Sturkie's Avian Physiology

Seventh Edition

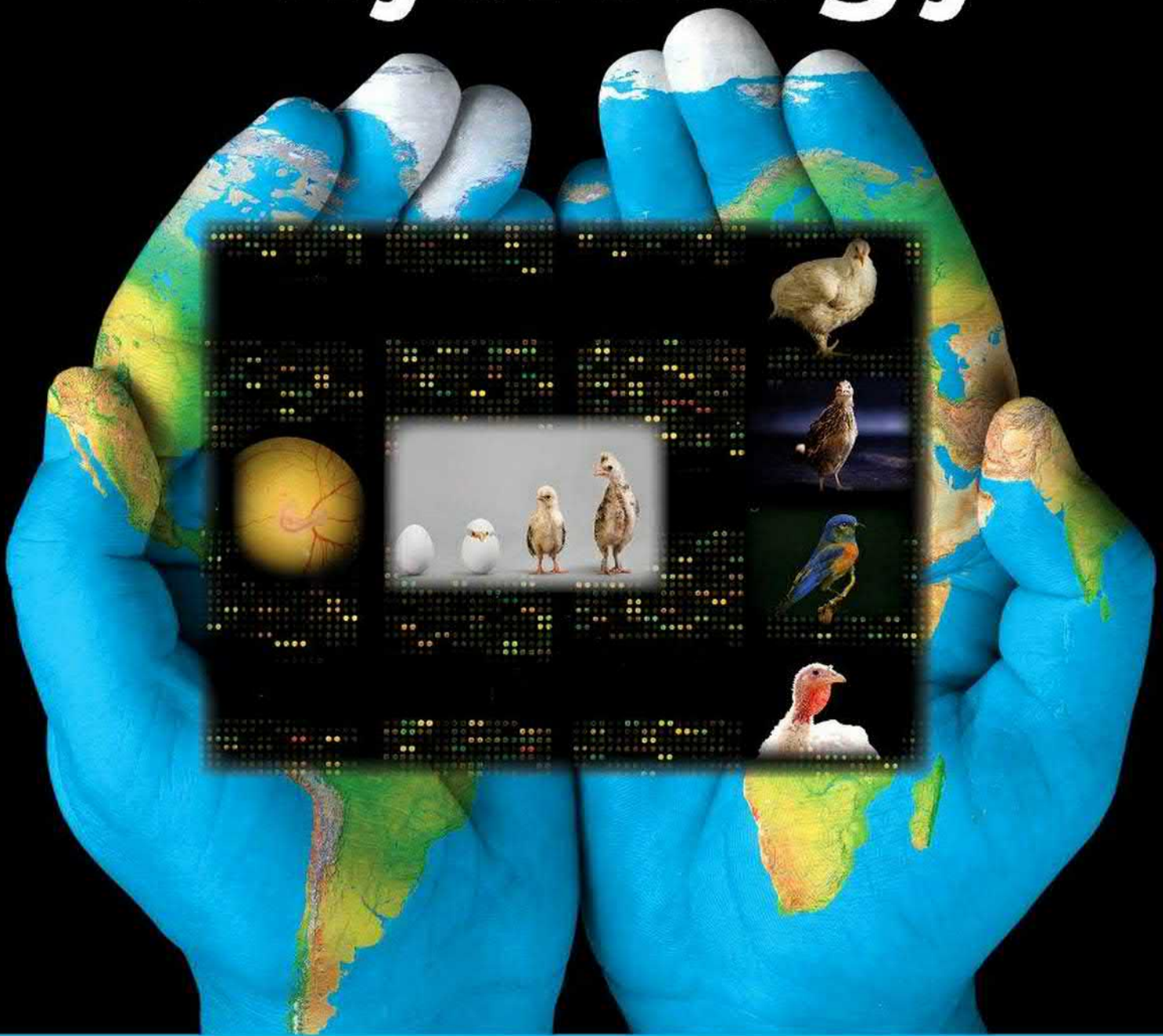

Edited by
Colin G. Scanes and Sami Dridi

Sturkie's Avian Physiology

Seventh Edition

Edited by
Colin G. Scanes
Department of Biological Science, University of Wisconsin, Milwaukee, WI, United States;
Center of Excellence for Poultry Science, University of Arkansas, Fayetteville, AR, United States
Sami Dridi
Center of Excellence for Poultry Science, University of Arkansas, Fayetteville, AR, United States

ACADEMIC PRESS
An imprint of Elsevier

Academic Press is an imprint of Elsevier
125 London Wall, London EC2Y 5AS, United Kingdom
525 B Street, Suite 1650, San Diego, CA 92101, United States
50 Hampshire Street, 5th Floor, Cambridge, MA 02139, United States
The Boulevard, Langford Lane, Kidlington, Oxford OX5 1GB, United Kingdom

Notices
Knowledge and best practice in this field are constantly changing. As new research and experience broaden our understanding, changes in research methods, professional practices, or medical treatment may become necessary.

Practitioners and researchers must always rely on their own experience and knowledge in evaluating and using any information, methods, compounds, or experiments described herein. In using such information or methods they should be mindful of their own safety and the safety of others, including parties for whom they have a professional responsibility.

To the fullest extent of the law, neither the Publisher nor the authors, contributors, or editors, assume any liability for any injury and/or damage to persons or property as a matter of products liability, negligence or otherwise, or from any use or operation of any methods, products, instructions, or ideas contained in the material herein.

Library of Congress Cataloging-in-Publication Data
A catalog record for this book is available from the Library of Congress

British Library Cataloguing-in-Publication Data
A catalogue record for this book is available from the British Library

ISBN: 978-0-12-819770-7

Publisher: Charlotte Cockle
Acquisitions Editor: Anna Valutkevich
Editorial Project Manager: Emerald Li
Production Project Manager: Selvaraj Raviraj
Cover Designer: Mark Rogers

Typeset by TNQ Technologies

To our mentors who have guided and inspired us and our families who have given us so much support.

Contributors

N.J. Beausoleil, Animal Welfare Science and Bioethics Centre, School of Veterinary Science, Massey University, Palmerston North, Manawatū, New Zealand

Charles M. Bishop, School of Natural Sciences, Bangor University, Bangor, Gwynedd, United Kingdom

Julio Blas, Department of Conservation Biology, Estación Biológica de Doñana, Consejo Superior de Investigaciones Científicas (CSIC), Seville, Spain

Walter Gay Bottje, Department of Poultry Science, Center of Excellence for Poultry Science, Division of Agriculture, University of Arkansas, Fayetteville, AR, United States

Kathleen R. Brazeal, School of Biological Sciences, University of Nebraska-Lincoln, Lincoln, NE, United States

Lindsay P. Brown, Department of Chemistry, University of Tennessee, Knoxville, TN, United States

Shane C. Burgess, College of Agriculture & Life Sciences, The University of Arizona, Tucson, AZ, United States

Warren W. Burggren, Developmental and Integrative Biology, Department of Biological Science, University of North Texas, Denton, TX, United States

Johan Buyse, Laboratory of Livestock Physiology, Department of Biosystems, Faculty of Bioscience Engineering, KU Leuven, Leuven, Belgium

Shawn R. Campagna, Department of Chemistry, University of Tennessee, Knoxville, TN, United States; Biological and Small Molecule Mass Spectrometry Core, University of Tennessee, Knoxville, TN, United States

Rocco V. Carsia, Department of Cell Biology and Neuroscience, Rowan University School of Osteopathic Medicine, Stratford, NJ, United States

Vincent M. Cassone, Department of Biology, University of Kentucky, Lexington, KY, United States

Natalia Cerón-Romero, Food and Animal Sciences, Alabama A&M University, Huntsville, AL, United States

Shira L. Cheled Shoval, Department of Animal Science, The Robert H. Smith Faculty of Agriculture, Food and Environment, The Hebrew University, Rehovot, Israel; Miloubar Feedmill, Ashrat Industrial Area, Israel

Hans H. Cheng, USDA, ARS, Avian Disease and Oncology Laboratory, East Lansing, MI, United States

Helen E. Chmura, Institute of Arctic Biology, University of Fairbanks, Fairbanks, AK, United States

Larry Clark, METIS, Ltd., Fort Collins, CO, United States

Mark A. Cline, Department of Animal and Poultry Sciences, Virginia Tech, Blacksburg, VA, United States

Jamie M. Cornelius, Department of Integrative Biology, Oregon State University, Corvallis, OR, United States

Dane A. Crossley, Department of Biological Sciences, University of North Texas, Denton, TX, United States

Veerle M. Darras, Department of Biology, KU Leuven, Leuven, Belgium

Karen D.M. Dean, University of Lethbridge, Lethbridge, AB, Canada

Eddy Decuypere, Laboratory of Livestock Physiology, Department of Biosystems, Faculty of Bioscience Engineering, KU Leuven, Leuven, Belgium

Mike Denbow, Department of Animal and Poultry Sciences, Virginia Tech, Blacksburg, VA, United States

Pierre Deviche, School of Life Sciences, Arizona State University, Tempe, AZ, United States

Sami Dridi, Center of Excellence for Poultry Science, University of Arkansas, Fayetteville, AR, United States

Joëlle Dupont, PRC (UMR 6175), INRA, Nouzilly, France; Unité de Physiologie de la Reproduction et des Comportements, Institut National de la Recherche Agronomique, Nouzilly, France

Vijay Durairaj, Huvepharma Inc., Lincoln, NE, United States

Edward M. Dzialowski, Department of Biological Sciences, University of North Texas, Denton, TX, United States

Nima K. Emami, Center of Excellence for Poultry Science, University of Arkansas, Fayetteville, AR, United States

Nadia Everaert, Precision Livestock and Nutrition Unit, TERRA Teaching and Research Centre, Gembloux Agro-Bio Tech, University of Liège, Gembloux, Belgium

Graham D. Fairhurst, School of Environment and Sustainability, University of Saskatchewan, Saskatoon, SK, Canada

Alison Ferver, Center of Excellence for Poultry Science, University of Arkansas, Fayetteville, AR, United States

Alexander R. Fisch, Department of Chemistry, University of Tennessee, Knoxville, TN, United States

Joel Gautron, BOA, INRAE, Université de Tours, Fonction et Régulation des protéines de l'œuf, Développement de l'œuf, Valorisation, Évolution, France

Elizabeth Gilbert, Department of Animal and Poultry Sciences, Virginia Tech, Blacksburg, VA, United States

David L. Goldstein, Department of Biological Sciences, Wright State University, Dayton, OH, United States

Elizabeth S. Greene, Center of Excellence for Poultry Science, University of Arkansas, Fayetteville, AR, United States

Christopher G. Guglielmo, Department of Biology, Advanced Facility for Avian Research, Western University, London, ON, Canada

Thomas P. Hahn, Department of Neurobiology, Physiology and Behavior, University of California, Davis, CA, United States

Orna Halevy, The Hebrew University of Jerusalem, Rehovot, Israel; The Ohio State University, Wooster, OH, United States

Maxwell Hincke, Department of Innovation in Medical Education; Department of Cellular and Molecular Medicine, Faculty of Medicine, University of Ottawa, Ottawa, ON, Canada

S.E. Holdsworth, Animal Welfare Science and Bioethics Centre, School of Veterinary Science, Massey University, Palmerston North, Manawatū, New Zealand

Christa F. Honaker, Department of Animal and Poultry Sciences, Virginia Tech, Blacksburg, VA, United States

Anna Hrabia, Department of Animal Physiology and Endocrinology, University of Agriculture in Krakow, Krakow, Poland

Alexander Jurkevich, Advanced Light Microscopy Core, University of Missouri, Columbia, MO, United States

John Kirby, College of the Environment and Life Sciences, The University of Rhode Island, Kingston, RI, United States

Michael H. Kogut, Southern Plains Agricultural Research Center, USDA-ARS, College Station, TX, United States

Daniel T. Ksepka, Bruce Museum, Greenwich, CT, United States

Christine Köppl, Cluster of Excellence "Hearing4all", Carl von Ossietzky University, Oldenburg, Germany; Research Center Neurosensory Science, Carl von Ossietzky University, Oldenburg, Germany; Department of Neuroscience, School of Medicine and Health Science, Carl von Ossietzky University, Oldenburg, Germany

Wayne J. Kuenzel, Poultry Science Center, University of Arkansas, Fayetteville, AR, United States

Vinod Kumar, Department of Zoology, University of Delhi, Delhi, India

H. Lehmann, Animal Welfare Science and Bioethics Centre, School of Veterinary Science, Massey University, Palmerston North, Manawatū, New Zealand

Scott A. MacDougall-Shackleton, Departments of Psychology and Biology, University of Western, London, ON, Canada

Graham R. Martin, School of Biosciences, University of Birmingham, Birmingham, United Kingdom

J.E. Martin, Royal (Dick) School of Veterinary Studies and the Roslin Institute, University of Edinburgh, Edinburgh, Scotland

Amanda L. May, Center for Environmental Biotechnology, University of Tennessee, Knoxville, TN, United States

Andrew E. McKechnie, South African Research Chair in Conservation Physiology, South African National Biodiversity Institute, Pretoria, Gauteng, South Africa; DSI-NRF Centre of Excellence at the FitzPatrick Institute, Department of Zoology and Entomology, University of Pretoria, Hatfield, Pretoria, Gauteng, South Africa

D.E.F. McKeegan, Institute of Biodiversity, Animal Health and Comparative Medicine, University of Glasgow, Glasgow, Scotland

Scott R. McWilliams, Department of Natural Resources Science, University of Rhode Island, Kingston, RI, United States

Henrik Mouritsen, Institut für Biologie und Umweltwissenschaften, Universität Oldenburg, Oldenburg, Germany; Research Centre for Neurosensory Sciences, University of Oldenburg, Oldenburg, Germany

Casey A. Mueller, Department of Biological Sciences, California State University San Marcos, San Marcos, CA, United States

Yves Nys, BOA, INRAE, Université de Tours, Fonction et Régulation des protéines de l'œuf, Développement de l'œuf, Valorisation, Évolution, France

Mary Ann Ottinger, Department of Biology and Biochemistry, University of Houston, Houston, TX, United States

Barbara J. Pierce, Department of Biology, Sacred Heart University, Fairfield, CT, United States

Tom E. Porter, Department of Animal and Avian Sciences, University of Maryland, College Park, MD, United States

Frank L. Powell, Department of Medicine Division of Pulmonary, Critical Care, Sleep Medicine, University of California, San Diego La Jolla, CA, United States

Monika Proszkowiec-Weglarz, United States Department of Agriculture, Agricultural Research Service, Animal Biosciences and Biotechnology Laboratory, Beltsville, MD, United States

Marilyn Ramenofsky, Department of Neurobiology, Physiology and Behavior, University of California, Davis, CA, United States

Narayan C. Rath, USDA/Agricultural Research Service and Department of Poultry Science, University of Arkansas, Fayetteville, AR, United States

Nicole Rideau, Recherches Avicoles, (UR 83), INRA, Nouzilly, France; Unité de Recherches Avicoles, Institut National de la Recherche Agronomique, Nouzilly, France

Alejandro B. Rodriguez-Navarro, Departmento de Mineralogia y Petrologia, Universidad de Granada, Spain

Colin G. Scanes, Center of Excellence for Poultry Science, University of Arkansas, Fayetteville, AR, United States; Department of Biological Sciences, University of Wisconsin, Milwaukee, WI, United States

Elizabeth M. Schultz, Department of Biology, Wittenberg University, Springfield, OH, United States

Paul B. Siegel, Department of Animal and Poultry Sciences, Virginia Tech, Blacksburg, VA, United States

Jean Simon, Recherches Avicoles, (UR 83), INRA, Nouzilly, France

Cynthia A. Smeraski, Science Education and Literacy Foundational Program, Fort Collins, CO, United States

Nurudeen Taofeek, Food and Animal Sciences, Alabama A&M University, Huntsville, AL, United States

Hiroshi Tazawa, Developmental and Integrative Biology, Department of Biological Science, University of North Texas, Denton, TX, United States

Zehava Uni, Department of Animal Science, The Robert H. Smith Faculty of Agriculture, Food and Environment, The Hebrew University, Rehovot, Israel

Sandra G. Velleman, The Hebrew University of Jerusalem, Rehovot, Israel; The Ohio State University, Wooster, OH, United States

Jorge A. Vizcarra, Food and Animal Sciences, Alabama A&M University, Huntsville, AL, United States

Brynn H. Voy, Department of Animal Science, University of Tennessee, Knoxville, TN, United States

Yajun Wang, Key Laboratory of Bio-resources and Eco-environment of Ministry of Education, College of Life Sciences, Sichuan University, Chengdu, Sichuan, PR China

Wesley C. Warren, Department of Animal Sciences, Bond Life Sciences Center, University of Missouri, Columbia, MO, United States

Heather E. Watts, School of Biological Sciences, Washington State University, Pullman, WA, United States

J. Martin Wild, Department of Anatomy and Medical Imaging, Faculty of Medical and Health Sciences, University of Auckland, Auckland, New Zealand

John C. Wingfield, Department of Neurobiology, Physiology and Behavior, University of California, Davis, CA, United States

Takashi Yoshimura, Laboratory of Animal Integrative Physiology, Graduate School of Bioagricultural Sciences, Institute of Transformative Bio-Molecules, Nagoya University, Nagoya, Aichi Prefecture, Japan

Huaijun Zhou, Department of Animal Science, University of California, Davis, CA, United States

Chapter 1

The importance of avian physiology

John C. Wingfield
Department of Neurobiology, Physiology and Behavior, University of California, Davis, CA, United States

The 20th century saw many revolutionary advances in the biological sciences. In 100 years, biology progressed from cataloging and describing species to sequencing the human genome. Along the way, astounding advances were made in cell and molecular biology, biomechanics, physiology, theoretical ecology, genetics, behavioral neurobiology, etc. These and other areas of the biological sciences continue to develop with Aves an important model group for links between environment and gene expression (e.g., Konishi et al., 1989). Environmental change including degradation, population, public health, food and energy production, education, and especially the public's understanding of science and technology are some of the most critical issues facing science and society. All of these pertain to biology. Technology and basic research in biological sciences have the potential to address the above issues, but they cannot be understood along traditional disciplinary lines. One enormous hurdle awaits 21st century biological research: how to integrate our knowledge of biology at all levels so we can pave the way for a deeper and broader understanding of how life on this planet works? This will also entail how to feed a still burgeoning population and educate future generations of undergraduates while conserving as much of the natural world as possible? If this were not enough, we must also deal with potentially catastrophic environmental problems resulting from climate change.

A major recurring problem with the spectacular success biology has experienced is that individual investigators have become so specialized and focused that in many cases they have, understandably, lost track of other disciplines. There is a growing consensus that biologists within disciplines have difficulty communicating with colleagues in other branches of biology. Clearly, the problems we face in the next decades will be solved only by taking broad integrative approaches involving expansive, multidisciplinary collaborations. In other words, molecular biology or theoretical ecology in isolation will not resolve problems that involve populations, their component individuals, as well as the complex interplay of physiology, behavior, cells, and molecules by which individuals function and interact. Management and control of these issues in relation to natural resources will also be difficult unless there are incentives to foster interdisciplinary research, integrate education, and maximize our potential to address problems by bringing to bear all of our knowledge in an effective way. Citing a report from the National Academy of Sciences, Jasanoff et al. (1997) assert that in the next decades, young scientists will be impeded in their advancement unless they are trained from an early age to diversify their expertise and career objectives.

As an example of the need to integrate ecology, behavior, and evolutionary biology with mechanisms at physiological, genetic, cell, and molecular levels, we can consider the functions of a differentiated cell in which complex interactions of many proteins occur. These functions can be modified by hormones that coordinate gene activity among various cells and tissues of the organism leading to the ultimate responses to internal and external environmental signals. A critical question is then how do hormones orchestrate transitions in morphology, physiology, and behavior of individual organisms in relation to a changing, and sometimes capricious environment? We can imagine observing an ecosystem and focusing on certain populations of individuals within it that have problems dealing with change in the environment triggered by, for example, human disturbance. It quickly becomes apparent that some populations, and individuals within them, deal with the environmental challenges better than others. It is reasonable to then ask what aspects of their physiology, behavior, and morphology are the causes of this failure, or success, and what the cell, molecular, and genetic bases of these differences might be. The investigation of interindividual variation will be another foundation for understanding how populations will evolve in response to environmental change. It is relatively simple to construct hypothetical scenarios whereby we traverse the spectrum of

Sturkie's Avian Physiology. https://doi.org/10.1016/B978-0-12-819770-7.00004-9

biological science from ecosystem to molecule in either direction, but it is not so intuitively obvious how we do this in practical terms. If such an interdisciplinary and integrative approach can be achieved, it will be possible to determine how we will deal with global changes already underway and ultimately prepare future generations to cope with ongoing changes.

Avian physiology has a long history of providing models for integration of disciplines, and it will continue in this role in the future (Konishi et al., 1989). In general, there are exceptionally broad data bases for birds on ecology and evolution across the globe. Match this with rapidly developing tools at genomic, transcriptomic, and epigenetic levels, then avian physiology is uniquely poised midway along the spectrum from genes to environmental to explore the molecular bases of adaptation and the integration of ecological and evolutionary aspects at the interfaces of morphology, physiology, and behavior. In addition, many wild avian species are abundant and easy to study making them ideal subjects for field observations and experiments in their natural environment, as well as in laboratory experimentation. Specific examples how avian physiology has played a major role in the development and integration of biological processes at many functional levels are discussed next.

1.1 Specific examples of the importance of avian physiology

Avian physiology has its roots in over 100 years of research on domesticated species, particularly the domestic fowl (*Gallus gallus*) as presented in the original version of Sturkie's Avian Physiology (Sturkie, 1954). Over the decades since there have been huge advances in avian physiology focused primarily on the poultry industry and food production. Then in the early 21st century, the chicken genome was sequenced and annotated (e.g., Burt, 2005; Burt and Pourquie, 2003). This opened up a new generation of biological studies at many of the interfaces outlined above, and was followed by sequencing the genome of a songbird, the zebra finch, *Taeniopygia guttata* (Warren et al., 2010). As technologies developed to sequence genomes more quickly and cheaply, the genomes of many other species have been sequenced as part of ambitious and exciting projects to eventually sequence the genomes of all the extant species of birds and some extinct ones as well (e.g., Zhang et al., 2014). If successful, such an unprecedented data base will allow analyses at so many levels of biological function. However, it should be borne in mind that the computational technologies to analyze such enormous amounts of data and integrate them with other diverse and unique data bases on morphology, physiology, behavior, and environment are huge challenges. Avian physiology will be a central focus for such integration. The examples given below are by no means all inclusive and new concepts and research directions are inevitable.

1.1.1 Physiology and poultry production

Physiological functions of domestic fowl from reproduction and growth to responses to diseases and stress such as weather factors (especially heat) also triggered thorough investigations of environmental biology and hormonal control of these processes (see Sturkie's Avian Physiology revised editions from 1954 to 2020). The domestic fowl and some other domesticated species (e.g., quail. duck, turkey) provide phenomenally broad data bases of physiology that rival those of mammals and fish. These in turn provide endless opportunities for other studies on wild species and gene-environment interactions—the foundations of understanding adaptation to a changing world.

1.1.2 Physiological ecology and birds, marine, freshwater, and terrestrial

Birds have played a central role in the development of physiological ecology, especially building on the vast array of data, techniques and tools made available from agricultural research (Phillips et al., 1985; Konishi et al., 1989). Avian physiological ecology is a thriving branch of biology that has provided a framework for other emerging topics such as environmental endocrinology, the regulation of seasonal changes in physiology, and individual differences and fitness. (e.g., Hau et al., 2010; Taff and Vitousek, 2016). Avian migration is a prime example of the integration of physiological systems that has benefitted enormously from avian physiology in general (Newton, 2010; Dingle, 2014; Ramenofsky and Wingfield, 2007). This has fueled investigations of one of the most integrative biological processes—the evolution, ecology, morphology, physiology, and behavior of movements across the environment in general.

Fundamental and applied research on domestic fowl has enriched development of avian physiology in relation to the comparative biology of environmental stress (Romero and Wingfield, 2016). All organisms must be able to cope with perturbations of the environment that are largely unpredictable, but require individuals to express facultative physiological and behavioral responses to cope. The "stress response" is common to most, if not all, organisms from bacteria and plants to invertebrate as well as vertebrate animals. Although the mechanisms involved vary fundamentally from plants to animals, they are well conserved within the vertebrates making avian systems excellent models. One aspect of climate change is the increase in frequency, duration, and intensity of extreme weather

events such as unseasonal storms, hurricanes, and typhoons. Understanding how some populations cope with these unpredictable events and others do not will have profound implications for understanding adaptation and consequences for conservation and agriculture.

New emerging avian models such as the zebra finch, great tit (*Parus major*, Santure et al., 2011), white-throated sparrow (*Zonotrichia albicollis*, Tuttle, 2003), and dark-eyed junco (*Junco hyemalis*, Ketterson and Atwell, 2016) and others, provide field and laboratory contexts for understanding physiological ecology as well as advancing basic research in neurobiology such as the physiology underlying behavioral patterns and avian song control systems (see Konishi et al., 1989; Pfaff and Joëls, 2017). These approaches using experiments both in the laboratory and the field have allowed the beginning of investigations of coping with climate change, shifts in habitat range, urbanization etc. (e.g., Partecke et al., 2006; Fokidis et al., 2009; Martin et al., 2010; Bonier, 2012; Caro et al., 2013; Visser and Gienapp, 2019). Birds have become important examples of models for conservation physiology (Wikelski and Cooke, 2006; Madlinger et al., 2016). For example, avian physiology is providing critical insights into one of the most important aspects of conservation—the impact of invasive species resulting from human activity as well as range expansions and contractions that have important and often devastating impacts on the survival of indigenous species from plants to mammals.

Another spin-off from avian physiology is the use of birds as sentinels of endocrine disruption—physiology, morphology, and behavior (National Research Council, 1999; Dawson, 2000; Norris and Carr, 2006; Carere et al., 2010). Although the responses of plants, invertebrates, as well as vertebrates, in general, are all important foci to document toxicology and endocrine disruption, the use of birds as models, and their well-known physiology both in the laboratory and field once again provide a useful model for understanding how organisms respond to disasters such as leakage of toxic chemicals, oil spills, etc. An example of a remaining critical issue of endocrine disruption is how organisms will cope with the now ubiquitous and global distribution of chemical mixtures in varying concentrations and how we may be able to ameliorate some of the effects of endocrine disruption by broad ranging "clean up" programs to levels of chemicals that organisms can at least tolerate?

1.2 Conclusions

Reading Sturkie's original avian physiology text (Sturkie, 1954), it is astonishing to learn how avian physiology has developed, expanded, and progressed in almost 70 years. The contributions of avian physiology to agriculture, biomedicine, veterinary science, and practice, as well as fundamental biology are vast. In the 21st century, with technologies until recently unimagined, these contributions will continue. What could not have been envisaged all those decades ago is how avian physiology has helped pioneer, initiate and develop new environmental aspects of biological sciences such as morphology and behavior at the interfaces with gene-environment interactions and coping with global change from urbanization, endocrine disrupting pollutants, and invasive species to the burgeoning effects of climate change. There is no question that avian physiology is very important and will continue to be at the cutting edge of so many branches of biological sciences. It will continue to influence not only basic research but also policy in managing planet Earth for future generations.

References

Bonier, F., 2012. Hormones in the city: endocrine ecology of urban birds. Horm. Behav. 61, 763–772.

Burt, D., 2005. Chicken genome: current status and future opportunities. Genome Res. 15, 1692–1698.

Burt, D., Pourquie, O., 2003. Chicken genome- science nuggets to come soon. Science 300, 1669.

Carere, C., Costantini, D., Sorace, A., Santucci, D., Alleva, E., 2010. Bird populations as sentinels of endocrine disrupting chemicals. Ann. 1st. Super Sanita 46, 81–88. https://doi.org/10.4415/ANN_10_01_10.

Caro, S.P., Schaper, S.V., Hut, R.A., Ball, G.F., Visser, M.E., 2013. The case of the missing mechanisms: how does temperature influence seasonal timing in Endotherms? PLoS Biol. 11, e1001517.

Dawson, A., 2000. Mechanisms of endocrine disruption with particular reference to occurrence in avian wildlife: a review. Ecotoxicology 9, 9–69.

Dingle, H., 2014. Migration: the Biology of Life on the Move, second ed. Oxford Univ Oxford.

Fokidis, H.B., Orchinik, M., Deviche, P., 2009. Corticosterone and corticosterone binding globulin in birds: relation to urbanization in a desert city. Gen. Comp. Endocrinol. 160, 259–270.

Hau, M., Ricklefs, R.E., Wikelski, M., 2010. Corticosterone, testosterone and life history strategies of birds. Proc. R. Soc. B 277, 3203–3212.

Jasanoff, S., Colwell, R., Dresselhaus, M.S., Goldman, R.D., Greenwood, M.R.C., Huang, A.S., Lester, W., Levin, S.I., Linn, M.C., Lubchenco, J., Novacek, M.J., Roosevelt, A.C., Taylor, J.E., Wexler, N., 1997. Conversations with the community: AAAS at the millennium. Science 278, 2066–2067.

Ketterson, E.D., Atwell, J.W., 2016. Snowbird: Integrative Biology and Evolutionary Diversity in the Junco. Univer Chicago Press, Chicago.

Konishi, M., Emlen, S., Ricklefs, R., Wingfield, J.C., 1989. Contributions of bird studies to biology. Science 246, 465–472.

Madlinger, C.L., Cooke, S.J., Crespi, E.J., Funk, J.L., Hultine, K.R., Hunt, K.E., Rohr, J.R., Sinclair, B.J., Suski, C.D., Willis, C.K.R., Love, O.P., 2016. Success stories and emerging themes in conservation physiology. Cons. Physiol. 4, 206. https://doi.org/10.1093/conphys/cov/057.

Martin, L.B., Hopkins, W.A., Mydlarz, L.D., Rohr, J.R., 2010. The effects of anthropogenic global changes on immune functions and disease resistance. Annals NY Acad. Sci. https://doi.org/10.1111/j.1749-6632.2010.05454.x.

National Research Council, 1999. Hormonally Active Agents in the Environment. National Academy Press, Washington DC.

Newton, I., 2010. The Migration Ecology of Birds. Academic Press (Elsevier), New York.

Norris, D.O., Carr, J.A. (Eds.), 2006. Endocrine Disruption. Oxford Univ Press, New York.

Partecke, J., Schwabl, I., Gwinner, E., 2006. Stress and the city: urbanization and its effects on the stress physiology in European blackbirds. Ecology 87, 1945–1952.

Pfaff, D.W., Joëls, M. (Eds.), 2017. Hormones, Brain and Behavior, third ed. Academic Press, New York.

Phillips, J.G., Butler, P.J., Sharp, P.J., 1985. Physiological Strategies in Avian Biology. Blackie and Son, Glasgow and London.

Ramenofsky, M., Wingfield, J.C., 2007. Regulation of migration. BioSci 57, 135–143.

Romero, L.M., Wingfield, J.C., 2016. Tempests, Poxes, Predators and People: Stress in Wild Animals and How They Cope. Oxford Univ Press, Oxford.

Santure, A.W., Gratten, J., Mossman, J.A., Sheldon, B.C., Slate, J., 2011. Characterization of the transcriptome of a wild great tit, *Parus major*, by next generation sequencing. BMC Genom. 12, 283.

Sturkie, P.D., 1954. Avian Physiology. Cornell University Press, Ithaca.

Taff, C.C., Vitousek, M.N., 2016. Optimizing phenotypes in a dynamic world? Trends Ecol. Evol. 31, 476–488. https://doi.org/10.1016/j.tree.2016.03.005.

Tuttle, E.M., 2003. Alternative reproductive strategies in the white-throated sparrow: behavioral and genetic evidence. Behav. Ecol. 14, 425–432.

Visser, M., Gienapp, P., 2019. Evolutionary and demographic consequences of phonological mismatches. Nat. Ecol. Evol. 3, 879–885. https://doi.org/10.1038/s41559-019-0880-8.

Warren, W.C., Clayton, D.F., Ellegren, H., Arnold, A.P., et al., 2010. The genome of a songbird. Nature 464. https://doi.org/10.1038/nature08819.

Wikelski, M., Cooke, S.J., 2006. Conservation physiology. Trends Ecol. Evol. 21, 38–46.

Integration of ecology and endocrinology in avian reproduction: a new synthesis. In: Wingfield, J.C., Visser, M.E., Williams, T.D. (Eds.), Phil. Trans. R. Soc. Ser. B 363.

Zhang, G., Li, B., Gilbert, M.T.P., Jarvis, E.D., Wang, J., 2014. Comparative genomic data of the avian phylogenomics project. Giga Sci. 3, 26. http://www.gigasciencejournal.com/content/3/1/26.

Chapter 2

Avian genomics

Hans H. Cheng[1], Wesley C. Warren[2] and Huaijun Zhou[3]
[1]USDA, ARS, Avian Disease and Oncology Laboratory, East Lansing, MI, United States; [2]Department of Animal Sciences, Bond Life Sciences Center, University of Missouri, Columbia, MO, United States; [3]Department of Animal Science, University of California, Davis, CA, United States

2.1 Introduction

All fields of biology have been greatly influenced by the generation of complete genome assemblies. This impact is most apparent with the findings and resulting applications from the Human Genome Project (HGP), which has transformed biomedical science (Green et al., 2015). Hoping for a similar transformation in agriculture, a genome assembly was first made for chicken in 2004 (International Chicken Genome Sequencing Consortium, 2004). More recently, as the feasibility and economics of generating a genome assembly increased, the number of species across all avian orders has increased dramatically (e.g., 48 were produced and analyzed in the landmark Zhang et al. (2014) paper), which strongly suggests that the field of genomics will only grow in its ability to shape the future direction for all fields of avian biology.

The original justification for having a genome assembly was to get a complete "parts list" of elements that contribute to an organism's phenotype with the primary goal being the identification and location of all genes. However, it soon become readily apparent that genomes were much more than just sequences that code for proteins; protein-coding regions account for ~1% of the human genome. Thus, current efforts have been focused on finding other relevant functional elements, such as noncoding elements that regulate when, where, and how much specific genes and/or particular isoforms are expressed. As these annotation efforts become more complete, the power and utility of genomes to inform other biological fields, like physiology, will become more apparent and enhanced.

Besides providing an incredible resource, genome assemblies and the field of genomics have fundamentally changed how experimental biology is conducted. It is now common to begin with discovery-based genomics science to build agnostic large datasets to analyze, which contrasts with traditional, reductionist hypothesis-based experiments. For example, many studies now start with transcriptome profiling (RNA sequencing) with the goal of generating hypotheses on what relevant genes and pathways to investigate further. Without genomics and its accompanying tools and resources, this approach would not have been possible. It is likely that this trend will only increase as more genomes are sequenced and functionally understood, along with the continuing development of more empowering and economical genomic-based technologies, and the desire to have and integrate multidimensional types of data to help understand complex biological problems. Having stated this, traditional experiments and the detailed information that they provide at many levels are still critical needs and inputs to truly empower avian genomes. In short, genomics adds another powerful approach to understanding biology.

Our target audience of this chapter is avian physiologists who might not be aware of the field of genomics. Specifically, we briefly summarize the current status of avian genome assemblies with the focus on chicken, as this is the most developed avian species to date, and common approaches that focus on DNA-based genomics. Key references are provided in each subsection to aid further reading.

2.2 Genome

2.2.1 Size

Eukaryotic genomes vary immensely, over 60,000-fold, from as small as 2.3 Mb for *Encephalitozoon intestinalis*, an intestinal parasite of humans and animals, to as large as 150 Gb found in the plant *Paris japonica* (Elliott and Gregory, 2015). This range in genome size, which does not correlate with organismal complexity (commonly referred to as the C-value paradox), has been recognized for a long time (Swift, 1950). However, genome size does seem to correlate positively with cell size and negatively with cell division rate (Elliott and Gregory, 2015). When considering

Sturkie's Avian Physiology. https://doi.org/10.1016/B978-0-12-819770-7.00047-5

only vertebrates, the size range (0.35−133 Gb) is less but still large (333-fold) (www.genomesize.com). In contrast to most other taxa, the interspecific variation for bird genome size is quite narrow − 0.9 Gb for the black-chinned hummingbird to 2.1 Gb for the ostrich; see Damas et al. (2019) for a more comprehensive review. The likely explanation for the relatively small genome size and stability of avian genomes is the low occurrence of transposable elements (TEs) and the loss of large segments that could counteract any TE expansion, which is the main driving force for the increase (Kapusta et al., 2017). Of interest to physiologists is the observation that genome size variation within bird species is associated with metabolism with smaller genomes having higher metabolic rates (Gregory, 2002).

2.2.2 Karyotype

Avian species are unique in having fairly high number of chromosomes. The majority of the species have 74 to 86 total chromosomes, which is equivalent to 37 to 43 pairs, though the reported range is 40 to 126 chromosomes (Griffin et al., 2007). The chicken karyotype is fairly typical (Fig. 2.1). It possesses 39 pairs of chromosomes, 38 pairs of autosomes and the Z and W sex chromosomes; unlike mammals, males are the homogametic sex (ZZ). An unusual feature of avian chromosomes is the variation in size distribution. Although arbitrarily defined as (1) macrochromosomes—autosomes one to five plus the Z chromosome are comparable in size to mammalian chromosomes, (2) intermediate microchromosomes—autosomes 6 to 10 and the W chromosome are similar in size to smaller human chromosomes, and (3) microchromosomes—all the remaining autosomes (11 to 38). The microchromosomes can be identified only through fluorescent in situ hybridization using specific probes (e.g., Romanov et al., 2005; Delany et al., 2009; Zhang et al., 2011). Due to their small size and the need for at least one recombination event during meiosis, microchromosomes are more gene dense, GC-rich in sequence content, and have higher recombination rates compared to macrochromosomes (International Chicken Genome Sequencing Consortium, 2004).

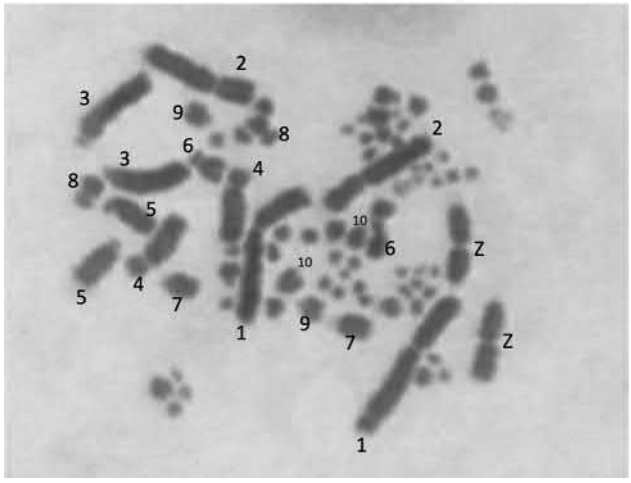

FIGURE 2.1 Mitotic metaphase chromosomes of a male (ZZ) chicken illustrating macro- and microchromosomes and the sex chromosomes. The cell shown was stained with the fluorochrome DAPI, which stains DNA and the image then inverted to black/white. Chromosome pairs one to nine and the Z are indicated by numbers. *Figure contributed by M.E. Delany, University of California, Davis, CA.*

2.3 Genome assemblies

2.3.1 Chicken legacy genomes

Since the first assembled chicken genome in 2004 (International Chicken Genome Sequencing Consortium, 2004) that used Sanger sequencing efforts, improvements in quality have closely followed the technological advancements in sequencing and mapping (Schmid et al., 2015). Furthermore, multiple upgrades (Gallus_gallus-2.1, 4.0, 5.0, GRCg6a) have greatly benefited from the better assembly of segmental duplications (SDs) (Eichler et al., 2004), closure of scaffold gaps, specialized approaches to resolve the complex sequence structure of the avian sex chromosomes (Bellott et al., 2018), and traditional bacterial artificial chromosome (BAC) clonal sequencing efforts that have improved sequence representation of chicken chromosome 16 (GGA16), which contains the major histocompatibility complex (MHC) (Miller and Taylor, 2016). Many of the genes, critical in governing immune responses, across species are clustered, multigenic families containing individual members that vary across haplotypes with intricate differences in sequence.

As with other vertebrate genomes, in chicken, a recurring hurdle to accurate computational experimentation is falsely collapsed or redundant SDs, repetitive elements and fragmented sex chromosome assemblies, mostly due to the organization of highly identical sequences that confuse de novo assembly attempts at constructing simple bifurcating graphs of each haplotype. Bellott et al. (2010) provide an exemplary case of the difficulties encountered where identification of a tandem array of four testis-expressed genes that constitutes ∼15% of the Z chromosome, one-fifth of all chicken SDs and in total about a third of the protein-coding genes on Z. Study of the W sex chromosome illustrates even more extreme heterochromatin stretches and a tandemly arranged gene with 40 copies (Bellott et al., 2017). It is well known that such duplications are frequently missed ("over-collapsed") in draft quality assemblies that they are common sites of copy number variation (CNV), and that such variation frequently have major phenotypic consequences (Conrad et al., 2010). Another example is that of the MHC-*B* complex in chicken on GGA16 (one of the smallest microchromosomes), a

region of great immunological importance with many gene duplications and CNVs. Directed sequencing of selected chicken BACs was critical to elucidate the partial organization of this region (Shiina et al., 2007), but in the future extreme sequence lengths (>500 Kb), such as the outcome of Oxford Nanopore sequencing technology, will be needed for gap-free genome sequence characterization.

Over the years, genetic linkage maps comprised of ordered and oriented molecular markers have helped to guide the genome assembly chromosome build. However, even though the consensus chicken genetic linkage map contains 50 linkage groups (Groenen et al., 2000), several microchromosomes were missing sequence marker alignments to a linkage group and still today chicken genome references have not captured the full autosome composition. This is of primary importance to the avian genome analysis process, especially given the high gene density per microchromosome. Recently improved sequencing and de novo assembly approaches or alternatively the use of advancing cytogenetic techniques will be crucial in efforts to assemble and assign these missing microchromosomes. In the current reference, GRCg6a, many of these unassigned sequences are likely found within the unplaced bin of chicken assembly reference files. However, in GRCg6a, there are only 14 Mb of unplaced contigs and scaffolds indicating there is also an inability to sequence or assemble some of these microchromosomes.

Ideally, the goal is to have complete sequence representation of all 40 chicken chromosomes, this includes Z and W sex chromosomes, but, of course, today this is not technically feasible for any vertebrate genomes, even human, although a recent telomere to telomere assembly of human X is encouraging (Miga et al., 2020). This study also highlights the incredible amount of manual curation that is needed to achieve this feat. Basically, automated methods to stitch together complex sequence structures still requires significant human intervention. Although the reasons for the breaks in vertebrate assembly contiguity "gaps" aren't always apparent, the usual culprits are repeats and base composition distortions, such as high GC homopolymers. In the chicken, we have observed assembly gap edges including elevated GC content approaching 75% in some regions and low-complexity sequences (International Chicken Genome Sequencing Consortium, 2004). Collectively this loss of sequence knowledge demonstrates more work is essential to not limit impending experiments. Of late, through longer read lengths, improved de novo assembly algorithmic methods and evolving mapping technology the ability to close ~80% of existing spanned gaps within assembled scaffolds, scaffolds defined as an ordered collection of contigs, are feasible (Bickhart et al., 2017; Koren et al., 2018).

2.3.2 Future chicken genome assembly

A need to represent the genome variation that exists within species has recently led to pangenome reference efforts (Computational Pan-Genomics Consortium, 2018). In chicken, a pangenome reference build must include mainstream and rare breeds, as well as commercially selected lines, both layers and broilers. De novo assembly methods, continue to evolve rapidly, where best practice is now, when possible, long-read sequencing of an F1 offspring and use of short reads from the parents to near fully phase haploid genomes of their offspring (Koren et al., 2018). In fact, the success of this approach has been recently documented for 16 vertebrate genomes, including bird species (Rhie et al., 2021). Assemblies created with this method offer more accurate assessments of complex structural variation (Kronenberg et al., 2018) and for some chromosomes gap-free starting points, such as human X that was spanned telomere-to-telomere (Miga et al., 2020).

In chicken, the primary objectives are to reduce sequence gaps and correct misassemblies that exist in the GRCg6a reference. Currently single haplotype genome references for an F_1 cross of a commercial layer (paternal) and broiler (maternal) line are under construction using this technique. Preliminary measures of sequence contiguity completeness show N50 contig "ungapped" lengths of 16 and 14 Mb in paternal and maternal genomes, respectively. After iterative scaffold builds with a long fragment physical map (BioNano) and chromosomal proximity ligation data, the near theoretical chromosome N50 scaffolds lengths of 60 and 89 Mb for paternal and maternal genomes is achieved, respectively. Further curation of these single haplotype assemblies promises to advance chicken genetic research by resolving much of the sequence structure presently fragmented and misappropriated in the GRCg6a reference.

2.3.3 Genes

The original chicken genome assembly estimated there were 20,000−23,000 protein-coding genes (International Chicken Genome Sequencing Consortium, 2004). However, more recent estimates from the comparison of 48 avian genomes indicates the number for bird genomes is lower at 15,000−16,000 (Zhang et al., 2014). Based on this number, this would reflect a ~30% reduction compared to the number found in mammals. At least 1241 of the loss in genes can be explained by large segmental deletions during the evolution of birds. However, ~70% of the lost genes show paralogs suggesting functional compensation. In addition, some of the gene loss may not be true but rather the inability to detect genes in high GC-rich regions (Bornelov et al., 2017).

Avian genes are ~50% smaller than their mammalian counterparts, mainly due to the shortening of introns and reduced distances between genes, which helps to account for the reduced size of avian genomes. Interestingly, with respect to avian-specific highly conserved elements, most are significantly associated with transcription factors associated with metabolism. Having a complete list of genes in many avian species has also enabled hypotheses on the evolution of flight, diets, vision, and reproductive traits (Zhang et al., 2014).

2.3.4 Transposons and endogenous viral elements

Avian genomes have a relatively low amount of TEs. In chicken, the most abundant TE is chicken repeat 1 (CR1), a long interspersed nucleotide element that with 200,000+ copies, comprises over 80% of all interspersed repeats in the chicken genome (International Chicken Genome Sequencing Consortium, 2004). A complete CR1 element is 4.5 kb in length, however, more than 99% of CR1 elements are truncated from their 5′ end, which is necessary for retrotransposition. Short interspersed nuclear element transposons are extremely rare, which contrasts to all other vertebrate genomes.

With respect to endogenous viral elements, analysis of 48 avian genomes has shown that there are five families of endogenous viruses—Retroviridae, Hepadnaviridae, Circoviridae, Parvoviridae, and Bornaviridae (Cui et al., 2014). However, over 99+% of these are endogenous retroviruses (ERVs), and the copy number of these elements range from 132 to 1032. There is great interest in ERVs as they are likely to contribute to evolution of gene expression and, thus, contributing to complex traits including ones for physiology. In humans, there are ~110,000 ERVs that contain over 300,000+ transcription factor binding sites (Buzdin et al., 2017). As many chicken ERVs are found in promoters and introns, they are likely to play a similar role.

2.3.5 Genome browsers

The chicken genome can be queried multiple ways using the major established genome browsers: Ensembl (https://useast.ensembl.org/index.html), NCBI (https://www.ncbi.nlm.nih.gov), and UCSC (https://genome.ucsc.edu/). Each genome browser offers a gateway to varied data types and search abilities for your sequence of interest. For example, using the UCSC genome browser any chicken chromosome can feature Ensembl or NCBI gene annotation, aligned mRNAs, conserved sequence chains against other vertebrates, simple repeats, CRISPR targets, and much more (Fig. 2.2). One can display a gene of interest, for example, the T cell receptor *CD3E*, and evaluate all putative targets for editing its gene structure as well as surrounding genes and their associated functional features. Future iterations of these browsers and new ones, such as FAANGMine.org for exploring sequence structures associated with gene regulation, will be of great value for researchers seeking information to design functional experiments in poultry. Another portal created by the Genome Reference Consortium (GRC; https://www.ncbi.nlm.nih.gov/grc) exists to report errors in the underlying chicken genome reference by the community. The GRC will ensure this resource continues to attain higher levels of reference quality and reporting accessibility with its readily useable web interface. All these public access points bode well for the continued use of this resource and advancing the knowledge of avian genome biology.

2.4 Connecting genome sequence to phenotype

2.4.1 Connecting genotype to phenotype

As discussed previously, a major driving force for generating genome assemblies was to accelerate the power of biology, and especially in the ability to identify the elements that define the makeup of an organism. Put another way, for few exceptions, while every cell in a chicken has the same DNA sequence, these cells vary greatly in many biological attributes primarily due to differences in gene expression. Couple this existing variation with genetic variation, then one begins to understand how the genome contributes to the wide diversity of traits observed within and between bird species. A mechanistic understanding of these processes can be harnessed to solve many important questions such as improvement of health, growth, reproduction, etc.

In the following sections, we briefly discuss the major approaches used to identify features in avian genomes that define trait variation observed in organisms.

2.4.2 Genome wide association study

It's been known for a long time that many traits have a genetic basis. A prime example is the tremendous progress made by poultry breeders to improve agronomic traits. However, prior to the genome sequence, identifying the underlying causative gene or genes was a very difficult task. Two contributing reasons for the lack of precision were (1) most traits are complex and controlled by many genes, each of which have can only have a small effect, and (2) there was a lack of known genetic markers that could survey the majority of the chicken genome.

The second deficiency was largely removed with the advent of the chicken genome assembly. More specifically, by sequencing additional chickens, millions of single nucleotide polymorphisms (SNPs) were identified that

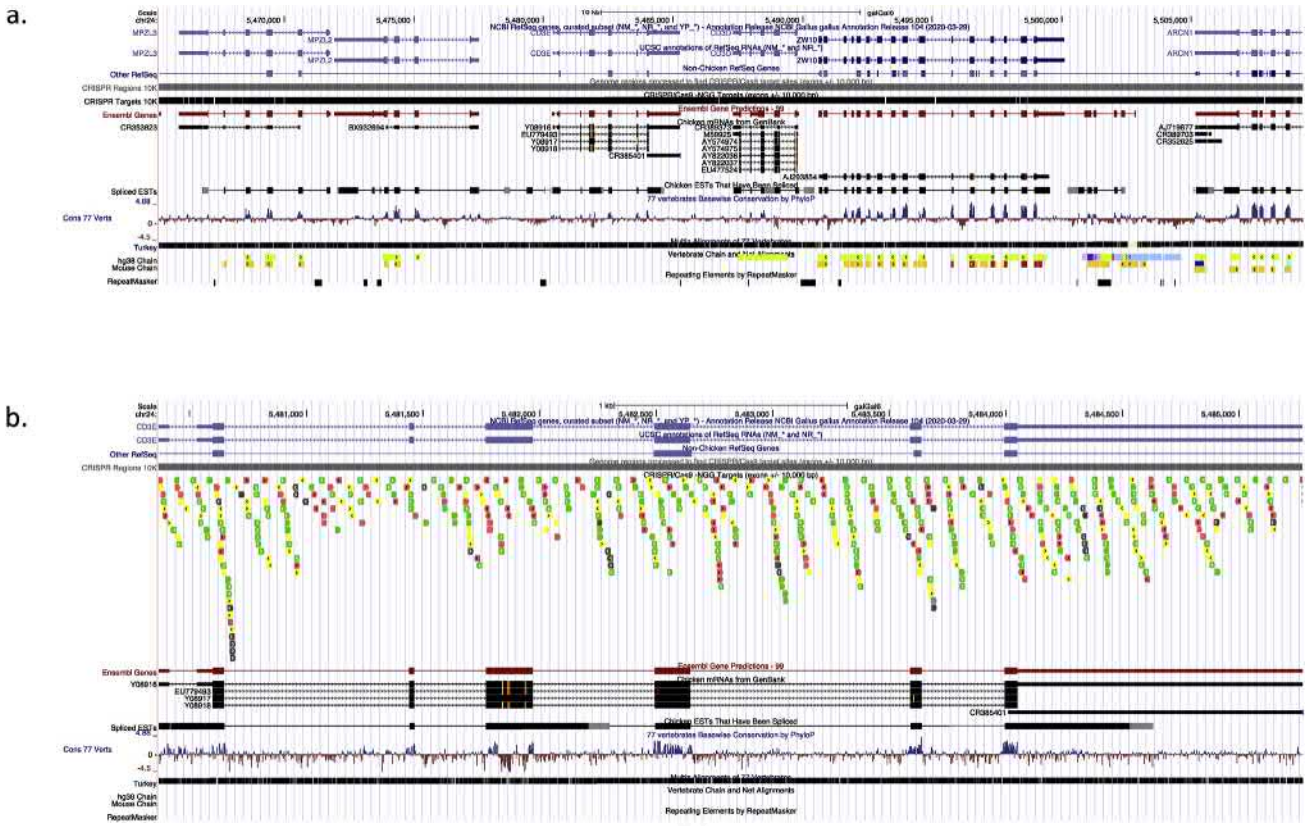

FIGURE 2.2 A UCSC Genome browser representation of GRCg6a chromosome 24. (A) regional overview at 44 kb window size that highlights the T cell receptor gene CD3E with other annotation tracks, (B) a higher resolution overview (4.9 kb) of the CD3E gene where the track is shown for CRISPR gene editing targets in this gene are represented by *multicolor boxes*.

could serve as genetic markers (International Chicken Polymorphism Map Consortium, 2004). Combined with affordable arrays that could determine the genotype tens to hundreds of thousands genetic variants, it was now feasible to survey the entire chicken genome. Studies that survey large numbers of birds with SNP chips are known as genome wide association studies or GWAS, for short; for more comprehensive reviews, see Uitterlinden (2016), Dehghan (2018), Tam et al. (2019). As a result, currently Animal QTLdb (animalgenome.org) lists 11,818 trait associations from 318 publications for chicken alone.

A typical GWAS experiment to dissect a complex trait requires thousands, if not tens of thousands of individuals, to have both genotype data from SNP chips and phenotypic data. Then statistical analysis is used to determine whether each SNP contributes to the trait of being studied. GWAS power is greatly enhanced by having more individuals surveyed and accurately measured phenotypes.

Like any genomic screen, the primary objective of GWAS is to identify candidate genes to interrogate further. Stated differently, while GWAS has revolutionized the genetic analysis of complex traits, any associated SNP is unlikely to be causative and only linked to the underlying causative genetic variant. Thus, further experimentation is needed to validate and better refine the association in order to identify the relevant gene or regulatory element.

Besides identifying trait associations, large-scale genotyping efforts can have other applications. One that might be more relevant to surveying avian diversity is the ability to define population structure. One of the first examples in birds was the study to examine whether heavily selected chicken populations were losing alleles (Muir et al., 2008).

2.4.3 Resequencing

Another major technological advancement that greatly impacted genomics was the development of next generation sequencing (NGS); for reviews on the NGS technologies, impact, and history see Koboldt et al. (2013), Goodwin et al. (2016), Heather and Chain (2016), Levy and Myers (2016), Slatko et al. (2018). Largely driven by the needs of the HGP, NGS is defined by highly parallel methods that produce extremely large amount of data. Existing platforms can easily provide reads that, when combined, cover the entire chicken genome many fold times at economical costs. With the widespread distribution of sequencing

machines, like SNP chips, NGS has enabled almost all laboratories to conduct large-scale sequencing efforts. This power continues to increase with the continuing declines in costs and, in particular, the increasing capability of "long read" platforms. And compared to SNP arrays, NGS allows for the interrogation of the entire genome and provides single base resolution. On the other hand, this increased power and sequence information comes at a cost mainly with the increased need for computational biology skills.

The great challenge in resequencing is in interpreting the results. This is because there are a large number of polymorphisms between any two individuals, of which only a small fraction will be associated with the trait of interest. For this reason, most resequencing efforts have been most successful in identifying genes of large effect, e.g., dermal hyperpigmentation (Dorshorst et al., 2011), polydactyly (Dunn et al., 2011), comb phenotypes (Wright et al., 2009; Dorshorst et al., 2015), sex-linked barring (Schwochow Thalmann et al., 2017), and talpid 2 (Chang et al., 2014). Typically, these efforts relied on mapping the mutations to a locus or having comparative knowledge from similar mutations in other organisms, which was then further characterized by whole genome resequencing. Analysis of the data revealed likely causative alleles.

2.4.4 Annotation

Functional characterization of genetic variants is often required to move from statistical association to causal variants and genes, especially in the noncoding genome. Recent studies have revealed that regulatory mutations in the noncoding regions are one of major drivers of phenotypic variations in complex traits (e.g., She and Jarosz, 2018). Therefore, functional annotation of regulatory elements in the chicken genome is essential in understanding biological mechanisms of physiological traits. In order to functionally annotate regulatory elements of genes, one must know the locations and functions of various sequence features such as promoters, enhancers, insulators, and silencers. In the past few years, the International Functional Annotation of Animal Genomes Consortium (FAANG.org) has developed core assays and bioinformatic pipelines that can be used to annotate these regulatory elements in the genomes of farm animals including chicken (Andersson et al., 2015; Giuffra et al., 2019).

Assays for characterizing chromatin accessibility and posttranslational histone modification can be used to identify and annotate regulatory elements. These posttranslational histone modifications can affect chromatin accessibility and gene expression. Chromatin immunoprecipitation sequencing (ChIP-seq) has been widely used to characterize histone modifications such as methylation and acetylation. For example, assays for histone H3 lysine 4 trimethylation (H3K4me3), H3 lysine 27 trimethylation (H3K27me3), H3 lysine 27 acetylation (H3K27ac), and H3 lysine 4 monomethylation (H3K4Me1) have been utilized to characterize chromatin state (ENCODE Project Consortium, 2012). An abundance of H3K4me3 correlates with promoters of active genes (Bernstein et al., 2002; Santos-Rosa et al., 2002; Xiao et al., 2012), while increased levels of H3K27me3 are associated with promoters of inactive genes (Heintzman et al., 2007). H3K27ac is a mark of active regulatory elements, and may distinguish active enhancers and promoters from their inactive counterparts (ENCODE Project Consortium, 2012). H3K4me1 is a mark of regulatory elements associated with enhancers and other distal elements, but also enriched downstream of transcription starts (ENCODE Project Consortium, 2012). High levels of H3K27ac and H3K4me1 are associated with enhancer regions and also correlate with areas of chromatin accessible sites (Greer and Shi, 2012). Insulators also play an essential role in regulating gene expression. The insulator-binding protein CCCTC-binding factor (CTCF) is the main insulator protein (Ong and Corces, 2014) for animal species. Chromatin accessibility provides a direct interpretation of epigenetic state, since chromatin organization and transcription factor binding together dictate the impact of regulatory elements on gene expression, determining cell-specific expression patterns and cell fate (Rivera and Ren, 2013). Assay for transposase-accessible chromatin (ATAC-seq) can be used to profile chromatin accessibility. Using the histone marks and CTCF binding sites in concert with ATAC-seq and RNA-seq can provide an unprecedented view of regulatory elements in the chicken genome. Active and inactive regulatory elements including promoters, enhancers, and insulators can be identified and annotated based on combinations of the assays above (Table 2.1).

Based on these assays of eight tissues in chickens, our results suggest that chicken genome has about half of the number of active regulatory elements including enhancers and promoters compared to mammals such as cattle and pig, especially on the number of enhancers, which may be due to same size of the chicken genome, one third that of a typical mammal (Kern et al., 2021).

2.4.5 CRISPR

Clustered, regularly interspaced, short palindromic repeats (CRISPR) is another revolutionary tool for genomic research that has very quickly become an indispensable tool for use in many organisms. Originally discovered in bacteria as a defense mechanism against invading viruses, CRISPR loci express small RNAs that complement viral genome sequences and when combined with associated CRISPR-associated nucleases (Cas) result in the enzymatic cleavage of both strands of the targeted viral DNA. Thus, only two components are required for DNA cleavage:

TABLE 2.1 Identification of promoter, enhancer, and insulator elements based on activation marks on ATAC-seq and ChIP-seq.

	Activation marks					
Regulatory element	ATAC-seq	H3K4me3	H3K27me3	H3K27ac	H3K4me1	CTCF
Active promoter	+	+	−	+	−	+/−
Inactive promoter	+	−	+	−	+	+/−
Active enhancer	+	+/−	+/−	+	+	+/−
Inactive enhancer	+	+/−	+/−	−	+	+/−
Insulator	+	−	−	−	−	+

+, indicates peaks on the marks; −, indicates no peaks on the marks; +/−, indicated poised peaks on marks depends on tissues, developmental or physiological status.

(1) an RNA molecule, called guide RNA (gRNA), which includes 17−20 bases that are complementary to the target DNA and (2) a Cas nuclease.

Recognizing the simplicity of the system, innovative scientists (Jinek et al., 2012; Cong et al., 2013) harnessed this system for widespread use in many other organisms including avians that allows for a programmable endonuclease, a feat that was previously difficult, if not impossible to achieve (Adli, 2018). After inducing double-stranded breaks in the genome, the resulting DNA damage must be repaired either by nonhomologous end-joining (NHEJ) or homology-directed recombination (HDR), resulting in a modified sequence. NHEJ can be used to cause small, random indel mutations, while HDR can generate precise replacement of targeted DNA or insertion of novel transgene cassettes up to many Kb in length. Given the power and simplicity of the system and different Cas proteins, there are many other new uses that are being employed including the ability to regulate gene expression, modify epigenetics, etc (Pickar-Oliver and Gersbach, 2019). In short, CRISPR allows for all groups to conduct gene editing and more in their cells or organism of interest.

With respect to avian systems, there are likely to be at least two key uses in the immediate future. The first is validation of the function of predicted genomic sites by knocking out the hypothesized DNA sequence and observing the phenotype. While this method is most amenable to cell lines (e.g., Chavali and Gergely, 2015), there are several reports on the deletion of various genes associated with chick development (e.g., Veron et al., 2015; Williams et al., 2018). The ultimate goal is to observe bioengineered birds (reviewed by Chojnacka-Puchta and Sawicka, 2020), which has recently been achieved using CRISPR to demonstrate that chickens lacking the receptor for avian leukosis virus subgroup J are resistant to viral infection (Koslová et al., 2020).

Another major approach that has not been reported yet for chickens is to use CRISPR in genomic screens. As stated by Neff (2020), genomic screens are comprised of three components: (1) the perturbation, (2) the model, and (3) the assay. With barcoded gRNAs and pooled cells, perturbations are clean and thorough as one can knockout the gene in every cell. The key is to have relevant cell types and ability to measure relevant phenotypic changes associated with loss of function.

2.5 Conclusions

Since the generation of the chicken genome assembly in 2004, the pace of genomics continues unabated. Due to the continued decline in sequencing costs and technologies, the ability to produce genome assemblies in other avian species or members within a species has grown immensely (Jarvis et al., 2014). These improvements have and will continue to greatly enhance of the power of genomics. Having stated this, the challenge is how to get parallel increases in other fields such as physiology. Although obtaining and accurately measuring many phenotypes is a difficult and time-consuming process, this new information will surely spur massive gains in our fundamental knowledge of genome structure, genetic variation, gene regulation, genome evolution, and many other areas of study.

References

Adli, M., 2018. The CRISPR tool kit for genome editing and beyond. Nat. Commun. 9, 1911.

Andersson, L., Archibald, A.L., Bottema, C.D., Brauning, R., Burgess, S.C., Burt, D.W., Casas, E., Cheng, H.H., Clarke, L., Couldrey, C., Dalrymple, B.P., Elsik, C.G., Foissac, S., Giuffra, E., Groenen, M.A., Hayes, B.J., Huang, L.S., Khatib, H., Kijas, J.W., Kim, H., Lunney, J.K., McCarthe, F.M., McEwan, J.C., Moore, S., Nanduri, B., Notredame, C., Palti, Y., Plastow, G.S., Reecy, J.M., Rohrer, G.A., Sarropoulou, E., Schmidt, C.J., Silverstein, J., Tellam, R.L., Tixier-Boichard, M., Tosser-Klopp, G., Tuggle, C.K., Vilkki, J., White, S.N., Zhao, S., Zhou, H., FAANG Consortium, 2015. Coordinated international action to accelerate genome-to-phenome with FAANG, the Functional Annotation of Animal Genomes project. Genome Biol. 16, 57.

Bellott, D.W., Cho, T.J., Hughes, J.F., Skaletsky, H., Page, D.C., 2018. Cost-effective high-throughput single-haplotype iterative mapping and sequencing for complex genomic structures. Nat. Protoc. 13, 787–809.

Bellott, D.W., Skaletsky, H., Cho, T.J., Brown, L., Locke, D., Chen, N., Galkina, S., Pyntikova, T., Koutseva, N., Graves, T., Kremitzki, C., Warren, W.C., Clark, A.G., Gaginskaya, E., Wilson, R.K., Page, D.C., 2017. Avian W and mammalian Y chromosomes convergently retained dosage-sensitive regulators. Nat. Genet. 49, 387–394.

Bellott, D.W., Skaletsky, H., Pyntikova, T., Mardis, E.R., Graves, T., Kremitzki, C., Brown, L.G., Rozen, S., Warren, W.C., Wilson, R.K., Page, D.C., 2010. Convergent evolution of chicken Z and human X chromosomes by expansion and gene acquisition. Nature 466, 612–616.

Bernstein, B.E., Humphrey, E.L., Erlich, R.L., Schneider, R., Bouman, P., Liu, J.S., Kouzarides, T., Schreiber, S.L., 2002. Methylation of histone H3 Lys 4 in coding regions of active genes. Proc. Natl. Acad. Sci. U. S. A. 99, 8695–8700.

Bickhart, D.M., Rosen, B.D., Koren, S., Sayre, B.L., Hastie, A.R., Chan, S., Lee, J., Lam, E.T., Liachko, I., Sullivan, S.T., Burton, J.N., Huson, H.J., Nystrom, J.C., Kelley, C.M., Hutchison, J.L., Zhou, Y., Sun, J., Crisà, A., Ponce de León, F.A., Schwartz, J.C., Hammond, J.A., Waldbieser, G.C., Schroeder, S.G., Liu, G.E., Dunham, M.J., Shendure, J., Sonstegard, T.S., Phillippy, A.M., Van Tassell, C.P., Smith, T.P., 2017. Single-molecule sequencing and chromatin conformation capture enable de novo reference assembly of the domestic goat genome. Nat. Genet. 49, 643–650.

Bornelöv, S., Seroussi, E., Yosefi, S., Pendavis, K., Burgess, S.C., Grabherr, M., Friedman-Eina, M., Andersson, L., 2017. Correspondence on Lovell et al.: identification of chicken genes previously assumed to be evolutionarily lost. Genome Biol. 18, 112.

Buzdin, A.A., Prassolov, V., Garazha, A.V., 2017. Friends-enemies: endogenous retroviruses are major transcriptional regulators of human DNA. Front. Chem. 5, 35.

Chang, C.F., Schock, E.N., O'Hare, E.A., Dodgson, J., Cheng, H.H., Muir, W.M., Edelmann, R.E., Delany, M.E., Brugmann, S.A., 2014. The cellular and molecular etiology of the craniofacial defects in the avian ciliopathic mutant talpid2. Development 141, 3003–3012.

Chavali, P.L., Gergely, F., 2015. Tackling centrosome biology through gene targeting in chicken B cells. Methods Cell Biol. 129, 83–102.

Chojnacka-Puchta, L., Sawicka, D., 2020. CRISPR/Cas9 gene editing in a chicken model: current approaches and applications. J. Appl. Genet. https://doi.org/10.1007/s13353-020-00537-9 (Online ahead of print.).

Computational Pan-Genomics Consortium, 2018. Computational pan-genomics: status, promises and challenges. Briefings Bioinf. 19, 118–135.

Cong, L., Ran, F.A., Cox, D., Lin, S., Barretto, R., Habib, N., Hsu, P.D., Wu, X., Jiang, W., Marraffini, L.A., Zhang, F., 2013. Multiplex genome engineering using CRISPR/Cas systems. Science 339, 819–823.

Conrad, D.F., Pinto, D., Redon, R., Feuk, L., Gokcumen, O., Zhang, Y., Aerts, J., Andrews, T.D., Barnes, C., Campbell, P., Fitzgerald, T., Hu, M., Ihm, C.H., Kristiansson, K., Macarthur, D.G., Macdonald, J.R., Onyiah, I., Pang, A.W., Robson, S., Stirrups, K., Valsesia, A., Walter, K., Wei, J., Wellcome Trust Case Control Consortium, Tyler-Smith, C., Carter, N.P., Lee, C., Scherer, S.W., Hurles, M.E., 2010. Origins and functional impact of copy number variation in the human genome. Nature 464, 704–712.

Cui, J., Zhao, W., Huang, Z., Jarvis, E.D., Gilbert, M.T., Walker, P.J., Holmes, E.C., Zhang, G., 2014. Low frequency of paleoviral infiltration across the avian phylogeny. Genome Biol. 15, 539.

Damas, J., O'Connor, R.E., Griffin, D.K., Larkin, D.M., 2019. Avian chromosomal evolution. In: Kraus, R.J.S. (Ed.), Avian Genomics in Ecology and Evolution. Springer Nature, Switzerland, pp. 69–92.

Dehghan, A., 2018. Genome-wide association studies. Methods Mol. Biol. 1793, 37–49.

Delany, M.E., Robinson, C.M., Goto, R.M., Miller, M.M., 2009. Architecture and organization of chicken microchromosome 16: order of the NOR, MHC-Y, and MHC-B subregions. J. Hered. 100, 507–514.

Dorshorst, B., Molin, A.M., Rubin, C.J., Johansson, A.M., Strömstedt, L., Pham, M.H., Chen, C.F., Hallböök, F., Ashwell, C., Andersson, L., 2011. A complex genomic rearrangement involving the endothelin 3 locus causes dermal hyperpigmentation in the chicken. PLoS Genet. 7, e1002412.

Dorshorst, B., Harun-Or-Rashid, M., Bagherpoor, A.J., Rubin, C.J., Ashwell, C., Gourichon, D., Tixier-Boichard, M., Hallböök, F., Andersson, L., 2015. A genomic duplication is associated with ectopic eomesodermin expression in the embryonic chicken comb and two duplex-comb phenotypes. PLoS Genet. 11, e1004947.

Dunn, I.C., Paton, I.R., Clelland, A.K., Sebastian, S., Johnson, E.J., McTeir, L., Windsor, D., Sherman, A., Sang, H., Burt, D.W., Tickle, C., Davey, M.G., 2011. The chicken polydactyly (Po) locus causes allelic imbalance and ectopic expression of Shh during limb development. Dev. Dynam. 240, 1163–1172.

Eichler, E.E., Clark, R.A., She, X., 2004. An assessment of the sequence gaps: unfinished business in a finished human genome. Nat. Rev. Genet. 5, 345–354.

Elliott, T.A., Gregory, T.R., 2015. What's in a genome? The C-value enigma and the evolution of eukaryotic genome content. Philos. Trans. R. Soc. Lond. B Biol. Sci. 370, 20140331.

ENCODE Project Consortium, 2012. An integrated encyclopedia of DNA elements in the human genome. Nature 489, 57–74.

Goodwin, S., McPherson, J.D., McCombie, W.R., 2016. Coming of age: ten years of next-generation sequencing technologies. Nat. Rev. Genet. 17, 333–351.

Greer, E.L., Shi, Y., 2012. Histone methylation: a dynamic mark in health, disease and inheritance. Nat. Rev. Genet. 13, 343–357.

Gregory, T.R., 2002. A bird's-eye view of the C-value enigma: genome size, cell size, and metabolic rate in the class Aves. Evolution 56, 121–130.

Green, E.D., Watson, J.D., Collins, F.S., 2015. Human genome project: twenty-five year of big biology. Nature 526, 29–31.

Griffin, D.K., Robertson, L.B.W., Tempest, H.G., Skinner, B.M., 2007. The evolution of the avian genome as revealed by comparative molecular cytogenetics. Cytogenet. Genome Res. 117, 64–77.

Groenen, M.A., Cheng, H.H., Bumstead, N., Benkel, B.F., Briles, W.E., Burke, T., Burt, D.W., Crittenden, L.B., Dodgson, J., Hillel, J., Lamont, S., de Leon, A.P., Soller, M., Takahashi, H., Vignal, A., 2000. A consensus linkage map of the chicken genome. Genome Res. 10, 137–147.

Giuffra, E., Tuggle, C.K., FAANG Consortium, 2019. Functional annotation of animal genomes (FAANG): current achievements and roadmap. Annu. Rev. Anim. Biosci. 7, 65–88.

Heather, J.M., Chain, B., 2016. The sequence of sequencers: the history of sequencing DNA. Genomics 107, 1–8.

Heintzman, N.D., Stuart, R.K., Hon, G., Fu, Y., Ching, C.W., Hawkins, R.D., Barrera, L.O., Van Calcar, S., Qu, C., Ching, K.A., Wang, W., Weng, Z., Green, R.D., Crawford, G.E., Ren, B., 2007. Distinct and predictive chromatin signatures of transcriptional promoters and enhancers in the human genome. Nat. Genet. 39, 311–318.

International Chicken Genome Sequencing Consortium, 2004. Sequence and comparative analysis of the chicken genome provide unique perspectives on vertebrate evolution. Nature 432, 695–716.

International Chicken Polymorphism Map Consortium, 2004. A genetic variation map for chicken with 2.8 million single-nucleotide polymorphisms. Nature 432, 717–722.

Jarvis, E.D., Mirarab, S., Aberer, A.J., Li, B., Houde, P., Li, C., Ho, S.Y., Faircloth, B.C., Nabholz, B., Howard, J.T., Suh, A., Weber, C.C., da Fonseca, R.R., Li, J., Zhang, F., Li, H., Zhou, L., Narula, N., Liu, L., Ganapathy, G., Boussau, B., Bayzid, M.S., Zavidovych, V., Subramanian, S., Gabaldón, T., Capella-Gutiérrez, S., Huerta-Cepas, J., Rekepalli, B., Munch, K., Schierup, M., Lindow, B., Warren, W.C., Ray, D., Green, R.E., Bruford, M.W., Zhan, X., Dixon, A., Li, S., Li, N., Huang, Y., Derryberry, E.P., Bertelsen, M.F., Sheldon, F.H., Brumfield, R.T., Mello, C.V., Lovell, P.V., Wirthlin, M., Schneider, M.P., Prosdocimi, F., Samaniego, J.A., Vargas Velazquez, A.M., Alfaro-Núñez, A., Campos, P.F., Petersen, B., Sicheritz-Ponten, T., Pas, A., Bailey, T., Scofield, P., Bunce, M., Lambert, D.M., Zhou, Q., Perelman, P., Driskell, A.C., Shapiro, B., Xiong, Z., Zeng, Y., Liu, S., Li, Z., Liu, B., Wu, K., Xiao, J., Yinqi, X., Zheng, Q., Zhang, Y., Yang, H., Wang, J., Smeds, L., Rheindt, F.E., Braun, M., Fjeldsa, J., Orlando, L., Barker, F.K., Jønsson, K.A., Johnson, W., Koepfli, K.P., O'Brien, S., Haussler, D., Ryder, O.A., Rahbek, C., Willerslev, E., Graves, G.R., Glenn, T.C., McCormack, J., Burt, D., Ellegren, H., Alström, P., Edwards, S.V., Stamatakis, A., Mindell, D.P., Cracraft, J., Braun, E.L., Warnow, T., Jun, W., Gilbert, M.T., Zhang, G., 2014. Whole-genome analyses resolve early branches in the tree of life of modern birds. Science 346, 1320–1331.

Jinek, M., Chylinski, K., Fonfara, I., Hauer, M., Doudna, J.A., Charpentier, E., 2012. A programmable dual-RNA-guided DNA endonuclease in adaptive bacterial immunity. Science 337, 816–821.

Kapusta, A., Suh, A., Feschotte, C., 2017. Dynamics of genome size evolution in birds and mammals. Proc. Natl. Acad. Sci. U. S. A. 114, E1460–E1469.

Kern, C., Wang, Y., Xu, X., Pan, Z., Halstead, M., Chanthavixay, G., Saelao, P., Waters, S., Xiang, R., Chamberlain, A., Korf, I., Delany, M.E., Cheng, H.H., Medrano, J.F., Van Eenennaam, A.L., Tuggle, C.K., Ernst, C., Flicek, P., Quon, G., Ross, P., Zhou, H., 2021. Functional annotations of three domestic animal genomes provide vital resources for comparative and agricultural research. Nat. Commun. 12, 1821. https://doi.org/10.1038/s41467-021-22100-8.

Koboldt, D.C., Steinberg, K.M., Larson, D.E., Wilson, R.K., Mardis, E.R., 2013. The next-generation sequencing revolution and its impact on genomics. Cell 155, 27–38.

Koren, S., Rhie, A., Walenz, B.P., Dilthey, A.T., Bickhart, D.M., Kingan, S.B., Hiendleder, S., Williams, J.L., Smith, T.P.L., Phillippy, A.M., 2018. De novo assembly of haplotype-resolved genomes with trio binning. Nat. Biotechnol. https://doi.org/10.1038/nbt.4277.

Koslová, A., Trefil, P., Mucksová, J., Reinišová, M., Plachý, J., Kalina, J., Kučerová, D., Geryk, J., Krchlíková, V., Lejčková, B., Hejnar, J., 2020. Precise CRISPR/Cas9 editing of the NHE1 gene renders chickens resistant to the J subgroup of avian leukosis virus. Proc. Natl. Acad. Sci. U. S. A. 117, 2108–2112.

Kronenberg, Z.N., Fiddes, I.T., Gordon, D., Murali, S., Cantsilieris, S., Meyerson, O.S., Underwood, J.G., Nelson, B.J., Chaisson, M.J.P., Dougherty, M.L., Munson, K.M., Hastie, A.R., Diekhans, M., Hormozdiari, F., Lorusso, N., Hoekzema, K., Qiu, R., Clark, K., Raja, A., Welch, A.E., Sorensen, M., Baker, C., Fulton, R.S., Armstrong, J., Graves-Lindsay, T.A., Denli, A.M., Hoppe, E.R., Hsieh, P., Hill, C.M., Pang, A.W.C., Lee, J., Lam, E.T., Dutcher, S.K., Gage, F.H., Warren, W.C., Shendure, J., Haussler, D., Schneider, VA., Cao, H., Ventura, M., Wilson, R.K., Paten, B., Pollen, A., Eichler, E.E., 2018. High-resolution comparative analysis of great ape genomes. Science 360 (6393), eaar6343. https://doi.org/10.1126/science.aar6343.

Levy, S.E., Myers, R.M., 2016. Advancements in next-generation sequencing. Annu. Rev. Genom. Hum. Genet. 17, 95–115.

Miga, K.H., Koren, S., Rhie, A., Vollger, M.R., Gershman, A., Bzikadze, A., Brooks, S., Howe, E., Porubsky, D., Logsdon, G.A., Schneider, V.A., Potapova, T., Wood, J., Chow, W., Armstrong, J., Fredrickson, J., Pak, E., Tigyi, K., Kremitzki, M., Markovic, C., Maduro, V., Dutra, A., Bouffard, G.G., Chang, A.M., Hansen, N.F., Thibaud-Nissen, F., Schmitt, A.D., Belton, J.-M., Selvaraj, S., Dennis, M.Y., Soto, D.C., Sahasrabudhe, R., Kaya, G., Quick, J., Loman, N.J., Holmes, N., Loose, M., Surti, U., ana Risques, R., Lindsay, T.A.G., Fulton, R., Hall, I., Paten, B., Howe, K., Timp, W., Young, A., Mullikin, J.C., Pevzner, P.A., Gerton, J.L., Sullivan, B.A., Eichler, E.E., Phillippy, A.M., 2020. Telomere-to-telomere assembly of a complete human X chromosome. Nature 585, 79–84. https://doi.org/10.1101/735928.

Miller, M.M., Taylor Jr., R.L., 2016. Brief review of the chicken Major Histocompatibility Complex: the genes, their distribution on chromosome 16, and their contributions to disease resistance. Poultry Sci. 95, 375–392.

Muir, W.M., Wong, G.K., Zhang, Y., Wang, J., Groenen, M.A., Crooijmans, R.P., Megens, H.J., Zhang, H., Okimoto, R., Vereijken, A., Jungerius, A., Albers, G.A., Lawley, C.T., Delany, M.E., MacEachern, S., Cheng, H.H., 2008. Genome-wide assessment of worldwide chicken SNP genetic diversity indicates significant absence of rare alleles in commercial breeds. Proc. Natl. Acad. Sci. U. S. A. 105, 17312–17317.

Neff, E.P., 2020. CRISPR takes genetic screens forward. Lab. Anim. 49, 13–16.

Ong, C.T., Corces, V.G., 2014. CTCF: an architectural protein bridging genome topology and function. Nat. Rev. Genet. 15, 234–246.

Pickar-Oliver, A., Gersbach, C.A., 2019. The next generation of CRISPR-Cas technologies and applications. Nat. Rev. Mol. Cell Biol. 20, 490–507.

Rhie, A., Rhie, A., McCarthy, S.A., Fedrigo, O., Damas, J., Formenti, G., Koren, S., Uliano-Silva, M., Chow, W., Fungtammasan, A., Kim, J., Lee, C., Ko, B.J., Chaisson, M., Gedman, G.L., Cantin, L.J., Thibaud-Nissen, F., Haggerty, L., Bista, I., Smith, M., Haase, B., Mountcastle, J., Winkler, S., Paez, S., Howard, J., Vernes, S.C., Lama, T.M., Grutzner, F., Warren, W.C., Balakrishnan, C.N., Burt, D., George, J.M., Biegler, MT., Iorns, D., Digby, A., Eason, D., Robertson, B., Edwards, T., Wilkinson, M., Turner, G., Meyer, A., Kautt, A.F., Franchini, P., Detrich, H.W. 3rd., Svardal ,H., Wagner, M., Naylor, G.J.P., Pippel, M.,

Malinsky, M., Mooney, M., Simbirsky, M., Hannigan, B.T., Pesout, T., Houck, M., Misuraca, A., Kingan, S.B., Hall, R., Kronenberg, Z., Sović, I., Dunn, C., Ning, Z., Hastie, A., Lee, J., Selvaraj, S., Green, R.E., Putnam, N.H., Gut, I., Ghurye, J., Garrison, E., Sims, Y., Collins, J., Pelan, S., Torrance, J., Tracey, A., Wood, J., Dagnew, R.E., Guan, D., London, S.E., Clayton, D.F., Mello, C.V., Friedrich, S.R., Lovell, P.V., Osipova, E., Al-Ajli, F.O., Secomandi, S., Kim, H., Theofanopoulou, C., Hiller, M., Zhou, Y., Harris, R.S., Makova, K.D., Medvedev, P., Hoffman, J., Masterson, P., Clark, K., Martin, F., Howe, K., Flicek, P., Walenz, B.P., Kwak, W., Clawson, H., Diekhans, M., Nassar, L., Paten, B., Kraus, R.H.S., Crawford, A.J., Gilbert, M.T.P., Zhang, G., Venkatesh, B., Murphy, R.W., Koepfli, K.P., Shapiro, B., Johnson, W.E., Di Palma, F., Marques-Bonet, T., Teeling, E.C., Warnow, T., Graves, J.M., Ryder, O.A., Haussler, D., O'Brien, SJ., Korlach, J., Lewin, H.A., Howe, K., Myers, E.W., Durbin, R., Phillippy, A.M., Jarvis, E.D., 2021. Towards complete and error-free genome assemblies of all vertebrate species. Nature 592, 737–746.

Rivera, C.M., Ren, B., 2013. Mapping human epigenomes. Cell 155, 39–55.

Romanov, M.N., Daniels, L.M., Dodgson, J.B., Delany, M.E., 2005. Integration of the cytogenetic and physical maps of chicken chromosome 17. Chromosome Res. 13, 215–222.

Santos-Rosa, H., Schneider, R., Bannister, A.J., Sherriff, J., Bernstein, B.E., Emre, N.C., Schreiber, S.L., Mellor, J., Kouzarides, T., 2002. Active genes are tri-methylated at K4 of histone H3. Nature 419, 407–411.

Schmid, M., Smith, J., Burt, D.W., Aken, B.L., Antin, P.B., Archibald, A.L., Ashwell, C., Blackshear, P.J., Boschiero, C., Brown, C.T., Burgess, S.C., Cheng, H.H., Chow, W., Coble, D.J., Cooksey, A., Crooijmans, R.P., Damas, J., Davis, R.V., de Koning, D.J., Delany, M.E., Derrien, T., Desta, T.T., Dunn, I.C., Dunn, M., Ellegren, H., Eöry, L., Erb, I., Farré, M., Fasold, M., Fleming, D., Flicek, P., Fowler, K.E., Frésard, L., Froman, D.P., Garceau, V., Gardner, P.P., Gheyas, A.A., Griffin, D.K., Groenen, M.A., Haaf, T., Hanotte, O., Hart, A., Häsler, J., Hedges, S.B., Hertel, J., Howe, K., Hubbard, A., Hume, D.A., Kaiser, P., Kedra, D., Kemp, S.J., Klopp, C., Kniel, K.E., Kuo, R., Lagarrigue, S., Lamon, S.J., Larkin, D.M., Lawal, R.A., Markland, S.M., McCarthy, F., McCormack, H.A., McPherson, M.C., Motegi, A., Muljo, S.A., Münsterberg, A., Nag, R., Nanda, I., Neuberger, M., Nitsche, A., Notredame, C., Noyes, H., O'Connor, R., O'Hare, E.A., Oler, A.J., Ommeh, S.C., Pais, H., Persia, M., Pitel, F., Preeyanon, L., Prieto, B.P., Pritchett, E.M., Rhoads, D.D., Robinson, C.M., Romanov, M.N., Rothschild, M., Roux, P.F., Schmidt, C.J., Schneider, A.S., Schwartz, M.G., Searle, S.M., Skinner, M.A., Smith, C.A., Stadler, P.F., Steeves, T.E., Steinlein, C., Sun, L., Takata, M., Ulitsky, I., Wang, Q., Wang, Y., Warren, W.C., Wood, J.M., Wragg, D., Zhou, H., 2015. Third report on chicken genes and chromosomes 2015. Cytogenet. Genome Res. 145, 78–179.

Schwochow Thalmann, D., Ring, H., Sundström, E., Cao, X., Larsson, M., Kerje, S., Höglund, A., Fogelholm, J., Wright, D., Jemth, P., Hallböök, F., Bed'Hom, B., Dorshorst, B., Tixier-Boichard, M., Andersson, L., 2017. The evolution of sex-linked barring alleles in chickens involves both regulatory and coding changes in CDKN2A. PLoS Genet. 13, e1006665.

She, R., Jarosz, D.F., 2018. Mapping causal variants with single-nucleotide resolution reveals biochemical drivers of phenotypic change. Cell 172, 478–490.

Shiina, T., Briles, W.E., Goto, R.M., Hosomichi, K., Yanagiya, K., Shimizu, S., Inoko, H., Miller, M., 2007. Extended gene map reveals tripartite motif., C-type lectin., and Ig superfamily type genes within a subregion of the chicken MHC-B affecting infectious disease. J. Immunol. 178, 7162–7172.

Slatko, B.E., Gardner, A.F., Ausubel, F.M., 2018. Overview of next-generation sequencing technologies. Curr. Protoc. Mol. Biol. 122, e59.

Swift, H., 1950. The constancy of deoxyribose nucleic acid in plant nuclei. Proc. Natl. Acad. Sci. U. S. A. 36, 643–654.

Tam, V., Patel, N., Turcotte, M., Bossé, Y., Paré, G., Meyre, D., 2019. Benefits and limitations of genome-wide association studies. Nat. Rev. Genet. 20, 467–484.

Uitterlinden, A.G., 2016. An introduction to genome-wide association studies: GWAS for dummies. Semin. Reprod. Med. 34, 196–204.

Véron, N., Qu, Z., Kipen, P.A., Hirst, C.E., Marcelle, C., 2015. CRISPR mediated somatic cell genome engineering in the chicken. Dev. Biol. 407, 68–74.

Williams, R.M., Senanayake, U., Artibani, M., Taylor, G., Wells, D., Ahmed, A.A., Sauka-Spengler, T., 2018. Genome and epigenome engineering CRISPR toolkit for in vivo modulation of cis-regulatory interactions and gene expression in the chicken embryo. Development 145, dev160333.

Wright, D., Boije, H., Meadows, J.R., Bed'hom, B., Gourichon, D., Vieaud, A., Tixier-Boichard, M., Rubin, C.J., Imsland, F., Hallböök, F., Andersson, L., 2009. Copy number variation in intron 1 of SOX5 causes the Pea-comb phenotype in chickens. PLoS Genet. 5, e1000512.

Xiao, S., Xie, D., Cao, X., Yu, P., Xing, X., Chen, C.C., Musselman, M., Xie, M., West, F.D., Lewin, H.A., Wang, T., Zhong, S., 2012. Comparative epigenomic annotation of regulatory DNA. Cell 149, 1381–1392.

Zhang, G., Li, C., Li, Q., Li, B., Larkin, D.M., Lee, C., Storz, J.F., Antunes, A., Greenwold, M.J., Meredith, R.W., Ödeen, A., Cui, J., Zhou, Q., Xu, L., Pan, H., Wang, Z., Jin, L., Zhang, P., Hu, H., Yang, W., Hu, J., Xiao, J., Yang, Z., Liu, Y., Xie, Q., Yu, H., Lian, J., Wen, P., Zhang, F., Li, H., Zeng, Y., Xiong, Z., Liu, S., Zhou, L., Huang, Z., An, N., Wang, J., Zheng, Q., Xiong, Y., Wang, G., Wang, B., Wang, J., Fan, Y., da Fonseca, R.R., Alfaro-Núñez, A., Schubert, M., Orlando, L., Mourier, T., Howard, J.T., Ganapathy, G., Pfenning, A., Whitney, O., Rivas, M.V., Hara, E., Smith, J., Farré, M., Narayan, J., Slavov, G., Romanov, M.N., Borges, R., Machado, J.P., Khan, I., Springer, M.S., Gatesy, J., Hoffmann, F.G., Opazo, J.C., Håstad, O., Sawyer, R.H., Kim, H., Kim, K.W., Kim, H.J., Cho, S., Li, N., Huang, Y., Bruford, M.W., Zhan, X., Dixon, A., Bertelsen, M.F., Derryberry, E., Warren, W., Wilson, R.K., Li, S., Ray, D.A., Green, R.E., O'Brien, S.J., Griffin, D., Johnson, W.E., Haussler, D., Ryder, O.A., Willerslev, E., Graves, G.R., Alström, P., Fjeldså, J., Mindell, D.P., Edwards, S.V., Braun, E.L., Rahbek, C., Burt, D.W., Houde, P., Zhang, Y., Yang, H., Wang, J., Avian Genome Consortium, Jarvis, E.D., Gilbert, M.T., Wang, J., 2014. Science 346, 1311–1320.

Zhang, Y., Zhang, X., O'Hare, T.H., Payne, W.S., Dong, J.J., Scheuring, C.F., Zhang, M., Huang, J.J., Lee, M.K., Delany, M.E., Zhang, H.B., Dodgson, J.B., 2011. A comparative physical map reveals the pattern of chromosomal evolution between the Turkey (*Meleagris gallopavo*) and chicken (Gallus gallus) genomes. BMC Genom. 12, 447.

Chapter 3

Transcriptomic analysis of physiological systems

Tom E. Porter

Department of Animal and Avian Sciences, University of Maryland, College Park, MD, United States

Abbreviations

ACTH Adrenocorticotropic hormone gene
ADRB2 Beta 2 adrenergic receptor gene
ALD Anterior latissimus dorsi
BDNF brain-derived neurotrophic factor gene
cDNA Complementary DNA
CGA Glycoprotein hormones, alpha subunit gene
DIO2 Thyroid hormone deiodinase 2 gene
DNA Deoxyribonucleic acid
ESTs Expressed sequence tags
FSH Follicle-stimulating hormone gene
FSHB FSH beta subunit gene
FSHR FSH receptor gene
GLUT1 Glucose transporter 1 gene
GRM8 Type 8 glutamate receptor gene
LH Luteinizing hormone
LHB LH beta subunit gne
LPS Lipopolysaccharide
MAPK Mitogen-activated protein kinase
miRNA Micro-RNA
MR mineralocorticoid receptor gene
mRNA Messenger RNA
NFκB Nuclear factor kappa B gene
NPYR5 Neuropeptide Y receptor type 5 gene
PLD Posterior latissimus dorsi
POMC Proopiomelanocortin gene
PPARγ Peroxisome proliferator-activated receptor gamma gene
RNA Ribonucleic acid
RNAseq Massively parallel sequencing of RNA
TTR Transthyretin gene
VIP vasoactive intestinal peptide gene

3.1 Introduction

How does the brain integrate environmental cues to control behavior, vocalization, and reproduction? How do the endocrine tissues respond to internal and external signals to coordinate physiological responses? What governs immune cell responses to pathogens? What are the mechanisms underlying muscle differentiation and development? How do hepatic, gastrointestinal, and adipose tissues respond to mediate nutrient uptake and metabolism? How does the cardiovascular system adjust to systemic and environmental needs? These questions have been asked by physiologists for decades. Multiple approaches have been taken to advance our knowledge in these areas. With the sequencing of the genomes for multiple avian species and the development of genome-wide tools for analysis of mRNA levels, physiologists have begun to address these still open questions on a genomic scale. Transcriptomics, also known as transcriptional profiling and functional genomics, involves large-scale and in many cases genome-wide analysis of mRNA levels in samples using DNA microarrays and massively parallel sequencing of RNA (RNAseq). The discussion below will highlight some of the efforts by avian physiologists to apply transcriptomics to the open questions noted above.

3.2 Early efforts

The first major effort in transcriptional profiling in avian species occurred with the chicken. A dramatic increase in the number of expressed sequence tags (ESTs) for chicken submitted to GenBank occurred between 1999 and 2002, prior to the release of the chicken genome sequence in 2004. During that four-year period, the number of ESTs for the chicken increased from a few hundred to more than 400,000. Assembly of these ESTs allowed for the production of more than a dozen DNA microarray platforms. Details on the production of these microarrays have been reviewed in detail (Cogburn et al., 2007; Gheyas and Burt, 2013). In 2001, three papers were published that marked the beginning of transcriptomics in birds (Liu et al., 2001; Morgan et al., 2001; Neiman et al., 2001). These first avian

Sturkie's Avian Physiology. https://doi.org/10.1016/B978-0-12-819770-7.00006-2

cDNA microarrays contained cDNAs representing approximately 2000 genes expressed in lymphoid tissues that were printed on nylon membranes. Several other tissue-specific cDNA microarrays were developed in the following few years (Bailey et al., 2003; Carre et al., 2006; Cogburn et al., 2003, 2004; Ellestad et al., 2006), and two groups produced cDNA microarrays representing more than half the expressed genes in the chicken (Burnside et al., 2005; Cogburn et al., 2004). These systems-wide cDNA microarrays were followed by oligonucleotide arrays representing the majority of expressed genes in the chicken (Affymetrix, ARK-Genomics/Operon, Agilent). Within five years of the foundation of functional genomics in the chicken and shortly after the release of the chicken genome sequence, tools were established for near genome-wide analysis of mRNA levels in chicken samples. Subsequent to these early efforts in the chicken, similar projects established resources for genomics studies in the zebra finch (Li et al., 2007) and Northern bobwhite quail (Rawat et al., 2010). These genomics tools were rapidly put to use in studies of physiological systems, which will be discussed below.

Early studies on transcriptomics in birds frequently resulted in long lists of genes that were either up-regulated or down-regulated in one set of samples relative to another. While these lists represented candidate genes for potential involvement in physiological responses, they did not add substantially to our understanding of the gene interactions mediating those responses. Many studies used hierarchical clustering, heat maps, or self-organizing maps to group genes based on their expression patterns in responses to treatments or during time-course studies. Examples of heat map and SOMS clustering are presented in Figs. 3.1 and 3.2, respectively. The rationale used was that genes that respond with similar patterns are likely regulated by shared mechanisms or even common transcription factors. More recent transcriptomic studies have placed differentially expressed genes into known or predicted gene networks and pathways based on reports in the literature (see example in Fig. 3.3). One commonly used pathway analysis software is Ingenuity Pathway Analysis. Taking multiple approaches to analyze transcriptomic results can lead to a broader understanding of the cellular pathways, gene networks, and transcriptional regulation of gene expression involved in physiological processes.

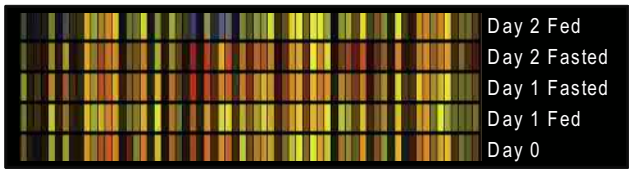

FIGURE 3.1 Heat map illustrating effects of fasting or feeding of newly hatched chickens on mRNA levels in the hypothalamus. Hypothalamic mRNA samples were analyzed using cDNA microarrays, and the results were clustered. Shown is a cluster of genes for which mRNA levels were increased (red) in response to fasting. Among these were *DIO2* and neuropeptide Y receptor type 5 (*NPYR5*). The data presented have been published previously (Higgins et al., 2010), but not in this format.

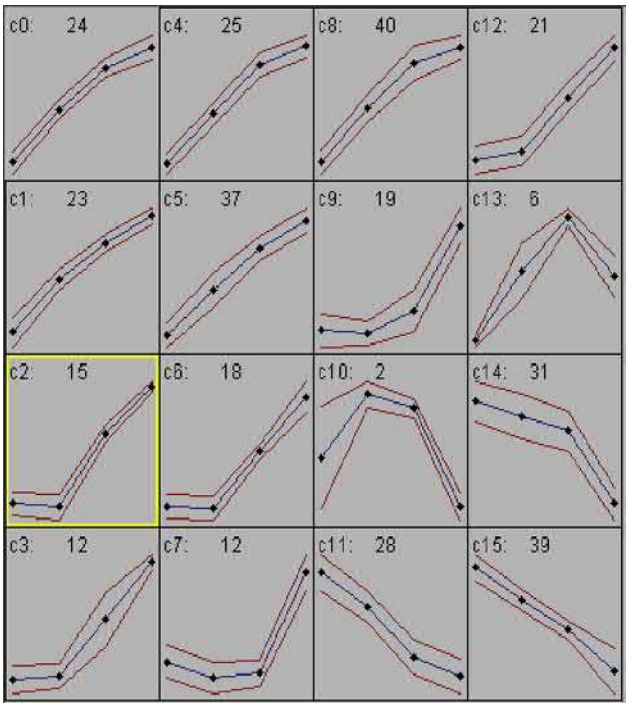

FIGURE 3.2 Self-organizing maps (SOMS) clustering of mRNA levels in the anterior pituitary gland during embryonic development. Pituitary gland mRNA samples from embryonic days 12, 14, 16, and 18 were analyzed using cDNA microarrays, and the results were clustered into SOMS based on mRNA level profiles during development. Cluster 2 (C2) outlined in yellow contains 15 genes whose expression increased on embryonic day 16. Growth hormone (*GH*) was among the genes in this cluster. These results have been published previously in a different format (Ellestad et al., 2006).

3.3 Nervous system

Vocalization in songbirds is part of the courtship ritual and an important neuroscience model for speech in humans and for sexual dimorphism in the central nervous system. However, the genes involved in establishing differences in vocalization between male and female songbirds were not known. Using microarray technology, differences in hypothalamic gene expression in response to territorial intrusion were found between the spring and autumn in free-living song sparrows (Mukai et al., 2009). Among the genes that were differentially expressed between the seasons were genes involved in thyroid hormone regulation and action, including genes encoding for the alpha subunit of thyroid-stimulating hormone (*CGA*) and transthyretin (*TTR*), supporting a role for thyroid hormones in modulating hypothalamic control of territorial aggression during seasonal reproduction. Gene express ion in the high-vocal

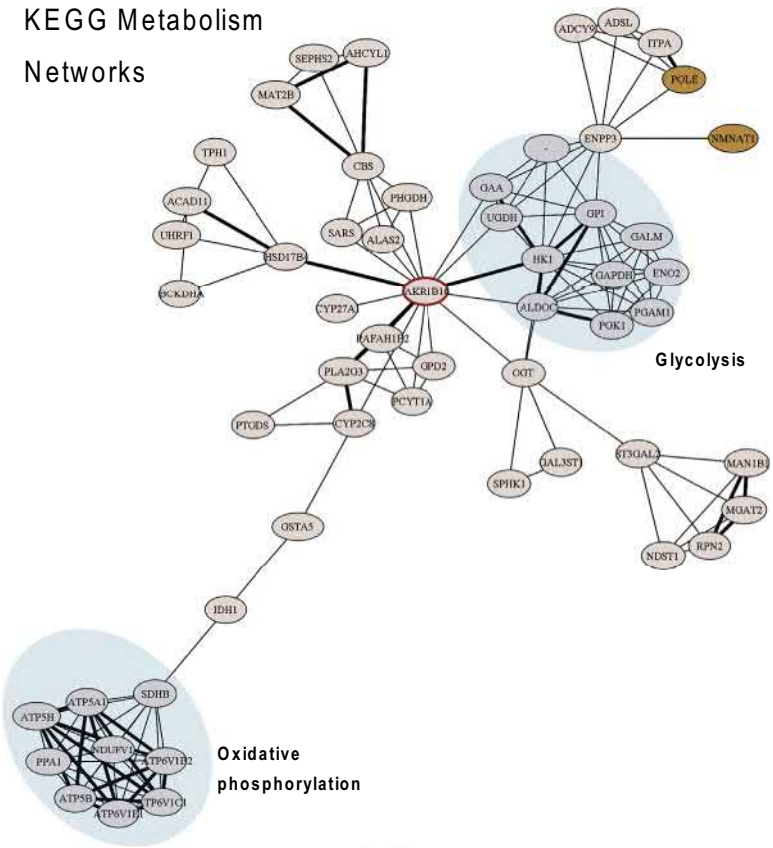

FIGURE 3.3 Network of genes that were differentially expressed in the hypothalamus of chickens genetically selected for high or low-body fat. Hypothalamic RNA samples from the two genetic lines were analyzed using cDNA microarrays, and the results were further analyzed using Ingenuity Pathway Analysis software. Genes involved in glycolysis and oxidative phosphorylation were among those that were differentially expressed in the hypothalamus of the fat and lean chickens. Additional details on these finding can be found in a previous publication (Byerly et al., 2010).

center (HVC) of zebra finches and canaries was similarly characterized (Li et al., 2007). Relative to a whole-brain reference RNA sample, expression of 190 genes was greater in the high vocal center of both zebra finch and canaries, suggesting that these genes might function in controlling vocalization. Genes expressed specifically within the song control nucleus (HVC) were also identified in the Bengalese finch using microarrays (Kato and Okanoya, 2010). In a more comprehensive study, microarray analysis of the basal ganglia identified thousands of genes differentially expressed in area X of singing zebra finches (Hilliard et al., 2012). Microarray analysis was also used to identify genes located on the Z chromosome that are expressed within the song control nucleus of the male zebra finch that are involved in cell survival (Tomaszycki et al., 2009), supporting their role in formation of the sexually dimorphic nucleus involved in masculinization of song. A similar microarray analysis of gene expression in the telencephalon of zebra finch and whitethroat indicated that most of the genes differentially expressed in males were linked to the Z chromosome (Naurin et al., 2011). However, only half of these were differentially expressed in males of both passerine species. Transcriptional profiling of the auditory lobe of zebra finches identified genes whose expression changed with the introduction of a novel song and reverted upon habituation of the birds to the introduced song (Dong et al., 2009; London et al., 2009). Interestingly, RNAseq revealed micro-RNAs (miRNA) in the auditory forebrain responsive to song that target genes whose expression changes with song (Gunaratne et al., 2011), indicating that expression of miRNAs likely contributes to song in birds.

The central nervous system plays an essential role in regulating metabolism, growth, and body composition. However, the full complement of genes expressed within the central nervous system that function in regulating these processes is not known. Transcriptomics has been used to identify genes and gene networks involved in these processes. Transcriptional profiling of the telencephalon of the white-crowned sparrow during the migratory and nonmigratory seasons revealed differences in expression of genes involved in glucose transport, including glucose transporter 1 (*GLUT1*) (Jones et al., 2008). These findings support an increased need by the nervous system for glucose during

the migratory season. In a study in which metabolism of newly hatched chickens was perturbed by fasting, microarray analysis revealed that fasting altered expression in the hypothalamus of genes involved in the regulation of metabolic rate, including thyroid hormone deiodinase 2 (*DIO2*) and proopiomelanocortin (*POMC*; Fig. 3.1), suggesting hypothalamic modulation of metabolic rate in order to compensate for decreased feed intake (Higgins et al., 2010). Genes not previously associated with hypothalamic regulation of feed intake and metabolism were also identified, including the beta 2 adrenergic receptor (*ADRB2*) and the type 8 glutamate receptor (*GRM8*). Functional relationships between *ADRB2*, *GRM8*, and *POMC* were confirmed in cultures of hypothalamic neurons, and effects were dependent on whether the neurons were derived from chicks that were previously fed or fasted. In two other reports, hypothalamic gene expression was profiled in genetic lines of chickens divergently selected for high or low-body fat (Byerly et al., 2010) or high or low-body weight (Ka et al., 2011). Differences in expression of genes associated with glucose sensing, transport, and metabolism were detected in the hypothalamus of birds selected for low or high-body fat, suggesting that differences in hypothalamic regulation of body fat in birds might involve the capacity of the hypothalamus to sense and metabolize glucose (Fig. 3.3). In contrast, selection for body weight did not affect hypothalamic expression of genes known to regulate feed intake and metabolism, even though the high body weight birds are hyperphagic. These studies demonstrated how involvement of novel gene pathways within the central nervous system in physiological processes can be identified using transcriptomics.

The central nervous system plays an integral role in stress responses. In an effort to define divergent mechanisms regulating long-term responses to stress occurring during embryonic and early posthatch development, corticosterone was administered to Japanese quail during pre- or postnatal development, and the effects on gene expression within the hippocampus and hypothalamus was assessed at adulthood using RNAseq (Marasco et al., 2016). Results indicated that effects depended on the developmental age of corticosterone treatment and on the region of the brain. Corticosterone-treated birds exhibited increased levels of mRNA for brain-derived neurotrophic factor and mineralocorticoid receptor (*MR*) in the hippocampus and corticotrophin-releasing hormone and serotonin receptors in the hypothalamus. Interestingly, mRNA levels in the hippocampus for the thyroid hormone transporter *TTR* were increased in response to prenatal but not postnatal corticosterone treatment. Conversely, levels of mRNA for the serotonergic system were up-regulated in the hypothalamus following postnatal but not prenatal corticosterone treatment. These findings indicate that early life stress can have prolonged effects within the central nervous system and that the effects are brain region and developmental stage dependent.

Maternal care of offspring is coordinated by the central nervous system, with particular involvement of the hypothalamus. Neuroendocrine regulation of brooding behavior in birds has been studied extensively. However, details on the molecular regulation of brooding behavior remain elusive. Transcriptional profiling of the hypothalamus of laying and brooding Muskovy ducks was performed using RNAseq analysis (Ye et al., 2019). Genes in the dopaminergic and serotonergic pathways, along with the principle regulator of prolactin secretion vasoactive intestinal peptide (*VIP*), were up-regulated in brooding birds. In contrast, genes in the glutamatergic pathway were down-regulated in brooding birds. Interestingly, *DIO2* and *TTR* mRNA levels were decreased in the hypothalamus of brooding ducks, implicating a potential role for thyroid hormones in the transition from laying to brooding states. Not all avian species brood their young. Some species are brood parasites, laying their eggs in the nests of another species to be brooded by the host. In a comparison of brood parasitic and nonparasitic blackbirds, transcriptional profiling of the preoptic area of the brain was conducted using RNAseq (Lynch et al., 2019). Two brood parasitic Icterids, brown-headed (Molothrus ater) and bronzed cowbirds (Molothrus aeneus), were compared with juvenile and adult red-winged blackbirds (*Agelaius phoeniceus*), a nonparasitic Icterid. Gene expression profiles for the parasitic birds more closely resembled those of the juvenile nonparasitic birds than the adult nonparasitic birds. These findings raise the intriguing possibility that the evolution of brood parasitism in birds might have involved a failure of the preoptic area to transition from the juvenile state to the reproductively mature state, a neotenic phenomenon.

3.4 Endocrine system

Transcriptomics has been used to characterize gene expression within endocrine tissues and the responses to hormonal treatments in birds. In one of the first microarray analyses in birds reported, transcriptional profiles were defined within the pineal gland of chicks during a light-dark circadian cycle (Bailey et al., 2003). Expression of hundreds of genes in the pineal gland oscillated during the light-dark cycle, including genes involved in melatonin synthesis. Importantly, this transcriptomics analysis revealed many genes associated with immune responses, stress responses, and hormone binding, suggesting other roles for these genes within the pineal gland or for the pineal gland within these other physiological systems. A similar analysis was subsequently performed in the chick retina (Bailey et al., 2004). Although some overlap in oscillating gene expression was found between the retina and the pineal gland, distinct differences were also noted,

suggesting that differences might exist in circadian regulation at the molecular level within the two tissues. Effects of thyroid hormone and growth hormone on hepatic gene expression have been characterized in the chicken using microarrays (Wang et al., 2007b). Dozens of thyroid hormone- and growth hormone-regulated genes were identified. Interestingly, cross talk between the two systems was noted, as thyroid hormone status affected mRNA levels for growth hormone receptor and insulin-like growth factor binding protein 1. Microarrays were used to characterize the response of the avian adrenal gland to adrenocorticotropic hormone (ACTH). Injection of ACTH increased mRNA levels for several steroidogenic genes but also genes with other functions, such as transcription, cell division, and electron transfer (Bureau et al., 2009). The effects of insulin immunoneutralization through administration of antiserum to insulin were evaluated in the chicken (Simon et al., 2012). Microarray analysis of mRNA samples from liver and muscle revealed that expression levels for more than 1000 genes were affected by decreased insulin levels or the elevated glucose levels associated with insulin immunoneutralization. The results demonstrated the wide range of effects of insulin on two of its target tissues. Microarrays were used to characterize changes in gene expression in the pituitary gland during chicken embryonic development (Ellestad et al., 2006). Numerous genes were identified with expression profiles that suggested involvement in differentiation of pituitary thyrotrophs, somatotrophs, and lactotrophs (Fig. 3.2). Effects of glucocorticoids on pituitary gene expression were also identified using cDNA microarrays. Treatment with corticosterone of chicken embryonic pituitary cells affected mRNA levels for hundreds of genes, and these were placed into networks of affected genes (Jenkins et al., 2013). The results were also used to identify putative glucocorticoid receptor targets in the chicken, demonstrating the power of pathway and network analysis of transcriptional profiles.

3.5 Reproductive system

Development and function of the reproductive system involves gonadal differentiation and hormonal effects on reproductive tissues, including testes, ovary, and oviduct. However, the full extent of the genetic mechanisms underlying these processes is not known. A number of studies have been reported in which investigators used transcriptomics to shed light on the underlying mechanisms controlling development and function of the reproductive system in birds. A comparison of gene expression in the shell glands of juvenile and laying chicken hens using cDNA microarrays identified hundreds of genes that are differentially expressed in the mature shell gland (Dunn et al., 2009). Similar transcriptional profiling of the uterus of the chicken using cDNA microarrays revealed genes expressed specifically in the magnum or the isthmus (Jonchère et al., 2010). Among these were genes encoding for antimicrobial proteins and ion transporters, respectively, supporting their role in antibacterial properties of the egg albumen and for eggshell formation. An analysis of the effects of a synthetic estrogen on gene expression in the oviduct demonstrated that estrogen affects expression of genes associated with epithelial differentiation and tissue remodeling (Song et al., 2011), consistent with the dramatic effects of estrogens on oviduct size and glandular development. Microarrays were used to identify genes expressed specifically within the germinal disk of the developing oocyte (Elis et al., 2008). These genes are likely to play a role in oocyte maturation or early embryonic development. Other genes found to be expressed in the granulosa cells are more likely involved in follicular maturation. Within the developing gonad of the chicken, miRNAs that were specific to the testes or ovary were identified using microarrays (Bannister et al., 2009), suggesting a role for miRNA expression in gonadal differentiation. One reproductive organ that is often overlooked is the pigeon crop that produces "crop milk" for the nutritional supply of offspring. A comparison of gene expression in nonlactating and lactating pigeon crop using oligonucleotide arrays identified genes that are differentially expressed in the lactating crop (Gillespie et al., 2011). Genes associated with extracellular matrix receptors, adherens tight junctions, and Wnt signaling were found. This finding supported hyperplasia and cellular release into the crop lumen in the formation of pigeon crop milk.

Several studies using transcriptional profiling of the hypothalamo-pituitary-ovarian axis have been reported. Transcriptional profiling of prehierarchical, preovulatory, and postovulatory ovarian follicles in the chicken using RNAseq identified genes involved in adherens junctions, apoptosis, and steroid biosynthesis (Zhu et al., 2015). RNAseq analysis was conducted on small white, large white, and small yellow ovarian follicles of laying and broody Zhedong white geese (Yu et al., 2016). Differentially expressed genes identified included many involved in hormone responses, follicular development, autophagy, and oxidation. Interestingly, those related to autophagy were up-regulated in ovarian follicles from broody hens, indicating that autophagy might play a significant role in follicular atresia associated with broodiness. RNAseq analysis of individual small yellow follicles with different levels of mRNA for the follicle-stimulating hormone (*FSH*) receptor (*FSHR*) was used to identify a novel mechanism for follicular recruitment (Wang et al., 2017). The Wnt signaling pathway was significantly up-regulated in the follicles with the highest levels of *FSHR* expression. Wnt4 was shown to stimulate proliferation of follicular granulosa cells and increase granulosa cell *FSHR* mRNA and decrease anti-Müllerian hormone mRNA levels, while FSH

was found to increase Wnt4 mRNA. These findings, based initially on transcriptional profiling, suggest that Wnt4 plays an important role in follicle selection in the chicken ovary. Transcriptomic analysis using RNAseq was performed on the hypothalamus and anterior pituitary gland of domestic turkey hens producing high or low numbers of eggs in a reproductive season. Pathway analysis of the differentially expressed genes revealed differences in thyroid hormone and estradiol signaling between the two groups of hens (Brady et al., 2020). Treatment of pituitary cells in culture confirmed that T_3 suppressed mRNA levels for the beta subunits of luteinizing hormone (*LHB*) and FSH (*FSHB*), with the effect being greater for cells from the high egg-producing hens. In contrast, treatment with E_2 increased mRNA levels for *LHB* and *FSHB*, with the effect being more pronounced for cells from the low egg-producing hens than the high egg-producing hens. These findings indicate that differences in thyroid hormone and estradiol signaling might account, in part, for differences in egg production rates. Moreover, they highlight how transcriptional profiling can uncover novel mechanisms governing physiological processes.

3.6 Immune system

Differences exist in immunological responses to pathogens among individuals in a species. However, the genes expressed within cells of the immune system that account for responses to pathogens and differences in responses among individuals are not entirely known. Microarray analysis was used to study gene expression in one lymphoid organ, the spleen, of susceptible and resistant lines of chickens in response to *Campylobacter jejuni* infection (Li et al., 2012b). Not surprisingly, expression of genes for lymphocyte activation and humoral responses, including immunoglobulin heavy and light chains, was increased following infection in the resistant line. Surprisingly, expression of genes related to erythropoiesis and apoptosis was affected in the susceptible line. These differences in genetic responses within the spleen to *Campylobacter jejuni* infection could contribute to susceptibility or resistance of individual birds to infection. In a similar study, transcriptional responses of the spleen to *Escherichia coli* infection were profiled (Sandford et al., 2011). Immunological pathways including cytokine signaling and Toll-like receptors were affected by *E. coli* challenge, and the magnitude of transcriptional changes was correlated with the severity of infection. Surprisingly, immunization prior to *E. coli* challenge had no significant effects on transcriptional profiles in response to *E. coli*. Similarly, transcriptional profiling of macrophage responses to *Salmonella*-derived endotoxins revealed effects on expression of genes for multiple cytokines and Toll-like receptors (Ciraci et al., 2010). In an earlier study of macrophage responses to lipopolysaccharide (LPS) or *E. coli*, downstream targets of the Toll-like receptor pathway were affected (Bliss et al., 2005). Transcriptional profiling of cecal gene expression in *Salmonella*-challenged neonatal chicks followed by pathway analysis revealed that expression of genes associated with the nuclear factor kappa B (*NFκB*) complex and apoptosis were affected by *Salmonella* administration (Higgins et al., 2011). In each of these studies, other genes not previously associated with immune responses were identified that might play a role in immunological responses to pathogens. In an analysis of miRNA expression within the spleen and the bursa of Fabricius of embryonic chicks, divergent expression of numerous miRNAs was noted, suggesting that these miRNAs might play diverse roles in the functions of the various tissues of the immune system (Hicks et al., 2009).

3.7 Muscle, liver, adipose, and gastrointestinal tissues

Multiple tissues are involved in nutrient absorption, metabolism, and partitioning into tissues for animal growth or energy storage. Among these are the intestine, liver, skeletal muscle, and adipose. However, all of the genes expressed in these tissues to regulate growth and nutrient partitioning are not known. In a comparison of skeletal muscle from slow-growing layer and fast-growing broiler chickens, transcriptional profiling using microarrays revealed differences in expression of genes encoding for muscle fiber proteins and regulators of satellite cell proliferation and differentiation (Zheng et al., 2009). Genes associated with slow muscle fibers were expressed at a greater level in breast muscle of layer than broiler chickens, while mRNA levels for genes associated with satellite cell growth were greater in muscle of broiler than layer chickens. In a similar analysis of gene expression in muscle types, microarray analysis was used to identify differentially expressed genes between the anterior latissimus dorsi (ALD) and posterior latissimus dorsi (PLD) muscles of turkeys (Nierobisz et al., 2011). Expression of genes encoding for extracellular matrix proteins was greater in the slow twitch, red ALD muscle than in the fast twitch, white PLD. In contrast, expression of genes involved in glycolysis was greater in the PLD than ALD. In a comparison of a random-bred turkey line with a line selected for increased body weight, microarray analysis of mRNA levels in breast muscle revealed alterations in expression of genes associated with extracellular matrix, apoptosis, Ca^{2+} signaling, and muscle function. Transcriptomics has been used to identify genes associated with meat quality of chicken breast muscle. Genes associated with lipid and carbohydrate metabolism were associated with meat quality (Sibut et al., 2011). In a similar study aimed at identifying genes involved in deposition of intramuscular fat in chickens,

transcriptional profiling of breast muscle from broiler chickens and a slow-growing Chinese breed using DNA microarrays revealed differential expression of genes involved in lipid metabolism and muscle development (Cui et al., 2012). DNA microarrays for chicken were also used to study pectoralis gene expression in juvenile and sea acclimated king penguins (Teulier et al., 2012). Genes associated with lipid metabolism were up-regulated, while genes associated with carbohydrate metabolism were down-regulated in older, sea acclimated penguins.

High environmental temperatures impair growth performance in chickens, but the molecular mechanisms involved have not been elucidated. Microarray analysis of gene expression in breast muscle of chickens exposed to chronic heat stress revealed changes in expression of genes involved in protein turnover, tumor necrosis factor signaling, and mitogen-activated protein kinase (*MAPK*) signaling (Li et al., 2011). Effects of acute and chronic heat stress on gene expression in the liver of broiler chickens were compared using RNAseq (Lan et al., 2016). The transcriptomic results indicated that acute heat stress had a greater impact on the broiler liver than chronic heat stress. Moreover, pathway analysis resulted in a novel network that combined the heat shock protein genes with immune response genes. In another study examining effects of heat stress on liver function in broiler chickens, transcriptomic and metabolomic analyses were combined (Jastrebski et al., 2017). Both analyses indicated that glycogenolysis and gluconeogenesis were elevated in the liver in response to heat stress. RNAseq was used to compare effects of acute and chronic heat stress on cardiac and skeletal muscle in two indigenous chicken ecotypes, from the lowland and highland regions of Kenya (Srikanth et al., 2019). The p53 and PPAR signaling pathways were enriched in both lowland and highland chickens, while MAPK signaling and protein processing in the endoplasmic reticulum were enriched only in the more heat-sensitive highland chickens. These results indicate that the ecotypes activated or suppressed different genes, demonstrating different underlying mechanisms in heat stress responses between the two ecotypes.

Domestic turkeys and broiler chickens have been bred for increased feed conversion and muscle growth. In studies aimed at identifying mechanisms responsible for differences in feed efficiency in broiler chickens, transcriptional profiling of breast muscle mRNA levels using microarrays indicated that an up-regulation of genes involved in anabolic processes and energy sensing and a down-regulation of genes involved in muscle fiber development and function are associated with high-feed efficiency (Bottje et al., 2012; Kong et al., 2011). Excessive deposition of body fat in commercial poultry leads to decreased conversion of feed into muscle for meat. However, the genetic mechanisms involved in accumulation of body fat in poultry are not known. Transcriptional profiling of adipose tissue from chicken lines divergently selected for low or high-body fat revealed that genes involved in lipid metabolism and endocrine function were differentially expressed between the genetic lines (Wang et al., 2007a). Genes identified included lipoprotein lipase (*LPL*), fatty acid binding protein, thyroid hormone-responsive protein (*Spot14*), and leptin receptor. In a more comprehensive study of a different pair of chicken lines genetically selected for low or high-abdominal fat, microarray analysis of adipose tissue was used to identify genes and gene networks involved in the observed differences in adiposity (Resnyk et al., 2013). Many genes involved in adipogenesis and lipogenesis were up-regulated in the fat line. Again, many genes involved in endocrine signaling were also differentially expressed between the two genetic lines, including *TTR*, *DIO1*, *DIO3*, *Spot14*, and chemerin. These findings suggest that differences in adiposity among individual birds might be related to differences in endocrine regulation of adipocyte differentiation and growth and lipid metabolism.

Lipogenesis in birds occurs primarily in the liver, and this process is regulated by the energy needs of the animal. Transcriptional profiling of newly hatched chicks that were fed or fasted revealed that the metabolic perturbation of fasting delayed the up-regulation of lipogenic genes in the liver (Richards et al., 2010). Expression of one gene that encodes for a transcription factor that regulates expression of the lipogenic genes, peroxisome proliferator-activated receptor gamma was also delayed, supporting coordinated regulation of lipogenesis. A similar analysis of transcriptional responses of the liver to fasting of older chickens has also been reported (Désert et al., 2008). In this study, fasting resulted in up-regulation of genes involved in ketogenesis, gluconeogenesis, and fatty acid beta-oxidation, while genes involved in fatty acid synthesis were down-regulated. These findings demonstrated the coordinated regulation of genes involved in nutrient partitioning by the liver in response to the metabolic perturbance of fasting.

Development of the intestine has also been studied using transcriptomics. Transcriptional profiles of the duodenum during embryonic development of the turkey were characterized using microarrays (de Oliveira et al., 2009). Results indicated that expression of peptidase and lipase genes (*LPL*) decreased toward hatch, while expression of genes encoding for peptide and glucose transporters (e.g., *PEPT1* and *SLC5AP*) increased toward hatch. Transcriptional profiles of the chicken jejunum were characterized during the first three weeks after hatch (Schokker et al., 2009). Microarray analysis indicated that genes involved in morphological and functional development were highly expressed immediately after hatch, while expression declined during later juvenile development.

3.8 Cardiovascular system

Chicken embryos are a widely used model for studies of cardiac development. As such, much is known about development of the heart in chickens. However, the complex relationships among genes necessary for cardiac development are not known. Gene expression profiling of early embryonic heart tissues was used to identify genes associated with cardiac development (Buermans et al., 2010). Results from this analysis included components of Wnt signaling. In another microarray analysis of heart development, differences in gene expression between the left and right ventricle were defined (Krejčí et al., 2012). Not surprisingly, the set of differentially expressed genes included genes associated with cardiac cell differentiation, heart development, and morphogenesis. However, many other genes not associated with these processes were also identified, providing a novel list of candidate genes for future research on the mechanisms underlying cardiac development. The cardiovascular system acclimates to life at higher altitudes and the associated hypoxia. However, the genes involved in cardiac acclimation in birds are not known. Microarray analysis of gene expression in the heart of the Tibetan chicken and chickens not adapted to life at high altitudes has been performed (Li and Zhao, 2009). Results provided a list of candidate genes that might function in chronic acclimation to high altitudes. Although not part of the cardiovascular system, microarray analysis of pectoral muscle was performed on rufous-collared sparrows sampled at 2000 and 4000 m above sea level in the Andes Mountains (Cheviron et al., 2008). Differentially expressed genes included those involved in oxidative phosphorylation and oxidative stress. Interestingly, none of the genes identified remained differentially expressed when high altitude and low-altitude birds were allowed to acclimate to life at sea level, supporting functional involvement of the candidate genes identified in acclimation of the birds to high altitudes.

3.9 Hurdles and future developments

One hurdle facing comparative physiologists in performing transcriptomics on nonmodel species is a lack of genomics resources. These include an assembled and well-annotated genome sequence. However, the number of avian genomes sequenced continues to grow, making functional genomics possible for investigators interested in nonmodel and wild species. Furthermore, the advent of RNAseq makes it possible to perform transcriptional profiling in species for which no DNA microarrays exist. With declining costs of RNAseq, this transcriptomics approach is now the preferred analysis for most studies of gene expression in physiological systems. A number of investigators have used RNAseq for characterization of mRNA and miRNA levels in the chicken (Goher et al., 2013; Hicks et al., 2010; Kang et al., 2013; Nie et al., 2012; Wang et al., 2011). Importantly, RNAseq has been used in nonmodel species to sequence and annotate the transcriptome in the dark-eyed junco (Peterson et al., 2012) and song sparrow (Srivastava et al., 2012), identify genes involved plumage coloring in ducks (Li et al., 2012a), study gene dosage compensation in the European crow (Wolf and Bryk, 2011), compare gene expression between the black carrion crow and the gray coated crow (Wolf et al., 2010), and identify genes differentially expressed between the ovaries of laying and broody geese (Xu et al., 2013). These studies using RNAseq were among the first transcriptomics studies in nonmodel avian species, and they demonstrate the utility of RNAseq for transcriptional profiling in physiological systems of any avian species. However, one major hurdle remains for comparative physiologists. Relatively few of the thousands of animal genomes now sequenced are well annotated. Prediction and annotation of genes in most genomes is based on sequence homology. With more than 10,000 avian species characterized, the possibilities for incorrect annotation of differentially expressed genes and, therefore, interpretation of transcriptional profiling results, are potentially equally as large as the number of species. Similarly, most commonly used pathway tools are based on the functions of genes determined from studies in mice and humans. Investigators and readers should use caution when interpreting transcriptomic results in avian species that have not been confirmed experimentally.

References

Bailey, M.J., Beremand, P.D., Hammer, R., Bell-Pedersen, D., Thomas, T.L., Cassone, V.M., 2003. Transcriptional profiling of the chick pineal gland, a photoreceptive circadian oscillator and pacemaker. Mol. Endocrinol. 17, 2084–2095.

Bailey, M., Beremand, P., Hammer, R., Reidel, E., Thomas, T., Cassone, V., 2004. Transcriptional profiling of circadian patterns of mRNA expression in the chick retina. J. Biol. Chem. 279, 52247–52254.

Bannister, S.C., Tizard, M.L.V., Doran, T.J., Sinclair, A.H., Smith, C., 2009. Sexually dimorphic microRNA expression during chicken embryonic gonadal development. Biol. Reprod. 81, 165–176.

Bliss, T.W., Dohms, J.E., Emara, M.G., Keeler, C.L., 2005. Gene expression profiling of avian macrophage activation. Vet. Immunol. Immunopathol. 105, 289–299.

Bottje, W.G., Kong, B.-W., Song, J.J., Lee, J.Y., Hargis, B.M., Lassiter, K., Wing, T., Hardiman, J., 2012. Gene expression in breast muscle associated with feed efficiency in a single male broiler line using a chicken 44K microarray. II. Differentially expressed focus genes. Poultry Sci. 91, 2576–2587.

Brady, K., Liu, H.-C., Hicks, J.A., Long, J.A., Porter, T.E., 2020. Transcriptome analysis of the hypothalamus and pituitary of Turkey hens with low and high egg production. BMC Genom. 21, 647.

Buermans, H.P.J., van Wijk, B., Hulsker, M.A., Smit, N.C.H., den Dunnen, J.T., van Ommen, G.B., Moorman, A.F., van den Hoff, M.J., 't Hoen, P.A.C., 2010. Comprehensive gene-expression survey identifies Wif1 as a modulator of cardiomyocyte differentiation. PLoS One 5, e15504.

Bureau, C., Hennequet-Antier, C., Couty, M., Guemene, D., 2009. Gene array analysis of adrenal glands in broiler chickens following ACTH treatment. BMC Genom. 10, 430.

Burnside, J., Neiman, P., Tang, J., Basom, R., Talbot, R., Aronszajn, M., Burt, D., Delrow, J., 2005. Development of a cDNA array for chicken gene expression analysis. BMC Genom. 6, 13.

Byerly, M.S., Simon, J., Cogburn, L.A., Le Bihan-Duval, E., Duclos, M.J., Aggrey, S.E., Porter, T.E., 2010. Transcriptional profiling of the hypothalamus during development of adiposity in genetically selected fat and lean chickens. Physiol. Genom. 42, 157–167.

Carre, W., Wang, X., Porter, T., Nys, Y., Tang, J., Bernberg, E., Morgan, R., Burnside, J., Aggrey, S., Simon, J., Cogburn, L., 2006. Chicken genomics resource: sequencing and annotation of 37,557 ESTs from single and multiple tissue cDNA libraries and CAP3 assembly of a chicken gene index. Physiol. Genom. 25, 514–524.

Cheviron, Z.A., Whitehead, A., Brumfield, R.T., 2008. Transcriptomic variation and plasticity in rufous-collared sparrows (*Zonotrichia capensis*) along an altitudinal gradient. Mol. Ecol. 17, 4556–4569.

Ciraci, C., Tuggle, C.K., Wannemuehler, M.J., Nettleton, D., Lamont, S.J., 2010. Unique genome-wide transcriptome profiles of chicken macrophages exposed to Salmonella derived-endotoxin. BMC Genom. 11, 545.

Cogburn, L.A., Porter, T.E., Duclos, M.J., Simon, J., Burgess, S.C., Zhu, J.J., Cheng, H.H., Dodgson, J.B., Burnside, J., 2007. Functional genomics of the chicken–a model organism. Poultry Sci. 86, 2059–2094.

Cogburn, L.A., Wang, X., Carre, W., Rejto, L., Aggrey, S.E., Duclos, M.J., Simon, J., Porter, T.E., 2004. Functional genomics in chickens: development of integrated-systems microarrays for transcriptional profiling and discovery of regulatory pathways. Comp. Funct. Genom. 5, 253–261.

Cogburn, L.A., Wang, X., Carre, W., Rejto, L., Porter, T.E., Aggrey, S.E., Simon, J., 2003. Systems-wide chicken DNA microarrays, gene expression profiling, and discovery of functional genes. Poultry Sci. 82, 939–951.

Cui, H.-X., Liu, R.-R., Zhao, G.-P., Zheng, M.-Q., Chen, J.-L., Wen, J., 2012. Identification of differentially expressed genes and pathways for intramuscular fat deposition in pectoralis major tissues of fast-and slow-growing chickens. BMC Genom. 13, 213.

de Oliveira, J.E., Druyan, S., Uni, Z., Ashwell, C.M., Ferket, P.R., 2009. Prehatch intestinal maturation of Turkey embryos demonstrated through gene expression patterns. Poultry Sci. 88, 2600–2609.

Désert, C., Duclos, M.J., Blavy, P., Lecerf, F., Moreews, F., Klopp, C., Aubry, M., Herault, F., Roy, P.L., Berri, C., Douaire, M., Diot, C., Lagarrigue, S., 2008. Transcriptome profiling of the feeding-to-fasting transition in chicken liver. BMC Genom. 9, 611.

Dong, S., Replogle, K.L., Hasadsri, L., Imai, B.S., Yau, P.M., Rodriguez-Zas, S., Southey, B.R., Sweedler, J.V., Clayton, D.F., 2009. Discrete molecular states in the brain accompany changing responses to a vocal signal. Proc. Natl. Acad. Sci. U. S. A. 106, 11364–11369.

Dunn, I.C., Wilson, P.W., Lua, Z., Bain, M.M., Crossan, C.L., Talbot, R.T., Waddington, D., 2009. New hypotheses on the function of the avian shell gland derived from microarray analysis comparing tissue from juvenile and sexually mature hens. Gen. Comp. Endocrinol. 163, 225–232.

Elis, S., Batellier, F., Couty, I., Balzergue, S., Martin-Magniette, M.-L., Monget, P., Blesbois, E., Govoroun, M.S., 2008. Search for the genes involved in oocyte maturation and early embryo development in the hen. BMC Genom. 9, 110.

Ellestad, L., Carre, W., Muchow, M., Jenkins, S., Wang, X., Cogburn, L., Porter, T., 2006. Gene expression profiling during cellular differentiation in the embryonic pituitary gland using cDNA microarrays. Physiol. Genom. 25, 414–425.

Gheyas, A.A., Burt, D.W., 2013. Microarray resources for genetic and genomic studies in chicken: a review. Genesis 51, 337–356.

Gillespie, M.J., Haring, V.R., McColl, K.A., Monaghan, P., Donald, J.A., Nicholas, K.R., Moore, R.J., Crowley, T.M., 2011. Histological and global gene expression analysis of the 'lactating' pigeon crop. BMC Genom. 12, 452.

Goher, M., Hicks, J.A., Liu, H.-C., 2013. The interplay between MDV and HVT affects viral miRNA expression. Avian Dis. 57, 372–379.

Gunaratne, P.H., Lin, Y.-C., Benham, A.L., Drnevich, J., Coarfa, C., Tennakoon, J.B., Creighton, C.J., Kim, J.H., Milosavljevic, A., Watson, M., Griffiths-Jones, S., Clayton, D.F., 2011. Song exposure regulates known and novel microRNAs in the zebra finch auditory forebrain. BMC Genom. 12, 277.

Hicks, J.A., Tembhurne, P.A., Liu, H.-C., 2009. Identification of microRNA in the developing chick immune organs. Immunogenetics 61, 231–240.

Hicks, J.A., Trakooljul, N., Liu, H.-C., 2010. Discovery of chicken microRNAs associated with lipogenesis and cell proliferation. Physiol. Genom. 41, 185–193.

Higgins, S.E., Ellestad, L.E., Trakooljul, N., McCarthy, F., Saliba, J., Cogburn, L.A., Porter, T.E., 2010. Transcriptional and pathway analysis in the hypothalamus of newly hatched chicks during fasting and delayed feeding. BMC Genom. 11, 162.

Higgins, S.E., Wolfenden, A.D., Tellez, G., Hargis, B.M., Porter, T.E., 2011. Transcriptional profiling of cecal gene expression in probiotic- and Salmonella-challenged neonatal chicks. Poultry Sci. 90, 901–913.

Hilliard, A.T., Miller, J.E., Fraley, E., Horvath, S., White, S.A., 2012. Molecular microcircuitry underlies functional specification in a basal ganglia circuit dedicated to vocal learning. Neuron 73, 537–552.

Jastrebski, S.F., Lamont, S.J., Schmidt, C.J., 2017. Chicken hepatic response to chronic heat stress using integrated transcriptome and metabolome analysis. PLoS One 12.

Jenkins, S.A., Ellestad, L.E., Mukherjee, M., Narayana, J., Cogburn, L.A., Porter, T.E., 2013. Glucocorticoid-induced changes in gene expression in embryonic anterior pituitary cells. Physiol. Genom. 45, 422–433.

Jonchère, V., Réhault-Godbert, S., Hennequet-Antier, C., Cabau, C., Sibut, V., Cogburn, L.A., Nys, Y., Gautron, J., 2010. Gene expression profiling to identify eggshell proteins involved in physical defense of the chicken egg. BMC Genom. 11, 57.

Jones, S., Pfister-Genskow, M., Cirelli, C., Benca, R.M., 2008. Changes in brain gene expression during migration in the white-crowned sparrow. Brain Res. Bull. 76, 536–544.

Ka, S., Albert, F.W., Denbow, D.M., Pääbo, S., Siegel, P.B., Andersson, L., Hallböök, F., 2011. Differentially expressed genes in hypothalamus in relation to genomic regions under selection in two chicken lines resulting from divergent selection for high or low body weight. Neurogenetics 12, 211–221.

Kang, L., Cui, X., Zhang, Y., Yang, C., Jiang, Y., 2013. Identification of miRNAs associated with sexual maturity in chicken ovary by Illumina small RNA deep sequencing. BMC Genom. 14, 352.

Kato, M., Okanoya, K., 2010. Molecular characterization of the song control nucleus HVC in Bengalese finch brain. Brain Res. 1360, 56–76.

Kong, B.-W., Song, J.J., Lee, J.Y., Hargis, B.M., Wing, T., Lassiter, K., Bottje, W., 2011. Gene expression in breast muscle associated with feed efficiency in a single male broiler line using a chicken 44K oligo microarray. I. Top differentially expressed genes. Poultry Sci. 90, 2535–2547.

Krejčí, E., Pesevski, Z., DeAlmeida, A.C., Mrug, M., Fresco, V.M., Argraves, W.S., Barth, J.L., Cui, X., Sedmera, D., 2012. Microarray analysis of normal and abnormal chick ventricular myocardial development. Physiol. Res. 61 (Suppl. 1), S137–S144.

Lan, X., Hsieh, J.C.F., Schmidt, C.J., Zhu, Q., Lamont, S.J., 2016. Liver transcriptome response to hyperthermic stress in three distinct chicken lines. BMC Genom. 17.

Li, C., Wang, X., Wang, G., Li, N., Wu, C., 2011. Expression analysis of global gene response to chronic heat exposure in broiler chickens (*Gallus gallus*) reveals new reactive genes. Poultry Sci. 90, 1028–1036.

Li, M., Zhao, C., 2009. Study on Tibetan Chicken embryonic adaptability to chronic hypoxia by revealing differential gene expression in heart tissue. Sci. China C Life Sci. 52, 284–295.

Li, S., Wang, C., Yu, W., Zhao, S., Gong, Y., 2012a. Identification of genes related to white and black plumage formation by RNA-seq from white and black feather bulbs in ducks. PLoS One 7, e36592.

Li, X., Swaggerty, C.L., Kogut, M.H., Chiang, H.-I., Wang, Y., Genovese, K.J., He, H., McCarthy, F.M., Burgess, S.C., Pevzner, I.Y., Zhou, H., 2012b. Systemic response to *Campylobacter jejuni* infection by profiling gene transcription in the spleens of two genetic lines of chickens. Immunogenetics 64, 59–69.

Li, X., Wang, X.-J., Tannenhauser, J., Podell, S., Mukherjee, P., Hertel, M., Biane, J., Masuda, S., Nottebohm, F., Gaasterland, T., 2007. Genomic resources for songbird research and their use in characterizing gene expression during brain development. Proc. Natl. Acad. Sci. U. S. A. 104, 6834–6839.

Liu, H.-C., Cheng, H.H., Tirunagaru, V., Sofer, L., Burnside, J., 2001. A strategy to identify positional candidate genes conferring Marek's disease resistance by integrating DNA microarrays and genetic mapping. Anim. Genet. 32, 351–359.

London, S.E., Dong, S., Replogle, K., Clayton, D.F., 2009. Developmental shifts in gene expression in the auditory forebrain during the sensitive period for song learning. Dev. Neurobiol. 69, 437–450.

Lynch, K.S., O'Connell, L.A., Louder, M.I.M., Balakrishnan, C.N., Fischer, E.K., 2019. Understanding the loss of maternal care in avian brood parasites using preoptic area transcriptome comparisons in brood parasitic and non-parasitic blackbirds. G3-Genes Genom. Genet. 9, 1075–1084.

Marasco, V., Herzyk, P., Robinson, J., Spencer, K.A., 2016. Pre- and post-natal stress programming: developmental exposure to glucocorticoids causes long-term brain-region specific changes to transcriptome in the precocial Japanese quail. J. Neuroendocrinol. 28.

Morgan, R.W., Sofer, L., Anderson, A.S., Bernberg, E.L., Cui, J., Burnside, J., 2001. Induction of host gene expression following infection of chicken embryo fibroblasts with oncogenic Marek's disease virus. J. Virol. 75, 533–539.

Mukai, M., Replogle, K., Drnevich, J., Wang, G., Wacker, D., Band, M., Clayton, D.F., Wingfield, J.C., 2009. Seasonal differences of gene expression profiles in song sparrow (Melospiza melodia) hypothalamus in relation to territorial aggression. PLoS One 4, e8182.

Naurin, S., Hansson, B., Hasselquist, D., Kim, Y.-H., Bensch, S., 2011. The sex-biased brain: sexual dimorphism in gene expression in two species of songbirds. BMC Genom. 12, 37.

Neiman, P.E., Ruddell, A., Jasoni, C., Loring, G., Thomas, S.J., Brandvold, K.A., Lee, R., Burnside, J., Delrow, J., 2001. Analysis of gene expression during myc oncogene-induced lymphomagenesis in the bursa of Fabricius. Proc. Nat. Acad. Sci. U. S. A. 98, 6378–6383.

Nie, Q., Sandford, E., Zhang, X., Nolan, L., Lamont, S., 2012. Deep sequencing-based transcriptome analysis of chicken spleen in response to avian pathogenic escherichia coli (APEC) infection. PLoS One 7, e41645.

Nierobisz, L.S., Sporer, K.R.B., Strasburg, G.M., Reed, K.M., Velleman, S.G., Ashwell, C.M., Felts, J.V., Mozdziak, P.E., 2011. Differential expression of genes characterizing myofibre phenotype. Anim. Genet. 43, 298–308.

Peterson, M.P., Whittaker, D.J., Ambreth, S., Sureshchandra, S., Buechlein, A., Podicheti, R., Choi, J.-H., Lai, Z., Mockatis, K., Colbourne, J., Tang, H., Ketterson, E.D., 2012. De novo transcriptome sequencing in a songbird, the dark-eyed junco (*Junco hyemalis*): genomic tools for an ecological model system. BMC Genom. 13, 305.

Rawat, A., Gust, K.A., Elasri, M.O., Perkins, E.J., 2010. Quail genomics: a knowledgebase for Northern bobwhite. BMC Bioinf. 11, S13.

Resnyk, C.W., Carré, W., Wang, X., Porter, T.E., Simon, J., Le Bihan-Duval, E., Duclos, M.J., Aggrey, S.E., Cogburn, L.A., 2013. Transcriptional analysis of abdominal fat in genetically fat and lean chickens reveals adipokines, lipogenic genes and a link between hemostasis and leanness. BMC Genom. 14, 557.

Richards, M.P., Proszkowiec-Weglarz, M., Rosebrough, R.W., McMurtry, J.P., Angel, R., 2010. Effects of early neonatal development and delayed feeding immediately post-hatch on the hepatic lipogenic program in broiler chicks. Comp. Biochem. Physiol. B 157, 374–388.

Sandford, E.E., Orr, M., Balfanz, E., Bowerman, N., Li, X., Zhou, H., Johnson, T.J., Kariyawasam, S., Liu, P., Nolan, L.K., Lamont, S.J., 2011. Spleen transcriptome response to infection with avian pathogenic *Escherichia coli* in broiler chickens. BMC Genom. 12, 469.

Schokker, D., Hoekman, A.J.W., Smits, M.A., Rebel, J.M.J., 2009. Gene expression patterns associated with chicken jejunal development. Dev. Comp. Immunol. 33, 1156–1164.

Sibut, V., Hennequet-Antier, C., LeBihan-Duval, E., Marthey, S., Duclos, M.J., Berri, C., 2011. Identification of differentially expressed genes in chickens differing in muscle glycogen content and meat quality. BMC Genom. 12, 112.

Simon, J., Milenkovic, D., Godet, E., Cabau, C., Collin, A., Métayer-Coustard, S., Rideau, N., Tesseraud, S., Derouet, M., Crochet, S., Cailleau-Audouin, E., Hennequet-Antier, C., Gespach, C., Porter, T.E., Duclos, M.J., Dupont, J., Cogburn, L.A., 2012. Insulin immuno-neutralization in fed chickens: effects on liver and muscle transcriptome. Physiol. Genom. 44, 283–292.

Song, G., Seo, H.W., Choi, J.W., Rengaraj, D., Kim, T.M., Lee, B.R., Kim, Y.M., Yun, T.W., Jeong, J.-W., Han, J.Y., 2011. Discovery of candidate genes and pathways regulating oviduct development in chickens. Biol. Reprod. 85, 306–314.

Srikanth, K., Kumar, H., Park, W., Byun, M., Lim, D., Kemp, S., Te Pas, M.F.W., Kim, J.M., Park, J.E., 2019. Cardiac and skeletal muscle transcriptome response to heat stress in Kenyan chicken ecotypes adapted to low and high altitudes reveal differences in thermal tolerance and stress response. Front. Genet. 10, 993.

Srivastava, A.J., Winker, K., Shaw, T.I., Jones, K.L., Glenn, T.C., 2012. Transcriptome analysis of a North American Songbird, Melospiza melodia. DNA Res. 19, 325−333.

Teulier, L., Dégletagne, C., Rey, B., Tornos, J., Keime, C., de Dinechin, M., Raccurt, M., Rouanet, J.-L., Roussel, D., Duchamp, C., 2012. Selective upregulation of lipid metabolism in skeletal muscle of foraging juvenile king penguins: an integrative study. Proc. R. Soc. Lond. Ser. B Biol. Sci. 279, 2464−2472.

Tomaszycki, M.L., Peabody, C., Replogle, K., Clayton, D.F., Tempelman, R.J., Wade, J., 2009. Sexual differentiation of the zebra finch song system: potential roles for sex chromosome genes. BMC Neurosci. 10, 24.

Wang, H.-B., Li, H., Wang, Q.-G., Zhang, X.-Y., Wang, S.-Z., Wang, Y.-X., Wang, X.-P., 2007a. Profiling of chicken adipose tissue gene expression by genome array. BMC Genom. 8, 193.

Wang, X., Carre, W., Saxton, A.M., Cogburn, L.A., 2007b. Manipulation of thyroid status and/or GH injection alters hepatic gene expression in the juvenile chicken. Cytogenet. Genome Res. 117, 174−188.

Wang, Y., Ghaffari, N., Johnson, C.D., Braga-Neto, U.M., Wang, H., Chen, R., Zhou, H., 2011. Evaluation of the coverage and depth of transcriptome by RNA-Seq in chickens. BMC Bioinf. 12 (Suppl. 10), S5.

Wang, Y.Y., Chen, Q.Y., Liu, Z.M., Guo, X.L., Du, Y.Z., Yuan, Z.J., Guo, M., Kang, L., Sun, Y., Jiang, Y.L., 2017. Transcriptome analysis on single small Yellow Follicles reveals that Wnt4 is involved in chicken Follicle selection. Front. Endocrinol. 8.

Wolf, J.B.W., Bayer, T., Haubold, B., Schilhabel, M., Rosenstiel, P., Tautz, D., 2010. Nucleotide divergence vs. gene expression differentiation: comparative transcriptome sequencing in natural isolates from the carrion crow and its hybrid zone with the hooded crow. Mol. Ecol. 19 (Suppl. 1), 162−175.

Wolf, J.B.W., Bryk, J., 2011. General lack of global dosage compensation in ZZ/ZW systems? Broadening the perspective with RNA-seq. BMC Genom. 12, 91.

Xu, Q., Zhao, W.M., Chen, Y., Tong, Y.Y., Rong, G.H., Huang, Z.Y., Zhang, Y., Chang, G.B., Wu, X.S., Chen, G.H., 2013. Transcriptome profiling of the goose (*Anser cygnoides*) ovaries identify laying and broodiness phenotypes. PLoS One 8, e55496.

Ye, P., Li, M., Liao, W., Ge, K., Jin, S., Zhang, C., Chen, X., Geng, Z., 2019. Hypothalamic transcriptome analysis reveals the neuroendocrine mechanisms in controlling broodiness of Muscovy duck (*Cairina moschata*). PLoS One 14, e0207050.

Yu, J., Lou, Y., Zhao, A., 2016. Transcriptome analysis of follicles reveals the importance of autophagy and hormones in regulating broodiness of Zhedong white goose. Sci. Rep. 6, 36877.

Zheng, Q., Zhang, Y., Chen, Y., Yang, N., Wang, X.-J., Zhu, D., 2009. Systematic identification of genes involved in divergent skeletal muscle growth rates of broiler and layer chickens. BMC Genom. 10, 87.

Zhu, G., Mao, Y., Zhou, W., Jiang, Y., 2015. Dynamic changes in the follicular transcriptome and promoter DNA methylation pattern of steroidogenic genes in chicken follicles throughout the ovulation cycle. PLoS One 10, e0146028.

Chapter 4

Avian proteomics

Alison Ferver[1], Shane C. Burgess[2], Colin G. Scanes[1] and Sami Dridi[1]

[1]*Center of Excellence for Poultry Science, University of Arkansas, Fayetteville, AR, United States;* [2]*College of Agriculture & Life Sciences, The University of Arizona, Tucson, AZ, United States*

Abbreviations

ACAA2 acetyl-CoA acyltransferase 2
ACE angiotensin I converting enzyme
ACOX1 acyl-CoA oxidase 1
AGR2 anterior gradient homolog 2
APEX ascorbic acid peroxidase
ATP adenosine triphosphate
AvBD10, AvBD9 avian β-defensin 10, avian β-defensin 9
BCO bacterial chondronecrosis with osteomyelitis
BirA bifunctional ligase/repressor A
Cas9 CRISPR associated protein 9
CD cluster differentiation
CECs chicken embryo cells
cGMP-PKG cyclic guanosine 3′, 5′-monophosphate-protein kinase G
CORT corticosterone
CPT1A carnitine palmitoyltransferase 1A
CRMP2 collapsin response mediator protein 2
CST3 Cystatin C
DNA deoxyribonucleic acid
eIF-2/eIF4 eukaryotic initiation factor 2
EOC epithelial ovarian cancer
FHN femur head necrosis
FSH follicle stimulating hormone
GaHV-2 Gallid herpesvirus 2
H5N1 hemagglutinin type 5 and neuraminidase type 1
HIF-1 alpha hypoxia-inducible-factor-1 alpha
HPLC high-performance liquid chromatography
Iba57 Iron-sulfur cluster assembly factor
ICATs isotope coded affinity tags
IFN interferon
IPA ingenuity pathway analysis
iTRAQ isobaric tags for relative and absolute quantification
LC liquid chromatography
LC-MS liquid chromatography tandem mass spectrometry
MALDI matrix assisted laser desorption/ionization
MALDI-TOF-MS matrix-assisted laser desorption ionization time of flight mass spectrometry
MD Marek's disease
MDV Marek's disease virus
Meq MDV EcoQ protein
mRNA messenger ribonucleic acid
MS mass spectrometry
mTOR mechanistic target of rapamycin
MudPIT multidimensional protein identification technology
NMR nuclear magnetic resonance
PAGE polyacrylamide gel electrophoresis
PCR polymerase chain reaction
PGAM1 phosphoglycerate mutase 1
pI isoelectric point
qPCR quantitative polymerase chain reaction
QTL quantitative trait locus
RNA ribonucleic acid
RP reversed-phase
SCX strong cation exchange
SDS-PAGE sodium dodecyl sulfate polyacrylamide gel electrophoresis
SILAC stable isotope labeling with amino acids in cell culture
SLC25A5 Solute carrier family 25 member 5
SM spaghetti meat
SPINK7 serine peptidase inhibitor kazal type 7
T-cells thymus cells
T-reg thymus cell regulatory
TD tibial dyschondroplasia
Th thymus cell helper
TSPO translocator protein
VEGFA vascular endothelial growth factor A
VLDLR very low density lipoprotein receptor
WB wooden breast
WS white striping
XIC extracted-ion chromatogram

4.1 Introduction

Whereas genomics provides and analyzes the entire set of functional elements encoded in a genome, and transcriptomics studies gene expression by measuring RNA levels, proteomics analyzes protein expression, modification, structure, localization, interaction, and function. Having a completed genome sequence of an organism is a

Sturkie's Avian Physiology. https://doi.org/10.1016/B978-0-12-819770-7.00001-3

key step toward understanding how that organism is built and maintained, and thus its complex biology. This information is stored in the genome in the form of genes, which are transcribed into RNA, and RNA is translated into proteins. The entire set of RNA transcripts and proteins encoded by the genome is called transcriptome and proteome, respectively (Velculescu et al., 1997; Wilkins et al., 1996). Although genes provide instructions, proteins are the functional units of almost all biological processes and the principal structural building blocks of all living organisms. Systems-level understanding of cell physiology is thus inevitably based on understanding the multifaceted interplay of gene expression and protein functional networks. An individual's genome sequence (with the exception of some regions dedicated to the adaptive immune system) is static, its epigenome (the methylation patterns on DNA) less so, and the transcriptome and proteome are extremely dynamic. These latter two differ from cell to cell, and change dramatically according to conditions that cells are exposed to. The transcriptome is more complicated than the genome because of both frame-shifting and alternative splicing. The proteome is even more complex because most proteins are co- and posttranslationally modified (Walsh, 2006). More than 200 different types of protein modifications are documented in vertebrates, and more than one of these modifications routinely occurs on most proteins (Walsh, 2006). Measurement of the proteome is also more challenging than that of the transcriptome because the dynamic range of proteins in tissues is higher than of transcripts, and can span over 11 orders of magnitude in body fluids (Anderson and Anderson, 2002), and most importantly, from a technical perspective, there is no equivalent of the polymerase chain reaction (PCR) for proteins—we must use very expensive machinery to directly identify proteins. Although mRNA quantities measured by quantitative (q)PCR, microarrays, or sequencing are often used as surrogates for protein quantities, and indirectly, protein activity, there is no or little correlation between mRNA and levels of its corresponding protein (Gygi et al., 1999a; Cullen et al., 2004; Nagaraj et al., 2011; Marguerat et al., 2012). This means that the presence or quantities of proteins in biological samples cannot be satisfactorily estimated solely through their mRNA levels. In addition, posttranslational modifications often profoundly affect protein activities. Though arguably less sensitive, proteomics methods are more specific for determining what is happening at the protein level—they can identify and quantify protein amounts and posttranslational modifications as well as be combined with other omics data to produce a complete biological picture of the organism or physiological state in question. Proteomics thus provides a direct measure of the predominant functional units responsible for cellular behavior. Although not absolutely essential, a sequenced and structurally annotated genome greatly facilitates proteomics. The more accurate the genome assembly and annotation, the more accurate the proteomics methodologies can be; this extends to the individual—the most accurate proteomics experiments will be done using the individual's own genome sequence and, to be more accurate still, the transcriptome that corresponds to the proteome. Conversely, proteomics can be used to improve the structural annotation of genomes (Nanduri et al., 2010; Jaffe et al., 2004). Red jungle fowl (*Gallus gallus*), the major wild ancestor of the domestic chicken, was the first avian and nonmammalian amniote to have its genome sequenced (International Chicken Genome Sequencing Consortium, 2004). The chicken is the principal nonmammalian vertebrate animal model for studying development, infectious disease, immunology, oncogenesis, and behavior. It is also one of the most important agricultural species for production of meat and eggs. Until additional avian complete genomes became available, the chicken genome served as de facto model bird genome, and most of the proteomics studies have utilized this model to study various aspects of bird biology. Complete or draft genomes of several other avian species have become available, including several lines of domestic chicken (*Gallus gallus domesticus*), zebra finch (*Taeniopygia guttata*), domestic turkey (*Meleagris gallopavo*), collared flycatcher (*Ficedula albicollis*), pied flycatcher (*Ficedula hypoleuca*), large ground finch (*Geospiza magnirostris*), scarlet macaw (*Ara macao*), mallard duck (*Anas platyrhynchos*), ground tit (*Pseudopodoces humilis*), Puerto Rican parrot (*Amazona vittata*), and budgerigar (*Melopsittacus undulatus*) (Ellegren et al., 2012; Warren et al., 2010; Oleksyk et al., 2012; Dalloul et al., 2010; Rands et al., 2013; Rubin et al., 2010; Huang et al., 2013; Cai et al., 2013; http://aviangenomes.org/, 2013). The turkey, duck, and domestic chicken were sequenced because they are economically important (Dalloul et al., 2010; Rubin et al., 2010; Rao et al., 2012). These species are also used as biomedical models, which is the reason that the zebra finch, scarlet macaw, and Puerto Rican amazon were sequenced—they are important in neuroscience for studying their behavioral, cognitive, and speech abilities (Warren et al., 2010; Oleksyk et al., 2012; Seabury et al., 2013). Darwin's finches are model organisms to study of various aspects of evolution and development (Rands et al., 2013). Flycatchers are important models for speciation (Ellegren et al., 2012), and the genome of the ground tit provides new opportunities to study adaptation mechanisms to extreme conditions (Cai et al., 2013). Collectively, the availability of these additional genomes is opening up new vistas for genome-wide research and studies of various aspects of bird biology both on the RNA and protein levels. It is expected that

large-scale analysis of the avian genome, transcriptome, and proteome will increase our understanding of complex molecular processes that determine phenotype.

4.2 Protein identification and analysis

Although traditional protein biochemistry focuses on studying properties of individual proteins, proteomics encompasses nearly any type of technology that enables studying proteins on a large scale. There have been numerous tools developed for identification of proteins, including two-hybrid systems (Fields and Song, 1989), protein/peptide microarrays (Haab, 2003; Panse et al., 2004), nuclear magnetic resonance (NMR) spectrometry, and mass spectrometry (MS)-based approaches (Fenn et al., 1989). The two-hybrid systems and peptide/peptide microarrays had limited applicability which although was alleviated through analytical capabilities of MS, resulted in more MS-based approaches taking over. MS, and occasionally NMR, are now being utilized in conjunction with bioinformatics for larger pathway annotations in high-throughput protein profiling and analysis (Aslam et al., 2017). NMR is less sensitive than MS; however, it benefits from more stable spectrometer, an absence of spectrum quenching, and its ability to use in a large range of experiments (Dona et al., 2016). The versatility of MS and modifications to its ionization method has made MS the most commonly used technique in large-scale proteomic and high-throughput analysis. In addition to its versatility, MS has also the ability to handle the difficulties associated with the complex and dynamic nature of proteomes (Han et al., 2008). MS simplifies and accelerates the analysis and characterization of proteins. MS-based proteomics refers to approaches that use MS for identifying, characterizing, and/or quantifying proteins in biological samples (Fig. 4.1). Mass spectrometers are used to detect, identify, and quantify small molecules based on their mass and charge (m/z) ratios with high precision, sensitivity, and speed. Many

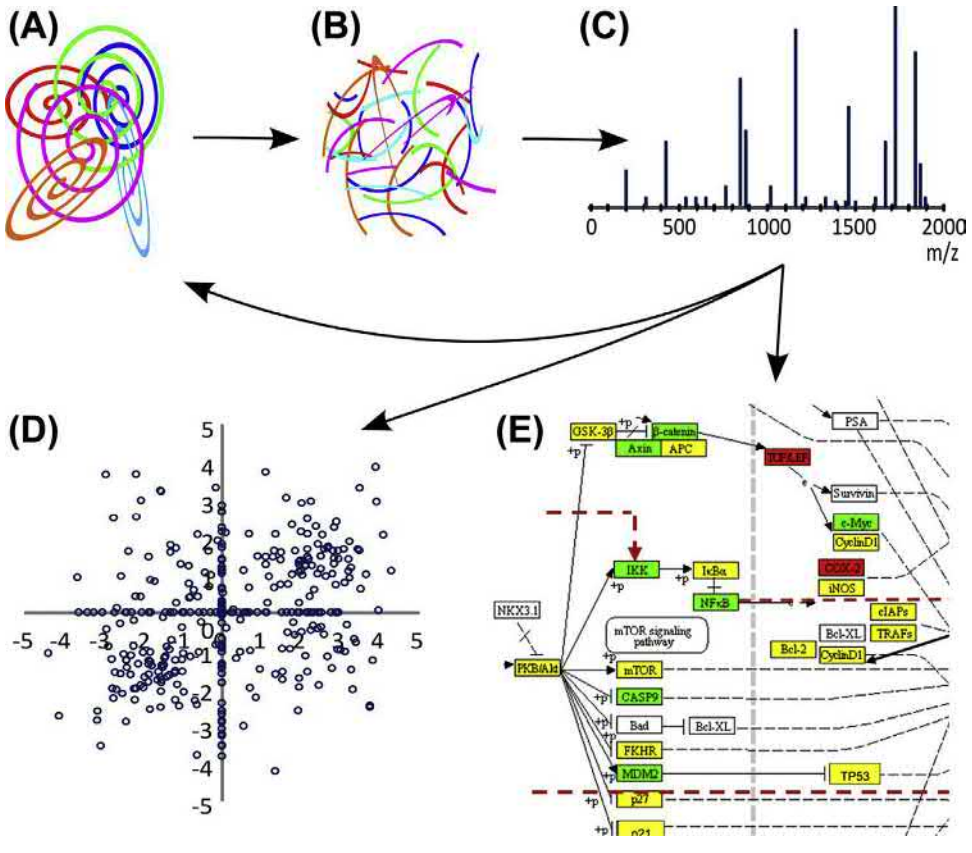

FIGURE 4.1 The workflow of mass spectrometry-based proteomics. The goal of proteomics is physical (protein identity, modifications, structure, localization) and functional (protein interactions, composition of protein complexes) characterization of the proteome. Proteomics denotes the collection of diverse technologies that enable the study of proteins on a large scale. In current proteomic research, mass spectrometry (MS) plays prime and indispensable role because several thousand proteins can be rapidly analyzed, correctly identified, and accurately quantified in a single MS-based experiment. Proteins (A) are typically too large for accurate mass determination by mass spectrometry, therefore, they are first digested into peptides (B), which are then analyzed by a mass spectrometer. The obtained peptide masses, peptide (tandem) mass spectra (C), are then searched against predicted peptide masses derived from DNA or protein sequence databases by using one or several different mass spectral search algorithms and their amino acid sequence is determined. The amino acid sequence of an identified peptide is often unique to its parental protein, and such peptides are used for unambiguous identification of proteins that were present in the analyzed sample. In addition to protein identification, MS enables accurate relative or absolute quantification of proteins. As a result, MS is commonly used to identify proteins that are qualitatively and/or quantitatively differentially expressed between studied conditions. The obtained proteomic information is integrated with existing knowledge and/or data from other large-scale studies (mRNA profiling, siRNA screens) to better understand cell or tissue biology at the system level. For example, protein expression levels are compared with mRNA levels (D), and differences in protein expression are analyzed in the context of biological pathways or interaction networks (E) in effort to identify the underlying causalities and mechanistic principles that give rise to a studied phenomenon or phenotype.

excellent reviews have been written that cover instrumentation and principles of protein identification by MS (Yates et al., 2009; Yates, 1998; Steen and Mann, 2004; Cottrell, 2011), and we will not replicate this information. Rather, we will introduce the key methods. A typical biological sample contains extremely complex proteomes. Because mass spectrometers can analyze only a limited number of different peptides at a time, the sample complexity must be reduced before MS. This has been historically done on the protein level by gel electrophoresis and more commonly done on the peptide level by various chromatography techniques.

4.2.1 Historical to current techniques

Two-dimensional (2D) polyacrylamide gel electrophoresis (PAGE) was the first technique that allowed truly complex proteomic analysis and was instrumental for the development of proteomics (O'Farrell, 1975; Rabilloud et al., 2010). 2D PAGE is the most widely used technique in gel-based proteomics; it simply deconvolutes a protein mixture in two dimensions. Proteins are first separated in the first dimension by their isoelectric point (pI), and then in the second dimension according to their electrophoretic mobility (which is a function of molecular weight and charge of a protein) in a polyacrylamide gel. Separated proteins are then stained and appear as spots in the gel. The amount of protein in a spot is determined by measuring the spot volume. This quantification is used as a screening process to select a limited number of corresponding spots that contain different amounts of protein on related gels. This technique is very useful for comparing two samples that have similar protein expression profiles in order to find proteins that differ between the samples in their expression levels or posttranslational modifications (Rabilloud et al., 2010). The major advantage of this method is that it is intrinsically quantitative. The major drawbacks are the limited capacity of protein separation; poor reproducibility of 2D gels; and low sensitivity, dynamic range, and throughput. Although efforts to overcome some of the shortcomings inherent to gel-based approaches resulted in the development of improved 2D gel methods, such as 2D fluorescence gel electrophoresis (Unlu et al., 1997), gel-free chromatographic approaches, which offer a number of advantages over gel-based methods, now completely dominate the field of proteomics. One of the most common approaches being multidimensional high-performance liquid chromatography (HPLC). Multidimensional HPLC quickly became the technique of choice for large-scale proteomic studies. Here, in contrast to gel-based approaches, the entire analyzed proteome is first digested, and the resulting peptides are then separated by multidimensional HPLC and further analyzed by MS. Digestion of a protein mixture generates a highly complex mixture of peptides, in which the connection between the peptide and the originating protein is lost. Peptides detected and identified by MS are then used to infer the presence of all original proteins in the sample, which is the principle of the "shotgun" proteomics named by an analogy to shotgun DNA sequencing. Multidimensional HPLC combines several separation steps to improve resolution of complex mixtures of peptides. One of the most popular multidimensional separation methods utilizes strong cation exchange and reversed-phase (RP) chromatography to separate peptides in two dimensions: first peptides are separated based on charge, and then on hydrophobicity (Washburn et al., 2001). This separation method is the basis of the shotgun proteomic strategy known as multidimensional protein identification technology (MudPIT) (Washburn et al., 2001). Another important chromatographic technique that is often used in gel-free approaches is affinity purification. Selective enrichment affinity materials are either used to enrich for peptides that contain certain posttranslational modifications, such as phosphorylation (Ficarro et al., 2002; Cao and Stults, 1999) or glycosylation (Geng et al., 2000; Durham and Regnier, 2006), or peptides that contain a specific selectable amino acid residue, such as cysteine (Wang and Regnier, 2001) or histidine (Wang et al., 2002). Affinity-enriched peptide mixtures are usually directly (online) or offline transferred to RP HPLC columns and further analyzed by MS. Gel-free approaches overcome many of the drawbacks that are inherent to gel-based methods (for example, proteins with extreme size, pI, or hydrophobicity are amenable for analysis); but more importantly, they allow a large number of proteins to be identified and quantified in a high-throughput manner and short time. The ability for high-throughput proteomics to detect low-abundance proteins was heavily investigated as it was a major drawback compared to gel-based approaches. Techniques on the front end of MS analysis that improve sensitivity include fractionation, affinity enrichment, and immune-depletion, depending on the sample (Shi et al., 2012). Improvements in statistical modeling of liquid chromatography tandem mass spectrometry (LC-MS/MS) in the MS-spectrum count label-free quantitative proteomic approach have also resulted in improved detection and attenuated bias toward low-abundance proteins (Lee et al., 2019). Recently, a combined approach of nanoparticles and MS, called Nanoproteomics, has shown to be an antibody-free, scalable and reproducible strategy to enable analysis of low-abundance proteins directly form samples such as serum (Tiambeng et al., 2020).

4.3 Quantitative proteomics

In addition to protein identification, mass spectrometry can quantify proteins in complex biological samples. The

proteome of a cell is highly dynamic and expressed proteins often change their locations, interactions, and modifications in response to different stimuli. The goal of quantitative proteomics is to obtain a snapshot of a proteome at a particular time. Accurate quantification of proteins is important for understanding of physiological or pathological phenomena, and for identification and modeling of functional networks. Traditionally, protein quantification has been based on the 2D PAGE approaches, but several gel-free methods allow accurate protein quantification solely by MS. Methods of quantitative proteomics are classified into two major categories: those that use stable isotopes and those that do not. The most popular stable isotope-labeling techniques either label peptides with isobaric tags for relative and absolute quantitation (iTRAQ) (Ross et al., 2004), or label proteins metabolically by incorporation of stable isotope labels with amino acids in cell culture (Ong et al., 2002) or enzymatically with isotope-coded affinity tags (Gygi et al., 1999b). Protein quantification by label-free approaches is based on the observation that the chromatographic peak area for any given peptide in an LC run (Bondarenko et al., 2002; Chelius and Bondarenko, 2002) and the number of tandem MS spectra of a given peptide (Liu et al., 2004) are proportional to peptide concentration in the analyzed sample. Thus, relative quantification by label-free approaches can be done by measuring and comparing the intensities of precursor ions, or by counting and comparing the number of tandem MS spectra derived from a particular protein in different experiments.

4.4 Structural proteomics

A protein's function is determined by its structure. The major goals of structural proteomics are to elucidate the three-dimensional (3D) protein structures and to determine the relationship between protein structure and function. Traditionally, static 3D protein structures are determined by X-ray crystallography (Sherwood et al., 2011) or NMR spectroscopy (Wuthrich, 1990). However, experimental determination of protein structure by these methods remains a difficult and laborious task in vitro but can be improved upon by utilizing current software for predictive models (Sherwood et al., 2011; Hyung and Ruotolo, 2012; Nealon et al., 2017). Alternatively, protein structures can be predicted computationally by homology modeling or ab initio (Flock et al., 2012). However, and despite decades of intensive research, these approaches do not always produce reliable models (Flock et al., 2012). Hydrogen-deuterium exchange (Wales and Engen, 2006), covalent labeling (Chance, 2001), or chemical cross-linking (Young et al., 2000; Petrotchenko and Borchers, 2010) have been coupled with MS to emerge as viable methods to probe 3D protein structure. Protein foot-printing methods modify the surface of the protein that is exposed to the solvent by exchanging amide protons with heavier deuterium atoms (Wales and Engen, 2006) or by different covalent modifications (Stocks and Konermann, 2009). The labeling changes the molecular weight of a protein, and this enables MS to identify the modified sites. Protein foot-printing methods are used to investigate protein conformation in solution. Chemical cross-linking covalently couples parts of a protein(s) that are close in space under native conditions. Subsequent MS analysis identifies the location and identity of the cross-linked sites, which provides important clues about the structural topology of the protein or protein complexes (Young et al., 2000; Petrotchenko and Borchers, 2010). Determining interacting partner proteins has become of increasingly high interest and poses additional challenges and is especially time consuming in *in-vitro* models. Predictive protein interaction software enables predictive models that alleviate the difficulty of protein interaction prediction in vitro. A fusion of experimental and predictive models allows the use of sparse experimental data to produce more accurate protein interactions. Numerous bioinformatic software have been developed to aid in predictive modeling approaches to protein structure and protein interactions, and there are extensive reviews covering the differences and uses of the software (Pagadala et al., 2017; Nealon et al., 2017; Aslam et al., 2017). Spatial proteomics is a relatively new method of determining proteins in the vicinity of a bait without a high affinity between interactors as long as they are in a defined region. Current techniques include an engineered version of ascorbic acid peroxidase (APEX) fused to proteins or involved in epitope tagging of Cas9. APEX fusion results in a hydroxyl radical when hydrogen peroxide and phenoxy biotin are added, labeling protein. In conjunction with Cas9, proteins surrounding a gene found using the Cas9 guide RNA can be labeled. Another strategy is BioID which uses biotin ligase enzyme BirA for similar data (Yates, 2019; Kim and Roux, 2016; Myers et al., 2018).

4.5 Application of proteomics in avian research

Until recently, red junglefowl, the ancestor of domestic chickens, was the only avian species with a sequenced genome (2004) (International Chicken Genome Sequencing Consortium, 2004). Because proteomics greatly depends on a complete and well-annotated genome sequence, most of the proteomics studies in birds have been done on this animal model. Since then, the complete genomes of zebra finch (2010) (Warren et al., 2010), turkey (2011) (Dalloul et al., 2010), and two flycatchers (2012) (Ellegren et al., 2012) have been sequenced and assembled and many more are underway (Oleksyk et al., 2012; Rands et al., 2013;

Rubin et al., 2010; Huang et al., 2013; Cai et al., 2013; Seabury et al., 2013). The increasing number of sequenced avian genomes expands the range of unique bird phenomena that can be studied on a global protein level, but more importantly, makes it possible to study avian proteomes directly through their genomes, obviating the need for cross-species peptide matching. A number of proteomic studies have been done to study various aspects of bird biology including egg production, embryogenesis, development, metabolism, behavior, cognition, immunity, cancer, disease, and infection.

4.5.1 Proteomics of egg physiology, embryonic development, and reproduction

A number of studies have focused on initial description and functional characterization of proteomes of different avian tissues, anatomical structures, or entire organs. The avian egg is a reproductive cell and a highly elaborate biological structure that protects and nourishes the developing embryo. The major components of the egg—the crystalline shell (Mann et al., 2006, 2007; Ahmed et al., 2017), albumen (egg white) (Mann and Mann, 2011; D'Ambrosio et al., 2008; Mann, 2007; Sun et al., 2017), yolk (Farinazzo et al., 2009; Mann and Mann, 2008; Liu et al., 2018), and the vitelline membrane (Mann, 2008)—have been extensively characterized by various proteomic approaches. Recent work combining transcriptome, QTL, and proteome data determined differentially expressed and significant genes and proteins from six different bird species (chicken, duck, goose, turkey, pigeon, and quail) in egg formation. Eleven common differentially expressed proteins were found in the egg white proteomes of all six species, but numerous genes and proteins were found to be uncommon in either the egg proteome of oviducts of the species (Zhang et al., 2020a,b,c). This type of large-scale, multifaceted research reveals key differences in proteomes across species while also highlighting the conservation of certain proteomes in egg formation. A key difference in Guinea Fowl compared to chicken eggs is the hardness of shell. A quantitative proteomic study using nano-LC-MS/MS identified 149 proteins, nine unique to Guinea Fowl, in the eggshell organic matrix at key stages of bio-mineralization. 61 of the proteins were found in the zone of microstructure shift, 17 were abundant in all zones, and some were involved in the control of calcite precipitation (Le Roy et al., 2019). This study provides potential biomarkers for selection of layers producing eggs with improved shell mechanical properties and therefore enhance food safety and potential decrease in vertical transmission of bacteria. Proteins involved in eggshell brownness were investigated via iTRAQ analysis with proteomics of the shell gland epithelium of hens laying dark and light brown eggs. About 147 differentially expressed proteins with 65 upregulated in light and 82 upregulated in dark egg layers. Functional analysis indicated that light brown egg layers produced less protoporphyrin IX for brownness, potentially via down-regulated Iba57 and up-regulated SLC25A5 with down-regulated TSPO (Li et al., 2016).

The chicken embryo is one of the most useful and investigated comparative and biomedical models for studying development, physiology, and pathogenesis. Proteomics has been used to characterize the proteome of a chicken embryonic cerebrospinal fluid (CSF) (Parada et al., 2006). This study identified, among others, 14 proteins that are also present in human CSF, and 12 of them are altered in neurodegenerative diseases and/or neurological disorders. Bon and co-workers identified and quantified selected proteomes of three different heart tissues and studied them at three different developmental stages (Bon et al., 2010). By comparing the identified proteomes, it was possible to study the changes in proteome expression and to identify proteins that were specific for particular heart structures or developmental stages. Grey et al. (2010) used an alternative approach, based on MALDI tissue imaging MS, to study spatial distribution of proteins in chicken heart structures such as vessels, valves, endocardium, myocardium, and septa. To better understand embryonic chicken bone formation, Balcerzak et al. applied proteomics to identify protein machinery of matrix vesicles, which is essential for the formation of hydroxyapatite (Balcerzak et al., 2008). Functional analysis of the matrix vesicle constituents suggested what roles these proteins might have in the mineralization process. The embryonic development of skeletal muscle has also been investigated in chicken using iTRAQ analysis and protein interaction network analyses (Ouyang et al., 2017). There were 19 up-regulated and 32 down-regulated proteins in embryonic age 11 versus 16, 238 up-regulated and 227 down-regulated proteins in embryonic age 11 and day 1 of age. The differentially expressed proteins were involved in pathways of protein synthesis, muscle contraction, and oxidative phosphorylation. By combining transcriptome data, results found 189 differentially expressed proteins correlating to mRNA levels and these proteins also were involved in muscle contraction and oxidative phosphorylation. A recent study on haptic proteins in embryonic and newly hatched chicks revealed 41% of the 3409 differentially expressed proteins were involved in metabolic processes and significant differences in haptic proteins from embryonic development to hatching (Peng et al., 2018). Most importantly, key factors controlling fat deposition during chicken embryonic development were elucidated to be ACAA2, CPT1A, and ACOX1. This study also revealed an alternative model using chicken for human obesity and insulin resistance. To better understand how birds are prepared for transition from a fat-rich diet *in ovo* to saccharide- and protein-based diet after hatch, Gilbert et al. (2010) analyzed the proteome of chicken small

intestine at hatch and during the early posthatch period in two different broiler lines (Gilbert et al., 2010). This study identified differences in expression of digestion and absorption-related proteins between different genetic lines.

A proteomic approach was also used to identify hypothalamic biomarkers associated with high-egg production in chickens (Kuo et al., 2005). Comparison of the hypothalamic proteomes from two related chicken lines selected for meat and high-egg production resulted in identification of six proteins that differed in their expression between the lines, and some of these proteins are involved in regulation of gene expression, signal transduction, and lipid metabolism. The heterogeneous nuclear ribonucleoprotein H3 was suggested as novel biomarker for high-egg production. A contributing factor in egg production is follicle selection. A study comparing transcriptome and proteome of small yellow follicles and hierarchical follicles in laying hens identified nine proteins and seven genes with VLDLR gene and protein being higher in hierarchical follicles as well as being stimulated by FSH in granulosa cells (Chen et al., 2020b). This study has implications for both laying hens and broilers as broiler breeders often undergo multiple follicle selection (Hocking and Robertson, 2000). 2D PAGE MS was used to compare expression profiles of proteins in the oviduct in chicken hens of different ages during the egg-laying period (Kim et al., 2007). The analysis revealed that anterior gradient homolog 2 (AGR2) protein was among the most differentially expressed proteins. Analysis of the mRNA showed that expression of AGR-2 was limited to the magnum and isthmus of the oviduct, and that this expression was approximately 900-fold higher in the mature oviduct in comparison to the premature one. Because AGR-2 is a secreted protein that shows estrogen dependent expression, and egg laying is strongly affected by estrogen, it was suggested that AGR-2 might be important for the development of the epithelial cells in the oviduct during the egg-laying period in chickens. 2D PAGE and MudPIT have been used to discover genetic and molecular mechanisms that compromise sperm mobility in chickens (Froman et al., 2011). Analysis of the sperm proteome from chicken lines of low or high-sperm mobility allowed deduction of a proteome-based model that explained well the differences in sperm mobility between lines, and confirmed the initial hypothesis that defects in ATP metabolism and glycolysis are responsible for premature mitochondrial failure, which results in sperm immobility. MALDI and top-down MS of chicken spermatozoa and seminal plasma along with comparative analysis using spectral count and XIC revealed unique profiles of most fertile males compared to least fertile male chickens (Labas et al., 2015). Over-represented enzymes in the most fertile males were involved in energy metabolism and respiratory chain activity and least fertile males differed in proteins including acrosin, ACE, AvBD10, and AvBD9. Selection for higher fertility was shown to impact proteomic profile of seminal fluid in white leghorn males compared to the red junglefowl ancestor (Atikuzzaman et al., 2017). 2DE and immunoassays were conducted on the seminal fluid of pooled males from each breed with statistics to cover intra- and intergroup variability. The results showed conserved proteins being serum albumin and ovotransferrin, but clear enrichment of proteins related to immune response regulation for sperm survival in female reproductive tract including less proinflammatory cytokines and an abundance of immunomodulatory/anti-inflammatory peptides. Taken together, these studies demonstrate the diverse application of proteomics in elucidating key pathways and proteins involved in avian reproduction and development.

4.5.2 Proteomics of behavior and plumage

The zebra finch is the dominant animal model for studying molecular mechanisms underlying learning, memory, vocalization, and social behavior. A natural perceptual experience, such as a sound of another bird singing, triggers rapid changes in expression of specific genes in the auditory region of the zebra finch brain (Mello et al., 1992). Repeated exposure to the same song leads to stimulus-specific habituation of the original response (Petrinovich and Patterson, 1979). To understand the process of habituation better, Dong et al. (2009) used DNA microarrays and 2D PAGE MS approaches to analyze global changes of gene expression at different stages in the development of habituation. This study showed that exposure to a song induces massive changes in gene expression, and that song response habituation is not a simple loss of the original responses but rather a change of neuronal responses underpinned by a novel and different gene expression profile. Analysis of protein expression showed that habituation is accompanied by a decrease in expression of cellular and mitochondrial proteins that are involved in biosynthesis and energy metabolism. Neuropeptides are signaling peptides found in neural tissue that modulate a wide range of physiological and behavioral processes including metabolism, reproduction, learning, and memory. Xie et al. (2010) used a combination of bioinformatics, MS, and biochemistry for prediction, identification, and localization of neuropeptidome of the zebra finch. Computational analysis of the zebra finch genome predicted 70 putative prohormones and 90 peptides derived from 24 putative pheromones identified in the zebra finch brain by two different MS approaches. The power of MS was further used for localization of a subset of peptides in the major song control nuclei of the zebra finch brain. Furthermore, gene expression of a subset of pheromone genes was anatomically mapped in selected zebra finch brain sections by in situ hybridization.

Birds display an enormous range of plumage colors, and this diversity rivals or exceeds that of plants (Stoddard and Prum, 2011). Still, bird plumage occupies only about 30% of the possible colors that birds can see (Stoddard and Prum, 2011). The molecular mechanisms that determine and drive the development of this diversity are largely unknown. The breeding plumage of male pied flycatchers varies from a brown to dark black. Leskinen et al. (2012) characterized and quantified the proteome of developing pied flycatcher feathers to advance understanding of physiological processes that underlay the variation in pigmentation. In total, 294 proteins were identified in the developing feathers. About 65 proteins were linked with epidermal development and/or pigmentation in the developing feathers, and 23 proteins were associated with pigment-containing organelles—melanosomes. The comparison of the brown- and black-specific proteomes revealed several proteins and functional networks that differed in expression between the two phenotypes and that are candidates for further studies. The most pronounced differences were detected in immunological signaling, oxidative stress, energy balance, and protein synthesis networks, and these differences might be responsible for differential feather growth and color pigmentation. A recent study tried to determine the molecular mechanism behind Columbian plumage feathers in the H line of the "Yufen I" commercial egg-layer (Wang et al., 2019). Both transcriptome and proteome were utilized in the analysis with 209 genes and 382 proteins differentially expressed in two locations. The melanogenesis pathway and melanin synthesis were involved via nine proteins that were differentially expressed. Melanogenesis, cardiomyocyte adrenergic, calcium, and cGMP-PKG were all activated pathways in Columbian plumage.

4.5.3 Proteomics of performance and physiology

Food products derived from farm animals, birds, and fish represent a significant part of the human diet. Understanding the nutrient metabolism, muscle accretion, and fat deposition in food birds provides practical knowledge that can be used to improve feed conversion efficiency, food quality, and the health and welfare of animals. Animal feed represents the major cost of poultry production. A balanced poultry diet is reflected in optimal growth and production at minimal nutrient expense. Because of the composition of poultry diet, where corn and soybeans are used as major sources of energy and proteins, respectively, some amino acids become more limited than others. Corzo et al. (2005) utilized the power of MS to understand amino acid requirements in chickens. Blood plasma proteome from chickens fed an adequate or lysine-deficient diet was analyzed to identify potential biomarkers of dietary lysine deficiency. The analysis revealed that lysine deficiency might not result in a simple overall reduction of protein synthesis in chickens fed with a lysine-deficient diet, but rather in reduced anabolism of specific proteins. Corzo et al. (2006) and Zhai et al. (2012) also evaluated the effect of dietary methionine on breast muscle accretion in broiler chickens (Corzo et al., 2006; Zhai et al., 2012). This study showed that four canonical pathways related to muscle development (citrate cycle, calcium signaling, actin cytoskeleton signaling, and clathrin-mediated endocytosis signaling) were differentially regulated between chickens that were fed with low- and high-methionine diets (Zhai et al., 2012). In addition, this study suggested that a methionine-rich diet preferably induced muscle accretion by sarcoplasmic over myofibrillar hypertrophy. A recent study concluded that changes in the diet composition can have large impacts on protein origins leaving the ileum by analyzing 160 Ross PM3 broilers fed either maize/soy-based diet as reference or the addition of 20% raw soy-meal to putatively cause changes in protein flow from the ileum (Cowieson et al., 2017). The raw soy-meal addition caused an increase in endogenous protein relative abundance and decrease in protein from soy and no effect on protein from maize. This study describes the ability of proteomics to be used to determine changes in digestion and secretion in chickens for a more in depth understanding of diet effects on the digestive tract. The blood plasma is an extremely complex tissue that contains thousands of distinct proteins. It is also the most common tissue used in diagnosis of disease and nutritional status. Several authors analyzed blood plasma protein composition to gain better understanding of protein dynamics during chicken development (Huang et al., 2006) or for discovery of plasma biomarkers that reflect nutritional conditions (Corzo et al., 2004, 2006). Muscle meat food products derived from birds, and in particular chickens, are important sources of essential nutrients and energy intake in the human diet. Proteomics has an obvious potential to study a broad range of aspects related to the meat production including nutrition, muscle formation, breed differentiation, meat quality, and meat contamination (Paredi et al., 2013; Schilling et al., 2017). Chicken strains selected for meat production show dramatic growth rates and accelerated accretion of the pectoralis (breast) major and minor muscles. The proteome of the chicken pectoralis muscle has been extensively profiled (Corzo et al., 2006; Zhai et al., 2012; Doherty et al., 2004; Teltathum and Mekchay, 2009), and another study identified over 5000 unique proteins in the pectoralis muscle of studied birds (Zhai et al., 2012). A complementary study identified the proteome of the pipping muscle, which is primarily used for breaking the egg's surface during hatching (Sokale et al., 2011). A recent study identified the potential role of mitochondria in the breast meat of feed efficient broilers through analysis of

152 differentially expressed proteins using IPA (Kong et al., 2016). A complementary study involving the proteogenomic analysis of breast meat in high-feed efficiency broiler males found those birds showed enrichment of ribosome assembly as well as proteasomes and autophagy processes for quality control and nuclear transport and protein translation compared to low-feed efficiency males (Bottje et al., 2017). This study is also a basis for phenotyping feed efficiency from a proteogenomic perspective and improving selection through a more well-defined phenotype. The identified proteins, 676 in all, were analyzed using the assigned Gene Ontology categories for molecular function, biological process, or cellular component. This analysis revealed which protein functions and cellular activities are important for rapid development of pipping muscle during embryogenesis.

McCarthy et al. (2006) analyzed the proteomes of the supporting stromal and B cells isolated from the chicken bursa of Fabricius, a unique bird organ and a common experimental system for B-cell development (McCarthy et al., 2006). Proteins were isolated from the two major functional cell types of bursa by a sequential detergent extraction procedure that increased proteome coverage and helped to localize known and previously unknown proteins to different cellular compartments. Functional modeling of the identified proteins provided insights about signaling pathways involved in programmed cell death, proliferation, and differentiation. In a similar study, van den Berg et al. (2007) applied whole organ proteomics to study frozen spleen. To gain a better understanding of B-cell development in the bursa of Fabricius, Korte et al. used a quantitative 2D PAGE approach to study bursal proteomes from the embryonic and posthatch developmental stages. They showed that enzymes of the retinoic acid metabolism play a crucial role in the early development of the primary avian B-cell organ (Korte et al., 2013). Similar observations were done in mammals, where vitamin A plays a similarly important role in the development of secondary lymphoid organs (van de Pavert et al., 2009). Proteomic analysis of the Harderian gland showed that Harderian gland is a site of active mucosal immunity also due to expression of hematopoietic prostaglandin D synthase (Scott et al., 2005), which is necessary for production of prostaglandin D2, the potent activator of inflammatory responses (Serhan et al., 2008). Several proteomic studies have used chicken embryos to study embryonic development of retina (Lam et al., 2006; Mizukami et al., 2008; Finnegan et al., 2008, 2010), face (Mangum et al., 2005), CSF (Parada et al., 2005, 2006), liver (Jianzhen et al., 2007), cardiovascular system (Bon et al., 2010), and vasculature (Soulet et al., 2013). Lam et al. (2006), Mizukami et al. (2008), and Finnegan et al. (2008) used 2D PAGE to catalog the most abundant proteins in young chicken retina and to identify those that were differentially expressed between different stages of retina development (Lam et al., 2006; Mizukami et al., 2008; Finnegan et al., 2008). These studies identified known and novel proteins that play roles in early ocular growth and neural development. The retinal dysplasia and degeneration (rdd) chick was used as a model to identify proteins that are differentially expressed during the onset of degeneration of retina (Finnegan et al., 2010). Mangum et al. (2005) studied the development of the first pharyngeal arch, an embryonic structure that is crucial for the formation of the face, as a model for the craniofacial defects in humans (Mangum et al., 2005). This study showed that expression of molecular chaperones, cytoskeletal proteins, and plasma proteins associated with vascularization was altered the most between the different stages of craniofacial development. Initial characterization of the zebra finch retina and optic tectum, a major structure of the midbrain, proteomes have been done using the one-dimensionl PAGE approach coupled with MS (Sloley et al., 2007a,b). Because these studies were done before the complete zebra finch genome was available, potential zebra finch proteins had to be identified by cross-species matching using the nonredundant NCBI, Ensemble, and Swissprot protein databases.

4.5.4 Proteomics of disease, myopathy, and infection

The recent explosion of animal and pathogen genomes has not only enabled identification of genes involved in the etiology and pathology of diseases (such as mutant gene variants or virulence factors) but also has opened up the door for proteomics to probe the pathogenesis and pathogen–host interactions on a global protein level. Proteomics has greatly improved understanding of diseases; it has been very valuable in diagnostic marker discovery, and it has a great potential in drug discovery. Despite its great value, disease proteomics remains to be one of the least-developed areas in avian research. Nevertheless, proteomics has been used to study the pathogenesis, etiology, and pathology of several avian (infectious) diseases. In addition, proteomics has been used to study various human diseases on chicken experimental models (Andrews Kingon et al., 2013).

4.5.4.1 Disease proteomics

The chicken is an ideal and unique animal model to probe the etiology and progression of spontaneous human epithelial ovarian cancer, largely because the domestic chicken has a high prevalence of spontaneous ovarian carcinomas. EOC remains the most lethal gynecologic malignancy in part because early detection and therapeutic strategies have been largely unsuccessful (Kurman and Shih, 2010). Hawkridge et al. (2010) used this model to study the onset and progression of EOC by a large-scale

biomarker discovery effort involving longitudinal sample collection and protein analysis by MS. Inter- and intra-individual measurement of proteins identified ovomacroglobulin (ovostatin) as a potential EOC biomarker because its levels in plasma were undetected in a healthy individual and significantly higher during later stages in an EOC bird. Pulmonary hypertension syndrome, or ascites syndrome, is a metabolic pathogenesis in meat-type chickens that is manifested by the formation of ascites. Ascites syndrome is one of the major problems in the chicken industry, and is caused by cardiopulmonary insufficiency during high-oxygen demands spurred by a rapid tissue growth (Currie, 1999). Proteomic analysis of the cardiac mitochondrial matrix proteomes of the ascites-resistant and ascites susceptible line broilers suggested that the mitochondria of susceptible chickens may respond inappropriately to hypoxia (Cisar et al., 2005). A complementary proteomic analysis of the hepatic proteomes of healthy birds and those with ascites suggested that insufficient energy generation in the liver is responsible for development of pulmonary hypertension syndrome (Wang et al., 2012).

4.5.4.2 Proteomics of muscle myopathy

Understanding the mechanism behind serious metabolic disorders is crucial for the development of treatment and preventative strategies. In the modern broiler, major metabolic disorders affecting producers and consumers are muscle myopathies in the form of wooden breast (WB), white striping (WS), and spaghetti meat (SM). In the case of WB, Cai et al. (2018) found eight differentially expressed proteins between normal and WB meat samples with differences indicating increased oxidative stress in addition to decreased glycolytic enzymes in WB muscle. When analyzing five different genetic strains of broilers, more abundant proteins in WB were involved in carbohydrate metabolism, oxidative stress, cytoskeleton structure, and signaling with regulated pathways involved in similar functions as well as cell death and survival and cellular organization (Zhang et al., 2020a,b,c). Postmortem proteomic analysis of WB affected tissue using 2D gel electrophoresis revealed changes in protein degradation, including desmin fragments, ovotransferrin chain A, and troponin I chain I degradation (Zhang et al., 2020a,b,c). Interestingly, some glycolytic proteins in WB showed evidence of posttranslational modification, including enolase, phosphoglucomutase-1, PGAM1, and pyruvate kinase. A study using a hybrid LTQ-OrbitrapXL LC-MS/MS compared proteomic profiles of normal breast and breast meat affected by WS or WB (Kuttappan et al., 2017). Using ingenuity pathway analysis (IPA) software, the 800 differentially expressed proteins were associated to biological pathways. IPA showed eIF-2 signaling, mTOR signaling, and regulation of eIF4 and $p70^{S6K}$ signaling were up-regulated in breast with severe myopathy compared to normal. The indication of increased protein synthesis pathways could be due to rapid growth and cellular stress due to degradation and attempted tissue repair. Down-regulated pathways included glycolysis and gluconeogenesis which coincided with higher pH. For WS, SDS-Page and further analysis of chemical composition of WS meat showed higher fat and lower protein content along with higher collagen and decreased protein quality (Petracci et al., 2014). SM meat was also analyzed in a similar study using SDS-PAGE and found that while the proteome profile varied little from SM to normal, the overall protein abundance was reduced as with other myopathies (Tasoniero et al., 2020).

4.5.4.3 Proteomics of infections

Some strains of the highly pathogenic avian influenza A subtype H5N1 cause severe acute encephalopathy and neurodegeneration in poultry and migratory birds. To reveal the mechanisms that cause the observed neuropathogenesis, Zou et al. (2010) used comparative proteomics to identify the proteins that were expressed differently in the brains of healthy and H5N1-infected chickens (Zou et al., 2010). Among the differentially expressed proteins were septin 5 and collapsin response mediator protein 2 (CRMP2). Septin 5 is dysregulated in Parkinson's disease and CRMP2 in Alzheimer's disease, Down syndrome, and human T-cell lymphotropic virus type I associated myelopathy (Vincent et al., 2005; Lubec et al., 1999; Son et al., 2005). This suggests that these proteins might also have a role in neurodegenerative pathologies associated with influenza H5N1 infection. Gallid herpesvirus 2 (GaHV-2) is an avian oncogenic herpesvirus that causes a highly infectious and rapidly progressive lymphomatous disease of chickens, Marek's disease (MD). GaHV-2 infects and transforms cells in all chicken genotypes, but some chickens are genetically resistant to gross lymphoma formation (Burgess and Davison, 2002). To better understand the molecular mechanisms of differential susceptibility to MD, spleen proteomes of MD susceptible and MD-resistant chickens were analyzed using the 2D PAGE MS approach (Thanthrige-Don et al., 2010). Among the differentially expressed proteins identified in this study were antioxidants; molecular chaperones; and proteins involved in the activation and migration of T lymphocytes, formation of cytoskeleton, protein degradation, and antigen presentation; and some of these were implicated as potential factors in MD resistance. In a similar study, analysis of the changes in the chicken spleen proteome induced by the GaHV-2 infections revealed that protein expression was the most altered during early stages of infection. Comparative analysis showed that proteins that were differentially

expressed at different timepoints postinfection were involved in a variety of cellular processes that are crucial for the host response to GaHV-2 infection and pathogenesis (Thanthrige-Don et al., 2009). To better understand how GaHV-2 infection changes the host protein expression, several proteomic profiling studies have been done to determine the proteome of GaHV-2-lytically infected chicken embryo cells (CECs) (Liu et al., 2006; Chien et al., 2011, 2012; Ramaroson et al., 2008) compare the phosphoproteomes of mock- and GaHV-2-infected CECs (Chien et al., 2011; Ramaroson et al., 2008); and quantify protein expression changes caused by GaHV-2 infection (Chien et al., 2012). Collectively, these studies revealed GaHV-2 infection dramatically changes the protein expression profile of infected cells. Overlaying quantitative and phosphorylation data revealed that GaHV-2 infection altered both protein expression and phosphorylation of proteins from several cellular pathways, and among the most affected processes were RNA transport, signal transduction, initiation of translation, and protein degradation. Perhaps the most interesting discovery of these studies is that GaHV-2 causes unique phosphorylation of the translation initiation factor 4E-binding protein 1, which is important for the assembly of the protein translation initiation complex after virus infection. In a complementary study, Buza and Burgess (2007) used MudPIT to profile the proteome of the GaHV-2-transformed lymphoblastoid cell line UA01. Functional modeling of the UA01 proteome showed that cells had a typical cancer phenotype. UA01 cells were activated, differentiated, and proliferative, but antagonistic to apoptosis, energy, quiescence, and senescence. Identified cytokines, cytokine receptors, and related proteins suggested that the UA01 proteome had a T-cell regulatory (T-reg) rather than T-helper (Th)-2 phenotype. MD, a CD4+ T cell lymphoma of chickens, and many human lymphomas overexpress the Hodgkin's disease antigen CD30 (CD30hi). MD lymphomas, like its human homologs, are formed by a minority of transformed (CD30hi) and a majority of nontransformed (CD30lo) cells (Burgess and Davison, 2002; Shack et al., 2008). Although the GaHV-2 gene meq is the principal oncogene, which acts as a transcription factor and transforms via the Jun pathway (Levy et al., 2005; Mescolini et al., 2019), the exact mechanism of neoplastic transformation and transition from CD30lo to CD30hi neoplastic phenotype is unknown. As described in this review, most of the proteomics work that has been done in aves has been descriptive, based on differential expression. Kumar et al. (2012), though, compared microRNA, mRNA, and protein levels and from this data imputed functional models. As described by many others in many different systems, there was poor overall correlation between mRNA and protein expression (Gygi et al., 1999a,b; Cullen et al., 2004). However, to identify the key regulatory proteins responsible for neoplastic transformation, all gene products which were differentially expressed in the same direction at both mRNA and protein levels (i.e., concordant) were selected for further analysis, and these did have an overall positive correlation. Those gene products with the greatest mRNA and protein correlation are known to be involved in human CD30-over expressing lymphomas. When ranked into pentiles based on protein expression levels, the Gene Ontology Biological Processes of cell cycle and proliferation to programmed cell death ratios were greatest in pentile 1. The authors then identified the numbers of putative canonical MDV Meq (the virus oncogene) binding sites in each of the 88 concordantly expressed genes' promoters; and genes in pentile 1 had the most Meq binding sites. Of the five concordant genes previously implicated in lymphomagenesis in other species most were in pentile 1 suggesting direct transcriptional regulation by Meq. In contrast, one gene product, CST3 was likely regulated by a micro-RNA. Recent proteomic MD research has revealed that MD viruses inhibit type I interferon in the thymus and bursa of Fabricius infected chickens and that strains of varying virulence affected type I IFNs differently (Sun et al., 2019). *Plasmodium gallinaceum* is a protozoal avian malaria parasite and the most relevant animal model of the human parasite *Plasmodium falciparum* sexual stages zygote and ookinete. The early stages of the *P. gallinaceum* life-cycle occur in its definitive host, the mosquito, but this process is largely unknown. To better understand the initial molecular mechanisms of *P. falciparum* vector interaction, Patra et al. (2008) used high-throughput proteomics to identify 966 orthologous proteins of *P. falciparum* present in the zygote and ookinete proteomes (Patra et al., 2008). About 40% of the identified proteins had hypothetical status, and the majority of these were transmembrane or secreted proteins. This suggests that these proteins might play important roles in parasite−host interactions. Coccidiosis of fowl, an intestinal disease caused by a protozoal parasite Eimeria, causes significant losses for the poultry industry. Plasma proteome profiles of two different chicken lines infected with one of three common Eimeria species were compared by the 2D PAGE MS (Gilbert et al., 2011). About 46 proteins displayed significantly changed expression in response to Eimeria infection. The differentially expressed proteins were found to participate in innate immunity, blood clotting, and iron and mitochondrial metabolism, and these processes fit well within the host acute-phase responses that are initiated when a tissue is invaded by a microorganism. Some of the identified proteins were suggested as candidate biomarkers for early diagnosis of Eimeria infection. A recent study investigating the interaction between *Eimeria maxima* and chicken jejunal epithelial cells utilized shotgun LC-MS/MS and Western blot analysis to reveal 35 annotated (Gene Ontology) peptides, 22 of which were associated with binding activity

and 15 with catalytic activity (Huang et al., 2018). This revealed novel findings of host-parasite interaction on a cellular level. Another protozoan parasite affecting poultry is *Histomonas meleagridis* which causes histomonosis or blackhead disease in poultry including turkeys. Proteomic study involving virulent and attenuated strain of *Histomonas* showed increased metabolism, in vitro adaptation and ameboid morphology pathways implicated in virulence based on MS analysis of 49 protein spots (Monoyios et al., 2018). Interestingly, MS also identified differential expression of *Escherichia coli* DH5α proteins indicating reciprocal interaction between two strains during monoxenic cultivation. *Salmonella enterica* subspecies enterica is a gram-negative enterobacterium and an important pathogen that infects a broad range of vertebrate species including chicken and man. The subspecies is routinely divided into more than 2500 serotypes (serovars) based on antigenic epitopes (Franklin et al., 2011). Salmonella serovars differ in host range and pathogenic potential, but molecular mechanisms underlying these differences are not well understood. Several proteomic studies compared proteomes of different avian Salmonella serovars and discovered possible molecular mechanisms responsible for the observed phenotypic differences (Encheva et al., 2005; Osman et al., 2009; Sun and Hahn, 2012).

4.5.5 Proteomics of avian welfare

Consumer concern for animal health and welfare has risen along with the popularity for chicken as a healthy protein source (Powers, 2020). The poultry industry now faces regulations as well as consumer preferences for birds raised in nonstressful and enriching environments. The ability for industry to measure and report factors that demonstrate good animal welfare has been limited with the definition of avian welfare itself left largely undefined. Proteomics has been utilized to determine novel biomarkers for and measurements of welfare in the modern broiler and other food animals with the major stress indicators being cortisol, creatine kinase, and lactate (Harkati et al., 2018; Sardi et al., 2020; Marco-Ramell et al., 2016; Bozzo et al., 2018). New research into improved techniques and specific markers for stressors such as heat stress, immobility, fasting, and ammonia exposure have been developed using the avian model and proteomics.

In the case of heat stress, understanding the mechanism behind physiological responses to heat stress in the high-metabolic, temperature-intolerant broiler is key, especially as global temperatures rise due to climate change. Proteomic work has resulted in the identification of novel molecular signatures for a bird's response to heat stress through measuring GRP75, a member of the heat-shock protein family (Dhamad et al., 2019). Another heat shock protein marker for heat stress was investigated, and most interestingly, was from a noninvasive source, the feather (Greene et al., 2019). HSP70 protein was detectable in the growing feather of heat-stressed Cobb500 broilers. This study is a direct example of proteomic technique providing noninvasive phenotypes and measures of welfare in the poultry industry. A study analyzing the proteomic response to heat stress in the avian hypothalamus revealed damage to the hypothalamus and provocation of pathways involved in attenuating protein destabilization and degradation and improving cytoskeleton integrity, oxygen transport, and neural development after acute heat stress (Tu et al., 2018). A study investigating response to heat stress during transportation found glycolysis pathway, calcium signaling, and molecular chaperones in the breast muscle of heat-stressed birds to be significantly different using iTRAQ proteomic analysis (Xing et al., 2017). Heat stress analysis on other tissues such as liver, spleen, and hypothalamus revealed differentially expressed proteins related to immune response, metabolism, and cellular processes including cell death (Tang et al., 2015; Ma et al., 2019; Tu et al., 2018). The ability for proteomic analysis to not only identify key signatures of responses but also annotate key proteins to a specified biological pathway makes advances in mechanistic understanding of animal welfare possible.

Although the modern broiler is extremely heat-intolerant, its high metabolism results in the fastest growth of almost any other food animal. This rapid growth is often associated with increased incidence of lameness and impaired mobility which is a major concern for animal welfare and health. Tonic immobility has been used to investigate the potential modulation of emotional reactivity on chronic stress-related behavior and physiological dysfunction in animals and corticosterone (CORT) delivered in drinking water is an established model for chronic stress in broilers. A study utilized these models conducted 2D gel electrophoresis and Western blot analysis of proteins in the breast muscle. Analysis showed CORT treatment, mimicking chronic stress, reduced growth of muscle by suppressing protein synthesis, and long tonic immobility had similar negative effects on muscle growth potentially via glucose metabolism (Fu et al., 2014). This along with similar studies demonstrates not only the physiological implications of immobility, but also the effect of chronic stress on health and performance (Hayward and Wingfield, 2004; Minvielle et al., 2002; Wang et al., 2013). A leading cause of lameness and immobility is bacterial chondronecrosis with osteomyelitis (BCO), also called femur head necrosis (FHN). Currently, identification of BCO requires necropsy of the femur head itself within the bird. However, proteomic research seeks to not only understand the mechanism behind this disorder but also identify a biomarker for earlier and easier phenotyping of BCO. To that end, a proteomic analysis used matrix-assisted laser desorption ionization time of flight mass spectrometry

(MALDI-TOF-MS) and liquid chromatography/electrospray ionization-tandem mass spectrometry (LC-MS/MS) to determine differential peptides in the plasma of FHN affected versus healthy broilers. Fibrinogen- and fetuin-derived peptides as well as alpha-1-acid glycoprotein, albumin, and SPINK7 were reduced in FHN affected birds with gallacin-9, apolipoprotein A1, and hemoglobin being elevated in the plasma of birds with FHN (Packialakshmi et al., 2016). The results of this study suggest tissue adhesion, proteolysis, and infection could be culpable for FHN. Although the study provides the basis for circulating biomarkers for FHN, more research is needed to determine the significance of these differential peptides and their efficacy as biomarkers. Tibial dyschondroplasia (TD) is another disorder which commonly causes lameness in fast-growing broilers. A proteomic analysis of high altitude Tibetan chickens, which have low incidence of TD, compared to low-altitude broilers revealed increased vascular distribution in the tibia accompanied by up-regulated hypoxia-inducible-factor-1 alpha as well as vascular endothelial growth factor A (VEGFA) and VEGF receptors. Hypoxia exposure of low-altitude broilers resulted in increased angiogenesis and upregulation of similar factors. This study describes the potential role in inhibition of angiogenesis in the pathology of TD and sets the ground work for potential target pathways in selection of broilers for resistance to TD.

A common practice in poultry production is fasting and has raised concerns by animal welfare advocates regarding detrimental effects on animal health not being considered. About 24 hour fasting has shown to impact broiler health by delaying growth and performance. A study using 2D electrophoresis and MALDI-TOF on intestinal samples of fasted chickens revealed differences in proteins related to fatty acid binding, stress response, and ion transport (Simon et al., 2019). The results of this study also revealed decreased intestinal absorption and differential expression of structural proteins. Studies of the hypothalamus revealed fasting induced differentially expressed enzymes involved in metabolic pathways between lines selected for low and high-body weights. Oxidative phosphorylation, citric acid cycle, and carbon metabolism were the major pathways connected to differentially expressed proteins. Fasting responsive proteins and their associated pathways were significantly over-expressed in high weight selected broilers in response to fasting (Liu et al., 2019). Taken together, these studies support the welfare effects of fasting on broilers and demonstrate proteomics capacity for identifying and defining pathways involved in welfare of fasting birds.

Ammonia is a major component of haze and often associated with certain management practices in the poultry industry and is often a cause of animal welfare concerns as birds are exposed to it low to the ground for long periods of time. Proteomics analysis in the thymus of chickens exposed to NH_3 had ultrastructural changes and 66 differentially expressed proteins involved in immune function, metabolic processes, and apoptosis. This proteomics analysis demonstrated ammonia toxicity mechanism in the thymus through immunosuppression, metabolic disruption, and apoptotic effect (Chen et al., 2020a). iTRAQ proteomic analysis revealed in a separate study that 30 differentially expressed proteins in the liver of ammonia exposed birds were related to nutrient metabolism, immune and stress response, as well as detoxification/biotransformation and transcriptional and translational regulation (Zhang et al., 2015). This resulted in differences in overall bird health and taken together, these studies suggest potential target pathways for measuring welfare in management related to ammonia exposure.

4.6 Conclusions

One of the primary goals of biology is to understand how organisms function on a molecular level. Because proteins are the "makers of life," understanding their functions is central to understanding biology. Proteomics is an extremely versatile and comprehensive platform to study proteins on a large scale. It offers a broad range of tools that can be used to determine the identity, structure, quantity, and quality of expressed proteins in biological systems as well as physiological responses to disease and environmental stressors. Proteomic data have also shown to be integral in the combined analysis of other omics technologies as the indicator of functional units in a given organism. Thus, while scientific questions in avian research remain essentially the same, proteomics has the potential to transform the form of biological inquiry.

References

Ahmed, T.A., Suso, H., Hincke, M.T., 2017. In-depth comparative analysis of the chicken eggshell membrane proteome. J. Proteomics 155, 49–62. https://doi.org/10.1016/j.jprot.2017.01.002. In this issue.

Anderson, N.L., Anderson, N.G., 2002. The human plasma proteome: history, character, and diagnostic prospects. Mol. Cell. Proteomics 1, 845–867.

Andrews Kingon, G.L., Petitte, J.N., Muddiman, D.C., Hawkridge, A.M., 2013. Multi-peptide nLC-PC-IDMS-SRM-based assay for the quantification of biomarkers in the chicken ovarian cancer model. Methods 61, 323–330.

Aslam, B., Basit, M., Nisar, M.A., Khurshid, M., Rasool, M.H., 2017. Proteomics: technologies and their applications. J. Chromatogr. Sci. 55, 182–196.

Atikuzzaman, M., Sanz, L., Pla, D., Alvarez-Rodriguez, M., Ruber, M., Wright, D., et al., 2017. Selection for higher fertility reflects in the seminal fluid proteome of modern domestic chicken. Comp. Biochem. Physiol. Genom. Proteonom. 21, 27–40.

Balcerzak, M., Malinowska, A., Thouverey, C., Sekrecka, A., Dadlez, M., Buchet, R., et al., 2008. Proteome analysis of matrix vesicles isolated from femurs of chicken embryo. Proteomics 8, 192–205.

van den Berg, B.H.J., Harris, T., McCarthy, F.M., Lamont, S.J., Burgess, S.C., 2007. Non-electrophoretic differential detergent fractionation proteomics using frozen whole organs. Rapid Commun. Mass Spectrom. 21, 3905–3909.

Bon, E., Steegers, R., Steegers, E.A.P., Ursem, N., Charif, H., Burgers, P.C., et al., 2010. Proteomic analyses of the developing chicken cardiovascular system. J. Proteome Res. 9, 268–274.

Bondarenko, P.V., Chelius, D., Shaler, T.A., 2002. Identification and relative quantitation of protein mixtures by enzymatic digestion followed by capillary reversed-phase liquid chromatography-tandem mass spectrometry. Anal. Chem. 74, 4741–4749.

Bottje, W.G., Lassiter, K., Piekarski-Welsher, A., Dridi, S., Reverter, A., Hudson, N.J., Kong, B.-W., 2017. Proteogenomics reveals enriched ribosome assembly and protein translation in pectoralis major of high feed efficiency pedigree broiler males. Front. Physiol. 8, 306.

Bozzo, G., Barrasso, R., Marchetti, P., Roma, R., Samoilis, G., Tantillo, G., Ceci, E., 2018. Analysis of stress indicators for evaluation of animal welfare and meat quality in traditional and jewish slaughtering. Animals (Basel) 8 (4). https://doi.org/10.3390/ani8040043. In this issue.

Burgess, S.C., Davison, T.F., 2002. Identification of the neoplastically transformed cells in Marek's disease herpesvirus-induced lymphomas: recognition by the monoclonal antibody AV37. J. Virol. 76, 7276–7292.

Buza, J.J., Burgess, S.C., 2007. Modeling the proteome of a Marek's disease transformed cell line: a natural animal model for CD30 overexpressing lymphomas. Proteomics 7, 1316–1326.

Cai, Q., Qian, X., Lang, Y., Luo, Y., Pan, S., Hui, Y., et al., 2013. The genome sequence of the ground tit *Pseudopodoces humilis* provides insights into its adaptation to high altitude. Genome Biol. 14, R29.

Cai, K., Shao, W., Chen, X., Campbell, Y.L., Nair, M.N., Suman, S.P., et al., 2018. Meat quality traits and proteome profile of woody broiler breast (pectoralis major) meat. Poultry Sci. 97, 337–346.

Cao, P., Stults, J.T., 1999. Phosphopeptide analysis by on-line immobilized metal-ion affinity chromatography-capillary electrophoresis-electrospray ionization mass spectrometry. J. Chromatogr. A 853, 225–235.

Chance, M.R., 2001. Unfolding of apomyoglobin examined by synchrotron footprinting. Biochem. Biophys. Res. Commun. 287, 614–621.

Chelius, D., Bondarenko, P.V., 2002. Quantitative profiling of proteins in complex mixtures using liquid chromatography and mass spectrometry. J. Proteome Res. 1, 317–323.

Chen, D.C., Hu, G.H., Zhang, S., Zhang, H.F., Teng, X.H., 2020a. Ammonia-triggered apoptosis via immune function and metabolic process in the thymuses of chickens by proteomics analysis. Ecotoxicol. Environ. Saf. 198, 9.

Chen, Q., Wang, Y., Liu, Z., Guo, X., Sun, Y., Kang, L., et al., 2020b. Transcriptomic and proteomic analyses of ovarian follicles reveal the role of VLDLR in chicken follicle selection. BMC Genom. 21, 486.

Chien, K.Y., Liu, H.C., Goshe, M.B., 2011. Development and application of a phosphoproteomic method using electrostatic repulsion-hydrophilic interaction chromatography (ERLIC), IMAC, and LC-MS/MS analysis to study Marek's Disease Virus infection. J. Proteome Res. 10, 4041–4053.

Chien, K.Y., Blackburn, K., Liu, H.C., Goshe, M.B., 2012. Proteomic and phosphoproteomic analysis of chicken embryo fibroblasts infected with cell culture-attenuated and vaccine strains of Marek's disease virus. J. Proteome Res. 11, 5663–5677.

Cisar, C.R., Balog, J.M., Anthony, N.B., Donoghue, A.M., 2005. Differential expression of cardiac muscle mitochondrial matrix proteins in broilers from ascites-resistant and susceptible lines. Poultry Sci. 84, 704–708.

Corzo, A., Kidd, M.T., Pharr, G.T., Burgess, S.C., 2004. Initial mapping of the chicken blood plasma proteome. Int. J. Poultry Sci. 3, 157–162.

Corzo, A., Kidd, M.T., Koter, M.D., Burgess, S.C., 2005. Assessment of dietary amino acid scarcity on growth and blood plasma proteome status of broiler chickens. Poultry Sci. 84, 419–425.

Corzo, A., Kidd, M.T., Dozier 3rd, W.A., Shack, L.A., Burgess, S.C., 2006. Protein expression of pectoralis major muscle in chickens in response to dietary methionine status. Br. J. Nutr. 95, 703–708.

Cottrell, J., 2011. Protein identification using MS/MS data. J. Proteomics 74 (10), 1842–1851. https://doi.org/10.1016/j.jprot.2011.05.014. In this issue.

Cowieson, A.J., Klausen, M., Pontoppidan, K., Faruk, M.U., Roos, F.F., Giessing, A.M.B., 2017. Identification of peptides in the terminal ileum of broiler chickens fed diets based on maize and soybean meal using proteomics. Anim. Prod. Sci. 57, 1738–1750.

Cullen, P., Lorkowski, S., Kratz, M., Werner, M., Marschall, C., Klein, H.-G., et al., 2004. Basic Concepts of Gene Expression. Analysing Gene Expression. Wiley-VCH Verlag GmbH & Co. KGaA, Darmstadt, Germany, pp. 1–95.

Currie, R.J., 1999. Ascites in poultry: recent investigations. Avian Pathol. 28, 313–326.

Dalloul, R.A., Long, J.A., Zimin, A.V., Aslam, L., Beal, K., Blomberg Le, A., et al., 2010. Multi-platform next-generation sequencing of the domestic Turkey (*Meleagris gallopavo*): genome assembly and analysis. PLoS Biol. 8.

Doherty, M.K., McLean, L., Hayter, J.R., Pratt, J.M., Robertson, D.H., El-Shafei, A., et al., 2004. The proteome of chicken skeletal muscle: changes in soluble protein expression during growth in a layer strain. Proteomics 4, 2082–2093.

Dhamad, A.E., Greene, E., Sales, M., Nguyen, P., Beer, L., Liyanage, R., et al., 2019. 75-kDa glucose-regulated protein (GRP75) is a novel molecular signature for heat stress response in avian species. Am. J. Physiol. Cell Physiol. 318, C289–C303.

Dona, A.C., Kyriakides, M., Scott, F., Shephard, E.A., Varchavi, D., Veselkov, K., et al., 2016. A guide to the identification of metabolites in NMR-based metabonomics/metabolomics experiments. Comput. Struct. Biotechnol. J. 14, 135–153.

Dong, S., Replogle, K.L., Hasadsri, L., Imai, B.S., Yau, P.M., Rodriguez Zas, S., et al., 2009. Discrete molecular states in the brain accompany changing responses to a vocal signal. Proc. Natl. Acad. Sci. U. S. A. 106, 11364–11369.

Durham, M., Regnier, F.E., 2006. Targeted glycoproteomics: serial lectin affinity chromatography in the selection of O-glycosylation sites on proteins from the human blood proteome. J. Chromatogr. A 1132, 165–173.

D'Ambrosio, C., Arena, S., Scaloni, A., Guerrier, L., Boschetti, E., Mendieta, M.E., et al., 2008. Exploring the chicken egg white proteome with combinatorial peptide ligand libraries. J. Proteome Res. 7, 3461–3474.

Ellegren, H., Smeds, L., Burri, R., Olason, P.I., Backstrom, N., Kawakami, T., et al., 2012. The genomic landscape of species divergence in *Ficedula flycatchers*. Nature 491, 756–760.

Encheva, V., Wait, R., Gharbia, S.E., Begum, S., Shah, H.N., 2005. Proteome analysis of serovars Typhimurium and Pullorum of *Salmonella enterica* subspecies I. BMC Microbiol. 5, 42.

Farinazzo, A., Restuccia, U., Bachi, A., Guerrier, L., Fortis, F., Boschetti, E., et al., 2009. Chicken egg yolk cytoplasmic proteome, mined via combinatorial peptide ligand libraries. J. Chromatogr. A 1216, 1241–1252.

Fenn, J.B., Mann, M., Meng, C.K., Wong, S.F., Whitehouse, C.M., 1989. Electrospray ionization for mass spectrometry of large biomolecules. Science 246, 64–71.

Ficarro, S.B., McCleland, M.L., Stukenberg, P.T., Burke, D.J., Ross, M.M., Shabanowitz, J., et al., 2002. Phosphoproteome analysis by mass spectrometry and its application to *Saccharomyces cerevisiae*. Nat. Biotechnol. 20, 301–305.

Fields, S., Song, O., 1989. A novel genetic system to detect protein-protein interactions. Nature 340, 245–246.

Finnegan, S., Robson, J.L., Wylie, M., Healy, A., Stitt, A.W., Curry, W.J., 2008. Protein expression profiling during chick retinal maturation: a proteomics-based approach. Proteome Sci. 6, 34.

Finnegan, S., Robson, J., Hocking, P.M., Ali, M., Inglehearn, C.F., Stitt, A., et al., 2010. Proteomic profiling of the retinal dysplasia and degeneration chick retina. Mol. Vis. 16, 7–17.

Flock, T., Venkatakrishnan, A., Vinothkumar, K., Babu, M.M., 2012. Deciphering membrane protein structures from protein sequences. Genome Biol. 13, 160.

Franklin, K., Lingohr, E.J., Yoshida, C., Anjum, M., Bodrossy, L., Clark, C.G., et al., 2011. Rapid genoserotyping tool for classification of *Salmonella serovars*. J. Clin. Microbiol. 49, 2954–2965.

Froman, D.P., Feltmann, A.J., Pendarvis, K., Cooksey, A.M., Burgess, S.C., Rhoads, D.D., 2011. Physiology and endocrinology symposium: a proteome-based model for sperm mobility phenotype. J. Anim. Sci. 89, 1330–1337.

Fu, W., Duan, Y., Wang, S., Ni, Y., Grossmann, R., Zhao, R., 2014. Comparative proteomic analysis of the breast muscle response to chronic corticosterone administration in broiler chickens showing long or short tonic immobility. Poultry Sci. 93, 784–793.

Geng, M., Ji, J., Regnier, F.E., 2000. Signature-peptide approach to detecting proteins in complex mixtures. J. Chromatogr. A 870, 295–313.

Gilbert, E.R., Williams, P.M., Ray, W.K., Li, H.F., Emmerson, D.A., Wong, E.A., et al., 2010. Proteomic evaluation of chicken Brush-Border membrane during the early posthatch period. J. Proteome Res. 9, 4628–4639.

Gilbert, E.R., Cox, C.M., Williams, P.M., McElroy, A.P., Dalloul, R.A., Ray, W.K., et al., 2011. Eimeria species and genetic background influence the serum protein profile of broilers with coccidiosis. PLoS One 6, e14636.

Greene, E.S., Rajaei-Sharifabadi, H., Dridi, S., 2019. Feather HSP70: a novel non-invasive molecular marker for monitoring stress induced by heat exposure in broilers. Poultry Sci. 98, 3400–3404.

Grey, A.C., Gelasco, A.K., Section, J., Moreno-Rodriguez, R.A., Krug, E.L., Schey, K.L., 2010. Molecular morphology of the chick heart visualized by MALDI imaging mass spectrometry. Anat. Rec. 293, 821–828.

Gygi, S.P., Rochon, Y., Franza, B.R., Aebersold, R., 1999a. Correlation between protein and mRNA abundance in yeast. Mol. Cell Biol. 19, 1720–1730.

Gygi, S.P., Rist, B., Gerber, S.A., Turecek, F., Gelb, M.H., Aebersold, R., 1999b. Quantitative analysis of complex protein mixtures using isotope-coded affinity tags. Nat. Biotechnol. 17, 994–999.

Haab, B.B., 2003. Methods and applications of antibody microarrays in cancer research. Proteomics 3, 2K116–2122.

Han, X., Aslanian, A., Yates 3rd, J.R., 2008. Mass spectrometry for proteomics. Curr. Opin. Chem. Biol. 12, 483–490.

Harkati, A., Boughellout, H., Fuente, G., Krid, F.A., Agli, A., Zidouner, M.N., Sentandreu, M.A., 2018. Effect of pre-slaughter handlings on broiler chicken welfare and relationship with meat quality. J. Vet. Sci. Technol. 9 (4) https://doi.org/10.4172/2157-7579.1000548. In this issue.

Hawkridge, A.M., Wysocky, R.B., Petitte, J.N., Anderson, K.E., Mozdziak, P.E., Fletcher, O.J., Horowitz, J.M., Muddiman, D.C., 2010. Measuring the intra-individual variability of the plasma proteome in the chicken model of spontaneous ovarian adenocarcinoma. Anal. Bioanal. Chem. 398, 737–749.

Hayward, L.S., Wingfield, J.C., 2004. Maternal corticosterone is transferred to avian yolk and may alter offspring growth and adult phenotype. Gen. Comp. Endocrinol. 135, 365–371.

Hocking, P.M., Robertson, G.W., 2000. Ovarian follicular dynamics in selected and control (relaxed selection) male- and female-lines of broiler breeders fed ad libitum or on restricted allocations of food. Br. Poultry Sci. 41, 229–234.

Huang, S.Y., Lin, J.H., Chen, Y.H., Chuang, C.K., Chiu, Y.F., Chen, M.Y., et al., 2006. Analysis of chicken serum proteome and differential protein expression during development in single-comb White Leghorn hens. Proteomics 6, 2217–2224.

Huang, Y., Li, Y., Burt, D.W., Chen, H., Zhang, Y., Qian, W., et al., 2013. The duck genome and transcriptome provide insight into an avian influenza virus reservoir species. Nat. Genet. 45, 776–783.

Huang, J., Liu, T., Li, K., Song, X., Yan, R., Xu, L., et al., 2018. Proteomic analysis of protein interactions between *Eimeria maxima* sporozoites and chicken jejunal epithelial cells by shotgun LC-MS/MS. Parasite. Vector. 11, 226.

Hyung, S.J., Ruotolo, B.T., 2012. Integrating mass spectrometry of intact protein complexes into structural proteomics. Proteomics 12, 1547–1564.

International Chicken Genome Sequencing Consortium, 2004. Sequence and comparative analysis of the chicken genome provide unique perspectives on vertebrate evolution. Nature 432, 695–716.

Jaffe, J.D., Berg, H.C., Church, G.M., 2004. Proteogenomic mapping as a complementary method to perform genome annotation. Proteomics 4, 59–77.

Jianzhen, H., Haitian, M., Liming, Y., Sixiang, Z., 2007. Developmental changes of protein profiles in the embryonic Sanhuang chicken liver. J. Vet. Med. A Physiol. Pathol. Clin. Med. 54, 464–469.

Kim, N.S., Shen, Y.N., Kim, T.Y., Byun, S.J., Jeon, I.S., Kim, S.H., 2007. Expression of AGR-2 in chicken oviduct during laying period. J. Biochem. Mol. Biol. 40, 212–217.

Kim, D.I., Roux, K.J., 2016. Filling the void: proximity-based labeling of proteins in living cells. Trends Cell Biol. 26, 804–817.

Kong, B.-W., Lassiter, K., Piekarski-Welsher, A., Dridi, S., Reverter-Gomez, A., Hudson, N.J., et al., 2016. Proteomics of breast muscle tissue associated with the phenotypic expression of feed efficiency within a pedigree male broiler line: I. Highlight on mitochondria. PLoS One 11, e0155679.

Korte, J., Frohlich, T., Kohn, M., Kaspers, B., Arnold, G.J., Hartle, S., 2013. 2D DIGE analysis of the bursa of Fabricius reveals characteristic proteome profiles for different stages of chicken B-cell development. Proteomics 13, 119–133.

Kumar, S., Kunec, D., Buza, J.J., Chiang, H.I., Zhou, H., Subramaniam, S., et al., 2012. Nuclear Factor kappa B is central to Marek's disease herpesvirus induced neoplastic transformation of CD30 expressing lymphocytes in-vivo. BMC Syst. Biol. 6, 123.

Kuo, Y.M., Shiue, Y.L., Chen, C.F., Tang, P.C., Lee, Y.P., 2005. Proteomic analysis of hypothalamic proteins of high and low egg production strains of chickens. Theriogenology 64, 1490–1502.

Kurman, R.J., Shih, I.M., 2010. The origin and pathogenesis of epithelial ovarian cancer: a proposed unifying theory. Am. J. Surg. Pathol. 34, 433–443.

Kuttappan, V.A., Bottje, W., Ramnathan, R., Hartson, S.D., Coon, C.N., Kong, B.-W., et al., 2017. Proteomic analysis reveals changes in carbohydrate and protein metabolism associated with broiler breast myopathy. Poultry Sci. 96, 2992–2999.

Lam, T.C., Li, K.K., Lo, S.C., Guggenheim, J.A., To, C.H., 2006. A chick retinal proteome database and differential retinal protein expressions during early ocular development. J. Proteome Res. 5, 771–784.

Lee, H.Y., Kim, E.G., Jung, H.R., Jung, J.W., Kim, H.B., Cho, J.W., et al., 2019. Refinements of LC-MS/MS spectral counting statistics improve quantification of low abundance proteins. Sci. Rep-UK 9, 13653.

Leskinen, P.K., Laaksonen, T., Ruuskanen, S., Primmer, C.R., Leder, E.H., 2012. The proteomics of feather development in pied flycatchers (*Ficedula hypoleuca*) with different plumage coloration. Mol. Ecol. 21, 5762–5777.

Levy, A.M., Gilad, O., Xia, L., Izumiya, Y., Choi, J., Tsalenko, A., et al., 2005. Marek's disease virus Meq transforms chicken cells via the v-Jun transcriptional cascade: a converging transforming pathway for avian oncoviruses. Proc. Natl. Acad. Sci. U. S. A. 102, 14831–14836.

Li, G., Sun, C., Wu, G., Shi, F., Liu, A., Yang, N., 2016. iTRAQ-based quantitative proteomics identifies potential regulatory proteins involved in chicken eggshell brownness. PLoS One 11 (12).

Liu, H.B., Sadygov, R.G., Yates, J.R., 2004. A model for random sampling and estimation of relative protein abundance in shotgun proteomics. Anal. Chem. 76, 4193–4201.

Liu, H.C., Soderblom, E.J., Goshe, M.B., 2006. A mass spectrometry based proteomic approach to study Marek's Disease Virus gene expression. J. Virol. Methods 135, 66–75.

Liu, Y., Qiu, N., Gao, D., Ma, M., 2018. Comparative proteomic analysis of chicken, duck, and quail egg yolks. Int. J. Food Prop. 21, 1311–1321.

Liu, L., Yi, J., Ray, W.K., Vu, L.T., Helm, R.F., Siegel, P.B., et al., 2019. Fasting differentially alters the hypothalamic proteome of chickens from lines with the propensity to be anorexic or obese. Nutr. Diabetes 9, 13.

Lubec, G., Nonaka, M., Krapfenbauer, K., Gratzer, M., Cairns, N., Fountoulakis, M., 1999. Expression of the dihydropyrimidinase related protein 2 (DRP-2) in Down syndrome and Alzheimer's disease brain is downregulated at the mRNA and dysregulated at the protein level. J. Neural. Transm. Suppl. 57, 161–177.

Ma, D., Liu, Q., Zhang, M., Feng, J., Li, X., Zhou, Y., et al., 2019. iTRAQ-based quantitative proteomics analysis of the spleen reveals innate immunity and cell death pathways associated with heat stress in broilers (*Gallus gallus*). J. Proteomics 196, 11–21.

Mangum, J.E., Farlie, P.G., Hubbard, M.J., 2005. Proteomic profiling of facial development in chick embryos. Proteomics 5, 2542–2550.

Mann, K., 2007. The chicken egg white proteome. Proteomics 7, 3558–3568.

Mann, K., 2008. Proteomic analysis of the chicken egg vitelline membrane. Proteomics 8, 2322–2332.

Mann, K., Mann, M., 2008. The chicken egg yolk plasma and granule proteomes. Proteomics 8, 178–191.

Mann, K., Mann, M., 2011. In-depth analysis of the chicken egg white proteome using an LTQ Orbitrap Velos. Proteome Sci. 9, 7.

Mann, K., Macek, B., Olsen, J.V., 2006. Proteomic analysis of the acid-soluble organic matrix of the chicken calcified eggshell layer. Proteomics 6, 3801–3810.

Mann, K., Olsen, J.V., Macek, B., Gnad, F., Mann, M., 2007. Phosphoproteins of the chicken eggshell calcified layer. Proteomics 7, 106–115.

Marco-Ramell, A., de Almeida, A.M., Cristobal, S., Rodrigues, S., Roncada, P., Bassols, A., 2016. Proteomics and the search for welfare and stress biomarkers in animal production in the one-health context. Mol. Biosyst. 12 (7), 2024–2235. https://doi.org/10.1039/c5mb00788g.

Marguerat, S., Schmidt, A., Codlin, S., Chen, W., Aebersold, R., Bahler, J., 2012. Quantitative analysis of fission yeast transcriptomes and proteomes in proliferating and quiescent cells. Cell 151, 671–683.

McCarthy, F.M., Cooksey, A.M., Wang, N., Bridges, S.M., Pharr, G.T., Burgess, S.C., 2006. Modeling a whole organ using proteomics: the avian bursa of Fabricius. Proteomics 6, 2759–2771.

Mello, C.V., Vicario, D.S., Clayton, D.F., 1992. Song presentation induces gene expression in the songbird forebrain. Proc. Natl. Acad. Sci. U. S. A. 89, 6818–6822.

Mescolini, G., Lupini, C., Davidson, I., Massi, P., Tosi, G., Fiorentini, L., Catelli, E., 2019. Molecular characterization of a Marek's disease virus strain detected in tumour-bearing turkeys. Avian Pathol. 49 (2), 202–207. https://doi.org/10.1080/03079457.2019.1691715. In this issue.

Minvielle, F., Mills, A.D., Faure, J.M., Monvoisin, J.L., Gourichon, D., 2002. Fearfulness and performance related traits in selected lines of Japanese quail (*Coturnix japonica*). Poultry Sci. 81, 321–326.

Mizukami, M., Kanamoto, T., Souchelnytskyi, N., Kiuchi, Y., 2008. Proteome profiling of embryo chick retina. Proteome Sci. 6, 3.

Monoyios, A., Patzl, M., Schlosser, S., Hess, M., Bilic, I., 2018. Unravelling the differences: comparative proteomic analysis of a clonal virulent and an attenuated *Histomonas meleagridis* strain. Int. J. Parasitol. 48, 145–157.

Myers, S.A., Wright, J., Peckner, R., Kalish, B.T., Zhang, F., Carr, S.A., 2018. Discovery of proteins associated with a predefined genomic locus via dCas9-APEX-mediated proximity labeling. Nat. Methods 15, 437–439.

Nagaraj, N., Wisniewski, J.R., Geiger, T., Cox, J., Kircher, M., Kelso, J., et al., 2011. Deep proteome and transcriptome mapping of a human cancer cell line. Mol. Syst. Biol. 7, 548.

Nanduri, B., Wang, N., Lawrence, M.L., Bridges, S.M., Burgess, S.C., 2010. Gene model detection using mass spectrometry. Methods Mol. Biol. 604, 137–144.

Nealon, J.O., Philomina, L.S., McGuffin, L.J., 2017. Predictive and experimental approaches for elucidating protein-protein interactions and quaternary structures. Int. J. Mol. Sci. 18, 2623.

Oleksyk, T.K., Pombert, J.F., Siu, D., Mazo-Vargas, A., Ramos, B., Guiblet, W., et al., 2012. A locally funded Puerto Rican parrot (*Amazona vittata*) genome sequencing project increases avian data and advances young researcher education. Giga Science 1, 14.

Ong, S.E., Blagoev, B., Kratchmarova, I., Kristensen, D.B., Steen, H., Pandey, A., et al., 2002. Stable isotope labeling by amino acids in cell culture, SILAC, as a simple and accurate approach to expression proteomics. Mol. Cell. Proteomics 1, 376–386.

Osman, K.M., Ali, M.M., Radwan, M.I., Kim, H.K., Han, J., 2009. Comparative proteomic analysis on *Salmonella gallinarum* and *Salmonella enteritidis* exploring proteins that may incorporate host adaptation in poultry. J. Proteomics 72, 815–821.

Ouyang, H., Wang, Z., Chen, X., Yu, J., Li, Z., Nie, Q., 2017. Proteomic analysis of chicken skeletal muscle during embryonic development. Front. Physiol. 8, 281.

O'Farrell, P.H., 1975. High resolution two-dimensional electrophoresis of proteins. J. Biol. Chem. 250, 4007–4021.

Packialakshmi, B., Liyanage, R., Lay, J.O., Okimoto, R., Rath, N.C., 2016. Proteomic changes in the plasma of broiler chickens with femoral head necrosis. Biomark. Insights 11. BMI.S38291.

Pagadala, N.S., Syed, K., Tuszynski, J., 2017. Software for molecular docking: a review. Biophys. Rev. 9, 91–102.

Panse, S., Dong, L., Burian, A., Carus, R., Schutkowski, M., Reimer, U., et al., 2004. Profiling of generic anti-phosphopeptide antibodies and kinases with peptide microarrays using radioactive and fluorescence based assays. Mol. Divers. 8, 291–299.

Parada, C., Gato, A., Bueno, D., 2005. Mammalian embryonic cerebrospinal fluid proteome has greater apolipoprotein and enzyme pattern complexity than the avian proteome. J. Proteome Res. 4, 2420–2428.

Parada, C., Gato, A., Aparicio, M., Bueno, D., 2006. Proteome analysis of chick embryonic cerebrospinal fluid. Proteomics 6, 312–320.

Paredi, G., Sentandreu, M.A., Mozzarelli, A., Fadda, S., Hollung, K., de Almeida, A.M., 2013. Muscle and meat: new horizons and applications for proteomics on a farm to fork perspective. J. Proteomics 88, 58–82.

Patra, K.P., Johnson, J.R., Cantin, G.T., Yates 3rd, J.R., Vinetz, J.M., 2008. Proteomic analysis of zygote and ookinete stages of the avian malaria parasite *Plasmodium gallinaceum* delineates the homologous proteomes of the lethal human malaria parasite *Plasmodium falciparum*. Proteomics 8, 2492–2499.

van de Pavert, S.A., Olivier, B.J., Goverse, G., Vondenhoff, M.F., Greuter, M., Beke, P., et al., 2009. Chemokine CXCL13 is essential for lymph node initiation and is induced by retinoic acid and neuronal stimulation. Nat. Immunol. 10, 1193-1U78.

Peng, M., Li, S., He, Q., Zhao, J., Li, L., Ma, H., 2018. Proteomics reveals changes in hepatic proteins during chicken embryonic development: an alternative model to study human obesity. BMC Genom. 19, 29.

Petracci, M., Mudalal, S., Babini, E., Cavani, C., 2014. Effect of white striping on chemical composition and nutritional value of chicken breast meat. Ital. J. Anim. Sci. 13, 3138.

Petrinovich, L., Patterson, T.L., 1979. Field studies of habituation. 1. Effect of reproductive condition, number of trials, and different delay intervals on responses of the white-crowned sparrow. J. Comp. Physiol. Psychol. 93, 337–350.

Petrotchenko, E.V., Borchers, C.H., 2010. Crosslinking combined with mass spectrometry for structural proteomics. Mass Spectrom. Rev. 29, 862–876.

Powers, R., 2020. Consumers' evaluation of animal welfare labels on poultry products. J. Appl. Commun. Res. 104 (1) https://doi.org/10.4148/1051-0834.2310.

Rabilloud, T., Chevallet, M., Luche, S., Lelong, C., 2010. Two-dimensional gel electrophoresis in proteomics: past, present and future. J. Proteomics 73, 2064–2077.

Ramaroson, M.F., Ruby, J., Goshe, M.B., Liu, H.C., 2008. Changes in the *Gallus gallus* proteome induced by Marek's disease virus. J. Proteome Res. 7, 4346–4358.

Rands, C.M., Darling, A., Fujita, M., Kong, L., Webster, M.T., Clabaut, C., et al., 2013. Insights into the evolution of Darwin's finches from comparative analysis of the *Geospiza magnirostris* genome sequence. BMC Genom. 14, 95.

Rao, M., Morisson, M., Faraut, T., Bardes, S., Feve, K., Labarthe, E., et al., 2012. A duck RH panel and its potential for assisting NGS genome assembly. BMC Genom. 13, 513.

Ross, P.L., Huang, Y.L.N., Marchese, J.N., Williamson, B., Parker, K., Hattan, S., et al., 2004. Multiplexed protein quantitation in *Saccharomyces cerevisiae* using amine-reactive isobaric tagging reagents. Mol. Cell. Proteomics 3, 1154–1169.

Labas, V., Grasseau, I., Cahier, K., Gargaros, A., Harichaux, G., Teixeira-Gomes, A.-P., et al., 2015. Qualitative and quantitative peptidomic and proteomic approaches to phenotyping chicken semen. J. Proteomics 112, 313–335.

Le Roy, N., Combes-Soia, L., Brionne, A., Labas, V., Rodriguez-Navarro, A.B., Hincke, M.T., et al., 2019. Guinea fowl eggshell quantitative proteomics yield new findings related to its unique structural characteristics and superior mechanical properties. J. Proteomics 209, 103511.

Rubin, C.J., Zody, M.C., Eriksson, J., Meadows, J.R., Sherwood, E., Webster, M.T., et al., 2010. Whole-genome resequencing reveals loci under selection during chicken domestication. Nature 464, 587–591.

Sardi, L., Gastaldo, A., Borciani, M., Bertolini, A., Musi, V., Martelli, G., Cavallini, D., Rubini, G., Nannoni, E., 2020. Identification of possible pre-slaughter indicators to predict stress and meat quality: a study on heavy pigs. Animals (Basel) 10 (6). https://doi.org/10.3390/ani10060945. In this issue.

Schilling, M.W., Suman, S.P., Zhang, X., Nair, M.N., Desai, M.A., Cai, K., et al., 2017. Proteomic approach to characterize biochemistry of meat quality defects. Meat Sci. 132, 131–138.

Scott, T.R., Messersmith, A.R., McCrary, W.J., Herlong, J.L., Burgess, S.C., 2005. Hematopoietic prostaglandin D2 synthase in the chicken Harderian gland. Vet. Immunol. Immunopathol. 108, 295–306.

Seabury, C.M., Dowd, S.E., Seabury, P.M., Raudsepp, T., Brightsmith, D.J., Liboriussen, P., et al., 2013. A multi-platform draft de novo genome assembly and comparative analysis for the Scarlet Macaw (*Ara macao*). PLoS One 8, e62415.

Serhan, C.N., Chiang, N., Van Dyke, T.E., 2008. Resolving inflammation: dual anti-inflammatory and pro-resolution lipid mediators. Nat. Rev. Immunol. 8, 349–361.

Shack, L.A., Buza, J.J., Burgess, S.C., 2008. The neoplastically transformed (CD30hi) Marek's disease lymphoma cell phenotype most closely resembles T-regulatory cells. Canc. Immunol. Immunother. 57, 1253–1262.

Sherwood, D., Cooper, J., Sherwood, D., 2011. Crystals, X-Rays, and Proteins: Comprehensive Protein Crystallography. Oxford University Press, New York.

Shi, T., Su, D., Liu, T., Tang, K., Camp, I., Camp, D.G., Qian, W.-J., et al., 2012. Advancing the sensitivity of selected reaction monitoring-based targeted quantitative proteomics. Proteomics 12, 1074–1092.

Simon, Á., Gulyás, G., Mészár, Z., Bhide, M., Oláh, J., Bai, P., et al., 2019. Proteomics alterations in chicken jejunum caused by 24 h fasting. Peer J. 7 e6588-e6588.

Sloley, S., Smith, S., Algeciras, M., Cavett, V., Busby, J.A., London, S., et al., 2007a. Proteomic analyses of songbird (Zebra finch; *Taeniopygia guttata*) retina. J. Proteome Res. 6, 1093–1100.

Sloley, S., Smith, S., Gandhi, S., Busby, J.A., London, S., Luksch, H., et al., 2007b. Proteomic analyses of zebra finch optic tectum and comparative histochemistry. J. Proteome Res. 6, 2341–2350.

Sokale, A., Peebles, E.D., Zhai, W., Pendarvis, K., Burgess, S., Pechan, T., 2011. Proteome profile of the pipping muscle in broiler embryos. Proteomics 11, 4262–4265.

Son, J.H., Kawamata, H., Yoo, M.S., Kim, D.J., Lee, Y.K., Kim, S., et al., 2005. Neurotoxicity and behavioral deficits associated with Septin 5 accumulation in dopaminergic neurons. J. Neurochem. 94, 1040–1053.

Soulet, F., Kilarski, W.W., Roux-Dalvai, F., Herbert, J.M., Sacewicz, I., Mouton-Barbosa, E., et al., 2013. Mapping the extracellular and membrane proteome associated with the vasculature and the stroma in the embryo. Mol. Cell. Proteomics 12 (8), 2293–2312.

Steen, H., Mann, M., 2004. The ABC's (and XYZ's) of peptide sequencing. Nat. Rev. Mol. Cell Biol. 5, 699–711.

Stocks, B.B., Konermann, L., 2009. Structural characterization of short lived protein unfolding intermediates by laser-induced oxidative labeling and mass spectrometry. Anal. Chem. 81, 20–27.

Stoddard, M.C., Prum, R.O., 2011. How colorful are birds? Evolution of the avian plumage color gamut. Behav. Ecol. 22, 1042–1052.

Sun, J.S., Hahn, T.W., 2012. Comparative proteomic analysis of *Salmonella enterica* serovars enteritidis, typhimurium and gallinarum. J. Vet. Med. Sci. 74, 285–291.

Sun, C., Liu, J., Li, W., Xu, G., Yang, N., 2017. Divergent proteome patterns of egg albumen from Domestic Chicken, Duck, Goose, Turkey, Quail and Pigeon. Proteomics 17, 1700145.

Sun, G.-R., Zhou, L.-Y., Zhang, Y.-P., Zhang, F., Yu, Z.-H., Pan, Q., et al., 2019. Differential expression of type I interferon mRNA and protein levels induced by virulent Marek's disease virus infection in chickens. Vet. Immunol. Immunopathol. 212, 15–22.

Tang, X., Meng, Q., Gao, J., Zhang, S., Zhang, H., Zhang, M., 2015. Label-free quantitative analysis of changes in broiler liver proteins under heat stress using SWATH-MS technology. Sci. Rep-UK. 5, 15119.

Tasoniero, G., Zhuang, H., Gamble, G.R., Bowker, B.C., 2020. Effect of spaghetti meat abnormality on broiler chicken breast meat composition and technological quality1. Poultry Sci. 99, 1724–1733.

Teltathum, T., Mekchay, S., 2009. Proteome changes in Thai indigenous chicken muscle during growth period. Int. J. Biol. Sci. 5, 679–685.

Thanthrige-Don, N., Abdul-Careem, M.F., Shack, L.A., Burgess, S.C., Sharif, S., 2009. Analyses of the spleen proteome of chickens infected with Marek's disease virus. Virology 390, 356–367.

Thanthrige-Don, N., Parvizi, P., Sarson, A.J., Shack, L.A., Burgess, S.C., Sharif, S., 2010. Proteomic analysis of host responses to Marek's disease virus infection in spleens of genetically resistant and susceptible chickens. Dev. Comp. Immunol. 34, 699–704.

Tiambeng, T.N., Roberts, D.S., Brown, K.A., Zhu, Y., Chen, B., Wu, Z., et al., 2020. Nanoproteomics enables proteoform-resolved analysis of low-abundance proteins in human serum. Nat. Commun. 11, 3903.

Tu, W.-L., Cheng, C.-Y., Chen, C.-J., Chan, H.-L., Wang, S.-H., Tang, P.-C., et al., 2018. Proteomic analysis of the hypothalamus of broiler-type Taiwan country chickens in response to acute heat stress. Anim. Sci. J. 89, 1475–1485.

Unlu, M., Morgan, M.E., Minden, J.S., 1997. Difference gel electrophoresis: a single gel method for detecting changes in protein extracts. Electrophoresis 18, 2071–2077.

Velculescu, V.E., Zhang, L., Zhou, W., Vogelstein, J., Basrai, M.A., Bassett Jr., D.E., et al., 1997. Characterization of the yeast transcriptome. Cell 88, 243–251.

Vincent, P., Collette, Y., Marignier, R., Vuaillat, C., Rogemond, V., Davoust, N., et al., 2005. A role for the neuronal protein collapsin response mediator protein 2 in T lymphocyte polarization and migration. J. Immunol. 175, 7650–7660.

Wales, T.E., Engen, J.R., 2006. Hydrogen exchange mass spectrometry for the analysis of protein dynamics. Mass Spectrom. Rev. 25, 158–170.

Walsh, C.T., 2006. Posttranslational Modification of Proteins: Expanding Nature's Inventory. Roberts and Company Publishers, Greenwood Village, CO.

Wang, S., Regnier, F.E., 2001. Proteomics based on selecting and quantifying cysteine containing peptides by covalent chromatography. J. Chromatogr. A 924, 345–357.

Wang, S., Zhang, X., Regnier, F.E., 2002. Quantitative proteomics strategy involving the selection of peptides containing both cysteine and histidine from tryptic digests of cell lysates. J. Chromatogr. A 949, 153–162.

Wang, Y., Guo, Y., Ning, D., Peng, Y., Cai, H., Tan, J., et al., 2012. Changes of hepatic biochemical parameters and proteomics in broilers with cold-induced ascites. J. Anim. Sci. Biotechnol. 3, 41.

Wang, S., Ni, Y., Guo, F., Fu, W., Grossmann, R., Zhao, R., 2013. Effect of corticosterone on growth and welfare of broiler chickens showing long or short tonic immobility. Comp. Biochem. Physiol. A 164, 537–543.

Wang, X., Li, D., Song, S., Zhang, Y., Li, Y., Wang, X., et al., 2019. Combined transcriptomics and proteomics forecast analysis for potential genes regulating the Columbian plumage color in chickens. PLoS One 14, e0210850.

Warren, W.C., Clayton, D.F., Ellegren, H., Arnold, A.P., Hillier, L.W., Kunstner, A., et al., 2010. The genome of a songbird. Nature 464, 757–762.

Washburn, M.P., Wolters, D., Yates 3rd, J.R., 2001. Large-scale analysis of the yeast proteome by multidimensional protein identification technology. Nat. Biotechnol. 19, 242–247.

Wilkins, M.R., Pasquali, C., Appel, R.D., Ou, K., Golaz, O., Sanchez, J.C., et al., 1996. From proteins to proteomes: large scale protein identification by two-dimensional electrophoresis and amino acid analysis. Biotechnology 14, 61–65.

Wuthrich, K., 1990. Protein structure determination in solution by NMR spectroscopy. J. Biol. Chem. 265, 22059–22062.

Xie, F., London, S.E., Southey, B.R., Annangudi, S.P., Amare, A., Rodriguez-Zas, S.L., et al., 2010. The zebra finch neuropeptidome: prediction, detection and expression. BMC Biol. 8, 28.

Xing, T., Wang, C., Zhao, X., Dai, C., Zhou, G., Xu, X., 2017. Proteome analysis using isobaric tags for relative and absolute analysis quantitation (iTRAQ) reveals alterations in stress-induced dysfunctional chicken muscle. J. Agric. Food Chem. 65, 2913–2922.

Yates 3rd, J.R., 1998. Mass spectrometry and the age of the proteome. J. Mass Spectrom. 33, 1–19.

Yates 3rd, J.R., 2019. Recent technical advances in proteomics. F1000Research 8. F1000 Faculty Rev-351.

Yates, J.R., Ruse, C.I., Nakorchevsky, A., 2009. Proteomics by mass spectrometry: approaches, advances, and applications. Annu. Rev. Biomed. Eng. 11, 49–79.

Young, M.M., Tang, N., Hempel, J.C., Oshiro, C.M., Taylor, E.W., Kuntz, I.D., et al., 2000. High throughput protein fold identification by using experimental constraints derived from intramolecular cross-links and mass spectrometry. Proc. Natl. Acad. Sci. U. S. A. 97, 5802–5806.

Zhai, W., Araujo, L.F., Burgess, S.C., Cooksey, A.M., Pendarvis, K., Mercier, Y., et al., 2012. Protein expression in pectoral skeletal muscle of chickens as influenced by dietary methionine. Poultry Sci. 91, 2548–2555.

Zhang, J., Li, C., Tang, X., Lu, Q., Sa, R., Zhang, H., 2015. High concentrations of atmospheric ammonia induce alterations in the hepatic proteome of broilers (*Gallus gallus*): an iTRAQ-based quantitative proteomic analysis. PLoS One 10, e0123596.

Zhang, X., Antonelo, D., Hendrix, J., To, V., Campbell, Y., Von Staden, M., et al., 2020. Proteomic characterization of normal and woody breast meat from broilers of five genetic strains. Meat Muscle Biol. 4, 1.

Zhang, F., Yin, Z.-T., Zhang, J.-F., Zhu, F., Hincke, M., Yang, N., Hou, Z.-C., 2020. Integrating transcriptome, proteome and QTL data to discover functionally important genes for duck eggshell and albumen formation. Genomics 112, 3687–3695.

Zhang, X., Zhai, W., Li, S., Suman, S.P., Chen, J., Zhu, H., et al., 2020. Early postmortem proteome changes in normal and woody broiler breast muscles. J. Agric. Food Chem. 68, 11000–11010.

Zou, W., Ke, J., Zhang, A., Zhou, M., Liao, Y., Zhu, J., et al., 2010. Proteomics analysis of differential expression of chicken brain tissue proteins in response to the neurovirulent H5N1 avian influenza virus infection. J. Proteome Res. 9, 3789–3798.

Further reading

Golub, E.E., 2009. Role of matrix vesicles in biomineralization. Biochim. Biophys. Acta 1790, 1592–1598.

Huang, J., Tang, X., Ruan, J., Ma, H., Zou, S., 2010. Use of comparative proteomics to identify key proteins related to hepatic lipid metabolism in broiler chickens: evidence accounting for differential fat deposition between strains. Lipids 45, 81–89.

Liu, Z.G., Song, L.Z., Lu, L.Z., Zhang, X.F., Zhang, F.M., Wang, K.H., et al., 2017. Comparative proteomics of matrix fractions between pimpled and normal chicken eggshells. J. Proteomics 167, 1–11.

Tu, W.-L., Cheng, C.-Y., Wang, S.-H., Tang, P.-C., Chen, C.-F., Chen, H.-H., et al., 2016. Profiling of differential gene expression in the hypothalamus of broiler-type Taiwan country chickens in response to acute heat stress. Theriogenology 85, 483–494 e8.

Zheng, A., Liu, G., Zhang, Y., Hou, S., Chang, W., Zhang, S., et al., 2012. Proteomic analysis of liver development of lean Pekin duck (*Anas platyrhynchos* domestica). J. Proteomics 75, 5396–5413.

Chapter 5

Avian metabolomics

Lindsay P. Brown[1], Amanda L. May[2], Alexander R. Fisch[1], Shawn R. Campagna[1,3] and Brynn H. Voy[4]
[1]Department of Chemistry, University of Tennessee, Knoxville, TN, United States; [2]Center for Environmental Biotechnology, University of Tennessee, Knoxville, TN, United States; [3]Biological and Small Molecule Mass Spectrometry Core, University of Tennessee, Knoxville, TN, United States; [4]Department of Animal Science, University of Tennessee, Knoxville, TN, United States

5.1 Introduction to metabolomics

Physiology is an emergent property produced from continual and dynamic interactions between an organism and its environment. The study of physiology relies on readouts, such as hormone levels or physical pressures, to monitor the inner workings of cells and tissues that maintain homeostasis. For centuries, these indicators of physiological function were made one analyte-at-a-time. Over the past few decades, however, revolutionary advances in technology, bioinformatics, and instrumentation enabled the development and use of "-omics" approaches, in which an organism's entire collection of genes, proteins, or other molecular phenotypes can be queried simultaneously, and with high sensitivity and throughput. Metabolomics refers to the comprehensive analysis of an organism's metabolome, the collection of small molecules, and intermediary metabolites that cells use and produce to function. Because the metabolome essentially records the results of upstream processes, it can be thought of as an ultimate phenotype that comprehensively capture's a snapshot of an organism's physiological state (Figure 5.1, Cui et al., 2018).

The first metabolomics study can be traced back to Linus Pauling in the late 1960s in which he used gas chromatography (GC) with flame ionization detection to monitor changes in the gut microbiota (Robinson et al., 1973). While metabolites were successfully detected, lengthy analysis times, lack of analytical resolution, and the inability to confirm metabolite identities or elucidate structures limited the overall utility of this technique. Still, this emerging technology was instrumental in helping Pauling and coworkers determine the inborn error in metabolism that leads to human disease (Robinson et al., 1973). Over the past two decades, advances in mass spectrometric instrumentation, improvements in sensitivity and reductions in cost have enabled widespread adoption of metabolomics, allowing researchers to monitor thousands of metabolites concurrently (Emwas et al., 2019). Accordingly the use of metabolomics has gained traction in a variety of disciplines, with applications to both human and animal physiology (Figure 5.2).

5.2 Methods of metabolomics

5.2.1 Instrumentation

The metabolome consists of small molecules (typically < 1500 Da) that span a range of polarities and structural types (Christians et al., 2016; Schrimpe-Rutledge et al., 2016). This chemical complexity creates a unique analytical challenge as compared to other -omics types, which tend to measure molecules of similar composition and structure. Metabolites can be divided into two major classes: polar (water-soluble) and nonpolar (lipid-like). Lipidomics is often used to describe the subclass of metabolomics methods that measure lipid-based metabolites (Figure 5.3). At their core, all metabolomics techniques rely on separation and measurement science to analyze highly complex mixtures. The most common metabolomics approaches are based on nuclear magnetic resonance (NMR) spectroscopy or mass spectrometry (MS), each of which has its advantages as well as intrinsic bias for detecting specific classes of metabolites (Grzybek et al., 2019). A typical metabolomics workflow for MS platforms is outlined in Figure 5.4.

5.2.1.1 Nuclear magnetic resonance spectroscopy

NMR spectroscopy poses significant advantages for some applications. NMR spectroscopy and imaging can quantify

Sturkie's Avian Physiology. https://doi.org/10.1016/B978-0-12-819770-7.00041-4

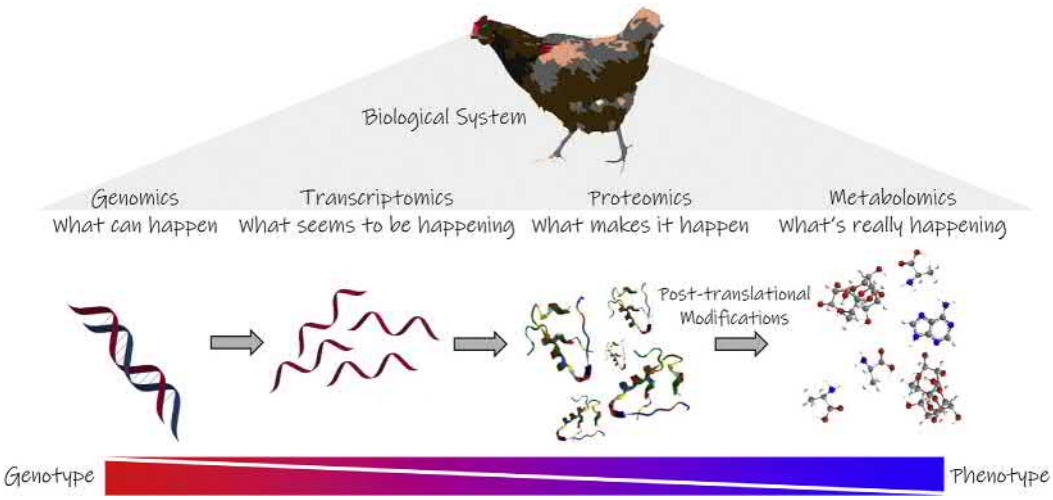

FIGURE 5.1 Concise overview of the "-omics" cascade. The cascade proceeds from tools that determine the blueprint of an organism to those that measure physiology directly. In reality, biological processes do not move in this manner as each component of the cascade may influence another.

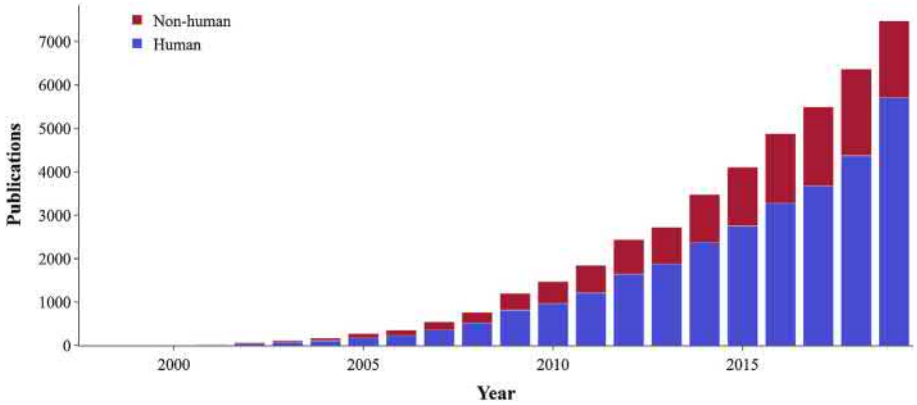

FIGURE 5.2 Number of publications per year available on PubMed.gov during 1998–2019 using search criteria "metabolomics" or "metabonomics." Results are filtered to include "Species: Nonhuman" and colored to delineate human versus nonhuman studies.

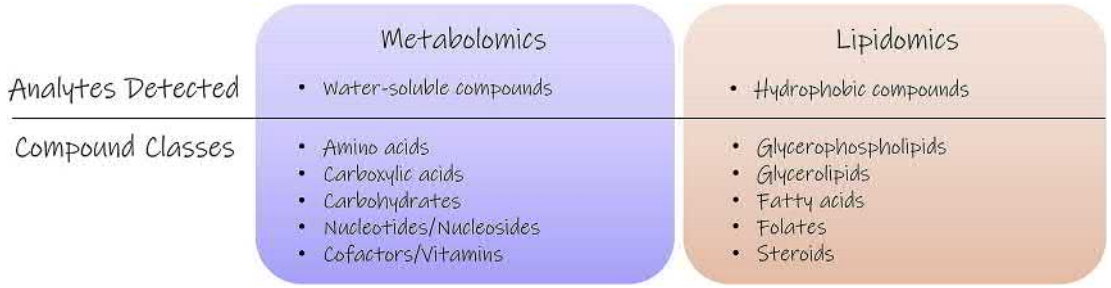

FIGURE 5.3 Overview of analyte types and typical compound classes measured in metabolomics and lipidomics experiments.

the most abundant compounds in a large variety of biological matrices, including biofluids, cells, or tissues, with minimal need for sample preparation. Structural isomers (or molecules with identical masses) can be differentiated and identified by NMR, whereas this is still challenging with MS. In addition, these techniques are nearly independent of the user or instrument used, allowing reproducibly and easy comparisons across platforms and studies (Emwas et al., 2019). Although NMR is a highly quantitative technique, it detects a fewer number of compounds due to metabolite signal overlap and the low-dynamic range of the instrument (Marshall and Powers, 2017).

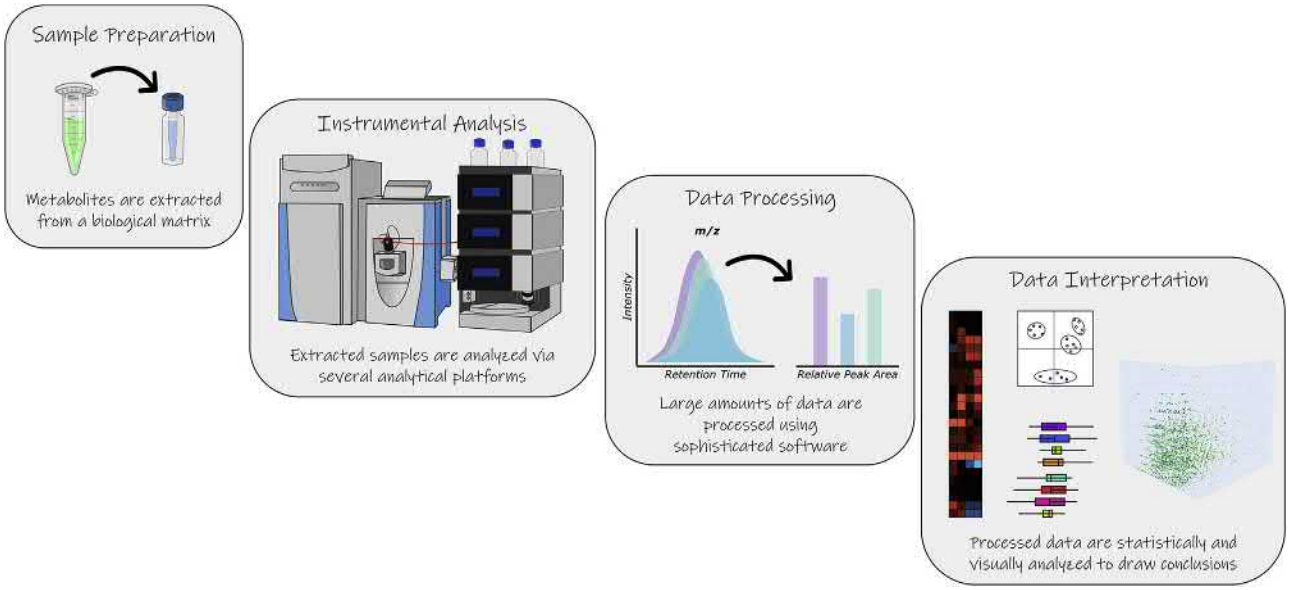

FIGURE 5.4 A simplified overview of the metabolomics experimental process. Samples are prepared via extraction of a diverse or specific set of analytes. The extracts are then analyzed by a variety of analytical platforms; a Thermo Fischer ® Orbitrap high-resolution mass spectrometer fitted with an liquid chromatography is shown. Processing consists of evaluating data for consistency and uniqueness. The final objective is to interpret data using various statistical or visualization options, such as heat maps, partial least squares discriminant analysis, multidimensional plots, and pathway maps.

NMR remains the analytical technique of choice for unknown structure identification, and the ability of two-dimensional (2D) NMR spectroscopy to correlate atoms belonging to the same compound greatly aids in these endeavors. Isotope tracing experiments that add metabolites or nutrients containing NMR active stable isotopes (typically ^{13}C or ^{15}N) to a sample allows the incorporation level of the isotope into metabolites to be measured and can also elucidate metabolic pathways as the dynamics of metabolite transformation can be traced (Tiziani et al., 2011). An interesting approach to isotope tracing is the combined analysis by NMR and MS. Detection of this type provides sensitive qualitative and quantitative information, exploiting the benefits of both detection methods (Bingol and Bruschweiler, 2015).

5.2.1.2 Mass spectrometry

MS-based metabolomics can detect many metabolites with a dynamic range of at least five orders of magnitude using a combination of chromatography, high-mass resolution, and/or tandem MS (Marshall and Powers, 2017). Each MS instrument consists of three main components: an ionization source, a mass analyzer, and an ion detector. These components allow the detection of various ions (i.e., molecules that have become charged), which are described by their mass-to-charge ratio (*m/z*). Based on its properties, a compound may ionize by the addition of a proton or loss of an electron to give a positive ion or vice versa to give a negative one. Modern instruments can switch between these two modes to cover a broader analytical range. Samples may undergo hard ionization, such as electron ionization (EI), which causes fragmentation of the molecule or soft ionization, such as electrospray or atmospheric pressure chemical ionization (APCI), which keeps the molecular structure intact. Of the available soft ionization sources, electrospray ionization (ESI) is most widely used because of its ability to generate intact ions via addition or removal of a proton and its analytical versatility over a broad range of compounds, i.e., small molecules (including metabolites), large molecules, surfactants, etc (Gross, 2004). In the event, ESI is not conducive for a particular analysis, for example, if ions formed during ESI are indicative of adducts or if the analytes being analyzed are low-polarity, APCI is often employed (Gross, 2004). Unlike ESI, APCI can generate ions from molecules that do not readily undergo acid-base reactions as ionization is accomplished by interactions with high-energy reactant gas species that are present in the corona discharge (Gross, 2004). As both sources operate at atmospheric pressure and are easily interchanged on most instruments, they are synergistic ionization techniques that are well suited for use with liquid chromatography (LC). On the other hand, most GC-MS utilize EI that results in fragmentation of analytes, although APPI and APCI sources for these instruments have been recently developed (Powers and Campagna, 2019). The fragmentation in most GC-MS metabolomics studies yields data that must be matched to existing spectral libraries or deconvoluted to predict structure and identify metabolites.

As many molecules possess similar *m/z,* the ability to distinguish between these compounds is necessary for

identification, and the chemical complexity of the metabolome highlights the utility of high-resolution mass analyzers and/or tandem techniques (see below). Low-resolution mass analyzers (such as quadrupoles or mass filters) are only capable of distinguishing ions ± 0.5 Da, which does not provide the resolution needed to distinguish among the thousands of compounds found a biological matrix (Jang et al., 2018). Conversely, high-resolution mass analyzers, such as ion cyclotron resonance, time-of-flight, and Orbitraps can routinely provide resolutions down to ±0.01−0.001 Da, which is sufficient to differentiate many molecules and isotopologues based on mass alone.

5.2.1.2.1 Separation

Despite its ability to resolve molecules based on mass, MS struggles as a stand-alone technique in the analysis of complex matrices due to the difficulty in ionizing and measuring many ions at once. Chromatographic separation is a synergistic technique that helps limit the complexity of the sample as it is introduced into the MS, which greatly aids in metabolite detection, quantitation, and identification (Johnson et al., 2016). Chromatography operates on a relatively simple basis: analytes dissolved in a *mobile phase* are allowed to interact with a *stationary phase*, and the affinity of a specific analyte for the stationary phase over the mobile phase leads to longer retention within the column. Differences in retention times among the metabolites are the foundation that provides separation. Though some alternatives such as capillary electrophoresis exist, the majority of metabolomics separation techniques rely on GC or LC (Lains et al., 2019). GC has been considered a workhorse in many laboratories since its implementation in the 1950s (Skoog et al., 2007). As expected, GC is particularly ideal for separation of thermally stable compounds that readily volatilize (i.e., molecules with low-boiling points). Therefore, GC analysis is generally used only for analyzing sugars, amino acids, fatty acids, or metabolites with compatible boiling points (Fiehn, 2016). Derivatization is necessary for many of these metabolite classes to aid in their volatilization to make them suitable for GC analysis (Fiehn, 2016).

LC instrumentation has seen significant advancement since its first use in the early 1900s, unlike GC which has largely remained the same (Skoog et al., 2007). The separation ability, sample efficiency, and broad applicability of modern LC instrumentation has made it an ideal choice for metabolomics analyses. Separations based on molecular size, polarity, hydrophilicity, and many other chemical properties are possible with modern columns. The most common columns used in metabolomics are those that separate a wide array of nonpolar and/or polar compounds, namely reverse phase (RP) and hydrophilic interaction liquid chromatography (HILIC), respectively. RP columns consist of a nonpolar stationary phase, often an alkane such as C_{18}, C_8, or C_4, attached to silica particles enclosed in a metal cylinder that can withstand high pressures (Huang et al., 2018). Compound separation is usually afforded by performing a gradient elution in which the mobile phase begins as a polar solvent and progressively becomes more nonpolar, thus allowing elution of compounds in decreasing order of polarity. HILIC stationary phases are generally more polar and rely on a mixture of chemical interactions to afford retention. Standard phase solvent gradients that progress from nonpolar to polar mobile phases are commonly used with HILIC separation, and studies have shown that the stationary phase particles surround themselves with a thin layer of water that interacts with the polar analytes to keep them retained longer that nonpolar molecules (McCalley, 2017).

Though not complete opposites, RP and HILIC methods of chromatography provide complementary separation chemistries to one another. Recent studies have utilized a technique called 2D-chromatography, in which two columns are used sequentially for separation in a single analysis. For example, this type of chromatography has been used for simultaneous detection of metabolites from both the metabolome and the lipidome, as well as metabolites that could not be separated using RP *or* HILIC alone (Wang et al., 2017). Despite its complex implementation, 2D-LC and 2D-GC have recently risen in popularity (Keppler et al., 2018).

5.2.1.2.2 Identification—targeted versus untargeted mass spectrometric analysis

Due to advancements in mass spectrometric capabilities, researchers can now either perform global analyses of the entire small molecule content of a sample (*untargeted metabolomics/lipidomics*) or focus on a predetermined set of molecules (*targeted metabolomics/lipidomics)* (Schrimpe-Rutledge et al., 2016; Bingol, 2018).Tandem MSs (e.g., the triple quadrupole) are used for targeted analyses. A target list of parent/fragment mass ions (i.e., knowns) is programmed into the instrument for these analyses that often rely on selective reaction monitoring to provide molecular identification. The use of a mass analyzer that selects for a parent ion and a second mass analyzer that selects for only fragments from a specific molecule affords separation in the mass domain and provides selectivity. These analyses are highly quantitative. However, they will not detect compounds for which the parent/fragment mass combination has not been programmed into the instrument, and these parameters are typically determined by injecting standards for each analyte of interest (Rabinowitz et al., 2011). This limits the ability of these methods to find novel biomarkers of biological activity, but data analysis is easier due to the lower number of metabolites detected (usually several hundred or fewer) and the high-confidence identifications.

Untargeted or global profiling experiments use a high-resolution MS (e.g., time-of-flight or Orbitrap

instruments) to detect parent ions with a high-mass accuracy to aid in metabolite identification, and tandem MS (MS/MS) is sometimes used to provide additional fragmentation data (Johnson et al., 2016). While global profiling experiments rarely increase the number of known compounds detected, they do allow for thousands of compounds of unknown structure and identity to be detected in a single analysis and provide an unbiased view of a larger portion of the metabolome (Su et al., 2017). However, compound identification can be difficult based on matching retention time, compound mass, and in some cases fragment mass, to a library of standards. This is further complicated due to differing performance among MS platforms and laboratories that often renders data incomparable among studies and facilities. Global profiling techniques are more labor- and analysis-intensive than targeted approaches; nonetheless, global metabolomics/lipidomics methods are the technique of choice for the discovery of novel metabolites and biomarkers (Vuckovic, 2018).

5.2.1.2.3 Data processing

Abundance of each detected metabolite is represented in raw data as a spectral peak, which must be aligned using known *m/z* and retention time information before being picked based on their intensities and peak shape. The *m/z*-retention time pair are used for metabolite naming or identification, and the intensity is proportional to concentration. Targeted analyses have become relatively streamlined, since metabolite identification is easier and more robust. Multiple software packages are available for data processing, and their usage varies depending on the approach (e.g., targeted vs. untargeted) (Jang et al., 2018).

5.2.2 Data analysis and interpretation

Regardless of whether NMR or MS is used, the core goal of metabolomics is to convert metabolite identifications and abundance to novel biological insight (Jang et al., 2018). The workflows used to accomplish this goal resembles those used for other 'omics platforms, in which biological signatures must be extracted from hundreds or thousands of data points. Clustering methods, such as hierarchical clustering and principle component analysis, are often used as a first analytical step to visualize distinctness of metabolite profiles between experimental groups (Heinemann, 2019). Univariate methods, such as t-tests and ANOVA, can be used to identify metabolites that differ statistically between experimental treatments (Ernest et al., 2012). Because of the hundreds of hypotheses that are typically tested simultaneously in these analyses, correction for multiple testing, for example using false discovery rate, should be included (Scheubert et al., 2017). Classical tools of statistics are often combined with multivariate analysis methods that reduce the dimensionality of the data and identify metabolites that most effectively discriminate groups. Supervised methods, such as partial least squares discriminant analysis (PLS-DA) and random forest, can be used to classify samples into groups based on patterns of metabolite abundance and to identify metabolites that are most effective at discriminating groups (Liebal et al., 2020, Figure 5.5).

Subsets of metabolites that emerge from these various winnowing methods can then be mined for biological insight and functional inference by mapping to known metabolic pathways. Bioinformatic resources such as the Kyoto Encyclopedia of Genes and Genomes Pathway Database (www.genome.jp), MAVEN, Metlin, and the Human Metabolome Database are highly valuable for functional interpretation of metabolite datasets (Xia et al., 2009; Clasquin et al., 2012; Guijas et al., 2018; O'Shea and Misra, 2020). A recent review of metabolomics tools, databases, and resources summarized over 100 published and nonpublished metabolomics tools and resources (O'Shea and Misra, 2020). Metaboanalyst (metaboanalyst.ca), a web server that contains a comprehensive set of analytical tools,

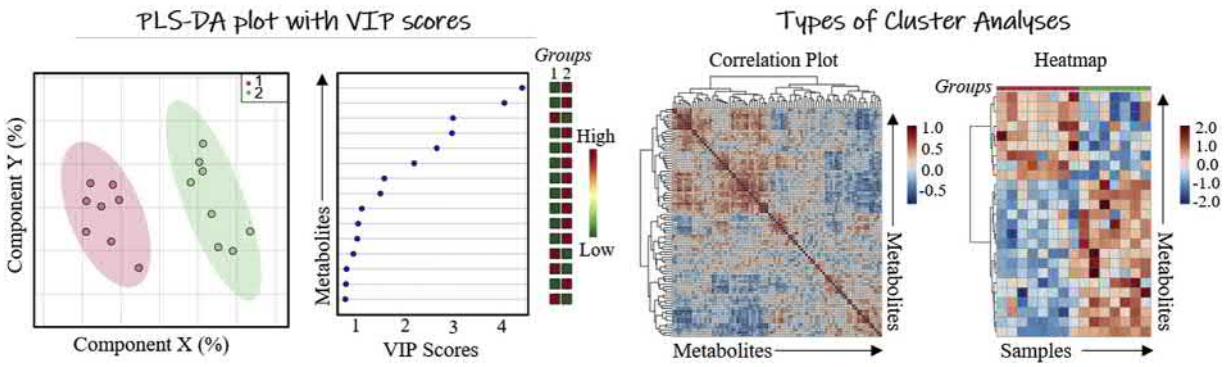

FIGURE 5.5 Examples of various visualization tools used in data analysis and interpretation. Partial least squares discriminant analysis (PLS-DA) plots, PLS-DA variable importance in projection scores, and cluster analyses including correlation plots and heat maps are common techniques to illustrate statistical significance and fold changes in large datasets. Illustrations were produced using the toolkit provided in Metaboanalyst (metaboanalyst.ca).

is particularly useful for quantitative and functional analyses of metabolomics datasets (Xia et al., 2009; Xia et al., 2012, 2015; Chong et al., 2018). Metabolomics data are often collected in the context of other physiological measurements, or alongside global measures of gene expression or other 'omics data types. Correlating metabolite abundance to other phenotypes can add additional insight into functional relationships and highlight metabolites that may be particularly relevant to a specific trait. As several studies that are summarized in the following section illustrate, connecting metabolome with transcriptome data yields synergistic insight that strengthens the biological value of both data types. Ultimately, metabolome data can be integrated into a systems biology approach, in which multiple types of 'omics data are integrated with phenotypic measurements using tools of correlation (Voy and Aronow, 2009; Voy, 2011). Genes, proteins, and metabolites are assembled into interconnected networks and mapped onto overlying phenotypes, providing mechanistic insight into pathways that underlie physiological functions. As discussed below, the emerging use of metabolomics and integration of metabolome data has begun to advance the study of avian physiology.

5.3 Applications of metabolomics to avian physiology

Although use of metabolomics is becoming more widespread, its application to avian physiology lags behind its role in more intensively studied areas, such as human disease. The majority of avian metabolomics studies to date have focused on issues relevant to the poultry industry, largely due to its economic importance and critical role in feeding a global population. A metabolomics toolkit is extremely well-suited to address these issues and physiological questions, as metabolism is inherently tied to growth and efficient utilization of feed that are critical for poultry production. In particular, modern broiler (meat-type) chickens are a metabolic marvel due to their incredible rates of growth and efficient conversion of dietary energy to tissue. The studies summarized below illustrate new insights into avian physiology that continue to emerge from use of metabolomics. In addition, they demonstrate the potential to use this platform to identify biomarkers of disease processes and desirable traits, using biological samples (e.g., serum) that are minimally invasive to collect yet can yield a global snapshot of a bird's physiological state.

5.3.1 Growth and efficiency

The ability to efficiently convert feed to lean tissue is a hallmark of modern broiler chickens. Commercial broiler lines have been produced by intensive selection for growth over the past several decades (Griffin and Goddard, 1994). As a result, growth rates of broilers increased approximately fourfold from 1957 to 2005 (Havenstein et al., 2003; Zuidhof et al., 2014). The efficiency with which broilers convert feed to tissue mass improved in parallel, cutting the amount of feed needed to support growth in half over the same time period (Havenstein et al., 2003; Zuidhof et al., 2014). Although the genetics and production environments of commercial broilers are tightly controlled, heterogeneity in feed efficiency still exists within flocks. Residual feed intake (RFI) is used to describe an individual bird's deviation in actual feed intake from what is predicted, based on the known relationship between weight of feed required per unit of weight gain (Romero et al., 2009). A negative RFI value reflects a higher than expected efficiency, while a positive value indicates reduced efficiency. RFI is heritable, making it a potential trait on which to select to improve efficiency. Circulating metabolites can feasibly be used as biomarkers of RFI, and some metabolites that are associated with higher feed efficiency in broilers have been identified. However, given that feed intake is a key component of RFI, it is difficult to discern metabolites that are affected by differences in feed intake per se from those that reflect intrinsic metabolic differences that underlie variation in efficiency.

To uncouple feed intake from RFI, Metzler-Zebeli et al. (2019) measured RFI and profiled serum metabolomes of broilers under both ad libitum and modestly restricted (85%) feeding. Serum metabolomes were profiled using a targeted ESI- LC/MS approach and a commercial kit (Absolute IDQ P180; BIOCRATES Life Sciences AG) that enabled absolute quantification of 188 known metabolites across various classes, including both small molecules and lipids. Using a mixed-model ANOVA, metabolites that were specifically affected by feed intake, RFI, and interaction of the two terms were identified. Feed efficiency was specifically associated with differences in serum amino acids. Levels of histidine, isoleucine, leucine, lysine, ornithine, proline, serine, threonine, and valines were lower, while tyrosine was higher, in birds with low RFI, independent of feed intake. Using a combination of PCA, regression modeling, and relevance networks, these authors identified metabolites that were specifically associated with RFI, feed intake, and total body weight gain. The amino acids isoleucine, lysine, valine, histidine, and ornithine were most closely associated with variation in RFI, while subsets of biogenic amines or glycerophospholipids were sufficient to discriminate birds based on feed intake and weight gain, respectively. This study illustrates the additional insight that can be gained when metabolomic data are integrated with other physiological measures.

Although improvements in feed efficiency over the past few decades have yielded remarkable advances in broiler growth, competing demands for soy, corn, and other major diet constituents make the cost of feed inputs increasingly

important. As for virtually any physiological trait, the ability to completely digest feedstuffs varies significantly between individual birds. Digestive efficiency contributes to RFI by affecting the amount of energy and nutrients that are extracted per unit of diet. Heritability estimates for digestive efficiency range from 0.33 to 0.47, making it an attractive target for genetic selection (Mignon-Grasteau et al., 2004). However, measuring efficiency is labor-intensive and low-throughput, requiring birds to be housed and fed individually. Metabolomics was used to identify biomarkers in serum that predict digestive efficiency, and to understand the metabolic relationships that contribute to efficiency in the digestive tract (Beauclercq et al., 2018).This study utilized two lines of chickens that had been derived through divergent selection for high (D+) or low (D−) digestive efficiency over eight generations, and for which various intensive measures of digestive efficiency (e.g., use of starch, lipids, dry matter) were measured from fecal samples. Metabolomes of both ileal and caecal contents, as well as serum, were quantified using NMR. Each sample type contained metabolites that contributed to a model predicting digestive efficiency. Although further effort is needed to validate biomarkers from this study, it provides foundational information about the metabolite pools that may reflect the capacity to fully digest feedstuffs in chicken.

Crude protein is both a costly component of poultry diets and an environmental concern due to emission and runoff of nitrogen. However, lowering the total crude protein content of diets without compromising growth is a significant challenge. Supplementing diets with glycine, a nonessential amino acid that can be reversibly metabolized to serine, has been shown to prevent compromised growth when crude protein levels are lowered, but the metabolic basis for this protection is poorly understood (Dean et al., 2006). To understand the metabolic basis for the growth supporting effects of glycine, broilers were fed a total of 12 diets containing varying levels of glycine and crude protein (Hofmann et al., 2019). Untargeted metabolomics of serum highlighted a somewhat unexpected association of phosphatidylcholine and sphingomyelin, rather than specific essential amino acids or glycine, with compromised growth under low crude protein intake. This study highlights the discovery potential of metabolomics when a platform capable of profiling broad classes of metabolites is used.

In addition to adequate total protein levels, specific amino acids must be optimized to support the unique physiological demands of rapid growth in broilers. Arginine is an essential amino acid that may have specific benefits for broiler physiology through its role as the precursor of nitric oxide (NO), an endogenous vasodilator. Improving basal levels of vasodilation may benefit broilers because tissue hypoxia contributes to development of breast muscle myopathies that currently challenge the broiler industry (Greene et al., 2019). Zampiga et al. (2018) tested the impact of dietary arginine supplementation on incidence of myopathies and profiled the effects on the breast muscle and serum metabolomes using NMR. Arginine supplementation significantly increased both circulating and tissue arginine content in broilers, confirming that local levels in muscle can be enhanced through the diet. Although incidence of breast myopathies was not affected by arginine supplementation, metabolite profiles indicated that arginine significantly enhanced both protein metabolism and energetic utilization of fatty acids, both of which are important for growth.

5.3.2 Consequences of selection

Many genes are pleiotropic, and the fundamental biochemical pathways that govern metabolism across tissues are inextricably linked. It is therefore not surprising that the intensive muscle growth of highly efficient broiler chickens has come with unintended physiological consequences (Griffin and Goddard, 1994). Metabolomics has proven useful for providing key insight into the metabolic tradeoffs that contribute to unintended and maladaptive traits in broilers.

5.3.2.1 Accretion of excess body fat

Although muscle and adipose tissue have divergent effects on body composition, selection for rapid growth inadvertently increased fat accretion in modern broiler chickens (Havenstein et al., 2003). Deposition of fat beyond what is physiologically necessary represents a waste of feed, the costliest component of production, and produces a byproduct with very little commercial value (Rauw et al., 1998; Baéza et al., 2015). Strategies to efficiently selected birds with a reduced tendency for fat accretion are therefore valuable to the poultry industry. Metabolomics (NMR) was employed to identify circulating biomarkers that could predict susceptibility to fat accretion (Baéza et al., 2015). Two lines of broilers (fat line and lean line) created using divergent selection were fed low and high-fat diets from three to nine weeks of age, creating a group of individuals with wide-ranging levels of adiposity. Chemometric methods identified metabolites that were associated with variation in adiposity, which were then used to develop regression models that predicted fat mass. A model containing free fatty acids, glutamine, methionine, phospholipids, cholesterol, and beta-hydroxybutyrate explained 74% of the variability in abdominal fat weight across the study population. Beta-hydroxybutyrate was inversely correlated with fat weight, indicating that increased levels of fatty acid oxidation contribute to leanness in broilers. Independent of diet, serum levels of glutamine, histidine, and betaine could discriminate between fat line and lean

line birds. This study demonstrates the biomarker potential of metabolites to predict fat accretion in broilers.

Mechanistic studies of susceptibility to accrete fat in broilers have largely focused on liver because of the clear contribution of hepatic delivery of triglyceride. As in humans, the liver is the primary site of de novo lipogenesis in avians (Leveille et al., 1968; O'Hea and Leveille, 1968), and divergent selection on serum VLDL levels yields birds with significant differences in adiposity (Hermier, 1997). Ji et al. investigated the role of adipose tissue in fat accretion using a combination of adipose tissue metabolomics and transcriptomics (Ji et al., 2014). To create a robust model of leanness, two genetically distinct lean lines of chickens (Leghorn (egg type) and Fayoumi (lean meat type)) were compared to a commercial broiler line. Untargeted tissue metabolomics using an LC/MS platform identified 47 (of 92 detected) metabolites that differed significantly in abundance between the three lines. Several components of the purine and pyrimidine metabolism pathway, which has been associated with resistance to obesity in mice (Tague et al., 2018), were significantly elevated in lean adipose tissue. In addition, tissue from both lean lines contained ~threefold more carnitine and acetylcarnitine than that of broilers, as well as increased levels of several amino acids. These changes in carnitine species corroborated parallel gene expression profiling which identified fatty acid oxidation in abdominal adipose tissue as a pathway associated with leanness. This relationship is also consistent with biomarkers of fatness identified by Baeza et al. (2015).

Insulin promotes adipocyte hypertrophy and fat accretion in many species, but its influence on avian adipocytes is unclear. Unlike in humans and most animals, the ability of insulin to stimulate glucose uptake and induce fatty acid synthesis in avian adipocytes is minimal (Tokushima et al., 2005). Metabolomics and transcriptomics were integrated in a study designed to clarify the effects of insulin in chicken adipose tissue (Ji et al., 2012). Broiler chicks (21 days of age) were fed ad libitum and administered an anti-insulin antibody, to neutralize circulating insulin, or vehicle for five hours. An additional group of chicks was fasted for five hours to serve as a metabolic control. Effects on the abdominal adipose tissue metabolome were determined using an untargeted LC/MS platform. No metabolites associated with glucose utilization were affected by insulin neutralization. However, tissue levels of free amino acids and their metabolites were significantly more abundant than in either the fed or fasted control groups. Fasting significantly decreased tissue amino acid levels, which was consistent with upregulation of genes that mediate amino acid metabolism in the fasted group. Relevance networks and hierarchical clustering demonstrated that many amino acids and their metabolites were closely correlated with expression of p85alpha, a regulatory subunit of phosphoinositide 3-kinase, which plays an important role in mediating insulin actions in adipose tissue (McCurdy et al., 2012). This use of metabolomics uncovered a potential role for insulin in regulating amino acid use, rather than glucose metabolism, in avian adipose tissue.

5.3.2.2 Muscle myopathies

The extremely rapid growth of breast muscle that characterizes modern broiler chickens may also be its Achilles heel. Highly efficient broilers are susceptible to develop degenerative muscle myopathies that compromise breast meat quality and consumer appeal (Mazzoni et al., 2015; Trocino et al., 2015; Kuttappan et al., 2016). Wooden breast (characterized by hardened, firm breast tissue) and white striping (fibrotic and lipid-laden regions that parallel muscle fibers) are the two most common lesions (Kuttappan et al., 2016). Both have arisen in the past decade, and they afflict flocks with a high rate of incidence worldwide (de Brot et al., 2016; Kuttappan et al., 2017). Histologically, lesions are characterized by signs of myodegeneration and regeneration, and by infiltration of fibroblasts, inflammatory cells, and adipocytes (Sihvo et al., 2014; Soglia et al., 2016; Chen et al., 2019). Myopathies are thought to develop in part when muscle growth outpaces vascular development, resulting in localized hypoxia and oxidative stress that disrupt cellular metabolism and damage myofibers (MacRae et al., 2006; Mutryn et al., 2015; Boerboom et al., 2018; Livingston et al., 2019). Several studies have used metabolomics to understand the metabolic basis for breast myopathies and to identify biomarkers that could be used to detect at-risk birds within a flock. An initial metabolomics investigation utilized a large library of commercially available annotated standards to quantify abundance of 282 compounds in breast muscle (Abasht et al., 2016). Birds affected or not with wooden breast were selected from two genetically distinct purebred broiler lines and from one commercial flock, creating a robust sample design. Random forest analysis was used to identify metabolites that most effectively discriminated affected from nonaffected tissue. The 30 top distinguishing metabolites mapped onto multiple metabolic pathways, including amino acid metabolism and oxidative stress. Affected tissue exhibited features of altered glycogen metabolism and glucose utilization. Tissue levels of glycolytic intermediates as well as lactate and pyruvate were significantly lower in affected birds, while components of the pentose phosphate pathway were increased compared to unaffected controls. The commercial platform that was used also queried lipids, which revealed that several fatty acids, phospholipids, signaling lipids (e.g., eicosanoids), and by-products of fatty acid oxidation were significantly elevated in affected wooden breast tissue. Changes in the circulating metabolome also support a role for aberrant fatty acid oxidation in this disorder. Both

carnitine and acetylcarnitine were among metabolites shown to be significantly elevated in serum of broiler affected with wooden breast compared to unaffected controls (Maharjan et al., 2019). These findings from use of metabolomics corroborate gene expression results and further implicate aberrant glucose and fatty acid metabolism as key factors in the etiology of wooden breast lesions (Mutryn et al., 2015; Zambonelli et al., 2016; Pampouille et al., 2018; Lake et al., 2019).

Breast muscle metabolomes have also been characterized in birds affected with white striping, the other major myopathy in broilers. Boerboom et al. (2018) classified white striping status of 51 broilers as either normal, moderate, or severe, based on examination of breast muscle at slaughter. Using a QTOF platform they measured abundance of 599 metabolites in breast muscle, including both lipids and small molecules. Upon comparing metabolomes of the three groups using ANOVA, 63 metabolites differed significantly between normal, moderate, and severe white striping status. Comparable to what was described for birds affected with wooden breast (Abasht et al., 2016), metabolome profiles highlighted fatty acid oxidation as a pathway linked to the disorder. Affected breast tissue contained higher levels of fatty acids and of certain carnitine esters, both of which are consistent with reduced fatty acid oxidation. Using pathway enrichment tools, they also found that the citric acid cycle, as well as glyoxylate, galactose, and taurine metabolism were affected in white striping. Wooden breast and white striping are described as distinct disorders, each with its characteristic histological features. However, both types of lesions can occur in the same muscle sample, which suggests that they may be different manifestations of the same underlying metabolic dysfunction in high-efficiency broilers (Lorenzi et al., 2014; Sihvo et al., 2014; Mutryn et al., 2015). In support of this concept, some metabolite changes (e.g., higher levels of taurine, malate, and certain fatty acids; imbalance in the TCA cycle) were found in both wooden breast and white striping. In addition, both studies related several of the disrupted pathways to hypoxia, which has been linked to extremely rapid growth in broilers (Livingston et al., 2019).

5.3.2.3 Ascites syndrome

Selection for rapid growth has also increased the susceptibility of modern broilers to ascites syndrome, in which excessive fluid accumulates in the peritoneal cavity from transudation of fluid from the vascular system (Peacock et al., 1989; Julian, 1993). In broilers, ascites is a consequence of right ventricular failure that is secondary to pulmonary hypertension. Pulmonary hypertension in broilers arises from a mismatch between oxygen demand and supply that is due to both metabolic demands of rapid growth and a relative reduction in heart and lung mass that developed over the course of selection (Kalmar et al., 2013). Eventually, right ventricular hypertrophy fails to compensate for hypoxemia, and the consequent increase in venous pressure drives fluid leak into the abdomen (Julian, 1993; Wideman et al., 2013). Mortality rates from ascites syndrome can be significant, and are exacerbated by production in low temperature or high-altitude environments (Ruiz-Feria and Wideman, 2001). Genetic background influences susceptibility/resistance to ascites, and heritability estimates (reaching 0.44) indicate the potential to select for resistance in commercial flocks (Lubritz et al., 1995). Serum metabolome profiling was used to identify biomarkers that could be used to identify birds resistant to ascites (Shi et al., 2017). Resistance was associated with increased abundance of various phospholipids. Species that discriminated susceptible from resistant birds contained choline, ethanolamine, serine, and inositol, and thus were not restricted to a specific class of phospholipids. Shao et al. used GC-MS to profile lung tissue metabolomes to gain new biochemical clues into the pathogenesis of pulmonary arterial hypertension in broilers (Shao et al., 2018). Affected birds were identified based on relative increase in right ventricular weight at slaughter. Clustering analyses indicated that lung metabolites clearly differentiated affected from unaffected birds. The set of metabolites with the highest discriminatory signals, based on variable importance in projection (VIP) values, was significantly enriched in components of amino acid metabolism, including increased lysine in lung tissue of birds affected with PAH. Lysine is notable because it inhibits uptake of arginine, which is the precursor for synthesis of the vasodilator NO. In addition, this metabolite set included ornithine and urea, which can limit NO production by competing with NO synthase for arginine. Insufficient synthesis of NO has been linked to development of pulmonary hypertension in broilers (Wideman et al., 2007). Interestingly, metabolome profiles also reflected differences in tissue fatty acid oxidation, just as hypoxia in breast muscle is associated with effects on this pathway (Mutryn et al., 2015; Abasht et al., 2016; Boerboom et al., 2018). Levels of the beta oxidation end-product beta-hydroxybutyrate were higher, and several fatty acids were lower, in lungs of affected birds (Shao et al., 2018). These similarities suggest that cellular hypoxia, through its impact on fatty acid metabolism, may be a common denominator to the consequences of rapid growth in broilers.

5.3.2.4 Heat stress/stress

Increased body size and the metabolic heat produced to accommodate rapid growth make modern broiler chickens more susceptible to heat stress (Deeb et al., 2002). Heat stress occurs when birds are no longer able to counteract elevated ambient temperatures and maintain a

thermoneutral body temperature. Paradoxically, heat stress suppresses feed intake but reallocates energy in a way that increases fat deposition (Geraert et al., 1996). Lu et al. used an experimental design that used pair-feeding to control for reduced feed intake and identify specific effects of heat stress on metabolism (Lu et al., 2018). Broilers were exposed to sustained heat stress (housed at 32°C) from 22 to 42 days of age. Pair feeding was used to create a control group that was housed under thermoneutral conditions (22°C) but with intake matched to heat stress birds. A total of 34 serum metabolites were identified as significantly altered by heat stress, based on a combination on ANOVA and OPLS-DA analyses. This set of metabolites was enriched in components of the TCA cycle, and in alanine, aspartate, glutamine, and tyrosine metabolism. Correlation analyses linked the circulating abundance of several amino acids, as well as pyruvate, with increased fat deposition in heat-stressed birds. Heat stress has been shown to rapidly alter hepatic lipid metabolism, which may contribute to increased fat accretion. Broilers were exposed to cyclical heat stress, in which ambient temperatures were increased for four hours/day, for one week (Jastrebski et al., 2017). Heat stress increased levels of glucose, glucose-6-phosphate, and fructose-6-phosphate, as well as components of gluconeogenesis, glycerol, and glycerol-3-phosphate. Most free amino acids were decreased by heat stress, which may be due to their use as substrates for gluconeogenesis. Effects of heat stress on glucose metabolism were corroborated by transcriptomics, which revealed differential expression of several enzymes in the glycolytic pathway. Stress in general has been shown to alter the metabolome profiles of poultry. Broilers consuming dexamethasone in their drinking water for four weeks exhibited significant increases in serum glucose, fatty acids, and amino acids, while components of the TCA cycle and beta-hydroxybutyrate were lower than in controls (Lv et al., 2018). In a related study, tissue metabolomes (liver, kidney, and breast muscle) were profiled in leghorn chickens consuming corticosterone in their drinking water for up to 12 days (Zaytsoff et al., 2019). This stress mimic significantly altered lipogenesis in the liver, and exerted tissue-specific effects on amino acid and glucose metabolism.

5.3.3 Mechanisms of antibiotic growth promoters

In addition to selective breeding, antibiotic growth promoters have contributed to the dramatic improvements in broiler chicken growth and performance (Dibner and Richards, 2005). When added to feed, subtherapeutic doses of certain antibiotics increase gain and feed conversion (Butaye et al., 2003). Despite their widespread use, the mechanisms through which antibiotics promote growth is not well understood. Because of the nature of antibiotics, an intuitively sound mechanism is that they increase availability of energy to the host by reducing the population of biota that scavenge nutrients in the gut (Visek, 1978). Evidence to date from both poultry and other species indicate that the mechanisms are more complex, and may result from a combination of selective metabolite enrichment and reduced gut inflammation, in addition to a net increase in energy (Engberg et al., 2000; Niewold, 2007; Lu et al., 2008; Khadem et al., 2014). Metabolomics as a platform is well-suited to yield insight into the mechanisms through which antibiotics promote growth. Gadde et al. (2018) utilized the breadth of untargeted metabolomics to characterize the effects of two widely used antibiotic growth promoters, virginiamycin, and bacitracin, on the intestinal metabolomes of broilers. Although both of these antibiotics are effective in promoting weight gain, their antimicrobial actions are distinct. Virginiamycin, a product of Streptomyces virginiae, inhibits bacterial protein synthesis by binding to the 50S ribosomal subunit (Butaye et al., 2003). Bacitracin is a combination of 10 peptides produced by two Bacillus species inhibits bacterial growth by disrupting lipid phosphorylation that is needed to synthesis of the bacterial wall (Butaye et al., 2003). Broiler chicks were fed either antibiotic from hatch to 21 days and compared to chicks receiving no growth promoters. Contents of the ileum were used for global metabolome profiling, and the composition of the microbiome was characterized by 16S sequencing. Both antibiotics had marked effects on the ileal metabolome. Of the 706 metabolites that were identified in ileal contents, 218 differed significantly between virginiamycin and controls, while 119 were significantly affected by bacitracin treatment. Although both increased weight gain to a comparable extent (10.1% for bacitracin and 7.9% for virginiamycin), gain was associated with distinct effects on the metabolome. The authors used random forest classification to identify the 30 metabolites with the most statistically significant ability to distinguish each treatment group. In comparison to controls, the metabolome of virginiamycin-treated birds was characterized by metabolites of amino acids (33%), fatty acids (30%), and nucleosides (23%). In contrast, lipid metabolites were the distinguishing feature of bacitracin metabolomes when compared to either controls (57%) or the virginiamycin group (66%). The lipid-enriched signature of bacitracin may reflect its interactions with cellular lipids, which confers its antimicrobial effects (Butaye et al., 2003). Despite these unique signatures, several metabolic pathways were commonly affected by both antibiotics, suggesting that there are some shared effects for growth promotion. Both bacitracin and virginiamycin significantly increased the levels of several lysine and tryptophan metabolites, including kynurenine, kynurenante, and quinolinate, which play important roles in regulation of inflammation (Chen et al., 2010). Changes in this pathway

also implicate effects on gut motility mediated through a reduction in serotonin. Serotonin is the main neurotransmitter used by the enteric nervous system, and a reduction in serotonin would be expected to increase gut transit time, allowing for enhanced nutrient and energy absorption from the diet. Several purine and pyrimidine metabolites were also commonly affected by both antibiotics, further supporting the concept that they share some outcomes on the intestinal metabolome.

A wide variety of plant-derived extracts show promise as alternatives to antibiotic growth promoters. Plant structural components can serve as probiotics, and endogenous phytochemicals can interact with the host immune and metabolic systems to influence energy utilization and gut health. Chen et al. (2020) combined microbial sequencing with metabolomics to compare the effects of virginiamycin to those of a plant essential oil (PEO) supplement in broiler chickens. Both supplements increased the relative abundance of bacteroidetes and decreased the abundance of Firmicutes in cecal samples, but each exerted unique effects at the genera level compared to control birds. Virginiamycin and PEO also exerted distinct influence on the cecal metabolome, with little overlap between the metabolites that were affected by each treatment compared to controls. However, both supplements significantly enriched the serum metabolomes in essential fatty acids, including linoleic and linolenic acids. Magnolia bark has shown promise in growth trials as a source of plant-derived chemicals that augment growth and feed utilization in broilers (Oh et al., 2018). Using a broad targeted metabolomics platform, Park et al. demonstrated diverse and relatively rapid effects of magnolia bark supplementation in broiler chicks (Park et al., 2020). Three weeks of supplementation (from hatch to 21 days of age) were sufficient to significantly alter the abundance of 278 metabolites in chick ileal contents. This set of metabolites spanned functional classes, including many components of macronutrient metabolism, as well as many more novel biochemicals and vitamin metabolites. Collectively, these studies illustrate the potential to exploit metabolome profiling to advance the search for new ways to enhance growth and health in poultry.

Across species, intrinsic variation in gut microbiomes influences growth and metabolism and is linked to inter-individual differences in body composition (Ridaura et al., 2013; Bergamaschi et al., 2020). Enterotype is used to describe distinct microbial community structures that can be detected in sets of individuals (Arumugam et al., 2011). Yuan et al. (2020) classified 206 broilers into three enterotypes, based on 16S RNA sequencing, and then used untargeted metabolomics to define and compare the resultant metabolomes in the duodenum. A total of 24 metabolites differed significantly between the three enterotype groups, reflecting the impact of different community structures on nutrients available to the host. This set included assorted sugars, as well as fatty acid metabolites and glutathione. Using correlation, the authors connected abundance of two specific genera, *Ochrobactrum* and *Rhodococcus*, which were more abundant in enterotype 2, with increased availability of simple sugars in the duodenum. Conversely, both were inversely correlated with beta-hydroxybutyrate, suggesting that provision of sugars by the microbiome may be associated with reduced oxidation of fatty acids. Interestingly, fat accretion was significantly higher in birds with this enterotype. The authors proposed that these two genera may contribute to increased weight gain by enhancing the bird's ability to utilize complex polysaccharides, which normally are poorly digested by chickens.

5.3.4 Toxicology

Many chemicals found in the environment (e.g., bisphenol A) can disrupt homeostatic metabolism and promote disease in both animals and humans (Heindel et al., 2017). The Deepwater Horizon oil spill exposed hundreds of avian species in the Gulf of Mexico to markedly increased levels of crude oil, resulting in large numbers of mortalities (Barron, 2012). In addition, sublethal exposures persisted for several months as the oil spread (Bursian et al., 2017). Follow-on, controlled studies demonstrated that exposure to sublethal levels of the same source of oil released during this spill affected function of multiple tissues and compromised energy balance (Bursian et al., 2017). Dorr et al. (2019) used metabolomics to identify specific metabolic pathways that are disrupted by sublethal oil exposure and may impact survivability of birds in the wild. Double-crested cormorants, a carnivorous aquatic bird that inhabits the Gulf, were experimentally housed in water containing oil collected from the Deep Water Horizon spill. Hepatic and plasma metabolomes of exposed and control birds were analyzed using NMR. Both sample types showed significant alterations in amino acid metabolism and use of fatty acids. Several branched chain, aromatic and essential amino acids increased significantly after seven days of exposure and remained elevated through completion at 22 days. Despite increased mobilization of amino acids, which cormorants normally rely on energetically as a fish-eating species, and sufficient glucose levels and feed intake, metabolomes suggested that oil exposure significantly increased fatty acid oxidation. Like amino acids, levels of beta-hydroxybutyrate, an end-product of fatty acid catabolism, increased significantly after only seven days exposure and remained elevated throughout the study. In addition, oil exposure altered the abundance of metabolites of bile acids in liver, further indicating effects on lipid metabolism. This use of metabolomics added a level of phenotypic granularity to understanding the consequences

of sublethal oil exposure in avians. Given the importance of lipid metabolism during seasonal adaptations, migration, and reproduction, this study provides an important foundation for studies of avian physiology in native environments.

Significant effects of environmental chemicals on avian lipid metabolism were also revealed in a separate study of laying hens and their offspring. Metabolome profiling was used to characterize the endogenous, tissue-specific metabolism of alpha-cypermethrin, a pyrethroid class insecticide, in laying hens (Liu et al., 2019). This class of compounds is lipid soluble and thus can thus be readily deposited in the yolk (Zheng et al., 2015). Avian embryos in the wild are therefore susceptible to its teratogenic effects (Uggini et al., 2012). Metabolome profiles of chicks that were newly hatched from hens exposed to alpha-cypermethrin exhibited significant effects on various lysophospholipids, as well as pantothenate. Tissue-specific differences in the time course and products of alpha-cypermethrin were also identified. This study highlights that metabolomics can serve dual purposes in toxicological studies by profiling both xenometabolites that are produced from breakdown of environmental chemicals and the corresponding disruptions to endogenous metabolomes.

5.4 Conclusions

Although metabolomics entered the 'omics field later than other players, rapid advances in technology and availability have accelerated its implementation in efforts to understand avian physiology. Its continued application to studies of both chickens and other species is expected to expand the global understanding of health, disease, and environmental adaptations? in avians.

References

Abasht, B., Mutryn, M.F., Michalek, R.D., Lee, W.R., 2016. Oxidative stress and metabolic perturbations in wooden breast disorder in chickens. PLoS One 11 (4), e0153750.

Arumugam, M., Raes, J., Pelletier, E., Le Paslier, D., Yamada, T., Mende, D.R., Fernandes, G.R., Tap, J., Bruls, T., Batto, J.M., Bertalan, M., Borruel, N., Casellas, F., Fernandez, L., Gautier, L., Hansen, T., Hattori, M., Hayashi, T., Kleerebezem, M., Kurokawa, K., Leclerc, M., Levenez, F., Manichanh, C., Nielsen, H.B., Nielsen, T., Pons, N., Poulain, J., Qin, J., Sicheritz-Ponten, T., Tims, S., Torrents, D., Ugarte, E., Zoetendal, E.G., Wang, J., Guarner, F., Pedersen, O., de Vos, W.M., Brunak, S., Dore, J., Meta, H.I.T.C., Antolin, M., Artiguenave, F., Blottiere, H.M., Almeida, M., Brechot, C., Cara, C., Chervaux, C., Cultrone, A., Delorme, C., Denariaz, G., Dervyn, R., Foerstner, K.U., Friss, C., van de Guchte, M., Guedon, E., Haimet, F., Huber, W., van Hylckama-Vlieg, J., Jamet, A., Juste, C., Kaci, G., Knol, J., Lakhdari, O., Layec, S., Le Roux, K., Maguin, E., Merieux, A., Melo Minardi, R., M'Rini, C., Muller, J., Oozeer, R., Parkhill, J., Renault, P., Rescigno, M., Sanchez, N., Sunagawa, S., Torrejon, A., Turner, K., Vandemeulebrouck, G., Varela, E., Winogradsky, Y., Zeller, G., Weissenbach, J., Ehrlich, S.D., Bork, P., 2011. Enterotypes of the human gut microbiome. Nature 473 (7346), 174–180.

Baéza, E., Jégou, M., Gondret, F., Lalande-Martin, J., Tea, I., Le Bihan-Duval, E., Berri, C., Collin, A., Métayer-Coustard, S., Louveau, I., Lagarrigue, S., Duclos, M.J., 2015. Pertinent plasma indicators of the ability of chickens to synthesize and store lipids. J. Anim. Sci. 93 (1), 107–116.

Barron, M.G., 2012. Ecological impacts of the deepwater horizon oil spill: implications for immunotoxicity. Toxicol. Pathol. 40 (2), 315–320.

Beauclercq, S., Nadal-Desbarats, L., Hennequet-Antier, C., Gabriel, I., Tesseraud, S., Calenge, F., Le Bihan-Duval, E., Mignon-Grasteau, S., 2018. Relationships between digestive efficiency and metabolomic profiles of serum and intestinal contents in chickens. Sci. Rep. 8 (1), 6678.

Bergamaschi, M., Maltecca, C., Schillebeeckx, C., McNulty, N.P., Schwab, C., Shull, C., Fix, J., Tiezzi, F., 2020. Heritability and genome-wide association of swine gut microbiome features with growth and fatness parameters. Sci. Rep. 10 (1), 10134.

Bingol, K., 2018. Recent advances in targeted and untargeted metabolomics by NMR and MS/NMR methods. High Throughput 7 (2).

Bingol, K., Bruschweiler, R., 2015. Two elephants in the room: new hybrid nuclear magnetic resonance and mass spectrometry approaches for metabolomics. Curr. Opin. Clin. Nutr. Metab. Care 18 (5), 471–477.

Boerboom, G., van Kempen, T., Navarro-Villa, A., Pérez-Bonilla, A., 2018. Unraveling the cause of white striping in broilers using metabolomics. Poultry Sci. 97 (11), 3977–3986.

Bursian, S.J., Alexander, C.R., Cacela, D., Cunningham, F.L., Dean, K.M., Dorr, B.S., Ellis, C.K., Godard-Codding, C.A., Guglielmo, C.G., Hanson-Dorr, K.C., Harr, K.E., Healy, K.A., Hooper, M.J., Horak, K.E., Isanhart, J.P., Kennedy, L.V., Link, J.E., Maggini, I., Moye, J.K., Perez, C.R., Pritsos, C.A., Shriner, S.A., Trust, K.A., Tuttle, P.L., 2017. Overview of avian toxicity studies for the deepwater horizon natural resource damage assessment. Ecotoxicol. Environ. Saf. 142, 1–7.

Butaye, P., Devriese, L.A., Haesebrouck, F., 2003. Antimicrobial growth promoters used in animal feed: effects of less well known antibiotics on gram-positive bacteria. Clin. Microbiol. Rev. 16 (2), 175–188.

Chen, L.R., Suyemoto, M.M., Sarsour, A.H., Cordova, H.A., Oviedo-Rondon, E.O., Wineland, M., Barnes, H.J., Borst, L.B., 2019. Temporal characterization of wooden breast myopathy ("woody breast") severity and correlation with growth rate and lymphocytic phlebitis in three commercial broiler strains and a random-bred broiler strain. Avian Pathol. 48 (4), 319–328.

Chen, Y., Stankovic, R., Cullen, K.M., Meininger, V., Garner, B., Coggan, S., Grant, R., Brew, B.J., Guillemin, G.J., 2010. The kynurenine pathway and inflammation in amyotrophic lateral sclerosis. Neurotox. Res. 18 (2), 132–142.

Chen, Y., Wang, J., Yu, L., Xu, T., Zhu, N., 2020. Microbiota and metabolome responses in the cecum and serum of broiler chickens fed with plant essential oils or virginiamycin. Sci. Rep. 10 (1), 5382.

Chong, J., Soufan, O., Li, C., Caraus, I., Li, S., Bourque, G., Wishart, D.S., Xia, J., 2018. MetaboAnalyst 4.0: towards more transparent and integrative metabolomics analysis. Nucleic Acids Res. 46 (W1), W486–W494.

Christians, U., Klawitter, J., Klawitter, J., 2016. Biomarkers in transplantation–proteomics and metabolomics. Ther. Drug Monit. 38 (Suppl. 1), S70−S74.

Clasquin, M.F., Melamud, E., Rabinowitz, J.D., 2012. LC-MS data processing with MAVEN: a metabolomic analysis and visualization engine. Curr. Protoc. Bioinf. (Chapter 14): Unit14.11.1-Unit14.11.23.

Cui, L., Lu, H., Lee, Y.H., 2018. Challenges and emergent solutions for LC-MS/MS based untargeted metabolomics in diseases. Mass Spectrom. Rev. 37 (6), 772−792.

de Brot, S., Perez, S., Shivaprasad, H.L., Baiker, K., Polledo, L., Clark, M., Grau-Roma, L., 2016. Wooden breast lesions in broiler chickens in the UK. Vet. Rec. 178 (6), 141.

Dean, D.W., Bidner, T.D., Southern, L.L., 2006. Glycine supplementation to low protein, amino acid-supplemented diets supports optimal performance of broiler chicks. Poultry Sci. 85 (2), 288−296.

Deeb, N., Shlosberg, A., Cahaner, A., 2002. Genotype-by-environment interaction with broiler genotypes differing in growth rate. 4. Association between responses to heat stress and to cold-induced ascites. Poultry Sci. 81 (10), 1454−1462.

Dibner, J.J., Richards, J.D., 2005. Antibiotic growth promoters in agriculture: history and mode of action. Poultry Sci. 84 (4), 634−643.

Dorr, B.S., Hanson-Dorr, K.C., Assadi-Porter, F.M., Selen, E.S., Healy, K.A., Horak, K.E., 2019. Effects of repeated sublethal external exposure to deep water horizon oil on the avian metabolome. Sci. Rep. 9 (1), 371.

Emwas, A.H., Roy, R., McKay, R.T., Tenori, L., Saccenti, E., Gowda, G.A.N., Raftery, D., Alahmari, F., Jaremko, L., Jaremko, M., Wishart, D.S., 2019. NMR spectroscopy for metabolomics research. Metabolites 9 (7).

Engberg, R.M., Hedemann, M.S., Leser, T.D., Jensen, B.B., 2000. Effect of zinc bacitracin and salinomycin on intestinal microflora and performance of broilers. Poultry Sci. 79 (9), 1311−1319.

Ernest, B., Gooding, J.R., Campagna, S.R., Saxton, A.M., Voy, B.H., 2012. MetabR: an R script for linear model analysis of quantitative metabolomic data. BMC Res. Notes 5, 596.

Fiehn, O., 2016. Metabolomics by gas chromatography-mass spectrometry: combined targeted and untargeted profiling. Curr. Protoc. Mol. Biol. 114, 30 34 31−30 34 32.

Gadde, U.D., Oh, S., Lillehoj, H.S., Lillehoj, E.P., 2018. Antibiotic growth promoters virginiamycin and bacitracin methylene disalicylate alter the chicken intestinal metabolome. Sci. Rep. 8 (1), 3592.

Geraert, P.A., Padilha, J.C., Guillaumin, S., 1996. Metabolic and endocrine changes induced by chronic heat exposure in broiler chickens: growth performance, body composition and energy retention. Br. J. Nutr. 75 (2), 195−204.

Greene, E., Flees, J., Dadgar, S., Mallmann, B., Orlowski, S., Dhamad, A., Rochell, S., Kidd, M., Laurendon, C., Whitfield, H., Brearley, C., Rajaram, N., Walk, C., Dridi, S., 2019. Quantum blue reduces the severity of woody breast myopathy via modulation of oxygen homeostasis-related genes in broiler chickens. Front. Physiol. 10, 1251.

Griffin, H.D., Goddard, C., 1994. Rapidly growing broiler (meat-type) chickens: their origin and use for comparative studies of the regulation of growth. Int. J. Biochem. 26 (1), 19−28.

Gross, J.H., 2004. Mass Spectrometry: A Textbook. Spring, New York, USA.

Grzybek, M., Palladini, A., Alexaki, V.I., Surma, M.A., Simons, K., Chavakis, T., Klose, C., Coskun, U., 2019. Comprehensive and quantitative analysis of white and brown adipose tissue by shotgun lipidomics. Mol. Metab. 22, 12−20.

Guijas, C., Montenegro-Burke, J.R., Domingo-Almenara, X., Palermo, A., Warth, B., Hermann, G., Koellensperger, G., Huan, T., Uritboonthai, W., Aisporna, A.E., Wolan, D.W., Spilker, M.E., Benton, H.P., Siuzdak, G., 2018. METLIN: a technology platform for identifying knowns and unknowns. Anal. Chem. 90 (5), 3156−3164.

Havenstein, G.B., Ferket, P.R., Qureshi, M.A., 2003. Carcass composition and yield of 1957 versus 2001 broilers when fed representative 1957 and 2001 broiler diets. Poultry Sci. 82 (10), 1509−1518.

Heindel, J.J., Blumberg, B., Cave, M., Machtinger, R., Mantovani, A., Mendez, M.A., Nadal, A., Palanza, P., Panzica, G., Sargis, R., Vandenberg, L.N., Vom Saal, F., 2017. Metabolism disrupting chemicals and metabolic disorders. Reprod. Toxicol. 68, 3−33.

Heinemann, J., 2019. Cluster analysis of untargeted metabolomic experiments. Methods Mol. Biol. 1859, 275−285.

Hermier, D., 1997. Lipoprotein metabolism and fattening in poultry. J. Nutr. 127 (5 Suppl.), 805S−808S.

Hofmann, P., Siegert, W., Kenéz, Á., Naranjo, V.D., Rodehutscord, M., 2019. Very low crude protein and varying glycine concentrations in the diet affect growth performance, characteristics of nitrogen excretion, and the blood metabolome of broiler chickens. J. Nutr. 149 (7), 1122−1132.

Huang, T.Y., Chi, L.M., Chien, K.Y., 2018. Size-exclusion chromatography using reverse-phase columns for protein separation. J. Chromatogr. A 1571, 201−212.

Jang, C., Chen, L., Rabinowitz, J.D., 2018. Metabolomics and isotope tracing. Cell 173 (4), 822−837.

Jastrebski, S.F., Lamont, S.J., Schmidt, C.J., 2017. Chicken hepatic response to chronic heat stress using integrated transcriptome and metabolome analysis. PLoS One 12 (7), e0181900.

Ji, B., Ernest, B., Gooding, J.R., Das, S., Saxton, A.M., Simon, J., Dupont, J., Metayer-Coustard, S., Campagna, S.R., Voy, B.H., 2012. Transcriptomic and metabolomic profiling of chicken adipose tissue in response to insulin neutralization and fasting. BMC Genom. 13, 441.

Ji, B., Middleton, J.L., Ernest, B., Saxton, A.M., Lamont, S.J., Campagna, S.R., Voy, B.H., 2014. Molecular and metabolic profiles suggest that increased lipid catabolism in adipose tissue contributes to leanness in domestic chickens. Physiol. Genom. 46 (9), 315−327.

Johnson, C.H., Ivanisevic, J., Siuzdak, G., 2016. Metabolomics: beyond biomarkers and towards mechanisms. Nat. Rev. Mol. Cell Biol. 17 (7), 451−459.

Julian, R.J., 1993. Ascites in poultry. Avian Pathol. 22 (3), 419−454.

Kalmar, I.D., Vanrompay, D., Janssens, G.P., 2013. Broiler ascites syndrome: collateral damage from efficient feed to meat conversion. Vet. J. 197 (2), 169−174.

Keppler, E.A.H., Jenkins, C.L., Davis, T.J., Bean, H.D., 2018. Advances in the application of comprehensive two-dimensional gas chromatography in metabolomics. Trends Anal. Chem. 109, 275−286.

Khadem, A., Soler, L., Everaert, N., Niewold, T.A., 2014. Growth promotion in broilers by both oxytetracycline and *Macleaya cordata* extract is based on their anti-inflammatory properties. Br. J. Nutr. 112 (7), 1110−1118.

Kuttappan, V.A., Hargis, B.M., Owens, C.M., 2016. White striping and woody breast myopathies in the modern poultry industry: a review. Poultry Sci. 95 (11), 2724−2733.

Kuttappan, V.A., Owens, C.M., Coon, C., Hargis, B.M., Vazquez-Anon, M., 2017. Incidence of broiler breast myopathies at 2 different ages and its impact on selected raw meat quality parameters. Poultry Sci. 96 (8), 3005−3009.

Lains, I., Gantner, M., Murinello, S., Lasky-Su, J.A., Miller, J.W., Friedlander, M., Husain, D., 2019. Metabolomics in the study of retinal health and disease. Prog. Retin. Eye Res. 69, 57–79.

Lake, J.A., Papah, M.B., Abasht, B., 2019. Increased expression of lipid metabolism genes in early stages of wooden breast links myopathy of broilers to metabolic syndrome in humans. Genes 10 (10).

Leveille, G.A., O'Hea, E.K., Chakbabarty, K., 1968. In vivo lipogenesis in the domestic chicken. Proc. Soc. Exp. Biol. Med. 128 (2), 398–401.

Liebal, U.W., Phan, A.N.T., Sudhakar, M., Raman, K., Blank, L.M., 2020. Machine learning applications for mass spectrometry-based metabolomics. Metabolites 10 (6).

Liu, X., Liu, C., Wang, P., Liang, Y., Zhan, J., Zhou, Z., Liu, D., 2019. Distribution, metabolism and metabolic disturbances of alpha-cypermethrin in embryo development, chick growth and adult hens. Environ. Pollut. 249, 390–397.

Livingston, M.L., Ferket, P.R., Brake, J., Livingston, K.A., 2019. Dietary amino acids under hypoxic conditions exacerbates muscle myopathies including wooden breast and white stripping. Poultry Sci. 98 (3), 1517–1527.

Lorenzi, M., Mudalal, S., Cavani, C., Petracci, M., 2014. Incidence of white striping under commercial conditions in medium and heavy broiler chickens in Italy. J. Appl. Poultry Res. 23 (4), 754–758.

Lu, J., Hofacre, C., Smith, F., Lee, M.D., 2008. Effects of feed additives on the development on the ileal bacterial community of the broiler chicken. Animal 2 (5), 669–676.

Lu, Z., He, X., Ma, B., Zhang, L., Li, J., Jiang, Y., Zhou, G., Gao, F., 2018. Serum metabolomics study of nutrient metabolic variations in chronic heat-stressed broilers. Br. J. Nutr. 119 (7), 771–781.

Lubritz, D.L., Smith, J.L., McPherson, B.N., 1995. Heritability of ascites and the ratio of right to total ventricle weight in broiler breeder male lines. Poultry Sci. 74 (7), 1237–1241.

Lv, Z.P., Peng, Y.Z., Zhang, B.B., Fan, H., Liu, D., Guo, Y.M., 2018. Glucose and lipid metabolism disorders in the chickens with dexamethasone-induced oxidative stress. J. Anim. Physiol. Anim. Nutr. 102 (2), e706–e717.

MacRae, V.E., Mahon, M., Gilpin, S., Sandercock, D.A., Mitchell, M.A., 2006. Skeletal muscle fibre growth and growth associated myopathy in the domestic chicken (*Gallus domesticus*). Br. Poultry Sci. 47 (3), 264–272.

Maharjan, P., Hilton, K., Weil, J., Suesuttajit, N., Beitia, A., Owens, C.M., Coon, C., 2019. Characterizing woody breast myopathy in a meat broiler line by heat production, microbiota, and plasma metabolites. Front. Vet. Sci. 6, 497.

Marshall, D.D., Powers, R., 2017. Beyond the paradigm: combining mass spectrometry and nuclear magnetic resonance for metabolomics. Prog. Nucl. Magn. Reson. Spectrosc. 100, 1–16.

Mazzoni, M., Petracci, M., Meluzzi, A., Cavani, C., Clavenzani, P., Sirri, F., 2015. Relationship between pectoralis major muscle histology and quality traits of chicken meat. Poultry Sci. 94 (1), 123–130.

McCalley, D.V., 2017. Understanding and manipulating the separation in hydrophilic interaction liquid chromatography. J. Chromatogr. A 1523, 49–71.

McCurdy, C.E., Schenk, S., Holliday, M.J., Philp, A., Houck, J.A., Patsouris, D., MacLean, P.S., Majka, S.M., Klemm, D.J., Friedman, J.E., 2012. Attenuated Pik3r1 expression prevents insulin resistance and adipose tissue macrophage accumulation in diet-induced obese mice. Diabetes 61 (10), 2495–2505.

Metzler-Zebeli, B.U., Siegerstetter, S.C., Magowan, E., Lawlor, P.G., O'Connell, N.E., Zebeli, Q., 2019. Feed restriction reveals distinct serum metabolome profiles in chickens divergent in feed efficiency traits. Metabolites 9 (2).

Mignon-Grasteau, S., Muley, N., Bastianelli, D., Gomez, J., Peron, A., Sellier, N., Millet, N., Besnard, J., Hallouis, J.M., Carre, B., 2004. Heritability of digestibilities and divergent selection for digestion ability in growing chicks fed a wheat diet. Poultry Sci. 83 (6), 860–867.

Mutryn, M.F., Brannick, E.M., Fu, W., Lee, W.R., Abasht, B., 2015. Characterization of a novel chicken muscle disorder through differential gene expression and pathway analysis using RNA-sequencing. BMC Genom. 16, 399.

Niewold, T.A., 2007. The nonantibiotic anti-inflammatory effect of antimicrobial growth promoters, the real mode of action? A hypothesis. Poultry Sci. 86 (4), 605–609.

O'Hea, E.K., Leveille, G.A., 1968. Lipogenesis in isolated adipose tissue of the domestic chick (*Gallus domesticus*). Comp. Biochem. Physiol. 26 (1), 111–120.

O'Shea, K., Misra, B.B., 2020. Software tools, databases and resources in metabolomics: updates from 2018 to 2019. Metabolomics 16 (3), 36.

Oh, S., Gadde, U.D., Bravo, D., Lillehoj, E.P., Lillehoj, H.S., 2018. Growth-promoting and antioxidant effects of magnolia bark extract in chickens uninfected or Co-infected with *Clostridium perfringens* and eimeria maxima as an experimental model of necrotic enteritis. Curr. Dev. Nutr. 2 (4), nzy009.

Pampouille, E., Berri, C., Boitard, S., Hennequet-Antier, C., Beauclercq, S.A., Godet, E., Praud, C., Jego, Y., Le Bihan-Duval, E., 2018. Mapping QTL for white striping in relation to breast muscle yield and meat quality traits in broiler chickens. BMC Genom. 19 (1), 202.

Park, I., Oh, S., Lillehoj, E.P., Lillehoj, H.S., 2020. Dietary supplementation with magnolia bark extract alters chicken intestinal metabolite levels. Front. Vet. Sci. 7, 157.

Peacock, A.J., Pickett, C., Morris, K., Reeves, J.T., 1989. The relationship between rapid growth and pulmonary hemodynamics in the fast-growing broiler chicken. Am. Rev. Respir. Dis. 139 (6), 1524–1530.

Powers, J.B., Campagna, S.R., 2019. Design and evaluation of a gas chromatograph-atmospheric pressure chemical ionization interface for an exactive Orbitrap mass spectrometer. J. Am. Soc. Mass Spectrom. 30 (11), 2369–2379.

Rabinowitz, J.D., Purdy, J.G., Vastag, L., Shenk, T., Koyuncu, E., 2011. Metabolomics in drug target discovery. Cold Spring Harb. Symp. Quant. Biol. 76, 235–246.

Rauw, W.M., Kanis, E., Noordhuizen-Stassen, E.N., Grommers, F.J., 1998. Undesirable side effects of selection for high production efficiency in farm animals: a review. Livest. Prod. Sci. 56 (1), 15–33.

Ridaura, V.K., Faith, J.J., Rey, F.E., Cheng, J., Duncan, A.E., Kau, A.L., Griffin, N.W., Lombard, V., Henrissat, B., Bain, J.R., Muehlbauer, M.J., Ilkayeva, O., Semenkovich, C.F., Funai, K., Hayashi, D.K., Lyle, B.J., Martini, M.C., Ursell, L.K., Clemente, J.C., Van Treuren, W., Walters, W.A., Knight, R., Newgard, C.B., Heath, A.C., Gordon, J.I., 2013. Gut microbiota from twins discordant for obesity modulate metabolism in mice. Science 341 (6150), 1241214.

Robinson, A.B., Partridge, D., Turner, M., Teranishi, R., Pauling, L., 1973. An apparatus for the quantitative analysis of volatile compounds in urine. J. Chromatogr. 85 (1), 19–29.

Romero, L.F., Zuidhof, M.J., Renema, R.A., Naeima, A., Robinson, F.E., 2009. Characterization of energetic efficiency in adult broiler breeder hens. Poultry Sci. 88 (1), 227–235.

Ruiz-Feria, C.A., Wideman Jr., R.F., 2001. Taurine, cardiopulmonary hemodynamics, and pulmonary hypertension syndrome in broilers. Poultry Sci. 80 (11), 1607–1618.

Scheubert, K., Hufsky, F., Petras, D., Wang, M., Nothias, L.F., Duhrkop, K., Bandeira, N., Dorrestein, P.C., Bocker, S., 2017. Significance estimation for large scale metabolomics annotations by spectral matching. Nat. Commun. 8 (1), 1494.

Schrimpe-Rutledge, A.C., Codreanu, S.G., Sherrod, S.D., McLean, J.A., 2016. Untargeted metabolomics strategies-challenges and emerging directions. J. Am. Soc. Mass Spectrom. 27 (12), 1897–1905.

Shao, F.J., Ying, Y.T., Tan, X., Zhang, Q.Y., Liao, W.T., 2018. Metabonomics profiling reveals biochemical pathways associated with pulmonary arterial hypertension in broiler chickens. J. Proteome Res. 17 (10), 3445–3453.

Shi, S., Shen, Y., Zhang, S., Zhao, Z., Hou, Z., Zhou, H., Zou, J., Guo, Y., 2017. Combinatory evaluation of transcriptome and metabolome profiles of low temperature-induced resistant ascites syndrome in broiler chickens. Sci. Rep. 7 (1), 2389.

Sihvo, H.K., Immonen, K., Puolanne, E., 2014. Myodegeneration with fibrosis and regeneration in the pectoralis major muscle of broilers. Vet. Pathol. 51 (3), 619–623.

Skoog, D.A., Holler, F.J., Nieman, T.A., 2007. Principles of Instrumental Analysis. Saunders College Pub. Harcourt Brace College Publishers, Philadelphia. Orlando, Fla.

Soglia, F., Mudalal, S., Babini, E., Di Nunzio, M., Mazzoni, M., Sirri, F., Cavani, C., Petracci, M., 2016. Histology, composition, and quality traits of chicken pectoralis major muscle affected by wooden breast abnormality. Poultry Sci. 95 (3), 651–659.

Su, X., Lu, W., Rabinowitz, J.D., 2017. Metabolite spectral accuracy on Orbitraps. Anal. Chem. 89 (11), 5940–5948.

Tague, E.D., Bourdon, A.K., MacDonald, A., Lookadoo, M.S., Kim, E.D., White, W.M., Terry, P.D., Campagna, S.R., Voy, B.H., Whelan, J., 2018. Metabolomics approach in the study of the well-defined poly-herbal preparation Zyflamend. J. Med. Food 21 (3), 306–316.

Tiziani, S., Kang, Y., Choi, J.S., Roberts, W., Paternostro, G., 2011. Metabolomic high-content nuclear magnetic resonance-based drug screening of a kinase inhibitor library. Nat. Commun. 2, 545.

Tokushima, Y., Takahashi, K., Sato, K., Akiba, Y., 2005. Glucose uptake in vivo in skeletal muscles of insulin-injected chicks. Comp. Biochem. Physiol. B Biochem. Mol. Biol. 141 (1), 43–48.

Trocino, A., Piccirillo, A., Birolo, M., Radaelli, G., Bertotto, D., Filiou, E., Petracci, M., Xiccato, G., 2015. Effect of genotype, gender and feed restriction on growth, meat quality and the occurrence of white striping and wooden breast in broiler chickens. Poultry Sci. 94 (12), 2996–3004.

Uggini, G.K., Patel, P.V., Balakrishnan, S., 2012. Embryotoxic and teratogenic effects of pesticides in chick embryos: a comparative study using two commercial formulations. Environ. Toxicol. 27 (3), 166–174.

Visek, W.J., 1978. Mode of growth promotion by antibiotics. J. Anim. Sci. 46 (5), 1447–1469.

Voy, B.H., 2011. Systems genetics: a powerful approach for gene-environment interactions. J. Nutr. 141 (3), 515–519.

Voy, B.H., Aronow, B.J., 2009. Embrace diversity! Systems genetics-enabled discovery of disease networks. Physiol. Genom. 39 (3), 169–171.

Vuckovic, D., 2018. Improving metabolome coverage and data quality: advancing metabolomics and lipidomics for biomarker discovery. Chem. Commun. 54 (50), 6728–6749.

Wang, S., Zhou, L., Wang, Z., Shi, X., Xu, G., 2017. Simultaneous metabolomics and lipidomics analysis based on novel heart-cutting two-dimensional liquid chromatography-mass spectrometry. Anal. Chim. Acta 966, 34–40.

Wideman, R.F., Chapman, M.E., Hamal, K.R., Bowen, O.T., Lorenzoni, A.G., Erf, G.F., Anthony, N.B., 2007. An inadequate pulmonary vascular capacity and susceptibility to pulmonary arterial hypertension in broilers. Poultry Sci. 86 (5), 984–998.

Wideman, R.F., Rhoads, D.D., Erf, G.F., Anthony, N.B., 2013. Pulmonary arterial hypertension (ascites syndrome) in broilers: a review. Poultry Sci. 92 (1), 64–83.

Xia, J., Mandal, R., Sinelnikov, I.V., Broadhurst, D., Wishart, D.S., 2012. MetaboAnalyst 2.0–a comprehensive server for metabolomic data analysis. Nucleic Acids Res. 40 (Web Server issue), W127–W133.

Xia, J., Psychogios, N., Young, N., Wishart, D.S., 2009. MetaboAnalyst: a web server for metabolomic data analysis and interpretation. Nucleic Acids Res. 37 (Web Server issue), W652–W660.

Xia, J., Sinelnikov, I.V., Han, B., Wishart, D.S., 2015. MetaboAnalyst 3.0–making metabolomics more meaningful. Nucleic Acids Res. 43 (W1), W251–W257.

Yuan, Z., Yan, W., Wen, C., Zheng, J., Yang, N., Sun, C., 2020. Enterotype identification and its influence on regulating the duodenum metabolism in chickens. Poultry Sci. 99 (3), 1515–1527.

Zambonelli, P., Zappaterra, M., Soglia, F., Petracci, M., Sirri, F., Cavani, C., Davoli, R., 2016. Detection of differentially expressed genes in broiler pectoralis major muscle affected by White Striping - Wooden Breast myopathies. Poultry Sci. 95 (12), 2771–2785.

Zampiga, M., Laghi, L., Petracci, M., Zhu, C., Meluzzi, A., Dridi, S., Sirri, F., 2018. Effect of dietary arginine to lysine ratios on productive performance, meat quality, plasma and muscle metabolomics profile in fast-growing broiler chickens. J. Anim. Sci. Biotechnol. 9, 79.

Zaytsoff, S.J.M., Brown, C.L.J., Montina, T., Metz, G.A.S., Abbott, D.W., Uwiera, R.R.E., Inglis, G.D., 2019. Corticosterone-mediated physiological stress modulates hepatic lipid metabolism, metabolite profiles, and systemic responses in chickens. Sci. Rep. 9 (1), 19225.

Zheng, X.B., Luo, X.J., Zeng, Y.H., Wu, J.P., Mai, B.X., 2015. Chiral polychlorinated biphenyls (PCBs) in bioaccumulation, maternal transfer, and embryo development of chicken. Environ. Sci. Technol. 49 (2), 785–791.

Zuidhof, M.J., Schneider, B.L., Carney, V.L., Korver, D.R., Robinson, F.E., 2014. Growth, efficiency, and yield of commercial broilers from 1957, 1978, and 2005. Poultry Sci. 93 (12), 2970–2982.

Chapter 6

Mitochondrial physiology—Sturkie's book chapter

Walter Gay Bottje

Department of Poultry Science, Center of Excellence for Poultry Science, Division of Agriculture, University of Arkansas, Fayetteville, AR, United States

6.1 Overview of mitochondria

6.1.1 Introduction

Mitochondria generate 90% of the energy in the form of adenosine triphosphate (ATP) within a cell by oxidative phosphorylation earning it the title of "powerhouse of the cell." The process of oxidative phosphorylation from the respiratory or electron transport chain (ETC) activity was first reported by Kennedy and Lehninger (1949). Energy production, however, is just one of many roles orchestrated by mitochondria. Mitochondria are the only organelle outside the nucleus with a discrete pool of DNA (mitochondrial, mtDNA). This distinction lead to the accepted theory of endosymbiotic origin of mitochondria in which an α-Proteobacteria took up a commensal residence within a eukaryotic cell with more recent evidence of co-evolution of an extant eukaryotic cell (Gray et al., 1999). According to Lehninger (1965), Rudolf Albert van Kolliker, a Swiss cytologist, first described mitochondria in 1857 and gave them the name of sarcosomes having a distinct granular structure surrounded by a membrane. Later, (Benda, 1898) renamed the structure the mitochondrion; a derivation from Greek for thread (*mitos*) and grain (*chondrion*) and the standard name for the organelle since the 1930s (Lehninger, 1965). The synthesis and import of nuclear (n)-encoded proteins that represent 98% of all mitochondrial protein is tightly coordinated with the synthesis of mtDNA-encoded proteins that is followed by the coordinated assembly needed for fully functional mitochondria. Mitochondria play a vital role in programmed cell death (apoptosis) and mitochondrial generated reactive oxygen species (ROS) at low levels is important in signal transduction whereas higher ROS generation makes the mitochondria a major site of endogenous oxidative stress. Mitochondria are dynamic organelles that change morphology and composition in response to physiological signals, e.g., variations in nutrition, O_2 levels, and metabolic demand (Aw and Jones, 1989). Mitochondria are not static structures (Hoppins et al., 2007) and undergo fusion and fission processes that are driven in part by the energetic status of the cell, e.g., Liesa and Shirihai (2013). Mitochondria also possess hormone receptors that have profound relevance on mitochondrial function (see reviews by Wyrutniak-Cabello et al. (2001), Chen et al. (2005), Psarra et al. (2006)). The first report of mitochondrial hormone receptors in avian muscle cells was provided by Lassiter et al. (2018).

6.1.2 Physical description

Under the electron microscope, mitochondria appear bean-shaped with striations that are visible due to folding of the inner mitochondrial membrane called cristae, which is where the ETC is located. Electron tomography revealed mitochondria as long tube-like structures that weave throughout the cytosol (Mannella, 2000). Sections of the mitochondrial membrane are contiguous with the endoplasmic and sarcoplasmic reticulum that facilitate shuttling of molecules such as ATP and ADP between the mitochondria and cytosol (Scheffler, 1999; Sharma et al., 2000). Mitochondria have an inner membrane that surround the mitochondrial matrix and an outer membrane that encloses an intramembranous space (Figs. 6.1 and 6.2). Cytochrome *c*, located in the intramembranous space, is critical for cellular respiration and for initiating normal cell turnover (apoptosis). Most mitochondrial proteins are found in the matrix and are associated with (a) the Kreb cycle, (b) β-oxidation of fats, (c) synthesis of heme proteins, and (d) iron-sulfur proteins prevalent in the ETC. Mitochondrial DNA is also present in the matrix.

Sturkie's Avian Physiology. https://doi.org/10.1016/B978-0-12-819770-7.00043-8

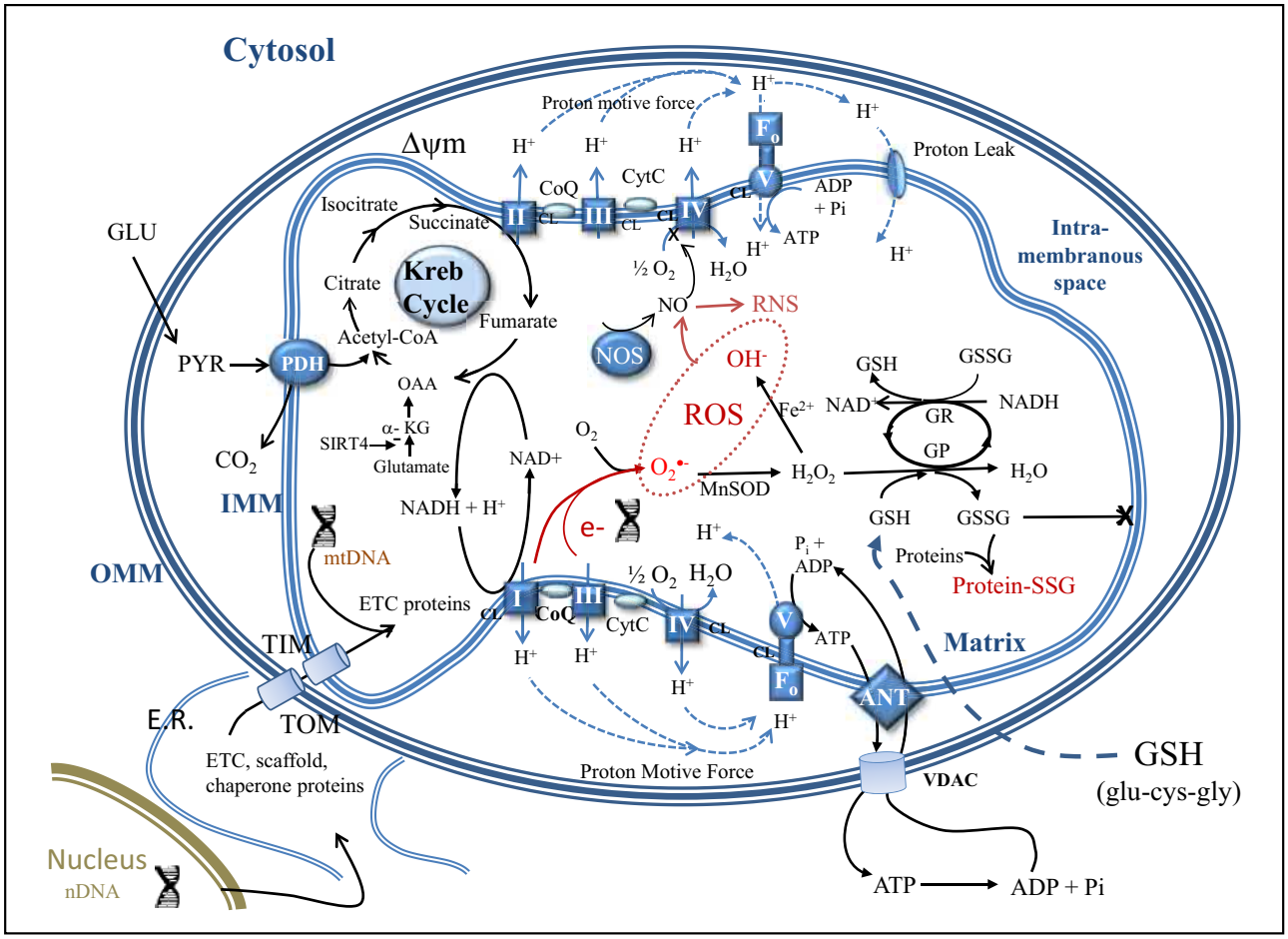

FIGURE 6.1 Overview of mitochondria. A stylized mitochondria with some of mitochondrial processes discussed in the text is presented. The mitochondria have both an outer (OMM) and inner (IMM) mitochondrial membrane with the electron transport chain (ETC) (I, II, III, IV, V) located on the IMM. The ETC toward the top shows electrons moving from succinate, an intermediate of the Kreb's Cycle, to Complex II, III, and IV. The ETC on the bottom shows NADH-linked energy substrates with electrons entering the ETC at Complex I. Electrons are passed between Complex II and III, and Complex I and III by coenzyme Q (CoQ). Cytochrome C (cyt *c*) shuttles electrons from complex III to Complex IV. The movement of electrons down the respiratory chain is accompanied by pumping of protons (H+), in the intramembranous space that sets up a proton motive force that drives ATP synthesis when protons flow through ATP synthase (Complex V). ATP is transported out of the mitochondria for use by the cell through the adenine nucleotide translocase (ANT) on the inner membrane and the VDAC on the outer membrane. A mitochondrial NOS produces NO that can compete with oxygen for the active site on cytochrome *c* oxidase. Protons may also move through the membrane at sites other than the ATP synthase in a process called proton leak. Proton leak dissipates the proton motive force without synthesis of ATP but can also attenuate formation of reactive oxygen species (ROS). Electrons (e−) that leak from the ETC can react with oxygen to form superoxide (O_2^-) that is normally converted to hydrogen peroxide (H_2O_2) by manganese superoxide dismutase (MnSOD). In the presence of free metal ions, H_2O_2 can be converted to the highly reactive hydroxyl radical (OH^-). Collectively, superoxide, H_2O_2 and OH^- are called ROS and can cause oxidative damage to cellular structures (e.g., proteins, lipids, DNA). ROS can react with NO to produce reactive nitrogen species that can damage these structures also. Glutathione (GSH) is an important endogenous antioxidant that is imported from the cytosol into the mitochondria. The active thiol in GSH is used to reduce lipid peroxides or H_2O_2 to water or lipid alcohols with the concomitant formation of oxidized glutathione (GSSG) that can be recycled to GSH reductase (GR) that utilizes reducing equivalents from NADH. Unlike cells, mitochondria cannot export GSSG and elevations in GSSG in mitochondria can lead to protein disulfides (protein-SSG) formation. This can be particularly detrimental to ETC activity due to the presence of reactive thiol groups in these proteins. The ETC is comprised of nuclear and mitochondrially encoded (mtDNA) proteins. The nuclear encoded proteins must be transported into the mitochondria which is facilitated by both outer membrane translocase (TOM) and inner membrane translocase (TIM) proteins. *This figure was adapted from Wallace (1999).*

The outer mitochondrial membrane is a simple phospholipid bilayer whereas the inner mitochondrial membrane is highly convoluted forming cristae that greatly increase its surface area. Due to the presence of the multiprotein complexes of the ETC, the inner mitochondrial membrane contains 70% protein and 30% lipid compared to a 50:50 ratio of proteins to lipids that is typically found in membranes. The inner mitochondrial membrane also contains cardiolipin, a unique lipid found primarily in mitochondria (Hatefi, 1985).

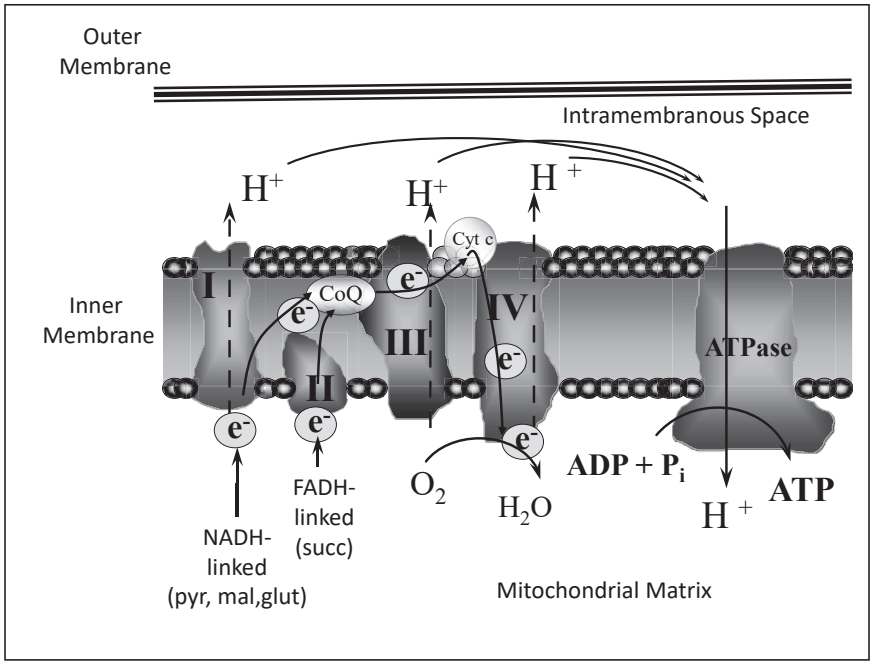

FIGURE 6.2 **Diagrammatic representation of the mitochondrial electron transport chain.** The respiratory chain consists of five multiprotein complexes (Complex I, II, III, IV, and V). Electrons (e−) enter the electron transport chain (ETC) either through Complex I from NADH-linked energy substrates (e.g., pyruvate, malate, glutamate), or at Complex II from FADH-linked substrates (e.g., succinate). The electrons are passed down the ETC (*solid arrows*) to the terminal electron acceptor, oxygen that is reduced to water. Coenzyme Q (CoQ, ubiquinone) is responsible for the transfer of electrons from Complex I and II to Complex III. Associated with the movement of electrons along the ETC is the movement of protons (H^+, *dashed arrows*) from the mitochondrial matrix into the intramembranous space, setting up a proton motive force. The movement of protons through the adenosine triphosphate synthase (ATP synthase, Complex V) provides the energy to support ATP synthesis. *Based on Lehninger et al. (1993).*

6.1.3 Mitochondrial and nuclear DNA interaction for assembly and function

Mitochondrial DNA, a circular molecule with over 16,000 base pairs, contains roughly 37 genes that code for two ribosomal RNA's, 22 transfer RNA's, and 13 proteins that combine with over 70 other n-encoded proteins to form the respiratory chain (Anderson et al., 1981). Transcription, translation, and mtDNA replication including synthesis of ribosomal proteins are all under nuclear regulation. Consequently, mitochondrial function depends upon the tightly coordinated interaction between nDNA and mtDNA-encoded proteins, protein assembly factors, and chaperone proteins involved in protein folding, protein scaffolding, and structural support (Nijtmans et al., 2002; Rabilloud et al., 2002; Ryan and Hoogenraad, 2007).

Nuclear encoded proteins destined for the mitochondria must be unfolded prior to transport through the outer (TOM) and inner (TIM) membrane translocase proteins (Ryan and Hoogenraad, 2007). After transit through these protein channels, the proteins are refolded within the mitochondria by chaperone proteins, e.g., heat shock proteins 70 (Hsp70), Hsp 60/10 (also called Chaperonin 60/10), Hsp78, and a number of proteases. Chaperone protein expression increases during stress (e.g., heat, oxidative, toxin-mediated) when they are particularly important in stabilizing and repairing damaged proteins.

The D loop of mtDNA contains regulators of mitochondrial transcription and replication. Differences in D loop mtDNA have been used to identify animals with different mitochondrial types. Some proteins are part of the mitochondrial import machinery, whereas others are needed for expression of the mitochondrial genome and metabolism. Other proteins are required for mitochondrial roles in apoptosis (Liu and Kitsis, 1996), redox cell signaling, and homeostasis (Bogoyevitch et al., 2000; Levonen et al., 2001; Droge, 2002). Rabilloud et al. (2002) indicated that "… *mitochondrial function in general, and mitochondrial protein synthesis in particular, depend on the conjugated and coordinated expression of both mitochondrial and nuclear genomes.*" A complex communication network between mitochondria and the nucleus also exists to coordinate mitochondrial biogenesis and function (Poyton and McEwen, 1996).

6.1.4 The respiratory chain and adenosine triphosphate synthesis

The ETC, first reported by Kennedy and Lehninger (1949), consists of five multiprotein enzyme complexes: Complex I (NADH: ubiquinone oxido-reductase), Complex II

(succinate: ubiquinone reductase), Complex III (ubiquinol: cytochrome *c* oxido-reductase), Complex IV (cytochrome *c* oxidase), and the F_1F_0 ATP synthase or ATPase (Complex V), and two mobile electron carriers, ubiquinone (Q) and cytochrome *c* (cyt *c*) (Figs. 6.1 and 6.2). Electrons enter the respiratory chain at Complex I for NADH-linked substrates (e.g., malate and pyruvate), or at Complex II for succinate, an $FADH_2$-linked substrate (Fig. 6.2). Ubiquinone carries electrons from Complex I and II to Complex III while cyt *c* shuttles electrons from Complex III to Complex IV. Electron transfer to O_2 (the terminal acceptor) results in full reduction of O_2 to water. Electron movement coincides with proton pumping to establish a proton motive force consisting of a membrane potential ($\Delta\psi_m$) and pH (proton) gradient that provide energy for ATP synthesis as protons flow back into the matrix through ATP synthase (Complex V). Protons can also cross the inner mitochondrial membrane at sites other than the ATP synthase due to anion carrier proteins (e.g., adenine nucleotide transporter, glutamate transporter), uncoupling proteins (UCPs), and intrinsic membrane characteristics (Brown and Brand, 1991; Brand et al., 1994, 2005; Rolfe and Brand, 1997; Brookes et al., 1997). Proton leak therefore consumes O_2 and dissipates the membrane potential without ATP synthesis. Uncoupling represents an inefficiency of mitochondrial function, but minimizes ROS production (see below). While mitochondrial uncoupling is important in heat generation in brown adipose fat tissue in mammals, brown adipose tissue has not been reported in any avian species and appears to have been lost early in evolution of the avian lineage from a common ancestor of birds and mammals (Mezentseva et al., 2008).

6.1.4.1 Ubiquinone (coenzyme Q)

Electron transfer from Complex I to Complex III and from Complex II to Complex III is carried out by ubiquinone (coenzyme Q; e.g., CoQ_9 and CoQ_{10}). Autooxidation of CoQ is a major source of mitochondrial ROS production (Chance et al., 1979; Turrens et al., 1985; Turrens and Boveris, 1980). Animals with relatively more CoQ_{10} had lower mitochondrial ROS production than those with higher CoQ_9 levels (Lass and Sohal, 1999), and CoQ content is highly correlated with Complex I and II activities (Ernster and Forsmark-Andree, 1993; Forsmark-Andree et al., 1997).

6.1.4.2 Cardiolipin

Cardiolipin (tetra-acyl-diphosphatidyl-glycerol) is a unique phosphorglyceride with four long-chain fatty acids compared to two side chains in typical phospholipids that is essential for membranes involved in coupled (oxidative) phosphorylation (Hoch, 1992). Full activity requires the interaction of each complex (I to V) with cardiolipin. Yeast lacking cardiolipin exhibit impaired mitochondrial function (Koshkin and Greenberg, 2000). Exogenously added cardiolipin depressed respiratory chain coupling but increased ATP synthase activity in isolated liver mitochondria (Bobyleva et al., 1997).

6.1.5 Assessing mitochondrial function

6.1.5.1 Polarographic method

A standard method of assessing mitochondrial function utilizes an O_2 electrode in a Warburg apparatus to measure O_2 consumption with different respiratory states in freshly isolated mitochondria (Estabrook, 1967). In the presence of NADH- and FADH-linked energy substrates, mitochondria exhibit an initial slow rate of O_2 consumption (State 2 respiration). The addition of ADP stimulates ETC activity and initiates rapid O_2 consumption that is followed by a slower rate of O_2 consumption (State 4 respiration) when ADP levels decline (i.e., ADP is limiting) due to oxidative phosphorylation and synthesis of ATP (from ADP and inorganic phosphorus). Functional indices calculated from these data include the respiratory control ratio (RCR) and ADP:O ratio (Estabrook, 1967). The RCR represents the degree of coupling or efficiency of respiratory chain activity and is calculated as State 3 (active respiration) divided by State 4 (resting) respiration rate. The ADP:O ratio is the amount of ADP phosphorylated per nanoatom of monomeric oxygen consumed during State 3 respiration and is an index of oxidative phosphorylation. Electron movement down the transport chain is coupled to proton pumping, setting up the proton motive force that synthesizes ATP as protons flow through the f_1f_0ATPase. The ADP:O ratio, an index of oxidative phosphorylation, is determined as ADP used per nmol monomeric oxygen during State 3 respiration. Theoretical ADP:O ratios are 2 (for succinate) and 3 (for malate) that enter at Complex I and II, respectively. ATP synthesis is not 100% efficient due in part to electron and proton leak. Decreases in the ADP:O ratio (increased O_2 use that is uncoupled from ATP synthesis) occur by (a) proton leakage across the inner mitochondrial membrane at sites other than the F_1F_0 ATPase (Brand et al., 1994) or (b) electron leakage from the respiratory chain that react with O_2 to form ROS such as superoxide and H_2O_2 (Boveris and Chance, 1973; Chance et al., 1979, see Section 6.1.5.2 below).

6.1.5.2 Flux analysis

A relatively new approach to assess mitochondrial function in intact cells using flux analysis of oxygen consumption rate was reported by Wu et al. (2007). The advantage of this method is that mitochondrial function can be assessed within intact cells which eliminates any artifacts (e.g., sheer

stress) that might be introduced from stirring that is a requirement of the polarographic method of Estabrook (1967). Assessment of glycolytic activity can also be determined simultaneously by assessment of extracellular acidification rate. Metabolic inhibitors will stimulate glycolytic activity.

Flux analysis was used to assess bioenergetic in response to 4-hydroxy 2-nonenal (4-HNE) induced oxidative stress in chicken embryo fibroblast (CEF) cells and a spontaneously immortalized CEF cell (DF-1) (Lassiter et al., 2014). It was determined that senescent CEF cells (passage 19) were more susceptible to 4-HNE-induced oxidative stress than younger (passage 8) CEF cells, but surprisingly, the immortal DF-1 cells were more sensitive to oxidant challenge than the CEF cells. Greater sensitivity to oxidant challenge following 4-HNE treatment may have been due to an inability of DF-1 cells to increase proton leak in comparison to CEF cells.

6.1.6 Mitochondrial role in apoptosis

Mitochondria are critical in initiating programmed cell death or apoptosis (Wallace, 1999). Between the inner and outer mitochondrial membranes are cytochrome *c*, apoptosis-inducing factor, and caspases (proteases) that contribute to apoptosis. Apoptosis is initiated by formation of the mitochondrial permeability transition pore (mtPTP) on the inner membrane. The mtPTP forms by the coalescing of the voltage-dependent anion channel (VDAC), adenine nucleotide translocase (ANT), BCL-2-associated X protein, and cyclophilin D. When the mtPTP is formed, the mitochondrial membrane potential is dissipated followed shortly thereafter by mitochondrial swelling and release of caspases and apoptosis initiating factor. The proteolytic caspases released into the cytoplasm degrades the cytoskeletal architecture. Events that trigger the opening of the mtPTP include (a) a decrease in energetic capacity of the mitochondria, (b) excessive influx of ionic calcium, and (c) increased ROS generation.

6.2 Mitochondrial inefficiencies, oxidative stress, and antioxidants

6.2.1 Electron transport defects and oxidative stress

6.2.1.1 Reactive oxygen species

Mitochondria are a major source of endogenous oxidative stress; 2−4% of O_2 used by mitochondria may be converted to ROS by univalent reduction of O_2 to form superoxide ($O_2\cdot^-$) following electron (e−) leak from the respiratory chain (Boveris and Chance, 1973; Chance et al., 1979; Turrens and Boveris, 1980). Superoxide dismutase (SOD) converts $O_2\cdot^-$ to H_2O_2 that is reduced to H_2O by GSH peroxidase (GPx). The relatively nonreactive H_2O_2 is converted to the highly reactive hydroxyl radical (•OH) in the presence of Fe^{2+} and Cu^{2+}, and due to its lipid solubility, is able to cross membranes and oxidize proteins, DNA, lipids, and carbohydrates throughout the cell (Yu, 1994, See Figs. 6.1 and 6.3).

6.2.1.2 Identification of site-specific defects in electron transport

Fig. 6.3 shows sites of e-leak that are accentuated by treatment with various chemical inhibitors. The use of these chemicals for identifying e−transport defects were pioneered by Boveris and Chance (1973), Chance et al. (1979), Turrens and Boveris (1980). Numerous reports followed that confirmed Complex I and III as predominant sites of mitochondrial e−leak and associated with numerous metabolic diseases in humans including Alzheimer, cancer, diabetes, and aging (Yu, 1994).

A criticism of the use of chemical inhibitors used in studies such as those mentioned above is that they cause maximum ROS production that can greatly exceed actual rates relative to basal noninhibited states (Goncalves et al., 2015; Brand, 2016). In their studies a total of 10 sites of electron leak were revealed in muscle mitochondria when media was used that mimicked skeletal muscle during rest and exercise states; generation of ROS was much greater in media mimicking muscular rest than in mild or intense exercise.

6.2.1.3 Nitric oxide and reactive nitrogen species

Nitric oxide (NO) produced by mitochondrial nitric oxide synthase (NOS) near the site of the ETC (Giulivi et al., 1998; Giulivi and Oursler, 2003) competitively inhibits cytochrome oxidase thus regulating mitochondrial O_2 consumption. The release of NO in the presence of ROS can produce a large number of reactive nitrogen species (RNS, e.g., peroxynitrite) that damage proteins by nitrosylation. Peroxynitrite was reported to be responsible for decreased activities of Complex I and II in mitochondria (Riobo et al., 2001).

6.2.1.4 DNA damage and respiratory chain complex activities

A correct balance of mtDNA- and nDNA-encoded proteins is needed for functional integrity of mitochondria (Nijtmans et al., 2002). Due to its proximity to the respiratory chain and a lack of protective histones, mtDNA is more susceptible to mitochondrial ROS-mediated oxidation than nDNA, and mtDNA oxidation can lead to mitochondrial

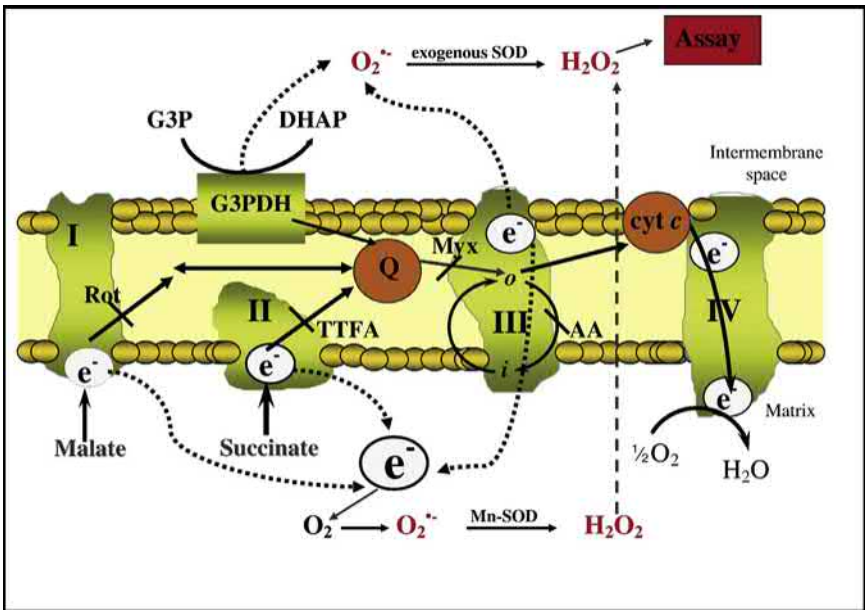

FIGURE 6.3 Diagrammatic representation of identification of site-specific defects in the electron transport chain using chemical inhibitor. The movement of electrons (e−) along the respiratory chain is shown by *solid arrows* from Complex I or Complex II to Complex III by the e−carrier, Coenzyme Q (Q) and to complex IV by cytochrome *c* (cyt *c*). The terminal step of electron transport is the full reduction of oxygen (O_2) to water by cytochrome *c* oxidase. Chemicals used to block e−transport and identify site-specific defects are rotenone (Rot) at Complex I, thenoyltrifluoroacetone (TTFA) at Complex II, and Myxothiazol (Myx) (at the outer membrane [*o*]) and antimycin A(AA) (at the inner membrane [*i*]) within Complex III. If a site-specific defect exists at any of these sites following chemical inhibition, e−leak (*dotted arrows*) results in the univalent reduction of O_2 to superoxide ($O^{\bullet}-$) that is reduced by hydrogen peroxide (H_2O_2) by superoxide dismutase (SOD). Topology of H_2O_2 formation (as in index of reactive oxygen species, ROS) can be determined by adding exogenous SOD to the media in isolated mitochondrial preparations that distinguishes it from endogenous ROS that is for by the mitochondrial located MnSOD (see Miwa et al. (2003)). Extramitochondrial e−leak can also occur when glyceraldehyde three- phosphate (GSP) is converted by G3P dehydrogenase (G3PDH) to dihyroxyacetone phosphate (DHAP). *Reprinted by permission Ojano-Dirain et al. (2007a).*

dysfunction (Kristal et al., 1994; Wei, 1998). Oxidant-medicated repression of mitochondrial transcription can exacerbate mitochondrial dysfunction by inhibiting respiratory protein synthesis (Kristal et al., 1997). Restricted availability of mt-encoded subunits or damaged proteins can lead to diminished complex activities and cell respiration (Wallace, 1999). There are also specific thiols in proteins of Complexes I, II, and IV that are particularly susceptible to oxidation that decrease complex activity upon exposure to oxidants (Lin et al., 2002b). Inverse relationships between oxidative stress and complex activity were noted in animals with low-feed efficiency (Ojano-Dirain et al., 2005; Bottje and Carstens, 2009).

6.2.1.5 Specific protein targets of mitochondrial reactive oxygen species

Mitochondrial ROS produced by Complex I (rotenone sensitive site) are exclusively released into the mitochondrial matrix whereas ROS produced at the ubiquinone-CIII site are confined to the intermembranous space (Han et al., 2001; St Pierre et al., 2002; Muller et al., 2004). Bleier et al. (2015) hypothesized that ROS generated at CI, which is in close proximity to mitochondrial DNA and redox sensitive proteins in the ETCs, would cause oxidation, whereas ROS from CIII would primarily participate in signal transduction reactions. Using two-dimensional gel electrophoresis with fluorescent detection, Bleier et al. (2015) identified specific proteins that were oxidized by ROS produced at CI (by reverse electron transport [RET] described below) differed from proteins oxidized by ROS generated at CIII (by forward electron transport) in isolated rat heart mitochondria. They concluded that there was a distinct difference in the proteins that were oxidized depending on the site of ROS production. Bleier et al. (2015) hypothesized that these proteins could " … *serve as biomarkers to study the generator-dependent dual role of mitochondrial ROS in redox signaling and oxidative stress*".

6.2.1.6 Mitochondrial reactive oxygen species generation in avian species

The use of chemical inhibitors shown in Fig. 6.3 has been used to assess mitochondrial ROS production in birds. In broilers, site-specific defects in e-leak at Complex I and III were identified in liver, lung, skeletal, and cardiac mitochondria obtained from birds exhibiting fulminant pulmonary hypertension syndrome (Cawthon et al., 2001; Iqbal et al., 2001; Tang et al., 2002). Greater ROS production due to site-specific defects in e−transport was also identified in

Complex I and III skeletal muscle, liver, and duodenal mitochondria associated with low-feed efficiency in broilers (Bottje et al., 2002; Iqbal et al., 2004; Ojano-Dirain et al., 2004, 2007a) as well as Complex II in duodenal tissue (Ojano-Dirain et al., 2004). Greater ROS production was likely responsible for higher oxidative stress and lower respiratory chain complex activities consistently observed in animals exhibiting a low-feed efficiency phenotype (Bottje and Carstens, 2009; Ojano-Dirain et al., 2007b) and may have been involved in differential gene expression in feed efficiency in broilers (Bottje and Kong, 2013). Mitochondrial ROS production has also been shown to play a role in heat stress (Abe et al., 2006; Mujahid et al., 2006, 2007, 2009).

Mitochondrial ROS production is generally lower in avian compared to comparable size mammalian species with an inverse relationship between longevity and mitochondrial ROS production (Herrero and Barja, 1997, 1998). Fig. 6.4 presents data of heart mitochondrial ROS production in comparable sized mammals and birds (Herrero and Barja, 1997, 1998) in the presence or absence of ETC inhibitors shown in Fig. 6.3. This species difference is even more remarkable since birds have a number of characteristics that should favor heightened mitochondrial radical production such as higher body temperatures, metabolic rates, and blood glucose concentrations (Holmes and Austad, 1995; Holmes et al., 2001). The fact that birds have much lower mitochondrial ROS production has been hypothesized to explain lower mitochondrial DNA diversity in avian compared to mammalian species (Hickey, 2008).

6.2.2 Mitochondrial uncoupling and attenuation of oxidative stress

Proton motive force provides the power that "drives" ATP synthesis when protons flow back into the matrix through ATP synthase (Complex V). However, protons that flow into the mitochondrial matrix at sites other than the ATP synthase (proton leak) dissipates proton motive force, diminishes mitochondrial membrane potential, and short circuits ATP synthesis (Brand et al., 1994). Oxygen consumption from proton leak can represent 25% of total basal metabolic rate in animals (Rolfe and Brand, 1997). Basal proton leak (or conductance) is facilitated by intrinsic characteristics of membranes and the presence of intramembranous proteins (e.g., UCPs, adenine nucleotide translocase [ANT]) (Brown and Brand, 1991; Rolfe and Brand, 1997; Brookes et al., 1997, 1998; Brand et al., 2005; Dilger et al., 1979). Free fatty acids enhance proton-translocating activities of ANT, UCPs, and phosphate and glutamate carrier proteins (Andreyev et al., 1988, 1989; Echtay et al., 2001; Samartsev et al., 1997; Jaburek et al., 1999). Proton leak is also stimulated by hyperthyroidism and diminished by hypothyroidism (Hafner et al., 1990).

Proton leak represents an energetic inefficiency, but plays an important role in attenuating mitochondrial ROS production and endogenous oxidative stress. A self-limiting

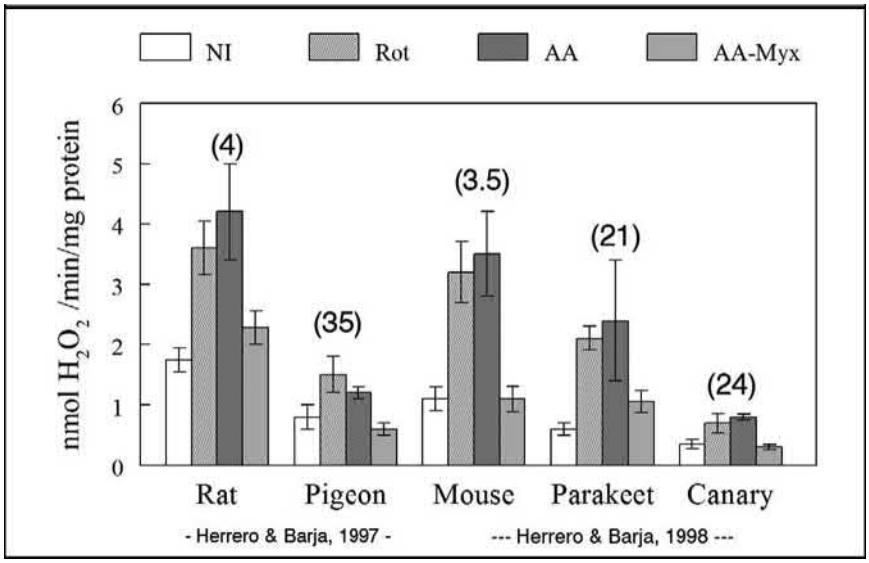

FIGURE 6.4 Hydrogen peroxide (H_2O_2) production rates (expressed as nmol/min/mg protein) in heart mitochondria isolated from mammals and birds of comparable body weights (rat vs. pigeon; mouse vs. parakeet and canary). Rates of H_2O_2 production are shown for mitochondria treated with no-inhibitor (NI, basal rate), and for mitochondria treated with inhibitors of Complex I (rotenone, Rot), and two inhibitors of Complex III (antimycin A, AA and myxothiazol, Myx, alone and in combination). The maximum life span for each animal species is shown in parentheses. *Data were obtained from Herrero and Barja (1997, 1998).*

feedback of superoxide on mitochondrial ROS production (Skulachev, 1996, 1997) is due to increased expression and activity of UCPs and ANT (Echtay et al., 2002; Murphy et al., 2003; Brand et al., 2004). This mechanism is depicted in Fig. 6.5 which is a composite of Figs. 6.1 and 6.2 from Brand et al. (2004).

Uncoupling to reduce mitochondrial ROS generation has been clearly demonstrated in several avian species. In birds, the initial sequencing of the avian uncoupling protein (avUCP) was reported by Raimbault et al. (2001) and confirmed shortly after by Toyomizu et al. (2002). Uncoupling of mitochondria represents an important physiological response to attenuate oxidative stress during both cold and heat stress conditions. Toyomizu et al. (2002) reported that ANT and UCP mRNA were upregulated in cold stressed chicken skeletal muscle. Increased UCP and ANT expression has been observed in skeletal muscle of chickens (Toyomizu et al., 2002), king penguins (Talbot et al., 2003, 2004), and in cold-acclimated ducks (Rey et al., 2010) that attenuates cold-induced increases in mitochondrial ROS production. Increased mitochondrial ROS and oxidative stress has also been observed in heat-stressed chicken skeletal muscle (Mujahid et al., 2007a,b). It was determined that olive oil attenuated mitochondrial ROS production during heat stress (Mujahid et al., 2009). The increased ROS production during heat stress was due to a combination of down-regulation of avUCP expression and an increase in inner mitochondrial membrane potential (Mujahid et al., 2006; Kikusato and Toyomizu, 2013).

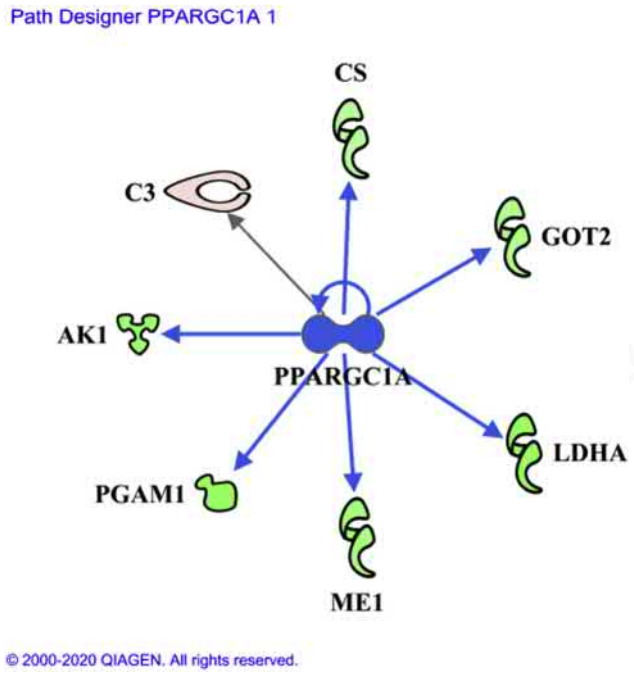

FIGURE 6.5 Attenuation of mitochondrial reactive oxygen species formation by increased uncoupling activity of adenine nucleotide translocase (ANT) and uncoupling protein (UCP). Shown in the figure are the outer and inner mitochondrial membranes (OMM and IMM) and intramembranous space (IS) within which proton motive force is generated by pumping of protons from the matrix into the IS. Proton leak occurs when protons move across the IMM at sites other than the ATP synthase. Electron leak from flavin and iron-sulfur centers in proteins of complex I, and from co-enzyme Q into the mitochondrial matrix causes univalent reduction of oxygen to superoxide ($O\cdot-$). In the presence of free iron (Fe^{2+}) that can be released from oxidative damage of matrix proteins (e.g., aconitase) results in the formation of hydroxyl radical ($\cdot OH$) that abstracts an electron from polyunsaturated fatty acid to form a carbon-centered fatty acid radical (FA radical) and an FA peroxyl radical in the presence of oxygen. This leads to the formation of a stable reactive alkenal, 4-hydroxy 2-nonenal (4-HNE) that stimulates uncoupling activity (proton leak) by ANT and UCP. Increased proton leak in turn dissipates proton motive force and mitochondrial membrane potential that reduces electron leak and mitochondrial reactive oxygen species formation. *Based on Echtay et al. (2002), Murphy et al. (2003), Brand et al. (2004).*

Differences in proton leak and mitochondrial membrane potential have also been linked to the phenotypic expression of feed efficiency in broilers (Ojano-Dirain et al., 2007a; Bottje et al., 2009). Enhanced ROS production was observed in muscle, liver, and duodenal mitochondria of broilers with low-feed efficiency compared to broilers with high-feed efficiency due to site-specific defects in electron transport (Ojano-Dirain et al., 2004; Bottje et al., 2004; Iqbal et al., 2005). Using a number of different chemical treatments, it was observed that proton leak in broilers with a high-feed efficiency phenotype exhibited proton leak that was either lower or equal to, but never higher than proton leak in broilers exhibiting a high-feed efficiency phenotype (Bottje et al., 2009). Observations of increased (<0.06) expression of avUCP and lower membrane potential in low feed efficiency mitochondria (Ojano-Dirain et al., 2004, 2007) are consistent with the model presented in Fig. 6.5 to minimize or attenuate mitochondrial ROS formation.

6.2.3 Antioxidants

It is difficult to discuss oxidation without also discussing antioxidants. Oxidative stress develops when the generation of ROS overwhelms antioxidant protection (Yu, 1994). Repair of damaged structures (e.g., lipids, proteins) is energetically expensive requiring considerable input of ATP to either repair or recycle materials within the cell. Mitochondrial ROS are normally metabolized by the enzymatic antioxidants, SOD, and glutathione peroxidase, as well as by nonenzymatic antioxidants GSH and α-tocopherol (Yu, 1994).

Glutathione is the major endogenous antioxidant system both in the cytosol and within mitochondria (Meister, 1984; Griffith and Meister, 1985; Martensson et al., 1993). Glutathione exists in either a reduced (GSH) or oxidized (GSSG; glutathione disulfide) form, and the GSSG:GSH ratio is used as an indicator of oxidative stress. The glutathione reduction-oxidation (redox) system consists of GSH

and the GSH recycling enzymes, GPx, and GSH reductase (GR) (Meister, 1984). The enzyme GPx metabolizes peroxides (e.g., H_2O_2) using reducing equivalents from GSH and catalyzes the reaction shown in Eq. (6.1):

$$2\ GSH + H_2O_2 \rightarrow GSSG + 2\ H_2O \quad (6.1)$$

Low levels of GSSG are maintained by GR, which utilizes nicotinamide adenine dinucleotide phosphate ($NADPH_2$) to reduce GSSG to GSH as shown in Eq. (6.2):

$$GSSG + NADPH_2 \rightarrow 2\ GSH + NADP^+ \quad (6.2)$$

The glutathione redox system is a vital defense mechanism of mitochondria against free radical damage as mitochondria lack catalase (Martensson et al., 1990), γ-glutamyl synthetase (the rate limiting enzyme in GSH synthesis) (Meister, 1984), and the ability to export GSSG (Olafsdottir and Reed, 1988). Martensson et al. (1990) noted that the mitochondrial GSH transport system might be designed to efficiently conserve mitochondrial GSH at the expense of cytosolic GSH.

During oxidative stress, toxic levels of GSSG can accumulate within mitochondria (Olafsdottir and Reed, 1988; Cawthon et al., 1999). Unlike cells, mitochondria are unable to export GSSG from the mitochondria leading to thiolation of critical proteins in the ETC and diminished activities for the respiratory chain complexes. Augustin et al. (1997) reported that mitochondria are not damaged by ROS as long as the mitochondria are in an energized state in which ROS production is minimized. Other research indicates that GSH levels are critical in maintaining or protecting respiratory chain complex activity from oxidation and positive correlations between GSH and respiratory chain activity have been reported (Ojano-Dirain et al., 2005; Bolanos et al., 1996; Cardoso et al., 1999).

6.3 Signal transduction and reverse electron transport

6.3.1 Low mitochondrial reactive oxygen species levels

Whereas high levels of ROS are detrimental, low levels of mitochondrial ROS act in signal transduction processes that are recognized as being vital for normal cell function processes (e.g, Giulivi and Oursler (2003), Crawford et al. (1997), Carper et al. (1999), Greiber et al. (2002), Li et al. (2002), Kemp et al. (2003)). Baughman and Mootha (2006) hypothesized "… *a homeostatic role for ROS in maintaining stable respiratory phenotypes across genetic variants of the mitochondrial genome.*" Finkel (2011) proposed that H_2O_2 stimulated several signaling pathways by oxidizing cysteine moieties of key regulatory proteins that are modulated by antioxidants such as peroxiredoxin (Rhee et al., 2005). Low levels of mitochondrial ROS contribute to mitochondrial-mediated signal transduction mechanisms (Finkel, 2011; Murphy et al., 2011) in a process designated as "mitochondrial hormesis (mitohormesis)" (Barbieri et al., 2013). Furthermore, whereas mitochondrial ROS generated from Complex I is associated with oxidative stress, ROS generated from Complex III is primarily involved in signal transduction (Sena and Chandel, 2012; Bleier et al., 2015). RET in the mitochondria is now recognized to be vital to a number of physiological conditions (see review by Scialo et al. (2017)).

6.3.2 Cellular nutrient utilization

Guaras et al. (2016) demonstrated that RET enables mitochondria to efficiently use different energy sources entering the transport chain. In this mechanism, the ratio of reduced coenzyme Q ($CoQH_2$) to oxidized CoQ[1] is a sensor that functions to optimize energy use by stimulating RET. The ETC is composed of five multiprotein complexes (see above) that can be arranged into supercomplexes consisting of CI + CIII + CIV and CI + CIII (Acin-Perez et al., 2008; Enriquez, 2016). It is proposed that these supercomplex arrangements creates two functional pools of CIII; one associated and another not associated with CI (Lapuente-Brun et al., 2013). When the energy source switches from glucose to fatty acids, ROS produced by RET degrade CI, the result of which increases mitochondrial fatty acid β-oxidation. Thus, remodeling of the ETC is a response to ubiquinone acting as a metabolic sensor that positions the mitochondria to efficiently oxidize different nutrients as they become available in the cell.

6.3.3 Macrophage function

Mitochondria enable macrophages to quickly shift from "attack and destroy" to a "heal and rebuild" cell needed for tissue repair after the initial foreign invasion or insult. In a bacterial infection, the ETC reorganizes resulting in a decrease in CI activity and an increase in CII activity (Garaude et al., 2016). The ability of macrophages to switch between these very different functional phenotypes occurs through a shift in mitochondrial energy production (from OXPHOS to glycolysis) concomitant with an increase in membrane potential that helps drive RET-derived ROS production and proinflammatory cytokine production (Mills et al., 2016). This redirection of mitochondrial function is a result of succinate accumulation with increased succinate dehydrogenase activity. Inhibition of proinflammatory cytokines in macrophages was achieved by (a) treating cells with dimethyl malonate to prevent succinate oxidation, (b) treating cells with rotenone to

1. CoQ transfers electrons from CI to CIII and CII to CIII.

block reverse electron flow from succinate, and (c) preventing CoQ reduction. RET from succinate is therefore essential for initiating an inflammatory response in macrophages.

6.3.4 Ischemia-reperfusion injury

When blood supply is interrupted (e.g., heart attack, stroke, or severe blood loss) and followed by blood flow restoration, oxidative damage of tissues occurs from a hyperimmune response and a burst of mitochondrial ROS production. Mitochondrial ROS generated during reperfusion was considered mainly a nonspecific response to increased oxygen levels (e.g., Murphy and Steenbergen (2008)). However, Chouchani et al. (2014) demonstrated that succinate accumulation during ischemia drives mitochondrial ROS generation during reperfusion due to RET from Complex II to Complex I. Ischemic damage of heart and brain tissue was prevented by rotenone (that blocks RET from CII to CI) and by inhibition of succinate dehydrogenase with dimethyl malonate.

6.3.5 Muscle differentiation

Many myogenic regulatory factors promote satellite cell differentiation to form myoblasts and myotubes in avian species (see Velleman and McFarland (2015)). Hydrogen peroxide produced by NADPH oxidase is instrumental for cardiac and muscle cell differentiation (Piao et al., 2005; Buggisch et al., 2007). Since H_2O_2 is lipid soluble, it readily crosses membranes in the various cell compartments. Using mitochondria specific antioxidants (MitoQ and MitoTEMPOL), it was determined that suppression of muscle differentiation was concomitant with decreased mitochondrial ROS production (Lee et al., 2011). This response was not due to inhibition of electron transport or ETC activity since these antioxidants had no effect on ATP production. During differentiation, there was an increase in mitochondrial content and increased expression and activity of CI. Treating cells with small inhibitory RNA or blockade of electron transport in CI inhibited muscle cell differentiation. It was concluded that superoxide produced by RET at CI was converted to H_2O_2 by MnSOD that stimulated muscle differentiation in response to NF-kB activation (Lee et al., 2011).

6.3.6 Aging and longevity

Examination of the mitoproteome that focused on CI assembly and stabilization produced a new insight into the role of mitochondria in aging (Miwa et al., 2003). CI is the largest complex of the respiratory chain containing ~40 proteins with two arms; one that extends into the mitochondrial matrix and a second arm that is found primarily within the inner mitochondrial membrane. The mitoproteome of young animals had reduced abundance of proteins in the matrix arm of CI in long-lived animals, but there was no difference in the abundance of the membrane arm of CI between short-lived and long-lived groups. Disruption of CI assembly reduced oxidative metabolism and elevated mitochondrial ROS production. Disruption of CI assembly resulted in premature senescence in primary hepatocytes. Miwa et al. (2003) hypothesized that decreased abundance of proteins in the catalytic component of CI improves assembly of the enzyme complex, improves substrate utilization while reducing mitochondrial ROS production and increasing longevity.

6.4 Matching energy production to energy need

6.4.1 Mitochondrial dynamics

Initial electron micrographs of mitochondria suggest that kidney shaped image of mitochondria as being a static organelle (Lehninger et al., 1993, p.39). Electron tomography (Mannella, 2000) provided a three-dimensional view of a sausage-like appearance of mitochondria extending through the cytosol with intimate connections to endoplasmic reticulum that could facilitate communication with the rest of the cell, protein transfer, and signaling. It is now apparent that mitochondrial fission and fusion events regulate mitochondrial function over a broad spectrum of available energy sources that can serve to cull defective organelles from the "mitochondrial herd" (see reviews by Hoppins et al. (2007), Archer (2013), Liesa and Shirihai (2013), Rambold and Pearce (2018)). In addition, it is clear that intimate connections of mitochondria with other organelles in the cell including the nucleus, endoplasmic reticulum, and lysosomes help in movement of proteins and as pathways for cell signaling to optimize cell function (Rambold and Pearce, 2018).

Liesa and Shirihai (2013) provided a review of fission and fusion events in a mitochondrial life cycle that is depicted in Fig. 6.6. In a nutrient limiting environment (e.g., starvation), mitochondria become elongated (fuse) and more efficient in producing ATP from energy substrates. In the face of excess nutrient availability, mitochondria divide (fragment) to become less efficient in oxidative phosphorylation and burning off excess fuel supply in the cell. In this fragmentation process, the endoplasmic reticulum targets the mitochondria with proteins, including mitofissin, dynamin, and dynamin-like 120 kDa—protein (**OPA-1** short) that split the mitochondria in two. Fission is part of the mitochondrial life cycle that allows mitochondria to adapt to different amounts of available nutrients. In the life cycle,

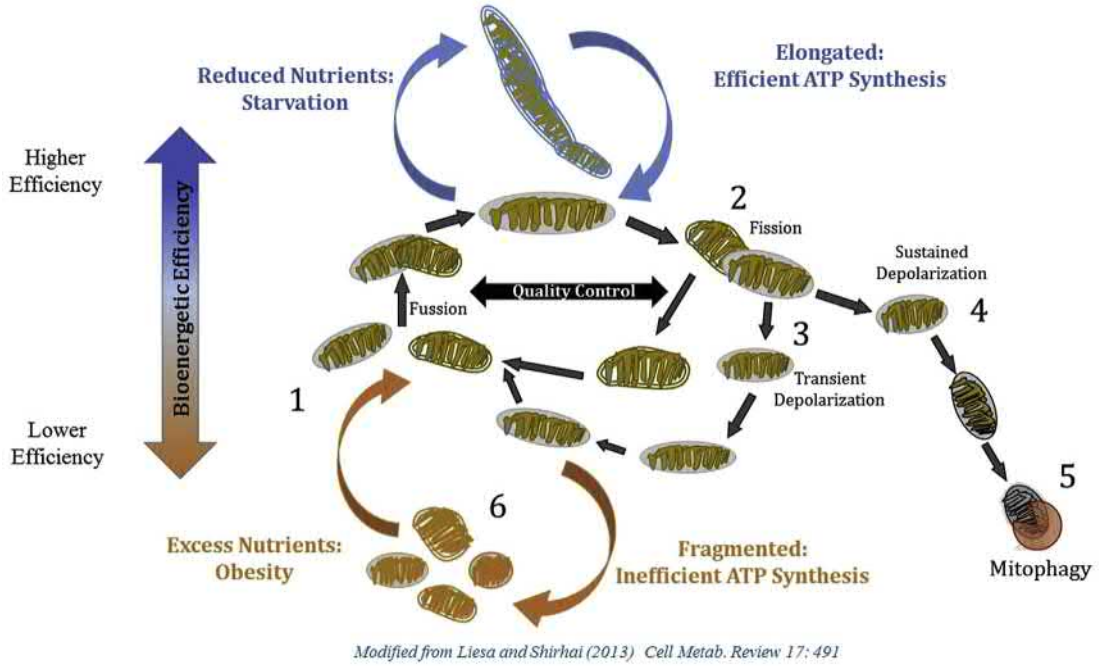

FIGURE 6.6 **Life cycle of mitochondria.** A mitochondrial life cycle was described by Liesa and Shirihai (2013). In this life cycle, mitochondria raise or lower energetic efficiency through biochemical and conformation changes in response to low or excess nutrient levels. In fusion events (1) two daughter cells can combine to form a single mitochondria. With nutrient limiting conditions (e.g., starvation, or possibly high energy demand such as muscle activity or rapid growth), mitochondria elongate and become more efficient in utilizing available substrate. Once nutrient levels are no longer limiting, the mitochondria return to normal size. Parts of the mitochondria may experience oxidative damage and increased mitochondrial reactive oxygen species (ROS) production with concomitant oxidation of mt-DNA. When this occurs, the endoplasmic reticulum will present specialized proteins (mitofissin, OPA-1, dynamin) to initiate mitochondrial fission (2). In this quality control process, the damaged or poorly functioning mitochondria with depolarized inner mitochondrial membrane will split from the optimal functioning mitochondria. If the mitochondria recover from depolarization, it will return to the mitochondrial life cycle (3). If mitochondria experience sustained membrane depolarization (4), it will be targeted for degradation by mitophagy (5). In response to excess nutrients (e.g., obesity), mitochondria fragment (6) and become less efficient in oxidative phosphorylation. Fragmentation is accompanied by increased mitochondrial ROS production that can have deleterious consequences to the cell. When cell nutrients levels decline, the mitochondria will return to the mitochondrial life cycle.

dysfunctional mitochondria are destined for removal by mitophagy (Fig. 6.6), thereby raising the collective function of the remaining mitochondrial population ("mitochondrial herd") in cells.

Regulation of mitochondrial dynamics by the orexin system in avian muscle cells was provided by Lassiter et al. (2015). After showing that orexin was secreted by quail muscle 7 (QM7) cells, it was determined that treating the cells with recombinant orexin A (rORX-A) and orexin B (rORX-B) down-regulated and upregulated mtDNA expression, respectively, indicating inhibition and stimulation of mitochondrial biogenesis. Furthermore, rORX-A inhibited genes associated with mitochondrial fusion (MFN1, OPA-1, and OMA1) and stimulated genes associated mitochondrial fission (MTFP1 and DNM1 and MTFR1) whereas rORX-B stimulated mitochondrial fusion by upregulating MFN2, OPA1, and OMA1. The findings by Lassiter et al. (2015) presented the first evidence of a physiological role of the orexin system in avian cells in regulating mitochondrial dynamics that could be hypothesized to play an important role in growth and development in birds if similar relationships occurred between orexin and mitochondria in vivo.

6.4.2 Mitochondrial biogenesis

Whereas mitochondria divide during mitosis to insure daughter cells are provided a full complement of functional mitochondria, mitochondrial biogenesis is stimulated in response to increased energy demand. An early demonstration of mitochondrial biogenesis was provided by Paul and Sperling (1952) who observed that there were more mitochondria in breast muscle from pigeons that are more active than the relatively sedentary commercial chicken. One of the first factors identified to increase mitochondrial biogenesis was peroxisome proliferator-activated gamma coactivator 1-alpha (PGC-1α) (Puigserver et al., 1998; Wu et al., 1999). Cold exposure increased the mRNA expression of PGC-1α that in turn increased the expression of several mitochondrial proteins including ATP synthase and cytochrome c-oxidases II and IV. PGC-1α as well as PGC-1β stimulate nuclear respiratory factors (NRF-1 and

NRF-2) and mitochondrial transcription factor A (TfamA) (Nisoli et al., 2003, 2004) that up-regulate mitochondrial transcription factor A (mtTFA) by independent mechanisms (Meirhaeghe et al., 2003; Lin et al., 2002a). NRF1 and NRF2 stimulate mitochondrial protein synthesis, e.g., ETC proteins, whereas mtTFA stimulates mitochondrial DNA transcription that is instrumental in synthesis of mitochondrial proteins during mitochondrial biogenesis. Because of its role in mitochondrial biogenesis, PGC-1α has been termed the master regulator of mitochondrial protein synthesis (Nisoli et al., 2003, 2004).

6.4.3 Adenosine monophosphate–activated protein kinase

Adenosine monophosphate (AMP)-activated protein kinase (AMPK) is critical for (a) sensing cellular energy (AMP/ATP) status and stimulating mitochondrial biogenesis (Zhou et al., 2001; Hardie et al., 2003; Hardie, 2007; Carling, 2004, 2005) and (b) in regulating animal food intake and overall energy balance (Minokoshi et al., 2004). Once AMPK is phosphorylated by serine-threonine kinase 11 (LKB1) (Hardie, 2005), the activated AMPK phosphorylates several proteins involved in carbohydrate, lipid, and protein metabolism (Kemp et al., 2003; Hardie, 2004, 2007). In general, AMPK reduces ATP-utilizing (anabolic) pathways (e.g., fatty acid synthesis) and increases ATP-generating (catabolic) pathways (e.g., fatty acid oxidation, glycolysis). AMPK is required for stimulating glucose uptake and glycolysis in skeletal muscle cells and astrocytes (Zhou et al., 2001; Almeida et al., 2004). AMPK also up-regulates PGC-1α expression (Ojuka, 2004) and therefore presumably plays a role in mitochondrial biogenesis. In conjunction with thyroid hormone receptor activation, PGC-1α up-regulates ANT and avUCP expression in chickens that uncouple mitochondrial oxidative phosphorylation (Masatoshi et al., 2005). Choi et al. (2001) presented evidence that AMPK and the AMPK cascade mechanisms are sensitive to ROS, particularly H_2O_2. Colombo and Moncada (2009) provided evidence that mitochondrial ROS-mediated upregulation of AMPK was associated with increased of several cellular antioxidants. Thus, AMPK is very important in sensing energy status in cells and could be a pivotal component in growth, development, and is responsive to mitochondrial generated ROS production. The expression of AMPK was higher in chickens exhibiting a high-feed efficiency phenotype (Bottje and Kong, 2013).

6.4.4 Sirtuins

The sirtuins are a family of conserved NAD-dependent deacetylases that regulate many cellular activities including stress response and energy metabolism (Haigis and Sinclair, 2010). SIRT4 is located mainly in mitochondria (Haigis et al., 2006) where it inactivates glutamate dehydrogenase by ADP-ribosylation. The inactivation of glutamate dehydrogenase that converts glutamate to α-ketoglutarate indicates that SIRT4 regulates entry of energy substrates into the Krebs cycle. Knockdown of SIRT 4 increased gene expression of mitochondrial and fatty acid metabolism enzymes in hepatocytes and myocytes, and changes in gene expression were associated with SIRT1-dependent fatty acid oxidation (Nasrin et al., 2010). Chau et al. (2010) reported that fibroblast growth factor 21 regulates energy homeostasis in adipocytes through phosphorylation and activation of AMPK by increasing cellular NAD + levels as well by deacetylation and activation of PGC-1α and histone 3. Activation of AMPK maintains energy balance by enhancing mitochondrial biogenesis and oxidative metabolism (Hardie, 2007). AMPK increased SIRT1 (NAD + -dependent type III deacetylase sirtuin 1) by increasing NAD + levels that modulate several downstream SIRT1 targets (Canto et al., 2009). AMPK and SIRT1 act in concert with PGC-1α to regulate energy homeostasis in response to differences in nutritional and environmental factors (Hardie, 2007; Reznick and Shulman, 2006).

Acknowledgments

I want to thank all of my students, postdocs, and collaborators that I have been so lucky to have come through my lab. None of this would have been possible without your hard work. I want to acknowledge funding sources especially USDA-NIFA and Arkansas Biosciences Institute. Finally, I want to thank you Jax William Bottje for teaching me so much about life in the short six months you were here with us—and his amazing parents, Kelsey and Tyler, who have taught me a lot about inner strength and grace.

References

Abe, T., Mujahid, A., Sato, K., Akiba, Y., Toyomizu, M., 2006. Possible role of avian uncoupling protein in down-regulating mitochondrial superoxide production in skeletal muscle of fasted chickens. FEBS (Fed. Eur. Biochem. Soc.) Lett. 580, 4815–4822.

Acin-Perez, R., Fernadez-Silva, P., Peleato, M.L., Perez-Martos, A., Enriquez, J.A., 2008. Respiratory active mitochondrial supercomplexes. Mol. Cell 32, 529–539.

Almeida, A., Moncada, S., Bolanos, J.P., 2004. Nitric oxide switches on glycolysis through the AMP protein kinase and 6-phosphofructo-2-kinase pathway. Nat. Cell Biol. 6, 45–51.

Anderson, S., Bankier, A.T., Barrell, B.G., Debruijn, M.L., Coulson, A.R., Drouin, J., et al., 1981. Sequence and organization of the human mitochondrial genome. Nature 290, 457–465.

Andreyev, A., Bondareva, T.O., Dedukhova, V.I., Mokhova, E.N., Skulachev, V.P., Tsofina, L.M., et al., 1989. The ATP/ADP-antiporter is involved in the uncoupling effect of fatty acids on mitochondria. Eur. J. Biochem. 182, 585–592.

Andreyev, A., Bondareva, T.O., Dedukhova, V.I., Mokhova, E.N., Skulachev, V.P., Volkov, N.I., 1988. Carboxyatractylate inhibits the uncoupling effect of free fatty acids. FEBS (Fed. Eur. Biochem. Soc.) Lett. 226, 265–269.

Archer, S.L., 2013. Mitochondrial dynamics - mitochondrial fission and fusion in human disease. N. Engl. J. Med. 369, 2236–2251.

Augustin, W., Wiswedel, I., Noack, J., Reinheckel, T., Reichelt, O., 1997. Role of endogenous antioxidants in defense against functional damage and lipid peroxidation in rat liver mitochondria. Mol. Cell. Biochem. 174, 199–205.

Aw, T.Y., Jones, D.P., 1989. Nutrient supply and mitochondrial function. Annu. Rev. Nutr. 9, 229–251.

Barbieri, E., Sestili, P., Vallorani, L., Guescini, M., Calcabrini, C., Gioacchini, A.M., et al., 2013. Mitohormesis in muscle cells a morphological, molecular and proteomic approach. Musc. Lig. Tend. 3, 254–266.

Baughman, J.M., Mootha, V.K., 2006. Buffering mitochondrial DNA variation. Nat. Genet. 38, 1232–1233.

Benda, C., 1898. Ueber die Spermatogenese der Vertebraten und höherer Evertebraten, II. Theil: Die Histiogenese der Spermien. Arch. Anat. Physiol. 73, 393–398.

Bleier, L., Wittig, I., Heide, H., Steger, M., Brandt, U., Dröse, S., 2015. Generator specific targets of mitochondrial ROS. Free Rad. Biol. Med. 78, 1–10.

Bobyleva, V., Bellei, M., Pazienza, T.L., Muscatello, U., 1997. Effect of cardiolipin on functional properties of isolated rat liver mitochondria. Biochem. Mol. Biol. Int. 41, 469–480.

Bogoyevitch, M.A., Ng, D.C., Court, N.W., Draper, K.A., Dhillon, A., Abas, L., 2000. Intact mitochondrial electron transport function is essential for signalling by hydrogen peroxide in cardiac myocytes. J. Mol. Cell. Cardiol. 32, 1469–1480.

Bolanos, J.P., Heales, J.R., Peuchen, S., Barker, J.E., Land, J.M., Clark, J.B., 1996. NO-mediated mitochondrial damage: a potential neuroprotective role for glutathione. Free Rad. Biol. Med. 21, 995–1001.

Bottje, W.G., Brand, M.D., Ojano-Dirain, C., Lassiter, K., Toyomizu, M., Wing, T., 2009. Mitochondrial proton leak kinetics and relationship with feed efficiency within a single genetic line of male broilers. Poultry Sci. 88, 1683–1693.

Bottje, W.G., Iqbal, M., Tang, Z., Cawthon, D.C., Okimoto, R., Wing, T., et al., 2002. Association of mitochondrial function with feed efficiency within a single genetic line of male broilers. Poultry Sci. 81, 546–555.

Bottje, W., Carstens, G.E., 2009. Association of mitochondrial function and feed efficiency in poultry and livestock species. J. Anim. Sci. 87, E48–E63.

Bottje, W., Kong, B.W., 2013. Feed efficiency: mitochondrial function to global gene expression. J. Anim. Sci. 91, 1582–1593.

Bottje, W., Iqbal, M., Pumford, N.R., Ojano-Dirain, C., Lassiter, K., 2004. Role of mitochondria in phenotypic expression of feed efficiency. J. Appl. Poultry Res. 13, 1–12.

Boveris, A., Chance, B., 1973. The mitochondrial generation of hydrogen peroxide. General properties and effect of hyperbaric oxygen. Biochem. J. 134 (3), 707–716.

Brand, M., 2016. Mitochondrial generation of superoxide and hydrogen peroxide as the source of mitochondrial redox signaling. Free Rad. Biol. Med. 100, 14–31.

Brand, M.D., Chien, L.F., Ainscow, E.K., Rolfe, D.F.S., Porter, R.K., 1994. The causes and functions of mitochondrial proton leak. Biochem. Biophys. Acta 1187, 132–139.

Brand, M.D., Pakay, J.L., Ocloo, A., Kokoszka, Z., Wallace, D.C., Brookes, P.S., et al., 2005. The basal proton conductance of mitochondria depends on adenine nucleotide translocase content. Biochem. J. 392, 353–362.

Brand, M.D., Affourtit, C., Esteves, T.C., Green, K., Lambert, A.J., Miwa, S., et al., 2004. Mitochondrial superoxide: production, biological effects, and activation of uncoupling proteins. Free Rad. Biol. Med. 37, 755–767.

Brookes, P.S., Buckingham, J.A., Tenreiro, A.M., Hulbert, A.J., Brand, M.D., 1998. The proton permeability of the inner membrane of liver mitochondria from ectothermic and endothermic vertebrates and from obese rats: correlation with standard metabolic rate and phospholipid fatty acid composition. Comp. Biochem. Physiol. 119B (2), 325–334.

Brookes, P.S., Rofle, D.F.S., Brand, M.D., 1997. The proton permeability of liposomes made from mitochondrial inner membrane phospholipids: comparison to isolated mitochondria. J. Membr. Biol. 155, 167–174.

Brown, G.C., Brand, M.D., 1991. On the nature of the mitochondrial proton leak. Biochem. Biophys. Acta 1059, 55–62.

Buggisch, M., Ateghang, B., Ruhe, C., Strobel, C., Lange, S., Wartenberg, M., et al., 2007. Stimulation of ES cell-derived cardiomyogenesis and neonatal cardiac cell proliferation by reactive oxygen species and NADPH oxidase. J. Cell Sci. 1, 885–894.

Canto, C., Gerhart-Hines, Z., Feige, J.N., Lagouge, M., Noriega, L., Milne, J.C., et al., 2009. AMPK regulates energy expenditure by modulating NAD+ metabolism and SIRT1 activity. Nature 458, 1056–1060.

Cardoso, S.M., Pereira, C., Oliveira, C.R., 1999. Mitochondrial function is differentially affected upon oxidative stress. Free Rad. Biol. Med. 26, 3–13.

Carling, D., 2004. The AMP-activated protein kinase cascade - a unifying system for energy control. Trends Biochem. Sci. 29, 18–24.

Carper, D.A., Sun, J.K., Iwata, T., Sigler, J.S.J., Ibaraki, N., Lin, L.R., et al., 1999. Oxidative stress induces differential gene expression in human lens epithelial cell line. Invest. Opthalmol. Vis. Sci. 40, 400–406.

Cawthon, D.C., McNew, R., Beers, K.W., Bottje, W.G., 2001. Electron transport chain defect and inefficient respiration may both underlie pulmonary hypertension syndrome (PHS)-associated mitochondrial dysfunction in broilers. Poultry Sci. 80, 474–484.

Cawthon, D., McNew, R., Beers, K.W., Bottje, W.G., 1999. Evidence of mitochondrial dysfunction in broilers with pulmonary hypertension syndrome (Ascites): effect of t-butyl hydroperoxide on function, glutathione and related thiols. Poultry Sci. 78, 114–125.

Chance, B., Sies, H., Boveris, A., 1979. Hydroperoxide metabolism in mammalian organs. Physiol. Rev. 59, 527–605.

Chau, M.D.L., Gap, K., Yang, Q., Wu, Z., Gromada, J., 2010. Fibroblast growth factor 21 regulates energy metabolism by activating the AMPK-SIRT1-PGC-1alpha pathway. Proc. Natl. Acad. Sci. U. S. A. 107, 12553–12558.

Chen, J.Q., Delannoy, M., Cooke, C., Yager, J.D., 2005. Regulation of mitochondrial respiratory chain structure and function by estrogens/estrogen receptors and potential physiological/patho-physiological implications. Biochim. Biophys. Acta 1746, 1–17.

Choi, S.L., Kim, S., Lee, K., Kim, J., Mu, J., Birnbaum, M.J., et al., 2001. The regulation of AMP-activated protein kinase by H_2O_2. Biochem. Biophys. Res. Commun. 287, 92–97.

Chouchani, E.T., Pell, V.R., Gaude, E., Aksentijevic, D., Sundier, S.Y., Robb, E.L., et al., 2014. Ischemic accumulation of succinate controls reperfusion injury through mitochondrial NOS. Nature 515, 431–435.

Colombo, S.L., Moncada, S., 2009. AMPKa1 regulates the antioxidant status of vascular endothelial cells. Biochem. J. 421, 163–169.

Crawford, D.R., Wang, Y., Schools, G.P., Kochheise, J., Davies, K.J., 1997. Down-regulation of mammalian mitochondrial RNAs during oxidative stress. Free Rad. Biol. Med. 22, 551–559.

Dilger, J.P., McLaughlin, S.G., McIntosh, T.J., Simon, A.S., 1979. The dielectric constant of phospholipid bilayers and the permeability of membranes to ions. Science 206, 1196–1198.

Droge, W., 2002. Free radicals in the physiological control of cell function. Physiol. Rev. 82, 47–95.

Echtay, K.S., Winkler, E., Fischmuth, K., Slingenberg, M., 2001. Uncoupling proteins 2 and 3 are highly active H^+ transporters and highly nucleotide sensitive when activated by coenzyme Q (ubiquinone). Proc. Natl. Acad. Sci. U. S. A. 98, 1416–1421.

Echtay, K., Roussel, D., Pierre, J.S., Jekabsons, M.B., Cadenas, S., Stuart, J.A., et al., 2002. Superoxide activates mitochondrial uncoupling proteins. Nature 415, 96–99.

Enriquez, J.A., 2016. Supramolecular organization of respiratory complexes. Annu. Rev. Physiol. 78, 533–561.

Ernster, L., Forsmark-Andree, P., 1993. Ubiquinol: an endogenous antioxidant in aerobic organisms. Clin. Invest. 71, S60–S65.

Estabrook, R.W., 1967. Mitochondrial respiratory control and polarographic measurement of ADP:O ratios. Methods Enzymol. 10, 41–47.

Finkel, T., 2011. Signal transduction by reactive oxygen species. J. Cell Biol. 194, 7–15.

Forsmark-Andree, P., Lee, C.P., Dallner, G., Ernster, L., 1997. Lipid peroxidation and changes in the ubiquinone content and the respiratory chain enzymes of submitochondrial particles. Free Rad. Biol. Med. 19, 749–757.

Garaude, J., Acin-Perez, R., Martinez-Cano, S., Enamorado, M., Ugolini, M., Nistal-Villan, M., et al., 2016. Mitochondrial respiratory chain adaptations in macrophages contribute to antibacterial host defense. Nat. Immunol. 17, 1037–1045.

Giulivi, C., Oursler, M.J., 2003. Role of mitochondrial oxygen and nitrogen reactive species in signaling. In: Forman, H.J., Fukuto, J., Torres, M. (Eds.), Signal Transduction by Reactive Oxygen and Nitrogen Species: Pathways and Chemical Principles. Kluwer Academic Publishers, The Netherlands, pp. 311–332.

Giulivi, C., Poderoso, J.J., Boveris, A., 1998. Production of nitric oxide by mitochondria. J. Biol. Chem. 273, 11038–11048.

Goncalves, R.L.S., Quinlan, C.L., Perevoshchikova, I.V., Hey-Mogensen, M., Brand, M.D., 2015. Sites of superoxide and hydrogen peroxide production by muscle mitochondria assess ex vivo under conditions mimicking rest and exercise. J. Biol. Chem. 290, 209–227.

Gray, M.W., Burger, G., Lang, B.F., 1999. Mitochondrial evolution. Science 5407, 1476–1481.

Greiber, S., Muller, B., Daemisch, P., Pavenstadt, H., 2002. Reactive oxygen species alter gene expression in podocyte: induction of granulocyte macrophage-colony stimulating factor. J. Am. Nephrol. 13, 86–95.

Griffith, O.W., Meister, A., 1985. Origin and turnover of mitochondrial glutathione in the isolated hepatocyte. Proc. Natl. Acad. Sci. U. S. A. 82, 4668–4672.

Guaras, A., Perales-Clemente, E., Calvo, E., Acõn-Perez, R., Loureiro-Lopez, M.A., Pujol, C., et al., 2016. The $CoQH_2$/CoQ ratio serves as a sensor of respiratory chain efficiency. Cell Rep. 15, 197–209.

Hafner, R.P., Brown, G.C., Brand, M.D., 1990. Analysis of the control of respiration rate, phosphorylation rate, proton leak rate and protonmotive force in isolated mitochondria using the 'top-down' approach of metabolic control theory. Eur. J. Biochem. 188, 313–319.

Haigis, M.C., Mostoslavsky, R., Haigis, K.M., Fahie, K., Christodoulou, D.C., Murphy, A.J., et al., 2006. SIRT4 inhibits glutamate dehydrogenase and opposes the effects of calorie restriction in pancreatic beta cells. Cell 126, 941–954.

Haigis, M.C., Sinclair, D.A., 2010. Mammalian sirtuins: biological insights and disease relevance. Ann. Rev. Pathol. 5, 253–295.

Han, D., Williams, E., Cadenas, W., 2001. Mitochondrial respiratory chain-dependent generation of superoxide anion and its release into the intermembrane space. Biochem. J. 353, 411–416.

Hardie, D.G., 2007. AMP- activated/SNF1 protein kinases: conserved guardians of cellular energy. Nat. Rev. Mol. Cell Biol. 8, 774–785.

Hardie, D.G., 2004. The AMP-activated protein kinase pathway-new players upstream, and downstream. J. Cell Sci. 117, 5479–5487.

Hardie, D.G., 2005. New roles for the LKB1-AMPK pathway. Curr. Opin. Cell Biol. 17, 167–173.

Hardie, D.G., Scott, J.W., Pan, D.A., Hudson, E.R., 2003. Management of cellular energy by the AMP-activated protein kinase system. FEBS (Fed. Eur. Biochem. Soc.) Lett. 546, 113–120.

Hatefi, Y., 1985. The mitochondrial electron transport and oxidative phosphorylation system. Annu. Rev. Biochem. 54, 1015–1069.

Herrero, A., Barja, G., 1997. Sites and mechanisms responsible for the low rate of free radical production of heart mitochondria in the long lived pigeon. Mech. Aging Devel. 98, 95–111.

Herrero, A., Barja, G., 1998. Hydrogen peroxide production of heart mitochondria and aging rate are slower in canaries and parakeets than in mice: sites of free radical generation and mechanisms involved. Mech. Aging Devel. 103, 133–146.

Hickey, A.J.R., 2008. An alternate explanation for low mtDNA diversity: an age-old solution? Heredity 100, 443.

Hoch, F., 1992. Cardiolipins and biomembrane function. Biochem. Biophys. Acta 1113, 71–133.

Holmes, D.J., Austad, S.N., 1995. Birds as models for the comparative biology of ageing: a prospectus. J. Gerontol. Biol. Sci. 50A, B59–B66.

Holmes, D.J., Fluckiger, R., Austad, S.N., 2001. Comparative biology of ageing in birds: an update. Exp. Gerentol. 36, 869–883.

Hoppins, S., Lackner, L., Nunnari, J., 2007. The machines that divide and fuse mitochondria. Annu. Rev. Biochem. 76, 751–780.

Iqbal, M., Cawthon, D., Wideman Jr., R.F., Bottje, W.G., 2001. Lung mitochondrial dysfunction in pulmonary hypertension syndrome. I. Site specific defects in electron transport chain. Poultry Sci. 80, 485–495.

Iqbal, M., Pumford, N.R., Tang, Z.X., Lassiter, K., Wing, T., Cooper, M., et al., 2004. Low feed efficient broilers within a single genetic line exhibit higher oxidative stress and protein expression in breast muscle with lower mitochondrial complex activity. Poultry Sci. 83, 474–484.

Iqbal, M., Pumford, N.R., Lassiter, K., Tang, Z., Wing, T., Cooper, M., et al., 2005. Compromised liver mitochondrial function and complex activity in low feed efficient broilers within a single genetic line associated with higher oxidative stress and differential protein expression. Poultry Sci. 84, 933–941.

Jaburek, M., Varecha, M., Gimeno, M., Dembski, M., Jezek, P., Zhang, M., et al., 1999. Transport function and regulation of mitochondrial uncoupling proteins 2 and 3. J. Biol. Chem. 274, 26003–26007.

Kemp, B.E., Stapleton, D., Campbell, D.J., Chen, Z.P., Murthy, S., Walter, M., et al., 2003. AMP-activated protein kinase, super metabolic regulator. Biochem. Soc. Trans. 31, 162–168.

Kennedy, E.P., Lehninger, A.L., 1949. Oxidation of fatty acids and tricarboxylic acid cycle intermediates by isolated rat liver mitochondria. J. Biol. Chem. 179, 957–963.

Kikusato, M., Toyomizu, M., 2013. Crucial role of membrane potential in heat stress-induced overproduction of reactive oxygen species in avian skeletal muscle. PLoS One 8 (5), 1–9.

Koshkin, V., Greenberg, M.L., 2000. Oxidative phosphorylation in cardiolipin-lacking yeast mitochondria. Biochem. J. 347, 687–691.

Kristal, B., Park, B., Yu, B.P., 1994. Antioxidants reduce peroxyl-mediated inhibition of mitochondrial transcription. Free Rad. Biol. Med. 16, 653–660.

Kristal, B., Koopmans, S., Jackson, C.T., Ikeno, Y., Par, B., Yu, B.P., 1997. Oxidant-mediated repression of mitochondrial transcription in diabetic rats. Free Rad. Biol. Med. 22, 813–822.

Lapuente-Brun, E., Moreno-Loshuertos, R., Acin-Perez, R., Latorre-Pellicer, A., Colas, C., Balsa, E., et al., 2013. Supercomplex assembly determines electron flux in the mitochondrial electron transport chain. Science 340, 1567–1570.

Lass, A., Sohal, R.S., 1999. Comparisons of coenzyme Q bound to mitochondrial membrane proteins among different mammalian species. Free Rad. Biol. Med. 27, 220–226.

Lassiter, K., Dridi, S., Piekarski, A., Greene, E., Hargis, B.M., Kong, B.-W., Bottje, W., 2014. Bioenergetics in chicken embryo fibroblast cells: evidence of lower proton leak in spontaneously immortalized chicken embryo fibroblast cells compared to young and senescent primary chicken embryo fibroblast cells. Comp. Biochem. Physiol. A 175, 115–123.

Lassiter, K., Greene, E., Piekarski, A., Faulkner, O.B., Hargis, B.M., Bottje, W., Dridi, S., 2015. Orexin system is expressed in avian muscle cells and regulates mitochondrial dynamics. Am. J. Physiol. Regul. Integr. Comp. Physiol. 308, R173–R187.

Lassiter, K., Dridi, S., Greene, E., Kong, B., Bottje, W.G., 2018. Identification of mitochondrial hormone receptors in avian muscle cells. Poultry Sci. 97, 2926–2933.

Lee, S., Tak, E., Lee, J., Rashid, M.A., Murphy, M.P., Ha, J., et al., 2011. Mitochondrial hydrogen peroxide generated from electron transport chain complex I stimulates muscle differentiation. Cell Res. 21, 817–834.

Lehninger, A.L., 1965. The Mitochondrion. W. A. Benjamin, Inc, New York, NY.

Lehninger, A.L., Nelson, D.L., Cox, M.M., 1993. Principles of Biochemistry. Worth Publishers, New York, NY.

Levonen, A.L., Patel, R.P., Brookes, P., Go, Y.M., Jo, H., Parthasarathy, S., et al., 2001. Mechanisms of cell signaling by nitric oxide and peroxynitrite: from mitochondria to MAP kinases. Antioxid. Redox Signal. 3, 215–229.

Li, J., Cai, Q., Zhou, H., Xiao, G.U., 2002. Effects of hydrogen peroxide on mitochondrial gene expression of intestinal epithelial cells. World J. Gastroenterol. 8, 1117–1122.

Liesa, M., Shirihai, O.S., 2013. Mitochondrial dynamics in the regulation of nutrient utilization and energy expenditure. Cell Metabol. 17, 491–506.

Lin, J., Puigserver, P., Donovan, J., Tarr, P., Spiegelman, B.M., 2002a. Peroxisome proliferator-activated receptor gamma coactivator 1Beta (PGC-1Beta), a novel PGC-1 related transcription coactivator associated with host cell factor. J. Biol. Chem. 277, 1645–1648.

Lin, T.K., Hughes, G., Muratovska, A., Blaikie, F.H., Brookes, P.S., Darley-Usmar, V., et al., 2002b. Specific modification of mitochondrial protein thiols in response to oxidative stress: a proteomics approach. J. Biol. Chem. 277, 17048–17056.

Liu, Y., Kitsis, R.N., 1996. Induction of DNA synthesis and apoptosis in cardiac myocytes by E1A oncoprotein. J. Cell Biol. 133, 325–334.

Mannella, C.A., 2000. Our changing views of mitochondria. J. Bioeng. Biomembr 32, 1–4.

Martensson, J., Han, J., Griffith, O.W., Meister, A., 1993. Glutathione ester delays the onset of scurvy in ascorbate-deficient Guinea pigs. Proc. Natl. Acad. Sci. U. S. A. 90, 317–321.

Martensson, J., Lai, J., Meister, A., 1990. High affinity transport of glutathione is part of a multicomponent system essential for mitochondrial function. Proc. Natl. Acad. Sci. U. S. A. 87, 7185–7189.

Masatoshi, U., Watanabe, K., Sato, K., Akiba, Y., Toyomizu, M., 2005. Possible role for avPGC-1alpha in the control of expression of fiber type, along with avUCP and avANT mRNA's in skeletal muscles of cold-exposed chickens. FEBS (Fed. Eur. Biochem. Soc.) Lett. 579, 11–17.

Meirhaeghe, A., Crowley, V., Lenaghan, C., Lelliott, C., Green, K., Stewart, A., et al., 2003. Characterization of the human, mouse and rat PGC1Beta (peroxisome-proliferator-activated receptor-gamma co-activator 1Beta)gene in vitro and in vivo. Biochem. J. 373, 155–165.

Meister, A., 1984. New aspects of glutathione biochemistry and transport: selective alteration of glutathione metabolism. Fed. Proc. 43, 3031–3042.

Mezentseva, N.V., Kumaratilake, J.S., Newman, S.A., 2008. The brown adipocyte differentiation pathway in birds: an evolutionary road not taken. BMC Biol. 6, 17.

Mills, E.L., Kelly, B., Logan, A., Costa, A.S.H., Varma, M., Bryant, C.E., et al., 2016. Succinate dehydrogenase supports metabolic repurposing of mitochondria to drive inflammatory macrophages. Cell 167, 457–470.

Minokoshi, Y., Alquier, T., Furukawa, N., Kim, Y.B., Lee, A., Xue, B., et al., 2004. AMP-Kinase regulates food intake by responding to hormonal and nutrient signals in the hypothalamus. Nature 428, 569–574.

Miwa, S., Pierre, J.S., Partridge, L., Brand, M.D., 2003. Superoxide and hydrogen peroxide production by drosophila mitochondria. Free Rad. Biol. Med. 35, 938–948.

Mujahid, A., Akiba, Y., Toyomizu, M., 2007a. Acute heat stress induces oxidative stress and decreases adaptation in young white leghorn cockerels by down regulation of avian uncoupling protein. Poultry Sci. 86, 364–371.

Mujahid, A., Sato, K., Akiba, Y., Toyomizu, M., 2006. Acute heat stress stimulates mitochondrial superoxide production in broiler skeletal muscle, possibly via down-regulation of uncoupling protein content. Poultry Sci. 85, 1259–1265.

Mujahid, A., Pumford, N.P., Bottje, W., Kiotaka, K., Miyazawa, T., Akiba, Y., et al., 2007b. Mitochondrial oxidative damage in chicken skeletal muscle induced by acute heat stress. J. Poultry Sci. 44, 439–445.

Mujahid, M., Akiba, Y., Toyomizu, M., 2009. Olive-oil supplemented diet alleviates acute heat stress-induced mitochondrial ROS production in chicken skeletal muscle. Am. J. Physiol. Regul. Integr. Comp. Physiol. 297, R690–R698.

Muller, F.L., Liu, Y.H., van Remmenn, H., 2004. Complex II releases superoxide to both sides of the inner mitochondrial membrane. J. Biol. Chem. 279, 49064–49073.

Murphy, E., Steenbergen, C., 2008. Mechanisms underlying acute protection from cardiac ischemia-reperfusion injury. Physiol. Rev. 88, 581–609.

Murphy, M.P., Echtay, K.S., Blaikie, F.H., Asin-Cayuela, J., Cocheme, H.M., Green, K., et al., 2003. Superoxide activates uncoupling proteins by generating carbon-centered radicals and initiating lipid peroxidation: studies using a mitochondria-targeted spin trap derived from a-phenyl-*N*-*tert*-butylnitrone. J. Biol. Chem. 278, 48534–48545.

Murphy, M.P., Holmgren, P.A., Larsson, N.G., Haliwell, B., Chang, C.J., Kalyanaraman, B., et al., 2011. Unraveling the biological roles of reactive oxygen species. Cell Metabol. 13, 361–366.

Nasrin, N., Wu, X., Fortier, E., Feng, Y., Bare, O.C., Chen, S., et al., 2010. SIRT4 regulates fatty acid oxidation and mitochondrial gene expression in liver and muscle cells. J. Biol. Chem. 285, 31995–32002.

Nijtmans, L.G.J., Sanz, A.M., Grivell, L.A., Coates, P.J., 2002. The mitochondrial PHB complex: roles in mitochondrial respiratory complex assembly, ageing and degenerative disease. Cell. Mol. Life Sci. 59, 143–155.

Nisoli, E., Clementi, E., Moncada, S., Carruba, M.O., 2004. Mitochondrial biogenesis as a cellular signaling framework. Biochem. Pharmacol. 67, 1–15.

Nisoli, E., Clementi, E., Paolucci, C., Cozzi, V., Tonello, C., Sciorati, C., et al., 2003. Mitochondrial biogenesis in mammals: the role of endogenous nitric oxide. Science 299, 896–899.

Ojano-Dirain, C., Tinsley, N.B., Wing, T., Cooper, M., Bottje, W.G., 2007a. Membrane potential and hydrogen peroxide production in duodenal mitochondria in broilers chicken (*Gallus gallus*) with low and high feed efficiency. Comp. Biochem. Physiol. 147, 934–941.

Ojano-Dirain, C., Bottje, W., Wing, T., Cooper, M., 2005. Glutathione and respiratory chain complex activities in duodenal mitochondria from broilers with low and high feed efficiency. Poultry Sci. 84, 782–788.

Ojano-Dirain, C., Iqbal, M., Cawthon, D., Swonger, S., Wing, T., Cooper, M., et al., 2004. Site-specific effects in electron transport in duodenal mitochondria is associated with low feed efficiency in broiler breeder males. Poultry Sci. 83, 1394–1403.

Ojano-Dirain, C., Pumford, N.R., Toyomizu, M., Bottje, W.G., 2007b. Association of mitochondrial function and feed efficiency. J. Poultry Sci. 44, 221–237.

Ojano-Dirain, C., Toyomizu, M., Wing, T., Cooper, M., Bottje, W.G., 2007. Gene expression in breast muscle and duodenum from low and high feed efficient broilers. Poultry Sci. 86, 372–381.

Ojuka, E.O., 2004. Role of calcium and AMP kinase in the regulation of mitochondrial biogenesis and GLUT4 levels in muscle. Proc. Nutr. Soc. 63, 275–278.

Olafsdottir, K., Reed, D.J., 1988. Retention of oxidized glutathione by isolated rat liver mitochondria during hydroperoxide treatment. Biochem. Biophys. Acta 964, 377–382.

Paul, M.H., Sperling, E.D., 1952. Cyclophorus system-XXIII. Correlation of cyclophorase activity and mitochondrial density in striated muscle. Proc. Soc. Exp. Biol. Med. 79, 352–354.

Piao, Y.J., Seo, Y.H., Hong, F., Kim, J.H., Kim, Y.J., Kang, M.H., et al., 2005. Nox_2 stimulates muscle differentiation via NF-kB/iNOS pathway. Free Rad. Biol. Med. 38, 989–1001.

Poyton, R.O., McEwen, J.E., 1996. Crosstalk between nuclear and mitochondrial genomes. Annu. Rev. Biochem. 65, 563–607.

Psarra, A.,G., Solakidi, S., Sekeris, C.E., 2006. The mitochondrion as a primary site of action of steroid and thyroid hormones: presence and action of steroid and thyroid hormone receptors in mitochondria of animal cells. Mol. Cell Endocrinol. 246, 21–33.

Puigserver, P., Wu, Z., Park, C.W., Graves, R., Wright, M., Spiegelman, B.M., 1998. A cold-inducible coactivator of nuclear receptors linked to adaptive thermogenesis. Cell 92, 829–839.

Rabilloud, T., Strub, J.M., Carte, N., Luche, S., van Dorsselaer, A., Lunardi, J., et al., 2002. Comparative proteomics as a new tool for exploring human mitochondrial tRNA disorders. Biochemist 41, 144–150.

Raimbault, S., Dridi, S., Denjean, F., Lachuer, J., Couplan, E., Bouillaud, F., et al., 2001. An uncoupling protein homologue putatively involved in facultative muscle thermogenesis in birds. Biochem. J. 353, 441–444.

Rambold, A.S., Pearce, E.L., 2018. Mitochondrial dynamics at the interface of immune cell metabolism and function. Trends Immunol. 39, 6–18.

Rey, B., Roussel, D., Romestaing, C., Belouze, M., Rouanet, J.L., Desplanches, D., et al., 2010. Up-regulation of avian uncoupling protein in cold-acclimated and hyperthyroid ducklings prevents reactive oxygen species production by skeletal muscle mitochondria. BMC Physiol. 10 (5), 1–12.

Reznick, R.M., Shulman, G.I., 2006. The role of AMP-activated protein kinase in mitochondrial biogenesis. J. Physiol. 574, 33–39.

Rhee, G., Kang, W., Jeong, W., Chang, T., Yang, K., Woo, H.A., 2005. Intracellular messenger function of hydrogen peroxide and its regulation by peroxiredoxins. Curr. Opin. Cell Biol. 17, 183–189.

Riobo, N.A., Clement, E., Melani, M., Boveris, A., Cadenas, E., Moncoda, S., et al., 2001. Nitric oxide inhibits mitochondrial NADH-ubiquinone reductase activity through the formation of peroxynitrite. Biochem. J. 359, 139–145.

Rolfe, D.F.S., Brand, M.D., 1997. The physiological significance of mitochondrial proton leak in animal cells and tissues. Biosci. Rep. 17, 9–16.

Ryan, M.T., Hoogenraad, N.J., 2007. Mitochondrial-nuclear communications. Annu. Rev. Biochem. 76, 701–722.

Samartsev, V.N., Smirnov, A.V., Zeldi, I.P., Markova, E.N., Mokova, E.N., Skulachev, V.P., 1997. Involvement of the aspartate/glutamate antiporter in fatty acid-induced uncoupling of liver mitochondria. Biochim. Biophys. Acta 1319, 251–257.

Scheffler, I., 1999. Mitochondria. Wiley-Liss Inc., New York, NY.

Scialo, F.D., Fernadez-Ayala, J., Sanz, A., 2017. Role of mitochondrial reverse electron transport in ROS signaling: potential roles in health and disease. Front. Physiol. 8, 1–7.

Sena, L.A., Chandel, N.S., 2012. Physiological roles of mitochondrial reactive oxygen species. Mol. Cell 48, 158−167.

Sharma, V.K., Ramesh, V., Franzini-Armstrong, C., Sheu, S., 2000. Transport of $Ca^{2+}$from sarcoplasmic reticulum to mitochondria in rat ventricular myocytes. J. Bioenerg. Biomembr. 32, 97−104.

Skulachev, V.P., 1996. Role of uncoupled and non-coupled oxidations in maintenance of safely low levels of oxygen and its one-electron reductants. Q. Rev. Biophys. 29, 169−202.

Skulachev, V.P., 1997. Membrane linked systems preventing superoxide formation. Biosci. Rep. 17, 347−366.

St Pierre, J., Buckingham, J.A., Roebuck, S.J., Brand, M.D., 2002. Topology of superoxide production from different sites in the mitochondrial electron transport chain. J. Biol. Chem. 277, 44784−44790.

Talbot, D.A., Duchamp, C., Rey, B., Hanuise, N., Rouanet, J.L., Sibille, B., et al., 2004. Uncoupling protein and ATP/ADP carrier increase mitochondrial proton conductance after cold adaptation of king penguins. J. Physiol. 558, 123−135.

Talbot, D.A., Hanuise, N., Rey, B., Rouanet, J., Duchamp, C., Brand, M.D., 2003. Superoxide activates a GDP-sensitive proton conductance in skeletal muscle mitochondria of king penguin (*Aptenodytes patagonicus)*. Biochem. Biophys. Acta 312, 983−988.

Tang, Z., Iqbal, M., Cawthon, D., Bottje, W.G., 2002. Heart and breast muscle mitochondrial dysfunction in pulmonary hypertension syndrome in broilers (*Gallus domesticus*). Comp. Biochem. Physiol. A132, 527−540.

Toyomizu, M., Ueda, M., Sato, S., Seki, Y., Sato, K., Akiba, Y., 2002. Cold-induced mitochondrial uncoupling and expression of chicken UCP and ANT mRNA in chicken skeletal muscle. FEBS (Fed. Eur. Biochem. Soc.) Lett. 529, 313−319.

Turrens, J.F., Alexander, A., Lehninger, A.L., 1985. Ubisemiquinone is the electron donor for superoxide formation by complex III of heart mitochondria. Arch. Biochem. Biophys. 237, 408−413.

Turrens, J.F., Boveris, A., 1980. Generation of superoxide anion by the NADH dehydrogenase of bovine heart mitochondria. Biochem. J. 191, 421−427.

Velleman, S.G., McFarland, S.D., 2015. Skeletal muscle. In: Scanes, C.G. (Ed.), Sturkie's Avian Physiology, sixth ed. Elesvier Academic Press, San Diego, CA 92101-4495, pp. 379−402.

Wallace, D., 1999. Mitochondrial diseases in man and mouse. Science 283, 1482−1488.

Wei, Y., 1998. Oxidative stress and mitochondrial DNA mutations in human aging. Exp. Biol. Med. 217, 53−63.

Wu, M., Neilson, A., Swift, A.L., Moran, R., Tamagnine, J., Parslow, D., et al., 2007. Multiparameter metabolic analysis reveals a close link between attenuated mitochondrial bioenergetic function and enhanced glycolysis dependency in human tumor cells. Am. J. Physiol. Cell Physiol. 292, C125−C136.

Wu, Z., Puigserver, P., Andersson, U., Zhang, C., Adelmant, G., Mootha, V., et al., 1999. Mechanisms controlling mitochondrial biogenesis and respiration through the thermogenic coactivator PGC-1. Cell 98, 115−124.

Wyrutniak-Cabello, C., Casas, F., Cabello, G., 2001. Thyroid hormone action in mitochondria. J. Mol. Endocrinol. 26, 67−77.

Yu, B.P., 1994. Cellular defenses against damage from reactive oxygen species. Physiol. Rev. 74, 139−162.

Zhou, G., Myers, R., Li, Y., Chen, Y., Shen, X., Fenyk-Melody, J., et al., 2001. Role of AMP-activated protein kinase in mechanism of metformin action. J. Clin. Invest. 108, 1167−1174.

Chapter 7

Evolution of birds

Daniel T. Ksepka
Bruce Museum, Greenwich, CT, United States

7.1 Introduction

Birds are the most diverse major clade of tetrapods, and also the youngest. From our human perspective, birds are intimately associated with concepts like feathers and flight, eggs and nests, and beauty and song. Understanding how birds evolved flight, survived one of the worst mass extinctions in Earth history, and ultimately radiated into the >10,000 species that exist today truly requires combining paleontological and neontological perspectives. This chapter provides an overview of major patterns in avian evolution with a focus on the fossil record. The relationships of modern birds, which are increasingly well resolved, thanks to genomic data, are touched on only briefly.

To appreciate the remarkable evolutionary journey that resulted in modern birds, it is best to begin with a cursory discussion of their place within the larger context of vertebrate evolution. Birds descended from theropod dinosaurs. Within a phylogenetic context, birds *are* dinosaurs, and so the term "nonavian dinosaur" is often employed to specify all dinosaurs except for birds, for example, in stating that nonavian dinosaurs went extinct at the end of the Cretaceous Period. For simplicity, "dinosaur" and "theropod" are used to refer only to the nonavian subset of those clades in this chapter.

7.2 The dinosaur–bird transition

7.2.1 Theropod dinosaurs

The dinosaur–bird transition has been reviewed in great detail elsewhere (e.g., Ostrom, 1975; Gauthier, 1986; Prum, 2002; Norell and Xu, 2005), and so will only be briefly summarized here. The closest theropod relatives of birds were small, feathered predators (Figure 7.1). Major branching patterns within the evolutionary tree of theropod dinosaurs are relatively well understood, though the precise relationships of certain taxa remain the subject of active research. Most recent analyses place birds within the clade Paraves, which unites the sickle-clawed dinosaur clades Dromaeosauridae and Troodontidae with Aves. Sequentially, the branches of the tree below Paraves are occupied by the beaked and crested Oviraptorosauria, the secondarily herbivorous Therizinosauria, the aberrant short-armed Alvarezsauridae, the ostrich-like Ornithomimosauria, and the small predatory Compsognathidae (Figure 7.2) (e.g., Turner et al., 2012; Brusatte et al., 2014). Debate remains over the relationships of the enigmatic bat-winged Scansoriopterygidae, which may represent relatives of Oviraptorosauria or the sister taxon of Paraves (Brusatte et al., 2014; O'Connor and Sullivan, 2014; Wang et al., 2019).

Many features closely associated with birds first arose within dinosaurs. These include feathers, the loss of digits resulting in a three-fingered hand, fusion of the clavicles into a furcula ("wishbone"), increasing hollowness of the limb bones, bipedal posture, and small body size. A great deal of convergent evolution took place in advanced theropods, and many seemingly key features evolved multiple times in distantly related theropods and birds. One such feature is the loss of teeth, which occurred independently in ornithomimosaurs, oviraptorosaurs, and multiple times in birds. Another is the shortening of the tail via fusion of multiple vertebrae into a pygostyle, which arose independently in oviraptorosaurs, scansoriopterygids, and birds.

7.2.2 Feathers first

The evolution of feathers was long linked with the origin of flight. The unveiling of the small feathered compsognathid dinosaur *Sinosauropteryx* (Figure 7.1A) rocked the paleontological and ornithological communities, effectively ending debate over the dinosaurian ancestry of birds and raising new questions about why feathers first evolved (Chen et al., 1998). The "proto-feathers" covering *Sinosauropteryx* are often described as unbranched monofilaments, but it is more likely that each feather was

Sturkie's Avian Physiology. https://doi.org/10.1016/B978-0-12-819770-7.00009-8

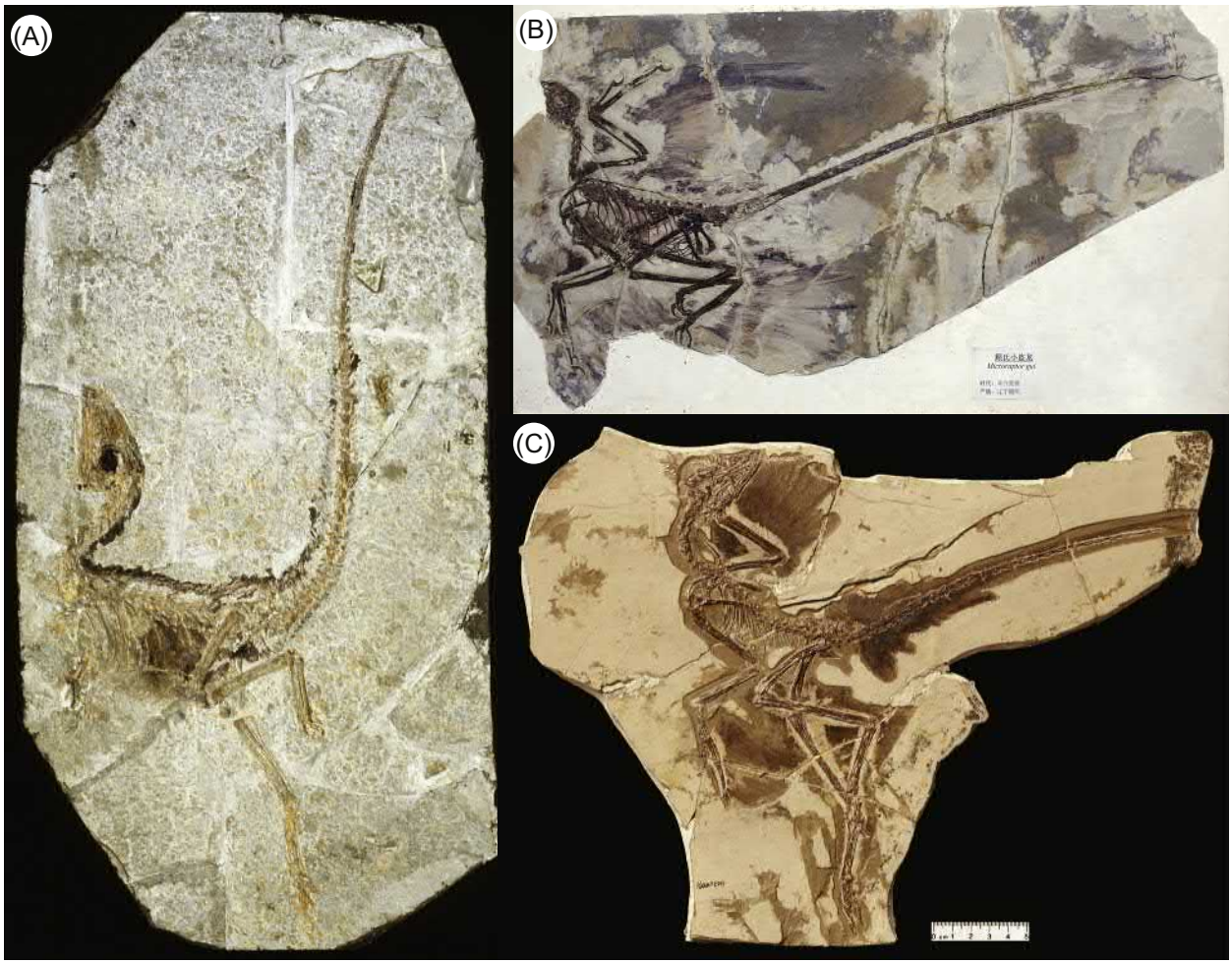

FIGURE 7.1 Feathered theropods. (A) Specimen of the compsognathid *Sinosauropteryx prima* (NIGP 127586) with filamentous feathers. (B) Specimen of the "four-winged" *Microraptor gui* (IVPP V 13352). (C) Specimen of the anchiornithid *Anchiornis huxleyi* (BMNHC PH804). *Credit: Photos by Mick Ellison, American Museum of Natural History.*

composed of multiple filaments joined either at a common base or a slender central shaft (Currie and Chen, 2001; Xu, 2020). A steady stream of new discoveries has confirmed that filamentous feathers were present in many other theropods (Norell and Xu, 2005; Qiang et al., 1998; Xu et al., 2003). More recent discoveries of ornithischian dinosaurs and pterosaurs with filamentous integument suggest that feathers have a deep history, extending back at least to the last common ancestor of all dinosaurs and possibly to the last common ancestor of dinosaurs and pterosaurs (Zheng et al., 2009; Yang et al., 2019).

Filamentous feathers would have failed miserably in forming an airfoil, but were useful for thermoregulatory insulation, especially in small dinosaurs. They also likely served to enhance display and camouflage patterning, functions that would have formerly been fulfilled by colored scales (Koschowitz et al., 2014). One major recent advance in paleobiology is the recognition that melanosomes, subcellular structures that store pigment, are often preserved in fossils and indeed may be largely responsible for feather preservation (Vinther et al., 2008). Melanosome aspect ratio can be used to infer melanin-based colors in extinct species, and has revealed display striping and countershading camouflage in dinosaurs (Zhang et al., 2010; Vinther et al., 2016).

Filamentous feathers differ markedly from the vaned pennaceous feathers we tend to imagine when we think of "a feather." These more complex feathers have a large central rachis and branching barbs, which are in turn held in place by smaller interlocking barbules, allowing them to form an airfoil in modern birds. The most basal theropods with pennaceous feathers were the clearly earthbound oviraptorosaurs. This suggests pennaceous feathers originally served a nonaerodynamic function, perhaps providing a more ordered "canvas" for display colors, as well as opening the door to structural color and complex ornamental feathers (Foth et al., 2014; Koschowitz et al., 2014). Paravian dinosaurs such as *Microraptor* and *Caihong* show

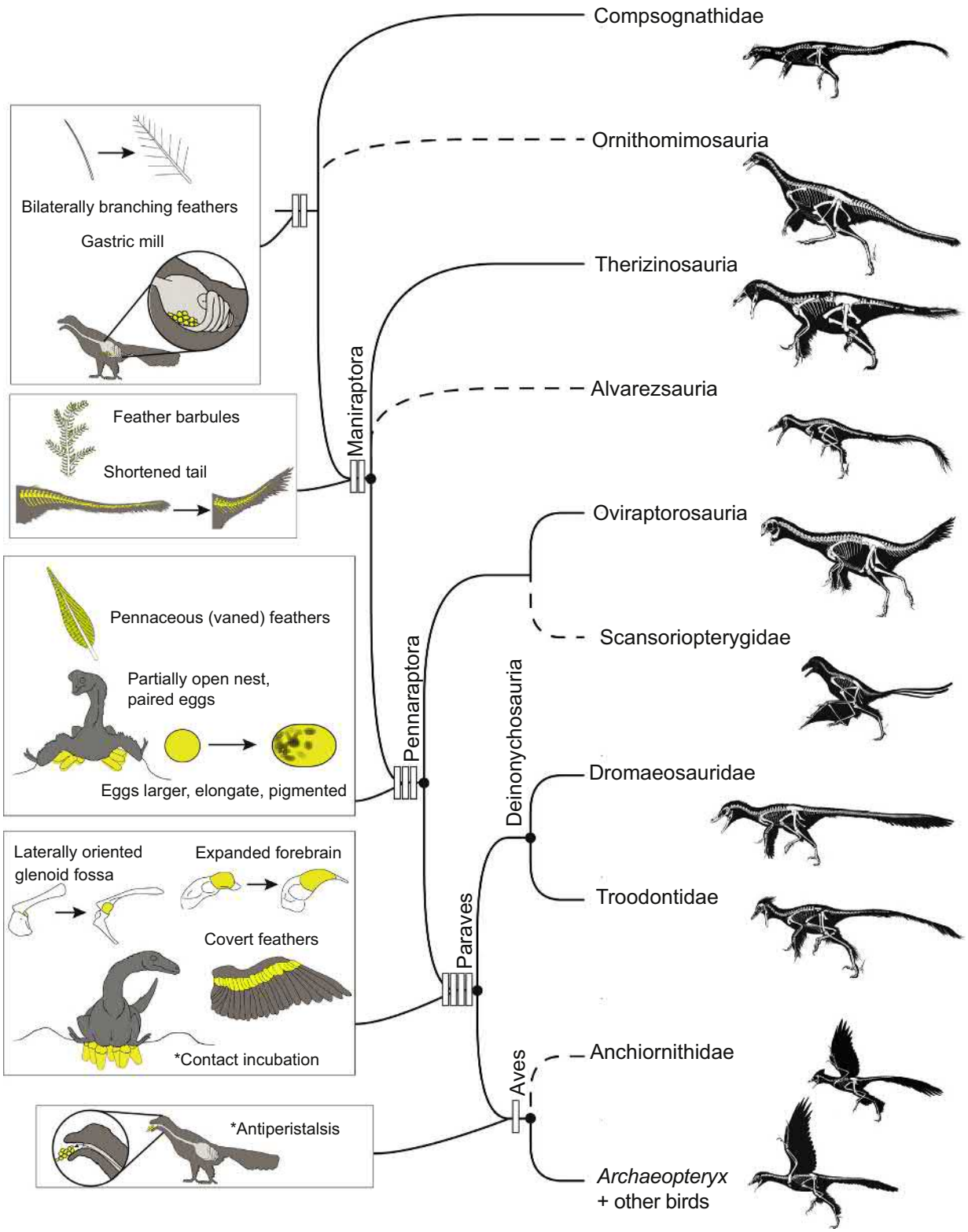

FIGURE 7.2 Phylogenetic tree depicting the relationships of birds to their theropod relatives. *Dashed lines* indicate uncertainty. Key synapomorphies discussed in this chapter are indicated. *Asterisks* indicate characters that evolve multiple times or for which placement remains uncertain. Skeletal silhouettes, top to bottom: *Sinosauropteryx prima*, *Ornithomimus edmontonicus*, *Beipiaosaurus inexpectatus*, *Shuvuuia deserti*, *Khaan mckennai*, *Ambopteryx longibrachium*, *Velociraptor mongoliensis*, *Sinornithosaurus millenii*, *Xiaotingia zhengi*, and *Archaeopteryx lithographica*. *Credit: Silhouette artwork by Jaime Headden, character illustrations by Kate Dzikiewicz.*

evidence of iridescent pennaceous feathers, indicating such structural coloration arose in theropods by the Late Jurassic (Li et al., 2012; Hu et al., 2018). Interlocking barbules have not yet been identified in theropod feathers, and their earliest occurrence is in *Archaeopteryx*. Plumulaceous (noninterlocking) barbules are known from feathers attached to a dinosaur tail preserved in amber which probably represents a basal maniraptoran (Xing et al., 2016).

Feathers with asymmetrical vanes arose in Paraves. The narrow leading vane and wide trailing vane of asymmetrical feathers aid in the formation of a lift-generating airfoil. Asymmetrical feathers occur universally in the wings and tails of volant modern birds. Thus, the presence of asymmetrical feathers in extinct species has been interpreted as evidence of flight capacity (Feduccia and Tordoff, 1979). However, the "flight" feathers of secondarily flightless birds typically retain asymmetrical vanes, reverting to symmetry only in birds with highly atrophied wings such as "ratites" (McGowen, 1989). Asymmetrical feathers have been reported in the wings of the dromaeosaurid *Microraptor* (see below) and the tail of the troodontid *Jianianhualong* (Xu et al., 2003, 2017). However, many other paravians appear to have had only symmetrical feathers (Lefèvre et al., 2017). This complex distribution suggests symmetrical feathers arose multiple times in concert with gliding ecology.

7.2.3 Taking wing

The earliest diverging theropod clade showing compelling evidence for some form of flight is Scansoriopterygidae. Scansoriopterygids can only be described as bizarre, and the discovery of "bat-winged" species ranks as one of the most startling fossil discoveries of the 21st century. The hyperelongate third finger of these small theropods initially puzzled paleontologists. Subsequently, the discovery of a specimen of *Yi xi* with preserved soft tissue revealed that the elongate finger combined with a novel rod-shaped wrist bone, dubbed the "styliform element," to anchor and control a membranous wing (Xu et al., 2015). Subsequent discovery of a second bat-winged species, *Ambopteryx longibrachium*, revealed that at least some scansoriopterygids had a pygostyle (Wang et al., 2019).

It is particularly remarkable that scansoriopterygids formed their wing from a membrane rather than feathers. Despite being nested within a clade of theropods that had pennaceous feathers, scansoriopterygids had only simple shaft-like wing feathers. The microstructure of these feathers suggests they represent a secondary simplification, with the role of potentially airfoil-forming pennaceous feathers made redundant by the membranous wing (Wang et al., 2019). *Yi* and *Ambopteryx* were well suited to gliding flight, though the lack of robust flight muscle insertions on the wing bones suggests they had little if any capacity for flapping (Xu et al., 2015). Marvelous as the scansoriopterygids were, they represent a now-extinct side branch of the theropod evolutionary tree and thus reveal little about the origin of avian flight.

Hints of what would later become a true bird wing (i.e., a feathered airfoil) first appear in large, flightless theropods. Although perplexing at face value, this simply suggests that incipient wings served no aerodynamic function, and were coopted for flight only later. The earliest diverging taxon to show potential evidence of a wing-like forelimb is the ornithomimosaur *Ornithomimus edmonticus* (Zelenitsky et al., 2012). In this species, juveniles show only filamentous feathers, whereas adults preserve carbonized markings that represent larger, potentially pennaceous feathers. However, because only shaft traces remain, it is uncertain whether these feathers were in fact branching, and they may instead represent broad monofilaments (Xu, 2020). More conclusive evidence for a wing-like forelimb is present in Oviraptorosauria. Several species are known to have had incipient wings, thanks to excellent fossil specimens with intact feathering (Ji et al., 1998). Oviraptorosaurians were clearly flightless, suggesting a nonaerodynamic function for the forelimb feathering, such as display or covering clutches during brooding (Hopp and Orsen, 2004).

The earliest "true" wing occurs in the dromaeosaurid *Microraptor* (Xu et al., 2003). This diminutive theropod possessed elongate asymmetrical wing feathers, as well as elongate pennaceous hind limb feathers (Figure 7.1B). This unexpected feather arrangement gave *Microraptor* the appearance of a dinosaurian biplane. Modeling suggests *Microraptor* was a proficient glider and this remarkable "four-winged" fossil provides perhaps the most compelling evidence for an intermediate gliding stage prior to the evolution of powered flight (Dyke et al., 2013). Once thought to be unique to *Microraptor*, feathered "trousers" extending from the hind limbs have since been reported in the dromaeosaurid *Sinornithosaurus* as well as early birds including *Archaeopteryx* and *Confuciusornis* (Ji et al., 2001; Longrich, 2006; Foth et al., 2014). Whether they served an aerodynamic or display function in these taxa remains debatable.

In modern bird wings, the elongate remiges are overlapped above and below by layers of shorter feathers called coverts. The incipient wings of oviraptorids appear to have lacked coverts, and thus to have been formed by a single layer of elongate feathers. Coverts have been identified in the *Microraptor* and the dromaeosaurid *Zhenyuanlong* (Lü and Brusatte, 2015), suggesting paravians shared a multilayered wing with improved airflow smoothing capabilities. The morphology of the coverts is poorly known in dromaeosaurids and troodontids, but those in *Anchiornis* differ from modern bird coverts in being poorly differentiated from the remiges (Longrich et al., 2012). This resulted in a

wing formed by stacked layers of relatively short feathers. *Archaeopteryx* was previously though to share this primitive arrangement, but new specimens reveal that it had short coverts and long primaries like modern birds (Foth et al., 2014). The combined presence of asymmetrical wing feathers, interlocking barbules, and elongate primaries suggests *Archaeopteryx* had substantially more advanced flight capabilities than the anchiornithids.

In summary, the balance of evidence suggests that although multiple theropod lineages acquired a capacity for gliding flight, *Archaeopteryx* is the earliest known taxon with the potential for powered flight. Nonetheless, drawing a bold line between *Archaeopteryx* and closely related groups in terms of flight capacity may never be possible to do with confidence, given phylogenetic uncertainty and the limits of inferring behavior in long-extinct species.

7.2.4 *Archaeopteryx*, the first bird?

For well over a century, there was little debate over the identity of the first bird. Originally named based on a single feather in 1861, *Archaeopteryx* is now known from 11 skeletons preserved in varying states of completeness (Rauhut et al., 2019). *Archaeopteryx* quickly became a linchpin of support for Darwin's theory of evolution—its status enhanced by the stunning quality of the "Berlin specimen," arguably the most beautiful fossil ever discovered. *Archaeopteryx* lived in an archipelago environment ~150 million years ago, when much of Europe was inundated by shallow ocean waters. Known specimens span a large range of sizes, from that of a small magpie to a large raven, contributing to debate over how many species are represented and whether the largest specimens should be placed in a separate genus (*Wellnhoferia*) (Elzanowski, 2001; Mayr et al., 2005; Rauhut et al., 2019).

Archaeopteryx long remained the key reference point for understanding the origin of birds because no serious challengers to its position at the base of the avian evolutionary tree arose for over a century. The brief promotion of the Triassic *Protoavis texensis* as an older rival to *Archaeopteryx* (Chatterjee, 1991) was nothing short of a debacle, with problems ranging from the veracity of reconstructed skeletal features to the chimeric nature of the type specimen (Witmer, 2001). The loneliness of *Archaeopteryx* ended dramatically when Mesozoic birds began to be unearthed in previously unfathomable numbers from eastern China near the turn of the 21st century. Thousands of individual fossils have emerged, revealing dozens of new species, ranging in age from roughly 110 to 160 million years old. As the floodgates opened, debate has started to swirl over candidates for the title of "first bird." Several small feathered theropods from the family Anchiornithidae (e.g., Figure 7.1C) have been proposed to occupy a branch one step below *Archaeopteryx* in some studies (Godefroit et al., 2013; Rauhut et al., 2019), which would make them the oldest and most primitive members of the bird line. However, the placement of these taxa remains controversial, and the possibility they instead represent small troodontid theropods or basal paravians is also plausible (Brusatte et al., 2014).

Other recent studies have called into question the placement of *Archaeopteryx* itself, shunting it off the bird branch to an alternate placement as sister taxon to Deinonychosauria (Mayr et al., 2005; Xu et al., 2011; Wang et al., 2019). This placement would imply *Archaeopteryx* was not a true bird, but rather an undersized cousin of *Velociraptor*—leaving the Early Cretaceous *Jeholornis* to inherit the title of first bird. The fact that each new study seems to yield a new reshuffling of advanced theropods, *Archaeopteryx*, and other primitive birds reflects the fact that these taxa split from one another in a relatively short time, making it likely we will always have some degree of uncertainty as to the branching patterns near the origin of birds. For purposes of this chapter, we will adopt the working hypotheses that anchiornithids occupy the branch immediately below *Archaeopteryx*, but that *Archaeopteryx* was the first bird with the potential for powered flight.

7.2.5 Flight in *Archaeopteryx*

The flight capabilities of *Archaeopteryx* have been subject to endless inquiry. Pectoral girdle morphology clearly indicates that *Archaeopteryx* was not capable of the same level of flight efficiency as modern birds. The absence of a bony sternum, which anchors the largest of the flight muscles in modern birds, immediately draws attention. However, this single feature cannot be considered surefire evidence against powered flight, as the sternum of *Archaeopteryx* may have been cartilaginous and thus not preserved in fossils (Bock, 2013). In addition, the pectoralis and supracoracoideus muscles may have attached primarily to the coracoid and/or furcula (Olson and Feduccia, 1979; Elzanowski, 2002), and so could have been well developed even in the absence of a bony sternum. However, other features, such as the lack of a triosseal canal and the lateral orientation of the shoulder joint, suggest a much weaker ability to elevate the wing than in modern birds (Ostrom, 1976; Senter, 2006).

The morphology of the wing is more congruent with powered flight. Recent data from wing bone cross-sectional geometry support the capacity for flapping flight (Voeten et al., 2018). Asymmetry of the flight feathers likewise suggests they served an aerodynamic function. On the other hand, lower trailing edge barb angles suggest the flight feathers of *Archaeopteryx* may have been less flexible than those of more advanced birds and thus less suited to maintaining a coherent airfoil under powered flight (Feo et al., 2015). Overall, skeletal and feather data suggest *Archaeopteryx* could fly, but surely lacked the sustained

flapping and sophisticated aerial maneuvering capabilities of modern birds.

7.3 The Mesozoic avifauna

7.3.1 Basal birds

Before attempting to summarize the early history of avian evolution, it is helpful to introduce the major groups of Mesozoic birds (Figure 7.3). Provided Anchiornithidae (provisionally eight species) ultimately prove to represent the branch on the avian tree below *Archaeopteryx*, they suggest the first birds were at best gliders. Anchiornithids were mostly crow-sized predators which retained teeth, had relatively long forearms, and lacked an ossified sternum. They possessed vaned feathers along both the forelimbs and hind limbs, but these appear to have largely been symmetrical and "shaggy" with limited aerodynamic efficiency (Saitta et al., 2018). The "silky" texture of the feathers in *Serikornis sungei* suggests the feathered "trousers" of anchiornithids served a display rather than aerodynamic function (Lefèvre et al., 2017). Display structures are also documented in the unique anchiornithid *Caihong juji*, which had both a pair of bony cranial crests and iridescent feathers (Hu et al., 2018).

After *Archaeopteryx,* the Jeholornithidae (three species) occupy the next branch of the evolutionary tree (Figure 7.4). These crow-sized birds had just six teeth, and at least one species, *Jeholornis prima*, consumed seeds and/or fruit (Zhou and Zhang, 2002a; O'Connor and Zhou, 2020). *Archaeopteryx* and *Jeholornis* retained a long bony tail like their theropod ancestors. Both had frond-like branching tail feathers, though in *Jeholornis* these were restricted to the distal part of the tail and a proximal fan of feathers was also present (O'Connor, 2020). Unlike *Archaeopteryx*, *Jeholornis* had a fused mandibular symphysis and partially fused carpometacarpus. The recently described short-tailed *Fukuipteryx prima* was proposed to represent an even more basal lineage than Jeholornithidae, which would require independent loss of the long bony tail in this species and more advanced birds (Imai et al., 2019). *Fukuipteryx* is known only from an incomplete skeleton representing an immature individual, so additional specimens are desirable before considering its phylogenetic placement resolved.

Confuciusornithidae, Jinguofortisidae, and *Sapeornis* occupy the next branches of the avian tree, though debate remains over their precise relationships. These groups differed from more basal birds in having a short bony tail ending in a pygostyle. Confuciusornithidae (five species) are the oldest birds that completely lacked teeth, though this loss occurred independently from the loss in crown birds (Chiappe et al., 1999). Confuciusornithids retained three long, clawed fingers like *Archaeopteryx* and Jeholornithidae, whereas in all other birds, the third digit is highly reduced. However, they were advanced in having a fully reversed hallux, which provided improved perching capabilities. The pigeon-sized species *Confuciusornis sanctus* is by far the best-represented Cretaceous bird, with thousands of specimens known. Because not one of these specimens preserves gut contents or gizzard stones, confuciusornithids likely consumed soft-bodied invertebrates (O'Connor and Zhou, 2020).

The recently named Jinguofortisidae unites two crow-sized species: *Jinguofortis perplexus* and *Chongmingia zhengi*. Jinguofortisidae show an unusual mix of features such as the fusion of the scapula and coracoid (also observed in many theropods and in Confuciusornithidae) and a strongly bowed minor metacarpal (resembling that of many crown birds but also Jeholornithidae). The low aspect ratio and low wing loading of *Jinguofortis* suggest this taxon had high maneuverability and occupied dense forest habitats (Wang et al., 2018). *Jinguofortis* at least had close-packed teeth in both the upper and lower jaws, and presence of gizzard stones in both *Jinguofortis* and *Chongmingia* suggests a plant-based diet for these birds (Wang et al., 2016, 2018).

Although a number of species have been assigned to *Sapeornis*, all are best considered junior synonyms of *Sapeornis chaoyangensis*. With a wingspan of approximately 1 m, this species was among the largest Cretaceous birds. *Sapeornis* retained a small number of teeth and lacked an ossified sternum. The large wingspan, primitive feather barb arrangement, and lack of an ossified sternum in *Sapeornis* suggest a soaring ecology, which would have allowed it to travel long distances via passive gliding (Zhou and Zhang, 2002b; Feo et al., 2015). Like *Jeholornis*, *Sapeornis* consumed seeds and/or fruits as at least part of its diet (O'Connor, 2019).

7.3.2 Enantiornithes: the opposite birds

While the abovementioned families were successful, the true diversification of birds is marked by the radiation of the Ornithothoraces, a clade that unites the extinct Enantiornithes and the Ornithuromorpha, which includes modern birds and their extinct relatives. Enantiornithes are known from nearly 100 named species (though some poorly defined species may prove invalid). They attained a global distribution and were the dominant birds of the Cretaceous, both in terms of abundance and ecological diversification. Enantiornithes are often referred to as "opposite birds" because their shoulder joint was formed by a convex ball on the coracoid inserting into a concave socket on the scapula, whereas the reverse is true in modern birds (Chiappe and Walker, 2002). With the exception of the toothless *Gobipteryx*, enantiornithines retained teeth. Most species were songbird sized and had more advanced flight capabilities than earlier birds based on their enlarged

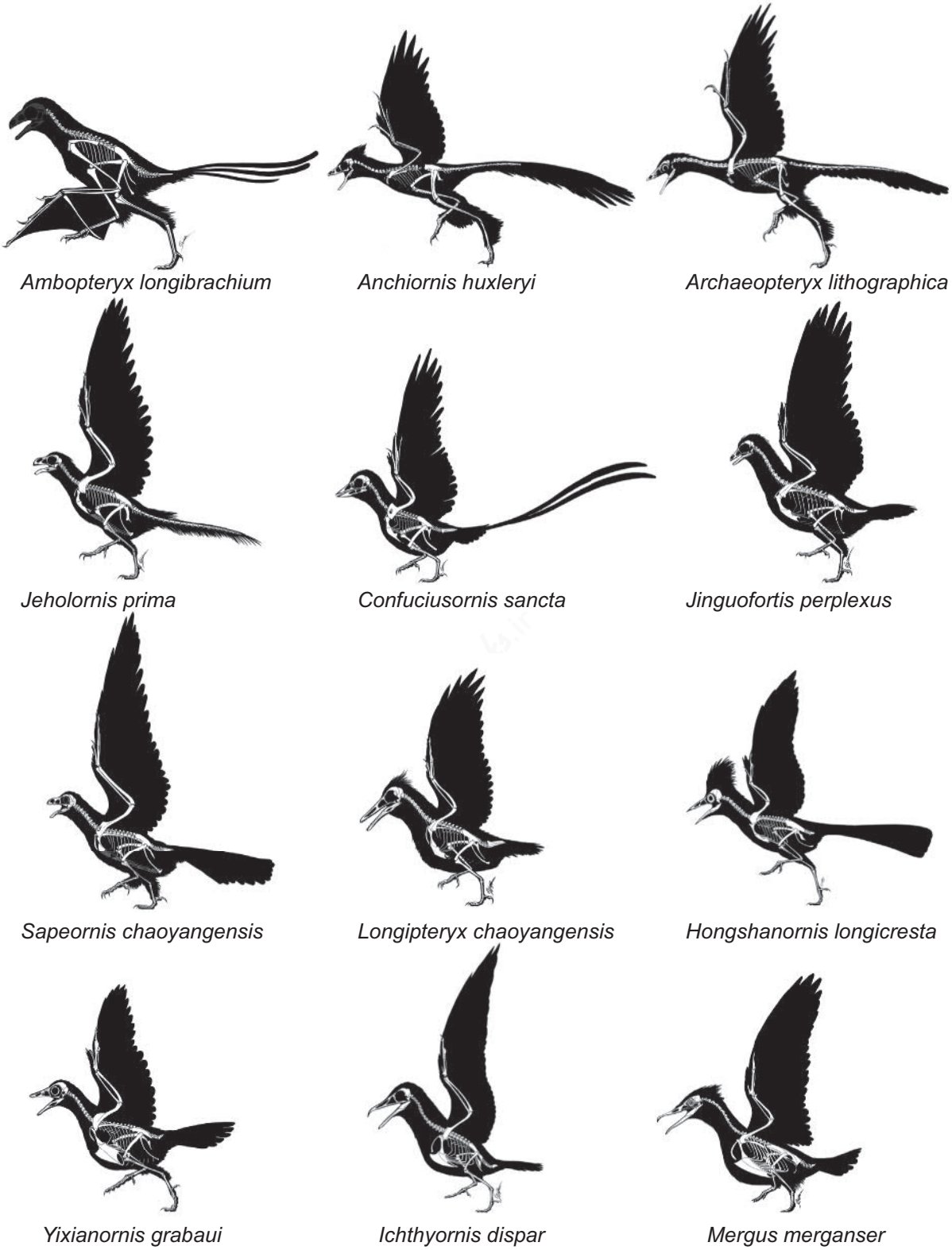

FIGURE 7.3 Reconstructions of the bat-winged scansoriopterygid *Ambopteryx longibrachium* and key avian taxa. *Credit: Artwork by Jaime Headden.*

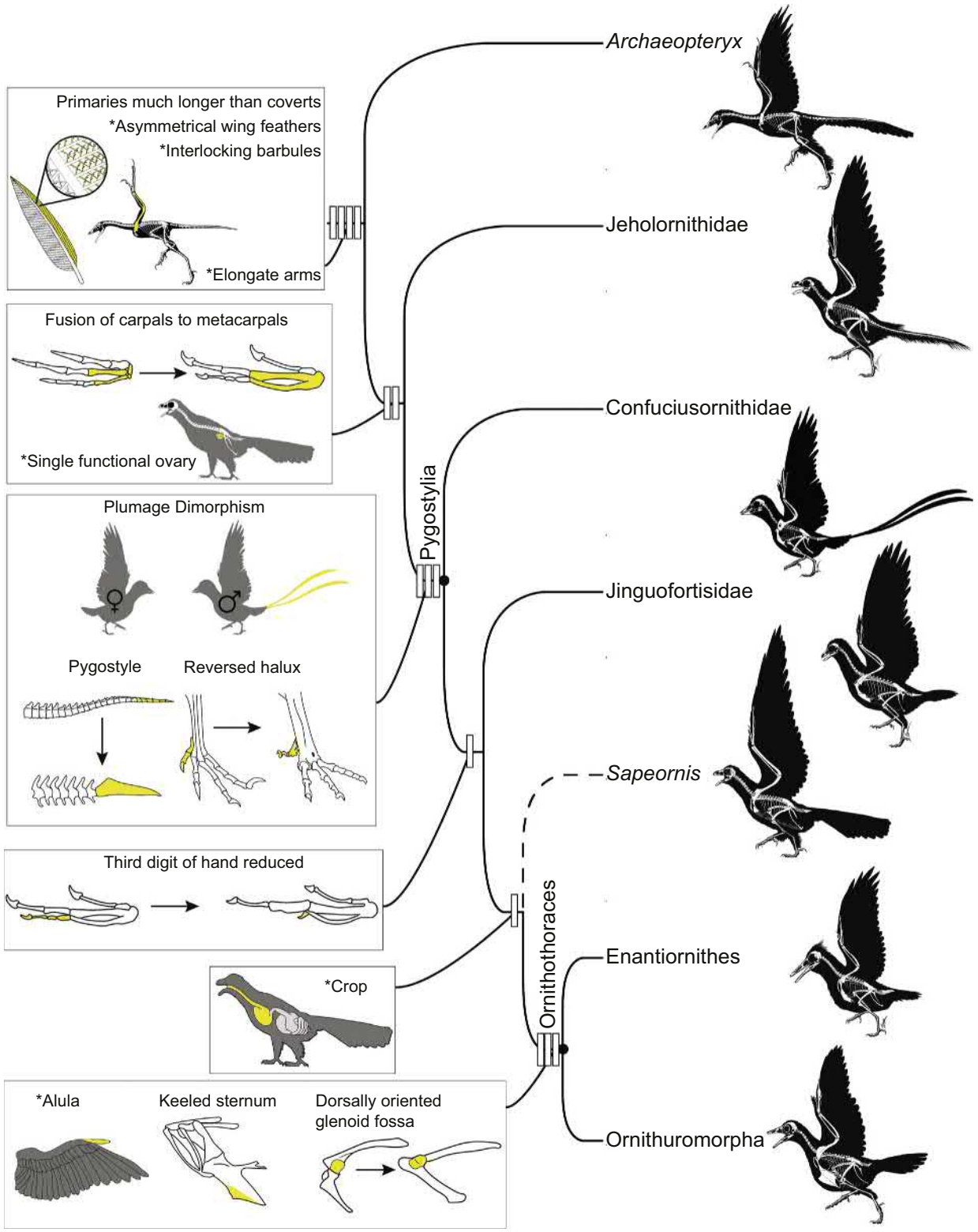

FIGURE 7.4 Phylogenetic tree depicting the relationships of early birds. *Dashed lines* indicate uncertainty. Key synapomorphies discussed in this chapter are indicated. Skeletal silhouettes, top to bottom: *Archaeopteryx lithographica*, *Jeholornis prima*, *Confuciusornis sanctus*, *Jinfengopteryx elegans*, *Sapeornis chaoyangensis*, *Longipteryx chaoyangensis*, and *Yixianornis grabaui*. *Credit: Silhouette artwork by Jaime Headden, character illustrations by Kate Dzikiewicz.*

sternum, wing bone proportions, and the presence of an alula (Chiappe and Walker, 2002). Together, these features suggest the capacity for sustained strong flapping and finer aerodynamic control. Enantiornithes were, for the most part, arboreal, as evidenced by a well-developed perching foot. Frustratingly, despite the wide array of tooth morphologies in Enantiornithes, fossilized gut contents are limited to single occurrence: fragments of a small crustacean in the rib cage of *Eoalulavis* (Sanz et al., 1996). The near-total lack of fossil gut contents in Enantiornithes suggests most species consumed prey with poor preservation potential, such as soft-bodied invertebrates (O'Connor, 2019).

The phylogeny of Enantiornithes is not yet fully resolved, but a few small clades are recognized. Pengornithidae (four species) represent one of the most basal enantiornithine families. They had many small teeth, stout legs, and a stubby pygostyle. The crow-sized *Pengornis houi* had blunt teeth suited for crushing soft arthropods (Zhou et al., 2008). The unique pygostyle of pengornithids helped anchor stiff, elongate tail feathers. *Parapengornis eurycaudatus* in particular may have used its tail feathers to prop itself against trees like a woodpecker (Hu et al., 2015).

Bohaiornithidae (six species) had robust beaks with an infratemporal bar, strong teeth, and stout feet with large claws on the middle toes. *Sulcavis geeorum* further had striations that presumably strengthened the enamel (O'Connor et al., 2013). These features suggest a tough diet, though the ecology of bohaiornithids remains the subject of debate. A raptorial ecology was proposed for the blunt-toothed *Bohaiornis guoi* (Figure 7.6B) in one study (Li et al., 2014), whereas others suggest bohaiornithids fed on hard-shelled invertebrates such as beetles and snails (O'Connor and Chiappe, 2011).

Longipterygidae (conservatively six species) were long-beaked enantiornithines. *Longirostravis* resembled a modern sandpiper except for the presence of a few small teeth near the tip of the beak, and may have had a similar probing ecology (O'Connor and Chiappe, 2011). *Longipteryx*, in contrast, bore several large blade teeth near the tip of its beak (Figure 7.6A). These powerful teeth would have been useless while probing, and instead appear to have been used to grasp slippery prey such as invertebrates and small fish (Chiappe and Qingjin, 2016).

The Late Cretaceous Avisauridae (conservatively six species) are an enigmatic group, with many species known only from a single bone. Whereas most enantiornithines were of modest size, a few avisaurid species reached the size range of turkeys (Atterholt et al., 2018). At least some avisaurids independently evolved features associated with advanced flight, such as a deep sternal keel and strong ulnar feather papillae, which are otherwise only seen in Ornithuromorpha (Atterholt et al., 2018) (Figure 7.4).

7.3.3 Cretaceous Ornithuromorpha: forerunners of modern birds

Ornithuromorpha include all modern birds along with their early relatives (Figure 7.5). Cretaceous ornithuromorphs show little evidence of arboreality: most species are inferred to have occupied ground-foraging or marine niches. Ornithuromorpha were a relatively minor part of the Cretaceous avifauna compared to the Enantiornithes, but the few ornithuromorphs that survived the Cretaceous–Paleogene (K-Pg) mass extinction gave rise to the >10,000 species of birds that live today. Space precludes a detailed survey of Cretaceous ornithuromorphs, but a few key taxa are mentioned briefly.

Archaeorhynchus spathula is the most primitive known ornithuromorph. The keeled sternum, short hind limb, and reduced hallux together suggest that, while *Archaeorhynchus* was a capable flier, it was unable to perch effectively and likely had a ground-feeding ecology. The toothless beak and spatulate lower jaw, along with the presence of gastroliths, suggest this species may have been herbivorous (Zhou et al., 2013) (Figure 7.6E). Hongshanornithidae (five species) represent another early branch of the ornithuromorph tree. These slender-beaked, plover-sized birds had elongate legs and toes that suggest a wading ecology (O'Connor et al., 2010). Though not the most basal member of Ornithuromorpha, the hongshanornithid *Archaeornithura meemannae* is the geologically oldest known representative of the clade at ~130 million years in age. Songlingornithidae (five species) are another shore-dwelling ornithuromorph clade. *Yanornis martini*, one of the best-known species, was a gull-sized bird with a moderately elongated beak, sharp teeth, and partially webbed feet. Many specimens of *Yanornis* preserve fish bones within the rib cage, providing direct evidence that this species was one of the earliest fish-eating birds (Zhou et al., 2002).

Gansus yumenensis and *Apsaravis ukhaana* each occupies branches of their own with no immediate relatives, intermediate between Songlingornithidae and more crownward birds. *Gansus* was the size of a small diving duck and likely had a similar foot-propelled diving ecology based on the prominent cnemial crest of the tibiotarsus and webbed toes (You et al., 2006). In contrast, the dove-sized *Apsaravis* provides an example of a presumably terrestrial Cretaceous ornithuromorph based on the discovery of the type specimen in a dune environment (Norell and Clarke, 2001).

Ichthyornis dispar merits special mention as the best-known volant species that occurs near the transition point between stem and crown birds (Clarke, 2004). This tern-sized bird had a skeleton that closely resembled modern birds with the notable exception of toothed jaws and a theropod-like adductor muscle chamber (Field et al., 2018b).

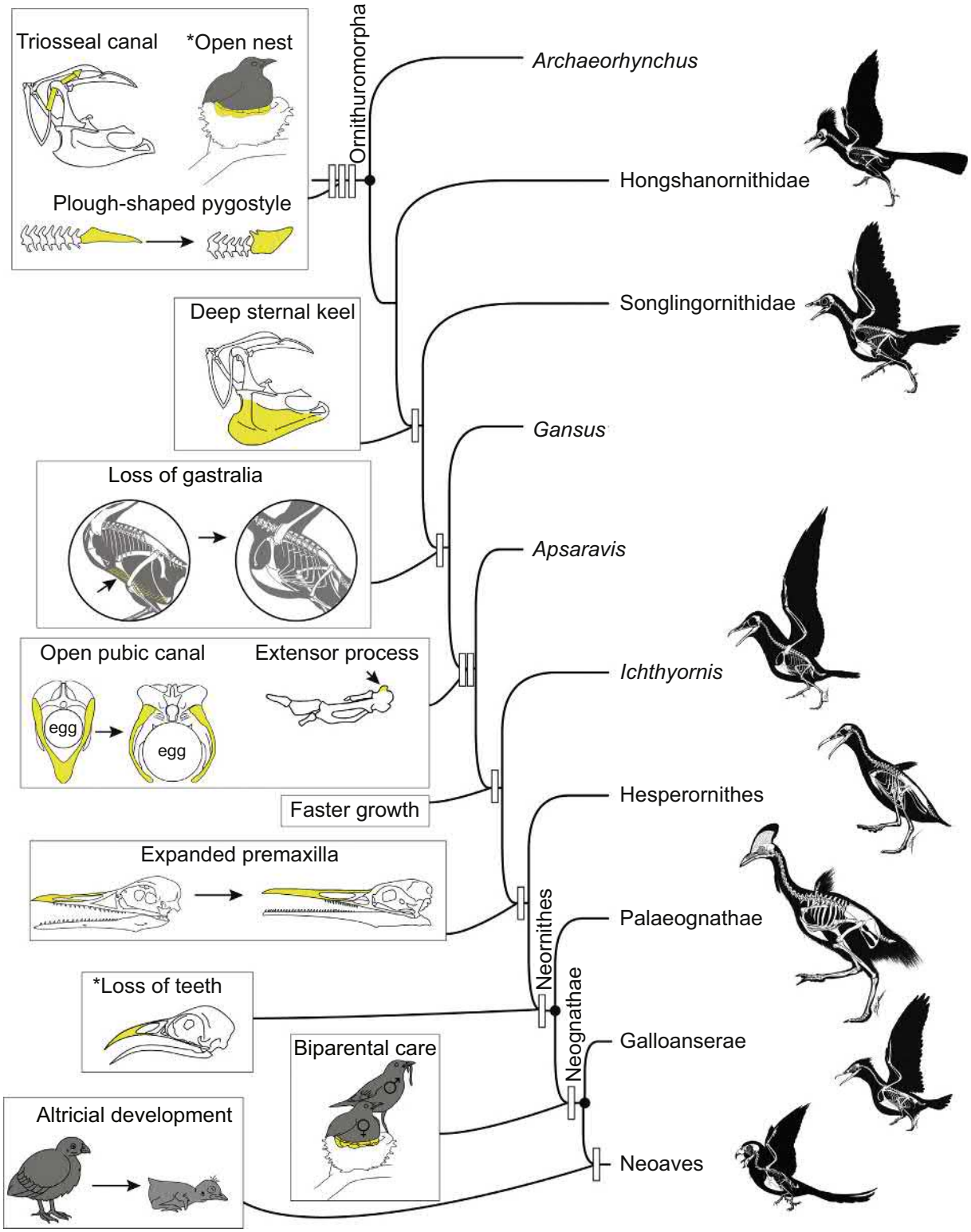

FIGURE 7.5 Phylogenetic tree depicting the relationships of ornithuromorph. Key synapomorphies discussed in this chapter are indicated. Skeletal silhouettes, top to bottom: *Hongshanornis longicresta*, *Yixianornis grabaui*, *Ichthyornis dispar*, *Hesperornis regalis*, *Casuarius casuarius*, *Mergus merganser*, and *Brotogeris chrysoptera*. *Credit: Silhouette artwork by Jaime Headden, character illustrations by Kate Dzikiewicz.*

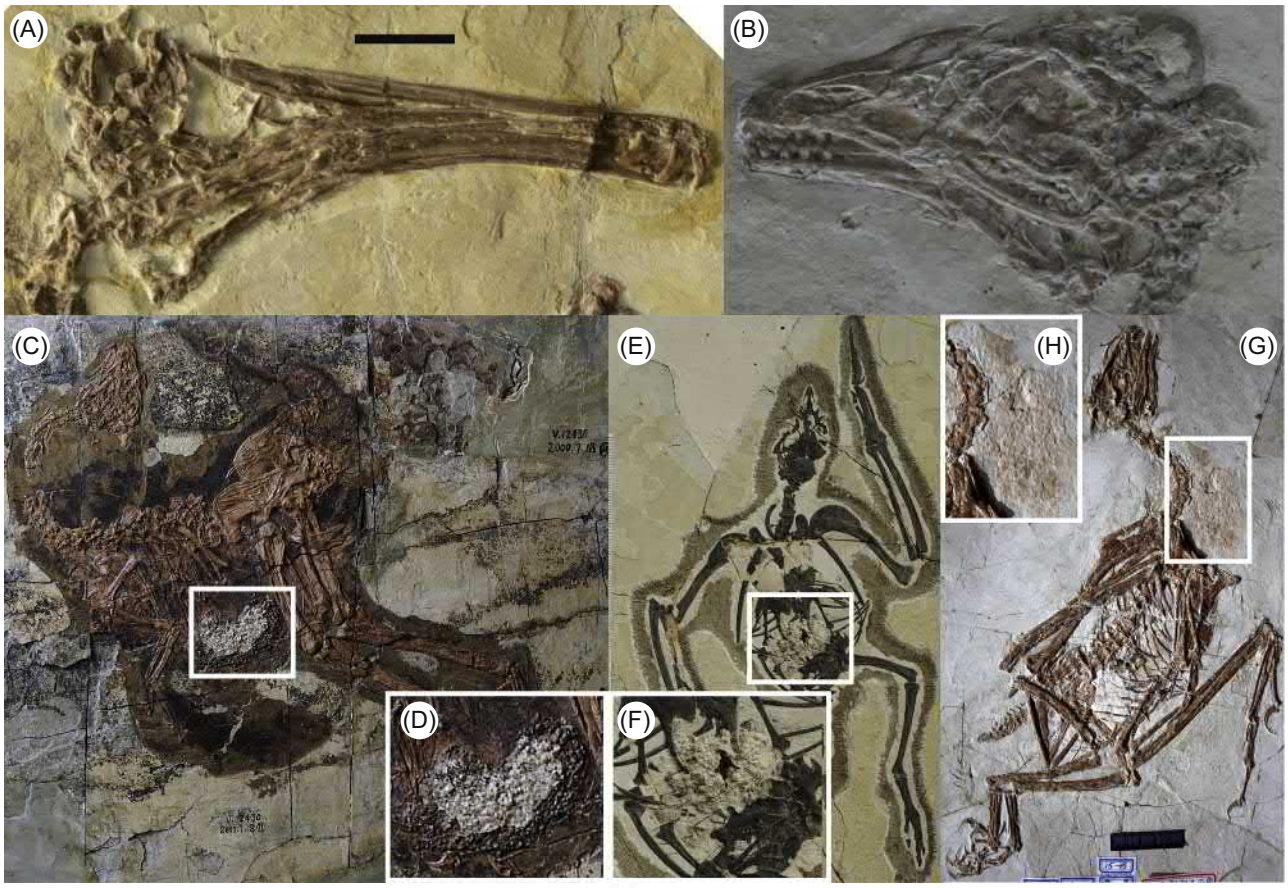

FIGURE 7.6 Fossil evidence for the evolution avian feeding and digestion. (A) Skull of the long-beaked enantiornithine *Longipteryx chaoyangensis* (DNHM D2889). (B) Skull of the blunt-toothed enantiornithine *Bohaiornis guoi* (IVPP V 17963). (C) Specimen of the oviraptorid *Caudipteryx* sp. (IVPP V12430) preserving gizzard stones, expanded in inset (D). (E) Specimen of the basal ornithuromorph *Archaeorhynchus spathula* (IVPP V17075) preserving gizzard stones, expanded in inset (F). (G) Specimen of *Sapeornis chaoyangensis* with fossil crop, expanded in inset (H). *Credit: Photos courtesy Dr. Jingmai O'Connor.*

Skeletal morphology, along with its shallow marine fossil environment, suggests *Ichthyornis* likely had a gull-like ecology, reinforcing the hypothesis that modern birds arose from shore-dwelling ancestors (Feduccia, 1995). Finally, the most fully aquatic Cretaceous birds were the diverse foot-propelled diving Hesperornithes, which occurred in freshwater and marine environments throughout the Northern Hemisphere in the Late Cretaceous, even extending north of the Arctic Circle (Wilson et al., 2016). Derived members of this clade reached large sizes (body lengths >1 m) and had wings reduced to only a small, splint-like humerus. Like modern grebes, hesperornithines had a massively expanded patella, mediolaterally compressed tarsometatarsus, and lobed toes. Despite these similarities, morphometric analyses suggest a diving ecology more similar to cormorants (Bell et al., 2019).

7.4 Assembling the modern bird

7.4.1 Freeing the tail for flight

With the Mesozoic aviary introduced, we can now trace the evolution of avian anatomy. Rather than moving from beak to tail, this section will proceed roughly from the root to the tip of the avian evolutionary tree. Although the evolution of the wing has historically commanded more attention, the pelvis, legs, and tail also underwent an earlier major transformation during the theropod–bird transition. Early theropods anchored the primary retractor muscle of the limb (caudofemoralis) to the base of their long muscular tails (Gatesy, 1990). Tail length accounts for roughly half of overall body length in early theropods, and thus appears to have played a major role in balance (Gatesy and Dial, 1996). Derived theropods evolved shorter and less robust tails, but a bony tail was still present in the earliest birds. In more advanced birds, the tail is reduced to a few vertebrae ending in a fused pygostyle, and plays little role in terrestrial locomotion. The caudofemoralis muscle is reduced or lost, with the function of retracting the hind limb taken over by the "hamstring" muscles, which anchor to the pelvis. This transition was accompanied by a shift from femoral retraction to knee flexion as the primary movement of the hind limb, which results in the nearly horizontal orientation of the femur in birds (Gatesy, 1990).

The decoupling of the tail and hind limb can be considered a major preadaptation for advanced flight. This freed the tail to take on the new role of aiding aerial

maneuvering, via the development of a fan-like spread of rectrices controlled by the musculature of the rectricial bulb system (Gatesy and Dial, 1996). In most Cretaceous birds, the pygostyle was rod-like and lacked a central dividing lamina, which, together with preserved feather evidence, suggests these taxa lacked a precisely controlled tail fan (Clarke et al., 2006; Wang and O' Connor, 2017). In contrast, ornithuromorphs exhibit a more ploughshare-shaped pygostyle, indicating the presence of left and right rectricial bulbs (Clarke et al., 2006). These would have anchored aerodynamic rectrices, imparting an important flight advantage to ornithuromorphs over their enantiornithine contemporaries.

7.4.2 Perfecting the wing

As detailed above, incipient feathered "wings" evolved in theropods prior to the advent of flight. Paravians, at least some of which had gliding flight, show some skeletal adaptations that are necessary for a true wing, including lengthening of the forelimb and reorientation of the glenoid fossa (articulation for the head of the humerus) to a more lateral position. This lateral orientation permitted a fuller range of forelimb elevation in Paraves, a capability that was further enhanced by the more dorsal glenoid orientation in Ornithothoraces (Jenkins, 1993; Senter, 2006). Interestingly, the sternum remained cartilaginous in *Archaeopteryx* and *Sapeornis*, despite being ossified in many theropods. All other birds (even flightless species) have an ossified sternum. A weakly developed midline ridge is present in some *Confuciusornis* specimens. Most enantiornithines possessed a true (albeit low) keel that was restricted to the caudal part of the sternum, and in these taxa, the pectoralis musculature may have attached in part to the furcula (Olson and Feduccia, 1979). In ornithuromorphs the keel extends to the cranial margin of the sternum and becomes progressively deeper, culminating in the powerfully developed keel of crown birds (Mayr, 2017a). Theropods and early birds had numerous gastralia ("belly ribs") caudal to their sternum, which are lost in advanced ornithuromorphs, possibly as a weight-reducing adaptation. The coracoid is plate-like in theropods but becomes progressively more elongated and strut-like in advanced birds. This culminates in the formation of the triosseal canal, an opening at the juncture of the furcula, coracoid, and scapula that serves as a pulley allowing the supracoracoideus muscle to lift the wing. The triosseal canal was once thought to be present in all Ornithothoraces, but recent fossil discoveries suggest enantiornithines lacked a true triosseal canal (Mayr, 2017a).

The distal wing elements were among the last features of the wing to evolve their modern form. The carpals and proximal ends of the second and third metacarpals remain free in theropods and *Archaeopteryx*. These became fused into an incipient carpometacarpus in Pygostylia, with further fusion of the metacarpals to one another within Ornithuromorpha. In *Apsaravis* and more advanced birds, the first metacarpal has a strongly projected extensor process for insertion of the ligaments that help automate the extension of the distal wing during the flight stroke (Norell and Clarke, 2001). Finally, the distal claws become modified into flattened phalanges in crown birds (a small alular claw remains in some species).

7.4.3 Neuroanatomy

Endocasts (natural or virtual casts of the inside of the braincase) provide a window into the sensory capabilities and cognition of extinct taxa. Theropod endocasts have revealed that the enlargement of the forebrain that characterizes modern birds first began in theropods (Larsson et al., 2000; Balanoff et al., 2013). Our understanding of early avian brain evolution is greatly hindered by the fact that almost all known Mesozoic bird skulls are preserved flattened on slabs. Thus, study of the early bird brains relies heavily on endocasts from *Archaeopteryx* and *Cerebavis*, a 93-million-year-old ornithuromorph bird. The holotype of *Cerebavis* was first described as a natural endocast (Kurochkin et al., 2007). Later recognized to be a skull, it was CT scanned to reveal the true endocast (Walsh et al., 2016). *Archaeopteryx* retained a theropod-like degree of forebrain expansion, whereas *Cerebavis* shows greater inflation, placing the latter within the range of modern birds (Balanoff et al., 2013; Walsh et al., 2016). It remains controversial whether early birds possessed a "Wulst," a mesopallial, and hyperpallial outgrowth of the forebrain associated with information processing and motor control (Balanoff et al., 2013; Beyrand et al., 2019). The primitive neuroanatomy of *Archaeopteryx* suggests that it either lacked a "flight-ready" brain or that, more plausibly, some theropods already had the neuroanatomical architecture necessary for flight (Balanoff et al., 2013).

Large relative brain sizes arose in crown birds. Early diverging crown birds such as Palaeognathae, Galloanserae, and basal Neoaves share the same ancestral brain–body size scaling pattern as advanced theropods, but within Neoaves, many shifts in the brain–body scaling relationship occurred rapidly after the K-Pg mass extinction (Ksepka, 2020). Relative brain sizes in some crows and parrots can rival those of primates, and it is interesting to note that the largest brained birds evolved only in the latter part of the Cenozoic.

7.4.4 Respiration and vocalization

The avian respiratory system consists of paired static lungs that serve as gas exchange surfaces and a system of connected air sacs that ventilate the lungs in a bellows-like fashion. This system allows unidirectional airflow, with oxygenated air passing over the gas exchange surfaces of

the lungs during both inhalation and exhalation. Unidirectional airflow was long thought to be associated with flight in birds, but recent work has shown it also occurs in crocodilians and lizards (Farmer and Sanders, 2010; Schachner et al., 2014). Air sacs, which are absent in living reptiles, have long been hypothesized to have been present in dinosaurs based on pneumatic fossae and foramina on the vertebrae. These features suggest dinosaurs possessed a dorsally immobile lung, which was divided into gas-exchanging and ventilating regions (Brocklehurst et al., 2020). Theropods likely had flexible air sacs, and at least some advanced taxa potentially had a fully decoupled lung and air sac system similar to modern birds (Brocklehurst et al., 2020). When this system evolved remains uncertain, as no theropod fossil preserves the lung structure. Remarkably, one specimen of the basal ornithuromorph bird *Archaeorhynchus* does preserve fossilized lung tissue. The intact tissue suggests the lungs were directly attached to the wall of the body cavity, indicating the respiratory system of early birds was similar to that of modern birds (Wang et al., 2018).

Modern bird vocalizations range from the simple grunts of emus to the intricate melodious songs of passerines. Whereas most tetrapods produce sound using the larynx, birds instead vocalize using a unique organ, the syrinx, which is located closer to the lungs. The syrinx is rarely preserved in fossil birds, and only two specimens have been reported to date (Clarke et al., 2016). Because both belong to crown birds, they shed little light on the timing of syrinx evolution. Cartilaginous (ossified in a few species) tracheal and bronchial rings support the passageways that connect the syrinx to the mouth and lungs in most birds. In contrast to the syrinx, these structures are relatively common in articulated fossil birds. Thus, the absence of preserved rings likely indicates the lack of a syrinx, and hence lack of song capabilities, in dinosaurs (Clarke et al., 2016).

Given the poor preservation potential of the syrinx, determining when and why this structure evolved remains a difficult question. One hypothesis holds that the elongation of the neck in birds, made possible by their derived respiratory system, created a situation in which a source of sound generation located closer to the lungs was more efficient (Riede et al., 2019). This would favor a transition from the larynx to the syrinx as the primary sound-generating organ, which begs the question of whether there was a stage in avian evolution during which both organs overlapped in function, or less plausibly a "quiet" phylogenetic interval during which dinosaurs lacked a functional larynx but had not yet evolved a syrinx (Kingsley et al., 2018).

While the timing of the origin of song remains a mystery, one innovation that appears restricted to crown birds is vocal learning. Most birds have an innate ability to perform their characteristic vocalizations, and will produce the same calls and songs even if raised in isolation (Kroodsma, 1984). Hummingbirds, parrots, oscine passerines (and perhaps a few suboscines), in contrast, are vocal learners: young birds learn specific vocalizations by listening to adults of their species (Nottebohm, 1972; Kroodsma, 2015). Vocal learning opens the door to mimicry. This is taken to the extreme in parrots, which can learn and utilize human words—obviously a most recent development (Pepperberg, 2009).

7.4.5 Teeth and beaks

Bird skulls resemble paedomorphic theropod skulls, with large orbits and short snouts that are likely ancestral juvenile traits carried into adulthood (Bhullar et al., 2012). Over the course of avian evolution, the skull became more consolidated. Theropod and early bird skulls retained visible sutures, whereas in crown birds, most of the cranial sutures are obliterated by adulthood. The avian beak is perhaps the most recognizable morphological hallmark of birds aside from feathers. Yet, the first birds lacked a true beak. Early birds retained premaxillary, maxillary, and dentary teeth. Reduction of the dentition occurred repeatedly, with independent losses of teeth in Confuciusornithidae, the enantiornithine *Gobipteryx*, several ornithuromorph lineages, and in crown birds.

The modern avian beak evolved within Ornithuromorpha, a process that began prior to the complete loss of teeth. In ornithuromorphs, loss of the premaxillary teeth preceded loss of maxillary and dentary teeth. Many ornithuromorphs possessed a small predentary ossification, interpreted as a biomechanically induced sesamoid, which articulated with the rostral tip of the mandible (Bailleul et al., 2019). The loss of premaxillary teeth and the evolution of this predentary ossification together played a crucial role in the origin of the modern avian beak, as the toothless, keratin-covered tips of the premaxilla and predentary together formed a pincher-like structure for fine manipulation (Field et al., 2018b). Theropods retained an upper temporal fenestra to accommodate the jaw adductor muscles, which are greatly reduced in modern birds. Somewhat surprisingly, this fenestra appears to have been retained in the near-crown bird *Ichthyornis*, demonstrating that the evolution of a transitional beak preceded reduction of the temporal musculature in the lineage leading to modern birds (Field et al., 2018b).

7.4.6 Digestive system

Lacking teeth, modern birds rely almost entirely on their digestive tract to process food. Most modern birds possess a crop for storing food, and all have a two-part stomach comprising a proventriculus and ventriculus (gizzard). Food swallowed directly or passed on from the crop enters

the proventriculus, where digestion is initiated via stomach acids and enzymes. The partially digested food then passes into the muscular gizzard where it is physically processed, often with the help of gastroliths (gizzard stones).

A two-chambered stomach with a gastric mill was present in theropods, as evidenced by gastroliths documented in Ornithomimosauria, Oviraptorosauria, and Scansoriopterygidae (Ji et al., 1998; Wang et al., 2019) (Figure 7.6C and D). Gastroliths have also been observed in some early bird lineages including Jeholornithidae and *Sapeornis*. They are conspicuously absent in Confuciusornithidae and Enantiornithes, suggesting these groups lacked a thick-walled gizzard capable of providing a gastric mill (O'Connor and Zhou, 2020). In modern birds, the gizzard varies in development from a thick-walled chamber capable of pulverizing tough food material to a thinly lined pouch incapable of accommodating gastroliths. The available evidence suggests a gizzard was ancestrally present in birds but that its development varied widely throughout avian evolution.

The crop is a more recent innovation. *Sapeornis* is the most primitive bird preserving a crop (Zheng et al., 2011) (Figure 7.6G and H), though the association of large numbers of undigested seeds preserved in some *Jeholornis* specimens suggests a crop could have been present in that taxon as well (Zhou and Zhang, 2002a). This timing suggests the crop may have evolved to increase food storage capacity beyond the limited stomach volume allowed by a rigid rib cage required for flight (O'Connor and Zhou, 2015).

Many modern birds can regurgitate difficult-to-digest material, such as bones and fur, in the form of pellets. Bone fragments in *Tyrannosaurus* coprolites suggest that theropods passed indigestible material completely through their digestive tract like modern crocodilians (Chin et al., 1998). The earliest evidence of antiperistalsis (the ability to regurgitate pellets) comes from intact, unexpelled pellets containing fish and lizard remains in *Anchiornis* (Zheng et al., 2018). Antiperistalsis may potentially have evolved earlier, given that pellets are unlikely to be preserved in the fossil record.

7.5 Reproduction and development

7.5.1 Sexual dimorphism

Birds provide some of the most striking examples of sexual dimorphism in the vertebrate world. Bony cranial ornamentation occurred in many theropods, but appears to have been present in both sexes. Bony ornaments occur in many modern birds, in which they may be identically developed in both sexes or more pronounced in males (Mayr, 2018). Convincing evidence for skeletal or size-based sexual dimorphism in dinosaurs is currently lacking (Mallon, 2017), though it remains possible dimorphism was manifested in a way not yet detected from the fossil record, such as dimorphic feather coloration or the presence of fleshy ornaments.

In modern birds, male-biased plumage dimorphism is common, whereas female-biased plumage dimorphism occurs only in a few groups (e.g., phalaropes). The earliest example of plumage dimorphism in birds occurs in the Confuciusornithidae, in which some individuals possess a pair of elongate ornamental rectrices (Figure 7.7A). The presence of putatuve ovarian follicles in one unornamented individual of *Eoconfuciusornis* suggests it was an adult female (Zheng et al., 2017). Thus, it seems likely that male-biased dimorphic plumage arose very early in the evolution of birds.

Males tend to be larger in bird species with size-based dimorphism, though some species show the opposite pattern (e.g., many falcons). The most remarkable example of size dimorphism occurs in the historically extinct moa *Dinornis*, in which females weighed almost three times as much as males (Bunce et al., 2003). Paternal brooding (see below) may have contributed to this wild size disparity, as males would have been restricted from attaining the same enormous sizes as females by the competing need to brood eggs without damaging them (Huynen et al., 2010).

7.5.2 Eggs

Major shifts in egg production and nesting occurred along the theropod—bird transition, spanning the full process from oogenesis to hatching. Dinosaurs, like most vertebrates, possessed two functional ovaries—a feature confirmed by the discovery of a pair of unlaid eggs within an oviraptorid dinosaur skeleton (Sato et al., 2005). Early dinosaurs laid large numbers of eggs per clutch, but derived theropods laid a single pair at a time, leading to clutches being completed via several discrete laying events. In modern birds, only the left ovary is typically functional. Reduction of the right ovary has been interpreted as an adaptation for reducing weight in egg-carrying females so as to maintain flight capacity (Taylor, 1970). Circular structures preserved in clusters near the life position of the left ovary in one specimen of *Jeholornis* and several enantiornithines have been identified as fossilized ovarian follicles, suggesting that the right ovary first became nonfunctional in early birds (Zheng et al., 2013) (Figure 7.7D and E). The nearly identical diameters of the follicles suggest simultaneous maturation, which is unexpected, as early bird body size would suggest only one egg could be stored in the body at a time (Zheng et al., 2013). However, the identity of these structures remains controversial and others have argued they instead represent plant propagules (Mayr et al., 2020).

Maniraptoran theropod eggs were elongate and small relative to body size compared to modern bird eggs. Rather than serving a specific function, the elongate shape may be

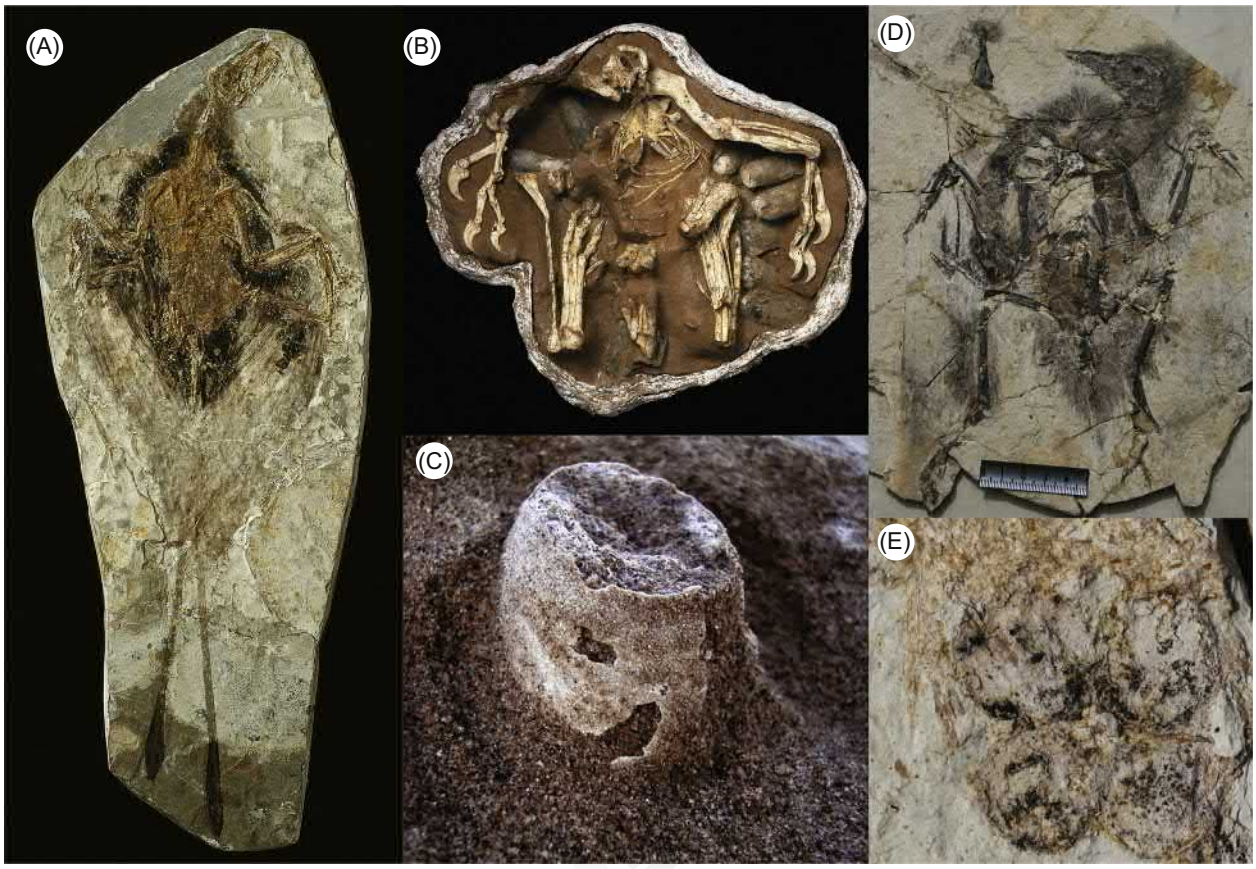

FIGURE 7.7 Fossil evidence for the evolution avian reproduction. (A) Sexually dimorphic tail plumage in a male specimen of *Confuciusornis sanctus* (GMV-2150). (B) Nesting oviraptorid *Citipati osmolskae* with eggs (IGM 100/979). (C) Partially buried enantiornithine egg (see Fernández et al., 2013). (D) Enantiornithine bird with putative ovarian follicles (STM29-8). (E) Close-up of putative ovarian follicles from another enantiornithine bird (STM10-45). *Credit: Photos in (A) and (B) by Mick Ellison, American Museum of Natural History, photo (C) courtesy Dr. Mariela S. Fernández, photos (D) and (E) courtesy of Dr. Jingmai O'Connor.*

a product of the ova being constricted in the oviduct as they expanded prior to shelling while absorbing the water required for development (Deeming and Ruta, 2014). At present, no eggs are known from the earliest birds. Enantiornithine eggs, however, are relatively well known, and were intermediate between theropods and modern birds in both size and shape (Varricchio and Jackson, 2016). Early ornithuromorph eggs have not yet been identified in the fossil record. However, osteology hints that larger egg sizes evolved relatively late in ornithuromorph history. The distal ends of the left and right pubis contact one another in basal birds and enantiornithines, constraining maximum egg diameter. In *Apsaravis* and more crownward birds, the pubes are widely separated, allowing for the passage of a larger egg (Dyke and Kaiser, 2010).

Like bird eggshell, theropod eggshell was hard and calcitic. Crocodilians mobilize calcium for shelling eggs directly from structural bone, whereas birds deposit an ephemeral layer of medullary bone to provide a rapidly accessible reservoir of calcium. Medullary bone appears to have first arisen in dinosaurs (Schweitzer et al., 2005; Lee and Werning, 2008). However, tissue resembling medullary bone may be deposited in non-egg-laying individuals for a variety of reasons including pathologies. One recent study considered nearly all reports of medullary bone in dinosaurs to be unconfirmed, due to the absence of one or more morphological characteristics (O'Connor et al., 2018). While these disparities should indeed raise caution, it must also be considered that medullary bone in dinosaurs may not have formed in exactly the same way as in modern birds. In particular, the much smaller egg size to body size ratio of large dinosaurs suggests that a smaller proportion of overall skeletal calcium needed to be mobilized to shell a clutch, in which case medullary bone may have had a more restricted skeletal distribution or lined a smaller region of a given bone's medullary cavity.

An overall trend toward smaller clutches occurs over the theropod–bird transition. Troodontid and oviraptorid clutches comprised 22–30 eggs (Varricchio et al., 1997). Given that theropods appear to have laid only two eggs

per cycle, such large clutches require either a greatly extended laying period or communal nesting (Horner, 1987). Intact clutches have not yet been uncovered from early birds, but the presence of 20 putative ovarian follicles in *Jeholornis* would suggests a very large clutch size (Zheng et al., 2013). Enantiornithine clutch size appears to have varied widely, based on evidence from putative follicles (5–14 as minimum estimates from two specimens) and an estimate of 8 eggs in one partial nest (Zheng et al., 2013; Varricchio and Barta, 2014). Clutch size varies tremendously in living birds, ranging from a single egg in many species such as albatrosses to over 20 eggs in gray partridges.

One fascinating recent discovery is the recovery of color patterns in dinosaur eggs. Birds are the only living amniotes that lay colored eggs. Modern bird eggs come in a variety of colors and patterns, ranging from plain white, to speckled, to the brilliant glossy eggs of some tinamous. In contrast, crocodilians lay plain, unpatterned eggs. Mass spectroscopy studies have revealed the presence of the pigments protoporphyrin and biliverdin in oviraptorid, troodontid, and dromaeosaurid eggs. This indicates some theropods laid blue-green eggs, and some laid eggs with speckled or spotted patterns (Wiemann et al., 2017). Sauropod and ornithischian dinosaur eggs lack evidence of color, suggesting colored eggs first evolved within theropods (Wiemann et al., 2018).

7.5.3 Nesting

Many dinosaurs buried their eggs in closed nests and so could not have brooded or manipulated them directly, whereas all modern birds, except for megapodes and brood parasites, directly incubate their eggs. Brooding, partially open nesting, contact incubation, and egg manipulation appear to have evolved in sequence across the theropod–bird transition.

Parallel pairing of eggs in oviraptorid nests corresponds to discrete laying events accommodating one egg from each ovary. Any subsequent movement would disrupt pairing, so it is unlikely that theropods manipulated their eggs (Varricchio et al., 1997). Nonetheless, the spectacular discovery of a "nesting oviraptorid" preserved at the center of a ring of eggs provides evidence for brooding in pennaraptoran theropods (Norell et al., 1995). The posture of the adult, with its arms (feathered in life) wrapped around the eggs, shows it was shielding the clutch when it perished (Figure 7.7B). Troodontids also brooded their eggs, and had a more advanced nest structure, with the eggs tightly positioned so that an adult could have covered the entire clutch with its abdomen (Varricchio et al., 1999). Because the eggs remained partially buried, it remains controversial whether nesting oviraptors and troodontids practiced true contact incubation or were only guarding their eggs (Deeming, 2006). An intermediate possibility is that adults raised egg temperatures somewhat via proximity and insulation, even without extensive direct contact. Indeed, oxygen isotope data indicate oviraptorid eggs were maintained at a temperature of 35–40°C, which, if accurate, implies at least some form of incubation (Amiot et al., 2017).

Intact enantiornithine nests show that at least some species partially buried their eggs vertically in sediment (Fernandez et al., 2013) (Figure 7.7C). Whether enantiornithines contact-incubated their eggs remains debated. Adult bones associated with a fossil clutch have been interpreted as belonging to brooding parents (Varricchio and Barta, 2014). However, estimates of enantiornithine egg strength and body mass have been used to argue that many species laid eggs too weak to support the weight of a brooding adult (Deeming and Mayr, 2018). Caution should be taken here, as these safety factor estimates apply to isolated eggs, whereas partially buried eggs would have been reinforced around their circumference by the presence of substrate and therefore able to resist greater stress. Dense concentrations of eggshells preserved alongside bones of nestlings and adults from Romania suggest colonial nesting was practiced by at least some enantiornithines (Dyke et al., 2012).

No direct fossil evidence exists for the presence or absence of chalazae, the membranes that anchor the yolk within an egg. However, because theropods and early birds appear not to have manipulated their eggs, chalazae may have been absent. If so, the evolution of chalazae may have allowed more open nesting strategies by protecting the embryo during egg movement and rotation (Varricchio and Barta, 2014). The evolution of colored eggs coincides with the evolution of partially open nests, and so may in turn have been driven by new selective pressures such as camouflage from predators or brood parasites (Wiemann et al., 2017).

Modern birds have a dazzling array of nest types. The shift from partially open to fully open nests occurred somewhere along the ornithuromorph lineage and likely played a major role in the radiation of crown birds by allowing them to brood their eggs in a variety of environments (Mayr, 2017b). Indeed, the inordinate success of passerines, which comprise the majority of extant bird species, may be due as much to nesting flexibility as complex song (Olson, 2001).

7.5.4 Development and growth

Increased contact incubation likely improved the efficiency of embryonic development along the theropod-to-bird transition. Incubation times in dinosaurs have recently been estimated based on growth lines preserved within teeth of embryos (Erickson et al., 2017; Varricchio et al., 2018). These data suggest troodontid eggs had an incubation time

of ~74 days, representing an intermediate condition between the long incubation times predicted by a crocodilian model (107.3 days) and the short incubation times predicted by an avian model (44.4 days) based on egg size (Varricchio et al., 2018).

Hatchlings of modern birds range from superprecocial (well-developed chicks needing no parental care) to superaltricial (weakly developed chicks hatching with closed eyes, few or no feathers, and capable of little movement aside from begging for food). Theropod hatchlings were well developed, at least from a skeletal perspective. Evidence of brooding, discussed above, suggests theropods practiced parental care. Thus, theropod hatchlings would most likely fall within the precocial category. Remarkable fossils of enantiornithine embryos suggest that enantiornithines were likewise precocial or superprecocial, exhibiting well-ossified skeletons, erupted teeth, and feather sheets (Elzanowski, 1981; Zhou and Zhang, 2004). The presence of flight feathers, along with early midline ossification of the sternum, suggests that enantiornithines may have been able to fly soon after hatching (O'Connor and Zhou, 2015). It has been hypothesized that the shift from arboreal to predominately aquatic or terrestrial habits in ornithuromorph birds facilitated a shift from fully independent superprecocial hatchlings to precocial hatchlings requiring some parental care (Mayr, 2017b). However, whether enantiornithine chicks were superprecocial *sensu stricto* (i.e., fully independent of parents) cannot be established or refuted based on available evidence. It is quite possible that chicks with strongly developed locomotor capabilities nevertheless relied on parents for protection, imprinting, or provisioning. Indeed, chicks of many extant bird species pursue their parents begging for food even after attaining flight capacity.

Crown birds likely shared a common ancestor exhibiting precocial development, as nearly all members of the early branching Palaeognathae and Galloanserae have precocial chicks, with the exception of the superprecocial Megapodiidae. Megapode chicks emerge from buried nests unassisted and astoundingly can fly the day that they hatch. Many shifts toward the altricial end of the spectrum occur within Neoaves, culminating in superaltricial chicks in at least eight clades (Botelho et al., 2015). Shifts in the opposite direction appear to be rare, with perhaps the most compelling example being loons, whose chicks can dive after just 2 or 3 days, though they often prefer to ride on their parents' backs.

Surprisingly, recent work suggests that paternal care characterized most early birds. Although direct evidence is lacking for the relative roles of males and females in theropod brooding, large clutch volume, lack of medullary bone in sampled nesting adults, and phylogenetic reconstructions all support the inference that males brooded eggs (Varricchio et al., 2008). Because paternal care also predominates in extant Palaeognathae, it is likely this was the primitive condition for crown birds (Moore and Varricchio, 2016). Thus, the shift to a predominantly biparental mode of care, which confers the advantage of additional protection and provisioning for chicks, may be considered a major innovation in Neognathae.

Theropods took several years to reach adult body size, and began breeding well before reaching maximum size (Lee and Werning, 2008). Extant birds grow much more rapidly, and almost all species reach their adult size in a matter of weeks or months. Moreover, most modern birds do not breed until after completing growth, in some cases delaying breeding until several years after reaching maximum size. Early birds like *Archaeopteryx* and *Confuciusornis* retained a slower growth curve, and thus grew in a manner similar to small dinosaurs. They reached maturity after 2 or 3 years with annual pauses in growth recorded by lines of arrested growth (LAGs), demarcations that are visible in thin sections of long bones (Erickson et al., 2009). The transition to more rapid maturation occurred within ornithuromorphs. The bone microstructure of the basal-most ornithuromorph *Archaeorhynchus* indicates it grew slowly like its enantiornithine contemporaries (Wang and Zhou, 2017). In contrast, the late Cretaceous *Ichthyornis* and Hesperornithes show more richly vascularized bone tissue and lack LAGs, suggesting they grew more rapidly and reached adult size in a single year (Chinsamy et al., 1998).

7.6 The rise of modern birds

7.6.1 The shallow Cretaceous roots of crown birds

By the end of the Cretaceous, crown birds (Neornithes) had evolved. When the crown bird radiation began remains a subject of perpetual debate, due to a sparse fossil record of Late Cretaceous birds and conflict between recent molecular divergence dating analyses. Regardless of when they first appeared, early crown birds were "modern" in that they had given up teeth once and for all, evolved a deep sternal keel for the pectoral muscles and precisely controlled tail fan, and acquired a development system in which they hatched from large eggs and achieved adult size rapidly. Despite these advantageous features, crown birds made up a relatively small proportion of the latest Cretaceous avifauna (Longrich et al., 2011).

The fossil record suggests that all crown birds descend from a handful of extinction boundary-crossing lineages, perhaps as few as four. Only a few convincing Cretaceous records of crown birds are known, all from very close to the K-Pg boundary. The oldest of these is the "wonder chicken" *Asteriornis maastrichtensis*, known from a 66.7–66.8-million-year-old skull and partial skeleton that

preserve features found in the otherwise disparate Galliformes (landfowl) and Anseriformes (waterfowl) (Field et al., 2020). *Asteriornis* was a small bird, about the size of the modern gray partridge, with a short, rounded beak, and large nostrils. This species probably branched off the avian evolutionary tree shortly before Galliformes and Anseriformes split from one another (Field et al., 2020).

Vegavis iaai is a slightly younger (~66.5 Ma) crown bird. Originally described from a partial postcranial skeleton, *Vegavis* was considered to be closely related to magpie geese and ducks, and thus the oldest species of crown Anseriformes (Clarke et al., 2005). However, the discovery of more complete material, together with the application of different phylogenetic models, has led to alternative hypotheses that *Vegavis* may instead represent a stem member of Anseriformes, or perhaps fall just outside the crown bird radiation (O'Connor et al., 2011; Worthy et al., 2017; Field et al., 2020). *Vegavis* possessed a strongly bowed femur, well-developed cnemial crests, and greatly enlarged patella (notably absent in most waterfowl, with the exception of a few diving taxa such as *Thalassornis*), which strongly suggest a diving ecology.

The putative Cretaceous Antarctic loon *Polarornis gregorii* shares numerous hind limb features with *Vegavis*, suggesting they are close relatives. However, the long and pointed bill of *Polarornis* would be unexpected if both taxa were nested within Anseriformes. Frustratingly, *Polarornis* remains an enigma despite being known from one of the most complete Late Cretaceous bird fossils. The type specimen was illustrated in great detail in a series of line drawings, which depict many fine details such as the location of cranial nerve foramina (Chatterjee, 2002). Regrettably, the skull has been so heavily reconstructed that few if any of these features can actually be observed in the fossil, begging the question of whether they were even there in the first place. Inexplicably for such a critical fossil, several bones described in the original monograph can no longer be located (see Clarke et al., 2016), leaving *Polarornis* to be considered by many avian paleontologists more of a cautionary tale than a keystone fossil.

Under a conservative phylogenetic framework considering *Asteriornis* to be a stem galloanserine and *Vegavis* to be a stem anseriform, the fossil record provides evidence that four major crown bird lineages diverged by the end of the Cretaceous, and thus survived the mass extinction: Palaeognathae ("ratites" and tinamous), Anseriformes, Galliformes, and Neoaves (all other crown birds). Whether any major groups of Neoaves had already diverged prior to the mass extinction remains unresolved—molecular divergence dating analyses yield conflicting results, and in most cases, the confidence intervals for multiple early splits overlap the K-Pg boundary, indicating statistical uncertainty (Ksepka and Phillips, 2015). Nonetheless, when the biological plausibility of a rapid radiation immediately prior to a mass extinction is weighed against that of a rapid radiation immediately following a mass extinction, it is hard to justify the former (Berv and Field, 2018).

7.6.2 Survival and extinction

A major asteroid impact at the end of the Cretaceous caused global devastation and wiped out close to 75% of all species (Alvarez et al., 1980). Following the impact, global wildfires caused by molten debris reentering the atmosphere burned a large proportion of existing forests, while smaller dust and soot particles remained suspended in the atmosphere leading to the temporarily shutdown of the photosynthesis-based food chain (Robertson et al., 2004). A few key factors set birds aside from their theropod relatives, which perished during the mass extinction. Small size would have been advantageous in the immediate aftermath of the asteroid impact, imparting lower energy requirements that would have been helpful in a resource-poor environment. However, large birds and small theropods overlapped in size, so this factor cannot fully explain differential survival. It is likely that the advanced beak and digestive system of birds played an important role, potentially allowing birds to sustain themselves with food sources such as seeds that remained available despite the temporary collapse of photosynthesis-based food chains (Larson et al., 2016). Flight may also have allowed birds to travel to less devastated areas, or to have occupied remote and less affected areas in the first place.

Perhaps a more compelling question is not why birds survived at all, but why some birds survived and others did not. As far as can be determined, the K-Pg mass extinction completely wiped out all stem birds, most notably the enantiornithines, leaving only crown birds to inherit the new landscape. Habitat preference provides the most plausible explanation for the survival of modern birds. Enantiornithes dominated arboreal ecosystems in the Cretaceous (O'Connor et al., 2011). Widespread deforestation during the extinction event may have led to the demise of birds that relied on canopy for feeding (Mayr, 2017c; Field et al., 2018a). Cretaceous crown birds, which preferred aquatic or ground-dwelling habitats, appear to have been less susceptible to the decimation of global forests (Field et al., 2018a, b). Notably, early crown birds presumably possessed a gizzard, whereas no known enantiornithines preserve evidence of gastric milling capacity, suggesting they may not have been able to access nonperishable food resources like seeds (O'Connor, 2019). While crown birds undoubtedly also suffered greatly during the mass extinction, their ancestral ecology ensured that a few lineages were able to hang on.

7.6.3 An explosive Paleogene radiation

Although avian fossils remain poorly sampled from early Paleocene localities, emerging evidence supports not only an explosive phylogenetic diversification but also a rapid ecological diversification. The two oldest Paleocene neoavians are indeed about as different from another as can be imagined. *Tsidiiyazhi abini*, a ~62.5-million-year-old mousebird, was a tiny species with a semizygodactyl grasping foot representing the oldest crown bird adapted to an arboreal existence (Ksepka et al., 2017). In contrast, the ~61-million-year-old *Waimanu manneringi* was a large penguin that had already made the transition to a flightless aquatic lifestyle (Slack et al., 2006). Molecular divergence analyses support an even wider radiation than the fossil record hints at, implying almost every order of modern birds had split from their sister taxa by the Eocene (Jarvis et al., 2014; Prum et al., 2015).

The mass extinction appears to have opened an array of new niches for crown birds by removing existing competitors. The most important of these was the complete opening of forest ecosystems vacated by enantiornithines. Crown birds rapidly diversified into arboreal niches, with an amazing variety of specialized groups ranging from owls to frogmouths and from rollers to passerines well represented in early Eocene lake deposits. Two major marine reptile groups, the plesiosaurs and mosasaurs, perished in the extinction along with the previously widespread and successful diving bird clade Hesperornithes. It is tempting to posit a link between the loss of these secondarily aquatic tetrapod clades and the rapid appearance of penguins shortly after the mass extinction. Likewise, the fact that Late Cretaceous pterosaurs tended toward very large sizes suggests that the dominance of pterosaurs may have prevented Cretaceous birds from moving into large soaring niches. Giant marine soaring forms first arose in crown birds, including the extinct bony-toothed Pelagornithidae and modern albatrosses, though the earliest representatives of both clades had relatively modest wingspans compared with their later descendants.

The closest that crown birds came to converging on the body plans of their extinct theropod relatives was in the terrestrial realm. Numerous lineages including the extant "ratites," the extinct giant waterfowl families Gastornithidae and Dromornithidae, and the extinct "terror bird" group Phorusrhacidae, all attained large sizes and reverted to flightlessness (Worthy et al., 2017). Ecologically, these groups essentially reoccupied niches vacated by theropod groups, e.g., with true ostriches converging on the Ornithomimosauria and terror birds converging on Deinonychosauria, with hooked beaks instead of serrated teeth.

7.7 The shape of modern bird diversity

For nearly a century and a half, ornithologists struggled to reconstruct the evolutionary tree of modern birds. Over time, morphological and molecular data led to support for three major divisions that are now recognized: Palaeognathae, Galloanserae, and Neoaves. Today, the rapidly advancing capacity for genomic-level sequencing is actively improving our understanding of finer level relationships within these clades (Jarvis et al., 2014; Prum et al., 2015; Reddy et al., 2017). It is beyond the scope of this chapter to provide more than a cursory review of the interrelationships and evolution of the >10,000 species of crown birds. Below, the three major branches are introduced with brief comments on patterns of diversity.

7.7.1 Palaeognathae

The basal split among all living birds separates the Palaeognathae and Neognathae (Galloanserae + Neoaves). These two branches led to wildly different evolutionary histories: Palaeognathae represent less than 1% of extant avian species as opposed to Neognathae accounting for more than 99%. Yet, Palaeognathae includes some of the most unusual birds ever to have lived, such as the nocturnal ground-probing kiwi and the enormous wingless moa. The long-held theory that "ratites" (ostrich, rhea, emu, cassowary, and kiwi) formed a clade guided hypotheses about palaeognath biogeography and flight loss for much of the 20th century. Surprisingly, molecular data have converged on a topology that nests the volant tinamous well within Palaeognathae (Phillips et al., 2010). Combined with geographical distribution, this requires a remarkable six losses of flight to have occurred in palaeognaths, with all but one leading to subsequent shifts to gigantism (Sackton et al., 2019).

The extinct volant Lithornithidae occurred in North America and Europe during the Paleogene. Controversy remains over whether Lithornithidae represent stem palaeognaths, crown palaeognaths, or even late-surviving stem birds (Houde, 1988; Livezey and Zusi, 2006; Nesbitt and Clarke, 2016). Olfactory bulb impressions in the skulls of lithornithids indicate they had a powerful sense of smell, and thus may have probed shoreline environments for food with their long beaks (Houde, 1988; Zelenitsky et al., 2011).

Ostriches are familiar as the largest living birds, but they would have been dwarfed by two major lineages of flightless palaeognaths that were wiped out by humans in the last millennium. The New Zealand Dinornithiformes (moa) and the Madagascar Aepyornithiformes (elephant birds) each attained gigantic sizes, with the aepyornithid

Vorombe titan believed to be the largest bird ever to have lived at ~650 kg (Hansford and Turvey, 2018). Remarkably, both of these clades of enormous birds are closely related to much smaller birds, with moa paired with tinamous, and elephant birds paired with kiwi in molecular phylogenies (Phillips et al., 2010; Mitchell et al., 2014). It is particularly perplexing that despite once occurring side by side in New Zealand, kiwi and moa share no close relationship.

7.7.2 Galloanserae

Galloanserae include the Galliformes (landfowl) and Anseriformes (waterfowl), two groups with extremely divergent ecologies. Galliformes are primarily ground dwelling, and many species have weak capacity for sustained flight, being instead adapted to rapid bursts of escape flight. Anseriformes are primarily aquatic and many species are capable of remarkable long-distance flight, such as the bar-headed goose, which flies over the Himalayas during migration. *Asteriornis*, the oldest crown bird, provides some insight into the ancestral ecology of Galloanserae. Long, slender hind limb bones suggest it dwelled near the shoreline. The small size and littoral ecology of this species, if general to early galloanserines, may have been key features helping them survive the K-Pg mass extinction (Field et al., 2020).

Although a full treatment of Galloanserae would require several additional chapters, it is worth noting that many of the most remarkable extinct clades of birds belong to this clade. On the Anseriformes side of the tree, the giant flightless Dromornithidae of Australia and Gastornithidae of the Northern Hemisphere were among the largest birds ever to have lived. Dromornithidae survived well into the Pleistocene before they were driven to extinction by humans (Roberts et al., 2001). On the Galliformes side, Sylviornithidae represent another family of giant flightless birds. They survived even closer to modern times, likely being wiped out soon after humans arrived in New Caledonia and Fiji approximately 500 years ago (Hume and Walters, 2012). Most unusual were the Pelagornithidae, marine soaring birds, whose place (or even inclusion) within Galloanserae remains uncertain. These remarkable birds had serried ranks of "pseudoteeth" lining their beaks, which were formed by bone covered by keratin rather than dentine and enamel. Pelagornithid pseudoteeth resemble first-generation crocodilian teeth, which begin as outgrowths of the jaw bones in the earliest developmental stages (Mayr and Rubilar-Rogers, 2010). Thus, pelagornithid pseudoteeth may actually be developmentally homologous to true teeth (Louchart et al., 2018). The largest flying bird ever to have lived was the pelagornithid species *Pelagornis sandersi*, which reached wingspans of ~6.4 m and likely had an albatross-like ecology (Ksepka, 2014).

7.7.3 Neoaves

Neoaves, by far the most diverse of the three major branches of the crown bird tree, includes over 10,000 species. Resolving the relationships of major groups within Neoaves has proven to be one of the most challenging puzzles of avian systematics, but much progress has been made in recent years. Phylogenomic analyses consistently recover the clades (1) Mirandornithes (grebes and flamingos), (2) Columbimorphae (pigeons, sandgrouse, and mesites), and (3) Strisores (nightbirds, swifts, and hummingbirds), but offer conflicting signals over which of these clades occupy the first branch of the neoavian tree (Jarvis et al., 2014; Prum et al., 2015; Reddy et al., 2017). Another early branching clade that is consistently supported is the Otidimorphae (cuckoos, turacos, and bustards). Subsequent branches are occupied by a number of aquatic clades. Strong support exists for a clade uniting the "core waterbirds" (e.g., loons, petrels, penguins, cormorants, pelicans, storks, herons, and tropicbirds), but it remains uncertain whether the Charadriiformes (shorebirds) are also part of this radiation or instead are closely related to the Gruiformes (cranes and rails).

The vast majority of Neoaves belong to the clade Telluraves ("higher land birds"), which contains all birds of prey (hawks, falcons, owls, and seriemas), a diverse array of mostly arboreal coraciimorph birds (mousebirds, courols, rollers, kingfishers, trogons, woodpeckers, and kin), parrots, and the hyperdiverse passerines, which account for more than half of all living bird species. Relationships within Telluraves have become increasingly well resolved, revealing a few interesting patterns. One example is that all four predatory clades occupy branches near the root of Telluraves, which implies the common ancestor of landbirds may have been predatory (Jarvis et al., 2014). Another is that parrots and passerines are sister taxa, which together with fossil evidence suggests passerines were ancestrally zygodactyl (Mayr, 2008).

7.8 The impact of humans on birds

The fossil record provides an ever-improving picture of the evolutionary history of birds, but it is important to remember that avian evolution did not stop when we reached the present day. Indeed, the rise of humans has arguably affected avian evolution as profoundly as the K-Pg mass extinction. Humans have long benefited from sharing the planet with birds, starting with the hunting, followed by domestication of birds for food, and even present-day bird watching which generates billions of dollars in economic activity. Yet, this relationship has rarely been mutually beneficial. Island species were initially the hardest hit types of birds, with more than 500 species, many flightless or with reduced flight capabilities, wiped

out as humans spread throughout the Pacific and Indian Oceans (Hume and Walters, 2012). These included many of the largest birds ever to have lived, such as the elephant bird and moa, thus greatly reducing not only the species diversity but also the morphological and ecological diversity of our remaining avifauna. By measure of raw abundance, the impact of humans is even more profound: domestic chickens now account for three times the biomass of all wild bird species on the planet (Bar-On et al., 2018). To a much less extreme degree, some of the more common wild bird species have also undergone population booms due to human-mediated introduction to new regions and habitat modification. For example, the combined population of Eurasian Starlings, Rock Pigeons, and House Sparrows in the United States rivals that of humans. A paleontologist from 10 million years in the future would infer an extinction event for birds, noting the loss especially of so many larger species, though they might be hard pressed to explain the appearance of a galliform disaster fauna with chickens spreading ubiquitously across the Earth like ferns rapidly recolonizing a posteruption volcanic island. Whether this hypothetical paleontologist ranks the extinction as minor or major will ultimately depend on our own response to overpopulation and attendant deforestation and climate change.

Acknowledgments

The author thanks Jaime Headden for creating the skeletal silhouette artwork, Kate Dzikiewicz for creating the character illustration line art, Mick Ellison, Jingmai O'Connor, and Mariela Fernandez for providing photos, and Daniel Field, Jingmai O'Connor, Steve Brusatte, and Kristin Lamm for helpful feedback.

References

Alvarez, L.W., Alvarez, W., Asaro, F., Michel, H.V., 1980. Extraterrestrial cause for the Cretaceous-Tertiary extinction. Science 208, 1095–1108.

Amiot, R., Wang, X., Wang, S., Lécuyer, C., Mazin, J.M., Mo, J., Flandrois, J.P., Fourel, F., Wang, X., Xu, X., 2017. δ18O-derived incubation temperatures of oviraptorosaur eggs. Palaeontology 60, 633–647.

Atterholt, J., Hutchison, J.H., O'Connor, J.K., 2018. The most complete enantiornithine from North America and a phylogenetic analysis of the *Avisauridae*. PeerJ 6, e5910.

Balanoff, A.M., Bever, G.S., Rowe, T.B., Norell, M.A., 2013. Evolutionary origins of the avian brain. Nature 501, 93–96.

Bailleul, A.M., Li, Z., O'Connor, J., Zhou, Z., 2019. Origin of the avian predentary and evidence of a unique form of cranial kinesis in Cretaceous ornithuromorphs. Proc. Natl. Acad. Sci. U.S.A. 116, 24696–24706.

Bar-On, Y.M., Phillips, R., Milo, R., 2018. The biomass distribution on Earth. Proc. Natl. Acad. Sci. U.S.A. 115, 6505–6511.

Bell, A., Wu, Y.H., Chiappe, L.M., 2019. Morphometric comparison of the Hesperornithiformes and modern diving birds. Palaeogeogr. Palaeoclimatol. Palaeoecol. 513, 196–207.

Berv, J.S., Field, D.J., 2018. Genomic signature of an avian Lilliput effect across the K-Pg extinction. Syst. Biol. 67, 1–13.

Beyrand, V., Voeten, D.F., Bureš, S., Fernandez, V., Janáček, J., Jirák, D., Rauhut, O., Tafforeau, P., 2019. Multiphase progenetic development shaped the brain of flying archosaurs. Sci. Rep. 9, 1–15.

Bhullar, B.-A.S., Marugán-Lobón, J., Racimo, F., Bever, G.S., Rowe, T.B., Norell, M.A., Abzhanov, A., 2012. Birds have paedomorphic dinosaur skulls. Nature 487, 223–226.

Bock, W.J., 2013. The furcula and the evolution of avian flight. Paleontol. J. 47, 1236–1244.

Botelho, J.F., Smith-Paredes, D., Vargas, A.O., 2015. Altriciality and the evolution of toe orientation in birds. Evol. Biol. 42, 502–510.

Brocklehurst, R.J., Schachner, E.R., Codd, J.R., Sellers, W.I., 2020. Respiratory evolution in archosaurs. Phil. Trans. Biol. Sci. 375, 20190140.

Brusatte, S.L., Lloyd, G.T., Wang, S.C., Norell, M.,A., 2014. Gradual assembly of avian body plan culminated in rapid rates of evolution across the dinosaur-bird transition. Curr. Biol. 24, 2386–2392.

Bunce, M., Worthy, T.H., Ford, T., Hoppitt, W., Willerslev, E., Drummond, A., Cooper, A., 2003. Extreme reversed sexual dimorphism in the extinct New Zealand moa Dinornis. Nature 425, 172–175.

Chatterjee, S., 1991. Cranial anatomy and relationships of a new Triassic bird from Texas. Phil. Trans. Biol. Sci. 332, 277–342.

Chatterjee, S., 2002. The morphology and systematics of *Polarornis*, a *Cretaceous loon* (Aves: Gaviidae) from Antarctica. In: Proceedings of the 5th Symposium of the Society of Avian Paleontology and Evolution, Beijing, pp. 125–155.

Chen, P.J., Dong, Z.M., Zhen, S.N., 1998. An exceptionally well-preserved theropod dinosaur from the Yixian Formation of China. Nature 391, 147–152.

Chiappe, L.M., Qingjin, M., 2016. Birds of Stone: Chinese Avian Fossils from the Age of Dinosaurs. Johns Hopkins University Press.

Chiappe, L.M., Ji, S.-A., Ji, Q., Norell, M.A., 1999. Anatomy and systematics of the *Confuciusornithidae* (Theropoda, Aves) from the late Mesozoic of Northeastern China. Bull. Am. Mus. Nat. Hist. 242, 1–89.

Chiappe, L.M., Walker, C.A., 2002. Skeletal morphology and systematics of the Cretaceous Euenantiornithes (Ornithothoraces: Enantiornithes). In: Chiappe, L.M., Witmer, L.M. (Eds.), Mesozoic Birds: Above the Heads of Dinosaurs. University of California Press, Berkeley, pp. 240–267.

Chin, K., Tokaryk, T.T., Erickson, G.M., Calk, L.C., 1998. A king-sized theropod coprolite. Nature 393, 680–682.

Chinsamy, A., Martin, L.D., Dodson, P., 1998. Bone microstructure of the diving *Hesperornis* and the volant *Ichthyornis* from the Niobrara Chalk of western Kansas. Cretac. Res. 19, 225–235.

Clarke, J.A., 2004. Morphology, phylogenetic taxonomy, and systematics of *Ichthyornis* and *Apatornis* (Avialae: ornithurae). Bull. Am. Mus. Nat. Hist. 2004, 1–179.

Clarke, J.A., Chatterjee, S., Li, Z., Riede, T., Agnolin, F., Goller, F., Isasi, M.P., Martinioni, D.R., Mussel, F.J., Novas, F.E., 2016. Fossil evidence of the avian vocal organ from the Mesozoic. Nature 538, 502–505.

Clarke, J.A., Tambussi, C.P., Noriego, J.I., Erickson, G.M., Ketcham, R.A., 2005. Definitive fossil evidence for the extant avian radiation in the Cretaceous. Nature 433, 305–308.

Clarke, J.A., Zhou, Z., Zhang, F., 2006. Insight into the evolution of avian flight from a new clade of early Cretaceous ornithurines from China and the morphology of *Yixianornis grabaui*. J. Anat. 208, 287–308.

Currie, P.J., Chen, P.-J., 2001. Anatomy of *Sinosauropteryx prima* from Liaoning, northeastern China. Can. J. Earth Sci. 38, 1705–1727.

Deeming, D.C., 2006. Ultrastructural and functional morphology of eggshells supports the idea that dinosaur eggs were incubated buried in substrate. Palaeontology 49, 171–185.

Deeming, C.D., Mayr, G., 2018. Pelvis morphology suggests that early Mesozoic birds were too heavy to contact incubate their eggs. J. Evol. Biol. 31, 701–709.

Deeming, D.C., Ruta, M., 2014. Egg shape changes at the theropod–bird transition, and a morphometric study of amniote eggs. Royal Soc. Open Sci. 1, 140311.

Dyke, G.J., De Kat, R., Palmer, C., Van Der Kindere, J., Naish, D., Ganapathisubramani, B., 2013. Aerodynamic performance of the feathered dinosaur *Microraptor* and the evolution of feathered flight. Nat. Commun. 4, 2489.

Dyke, G.J., Kaiser, G.W., 2010. Cracking a developmental constraint: egg size and bird evolution. Record Aust. Mus. 62, 207–216.

Dyke, G.J., Vremir, M., Kaiser, G., Naish, D., 2012. A drowned Mesozoic bird breeding colony from the late Cretaceous of Transylvania. Naturwissenschaften 99, 435–442.

Elzanowski, A., 1981. Embryonic bird skeletons from the late Cretaceous of Mongolia. Palaeontol. Pol. 42, 147–176.

Elzanowski, 2001. A new genus and species for the largest specimen of *Archaeopteryx*. Acta Palaeontol. Pol. 46, 519–532.

Elzanowski, A., 2002. Archaeopterygidae (upper Jurassic of Germany). In: Chiappe, L.M., Witmer, L.M. (Eds.), Mesozoic Birds: Above the Heads of Dinosaurs. University of California Press, Berkeley, pp. 129–159.

Erickson, G.M., Rauhut, O.W., Zhou, Z., Turner, A.H., Inouye, B.D., Hu, D., Norell, M.A., 2009. Was dinosaurian physiology inherited by birds? Reconciling slow growth in *Archaeopteryx*. PLoS One 4, e7390.

Erickson, G.M., Zelenitsky, D.K., Kay, D.I., Norell, M.A., 2017. Dinosaur incubation periods directly determined from growth-line counts in embryonic teeth show reptilian-grade development. Proc. Natl. Acad. Sci. U.S.A. 114, 540–545.

Farmer, C., Sanders, K., 2010. Unidirectional airflow in the lungs of alligators. Science 327, 338–340.

Feduccia, A., 1995. Explosive evolution in Tertiary birds and mammals. Science 267, 637–638.

Feduccia, A., Tordoff, H.B., 1979. Feathers of *Archaeopteryx*: asymmetric vanes indicate aerodynamic function. Science 203, 1021–1022.

Feo, T.J., Field, D.J., Prum, R.O., 2015. Barb geometry of asymmetrical feathers reveals a transitional morphology in the evolution of avian flight. Proc. Biol. Sci. 282, 20142864.

Fernández, M.S., García, R.A., Fiorelli, L., Scolaro, A., Salvador, R.B., Cotaro, C.N., Kaiser, G.W., Dyke, G.J., 2013. A large accumulation of avian eggs from the Late Cretaceous of Patagonia (Argentina) reveals a novel nesting strategy in Mesozoic birds. PLoS One 8, e61030.

Field, D.J., Benito, J., Chen, A., Jagt, J.W., Ksepka, D.T., 2020. Late Cretaceous neornithine from Europe illuminates the origins of crown birds. Nature 579, 397–401.

Field, D.J., Bercovici, A., Berv, J.S., Dunn, R., Fastovsky, D.E., Lyson, T.R., Vajda, V., Gauthier, J.A., 2018a. Early evolution of modern birds structured by global forest collapse at the end-Cretaceous mass extinction. Curr. Biol. 28, 1825–1831.

Field, D.J., Hanson, M., Burnham, D., Wilson, L.E., Super, K., Ehret, D., Ebersole, J.A., Bhullar, B.-A.S., 2018b. Complete *Ichthyornis* skull illuminates mosaic assembly of the avian head. Nature 557, 96–100.

Foth, C., Tischlinger, H., Rauhut, O.W.M., 2014. New specimen of *Archaeopteryx* provides insights into the evolution of pennaceous feathers. Nature 511, 79–82.

Gatesy, S.M., 1990. Caudofemoral musculature and the evolution of theropod locomotion. Paleobiology 16, 170–186.

Gatesy, S.M., Dial, K.P., 1996. Locomotor modules and the evolution of avian flight. Evolution 50, 331–340.

Gauthier, J., 1986. Saurischian monophyly and the origin of birds. Memoir. Calif. Acad. Sci. 8, 1–55.

Godefroit, P., Cau, A., Dong-Yu, H., Escuillié, F., Wenhao, W., Dyke, G., 2013. A Jurassic avialan dinosaur from China resolves the early phylogenetic history of birds. Nature 498, 359–362.

Hansford, J.P., Turvey, S.T., 2018. Unexpected diversity within the extinct elephant birds (Aves: Aepyornithidae) and a new identity for the world's largest bird. Royal Soc. Open Sci. 5, 181295.

Hopp, T.P., Orsen, M.J., 2004. Dinosaur brooding behavior and the origin of flight feathers. In: Currie, P.J., Koppelhus, E.B., Shugar, M.A., Wright, J.L. (Eds.), Feathered Dragons: Studies on the Transition from Dinosaurs to Birds. Indiana University Press, Bloomington, pp. 234–254.

Horner, J.R., 1987. Ecologic and behavioral implications derived from a dinosaur nesting site. In: Czerkas, S.J., Olson, E.C. (Eds.), Dinosaurs Past and Present, vol. 2. Natural History Museum of Los Angeles County, Los Angeles, pp. 50–63.

Houde, P.W., 1988. Paleognathous Birds from the Early Tertiary of the Northern Hemisphere. Nuttall Ornithological Club, Cambridge.

Hu, D., Clarke, J.A., Eliason, C.M., Qiu, R., Li, Q., Shawkey, M.D., Zhao, C., D'alba, L., Jiang, J., Xu, X., 2018. A bony-crested Jurassic dinosaur with evidence of iridescent plumage highlights complexity in early paravian evolution. Nat. Commun. 9, 217.

Hu, H., O'Connor, J.K., Zhou, Z., 2015. A new species of Pengornithidae (Aves: Enantiornithes) from the Lower Cretaceous of China suggests a specialized scansorial habitat previously unknown in early birds. PLoS One 10, e0126791.

Hume, J.P., Walters, M., 2012. Extinct Birds. T. & A. D. Poyser, London.

Huynen, L., Gill, B.J., Millar, C.D., Lambert, D.M., 2010. Ancient DNA reveals extreme egg morphology and nesting behavior in New Zealand's extinct moa. Proc. Natl. Acad. Sci. U.S.A. 107, 16201–16206.

Imai, T., Azuma, Y., Kawabe, S., Shibata, M., Miyata, K., Wang, M., Zhou, Z., 2019. An unusual bird (Theropoda, Avialae) from the Early Cretaceous of Japan suggests complex evolutionary history of basal birds. Commun. Biol. 2, 1–11.

Jarvis, E.D., et al., 2014. Whole-genome analyses resolve early branches in the tree of life of modern birds. Science 346, 1320–1331.

Jenkins, F.A., 1993. The evolution of the avian shoulder joint. Am. J. Sci. 293, 253.

Ji, Q., Currie, P.J., Norell, M.A., Shu-An, J., 1998. Two feathered dinosaurs from northeastern China. Nature 393, 753–761.

Ji, Q., Norell, M.A., Gao, K.Q., Ji, S.A., Ren, D., 2001. The distribution of integumentary structures in a feathered dinosaur. Nature 410, 1084–1088.

Kingsley, E.P., Eliason, C.M., Riede, T., Li, Z., Hiscock, T.W., Farnsworth, M., Thomson, S.L., Goller, F., Tabin, C.J., Clarke, J.A., 2018. Identity and novelty in the avian syrinx. Proc. Natl. Acad. Sci. U.S.A. 115, 10209–10217.

Koschowitz, M.C., Fischer, C., Sander, M., 2014. Beyond the rainbow. Science 346, 416–418.

Kroodsma, D.E., 2015. The Singing Life of Birds: The Art and Science of Listening to Birdsong. Houghton Mifflin Harcourt, New York.

Kroodsma, D.E., 1984. Songs of the Alder Flycatcher (*Empidonax alnorum*) and Willow Flycatcher (*Empidonax traillii*) are innate. Auk 101, 13–24.

Ksepka, D.T., 2014. Flight performance of the largest volant bird. Proc. Natl. Acad. Sci. U.S.A. 111, 10624–10629.

Ksepka, D.T., et al., 2020. Tempo and pattern of avian brain size evolution. Curr. Biol. 30, 2026–2036.

Ksepka, D.T., Phillips, M.J., 2015. Avian diversification patterns across the K-Pg boundary: influence of calibrations, datasets, and model Misspecification. Ann. Mo. Bot. Gard. 100, 300–328.

Ksepka, D.T., Stidham, T.A., Williamson, T.E., 2017. Early Paleocene landbird supports rapid phylogenetic and morphological diversification of crown birds after the K-Pg mass extinction. Proc. Natl. Acad. Sci. U.S.A. 114, 8047–8052.

Kurochkin, E.N., Dyke, G.J., Saveliev, S.V., Pervushov, E.M., Popov, E.V., 2007. A fossil brain from the Cretaceous of European Russia and avian sensory evolution. Biol. Lett. 3, 309–313.

Larson, D.W., Brown, C.M., Evans, D.C., 2016. Dental disparity and ecological stability in bird-like dinosaurs prior to the end-Cretaceous mass extinction. Curr. Biol. 26, 1325–1333.

Larsson, H.C.E., Sereno, P.C., Wilson, J.A., 2000. Forebrain enlargement among theropod dinosaurs. J. Vertebr. Paleontol. 20, 615–618.

Lee, A.H., Werning, S., 2008. Sexual maturity in growing dinosaurs does not fit reptilian growth models. Proc. Natl. Acad. Sci. U.S.A. 105, 582–587.

Lefèvre, U., Cau, A., Cincotta, A., Hu, D., Chinsamy, A., Escuillié, F., Godefroit, P., 2017. A new Jurassic theropod from China documents a transitional step in the macrostructure of feathers. Sci. Nat. 104, 74.

Li, Q., Gao, K.Q., Meng, Q., Clarke, J.A., Shawkey, M.D., D'Alba, L., Pei, R., Ellison, M., Norell, M.A., Vinther, J., 2012. Reconstruction of *Microraptor* and the evolution of iridescent plumage. Science 335, 1215–1219.

Li, Z., Zhou, Z., Wang, M., Clarke, J.A., 2014. A new specimen of large-bodied basal enantiornithine *Bohaiornis* from the early Cretaceous of China and the inference of feeding ecology in Mesozoic birds. J. Paleontol. 88, 99–108.

Livezey, B.C., Zusi, R.L., 2006. Higher-order phylogenetics of modern birds (Theropoda, Aves: Neornithes) based on comparative anatomy. I. Methods and characters. Bull. Carnegie Mus. Nat. Hist. 37, 1–544.

Longrich, N.R., 2006. Structure and function of hindlimb feathers in *Archaeopteryx lithographica*. Paleobiology 32, 417–431.

Longrich, N.R., Tokaryk, T., Field, D.J., 2011. Mass extinction of birds at the Cretaceous–Paleogene (K–Pg) boundary. Proc. Natl. Acad. Sci. U.S.A. 108, 15253–15257.

Longrich, N.R., Vinther, J., Meng, Q., Li, Q., Russell, A.P., 2012. Primitive wing feather arrangement in *Archaeopteryx lithographica* and *Anchiornis huxleyi*. Curr. Biol. 22, 2262–2267.

Louchart, A., De Buffrénil, V., Bourdon, E., Dumont, M., Viriot, L., Sire, J.-Y., 2018. Bony pseudoteeth of extinct pelagic birds (Aves, Odontopterygiformes) formed through a response of bone cells to tooth-specific epithelial signals under unique conditions. Sci. Rep. 8, 12952.

Lü, J., Brusatte, S.L., 2015. A large, short-armed, winged dromaeosaurid (Dinosauria: Theropoda) from the early Cretaceous of China and its implications for feather evolution. Sci. Rep. 5, 11775.

Mallon, J.C., 2017. Recognizing sexual dimorphism in the fossil record: lessons from nonavian dinosaurs. Paleobiology 43, 495–507.

Mayr, G., 2008. Phylogenetic affinities of the enigmatic avian taxon *Zygodactylus* based on new material from the early Oligocene of France. J. Syst. Palaeontol. 6, 333–334.

Mayr, G., 2017a. Pectoral girdle morphology of Mesozoic birds and the evolution of the avian supracoracoideus muscle. J. Ornithol. 158, 859–867.

Mayr, G., 2017b. Evolution of avian breeding strategies and its relation to the habitat preferences of Mesozoic birds. Evol. Ecol. 31, 131–141.

Mayr, G., 2017c. Avian Evolution: The Fossil Record of Birds and its Paleobiological Significance. John Wiley & Sons.

Mayr, G., 2018. A survey of casques, frontal humps, and other extravagant bony cranial protuberances in birds. Zoomorphology 137, 457–472.

Mayr, G., Kaye, T.G., Pittman, M., Saitta, E.T., Pott, C., 2020. Reanalysis of putative ovarian follicles suggests that Early Cretaceous birds were feeding not breeding. Scientific Reports 10, 19035.

Mayr, G., Pohl, B., Peters, D.S., 2005. A feathered specimen of *Archaeopteryx* with theropod features. Science 310, 1483–1486.

Mayr, G., Rubilar-Rogers, D., 2010. Osteology of a new giant bony-toothed bird from the Miocene of Chile, with a revision of the taxonomy of Neogene Pelagornithidae. J. Vertebr. Paleontol. 30, 1313–1330.

McGowan, C., 1989. Feather structure in flightless birds and its bearing on the question of the origin of feathers. J. Zool. 218, 537–547.

Mitchell, K.J., Llamas, B., Soubrier, J., Rawlence, N.J., Worthy, T.H., Wood, J., Lee, M.S.Y., Cooper, A., 2014. Ancient DNA reveals elephant birds and kiwi are sister taxa and clarifies ratite bird evolution. Science 344, 898–900.

Moore, J.R., Varricchio, D.J., 2016. The evolution of diapsid reproductive strategy with inferences about extinct taxa. PLoS One 11.

Nesbitt, S.J., Clarke, J.A., 2016. The anatomy and taxonomy of the exquisitely preserved Green River formation (early Eocene) Lithornithids (Aves) and the relationships of Lithornithidae. Bull. Am. Mus. Nat. Hist. 406, 1–91.

Norell, M.A., Clarke, J.A., 2001. Fossil that fills a critical gap in avian evolution. Nature 409, 181–184.

Norell, M.A., Clarke, J.M., Chiappe, L.M., Dashzeveg, D.A., 1995. A nesting dinosaur. Nature 378, 774–776.

Norell, M.A., Xu, X., 2005. Feathered dinosaurs. Annu. Rev. Earth Planet Sci. 33, 277–299.

Nottebohm, F., 1972. The origins of vocal learning. Am. Nat. 106, 116–140.

O'Connor, J.K., 2019. The trophic habits of early birds. Palaeogeogr. Palaeoclimatol. Palaeoecol. 513, 178–195.

O'Connor, J.K., 2020. The plumage of basal birds. In: Foth, C., Rauhut, O.W.M. (Eds.), The Evolution of Feathers. Springer, Cham, pp. 147–172.

O'Connor, J.K., Chiappe, L.M., 2011. A revision of enantiornithine (Aves: Ornithothoraces) skull morphology. J. Syst. Palaeontol. 9, 135–157.

O'Connor, J.K., Chiappe, L.M., Bell, A., 2011. Pre-modern birds: avian divergences in the Mesozoic. In: Dyke, G., Kaiser, G. (Eds.), Living Dinosaurs: The Evolutionary History of Modern Birds. Wiley Blackwell, Chichester, pp. 39–114.

O'Connor, J.K., Erickson, G.M., Norell, M., Bailleul, A.M., Hu, H., Zhou, Z., 2018. Medullary bone in an Early Cretaceous enantiornithine bird and discussion regarding its identification in fossils. Nat. Commun. 9, 1–8.

O'Connor, J.K., Gao, K.Q., Chiappe, L.M., 2010. A new ornithuromorph (Aves: Ornithothoraces) bird from the Jehol Group indicative of higher-level diversity. J. Vertebr. Paleontol. 30, 311–321.

O'Connor, J.K., Sulivan, C., 2014. Reinterpretation of the Early Cretaceous maniraptoran (Dinosauria: Theropoda) *Zhongornis haoae* as a scansoriopterygid-like non-avian, and morphological resemblances between scansoriopterygids and basal oviraptorosaurs. Vertebr. Palasiat. 52, 3–30.

O'Connor, J.K., Zhang, Y., Chiappe, L.M., Meng, Q., Quanguo, L., Di, L., 2013. A new enantiornithine from the Yixian Formation with the first recognized avian enamel specialization. J. Vertebr. Paleontol. 33, 1–12.

O'Connor, J.K., Zhou, Z., 2015. Early evolution of the biological bird: perspectives from new fossil discoveries in China. J. Ornithol. 156, 333–342.

O'Connor, J.K., Zhou, Z., 2020. The evolution of the modern avian digestive system: insights from paravian fossils from the Yanliao and Jehol biotas. Palaeontology 63, 13–27.

Olson, S.L., 2001. Why so many kinds of passerine birds? Bioscience 51, 268–269.

Olson, S.L., Feduccia, A., 1979. Flight capability and the pectoral girdle of *Archaeopteryx*. Nature 278, 247–248.

Ostrom, J.H., 1975. The origin of birds. Annu. Rev. Earth Planet Sci. 3, 55–77.

Ostrom, J.H., 1976. *Archaeopteryx* and the origin of birds. Biol. J. Linn. Soc. 8, 91–182.

Pepperberg, I.M., 2009. The Alex Studies: Cognitive and Communicative Abilities of Grey Parrots. Harvard University Press, Cambridge.

Phillips, M.J., Gibb, G.C., Crimp, E.A., Penny, D., 2010. Tinamous and moa flock together: mitochondrial genome sequence analysis reveals independent losses of flight among ratites. Syst. Biol. 59, 90–107.

Prum, R.O., 2002. Why ornithologists should care about the theropod origin of birds. Auk 119, 1–17.

Prum, R.O., et al., 2015. A comprehensive phylogeny of birds (Aves) using targeted next-generation DNA sequencing. Nature 526, 569–573.

Qiang, J., Currie, P.J., Norell, M.A., Shu-An, J., 1998. Two feathered dinosaurs from northeastern China. Nature 393, 753–761.

Rauhut, O.W., Tischlinger, H., Foth, C., 2019. A non-archaeopterygid avialan theropod from the Late Jurassic of southern Germany. eLife 8, e43789.

Reddy, S., Kimball, R.T., Pandey, A., Hosner, P.A., Braun, M.J., Hackett, S.J., Han, K.-L., Harshman, J., Huddleston, C.J., Kingston, S., 2017. Why do phylogenomic data sets yield conflicting trees? Data type influences the avian tree of life more than taxon sampling. Syst. Biol. 66, 857–879.

Riede, T., Thomson, S.L., Titze, I.R., Goller, F., 2019. The evolution of the syrinx: an acoustic theory. PLoS Biol. 17, e2006507.

Roberts, R.G., Flannery, T.F., Ayliffe, L.K., Yoshida, H., Olley, J.M., Prideaux, G.J., Laslett, G.M., Baynes, A., Smith, M.A., Jones, R., 2001. New ages for the last Australian megafauna: continent-wide extinction about 46,000 years ago. Science 292, 1888–1892.

Robertson, D.S., McKenna, M.C., Toon, O.B., Hope, S., Lillegraven, J.A., 2004. Survival in the first hours of the Cenozoic. Geol. Soc. Am. Bull. 116, 760–768.

Sackton, T.B., Grayson, P., Cloutier, A., Hu, Z., Liu, J.S., Wheeler, N.E., Gardner, P.P., Clarke, J.A., Baker, A.J., Clamp, M., 2019. Convergent regulatory evolution and loss of flight in paleognathous birds. Science 364, 74–78.

Saitta, E.T., Gelernter, R., Vinther, J., 2018. Additional information on the primitive contour and wing feathering of paravian dinosaurs. Palaeontology 61, 273–288.

Sanz, J.L., Chiappe, L.M., Pérez-Moreno, B.P., Buscalioni, A.D., Moratalla, J.J., Ortega, F., Poyato-Ariza, F.J., 1996. An Early Cretaceous bird from Spain and its implications for the evolution of avian flight. Nature 382, 442–445.

Sato, T., Cheng, Y.-N., Wu, X.-C., Zelenitsky, D.K., Hsiao, Y.-F., 2005. A pair of shelled eggs inside a female dinosaur. Science 308, 375.

Schachner, E.R., Cieri, R.L., Butler, J.P., Farmer, C., 2014. Unidirectional pulmonary airflow patterns in the savannah monitor lizard. Nature 506, 367–370.

Schweitzer, M.H., Wittmeyer, J.L., Horner, J.R., 2005. Gender-specific reproductive tissue in ratites and *Tyrannosaurus rex*. Science 308, 1456–1460.

Senter, P., 2006. Scapular orientation in theropods and basal birds, and the origin of flapping flight. Acta Palaeontol. Pol. 51, 305–313.

Slack, K.E., Jones, C.M., Ando, T., Harrison, G.L., Fordyce, R.E., Arnason, U., Penny, D., 2006. Early penguin fossils, plus mitochondrial genomes, calibrate avian evolution. Mol. Biol. Evol. 23, 1144–1155.

Taylor, T.G., 1970. How an eggshell is made. Sci. Am. 222, 88–95.

Turner, A.H., Makovicky, P.J., Norell, M.A., 2012. A review of dromaeosaurid systematics and paravian phylogeny. Bull. Am. Mus. Nat. Hist. 371, 1–206.

Varricchio, D.J., Barta, D.E., 2014. Revisiting Sabath's "larger avian eggs" from the Gobi Cretaceous. Acta Palaeontol. Pol. 60, 11–25.

Varricchio, D.J., Jackson, F.D., 2016. Reproduction in Mesozoic birds and evolution of the modern avian reproductive mode. Auk 133, 654–684.

Varricchio, D.J., Jackson, F., Borkowski, J.J., Horner, J.R., 1997. Nest and egg clutches of the dinosaur *Troodon formosus* and the evolution of avian reproductive traits. Nature 385, 247–250.

Varricchio, D.J., Jackson, F., Trueman, C.N., 1999. A nesting trace with eggs for the Cretaceous theropod dinosaur *Troodon formosus*. J. Vertebr. Paleontol. 19, 91–100.

Varricchio, D.J., Kundrát, M., Hogan, J., 2018. An intermediate incubation period and primitive brooding in a theropod dinosaur. Sci. Rep. 8, 1–6.

Varricchio, D.J., Moore, J.R., Erickson, G.M., Norell, M.A., Jackson, F.D., Borkowski, J.J., 2008. Avian paternal care had dinosaur origin. Science 5909, 1826–1828.

Vinther, J., Briggs, D.E.G., Prum, R.O., Saranathan, V., 2008. The colour of fossil feathers. Biol. Lett. 4, 522–525.

Vinther, J., Nicholls, R., Lautenschlager, S., Pittman, M., Kaye, T.G., Rayfield, E., Mayr, G., Cuthill, I.C., 2016. 3D camouflage in an ornithischian dinosaur. Curr. Biol. 26, 2456–2462.

Voeten, D.F.A.E., Cubo, J., De Margerie, E., Röper, M., Beyrand, V., Bureš, S., Tafforeau, P., Sanchez, S., 2018. Wing bone geometry reveals active flight in *Archaeopteryx*. Nat. Commun. 9, 923.

Walsh, S.A., Milner, A.C., Bourdon, E., 2016. A reappraisal of *Cerebavis cenomanica* (Aves, ornithurae), from Melovatka, Russia. J. Anat. 229, 215–227.

Wang, W., O'Connor, J.K., 2017. Morphological coevolution of the pygostyle and tail feathers in early Cretaceous birds. Vertebr. Palasiat. 55, 289–314.

Wang, M., O'Connor, J.K., Xu, X., Zhou, Z., 2019. A new Jurassic scansoriopterygid and the loss of membranous wings in theropod dinosaurs. Nature 569, 256–259.

Wang, M., Stidham, T.A., Zhou, Z., 2018. A new clade of basal Early Cretaceous pygostylian birds and developmental plasticity of the avian shoulder girdle. Proc. Natl. Acad. Sci. U.S.A. 115, 10708–10713.

Wang, M., Wang, X., Wang, Y., Zhou, Z., 2016. A new basal bird from China with implications for morphological diversity in early birds. Scientific Reports 6, 19700.

Wang, M., Zhou, Z., 2017. A new adult specimen of the basalmost ornithuromorph bird *Archaeorhynchus spathula* (Aves: Ornithuromorpha) and its implications for early avian ontogeny. J. Syst. Palaeontol. 15, 1–18.

Wiemann, J., Yang, T.-R., Norell, M.A., 2018. Dinosaur egg colour had a single evolutionary origin. Nature 563, 555–558.

Wiemann, J., Yang, T.-R., Sander, P.N., Schneider, M., Engeser, M., Kath-Schorr, S., Müller, C.E., Sander, P.M., 2017. Dinosaur origin of egg color: oviraptors laid blue-green eggs. PeerJ 5, e3706.

Wilson, L.E., Chin, K., Cumbaa, S.L., 2016. A new hesperornithiform (Aves) specimen from the late Cretaceous Canadian High Arctic with comments on high-latitude hesperornithiform diet. Can. J. Earth Sci. 53, 1476–1483.

Witmer, L.M., 2001. The role of *Protoavis* in the debate on avian origins. In: Gauthier, J.A., Gall, L.F. (Eds.), New Perspectives on the Origin and Evolution of Birds: Proceedings of the International Symposium in Honor of John H. Ostrom. Yale University Press, New Haven, pp. 537–548.

Worthy, T.H., Degrange, F.J., Handley, W.D., Lee, M.S., 2017. The evolution of giant flightless birds and novel phylogenetic relationships for extinct fowl (Aves, Galloanseres). Royal Soc. Open Sci. 4, 170975.

Xing, L., et al., 2016. A feathered dinosaur tail with primitive plumage trapped in mid-Cretaceous amber. Curr. Biol. 26, 3352–3360.

Xu, X., 2020. Filamentous integuments in nonavialan theropods and their kin: advances and future perspectives for understanding the evolution of feathers. In: Foth, C., Rauhut, O.W.M. (Eds.), The Evolution of Feathers. Springer, Cham, pp. 67–78.

Xu, X., Currie, P., Pittman, M., Xing, L., Meng, Q., Lü, J., Hu, D., Yu, C., 2017. Mosaic evolution in an asymmetrically feathered troodontid dinosaur with transitional features. Nat. Commun. 8, 14972.

Xu, X., You, H., Du, K., Han, F., 2011. An *Archaeopteryx*-like theropod from China and the origin of Avialae. Nature 475, 465–470.

Xu, X., Zheng, X., Sullivan, C., Wang, X., Xing, L., Wang, Y., Zhang, X., O'Connor, J.K., Zhang, F., Pan, Y., 2015. A bizarre Jurassic maniraptoran theropod with preserved evidence of membranous wings. Nature 521, 70–73.

Xu, X., Zhou, Z., Wang, X., Kuang, X., Zhang, F., Du, X., 2003. Four-winged dinosaurs from China. Nature 421, 335–340.

Yang, Z., Jiang, B., McNamara, M.E., Kearns, S.L., Pittman, M., Kaye, T.G., Orr, P.J., Xu, X., Benton, M.J., 2019. Pterosaur integumentary structures with complex feather-like branching. Nat. Ecol. Evol. 3, 24–30.

You, H.-L., Lamanna, M.C., Harris, J.D., Chiappe, L.M., O'Connor, J., Ji, S.-A., Lü, J.-C., Yuan, C.-X., Li, D.-Q., Zhang, X., 2006. A nearly modern amphibious bird from the Early Cretaceous of northwestern China. Science 312, 1640–1643.

Zelenitsky, D.K., Therrien, F., Erickson, G.M., Debuhr, C.L., Kobayashi, Y., Eberth, D.A., Hadfield, F., 2012. Feathered non-avian dinosaurs from North America provide insight into wing origins. Science 338, 510–514.

Zelenitsky, D.K., Therrien, F., Ridgely, R.C., McGee, A.R., Witmer, L.M., 2011. Evolution of olfaction in non-avian theropod dinosaurs and birds. Proc. Royal Soc. B 1725, 3625–3634.

Zhang, F., Kearns, S.L., Orr, P.J., Benton, M.J., Zhou, Z., Johnson, D., Xu, X., Wang, X., 2010. Fossilized melanosomes and the colour of Cretaceous dinosaurs and birds. Nature 463, 1075–1078.

Zheng, X., O'Connor, J.K., Huchzermeyer, F., Wang, X., Wang, Y., Wang, M., Zhou, Z., 2013. Preservation of ovarian follicles reveals early evolution of avian reproductive behaviour. Nature 495, 507–511.

Zheng, X.-T., O'Connor, J.K., Wang, X.-L., Pan, Y.-H., Wang, Y., Wang, M., Zhou, Z.-H., 2017. Exceptional preservation of soft tissue in a new specimen of *Eoconfuciusornis* and its biological implications. Natl. Sci. Rev. 4, 441–452.

Zheng, X., Martin, L.D., Zhou, Z., Burnham, D.A., Zhang, F., Miao, D., 2011. Fossil evidence of avian crops from the Early Cretaceous of China. Proc. Natl. Acad. Sci. U.S.A. 108, 15904–15907.

Zheng, X., Wang, X., Sullivan, C., Zhang, X., Zhang, F., Wang, Y., Li, F., Xu, X., 2018. Exceptional dinosaur fossils reveal early origin of avian-style digestion. Sci. Rep. 8, 1–8.

Zheng, X.T., You, H.L., Xu, X., &Dong, Z.M., 2009. An Early Cretaceous heterodontosaurid dinosaur with filamentous integumentary structures. Nature 458, 333–336.

Zhou, S., Zhou, Z., O'Connor, J.K., 2013. Anatomy of the basal ornithuromorph bird *Archaeorhynchus spathula* from the early Cretaceous of Liaoning, China. J. Vertebr. Paleontol. 33, 141–152.

Zhou, Z., Clarke, J.A., Zhang, F., 2002. *Archaeopraptor's* better half. Nature 420, 285.

Zhou, Z., Clarke, J.A., Zhang, F., 2008. Insight into diversity, body size and morphological evolution from the largest Early Cretaceous enantiornithine bird. J. Anat. 212, 565–577.

Zhou, Z., Zhang, F., 2002a. A long-tailed, seed-eating bird from the Early Cretaceous of China. Nature 418, 405–409.

Zhou, Z., Zhang, F., 2002b. Largest bird from the Early Cretaceous and its implications for the earliest avian ecological diversification. Naturwissenschaften 89, 34–38.

Zhou, Z., Zhang, F., 2004. A precocial avian embryo from the Lower Cretaceous of China. Science 306, 653.

Chapter 8

Domestication of poultry

Paul B. Siegel[1], Christa F. Honaker[1] and Colin G. Scanes[2]
[1]Department of Animal and Poultry Sciences, Virginia Tech, Blacksburg, VA, United States; [2]Center of Excellence for Poultry Science, University of Arkansas, Fayetteville, AR, United States

8.1 Introduction

Birds, from a range of species, were domesticated for numerous reasons including sport, communication, ceremony, and food. The focus here will be on domesticated birds or "poultry", namely chickens, ducks, geese, guinea fowl, Japanese quail, ostriches, pigeons, and turkeys. Chickens, ducks, and turkeys have been much studied and are important sources of food for their domesticators, namely humans. Crawford (1990) and Appleby et al. (2004) provide brief overviews for other domesticated birds, including pigeons, quail, and ratites. Domestication of chickens commenced during the Neolithic period (Stevens, 1991) about midway during the First Agricultural Revolution (see Table 8.1). Domestication of ducks commenced at least several centuries BCE (McKinney, 1969), while in more recent times, turkeys were domesticated in the Americas.

8.2 Domestication

Domestication is dependent on human intervention and actions, be they intentional (e.g., artificial incubation of eggs) or indirect (e.g., environmental changes). Thus, modifications of the process may be abrupt or gradual. Domestication is considered as directed evolution with humans deciding which individuals are chosen to produce the next generation. Changes in the phenotypes reflect shifts in genotypes as they interact with internal and external environments, including multiple physiological processes. The effects may be short-term or generational because of mate choice and sexual reproduction.

Domestication of plants and animals is a continuing process that may be viewed historically in a time and geographical context (Diamond, 1999; Zeder, 2015). Table 8.1 summarizes the domestication of birds. The Neolithic Revolution was a major turning point in the development of human society with many plants and animals domesticated. Domestication is arguably considered as one of the great innovations in human history. Adapting the Merriam-Webster definition of domestication, domestication of birds is the adaptation of an avian species "*from a wild or natural state (as by selective breeding) to life in close association with humans.*" Zeder (2015) defined domestication as "*a sustained multigenerational, mutualistic relationship in which one organism assumes a significant degree of influence over the reproduction and care of another organism in order to secure a more predictable supply of a resource of interest, and through which the partner organism gains advantage over individuals that remain outside this relationship, thereby benefitting and often increasing the fitness of both the domesticator and the target domesticate.*" Domestication involves changes whereby the breeding and care of animals are directly or indirectly controlled by humans and is more than simply taming (Darwin, 1868). In comparison to plants, the domestication of poultry is very recent in terms of human history (see Table 8.1). To put it into perspective, Craig and Crawford (1981) wrote, "*a crude calculation suggests that man has lived alongside domesticated animals for only about one-half of 1% as long as he has been a toolmaker.*"

In recent centuries, knowledge and technologies in the life sciences (e.g., rediscovery of Mendelism, DNA, and genomics) have and continue to have major impacts on the paths taken to direct residual and "new" genetic variation via intercrosses, which in turn influence physiological and behavioral mechanisms and phenotypes. Such techniques address the evolutionary process of domestication and selection. Rubin et al. (2010) used whole genome sequencing to trace the origin of the domestic fowl. Corso et al. (2017) reported that while the domestic turkey came in plumage colors controlled by at least five genetic loci, only the bronze has been precisely identified. Deng et al. (2019) used genome-wide association studies to detect novel loci in Pekin ducks. Another example of the use of genomic approaches has been study of the development of a "new" genetic breed of chicken, the White Plymouth Rock; this being a breed that was a large contributor to today's meat-

Sturkie's Avian Physiology. https://doi.org/10.1016/B978-0-12-819770-7.00026-8

TABLE 8.1 Domestication of avian species.

Species	Number of domestic-cation events	Ancestor(s)	Location(s) of domestication	Putative time of domestication	References
Chickens (*Gallus gallus*)	Multiple	Red junglefowl (*Gallus gallus*) with introgressions from other species	East Asia (present-day China), South East Asia, and the Indian subcontinent	~6000–8000 BCE	Darwin (1868), Liu et al. (2006), Kangina-kudru et al. (2008), Rubin et al. (2010), Miao et al. (2013), Xiang et al. (2014, 2015) but disputed by Peters et al. (2015)
Ducks (Chinese breeds)	1?	Mallard ducks (*Anas platyrhyn-chos*) with some contribution from the spot-billed duck (*Anas zonorhyncha*)	East Asia (present-day China)	~1000–2000 BCE	Cherry and Morris (2008), Qu et al. (2009), Li et al. (2010)
Ducks (European breeds) (*Anas platyrhynchos*)	1	Mallard ducks (*Anas platyrhynchos*)	Unclear whether separate domestication or multiple introgressions	~0–2000 BCE	Cherry and Morris (2008), Qu et al. (2009), Li et al. (2010)
Geese (European breeds plus Yili goose)	1 (or 2?)	Greylag goose (*Anser anser*)	Eastern Mediterranean region/"Fertile Crescent"	~3000 BCE	Shi et al. (2006), Li et al. (2011), Heikkinen et al. (2015)
Geese (25 of 26 Chinese breeds)	1	Swan goose (*Anser cygnoides*)	East Asia (present-day China)	~3000 BCE	Shi et al. (2006), Li et al. (2011), Heikkinen et al. (2015)
Guinea fowl (*Numida meleagris*)	1	Helmeted guinea fowl (*Numida meleagris*	North Africa (present-day Mali and Sudan)	2000 years BP	Vignal et al. (2019)
Japanese quail (*Coturnix japonica*)	1 or 2	Japanese quail (*Coturnix japonica*)	China plus latter in Japan	~1000 CE	Chang et al. (2005)
Muscovy duck (*Cairina moschata*)	1	Muscovy duck (*Cairina moschata*)	Central America and/or the North of South America	500 CE	Wetmore (1956), Hesse (1980), Stahl et al. (2006)
Ostriches (*Struthio camelus*)	1	Hybrid of South African (*S. c. australis*) and North African (*S. c. camelus*) ostriches	South Africa	1850–1900 CE	Duerden (1906), Spinu et al. (1999)
Pigeons (*Columba livia*)	1	Rock pigeons (*Columba livia*)	Eastern Mediterranean region	~1000–3000 BCE	Darwin (1868), Stringham et al. (2012)
Turkey (*Meleagris gallopavo*)	1 or more	Wild turkeys (*Meleagris gallopavo*)	North America (present-day Mexico and perhaps South West U.S.A.)	800 BCE	Speller et al. (2010), Padilla-Jacobo et al. (2018)

BCE Before common era (equivalent to BC).
CE Common era (equivalent to AD).

type broiler chickens. Using current genetic tools, Guo et al. (2019), via genomic analysis, revealed not only genome-wide contributions from the foundation breeds (Dominique [sire] and both Black Cochin or Black Java [dams] together with contributions from Brahma, Langshan, and Black Minorca breeds), but also differences in contributions to each of 29 chromosome pairs of the White Plymouth Rock.

Although unaware of Mendel, Darwin (1868) wrote of the importance of variation in domestication. The same thinking may be seen in the writings of Fritz Muller (West, 2003, 2016). Certain behaviors that facilitated the domestication of poultry that were important at one point in time (e.g., escape behaviors) may be redundant today when animals are kept in confinement. Also, the behavioral and physiological processes involved may not be all or none, but modified by the degree of stimuli, response thresholds, point in the life cycle, heritability, and epigenetics. Conditioning may influence both the behavior and response of an animal, an example being nest locations and adaptation responses between the first and subsequent ovipositions (Beuving, 1980). A recent and quite different example is the "henny feathering" phenotype in the Seabright chicken (Li et al., 2019). Although the presence of female-like plumage on males is known to be caused by a dominant mutation, the mechanisms involved have been elusive. Today we know that, physiologically, the phenotype was caused by ectopic expression of *CYP19A1* encoding aromatase in the skin, thus precluding development of male-specific plumage, but not sexual behavior.

8.2.1 Chickens

Today, the domestic chicken (*Gallus gallus domesticus*), which originated during the First Agricultural Revolution from the junglefowl of Southeast Asia, is found throughout the world (Robinson et al., 2014, Fig. 8.1). Charles Darwin (1868) considered that chickens were domesticated exclusively from red junglefowl (*Gallus gallus*). In contrast, Hutt (1949) proposed that modern chickens were derived from four species of junglefowl, specifically, red junglefowl native to Indochina, gray junglefowl (*Gallus sonneratii*) native to the Indian subcontinent, Ceylon or Sri Lanka junglefowl (*Gallus lafayetti*) native to Sri Lanka, and green junglefowl (*Gallus varius*) native to Java. Genomic studies have demonstrated that the chickens are derived from the red junglefowl in a monophyletic manner (Fumihito et al., 1994, 1996). There is also evidence that there has been introgression of genes from other species. For instance, if the trait of yellow legs due to carotenes in the skin and a mutation depressing expression of beta-carotene dioxygenase 2 is considered. This appears to have been introgressed from gray junglefowl (Eriksson et al., 2008). There is also evidence of introgression from *Gallus lafayetti* based on mitochondrial DNA (Nishibori et al., 2005). Conversely, there have been intrusion of chicken genes into the green junglefowl (Sawai et al., 2010). Within diverse environments, chickens have adapted to conditions ranging from that of scavengers to highly intensive production systems that focus on intense and persistent year-round egg production and rapid growth. In the case of the latter, although the individuals are marketed prior to sexual maturity, their parents must be capable of reproduction (Siegel, 2014).

Do the differences between the junglefowl and today's commercial egg or meat-type chickens go beyond plumage color (although not all egg-type commercial chickens have white plumage), and, respectively, numbers of eggs laid or body size? It is noteworthy that among domestic farm animals, the chicken has increased in size while that of mammals has decreased (Diamond, 1999). Sutherland et al. (2018) reported body weights of <100 g for Red junglefowl at 35 days of age. The commercial chicken industry, developed with breeding programs in the post-World War II period, focused on either egg or meat production. This resulted in dramatic increases in body size of meat-type chickens. Body weights at 35 days, typically 1400 g in 1985 were, in 2010, slightly in excess of 2400 g (Siegel, 2014), and have since increased at 40 to 50 g per year (also see Table 8.2). For commercial egg laying stocks, the neuroendocrine cascade for the onset and persistency of egg production is well documented (Scanes et al., 1992). Also needed for the onset of egg production are minimum age, body weight, and body composition, which may be stock specific (Zelenka et al., 1987). This knowledge has allowed the development of breeding and husbandry programs so that stocks routinely peak at greater than 95% and maintain intensity and persistency of egg production for extended periods (Preisinger, 2017; Fernyhough et al., 2020).

Plumage colors for breeds of chickens are summarized in The American Standard of Perfection (American Poultry Association, 1947). Because white plumage color is inherited as recessive white (*cc*) or as dominant white (*II*) (Hutt, 1949), it masks the phenotypic expression of genes responsible for other colors, although feathers of chickens that are *Ii* may have some colored spots. Thus, the changes are in conformation, not structure. Male junglefowl have "showy" plumage while the females are drab, which provides camouflage to reduce predation during incubating eggs and chick rearing. Both junglefowl and domestic chickens are ground nesters. The colorful plumage of junglefowl males may be viewed as a compromise between sexual selection (female choice) and predation. The introduction of *cc* and *II* in commercial flocks facilitated processing (no dark pin feathers) for marketing.

Behaviors that favored domestication of poultry are intertwined with physiological mechanisms at any point in the life history of the individual. Examples include the

FIGURE 8.1 Junglefowl and domestic chicken examples, as represented by female and male (top) Red Junglefowl, (middle) White Leghorn egg-type chickens selected for antibody production, and (bottom) White Plymouth Rock meat-type chickens selected for high body weight. *Photos courtesy of (top) Dez-Ann Sutherland and Jingyi Li and (middle and bottom) Christa Honaker.].*

neuroendocrine behavioral aspects of reproduction and responses to acute and chronic stressors (the general adaptation syndrome). Although the adaptability of the chicken is a function of its behavioral and physiological makeup, Price (1984) pointed-out that the influence of domestication has been mostly quantitative rather than qualitative. Over the years, stimuli may have been altered as have the thresholds of responses to stimuli. Whole genome sequencing has provided a schematic tree on the domestication of the chicken and its breeding history with experimental and commercial populations as examples (Rubin et al., 2010).

Scavenging domestic chickens capitalize on those behaviors and the underlying physiological mechanisms that facilitated their domestication. Although under intensive husbandry, as the physiological processes remain, some of

TABLE 8.2 Anthropogenic influences on domesticated poultry species.

Phenomenon	Example	References
1 Introgressions		
a. From other species	Yellow legs in chickens from gray junglefowl (*Gallus sonneratii*) Introgression from the Sri Lankan or Ceylon junglefowl (*Gallus lafayetti*)	Eriksson et al. (2008) Lawal et al. (2020)
b. From wild birds of the same species	Ducks	
2 Relaxed selection	**i.** Domestic geese have reduced ability to fly due to relaxation of constraints **ii.** Wild pigeons have small body weight in desert conditions	Wang et al. (2017) Marom et al. (2018)
3 Selection of desired traits		
a. Selection prior to scientific selection	**i.** During late medieval period in Europe, both the yellow legs trait and the TSHR variant in chickens became fixed **ii.** Pekin ducks selected for growth and white plumage **iii** Japanese quail selected for growth **iv.** Selection pressure in village chickens to resistance to elevated temperatures	Girdland et al. (2014) Zhou et al. (2018) Chang et al. (2005) Lawal et al. (2018)
b. Scientific selection	Predominantly applied to chickens, ducks, geese, and turkeys with improved growth such as a 4.62-fold increase in body weight between 2005 commercial chickens and 1957 birds	Zuidhof et al. (2014)
4 Narrow genetic base and drift		
a. Trading with small numbers of birds	**i.** Zimbabwean village chickens having either Southeast Asian or Indian ancestry **ii.** Dutch breeds have some East Asian elements	Muchadeyi et al. (2008) Dana et al. (2011)
b. Geographical isolation	**i.** Village chickens in South Africa **ii.** Native chickens on the Samar Island, Philippines	Godinez et al. (2019) Mtileni et al. (2016)
c. Commercial poultry	Genome of commercial turkeys exhibits markedly lower diversity than that in chickens	Aslam et al. (2012)
5 Presence of deleterious missense variants	Reported in commercial chickens	Derks et al. (2018)

TSHR, thyroid stimulating hormone/thyrotropin receptor.

the behaviors that facilitated domestication of the chicken have become redundant. Hale (1969) and Price (1984) summarized and discussed traits that initially favored domestication of the chicken. Chickens were not a migratory species, thus while they may exhibit escape behaviors, flight was not an issue. Other traits that favored domestication included a social structure that allowed grouping of males and females. In addition, within sexes, in small groups, the social structure was stable (Guhl, 1953), inferring a capacity for recognition and memory. Other behaviors considered included promiscuity, incubation behavior, precocial young, omnivorous dietary habits, and adaptation to a range of environments.

Although at oviposition the embryo has proceeded to a multicellular stage and the second of the three primary "germ layers" have usually begun to appear (Romanoff, 1960), the embryo essentially develops outside the body of the dam. Upon hatching, the chick transitions over a brief period from cold to warm blooded, thus providing opportunity for an interface between hen and human intervention. In the natural state, parental care is by the hen, however, males will express maternal behavior under certain conditions (Kovach, 1967). The intervention by humans in the domestication process accelerated during the transition from the Agricultural to the Scientific Revolution. This was further enhanced during the 20th century with the rediscovery of Mendelism, recognition of B and T cell immunity, advances in nutrition, and their interface with the dynamics and relationships among physiological systems. For example, although the development of the force-draft incubator made incubation behavior irrelevant, it took generations of selection to modify neuroendocrine thresholds to preclude broody behavior. The implementation of group rearing of precocial chicks also removed the need for

maternal behavior. Although artificial incubation can be traced to at least the Ch'in period of 246–207 BCE (Landauer, 1951), its development became suddenly abrupt via a technological breakthrough. Namely, large scale forced-air incubation did not become routine until the 20th century with the discovery of electricity. This led to the control of brooding and selection for the onset and persistence of egg production by manipulation of the photoperiod and genetics (Siegel, 2014).

The evolutionary tree of the domestic chicken has branches where, over time, behavioral and physiological characteristics may have or had different relevance. That we may no longer observe chickens exhibiting certain behaviors does not imply that they no longer exist. Rather, the normal cascading of physiological processes may have been disrupted and thus altered thresholds for responses. An example is polygenic trait broodiness (Saeki, 1957). This may be because it is rarely expressed in populations bred for high egg production and rapid growth. Pedigrees for scavengers are seldom known, and the sizes of pedigree populations for show and fancier stocks are too small for the necessary statistical reliability. Yet, we know that broodiness is a threshold trait with at least two components (i.e., initiate incubation and to persist throughout the period). These behavioral and physiological dynamics are well documented, as are those involved with posthatching relationships.

Overall, the domestic chicken may be viewed in numerous forms with a multitude of uses, from the Neolithic period to the present day. Yet, much of the standing genetic variation from the junglefowl remains. Namely, the physiological processes involved and morphological structures, while altered, remain fundamentally the same, and this holds true not only for chickens but also other domestic species as well.

8.2.2 Turkeys

The turkey (*Meleagris gallopavo*) has a rich history in the United States beginning with the settlements at Jamestown in 1607 and Plymouth Rock in 1620 and with it being the "center of the table" for the Thanksgiving holiday. The turkeys of lore from Virginia and Massachusetts were wild, not the domestic turkeys that Hernán Cortés observed a century earlier in the conquered Aztec empire (Schorger, 1966). His classic, "The Wild Turkey: Its History and Domestication," is generally considered the primary source for what has been written on the early history of the domestication of the turkey. About 25 years later, Buss (1990) provided history and insights on the metabolism, neuroendocrinology, and muscle physiology in the development of the "broad breasted" domestic turkey that is common in America, Europe, and the Middle East. His history of the "broad breasted" turkey compliments and is not independent of the behaviors described by Hale et al. (1969).

The turkey was already domesticated when Cortés arrived in the Yucatan Peninsula in Central America before conquering the Aztec Empire in 1519 (see Table 8.1). There is evidence from Mayan archaeological sites dating to 300 BCE–100 CE of the presence of domesticated turkeys (Thornton et al., 2012). These were genetically distinct from local turkeys suggesting trading of domestic turkeys (Thornton et al., 2012). The turkey, unlike the chicken and duck, has unique head and neck appendages that lack feathers (Scanes et al., 1992). These anatomical features (Fig. 8.2) are consistent with initial domestications in hot, dry climates. A lack of feathers is beneficial to aid in dissipation of heat and thermoregulation.

This domesticated turkey was taken to Europe and returned to the Americas several times, resulting in a series of domestications with introgressions from wild turkeys (Schorger, 1966). Schorger (1966) also writes that there is evidence of turkey domestication in Arizona and New Mexico during Pueblo I (700–900 CE) and perhaps two centuries earlier (500–700 CE), as well as later in Pueblo II and III (900–1100 CE) (Schorger, 1966, Table 8.1).

Fundamental to acceleration of the process of turkey domestication during the 20th, and now into the 21st, century was further understanding of the physiological-behavioral interface described for the chicken. Commercial turkey breeds are more closely related to three of the heritage breeds, the Blue Slate, Bourbon Red, and Narragansett, than to either Royal Palm or Spanish Black breeds (Kamara et al., 2007), and the turkey genome exhibits markedly lower diversity than the chicken (Aslam et al., 2012).

Human interventions on reproduction in the domestication of the turkey involved primarily neuroendocrine relationships associated with onset and persistence of egg

FIGURE 8.2 A Bourbon Red tom turkey. *Photo courtesy of Audrey McElroy.*

and sperm production, incubation, and maternal behaviors. The high heritability and intense selection for growth and breast meat yield resulted in considerable changes in motor ability as well as sexual dimorphism in body weights of males and females. Although the adult female to male body weight ratio may have remained constant at approximately two-thirds, a dimorphism in body weight per se of 6 and 9 kg to 12 and 18 kg has been considerable. Thus, unlike the chicken and duck, artificial insemination (Bakst and Dymond, 2013) has become routine in commercial turkey production. This dimorphism requires sex separate breeding flocks of domestic high meat yielding turkey populations for the procedure to be successful. The photoperiod response is not only important for the onset and persistency of egg and sperm production but also remains unchanged. While on the topic of reproduction, we would be remiss in not pointing out that a considerable literature exists on parthenogenesis in the turkey (e.g., Olsen and Marsden, 1968). This phenomenon was recently reviewed for several avian species (Ramachandran and McDaniel, 2018).

8.2.3 Ducks

The mallard, or mallard duck (*Anas platyrhynchos*), and the Muscovy (*Cairina moschata*) are the progenitors of domestic ducks (McKinney, 1969, 1975; Dohner, 2001). The literature is unclear as to when and where ducks were first domesticated. When viewed in the context of traits that favored domestication (Hale, 1969), the aspects of flight and migration were probably major factors in multiple initial domestications, especially for the mallard. Most domestic ducks trace back to mallards, whose early domestication occurred during the Iron Age in Southeast Asia and China (Crawford, 1990; Zhou et al., 2018, Table 8.1). Chinese breeds of domestic ducks are predominantly derived from mallard ducks, with some contribution from the spot-billed duck (*Anas zonorhyncha*) (Qu et al., 2009; Li et al., 2010). Domesticated ducks moved on to Europe, being farmed by the Romans in about 50 BCE (Cherry and Morris, 2008). In contrast, the domesticated Muscovy was present in present-day Latin America when the Europeans first arrived during the 15th century (Table 8.1).

There are numerous distinguishing characteristics between mallard and Muscovy ducks, and their routes to domestication differed in time and source. The incubation periods are 28 and 35 days for mallards and Muscovy, respectively. Although they will mate naturally, the incubation period of about 32 days is intermediate. The resulting progeny are sterile (Dohner, 2001), with those between a Muscovy male and mallard female called "mules," while those from the reciprocal cross are called "hennies."

Mallards are wildly distributed in the Northern hemisphere including Eurasia, North America, and North Africa and exhibit migration (e.g., Yamaguchi et al., 2008; van Toor et al., 2013; Bengtsson et al., 2014). Up until commercial production with confinement husbandry (Cherry and Morris, 2008), matings frequently occurred between wild and domestic ducks, resulting in introgression of genes from their wild ancestors. This may have facilitated the development of ducks that are highly recognized for meat characteristics such as the Pekin or prolific egg production such as the Khaki Campbell (American Poultry Association, 1947; Qu et al., 2009). Although there are numerous genes associated with plumage color, among duck populations, the white feathers and down relevant in the processing of meat-type ducks are *cc* (recessive white), which is an epistatic genotype for color, thus masking plumage color expression. While major loci, such as recessive white, may have remained a constant and precluded expression of other genes, we must recognize that most physiological traits are quantitatively inherited with inter- and intralocus interactions. Human intervention may have had a considerable effect in the formation of breeds developed from mallards and Muscovy, but branching may have been considerable with the two species. For example, within the Chinese breeds, the Pekin haplotypes are distinctly different from those of other domestic breeds originating from the wild mallard (Qu et al., 2009).

As with the chicken, human intervention has replaced, via artificial incubation, the need for incubation and parental behaviors, altering thresholds and cascades necessary for development and physiological processes. An example was provided by Lockner and Youngren (1976) in their detailed description of the neuromuscular development and sound production in mallards. Their experiments on the structural development and physiological interface of sound production in ducks are classics. Although highly domesticated from dual sources and locations, a duck is still a duck. The female "quacks," while the male remains relatively silent.

8.2.4 Geese

European and Chinese domestic geese originated from independent domestication events, respectively, in the eastern Mediterranean region/"Fertile Crescent" and in East Asia (Shi et al., 2006; Heikkinen et al., 2015, Table 8.1). European breeds of domestic geese are derived from the Greylag goose (*Anser anser*) (Heikkinen et al., 2015). In contrast, almost all Chinese breeds originated from the swan goose (*Anser cygnoides*). Of 26 breeds of Chinese domestic geese, the maternal lines of 25 are the swan goose while one (the Yili goose) was derived from the Greylag goose (Li et al., 2011).

8.2.5 Other domesticated birds

For details of the domestication of other birds, see Table 8.1. Pigeons were domesticated from rock pigeons (*Columba livia*) between 1000 and 3000 BCE, probably in the Eastern Mediterranean region (discussed Darwin, 1868; Stringham et al., 2012, Table 8.1). The breeds fall into categories such as tumblers and rollers, fan-tails, owls, pouters and croppers, and mane pigeons, with their genetics having been characterized (Stringham et al., 2012).

Farmed ostriches (*Struthio camelus*) were developed in the second part of the 19th century from a cross between two subspecies of ostriches, respectively, the South African (*S. c. australis*) and North African (*S. c. camelus*) ostriches (reviewed: Spinu et al., 1999). While they have been subjected to considerable selection (reviewed: Spinu et al., 1999), it not clear whether they should be considered as domesticated or tamed; with 300,000 tame ostriches (*Struthio camelus*) being farmed in the Cape province of South Africa in the first decade of the 20th century (Duerden, 1906, Table 8.1).

The guinea fowl was domesticated from the helmeted guinea fowl (*Numida meleagris*) about 2000 years BP in North Africa in present-day Mali and Sudan as a food resource (Vignal et al., 2019, Table 8.1). Japanese quail (*Coturnix japanica*) were domesticated in about 1000 CE in China and later in Japan (Chang et al., 2005, Table 8.1).

8.3 Conclusions

Table 8.2 summarizes multiple factors influencing domesticated birds and consequently their physiological and anatomical phenotypes. The corollary to this is that there are effects on wild birds that are directly or indirectly anthropogenic in nature. This includes the following: (1). invasive and introduced species, (2). feral birds, and (3). introgressions from domesticated birds to wild species.

It may be questioned whether we should consider that a chicken is still anatomically, behavioral and physiologically, a chicken, be it a junglefowl, fighting cock, broiler, layer, etc. In an evolutionary context, this may be considered minor because matings between individuals of each of these groups can produce fertile progeny (e.g., Sutherland et al., 2018; Godinez et al., 2019). Differences in body size may preclude natural matings between wild birds and commercial poultry (chickens: Blohowiak et al., 1980; turkeys: Bakst and Dymond, 2013), however, they produce fertile progeny via artificial insemination. There are, however, caveats as recently discussed by Bennett et al. (2018). The caveats may vary because populations of chickens, ducks, and turkeys may vary in their degree of domestication. There are populations of chickens, for example, bred for sport, feathers, meat, or egg production. The same may be the case for ducks and turkeys. Thus, one cannot generalize without consideration of the process in reverse (i.e., feralization). Namely, what is the capacity of the domestic bird to survive and reproduce in nature? This will depend on several factors and is not independent of the weakest link in the biological process for adaptation to the environment into which it has been released. For the chicken, perhaps the example most intensively studied is that of McBride et al. (1969) for the feral fowl.

There are genotypic and phenotypic effects of domestication, introgressions, and selection (Zeder, 2015). For instance, marked differences in brain anatomy have been reported between red junglefowl and modern chickens (Kawabe et al., 2017). Similarly, brain size is reduced in red junglefowl selected for tameness (Agnvall et al., 2017). Selective breeding led to the development of White Leghorn chickens exhibiting persistent egg production due to the absence of incubation behavior; this being due to shifts in prolactin physiology (Hutt, 1949; Zhou et al., 2008; Basheer et al., 2015).

Examination of chicken bones from archaeological sites and comparison with modern commercial chickens and red junglefowl indicates four important aspects of the development of today's commercial chickens. There was little difference between maximal breadth of tibiotarsus between red junglefowl and either ancient or more recent chickens (Bennett et al., 2018). In contrast, there was a marked increase in maximal breadth in modern meat-type chickens (Bennett et al., 2018). Another major shift is the diet with chickens prior 1900 being omnivorous while today's commercial chickens are almost exclusively granivorous (Bennett et al., 2018).

It is important to recognize that the scientific consensus changes with new information, and every study should not be viewed as necessarily conclusive. It was supposed that a mutation of the thyrotropin receptor (TSHR) (residue 558 is arginine in chickens and glycine in red junglefowl) (Grottesi et al., 2020) was linked to the domestication of chickens about 8000 years ago (Rubin et al., 2010). It was argued, as it permits year-round production of eggs (Rubin et al., 2010). However, based on examination of DNA extracted from ancient chicken specimens from archaeological sites (280 BCE−1800 CE) in Europe, it was concluded that the mutated TSHR gene was only fixed in poultry populations in the last 500 years (Girdland et al., 2014). Among the physiological consequences of the mutation are shifts in hypothalamic TSHR expression and reduced plasma concentrations of thyroxine but not triiodothyronine (Karlsson et al., 2016). What is not clear is to what extent the arginine 558 form is found in the exotic breeds or village/indigenous chickens.

Another change with domestication and selection is plumage. Although colored plumage has an advantage in the wild regarding predator-prey, current commercial meat poultry predominantly have white plumage for processing

purposes. It is the result of the recessive genotype (*cc*), which precludes expression of plumage color (Somes, 1984). Our sense is that *c* was a "spot" mutation and, unlike albinism, the expression was essentially limited to preclusion of plumage color expression. Initially, humans were interested in white plumage as a "sport" that could be easily introgressed into their population because the phenotype was recessive. During pre-Mendelian periods, matings of like to like allowed for simply inherited traits to form "new" strains.

It has been hypothesized that decreased fear of humans was important to domestication. In red junglefowl selected for either high or low fear, there were shifts in brain gene expression (Bélteky et al., 2016). There were, however, no differences in baseline and stressed bird circulating concentrations of the stress hormone, corticosterone, between red junglefowl selected for either low or high fear of humans (Agnvall et al., 2015).

In conclusion, the initial domestication of different species of birds, including chickens, ducks, and turkeys, occurred during different time periods (Table 8.1), and this should be viewed as a continuing process. Thus, the involvement of humans in the process may be considered as directed evolution. Although today, domesticated and wild birds are distinguished by phenotypic characteristics, their basic anatomy and physiology have much in common. It is also noted that there are effects on wild birds that are both anthropogenic and avian in nature. This includes the following: (1). invasive and introduced species, (2). feral birds and (3). introgressions from domesticated birds to wild species together with obviously (4). habitat loss.

References

American Poultry Association, 1947. The American Standard of Perfection. Am. Poult. Assoc., Davenport, IA.

Agnvall, B., Katajamaa, R., Altimiras, J., Jensen, P., 2015. Is domestication driven by reduced fear of humans? Boldness, metabolism and serotonin levels in divergently selected red junglefowl (*Gallus gallus*). Biol. Lett. 11, 20150509.

Agnvall, B., Bélteky, J., Jensen, P., 2017. Brain size is reduced by selection for tameness in Red junglefowl- correlated effects in vital organs. Sci. Rep. 7, 3306.

Appleby, M.C., Mench, J.A., Hughes, B.O., 2004. Poultry Behaviour and Welfare. CABI Pub., Cambridge, MA.

Aslam, M.L., Bastiaansen, J.W., Elferink, M.G., Megens, H.J., Crooijmans, R.P., Blomberg, L.A., Fleischer, R.C., Van Tassell, C.P., Sonstegard, T.S., Schroeder, S.G., Groenen, M.A., Long, J.A., 2012. Whole genome SNP discovery and analysis of genetic diversity in Turkey (*Meleagris gallopavo*). BMC Genom. 13, 391.

Bakst, M.R., Dymond, J.S., 2013. Artificial insemination in poultry. In: Lemma, A. (Ed.), Success in Artificial Insemination: Quality of Semen and Diagnostics Employed. IntechOpen. https://doi.org/10.5772/54918.

Basheer, A., Haley, C.S., Law, A., Windsor, D., Morrice, D., Talbot, R., Wilson, P.W., Sharp, P.J., Dunn, I.C., 2015. Genetic loci inherited from hens lacking maternal behaviour both inhibit and paradoxically promote this behaviour. Genet. Sel. Evol. 47, 100.

Bélteky, J., Agnvall, B., Johnsson, M., Dominic Wright, D., Jensen, P., 2016. Domestication and tameness: brain gene expression in red junglefowl selected for less fear of humans suggests effects on reproduction and immunology. R. Soc. Open Sci. 3, 160033.

Bengtsson, D., Avril, A., Gunnarsson, G., Elmberg, J., Söderquist, P., Norevik, G., Tolf, C., Safi, K., Fiedler, W., Wikelski, M., Olsen, B., Waldenström, J., 2014. Movements, home-range size and habitat selection of mallards during autumn migration. PLoS One 9, e100764.

Bennett, C.E., Thomas, R., Williams, M., Zalasiewicz, J., Edgeworth, M., Miller, H., Coles, B., Foster, A., Burton, E.J., Marume, U., 2018. The broiler chicken as a signal of a human reconfigured biosphere. R. Soc. Open Sci. https://doi.org/10.1098/rsos.180325.

Beuving, G., 1980. Corticosteroids in laying hens. In: Moss, R. (Ed.), The Laying Hen and its Environment. Martinus Nijhoff Pub., The Hague, pp. 65–82.

Blohowiak, C.C., Siegel, P.B., Van Krey, H.P., 1980. Sexual behavior of dwarf and normal genotypes in divergent growth lines of chickens. Appl. Anim. Ethol. 6, 189–201.

Buss, E.G., 1990. Genetics of growth and meat production in turkeys. In: Crawford, R.D. (Ed.), Poultry Breeding and Genetics. Elsevier, Amsterdam, pp. 645–675.

Chang, G.B., Chang, H., Liu, X.P., Xu, W., Wang, H.Y., Zhao, W.M., Olowofeso, O., 2005. Developmental research on the origin and phylogeny of quails. World's Poult. Sci. J. 61, 105–112.

Cherry, P., Morris, T.M., 2008. Domestic Duck Production: Science and Practice. CABI Wallingford, Oxfordshire, UK.

Corso, J., Hepp, D., Ledur, M.C., Peixoto, J.O., Fagundes, N.J.R., Freitas, T.R.O., 2017. Genetic variation of the bronze locus (*MC1R*) in turkeys from Southern Brazil. Genet. Mol. Biol. 40, 104–108.

Craig, J.V., 1981. Domestic Animal Behavior. Prentice-Hall Inc., Englewood Cliffs, NJ.

Crawford, R.D., 1990. Origin and history of poultry species. In: Crawford, R.D. (Ed.), Poultry Breeding and Genetics. Elsevier, Amsterdam, pp. 1–41.

Dana, N., Megens, H.J., Crooijmans, R.P., Hanotte, O., Mwacharo, J., Groenen, M.A., van Arendonk, J.A., 2011. East Asian contributions to Dutch traditional and western commercial chickens inferred from mtDNA analysis. Anim. Genet. 42, 125–133.

Darwin, C., 1868. The Variation of Animals and Plants under Domestication. John Murray, London.

Deng, M.-T., Zhu, F., Yang, Y.Z., Yang, F.X., Hao, J., Chen, S.R., Hou, Z.C., 2019. Genome-wide association study reveals novel loci associated with body size and carcass yields in Pekin ducks. BMC Genom. 20 https://doi.org/10.1186/s12864-018-5379-1.

Derks, M.F.L., Megens, H.J., Bosse, M., Visscher, J., Peeters, K., Bink, M.C.A.M., Vereijken, A., Gross, C., de Ridder, D., Reinders, M.J.T., Groenen, M.A.M., 2018. A survey of functional genomic variation in domesticated chickens. Genet. Sel. Evol. 50, 17.

Diamond, J., 1999. Guns, Germs, and Steel: The Fates of Human Societies. W.W. Norton and Co., New York, NY.

Dohner, J.V., 2001. The Encyclopedia of Historic and Endangered Livestock and Poultry Breeds. Yale Univ. P., New Haven, CT.

Duerden, J., 1906. Defects in ostrich feathers in South Africa. Nature 74, 55–56.

Eriksson, J., Larson, G., Gunnarsson, U., Bed'hom, B., Tixier-Boichard, M., Strömstedt, L., Wright, D., Jungerius, A., Vereijken, A., Randi, E., Jensen, P., Andersson, L., 2008. Identification of the yellow skin gene reveals a hybrid origin of the domestic chicken. PLoS Genet. 4, e1000010.

Fernyhough, M., Nicol, C., van de Braak, T., Toscano, M.J., Tønnessen, M., 2020. The ethics of laying hen genetics. J. Ag. Env. Ethics 33, 15–36.

Fumihito, A., Miyake, T., Sumi, S., Takada, M., Ohno, S., Kondo, N., 1994. One subspecies of the red junglefowl (Gallus gallus gallus) suffices as the matriarchic ancestor of all domestic breeds. Proc. Natl. Acad. Sci. U. S. A. 91, 12505–12509.

Fumihito, A., Miyake, T., Takada, M., Shingu, R., Endo, T., Gojobori, T., Kondo, N., Ohno, S., 1996. Monophyletic origin and unique dispersal patterns of domestic fowls. Proc. Natl. Acad. Sci. U. S. A. 93, 6792–6795.

Girdland, F.L., Allen, R., Barnett, R., Malmström, H., Peters, J., Eriksson, J., Andersson, L., Dobney, K., Larson, G., 2014. Establishing the validity of domestication genes using DNA from ancient chickens. Proc. Natl. Acad. Sci. U. S. A. 111, 6184–6189.

Godinez, C.J.P., Nishibori, M., Matsunaga, M., Espina, D.M., 2019. Phylogenetic studies on Red junglefowl (*Gallus gallus*) and native chicken (*Gallus domesticus*) in Samar Island, Philippines using the mitochondrial DNA D-loop region. J. Poultry Sci. 56, 237–244.

Grottesi, A., Gabbianelli, F., Valentini, A., Chillemi, G., 2020. Structural and dynamic analysis of G558R mutation in chicken TSHR gene shows altered signal transduction and corroborates its role as a domestication gene. Anim. Genet. 51, 51–57.

Guhl, A.M., 1953. Social behavior of the domestic fowl. Kan. Agr. Expt. Sta. Tech. Bul. 73 (Manhattan, KS).

Guo, Y., Lillie, M., Zan, Y., Beranger, J., Martin, A., Honaker, C.F., Siegel, P.B., Carlborg, Ö., 2019. A genomic inference of the White Plymouth Rock genealogy. Poultry Sci. 98, 5272–5280.

Hale, E.B., 1969. Domestication and the evolution of behavior. In: Hafez, E.S.E. (Ed.), The Behavior of Domestic Animals. Williams and Wilkins Co., Baltimore, MD, pp. 22–44.

Hale, E.B., Schleidt, W.M., Schein, M.W., 1969. The behavior of turkeys. In: Hafez, E.S.E. (Ed.), The Behavior of Domestic Animals. Williams and Wilkins Co., Baltimore, MD, pp. 554–592.

Heikkinen, M.E., Ruokonen, M., Alexander, M., Aspi, J., Pyhäjärvi, T., Searle, J.B., 2015. Relationship between wild greylag and European domestic geese based on mitochondrial DNA. Anim. Genet. 46, 485–497.

Hesse, B., 1980. Archaeological evidence for muscovy duck in Ecuador. Curr. Anthropol. 21, 139–140.

Hutt, F.B., 1949. Genetics of the Fowl: The Classic Guide to Poultry Breeding and Chicken Genetics. McGraw Hill, New York, NY.

Kamara, D., Gyenai, K.G., Geng, T., Hammade, H., Smith, E.J., 2007. Microsatellite marker-based genetic analysis of relatedness between commercial and heritage turkeys (*Meleagris gallopavo*). Poultry Sci. 86, 46–49.

Kanginakudru, S., Metta, M., Jakati, R.D., Nagaraju, J., 2008. Genetic evidence from Indian red jungle fowl corroborates multiple domestication of modern day chicken. BMC Evol. Biol. 8, 174.

Karlsson, A.C., Fallahshahroudi, A., Johnsen, H., Hagenblad, J., Wright, D., Andersson, L., Jensen, P., 2016. A domestication related mutation in the thyroid stimulating hormone receptor gene (TSHR) modulates photoperiodic response and reproduction in chickens. Gen. Comp. Endocrinol. 228, 69–78.

Kawabe, S., Tsunekawa, N., Kudo, K., Tirawattanawanich, C., Akishinonomiya, F., Endo, H., 2017. Morphological variation in brain through domestication of fowl. J. Anat. 231, 287–297.

Kovach, J.K., 1967. Maternal behavior in the domestic cock under the influence of alcohol. Science 156, 835–837.

Landauer, W., 1951. The Hatchability of Chicken Eggs as Influenced by Environment and Heredity. Storrs Agr. Expt. Sta. Bul. 262 (Revised), Storrs, CT.

Lawal, R.A., Al-Atiyat, R.M., Aljumaah, R.S., Silva, P., Mwacharo, J.M., Hanotte, O., 2018. Whole-genome resequencing of red junglefowl and indigenous village chicken reveal new insights on the genome dynamics of the species. Front. Genet. 9, 264.

Lawal, R.A., Martin, S.H., Vanmechelen, K., Vereijken, A., Silva, P., Al-Atiyat, R.M., Aljumaah, R.S., Mwacharo, J.M., Wu, D.D., Zhang, Y.P., Hocking, P.M., Smith, J., Wragg, D., Hanotte, O., 2020. The wild species genome ancestry of domestic chickens. BMC Biol. 18, 13.

Li, H.F., Zhu, W.Q., Song, W.T., Shu, J.T., Han, W., Chen, K.W., 2010. Origin and genetic diversity of Chinese domestic ducks. Mol. Phylogenet. Evol. 57, 634–640.

Li, H.F., Zhu, W.Q., Chen, K.W., Xu, W.J., Song, W., 2011. Two maternal origins of Chinese domestic goose. Poultry Sci. 90, 2705–2710.

Li, J., Davis, B.W., Jern, P., Dorshorst, B.J., Siegel, P.B., Andersson, L., 2019. Characterization of the endogenous retrovirus insertion in *CYP19A1* associated with henny feathering in chicken. Mobile DNA. https://doi.org/10.1186/s13100-019-0181-4.

Liu, Y.P., Wu, G.S., Yao, Y.G., Miao, Y.W., Luikart, G., Baig, M., Beja-Pereira, A., Ding, Z.L., Palanichamy, M.G., Zhang, Y.P., 2006. Multiple maternal origins of chickens: out of the Asian jungles. Mol. Phylogenet. Evol. 38, 12–19.

Lockner, F.R., Youngren, O.M., 1976. Functional syringeal anatomy of the Mallard. I. In situ electromyograms during ESB elicited calling. Auk 93, 324–342.

Marom, N., Rosen, B., Tepper, Y., Bar-Oz, G., 2018. Pigeons at the edge of the empire: bioarchaeological evidences for extensive management of pigeons in a Byzantine desert settlement in the southern Levant. PLoS One 13, e0193206.

McBride, G., Parer, I.P., Foenander, F., 1969. The social organization and behaviour of the feral domestic fowl. Anim. Behav. Mongr. 2, 127–181.

McKinney, F., 1969. The behavior of ducks. In: Hafez, E.S.E. (Ed.), The Behavior of Domestic Animals. Williams and Wilkins Co., Baltimore, MD, pp. 593–626.

McKinney, F., 1975. The behavior of ducks. In: Hafez, E.S.E. (Ed.), The Behavior of Domestic Animals. Williams and Wilkins Co., Baltimore, MD, pp. 490–519.

Miao, Y.W., Peng, M.S., Wu, G.S., Ouyang, Y.N., Yang, Z.Y., Yu, N., Liang, J.P., Pianchou, G., Beja-Pereira, A., Mitra, B., Palanichamy, M.G., Baig, M., Chaudhuri, T.K., Shen, Y.Y., Kong, Q.P., Murphy, R.W., Yao, Y.G., Zhang, Y.P., 2013. Chicken domestication: an updated perspective based on mitochondrial genomes. Heredity 110, 277–282.

Mtileni, B., Dzama, K., Nephawe, K., Rhode, C., 2016. Estimates of effective population size and inbreeding in South African indigenous chicken populations: implications for the conservation of unique genetic resources. Trop. Anim. Health Prod. 48, 943–950.

Muchadeyi, F.C., Eding, H., Simianer, H., Wollny, C.B., Groeneveld, E., Weigend, S., 2008. Mitochondrial DNA D-loop sequences suggest a Southeast Asian and Indian origin of Zimbabwean village chickens. Anim. Genet. 39, 615–622.

Nishibori, M., Shimogiri, T., Hayashi, T., Yasue, H., 2005. Molecular evidence for hybridization of species in the genus Gallus except for Gallus varius. Anim. Genet. 36, 367–375.

Olsen, M.W., Marsden, S.J., 1968. Incidence of parthenogenesis in eggs of various strains of domestic turkeys, Meleagris Gallopavo. Poult. Sci. 47, 1030–1032.

Padilla-Jacobo, G., Cano-Camacho, H., López-Zavala, R., Cornejo-Pérez, M.E., Zavala-Páramo, M.G., 2018. Evolutionary history of Mexican domesticated and wild *Meleagris gallopavo*. Genet. Sel. Evol. 50, 19.

Peters, J., Lebrasseur, O., Best, J., Miller, H., Fothergill, T., Dobney, K., Thomas, R.M., Maltby, M., Sykes, N., Hanotte, O., O'Connor, T., Collins, M.J., Larson, G., 2015. Questioning new answers regarding Holocene chicken domestication in China. Proc. Natl. Acad. Sci. U. S. A. 112, E2415.

Preisinger, R., 2017. Innovative layer genetics to handle global challenges in egg production. Br. Poultry Sci. 59 https://doi.org/10.1080/00071668.2018.1401828.

Price, E.O., 1984. Behavioral aspects of animal domestication. Q. Rev. Biol. 59, 1–32.

Qu, L., Liu, W., Yang, F., Hou, Z., Zheng, J., Xu, G., Yang, N., 2009. Origin and domestication history of Peking ducks determined through microsatellite and mitochondrial marker analysis. Sci. China C Life Sci. 52, 1030–1035.

Ramachandran, R., McDaniel, C.D., 2018. Parthenogenesis in birds: a review. Reproduction 155, R245–R257.

Robinson, T.P., Wint, G.R.W., Conchedda, G., Van Boeckel, T.P., Ercoli, V., Palamara, E., Cinardi, G., Aietti, L.D., Hay, S.I., Gilbert, M., 2014. Mapping the global distribution of livestock. PLoS One 9, e96084.

Romanoff, A.L., 1960. The Avian Embryo: Structural and Functional Development. Macmillan, New York, NY.

Rubin, C.-J., Zody, M.C., Siegel, P.B., Lindblad-Toh, K., Andersson, L., 2010. Whole-genome resequencing reveals loci under selection during chicken domestication. Nature 464, 587–591.

Saeki, Y., 1957. Inheritance of broodiness in Japanese Nagoya fowl, with special reference to sex-linkage and notice in breeding practice. Poultry Sci. 36, 378–383.

Sawai, H., Kim, H.L., Kuno, K., Suzuki, S., Gotoh, H., Takada, M., Takahata, N., Satta, Y., Fumihito, A., 2010. The origin and genetic variation of domestic chickens with special reference to junglefowls Gallus g. gallus and G. varius. PLoS One 5, e10639.

Scanes, C.G., Brant, G., Ensminger, M.E., 1992. Poultry Science. Prentice Hall, Upper Saddle River, NJ.

Schorger, A.W., 1966. The Wild Turkey: Its History and Domestication. Univ. Okl. P., Norman, OK.

Shi, X.-W., Wang, J.-W., Zeng, F.-T., Qiu, X.-P., 2006. Mitochondrial DNA cleavage patterns distinguish independent origin of Chinese domestic geese and western domestic geese. Biochem. Genet. 44, 237–245.

Siegel, P.B., 2014. Evolution of the modern broiler and feed efficiency. Annu. Rev. Anim. Biosci. 2, 375–385.

Somes, R.G., 1984. International registry of poultry genetic stocks. Storrs Agr. Expt. Sta. Bul. 469.

Speller, C.F., Kemp, B.M., Wyatt, S.D., Monroe, C., Lipe, W.D., Arndt, U.M., Yang, D.Y., 2010. Ancient mitochondrial DNA analysis reveals complexity of indigenous North American turkey domestication. Proc. Natl. Acad. Sci. U. S. A. 107, 2807–2812.

Spinu, M., Spinu, O., Degen, A.A., 1999. Haematological and immunological variables in a domesticated and wild subspecies of ostrich (*Struthio camelus*). Br. Poultry Sci. 40, 613–618.

Stahl, P.W., Muse, M.C., Delgado-Espinoza, F., 2006. New evidence for pre-columbian muscovy duck *Cairina moschata* from Ecuador. Ibis 148, 657–663.

Stevens, L., 1991. Genetics and Evolution of the Domestic Fowl. Cambridge Univ. P., Cambridge, UK.

Stringham, S.A., Mulroy, E.E., Xing, J., Record, D., Michael, W., Guernsey, M.W., Aldenhoven, J.T., Osborne, E.J., Shapiro, M.D., 2012. Divergence, convergence, and the ancestry of feral populations in the domestic rock pigeon. Curr. Biol. 22, 302–308.

Sutherland, D.A.T., Honaker, C.F., Dorshorst, B., Andersson, L., Brisbane, I.L., Siegel, P.B., 2018. Growth patterns for three generations of an intercross between Red junglefowl and chickens selected for low body weight. J. Anim. Breed. Genet. 135, 300–310.

Thornton, E.K., Emery, K.F., Steadman, D.W., Speller, C., Matheny, R., Yang, D., 2012. Earliest Mexican turkeys (*Meleagris gallopavo*) in the Maya region: implications for pre-Hispanic animal trade and the timing of Turkey domestication. PLoS One 7, e42630.

van Toor, M.L., Hedenström, A., Waldenström, J., Fiedler, W., Holland, R.A., Thorup, K., Wikelski, M., 2013. Flexibility of continental navigation and migration in European mallards. PLoS One 8, e72629.

Vignal, A., Boitard, S., Thébault, N., Dayo, G.K., Yapi-Gnaore, V., Youssao Abdou Karim, I., Berthouly-Salazar, C., Pálinkás-Bodzsár, N., Guémené, D., Thibaud-Nissen, F., Warren, W.C., Tixier-Boichard, M., Rognon, X., 2019. A Guinea fowl genome assembly provides new evidence on evolution following domestication and selection in galliformes. Mol. Ecol. Resour. 19, 997–1014.

Wang, Y., Hu, Y., He, D., Chen, S., Li, S., Lan, D., Ren, P., Lin, Z., Liu, Y., 2017. Contribution of both positive selection and relaxation of selective constraints to degeneration of flyability during geese domestication. PLoS One 12, e0185328.

West, D.A., 2003. Fritz Müller: A Naturalist in Brazil. Pocahontas P. Inc., Blacksburg, VA.

West, D.A., 2016. Darwin's Man in Brazil: The Evolving Science of Fritz Müller. Univ. P. of Florida, Gainesville, FL.

Wetmore, A., 1956. The muscovy duck in the Pleistocene of Panamá. Wilson Bull. 68, 327.

Xiang, H., Gao, J., Yu, B., Zhou, H., Cai, D., Zhang, Y., Chen, X., Wang, X., Hofreiter, M., Zhao, X., 2014. Early Holocene chicken domestication in northern China. Proc. Natl. Acad. Sci. U. S. A. 111, 17564–17569.

Xiang, H., Gao, J., Yu, B., Hofreiter, M., Zhao, X., 2015. Reply to Peters et al.: further discussions confirm early Holocene chicken domestication in northern China. Proc. Natl. Acad. Sci. U. S. A. 112, E2416.

Yamaguchi, N., Hiraoka, E., Fujita, M., Hijikata, N., Ueta, M., Takagi, K., Konno, S., Okuyama, M., Watanabe, Y., Osa, Y., Morishita, E., Tokita, K., Umada, K., Fujita, G., Higuchi, H., 2008. Spring migration routes of mallards (*Anas platyrhynchos*) that winter in Japan, determined from satellite telemetry. Zool. Sci. 25, 875–881.

Zeder, M.A., 2015. Core questions in domestication research. Proc. Natl. Acad. Sci. U. S. A. 112, 3191–3198.

Zelenka, D.J., Jones, D.E., Dunnington, E.A., Siegel, P.B., 1987. Selection for body weight at eight weeks of age. 18. Comparisons between mature and immature pullets at the same live weight and age. Poultry Sci. 66, 41–46.

Zhou, M., Lei, M., Rao, Y., Nie, Q., Zeng, H., Xia, M., Liang, F., Zhang, D., Zhang, X., 2008. Polymorphisms of vasoactive intestinal peptide receptor-1 gene and their genetic effects on broodiness in chickens. Poultry Sci. 87, 893–903.

Zhou, Z., Li, M., Cheng, H., Fan, W., Yuan, Z., Gao, Q., Xu, Y., Guo, Z., Zhang, Y., Hu, J., Liu, H., Liu, D., Chen, W., Zheng, Z., Jiang, Y., Wen, Z., Liu, Y., Chen, H., Xie, M., Zhang, Q., Huang, W., Wang, W., Hou, S., Jiang, Y., 2018. An intercross population study reveals genes associated with body size and plumage color in ducks. Nat. Commun. 9, 2648.

Zuidhof, M.J., Schneider, B.L., Carney, V.L., Korver, D.R., Robinson, F.E., 2014. Growth, efficiency, and yield of commercial broilers from 1957, 1978, and 2005. Poultry Sci. 93, 2970–2982.

Chapter 9

The avian somatosensory system: a comparative view

J. Martin Wild

Department of Anatomy and Medical Imaging, Faculty of Medical and Health Sciences, University of Auckland, Auckland, New Zealand

Abbreviations

0I Nucleus olivaris inferior
A Arcopallium
Bas Nucleus basorostralis
CN IX Glossopharyngeal nerve
CN XII Hypoglossal nerve
CTB Cholera toxin B-chain
DCN Dorsal column nuclei; nuclei gracilis, cuneatus et cuneatus externus
DIVA Nucleus dorsalis intermedius ventralis anterior
DLP Nucleus dorsolateralis posterior thalami
DLPc Nucleus dorsolateralis posterior thalami, pars caudalis
DLPr Nucleus dorsolateralis posterior thalami, pars rostralis
DRG Dorsal root ganglion
EM Electron microscopy
FLM Fasciculus longitudinalis medialis
HA Hyperpallium apicale
HRP Horseradish peroxidase
HVC HVC (proper name)
ICc Central nucleus of the inferior colliculus
ICo Nucleus intercollicularis
IHA Interstitial hyperstriatum accessorium
LLDa Anterior division of the dorsal lateral lemniscal nucleus
LLDp Posterior division of the dorsal lateral lemniscal nucleus
LLI Intermediate nucleus of the lateral lemniscus
LLir Rostral part of the intermediate nucleus of the lateral lemniscus
LLIc Caudal part of the intermediate nucleus of the lateral lemniscus
LLV Ventral nucleus of the lateral lemniscus
LPS Lamina palliosubpallialis
M Mesopallium
MLd Nucleus mesencephalicus lateralis, pars dorsalis
N Nidopallium
NCL Nidopallium caudolaterale
NI/NC Neostriatum intermedium/neostriatum caudale
Nlf Nucleus interface
nTTD Nucleus tractus descendens nervi trigemini; nTTDc caudalis; nTTDi interpolaris; nTTDo oralis
nVI Nucleus nervi abducentis
NVI Nervus abducens
nVII Nucleus nervi facialis
nXIIts Nucleus nervi hypoglossi, pars tracheosyringealis
Ov Nucleus ovoidalis
PE Nucleus pontis externus
PrV Nucleus sensorius principalis nervi trigemini
RPcvm Ventromedial part of the parvocellular reticular formation
Rt Nucleus rotundus
SCi Intermediate part of the core nucleus of the preisthmic region (Puelles et al., 1994)
SI Primary somatosensory cortex
SII Secondary somatosensory cortex
sP Nucleus subprincipalis
SS Synsacral segment
SSp Nucleus supraspinalis
St Striatum
Uva Nucleus uvaeformis
VB Ventrobasal complex

9.1 Introduction

Once thought to be a meager sensory system (Ariens Kappers et al., 1936), the avian somatosensory system has in more recent times been shown to be every bit as detailed and complicated in its anatomical and functional organization as in mammals (reviews in Necker, 2000a,b; Wild, 2015). Necker (2000a) provided a concise overview of the system's basic organization, from the types, distribution, and physiology of mechanoreceptors and other sensory receptors found in avian skin, to the synaptic and functional connectivity of the somatosensory pathways ascending throughout the neuraxis (Fig. 9.1). He divided the avian somatosensory system into two parts, spinal and trigeminal, noting that the former innervates the body surface and extremities, minus the head, and the latter mainly the beak. However, with regard to ascending systems, "spinal" usually implies an origin in the spinal cord itself, rather than in the periphery, and "trigeminal" excludes other primary afferent projections from the head, such as the tongue,

Sturkie's Avian Physiology. https://doi.org/10.1016/B978-0-12-819770-7.00018-9

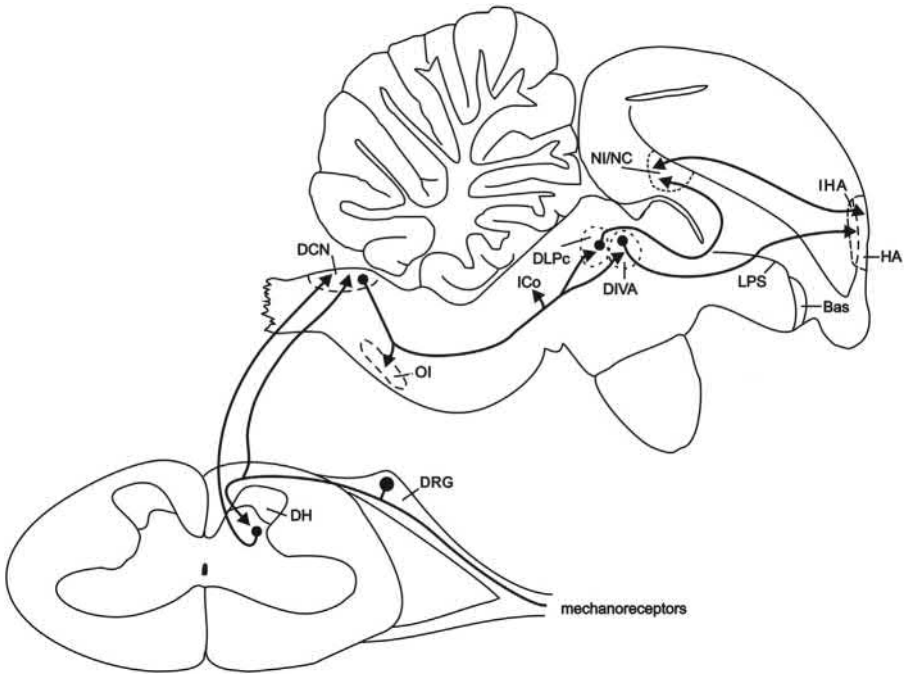

FIGURE 9.1 **Schematic parasagittal view of the brain of a pigeon showing the main somatosensory pathways from the body (minus the head).** *Filled circles* denote cell bodies, *arrows* denote terminations. Note that there are substantial deviations from this plan in some other species (see text and Figs. 9.3 and 9.5). *Adapted from Necker (2000a).*

which is not innervated by the trigeminal nerve in birds, but which plays a major somatosensorimotor role in feeding. In the present chapter, therefore, as in the previous (Wild, 2015), we make a preferred division of somatosensory origins into, on the one hand, those from the body (including feathered or unfeathered integument of the neck, thorax, abdomen, pelvis, wings, lower limb, and reproductive organs), and, on the other, those from the head (beak and mouth, tongue, head skin, and cornea). At a stretch, somatosensory input may also be provided by joint and muscle receptors, and in birds by receptors in the air sacs and syrinx (Kubke et al., 2004; Suthers et al., 2002).

9.2 Body somatosensory primary afferent projections in different species

9.2.1 Spinal cord

Our knowledge of primary afferent projections to the bird's spinal cord is based on a variety of techniques, such as tracing degenerating fibers following dorsal rhizotomy (van den Akker, 1970; Leonard and Cohen, 1975a), injecting tracer into dorsal root ganglia or applying it to the cut ends of dorsal roots (Necker, 2001), injecting tracer into feather follicles, whole wing or leg nerves (Wild, 1985; Necker and Schermuly, 1985; Schulte and Necker, 1994; Ohmori and Necker, 1995), applying tracer to cutaneous nerves and skin (Woodbury and Scott, 1991), and injecting ankle joint receptors (Gentle et al., 1995) or muscles (Wild, 1985) in pigeons and chickens. Neurophysiological analyses of pigeon dorsal horn responses have been provided by Necker (1985a,b; 1990) for pigeons and by Woodbury (1992) for chickens.

Although the different techniques provide different patterns of projections to the cord and brainstem, it is clear that primary afferent fibers enter and terminate in the cord differently depending on their diameter, as in mammals. Necker (2001) found that at the entry level of C5, for instance, large-diameter fibers entered the dorsal horn from its medial aspect, between laminae IV and V. These fibers continued into the ventral horn, where they terminated densely, and some continued laterally to terminate in the marginal nuclei. Fine-diameter fibers entered the dorsal horn laterally and terminated in various parts of the horn at the level of entry, whereas other fine fibers extended as far as C1 rostrally and at least as far as C8 caudally. Intermediate diameter fibers entered the dorsal horn from dorsal and medial positions to terminate, from Cl to C8, in lamina IV and medial lamina V. Some fibers crossed in the dorsal commissure to terminate in similar areas on the contralateral side.

That the primary afferent projections are somatotopically organized is indicated by the fact that the follicles or primary flight feathers and their coverts of the wing are represented in lamina I and medial lamina II, whereas the

follicles of secondary flight feathers and their coverts are represented at the lateral edge of the dorsal horn (Wild, 1985; Necker, 1990). Terminal fields of chicken ankle afferents are found in laminae I–III and VI, with a few terminals in deeper laminae (Gentle et al., 1995), which is similar to the projections from the cutaneous nerves of the leg in chicks (Woodbury and Scott, 1991). It should be remembered, however, that in birds as well as in mammals, different types of tracer tend to produce labeling in different laminae, with wheat germ agglutinin tending to produce labeling in laminae I and II, and cholera toxin B (CTB)-chain producing labeling predominantly in lamina III and IV (Robertson and Grant, 1985).

Primary afferent terminations in the dorsal horn can extend over several segments and are not necessarily heaviest at the level of entry of the dorsal root fibers. Gentle et al. (1995), for instance, found that although ankle joint afferents entered the cord predominantly over synsacral level SS5-7, terminations were split such that there was a small field in SS7 and 8 and a larger field in SS3 and 4. Split terminal fields were also found for whole nerve inputs (Woodbury and Scott, 1991). Terminations of wing nerve fibers extend well beyond the rostrocaudal extent of incoming rootlets, although the density of terminations declines with increasing distance from the entry zone (Leonard and Cohen, 1975a; Wild, 1985). These terminations are likely collaterals of fibers ascending or descending to more distant levels. In the case of wing nerve afferents, at least, fibers ascending in the dorsal column to the medulla provide collaterals to the dorsal horn of most, if not all, of the dozen or so cervical segments (Wild, unpublished observations in pigeons). In the greenfinch wing, nerve afferent terminations in the cervical cord are concentrated in medial lamina V (Wild, 1997), as are primary afferent fibers in budgerigars (Wild et al., 1997). Neurons at similar locations and in the nucleus of Bischoff in the upper cervical spinal cord of pigeons can be retrogradely labeled from injections of tracer into either a dorsal thalamic somatosensory nucleus (DIVA; see below) or a multimodal thalamic nucleus (DLP; see below) (Wild, 1989), which could suggest the presence of a spinothalamic projection from medial lamina V of upper cervical spinal cord segments. These findings should be contrasted with those of Schneider and Necker (1989), who found that DIVA injections retrogradely labeled very few cells in the brachial spinal cord intermediate region, but many cells at lumbar levels, suggesting a spinothalamic projection mediating lower limb somatosensory input, but the virtual absence of one from the wing.

Apart from the limbs and neck, there is little information about input from other parts of the body. Recent interest in the neural control of avian reproductive behavior, however, has involved making injections of fluorescent tracers (e.g., CTB) into the cloaca of quail and canary, a procedure that has revealed a major terminal field in the medial part of the dorsal horn throughout several sacral segments (Fig. 9.2), roughly co-extensive with the rostrocaudal distribution of retrogradely labeled cloacal motoneurons (see Wild and Balthazart, 2013; Wild, 2015). Although the supraspinal and reflex connectivity of neurons in this medial part of the sacral dorsal horn has not been determined, the data could suggest an important somatosensory role of the input from principal structures involved in reproductive behavior and voiding.

9.2.2 Brainstem

Primary afferent projections from the body to the brainstem were first visualized in pigeons by van den Akker (1970) using degeneration techniques following dorsal rhizotomies, and later using the transganglionic horseradish peroxidase (HRP) technique by Wild (1985). Neck primary afferents were also visualized in pigeons by Necker (2001), and limb primary afferents have been visualized in pigeons, chickens, greenfinches, and barn owls (Schulte and Necker, 1994; Necker and Schermuly, 1985; Gentle et al., 1995; Wild et al., 1997; Wild et al., 2001).

At caudal levels of the dorsal column nuclei (DCN, i.e., gracile, cuneate, and external cuneate nuclei) in pigeons, leg afferent terminations in the gracile nucleus lie medial to those of the wing in the cuneate nucleus, but more rostrally there is substantial overlap of leg and wing inputs throughout the DCN, although wing inputs extend further laterally around the periphery of the medulla than leg inputs. A picture of the representation of the wings can be gained by imagining them spread out and extending over the dorsal and dorsolateral periphery of the medulla. Only in the barn owl have terminations from the wing and leg been seen to be confined to clearly separate gracile and cuneate nuclei (Wild et al., 2001). In pigeons, neck primary afferents were found by Necker (2001) to project rostrally and ventrolaterally in the DCN complex, where they terminated in the external cuneate nucleus[1] (CuE), in a nucleus that he compared with the intermediate nucleus of Cajal, as well as in another nucleus he thought comparable to nucleus *x* located lateral to the nucleus of the descending trigeminal tract (nTTD) and ventral to the descending vestibular nucleus, well rostral to the obex. As in mammals, primary afferent projections to the DCN are supplemented by a dorsal column postsynaptic system (Fig. 9.1), which in pigeons takes its origin from lamina IV of the brachial spinal cord, where mechanosensitive neurons have been located (Necker, 1985a,b, 1991).

1. The avian external cuneate nucleus is not the equivalent of the same named nucleus in mammals because its inputs are not confined to upper limb proprioceptors and, at least in pigeons, it does not project to the cerebellum (Wild, 1985; Reinke and Necker, 1996).

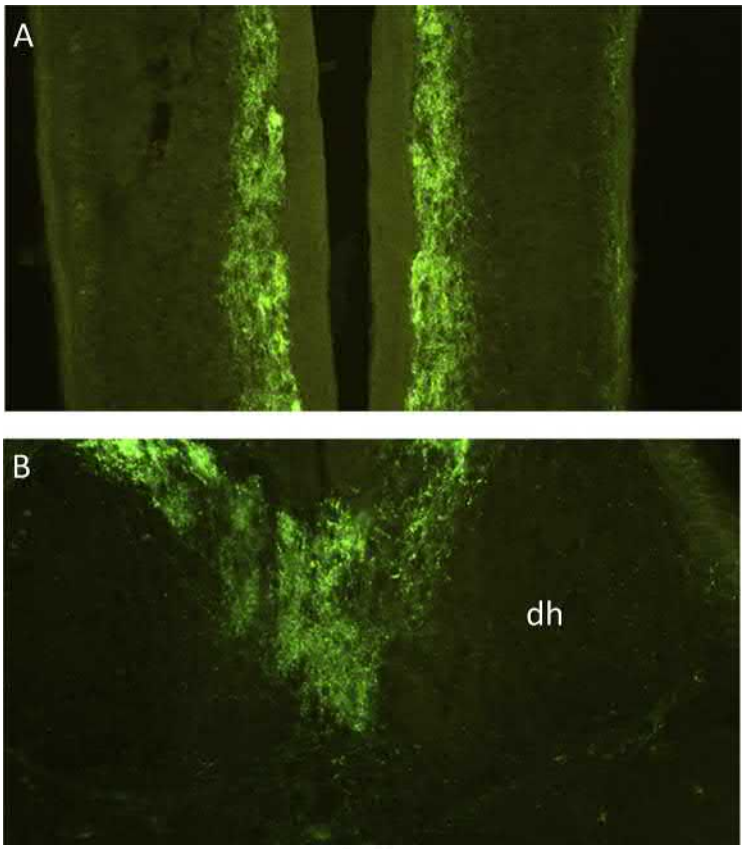

FIGURE 9.2 Cloacal afferent terminations in the sacral spinal cord. (A) Horizontal section, (B) transverse section (dorsal is up). These terminations, which were visualised following subcutaneous injection of green flourescent CTB (CTB-488) into the cloaca of male canaries, were localised to the medial aspect of each dorsal horn.

In pigeons, finches and barn owls primary afferent projections extend ipsilaterally throughout the medulla and into the pons, where they terminate sparsely in proximity to PrV (Wild, 1985, 1997). In the Australian budgerigar (*Melopsittacus undulatus*) (Wild et al., 1997) and possibly other psittaciforms (Wild, 1981), primary afferents from both wing and leg also reach pontine levels, where they terminate densely and topographically in nucleus subprincipalis (sP), immediately subjacent to PrV (Fig. 9.3). One implication of these findings in the budgerigar is that here at pontine levels there is a striking instance of a complete, somatotopic representation of the whole body, with the beak and tongue and possibly some other parts of the head being represented massively in PrV (see below) and, ventral to PrV, a smaller representation of the rest of the body in sP (Fig. 9.3).

9.3 Ascending projections of the dorsal column nuclei

As in mammals (Berkley et al., 1986), the DCN in birds project predominantly contralaterally to several more rostral nuclei via a medial lemniscus, en route to their final targets in the thalamus (Fig. 9.1, Wild, 1989, 1997). The inferior olive (0I) in the caudal brainstem is the first target, which then projects to the cerebellum via the inferior cerebellar peduncle. Because in pigeons, at least, the DCN do not project directly to the cerebellum, the route to the cerebellum via the OI may be one way that somatosensory inputs serve sensorimotor control.

Another significant target of the DCN is the midbrain, where there are terminations not only in intercollicular regions surrounding the auditory nucleus mesencephalicus lateralis, pars dorsalis (MLd) but also within it (Karten, 1967; Leibler, 1975; Wild, 1989, 1995, 1997). Units recorded electrophysiologically in the region between the dorsal border of MLd and the tectal ventricle respond to both somatosensory and visual stimuli (Ballam, 1982). The region ventral to more caudomedial regions of MLd forms a distinct nucleus called the intermediate part of the core nucleus of the preisthmic region (SCi; Puelles et al., 1994). Its neurons are exquisitely sensitive to tactile stimuli applied to feathers and body surface and respond with large-amplitude action potentials (Wild, 1995). Its ascending projections require further definition, but the location of terminations around the ventral periphery of the

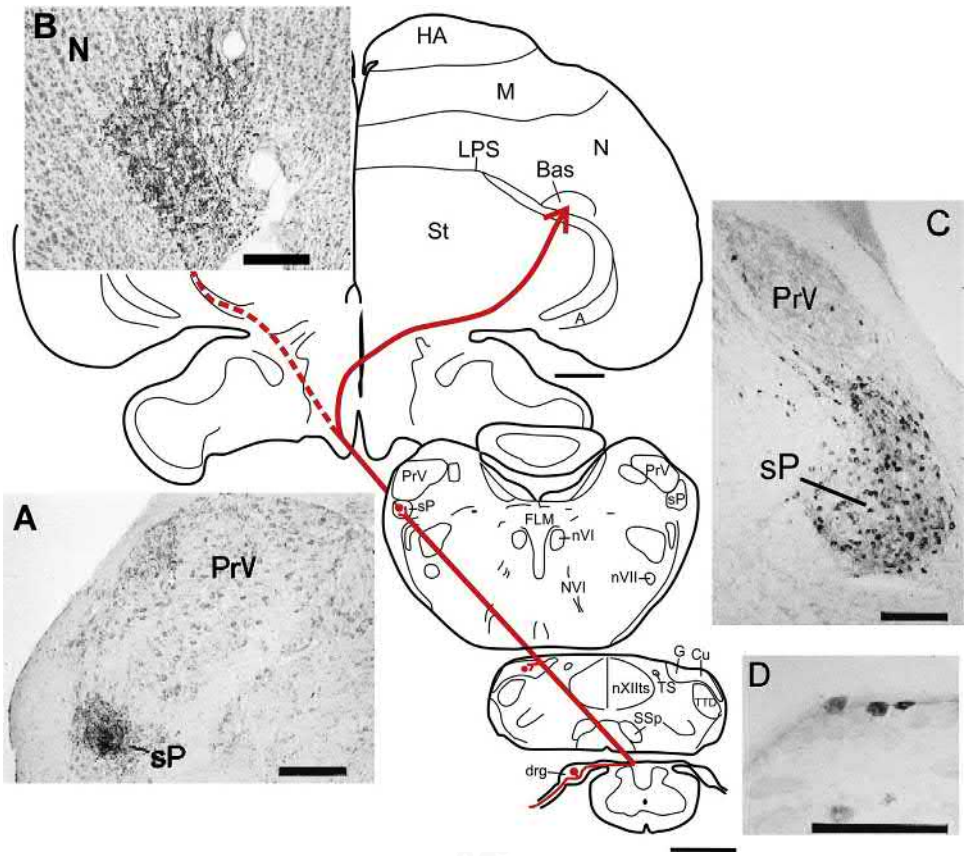

FIGURE 9.3 **Somatosensory pathway in the budgerigar (parakeet).** Primary afferent fibers project to and terminate in the ipsilateral nucleus subprincipalis (sP), cell bodies of which project their axons to the body regions of Bas, predominantly contralaterally (*solid lines*). Scale bars for schematics: 1 mm. (AJ Terminal field in sP fo1lowing an injection of horseradish peroxidase-conjugated cholera toxin B (CTB)-chain in the ipsilateral radial nerve. The terminal field of sciatic fibers (not shown) is located ventrolateral to that of the wing. (B) Terminal field (note its precise borders) in the body part of Bas following an injection of biotinylated dextran amine (BDA) in the contralateral sP. (C) Retrogradely labeled cells in sP following an injection of CTB in the contralateral body part of Bas. (D) Retrogradely labeled cells in a dorsal root ganglion of a spinal segment from the brachial enlargement, following an injection of BDA in the ipsilateral sP. Note that the gracile (G) and Cuneate (C) nuclei of the dorsal columns also project to sP. Scale bars = 200 μm for photomicrographs. *Adapted from Wild et al. (1997).*

thalamic auditory nucleus ovoidalis (Ov), Ov being the main target of MLd projections (Karten, 1967), closely mirrors the location of SCi with respect to MLd (Wild and Williams, 2000). In pigeons and finches, it appears that the DCN also project directly to MLd, where diffuse terminations overlap the much denser terminations of projections from brainstem auditory nuclei (Wild, 1989, 1995, 1997). Speculations concerning the functions of the somatosensory projection to MLd can be found in Wild (1995). In the barn owl, there is a similar but more restricted DCN projection to rostrodorsal parts of MLd (known in barn owls as the central nucleus of the inferior colliculus; Wild et al., 2008). These findings represent but one of the several instances in the avian brain of somatosensory and auditory proximity or overlap.

At caudal thalamic levels, the DCN project upon the medial spiriform nucleus, which then projects to the cerebellum (Karten and Finger, 1976; Wild, 1992). Next, the DCN target a nucleus called dorsolateral posterior thalami (DLP), the caudal part of which in pigeons (DLPc) has been considered comparable with nucleus uvaeformis (Uva) in finches (Wild, 1987, 1994; Funke, 1989a). DLPc and Uva tend to be multimodal (Korzeniewski, 1987; Korzeniewski and Güntürkün, 1990; Wild, 1994), and in this respect are perhaps similar to the posterior group of thalamic nuclei of mammals (Gamlin and Cohen, 1986). Both beak and body responses have been found in DLP in pigeons (Korzeniewski, 1987), but beak responses are likely to arise from the nTTD (Korzeniewski and Güntürkün, 1990) rather than from the DCN (see also Wild, 1989; Faunes and Wild, 2017a). Rostral to DLP, the DCN target the nucleus DIVA, which lies immediately dorsal and lateral to the auditory nucleus Ov and the visual nucleus rotundus (Wild, 1989, 1997; Faunes and Wild, 2017a). Unlike DLP, DIVA is specifically somatosensory; although it contains a representation of most body parts (including toes, but not the beak), it is weakly somatotopically organized (Schneider and Necker, 1996). DIVA is probably

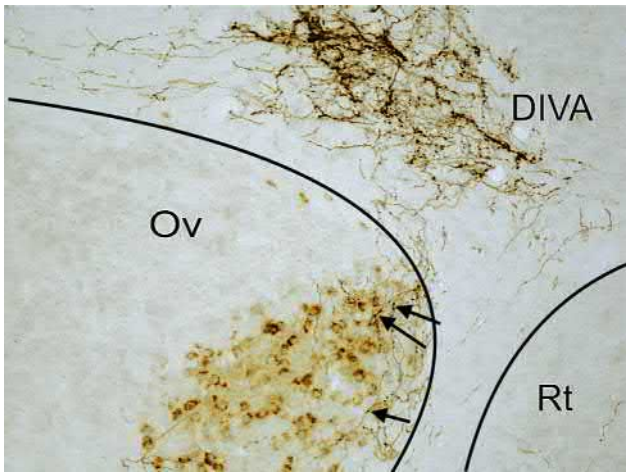

FIGURE 9.4 Dorsal column nuclei projections to nucleus ovoidalis and DIVA. Labeled fibers and varicosities (black, e.g., at *arrows*) in the lateral part of nucleus ovoidalis (Ov) and the overlying dorsal thalamic somatosensory nucleus DIVA in the zebra finch, following an iontophoretic injection of BDA in the dorsal column nucleus (section midline is to the left). Neurons in the lateral part of Ov (brown) were retrogradely labeled by an injection of cholera toxin B-chain in the lateral part of Field L, the primary thalamorecipient auditory field in the telencephalon. Rt: nucleus rotundus. *Wild, unpublished observations.*

homologous to part of the ventrobasal complex (VB) of mammals. In zebra finches, there is a small but distinct projection from the DCN to a lateral part of Ov, as fibers pass to the overlying DIVA (Fig. 9.4). This is yet another instance in the avian brain of somatosensory and auditory proximity or overlap.

Unlike the case for mammals (Berkley et al., 1986), there is some evidence in finches, at least, that single DCN neurons project to more than one more rostral nucleus (e.g., intercollicular nucleus and DIVA) via branched axons (Wild, 1997).

To complete this section, again in the curious case of the budgerigar, the DCN project ipsilaterally to sP in the pons (Wild et al., 1997), as do primary afferents from the wings and legs (Figs. 9.3 and 9.5). Whether the DCN also project to the thalamus in this species is not known. Another variation on the DCN projections occurs in the barn owl, in which there is a projection from both gracile and cuneate nuclei to a large nucleus at the lateral edge of the pons called pontis externus (PE) (Wild et al., 2001). Such a nucleus, which in the barn owl does not receive primary afferent projections directly from the body surface, has thus far not been described for any other species. PE may, however, be the functional equivalent of sP in budgerigar because, like sP, it provides a major body somatosensory and topographically organized input to nucleus basorostralis pallii (Bas) (see below). The various ascending somatosensory pathways are depicted for four species in Fig. 9.5.

9.4 Telencephalic projections of thalamic nuclei receiving somatosensory input

The ascending projections of DLP/Uva and DIVA are quite separate. In pigeons, DLP projects to the intermediate and caudal parts of the nidopallium (NI/NC: Gamlin and Cohen, 1986; Funke, 1989a; Wild, 1987). The terminal field of more rostral parts of DLP (DLPr) lies medially adjacent to the visual entopallium, whereas the terminal field of DLPc lies more caudally, closer to the thalamorecipient auditory field L, and is predominantly somatosensory (Wild, 1987; Funke, 1989b). In finches, which are songbirds, the equivalent region of the nidopallium to which Uva projects is called nucleus interface (NIf), which is usually regarded as belonging to the song system (Nottebohm et al., 1982). It is possible, however, that following a sufficiently fine-grained electophysiological and anatomical analysis, this region of the nidopallium may be subdivided into visual, somatosensory, and auditory components (Wild, unpublished observations), with the auditory component in songbirds then providing the predominant input to HVC of the song control system (Nottebohm et al., 1982; Wild, 1994; Vates, 1996; Lewandowski et al., 2013).

In both pigeons and finches, the ascending projections of DIVA are specifically to the interstitial hyperstristum accessorium (IHA) of the rostral, somatosensory Wulst (Wild, 1987, 1997; Funke, 1989a). In finches, the input to IHA is distinctly and regularly patchy, but a somatotopic organization has not been examined. In pigeons, there is a very weak somatotopic organization of this region (Funke, 1989b).

It has been suggested that the somatosensory area in the rostral Wulst of birds may be equivalent to SI in mammals, whereas the more caudal somatosensory area in NI/NC is equivalent to SII (Wild, 1987). The two regions are reciprocally connected (Wild and Williams, 1999). Unlike the somatosensory inputs to SI in mammals, however, the avian classical three-neuron sequence of somatosensory projections from the body surface to the telencephalon via primary afferent projections to the DCN, contralateral DCN projections to the dorsal thalamus, and DIVA projections to the rostral Wulst, mediates a decreasingly specific somatotopic organization as it ascends. In the spinal dorsal horn, the somatotopy is both anatomically and electrophysiologically clear cut (see above; Necker, 1990; Woodbury, 1992); in the caudal parts of the DCN, it is reasonably clear, but much less clear in more rostral parts of the DCN (Wild, 1985). In DIVA, the somatotopy is unimpressive (Schneider and Necker, 1996), as it is in the rostral Wulst (Funke, 1989b). Furthermore, the beak appears not to be represented in DIVA, but the toes and foot joints are (Schneider and Necker, 1996).

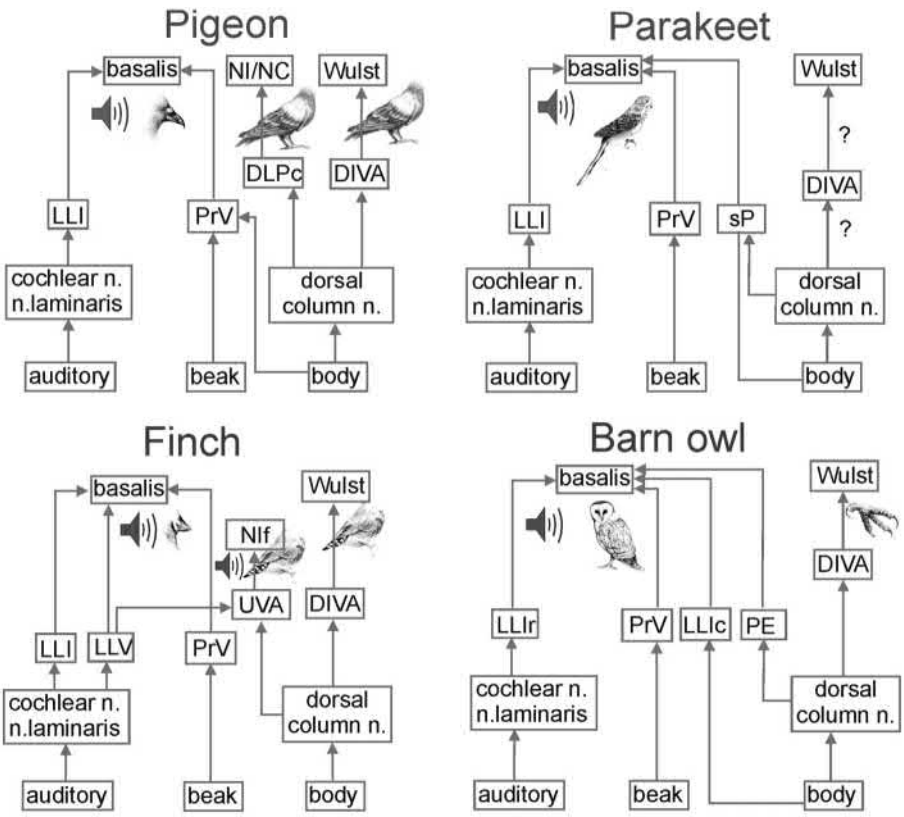

FIGURE 9.5 **Comparative schematic of ascending somatosensory and auditory projections to the telencephalon via thalamic and nonthalamic pathways in four different species.** Note the "beakless" representation of the body in the rostral Wulst of pigeons and finches and the complete body + beak + auditory representation in Bas of parakeets (budgerigars) and barn owls (auditory representations are symbolized by speakers). Note also the auditory projection to nucleus interface of finches, which is relayed via projections of the ventral nucleus of the lateral lemniscus to nucleus uvaeformis (Coleman et al., 2007), and perhaps by projections of ovoidalis to the nucleus interface (not shown; Wild, unpublished observations). *Adapted from Wild et al. (2008).*

At the frontal pole of the brain of the barn owl, rostral to what would be the rostral Wulst of other birds, there is an apparently unique bulge that contains a detailed somatotopic representation of the contra1ateral claw (Manger et al., 2002; Wild et al., 2008, Fig. 9.6). Curiously, a representation of more proximal parts of the lower limb, or of any other body part, was not found in or near this bulge, but the foot and other parts of the body are also represented in what is now called Bas (Reiner et al., 2004, and see below). Apparently, sensory input from the claw is all-important for the predatory barn owl. It would be most interesting to determine the representation of the claw in other predatory avian species that strike and capture their prey in a similar way to barn owls, such as eagles.

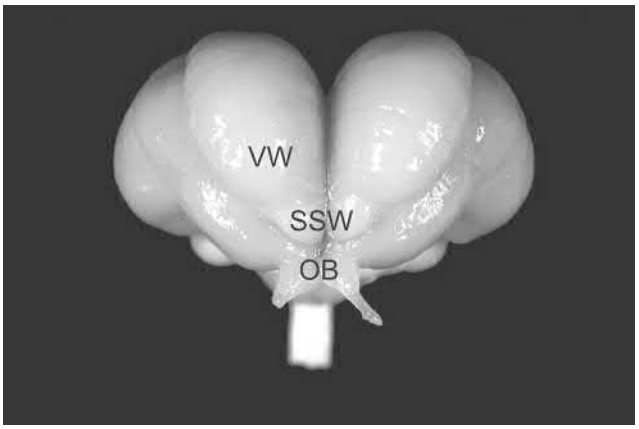

FIGURE 9.6 **The brain of a barn owl viewed from in front.** *OB*, olfactory bulb; *SSW*, somatosensory Wulst (claw area); *VW*, visual Wulst. *From Wild et al. (2008).*

9.5 Somatosensory primary afferent projections from the beak, tongue, and syrinx to the trigeminal column

9.5.1 The principal sensory trigeminal nucleus

The bird's beak or bill varies hugely in shape and size between different species (e.g., compare the beaks of pelican, spoonbill, tucan, kiwi, flamingo, duck, cockatoo, wren)—a variation that is generally correlated with the different feeding habits and preferred foods, on the one hand, and on the other with the size and morphological

complexity of the principal sensory trigeminal nucleus (PrV, to which trigeminal beak afferents project) (Stingelin, 1961). As an instance of microevolutionary processes at work, the size and shape of the beaks of Galapagos finches may even vary according to the annual availability of preferred types of food (Weiner, 1995).

In many species, there are specializations of the beak for various feeding strategies or for probing the substrate. For instance, ducks have an elaborate bill tip organ packed with mechanoreceptors (Berkhoudt, 1980), which enable the discrimination of food items through dabbling and sifting. Many shorebirds, such as sandpipers (Scolopacidae), possess Herbst corpuscles densely packed into honeycomb-like cavities in the bill, which enable the detection of food items even remote from the bill (Gerritsen and Meiboom, 1986). This is similar in kiwi, for probing the substrate during their night time foraging (Cunningham et al., 2007; Martin et al., 2007). In many other species, such as parrots and finches, however, the mechanoreceptors are not in the bone but lie more superficially, nearer the bill surface for the detection, manipulation, and guidance of food items within the mouth (Demery et al., 2011; Krulis, 1978). During feeding, these processes are aided by tongue movements, but differently in different species. Again in parrots and finches, the tongue is loaded with mechanoreceptors (Herbst and Grandry corpuscles) that enhance the efficiency of the cracking and husking of seeds in conjunction with the beak (Krulis, 1978; Wild, 1990; Demery et al., 2011). In contrast, in pigeons, the beak functions as a simple grasper, like the combination of forefinger and thumb of humans (Fig. 9.7). Once the food object is grasped, the tongue aids the transport of food objects, such as peas or grain, from the beak tip lo the back of the mouth, and these items are then swallowed whole (Zweers, 1982).

PrV receives topographic projections from the beak by way of ophthalmic (upper beak), maxillary (palate, lower eyelid), and mandibular (lower beak) branches of the trigeminal nerve (Dubbeldam, 1980; Dubbeldam and Karten, 1978; Wild and Zeigler, 1996; Faunes and Wild, 2017b). Depending on the species, PrV may also receive projections from the tongue, but unlike the case for mammals, not by way of the trigeminal nerve. In pigeons, there does not appear to be a representation of the tongue in PrV (Wild, unpublished observations), but in finches, parrots, and ducks, there is a substantial lingual representation in PrV. In ducks, lingual afferents are carried by the glossopharyngeal nerve and terminate in a dorsomedial portion of PrV (Dubbeldam et al., 1979; Dubbeldam, 1980). In finches and parrots, they are carried by the hypoglossal nerve and terminate in a dorsolateral portion of PrV (Wild, 1981, 1990; Faunes and Wild, 2017b). These afferents are unlikely to be trigeminal afferents that hitchhike via other nerves because their cell bodies are not located in the trigeminal ganglion, but in a combined "jugular" ganglion (Dubbeldam et al., 1979; Wild, 1981). The innervation of the orderly arrays of sensory receptors (Herbst and Grandry corpuscles; Berkhoudt, 1980; Gottschaldt, 1985) in the tongue can be visualized by injecting the hypoglossal nerve with CTB-chain (Fig. 9.8) or staining tongue sections with a trichrome stain (Wild, 1990). These receptors have also been visualized with electron microscopy (Toyoshima and Shimamura, 1991), although the source of their innervation was apparently not known to these authors.

The tracheosyringeal nerve, the other major branch of the hypoglossal nerve (CN XII) in birds, also has a sensory component, and this projects upon a lateral aspect of PrV, at least in zebra finches (Bottjer and Arnold, 1982; Faunes et al., 2017). The fibers have been identified as substance P-immunopositive syringeal muscle afferents, a finding that may be of particular interest in the context of the sensory control of vocalization in general and singing in particular, especially in view of the absence of muscle spindles in avian syringeal muscles generally (Faunes et al., 2017)—see nTTD below.

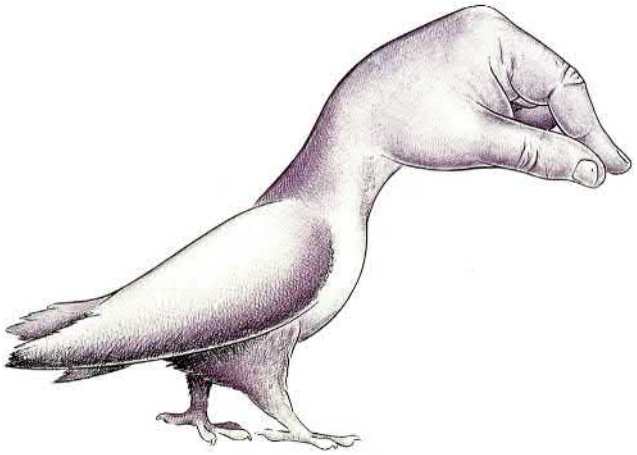

FIGURE 9.7 Drawing of the pigeon body and human hand to illustrate the functional nature of the bird's beak as a combined thumb-and-forefinger grasper and mouth.

9.5.2 Nucleus of the descending trigeminal tract

Because PrV is the predominant origin of trigeminal projections to the telencephalon (Fig. 9.9), the descending component of the trigeminal column (nTTD) has traditionally been studied only sporadically, in ducks and pigeons (Silver and Witkovsky, 1973; Dubbeldam and Karten, 1978; Arends and Dubbeldam, 1984; Arends et al., 1984). More recent and specific analyses of the central projections of trigeminal nerve branches or their innervated peripheral territories have used injections of either HRP-conjugated CTB or unconjugated CTB in pigeons, chickens, and zebra finches (Wild and Zeigler, 1996; Wild and Krutzfeldt, 2012; Faunes and Wild, 2017b). These studies show a fairly consistent pattern of descending

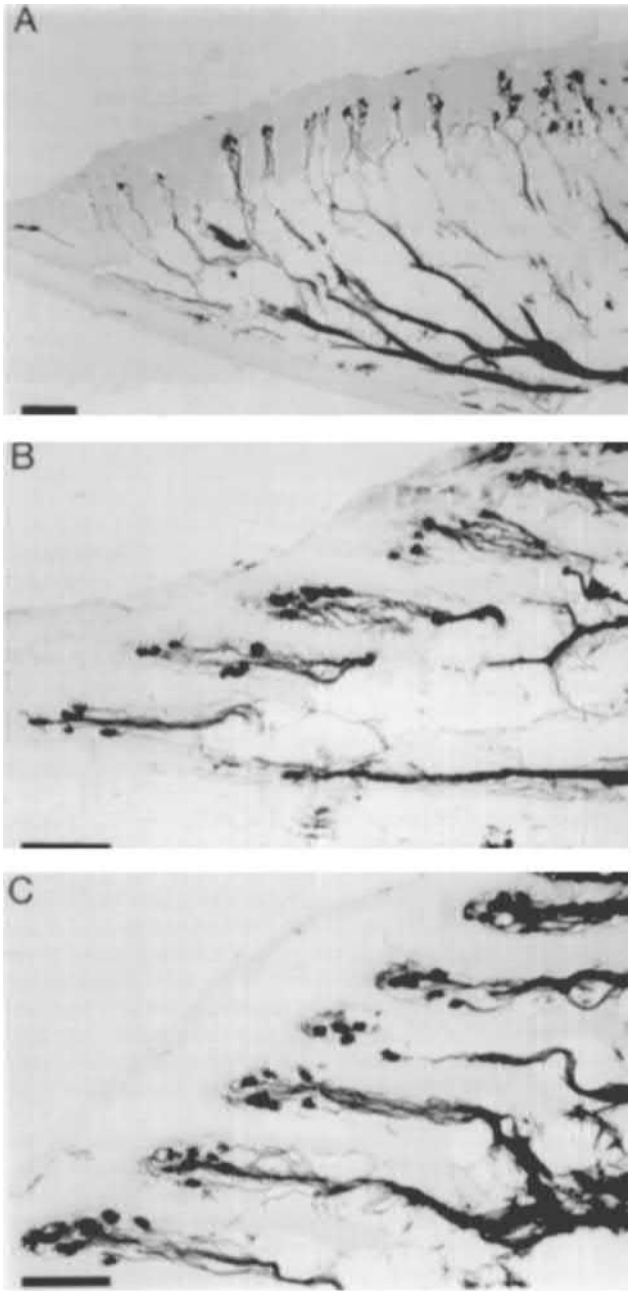

FIGURE 9.8 Photomicrographs of horseradish peroxidase-conjugated cholera toxin B-chain labeled hypoglossal nerve branches innervating the papillae of the tongue in zebra finch (A), a greenfinch (B), and a gold finch (C), anterior to the left. The terminal "blobs" visible at this magnification (bars = 200 μm) are terminal cell receptors at the sides and apices of the bowls of flask-shaped papillae. Note how the papillae of the zebra finch tongue are perpendicular to the surface, whereas those of the other two species lie in the horizontal plane and are hence at approximately 45″ to the surface. *From Wild (1990).*

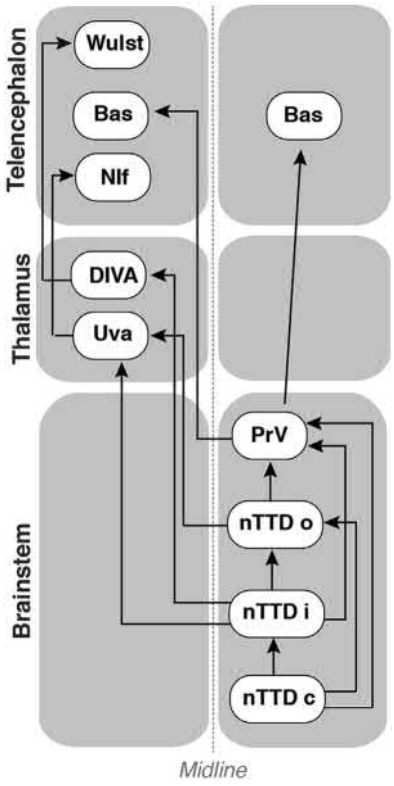

FIGURE 9.9 Schematic depiction of the ascending projections of the sensory trigeminal complex in the zebra finch. *From Faunes and Wild (2017b).*

projections throughout the three subdivisions of the nTTD, there being a roughly inverted representation of mandibular, maxillary, and ophthalmic afferents throughout pars interpolaris and parts of caudalis, but a clear-cut mediolateral representation at upper cervical spinal levels. Corneal afferents terminate specifically in a ventral portion of the ophthalmic representation in pars caudalis and in the laterally adjacent external cuneate nucleus (Wild, 1999), and in the zebra finch, the corneal afferents in nTTD have been shown to be calbindin-like immunopositive (Faunes and Wild, 2017b). Dubbeldam and Karten (1978) also described a lateral descending tract in the pigeon, which is also present in certain snakes possessing infrared detection. It is possible, therefore, that in birds this tract might carry thermosensitive afferents (see Wild and Zeigler, 1996).

As in mammals, mechanosensitive afferents that terminate in nTTD in birds arrive over other nerves in addition to the trigeminal. In the mallard duck, lingual afferents traveling in the glossopharyngeal nerve terminate dorsomedially in nTTD (Dubbeldam et al., 1979). In finches, lingual afferents traveling in the lingual branch of the hypoglossal nerve terminate dorsolaterally in pars interpolaris and pars caudalis of nTTD, but most medially at upper cervical spinal cord levels (Wild, 1990; Faunes and Wild, 2017b). This suggests that although the tongue makes contact with both upper and lower beaks during feeding, in the brainstem, lingual afferents are aligned with mandibular afferents (which innervate the lower beak) rather than with ophthalmic ones (which innervate the upper beak). As in PrV, some substance P-immunopositive

syringeal muscle afferents in finches terminate in a dorsolateral part of the interpolaris portion of nTTD, having arrived there by way of the tracheosyringeal nerve (Faunes et al., 2017). This finding gains further importance in the context of hypothesized feedback from the syrinx during singing (Bottjer and Arnold, 1982, 1984), especially now that a projection from nTTD to nucleus Uva of the songbird song system has been identified (Faunes and Wild, 2017a, Fig. 9.9).

9.6 Nucleus basorostralis

Anatomical knowledge of trigeminal components of the avian somatosensory system has existed for much longer than knowledge of its spinal components, Wallenberg describing a direct projection from PrV to a nucleus in the rostrobasal part of the avian forebrain via the quintofrontal tract as early as 1903. Although considerable anatomical and physiological attention has been directed to Bas in several species in the last 40 years, the nucleus remains enigmatic from both an anatomical and to some extent from a functional point of view. The absence of a thalamic relay in the PrV projection to Bas remains puzzling, at least in comparison with the organization of the somatosensory system in mammals (Cohen and Karten, 1974). Although Bas has been known for decades to play a major function in the sensory control of feeding in pigeons and ducks, it is now known to be more than a forebrain nucleus dedicated solely to the somatosensory representation of the beak (Witkovsky et al., 1973). Dubbeldam and colleagues in the 1980s used the mallard to investigate the functional morphology of Bas in relation to the duck's feeding apparatus and its various mechanoreceptors involved in the different sensory phases of feeding (Berkhoudt, 1980). The projections of PrV subnuclei were traced to Bas (Dubbeldam et al., 1981), and the nucleus was mapped electrophysiologically to reveal a distinct functional topography based on the representations of the glossopharyngeal and trigeminal nerve branches innervating the tongue and beak, respectively (Berkhoudt et al., 1981). Projections of PrV to Bas were also traced in pigeons (Wild et al., 1985) and in zebra finches (Wild and Farabaugh, 1996), but Bas is much smaller in these species than in ducks and does not lend itself so readily to detailed electrophysiological mapping. In budgerigars, as in ducks, however, Bas lies atop the pallial-subpallial border rather that lateral to it, so a complete mapping of the representations of beak and tongue has been performed (Wild et al., 1997, Fig. 9.10). As in ducks, a large lingual representation is present rostrally in Bas, but this is hypoglossal territory rather than glossopharyngeal. Behind is an even larger representation of the beak, followed by a smaller one of the head. On the lateral aspect of the head representation is an indentation that includes a representation of the cochlea and possibly of the semicircular canals; these representations seemingly mirroring the position on the lateral aspect of the skull of the cochlear and vestibular apparatus at the medial end of an external auditory meatus. Progressively more caudal to the representation of the head are representations of the wings, body, and legs and feet. These body inputs are relayed predominantly by the contralateral nucleus sP, ventral to PrV, which supplies the inputs from beak and tongue. Thus, in the budgerigar, there is a complete representation of the body in Bas, much as there is at pontine levels (see above).

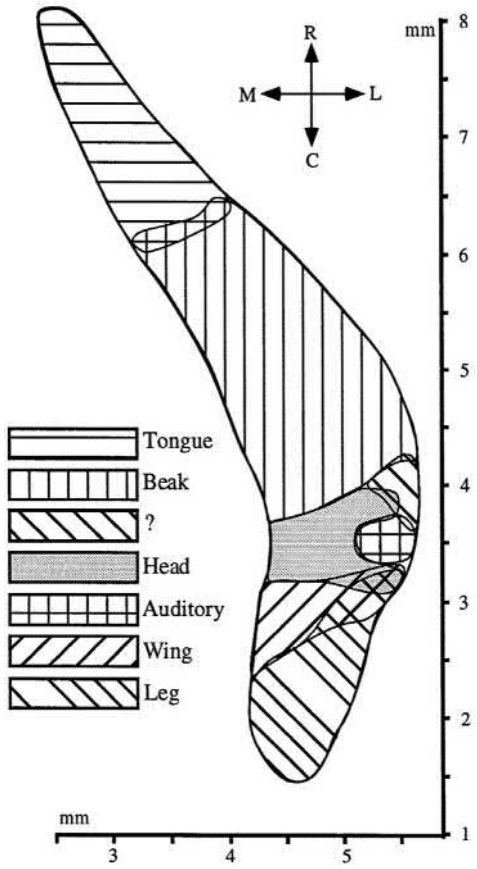

FIGURE 9.10 A two-dimensional map of Bas on the right side of the brain of the budgerigar (parakeet). The map is based primarily on recordings of evoked multiple-unit activity in Bas. The area rostral to the auditory area possibly receives inputs from a vestibular nucleus. *From Wild et al. (1997).*

The auditory representation in Bas of all species thus far examined reflects its input from the intermediate nucleus of the lateral lemniscus (LLI, which lies close to PrV), a projection first defined in pigeons (Arends and Zeigler, 1986) and later in zebra finches (Wild and Farabaugh, 1996). In these last two species, however, complete body representations have not been found in Bas, although in finches, as in parrots, there is a large lingual (hypoglossal) representation rostrally in the nucleus.

The largest Bas thus far encountered is that of the barn owl, in which there also appears to be a complete body representation, including a tonotopically organized auditory component (Wild et al., 2001). Injections of tracers in Bas retrogradely label neurons in the massive PE nucleus that forms a bulge on the lateral aspect of the pons and lies ventrolateral to the equally large anterior and posterior divisions of the dorsal nucleus of the lateral lemniscus (LLda and LLDp). In turn, injections in PE retrogradely label neurons in the DCN, thereby completing a three-neuron sequence of somatosensory projections from the body periphery, but one that is quite different from the classical sequence in mammals that projects via the thalamus. Medially adjacent to PE is a smaller LLI that presumably provides most of the auditory input to Bas, although Bas seems also to receive a small auditory projection from LLDa.

9.7 The meeting of the spinal and trigeminal systems

In his chapter on the spinal cord, Necker (2000b) briefly mentioned a difference between pigeons and chickens in the laminar organization of the dorsal horn, a difference that has received further examination (Wild et al., 2010). In pigeons, the dorsal horn laminae are arranged in mammalian fashion, with lamina II lying dorsal to lamina III; however, in chickens the latter lies medial, not ventral, to the former (cf. Brinkman and Martin, 1974; Leonard and Cohen, 1975b). In fact, as Woodbury (1998) showed, the majority of bird species resemble chickens, rather than pigeons, in the bifid, side-by-side arrangement of laminae II and III. Nevertheless, the functional organization of these laminae in chickens and their kin is not dissimilar to that in pigeons and their kin, in that smaller diameter and unmyelinated primary afferents terminate in lamina I and II, whereas larger diameter, myelinated primary afferents terminate in lamina III (Woodbury and Scott, 1991; Wild, 1985).

Many years ago, Woodbury asked a related, interesting question about the organization of the trigeminal dorsal horn: since this was generally considered to be a direct continuation of the spinal dorsal horn, and to have a similar organization, did this organization reflect the organization present at spinal levels in species in which II and III were side by side rather than arranged in mammalian-type laminar fashion? In other words, was the trigeminal dorsal horn also split in chickens, etc., with a side-by-side arrangement of superficial and deeper laminae? This question has been answered, and the findings compared with those in pigeons (Wild and Zeigler, 1996; Wild et al., 2010). It was found that the trigeminal dorsal horn in chickens was organized in a laminar fashion, as it is in pigeons, and remained laminar down to about the level of C3. Thereafter, however, lamina III gradually, over a couple of segments, shifted medially, until from C5 caudally laminae II and III came to lie side by side. It was also shown that, although the three branches or the trigeminal nerve in the chicken terminated throughout the dorsal horn in a similar fashion to that in pigeons—with ophthalmic afferents laterally, mandibular afferents medially and maxillary afferents in between—they did not extend further caudally than about C3, in contrast to C6 or C7 in pigeons. Thus, it appears that trigeminal primary afferents in the chicken do not terminate at cervical spinal levels that have a side-by-side arrangement of dorsal horn laminae. These findings suggest a discontinuity of spinal and trigeminal dorsal horn organization, the reason for which remains obscure. What is clear, however, is that Woodbury's (1998) hypothesis of a side-by-side arrangement of laminae II and III defining a novel clade of birds is not supported, for when an appropriate phylogenetic analysis is performed, a reversion to the mammalian type of arrangement of dorsal horn lamina is seen to have occurred several times in avian evolution (Wild et al., 2010).

9.8 The somatosensorimotor system in birds

In mammals, somatosensory inputs to the cortex initiate somatomotor responses that reach brainstem and spinal targets via corticobulbar and corticospinal components of the pyramidal tract. Such a tract in birds originating in the rostral part of the Wulst was proposed by Zecha (1962) and shown with contemporary tracing techniques in pigeons and zebra finches by Wild and Williams (2000). The pyramidal tract equivalent originates in the hyperpallium apicale (HA) of the rostral Wulst, implying rather direct connections between somatosensory inputs to IHA and somatomotor outputs from HA. The tract and its terminations are far from meager. As in mammals, the red nucleus is a prime target, which then projects to all levels of the spinal cord (Wild et al., 1979). Further caudally, the tract terminates profusely throughout wide regions of the brainstem reticular formation and secondary sensory nuclei, such as the external cuneate nucleus, but does not proceed further caudally than upper cervical levels.

An interesting but little-known somatosensorimotor link in the brainstem reflects control of the lower eyelid, which relaxes during sleep to cover the eye, in contrast to the descent of the upper lid in mammals. During waking hours, the lower eyelid appears to be under tonic control to keep the eye open, until a corneal stimulus initiates a defensive reaction. These actions are mediated via corneal afferent input to the ophthalmic part of nTTD and projections of nTTD to the dorsal motor nucleus of the trigeminal motor complex that innervates the two muscles of the lower eyelid (Wild and Williams, 1999).

In contrast to motor output from rostral HA via the pyramidal tract, outputs of Bas exit the telencephalon from the arcopallium at the caudal pole of the brain. They reach the arcopallium indirectly via an overlying part of the frontal nidopallium and the caudolateral part of the nidopallium caudolaterale (Wild et al., 1985; Dubbeldam and Visser, 1987). In finches, beak and auditory components of Bas were shown to follow this route independently (Wild and Farabaugh, 1996). The descending projections of different major parts of the arcopallium were originally described by Zeier and Karten (1971) in pigeons and shown to include secondary sensory nuclei in the brainstem. This was specifically confirmed using contemporary tracing techniques in zebra finches, in which Bas-recipient components of the lateral arcopallium were shown to target the nTTD (Wild and Farabaugh, 1996) and the ventromedial part of the parvocellular reticular formation (RPcvm), which is a major nexus of premotor projections to the jaw and other upper vocal tract motor nuclei (Wild and Krutzfeldt, 2012).

9.9 Somatosensory projections to the cerebellum

In the pigeon cerebellum, there are two somatosensory areas, one rostrally (lobules I–VI) and another caudally (lobule IX) (Necker, 2000a; see also Whitlock, 1952). Somatosensory projections to these regions are relayed from the spinal cord (Necker, 1992, 2000a; Okado et al., 1987). Spinal inputs to the anterior cerebellum arise predominantly from neurons in Clarke's column and hence are proprioceptive. Spinal inputs to the posterior cerebellum arise primarily from cervical lamina IV neurons, which are mechanosensitive (Necker, 1992). Another source of putative mechanosensitive spinocerebellar fibers is the paragriseal cells, which in the lumbosacral spinal cord are contacted by the axons of neurons in the contralateral accessory lobes of Lachi (marginal nuclei) (Necker, 1997). These lobes comprise a sensory component of a lumbosacral specialization involved in a sense of equilibrium (Necker, 1999; Necker et al., 2000; Rosenberg and Necker, 2000).

9.10 Magnetoreception and the trigeminal system

The link between magnetoreception and the trigeminal system in birds is historically highly controversial (Mouritsen, 2015, 2018; Wild, 2015). In European robins experimentally induced rapid changes in magnetic field intensity, horizontal direction, and inclination were shown to lead to neuronal activation in parts of the nTTD and in a ventral crescent of the principal nucleus (PrV; Heyers et al., 2010). Such activation was significantly reduced by section of the ophthalmic nerve (V1), which innervates the upper beak where magnetoreceptors have been thought to lie (see Treiber et al., 2012 for negative evidence from pigeon beak analysis). It is never the less interesting that in another migrant songbird (the Eurasian blackcap, Kobylkov et al., 2020) has shown that some neurons in a similar ventral crescent of PrV can be retrogradely labeled from a region of the nidopallium close to, but separate from, Bas, to which the main, dorsal part of PrV projects (Wild and Zeigler, 1996; Wild and Farabaugh, 1996); and some of these labeled neurons were also shown to be neuronally activated by experimentally induced magnetic field changes. Widely distributed projections from the frontal nidopallium could ensure appropriate connections with other parts of the brain involved in the computation of parameters underlying long-distance migration.

9.11 Summary and conclusions

It is hoped that this chapter will lead to the realization and appreciation of considerable diversity in the organization of the somatosensory system in birds. Even within the few species so far examined, there seem to be major deviations from the commonly accepted mammalian-type sequence of somatosensory projections throughout the brain. Of course, within mammals also, there are huge differences in the species-specific representation of the integument and of parts of the head-representations that, as in birds, reflect the functional importance of the body part in the everyday behavior of the animal. However, these distorted representations in mammals are the end stations of a common three-neuron sequence of somatosensory projections from the periphery to the cortex, via the DCN and the thalamus. In contrast, in some species of birds, even the DCN are not an obligatory relay in the sequence of ascending projections from the periphery. Furthermore, in parrots, at least, there appears to be a complete representation of the body and head at pontine levels-a phenomenon not encountered in mammals, or probably in many other species of birds. Another striking and equally puzzling feature of the somatosensory projections in birds is the complete or partial separation of the representations of the beak and body in Bas or in the rostral Wulst. The great majority of beak inputs are relayed via PrV to Bas. In barn owls and budgerigars, the representation of the beak in Bas is but one part, albeit a major part, of a complete representation of the whole body. In ducks, pigeons, and finches, a representation of the rest of the body is apparently absent in Bas (or has not yet been found), except for that of the cochlea.

In pigeons, the somatosensory, rostral part of the Wulst comprises a weakly somatotopic representation of the body minus the beak, with a second nonsomatotopic body representation further caudally in NI/NC of the nidopallium

(Wild, 1987; Funke, 1989a). Whether there is a somatosensory representation of the body in the rostral Wulst of ducks and parrots remains to be determined. In barn owls, the claw—and only the claw—is represented in what may be a specialization of the rostral Wulst. In the dunlin (Pettigrew and Frost, 1985), the finding of a tactile fovea in the rostral part of the telencephalon, representing the specialized probing beak tips, is intriguing, but whether the recording electrodes were in Bas or a body representation in another part of the telencephalon is not clear.

In the final analysis, we should remind ourselves—obvious though it may be—that one of the main functions of the body somatosensory system, at least for most birds, is to enable flight. Once underrated as a somatosensory system (Ariens Kappers et al., 1936), its complex organization can now be appreciated with the help of the tools of modern neuroanatomy and electrophysiology; and with the help of cameras fixed to flying birds (jdp.co.uk/programmes/earthflight), we can also marvel at the feedback from feathers this system must provide to guide the birds through their aerial worlds (Bilo and Bilo, 1983; Necker, 1985c).

References

van den Akker, L.M., 1970. An Anatomical Outline of the Spinal Cord of the Pigeon. Royal Van Gorcum Ltd, Assen: The Netherlands.

Arends, J.J.A., Dubbeldam, J.L., 1984. The subnuclei and primary afferents of the descending trigeminal system in the mallard. Neuroscience 13, 781–795.

Arends, J.J.A., Zeigler, H.P., 1986. Anatomical identification of an auditory pathway from a nucleus of the lateral lemniscus to the frontal telencephalon (nucleus basalis) of the pigeon. Brain Res. 398, 375–381.

Arends, J.J.A., Woelders-Blok, A., Dubbeldam, J.L., 1984. The efferent connections of the nuclei of the descending trigeminal tract in the mallard (*Anas platyrhyncos* L.). Neuroscience 13, 797–817.

Ariëns Kappers, C.U., Huber, G.C., Crosby, E.C., 1936. The Comparative Anatomy of the Nervous System of Vertebrates, Including Man. The Macmillan Company, New York.

Ballam, G.O., 1982. Bilateral and multimodal semsory interactions of single cells in the pigeon's midbrain. Brain Res. 245, 27–35.

Berkhoudt, H., 1980. The morphology and distribution of cutaneous mechanoreceptors (Herbst and Grandry corpuscles) in the bill and tongue of the mallard (*Anas platyrhynchos* L.). Neth. J. Zool. 30, 1–34.

Berkhoudt, H., Dubbeldam, L., Zeilstra, S., 1981. Studies on the somatotopy of the trigeminal system in the mallard, *Anas platyrhynchos* L. IV. Tactile representation in the nucleus basalis. An electrophysiological study. J. Comp. Neurol. 196, 407–420.

Berkley, K.J., Budell, R.J., Blomqvist, A., Bull, M., 1986. Output systems of the dorsal column nuclei in the cat. Brain Res. Rev. 11, 199–225.

Bilo, D., Bilo, A., 1983. Neck flexion related activity of flight control muscles in the flow-stimulated pigeon. J. Comp. Physiol. 53, 111–122.

Bottjer, S.W., Arnold, A., 1982. Afferent neurons in the hypoglossal nerve of the zebra finch (*Poephila guttata*): localization with horseradish peroxidase. J. Comp. Neurol. 210, 190–198.

Bottjer, S.W., Arnold, A., 1984. The role of feedback from the vocal organ. I. Maintenance of stereotypical vocalizations by adult zebra finches. J. Neurosci. 4, 2387–2396.

Brinkman, R.W., Martin, A.H., 1974. A cytoarchitectonic study of the spinal cord of the domestic fowl *Gallus gallus domesticus*. I. Brachial region. Brain Res. 56, 43–62.

Cohen, D.H., Karten, H.J., 1974. The structural organization of avian brain: an overview. In: Goodman, I.J., Schein, M. (Eds.), Birds: Brain and Behavior. Academic Press, New York, pp. 29–73.

Coleman, M.J., Roy, A., Wild, J.M., Mooney, R., 2007. Thalamic gating of auditory responses in telencephalic song control nuclei. J. Neurosci. 27, 10024–10036.

Cunningham, S., Castro, I., Alley, M., 2007. A new prey-detection mechanism for kiwi (*Apteryx* spp.) suggests convergent evolution between paleognathous and neognathous birds. J. Anat. 211, 493–502.

Demery, Z.P., Chappell, J., Martin, G.R., 2011. Vision, touch and object manipulation in Senegal parrots *Poicephalus senegalus*. Proc. R. Soc. B. 278, 3687–3693.

Dubbeldam, J.L., 1980. Studies on the somatotopy of the trigeminal system in the mallard, *Anas platyrhynchos* L. II. Morphology of the principal sensory nucleus. J. Comp. Neurol. 191, 557–571.

Dubbeldam, J.L., Karten, H.J., 1978. The trigeminal system in the pigeon (*Columba livia*). I. Projections of the gasserian ganglion. J. Comp. Neurol. 180, 661–678.

Dubbeldam, J.L., Visser, A.M., 1987. The organization of the nucleus basalis-neostriatum complex of the mallard (*Anas platyrhynchos* L.) and its connections with the archistriatum and the paleostriatum complex. Neuroscience 21, 487–517.

Dubbeldam, J.L., Brus, E.R., Menken, S.B.J., Zeilstra, S., 1979. The central projections of the glossopharyngeal and vagus ganglia in the mallard, *Anas platyrhynchos* L. J. Comp. Neurol. 183, 149–168.

Dubbeldam, J.L., Brauch, C.S.M., Don, A., 1981. Studies on the somatotopy of the trigeminal system in the mallard, Anas platyrhyncos L. III. Afferents and organization of the nucleus basalis. J. Comp. Neurol. 196, 391–405.

Faunes, M., Wild, J.M., 2017a. The ascending projections of the nuclei of the descending trigeminal tract (nTTD) in the zebra finch (*Taeniopygia guttata*). J. Comp. Neurol. 525, 2832–2846.

Faunes, M., Wild, J.M., 2017b. The sensory trigeminal complex and the organization of its primary afferents in the zebra finch (*Taeniopygia guttata*). J. Comp. Neurol. 525, 2820–2831.

Faunes, M., Botelho, J.F., Wild, J.M., 2017. Innervation of the syrinx of the zebra finch (*Taeniopygia guttata*). J. Comp. Neurol. 25, 2847–2860. https://doi.org/10.1002/cne.24236.

Funke, K., 1989a. Somatosensory areas in the telencephalon of the pigeon. II. Spinal pathways and afferent connections. Exp. Brain Res. 76, 620–638.

Funke, K., 1989b. Somatosensory areas in the telencephalon of the pigeon. I. Response characteristics. Exp. Brain Res. 76, 603–619.

Gamlin, P.D.R., Cohen, D.H., 1986. A second ascending visual pathway from the optic tectum to the telencephalon in the pigeon (*Columba livia*). J. Comp. Neurol. 250, 296–310.

Gentle, M.J., Hunter, L.N., Sterling, R.J., 1995. Projections of ankle joint afferents to the spinal cord and brainstem of the chicken (*Gallus g. domesticus*). J. Comp. Neurol. 361, 669–680.

Gerritsen, A.F.C., Meiboom, A., 1986. The role of touch in prey density estimation by *Calidris alba*. Neth. J. Zool. 36, 530–562.

Gottschaldt, K.-M., 1985. Structure and function of avian somatosensory receptors. In: King, A.S., McLelland, J. (Eds.), Form and Function in Birds, vol. 3. Academic Press, London, pp. 375–461.

Heyers, D., Zapka, M., Hoffmeister, M., Wild, J.M., Mouritsen, H., 2010. Magnetic field changes activate the trigeminal brainstem complex in a migratory bird. Proc. Natl. Acad. Sci. U. S. A. 107, 9394–9399.

Karten, H.J., 1967. The organization of the ascending auditory pathway in the pigeon (*Columba livia*). I. Diencephalic projections of the inferior colliculus (nucleus mesencehalicus lateralis, pars dorsalis). Brain Res. 6, 409–427.

Karten, H.J., Finger, T.H., 1976. A direct thalamo-cerebellar pathway in pigeon and catfish. Brain Res. 102, 335–338.

Kobylkov, D., Schwarze, S., Michalik, B., Winklhofer, M., Mouritsen, H., Heyers, D., 2020. A newly identified trigeminal brain pathway in a night-migratory bird could be dedicated to transmitting magnetic map information. Proc. R. Soc. B 287, 20192788. https://doi.org/10.1098/rspb.2019.2788.

Korzeniewski, E., 1987. Multisensory convergence in the thalamus of the pigeon (*Columba livia*). Neurosci. Lett. 80, 55–60.

Korzeniewski, E., Güntürkün, O., 1990. Sensory properties and afferents of the N. dorsolateralis posterior thalami of the pigeon. J. Comp. Neurol. 292, 457–479.

Krulis, V., 1978. Struktur und Verteilung von Tastrezeptoren im Schnabel-Zungenbereich von Singvögeln, im besonderen der Fringillidae. Rev. Suisse Zool. 85, 385–447.

Kubke, M.F., Ross, J.M., Wild, J.M., 2004. Vagal innervation of the air sacs in a songbird, *Taenopygia guttata*. J. Anat. 204, 283–292.

Leibler, L., 1975. Ascending Binaural and Monaural Pathways to Mesencephalic and Diencephalic Auditory Nuclei in the Pigeon, *Columba livia* (Ph.D. thesis). Massachusetts Institute of Technology, Cambridge, Mass., USA.

Leonard, R.B., Cohen, D.H., 1975a. Spinal terminal fields of dorsal root fibers in the pigeon (*Columba livia*). J. Comp. Neurol. 163, 181–192.

Leonard, R.B., Cohen, D.H., 1975b. A cytoarchitectonic analysis of the spinal cord of the pigeon (*Columba livia*). J. Comp. Neurol. 163, 159–180.

Lewandowski, B.C., Alexei, A., Hahnloser, R., Schmidt, M.F., 2013. At the interface of the auditory and vocal motor systems: NIf and its role in vocal processing, production and learning. J. Physiol. 107, 178–192.

Manger, P.R., Elston, G.N., Pettigrew, J.D., 2002. Multiple maps and activity-dependent representational plasticity in the anterior Wulst of the adult barn owl (*Tyto alba*). Eur. J. Neurosci. 16, 743–750.

Martin, G.R., Wilson, K.-J., Wild, J.M., Parsons, S., Kubke, M.F., Corfield, J., 2007. Kiwi forego vision in the guidance of their nocturnal activities. PLoS One 2 (2), e198. https://doi.org/10.1371/journal.pone.0000198.

Mouritsen, H., 2015. Magnetoreception in birds and its use for long-distance migration. In: Sturkie's Avian Physiology, sixth ed., pp. 113–133 ch. 8.

Mouritsen, H., 2018. Long-distance navigation and magnetoreception in migratory animals. Nature 558, 50–59. https://doi.org/10.1038/s41586-018-0176-1.

Necker, R., 1985a. Projection of a cutaneous nerve to the spinal cord of the pigeon. I. Evoked field potentials. Exp. Brain Res. 59, 338–343.

Necker, R., 1985b. Projection of a cutaneous nerve to the spinal cord of the pigeon. II. Responses of dorsal horn neurons. Exp. Brain Res. 59, 344–352.

Necker, R., 1985c. Observations on the function of a slowly-adapting mechanoreceptor associated with filoplumes in the feathered skin of pigeons. J. Comp. Physiol. A. 156, 391–394.

Necker, R., 1990. Sensory representation of the wing in the spinal dorsal horn of the pigeon. Exp. Brain Res. 81, 403–412.

Necker, R., 1991. Cells of origin of avian postsynaptic dorsal column pathways. Neurosci. Lett. 126, 91–93.

Necker, R., 1992. Spinal neurons projecting to anterior or posterior cerebellum in the pigeon. Anat. Embryol. 185, 325–334.

Necker, R., 1997. Projections of the marginal nuclei in the spinal cord of the pigeon. J. Comp. Neurol. 377, 95–104.

Necker, R., 1999. Specializations in the lumbosacral spinal cord of birds: morphological and behavioural evidence for a sense of equilibrium. Eur. J. Morphol. 37, 211–214.

Necker, R., 2000a. The somatosensory system. In: Sturkie's Avian Physiology, fifth ed., pp. 57–69.

Necker, R., 2000b. Functional organization of the spinal cord. In: Sturkie's Avian Physiology, fifth ed., pp. 71–81.

Necker, R., 2001. Spinocerebellar projections in the pigeon with special reference to the neck region of the body. J. Comp. Neurol. 429, 403–418.

Necker, R., Schermuly, C., 1985. Central projections of the radial nerve and one of its cutaneous branches in the pigeon. Neurosci. Lett. 58, 271–276.

Necker, R., Janssen, A., Beissenhirtz, T., 2000. Behavioural evidence of the role of lumbosacral anatomical specializations in pigeons in maintaining balance during terrestrial locomotion. J. Comp. Physiol. A Sens. Neural Behav. Physiol. 186, 409–412.

Nottebohm, F., Kelley, D.B., Paton, J.A., 1982. Connections of vocal control nuclei in the canary telencephalon. J. Comp. Neurol. 207, 344–357.

Ohmori, Y., Necker, R., 1995. Central projections of primary afferents from the interosseus nerve in the pigeon. Brain Res. Bull. 38, 269–274.

Okado, N., Ito, R., Homma, S., 1987. The terminal distribution pattern of spinocerebellar fibers: an anterograde labelling study in the post-hatching chick. Anat. Embryol. 176, 175–182.

Pettigrew, J.D., Frost, B.J., 1985. A tactile fovea in the Scolopacidae? Brain Behav. Evol. 26, 185–195.

Puelles, L., Rrobles, M., Martínez-de-la-Torre, M., Martínez, S., 1994. New subdivision schema for the avian torus semicircularis: neurochemical maps in the chick. J. Comp. Neurol. 340, 98–125.

Reiner, A., Bruce, L., Butler, A., Csillag, A., Kuenzel, W., Medina, L., Paxinos, G., Perkel, D., Shimizu, T., Striedter, G., Wild, J.M., Ball, G., Durand, S., Gunturkun, O., Lee, D., Mello, C.V., Power, A., White, S.,A., Hough, G., Kubikova, L., Smulder, T.V., Wada, K., Dugas-Ford, J., Husband, S., Yamamoto, K., Yu, J., Siang, C., Jarvis, E.D., 2004. Revised nomenclature for avian telencephalon and some related hrainstem nuclei. J. Comp. Neurol. 473, 377–414.

Reinke, H., Necker, R., 1996. Coding of vibration by neurons of the dorsal column nuclei in the pigeon. J. Comp. Physiol. A. 179, 263–276.

Robertson, B., Grant, G., 1985. A comparison between wheat germ agglutinin and choleragenoid-horseradish peroxidise as anterogradely transported markers in central branches of primary sensory neurons in rat with some observations in the cat. Neuroscience 14, 895–905.

Rosenberg, J., Necker, R., 2000. Fine structural evidence of mechanoreception in spinal lumbosacral accessory lobes of pigeons. Neurosci. Lett. 285, 13–16.

Schneider, A., Necker, R., 1989. Spinothalamic projections in the pigeon. Brain Res 484, 139–149.

Schneider, A., Necker, R., 1996. Electrophysiological investigations of the somatosensory thalamus of the pigeon. Exp. Brain Res. 109, 377–383.

Schulte, M., Necker, R., 1994. Projection of wing nerves to spinal cord and brain stem of he pigeon a studies by transganglionic transport of Fast Blue. J. Brain Res. 35, 313–325.

Silver, R., Witkovsky, P., 1973. Functional characteristics of single units in the spinal trigeminal nucleus of the pigeon. Brain Behav. Evol. 8, 287–303.

Stingelin, W., 1961. Grossenunterschiede des sensiblen Trigeminuskerns bei verschiedenen Vögeln. Rev. Suisse Zool. 68, 247–251.

Suthers, R.A., Goller, F., Wild, J.M., 2002. Somatosensory feedback modulates the respiratory motor program of crystallized birdsong. Proc. Natl. Acad. Sci. U. S. A. 99, 5680–5685.

Toyoshima, K., Shimamura, A., 1991. Ultrastructure of Merkel corpuscles in the tongue of the finch, *Lonchura striata*. Cell Tissue Res. 264, 427–436.

Treiber, C.D., Salzer, M.C., Riegler, J., Edelman, N., Sugar, C., Breuss, M., Pichler, P., Cadiou, H., Saunders, M., Lythgoe, M., Shaw, J., Keays, D.A., 2012. Clusters of iron-rich cells in the upper beak of pigeons are macrophages not magnetosensitive neurons. Nature. https://doi.org/10.1038/nature11046.

Vates, E.G., 1996. Auditory pathways of caudal telencephalon and their relation to the song system of adult male zebra finches (*Taenopygia guttata*). J. Comp. Neurol. 366, 513-442.

Weiner, J., 1995. The Beak of the Finch. Vintage.

Whitlock, D.G., 1952. A neurohistological and neurophysiological study of afferent fiber tracts and receptive areas of the avian cerebellum. J. Comp. Neurol. 97, 567–635.

Wild, J.M., 1981. Identification and localization of the motor nuclei and sensory projections of the glossopharyngeal, vagus and hypoglossal nerves in the cockatoo (*Cacatua roseicapilla*), Cacatuidae. J. Comp. Neurol. 203, 352–378.

Wild, J.M., 1985. The avian somatosensory system. I. Primary spinal afferent input to the spinal cord and brainstem in the pigeon (*Columba livia*). J. Comp. Neurol. 240, 377–395.

Wild, J.M., 1987. The avian somatosensory system: connections of regions of body representation in the forebrain of the pigeon. Brain Res. 412, 205–223.

Wild, J.M., 1989. The avian somatosensory system. II. Ascending projections of the dorsal column and external cuneate nuclei in the pigeon. J. Comp. Neurol. 287, 1–18.

Wild, J.M., 1990. Peripheral and central terminations of hypoglossal afferents innervating lingual tactile mechanoreceptor complexes in *Fringillidae*. J. Comp. Neurol. 298, 157–171.

Wild, J.M., 1992. Direct and indirect "cortico"-rubral and rubrocerebellar cortical projections in the pigeon. J. Comp. Neurol. 326, 623–636.

Wild, J.M., 1994. Visual and somatosensory projections to the avian song system via nucleus uvaeformis (Uva) and a comparison with the projections of a similar thalamic nucleus in a non-songbird (*Columba livia*). J. Comp. Neurol. 349, 512–535.

Wild, J.M., 1995. Convergence of somatosensory and auditory projections in the avian torus semicircularis, including the central auditory nucleus. J. Comp. Neurol. 358, 465–486.

Wild, J.M., 1997. The avian somatosensory system: the pathway from wing to Wulst in a passerine (*Chloris chloris*). Brain Res. 759, 122–134.

Wild, J.M., 1999. Trigeminal disynaptic circuit mediating corneal afferent input to M. depressor palpebrae inferioris motoneurons in the pigeon (*Columba livia*). J. Comp. Neurol. 403, 391–406.

Wild, J.M., 2015. The avian somatosensory system: a comparative view. In: Sturkie's Avian Physiology, sixth ed., pp. 55–69.

Wild, J.M., Farabaugh, S.M., 1996. Organization of afferent and efferent projections of nucleus basalis prosencephali in a passerine (*Taeneopygia guttata*). J. Comp. Neurol. 365, 306–328.

Wild, J.M., Zeigler, H.P., 1996. Central projections and somatotopic organization of trigeminal primary afferents in the pigeon (*Columba livia*). J. Comp. Neurol. 368, 136–152.

Wild, J.M., Williams, M.N., 1999. Rostral Wulst in passerine birds. II. Intratelencephalic projections to nuclei associated with the auditory and song systems. J. Comp. Neurol. 413, 520–534.

Wild, J.M., Williams, M.N., 2000. Rostral Wulst in passerine birds. I. Origin, course and terminations of an avian 'pyramidal tract'. J. Comp. Neurol. 416, 429–450.

Wild, J.M., Krützfeldt, N.O.E., 2012. Trigeminal and telencephalic projections to jaw and other upper vocal tract premotor neurons in songbirds: sensorimotor circuitry for beak movements during singing. J. Comp. Neurol. 520, 590–605.

Wild, J.M., Balthazart, J., 2013. Neural pathways mediating control of reproductive behavior in male Japanese quail. J. Comp. Neurol. 521, 2067–2087.

Wild, J.M., Arends, J.J.A., Zeigler, H.P., 1985. Telencephalic connections of the trigeminal system in the pigeon (*Columba livia*): a trigeminal sensorimotor circuit. J. Comp. Neurol. 234, 441–464.

Wild, J.M., Reinke, H., Farabaugh, S.M., 1997. A non-thalamic pathway contributes to a whole body map in the brain of the budgerigar. Brain Res. 755, 137–141.

Wild, J.M., Kubke, M.F., Carr, C.E., 2001. Tonotopic and somatotopic representation in nucleus basalis of the barn owl, *Tyto alba*. Brain Behav. Evol. 57, 39–62.

Wild, J.M., Kubke, M.F., Pena, J.L., 2008. A pathway for predation in the brain of the barn owl: projections of the gracile nucleus to the 'claw area' of the rostral Wulst, via the dorsal thalamus. J. Comp. Neurol. 509, 156–166.

Wild, J.M., Krützfeldt, N.O.E., Altshuler, D., 2010. Trigeminal and spinal dorsal horn (dis)continuity and avian evolution. Brain Behav. Evol. 76, 11–19.

Wild, J.M., Cabot, J.B., Cohen, D.H., Karten, H.J., 1979. Origin, course and terminations of the rubrospinal tract in the pigeon (*Columba livia*). J. Comp. Neurol. 197, 639–654.

Witkovsky, P., Zeigler, H.P., Silver, R., 1973. The nucleus basalis of the pigeon: a single unit analysis. J. Comp. Neuol. 147, 119–128.

Woodbury, C.J., 1992. Physiological studies of cutaneous inputs to dorsal horn laminae I-IV of adult chickens. J. Neurophysiol. 67, 241–254.

Woodbury, C.J., 1998. Two spinal cords in birds: novel insights into early avian evolution. Proc. Roy. Soc. Lond. B. 265, 1721–1729.

Woodbury, C.J., Scott, S.A., 1991. Somatotopic organization of hindlimb skin sensory inputs to the dorsal horn of hatchling chicks (*Gallus g. domesticus*). J. Comp. Neurol. 314, 237–256.

Zeier, H., Karten, H.J., 1971. The archistriatum of the pigeon: organization of afferent and efferent connections. Brain Res. 31, 313–326.

Zecha, A., 1962. The 'pyramidal tract' and other telencephalic efferents in birds. Acta Morphol. Neerl-Scand 5, 194–195.

Zweers, G., 1982. The feeding system of the pigeon (*Columba livia*). Adv. Anat. Embryol. Cell Biol. 73, 1–108.

Chapter 10

Avian vision

Graham R. Martin
School of Biosciences, University of Birmingham, Birmingham, United Kingdom

10.1 Introduction

The primary reliance of birds on vision is readily and frequently asserted. Casual observations of birds completing their everyday behaviors is sufficient to convince most observers that birds are using vision to control their key behaviors. This assertion is supported by evidence that in most bird species relatively large portions of their brains are devoted to the analysis of information from vision (Reiner et al., 2005). Also, the so-called intelligent behaviors of birds seem to be based primarily upon visual information (Emery, 2006). Thus, gaining information from vision and using it to guide sophisticated behaviors, seems to be the essential function of the brains of most birds.

Only in a handful of extant bird species does vision appear not to be the primary sense. The prime examples of "nonvisual" birds are the five species of flightless Kiwi (Apterygidae), whose vision seems to have regressed as they evolved in the absence of mammalian predators (Martin et al., 2007b). Even blind individual Kiwi have been recorded living healthy lives in the wild (Moore et al., 2017), presumably guided exclusively by olfaction, touch, and hearing. In some bird species, these senses play a complementary role to vision. This is found among some of the petrels (Procellariidae), shorebirds (Scolopacidae), and owls (Strigidae), in which olfaction, touch, and hearing play a key role in finding food items (Martin, 2017a). However, in these birds, vision is probably the primary guide for locomotion.

The importance of vision in birds was encapsulated in the phrase "a bird is a wing guided by an eye." Coined almost 80 years ago by Rochon-Duvigneaud in his influential survey of the eyes and vision of vertebrates (Rochon-Duvigneaud, 1943), this phrase captured the essence of birds from a sensory ecology perspective. Rochon-Duvigneaud's inspiration sprang from the idea that the dominant feature of bird biology is flight, and that the key features of birds can be explained by considering them as "flying machines" (King and King, 1980). This provided a unified framework for thinking about birds as vertebrates in which low body mass is combined with muscles, respiratory, and digestive systems capable of generating high power output. If adaptations to facilitate flight could be considered dominant in shaping core aspects of bird biology, it was a small step to assume that the control of flight would also make particular demands on the information that birds gather from their environment, hence birds could be succinctly summed up as "wings guided by eyes."

It now seems, however, that this assumption may have been misplaced. As more has been learned about the sensory ecology of birds, it seems that controlling flight may not be the prime driver of their vision (Martin, 2017b). The key driver of bird senses is now best regarded as stemming from the demands of foraging, that is the detection, acquisition, screening, and ingestion of food items, with vision being driven primarily by the demands of detection and acquisition. The second key driver that has shaped bird vision is the detection of predators. However, the visual tasks of foraging and predator detection can make antagonist demands for information, and these demands can be seen played out in the eyes of most birds (Martin, 2014). The informational demands for controlling flight can perhaps best be considered as met within the requirements set by the primary sensory challenges of foraging and predator detection.

It is now argued that it is more appropriate to regard a bird as "a bill guided by an eye" (Martin, 2017b). This is because the bill is the prime tool with which a bird interacts intimately with its environment. In the majority of species, survival depends upon bringing the bill unfailingly to "the right place at the right time." For some species, particularly some of the birds of prey, it might be better to suggest that they are primarily "feet guided by an eye." This is because it is the feet that do the crucial act of prey acquisition and so have to be positioned accurately in space and time,

Sturkie's Avian Physiology. https://doi.org/10.1016/B978-0-12-819770-7.00023-2

although even these birds also need to place their bills accurately when manipulating items.

This change in the short-hand way of describing birds is important because it changes how we might think about birds in an everyday sense. It indicates that the main task of a bird, day-in-day-out is getting its bill (or feet) to the right-place at the right-time, over-and-over again. The informational control of these tasks is subject to constant selective pressure. In foraging, getting the right information to control the bill is as important as having a bill of the right shape. It is argued that bill shape is likely to be under constant selective pressure (Grant and Grant, 2014) and so it seems likely that controlling the bill is also subject to similar levels of selection. There is no value in having a tool that cannot be effectively controlled. Making a sensory-based error when flying may be important, but it is not as important as being unable to explore the environment at close range and use the bill to acquire food.

10.2 What vision does?

The essence of vision is simple; it is the determination of the direction from which light has traveled to reach the observer (Land and Nilsson, 2012). All aspects of vision are elaborations of this basic ability.

The light sensitive patches found on the surfaces of early animals could record only the presence of light. What marked the evolution of those patches into eyes 500 million years ago was the ability to determine where light was coming from (Nilsson, 2009; Nilsson and Pelger, 1994). Once this basic ability had evolved there followed rapid selection for eyes with ever more accurate spatial resolution (Nilsson and Pelger, 1994; Parker, 2003).This was coupled with the evolution of the ability to detect light over an increasingly wider range of intensities, eventually resulting in eyes that could function from bright sunlight to dim moonlight. Spatial resolution was further enhanced through the evolution of color vision, the ability to differentiate between light of different wavelengths.

Vision in some modern birds is arguably at the pinnacle of eye performance. In some bird species, spatial resolution is close to the very limits of what is theoretically possible for a vertebrate eye, dictated by the physical properties of light (Land and Nilsson, 2012). The highest known spatial resolution of any animal has been recorded in eagles and vultures (Fischer, 1969; Reymond, 1985). In these birds, resolution reaches close to the limits set by the physical properties of light.

Color vision enables many birds to differentiate between lights of very similar wavelengths, perhaps giving some species the highest levels of spectral resolution among vertebrates (Wright, 1972, 1979). However, even with high-spectral resolution, the ability to resolve spatial detail using colored light is below that of spatial resolution involving achromatic patterns (Potier et al., 2018).

Many birds, perhaps the majority of species, achieve spectral resolution across a broad light spectrum, from ultraviolet to far red (Cuthill et al., 2000). However, it should be noted that contrary to popular belief, birds are not exceptional in this, the same broad spectral range of vision is found in many mammals (Douglas and Geffery, 2014) and invertebrates (Cronin, 2008). Furthermore, vision in the ultraviolet region of the spectrum is not a property of vision in all birds. The majority of nonpasserine species cannot be considered as truly ultraviolet sensitive in that they do not have a photoreceptor that is maximally sensitive in that region (Odeen and Hastad, 2013), and in some birds (notably diurnal birds of prey), ultraviolet light is filtered out by the lens and cornea and does not reach the retina (Lind et al., 2013, 2014).

The vision of birds can also function within the full range of naturally occurring light levels, a range of 100 million-fold. This allows birds to use visual information in both bright daylight and in low-light level environments, for example, in nocturnal forests and deep water habitats (Martin, 2017a).

Another remarkable performance of the vision of most bird eyes it that they can extract spatial information simultaneously across a wide sector of space about the bird. Most bird eyes have an extensive visual field and because there are always two eyes in the skull, the total visual field is typically very extensive. In some species, eye placement and visual fields combine to give complete panoramic vision without blind areas above and behind the head (Martin, 2014). Such total panoramic vision is, however, not unique to birds; it is also found in some mammals, most notably in the Lagomorpha, rabbits, and hares (Hughes, 1977).

10.3 Variations in avian vision

While examples of outstanding visual performance are fascinating, general descriptions of visual performance must be couched with uncertainty. Qualifications of "most" or "some" when describing the visual performance of bird species are essential. It is not possible to talk about "avian vision" in a unified way; there is much variation between species (Martin, 2017a). Differences in visual performance apply especially with respect to resolution (acuity), visual fields, and absolute sensitivity. For example, an owl's eye may be approximately 100 times more sensitive than that of a dove, and a falcon may have visual acuity four times greater than that of the dove it is pursuing. Some ducks can see all around their heads, while vultures have extensive blind areas above and behind their heads. Clearly, such differences in vision need both functional and mechanistic explanations.

The ability of eyes to extract accurate and precise information from the world is not without cost. Eyes, and the processing of information by the visual system, are metabolically expensive (Laughlin, 2001), and the eyes of no one species can do everything (Land and Nilsson, 2012). Like all evolved structures, there are compromises and trade-offs, and these may be dictated by both physics and biology. For example, it is well understood that the nature of light itself means that adaptations of eye structures that can achieve high resolution run counter to adaptations that enhance high sensitivity (Land and Nilsson, 2012).

It is these metabolic and physical limitations that have led to the specializations of eyes across species. Much of the fascination of avian vision lies in understanding these specializations. They are perhaps best understood as the result of natural selection for eyes that can extract information which is finely tuned to the sensory challenges presented by the execution of particular tasks in particular environments. Regarding the evolution of eyes as being "task-led" (Nilsson, 2009) has provided a valuable explanatory framework with which to account for the diversity of bird eyes found today (Martin, 2017a). Metabolic considerations can provide a basis for explaining the apparently suboptimal and near loss of vision in some bird species, such as Kiwi, Apterygidae (Martin et al., 2007b).

10.4 Variations in eyes

All bird eyes are based upon the same basic anatomy and physiology. Variations in visual performance between species are derived from relatively simple differences in structure. These include differences in absolute eye size, differences in optical performance, and differences in the relative numbers and distributions of photoreceptors types across the retina. These differences can be large but even subtle variations are functionally significant, and they can all be interpreted as specializations for the extraction of particular information related to the conduct of particular tasks, in particular, light environments.

Just what those tasks are requires detailed understanding of the behavior and ecology of particular species. Although these are well studied in some species, knowledge is still partial or nonexistent for many species. Some interspecies variations in vision can be attributed to trade-offs between visual information and information provided by other senses. These can include hearing, touch, and taste. Understanding how they are used in the conduct of specific tasks in particular environments may be necessary to develop a full understanding of a species' visual capacities. Such trade-offs between vision and other sources of information have been well demonstrated in examples of underwater foraging in cormorants (Phalacrocoracidae) and penguins (Spheniscidae) (Martin, 1999; White et al., 2007), and in the nocturnal foraging behavior of a range of species including owls (Strigidae, Tytonidae), shorebirds (Charadriidae, Scolopacidae), kiwi (Apterygidae), and oilbirds (Steatornithidae) (Martin et al., 2004; Martin, 2017a).

10.5 Bird eyes: function, structure, and variations

Precise and accurate spatial resolution is achieved in vertebrate eyes through two anatomically linked but functionally separate systems. The *optical system* receives light and creates an image of the world. This image is projected onto a surface, the retina, which is the *image analysis system*. It is here that analysis of the image begins, and information is extracted and sent to the brain for further processing (Fig. 10.1). High resolution requires the production of an image which is a spatially accurate representation of the world. The image must be distortion free and sharply focused, but the physical nature of light and optics place fundamental limits on image properties, an image can never be an exact representation of the physical world (Land and Nilsson, 2012).

Although the two main functional systems of an eye are physically linked, they are subject to independent evolution. Even if the eyes of two different species have similar optical systems, they may analyze their images in different ways. Similarly, eyes which have the same overall dimensions can have different optical systems which present different images for analysis by their retinas. It seems unlikely that the eyes of any two species are exactly the same. This means that birds of two different species sitting side-by-side will extract different visual information from the environment which they share. Indeed it is subtle variations between eyes of individuals, not just species, which provides the raw material that drives the evolution of vision (Nilsson and Pelger, 1994).

The visual information extracted from the environment by different species can also differ markedly because eyes never occur singly, they are always paired. Although bird eyes are arranged symmetrically in the skull with respect to its median sagittal plane, their positions can differ markedly between species. These differences in eye positions can result in significant differences in the visual fields of birds (Martin, 2014). These are the regions of space about the head from which visual information can be retrieved at any one instant. It includes the degree to which there is overlap between the fields of each eye, the binocular field. Differences in visual field configurations have important implications for what information is made available at any one instant and therefore how vision can influence a bird's behavior.

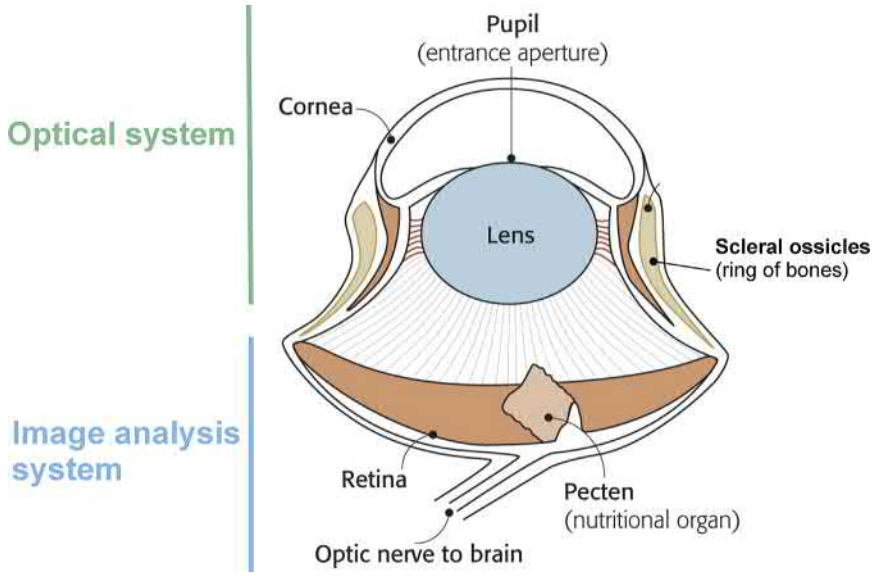

FIGURE 10.1 The two main functional systems of a bird's eye illustrated by a sectional diagram of the eye of an owl. The optical system has two components: cornea and the lens. These produce a focused image projected onto the retina which is where the first stage of image analysis begins, and from where information is sent via the optic nerve to the brain. In different eyes, the lens and cornea can have different optical properties depending upon their shape and size. These produce images with different properties (size, brightness, contrast) in different eyes. The image analysis system in different species exhibit large variations in the way photoreceptors and ganglion cells are arrayed across the retina, influencing markedly the way that images in different eyes are analyzed. *Drawing by Nigel Hawtin (Nigelhawtin.com) based upon an original drawing by the author.*

10.5.1 The optical system

The properties of the optical system of an eye can affect four key parameters of the image: brightness (how much light is captured to make the image), size (the area over which the image is spread), angular size of the image (how wide a field of view is captured in the image), and quality (the precision with which light from a point in the world is brought to a focus in the image). Variation in each one of these parameters can alter the information that an eye can extract from its environment.

The optical system has two main elements: cornea and lens (Fig. 10.1). The cornea, the curved surface at the front of the eye essentially functions to provide a boundary between media of two different refractive index; air and the fluid-filled chamber of the eye. The radius of curvature of the cornea is the key to its image-forming properties. A more highly curved surface produces a smaller image than a more shallowly curved one. The lens, suspended in the fluids that fill the two chambers of the eye, derives its primary optical function by virtue of its two convex surfaces. The overall refractive index of the lens is greater than that of the surrounding fluids, enabling it to bend light that passes into and out of it. The lens surfaces can vary in their curvature, and in whether curvatures are uniform or become flatter or more curved toward the equator of the lens. The refractive index of the lens is not uniform, but rather it varies with position within the lens. Combined, the properties of the cornea and lens determine the size of the image, how far behind the lens it is focused (the focal length of the eye), its quality (how sharply it is focused), over how much of the image best focus is maintained, and how much of the scene is contained in the image (the field of view).

In vertebrate eyes, the lens also has a role in adjusting the focus of the image so that objects at different distances from the eye can be brought into sharp focus, that is, the eye can "accommodate." In larger eyes with wider pupils, accommodation becomes increasingly important compared with small eyes. In mammals and reptiles, accommodation is achieved primarily by deformation of the lens surface curvatures, while in fish the lens is moved but not deformed (Land and Nilsson, 2012). In birds, the curvatures of both the cornea and lens surfaces can be altered during accommodation (Glasser et al., 1994; Schaeffel and Howland, 1987).

10.5.1.1 Variation in the optical systems of bird eyes

The relative amount of focusing contributed by the lens and the cornea in forming the image upon the retina can differ quite significantly in different eyes. This is clearly seen when comparing the optical systems of eyes of the same overall size. A good example is provided by comparison of the eyes of Rock Doves *Columba livia* and Manx Shearwaters *Puffinus puffinus* (Fig. 10.2). Although these eyes have the same axial lengths ($\approx$12 mm), the curvature of

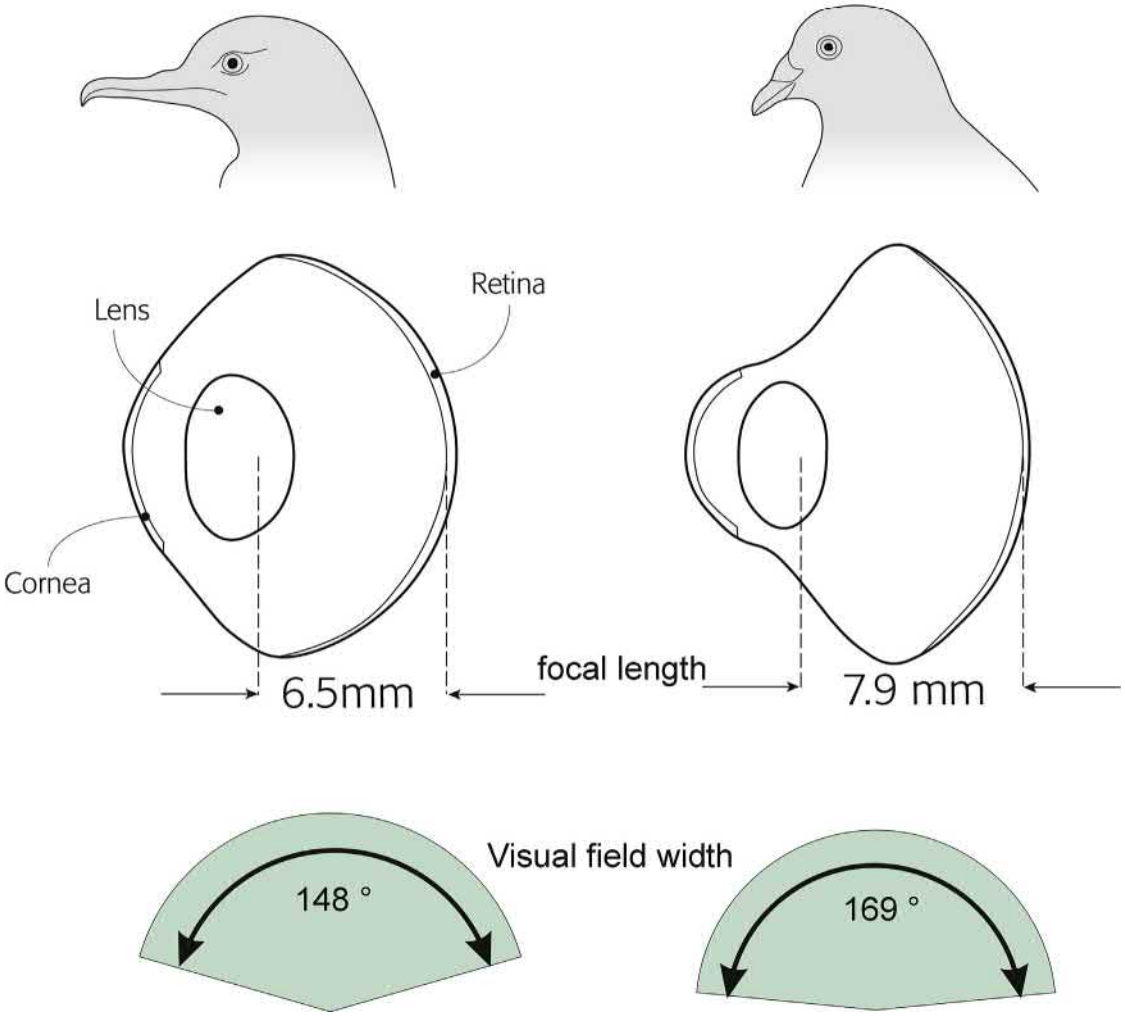

FIGURE 10.2 **Diagrams of sections through the eyes of Manx Shearwaters and Rock Doves.** The eyes of these birds are of the same overall size (both in length and diameter), but their corneas and lenses have quite different characteristics. The result of these differences is that the images produced by them have quite different properties. The image is smaller in Shearwaters (indicated by a shorter focal length) and brighter. Also, the visual field of a Shearwater's eye is significantly narrower than in a Dove. *Original diagram by the author from* Bird Senses *(2020).*

their corneas, and the curvatures of their lens surfaces, differ. Although these are relatively small differences, they result in important differences in the image properties in these two eyes. In shearwaters, the shorter focal length of the optical system results in a smaller but brighter image compared with doves (Martin and Brooke, 1991). These differences can be interpreted by reference to the frequent night-time activities of shearwaters whereas doves usually go to roost at twilight. The narrower visual field width of Shearwater eyes (Fig. 10.2) is a consequence of the shorter focal length of their optics and reduces the space around the head from which shearwaters can gain information, compared with doves.

Vertebrate eyes can also vary greatly in size. This is captured in Fig. 10.3 which compares the overall size and basic optical parameters of the eyes of Common Starlings *Sturnus vulgaris*, Tawny Owls *Strix aluco*, and Common Ostriches *Struthio camelus*. As in any optical system, absolute size inevitably determines the size of the image that it produces, and a larger sized image of a given scene can contain more detailed spatial information than a smaller image. Furthermore, a large entrance pupil determines the upper limit on the quality of the image, with respect to how sharp the focus of the image can be. This is driven by the wave nature of light and to achieve the sharpest focus requires an absolutely large entrance aperture (Land, 1981; Shlaer, 1972). However, absolute size also determines the maximum amount of light that can be gathered and hence the brightness of the image, and this is especially important when viewing small discrete sources of light in a scene (Land, 1981). A consequence of this is that eyes which have evolved for high sensitivity rather than high resolution

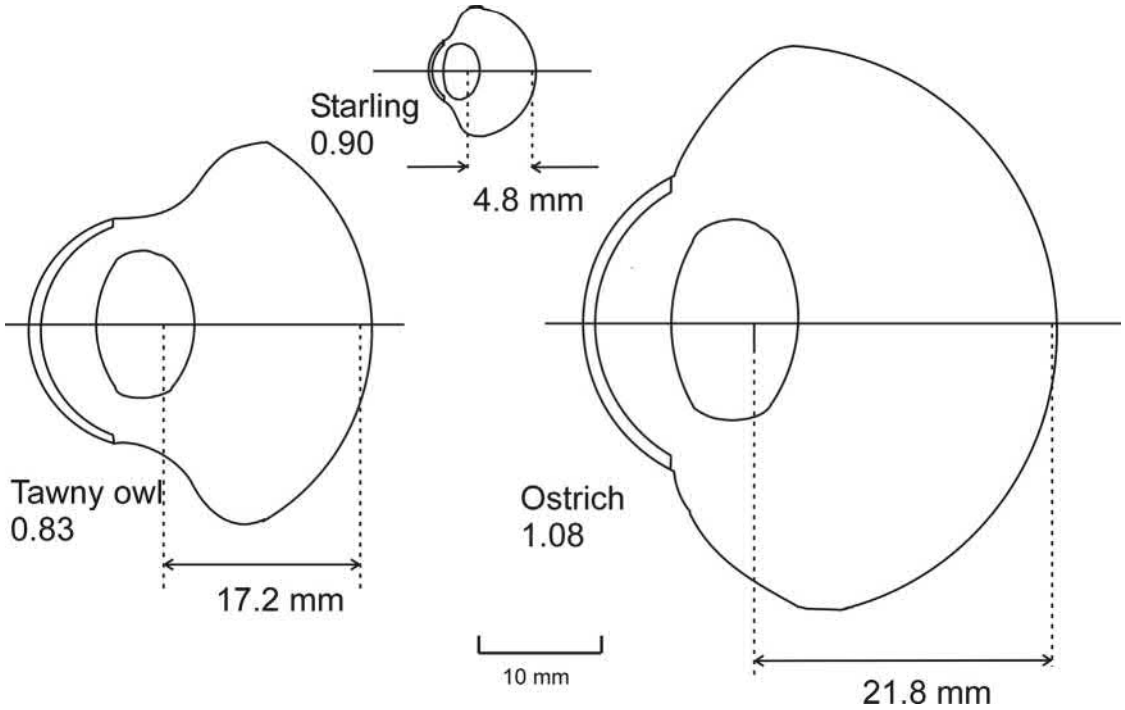

FIGURE 10.3 Sectional diagrams of schematic models of the eyes and optics of Tawny Owls, Common Starlings, and Ostriches. These diagrams are to scale and show the large size variation found in the eyes of birds. Also indicated are the focal lengths of these eyes and the ratio of the power of the lens to the power of the cornea. The longer the focal length, the larger the image of the same object when viewed by each eye. The ratio of lens to corneal power is another key descriptor of the optics of vertebrate eyes. *Original diagram by the author from* Bird Senses *(2020).*

also have absolutely large eyes, as is the case in some owl species (Fig. 10.3).

Large eye size, however, does not guarantee high resolution. That also requires that the image analysis system is matched to the task of extracting fine details that the image may contain (see section below). The Ostrich eye is an important example of this (Fig. 10.3). Despite it being probably the largest eye of any terrestrial vertebrate, its spatial resolution is not the highest. In fact, maximum acuity of Ostriches is estimated to be similar to that found in birds with much small eyes, including Indian Peafowl *Phasianus colchicus*, Rock Doves, and Silver Eyes *Zosterops lateralis* (Boire et al., 2001; Coimbra et al., 2015; Hodos et al., 1976). Thus, the functional significance of the Ostrich eye's large size may lie in the enhancement of sensitivity rather than resolution, which is correlated with ostriches' vulnerability to large mammalian predators at night.

10.5.2 Vision under water

Many bird species habitually forage under water. However, when an eye is immersed, its cornea loses it optical function because it no longer separates two surfaces of different refractive index. It is reasonable to assume that the eyes of amphibious species should operate effectively in both air and underwater, although evidence for this is limited. There is evidence that both Great Cormorants *Phalacrocorax carbo* and Australasian Gannets *Morus serrator* are equally focused in both air and water (Katzir and Howland, 2003; Machovsky-Capuska et al., 2012). However, it has been shown that underwater the eyes of Great Cormorants have very low acuity, the lowest recorded in any bird under daytime light levels (White et al., 2007).

Two possible mechanisms of how the optical effects of immersion might be mitigated in amphibious birds have been proposed (Fig. 10.4). The first mechanism is suggested by the observation that some penguins have corneas that are relatively flat and hence of low refractive power (Sivak and Millodot, 1977). This means that the loss of focusing power upon immersion is not large, and the lost power can be compensated for by a more spherical lens whose power is increased upon immersion. There is evidence that this type of mechanism does occur in some penguin species (Howland and Sivak, 1984; Martin and Young, 1984).

The second mechanism is proposed to occur in species whose eyes have a more typically curved cornea. It is suggested that loss of their higher refractive power upon immersion is compensated by the eye having a mechanism that combines a highly malleable lens with a rigid iris. Upon immersion, it is suggested that the lens is pushed up

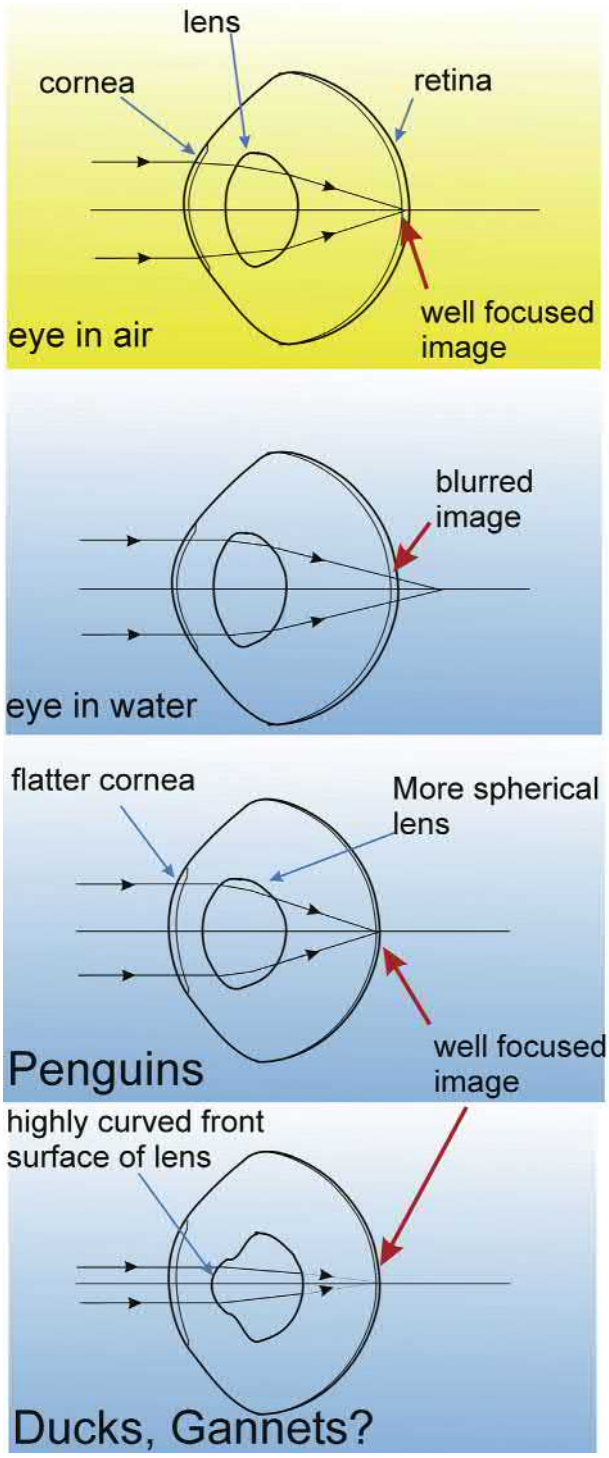

FIGURE 10.4 The problems of immersion and how it might be overcome in birds. An eye that is well focused in air loses the power of the cornea upon immersion. An image instead of being well focused on the retina is in effect focused behind the eye and the image appears blurred. Two possible mechanisms may have evolved to overcome this problem in amphibious birds. In some amphibious species, the cornea is relatively flat and therefore its loss upon immersion is less of a problem. The extra power needed to focus the image on the retina when the eye is immersed can be achieved by a more spherical lens whose power needs to change little. This type of mechanism may be a feature of the eyes of penguins and albatrosses. An alternative mechanism employs a malleable lens which upon immersion is pushed against a stiffened iris and the lens' front surface bulges through the pupil to make a highly curved, and hence powerful, lens. There is some evidence that this may occur in some ducks, gannets, and cormorants. However, the bulging lens may be an artifact of the investigation procedure which has over driven the muscles of the eye that control lens position and the iris. *Original diagram by the author from* Bird Senses *(2020).*

against the iris. The front surface of the lens bulges through the pupil to make a highly curved surface and hence a powerful lens (Fig. 10.4). It is suggested that this mechanism occurs in some diving ducks (Anatidae), and in gannets and cormorants (Sulidae) (Cronin, 2012; Hess, 1909; Levy and Sivak, 1980). However, the mechanism has not been optically modeled, and the evidence is not compelling. The bulging lens seen in the experimental work with ducks may be an artifact of the investigative procedure which used drugs applied to the eye. These may have over-driven the muscles that control lens position, pupil size, and iris rigidity.

As well as effects on focus, the loss of corneal refractive power upon immersion has two other important effects. First, the effective diameter of the pupil decreases. This is because it is no longer magnified by the cornea. This reduction in effective pupil size results in a decrease in the brightness of the image. In Humboldt Penguins, the decrease in image brightness has been shown to be nearly threefold (Martin and Young, 1984). Second, abolishing the magnifying power of the cornea also moves the margins of the field of view toward the axis of the eye. The effect is that a smaller section of the world is projected onto the retina, and so the total visual field shrinks. These changes are also not trivial, for example, in Humboldt Penguins, the visual field width of an eye may shrink in width by more than 30 degrees which is sufficient to abolish binocularity in all but a small section of the frontal visual field (Martin and Young, 1984). Such changes are significant for understanding the extent of the environment that an amphibious bird can see upon immersion. Certainly, measures of a bird's visual field in air cannot be applied directly to understanding its behavior underwater.

10.5.3 The image analysis system

10.5.3.1 Photoreceptors and visual pigments

Image analysis in vertebrate eyes begins with the detection of light by the photoreceptors of the retina. These are the familiar rods and cones which are found in all vertebrate eyes. Each photoreceptor signals the absorption of light photons by the photopigment molecules in their outer segment. These signals are collated by ganglion cells, which in turn send a signal along the optic nerve to the

brain where they are integrated with signals from the many millions of photoreceptors which are distributed across the retina. While differences between species in the type of photoreceptors is very limited, the number of photoreceptors and the way they are distributed across retinas, differ significantly. The result is that even if identical mages were present in the eyes of two species, the information that is extracted from them is likely to be significantly different.

The rods of bird retinas are of similar structure, and contain a similar photopigment, to those found in the retinas of other vertebrate taxa. The cones, however, differ from those of other vertebrates in respect of both their structure and the wavelengths of light to which their photopigments are maximally sensitive (referred to as their λmax). In birds, two types of cones occur, "single" and "double," which refers to the number of outer segments (Fig. 10.5). Double cones are not unique to birds; they are widespread in vertebrates but are absent from mammals (Bowmaker and Loew, 2008; Cronin, 2008; Walls, 1942). Double cones contain the same photopigment in both of their outer segments. Single cones in bird retinas are usually of four types, classified according to the λmax of the photopigment they contain (Cserhati et al., 1989; Hart et al., 2000a). Thus, most avian retinas contain a total of six photoreceptor types: double cones, four types of single cones, and rods (Martin and Osorio, 2008) (Fig. 10.5). By contrast, most mammalian retinas, including humans, have four types of photoreceptors (three single cones, plus rods).

As in other vertebrate retinas, the important functional difference between rods and cones is that rods function primarily at low-light levels (twilight and below), while cones function at higher light levels (twilight and above).

The types of photopigments found in bird photoreceptor outer segments show a high degree of similarity across species. This suggests that these pigment types arose early in the linage leading to modern birds and that their properties have been highly conserved. Birds regarded as distantly related (Hackett et al., 2008; Prum et al., 2015) have been shown to have very similar photoreceptor pigments. For example, the visual pigments found in the eyes of a species of pelagic seabird (Wedge-tailed Shearwaters *Ardenna pacifica*, Procellariiformes) are very similar to those found in a phylogenetically distant species that is terrestrial and lives in open forest habitats (Indian Peafowl *Pavo cristatus*, Galliformes) (Hart, 2002, 2004; Hart and Hunt, 2007). This suggests that visual pigments in birds have general properties that are not tuned to the performance of specific tasks or to differences in the types of habitat that birds exploit. However, what does differ between species is the number and distributions within the retinas of receptors containing the different photopigment types.

The five types of visual pigments of birds are labeled and characterized by their λmax as follows:

RH1: rhodopsin type 1 (λmax 500 nm), found in the rod receptors

RH2: rhodopsin type 2 (λmax 505 nm), found in single cone receptors

SWS2: short wave type 2 (λmax 470 nm), found in single cone receptors

LWS: long wave (λmax 565 nm), found in both single and double cone receptors

SWS1: short wave type 1—This pigment is also found in single cone receptors but occurs in two types that are found in different species. Pigments with λmax at 365 nm are referred to as ultraviolet sensitive (UVS pigment); those in which λmax is at 410 nm are referred to as violet sensitive (VS pigment) (Wilkie et al., 2000).

Cone receptors containing UVS pigment are found in gulls (Laridae, Charadriiformes), ostriches (Struthioniformes), parrots (Psittaciformes), and oscine passerines (but not in Corvidae) (Odeen et al., 2010, 2011; Odeen and Hastad, 2013). It is only these species which have true UV vision. Other species have the VS pigment, their spectral sensitivity extends into the violet-near UV part of the spectrum, but they lack specific UV sensitivity. It is worth noting that human retinas contain a cone pigment (λmax in the 420−440 nm range) which has peak sensitivity close to that of the avian VS pigment.

The spectral sensitivity characteristics of avian cone receptors are complicated by the presence in each cone of an oil droplet (Fig. 10.5). Each droplet sits in the proximal part of the outer segment so that light must pass through it before it reaches the photopigment in the outer segment (Cserhati et al., 1989). Oil droplets are also found in the photoreceptors of reptiles but are absent from most mammal species.

The droplets contain carotenoid pigments that are derived from the bird's diet. These pigments occur at a high density and give the droplets a bright color when observed using a light microscope. They appear as reds, greens, and yellows, but colorless droplets also occur. The pigments in the oil droplets are not photosensitive, they simply absorb and transmit light in different parts of the spectrum and so do not contribute directly to vision. However, because light must travel through the droplets before reaching the outer segment, they serve an important filtering function and sharpen the spectral sensitivity of the LWS, MWS, and SWS cones (Hart and Vorobyev, 2005). The resultant spectral sensitives (photopigment plus oil droplet filtering) of the different receptor types are shown in Fig. 10.5. The peak sensitivities of the four receptor types are spaced approximately equally across the birds' visible spectrum.

Sharpening the spectral sensitivity does not occur in the double cones because their oil droplets are transparent over the wavelengths that the photopigment is sensitive to. However, these droplets do block UV light from reaching

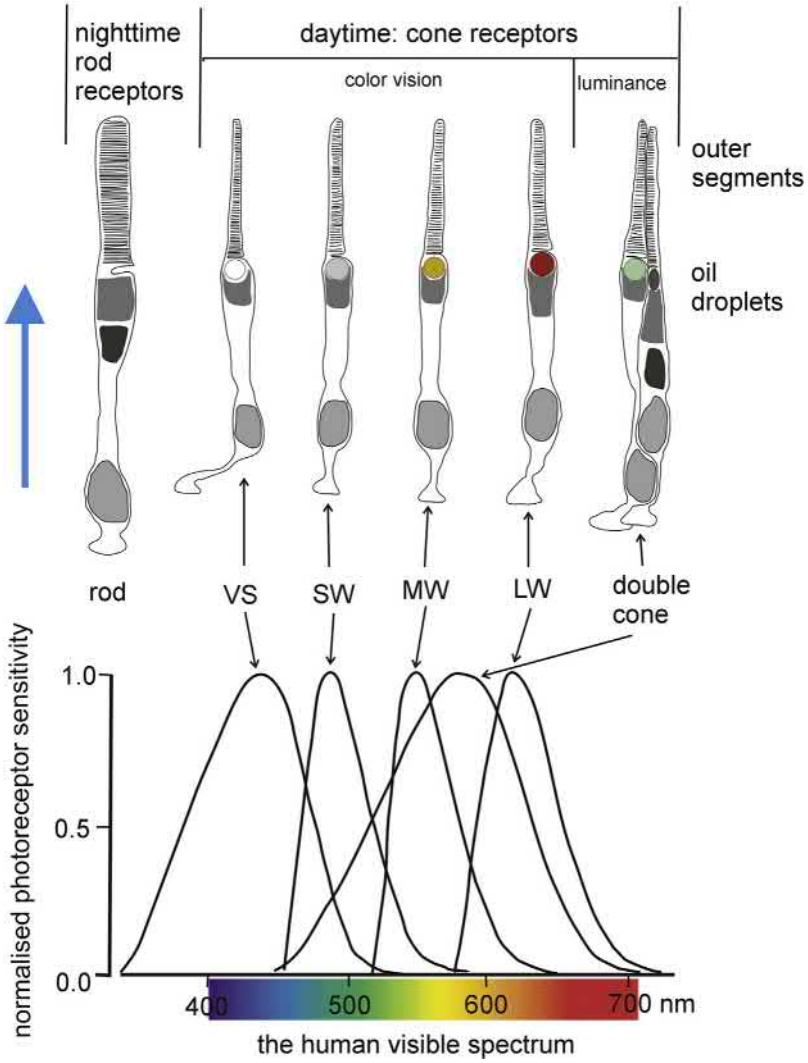

FIGURE 10.5 **The photoreceptors of bird retinas are of few types and are similar in all bird species.** What varies between species are the relative numbers and distributions of the different receptors types across the retinas of different species. In birds, rods are of one type, but the cones are of five different types; four types of single cones and double cones. The different types of single cones are classified by reference to the position in the spectrum of the peak sensitivity of the photopigments that they contain. The top portion of the diagram depicts the types of retinal photoreceptors as they appear when viewed through a light microscope. The outer segments are extremely narrow, generally between 1 and 2 microns in diameter, but they are relatively long. Each outer segment contains many millions of photosensitive pigment molecules. The four types of single cones provide the fundamental mechanism upon which color vision is based. The double cones provide a neural channel that is thought to signal luminance (brightness), and they are not part of the color vision system. Within all cone types there is an oil droplet. The arrow on the left indicates the direction in which light travels from the optics of the eye to the focused image on the retina. This means that the light that makes up the retinal image must pass through the oil droplets before it enters the outer segments. Oil droplets that are colored act as cut-off filters and allow light only above particular wavelengths to pass through to the photopigment molecules. The combination of photopigment types and oil droplet types results in their being four main types of single cone photoreceptors in birds' retinas with each cone type able to absorb light only within a particular part of the spectrum, although there is overlap between them. The lower section of the diagram shows the resultant photoreceptor sensitivities and the labels used to describe them. These are LW (long wave) which absorb light at the orange-red end of the visible spectrum; MW (middle wave), absorbing light in the green-yellow spectral region; SW (short wave) absorbing light in the blue-green spectral region; VS, which absorbs light in the violet-ultraviolet spectral region. *Redrawn from illustration provided by Peter Olsson Lund Vision Group, Sweden, and Daniel Osorio (University of Sussex, UK).*

the photopigment. The oil droplets in the UV/VS cones are also transparent, but they also allow UV light to reach the photopigments.

The key function of the single cone types lies in providing the foundation of color vision; the ability to differentiate between light sources based upon their spectral composition, not just upon their brightness. There is good evidence from behavioral investigations, as well as from retinal physiology that bird color vision should be viewed as based on the four single cone receptor types. It is

therefore referred to as a tetrachromatic system, as opposed to the cone system underlying human color vision, which is based on three cone receptor types, trichromatic vision. A range of investigative techniques (Jones and Osorio, 2004; Osorio et al., 1999) have indicated that double cones are not part of the color vision mechanism and probably constitute a separate channel that signals luminance at daytime light levels.

Because cone photoreceptors do not function at lower twilight and night-time light levels color vision is functional during higher twilight and daytime only. At lower light levels, only the rod receptors are functional and since there is only one type of rod receptor there is no basis for color vision. Furthermore, the photopigments found in rods, the RH1 pigment, have very similar characteristics across all birds and indeed across other animal taxa. The result is that spectral sensitivity at night is likely to be very similar across all bird species, and indeed is similar across most terrestrial vertebrates, with a peak at around 500 nm.

Such similarity in spectral sensitivity is, however, not the case at higher light levels. Under these conditions, spectral sensitivity is determined by the combined functioning of the cone photoreceptors. Although the sensitivity of the cones types does not vary markedly across species, their relative numbers in each retina do vary. Spectral sensitivity functions at high light levels show variations between individual birds and between different measuring techniques and conditions (Wright, 1979). In Rock Doves, maximum sensitivity has been found to lie between 560 and 620 nm in different studies, and all studies also showed an increase in sensitivity (but not a maximum) below 420 nm. Despite this variability, it was possible to model the overall spectral sensitivity of doves by making assumptions as to the relative abundance of cone photoreceptor types found across the whole of the retina (Bowmaker, 1977). This technique has been used to predict spectral sensitivities in other species based upon knowledge of their cone visual pigments and oil droplets characteristics (Hart et al., 1999).

10.5.3.2 Variation in the image analysis systems of bird eyes

Although there is little variation in the suite of photoreceptor types found in the retinas of different bird species, there are known to be very marked differences in the relative abundance of receptor types and in their distributions within the retinas of different species (Hart et al., 1998, 2000a; Hart, 2001, 2004). The result of this is twofold. First, in any eye, the image projected onto the retina is not analyzed in a uniform way across the whole of its area. Second, there can be very marked differences in patterns of analysis between eyes of different species. The result is that an image of the same scene in the eye of one bird species will be subject to different analysis by the eye of another species.

10.5.3.3 Variation in the distribution of receptor types

Variations in the distributions of cone receptor types across the retina can be striking, and it seems likely that they result in differences in spectral sensitivity and probably color vision in different parts of the visual field of a single eye, and there is some evidence to support this (Martin and Muntz, 1978). A striking example of variation in the types of receptors within the retina is found in Rock Doves, in which a large area is dominated by receptors containing red oil droplets (LW-sensitive cones), known as the "red-field" (Galifret, 1968). This area looks downward within the visual field, while receptors containing yellow oil droplets (MW-sensitive cones, the "yellow field") predominate in areas that look laterally and upward. These different areas are obvious even to the naked eye in a trans-illuminated excised retina; there is a very clear boundary between the areas (Fig. 10.6). The visual ecology and function of this striking regional specialization within dove eyes is not understood, although it has been suggested that the yellow field in some way enhances the contrast of objects seen against the blue of the sky (Lythgoe, 1979). Other species show systematic differences in the distribution of cone receptor types (Galifret, 1968), but there is a gradient in the relative abundance of different receptor types across the retina, rather than clearly demarked fields.

10.5.3.4 Variation in the densities of receptor types

Variations in the relative densities of photoreceptors and ganglion cells are also very striking. These differences in the density of cells may be overlaid on patterns of cone receptor types (Fig. 10.6). Very distinct patterns in ganglion cell density have been discerned with light microscopy across a diverse range of species. For example, clear patterns of ganglion cell distribution have been described in doves (Bingelli and Paule, 1969), Ostrich (Boire et al., 2001), waterfowl (Fernandez-Juricic et al., 2011; Lisney et al., 2013a), Procellariiform seabirds (Hayes and Brooke, 1990; Mitkus et al., 2016), penguins (Coimbra et al., 2012), flamingos (Lisney et al., 2020), new world vultures (Lisney et al., 2013b), passerines (Coimbra et al., 2006, 2015), and parrots (Coimbra et al., 2014; Mitkus et al., 2014).

In all of these species, clear patterns of photoreceptor and ganglion cell concentrations occur (Fig. 10.7). These patterns may be roughly circular, with a very high concentration at the center and a gradual decline of cell density away from the center. In some species more than one region of high concentration can occur, while in others high

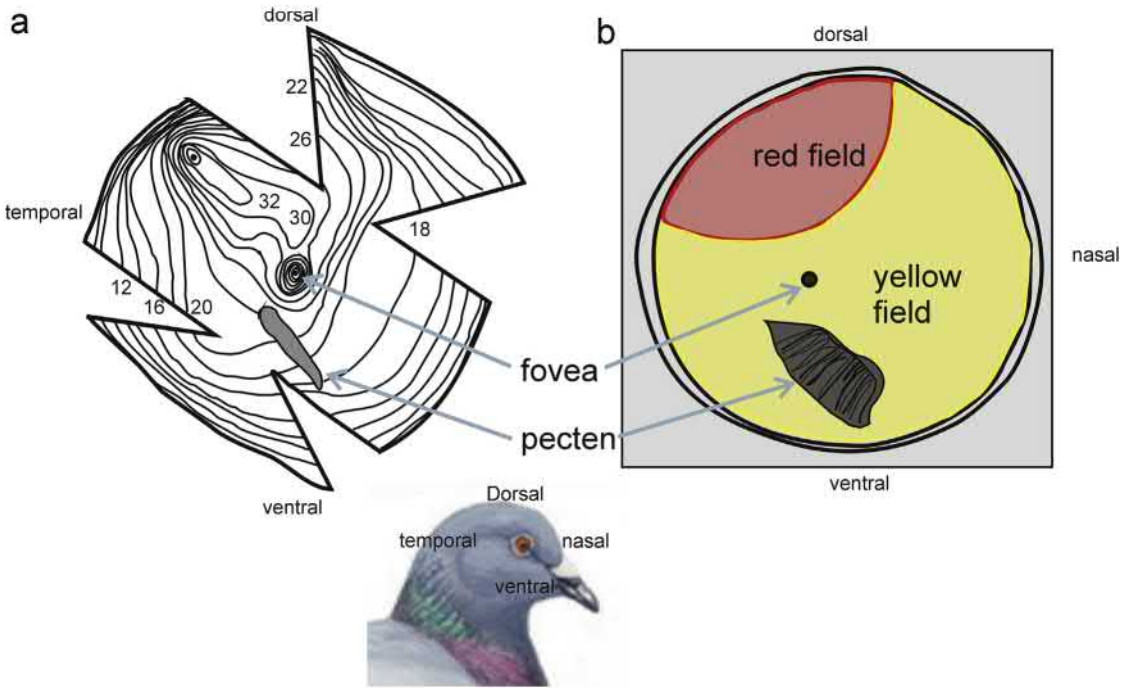

FIGURE 10.6 An indication of the complex way in which image analysis can vary across an individual retina provided by the example of the retina of Rock Doves *Columba livia*. Diagram (A) shows the topography of ganglion cell density in the right eye with the orientation of the retina as in the sketch of the bird. The lines are isodensity contours that join regions in which ganglions cells have the same density (the numbers by contours indicate ganglion cell density as × 1000 per mm^2). A distinct contour pattern is obvious, with low densities of ganglion cells at the periphery in the ventral and nasal sections of the retina (which looks upwards and backwards), and two distinct areas of very high ganglion cell density, one in the central retina (which projects laterally) and another in the temporal-dorsal retina, which looks downwards, possibly in the direction of the bill. The central region of high-cell density is also associated with a fovea. Diagram (B) indicates that the density of photoreceptor types also differs across the retina. The orientation of the retina is the same and so the two diagrams could be overlaid. In the temporal-dorsal retina, there is a region "the red field" in which LW type cones containing red oil droplets (Fig. 10.6) dominate. The rest of the retina is dominated by MW type cones which contain yellow oil droplets. *Diagrams redrawn and modified from originals in (Bingelli and Paule 1969) and (Galifret 1968).*

densities of receptors may occur in a linear band that is typically arranged so that it projects approximately horizontally when the bird's head is held in its usual resting posture. The usual interpretation of these patterns is that areas of high receptor concentration are regions of heightened spatial resolution within the visual field of the eye. These regions may take the form of an elongated band that projects toward the horizon, or they may indicate a direction of elevated resolution projecting in a particular direction.

Areas of the highest cell density may be associated with a fovea. This is a highly localized region in which the outer layers of the retinal cells are displaced to form a small pit or depression in the surface of the retina (Bringmann, 2019) (Fig. 10.8). Displacing the layers of the retina in this way ensures that the highest quality optical image is received directly by the photoreceptors, thus avoiding any image degradation that might be caused by passing through the layers of the retina. A number of hypotheses have been proposed concerning the function of foveas, including image magnification and image fixation mechanisms (Bringmann, 2019; Potier et al., 2020). However, strong evidential support for any of these hypotheses is lacking. Thus, beyond the general observation that displacing the retinal layers enhances spatial resolution by allowing the highest quality image to be received directly at the photoreceptors, it is not clear what the actual form of a fovea does.

It is clear that patterns of photoreceptor and ganglion cell distribution can vary not only between species but also between individuals within a species (Mitkus et al., 2014). Furthermore, differences in cell density and distributions between the eyes of the same individual have also been demonstrated (Hart et al., 2000b), and the shape and size of foveas have been shown to vary between individuals and probably change over an individual's life time (Potier et al., 2020). Such variations provide a very rich substrate for not only interspecific but also interindividual differences in analysis of the retinal image. It is upon such differences that natural selection is likely to be continually acting, resulting in visual capacities which can be considered to have become tuned in different species to informational requirements for the conduct of particular tasks in particular environments.

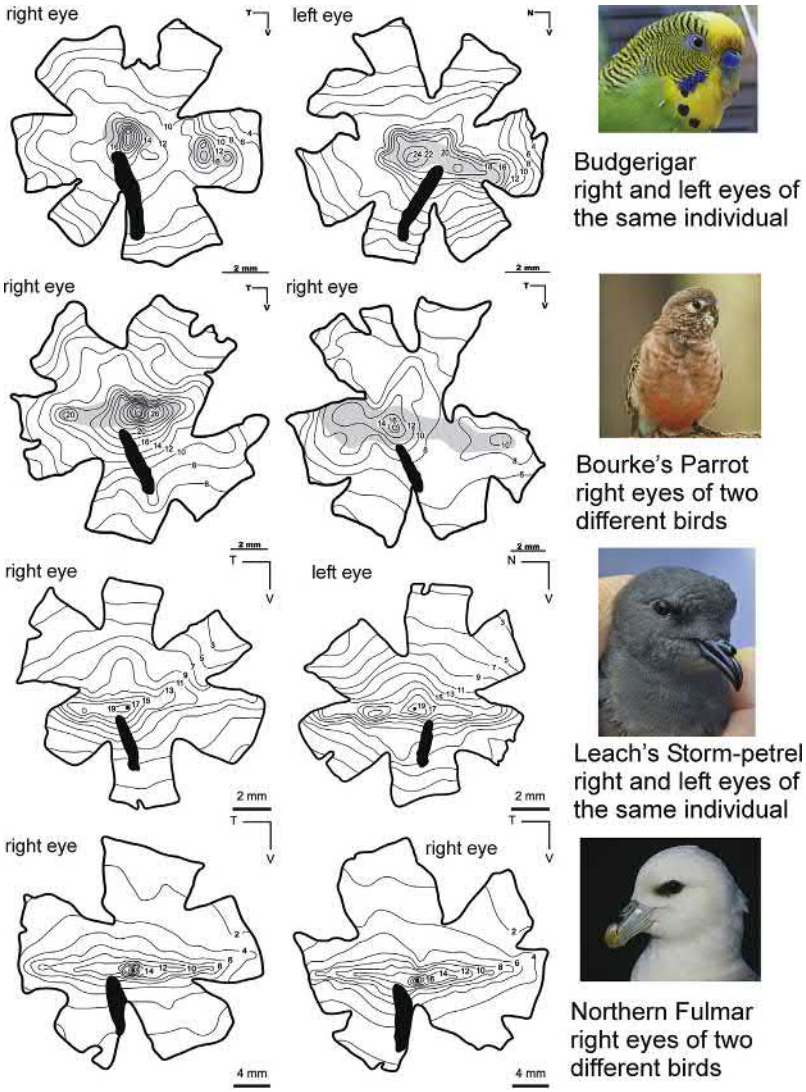

FIGURE 10.7 **Patterns of retinal ganglion cells in birds.** Each diagram shows the contours of equal ganglion cells densities (× 1000 cells mm^{-2}) on a flattened retina, the pecten (indicated by the black shading) creates a blind area in the eye and is a prominent landmark. The two examples from a Budgerigar show the left and right eyes from the same individual. They show a high concentration of ganglion cells in the center of the retina which indicate well demarked regions of high acuity that look out laterally from the eye, approximately in the center of the field of view. There is a second concentration in the retina toward the bill which looks slightly backwards. However, there are also marked differences between the two eyes. In Bourke's Parrots, the two diagrams are for the same eyes from different birds and show marked differences between the individuals. Both have a high concertation of cells in the center of the retina, but in one bird, there is a second concentration which looks forwards while in the other the overall density is much lower and the second area of concentration looks backwards in the field of view. In the two seabird species, clear linear bands of high ganglion cell concentrations are found running across the retina and project laterally toward the direction of the horizon. However, as in the parrots, there are differences between the left and right eyes of the same individual and differences between individuals. *Ganglion cells maps of Budgerigars and Bourke's Parrot are from (Mitkus et al., 2014), Fulmar and Storm-petrel (Mitkus et al., 2015). Photographs, Budgerigar, Michael Cole; Bourke's Parrot, Daniela Parra; Leach's Storm-petrel, Peter R. Flood; Northern Fulmar, Steve Garvie.*

10.6 The visual fields of birds

Differences in optical structure affect not only the size and brightness of the image but also determine the extent of the world that is imaged. This is important, since it determines the extent of a bird's visual world from which it can gain information. In birds, the field of view of a single eye can be as narrow as 124 degrees (owls) and as wide as 180 degrees (ducks and shorebirds) (Martin, 2007).

When the fields of two eyes are combined, variations in the birds' total visual field are considerable (Martin, 2007). Thus, in a horizontal plane, the total width of the visual field in owls is about 200 degrees, while in some shorebirds and ducks, the field provides a total 360 degrees panorama. Associated with these are marked differences in the extent of visual fields above, behind, and below the head. The axes of the two eyes may diverge by a relatively small

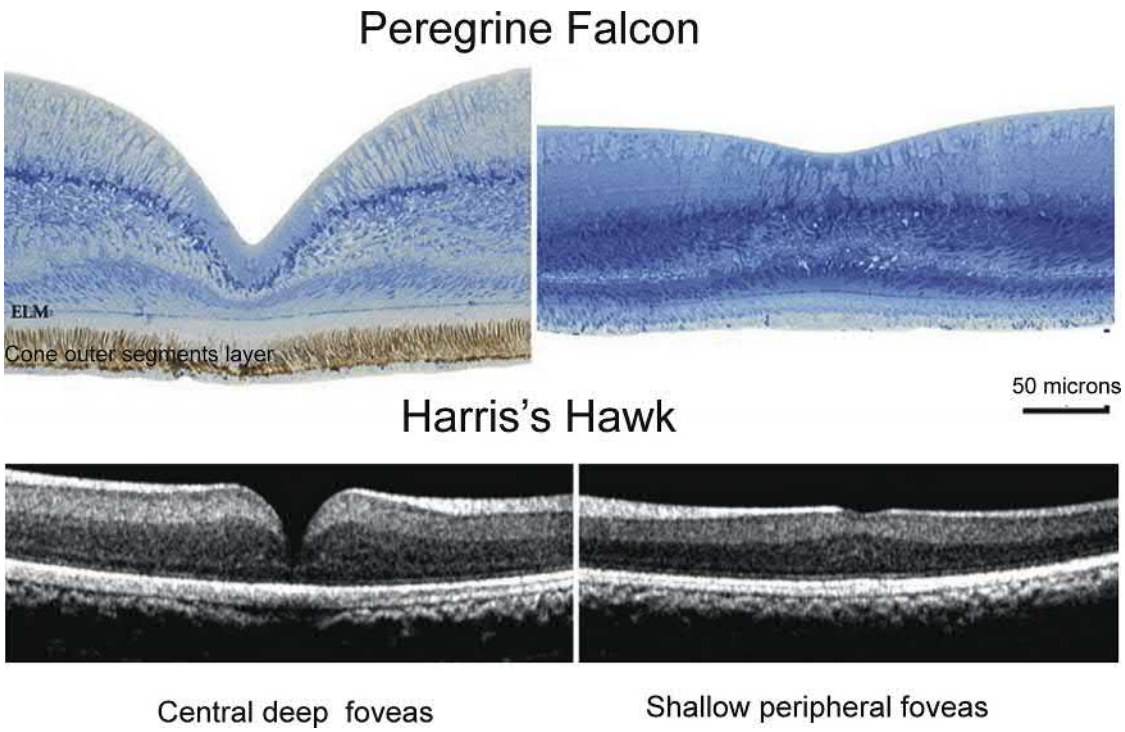

FIGURE 10.8 **Sections through the retinas of a Peregrine Falcon and a Harris's Hawk showing foveas.** In both species, there are two foveas. One is placed more-or-less centrally in the retina and looks out laterally in the bird's field of view. The other is placed toward the periphery of the retina and looks more forwards, although it does not look directly forward. The central foveas are deep and have sharply curved sides, the shallow foveas are more bowl shaped, both are locations where acuity is enhanced compared with the rest of the retina. Note that light making up the image travels from top to bottom in these diagrams and the photoreceptors are in the bottom layers in each illustration. They can be clearly seen in the picture of the Peregrine's deep fovea (top left). *Illustrations courtesy of Mindaugus Mitkus (Peregrine Falcon) and Simon Potier (Harris's Hawk) both University of Lund Vision Group, Sweden.*

amount (e.g., in owls, eyes diverge by about 55 degrees), or they can be almost diametrically opposed (ducks and shorebirds). Thus, the fields of the two eyes have become combined in many ways and so provide a wide range of different total fields of view, as well as markedly different degrees by which the two eyes overlap and provide binocular coverage of part of the total field (Fig. 10.9).

Humans are unusual animals in having two eyes placed on the front of the skull. This results in each eye seeing almost the same sector of space. This arrangement is quite different from that found in birds (Martin, 2007, 2012). In most species, eye position is such that each eye sees something different from what is seen by the other eye. Frontal eye placement in humans leaves us with the subjective experience that the world lies in front of us and that we move into it. For most birds, the world surrounds them, and they flow through it. Birds can extract information from a scene receding behind them while simultaneously gaining information from the world into which they are traveling.

At one extreme are the visual fields of some ducks and some shorebirds, which can see the whole of the hemisphere above and around their head (Martin, 2007, 2014). In fact, the only place from which they cannot retrieve information is the part obscured by their own bodies. The utility of such broad visual coverage for the detection of conspecifics and predators has been demonstrated (Guillemain et al., 2002).

Differences in visual field configuration can occur between closely related species suggesting that visual fields can be finely tuned to subtle differences in the perceptual challenges of different foraging tasks. For example, there are significant differences in the visual fields of different species of ibises in the same family (Threskiornithidae) that depend on whether the birds probe their bills into soft substrata or take items from dry surfaces (Martin and Portugal, 2011). There are differences in the visual fields of closely related ducks which have been accounted for by whether the species feeds by selective grazing or filter feeding (Guillemain et al., 2002), and differences among sandpipers (Scolopacidae) which have been accounted for by whether the species employs tactile cues from the bill rather that visual cues when foraging (Martin and Piersma, 2009; Piersma et al., 1998).

These examples indicate that the vision of different bird species, even within the same family, have been subtly tuned by natural selection primarily to the perceptual

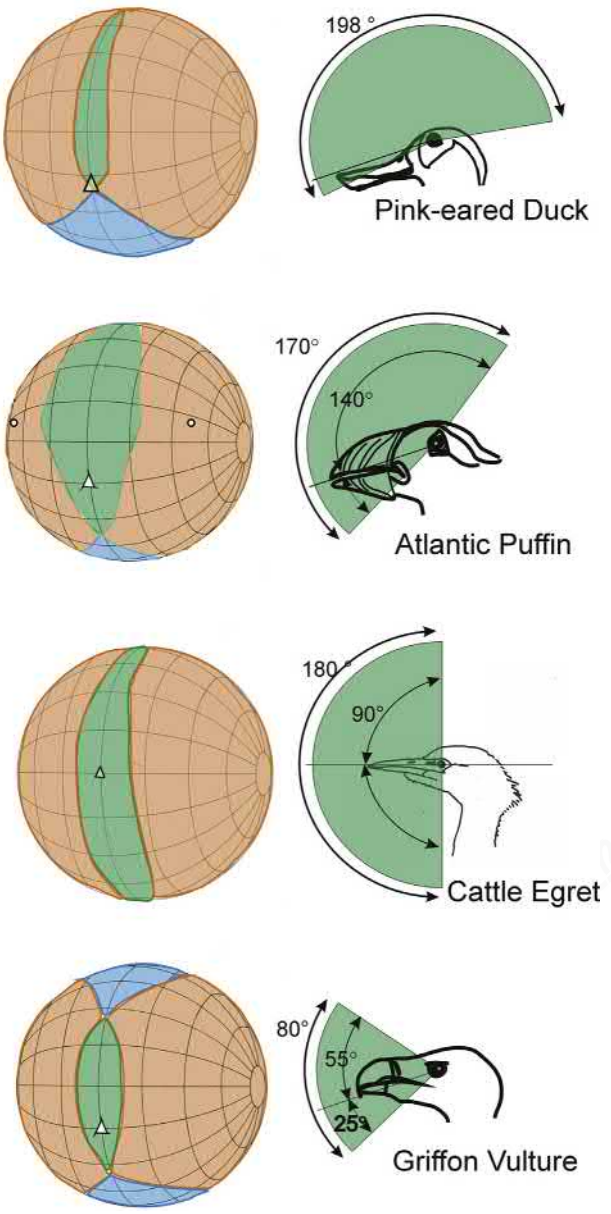

FIGURE 10.9 Diversity in the visual fields of birds. The visual fields of four species are shown with two diagrams for each species. The left hand column shows the visual fields as projected onto the surface of a globe that surrounds the bird's head. This is a perspective view of the head with the bill projecting in the directions indicated by the white triangles. The green sector is the region of binocular overlap, the blue is the blind sector, and the orange sector shows the area covered by each eye alone to the left and right of the head. There are clear differences in the position, width, and vertical extent of the regions of binocular overlap and in the extent of blind regions about the head. The right hand column of diagrams shows the vertical extend of the binocular regions in the median sagittal plane of the head (the plane which divides the head in two vertically). In Pink-eared Ducks *Malacorhynchus membranaceus*, the binocular area extends from the bill through more than 180degrees, hence there is no blind region about the head. In Atlantic Puffins *Fratercula arctica*, the binocular region is broader and oriented upwards but not sufficiently to allow the birds to see fully behind their heads. In Cattle Egrets *Bubulcus ibis*, the binocular region is also long and narrow but is orientated so that the birds can see directly below them in the frontal field and there is a small blind area behind the head. In Griffon Vultures *Gyps fulvus*, the region of binocular overlap is very small in width, and in vertical extent, there is a large blind area above and behind the head. *Drawings by the author based upon originals in (Katzir and Martin, 1994; Martin et al., 2007a, 2012; Martin and Wanless, 2015).*

challenges of particular foraging tasks. It has been argued that such subtle tuning of visual fields should be considered as important as the fine-tuning of bill structures as a means of meeting the physical challenges posed by the exploitation of different foods in these same species (Martin, 2014).

The full range of factors that are considered to play a role in the evolution of visual field configurations in birds have been discussed in some detail (Martin, 2014, 2017b). Data are available on visual field configurations in more than 100 species across a wide range of taxa. It is argued that visual field configurations are driven primarily by two competing informational demands posed by the tasks of foraging and predator detection. The primary demand is for the control of bill position during foraging (or in some predatory species, feet position).

The key requirement, regardless of whether a bird forages by pecking, lunging, or grabbing items with their feet, is the control of direction of travel and the time to contact with a target. As such it is concerned with objects that lie relatively close to the bird, broadly within its frontal field of view. Predator detection requires the detection of objects that are relatively remote from the bird that lie in its lateral or peripheral field of view. Visual field configurations can thus be considered the result of a trade-off between those demands as they occur in different species.

In species with large eyes that have evolved to provide high-acuity vision, a third demand also influences their visual field, avoiding imaging the sun on the retina (Martin and Coetzee, 2004). The image of such a bright light source compromises high-spatial resolution and so these birds, which include eagles, hornbills, bustards, and cranes, have extensive blind regions to the front and above their heads. This can render them vulnerable to collisions when in flight and surveying the land below (Martin and Shaw, 2010).

10.7 Spatial resolution in birds

Spatial resolution in vertebrate eyes is determined by the characteristics of both the image producing and image analyzing mechanisms. To achieve high resolution requires an image that is of high quality, well focused, and large. This requires an optical system which has a long focal length and a large entrance pupil. Pupil size is important since it determines the limit on the quality of the image (Land and Nilsson, 2012). Image size is important since it determines the number of photoreceptors/ganglion cells

over which the image is spread, and hence are available to analyze the image.

The "best" estimate of an animal's spatial resolution is gained by interrogating it, using behavioral training psychophysical techniques. These can be used to determine the limits of visual performance under a range of ambient conditions (Lind et al., 2012; Potier et al., 2016; Reymond, 1985; White et al., 2007). Such investigations are difficult and laborious but they can be substituted using data based upon eye anatomy. This provides an estimate of maximum spatial resolution of an eye but only at high light levels. It requires knowledge of the spatial separation of photoreceptors and/or ganglion cells at their maximum density within the retina. This can be combined with a measure or estimate of the focal length of the eye's optics. The result is an estimate of the maximum resolution of an eye for high contrast stimulus patterns, at high light levels. This anatomical technique has been used to estimate acuity for more than 25 bird species, and behavioral data have been gathered on an equal number of species. Some examples of acuity using behavioral and anatomical techniques are given in Table 10.1. A more comprehensive table of acuity in over 50 species from 25 avian families can be found in (Martin, 2017a).

Crucially, there have been some detailed studies which show that anatomically estimated acuity correlates well with acuity determined at daytime light levels using behavioral psychophysical tests. This was first demonstrated in eagles and falcons (Reymond, 1985, 1987). It should be noted, however, that the anatomical technique

TABLE 10.1 Spatial resolution in a sample of bird species and in young humans.

Order	Family	Species	Spatial resolution cycles/degree	Acuity minutes of arc	Method	Source
Accipitriformes	Accipitridae	Wedge-tailed eagle *Aquila audax*	142	0.2	Anatomy and behavior	Reymond (1985)
Accipitriformes	Accipitridae	Indian vulture *Gyps indicus*	135	0.2	Behavior	Fischer (1969)
Falconiformes	Falconidae	Brown falcon *Falco berigora*	73	0.4	Anatomy and behavior	Reymond (1987)
Columbiformes	Columbidae	Rock dove *Columba livia*	18	1.7	Behavior	Hodos et al. (1976)
Anseriformes	Anatidae	Canada goose *Branta canadensis*	9.6	3.1	Anatomy	Fernandez-Juricic et al. (2011)
Galliformes	Phasianidae	Red jungle fowl *Gallus gallus*	8.3	3.6	Anatomy	Ehrlich (1981)
Strigiformes	Strigidae	Great horned owl *Bubo virginianus*	7.5	4	Behavior	Fite (1973)
Passeriformes	Passeridae	House sparrow *Passer domesticus*	4.8	6.3	Anatomy	Dolan and Fernandez-Juricic (2010)
Passeriformes	Fringillidae	House finch *Haemorhous mexicanus*	4.7	6.4	Anatomy	Dolan and Fernandez-Juricic (2010)
Suliformes	Phalacrocoracidae	Great cormorant *Phalacrocorax carbo* (underwater)	3.3	9.1	Behavior	White et al. (2007)
		Human	72	0.4	Behavior	Land and Nilsson (2012)

Resolution is shown as both cycles per degree and minutes of arc. The two measures are interchangeable. Older studies tended to use acuity, while more recent studies prefer to express resolution in cycles per degree. All behavioral measures were made at high daytime light levels and indicate the best performance (finest spatial detail that can be resolved)

cannot provide estimates of spatial resolution at lower levels of illumination, when spatial resolution inevitably decreases (Land and Nilsson, 2012). Such decreases in acuity with decreasing light levels have been confirmed using behavioral techniques in a number of bird species including chickens *Gallus gallus* (Gover et al., 2009), doves *Columba livia* (Blough, 1971), wedge-tailed eagles (Reymond, 1985), great horned owls *Bubo virginianus* (Fite, 1973), and barn owls *Tyto alba* (Orlowski et al., 2012).

Table 10.1 illustrates that maximum spatial resolution across bird species can vary over a range of at least 30-fold. The acuity of an eagle is eight times higher than that of a dove, and 18 times that of a chicken. Another way to compare these acuities is that an eagle should be able to detect a given object 8 times further away than a dove, and 18 times further away than a chicken.

It is worth noting that the low acuity of Great Cormorants underwater (Table 10.1) is close to the highest acuity measured underwater in humans without face masks (Gislen et al., 2003), found in children from the Moken people (West coast of Thailand). These children forage underwater guided by vision and although their underwater acuity is high compared to that of Europeans, it is considerably lower than their own acuity in air. Furthermore, the similarity between the underwater acuity of cormorants and this human population indicates that high acuity is not a requirement for successful underwater foraging. In both humans and cormorants, it seems that the relatively poor acuity when immersed is complemented by the employment of specific foraging techniques aimed at particular quarry (White et al., 2007).

As shown in Table 10.1, acuity provides a useful metric with which to compare vision across species. It is also useful to estimate the distances at which high-contrast stimuli can be detected. For example, it is possible to use acuity values to estimate the maximum distance at which typical prey or a carcass could be detected by a foraging predator or scavenger. Acuity data have also been used in a similar way to determine the likely maximum distance at which an obstacle could be detected by a bird. This can also be used to estimate the optimum size and positioning of a pattern designed to function as a warning to a bird that an obstacle, such as a power line, lies ahead (Martin, 2011).

Extrapolations from acuity data to field situations also make it clear that the most conspicuous stimuli are likely to be high contrast (black and white) patterns, rather than colored patterns. Although particular colors may have salience for particular species in the mediation of specific behaviors (Endler et al., 2005, 2014), acuity for colored patterns has been shown to be significantly lower than for black and white patterns. This has been demonstrated recently in Budgerigars *Melopsittacus undulatus* (Lind and Kelber, 2011) and in Harris's Hawks *Parabuteo unicinctus* (Potier et al., 2018). Given the phylogenetic distance between these species and their marked differences in ecology, lower acuity for chromatic stimuli is likely to be a feature of the vision of all bird species, probably a feature of all visual systems. It is well established in humans (Mullen, 1985).

10.8 Contrast sensitivity

Although it is possible to manufacture high-contrast stimuli to act as warnings for birds, natural stimuli are rarely of high contrast. Most avian real-world tasks require the detection of stimuli that of low contrast. The ability to detect stimuli of low contrast is summarized by the determination of a contrast sensitivity function (Ghim and Hodos, 2006). This determines the minimum amount of contrast that can be detected for stripes of different widths when they are presented as gratings of different spatial frequencies. High-contrast gratings of the kind used to determine maximum acuity are one extreme of the contrast sensitivity function. To detect very fine gratings, high contrast is essential, but coarser gratings can be detected at relatively low contrast (Fig. 10.10). A full contrast sensitivity function indicates how wide stripe patterns must be for the smallest difference in contrast to be visible across a range of grating frequencies.

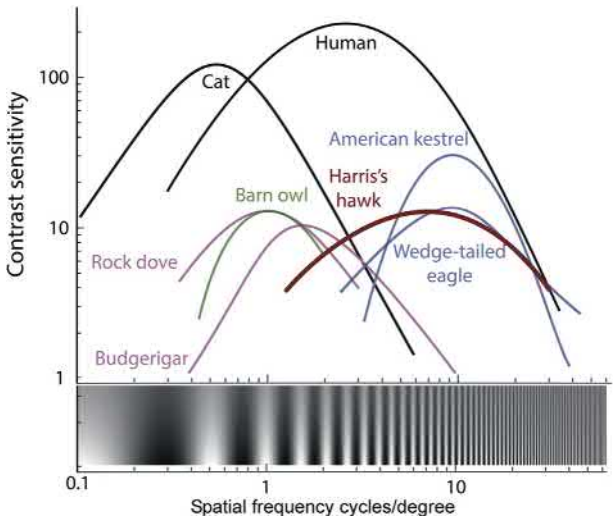

FIGURE 10.10 Contrast sensitivity functions of birds and mammals. At each grating frequency (as indicated across the lower part of the diagram), the contrast of the pattern is varied and the minimum contrast that the bird can detect at that frequency is determined. For each species, there is a range of spatial frequencies in which sensitivity to contrast is high. However, sensitivity drops off rapidly at both higher and lower spatial frequencies. Bird species differ markedly in their sensitivity to contrast, and all birds are much less sensitive to contrast than humans and cats. This means that scenes must have higher degrees of contrast for birds to be able to detect detail within them compared with mammals. *Redrawn from an original figure by Simon Potier of the University of Lund Vision Group.*

Although contrast sensitivity functions are not available for many bird species, they indicate that birds have lower contrast sensitivity compared with mammals, including humans. That is, at a given stripe width, contrast has to be higher in birds than in mammals before it can be detected (Harmening et al., 2007, 2009; Hodos et al., 2002; Lind et al., 2012; Lind and Kelber, 2011).

In all vertebrate species tested to date, contrast sensitivity declines as stripe widths either increase or decrease away from the widths where contrast sensitivity is highest (Fig. 10.10). Thus, there is a middle range of stripe widths where small amounts of contrast differences are relatively easily detected. Most importantly, these studies demonstrate that when stimuli are of low contrast, the optimal size at which they are most likely to be detected is relatively large, much broader than the stripes that are detectable at high contrast. This emphasizes that measures of maximum acuity (of the kind shown in Table 10.1) may have limited application for understanding what spatial information a bird is able to retrieve from within its natural environment.

An illustration of the importance of this is provided by an attempt to use information on how the resolution of Great Cormorants is affected by target contrast. This modeled a "cormorant's eye view" to simulate how a typical prey item would appear at different distances and with different degrees of contrast (Fig. 10.11). The model showed that only at less than 1 m can a fish, of the size typically taken by Great Cormorants, be seen in any detail. Beyond this distance, a prey fish will appear as no more than a faint blur. However, cormorants are able to use this information to forage efficiently by employing specialized foraging behaviors (White et al., 2007).

10.9 Closing remarks

As outlined in the introduction, vision is fundamentally about spatial information, about where light is coming from in the world that surrounds the observer. The remarkable accuracy and precision of vision in birds is built upon finely tuned optics and image analysis mechanisms. Vision in birds is, however, far from uniform. Natural selection has built upon the inherent flexibility of the vertebrate eye's optical system, the flexibility in the way retinal receptors can be arranged, and the flexibility with which eyes can be placed in the skull to give each species a different suite of visual information. There is not one "bird's eye view" but many.

Well-founded comparisons between the vision of different bird species are, however, limited. Only for those species for which there is detailed information on physiology and anatomy of the eyes, or the visual capacities of the whole animal, can reliable comparisons be made. These are but a handful of species compared with the more than 10,000 bird species that exist today.

Even among this handful of species there is wide diversity in the information that their vision provides. Each species appears to have a unique suite of information that guides them in the execution of different tasks in different light environments; from pecking to lunging at food items, from bright sunlight to woodlands at night, from the open skies to below water. It should also be remembered that visual information is complemented by equally diverse sources of information from other senses, and that information provided by vision and other senses are usually used in complementary ways to guide behavior (Martin,

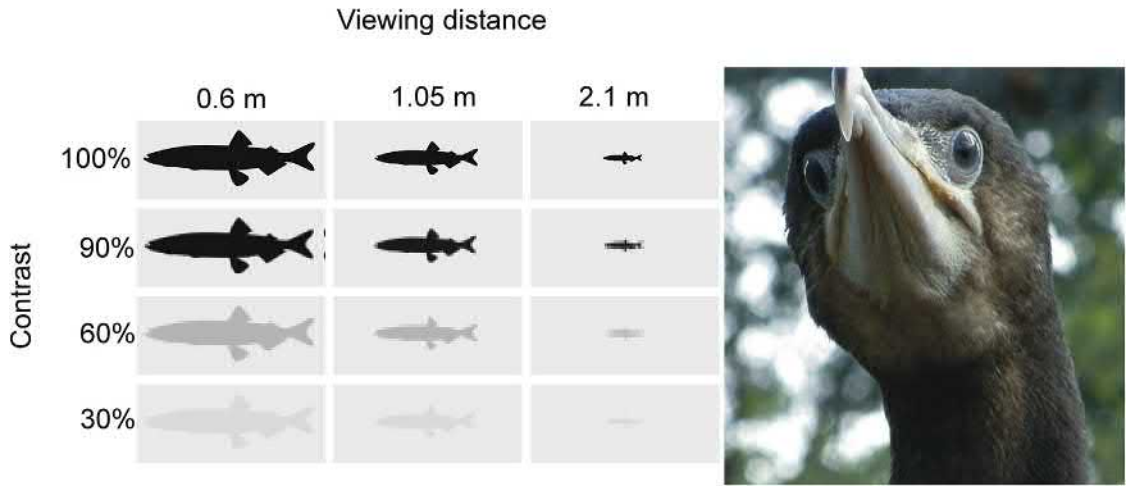

FIGURE 10.11 A simulation of how a fish model might appear to a cormorant at different viewing distance and at different degrees of contrast with the background. The model fish is based upon a 10 cm long Capelin, a species commonly taken by Great Cormorants. The acuity of the cormorant is based upon behavioral measures and assumes the highest acuity of this species underwater. The water is clear, and the light level is 10 lux, which is at the lower end of the daylight range. The simulation shows that apart from the high contrast fish viewed at close range, all target fish will appear quite indistinct. This gives rise to the idea that cormorants will frequently be lunging at an escaping blur when foraging, especially when water is turbid, rather than lunging at a distinct fish shape. *Redrawn from White et al. (2007).*

2017a, 2020). The result of this diversity in sensory information is that while different bird species can share the same environment, they live in different worlds.

Clearly, understanding both the fundamental mechanisms of the eye and visual system, and how these have been elaborated in each species, is vital for understanding the very essence and diversity of birds. While the foundations of our knowledge of avian vision can be considered secure, much remains to be done. Filling in the comparative details, elucidating general principles that explain the diversity of avian vision, and building knowledge of the information that birds extract from the world; these are all fundamental tasks in ornithology.

References

Bingelli, R.L., Paule, W.J., 1969. The pigeon retina: quantitative aspects of the optic nerve and ganglion cell layer. J. Comp. Neurol. 137, 1–18.

Blough, D.S., 1971. The visual acuity of the pigeon for distant targets. J. Exp. Anal. Behav. 15, 57–68.

Boire, D., Dufour, J.S., Theoret, H., Ptito, M., 2001. Quantitative analysis of the retinal ganglion cell layer in the ostrich, *Struthio camelus*. Brain Behav. Evol. 58, 343–355.

Bowmaker, J.K., 1977. The visual pigments, oil droplets and spectral sensitivity of the pigeon. Vis. Res. 17, 1129–1138.

Bowmaker, J.K., Loew, E., 2008. Vision in fish. In: Basbaum, A.I., et al. (Eds.), The Senses: A Comprehensive Reference, vol. 1. Elsevier, Amsterdam, pp. 54–76.

Bringmann, A., 2019. Structure and function of the bird fovea. Anat. Histol. Embryol. 48, 177–200.

Coimbra, J.P., Collin, S.P., Hart, N.S., 2014. Topographic specializations in the retinal ganglion cell layer correlate with lateralized visual behavior, ecology, and evolution in cockatoos. J. Comp. Neurol. 522, 3363–3385.

Coimbra, J.P., Collin, S.P., Hart, N.S., 2015. Variations in retinal photoreceptor topography and the organization of the rod-free zone reflect behavioral diversity in Australian passerines. J. Comp. Neurol. 523, 1073–1094.

Coimbra, J.P., Marceliano, M.L.V., Andrade-da-Costa, B.L.D., Yamada, E.S., 2006. The retina of tyrant flycatchers: topographic organization of neuronal density and size in the ganglion cell layer of the great kiskadee *Pitangus sulphuratus* and the rusty margined flycatcher *Myiozetetes cayanensis* (Aves: Tyrannidae). Brain Behav. Evol. 68, 15–25.

Coimbra, J.P., Nolan, P.M., Collin, S.P., Hart, N.S., 2012. Retinal ganglion cell topography and spatial resolving power in penguins. Brain Behav. Evol. 80, 254–268.

Cronin, T.W., 2008. Visual ecology. In: Basbaum, A.I., et al. (Eds.), The Senses: A Comprehensive Reference, vol. 1. Elsevier, Amsterdam, pp. 211–245.

Cronin, T.W., 2012. Visual optics: accommodation in a splash. Curr. Biol. 22, R871–R873.

Cserhati, P., Szel, A., Rohlich, P., 1989. Four cone types characterized by anti-visual pigment antibodies in the pigeon retina. Invest. Ophthalmol. Vis. Sci. 30, 74–81.

Cuthill, I.C., Partridge, J.C., Bennett, A.T.D., Church, S.C., Hart, N.S., Hunt, S., 2000. Ultraviolet vision in birds. Adv. Stud. Behav. 29, 159–214.

Dolan, T., Fernandez-Juricic, E., 2010. Retinal ganglion cell topography of five species of ground-foraging birds. Brain Behav. Evol. 75, 111–121.

Douglas, R.H., Geffery, G., 2014. The spectral transmission of ocular media suggests that ultraviolet sensitivity is widespread among mammals. Proc. R. Soc. Biol. Sci. Ser. B 281, 20132995.

Ehrlich, D., 1981. Regional specialization of the chick retina as revealed by the size and density of neurons in the ganglion cell layer. J. Comp. Neurol. 195, 643–657.

Emery, N.J., 2006. Cognitive ornithology: the evolution of avian intelligence. Phil. Trans. R. Soc. B Biol. Sci. 361, 23–43.

Endler, J.A., Gaburro, J., Kelley, L.A., 2014. Visual effects in great bowerbird sexual displays and their implications for signal design. Proc. R. Soc. Biol. Sci. Ser. B 281. https://doi.org/10.1098/rspb.2014.0864.

Endler, J.A., Westcott, D.A., Madden, J.R., Robson, T., 2005. Animal visual systems and the evolution of color patterns: sensory processing illuminates signal evolution. Evolution 59, 1795–1818.

Fernandez-Juricic, E., Moore, B.A., Doppler, M., Freeman, J., Blackwell, B.F., Lima, S.L., DeVault, T.L., 2011. Testing the terrain hypothesis: Canada Geese see the world laterally and obliquely. Brain Behav. Evol. 77, 147–158.

Fischer, V.A.B., 1969. Laboruntersuchungen und Freiland beobachtungen zum Sehvermogen und Verhalten von Altweltgeiern. Zoologische Jahrbuecher Abteilung fuer Systematik Biologie 96, S81–S132.

Fite, K.V., 1973. Anatomical and behavioral correlates of visual acuity in the Great Horned Owl. Vis. Res. 13, 219–230.

Galifret, Y., 1968. Les diverse aires fonctionelles de la retine du pigeon. Zeitschrift fur Zellforschung und Mikroskopische Anatomie 86, 535–545.

Ghim, M.M., Hodos, W., 2006. Spatial contrast sensitivity of birds. J. Comp. Physiol. A 192, 523–534.

Gislen, A., Dacke, M., Kroger, R.H.H., Abrahamsson, M., Nilsson, D.-E., Warrant, E., 2003. Superior underwater vision in a human population of sea gypsies. Curr. Biol. 13, 833–836.

Glasser, A., Troilo, D., Howland, H.C., 1994. The mechanism of corneal accommodation in chicks. Vis. Res. 34, 1549–1566.

Gover, N., Jarvis, J.R., Abeyesinghe, S.M., Wathes, C.M., 2009. Stimulus luminance and the spatial acuity of domestic fowl (Gallus. g. domesticus). Vis. Res. 49, 2747–2753.

Grant, P.R., Grant, B.R., 2014. Forty Years of Evolution: Darwin's Finches on Daphne Major Island. Prinecton University Press, Princeton.

Guillemain, M., Martin, G.R., Fritz, H., 2002. Feeding methods, visual fields and vigilance in dabbling ducks (Anatidae). Funct. Ecol. 16, 522–529.

Hackett, S.J., Kimball, R.T., Reddy, S., Bowie, R.C., Braun, E.L., Braun, M.J., Chojinowski, J.L., Cox, A., Han, K.-L., Harshman, J., Huddleston, C.J., Marks, B.D., Miglia, K.J., Moore, W.S., Sheldon, F.H., Steadman, D.W., Witt, C.C., Yuri, T., 2008. A phylogenomic study of birds reveals their evolutionary history. Science 1763–1768.

Harmening, W.M., Nikolay, P., Orlowski, J., Wagner, H., 2007. Contrast sensitivity in the barn owl. Perception 36, 77.

Harmening, W.M., Nikolay, P., Orlowski, J., Wagner, H., 2009. Spatial contrast sensitivity and grating acuity of barn owls. J. Vis. 9 https://doi.org/10.1167/9.7.13.

Hart, N.S., 2001. Variations in cone photoreceptor abundance and the visual ecology of birds. J. Comp. Physiol. A Sensory Neural Behav. Physiol. 187, 685–697.

Hart, N.S., 2002. Vision in the peafowl (Aves: *Pavo cristatus*). J. Exp. Biol. 205, 3925–3935.

Hart, N.S., 2004. Microspectrophotometry of visual pigments and oil droplets in a marine bird, the wedge-tailed shearwater Puffinus pacificus: topographic variations in photoreceptor spectral characteristics. J. Exp. Biol. 207, 1229–1240.

Hart, N.S., Hunt, D., 2007. Avian visual pigments: characteristics, spectral tuning, and evolution. Am. Nat. 169, S7–S26.

Hart, N.S., Partridge, J.C., Bennett, A.T.D., Cuthill, I.C., 2000a. Visual pigments, cone oil droplets and ocular media in four species of *Estrildid Finch*. J. Comp. Physiol. A Sensory Neural Behav. Physiol. 186, 681–694.

Hart, N.S., Partridge, J.C., Cuthill, I.C., 1998. Visual pigments, oil droplets and cone photoreceptor distribution in the European Starling (*Sturnus vulgaris*). J. Exp. Biol. 201, 1433–1446.

Hart, N.S., Partridge, J.C., Cuthill, I.C., 1999. Visual pigments, cone oil droplets, ocular media and predicted spectral sensitivity in the Domestic Turkey (*Meleagris gallopavo*). Vis. Res. 39, 3321–3328.

Hart, N.S., Partridge, J.C., Cuthill, I.C., 2000b. Retinal asymmetry in birds. Curr. Biol. 10, 115–117.

Hart, N.S., Vorobyev, M., 2005. Modelling oil droplet absorption spectra and spectral sensitivities of bird cone photoreceptors. J. Comp. Physiol. A 191, 381–392.

Hayes, B.P., Brooke, M.d.L., 1990. Retinal ganglion cell distribution and behaviour in procellariiform seabirds. Vis. Res. 30, 1277–1289.

Hess, C., 1909. Die Akkommodation bei Tauchervogeln. Arch vergleich Opthal 1, 153–164.

Hodos, W., Ghim, M., Potocki, A., Fields, J., Storm, T., 2002. Contrast sensitivity in pigeons: a comparison of behavioral and pattern ERG methods. Doc. Ophthalmol. 104, 107–118.

Hodos, W., Leibowitz, R.W., Bonbright, J.C., 1976. Near-field visual acuity of pigeons: effects of head location and stimulus luminance. J. Exp. Anal. Behav. 25, 129–141.

Howland, H.C., Sivak, J.G., 1984. Penguin vision in air and water. Vis. Res. 24, 1905–1909.

Hughes, A., 1977. The topography of vision in mammals of contrasting life style: comparative optics and retinal organization. In: Crescitelli, F. (Ed.), Handbook of Sensory Physiology, Vol VII/5. Springer-Verlag, Berlin, pp. 613–756.

Jones, C.D., Osorio, D., 2004. Discrimination of oriented visual textures by poultry chicks. Vis. Res. 44, 83–89.

Katzir, G., Howland, H.C., 2003. Corneal power and underwater accommodation in great cormorants (*Phalacrocorax carbo* sinensis). J. Exp. Biol. 206, 833–841.

Katzir, G., Martin, G.R., 1994. Visual fields in herons (Ardeidae) - panoramic vision beneath the bill. Naturwissenschaften 81, 182–184.

King, A.S., King, D.Z., 1980. Avian morphology: general principles. In: King, A.S., McLelland, J. (Eds.), Form and Function in Birds. Academic Press, London, pp. 10–89.

Land, M.F., 1981. Optics and vision in invertebrates. In: Autrum, H. (Ed.), Handbook of Sensory Physiology, Vol VII/6B. Springer-Verlag, Berlin, pp. 471–592.

Land, M.F., Nilsson, D.-E., 2012. Animal Eyes, second ed. Oxford University Press, Oxford.

Laughlin, S.B., 2001. The metabolic cost of information- a fundamental factor in visual ecology. In: Barth, F.G., Schmid, A. (Eds.), Ecology of Sensing. Springer, Berlin, pp. 170–185.

Levy, B., Sivak, J.G., 1980. Mechanisms of accommodation in the bird eye. J. Comp. Physiol. A Sensory Neural Behav. Physiol. 137, 267–272.

Lind, O., Mitkus, M., Olsson, O., Kelber, A., 2013. Ultraviolet sensitivity and colour vision in raptor foraging. J. Exp. Biol. 216, 1819–1826.

Lind, O., Mitkus, M., Olsson, P., Kelber, A., 2014. Ultraviolet vision in birds: the importance of transparent eye media. Proc. R. Soc. Biol. Sci. Ser. B 281, 20132209.

Lind, O., Kelber, A., 2011. The spatial tuning of achromatic and chromatic vision in budgerigars. J. Vis. 11 https://doi.org/10.1167/11.7.2.

Lind, O., Sunesson, T., Mitkus, M., Kelber, A., 2012. Luminance-dependence of spatial vision in budgerigars (*Melopsittacus undulatus*) and Bourke's parrots (*Neopsephotus bourkii*). J. Comp. Physiol. A Neuroethol. Sens. Neural Behav. Physiol. 198, 69–77.

Lisney, T.J., Potier, S., Isard, P.-F., Mentek, M., Mitkus, M., Collin, S.P., 2020. Retinal topography in two species of flamingo (Phoenicopteriformes: Phoenicopteridae). J. Comp. Neurol. https://doi.org/10.1002/cne.24902.

Lisney, T.J., Stecyk, K., Kolominsky, J., Schmidt, B.K., Corfield, J.R., Iwaniuk, A.N., Wylie, D.R., 2013a. Ecomorphology of eye shape and retinal topography in waterfowl (Aves: Anseriformes: Aanatidae) with different foraging modes. J. Comp. Physiol. A 199, 385–402.

Lisney, T.J., Stecyk, K., Kolominsky, J., Graves, G.R., Wylie, D.R., Iwaniuk, A.N., 2013b. Comparison of eye morphology and retinal topography in two species of New World Vultures (Aves: Cathartidae). Anat. Rec. 296, 1954–1970.

Lythgoe, J.N., 1979. The Ecology of Vision. Clarendon Press, Oxford.

Machovsky-Capuska, G.E., Howland, H.C., Rabenheimer, D., Vaughn-Hirschorn, R., Wursig, B., Hauber, M.E., Katzir, G., 2012. Visual accommodation and active pursuit of prey underwater in a plunge-diving bird: the Australasian gannet. Proc. R. Soc. B Biol. Sci. 279, 4118–4125.

Martin, G.R., 1999. Eye structure and foraging in king penguins *Aptenodytes patagonicus*. Ibis 141, 444–450.

Martin, G.R., 2007. Visual fields and their functions in birds. J. Ornithol. 148 (Suppl. 2), 547–562.

Martin, G.R., 2011. Understanding bird collisions with man-made objects: a sensory ecology approach. Ibis 153, 239–254.

Martin, G.R., 2012. Through Birds' Eyes: insights into avian sensory ecology. J. Ornithol. 153 (Suppl. 1), S23–S48.

Martin, G.R., 2014. The subtlety of simple eyes: the tuning of visual fields to perceptual challenges in birds. Phil. Trans. R. Soc. B. Biol. Sci. 369 https://doi.org/10.1098/rstb.2013.0040.

Martin, G.R., 2017a. The Sensory Ecology of Birds. Oxford University Press, Oxford.

Martin, G.R., 2017b. What drives bird vision? Bill control and predator detection overshadow flight. Front. Neurosci. 11, 619.

Martin, G.R., 2020. Bird Senses. Exeter. Pelagic Press.

Martin, G.R., Brooke, M.D.L., 1991. The eye of a procellariiform seabird, the Manx shearwater, *Puffinus puffinus*: visual fields and optical structure. Brain Behav. Evol. 37, 65–78.

Martin, G.R., Coetzee, H.C., 2004. Visual fields in Hornbills: precision-grasping and sunshades. Ibis 146, 18–26.

Martin, G.R., Jarrett, N., Williams, M., 2007a. Visual fields in blue ducks and pink-eared ducks: visual and tactile foraging. Ibis 149, 112–120.

Martin, G.R., Muntz, W.R.A., 1978. Spectral sensitivity of the red and yellow oildroplet fields of the pigeon (*Columba livia*). Nature 274, 620–621.

Martin, G.R., Osorio, D., 2008. Vision in birds. In: Basbaum, A.I., et al. (Eds.), The Senses: A Comprehensive Reference, vol. 1. Elsevier, Amsterdam, pp. 25–52.

Martin, G.R., Piersma, T., 2009. Vision and touch in relation to foraging and predator detection: insightful contrasts between a plover and a sandpiper. Proc. R. Soc. Lond. Ser. B Biol. Sci. 276, 437–445.

Martin, G.R., Portugal, S.J., 2011. Differences in foraging ecology determine variation in visual field in ibises and spoonbills (Threskiornithidae). Ibis 153, 662–671.

Martin, G.R., Portugal, S.J., Murn, C.P., 2012. Visual fields, foraging and collision vulnerability in Gyps vultures Ibis. Ibis 154, 626–631.

Martin, G.R., Rojas, L.M., Ramirez, Y., McNeil, R., 2004. The eyes of oilbirds (*Steatornis caripensis*): pushing at the limits of sensitivity. Naturwissenschaften 91, 26–29.

Martin, G.R., Shaw, J.M., 2010. Bird collisions with power lines: failing to see the way ahead? Biol. Conserv. 143, 2695–2702.

Martin, G.R., Wanless, S., 2015. The visual fields of Common Guillemots *Uria aalge* and Atlantic Puffins *Fratercula arctica*: foraging, vigilance and collision vulnerability. Ibis 157, 798–807.

Martin, G.R., Wilson, K.J., Wild, M.J., Parsons, S., Kubke, M.F., Corfield, J., 2007b. Kiwi forego vision in the guidance of their nocturnal activities. PLoS One 2 (2), e198. https://doi.org/10.1371/journal.pone.0000198.

Martin, G.R., Young, S.R., 1984. The eye of the Humboldt Penguin, *Spheniscus humboldti*: visual fields and schematic optics. Proc. R. Soc. Lond. Ser. B Biol. Sci. 223, 197–222.

Mitkus, M., Chaib, S., Lind, O., Kelber, A., 2014. Retinal ganglion cell topography and spatial resolution of two parrot species: budgerigar *Melopsittacus undulatus* and Bourke's parrot *Neopsephotus bourkii*. J. Comp. Physiol. A 200, 371–384.

Mitkus, M., Nevitt, G.A., Danielsen, J., Kelber, A., 2015. Spatial resolution and optical sensitivity of a DMS-responder and a non-responder: leach's storm-petrel and Northern fulmar. Doctoral dissertation. In: Mitkus, M. (Ed.), Spatial Vision in Birds: Anatomical Investigation of Spatial Resolving Power. Lund University, Lund, pp. 75–88.

Mitkus, M., Nevitt, G.A., Danielsen, J., Kelber, A., 2016. Vision on the high seas; spatial resolution and optical sensitivity in two procellariiform seabirds with different foraging strategies. J. Exp. Biol. 219, 3329–3338.

Moore, B.A., Paul-Murphy, J.R., Tennyson, A.J.D., Murphy, C.J., 2017. Blind free-living kiwi offer a unique window into the ecology and evolution of vertebrate vision. BMC Biol. 15, 85.

Mullen, K.T., 1985. The contrast sensitivity of human colour vision to red-green and blue-yellow chromatic gratings. J. Physiol. 359, 381–400.

Nilsson, D.-E., 2009. The evolution of eyes and visually guided behaviour. Phil. Trans. R. Soc. B Biol. Sci. 364, 2833–2847.

Nilsson, D.-E., Pelger, R.F., 1994. A pessimistic estimate of the time required for an eye to evolve. Proc. R. Soc. Lond. Ser. B Biol. Sci. 256, 53–58.

Odeen, A., Hastad, O., 2013. The phylogenetic distribution of ultraviolet sensitivity in birds. BMC Evol. Biol. 13 https://doi.org/10.1186/1471-2148-13-36.

Odeen, A., Hastad, O., Alstrom, P., 2010. Evolution of ultraviolet vision in shorebirds (Charadriiformes). Biol. Lett. 6, 370–374.

Odeen, A., Hastad, O., Alstrom, P., 2011. Evolution of ultraviolet vision in the largest avian radiation - the passerines. BMC Evol. Biol. 11 https://doi.org/10.1186/1471-2148-11-313.

Orlowski, J., Harmening, W., Wagner, H., 2012. Night vision in barn owls: visual acuity and contrast sensitivity under dark adaptation. J. Vis. 12, 1–8. https://doi.org/10.1167/12.13.4.

Osorio, D., Vorobyev, M., Jones, C.D., 1999. Colour vision of domestic chicks. J. Exp. Biol. 202, 2951–2959.

Parker, A., 2003. In the Blink of an Eye. Persus Books, Cambridge, Massachusetts.

Piersma, T., van Aelst, R., Kurk, K., Berkhoudt, H., Maas, L.R.M., 1998. A new pressure sensory mechanisms for prey detection in birds: the use of principles of seabed dynamics? Proc. R. Soc. Lond. Ser. B Biol. Sci. 265, 1377–1383.

Potier, S., Bonadonna, F., Kelber, A., Duriez, O., 2016. Visual acuity in an opportunistic raptor, the chimango caracara (*Milvago chimango*). Physiol. Behav. 157, 125–128.

Potier, S., Mitkus, M., Kelber, A., 2018. High resolution colour vision, but low contrast sensitivity in a diurnal raptor. Proc. Biol. R Soc. B Sci. 285, 20181036. https://doi.org/10.1098/rspb.2018.1036.

Potier, S., Mitkus, M., Lisney, T.J., Isard, P.-F., Dulaurent, T., Mentek, M., Cornette, R., Schikorski, D., Kelber, A., 2020. Inter-individual differences in foveal shape in a scavenging raptor, the black kite *Milvus migrans*. Sci. Rep. https://doi.org/10.1038/s41598-020-63039-y.

Prum, R.O., Berv, J.S., Dornburg, A., Field, D.J., Townsend, J.P., Lemmon, E.M., Lemmon, A.R., 2015. A comprehensive phylogeny of birds (Aves) using targeted next-generation DNA sequencing. Nature 526. 569-U247.

Reiner, A., Yamamoto, K., Karten, H.J., 2005. Organization and evolution of the avian forebrain. Anat. Rec. Part A 287A, 1080–1102.

Reymond, L., 1985. Spatial visual acuity of the eagle *Aquila audax*: a behavioural, optical and anatomical investigation. Vis. Res. 25, 1477–1491.

Reymond, L., 1987. Spatial visual acuity of the falcon, *Falco berigora*: a behavioural, optical and anatomical investigation. Vis. Res. 27, 1859–1974.

Rochon-Duvigneaud, A., 1943. Les yeux et la vision des vertébrés. Masson, Paris.

Schaeffel, F., Howland, H.C., 1987. Corneal acommodation in chick and pigeon. J. Comp. Physiol. A 160, 375–384.

Shlaer, R., 1972. An eagle's eye: quality of retinal image. Science 176, 920–922.

Sivak, J.G., Millodot, M., 1977. Optical performance of the penguin eye in air and water. J. Comp. Physiol. A Sensory Neural Behav. Physiol. 119, 241–247.

Walls, G.L., 1942. The Vertebrate Eye and its Adaptive Radiation. Cranbrook Institute of Science, Michigan.

White, C.R., Day, N., Butler, P.J., Martin, G.R., 2007. Vision and foraging in cormorants: more like herons than Hawks? PLoS One i2 (7), e639. https://doi.org/10.1371/journal.pone.0000639.

Wilkie, S.E., Robinson, P.R., Cronin, T.W., Poopalasun-daram, S., Bowmaker, J.K., Hunt, D.M., 2000. Spectral tuning of avian violet- and ultraviolet-sensitive visual pigments. Biochemistry 39, 7895–7901.

Wright, A.A., 1972. The influence of ultraviolet radiation on the pigeon's color discrimination. J. Exp. Anal. Behav. 17, 325–337.

Wright, A.A., 1979. Color-vision psychophysics. In: Granda, A.M., Maxwell, J.H. (Eds.), Neural Mechanisms of Behavior in the Pigeon. Plenum Press, New York.

Chapter 11

Avian hearing

Christine Köppl[1,2,3]

[1]Cluster of Excellence "Hearing4all", Carl von Ossietzky University, Oldenburg, Germany; [2]Research Center Neurosensory Science, Carl von Ossietzky University, Oldenburg, Germany; [3]Department of Neuroscience, School of Medicine and Health Science, Carl von Ossietzky University, Oldenburg, Germany

Abbreviations

Aivm ventromedial portion of the intermediate arcopallium
CM caudal nidopallium
ICc central nucleus of the inferior colliculus
ICx external nucleus of the inferior colliculus
ILD interaural level difference
ITD interaural time difference
LLDp posterior part of the ventral nucleus of the lateral lemniscus
MLd nucleus mesencephalicus lateralis pars dorsalis
NA nucleus angularis
NCM caudal medial nidopallium
Nd dorsal nidopallium
NL nucleus laminaris
NM nucleus magnocellularis

11.1 Introduction: what do birds hear?

Birds are very vocal. They communicate by a multitude of vocalisations, ranging from simple calls and cries to extremely varied songs, often also beautiful to our ears. Unlike simple calls and like human speech, birdsong must be learned and can serve to recognize other birds individually. Even beyond communication, the sense of hearing has special meaning to many birds. Owls that hunt hidden prey or at night rely on their keen sense of hearing. Some birds use echolocation to find their way in dark caves. However, some myths about the hearing of birds also abound. Perhaps the most notorious is the assertion that they hear ultrasound, that is, frequencies too high for humans to hear. Bird scare devices based on broadcasting ultrasound might scare a lot of mammals but they are inaudible to birds. Although some birds' songs may contain ultrasonic components (e.g., Pytte et al., 2004), they do not hear those themselves. Avian hearing typically remains restricted to below 10 kHz (Fig. 11.1), somewhat lower than human hearing. As a rule of thumb, small birds hear better at high frequencies than larger birds and vice versa (Dooling et al., 2000; Gleich and Langemann, 2011). Some birds, most notably owls, are exquisitely sensitive and able to hear fainter sounds than we can (Fig. 11.1).

In many standard behavioral auditory tests, such as frequency or intensity discrimination, birds do just as well as a typical mammal, including humans (Dooling et al., 2000; Moss and Carr, 2013). On some measures of temporal resolution, especially tasks that require the perception of fast fluctuating fine-structure, birds often outperform mammals (Dooling et al., 2000). Localizing sounds is more of a problem for birds because of their generally small head size which, in combination with their restricted upper hearing range, offers only small interaural cues (Klump, 2000; Köppl, 2009). As a rule, birds can localize sounds in azimuth as well as any mammal of comparable size (Moss and Carr, 2013). However, they cannot localize in elevation. The only exception to this are several owl species, which show extraordinary localization performance and prominent specializations associated with that (Klump, 2000). In more naturalistic auditory tasks, birds have been shown to group complex sounds into perceptual categories and patterns, much like humans do with, e.g., speech syllables (Dooling et al., 2000). Birds also form "auditory objects," that is, they group concurrent sounds in a complex scene into perceptual objects, e.g., different individual birds singing or tonal patterns forming galloping rhythms (Dooling et al., 2000; Moss and Carr, 2013).

Obviously, the auditory world of birds is rich, and hearing plays an important part in their lives. This chapter will summarize the sensory aspects of hearing in birds. How do birds' ears work, and how is sound processed in the brain? It should be pointed out that, although not the focus of this chapter, much of what is discussed below also applies to crocodilians that, together with birds (and a lot of extinct forms), are classified as archosaurs (Carroll, 1988;

Sturkie's Avian Physiology. https://doi.org/10.1016/B978-0-12-819770-7.00029-3

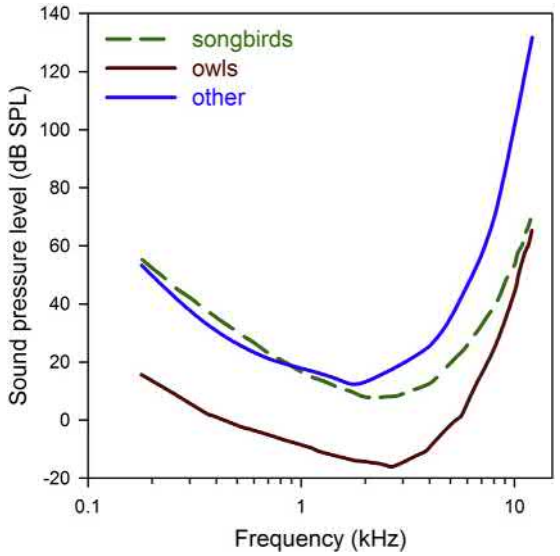

FIGURE 11.1 Median behavioral audiograms for three groups of birds. Note that owls hear sounds below 0 dB SPL, i.e., below the best human thresholds. *Modified Figure 7.1 from Dooling et al. (2000), with kind permission from Springer Science + Business Media B.V.*

Nesbitt, 2011). Like birds, crocodilians are quite vocal, and their auditory system is very similar (Vergne et al., 2009; Young et al., 2013).

11.2 Outer and middle ear

11.2.1 No specialized outer ear structures except in owls

Birds, like all nonmammals, do not have external ears or pinnae. This is easily explained by their generally small body (and consequently head) size in combination with a range of hearing limited to frequencies below about 10 kHz. The mammalian pinna is a sound reflection and filtering device that provides cues about the direction of a sound source relative to the head (Pickles, 2008). For this to be effective, sound wavelength, as a rule of thumb, must be smaller than head diameter, a condition which is generally not met in birds within their limits of hearing. Some very specialized owls, however, exploit similar principles, by bearing asymmetrical outer ears consisting of a facial ruff, skin flaps, and/or even asymmetrical bony ear canals (Norberg, 2002). Effectively, one of the outer ears is pointing slightly upwards, and the other downwards, which differentially reflects frequencies above 4 kHz or so (Keller et al., 1998). If the inputs from both ears are compared, this conveys a sensitivity for sound source elevation (see Section 11.4.2). Remarkably, such asymmetrical outer ears arose several times independently, in different owl genera, as an adaptation to hunting by auditory cues (Norberg, 2002).

11.2.2 The single-ossicle middle ear

Middle ears arose independently in a number of land vertebrate lineages during the Triassic period (Clack and Allin, 2004). In all nonmammalian lineages, the middle ear consists of a simple, piston-like device. It is for the most part homologous with the mammalian stapes (Manley and Sienknecht, 2013). The middle ear of birds consists of an elongate, mostly bony columella that bears a footplate on its medial end that abuts the bony inner-ear capsule. At its peripheral end, the columella grades into the mainly cartilaginous extracolumella that, with one of its several projections, makes close contact to the eardrum (Fig. 11.2). The most important part of the extracolumella is the inferior process, which connects the edge of the eardrum to somewhere close to its center. About half way along its length, the extracolumella is connected almost at a right angle to the columella; the flexible cartilage connection permits the columella to move in a piston-like fashion. Eardrum motion causes the inferior process to tilt on its fulcrum (at the edge of the eardrum), which exerts a force on the columella (Fig. 11.3). The force at the columellar footplate greatly exceeds that of the sound arriving at the eardrum since (a) the columella inserts at (roughly) half the length of the extracolumella and (b) the surface area of the eardrum is much larger than that of the footplate (Saunders et al., 2000). By these means, the middle ear acts

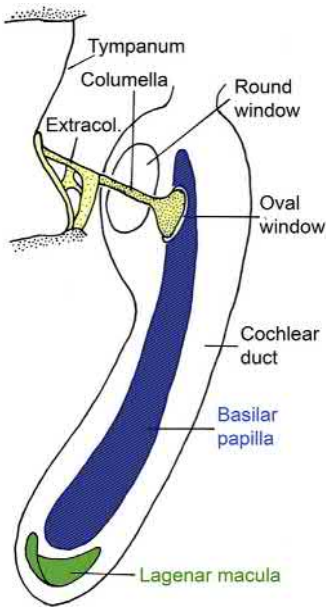

FIGURE 11.2 Schematic drawing of the cochlear duct of a typical bird, and its connection to the eardrum (tympanum) via the columella and extracolumella (yellow) of the middle ear. The dorsal, vestibular part of the inner ear is not shown. Two sensory hair cell organs are located in the cochlear duct: the auditory basilar papilla (blue) and the vestibular lagenar macula (green).

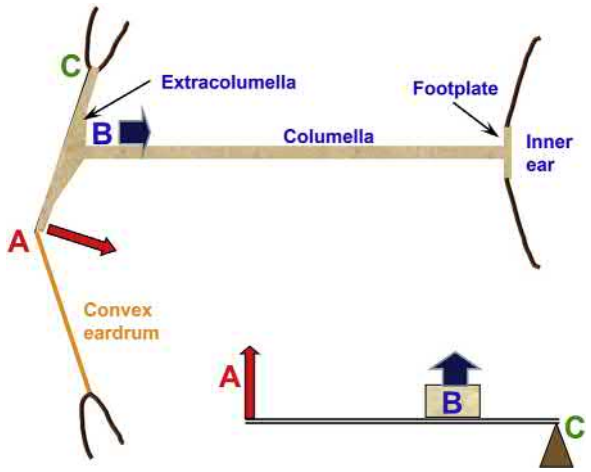

FIGURE 11.3 A schematic diagram of the middle ear of birds and its function. The extracolumella is attached flexibly to the columella, such that movement of the eardrum inwards results in a piston-like movement of the columellar footplate. The illustration at the lower right shows that these structures together build a lever of second order. The arrow length is proportional to the displacement amplitude, the arrow width to the force behind the movement. Thus at point B, the displacement is smaller than at A, but the force proportionately larger. C is the fulcrum, the axis of rotation of the lever.

as an impedance-matching device allowing sound from the low-impedance medium air to very effectively change the pressure in the high-impedance fluids of the inner ear (Fig. 11.3). Without it, the inner ear would be about 40 dB less sensitive (Gummer et al., 1989).

An enigma remains the paratympanic organ, a receptor patch almost exclusively found in birds and crocodiles, situated on the wall of the tympanic cavity (von Bartheld and Gianessi, 2011). It is made up of hair cells that are innervated by the facial nerve. However, its function is unknown. It has been speculated to act as a barometric device.

11.2.3 Internally coupled middle ears

The middle ears of birds are not enclosed in bullae as they are typically in mammals, but are acoustically connected through skull spaces. A prominent part of this connection is formed by wide Eustachian tubes that open into the buccal cavity (Christensen-Dalsgaard, 2011). However, there are very likely multiple routes through the highly trabeculated avian skull that have been difficult to visualize (Larsen et al., 2016). The functional implication of interaural coupling is that the ears function as pressure difference receivers, with sound reaching each eardrum from both sides. Depending on the physical dimensions of the head, the wavelength and the attenuation across the head, significant interactions between the sounds reaching the eardrum from both sides may result in increased directional cues. Although agreed in principle that this helps birds in localizing sound sources, the precise extent to which this happens in different species is still controversial and measurements by different laboratories vary (recent reviews in Christensen-Dalsgaard, 2011; Köppl, 2019; Larsen et al., 2016). Small birds probably experience more of such acoustic cross-talk while larger birds experience less, and limited to lower frequencies. Indeed, in the barn owl, internal coupling of the middle ears appears to play no role in the high-frequency range that the owl uses for prey localization (Calford and Piddington, 1988; Moiseff and Konishi, 1981b).

11.3 Basilar papilla (cochlea)

11.3.1 General morphology and physiology

The inner ear or labyrinth houses both the vestibular organs and the auditory organ, the basilar papilla. The hearing part is commonly referred to as cochlea or cochlear duct, which is correct in the sense that it is homologous to the mammalian cochlea (Manley and Clack, 2004). However, the avian version is not coiled and the term cochlea ("snail") thus not entirely appropriate. The cochlear duct houses the auditory basilar papilla and the vestibular lagenar macula, which forms the apical tip of the labyrinth (Fig. 11.2). This is another salient difference to mammals, which have lost the lagenar macula. In spite of earlier evidence to the contrary, the avian lagenar macula does not respond to sound (Manley et al., 1991) and does not send afferent fibers to the cochlear nuclei (Kaiser and Manley, 1996).

The avian basilar is typically only slightly curved and a few millimeters long; it tapers from being wide near the apical end to narrow at the basal end (Figs. 11.2 and 11.4A) (Gleich and Manley, 2000). It is composed of several thousand sensory hair cells, plus supporting cells surrounding each hair cell in a roughly hexagonal pattern (Fig. 11.4C and D). The epithelium sits on a basilar membrane that is largely suspended over the fluid of scala tympani. At both edges, the structure is anchored to the cartilaginous limbus and at the inner (or neural) edge, a varying proportion of hair cells actually sits atop this solid tissue, not on the basilar membrane (Fig. 11.5). There are two types of hair cells, tall and short (see Section 11.3.2). All hair cells are covered by the tectorial membrane, an acellular, proteinaceous structure (Goodyear and Richardson, 2002). Sound sets the basilar papilla in motion, which ultimately deflects the mechanosensitive bundles of its hair cells through a shear motion between them and the tectorial membrane. However, the precise modes of mechanical excitation in the avian papilla are still unclear. The basilar papilla is tonotopically organized, such that hair cells at apical locations are maximally sensitive to low frequencies, typically down to about 100 Hz, and those at basal locations maximally sensitive

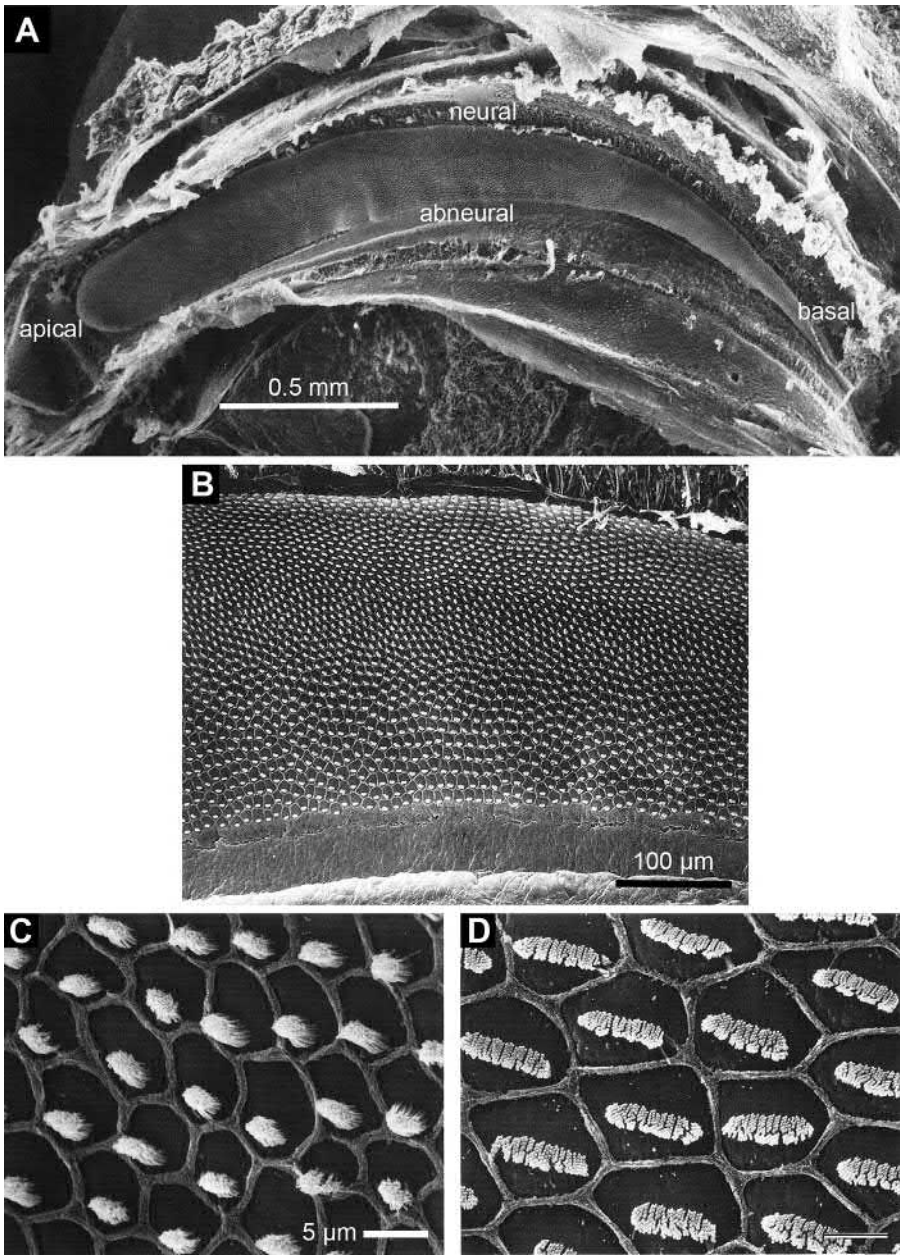

FIGURE 11.4 Surface morphology of the basilar papilla. (A): Low-magnification scanning electron micrograph of the exposed papilla of a chicken, after removal of the overlying tegmentum vasculosum and tectorial membrane. (B): View onto a segment of basilar papilla. Individual hair bundles are identifiable as white structures whose orientation changes across the epithelium. (C, D): High-magnification view onto a small group of hair cells. Note the hexagonal fringe of supporting cells surrounding each hair cell and the mechanosensitive hair bundles composed of tightly packed stereovilli. Note also that hair cells from apical regions (C) have smaller but taller bundles than those from basal regions (D). *Figure 1 from Cotanche et al. (1994), reproduced with kind permission from Springer Science + Business Media.*

to high frequencies, typically 5−8 kHz (Gleich et al., 2004). A traveling wave has been observed at the level of the basilar membrane (Gummer et al., 1987; Xia et al., 2016). However, unlike in the mammalian cochlea, its frequency resolution does not approximate the known selectivity at the neural level. Furthermore, the hair cells conveying the most sensitive responses appear to sit on or at the edge of the solid limbus (Gleich, 1989; Smolders et al., 1995), suggesting that basilar-membrane motion does not directly mediate the hair cells' mechanical stimulation. Hair cells in the avian basilar papilla show a very unique and complex pattern of bundle orientation (Gleich and Manley, 2000, Fig. 11.4B) that has prompted speculation about excitation waves moving obliquely across the tectorial membrane (Tilney et al., 1987), but this remains experimentally untested.

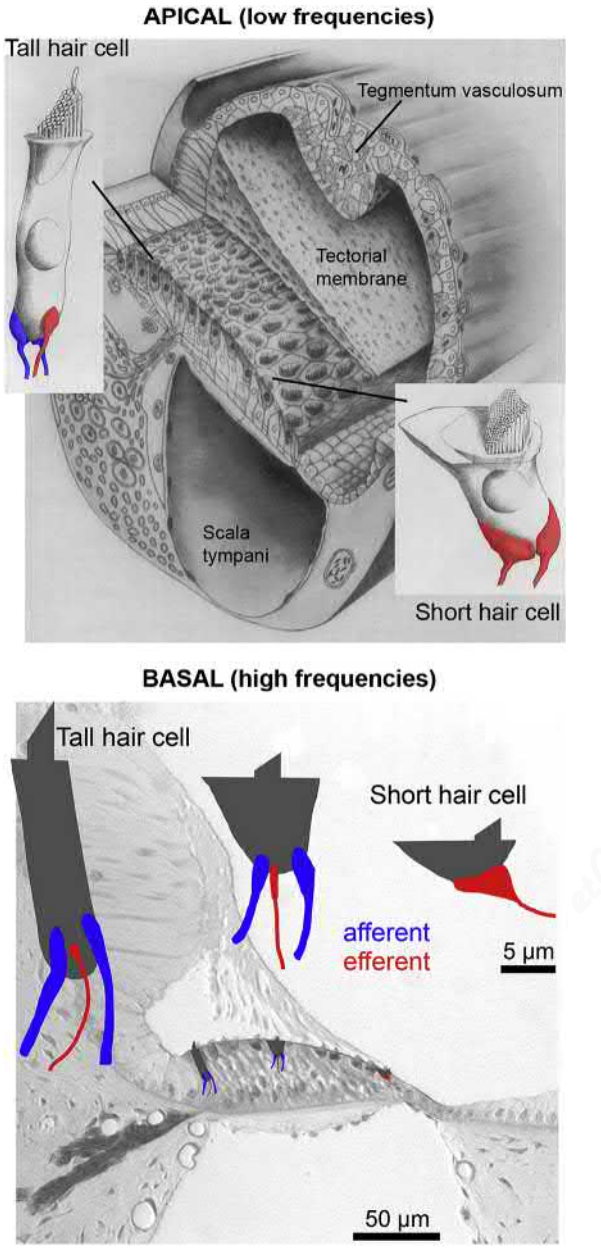

FIGURE 11.5 Overview of basilar papilla morphology and innervation. The top panel shows a three-dimensional (3D) rendering of a typical cross-section through the apical, low-frequency part. The papilla is wide, with many hair cells across, most of which are tall hair cells. Insets are 3D drawings of two representative hair cells, with afferent (blue) and efferent (red) nerve terminals attached. The lower panel shows a light-microscopical cross-section through the basal, high-frequency part, with some hair cells schematically highlighted and also shown enlarged. The lower scale bar applies to the histological image, the upper one to the drawings. The schematic drawings also show the typical innervation pattern, with afferent terminals drawn in blue and efferent terminals in red. *Figure 1 from Takasaka and Smith (1971), reproduced with permission from Academic Press; Figure 7 from Manley and Ladher (2008), reproduced with kind permission from the artist, Johanna Kraus; Figure 1A from Köppl (2011a), reproduced with permission of Elsevier BV.*

Transduction by the hair cells can be assumed to work according to the "gating-spring" principle established in other hair cell systems (Fettiplace and Ricci, 2006). Deflection of the mechanosensitive hair bundle directly modulates the open probability of transduction channels associated with the tip links in the bundle. Opening of the transduction channels leads to the depolarizing influx of cations, chiefly K^+ and Ca^{2+}. The movement of K^+ into the cell is due to the unusual ionic composition and electrical potential in the endolymphatic environment facing the apical surfaces of the hair cells. As is typical for the inner ear of all vertebrates, a high K^+ concentration and low Na^+ concentration, close to intracellular conditions, are maintained in endolymph, together with a slight to moderate, positive potential, the endocochlear potential (reviewed in Köppl et al., 2018). In the cochlear duct of birds, this metabolically demanding task is carried out by the tegmentum vasculosum, the tissue separating scala vestibuli and scala media and thus directly overhanging the basilar papilla (Fig. 11.5). An endocochlear potential of about +15 mV is maintained in avian endolymph (Necker, 1970), much lower than in the mammalian cochlea but higher than in the vestibular parts of the inner ear (Köppl et al., 2018).

Hair bundle morphology varies characteristically along the basilar papilla and thus along the tonotopic gradient. Hair cells at apical locations have relatively tall bundles composed of relatively few stereovilli, while hair cells at basal locations have shorter bundles with many stereovilli (Gleich and Manley, 2000, Fig. 11.4C and D). This morphology is a major determinant of bundle stiffness and, as in all vertebrates, it is believed that this contributes to tune a hair cell's mechanical frequency response. In addition, avian hair cells are electrically tuned to respond preferentially to different frequencies. This is achieved by varying the number and/or kinetics of two principal ion channels in the cell membrane, voltage-gated Ca^{2+} channels and Ca^{2+}-activated K^+ channels (reviewed in Fettiplace, 2020). However, electrical tuning is likely to be less effective or even absent at the highest frequencies (Wu et al., 1995).

One of the most fascinating aspects of hair cell function is the ability for reverse transduction, i.e., the ability to generate mechanical forces and thus to actively amplify low-level stimuli. Active movements of hair bundles have indeed been observed in isolated hair cells in vitro, and it is currently believed that this ability is inherent to the hair cells' transduction mechanism (review in Martin, 2008). In mammalian cochlear outer hair cells, an additional mechanism evolved, conveying somatic motility through the voltage-sensitive protein prestin in the cell membrane (review in Russell, 2013). This appears to dominate amplification in the high-frequency range of several kHz and above in mammals. Hair cells of the avian basilar

papilla have been suggested to represent an intermediate case in which reverse transduction and somatic motility may literally join forces (Beurg et al., 2013). However, this is controversial (Tan et al., 2011; Xia et al., 2016) and much remains to be learned about the precise mechanisms of active amplification in the bird inner ear. Nevertheless, the presence of amplification is undisputed. One of its indirect manifestations is the occurrence of otoacoustic emissions, faint sounds emitted by the inner ear that are believed to be an epiphenomenon of the active processes. Otoacoustic emissions are only measurable under shielded, very quiet laboratory conditions. They may be present spontaneously or can be evoked by a range of stimulation protocols, and have been observed in a wide range of vertebrates, including birds (Bergevin et al., 2015; Engler et al., 2019; Manley and Van Dijk, 2008; Taschenberger and Manley, 1997).

Hair cells are secondary sensory cells, they thus do not form an axon. They are contacted by two basic types of neurones, afferent and efferent to the central nervous system (Fig. 11.5). Afferent neurons have their cells bodies located in a compact ganglion close to the basilar papilla. Their peripheral fibers enter the basilar papilla at its inner or neural edge and contact typically only one hair cell each. The afferent synapses are of the specialized ribbon synapse type, which occurs only in vertebrate hair cells and photoreceptors and in retinal bipolar cells. They are believed to enable high, sustained rates of transmitter release (review in Moser et al., 2020). The central axons of the afferents collectively form the auditory nerve and terminate on the brainstem neurones comprising the cochlear nucleus. A truly unique feature of the avian auditory papilla is that typically 20–25% of the hair cells receive no afferent contacts (see also Section 11.3.2). In contrast, all hair cells receive efferent input from neurons located in the ventral brainstem (review in Köppl, 2011b). The predominant effect of evoked efferent activity on the hair cells is inhibitory. However, very little is known about the behavioral contexts in which efferents are active and, consequently, about their broader role in hearing.

11.3.2 Hair cell types: a remarkable example of evolutionary convergence in birds and mammals

When the ancestors of birds and mammals separated, their common heritage included a dedicated auditory hair cell field, the basilar papilla. This ancestral basilar papilla is likely to have been small, with a uniform hair cell type and sensitive to low frequencies only (Manley and Köppl, 1998). Thus, although the basilar papilla itself is homologous between the groups, its specializations are not. The auditory hair cell types in particular represent remarkable convergent evolutionary developments.

Cross-sections of avian basilar papillae, at first glance, do not show any of the prominent and uniquely mammalian features, such as the tunnel of Corti or the strict arrangement of one row of inner and three rows of outer hair cells. However, looking more closely at the fine structure of the hair cells and especially their innervation, a very salient analogy emerges. Like mammals, birds have two types of hair cells, here called tall and short hair cells. Unlike in mammals, those types are not sharply separated. The extremes are clearly different and well defined, but the two types grade into each other (Gleich and Manley, 2000). Tall hair cells are found on the inner (neural) side of the epithelium and gradually transition into short hair cells toward the outer (abneural) edge (Fig. 11.5). Furthermore, the relative numbers of tall and short hair cells are not fixed in the manner of inner and outer hair cells in mammals, but change along the tonotopic gradient. Basal, high-frequency regions show a predominance of short hair cells and vice versa. Most strikingly, short hair cells receive large efferent terminals but are devoid of afferent innervation (Fischer, 1994a, Fig. 11.5). This may be the only example of a sensory cell entirely losing its primary function. It is even more extreme than the innervation of mammalian outer hair cells, which also receive large efferent terminals but retain a sparse afferent innervation (review in Fettiplace, 2017). Clearly, avian short hair cells are not the principal sensory cells for hearing. The analogy to the mammalian cochlea, in which inner hair cells take most of the classical sensory role and outer hair cells are specialized for mechanical amplification (Dallos, 1996) is palpable. However, much remains to be learned about the assumed amplificatory role of short hair cells, as there is currently little direct evidence for it. Although short hair cells do exhibit bundle motility in vitro, tall hair cells do as well (Beurg et al., 2013), so it remains unclear what the specific role(s) of short hair cells may be.

11.3.3 Hair cell regeneration: birds never lose their hearing

Since human hearing loss often involves damage to and ultimately death of hair cells through noise or ototoxic medication, similar treatments were used on birds in order to find a good preparation to study the underlying phenomena. This led to the remarkable discovery that adult birds are able to regenerate functional hair cells (review in Rubel et al., 2013). It very quickly became apparent that, in contrast to humans, birds did not necessarily suffer permanent hearing loss. Instead, and unexpectedly, hearing thresholds returned to normal or near-normal within a matter of weeks following damage. This discovery initiated an excited search for the underlying cellular and genetic processes. It is now known that after insult and hair cell death, new hair cells are regenerated from the surviving supporting cells, either by rekindled cell division or by

direct transdifferentiation into hair cells (review in Stone and Cotanche, 2007). The regeneration process is extensive and detailed. Specific, local hair cell characteristics such as hair cell shape, bundle shape, and orientation are so well matched to the surviving adjacent areas that it can be difficult to distinguish an undamaged cochlea from a recovered one. In addition, nerve fibers reconnect with the new hair cells, and the overlying tectorial membrane is at least partly replaced (Cotanche, 1999), in total leading to an impressive functional recovery (Ryals et al., 2013; Smolders, 1999). Regeneration reaches its limits, however, if the damage extends over very large areas of the basilar papilla and includes supporting cells (Cotanche, 1999; Smolders, 1999).

Even without severely damaging experience, the avian basilar papilla appears to continuously regenerate hair cells at a low level (Gleich et al., 1997; Ryals and Westbrook, 1990). Thus, there is probably no such thing as age-related hearing loss in birds. Indeed, birds in captivity often reach ages that are multiples of their expected lifetime in the wild, and tests on starlings and barn owls showed that they can still have close-to-normal hearing thresholds at such ripe old ages (Krumm et al., 2017; Langemann et al., 1999). It is not without irony that human breeding of certain races of song birds for their loud songs unknowingly involved these mechanisms. Belgian Waterslager canaries have an inherited high frequency hearing loss and sing a louder and lower-pitched song than normal canaries (Okanoya and Dooling, 1985). In the basilar papilla of those birds, hair cells continuously die at abnormal rates, a process that is incompletely offset by ongoing regeneration of new hair cells (Gleich et al., 1997; Wilkins et al., 2001). Unfortunately, the hope of initiating the same kind of regeneration of hair cells in mammalian cochleae has so far not been fulfilled (Brigande and Heller, 2009; Zheng and Zuo, 2017).

11.3.4 Cochlear specializations: auditory foveae, infrasound hearing

As mentioned above, the basilar papilla is tonotopically organized. Apical regions respond most sensitively to low frequencies, and the characteristic frequency gradually increases toward the basal end. In a typical avian basilar papilla, this tonotopic map is well described by a near-logarithmic function, i.e., each doubling of frequency (equivalent to one octave) corresponds to an approximately equal length of papilla (Fig. 11.6, Gleich et al., 2004). However, there are interesting exceptions to this rule. In analogy to visual foveae, regions of enhanced frequency representation, where some frequencies occupy disproportionally more space along the basilar papilla, have been termed auditory foveae. In birds, the best known example of such an auditory fovea is the barn owl, and a similar case

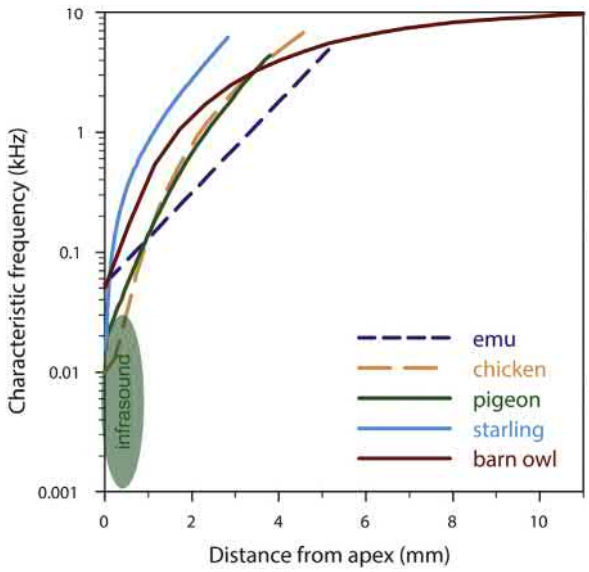

FIGURE 11.6 Tonotopic frequency representation along the avian basilar papilla. The differently colored curves show the mapping functions for several species of birds, as determined from labeling physiologically characterized auditory nerve fibers to reveal their innervation sites in the papilla. Note the exceptional length of the barn owl basilar papilla and the shallow slope of its frequency map over most of its extent, indicating an auditory fovea, i.e., expanded spatial representation of a narrow, high-frequency band. Infrasound sensitivity in the pigeon was found over the most apical mm, but it may not be strictly tonotopic and is therefore represented by the green area. *Data from Chen et al. (1994), Gleich et al. (2004), Köppl et al. (1993), Köppl and Manley (1997), Smolders et al. (1995).*

has been suggested for the kiwi. In the barn owl, the frequencies of the highest octave perceived (5 to 10 kHz) fully occupy the basal half of the basilar papilla (Köppl et al., 1993), as much space as the lower five or six octaves together (Fig. 11.6, red curve). These are the frequencies shown behaviorally to be the most useful for prey localization (Payne, 1971). The anatomical gradients of the owl cochlea, that at least partially determine the frequency response of the hair cells, hardly change along the basal half of the cochlea, concordant with a large expansion of the area processing higher frequencies (Fischer et al., 1988). As a visual fovea is associated with improved acuity, a larger cochlear representation is often assumed to correlate with enhanced frequency resolution. Interestingly, this is not the case in the barn owl (Köppl et al., 1998), suggesting that the role of the fovea instead may be to lay the foundation for massive parallel processing, by increasing the numbers of afferent fibers from this behaviorally important frequency region (Fischer, 1994b; Köppl, 1997b). While there are no physiological data from the ear of the kiwi, studies of hair cell morphology also suggested a foveal expansion of frequency representation in the upper range of kiwi hearing, estimated at 4 to 6 kHz (Corfield et al., 2011).

An equally amazing specialization for extremely low-frequency hearing has been found in pigeons. For some time, it had been known from behavioral experiments that pigeons are sensitive to infrasound, defined as frequencies below those audible to humans, that is < 15 Hz (Kreithen and Quine, 1979). Schermuly and Klinke (1990b) traced the origin of this sensitivity to hair cells located in the extreme apical-abneural regions of the pigeon basilar papilla. The afferent fibers connecting to these hair cells did not respond to normal acoustic frequencies, but showed responses to infrasound at levels comparable to the behavioral thresholds shown previously (Schermuly and Klinke, 1990a). Quite in contrast to the high-frequency foveae discussed above, the infrasound receptive region appears to co-exist, over the most apical 1 mm of the basilar papilla, alongside a conventional logarithmic frequency representation (Fig. 11.6, green) (Smolders et al., 1995). The behavioral significance of infrasound hearing remains unknown. Although it has been suggested that pigeons use it as a navigational cue (Hagstrum, 2000; Kreithen and Quine, 1979), conclusive evidence is lacking. Infrasound sensitivity may be more widespread among birds but remains poorly explored (review in Zeyl et al. 2020). Behavioral sensitivity to infrasound was recently confirmed for chickens (Hill et al., 2014), supporting previous evidence of best response frequencies at least as low as 10 Hz in some neurones in the cochlear nucleus of the chicken (Warchol and Dallos, 1989).

11.3.5 Auditory nerve: what the ear conveys to the brain

All information that the brain receives about the outside acoustic world is encoded in the activity of the auditory nerve fibers. Beginning with Sachs et al. (1974), who recorded single-unit activity in the pigeon auditory nerve, there have been numerous studies on the responses of afferent fibers in various bird species to simple, well-controlled stimuli. Here, I will briefly summarize the encoding of frequency, sound level, and temporal fine structure.

All avian auditory nerve fibers are spontaneously active. Mean spontaneous rates vary between 45 and 90 spikes/s, depending on species, in adult birds (Köppl, 1997a). Unlike in mammals, there is no consistent, strong correlation in birds between spontaneous rate and sensitivity to tonal stimulation, and there is no population of fibers with very low-spontaneous activity (<1 spike/s). Spontaneous activity is irregular, and the interspike interval distribution is typically Poisson-like, modified by the refractory period (Gleich and Manley, 2000; Neubauer et al., 2009). Interestingly, a significant number of fibers show preferred intervals whose period is at or close to their characteristic frequency for tonal stimulation. Although some of this activity for very sensitive fibers may be attributable to inadequate sound shielding during experiments, the bulk of evidence points to this being a genuine phenomenon which reflects spontaneous oscillations of the hair cell membrane potential due to electrical tuning and/or active mechanical amplification processes in the avian cochlea (Gleich and Manley, 2000; Taschenberger and Manley, 1997).

Sound frequency is, of course, collectively coded according to the place principle, where the tonotopic gradient along the basilar papilla is preserved in the projections to the brain. Upon tonal stimulation, each auditory nerve fiber responds most sensitively to one particular frequency, its characteristic frequency. At increasingly lower and higher frequencies, the fiber's sensitivity decreases rapidly, so that its response area forms a narrow, V-shaped frequency tuning curve (Fig. 11.7A). In birds, these curves are very sharply tuned, with higher mean quality factors than mammalian responses at equivalent frequencies, and typically almost symmetrical (Gleich and Manley, 2000). However, the best thresholds of fibers within any narrow range of characteristic frequencies in an individual ear vary in birds more widely than in mammals, by as much as 50 dB (Fig. 11.7B).

Sound level is encoded in the discharge rates of auditory nerve fibers. The dynamic ranges over which individual fibers are able to encode have been studied in depth in response to short tonal stimuli of 50 to 100 ms and vary characteristically. There are: (1) saturating fibers, whose discharge rate rises rapidly above threshold, then also levels off abruptly at a break point, (2) sloping-saturating fibers, whose rate does not show an abrupt saturation but continues to rise more slowly above the break point (Fig. 11.7C), and (3) straight fibers, whose discharge rate slowly rises with a nearly uniform, shallow slope over a broad range of sound levels (Gleich and Manley, 2000; Köppl, 2011a). This shows remarkable parallels to mammals, where the same three types were originally described. However, in contrast to mammals, there are no correlations with other fiber properties in birds. It is believed that in both cases, the discharge behavior of auditory nerve fibers with sound level is shaped by the underlying processes of active amplification, effecting a compressive nonlinearity. However, in birds, the nonlinearity is suggested to develop and vary locally, perhaps at the level of individual hair cells, while in mammals stronger coupling leads to a shared nonlinear response of larger groups of hair cells (Köppl, 2011a). The wide range of thresholds and the different dynamic ranges together ensure that the avian auditory nerve is able to encode a very wide range of sound levels indeed.

Finally, temporal information is encoded by phase locking of auditory nerve fibers, i.e., spikes are discharged preferentially at a specific phase of a sinusoidal or near-sinusoidal stimulus. It is important to point out that a spike need not occur in every cycle of the stimulus

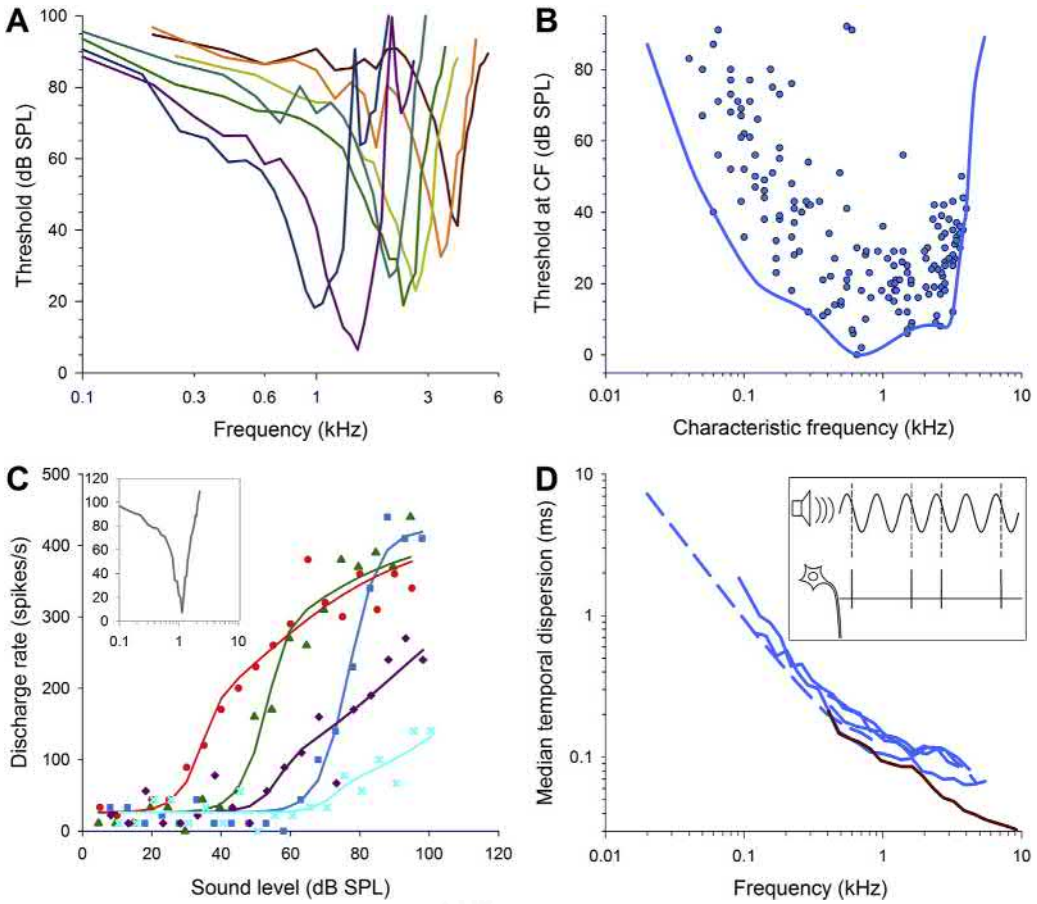

FIGURE 11.7 Salient characteristics of single auditory nerve fiber activity. (A): Examples of frequency tuning curves from the emu (Manley et al., 1997). (B): Distribution of the most sensitive thresholds of a population of fibers from the emu (Manley et al., 1997), as a function of characteristic frequency. Note the large range of thresholds at any one frequency, which is typical and not due to damage. The solid line joins data from the most sensitive fibers, which gives an approximation of the emu's audiogram. (C): Rate-level functions for one particular auditory nerve fiber in the emu, in response to several different frequencies within the fiber's response area shown in the inset. Note the pronounced sloping-saturating behavior at the most sensitive, characteristic frequency (shown in red). (D): The inset illustrates schematically the temporal relationship between a sinusoidal stimulus and phase-locked action potentials. In real auditory nerve fibers, individual spikes vary in their timing around a mean preferred phase. Median values for this temporal jitter or dispersion are shown in the main graph, as a function of frequency, for several bird species: barn owl red (Köppl, 1997c), emu *dashed blue* (Manley et al., 1997), and, all in blue, chicken (Salvi et al., 1992), pigeon (Hill et al., 1989), starling (Gleich and Narins, 1988), redwing blackbird (Sachs et al., 1980). *(C) Data from Yates et al. (2000).*

(Fig. 11.7D inset). Indeed, at frequencies above 300–400 Hz, which is the upper range of sustained discharge rates, many cycles may be skipped but phase locking still persists into the kHz range. Phase locking critically depends on the ability to control spike timing within the temporal window of one stimulus cycle. Thus, the requirement for temporal precision rises with increasing frequency (and shorter cycles), and phase locking invariably fails above a species-specific frequency limit. Avian auditory nerve fibers typically phase lock up to 3–4 kHz (Fig. 11.7D) which compares favorably to other vertebrates, including mammals. A famous exception is the barn owl where phase locking persists to frequencies near 10 kHz, corresponding to a precision of spiking, or temporal jitter, of only 20–30 μs (Fig. 11.7D, red curve) (Köppl, 1997c). Although it remains unknown what cellular mechanisms enable this extraordinary precision, it is clearly an adaptation and prerequisite for the superb sound localization abilities of the barn owl (see Section 11.4.2).

11.4 The auditory brain

11.4.1 Basic organization of auditory pathways

The principal pathways of the avian auditory brain follow a general layout shared by all land vertebrates (Fig. 11.8, Carr et al., 2017; Grothe et al., 2004). The major afferent pathways flow from the cochlear nucleus, either directly or indirectly, through the brainstem areas of the superior olive and lateral lemniscus, to the midbrain inferior colliculus [also termed torus semicircularis, or nucleus mesencephalicus lateralis pars dorsalis (MLd)]. From there,

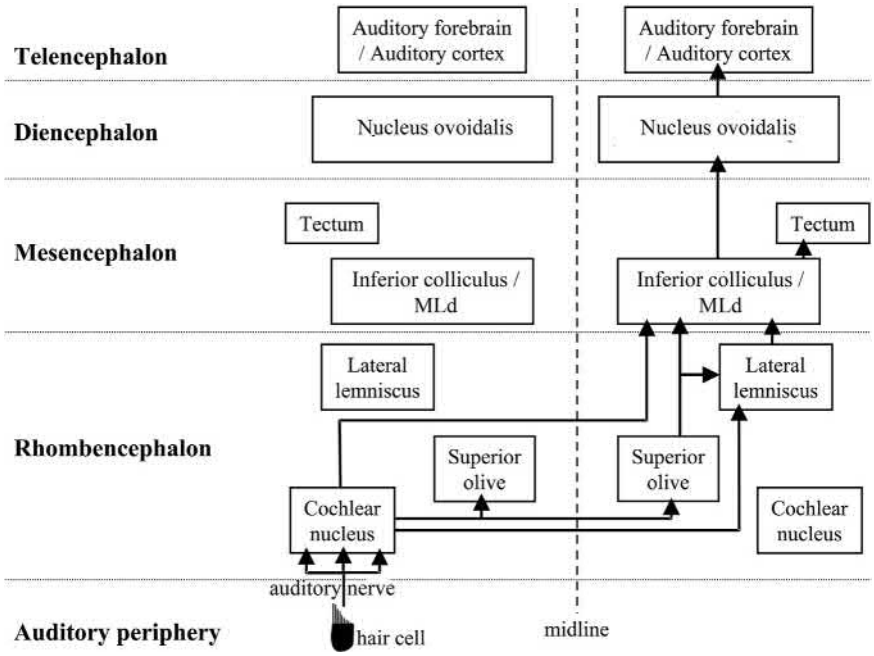

FIGURE 11.8 Principal wiring diagram of the central ascending auditory pathway of birds. Each *box* represents a major center that may contain multiple subareas. *Modified Figure 10.1 from Grothe et al. (2004), with kind permission from Springer Science + Business Media B.V.*

projections go to multimodal layers of the optic tectum (or superior colliculus) and to the auditory thalamus and from the latter on to the auditory forebrain. Beyond this very general pattern, however, the specific nuclei or subdivisions of nuclei can differ substantially between the major vertebrate groups and the evolutionary origin and homology of many auditory areas beyond the broad categories outlined above is quite controversial. In general, differences in the central auditory pathways mirror the major types of basilar papilla specializations and thus are now believed to also be the result of independent evolution (Carr et al., 2017; Grothe et al., 2004). Birds follow an archosaurian pattern that they share with crocodilians; it is also most similar to that of other, more distantly related, "reptiles."

The cochlear nucleus of birds has two major subdivisions, nucleus magnocellularis (NM) and nucleus angularis (NA), both of which receive a shared input by collaterals of each auditory nerve fiber. NM and NA probably form the starting points of several auditory processing streams that specialize in different aspects. NM is the relatively more simple of the two, containing one predominant neuron type that is clearly specialized for preserving or even enhancing the temporal information conveyed through phase locking from the auditory nerve (Carr and Boudreau, 1993; Sullivan and Konishi, 1984). NM is thus the starting point of a "time pathway." The best known function of this time pathway is the extraction of interaural time differences (ITDs) used in sound localization (see Section 11.4.2). NA then appears to be the origin for everything else, although commonly referred to simply as the "intensity pathway," which does not do justice to the complexity already seen at this level. NA contains a range of cell types having distinct anatomical and physiological properties (reviews in Grothe et al., 2004; MacLeod and Carr, 2007). Although cell-specific connection patterns have not yet been investigated, NA neurones collectively have several projection targets in the superior olive and lemniscal nuclei, as well as direct projections to the inferior colliculus. Thus, the potential for different functional processing streams is present. In the barn owl, a specific involvement in deriving interaural level differences (ILDs) for sound localization has been demonstrated (see Section 11.4.2).

While the cochlear nuclei are still strictly monaural, all higher levels show more or less pronounced binaural interaction. A tonotopic organization is, however, retained in the brainstem nuclei. All afferent auditory information then converges again in the midbrain nucleus MLd, which is considered homologous to the mammalian inferior colliculus (Carr and Code, 2000). The definition of MLd subdivisions differs between authors but, in general, a "core and belt"-type organization is recognized and common terms used for those are central and external nucleus, or, abbreviated, ICc and ICx. Brainstem projections terminate in the ICc regions which, in turn, project to ICx. The physiology of the avian auditory midbrain has mostly been studied in the context of sound localization (see Section 11.4.2). In the barn owl, successive processing steps culminate in the formation of a neural map of auditory space in the ICx (review in Konishi, 2003). It is currently

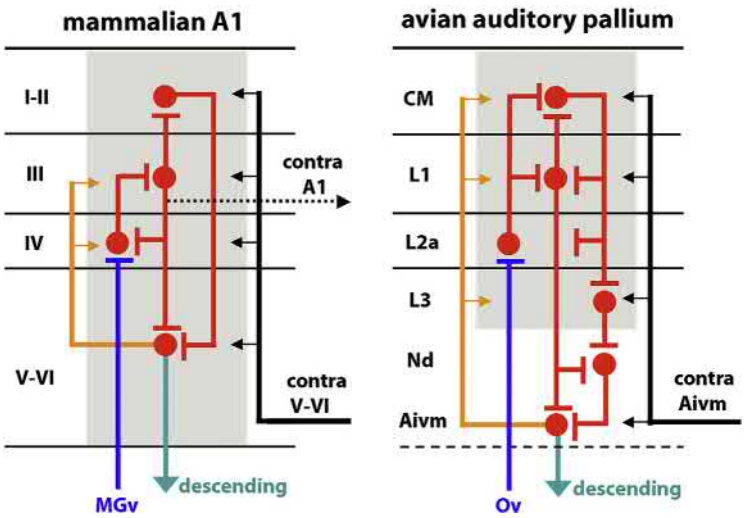

FIGURE 11.9 Suggested analogy in the circuitry between the different layers of mammalian auditory cortex and the principal nuclei of the avian auditory pallium. Thalamic inputs, intrinsic connections, and descending projections are shown in blue, red and turquoise, respectively. *Orange lines* and *arrows* indicate recurrent projections from the deep layers to the more superficial layers. Reentrant projections from the other side of the brain are drawn in black. *Figure 4 from Wang et al. (2010).*

unclear to what extent this generalizes to other birds. In a songbird, the zebra finch, responses of MLd neurones cluster into functional groups that were suggested to represent cues for fundamental acoustic percepts, such as pitch, timbre, and rhythm (Woolley et al., 2009). As a general principle in vertebrates, although a tonotopic representation is maintained in parts of the auditory midbrain, pure tones are often not the most effective stimuli. Instead, selectivity for other, derived sound features, such as location or temporal modulation, begins to predominate.

In parallel to the connections from the ICc to the ICx (and on to the superior colliculus), the ICc also initiates the forebrain ascending auditory pathway, by projecting to the thalamic nucleus ovoidalis (Fig. 11.8, Carr and Code, 2000). The morphology and connections of nucleus ovoidalis are quite well characterized, but its functional role remains unclear and few studies have probed it physiologically (Carr and Code, 2000; Ondracek and Hahnloser, 2013; Proctor and Konishi, 1997). Nucleus ovoidalis projects on to the primary auditory forebrain area in birds. It is important to point out that the nomenclature used in the avian forebrain has seen major revision quite recently, driven by growing evidence that early interpretations of avian forebrain organization had been erroneous and that the classic nomenclature derived from it was seriously misleading (Jarvis et al., 2005). According to the revised nomenclature, the avian auditory forebrain consists of Field L in the caudal nidopallium, the caudal mesopallium (CM), the dorsal nidopallium, and the ventromedial portion of the intermediate arcopallium (Aivm) (Wang et al., 2010). Field L is further divided into subregions with only L2 being the primary, thalamorecipient layer. It has been argued recently that all four avian auditory forebrain areas together form a circuit highly similar in both its columnar and laminar organization to the mammalian auditory cortex (Fig. 11.9, Wang et al., 2010). The physiology of the avian auditory forebrain has been studied most extensively in songbirds (see also Section 11.4.4). Here, a hierarchy of responses is apparent, with a clear tonotopic organization and spectrally defined responses in thalamorecipient neurons, and striking specificities to species-specific vocalisations emerging in higher-order neurons. Also, correlates of perceptual categories of auditory streaming, such as galloping rhythms, have been found in the responses of Field L neurones (Bee and Klump, 2005; Itatani and Klump, 2011). In the barn owl, the forebrain ascending auditory pathway appears to independently generate a second representation of auditory space that resides in the arcopallium. However, the forebrain representation is different in several salient aspects and probably serves different functions to the midbrain topographical map of space (Cohen and Knudsen, 1999; Peña et al., 2019; Vonderschen and Wagner, 2014).

11.4.2 The generation of an auditory space map in the barn owl

Beginning with the classic studies of Roger Payne (1971), who first demonstrated that barn owls use acoustic cues to precisely locate and strike their prey in the dark, many general principles about how the location of sounds in the environment is reconstructed by the brain have been learned from this bird. Unlike vision, the sense of hearing cannot rely on a spatial image of the external world being projected onto the primary receptor surface and relayed to the brain. Sound localization requires central auditory computation, using indirect cues. For birds, these cues are

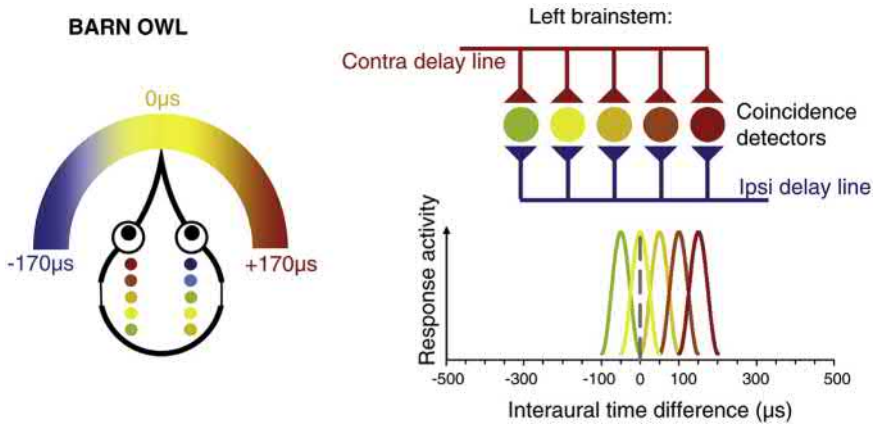

FIGURE 11.10 Schematic illustration of the coding of interaural time differences according to the Jeffress model (1948) and as seen in the barn owl. Each half of the brainstem contains a representation of interaural time differences, corresponding to sound sources mostly in the contralateral acoustic hemifield. This map is created by the basic circuit of delay lines and coincidence detectors illustrated for the left side of the brainstem. Typical responses of barn owl coincidence detector neurones in nucleus laminaris are shown below the circuit diagram, as a function of interaural time difference. Together they cover the interaural time difference range experienced by the owl and form a topographic representation of the auditory azimuth. *Figure 2A from Köppl (2009), reproduced with permission from Cell Press.*

largely binaural in nature, i.e., the inputs from both ears are compared for the minute differences in timing and level that arise from different path lengths of the sound to both ears and from sound shadowing effects of the head and body (Klump, 2000). While for most birds, both ITDs and ILDs are cues for sound source azimuth, the asymmetrical facial ruff of the barn owl (see Section 11.2.1) generates ILDs as a function of sound source elevation. This changes the meaning of ILDs but not necessarily the neural processing steps to derive them. Much of what has been learned from the barn owl is believed to reflect general principles of the neural computation of sound location in birds, if not vertebrates (Aralla et al., 2020; Grothe et al., 2010; Konishi, 2003; Takahashi, 2010). In the barn owl, the binaural comparisons of time and level are carried out in parallel processing streams in brainstem nuclei that are specialized for each task. At the midbrain level, this information is then combined and used to create a "space map," i.e., a two-dimensional (2D) representation of auditory space in azimuth and elevation.

Contrary to intuition, the computation of ITD is not based on a comparison of sound onset at the two ears, but largely relies on ongoing temporal information from neural phase locking in the auditory nerve (see Section 11.3.5). This was shown by clever behavioral experiments with owls wearing headphones that allow for the presentation of stimuli that artificially dissociate onset and ongoing ITDs (Moiseff and Konishi, 1981a). The phase locking of auditory nerve fibers is preserved by the monaural cochlear NM, which then projects to the binaural nucleus laminaris (NL). NL neurones perform arguably one of the most challenging and extreme tasks in the nervous system: they receive the phase-locked inputs from each side and fire selectively if their inputs coincide within a very narrow, submillisecond time window (Funabiki et al., 2011; Kuba, 2007). Of course, such coincidence naturally occurs only when sounds originate directly in front (or back) of the animal. To encode more lateral sound locations, the incoming NM axons contact several NL neurones serially, thus forming functional delay lines that match and compensate for the range of natural acoustic interaural delays (Fig. 11.10). This principle of an array of coincidence detectors, receiving temporal information by delay lines from both sides to create a topographical map of auditory azimuth, was originally formulated by Jeffress (1948). It appears beautifully implemented in the NM-NL circuit of birds in general (Burger and Rubel, 2008; Kubke and Carr, 2006), with the owl displaying a hypertrophied form and achieving the highest temporal resolution (Carr and Boudreau, 1993; Funabiki et al., 2011). The initial topographic map of auditory azimuth is created many times over in NL, separately in each frequency band of the tonotopically organized nucleus (Carr et al., 2015). An important task of subsequent processing steps within the ICc of the midbrain is to converge this information across frequencies and thus remove inherent ambiguities due to the cyclic nature of the phase code underlying it (Konishi, 2003; Singheiser et al., 2012).

The first binaural comparison of sound level occurs in the posterior part of the ventral nucleus of the lateral lemniscus (LLDp, formerly also called VLVp). Here, excitatory inputs from the contralateral ear (coming in via the cochlear nucleus angularis, NA) compete with inhibitory inputs from the ipsilateral ear (coming in via NA and the contralateral LLDp). Depending on the relative strengths of excitation and inhibition, the responses of individual LLDp neurones decrease at different relative levels of ipsi- and contralateral sound, or ILD. Inhibitory

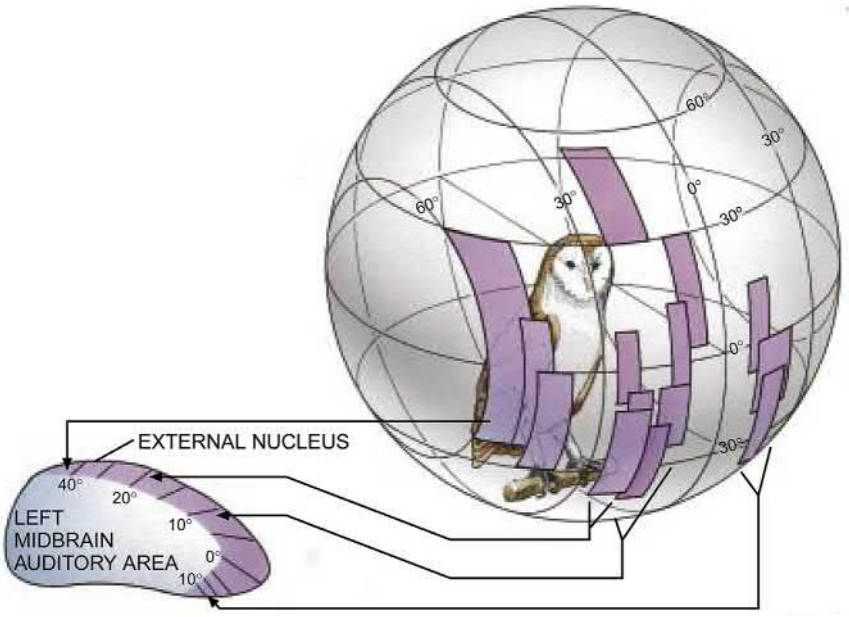

FIGURE 11.11 Auditory space map in the midbrain of barn owls. In the external nucleus of the inferior colliculus (colored purple) the auditory spatial receptive fields of neurones change systematically with position along the nucleus. Some examples of receptive fields are illustrated as purple rectangles on a sphere surrounding the owl. This spatial map is synthesized from auditory responses selective for specific interaural time and level differences. *From Konishi (1993), with kind permission from Jana Brennings.*

strength systematically decreases along the dorsoventral axis of the nucleus, and thus establishes a first topographic representation of ILD (review in Konishi, 2003). At the level of the ICc, the sigmoidal response functions of inputs from LLDp neurones sharpen into bell-like curves only showing responses to a restricted range of ILDs (Konishi, 2003; Singheiser et al., 2012).

Finally, in the ICx, a 2D map of space-specific neurones with receptive fields bounded both in azimuth and elevation is synthesized (Fig. 11.11, Knudsen and Konishi, 1978), where the azimuthal axis is based on the selectivity for ITD and the elevational axis on the selectivity for ILD (Konishi, 2003; Takahashi et al., 2003). At the level of the individual space-specific neurones, both inputs are combined by a multiplicative process that further sharpens their resulting receptive field (Peña and Konishi, 2001). This auditory space map is relayed from ICx to bimodal neurones of the optic tectum (or superior colliculus), forming a combined auditory-visual spatial representation that contributes to stereotypical orienting behaviors (Knudsen, 2002; Peña and Gutfreund, 2014).

11.4.3 Developmental plasticity: auditory space is calibrated by vision

As just outlined, the auditory space representation in the barn owl's midbrain is a computational map generated from indirect cues (ITD and ILD) to sound location. These cues vary with details of head size and shape and are thus to some extent individual (Keller et al., 1998). How does the bird know which ITD and ILD values to associate with precise locations in space? Experiments manipulating the auditory cues of young owls by plugging one ear showed that owls learned, over some weeks, to again precisely localize sounds under these conditions. If instead their visual world was shifted by fitting prism spectacles, it was still the sound localization behavior that slowly adapted to match the changed visual environment (Knudsen, 2002; Peña and Gutfreund, 2014). Thus, owls use vision to learn to associate certain ITDs and ILDs with the correct locations in space. The visual system, with its direct projection map of the retinal image provides the objective spatial representation of the outside world against which the computational map of the auditory system is calibrated. The site of this plasticity has been identified as the ICx, the site where the auditory space map is first synthesized (Fig. 11.12). Additional anatomical connections from the ICc can be induced here whose ITD selectivity matches the corresponding visual receptive field in the optic tectum, and those new connections come to dominate the response of ICx neurones over previously formed, now mismatched inputs (Knudsen, 2002). The required error signal appears to be provided by reciprocal projections from the optic tectum to the ICx, an area traditionally thought to be exclusively auditory. Like many forms of experience-dependent plasticity, this learning of the meaning of auditory cues is limited to young owls and gradually diminishes in early adult life (Knudsen, 2002). Many of the principles

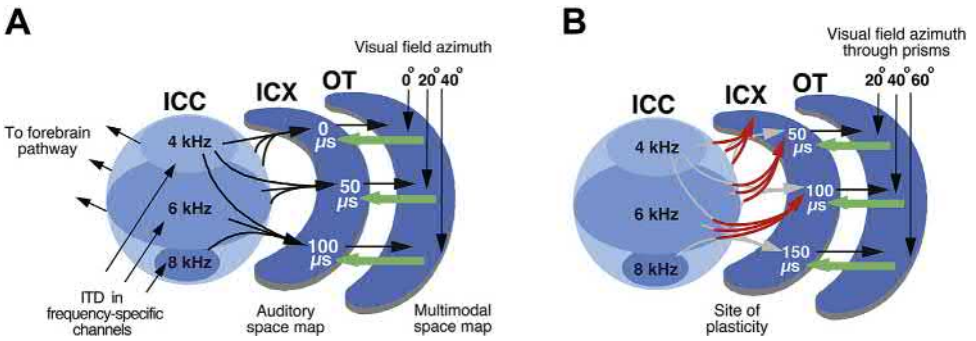

FIGURE 11.12 Schematic summary of adaptive plasticity in the auditory space map of the barn owl, after modified visual experience in early life. (A): Normally, different tonotopic regions from the ICc that share selectivity for a common interaural time difference converge in the ICx. Together, many such convergent projections contribute the azimuthal axis of the space map that is relayed and combined with matching visual receptive fields in the optic tectum (OT). (B): When visual receptive fields are artificially shifted by fitting prims goggles to the owl, the auditory space map shifts accordingly, by forming new and matching connections between ICc and ICx (*red arrows*). *Green arrows* represent an instructive feedback projection from the OT to ICx. *Figure 7 from Knudsen (2002), reprinted by permission from Macmillan Publishers Ltd.*

shown for the learning of auditory localization in the owl also apply to the mammalian auditory system (King et al., 2000; Keating and King, 2015).

11.4.4 The special processing of birdsong

Much of the research on higher-order auditory processing in birds has concentrated on songbirds, for two reasons. First, the behaviorally most relevant acoustic signals are clearly defined and can guide the design of stimuli to test. Second, birdsong is a learned vocalization, a rare trait shared only with human speech and few other avian and mammalian vocalizations (Bolhuis et al., 2010; Jarvis, 2004). Together, this makes the songbird auditory system a rich source for unraveling how vocalisations are processed and learned. Not surprisingly, songbirds have very well-developed auditory forebrain areas (Fig. 11.13A). However, in addition to that, a whole set of sensorimotor "song nuclei" is present, which are involved in vocal learning and plasticity and which have no clear equivalent in vocal nonlearning birds (Fig. 11.13B, review in Farries, 2004). Of central importance is the nucleus HVC, which appears to be the pivotal interface between the auditory input and the motor output for singing. It is also the nucleus where neurogenesis in adult animals was first shown to produce functional neurons, in this case seasonally (Nottebohm, 2004). In HVC, extremely selective auditory responses, not just for species-specific vocalisations but for the individual bird's own song, appear for the first time (Konishi, 2004). HVC is then the starting point of two major motor pathways (Fig. 11.13B): First, a fairly direct, posterior pathway projects to the robust nucleus of the arcopallium (RA) and from there to various brainstem motor nuclei controlling the syrinx and respiration (Farries, 2004). Second, the so-called anterior forebrain pathway eventually also leads to RA but via a whole set of intermediate nuclei that are believed to be homologous to the mammalian basal ganglia (Perkel, 2004). The anterior forebrain pathway has been shown to be critical for song learning in young birds (Brainard, 2004). In addition, there is evidence for an involvement in the plastic control of song, even in species that do not normally learn new songs as adults (Konishi, 2004). Therefore, it is believed that the anterior forebrain pathway, although not strictly necessary to produce song in an adult, continuously monitors what the bird actually sings and initiates corrections when necessary.

The purely auditory ascending forebrain pathway (Fig. 11.13A), which eventually feeds into the specialized sensorimotor song nuclei system, comprises the primary field L and the secondary CM, both shared with other birds, and the secondary NCM (caudal medial nidopallium), an area unique to songbirds. Responses in these auditory areas never show the particular selectivity for the individual bird's own song (Theunissen et al., 2004). However, selectivity for conspecific song arises. As a rule, neurones in the primary auditory area Field L are poorly driven by simple tones or noise but respond selectively to spectrotemporal features that characterize conspecific song and other natural sounds (Theunissen and Shaevitz, 2006). Many individual neurons appear to specialize in either spectral or temporal modulation selectivity and cluster accordingly in specific subregions (Nagel et al., 2011). The secondary auditory forebrain areas NCM and CM may add selectivity for familiar songs versus novel songs and have thus been implicated in auditory memory formation (Ondracek and Hahnloser, 2013; Theunissen and Shaevitz, 2006).

11.4.5 Echolocating birds

Among the fascinating curiosities of the bird world are some species that use echolocation. These are the neotropical oilbird, *Steatornis caripensis*, and the paleotropical swiftlets of the genera *Aerodramus* and *Collocalia*. Both groups have independently evolved echolocation as a

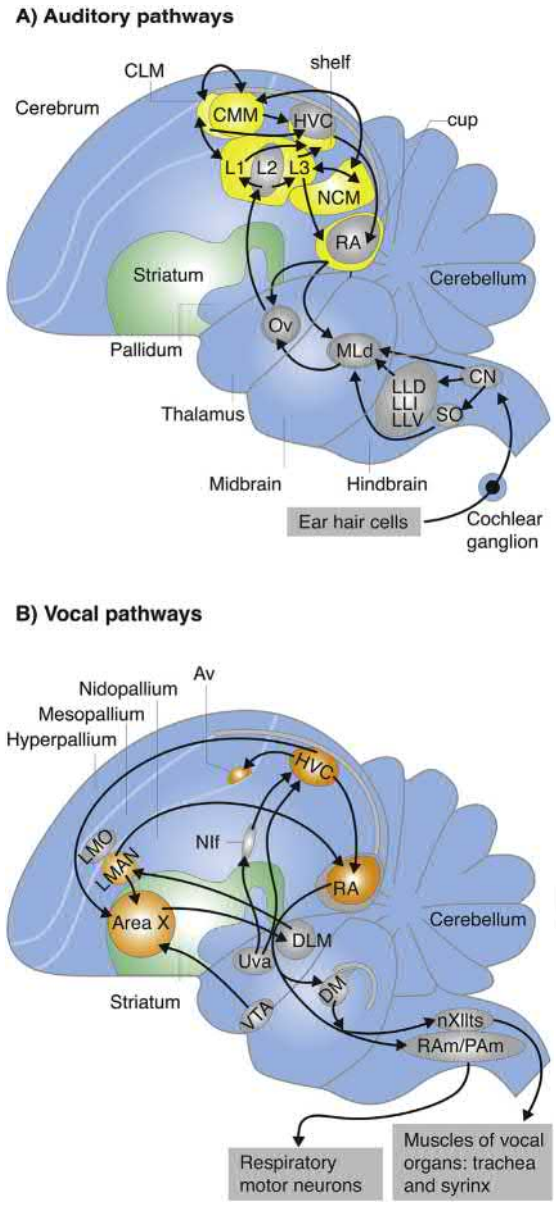

FIGURE 11.13 Schematic diagram of a composite view of parasagittal sections of a songbird brain, giving approximate positions of nuclei and brain regions. (A): Auditory ascending pathways, with brain regions that show increased neuronal activation when the bird hears song highlighted in yellow. (B): Vocal motor pathways. Depicted are connections between the nuclei, of both the direct posterior pathway and the anterior forebrain pathway. Both pathways together form the so-called song system. The orange nuclei in the song system show substantially enhanced neuronal activation when the bird itself is singing. Area X, Area X of the striatum; *Av*, avalanche; *CLM*, caudo-lateral mesopallium; *CN*, cochlear nucleus; *DLM*, medial subdivision of the dorsolateral nucleus of the anterior thalamus; *DM*, dorsomedial subdivision of nucleus intercollicularis of the mesencephalon; *HVC*, a letter-based name; *L1*, *L2*, and *L3* are subdivisions of Field L; *LLD*, lateral lemniscus, dorsal nucleus; *LLI*, lateral lemniscus, intermediate nucleus; *LLV*, lateral lemniscus, ventral nucleus; *LMAN*, lateral magnocellular nucleus of the anterior nidopallium; *LMO*, lateral oval nucleus of the mesopallium; *MLd*, dorsal part of the lateral nucleus of the mesencephalon; *NIf*, interfacial nucleus of the nidopallium; *nXIIts*, tracheosyringeal portion of the nucleus hypoglossus (nucleus XII); *Ov*, nucleus ovoidalis; *PAm*, nucleus paraambiguus medullaris; *RA*, robust nucleus of the arcopallium; *RAm*, nucleus retroambiguus medullaris; *SO*, superior olive; *Uva*, nucleus uvaeformis; *VTA*, ventral tegmental area. *Figure 1 from Moorman et al. (2011), updated after Figure 1 in Bolhuis et al. (2010), reprinted with kind permission from John Wiley and Sons and from Macmillan Publishers Ltd.*

means of navigating in the dark caves where they roost and nest (review in Brinkløv et al., 2013). This lifestyle has many superficial similarities with bats. However, the birds' echolocation calls are not ultrasonic but fall well within the typical avian hearing range. Due to this lower frequency range of the calls, avian echolocation cannot approach the spatial resolution of bat ultrasonic navigation, but few rigorous tests have been conducted (Griffin and Thompson, 1982; Konishi and Knudsen, 1979). Furthermore, the birds were reported to use echolocation only under conditions where they were unable to navigate by vision (Griffin, 1953; Novick, 1959), although anecdotal observations of foraging birds suggest this may be worth re-examining (Brinkløv et al., 2013).

Both the oilbird and the cave swiftlets use brief clicks that are produced by the syrinx (Suthers and Hector, 1982, 1985) and typically emitted in pairs or short trains (Konishi and Knudsen, 1979; Thomassen and Povel, 2006). The dominant frequencies in the clicks are in the range of several kHz and appear to match the birds' sensitive hearing range. However, due to their remote geographical distributions, very few species and individuals have been tested. From the studies available, it appears that the hearing capabilities of echolocating birds are unremarkable (Coles et al., 1987; Konishi and Knudsen, 1979). Anatomical data on the relative size of the auditory midbrain suggest a slight enlargement, which may indicate moderate specializations for echolocation processing (Cobb, 1968; Iwaniuk et al., 2006).

11.5 Summary

The sense of hearing has special meaning to many birds, be it for communication, hunting, or orienting in the dark. Avian hearing typically remains restricted to below 10 kHz, somewhat lower than human hearing and much lower than in a typical mammal. However, within that range, avian hearing is just as sensitive and discriminative. Important insights into auditory physiology have come from studies on birds, such as the mechanisms of regeneration of sensory hair cells after damage, the neural computations underlying sound localization or the neural processing, and learning of vocalizations. Some fascinating auditory specializations in birds are infrasound hearing in pigeons, asymmetric ears in owls, and echolocation in oilbirds and swiftlets.

References

Aralla, R., Ashida, G., Köppl, C., 2020. Binaural responses in the auditory midbrain of chicken (*Gallus gallus*). Eur. J. Neurosci. 51, 1290–1304.

Bee, M.A., Klump, G.M., 2005. Auditory stream segregation in the songbird forebrain: effects of time intervals on responses to interleaved tone sequences. Brain Behav. Evol. 66, 197–214.

Bergevin, C., Manley, G.A., Köppl, C., 2015. Salient features of otoacoustic emissions are common across tetrapod groups and suggest shared properties of generation mechanisms. PNAS 112, 3362–3367.

Beurg, M., Tan, X., Fettiplace, R., 2013. A prestin motor in chicken auditory hair cells: active force generation in a nonmammalian species. Neuron 79, 69–81.

Bolhuis, J.J., Okanoya, K., Scharff, C., 2010. Twitter evolution: converging mechanisms in birdsong and human speech. Nat. Rev. Neurosci. 11, 747–759.

Brainard, M.S., 2004. Contributions of the anterior forebrain pathway to vocal plasticity. Ann. N. Y. Acad. Sci. 1016, 377–394.

Brigande, J.V., Heller, S., 2009. Quo vadis, hair cell regeneration? Nat. Neurosci. 12, 679–685.

Brinkløv, S., Fenton, M.B., Ratcliffe, J.M., 2013. Echolocation in oilbirds and swiftlets. Front. Physiol. 4, 123.

Burger, R.M., Rubel, E.W., 2008. Encoding of interaural timing for binaural hearing. In: Basbaum, A.I., Kaneko, A., Shepherd, G.M., Westheimer, G. (Eds.), The Senses: A Comprehensive Reference. Academic Press, San Diego, pp. 613–630.

Calford, M.B., Piddington, R.W., 1988. Avian interaural canal enhances interaural delay. J. Comp. Physiol. A Sens. Neural Behav. Physiol. 162, 503–510.

Carr, C.E., Boudreau, R.E., 1993. Organization of the nucleus magnocellularis and the nucleus laminaris in the barn owl: encoding and measuring interaural time differences. J. Comp. Neurol. 334, 337–355.

Carr, C.E., Code, R.A., 2000. The central auditory system of reptiles and birds. In: Dooling, R.J., Fay, R.R., Popper, A.N. (Eds.), Comparative Hearing: Birds and Reptiles. Springer Verlag, New York, pp. 197–248.

Carr, C.E., Shah, S., McColgan, T., Ashida, G., Kuokkanen, P.T., Brill, S., Kempter, R., Wagner, H., 2015. Maps of interaural delay in the owl's nucleus laminaris. J. Neurophysiol. 114, 1862–1873.

Carr, C.E., Christensen-Dalsgaard, J., Edds-Walton, P., Köppl, C., Tang, Y., Young, B.A., Willis, K.L., 2017. Evolutionary trends in hearing in nonmammalian vertebrates. In: Striedter, G. (Ed.), The Evolution of the Nervous Systems in Nonmammalian Vertebrates, 2 ed. Elsevier, Oxford, pp. 291–308.

Carroll, R.L., 1988. Vertebrate Paleontology and Evolution. Freeman, New York.

Chen, L., Salvi, R., Shero, M., 1994. Cochlear frequency-place map in adult chickens: intracellular biocytin labeling. Hear. Res. 81, 130–136.

Christensen-Dalsgaard, J., 2011. Vertebrate pressure-gradient receivers. Hear. Res. 273, 37–45.

Clack, J.A., Allin, E., 2004. The evolution of single- and multiple-ossicle ears in fishes and tetrapods. In: Manley, G.A., Popper, A., Fay, R.R. (Eds.), Evolution of the Vertebrate Auditory System. Springer Verlag, New York, pp. 128–163.

Cobb, S., 1968. On the size of the auditory nuclei in some Apodiformes and Caprimulgiformes. Auk 85, 132–133.

Cohen, Y.E., Knudsen, E.I., 1999. Maps versus clusters: different representations of auditory space in the midbrain and forebrain. Trends Neurosci. 22, 128–135.

Coles, R.B., Konishi, M., Pettigrew, J.D., 1987. Hearing and echolocation in the Australian grey swiftlet, *Collocalia spodiopygia*. J. Exp. Biol. 129, 365–371.

Corfield, J., Kubke, M.F., Parsons, S., Wild, J.M., Köppl, C., 2011. Evidence for an auditory fovea in the New Zealand kiwi (*Apteryx mantellii*). PLoS One 6, e23771.

Cotanche, D.A., 1999. Structural recovery from sound and aminoglycoside damage in the avian cochlea. Audiol. Neuro. Otol. 4, 271–285.

Cotanche, D.A., Lee, K.H., Stone, J.S., Picard, D.A., 1994. Hair cell regeneration in the bird cochlea following noise damage or ototoxic drug damage. Anat. Embryol. 189, 1–18.

Dallos, P., 1996. Overview: cochlear neurobiology. In: Dallos, P., Popper, A.N., Fay, R.R. (Eds.), The Cochlea. Springer Verlag, New York, pp. 1–43.

Dooling, R.J., Lohr, B., Dent, M.L., 2000. Hearing in birds and reptiles. In: Dooling, R.J., Fay, R.R., Popper, A.N. (Eds.), Comparative Hearing: Birds and Reptiles. Springer Verlag, New York, pp. 308–359.

Engler, S., Köppl, C., Manley, G.A., de Kleine, E., van Dijk, P., 2019. Suppression tuning of spontaneous otoacoustic emissions in the barn owl (*Tyto alba*). Hear Res. 385, 107835.

Farries, M.A., 2004. The avian song system in comparative perspective. Ann. N. Y. Acad. Sci. 1016, 61–76.

Fettiplace, R., 2017. Hair cell transduction, tuning, and synaptic transmission in the mammalian cochlea. Comp. Physiol. 7, 1197–1227.

Fettiplace, R., 2020. Diverse mechanisms of sound frequency discrimination in the vertebrate cochlea. Trends Neurosci. 43, 88–102.

Fettiplace, R., Ricci, A.J., 2006. Mechanoelectrical Transduction in Auditory Hair Cells, Vertebrate Hair Cells, pp. 154–203.

Fischer, F.P., 1994a. General pattern and morphological specializations of the avian cochlea. Scanning Microsc. 8, 351–364.

Fischer, F.P., 1994b. Quantitative TEM analysis of the barn owl basilar papilla. Hear. Res. 73, 1–15.

Fischer, F.P., Köppl, C., Manley, G.A., 1988. The basilar papilla of the barn owl *Tyto alba*: a quantitative morphological SEM analysis. Hear. Res. 34, 87–102.

Funabiki, K., Ashida, G., Konishi, M., 2011. Computation of interaural time difference in the owl's coincidence detector neurons. J. Neurosci. 31, 15245–15256.

Gleich, O., 1989. Auditory primary afferents in the starling: correlation of function and morphology. Hear. Res. 37, 255–267.

Gleich, O., Langemann, U., 2011. Auditory capabilities of birds in relation to the structural diversity of the basilar papilla. Hear. Res. 273, 80–88.

Gleich, O., Manley, G.A., 2000. The hearing organ of birds and crocodilia. In: Dooling, R.J., Fay, R.R., Popper, A.N. (Eds.), Comparative Hearing: Birds and Reptiles. Springer Verlag, New York, pp. 70–138.

Gleich, O., Narins, P.M., 1988. The phase response of primary auditory afferents in a songbird (*Sturnus vulgaris* L.). Hear. Res. 32, 81–92.

Gleich, O., Dooling, R.J., Presson, J.C., 1997. Evidence for supporting cell proliferation and hair cell differentiation in the basilar papilla of adult Belgian Waterslager canaries (*Serinus canarius*). J. Comp. Neurol. 377, 5–14.

Gleich, O., Fischer, F.P., Köppl, C., Manley, G.A., 2004. Hearing organ evolution and specialization: *Archosaurs*. In: Manley, G.A., Popper, A., Fay, R.R. (Eds.), Evolution of the Vertebrate Auditory System. Springer Verlag, New York, pp. 224–255.

Goodyear, R.J., Richardson, G.P., 2002. Extracellular matrices associated with the apical surfaces of sensory epithelia in the inner ear: molecular and structural diversity. J. Neurobiol. 53, 212–227.

Griffin, D.R., 1953. Acoustic orientation in the oil bird, Steatornis. Proc. Natl. Acad. Sci. U. S. A. 39, 884–893.

Griffin, D.R., Thompson, D., 1982. Echolocation by cave swiftlets. Behav. Ecol. Sociobiol. 10, 119–123.

Grothe, B., Carr, C.E., Cassedy, J.H., Fritzsch, B., Köppl, C., 2004. The evolution of central pathways and their neural processing patterns. In: Manley, G.A., Popper, A., Fay, R.R. (Eds.), Evolution of the Vertebrate Auditory System. Springer Verlag, New York, pp. 289–359.

Grothe, B., Pecka, M., McAlpine, D., 2010. Mechanisms of sound localization in mammals. Physiol. Rev. 90, 983–1012.

Gummer, A.W., Smolders, J.W.T., Klinke, R., 1987. Basilar membrane motion in the pigeon measured with the Mössbauer technique. Hear. Res. 29, 63–92.

Gummer, A.W., Smolders, J.W.T., Klinke, R., 1989. Mechanics of a single-ossicle ear: I. The extra-stapedius of the pigeon. Hear. Res. 39, 1–14.

Hagstrum, J., 2000. Infrasound and the avian navigational map. J. Exp. Biol. 203, 1103–1111.

Hill, K.G., Stange, G., Mo, J., 1989. Temporal synchronization in the primary auditory response in the pigeon. Hear. Res. 39, 63–74.

Hill, E.M., Koay, G., Heffner, R.S., Heffner, H.E., 2014. Audiogram of the chicken (*Gallus gallus domesticus*) from 2 Hz to 9 kHz. J. Comp. Physiol. 200, 863–870.

Itatani, N., Klump, G.M., 2011. Neural correlates of auditory streaming of harmonic complex sounds with different phase relations in the songbird forebrain. J. Neurophysiol. 105, 188–199.

Iwaniuk, A.N., Clayton, D.H., Wylie, D.R.W., 2006. Echolocation, vocal learning, auditory localization and the relative size of the avian auditory midbrain nucleus (MLd). Behav. Brain Res. 167, 305–317.

Jarvis, E.D., 2004. Learned birdsong and the neurobiology of human language. Ann. N. Y. Acad. Sci. 1016, 749–777.

Jarvis, E., Gunturkun, O., Bruce, L., Csillag, A., Karten, H., Kuenzel, W., Medina, L., Paxinos, G., Perkel, D.J., Shimizu, T., Striedter, G., Wild, J.M., Ball, G.F., Dugas-Ford, J., Durand, S.E., Hough, G.E., Husband, S., Kubikova, L., Lee, D.W., Mello, C.V., Powers, A., Siang, C., Smulders, T.V., Wada, K., White, S.A., Yamamoto, K., Yu, J., Reiner, A., Butler, A.B., Avian Brain Nomenclature Consortium, 2005. Avian brains and a new understanding of vertebrate brain evolution. Nat. Rev. Neurosci. 6, 151–159.

Jeffress, L.A., 1948. A place theory of sound localization. J. Comp. Physiol. & Psychol. 41, 35–39.

Kaiser, A., Manley, G.A., 1996. Brainstem connections of the macula lagenae in the chicken. J. Comp. Neurol. 374, 108–117.

Keating, P., King, A.J., 2015. Sound localization in a changing world. Curr. Opin. Neurobiol. 35, 35–43.

Keller, C.H., Hartung, K., Takahashi, T.T., 1998. Head-related transfer functions of the barn owl: measurement and neural responses. Hear. Res. 118, 13–34.

King, A.J., Parsons, C.H., Moore, D.R., 2000. Plasticity in the neural coding of auditory space in the mammalian brain. Proc. Natl. Acad. Sci. U. S. A. 97, 11821–11828.

Klump, G.M., 2000. Sound localization in birds. In: Dooling, R.J., Fay, R.R., Popper, A.N. (Eds.), Comparative Hearing: Birds and Reptiles. Springer Verlag, New York, pp. 249–307.

Knudsen, E.I., 2002. Instructed learning in the auditory localization pathway of the barn owl. Nature 417, 322–328.

Knudsen, E.I., Konishi, M., 1978. A neural map of auditory space in the owl. Science 200, 795–797.

Konishi, M., 1993. Listening with two ears. Sci. Am. 268, 66–73.

Konishi, M., 2003. Coding of auditory space. Annu. Rev. Neurosci. 26, 31–55.

Konishi, M., 2004. The role of auditory feedback in birdsong. Ann. N. Y. Acad. Sci. 1016, 463–475.

Konishi, M., Knudsen, E.I., 1979. The oilbird: hearing and echolocation. Science 204, 425–427.

Köppl, C., 1997a. Frequency tuning and spontaneous activity in the auditory nerve and cochlear nucleus magnocellularis of the barn owl, *Tyto alba*. J. Neurophysiol. 77, 364–377.

Köppl, C., 1997b. Number and axon calibres of cochlear afferents in the barn owl. Int. J. Oper. Res. 3, 313–334.

Köppl, C., 1997c. Phase locking to high frequencies in the auditory nerve and cochlear nucleus magnocellularis of the barn owl, *Tyto alba*. J. Neurosci. 17, 3312–3321.

Köppl, C., 2009. Evolution of sound localisation in land vertebrates. Curr. Biol. 19, R635–R639.

Köppl, C., 2011a. Birds - same thing, but different? Convergent evolution in the avian and mammalian auditory systems provides informative comparative models. Hear. Res. 273, 65–71.

Köppl, C., 2011b. Evolution of the octavolateral efferent system. In: Ryugo, D., Fay, R.R., Popper, A.N. (Eds.), Auditory and Vestibular Efferents. Springer Science+Business Media, LLC, New York, pp. 217–259.

Köppl, C., 2019. Internally coupled middle ears enhance the range of interaural time differences heard by the chicken. J. Exp. Biol. 222, jeb199232.

Köppl, C., Manley, G.A., 1997. Frequency representation in the emu basilar papilla. J. Acoust. Soc. Am. 101, 1574–1584.

Köppl, C., Gleich, O., Manley, G.A., 1993. An auditory fovea in the barn owl cochlea. J. Comp. Physiol. A Sens. Neural Behav. Physiol. 171, 695–704.

Köppl, C., Klump, G.M., Taschenberger, G., Dyson, M., Manley, G.A., 1998. The auditory fovea of the barn owl - no correlation with enhanced frequency resolution. In: Palmer, A.R., Rees, A., Summerfield, A.Q., Meddis, R. (Eds.), Psychophysical and Physiological Advances in Hearing. Whurr Publishers Ltd, London, pp. 153–161.

Köppl, C., Wilms, V., Russell, I.J., Nothwang, H.G., 2018. Evolution of endolymph secretion and endolymphatic potential generation in the vertebrate inner ear. Brain Behav. Evol. 92, 1–31.

Kreithen, M.L., Quine, D.B., 1979. Infrasound detection by the homing pigeon:a behavioral audiogram. J. Comp. Physiol. 129, 1–4.

Krumm, B., Klump, G., Köppl, C., Langemann, U., 2017. Barn owls have ageless ears. Proc. R. Soc. B 284, 20171584.

Kuba, H., 2007. Cellular and molecular mechanisms of avian auditory coincidence detection. Neurosci. Res. 59, 370–376.

Kubke, M.F., Carr, C.E., 2006. Morphological variation in the nucleus laminaris of birds. Int. J. Comp. Psychol. 19, 83–97.

Langemann, U., Hamann, I., Friebe, A., 1999. A behavioral test of presbycusis in the bird auditory system. Hear. Res. 137, 68–76.

Larsen, O.N., Christensen-Dalsgaard, J., Jensen, K.K., 2016. Role of intracranial cavities in avian directional hearing. Biol. Cybern. 110, 319–331.

MacLeod, K.M., Carr, C.E., 2007. Beyond timing in the auditory brainstem: intensity coding in the avian cochlear nucleus angularis. Prog. Brain Res. 165, 123–133.

Manley, G.A., Clack, J.A., 2004. An outline of the evolution of vertebrate hearing organs. In: Manley, G.A., Popper, A., Fay, R.R. (Eds.), Evolution of the Vertebrate Auditory System. Springer Verlag, New York, pp. 1–26.

Manley, G.A., Köppl, C., 1998. Phylogenetic development of the cochlea and its innervation. Curr. Opin. Neurobiol. 8, 468–474.

Manley, G.A., Ladher, R., 2008. In: Dallos, P., Oertel, D. (Eds.), Phylogeny and Evolution of Ciliated Mechanoreceptor Cells, Audition. Academic Press, San Diego, pp. 1–34.

Manley, G.A., Sienknecht, U., 2013. The evolution and development of middle ears in land vertebrates. In: Puria, S., Popper, A.N., Fay, R.R. (Eds.), The Middle Ear. Science, Otosurgery, and Technology. Springer Science+Business Media, LLC, New York, pp. 7–30.

Manley, G.A., Van Dijk, P., 2008. Otoacoustic emissions in Amphibians, Lepidosaurs, and Archosaurs. In: Manley, G.A., Fay, R.R., Popper, A.N. (Eds.), Active Processes and Otoacoustic Emissions in Hearing. Springer Science+Business Media, LLC, New York, pp. 211–260.

Manley, G.A., Haeseler, C., Brix, J., 1991. Innervation patterns and spontaneous activity of afferent fibres to the lagenar macula and apical basilar papilla of the chick's cochlea. Hear. Res. 56, 211–226.

Manley, G.A., Köppl, C., Yates, G.K., 1997. Activity of primary auditory neurones in the cochlear ganglion of the Emu *Dromaius novaehollandiae* I: spontaneous discharge, frequency tuning and phase locking. J. Acoust. Soc. Am. 101, 1560–1573.

Martin, P., 2008. Active hair-bundle motility of the hair cells of vestibular and auditory organs. In: Manley, G.A., Fay, R.R., Popper, A.N. (Eds.), Active Processes and Otoacoustic Emissions in Hearing. Springer Science+Business Media, LLC, New York, pp. 93–144.

Moiseff, A., Konishi, M., 1981a. Neuronal and behavioral sensitivity to binaural time differences in the owl. J. Neurosci. 1, 40–48.

Moiseff, A., Konishi, M., 1981b. The owl's interaural pathway is not involved in sound localization. J. Comp. Physiol. A Sens. Neural Behav. Physiol. 144, 299–304.

Moorman, S., Mello, C.V., Bolhuis, J.J., 2011. From songs to synapses: molecular mechanisms of birdsong memory. Molecular mechanisms of auditory learning in songbirds involve immediate early genes, including zenk and arc, the ERK/MAPK pathway and synapsins. Bioessays 33, 377–385.

Moser, T., Grabner, C.P., Schmitz, F., 2020. Sensory processing at ribbon synapses in the retina and the cochlea. Physiol. Rev. 100, 103–144.

Moss, C.F., Carr, C.E., 2013. Comparative audition. In: Weiner, I.B. (Ed.), Handbook of Psychology, second ed. John Wiley & Sons, Inc., pp. 115–156

Nagel, K., Kim, G., McLendon, H., Doupe, A., 2011. A bird brain's view of auditory processing and perception. Hear. Res. 273, 123–133.

Necker, R., 1970. Zur Entstehung der Cochleapotentiale von Vögeln: Verhalten bei O_2-Mangel, Cyanidvergiftung und Unterkühlung sowie Beobachtungen über die räumliche Verteilung. Z. für Vgl. Politikwiss. (ZfVP) 69, 367–425.

Nesbitt, S.J., 2011. The early evolution of archosaurs: relationship and the origin of major clades. Bull. Am. Mus. Nat. Hist. 2011, 1–292.

Neubauer, H., Köppl, C., Heil, P., 2009. Spontaneous activity of auditory nerve fibers in the barn owl (*Tyto alba*): analyses of interspike interval distributions. J. Neurophysiol. 101, 3169–3191.

Norberg, R.A., 2002. Independent evolution of outer ear asymmetry among five owl lineages: morphology, function and selection. In: Newton, I., Kavanagh, R., Olsen, J., Taylor, I. (Eds.), Ecology and Conservation of Owls. CSIRO Publishing, Collingwood, Victoria, Australia, pp. 329–342.

Nottebohm, F., 2004. The road we travelled: discovery, choreography, and significance of brain replaceable neurons. Ann. N. Y. Acad. Sci. 1016, 628–658.

Novick, A., 1959. Acoustic orientation in the cave swiftlet. Biol. Bull. Mar. Biol. Lab. Woods Hole 117, 497–503.

Okanoya, K., Dooling, R.J., 1985. Colony differences in auditory thresholds in the canary (*Serinus canarius*). J. Acoust. Soc. Am. 78, 1170–1176.

Ondracek, J.M., Hahnloser, R.H.R., 2013. Advances in understanding the auditory brain of songbirds. In: Köppl, C., Manley, G.A., Popper, A.N., Fay, R.R. (Eds.), Insights from Comparative Hearing Research. Springer Science+Business Media, LLC, New York (in press).

Payne, R.S., 1971. Acoustic location of prey by barn owls (*Tyto alba*). J. Exp. Biol. 54, 535–573.

Peña, J.L., Gutfreund, Y., 2014. New perspectives on the owl's map of auditory space. Curr. Opin. Neurobiol. 24, 55–62.

Peña, J.L., Konishi, M., 2001. Auditory spatial receptive fields created by multiplication. Science 292, 249–252.

Peña, J.L., Cazettes, F., Beckert, M.V., Fischer, B.J., 2019. Synthesis of hemispheric ITD tuning from the readout of a neural map: commonalities of proposed coding schemes in birds and mammals. J. Neurosci. 39, 9053–9061.

Perkel, D.J., 2004. Origin of the anterior forebrain pathway. Ann. N. Y. Acad. Sci. 1016, 736–748.

Pickles, J.O., 2008. An Introduction to the Physiology of Hearing, third ed. Emerald Group Publishing Ltd., Bingley, UK.

Proctor, L., Konishi, M., 1997. Representation of sound localization cues in the auditory thalamus of the barn owl. Proc. Natl. Acad. Sci. U. S. A. 94, 10421–10425.

Pytte, C.L., Ficken, M.S., Moiseff, A., 2004. Ultrasonic singing by the blue-throated hummingbird: a comparison between production and perception. J. Comp. Physiol. A Neuroethol. Sens. Neural. Behav. Physiol. 190, 665–673.

Rubel, E.W., Furrer, S.A., Stone, J.S., 2013. A brief history of hair cell regeneration research and speculations on the future. Hear. Res. 297, 42–51.

Russell, I.J., 2013. Roles for prestin in harnessing the basilar membrane to the organ of Corti. In: Köppl, C., Manley, G.A., Popper, A.N., Fay, R.R. (Eds.), Insights from Comparative Hearing Research. Springer Science+Business Media, LLC, New York (in press).

Ryals, B.M., Westbrook, E.W., 1990. Hair cell regeneration in senescent quail. Hear. Res. 50, 87–96.

Ryals, B.M., Dent, M.L., Dooling, R.J., 2013. Return of function after hair cell regeneration. Hear. Res. 297, 113–120.

Sachs, M.B., Young, E.D., Lewis, R.H., 1974. Discharge patterns of single fibers in the pigeon auditory nerve. Brain Res. 70, 431–447.

Sachs, M.B., Woolf, N.K., Sinnott, J.M., 1980. Response properties of neurons in the avian auditory system: comparisons with mammalian homologues and consideration of the neural encoding of complex stimuli. In: Popper, A.N., Fay, R.R. (Eds.), Comparative Studies of Hearing in Vertebrates. Springer-Verlag, New York, Heidelberg, Berlin, pp. 323–353.

Salvi, R.J., Saunders, S.S., Powers, N.L., Boettcher, F.A., 1992. Discharge patterns of cochlear ganglion neurons in the chicken. J. Comp. Physiol. A Sens. Neural Behav. Physiol. 170, 227–241.

Saunders, J.C., Duncan, R.K., Doan, D.E., Werner, Y.L., 2000. The middle ear of reptiles and birds. In: Dooling, R.J., Fay, R.R., Popper, A.N. (Eds.), Comparative Hearing: Birds and Reptiles. Springer Verlag, New York, pp. 13–69.

Schermuly, L., Klinke, R., 1990a. Infrasound sensitive neurones in the pigeon cochlear ganglion. J. Comp. Physiol. A Sens. Neural Behav. Physiol. 166, 355–363.

Schermuly, L., Klinke, R., 1990b. Origin of infrasound sensitive neurones in the papilla basilaris of the pigeon: an HRP study. Hear. Res. 48, 69–78.

Singheiser, M., Gutfreund, Y., Wagner, H., 2012. The representation of sound localization cues in the barn owl's inferior colliculus. Front. Neural Circ. 6, 45.

Smolders, J.W.T., 1999. Functional recovery in the avian ear after hair cell regeneration. Audiol. Neuro. Otol. 4, 286–302.

Smolders, J.W.T., Ding-Pfennigdorff, D., Klinke, R., 1995. A functional map of the pigeon basilar papilla: correlation of the properties of single auditory nerve fibres and their peripheral origin. Hear. Res. 92, 151–169.

Stone, J.S., Cotanche, D.A., 2007. Hair cell regeneration in the avian auditory epithelium. Int. J. Dev. Biol. 51, 633–647.

Sullivan, W.E., Konishi, M., 1984. Segregation of stimulus phase and intensity coding in the cochlear nucleus of the barn owl. J. Neurosci. 4, 1787–1799.

Suthers, R.A., Hector, D.H., 1982. Mechanism for the production of echolocating clicks by the grey swiftlet, *Collocalia spodiopygia*. J. Comp. Physiol. 148, 457–470.

Suthers, R.A., Hector, D.H., 1985. The physiology of vocalization by the echolocating oilbird, *Steatornis caripensis*. J. Comp. Physiol. 156, 243–266.

Takahashi, T.T., 2010. How the owl tracks its prey – II. J. Exp. Biol. 213, 3399–3408.

Takahashi, T.T., Bala, A.D.S., Spitzer, M.W., Euston, D.R., Spezio, M.L., Keller, C.H., 2003. The synthesis and use of the owl's auditory space map. Biol. Cybern. 89, 378–387.

Takasaka, T., Smith, C.A., 1971. The structure and innervation of the pigeon's basilar papilla. J. Ultra. Res. 35, 20–65.

Tan, X., Pecka, J.L., Tang, J., Okoruwa, O.E., Zhang, Q., Beisel, K.W., He, D.Z.Z., 2011. From zebrafish to mammal: functional evolution of prestin, the motor protein of cochlear outer hair cells. J. Neurophysiol. 105, 36–44.

Taschenberger, G., Manley, G.A., 1997. Spontaneous otoacoustic emissions in the barn owl. Hear. Res. 110, 61–76.

Theunissen, F.E., Shaevitz, S.S., 2006. Auditory processing of vocal sounds in birds. Curr. Opin. Neurobiol. 16, 400–407.

Theunissen, F.E., Amin, N., Shaevitz, S.S., Woolley, S.M., Fremouw, T., Hauber, M.E., 2004. Song selectivity in the song system and in the auditory forebrain. Ann. N. Y. Acad. Sci. 1016, 222–245.

Thomassen, H.A., Povel, G.D.E., 2006. Comparative and phylogenetic analysis of the echo clicks and social vocalizations of swiftlets (Aves: Apodidae). Biol. J. Linn. Soc. 88, 631–643.

Tilney, M.S., Tilney, L.G., DeRosier, D.J., 1987. The distribution of hair cell bundle lengths and orientations suggests an unexpected pattern of hair cell stimulation in the chick cochlea. Hear. Res. 25, 141–151.

Vergne, A.L., Pritz, M.B., Mathevon, N., 2009. Acoustic communication in crocodilians: from behaviour to brain. Biol. Rev. 84, 391–411.

von Bartheld, C.S., Gianessi, F., 2011. The paratympanic organ: a barometer and Altimeter in the middle ear of birds? J. Exp. Zool. B Mol. Dev. Evol. 316, 402–408.

Vonderschen, K., Wagner, H., 2014. Detecting interaural time differences and remodeling their representation. Trends Neurosci. 37, 289–300.

Wang, Y., Brzozowska-Prechtl, A., Karten, H., 2010. Laminar and columnar auditory cortex in avian brain. Proc. Natl. Acad. Sci. U. S. A. 107, 12676–12681.

Warchol, M.E., Dallos, P., 1989. Neural response to very low-frequency sound in the avian cochlear nucleus. J. Comp. Physiol. A Sens. Neural Behav. Physiol. 166, 83–95.

Wilkins, H.R., Presson, J.C., Popper, A.N., Ryals, B.M., Dooling, R.J., 2001. Hair cell death in a hearing-deficient canary. Jaro 2, 79–86.

Woolley, S.M., Gill, P.R., Fremouw, T., Theunissen, F.E., 2009. Functional groups in the avian auditory system. J. Neurosci. 29, 2780–2793.

Wu, Y.-C., Art, J.J., Goodman, M.B., Fettiplace, R., 1995. A kinetic description of the calcium-activated potassium channel and its application to electrical tuning of hair cells. Prog. Biophys. Mol. Biol. 63, 131–158.

Xia, A., Liu, X., Raphael, P.D., Applegate, B.E., Oghalai, J.S., 2016. Hair cell force generation does not amplify or tune vibrations within the chicken basilar papilla. Nat. Commun. 7, 13133.

Yates, G.K., Manley, G.A., Köppl, C., 2000. Rate-intensity functions in the emu auditory nerve. J. Acoust. Soc. Am. 107, 2143–2154.

Young, B.A., Mathevon, N., Tang, Y., 2013. Reptile auditory neuroethology: what do reptiles do with their hearing? In: Köppl, C., Manley, G.A., Popper, A.N., Fay, R.R. (Eds.), Insights from Comparative Hearing Research. Springer Science+Business Media, LLC, New York (in press).

Zeyl, J.N., den Ouden, O., Köppl, C., Assink, J., Christensen-Dalsgaard, J., Patrick, S.C., Clusella-Trullas, S., 2020. Infrasonic hearing in birds: a review of audiometry and hypothesized structure-function relationships. Biol. Rev. Camb. Phil. Soc. 95, 1036–1054.

Zheng, F., Zuo, J., 2017. Cochlear hair cell regeneration after noise-induced hearing loss: does regeneration follow development? Hear. Res. 349, 182–196.

Chapter 12

Chemesthesis and olfaction

Larry Clark[1] and Cynthia A. Smeraski[2]
[1]METIS, Ltd., Fort Collins, CO, United States; [2]Science Education and Literacy Foundational Program, Fort Collins, CO, United States

12.1 Chemical senses

The chemical senses generally fall into three categories: (1) chemesthesis (irritation and pain), (2) olfaction (smell), and (3) gustation (taste). Traditional emphasis in describing responsiveness to chemical stimuli has been placed on taste and smell. The reality is more complex. For example, the sensory afferents for chemesthetic perception are in close proximity with olfactory receptors in the nasal cavity and with gustatory receptors in the oral cavity. Because external chemical stimuli can be processed by multiple sensory systems, there has been a great deal of confusion in the behavioral and ecological literature on the importance of individual sensory modalities. Generally, the principal mediating sensory modality may be related to stimulus type, concentration, and presentation (i.e., nose, eyes, mouth). However, when perception of external chemical stimuli occurs across modalities, the combined perceptual quality is commonly referred to as flavor, which is a reflection of the cognitive integration of all inputs.

Early studies of bird chemosensory systems were descriptive from a neuroanatomical, physiological, and behavioral perspective. As methodologies have expanded, insights into behavioral and physiological mechanisms have been augmented with genomic and molecular studies. The later have formed the basis of most avian chemesthetic studies over the past 15 years. We follow this general pattern of organization in this chapter, realizing that from an information processing perspective at the animal systems and ecological levels, chemical signals may be simultaneously processed by multiple sensory systems and be further integrated with other sensory inputs before the bird behaviorally responds. Gustation is covered separately in this volume.

12.2 Chemesthesis

Nociception is the detection of potential or actual harmful stimuli (Julius, 2013). Nociceptors have three functions: (1) detection of endogenous inflammatory stimuli which is useful in initiating and promoting behaviors conducive to healing and repair, (2) detection of potentially damaging external noxious stimuli which is useful in warning an animal to the risk of injury, and (3) detection of neural damage and ectopic firing. This later function is a pathological condition of chronic pain. Nociceptors have high thresholds for exogenous stimuli presumably because it would be maladaptive to defensively respond to every external assault. Nociceptors also have low thresholds for endogenous stimuli. This is an adaptive response to promote healing once tissue damage has occurred (Patapoutian et al., 2009).

Chemesthesis is a subcategory of nociception and is the perception of chemically induced irritation. Examples of other nociceptive stimuli are temperature and pressure and are covered elsewhere in this volume. Generally, chemesthetic stimuli result in reflexive withdraw by the animal and does not require learning for the defensive action. In contrast, prolonged postingestional discomfort, malaise, or illness may involve chemosensory and other sensory systems and set up conditions for learned avoidance (Clark and Avery, 2013). Pain is the perception and integration of processes involved in nociception, malaise, or illness that result in behavior modifications by the animal (Sneddon et al., 2014).

Interest in chemesthetic function and properties in birds has largely been focused in four areas: (1) the evolutionary phylogenetic relationships of receptor mediated perception of noxious stimuli and its consequence to the foraging ecology of birds (Clark, 1998a; Saito and Tominaga, 2015); (2) the applicability of using aversive compounds in modulating feeding behavior of birds to develop repellents for prevention of crop damage or otherwise mitigating against damage caused by birds (Mason and Clark, 1997); (3) promotion of animal welfare in domestic poultry production (Kuenzel, 2007; Gentle, 2011); and (4) to gain a better understanding of pathologic pain and for the development of appropriate analgesics (Julius, 2013; Szolcsanyi, 2014).

Sturkie's Avian Physiology. https://doi.org/10.1016/B978-0-12-819770-7.00035-9

12.3 Neural organization

The perception of noxious stimuli begins with activation of primary sensory nociceptors (Woolf and Ma, 2007). The primary sensory neurons are the interface between the internal and external environments. Nociceptors have cell bodies located in the dorsal root ganglion, a peripheral axon that innervates tissues, and a central axon that enters the spinal cord to transfer information to the central nervous system (Figure 12.1). Many nociceptive neurons respond to multiple stimuli (e.g., thermal and chemical). These are referred to as polymodal nociceptors.

A major component for the mediation of chemical nociception is the trigeminal nerve (TN). The TN is the principal somatic sensory nerve of the head, and its primary function is the coding of mechanical and thermal stimuli. However, the TN also contains chemoreceptive fibers that mediate the detection of chemical irritants (Silver and Maruniak, 1980). The somatosensory nerves are the primary somatic sensory system of the rest of the body. Like the TN, the somatosensory nerves in birds primarily code for mechanical and thermal stimuli, but they do have sensory afferents that are chemosensory (Gentle, 2011; Wild, 1985). Aspects of the avian TN neural architecture related to navigation and mechanoreception are reviewed elsewhere (Kishkinev and Chernetsov, 2014; Schneider et al., 2017; Wiltschko and Wiltschko, 2019).

In birds, chemosensitive fibers in the TN and somatosensory nerves are similar to mammalian afferents. Most are unmyelinated C-type polymodal nociceptors with conduction velocities of 0.3−1 m/s. However, some myelinated A-delta high-threshold mechanoreceptors with

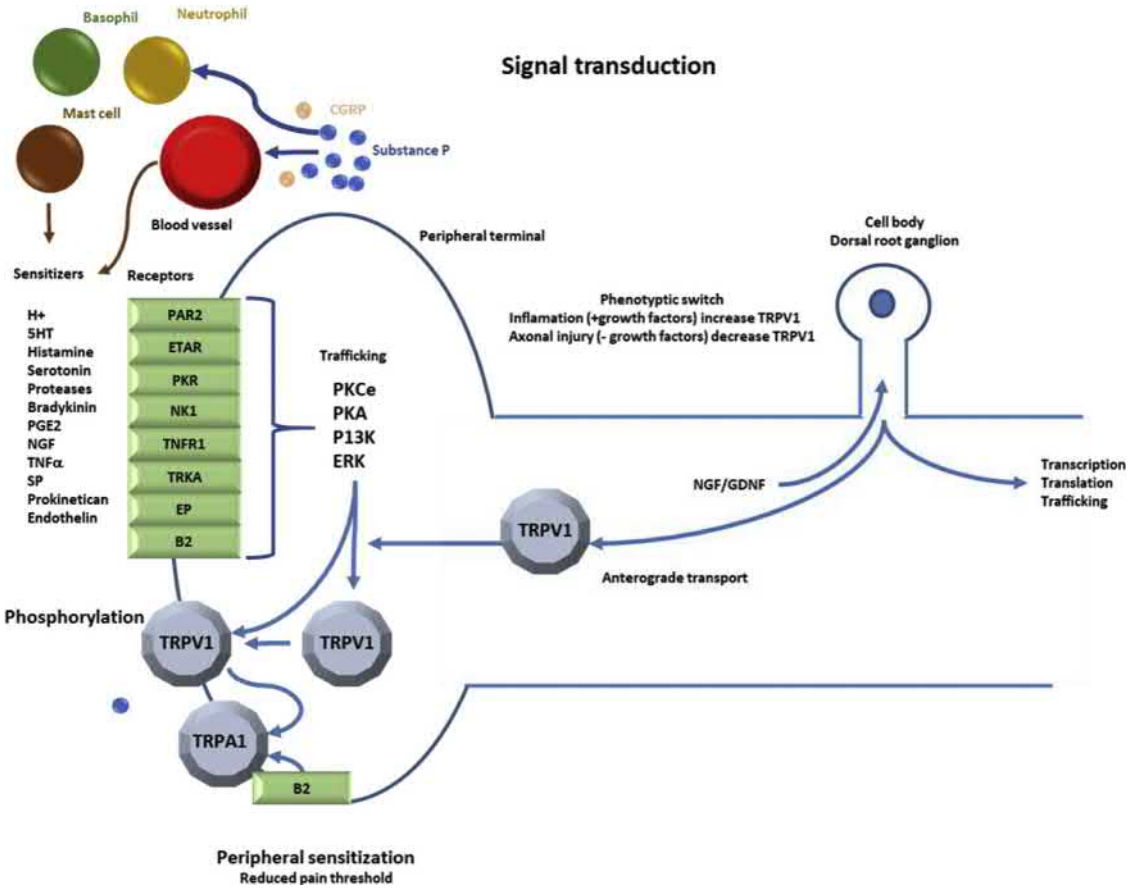

FIGURE 12.1 Sensitization and activation of primary afferent nociceptor. Nociceptors not only transmit peripheral signals but may also affect vasodilation and other responses from nearby cells, initiating a variety of local signaling (neurogenic inflammation), which enhances sensitivity to exogenous and mechanical stimuli. These endogenous sensitizers act on receptors expressed by nociceptors to activate intracellular signal transduction pathways that alter trafficking to the membrane, thresholds, and kinetics. Growth factors, e.g., nerve growth factor, are retrogradely transported to the cell body of the nociceptors. Through intracellular signaling pathways, expression of TRP channels is increased and they are transported to the peripheral terminal. Changes in transcription and translation of TRP channels and other proteins can switch the chemical phenotype of the neurons from their state in naive conditions to an altered state during inflammation. *B2*, bradykinin receptor; *ERK*, extracellular signal-regulated kinase; *ETAR*, endothelin receptor type A; *GDNF*, glial-cell-derived neurotrophic factor; *NK1*, neurokinin receptor 1; *PAR2*, protease-activated receptor 2; *PGE2*, prostaglandin E2; *PI3K*, phosphoinositide 3-kinase; *PK*, protein kinase; *PKR*, prokineticin receptor; *TNFα*, tumor necrosis factor α; *TNFR1*, TNF receptor 1; *TRKA*, tyrosine kinase receptor A. *Adapted from Patapoutian et al. (2009) and Julius (2013).*

conduction velocities of 5−40 m/s also respond to chemical stimuli. The discharge patterns and conduction velocities for the chicken, mallard (*Anas platyrhynchos*), and pigeon (*Columba livia*) are similar to those observed in mammals (Necker, 1974; Gentle, 1989).

The morphological organization of the peripheral TN in birds is similar to mammals (Dubbeldam and Karten, 1978; Dubbeldam and Veenman, 1978; Gottschaldt, 1985; Douglas and Paul Murphy, 2017; Faunes and Wild, 2017). The TN is the VIth cranial nerve in birds, arising from the rostrolateral medulla near the caudal surface of the optic lobe (Getty, 1975; Schrader, 1970).The TN travels along the trochlear nerve (IV), entering a fossa in the floor of the cranial cavity where the trigeminal ganglion (TG) is found. The TG is subdivided into a smaller medial ophthalmic region and a larger lateral maxillomandibular region from which the nerve splits into three branches. In the chicken (*Gallus gallus domesticus*), the ophthalmic branch innervates the frontal region, the eyeball, upper eyelid, conjunctiva, glands in the orbit, the rostrodorsal part of the nasal cavity, and the tip of the upper jaw. The ophthalmic branch as a communicating ramus with the trochlear nerve serves for motor control of the eye region. This aspect can provide for reflexive response to irritating stimuli to the ocular region. The larger medial ramus accompanies the olfactory nerve into the nasal fossa via the medial orbitonasal foramen. The maxillary branch provides sensory input from the integument of the crown, temporal region, rostral part of the external ear, upper and lower eyelids, the region between the nostrils and eye, conjunctival mucosa, the mucosal part of the palate, and the floor of the medial wall of the nasal cavity. The mandibular branch provides sensory input from the skin and rhamphotheca of the lower jaw, intermandibular skin, wattles, oral mucosa of rostral floor of the mouth, and the palate near the angle of the mouth (Getty, 1975; Schrader, 1970).

12.3.1 Peptides involved in pain perception

Though birds have slightly different neural architecture relative to mammals, the underlying functions of neural connections have been evolutionarily preserved (Butler and Cotterill, 2006; Dugas-Ford et al., 2012; Güntürkün, 2012). This also applies to the underlying physiological and biochemical processes of chemically induced pain. Generally, birds have the same classes of neuropeptides as mammals that serve similar functions, but their structures are not 100% homologous. Avian endogenous pain-promoting substances such as substance P, 5-HT, histamine, bradykinin, and acetylcholine evoke inflammation and pain-related behaviors in chickens, pigeons, rats, dogs, and guinea pigs (Figure 12.1; Szolcsanyi et al., 1986; Gentle and Hill, 1987; Gentle and Hunter, 1993; Koda et al., 1996; Hu et al., 2002; Ohta et al., 2006). In *Coturnix* quail, aromatase neurons were associated with the neurokinin 1 receptor and in is proximity to substance P-immunoreactive fibers, suggestive that aromatase neurons may participate in the control of nociception as well (Evrard et al., 2003). Prostaglandins that modulate the pain response in mammals also serve this function in birds, and their effects can be abolished by prostaglandin biosynthase inhibitors such as aspirin-like analgesics (Clark, 1995). Despite these physiologically mediated similarities, there are differences in how birds and mammals respond to some exogenous chemical stimuli. In mammals, chemicals such as capsaicin are potent trigeminal irritants. These irritants deplete substance P from afferent terminals and the dorsal root ganglion, producing an initial sensitization followed by desensitization to further chemical stimulation (Szolcsanyi, 1982). In contrast, birds are behaviorally insensitive to capsaicin (Mason and Maruniak, 1983). Peripheral presentation of capsaicin to pigeons and chickens does not cause release of substance P in avian sensory afferents (Pierau et al., 1986; Szolcsanyi et al., 1986; Sann et al., 1987). These taxon-specific responses to exogenous chemical stimuli underscore taxonomic differences in both endogenous neuropeptides and receptors whose significance has been implicated in the evolutionary ecology of the taxa (Mason et al., 1991).

12.3.2 Responses to chemicals

Birds consuming experimental solutions demonstrate an ability to detect acids, and their responses vary depending upon the acid and its concentration (Kare, 1954; Berkhoudt, 1985). Most birds are tolerant of acetic acid and hydrochloric acid (Rensch and Neunzig, 1925; Kare and Rogers, 1976). However, chickens, *Gallus domesticus,* may only experience weak pain from acid stimulation. The relative weak response of the chicken TRPV1 (cTRPV1) receptor as compared to the mouse TRPV1 (mTRPV1) appears to be related to differences at the C-terminal CaM binding site (Liang et al., 2019). This weak receptor response is consistent with the behavioral observations indicating chickens only experience mild discomfort or pain to acid stimulation.

Exposure to noxious vapors also evokes responses in birds. Ammonia gas, acetic acid vapor, and carbon dioxide administered to oral and nasal cavities evoke neural and behavioral responses in the chicken (Soudek, 1929; McKeegan, 2004). Changes in carbon dioxide concentration in the nasopharynx region can cause species-specific changes in reflexive breathing in birds (Hiestand and Randall, 1941). However, concentrations of carbon dioxide that are sufficiently high to be irritating to mammals have no effect on blood pressure, heart rate, tidal volume, breathing frequency, upper airway resistance, or lower airway resistance in geese and chickens. This is consistent

with the relative acid insensitivity of the cTRPV1 receptor (Liang et al., 2019). Geese and chickens respond differently than mammals to exposure to sulfur dioxide, but in a similar manner when exposed to ammonia and phenyl diguanide (Callanan et al., 1974; McKeegan et al., 2005).

Many aromatic molecules are aversive to birds when ingested orally (Kare, 1961; Mason et al., 1989; Crocker and Perry, 1990; Clark and Shah, 1991, 1993; Crocker et al., 1993). Direct contact with receptors through solution may occur or odor volatiles may diffuse into the epithelium and act through TN nociceptors in the mouth, or through retronasal stimulation of TN nociceptors in the olfactory cavity (Tucker, 1971; Silver and Maruniak, 1980; Keverne et al., 1986). Electrophysiological evidence shows that the TN responds to odors albeit generally with less sensitivity than the olfactory nerve (Tucker, 1963). Behavioral assays yield similar results. Pigeons trained to respond to odors fail to respond after olfactory nerve transections. However, odor responding can be reinstated if the odor concentration is increased (Michelsen, 1959; Henton, 1969; Henton et al., 1966). Odor sensitivity of pigeons decreased by two to four log units (vapor saturation) after olfactory nerve transaction (Walker et al., 1979). In European starlings, avoidance of anthranilate compounds was partially a consequence of olfactory cues. When the olfactory nerves were transected, avoidance was only mildly diminished. When the ophthalmic branches of the TN were transected, the starlings became insensitive to the aversive properties of the anthranilates (Mason et al., 1989; Clark, 1996). Thus, caution must be exercised in categorizing volatile chemicals as being mediated through olfactory or chemesthetic systems. A vapor could be mediated by both systems, with the primary effect being determined by concentration.

Several lines of evidence suggest that a variety of chemicals have intrinsic properties that cause them to be aversive on a purely chemesthetic sensory basis. First the aversive quality is unlearned, that is, avoidance occurs upon initial contact. Second, there is no evidence that consumption is altered by gastrointestinal feedback, i.e., intake of fluid treated with those sensory stimuli is constant over time. Third, unlike mammals, birds seem unable to associate aversive quality of the stimulus with other chemosensory cues, suggesting that conditioned flavor avoidance learning does not occur. Fourth, birds do not habituate to the stimulus, thus, avoidance persists in the absence of reinforcement (Clark and Mason, 1993; Clark and Shah, 1994; Clark, 1996; Clark and Avery, 2013).

Another area of research has been the investigation of plant compounds as either flavorings for feed additives or for their repellent properties (Clark, 1998c; Zeng et al., 2015). While many plant compounds are aversive across taxa, some mammalian irritants are not effective against birds and vice versa. The prototypical example is capsaicin, a plant derived compound first isolated by Thresh (1876), with pungency attributes to humans developed by Scoville (1912) and Nelson (1920), and structurally elucidated by Nelson and Dawson (1923). Birds are behaviorally insensitive to capsaicin (Mason and Maruniak, 1983; Szolcsanyi et al., 1986), whereas mammals are not (Figure 12.2). The possible ecological consequence to the pepper plant was presumably selective pressure favoring evolutionary incorporation of a chemical for protection against a seed predator (rodents), but non-noxious to a seed disperser (birds; Mason et al., 1991; Tewksbury and Nabhan, 2001).

12.3.3 Structure-activity relationships

The historical search for bird repellents has generally been opportunistic in the identification of compounds, with over 10,000 compounds having been evaluated over time (O'Hare et al., 2012). Clark (1998c) and colleagues took a more systematic approach. Using core structures, substituents with differing structural, electronic, and physicochemical attributes were systematically evaluated for repellency in feeding and drinking trial for 113 compounds. Within chemical classes (with a few exceptions, see below) European starlings (*Sturnus vulgaris*) demonstrated aversive responses to acetophenones, anthranilates, anilines, benzyl alcohols, and veratryl amines; whereas starlings were largely indifferent to benzaldehydes, thiozoles, N-heteocycles, acetates, benzoates, veratryls benzamides, and preferred benzoic acids, and amino acids (Figure 12.3). Pulegone has been identified as a potent bird repellent (Mason, 1990), but starlings were indifferent to 12 other menthone derivatives (Mason and Primus, 1996). Watkins et al. (1999) demonstrated repellency and indifference of cinnamaldehyde and their derivatives based on chemical structure. Such behavioral differences in response pose interesting evolutionary questions, but also provide background for using these exogenous chemical probes to elucidate structure-activity relationships and receptor mechanisms which might prove useful for rational design of species-specific repellents and analgesics (Clark, 1998a,b,c; Maatuf et al., 2019).

Despite the well-known behavioral insensitivity of birds to capsaicin, birds are averse to other vanilloid compounds, reflexively avoiding them (Figure 12.2). Aromatic compounds that are considered aversive by birds are qualitatively characterized as having an aromatic heterocyclic core, high degree of basicity, high degree of lipophilicity, and a high degree of electronegativity (Figure 12.3). The core aromatic heterocycle of a repellent compound is enhanced by substitutions that affect electron donation: amino > methoxy > methyl > hydroxyl groups. Resonance of lone pairs of electrons enhances repellency as a function of substituent position: ortho > para > meta. Acidic substituents in the electron withdrawing group detract from aversive qualities of the compound. Steric

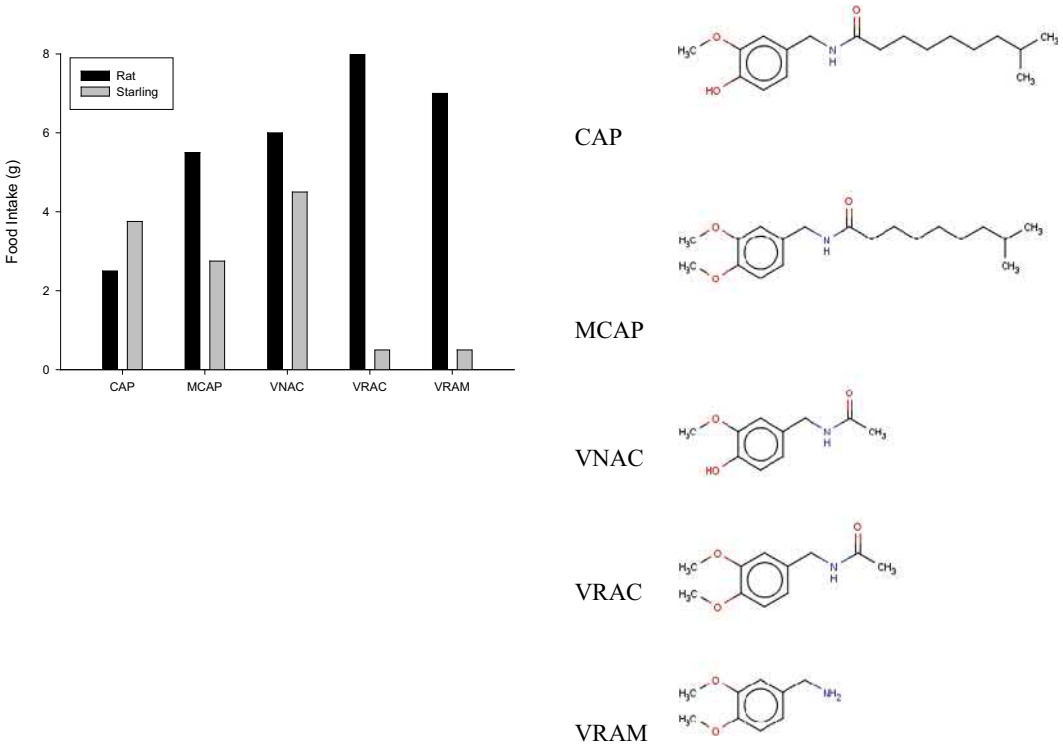

FIGURE 12.2 **Consumption of food treated with capsaicin (CAP), methyl capsaicin (MCAP), vanillyl acetamide (VNAC), veratryl acetamide (VRAC), and veratryl amine (VRAM) in rats and starlings.** Note the general inverse relationship of consumption as structure changes, suggesting functional receptor differences in the two taxa. Bird repellents are more basic and rigid (planar) than mammal aversive compounds. Concentration applied was 1000 ppm. Consumption of 4 g of untreated food is control baseline intake for both species. Compound structures from top to bottom are CAP, MCAP, VNAC, VRAC, and VRAM. *Data adapted from Mason et al. (1991).*

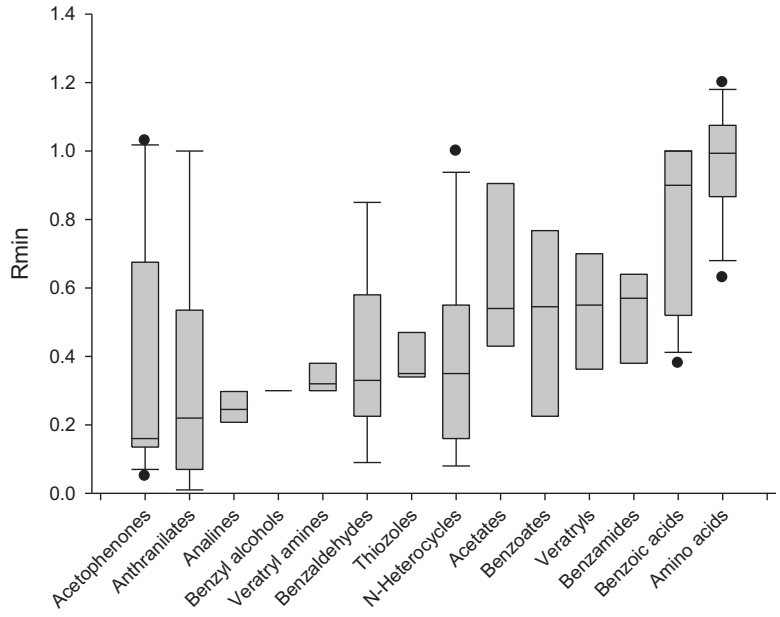

FIGURE 12.3 **The relative reduction of fluid intake for solutions as a function of chemical class, which assumes a benzene parent structure with the nomenclatural taxonomy defined by the principal electron withdrawing group.** Fluid intake is the asymptotic minimum intake in one-bottle six hour drinking trials (R_{min}). Stongly aversive solutions (where R_{min} is not statistically distinguishable from zero) have $R_{min} < 0.2$. Moderately aversive solutions have $0.2 < R_{min} < 0.4$, weakly aversive solutions have $0.4\ R_{min} < 0.6$, and solutions with $R_{min} > 0.6$ are not aversive at all (not statistically different from water controls). Median R_{min} (solid bars), R_{min} 25th−75th percentile (shaded box), R_{min} 5th−95th percentile (capped line), and the range of R_{min} (open symbols). *Adapted from Clark (1997).*

effects and extreme delocalization of lone pairs of electrons, as might occur in meta isomers and aromatic structures with multiple substituted electron donating groups, tend to interfere with repellency (Mason et al., 1989; Clark and Shah, 1991, 1994; Clark et al., 1991; Shah et al., 1991). In addition, good bird repellents tend to be lipophilic, presumably to gain better access to the lipid bilayer membrane (Mason et al., 1989).

Quantitative structure-activity relationships of aromatic compounds and repellency are consistent with earlier qualitative studies. The aversive properties of 14 derivatives of cinnamic acid compounds are characterized by heat of formation (DH(f)), polarizability (XY and YY), and super delocalizability (Sr). All of these descriptors are electronic (Watkins et al., 1999). These findings generally align with a reanalysis of the QSAR relationships of the 117 compounds described above. Canonical analysis of the relationship of physicochemical, topological, and electrostatic descriptors and the concentration-response shape of thefour-parameter fluid intake curve showed that 94% of variance in the response profile could be accounted for by five parameters: polarizability, ES2, ANC, KAPPA2, and CHI2. Polarizability is the relative susceptibility of the electron cloud of a molecule to be distorted by the presence of an external electric field. Owing to distortion, an induced electric dipole moment appears. Temporary dipoles induce dipoles in other molecules resulting in van der Waals intermolecular forces by orienting the temporary and induced dipoles with each other. ES2 is an electrotopological descriptor that describes electronic interactions between molecules. ANC is a partial negative electronic charge descriptor of electrostatic potential that influences molecular interactions (Clark, 1997). CHI2 and KAPP2 are valence connectivity and shape descriptors that may describe the rigidity of the molecule and accessibility of the molecule to receptor pockets (Chu et al., 2020).

12.3.4 Transient receptor potential channels

The almost ubiquitous responsiveness of species to acids across taxonomic orders suggests evolutionary conservation of this trait (Pattison et al., 2019). The ability to detect protons is critical for the regulation of ionic homeostasis so important for cell function, as is the ability to detect exogenous chemical conditions. This detection is accomplished through different mechanisms, i.e., acid sensing ion channels, proton sensing G protein-coupled receptors (GPCR; Ludwig et al., 2003) and two-pore potassium channels. While there is a strong conservation of histidine residues in extracellular portions of the GPCR receptor, some portions differ among species. Relative to mammals and amphibians, chicken GPCR-68 also responds to protons. However, unlike mammals and amphibia, chicken GPCR-65 is not proton sensitive (Mochimaru et al., 2018; Musha et al., 2019).

Nonselective transient receptor potential (TRP) cation channels are evolutionarily conserved membrane proteins involved in sensory neuron activation events, neurotransmitter release, release of inflammatory mediators, and other aspects of pain transduction (Julius, 2013, Figure 12.4). At least 28 such channels, divided into six subtypes based on sequence homology have been identified: vanilloid (TRPV1-6), ankyrin (TRPA1), canonical (TRPC1-7), melastatin (TRPM1-8), mucolipin (TRPML1-1-3), and polycystin (TRPP1-3) (Samanta et al., 2018). For taxa studied to date, TRP channels share six transmembrane across regions S1−S6 and a pore-forming loop between S5 and S6 (Moran and Szallasi, 2018). Because the subfamilies are based on homology, functional attributes of channels are dispersed across receptor type subfamilies (Figure 12.4). TRP receptor channels (TRPA1, TRPV1-4, TRPM-2, 4, 5, 8) serve a valuable function as thermal sensors important to a species' ecology and are activated across different temperature ranges across species (Saito and Tominaga, 2015; Oda et al., 2017). Moreover, many of these channels are polymodal (e.g., responding to temperature, endogenous chemicals, and exogenous chemicals). In particular, TRPA1 and TRPV1 have been extensively studied with respect to chemical sensitivity across taxa. While most of what is known about TRP channels is derived from work done on mammals (Holzer, 2011), a thorough and dynamic database is maintained on line that increasingly incorporates characterizations of other taxa (https://www.guidetopharmacology.org/index.jsp) (Startek et al., 2019; Walters and Williams, 2019).

TRPV1 (initially called VR1) was first cloned in mammals and found to respond to the exogenous vanilloid, capsaicin (Caterina et al., 1997), as well as endogenous agonists, anandamide, and 12-HPETE, which are structurally similar to capsaicin (Zygmunt et al., 1999; Hwang et al., 2000). TRPV1 is also activated by heat (>43°C) and acid (<pH 6). The sensation that TRPV1 activation evokes in humans via these polymodal nociceptors is one of tingling and burning, e.g., the sensation produced by capsaicin found in chili peppers (Jordt and Julius, 2002). Like its mammalian counterpart, the TRP receptor in birds (cTRPV1, chick dorsal root ganglion) responds to high temperature (>45°C) and extracellular acid solution (pH < 4). However, cTRPV1 is different, showing a 68% identity and 79% similarity to rat TRPV1.

Digital fluorescence imaging of intracellular calcium $[Ca^{2+}]_i$ in vitro preparations of chicken and rat trigeminal dorsal root ganglia show that there are separate and overlapping populations of neurons that are sensitive to the well-described avian irritant, methyl anthranilate, and capsaicin (Kirifides et al., 2004). In the chicken, 48% of

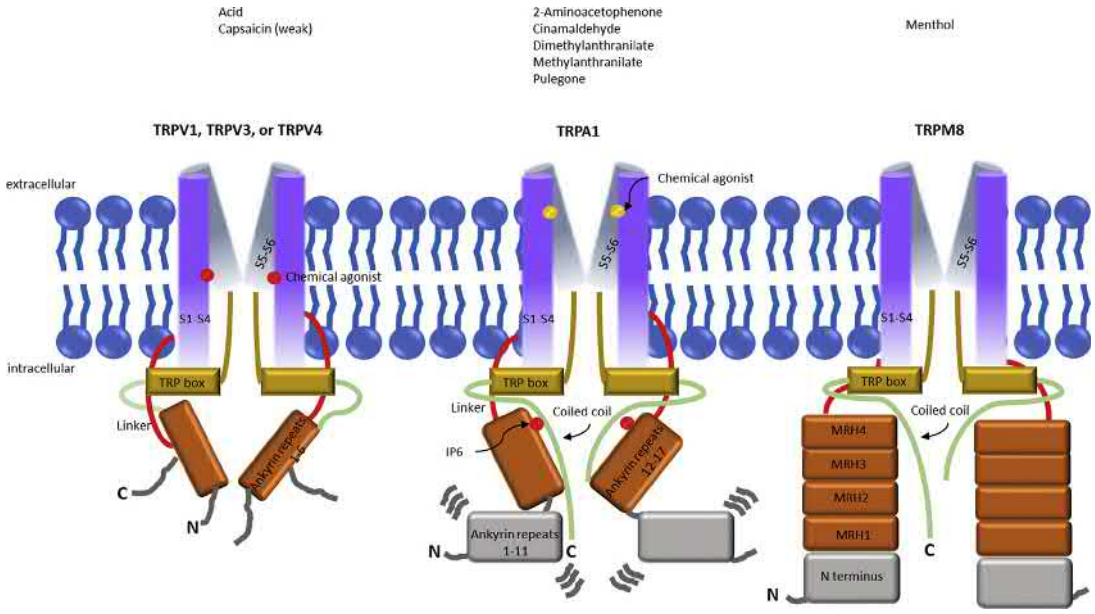

FIGURE 12.4 **Schematic diagrams of transient receptor potential (TRP) channels identified in avian chemesthesis.** Chemicals above the channels are known agonists for avian TRP channels. All follow the same color scheme from N- to C-terminus: N-terminal cytoplasmic domain, orange; linker, green; S1−S4, lilac; S5−S6, blue; TRP-box helix, gold; C-terminus, red; and flexible N- or C-terminal extensions, gray. TRPV1, TRPV3, and TRPV4 proteins contain six ankyrin repeats in their N-terminus. The C-terminus interacts with the ankyrin repeats, connecting the cytoplasmic regions. A chemical agonist (e.g., capsaicin or resiniferatoxin for TRPV1) binding site was identified at the interface of the S1−S4 and S5−S6 regions. TRPV4 contains a proline-rich region in its flexible N-terminal extension. TRPA1's unique structural features include a C-terminal coiled-coil region and 17 ankyrin repeats in the N-terminus; repeats 1−11 were not modeled in the cryoEM structure and are likely to connect to repeats 12−17 through a flexible link. An IP6 molecule bridges the N-terminal ankyrin repeats to the C-terminal coiled-coil. A chemical antagonist, A967079, binds within the S5−S6 pore region (*yellow circle*). Cysteines sensing reactive electrophiles are represented as black circles in the membrane-proximal N-terminal linker region that surrounds the TRP-box helix (red). No structure is yet available for TRPM8, but its transmembrane domain is homologous to that of TRPV1 and TRPA1. The N-terminal region contains "melastatin homology regions," and its C-terminus contains a predicted coiled coil (Moran and Sazalli, 2018).

neurons responded to methyl anthranilate, while only 16% responded to capsaicin. Moreover, there was a greater change in $[Ca^{2+}]_i$ to equimolar concentrations of methyl anthranilate (78%) relative to capsaicin (43%). Increases in $[Ca^{2+}]_i$ were dependent upon extracellular calcium for both methyl anthranilate and capsaicin. Like mammals, extracellular Na^+ can regulate TRPV1 activity in chickens presumably by inactivation of TRPV1 protein binding sites (Saito et al., 2014; Uzura et al., 2020). Birds certainly seem to be able to perceive capsaicin, however, they do not perceive it as painful. Mason and Clark (1995) showed that European starlings were indifferent to capsaicin but could be trained to responds to capsaicin in a behavioral conditioned avoidance paradigm. The response was mediated by the TN because the conditioned response did not occur with transection of the ophthalmic branch of the TN. Bilateral olfactory nerve cuts had no effect on shaping the response.

Substitution of glutamic acid (in the chicken) for analine (in the rat) at the 578 position of the S4−S5 helix was sufficient to induce sensitivity in cTRPV1. Substitutions of lysine, glutamine, or proline at residue A578 also resulted in capsaicin sensitivity in cTRPV1. The hydrophilic analog, Cap-EA, the cTRzPV1-A578E mutant suggesting that A578 may be involved in vanilloid binding. The hydrophilic zingerone did not activate A578 mutants, indicating the core vanilloid structure is not involved in binding (Chu et al., 2020). These results are consistent with the behavioral structure-activity behavioral studies of avian vanilloid responses (Mason et al., 1991; Shah et al., 1991).

Other common mammalian irritants that activate TRPV1 receptors have been examined. But birds remain largely unresponsive. cTRPV1 is not activated by allylisothiocynate (mustard oil) in chickens, This difference is due to the eight chicken-specific amino acid residues around transmembrane 3, which is the main site of capsaicin-binding in rat TRPV1 (Kawabata et al., 2017).

The transient receptor potential ankyrin 1 (TRPA1) is a phylogenetically ancient receptor ubiquitously found across taxa (Saito and Shingai, 2006). TRPA1 is a nonselective cation permeable receptor that responds to temperature as well as a variety of chemical stimuli in mammals (Gupta et al., 2016). TRPA1 responds to heat in frogs, reptiles, and birds, while it responds to noxious cold in mammals (Saito et al., 2012). In chickens, TRPA1 is highly co-expressed with TRPV1 (Saito et al., 2014). Similar to other taxa (Oda et al., 2017), avian TRPA1 is also responsive to a variety of exogenous chemicals. Chicken TRPA1 is responsive to the avian behavioral irritants, methyl

anthranilate, dimethyl anthranilate, 2-aminoacetophenone, cinnamaldehyde, and pulegone (Clark et al., 1991; Watkins et al., 1999; Banzawa et al., 2014; Saito et al., 2014; Majikina et al., 2018). cTRPA1 is not responsive to the bird irritant veratrylamine, which is structurally related to capsaicin (Shah et al., 1991; Saito et al., 2014). TRP channel activation was found to be more dependent on chemical reactivity relative to molecular shape (Hinman et al., 2006; Macpherson et al., 2007). However, the importance of gaining access to proximity of the TRP channels owing to influences of molecular flexibility and shape still remains to be more fully explored. As in other taxa, charged amino acid residues near the outer pore regulate intracellular Ca^{2+} concentration ($[Ca^{2+}]_i$) (Saito et al., 2014; Kurganov et al., 2017; Marsakova et al., 2017; Majikina et al., 2018). Agonistic and antagonistic actions are regulated by multiple amino acid residues in the TM domain and variations in these residues in part explain differential responsiveness among species (Banzawa et al., 2014).

Melastatin transient receptor potential (TRPM) receptors are involved in temperature sensing, chemosensation, ion homeostasis, and redox sensing across taxa (Clapham, 2003). For vertebrates, TRPM8 has been shown to be important for temperature and chemoreception that demonstrate diverse adaptation across species for fine-tuned sensation of environmental stimuli (Myers et al., 2009). Rat TRPM8 is activated by temperature <26°C and by menthol and eucalyptol (Behrendt et al., 2004). In chicken TRPM8, the activation is slightly higher (34°C), and the receptor was also responsive to menthol. In contrast, the cTRPM8 receptor was insensitive to the mammalian super stimulus, icilin. A series of chimera studies showed that the differences between rTRPM8 and cTRPM8 were attributable to small amino acid differences in the TM2 and TM3 regions (Chuang et al., 2004; Pertusa et al., 2014; Yin et al., 2019). The incilin insensitive cTRPM8 receptor is also insensitive to camphor whereas the rTRPM8 receptor is not (Selescu et al., 2013). It is noteworthy that cTRPm8 receptors are abundant in chickens and that cTRPM8 are sensitive to menthol (Yamamoto et al., 2016), yet birds seem to be behaviorally indifferent to this chemical as an irritating signal (Mason and Primus, 1996). Thus, the bird TRPM8 receptor may be a thermal and chemoreceptor, but it is unclear whether it is important as a nociceptor.

In summary, it appears that the TRPA1 receptor has been implicated in most of the avian responsiveness to exogenous chemical irritants in birds, though a better systematic coupling of the compound classes identified by structure-activity studies with molecular receptors studies seems warranted in order to more thoroughly evaluate the importance of other chemically activated nociceptive receptor channels in birds.

12.4 Olfaction

Birds have a well-developed functional sense of smell as evidenced by multiple research areas from the past 60 years. Fundamental platforms of neuroanatomical, morphological, neurophysiological, behavioral, and genomic studies have investigated a variety of avian species. Generally, the overall components of the avian olfactory system are like that of other vertebrates. As in other taxa, the avian olfactory literature exemplifies the variation in olfactory neural substrates (e.g., number of olfactory receptors/genes, olfactory bulb size/divisions, nasal cavity morphology, location of nares) as well as differences in olfactory behavioral capabilities of birds across and within avian families.

12.4.1 Olfactory morphology, neural architecture, and transduction of chemical signals

Air entering a bird's nasal cavity passes through a series of mucus-covered, invaginated chambers, called nasal conchae. Nasal conchae influence air flow dynamics and direct odors to the caudal-most chamber, which contains the chemically sensitive olfactory epithelium (Bang, 1960, 1961, 1963, 1964, 1965, 1966, 1971; Bang and Cobb, 1968; Cevik-Dermirkan et al., 2007; Farouk et al., 2017; Harem et al., 2018). As in other vertebrates, embedded in the olfactory epithelium are the goblet-shaped olfactory sensory neurons, which are surrounded by clusters of supporting cells and basal cells. Unlike amphibians, reptiles, and mammals, birds do not possess a vomeronasal organ or accessory olfactory system (Rieke and Wenzel, 1978). Odorant molecules that have dissolved into and diffused through the nasal mucus are detected by the olfactory receptors of the sensory neurons. Olfactory receptors are embedded in the 6–15 cilia that extend from the olfactory neuron's apical dendritic knob that projects to the mucus-nasal cavity interface. Length of olfactory cilia can vary by species, and perhaps by location in the epithelium. Black vultures, for example, have cilia of 40–50 μm, while domestic fowl have cilia of 7–10 μm (Shibuya and Tucker, 1967). A recent study in mice, however, found that cilia length is dependent on their location in the olfactory epithelium, with longer cilia located in regions with higher odor absorption (Challis et al., 2015). Whether this is also true in the avian olfactory epithelium remains to be seen. Mucous secretions covering cilia provide rapid flow for odor molecules. Mucous secretions from the olfactory glands (Bowman's) must be removed and replaced to maintain diffusion and avoid receptor habituation to odorant molecules. The traction of nearby respiratory cilia on epithelial cells facilitates movement of secretions.

In vertebrates, the binding of odorants to the olfactory receptors in the ciliary membrane is the first step of the olfactory transduction cascade. Olfactory receptors belong to the superfamily of guanine nucleotide-binding protein (G protein)-coupled receptors (seven-transmembrane receptors). Each olfactory sensory neuron expresses one type of G protein-coupled olfactory receptor. When an odorant binds to a G protein-coupled receptor, its activation alters the G protein conformation. This conformational change causes GDP to split from the subunit of the G protein, which then binds to GTP, with subsequent activation of adenylyl cyclase III and the formation of cyclic AMP. Increases in the second messenger cyclic AMP open cyclic nucleotide gated channels, allowing extracellular cations (calcium and sodium) to enter. Increases in intracellular cations generates local depolarization of the ciliary membrane (receptor potential), and opens calcium-activated chloride channels resulting in the flow of chloride anions to extracellular space causing further depolarization (Gomez and Celli, 2008; Antunes and de Souza, 2016). Sufficient membrane depolarization via several odorant/ligand binding events that reach the neuronal cell body will trigger action potentials in olfactory neurons' axons, and thus transmit odor signal directly to the brain via the olfactory nerves. Note that the formation of other second messengers (e.g., 1, 4, 5-triphosphate, IP3) by activation of different G proteins to increase intracellular calcium may additionally/alternatively be involved (Jung et al., 2005; Gomez and Celli, 2008). Thus, an extracellular chemical signal (odorant) is transduced to an intracellular electrical signal that travels to the next neuron located in the brain's olfactory bulb.

As noted above, axons of each olfactory receptor neuron directly innervate the olfactory bulb, located in the anterior region of the brain. The olfactory bulb is composed of concentric cell layers, with incoming olfactory nerve fibers constituting the outermost layer in birds. The endings of axons from olfactory receptor neurons that express the same type of olfactory receptor converge to form spherical structures called glomeruli in the outer layer of the olfactory bulb. Thus, each glomerulus may represent a subset of primary sensory neurons of a given receptor type. A given odorant may activate several different olfactory receptor types causing a unique pattern of activation across glomeruli specific to that odorant. Through using a combination of calcium imaging and single-cell RT−PCR to identify odorant receptors for odorants with related structures, Malnic et al. (1999) observed that one odorant receptor can recognize multiple odorants, and that one odorant is recognized by multiple olfactory receptors. Mitral and tufted cell bodies are located in the olfactory bulbs' deeper layers, but extend their dendrites into the glomerular layer, where they receive synaptic input from the primary olfactory neurons. In general, the cytoarchitecture of the avian olfactory bulb is similar to that of other vertebrates, with the exception that some layers may be less distinctive than in the mammals (Allison, 1953; Andres, 1970; Lee et al., 2019, Figure 12.5). Avian olfactory bulbs can appear a) fused, as in songbirds, b) sheetlike, covering the anterior portion of the telencephalon, as in the Kiwi, or c) appear as two separate lobes, continuous or separate from the telencephalon (Corfield et al., 2014, 2015, Figure 12.6). Corfield and colleagues additionally found that the organization of olfactory bulb layers are typically conserved across avian species they examined (Figure 12.6B). However, it was also observed that there were notable differences across species in the relative thickness and cell density of some layers. It appears that olfactory bulb size may relate to the relative thickness of layers, whether the layers are clearly defined, and whether the cells (e.g., mitral) are closely packed together.

Mitral cells are the main projections from the olfactory bulb to piriform cortex and other processing brain regions that integrate sensory information (Rieke and Wenzel, 1978; Reiner and Karten, 1985; Patzke et al., 2011; Atoji and Wild, 2014). The olfactory bulb is the first relay station in the brain for processing olfactory information. As such, there has recently been an increase in understanding the neuronal diversity and interconnections within the bulb itself (Nagayama et al., 2014). In the pigeon, bilateral projections from the olfactory bulb are to the prepiriform cortex, the piriform cortex, the dorsolateral corticoid area, and nucleus taeniae of the amygdala, while ipsilateral projections are to the medial septum (Patzke et al., 2011; Atoji and Wild, 2014).

12.4.2 Olfactory bulb size, olfactory acuity, and genomics of olfactory receptors

The extent of scrolling of caudal conchae correlates with the surface area of olfactory epithelium and the relative size of the olfactory bulb (Bang and Cobb, 1968; Bang, 1971; Bang and Wenzel, 1986; Roper, 1999; Hagelin, 2007a). Avian orders with relatively larger olfactory bulbs have lower detection thresholds, indicating they may be more sensitive to certain odorous compounds than those with relatively small olfactory bulbs (Clark et al., 1993, Table 12.1, Figure 12.7). However, this does not indicate that birds with small olfactory bulbs, such as passerines, have little olfactory capabilities. Passerines, for example, have detection values comparable to macrosmatic mammals such as rats and rabbits (Davis, 1973). While a larger olfactory bulb size or greater scrolling of receptor epithelium likely indicates greater functional capacity (e.g., more cells and neural circuits; Meisami, 1991), it is important not to dismiss avian species with relatively "unelaborate" olfactory systems (Hagelin, 2007b). Both field and laboratory tests indicate several taxa with relatively small olfactory

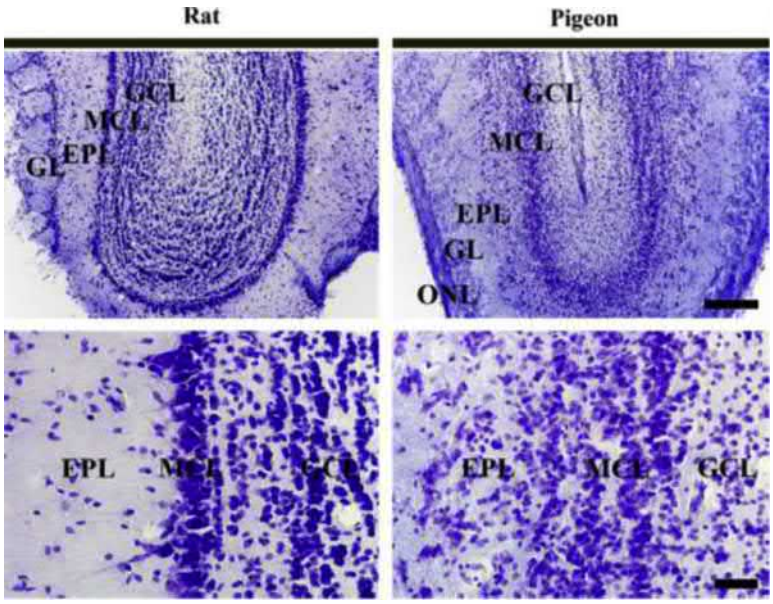

FIGURE 12.5 CV staining of the rat (A and a) and pigeon (B and b) OB. Layers in the pigeon olfactory bulb (OB) are not clear like those in the rat OB: although each layer can be identified. *EPL*, external plexiform layer; *GCL*, granule cell layer; *GL*, glomerular layer; *IPL*, internal plexiform layer; *MCL*, mitral cell layer; *ONL*, olfactory nerve layer. Scale bar = 200 μm (A and B) and 40 μm (a and b) (Lee et al., 2019).

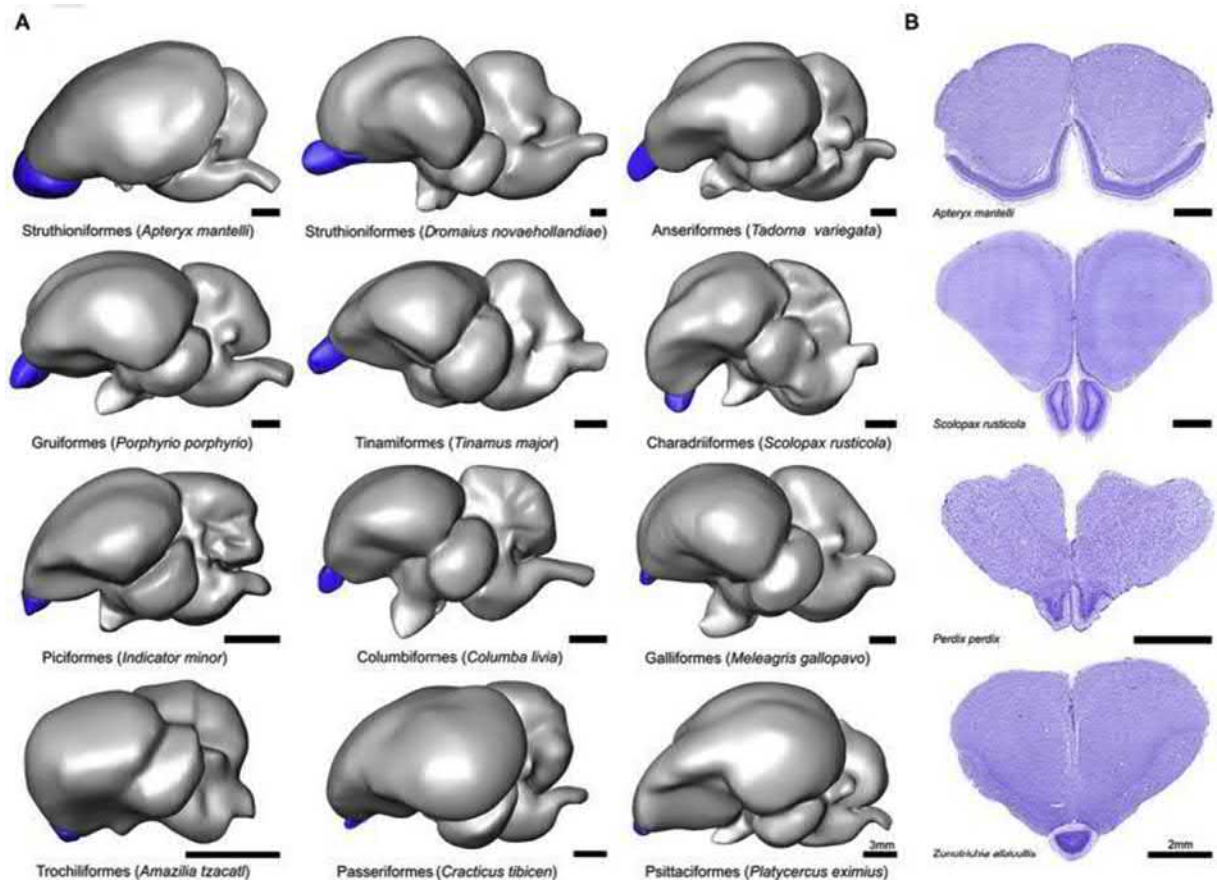

FIGURE 12.6 Gross morphology of the olfactory bulbs (OBs) in birds. (A) Lateral view of three-dimensional models of 12 representative avian species. Blue denotes the OBs and models are organized from largest to smallest. Scale bar = 3 mm. (B) Coronal Nissl stained sections showing the OBs in four representative avian species and illustrating the cytoarchitectural and cross species variation. Scale bar = 2 mm (Corfield et al., 2015).

TABLE 12.1 Summary of mean ratios of ipsilateral olfactory bulb diameter to cerebral hemisphere diameter and their standard errors for several orders of birds.

Order	*N*	Ratio	SE	Order	*N*	Ratio	SE
Anseriformes	4	19.4	1.5	Psittaciformes	2	8.0	1.4
Apodiformes	8	12.3	1.9	Falconiformes	5	17.4	2.6
Apterygiformes	1	34.0	0.0	Charadriiformes	9	16.4	0.9
Caprimlgiformes	3	23.3	0.7	Galliformes	3	14.2	1.4
Columbiformes	2	20.0	1.4	Piciformes	5	11.4	1.3
Cuculiformes	4	19.5	0.6	Passeriformes	25	13.3	0.7
Gruiformes	14	22.2	0.9	Pelecaniformes	4	12.1	1.6
Gaviiformes	1	20.0	0.0	Coraciiformes	5	14.5	1.6
Podicipediformes	2	24.5	1.8	Sphenisciformes	1	17.0	0.0
Procellariiformes	10	29.1	1.4				

Sample sizes indicate the number of species (*N*).
Data adapted from Bang and Cobb (1968).

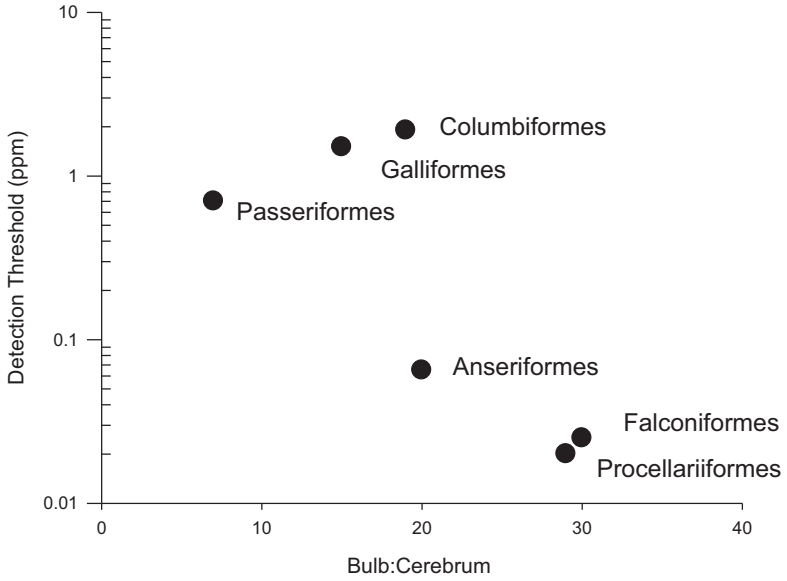

FIGURE 12.7 Relationship between olfactory detection threshold and relative size of the olfactory bulb for different orders of birds. *Adapted from Clark and Shah (1992).*

bulbs can discriminate between and/or adaptively employ certain odors, such as those related to breeding and nesting, or individual/conspecific recognition (e.g., crested auklets [*Aethia cristatella*] Hagelin et al., 2003; European starlings Clark and Mason, 1985, 1987, 1988; Gwinner and Berger, 2005, 2008; Corsican Blue Tit [*Parus caeruleus ogliastrae*] Petit et al., 2002; Zebra finch Caspers et al., 2017; Krause et al., 2018).

Olfactory bulbs vary in relative size across vertebrates, and the relative size is independent of the size of the rest of the brain in fish and mammals. In birds, the relative size of olfactory bulbs is typically described as size of bulb relative to size of brain, cerebral hemispheres, or specific brain regions (Bang and Cobb, 1968; Healy and Guilford, 1990; Zelenitsky et al., 2009; 2011; Corfield et al., 2015; Supplementary Material in Avilés and Amo, 2018). With the aforementioned caveats in mind, the olfactory bulb ratio has been used as a proxy for olfactory capabilities because it estimates the amount of forebrain or brain devoted to olfactory perception. Elaborated olfactory

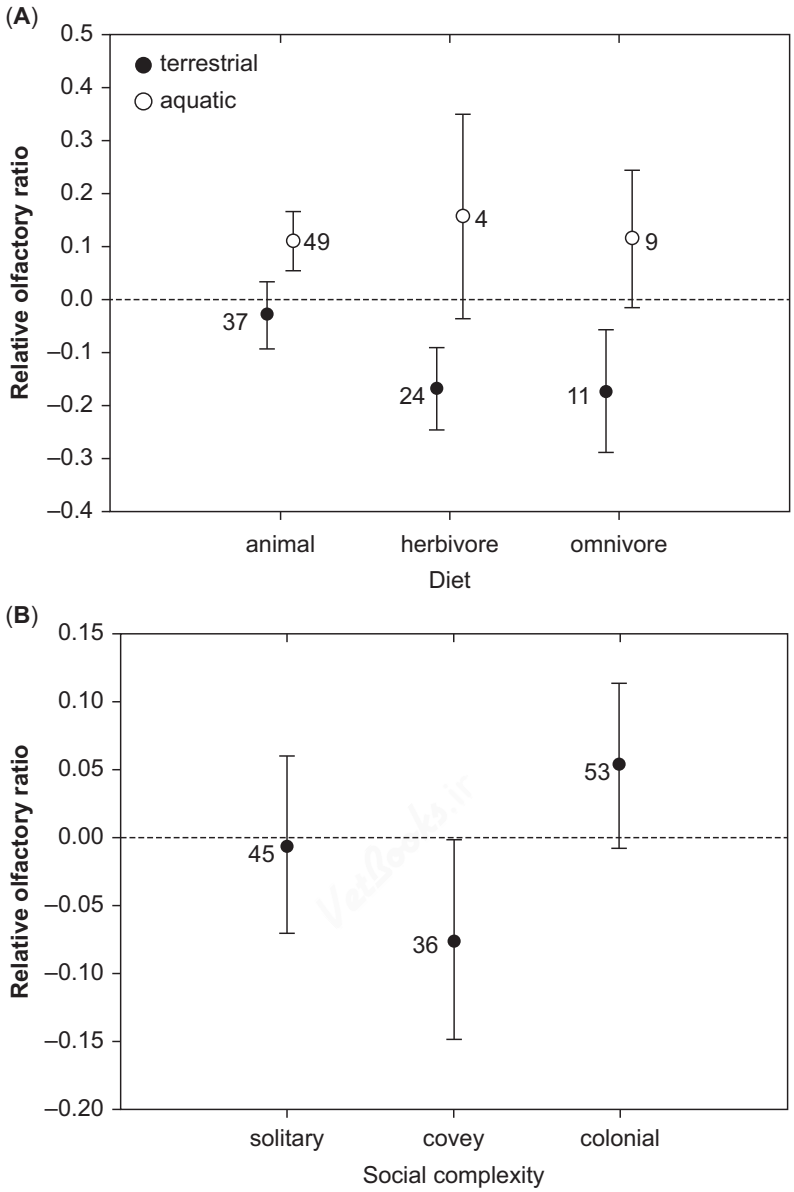

FIGURE 12.8 **Avian olfactory ratio (mean + SE) of aquatic and terrestrial species in relation to (A) diet and (B) social complexity (Aviles and Amos, 2018).**

systems typically belong to species with demonstrated reliance on odor cues in the field (Stager, 1964; Hutchison and Wenzel, 1980; Hagelin, 2004; Cunningham et al., 2009; Corfield et al., 2014; Grigg et al., 2017; Silva et al., 2020), and in some species, correlate positively with the absolute number of olfactory receptor genes (Steiger et al., 2008). Fossil evidence also indicates olfactory bulb size was relatively large early in bird evolution, revealing a previously unrecognized emphasis on smell (Zelenitsky et al., 2011). Evolutionary mechanisms that contribute to the diversity of bulb size remains a discipline of active research. Recent studies focus on the correlations between behavior, relative bulb size, phylogeny, habitat, and ecology (Corfield et al., 2015; Avilés and Amo, 2018). Corfield found that habitat (living and foraging in semi-aquatic environments) was strongly related to driving larger olfactory bulbs, while Avilés and Amo (2018) suggest that an interactive effect of aquatic habitat and diet is the driving force in the evolution of the olfactory apparatus (Figure 12.8). These scenarios may not be mutually exclusive, and the studies may differ in the sample size of species used in described environments and phylogeny used in analysis. Foraging behavior is contingent on ecological conditions, and therefore the interaction between ecological and behavioral characters that may be driving the olfactory bulb size.

Another metric that is reasonably correlated to olfactory bulb ratio and thus olfactory sensitivity is the number of potentially functional olfactory receptors. The number of olfactory receptor neurons (on one side of the nasal cavity) varies widely across avian species: from approximately 5,800,0000 in ducks, 2,700,000 gulls, 570,000 in quails, and 130,0000 in budgerigar, to 110,000 in the bengalee (Matsuzaki, 1995). In comparison, the approximate number in the rodent nose is five million olfactory receptor neurons (De Castro, 2009). The number of genes coding the olfactory receptors in the rat and mouse is estimated to be 1000−1300 (with 20% pseudogenes), ∼100−150 in fish, and approximately 100−650 in birds, depending on the species (Buck and Axel 1991; Ngai et al., 1993; Zhang and Firestein, 2002; Steiger et al., 2008, 2009a,b). For example, in the chicken, 479 gene homologs (with 111 pseudogenes) were identified and in the zebra finch there are 553 gene homologs (with 221 pseudogenes) (Steiger et al., 2009b). However, the range of olfactory receptors in similar diurnal species is only 55−109 (Steiger et al., 2009a). Nocturnal species known to rely on their sense of olfaction in foraging, such as the brown kiwi (*Apteryx australis*), and kakapo (*Strigops habroptilus*), respectively, have 478 and 312 genes identified (Steiger et al., 2009a). The greater the repertoire of olfactory receptors that a species possesses, the more glomeruli that are formed, which results in a larger olfactory bulb ratio, and subsequent olfactory sensibility. Identifying the repertoire of olfactory receptor genes across species may provide evidence of adaptive evolution for specialized olfactory functions. By comparing the functional olfactory receptor subgenome repertoire across a number of phylogenetically and ecological diverse birds, studies can identify which olfactory gene families are important for given ecological niche or behavior.

The olfactory receptor proteins in the primary sensory neurons are encoded by single-exon (intron-less) olfactory receptor genes that are divided into two major types: Type I includes Class I (α, β, δ, ε, and ζ groups) and Class II (γ group) genes, and Type II includes (η) (Figure 12.9). Within these classes, olfactory receptor genes are further grouped into families based on genetic similarity. Class I families code for receptor proteins that are thought to principally bind to water-borne molecules, and Class II families bind to air-borne molecules (Glusman et al., 2000; Hayden et al., 2010).

Molecular mechanisms shaping the patterns of avian diversification of olfactory abilities have been recently been revisited (Khan et al., 2015; Silva et al., 2020). There are 11 olfactory receptor gene families in birds and reptiles (1/3/7, 2/13, 4, 5/8/9, 6, 10, 11, 12, 14, 51, and 52) (Khan et al., 2015). The olfactory receptor gene family 14 was most abundant in birds (Steiger et al., 2009a,b). Overall, complete characterization of avian olfactory receptor genes into functional and nonfunctional genes point to patterns of gene gains and losses that had a crucial role in determining the olfactory receptor gene repertoires in individual species, and thus shape patterns of diversification of olfactory abilities (Supplementary Material online in Khan et al., 2015). For example, as stated above, chick and zebra finch, along with the budgerigar, have larger olfactory receptor repertoires which may reflect species-specific recent rapid expansion and positive selection of OR14 family. Phylogenetic analysis in Cory's Shearwater showed that a majority (85%) of the olfactory receptor genes identified belong to the avian-specific γ-c clade, pointing to gene duplication/conversion events (Silva et al., 2020). The application of olfactory receptor genomics has expanded our understanding of the potential interactive measures of ecology, habitat, and behavioral traits in relation to olfactory sense in birds and its adaption to different ecosystems.

12.4.3 Laboratory detection thresholds, discrimination, and seasonal change

It is no surprise that avian responsiveness to odors has been demonstrated using a variety of methods, stimuli, and species (Tables 12.2 12.3). Birds certainly have the anatomical organization that is suggestive of olfactory

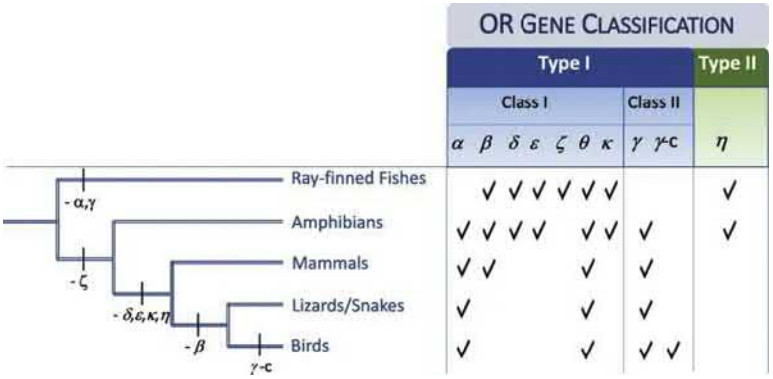

FIGURE 12.9 **Classification and schematic distribution of olfactory receptor genes in major vertebrate lineages (Silva et al., 2020).**

TABLE 12.2 Summary of behavioral olfactory threshold data for different species of birds.

Species	Method	Stimulus	Response range (ppm)	Source
Domestic pigeon, *Columbia livia*	CC, OC	Amyl acetate	0.31–29.80	5,6,11,12,13,14
	CC	Benzaldehyde	0.47–0.75	14
	USR	Butanethiole	13,820	9
	CC	Butanoic acid	2.59	5
	CC	Butanol	0.17	14
	CC	n-butyl acetate	0.11–2.59	5,14
	CC	Ethanethiol	10,080	9
	OC	Heptane	0.29–0.38	10
	OC	Hexane	1,53–2.98	10
	USR	Menthol	0.10	9
	OC	Pentane	16.45–20.76	10
Chicken, *Gallus domesticus*	OC	Heptane	0.31–0.57	10
	OC	Hexane	0.64–1.00	10
	OC	Pentane	1,58–2.22	10
Northern bobwhite quail, *Colinus virginianus*	OC	Heptane	2.14–3.49	10
	OC	Hexane	3.15–4.02	10
	OC	Pentane	7.18–10.92	10
Magpie, *Pica pica*	USR	Butanethiol	13,416	9
	USR	Ethanethiol	8400	9
	USR	Menthol	0.25	9
Turkey vulture, *Cathartes aura*	USR	Butanoic acid	0.01	8
	USR	Ethanethiol	0.06	8
	USR	Trimethylamine	0.59	7
Black-tailed gull, *Larus crossirostris*	EP	Amyl acetate	0.82	7
European starling, *Sturnus vulgaris*	CC	Cyclohexanone	2.50	3
Cedar waxwing, *Bombycilla cedrorum*	CC	Cyclohexanone	6.80	1
Tree swallow, *Tachycineta bicolor*	CC	Cyclohexanone	73.42	1
Brown-headed cowbird, *Molothrus ater*	CC	Ethyl butyrate	0.76	2
Catbird, *Dumatella carolinensis*	CC	Cyclohexanone	35.14	4
Eastern phoebe, *Sayornis phoebe*	CC	Cyclohexanone	35.61	4
Goldfinch, *Carduelis carduelis*	CC	Cyclohexanone	13.05	4
Great tit, *Parus major*	CC	Cyclohexanone	34.10	4
Black-capped chickadee, *Parus atricapillus*	CC	Cyclohexanone	59.95	4

CC, cardiac conditioning; *E*, electrophysiology; *OC*, operant conditioning; *USR*, unconditional somatic response. [1]Clark, 1991a; [2]Clark and Mason, 1989; [3]Clark and Smeraski, 1990; [4]Clark et al., 1993; [6]Henton, 1969; [7]Henton et al., 1966; [8]Shibuya and Tucker, 1967; [9]Smith and Paselk, 1986; [10]Snyder and Peterson, 1979; [11]Stattleman et al., 1975; [12]Walker, 1983, [13]Walker et al., 1979; [14]Walker et al., 1986

ability (above). Evidence from studies from single neurons, olfactory nerve fibers, and electroencephalograms all indicate odor signals are transmitted to the brain (Tucker, 1965; Sieck and Wenzel, 1966; Shibuya and Tucker, 1967, Shibuya and Tonosaki, 1972; Wenzel and Sieck, 1972; Shallenberger, 1975; Hutchison and Wenzel, 1980; Macadar et al., 1980; McKeegan, 2002, 2009). This odor stimulation, whether pure reagents, or volatile mixtures that

TABLE 12.3 Some avian orders considered to be very odorous by ornithologists.[1]

Order	Common Name	Number of Species
Procellariiformes	Petrels, shearwaters, diving petrels	16
Ciconiiformes	Herons, storks, new world vultures	12
Anseriformes	Ducks, geese, swans, screamers	49
Charadriiformes	Sandpipers, gulls, auks	23
Psittaciformes	Parrots	14
Cuculiformes	Cuckoos	16
Coraciiformes	Kingfishers, rollers, hoopoes, woodhoopoes	14
Piciformes	Woodpeckers, barbets, tucans	33
Passeriformes	Grackles, starlings, ravens, finches, honeycreepers	46

[1]*Data compiled from Weldon and Rappole (1997).*

may be ecologically relevant, generates spontaneous physiological reactions such as changes in respiration and heart rate and have been observed in: wedged-tailed shearwaters, *Puffinus pacificus;* Manx shearwater, *Puffinus puffinus*; black-footed albatross, *Diomedea nigripes*; mallard, *Anas platyrhynchos*; turkey vulture, *Cathartes aura*; bobwhite quail, *Colinus virginianus*; chickens; pigeons, *Columbia livia*; and kiwi, *Apteryx australis* (Neuhaus, 1963; Snyder and Peterson, 1979; Smith and Paselk, 1986; Wenzel, 1967, 1971; Wenzel and Sieck, 1972). The yellow-headed Amazon parrot, *Amazona ochrocephala*; raven, *Corvus corax*; and canary, *Serinus canaria* did not exhibit spontaneous responses. Habituation to the stimulus under this paradigm, however, is problematic.

Less invasive studies that allow birds to freely feed, drink, or choose a location based on olfactory training can be useful. Operant conditioning (Michelsen, 1959, ; Henton et al., 1966; Henton, 1969) and poison avoidance learning (Clark and Mason, 1987) have proved to be more reliable assays for response relative to spontaneous response metrics (Passe, 1985). Hummingbirds can be trained to make discriminative fluid selections based on associated odors (Goldsmith and Goldsmith, 1982; Ioale and Papi, 1989). Similarly, domestic chicks can discriminate between palatable and unpalatable food based on associated odor cues (Marples and Roper, 1997; Roper and Marples, 1997). Care must be given when testing volatile compounds, however. Learned and nonlearned responses to methyl anthranilate are modulated by olfaction, but the principal response is mediated through avoidance of the irritating properties (Mason et al., 1989; Clark 1996; Burne and Rogers, 1999; Marples and Roper 1997).

Two process learning paradigms, such as cardiac conditioning, have proven to be a reliably successful technique for detection, discrimination, and threshold testing (Rescorla and Solomon, 1967; Walker et al., 1986; Clark and Mason, 1989; Clark and Smeraski, 1990; Clark, 1991a; Clark et al., 1993). For cardiac conditioning, an odor (the conditional stimulus) is paired with an aversive experience, for example, a shock (the unconditional stimulus). Heart rate is compared pre- and poststimulus presentation during training, until a level of cardiac acceleration is reliably achieved, indicating a bird has learned to associate the odor in anticipation of a shock. Thereafter, tests on detection or odor discrimination can proceed. Most birds tested with this paradigm have shown olfactory capabilities comparable to mammals (Davis, 1973). Even passerines, with the least developed olfactory system, demonstrate behavioral responsiveness to odors (Clark, 1991a; Clark et al., 1993).

European starlings offer an interesting case study of olfactory structure, function, and seasonality. Male starlings incorporate green plants rich in aromatic volatiles into nests, some of which act as a fumigant against parasites and pathogens (e.g., Clark and Mason, 1985, 1987, 1988; Clark, 1991b; Gwinner, 1997; Gwinner et al., 2000; Gwinner and Berger, 2005). Using conditioned avoidance learning, Clark and Mason (1987) showed that European starlings could discriminate between volatiles derived from plants and that after bilateral olfactory nerve cuts; they could no longer make odor-based discriminations. Starlings are most sensitive to, and can discriminate between, plant odors during spring only, rather than in summer and fall. Spring is coincident with nest building and suggests a hormonal influence (Clark and Smeraski, 1990). Birds treated with testosterone (T), a hormone that enlarges song-learning nuclei of the brain and alters behavior, exhibited enlarged olfactory bulbs year-round, indicating a proximate effect on bulb structure. However, perception of plant odor in T-implanted males was greatest during spring only,

indicating that perception was independent of T-treatment and olfactory bulb volume. One hypothesized but untested mechanism is that an increase in receptor cell density in starling olfactory epithelium occurs in spring (DeGroof et al., 2010).

12.4.4 Odor detection during development

Volatile compounds diffuse through avian eggshell (Rahn et al., 1979), providing an opportunity for odor exposure within the egg (Tolhurst and Vince, 1976; Sneddon et al., 1998). Many vertebrates, including birds, detect and learn chemical information as embryos (e.g., humans: Schaal et al., 2000; Mennella et al., 2001; other mammals: Hepper, 1988; Bilko et al., 1994; amphibians: Mathis et al., 2008; birds: Porter and Picard, 1998; Bertin et al., 2012). Zebra finch chicks transferred to another nest while still in the egg retain the chemosensory sense of their mother (Caspers et al., 2017) and provides further evidence that odors can transmit into the eggs and that sensory cues can be learned during the embryonic period (Caspers et al., 2015; Hagelin et al., 2013). Early exposure to chemical signals can cause changes in neuroanatomy, which alters chemosensory perception in a way that may adaptively shape responses later in life (e.g., to food, mates; Todrank et al., 2011).

Studies of domestic chickens, the avian model for development, indicate that odor detection can occur before or after young pierce the egg's air sac and begin breathing air (e.g., Tolhurst and Vince, 1976; Bertin et al., 2012; Hagelin et al., 2013). Olfactory receptor neurons are functional six days prior to air-breathing (on embryonic developmental day 13; Lalloué et al., 2003), when nasal passages are full of amniotic fluid. Embryos at this stage swallow frequently, facilitating fluid movement, which is similar to mammals in utero (Sneddon et al., 1998). Air-breathing begins two days prior to hatching during embryonic developmental day 19 (Tolhurst and Vince, 1976).

The magnitude of embryonic response varies relative to stimulus concentration and timing of exposure (Bertin et al., 2010). Later developmental stages show relatively greater responses to odors (Gomez and Celli, 2008; Bertin et al., 2012). Detectable stimuli include artificial odors (Sneddon et al., 1998), as well as naturally occurring scents, such nest materials (Gwinner and Berger, 2008), food-related odors (Burne and Rogers, 1999; Cunningham and Nevitt, 2011), and compounds found in plumage scent of at least one alcid species (Hagelin et al., 2013).

12.4.5 How do birds use olfactory cues?

While not physiological per se, it is important to summarize the different types of behaviors and ecological context for use of olfactory cues by birds. Appreciation of the diversity of behaviors and their context will help guide mechanistic studies on how odor information is received, processed, and acted upon. Olfaction has been shown to play an important role in foraging, food identification, navigation/homing, mate selection and advertisement, individual and species recognition, predatory avoidance, territorial scent marking, and social communication. Hagelin (2007a) made a distinction between environmentally derived odors (e.g., food, predators) and those produced by birds themselves (e.g., body odors, fecal odor, preen gland secretions). The latter can have social and reproductive implications. Below we provide some examples of the role of environmental chemical signals and odors derived from avian chemical substances, but how the chemical signals/cues are translated into adaptive behavior at the physiological level remains elusive. We provide this sampling of avian behaviors to inspire further studies in the physiology of behavior guided by olfactory cues.

The use of olfactory cues for locating food has been documented for numerous species, such as procellariids, vultures, corvids, hummingbirds, honeyguides, parrots, and kiwis (reviewed in Roper, 1999). Turkey vultures (*Cathartes aura*), for example, are attracted to ethyl-mercaptan, a volatile associated with decomposed carcasses (Stager, 1964, 1967), and can locate food without visual cues (Houston, 1987; Potier et al., 2019). Procellariforms also forage over considerable distances. Black-footed albatrosses *(Diomedea nigripes*) respond to bacon grease over 31 km away (20 miles; Miller, 1942), whereas Leach's storm petrel (*Oceanodroma leucorhoa*) theoretically home to scent targets at a distance of 1−12 km (Clark and Shah, 1992).

With regard to predators, scent of urine and/or feces has an aversive effect on some avian species (blue tits [*Cyanistes caeruleus*], Amo et al., 2008; house finches [*Carpodacus mexicanus*], Roth et al., 2008; red junglefowl [*Gallus gallus*], Zidar and Løvlie, 2012; house sparrows [*Passer domesticus*], Griggio et al., 2016), but not all (eastern blue birds [*Sialia sialis*], Godard et al., 2007; house wren [*Troglodytes aedon*], Johnson et al., 2011). Application of predator odor can deter breeding ducks and songbirds (Eicholz et al., 2012; Forsman et al., 2013) as well as evoke avoidance behavior in red-legged partridges (Mahr and Hoi, 2018). Responses appear to be innate, rather than learned (Amo et al., 2011b), though sleeping birds are unreactive (Amo et al., 2011a).

Odors are also germane to avian orientation and navigation (reviewed in Wallraff, 2005; Gagliardo, 2013). Homing pigeons, for example, exhibit larger olfactory bulbs than nonhoming breeds (Rehkämper et al., 1988, 2008). Investigators have also altered pigeon homing

behavior via experimental disruption of the olfactory system. Manipulations include olfactory nerve transection (Papi et al., 1971; Gagliardo et al., 2006, 2009), anesthesia of olfactory mucosa (Wallraff, 1988), ablating the central piriform cortex of the brain (Papi and Casini, 1990), and nostril plugging. The last of these manipulations indicates pigeons rely more on their right nostril for olfactory information (Gagliardo et al., 2007, 2011). ZENK, an immediate early gene expressed in olfactory neurons, also implicates the use of olfaction during the process of homing (Patzke et al., 2010) and may exhibit seasonal differences in migratory and nonmigratory songbirds (Rastogi et al., 2016). Emerging evidence for passerines species also supports olfaction during migration. For example, adult gray catbirds (*Dumetella carolinensis*) rendered temporarily anosmic (by washing the olfactory tissues with zinc-sulfate) oriented differently from adult controls, but similarly to juvenile birds, which were migrating for the first time and therefore unable to navigate (Holland et al., 2009). With regard to cellular mechanisms, black-headed buntings (*Emberiza melanocephala*) increase activation of olfactory tissues (as measured by c-fos immunoreactivity) during migration. These birds exhibit a seasonally enhanced emphasis on olfaction while migrating, compared to visual systems (Rastogi et al., 2011, 2016).

Many birds produce a variety of odorous compounds (reviewed in Campagna et al., 2012). For example, a seabird colony, with its dense numbers of birds, burrows, and feces, makes for a potent chemosensory experience. Pioneering work by Grubb (1974) on Leach's storm petrel showed differential return rates to nest sites after surgical manipulation, indicative of olfactory-based homing: controls = 91%, sham surgery: 74%, olfactory nerve section: 0%. Several petrel species have since been shown to discriminate between the odor of their own nest and conspecific burrows (Mínguez, 1997; De Léon et al., 2003; Bonadonna et al., 2003a,b). Attraction to home nest odor is also reported for passerines (Caspers and Krause, 2010; Krause and Caspers, 2012). More recently, there is a focus on the role of microbiota on the chemical cues used in olfactory evoked social communication (Maraci et al., 2018).

Avian chemical substances are linked with a variety of social contexts (reviewed in Hagelin, 2007a; Hagelin and Jones, 2007; Balthazart and Taziaux, 2009; Caro and Balthazart, 2010). Uropygial gland secretions, for example, show some level of hormonal control, and exhibit individual, sex, and age-specific patterns (e.g., Procellariiformes: Mardon et al., 2010, 2011; Anseriformes: Kolattukudy et al., 1987; Galliformes: Karlsson et al., 2010; passerines: Whittaker et al., 2010; Whelan et al., 2010; Shaw et al., 2011; Amo et al., 2012a). Pioneering work by Balthazart and Schoffeniels (1979) indicated male mallards decreased social displays and sexual behavior toward females when their olfactory nerves were sectioned, suggesting that an intact olfactory system is critical to courtship and mating. Crested auklets produce a seasonally elevated scent associated with a stereotyped behavior that focuses on the scented region of the body (the nape). Auklets are attracted to natural feather odor, a chemical cocktail of odor compounds, and to scented decoys, which suggests odor has a social function (Hagelin et al., 2003; Jones et al., 2004; Hagelin, 2007a). Mounting evidence suggests that preen gland secretions likely play a leading role in intraspecific communication (Campagna et al., 2012; Caro and Balthazart, 2010; Caro et al., 2015; Hagelin and Jones, 2007; Moreno-Rueda, 2017) even in song sparrows, a relatively nonsocial bird (Grieves et al., 2019).

Procellariiform seabirds show a surprising level of body odor discrimination of conspecifics, in that they are attracted to mate odors and avoid self-odor (Antarctic petrel [*Pachyptila desolata*] Bonadonna and Nevitt, 2004; blue petrels [*Halobaena caerulea*], Mardon and Bonadonna, 2009). Furthermore, preference for the odor of unrelated individuals over those of kin suggests body odors could provide a mechanism for inbreeding avoidance, known as self-referent phenotype matching (Mateo and Johnston, 2000; European storm petrel [*Hydrobates pelagicus*], Bonadonna and Sanz-Aguilar, 2012). This may be particularly important in petrels, as they are long-lived, philopatric species that mate for life. Petrels are also likely to encounter kin on their natal breeding grounds that they have never met before (Bonadonna and Nevitt, 2004; Bonadonna and Sanz-Aguilar, 2012). Responses of passerines to conspecific odor also appear to provide complex information, in that they correlate with social rank (house finch, Amo et al., 2012b), sex (European starling, Amo et al., 2012a), and body size (dark-eyed junco [*Junco hyemalis*], Whittaker et al., 2011).

12.5 Summary

The chemical senses across taxa have always seemed to be a side branch of sensory science. This is understandable in that auditory and visual cues have relatively more easily quantifiable signals that are largely received by well-defined sensory systems. Even taste (for birds) is a bit more straightforward in that sensory cues are brought to the mouth and involve more or less straightforward processes of interacting with receptors. In contrast, volatile cues, at lower concentrations for olfaction and higher concentrations for chemesthesis, emanate from a chaotic environment often making it difficult to precisely know what is in the signal and at what concentration, let alone the potential myriads of signals that are present and need processing. For the most part, scientists in this field "black box" the signal into broad categories, or deal with simplifying mixtures

down to one or two sensory cues. This is a difficult enough science for the well described human food and flavor industries, let alone the under studied field of avian chemical senses. Nonetheless, great strides have been made over time in our understanding how birds use chemical cues and what mechanisms they use to process these cues. In part this progress is owing to advances in technological capabilities. Beyond that, however, the current trends for multidisciplinary approaches to address scientific questions have allowed us to ask more interesting and complex questions. Together, we have a profoundly new appreciation of the role chemical signals play in the ecology and evolution of birds.

References

Allison, A.C., 1953. Morphology of olfaction in vertebrates. Biol. Rev. 28, 195–244.

Amo, L., Caro, S.P., Visser, M.E., 2011a. Sleeping birds do not respond to predator odour. PLoS One 6, e27576.

Amo, L., Visser, M.E., van Oers, K., 2011b. Smelling out predators is innate in birds. Ardea 99, 177–184.

Amo, L., Galvan, I., Tomas, G., Sanz, J.J., 2008. Predator odour recognition and avoidance in a songbird. Funct. Ecol. 22, 289–293.

Amo, L., Avielé, J.M., Jarejo, D., Aránzazu, P., Rodríguez, J., Gustavo, T., 2012a. Sex recognition by odour and variation in the uropygial gland secretion in starlings. J. Anim. Ecol. 81, 605–613.

Amo, L., López-Rull, I., Pagán, I., Garcia, C.M., 2012b. Male quality and conspecific scent preferences in the house finch, *Carpodacus mexicanus*. Anim. Behav. 84, 1483–1489.

Andres, K.H., 1970. Anatomy and ultrastructure of the olfactory bulb in fish, amphibians, reptiles, birds and mammals. In: Wolstenhome, G.E.W., Knight, J. (Eds.), Taste and Smell in Vertebrates. JandA Churchill, London, pp. 177–193.

Antunes, G., de Souza, F.M.S., 2016. Olfactory receptor signaling. In: Methods in Cell Biology, vol. 132. Academic Press, pp. 127–145.

Atoji, Y., Wild, J.M., 2014. Efferent and afferent connections of the olfactory bulb and prepiriform cortex in the pigeon (*Columba livia*). J. Comp. Neurol. 522, 1728–1752.

Avilés, J.M., Amo, L., 2018. The evolution of olfactory capabilities in wild birds: a comparative study. Evol. Biol. 45, 27–36.

Balthazart, J., Schoffeniels, E., 1979. Pheromones are involved in the control of sexual behaviour in birds. Naturwissenschaften 66, 55–56.

Balthazart, J., Taziaux, M., 2009. The underestimated role of olfaction in avian reproduction. Behav. Brain Res. 200, 248–259.

Bang, B.G., 1960. Anatomical evidence for olfactory function some species of birds. Nature 188, 547–549.

Bang, B.G., 1961. The surface pattern of the nasal mucosa and its relation to mucous flow—a study of chicken and herring gull nasal mucosae. J. Morphol. 109, 57–72.

Bang, B.G., 1963. Comparative studies of the nasal organs of birds: a study of 28 species of birds of West Bengal. Pavo 1, 79–89.

Bang, B.G., 1964. The nasal organs of the Black and Turkey Vultures: a comparative study of the cathartid species *Coragyps atratus atratus* and *Canhartes aura septentrionalis* (with notes on *Cathartes aura falklandica, Pseudogyps bengalensis,* and *Neophron percnopterus).* J. Morphol. 115, 153–184.

Bang, B.G., 1965. Anatomical adaptations for olfaction in the snow petrel. Nature 205, 513–515.

Bang, B.G., 1966. The olfactory apparatus of tube-nosed birds (Procellariiformes). Acta Anat. 65, 391–415.

Bang, B.G., 1971. Functional anatomy of the olfactory system in 23 orders of birds. Acta Anat. Suppl. 58, 1–71.

Bang, B.G., Cobb, S., 1968. The size of the olfactory bulb in 108 species of birds. Auk 85, 55–61.

Bang, B., Wenzel, B.M., 1986. Nasal cavity and olfactory system. In: King, A.S., McLellan, J. (Eds.), Form and Function in Birds III. Academic Press, London, pp. 195–225.

Banzawa, N., Saito, S., Imagawa, T., Kashio, M., Takahashi, K., Tominaga, M., Ohta, T., 2014. Molecular basis determining inhibition/activation of nociceptive receptor TRPA1 protein a single amino acid dictates species-specific actions of the most potent mammalian TRPA1 antagonist. J. Biol. Chem. 289, 31927–31939.

Behrendt, H.J., Germann, T., Gillen, C., Hatt, H., Jostock, R., 2004. Characterization of the mouse cold-menthol receptor TRPM8 and vanilloid receptor type-1 VR1 using a fluorometric imaging plate reader (FLIPR) assay. Br. J. Pharmacol. 141, 737–745.

Berkhoudt, H., 1985. The role of oral exteroceptive sense organs in avian feeding behavior. Fortschritte der Zoologie 30.

Bertin, A., Calandreau, L., Arnould, C., Lèvy, F., 2012. The developmental stage of chicken embryos modulates impact of *in ovo* olfactory stimulation on food preferences. Chem. Senses 37, 253–261.

Bertin, A., Calandreau, L., Arnould, C., Nowak, R., Lèvy, F., Noirot, V., Bouvarela, I., Leterrier, C., 2010. *In ovo* olfactory experience influences post-hatch feeding behaviour in young chickens. Ethology 116, 1027–1037.

Bilko, A., Altbacker, V., Hudson, R., 1994. Transmission of food preference in the rabbit— the means of information-transfer. Physiol. Behav. 56, 907–912.

Bonadonna, F., Nevitt, G.A., 2004. Partner-specific odor recognition in an Antarctic seabird. Science 306, 835.

Bonadonna, F., Cunningham, G.B., Jouventin, P., Hesters, F., Nevitt, G.A., 2003. Evidence for nest-odour recognition in two species of diving petrel. J. Exp. Biol. 206, 3719–3722.

Bonadonna, F., Hesters, F., Jouventin, P., 2003. Scent of a nest: discrimination of own nest odours in Antarctic prions, *Pachyptila desolata*. Behav. Ecol. Sociobiol. 54, 174–178.

Bonadonna, F., Sanz-Aguilar, A., 2012. Kin recognition and inbreeding avoidance in wild birds: the first evidence for individual kin-related odour recognition. Anim. Behav. 84, 509–513.

Burne, T.H., Rogers, L.J., 1999. Changes in olfactory responsiveness by the domestic chick after early exposure to odorants. Anim. Behav. 58, 329–336.

Buck, L., Axel, R., 1991. A novel multigene family may encode odorant receptors: a molecular basis for odor recognition. Cell 65, 175–187.

Butler, A.B., Cotterill, R.M.J., 2006. Mammalian and avian neuroanatomy and the question of consciousness in birds. Biol. Bull. 211, 106–127.

Callanan, D., Dixon, M., Widdicombe, J.G., Wise, J.C.M., 1974. Responses of geese to inhalation of irritant gases and injection of phenyl diguanide. Tresp. Physiol. 22, 157–166.

Campagna, S., Mardon, J., Celerier, A., Bonadonna, F., 2012. Potential semiochemical molecules from birds: a practical and comprehensive compilation of the last 20 years studies. Chem. Senses 37, 3–25.

Caro, S.P., Balthazart, J., 2010. Pheromones in birds: myth or reality? J. Comp. Physiol. A. 196, 751–766.

Caro, S.P., Balthazart, J., Bonadonna, F., 2015. The perfume of reproduction in birds: chemosignaling in avian social life. Horm. Behav. 68, 25–42.

Caspers, B.A., Krause, E.T., 2010. Odour-based natal nest recognition in the zebra finch (*Taeniopygia guttata*), a colony-breeding songbird. Biol. Lett. 7, 184–186.

Caspers, B.A., Hagelin, J., Bock, S., Krause, E.T., 2015. An easy method to test odour recognition in songbird hatchlings. Ethology 121, 882–887.

Caspers, B.A., Hagelin, J.C., Paul, M., Bock, S., Willeke, S., Krause, E.T., 2017. Zebra Finch chicks recognise parental scent, and retain chemosensory knowledge of their genetic mother, even after egg cross-fostering. Sci. Rep. 7, 1–8.

Caterina, M.J., Schumacher, M.A., Tominaga, M., Rosen, T.A., Levine, J.D., Julius, D., 1997. The capsaicin receptor: a heat-activated ion channel in the pain pathway. Nature 389, 816–824.

Cevik-Dermirkan, A., Kurtul, I., Haziroglu, R.M., 2007. Gross morphological features of the nasal cavity in the Japanese quail. Ankara Üniversitesi Veteriner Fakültesi Dergisi 54, 1–5.

Challis, R.C., Tian, H., Wang, J., He, J., Jiang, J., Chen, X., Yin, W., Connelly, T., Ma, L., Yu, C.R., Pluznick, J.L., Storm, D.R., Huang, L., Zhao, K., Ma, M., 2015. An olfactory cilia pattern in the mammalian nose ensures high sensitivity to odors. Curr. Biol. 25, 2503–2512.

Chu, Y., Cohen, B.E., Chuang, H.H., 2020. A single TRPV1 amino acid controls species sensitivity to capsaicin. Sci. Rep. 10, 1–12.

Chuang, H.H., Neuhausser, W.M., Julius, D., 2004. The super-cooling agent icilin reveals a mechanism of coincidence detection by a temperature-sensitive TRP channel. Neuron 43, 859–869.

Clapham, D.E., 2003. TRP channels as cellular sensors. Nature 426, 517–524.

Clark, L., 1991a. Odor detection thresholds in tree swallows and cedar waxwings. Auk 108, 177–180.

Clark, L., 1991b. The nest protection hypothesis: the adaptive use of plant secondary compounds by European starlings. In: Loye, J.E., Zuk, B. (Eds.), Bird-Parasite Interactions: Ecology Evolution and Behaviour. Oxford University Press, Oxford, pp. 205–221.

Clark, L., 1995. Modulation of avian responsiveness to chemical irritants: effects of prostaglandin E1 and analgesics. J. Exp. Zool. 271, 432–440.

Clark, L., 1996. Trigeminal repellents do not promote conditional odor avoidance in European starlings. Wilson Bull. 108, 36–52.

Clark, L., 1997. A review of the bird repellent effects of 117 carbocylic compounds. In: Mason, J.R. (Ed.), Repellents in Wildlife Management. National Wildlife Research Center, Fort Collins, CO, pp. 343–352.

Clark, L., 1998a. The physiological, ecological, and evolutionary bases for the avoidance of chemical irritants by birds. In: Nolan, V. (Ed.), Current Ornithology, vol. 14. Plenum Press, New York, pp. 1–37.

Clark, L., 1998b. Bird repellents: interaction of chemical agents in mixtures. Physiol. Behav. 64, 689–695.

Clark, L., 1998c. Review of bird repellents. Proc. Vertebr. Pest Conf. 18, 330–337.

Clark, L., Avery, M.L., 2013. Factors influencing the effectiveness of chemical repellents in management of birds on airports. In: DeVault, T.L., Blackwell, B.F., Belant, J.L. (Eds.), Wildlife in Airport Environments. Johns Hopkins University Press, Baltimore.

Clark, L., Mason, J.R., 1985. Use of nest material as insecticidal and anti-pathogenic agents by the European starling. Oecologica 67, 169–176.

Clark, L., Mason, J.R., 1987. Olfactory discrimination of plant volatiles by the European Starling. Anim. Behav. 35, 227–235.

Clark, L., Mason, J.R., 1988. Effect of biologically active plants used as nest material and the derived benefit to starling nestlings. Oecologica 77, 174–180.

Clark, L., Mason, J.R., 1989. Sensitivity of brown-headed cowbirds to volatiles. Condor 91, 922–932.

Clark, L., Mason, J.R., 1993. Interactions between sensory and post-ingestional repellents in starlings: methyl anthranilate and sucrose. Ecol. Appl. 3, 262–270.

Clark, L., Shah, P., 1991. Nonlethal bird repellents: in search of a general model relating repellency and chemical structure. J. Wild. Manag. 55, 538–545.

Clark, L., Shah, P.S., 1992. Information content of prey odor plumes: what do foraging Leach's storm petrels know? In: Doty, R.L., Müller-Schwartze, D. (Eds.), Chemical Signals in Vertebrates. Plenum Press, New York, pp. 421–428.

Clark, L., Shah, P., 1994. Tests and refinements of a general structure-activity model for avian repellents. J. Chem. Ecol. 20, 321–339.

Clark, L., Smeraski, C.A., 1990. Seasonal shifts in odor acuity by starlings. J. Exp. Zool. 177, 673–680.

Clark, L., Avilova, K.V., Bean, N.J., 1993. Odor thresholds in passerines. Comp. Biochem. Physiol. A 104, 305–312.

Clark, L., Shah, P., Mason, J.R., 1991. Chemical repellency in birds: relationship between chemical structure and avoidance response. J. Exp. Zool. 260, 310–322.

Corfield, J.R., Eisthen, H.L., Iwaniuk, A.N., Parsons, S., 2014. Anatomical specializations for enhanced olfactory sensitivity in kiwi, *Apteryx mantelli*. Brain Behav. Evol. 84, 214–226.

Corfield, J.R., Price, K., Iwaniuk, A.N., Gutierrez-Ibañez, C., Birkhead, T., Wylie, D.R., 2015. Diversity in olfactory bulb size in birds reflects allometry, ecology, and phylogeny. Neuroanatomy 9, 102. https://doi.org/10.3389/fnana.2015.00102.

Crocker, D.R., Perry, S.M., 1990. Plant chemistry and bird repellents. Ibis 132, 300–308.

Crocker, D.R., Perry, S.M., Wilson, M., Bishop, J.D., Scanlon, C.D., 1993. Repellency of cinnamic acid derivatives to captive rock doves. J. Wildl. Manag. 57, 113–122.

Cunningham, S.J., Castro, I., Potter, M.A., 2009. The relative importance of olfaction and remote touch in prey detection by North Island brown kiwis. Anim. Behav. 78, 899–905.

Cunningham, G.B., Nevitt, G.A., 2011. Evidence for olfactory learning in procellariform seabird chicks. J. Avian Biol. 42, 85–88.

Davis, R.G., 1973. Olfactory psychophysical parameters in man, rat, dog and pigeon. J. Comp. Physiol. Psychol. 85, 221–232.

De León, A., Mínguez, E., Belliure, B., 2003. Self-odour recognition in European storm-petrel chicks. Beyond Behav. 140, 925–933.

De Castro, F., 2009. Wiring olfaction: the cellular and molecular mechanisms that guide the development of synaptic connections from the nose to the cortex. Front. Neurosci. 3, 4.

DeGroof, G., Gwinner, H., Steiger, S., Kempenaers, B., van der Linden, A., 2010. Neural correlates of behavioural olfactory sensitivity changes seasonally in European Starlings. PLoS One 5, e14337.

Douglas, J.M., Paul-Murphy, J.R., 2017. Pain in birds. In: Exotic Animal Neurology, an Issue of Veterinary Clinics of North America: Exotic Animal Practice, vol. 21. E-Book, pp. 17–31.

Dubbeldam, J.L., Karten, H.J., 1978. The trigeminal system in the pigeon (*Columba livia*). I. Projections of the Gasserian ganglion. J. Comp. Neurol. 180, 661–678.

Dubbeldam, J.L., Veenman, C.L., 1978. Studies on the somatopy of the trigeminal system in the mallard, *Anas platyrhynchos* L: the Ganglion trigeminale. Neth. J. Zool. 28, 150–160.

Dugas-Ford, J., Rowell, J.J., Radsdale, C.W., 2012. Cell-type homologies and the origins of the neocortex. Proc. Natl. Acad. Sci. U.S.A. 109, 16974–16979. https://doi.org/10.1073/pnas.1204773109.

Eicholz, M.W., Dassow, J.A., Stafford, J.D., Weatherhead, P.J., 2012. Experimental evidence that nesting ducks use mammalian urine to assess predator abundance. Auk 129, 638–644.

Evrard, H.C., Willems, E., Harada, N., Balthazart, J., 2003. Specific innervation of aromatase neurons by substance P fibers in the dorsal horn of the spinal cord in quail. J. Comp. Neurol. 465, 309–318.

Farouk, S.M., Hassan, S.A., Emam, M.A., 2017. Histochemical and surface ultrastructural characteristics of the nasal cavity of laughing dove. Anat. Histol. Embryol. 46, 592–599.

Faunes, M., Wild, J.M., 2017. The ascending projections of the nuclei of the descending trigeminal tract (nTTD) in the zebra finch (*Taeniopygia guttata*). J. Comp. Neurol. 525, 2832–2846.

Forsman, J.T., Monkkonen, M., Thomson, R.L., 2013. Mammalian nest predator feces as a cue in avian habitat selection decisions. Behav. Ecol. 24, 262–266.

Gagliardo, A., 2013. Forty years of olfactory navigation in birds. J. Exp. Biol. 216, 2165–2171.

Gagliardo, A., Filannino, C., Ioalè, P., Pecchia, T., Wikelski, M., Vallortigara, G., 2011. Olfactory lateralization in homing pigeons: a GPS study on birds released with unilateral olfactory inputs. J. Exp. Biol. 214, 593–598.

Gagliardo, A., Ioalè, P., Savini, M., Wild, J.M., 2006. Having the nerve to home: trigeminal magneto receptor versus olfactory mediation of homing in pigeons. J. Exp. Biol. 209, 2888–2892.

Gagliardo, A., Ioalè, P., Savini, M., Wild, J.M., 2009. Navigational abilities of adult and experienced homing pigeons deprived of olfactory or trigeminally mediated magnetic information. J. Exp. Biol. 212, 3119–3124.

Gagliardo, A., Pecchia, T., Savini, M., Odetti, F., Ioalè, P., Vallortigara, G., 2007. Olfactory lateralization in homing pigeons: initial orientation of birds receiving a unilateral olfactory input. Eur. J. Neurosci. 25, 1511–1516.

Gentle, M.J., 1989. Cutaneous sensory afferents recorded from the *nervus intramandibularis* of *Gallus gallus vardomesticus*. J.Compar. Physiol. A 164, 763–774.

Gentle, M.J., 2011. Pain issues in poultry. Appl. Anim. Behav. Sci. 135, 252–258.

Gentle, M.J., Hill, F.L., 1987. Oral lesions in the chicken: behavioural responses following nociceptive stimulation. Physiol. Behav. 40, 781–783.

Gentle, M.J., Hunter, L.N., 1993. Neurogenic inflammation in the chicken (*Gallus gallus* var *domesticus*). Comp. Biochem. Physiol. C 105, 459–462.

Getty, R., 1975. Sisson and Grossman's the Anatomy of the Domestic Animals. W.B. Saunders Company, Philadelphia.

Glusman, G., Bahar, A., Sharon, D., Pilpel, Y., White, J., Lancet, D., 2000. The olfactory receptor gene superfamily: data mining, classification, and nomenclature. Mamm. Genome 11, 1016–1023.

Godard, R.D., Bowers, B.B., Wilson, C.M., 2007. Eastern Bluebirds *Sialia sialis* do not avoid nest boxes with chemical cues from two common nest predators. J. Avian Biol. 38, 128–131.

Goldsmith, K.M., Goldsmith, T.H., 1982. Sense of smell in the black-chinned hummingbird. Condor 84, 237–238.

Gomez, G., Celli, A., 2008. The peripheral olfactory system of the domestic chicken: physiology and development. Brain Res. Bull. 76, 208–216.

Grieves, L.A., Bernards, M.A., MacDougall-Shackleton, E.A., 2019. Behavioural responses of songbirds to preen oil odour cues of sex and species. Anim. Behav. 156, 57–65.

Grigg, N.P., Krilow, J.M., Gutierrez-Ibanez, C., Wylie, D.R., Graves, G.R., Iwaniuk, A.N., 2017. Anatomical evidence for scent guided foraging in the Turkey vulture. Sci. Rep. 7, 1–10.

Griggio, M., Fracasso, G., Mahr, K., Hoi, H., 2016. Olfactory assessment of competitors to the nest site: an experiment on a passerine species. PLoS One 11, e0167905.

Grubb, T.C., 1974. Olfactory navigation to the nesting burrow in Leach's petrel *Oceanodroma leucorrhoa*. Anim. Behav. 22, 192–202.

Gottschaldt, K.–M., 1985. Structure and function of avian somatosensory receptors. In: King, A.S., McLelland, J. (Eds.), Form and Function in Birds, vol. 3. Academic Press, London, pp. 375–461.

Gupta, R., Saito, S., Mori, Y., Itoh, S.G., Okumura, H., Tominaga, M., 2016. Structural basis of TRPA1 inhibition by HC-030031 utilizing species-specific differences. Sci. Rep. 6, 37460.

Güntürkün, O., 2012. The convergent evolution of neural substrates for cognition. Psychol. Res. 2, 212–219.

Gwinner, H., 1997. The function of green plants in nests of European starlings (*Sturnis vulgaris*). Beyond Behav. *1***34**, 337–351.

Gwinner, H., Oltrogge, M., Trost, L., Nienaber, U., 2000. Green plants in starling nests: effects on nestlings. Anim. Behav. 59, 301–309.

Gwinner, H., Berger, S., 2005. European starlings: nestling condition, parasites and green nest material during the breeding season. J. Ornithol. 146, 365–371.

Gwinner, H., Berger, S., 2008. Starling males select green nest material by olfaction using experience-independent and experience-dependent cues. Anim. Behav. 75, 971–976.

Hagelin, J.C., 2004. Observations on the olfactory ability of an endangered nocturnal parrot: the New Zealand Kakapo. Ibis 146, 161–164.

Hagelin, J.C., 2007a. Odors and chemical signaling. In: Jamieson, B.G.M. (Ed.), Reproductive Biology and Phylogeny of Birds, Vol. 6B. Science Publishers, Enfield, NH, pp. 75–119.

Hagelin, J.C., 2007b. The citrus-like scent of crested auklets: reviewing the evidence for an avian olfactory ornament. J. Ornithol. 148, S195–S201.

Hagelin, J.C., Jones, I.L., 2007. Bird odors and other chemical substances: a defense mechanism or overlooked mode of intraspecific communication? Auk 124, 741–761.

Hagelin, J.C., Jones, I.L., Rasmussen, L.E.L., 2003. A tangerine-scented social odor in a monogamous seabird. Proc. R. Soc. Ser. B 270, 1323–1329.

Hagelin, J.C., Simonet, J.C., Lyson, T.R., 2013. Embryonic domestic chickens can detect compounds in an avian chemosignal before breathing air. In: East, M.L., Dehnhard, M. (Eds.), Chemical Signals in Vertebrates, vol. 12. Springer, New York, pp. 363–377.

Harem, İ.S., Kocak, M., Sari, E.K., 2018. The histological structure and histochemistry of the mucosa of the nasal conchae in geese, Anser anser. Biotech. Histochem. 93, 432–441.

Healy, S., Guilford, T., 1990. Olfactory-bulb size and nocturnality in birds. Evolution 44, 339–346.

Hayden, S., Bekaert, M., Crider, T.A., Mariani, S., Murphy, W.J., Teeling, E.C., 2010. Ecological adaptation determines functional mammalian olfactory subgenomes. Genome Res. 20, 1–9.

Henton, W.W., 1969. Conditioned suppression to odorous stimuli in pigeons. J. Exp. Anal. Behav. 12, 175–185.

Henton, W.W., Smith, J.C., Tucker, D., 1966. Odor discrimination in pigeons. Science 153, 1138–1139.

Hepper, P.G., 1988. Adaptive fetal learning: prenatal exposure to garlic affects postnatal preferences. Anim. Behav. 36, 935–936.

Hiestand, W.A., Randall, W.C., 1941. Species differentiation in the respiration of birds following carbon dioxide administration and the location of inhibitory receptors in the upper respiratory tract. J. Cell. Comp. Physiol. 17, 333–340.

Hinman, A., Chuang, H., Bautista, D.M., Julius, D., 2006. TRP channel activation by reversible covalent modification. Proc. Natl. Acad. Sci. U.S.A. 103, 19564–19568.

Holland, R.A., Thorup, K., Gagliardo, A., Bisson, I.-A., Knecht, E., Mizrahi, D., Wikelski, M., 2009. Testing the role of sensory systems in the migratory heading of a songbird. J. Exp. Biol. 212, 4065–4071.

Holzer, P., 2011. Transient receptor potential (TRP) channels as drug targets for diseases of the digestive system. Pharmacol. Ther. 131, 142–170.

Houston, D.C., 1987. Scavenging efficiency of Turkey vultures in tropical forests. Condor 88, 318–323.

Hu, H.J., Bhave, G., Gereau, R.W., 2002. Prostaglandin and protein kinase A-dependent modulation of vanilloid receptor function by metabotropic glutamate receptor 5: potential mechanism for thermal hyperalgesia. J. Neurosci. 22, 7444–7452.

Hutchison, L.V., Wenzel, M., 1980. Olfactory guidance in foraging by procellariifoms. Condor 82, 314–319.

Hwang, S.W., Cho, H., Kwak, J., Lee, S.-Y., Kang, C.J., Jung, J., Cho, S., Min, K.H., Suh, Y.G., Kim, D., Oh, U., 2000. Direct activation of capsaicin receptors by products of lipoxygenases: endogenous capsaicin-like substances. Proc. Natl. Acad. Sci. U.S.A. 97, 6155–6160.

Ioalé, P., Papi, F., 1989. Olfactory bulb size, odor discrimination and magnetic insensitivity in hummingbirds. Physiol. Behav. 45, 995–999.

Johnson, J.S., Murphy, S.M., Parrish, G.W., 2011. Lack of predator-odor detection and avoidance in a songbird, the House Wren. J. Field Ornithol. 82, 150–157.

Jones, I.L., Hagelin, J.C., Major, H.L., Rasmussen, L.E.L., 2004. An experimental field study of the function of Crested Auklet feather odor. Condor 106, 71–78.

Jordt, S.-E., Julius, D., 2002. Molecular basis for species-specific sensitivity to "hot" chili peppers. Cell 108, 421–430.

Julius, D., 2013. TRP channels and pain. Ann. Rev. Cell Dev. Biol. 29, 355–384.

Jung, Y., Wirkus, D., Amendola, D., Gomez, G., 2005. Characteristics of odorant elicited calcium fluxes in acutely-isolated chick olfactory neurons. J. Comp. Physiol. A. 191, 511–520.

Khan, I., Yang, Z., Maldonado, E., Li, C., Zhang, G., Gilbert, M.T.P., Antunes, A., 2015. Olfactory receptor subgenomes linked with broad ecological adaptations in Sauropsida. Mol. Biol. Evol. 32 (11), 2832–2843.

Kare, M.R., 1954. In: Sturkie, P.D. (Ed.), The Special Senses. Cornell University Press, Ithaca, pp. 406–446.

Kare, M.R., 1961. Comparative aspects of taste. In: Kare, M.R., Halpern, B.P. (Eds.), Physiological and Behavioral Aspects of Taste. University of Chicago Press, Chicago, pp. 13–23.

Kare, M.R., Rogers, J.G., 1976. Sense organs. In: Avian Physiology. Springer, Berlin, Heidelberg, pp. 29–52.

Karlsson, A.C., Jensen, P., Elgland, M., Laur, K., Fyrner, T., Konradsson, P., Laska, M., 2010. Red junglefowl have individual odors. J. Exp. Biol. 213, 1619–1624.

Kawabata, F., Kawabata, Y., Liang, R., Nishimura, S., Tabata, S., 2017. Comparative analysis of allyl isothiocyanate (AITC)-induced carbohydrate oxidation changes via TRPV1 between mice and chickens. Biomed. Res. 38 (3), 149–155.

Keverne, E.B., Murphy, C.L., Silver, W.L., Wysocki, C.J., Meredith, M., 1986. Non-olfactory chemoreceptors of the nose: recent advances in understanding the vomeronasal and trigeminal systems. Chem. Senses 11, 119–133.

Kirifides, M.L., Kurnellas, M.P., Clark, L., Bryant, B.P., 2004. Calcium responses of chicken trigeminal ganglion neurons to methyl anthranilate and capsaicin. J. Exp. Biol. 207, 715–722.

Kishkinev, D.A., Chernetsov, N.S., 2014. Magnetoreception systems in birds: a review of current research. Zhurnal obshchei biologii 75, 104–123.

Koda, H., Minagawa, M., Si-Hong, L., Mizumura, K., Kumazawa, T., 1996. H1-receptor-mediated excitation and facilitation of the heat response by histamine in canine visceral polymodal receptors studied in vitro. J. Neurophysiol. 76, 1396–1404.

Kolattukudy, P.E., Bohnet, S., Rogers, L., 1987. Diesters of 3-hydroxy fatty acids produced by the uropygial glands of female mallards uniquely during the mating season. J. Lipid Res. 28, 582–588.

Krause, E.T., Bischof, H.J., Engel, K., Golueke, S., Maraci, O., Mayer, U., Caspers, B.A., 2018. Olfaction in the zebra finch (Taeniopygia guttata): what is known and further perspectives. In Advances in the study of behavior, 50. Academic Press, pp. 37–85.

Krause, E.T., Caspers, B.A., 2012. Are olfactory cues involved in nest recognition in two social species of estrildid finches? PLoS One 7, e36615.

Kuenzel, W.J., 2007. Neurobiological basis of sensory perception: welfare implications of beak trimming. Poultry Sci. 86, 1273–1282.

Kurganov, E., Saito, S., Tanaka Saito, C., Tominaga, M., 2017. Requirement of extracellular Ca^{2+} binding to specific amino acids for heat-evoked activation of TRPA1. J. Physiol. 595, 2451–2463.

Lalloué, F.L., Ayer-Le-Lièvre, C.S., Sicard, G., 2003. Analysis of the functional maturation of olfactory neurons in chicks before and after birth. Chem. Senses 28, 729–737.

Lee, T.K., Park, J.H., Ahn, J.H., Park, Y.E., Park, C.W., Lee, J.C., Go, S., 2019. Parvalbumin-immunoreactive cells in the olfactory bulb of the pigeon: comparison with the rat. Anat. Histol. Embryol. 48, 334–339.

Liang, R., Kawabata, Y., Kawabata, F., Nishimura, S., Tabata, S., 2019. Differences in the acidic sensitivity of transient receptor potential vanilloid 1 (TRPV1) between chickens and mice. Biochem. Biophys. Res. Commun. 515, 386–393.

Ludwig, M.-G., Vanek, M., Guerin, I.D., Gasser, J.A., Jones, C.E., Junker, U., Hofstetter, H., Wolf, R.M., Seuwen, K., 2003. Proton-sensing G-protein-coupled receptors. Nature 425, 93–98.

Maatuf, Y., Geron, M., Priel, A., 2019. The role of toxins in the pursuit for novel analgesics. Toxins 11, 131.

Macadar, A.W., Rausch, L.J., Wenzel, B.M., Hutchison, L.V., 1980. Electrophysiology of the olfactory pathway in the pigeon. J. Comp. Physiol. 137, 39–46.

Macpherson, L.J., Dubin, A.E., Evans, M.J., Marr, F., Schultz, P.G., Cravatt, B.F., Patapoutian, A., 2007. Noxious compounds activate TRPA1 ion channels through covalent modification of cysteines. Nature 445, 541–545.

Mahr, K., Hoi, H., 2018. Red-legged partridges perceive the scent of predators and alarm scents of an avian heterospecific. Anim. Behav. 144, 109–114.

Majikina, A., Takahashi, K., Saito, S., Tominaga, M., Ohta, T., 2018. Involvement of nociceptive transient receptor potential channels in repellent action of pulegone. Biochem. Pharmacol. 151, 89–95.

Malnic, B., Hirono, J., Sato, T., Buck, L.B., 1999. Combinatorial receptor codes for odors. Cell 96, 713–723.

Maraci, Ö., Engel, K., Caspers, B.A., 2018. Olfactory communication via microbiota: what is known in birds? Genes 9, 387.

Mardon, J., Bonadonna, F., 2009. Atypical homing or self-odour avoidance? Blue petrels (*Halobaena caerulea*) are attracted to their mate's odour but avoid their own. Behav. Ecol. Sociobiol. 63, 537–542.

Mardon, J., Saunders, S.M., Anderson, M.J., Couchoux, C., Bonadonna, F., 2010. Species, gender, and identity: cracking petrels' sociochemical code. Chem. Senses 35, 309–321.

Mardon, J., Saunders, S.M., Bonadonna, F., 2011. From preen secretions to plumage: the chemical trajectory of blue petrels' *Halobaena caerulea* social scent. J. Avian Biol. 42, 29–38.

Marsakova, L., Barvik, I., Zima, V., Zimova, L., Vlachova, V., 2017. The first extracellular linker is important for several aspects of the gating mechanism of human TRPA1 channel. Front. Mol. Neurosci. 10, 16.

Marples, N.M., Roper, T.J., 1997. Response of domestic chicks to methyl anthranilate odour. Anim. Behav. 53 (6), 1263–1270.

Matsuzaki, O., 1995. Numbers of olfactory receptor cells and fine structure of olfactory nerves in various birds. Zool. Sci. 12, 117–123.

Mason, J.R., 1990. Evaluation of d-pulegone as an avian repellent. J. Wildl. Manag. **54**, 130–135.

Mason, J.R., Clark, L., 1995. Capsaicin detection in trained starlings: the importance of olfaction and trigeminal chemoreception. Wilson Bull. 107, 165–169.

Mason, J.R., Clark, L., 1997. Avian repellents: options, modes of action, and economic considerations. In: Mason, J.R. (Ed.), Repellents in Wildlife Management. USDA, National Wildlife Research Center, Fort Collins, CO, pp. 371–382.

Mason, J.R., Maruniak, J.A., 1983. Behavioral and physiological effects of capsaicin in red-winged blackbirds. Pharmacol. Biochem. Behav. 19, 857–862.

Mason, J.R., Primus, T., 1996. Response of European starlings to menthone derivatives: evidence for stereochemical differences in repellency. Crop Protect. 15, 723–726.

Mason, J.R., Adams, M.A., Clark, L., 1989. Anthranilate repellency to starlings: chemical correlates and sensory perception. J. Wildl. Manag. 53, 55–64.

Mason, J.R., Bean, N.J., Shah, P., Clark, L., 1991. Taxon-specific differences in responsiveness to capsaicin and several analogues: correlates between chemical structure and behavioral aversivenesss. J. Chem. Ecol. 17, 2539–2551.

Mathis, A., Ferrari, M.C.O., Windel, N., Messier, F., Chivers, D.P., 2008. Learning by embryos and the ghost of predation future. Proc. R. Soc. B. 275, 2603–2607.

Mateo, J.M., Johnston, R.E., 2000. Kin recognition and the 'armpit effect': evidence of self-referent phenotype matching. Proc. R. Soc. B. 267, 695–700.

McKeegan, D.E.F., 2002. Spontaneous and odour evoked activity in single avian olfactory bulb neurons. Brain Res. 929, 48–58.

McKeegan, D.E., 2004. Mechano-chemical nociceptors in the avian trigeminal mucosa. Brain Res. Rev. 46, 146–154.

McKeegan, D.E.F., 2009. Avian chemoreception: an electrophysiological approach. International symposium on olfaction and taste. Ann. N. Y. Acad. Sci. 1170, 438–441.

McKeegan, D.E.F., Smith, F.S., Demmers, T.G.M., Wathes, C.M., Jones, R.B., 2005. Behavioral correlates of olfactory and trigeminal gaseous stimulation in chickens, Gallus domesticus. Physiol. Behav. 84, 761–768.

Meisami, E., 1991. Chemoreception. In: Prosser, D.L. (Ed.), Neural and Integrative Animal Physiology. John Wiley and Sons, New York, NY, pp. 335–362.

Mennella, J.A., Jagnow, C.P., Beauchamp, G.K., 2001. Prenatal and postnatal flavor learning by human infants. Pediatrics. https://doi.org/10.1542/peds.107.6.e88.

Michelsen, W.J., 1959. Procedure for studying olfactory discrimination in pigeons. Science 130, 630–631.

Miller, L., 1942. Some tagging experiments with black-footed albatrosses. Condor 44, 3–9.

Mínguez, E., 1997. Olfactory nest recognition by British storm-petrel chicks. Anim. Behav. 53, 701–707.

Mochimaru, Y., Negishi, J., Murakami, S., Musha, S., Sato, K., Okajima, F., Tomura, H., 2018. Metals differentially activate ovarian cancer G protein-coupled receptor 1 in various species. Zool. Sci. 35, 109–114.

Moran, M.M., Szallasi, A., 2018. Targeting nociceptive transient receptor potential channels to treat chronic pain: current state of the field. Br. J. Pharmacol. 175, 2185–2203.

Moreno-Rueda, G., 2017. Preen oil and bird fitness: a critical review of the evidence. Biol. Rev. 92, 2131–2143.

Musha, S., Nagayama, S., Murakami, S., Kojima, R., Deai, M., Sato, K., Okajima, F., Ueharu, H., Tomura, H., 2019. Protons differentially activate TDAG8 homologs from various species. Zool. Sci. 36, 105–111.

Myers, B.R., Sigal, Y.M., Julius, D., 2009. Evolution of thermal response properties in a cold-activated TRP channel. PLoS One 4, e5741.

Nagayama, S., Homma, R., Imamura, F., 2014. Neuronal organization of olfactory bulb circuits. Front. Neural Circ. 8, 98.

Necker, R., 1974. Dependence of mechanoreceptor activity on skin temperature in sauropsid. II. Pigeon and duck. J. Comp. Physiol. 92, 75–83.

Nelson, E.K., 1920. The constitution of capsaicin, the pungent principle of Capsicum. II. J. Am. Chem. Soc. 42, 597–599.

Nelson, E.K., Dawson, L.E., 1923. The constitution of capsaicin, the pungent principle of capsicum III. J. Am. Chem. Soc. 45, 2179–2181. https://doi.org/10.1021/ja01662a023.

Neuhaus, W., 1963. On the olfactory sense of birds. In: Zotterman, Y. (Ed.), Olfaction and Taste, pp. 111–123.

Ngai, J., Dowling, M.M., Buck, L., Axel, R., Chess, A., 1993. The family of genes encoding odorant receptors in the channel catfish. Cell 72, 657–666.

Oda, M., Saito, K., Hatta, S., Kubo, Y., Saitoh, O., 2017. Chemical and thermal sensitivity of medaka TRPA1 analyzed in heterologous expression system. Biochem. Biophys. Res. Commun. 494, 194–201.

Ohta, T., Ikemi, Y., Murakami, M., Imagawa, T., Otsuguro, K., Ito, S., 2006. Potentiation of transient receptor potential V1 functions by the

activation of metabotropic 5_HT receptors in rat primary sensory neurons. J. Physiol. 576, 809–822.

O'Hare, J.R., Eisemann, J.D., Bowles Jr., W.A., Schafer Jr., E.W., Fagerstone, K.A., 2012. NWRC chemical effects database—what's old is new again. Proc. Vertebr. Pest Conf. 25, 134–138.

Papi, F., Casini, G., 1990. Pigeons with ablated pyriform cortex home from familiar but not from unfamiliar sites. Proc. Natl. Acad. Sci. U.S.A. 87, 3783–3787.

Papi, F., Fiore, L., Fiaschi, V., Benvenuti, S., 1971. The influence of olfactory nerve section on the homing capacity of carrier pigeons. Monit. Zool. Ital. 5, 265–267.

Passe, D.H., Walker, J.C., 1985. Odor psychophysics in vertebrates. Neurosci. Biobehav. Rev. 9, 431–467.

Pattison, L.A., Callejo, G., St John Smith, E., 2019. Evolution of acid nociception: ion channels and receptors for detecting acid. Philos. Trans. R. S. B. 374 (1785), 20190291.

Patapoutian, A., Tate, s., Woolf, J., 2009. Transient receptor potential channels: targeting pain at the source. Nat. Rev. Drug Discov. 8, 55–68.

Patzke, N., Manns, M., Güntürkün, O., Ioalè, P., Gagliardo, A., 2010. Navigation-induced ZENK expression in the olfactory system of pigeons (*Columba livia*). Eur. J. Neurosci. 31, 2062–2072.

Patzke, N., Manns, M., Güntürkün, O., 2011. Telencephalic organization of the olfactory system in homing pigeons (*Columba livia*). Neuroscience 194, 53–61.

Petit, C., Hossaert-McKey, M., Perret, P., Blondel, J., Lambrechts, M.M., 2002. Blue tits use selected plants and olfaction to maintain an aromatic environment for nestlings. Ecol. Lett. 5, 585–589.

Pertusa, M., González, A., Hardy, P., Madrid, R., Viana, F., 2014. Bidirectional modulation of thermal and chemical sensitivity of TRPM8 channels by the initial region of the N-terminal domain. J. Biol. Chem. 289, 21828–21843.

Pierau, F.-K., Sann, H., Garti, G., 1986. Resistance of birds to capsaicin and differences in their substance P (SP) system. Proc. Int. Uni. Physiol. Sci. 36, 207–211.

Porter, R.H., Picard, M., 1998. Effects of early odor exposure in domestic chicks. Reprod. Nutr. Dev. 38, 441–448.

Potier, S., Duriez, O., Célérier, A., Liegeois, J.L., Bonadonna, F., 2019. Sight or smell: which senses do scavenging raptors use to find food? Anim. Cognit. 22, 49–59.

Rahn, H., Paganelli, A., Paganelli, C.V., 1979. How bird eggs breathe. Sci. Am. 240, 46–55.

Rastogi, A., Kumari, Y., Rani, S., Kumar, V., 2011. Phase inversion of neural activity in the olfactory and visual systems of a night-migratory bird during migration. Eur. J. Neurosci. 34, 99–109.

Rastogi, A., Malik, S., Rani, S., Kumar, V., 2016. Annual life-history dependent seasonal differences in neural activity of the olfactory system between non-migratory and migratory songbirds. Behav. Brain Res. 296, 233–239.

Rehkämper, G., Frahm, H.D., Cnotka, J., 2008. Mosaic evolution and adaptive brain component alteration under domestication seen on the background of evolutionary theory. Brain Behav. Evol. 71, 115–126.

Rehkämper, G., Haase, E., Frahm, H.D., 1988. Allometric comparison of brain weight and brain structure volumes in different breeds of the domestic pigeon, *Columba livia* f.d. (fantails, homing pigeons, strassers). Brain Behav. Evol. 31, 141–149.

Reiner, A., Karten, H.J., 1985. Comparison of olfactory bulb projections in pigeons and turtles. Brain Behav. Evol. 27, 11–27.

Rensch, B., Neunzig, R., 1925. Experimentelle Untersuchungen über den Geschmackssinn der Vögel II. J. Ornithol. 73, 633–646.

Rescorla, R.A., Solomon, R.L., 1967. Two-process learning theory: relationships between Pavlovian conditions and instrument training. Psychol. Rev. 74, 151–183.

Rieke, G.K., Wenzel, B.M., 1978. The forebrain projections of the pigeon olfactory bulb. J. Morphol. 158, 41–56.

Roper, T.J., 1999. Olfaction in birds. In: Snowden, T., Roper, T.J. (Eds.), Advances in the Study of Behaviour, vol. 28. Academic Press, Boston, MA, pp. 247–332.

Roper, T.J., Marples, N.M., 1997. Odour and colour as cues for taste-avoidance learning in domestic chicks. Anim. Behav. 53, 1241–1250.

Roth, T.C., Cox, J.G., Lima, S.L., 2008. Can foraging birds assess predation risk by scent? Anim. Behav. 76, 2021–2027.

Saito, S., Shingai, R., 2006. Evolution of thermo TRP ion channel homologs in vertebrates. Physiol. Genom. 27, 219–230.

Saito, S., Tominaga, M., 2015. Functional diversity and evolutionary dynamics of thermoTRP channels. Cell Calcium 57, 214–221.

Saito, S., Banzawa, N., Fukuta, N., Saito, C.T., Takahashi, K., Imagawa, T., Ohta, T., Tominaga, M., 2014. Heat and noxious chemical sensor, chicken TRPA1, as a target of bird repellents and identification of its structural determinants by multispecies functional comparison. Mol. Biol. Evol. 31, 708–722.

Saito, S., Nakatsuka, K., Takahashi, K., Fukuta, N., Imagawa, T., Ohta, T., Tominaga, M., 2012. Analysis of transient receptor potential ankyrin 1 (TRPA1) in frogs and lizards illuminates both nociceptive heat and chemical sensitivities and coexpression with TRP vanilloid 1 (TRPV1) in ancestral vertebrates. J. Biol. Chem. 287, 30743–30754.

Samanta, A., Hughes, T.E., Moiseenkova-Bell, V.Y., 2018. Transient receptor potential (TRP) channels. In: Membrane Protein Complexes: Structure and Function. Springer, Singapore, pp. 141–165.

Sann, H., Harti, G., Pierau, F.-K., Simon, E., 1987. Effect of capsaicin upon afferent and efferent mechanisms of nociception and temperature regulation in birds. Can. J. Physiol. Pharmacol. 65, 1347–1354.

Shallenberger, R.J., January 1975. Olfactory use in the wedge-tailed shearwater (*Puffinus pacificus*) on Manana is. Hawaii. In: Olfaction and Taste: 5th Symposium. Academic Press, pp. 355–359.

Schaal, B., Marlier, L., Soussignan, R., 2000. Human foetuses learn odours from their pregnant mother's diet. Chem. Senses 25, 729–737.

Schneider, E.R., Anderson, E.O., Mastrotto, M., Matson, J.D., Schulz, V.P., Gallagher, P.G., LaMotte, R.H., Gracheva, E.O., Bagriantsev, S.N., 2017. Molecular basis of tactile specialization in the duck bill. Proc. Acad. Nat. Sci. 1**14**, 13036–13041.

Schrader, E., 1970. Die Topographie der Kopfnerven vom Huhn. Ph.D. Dissertation. Freien University, Berlin.

Scoville, W.L., 1912. Note on capsicums. J. Am. Pharm. Assoc. 1, 1. https://doi.org/10.1002/pjs.3080010520.

Selescu, T., Ciobanu, A.C., Dobre, C., Reid, G., Babes, A., 2013. Camphor activates and sensitizes transient receptor potential melastatin 8 (TRPM8) to cooling and icilin. Chem. Senses 38, 563–575.

Shah, P., Clark, L., Mason, J.R., 1991. Prediction of avian repellency from chemical structure: the aversiveness of vanillin, vanillyl alcohol and veratryl alcohol. Pestic. Biochem. Physiol. 40, 169–175.

Shaw, C.L., Rutter, J.E., Austin, A.L., Garvin, M.C., Whelan, R.J., 2011. Volatile and semivolatile compounds in gray catbird uropygial secretions vary with age and between breeding and wintering grounds. J. Chem. Ecol. 37, 329–339.

Shibuya, T., Tucker, D., 1967. Single unit responses of olfactory receptors in vultures. In: Hayashi, T. (Ed.), Olfaction-and Taste. Pergamon Press, Oxford, pp. 219–220.

Shibuya, T., Tonosaki, K., 1972. Electrical responses of single olfactory receptor cells in some vertebrates. In: Schneider, D. (Ed.), Olfaction and Taste. Wissenschaftliche Verlagsgesellschaft MBH, Stuttgart, pp. 102–108.

Sieck, M.H., Wenzel, B.M., January 1966. EEG correlates of avian olfaction. Fed. Proc. 25, 463.

Silva, M.C., Chibucos, M., Munro, J.B., Daugherty, S., Coelho, M.M., Silva, J.C., 2020. Signature of adaptive evolution in olfactory receptor genes in Cory's Shearwater supports molecular basis for smell in procellariiform seabirds. Sci. Rep. 10, 1–11.

Silver, W.L., Maruniak, J.A., 1980. Trigeminal chemoreception in the nasal and oral cavities. Chem. Senses 6, 295–305.

Smith, S.A., Paselk, R.A., 1986. Olfactory sensitivity of the Turkey vulture (*Cathartes aura*) to three carrion-associated odorants. Auk 103, 586–592.

Soudek, S., 1929. The sense of smell in birds. Int. Congrss Zool. 10, 755.

Sneddon, H., Hadden, R., Hepper, P.G., 1998. Chemosensory learning in the chicken embryo. Physiol. Behav. 64, 133–139.

Sneddon, L.U., Elwood, R.W., Adamo, S.A., Leach, M.C., 2014. Defining and assessing animal pain. Anim. Behav. 97, 201–212.

Snyder, G.K., Peterson, T.T., 1979. Olfactory sensitivity in the black-billed magpie and in the pigeon. Comp. Biochem. Physiol. A 62, 921–925.

Stager, K.E., 1964. The role of olfaction in food location by the Turkey Vulture (*Cathartes aura*). Los. Ang. Cty. Mus. Contrib. Sci. 81, 1–63.

Stager, K.E., 1967. Avian olfaction. Am. Zool. 7, 415–420.

Startek, J.B., Voets, T., Talavera, K., 2019. To flourish or perish: evolutionary TRiPs into the sensory biology of plant-herbivore interactions. Pflügers Archiv-Eur. J. Physiol. 471, 213–236.

Stattelman, A.J., Talbot, R.B., Coulter, D.B., 1975. Olfactory thresholds of pigeons (*Columba liva*), quail (*Colinus virginianus*) and chickens (*Gallus gallus*). Comp. Biochem. Physiol. A 50, 807–809.

Steiger, S.S., Fidler, A.E., Valcu, M., Kempenaers, B., 2008. Avian olfactory receptor gene repertoires: evidence for a well-developed sense of smell in birds? Proc. R. Soc. Ser. B 275, 2309–2317.

Steiger, S.S., Fidler, A.E., Kempenaers, B., 2009a. Evidence for increased olfactory receptor gene repertoire size in two nocturnal bird species with well-developed olfactory ability. BMC Evol. Biol. 9, 1–11.

Steiger, S.S., Kuryshev, V.Y., Stensmyr, M.C., Kempenaers, B., Mueller, J.C., 2009b. A comparison of reptilian and avian olfactory receptor gene repertoires: species-specific expansion of group γ genes in birds. BMC Genom. 10, 446.

Szolcsanyi, J., 1982. Capsaicin type pungent agents producing pyrexia. In: Milton, A.S. (Ed.), Handbook of Experimental Pharmacology. Springer-Verlag, Berlin, pp. 437–478.

Szolcsányi, J., 2014. Capsaicin and sensory neurones: a historical perspective. In: Capsaicin as a Therapeutic Molecule. Springer, Basel, pp. 1–37.

Szolcsanyi, J., Sann, H., Pierau, F.-K., 1986. Nociception is not impaired by capsaicin. Pain 27, 247–260.

Tewksbury, J.J., Nabhan, G.P., 2001. Seed dispersal-directed deterrence by capsaicin in chilies. Nature 412, 403–404.

Thresh, J.C., 1876. Isolation of capsaicin. Pharm. J. Trans. 6, 941–947.

Todrank, J., Heth, G., Restrepo, D., 2011. Effects of *in utero* odorant exposure on neuroanatomical development of the olfactory bulb and odour preferences. Proc. R. Soc. B. 278, 1949–1955.

Tolhurst, B.E., Vince, M.A., 1976. Sensitivity to odours in the embryo of the domestic fowl. Anim. Behav. 24, 772–779.

Tucker, D., 1963. Olfactory, vomeronasal and trigeminal receptor responses to odorants. In: Zotterman, Y. (Ed.), Olfaction and Taste. Pergamon, New York, pp. 45–69.

Tucker, D., 1965. Electrophysiological evidence for olfactory function in birds. Nature 2**07**, 34–36.

Tucker, D., 1971. Nonolfactory responses from the nasal cavity: Jacobson's organ and the trigeminal system. In: Beidler, L.M. (Ed.), Handbook of Sensory Physiology IV: Chemical Senses Olfaction. Springer-Verlag, Berlin, pp. 151–181.

Uzura, R., Takahashi, K., Saito, S., Tominaga, M., Ohta, T., 2020. Reduction of extracellular sodium evokes nociceptive behaviors in the chicken via activation of TRPV1. Brain Res. 147052.

Walker, J.C., 1983. An operant procedure for testing olfactory capacities in restrained pigeons. Physiol. Behav. 30, 165–168.

Walker, J.C., Tucker, D., Smith, J.C., 1979. Odor sensitivity mediated by trigeminal nerve in pigeon. Chem. Senses Flavor 4, 107–116.

Walker, J.C., Walker, D.B., Tambiah, C.R., Gilmore, K.S., 1986. Olfactory and nonolfactory odor detection in pigeons: elucidation by a cardiac acceleration paradigm. Physiol. Behav. 38, 575–580.

Wallraff, H.G., 1988. Olfactory deprivation in pigeons: examination of methods applied in homing experiments. Comp. Biochem. Physiol. A Comp. Physiol. 89, 621–629.

Wallraff, H., 2005. Beyond familiar landmarks and integrated routes: goal-oriented navigation by birds. Connect. Sci. 17, 91–106.

Walters, E.T., Williams, A.C. de C., 2019. Evolution of mechanisms and behaviour important for pain. Phil. Trans. R. Soc. B. https://doi.org/10.1098/rstb.2019.0275.

Watkins, R.W., Lumley, J.A., Gill, E.L., Bishop, J.D., Langton, S.D., MacNicoll, A.D., Price, N.R., Drew, M.G.B., 1999. Quantitative structure-activity relationships (QSAR) of cinnamic acid bird repellents. J. Chem. Ecol. 25, 2825.

Weldon, P.J., Rappole, J.H., 1997. A survey of birds odorous or unpalatable to humans: possible indications of chemical defense. J. Chem. Ecol. 23, 2609–2633.

Wenzel, B.M., 1967. Olfactory perception in birds. Olfac. Taste 2, 203–217.

Wenzel, B.M., 1971. Olfactory sensation in the kiwi and other birds. NYASA 188, 183–192.

Wenzel, B.M., Sieck, M.H., 1972. Olfactory perception and bulbar electrical activity in several avian species. Physiol. Behav. 9, 287–293.

Whelan, R.J., Levin, T.C., Owen, J.C., Garvin, M.C., 2010. Short-chain carboxylic acids from gray catbird (*Dumetella carolinensis*) uropygial secretions vary with testosterone levels and photoperiod. Comp. Biochem. Physiol. B 156, 183–188.

Whittaker, D.J., Soini, H.A., Atwell, J.W., Hollars, C., Novotny, M.V., Ketterson, E.D., 2010. Songbird chemosignals: volatile compounds in preen gland secretions vary among individuals, sexes and populations. Behav. Ecol. 21, 608–614.

Whittaker, D.J., Richmond, K.M., Miller, A.K., Kiley, R., Burns, C.B., Atwell, J.W., Ketterson, E.D., 2011. Intraspecific preen oil preferences in dark-eyed juncos (*Junco hyemalis*). Behav. Ecol. 22, 1256–1263.

Wild, J.M., 1985. The avian somatosensory system. I. Primary spinal afferent input to the spinal cord and brainstem in the pigeon (*Columba livia*). J. Comp. Neurol. 240, 377–395.

Wiltschko, R., Wiltschko, W., 2019. Magnetoreception in birds. J. R. Soc. Interface 16, 20190295.

Woolf, C.J., Ma, Q., 2007. Nociceptors-noxious stimulus detectors. Neuron 55, 353–364.

Yamamoto, A., Takahashi, K., Saito, S., Tominaga, M., Ohta, T., 2016. Two different avian cold-sensitive sensory neurons: transient receptor potential melastatin 8 (TRPM8)-dependent and-independent activation mechanisms. Neuropharmacology 111, 130–141.

Yin, Y., Le, S.C., Hsu, A.L., Borgnia, M.J., Yang, H., Lee, S.Y., 2019. Structural basis of cooling agent and lipid sensing by the cold-activated TRPM8 channel. Science 363 (6430).

Zelenitsky, D.K., Therrien, F., Kobayashi, Y., 2009. Olfactory acuity in theropods: palaeobiological and evolutionary implications. Proc.Royal Soc. B: Biol. Sci. 276, 667–673.

Zelenitsky, D.K., Therrien, F.O., Ridgely, R.C., McGee, A.R., Witmer, L.M., 2011. Evolution of olfaction in non-avian theropod dinosaurs and birds. Proc. R. Soc. Ser. B 278, 3625–3634.

Zeng, Z., Zhang, S., Wang, H., Piao, X., 2015. Essential oil and aromatic plants as feed additives in non-ruminant nutrition: a review. J. Anim. Sci. Biotechnol. 6, 7.

Zhang, X., Firestein, S., 2002. The olfactory receptor gene superfamily of the mouse. Nat. Neurosci. 5, 124–133.

Zidar, J., Løvlie, H., 2012. Scent of the enemy: behavioral responses to predator faecal odour in the fowl. Anim. Behav. 84, 547–554.

Zygmunt, P.M., Petersson, J., Andersson, D.A., Chuang, H., Sørgård, M., Di Marzo, V., Julius, D., Högestätt, E.D., 1999. Vanilloid receptors on sensory nerves mediate the vasodilator action of anandamide. Nature 400, 452–457.

Chapter 13

Taste in birds

Shira L. Cheled Shoval[1,2], Zehava Uni[1] and Colin G. Scanes[3,4]

[1]Department of Animal Science, The Robert H. Smith Faculty of Agriculture, Food and Environment, The Hebrew University, Rehovot, Israel; [2]Miloubar Feedmill, Ashrat Industrial Area, Israel; [3]Department of Biological Sciences, University of Wisconsin, Milwaukee, WI, United States; [4]Center of Excellence for Poultry Science, University of Arkansas, Fayetteville, AR, United States

Abbreviations

2-AFC 2 alternative forced choice
AC Adenylyl cyclase
Bp Base pair
BW Body weight
D Day
DOH Day of hatch
E19 Embryonic day 19
EEG Electroencephalogram analysis
Gg *Gallus gallus*
GIT Gastro-intestinal tract
GPCR G-protein coupled receptor
GPR120 G-protein-coupled receptor 120
IMP Inosine 5′-monophosphate
IP3 Inositol triphosphate
L-MSG Mono-sodium L-glutamate
PCR Polymerase chain reaction
PDE Phosphodiesterase
Pkd2l1 (PKD2L1 gene) Polycystin 2 Like 1, Transient Receptor Potential Cation Channel
PLCβ2 Phospholipase Cβ2
QH Quinine HCl
qPCR Quantitative PCR (real-time PCR)
RT-PCR Reverse transcription PCR
Scnn (SCNN genes) sodium channel family of genes
TAS1R/TAS2R Taste 1 receptor/Taste 2 receptor
TRCs Taste receptor cells
TRPM5 transient receptor potential melastatin 5

13.1 Introduction

13.1.1 What is taste?

Taste perception enables the animal to evaluate nutritional value and potential toxicity of food, and converts taste stimuli into physiological stimuli which in turn promote or suppress feed consumption. Taste research traditionally focused on mammalian model species, where taste research in avian was for the most part neglected and mainly descriptive. However, in the past two decades, we witness the emergence of new avian histological, molecular, and behavioral taste research using innovative techniques together with recent genomic data.

This chapter will discuss taste perception and mechanisms in birds in the following categories: the different taste modalities, taste buds anatomy, taste receptors and signaling molecules, measuring taste behavior in animals, extra gustatory taste receptors, and taste perception variation between different birds.

13.1.2 Taste perception

13.1.2.1 Role of taste

The sense of taste, a specialized chemosensory system, is the mechanism responding to specific chemicals in food and/or water. Why do birds have the ability to taste? Taste perception has evolved as a self-survival mechanism, which enables the bird the nutritional evaluation of food and water with its consumption. Research supports a direct relationship between taste signals and nutrition, by that all main natural taste agonists currently known are either nutrients or anti-nutritional factors. Avian are immensely diverse in habitats and dietary niches, which in turn creates a broad range of potential nutrients and toxins birds are encountered with in their diets. While some avian species rely in their diet on grains, plants, and insects (like wild chicken), other birds consume nectars and fruits containing sugars such as sucrose (Rowland et al., 2015).

13.1.2.2 The five taste modalities

Today, it is the consensus that sense of taste can be divided to five different taste modalities: sweet, umami, bitter, salty, and sour. While sweet and umami taste modalities indicate carbohydrates and several L-amino acids are palatable and as so encourage consumption, sour and bitter indicates

Sturkie's Avian Physiology. https://doi.org/10.1016/B978-0-12-819770-7.00051-7

potential spoilage or toxicity of the food ingested, causing an aversive and rejection responses. The fifth salty taste results from sodium salts (and some nonsodium salts) and is most likely representative for sodium and some other minerals in the food. This taste's palatability however is somewhat different and unique from the previously described, where it depends on the animal physiological state and needs together with salt concentrations in the food itself (Bachmanov and Beauchamp, 2007; Yarmolinsky et al., 2009; Roura et al., 2013; Liman et al., 2014). In the recent years, there is an increasing agreement on the existence of a sixth taste modality—fat or fatty acid taste. Furthermore, other potential new nonclassical taste qualities have been suggested such as calcium and water, which potentially work through taste perception mechanisms (Bachmanov and Beauchamp, 2007).

13.1.3 Anatomy of taste buds

13.1.3.1 Taste buds

What are the tissues responsible for taste sensation? Tastants (taste molecules) are recognized by taste receptors found in taste receptor cells (TRCs). TRCs are organized in an epithelial structures named taste buds located in the oral cavity of the animal. Avian taste buds, like mammalians, contain a group of fusiform cells which have a pear-like shape (reviewed Liu et al., 2018), with their longitudinal axis oriented vertically to the epithelium and the apical side composed of receptors situated in TRCs containing small or large receptor villi. These TRCs are compact modified epithelial cells extending taste perception into the apical surface of the epithelium, where taste buds pores enable the direct interaction of tastants present in the oral cavity (Liman et al., 2014).

13.1.3.2 Morphology

The morphology of avian taste buds has been described in crows, mallard ducks, pigeons, grebes, and starlings (Berkhoudt, 1992); however, the most researched avian on the topic of taste perception is the domestic chicken. Avian taste buds differ from mammals morphologically mainly by not being associated with gustatory papillae.

13.1.3.3 Types of taste buds

Taste buds can be divided into three types based on morphology (mainly shape)—Type I buds characterized as ovoid structures comprised of a central core of sensory and structural supporting cells called sustentacular cells surrounded by follicular cells. These can be found in chickens, pigeons, and songbirds (Berkhoudt, 1985, 1992; Rowland et al., 2015). Type II buds possess similar supporting follicular cells, are characterized by a more narrow-elongated morphology and can be found in ducks and waders (Rowland et al., 2015). The type III buds, which can be found only in parrots, are similar to mammalian taste buds but the supporting follicular cells are missing (Rowland et al., 2015).

13.1.3.4 Taste buds markers in chickens

Advances in histology and molecular biology together with new genomic data available enabled to shed more light into taste structures in birds. Recently markers such as Epcam, α-Gustducin, and Vimentin (intermediate filaments) have been used to identify taste bud cells in chickens (Venkatesan et al., 2016). There is a bimodal distribution of taste bud widths with diameters of around either 45 or 65 μm with an area and developmental stage association (Ganchrow and Ganchrow, 1985). Taste buds are in communication with the oral cavity via circular openings called taste pores (2−10 μm in diameter) in the epithelium (Kudo et al., 2008; Rajapaksha et al., 2016; reviewed Liu et al., 2018).

13.1.3.5 Taste bud number and distribution

13.1.3.5.1 Distribution in different vertebrates

In mammals, taste buds are located mostly in the tongue and in some cases soft palate (Liman et al., 2014); however, they can be found in other parts of the oral cavity in different vertebrates. Traditionally birds were thought of possessing poor sense of taste, mainly due to lower number of taste buds compared to other vertebrates. However, due to research in new oral cavity areas (areas beyond the tongue) which were not examined before it is known by now that birds have more taste buds than previously thought (Kudo et al., 2008; Rajapaksha et al., 2016).

Taste buds' morphology, count, and distribution holds great inter- and intraspecies variation (Northcutt, 2004)—from only 56 and 62 taste buds in pigeons and quails respectively, through 2000−8000 in humans (Roper, 2013; Roura et al., 2013) and up to ∼20,000 in cows and pigs (Roura et al., 2013, Table 13.1). Due to the nature of feeding in birds (no mastication and lower saliva secretion), taste buds in birds are uncommon on the tongue, but rather are most abundant in the anteroposterior extent of the upper beak epithelium (upper palate), the lower palate, and usually in proximity with salivary gland ducts (Ganchrow and Ganchrow, 1985, Figure 13.1).

13.1.3.5.2 Distribution in birds

The number and distribution of taste buds in chicken has been reported (Ganchrow and Ganchrow, 1985; Ganchrow et al., 1993). Chicken taste buds are found mainly around salivary glands in the soft epithelium of the palate, the base of the tongue and the pharynx with unique distribution where the majority of taste buds are located on the upper palate (69%) and lower palate (29%), and only small

TABLE 13.1 Abundance of taste buds in different vertebrates[a].

Species			Number of taste buds	Sweet/umami receptor genes	Number of *TAS2R* genes
Chicken (*Gallus gallus*)	Broiler	Embryo (E19)	~80		
		Adult	312–770	T1R1/T1R3	3
	Laying type: White Leghorn		192		
	Rhode Island		253		
Turkey (*Meleagris gallopavo*)			200	T1R1/T1R3	18
Quail (*Coturnix japonica*)			62		
Duck (Anatidae spp.)			350		
Parrot (Psittacidae spp.)			350		
Zebra finch (*Taeniopygia guttata*)				T1R1/T1R3	8
Medium ground finch (*Geospiza fortis*)					9
Sparrow (*Zonotrichia albiocollis*)					15
European starling (*Sturnus vulgaris*)			200	T1R1/T1R3	7
Blue tit (*Cyanistes caeruleus*)			24		
Human (*Homo sapiens*)			7902	T1R1/T1R2/T1R3	10
Pig (*Sus scrofa*)			19,904	T1R1/T1R2/T1R3	25

[a]*Adapted from Ganchrow and Ganchrow (1985), Roura et al. (2013), Li and Zhang (2014), Rajapaksha et al. (2016).*

percentage are found in the poster ventrolateral region of the anterior tongue (2%). Until recently, studies using standard morphological techniques showed counts of 250–350 taste buds in adult chickens (Berkhoudt, 1985; Kudo et al., 2010); however, recently the use of new and innovative techniques demonstrated the number to be a bit higher (~800) (Rajapaksha et al., 2016; Venkatesan et al., 2016). Other reports on bird's taste bud counts reveal similar lower numbers (Table 13.1). Yet, it seems that despite a lower number of taste buds compared to mammals (~10–30 times lower), birds oral cavity size scale is much smaller compared to mammals (~200 times), indicative that in birds a higher ratio of number of taste buds/gram of food ingested in a single bite. This can lead to the assumption that the capacity to taste consumed food is not compromised by taste buds distribution in birds (Roura et al., 2013).

13.1.3.6 Afferent nerves from the taste buds

As in mammals, there are three taste-related afferent nerves which transfer taste information from the oral cavity of the bird into the brain: (1). the chorda tympani in the mandibular, (2). greater superficial petrosal from the soft palate, and (3). the lingual branch of the glossopharyngeal nerves. These transmit information to the nucleus of the solitary tract (brain stem) then though the parabrachial nucleus and the ventral postermedial nucleus (VPM) to the primary gustatory cortex in the insula (Mason and Clark, 2000); reviewed (Yarmolinsky et al., 2009).

13.1.3.7 Changes in taste buds during growth and development

Based on electron microscopy, there are no changes in the number of TRCs during growth and development in chickens between hatching and adulthood (up to 140 days) (Kudo et al., 2008). Taste buds are first identified at day 17 of embryonic development. Numbers of taste buds increase rapidly between days 17E and 19E of the development of the chick embryo chicken (Ganchrow and Ganchrow, 1987, see Table 13.1).

13.1.4 Taste receptors

13.1.4.1 Overview

Taste receptors are chemoreceptors interacting with tastants initiating an afferent signal transmitted to the brain resulting in taste perception (Bachmanov and Beauchamp, 2007).

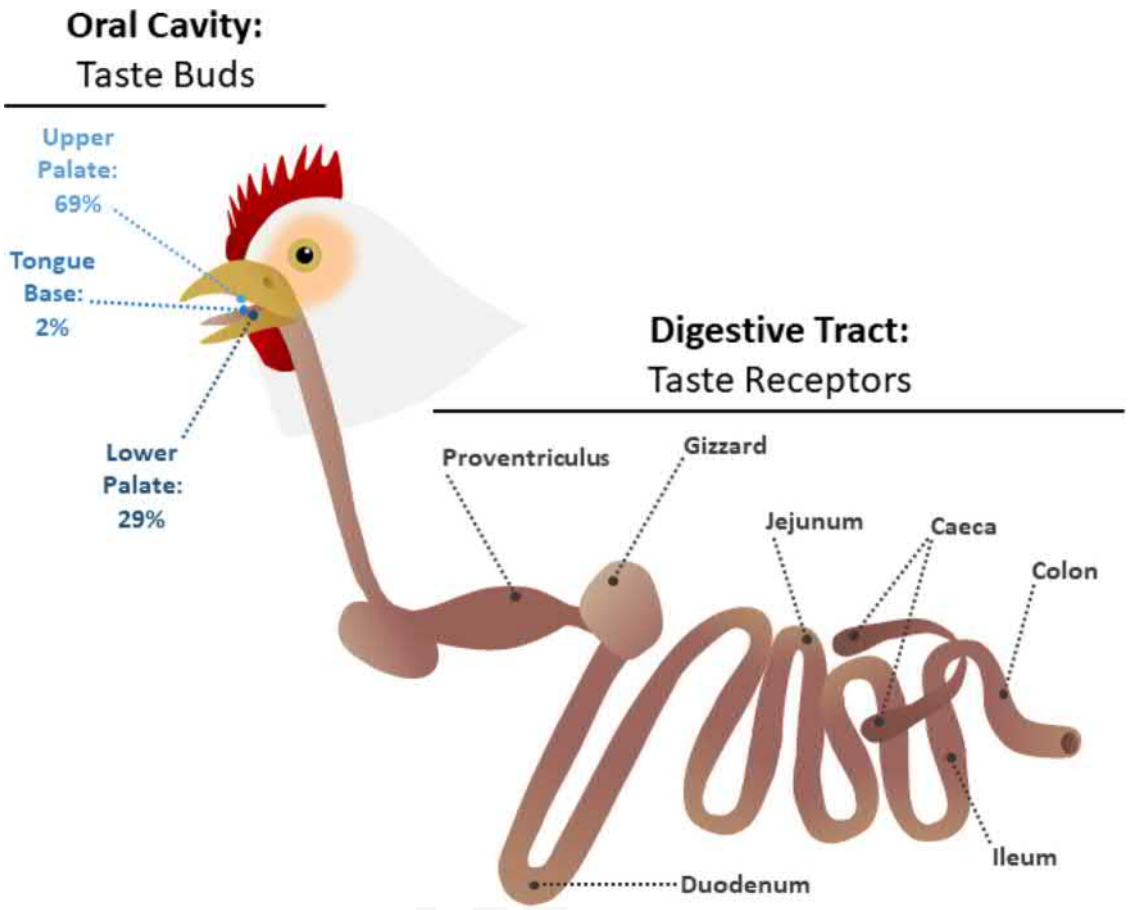

FIGURE 13.1 Taste buds distribution in the chicken oral cavity (as published by [Ganchrow and Ganchrow, 1985]) and gastrointestinal tract taste receptor expression sites (as published in [Cheled-Shoval et al., 2015]).

In the presence of the specific tastant, brain sites are ultimately signaled following binding to the receptors and subsequent signal transduction mechanism. It was shown that G-protein coupled receptors (GPCRs) are involved in the perception of sweet, umami, and bitter taste (as well as the potential sixth taste of fat) (Cygankiewicz et al., 2014), while salty and sour tastes are perceived by ion channels (sodium, potassium, or hydrogen) or ion exchanges (Mombaerts, 2004; Cygankiewicz et al., 2014). Based on mammalian studies, TRCs in the taste buds only express specific receptors for one tastant, respectively, sweet or bitter or umami or sour or salty tastants (reviewed Yarmolinsky et al., 2009). Based on the situation in mammals, taste buds contain 50 to 100 TRCs and can detect multiple tastants as the cells respond to different tastants (reviewed Yarmolinsky et al., 2009).

13.1.4.2 Caveat on taste receptors

The names employed for the taste receptors in this chapter will follow those employed by the authors of the papers cited. It is recognized that there are discrepancies with this approach with homologous proteins having different names.

13.1.4.3 Taste receptor type 1 receptors (tas1r family)

Taste receptor type 1 receptors (Tas1r) are G-protein coupled proteins consisting of three known receptors: Tas1R1, Tas1R2, and Tas1R3 (Li, 2009). This three receptors are responsible for the perception of sweet and umami as heterodimeric assembly by the arrangement of Tas1R1/Tas1R3 (a heterodimer receptor composed of Tas1R1 and Tas1R3 subunits) for umami and Tas1r2/Tas1R3 for sweet (Nelson et al., 2001, 2002; Li et al., 2002; Damak et al., 2003; Zhao et al., 2003).

13.1.5 Sweet taste

13.1.5.1 Overview

With the advances in genomic sequencing, it has been established that birds lack completely the Tas1R2 monomer (of the sweet taste heterodimer Tas1R2/Tas1R3) in their genome (chickens (Shi and Zhang, 2006); multiple avian species (Baldwin et al., 2014; Zhao et al., 2015)). Therefor it is not surprising that chickens nor jungle fowl can detect the sweet tastants, glucose, sucrose, and fructose at

concentrations mammals do (Halpern, 1962; Maller and Kare, 1967), or alternatively reject them at very high concentrations (Gentle, 1972; Cheled-Shoval et al., 2017b). Both suggesting insensitivity to sweet in galliforms and possibly alternative mode of sweet perception with different sweet tastants in these species (Table 13.2).

13.1.5.2 Sweet preferences in birds

Certain types of birds such as hummingbirds and sunbirds rely in their diets on nectar and fruits containing the disaccharide *sucrose*, the hexose monosaccharides *glucose* and *fructose,* and some more complex sugars (Vanwyk and Nicolson, 1995; Rowland et al., 2015). While in chicken and other galliforms, taste-related studies were mainly threshold related, in bird species that consume nectar and fruits; the studies focuses mainly on sugar type preferences at different concentrations. Sugar preferences in nectarivorous and frugivorous species can be concentration-dependent (Rowland et al., 2015). Even though Fleming et al. (2004) reported two nectivores—broad-tailed humming bird (*Selasphorus platycercus*) and white-bellied sunbird (*Nectarinia talatala*)—demonstrated very little discrimination between sucrose and hexose monosaccharides solutions, later on, different researches studying nectarivorous birds reported a shift from sucrose to hexose monosaccharides preference in lower solution concentrations (Lotz and Schondube, 2006, Fleming, 2008; Brown et al., 2010a,b). Village weavers (*Ploceus cucullatus*), a generalist passerine nectivores, demonstrated hexose solution preference at 5 and 10% over sucrose, but not at higher concentrations up to 25% (Odendaal et al., 2010). However, in the opportunistic nectivores, dark-capped bulbuls (*Pycnonotus tricolor*) a nonconcentration-related preference to hexose was demonstrated (Brown et al., 2008). These concentration-dependent shifts in preference may result from physiological causes as suggested by Lotz and Schondube (2006). It can be hypothesis that birds may prefer the easily absorbed hexose monosaccharides due to the extra energetically costs of sucrose hydrolyzes (Martínez del Rio, 1990).

Unlike specialist nectivores, generalist nectivores species usually display a nonconcentration-related preference for hexose monosaccharides (Rowland et al., 2015).

In frugivorous species, we can address two types—specialist and seasonal-generalist frugivores. In fruits, the most common sugars are hexose monosaccharides, fructose and glucose, while sucrose is accountable for only 8% of

TABLE 13.2 Different sweet taste responses in chicken.

Test (behavioral/electrophysiological)	Tastant	Concentration	Response
Behavioral	Glucose	>2.5%	None[a]
		5–30%	Rejection[a]
		30%	Rejection[b]
	Fructose	10%	Indifferent or rejection[b]
		20%	
		30%	
	Sucrose	1–30%	Preference[b]
		2.5–25%	Indifference[c]
		34.2%	Rejection[a]
Electrophysiological	Dextrose	2.5–25%	Indifference[c]
	Xylose	2.5–25%	Rejection
	Glucose	>2.5%	None[b]
	Fructose	10%	None[b]
		20%	
	Sucrose	1%	Rare response[b]
		10%	

[a] *Cheled-Shoval et al. (2017b).*
[b] *Gentle (1972).*
[c] *Kare and Medway (1959).*

total sugar content (Baker et al., 1998; Rowland et al., 2015). Some frugivores show preference to hexose monosaccharides over sucrose (Del Rio and Stevens, 1989; Brugger and Nelms, 1991; Del Rio et al., 1992).

Seasonal frugivores which do not rely on fruits as a main source of food seems to be less sensitive to solution concentrations (Rowland et al., 2015). Research done on red-winged blackbirds (relies more on grains) and starlings (relies on insects and fruits) showed insensitivity of the blackbird to fructose fitting their dietary niche while the starlings demonstrated a correlation between fruits and sugar preference (Espaillat and Mason, 1990; Rowland et al., 2015).

Regarding insectivore, omnivore and carnivore birds, ravens, as excepted from carrion eaters, did not show preference to five different sugar solutions compared to water (Harriman and Fry, 1990). Similarly, ducks and nonfrugivorous owls showed either rejection or indifference to sugar (Rowland et al., 2015). On the other hand, a preference for 7 and 14% glucose solutions was demonstrated in the great tit (*Parus major*) (Warren and Vince, 1963). It should be noted that the test conducted in this study was carried with choice, implying acceptance rather than preference. Similarly, other taste studies in these nonnectar or fruit eaters were done in manner that results demonstrate either acceptance, tolerance, or absorption rather than preference.

To that point, it is highly important, when talking on taste preference or taste threshold tests, to take into consideration the great variety of tests and the fact that most studies do not address the issues of viscosity (highly relevant in sweet taste), postingestive effects, and other important factors. This will be reviewed broadly later on.

13.1.5.3 The sweet dilemma

Despite the lack of Tas1R2 subunit in birds, we do see sweet taste perception in different birds as discussed above. So how do birds taste sweet? Baldwin et al. (2014) reported the hummingbirds anna's hummingbird (*Calypte anna*) and ruby-throated hummingbirds (*Archilochus colubris*) respond to sucrose due to repurposing their umami taste receptor Tas1R1/Tas1R3 such that it binds sucrose as well (discussed in more detail in Section 13.1.6 about the umami taste). In addition, birds might sense sweet tastants through only one of the sweet taste receptors subunit (Tas1R3) as suggested in mice (Treesukosol et al., 2011) or have an alternative mode of sensation for sweet tastants. This question warrants further study.

13.1.5.4 Evolutionary considerations of Tas1r2

It has been proposed that the loss of *Tas1r2* occurred in the carnivorous theropod dinosaurs that were ancestral to the avian lineage; carnivorous mammals having also lost (Beauchamp and Jiang, 2015; Antinucci and Risso, 2017). It is assumed that this is due to the relaxation of the selection pressure for maintaining a functioning TAS1R2 gene (Antinucci and Risso, 2017). When examining the evolutionary process, we see that the nonavian reptiles gained the Tas1R2 back, another hint that the loss occurred within Dinosauria. Taking into consideration the previous section, it seems that birds who rely mainly on nectar or fruit in their diets developed a Tas1R2-independent sweet taste perception mechanism (Baldwin et al., 2014).

13.1.6 Umami taste

13.1.6.1 Overview

Umami taste is related to dietary protein and senses some amino acids (AAs), such as glutamic acid (Glu). Similarly to the sweet and bitter taste, the umami taste is mediated by GPCRs. Avian umami taste receptor is a heterodimer composed of two GPCR subunits: Tas1r1 and Tas1r3. The umami taste receptors shares the same three-dimensional architecture described for the sweet taste receptor (Pin, 2013) and switches between an "open-open/inactive" conformation to a "closed-open/active" conformation (Cascales et al., 2010).

The Tas1r1 and, therefore, the ability to detect umami is not present in all avian species. Reports on the Adelie penguin (*Pygoscelis adeliae*) and emperor penguin (*Aptenodytes forsteri*) show that Tas1r1 is a pseudogene (Zhao et al., 2015). Similarly, the Tas1r1 is not found in the red-throated loon (*Gavia stellata*) (Zhao et al., 2015).

The chicken umami receptor responds to *alanine* and *serine* (known to stimulate the umami receptor in rodents and fish). Studies on European starling (*Sturnus vulgaris*) and red-winged blackbird (*Agelaius phoeniceus*) demonstrated the ability to taste L-alanine (Espaillat and Mason, 1990; Werner et al., 2008). Response to alanine, and to a less extent serine, is detected in the insectivorous chimney swift (*Chaetura pelagica*) and in chicken (Baldwin et al., 2014). In contrast, the umami receptor in hummingbirds (Anna's hummingbirds [*Calypte anna*]) responds to sugars (sucrose > fructose >> glucose) and to alanine, albeit poorly (Baldwin et al., 2014). Thus, it is suggested that the umami receptor in birds has acquired the ability to respond to sugars while losing their ability to respond to alanine or serine (Baldwin et al., 2014).

The chicken umami receptor responds to L-glutamate (L-Glu), first discovered as an umami tastant in by Ikeda (1909). Glutamate umami taste intensity can be strongly potentiated by purine ribonucleotides, such as 5′-monophosphate (IMP) and guanosine 5′-monophosphate (GMP) (Zhang et al., 2008; Dang et al., 2014). Glutamate, IMP, and GMP are the most renowned modulators of the umami taste receptor, but many other substances, including peptides and free AAs, can elicit and/or enhance the umami taste (Yu et al., 2017; Zhang et al., 2019).

A functional umami taste receptor heterodimer (Tas1r1/Tas1r3) has been predicted in most mammalian, bird, and fish with some exceptions (Shi and Zhang, 2006; Roura et al., 2008; Zhao et al., 2010; Jiang et al., 2012). This wide distribution across vertebrate species makes the umami taste an important and highly conserved taste. Accordingly, it is rational to hypnotize that the chicken umami taste might be activated by a broad array of AA. Identifying the umami compounds that might be driving protein-specific appetite in chickens is a fundamental question to improve feed intake and efficiency of feed utilization in poultry diets and to adopt new alternative feedstuff to poultry diet.

13.1.6.2 Umami preference test in birds

Preference for Glu has been described in several animal species including chickens (Roura et al., 2008, 2013). Moran and Stilborn (1996) found that L-Glu increased feed intake and growth in broiler chickens fed minimal crude protein with adequate essential AA (Moran and Stilborn, 1996). Similar results are reported for turkey poults (Boling and Firman, 1997). However, supplemental Glu to broiler diets without adequate AA balance may have a negative impact on appetite (Kerr and Kidd, 1999).

Sensing of lysine, methionine, and tryptophan was demonstrated in a choice-feeding situation, were broiler chicks showed an immediate preference for a balanced diet containing synthetic AA compared to a similar diet deficient in lysine, methionine, and tryptophan (Picard et al., 1993).

13.1.7 Taste receptor type 2 receptors

Bitter taste receptors are seven transmembrane domain GPCR family termed taste 2 receptors (TAS2Rs) which was identified in 2000 (Adler et al., 2000; Matsunami et al., 2000) and their downstream signaling components (Sanematsu et al., 2014). This gene family varies widely between species from none to ~80 (Li and Zhang, 2014), with ~25 functioning genes in humans, and only 1 in turkeys (see Table 13.1). Within avian, the number of TAS2R genes also varies markedly:

- *Galliformes*: chicken (*Gallus gallus*)—3, respectively TAS2R1, TAS2R2, and TAS2R7 (Zhao et al., 2015).
- *Sphenisciformes*: penguins—0 (Zhao et al., 2015).
- *Passeriformes*: white-throated sparrow—17 (15 para-orthologs of zebra finch *TAS2R1 resulting from gene duplication* [Davis et al., 2010]).

TAS2R genes are unusual in lacking introns (reviewed Antinucci and Risso, 2017) and are ~900 base pairs. TAS2Rs have short extracellular N-terminal domain (Maehashi and Huang, 2009) and are characterized by highly conserved motifs in the transmembrane domains, while variable in the extracellular region enabling the recognition and binding of chemically divers bitter substances (Maehashi and Huang, 2009; Yarmolinsky et al., 2009). Following its complete sequencing in recent years, it was shown that the chicken genome contains only three TAS2Rs—ggTAS2R1, ggTAS2R2 (both similar to the human hTAS2R39 and hTAS2R40 gene groups), and TAS2R7 (similar to the human hTAS2R7 and hTAS2R9 gene groups) (Go and SMBE Tri-National Young Investigators, 2006; Lagerstrom et al., 2006).

13.1.8 GPCRs' taste signal transduction

13.1.8.1 Overview

Studies in mammalians demonstrate that TAS1R and TAS2R receptors share a similar signaling pathway following the activation of the receptors although TRCs can express only one type of receptor, i.e., bitter, sweet, or umami taste receptors but not simultaneously together (Ishimaru, 2009; Cygankiewicz et al., 2014). The binding of a taste molecule (or a tastant) to either TAS1Rs or TAS2R receptors found on the apical membrane of TRCs leads to the activation and dissociation of the heterotrimeric G-protein subunits, which include α-gustducins Gαi2, Gα14, Gβ3, and Gγ13, and are co-expressed together with bitter, sweet, and umami receptors in TRCs (Ishimaru, 2009). This leads to the activation of two major signaling pathways: (i) the dissociated Gα14 and/or Gβ3/Gγ13 activate phospholipase C (**PLC**)-β2. This initiates the hydrolysis of phosphatidylinositol 4,5-biphosphate (PI(4,5)P_2) to inositol triphosphate (**IP_3**) and di-acylglycerol, followed by binding of IP_3 to IP_3R3 (IP_3 receptor 3). This binding causes the release of Ca^{2+} from intracellular stores and the subsequent opening of transient receptor potential melastatin 5 (**TRPM5**) channels, Na^+ influx, and the final depolarization of the TRCs (Yamamoto and Ishimaru, 2013). (ii) in the second pathway, which involves **cAMP**, it is suggested that the α subunit causes two opposite reactions: increase of cAMP levels by the activation of adenylyl cyclase (**AC**) and decrease of cAMP level by phosphodiesterase activation. While the decreased cAMP levels are thought to lead to Ca^{2+} release as well together with the PLCβ2 pathway, the elevated cAMP levels from AC activate PKA kinase which in turn phosphorylate K^+ channels which inhibits them causing the TRCs membrane polarization and neurotransmitter secretion (Cygankiewicz et al., 2014, see Figure 13.2).

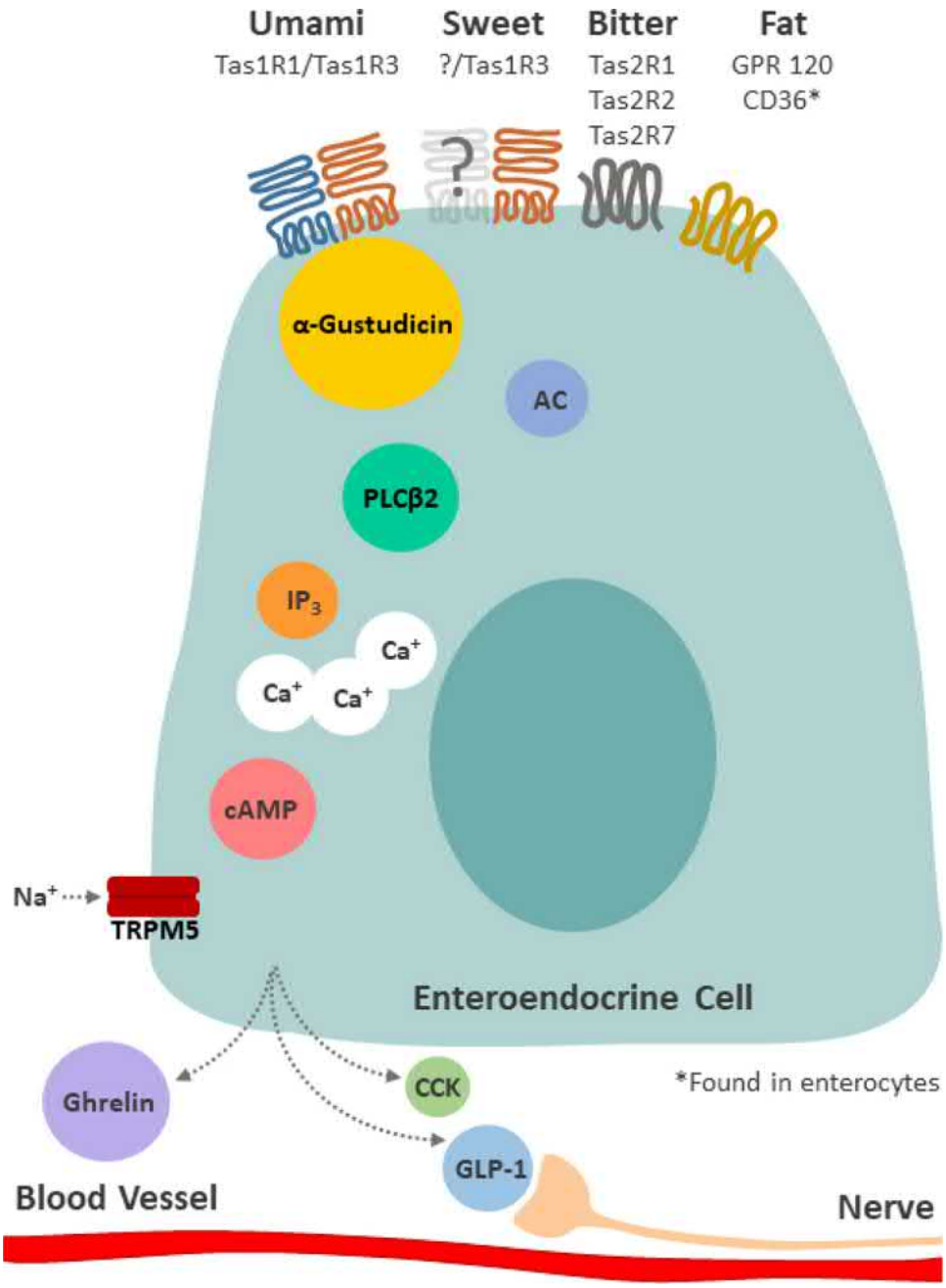

FIGURE 13.2 Basic illustration of extra-gustatory taste-receptors' chemosensory pathways, located in enteroendocrine cell of chicken GIT. Tastants are recognized by different taste receptors (sweet, bitter, amino-acids), inducing signaling pathways which in turn initiates, with the gustducin/transducin protein, the PLCβ2-mediated synthesis of IP3, causing the release of Ca^{2+} from intracellular storage together with reduction in cAMP levels through phosphodiestrases, all leading to the release of GI peptides involved in food intake and gut functionality regulation. *Adapted from Rozengurt (2006), Janssen and Depoortere (2013).*

13.1.8.2 Sequencing of taste receptor type 2 receptors (TAS2R) in birds

13.1.8.2.1 TAS2R1 and TAS2R2

Wang and Zhao (2015) examined 48 genomes of birds representing all but three avian orders for bitter taste receptor genes. The number of TAS2R genes ranged from 1 in the domestic pigeon to 12 in the bar-tailed trogon. An average of four TAS2Rs repertoire was identified. Interestingly, the diet of the birds and number of putative functional TAS2Rs showed positive correlation, with herbivorous and insectivorous having more functional TAS2Rs than carnivorous, with less potential toxins in their diets.

The sequences of both TAS2R1 and TAS2R2 in birds have been reported:

- TAS2R1 [*Galliformes*: chicken—Genbank KT377152; *Casuariiformes*: emu (*Dromaius novaehollandiae*)—Genbank AB608217; Northern fulmar (*Fulmarus glacialis*)—Genbank KP121490; *Gaviiformes*: red-throated loon (*Gavia stellata*)—Genbank KP121495; *Passeriformes*: western yellow wagtail (Motacilla flava)—Genbank GU815912]
- TAS2R2 [*Galliformes*: chicken—Genbank KT377157; *Casuariiformes*: emu (*Dromaius novaehollandiae*)—Genbank AB630153; *Procellariiformes*: e.g., Hawaiian black-footed albatross (*Phoebastria nigripes*)—Genbank KP121501; Northern fulmar (*Fulmarus glacialis*)—Genbank KP121500]

13.1.8.2.2 Other TAS2R genes

The sequences of amino acid residues for other TAS2R proteins have been reported in birds: namely, chicken TAS2R7 (NM_001080719); turkey TAS2R9 like (Genebank XM_003204660) and mallard duck TAS2R9 like (XM_027455347). These TAS2R proteins exhibit marked homologies (see Figure 13.3) suggesting the terminology needs revision.

13.1.8.2.3 Evolutionary aspects of taste receptor type 2 receptors

With the emergence of genomic data availability, it can be concluded that the avian TAS2R genes repertoire was submitted to vigorous changes (either expansions or deletions) through evolution (Go and SMBE Tri-National Young Investigators, 2006; Dong et al., 2009; Wang and Zhao, 2015). Despite the lower average TAS2R numbers in birds, it has been demonstrated using in vitro cell-based models, that the promiscuity of the receptors enables the recognition of a broad bitter tastant repertoire, similar to that in other vertebrates with higher numbers of putative functional TAS2Rs (Behrens et al., 2014).

In Passeriform birds, the TAS2R1 gene has undergone multiple gene duplications resulting in the increases in the number of TAS2R genes (see Table 13.1 and Figure 13.4). Moreover, the white-throated sparrow has 15 para-orthologs of zebra finch TAS2R1 (Davis et al., 2010). Similarly, it would appear that the TAS2R1 gene underwent multiple (four) gene duplications in humming birds (Anna's humming bird [*Calypte anna*]) (Wang and Zhao, 2015; Wang et al., 2019).

Bitter taste receptors are not present in either penguins or gaviiform birds with all the TASR2 genes having undergone pseudogenization in the ancestors to penguins and/or gaviiform birds (Zhao et al., 2015). The loss of functioning TAS2R in these two avian groups may be independent. Similarly, in aquatic mammals, there are no functioning TAS2R genes in cetacean species (Li and Zhang, 2014).

13.1.9 Bitter taste

13.1.9.1 Overview

Bitter tastants are a part of birds' nutrition originating in plants, insects, and even nectars. Studies on bitter taste thresholds focused mainly on more traditional bitter tastants

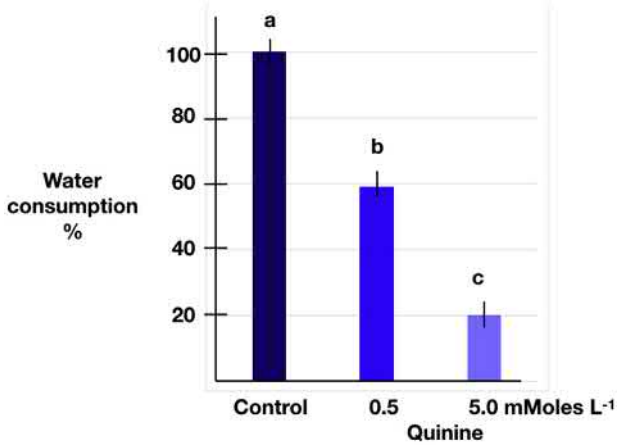

FIGURE 13.3 Comparison of the sequence of amino acid residues in chicken TAS2R7 (NM_001080719) with turkey TAS2R9 like (Genebank XM_003204660) and mallard duck TAS2R9 like (XM_027455347). [Yellow Chicken and identical to chicken in turkey and duck; Green identical between turkey and duck; Blue Difference between turkey and chicken; Red Difference between duck and chicken].

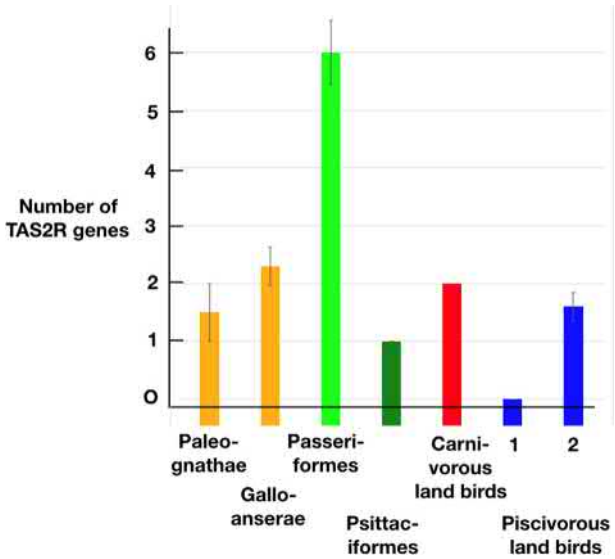

FIGURE 13.4 Number of TAS2R genes in avian groups. Vertical bars indicate SEM. Remark- Colin, the lines of the graph are shifted. Need editing. Carnivorous landbirds — Accipitriformes, Cathartiformes, Strigiformes, Falconiformes; Piscivorous waterbirds 1. Gaviiformes and Sphenisciformes, 2. Ciconiiformes, Pelecaniformes, Procellariiformess and Suliformes. *Calculated from data in Wang and Zhao (2015).*

in mammals such as quinine. Chickens, probably the most researched bird regarding bitter taste, demonstrates a dose-dependent and strain-dependent behavioral aversion responses to bitter tastants from embryo to adult (Gentle, 1975; Vince, 1977; Ganchrow et al., 1990; Kudo et al., 2010; Cheled-Shoval et al., 2014, 2017b). Quinine threshold, based on in vivo trials, was identified by Matson et al. (2004) to be 100 μM for quinine in cockatiels. In the egg laying type chickens, White Leghorn and Rhode Island Red chicken, quinine threshold was 2.0 mM (Kudo et al., 2010), while broilers demonstrated a lower threshold of 0.3 mM (Cheled-Shoval et al., 2014). Electrophysiological tests demonstrated lingua nerve responses between 0.01 and 0.02 M (Kitchell et al., 1959; Halpern, 1962) and chorda tympani responses to higher quinine concentration of 0.1 and 0.05 M (Gentle, 1981, 1983). In vivo quinine thresholds in chickens, also confirmed by in vitro cell-based techniques, demonstrated 0.01 mM threshold (Cheled-Shoval et al., 2014, Table 13.3). These variations in threshold emphasize the need of a unified and clear protocol for threshold termination tests, as suggested and reviewed in depth by Cheled-Shoval et al. (2017b).

13.1.9.2 Agonists of bitter receptors (TAS2R)

Different TAS2R exhibits differential responsiveness to various TAS2R agonists (Behrens et al., 2014), information regarding chicken bitter ligands also accessible via the BitterDB database http://bitterdb.agri. huji.ac.il/dbbitter.php (Wiener et al., 2012). Although quinine is viewed as the "classical" agonist for TAS2R, there are TAS2R agonists that are more potent (Table 13.4).

In chicken, several ggTAS2s ligands were identified by using both in vitro and in vivo methods, such as quinine, (+)-catechin, (−)-epicatechin and epicatechin gallate (Cheled-Shoval et al., 2017a).

In addition, a comprehensive study (Behrens et al., 2004) using cell-based methods specifying the chicken three ggTAS2Rs ligand repertoires, with three compounds are conserved between all three ggTAS2R2. Comparing these ligands to their human homologous receptors, it is evident that while ggTAS2R1 and ggTAS2R2 repertoires are similar in sizes to their human homologs, they are also mostly different in the identity of their ligands. The ggTAS2R7 repertoire, however, differs both in ligand numbers (higher number of ligands) and in their identity (Di Pizio and Niv, 2015). These changes in the chicken receptors in ligands suggest a possible positive selection acting on the ligand recognition and binding regions of the ggTAS2R7 receptor, which may explain this diversification in ligand phenomenon.

Similarly, Wang et al. (2019) demonstrated in hummingbirds a different level of sensitivity together with new functions in the hummingbird TAS2R gene copies proposing positive selection in these genes. The study suggested the hummingbird bitter taste evolution enabled increased sensitivities and specialized abilities to detect bitter-tasting nectar in order to maintain specificity of pollinators.

13.1.9.3 Ecological influence on bitter taste

It has been argued that the retention of multiple functioning TAS2R genes in hummingbirds is advantageous facilitating

TABLE 13.3 In vivo thresholds for sweet, umami, and bitter in chickens and different mammals

Tastant	Taste	Chicken	Human	Rat	Mouse
Quinine	Bitter	≥0.0003M[a]	0.0008M[c]	0.000012M[c]	0.0001M[g]
Sucrose	Sweet	≥1M[a]	0.00023−0.1538M[c]	0.0025−0.004M[g]	0.00193M[j]
		0.06−0.9M[b]			
MSG	Umami	≥0.3M[a]	0.001−0.05M[d]	0.001−0.0025[h]	0.0024M[i]
MSG + IMP	Umami	≥0.3M MSG[a]	Response to MSG is eightfold stronger[e]	Response to MSG is 1.7-fold stronger[i]	
			MSG threshold is lowered 100-fold[f]		

[a] *Cheled-Shoval et al. (2017b).*
[b] *Kudo et al. (2010).*
[c] *Purves et al. (2001).*
[d] *Pepino et al. (2010).*
[e] *Yamaguchi (1991).*
[f] *Yamaguchi (1979).*
[g] *Koh and Teitelbaum (1961).*
[h] *Stapleton et al. (2002).*
[i] *Kurihara (2015).*
[j] *Delay et al. (2006).*
Adapted from Cheled-Shoval et al. (2017b).

TABLE 13.4 Chemical agents that evoke changes in fluorescence indicating increases in intracellular calcium in cells transfected with chicken or turkey bitter taste receptors (Behrens et al., 2014).

Bitter taste receptors	Chemical agents that evoke a response
Chicken	
TAS2R1	Chloramphenicol > chloroquine > chlorpheniramine ≈ diphenidol ≈ quinine sulfate > nicotin ≈ picotoxin
TAS2R2	Caffeine > coumarin ≈ parthenolide ≈ quinine sulfate > chloramphenicol ≈ diphenidol ≈ yohimbine
TAS2R7[a]	Amargenin ≈ colchicine > andrographolide ≈ chloramphenicol ≈ carisoprodol > diphenidol ≈ picotoxin ≈ quinine sulfate
Turkey	
TAS2R3[a]	Limonin > thujone > picrotoxin > cholicine,
TAS2R4[a]	Caffeine > chloramphenicol ≈ coumarin ≈ parthenolide > colchicine ≈ diphenidol ≈ erythromycin ≈ picotoxin ≈ quinine sulfate

[a]*employing terminology of Behrens et al. (2014).*

detection of nectar that is bitter containing deleterious toxicants, e.g., plant alkaloids or polyphenolic tannins or insect secretions or is spoiled (Glendinning, 1994; Wang and Zhao, 2015). The absence of a functioning TAS2R in sphenisciform or gaviiform birds presumably reflects a lack of utility of detecting bitter tastants in these waterbirds.

The threshold for rejection of bitter-tasting potential foods varies with the species of bird's diet (Glendinning, 1994). Carnivores have a low threshold and reject foods with even low concentrations of bitter-tasting chemical agents. In contrast, herbivores have a high threshold to bitter tastes (Glendinning, 1994).

13.1.10 Salt and sour taste

Different from sweet, bitter, and umami tastes which are mediated by GPCRs, gustducin, and downstream signaling cascades, the salty and sour tastes modulate taste function by direct entry of H+ and Na+ ions through specialized membrane ion channels. For sensing salty and sour, the epithelial sodium channel (ENaC), the polycystic kidney disease (PKD) channels, the transient receptor potential (TRP) channel M5 (Trpm5) are utilized.

13.1.10.1 Salt taste receptor in birds

The receptor for salty taste is a heteromer consisting of subunit sodium channel monomers, specifically Scnn1a, Scnn1b, and Scnn1g (Zhao et al., 2015; Antinucci and Risso, 2017). These are members of the sodium channel gene family (SCNN) (Zhao et al., 2015). Salty taste receptors are present in all avian species including penguins (Zhao et al., 2015).

Deduced sequences of Scnn1a have been reported in multiple avian species: *Anseriformes*: black swan (*Cygnus atratus*)—Genbank XM_035571576; *Galliformes*: chicken—Genbank NM_205145; *Pelecaniformes*: little egret (*Egretta garzetta*)—Genbank XM_009639112; *Passeriformes*: New Caledonian crow (*Corvus moneduloides*)—Genbank XM_032098703. The SCNN1a gene is located on chromosome 1 (chicken (Habermann et al., 2001)).

13.1.10.2 Salty preferences tests

Preferences tests show that birds respond to sodium chloride (NaCl). High concentrations elicit aversion, whereas low concentrations are usually attractive, particularly after sodium depletion (Kare and Mason, 1986). In a diet choice situation, chickens on Na-deficient diet will select NaCl solutions up to 9 g/L while higher Na concentrations are rejected. Aversion starts with solutions of 250 mM while preferences are between 85 and 100 mM (Duncan, 1962). Avoidance to a 5% NaCl inclusion (870 mM) was reported by Balog and Millar (1989).

13.1.10.3 Sour taste receptor in birds

The receptors for sour taste are the transmembrane channels that are selective for H+ ions. Several of these channels have been identified in mammals (Bachmanov and Beauchamp, 2007). Both ENaC and H+ ion channels orthologous genes are present in chicken genome databases. The sour sensing is mediated by Pkd2l1 (PKD2L1 gene) and HCN1 receptor proteins. PKD2L1 was identified in each of the 16 bird genomes examined (Zhao et al., 2015) and is a member of the TRP channel gene family.

13.1.10.4 Sour preferences tests

Sensitivity to acids changes with avian species and with age (Mason and Clark, 2000). Chickens were tolerant to medium acidic or alkaline solutions but avoided solutions with

extreme pH (acid or alkaline) (Fuerst Jr and Kare, 1962). Chicken also avoid 0.2 M (or higher) hydrochloric and acetic acid solutions (Gentle, 1972) and avoid as well high concentrations (6%) of citric acid (Balog and Millar, 1989) and some acid blends (Viola et al., 2008). It might be interesting to reconsider the sour taste modality since there are indications on some positive preferences for acidic pH in chickens (Kare and Mason, 1986; Mason and Clark, 2000).

13.1.11 Fatty acid taste

Evidence in human and rodents supports the existence of a unique taste for fat and suggest that oral perception of fatty acid is a sixth basic taste quality (Gaillard and Kinnamon, 2019). Fat taste starts when triglycerides in the oral cavity are hydrolyzed into free fatty acids (FFAs), by lingual lipases, which in turn stimulates taste cells in the taste buds. At the surface of the cell membrane, the FFA ligand binds to two types of proteins, a G-protein-coupled receptor 120 (GPR120) and CD36 (Cartoni et al., 2010). This binding triggers a cascade of signaling events, leading to an increase in intracellular calcium which in turn mediates the depolarization of the cell and the release of neurotransmitters onto gustatory nerve fibers (Reed and Xia, 2015).

There is evidence that birds can detect fat. The structure of one of the putative receptors for fatty acids, GPR120, has been reported in chickens (Sawamura et al., 2015).

As for fat taste preference, gustation plays a key role in determining oil preferences in chickens (Furuse et al., 1996). Furthermore, chickens prefer feed containing oleic acid and linoleic acids than feed with mineral oil added instead (Sawamura et al., 2015).

13.1.12 Extra gustatory taste in birds

13.1.12.1 Overview

One of the major breakthroughs of taste research in the past two decades is the revelation of taste receptors and taste signaling components such as TRPM5, PLCβ2 and the G-protein subunits in extra-gustatory tissues. These taste-related molecules were found to be expressed not only in taste buds but also on varied extra-oral cells such as brush cells or enteroendocrine cells in different tissues such as the respiratory system, testis, heart, liver, pancreas, brain, and the gastrointestinal tract (GIT). Even though their exact function in each tissue is still to be determined, it is clear that taste receptors sense nutrients in these extra-gustatory tissues and that the signaling components participate in transduction pathways similarly to those in gustatory tissues (Yamamoto and Ishimaru, 2013) suggesting these pathways are not restricted to taste perception per se alone (Figure 13.2). Indeed, these sweet, bitter, and umami taste pathways were shown to be involved in many gut physiological mechanisms (Jang et al., 2007; Jeon et al., 2008; Janssen et al., 2011; Shirazi-Beechey et al., 2014; San Gabriel, 2015), all are key factors in gut functionality and feed intake regulation.

Despite the importance of taste pathways in these intestinal pathways and its great potential implications in birds in general and chicken production and nutrition as an agriculture animal particularly, the research of avian taste perception in the GIT has only started to thrive very recently, with focus on chicken.

13.1.12.2 Gene expression of taste receptors and signaling molecules in extra-gustatory tissues in chicken

With the release of the chicken full genome (Hillier et al., 2004), the three bitter taste receptors were identified in its genome, together with the lack of Tas1r2 (Lagerstrom et al., 2006; Shi and Zhang, 2006). The identification of taste-related genes outside of the oral cavity in chickens was reported only almost a decade later. In 2010, Byerly et al. identified T1R1 expression in the chicken hypothalamus, with higher expression in fat broilers compared to lean. Between 2014 and 16, publication reported the expression of the three chicken bitter taste T2Rs—*ggTAS2R1*, *ggTAS2R2,* and *ggTAS2R7*, 2 sweet/umami T1Rs—*ggTAS1R1* and *ggTAS1R3*, and the downstream signaling effectors *α-gustducin*, *PLCβ2,* and *TRPM5* along the chicken GIT (Cheled-Shoval et al., 2014, 2015), the expression of the umami taste receptor *mGluR* in the chicken GIT (Yoshida et al., 2015) and the expression of the fatty acid receptors GP43 GPR120 and CD36, suggesting that taste pathways are involved in the chicken GIT's sensing of different nutrients such as carbohydrates, amino-acids, and bitter compounds (potential toxins). These taste-related genes, detected by real-time PCR, were found at different expression levels in the GIT's different sections, palate, tongue, ventriculus (gizzard), duodenum, jejunum, ileum, cecum, and colon (Figure 13.1). In recent years, more publications reported the expression on additional taste-related genes in both the oral cavity and extra-gustatory tissues in birds (Mazzoni et al., 2016). Differences in taste-related genes expression were observed between two developmental stages (embryo ver. mature broiler), both in the oral cavity and in the GIT.

13.1.12.3 Effect of tastants on gene expression

Investigation on how taste-related genes expression is affected by tastants in both oral cavity and extra-gustatory tissues such as the GIT or in cell-based methods is scarce. Cheled-Shoval reported an elevation in *ggTAS2Rs*, *PLCβ2*,

and *α-gustducin* expression in the palate and duodenum of chickens following bitter tastant administration together with a subsequential elevation in sensitivity to the tastant (Cheled-Shoval et al., 2014).

13.1.13 Measuring taste perception in birds: aversion or preference testing

13.1.13.1 Methods for taste perception tests

Methods include (i) gustatory nerve recordings following chemical stimuli and electroencephalogram (EEG) analysis of arousal patterns (Halpern, 1962; Gentle, 1972, 1983) (ii) cell-based assays using Ca^{2+} imaging technology (Behrens et al., 2014; Cheled-Shoval et al., 2014; Dey et al., 2017; Su et al., 2019) (iii) behavioral responses to oral stimulation such as beak movements, head shaking, beak clapping, etc., in both embryos and mature chickens (Vince, 1977; Gentle and Harkin, 1979; Gentle, 1981; Ganchrow et al., 1990), and (iv) detection or preference taste threshold determination using aqueous solutions via no-choice, double choice, or multiple choice. In these tests, the tastants are dissolved in distilled water usually and consumption is recorded throughout the trial (Pfaffmann, 1956; Jacobs and Scott, 1957; Kare and Medway, 1959; Fuerst Jr and Kare, 1962; Gentle, 1972; Kudo et al., 2010).

These methods, mainly examining sweet, bitter, and sour tastes varied greatly in their choice manner (no-choice, 2-AFC, or multiple choice), their length (min, h, days, or weeks), their developmental stage (embryos, young chicks, or mature chickens), strains tested (hens vs. broilers) and included various perception measurements including behavioral indications, consumption sometimes together EEG analysis of arousal patterns. Notably, choice tests results are not considered as an acuity threshold but only a preference/avoidance threshold representing a changed behavior (preferring or aversion) to a stimulus solution over water.

It is highly important to note that due to this high diversity of methods (behavioral, consumption, and physiological responses) and the use of different strains, ages, and tests-length, the results of these studies of taste perception in birds show inconsistency and great variability.

13.1.13.2 Preference tests in birds

Choice or preference systems have demonstrated that generally birds avoid water containing bitter tastants, while in nectar consuming birds increased consumption of sucrose containing water was identified. Given a choice between water and water containing quinine hydrochloride, chickens avoid the quinine water in a concentration-dependent manner (Cheled-Shoval et al., 2017b, see Figure 13.5). The threshold for this effect is between 0.1 and 0.2 mM (Cheled-Shoval et al., 2017b). In contrast, the threshold for chickens avoiding water containing monosodium glutamate is between 300 and 500 mM (Cheled-Shoval et al., 2017b). Moreover, there was preference for plain water or avoidance for inosine 5′-monophosphate containing water (Cheled-Shoval et al., 2017b). In choice studies, chickens avoided solutions containing the umami tastes, serine, alanine, and glutamate together with inosine 5′-monophosphate (Yoshida et al., 2018). Chickens exhibited a preference for water rather than water containing bitter tasting, TAS2R agonists, with marked differences in the threshold (Table 13.5, Cheled-Shoval et al., 2017a). Hummingbirds exhibit increased drinking of water when it contains sucrose or fructose broad-billed hummingbird (*Cynanthus latirostris*) (Medina-Tapia et al., 2012); ruby-throated hummingbird (*Archilochus colubris*), Anns's hummingbirds (*Calypte anna* (Baldwin et al., 2014). Comparisons of chicken thresholds to humans and rat showed that while bitter threshold is similar, chickens are less sensitive to umami and even less sweet tastes, which is in agreement with the lacking of the Tas1R2 unit from the chicken genome (Table 13.4).

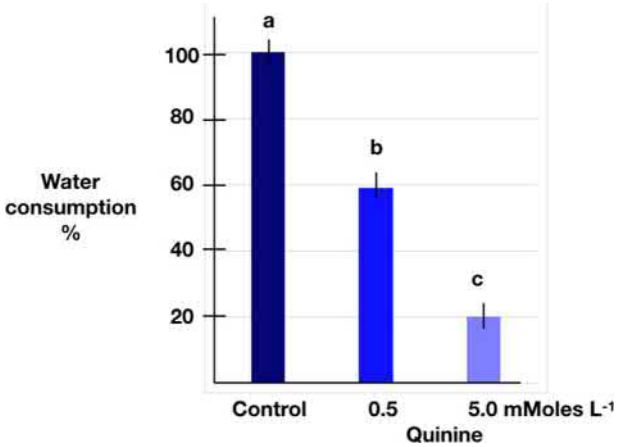

FIGURE 13.5 Consumption of quinine containing water in chicks in a preference system (provided with a choice between water and quinine containing water expressed as a percentage [a, b, c difference letters indicate difference $P < .05$]. *Adapted from Cheled-Shoval et al. (2017a).*

TABLE 13.5 Preference for water compared to agonist containing water by chickens (Cheled-Shoval et al., 2017a).

Receptor activated in vitro	Specific agonist	In vivo threshold mM
TAS2R1	Nicotine	0.33
TAS2R2	Caffeine	10
TAS2R7	(+)-catechin	3
TAS2R7	Erythromycin	0.1
TAS2R1,R2,R7	Quinine HCl	0.3

13.1.13.3 In vivo versus in vitro thresholds

In recent years, one of the most common in vitro method used in taste perception studies of birds is the cell-based functional expression assays for the determination of a receptors' activation by taste potential ligands (Behrens et al., 2004, 2009, 2014; Brockhoff et al., 2007, 2010; Reichling et al., 2008; Meyerhof et al., 2010; Dey et al., 2017). These in vitro cell-based threshold tests indicate only activation of the receptor and not guaranteed actual perception threshold of the bird. Taste receptors can be either broad (activated by a large number of ligands) or narrow (activated by a small number of ligands) or even singular (activated by a single ligand). A comparison of chicken in vivo and in vitro thresholds between TAS2R-selective and TAS2R-promiscuous ligands and the difference between ligands activating individual ggTAS2Rs showed that no simple relationship between in vivo and in vitro thresholds exist. Even same-receptor activators with similar in vitro thresholds (for example, (+)-catechin and erythromycin for ggTAS2R7) had different in vivo avoidance thresholds Cheled-Shoval et al. (2017a).

These results demonstrate that even in the simplest possible TAS2R system such as chicken, the relation of these two methods is complicated and the strength of the in vivo response could not be accurately predicted from cellular data.

13.1.14 Conclusions

It was commonly assumed birds have limited sense of taste mainly as a result of lower numbers of taste buds and of bitter taste receptors and the lack of the sweet taste receptor subunit Tas1R2 in the avian linage. However, accumulating data including behavioral, genomic, genetic, and molecular studies demonstrates clearly that birds possess a well-developed sense of taste governing nutritional evaluation and feed choices as in other vertebrates (see Table 13.3). In addition to taste perception, per-se taste receptors and their downstream proteins signals have been identified in birds outside the oral cavity, mainly along the GIT as well as in other extra-gustatory tissues such as the airways. These taste receptors, which are located in enteroendocrine cells in the GIT (Figure 13.2), have been shown to be involved in different gut functionality, metabolic and endocrinic pathways in mammals, and it can be assumed to be involved in a similar manner in birds.

There is substantial scope for future research on taste in birds. Questions that may be poised include the following:

- Why have birds so few taste buds? Is it related to the lack of chewing?
- What is the correct terminology for avian TAS2R genes?
- When did the sweet receptor lost in avian evolution?
- Why is advantageous to have more than one bitter taste receptors?
- Why are there more functioning TAS2R2 genes in passerine birds?
- Can the ability of poultry to detect different tastants be employed to increase feed intake?
- What is the relevance of taste receptors in the gastrointestinal tract and other organs?

Future research on the molecular mechanisms governing eating behavioral responses, taste perception and intestinal functionality and their interactions, all key features in both wild and domesticated avian nutrition and production, will help elucidate the role of taste in avian feed-intake regulation, feed choice, and acceptance, both ecologically and evolutionary.

References

Adler, E., Hoon, M.A., Mueller, K.L., Chandrashekar, J., Ryba, N.J., Zuker, C.S., 2000. A novel family of mammalian taste receptors. Cell 100 (6), 693–702.

Antinucci, M., Risso, D., 2017. A matter of taste: lineage-specific loss of function of taste receptor genes in vertebrates. Front. Mol. Biosci. 4, 81.

Bachmanov, A.A., Beauchamp, G.K., 2007. Taste receptor genes. Annu. Rev. Nutr. 27, 389–414.

Baker, H.G., Baker, I., Hodges, S.A., 1998. Sugar composition of nectars and fruits consumed by birds and bats in the tropics and subtropics 1. Biotropica 30 (4), 559–586.

Baldwin, M.W., Toda, Y., Nakagita, T., O'Connell, M.J., Klasing, K.C., Misaka, T., Edwards, S.V., Liberles, S.D., 2014. Sensory biology. Evolution of sweet taste perception in hummingbirds by transformation of the ancestral umami receptor. Science 345 (6199), 929–933.

Balog, J., Millar, R., 1989. Influence of the sense of taste on broiler chick feed consumption. Poult. Sci. 68 (11), 1519–1526.

Beauchamp, G.K., Jiang, P., 2015. Comparative biology of taste: insights into mechanism and function. Flavour 4 (1), 1–3.

Behrens, M., Brockhoff, A., Batram, C., Kuhn, C., Appendino, G., Meyerhof, W., 2009. The human bitter taste receptor hTAS2R50 is activated by the two natural bitter terpenoids andrographolide and amarogentin. J. Agric. Food Chem. 57 (21), 9860–9866.

Behrens, M., Brockhoff, A., Kuhn, C., Bufe, B., Winnig, M., Meyerhof, W., 2004. The human taste receptor hTAS2R14 responds to a variety of different bitter compounds. Biochem. Biophys. Res. Commun. 319 (2), 479–485.

Behrens, M., Korsching, S.I., Meyerhof, W., 2014. Tuning properties of avian and frog bitter taste receptors dynamically fit gene repertoire sizes. Mol. Biol. Evol. 31 (12), 3216–3227.

Berkhoudt, H., 1985. Structure and function of avian taste receptors. In: King, A.S., McLelland, J. (Eds.), Form and Function in Birds, vol. 3. Academic Press, London, pp. 463–496.

Berkhoudt, H., 1992. Avian taste buds: topography, structure and function. In: Chemical Signals in Vertebrates 6. Springer, pp. 15–20.

Boling, S.D., Firman, J.D., 1997. A low-protein diet for Turkey poults. Poult. Sci. 76 (9), 1298–1301.

Brockhoff, A., Behrens, M., Massarotti, A., Appendino, G., Meyerhof, W., 2007. Broad tuning of the human bitter taste receptor hTAS2R46 to various sesquiterpene lactones, clerodane and labdane diterpenoids, strychnine, and denatonium. J. Agric. Food Chem. 55 (15), 6236–6243.

Brockhoff, A., Behrens, M., Niv, M.Y., Meyerhof, W., 2010. Structural requirements of bitter taste receptor activation. Proc. Natl. Acad. Sci. U. S. A. 107 (24), 11110–11115.

Brown, M., Downs, C.T., Johnson, S.D., 2008. Sugar preferences of nectar feeding birds–a comparison of experimental techniques. J. Avian Biol. 39 (5), 479–483.

Brown, M., Downs, C.T., Johnson, S.D., 2010a. Concentration-dependent sugar preferences of the Malachite Sunbird (*Nectarinia famosa*). Auk 127 (1), 151–155.

Brown, M., Downs, C.T., Johnson, S.D., 2010b. Sugar preferences and digestive efficiency in an opportunistic avian nectarivore, the Dark-capped Bulbul Pycnonotus tricolor. J. Ornithol. 151 (3), 637–643.

Brugger, K.E., Nelms, C.O., 1991. Sucrose avoidance by American robins (*Turdus migratorius*): implications for control of bird damage in fruit crops. Crop Protect. 10 (6), 455–460.

Cartoni, C., Yasumatsu, K., Ohkuri, T., Shigemura, N., Yoshida, R., Godinot, N., le Coutre, J., Ninomiya, Y., Damak, S., 2010. Taste preference for fatty acids is mediated by GPR40 and GPR120. J. Neurosci. 30 (25), 8376–8382.

Cascales, J.L., Costa, S.O., de Groot, B.L., Walters, D.E., 2010. Binding of glutamate to the umami receptor. Biophys. Chem. 152 (1–3), 139–144.

Cheled-Shoval, S., Behrens, M., Korb, A., Di Pizio, A., Meyerhof, W., Uni, Z., Niv, M.Y., 2017a. From cell to beak: in-vitro and in-vivo characterization of chicken bitter taste thresholds. Molecules 22 (5), 821.

Cheled-Shoval, S.L., Behrens, M., Meyerhof, W., Niv, M.Y., Uni, Z., 2014. Perinatal administration of a bitter tastant influences gene expression in chicken palate and duodenum. J. Agric. Food Chem. 62 (52), 12512–12520.

Cheled-Shoval, S.L., Druyan, S., Uni, Z., 2015. Bitter, sweet and umami taste receptors and downstream signaling effectors: expression in embryonic and growing chicken gastrointestinal tract. Poult. Sci. 94 (8), 1928–1941.

Cheled-Shoval, S.L., Reicher, N., Niv, M.Y., Uni, Z., 2017b. Detecting thresholds for bitter, umami, and sweet tastants in broiler chicken using a 2-choice test method. Poult. Sci. 96 (7), 2206–2218.

Cygankiewicz, A.I., Maslowska, A., Krajewska, W.M., 2014. Molecular basis of taste sense: involvement of GPCR receptors. Crit. Rev. Food Sci. Nutr. 54 (6), 771–780.

Damak, S., Rong, M., Yasumatsu, K., Kokrashvili, Z., Varadarajan, V., Zou, S., Jiang, P., Ninomiya, Y., Margolskee, R.F., 2003. Detection of sweet and umami taste in the absence of taste receptor T1r3. Science 301 (5634), 850–853.

Dang, Y., Gao, X., Xie, A., Wu, X., Ma, F., 2014. Interaction between umami peptide and taste receptor T1R1/T1R3. Cell Biochem. Biophys. 70 (3), 1841–1848.

Davis, J.K., Lowman, J.J., Thomas, P.J., ten Hallers, B.F., Koriabine, M., Huynh, L.Y., Maney, D.L., de Jong, P.J., Martin, C.L., Thomas, J.W., 2010. Evolution of a bitter taste receptor gene cluster in a New World sparrow. Genome Biol. & Evol. 2, 358–370.

Del Rio, C.M., Baker, H., Baker, I., 1992. Ecological and evolutionary implications of digestive processes: bird preferences and the sugar constituents of floral nectar and fruit pulp. Experientia 48 (6), 544–551.

Del Rio, C.M., Stevens, B.R., 1989. Physiological constraint on feeding behavior: intestinal membrane disaccharidases of the starling. Science 243 (4892), 794–796.

Delay, E., Hernandez, N., Bromley, K., Margolskee, R., 2006. Sucrose and monosodium glutamate taste thresholds and discrimination ability of T1R3 knockout mice. Chem. Senses 31 (4), 351–357.

Dey, B., Kawabata, F., Kawabata, Y., Yoshida, Y., Nishimura, S., Tabata, S., 2017. Identification of functional bitter taste receptors and their antagonist in chickens. Biochem. Biophys. Res. Commun. 482 (4), 693–699.

Di Pizio, A., Niv, M.Y., 2015. Promiscuity and selectivity of bitter molecules and their receptors. Bioorg. Med. Chem. 23 (14), 4082–4091.

Dong, D., Jones, G., Zhang, S., 2009. Dynamic evolution of bitter taste receptor genes in vertebrates. BMC Evol. Biol. 9, 12.

Duncan, C., 1962. Salt preferences of birds and mammals. Physiol. Zool. 35 (2), 120–132.

Espaillat, J.E., Mason, J.R., 1990. Differences in taste preference between red-winged blackbirds and European starlings. Wilson Bull. 292–299.

Fleming, R.H., 2008. Nutritional factors affecting poultry bone health. Proc. Nutr. Soc. 67 (2), 177–183.

Fleming, P.A., Bakken, B.H., Lotz, C.N., Nicolson, S.W., 2004. Concentration and temperature effects on sugar intake and preferences in a sunbird and a hummingbird. Funct. Ecol. 18, 223–232.

Fuerst Jr., W.F., Kare, M.R., 1962. The influence of pH on fluid tolerance and preferences. Poult. Sci. 41 (1), 71–77.

Furuse, M., Choi, Y.H., Satoh, S., Okumura, J., 1996. The action of the cholecystokinin-A receptor antagonist, devazepide, on the digestive system of the chicken. Experientia 52 (4), 353–356.

Gaillard, D., Kinnamon, S.C., 2019. New evidence for fat as a primary taste quality. Acta Physiol. 226 (1), e13246.

Ganchrow, D., Ganchrow, J.R., 1985. Number and distribution of taste buds in the oral cavity of hatchling chicks. Physiol. Behav. 34 (6), 889–894.

Ganchrow, J.R., Ganchrow, D., 1987. Taste bud development in chickens (*Gallus gallus domesticus*). Anat. Rec. 218 (1), 88–93.

Ganchrow, J.R., Ganchrow, D., Royer, S.M., Kinnamon, J.C., 1993. Aspects of vertebrate gustatory phylogeny: morphology and turnover of chick taste bud cells. Microsc. Res. Tech. 26 (2), 106–119.

Ganchrow, J.R., Steiner, J.E., Bartana, A., 1990. Behavioral reactions to gustatory stimuli in young chicks (*Gallus gallus domesticus*). Dev. Psychobiol. 23 (2), 103–117.

Gentle, M., 1972. Taste preference in the chicken (*Gallus domesticus* L.). Br. Poult. Sci. 13 (2), 141–155.

Gentle, M., 1983. The chorda tympani nerve and taste in the chicken. Experientia 39 (9), 1002–1003.

Gentle, M.J., 1975. Using arousal changes in the electroencephalogram to measure taste sensitivity in the chicken. J. Physiol. 244 (1), 9P–10P.

Gentle, M.J., 1981. Oral behaviour following forebrain ablations in *Gallus domesticus*. Behav. Process. 6 (2), 109–120.

Gentle, M.J., Harkin, C., 1979. The effect of sweet stimuli on oral behaviour in the chicken. Chem. Senses 4 (3), 183–190.

Glendinning, J.I., 1994. Is the bitter rejection response always adaptive? Physiol. Behav. 56 (6), 1217–1227.

Go, Y., SMBE Tri-National Young Investigators, 2006. Proceedings of the SMBE Tri-National Young Investigators' Workshop 2005. Lineage-specific expansions and contractions of the bitter taste receptor gene repertoire in vertebrates. Mol. Biol. Evol. 23 (5), 964–972.

Habermann, F.A., Biet, C., Fries, R., 2001. Chromosomal localization of the genes encoding SCNN1A, BTG1, IFNG and MAOA on chicken chromosome 1 by fluorescence in-situ hybridization. Chromosome Res. 9 (6), 515–518.

Halpern, B.P., 1962. Gustatory nerve responses in the chicken. Am. J. Physiol. 203, 541–544.

Harriman, A.E., Fry, E.G., 1990. Solution acceptance by common ravens (*Corvus corax*) given two-bottle preference tests. Psychol. Rep. 67 (1), 19–26.

Hillier, L., Miller, W., Birney, E., Warren, W., Hardison, R., Ponting, C., Bork, P., Burt, D., Groenen, M., Delany, M., 2004. International Chicken Genome Sequencing Consortium: sequence and comparative analysis of the chicken genome provide unique perspectives on vertebrate evolution. Nature 432 (7018), 69–716.

Ikeda, K., 1909. On a new seasoning. J. Tokyo Chem. Soc. 30, 820–836.

Ishimaru, Y., 2009. Molecular mechanisms of taste transduction in vertebrates. Odontology 97 (1), 1–7.

Jacobs, H.L., Scott, M., 1957. Factors mediating food and liquid intake in chickens: 1. Studies on the preference for sucrose or saccharine solutions. Poult. Sci. 36 (1), 8–15.

Jang, H.-J., Kokrashvili, Z., Theodorakis, M.J., Carlson, O.D., Kim, B.-J., Zhou, J., Kim, H.H., Xu, X., Chan, S.L., Juhaszova, M., 2007. Gut-expressed gustducin and taste receptors regulate secretion of glucagon-like peptide-1. Proc. Natl. Acad. Sci. U. S. A. 104 (38), 15069–15074.

Janssen, S., Depoortere, I., 2013. Nutrient sensing in the gut: new roads to therapeutics? Trends Endocrinol. Metabol. 24 (2), 92–100.

Janssen, S., Laermans, J., Verhulst, P.-J., Thijs, T., Tack, J., Depoortere, I., 2011. Bitter taste receptors and α-gustducin regulate the secretion of ghrelin with functional effects on food intake and gastric emptying. Proc. Natl. Acad. Sci. U. S. A. 108 (5), 2094–2099.

Jeon, T.-I., Zhu, B., Larson, J.L., Osborne, T.F., 2008. SREBP-2 regulates gut peptide secretion through intestinal bitter taste receptor signaling in mice. J. Clin. Invest. 118 (11), 3693–3700.

Jiang, P., Josue, J., Li, X., Glaser, D., Li, W., Brand, J.G., Margolskee, R.F., Reed, D.R., Beauchamp, G.K., 2012. Major taste loss in carnivorous mammals. Proc. Natl. Acad. Sci. U. S. A. 109 (13), 4956–4961.

Kare, M., Mason, J., 1986. The chemical senses in birds. In: Sturkie, P.D. (Ed.), Avian Physiology. Springer-Verlag, New York.

Kare, M.R., Medway, W., 1959. Discrimination between carbohydrates by the fowl. Poult. Sci. 38 (5), 1119–1127.

Kerr, B., Kidd, M., 1999. Amino acid supplementation of low-protein broiler diets: 1. Glutamic acid and indispensable amino acid supplementation. J. Appl. Poultry Res. 8 (3), 298–309.

Kitchell, R., Ström, L., Zotterman, Y., 1959. Electrophysiological studies of thermal and taste reception in chickens and pigeons. Acta Physiol. Scand. 46 (2-3), 133–151.

Koh, S.D., Teitelbaum, P., 1961. Absolute behavioral taste thresholds in the rat. J. Comp. Physiol. Psychol. 54 (3), 223.

Kudo, K., Shiraishi, J., Nishimura, S., Bungo, T., Tabata, S., 2010. The number of taste buds is related to bitter taste sensitivity in layer and broiler chickens. Anim. Sci. J. 81 (2), 240–244.

Kudo, K., Nishimura, S., Tabata, S., 2008. Distribution of taste buds in layer-type chickens: scanning electron microscopic observations. Anim. Sci. J. 79 (6), 680–685.

Kurihara, K., 2015. Umami the fifth basic taste: history of studies on receptor mechanisms and role as a food flavor. BioMed. Res. Int. 2015.

Lagerstrom, M.C., Hellstrom, A.R., Gloriam, D.E., Larsson, T.P., Schioth, H.B., Fredriksson, R., 2006. The G protein-coupled receptor subset of the chicken genome. PLoS Comput. Biol. 2 (6), e54.

Li, D., Zhang, J., 2014. Diet shapes the evolution of the vertebrate bitter taste receptor gene repertoire. Mol. Biol. Evol. 31 (2), 303–309.

Li, X., 2009. T1R receptors mediate mammalian sweet and umami taste. Am. J. Clin. Nutr. 90 (3), 733S–737S.

Li, X., Staszewski, L., Xu, H., Durick, K., Zoller, M., Adler, E., 2002. Human receptors for sweet and umami taste. Proc. Natl. Acad. Sci. U. S. A. 99 (7), 4692–4696.

Liman, E.R., Zhang, Y.V., Montell, C., 2014. Peripheral coding of taste. Neuron 81 (5), 984–1000.

Liu, H.-X., Rajapaksha, P., Wang, Z., Kramer, N.E., Marshall, B.J., 2018. An update on the sense of taste in chickens: a better developed system than previously appreciated. J. Nutr. Food Sci. 8 (2).

Lotz, C.N., Schondube, J.E., 2006. Sugar preferences in nectar-and fruit-eating birds: behavioral patterns and physiological causes 1. Biotropica: J. Biol. & Conserv. 38 (1), 3–15.

Maehashi, K., Huang, L., 2009. Bitter peptides and bitter taste receptors. Cell. Mol. Life Sci. 66 (10), 1661–1671.

Maller, O., Kare, M.R., 1967. Observations on the sense of taste in the armadillo (*Dasypus novemcinctus*). Anim. Behav. 15 (1), 8–10.

Martínez del Rio, C., 1990. Dietary, phylogenetic, and ecological correlates of intestinal sucrase and maltase activity in birds. Physiol. Zool. 63 (5), 987–1011.

Mason, J., Clark, L., 2000. The chemical senses in birds. In: Sturkie's Avian Physiology, fifth ed. Academic Press, New York, New York, USA, pp. 39–56.

Matson, K.D., Millam, J.R., Klasing, K.C., 2004. Cockatiels (*Nymphicus hollandicus*) reject very low levels of plant secondary compounds. Appl. Anim. Behav. Sci. 85 (1–2), 141–156.

Matsunami, H., Montmayeur, J.P., Buck, L.B., 2000. A family of candidate taste receptors in human and mouse. Nature 404 (6778), 601–604.

Mazzoni, M., Bombardi, C., Vallorani, C., Sirri, F., De Giorgio, R., Caio, G., Grandis, A., Sternini, C., Clavenzani, P., 2016. Distribution of alpha-transducin and alpha-gustducin immunoreactive cells in the chicken (*Gallus domesticus*) gastrointestinal tract. Poult. Sci. 95 (7), 1624–1630.

Medina-Tapia, N., Ayala-Berdon, J., Morales-Perez, L., Melo, L.M., Schondube, J.E., 2012. Do hummingbirds have a sweet-tooth? Gustatory sugar thresholds and sugar selection in the broad-billed hummingbird Cynanthus latirostris. Comp. Biochem. Physiol. Mol. Integr. Physiol. 161 (3), 307–314.

Meyerhof, W., Batram, C., Kuhn, C., Brockhoff, A., Chudoba, E., Bufe, B., Appendino, G., Behrens, M., 2010. The molecular receptive ranges of human TAS2R bitter taste receptors. Chem. Senses 35 (2), 157–170.

Mombaerts, P., 2004. Genes and ligands for odorant, vomeronasal and taste receptors. Nat. Rev. Neurosci. 5 (4), 263–278.

Moran Jr., E.T., Stilborn, H.L., 1996. Effect of glutamic acid on broilers given submarginal crude protein with adequate essential amino acids using feeds high and low in potassium. Poult. Sci. 75 (1), 120–129.

Nelson, G., Chandrashekar, J., Hoon, M.A., Feng, L., Zhao, G., Ryba, N.J., Zuker, C.S., 2002. An amino-acid taste receptor. Nature 416 (6877), 199–202.

Nelson, G., Hoon, M.A., Chandrashekar, J., Zhang, Y., Ryba, N.J., Zuker, C.S., 2001. Mammalian sweet taste receptors. Cell 106 (3), 381–390.

Northcutt, R.G., 2004. Taste buds: development and evolution. Brain Behav. Evol. 64 (3), 198–206.

Odendaal, T.C., Brown, M., Downs, C.T., Johnson, S.D., 2010. Sugar preferences and digestive efficiency of the village weaver: a generalist avian pollinator of African plants. J. Exp. Biol. 213 (Pt 14), 2531–2535.

Pepino, M.Y., Finkbeiner, S., Beauchamp, G.K., Mennella, J.A., 2010. Obese women have lower monosodium glutamate taste sensitivity and prefer higher concentrations than do normal-weight women. Obesity 18 (5), 959–965.

Pfaffmann, C., 1956. Taste and smell. Annu. Rev. Psychol. 7, 391–408.

Picard, M.L., Uzu, G., Dunnington, E.A., Siegel, P.B., 1993. Food intake adjustments of chicks: short term reactions to deficiencies in lysine, methionine and tryptophan. Br. Poult. Sci. 34 (4), 737–746.

Pin, J.P., 2013. Tuning synaptic activity with light-controlled GPCRs. Nat. Neurosci. 16 (4), 377–379.

Purves, D., Augustine, G., Fitzpatrick, D., Katz, L., Lamantia, A., McNamara, J., Williams, S., 2001. Taste Perception in Humans. Neuroscience, second ed. Sinauer Associates, Sunderland MA.

Rajapaksha, P., Wang, Z., Venkatesan, N., Tehrani, K.F., Payne, J., Swetenburg, R.L., Kawabata, F., Tabata, S., Mortensen, L.J., Stice, S.L., 2016. Labeling and analysis of chicken taste buds using molecular markers in oral epithelial sheets. Sci. Rep. 6 (1), 1–10.

Reed, D.R., Xia, M.B., 2015. Recent advances in fatty acid perception and genetics. Adv. Nutr. 6 (3), 353S–360S.

Reichling, C., Meyerhof, W., Behrens, M., 2008. Functions of human bitter taste receptors depend on N-glycosylation. J. Neurochem. 106 (3), 1138–1148.

Roper, S.D., 2013. Taste buds as peripheral chemosensory processors. Semin. Cell Dev. Biol. 24 (1), 71–79.

Roura, E., Andres-Lacueva, C., Estruch, R., Lourdes Mata Bilbao, M., Izquierdo-Pulido, M., Lamuela-Raventos, R.M., 2008. The effects of milk as a food matrix for polyphenols on the excretion profile of cocoa (-)-epicatechin metabolites in healthy human subjects. Br. J. Nutr. 100 (4), 846–851.

Roura, E., Baldwin, M.W., Klasing, K., 2013. The avian taste system: potential implications in poultry nutrition. Anim. Feed Sci. Technol. 180 (1–4), 1–9.

Rowland, H.M., Parker, M.R., Jiang, P., Reed, D.R., Beauchamp, G.K., 2015. Comparative taste biology with special focus on birds and reptiles. Handb. Olfaction & Gust. 957–982.

Rozengurt, E., 2006. Taste receptors in the gastrointestinal tract. I. Bitter taste receptors and alpha-gustducin in the mammalian gut. Am. J. Physiol. Gastrointest. Liver Physiol. 291 (2), G171–G177.

San Gabriel, A.M., 2015. Taste receptors in the gastrointestinal system. Flavour 4 (1), 1–4.

Sanematsu, K., Yoshida, R., Shigemura, N., Ninomiya, Y., 2014. Structure, function, and signaling of taste G-protein-coupled receptors. Curr. Pharmaceut. Biotechnol. 15 (10), 951–961.

Sawamura, R., Kawabata, Y., Kawabata, F., Nishimura, S., Tabata, S., 2015. The role of G-protein-coupled receptor 120 in fatty acids sensing in chicken oral tissues. Biochem. Biophys. Res. Commun. 458 (2), 387–391.

Shi, P., Zhang, J., 2006. Contrasting modes of evolution between vertebrate sweet/umami receptor genes and bitter receptor genes. Mol. Biol. Evol. 23 (2), 292–300.

Shirazi-Beechey, S.P., Daly, K., Al-Rammahi, M., Moran, A.W., Bravo, D., 2014. Role of nutrient-sensing taste 1 receptor (T1R) family members in gastrointestinal chemosensing. Br. J. Nutr. 111 (S1), S8–S15.

Stapleton, J., Luellig, M., Roper, S., Delay, E.R., 2002. Discrimination between the tastes of sucrose and monosodium glutamate in rats. Chem. Senses 27 (4), 375–382.

Su, Y., Jie, H., Zhu, Q., Zhao, X., Wang, Y., Yin, H., Kumar Mishra, S., Li, D., 2019. Effect of bitter compounds on the expression of bitter taste receptor T2R7 downstream signaling effectors in cT2R7/pDisplay-Galpha16/gust44/pcDNA3.1 (+) cells. BioMed Res. Int. 2019, 6301915.

Treesukosol, Y., Smith, K.R., Spector, A.C., 2011. Behavioral evidence for a glucose polymer taste receptor that is independent of the T1R2+3 heterodimer in a mouse model. J. Neurosci. 31 (38), 13527–13534.

Vanwyk, B., Nicolson, S., 1995. Xylose Is a Major Nectar Sugar in Protea and Faurea, vol. 91. Bureau Scientific Publ Po Box 1758, Pretoria 0001, South Africa, pp. 151–153.

Venkatesan, N., Rajapaksha, P., Payne, J., Goodfellow, F., Wang, Z., Kawabata, F., Tabata, S., Stice, S., Beckstead, R., Liu, H.-X., 2016. Distribution of α-gustducin and vimentin in premature and mature taste buds in chickens. Biochem. Biophys. Res. Commun. 479 (2), 305–311.

Vince, M.A., 1977. Taste sensitivity in the embryo of the domestic fowl. Anim. Behav. 25, 797–805.

Wang, K., Zhao, H., 2015. Birds generally carry a small repertoire of bitter taste receptor genes. Genome. Biol. Evol. 7 (9), 2705–2715.

Viola, E.S., Vieira, S.L., Torres, C.A., de Freitas, D.M., Berres, J., 2008. Performance of broilers supplemented with blends of lactic, formic, acetic, and phosphoricacids in the feed or water. Braz. J. Anim. Sci. 37, 296–302.

Wang, Y., Jiao, H., Jiang, P., Zhao, H., 2019. Functional divergence of bitter taste receptors in a nectar-feeding bird. Biol. Lett. 15 (9), 20190461.

Warren, R.P., Vince, M.A., 1963. Taste discrimination in the great tit (Parus major). J. Comp. Physiol. Psychol. 56, 910–913.

Werner, S.J., Kimball, B.A., Provenza, F.D., 2008. Food color, flavor, and conditioned avoidance among red-winged blackbirds. Physiol. Behav. 93 (1–2), 110–117.

Wiener, A., Shudler, M., Levit, A., Niv, M.Y., 2012. BitterDB: a database of bitter compounds. Nucleic Acids Res. 40, D413–D419 (Database issue).

Yamaguchi, S., 1979. The Umami Taste. ACS Publications.

Yamaguchi, S., 1991. Basic properties of umami and effects on humans. Physiol. Behav. 49 (5), 833–841.

Yamamoto, K., Ishimaru, Y., 2013. Oral and extra-oral taste perception. Semin. Cell Dev. Biol. 24 (3), 240–246.

Yarmolinsky, D.A., Zuker, C.S., Ryba, N.J., 2009. Common sense about taste: from mammals to insects. Cell 139 (2), 234–244.

Yoshida, Y., Kawabata, F., Kawabata, Y., Nishimura, S., Tabata, S., 2018. Expression levels of taste-related genes in palate and tongue tip, and involvement of transient receptor potential subfamily M member 5 (TRPM5) in taste sense in chickens. Anim. Sci. J. 89 (2), 441–447.

Yoshida, Y., Kawabata, Y., Kawabata, F., Nishimura, S., Tabata, S., 2015. Expressions of multiple umami taste receptors in oral and gastrointestinal tissues, and umami taste synergism in chickens. Biochem. Biophys. Res. Commun. 466 (3), 346–349.

Yu, X., Zhang, L., Miao, X., Li, Y., Liu, Y., 2017. The structure features of umami hexapeptides for the T1R1/T1R3 receptor. Food Chem. 221, 599–605.

Zhang, F., Klebansky, B., Fine, R.M., Xu, H., Pronin, A., Liu, H., Tachdjian, C., Li, X., 2008. Molecular mechanism for the umami taste synergism. Proc. Natl. Acad. Sci. U. S. A. 105 (52), 20930–20934.

Zhang, J., Zhao, M., Su, G., Lin, L., 2019. Identification and taste characteristics of novel umami and umami-enhancing peptides separated from peanut protein isolate hydrolysate by consecutive chromatography and UPLC-ESI-QTOF-MS/MS. Food Chem. 278, 674–682.

Zhao, G.Q., Zhang, Y., Hoon, M.A., Chandrashekar, J., Erlenbach, I., Ryba, N.J., Zuker, C.S., 2003. The receptors for mammalian sweet and umami taste. Cell 115 (3), 255–266.

Zhao, H., Li, J., Zhang, J., 2015. Molecular evidence for the loss of three basic tastes in penguins. Curr. Biol. 25 (4), R141–R142.

Zhao, H., Yang, J.R., Xu, H., Zhang, J., 2010. Pseudogenization of the umami taste receptor gene Tas1r1 in the giant panda coincided with its dietary switch to bamboo. Mol. Biol. Evol. 27 (12), 2669–2673.

Chapter 14

Avian nociception and pain

N.J. Beausoleil, S.E. Holdsworth and H. Lehmann
Animal Welfare Science and Bioethics Centre, School of Veterinary Science, Massey University, Palmerston North, Manawatū, New Zealand

14.1 Introduction

14.1.1 What is pain and what is it for?

Animal pain is defined as "*an aversive sensory and emotional experience representing an awareness by the animal of damage or threat to the integrity of its tissues … it changes the animal's physiology and behavior to reduce or avoid damage, to reduce the likelihood of recurrence and to promote recovery*" (Molony and Kent, 1997). Thus, the ultimate function of pain is to protect the animal from current and future tissue damage (Viñuela-Fernández et al., 2007). This function is achieved through two inter-related processes: nociception and the emotional experience of pain. Nociception is the sensory component and involves the sensory and motor systems that detect and respond to damaging or potentially damaging (noxious) stimuli (Dubin and Patapoutian, 2010). The emotional component of pain, the unpleasant "pain experience", arises only when nociceptive signals are transmitted to areas of the brain associated with generating emotions and with motivational learning (Bateson, 1991, Fig. 14.1). The emotional and cognitive components of pain are proposed to provide the animal with long-lasting motivation to avoid noxious stimuli and better protect itself from damage in the future (Bateson, 1991; Elwood, 2011).

14.1.2 Why does pain matter?

Birds are exposed to many situations, conditions, and procedures that result in tissue damage and thus have the potential to cause pain. Clinically, common causes of damage in wild and pet birds are predator attacks, vehicle collisions, self-mutilation, and diseases (Malik and Valentine, 2018). In production systems, birds are subject to damage due to husbandry procedures such as debeaking and dubbing, injuries related to transport, shackling and feather pecking, and conditions such as keel fractures, osteoarthritis, footpad dermatitis, and myopathies associated with breeding for production traits and/or management conditions (e.g., Gentle, 2011; Hothersall et al., 2016; Norring et al., 2018; Thøfner et al., 2020). Thus, there is clearly scope for many birds to experience pain, which may impact on their welfare, productivity, and behavior.

Because of the inherent unpleasantness of the pain experience, understanding and avoiding animal pain is important for safeguarding their welfare. An animal's welfare state represents the sum of all its mental experiences; these arise due to interpretation, by the animal's brain, of sensory information about its internal and external environment (Beausoleil and Mellor, 2017). Unpleasant experiences motivate the animal to act to rectify the problem and/or reduce the risk of future reoccurrence (Elwood, 2011; Williams et al., 2019). Problems that cannot be effectively rectified through behavioral and physiological responses will have a greater detrimental impact on welfare than acute experiences. Thus, chronic pain is of greater concern for bird welfare than acute pain, which is relatively short-lived. Chronic pain arises when the nociceptive pathways are sensitized following damage, resulting in hyperalgesia (noxious stimuli are more painful) and/or allodynia (innocuous stimuli are painful) (Dubin and Patapoutian, 2010). This state can last long after the original damage has healed. Because of its greater significance to the animal, chronic pain is more likely than acute pain to result in long-term changes in behavior and motivation and to confer survival benefits in terms of reducing the likelihood of future damage (Crook et al., 2014).

Likewise, longer-lasting pain will have greater impacts on productivity. These arise because of pain-related alterations in behavior (e.g., reduced feeding Gentle et al., 1997; Davis et al., 2004) or because prolonged physiological stress responses cause a metabolic shift, sacrificing growth, immune and reproductive functions (Virden and Kidd, 2009; Williams et al., 2019). Finally, pain can affect important behaviors, sometimes in ways that impair

Sturkie's Avian Physiology. https://doi.org/10.1016/B978-0-12-819770-7.00028-1

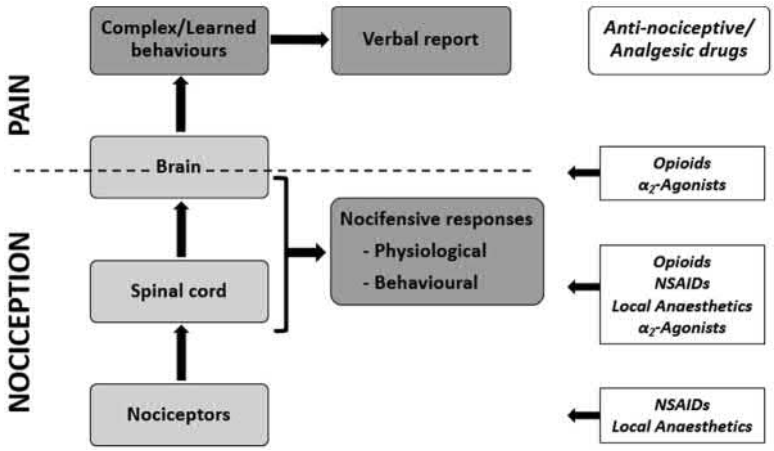

FIGURE 14.1 Generic schema of the neuroanatomical structures and pathways necessary to sense, transmit, integrate, and modulate nociceptive information to generate the experience of pain and observable responses. Verbal report is possible only from humans. Types of exogenous anti-nociceptive/analgesic drugs acting at different levels of the pathway are noted: nonsteroidal anti-inflammatory drugs (NSAIDs), alpha-2 adrenoreceptor agonist drugs (α_2-agonists).

recovery (Paul-Murphy and Hawkins, 2015). For example, animals in pain may become more aggressive or reluctant to interact with conspecifics or their human carers. Thus, there are ethical, economic, and conservation reasons for considering avian pain.

14.2 What evidence is required to demonstrate the capacity for pain?

The capacity of birds to experience pain is usually assumed. For example, birds are considered to be sentient in the animal welfare legislation of many jurisdictions (e.g., New Zealand Government, 2015; McCulloch, 2018; Australian Capital Territory, 2019), implying that they have the capacity for mental experiences, including pain (Mellor, 2019). However, many claims about birds' capacity for, and experience of, pain are based largely on extrapolation from mammals. Because of potentially relevant differences in neuroanatomy and physiology (Kuenzel, 2007; Shanahan et al., 2013; Zehnder et al., 2014) and the fact that we are apparently less well able to recognize indicators of pain in birds (Hawkins, 2006; Paul-Murphy and Hawkins, 2015), such extrapolation may not be appropriate. In fact, central processing of information about noxious stimuli, and thus the potential for the pain experience, is less well understood in birds than it is in fish (Williams et al., 2019).

Recent reviews provide detail of the physiology and expression of nociception and pain in birds (Gentle, 2011; Machin, 2014; Douglas et al., 2018; Baker et al., 2019). Here, we present a brief, systematic summary of the evidence that birds are capable of both the sensory and emotional components of pain (Bateson, 1991; Elwood, 2011; Sneddon et al., 2014; Burrell, 2017). The evidence is organized according to the neural apparatus required for nociception and observable evidence that nociception is occurring, followed by the structures and processes required to generate the emotional and cognitive components of the pain experience and the kind of evidence required to demonstrate the capacity for pain per se. General explanation of each component is followed by a summary of the specific evidence that birds do, in fact, possess that particular function. Table 14.1 summarizes key literature for different types of evidence supporting, or failing to support, each component in birds. We also consider evidence of how nociception or pain would be modified through the application of mitigation strategies such as analgesic drugs.

14.2.1 What is needed for nociception?

The required components for nociception are sensory receptors to detect damaging stimuli and transduce those inputs into electrical impulses, neural pathways to transmit those impulses from the periphery to CNS, and from there to integrating centers within the CNS to facilitate generation of reflex protective (nocifensive) responses.

14.2.1.1 Transduction, transmission, and modulation of nociceptive information

Nociceptors are free (unspecialized) nerve endings of peripheral fibers that act as sensory receptors for noxious stimuli. Found in various tissues, they encode the stimulus modality, intensity, and duration. Fast pain is associated with rapid transmission of impulses from the periphery to the spinal cord in large diameter, myelinated Aδ fibers while slower-arising and longer-lasting pain (dull/aching) is due to transmission in smaller, unmyelinated C fibers

TABLE 14.1 Key evidence of the presence and activation of each level of the nociceptive and pain pathways in birds.

Level of evidence	Kind of evidence	Key references
Nociceptors		
	Immunohistochemical	Jordt and Julius (2002), Saito et al. (2014)
	Electrophysiological	Necker and Reiner (1980), Gentle (1989), Gentle (1991), Gentle and Thorp (1994), Gentle and Tilston (2000), Gentle et al. (2001), McKeegan et al. (2002), McKeegan (2004), Sandercock (2004)
Pathway to spinal cord and brainstem		
	Immunohistochemical or Immunocytochemical	Lavalley and Ho (1983), Gentle et al. (1995), Den Boer-Visser and Dubbeldam (1996), Zhai and Atsumi (1997), Dubbeldam (1998), Kawate et al. (2005), Li et al. (2005), Wild et al. (2010)
	Electrophysiological	Delius and Bennett (1972), Holloway et al. (1980)
	Endogenous and exogenous modulation	Reiner et al. (1989), Sufka et al. (1991), Nicol et al. (1992), Gentle and Thorp (1994), Kawate et al. (2005), Sheehan et al. (2010)
Nocifensive responses		
	Behavioral withdrawal/escape	Gentle and Wood-Gush (1976), Gentle (1981), Hughes (1990), Gentle and Hunter (1991), Paul-Murphy et al. (1999a), Paul-Murphy et al. (1999b), Evrard and Balthazart (2002), Hoppes et al. (2003), Sladky et al. (2006), Hothersall et al. (2011), Sanchez-Migallon Guzman et al. (2011), Sanchez-Migallon Guzman et al. (2012), Caplen et al. (2013a), Geelen et al. (2013), Hothersall et al. (2014)
	Physiological	Glatz (1987), Woolley and Gentle (1987), Glatz and Lunam (1994), Machin and Livingston (2002), Davis et al. (2004), Moneva et al. (2008)
	Endogenous and exogenous modulation	Hughes (1990), Paul-Murphy et al. (1999b), Machin and Livingston (2002), Hoppes et al. (2003), Roach and Sufka (2003), Sladky et al. (2006), Sanchez-Migallon Guzman et al. (2011), Sanchez-Migallon Guzman et al. (2012), Caplen et al. (2013a), Geelen et al. (2013), Hothersall et al. (2014)
Higher brain processing		
	Neuroanatomical or Electrophysiological	Dubbeldam (1998), Dubbeldam (2009)
	Electroencephalogram	Woolley and Gentle (1987)*, Gentle and Hunter (1991), Trebilcock (2015)*, McIlhone et al. (2018)*
Complex behaviour		
	Spontaneous expression	Duncan et al. (1989), Gentle et al. (1990), Duncan et al. (1991), Gentle et al. (1991), Hughes and Sufka (1991), Glatz et al. (1992), Gentle (1997)*, Gentle et al. (1997), Reiter and Bessei (1997), Buchwalder and Huber-Eicher (2005), Hocking et al. (2005), Freire et al. (2011)*, Desmarchelier et al. (2012), Nasr et al. (2012), Caplen et al. (2013b), Sinclair et al. (2015), Weber Wyneken et al. (2015)
	Motivational trade-offs	McGeown et al. (1999), Berg and Sanotra (2003), Caplen et al. (2014), Hothersall et al. (2016), Singh et al. (2017)
	Exogenous modulation of spontaneous behavior	Hughes and Sufka (1991), Glatz et al. (1992), McGeown et al. (1999), Buchwalder and Huber-Eicher (2005), Hocking et al. (2005), Nasr et al. (2012), Caplen et al. (2013b), Hothersall et al. (2016), Singh et al. (2017), Bailey et al. (2019)
	Endogenous modulation	Gentle and Corr (1995), Wylie and Gentle (1998), Gentle and Tilston (1999)
	Associative learning tests	Danbury et al. (2000), Freire et al. (2008)*, Nasr et al. (2013)

*indicates evidence that fails to support the existence of a particular component or manifestation of nociception or pain in birds.

(Dubin and Patapoutian, 2010). Nociceptive fibers synapse onto spinal cord neurons in the outermost layers of the dorsal horn. Here, the release of neurotransmitters activates neurons which project up the spinal cord to the brainstem and other structures (Willis, 1985; Cortelli et al., 2013).

Following injury or infection, nociceptors become sensitized by inflammatory chemicals released by immune cells (Burrell, 2017). Peripheral "anti-nociception" can be achieved using anti-inflammatory drugs to reduce the production of these chemicals or using local anaesthetics to block transmission in the nociceptive fibers; both reduce inputs to the spinal cord (Williams et al., 2019, Fig. 14.1). Centrally, the dorsal horn of the spinal cord is the primary site for modulation of nociceptive signals. Ascending spinal nociceptive fibers, as well as neurons from higher brain regions, stimulate modulation centers in the brainstem and hypothalamus which then exert descending control on dorsal horn neurons (Cortelli et al., 2013). Opioids and endocannabinoids produced by the brain in response to nociceptive inputs or other "stressors" bind to receptors in other parts of the brain and spinal cord to reduce subsequent signals reaching the brain, i.e., endogenous analgesia (Baker et al., 2019). Many drugs that produce central anti-nociception or analgesia act on these opioid receptors or stimulate other components of the descending inhibitory pathways (Burrell, 2017, Fig. 14.1).

The capacity of birds for nociception and modulation of nociceptive signals is well-established (reviewed by Machin, 2014; Sneddon et al., 2014; Douglas et al., 2018; Baker et al., 2019; Williams et al., 2019). Briefly, various nociceptors have been found in the skin, ankle joints, skeletal muscles, nasal and oral epithelium, and other beak structures of poultry, waterfowl, or starlings (Table 14.1). Mechanical, thermal, and polymodal (mechanothermal and mechanochemical) nociceptors have been identified (Dubbeldam, 2009). These respond similarly to those of mammals, although there are differences in sensitivity to chemicals (e.g., capsaicin) and in the high and low temperatures that activate thermal receptors (Machin, 2005; Saito et al., 2014).

Likewise, the organization of the ascending sensory pathways up to the brainstem and thalamus appears to be similar in birds and mammals (Shanahan et al., 2013; Douglas et al., 2018), although there is little specific information on nociceptive pathways within the brain and that from only a few avian species (Table 14.1). The neurochemicals and receptors required for endogenous modulation have been demonstrated in birds; the proportions of the various opioid receptors differ from those of mammals, and this influences the efficacy of opioid drugs in birds (Singh et al., 2017; Douglas et al., 2018). Overall, birds and mammals seem to have similar capacities to detect, transduce, transmit, and modulate noxious signals.

14.2.1.2 Nocifensive responses

Nocifensive responses are the immediate, automatic (reflex) behavioral and physiological responses to noxious stimulation designed to remove the animal from immediate danger and restore homeostasis (Cortelli et al., 2013). These responses are facilitated by multiple interactions between ascending nociceptive neurons and neurons in other systems at both spinal and supraspinal levels. Inputs from the spinal cord and trigeminal nerves activate multiple areas in the brainstem, hypothalamus, thalamus, and amygdala. These "subcortical reflex centers" stimulate physiological responses from the autonomic nervous system and hypothalamic pituitary adrenal axis and behavioral responses such as limb withdrawal and other rapid avoidance or defensive movements (Cortelli et al., 2013; Baker et al., 2019).

Birds demonstrate nocifensive behavioral and physiological responses to potential or actual tissue damage (Table 14.1). Behavioral withdrawal reflexes can be elicited by noxious thermal, electrical, and mechanical stimuli in various species, even when the birds are anesthetized (e.g., Machin and Livingston, 2002). Coordinated escape behaviors to some noxious events are shown even by chickens lacking a forebrain (Gentle and Wood-Gush, 1976; Gentle, 1981), supporting the idea that these behaviors are organized in the brainstem. Likewise, rapid changes in heart and respiratory rates and blood pressure follow feather removal, comb pinching, beak trimming, and other noxious stimuli in chickens and ducks. Beak trimming and formalin injection elicited sustained increases in circulating stress hormones (corticosterone) in chickens.

There is also evidence of exogenous modulation of nocifensive responses in birds. Behaviorally, birds become less responsive in withdrawal threshold tests after administration of opioid drugs and more responsive following inflammation; the latter sensitization can be reversed by both anti-inflammatory drugs and opioids. Similarly, nonsteroidal anti-inflammatory drugs (NSAIDs) and opioids reduced cardiorespiratory responses to noxious stimulation in ducks and parrots. In summary, birds demonstrate both the necessary neural anatomy and the behavioral and physiological manifestations of nociception, which is supported by evidence of anti-nociception.

14.2.2 What is needed for pain?

For animals to become aware of noxious sensations and experience the unpleasant emotion proposed to give pain its adaptive value, further brain processing of nociceptive inputs is required. Evidence of that processing comes from the presence and activation of the necessary brain areas and from the flexible expression of behavior indicative of

complex integration of information, learning, and memory, and changes in motivation due to the unpleasant nature of the experience (Elwood, 2011; Sneddon et al., 2014).

14.2.2.1 Higher brain processing of nociceptive inputs

In general terms, the required components are ascending pathways from the thalamus to telencephalic (forebrain) areas involved in sensory processing and generation of emotion, memory, and avoidance learning that are activated by noxious stimulation and that exert descending control on other brain areas involved in producing motor responses and modulating nociception. In humans and other mammals, a network of cortical areas, referred to as the "pain matrix," is considered to be responsible for generating pain from nociception (reviewed by Cortelli et al., 2013); measuring activity in this network using neuroimaging may provide an objective reflection of the pain experience (Borsook et al., 2010; Da Silva and Seminowicz, 2019).

The architecture of the avian forebrain is very different from that of mammals, and the brain structures that might be involved in a "pain matrix" are not yet known (Dubbeldam, 2009; Williams et al., 2019). However, some functional homologies (Kuenzel, 2007; Baker et al., 2019) and similar connectivity among brain areas involved in sensory association and executive and motor functions have been found in pigeon and mammalian brains, including a network resembling the human subnetwork for processing internal sensory information (Shanahan et al., 2013). This suggests similar forebrain organization for processing of sensory information and higher cognitive functions in birds and mammals (Güntürkün, 2012), which may include generation of pain.

Several studies have explored the global electrical responses of the chicken brain to nociceptive inputs using the electroencephalogram (EEG). Thus far, these methods have failed to detect changes in the EEG like those observed in mammals (Murrell and Johnson, 2006). While Gentle and Hunter (1991) reported qualitative changes in the EEG response of chickens to feather removals, these were in the opposite direction to those expected and correlated with periods of behavioral immobility rather than with stimulus application per se. In contrast, Woolley and Gentle (1987) found no responses to a comb pinch or noxious thermal stimulus. Likewise, neither surface recordings (McIlhone et al., 2018) nor recordings from electrodes placed in subregions of the hyperpallium and nidopallium (Trebilcock, 2015) revealed quantitative EEG responses to noxious electrical, mechanical, or thermal stimulation. The difference may relate to the differences in forebrain architecture, particularly the deeper location of relevant structures in birds (Williams et al., 2019). Further neuroimaging studies are required to elucidate the brain networks involved in avian pain processing.

14.2.2.2 Complex behavioral responses

Because nociception can cause a range of acute physiological and behavioral responses that don't require higher brain processing (Cortelli et al., 2013), these nocifensive responses by themselves provide weak evidence of the cognitive and emotional aspects of pain. Stronger evidence comes from behaviors which are more complex and prolonged and the expression of which is influenced by other motivational states and vice versa, i.e., motivational tradeoffs (Gentle and Corr, 1995). Examples include changes in the animal's normal behavioral repertoire or the expression of specific behaviors that reflect awareness of the site of damage or reduce further stimulation of that area (Bateson, 1991). However, care is required in interpreting these "pain-related" behaviors as some have been observed in animals lacking a forebrain (Matthies and Franklin, 1992; Gentle, 1997), suggesting that they can be organized in the brainstem without the higher processing necessary for the pain experience. Thus, observing the effects of manipulating other motivations (e.g., hunger) on such responses can provide stronger evidence of pain. Examples include stress-induced and attentional analgesia, in which stress or a shift in attentional focus reduces responsiveness to noxious stimulation (Baker et al., 2019). Perhaps even more compelling are tests of associative learning and memory, in which animals are asked to demonstrate their unpleasant experience of a noxious event or condition through their subsequent responses to places or signals associated with that event/condition or its relief (Gao et al., 2004; Dunlop et al., 2006; Elwood, 2011; Gerber et al., 2014; Sneddon et al., 2014).

Most of the avian research on complex behavioral responses has been done on poultry following procedures, or with conditions, expected to cause chronic pain. Following debeaking, chickens show prolonged changes in general activity, locomotion, feeding, drinking, preening, and pecking at objects (Table 14.1); such changes can persist for many weeks depending on trimming age, method, and severity. Broiler chickens and turkeys with naturally occurring or induced inflammatory arthritis show changes in gait (limping) or weight-bearing (e.g., one-legged standing). Altered behavior following debeaking and abnormal gait due to arthritis is improved by the administration of local anaesthetics, NSAIDs or opioids.

Tests explicitly designed to create motivational conflict provide support for chickens' ability to weigh the unpleasantness of pain against other priorities (Table 14.1). For example, lame broilers were slower to traverse an obstacle course to access food and sat more quickly in a

mildly aversive water bath than did sound birds. NSAIDs improved the performance of lame birds, suggesting they were able to attend to the other motivational priorities when pain was reduced. While little work has been done on stress-induced or attentional analgesia in birds, there is some evidence that it occurs and is mediated by endogenous opioids. Introduction into a novel environment suppressed the pain behavior of layer hens with induced arthritis (Gentle and Tilston, 1999). Likewise, increased feeding motivation and preparation to egg-lay suppressed arthritis-related pain behavior, and this effect was reversed by naloxone (Wylie and Gentle, 1998).

Little work on associative learning and memory related to tissue damage has been undertaken on birds. Of three studies, two provide compelling evidence that chickens with injuries likely to cause chronic pain learned to associate a place or color with analgesia (relief learning), supporting the cognitive and emotional significance of their experience. In one study, layer hens with healed keel fractures showed a preference for a place they had learned to associate with injection of an opioid analgesic, while sound hens showed no preference (Nasr et al., 2013). Similarly, naturally lame broilers preferentially selected colored feed treated with an NSAID shown to improve lameness, and the amount of feed consumed increased with the degree of lameness (Danbury et al., 2000). In contrast, Freire et al. (2008) found no evidence of a learned preference for an NSAID-treated food by debeaked layer hens, despite birds showing pain-guarding behavior, and the observation that consumption of large doses of carprofen reduced this behavior. It is possible that the type or consumed dose of analgesic was not effective in facilitating a learned association for that type of chronic pain.

Overall, the results of various behavioral studies examining motivational trade-offs and associative learning support the capacity of chickens to experience an unpleasant emotion due to noxious stimulation that alters their subsequent decision-making and behavior; however, direct evidence of the brain processing facilitating that capacity has not yet been demonstrated.

14.3 Conclusions

Thus far, nociception and pain have been studied in only around 15 of the estimated 10,000 bird species in 6 of 40 avian orders. Relevant differences exist among species, for example, in the neural pathways carrying sensory information to the forebrain (Kuenzel, 2007), thus pain studies should be extended within the Aves class. In those species studied, the capacity for nociception is well-established, supported by evidence of the neuroanatomical and neurochemical substrates for nociceptive signaling and modulation, and by observation of nocifensive responses to potential or actual tissue damage. Most of the neurological research has been undertaken in chickens and pigeons, probably because of the availability and low value of individuals of these species, the potential for welfare compromise in the poultry industry and because the pigeon brain atlas is the most detailed and accurate.

Evidence of the cognitive and emotional components of pain comes largely from behavioral studies on chickens; most explore spontaneous expression of complex behaviors following tissue damage and its mitigation by analgesics. Very few studies have been undertaken to provide evidence of higher brain processing of nociceptive information in birds, and more of these kinds of studies are needed. A few demonstrate endogenous alterations in pain sensitivity reflective of cognitive processing or associative learning indicative of the unpleasantness of chronic pain. While neuroimaging evidence of higher brain processing of nociceptive inputs has not yet been found, the available behavioral evidence supports the capacity of chickens, at least, to experience pain emotionally. As pain, particularly when chronic, can impact detrimentally on animal welfare and productivity, there is a need for continued research into pain and its alleviation in a wider range of avian species.

References

Australian Capital Territory, 2019. Animal Welfare Legislation Amendment Bill 2019 (Canberra, ACT, Australia).

Bailey, R.S., Sheldon, J.D., Allender, M.C., Adkesson, M.J., Chinnadurai, S.K., 2019. Analgesic efficacy of tramadol compared with meloxicam in ducks (*Cairina moschata domestica*) evaluated by ground-reactive forces. J. Avian Med. Surg. 33, 133–140.

Baker, B.I., Machin, K.L., Schwean-Lardner, K., 2019. When pain and stress interact: looking at stress-induced analgesia and hyperalgesia in birds. World Poultry Sci. J. 75, 457–468.

Bateson, P., 1991. Assessment of pain in animals. Anim. Behav. 42, 827–839.

Beausoleil, N.J., Mellor, D.J., 2017. Validating indicators of sheep welfare. In: Greyling, J. (Ed.), Achieving Sustainable Production of Sheep. Burleigh Dodds Publishing, Cambridge, U.K., pp. 327–343

Berg, C., Sanotra, G.S., 2003. Can a modified latency-to-lie test be used to validate gait-scoring results in commercial broiler flocks? Anim. Welf. 12, 655–659.

Borsook, D., Sava, S., Becerra, L., 2010. The pain imaging revolution: advancing pain into the 21st century. Neuroscientist 16.

Buchwalder, T., Huber-Eicher, B., 2005. Effect of the analgesic butorphanol on activity behaviour in turkeys (*Meleagris gallopavo*). Res. Vet. Sci. 79, 239–244.

Burrell, B.D., 2017. Comparative biology of pain: what invertebrates can tell us about how nociception works. J. Neurophysiol. 117, 1461–1473.

Caplen, G., Baker, L., Hothersall, B., McKeegan, D.E.F., Sandilands, V., Sparks, N.H.C., Waterman-Pearson, A.E., Murrell, J.C., 2013a. Thermal nociception as a measure of non-steroidal anti-inflammatory drug effectiveness in broiler chickens with articular pain. Vet. J. 198.

Caplen, G., Colborne, G.R., Hothersall, B., Nicol, C.J., Waterman-Pearson, A.E., Weeks, C.A., Murrell, J.C., 2013b. Lame broiler chickens respond to non-steroidal anti-inflammatory drugs with objective changes in gait function: a controlled clinical trial. Vet. J. 196, 477–482.

Caplen, G., Hothersall, B., Nicol, C.J., Parker, R.M., Waterman-Pearson, A.E., Weeks, C.A., Murrell, J.C., 2014. Lameness is consistently better at predicting broiler chicken performance in mobility tests than other broiler characteristics. Anim. Welf. 23, 179–187.

Cortelli, P., Giannini, G., Favoni, V., Cevoli, S., Pierangeli, G., 2013. Nociception and autonomic nervous system. Neurol. Sci. 34, 41–46.

Crook, R.J., Dickson, K., Hanlon, R.T., Walters, E.T., 2014. Nociceptive sensitization reduces predation risk. Curr. Biol. 24, 1121–1125.

Da Silva, J.T., Seminowicz, D.A., 2019. Neuroimaging of pain in animal models: a review of recent literature. Pain Rep. 4, 1–9.

Danbury, T.C., Weeks, C.A., Waterman-Pearson, A.E., Kestin, S.C., Chambers, J.P., 2000. Self-selection of the analgesic drug carprofen by lame broiler chickens. Vet. Rec. 146, 307–311.

Davis, G.S., Anderson, K.E., Jones, D.R., 2004. The effects of different beak trimming techniques on plasma corticosterone and performance criteria in Single Comb White Leghorn hens. Poultry Sci. 83, 1624–1628.

Delius, J.D., Bennett, K., 1972. Cutaneous sensory projections to the avian forebrain. Brain Res. 37, 205–221.

Den Boer-Visser, A.M., Dubbeldam, J.L., 1996. The distribution of acetylcholinesterase reactivity and substance P, serotonin and met-enkephalin immunoreactivity in the myelencephalon of normal chickens (*Gallus gallus domesticus*) and after debeaking. Neth. J. Zool. 47, 289–312.

Desmarchelier, M., Troncy, E., Beauchamp, G., Paul-Murphy, J.R., Fitzgerald, G., Lair, S., 2012. Evaluation of a fracture pain model in domestic pigeons (*Columba livia*). Am. J. Vet. Res. 73, 353–360.

Douglas, J.M., Sanchez-Migallon Guzman, D., Paul-Murphy, J.R., 2018. Pain in birds: the anatomical and physiological basis. Vet. Clin. N. Am. Equine Pract. 21, 17–31.

Dubbeldam, J.L., 1998. The sensory trigeminal system in birds: input, organization and effects of peripheral damage: a review. Arch. Physiol. Biochem. 106, 338–345.

Dubbeldam, J.L., 2009. The trigeminal system in birds and nociception. Cent. Nerv. Syst. Agents Med. Chem. 9, 150–158.

Dubin, A.E., Patapoutian, A., 2010. Nociceptors: the sensors of the pain pathway. J. Clin. Invest. 120, 3760–3772.

Duncan, I.J.H., Beatty, E.R., Hocking, P.M., Duff, S.R.I., 1991. Assessment of pain associated with degenerative hip disorders in adult male turkeys. Res. Vet. Sci. 50, 200–203.

Duncan, I.J.H., Slee, G.S., Seawright, E., Breward, J., 1989. Behavioural consequences of partial beak amputation (beak trimming) in poultry. Br. Poultry Sci. 30, 479–488.

Dunlop, R., Millsopp, S., Laming, P., 2006. Avoidance learning in goldfish (*Carassius auratus*) and trout (*Oncorhynchus mykiss*) and implications for pain perception. Appl. Anim. Behav. Sci. 97, 255–271.

Elwood, R.W., 2011. Pain and suffering in invertebrates? ILAR J. 52, 175–184.

Evrard, H.C., Balthazart, J., 2002. The assessment of nociceptive and non-nociceptive skin sensitivity in the Japanese quail (*Coturnix japonica*). J. Neurosci. Methods 116, 135–146.

Freire, R., Eastwood, M.A., Joyce, M., 2011. Minor beak trimming in chickens leads to loss of mechanoreception and magnetoreception. J. Anim. Sci. 89, 1201–1206.

Freire, R., Glatz, P.C., Hinch, G., 2008. Self-administration of an analgesic does not alleviate pain in beak trimmed chickens. Asian-Aus. J. Sci. 21, 443–448.

Gao, Y.J., Ren, W.H., Zhang, Y.Q., Zhao, Z.Q., 2004. Contributions of the anterior cingulate cortex and amygdala to pain-and fear-conditioned place avoidance in rats. Pain 110, 343–353.

Geelen, S., Sanchez-Migallon Guzman, D., Souza, M.J., Cox, S.K., Keuler, N.S., Paul-Murphy, J.R., 2013. Antinociceptive effects of tramadol hydrochloride after intravenous administration to Hispaniolan Amazon parrots (*Amazona ventralis*). Am. J. Vet. Res. 74, 201–206.

Gentle, M., Tilston, V., 2000. Nociceptors in the legs of poultry: implications for potential pain in pre-slaughter shackling. Anim. Welf. 9, 227–236.

Gentle, M., Tilston, V., McKeegan, D., 2001. Mechanothermal nociceptors in the scaly skin of the chicken leg. Neuroscience 106, 643–652.

Gentle, M.J., 1981. Oral behaviour following forebrain ablations in *Gallus domesticus*. Behav. Process. 6, 109–120.

Gentle, M.J., 1989. Cutaneous sensory afferents recorded from the nervus intramandibularis of *Gallus gallus* var domesticus. J. Comp. Physiol. B 164, 763–774.

Gentle, M.J., 1991. The acute effects of amputation on peripheral trigeminal afferents in *Gallus gallus* var domesticus. Pain 46, 97–103.

Gentle, M.J., 1997. Pain-related behaviour following sodium urate arthritis is expressed in decerebrate chickens. Physiol. Behav. 62, 581–584.

Gentle, M.J., 2011. Pain issues in poultry. Appl. Anim. Behav. Sci. 135, 252–258.

Gentle, M.J., Corr, S.A., 1995. Endogenous analgesia in the chicken. Neurosci. Lett. 201, 211–214.

Gentle, M.J., Hunter, L.N., 1991. Physiological and behavioural responses associated with feather removal in *Gallus gallus* var domesticus. Res. Vet. Sci. 50, 95–101.

Gentle, M.J., Hunter, L.N., Corr, S.A., 1997. Effects of caudolateral neostriatal ablations on pain-related behaviour in the chicken. Physiol. Behav. 61, 493–498.

Gentle, M.J., Hunter, L.N., Sterling, R.J., 1995. Projections of ankle joint afferents to the spinal cord and brainstem of the chicken (*Gallus g.* domesticus). J. Comp. Neurol. 361, 669–680.

Gentle, M.J., Hunter, L.N., Waddington, D., 1991. The onset of pain related behaviours following partial beak amputation in the chicken. Neurosci. Lett. 128, 113–116.

Gentle, M.J., Thorp, B.H., 1994. Sensory properties of ankle joint capsule mechanoreceptors in acute monoarthritic chickens. Pain 57, 361–374.

Gentle, M.J., Tilston, V.L., 1999. Reduction in peripheral inflammation by changes in attention. Physiol. Behav. 66, 289–292.

Gentle, M.J., Waddington, D., Hunter, L.N., Jones, R.B., 1990. Behavioural evidence for persistent pain following partial beak amputation in chickens. Appl. Anim. Behav. Sci. 27, 149–157.

Gentle, M.J., Wood-Gush, G.M., 1976. Observations of the behaviour of *Gallus domesticus* following telencephalic removal. Behav. Biol. 1, 223–231.

Gerber, B., Yarali, A., Diegelmann, S., Wotjak, C.T., Pauli, P., Fendt, M., 2014. Pain-relief learning in flies, rats, and man: basic research and applied perspectives. Learn. Mem. 21, 232–252.

Glatz, P.C., 1987. Effects of beak trimming and restraint on heart rate, food intake, body weight and egg production in hens. Br. Poultry Sci. 28, 601–611.

Glatz, P.C., Lunam, C.A., 1994. Production and heart rate responses of chickens beak-trimmed at hatch or at 10 or 42 days of age. Aust. J. Exp. Agric. 34, 443–447.

Glatz, P.C., Murphy, L.B., Reston, A.P., 1992. Analgesic therapy of beak-trimmed chickens. Aust. Vet. J. 69, 18-18.

Güntürkün, O., 2012. The convergent evolution of neural substrates for cognition. Psychol. Res. 76, 212–219.

Hawkins, M.G., 2006. The use of analgesics in birds, reptiles, and small exotic mammals. J. Exot. Pet Med. 15, 177–192.

Hocking, P.M., Robertson, G.W., Gentle, M., 2005. Effects of non-steroidal anti-inflammatory drugs on pain-related behaviour in a model of articular pain in the domestic fowl. Res. Vet. Sci. 78, 69–75.

Holloway, J.A., Trouth, C.O., Wright, L.E., Keyser, G.F., 1980. Cutaneous receptive field characteristics of primary afferents and dorsal horn cells in the avian (*Gallus domesticus*). Exp. Neurol. 68, 477–488.

Hoppes, S., Flammer, K., Hoersch, K., Papich, M., Paul-Murphy, J.R., 2003. Disposition and analgesic effects of fentanyl in white cockatoos (*Cacatua alba*). J. Avian Med. Surg. 17, 124–130.

Hothersall, B., Caplen, G., Nicol, C.J., Taylor, P.M., Waterman-Pearson, A.E., Weeks, C.A., Murrell, J.C., 2011. Development of mechanical and thermal nociceptive threshold testing devices in unrestrained birds (broiler chickens). J. Neurosci. Methods 201, 220–227.

Hothersall, B., Caplen, G., Parker, R.M., Nicol, C.J., Waterman-Pearson, A.E., Weeks, C.A., Murrell, J.C., 2016. Effects of carprofen, meloxicam and butorphanol on broiler chickens' performance in mobility tests. Anim. Welf. 25.

Hothersall, B., Caplen, G., Parker, R.M.A., Nicol, C.J., Waterman-Pearson, A.E., Weeks, C.A., Murrell, J.C., 2014. Thermal nociceptive threshold testing detects altered sensory processing in broiler chickens with spontaneous lameness. PLoS One 9, e97883.

Hughes, R.A., 1990. Strain-dependent morphine-induced analgesic and hyperalgesic effects on thermal nociception in domestic fowl (*Gallus gallus*). Behav. Neurosci. 104.

Hughes, R.A., Sufka, K.J., 1991. Morphine hyperalgesic effects on the formalin test in domestic fowl (*Gallus Gallus*). Pharmacol. Biochem. Behav. 38, 247–251.

Jordt, S.E., Julius, D., 2002. Molecular basis for species-specific sensitivity to "hot" chili peppers. Cell 108, 421–430.

Kawate, T., Sakamoto, H., Yang, C., Li, Y., Shimada, O., Atsumi, S., 2005. Immunohistochemical study of delta and mu opioid receptors on synaptic glomeruli with substance P-positive central terminals in chicken dorsal horn. Neurosci. Res. 53, 279–287.

Kuenzel, W.J., 2007. Neurobiological basis of sensory perception: welfare implications of beak trimming. Poultry Sci. 86, 1273–1282.

Lavalley, A.L., Ho, R.H., 1983. Substance P, somatostatin, and methionine enkephalin immunoreactive elements in the spinal cord of the domestic fowl, *Gallus domesticus*. J. Comp. Neurol. 213, 406–413.

Li, Y.N., Sakamoto, H., Kawate, T., Cheng, C.X., Li, Y.C., Shimada, O., Atsumi, S., 2005. An immunocytochemical study of calbindin-D28K in laminae I and II of the dorsal horn and spinal ganglia in the chicken with special reference to the relation to substance P-containing primary afferent neurons. Arch. Histol. Cytol. 68, 57–70.

Machin, K.L., 2005. Avian pain: physiology and evaluation. Compendium 27, 98–108.

Machin, K.L., 2014. Recognition and treatment of pain in birds. In: Egger, C.M., Love, L., Doherty, T. (Eds.), Pain Management in Veterinary Practice. John Wiley & Sons, Inc, New Jersey, USA, pp. 407–415.

Machin, K.L., Livingston, A., 2002. Assessment of the analgesic effects of ketoprofen in ducks anesthetized with isoflurane. Am. J. Vet. Res. 63, 821–826.

Malik, A., Valentine, A., 2018. Pain in birds: a review for veterinary nurses. Vet. Nurse J. 33, 11–25.

Matthies, B.K., Franklin, K.B., 1992. Formalin pain is expressed in decerebrate rats but not attenuated by morphine. Pain 51, 199–206.

McCulloch, S.P., 2018. Brexit and animal protection: legal and political context and a framework to assess impacts on animal welfare. Animals 8, 213.

McGeown, D., Danbury, T.C., Waterman-Pearson, A.E., Kestin, S.C., 1999. Effect of carprofen on lameness in broiler chickens. Vet. Rec. 144, 668–671.

McIlhone, A.E., Beausoleil, N.J., Kells, N.J., Mellor, D.J., Johnson, C.B., 2018. Effects of noxious stimuli on the electroencephalogram of anaesthetised chickens (*Gallus gallus domesticus*). PLoS One 13, e0196454.

McKeegan, D.E.F., 2004. Mechano-chemical nociceptors in the avian trigeminal mucosa. Brain Res. Rev. 46, 146–154.

McKeegan, D.E.F., Demmers, T.G.M., Wathes, C.M., Jones, R.B., Gentle, M.J., 2002. Response characteristics of nasal trigeminal nociceptors in *Gallus domesticus*. Neuroreport 13, 1033–1035.

Mellor, D.J., 2019. Welfare-aligned sentience: enhanced capacities to experience, interact, anticipate, choose and survive. Animals 9.

Molony, V., Kent, J., 1997. Assessment of acute pain in farm animals using behavioral and physiological measurements. J. Anim. Sci. 75, 266–272.

Moneva, P., Popova-Ralcheva, S., Gudev, D., Sredkova, V., Yanchev, I., 2008. Stress response dynamics in ACTH and formalin treated chickens. Bulg. J. Ag. Sci. 14, 598–605.

Murrell, J.C., Johnson, C.B., 2006. Neurophysiological techniques to assess pain in animals. J. Vet. Pharmacol. Therapeut. 29, 325–335.

Nasr, M.A.F., Browne, W.J., Caplen, G., Hothersall, B., Murrell, J.C., Nicol, C.J., 2013. Positive affective state induced by opioid analgesia in laying hens with bone fractures. Appl. Anim. Behav. Sci. 147, 127–131.

Nasr, M.A.F., Nicol, C.J., Murrell, J.C., 2012. Do laying hens with keel bone fractures experience pain? PLoS One 7, e42420.

Necker, R., Reiner, B., 1980. Temperature-sensitive mechanoreceptors, thermoreceptors and heat nociceptors in the feathered skin of pigeons. J. Comp. Physiol. B 135, 201–207.

New Zealand Government, 2015. Animal Welfare Amendment Act (No 2) (Wellington, New Zealand).

Nicol, G.D., Klingberg, D.K., Vasko, M.R., 1992. Prostaglandin E2 increases in calcium conductance and stimulates release of substance P in avian sensory neurons. J. Neurosci. 12, 1917–1927.

Norring, M., Valros, A., Valaja, J., Sihvo, H.K., Immonen, K., Puolanne, E., 2018. Wooden breast myopathy links with poorer gait in broiler chickens. Animal 1–6.

Paul-Murphy, J., Hawkins, M.G., 2015. Bird-specific considerations: recognizing pain behavior in pet birds. In: Gaynor, J., Muir, W. (Eds.), Handbook of Veterinary Pain Management, third ed. Elsevier, Amsterdam, Netherlands, pp. 536–554.

Paul-Murphy, J.R., Brunson, D.B., Miletic, V.A., 1999a. A technique for evaluating analgesia in conscious perching birds. Am. J. Vet. Res. 60, 1213–1217.

Paul-Murphy, J.R., Brunson, D.B., Miletic, V.A., 1999b. Analgesic effects of butorphanol and buprenorphine in conscious African grey parrots (*Psittacus erithacus* and *Psittacus erithacus* timneh). Am. J. Vet. Res. 60, 1218–1221.

Reiner, A., Brauth, S.E., Kitt, C.A., Quirion, R., 1989. Distribution of mu, delta, and kappa opiate receptor types in the forebrain and midbrain of pigeons. J. Comp. Neurol. 280, 359–382.

Reiter, K., Bessei, W., 1997. Gait analysis in laying hens and broilers with and without leg disorders. Equine Vet. J. 29, 110–112.

Roach, J.T., Sufka, K.J., 2003. Characterization of the chick carrageenan response. Brain Res. 994, 216–225.

Saito, S., Banzawa, N., Fukuta, N., Saito, C.T., Takahashi, K., Imagawa, T., Ohta, T., Tominaga, M., 2014. Heat and noxious chemical sensor, chicken TRPA1, as a target of bird repellents and identification of its structural determinants by multispecies functional comparison. Mol. Biol. Evol. 31, 708–722.

Sanchez-Migallon Guzman, D., Kukanich, B., Keuler, N.S., Klauer, J.M., Paul-Murphy, J.R., 2011. Antinociceptive effects of nalbuphine hydrochloride in Hispaniolan Amazon parrots (*Amazona ventralis*). Am. J. Vet. Res. 72, 736–740.

Sanchez-Migallon Guzman, D.S.M., Souza, M.J., Braun, J.M., Cox, S.K., Keuler, N.S., Paul-Murphy, J.R., 2012. Antinociceptive effects after oral administration of tramadol hydrochloride in Hispaniolan Amazon parrots (*Amazon ventralis*). Am. J. Vet. Res. 73, 1148–1152.

Sandercock, D.A., 2004. Putative nociceptor responses to mechanical and chemical stimulation in skeletal muscles of the chicken leg. Brain Res. Rev. 46, 155–162.

Shanahan, M., Bingman, V.P., Shimizu, T., Wild, M., O, G., 2013. Large-scale network organization in the avian forebrain: a connectivity matrix and theoretical analysis. Front. Comput. Neurosci. 7, 1–17.

Sheehan, M.H., Kream, R.M., Stefano, G.B., 2010. Biological indications of a novel "short" μ opiate receptor in domestic chicken. Arch. Med. Sci. 6, 478–482.

Sinclair, A., Weber Wyneken, C., Veldkamp, T., Vinco, L.J., Hocking, P.M., 2015. Behavioural assessment of pain in commercial turkeys (*Meleagris gallopavo*) with foot pad dermatitis. Br. Poultry Sci. 56, 511–521.

Singh, P.M., Johnson, C.B., Gartrell, B., Mitchinson, S., Jacob, A., Chambers, P., 2017. Analgesic effects of morphine and butorphanol in broiler chickens. Vet. Anaesth. Analg. 44, 538–545.

Sladky, K.K., Krugner-Higby, L., Meek-Walker, E., Heath, T.D., Paul-Murphy, J.R., 2006. Serum concentrations and analgesic effects of liposome-encapsulated and standard butorphanol tartrate in parrots. Am. J. Vet. Res. 67, 775–781.

Sneddon, L.U., Elwood, R.W., Adamo, S.A., Leach, M.C., 2014. Defining and assessing animal pain. Anim. Behav. 97, 201–212.

Sufka, K.J., Hughes, R.A., Giordano, J., 1991. Effects of selective opiate antagonists on morphine-induced hyperalgesia in domestic fowl. Pharmacol. Biochem. Behav. 38, 49–54.

Thøfner, I., Hougen, H.P., Villa, C., Lynnerup, N., Christensen, J.P., 2020. Pathological characterization of keel bone fractures in laying hens does not support external trauma as the underlying cause. PLoS One 15, e0229735.

Trebilcock, P.D., 2015. Investigating the Electrical Response of the Brain of the Domestic Chicken (*Gallus gallus domesticus*) to Nociception through the Use of Depth Electroencephalography (dEEG). Masters dissertation, Massey University, Manawatū, New Zealand.

Viñuela-Fernández, I., Jones, E., Welsh, E.M., Fleetwood-Walker, S.M., 2007. Pain mechanisms and their implication for the management of pain in farm and companion animals. Vet. J. 174, 227–239.

Virden, W.S., Kidd, M.T., 2009. Physiological stress in broilers: ramifications on nutrient digestibility and responses. J. Appl. Poultry Res. 18, 338–347.

Weber Wyneken, C., Sinclair, A., Veldkamp, T., Vinco, L.J., Hocking, P.M., 2015. Footpad dermatitis and pain assessment in Turkey poults using analgesia and objective gait analysis. Br. Poultry Sci. 56, 522–530.

Wild, J.M., Krützfeldt, N.O.E., Altshuler, D.L., 2010. Trigeminal and spinal dorsal horn (dis)continuity and avian evolution. Brain Behav. Evol. 76 (1), 11–19.

Williams, C.J.A., James, L.E., Bertelsen, M.F., Wang, T., 2019. Analgesia for non-mammalian vertebrates. Curr. Opin. Physiol. 11, 75–84.

Willis, W.D., 1985. Nociceptive pathways: anatomy and physiology of nociceptive ascending pathways. Philos. Trans. R. Soc. Lond. Ser. B Biol. Sci. 308, 253–268.

Woolley, S.C., Gentle, M.J., 1987. Physiological and behavioural responses in the hen (*Gallus domesticus*) to nociceptive stimulation. Comp. Biochem. Physiol., A: Mol. Integr. Physiol. 88, 27–31.

Wylie, L.M., Gentle, M.J., 1998. Feeding-induced tonic pain suppression in the chicken: reversal by naloxone. Physiol. Behav. 64, 27–30.

Zehnder, A.M., Hawkins, M.G., Pascoe, P.J., 2014. Avian anatomy and physiology. In: West, G., Heard, D., Caulkett, N.A. (Eds.), Zoo Animal and Wildlife Immobilization and Anesthesia, second ed. John Wiley & Sons, Inc., New Jersey, USA, pp. 389–398.

Zhai, X.Y., Atsumi, S., 1997. Large dorsal horn neurons which receive inputs from numerous substance P-like immunoreactive axon terminals in the laminae I and II of the chicken spinal cord. Neurosci. Res. 28, 147–154.

Chapter 15

Magnetoreception in birds and its use for long-distance migration*

Henrik Mouritsen[1,2]

[1]Institut für Biologie und Umweltwissenschaften, Universität Oldenburg, Oldenburg, Germany; [2]Research Centre for Neurosensory Sciences, University of Oldenburg, Oldenburg, Germany

15.1 Introduction

The Earth's magnetic field provides potentially useful information, which birds and other animals could use for directional and/or positional information. It has been clearly demonstrated that many birds are able to sense the compass direction of the Earth's magnetic field and that they can use this information as part of a compass sense. More recently, it has also been demonstrated that at least some birds can use magnetic information to determine their approximate position on the Earth based on magnetic cues. In addition to direct uses for orientation and navigation, magnetic information also seems to be able to influence other physiological processes such as fattening and migratory motivation as a trigger for changes in behavior. While the behavioral responses to geomagnetic cues are relatively well understood, the physiological mechanisms enabling birds to sense the Earth's magnetic field are only starting to be understood and understanding the magnetic sense(s) of animals including birds remains one of the most significant unsolved problems in biology. It is very challenging to sense magnetic fields as weak as that of the Earth using only biologically available materials. Only two basic mechanisms are considered theoretically viable in small terrestrial animals: iron-particle–based magnetoreception and radical-pair–based magnetoreception. Based on current scientific evidence, both iron-particle–based magnetoreception and radical-pair–based magnetoreception mechanisms seem to exist in birds, but they seem to be used for different purposes. Plausible primary sensory molecules and a few brain areas involved in processing magnetic information have been identified in birds for each of these two types of magnetic senses. Nevertheless, we are still far away from understanding the detailed function of any of the at least two different magnetic senses existing in at least some bird species, and, at present, no primary sensory structure has been identified beyond reasonable doubt to be the source of avian magnetoreception. This is an exciting but challenging field requiring a highly multidisciplinary, stringent, scientific approach in which a number of major discoveries are likely to be made in the next one–two decades.

15.2 Magnetic fields

Moving electric charges such as electrons produce magnetic fields. On the microscopic scale, electron (and nuclear) spins can generate magnetic fields. On the macroscopic scale, a magnetic field, **B**, is, for instance, generated around a wire when current runs through it. The magnetic field at a given location can be described as a three-dimensional (3D) vector, whose strength, **B**, is measured as magnetic flux density using the unit "Tesla [T]" $1T = 1(V*s)/m^2 = 1\ (N*s)/(C*m) = 10{,}000$ Gauss [V = Volt, s = second, m = meter, N = Newton, C = Coulomb]. Some materials, which are called "ferromagnetic," can be permanently magnetized by a magnetic field, and this magnetization remains after the magnetizing field

* Since the classical findings in magnetoreception do not change, there is significant text and content overlap between the present edited chapter and the original chapter as well as with another book chapter focusing on magnetoreception in all kinds of organisms titled "The Magnetic Senses," which I wrote for the textbook "Neurosenses": Mouritsen, H., 2013. The Magnetic senses. In: Galizia, C.G., Lledo, P.M. (Eds.), Neurosciences—From Molecule to Behavior: A University Textbook. https://doi.org/10.1007/978-3-642-10,769-6_20, © Springer-Verlag Berlin Heidelberg, pp. 427–443. The Springer Verlag has permitted the reuse of significant parts of the "Neurosenses" textbook chapter text in the present chapter. Specific references to this text is not given at every location where text is reused, since such references would compromise readability, and could be misunderstood to be referring to primary research findings.

Sturkie's Avian Physiology. https://doi.org/10.1016/B978-0-12-819770-7.00040-2

has been removed. Magnetite [Fe_3O_4], an iron-oxide, is a well-known example of a ferromagnetic mineral (Mouritsen, 2013).

15.3 The Earth's magnetic field

The Earth generates its own magnetic field (the geomagnetic field), which is mostly caused by electric currents in the liquid outer core of the Earth (the "dynamo effect"). The magnetic field measured at the Earth's surface is similar to the magnetic field one would expect to see if a large dipole magnet was placed in the center of the Earth (see Fig. 15.1). The Earth's magnetic field currently has a magnetic field South pole near the Earth's geographic north pole (referred to as "Magnetic North" or "Magnetic North Pole" in biology). Throughout this chapter, I will follow the convention used in the bird orientation research literature and use the term "Magnetic North" or "Magnetic North Pole" to refer, not to the physical magnetic North Pole, but to the magnetic pole located closest to the geographic North Pole. Likewise, the magnetic field North Pole near the Earth's geographic South Pole will be referred to as "Magnetic South" or "Magnetic South Pole" (Mouritsen, 2013).

The magnetic field lines leave the Magnetic South Pole and re-enter the Magnetic North Pole. The polarity of the magnetic field lines on the Earth's surface always points toward magnetic North, and they can therefore provide a highly reliable directional reference, which can be used as the basis for a magnetic compass anywhere on planet Earth except at the magnetic poles. At the magnetic poles, the field lines point directly into the sky (at the Magnetic South Pole) or directly into the Earth (at the Magnetic North Pole). At the magnetic equator, the magnetic field lines are parallel to the Earth's surface. The angle between the magnetic field lines and the Earth's surface is called "magnetic inclination." Thus, magnetic inclination changes gradually from −90 degrees at the magnetic South Pole to zero degrees at the magnetic equator to +90 degrees at the magnetic North pole (see Fig. 15.1). The Earth's magnetic field intensity ranges from ca. 30,000 nT (nano-Tesla = 10^{-9} T; 1 T = 1 V m^{-2}; 1 nT = 10^{-5} Gauss) near

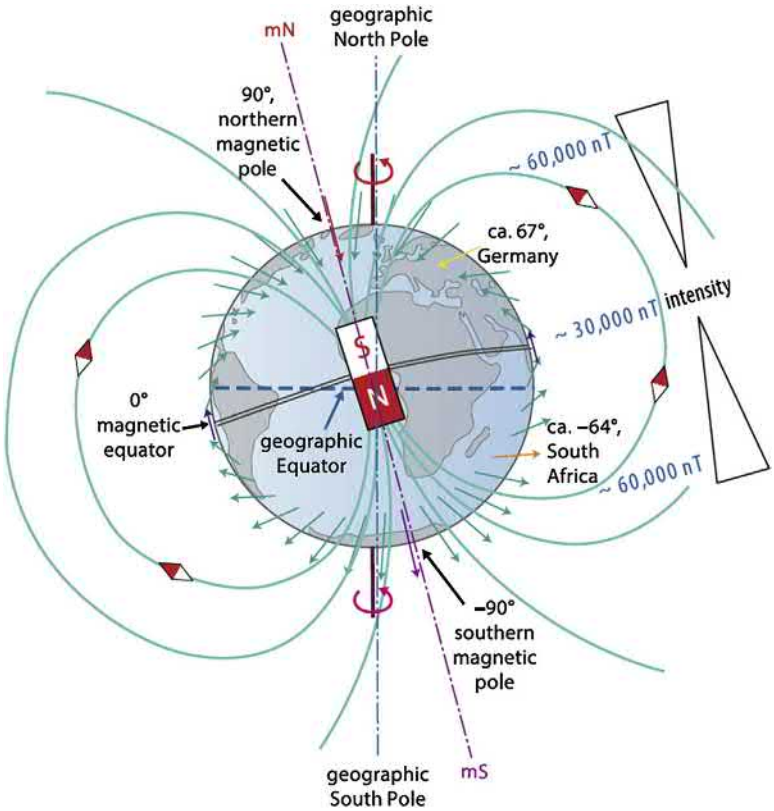

FIGURE 15.1 The Earth's magnetic field (the geomagnetic field). Notice that the southern and northern magnetic poles and the Magnetic Equator do not coincide with the geographical poles and the Geographic Equator. Also notice that the magnetic field lines intersect the Earth's surface at different angles depending on the magnetic latitude (*blue-green lines and vectors*). The intersection angle is called the magnetic inclination. Magnetic inclination is, for instance, +90 degrees at the magnetic North Pole (*red vector*), ~+67 degrees at the latitude of Germany (*yellow vector*), 0 degree at the magnetic equator (*dark blue vectors*), ~−64 degrees at the latitude of South Africa (*orange vector*), and −90 degrees at the magnetic South Pole (*magenta vector*). The magnetic intensity varies from ca. 60,000 nT near the magnetic poles to ca. 30,000 nT along the magnetic equator. *Adapted with permission after Wiltschko and Wiltschko (1996) and Mouritsen (2013).*

the magnetic equator to ca. 60,000 nT at the magnetic poles. Earth-strength magnetic fields are usually measured with a calibrated 3-axial Flux-Gate magnetometer. Both magnetic inclination and magnetic intensity can, in theory, be useful for determining one's position, but, on most parts of the Earth, magnetic inclination and intensity changes predominantly from North to South but not much from East to West. It therefore seems easier to determine latitude than longitude from geomagnetic field information (Mouritsen, 2003, 2013), even though recent studies have shown that Eurasian reed warblers, *Acrocephalus scirpaceus* (a night-migratory songbird), can also use magnetic cues to compensate for East−West displacements (Kishkinev et al., 2015; Chernetsov et al., 2017; Pakhomov et al., 2018).

The Magnetic North Pole is currently located in Northern Canada, and the Magnetic South Pole is currently located south of Australia. Consequently, the geographic and magnetic poles do not coincide (see Fig. 15.1). The deviation between geographic and magnetic North is called the "magnetic declination." Magnetic declination is the angle between magnetic north, i.e., the direction in which the north end of a compass needle points in, and geographic north. The declination is positive when Magnetic North is east of geographic North and negative when Magnetic North is west of geographic North. Declination is mostly small, but near the magnetic poles, declination can pose a serious problem for navigating birds using a magnetic compass, unless they find a way to compensate for it. On the other hand, magnetic declination could be a useful parameter to determine, e.g., East−West position if it would be combined with other map cues (Mouritsen, 2013; Kishkinev et al., 2021; Chernetsov et al., 2017, 2020).

15.4 Changing magnetic fields for experimental purposes

The direction of the magnetic field around a wire can be determined by the "right hand rule": if you grasp around the wire with your right hand so that your thumb is pointing in the direction of the current, the magnetic field around the wire runs in the direction in which your fingers are pointing. The magnetic field decreases with distance as you move away from the wire. If you create a coil of wire, the magnetic field created is much stronger inside the coil than on the outside of the coil because many parallel magnetic field lines created by different parts of the wire coincides and thus add up in the center of the coil. This is the reason why coil constructions are typically used to produce and alter magnetic fields (Mouritsen, 2013).

The typical coil constructions, which are used to produce Earth-strength magnetic fields for scientific experiments, are so-called "Helmholtz coils": a pair of parallel coils placed one radius apart from each other (Kirschvink, 1991). In a pair of Helmholtz coils, the magnetic field is very homogeneous within a central space of ca. 60% of the radius of the coils (Kirschvink, 1991). The magnetic field generated in the center of a pair of Helmholtz coils is $\mathbf{B} = (0.9*10^{-6}$ T m/A * n *I)/R; where T is the unit Tesla, n is the number of turns in each coil, I is the current flowing through the coils measured in Ampere (A), and R is the radius of the coils measured in meters (m) (Kirschvink, 1991). One pair of Helmholtz coils can alter the magnetic field along one axis only. To make any desired 3D magnetic field, ideally three pairs of Helmholtz coils oriented perpendicular to each other are needed. If one adds an artificially created field to an existing field (such as that of the Earth), the resultant field is calculated by simple vector addition of the two fields (see Fig. 15.2; Kirschvink, 1991). Therefore, it is also possible to use a single pair of Helmholtz coils to make any 3D magnetic field, but in that case, this single pair of coils must be oriented very precisely in 3D space (see Fig. 15.2, Mouritsen, 2013).

While the Helmholtz arrangement is easy to calculate and construct, the central homogeneous space can be increased to ca. 110% of the radius of the coils by using more elaborate coil designs such as the Merritt-4-coil system (Kirschvink, 1991; Zapka et al., 2009, Figure 20.2 in Mouritsen, 2013; Schwarze et al., 2016). To control for artifacts, one would—independent of the coil design chosen—expect the coils to be "double wound" (Kirschvink, 1991; Kirschvink et al., 2010). This means that during construction of the coils, each coil contains two separate, but identically wounded, wires each with separate connectors, so that one can either run current through both halves of the windings in the same direction (then the magnetic field in the center of the coil will change), or one can run the current through one half of the coils in one direction but in the opposite direction through the second half of the windings. In that case, the current running through one half of the windings will create a magnetic field, which exactly cancels the magnetic field produced by the other half of the windings, and the background field is not changed. By using double wound coils, exactly the same amount of current is sent through the coils whether the magnetic field is being changed or not. Double-wounded coils also allow for truly double-blinded experiments (Kirschvink, 1991; Zapka et al., 2009; Harris et al., 2009; Hein et al., 2010, 2011; Engels et al., 2012; Mouritsen, 2018). An excellent presentation of the theoretical background as well as practical instructions on how to construct various coil designs for changing Earth-strength magnetic fields can be found in Kirschvink (1991).

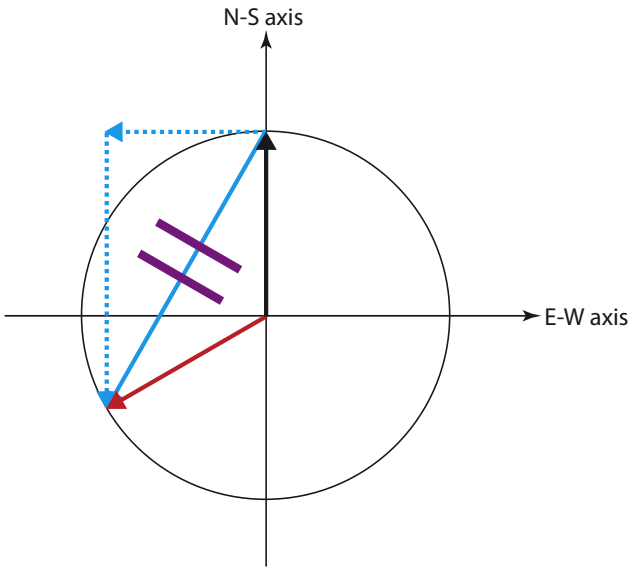

FIGURE 15.2 Magnetic fields are vector fields and can easily be turned with pairs of coils. If we consider the geomagnetic field, it will point toward North (0 degree) and have a vertical and a horizontal component. Let's say that we want to create a magnetic field with the same strength and inclination as the geomagnetic field but which is turned horizontally 120 degrees counterclockwise. In that case, the vertical component of the field should remain unchanged, and we only have to consider the two dimensions in the horizontal plane. Let's say that the Earth's magnetic field at the relevant location has a horizontal field component of 18,000 nT pointing toward magnetic North (*black vector*). If we want to turn the field to point toward 240 degrees (a 120 degrees counterclockwise turn, *red vector*), we need to produce a magnetic field vector (the *blue vector*) that connects the tip of the *black vector* to the tip of the *red vector*. The needed field can be produced by a single pair of Helmholtz coils (symbolized by the *violet lines*) if the coil frames are oriented on the axis defined by half the wanted angular turn (in this case 120 degrees/2 = 60 degrees) given that the final wanted intensity remains unchanged. Simple trigonometry can be used to calculate the needed field strength, B_{blue}, of the *blue vector*. In this case: $B_{blue} = (((\cos(\alpha_{black})*B_{black}) - (\cos(\alpha_{red})*B_{red}))^2 + ((\sin(\alpha_{black})*B_{black}) - (\sin(\alpha_{red})*B_{red}))^2)^{1/2}$, where $\alpha_{black} = 360$ degrees, $\alpha_{red} = 240$ degrees and $B_{black} = B_{red} = 18{,}000$ nT => $B_{blue} = ((\cos(360 \text{ degrees})*18{,}000 \text{ nT} - \cos(240 \text{ degrees})*18{,}000 \text{ nT})^2 + (\sin(360\text{degrees})*18{,}000 \text{ nT} - \sin(240 \text{ degrees})*18{,}000 \text{ nT})^2)^{1/2} = (((27{,}000 \text{ nT})^2 + (-15{,}588 \text{ nT})^2)^{1/2} = 31{,}177$ nT. If the strength of the final vector should have a different intensity than the original vector, or if the vertical component needs to be changed as well, again a single pair of coils can in principle do the job (the needed calculations are three-dimensional [3D]), but accurately orienting this pair of coils is very difficult in real life. Therefore, if excellent control of static magnetic fields is required, usually 3D systems of perpendicularly oriented coils are used. Since magnetic fields are vector fields, which all need to be added up to get the total resultant field, instead of producing the direct vector (the *blue vector*) that connects the tip of the *black vector* to the tip of the *red vector*, we can produce two vectors (the *dashed blue vectors*) along the two coil axes, which in total connects the tip of the *black vector* to the tip of the *red vector*. With such systems, each of the needed vectors are much more easy to calculate. The needed N−S component is: $\cos(\alpha_{black})*B_{black} - \cos(\alpha_{red})*B_{red}$ and the needed E−W component is $\sin(\alpha_{black})*B_{black} - \sin(\alpha)*B_{red}$. If one uses a 3D magnetometer oriented with the x-axis toward North and the Y-axis toward East, and one just wants to calculate the values that should be on the display when the wanted field is present, X should read $\cos(\alpha_{red})*B_{red}$ and Y should read $\sin(\alpha)*B_{red}$. In the case of a 120 degrees counterclockwise turn of the above-mentioned field, X should thus read cos(240 degrees)*18,000 nT = −9000 nT, and Y should read sin(240 degrees)*18,000 nT = −15,588 nT. All formulas presented here are valid for geographical angles (North = 0 degree = 360 degrees; East = 90 degrees, South = 180 degrees; and West = 270 degrees) but have to be modified if mathematical angles are used (East = 0 degree; North = 90 degrees; West = 180 degrees; and South = 270 degrees). What should the same magnetometer read on X and Y, if the same geomagnetic field is turned horizontally to 165 degrees? (X = −17,387 nT; Y = +4659 nT).

15.5 Birds use information from the Earth's magnetic field for various behaviors

15.5.1 Orientation and navigation

Orientation and navigation skills are essential for the survival of all migratory birds. All first-time migrants are faced with the challenge of finding an unfamiliar wintering area, often thousands of kilometers away (Berthold, 1991; Mouritsen and Mouritsen, 2000; Mouritsen, 2003, 2018). Many bigger birds are day migratory and travel in groups, which means that young birds of these species might simply follow experienced birds that know the way. However, most small songbirds are night-migratory and travel alone without contact to their parents. Consequently, all their navigational skills must be based on inherited sensory capabilities and strategies (Mouritsen, 2003; Holland, 2014). No cues requiring previous experience with the goal can be involved in the orientation strategies of solitary, first-year migrants. These considerations strongly limit the number of possible orientation cues to a few classes of globally or at least regionally consistent cues (Mouritsen, 2003; Holland, 2014):

(a) celestial cues, including the sun, the stars, and maybe the polarized light pattern of the sky

and

(b) geomagnetic cues

In addition to these cues, some authors have suggested that chemical cues (odors, Wallraff and Andreae, 2000; Wallraff, 2005; Gagliardo et al., 2006, 2008, 2009; Gagliardo, 2013), infrasound (sound with frequency below ca. 20 Hz; Hagstrum, 2013, but see Wallraff, 1972 and Holland, 2014), and/or Coriolis forces (The phenomenon that moving liquids and moving air are deflected slightly to the right on the Northern Hemisphere and slightly to the left on the Southern Hemisphere because of the Earth's rotation; Coriolis, 1835) might also be used for orientation and navigation.

However, there seems to be no physiological structure inside birds, which would enable them to detect the

Coriolis effect with a reasonable signal-to-noise ratio (Rosenblum et al., 1985; Adair, 1991; Kirschvink et al., 2010). Likewise, it is difficult to imagine how an inexperienced migrant could know, in advance, what the infrasound or odor "landscapes" along its migratory path looks like, and it is difficult to imagine that the infrasound and/or odor landscapes would be simple and consistent enough to be used by inexperienced birds as a primary map cue over thousands of kilometers (but see Wallraff and Andreae, 2000). Furthermore, because the width of the bird's head is much smaller than the wavelength of infrasound, it would be challenging for a small bird with a 2 cm wide head to determine from which direction infrasound originates (Mouritsen, 2013).

Thus, the primary orientation system of young inexperienced migrants on their first autumn migration is likely to be based primarily on celestial and magnetic cues, and it is known that when first-time autumn migrants are displaced away from their migration route, they are unable to correct for displacements (e.g., Drost, 1938; Perdeck, 1958; Mouritsen and Larsen, 1998; Mouritsen, 2003; Thorup et al., 2007; Holland, 2014). Instead, they choose a migration route parallel to their normal route and thus do not seem to possess a map sense (see Fig. 15.3). The migratory program of first-season solitary migrants can be described as a "clock-and-compass," "calendar-and-compass," or "vector navigation" strategy (Mayr, 1952; Perdeck, 1958; Schmidt-König, 1965; Rabøl, 1978; Berthold, 1991; Mouritsen, 1998b, 2003; Mouritsen and Mouritsen, 2000), where the birds fly in a specific direction for a given amount of time independent of their present location. Since the system include little (see below under magnetic signposts) or no location-related feedback, the orientation strategy of first-time solitary migrants can be mathematically described as a directed random walk: the birds choose their flight direction randomly from a normal-like distribution pointing in their mean migratory direction each evening independent of previous events (Mouritsen, 1998b; Mouritsen and Mouritsen, 2000; Mouritsen et al., 2013). This strategy predicts that the statistical distribution of first-time migrants should be parabolic, and it has been shown that this prediction fits very well with the actual distribution of ringing recoveries of free-flying, first-time migrants in Western Europe (Mouritsen, 1998b; Mouritsen and Mouritsen, 2000).

The orientation task facing adult migrants and young migrants on their first spring migration is fundamentally different from the task faced during their first autumn migration (Kramer, 1957; Rabøl, 1978; Berthold, 1991; Mouritsen, 2003, 2018; Holland, 2014). Adult migrants and young migrants on their first spring migration are migrating back toward a region they have had previous experience with and therefore their orientation system is likely to include local (map) information gained through previous migration experience. Birds that would use sensory information from all useful senses, which would improve their ability to find their way (e.g., magnetic sense, olfaction, vision, and hearing), should have an evolutionary advantage over birds that would only use a single cue or sense. Thus, it is likely that the orientation strategies of experienced migrants are multisensory and involves learned maps (Mouritsen, 2003, 2013, 2018; Holland, 2014).

Indeed, in contrast to first-time migrants, experienced migrants are able to correct for displacements (Perdeck, 1958; Mewaldt, 1964; Thorup et al., 2007; Chernetsov et al., 2008, 2017; Kishkinev et al., 2010, 2013, 2015; Pakhomov et al., 2018) and thus have added a learned map to their orientation program (see Fig. 15.3). Interestingly, this map is also functional at locations that have not been visited previously: birds can correct their orientation appropriately when they are experimentally displaced to far away locations, where they have certainly never been before (Perdeck, 1958; Mewaldt, 1964; Thorup et al., 2007; Chernetsov et al., 2008, 2017; Kishkinev et al., 2010, 2013, 2015; Kishkinev et al., 2021). If their learned map would have been based exclusively on previously experienced local landmarks, it should not have worked at unfamiliar locations.

Even though the functional basis of this map sense is not yet understood (Holland, 2014; Mouritsen, 2018), it is almost certainly based on multiple cues and it must involve the detection of larger scale gradients, which can be extrapolated and thus enable birds to return from unfamiliar locations. Furthermore, it is important to stress that navigational cues that can be used over thousands of kilometers differ from those that are useful over a few kilometers, meters, or centimeters over time-scales of a few seconds, minutes, or hours (Mouritsen, 2018). In fact, any long-distance navigational journey to a previously visited location consists of at least three different phases: a long-distance phase, a homing phase, and a pinpointing-the-goal phase (see Fig. 15.4; Mouritsen, 2018). The cues used during these three phases mostly differ. For instance, magnetic fields or global celestial cues will in most cases be of no use during the pinpointing-the-goal phase. It is therefore clear that no single cue or mechanism can explain how a long-distance migratory bird finds its way back to a known breeding or wintering location (Mouritsen, 2018).

15.6 The magnetic compass of birds

Friedrich W. Merkel and Wolfgang Wiltschko discovered that birds have a magnetic compass sense in the mid-1960s (Merkel and Wiltschko, 1965; Wiltschko, 1968). When birds are placed in a round cage at night, they show migratory restlessness (or "Zugunruhe" in Kramer, 1949): the birds primarily jump/flutter in their migratory direction, and when the magnetic field is rotated horizontally in the absence of celestial cues, the birds turn their orientation

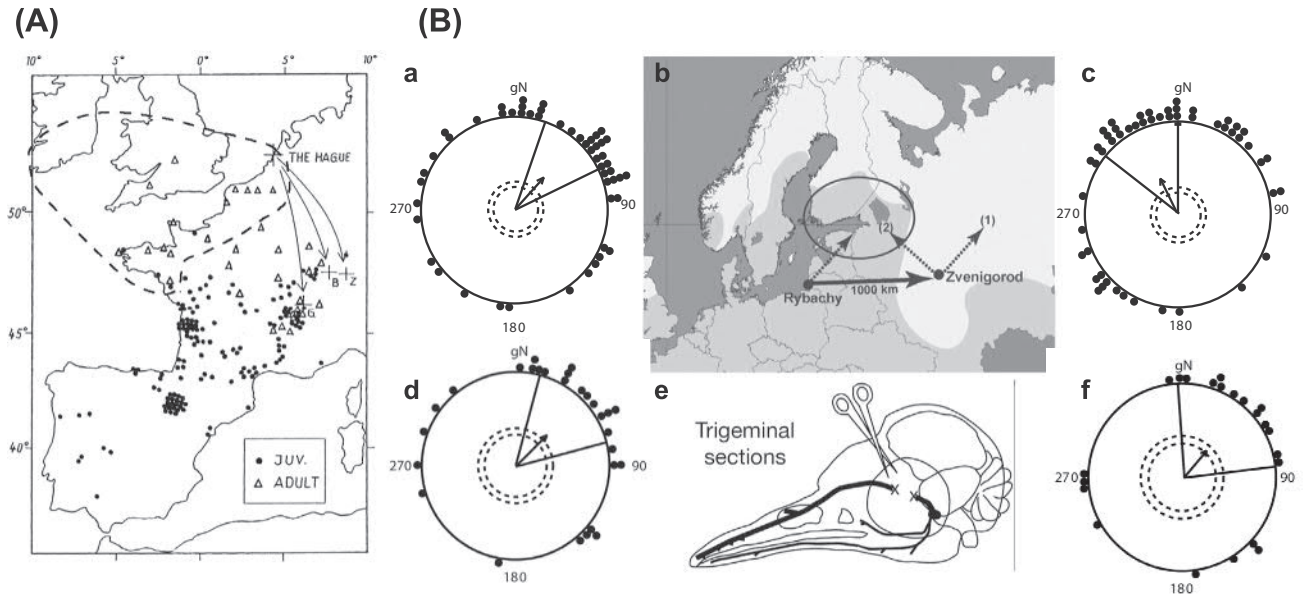

FIGURE 15.3 Displacement experiments provide key evidence for understanding the spatiotemporal orientation strategies of migratory birds. (A) Perdeck's classical experiments where he displaced >10,000 starlings from Holland S/SSE (→) to Switzerland during autumn migration showed that young starlings (●) on their first autumn were unable to correct for the displacement. The young birds show a parallel-displaced migration pattern relative to the wintering area of nondisplaced controls (*Dashed area*), whereas adult starlings (Δ) orient directly back to the normal population-specific wintering area of non-displaced controls. (B) Displacement experiments (Chernetsov et al., 2008; Kishkinev et al., 2013), in which Eurasian reed warblers (Acrocephalus scirpaceus) were tested in Emlen funnels (Emlen and Emlen, 1966; Mouritsen et al., 2009) before and after displacement, showed that young birds on their first spring migration are already able to correct for a 1000 km eastward displacements to a location where they have certainly never been before (b). (a) Orientation of birds at the capture site (Rybachy). (c) Orientation of the same birds after the 1000 km eastward translocation to Zvenigorod. Each *dot* at the circular diagram periphery indicates the mean orientation of one individual bird. The arrows show group mean directions and vector lengths. The *dashed circles* indicate the length of the group mean vector needed for significance according to the Rayleigh test (5 and 1% level for inner and outer *dashed circles*, respectively). The *lines* flanking group mean vectors indicate the 95% confidence intervals for the mean direction. gN—geographic North. On (b), a map of the displacement region is shown. The *shaded light gray* zone represents the breeding range of Eurasian reed warblers, and the *dashed arrows* show the expected results in case of (1): no compensation for the displacement, or (2): compensation toward the eastern part of the breeding range. Notice that intact birds compensate for the displacement, whereas birds which had the ophthalmic branch of the trigeminal nerve cut (d-f) could no longer compensate for the displacement (re-assembled after Chernetsov et al., 2008 and Kishkinev et al., 2013). The same results were obtained in virtual displacement experiments where the birds were exposed to the magnetic parameters of Zvenigorod inside coil systems but without being physically moved from Rybachy (Kishkinev et al., 2015; Pakhomov et al., 2018). *(A) From Mouritsen (2003) after Schmidt-Koenig (1965) and Perdeck (1958).*

with the magnetic field (see Fig. 15.5). This is the behavioral evidence required to show that a migratory bird species possesses and is able to use a magnetic compass (Wiltschko and Wiltschko, 1995). A magnetic compass has been found in more or less every migratory bird species properly tested for it (Wiltschko and Wiltschko, 1995), and it is therefore quite safe to presume that at least all night-migratory songbirds and potentially birds in general possess a magnetic compass.

It is important to note that there are at least two different magnetic field properties, which could potentially be used as input for a magnetic compass sense. A magnetic *polarity* compass (like the human ship compass) uses only the horizontal component of the field lines, which points toward magnetic North anywhere on Earth. Alternatively, a magnetic *inclination* compass detects only the angle between the geomagnetic field lines and the Earth's surface or gravity—not the polarity of the field lines. The smallest angle between the Earth's surface and the geomagnetic field lines indicates the direction "toward the magnetic equator," whereas the greatest angle indicates "toward the magnetic pole." Since the inclination is opposite on the northern and southern hemisphere, respectively, this holds on both hemispheres. All bird species properly tested so far have a magnetic inclination compass (Wiltschko and Wiltschko, 1972, 1995; see Fig. 15.5). Thus, the magnetic compass of night-migratory birds does not separate between North and South like our ship compass, but distinguishes between "toward the magnetic equator" and "toward the magnetic pole" (The Magnetic North Pole in the Northern Hemisphere and the magnetic South Pole in the Southern Hemisphere). Furthermore, the birds' magnetic compass sense seems to have a rather narrow functional intensity window, but this window seems to be extendable to new intensities after a few hours of adaptation to a changed magnetic field intensity (Wiltschko, 1978).

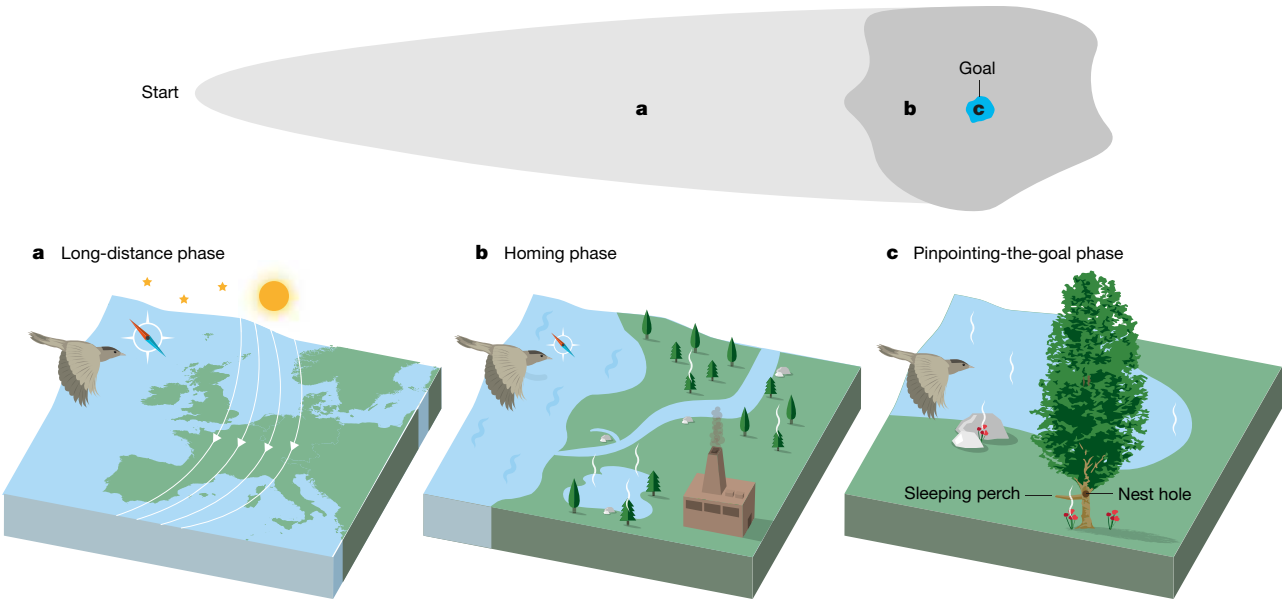

FIGURE 15.4 **Long-distance navigational tasks back to a previously visited location usually involve at least three different phases.** (A) During the long-distance phase, celestial and magnetic compass and map cues are usually important and landmarks such as coastlines can function as physical constraints. (B) During the homing phase, compasses still tends to be important and regional map cues such as olfactory and visual landmarks, olfactory gradients, strong magnetic anomalies, and maybe even soundscapes become important. (C) During the pinpointing-the-goal phase, very local cues such as a specific tree, a cave entrance, or a smelly swamp can help locate, for example, a sleeping perch or nest hole. *From Mouritsen (2018).*

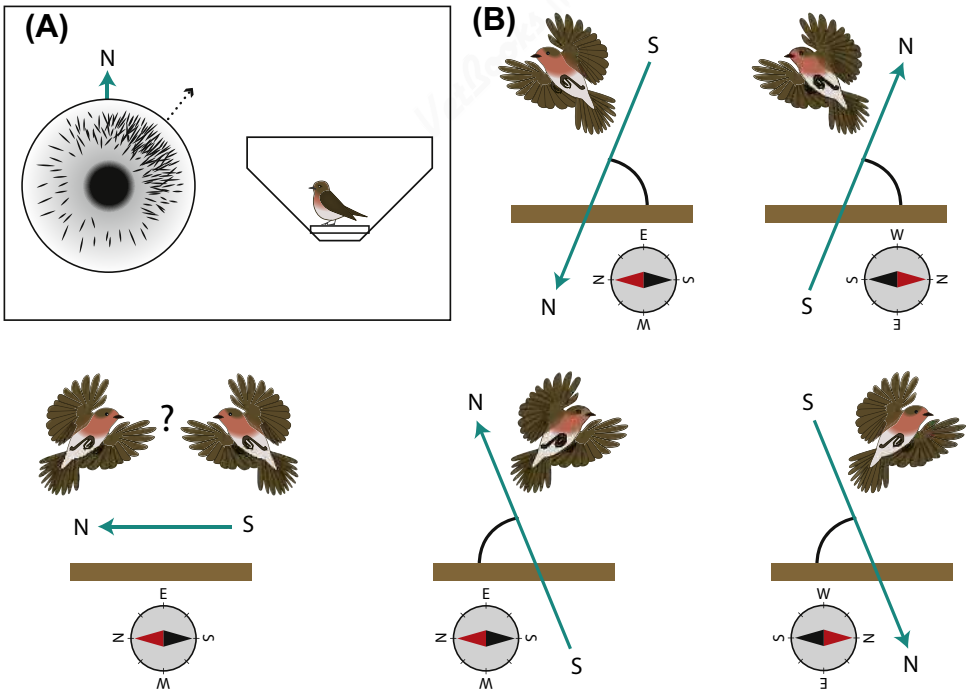

FIGURE 15.5 **The Emlen funnel and the inclination compass.** (A) The so-called Emlen funnel is the most commonly used orientation cage (Emlen and Emlen, 1966). The mean jumping direction of the birds are recorded on scratch-sensitive paper lining the inclined wall of the funnel (Mouritsen et al., 2009). (B) Early experiments by Wiltschko and Wiltschko (1972) have shown that night-migratory birds have an inclination compass, which means that they measure the angle between the magnetic field lines and the Earth's surface or gravity. Thereby, the birds separate between poleward and equatorward, not between North and South like a polarity compass would do (if birds use a polarity compass, they should have oriented in the direction indicated by the red end of the inserted technical compass). Birds are disoriented in a horizontal magnetic field like the one occurring at the magnetic equator. The flight direction of the inserted bird indicates the springtime mean direction chosen by all bird species tested so far in the given magnetic field (Wiltschko and Wiltschko, 1995). The *green arrows* indicate the direction if the magnetic field lines. Brown bar = The Earth's surface. N = geographic North. S = geographic South. *Figure and legend is reused from Mouritsen (2013).*

15.7 Do birds possess a magnetic map?

Many studies have reported that magnetic cues play an important role in birds' sense of position, i.e., that birds have a "magnetic map." However, the existence of a magnetic map used to be heavily debated and the views among researchers ranged from a magnetic map with a precision of a few kilometers being an established fact (e.g., Walcott, 1991; Wiltschko and Wiltschko, 1995; Wiltschko et al., 2010a) to a magnetic map sense being an evergreen phantom (Wallraff, 2001; Gagliardo et al., 2009). Recent virtual displacements to simulated magnetic locations, which were usually matched to previous actual displacements (Chernetsov et al., 2008; Kishkinev et al., 2013), have now demonstrated that at least some long-distance night-migratory songbirds are able to use magnetic information to determine their approximate large-scale position on the globe (Kishkinev et al., 2015, 2021; Chernetsov et al., 2017; Pakhomov et al., 2018). Furthermore, by correlating yearly changes in magnetic inclination with >60 years of colony recruitment data from Manx shearwaters (Puffinus puffinus) banded as chicks, this tube-nosed seabird seems to imprint on the magnetic inclination of their natal colony and to use this cue when they return to breed (Wynn et al., 2020), as do Pacific salmon (Putman et al., 2013).

Pigeons with opaque lenses that prevented them from detecting any local visual landmarks can return to within ca. 5 km of their loft (Schmidt-Koenig and Walcott, 1978). Thus, the precision of non-landmark-based navigation seems to be a few kilometers, but which cue(s) enable pigeons to home to within about 5 km of their loft without being able to use visual landmarks? At present, informed neutral observers of the olfaction contra magnetic map controversy agree (e.g., Able, 1996; Mouritsen, 2013 [both are orientation researchers who have never performed a pigeon release and thus have no vested interest in any of the camps]) that the evidence suggesting that chemical cues (odors) play an important role in the non-landmark-based part of pigeons' map sense (e.g., Papi, 1991, Wallraff and Andreae, 2000; Wallraff, 2001, 2005; Gagliardo et al., 2006, 2008, 2009) is much more convincing than the evidence supporting an important role of magnetic cues in the pigeons' map used during the homing phase (e.g., Walcott, 1991; Wiltschko and Wiltschko, 1995; Dennis et al., 2007; Wiltschko et al., 2010a; Holland, 2010). But remember, in the end, both camps may be right. The map will be multifactorial since a bird using all available input from all its senses will have an evolutionary advantage over a bird using only a single cue for a task so essential for the survival (Mouritsen, 2018). In any case, it remains very difficult to understand how a magnetic field-based map sense should be able to function on a scale <10 km. Why is that?

The problem for a bird wanting to use a magnetic map is that the average change in magnetic field intensity is only ca. 3 nT/km on the North–South axis: the geomagnetic field changes ca. 30,000 nT (nT) from one of the magnetic poles to the magnetic equator, which are ca. 10,000 km apart. Likewise, magnetic inclination changes only about 0.009 degrees/km along the North–South axis (a 90° change over 10,000 km). On the East–West axis, there is mostly very little change in magnetic field intensity and magnetic inclination. Thus, any magnetic field-based input to a reasonably precise map would require a very accurate magnetic sensory system and a very accurate sense of gravity. However, even if birds have such a system, daily, partly stochastic, natural variations in the geomagnetic field in the order of 30–100 nT in more or less random directions mean that it is very difficult to imagine, how a magnetic-field-based map sense could have a precision <10–30 km (Mouritsen, 2013, 2018) (during magnetic storms generated primarily by the sun, the geomagnetic field variability can reach 1000 nT; Courtillot and Mouël, 1988).

It is therefore expected that magnetic parameters can help determine position only where the expected differences in the magnetic field parameters are consistently larger than the daily magnetic variations (Mouritsen, 2013). Thus, even though a few studies have suggested that more accurate magnetic maps can be realized (Phillips et al., 2002; Dennis et al., 2007), magnetic maps are most likely only relevant during the long-distance navigation phase and maybe during part of the homing phase, at least in fast-moving animals (Mouritsen, 2018). Other cues such as odors and familiar landmarks may be more significant map parameters at shorter distances.

Intriguing data also exists that suggest that some songbirds can use magnetic cues as approximate geographic "signposts," which, for example, tells the birds when to increase their fat reserves before crossing the Sahara Desert (Fransson et al., 2001) or when to change their migratory heading (Henshaw et al., 2010). Cases, where specific magnetic parameters trigger a change in behavior is referred to as a magnetic "signpost" (Mouritsen, 2013).

15.8 Interactions with other cues

As mentioned previously, in most orientation-related contexts, magnetic cues interact with several other sources of similar and/or conflicting information. For instance, night-migratory songbirds do not only have a magnetic compass but also have a sun compass and a star compass (Emlen, 1975; Schmidt-König et al., 1991; Mouritsen and Larsen, 2001; Cochran et al., 2004; Zapka et al., 2009). They only need information from any one of these compasses to orient in the appropriate direction

(e.g., Mouritsen, 1998a; Muheim et al., 2006b; Chernetsov et al., 2011; Liu and Chernetsov, 2012). If the three compasses provide conflicting information, it is not consistent which compass the birds prefer. The preference is probably dependent on the ecological context and on details of the experimental setup and the conditions under which the birds were housed and tested, and it is likely that calibrations are taking place in nature, see Fig. 15.6 (Cochran et al., 2004; Muheim et al., 2006a; Liu and Chernetsov, 2012). The few experiments with truly free-flying birds performed so far suggested that two species of North American, night-migratory songbirds used the magnetic compass as their primary compass in midair during spring migration, but that they calibrate this compass based on celestial cues during the sunset period (Cochran et al., 2004; but this mechanism is not universal (Chernetsov et al., 2011)). Other evidence suggests that polarized light cues might be crucial for this calibration (Muheim et al., 2006a), but so far, it is not understood how a bird's eyes can detect polarized light.

In pigeon homing or any other shorter-distance, map-related task, the interactions between different cues seem to be even more complicated. Homing pigeons have been shown to use olfactory cues (Papi, 1991; Wallraff and Andreae, 2000; Wallraff, 2001, 2005; Gagliardo et al., 2006, 2008, 2009, 2018), visual landmarks of various kinds (e.g., Guilford et al., 2004), outward journey information (reviews in Wiltschko and Wiltschko, 1995; Wallraff, 2005), and maybe magnetic cues (Walcott, 1991; Wiltschko and Wiltschko, 1995; Dennis et al., 2007; Wiltschko et al., 2010a) to estimate their position relative to home when released from a previously unknown location. The relative importance of these map cues is hotly debated with many apparently contradictory results occurring in the literature. One reason may very well be that in one location, one type of cue may be particularly reliable; whereas another cue is more reliable in a different location and that the animals therefore predominantly rely on different cues in different locations. The most convincing experiments performed to date involved cutting of the olfactory nerves or cutting of the ophthalmic branch of the trigeminal nerves in both experienced and inexperienced pigeons. The experiments showed that homing pigeons tested in Italy need intact olfactory nerves but not intact "magnetic" nerves (see below) to home (Gagliardo et al., 2006, 2008, 2009; Gagliardo, 2013). In procellariiform seabirds such as albatrosses and shearwaters, olfactory cues also seem to be much more important for navigation than magnetic cues (Mouritsen et al., 2003; Nevitt and Bonadonna, 2005; Bonadonna et al., 2005; Gagliardo et al., 2013; Pollonara et al., 2015; Padget et al., 2017). However, recent data suggest that Manx Shearwaters do use magnetic inclination to imprint on and return to their natal colony (Wynn et al., 2020).

15.9 How do birds sense the Earth's magnetic field?

It is challenging to detect the weak geomagnetic field with biological materials. Considering the anatomical constraints and known structures found within small birds, careful models of putative sensory mechanisms often find it hard to explain how a 50,000 nT magnetic field can result in reliable signals in the presence of thermal fluctuations (kT) and other sources of noise. In fact, any biological mechanism that can, in principle, allow detection of 50,000 nT fields is noteworthy (Ritz et al., 2010; Mouritsen, 2013, 2018; Hore and Mouritsen, 2016; Hore, 2012). Only three basic mechanisms are currently considered to be physically viable: (1) induction in highly sensitive electric sensors, (2) iron-particle–based magnetoreception, and (3) radical-pair–based magnetoreception.

15.10 The induction hypothesis

Electromagnetic induction is the production of voltage across an electric conductor situated in a changing magnetic field or a conductor moving through a stationary magnetic field. Thus, in practical terms, if one has an electric wire and one moves this through a magnetic field, a current will be generated in the wire. If this wire is ring or coil-shaped, directional sensitivity can be achieved. In biological tissues, one would need conductive, liquid-filled, ring-like structures of sufficient size and diameter to generate measurable electrical signals, which can be picked up by an electrically sensitive receptor cell. For electromagnetic induction, Lorenzini ampullae are a concrete realization of an electrically sensitive cell operating in saltwater fish (von der Emde, 2013; Newton et al., 2019). Their function uses the fact that saltwater is electrically conductive, and aquatic animals could potentially use induction to sense the geomagnetic field (Kalmijn, 1981; Molteno and Kennedy, 2009). However, no strong evidence currently exists that fish actually use their electric sense to deduce information from the geomagnetic field (Kirschvink et al., 2010; Mouritsen, 2013). In land-based animals, it is difficult to imagine how induction could be used to sense the geomagnetic field since air has low conductivity and the needed structures therefore would have to be realized inside the animals themselves. Several authors have stated that the required physiological structures filled with conductive liquid in birds are too small to function as magnetic induction sensors (Kirschvink et al., 2010; Mouritsen, 2013). However, some recent calculations have suggested that the semicircular canals of pigeons might just be large enough if very fast head movement speeds are assumed (Nimpf et al., 2019). The semicircular canals of almost all night-migratory songbirds, which navigate better over large distances than pigeons, would, however, have too small

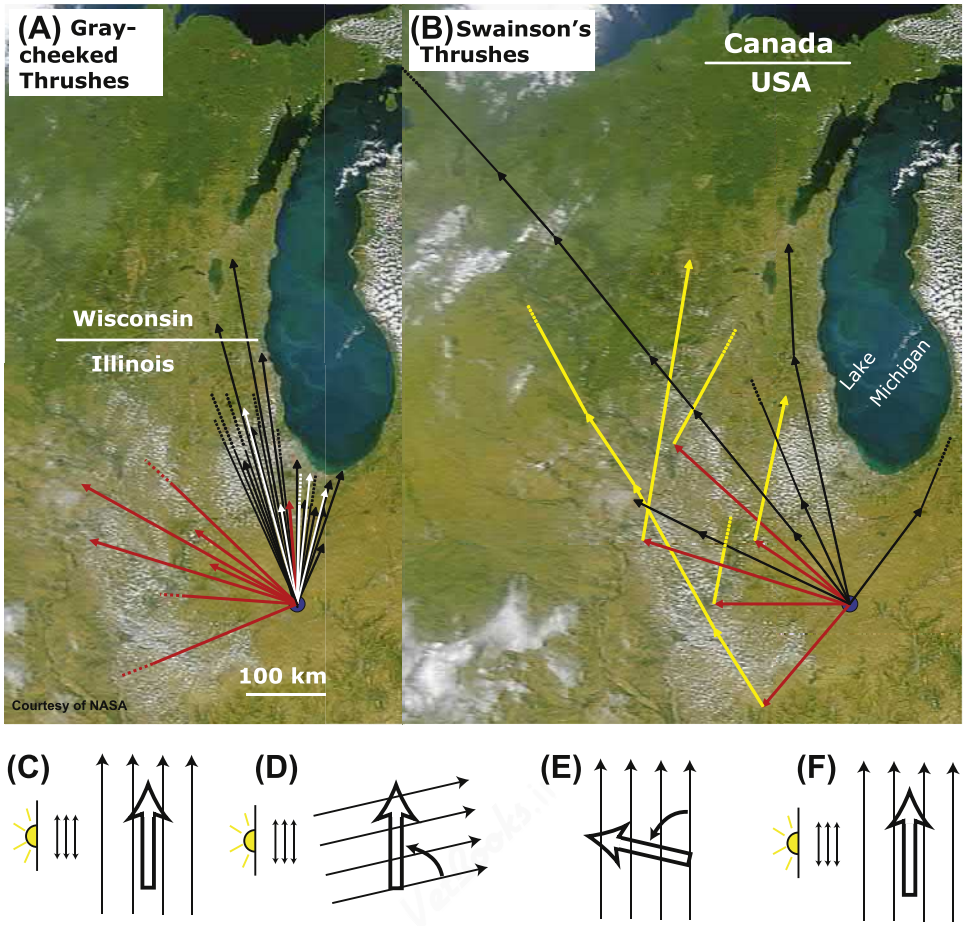

FIGURE 15.6 Some birds calibrate their magnetic compass from celestial cues around sunset. Tracks of free-flying Gray-cheeked Thrushes (A) and Swainson's Thrushes (B) released from Champaign, Illinois are shown. The *arrows* indicate the direction and ground tracks of migratory flights when wind effects were discarded. *Black arrows* indicate migratory flights of nonmanipulated individuals. *Red arrows* indicate migratory flights of experimental birds that had experienced a magnetic field turned to 80 degrees East prior to takeoff, and *yellow arrows* indicate the migratory flights of the experimental birds during subsequent nights. *White arrows* indicate the migratory flight paths of experimental birds that did not migrate on the night of magnetic treatment, but did so 1−6 days later. *Connected arrows* show flights of the same individual during successive nights. Data are depicted differently in (A) and (B) because for Gray-cheeked thrushes, experimental and control birds are different individuals while in Swainson's thrushes, the same experimental individuals were followed for at least two successive nocturnal migrations (due to the large spread in natural headings). *Broken lines* indicate that birds were lost during tracking at the site where the broken lines start. Notice that the birds that experienced a magnetic field turned 80 degrees to the east during sunset and which were released after all light from the sun had disappeared, migrated toward the west when they embarked on migration on the same night. On later nights, they migrated in the appropriate northerly spring migratory direction. These results mean that the birds had calibrated their magnetic compass from their sun compass prior to take-off and that this calibration happens daily. The reasons are illustrated in (C−F). (C) situation for control birds. (D): the turned field is calibrated by the sun during sunset. (E): after release, the birds experience the natural field lines and since all light from the sun had disappeared at time of release, their sunset-calibrated magnetic compass makes them fly wrong for the rest of the first night. (F): on the second night after release, sun and magnetic cues are in agreement and the birds will reorient into their intended migratory direction. The four *thin parallel arrows* (C−F) indicate the horizontal direction of the magnetic field lines experienced by the birds. The *thick arrow* indicates the expected orientation of the birds. The setting sun and the three lines with *double arrowheads* indicate whether sun and polarized light cues were available for calibration. *Figure and parts of the legend from Cochran et al. (2004).*

semicircular canals for induction to work. Thus, for many birds, another mechanism must be responsible for magnetoreception.

15.11 The magnetic-particle−based hypothesis

When human beings want to use the direction of the geomagnetic field for orientation, we use a technical compass based on a needle made of magnetized iron or a magnetic iron compound that moves in the horizontal plane. Therefore, the first suggestion almost any human thinks of when one asks them how birds may detect the geomagnetic field is: "Maybe they have little compass needles in their head." A compass-needle-like structure has been realized inside magnetotactic bacteria, see Fig. 15.7A (Blakemore, 1975; Frankel and Blakemore, 1989). Not surprisingly, this suggestion was also the first suggestion

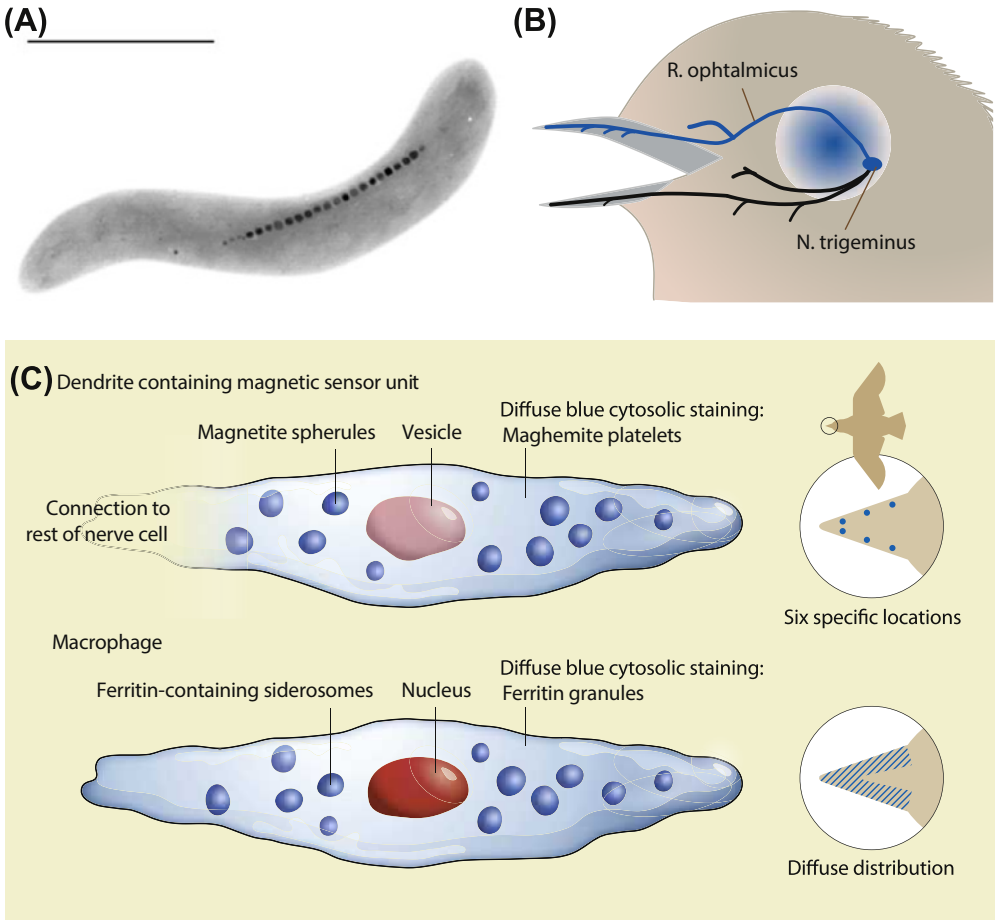

FIGURE 15.7 **Iron-particle structures in birds.** (A) Transmission electron micrograph of the magnetotactic bacteria, *Magnetospirillum magnetotacticum*, showing the magnetosome chain inside the cell. Scale bar: 1 μm. Magnetosomes would be the most straightforward solution for a magnetic field sensor in the nervous system of a bird, but, so far, magnetosomes have not been proven to occur in any bird. (B) Bird head schematically illustrating the anatomical location of the three branches of the trigeminal nerve. (C) Schematic drawing of iron-containing structures in birds' upper beak illustrating the opposing interpretations of Fleissner et al. (2003) and Treiber et al. (2012). *(A) Photograph © Richard B. Frankel. (C) Figure reproduced with permission from Nature: Mouritsen (2012) Nature 484: 320–321. Reproduced from Mouritsen (2013).*

scientists came up with. A chain of single domain magnetite particles (Blakemore, 1975; Frankel and Blakemore, 1989; Kirschvink et al., 2010) or other very similar iron oxides (Falkenberg et al., 2010) would be the easiest realization of a small compass-needle-like structure inside a bird, but other arrangements of iron-based particles could also work as a magnetic field detector (Solov'yov and Greiner, 2009; Kirschvink et al., 2010). Any such magnetic particles are expected to transduce the magnetic signal by opening or closing pressure-sensitive ion channels (Johnsen and Lohmann, 2005; Cadiou and McNaughton, 2010; Shaw et al., 2015).

Many studies have documented the presence of magnetite or other kinds of iron-based compounds in almost any animal, where researchers have seriously looked (e.g., in *Caenorhabditis elegans*, mollusks, insects, crustaceans, and various vertebrates; Mouritsen, 2013, 2018; Shaw et al., 2015). However, the mere existence of iron-containing compounds, particles, or even magnetite does not represent significant evidence by itself that such structures have any relevance to magnetoreception (Mouritsen, 2013, 2018; Malkemper et al., 2019). Iron is an important element required for proper function of most organisms. Consequently, iron homeostasis is important, and iron-containing deposits may just be a way for an organism to get rid of excess iron. Therefore, only if iron-containing particle structures are found at consistent, specific locations and are associated with the nervous system, the iron-containing structures qualify as serious magnetosensory candidates (Mouritsen, 2013, 2018). The existence of magnetite particle chains, which lead to a magnetically oriented swimming behavior in so-called magnetotactic bacteria (Blakemore, 1975; Frankel and Blakemore, 1989; Bazylinski and Frankel, 2004), unequivocally proves that

living cells can, in principle, synthesize magnetite that will align with the geomagnetic field. However, the magnetite particles in these bacteria are not part of an active sensory system, they only lead to passive alignment (Wiltschko and Wiltschko, 1995; Mouritsen, 2013).

For a while, the most promising, active, magnetic-particle–based magnetoreceptor candidate structures in vertebrates were those reported from the olfactory epithelium of fish (Walker et al., 1997; Eder et al., 2012) and in the upper beak of birds (Fleissner et al., 2003; Falkenberg et al., 2010). However, recent findings suggest that these structures were contamination artifacts (Edelman et al., 2015) and macrophages involved in iron homeostasis (Treiber et al., 2012), respectively. Thus, at present, no convincingly documented, magnetic-particle–based, magnetoreceptive candidate structures are known from birds, see Fig. 15.7C (Mouritsen, 2012, 2018).

Conditioning of birds to magnetic stimuli has also proven to be very difficult, and independent replication is rare. It has been reported that homing pigeons, *Colomba livia*, can be conditioned to respond to strong magnetic fields (Mora et al., 2004; Mora and Bingman, 2013). The conditioned response to a very strong magnetic field (around two times the strength of the geomagnetic field) required intact trigeminal nerves (Mora et al., 2004). Consequently, pigeons seem to, in principle, be able to detect strong magnetic field changes via the ophthalmic branch of the trigeminal nerve. However, in order to use geomagnetic information for a map, animals must be sensitive to changes in the geomagnetic field, which are three to five orders of magnitude smaller than the anomalies used in the successful conditioning experiments. Using a very similar paradigm adapted for European robins and using weaker fields resulted in nicely conditioned responses to auditory stimuli but failed to produce a conditioned response to magnetic field stimuli (Kishkinev et al., 2012).

The ophthalmic branch of the trigeminal nerve (see Fig. 15.8) terminates in the principal (PrV) and spinal tract (SpV) nuclei of the trigeminal brainstem complex (Williams and Wild, 2001; Heyers et al., 2010, see Fig. 15.8). Neuronal activation studies show that sub-populations of neurons both in the ventral PrV and in parts of SpV in European robins (*Erithacus rubecula*), Pigeons (*Columba livia*), Northern Wheatears (*Oenanthe oenanthe*), and Eurasian Blackcaps (*Sylvia atricapilla*) are activated by changing magnetic field stimuli, but not by a zero magnetic field (Heyers et al., 2010; Lefeldt et al., 2014; Elbers et al., 2017; Kobylkov et al., 2020a). Furthermore, the activation seen in the changing magnetic field is strongly reduced when the ophthalmic branch of the trigeminal nerve is severed (see Fig. 15.8B and C). Neuronal tracing experiments have shown that SpV projects to PrV (Arends et al., 1984; Faunes and Wild, 2017), and that the magnetically activated ventral part of PrV forms a separate, previously unknown, connection to the ipsilateral trigeminal frontal nidopallium (NFT) in the forebrain that is likely to be a key processing pathway for trigeminally mediated magnetoreception (see Fig. 15.8A; Kobylkov et al., 2020a). These findings suggest that the ophthalmic branches of the trigeminal nerves carry magnetic information in birds (Heyers et al., 2010; Lefeldt et al., 2014; Elbers et al., 2017; Kobylkov et al., 2020a). However, the sensory origin (most

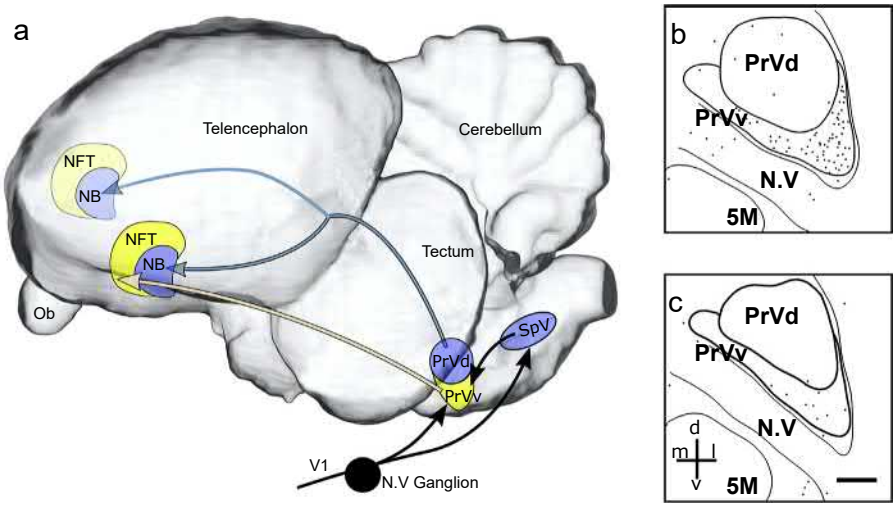

FIGURE 15.8 Magnetically activated neurons in two hindbrain-regions, SpV and ventral PrV, receive sensory input from the ophthalmic branch of the trigeminal nerve (V1) and passes this information onto the NFT in the forebrain of night-migratory birds. (A) schematic drawing of the currently known parts of the pathway processing magnetic information received via the ophthalmic branch of the trigeminal nerve in night-migratory songbirds. (B) Neurons in the ventral part of PrV are activated by magnetic stimuli (activated neurons are indicated by the *black dots* in (B) and (C); after Heyers et al., 2010). (C) The neuronal activation in PrVv significantly drops after bilateral V1 ablation or removal of the magnetic stimuli (after Heyers et al., 2010). *Figure modified after Kobylkov et al. (2020b).*

likely magnetic-particle–based) of the trigeminally mediated magnetic information are unclear at present (see Fig. 15.7C; Mouritsen, 2012).

Information from the ophthalmic branch of the trigeminal nerve is neither required nor sufficient for magnetic compass orientation in several night-migrating songbird species (e.g., Zapka et al., 2009, see Fig. 15.13). Homing experiments with pigeons have shown that pigeons tested around Pisa (Italy) need intact olfactory nerves but not intact trigeminal nerves to home (Gagliardo et al., 2006, 2008, 2009). The most likely function of the trigeminal nerve-related magnetic sense is to detect large-scale changes in magnetic field strength and/or magnetic inclination, which could be used to determine approximate position. Real displacement experiments have shown that Eurasian Reed Warblers, *Acrocephalus Scirpaceus*, are capable of correcting for a 1000 km eastward displacement (Chernetsov et al., 2008), but that this ability disappears when the ophthalmic branch of the trigeminal nerve is cut (Kishkinev et al., 2013, see Fig. 15.3). Eurasian Reed Warblers also correct for virtual magnetic displacements in which all the magnetic field parameters are set to match the real displacement location of previous experiments, but in which the birds were not actually moved (Kishkinev et al., 2015). Because all other cues such as olfactory and celestial cues are identical before and after virtual displacements, virtual magnetic displacement experiments demonstrate that magnetic parameters can play a decisive role in the map sense of long-distance, night-migratory songbirds (Kishkinev et al., 2015; Chernetsov et al., 2017; Pakhomov et al., 2018). Intact ophthalmic branches of the trigeminal nerves are required for these birds' abilities to correct for virtual magnetic displacements (Pakhomov et al., 2018). Furthermore, experiments with night-migratory songbirds exposed to strong magnetic pulses, which are thought to disturb any magnetite-based magnetic sense for days to weeks, but which should not have any effect after the treatment itself on a light-dependent magnetoreception mechanism (see next section), support the idea that the magnetic map or signpost sense could be magnetic-particle–based (Wiltschko et al., 2009; Holland, 2010; Holland and Helm, 2013).

It has also been suggested that the avian lagena (a part of the birds' vestibular system) and/or the semicircular canals play a role in magnetodetection (Wu and Dickman, 2011, 2012; Malkemper et al., 2019; Nimpf et al., 2019). Whether the inner ear provides the primary magnetic information or gravity information to the magnetic sense is not yet clear (Malkemper et al., 2019), but if the electrophysiological data (Wu and Dickman, 2012) can be independently replicated, the role of the lagena in magnetoreception is very significant indeed and the vestibular brainstem nuclei would be a very important processing station for magnetic field information.

15.12 The light-dependent hypothesis

The magnetic compass behavior of newts (Phillips and Borland, 1992) and birds (Wiltschko et al., 1993, 2010b; Muheim et al., 2002) is dependent on the wavelengths of light being available during behavioral tests. Already in the late 1970s, theoretical considerations led Klaus Schulten to suggest that chemical reactions based on radical-pairs in photosensitive molecules could form the basis of a magnetic compass sense (Schulten et al., 1978). An extensive tutorial review on the radical-pair mechanism of magnetoreception can be found in Hore and Mouritsen (2016).

The principles of the suggested light-dependent magnetic sensing mechanism are illustrated in Fig. 15.9. A light-sensitive molecule absorbs light and uses the light energy to transfer an electron within a molecule or between associated molecules. Thereby, a radical pair is produced. If this radical pair is long-lived ($\sim$1–10 μs), it can, depending on the spin of the electrons, exist in one of two states, a singlet state (spins antiparallel) or a triplet state (spins mostly parallel). It is known from chemistry that singlet and triplet states have different chemical properties and thus often result in different chemical end products. Earth-strength magnetic fields can theoretically affect the relative likelihoods of the molecule being in the singlet or triplet states, and thereby modulate a presently unknown biochemical pathway (Schulten et al., 1978; Ritz et al., 2000; Rodgers and Hore, 2009; Hore and Mouritsen, 2016), but see Wu et al. (2020).

How can we imagine that a bird using a light-induced, radical-pair mechanism would detect the magnetic field? It is possible that a virtual visual image would literally enable birds to "see" the direction of the magnetic field lines. Various specific virtual images have been suggested (see e.g., Fig. 15.10; Ritz et al., 2000, 2010; Solov'yov et al., 2010). However, all these images are for illustrative purposes only because we have much too little information available at present to know how an actual magnetically modulated light pattern seen by a bird would look like (Mouritsen, 2013; Hore and Mouritsen, 2016). It is almost certain, however, that the mechanism would require two neighboring sensors oriented in such a way relative to each other that they would calculate out light intensity and light polarization angle (Hore and Mouritsen, 2016; Worster et al., 2017). The outer or inner segments of cone photoreceptor cells, most likely the double cones (Günther et al., 2018, 2021), would be ideal locations for the light-dependent, radical-pair–based, magnetic field sensors (Hore and Mouritsen, 2016; Mouritsen, 2018; Xu et al., 2021).

If the radical-pair mechanism is responsible for magnetoreception, it means that it is based on a quantum mechanical effect (Rodgers and Hore, 2009; Ball, 2011; Hogben et al., 2012; Solov'yov et al., 2014; Hore and

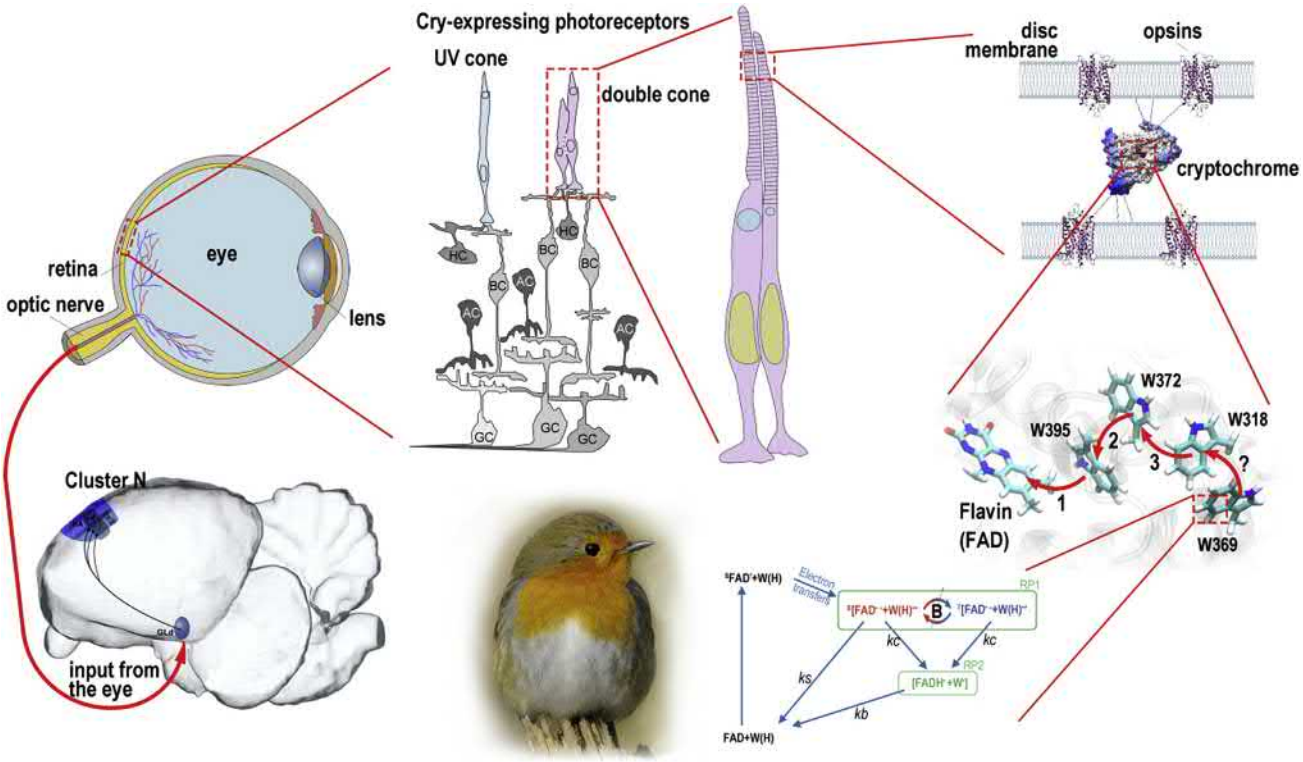

FIGURE 15.9 Summary of the proposed light-dependent magnetic compass sensing hypothesis in birds. Most of the experiments reviewed here were performed on European robins, *Erithacus rubecula*. The reference direction provided by the Earth's magnetic field is detected in the birds' eyes. It is hypothesized that cryptochrome proteins are the light-dependent magnetic sensory molecules. Light absorption is thought to generate long-lived flavin-tryptophan radical pairs generated by sequential electron transfers within cryptochromes in the retina, whose reaction yields are determined by the orientation of the molecule with respect to the magnetic field vector. If the cryptochromes were associated with the membrane disks of the outer segments of the photoreceptors, then an ordered structure could result, and different reaction yields in different parts of the retina or between neighboring cells could be compared to provide a visual impression of the compass bearing (see Fig. 15.10). The most likely magnetoreceptive candidate molecule at present is cryptochrome 4 which is located in the outer segments of the double cones and long-wavelength single cones. Light-dependent magnetic compass information is transmitted from the retina through the optic nerve to the visual thalamus and from there to Cluster N in the forebrain, via the thalamofugal visual pathway (Fig. 15.12). If Cluster N is destroyed, European robins can no longer use their magnetic compass (Fig. 15.13). The illustration of the cryptochromes bound to photoreceptor membranes is modified from Solov'yov et al. (2010). The brain illustration originates from Mouritsen et al. (2016). The compound illustration was created by Ilia Solov'yov. *Photo by Henrik Mouritsen.*

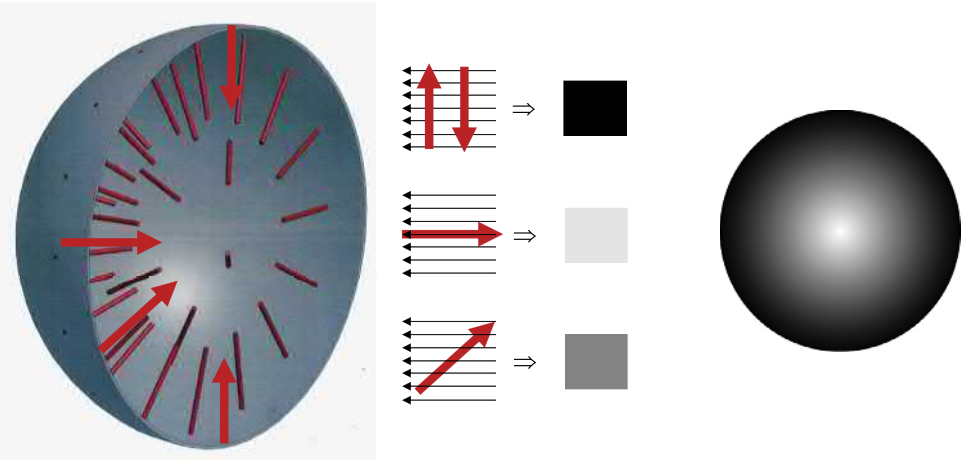

FIGURE 15.10 How the light-dependent, radical-pair–based, magnetic sensing mechanism could lead to perception of a visual image. Principal illustration suggesting how birds could, in principle, convert a magnetic stimulus into a putative visual image. Left: three-dimensional illustration of the half-sphere of an eyeball. Red pins simulate cryptochrome orientation all pointing toward the center of the eyeball. If a bird's eye would be looking in the direction of the magnetic field lines, one could imagine that the birds would see a pattern similar to the one illustrated on the right because the light-sensitivity of one or more cryptochromes would depend on their orientation relative to the axis of the magnetic field lines. *Redrawn after Mouritsen (2013) inspired by Ritz et al. (2000).*

Mouritsen, 2016; Mouritsen, 2018). It might in fact be the only sensory mechanism in biology to be inherently quantum in nature. Critics of the radical-pair mechanism have pointed out that the interaction energy between a geomagnetic field and a radical is typically several orders of magnitude below the background thermal energy, k_BT (e.g., Kirschvink et al., 2010). At first glance, this might seem critical, but because the spins in the relevant radicals are very far from equilibrium this is not a fundamental problem. Very weak magnetic interactions can affect radical pair reactions essentially for three reasons (Hore, 2011; Hore and Mouritsen, 2016). (a) Radical pair chemistry is controlled by the electron spins in the radicals. (b) The electron spins are not at thermal equilibrium. (c) The electron spins behave quantum mechanically. Weak magnetic fields affect the coherent behavior of the electron spins in a fundamentally quantum manner in which k_BT plays no role. Instead of comparing interaction energies to k_BT, one must compare the time required for a magnetic interaction to have an effect with the time required for the system to reach thermal equilibrium, the so-called spin-correlation time (Hore, 2011; Hore and Mouritsen, 2016). If the former is shorter than the latter, then the magnetic field can have an effect (Hore, 2011), and if the spin-correlation time is at least 2−10 μs, a so-called quantum-needle effect appears, which could improve the directional accuracy of a radical-pair–based magnetoreceptor system very substantially (Hiscock et al., 2016). As an excellent analogy (Hore, 2011; Hore and Mouritsen, 2016), one can imagine a fly and a rectangular granite block. If the granite block is standing on one of its sides (conventional physics, equilibrium), the fly has no chance to flip the granite block, but if the granite block is balancing on one of its sharp corners (quantum mechanics, nonequilibrium), depending on where the fly lands, it might flip the granite block to one or the other side (Fig. 15.11).

Which molecule can be responsible for light-dependent magnetoreception? Opsins cannot function as radical-pair–based magnetoreceptors because opsins use the light energy to change a chemical bond, not to transfer an electron. The only currently known photoreceptor molecules found in vertebrates, which can use light energy to form long-lived radical pairs are the cryptochromes (Ahmad and Cashmore, 1993; Cashmore et al., 1999; Ritz et al., 2000, 2010; Giovani et al., 2003; Liedvogel et al., 2007a; Biskup et al., 2009; Rodgers and Hore, 2009; Liedvogel and Mouritsen, 2010; Nießner et al., 2011, 2016, 2018; Bolte et al., 2016; Sheppard et al., 2017; Günther et al., 2018; Zoltowski et al., 2019; Xu et al., 2021). Some cryptochromes are known to be involved in circadian clocks (Cashmore et al., 1999; Sancar, 2003). However, in birds, more cryptochromes than the ones thought to be involved in the clock occur, so it is easy to imagine that they can play a role in other biochemical processes (Liedvogel and Mouritsen, 2010; Günther et al., 2018; Xu et al., 2021). Cryptochromes are related to the DNA repair

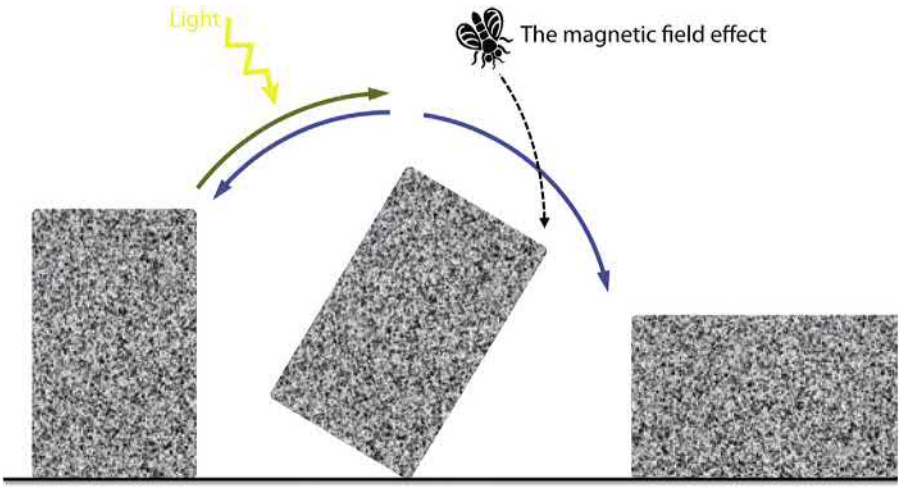

FIGURE 15.11 Granite block analogy of light-dependent magnetoreception. A granite block analogy can help understand how a radical-pair–based mechanism can theoretically be used to sense Earth-strength magnetic fields, even though the energy exerted by the magnetic field on the radical is much lower than thermal energy, k_BT. Imagine a granite block standing on one of its sides (the system is in equilibrium). If a fly lands on the granite block while it is in this position, there is no way the fly can make the granite block flip over. In fact, quite a lot of energy is needed to move the granite block onto one of its sharp corners (a state very far from equilibrium), but once it is on one of its sharp corners, a very small amount of energy can influence which way the granite block falls. Now even a fly landing on the granite block may make it flip over to one or the other side. In the light-dependent, radical-pair–based magnetoreception hypothesis, light has much more energy than the magnetic field. It is the absorption of light that brings a photoreceptor molecule (probably a cryptochrome) into an exited state (moves the granite block onto its sharp corner in the analogy). This excited state is highly sensitive to even very small magnetic field effects (the fly landing onto the granite block in the analogy). *After Hore (2011) and Hore and Mouritsen (2016).*

enzymes called photolyases (Cashmore et al., 1999; Sancar, 2003) and consist of a photolyase homology region and a C-terminal end, which varies greatly between different cryptochromes (Cashmore et al., 1999; Sancar, 2003; Müller and Carell, 2009; Liedvogel and Mouritsen, 2010; Chaves et al., 2011; Ozturk, 2017; Zoltowski et al., 2019). Many cryptochromes, including at least bird cryptochrome 4, noncovalently bind the cofactor flavin (Ozturk et al., 2009; Xu et al., 2021; Zoltowski et al., 2019). The light-induced electron transfer takes place between the flavin and three or four tryptophan residues within the cryptochrome protein (Gindt et al., 1999; Biskup et al., 2009; Rodgers and Hore, 2009; Solov'yov et al., 2012; Maeda et al., 2012; Hore and Mouritsen, 2016; Sheppard et al., 2017; Zoltowski et al., 2019; Xu et al., 2021). Very recently, it was shown that Cryptochrome 4 from night-migratory European robins is very magnetically sensitive in vitro, and more so than cryptochrome 4 from non-migratory pigeons and chickens (Xu et al., 2021).

Cryptochromes are predominantly found within photoreceptor cells and ganglion cells in the eyes of birds (Mouritsen et al., 2004; Möller et al., 2004; Nießner et al., 2011, 2016; Bolte et al., 2016, 2021; Günther et al., 2018). At present, cryptochromes are the only seriously considered candidate molecules for radical-pair–based magnetoreception in birds (Mouritsen and Ritz, 2005; Rodgers and Hore, 2009; Ritz et al., 2010; Hore and Mouritsen, 2016; Mouritsen, 2018), and Earth-strength magnetic fields effects on a radical pair reaction in an artificially produced molecule mimicking the reaction principle thought to take place in cryptochrome have been observed and thus support the theoretical feasibility of the suggested mechanism (Maeda et al., 2008; reviewed in Mouritsen and Hore, 2012).

Following the suggestion of Klaus Schulten et al. (1978), it was shown that the compass orientation behavior of night-migrating songbirds is influenced by the color (i.e., wavelengths) of the light available in the room in which the orientation tests are performed (Wiltschko et al., 1993, 2010b). This wavelength dependence is difficult to explain if the eyes and/or pineal organ are not somehow involved in the magnetic compass. In birds, the pineal organ is not needed for magnetic compass orientation (Schneider et al., 1994), whereas photoreceptor molecules in the pineal organ seem to be essential for magnetic compass orientation in newts (Phillips et al., 2001).

The radical-pair mechanism of magnetoreception should be disturbed by oscillating radio frequency (RF) magnetic fields with frequencies in resonance with one or more of the singlet-triplet oscillation frequencies, which are determined by the possible energy-level splits of the radical pair, because such fields could override the effect of the external magnetic field and thus alter the reaction yield (Henbest et al., 2004). On the contrary, weak RF magnetic fields are both too weak and too fast to interfere with any induction- or magnetite-based magnetoreceptors (Hore and Mouritsen, 2016).

Oscillating, RF magnetic fields in the low MHz range as weak as a few nT (ca. 0.01–0.1% of the geomagnetic field strength) disrupt the magnetic compass orientation capabilities of night-migratory songbirds (Ritz et al., 2004, 2009; Engels et al., 2014; Schwarze et al., 2016; Pakhomov et al., 2017; Kobylkov et al., 2019). At first, it was claimed that only an RF magnetic field at the so-called Larmor frequency could disrupt the orientation of birds (Ritz et al., 2009), but later it was shown that broadband RF fields are much more effective in disrupting the birds' magnetic compass (Engels et al., 2014; Schwarze et al., 2016). Broadband RF effects are much easier to understand than the claimed Larmor frequency-specific effects because any realistic organic radical-pair that could occur inside a bird will have magnetic nuclei such as hydrogens and/or nitrogen near the unpaired electrons, and this leads to multiple energy level splits and thus to a predicted broadband RF effect (for a detailed explanation, see Hore and Mouritsen, 2016). While it can be understood based on quantum mechanical theory why broadband RF fields can affect a radical-pair–based magnetoreception mechanism, it remains a challenge to explain how RF fields as weak as a few nT can have the effects observed in behavioral tests (Hore and Mouritsen, 2016; Hiscock et al., 2017; Mouritsen, 2018).

On the neuroanatomical level, a region named Cluster N (Fig. 15.12) is by far the most active forebrain region when night-migrating birds perform magnetic compass orientation, and this activation disappears when the birds' eyes are covered (Mouritsen et al., 2005; Feenders et al., 2008; Zapka et al., 2010; Hein et al., 2010). Cluster N receives its neuronal input from the eyes via the thalamofugal visual pathway (Heyers et al., 2007; Mouritsen et al., 2016). The presence and activation of Cluster N at night has been independently replicated in other night-migratory songbirds (Rastogi et al., 2011). Could Cluster N be a processing center of light-dependent magnetic compass information?

Double-blind experiments (Fig. 15.13) with European robins have shown that birds with bilateral Cluster N lesions were unable to orient using their magnetic compass (Zapka et al., 2009). In contrast, sham Cluster N lesions or bilateral sections of the ophthalmic branch of the trigeminal nerves did not influence the robins' ability to use their magnetic compass for orientation (Zapka et al., 2009). Cluster N lesions only affect the magnetic compass, since Cluster N lesioned robins orient well using their sun and star compasses (Zapka et al., 2009). These data (a) show that Cluster N is required for magnetic compass orientation in this species; (b) indicate that Cluster N may be specifically involved in processing magnetic compass information; (c) strongly suggest that a vision-mediated mechanism

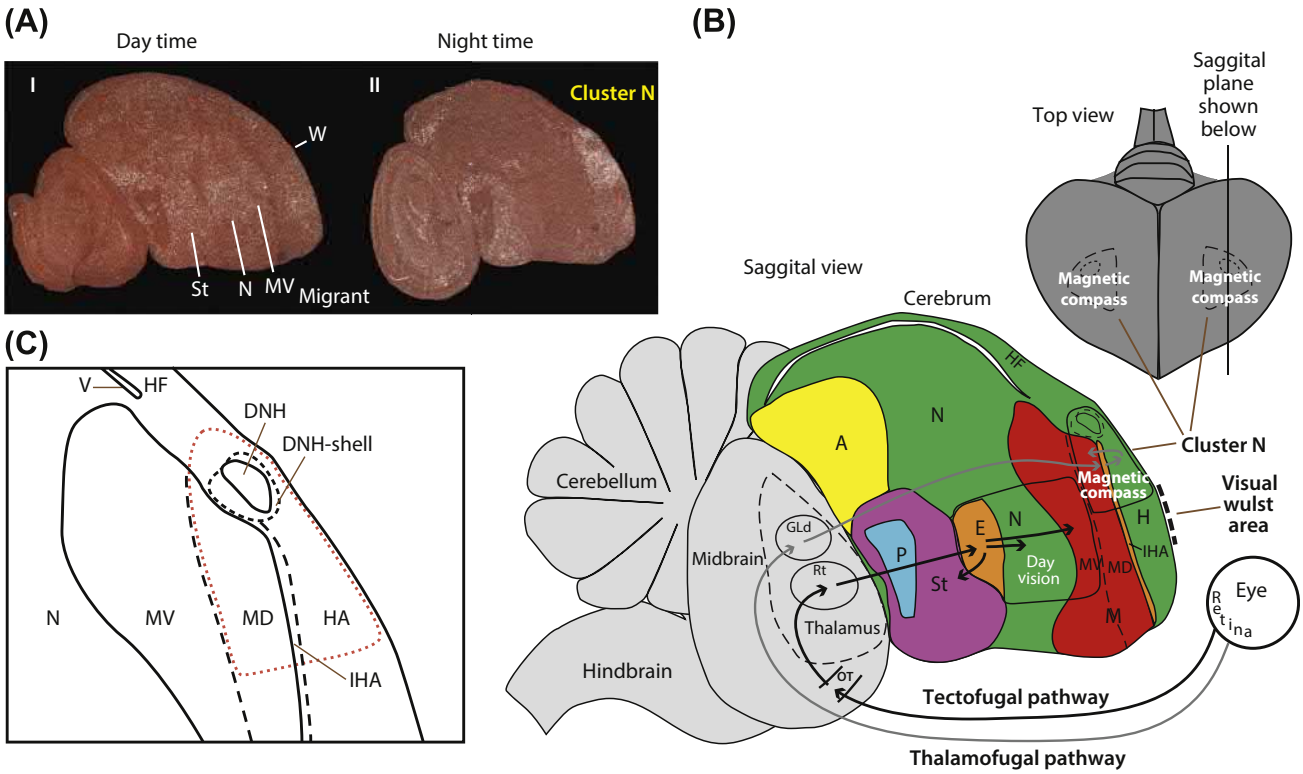

FIGURE 15.12 **Cluster N.** (A) Cluster N is the most active brain area when migratory birds perform magnetic sensing and/or compass orientation at night (white signal in the brain slices indicate activated neurons) and Cluster N is required for magnetic compass orientation (see Fig. 15.13). (B) Cluster N is a part of the visual Wulst and receives input from the eyes via the thalamofugal visual pathway (Heyers et al., 2007). Top view of the brain in gray indicates the medial-lateral and the frontal-caudal extent of Cluster N and the DNH and DNH-shell. (C) Cluster N is a functional unit consisting of a part of the hyperpallium, maybe a part of the dorsal mesopallium (Jarvis et al., 2013), and a nucleus embedded within the hyperpallium named DNH with a shell of cells around the DNH. Anatomy: *A*, arcopallium; *DNH*, dorsal nucleus of the hyperpallium; *DNH-shell*, shell around the DNH; *E*, entopallium; *H*, hyperpallium; *HF*, hippocampal formation; *IHA=HI*, interstitial region of the hyperpallium intercalatum; *LGd*, Lateral geniculate nucleus, dorsal part; *M*, mesopallium; *MD*, mesopallium dorsale; *MV*, mesopallium ventrale; *N*, nidopallium; *OT*, optic tectum; *P*, pallidum; *Rt*, nucleus rotundus; *St*, striatum; *v*, ventricle; *W*, visual Wulst. *From Mouritsen (2013) after Mouritsen et al. (2005).*

underlies the magnetic compass in this migratory songbird; (d) indicate that input from the lagena is not sufficient for magnetic compass orientation in robins; and (e) show that the proposed magnetic input to the brain transmitted via the trigeminal nerve is neither necessary nor sufficient for magnetic compass orientation of European robins tested in an orientation cage (Zapka et al., 2009; Mouritsen, 2013, 2018). The exact role of Cluster N within the magnetic compass information processing circuit has not been determined, but the existing results raise the distinct possibility that this small part of the visual system enables birds to "see" magnetic compass information (Mouritsen, 2013, 2018).

Do these results exclude the possibility that magnetic-particle–based and/or trigeminally mediated and/or lagena-mediated magnetoreception exists? Absolutely not. In birds, magnetic-particle–based magnetoreception may very well exist, and magnetic field–dependent neuronal activation in trigemino-recipient and lagena-recipient regions has been documented (see above). Trigeminally mediated magnetoreception just does not seem to be the primary mechanism for the magnetic compass of night-migratory songbirds (Zapka et al., 2009), but is likely to be a primary source for magnetic positional information (Mora et al., 2004; Kishkinev et al., 2013; Pakhomov et al., 2018). In fact, it is likely that light-mediated, radical-pair–based magnetoreception and magnetic-particle–based magnetoreception mechanisms exist side by side in several animal species and that they may provide the animals with different types of magnetic information (Wiltschko and Wiltschko, 2007; Hore and Mouritsen, 2016; Mouritsen, 2018).

As so often in biology, when there are two hypotheses how something works, it often turns out that both of them are correct to a certain degree. Furthermore, seemingly unnecessary redundancy seems to be a very common occurrence in biology, probably because organisms that can perform an important function in several ways will be more robust to changes and thus be favored by evolution (Mouritsen, 2013).

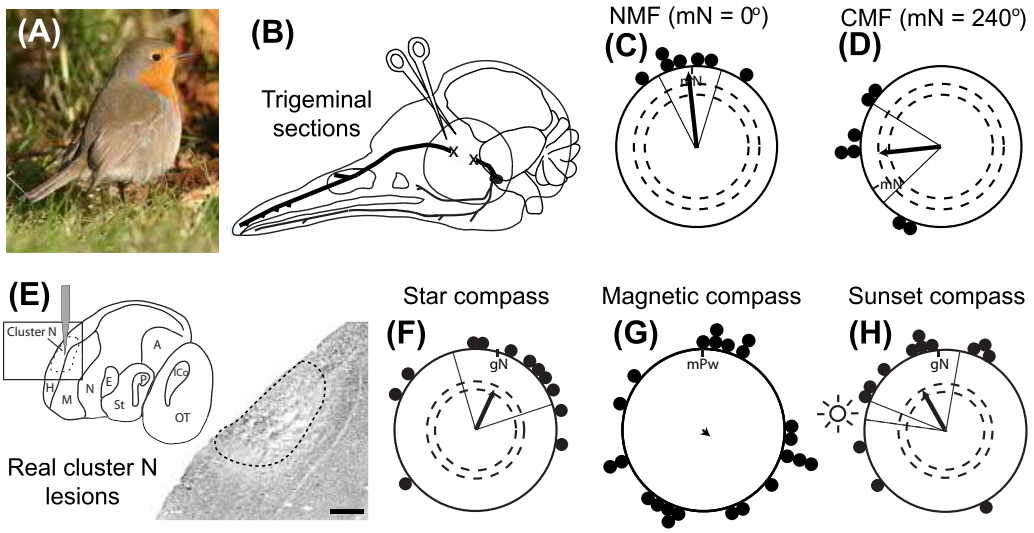

FIGURE 15.13 The brain region Cluster N is necessary for magnetic compass orientation behavior, but not for star and sun compass orientation. The trigeminal nerve is neither necessary nor sufficient for magnetic compass orientation in European Robins. (A) The European Robin. (B–D): Bilateral sectioning of the ophthalmic branch of the trigeminal nerve (B) does not affect the birds' magnetic compass orientation capabilities (C–D; mN = magnetic North). (E–H) Bilateral chemical lesions of Cluster N (E) destroyed the magnetic compass capabilities of the birds (G), whereas star compass orientation in a planetarium (F) and sun compass orientation outdoors with view of the setting sun (H) was unaffected by Cluster N lesions. The circular diagrams are explained in the legend of Fig. 15.3. (E) shows a schematic drawing and an example part of a brain section saggitally cut through the center of Cluster N and stained with a neuronal marker. Scale bar 500 µm. Rostral is left, caudal is right. Note that the tissue where Cluster N should have been in the lesioned bird (E) is destroyed. Anatomy: *A*, arcopallium; *E*, entopallium; *H*, hyperpallium; *ICo*, intercollicular complex; *M*, mesopallium; *MD*, mesopallium dorsale; *MV*, mesopallium ventrale; *N*, nidopallium; *OT*, optic tectum; *P*, pallidum. *(A) Photo © Henrik Mouritsen. From Mouritsen (2013) after Zapka et al. (2009).*

15.13 Irreproducible results and the urgent need for independent replication

Magnetic sense research is strongly influenced by a number of claims, which nobody has ever been able to independently replicate. This is particularly true for electrophysiological evidence (e.g., Semm and Demaine, 1986; Beason and Semm, 1987; Ramirez et al., 2014), but there are also many other examples of contradicting and/or seemingly irreproducible results in the literature including the effects of lidocaine treatment on upper beak receptors (Engels et al., 2018), many claims that humans have a magnetic sense (Westby and Partridge, 1986; Baker, 1989), and the claim that the magnetic compass of birds should only be in the right eye of birds (Wiltschko et al., 2002, 2003; Liedvogel et al., 2007b; Stapput et al., 2010; Hein et al., 2010, 2011; Engels et al., 2012). These problems with reproducibility do not necessarily mean that the original claims were wrong. However, it means that any result in magnetoreception—and in any other field for that matter—should be treated with caution until a given finding has been independently replicated.

This lack of reproducibility in magnetic sense–related research is, unfortunately, accompanied by an almost complete lack of double-blind procedures. Considering this history and the fact that humans have no intuitive feel for magnetic stimuli (and therefore are less likely to detect even obvious artifacts), double-blind procedures should become the standard. Studies representing the first independent, double-blind, replication of key findings in magnetoreception are therefore almost as important as the original finding (Mouritsen, 2013, 2018).

15.14 Where do we go from here?

Even though the magnetic senses are still not completely understood, many studies from different fields support both the magnetic-particle–based and the light-dependent magnetoreception hypotheses. However, fundamental questions remain in all relevant fields.

For instance, functional understanding of any particular magnetic-particle–based structure proven to be involved in an active sensory system is lacking (Mouritsen, 2012, 2018). Likewise, we yet have to understand biophysically how nature designed radical-pair receptors so that they can be sensitive to Earth-strength magnetic fields at physiological temperatures, a feat that has been approximated, but not yet fully accomplished in manmade radical-pair reactions (Maeda et al., 2008; Rodgers and Hore, 2009; Hore and Mouritsen, 2016). Furthermore, studies at the protein level in vitro suggest that cryptochromes from night-migratory songbirds, but seemingly not those from nonmigratory chicken and pigeons, have properties optimal

for magnetic sensing (Xu et al., 2021), but we yet have to demonstrate magnetic field effects on bird cryptochromes in vivo.

On the neuroanatomical level, we have just begun to explore the brain circuits processing magnetic information, but we are still far from understanding how a bird gets from the detection of magnetic information to a directional choice, which is made, based on integration of information from multiple sensory systems (reviewed in Mouritsen et al., 2016). Also, so far, none of the reported responses of single neurons to magnetic stimuli have been independently replicated. Even at the behavioral level, where most studies about magnetic senses have been published, a clear separation of experimental parameters has proven difficult, and many behaviors appear to be multimodal, or at least modulated by other modalities, such as vision and olfaction (Mouritsen, 2013, 2018).

In conclusion, magnetoreception is an important part of life for birds and a wide variety of other animals, and there are still many opportunities to perform new, groundbreaking research on the molecules, cells, and neural processes underlying any kind of magnetoreception.

References

Able, K.P., 1996. The debate over olfactory navigation by homing pigeons. J. Exp. Biol. 199, 121–124.

Adair, R.K., 1991. Constraints on biological effects of weak extremely-low frequency electromagnetic fields. Phys. Rev. 43, 1039–1048.

Ahmad, M., Cashmore, A.R., 1993. HY4 gene of *A. thaliana* encodes a protein with characteristics of a blue-light photoreceptor. Nature 366, 162–166.

Arends, J.J., Woelders-Blok, A., Dubbeldam, J.L., 1984. The efferent connections of the nuclei of the descending trigeminal tract in the mallard (*Anas platyrhynchos* L.). Neuroscience 13, 797–817.

Baker, R.R., 1989. Human Navigation and Magnetoreception. Manchester University Press, Manchester.

Ball, P., 2011. Physics of life: the dawn of quantum biology. Nature 474, 272–274.

Bazylinski, D.A., Frankel, R.B., 2004. Magnetosome formation in prokaryotes. Nat. Rev. Microbiol. 2, 217–230.

Beason, R.C., Semm, P., 1987. Magnetic responses of the trigeminal nerve system of the bobolink (*Dolichonyx oryzivorus*). Neurosci. Lett. 80, 229–234.

Berthold, P., 1991. Spatiotemporal programmes and genetics of orientation. In: Berthold, P. (Ed.), Orientation in Birds. Birkhäuser Verlag, Basel, pp. 86–105.

Biskup, T., Schleicher, E., Okafuji, A., Link, G., Hitomi, K., Getzoff, E.D., Weber, S., 2009. Direct observation of a photoinduced radical-pair in a cryptochrome blue-light photoreceptor. Angew. Chem. Int. Ed. 48, 404–407.

Blakemore, R., 1975. Magnetotactic bacteria. Science 190, 377–379.

Bolte, P., Bleibaum, F., Einwich, A., Günther, A., Liedvogel, M., Heyers, D., Depping, A., Wöhlbrand, L., Rabus, R., Janssen-Bienhold, U., Mouritsen, H., 2016. Localisation of the putative magnetoreceptor cryptochrome 1b in the retinae of migratory birds and homing pigeons. PLoS One 11, e0147819.

Bolte, P., Einwich, A., Seth, P.K., Chetverikova, R., Heyers, D., Wojahn, I., Janssen-Bienhold, U., Feederle, R., Hore, P.J., Dedek, K., Mouritsen, H., 2021. Cryptochrome 1a localisation in light- and dark-adapted retinae of several migratory and non-migratory bird species: No signs of light-dependent activation. Ethol. Ecol. Evol. https://doi.org/10.1080/03949370.2020.1870571. In press.

Bonadonna, F., Bajzak, C., Benhamou, S., Igloi, K., Jouventin, P., Lipp, H.P., Dell'Omo, G., 2005. Orientation in the wandering albatross: interfering with magnetic perception does not affect orientation performance. Proc. Roy. Soc. Lond. B 272 (1562), 489–495.

Cadiou, H., McNaughton, P.A., 2010. Avian magnetite-based magnetoreception: a physiologist's perspective. J. R. Soc. Interface 7, S193–S205.

Cashmore, A.R., Jarillo, J.A., Wu, Y.-J., Liu, D., 1999. Cryptochromes: blue light receptors for plants and animals. Science 284, 760–765.

Chaves, I., et al., 2011. The cryptochromes: blue light photoreceptors in plants and animals. Annu. Rev. Plant Biol. 62, 335–364.

Chernetsov, N., Kishkinev, D., Mouritsen, H., 2008. A long-distance avian migrant compensates for longitudinal displacement during spring migration. Curr. Biol. 18, 188–190.

Chernetsov, N., Kishkinev, D., Kosarev, V., Bolshakov, C.V., 2011. Not all songbirds calibrate their magnetic compass from twilight cues: a telemetry study. J. Exp. Biol. 214, 2540–2543.

Chernetsov, N., Pakhomov, A., Kobylkov, D., Kishkinev, D., Holland, R.A., Mouritsen, H., 2017. Migratory Eurasian reed warblers can use magnetic declination to solve the longitude problem. Curr. Biol. 27, 2647–2651.

Chernetsov, N., Pakhomov, A., Davydov, A., Cellarius, F., Mouritsen, H., 2020. No evidence for the use of magnetic declination for migratory navigation in two songbird species. PLoS One 15, e0232136. https://doi.org/10.1371/journal.pone.0232136.

Cochran, W.W., Mouritsen, H., Wikelski, M., 2004. Migrating songbirds recalibrate their magnetic compass daily from twilight cues. Science 304, 405–408.

Coriolis, G., 1835. Sur les équations du mouvement relatif des systèmes de corps. Journal de l'École polytechnique 15, 142–154.

Courtillot, V., Le Mouël, J.L., 1988. Time variations of the Earth's magnetic field: from daily to secular. Annu. Rev. Earth Planet Sci. 16, 389–476.

Dennis, T.E., Rayner, M.J., Walker, M.M., 2007. Evidence that pigeons orient to geomagnetic intensity during homing. Proc. R. Soc. B 274, 1153–1158.

Drost, R., 1938. Über den Einfluss von Verfrachtungen zur Herbstzugzeit auf den Sperber, *Accipiter nisus* (L.). Zugleich ein Beitrag zur Frage nach der Orientierung der Vögel auf dem Zuge ins Winterquartier. Proc. Int. Ornithol. Congr. 9, 502–521 (Rouen).

Edelman, N.B., Fritz, T., Nimpf, S., Pichler, P., Lauwers, M., Hickman, R.W., et al., 2015. No evidence for intracellular magnetite in putative vertebrate magnetoreceptors identified by magnetic screening. Proc. Natl. Acad. Sci. U. S. A. 112, 262–267.

Eder, S.H.K., Cadiou, H., Muhamad, A., McNaughton, P.A., Kirschvink, J.L., Winklhofer, M., 2012. Magnetic characterization of isolated candidate vertebrate magnetoreceptor cells. Proc. Natl. Acad. Sci. U. S. A. 109, 12022–12027.

Elbers, D., Bulte, M., Bairlein, F., Mouritsen, H., Heyers, D., 2017. Magnetic activation in the brain of the migratory northern wheatear (*Oenanthe oenanthe*). J. Comp. Physiol. 203, 591–600.

von der Emde, G., 2013. Electroreception. In: Galizia, C.G., Lledo, P.-M. (Eds.), Neurosciences - from Molecule to Behavior: A University Textbook. Springer-Verlag Berlin Heidelberg, pp. 409–425.

Emlen, S.T., 1975. The stellar-orientation system of a migratory bird. Sci. Am. 233, 102–111.

Emlen, S.T., Emlen, J.T., 1966. A technique for recording migratory orientation of captive birds. Auk 83, 361–367.

Engels, S., Hein, C.M., Lefeldt, N., Prior, H., Mouritsen, H., 2012. Night-migratory songbirds possess a magnetic compass in both eyes. PLoS One 7 (9), e43271.

Engels, S., Schneider, N.-L., Lefeldt, N., Hein, C.M., Zapka, M., Michalik, A., Elbers, D., Kittel, A., Hore, P.J., Mouritsen, H., 2014. Anthropogenic electromagnetic noise disrupts magnetic compass orientation in a migratory bird. Nature 509, 353–356.

Engels, S., Treiber, C.D., Salzer, M.D., Michalik, A., Ushakova, L., Keays, D.A., Mouritsen, H., Heyers, D., 2018. Lidocaine is a nocebo treatment for trigeminally mediated magnetic orientation in birds. J. R. Soc. Interface 20180124.

Falkenberg, G., Fleissner, G., Schuchardt, K., Kuehbacher, M., Thalau, P., Mouritsen, H., Heyers, D., Wellenreuther, G., Fleissner, G., 2010. Avian magnetoreception: elaborate iron mineral containing dendrites in the upper beak seem to be a common feature of birds. PLoS One 5 (2), e9231.

Faunes, M., Wild, J.M., 2017. The ascending projections of the nuclei of the descending trigeminal tract (nTTD) in the zebra finch (*Taeniopygia guttata*). J. Comp. Neurol. 525, 2832–2846.

Feenders, G., Liedvogel, M., Rivas, M., Zapka, M., Horita, H., Hara, E., Wada, K., Mouritsen, H., Jarvis, E.D., 2008. Molecular mapping of movement-associated areas in the avian brain: a motor theory for vocal learning origin. PLoS One 3 (3), e1768.

Fleissner, G., Holtkamp-Rötzler, E., Hanzlik, M., Winklhofer, M., Fleissner, G., Petersen, N., Wiltschko, W., 2003. Ultrastructural analysis of a putative magnetoreceptor in the beak of homing pigeons. J. Comp. Neurol. 458, 350–360.

Frankel, R.B., Blakemore, R.P., 1989. Magnetite and magnetotaxis in microorganisms. Bioelectromagnetics 10, 223–237.

Fransson, T., Jakobsson, S., Johansson, P., Kullberg, C., Lind, J., Vallin, A., 2001. Bird migration - magnetic cues trigger extensive refuelling. Nature 414, 35–36.

Gagliardo, A., 2013. Forty years of olfactory navigation in birds. J. Exp. Biol. 216, 2165–2171.

Gagliardo, A., Ioalè, P., Savini, M., Wild, J.M., 2006. Having the nerve to home: trigeminal magnetoreceptor versus olfactory mediation of homing in pigeons. J. Exp. Biol. 209, 2888–2892.

Gagliardo, A., Ioalè, P., Savini, M., Wild, M., 2008. Navigational abilities of homing pigeons deprived of olfactory or trigeminally mediated magnetic information when young. J. Exp. Biol. 211, 2046–2051.

Gagliardo, A., Ioalé, P., Savini, M., Wild, M., 2009. Navigational abilities of adult and experienced homing pigeons deprived of olfactory or trigeminally mediated magnetic information. J. Exp. Biol. 212, 3119–3124.

Gagliardo, A., Bried, J., Lambardi, P., Luschi, P., Wikelski, M., Bonadonna, F., 2013. Oceanic navigation in Cory's shearwaters: evidence for a crucial role of olfactory cues for homing after displacement. J. Exp. Biol. 216, 2798–2805.

Gagliardo, A., Pollonara, E., Wikelski, M., 2018. Only natural local odours allow homeward orientation in homing pigeons released at unfamiliar sites. J. Comp. Physiol. 204, 761–771.

Gindt, Y.M., Vollenbroek, E., Westphal, K., Sackett, H., Sancar, A., Babcock, G.T., 1999. Origin of the transient electron paramagnetic resonance signals in DNA photolyase. Biochemistry 38, 3857–3866.

Giovani, B., Byrdin, M., Ahmad, M., Brettel, K., 2003. Light-induced electron transfer in a cryptochrome blue-light photoreceptor. Nat. Struct. Biol. 10, 489–490.

Guilford, T., Roberts, S., Biro, D., Rezek, I., 2004. Positional entropy during pigeon homing II: navigational interpretation of Bayesian latent state models. J. Theor. Biol. 227, 25–38.

Günther, A., Dedek, K., Haverkamp, S., Irsen, S., Briggman, K., Mouritsen, H., 2021. Double cones and the diverse connectivity of photoreceptors and bipolar cells in an avian retina. J. Neurosci. https://doi.org/10.1523/JNEUROSCI.2495-20.2021. In press.

Günther, A., Einwich, A., Sjulstok, E., Feederle, R., Bolte, P., Koch, K.-W., Solov'yov, I.A., Mouritsen, H., 2018. Double-cone localization and seasonal expression pattern suggest a role in magnetoreception for European robin cryptochrome 4. Curr. Biol. 28, 211–223.

Hagstrum, J.T., 2013. Atmospheric propagation modeling indicates homing pigeons use loft-specific infrasonic 'map' cues. J. Exp. Biol. 216, 687–699.

Harris, S.-R., Henbest, K.B., Maeda, K., Pannell, J.R., Timmel, C.R., Hore, P.J., Okamoto, H., 2009. Effect of magnetic fields on cryptochrome-dependent responses in *Arabidopsis thaliana*. J. R. Soc. Interface 6, 1193–1205.

Hein, C.M., Zapka, M., Heyers, D., Kutzschbauch, S., Schneider, N.-L., Mouritsen, H., 2010. Night-migratory garden warblers can orient with their magnetic compass using the left, the right or both eyes. J. R. Soc. Interface 7, S227–S233.

Hein, C.M., Engels, S., Kishkinev, D., Mouritsen, H., 2011. Robins have a magnetic compass in both eyes. Nature 471, E11. https://doi.org/10.1038/nature09875.

Henbest, K.B., Kukura, P., Rodgers, C.T., Hore, P.J., Timmel, C.R., 2004. Radio frequency magnetic field effects on a radical recombination reaction: a diagnostic test for the radical pair mechanism. J. Am. Chem. Soc. 126, 8102–8103.

Henshaw, I., Fransson, T., Jakobsson, S., Kullberg, C., 2010. Geomagnetic field affects spring migratory direction in a long distance migrant. Behav. Ecol. Sociobiol. 64, 1317–1323.

Heyers, D., Manns, M., Luksch, H., Güntürkün, O., Mouritsen, H., 2007. A visual pathway links brain structures active during magnetic compass orientation in migratory birds. PLoS One 2 (9), e937.

Heyers, D., Zapka, M., Hoffmeister, M., Wild, J.M., Mouritsen, H., 2010. Magnetic field changes activate the trigeminal brainstem complex in a migratory bird. Proc. Natl. Acad. Sci. U. S. A. 107, 9394–9399.

Hiscock, H.G., Worster, S., Kattnig, D.R., Steers, C., Jin, Y., Manolopoulos, D.E., Mouritsen, H., Hore, P.J., 2016. The quantum needle of the avian magnetic compass. Proc. Natl. Acad. Sci. U. S. A. 113, 4634–4639.

Hiscock, H.G., Mouritsen, H., Manolopoulos, D.E., Hore, P.J., 2017. Disruption of magnetic compass orientation in migratory birds by radiofrequency electromagnetic fields. Biophys. J. 113, 1475–1484.

Hogben, H.J., Biskup, T., Hore, P.J., 2012. Entanglement and sources of magnetic anisotropy in radical pair-based avian magnetoreceptors. Phys. Rev. Lett. 109, 220501.

Holland, R.A., 2010. Differential effects of magnetic pulses on the orientation of naturally migrating birds. J. R. Soc. Interface 7, 1617–1625.

Holland, R.A., 2014. True navigation in birds: from quantum physics to global migration. J. Zool. 293, 1–15. https://doi.org/10.1111/jzo.12107.

Holland, R.A., Helm, B., 2013. A strong magnetic pulse affects the precision of departure direction of naturally migrating adult but not juvenile birds. J. R. Soc. Interface 10, 20121047.

Hore, P.J., 2011. The quantum robin. Navig. News 2011 (10), 19–21.

Hore, P.J., 2012. Are biochemical reactions affected by weak magnetic fields? Proc. Nat. Acad. Sci. U. S. A. 109, 1357–1358.

Hore, P.J., Mouritsen, H., 2016. The radical-pair mechanism of magnetoreception. Annu. Rev. Biophys. 45, 299–344.

Jarvis, E.D., Yu, J., Rivas, M.V., Horita, H., Feenders, G., Whitney, O., Jarvis, S.C., Jarvis, E.R., Kubikova, L., Puck, A.E.P., Siang-Bakshi, C., Martin, S., McElroy, M., Hara, E., Howard, J., Pfenning, A., Mouritsen, H., Chen, C.-C., Wada, K., 2013. Global view of the functional molecular organization of the avian cerebrum: mirror images and functional columns. J. Comp. Neurol. 521, 3614–3665.

Johnsen, S., Lohmann, K.J., 2005. The physics and neurobiology of magnetoreception. Nat. Rev. Neurosci. 6, 703–712.

Kalmijn, A.J., 1981. Biophysics of geomagnetic field detection. IEEE Trans. Magn. 17, 1113–1124.

Kishkinev, D., Chernetsov, N., Mouritsen, H., 2010. A double clock or jetlag mechanism is unlikely to be involved in detection of east-west displacements in a long-distance avian migrant. Auk 127, 773–780.

Kishkinev, D., Mouritsen, H., Mora, C.V., 2012. An attempt to develop an operant conditioning paradigm to test for magnetic discrimination behaviour in a migratory songbird. J. Ornithol. 153, 1165–1177.

Kishkinev, D., Chernetsov, N., Heyers, D., Mouritsen, H., 2013. Migratory reed warblers need intact trigeminal nerves to correct for a 1,000 km eastward displacement. PLoS One 8 (6), e65847.

Kishkinev, D., Chernetsov, N., Pakhomov, A., Heyers, D., Mouritsen, H., 2015. Eurasian reed warblers compensate for virtual magnetic displacement. Curr. Biol. 25, R822–R824.

Kirschvink, J.L., 1991. Uniform magnetic fields and double-wrapped coil systems: improved techniques for the design of bioelectromagnetic experiments. Bioelectromagnetics 13, 401–411.

Kirschvink, J.L., Winklhofer, M., Walker, M.M., 2010. Biophysics of magnetic orientation: strengthening the interface between theory and experimental design. J. R. Soc. Interface 7, 179–191.

Kobylkov, D., Wynn, J., Winklhofer, M., Chetverikova, R., Xu, J., Hiscock, H., et al., 2019. Electromagnetic 0.1–100 kHz noise does not disrupt orientation in a night-migrating songbird implying a spin coherence lifetime of less than 10 μs. J. R. Soc. Interface 16, 20190716.

Kobylkov, D., Schwarze, S., Michalik, B., Winklhofer, M., Mouritsen, H., Heyers, D., 2020a. A newly identified trigeminal brain pathway in a night-migratory bird could be dedicated to transmitting magnetic map information. Proc. R. Soc. B 287, 20192788.

Kobylkov, D., 2020b. Transduction mechanisms in magnetoreception. In: Fritzsch, B. (Ed.), The Senses: A Comprehensive Reference, 2 ed. Elsevier, pp. 459–478. https://doi.org/10.1016/B978-0-12-805408-6.00004-X.

Kishkinev, D., Packmor, F., Zechmeister, T., Winkler, H.-C., Chernetsov, N., Mouritsen, H., Holland, R., 2021. Navigation by extrapolation of geomagnetic cues in a migratory songbird. Curr. Biol. 31, 1563–1569.

Kramer, G., 1949. Über Richtungstendenzen bei der nächtlichen Zugunruhe gekäfigter Vögel. In: Mayr, E., Schüz, E. (Eds.), Ornithologie als Biologische Wissenschaft, pp. 269–283 (Heidelberg).

Kramer, G., 1957. Experiments on bird orientation and their interpretation. Ibis 99, 196–227.

Lefeldt, N., Heyers, D., Schneider, N.-L., Engels, S., Elbers, D., Mouritsen, H., 2014. Magnetic field-driven induction of ZENK in the trigeminal system of pigeons (*Columba livia*). J. R. Soc. Interface 11, 20140777.

Liedvogel, M., Mouritsen, H., 2010. Cryptochromes – a potential magnetoreceptor: what do we know and what do we want to know? J. R. Soc. Interface 7, S147–S162.

Liedvogel, M., Maeda, K., Henbest, K., Schleicher, E., Simon, T., Timmel, C.R., Hore, P.J., Mouritsen, H., 2007a. Chemical magnetoreception: bird cryptochrome 1a is excited by blue light and forms long-lived radical-pairs. PLoS One 2 (10), e1106.

Liedvogel, M., Feenders, G., Wada, K., Troje, N.F., Jarvis, E.D., Mouritsen, H., 2007b. Lateralized activation of Cluster N in the brains of migratory songbirds. Eur. J. Neurosci. 25, 1166–1173.

Liu, X., Chernetsov, N., 2012. Avian orientation: multi-cue integration and calibration of compass systems. Chinese Birds 3, 1–8.

Maeda, K., Henbest, K.B., Cintolesi, F., Kuprov, I., Rodgers, C.T., Liddell, P.A., Gust, D., Timmel, C.R., Hore, P.J., 2008. Chemical compass model of avian magnetoreception. Nature 453, 387–390.

Maeda, K., et al., 2012. Magnetically sensitive light-induced reactions in cryptochrome are consistent with its proposed role as a magnetoreceptor. Proc. Natl. Acad. Sci. U. S. A. 109, 4774–4779.

Malkemper, E.P., Kagerbauer, D., Ushakova, L., Nimpf, S., Pichler, P., Treiber, C.D., et al., 2019. No evidence for a magnetite-based magnetoreceptor in the lagena of pigeons. Curr. Biol. 29, R14–R15.

Mayr, E., 1952. German experiments on orientation of migrating birds. Biol. Rev. Camb. Phil. Soc. 27, 394–400.

Merkel, F.W., Wiltschko, W., 1965. Magnetismus und Richtungsfinden zugunruhiger Rotkehlchen (*Erithacus rubecula*). Vogelwarte 23, 71–77.

Mewaldt, R., 1964. California sparrows return from displacement to Maryland. Science 146, 941–942.

Möller, A., Sagasser, S., Wiltschko, W., Schierwater, B., 2004. Retinal cryptochrome in a migratory passerine bird: a possible transducer for the avian magnetic compass. Naturwissenschaften 91, 585–588.

Molteno, T.C.A., Kennedy, W.L., 2009. Navigation by induction-based magnetoreception in elasmobranch fishes. J. Biophys. 380976.

Mora, C.V., Davison, M., Wild, J.M., Walker, M.M., 2004. Magnetoreception and its trigeminal mediation in the homing pigeon. Nature 432, 508–511.

Mora, C.V., Bingman, V.P., 2013. Detection of magnetic field intensity gradient by homing pigeons (*Columba livia*) in a novel "virtual magnetic map" conditioning paradigm. PLoS One 8 (9), e72869.

Mouritsen, H., 1998a. Redstarts, *Phoenicurus phoenicurus*, can orient in a true-zero magnetic field. Anim. Behav. 55, 1311–1324.

Mouritsen, H., 1998b. Modelling migration: the clock-and-compass model can explain the distribution of ringing recoveries. Anim. Behav. 56, 899–907.

Mouritsen, H., 2003. Spatiotemporal orientation strategies of long-distance migrants. In: Berthold, P., Gwinner, E., Sonnenschein, E. (Eds.), Avian Migration. Springer, Berlin, pp. 493–513.

Mouritsen, H., 2012. Sensory biology: search for the compass needles. Nature 484, 320–321.

Mouritsen, H., 2013. The magnetic senses. In: Galizia, C.G., Lledo, P.-M. (Eds.), Neurosciences - from Molecule to Behavior: A University Textbook. Springer-Verlag Berlin Heidelberg, pp. 427–443.

Mouritsen, H., 2018. Long-distance navigation and magnetoreception in migratory animals. Nature 558, 50–59.

Mouritsen, H., Larsen, O.N., 1998. Migrating young pied flycatchers *Ficedula hypoleuca* do not compensate for geographical displacements. J. Exp. Biol. 201, 2927–2934.

Mouritsen, H., Larsen, O.N., 2001. Migrating songbirds tested in computer-controlled Emlen funnels use stellar cues for a time-independent compass. J. Exp. Biol. 204, 3855–3865.

Mouritsen, H., Hore, P.J., 2012. The magnetic retina: light-dependent and trigeminal magnetoreception in migratory birds. Curr. Opin. Neurobiol. 22, 343–352.

Mouritsen, H., Mouritsen, O., 2000. A mathematical expectation model for bird navigation based on the clock-and-compass strategy. J. Theor. Biol. 207, 283–291.

Mouritsen, H., Ritz, T., 2005. Magnetoreception and its use in bird navigation. Curr. Opin. Neurobiol. 15, 406–414.

Mouritsen, H., Huyvaert, K.P., Frost, B.J., Andersson, D.J., 2003. Waved albatrosses can navigate with strong magnets attached to their head. J. Exp. Biol. 206, 4155–4166.

Mouritsen, H., Janssen-Bienhold, U., Liedvogel, M., Feenders, G., Stalleicken, J., Dirks, P., Weiler, R., 2004. Cryptochromes and Neuronal-Activity Markers Colocalize in the Retina of Migratory Birds.

Mouritsen, H., Feenders, G., Liedvogel, M., Wada, K., Jarvis, E.D., 2005. Night-vision brain area in migratory songbirds. Proc. Natl. Acad. Sci. U. S. A. 102, 8339–8344.

Mouritsen, H., Feenders, G., Hegemann, A., Liedvogel, M., 2009. Thermal paper can replace typewriter correction paper in Emlen funnels. J. Ornithol. 150, 713–715.

Mouritsen, H., Derbyshire, R., Stalleicken, J., Mouritsen, O.Ø., Frost, B.J., Norris, R.D., 2013. An experimental displacement and over 50 years of tag-recoveries show that monarch butterflies are not true navigators. Proc. Natl. Acad. Sci. U. S. A. 110, 7348–7353.

Mouritsen, H., Heyers, D., Güntürkün, O., 2016. The neural basis of long-distance navigation in birds. Annu. Rev. Physiol. 78, 133–154.

Muheim, R., Bäckman, J., Akesson, S., 2002. Magnetic compass orientation in European robins is dependent on both wavelength and intensity of light. J. Exp. Biol. 205, 3845–3856.

Muheim, R., Phillips, J.B., Åkesson, S., 2006a. Polarized light cues underlie compass calibration in migratory songbirds. Science 313, 837–839.

Muheim, R., Moore, F.R., Phillips, J.B., 2006b. Calibration of magnetic and celestial compass cues in migratory birds—a review of cue-conflict experiments. J. Exp. Biol. 209, 2–17.

Müller, M., Carell, T., 2009. Structural biology of DNA photolyases and cryptochromes. Curr. Opin. Struct. Biol. 19, 277–285.

Nevitt, G.A., Bonadonna, F., 2005. Sensitivity to dimethyl sulphide suggests a mechanism for olfactory navigation by seabirds. Biol. Lett. 1, 303–305.

Newton, K.C., Gill, A.B., Kajiura, S.M., 2019. Electroreception in marine fishes: chondrichthyans. J. Fish. Biol. 95, 135–154.

Nießner, C., Denzau, S., Gross, J.C., Peichl, L., Bischof, H.J., Fleissner, G., Wiltschko, W., Wiltschko, R., 2011. Avian ultraviolet/violet cones identified as probable magnetoreceptors. PLoS One 6 (5), e20091.

Nießner, C., Gross, J.C., Denzau, S., Peichl, L., Fleissner, G., Wiltschko, W., Wiltschko, R., 2016. Seasonally changing cryptochrome 1b expression in the retinal ganglion cells of a migrating passerine bird. PLoS One 11, e0150377.

Nießner, C., Denzau, S., Peichl, L., Wiltschko, W., Wiltschko, R., 2018. Magnetoreception: activation of avian cryptochrome 1a in various light conditions. J. Comp. Physiol. 204, 977–984.

Nimpf, S., Nordmann, G.C., Kagerbauer, D., Malkemper, E.P., Landler, L., Papadaki-Anastasopoulou, A., et al., 2019. A putative mechanism for magnetoreception by electromagnetic induction in the pigeon inner ear. Curr. Biol. 29, 4052–4059.

Ozturk, N., 2017. Phylogenetic and functional classification of the photolyase/cryptochrome family. Photochem. Photobiol. 93, 104–111.

Ozturk, N., Selby, C.P., Song, S.H., Ye, R., Tan, C., Kao, Y.T., Zhong, D.P., Sancar, A., 2009. Comparative photochemistry of animal Type 1 and Type 4 cryptochromes. Biochemistry 48, 8585–8593.

Padget, O., Dell'Ariccia, G., Gagliardo, A., González-Solís, J., Guilford, T., 2017. Anosmia impairs homing orientation but not foraging behaviour in free-ranging shearwaters. Sci. Rep. 7, 9668.

Pakhomov, A., Bojarinova, J., Cherbunin, R., Chetverikova, R., Grigoryev, P.S., Kavokin, K., et al., 2017. Very weak oscillating magnetic field disrupts the magnetic compass of songbird migrants. J. R. Soc. Interface 14, 20170364.

Pakhomov, A., Anashina, A., Heyers, D., Kobylkov, D., Mouritsen, H., Chernetsov, N., 2018. Magnetic map navigation in a migratory songbird requires trigeminal input. Sci. Rep. 8, 11975.

Papi, F., 1991. Olfactory navigation. In: Berthold, P. (Ed.), Orientation in Birds. Birkhäuser, Basel, pp. 52–85.

Perdeck, A.C., 1958. Two types of orientation in migrating starlings, *Sturnus vulgaris* L., and chaffinches, *Fringilla coelebs* L., as revealed by displacement experiments. Ardea 46, 1–37.

Phillips, J.B., Borland, S.C., 1992. Behavioural evidence for use of a light-dependent magnetoreception mechanism by a vertebrate. Nature 359, 142–144.

Phillips, J.B., Deutschlander, M.E., Freake, M.J., Borland, S.C., 2001. The role of extraocular photoreceptors in newt magnetic compass orientation: parallels between light-dependent magnetoreception and polarized light detection in vertebrates. J. Exp. Biol. 204, 2543–2552.

Phillips, J.B., Freake, M.J., Fischer, J.H., Borland, C., 2002. Behavioral titration of a magnetic map coordinate. J. Comp. Physiol. 188, 157–160.

Pollonara, E., Luschi, P., Guilford, T., Wikelski, M., Bonadonna, F., Gagliardo, A., 2015. Olfaction and topography, but not magnetic cues, control navigation in a pelagic seabird: displacements with shearwaters in the Mediterranean Sea. Sci. Rep. 5, 16486.

Putman, N.F., Lohmann, K.J., Putman, E.M., Quinn, T.P., Klimley, A.P., Noakes, D.L.G., 2013. Evidence for geomagnetic imprinting as a homing mechanism in Pacific salmon. Curr. Biol. 23, 312–316.

Rabøl, J., 1978. One-direction orientation versus goal area navigation in migratory birds. Oikos 30, 216–223.

Ramírez, E., Marín, G., Mpodozis, J., Letelier, J.C., 2014. Extracellular recordings reveal absence of magneto sensitive units in the avian optic tectum. J. Comp. Physiol. 200, 983–996.

Rastogi, A., Kumari, Y., Rani, S., Kumar, V., 2011. Phase inversion of neural activity in the olfactory and visual systems of a night-migratory bird during migration. Eur. J. Neurosci. 34, 99–109.

Ritz, T., Adem, S., Schulten, K., 2000. A model for photoreceptor-based magnetoreception in birds. Biophys. J. 78, 707–718.

Ritz, T., Thalau, P., Phillips, J.B., Wiltschko, R., Wiltschko, W., 2004. Resonance effects indicate a radical-pair mechanism for avian magnetic compass. Nature 429, 177–180.

Ritz, T., Wiltschko, R., Hore, P.J., Rodgers, C.T., Stapput, K., Thalau, P., Timmel, C.R., Wiltschko, W., 2009. Magnetic compass of birds is based on a molecule with optimal directional sensitivity. Biophys. J. 96, 3451–3457.

Ritz, T., Ahmad, M., Mouritsen, H., Wiltschko, R., Wiltschko, W., 2010. Photoreceptor-based magnetoreception: optimal design of receptor molecules, cells, and neuronal processing. J. R. Soc. Interface 7, S135–S146.

Rodgers, C.T., Hore, P.J., 2009. Chemical magnetoreception in birds: the radical pair mechanism. Proc. Natl. Acad. Sci. U. S. A. 106, 353–360.

Rosenblum, B., Jungerman, R.L., Longfellow, L., 1985. Limits to induction-based magnetoreception. In: Kirschvink, J.L., Jones, D.S., MacFadden, B.J. (Eds.), Magnetite Biomineralization and Magnetoreception in Organisms: a New Biomagnetism. Plenum Press, New York, NY, pp. 223–232.

Sancar, A., 2003. Structure and function of DNA photolyases and cryptochrome blue-light photoreceptors. Chem. Rev. 103, 2203–2237.

Schmidt-Koenig, K., 1965. Current problems in bird orientation. In: Advances in the Study of Behaviour, vol. 1, pp. 217–272.

Schmidt-Koenig, K., Walcott, C., 1978. Tracks of pigeons homing with frosted lenses. Anim. Behav. 26, 480–486.

Schmidt-Koenig, K., Ganzhorn, J.U., Ranvaud, R., 1991. The sun compass. In: Berthold, P. (Ed.), Orientation in Birds. Birkhäuser, Basel, pp. 1–15.

Schneider, T., Thalau, H.P., Semm, P., Wiltschko, W., 1994. Melatonin is crucial for the migratory orientation of pied flycatchers (*Ficedula-hypoleuca pallas*). J. Exp. Biol. 194, 255–262.

Schulten, K., Swenberg, C.E., Weller, A., 1978. A biomagnetic sensory mechanism based on magnetic field modulated coherent electron spin motion. Zeitschrift für Physikalische Chemie, Neue Folge 111, 1–5.

Schwarze, S., Schneider, N.-L., Reichl, T., Dreyer, D., Lefeldt, N., Engels, S., Baker, N., Hore, P.J., Mouritsen, H., 2016. Weak broadband electromagnetic fields are more disruptive to magnetic compass orientation in a night-migratory songbird (*Erithacus rubecula*) than strong narrow-band fields. Front. Behav. Neurosci. 10, 55.

Semm, P., Demaine, C., 1986. Neurophysiological properties of magnetic cells in the pigeon's visual system. J. Comp. Physiol. 159, 619–625.

Shaw, J., Boyd, A., House, M., Woodward, R., Mathes, F., Cowin, G., et al., 2015. Magnetic particle-mediated magnetoreception. J. R. Soc. Interface 12, 20150499.

Sheppard, D.M., Li, J., Henbest, K.B., Neil, S.R., Maeda, K., Storey, J., et al., 2017. Millitesla magnetic field effects on the photocycle of an animal cryptochrome. Sci. Rep. 7, 42228.

Solov'yov, I.A., Greiner, W., 2009. Micromagnetic insight into a magnetoreceptor in birds: existence of magnetic field amplifiers in the beak. Phys. Rev. 80, 041919.

Solov'yov, I.A., Mouritsen, H., Schulten, K., 2010. Acuity of a cryptochrome and vision-based magnetoreception system in birds. Biophys. J. 99, 40–49.

Solov'yov, I.A., Domratcheva, T., Shahi, A.R.M., Schulten, K., 2012. Decrypting cryptochrome: revealing the molecular identity of the photoactivation reaction. J. Am. Chem. Soc. 134, 18046–18052.

Solov'yov, I.A., Ritz, T., Schulten, K., Hore, P.J., 2014. A chemical compass for bird navigation. In: Mohseni, M., Omar, Y., Engel, G., Plenio, M. (Eds.), Quantum Effects in Biology. Cambridge University Press, pp. 216–236 (in press).

Stapput, K., Güntürkün, O., Hoffmann, K.-P., Wiltschko, R., Wiltschko, W., 2010. Magnetoreception of directional information in birds requires nondegraded vision. Curr. Biol. 20, 1259–1262.

Thorup, K., Bisson, I.-A., Bowlin, M.S., Holland, R.A., Wingfield, J.C., Ramenofsky, M., Wikelski, M., 2007. Evidence for a navigational map stretching across the continental U.S. in a migratory songbird. Proc. Natl. Acad. Sci. U. S. A. 104, 18115–18119.

Treiber, C.D., Salzer, M.C., Riegler, J., Edelman, N., Sugar, C., Breuss, M., Pichler, P., Cadiou, H., Saunders, M., Lythgoe, M., Shaw, J., Keays, D.A., 2012. Clusters of iron-rich cells in the upper beak of pigeons are macrophages not magnetosensitive neurons. Nature 484, 367–370.

Walcott, C., 1991. Magnetic maps in pigeons. In: Berthold, P. (Ed.), Orientation in Birds. Birkhäuser, Basel, pp. 38–51.

Walker, M.M., Diebel, C.E., Haugh, C.V., Pankhurst, P.M., Montgomery, J.C., Green, C.R., 1997. Structure and function of the vertebrate magnetic sense. Nature 390, 371–376.

Wallraff, H.G., 1972. Homing of pigeons after extirpation of their cochleae and lagenae. Nat. New Biol. 236, 223–224.

Wallraff, H.G., 2001. Navigation by homing pigeons: updated perspective. Ethol. Ecol. Evol. 13, 1–48.

Wallraff, H.G., 2005. Avian Navigation: Pigeon Homing as a Paradigm. Springer Verlag, Berlin.

Wallraff, H.G., Andreae, M.O., 2000. Spatial gradients in ratios of atmospheric trace gases: a study stimulated by experiments on bird navigation. Tellus 52B, 1138–1157.

Westby, G.W.M., Partridge, K.J., 1986. Human homing: still no evidence despite geomagnetic controls. J. Exp. Biol. 120, 325–331.

Williams, M.N., Wild, J.M., 2001. Trigeminally innervated iron-containing structures in the beak of homing pigeons, and other birds. Brain Res. 889, 243–246.

Wiltschko, W., 1968. Über den Einfluss statischer Magnetfelder auf die Zugorientierung der Rotkehlchen (*Erithacus rubecula*). Zeitschrift für Tierpsychology 25, 537–558.

Wiltschko, W., 1978. Further analysis of the magnetic compass of migratory birds. In: Schmidt-Koenig, K., Keeton, W.T. (Eds.), Animal Migration, Navigation and Homing. Springer, Berlin Heidelberg New York, pp. 302–310.

Wiltschko, W., Wiltschko, R., 1972. Magnetic compass of European robins. Science 176, 62–64.

Wiltschko, R., Wiltschko, W., 1995. Magnetic Orientation in Animals. Springer Verlag, ISBN 978-3-642-79751-4, 298pp.

Wiltschko, W., Wiltschko, R., 1996. Magnetic orientation in birds. J. Exp. Biol. 199, 29–38.

Wiltschko, W., Wiltchko, R., 2007. Magnetoreception in birds: two receptors for two different tasks. J. Ornithol. 148, S61–S76.

Wiltschko, W., Munro, U., Ford, H., Wiltschko, R., 1993. Red light disrupts magnetic orientation of migratory birds. Nature 364, 525–527.

Wiltschko, W., Traudt, J., Güntürkün, O., Prior, H., Wiltschko, R., 2002. Lateralization of magnetic compass orientation in a migratory bird. Nature 419, 467–470.

Wiltschko, W., Munro, U., Ford, H., Wiltschko, R., 2003. Lateralisation of magnetic compass orientation in silvereyes, *Zosterops lateralis*. Aust. J. Zool. 51, 597–602.

Wiltschko, W., Munro, U., Ford, H., Wiltschko, R., 2009. Avian orientation: the pulse effect is mediated by the magnetite receptors in the upper beak. Proc. Roy. Soc. Lond. B 276, 2227–2232.

Wiltschko, R., Schiffner, I., Fuhrmann, P., Wiltschko, W., 2010a. The role of magnetite-based receptors in the beak in pigeon homing. Curr. Biol. 20, 1534–1538.

Wiltschko, R., Stapput, K., Thalau, P., Wiltschko, W., 2010b. Directional orientation of birds by the magnetic field under different light conditions. J. R. Soc. Interface 7, 163–177.

Worster, S., Mouritsen, H., Hore, P.J., 2017. A light-dependent magnetoreception mechanism insensitive to light intensity and polarization. J. R. Soc. Interface 14, 20170405.

Wu, L.Q., Dickman, J.D., 2011. Magnetoreception in an avian brain in part mediated by inner ear lagena. Curr. Biol. 21, 418–423.

Wu, L.Q., Dickman, J.D., 2012. Neural correlates of a magnetic sense. Science 336, 1054–1057.

Wu, H., Scholten, A., Einwich, A., Mouritsen, H., Koch, K.-W., 2020. Protein-protein interaction of the putative magnetoreceptor cryptochrome 4 expressed in the avian retina. Sci. Rep. 10, 7364 https://doi.org/10.1038/s41598-020-64429-y.

Wynn, J., Padget, O., Mouritsen, H., Chris Perrins, C., Guilford, T., 2020. Natal imprinting to the Earth's magnetic field in a pelagic seabird. Curr. Biol. 30, R802–R804. https://doi.org/10.1016/j.cub.2020.05.039.

Xu, J., et al., 2021. Magnetic sensitivity of cryptochrome 4 from a migratory songbird. Nature. https://doi.org/10.1038/s41586-021-03618-9. In press.

Zapka, M., Heyers, D., Hein, C.M., Engels, S., Schneider, N.-L., Hans, J., Weiler, S., Dreyer, D., Kishkinev, D., Wild, J.M., Mouritsen, H., 2009. Visual but not trigeminal mediation of magnetic compass information in a migratory bird. Nature 461, 1274–1277.

Zapka, M., Heyers, D., Liedvogel, M., Jarvis, E.D., Mouritsen, H., 2010. Night-time neuronal activation of Cluster N in a day- and night-migrating songbird. Eur. J. Neurosci. 32, 619–624.

Zoltowski, B.D., Chelliah, Y., Wickramaratne, A., Jarocha, L., Karki, N., Xu, W., Mouritsen, H., Hore, P.J., Hibbs, R.E., Green, C.B., Takahashi, J.S., 2019. Chemical and structural analysis of a photoactive vertebrate cryptochrome from pigeon. Proc. Natl. Acad. Sci. U. S. A. 116, 19449–19457.

Chapter 16

The avian subpallium and autonomic nervous system

Wayne J. Kuenzel[1] and Alexander Jurkevich[2]

[1]Poultry Science Center, University of Arkansas, Fayetteville, AR, United States; [2]Advanced Light Microscopy Core, University of Missouri, Columbia, MO, United States

16.1 Introduction

The telencephalon of vertebrates comprises two major formations, the dorsal part or pallium (cortex in mammals) and the basal part or subpallium. The last two decades revolutionized our understanding of the structural organization of these two telencephalic divisions. Discovery of evolutionally conserved homeobox genes, a group of transcription factors regulating the development of the telencephalon, and analysis of their expression patterns provided the conceptual molecular framework for accurate identification of homologs of pallial and subpallial structures in morphologically diverse brains of various classes of vertebrates (Puelles et al., 2007, 2019; Abellán and Medina, 2009, 2010; Medina and Abellán, 2012; Gonzalez et al., 2014; Pauly et al., 2014; Vicario et al., 2017. These findings were complemented with developmental studies of other neurochemical markers (acetylcholinesterase, tyrosine hydroxylase, gamma-aminobutyric acid, substance P (SP), encephalin, CART, and other neuropeptides) that revealed the extent of structural subdivisions of the subpallium (Reiner et al., 1984a,b; Goodson et al., 2004; Bálint et al., 2011; Bruce et al., 2016; Gutierrez-Ibanez et al., 2016).

The subpallium comprises the basal ganglia (BG) and other anatomical components critical to the survival of a particular species. Specifically, it includes structures and pathways that help to regulate movements and complex ingestive, reproductive, and defensive behaviors. Indeed, those functions listed require close coordination with the autonomic nervous system (ANS). Importantly, some neuronal groups residing in the subpallium project directly to central structures that serve as premotor nuclei of the ANS. Therefore the overall purpose of this review is to provide an overview of the structures and functions of the subpallium and indicate how that basal forebrain region connects with components of the ANS. The last section of the chapter includes specific examples and hypotheses about how the subpallial nervous system, ANS, and neuroendocrine systems are interconnected and integrated to regulate the reproductive system, ingestive behavior, stress, and selected ethophysiological events of the annual cycle of birds. By focusing on central neural structures, it is hoped that readers will be directed to brain regions or neural pathways that regulate functions or behaviors of interest and will recognize areas where research is greatly needed due to large gaps in our knowledge.

16.2 Components of the subpallium

The subpallium includes six major components: (1) dorsal somatomotor basal ganglia (DSBG), (2) ventral visceroolimbic basal ganglia (VVBG), (3) extended amygdala, (4) basal telencephalic cholinergic (Ch) and noncholinergic corticopetal system, (5) septum, and (6) preoptic area (POA) (Figure 16.1). Note that since the publication of the previous edition of this chapter (Kuenzel, 2015), an additional component, the POA, has been added to the groups comprising the avian subpallium. The reason for adding the POA is that developmental genes used to compare the mouse and chick forebrains during embryogenesis, showed evidence that the POA displayed markers of subpallial origin. Specifically the POA showed expression of *Dlx-2* and *Nkx-2.1* considered as striatum and pallidum gene markers, respectively, in tissues regarded as subpallial (Rubenstein et al., 1998; Puelles et al., 2000). Additionally, in both editions of the Chick Brain in Stereotaxic Coordinates (Puelles et al., 2007, 2019), it was stated that some structures in the POA should be regarded as subpallial. We concur with this view; however, there are no data indicating what specific structures within that area are subpallial. A major structure that nicely separates the subpallium from the overlying pallium is the

Sturkie's Avian Physiology. https://doi.org/10.1016/B978-0-12-819770-7.00031-1

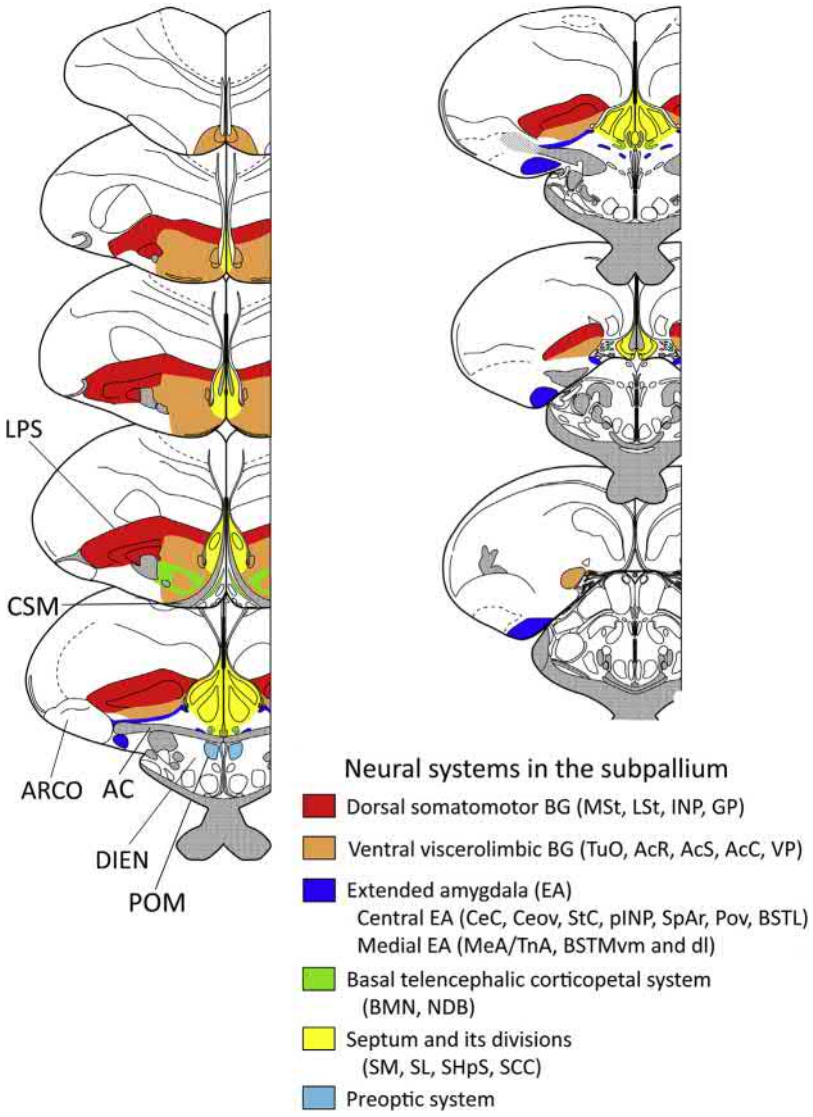

FIGURE 16.1 Six neural components of the avian subpallium. **(1)** Dorsal somatomotor basal ganglia (shown in red) include the medial striatum (MSt), lateral striatum (LSt), intrapeduncular nucleus (INP), and globus pallidus (GP). The pallial-subpallial lamina (LPS) marks the dorsal border of the avian subpallium. **(2)** Ventral viscerolimbic basal ganglia (shown in tan) include the olfactory tubercle (TuO), nucleus accumbens (rostral pole, shell and core, AcR, AcS, and AcC), and ventral pallidum (VP). **(3)** Extended amygdala and bed nuclei of the stria terminalis (shown in dark blue) include the central extended amygdala (Central EA) and medial extended amygdala (Medial EA). The Central EA is composed of the CeC, Ceov, StC, pINP, SpAr, Pov, and BSTL (see also Figure 16.7A). The Medial EA comprises the MeA/TnA and BSTMvm, BSTMdl (see also Figure 16.7B). **(4)** Basal telencephalic corticopetal system (shown in green) includes the basal magnocellular nucleus (BMN) and diagonal band nucleus (NDB). **(5)** Septum and its divisions (shown in yellow) comprise the medial septal, lateral septal, septohippocampal septal (SHpS), and caudocentral septal divisions. **(6)** Preoptic system (shown in light blue) comprises the POM and probably additional, unidentified structures. Abbreviations: *AC*, anterior commissure; *ARCO*, arcopallium; *CSM*, corticoseptomesencephalic tract; *DIEN*, diencephalon; *LPS*, pallial-subpallial lamina; *POM*, medial preoptic nucleus. SL. lateral septum; SM, medial septum. Abbreviations of extended amygdala structures. Central EA: *BSTL*, lateral bed nucleus of the stria terminalis; *CeC*, capsular extended amygdala; *Ceov*, oval central amygdalar nucleus; *pINP*, peri-intrapeduncular nucleus island field; *Pov*, perioval zone; *SpAr*, rostral division of the subpallial amygdala; *StC*, striatal capsule. Medial EA: *MeA*, medial amygdala/TnA, nucleus taeniae amygdala, BSTMvm, dl, ventromedial (vm) and dorsolateral (dL) portions of the medial bed nucleus of the stria terminalis. *Modified from Kuenzel (2015).*

pallial-subpallial lamina (LPS, Figure 16.1). This lamina when visualized in coronal sections in anterior regions of the forebrain clearly defines the subpallium. When coronal sections of an avian brain reach the level of the hypothalamus, as evidenced by the appearance of the anterior commissure (AC), the neural structures ventral and posterior to that fiber tract are regarded as hypothalamic in avian and other vertebrate species. Note that in Figures 14 and 15 of Puelles et al. (2007, 2019), the LPS, abbreviated "psp" in both figures, dips ventrally, below the AC, into both the hypothalamic and POAs. Hence, if the LPS is regarded as an effective, structural marker of the subpallium, then currently a more extensive group of structures within the preoptic and hypothalamic regions have been proposed to be included in the subpallium. Further research will be required to obtain a consensus regarding which preoptic structures should be included in the sixth component of the subpallium.

Significant advances have been made in understanding the embryonic development of the subpallial region of the avian brain from known proliferative zones based upon gene expression and fate mapping data. Details about the histogenetic zones can be obtained in the following references (Puelles et al., 2000, 2007; Cobos et al., 2001a,b; Marín and Rubenstein, 2001; Redies et al., 2001; Flames et al., 2007; Abellán and Medina, 2008; 2009; García-López et al., 2008; Abellán et al., 2010; Kuenzel et al., 2011; Vicario et al., 2017). Each of the six subpallial components in posthatching and adult birds is discussed in the following sections of this chapter.

16.2.1 Dorsal somatomotor basal ganglia

16.2.1.1 Structures

The BG are composed of dorsal somatomotor and ventral viscerolimbic components. Discovery of the abundance of dopamine and acetylcholinesterase in the avian subpallium in the 1960s (Spooner and Winters, 1966; Juorio and Vogt, 1967; Karten, 1969; Nauta and Karten, 1970) showed the avian BG occupied the ventromedial portion of the forebrain (Figure 16.2) and not its extent throughout the entire forebrain as previously thought. The pallial-subpallial lamina (LPS; Figure 16.2C) marks the boundary between the pallium and BG. Importantly the use of immunohistochemistry and an antibody to tyrosine hydroxylase (an indicator of dopamine) and choline acetyltransferase (ChAT) [synthesizes acetylcholine (ACh)] clearly showed how similar the avian BG were to those of mammals regarding their location and relative size compared with the rest of the telencephalon.

Key structures of the DSBG include the dorsal and ventral parts of the medial striatum (MSt), lateral striatum (LSt), nucleus intrapeduncularis (INP), and globus pallidus (GP) (Figure 16.2). Based on gene expression pattern shared with other striatal (st) structures, the INP has been suggested to be renamed the intermediate striatum (Jarvis et al., 2013). In songbirds, the dorsal somatomotor BG include also Area X, a structure involved in the control of vocal motor functions (Gale and Perkel, 2010). The MSt and LSt are generally considered homologous to the mammalian caudate-putamen (Reiner et al., 2004). The MSt (previously called the lobus parolfactorius) and LSt are each further divided into medial and lateral zones. For neurochemical details of comparisons among birds, mammals, reptiles, amphibians, and other vertebrates see Reiner et al. (1998), Smeets et al. (2000), Bruce et al. (2016). Detailed neurochemistry of the BG focusing particularly on neuropeptides and neurotransmitters in specific neuroanatomical regions has been published in birds (Wynne and Güntürkün, 1995; Reiner et al., 1998; Abellán and Medina, 2009; Kuenzel et al., 2011; Bruce et al., 2016).

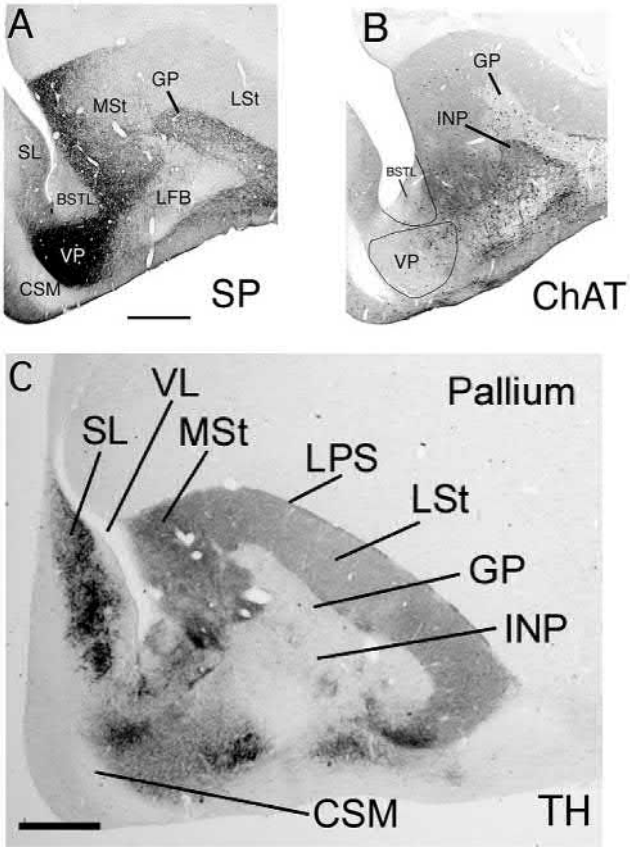

FIGURE 16.2 Components of the dorsal somatomotor basal ganglia. Images of transverse sections of pigeon brain showing immunoreactivity for (A) substance P (SP) and (B) choline acetyltransferase (ChAT). A transverse section of chicken brain shows immunolabeling for (C) tyrosine hydroxylase (TH). The use of TH, an indicator of dopaminergic input, identifies striatal structures of the dorsal somatomotor basal ganglia, particularly the lateral (LSt) and medial striatum (MSt). Note also the increased immunoreactivity of SP fibers in the ventral pallidum (VP) as well as portions of the VP showing increased levels of ChAT neurons and TH fibers. In B, the field of cholinergic neurons spanning the VP and lateral forebrain bundle (LFB) represents the basal magnocellular cholinergic cell group (BMN). There exists a paucity of ChAT neurons and SP immunoreactivity in the lateral bed nucleus of the stria terminalis (BSTL). Other abbreviations: *CSM*, corticoseptomesencephalic tract; *GP*, globus pallidus; *INP*, intrapeduncular nucleus; *LPS*, pallial-subpallial lamina; *SL*, lateral septum; *VL*, lateral ventricle. Scale bar = 1 mm in (A) and (C) (scale bar in A applies to A, B). *Modified from Kuenzel (2015).*

16.2.1.2 Functions

Models of the functional organization of the somatic BG, first developed in mammals, comprised two parallel output circuits that had opposing functions in motor control as well as interactions between them (Albin et al., 1989; DeLong, 1990; Gerfen, 1992). Birds have been shown to have similar direct and indirect pathways (Reiner et al., 1998). A modified representation of the direct and indirect motor pathways involving the avian DSBG is shown in Figure 16.3. The direct pathway (Figure 16.3A) promotes movement of birds (head, wings, legs). Input into the avian striatum (homologous to mammalian caudate-putamen) occurs via the "corticostriatal" projections (from pallium), shown here as glutamatergic excitatory (+) input to the lateral and MSt (Veenman and Reiner, 1996; Csillag et al., 1997; Reiner et al., 2001; Ding et al., 2003; Ding and Perkel, 2004; Farries et al., 2005). Modulatory dopaminergic input to the striatum likewise occurs from the substantia nigra, pars compacta (SNc) [A9 catecholaminergic (CA) cell group], ventral tegmental area (VTA; A10 CA group) and retrorubral field (A8 CA group)

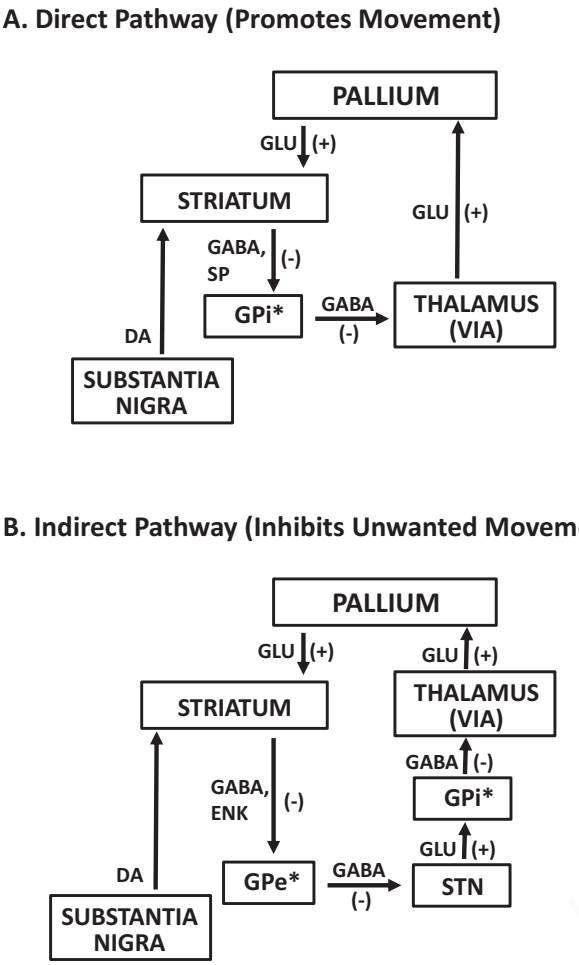

FIGURE 16.3 Schematic diagram showing a direct pathway where excitatory inputs (+) from the pallium and modulatory inputs from the substantia nigra promote skeletal muscle movements in birds. In parallel, an indirect pathway functions to inhibit unwanted movement thereby facilitating the movement initiated by the direct pathway. Abbreviations: *DA*, dopamine; *ENK*, encephalin; *GABA*, gamma-aminobutyric acid; *GLU*, glutamic acid; *GPe*, globus pallidus externa (lateral portion of GP); *GPi*, globus pallidus internus (medial portion of GP); *SP*, substance P; *STN*, subthalamic nucleus; *VIA*, ventrointermediate thalamic area. *From Kuenzel (2015).*

(Brauth et al., 1978; Kitt and Brauth, 1986b; Bailhache and Balthazart, 1993; Moons et al., 1994; Reiner et al., 1994; Wynne and Güntürkün, 1995, Figure 16.4). Both the lateral and MSt receive excitatory inputs from the pallium. The striatum, in turn, projects inhibitory neurons containing both GABA and SP to the medial (interna) region of GP (Figure 16.3A), indicated by globus pallidus internus (GPi) (Anderson and Reiner, 1990, 1991; Reiner, 1986; Reiner and Anderson, 1990; Veenman and Reiner, 1994). The medial area of the GP projects inhibitory GABAergic neurons to a small thalamic region called the ventrointermediate thalamic area (VIA; Karten and Dubbeldam, 1973; Kitt and Brauth, 1982; Medina et al., 1997). The VIA contains glutamatergic neurons which are excitatory and project to the Wulst in the dorsal region of the pallium that appears comparable to the mammalian primary somatosensory/somatomotor cortex (Wild, 1987; Korzeniewska and Güntürkün, 1990; Medina and Reiner, 2000).

In addition to the previously described direct pathway facilitating body movement, there is an antagonistic pathway that inhibits bird movements (Figure 16.3B). This parallel pathway, distinct from the direct pathway, is called the indirect pathway. It originates from the striatum, comprises neurons co-localized with GABA and encephalin (ENK), and functions to inhibit unwanted body movements. Nonetheless it has the same excitatory inputs shown previously for the direct motor pathway (Figure 16.3B). Those striatal (st) projection neurons are inhibitory and innervate the lateral (externa) portion of the globus pallidus (Figure 16.3B; Brauth, 1984; Reiner et al., 1984a,b; Reiner, 1987; Anderson and Reiner, 1990; Veenman and Reiner, 1994; Veenman et al., 1994). Inhibitory GABAergic neurons project to the avian equivalent of the subthalamic nucleus (STN) which contains excitatory glutamatergic neurons that in turn project back to the GP interna (Jiao et al., 2000). The medial GP comprises predominantly GABAergic inhibitory neurons that project to a ventral tier thalamic region called the VIA. The VIA contains excitatory glutamatergic neurons projecting to the pallium (Figure 16.3B). In summary, activation of ENK and GABA containing neurons in the striatum produces inhibition of neurons in the GPe ultimately resulting in release of GABA from the GPi. GABA release inhibits the thalamic VIA thereby decreasing glutamate output into specific pallial projection sites. The overall effect of this pathway is to promote suppression of unwanted movements that potentially would conflict with the movements being promoted by the direct pathway (Figure 16.3A). Behavioral data supporting the function of the indirect pathway were obtained in rats following unilateral lesions to the STN (Kafetzopoulos and Papadopoulos, 1983; Piallat et al., 1996) and later in pigeons following unilateral surgical lesions directed to the anterior nucleus of the ansa lenticularis, the avian homolog of the mammalian STN (Jiao et al., 2000), that produced hyperkinesia and rotation due to blocking glutamatergic input into the internal part of the GPi. Therefore the GPi projection neurons produced little GABA and the VIA released elevated glutamate. The lesioned pigeons showed enhanced motor movements on one side of the body, and thereby rotation movements were observed.

Recently the model of direct and indirect pathways of the BG was re-examined, and subsequently more dynamic interactions between the two pathways have been proposed in mammals (Calabresi et al., 2014). Additional data will need to be obtained in birds to determine if a similar level of plasticity exists in the avian BG.

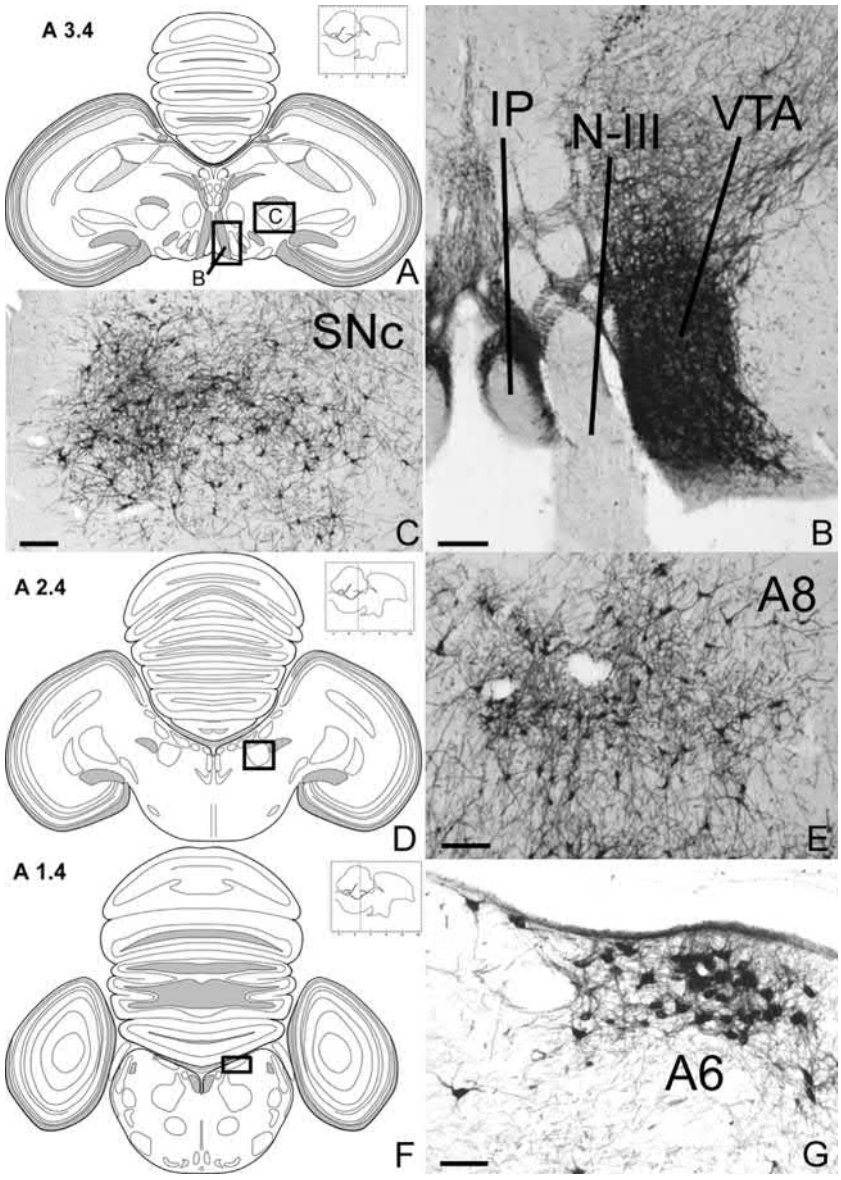

FIGURE 16.4 Sources of modulatory afferent inputs to the basal ganglia in chick brain. (A) Brain atlas plate A3.4 (Kuenzel and Masson, 1988). Boxed in areas show location of images for 4B and 4C. (B) Ventral tegmental area (VTA) or A10 dopaminergic cell group. (C) Substantia nigra pars compacta (SNc) or A9 dopaminergic cell group. (D) Chick brain atlas plate A2.4; *boxed area* shows location of digital image, (E), A8 dopaminergic cell group. (F) Chick brain atlas plate A1.4. *Boxed area* shows location of image 4G. (G) Locus coeruleus or A6 noradrenergic cell group. Scale bar for B, C, E = 200 μm and for G = 100 μm. Other abbreviations: *IP*, interpeduncular nucleus; *N-III*, oculomotor nerve. *From Kuenzel (2015).*

Data obtained in lampreys (jawless vertebrates) have shown that this species likewise contains all the major components of the BG including striatum, GP, and STN suggesting that this phylogenetically old group of vertebrates had similar, functional direct and indirect pathways forming a core network regulating motor function (Stephenson-Jones et al., 2011). Data support the general hypothesis that the BG circuits evolved in vertebrates to support selection of motor actions (Redgrave et al., 1999). Further research has shown the marked conservation of the dual-output pathways throughout vertebrate phylogeny (Stephenson-Jones et al., 2012). Additionally, a neural structure in lampreys found to be homologous to the mammalian pedunculopontine nucleus (PPN), located in the midbrain near the substantia nigra and VTA, has been identified (Stephenson-Jones et al., 2012). The PPN is thought to be involved in the initiation and modulation of gait and other stereotyped movements in mammals (Pahapill and Lozano, 2000). In birds, the ventral mesencephalic profundus nucleus identified in avian brain atlases (Karten and Hodos, 1967; Kuenzel and Masson, 1988) was renamed the pedunculopontine tegmental nucleus (PPT or PPN; Reiner et al., 2004) due to the presence of cholinergic (Ch) neurons and its association with components comprising the BG. The PPN has been proposed to be an extended part of the BG among vertebrates due to its connectivity with BG structures (Mena-Segovia et al., 2004).

16.2.2 Ventral viscerolimbic basal ganglia

16.2.2.1 Structures

The VVBG are organized structurally similar to the DSBG in that it has a dorsal st and a ventral pallidal subdivision. The VVBG comprises the ventral portion of the MSt, nucleus accumbens (core, shell, and rostral pole), olfactory tubercle, and ventral pallidum (VP) (Figure 16.5, 16.6). The st subdivision consists of the ventral portion of the MSt, shell, and core of the nucleus accumbens and superficial part of the olfactory tubercle. Striatal components, particularly nucleus accumbens, receive excitatory pallial inputs, most likely glutamatergic (Veenman and Reiner, 1996; Csillag et al., 1997; Reiner et al., 2001; Ding et al., 2003; Ding and Perkel, 2004; Farries et al., 2005). Pallial inputs to the olfactory tubercle come from the olfactory bulb (Figure 16.5A), piriform cortex (Bingman et al., 1994), and dorsomedial hippocampus (Atoji and Wild, 2004). Dopaminergic st, modulatory input largely originates from the VTA A10 cell group (Figure 16.4B) and also from the substantia nigra (Figure 16.4C; Kitt and Brauth, 1986b; Moons et al., 1994; Panzica et al., 1994, 1996). Striatal structures have been shown to have interneurons containing NADPH-diaphorase and nitric oxide synthase (NOS; Vincent et al., 1983; Brüning, 1993; Brüning et al., 1994; Panzica et al., 1994), as well as calcitonin gene-related peptide fibers (Lanuza et al., 2000; Roberts et al., 2002) and thyroid hormone releasing hormone-containing fibers (Jozsa et al., 1988). As stated previously, the st subdivision of the ventral viscerolimbic BG, regarding its inputs and outputs, is structurally similar to the DSBG as it receives excitatory glutamatergic input from the pallium and modulatory dopaminergic input largely from the VTA or A10 cell group and some input from the SNc. Additionally, the MSt, nucleus accumbens, and olfactory tubercle of the st subdivision, similar to the DSBG, have GABAergic projection neurons co-localized with either SP or ENK. The viscerolimbic pallidal subdivision includes the VP and deep olfactory tubercle (Figure 16.5A and B).

A prominent, major structure of the VVBG is the nucleus accumbens. The mammalian nucleus accumbens (Ac) comprises a central core (AcC) surrounded on its medial, ventral, and lateral sides by a shell (AcS; Herkenham et al., 1984; Záborszky et al., 1985). A third subterritory of the mammalian accumbens has also been identified (Zahm, 2000; Zahm and Brog, 1992; Zahm and Heimer, 1993). Similarly, in avian species, three sub-territories of the Ac have been defined utilizing antibodies to SP, neuropeptide Y (NPY), dopamine and cAMP-regulated phosphoprotein (DARPP-32), calcium-binding proteins, and neurotensin (NT) (Roberts et al., 2002; Bálint and Csillag, 2007; Abellán and Medina, 2009; Bálint et al., 2011, 2016; Husband and Shimizu, 2011). The rostral pole (AcR), core (AcC), and shell (AcS) subdivisions of accumbens in the chick brain have been documented (Balínt and Csillag, 2007; Balínt et al., 2011) and are shown in Figure 16.6 (Balínt et al., 2011). Recently using 12 different antibodies of neuropeptides (calcium-binding proteins or neuromodulator-related enzymes) the AcR, AcC, and AcS and other structures within the BG have been studied in pigeons (right side of Figure 16.6, Bruce et al., 2016), and specific accumbens boundaries of subunits have been shown to differ from previous studies completed in the chicken (Bálint and Csillag, 2007). The AcC and AcS in

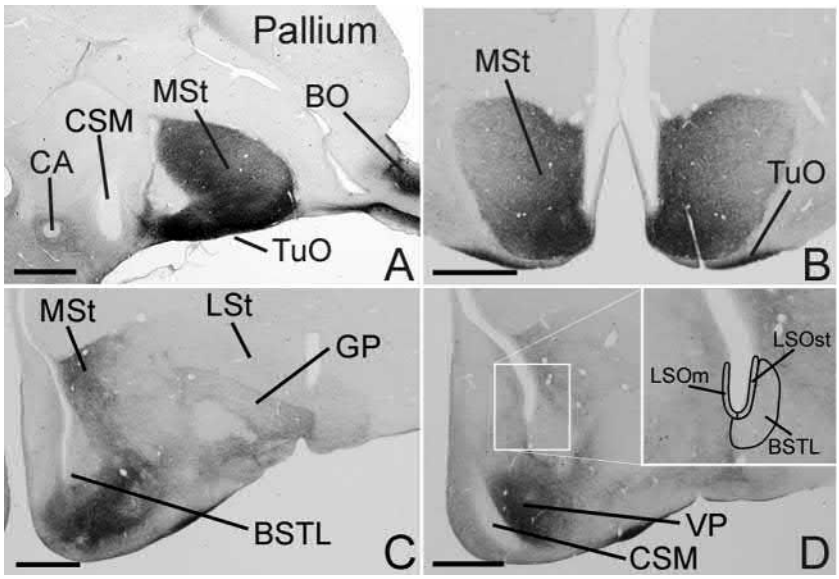

FIGURE 16.5 Sections of chick brain showing components of the viscerolimbic basal ganglia (BG) immunolabeled with an antibody to substance P. (A) Sagittal section near midline showing the ventral portion of medial striatum (MSt) and tuberculum olfactorium (TuO). Note projections from the olfactory bulb (BO) reaching the TuO. (B–D). Transverse sections of BG depicting the MSt, TuO, and VP. The insert in 5D shows the location of one of the circumventricular organs, the lateral septal organ (LSO), that is associated with the septum and its divisions. Other abbreviations: *BSTL*, lateral bed nucleus of the stria terminalis; *CA*, anterior commissure; *CSM*, corticoseptomesencephalic tract; *GP*, globus pallidus, LSOm, LSO st, lateral septal organ, medial(m) striatal(st). Scale bars for 5A-D = 1.0 mm. *Modified from (Kuenzel, 2015).*

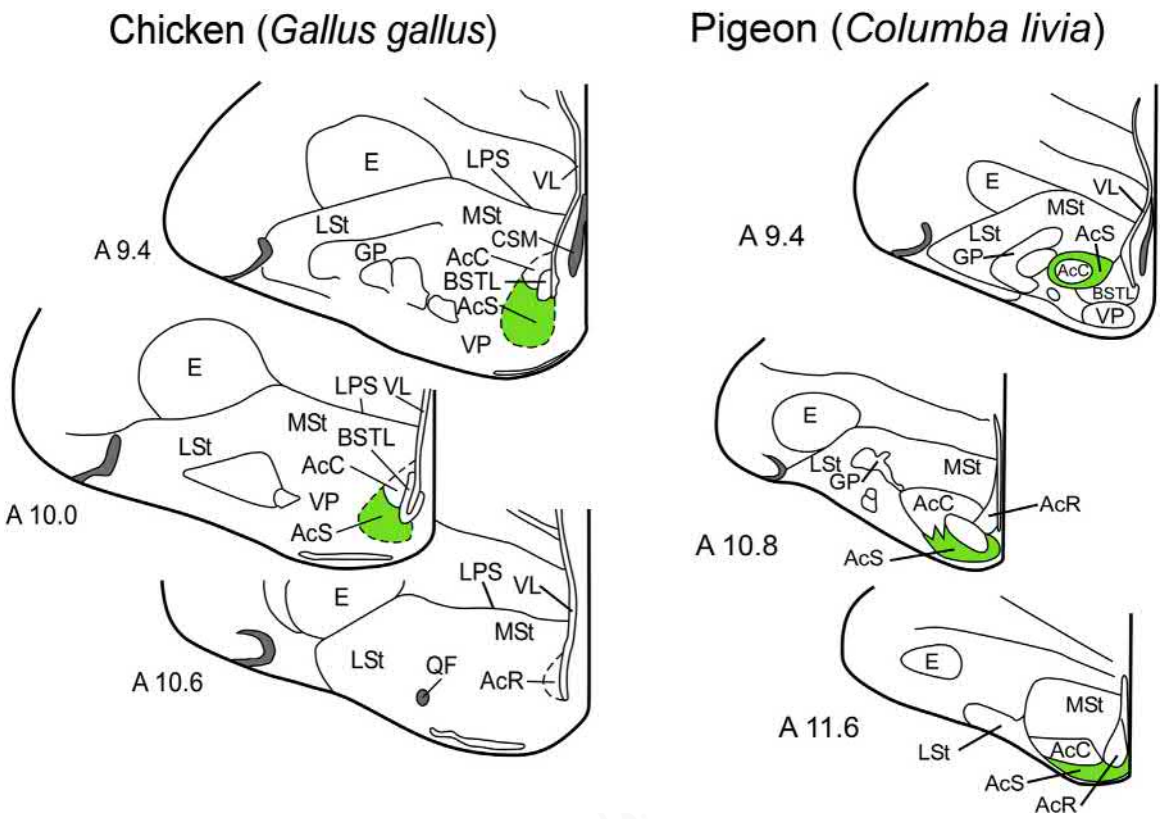

FIGURE 16.6 Comparison of the extent and size of subdivisions of the nucleus accumbens in two avian species. Coronal sections of chick brain showing atlas plate A9.4 (posterior forebrain) to plate A10.6 (more anterior section). Shown is the rostral-caudal extent of subdivisions of the nucleus accumbens (AcR, AcC, and AcS). Modified sections of pigeon brain, mapped on estimated, equivalent locations on chick brain atlas plates in order to compare sizes of accumbens subdivisions (AcR, AcC, and AcS) and their rostral-caudal extent in forebrain. Abbreviations: *AcC, AcR, AcS*, accumbens core, rostral pole, shell, respectively; *BSTL*, lateral bed nucleus of the stria terminalis; *CSM*, corticoseptomesencephalic tract; *E*, entopallium; *GP*, globus pallidus; *LPS*, pallial-subpallial lamina; *LSt*, lateral striatum; *MSt*, medial striatum; *QF*, quintofrontal tract; *VL*, lateral ventricle; *VP*, ventral pallidum. *Modified from Bálint and Csillag (2007) and Bruce et al. (2016). Atlas plates modified from Kuenzel and Masson (1988).*

the pigeon extend to more rostral levels of the forebrain than noted in chickens. Nonetheless, there is overall agreement of the positions of the three components within the BG showing that their subdivisions are somewhat conserved.

The complex accumbens structure is important to understand due to its diverse reciprocal connections with limbic and visceral structures including the hippocampal formation, arcopallium/amygdala, VP, lateral hypothalamus, and VTA and its multiple functions (reviewed in Husband and Shimizu, 2011). It also receives input from central components of the ANS including the lateral hypothalamus (Berk and Hawkin, 1985), lateral bed nucleus of the stria terminalis (BSTL) (Atoji et al., 2006), parabrachial nucleus (Wild et al., 1990), nucleus tractus solitarius (NTs) (Arends et al., 1988; Bálint and Csillag, 2007), and dorsal motor nucleus of the vagus (Arends et al., 1988). As noted previously, st subdivisions have dopaminergic input from the VTA and substantia nigra. In addition, the nucleus accumbens receives dense noradrenergic input from the A6 area (locus coeruleus; Fig. 16.4F and G), particularly in the AcS (Kitt and Brauth, 1986a; von Bartheld and Bothwell, 1992; Bailhache and Balthazart, 1993; Reiner et al., 1994; Moons et al., 1995; Mello et al., 1998). Output of the st accumbens nucleus as well as that from some neurons of the st olfactory tubercle is to the VP. The avian VP in turn projects to several diencephalic sites including the STN, paraventricular nucleus (PVN), lateral hypothalamic area, thalamic reticular nucleus, dorsomedial thalamus, and habenular nucleus (Kitt and Brauth, 1981; Berk and Hawkin, 1985; Veenman et al.,1995; Medina and Reiner, 1997). Additionally, the AcC and AcR subdivisions project via neurotensinergic neurons to the parabrachial nucleus, the NTs, and vagal motor nucleus that are regarded as unique to chickens at this time (Balínt et al., 2016).

16.2.2.2 Functions

The mammalian nucleus accumbens has been described as a limbic-motor integrator because it receives inputs from diverse structures that contribute to an organism's affective and motivational states, including the basolateral amygdala,

hippocampus, prefrontal cortex, and midbrain monoamine and brainstem autonomic systems. Early studies showed that the accumbens is involved in reward-seeking behaviors. A useful definition of reward in animal experiments is a demonstration that an unconditioned stimulus can initiate appetitive behavior and evoke "approach" behavioral effects (Ikemoto and Panksepp, 1999). The extensive data in mammals show that rats will self-administer dopamine, amphetamine, or electrical stimulation (each of these is initially an unconditioned stimulus) in the region of the Ac (Broekkamp et al., 1975; Cador et al., 1991). However, emerging new evidence suggests that the function of the Ac is not limited to "a center of reward" but also includes "action selection" facilitating goal-seeking appetitively or aversively motivated behaviors (Floresco, 2015). Striking differences in afferent and efferent projections of the core and shell subdivisions of Ac (Heimer and Alheid, 1991; Zahm and Brog, 1992; Bálint and Csillag, 2007) imply that they may have different functional roles. The AcC has similarities to the overlying caudate-putamen and therefore more allied with voluntary motor functions. Research by Alheid and Heimer (1988), Heimer and Alheid (1991), and Zahm and Brog (1992) suggested that the AcC mediates appetitive instrumental learning or learning of new motor skills. In contrast, the AcS due to its connections with the extended amygdala (Alheid and Heimer, 1988) is associated with visceral or motivational mechanisms. Specifically, blockade of AMPA/kainite receptors within the AcS, but not the AcC, induced marked and prolonged feeding in satiated rats (Maldonado-Irizarry et al., 1995). Hence the AcS was thought to be responsible for integrating basic drives and visceroendocrine mechanisms. The shell appears to have a role in regulating both appetitive and aversively motivated behavior since expression of Fos in the shell is activated by both stressful and reinforcing stimuli (Kelley, 1999). The Ac, and the shell region in particular, displays significant changes to stress (Kalivas and Duffy, 1995; King et al., 1997). In mammals, the medial shell region of accumbens has shown stress responsivity (Castro and Bruchas, 2019) and modulates social stress behaviors (Russo and Nestled, 2013).

In mammals, reinforcement-based learning involving reward or punishment has been shown to include parts of the dorsal and ventral striatum and other BG nuclei receiving dopaminergic input from the VTA (Graybiel and Grafton, 2015). The ventral striatum appears necessary for initial learning of motivated behaviors that could become habitual (Atallah et al., 2014). It has been suggested that addictive behavior may be an extreme form of habits involving a sequence of motor behaviors developed by trial-and-error learning (Graybiel and Grafton, 2015). Studies with songbirds indicate that the BG, including the ventral viscerolimbic division, may be involved in integration of the three key components of reinforcement learning: motor exploration or variability, error and evaluation signals, and biasing signals to adjust future actions (Gale and Perkel, 2010; Woolley and Kao, 2015; Xiao et al., 2018). In female songbirds, the Ac is involved in discrimination of conspecific courtship vocalization. Importantly, the neural activation of Ac in response to male courtship song appears to be estradiol-dependent (Maney, 2013).

In chicks, the MSt has been suggested to be a storage site for memory traces (Rose, 2000). Chicks that were trained to avoid bitter-tasting beads of particular color in a passive avoidance learning paradigm showed retrograde amnesia following the MSt lesions that also included at least some of the Ac (Gilbert et al., 1991; Patterson and Rose, 1992). Furthermore, passive avoidance training resulted in a series of metabolic and morphological changes in the MSt, such as increased glucose uptake and changing synaptic ultrastructure (Rose and Stewart, 1999). By contrast, other studies employing chemical lesions of the caudal MSt in chicks indicated that this structure is unlikely to be a principal site for permanent storage of memory. In these studies, chicks were trained to discriminate color beads associated with food reward. Posttraining lesion of the caudal MSt impaired subsequent novel learning but did not interfere with memorized association of color (Izawa et al., 2002, 2003; Matsushima et al., 2003). Bilateral electrical lesion of the Ac in chicks resulted in increased vocalization or distressed calls, when placed in an open field environment (Zachar et al., 2017).

16.2.3 Extended amygdaloid complex: central extended amygdala and medial extended amygdala

Heimer and coworkers recognized that the mammalian amygdaloid complex comprised two major groups, each of which had associated neuronal structures that extended from them forming a neuronal corridor. The two corridors were named the extended amygdala, one originating from the central nucleus of the amygdala (CeM) while the second was continuous with the medial amygdaloid nucleus. Both passed through a territory ventral to the GP (anatomically referred to as sublenticular), and the neuronal corridors ended in different components of the bed nuclei of the stria terminalis (Alheid and Heimer, 1988; Alheid et al., 1995). Each corridor possessed similar neurochemical characteristics of the amygdaloid nucleus from which they were confluent. Functionally, the central and medial amygdaloid nuclei and their respective sub-nuclei of the complex bed nuclei of the stria terminalis represent the major output nuclei of the amygdala of mammals (Swanson and Petrovich, 1998; Swanson, 2000; Paré et al., 2004).

Developmental, neurohistochemical, hodological, and behavioral data suggest strongly that comparable structures

forming a subpallial amygdaloid complex exist in birds (Jurkevich et al., 1997, 1999; Aste et al., 1998; Cheng et al., 1999; Panzica et al., 1999; Absil et al., 2002a,b; Roberts et al., 2002; Reiner et al., 2004; Yamamoto et al., 2005; Abellán and Medina, 2009; Xie et al., 2010, 2011; Vicario et al., 2014, 2015, 2017). For clarification of the structures and functions of the subpallial amygdaloid complex, each of its two basic components will be discussed, first in mammals and then in birds.

16.2.3.1 Central extended amygdala

16.2.3.1.1 Structures

The CeM, cells within the corridor of the central extended amygdala, and the lateral BSTL comprise structures of the central extended amygdaloid complex in mammals. Associated with the CeM are groups of intercalated cells positioned between the lateral amygdala and the CeM (Paré et al., 2004). The major group of neurons projecting from the central extended amygdaloid complex is GABAergic, similar to the dorsal somatomotor and VVBG discussed previously. A difference is that the GABAergic neurons are typically enriched with one of several neuropeptides including corticotropin-releasing hormone (CRH), NT, somatostatin, or ENK (Moga and Gray, 1985; Swanson and Petrovich, 1998; Paré and Smith, 1994; Alheid et al., 1995; Poulin and Timofeeva, 2008; Panguluri et al., 2009). The major descending projections of the central extended amygdaloid complex are to the lateral hypothalamus, central gray (GCt), parabrachial nucleus, and nucleus of the solitary tract, all of which are structures in the diencephalon and brainstem associated with of the ANS. Functionally the structures and their connections to the ANS regulate physiological processes and behaviors related to ingestion, and fear/anxiety/stress (Alheid and Heimer, 1988; Alheid et al., 1995; Swanson, 2000; de Olmos et al., 2004).

In birds, a major component of the central extended amygdaloid complex, positioned directly below the GP, was previously termed the subpallial amygdaloid area (SpA; Reiner et al., 2004). Thereafter, it was proposed that the SpA and its lateral continuation directly ventral to the LSt be renamed the central extended amygdala (EAce, Figure 16.7A, Abellán and Medina, 2009; Vicario et al., 2014). It was also suggested that part of the caudolateral striatum and lateral continuation of the SpA may be the avian structure homologous to the mammalian CeM (Abellán and Medina, 2009). Another avian structure that has been suggested to be homologous to the mammalian central amygdaloid nucleus is the compact division of the posterior pallial amygdaloid nucleus (Atoji and Wild, 2006). A structure, recently termed the st capsule (StC) (composed of a thin group of subpallial neurons) located between the nidopallium and LSt (Puelles et al., 2007), has been proposed to be comparable to the intercalated cell masses of the mammalian amygdala (Abellán and Medina, 2009) that occur juxtapositioned to central amygdaloid

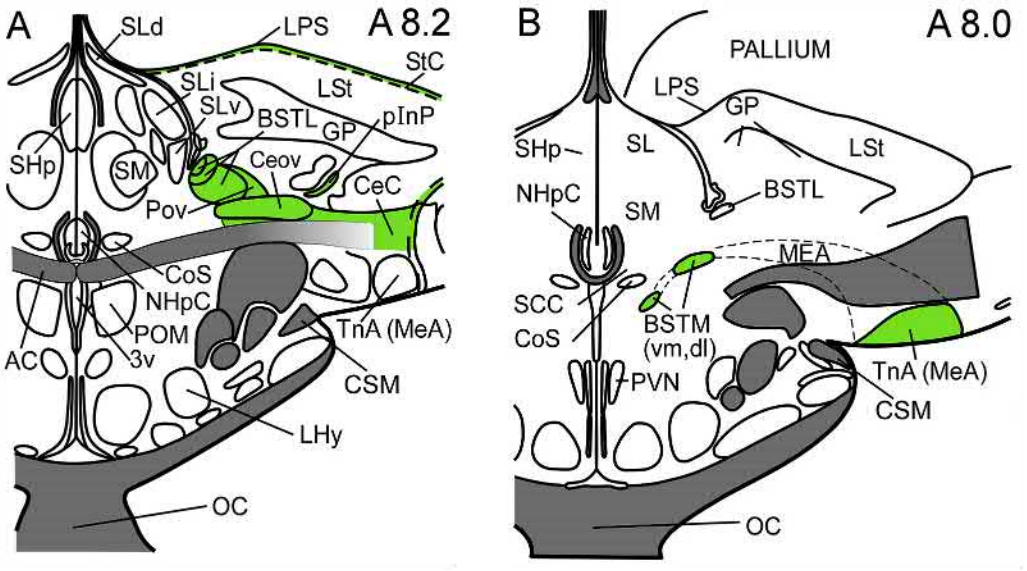

FIGURE 16.7 Central and medial extended amygdala in the chicken brain. The central extended amygdaloid complex is shown in green (A) and comprises the CeC, StC, pInP, SpAr (not shown), Ceov, Pov, and BSTL. The medial extended amygdaloid complex, shown in green (B) consists of the TnA/(MeA), BSTMvm, and BSTMdl (refer to Fig. 16.1 for names of abbreviations). Other abbreviations: *AC*, anterior commissure; *CoS*, commissural septal nucleus; *CSM*, corticoseptomesencephalic tract; *GP*, globus pallidus; *LHy*, lateral hypothalamic nu.; *LPS*, pallial-subpallial lamina; *LSt*, lateral striatum, *NHpC*, nucleus of hippocampal commissure; *OC*, optic chiasma; *POM*, medial preoptic nucleus; *PVN*, paraventricular nucleus; *SCC*, caudo-central septum; *SHp*, septohippocampal septum; *SLd*, dorsal lateral septal nucleus; *SLi*, intermediate lateral septal nucleus; *SLv*, ventral lateral septal nucleus; *SM*, medial septal nucleus; *3v*, third ventricle. *Modified from Abellán and Medina (2009) and Vicario et al. (2014).*

nucleus of mammals (Paré et al., 2004). An important component of the central extended amygdaloid complex is the lateral BSTL (Figure 16.7A) that is regarded as comparable to the mammalian BSTL due to the presence of CRH (Panzica et al., 1986; Ball et al., 1989; Richard et al., 2004), neurotensinergic (Reiner and Carraway, 1987; Atoji et al., 1996; Reiner et al., 2004) and enkephalinergic (Molnar et al., 1994) neurons. The avian BSTL has been shown to have direct connections to components of the ANS including hypothalamic structures, parabrachial nucleus, nucleus of the solitary tract, and dorsal motor nucleus of the vagus (Berk, 1987; Arends et al., 1988; Wild et al., 1990; Atoji et al., 2006; Bálint et al., 2011). In summary, the structures that comprise the avian EAce along primarily a sublenticular corridor include the following: (1) capsular central amygdala, (2) StC, (3) peri-intrapeduncular nuclear island field, (4) oval central amygdalar nucleus (Ceov), (5) rostral division of the subpallial amygdala, (6) perioval zone, and (7) dorsal part of the lateral BSTL (Figure 16.7A, Abellán and Medina, 2009; Vicario et al., 2014).

16.2.3.1.2 Functions

In mammals, the central extended amygdaloid complex is thought to be involved in food intake and fear/anxiety/stress behavior due to its connectivity to central components of the ANS located in the hypothalamus and caudal brainstem (van der Kooy et al., 1984; Luiten et al., 1987; Paré et al., 2004). In particular, CRH neurons in the BSTL can affect the regulation of appetite (Heimer and Alheid, 1991; Clark and Kaiyala, 2003; Gallagher et al., 2008; Krogh et al., 2008). The stria terminalis is known to have connections with the lateral hypothalamic area, parabrachial nucleus, nucleus of the solitary tract, and dorsal motor nucleus of the vagus, all of the previously listed structures have connectivity to the ANS. In birds, similar central connections with the ANS have been demonstrated showing that neural pathways regulating ingestive behavior in mammals and birds are conserved (reviewed in Kuenzel and Blähser, 1993; Kuenzel, 1994, 2000; Kuenzel et al., 2011). Furthermore, CRH has been shown to be an important regulator of stress and anxiety in mammals (Paré et al., 2004) and causes distress vocalizations in chicks (Zhang et al., 2004).

16.2.3.2 Medial extended amygdala

16.2.3.2.1 Structures

The medial extended amygdaloid complex in mammals comprises the medial amygdala (MeA), the neuronal corridor emerging from the MeA, and the medial nuclear complex of the BSTL. The main input to the MeA originates in the olfactory bulb as well as in the accessory olfactory system and its vomeronasal organ. It is rich in gonadal steroid receptors and projects to various hypothalamic structures involved with reproductive behavior, aggression, and defense (Alheid et al., 1994; Swanson, 2000). Similar to other projection neurons comprising the subpallial structures, the medial extended amygdala (MEA) has predominantly GABAergic neurons (Alheid et al., 1994, 1995; Swanson, 2000). Glutamatergic neurons have also been identified (Choi et al., 2005).

The composition of the MEA in birds was established relatively recently. The nucleus taeniae was proposed for some time to be comparable to the mammalian MeA (Cheng et al., 1999) and was renamed the nucleus taeniae of the amygdala (Reiner et al., 2004). Controversy persists, however, and recently it was proposed that the name nucleus taeniae of the amygdala be changed to medial ventral arcopallium due to several, diverse in situ hybridization results in the zebra finch showing that the songbird arcopallium is primarily pallial (Mello et al., 2019). Nonetheless, over the years, data in other avian species have supported the concept that birds have a MeA and an extended amygdala (Yamamoto et al., 2005). Birds also have the medial BSTL (Figure 16.7B, Jurkevich et al., 1997, 1999; Aste et al., 1998). In addition to arginine vasotocin (AVT), neurons of the BSTM of chickens contain galanin (Klein et al., 2006). Embryological studies showed that birds have a subpallial MeA with a corridor of neurons that extends to the BSTM, and therefore it was proposed that birds have a MEA (Figure 16.7B) complex (Abellán and Medina, 2009). Recently binding site densities of 11 receptors were studied to map their distribution in specific subregions of the arcopallium/amygdaloid complex of pigeons in order to compare their subregions with mammalian counterparts (Herold et al., 2018). In addition to GABAergic and glutamatergic neurons, the MEA complex likewise has nitrergic neurons (Panzica et al., 1994; Balthazart et al., 2003) resembling comparable findings of GABAergic and nitrergic neurons in the mammalian medial amygdalar nucleus (Tanaka et al., 1997; Swanson, 2000). In addition to inputs from the olfactory bulbs, the avian subpallial amygdala receives projections from the piriform cortex (Bingman et al., 1994; Veenman et al., 1995). Vasotocin neurons of the BSTM component of the medial extended amygdaloid complex project to the medial preoptic nucleus (POM) (Absil et al., 2002a). The avian MeA is reciprocally connected to the hippocampal formation (Atoji et al., 2002; Atoji and Wild, 2004). A detailed account of transcription factors that have played a role in the development of the MEA in zebra finches has recently been published (Vicario et al., 2017). Importantly, the medial extended amygdaloid complex contains high concentrations of androgen and estrogen receptors as well as the enzyme aromatase which converts testosterone to estradiol (Balthazart et al., 1998b; Foidart et al., 1999). The

abundance of sex steroid receptors is greater in males in this region (Watson and Adkins-Regan, 1989). A more detailed account of aromatase and steroid receptors is reviewed under the subheading *Septal and preoptic neuroendocrine systems.*

16.2.3.2.2 Functions

As stated previously, in mammals, the medial extended amygdaloid complex plays a key role in mating, sexual, defensive, and aggressive behaviors. Olfactory inputs from the main and accessory olfactory systems are important signals to the complex (Swanson, 2000; Choi et al., 2005). Hodological and behavioral data suggest that the BSTM and MeA play a similar role in birds (Panzica et al., 1998; Thompson et al., 1998; Absil et al., 2002a; Abellán and Medina, 2009; Xie et al., 2010, 2011; Vicario et al., 2017). Due to a lack of a defined accessory olfactory system and small olfactory bulbs in most avian species, it has been thought that pheromones and odors do not serve a critical function in this vertebrate class. Nonetheless, it has been shown that chemosensory communication plays a role in avian social and sexual behavior (Balthazart and Schoffeniels, 1979; Caro et al., 2015) and navigation in homing pigeons (Wiltschko and Wiltschko, 2017). A tract-tracing study in pigeons revealed bilateral projections from the olfactory bulbs to the nucleus of the taeniae of the amygdala and ipsilateral projections to the medial septum suggesting that olfactory cues in birds can be relayed to the limbic system (Patzke et al., 2011). Furthermore, electrophysiological responses in the avian olfactory bulb to odorants are comparable to those in mammals (McKeegan, 2002). Importantly, structures in the medial extended amygdaloid complex have been shown to be sexually dimorphic in avian species. Specifically, the BSTM has been shown to be larger in males, is steroid-responsive and plays a role in copulatory behavior in mammals (Del Abril et al., 1987; Guillamón and Segovia, 1997) and birds (Kiss et al., 1987; Voorhuis et al., 1988; Panzica et al., 1998; Viglietti-Panzica et al., 1992; Aste et al., 1998; Jurkevich et al., 1999). A subnucleus of the BSTM in chickens, the BSTM2 (ventromedial BSTM) functions in male appetitive sexual behavior (Xie et al., 2010, 2011).

16.2.4 Basal telencephalic cholinergic and noncholinergic corticopetal system

16.2.4.1 Structures

The basal corticopetal system, sets of neurons at the base of the forebrain that project to the cortex in mammals, or pallium in birds and other vertebrates, is composed mostly of Ch neurons that in mammals are found overlapping other neuronal types located in the GP and VP of the BG and medial septum-diagonal band nuclei. Specifically Ch neurons are located in three main areas: anteromedial (medial septal nucleus or Ch1), intermediate [vertical and horizontal limbs of the diagonal band nuclei (NDBv and NDBh, respectively) or Ch2/Ch3], and caudolateral [nucleus basalis of Meynert (NBM) or Ch4] (Mesulam et al., 1984; Mesulam, 1990). In birds, three nuclei have been grouped together that comprise this telencephalic corticopetal system: basal magnocellular nucleus (BMN), nuclei of the diagonal band, vertical limb (NDBv), and horizontal limb (NDBh) (Figure 16.1). All three avian nuclei have in common the presence of Ch neurons (Reiner et al., 2004). In the first nucleus listed, the NBM, the Ch neurons are found in and about the ventral GP, VP (Figure 16.2B), intrapeduncular nucleus and in and about the lateral and medial forebrain bundle (MFB) (Medina and Reiner, 1994; Reiner et al., 2004). The darkly stained circular dots scattered between the VP and GP structures on Figure 16.2B are cell bodies of Ch neurons immunolabeled with an antibody to ChAT. Of interest is that the avian NBM is considered equivalent to the mammalian nucleus basalis of Meynert which contains Ch neurons that project to neocortex, hippocampus, and amygdala (Záborsky et al., 1999). In birds, the NBM receives input from the VVBG, including the nucleus accumbens, as well as the subpallial amygdaloid complex including the arcopallium (Veenman et al., 1995; Medina and Reiner, 1997). Another two avian Ch nuclei, the NDBv and NDBh, are comparable to groups of Ch neurons located in the nucleus of the diagonal band in the mammalian basal forebrain region (Woolf, 1991). The avian NDB projects heavily to the hippocampal and parahippocampal areas (Benowitz and Karten, 1976; Casini et al., 1986; Atoji et al., 2002; Montagnese et al., 2004).

16.2.4.2 Functions

In mammals, the basal forebrain, particularly the nucleus basalis of Meynert, has been implicated in learning and memory. Evidence from clinical geriatric studies resulted in the "Ch hypothesis" that memory dysfunction was the result of pathological changes to Ch neurons (Bartus et al., 1982). Specifically, corticopetal Ch neurons have been shown to play a role in modulating cortical activity and in attentional and arousal processes (Zaborszky et al., 1999) that affect learning and memory (Mesulam and Geula, 1988; Metherate et al., 1988, 1992; Cape and Jones, 2000; Cape et al., 2000). There exists a high correlation between the loss of memory and loss of Ch neurons in humans, e.g., Alzheimer's disease (Auld et al., 2002). It has been hypothesized that a different pattern of neuronal loss occurs within the nucleus basalis of Meynert (NBM) in different neuronal diseases and that understanding the functional significance of subregions of the NBM would prove

important in elucidating the pathogenesis of dementia in other neuropsychiatric disorders such as Parkinson's disease (Liu et al., 2015).

Little is known about the role of basal forebrain Ch neurons in cognitive processes in birds. Nonetheless pharmacological blockage of muscarinic Ch receptors results in impaired learning and memory in diverse avian species (Patterson et al., 1990; Mineau et al., 1994; Savage et al., 1994; Kohler et al., 1996; Zhao et al., 1997). Additionally, beta-amyloid toxicity, known to damage the basal forebrain Ch system in mammals, impairs memory in chicks (Gibbs et al., 2010). Of interest, previous studies in mammals have reported basal forebrain Ch neurons originate from the subpallium (Marin et al., 2000; Xu et al., 2008), however more recently, it has been suggested that they originate from the pallium (Pombero et al., 2011). Pombero et al. (2011) analyzed pallial implants in mice just caudal and ventral to the olfactory bulb. The cells migrated caudally and ventrally into the subpallium and were detected in the basal forebrain region. The original pallial cells that reached the ventral forebrain were shown to express choline acetyltransferease therefore differentiated into Ch neurons. Olfactory alterations have been identified as a risk factor and an early marker of neurodegenerative diseases, such as Alzheimer's disease. Hence this long-distance migration from the caudal region of the olfactory bulbs to the basal forebrain may be one reason for the cause of some neurodegenerative diseases affecting cognitive function (Pombero et al., 2011). It would be of interest to determine whether the origin of Ch cells in the basal forebrain of chick embryos likewise occurs in the anterior pallial region.

16.2.5 Septum and septal neuroendocrine systems

16.2.5.1 Divisions and structures

The avian septum lies dorsal and anterior to the diencephalon and comprises all neural structures medial to the ventral horns of the lateral ventricle (Figures 16.1 and 16.7). It first appears in rostral coronal sections of forebrain as the ventral horns of the lateral ventricle begin to move apart laterally from midline. The corticoseptomesencephalic tract (CSM, Figure 16.1), previously called the tractus septopalliomesencephalicus begins to descend from the hippocampal region into the septum (Figure 16.1, vertical set of images #3 & 4 in left column). The CSM comprises two parallel symmetrical tracts descending at midline, one on each side of the brain. Each tract gradually moves away from midline as it descends to the base of the brain. The brain region medial to the CSM contains preoptic structures (Figure 16.1, fourth vertical image from the top, white area) while the territory lateral to the CSM on both sides of the brain and extending to the lateral, descending horns of the lateral ventricle is the septal region (Figure 16.1, yellow in color). Posteriorly, the AC delineates the ventral boundary of the septal region (AC, Figure 16.1). Structures ventral to the AC are regarded as preoptic or hypothalamic (Figure 16.1). Moving caudally beyond the AC, the top of the third ventricle (3V) marks the floor of the septum (Figure 16.7B). Posteriorly, the septum gradually decreases in size, but before the septum disappears, the corticohabenular and corticoseptal tract becomes one of the last visible traces of the septum.

The septum of mammals has been parcellated into numerous chemoarchitectonic zones that can be grouped into four major divisions (Jakab and Leranth, 1995; Risold and Swanson, 1997a,b). A comparative study was completed using a variety of songbird species and antibodies against 10 neuropeptides and enzymes in order to develop a nomenclature and framework to establish homologous septal zones among tetrapods (Goodson et al., 2004). Results suggested that the avian septum is comparable to the mammalian structure and can be divided into four major divisions: lateral septum (SL), medial septum (SM), septohippocampal septum (SHpS), and caudocentral septum (SCC). Coupled with recent developmental (Puelles et al., 2007; Abellán and Medina, 2009; Abellán et al., 2010) and hodological (Atoji and Wild, 2004; Montagnese et al., 2004, 2008) studies, homologous divisions and structures have been proposed which will be detailed below.

16.2.5.1.1 Lateral septal division

The developing avian lateral septum (SL, Figure 16.7A) comprises three nuclei, the dorsal (SLd) and intermediate are st derivatives based upon expression of Pax6 and LIM-only gene *Lmo4,* while the ventral one is a pallidal derivative due to expression of the *Nkx2.1* gene (Garcia-López et al., 2008; Abellán and Medina, 2009; Medina and Abellán, 2009). In roosters, a suggested location of the three SL structures using AVT and CRH immunostaining is shown in Figure 16.8. Hodological studies have shown four major inputs to the lateral septum including the hippocampal formation, arcopallium/amygdala, diencephalon, and brainstem. Different hippocampal domains project preferentially to different SL regions of birds (Atoji and Wild, 2004; Montagnese et al., 2004, 2008) as well as mammals (Risold and Swanson, 1997b). In addition, in mammals, major glutamatergic inputs to the SL have been documented from pyramidal neurons in the hippocampus (Jakab and Leranth, 1995; Risold and Swanson, 1997b). The caudal intermediate arcopallium and nucleus taeniae of the amygdala (MeA) have been shown to project to the avian SL (Atoji and Wild, 2004; Montagnese et al., 2004, 2008). The mammalian MeA, proposed to be homologous to the avian nucleus taeniae of

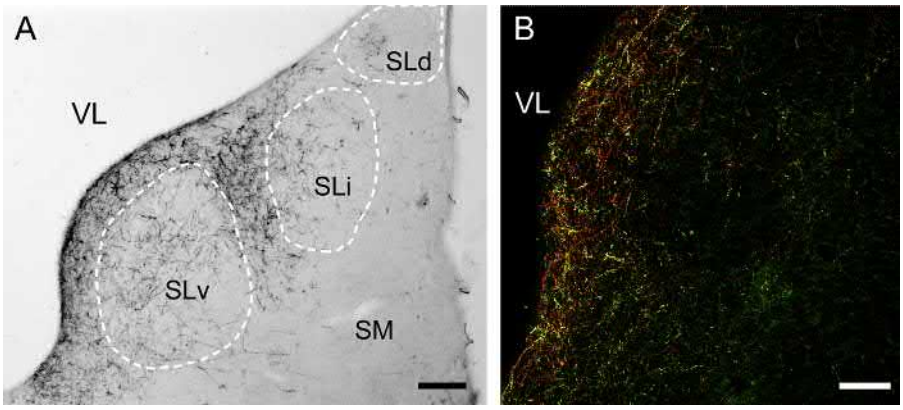

FIGURE 16.8 The septum of the chicken. (A) Coronal section of the septal area of a rooster brain showing immunoreactivity for arginine vasotocin with outlined proposed locations of three structures in the lateral area of the lateral septal division. (B) Coronal section of the septal area of a rooster showing arginine vasotocin (red) and corticotropin releasing hormone (green) innervation. Scale bar for 16,8A = 200 μm, 16,8B = 100 μm. Abbreviations: *SLd, SLi, SLv*, dorsal, intermediate and ventral nuclei of lateral septum; *SM*, medial septum; *VL*, lateral ventricle.

the amygdala (Thompson et al., 1998; Cheng et al., 1999; Yamamoto et al., 2005), sends projections to the SL (Canteras et al., 1995). Extensive input to the SL originates from the rostral-caudal extent of the ventral diencephalon including the POA (POM) (Berk and Butler, 1981; Panzica et al., 1992; Balthazart et al., 1994; Balthazart and Absil, 1997; Atoji and Wild, 2004; Montagnese et al., 2008), hypothalamus (anterior and lateral hypothalamic area), tuberal and mammillary region (Atoji and Wild, 2004, 2006). Similar projections have been demonstrated in the rat (Canteras et al., 1992, 1994; Risold and Swanson, 1997b). A major output from the mammalian SL descends via the MFB and innervates the medial septal nucleus, nucleus of the diagonal band, lateral hypothalamic area, medial preoptic, anterior hypothalamic, ventral premammillary, and mammillary nuclei (Risold and Swanson, 1997b). The avian SL sends similar projections to the POM, anterior and ventromedial hypothalamic nucleus, lateral hypothalamic area, and lateral mammillary nucleus (Atoji and Wild, 2004) thereby showing numerous reciprocal projections between hypothalamic nuclei and SL in birds and mammals. Finally, a fourth, extensive set of projections to the mammalian and avian SL originate from the brainstem, specifically from the VTA (Kitt and Brauth, 1986b), locus coeruleus (Kitt and Brauth, 1986a), and nucleus raphe/linear caudalis (Cozzi et al., 1991; Atoji and Wild, 2004). Those projections to the SL have been reported to be dopaminergic (Bailhache and Balthazart, 1993; Bottjer, 1993; Moons et al., 1994; Wynne and Güntürkün, 1995), noradrenergic (Bailhache and Balthazart, 1993; Moons et al., 1995; Mello et al., 1998), and serotonergic (Challet et al., 1996), respectively.

Additional chemoarchitectonic studies have shown dense neural terminals containing AVT and its mammalian homolog vasopressin in the caudal and ventrolateral region of the SL among various vertebrate taxa (De Vries and Panzica, 2006). The density of these projections in vertebrates is testosterone-dependent and sexually dimorphic (Moore and Lowry, 1998; Goodson and Bass, 2001). The sexual dimorphic expression has been demonstrated in several avian species (Voorhuis et al., 1988; Viglietti-Panzica et al., 1992; Jurkevich et al., 1997; Panzica et al., 1999). The SL is also rich in androgen-concentrating cells (Arnold et al., 1976; Barfield et al., 1978) and in estrogen receptors (Panzica et al., 2001). Other chemoarchitectonic studies have shown that galanin fibers occur in the lateral wall of the septum in Japanese quail (Azumaya and Tsutsui, 1996), collared dove (Dubbeldam et al., 1999), songbirds (Goodson et al., 2004), chickens (Klein et al., 2006), anuran amphibians (Lazar et al., 1991), and mammals (Melander et al., 1986; Risold and Swanson, 1997a; Chaillou et al., 1999). Of interest is that the distribution of galanin fibers in the lateral septum and perikarya in the medial BSTL have been shown to be sexually dimorphic in chickens (Klein et al., 2006) as previously demonstrated for AVT. Both the SL and SM of chickens contain numerous CRH-immunoreactive terminals. Interestingly, the density of these terminals increases in adult chickens (Richard et al., 2004).

16.2.5.1.2 Medial septal division

The medial septal division in the developing mouse and chicken expresses Tbr1 (Puelles et al., 2000), Lhx6, Lhx7/8, GAD67, and VGLUT2 (Flames et al., 2007; Abellán and Medina, 2009; Abellán et al., 2010) and consists of glutamatergic, GABAergic, Ch neurons, and some neurons from pallial septal and pallido-preoptic subdivisions, the latter in the ventral region of the SM expresses some GABAergic neurons (Abellán et al., 2010). Similar to the lateral septum, the SM (Figure 16.7) has inputs from the hippocampal complex, entire rostral-caudal extent of the ventral diencephalon including nuclei from the preoptic, anterior hypothalamus, mammillary, and tuberal regions as well as

receives projections from the VTA, locus coeruleus, and linear caudalis (Kitt and Brauth, 1986a,b; Atoji and Wild, 2004; Montagnese et al., 2008). Other inputs documented include the nucleus of the diagonal band (Atoji and Wild, 2004; Montagnese et al., 2008), medial division of the BSTL (Montagnese et al., 2008), and the dorsal lateral nucleus of the anterior, medial thalamus (Atoji and Wild, 2004). The SM sends projections to the hippocampal complex (Atoji and Wild, 2004), olfactory tubercle, VP, lateral septum, nucleus of the diagonal band, and commissural septal nucleus (Atoji and Wild, 2004; Montagnese et al., 2008). Chemoarchitectonic studies show that most peptidergic and aminergic neurons and fibers show less immunoreactivity (ir) compared to the SL. The one exception appears to be the presence of Ch neurons which show their greatest concentration in the medial septum, particularly at caudal levels not only in a variety of bird species but also the ventromedial septum of most tetrapod groups (Goodson et al., 2004). Refer to the previous Section 16.2.4 covering the "Basal telencephalic cholinergic and noncholinergic corticopetal system."

16.2.5.1.3 Septohippocampal septal division

A septohippocampal nucleus occurs in mammals (Jakab and Leranth, 1995; Risold and Swanson, 1997a,b) and a similar nucleus, the SHpS (Figure 16.7A), has been proposed to exist in birds comprising a small, thin vertical area located above the AC and extending to the dorsal region of the septum (Goodson et al., 2004). Developmental studies utilizing the pallial marker Emx-1 initially suggested that a discrete, dorsal area of the SHpS was pallial (Puelles et al., 2007). More recent data using a gene *Lhx5* encoding a transcription factor showed that the entire medial portion of the septohippocampal division from its most dorsal extent ventral to the nucleus of the hippocampal commissure comprises a pallial portion of the septum (Abellán et al., 2010). Chemoarchitectonic data displayed VGLUT2 transporter surrounding the nucleus of the hippocampal commissure suggesting that the neurons were glutamatergic providing additional support that the SHpS is a pallial derivative (Abellán et al., 2010). Another source of evidence for its pallial origin comes from the well-known migration of gonadotropin-releasing hormone, type one (GnRH-1) neurons from the embryonic olfactory placode into the pallium behind the olfactory bulb and their subsequent migration toward the preoptic, hypothalamic, and septal regions (Figure 16.9A). The unusual neuronal migration has been demonstrated in amphibians (Muske and Moore, 1988), mammals (Schwanzel-Fukuda and Pfaff, 1989; Wray et al., 1989) and birds (Murakami et al., 1991; Norgren and Lehman, 1991). Of interest is that for mammalian species, a major portion of the GnRH-1 neurons finally reside in the POA and arcuate nucleus of the hypothalamus (Silverman et al., 1994) while in the avian brain such as the chick, 73% of the total GnRH-1 neurons remain in the septum between the medial and lateral septal divisions and surrounding the nucleus of the hippocampal commissure (NHpC, Figure 16.9B, Kuenzel and Golden, 2006). Within the core region of the nucleus of the hippocampal commissure are dense plexuses of galanin (Figure 16.9C, Klein et al., 2006) and CRH fibers (Richard et al., 2004). Recent studies revealed a large group of CRH neurons in the NHpC (Figure 16.9D–F, Nagarajan et al., 2014) and demonstrated that they are involved in the neuroendocrine regulation of stress (Nagarajan et al., 2017a,b; Kadhim et al., 2019). The avian SHpS is also characterized by SP, NPY, and vasoactive intestinal peptide (VIP) fibers (Goodson et al., 2004). The latter two peptides (NPY and VIP) are associated with reproductive function. Similarly, the septohippocampal nucleus of rats has been shown to express NPY mRNA in cell perikarya and SP in fibers (Risold and Swanson, 1997a).

16.2.5.1.4 Caudocentral septal division

The fourth major septal area of mammals is the posterior septum which contains the septofimbrial and triangular nuclei (Jakab and Laranth, 1995; Risold and Swanson, 1997a,b). It has been proposed that birds have a caudocentral septal division that is topographically comparable to the mammalian septofimbrial nucleus and appears to be a caudal expansion of the ventrolateral SL (Goodson et al., 2004). The most posterior aspect of the caudocentral septum contains the corticohabenularis and corticoseptal tract. In the rat, a similarly located fiber tract is termed the fimbria of hippocampus and connects the septofibrial nucleus with the hippocampus (Risold and Swanson, 1997b). It has therefore been proposed that the corticohabenularis and corticoseptal tract be renamed the fimbria of hippocampus (Goodson et al., 2004; Puelles et al., 2007, 2019). In the ventral region of the avian caudocentral septal division occur GnRH-1 neurons that are a continuation of the major group of GnRH-1 found in and about the nucleus of the hippocampal commissure (Kuenzel and Golden, 2006). On the ventral side of the NHpC displaying a projection into the 3V (Figure 16.9E) is the subseptal organ (SSO) homologous to the mammalian subfornical organ (SFO) that plays a role in the regulation of water intake.

16.2.5.2 Functions

16.2.5.2.1 Septal-hypothalamic-pituitary-gonadal neuroendocrine system

As previously stated, during embryonic development, GnRH-1 neurons migrate into the brain just behind the olfactory bulbs and migrate from the pallium to the septal and diencephalic regions. In chicks, most of the GnRH-1

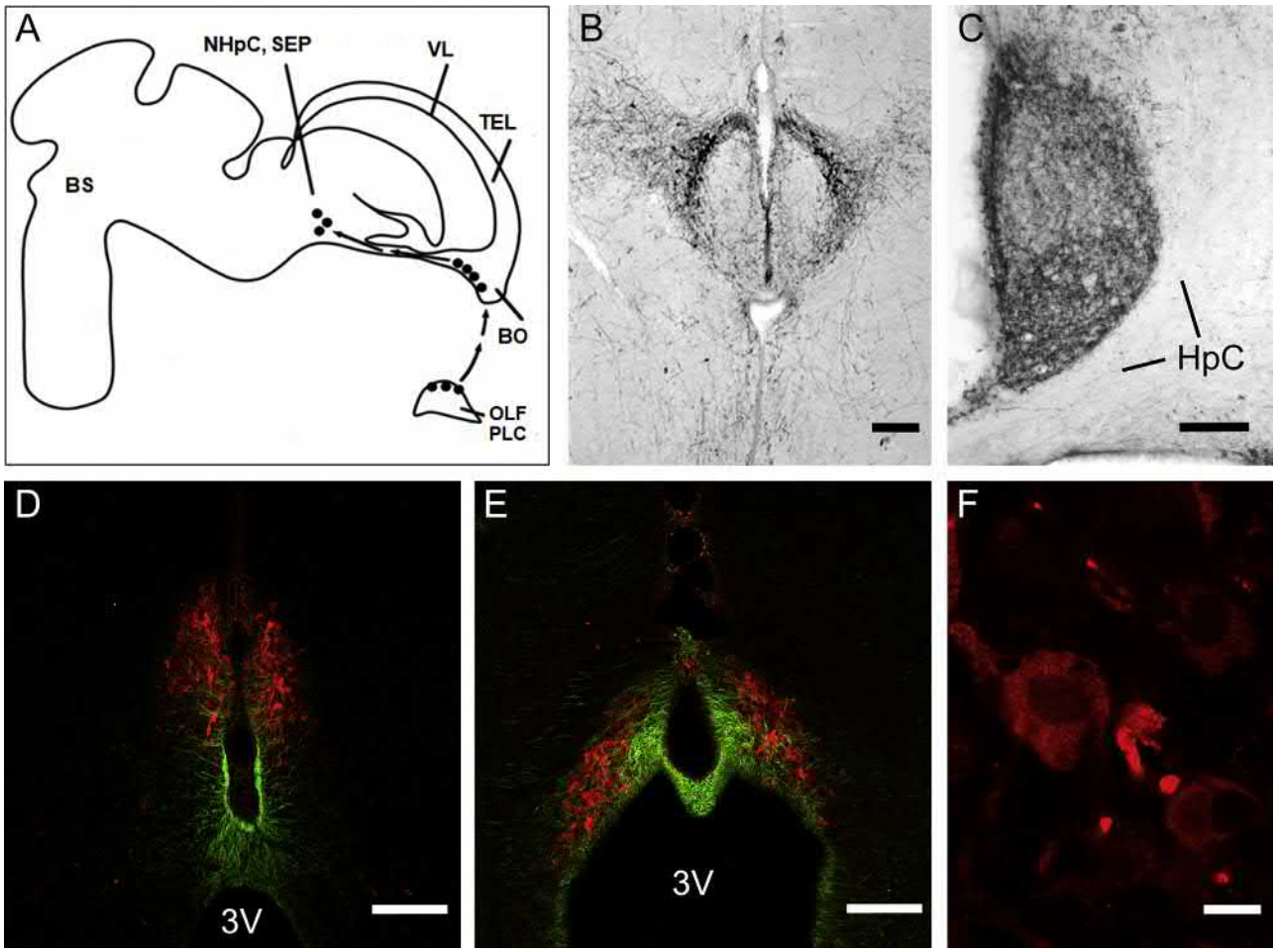

FIGURE 16.9 Neuroendocrine neurons in and around the nucleus of the hippocampal commissure. (A) GnRH-1 neurons originate outside the brain in the olfactory placode (OLF PLC) and migrate into the brain. (B) A septal area surrounding the nucleus of the hippocampal commissure (NHpC) receives a major, migrating group of GnRH-1 neurons. (C) Galanin fibers within the NHpC are surrounded by the (HpC). (D) and (E) show anterior and posterior images of the NHpC immunostained for corticotropin releasing hormone (red) and the avian vasotocin 1a receptor (V1aR, green). (F) High magnification image of CRH neurons within the NHpC. Scale bar for 16,9B = 300 μm, scale bars for 16.9C, D, and E = 100 μm, and 16,9F = 10 μm. Abbreviations: *BO*, olfactory bulb; *BS*, brainstem; *HpC*, hippocampal commissure; *SEP*, septum; *TEL*, telencephalon; *VL*, lateral ventricle; *3V*, third ventricle. *A and B from Kuenzel (2015).*

neurons reside in the septum, particularly around the periphery of the NHpC. We have proposed to name the region, the belt (b) of the NHpC (NHpCb, Figure 16.9B). The NHpC extends a significant rostral-caudal distance thereby residing within three divisions of the septum, the medial septum (SM), SHpS, and caudocentral septum (SCC). Moreover, the NHpC is located in a close apposition to four circumventricular organs (CVOs) making this nucleus an important hub for neuroendocrine communication between the septum and the rest of the brain via the cerebrospinal fluid.

What are CVOs? CVOs are found in the brain of all vertebrate classes. As the name implies, they occur adjacent to the ventricles of the brain in specific regions. Four CVOs are associated with the avian septum including the lateral septal organ (LSO), organum vasculosum of the lamina terminalis (OVLT), SSO, and choroid plexus (ChP). There are general characteristics that many CVOs possess including specialized ependymal cells, a vascular area that lacks a blood-brain barrier and cerebrospinal fluid-contacting neurons (Vigh, 1971). Due to their known neuroendocrine function for sustained and integrated activities of vital importance to the survival of a given vertebrate species (Weindl, 1973), four CVOs that border the avian septum will be briefly discussed, beginning with the LSO.

The avian LSO was named and shown located at the base of each lateral ventricle in chickens (Kuenzel and van Tienhoven, 1982) and later characterized as comprising two components, a lateral and medial part (Kuenzel and Blähser, 1994; Kuenzel et al., 1997). The medial LSO (LSOm) is located at the base of the lateral ventricle in the

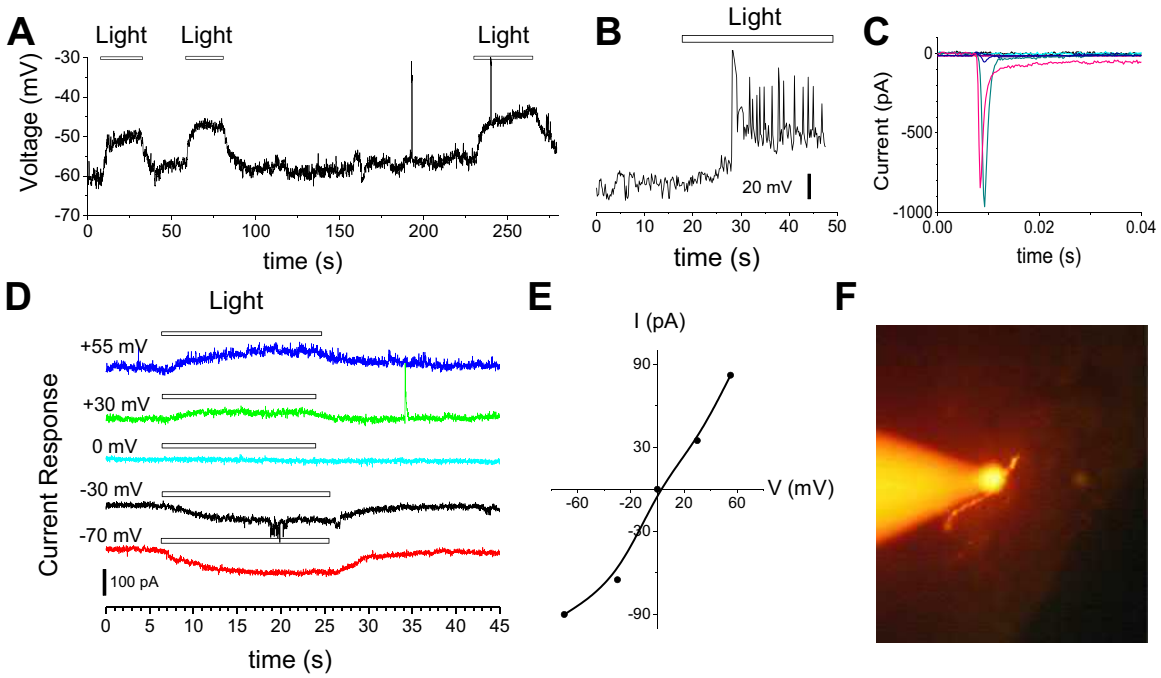

FIGURE 16.10 (A) Light-evoked responses from a neuron in the lateral septal organ, showing slowly rising subthreshold depolarization under current clamp. (B) Light-evoked response from another cell under current clamp, showing a light-evoked slow depolarization, which led to delayed suprathreshold spikes. (C) Voltage-gated Na currents (shown after leak subtraction) from the same cell as in B, in response to a series of depolarizing voltage steps of increasing amplitude from a holding potential of −70mV. (D). Light-evoked current responses recorded at various holding potentials under voltage clamp, showing a reversal potential near 0 mV. (E) Current:voltage (I−V) relation of light-evoked currents in (D). (F) Digital image of an Alexa Fluor 594-filled neuron near the ventricular surface of a septal slice under whole-cell patch showing a bipolar morphology. The intensity of full-field light stimulation was 0.04 nW/μm^2. *From Kuenzel et al. (2015).*

ventral portion of the lateral septum. It has cerebrospinal fluid-contacting neurons that contain and synthesize vasoactive intestinal peptide (VIP) as well as other neurochemical types, and specialized ependyma. The lateral component of LSO occupies a location at the base of the lateral ventricle in the st brain region and therefore is currently referred to as the st part of the LSO (LSOst, Figure 16.5D). The LSOst has layers of highly modified ependymal cells, VIP receptors, and lacks a complete blood-brain barrier (Kuenzel and Blähser, 1994; Kuenzel et al., 1997). VIP containing neurons in the avian (Silver et al., 1988; Wada et al., 2000) and reptilian (Foster et al., 1994; Foster and Soni, 1998) lateral septum have also been shown to contain opsin-like compounds suggesting that those neurons or others in that organ may serve as deep brain photoreceptors involved in monitoring seasonal time by sensing exposure to daylight. Our laboratory was the first to record currents from LSO neurons that responded to light using the patch-clamp technique. Results showed light-evoked responses from bipolar neurons in the LSOm displaying slowly rising subthreshold depolarization under current clamp (Kuenzel et al., 2015). When recorded under voltage clamp at various holding potentials, these cells responded to light with slowly developing current responses that reversed direction at approximately 0 mV (Figure 16.10D), suggesting that they were mediated by nonselective cation channels. The electrophysiological data, notably the slowness, 5 s in rise time (Figure 16.10A) following light stimulation, and most interestingly, its polarity, depolarization (Figures 16.10A and B) rather than the characteristic hyperpolarization found in rods and cones, and the cation-selective nature of the underlying ion channels all share a remarkable similarity with the intrinsically photosensitive (ip) retinal ganglion cells (RGCs) examined in the mammalian retina (Berson et al., 2002; Berson, 2003). The seminal data of Berson et al. (2002) have shown that the mammalian ipRGC is a primitive form of photoreceptor and has been proposed to use an invertebrate-like phototransduction cascade (Qiu et al., 2005). Data suggest that neurons in the LSO of chicks contain photoreceptors with similar electrophysiological responses to light as found in the mammalian ipRGC. Unknown is what photopigment is contained in the light responsive bipolar cells within the avian LSOm. Recent data have shown that dissected brain areas containing the LSOm show significantly increased gene expression of both opsin 4 (melanopsin) and opsin 5 (neuropsin). Birds were sampled at both three and seven days following exposure to long-day photostimulation. Data suggest that neurons within the dissected area contain one or both opsin-

type receptor neurons and display increased photopigment gene expression that persists through at least seven days following long-day photoperiods (Kang and Kuenzel, 2015). Notably, gonadal development in birds subjected to an increase in photoperiod was significantly attenuated by bilateral lesions directed to the LSO suggesting that this structure could be a functional site of deep brain photoreceptors (Rathinam and Kuenzel, 2005). In agreement with these findings, VIP within the septal region showed significant gene activation following photostimulation (Li and Kuenzel, 2008) and an opsin-containing neuron located in the avian lateral septum was shown at the light and electron microscopic level to innervate dendrites of a GnRH neuron (Saldanha et al., 2001). Nonetheless, all data to date have not provided direct evidence that the LSO contains a key group of deep brain photoreceptors.

The other three CVOs that contact the NHpC include two residing in the 3V, the OVLT, and SSO, homologous to the mammalian SFO, and ChP located primarily in the terminal region of the NHpC where the two lateral ventricles join the dorsal 3V. The avian OVLT first appears near the rostral wall of the 3V, termed the lamina terminalis where the POA begins. At this location, the OVLT is a highly vascular structure on both sides of the 3V. In rodents, the OVLT is restricted to the anterior, ventral preoptic/hypothalamic region, and it is found near the suprachiasmatic nucleus (Duvernoy and Risold, 2007). In contrast, the OVLT of birds is more extensive and comprises a prechiasmatic segment located between the anterior part of the optic chiasma and base of the brain. The vascular OVLT extends dorsally on both sides of the anterior region of the 3V, continues as a subcommissural segment and passes in front of and dorsal to the AC to form a precommissural and supracommissural segment, respectively (Dellmann, 1964; Mikami, 1976). The avian OVLT therefore occupies a strategic position between the anterior roof of the diencephalon and floor of the septum along midline. In mammals, GnRH neurons are found in the preoptic region adjacent to the OVLT, and GnRH fibers are found in and about the OVLT (Foster and Younglai, 1991; Silverman et al., 1994). In the chick, a terminal field of GnRH-1 neurons has been observed throughout the entire extent of the OVLT (shown in red in Fig. 5 of Kuenzel, 2018) and continues along midline to become another CVO, the SSO (shown in green in Fig. 5 of Kuenzel (2018) (Figure 16.9E). Anatomical data suggest a large terminal field of GnRH-1 neurons occurs along the midline floor of the septal region where GnRH-1 hormone can be secreted into the cerebrospinal fluid of the 3V and/or into the capillaries of the CVOs (Kuenzel, 2018). The final CVO associated with the NHpC is the ChP, an extensive capillary complex, which surrounds the caudal terminal end of the septum. Hence, the septal complex of GnRH-1 neurons has the capability of sending well-known projections to the median eminence above the anterior pituitary (APit), but also secreting GnRH-1 within the dorsal region of ventricular system into cerebrospinal fluid.

16.2.5.2.2 Septal-hypothalamic-pituitary-adrenal neuroendocrine system

The core of the NHpC contains CRH neurons (Figure 16.9D–F) and appears to be involved in the regulation of stress in birds (Nagarajan et al., 2014, 2017b; Kadhim et al., 2019). The major, evolutionally conserved group of CRH neurons regulating stress is localized in the hypothalamic PVN of birds and mammals. It is of particular interest to understand how these two groups of CRH neurons contribute to the avian stress response. Recent work provided some insights into the time course of neuronal activation in the NHpC and PVN following exposure to a stressor, food deprivation. It appeared that in response to food deprivation the earliest increase in CRH gene expression occurred in the NHpC followed by an increase in CRH gene expression in the PVN (Nagarajan et al., 2017b). Another study using the same stressor showed that both the NHpC and PVN displayed an increase in CRH gene expression at the first sampling time, 2 h (hr.) after stress, however, the rate of increase in the NHpC was 70% from non-stressed controls, while in the PVN the CRH gene expression showed a modest 33% increase. Importantly, the expression of the CRH gene in the NHpC matched the output of the pituitary stress hormone POMC. Specifically, both the CRH gene expression in the NHpC and the expression of the POMC gene in the APit peaked at 2 h following exposure to stress. Moreover, the levels of CRH mRNA in the NHpC and POMC mRNA in the APit returned to control values at 8 h after beginning of food deprivation. In contrast, the CRH gene expression in the PVN showed a slow but steady increase that peaked at 8 h, maintaining the stress response (Kadhim et al., 2019). Results suggested that CRH mRNA produced by the NHpC was a significant contributor, and appeared to be the earliest one that influenced APit production of POMC resulting in a significant increase of the stress hormone CORT (Kadhim et al., 2019).

Food deprivation used in the previous, cited studies is a gradual stressor that increases in time due to the intensity of hunger. Immobilization or restraint is another common experimental model to study stress-related mechanisms. In contrast to food deprivation, immobilization stress is immediately perceived by a bird that is restricted to move and spread its wings. Therefore a different stressor of this type could test whether an early response of CRH neurons in the NHpC was stressor specific or a general avian response to stress. Immobilization induced a significant increase in CRH gene expression in the NHpC and PVN at 15 min, the first sampling point. Of interest, the pattern of

response was the same as in the study with food deprivation. A more than 100% increase in gene expression by CRH mRNA transcripts in the NHpC occurred compared to a 30% increase in gene expression of CRH mRNA transcripts within the PVN at the 15 min sampling point (Kadhim et al., 2021). Similarly, the pattern of APit POMC gene expression also peaked at the 15 min sampling point matching closely the previous experiment using food deprivation stress.

To determine more directly whether the NHpC and its CRH neurons are truly early responders to stress and contribute to the traditional hypothalamic HPA axis, an experiment was designed to surgically implant an electrode into the septum using a stereotaxic instrument to target the NHpC and produce a small electrolytic lesion to down regulate the structure. A group with lesions directed to the NHpC and control birds were subjected to food deprivation stress and sampled at the 2 h sampling point previously shown to be the peak response of the NHpC from that stressor. Results showed a significant reduction in CRH gene expression in the NHpC, significant reduction in APit POMC and plasma CORT (Kidd et al., 2019). Results suggest that the NHpC appears to function in the traditional HPA axis of poultry and appears to be an early responder to stressors. Perhaps a comparable neural structure exits in other vertebrate species as well.

16.2.5.2.3 Other functions related to structures within the septum

The septum has major connections with the hippocampus, amygdala, diencephalon, and brainstem. Functions attributed to this brain subpallial region include ingestive, defensive, and reproductive behaviors that are fundamental to sustainability of vertebrate species (Swanson, 2000). With respect to inputs from the hippocampus, food caching has been associated with the septum. Specifically, black-capped chickadees are known to display food-storing behavior, a seasonally related activity. A significant increase in septal as well as hippocampal volume occurred during the time of year storing behavior was at its peak (Shiflett et al., 2002). Another seasonal activity displayed by birds is reproductive behavior that usually occurs in the spring when day length increases. The septum plays a major role in courtship and aggressive behavior in a variety of avian species (Ramirez et al., 1988; Goodson, 1998; Goodson and Adkins-Regan, 1999; Panzica et al., 2001). Lesions of the septal region produced a facilitation of male courtship behavior and vocalization in ring doves (Cooper and Erickson, 1976) and facilitated both overt aggression and the number of simple, multipurpose songs in territorial field sparrows (Goodson et al., 1999). When brain sections are immunostained for AVT, the lateral septum of male Japanese quail when compared with females shows significantly greater immunostaining of AVT fibers (Panzica et al., 2001). Similarly, AVT and galanin fibers in male chickens (Jurkevich et al., 1997; Klein et al., 2006) display increased density within the lateral septum. During both courtship and mating behavior between roosters and hens as well as agonistic behavior between two males, significantly greater amounts of Fos protein produced by the immediate early gene *c-fos* occurred in the lateral septum of males (Xie et al., 2010). Increased expression of the gene *c-fos* in neurons is a marker of activation of those cells.

Hodological studies in birds involving the septum have shown that not only is there a descending neuroendocrine system affecting hypothalamic function but also ascending pathways from key diencephalic structures back to the septum suggesting that the downstream motor pathways have a number of feedback loops (Berk and Butler, 1981; Berk and Finkelstein, 1983; Atoji and Wild, 2004; Montagnese et al., 2004, 2008). Several hypothalamic structures with direct connections to the septum have been shown in previous studies to be involved with food intake and the regulation of the ANS. The reciprocal connections of the septum to hypothalamic structures as well as the presence of the SSO at the floor of the septum shown to contain angiotensin II receptors, provides evidence that the septum is involved in the regulation of food and water intake, respectively. Chicks subjected to osmotic stress showed increased avian V1aR, angiotensin II type 1 receptor, and transient receptor potential vanilloid receptor 1 (TRPV1) mRNA levels in the SSO/SFO (Aman et al., 2016) located in the ventral portion of the NHpC. The avian V1aR is found in abundance in the OVLT and SSO as well as other CVOs (Selvam et al., 2015). When the Manning compound (SR-49,059), a specific blocker of the avian V1aR is applied intracerebroventricularly prior to the injection of NPY, food intake was significantly increased compared to a treatment group with NPY alone. Results showed that the V1aR functions in appetite regulation by mediating an anorexigenic effect (Kuenzel et al., 2016). There exists structural and functional evidence that the septum possesses a descending neuroendocrine and integration system involved with basic social and ingestive behaviors and functions.

16.2.6 Preoptic area

16.2.6.1 Structures

There was a long-standing tradition among neuroanatomists of attributing the POA to the hypothalamus. Introduction of genetic molecular markers and developmental analysis of subpallial *Nkx-2.1* and *Shh* gene expression patterns demonstrated striking similarity between the POA and the adjacent subpallial telencephalic areas of the

chicken, zebra finch, and mouse suggesting that the POA has to be considered as a part of the subpallium (Rubenstein et al., 1998; Puelles et al., 2007; Abellan and Medina, 2009; Shimogori et al., 2010; Medina and Abellan, 2012; Vicario et al., 2014, 2017; Puelles and Rubenstein, 2015). In the developing mouse, a narrow dorsoventral belt of Shh-expressing cells forms a clear molecular boundary between the POA and the neighboring paraventricular area of the hypothalamus (Shimogori et al., 2010; Puelles and Rubenstein, 2015). Additional analysis of gene expression patterns revealed two subdivision of the POA—the commissural preoptic area (POC) and the basal preoptic are (POB). In birds, the POC is characterized by strong expression of *Lhx7/8* and *Shh* genes and lack of the pro-*ENK* gene expression, while the POB shows strong expression of the pro-*ENK* and *Shh* genes and lacks the *Lhx7/8* expression in most of its cells (Abellan and Medina, 2009; Vicario et al., 2017). In the mouse and birds, the POC bends around the ventral surface of the AC and includes at least one nucleus, the median preoptic nucleus (MnPO, Medina and Abellan, 2012); however, in birds the boundaries and function/s of this nucleus remain unclear. The POB appears to occupy the ventral portion of the POA and includes the POM and probably some other neural cell groups that have not been defined. Due to insufficient data and lack of consensus regarding localization and functions of neuronal groups within POA subdivisions of the avian brain, only the POM will be discussed here.

The POM is currently the most prominent structure within the POC of birds. Neurons in the POM produce aromatase, a testosterone-converting enzyme, and therefore aromatase immunoreactivity serves as a neurochemical marker of this nucleus (Figure 16.11) (Balthazart et al., 1990; Riters et al., 2000; Xie et al., 2011). Japanese quail males have larger volumes of the POM than females, and this sex difference is testosterone-dependent. Reduction of testosterone levels by castration or by transitioning birds to short daylength results in gonadal regression and a decrease in POM volume in males (Balthazart and Ball, 2007). In male starlings, the size of the POM is largest during the spring breeding season when testosterone concentration peaks and shows a significant reduction during the following nonbreading period (Riters et al., 2000).

The POM of quail receives projections from a component of the medial extended amygdala, namely the BSTM, PVN, and supraoptic nucleus. Specifically, sexually dimorphic vasotocinergic innervation of the POM in males originates from the BSTM (Absil et al., 2002a). More recent neuroanatomical studies in male quail have identified a presumptive polysynaptic pathway from the POM down to the cloacal muscle involved in copulatory behavior. The pathway includes a projection from the POM to the intercollicular complex (ICo; Wild and Balthazart, 2013). Within the ICo was found a distinct, elongated nucleus, the

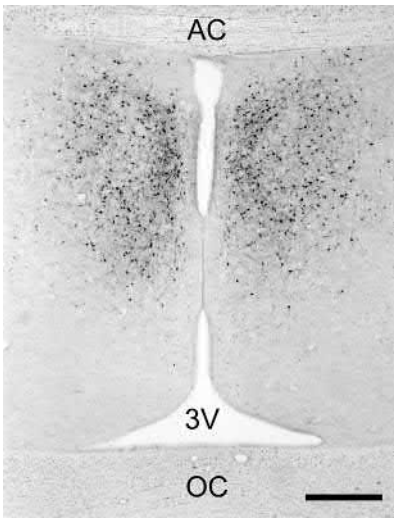

FIGURE 16.11 Coronal brain section showing the medial preoptic nucleus (POM) immunoreactive for aromatase located directly ventral to the AC. Abbreviations: *AC*, anterior commissure; *OC*, optic chiasma; *3V*, third ventricle. Scale Bar = 500 μm.

dorsomedial nucleus (DM). The DM was shown to project to the caudal brainstem nucleus called the nucleus retroambigualis (RAm; Wild et al., 1997; Wild and Balthazart, 2013). Anterograde tracing from the RAm showed a continuous projection from that caudal brainstem nucleus through the entire length of the spinal cord to the sacral region of spinal cord. The motor neurons in the ventral horn at that spinal cord level innervate the large cloacal sphincter muscle (mSC; Wild and Balthazart, 2013).

16.2.6.2 Functions

The POM is a member of the social behavior network and a pathway from that structure to the lumbar region of the ANS has been mapped showing its involvement in consummatory, sexual behavior.

A social behavior network was proposed to exist in mammals that functioned to regulate male reproductive behavior (Newman, 1999). Birds likewise were shown to have a neuroendocrine social behavior network (Goodson, 2005). The social behavior network comprises six nodes: (1) POA, (2) lateral septum (SL), (3) extended MeA and medial bed nucleus of stria terminalis BSTM, (4) anterior hypothalamus (AHy), (5) ventromedial hypothalamus (VMN), and (6) midbrain [periaqueductal gray (PAG), also known as central gray (GCt)]. Each node binds sex steroid hormones and has been implicated in control of social behavior, particularly appetitive/consummatory reproductive and aggressive behavior (Newman, 1999; Goodson, 2005). Interestingly, using FOS ir (immediate, early gene data), each behavioral context is associated with a distinct *pattern* of activation across nodes (Goodson, 2005). The POA is more responsive in males, particularly the POM and

shows differentially regulated subregions of the POM for appetitive and consummatory sexual behavior in Japanese quail (Balthazart et al., 1998a). The POM was found to be sexually dimorphic (Viglietti-Panzica et al., 1986; Adkins-Regin and Watson, 1990). As mentioned previously under subheading (C. Extended Amygdaloid Complex, MEA, 2. Functions), the MeA projects to the BSTM complex, and the BSTM has been shown to be sexually dimorphic, larger in males, steroid-responsive and affects copulatory behavior in birds (Kiss et al., 1987; Voorhuis et al., 1988; Panzica et al., 1998; Viglietti-Panzica et al., 1992; Aste et al., 1998; Jurkevich et al., 1999). The rooster ventromedial BSTM functions in appetitive sexual behavior (Xie et al., 2010, 2011). Importantly, vasotocin neurons in the BSTM project to the POM (Absil et al., 2002b).

The avian POM is one of the largest and best-documented group of neurons expressing aromatase (Figure 16.11). Estrogen synthesis by the enzyme aromatase within the POM has been known for some time to activate male sexual behavior (Panzica et al., 1996; Balthazart et al., 2004) and interestingly, rapid changes in aromatase within the POM have been documented within minutes following a sexual interaction with a female (de Bournonville et al., 2013).

Using FOS-immunoreactivity (FOS-ir) as an indicator on neuronal activation, Xie et al. (2010) have observed a prominent increase of FOS-ir cell number in the POM of chicken males following copulation with a female. Curiously, a similar increase in FOS-ir cell number was observed in the POM of males that interacted with another male. These data confirmed previous observations regarding a key role of the POM in controlling male copulatory behavior in many vertebrate species (Crews, 2005; Balthazart and Ball, 2007), and also extended the function of POM to the regulation of male aggression. Several previous studies revealed differential FOS expression in the avian rostral and caudal POM following appetitive (courtship) or consummatory (copulation) sexual behavior (Riters et al., 2004; Balthazart and Ball, 2007). The caudal POM in quail sends sexually dimorphic descending projections to the midbrain PAG forming a pathway controlling male copulatory reflexes (Absil et al., 2002b). It could explain the induction of FOS expression in the caudal POM following copulation observed in the chicken. In contrast to the well-documented function of POM in sexual behavior, the role of this structure in agonistic behavior of avian males has received less attention (Barfield, 1971; Schlinger and Callard, 1990). An induction of IEGs in the POM after male−male interactions was observed in songbirds during the breeding season (Goodson et al., 2005). The latter studies support observations showing an increase in FOS expression in the POM following intermale interactions and suggest that the POM may play a more complex role in social encounters than just controlling consummatory copulation.

16.3 Components of the autonomic nervous system

The avian ANS, characteristic of all vertebrate systems, comprises two basic arms: (1) the sympathetic nervous system (SNS) and (2) parasympathetic nervous systems (PNS). Structural components of the SNS and PNS along with targets of their projections are schematically presented (Figure 16.12). The following short review focuses on the main structures of the ANS and a few key central neuronal structures that serve as components of the central nervous system providing connectivity from subpallial structures to the ANS for its continuous functional regulation. Overall, the ANS is responsible for motor functions and secretions that occur automatically on a daily, seasonal, and annual basis. It involves the integration of sensory information such that smooth muscle, cardiac muscle, and secretory cells located in visceral organs provide the appropriate output to maintain homeostasis of bodily functions such as heart and lungs to regulate blood pressure and respiratory rate thereby affecting osmotic and pH balance, body temperature (particularly in homoiotherms), gastrointestinal movements, reproductive processes, circadian rhythms, and other essential circannual rhythmic functions that are continuously regulated. To balance the regulatory output, two antagonistic systems are in place—the sympathetic and parasympathetic arms of the ANS. More detailed information is available in a number of reviews (Akester, 1979; Bubien-Waluszewska, 1981; Kuenzel, 2000; Yasuda, 2002; Nilsson, 2011).

16.3.1 Sympathetic nervous system

Similar to mammals, a chain of ganglia exists on both sides of the vertebral column in the thoracolumbar region of the spinal cord of birds (Figure 16.12). A marked difference, however, exists in avian species. Most of the vertebrae are fused, due to the function of flight requiring a stable, solid structure to protect the spinal cord during rapid initiation of flight and particularly during landing. Due to the extensive fusion of bones, it requires considerable skills to dissect the entire spinal cord, spinal nerves, and ganglia associated with each segment of the spinal cord. More than one system of numbering the spinal nerves and ganglia exists due to the variable number of vertebrae occurring among various avian species. Additionally, two different methods have been developed which either number the spinal segments and nerves sequentially beginning with the cervical region and ending with the last coccygeal vertebra (Dubbeldam, 1993; Yasuda, 2002) or number the vertebrae, spinal segments, and their associated spinal nerves, dorsal root

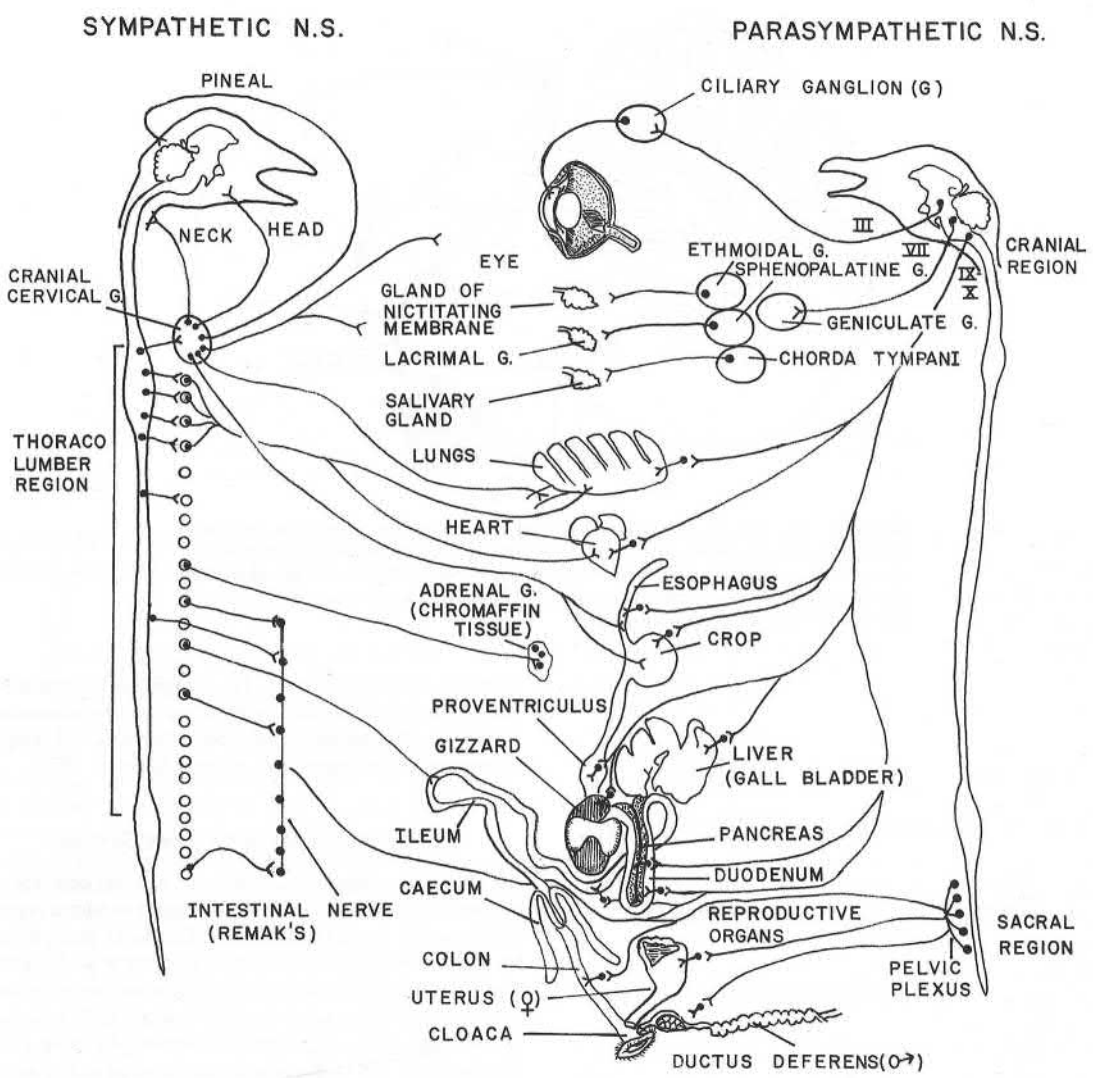

FIGURE 16.12 The motor component of the avian autonomic nervous system (ANS). The sympathetic and parasympathetic arms of the ANS are shown on the left and right sides, respectively.

ganglia, and the chain of autonomic ganglia to a regional group of vertebrae (Nickel et al., 1977; Landmesser, 1978). The usual, traditional regional terms cervical, thoracic, lumbar, and sacral (or synsacral and coccygeal) nerves (and ganglia) have been utilized, but the transitional zones may be problematic to ascribe a ganglion or spinal nerve to the appropriate region when the synsacral bone is dissected to reveal the caudal spinal cord (Dubbeldam, 1993). Therefore, documentation with images is most helpful for each species, particularly when referencing a specific segment, ganglion, or spinal nerve in a study.

Within each segment of the thoracolumbar region of the spinal cord is a nucleus that identifies the central nervous system origin of the SNS. The intermediomedial nucleus, previously termed the column of Terni, contains the preganglionic motor neurons of the SNS. The nucleus is located at midline of a cross-section of spinal cord, directly dorsal to the central canal (see Figure 16.5 in Kuenzel, 2000). The axonal processes of the neurons move laterally a short distance and innervate one of the autonomic ganglia. A major neurotransmitter released is ACh that binds to nicotinic receptors present on postganglionic neurons. The long postganglionic axons project to specific visceral organs and release primarily the neurotransmitter norepinephrine which binds to subtypes of alpha or beta adrenergic receptors.

An autonomic, ganglionated nerve unique to birds is Remak's nerve (Figure 16.12). It appears at the end of the duodenum, running parallel to the intestinal tract and ending at the cloaca. Remak's nerve plays a role in the regulation of gut motility (Hodgkiss, 1984a,b). Microinjections of a neurotracer into individual neurons within

ganglia of Remak's nerve in the chicken revealed four distinct morphological types of neurons. The function of each neuronal type remains unknown (Lunam and Smith, 1996). Previous research into gastrointestinal motility by the late Dr. Gary Duke's laboratory discovered that sections of the avian gastrointestinal tract showed clear antiperistalsis or reversed peristalsis, that is smooth muscle movement resulting in a sequential movement of food or "owl pellets" in an adoral direction (Duke et al., 1977; Lai and Duke, 1978). His research and videos clearly show retro- and/or antiperistalsis which is a characteristic of avian species. The research from the lab of Hodgkiss does not cite any of Duke's publications, where Hodgkiss has suggested that Remak's nerve may function in gut antiperistalsis (Hodgkiss, 1984a,b). It is a pity their two labs did not interact as this area appears to be a fertile area of investigation for determining the mechanism of antiperistalsis in birds.

16.3.2 Parasympathetic nervous system

The PNS has a system divided into two sets of preganglionic neurons, one originating in the brain and a second set located in the sacral region of the spinal cord (Figure 16.12). Preganglionic neurons in the brain are found in motor nuclei of the oculomotor (III), facial (VII), glossopharyngeal (IX), and vagus (X) nerves (Akester, 1979; Dubbeldam, 1993). The cranial nerve that has a major impact on a diverse number of visceral organs regarding parasympathetic regulation of function is the vagus. Those in the sacral region have processes that form a pelvic plexus. In contrast to the SNS, the preganglionic neurons of the PNS project long processes to specific ganglia located within or adjacent to visceral organs or tissues regulated by the preganglionic neurons. Similar to the SNS, the preganglionic neurons secrete the neurotransmitter ACh. Nicotinic receptors on postganglionic neurons bind ACh and, in turn, the major neurotransmitter released from postganglionic neurons is ACh which binds to muscarinic receptors found within the targeted visceral organ.

16.4 Integration of the subpallium and ANS in complex neural circuits in birds: two examples involving vasoactive intestinal polypeptide as a regulator

16.4.1 The social behavior network

Newman (1999) proposed that three subpallial structures, the POA, the lateral septum (LS), and the medial extended amygdala (MeA and BSTM); along with the anterior hypothalamus, ventromedial hypothalamic area, and the periaqueductal gray of the midbrain are implicated in the control of various forms of social behavior in mammals. These six regions or "nodes" were grouped together based on their properties to be involved in modulation of several social behaviors, their interconnectivity, and their sensitivity to steroid hormones. It was suggested that social behaviors emerge from complex, dynamic temporary patterns of activity generated by all components of the SBN. Different social contexts result in unique patterns of activation producing different behavioral outcomes. A similar six-node SBN was shown to occur neuroanatomically and functionally in fish and birds (Goodson, 2005), and subsequent studies suggested an evolutionally conserved nature of the SBN (O'Connell and Hofmann, 2012). Recent findings revealed vasoactive intestinal polypeptide (VIP) and VIP receptors throughout the SNB of songbirds (Kingsbury and Wilson, 2016). Functionally, VIP has been shown to be the major neuroendocrine releaser of prolactin from the APit in birds (Macnamee et al., 1986; Opel and Proudman, 1988; Mauro et al., 1989). In ring doves, VIP initiated parental feeding (Buntin et al., 1991) and initiation of egg incubation in bantam hens (Sharp et al., 1989) and turkeys (El Halawani et al., 1996). Utilizing a number of songbird species, VIP neural "hotspots" were described in the SBN where VIP signaling appears to contribute to regulating a given social behavior. VIP and its receptors within the LS and BSTM appeared to play important roles in social affiliation and gregariousness (Kingsbury and Wilson, 2016). Interestingly, the study examined two species, field sparrow (*Spizella pusilla)* and dark-eyed junco (*Junco hyemalis*) showing a territorial phenotype during the breeding season and a flocking phenotype in winter compared to two species not displaying winter flocking. Interestingly, more robust VIP ir of the BSTM was reported in the two species that flock during the winter compared to the two not displaying seasonal wintering flocking. Results suggested that greater VIP-ir fiber density is associated with a winter flocking phenotype (Kingsbury and Wilson, 2016). Based upon their results in variation of VIP fiber and receptor density in three subpallial structures—LS, BSTM, and MeA, it was proposed that species differences in grouping behavior is modulated by VIP signaling throughout the SNB and the three nodes are regarded as hotspots for the regulation of avian affiliative behavior.

In contrast, VIP signaling in the anterior hypothalamus (AHy) and caudal septum, specifically the caudocentral septum (CcS) mediated aggression. Infusions of VIP targeting the caudal septum significantly increased aggressive behavior (Goodson, 1998). The avian septum receives projections from the AHy (Atoji and Wild, 2004), a hypothalamic area in mammals that mediates agonistic behavior (Nelson and Trainor, 2007). The avian AHy has been shown to contain VIP neurons and knockdown of the

VIP peptide using antisense oligonucleotides significantly decreased nest defense aggressive behavior in zebra finches (Goodson et al., 2012).

16.4.2 Poikilostasis or shifts in homeostasis: an hypothesis involving the visceral forebrain system

16.4.2.1 Regulation of annual cycles of avian species

Essentially all previously stated functions of the subpallium and ANS—regulation of bodily movement, reward, reproductive, social and related behaviors, memory, neuroendocrine and autonomic function—are developed to achieve one outcome, homeostasis, not only on a daily basis but also throughout the year to regulate the entire annual cycle of vertebrates. An hypothesis was introduced nearly 30 years ago that appears relevant to both wild and domestic avian species (Kuenzel and Blähser, 1993). It was based upon the neuropeptide distribution and gene expression of VIP mapped throughout the chick brain (Kuenzel and Blähser, 1994; Kuenzel et al., 1997). The unique VIP distribution identified an avian CVO (the LSO), subpallial structures, and central components of the ANS, a majority of which were previously grouped together and proposed to function as a visceral forebrain system in mammals (van der Kooy et al., 1984). The mammalian visceral forebrain system comprised the medial and lateral prefrontal cortex, paraventricular, arcuate and posterolateral hypothalamic nuclei, BSTL, central nucleus of the amygdalal, and nucleus tractus solitarius (NTs). It was hypothesized that the system influenced autonomic functions and could override brainstem homeostatic mechanisms during periods of stress or emotional activity (van der Kooy et al., 1984). A key structure within the visceral forebrain system was the NTs. The NTs immunostains intensely with an antibody to VIP and is a key brainstem structure connected to the parasympathetic arm of the ANS. Some birds display dramatic physiological and behavioral changes throughout their annual cycle, therefore the term poikilostasis, meaning shifts in homeostasis (Kuenzel et al., 1997; Kuenzel, 2000) could explain the remarkable seasonal behaviors displayed by migratory birds. In other words, poikilostasis means that the set point for homeostatsis or the balance between the SNS and PNS does not stay constant, rather the set point shifts either in favor of the PNS or SNS dependent upon the season throughout the year.

Migratory birds, particularly those in temperate zones that migrate north each spring generally forage in flocks prior to migration and need to shift to an anabolic state where rapid body weight gains are essential in order to deposit the necessary fat reserves to make the demanding migratory journey to the breeding grounds. Upon arrival, there occurs a shift to a catabolic state as birds enter a new phase of their annual cycle. Birds become territorial and aggressive in order to defend their selected space, attract and find a mate, and build a nest during the breeding season. The physiological and behavioral processes required for successful reproduction, incubation behavior, and the rearing of young are metabolically demanding. Thereafter birds undergo a major molt that continues their catabolic state resulting in the utilization of considerable lipid reserves. A shift to an anabolic state then follows, resulting in increased food intake to prepare birds for a rigorous return migratory flight to the wintering grounds. Due to the marked changes in metabolic states that birds undergo coupled with short time periods for each particular phase of their annual cycles, birds would unlikely be able to complete their seasonal life history requirements if set points for energy homeostasis were fixed throughout the year. Hence shifts in homeostasis (poikilostasis) would allow the PNS to dominate when anabolic processes were critical for rapid body weight gains and conversely, a shift to greater activity of the sympathetic arm of the ANS could occur when energy demands were high and sustained. The hypothesis of poikilostasis suggests that there exists in birds, and perhaps other vertebrate species, the capacity for dynamic shifts in the balance or set points of the ANS in order to successfully complete their annual cycles. A key neuropeptide, VIP and its receptors appear to play a role in changing the behavior, neuroendocrine regulation, and balance of the ANS to shift the birds from one phase to the sequential one in their annual cycle. The recent molecular models involving neural pathways, energy sensors, and the ability to integrate nutrient and hormonal signaling at the level of the hypothalamus may provide additional key markers for testing the validity of this hypothesis by focusing upon signals and processes associated with shifts in the balance of the ANS.

16.4.2.2 Some current metabolic and behavioral issues with breeding stock of broilers and turkeys

With the continued use of genetic selection programs in broilers as well as turkeys for increased growth rate and better feed conversion, the result has been a modern bird showing a high efficiency for the conversion of feed to a quality meat product. A cost, however, for managers of broiler and turkey breeders has been a feed restriction program that requires careful monitoring throughout the life span of birds in order to insure that parent stock remain healthy and continue to produce an acceptable rate of fertilized eggs (Richards et al., 2010). Data over many years have shown that broilers compared to layers display increased food intake, less overall activity, and a lower

basal metabolic rate. Data suggest an imbalance of the ANS, pointing to a physiological system with high parasympathetic and low sympathetic activity in current meat-type birds. It would be worthwhile to examine VIP and its receptors in combination with the advances in the understanding of the neural regulation of food intake, metabolic signals, energy homeostasis, and genes involved (Richards and Proszkowiec-Weglarz, 2007; Byerly et al., 2009; Yuan et al., 2009). The time may be appropriate to examine gene expression of VIP, its receptors, and related genes affecting subpallial function and ANS in order to develop an objective PNS/SNS ratio indicative of an effective balance between acceptable growth rate, lifetime welfare, and sustained reproductive output for birds selected as parent stock.

16.5 Summary and conclusions

Neural structures that comprise six distinct regions in the subpallium of the avian forebrain (Figure 16.1) as well as the basic components of the ANS were reviewed. Noteworthy is the evidence that the regions are evolutionarily conserved among vertebrates. Therefore data obtained in mammalian and other vertebrate classes can be cautiously utilized to help understand the function of systems that have not been examined extensively in birds. Subpallial structures are important as several have been shown to have connectivity to pallial (cortical-like) brain regions as well as to key hypothalamic and brainstem structures that are part of the cognitive, neuroendocrine, and ANSs. Importantly, the latter two systems involve the production of hormones that can modulate the physiology and behavior of organisms for hours, days, and even weeks indicating processes regulating seasonal activities of birds.

Some of the functions associated with subpallial and ANS components include the neural regulation of feeding, reproductive, voluntary movement, affiliative, agonistic, and stress behaviors. Additional functions associated with the subpallium and ANS include reward, memory, and learning. It is hoped that the review will stimulate further reading and expand discussion of structural and functional aspects of the avian subpallium, as well as help suggest future research that can advance the understanding of the avian central nervous system, its neural pathways, and functions among various wild and domestic avian species.

Acknowledgments

Supported in part by NSF Grant #IOS-0842937, a grant from the Arkansas Biosciences Institute (ABI), the Arkansas Division of Agriculture, and USDA/NIFA Sustainable Agricultural Systems #2019-69012-29905. We wish to thank John Wray for completing Figures 16.6 and 16.7 in the chapter.

References

Abellán, A., Medina, L., 2008. Expression of cLhx6 and cLhx7/8 suggests a pallido-pedunculo-preoptic origin for the lateral and medial parts of the avian bed nucleus of the stria terminalis. Brain Res. Bull. 75, 299–304.

Abellán, A., Medina, L., 2009. Subdivisions and derivatives of the chicken subpallium based on expression of LIM regulatory genes and markers of neuron subpopulations during development. J. Comp. Neurol. 515, 465–501.

Abellán, A., Vernier, B., Rétaux, S., Medina, L., 2010. Similarities and differences in the forebrain expression of Lhx1 and Lhx5 between chicken and mouse: insights for understanding telencephalic development and evolution. J. Comp. Neurol. 518, 3512–3528.

Absil, P., Braquenier, J.B., Balthazart, J., Ball, G.F., 2002a. Effects of lesions of nucleus taeniae on appetitive and consummatory aspects of male sexual behavior in Japanese quail. Brain Behav. Evol. 60, 13–35.

Absil, P., Papello, M., Viglietti-Panzica, C., Balthazart, J., Panzica, G.C., 2002b. The medial preoptic nucleus receives vasotocinergic inputs in male quail: a tract-tracing and immunocytochemical study. J. Chem. Neuroanat. 24, 27–39.

Adkins-Regan, E., Watson, J.T., 1990. Sexual dimorphism in the avian brain is not limited to the song system of songbirds: a morphometric analysis of the brain of the quail (*Coturnix japonica*). Brain Res. 514, 320–326.

Akester, A.R., 1979. The autonomic nervous system. In: King, A.S., McLelland, J. (Eds.), Form and Function in Birds, vol. 1. Academic Press, London, pp. 381–441.

Albin, R.L., Young, A.B., Penney, J.B., 1989. The functional anatomy of basal ganglia disorders. Trends Neurosci. 12, 366–375.

Alheid, G.F., Heimer, L., 1988. New perspectives in basal forebrain organization of special relevance for neuropsychiatric disorders: the striatopallidal, amygdaloid, and corticopetal components of substantia innominata. Neuroscience 27, 1–39.

Alheid, G.F., Beltramino, C., Braun, A., Miselis, R.R., Francois, C., de Olmos, J.S., 1994. Transition areas of the striatopallidal system with the extended amygdala in the rat and primate: observations from histochemistry and experiments with mono- and trans-synaptic tracers. In: Percheron, G., McKenzie, J.S., Feger, J. (Eds.), The Basal Ganglia IV. New Ideas and Data on Structure and Function, Advances in Behavioral Biology, vol. 41. Plenum Press, NY, pp. 95–107.

Alheid, G.F., de Olmos, J.S., Beltramino, C.A., 1995. Amygdala and extended amygdala. In: Paxinos, G. (Ed.), The Rat Nervous System. Academic Press, San Diego, pp. 495–578.

Aman, N.A., Nagarajan, G., Kang, S.W., Hancock, M., Kuenzel, W.J., 2016. Differential responses of the vasotocin 1a receptor (V1aR) and osmoreceptors to immobilization and osmotic stress in sensory circumventricular organs of the chicken (*Gallus gallus*) brain. Brain Res. 1649, 67–78.

Anderson, K.D., Reiner, A., 1990. Extensive co-occurrence of substance P and dynorphin in striatal projection neurons: an evolutionarily conserved feature of basal ganglia organization. J. Comp. Neurol. 295, 339–369.

Anderson, K.D., Reiner, A., 1991. Striatonigral projection neurons: a retrograde labeling study of the percentages that contain substance P or enkephalin in pigeons. J. Comp. Neurol. 303, 658–673.

Arends, J.J., Wild, J.M., Zeigler, H.P., 1988. Projections of the nucleus of the tractus solitarius in the pigeon (*Columba livia*). J. Comp. Neurol. 278, 405–429.

Arnold, A.P., Nottebohm, F., Pfaff, D.W., 1976. Hormone concentrating cells in vocal control and other areas of the brain of the zebra finch (*Poephila guttata*). J. Comp. Neurol. 165, 487–511.

Aste, N., Balthazart, J., Absil, P., Grossmann, R., Mülhbauer, E., Viglietti-Panzica, C., Panzica, G.C., 1998. Anatomical and neurochemical definition of the nucleus of the stria terminalis in Japanese quail (*Coturnix japonica*). J. Comp. Neurol. 396, 141–157.

Atallah, H.E., McCool, A.D., Howe, M.W., Graybiel, A.M., 2014. Neurons in the ventral striatum exhibit cell-type-specific representations of outcome during learning. Neuron 82, 1145–1156.

Atoji, Y., Saito, S., Wild, J.M., 2006. Fiber connections of the compact division of the posterior pallial amygdala and lateral part of the bed nucleus of the stria terminalis in the pigeon (*Columba livia*). J. Comp. Neurol. 499, 161–182.

Atoji, Y., Shibata, N., Yamamoto, Y., Suzuki, Y., 1996. Distribution of neurotensin-containing neurons in the central nervous system of the pigeon and the chicken. J. Comp. Neurol. 375, 187–211.

Atoji, Y., Wild, J.M., 2004. Fiber connections of the hippocampal formation and septum and subdivisions of the hippocampal formation in the pigeon as revealed by tract tracing and kainic acid lesions. J. Comp. Neurol. 475, 426–461.

Atoji, Y., Wild, J.M., 2006. Anatomy of the hippocampal formation. Rev. Neurosci. 17, 3–15.

Atoji, Y., Wild, J.M., Yamamoto, Y., Suzuki, Y., 2002. Intratelencephalic connections of the hippocampus in pigeons (*Columba livia*). J. Comp. Neurol. 447, 177–199.

Auld, D.S., Kornecook, T.J., Bastianetto, S., Quirion, R., 2002. Alzheimer's disease and the basal forebrain cholinergic system: relations to beta-amyloid peptides, cognition, and treatment strategies. Prog. Neurobiol. 68, 209–245.

Azumaya, Y., Tsutsui, K., 1996. Localization of galanin and its binding sites in the quail brain. Brain Res. 727, 187–195.

Bailhache, T., Balthazart, J., 1993. The catecholaminergic system of the quail brain: immunocytochemical studies of dopamine beta-hydroxylase and tyrosine hydroxylase. J. Comp. Neurol. 329, 230–256.

Bálint, E., Csillag, A., 2007. Nucleus accumbens subregions: hodological and immunohistochemical study in the domestic chick (*Gallus domesticus*). Cell Tissue Res. 327, 221–230.

Bálint, E., Mezey, S., Csillag, A., 2011. Efferent connections of nucleus accumbens subdivisions of the domestic chicken (*Gallus domesticus*): an anterograde pathway tracing study. J. Comp. Neurol. 519, 2922–2953.

Bálint, E., Balazsa, T., Zachar, G., Mezey, S., Csillag, A., 2016. Neurotensin: revealing a novel neuromodulator circuit in the nucleus accumbens-parabrachial nucleus projection of the domestic chick. Brain Struct. Funct. 221, 605–616.

Ball, G.F., Nock, B., McEwen, B.S., Balthazart, J., 1989. Distribution of alpha 2-adrenergic receptors in the brain of the Japanese quail as determined by quantitative autoradiography: implications for the control of sexually dimorphic reproductive processes. Brain Res. 491, 68–79.

Balthazart, J., Absil, P., Fiasse, V., Ball, G.F., 1994. Effects of the aromatase inhibitor R76713 on sexual differentiation of brain and behaviour in zebra finches. Behaviour 131, 225–260.

Balthazart, J., Ball, G.F., 2007. Topography in the preoptic region: differential regulation of appetitive and consummatory male sexual behaviors. Front. Neuroendocrinol. 28, 161–178.

Balthazart, J., Absil, P., 1997. Identification of catecholaminergic inputs to and outputs from aromatase-containing brain areas of the Japanese quail by tract tracing combined with tyrosine hydroxylase immunocytochemistry. J. Comp. Neurol. 382, 401–428.

Balthazart, J., Schoffeniels, E., 1979. Pheromones are involved in the control of sexual behaviour in birds. Naturwissenschaften 66, 55–56.

Balthazart, J., Absil, P., Gerard, M., Appeltants, D., Ball, G.F., 1998a. Appetitive and consummatory male sexual behavior in Japanese quail are differentially regulated by subregions of the preoptic medial nucleus. J. Neurosci. 18, 6512–6527.

Balthazart, J., Baillien, M., Cornil, C.A., Ball, G.F., 2004. Preoptic aromatase modulates male sexual behavior: slow and fast mechanisms of action. Physiol. Behav. 83, 247–270.

Balthazart, J., Foidart, A., Surlemont, C., Vockel, A., Harada, N., 1990. Distribution of aromatase in the brain of the Japanese quail, ring dove, and zebra finch: an immunocytochemical study. J. Comp. Neurol. 301, 276–288.

Balthazart, J., Foidart, A., Baillien, M., Harada, N., Ball, G.F., 1998b. Anatomical relationships between aromatase and tyrosine hydroxylase in the quail brain: double-label immunocytochemical studies. J. Comp. Neurol. 391, 214–226.

Balthazart, J., Panzica, G.C., Krohmer, R.W., 2003. Anatomical relationships between aromatase-immunoreactive neurons and nitric oxide synthase as evidenced by NOS immunohistochemistry or NADPH diaphorase histochemistry in the quail forebrain. J. Chem. Neuroanat. 25, 39–51.

Barfield, R.J., 1971. Activation of sexual and aggressive behavior by androgen implanted into the male ring dove brain. Endocrinology 89, 1470–1476.

Barfield, R.J., Ronay, G., Pfaff, D.W., 1978. Autoradiographic localization of androgen-concentrating cells in the brain of the male domestic fowl. Neuroendocrinology 26, 297-211.

Bartus, R.T., Dean, R.L., Beer, B., Lippa, A., 1982. The cholinergic hypothesis of geriatric memory dysfunction. Science 217, 408–414.

Benowitz, L.I., Karten, H.J., 1976. Organization of the tectofugal visual pathway in the pigeon: a retrograde transport study. J. Comp. Neurol. 167, 503–520.

Berk, M.L., Butler, A.B., 1981. Efferent projections of the medial preoptic nucleus and medial hypothalamus in the pigeon. J. Comp. Neurol. 203, 379–399.

Berk, M.L., Finkelstein, J.A., 1983. Long descending projections of the hypothalamus in the pigeon, *Columba livia*. J. Comp. Neurol. 220, 127–136.

Berk, M.L., 1987. Projections of the lateral hypothalamus and bed nucleus of the stria terminalis to the dorsal vagal complex in the pigeon. J. Comp. Neurol. 260, 140–156.

Berk, M.L., Hawkin, R.F., 1985. Ascending projections of the mammillary region in the pigeon: emphasis on telencephalic connections. J. Comp. Neurol. 239, 330–340.

Berson, D.M., 2003. Strange vision: ganglion cells as circadian photoreceptors. Trends Neurosci. 26, 314–320.

Berson, D.M., Dunn, F.A., Takao, M., 2002. Phototransduction by retinal ganglion cells that set the circadian clock. Science 295, 1070–1073.

Bingman, V.P., Casini, G., Nocjar, C., Jones, T.J., 1994. Connections of the piriform cortex in homing pigeons (*Columba livia*) studied with fast blue and WGA-HRP. Brain Behav. Evol. 43, 206–218.

Bottjer, S.W., 1993. The distribution of tyrosine hydroxylase immunoreactivity in the brains of male and female zebra finches. J. Neurobiol. 24, 51–69.

Brauth, S.E., 1984. Enkephalin-like immunoreactivity within the telencephalon of the reptile *Caiman crocodilus*. Neuroscience 11, 345–358.

Brauth, S.E., Ferguson, J.L., Kitt, C.A., 1978. Prosencephalic pathways related to the paleostriatum of the pigeon (*Columba livia*). Brain Res. 147, 205–221.

Broekkamp, C.L.E., Pijnenburg, A.J.J., Cools, A.R., Van Rossum, J.M., 1975. The effect of microinjections of amphetamine into the neostriatum and the nucleus accumbens on self-stimulation behavior. Psycopharmacologia 42, 179–183.

Bruce, L.L., Erichsen, J.T., Reiner, A., 2016. Neurochemical compartmentalization within the pigeon basal ganglia. J. Chem. Neuroanat. 78, 65–86.

Brüning, G., 1993. Localization of NADPH-diaphorase in the brain of the chicken. J. Comp. Neurol. 334, 192–208.

Brüning, G., Funk, U., Mayer, B., 1994. Immunocytochemical localization of nitric oxide synthase in the brain of the chicken. Neuroreport 5, 2425–2428.

Bubien-Waluszewska, A., 1981. The cranialnerves. In: King, A.S., McLelland, J. (Eds.), Form and Function in Birds, vol. 2. Academic Press, London, pp. 385–438.

Buntin, J.D., Becker, G.M., Ruzycki, E., 1991. Facilitation of parental behavior in ring doves by systemic or intracranial injections of prolactin. Horm. Behav. 25, 424–444.

Byerly, M.S., Simon, J., Lebihan-Duval, E., Duclos, M.J., Cogburn, L.A., Porter, T.E., 2009. Effects of BDNF, T3, and corticosterone on expression of the hypothalamic obesity gene network in vivo and in vitro. Am. J. Physiol. Regul. Integr. Comp. Physiol. 296, R1180–R1189.

Cador, M., Taylor, J.R., Robbins, T.W., 1991. Potentiation of the effects of reward-related stimuli by dopaminergic-dependent mechanisms in the nucleus accumbens. Psychopharmacology (Berlin) 104, 377–385.

Calabresi, P., Picconi, B., Tozzi, A., Ghiglieri, V., Di, F.M., 2014. Direct and indirect pathways of basal ganglia: a critical reappraisal. Nat. Neurosci. 17, 1022–1030.

Canteras, N.S., Simerly, R.B., Swanson, L.W., 1992. Connections of the posterior nucleus of the amygdala. J. Comp. Neurol. 324, 143–179.

Canteras, N.S., Simerly, R.B., Swanson, L.W., 1995. Organization of projections from the medial nucleus of the amygdala: a PHAL study in the rat. J. Comp. Neurol. 360, 213–245.

Canteras, N.S., Simerly, R.B., Swanson, L.W., 1994. Organization of projections from the ventromedial nucleus of the hypothalamus: a Phaseolus vulgaris-leucoagglutinin study in the rat. J. Comp. Neurol. 348, 41–79.

Cape, E.G., Jones, B.E., 2000. Effects of glutamate agonist versus procaine microinjections into the basal forebrain cholinergic cell area upon gamma and theta EEG activity and sleep-wake state. Eur. J. Neurosci. 12, 2166–2184.

Cape, E.G., Manns, I.D., Alonso, A., Beaudet, A., Jones, B.E., 2000. Neurotensin-induced bursting of cholinergic basal forebrain neurons promotes gamma and theta cortical activity together with waking and paradoxical sleep. J. Neurosci. 20, 8452–8461.

Caro, S.P., Balthazart, J., Bonadonna, F., 2015. The perfume of reproduction in birds: chemosignaling in avian social life. Horm. Behav. 68, 25–42.

Casini, G., Bingman, V.P., Bagnoli, P., 1986. Connections of the pigeon dorsomedial forebrain studied with WGA-HRP and 3H-proline. J. Comp. Neurol. 245, 454–470.

Castro, D.C., Bruchas, M.R., 2019. A Motivational and neuropeptidergic hub: anatomical and functional diversity within the nucleus accumbens shell. Neuron 102, 529–552.

Chaillou, E., Tramu, G., Tillet, Y., 1999. Distribution of galanin immunoreactivity in the sheep diencephalon. J. Chem. Neuroanat. 17, 129–146.

Challet, E., Miceli, D., Pierre, J., Repérant, J., Masicotte, G., Herbin, M., Vesselkin, N.P., 1996. Distribution of serotonin-immunoreactivity in the brain of the pigeon (*Columba livia*). Anat. Embryol. 193, 209–227.

Cheng, M., Chaiken, M., Zuo, M., Miller, H., 1999. Nucleus taenia of the amygdala of birds: anatomical and functional studies in ring doves (*Streptopelia risoria*) and European starlings (*Sturnus vulgaris*). Brain Behav. Evol. 53, 243–270.

Choi, G.B., Dong, H.-W., Murphy, A.J., Valenzuela, D.M., Yancopoulos, G.D., Swanson, L.W., Anderson, D.J., 2005. Lhx6 delineates a pathway mediating innate reproductive behaviors from the amygdala to the hypothalamus. Neuron 46, 647–660.

Clark, M.S., Kaiyala, K.J., 2003. Role of corticotropin-releasing factor family peptides and receptors in stress-related psychiatric disorders. Semin. Clin. Neuropsychiatry 8, 119–136.

Cobos, I., Puelles, L., Martinez, S., 2001a. The avian telencephalic subpallium originates inhibitory neurons that invade tangentially the pallium (dorsal ventricular ridge and cortical areas). Dev. Biol. 239, 30–45.

Cobos, I., Shimamura, K., Rubenstein, J.L., Martinez, S., Puelles, L., 2001b. Fate map of the avian anterior forebrain at the four-somite stage, based on the analysis of quail-chick chimeras. Dev. Biol. 239, 46–67.

Cooper, R.L., Erickson, C.J., 1976. Effects of septal lesions on the courtship behavior of male ring doves (*Streptopelia risoria*). Horm. Behav. 7, 441–450.

Cozzi, B., Viglietti-Panzica, C., Aste, N., Panzica, G.C., 1991. The serotoninergic system in the brain of the Japanese quail. An immunohistochemical study. Cell Tissue Res. 263, 271–284.

Crews, D., 2005. Evolution of neuroendocrine mechanisms that regulate sexual behavior. Trends Endocrinol. Metabol. 16, 354–361.

Csillag, A., Székely, A.D., Stewart, M.G., 1997. Synaptic terminals immunolabeled against glutamate in the lobus parolfactorius of domestic chicks (*Gallus domesticus*) in relation to afferents from the archistriatum. Brain Res. 750, 171–179.

De Bournonville, C., Dickens, M.J., Ball, G.F., Balthazart, J., Cornil, C.A., 2013. Dynamic changes in brain aromatase activity following sexual interactions in males: where, when and why? Psychoneuroendocrinology 38, 789–799.

de Olmos, J.S., Beltramino, C.A., Alheid, G., 2004. Amygdala and extended amygdala of the rat: a cytoarchitectonical, fibroarchitectonical, and chemoarchitectonical survey. In: Paxinos, G. (Ed.), The Rat Nervous System, third ed. Elsevier Academic Press, San Diego, pp. 509–603.

De Vries, G.J., Panzica, G.C., 2006. Sexual differentiation of central vasopressin and vasotocin systems in vertebrates: different mechanisms, similar endpoints. Neuroscience 138, 947–955.

Del Abril, A., Segovia, S., Guillamón, A., 1987. The bed nucleus of the stria terminalis in the rat: regional sex differences controlled by gonadal steroids early after birth. Brain Res. 429, 295–300.

Dellmann, H.D., 1964. On the structure of the vascular organ of the terminal lamina in poultry. Anat. Anzeiger 115, 174–183.

DeLong, M.R., 1990. Primate models of movement disorders of basal ganglia origin. Trends Neurosci. 13, 281–285.

Ding, L., Perkel, D.J., 2004. Long-term potentiation in an avian basal ganglia nucleus essential for vocal learning. J. Neurosci. 24, 488–494.

Ding, L., Perkel, D.J., Farries, M.A., 2003. Presynaptic depression of glutamatergic synaptic transmission by D1-like dopamine receptor activation in the avian basal ganglia. J. Neurosci. 23, 6086–6095.

Dubbeldam, J.L., 1993. Systema nervosum periphericum. Nuttall Ornithological Club. In: Handbook of Avian Anatomy: Nomina Anatomica Avian Mus. Comp. Zool. Harvard Univ., Cambridge, MA, pp. 555–584.

Dubbeldam, J.L., van Ommen, M.H., den Boer-Visser, A.M., 1999. Immunohistochemical characterization of forebrain areas in the collared dove (*Streptopelia decaocto*). Eur. J. Morphol. 37, 134–138.

Duke, G.E., Dziuk, H.E., Evanson, O.A., Miller, J.E., 1977. Studies of methods for in situ observation of gastric motility in domestic turkeys. Poultry Sci. 56, 1575–1578.

Duvernoy, H.M., Risold, P.Y., 2007. The circumventricular organs: an atlas of comparative anatomy and vascularization. Brain Res. Rev. 56, 119–147.

El Halawani, M.E., Pitts, G.R., Sun, S., Silsby, J.L., Sivanandan, V., 1996. Active immunization against vasoactive intestinal peptide prevents photo-induced prolactin secretion in turkeys. Gen. Comp. Endocrinol. 104, 76–83.

Farries, M.A., Ding, L., Perkel, D.J., 2005. Evidence for "Direct" and "Indirect" pathways through the song system basal ganglia. J. Comp. Neurol. 484, 93–104.

Flames, N., Pla, R., Gelman, D.M., Rubenstein, J.L., Puelles, L., Marín, O., 2007. Delineation of multiple subpallial progenitor domains by the combinatorial expression of transcriptional codes. J. Neurosci. 27, 9682–9695.

Floresco, S.B., 2015. The nucleus accumbens: an interface between cognition, emotion, and action. Annu. Rev. Psychol. 66, 25–52.

Foidart, A., Lakaye, B., Grisar, T., Ball, G.F., Balthazart, J., 1999. Estrogen receptor-beta in quail: cloning, tissue expression and neuroanatomical distribution. J. Neurobiol. 40, 327–342.

Foster, R.G., Grace, M.S., Provencio, I., Degrip, W.J., Garcia-Fernandez, J.M., 1994. Identification of vertebrate deep brain photoreceptors. Neurosci. Biobehav. Rev. 18, 541–546.

Foster, R.G., Soni, B.G., 1998. Extraretinal photoreceptors and their regulation of temporal physiology. Rev. Reprod. 3, 145–150.

Foster, W.G., Younglai, E.V., 1991. An immunohistochemical study of the GnRH neuron morphology and topography in the adult female rabbit hypothalamus. Am. J. Anat. 191, 293–300.

Gale, S.D., Perkel, D.J., 2010. Anatomy of a songbird basal ganglia circuit essential for vocal learning and plasticity. J. Chem. Neuroanat. 39, 124–131.

Gallagher, J.P., Orozco-Cabal, L.F., Liu, J., Shinnick-Gallagher, P., 2008. Synaptic physiology of central CRH system. Eur. J. Pharmacol. 583, 215–225.

García-López, M., Abellán, A., Legaz, I., Rubenstein, J.L.R., Puelles, L., Medina, L., 2008. Histogenetic compartments of the mouse centromedial and extended amygdala based on gene expression patterns during development. J. Comp. Neurol. 506, 46–74.

Gerfen, C.R., 1992. The neostriatal mosaic: multiple levels of compartmental organization. Trends Neurosci. 15, 133–139.

Gibbs, M.E., Maksel, D., Gibbs, Z., Hou, X., Summers, R.J., Small, D.H., 2010. Memory loss caused by β-amyloid protein is rescued by a β_3-adrenoceptor agonist. Neurobiol. Aging 31, 614–624.

Gilbert, D.B., Patterson, T.A., Rose, S.P., 1991. Dissociation of brain sites necessary for registration and storage of memory for a one-trial passive avoidance task in the chick. Behav. Neurosci. 105, 553–561.

Gonzalez, A., Morona, R., Moreno, N., Bandin, S., Lopez, J.M., 2014. Identification of striatal and pallidal regions in the subpallium of anamniotes. Brain Behav. Evol. 83, 93–103.

Goodson, J.L., 1998. Vasotocin and vasoactive intestinal polypeptide modulate aggression in a territorial songbird, the violet-eared waxbill (Estrildidae: *Uraeginthus granatina*). Gen. Comp. Endocrinol. 111, 233–244.

Goodson, J.L., 2005. The vertebrate social behavior network: evolutionary themes and variations. Horm. Behav. 48, 11–22.

Goodson, J.L., Adkins-Regan, E., 1999. Effect of intraseptal vasotocin and vasoactive intestinal polypeptide infusions on courtship song and aggression in the male zebra finch (*Taeniopygia guttata*). J. Neuroendocrinol. 11, 19–25.

Goodson, J.L., Bass, A.H., 2001. Social behavior functions and related anatomical characteristics of vasotocin/vasopressin systems in vertebrates. Brain Res. Rev. 35, 246–265.

Goodson, J.L., Eibach, R., Sakata, J., Adkins-Regan, E., 1999. Effect of septal lesions on male song and aggression in the colonial zebra finch (*Taeniopygia guttata*) and the territorial field sparrow (*Spizella pusilla*). Behav. Brain Res. 98, 167–180.

Goodson, J.L., Evans, A.K., Lindberg, L., 2004. Chemoarchitectonic subdivisions of the songbird septum and a comparative overview of septum chemical anatomy in jawed vertebrates. J. Comp. Neurol. 473, 293–314.

Goodson, J.L., Evans, A.K., Lindberg, L., Allen, C.D., 2005. Neuroevolutionary patterning of sociality. Proc. R. Soc. B 272, 227–235.

Goodson, J.L., Wilson, L.C., Schrock, S.E., 2012. To flock or fight: neurochemical signatures of divergent life histories in sparrows. Proc. Natl. Acad. Sci. U. S. A 109 (Suppl. 1), 10685–10692.

Graybiel, A.M., Grafton, S.T., 2015. The striatum: where skills and habits meet. Cold Spring Harb. Perspect. Biol. 7, a021691.

Guillamón, A., Segovia, S., 1997. Sex differences in the vomeronasal system. Brain Res. Bull. 44, 377–382.

Gutierrez-Ibanez, C., Iwaniuk, A.N., Jensen, M., Graham, D.J., Pogany, A., Mongomery, B.C., Stafford, J.L., Luksch, H., Wylie, D.R., 2016. Immunohistochemical localization of cocaine- and amphetamine-regulated transcript peptide (CARTp) in the brain of the pigeon (*Columba livia*) and zebra finch (*Taeniopygia guttata*). J. Comp. Neurol. 524, 3747–3773.

Heimer, L., Alheid, G.F., 1991. Piecing together the puzzle of basal forebrain anatomy. In: Napier, T.C., Kaliavs, P.W., Hanin, I. (Eds.), The Basal Forebrain: Anatomy to Function. Plenum Press, New York, pp. 1–42.

Herkenham, M., Moon-Edley, S., Stuart, J., 1984. Cell clusters in the nucleus accumbens of the rat and the mosaic relationship of opiate receptors, acetylcholinesterase and subcortical afferent terminations. Neuroscience 11, 561–593.

Herold, C., Paulitschek, C., Palomero-Gallagher, N., Güntürkün, O., Zilles, K., 2018. Transmitter receptors reveal segregation of the arcopallium/amygdala complex in pigeons (*Columba livia*). J. Comp. Neurol. 526, 439–466.

Hodgkiss, J.P., 1984a. Evidence that enteric cholinergic neurons project orally in the intestinal nerve of the chicken. Q. J. Exp. Physiol. 69, 797–807.

Hodgkiss, J.P., 1984b. Peristalsis and antiperistalsis in the chicken caecum are myogenic. Q. J. Exp. Physiol. 69, 161–170.

Husband, S.A., Shimizu, T., 2011. Calcium-binding protein distributions and fiber connections of the nucleus accumbens in the pigeon (*Columba livia*). J. Comp. Neurol. 519, 1371–1394.

Ikemoto, S., Panksepp, J., 1999. The role of nucleus accumbens dopamine in motivated behavior: a unifying interpretation with special reference to reward-seeking. Brain Res. Brain Res. Rev. 31, 6–41.

Izawa, E., Zachar, G., Aoki, N., Koga, K., Matsushima, T., 2002. Lesions of the ventro-medial basal ganglia impair the reinforcement but not the recall of memorized color discrimination in domestic chicks. Behav. Brain Res. 136, 405–414.

Izawa, E., Zachar, H., Yanagihara, S., Matsushima, T., 2003. Localized lesion of lobus parolfactorius caused impulsive choice in the domestic chick: evolutionarily conserved function of ventral striatum. J. Neurosci. 23, 1894–1902.

Jakab, R.L., Leranth, C., 1995. Septum. In: Paxinos, G. (Ed.), The Rat Nervous System, second ed. Academic Press, San Diego, pp. 405–442.

Jarvis, E.D., Yu, J., Rivas, M.V., Horita, H., Feenders, G., Whitney, O., Jarvis, S.C., Jarvis, E.R., Kubikova, L., Puck, A.E.P., Siang-Bakshi, C., Martin, S., McElroy, M., Hara, E., Howard, J., Pfenning, A., Mouritsen, H., Chen, C.-C., Wada, K., 2013. Global view of the functional molecular organization of the avian cerebrum: mirror images and functional columns. J. Comp. Neurol. 521, 3614–3665.

Jiao, Y., Medina, L., Veenman, C.L., Toledo, C., Puelles, L., Reiner, A., 2000. Identification of the anterior nucleus of the ansa lenticularis in birds as the homolog of the mammalian subthalamic nucleus. J. Neurosci. 20, 6998–7010.

Jozsa, R., Korf, H.W., Csernus, V., Mess, B., 1988. Thyrotropin-releasing hormone (TRH)-immunoreactive structures in the brain of the domestic mallard. Cell Tissue Res. 251, 441–449.

Juorio, A.V., Vogt, M., 1967. Monoamines and their metabolites in the avian brain. J. Physiol. 189, 489–518.

Jurkevich, A., Barth, S.W., Grossmann, R., 1997. Sexual dimorphism of arg-vasotocin gene expressing neurons in the telencephalon and dorsal diencephalon of the domestic fowl. An immunocytochemical and in situ hybridization study. Cell Tissue Res. 287, 69–77.

Jurkevich, A., Barth, S.W., Kuenzel, W.J., Kohler, A., Grossman, R., 1999. Development of sexually dimorphic vasotocinergic system in the bed nucleus of stria terminalis in chickens. J. Comp. Neurol. 408, 46–60.

Kadhim, H.J., Kang, S.W., Kuenzel, W.J., 2019. Differential and temporal expression of corticotropin releasing hormone and its receptors in the nucleus of the hippocampal commissure and paraventricular nucleus during the stress response in chickens (*Gallus gallus*). Brain Res. 1714, 1–7.

Kadhim, H., Kang, S.W., Kuenzel, W.J., 2021. Possible roles of brain derived neurotrophic factor and corticotropin releasing hormone neurons in the nucleus of hippocampal commissure functioning within the avian neuroendocrine regulation of stress. Stress. https://doi.org/10.1080/10253890.2021.1929163. In press.

Kafetzopoulos, E., Papadopoulos, G., 1983. Turning behavior after unilateral lesion of the subthalamic nucleus in the rat. Behav. Brain Res. 8, 217–223.

Kalivas, P.W., Duffy, P., 1995. Selective activation of dopamine transmission in the shell of the nucleus accumbens by stress. Brain Res. 675, 325–328.

Kang, S.W., Kuenzel, W.J., 2015. Deep-brain photoreceptors (DBPs) involved in the photoperiodic gonadal response in an avian species, Gallus gallus. Gen. Comp. Endocrinol. 211, 106–113.

Karten, H.J., Hodos, W., 1967. A Stereotaxic Atlas of the Brain of the Pigeon (*Columba livia*). The Johns Hopkins University Press, Baltimore, MD.

Karten, H.J., 1969. The organization of the avian telencephalon and some speculations on the phylogeny of the amniote telencephalon. Ann. N. Y. Acad. Sci. 167, 146–179.

Karten, H.J., Dubbeldam, J.L., 1973. The organization and projections of the paleostriatal complex in the pigeon (*Columba livia*). J. Comp. Neurol. 148, 61–89.

Kelley, A.E., 1999. Neural integrative activities of nucleus accumbens subregions in relation to learning and motivation. Psychobiology 27, 198–213.

Kidd Jr., M., Kadhim, H.J., Kang, S.W., Kuenzel, W.J., 2019. Surgical disruption of corticotropin releasing hormone neurons in the nucleus of the hippocampal commissure reduces HPA axis activity in birds. Neuroscience Meeting Planner, No. 767.05.

King, D., Zigmond, M.J., Finlay, J.M., 1997. Effects of dopamine depletion in the medial prefrontal cortex on the stress-induced increase in extracellular dopamine in the nucleus accumbens core and shell. Neuroscience 77, 141–153.

Kingsbury, M.A., Wilson, L.C., 2016. The role of VIP in social behavior: neural hotspots for the modulation of affiliation, aggression, and parental care. Integr. Comp. Biol. 56, 1238–1249.

Kiss, J.Z., Voorhuis, T.A., van Eekelen, J.A., de Kloet, E.R., de, Wied, D., 1987. Organization of vasotocin-immunoreactive cells and fibers in the canary brain. J. Comp. Neurol. 263, 347–364.

Kitt, C.A., Brauth, S.E., 1982. A paleostriatal-thalamic-telencephalic path in pigeons. Neuroscience 7, 2735–2751.

Kitt, C.A., Brauth, S.E., 1981. Projections of the paleostriatum upon the midbrain tegmentum in the pigeon. Neuroscience 6, 1551–1566.

Kitt, C.A., Brauth, S.E., 1986a. Telencephalic projections from midbrain and isthmal cell groups in the pigeon. I. Locus coeruleus and subcoeruleus. J. Comp. Neurol. 247, 69–91.

Kitt, C.A., Brauth, S.E., 1986b. Telencephalic projections from midbrain and isthmal cell groups in the pigeon. II. The nigral complex. J. Comp. Neurol. 247, 92–110.

Klein, S., Jurkevich, A., Grossmann, R., 2006. Sexually dimorphic immunoreactivity of galanin and colocalization with arginine vasotocin in the chicken brain (*Gallus gallus domesticus*). J. Comp. Neurol. 499, 828–839.

Kohler, E.C., Riters, L.V., Chaves, L., Bingman, V.P., 1996. The muscarinic acetylcholine receptor antagonist scopoloamine impairs short-distance homing pigeon navigation. Physiol. Behav. 60, 1057–1061.

Korzeniewska, E., Gunturkun, O., 1990. Sensory properties and afferents of the N. dorsolateralis posterior thalami of the pigeon. J. Comp. Neurol. 292, 457–479.

Krogh, K., Ostergaard, K., Sabroe, S., Laurberg, S., 2008. Clinical aspects of bowel symptoms in Parkinson's disease. Acta Neurol. Scand. 117, 60–64.

Kuenzel, W.J., Blähser, S., 1994. Vasoactive intestinal polypeptide (VIP)-containing neurons: distribution throughout the brain of the chick (*Gallus domesticus*) with focus upon the lateral septal organ. Cell Tissue Res. 275, 91–107.

Kuenzel, W.J., Golden, C.D., 2006. Distribution and change in number of gonadotropin-releasing hormone-1 neurons following activation of the photoneuroendocrine system in the chick, *Gallus gallus*. Cell Tissue Res. 325, 501–512.

Kuenzel, W.J., Hancock, M., Nagarajan, G., Aman, N.A., Kang, S.W., 2016. Central effect of vasotocin 4 receptor (VT4R/V1aR) antagonists on the stress response and food intake in chicks given neuropeptide Y (NPY). Neurosci. Lett. 620, 57–61.

Kuenzel, W.J., Kang, S.W., Zhou, Z.J., 2015. Exploring avian deep-brain photoreceptors and their role in activating the neuroendocrine regulation of gonadal development. Poultry Sci. 94, 786–798.

Kuenzel, W.J., McCune, S.K., Talbot, R.T., Sharp, P.J., Hill, J.M., 1997. Sites of gene expression for vasoactive intestinal polypeptide throughout the brain of the chick (*Gallus domesticus*). J. Comp. Neurol. 381, 101–118.

Kuenzel, W.J., Medina, L., Csillag, A., Perkel, D.J., Reiner, A., 2011. The avian subpallium: new insights into structural and functional subdivisions occupying the lateral subpallial wall and their embryological origins. Brain Res. 1424, 67–101.

Kuenzel, W.J., van Tienhoven, A., 1982. Nomenclature and location of avian hypothalamic nuclei and associated circumventricular organs. J. Comp. Neurol. 206, 293–313.

Kuenzel, W.J., 1994. Central neuroanatomical systems involved in the regulation of food intake in birds and mammals. J. Nutr. 124, 1355S–1370S.

Kuenzel, W.J., 2000. The autonomic nervous system of birds. In: Whittow, G.C. (Ed.), Sturkie's Avian Physiology. Academic Press, San Diego, pp. 101–122.

Kuenzel J, W, 2015. The avian subpallium and autonomic nervous system. In: Scanes G., C. (Ed.), Sturkie's Avian Physiology, 6th. Elsevier, San Diego, CA, pp. 135–163.

Kuenzel, W.J., 2018. Mapping the brain of the chicken (*Gallus gallus*), with emphasis on the septal-hypothalamic region. Gen. Comp. Endocrinol. 256, 4–15.

Kuenzel, W.J., Blähser, S., 1993. The visceral forebrain system in birds: its proposed anatomical components and functions. Poultry Avian Biol. Rev. 5, 29–36.

Kuenzel, W.J., Masson, M., 1988. A Stereotaxic Atlas of the Brain of the Chick (*Gallus domesticus*). Johns Hopkins University Press, Baltimore.

Lai, H.C., Duke, G.E., 1978. Colonic motility in domestic turkeys. Am. J. Dig. Dis. 23, 673–681.

Landmesser, L., 1978. The development of motor projection patterns in the chick hind limb. J. Physiol. 284, 391–414.

Lanuza, E., Davies, D.C., Landete, J.M., Novejarque, A., Martínez-García, F., 2000. Distribution of CGRP-like immunoreactivity in the chick and quail brain. J. Comp. Neurol. 421, 515–532.

Lazar, G.Y., Liposits, Z.S., Toth, P., Trasti, S.L., Maderdrut, J.L., Merchenthaler, I., 1991. Distribution of galanin-like immunoreactivity in the brain of *Rana esculenta* and *Xenopus laevis*. J. Comp. Neurol. 310, 45–67.

Li, H., Kuenzel, W.J., 2008. A possible neural cascade involving the photoneuroendocrine system (PNES) responsible for regulating gonadal development in an avian species, Gallus gallus. Brain Res. Bull. 76, 586–596.

Liu, A.K.L., Chang, R.C.-C., Pearce, R.K.B., Gentleman, S.M., 2015. Nucleus basalis of Meynert revisited: anatomy,history and differential involvement in Alzheimer's and Parkinson's disease. Acta Neuropathol. 129, 527–540.

Luiten, P.G., ter Horst, G.J., Steffens, A.B., 1987. The hypothalamus, intrinsic connections and outflow pathways to the endocrine system in relation to the control of feeding and metabolism. Prog. Neurobiol. 28, 1–54.

Lunam, C.A., Smith, T.K., 1996. Morphology and projections of neurons in Remak's nerve of the domestic fowl revealed by intracellular injection of biocytin. Cell Tissue Res. 284, 215–222.

Macnamee, M.C., Sharp, P.J., Lea, R.W., Sterling, R.J., Harvey, S., 1986. Evidence that vasoactive intestinal polypeptide is a physiological prolactin-releasing factor in the bantam hen. Gen. Comp. Endocrinol. 62, 470–478.

Maldonado-Irizarry, C.S., Swanson, C.J., Kelley, A.E., 1995. Glutamate receptors in the nucleus accumbens shell control feeding behavior via the lateral hypothalamus. J. Neurosci. 15, 6779–6788.

Maney, D.L., 2013. The incentive salience of courtship vocalizations: hormone-mediated 'wanting' in the auditory system. Hear. Res. 305, 19–30.

Marín, O., Anderson, S.A., Rubenstein, J.L., 2000. Origin and molecular specification of striatal interneurons. J. Neurosci. 20, 6063–6076.

Marín, O., Rubenstein, J.L., 2001. A long, remarkable journey: tangential migration in the telencephalon. Nat. Rev. Neurosci. 2, 780–790.

Matsushima, T., Izawa, E., Aoki, N., Yanagihara, S., 2003. The mind through chick eyes: memory, cognition and anticipation. Zool. Sci. 20, 395–408.

Mauro, L.J., Elde, R.P., Youngren, O.M., Phillips, R.E., El Halawani, M.E., 1989. Alterations in hypothalamic vasoactive intestinal peptide-like immunoreactivity are associated with reproduction and prolactin release in the female Turkey. Endocrinology 125, 1795–1804.

McKeegan, D.E., 2002. Spontaneous and odour evoked activity in single avian olfactory bulb neurones. Brain Res. 929, 48–58.

Medina, L., Reiner, A., 2000. Do birds possess homologues of mammalian primary visual, somatosensory and motor cortices? Trends Neurosci. 23, 1–12.

Medina, L., Veenman, C.L., Reiner, A., 1997. Evidence for a possible avian dorsal thalamic region comparable to the mammalian ventral anterior, ventral lateral, and oral ventroposterolateral nuclei. J. Comp. Neurol. 384, 86–108.

Medina, L., Abellán, A., 2009. Development and evolution of the pallium. Semin. Cell Dev. Biol. 20, 698–711.

Medina, L., Abellan, A., 2012. Subpallial structures. In: Watson, C., Paxinos, G., Puelles, L. (Eds.), The Mouse Nervous System. Academic Press, San Diego, pp. 173–220.

Medina, L., Reiner, A., 1994. Distribution of choline acetyltransferase immunoreactivity in the pigeon brain. J. Comp. Neurol. 342, 497–537.

Medina, L., Reiner, A., 1997. The efferent projections of the dorsal and ventral pallidal parts of the pigeon basal ganglia, studied with biotinylated dextran amine. Neuroscience 81, 773–802.

Melander, T., Hokfelt, T., Rokaeus, A., 1986. Distribution of galaninlike immunoreactivity in the rat central nervous system. J. Comp. Neurol. 248, 475–517.

Mello, C.V., Kaser, T., Buckner, A.A., Wirthlin, M., Lovell, P.V., 2019. Molecular architecture of the zebra finch arcopallium. J. Comp. Neurol. 527, 2512–2556.

Mello, C.V., Pinaud, R., Ribeiro, S., 1998. Noradrenergic system of the zebra finch brain: immunocytochemical study of dopamine-beta-hydroxylase. J. Comp. Neurol. 400, 207–228.

Mena-Segovia, J., Bolam, J.P., Magill, P.J., 2004. Pedunculopontine nucleus and basal ganglia: distant relatives or part of the same family? Trends Neurosci. 27, 585–588.

Mesulam, M.M., 1990. Human brain cholinergic pathways. Prog. Brain Res. 84, 231–234.

Mesulam, M.M., Geula, C., 1988. Nucleus basalis (Ch4) and cortical cholinergic innervation in the human brain: observations based on the distribution of acetylcholinesterease and choline acetyltransferase. J. Comp. Neurol. 275, 216–240.

Mesulam, M.M., Mufson, E.J., Levey, A.I., Wainer, B.H., 1984. Atlas of cholinergic neurons in the forebrain and upper brainstem of the macaque based on monoclonal choline acetyltransferase immunohistochemistry and acetylcholininesterease histochemistry. Neuroscience 12, 669–686.

Metherate, R., Cox, C.L., Ashe, J.H., 1992. Cellular bases of neocortical activation: modulation of neural oscillations by the nucleus basalis and endogenous acetylcholine. J. Neurosci. 12, 4701–4711.

Metherate, R., Tremblay, N., Dykes, R.W., 1988. Transient and prolonged effects of acetylcholine on responsiveness of cat somatosensory cortical neurons. J. Neurophysiol. 59, 1253–1276.

Mikami, S., 1976. Ultrastructure of the organum vasculosum of the lamina terminalis of the Japanese quail, *Coturnix coturnix* japonica. Cell Tissue Res. 172, 227–243.

Mineau, P., Boag, P.T., Beninger, R.J., 1994. The effects of physostigmine and scopolamine on memory for food caches in the black-capped chickadee. Pharmacol. Biochem. Behav. 49, 363–370.

Moga, M.M., Gray, T.S., 1985. Peptidergic efferents from the intercalated nuclei of the amygdala to the parabrachial nucleus in the rat. Neurosci. Lett. 61, 13–18.

Molnar, M., Casini, G., Davis, B.M., Bagnoli, P., Brecha, N., 1994. Distribution of proenkephalin mRNA in the chicken and pigeon telencephalon. J. Comp. Neurol. 348, 419–432.

Montagnese, C.M., Zachar, G., Balint, E., Csillag, A., 2008. Afferent connections of septal nuclei of the domestic chick (*Gallus domesticus*): a retrograde pathway tracing study. J. Comp. Neurol. 511, 109–150.

Montagnese, C.M., Szekely, A.D., Adam, A., Csillag, A., 2004. Efferent connections of septal nuclei of the domestic chick (*Gallus domesticus*): an anterograde pathway tracing study with a bearing on functional circuits. J. Comp. Neurol. 469, 437–456.

Moons, L., D'Hondt, E., Pijcke, K., Vandesande, F., 1995. Noradrenergic system in the chicken brain: immunocytochemical study with antibodies to noradrenaline and dopamine-beta-hydroxylase. J. Comp. Neurol. 360, 331–348.

Moons, L., Van, G.J., Ghijsels, E., Vandesande, F., 1994. Immunocytochemical localization of L-dopa and dopamine in the brain of the chicken (*Gallus domesticus*). J. Comp. Neurol. 346, 97–118.

Moore, F.L., Lowry, C.A., 1998. Comparative neuroanatomy of vasotocin and vasopressin in amphibians and other vertebrates. Comp. Biochem. Physiol. C Pharmacol. Toxicol. Endocrinol. 119, 251–260.

Murakami, S., Seki, T., Wakabayashi, K., Arai, Y., 1991. The ontogeny of luteinizing hormone-releasing hormone (LHRH) producing neurons in the chick embryo: possible evidence for migrating LHRH neurons from the olfactory epithelium expressing a highly polysialylated neural cell adhesion molecule. Neurosci. Res. 12, 421–431.

Muske, L.E., Moore, F.L., 1988. The nervus terminalis in amphibians: anatomy, chemistry and relationship with the hypothalamic gonadotropin-releasing hormone system. Brain Behav. Evol. 32, 141–150.

Nagarajan, G., Jurkevich, A., Kang, S.W., Kuenzel, W.J., 2017a. Anatomical and functional implications of corticotrophin-releasing hormone neurones in a septal nucleus of the avian brain: an emphasis on glial-neuronal interaction via V1a receptors in vitro. J. Neuroendocrinol. 29, 1–11.

Nagarajan, G., Kang, S.W., Kuenzel, W.J., 2017b. Functional evidence that the nucleus of the hippocampal commissure shows an earlier activation from a stressor than the paraventricular nucleus: implication of an additional structural component of the avian hypothalamo-pituitary-adrenal axis. Neurosci. Lett. 642, 14–19.

Nagarajan, G., Tessaro, B.A., Kang, S.W., Kuenzel, W.J., 2014. Identification of arginine vasotocin (AVT) neurons activated by acute and chronic restraint stress in the avian septum and anterior diencephalon. Gen. Comp. Endocrinol. 202, 59–68.

Nauta, W.J.H., Karten, H.J., 1970. A general profile of the vertebrate brain, with sidelights on the ancestry of the cerebral cortex. In: Schmitt, F.O. (Ed.), The Neurosciences, Second Study Program. Rockefeller University Press, New York, pp. 7–26.

Nelson, R.J., Trainor, B.C., 2007. Neural mechanisms of aggression. Nat Rev Neurosci 8, 536–546.

Newman, S.W., 1999. The medial extended amygdala in male reproductive behavior: a node in the mammalian social behavior network. Ann. N. Y. Acad. Sci. 877, 242–257.

Nickel, R., Schummer, A., Seiferle, E., Siller, W.G., Wight, P.A.L., 1977. In: Anatomy of the Domestic Birds. Springer-Verlag, New York.

Nilsson, S., 2011. Comparative anatomy of the autonomic nervous system. Auton. Neurosci. 165, 3–9.

Norgren Jr., R.B., Lehman, M.N., 1991. Neurons that migrate from the olfactory epithelium in the chick express luteinizing hormone-releasing hormone. Endocrinology 128, 1676–1678.

O'Connell, L.A., Hofmann, H.A., 2012. Evolution of a vertebrate social decision-making network. Science 336, 1154–1157.

Opel, H., Proudman, J.A., 1988. Stimulation of prolactin release in turkeys by vasoactive intestinal peptide. Proc. Soc. Exp. Biol. Med. 187, 455–460.

Pahapill, P.A., Lozano, A.M., 2000. The pedunculopontine nucleus and Parkinson's disease. Brain 123, 1767–1783.

Panguluri, S., Saggu, S., Lundy, R., 2009. Comparison of somatostatin and corticotrophin-releasing hormone immunoreactivity in forebrain neurons projecting to taste-responsive and non-responsive regions of the parabrachial nucleus in rat. Brain Res. 1298, 57–69.

Panzica, G.C., Aste, N., Vigietti-Panzica, C., Fasolo, A., 1992. Neuronal circuits controlling quail sexual behavior. Chemical neuroanatomy of the septo-preoptic region. Poultry Avian Biol. Rev. 4, 249–259.

Panzica, G.C., Aste, N., Castagna, C., Viglietti-Panzica, C., Balthazart, J., 2001. Steroid-induced plasticity in the sexually dimorphic vasotocinergic innervation of the avian brain: behavioral implications. Brain Res. Rev. 37, 178–200.

Panzica, G., Pessatti, M., Viglietti-Panzica, C., Grossmann, R., Balthazart, J., 1999. Effects of testosterone on sexually dimorphic parvocellular neurons expressing vasotocin mRNA in the male quail brain. Brain Res. 850, 55–62.

Panzica, G.C., Arévalo, R., Sánchez, F., Alonso, J.R., Aste, N., Viglietti-Panzica, C., Aijón, J., Vázquez, R., 1994. Topographical distribution of reduced nicotinamide adenine dinucleotidde phosphate-diaphorase in the brain of the Japanese quail. J. Comp. Neurol. 342, 97–114.

Panzica, G.C., Castagna, C., Viglietti-Panzica, C., Russo, C., Tlemçani, O., Balthazart, J., 1998. Organizational effects of estrogens on brain vasotocin and sexual behavior in quail. J. Neurobiol. 37, 684–699.

Panzica, G.C., Garzino, A., García-Ojeda, E., 1996. Coexistence of NADPH-diaphorase and tyrosine hydroxylase in the mesencephalic catecholaminergic system of the Japanese quail. J. Chem. Neuroanat. 11, 37–47.

Panzica, G.C., Viglietti-Panzica, C., Fasolo, A., Vandesande, F., 1986. CRF-like immunoreactive system in the quail brain. J. Hirnforsch. 27, 539–547.

Paré, D., Quirk, G.J., Ledoux, J.E., 2004. New vistas on amygdala networks in conditioned fear. J. Neurophysiol. 92, 1–9.

Paré, D., Smith, Y., 1994. GABAergic projection from the intercalated cell masses of the amygdala to the basal forebrain in cats. J. Comp. Neurol. 344, 33–49.

Patterson, T.A., Lipton, J.R., Bennett, E.L., Rozenzweig, M.R., 1990. Cholinergic receptor antagonists impair formation of intermediate-term memory in the chick. Behav. Neural. Biol. 54, 63–74.

Patterson, T.A., Rose, S.P., 1992. Memory in the chick: multiple cues, distinct brain locations. Behav. Neurosci. 106, 465–470.

Patzke, N., Manns, M., Güntürkün, O., 2011. Telencephalic organization of the olfactory system in homing pigeons (*Columba livia*). Neuroscience 194, 53–61.

Pauly, M.C., Dobrossy, M.D., Nikkhah, G., Winkler, C., Piroth, T., 2014. Organization of the human fetal subpallium. Front. Neuroanat. 7, 54.

Piallat, B., Benazzouz, A., Benabid, A.L., 1996. Subthalamic nucleus lesion in rats prevents dopaminergic nigral neuron degeneration after striatal 6-OHDA injection: behavioural and immunohistochemical studies. Eur. J. Neurosci. 8, 1408–1414.

Pombero, A., Bueno, C., Saglietti, L., Rodenas, M., Guimera, J., Bulfone, A., Martinez, S., 2011. Pallial origin of basal forebrain cholinergic neurons in the nucleus basalis of Meynert and horizontal limb of the diagonal band nucleus. Development 138, 4315–4326.

Poulin, A.-M., Timofeeva, E., 2008. The dynamics of neuronal activation during food anticipation and feeding in the brain of food-entrained rats. Brain Res. 1227, 128–141.

Puelles, L., 2019. Survey of midbrain, diencephalon, and hypothalamus neuroanatomic terms whose prosomeric definition conflicts with columnar tradition. Front. Neuroanat. 13, 20.

Puelles, L., Kuwana, E., Puelles, E., Bulfone, A., Shimamura, K., Keleher, J., Smiga, S., Rubenstein, J.L., 2000. Pallial and subpallial derivatives in the embryonic chick and mouse telencephalon, traced by the expression of the genes *D1x-2, Emx-1, Nkx*-2,1, *Pax-6*, and *Tbr-1*. J. Comp. Neurol. 424, 409–438.

Puelles, L., Martínez-de-la-Torre, M., Paxinos, G., Watson, C., Martínez, S., 2007. The Chick Brain in Stereotaxic Coordinates. Academic Press, San Diego.

Puelles, L., Martinez-de-la-Torre, M., Martínez, S., Watson, C., Paxinos, G., 2019. The Chick Brain in Stereotaxic Coordinates and Alternate Stains, second ed. Elsevier, Academic Press, San Diego.

Puelles, L., Rubenstein, J.L., 2015. A new scenario of hypothalamic organization: rationale of new hypotheses introduced in the updated prosomeric model. Front. Neuroanat. 9, 27.

Qiu, X., Kumbalasiri, T., Carlson, S.M., Wong, K.Y., Krishna, V., Provencio, I., Berson, D.M., 2005. Induction of photosensitivity by heterologous expression of melanopsin. Nature 433, 745–749.

Ramirez, J.M., Salas, C., Portavella, M., 1988. Offense and defense after lateral septal lesions in *Columba livia*. Int. J. Neurosci. 41, 241–250.

Rathinam, T., Kuenzel, W.J., 2005. Attenuation of gonadal response to photostimulation following ablation of neurons in the lateral septal organ of chicks. Brain Res. Bull. 64, 455–461.

Redgrave, P., Prescott, T.J., Gurney, K., 1999. The basal ganglia: a vertebrate solution to the selection problem? Neuroscience 89, 1009–1023.

Redies, C., Medina, L., Puelles, L., 2001. Cadherin expression by embryonic subdivisions and derived gray matter structures in the telencephalon of the chicken. J. Comp. Neurol. 438, 253–285.

Reiner, A., 1986. The co-occurrence of substance P-like immunoreactivity and dynorphin-like immunoreactivity in striatopallidal and striatonigral projection neurons in birds and reptiles. Brain Res. 371, 155–161.

Reiner, A., 1987. The distribution of proenkephalin-derived peptides in the central nervous system of turtles. J. Comp. Neurol. 259, 65–91.

Reiner, A., Anderson, K.D., 1990. The patterns of neurotransmitter and neuropeptide co-occurrence among striatal projection neurons: conclusions based on recent findings. Brain Res. Rev. 15 (3), 251–265.

Reiner, A., Carraway, R.E., 1987. Immunohistochemical and biochemical studies on Lys8-Asn9-neurotensin 8-13 (LANT6)-related peptides in the basal ganglia of pigeons, turtles, and hamsters. J. Comp. Neurol. 257, 453–476.

Reiner, A., Brauth, S.E., Karten, H.J., 1984a. Evolution of the amniote basal ganglia. Treands Neurosci. 7, 320–325.

Reiner, A., Davis, B.M., Brecha, N.C., Karten, H.J., 1984b. The distribution of enkephalinlike immunoreactivity in the telencephalon of the adult and developing domestic chicken. J. Comp. Neurol. 228, 245–262.

Reiner, A., Karle, E.J., Anderson, K.D., Medina, L., 1994. Catecholaminergic perikarya and fibers in the avian nervous system. In: Smeets, W.J.A.J., Reiner, A. (Eds.), Phylogeny and Development of Catecholaminergic Systems in the CNS of Vertebrates. Cambridge University Press, Cambridge, pp. 135–181.

Reiner, A., Medina, L., Veenman, C.L., 1998. Structural and functional evolution of the basal ganglia in vertebrates. Brain Res. Rev. 28, 235–285.

Reiner, A., Perkel, D.J., Bruce, L.L., Butler, A.B., Csillag, A., Kuenzel, W., Medina, L., Paxinos, G., Shimizu, T., Striedter, G., Wild, M., Ball, G.F., Durand, S., Güntürkün, O., Lee, D.W., Mello, C.V., Powers, A., White, S.A., Hough, G., Kubikova, L., Smulders, T.V., Wada, K., Dugas-Ford, J., Husband, S., Yamamoto, K., Yu, J., Siang, C., Jarvis, E.D., 2004. Revised nomenclature for avian telencephalon and some related brainstem nuclei. J. Comp. Neurol. 473, 377–414.

Reiner, A., Stern, E.A., Wilson, C.J., 2001. Physiology and morphology of intratelencephalically projecting corticostriatal-type neurons in pigeons as revealed by intracellular recording and cell filling. Brain Behav. Evol. 58, 101–114.

Richard, S., Martinez-Garcia, F., Lanuza, E., Davies, D.C., 2004. Distribution of corticotropin-releasing factor-immunoreactive neurons in the central nervous system of the domestic chicken and Japanese quail. J. Comp. Neurol. 469, 559–580.

Richards, M.P., Proszkowiec-Weglarz, M., 2007. Mechanisms regulating feed intake, energy expenditure, and body weight in poultry. Poultry Sci. 86, 1478–1490.

Richards, M.P., Rosebrough, R.W., Coon, C.N., McMurtry, J.P., 2010. Feed intake regulation for the female broiler breeder: in theory and in practice. J. Appl. Poultry Res. 19, 182–193.

Risold, P.Y., Swanson, L.W., 1997a. Chemoarchitecture of the rat lateral septal nucleus. Brain Res. Brain Res. Rev. 24, 91–113.

Risold, P.Y., Swanson, L.W., 1997b. Connections of the rat lateral septal complex. Brain Res. Brain Res. Rev. 24, 115–195.

Riters, L.V., Eens, M., Pinxten, R., Duffy, D.L., Balthazart, J., Ball, G.F., 2000. Seasonal changes in courtship song and the medial preoptic area in male European starlings (*Sturnus vulgaris*). Horm. Behav. 38, 250–261.

Riters, L.V., Teague, D.P., Schroeder, M.B., Cummings, S.E., 2004. Vocal production in different social contexts relates to variation in immediate early gene immunoreactivity within and outside of the song control system. Behav. Brain Res. 155, 307–318.

Roberts, T.F., Hall, W.S., Brauth, S.E., 2002. Organization of the avian basal forebrain: chemical anatomy in the parrot (*Melopsittacus undulatus*). J. Comp. Neurol. 454, 383–408.

Rose, S.P., 2000. God's organism? The chick as a model system for memory studies. Learn. Mem. 7, 1–17.

Rose, S.P., Stewart, M.G., 1999. Cellular correlates of stages of memory formation in the chick following passive avoidance training. Behav. Brain Res. 98, 237–243.

Rubenstein, J.L.R., Shimamura, K., Martinez, S., Puelles, L., 1998. Regionalization of the prosencephalic neural plate. Annu. Rev. Neurosci. 21, 445–478.

Russo, S.J., Nestler, E.J., 2013. The brain reward circuitry in mood disorders. Nat. Rev. Neurosci. 14, 609–625.

Saldanha J., C., Silverman, A.-J., Silver, R., 2001. Direct innervation of GnRH neurons by encephalic photoreceptors in birds. J. Biol. Rhythms 16, 39–49.

Savage, L.M., Stanchfield, M.A., Overmeier, J.B., 1994. The effects of scopolamine, diazepam, and lorazepam on working memory in pigeons: an analysis of reinforcement procedures and sample problem type. Pharmacol. Biochem. Behav. 48, 183–191.

Schwanzel-Fukuda, M., Pfaff, D.W., 1989. Origin of luteinizing hormone-releasing hormone neurons. Nature 338, 161–164.

Selvam, R., Jurkevich, A., Kuenzel, W.J., 2015. Distribution of the vasotocin type 4 receptor throughout the brain of the chicken, *Gallus gallus*. J Comp Neurol 523 (2), 335–358.

Sharp, P.J., Sterling, R.J., Talbot, R.T., Huskisson, N.S., 1989. The role of hypothalamic vasoactive intestinal polypeptide in the maintenance of prolactin secretion in incubating bantam hens: observations using passive immunization, radioimmunoassay and immunohistochemistry. J. Endocrinol. 122, 5–13.

Shiflett, M.W., Gould, K.L., Smulders, T.V., DeVoogd, T.J., 2002. Septum volume and food-storing behavior are related in parids. J. Neurobiol. 51, 215–222.

Shimogori, T., Lee, D.A., Miranda-Angulo, A., Yang, Y., Wang, H., Jiang, L., Yoshida, A.C., Kataoka, A., Mashiko, H., Avetisyan, M., Qi, L., Qian, J., Blackshaw, S., 2010. A genomic atlas of mouse hypothalamic development. Nat. Neurosci. 13, 767–775.

Schlinger, B.A., Callard, G.V., 1990. Aromatization mediates aggressive behavior in quail. Gen. Comp. Endocrinol. 79, 39–53.

Silver, R., Witkovsky, P., Horvath, P., Alones, V., Barnstable, C.J., Lehman, M.N., 1988. Coexpression of opsin- and VIP-like-immunoreactivity in CSF-contacting neurons of the avian brain. Cell Tissue Res. 253, 189–198.

Silverman, A.J., Livne, I., Witkin, J.W., 1994. The gonadotropin-releasing hormone (GnRH), neuronal systems: immunocytochemistry and in situ hybridization. In: Knobil, E., Neill, J.D. (Eds.), The Physiology of Reproduction, vol. 2e. Raven Press Ltd, New York, pp. 1683–1709.

Smeets, W.J., Marin, O., Gonzalez, A., 2000. Evolution of the basal ganglia: new perspectives through a comparative approach. J Anat 196, 501–517.

Spooner, C.E., Winters, W.D., 1966. Neuropharmacological profile of the young chick. Int. J. Neuropharmacol. 5, 217–236.

Stephenson-Jones, M., Ericsson, J., Robertson, B., Grillner, S., 2012. Evolution of the basal ganglia: dual-output pathways conserved throughout vertebrate phylogeny. J. Comp. Neurol. 520, 2957–2973.

Stephenson-Jones, M., Samuelsson, E., Ericsson, J., Robertson, B., Grillner, S., 2011. Evolutionary conservation of the basal ganglia as a common vertebrate mechanism for action selection. Curr. Biol. 21, 1081–1091.

Swanson, L.W., 2000. Cerebral hemisphere regulation of motivated behavior. Brain Res. 886, 113–164.

Swanson, L.W., Petrovich, G.D., 1998. What is the amygdala? Trends Neurosci. 21, 323–331.

Tanaka, M., Ikeda, T., Hayashi, S., Iijima, N., Amaya, F., Hisa, Y., Ibata, Y., 1997. Nitrergic neurons in the medial amygdala project to the hypothalamic paraventricular nucleus of the rat. Brain Res. 777, 13–21.

Thompson, R.R., Goodson, J.L., Ruscio, M.G., Adkins-Regan, E., 1998. Role of the archistriatal nucleus taeniae in the sexual behavior of male Japanese quail (*Coturnix japonica*): a comparison of function with the medial nucleus of the amygdala in mammals. Brain Behav. Evol. 51, 215–229.

van der Kooy, D., Koda, L.Y., McGinty, J.F., Gerfen, C.R., Bloom, F.E., 1984. The organization of projections from the cortex, amygdala, and hypothalamus to the nucleus of the solitary tract in rat. J. Comp. Neurol. 224, 1–24.

Veenman, C.L., Albin, R.L., Richfield, E.K., Reiner, A., 1994. Distributions of $GABA_A$, $GABA_B$, and benzodiazepine receptors in the forebrain and midbrain of pigeons. J. Comp. Neurol. 344, 161–189.

Veenman, C.L., Reiner, A., 1994. The distribution of GABA-containing perikarya, fibers, and terminals in the forebrain and midbrain of pigeons, with particular reference to the basal ganglia and its projection targets. J. Comp. Neurol. 339, 209–250.

Veenman, C.L., Reiner, A., 1996. Ultrastructural morphology of synapses formed by corticostriatal terminals in the avian striatum. Brain Res. 707, 1–12.

Veenman, C.L., Wild, J.M., Reiner, A., 1995. Organization of the avian "corticostriatal" projection system: a retrograde and anterograde pathway tracing study in pigeons. J. Comp. Neurol. 354, 87–126.

Vicario, A., Abellán, A., Desfilis, E., Medina, L., 2014. Genetic identification of the central nucleus and other components of the central extended amygdala in chicken during development. Front. Neuroanat. 8, 90.

Vicario, A., Abellán, A., Medina, L., 2015. Embryonic origin of the Islet1 and Pax6 neurons of the chicken central extended amygdala using cell migration assays and relation to different neuropeptide-containing cells. Brain Behav. Evol. 85, 139–169.

Vicario, A., Mendoza, E., Abellán, A., Scharff, C., Medina, L., 2017. Genoarchitecture of the extended amygdala in zebra finch, and expression of FoxP2 in cell corridors of different genetic profile. Brain Struct. Funct. 222, 481–514.

Vigh, B., 1971. Das Paraventrikularorgan und das zirkumventrikuläre System des Gehirns. Stud. Biol. Hung. 10 (Akad Kiadó, Budapest).

Viglietti-Panzica, C., Panzica, G.C., Fiori, M.G., Calcagni, M., Anselmetti, G.C., Balthazart, J., 1986. A sexually dimorphic nucleus in the quail preoptic area. Neurosci. Lett. 64, 129–134.

Viglietti-Panzica, C., Anselmetti, G.C., Balthazart, J., Aste, N., Panzica, G.C., 1992. Vasotocinergic innervation of the septal region in the Japanese quail: sexual differences and the influence of testosterone. Cell Tissue Res. 267, 261–265.

Vincent, S.R., Johansson, O., Hökfelt, T., Skirboll, L., Elde, R.P., Terenius, L., Kimmel, J., Goldstein, M., 1983. NADPH-diaphorase: a selective histochemical marker for striatal neurons containing both somatostatin- and avian pancreatic polypeptide (APP)-like immunoreactivities. J. Comp. Neurol. 217, 252–263.

von Bartheld, C.S., Bothwell, M., 1992. Development and distribution of noradrenergic and cholinergic neurons and their trophic phenotypes in the avian ceruleus complex and midbrain tegmentum. J. Comp. Neurol. 320, 479–500.

Voorhuis, T.A.M., Kiss, J.Z., de Kloet, E.R., de Wied, D., 1988. Testosterone-sensitive vasotocin-immunoreactive cells and fibers in the canary brain. Brain Res. 442, 139–146.

Wada, Y., Okano, T., Fukada, Y., 2000. Phototransduction molecules in the pigeon deep brain. J. Comp. Neurol. 428, 138–144.

Watson, J.T., Adkins-Regan, E., 1989. Neuroanatomical localization of sex steroid concentrating cells in the Japanese quail (*Coturnix japonica*): autoradiography with (^{3}H)-estradiol, (^{3}H)-testosterone and (^{3}H)-dihydrotestosterone. Neuroendocrinology 49, 51–64.

Weindl, A., 1973. Neuroendocrine aspects of circumventricular organs. In: Ganong, W.E., Martini, L. (Eds.), Frontiers in Neuroendocrinology. Oxford Univ. Press, London and New York, pp. 3–32.

Wild, J.M., Balthazart, J., 2013. Neural pathways mediating control of reproductive behavior in male Japanese quail. J. Comp. Neurol. 521, 2067–2087.

Wild, J.M., Li, D., Eagleton, C., 1997. Projections of the dorsomedial nucleus of the intercollicular complex (DM) in relation to respiratory-vocal nuclei in the brainstem of pigeon (*Columba livia*) and zebra finch (*Taeniopygia guttata*). J. Comp. Neurol. 377, 392–413.

Wild, J.M., 1987. Thalamic projections to the paleostriatum and neostriatum in the pigeon (*Columba livia*). Neuroscience 20, 305–327.

Wild, J.M., Arends, J.J., Zeigler, H.P., 1990. Projections of the parabrachial nucleus in the pigeon (*Columba livia*). J. Comp. Neurol. 293, 499–523.

Wiltschko, R., Wiltschko, W., 2017. Considerations on the role of olfactory input in avian navigation. J. Exp. Biol. 220, 4347–4350.

Woolf, N.J., 1991. Cholinergic systems in mammalian brain and spinal cord. Prog. Neurobiol. 37, 475–524.

Woolley, S.C., Kao, M.H., 2015. Variability in action: contributions of a songbird cortical-basal ganglia circuit to vocal motor learning and control. Neuroscience 296, 39–47.

Wray, S., Nieburgs, A., Elkabes, S., 1989. Spatiotemporal cell expression of luteinizing hormone-releasing hormone in the prenatal mouse: evidence for an embryonic origin in the olfactory placode. Brain Res. Dev. Brain Res. 46, 309–318.

Wynne, B., Güntürkün, O., 1995. Dopaminergic innervation of the telencephalon of the pigeon (*Columba livia*): a study with antibodies against tyrosine hydroxylase and dopamine. J. Comp. Neurol. 357, 446–464.

Xiao, L., Chattree, G., Oscos, F.G., Cao, M., Wanat, M.J., Roberts, T.F., 2018. A basal ganglia circuit sufficient to guide birdsong learning. Neuron 98, 208–221.

Xie, J., Kuenzel, W.J., Anthony, N.B., Jurkevich, A., 2010. Subpallial and hypothalamic areas activated following sexual and agonistic encounters in male chickens. Physiol. Behav. 101, 344–359.

Xie, J., Kuenzel, W.J., Sharp, P.J., Jurkevich, A., 2011. Appetitive and consummatory sexual and agonistic behavior elicits FOS expression in aromatase and vasotocin neurons within the preoptic area and bed nucleus of the stria terminalis of male domestic chickens. J. Neuroendocrinol. 23, 232–243.

Xu, Q., Tam, M., Anderson, S.A., 2008. Fate mapping Nkx2.1-lineage cells in the mouse telencephalon. J. Comp. Neurol. 506, 16–29.

Yamamoto, K., Sun, Z., Wang, H.B., Reiner, A., 2005. Subpallial amygdala and nucleus taeniae in birds resemble extended amygdala and medial amygdala in mammals in their expression of markers of regional identity. Brain Res. Bull. 66, 341–347.

Yasuda, M., 2002. The Anatomical Atlas of Gallus. University of Tokyo Press, Tokyo.

Yuan, L., Ni, Y., Barth, S., Wang, Y., Grossmann, R., Zhao, R., 2009. Layer and broiler chicks exhibit similar hypothalamic expression of orexigenic neuropeptides but distinct expression of genes related to energy homeostasis and obesity. Brain Res. 1273, 18–28.

Záborszky, L., Alheid, G.F., Beinfeld, M.C., Eiden, L.E., Heimer, L., Palkovits, M., 1985. Cholecystokinin innervation of the ventral striatum: a morphological and radioimmunological study. Neuroscience 14, 427–453.

Záborszky, L., Pang, K., Somogyi, J., Nadasdy, Z., Kallo, I., 1999. The basal forebrain corticopetal system revisited. Ann. N. Y. Acad. Sci. 877, 339–367.

Zachar, G., Toth, A.S., Balogh, M., Csillag, A., 2017. Effect of nucleus accumbens lesions on socially motivated behaviour of young domestic chicks. Eur. J. Neurosci. 45, 1606–1612.

Zahm, D.S., 2000. An integrative neuroanatomical perspective on some subcortical substrates of adaptive responding with emphasis on the nucleus accumbens. Neurosci. Biobehav. Rev. 24, 85–105.

Zahm, D.S., Brog, J.S., 1992. On the significance of subterritories in the "accumbens" part of the rat ventral striatum. Neuroscience 50, 751–767.

Zahm, D.S., Heimer, L., 1993. Specificity in the efferent projections of the nucleus accumbens in the rat: comparison of the rostral pole projection patterns with those of the core and shell. J. Comp. Neurol. 327, 220–232.

Zhang, R., Tachibana, T., Takagi, T., Koutoku, T., Denbow, D.M., Furuse, M., 2004. Serotonin modifies corticotropin-releasing factor-induced behaviors of chicks. Behav. Brain Res. 151, 47–52.

Zhao, W.Q., Feng, H., Bennett, P., Ng, K.T., 1997. Inhibition of intermediate-term memory following passive avoidance training in neonate chicks by a presynaptic cholinergic blocker. Neurobiol. Learn. Mem. 67, 207–213.

Further reading

Doupe, A.J., Perkel, D.J., Reiner, A., Stern, E.A., 2005. Birdbrains could teach basal ganglia research a new song. Trends Neurosci. 28, 353–363.

Dubbeldam, J.L., den Boer-Visser, A.M., 2002. The central mesencephalic grey in birds: nucleus intercollicularis and substantia grisea centralis. Brain Res. Bull. 57, 349–352.

El Halawani, M.E., Kang, S.W., Leclerc, B., Kosonsiriluk, S., Chaiseha, Y., 2009. Dopamine-melatonin neurons in the avian hypothalamus and their role as photoperiodic clocks. Gen. Comp. Endocrinol. 163, 123–127.

Gale, S.D., Person, A.L., Perkel, D.J., 2008. A novel basal ganglia pathway forms a loop linking a vocal learning circuit and its dopaminergic input. J. Comp. Neurol. 508, 824–839.

González, A., Morona, R., Moreno, N., Bandan, S., López, J.M., 2014. Identification of striatal and pallidal regions in the subpallium of anamniotes. Brain Behav Evol 83, 93–103.

Güntürkün, O., Stacho, M., Ströckens, F., 2017. The brains of reptiles and birds. In: Kaas, J. (Ed.), Evolution of Nervous Systems, vol. 1. Elsevier, Oxford, pp. 171–221.

Jarvis, E.D., Gunturkun, O., Bruce, L., Csillag, A., Karten, H., Kuenzel, W., Medina, L., Paxinos, G., Perkel, D.J., Shimizu, T., Striedter, G., Wild, J.M., Ball, G.F., Dugas-Ford, J., Durand, S.E., Hough, G.E., Husband, S., Kubikova, L., Lee, D.W., Mello, C.V., Powers, A., Siang, C., Smulders, T.V., Wada, K., White, S.A., Yamamoto, K., Yu, J., Reiner, A., Butler, A.B., 2005. Avian brains and a new understanding of vertebrate brain evolution. Nat. Rev. Neurosci. 6, 151–159.

Kingsbury, M.A., Kelly, A.M., Schrock, S.E., Goodson, J.L., 2011. Mammal-like organization of the avian midbrain central gray and a reappraisal of the intercollicular nucleus. PloS One 6, e20720.

Moreno, N., González, A., Rétaux, S., 2009. Development and evolution of the subpallium. Semin Cell Dev Biol 20, 735–743.

Nilsson, S., 2011. Comparative anatomy of the autonomic nervous system. Auton Neurosci 165, 3–9.

Nomura, T., Izawa, E.I., 2017. Avian brains: Insights from development, behaviors and evolution. Dev Growth Differ 59, 244–257.

Perry, S.F., Capaldo, A., 2011. The autonomic nervous system and chromaffin tissue: neuroendocrine regulation of catecholamine secretion in non-mammalian vertebrates. Auton Neurosci 165, 54–66.

Prounis, G.S., Ophir, A.G., 2020. One cranium, two brains not yet introduced: Distinct but complementary views of the social brain. Neurosci Biobehav Rev 108, 231–245.

Sharp, P.J., Ciccone, N.A., 2005. The gonadotrophin releasing hormone neurone: key to avian reproductive function. In: Dawson, A., Sharp, P.J. (Eds.), Functional Avian Endocrinology. Narosa Publishing House Pvt Ltd, India, pp. 59–72.

Chapter 17

Blood

Colin G. Scanes
Center of Excellence for Poultry Science, University of Arkansas, Fayetteville, AR, United States

17.1 Introduction

Blood consists of the following components:

- Plasma
- Formed elements or cells containing nuclei and mitochondria.
  - Erythrocytes (red blood cells)
  - Leukocytes (white blood cells)
  - Thrombocytes (equivalent to platelets in mammals).

Blood is critically important to the physiology of birds. The functions of blood include the following:

- Transportation of the following:
  - Respiratory gases (oxygen and carbon dioxide)
  - Electrolytes (e.g., Na^+, K^+, Ca^{2+}, Mg^{2+}, PO_4^{3-})
  - Nutrients (e.g., glucose, fatty acids, amino acids)
  - Metabolites (e.g., lactate)
  - Waste compounds (urate, urea)
  - Hormones
  - Heat
- Protection via antibodies, leukocytes, and thrombocytes
- Water, glucose, and electrolyte homeostasis
- Clotting in the event of injury of blood vessels.

Blood also carries pathogens and toxicants.

Blood is more viscous than water. The viscosity of chicken blood is calculated as 27.6×10^{-4} Pa s or 3.1-fold that of water while the viscosity of blood from domestic ducks and geese is 4.2-fold that of water (reviewed Sturkie, 1986). While blood viscosity is increased in broiler chickens with ascites, plasma viscosity was reduced (Maxwell et al., 1992a; Fedde and Wideman, 1996).

17.2 Plasma

Table 17.1 summarizes mean concentrations of the constituents of plasma of birds while Table 17.2 compares the plasma volume with the volumes of other fluids in the body of birds. The osmotic pressure of avian plasma comes the following (Peltonen and Sankarri, 2011):

- Electrolytes: 95% (see Table 17.1)
- Glucose, amino acids, urea, and other organic molecules: 5%
- Proteins: 0.5% of colloidal osmotic pressure.

Plasma is 40% more viscous than water (chickens, ostriches, domestic ducks, geese—reviewed Sturkie, 1986).

The circulating concentrations of electrolytes vary with physiological state. Venous plasma concentrations of sodium and plasma osmolarity are elevated by either dehydration or hyperthermia (chickens: Arad et al., 1983). Hyperthermia also results in elevated concentrations of chloride ions, blood urea nitrogen, and uric acid (chickens: Arad et al., 1983).

17.2.1 Circulating electrolytes

The concentrations of individual electrolytes are maintained within strict limits in view of their critical role in blood osmotic pressure and polarization/depolarization of nerves and muscles. The mean circulating concentrations of electrolytes such as sodium, potassium, and chloride across a large number of avian species are summarized in Table 17.1. There are shifts in the circulating concentration of electrolytes with physiological state. For instance, acute heat stress is followed by decreases in the plasma concentrations of sodium and potassium ions (chickens: Borges et al., 2004). Moreover, plasma concentrations of sodium are reduced with fasting and the concomitant reduction in metabolism (Christensen et al., 2012). There are differences in venous plasma concentrations of sodium and chloride between migratory and nonmigratory species of passeriform birds (Heatley et al., 2013).

Circulating concentrations of bicarbonate changes with pCO_2 (see Section 17.4). For instance, there are decreases in the plasma concentrations of bicarbonate ions due to

Sturkie's Avian Physiology. https://doi.org/10.1016/B978-0-12-819770-7.00044-X

TABLE 17.1 Mean concentrations of constituents of plasma in birds.

Parameter	Number of species	Plasma concentration +SEM	Units
Protein	100	39.6 ± 0.74	g/L
Albumen	63	15.9 ± 0.55	g/L
Globulin	55	18.8 ± 0.96	g/L
Glucose	139	15.4 ± 0.32	mM or mmol./L
Sodium	47	152.5 ± 1.13	mequiv./L
Chloride	43	112.6 ± 1.28	mequiv./L
Calcium	49	2.56 ± 0.10	mequiv./L
Potassium	46	3.21 ± 0.19	mequiv./L
Uric acid	60	0.50 ± 0.04	mM or mmol./L
Blood urea nitrogen	43	1.11 ± 0.09	mM or mmol./L

For details of circulating concentrations of serum/plasma constituents in individual avian species, see Table 1 in the companion website.

TABLE 17.2 Blood and other fluid components of birds.

	Volume as a % of body weight	
	Mallard ducks	Chickens (laying hen)
Plasma[a]	4.3	4.6
Interstitial fluid[a]	15.7	21.7
Intracellular fluid	43.6	31.1
Reference	Ruch and Hughes (1975), Keijer and Butler (1982)	Medway and Kare (1959a,b)

[a] *Plasma + Interstitial fluid = extracellular fluid.*

panting associated with acute heat stress (chickens: Borges et al., 2004) and with the hyperventilation of exercise (chickens: Gleeson and Brackenberry, 1984). Differences have been reported for venous plasma concentrations of bicarbonate between migratory and nonmigratory species of passeriform birds (Heatley et al., 2013).

17.2.2 Circulating nutrients and other small organic molecules

The mean circulating concentrations of glucose, uric acid, and urea across a large number of wild bird species are summarized in Table 17.1.

17.2.2.1 Plasma concentrations of glucose

The plasma concentrations of glucose are more than double those in mammals (Table 17.1). In chickens, plasma concentrations of glucose are relatively refractory to physiological changes such as insulin administration or fasting (see Chapter 25). In contrast in wild birds, there are shifts in plasma concentrations of glucose. Plasma concentrations of glucose are depressed after flight (American robins: Gerson and Guglielmo, 2013) but elevated during captivity (rufous-collared sparrow: Ruiz et al., 2009).

17.2.2.2 Plasma concentrations of fatty acids

At times of starvation and other times when additional energy is required, adipose triglyceride is hydrolyzed to fatty acids and glycerol in the process of lipolysis. The fatty acids transit into the plasma and provide an energy source for tissues such as skeletal muscle (see Chapter 23). Plasma concentrations of nonesterified fatty acids (NEFAs) are increased following fasting (chicken: Lepkovsky et al., 1967; Langlow et al., 1970; Serr et al., 2009). In a concomitant manner, plasma concentrations of NEFA are reduced following feeding (chicken: Sato et al., 2008). In contrast, plasma concentrations of NEFA were unaffected by fasting in white-throated sparrow (Smith et al., 2007). In addition, plasma concentrations of NEFA are increased following flying (American robin: Gerson and Guglielmo, 2013).

Plasma concentrations of NEFA are influenced by endocrine status. In chickens, there are increases following insulin challenge (Lepkovsky et al., 1967; Langlow et al., 1970), goitrogen administration causing hypothyroidism

(Hamano, 2012), glucagon administration (Langlow et al., 1970), and the synthetic glucocorticoid, dexamethasone (Serr et al., 2011). Similarly, plasma concentrations of NEFA were elevated following glucagon administration in emperor penguins (Groscolas and Bézard, 1977). In contrast, plasma concentrations of NEFA are decreased by neuropeptide Y (chicken: Liu et al., 2017).

17.2.2.3 Plasma concentrations of lactate

Anaerobic metabolism generates lactic acid. It is, therefore, no surprising that plasma concentrations of lactate are increased during exercise in birds. For example, increased plasma concentrations of lactate have been reported from chickens on a treadmill (from 2.1 to 8.4 mMoles/L in Gleeson and Brackenberry, 1984), within 2 min of flight in captive peregrine falcons and brown goshawks (Holz et al., 2006) and in free-flying migrating northern bald ibis (Bairlein et al., 2015).

17.2.2.4 Uric acid and urea

Nitrogenous waste is carried in the circulation in birds as uric acid and urea (see Chapter 27). Plasma concentrations of uric acid and urea in birds are summarized in Table 17.1. It is assumed that the circulating concentrations of uric acid and urea are very similar in birds (Sturkie, 1986). However, this is only the case when expressed as mg/dL but not on a millimolar (mmole/L) basis. Circulating concentrations of nitrogenous waste are influenced by physiological state. For example, heat stress reduces circulating concentrations of urate (chickens: Lin et al., 2006). Moreover, plasma concentrations of urate increase in a linear with duration of flight (American robin: Gerson and Guglielmo, 2013). This may reflect nitrogen from deamination of amino acids and gluconeogenic production of glucose. Similarly, circulating concentrations of urate are greater in birds consuming an insect diet (high protein) than a grain diet (white-throated sparrow: Smith et al., 2007).

17.2.2.5 Circulating antioxidants

Antioxidants have a protective role, reducing damage from free radicals and the immune-related respiratory burst. The major antioxidant in the plasma is uric acid with vitamin E and four carotenoids together with vitamin C and malondialdehyde also being antioxidants. There are changes in the circulating antioxidant capacity with stress and diet (Cohen et al., 2007, 2009). Moreover, there are decreases in the blood concentration of vitamin A, carotene, malondialdehyde, and vitamin C in chickens challenged with *Eimeria acervulina* (Koinarski et al., 2005). Moreover, enzymes including peroxide dismutase and catalase acts effectively as antioxidants; their activities are depressed in broiler chickens infected with *Eimeria acervuline* (Koinarski et al., 2005).

17.2.2.6 Carotenoids

Carotenoids (e.g., lutein and zeaxanthin) are transported in the blood to tissues near the surface of birds requiring coloration. The dietary hydroxycarotenoids per se provide yellow coloration while red color is the result of biotransformation to ketocarotenoids. This has been studied in the red-legged partridge with their red ornamentation of the legs, eye rings, and bill (García-de Blas et al., 2016).

17.2.3 Plasma proteins

The mean circulating concentrations of protein, albumen, and globulin across a large number of avian species are summarized in Table 17.1. The mean circulating concentrations of protein, albumin, and globulin across a large number of avian species (Table 1: Appendix 1) are the following:

- Protein 36.2 g/L
- Albumin 13.4 g/L
- Globulin 13.9 g/L.

The colloidal osmotic pressure due to plasma proteins is much lower than that exerted by electrolytes and small organic molecules, such as glucose, and lower than that in mammals (Peltonen and Sankari, 2011). Based on electrophoretic analysis, the major proteins in serum are the following:

- Prealbumin (with transthyretin binding thyroid hormones)
- Albumen (binding fatty acids, lipophilic hormones, etc.)
- Globulins (α, β, and γ).

In the reproductively active female birds, there are high concentrations of yolk precursors. In the avian embryo, the major plasma protein is α-fetoprotein. This binds metals. The α-fetoprotein has been isolated from chick embryos but does not appear to bind steroid hormones, unlike its mammalian counterpart (Ido and Matsuno, 1982).

17.2.3.1 Extracellular fluid

Extracellular fluid is comprised of plasma and interstitial fluid. The volume of interstitial fluid is marked greater quantitatively than plasma (Table 17.2). Based on studies with suction blister fluids, the concentrations of proteins in interstitial fluid (extracellular fluid excluding plasma) are about half those in plasma (Peltonen and Sankari, 2011).

17.2.3.2 Albumin

Serum albumin is synthesized in the liver (chicken: Fujii et al., 1996). The functions of albumin include providing a colloidal osmotic effect and facilitating transport of nutrients and lipophilic hormones. For instance, albumin binds to, transports, and distributes lipids, including fatty acids.

In the presence of albumin, there is increased update of saturated fatty acids, such as palmitate, by chick embryo cardiac cells (Paris et al., 1978).

There are changes in the plasma concentrations of albumen during development with increases during late embryonic development and early chick life (Grieninger et al., 1986). Moreover, there are some changes in the plasma concentrations of albumin with physiological state. For instance, induction of early molt by reduced photoperiod and feed withdrawal for 48 h results in reductions in albumin concentrations in the plasma (chickens: Gildersleeve et al., 1983a). There are marked diurnal changes in plasma concentrations of albumin (chickens: Gildersleeve et al., 1983a). Moreover, plasma concentrations of albumin are decreased in laying females (Morgan, 1975). Administration of turpentine evokes an acute phase response with decreased plasma concentrations of albumin (chicken: Grieninger et al., 1986).

17.2.3.3 Globulins

There are multiple proteins in the globulin groupings. Broadly, globulins can be divided into three categories based on electrophoretic mobility:

- Alpha-globulins
  - α_1-globulin, including apolipoprotein A-1, which binds lipids (chickens: Roman et al., 2009), transcortin, and retinol binding protein
  - α_2-globulin including angiotensin (precursor of angiotensin I and II) and ceruloplasmin.
- Beta-globulins
  - β_1-globulin
  - β_1-globulin, including transferrin in mammals but not in birds.
- Gamma-globulin
  - Nonimmunoglobulin fraction containing transferrin in at least some birds (Torres-Medina et al., 1971). Fujii et al. (1996) and McKnight et al. (1980) reported that transferrin is expressed in the liver and oviduct, and it is secreted into the blood.
  - Immunoglobulins (Igs):
    - IgA
    - IgM
    - IgY (equivalent to IgG in mammals).

The structures of plasma proteins from avian species have been predicted from mRNA and cDNA sequencing including the following:

- Albumin [chicken (*Gallus gallus*): NCBI Reference Sequence: NM_205261.1]
- Alpha fetoprotein (chicken: NCBI Reference Sequence: XM_003641200.1)
- Ceruloplasmin [chicken: NCBI Reference Sequence: XM_001235148.2; turkey (*Meleagris gallopavo*): NCBI Reference Sequence: XM_003209288.1; zebra finch (*Taeniopygia guttata*): NCBI Reference Sequence: XM_002188284.2].
- Transferrin receptors (chicken: NCBI Reference Sequence: NM_205256.1).

Globulin concentrations are influenced by physiological state. For instance, induction of early molting, by reduced photoperiod and feed withdrawal, is followed by increases in the circulating concentrations of total globulin (chickens: Gildersleeve et al., 1983a). Serum concentrations of α_1-globulin decline during growth in male chickens (Peltonin and Sankari, 2011).

17.2.3.4 Specific proteins including vitamin and cation binding proteins

17.2.3.4.1 Ceruloplasmin

The principal circulating transporter protein that binds copper ions is ceruloplasmin. This glycoprotein is produced by the liver. Avian ceruloplasmin has been purified and partially characterized (chicken: Calabrese et al., 1988; Disilvestro and Harris, 1985; Hilewicz-Grabska et al., 1988). Chicken ceruloplasmin binds five atoms of copper per molecule (Calabrese et al., 1988).

Plasma concentrations of ceruloplasmin are influenced by physiological and nutritional status. Concentrations of ceruloplasmin are affected by copper status being depressed by copper deficiency (chicken: Baumgartner et al., 1978; Kaya et al., 2006) and elevated by dietary copper supplementation (chicken: Koh et al., 1996; Jarosz et al., 2018). Plasma concentrations of ceruloplasmin are also elevated acutely following injection of *Escherichia coli* endotoxin/lipopolysaccharide (LPS) (chicken: Curtis and Butler, 1980; Lin et al., 2006; Wang et al., 2016) and by glucocorticoids (chicken: Lin et al., 2004). Circulating concentrations of ceruloplasmin are depressed in birds receiving dietary supplementation with 5-aminolevulinic acid, a precursor for porphyrin and then heme (chicken: Sato et al., 2012).

17.2.3.4.2 Retinol-binding protein

Vitamin A is transported bound to retinol-binding protein (RBP) which can complex with prealbumin (chicken: Abe, 1975). The only circulating RBP is RBP 4 in birds (Yin et al., 2013). Avian RBP has been purified and its crystal structure characterized (chicken: Zanotti et al., 2001). Transthyretin also binds RBP (Eguchi et al., 2008).

The liver has the highest expression of RBP 4, but it is also expressed in the small intestine, ovary, kidney, and heart (chicken: Yin et al., 2013). Synthesis of RBP 4 by the liver is inhibited in vivo by vitamin E in the feed or in vitro by α-tocopherol in the incubation media (chicken: Zhou et al., 2012).

17.2.3.4.3 Transferrin

Transferrin transports iron (two molecules of iron for each molecule of transferrin) in the blood (reviewed Lambert et al., 2005) with, in turn, there being at least some of the transferrin bound to transferrin receptor. The circulating concentrations of iron are reported as ~2 μg/mL (Morgan, 1975). Iron bound to transferrin can be transferred to the other major iron-binding protein, the yolk precursor phosvitin (Morgan, 1975).

The structure of avian transferrin has been reported (chicken: Guha Thakurta et al., 2003; Lambert et al., 2005). In addition to transporting iron, transferrin facilitates the uptake of ferrous iron during development of erythrocytes (chick embryo blood cells: van Bockxmeer and Morgan, 1982). Transferrin also binds a circulating enzyme, butyrylcholinesterase (chicken: Weitnauer et al., 1999).

Transferrin is synthesized by liver and secreted into the blood (chicken: Fujii et al., 1996). In birds, expression of the transferrin gene is restricted to the liver and oviduct (McKnight et al., 1980). The chicken transferrin receptor has been characterized based on the cDNA (chicken: Gerhardt et al., 1991). The transferrin receptor can induce programmed cell death or apoptosis (chicken: Ohno et al., 2008).

The circulating concentrations of transferrin and the transferrin receptor are reported as respectively 2.4 mg/mL (Morgan, 1975) and 1.2 μg/mL (chicken: Wiwanitkit et al., 2007). Plasma transferrin receptor concentrations reflect erythropoietic activity.

There are effects of physiology on circulating concentrations of transferrin. Circulating concentrations of transferrin are elevated by either estrogen or iron deficiency (chicken: McKnight et al., 1980). Hepatic expression of transferrin increased by estrogen and glucocorticoids (chicken: McKnight et al., 1980). Plasma concentrations of transferrin are also increased in chickens with a *Staphylococcus aureus* infection (Chamanza et al., 1999). Similarly, there is a strong tendency for plasma concentrations of transferrin receptor to be increased in birds infected with *Plasmodium gallinaceum*, the protozoan that causes malaria in poultry (chicken: Wiwanitkit et al., 2007).

17.2.3.4.4 Proteins protecting against tissue damage from hemoglobin

When erythrocytes are lysed or the cell membrane is destablized, hemoglobin is released. In the absence of defense mechanisms, there is oxidation of lipids and proteins by the hemoglobin. The hemoglobin binding protein, haptoglobin, is part of the defensive mechanism in mammals and some avian species. Haptoglobin is absent from chickens where there is an alternative hemoglobin binding protein, PIT54 (Wicher and Fries, 2006). The structure of haptoglobin has been deduced from cDNA from multiple avian species [Infraclass: *Palaeognathae* e.g., emu (*Dromaius novaehollandiae*) XM_026104274; Infraclass: *Neognathae* Superorder *Neoaves* e.g., Anna's hummingbird (*Calypte anna*) Genbank Accession number XM_030458019.1; golden-collared manakin (*Manacus vitellinus*) XM_008927555.2; willow flycatcher (*Empidonax traillii*) XM_027904202; peregrine falcon (*Falco peregrinus*) XM_005235439; rock pigeon (*Columba livia*) XM_005504706 and Adelie penguin (*Pygoscelis adeliae*) XM_009335253].

In contrast, the haptoglobin gene appears to be missing in the Superorder *Galloanserae* (ducks, geese, chickens, turkeys, etc.). Haptoglobin like activity, as determined by its ability to prevent hemoglobin peroxidase activity, is increased in chickens challenged with infectious bronchitis virus infection as part of the acute phase response (Asasi et al., 2013). Another protective protein is hemopexin, an α_1-globulin and hemoglobin-binding protein (chicken: Grieninger et al., 1986). There is a 1000-fold increase in plasma concentrations of hemopexin beginning day 21 of embryonic development rising rapidly during early chick life (Grieninger et al., 1986). Moreover, administration of turpentine evokes an acute phase response with increased plasma concentrations of hemopexin.

17.2.3.4.5 Hormone binding proteins

Lipophilic hormones including the steroid hormones are transported in the plasma bound to proteins including albumin and specific binding proteins. The rationale for lipophilic hormones having binding proteins in the circulation is to facilitate the distribution of the hormones throughout their target organ(s) (Richardson et al., 2005).

17.2.3.4.6 Sex hormone–binding protein

While sex steroid–binding globulin is present in mammals [e.g., from Genbank: rat (*Rattus norvegicus*) NM_012650] and reptiles [e.g., from Genbank: Chinese alligator (*Alligator sinensis*) XM_025195189.1; green anole (*Anolis carolinensis*) XM_016998039], it is not present in birds (Wingfield et al., 1984; Breuner and Orchinik, 2009; Malisch and Breuner, 2010) with none recorded in Genbank.

17.2.3.4.7 Thyroid hormones/transthyretin

Homologs of mammalian thyroxine-binding globulin are not present in birds (Schreiber and Richardson, 1997). Thyroid hormones bind to both albumin (Schreiber and Richardson, 1997) and transthyretin in birds as in all other vertebrate classes (Schreiber and Richardson, 1997; Richardson et al., 2005). Avian transthyretin has been purified as a 15 KDa protein (chicken: Eguchi et al., 2008). In contrast with the situation with mammalian transthyretin, there is greater binding of T_3 than T_4 to avian transthyretin

[chicken: Duan et al., 1991; glaucous gull (*Larus hyperboreus*) and herring gull (*Larus argentatus*): Ucán-Marin et al., 2009, 2010]. Transthyretin also binds retinol binding protein (Eguchi et al., 2008).

17.2.3.4.8 Transcortin (corticosteroid bonding globulin)

Birds have a corticosteroid-binding globulin (CBG) or transcortin. This α1 globulin binds and transports corticosterone in the plasma, for example, in the American kestrel (Whitman et al., 2011), chicken (Murakami, 1991), white crowned sparrow (Breuner and Orchinik, 2009), and zebra finch (Schmidt et al., 2010). CBG has been characterized in birds (chicken and zebra finch: Vashchenko et al., 2016). Not only does CBG bind corticosterone, cortisol, and progesterone but also multiple androgens (dark-eyed juncos: Deviche et al., 2001; chicken and zebra finch: Vashchenko et al., 2016). Circulating concentrations of CBG are influenced by reproductive state (e.g., either testosterone treatment or breeding season in male dark-eyed juncos: Deviche et al., 2001) and stress (American kestrel: Whitman et al., 2011).

17.2.3.5 Gamma globulins

Gamma globulins include IgA, IgM, and IgY (equivalent to IgE and IgG in mammals). In growing chickens, the concentrations of Igs are the following:

- Immunoglobulin A (IgA): 0.3 g/L
- Immunoglobulin M (IgM): 2.7 g/L
- Immunoglobulin Y (IgY): 5.5 g/L

(based on Klasing 1998). The concentrations of IgY are markedly lower in laying hens (0.8 g/L) (Cetin et al., 2010) probably reflecting transfer into the yolk-filled oocyte.

In birds, there is transfer of Ig into eggs with, for instance, amounts being 99% of IgY in the yolk and less than 1% in the egg white (see Table 17.3) (chicken: Hamal et al., 2006). Yolk concentrations of IgY are 36% of those of plasma. In contrast, IgA and IgM are only about 5% of plasma concentrations. Chick embryos take up IgY via the yolk sac (see Table 17.3) (chicken: Hamal et al., 2006). This provides passive or maternal immunity. The hatched chicks have maternal antibodies in their circulation as is evident for the decline in plasma concentrations of IgY but not IgA or IgM in posthatching development (see Table 17.3) (chicken: Hamal et al., 2006). Moreover, vaccination of the dam results in important passive immunity to pathogens in the first weeks of life (e.g., Maas et al., 2011; Lardinois et al., 2014). Similarly, transfer of antibodies has been demonstrated in zebra finches (Martyka et al., 2011).

17.2.3.6 Enzymes

There are multiple enzymes in the plasmas of birds including the following: alkaline phosphatase, glutamic oxaloacetic transaminase (GOT), and lactic acid dehydrogenase (LDH) (also see above). The activities of aspartate aminotransferase and creatine phosphotransferase are most frequently determined in hematological studies. Circulating antioxidant enzymes include superoxide dismutase, catalase, and glutathione peroxidase.

The activity of enzymes is reported to be influenced by both physiology and the external environment. For instance, alanine transferase activity in venous plasma is elevated by either dehydration or hyperthermia (Arad et al., 1983). Histidine supplementation increased the activity of the antioxidant enzyme, glutathione peroxidase but decreased reactivity of superoxide dismutase in plasma (turkeys: Kopec et al., 2016). Induction of an early molt by

TABLE 17.3 Demonstration of transfer of maternal IgY but not IgA or IgM via the yolk.

	IgY	IgA	IgM
Plasma concentration (dam[a]) mg mL^{-1}	4.64	0.32	0.92
Egg total in mg (mg mL^{-1})			
Yolk	33.2 (1.70)	0.37 (0.02)	0.40 (0.02)
White	0.24 (0.01)	0.37 (0.01)	0.23 (0.01)
Chick plasma mg mL^{-1}			
Three days	1.25	0.00	0.01
Seven days	0.74	0.02	0.11
14 days	0.59	0.15	0.14
21 days	0.69	0.19	0.22

[a]*Broiler breeder hens.*
Calculated from Hamal et al. (2006).

reduced photoperiod and withdrawing feed results in changes in plasma activities of the following: glutamic pyruvic transaminase (decreased), alkaline phosphatase, LDH, and GOT (increased) (chickens: Gildersleeve et al., 1983a). Moreover, depressed plasma cholinesterase activity has been used as a biomarker for exposure to organophosphate pesticides (Santos et al., 2012). However, it is critically important to have a baseline for cholinesterase activity in plasma of the specific species (Santos et al., 2012).

17.2.3.7 Yolk precursors

The major yolk precursors are transported in the blood of the laying female bird and are the following:

- Vitellogenin
- Very low-density lipoprotein (VLDL).

Both vitellogenin and VLDL are synthesized in the liver with synthesis induced by estrogen (Deeley et al., 1975). In the circulation, VLDL has the following characteristics:

- Globular micelle-like
- Nonpolar core of triglycerides and cholesterol esters
- Coated with amphiphilic mix of phospholipid, free cholesterol, and apolipoprotein.

(reviewed Loh et al., 2011).

Vitellogenin and VLDL are transported across the oocyte cell membrane by a receptor-mediated process (chickens: Stifani et al., 1990). The half-life of VLDL in female turkeys is 5.05 h (Bacon, 1981). There is little variation in the circulating concentration of vitellogenin during the ovulation cycle of the hen (calculated from Redshaw and Follett, 1976). Within the oocyte, vitellogenin is cleaved to lipovitellin and phosvitin (Deeley et al., 1975).

17.3 Erythrocytes

Table 17.4 summarizes multiple erythrocyte characteristics including number, hematocrit, and erythrocyte size in wild birds and adult poultry. The percentage of plasma trapped in formed elements in hematocrit is estimates as 1.7% (Brahm and Wieth, 1977).

17.3.1 Structure of the erythrocyte

Unlike mammalian erythrocytes, avian erythrocytes have nuclei and other intracellular organelles such as mitochondria (e.g., Stier et al., 2013, 2014). Avian erythrocytes exhibit lower permeability to urea than mammalian erythrocytes (Brahm and Wieth, 1977).

Avian erythrocytes are ovoid cells (Figure 17.1) with an average volume of 145 fL across multiple avian species with consistent sizes (Scanes, 2015) (Table 17.4):

- Long diameter: ~ 12.5 μm
- Short diameter: 6.8 μm
- Thickness: 3.2 μm.

The volume of erythrocytes declines during the development from 170 fL at day 10−140 fL at day 18 (chicken: Tazawa et al., 2011). There is marked asymmetry, with a ratio of erythrocyte length to width of 1.7 in chickens and 1.8 in wild birds. The surface area of chicken erythrocytes was reported as 149 μm^2 (Bulliman and Kuchel, 1988).

TABLE 17.4 Characteristics of erythrocytes in wild birds (excluding poultry species) and chickens.

Parameter	Wild birds		Chickens[a]	Units
	Number of species	Data		
PCV[b]/Hematocrit	158	44.0	44.0	%
Hemoglobin	134	14.5	10.1	%
Erythrocytes				
Concentration	164	3.33	3.2	$10^6\ \mu L^{-1}$ or $10^6\ mm^{-3}$
Volume	81	149.6	149.4	fL
Length	364	12.5	12.2	μM
Width	362	6.8	7.1	μM
Ratio of length to width	362	1.844	1.718	
Cross-sectional area[c]	362	68.3	68.0	μM[b]
Hemoglobin amount	23	50.8	32.0	fg

For additional materials, see the companion website.
[a]*Summarized from early data from mature adult chickens (Sturkie, 1986).*
[b]*PCV or packed cell volume.*
[c]*Area = π × ½ length × ½ width.*

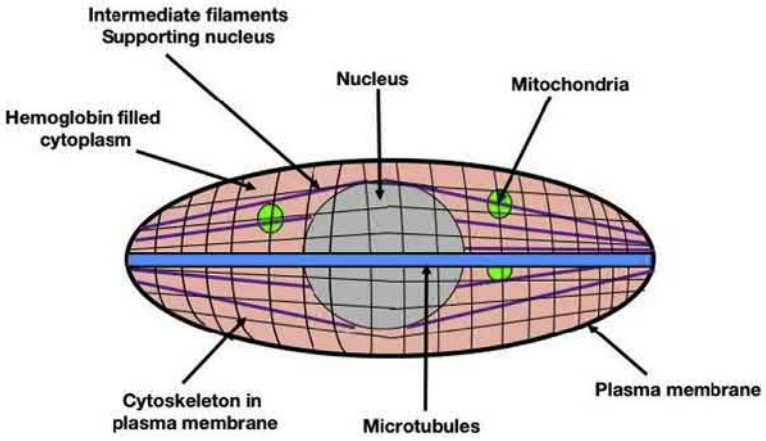

FIGURE 17.1 **Avian erythrocytes.** (A) Schematic view of avian erythrocyte showing nucleus, hemoglobin filled cytoplasm, mitochondria (green), marginal band of microtubules (blue), membrane cytoskeleton (shown as cross-hatch) maintaining shape of the cell and intermediate filaments (purple) support the nucleus. (B) Electron microscopy of chicken bone marrow cells showing developing erythrocytes with electron dense hemoglobin (bar 5 μm). *Reproduced from Shini et al. (2008).*

17.3.1.1 Nucleus

There is a centrally located nucleus (long diameter ~6.5 μm, short diameter ~2.8 μm). The avian erythrocyte differs from that in mammals by the presence of a nucleus and mitochondria and by being larger. The most abundant protein is hemoglobin (Figure 17.1). Nuclear abnormalities such as micronuclei, nuclear buds, notched nuclei, binucleated cells, nuclear tails, and nucleoplasmic bridges are observed in avian erythrocytes (Quero et al., 2016). Erythrocytes of wild birds contain more hemoglobin than those of chickens (Table 17.4). The nuclei of avian erythrocytes contain hemoglobin (Davis, 1961). This is contiguous with cytoplasmic hemoglobin via pores in the nucleus membrane (Davis, 1961).

17.3.1.2 Plasma and nuclear membranes

There is a similar surface area for the plasma and nuclear membranes per cell (Zentgraf et al., 1971). The structures of the plasma and nuclear membranes of chicken erythrocytes have been investigated. Water permeability of avian erythrocytes was reported as 1.35 cm/s (Brahm and Wieth, 1977).

17.3.1.2.1 Lipid composition

Plasma and nuclear membranes differ in composition (see Table 17.5). The fatty acid composition of the cell membrane of avian erythrocytes is modified in the diet (e.g., cockatiel—Heinze et al., 2012). The plasma membrane contains ATPase (Zentgraf et al., 1971) including Na^+/K^+ ATPase (Watts and Wheeler, 1978) and Ca^{2+}-ATPase (Alves-Ferreira et al., 1999; Li et al., 2011) while the nuclear membrane contains lamin B receptor (Simos et al., 1996). The osmotic fragility of avian erythrocytes is reduced by the flavonoid, fisetin (Ogbuagu et al., 2018).

17.3.1.2.2 Carbohydrates in the erythrocyte plasma membrane

N-glycans on the surface of avian erythrocytes have been characterized (chicken: Aich et al., 2011).

17.3.1.2.3 Proteins in the erythrocyte plasma membrane

There are multiple proteins in the plasma membrane of birds including class I molecules. Expression of class I molecules varies markedly in chicken erythrocytes by different chicken MHC haplotypes (Tregaskes et al., 2016). There are also receptors in the erythrocyte plasma membrane. Peptides representing variants of a putative hemagglutination motif bind to a sialylated receptors on avian erythrocytes plasma membranes (chicken: May et al., 2014). Desialylated erythrocyte membranes show much reduced binding of these peptides (May et al., 2014).

17.3.1.3 Microtubules

Microtubules stabilize the asymmetric structure of erythrocytes (Winckler and Solomon, 1991). They are composed of tubulin, with 95% of the tubulin from chicken erythrocytes being tubulin-βVI (Sharma et al., 2010). The erythrocyte anion transport protein (erythrocyte band 3) is the major transport protein in the erythrocyte. It has two functions:

- An anchor for the intracellular cytoskeleton
- The key anion transporter exchanging bicarbonate (HCO_3^-) for chloride (Cl^-) ions.

TABLE 17.5 Lipid composition of cell membranes of avian erythrocytes.

Lipids[a]	Lipid composition of chicken (pigeon) erythrocyte membranes	
	Plasma membrane	Nuclear membrane
Cholesterol	1.04	0.42
Cholesterol esters	0.02	0.11
Phospholipids	1.00	1.00
• Phosphatidylcholine	0.30 (0.33)	0.53
• Phosphatidylethanolamine	0.31 (0.30)	0.26
• Sphingomyelin	… 0.31 (0.19)	0.13
• Phosphatidylinositol	0.04 (0.04)	0.07

[a]*Data are expressed as a molar ratio relative to total phospholipids.*
Data from Kleinig et al. (1971), Watts and Wheeler (1978).

17.3.1.4 Mitochondria

Mitochondria have been demonstrated to be present in erythrocytes by transmission electron microscopy (e.g., zebra finch: Stier et al., 2013, 2014). The mitochondria are functional producing the reactive oxygen species (ROS) and mitochondrial superoxide (zebra finch: Stier et al., 2013).

17.3.2 Erythrocyte chromatin and transcription

Chromatin is composed of DNA with associated proteins. The chromatin structure is critical in the control of DNA replication, repair, and transcription. It is reasonable to conclude that the chromatin is in a decondensed state (Morera et al., 2011). The 30-nm fiber is the "first hierarchical level of chromatin folding" allows transcription and access by regulatory factors but not DNA replication in chicken erythrocytes (Scheffer et al., 2011). There are also strong associations between linker histones and chromatin in chicken erythrocyte nuclei (Koutzamani et al., 2002). The histones associated with the DNA in the nuclei within avian erythrocytes can undergo post-translational modification including acetylation, formylation, phosphorylation, and oxidation (Sarg et al., 2015; Jahan et al., 2016). This influences expression of specific genes.

17.3.2.1 Transcription and translation

There is both transcription and translation in avian erythrocytes (e.g., chicken: Morera et al., 2011; St. Paul et al., 2013). The ratio of RNA to hemoglobin decreases rapidly in a linear manner from about 240 μg per mg on day 3−35 μg per mg at day 6 (chicken: Baumann et al., 2003). Subsequently, the ratio of RNA to hemoglobin declines at a much slower rate to less than 10 μg per mg at day 17 (chicken: Baumann et al., 2003). There are large reductions in the erythrocyte ATP content decreasing from a molar ratio of RNA to Hb from 6.8 (day 3) to 0.5 (day 17) (chicken: Baumann et al., 2003).

Avian erythrocytes have also been demonstrated to express innate immune system genes including toll-like receptor (TLR) 2, 3, 4, 5, 9, and 21 together with type 1 interferon (IFN), myxovirus resistance 1, and interleukin (IL)-8 (Morera et al., 2011; St. Paul et al., 2013). Expression in antimicrobials influenced after infection with Marek's disease virus (AvBD2, 4, 7 ↑; AvBD1, 6, 9 ↓) (Niu et al., 2018). Selenium deficiency influenced the expression of 24 selenoproteins and 10 cytokines (chicken: Luan et al., 2016).

17.3.2.2 Stress and erythrocyte DNA

Stress increases DNA damage in avian erythrocytes with this correlating with both plasma concentrations of corticosterone (captivity in house sparrows: Gormally et al., 2019). Oxidative damage to DNA is reported in erythrocytes from birds (European starling Nettle et al., 2017). Stress has also been reported to influence both methylation and hydroxymethylation of specific genes in the avian erythrocytes (Pértille et al., 2017).

17.3.2.3 Telomeres

Telomeres protect the ends of chromosomes. The length of telomeres decreases with age in multiple species with telomere rate of change being a predictor of lifespan (Tricola et al., 2018). There are exceptions with the decrease in telomere with age not being seen in all birds, e.g., great spotted cuckoos (Soler et al., 2015).

17.3.3 Metabolism of erythrocytes

Surprisingly, metabolism and expression of metabolic enzymes in avian erythrocyte has received relatively little attention. It has been assumed that glucose is the major substrate for energy needs of the erythrocyte. However, glucose failed to maintain erythrocyte ATP in vitro (chicken: Mathew et al., 1993). In contrast, glutamine was effective (chicken: Mathew et al., 1993). Moreover, chicken erythrocytes can employ glycine as a substrate (Dajani and Orten, 1959).

There is evidence that the avian erythrocyte employs the citric acid cycle based on older literature (chicken: Dajani and Orten, 1958). However, there was no detectable activity of TCA cycle enzymes in the pigeon erythrocyte (Kalomenopoulou and Beis, 1990). Metabolic enzymes activities (including the following hexokinase, phosphofructokinase, and pyruvate kinase) are reported in pigeon erythrocytes (Kalomenopoulou and Beis, 1990). High activities for the following enzymes have been reported for erythrocytes from the little penguin (*Eudyptula minor*): triphosphate isomerase, lactate dehydrogenase, glyceraldehyde phosphate dehydrogenase, and phosphoglycerate kinase (Nicol et al., 1988). In the little penguin (*Eudyptula minor*) erythrocytes, about half glucose is metabolized to lactate (Nicol et al., 1988).

Erythrocytes have a high concentration of ATP in early embryonic development e.g., 15 mmol per liter at day three of incubation (chicken: Baumann et al., 2003). Erythrocytes from chick embryos also have significant levels of CTP and UTP (chicken: Baumann et al., 2003). In addition, erythrocytes from chick embryos contain another high-energy compound, 2,3-bisphosphoglycerate (2,3-BPG) (chicken: Baumann et al., 2003). In vitro, ATP concentrations are depressed by hypoxia in erythrocytes from 10-day embryos (chicken: Baumann et al., 2003).

17.3.3.1 Mitochondrial functioning in avian erythrocytes

Mitochondria are not only present in erythrocytes (e.g., zebra finch: Stier et al., 2013) but also exhibit both oxygen consumption together with both basal production of superoxide and elevated superoxide production in the presence of antimycin (Stier et al., 2013).

The important mitochondrial inner membrane phospholipid, cardiolipin, is found in erythrocytes from 21 species of birds from the orders *Accipriformes*, *Anseriformes*, *Columbiformes*, *Faconiformes*, *Galliformes*, *Passeriformes*, and *Strigiformes* (Delhaye et al., 2016). Interestingly, longevity of avian species was reported to be related to both production of ROS by erythrocyte mitochondria and to mitochondrial cardiolipin content (Montgomery et al., 2012; Delhaye et al., 2016).

17.3.3.2 Enzymes in erythrocytes

Antioxidant enzymes are present in erythrocytes. Histidine supplementation decreased the activity of the antioxidant enzyme, superoxide dismutase in erythrocytes (turkeys: Kopec et al., 2016).

17.3.4 Number of avian erythrocytes and packed cell volume

There are physiological effects on both hematocrit and erythrocyte concentrations. These are, for instance, reduced from prior to breeding to egg production (zebra finches: Wagner et al., 2008). Cobalt increases erythrocyte numbers and can cause polycythemia (Diaz et al., 1994). Fair et al. (2007) concluded that hematocrits were greater in adult than immature or nestling birds. In contrast, there was no difference in the hematocrit between males and female birds based on a meta-analysis of 36 studies of wild bird species (Fair et al., 2007). Erythrocyte numbers were greater in January in Belize prior to migration than in summer in Connecticut (gray catbirds: Booth and Elliott, 2003). Similarly, hematocrit was greater in migratory than sedentary Passerine species (Pistone et al., 2017).

Table 17.4 summarizes the mean packed cell volume (hematocrit) and erythrocyte concentrations across multiple avian species and a comparison with earlier data in chickens. Across avian species, hematocrit is inversely proportional to $\log_{10}$ body weight declining from 52% on average in birds at 10 g to 40% in birds at 1 kg (Bishop and Butler, 1995). When erythrocytes are removed, the hematocrit declines as the plasma volume is more rapidly restored. Following removal of 30% of the blood, there is an almost immediate decrease in hematocrit and erythrocyte concentration (Japanese quail: Schindler et al., 1987).

When oxygen partial pressure is low, there is an increase in erythrocyte concentrations and hematocrit. For instance, hypoxia increases hematocrit (Japanese quail: Rosse and Waldmann, 1966; chickens: Maxwell et al., 1987). Similarly following removal of 30% of the blood and the immediate decrease in erythrocyte concentration, there is then a rapid recovery with 72 h (Japanese quail: Schindler et al., 1987). Indicative of the acceleration of erythropoiesis, there are parallel increases in the number of immature red blood cells, namely reticulocytes, in the blood and bone marrow (Japanese quail: Gildersleeve et al., 1985a,b; Schindler et al., 1987). In an analogous manner, erythropoiesis is depressed in polycythemic birds (Japanese quail: Rosse and Waldmann, 1966).

There are marked increases in the concentration of erythrocytes during embryonic development (chicken: Tazawa et al., 2011). These changes are illustrated in Figure 17.2. As might be expected, the concentration of erythrocytes is increased in response to high altitude

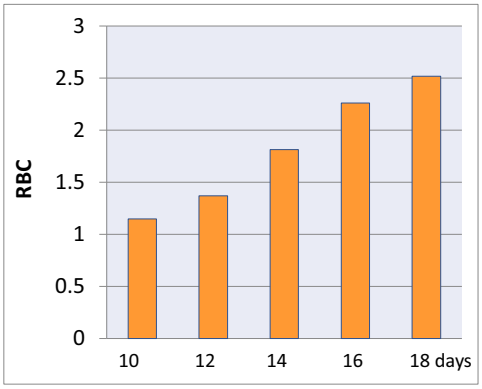

FIGURE 17.2 Changes in erythrocyte numbers (number × 10^6 per µl) during embryonic development of the chicken. *Data from Tazawa et al. (2011).*

(e.g., turkey embryos: Bagley et al., 1990). Similarly, and not unexpectedly, hematocrit is reduced with copper deficiency (chicken: Baumgartner et al., 1978). In chickens, there appears to be a sex difference in hematocrit and erythrocyte number between breeding males and females (Table 17.6), presumably due to the high concentrations of yolk precursors in the plasma.

There are also decreases in erythrocyte concentrations by some toxicants, e.g., following *in ovo* administration of 1-(2-chlorophenyl)-1-(4-chlorophenyl)-2,2,2-trichloroethane o,p'-DDT (Japanese quail: Bryan et al., 1989), chemicals such as acetophenylhydrazine and the organophosphorus pesticide, foschlor, reduce the circulating concentration of erythrocytes, inducing anemia in chickens (Coll and Ingram, 1978; Gromysz-Kałkowska et al., 1985). Moreover, petroleum oil decreases packed cell volume (mallard ducks: Lee et al., 2012). Some chemicals such as acetophenylhydrazine and foschlor reduce the circulating concentration of erythrocytes, inducing anemia in chickens (Coll and Ingram, 1978; Gromysz-Kałkowska et al., 1985). Similarly, hematocrit is depressed in seabirds from sites contaminated with petroleum oil (Fallon et al., 2018).

17.3.5 Production

Avian erythrocytes are produced in the bone marrow. In vitro, embryonic bone marrow cells have been demonstrated as capable of developing into erythrocytes (e.g., Japanese quail: Brandon et al., 2000).

The avian erythrocyte series can be summarized as follows:

- Erythroblasts (cell proliferation) →
- Polychromatic erythroblasts (reduce cell volume with hemoglobin synthesis initiated) → Reticulocytes (further reduce cell volume with hemoglobin synthesis) →
- Mature erythrocytes

(based on Williams, 1972).

17.3.6 Erythropoietin

Evidence for an avian erythropoietin (EPO) comes from the ability of chicken plasma to stimulate heme accumulation in chicken erythroid cells in vitro with plasma from anemic chickens being more effective (Coll and Ingram, 1978). Moreover, in vivo the rate of erythropoiesis changes in a manner consistent with control by EPO; being increased in anemia (chicken: Rosse and Waldmann, 1966) and depressed by polycythemia (Japanese quail: Rosse and Waldmann, 1966). During development of bone air sacs in the bones of posthatching pigeons, there are decreases in hemopoietic bone marrow as a percentage of body weight and increased distribution in ulna, radius, femur, tibiotarsus, scapula, furcula, and the caudal vertebrae (Schepelmann, 1990).

The structure of avian EPO has been deduced from cDNA [e.g., budgerigar (*Melopsittacus undulatus*)—XM_034073494.1; chicken (*Gallus gallus*)—KR063574.1; kakapo (*Strigops habroptila*)—XM_030474553.2; kiwi (*Apteryx rowi*)—XM_026063843.1; Swainson's thrush (*Catharus ustulatus*)—XM_033084268.1; Tibetan groundtit (*Pseudopodoces humilis*)—XM_014262263.1; wire-tailed manakin (*Pipra filicauda*)—Genbank XM_027712402; Zebra finch (*Taeniopygia guttata*)—XM_032745377].

EPO acts by binding to the EPO receptor (EpoR). The structures of the EpoR have been deduced (chicken: Hron et al., 2015). There is increased proliferation of avian erythroblasts with over-expression of EpoR (Mikulits et al., 2000). Moreover, iron repression of ferritin heavy chain expression is prevented by over-expression of both EpoR and c-Kit, another cytokine growth factor receptor (Mikulits et al., 2000).

TABLE 17.6 Comparison of erythrocyte concentrations and hematocrit in male and female chickens.

Gender of reproductively mature chickens	Erythrocyte concentration 10^6 µL^{-1} or 10^6 mm^{-3}	PCV/Hematocrit %
Male (rooster)	3.6	42.9
Females (laying hen)	2.8	29.8

17.3.7 Lifespan

Despite having a nucleus, avian erythrocytes do not divide failing to enter a new S phase (Williams, 1972). Bird erythrocytes have a very limited lifespan that is much less than in mammals (e.g., Brace and Atland, 1956; reviewed Beuchat and Chong, 1998) with all labeled cells disappearing in 42 days (ducks), 35 days (chickens—*Gallus gallus*) and 48 days (pigeons—*Columba livia*) (Rodman et al., 1957) and a mean survival time of 34 days in the (Japanese quail *Coturnix coturnix*: Nirmallan and Robinson, 1973).

The lifespan of avian erythrocytes is calculated as mean = 39.7 + (n = 4 species) S.E.M. 3.3 days. In contrast, the longevity of mammalian erythrocytes is longer at 85.6 + (n = 11 species) S.E.M. 10.5 days (Calculated from Röhme, 1981).

17.3.8 Hemoglobin

Hemoglobin binds to oxygen at the lungs and releases oxygen at the tissues. Avian hemoglobin has been purified (Chicken: Matsuda and Takae, 1963), crystallized, and characterized including X-ray analysis (e.g., bar-headed goose: greylag goose: Liang et al., 2001; ostrich: Sundaresan et al., 2009). As with mammals, hemoglobin is a tetrameric protein with four heme units. There are two α-globin and two β-globin together with four heme units, each containing ferrous iron ions in each hemoglobin molecule.

The molecular basis of the greater oxygen affinity and a lower Bohr effect of early embryonic hemoglobin has been established (Chapman et al., 1980). ATP and other nucleotides major determinants of oxygen saturation (chicken: Baumann et al., 2003).

There are multiple forms of avian hemoglobin with six forms in the chicken, four embryonic and two in the adult:

Embryo

Major forms

- Hb P with π α globin and ρ β
- Hb P′

Minor forms

- Hb M α^D globin
- Hb E α^A globin

Adult

Major form

- Hb A α^A globin

Minor form

- Hb D α^D globin

In the chicken, the relative contribution of two major embryonic hemoglobins peaks at four days of embryonic development and then decreases gradually. They are no longer detectable from 15 days. The two minor ones increase up to 6–7 days and then decrease but are still present in the blood at hatching (Cirotto et al., 1975). The shifts in composition of composition of α globin in chick embryo blood are summarized in Figure 17.3. During development, there are switches in which globin genes are expressed with for instance inactivation/silencing of the π gene for early embryonic hemoglobin in adult erythroblasts (chicken: Rincón-Arano et al., 2009; Ioudinkova et al., 2011) with methylation of the promoter region of the gene (chicken: Singal et al., 2002).

Inositol hexaphosphate and 2,3-BGP bind to a specific binding site in both oxygenated and deoxygenated avian

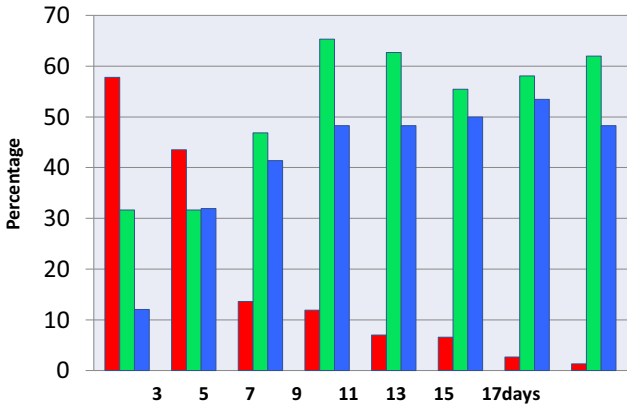

FIGURE 17.3 **Shifts in the proportion of α globins during embryonic development of the chicken (red π α globin, green α A globin, and blue α D globin).**

hemoglobin (chicken: Brygier et al., 1975). The binding of oxygen to hemoglobin is markedly affected by organic phosphates in the avian erythrocyte. In most birds, it is thought that the major regulator is inositol pentaphosphate, but in ostriches, there is evidence that inositol tetrakisphosphate (inositol-P_4) plays a critical role (Sundaresan et al., 2009). Inositol hexakisphosphate (inositol P_6) decreases the affinity of chicken or pigeon hemoglobin for oxygen (Vandecasserie et al., 1971). Similarly, inositol-P_5 lowers the oxygen affinity of hemoglobin (Isaacks et al., 1977).

Arteriovenous differences in the blood concentration of oxygen are constant in either resting or exercising birds being independent of body mass (Bishop and Butler, 1995).

17.3.8.1 Hemoglobin genes

In birds as in mammals, there are multiple hemoglobin genes: seven in the chicken (Reitman et al., 1993) and six in the zebra finch (Alev et al., 2009). These represent a small family of genes encoding α and β globins. The avian hemoglobin genes can be summarized as follows:

- Chicken π (Pi) α—homologous to duck π and orthologous to α1 in zebra finch
- Chicken α D—homologous to turkey, ostrich quail α D and orthologous to α2 in zebra finch
- Chicken α A—homologous to turkey, ostrich quail α A and orthologous to α3 in zebra finch
- Chicken ρ (Rho or P) β—possibly orthologous to β1 in zebra finch
- Chicken βH—possibly orthologous to β2 in zebra finch
- Chicken βA—homologous to turkey, duck, flamingo, condor, macaw, pigeon, and ostrich β major and orthologous to β3 in zebra finch
- Chicken β ε (Epsilon or E) with marked homologies to chicken ρ.

In adult zebra finches, hemoglobin consists of 74% α3 and 26% α2 and all β3 globin while in the embryo, hemoglobin consists of 28% α1, 55% α2, 16% α3, and 44% β1, 33% β2, and 24% β3 (Alev et al., 2009).

The α globin genes are located on chromosome 14 in the chicken. In embryonic erythrocytes, the region containing the α globin genes is located in a crown of DNA loops surrounding the nuclear matrix (Iarovaia et al., 2009).

17.3.8.2 Adaptations of hemoglobin to flight at high altitudes

The structures of hemoglobin in birds that fly at high altitudes have increased affinity for oxygen (see Figure 17.4). For instance, there are subtle changes to the protein structure (single substitutions in α globin) in both the bar-headed goose, a species that migrates across the Himalayas and the Andean goose (Jessen et al., 1991). Similarly, the oxygen affinity of hemoglobin in driving birds such as emperor penguins is increased (Meir and Ponganis, 2009). This can be readily seen from the left shift in the O_2—Hb dissociation curve for the bar-headed goose and the emperor penguin compared with the domestic duck (and most other birds) (see Figure 17.4).

17.3.8.3 Glycation of hemoglobin

Despite elevated circulating concentrations of glucose, the percentage of hemoglobin that is glycated is lower in most birds examined than in mammals, for example, <2% in rooks (*Corvus frugilegus*) and mute swans (*Cygnus olor*) (Miksik and Hodný, 1992; also reviewed: Beuchat and

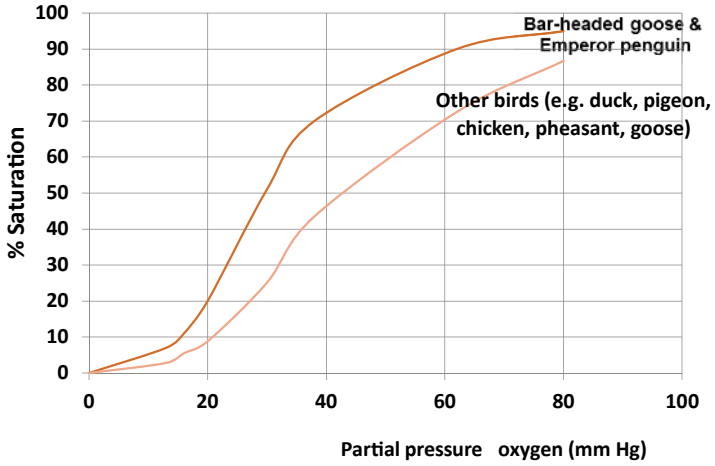

FIGURE 17.4 Oxygen dissociation curves for hemoglobin in avian erythrocytes. Data for calculated pigeon, domestic ducks and geese, Mucovy duck, chicken and red-necked pheasant from Christensen and Dill (1935) and for domestic goose, bar-headed geese and emperor penguins from Meir and Ponganis (2009).

Chong, 1998). Even in hummingbirds where plasma concentrations of glucose can be over 40 mmol/L, glycated hemoglobin is within the mammalian range (3.5–5.0) (Beuchat and Chong, 1998).

17.3.8.4 Hemoglobin and nutrition

In birds as might be expected, with low-iron availability, circulating concentrations of hemoglobin are reduced. Chickens together with the stable isotope ^{58}Fe have been proposed as a model for investigating iron availability (Tako et al., 2010).

17.3.9 Carbonic anhydrase

Carbonic anhydrase in erythrocytes catalyzes the reaction between carbon dioxide and water to yield carbonic acid. This in turn forms bicarbonate (HCO_3^-) and protons (H^+) reversibly.

$$CO_2 + H_2O \leftrightarrow H_2CO_3 \leftrightarrow HCO_3^- + H^+$$

Carbonic anhydrate (CA, EC 4.2.1.1) has been purified from avian erythrocytes (e.g., chicken: Bernstein and Schraer, 1972; ostrich: Ozensoy et al., 2005; pigeon: Ozensoy et al., 2011). Carbonic anhydrase activity is increased by β adrenergic agonists based on studies with Japanese quail erythrocytes (Igbo et al., 1994). Moreover, hypoxia increases carbonic anhydrase activity in avian erythrocytes (Glombitza et al., 1996).

There are increases in the amount of carbonic anhydrase II (CAII) and the isoenzyme CAIII relative to hemoglobin as female chickens commences egg production (Nishita et al., 2011a,b). Ferrous iron increases the activity of carbonic anhydrase from avian erythrocytes (Wu et al., 2007).

17.3.9.1 Intracellular pH

The intracellular pH in chicken erythrocytes is pH 7.219 (Kozma et al., 1995; Richardson and Swietach, 2016).

17.3.10 Transporters in erythrocyte plasma membrane

17.3.10.1 Anion transporter

The key anion transporter exchanges bicarbonate (HCO_3^-) for chloride (Cl^-) ions. The transcripts for the anion transporter have been characterized in the chicken with chicken erythroid cells having been demonstrated to express anion transport proteins (band 3) (Kim et al., 1988). The v-erbA oncogene suppresses expression of anion transport proteins (band 3) by chicken erythroid cells (Zenke et al., 1988). There are oxygen-sensitive membrane transporters in avian erythrocytes (Gibson et al., 2000). Another plasma membrane protein in the turkey erythrocyte is goblin, which is phosphorylated in the presence of β-adrenergic agonists (Alper et al., 1980).

17.3.10.2 Sodium and potassium transport

There is considerable movement of sodium (Na^+) and potassium (K^+) across the erythrocyte plasma membrane. The flux of sodium ions across the plasma membrane of erythrocytes from turkeys is two- to threefold that in humans (Palfrey and Greengard, 1981). The $Na^+/K^+/2Cl^-$ cotransporter in avian erythrocytes exhibits sensitivity to β-adrenergic agonists and to oxygen concentrations (reviewed in Gibson et al., 2000). Transport of potassium into chicken erythrocytes declines with age (Drew et al., 2002).

17.3.11 Glucose

Glucose entry into avian erythrocytes is low, being both nonsaturable and saturable carrier mediated; it can be inhibited by cytochalasin (Simons, 1983a,b). The 3-0-methylglucose uptake by pigeon erythrocytes that can be inhibited by cytochalasin B is low as there are only about 200 copies of the GLUT-1 protein per erythrocyte (compared to 300,000 in humans) (Diamond and Carruthers, 1993). Erythrocyte expression of GLUT-1 and GLUT-3 declines during differentiation of erythrocytes (Matthew et al., 1994).

17.3.11.1 Amino acids and urea

Amino acids are transported across the plasma membrane of the avian erythrocyte with uptake of glycine, leucine, and lysine being sodium dependent (Somes et al., 1981; Lerner et al., 1984). Lines of chickens have been selected with high and low amino acid transport phenotypes (Vargas and Devés, 2001; Angelo et al., 2005). Avian erythrocytes are reported to have little expression of urea-transporter-B (Liu et al., 2011).

17.3.12 Hormonal effect on erythrocytes

There are at least three β-adrenergic receptors in the cell membrane of the avian erythrocyte, namely βtrunc, β3C, and β4C-receptors (turkey: Chen et al., 1994; Baker, 2010). The turkey has been used as a model for β-adrenergic receptors. These are functional with β adrenergic receptor agonists increasing adenylate cyclase activity (Stadel et al., 1982; Peters et al., 1984). Avian β adrenergic receptors are desensitized by β adrenergic receptor agonists and sensitized by β adrenergic receptor antagonists due to structural changes (Stadel et al., 1982; Peters et al., 1984). The beta-adrenergic receptors on avian erythrocytes activate adenylate cyclase via G_s proteins (turkey: Ugur and Onaran, 1997).

Chick embryo erythrocytes have A2α adenosine receptors that also activate adenylate cyclase (Glombitza et al., 1996). There are progressive reductions in the erythrocyte responses to beta-adrenergic and A2 receptor agonists during embryonic development due to cGMP-inhibited phosphodiesterase 3 (Baumann et al., 1999).

At the beginning of second half of embryonic development, there is progressive hypoxia with release of norepinephrine. Carbonic anhydrase II activity and expression in embryonic avian erythrocytes is increased by norepinephrine, acting via β adrenergic receptors and cyclic adenosine monophosphate (cAMP) as the signal transducer (chicken: Dragon et al., 1996; Dragon and Baumann, 2001). In addition, cAMP increases 2,3-BPG (chicken: Dragon et al., 1996). Moreover, with hypoxia, erythrocyte ATP declines and oxygen affinity increases. There are similar effects of adenosine on avian erythrocytes acting via A_2 receptors and cAMP (white-tailed ptarmigan: Dragon et al., 1999; chicken: Glombitza et al., 1996; Dragon and Baumann, 2001). There is activation of Na^+-K^+-Cl^- co-transporters by cAMP leading to increases in avian erythrocyte volume (duck: Lytle, 1997).

There are multiple receptors to cytokines in the plasma membrane of avian erythrocyte. Receptors related to innate immunity are briefly covered in Section 17.3.11.

17.3.13 Effect of stressors of erythrocytes

There are, however, effects of stressors on the avian erythrocyte. For instance, exposure to crude oil is followed by degeneration of the erythrocyte mitochondria in herring gulls (*Larus argentatus*) and Atlantic puffins (*Fratercula arctica*) (Leighton, 1985). Avian erythrocytes exhibit marked increases in production of both hydrogen peroxide and super oxide in vitro in response to glucose or glucose 6-phosphate together with shifts in the oxygen dissociation curve for hemoglobin (Zhang et al., 2011). In contrast, the effects on either ROS or hemoglobin are not observed with mammalian red blood cells (Zhang et al., 2011). Similarly ROS are produced by mitochondria from avian erythrocyte for instance from quail or parrots (Montgomery et al., 2012). These effects may explain the shorter lifespan of avian erythrocytes (see above).

17.3.14 Avian erythrocytes and the innate immune system

Avian erythrocytes are part of the innate immune system. Chicken erythrocytes express transcripts including TLR 3, 9, and 21 and myxovirus resistance in a specific pathogen-associated molecular pattern (PAMP) manner as part of the innate immune response (Morera et al., 2011). In addition, not only do they express TLR and cytokines [IL-1γ, IL-2, IL-4, IL-6, IL-7, IL-8, IL-10, IL-12β, IFN-γ (Luan et al., 2016)] but also there is increased release of nitrite together with IL-8 after stimulation of TLR3 and of IFNs after stimulation of TLR21 (St. Paul et al., 2013). Chicken erythrocytes also express avian β-defensins (AvBDs) (AvBD1 to 7 together with AvBD9) and liver-expressed antimicrobial peptide-2 (Niu et al., 2018). Moreover, after activation by the opportunistic pathogenic yeast, *Candida albicans*, chicken erythrocytes release cytokines including IFN-gamma-like and migration inhibitory factor activities (Passantino et al., 2007). Another example of protective effects of avian erythrocytes is antifilm activity of histone from avian erythrocytes against *Staphylococcus aureus* (Rose-Martel et al., 2017).

17.4 Blood gases

Table 17.7 summarizes arterial and venous pO_2 in multiple species of resting birds. There is no change in arterial pO_2 during short-term (pigeon: Butler et al., 1977) or long-term flight (northern bald ibis: Bairlein et al., 2015). This is presumably due to the increased rate of respiration. Moreover, in chickens exercising on a treadmill, arterial pO_2 paradoxically increases (Gleeson and Blackenbury, 1984), again presumable due to increased respiration. In contrast, both arterial and venous pO_2 is decreased during a dive (Emperor penguin: Meir and Ponganis, 2009) and during the hypoxia resulting from high altitudes (Scott and Milsom, 2006). There are changes in pO_2 and pCO_2 during growth of chickens (Table 17.7). There is a decline in venous pO_2 during growth of meat-type (rapid growing) chickens, presumably reflecting the requirements of metabolism.

Arterial pCO_2 is influenced by respiration, particularly with panting. For instance, pCO_2 is reduced at elevated environmental temperatures (30°C) and exercise with the effect of exercise much greater at elevated temperatures (chickens running on a treadmill: Gleeson and Blackenbury, 1984). Moreover, pCO_2 is decreased in heat-stressed emus that are panting (Jones et al., 1983). However, venous pCO_2 is increased during the rapid growth phase (Table 17.8) and reduced during fasting in chickens (Christensen et al., 2012). It is reasonable to assume that these changes are due to shifts in metabolism.

17.5 Leukocytes

There are five types of leukocytes in birds:

- Heterophils (granulocyte or polymorphonuclear leukocytes)
- Lymphocytes
- Eosinophils (granulocyte or polymorphonuclear leukocytes)
- Monocytes
- Basophils (granulocyte or polymorphonuclear leukocytes).

TABLE 17.7 Examples of arterial and venous pO_2, pCO_2, and pH in rest birds.

Species	Arterial	Venous	References
pO_2			
Amazon parrot	98		Valéria et al. (2008)
Boat tailed grackle		47	Harms and Harms (2012)
Chicken	102		Gleeson and Brachenberry (1984)
Duck	82		Kawashiro and Scheid (1975)
Emperor penguin	96	74	Meir and Ponganis (2009)
Frigate birds		52	Valle et al. (2018)
Mourning dove		49	Harms and Harms (2012)
House sparrow		40	Harms and Harms (2012)
Pigeon	87	57	Butler et al. (1977)
Southern crested caracaras	99		Escobar et al. (2011)
Mean	**94 + 3.2**	**53 + 4.8**	
pCO_2			
Amazon parrot	22		Valéria et al. (2008)
Boat tailed grackle		29	Harms and Harms (2012)
Chicken	25		Gleeson and Brachenberry (1984)
Duck	38		Kawashiro and Scheid (1975)
Eurasian black vultures		29	Kenny et al. (2015)
Frigate birds		38	Valle et al. (2018)
Gyr falcons	37	35	Raghav et al. (2015)
House sparrow		38	Harms and Harms (2012)
Mottled duck		35	Ratliff et al. (2017)
Mourning dove		29	Harms and Harms (2012)
Pigeon	27	35	Butler et al. (1977)
Quaker parrot		29	Rettenmund et al. (2014)
Mean	**30 + 3.2**	**33 + 1.3**	
pH			
Boat-tailed grackle		7.43	Harmes et al. (2016)
Chicken		7.42	Martin et al. (2010)
Eurasian black vultures		7.41	Kenny et al. (2015)
Frigate birds		7.35	Valle et al. (2018)
Gyr falcons	7.42	7.48	Raghav et al. (2015)
House sparrow		7.36	Harmes et al. (2016)
Mourning dove		7.39	Harms et al. (2016)
Pigeon		7.36	Butler et al. (1977)
Quaker parrot		7.43	Rettenmund et al. (2014)
Southern crested caracaras	7.54		Escobar et al. (2011)
Mean	**7.48**	**7.40 + 0.01**[a]	

[a]*Coefficient of variation 0.57% across nine avian species.*

TABLE 17.8 Changes in venous pO_2 and pCO_2 during growth in broiler chickens.

Age of chickens	pO_2	pCO_2	References
11 d	58	48	Van As et al. (2010)
33 d	48	59	Van As et al. (2010)
47 d	35	69	Van As et al. (2010)
Adult[a]	46	38	Martin et al. (2010)

[a]*Broiler breeder (female meat-type chicken).*

Figure 17.6. shows the structure of avian leukocytes. Table 17.7 summarizes the concentrations of leukocytes and differential counts in both wild poultry and poultry. Klasing and colleagues estimated that chickens produce 0.76 g leukocytes per kilogram per day. Leukocytes are found in the "buffy" layer when the hematocrit of avian blood is being determined.

17.5.1 Number of leukocytes

There are physiological or pathological shifts in the circulating concentrations of leukocytes. For example, the blood concentration of leukocytes are almost half of adult levels in juvenile stork (white stork: Han et al., 2016). In addition, infecting chickens with *Plasmodium juxtanucleare* is followed by increase blood concentrations of leukocytes (Siveira et al., 2009). Similarly, there are increases in leukocyte concentrations with botulism (black-faced spoonbills: Chou et al., 2008) and following hypoxia (chickens: Maxwell et al., 1987). In contrast, leukocyte concentrations are depressed in captive compared to wild birds (Amazon parrots: Deem et al., 2005) and with mycotoxin ingestion (chickens: Andretta et al., 2012).

17.5.2 Heterophils

Heterophils are the functional equivalent of neutrophils in mammals (Harmon, 1998). There have been 78 proteins identified that are characteristic for heterophils (Sekelova et al., 2017). These include antibacterial proteins, calprotectin (MRP126), myeloid protein 1, Cathelicidin (CATHL)1, CATHL2, CATHL3, lysozyme G, lysozyme, and ribonuclease homolog (RSFR) (Sekelova et al., 2017).

17.5.2.1 Structure

Heterophils are polymorphonuclear leukocytes (Figure 17.6). They have a diameter of 10−15 μm (Sturkie, 1986). Avian heterophils are weakly basophilic and pseudoeosinophilic, staining brilliant red with Wright's stain (Sturkie, 1986). Based on electron microscopy studies, avian heterophils have the following structures:

- Nuclei with two or three lobes
- Sparse mitochondria
- Two types of granules
  - Dense oval or spherical granules with diameters between 0.4 and 1.8 μm
  - Less dense granules.

(ducks and geese: Maxwell, 1973).

Stressors such as corticosterone or LPS influence heterophil structure with reduced cross-sectional area and increased granule diameter (chickens: Shini et al., 2008).

17.5.2.2 Function

Heterophils play an important role in innate immunity with the following actions:

- Phagocytizing bacteria
- Attracting lymphocytes
- Releasing antimicrobial peptides
- Killing pathogens by oxidative bursts
- Exerting acute inflammatory responses

(reviewed Harmon, 1998).

17.5.2.2.1 Heterophils and phagocytosis

Heterophils are the major phagocytic leukocytes in birds (reviewed Harmon, 1998). Avian heterophils exhibit a superior ability to both phagocytize and kill bacteria than that of monocytes (Stabler et al., 1994). Moreover, phagocytosis is enhanced by opsonization of bacteria (Stabler et al., 1994). The phagocytic activity of heterophils is increased following priming with IFN γ (chicken: Kogut et al., 2005) or interleukin (IL)-2 (chicken: Kogut et al., 2002, 2003). The phagocytic activity of avian heterophils is influenced by both internal and external factors. For instance, avian heterophils show decreased phagocytic activity with age (ring dove: Terrón et al., 2004) and after feeding aflatoxin (chicken: Chang and Hamilton, 1979a).

Chicken heterophils that are infected with bacteria attract lymphocytes (Lam, 2002). Avian heterophils release superoxide (chicken and turkey: Stabler et al., 1994). Heterophils produce reactive oxygen following agonists

bind to Dectin-1; this latter being pattern recognition receptors for exogenous β-glucan (found on bacterial cell walls) (chicken: Nerren and Kogut, 2009). Activation of heterophils by ligand binding to TLR2 and TLR4 is followed by oxidative bursts (Guriec et al., 2018).

17.5.2.2.2 Heterophils and cytokines

Activation of heterophils include degranulation, and marked increased transcription of the proinflammatory cytokines, IL1β, IFNα, and IFNγ, together with some increase in IL8 and IL18 expression (Guriec et al., 2018). Binding of agonists to TLR2 (e.g., PAMPs) and TLR4 (LPS) activate heterophils while antagonists to TLR2 and TLR4 reduce heterophil activation (Guriec et al., 2018). Heterophils express activating triggering receptor expressed on myeloid cells (TREM) A (chicken: Viertlboeck et al., 2013).

17.5.2.2.3 Heterophils and antimicrobial peptides

Avian heterophils produce host antimicrobial peptides, specifically β-defensins, for instance, chicken heterophil peptide (CHP) 1 and CHP 2 (Sugiarto and Yu, 2004). Other antibacterial proteins produced by avian heterophils include calprotectin (MRP126), myeloid protein 1, cathelicidin (CATHL)1, CATHL2, CATHL3, lysozymeG, lysozyme, and RSFR (chicken: Sekelova et al., 2017). Both defensins and cathelicidins are highly cationic and antimicrobial.

There have been changes in the number of cathelicidins during avian evolution. The *CATHL1* gene has been duplicated in galliform birds. In contrast, the *CATHL2* gene is lost in birds of the orders *Sphenisciformes* and *Ciconiiformes*. In addition, the *CATHL1* gene is a pseudogene in falconiform birds and lost from birds in the orders *Passeriformes*, *Sphenisciformes*, and *Ciconiiformes* (Cheng et al., 2015).

17.5.2.2.4 Toll-like receptors and heterophils

Chicken heterophils express TLR1 type 1, TLR1 type 2, TLR1 type 3, TLR1 type 4, TLR2, TLR3, TLR4, TLR5, TLR7, TLR21, and TLR21 (Kogut et al., 2012). These can be activated by specific TLR agonists and bacteria (Farnell et al., 2003). Moreover, expression of TLR4 and TLR15 is up-regulated after *Eimeria tenella* challenge (Zhou et al., 2013).

17.5.2.2.5 Stressors and heterophil functioning

Stressors influence heterophil functioning. For instance, the magnitude of the oxidative bursts from heterophils is increased following stress (transportation in turkeys: Huff et al., 2010).

17.5.2.3 Number

Heterophils numbers in the blood are influenced by stressors with corticosterone increasing heterophil concentrations (chickens: Gross and Siegel, 1983) (Figure 17.7). Increases in the concentration of heterophils have been reported after the following stresses: hypoxia (exposure to low partial pressure of oxygen in chickens: Maxwell et al., 1987; removal of 30% blood in Japanese quail: Schindler et al., 1987), heat stress (chickens: Atlan et al., 2000), handling and transportation (Amazon parrots: McRee et al., 2018), and pesticide administration in Japanese quail (paraquat: Clark et al., 1988; chlorphenvinphos and foschlor: Gromysz-Kałkowski et al., 1985).

There is movement of heterophils out of the circulation into tissues. For instance, there are large increases in heterophils infiltrating the pulp of growing feathers injected with phytohemagglutinin-P (Sullivan and Erf, 2017). Heterophils accumulate in the peritoneal cavity in chickens that have been challenged i.p. with *Salmonella enteritis* (Kogut et al., 1995).

17.5.2.4 Production

Heterophils are produced in the bone marrow. In vitro embryonic bone marrow cells have been demonstrated to be capable of developing into heterophils (Japanese quail: Brandon et al., 2000).

17.5.3 Lymphocytes

Avian lymphocytes can be isolated using specific monoclonal antibodies. There are two types of B and T lymphocytes with B and T precursor cells developing, respectively, in the bursa Fabricius and thymus. The proportion of B and T lymphocytes in broiler chickens is the following:

- T type lymphocytes
  - $CD3^+$ 93.4%
  - $CD4^+$ $CD25^+$ 41.6%
  - $CD8^+$ $CD25^+$ 27.3%
- B type lymphocytes
  - $BU\text{-}1^+$ 19.3%
  - $BU\text{-}1^+$ MHC Class II^+ 2.7%

(broiler chicken: Jarosz et al., 2017). Chicken $CD4^+CD25^+$ cells are equivalent to regulatory T cells in mammals (formerly known as T suppressor cells) (Shanmugasundaram and Selvaraj, 2011). T and B lymphocytes express TREM A (chicken: Viertlboeck et al., 2013).

17.5.3.1 Structure

Avian lymphocytes are weakly basophilic. The structure of circulating avian lymphocytes was characterized by electron microscopy (ducks, geese, pigeons, turkeys, and Japanese quail: Maxwell, 1974) (see Figure 17.5). Avian lymphocytes have a nonlobed nucleus with a high nuclear: cytoplasmic ratio.

There are two structural types of lymphocytes in the circulation of birds, namely small and medium size

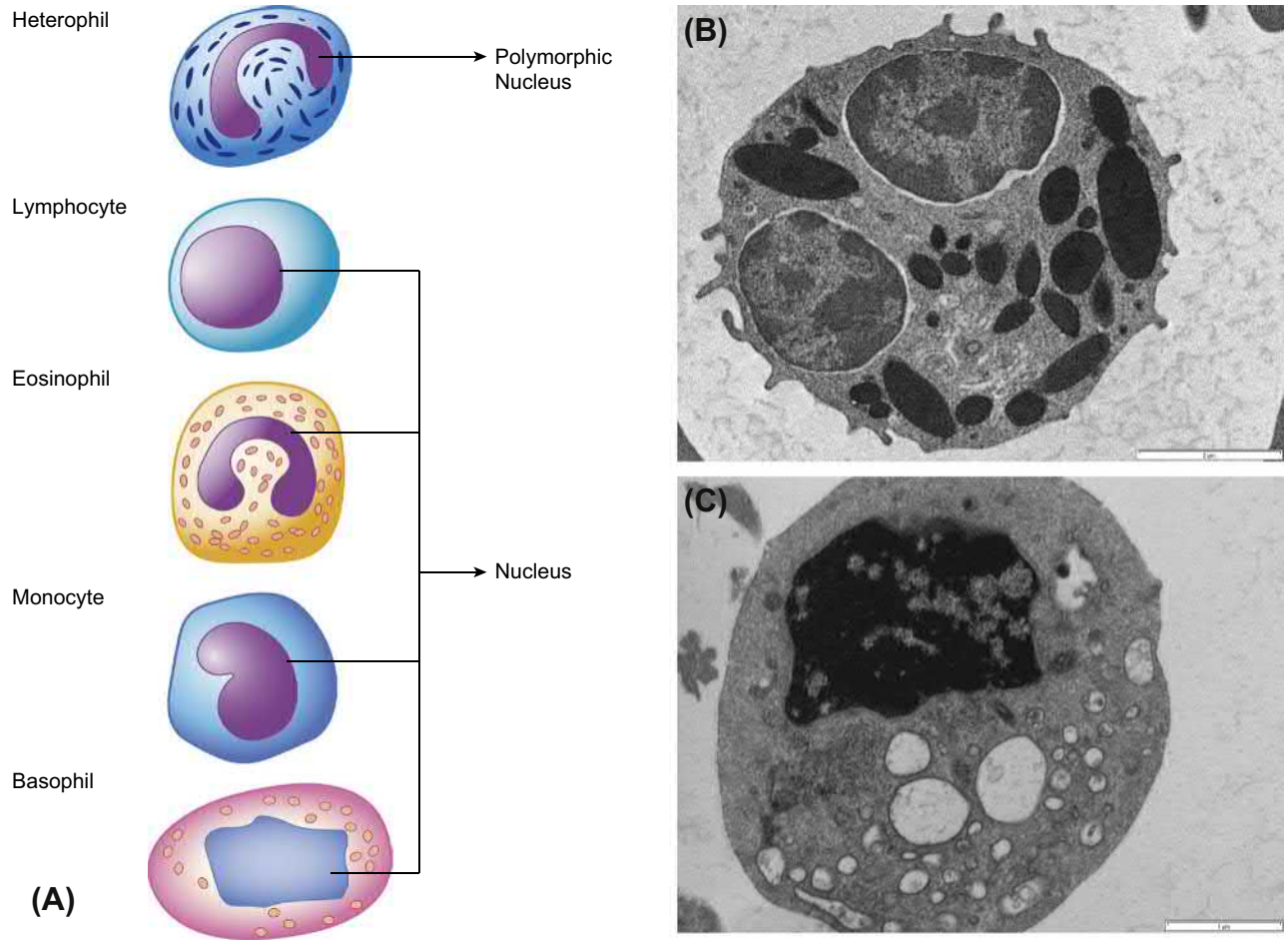

FIGURE 17.5 **Avian leukocytes.** (A) Schematic images of leukocytes. (B) Electron micrographs of heterophils from chicken peripheral blood. (C) Electron micrographs of agranular lymphocytes from chicken peripheral blood. *Reproduced from Shini et al. (2008).*

(Maxwell, 1974). In the small lymphocytes, the nucleus is pleomorphic in shape. The cytoplasm contains multiple mitochondria, Golgi apparatus, some endoplasmic reticulum, and a few granules. The small lymphocytes have extensive pseudopodia. The medium-sized lymphocytes are oval with a spherical nucleus. They have relatively few intracellular organelles (mitochondria, endoplasmic reticulum) and a few pseudopodia.

There are shifts in the structure of lymphocytes with physiology. Challenge with LPS is followed by reduced size (diameter and cross-sectional area) of circulating lymphocytes (chicken: Shini et al., 2008).

17.5.3.2 Function

Lymphocytes play important roles in both humoral and cell-mediated immunity. This is discussed in detail in Chapter 24.

Stressors influence lymphocyte functioning. For instance, lymphocyte expression of (heat shock protein) HSP 70 and HSP 90 is increased in chickens subjected to psychological stress for seven days (Pusch et al., 2018). Corticosterone suppresses proliferation of both T and B lymphocytes (Mehaisen et al., 2017).

17.5.3.3 Numbers

Circulating concentrations of lymphocytes are influenced by stresses. Administration of corticosterone is followed by decreases in blood concentrations of lymphocytes (chicken: Gross and Siegel) (Figure 17.7). In contrast, hypoxia increases lymphocytes numbers (Maxwell et al., 1987). Moreover, a transient increase in the blood concentration of lymphocytes occurs in turkeys after seven days after challenge with protozoan, *Eimeria adenoeides* (Gadde et al., 2009). There is movement of lymphocytes out of the circulation into tissues. There are large increases in lymphocytes (predominately $CD4^+$ T lymphocytes) infiltrating the pulp of growing feathers injected with phytohemagglutinin-P (Sullivan and Erf, 2017).

17.5.4 Eosinophils

17.5.4.1 Structure

Avian eosinophils are ovoid granulocytes with considerable cytoplasm (Figure 17.6). The round granules stain red after the uptake of the stain/dye eosin in histological slide preparation. The nucleus has two lobes (i.e., bilobed) (Sturkie, 1986). Electron microscopy revealed that avian eosinophils have multiple dense granules (0.1−1.6 μm diameter) with crystalline cores (Maxwell and Stiller, 1972).

17.5.4.2 Function

The functions of avian eosinophils are not well established (e.g., Campbell and Ellis, 2007). It is likely that avian eosinophils release specific cytokines in response to challenges.

17.5.4.3 Number

The numbers of eosinophils in the blood are elevated after some stresses. For instance, circulating concentrations of eosinophils were increased after handling and transportation (Amazon parrots: McRee et al., 2018) and in birds in captivity (rufous-collared sparrows: Ruiz et al., 2002). Similarly, infection with schistosomes, *Austrobilharzia variglandis*, is followed by consistent increases in the number of eosinophils per unit blood volume (chickens: Ferris and Bacha, 1986). In contrast, the concentrations of basophils are decreased after exposure to the pesticides, chlorphenvinphos, and foschlor (Japanese quail: Gromysz-Kałkowska et al., 1985). There were no effects of hypoxia on eosinophil numbers (chicken: Maxwell et al., 1987).

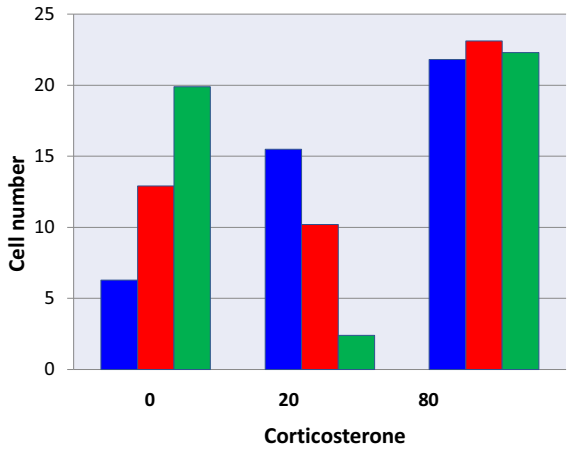

FIGURE 17.6 Effect of corticosterone (in diet in ppm) on heterophils (blue), lymphocytes (red), and total leukocytes (green) in young chickens. *Data from Gross and Siegel (1983).*

17.5.5 Monocytes

17.5.5.1 Structure

Avian monocytes are oval cells with considerable cytoplasm. Electron microscopy reveals that avian monocytes have multiple small granules (0.1−1.6 μm) with crystalline cores (Maxwell and Stiller, 1972). They have kidney-shaped nuclei and extensive cytoplasm containing a well-developed Golgi apparatus, rough endoplasmic reticulum, microtubules, vesicles, and mitochondria (ducks, geese, pigeons, turkeys, and Japanese quail: Maxwell, 1974).

17.5.5.2 Function

The functioning of avian monocytes is becoming understood. Monocytes are phagocytic, exert a chemotaxic effect on other leukocytes, release cytokines, produce nitric oxide (NO) and, in tissues, transform to macrophage (Grecchi et al., 1980). Opsonization of bacteria enhances their phagocytosis by avian monocytes (chicken: Stabler et al., 1994). Avian monocytes exert a chemitaxic on heterophils and lymphocytes due to their releasing macrophage inflammatory protein (MIP)-1β (Lam et al., 2002).

In response to LPS, monocytes release NO with increased expression of inducible NO synthase (chickens: Bowen et al., 2009). In turn, NO induces vasodilation. Moreover, in the presence of activators of TLR-2 and TLR-4, there is release of NO and increased expression of cytokines, IL-1β, IFNα, IFNγ, IL-8, and IL-13 together with the important receptors, TLR2 and TLR4 by monocytes (chicken: Guriec et al., 2018). Monocytes express TREM A (chicken: Viertlboeck et al., 2013).

Stressors influence monocyte functioning. Aflatoxins decrease the phagocytic activity of monocytes (chicken: Chang and Hamilton, 1979b).

17.5.5.3 Number

The blood concentration of monocytes is increased after vaccination against Newcastle disease virus (chicken: Taebipour et al., 2017). There are effects of some stressors on blood monocyte numbers. There are large increases (>threefold) in the blood concentrations of monocytes (monocytosis) in zinc deficient birds (chickens, turkeys, and quail—Wight et al., 1980). In addition, the percentage of monocytes is increased following stress (transportation in turkeys: Huff et al., 2010). Moreover, infection with schistosomes (*Austrobilharzia variglandis*) is followed by consistent increases in the number of monocytes per unit blood volume (chickens: Ferris and Bacha, 1986). Conversely, there were no effects of hypoxia on circulating monocyte numbers (chicken: Maxwell et al., 1987). There is movement of monocytes out of the circulation into tissues. For instance, there are increases in the number of

monocytes in intestinal villi of mallard ducks infected with the trematode intestinal fluke, *Sphaeridiotrema globulus* (Mucha and Huffman, 1991).

17.5.5.4 Production

Monocytes are produced in the bone marrow. In vitro, embryonic marrow cells have been reported as capable of developing into monocytes (e.g., Brandon et al., 2000).

17.5.6 Basophils

17.5.6.1 Structure

The nuclei and cytoplasmic granules take up basic stains, such as hematoxylin, giving a pale purple appearance (Sturkie, 1986). The ultrastructure of avian basophils has been reported (ducks and geese: Maxwell, 1973). Basophils are granulocytes. They contain cytoplasmic granules (see Figure 17.6). These vary in diameter from 0.1 to 0.8 µm diameter in ducks and geese and up to 1.0 µm diameter in turkeys (Maxwell, 1973). The nuclei of basophils are reported as polymorphic (Sturkie, 1986) or nonlobulated (ducks and geese) (Maxwell, 1973).

17.5.6.2 Function

Based on the situation in mammals (Voehringer, 2017), avian basophils are part of the innate immune system being proinflammatory cells associated with allergies and helminth infection. Like mast cells, basophils have receptors for IgE and release histamine.

17.5.6.3 Number

Basophil numbers in the blood are influenced by some stressors. Basophil cell number in the blood is increased with feed restriction (chickens: Maxwell et al., 1990, 1992a,b; ducks: Maxwell et al., 1992b). In addition, some other stresses influence the number of basophils in the blood of birds. The number of basophils in broiler chickens is increased by intermittent noise (Bedanova et al., 2010), by heat stress (Atlan et al., 2000) and after challenges with *P. juxtanucleare* (Siveira et al., 2009). In addition, the concentrations of basophils are increased after exposure to the insecticide chlorphenvinphos (Japanese quail: Gromysz-Kałkowska et al., 1985). In contrast, there were decreases in circulating basophil numbers in skylarks (*Alauda arvensis*) after LPS challenge (Hegemann et al., 2013). However, there was no effect of some stresses on the number of basophils per unit volume in the blood (handling and transportation in Amazon parrots: McRee et al., 2018; hypoxia in chickens: Maxwell et al., 1987). Basophils can move from the circulation to tissues. For instance, there are large increases in the number of basophils infiltrating the pulp of growing feathers injected with phytohemagglutinin-P (Sullivan and Erf, 2017).

17.5.7 Heterophil: lymphocyte ratios

The heterophil: lymphocyte (H:L) ratio as an indicator of stress in birds. The adrenal glucocorticoid, corticosterone, increases the H:L ratio (Gross and Siegel, 1983) (see Figure 17.7). As might be expected, H:L ratios are

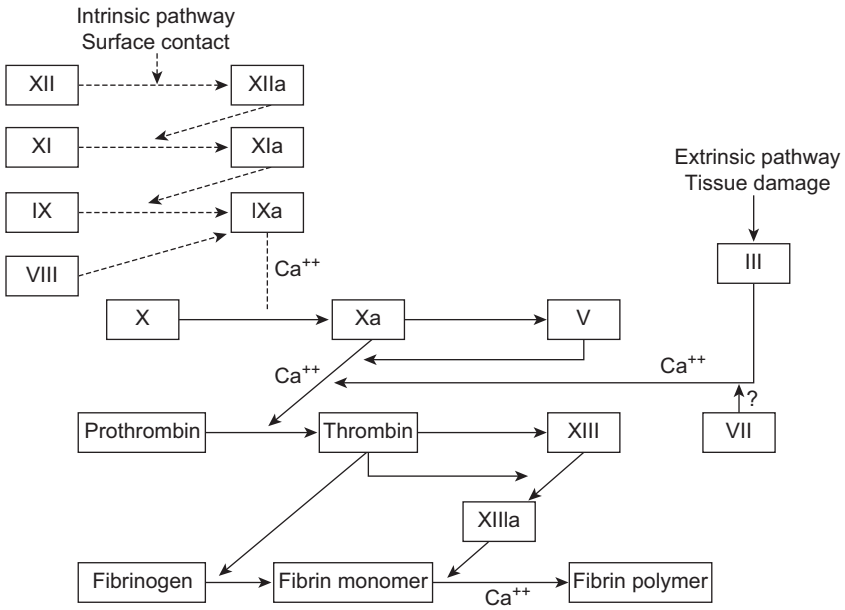

FIGURE 17.7 Cascade of coagulation of avian blood with a series of clotting factors.

increased by stress. The H:L ratio is increased with psychological stresses in multiple studies:

- Feeding at random times (chickens: Pusch et al., 2018).
- Social disruption (mixing two groups of birds) (chickens: Gross, 1990)
- Handling and transportation (Amazon parrots: McRee et al. (2018); chickens: Yalcin and Güler, 2012; turkeys (Huff et al., 2010).
- Intensive versus extensive systems in indigenous ducks (Kolluri et al., 2014).

The H:L ratio is also increased with physical stresses, albeit without complete consistency:

- Glucocorticoid administration (corticosterone: Gross and Siegel, 1983; Gross, 1990; Mehaisen et al., 2017; Weimer et al., 2018; dexamethasone: Huff et al., 2011).
- Ammonia (broiler chicks: McFarlane and Curtis)
- Disease (multiple passerine species: Wilcoxen et al., 2015)
- Electric shocking (chicken: McFarlane and Curtis, 1989)
- Fasting (Gross and Siegel, 1983; Gross, 1990) or feed restriction (chickens: Zulkifli et al., 2000; Azis, 2012)
- Heat stress (laying hens: Mashaly et al., 2004; broiler chicks: McFarlane and Curtis, 1989; in one line of broiler chicks but not another: Xu et al., 2018).
- Hypoxia (chickens: Maxwell et al. (1987).
- Injury (Adélie penguins: Vleck et al., 2000)
- Intermittent noise (broiler chickens: Bedanova et al., 2010).
- Killed *E. coli* (chickens: Gross and Siegel, 1983).
- LPS challenge on the H:L ratio (skylarks: Hegemann et al., 2013).
- Received feed contaminated with the mycotoxin, deoxynivalenol (chickens: Ghareeb et al., 2011, 2014).

In contrast, H:L ratios are depressed in the pesticide, malathion (chicken: Gross and Siegel, 1983).

17.6 Thrombocytes

In birds, thrombocytes are the functional equivalent of platelets in mammals. They, like leukocytes, are found in the "buffy" layer when the hematocrit of avian blood is being determined. Avian thrombocytes play important roles in both blood clotting and immune functioning. They should be considered as subtype of leukocytes (Seliger et al., 2012).

17.6.1 Structure

Avian thrombocytes have the following characteristics:

- Cell diameter 5.4 μm (Japanese quail: Belleville et al., 1982)—8.5 μm (Rhea: Gallo et al., 2015)
- Nuclear diameter 4.2 μm (Japanese quail: Belleville et al., 1982).

Avian thrombocytes can be confused with lymphocytes but are readily recognized using specific monoclonal antibodies (e.g., chicken: Horiuchi et al., 2004) or by expression of αVβ3 (Windau et al., 2013). The ultrastructure of the avian thrombocyte has been characterized (ducks, geese, pigeons, turkeys, and Japanese quail: Maxwell, 1974). Avian thrombocytes have an irregular shape with multiple pseudopodia. Similarly, the nucleus is irregular in shape. There is more cytoplasm than is seen in small lymphocytes. There are multiple small mitochondria, an endoplasmic reticulum, prominent microtubules, and a few dense granules.

17.6.2 Function

Like platelets in mammals, thrombocytes play an important role in hemostasis in birds. Avian thrombocytes have been demonstrated to form aggregates (chickens: Grant and Zucker, 1973; pigeon: O'Toole et al., 1994) with aggregation stimulated by serotonin (domestic ducks: Belamarich and Simoneit, 1973) and contact with collagen (duck: Stiller et al., 1975). Moreover, avian thrombocytes adhere to collagen with this stimulating degranulation and release of serotonin (chicken: Schmaier et al., 2011). Avian thrombocytes express α2bβ3 integrins, albeit at a lower level than in mammalian platelets (chicken: Schmaier et al., 2011). However, vaso-occlusion thrombosis is not observed in birds (Australian budgerigars: Schmaier et al., 2011).

Avian thrombocytes are part of the innate immune system. Evidence for this comes from the following. They are phagocytic (Carlson et al., 1968) with bacteria but probably not protozoa (chicken: Chang and Hamilton, 1979c; DaMatta et al., 1998). Chicken thrombocytes have been reported to exhibit increase phagocytosis in response to LPS (St Paul, 2012). Moreover, like leukocytes, produce TLR, inflammatory cytokines and other agents. There is marked expression of TLR2, TLR3, and TLR4 by chicken thrombocytes together with some expression of TLR5, TLR7, and TLR21 (St. Paul et al., 2012). In response to stimulation by LPS acting via TLR, there is increased expression of proinflammatory cytokines IL-1β, IL-6, and IL-8 together with the antiviral cytokines, IL12, and IFN-alpha by avian thrombocytes (chickens: Ferdous et al., 2008; St. Paul et al., 2012; Winkler et al., 2017). In addition, chicken thrombocytes release nitrite in response to LPS (St. Paul et al., 2012). Avian thrombocytes express both the activating TREM A (chicken: Viertlboeck et al., 2013) and the inhibitory TREM B (chicken: Turowski et al., 2016). Avian thrombocytes also have been reported to produce leukotriene B_4 (Jha et al., 2005) and prostaglandin E_2 (Scott and Owens, 2008). In addition, activating chicken Ig-like receptors are found in avian thrombocytes (Windau et al., 2013).

17.6.3 Number

Table 17.7. summarizes thrombocyte concentrations in wild birds and poultry. The number of thrombocytes in the

blood can be influenced by environmental factors. The number of thrombocytes per unit blood volume is also elevated by feed restriction (chickens: Maxwell et al., 1990). The circulating concentrations of thrombocytes is decreased (thrombocytopenia) with viral infections such as by bursal disease virus in chickens (Lima et al., 2005). Moreover, there are marked decreases in the concentration of thrombocytes in chickens with experimentally induced malaria following challenge with *P. juxtanucleare* (Siveira et al., 2009) or *P. gallinaceum* (de Macchi et al., 2013). Similarly, there are decreases in the number of thrombocytes following intravenous administration of cellulose microparticles (Wang et al., 2003). In contrast, thrombocyte numbers increase following challenge with LPS (chicken: Gehad et al., 2002). Pesticides can influence thrombocyte concentrations, being increased by foschor but decreased by chlorphenvinphos (Japanese quail: Gromysz-Kałkowska et al., 1985).

17.6.4 Production

Thrombocytes are produced from thromboblasts in the bone marrow. In vitro, embryonic marrow cells have been demonstrated to be capable of developing into thrombocytes (Japanese quail: Brandon et al., 2000). Thrombocyte production is stimulated by thrombopoietin (TPO) with avian TPO and its receptor c-Mpl proto-oncogene having been characterized (chickens: Bartunek et al., 2008). Expression of TPO is restricted to the liver and spleen while its receptor is expressed in bone marrow, lungs, and spleen (Bartunek et al., 2008).

17.6.5 Thrombopoietin

TPO stimulates production of thrombocytes. The structure of avian TPO has been deduced from cDNA [e.g., budgerigar (*Melopsittacus undulatus*)—Genbank XM_005146962.1; chicken: Bartunek et al., 2008]. It is expressed in the liver and spleen while its receptor is expressed in bone marrow together with lungs and spleen (chicken: Bartunek et al., 2008).

17.7 Other cells types in avian plasma

17.7.1 Reticulocytes

Reticulocytes are immature erythrocytes that can be found in the circulation of birds (e.g., red-tailed hawk: Johns et al., 2008; Japanese quail with 0.25×10^{-6} cells per mm^3: Gildersleeve et al.,1983b). These vary with physiological, toxicological, and pathological state. At the end of incubation, there is a marked increase in the reticulocyte (immature erythrocytes) index (zebra finches: Wagner et al., 2008). Low levels of reticulocytemia (maximum 4.5%) in chickens were induced by withdrawal of blood but higher concentrations of reticulocytes were induced by withdrawal of blood from birds infected with *Leucocytozoon caulleryi* (Ohnishi and Nishimura, 2001). There are marked increases in the number of reticulocytes in the circulation of American oystercatchers contaminated with oil (Fallon et al., 2018). Similarly, the number of reticulocytes are increased following intoxication with zinc (mallard ducks: Levengood et al., 2000) and fenitrothion (Szubartowska and Gromysz-Kałkowska, 1992).

17.7.2 Mott cells

Mott cells are detected in blood from laying hens (Cotter, 2015). These plasma cells contain both cytoplasmic and nuclear vacuoles and exhibit phagocytosis (Cotter, 2015).

17.7.3 Natural killer cells

Natural killer cells are also observed in avian blood (Cotter, 2015).

17.8 Parasites and blood cells

Parasites can infect blood cells in birds. *P. gallinaceum* organisms are found in erythrocytes, thrombocytes, and leukocytes in chickens infected with malaria (de Macchi et al., 2013; Granthon and Williams, 2017). Similarly, both avian erythrocytes and thrombocytes can be infected with *Toxoplasma gondii* organisms (Malkwitz et al., 2017). In contrast, *Leucocytozoon sabrazesi* infect thrombocytes but not other blood cells (chickens: Zhao et al., 2015).

Parasites also influence the numbers of leukocytes and thrombocytes. For instance, infection of pigeons with the erythrocyte parasite, *Haemoproteus columbae*, is accompanied by increases in leukocytes, decreases in lymphocytes, and increases in both basophils and eosinophils (Samani et al., 2016). Leukocyte numbers, specifically of heterophils, eosinophils, and monocytes, are increased in chickens infected with schistosome, *Austrobilharzia variglandis* (Ferris and Bacha, 1986).

17.9 Clotting

The overall scheme for clotting in birds is similar to that in mammals but clotting factors XI and XII appear to be missing in birds (reviewed Buzula et al., 2017). There are both extrinsic and intrinsic clotting systems (Doerr and Hamilton, 1981). Fibrinogen is cleaved by the protease, thrombin, to fibrin (Weissbach et al., 1991), which is then polymerizes. Prothrombin is activated to thrombin by a cascade of clotting factors.

The sequences of some of the avian clotting factors have been deduced from their genes or cDNA or following purification:

- Fibrinogen α chain [chicken: Gene ID: 396307]
- Fibrinogen β chain [chicken- Gene ID: 373926]
- F2 coagulation factor II/thrombin [chicken—Gene ID: 395306; ostrich: Frost et al., 2000].
- Thrombin [Japanese quail: Belleville et al., 1982]

The tertiary protein structure of the fibrinogen has been reported (chicken: Yang et al., 2000).

Clotting factors are produced by the liver (fibrinogen—chicken: Grieninger et al., 1989; prothrombin—ostrich: Frost et al., 2000). Plasma concentrations of fibrinogen have been reported as 1.8 g/L (Roy et al., 2014) and 3.1 g/L (chicken: Pliszczak-Krol et al., 2012). Fibrinogen concentrations are increased in laying hens infected with *Streptococcus equi* (Roy et al., 2014). Administration of turpentine evokes an acute phase response with increased plasma concentrations of fibrinogen (chicken: Grieninger et al., 1986). There are age-related shifts in circulating concentrations of clotting factors including plasminogen and fibrinogen but not tissue factor or tissue factor pathway inhibitor (Buzala et al., 2016).

Avian blood appears to clot more slowly than does mammalian blood (Japanese quail: Belleville et al., 1982). For instance, the whole blood clotting time is 38 min for Japanese quail compared to 8 min for human blood (Belleville et al., 1982). Avian blood does not clot in response to glass activation (Japanese quail: Belleville et al., 1982). Table 17.8 provides examples of clotting times in birds. Clotting times are increased in chickens receiving aflatoxin in their diet (Doerr et al., 1974).

References

Abe, T., Muto, Y., Hosoya, N., 1975. Vitamin A transport in chicken plasma: isolation and characterization of retinol-binding protein (RBP), prealbumin (PA), and RBP-PA complex. J. Lipid Res. 16, 200–210.

Aich, U., Beckley, N., Shriver, Z., Raman, R., Viswanathan, K., Hobbie, S., Sasisekharan, R., 2011. Glycomics-based analysis of chicken red blood cells provides insight into the selectivity of the viral agglutination assay. FEBS J. 278, 1699–1712.

Alev, C., Shinmyozu, K., McIntyre, B.A., Sheng, G., 2009. Genomic organization of zebra finch alpha and beta globin genes and their expression in primitive and definitive blood in comparison with globins in chicken. Dev. Gene. Evol. 219, 353–360.

Alper, S.L., Palfrey, H.C., DeRiemer, S.A., Greengard, P., 1980. Hormonal control of protein phosphorylation in Turkey erythrocytes. Phosphorylation by cAMP-dependent and Ca^{2+}-dependent protein kinases of distinct sites in goblin, a high molecular weight protein of the plasma membrane. J. Biol. Chem. 255, 11029–11039.

Alves-Ferreira, M., Scofano, H.M., Ferreira-Pereira, A., 1999. Ca(2+)-ATPase from chicken (*Gallus domesticus*) erythrocyte plasma membrane: effects of calmodulin and taurine on the Ca(2+)-dependent ATPase activity and Ca^{2+} uptake. Comp. Biochem. Physiol. B 22, 269–276.

Andretta, I., Kipper, M., Lehnen, C.R., Lovatto, P.A., 2012. Meta-analysis of the relationship of mycotoxins with biochemical and hematological parameters in broilers. Poult. Sci. 91, 376–382.

Angelo, S., Cabrera, S., Rojas, A.M., Rodríguez, N., Devés, R., 2005. Testing the hypothesis that system y(+)L accounts for high- and low-transport phenotypes in chicken erythrocytes using L-leucine as substrate. J. Membr. Biol. 204, 93–100.

Arad, Z., Marder, J., Eklat, U., 1983. Serum electrolytes and enzyme responses to heat stress and dehydration in the fowl (*Gallus domesticus*). Comp. Biochem. Physiol. A 74A, 448–453.

Asasi, K., Mohammadi, A., Boroomand, Z., Hosseinian, S.A., Nazifi, S., 2013. Changes of several acute phase factors in broiler chickens in response to infectious bronchitis virus infection. Poultry Sci. 92, 1989–1996.

Atlan, Ö., Atlan, A., Bayraktar, Ö.H., 2000. Effects of heat stress on some blood parameters in broilers. Turk. J. Vet. Anim. Sci. 24, 145–148.

Azis, A., 2012. Performance and heterophil to lymphocyte (H/L) ratio profile of broiler chickens subjected to feeding time restriction. Int. J. Poultry Sci. 11, 153–157.

Bacon, W., 1981. Metabolism of lipid labeled very low density lipoprotein from laying Turkey hens in laying Turkey hens and immature turkeys. Poultry Sci. 60, 1525–1536.

Bagley, L.G., Christensen, V.L., Gildersleeve, R.P., 1990. Hematological indices of Turkey embryos incubated at high altitude as affected by oxygen and shell permeability. Poultry Sci. 69, 2035–2039.

Bairlein, F., Fritz, J., Scope, A., Schwendenwein, I., Stanclova, G., van Dijk, G., Meijer, H.A.J., Verhulst, S., Dittami, J., 2015. Energy expenditure and metabolic changes of free-flying migrating northern bald ibis. PLoS One 10, e0134433.

Baker, J.G., 2010. A full pharmacological analysis of the three Turkey β-adrenoceptors and comparison with the human β-adrenoceptors. PLoS One 5, e15487.

Bartunek, P., Karafiat, V., Bartunkova, J., Pajer, P., Dvorakova, M., Kralova, J., Zenke, M., Dvorak, M., 2008. Impact of chicken thrombopoietin and its receptor c-Mpl on hematopoietic cell development. Exp. Hematol. 36, 495–505.

Baumann, R., Blass, C., Götz, R., Dragon, S., 1999. Ontogeny of catecholamine and adenosine receptor-mediated cAMP signaling of embryonic red blood cells: role of cGMP-inhibited phosphodiesterase 3 and hemoglobin. Blood 94, 4314–4320.

Baumann, R., Gotz, R., Dragon, S., 2003. NTP pattern of avian embryonic red cells: role of RNA degradation and AMP deaminase/5'-nucleotidase activity. Am. J. Physiol. 284, R771–R779.

Baumgartner, S., Brown, D.J., Salevsky Jr., E., Leach Jr., R.M., 1978. Copper deficiency in the laying hen. J. Nutr. 108, 804–811.

Bedanova, I., Chloupek, J., Chloupek, P., Knotkova, Z., Voslarova, E., Pistekova, V., Vecerek, V., 2010. Responses of peripheral blood leukocytes to chronic intermittent noise exposure in broilers. Berl. Munch. Tierarztl Wochenschr 123, 186–191.

Belamarich, F.A., Simoneit, L.W., 1973. Aggregation of duck thrombocytes by 5- hydroxytryptamine. Microvasc. Res. 6, 229–234.

Belleville, J., Cornillon, B., Paul, J., Baguet, J., Clendinnen, G., Eloy, R., 1982. Haemostasis, blood coagulation and fibrinolysis in the Japanese quail. Comp. Biochem. Physiol. A 71, 219–230.

Bernstein, R.S., Schraer, R., 1972. Purification and properties of an avian carbonic anhydrase from the erythrocytes of *Gallus domesticus*. J. Biol. Chem. 247, 1306–1322.

Beuchat, C.A., Chong, C.R., 1998. Hyperglycemia in hummingbirds and its consequences for hemoglobin glycation. Comp. Biochem. Physiol. A 20, 409–416.

Bishop, C., Butler, P., 1995. Physiological modelling of oxygen consumption in birds during flight. J. Exp. Biol. 198, 2153–2163.

Booth, C.E., Elliott, P.F., 2003. Hematological responses to hematozoa in North American and neotropical songbirds. Comp. Biochem. Physiol. 133A, 451–467.

Borges, S.A., Fischer da Silva, A.V., Majorka, A., Hooge, D.M., Cummings, K.R., 2004. Physiological responses and dietary electrolyte balance (sodium plus potassium minus chloride, milliequivalent per kilogram). Poultry Sci. 83, 1551–1558.

Bowen, O.T., Dienglewicz, R.L., Wideman, R.F., Erf, G.F., 2009. Altered monocyte and macrophage numbers in blood and organs of chickens injected i.v. with lipopolysaccharide. Vet. Immunol. Immunopathol. 131, 200–210.

Brace, K., Atland, P.D., 1956. Lifespan of the duck and chicken erythrocytes as determined with C-14. Proc. Soc. Exp. Biol. Med. 92, 615–617.

Brandon, C., Eisenberg, L.M., Eisenberg, C.A., 2000. WNT signaling modulates the diversification of hematopoietic cells. Blood 96, 4132–4141.

Breuner, C.W., Orchinik, M., 2009. Pharmacological characterization of intracellular, membrane, and plasma binding sites for corticosterone in house sparrows. Gen. Comp. Endocrinol. 163, 214–224.

Brahm, J., Wieth, J.O., 1977. Separate pathways for urea and water, and for chloride in chicken erythrocytes. J. Physiol. 266, 727–747.

Bryan, T.E., Gildersleeve, R.P., Wiard, R.P., 1989. Exposure of Japanese quail embryos to o,p'-DDT has long-term effects on reproductive behaviors, hematology, and feather morphology. Teratology 39, 525–535.

Brygier, J., De Bruin, S.H., Van Hoof, M.K., Rollema, H.S., 1975. The interaction of organic phosphates with human and chicken hemoglobin. Eur. J. Biochem. 60, 379–383.

Bulliman, B.T., Kuchel, P.W., 1988. A series expression for the surface area of an Ellipsoid and its application to the computation of the surface area of avian erythrocytes. J. Theor. Biol. 134, 113–123.

Butler, P.J., West, N.H., Jones, D.R., 1977. Respiratory and cardiovascular responses of the pigeon to sustain level flight in a wind-tunnel. J. Exp. Biol. 71, 7–26.

Buzala, M., Ponczek, M.B., Slomka, A., Roslewska, A., Janicki, B., Zekanowska, E., Bednarczyk, M., 2016. A pilot study of tissue factor-tissue factor pathway inhibitor axis and other selected coagulation parameters in broiler chickens administered *in ovo* with selected prebiotics. Folia Biol. (Krakow) 64, 213–224.

Buzalaa, M., Słomkab, A., Janickia, B., Ponczekc, M.B., Zekanowskab, E., 2017. The mechanism of blood coagulation, its disorders and measurement in poultry. Livest. Sci. 195, 1–8.

Calabrese, L., Carbonaro, M., Musci, G., 1988. Chicken ceruloplasmin. Evidence in support of a trinuclear cluster involving type 2 and 3 copper centers. J. Biol. Chem. 263, 6480–6483.

Campbell, T.W., Ellis, C.K., 2007. Hematology. In: Ritchie, W.B., Harrison, G.J., Harrison, L.R. (Eds.), Avian Medicine: Principles and Application. Wingers Publishing, Lake Worth, Florida, pp. 176–198.

Carlson, H.C., Sweeny, P.R., Tokaryk, J.M., 1968. Demonstration of phagocytic and trephocytic activities by chicken thrombocytes by microscopy and vital staining techniques. Avian Dis. 12, 700–715.

Cetin, E., Silici, S., Cetin, N., Güçlü, B.K., 2010. Effects of diets containing different concentrations of propolis on hematological and immunological variables in laying hens. Poult. Sci. 89, 1703–1708.

Chamanza, R., Toussaint, M.J., van Ederen, A.M., van Veen, L., Hulskamp-Koch, C., Fabri, T.H., 1999. Serum amyloid A and transferrin in chicken. A preliminary investigation of using acute-phase variables to assess diseases in chickens. Vet. Q. 21, 158–162.

Chang, C.F., Hamilton, P.B., 1979a. Impaired phagocytosis by heterophils from chickens during aflatoxicosis. Toxicol. Appl. Pharmacol. 48, 459–466.

Chang, C.F., Hamilton, P.B., 1979b. Impaired phagocytosis by heterophils from chickens during aflatoxicosis. Poultry Sci. 58, 562–566.

Chang, C.F., Hamilton, P.B., 1979c. The thrombocyte as the primary circulating phagocyte in chickens. J. Reticuloendothel. Soc. 25, 585–590.

Chapman, B.S., Tobin, A.J., Hood, L.E., 1980. Complete amino acid sequences of the major early embryonic alpha-like globins of the chicken. J. Biol. Chem. 255, 9051–9059.

Chen, X.H., Harden, T.K., Nicholas, R.A., 1994. Molecular cloning and characterization of a novel beta-adrenergic receptor. J. Biol. Chem. 269, 24810–24819.

Cheng, Y., Prickett, M.D., Gutowska, W., Kuo, R., Belov, K., Burt, D.W., 2015. Evolution of the avian β-defensin and cathelicidin genes. BMC Evol. Biol. 15, 188.

Chou, S.J., Shieh, Y.C., Yu, C.Y., 2008. Hematological and biochemistry values for black-faced spoonbills (*Platalea minor*) with and recovering from botulism. J. Wildl. Dis. 44, 781–784.

Christensen, E.H., Dill, D.B., 1935. Oxygen dissociation curves of bird blood. J. Biol. Chem. 109, 443–448.

Christensen, K., Vizzier-Thaxton, Y., Thaxton, J.P., Scanes, C.G., 2012. Changes in body tempteratures during growth and in response to fasting in growing modern meat type chickens. Brit. Poult. Sci. 53, 531–537.

Cirotto, C., Di Tella, A.S., Geraci, G., 1975. The hemoglobins of the developing chicken embryos. Fractionation and globin composition of the individual component of total erythrocytes and of a single erythrocyte type. Cell Differ. 4, 87–99.

Clark, M.W., Gildersleeve, R.P., Thaxton, J.P., Parkhurst, C.R., McRee, D.I., 1988. Hematological effects of ethyl methanesulfonate, paraquat and phenylhydrazine in Japanese quail. Comp. Biochem. Physiol. C 89, 15–30.

Cohen, A., Klasing, K., Ricklefs, R., 2007. Measuring circulating antioxidants in wild birds. Comp. Biochem. Physiol. B 147, 110–121.

Cohen, A.A., McGraw, K.J., Robinson, W.D., 2009. Serum antioxidants levels in wild birds vary in relation to diet, season, life history strategy, and species. Oecologia 161, 673–683.

Coll, J., Ingram, V.M., 1978. Stimulation of heme accumulation and erythroid colony formation in cultures of chick bone marrow cells by chicken plasma. J. Cell Biol. 76, 184–190.

Cotter, P.F., 2015. Are peripheral Mott cells an indication of stress or inefficient immunity. Poultry Sci. 94, 1433–1438.

Curtis, M.J., Butler, E.J., 1980. Response of caeruloplasmin to *Escherichia coli* endotoxins and adrenal hormones in the domestic fowl. Res. Vet. Sci. 28, 217–222.

Dajani, R., Orten, J.M., 1958. A study of the citric acid cycle in erythrocytes. J. Biol. Chem. 231, 913–924.

Dajani, R., Orten, J.M., 1959. The utilization of glycine by the nucleated erythrocyte. J. Biol. Chem. 234, 877–879.

DaMatta, R.A., Seabra, S.H., de Souza, W., 1998. Further studies on the phagocytic capacity of avian thrombocytes. Submicrosc. Cytol. Path. 30, 271–277.

Davis, H.G., 1961. Structure of nucleated erythrocytes. J. Biophys. Biochem. Cytol. 9, 671–687.

Deeley, R.G., Mullinix, D.P., Wetekam, W., Kronenberg, H.M., Meyers, M., Eldridge, J.D., Goldberger, R.F., 1975. Vitellogenin synthesis in the avian liver. Vitellogenin is the precursor of the egg yolk phosphoproteins. J. Biol. Chem. 250, 9060–9066.

de Macchi, B.M., Miranda, F.J.B., de Souza, F.S., de Carvalho, E.C.Q., Albernaz, A.P., do Nascimento, J.L.M., DaMatta, R.A., 2013. Chickens treated with a nitric oxide inhibitor became more resistant to *Plasmodium gallinaceum* infection due to reduced anemia, thrombocytopenia and inflammation. Vet. Res. 44, 8.

Deem, S.L., Noss, A.J., Cuéllar, R.L., Karesh, W.B., 2005. Health evaluation of free-living and captive blue-fronted Amazon parrots (*Amazona aestiva*) in the Gran Chaco. Bolivia. J. Zoo Wildl. 36, 598–605.

Delhaye, J., Salamin, N., Roulin, A., Criscuolo, F., Bize, P., Christe, P., 2016. Interspecific correlation between red blood cell mitochondrial ROS production, cardiolipin content and longevity in birds. Age (Dordr.) 38, 433–443.

Deviche, P., Breuner, C., Orchinik, M., 2001. Testosterone, corticosterone, and photoperiod interact to regulate plasma levels of binding globulin and free steroid hormone in dark-eyed juncos, *Junco hyemalis*. Gen. Comp. Endocrinol. 122, 67–77.

Diamond, D.L., Carruthers, A., 1993. Metabolic control of sugar transport by derepression of cell glucose transporters. An insulin recruitment-independent mechanism of regulation. J. Biol. Chem. 268, 6437–6444.

Diaz, G.J., Julian, R.J., Squires, E.J., 1994. Cobalt-induced polycythaemia causing right ventricular hypertrophy and ascites in meat-type chickens. Avian Pathol. 23, 91–104.

Disilvestro, R.A., Harris, E.D., 1985. Purification and partial characterization of ceruloplasmin from chicken serum. Arch. Biochem. Biophys. 241, 438–446.

Doerr, J.A., Hamilton, P.B., 1981. New evidence for intrinsic blood coagulation in chickens. Poultry Sci. 60, 237–242.

Doerr, J.A., Huff, W.E., Tung, H.T., Wyatt, R.D., Hamilton, P.B., 1974. A survey of T-2 toxin, ochratoxin, and aflatoxin for their effects on the coagulation of blood in young broiler chickens. Poultry Sci. 53, 1728–1734.

Dragon, S., Baumann, R., 2001. Erythroid carbonic anhydrase and hsp70 expression in chick embryonic development: role of cAMP and hypoxia. Am. J. Physiol. 280, R870–R878.

Dragon, S., Glombitza, S., Götz, R., Baumann, R., 1996. Norepinephrine-mediated hypoxic stimulation of embryonic red cell carbonic anhydrase and 2,3-DPG synthesis. Am. J. Physiol. 271, R982–R988.

Dragon, S., Carey, C., Martin, K., Baumann, R., 1999. Effect of high altitude and in vivo adenosine/β adrenergic receptor blockade on ATP and 2,3BPG concentrations in red blood cells of avian embryos. J. Exp. Biol. 202, 2787–2795.

Drew, C., Lapaix, F., Egee, S., Thomas, S., Ellory, J.C., Staines, H.M., 2002. Age-dependent changes in cation transport in the chicken erythrocyte. Comp. Biochem. Physiol. A 133, 169–178.

Duan, W., Achen, M.G., Richardson, S.J., Lawrence, M.C., Wettenhall, R.E., Jaworowski, A., Schreiber, G., 1991. Isolation, characterization, cDNA cloning and gene expression of an avian transthyretin. Implications for the evolution of structure and function of transthyretin in vertebrate. Eur. J. Biochem. 200, 679–687.

Eguchi, R., Ishihara, A., Yamauchi, K., 2008. Interaction of diethylstilbestrol and ioxynil with transthyretin in chicken serum. Comp. Biochem. Physiol. C 147, 345–350.

Escobar, A., Thiesen, R., Vitaliano, S.N., Belmonte, E.A., Werther, K., Valadã0, C.A., 2011. Cardiorespiratory effects of isoflurane anesthesia in crested caracaras (*Caracara plancus*). J. Zoo. Wildl. Med. 42, 12–17.

Fair, J., Whitaker, S., Pearson, B., 2007. Sources in the variation in haematocrit in birds. Ibis 149, 535–552.

Fallon, J.A., Smith, E.P., Schoch, N., Paruk, J.D., Adams, E.A., Evers, D.C., Jodice, P.G.R., Perkins, C., Schulte, S., Hopkins, W.A., 2018. Hematological indices of injury to lightly oiled birds from the Deepwater Horizon oil spill. Environ. Toxicol. Chem. 37, 451–461.

Farnell, M.B., Crippen, T.L., Haiqi, H., Swaggerty, C.L., Kogut, M.H., 2003. Oxidative burst mediated by Toll-like receptors (TLR) and CD14 on avian heterophils stimulated with bacterial Toll agonists. Dev. Comp. Immunol. 27, 423–429.

Fedde, M.R., Wideman, R.F., 1996. Blood viscosity in broilers: influence of pulmonary hypertension syndrome. Poultry Sci. 75, 1261–1267.

Ferdous, F., et al., 2008. Broiler chicken thrombocyte response to lipopolysaccharide. Poultry Sci. 87, 61–63.

Ferris, M., Bacha Jr., W.J., 1986. Response of leukocytes in chickens infected with the avian schistosome *Austrobilharzia variglandis* (Trematoda). Avian Dis. 30, 683–686.

Frost, L., Naudé, R., Oelofsen, W., Muramoto, K., Naganuma, T., Ogawa, T., 2000. Purification and characterization of ostrich prothrombin. Int. J. Biochem. Cell Biol. 32, 1151–1159.

Fujii, M., Yoshino, I., Suzuki, M., Higuchi, T., Mukai, S., Aoki, T., Fukunaga, T., Sugimoto, Y., Inoue, Y., Kusuda, J., Saheki, T., Sato, M., Hayashi, S., Tamaki, M., Sugano, T., 1996. Primary culture of chicken hepatocytes in serum-free medium (pH 7.8) secreted albumin and transferrin for a long period in free gas exchange with atmosphere. Int. J. Biochem. Cell Biol. 28, 1381–1391.

Gadde, U., Chapman, H.D., Rathinam, T.R., Erf, G.F., 2009. Acquisition of immunity to the protozoan parasite *Eimeria adenoeides* in Turkey poults and the peripheral blood leukocyte response to a primary infection. Poultry Sci. 88, 2346–2452.

Gallo, S.S., Ederli, N.B., Bôa-Morte, M.O., Oliveira, F.C., 2015. Hematological, morphological and morphometric characteristics of blood cells from rhea, Rhea Americana (Struthioniformes: rheidae): a standard for Brazilian birds. Braz. J. Biol. 75, 953–962.

García-de Blas, E., Mateo, R., Alonso-Alvarez, C., 2016. Specific carotenoid pigments in the diet and a bit of oxidative stress in the recipe for producing red carotenoid-based signals. Peer J. 4, e2237.

Gehad, A.E., Lillehoj, H.S., Hendricks 3rd, G.L., Mashaly, M.M., 2002. i. Initiation of humoral immunity. ii. The effects of t-independent and t-dependent antigens on the distribution of lymphocyte populations. Dev. Comp. Immunol. 26, 761–771.

Gerhardt, E.M., Chan, L.N., Jing, S.Q., Qi, M.Y., Trowbridge, I.S., 1991. The cDNA sequence and primary structure of the chicken transferrin receptor. Gene 102, 249–254.

Gerson, A.R., Guglielmo, C.G., 2013. Energetics and metabolite profiles during early flight in American robins (*Turdus Migratorius*). J. Comp. Physiol. B. 183, 983–991.

Ghareeb, K., Awad, W.A., Böhm, J., 2011. Mycotoxin Contamination of Feedstuffs - an Additional Stress Factor for Broiler chickens.403-406.-XVth International Congress on Animal Hygiene; Jul 3−7, 2011; Vienna, Austria.

Ghareeb, K., Awad, W.A., Sid-Ahmed, O.E., Böhm, J., 2014. Insights on the host stress, fear and growth responses to the deoxynivalenol feed contaminant in broiler chickens. PLoS One 9, e87727.

Gibson, J.S., Cossins, A.R., Ellory, J.C., 2000. Oxygen-sensitive membrane transporters in vertebrate red cells. J. Exp. Biol. 203, 1395−1407.

Gildersleeve, R.P., Galvin, M.J., Thaxton, J.P., McRee, D.I., 1985a. Hematological response of Japanese quail to acute hemorrhagic stress. Comp. Biochem. Physiol. A 81, 403−409.

Gildersleeve, R.P., Phelps, P.V., Thaxton, J.P., McRee, D.I., 1983. Effect of phlebotomy on reticulocyte numbers in Japanese. Quail. Poult. Sci. 64, 1990−1995.

Gildersleeve, R.P., Phelps, P.V., Thaxton, J.P., McRee, D.I., 1985b. Effect of phlebotomy on reticulocyte numbers in Japanese Quail. Poultry Sci. 64, 1990−1995.

Gildersleeve, R.P., Satterlee, D.G., Johnson, W.A., Scott, T.R., 1983. The effects of forced molt treatment on blood biochemicals in hens. Poultry Sci. 62, 755−762.

Gleeson, M., Brackenberry, J.H., 1984. Effects of body temperature on ventilation, blood gases, and acid-base balance in exercising fowl. Q. J. Exp. Physiol 69, 61−72.

Glombitza, S., Dragon, S., Berghammer, M., Pannermayr, M., Baumann, R., 1996. Adenosine causes cAMP-dependent activation of chick embryo red cell carbonic anhydrase and 2,3-DPG synthesis. Am. J. Physiol. 271, R973−R981.

Gormally, B.M.G., Fuller, R., McVey, M., Romero, L.M., 2019. DNA damage as an indicator of chronic stress: correlations with corticosterone and uric acid. Comp. Biochem. Physiol. A 227, 116−122.

Grant, R.A., Zucker, M.B., 1973. Avian thrombocyte aggregation and shape change *in vitro*. Am. J. Physiol. 225, 340−343.

Granthon, C., Williams, D.A., 2017. Avian malaria, body condition, and blood parameters in four species of songbirds. Wilson J. Ornithol. 129, 492−509.

Grecchi, R., Salida, A.M., Mariano, M., 1980. Morphological changes, surface receptors and phagocytic potential of fowl mono-nuclear phagocytes and thrombocytes in vivo and in vitro. J. Pathol. 130, 23−31.

Grieninger, G., Liang, T.J., Beuving, G., Goldfarb, V., Metcalfe, S.A., Muller-Eberhard, U., 1986. Hemopexin is a developmentally regulated, acute-phase plasma protein in the chicken. J. Biol. Chem. 261, 15719−15724.

Grieninger, G., Oddoux, C., Diamond, L., Weissbach, L., Plant, P.W., 1989. Regulation of fibrinogen synthesis and secretion by the chicken hepatocyte. Ann. N. Y. Acad. Sci. 557, 257−270.

Groscolas, R., Bézard, J., 1977. Effect of glucagon and insulin on plasma free fatty acids and glucose in the Emperor penguin, *Aptenodytes forsteri*. Gen. Comp. Endocrinol. 32, 230−235.

Gromysz-Kałkowska, K., Szubartowska, E., Kaczanowska, E., 1985. Peripheral blood in the Japanese quail (*Coturnix coturnix japonica*) in acute poisoning by different insecticides. Comp. Biochem. Physiol. C 81, 209−212.

Gross, W.B., 1990. Effect of adrenal blocking chemicals on the responses of chickens and turkeys to environmental stressors and ACTH. Avian Pathol. 9, 295−304.

Gross, W.B., Siegel, H.S., 1983. Evaluation of the heterophil:lymphocyte ratio as a measure of stress in chickens. Avian Dis. 27, 972−979.

Guha Thakurta, P., Choudhury, D., Dasgupta, R., Dattagupta, J.K., 2003. Structure of diferric hen serum transferrin at 2.8 A resolution. Acta Crystallogr. D 59, 1773−1781.

Guriec, N., Bussy, F., Gouin, C., Mathiaud, O., Quero, B., Le Goff, M., Collén, P.N., 2018. Ulvan activates chicken heterophils and monocytes through toll-like receptor 2 and toll-like receptor 4. Front. Immunol. 9, 2725.

Hamano, Y., 2012. Alleviative effects of α-lipoic acid supplementation on acute heat stress-induced thermal panting and the level of plasma nonesterified fatty acids in hypothyroid broiler chickens. Br. Poultry Sci. 53, 125−133.

Hamal, K.R., Burgess, S.C., Pevzner, I.Y., Erf, G.F., 2006. Maternal antibody transfer from dams to their egg yolks, egg whites, and chicks in meat lines of chickens. Poultry Sci. 85, 1364−1372.

Han, J.I., Jang, H.J., Na, K.J., 2016. Hematologic and serum biochemical reference intervals of the Oriental white stork (*Ciconia boyciana*) and the application of an automatic hematologic analyzer. J. Vet. Sci. 17, 399−405.

Harmon, B.G., 1998. Avian heterophils in inflammation and disease resistance. Poultry Sci. 77, 972−977.

Harms, C.A., Harms, R.V., 2012. Venous blood gas and lactate values of mourning doves (*Zenaida macroura*), boat-tailed grackles (*Quiscalus major*) and house sparrows (*Passer domestricus*) after capture by mist netting, banding and venipuncture. J. Zoo. Wildl. Med. 43, 77−84.

Harms, C.A., Jinks, M.R., Harms, R.V., 2016. Blood gas, lactate, and hematology effects of venipuncture timing and location after mist-net capture of mourning doves (*Zenaida macroura*), boat tailed grackles (*Quiscalus major*), and house sparrows (*Passer domesticus*). J. Wildl. Dis. 52 (2 Suppl. l), S54−S64.

Heatley, J.J., Cary, J., Russell, K.E., Voelker, G., 2013. Clinicopathologic analysis of passeri form venous blood reflects transitions in elevation and altitude. Vet. Med. Res. 4, 21−29.

Heinze, C.R., Hawkins, M.G., Gillies, L.A., Wu, X., Walzem, R.I., German, J.B., Klasing, K.C., 2012. Effect of dietary omega-3 fatty acids on red blood cell lipid composition and plasma metabolites in the cockatiel, *Nymphicus hollandicus*. J. Anim. Sci. 90, 3068−3079.

Hegemann, A., Matson, K.D., Versteegh, M.A., Villegas, A., Tieleman, B.I., 2013. Immune response to an endotoxin challenge involves multiple immune parameters and is consistent among the annual-cycle stages of a free-living temperate zone bird. J. Exp. Biol. 216, 2573−2580.

Hilewicz-Grabska, M., Zgirski, A., Krajewski, T., Plonka, A., 1988. Purification and partial characterization of goose ceruloplasmin. Arch. Biochem. Biophys. 260, 18−27.

Holz, P., Naisbitt, R., Mansell, P., 2006. Fitness level as a determining factor in the survival of rehabilitated peregrine falcons (*Falco peregrinus*) and brown goshawks (*Accipiter fasciatus*) released back into the wild. J. Avian Med. Surg. 20, 15−20.

Horiuchi, H., Tanaka, K., Shigeta, A., Yoshida, K., Kushima, K., Ohta, H., Furusawa, S., Matsuda, H., 2004. A monoclonal antibody against chicken thrombocytes reacts to cells in the thrombocyte lineage. J. Vet. Med. Sci. 66, 243−250.

Hron, T., Pajer, P., Paces, J., Bartunek, P., Elleder, D., 2015. Hidden genes in birds. Genome Biol. 16, 164.

Huff, G.R., Dutta, V., Huff, W.E., Rath, N.C., 2011. Effects of dietary yeast extract on turkey stress response and heterophil oxidative burst activity. Br. Poult. Sci. 52, 446−455.

Huff, G.R., Huff, W.E., Farnell, M.B., Rath, N.C., Solis de los Santos, F., Donoghue, A.M., 2010. Bacterial clearance, heterophil function, and

hematological parameters of transport-stressed Turkey poults supplemented with dietary yeast extract. Poultry Sci. 89, 447–456.

Iarovaia, O.V., Borounova, V.V., Philonenko, E.S., Kantidze, O.L., Vassetzky, Y.S., Razin, S.V., 2009. In embryonic chicken erythrocytes actively transcribed alpha globin genes are not associated with the nuclear matrix. J. Cell. Biochem. 106, 170–178.

Ido, E., Matsuno, T., 1982. Purification and physicochemical and immunological analysis of chicken alpha-fetoprotein. Jpn. J. Med. Sci. Biol. 35, 87–96.

Igbo, I.N., Reigel Jr., C.E., Greene, I.M., Kenny, A.D., 1994. Effect of reserpine pretreatment on avian erythrocyte carbonic anhydrase activation by isoproterenol. Pharmacology 49, 112–120.

Ioudinkova, E.S., Ulianov, S.V., Bunina, D., Iarovaia, O.V., Gavrilov, A.A., Razin, S.V., 2011. The inactivation of the π gene in chicken erythroblasts of adult lineage is not mediated by packaging of the embryonic part of the α-globin gene domain into a repressive heterochromatin-like structure. Epigenetics 6, 1481–1488.

Isaacks, R., Harkness, D., Sampsell, R., Adler, J., Roth, S., Kim, C., Goldman, P., 1977. Studies on avian erythrocyte metabolism. Inositol tetrakisphosphate: the major phosphate compound in the erythrocytes of the ostrich (*Struthio camelus camelus*). Eur. J. Biochem. 77, 567–574.

Jahan, S., Xu, W., He, S., Gonzalez, C., Delcuve, G.P., Davie, J.R., 2016. The chicken erythrocyte epigenome. Epigenet. Chromatin 9, 19.

Jarosz, L., Stepien-Pysniak, D., Gradzki, Z., Kapica, M., Gacek, A., 2017. The effect of feed supplementation with Zakarpacki zeolite (clinoptilolite) on percentages of T and B lymphocytes and cytokine concentrations in poultry. Poultry Sci. 96, 2091–2097.

Jarosz, Ł.S., Marek, A., Grądzki, Z., Kwiecień, M., Kaczmarek, B., 2018. The effect of feed supplementation with a copper-glycine chelate and copper sulphate on selected humoral and cell-mediated immune parameters, plasma superoxide dismutase activity, ceruloplasmin and cytokine concentration in broiler chickens. J. Anim. Physiol. Anim. Nutr. 102, e326–e336.

Jessen, T.H., Weber, R.E., Fermi, G., Tame, J., Braunitzer, G., 1991. Adaptation of bird hemoglobins to high altitudes: demonstration of molecular mechanism by protein engineering. Proc. Natl. Acad. Sci. U.S.A 88, 6519–6522.

Jha, S., Hall, J.A., Cherian, G., Henry, L.R., Schlipf, J.W., 2005. Optimization of assay conditions for leukotriene B4 synthesis by neutrophils or platelets isolated from peripheral blood of monogastric animals. Prostaglandins Leukot. Essent. Fatty Acids 72, 423–430.

Johns, J.L., Shooshtari, M.P., Christopher, M.M., 2008. Development of a technique for quantification of reticulocytes and assessment of erythrocyte regenerative capacity in birds. Am. J. Vet. Res. 69, 1067–1072.

Jones, J.H., Grubb, B., Schmidt-Nielsen, K., 1983. Panting in the emu causes arterial hypoxemia. Respir. Physiol. 54, 189–195.

Kalomenopoulou, M., Beis, I., 1990. Studies on the pigeon red blood cell metabolism. Comp. Biochem. Physiol. B 95, 677–684.

Kawashiro, T., Scheid, P., 1975. Arterial blood gases in undisturbed resting birds: measurements in chicken and duck. Respir. Physiol. 23, 337–342.

Kaya, A., Altiner, A., Ozpinar, A., 2006. Effect of copper deficiency on blood lipid profile and haematological parameters in broilers. J. Vet. Med. A 53, 399–404.

Keijer, E., Butler, P.J., 1982. Volumes of the respiratory and circulatory systems in tufted and mallard ducks. J. Exp. Biol. 101, 213–220.

Kenny, D., Reading, R., Lee, H.-s, 2015. Blood-gas analysis from free-ranging Eurasian black vultures (*Aegypius monachus*) in Mongolia and the Republic of Korea. J. Vet. Sci. 1, 1–9.

Kim, H.R., Yew, N.S., Ansorge, W., Voss, H., Schager, C., Vennström, B., Zenke, M., Engel, J.D., 1988. Two different mRNAs are transcribed from a single genomic locus encoding the chicken erythrocytes anion transport oprotein (band 3). Mol. Cell. Biol. 8, 4416–4424.

Klasing, K.C., 1998. Nutritional modulation of resistance to infectious diseases. Poult. Sci. 77, 1119–1125.

Kleinig, H., Zentgraf, H., Comes, P., Stadler, J., 1971. Nuclear membranes and plasma membranes from hen erythrocytes: lipid composition. J. Biol. Chem. 246, 2996–3000.

Kogut, M.H., McGruder, E.D., Hargis, B.M., Corrier, D.E., Deloach, J.R., 1995. Characterization of the pattern of inflammatory cell influx in chicks following the intraperitoneal administration of live *Salmonella enteritidis* and *Salmonella enteritidis*-immune lymphokines. Poultry Sci. 74, 8–17.

Kogut, M.H., Rothwell, L., Kaiser, P., 2002. Differential effects of age on chicken heterophil functional activation by recombinant chicken interleukin-2. Dev. Comp. Immunol. 26, 817–830.

Kogut, M.H., Rothwell, L., Kaiser, P., 2003. Priming by recombinant chicken interleukin-2 induces selective expression of IL-8 and IL-18mRNA in chicken heterophils during receptor-mediated phagocytosis of opsonized and nonopsonized *Salmonella enterica* serovar *enteritidis*. Mol. Immunol. 40, 603–610.

Kogut, M.H., Rothwell, L., Kaiser, P., 2005. IFN-gamma priming of chicken heterophils upregulates the expression of proinflammatory and Th1 cytokine mRNA following receptor -mediated phagocytosis of *Salmonella enterica* serovar *enteritidis*. J. Interferon Cytokine Res. 25, 73–81.

Kogut, M.H., Chiang, H.I., Swaggerty, C.L., Pevzner, I.Y., Zhou, H., 2012. Gene expression analysis of Toll-Like Receptor pathways in heterophils from genetic chicken lines that differ in their susceptibility to Salmonella enteritidis. Front. Genet. 3, 121.

Koh, T.S., Peng, R.K., Klasing, K.C., 1996. Dietary copper level affects copper metabolism during lipopolysaccharide-induced immunological stress in chicks. Poultry Sci. 75, 867–872.

Koinarski, V., Georgieva, N., Gadjeva, V., Petkov, P., 2005. Antioxidant status of broiler chickens, infected with *Eimeria acervulina*. Revue Méd. Vet. 156, 498–502.

Kolluri, G., Ramamurthy, N., Churchil, R.R., Raj, G.D., Kannaki, T.R., 2014. Influence of age, sex and rearing systems on Toll-like receptor 7 (*TLR7*) expression pattern in gut, lung and lymphoid tissues of indigenous ducks. Br. Poultry Sci. 55, 59–67.

Kopec, W., Wiliczkiewicz, A., Jamroz, D., Biazik, E., Pudlo, A., Hikawczuk, T., Skiba, T., Korzeniowska, M., 2016. Antioxidant status of Turkey breast meat and blood after feeding a diet enriched with histidine. Poultry Sci. 95, 53–61.

Koutzamani, E., Loborg, H., Sarg, B., Lindner, H.H., Rundquist, I., 2002. Linker histone subtype composition and affinityfor chromatin in situ in nucleated mature erythrocytes. J. Biol. Chem. 277, 44688–44694.

Kozma, T.G., Omana, F., Ducoff, H.S., Dawson, M.J., 1995. Thermotolerance in chicken red blood cells studied by 31P NMR spectroscopy. Int. J. Hyperther. 11, 647–662.

Lam, K.M., 2002. The macrophage inflammatory protein-1beta in the supernatant of *Mycoplasma gallisepticum*-infected chicken leukocytes attracts the migration of chicken heterophils and lymphocytes. Dev. Comp. Immunol. 26, 85–93.

Lambert, L.A., Perri, H., Halbrooks, P.J., Mason, A.B., 2005. Evolution of the transferrin family: conservation of residues associated with iron and anion binding. Comp. Biochem. Physiol. B 142, 129–141.

Langslow, D.R., Butler, E.J., Hales, C.N., Pearson, A.W., 1970. The response of plasma insulin, glucose and non-esterified fatty acids to various hormones, nutrients and drugs in the domestic fowl. J. Endocrinol. 46, 243–260.

Lardinois, A., van den Berg, T., Lambrecht, B., Steensels, M., 2014. A model for the transfer of passive immunity against Newcastle disease and avian influenza in specific pathogen free chickens. Avian Pathol. 43, 118–124.

Lee, K.A., Tell, L.A., Mohr, F.C., 2012. Inflammatory markers following acute fuel oil exposure or bacterial lipopolysaccharide in mallard ducks (*Anas platyrhynchos*). Avian Dis. 56, 704–710.

Leighton, F.A., 1985. Morphological lesions in red blood cells from herring gulls and Atlantic puffins ingesting Prudhoe Bay crude oil. Vet. Pathol. 22, 393–402.

Lepkovsky, S., Dimick, M.K., Furuta, F., Snapir, N., Park, R., Narita, N., Komatsu, K., 1967. Response of blood glucose and plasma free Fatty acids to fasting and to injection of insulin and testosterone in chickens. Endocrinology 81, 1001–1006.

Lerner, J., Smagula, R.M., Somes Jr., R.G., 1984. Sodium-ion dependence of glycine and lysine transport in chicken erythrocytes genetically selected for high and low leucine transport activity. Comp. Biochem. Physiol. A 78, 277–278.

Levengood, J.M., Sanderson, G.C., Anderson, W.L., Foley, G.L., Brown, P.W., Seets, J.W., 2000. Influence of diet on the hematology and serum biochemistry of zinc-intoxicated mallards. J. Wildl. Dis. 36, 111–123.

Li, K., Zhao, L., Geng, G., Ma, L., Dong, S., Xu, T., Wang, J., Wang, H., Tian, Y., Qiao, J., 2011. Increased calcium deposits and decreased Ca^{2+} -ATPase in erythrocytes of ascitic broiler chickens. Res. Vet. Sci. 90, 468–473.

Liang, Y.H., Liu, X.Z., Liu, S.H., Lu, G.Y., 2001. The structure of greylag goose oxy haemoglobin: the roles of four mutations compared with bar-headed goose haemoglobin. Acta Crystallogr. D Biol. Crystallogr. 57, 1850–1856.

Lima, A., Fehervari, T., Paasch, L.H., Calderón, N.L., 2005. Haematological and histological findings in Leghorn chickens infected with infectious bursal disease virus strain 73688. Acta Vet. Hung. 53, 501–506.

Lin, H., Decuypere, E., Buyse, J., 2004. Oxidative stress induced by corticosterone administration in broiler chickens (*Gallus gallus domesticus*) 1. Chronic exposure. Cokmp. Biochem. Physiol. B. Biochem. Mol. Biol. 139, 737–744.

Lin, H., Decuypere, E., Buyse, J., 2006. Acute heat stress induces oxidative stress in broiler chickens. Comp. Biochem. Physiol. A 144, 11–17.

Liu, L., Lei, T., Bankir, L., Zhao, D., Gai, X., Zhao, X., Yang, B., 2011. Erythrocyte permeability to urea and water: comparative study in rodents, ruminants, carnivores, humans, and birds. J. Comp. Physiol. B. 181, 65–72.

Liu, L., Wang, G., Xiao, Y., Shipp, S.L., Siegel, P.B., Cline, M.A., Gilbert, E.R., 2017. Peripheral neuropeptide Y differentially influences adipogenesis and lipolysis in chicks from lines selected for low or high body weight. Comp. Biochem. Physiol. A 213, 1–10.

Loh, T.C., Tan, B.K., Foo, H.L., Norhani, A., Zulkifli, I., 2011. Relationships of plasma and very-low-density lipoprotein lipids and subfractions with abdominal fat in chickens. Asian-Australas. J. Anim. Sci. 24, 82–87.

Luan, Y., Zhao, J., Yao, H., Zhao, X., Fan, R., Zhao, W., Zhang, Z., Xu, S., 2016. Selenium deficiency influences the mRNA expression of selenoproteins and cytokines in chicken erythrocytes. Biol. Trace Elem. Res. 171, 427–436.

Lytle, C., 1997. Activation of the avian erythrocyte Na-K-Cl cotransport protein by cell shrinkage, cAMP, fluoride, and calyculin-A involves phosphorylation at common sites. J. Biol. Chem. 272, 15069–15077.

Maas, R., Rosema, S., van Zoelen, D., Venema, S., 2011. Maternal immunity against avian influenza H5N1 in chickens: limited protection and interference with vaccine efficacy. Avian Pathol. 40, 87–92.

Malkwitz, I., Berndt, A., Zhang, R., Daugschies, A., Bangoura, B., 2017. Replication of *Toxoplasma gondii* in chicken erythrocytes and thrombocytes compared to macrophages. Parasitol. Res. 116, 123–131.

Malisch, J.L., Breuner, C.W., 2010. Steroid-binding proteins and free steroids in birds. Mol. Cell. Endocrinol. 316, 42–52.

Martin, M.P., Wineland, M., Barnes, H.J., 2010. Selected blood chemistry and gas reference ranges for broiler breeders using the i-STAT handheld clinical analyzer. Avian Dis. 54, 1016–1020.

Martyka, R., Joanna Rutkowska, J., Cichoń, M., 2011. Sex-specific effects of maternal immunization on yolk antibody transfer and offspring performance in zebra finches. Biol. Lett. 7, 50–53.

Mashaly, M.M., Hendricks 3rd, G.L., Kalama, M.A., Gehad, A.E., Abbas, A.O., Patterson, P.H., 2004. Effect of heat stress on production parameters and immune responses of commercial laying hens. Poultry Sci. 83, 889–894.

Mathew, A., Grdisa, M., Johnstone, R.M., 1993. Nucleosides and glutamine are primary energy substrates for embryonic and adult chicken red cells. Biochem. Cell. Biol. 71, 288–295.

Matsuda, G., Takae, H., 1963. The studies on the structure of chicken hemoglobin: 1. Chromatographic purification of chicken hemoglobin. J. Biochem. 54, 156–160.

Matthew, A., Grdisa, M., Robbins, P.J., White, M.K., Johnstone, R.M., 1994. Loss of glucose transporters is an early event in differentiation of HD3 cells. Am. J. Physiol. 266, C1222–C1230.

Maxwell, M.H., 1973. Comparison, of heterophil and basophil ultrastructure in six species of domestic birds. J. Anat. 115, 187–202.

Maxwell, M.H., Stiller, W.G., 1972. The ultrastructure characteristics of the eosinophil granules in six species of domestic bird. J. Anat. 112, 289–303.

Maxwell, M.H., Tullett, S.G., Burton, F., 1987. A haematological and morphological study of young broiler chicks with experimentally-induced hypoxia. Res. Vet. Sci. 43, 331–338.

Maxwell, M.H., Robertson, G.W., Spence, S., McCorquodale, C.C., 1990. Comparison of haematological values in restricted and *ad libitum*-fed domestic fowls: white blood cells and thrombocytes. Br. Poultry Sci. 31, 399–405.

Maxwell, M.H., Robertson, G.W., McCorquodale, C.C., 1992a. Whole blood and plasma viscosity values in normal and ascitic broiler chickens. Br. Poultry Sci. 33, 871–877.

Maxwell, M.H., 1974. An ultrastructural comparison, of the mononuclear leucocytes and thrombocytes in six species of domestic bird. J. Anat. 117, 69–80.

Maxwell, M.H., Hocking, P.M., Robertson, G.W., 1992b. Differential leucocyte responses to various degrees of food restriction in broilers, turkeys and ducks. Br. Poultry Sci. 33, 177–187.

May, M., Dunne, D.W., Brown, D.R., 2014. A sialoreceptor binding motif in the *Mycoplasma synoviae* adhesin VlhA. PLoS One 9, e110360.

McFarlane, J.M., Curtis, S.E., 1989. Multiple concurrent stressors in chicks: 3. Effects on plasma corticosterone and the H/L ratio. Poultry Sci. 68, 522–527.

McKnight, G.S., Lee, D.C., Palmiter, R.D., 1980. Transferrin gene expression: regulation of mRNA transcription in chick liver by steroid hormones and iron deficiency. J. Biol. Chem. 255, 148–153.

McRee, A.E., Tully Jr., T.N., Nevarez, J.G., Beaufrere, H., Ammersbach, M., Gaunt, S.D., Fuller, R.G., Romero, L.M., 2018. Effect of routine handling and transportation on blood leukocyte concentrations and plasma corticosterone in captive Hispaniolan Amazon parrots (*Amazona ventralis*). J. Zoo. Wildl. Med. 49, 396–403.

Medway, W., Kare, M.R., 1959a. Blood and plasma volume, hematocrit, blood specific gravity and serum protein electrophoresis of the chicken. Poultry Sci. 38, 624–631.

Medway, W., Kare, M.R., 1959b. Water metabolism of the growing domestic fowl with special reference to water balance. Poultry Sci. 38, 631–637.

Mehaisen, G.M.K., Eshak, M.G., Elkaiaty, A.M., Atta, A.-R.M.M., Mashaly, M.M., Abass, A.O., 2017. Comprehensive growth performance, immune function, plasma biochemistry, gene expressions and cell death morphology responses to a daily corticosterone injection course in broiler chickens. PLoS One 12, e0172684.

Meir, J.U., Ponganis, P.J., 2009. High-affinity hemoglobin and blood oxygen saturation in diving emperor penguins. J. Exp. Biol. 212, 3330–3338.

Miksik, I., Hodný, Z., 1992. Glycated hemoglobin in mute swan (*Cygnus olor*) and rook (*Corvus frugilegus*). Comp. Biochem. Physiol. B 103, 553–559.

Mikulits, W., Schranzhofer, M., Deiner, E.M., Beug, H., Müllner, E.W., 2000. Regulation of ferritin mRNA translation in primary erythroblasts: exogenous c-Kit plus EpoR signaling mimics v-ErbA oncoprotein activity. Biochem. Biophys. Res. Commun. 275, 292–294.

Montgomery, M.K., Hulbert, A.J., Buttemer, W.A., 2012. Does the oxidative stress theory of aging explain longevity differences in birds? I. Mitochondrial ROS production. Exp. Gerontol. 47, 203–210.

Morera, D., Roher, N., Ribas, L., Balasch, J.C., Doñate, C., Callol, A., Boltaña, S., Roberts, S., Goetz, G., Goetz, F.W., MacKenzie, S.A., 2011. RNA-Seq reveals an integrated immune response in nucleated erythrocytes. PLoS One 6, e26998.

Morgan, E.H., 1975. Plasma iron transport during egg laying and after oestrogen administration in the domestic fowl (*Gallus domesticus*). Q. J. Exp. Physiol. Cogn. Med. Sci. 60, 233–247.

Mucha, K.H., Huffman, J.E., 1991. Inflammatory cell stimulation and wound healing in *Sphaeridiotrema globulus* experimentally infected mallard ducks (*Anas platyrhynchos*). J. Wildl. Dis. 27, 428–434.

Murakami, T., 1991. Positive cooperativity of [3H]dexamethasone binding to chick corticosteroid-binding globulin. Comp. Biochem. Physiol. A 100, 361–364.

Nerren, J.R., Kogut, M.H., 2009. The selective Dectin-1 agonist, curdlan, induces an oxidative burst response in chicken heterophils and peripheral blood mononuclear cells. Vet. Immunol. Immunopathol. 127, 162–166.

Nettle, D., Andrews, C., Reichert, S., Bedford, T., Kolenda, C., Parker, C., Martin-Ruiz, C., Monaghan, P., Bateson, M., 2017. Early-life adversity accelerates cellular ageing and affects adult inflammation: experimental evidence from the European starling. Sci. Rep. 7, 40794.

Nicol, S.C., Melrose, W., Stahel, C.D., 1988. Haematology and metabolism of the blood of the little penguin, *Eudyptula minor*. Comp. Biochem. Physiol. 89A, 383–386.

Nirmallan, G.P., Robinson, G.A., 1973. The survival time of erythrocytes (DF^{32} P-label) in the Japanese quail. Poultry Sci. 52, 355–359.

Nishita, T., Tomita, Y., Imanari, T., Ichihara, N., Orito, K., Arishima, K., 2011a. Biochemical and developmental characterization of carbonic anhydrase II from chicken erythrocytes. Acta Vet. Scand 53, 16.

Nishita, T., Tomita, Y., Yorifuji, D., Orito, K., Ochiai, H., Arishima, K., 2011b. Purification of chicken carbonic anhydrase isozyme-III (CA-III) and its measurement in White Leghorn chickens. Acta Vet. Scand 53, 63.

Niu, S., Jahejo, A.R., Jia, F.J., Li, X., Ning, G.B., Zhang, D., Ma, H.L., Hao, W.F., Gao, W.W., Zhao, Y.J., Gao, S.M., Li, G.L., Li, J.H., Yan, F., Gao, R.K., Bi, Y.H., Han, L.X., Gao, G.F., Tian, W.X., 2018. Transcripts of antibacterial peptides in chicken erythrocytes infected with Marek's disease virus. BMC Vet. Res. 14363.

Ogbuagu, N.E., Aluwong, T., Ayo, J.O., Sumanu, V.O., 2018. Effect of fisetin and probiotic supplementation on erythrocyte osmotic fragility, malondialdehyde concentration and superoxide dismutase activity in broiler chickens exposed to heat stress. J. Vet. Med. Sci. 80, 1895–1900.

Ohnishi, Y., Nishimura, K., 2001. The role of reticulocytes on gametocytogenesis in chickens infected with *Leucocytozoon calleryi*. J. Vet. Med. Sci. 63, 797–800.

Ohno, Y., Yagi, H., Nakamura, M., Masuko, K., Hashimoto, Y., Masuko, T., 2008. Cell-death-inducing monoclonal antibodies raised against DT40 tumor cells: identification of chicken transferrin receptor as a novel cell-death receptor. Cancer Sci. 99, 894–900.

O'Toole, E.T., Hantgan, R.R., Lewis, J.C., 1994. Localization of fibrinogen during aggregation of avian thrombocytes. Exp. Mol. Pathol. 61, 175–190.

Ozensoy, O., Arslan, M., Supuran, C.T., 2011. Carbonic anhydrase inhibitors: purification and inhibition studies of pigeon *(Columba livia*var.*domesticus*) red blood cell carbonic anhydrase with sulfonamides. J. Enzyme Inhib. Med. Chem. 26, 749–753.

Ozensoy, O., Isik, S., Arslan, O., Arslan, M., Scozzafava, A., Supuran, C.T., 2005. Carbonic anhydrase inhibitors. Inhibition of red blood cell ostrich (*Struthio camelus*) carbonic anhydrase with a series of aromatic and heterocyclic sulfonamides. J. Enzym. Inhib. Med. Chem. 20, 383–387.

Palfrey, H.C., Greengard, P., 1981. Hormone-sensitive ion transport systems in erythrocytes as models for epithelial ion pathways. Ann. N. Y. Acad. Sci. 372, 291–308.

Paris, D., Samuel, D., Jacques, Y., Gache, C., Franchi, A., Ailhaud, G., 1978. The role of serum albumin in the uptake of fatty acids by cultured cardiac cells from chick embryo. Eur. J. Biochem. 83, 235–243.

Passantino, L., Massaro, M.A., Jirillo, F., Di Modugno, D., Ribaud, M.R., Modugno, G.D., Passantino, G.F., Jirillo, E., 2007. Antigenically activated avian erythrocytes release cytokine-like factors: a conserved

phylogenetic function discovered in fish. Immunopharmacol. Immunotoxicol. 29, 141–152.

Peltonen, L.M., Sankarri, S., 2011. Ott's protein osmotic pressure of serum and interstitial fluid in chickens (*Gallus gallus*): effect of age and gender. J. Exp. Biol. 214, 599–606.

Pértille, F., Brantsæter, M., Nordgreen, J., Coutinho, L.L., Janczak, A.M., Jensen, P., Guerrero-Bosagna, C., 2017. DNA methylation profiles in red blood cells of adult hens correlate with their rearing conditions. J. Exp. Biol. 220, 3579–3587.

Peters, J.R., Nambi, P., Sibley, D.R., Lefkowitz, R.J., 1984. Enhanced adenylate cyclase activity of Turkey erythrocytes following treatment with beta-adrenergic receptor antagonists. Eur. J. Pharmacol. 107, 43–52.

Pistone, J., Heatley, J.J., Campbell, T.A., Voelker, G., 2017. Assessing Passeriformes health in South Texas via select venous analytes. Comp. Biochem. Physiol. B 210, 64–71.

Pliszczak-Krol, A., Graczyk, S., Gemra, M., Iwaszko-Simonik, A., Krol, J., 2012. The influence of bacterial lipopolysaccharide (LPS) and adrenocorticotropic hormone (ACTH) administration on coagulation processes in chickens. Bull. UASMV. Vet. Med. 69, 224–225.

Pusch, E.A., Bentz, A.B., Becker, D.J., Navara, K.J., 2018. Behavioral phenotype predicts physiological responses to chronic stress in proactive and reactive birds. Gen. Comp. Endocrinol. 255, 71–77.

Quero, A.A.M., Ferré, D.M., Zarco, A., Cuervo, P.F., Gorla, N.B.M., 2016. Erythrocyte micronucleus cytome assay of 17 wild bird species from the central Monte desert, Argentina. Environ. Sci. Pollut. Res. Int. 23, 25224–25231.

Raghav, R., Middleton, R., Ahamed, R., Arjunan, R., Caliendo, V., 2015. Analysis of arterial and venous blood gases in healthy gyr falcons (*Falco rusticolus*) under anesthesia. J. Avian Med. Surg. 29, 290–298.

Ratliff, C., Gentry, J., Kusmierczyk, J., Hartke, K.M., Acierno, M.J., Musser, J.M., Russell, K.E., Heatley, J.J., 2017. Venous blood gas, electrolyte, and hematologic analytes of the mottled duck, Anas fulvigula. J. Wildl. Dis. 53, 159–164.

Redshaw, M.R., Follett, B.K., 1976. Physiology of egg yolk production by the fowl: the measurement of circulating levels of vitellogenin employing a specific radioimmunoassay. Comp. Biochem. Physiol. A 55, 399–405.

Reitman, M., Grasso, J.A., Blumenthal, R., Lewit, P., 1993. Primary sequence, evolution, and repetitive elements of the *Gallus gallus* (chicken) beta-globin cluster. Genomics 18, 616–626.

Rettenmund, C.L., Heatley, J.J., Russell, K.E., 2014. Comparison of two analyzers to determine selected venous blood analytes of Quaker parrots (*Myiopsitta monachus*). J. Zoo Wildl. Med. 45, 256–262.

Richardson, S.L., Swietach, P., 2016. Red blood cell thickness is evolutionarily constrained by slow, hemoglobin-restricted diffusion in cytoplasm. Sci. Rep. 6, 36018.

Richardson, S.J., Monk, J.A., Shepherdley, C.A., Ebbesson, L.O., Sin, F., Power, D.M., Frappell, P.B., Köhrle, J., Renfree, M.B., 2005. Developmentally regulated thyroid hormone distributor proteins in marsupials, a reptile, and fish. Am. J. Physiol. 288, R1264–R1272.

Rincón-Arano, H., Guerrero, G., Valdes-Quezada, C., Recillas-Targa, F., 2009. Chicken alpha-globin switching depends on autonomous silencing of the embryonic pi globin gene by epigenetics mechanisms. J. Cell Biochem. 108, 675–687.

Rodman, G.P., Ebaugh Jr., F.G., Fox, M.R.S., 1957. Life span of red blood cells of the chicken, pigeon, and duck as estimated by use of $Na_2Cr^{51}O_4$with observations of red cell turnover in mammal, birds and reptile blood. J. Hematol. 12, 355–366.

Röhme, D., 1981. Evidence for a relationship between longevity of mammalian species and life spans of normal fibroblasts *in vitro* and erythrocytes *in vivo*. Proc. Natl. Acad. Sci. U.S.A. 78, 5009–5013.

Roman, Y., Bed'hom, B., Guillot, A., Levrier, J., Chaste-Duvernoy, D., Bomsel-Demontoy, M.C., Jalme, M.S., 2009. Identification of apolipoprotein A-I in the alpha-globulin fraction of avian plasma. Vet. Clin. Pathol. 38, 206–212.

Rose-Martel, M., Kulshreshtha, G., Ahferom Berhane, N., Jodoin, J., Hincke, M.T., 2017. Histones from avian erythrocytes exhibit antibiofilm activity against methicillin-sensitive and methicillin-resistant *Staphylococcus aureus*. Sci. Rep. 7, 45980.

Rosse, W.F., Waldmann, T.A., 1966. Factors controlling erythropoiesis in birds. Blood 27, 654–661.

Roy, K., Bertelsen, M.F., Pors, S.E., Johansen, K.W., Kristensen, A.T., Kjelgaard-Hansen, M., Andreasen, E.B., Christensen, J.P., Biswas, P.K., Bojesen, A.M., 2014. Inflammation-induced haemostatic response in layer chickens infected with *Streptococcus equi* subsp. *zooepidemicus* as evaluated by fibrinogen, prothrombin time and thromboelastography. Avian Pathol. 43, 364–370.

Ruch, F.E., Hughes, M.R., 1975. The effects of hypertonic sodium chloride injection in ducks (*Anas platyrhynchos*), gulls (*Larus glaucesens*) and roosters (*Gallus domesticus*). Comp. Biochem. Physiol. 52A, 21–28.

Ruiz, G., Rosenmann, M., Fernado Novoa, F., Sabat, P., 2002. Hematological parameters and stress index in Rufous-collared sparrows dwelling in urban environments. Condor 104, 162–166.

Ruiz, G., Rosenmann, M., Novoa, F.F., Sabat, P., 2009. Hematological parameters and stress index in rufous-collared sparrows dwelling in urban environments. Condor 104, 162–166.

Samani, A.D., Kheirabadi, K.P., Mohebbi, A., 2016. Effect of *Haemoproteus columbae* infection on the hemogram of the pigeons (*Columba livia domestica*). J. Parasit. Dis. 40, 1406–1410.

Sarg, B., Lopez, R., Lindner, H., Ponte, I., Suau, P., Roque, A., 2015. Identification of novel post-translational modifications in linker histones from chicken erythrocytes. J. Proteom. 113, 162–177.

Sato, T., Soeda, S., Ohta, Y., Katayama, K., Arai, T., Tazaki, H., 2008. Plasma glucose, mannose, and non-esterified fatty acid concentrations in layer-type chickens. Br. Poultry Sci. 49, 731–735.

Sato, K., Matsushita, K., Takahashi, K., Aoki, M., Fuziwara, J., Miyanari, S., Kamada, T., 2012. Dietary supplementation with 5-aminolevulinic acid modulates growth performance and inflammatory responses in broiler chickens. Poultry Sci. 91, 1582–1589.

Scanes, C.G., 2015. Blood. In: Scanes, C.G. (Ed.), Sturkie's Avian Physiology, sixth ed. Elsevier, Amsterdam, pp. 167–191.

Schepelmann, K., 1990. Erythropoietic bone marrow in the pigeon: development of its distribution and volume during growth and pneumatization of bones. J. Morph. 203, 21–34.

Scheffer, M.P., Eltsov, M., Frangakis, A.S., 2011. Evidence for short-range helical order in the 30-nm chromatin fibers of erythrocyte nuclei. Proc. Natl. Acad. Sci. U.S.A 108, 16992–16997.

Schindler, S.L., Gildersleeve, R.P., Thaxton, J.P., McRee, D.I., 1987. Hematological responses of hemorrhaged Japanese quail after blood volume replacement with saline. Comp. Biochem. Physiol. A 87, 933–945.

Schmaier, A.A., Stalker, T.J., Runge, J.J., Lee, D., Nagaswami, C., Mericko, P., Chen, M., Cliché, S., Gariépy, C., Brass, L.F.,

Hammer, D.A., Weisel, J.W., Rosenthal, K., Kahn, M.L., 2011. Occlusive thrombi arise in mammals but not birds in response to arterial injury: evolutionary insight into cardiovascular disease. Blood 118, 3661–3669.

Schmidt, K.L., Malisch, J.L., Breuner, C.W., Soma, K.K., 2010. Corticosterone and cortisol binding sites in plasma, immune organs and brain of developing zebra finches: intracellular and membrane-associated receptors. Brain Behav. Immun. 24, 908–918.

Schreiber, G., Richardson, S.J., 1997. The evolution of gene expression, structure and function of transthyretin. Comp. Biochem. Physiol. B 116, 137–160.

Scott, G.R., Milsom, W.K., 2006. Flying high: a theoretical analysis of the factors limiting exercise performance in birds at altitude. Respir. Physiol. Neurobiol. 154, 284–301.

Scott, T., Owens, M.D., 2008. Thrombocytes respond to lipopolysaccharide through Toll-like receptor-4, and MAP kinase and NF-kappaB pathways leading to expression of interleukin-6 and cyclooxygenase-2 with production of prostaglandin E2. Mol. Immunol. 45, 1001–1008.

Sekelova, Z., Stepanova, H., Polansky, O., Varmuzova, K., Faldynova, M., Fedr, R., Rychlik, I., Vlasatikova, L., 2017. Differential protein expression in chicken macrophages and heterophils in vivo following infection with *Salmonella Enteritidis*. Vet. Res. 48, 35.

Seliger, C., Schaerer, B., Kohn, M., Pendl, H., Weigend, S., Kaspers, B., Härtle, S., 2012. A rapid high-precision flow cytometry based technique for total white blood cell counting in chickens. Vet. Immunol. Immunopathol. 145, 86–99.

Serr, J., Suh, Y., Lee, K., 2009. Regulation of adipose triglyceride lipase by fasting and refeeding in avian species. Poultry Sci. 88, 2585–2591.

Serr, J., Suh, Y., Oh, S.A., Shin, S., Kim, M., Latshaw, J.D., Lee, K., 2011. Acute up-regulation of adipose triglyceride lipase and release of non-esterified fatty acids by dexamethasone in chicken adipose tissue. Lipids 46, 813–820.

Shanmugasundaram, R., Selvaraj, R.K., 2011. Regulatory T cell properties of chicken $CD4^{+}CD25^{+}$ cells. J. Immunol. 186, 1997–2002.

Sharma, S., Poliks, B., Chiauzzi, C., Ravindra, R., Blanden, A.R., Banes, S., 2010. Characterization of the colchicine binding site on avian tubulin isotype VI. Biochemistry 49, 2932–2942.

Shini, S., Kaiser, P., Shini, A., Bryden, W.L., 2008. Differential alterations in ultrastructural morphology of chicken heterophils and lymphocytes induced by corticosterone and lipopolysaccharide. Vet. Immunol. Immunopathol. 122, 83–93.

Simons, T.J., 1983a. Characterization of sugar transport in the pigeon red blood cells. J. Physiol. 338, 477–499.

Simons, T.J., 1983b. The role of calcium in the regulation of sugar transport in the pigeon red blood cell. J. Physiol. 338, 501–526.

Simos, G., Maison, C., Georgatos, S.D., 1996. Characterization of p18, a component of the lamin B receptor complex and a new integral membrane protein of the avian erythrocyte nuclear envelope. J. Biol. Chem. 271, 12617–12625.

Singal, R., vanWert, J.M., Ferdinand Jr., L., 2002. Methylation of alpha-type embryonic globin gene alpha pi represses transcription in primary erythroid cells. Blood 100, 4217–4222.

Siveira, P., Damatta, R.A., Dagusto, M., 2009. Hematological changes of chickens experimentally infected with *Plasmodium (Bennettinia) juxtanucleare*. Vet. Parasitol. 162, 257–262.

Soler, J.J., Ruiz Castellano, C., Martínez-de la Puente, J., Tomás, G., Ruiz-Rodríguez, M., Figuerola, J., 2015. Telomere dynamics in parasitic great spotted cuckoos and their magpie hosts. J. Evol. Biol. 28, 1610–1617.

Somes, R.G., Smagula, R.M., Lerner, J., 1981. Selective breeding of chickens for erythrocytes with high and low leucine transport activity. Am. J. Physiol. 241, C233–C242.

Smith, S.B., McWilliams, S.R., Guglielmo, C.G., 2007. Effect of diet composition on plasma metabolite profiles in a migratory songbird. The Condor 109, 48–58.

Stabler, J.G., McCormick, T.W., Powell, K.C., Kogut, M.H., 1994. Avian heterophils and monocytes: phagocytic and bactericidal activities against *Salmonella enteritidis*. Vet. Microbiol. 38, 293–305.

Stadel, J.M., Nambi, P., Lavin, T.N., Heald, S.L., Caron, M.G., Lefkowitz, R.J., 1982. Catecholamine-induced desensitization of Turkey erythrocyte adenylate cyclase. Structural alterations in the beta-adrenergic receptor revealed by photoaffinity labeling. J. Biol. Chem. 257, 9242–9245.

Stifani, S., Barber, D.L., Nimpf, J., Schneider, W.J., 1990. A single chicken oocyte plasma membrane protein mediates uptake of very-low-density lipoprotein and vitellogenin. Proc. Natl. Acad. Sci. U.S.A. 87, 1955–1959.

Stiller, R.A., Belamarich, F.A., Shepro, D., 1975. Aggregation and release in thrombocytes of the duck. Am. J. Physiol. 229, 206–210.

St Paul, M., Paolucci, S., Barjesteh, N., Wood, R.D., Schat, K.A., Sharif, S., 2012. Characterization of chicken thrombocyte responses to Toll-like receptor ligands. PLoS One 7, e43381.

St Paul, M., Paolucci, S., Barjesteh, N., Wood, R.D., Sharif, S., 2013. Chicken erythrocytes respond to Toll-like receptor ligands by up-regulating cytokine transcripts. Res. Vet. Sci. 95, 87–91.

Stier, A., Bize, P., Schull, Q., Zoll, J., Singh, F., Geny, B., Gros, F., Royer, C., Massemin, S., Criscuolo, F., 2013. Avian erythrocytes have functional mitochondria, opening novel perspectives for birds as animal models in the study of ageing. Front. Zool. 10, 33.

Stier, A., Bize, P., Roussel, D., Schull, Q., Massemin, S., Criscuolo, F., 2014. Mitochondrial uncoupling as a regulator of life-history trajectories in birds: an experimental study in the zebra finch. J. Exp. Biol. 217, 3579–3589.

Sturkie, P.D., 1986. Avian Physiology. Springer Verlag, New York.

Sugiarto, H., Yu, P.-L., 2004. Avian antimicrobial peptides: the defense role of b-defensins. Biochem. Biophys. Res. Commun. 323, 721–727.

Sullivan, K.S., Erf, G.F., 2017. CD4+ T cells dominate the leukocyte infiltration response initiated by intra-dermal injection of phytohemagglutinin into growing feathers in chickens. Poultry Sci. 96, 3574–3580.

Sundaresan, S.S., Ramesh, P., Sivakumar, K., Ponnuswamy, M.N., 2009. Purification, crystallization and preliminary X-ray analysis of haemoglobin from ostrich (*Struthio camelus*). Acta Crystallogr. F 65, 681–683.

Szubartowska, E., Gromysz-Kałkowska, K., 1992. Blood morphology in quails after poisoning with fenitrothion. Comp. Biochem. Physiol. C 101, 263–267.

Taebipour, M.J., Dadras, H., Nazifi, S., Afsar, M., Ansari-Lari, M., 2017. Evaluation of blood monocyte and lymphocyte population in broiler chicken after vaccination and experimental challenge with Newcastle disease virus. Vet. Immunol. Immunopathol. 190, 31–38.

Tako, E., Rutzke, M.A., Glahn, R.P., 2010. Using the domestic chicken (*Gallus gallus*) as an in vivo model for iron bioavailability. Poultry Sci. 89, 514–521.

Tazawa, H., Andrewartha, S.J., Burggren, W.W., 2011. Development of hematological respiratory variables in late chicken embryos: the relative importance of incubation time and embryo mass. Comp. Biochem. Physiol. A 159, 225–233.

Torres-Medina, A., Rhodes, M.B., Mussman, H.C., 1971. Chicken serum proteins: comparison of electrophoretic techniques and localization of transferrin. Poultry Sci. 50, 1115–1121.

Terrón, M.P., Paredes, S.D., Barriga, C., Ortega, E., Rodríguez, A.B., 2004. Comparative study of the heterophil phagocytic function in young and old ring doves (*Streptopelia risora*) and its effects of melatonin. J. Neuroendocril. 15, 1111–1115.

Tregaskes, C.A., Harrison, M., Sowa, A.K., van Hateren, A., Hunt, L.G., Vainio, O., Kaufman, J., 2016. Surface expression, peptide repertoire, and thermostability of chicken class I molecules correlate with peptide transporter specificity. Proc. Natl. Acad. Sci. U.S.A. 113, 692–697.

Tricola, G.M., Simons, M.J.P., Atema, E., Boughton, R.K., Brown, J.L., Dearborn, D.C., Divoky, G., Eimes, J.A., Huntington, C.E., Kitaysky, A.S., Juola, F.A., Lank, D.B., Litwa, H.P., Mulder, E.G.A., Nisbet, I.C.T., Okanoya, K., Safran, R.J., Schoech, S.J., Schreiber, E.A., Thompson, P.M., Verhulst, S., Wheelwright, N.T., Winkler, D.W., Young, R., Vleck, C.M., Haussmann, M.F., 2018. The rate of telomere loss is related to maximum lifespan in birds. Phil. Trans. Roy. Soc. Lond. B 373, 20160445.

Turowski, V., Sperling, B., Hanczaruk, M.A., Göbel, T.W., Viertlboeck, B.C., 2016. Chicken TREM-B1, an inhibitory Ig-like receptor expressed on chicken thrombocytes. PLoS One 11, e0151513.

Ucán-Marín, F., Arukwe, A., Mortensen, A., Gabrielsen, G.W., Fox, G.A., Letcher, R.J., 2009. Recombinant transthyretin purification and competitive binding with organohalogen compounds in two gull species (*Larus argentatus* and *Larus hyperboreus*). Toxicol. Sci. 107, 440–450.

Ucán-Marin, F., Arukwe, A., Mortensen, A.S., Gabrielsen, G.W., Letcher, R.J., 2010. Recombinant albumin and transthyretin transport proteins from two gull species and human: chlorinated and brominated contaminant binding and thyroid hormones. Environ. Sci. Technol. 44, 497–504.

Ugur, O., Onaran, H.O., 1997. Allosteric equilibrium model explains steady-state coupling of beta-adrenergic receptors to adenylate cyclase in Turkey erythrocyte membranes. Biochem. J. 323, 765–776.

Valéria, V.P., Fantoni, D.T., Otsuk, D.A., Auler Jr., J.O.C., 2008. Blood-gas and electrolyte values for Amazon parrots (*Amonzona aestiva*). Pesqui. Vet. Bras. 28, 108–112.

Valle, C.A., Ulloa, C., Deresienski, D., Regalado, C., Muñoz-Pérez, J.P., Garcia, J., Hardesty, B.D., Skehel, A., Lewbart, G.A., 2018. Health status of great frigatebirds (*Fregata minor*) determined by haematology, biochemistry, blood gases, and physical examination. Conserv. Physiol. 6 coy034.

Van As, P., Elferin, M.G., Closter, A.M., Vereijken, A., Bovenhuis, H., Croojmans, R.P., Decuyper, E., Groenen, M.A., 2010. The use of blood gas parameters to predict ascites susceptibility in juvenile broilers. Poultry Sci. 89, 1684–1691.

van Bockxmeer, F.M., Morgan, E.H., 1982. Comparative aspects of transferrin-reticulocyte interactions: membrane receptors and iron uptake. Comp. Biochem. Physiol. A 71, 211–218.

Vandecasserie, C., Schnek, A.G., Léonis, J., 1971. Oxygen-affinity studies of avian hemoglobins. Chicken and pigeon. Eur. J. Biochem. 24, 284–287.

Vargas, M., Devés, R., 2001. System y+L-like activities account for high and low amino-acid transport phenotypes in chicken erythrocytes. J. Membr. Biol. 183, 183–193.

Vashchenko, G., Das, S., Moon, K.-M., Rogalski, J.C., Taves, M.D., Soma, K.K., Van Petegem, F., Foster, L.J., Hammond, G.L., 2016. Identification of avian corticosteroid-binding globulin (SerpinA6) reveals the molecular basis of evolutionary adaptations in serpinA6 structure and function as a steroid-binding protein. J. Biol. Chem. 291, 11300–11312.

Viertlboeck, B.C., Hanczaruk, M.A., Amann, B., Bader, S.R., Schmitt, R., Sperling, B., Schwarz, S.C., Schmahl, W., Deeg, C.A., Göbel, T.W., 2013. Chicken immunoregulatory Ig-like receptor families: an overview and expression details on ggTREM-A1. Dev. Comp. Immunol. 41, 403–412.

Vleck, C.M., Vertalino, N., Vleck, D., bucher, T.L., 2000. Stress, corticosterone, and heterophil to lymphocyte ratios in free-living Adélie penguins. Condor 102, 392–400.

Voehringer, D., 2017. Recent advances in understanding basophil functions in vivo. V1000Res 6, 1464.

Wagner, E.C., Stables, C.A., Williams, T.D., 2008. Hematological changes associated with egg production: direct evidence for changes in erythropoiesis but a lack of resource dependence? J. Exp. Biol. 211, 2960–2968.

Wang, W., Wideman Jr., R.F., Bersi, T.K., Erf, G.F., 2003. Pulmonary and hematological inflammatory responses to intravenous cellulose microparticles in broilers. Poultry Sci. 82, 771–780.

Wang, W., Li, Z., Ren, W., Yue, Y., Guo, Y., 2016. Effects of live yeast supplementation on lipopolysaccharide-induced inflammatory responses in broilers. Poultry Sci. 95, 2557–2564.

Watts, C., Wheeler, K.P., 1978. Protein and lipid components of the pigeon erythrocyte membrane. Biochem. J. 173, 899–907.

Weimer, S.L., Wideman, R.F., Scanes, C.G., Mauromoustakos, A., Christensen, K.D., Vizzier-Thaxton, Y., 2018. An evaluation of methods for measuring stress in broiler chickens. Poultry Sci. 97, 3381–3389.

Weissbach, L., Oddoux, C., Procyk, R., Grieninger, G., 1991. The beta chain of chicken fibrinogen contains an atypical thrombin cleavage site. Biochemistry 30, 3290–3294.

Weitnauer, E., Ebert, C., Hucho, F., Robitzki, A., Weise, C.,P.G., 1999. Butyrylcholinesterase is complexed with transferrin in chicken serum. J. Protein Chem. 18, 205–214.

Whitman, B.A., Breuner, C.W., Dufty Jr., A.M., 2011. The effects of neonatal handling on adrenocortical responsiveness, morphological development and corticosterone binding globulin in nestling American kestrels (*Falco sparverius*). Gen. Comp. Endocrinol. 172, 260–267.

Wicher, K.B., Fries, E., 2006. Haptoglobin, a hemoglobin-binding plasma protein, is present in bony fish and mammals but not in frog and chicken. Proc. Natl. Acad. Sci. U.S.A. 103, 4168–4173.

Wight, P.A.L., Dewar, W.A., MacKenzie, G.M., 1980. Monocytosis in experimental zinc deficiency of domestic birds. Avian Pathol. 9, 61–66.

Wilcoxen, T.E., Horn, D.J., Hogan, B.M., Hubble, C.N., Huber, S.J., Flamm, J., Knott, M., Lundstrom, L., Salik, F., Wassenhove, S.J., Wrobel, E.R., 2015. Effects of bird-feeding activities on the health of wild birds. Conserv. Physiol. 3 cov058.

Williams, A.F., 1972. DNA synthesis in purified populations of avian erythroid cells. J. Cell Sci. 10, 27–46.

Winckler, B., Solomon, F., 1991. A role of microtubule bundles in the morphogenesis of chicken erythrocytes. Proc. Natl., Acad. Sci. U.S.A. 88, 6033–6027.

Windau, K., Viertlboeck, B.C., Göbel, T.W., 2013. The Turkey Ig-like receptor family: identification, expression and function. PLoS One 8, e59577.

Wingfield, J.C., Matt, K.S., Farner, D.S., 1984. Physiologic properties of steroid hormone-binding proteins in avian blood. Gen. Comp. Endocrinol. 53, 281–292.

Winkler, C., Ferdous, F., Dimmick, M., Scott, T., 2017. Lipopolysaccharide induced Interleukin-6 production is mediated through activation of ERK 1/2, p38 MAPK, MEK, and NFκB in chicken thrombocytes. Dev. Comp. Immunol. 73, 124–130.

Wiwanitkit, V., Paritpokee, N., Nithiuthai, S., Boonchalermvichian, C., Bhokaisawan, N., 2007. Change of serum transferrin receptor due to malarial infection, an experiment in Plasmodium gallinaceum infected chicken model. J. Vector Borne Dis. 44, 255–258.

Wu, Y., Zhao, X., Li, P., Huang, H., 2007. Impact of Zn, Cu, and Fe on the activity of carbonic anhydrase of erythrocytes in ducks. Biol. Trace Elem. Res. 118, 227–232.

Xu, Y., Lai, X., Li, Z., Zhang, X., Luo, Q., 2018. Effect of chronic heat stress on some physiological and immunological parameters in different breed of broilers. Poultry Sci. 97, 4073–4082.

Yalçin, S., Güler, H.C., 2012. Interaction of transport distance and body weight on preslaughter stress and breast meat quality of broilers. Br. Poult. Sci. 53, 175–182.

Yang, Z., Mochalkin, I., Veerapandian, L., Riley, M., Doolittle, R.F., 2000. Crystal structure of native chicken fibrinogen at 5.5-A resolution. Proc. Natl. Acad. Sci. U.S.A. 97, 3907–3912.

Yin, H.D., Gilbert, E.R., Chen, S.Y., Li, D.Y., Zhang, Z.C., Wang, Y., Liu, Y.P., Zhu, Q., 2013. Ontogenic expression pattern and genetic polymorphisms of the retinol-binding protein 4 (RBP4) gene in Erlang mountainous chickens. Gene 526, 170–175.

Zenke, M., Kahn, P., Disela, C., Vennström, B., Leutz, A., Keegan, K., Hayman, M.J., Choi, H.R., Yew, N., Engel, J.D., Beug, H., 1988. V-erbA specifically suppresses transcription of the avian erythrocyte anion transporter (band 3) gene. Cell 52, 107–119.

Zentgraf, H., Deumling, B., Jarasch, E.-D., Franke, W.W., 1971. Nuclear membranes and plasma membranes from hen erythrocytes. I. Isolation, characterization and comparison. J. Biol. Chem 246, 2986–2995.

Zanotti, G., Calderone, V., Beda, M., Malpeli, G., Folli, C., Berni, R., 2001. Structure of chicken plasma retinol-binding protein. Biochim. Biophys. Acta 1550, 64–69.

Zhao, W., Liu, J., Xu, R., Zhang, C., Pang, Q., Chen, X., Liu, S., Hong, L., Yuan, J., Li, X., Chen, Y., Li, J., Su, X.Z., 2015. The gametocytes of *Leucocytozoon sabrazesi* infect chicken thrombocytes, not other blood cells. PLoS One 10, e0133478.

Zhang, Z.W., Cheng, J., Xu, F., Chen, Y.E., Du, J.B., Yuan, M., Zhu, F., Xu, X.C., Yuan, S., 2011. Red blood cell extrudes nucleus and mitochondria against oxidative stress. IUBMB Life 63, 560–565.

Zhou, X.D., Dong, X.F., Tong, J.M., Xu, P., Wang, Z.M., 2012. High levels of vitamin E affect retinol binding protein but not CYP26A1 in liver and hepatocytes from laying hens. Poultry Sci. 91, 1135–1141.

Zhou, Z., Wang, Z., Cao, L., Hu, S., Zhang, Z., Qin, B., Guo, Z., Nie, K., 2013. Upregulation of chicken TLR4, TLR15 and MyD88 in heterophils and monocyte-derived macrophages stimulated with *Eimeria tenella in vitro*. Exp. Parasitol. 133, 427–433.

Zulkifli, I., Che Norma, M.T., Chong, C.H., Loh, T.C., 2000. Heterophil to lymphocyte ratio and tonic immobility reactions to preslaughter handling in broiler chickens treated with ascorbic acid. Poultry Sci. 79, 402–406.

Further reading

Bedanova, I., Voslarova, E., Chloupek, P., Pistekova, V., Suchy, P., Blahova, J., Dobsikova, R., Vecerek, V., 2007. Stress in broilers resulting from shackling. Poultry Sci. 86, 1065–1069.

Ching, K.H., Collarini, E.J., Abdiche, Y.N., Bedinger, D., Pedersen, D., Izquierdo, S., Harriman, R., Zhu, L., Etches, R.J., van de Lavoir, M.C., Harriman, W.D., Leighton, P.A., 2018. Chickens with humanized immunoglobulin genes generate antibodies with high affinity and broad epitope coverage to conserved targets. MAbs 10, 71–80.

Hill, K.L., Mortensen, Å.K., Teclechiel, D., Willmore, W.G., Sylte, I., Jenssen, B.M., Letcher, R.J., 2018. *In vitro* and *in silico* competitive binding of brominated polyphenyl ether contaminants with human and gull thyroid hormone transport proteins. Environ. Sci. Technol. 52, 1533–1541.

Ouyang, X., Froment, J., Leonards, P.E.G., Christensen, G., Tollefsen, K.E., de Boer, J., Thomas, K.V., Lamoree, M.H., 2017. Miniaturization of a transthyretin binding assay using a fluorescent probe for high throughput screening of thyroid hormone disruption in environmental samples. Chemosphere 171, 722–728.

Tazawa, H., Ono, T., Mochizuki, M., 1976. Oxygen dissociation curve for chorioallantoic capillary blood of chicken embryo. J. Appl. Physiol. 40, 393–398.

Zhang, J., Hua, Z., Tame, J.R., Lu, G., Zhang, R., Gu, X., 1996. The crystal structure of a high oxygen affinity species of haemoglobin (bar-headed goose haemoglobin in the oxy form). J. Mol. Biol. 255, 484–493.

Chapter 18

The cardiovascular system

Edward M. Dzialowski and Dane A. Crossley
Department of Biological Sciences, University of North Texas, Denton, TX, United States

18.1 Introduction

Birds have evolved a high-performance cardiovascular system to meet the rigorous demands of running, flying, swimming, or diving in a variety of environments, some of them very harsh. Sustained high levels of activity in these environments place severe demands on the transport capabilities of the cardiovascular system to provide adequate delivery of oxygen to working vascular beds and to provide efficient removal of metabolic products. Furthermore, birds are homeothermic organisms, and the cardiovascular system plays a major role in conserving or removing body heat. The descriptions of the component parts of the circulatory system in this chapter illustrate that these transport requirements are met in a variety of ways in birds inhabiting particular environmental niches. This chapter describes the morphology and functional aspects of the avian heart (Section 18.2), circulatory hemodynamics (Section 18.3), and the vascular tree (Section 18.4). A common thread running through this discussion is that the component parts of the circulation must cooperate in an integrated fashion in order to ensure tissue oxygen delivery matches tissue demands. This is done through the integrative control of the avian circulation by autoregulatory, humoral, and neural mechanisms (Section 18.5). Significant number of studies has examined the development of cardiovascular control in avian embryos (Section 18.5) which have expanded our understanding of this system throughout ontogeny. Finally, the cardiovascular system functions within a complex animal which interacts with the environment (Section 18.6).

Modern birds are derived from theropod dinosaurs (Padian and de Ricqles, 2009), while mammals have descended from a group of carnivorous reptiles, the cynodonts. These ancestral lines originated in the Triassic more than 200 million years ago, so in evolutionary terms, avian and mammalian stocks have been separated for a substantial period of time. As one might expect, significant differences in cardiovascular structure and function have arisen in the two groups since their separation, yet a number of similarities in their circulatory systems are also evident. Such similarities probably represent both the conservation of characteristics common to organisms ancestral to the two groups, a shared endothermic phenotype, and the results of convergent evolution once the stocks had divided. Unfortunately, our knowledge of cardiovascular structure and function remains far more limited in birds than in mammals. This review of the avian cardiovascular system encompasses the chapter from a previous edition of this volume (Whittow, 2000) that drew from a number of excellent previous reviews, including major works by Akester (1971), Jones and Johansen (1972), Bennett (1974), Baumel (1975), Akester (1979), Cabot and Cohen (1980), West et al. (1981), and Benzo (1986). We have updated and extended these works and summarize recent contributions in additional areas.

18.2 Heart

18.2.1 Gross structure and function

18.2.1.1 Functional anatomy

The avian heart, like that of the mammal, is a four-chambered, muscular fluid pump that intermittently pressurizes the central arteries, inducing blood flow to the capillary beds of both the systemic and pulmonary circulations. Functionally, these circuits lie in series with each other, and blood returns to the heart to be pressurized before entering either circuit. As in mammals, the right ventricle pressurizes the pulmonary circulation, and the left ventricle pressurizes the systemic circulation. In each case, the pressure differential between the central mean arterial pressure and the central venous pressure drives blood flow [the cardiac output (CO)] through the resistance to flow offered by the microvessels of the circulation. The left and right atria receive blood at central venous pressure before it enters the ventricles. In common with the atria of mammals, these chambers probably function more as blood reservoirs for their respective ventricles than as important "superchargers" for ventricular pressure. The resistance to blood flow, the peripheral resistance, is lower in the pulmonary

Sturkie's Avian Physiology. https://doi.org/10.1016/B978-0-12-819770-7.00042-6

than in the systemic circuit, so the right ventricle is required to generate less pressure than the left ventricle to produce the same volume flow rate. This difference in ventricular pressure is reflected in the gross anatomy of the ventricles, the myocardium of the right ventricle being thinner than that of the more powerful left ventricle.

In birds, the heart is located in the cranial part of the common thoracoabdominal cavity, with its long axis slightly to the right of the midline. It is partly enclosed dorsally and laterally by the lobes of the liver. A very thin but tough, fibrous pericardial sac encloses the heart.

This sac contains a small volume of serous fluid that provides lubrication for the rhythmic motion of the cardiac contraction cycle. The pericardium is loosely attached to the dorsal surface of the sternum and the surrounding air sacs and more firmly to the liver. It is also attached, via the peritoneum of the hepatic peritoneal cavities, to the vertebral column. These attachments secure the apex of the heart within the median incisura of the liver and in the caudoventral axis of the thoracoabdominal cavity. The outer fibrous layer of the pericardial sac is continuous with the outer adventitial layer of the large central blood vessels. The pericardial membrane is relatively noncompliant and therefore strongly resists large, rapid increases in cardiac size which might be caused by volume overload of a heart chamber. The noncompliant nature of the pericardial sac may result in some degree of mechanical coupling between the ventricles via the contained incompressible lubricating fluid. For example, an increase in diastolic pressure in one ventricle may be transmitted to the other, increasing pressure and decreasing compliance.

18.2.1.2 Heart size

In birds, heart mass scales in respect to body mass as $M_h = 0.014\ M_b^{0.91}$ (Bishop and Butler, 1995). In mammals, the relationship is $M_h = 0.0058 M_b^{0.98}$ (Prothero, 1979), where M_h is heart mass and M_b body mass. When compared with mammals, birds of a given body mass have a significantly heavier heart. This may be due to the high aerobic power output needed to sustain flapping flight. Furthermore, unlike mammals in which heart mass is almost directly proportional to body mass, in birds the exponent denoting proportionality is significantly less than one. This means that larger birds like swans, ducks, and geese tend to have proportionally smaller hearts in relation to their body mass than do smaller birds. Thus, heart mass represents about 1.1% of body mass for a bird like the racing pigeon (421 g), compared with 0.8% for the 2.95 kg Pekin duck (Grubb, 1983; Bishop and Butler, 1995). Heart size has also been shown to vary with flight capacity, with birds that continuously hover during flight having the largest hearts and poor fliers having the smallest hearts (Nespolo et al., 2018). For example, hummingbirds have proportionally larger hearts than all other birds (Bishop and Butler, 1995), reflecting the high aerobic demands of hovering flight. For 25 species of hummingbirds: $M_h = 0.025 M_b^{0.95}$ (Hartman, 1961). In contrast, the ornate tinamou (*Nothoprocta ornate*) and Chilean tinamou (*Nothoprocta perdicaria*) have heart masses that represent only 0.24 and 0.28% of body mass, respectively (Altimiras et al., 2017). In a number of migrating species, the heart hypertrophies before migration supporting morphological plasticity (see Section 18.6.1.2). Migrating birds have transcriptomic plasticity allowing changes in heart size, and therefore CO, that could be induced by seasonal humoral mechanisms.

Heart mass as a fraction of body mass is age dependent. Prior to hatching, the ventricles of pekin ducks (*Anas platyrhynchos domestica*) represents about 0.4% of body mass and increase significantly upon hatching to 0.75% of body mass (Sirsat et al., 2016). This increase in heart mass coincides with an increase in aerobic capacity of the hatchling. Similar increases have been observed in the chicken, Pekin duck, and emu after hatching (Price and Dzialowski, 2018). Of note species of the avian order Tinamiformes have lower heart to body mass ratio and heart growth is similar to American alligators (*Alligator mississippiensis*; Altimiras et al., 2017).

18.2.1.3 Cardiac chambers

The avian heart has two completely divided atria and ventricles. These chambers are functionally equivalent to those of the mammalian heart, serving to distribute CO to the systemic circulation and to the lungs. In life, the atria are rounded chambers, distended with blood during atrial diastole. In excised hearts they may collapse, causing auricles to appear. The right atrium tends to be much larger than the left. The wall of the avian atria and ventricles, as in mammals, consists of endocardial, myocardial, and epicardial layers. The atrial walls are generally thin, although atrial muscle is arranged in thick bundles forming muscular arches. The right and left transverse arches are arranged at right angles to the dorsal longitudinal arch and the interatrial septum. The transverse arches branch into smaller bundles which fuse with a circular muscle band (muscularis basianularis atrii) at the ventral limits of the atria. Contraction of atrial muscle nearly empties the atria. In many species, the atria lack functional inflow valves, so the importance of atrial contraction for ventricular filling may be slight.

The muscular architecture of the ventricles is more complex than that of the atria and includes a superficial layer, longitudinal muscle of the right ventricle, and sinuspiral and bulbospiral muscles. The left ventricle is cone-shaped and extends to the apex of the heart. Its right wall forms the interventricular septum. The free wall of the right ventricle is continuous with the outer portion of the wall of the left ventricle and wraps around the right side of the heart to enclose a crescent-shaped cavity which does not reach the apex of the heart. The muscular walls of the

two ventricles are differentially developed, the wall of the left ventricle being two to three times thicker than that of the right. In addition, the radius of curvature of the left venticle wall is smaller than that of the right (Figure 18.1). This implies both a greater mechanical advantage for pressure generation in the left than in the right ventricle and, according to LaPlace's law, a smaller wall tension for a given left ventricular pressure increment. Therefore, contraction of the myocardial layers of the thick, small radius wall of the left ventricle enables it to generate systolic pressures four–five times higher than those produced by the right ventricle, without rupturing. The larger radius of curvature and thinner free ventricular wall of the right ventricle reflects the lower systolic pressures generated by this chamber, made possible by the low-vascular resistance of the avian lungs. Another consequence of this geometry is that relatively large changes in stroke volume can be made by small changes in the degree of shortening of right ventricular muscle fibers.

18.2.1.4 Valves

Blood entering the left ventricle from the left atrium during atrial systole passes through an orifice guarded by a membranous atrioventricular (AV) valve, similar in general structure to a mammalian AV valve. The valve forms a continuous membrane around the aperture. The valve is tricuspid, not bicuspid as it is in mammals, but in the avian heart, the cusps of this valve are poorly defined. The anterior and posterior leaflets are small. The large aortic (medial) leaflet is connected to the bases of the left and noncoronary cusps of the adjacent aortic outflow valve by fibrous tissue. The free margin of the valve is well secured to the left ventricular endocardium by numerous inextensible chordae tendineae. This arrangement prevents valve eversion during ventricular systole.

Blood passing from the right atrium to the right ventricle enters through an orifice guarded by a muscular valve that is structurally unique to birds. In pronounced contrast to the fibrous structure characteristic of the mammalian tricuspid valve, in birds, the right AV valve consists of a single spiral flap of myocardium attached obliquely to the free wall of the right ventricle and the interventricular septum (Figure 18.2; Prosheva et al., 2015, 2016; Lu et al., 1993a). This spiral flap is apposed to a downward extension of the free wall of the right atrium. The atrial component of the valve extends toward the apex of the ventricle for a shorter distance than does the right ventricular flap. Most of the valve is made of ventricular myocardium and is bilaminar only in its upper portion. The mechanism of valve closure at the start of ventricular systole is unknown. It appears to close in part by active contraction of the muscular flap attached to the wall of the right ventricle (Prosheva et al., 2015). The muscular AV value is predicted to separate the two right atria and ventricle and contribute to right ventricular pressure generation (Prosheva et al., 2015).

The idea of valve closure depending at least partially on active muscular contraction is supported by evidence that at the cellular level both AV valves are closely approached by the electrical conducting system of the myocardium. A complete ring of Purkinje fibers encircles the right AV orifice and connects to the muscular AV valve (Lu et al., 1993a,b). An exception to this anatomical arrangement may be the penguin, in which Adams (1937) did not find a Purkinje ring. The majority of studies, summarized by Lu et al. (1993a,b), support the idea that both the atrial and ventricular muscular components of the right AV valve are excited to contract via the Purkinje system. However, Szabo et al. (1986) thought that there was an insulating layer of connective tissue between the Purkinje AV ring system and the left ventricular myocardium, suggesting that

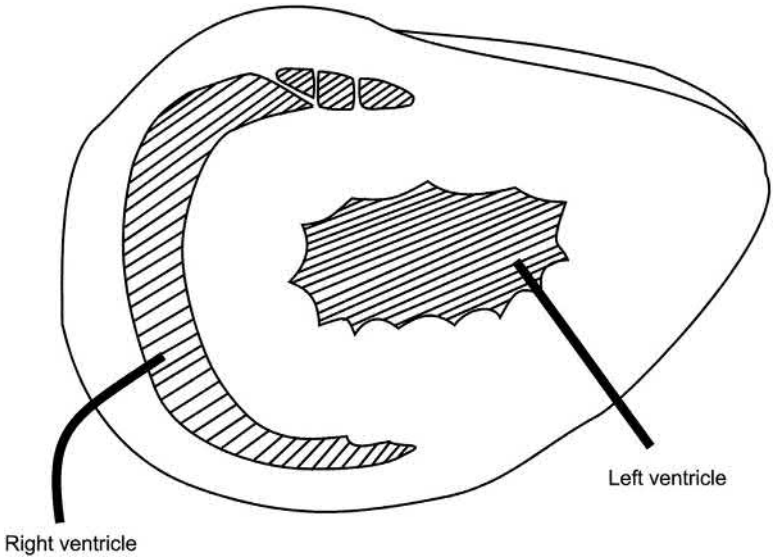

FIGURE 18.1 Transverse section through the ventricles of the avian heart. The lumen of each ventricle is shaded. *Reprinted from West et al. (1981).*

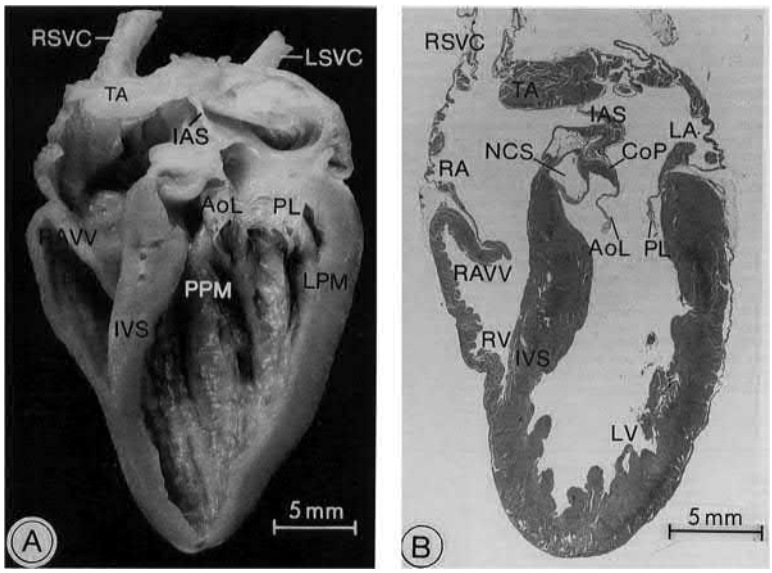

FIGURE 18.2 Anterior frontal views through the atria and ventricles of a chicken heart, showing both the right and left atrioventricular (AV) valves. (A) Anterior view of heart dissected in the frontal plane. (B) Frontal histological section of 8 μm thickness, Goldner trichrome stain. *AOL*, aortic leaflet of left AV valve; *COP*, connecting part of muscle arch; *IAS*, interatrial septum; *IVS*, interventricular septum; *LA*, left atrium; *LPM*, left papillary muscle; *LSVC*, left superior vena cava; *LV*, left ventricle; *NCS*, noncoronary sinus of the aorta; *PL*, posterior leaflet of left AV valve; *PPM*, posterior papillary muscle; *RA*, right atrium; *RAVV*, right AV valve; *RSVC*, right superior vena cava; *RV*, right ventricle. *From Lu et al. (1993a).*

the muscle flap derived from the left ventricle may work passively. Definitive physiological experiments have not been performed to resolve this issue, but the balance of current evidence suggests that both portions of the valve are electrically activated before the ventricular myocardium to dynamically contract and close the AV orifice at the start of ventricular systole (Lu et al., 1993b). This is clearly very different from the closure mechanism in mammals, in which the leaflets of the tricuspid valve float up into the right AV orifice, moved by the AV pressure differential generated during ventricular systole itself.

The outflow valves from the right and left ventricles are, at first glance, more conventional (mammalian) in nature. The pulmonary outflow valve consists of three semilunar cusps. It prevents regurgitation from the pulmonary artery into the right ventricle, the valvules opening as pressure in the ventricle falls below that in the pulmonary trunk on ventricular diastole. There are also three semilunar cusps in the aortic outflow valve, but they are much more rigid than those of the pulmonary outflow valve and are firmly attached to underlying myocardium. The cusps are linked by a ring of fibrous tissue that lies within a complete ring of underlying, circumferentially arranged, myocardial cells. The ring is completed by an arch of cardiac muscle that lies between the left coronary cusp of the aortic outflow valve and the aortic leaflet of the left AV valve as shown in Figure 18.3 (Lu et al., 1993a). This anatomical arrangement contrasts with that in the mammalian heart, in which there is only connective tissue, not myocardium, between that

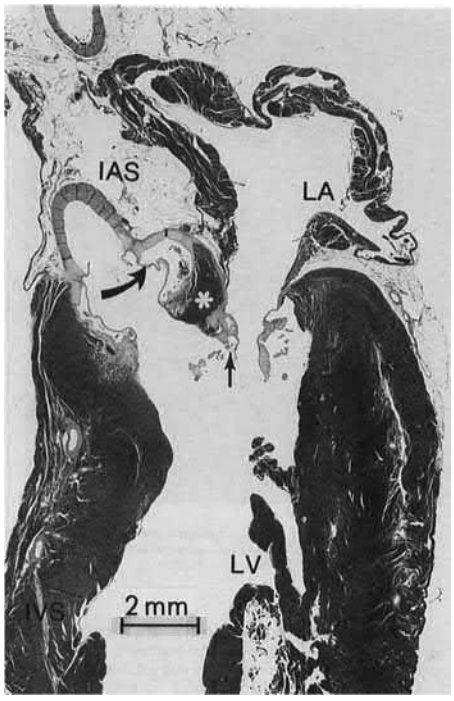

FIGURE 18.3 Photomicrograph of a histological section of the chicken heart, taken in a modified sagittal plane through the anterior column of the muscle arch, indicated by an asterisk. The muscle arch lies between the left coronary aortic valve cusp (*curved arrow*) and the aortic leaflet of the left AV valve (*straight arrow*). *IAS*, interatrial septum; *LA*, left atrium; *LV*, left ventricle. *From Lu et al. (1993a).*

part of the muscular ring lying between the aortic wall and the adjacent mitral valve; in mammals, the myocardial ring is incomplete. In the bird, however, this sphincter-like myocardial cylinder is potentially capable, on contraction, of constricting the left ventricular outflow tract. Lu et al. (1993a) propose that the muscular ring could act as a sphincter controlling the rate of left ventricular outflow by modulating outflow resistance. Another attractive possibility is that muscular contraction of the myocardial ring could close the relatively rigid cusps of the aortic outflow valve. The middle bundle branch of the Purkinje system is connected to the arch of muscle, so its contraction may start relatively early in the cardiac cycle. Obviously, physiological studies are needed to determine whether either of these intriguing mechanisms operates in the avian heart.

18.2.1.5 Coronary circulation

Oxygenated blood destined to supply the avian myocardium via the right and left coronary arteries enters the right ventral and left aortic sinuses, which lie immediately downstream from the cusps of the aortic outflow valve. Most birds have two entrances to the coronary circulation, although there is individual variation so that up to four openings have been observed. In chickens, the right ventral sinus leads into the right coronary artery, which then divides immediately into a superficial and a deep branch (Figure 18.4). The superficial branch follows the groove (coronary sulcus) between the right ventricle and atrium

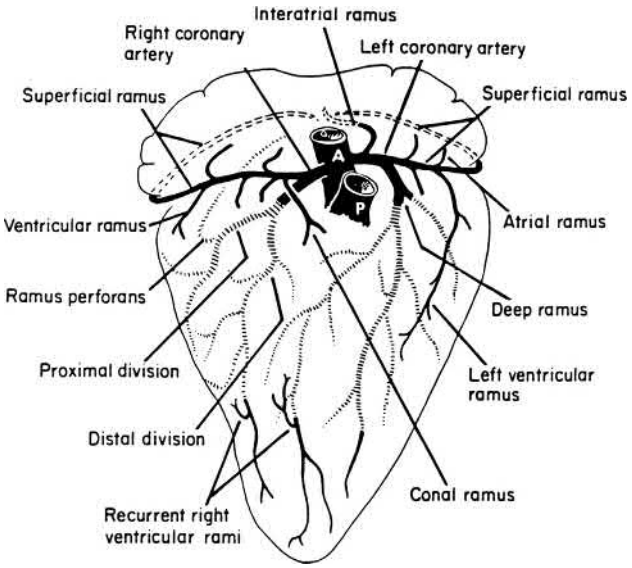

FIGURE 18.4 Arrangement of the coronary arteries of the chicken, *Gallus*, drawn from the cranioventral aspect. *Solid black and dashed lines* represent superficial portions of arteries. *Cross-hatched lines* represent deep arteries embedded in the myocardium of the ventral and right side of the interventricular septum. *A*, aorta; *P*, pulmonary trunk. *From West et al. (1981).*

and supplies the cardiac muscle of both chambers. The larger deep branch supplies the ventral wall of the right ventricle, the dorsal walls of both atria, and the muscular right AV valve. In most species, the right coronary artery is dominant and also supplies the ventricular septum, the heart apex, and much of the left ventricular myocardium. The left coronary artery arises from the left aortic sinus and also has a superficial branch which follows the left coronary sulcus. Another superficial branch gives off atrial and ventricular tributaries, and a deep branch supplies the ventral myocardium of the left ventricle. It is not uncommon in chickens for the left coronary artery to be dominant, in which case it supplies almost all of the left ventricular myocardium and the heart apex. There are frequent anastomoses between the branches of the coronary arteries, particularly near the coronary sulcus.

Five groups of cardiac veins, with frequently anastomosing small tributaries, return venous blood from the myocardium into the right atrium via a coronary sinus. Small cardiac veins open directly into the atria and the right ventricle. This basic anatomical pattern of coronary circulation is described in birds ranging from chicken, duck, and pigeon (West et al., 1981), quail (Kato et al., 2018), and ostrich (Bezuidenhout, 1984).

The rate of perfusion of avian myocardium is high compared with perfusion rates of most other avian tissues receiving around 8% of CO (see Section 18.4.2.3; Johansen, 1964; Jones et al., 1979; Ellerby et al., 2005). The constantly active cardiac muscle is perfused at a higher rate than resting skeletal muscle. During exercise in the guinea fowl, flow to the ventricles more than doubled (Ellerby et al., 2005). Presumably, as in mammals, the majority of avian coronary blood flow occurs in diastole, so we might expect coronary flow to increase if the diastolic interval is prolonged, provided arterial driving pressure does not fall.

18.2.2 Cardiac variables

The avian cardiovascular system is not merely a replica of the arrangement in mammals, despite similarities in performance between the two systems. Birds have larger hearts, bigger stroke volumes, lower heart rates, and higher CO than mammals of corresponding body mass (Grubb, 1983). In addition, in many avian species, mean arterial pressure is higher than that found in mammals of comparable body mass (see Smith, 1994). CO, the product of stroke volume and heart rate, is of particular interest because it is a major determinant of the rate of oxygen delivery to tissues.

In resting birds, left ventricular stroke volume (V_s) scales almost directly proportional with body mass (M_b) (Grubb, 1983; Seymour and Blaylock, 2000). For nine species of birds ranging in body mass from 0.035 kg (budgerigar) to 37.5 kg (emu), Grubb found that $V_s = 1.72M_b^{0.97}$, where

V_s is in milliliters and M_b is in kilograms. Seymour and Blaylock (2000) found a similar relationship in birds and $V_s = 0.99M_b^{1.03}$ in mammals. Heart rate (f_H, beats min^{-1}) at rest was found to be slower in larger birds: $f_H = 178.5M_b^{-0.282}$. CO (CO, mL kg^{-1} min^{-1}) at rest, the product of stroke volume and heart rate, therefore scaled with the mass of the bird as: $CO = 307.0M_b^{0.69}$. The corresponding relationship for mammalian CO is $CO = 166M_b^{0.79}$ (Holt et al., 1968). These results show that birds have a proportionally larger CO compared with a mammal of the same body mass. In larger birds, resting heart rate is slower than in smaller birds. Bishop and Butler (1995) found that for 49 species the allometric relationship for heart rate at rest was $f_H = 125M_b^{-0.37}$, while for birds in flight it was $f_H = 480M_b^{-0.19}$. It is interesting that the heart rate–body mass relationship during flight has a shallower slope than in resting animals, indicating larger species show a greater increase in heart rate in absolute terms in the transition from rest to flight. Bishop and Butler (1995) suggest that the body mass exponent of stroke volume in flight should be similar to that at rest ($M_b^{0.96}$), even though the absolute value of stroke volume may increase during flight. Therefore, in flight, it is predicted that CO will scale to body mass as the sum of the exponents for stroke volume and heart rate ($M_b^{0.77}$).

In flight, as at rest, larger species show lower coronary perfusion rates per mass of body tissue. It is likely that this reflects an optimization of the arterial oxygen supply at the tissue level, the body mass exponent for CO being very similar to the exponent for mass-specific oxygen consumption. Thus, natural selection probably acts on CO to maintain the arteriovenous O_2 difference at a similar level across different avian species. Stroke volume is constrained by cardiac geometry such that, on theoretical grounds, V_s should be closely proportional to M_h and M_b (Schmidt-Nielsen, 1984; Astrand and Rodahl, 1986). Therefore, the lower mass–specific CO of larger avian species, matching their lower mass–specific VO_2 levels, are reflected in their lower heart rates.

18.2.3 Fine structure and cardiac electrophysiology

18.2.3.1 Fine structure

Histologically the atria and ventricles are quite similar consisting of an external layer, the epicardium, which is separated from an inner endocardium by the mass of heart muscle, the myocardium. Ventricles are much thicker than the atria due to extensive proliferation of the myocardial layer. The epicardial and endocardial layers are morphologically similar, consisting of loose connective tissue and elastic fibers bordered by a single layer of squamous epithelial or endothelial cells, respectively. The atrial and ventricular septa have endocardial layers facing the lumens of their respective cavities with myocardial cells between them. In the sparrow and stork, the atrial septum is very thin and in some regions consists only of two apposed layers of endocardium.

The atrial and ventricular myocardia consist of striated muscle fibers, differing from those of mammals in three notable respects (Sommer and Johnson, 1969, 1970; Hirakow, 1970). (1) Striated muscle bands are prominent in mammalian cardiac muscle are also present in bird hearts, with the exception of the M-band. In mammalian cardiac muscle, the M-band is a line of protein molecules connecting adjacent myosin filaments. The significance of the lack of an M-band on the contractile properties of avian myocytes is unknown. (2) Avian cardiac muscle fibers are much smaller in diameter than mammalian fibers and hence there are many more of them in similarly sized hearts. Avian myocardial cells are typically 2–7 μm in diameter compared with the 10–15 μm diameter of mammalian cells. (3) Myocardial cells of all fish and reptiles (Shiels and Galli, 2014), including avian species lack transverse tubules (T-tubules) which are prominent in mammalian cardiac muscle. The membrane surrounding the muscle fibers (sarcolemma) consists of two parts, a cell membrane (plasmalemma) and an external layer interconnected with an interstitial network of collagenous fibers. In mammalian cardiac muscle, T-tubules form as invaginations of the plasmalemma, perpendicular to the long axis of the myofilaments. T-tubules lie next to, and form junctions with, sections of the sarcoplasmic reticulum (SR) (diads or triads). In mammals, the T-tubule system increases the surface area of the myocardial cells to the extent that the surface-to-volume ratio of a mouse cardiac cell (15 μm diameter) is the same as that of a finch (8 μm diameter). The finch and the mouse have similar cardiac frequencies (Bossen et al., 1978).

The connection between the SR and the sarcolemma occurs through "couplings" and in birds that lack a T-tubule system these couplings occur at the surface of the cell (Figure 18.5). Peripherial couplings are affected by junctional processes that extend from the cytoplasmic face of the SR (junctional sarcoplasmic reticulum, JSR) that are very closely opposed to the inner surface of the sarcolemma. Birds and the other reptiles possess an extended junctional sarcoplasmic reticulum or corbular JSR that is not associated with the sarcolemma (Perni et al., 2012; Shiels and Galli, 2014). Corbular JSR is much less developed in chicken than in passerine birds (Sommer et al., 1991). The volume of peripheral JSR in mouse hearts and the total volume of peripheral JSR (20%) and corbular JSR (80%) in the finch are virtually identical (Bossen et al., 1978).

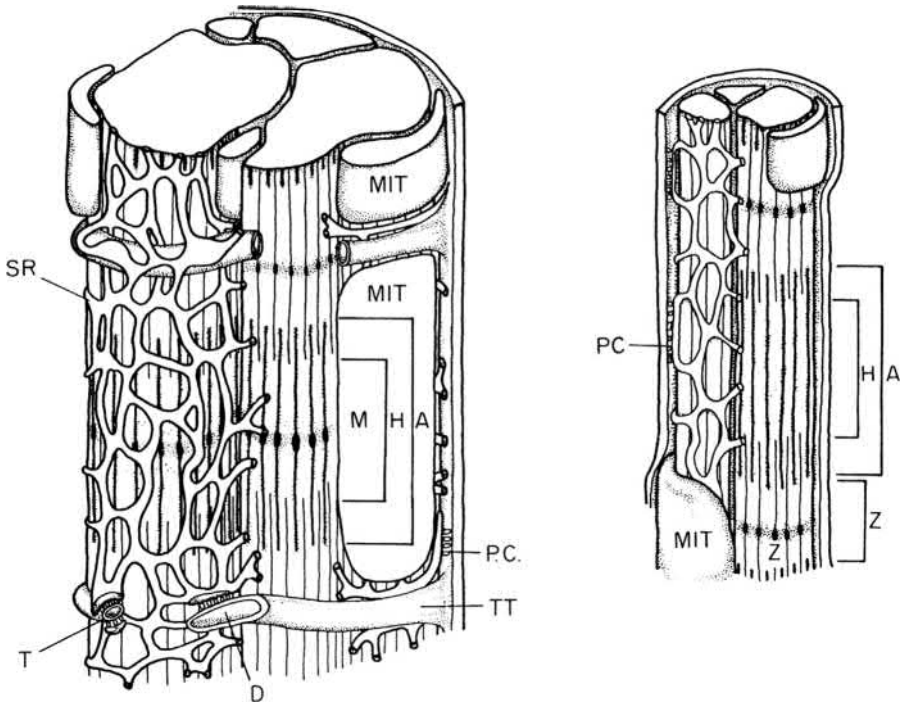

FIGURE 18.5 Comparison of mammalian (left) and avian (right) myocardial cells. The major distinguishing features of avian fibers are smaller cell diameters and absence of M bands and transverse (T)-tubules. *D*, diad junction; *M, H, A, I, Z*, bands of striated muscle; *MIT*, mitochondria; *PC*, peripheral coupling site; *SR*, sarcoplasmic reticulum; *T*, triad junction; *TT*, transverse tubule. *From Sommer and Johnson (1969).*

18.2.3.2 Excitation–contraction coupling

Excitation–contraction coupling describes how an electrical signal, the action potential (AP), traveling along the sarcolemma evokes calcium release from the SR in the region of the myofibrils, causing a change in actin–myosin interactions leading to muscle contraction. In cardiomyocytes, the transduction between the electrical signal and Ca^{2+} release from the JSR is affected by a transmitter which is, in fact, calcium itself. In the first step of this process, the AP causes voltage-gated L-type Ca^{2+} channels to open in the sarcolemmal membrane through a conformational change in the channels. Ca^{2+} enters the cell and diffuses to ryanodine receptor channels on the junctional processes where it acts as a ligand, opening Ca^{2+}-dependent Ca^{2+} channels which in turn release sequestered Ca^{2+} from the SR. The Ca^{2+}-dependent Ca^{2+} channels are Ryanodine receptor channels clustered in subcellular of Ca^{2+} release units (CRUs; Shiels and Galli, 2014). In the avian myocyte, CRUs are found either on the peripheral JSR near the L-type Ca^{2+} channels or at corbular JSR not associated with the sarcolemma. The release of Ca^{2+} from the corbular JSR CRUs is responsible for the rapid propagation of the Ca^{2+} signal to the center of the contracting myocyte (Sheard et al., 2019). This Ca^{2+}-induced Ca^{2+} release (CICR) is crucial for the physiological function of the bird heart in which the corbular JSR is the majority of the junctional SR. Furthermore, CICR allows exquisitely fine regulation of force generation in myocytes. Relaxation of the myocytes is due to the uptake of Ca^{2+} into the SR via sarco/endoplasmic reticulum Ca^{2+} ATPase (SERCA) and extrusion by Na^{+}/Ca^{2+} exchange. In cardiac muscle, contraction is "all or none," and force modulation must be done at the cellular level by regulating not only the amount of Ca^{2+} entering through the sarcolemma but also its effect on Ca^{2+} release from the SR.

18.2.3.3 Conduction system

The cardiac conduction system of the avian heart consists of the sinoatrial (SA) node, AV node, AV Purkinje ring, His bundle, and three bundle branches (Figure 18.6). Histologically, three types of cells are associated with the conducting system. (1) Pacemaker cells (P-cells) are small and spherical in shape and are found in both the SA and AV nodes. P-cells have the property of repetitive spontaneous depolarization. (2) Transitional cells (T-cells) are much smaller and have fewer microfibrils than cardiac muscle cells; their structure is intermediate between normal cardiac muscle cells and Purkinje fibers. (3) Purkinje fibers are large, elongated, brick-shaped cells containing few myofibrils. Many Purkinje cells, however, contain longitudinal fibers called intermediate filaments; these are part of the cytoskeleton, serving to maintain cell shape as the myocardium contracts. Purkinje cells may be up to five times the diameter of myocardial cells.

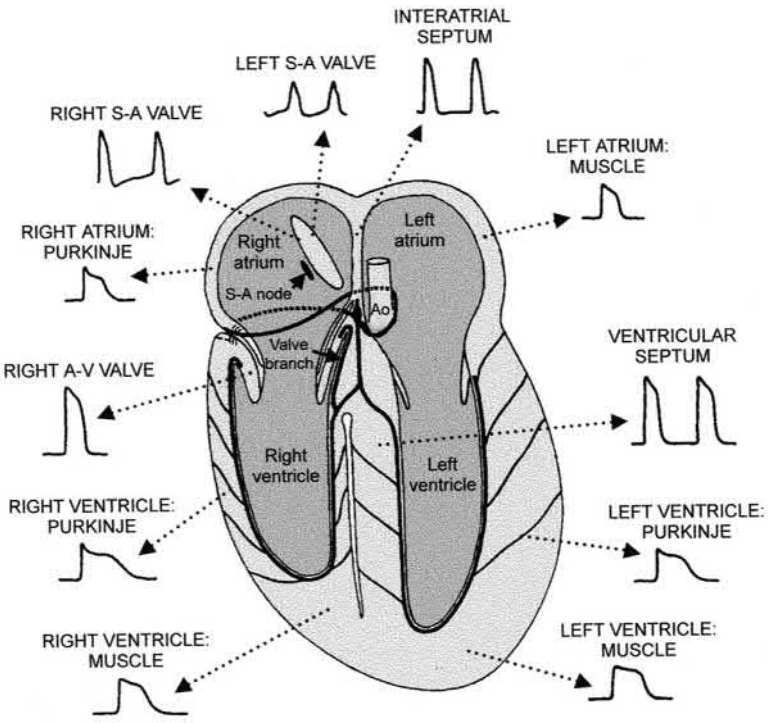

FIGURE 18.6 The Purkinje system of the bird heart and transmembrane action potentials recorded from cells at the indicated sites in chicken and turkey. *From Jones and Johansen (1972).*

The SA node is located close to the opening of the venae cavae into the right atrium although there is considerable species variation in birds. The SA node consists of P-cells and many T-cells enclosed in a loosely organized connective tissue sheath. The T-cells transmit impulses from the pacemaker to atrial muscle cells. The SA node morphologically, and perhaps physiologically, diffuses in birds, and the primary electrical pacemaker region appears to change position spontaneously within the node (Hill and Goldberg, 1980).

For normal cardiac function, all cardiac muscle fibers within a given cardiac chamber should contract more or less simultaneously, while it is essential that the atria contract before the ventricles. The wave of excitation initiated in the SA node is delayed at the AV node allowing the atria to empty before ventricular contraction begins. The electrical impulse which initiates contraction spreads through the atria and ventricles at rates in excess of 1 m s^{-1}, whereas conduction through the AV node is two to three orders of magnitude slower. Spread of excitation through myocardial muscle occurs from one muscle cell to the next as well as along specialized conducting pathways. Individual muscle cells are discrete entities, but they behave electrically as if they were all joined together to form a syncytium. This property results from low-electrical resistance in parts of the cell membrane where cell apposition is very close. Junctional complexes, the intercalated disks, commonly join myocytes end-to-end in avian myocardium, occurring at right angles to the long axis of the myofibrils. Intercalated disks consist of two components, desmosomes, which mechanically couple the cells together, and nexuses, which couple cells electrically. A nexus may be viewed as an array of unit electrical resistors with their number being inversely proportional to the electrical resistance between the cells (Sommer, 1983). Interestingly, there are few nexuses along the longitudinal axes of myocardial cells.

The speed at which the wave of electrical excitation propagates through the ventricles is enhanced by a specialized conducting system of Purkinje fibers but whether a specialized conducting system also exists in the atria of birds is controversial. In the atrium, waves of electrical and contractile activity proceed in the same direction, from the SA to AV nodes, which may mean that a specialized conducting system is unnecessary here. However, both atria contain Purkinje cells, and these have been described both morphologically and physiologically as being organized to preferentially direct the wave of activation toward the AV node (Davies, 1930; Hill and Goldberg, 1980). The contrarian view is that since the Purkinje cells in the atria are mixed diffusely among the normal myocardial cells then they may represent the remnants of an embryological anlage left over from the time when that anlage was building the ventricular conducting system (Sommer, 1983).

The atrial wave of excitation crosses to the ventricle through the AV node which, in birds, is a somewhat controversial structure because many morphological investigations have failed to locate it, although its presence

has been established in functional studies. In the chicken, the AV node is located in the right side of the base of the interatrial septum (Davies, 1930; Lu et al., 1993b; Ying et al., 1993) although in Indian fowl, *Pycnonotus cafer*, house sparrow, *Passer domesticus*, and in *Bubo bengalensis*, it is located in the left AV junction (Mathur, 1973). A right AV ring bundle with pacemaker properties is located in the right AV-junction associated with the AV node in the avian heart (Prosheva and Kaseva, 2016). The His bundle and its three bundle branches of Purkinje cells arise from the AV node. The right and left bundle branches emerge from the septum to form a network in the subendocardium of the right and left ventricles, respectively, penetrating the myocardium along the tracts of the coronary arteries (periarterial Purkinje fibers).

An indication of the theropod ancestry of birds can be inferred from the conducting system of the heart. Birds, unlike mammals, possess an AV ring of P-cells on the right side of the heart which runs up and around the right AV valve (Figure 18.7; Prosheva and Kaseva, 2016; and see Section 18.2.1.4). The middle bundle branch, after separating from the others, runs around the aorta and connects to the AV ring forming a figure eight (Lu et al., 1993b).

Purkinje cells conduct electrical impulses much faster than cardiac myocytes. In mammals, part of the reason for this high-conduction speed is that Purkinje cells lack a T-tubule system. T-tubules increase the surface area of the cell and therefore membrane capacitance (increasing the length of time a given amount of electrical charge will take to alter membrane potential); a high capacitance thus slows conduction velocity. However, in birds, there is no T-tubule system associated with either myocardial or Purkinje cells, yet the latter still conduct impulses at a faster rate. This is because conduction velocity varies directly with cell diameter, and avian Purkinje cells are much larger than myocardial cells. Furthermore, a higher conduction velocity may be fostered in Purkinje cells by intermediate filaments which serve to keep the cell round. Also, the electrical resistance between Purkinje cells is lower than that between myocardial cells because nexus size also increases with cell diameter, acting to further increase conduction velocity. Finally, in mammals with extremely large hearts (i.e., ungulates), the Purkinje cells within a bundle are tightly packed together and surrounded by an insulating membrane so that they behave electrically as a single fiber of a diameter equal to that of the whole bundle. Purkinje cells are likewise bundled in the avian heart but whether this enhances conduction velocity is uncertain because the bundles lack a connective tissue sheath and are therefore not insulated from surrounding tissues.

18.2.3.4 Electrophysiology

The Purkinje fibers follow the coronary arteries and therefore take a relatively short course through the thick left myocardium. This accounts for the rapidity of arrival of the wave of excitation at a given point on the surface of the left ventricular wall in the avian heart (Lewis, 1916). The sequence of depolarization is, according to Kisch (1951): right ventricle apex, right ventricle base, left ventricle base, and left ventricle apex. Moore (1965) mapped epicardial activation in the turkey and suggests that the apical third of the right ventricular epicardium is activated earliest, the upper basilar third is intermediate, and the pulmonary

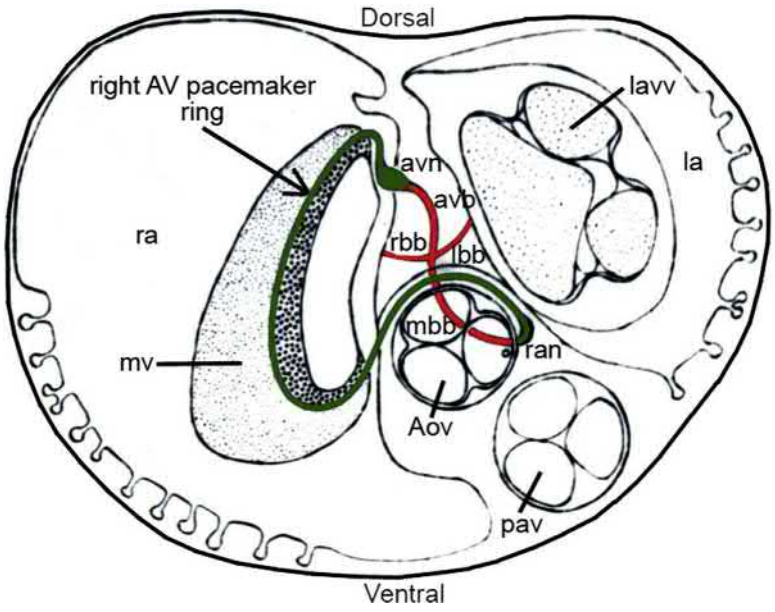

FIGURE 18.7 Diagram of the right atrioventricular pacemaker ring (green) and atrioventricular bundle (red) in the chicken heart. *Aov*, aortic valve; *avb*, atrioventricular bundle; *avn*, atrioventricular node; *la*, left atrium; *lavv*, left atrioventricular valve; *lbb*, left bundle branch; *mbb*, middle bundle branch; *mv*, muscular valve; *pav*, pulmonary artery valve; *ra*, right atrium; *ran*, retroaortic node; *rbb*, right bundle branch. *From Prosheva and Kaseva (2016).*

outflow tract is the last region activated in the whole heart. The anterior one-third of the septal region and the middle region of the left ventricle are activated before the basilar regions, the whole left ventricular epicardium being activated in 12.5 ms. Others have found somewhat different sequences of activation (Lewis, 1916; Mangold, 1919). Kisch suggests that the conducting system stimulates heart muscle only at places of direct contact between its terminal fibers and heart muscle and not along the entire course of the conducting system (Kisch, 1951) showing that subendocardial muscle is activated about 20 ms later than the earliest activated subepicardial muscle, which in turn suggests short cuts of the conductive system to subepicardial muscle. However, Davies (1930), Lu et al. (1993b), and Kharin (2004) suggest that since the bundle branches lack a fibrous sheath, there will be early and widespread propagation of the impulse in the septal region and thence along the bundle to all parts of the ventricles. Kharin (2004) mapping activation patterns with 64 electrodes in the chicken ventricle found earliest activation in both the right and left ventricle in a mosaic-like pattern. Repolarization of the ventricle follows a different pattern from that observed during depolarization (Kharin, 2004). Repolarization starts at the right ventricle apex and moves down to the left ventricle apex. This is then followed by repolarization of the left ventricle base and finally the right ventricle base.

The conducting system of the bird heart has been investigated by recording transmembrane potentials from cells in the heart of the chicken and turkey (Moore, 1965, 1967). The P-cells of the SA node, in the absence of any extrinsic influences, set the heart rate. Cells that function as pacemakers show a characteristic slow depolarization during diastole, the steepness of the depolarization being related to the degree of automaticity inherent in the cell (the fastest cells to depolarize drive the slower cells), whereas cells not spontaneously active show a steady membrane potential during diastole (Figure 18.6). APs recorded from the junction of the left SA valve with the sinus venosus show diastolic depolarization (prepotentials) with a slow transition to the ascending phase of the actual AP (Figure 18.6), in contrast to the relatively more rapid rise of the AP recorded in the right SA valve itself, indicating that cells in the right SA valve are triggered by the P-cells. The duration of APs recorded from ventricular muscle cells is longer than those recorded from atrial muscle cells (Figure 18.6). Purkinje fibers display a prominent sharp peak to their APs, which is followed by a distinct plateau, a feature not seen in APs from atrial or ventricular muscle cells. The duration of depolarization is also much longer in Purkinje fibers although diastolic depolarizations have not been recorded from avian Purkinje fibers. The longer duration of the Purkinje APs as compared with those of ventricular myocytes indicates a long refractory period which would tend to prevent extrasystole and possible fibrillation by assuring a concerted depolarization of the ventricular muscle (Moore, 1965). The myocytes of the right AV-valve also exhibit the characteristic depolarization of P-cells (Prosheva and Kaseva, 2015, 2016).

An electrocardiogram (ECG) shows the summed electrical activity of the heart (Figure 18.8). An ECG is recorded indirectly with electrodes placed on the body surface or just under the skin. (A direct ECG recording would be made by dividing the sternum and placing recording electrodes directly on the surface of the heart). In birds, as in mammals, three standard leads (I, II, and III) are used, following the model first conceived by Einthoven over 100 years ago. The body is a volume conductor of electricity, and the depolarization and repolarization waves that sweep across the heart can be reduced to a single electrical dipole. The dipole has magnitude (volts), direction, and sense (positive or negative), so it is a vector quantity. In Einthoven's concept, the cardiac vector is situated at the center of an equilateral triangle formed by the bipolar lead connections. Lead I connects across the thorax from the right (negative electrode) to the left (positive electrode) wing bases. Lead II is recorded between right wing base (negative electrode) and left thigh (positive electrode). Lead III is connected between the left wing base (negative electrode) and the left thigh (positive electrode). The arrangement of these leads is such that, in humans and many other mammals, the polarity of the recorded signals is positive. In contrast, in birds, the polarity of the major component of the ECG (ventricular contraction) is negative (Boukens et al., 2019, Figure 18.8).

There has been some controversy over what the typical avian ECG looks like (Figure 18.8). For instance, Kisch (1951) reported the presence of P, QRS, and T waves, whereas Mangold (1919) reported that the ECG of birds has no R component, but instead a deep S wave. Sturkie (1986) reported the presence of P, a dominant S, and T waves, a small R, but no Q wave. There is general agreement that it is absent in the chicken (Goldberg and Bolnick, 1980; Liu and Li, 2005), small in the turkey (McKenzie et al., 1971), and prominent in some duck ECGs (Cinar et al., 1996). Aside from being useful in monitoring heart rate, the ECG can also be used to access the timing of the various phases of the cardiac cycle, since components of the ECG can be identified with atrial (P wave) and ventricular (QRS or RS) depolarization as well as repolarization of the ventricles (T wave). The duration of the P wave is the period of atrial depolarization and repolarization while the P–R duration includes the conduction delay at the AV node. QRS or RS represents ventricular activation, and the T wave is the period in which the heart is completely depolarized. QT or RT duration represents the duration of a complete cycle of activation and relaxation of the ventricle. Most of these intervals are fixed, so it is primarily the period between the T and P waves (i.e., interbeat interval), which shortens and

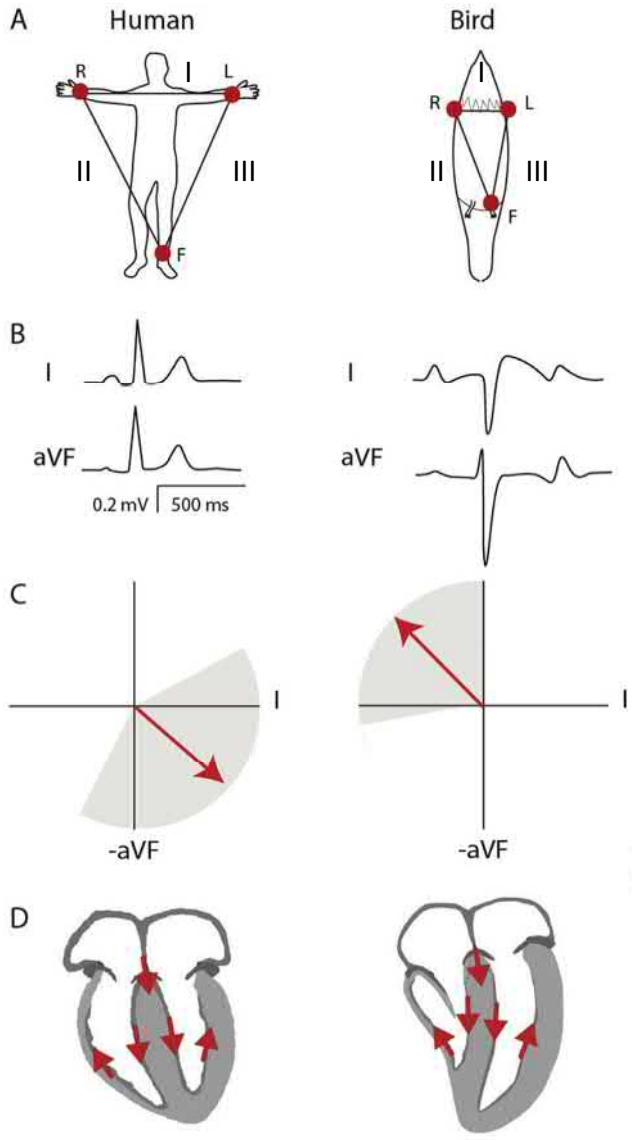

FIGURE 18.8 (A) Relationship of the three standard electrical leads (I, II, and III) as conceived by Einthoven in a human and a bird. (B) Electrocardiogram measured from Lead I and aVF of a human and a chicken (C). Vectorgrams based on Lead I and aVF for a human and a bird. (D). The pattern of ventricle electrical activation of the mammalian and avian ventricles. *From Boukens et al., 2019.*

lengthens with increases and decreases in heart rate, respectively. In fact, at very high-heart rates, the T wave of one beat may come to overlie the P wave of the next.

Bipolar recording of the standard limb leads means that the cardiac vector is projected along the line between the two electrodes (Figure 18.8). When all leads are used, then it is possible to reconstruct the orientation of the vectorcardiogram for any of the events of the cardiac cycle with respect to the plane of orientation of the leads. Standard leads lie in the frontal plane and, in mammals, the vectorcardiogram of the QRS is oriented downward (inferiorly) and to the left (Figure 18.8). In contrast, the vectorcardiogram of the QRS wave in the bird heart is close to −90 degrees, being oriented along the long axis of the body, and superior to the frontal plane. Hence, the QRS or RS wave is of negative polarity and barely represented in lead I with the highest voltages being recorded by leads II or III. The mean electrical axes of the P and T waves can be calculated in a similar fashion. By using other cardiac leads in addition to the standard limb lead I, Szabuniewicz and McCrady (1967) were able to determine the vectorcardiogram of the QRS or RS, P, and T waves of the heart in the chicken not only in the frontal plane (−77.1 degree) but also in the horizontal (+72.4 degrees) and sagittal (−55.4 degrees) planes.

As the mean electrical axis of the ventricular depolarization phase is negative while that for the repolarization phase is positive, then the QRS or RS component deflects downward or negatively while the T wave is upright or positive (Figure 18.8). Obviously, the heart does not markedly change its position in the chest with each beat. The waves deflect in opposite directions because depolarization causes the ventricular myocardium to become negative and repolarization drives the myocardium positive. Also, the time courses of these waves are different. Repolarization is slower than depolarization, so the T wave is more spread out than the QRS or RS wave. In this context, it should be noted that when the ECG is recorded just for purposes of monitoring heart rate, using a single pair of leads (usually II), the RS wave is often presented as deflecting positively. This is achieved by reversing the polarity of the lead II bipolar electrodes (inverting Einthoven's triangle, Figure 18.8) and is done for artistic reasons.

Further interpretation of the ECG of birds is complicated by variability in electrode recording sites, anatomical differences between species, and the absence of a large bank of data such as has been accumulated for humans and, to a lesser extent, other mammals. In fact, it seems most unlikely that rigorous, detailed investigation of the ECG of birds will ever be used for clinical diagnosis. Boulianne et al. (1992) suggest that only diseases that cause a shift in position of the heart in the torso, and therefore alter the MEA, can be successfully diagnosed by two-dimensional electrocardiography.

18.3 General circulatory hemodynamics

The three major constituents of the pulmonary and systemic circulations are (1) the arteries or distributing vessels, (2) the capillaries or exchange vessels, and (3) the veins which act as storage and return vessels. Arterioles and venules are muscular vessels located upstream and downstream of the capillary beds, respectively. They are regulatory vessels,

directly controlling blood flow distribution and indirectly controlling exchange of materials across capillary walls by adjustment of capillary pressure.

The major arteries bifurcate many times before the capillary beds and at each bifurcation vascular resistance increases (McDonald, 1974). Volume flow in the parent and daughter vessels remains the same in the steady state but flow velocity in the daughters falls to about 80% of that in the parent vessel. Therefore, the sum of the cross-sectional areas (πr^2, where r is internal radius) of both daughter vessels is greater than that of the parent vessel by about 25%. Hence as the vessels divide, flow velocity falls resulting in exceptionally low-capillary circulation flow velocity. This allows adequate time for exchange of blood gases, nutrients, and metabolites with the surrounding cells.

Pressure, generated by ventricle contraction, drives blood flow around the circulation. Poiseuille's law relates volume flow (Q) to the pressure drop ($P_1 - P_2$) along a tube of radius (r) and length (L) during steady flow, as follows:

$$\dot{Q} = (P_1 - P_2) \times \frac{\pi r^4}{8\,\mu L} \tag{18.1}$$

where μ is blood viscosity. Rearrangement of Eq. (18.1) provides a somewhat more familiar form,

$$\frac{\pi r^4}{8\,\mu L} = P_1 - P_2 \frac{}{\dot{Q}} \tag{18.2}$$

because the term on the left-hand side of Eq. (18.2) is vascular resistance (R). Consequently,

$$R = P_1 - P_2 \frac{}{\dot{Q}} \tag{18.3}$$

or, for the whole body, total peripheral resistance (TPR, kPa ml^{-1} min),

$$TRP = \frac{MAP - MVP}{CO} \tag{18.4}$$

where MAP is mean arterial pressure (kPa), MVP is mean venous pressure (kPa), and CO is CO (ml min^{-1}). In order to compare animals of different sizes, CO may be expressed on a unit weight basis (i.e., ml min^{-1} kg^{-1}).

Because the length (L) of any vascular channel is anatomically fixed and blood viscosity only varies by two to three times, the radius of the vessels dominate vascular resistance (Eq. 18.2). Consequently, with a given pressure drop, halving vessel radius will reduce flow to one 16th, as shown in Figure 18.9, for a change in vessel radius from, for instance, two units (center profile) to one (left profile). This has important implications for the control of blood flow distribution.

Poiseuille's Law (Eq. 18.1) applies to steady flow but in the major arteries flow is highly pulsatile. In pulsatile flow, due to the inertia of the blood and high heartbeat frequencies, flow amplitude may no longer vary linearly with the pressure gradient. Nevertheless, the extent of the deviation from Poiseuille's law can be assessed from a nondimensional constant α (Womersley, 1957)

$$\alpha = r\sqrt{\frac{2\pi f \rho}{\mu}} \tag{18.5}$$

where r is radius, f is heart rate, ρ is blood density, and μ is blood viscosity.

When $\alpha < 0.5$ for the fundamental frequency (i.e., heartbeat frequency), the phase lag is negligible and flow conforms approximately with that predicted by Poiseuille's equation. Calculations for the aorta of a duck give a value for α of 6.0–7.0 for the fundamental frequency (about 3 sec^{-1}) so that estimation of flow by the Poiseuille formula is not reliable. However, it is obvious that for any given heart frequency, the value of α is directly dependent on the size of the vessel. Hence, in the femoral artery, α is certainly below 1, and flow will vary approximately linearly with the pressure gradient in this vessel. The vessels of

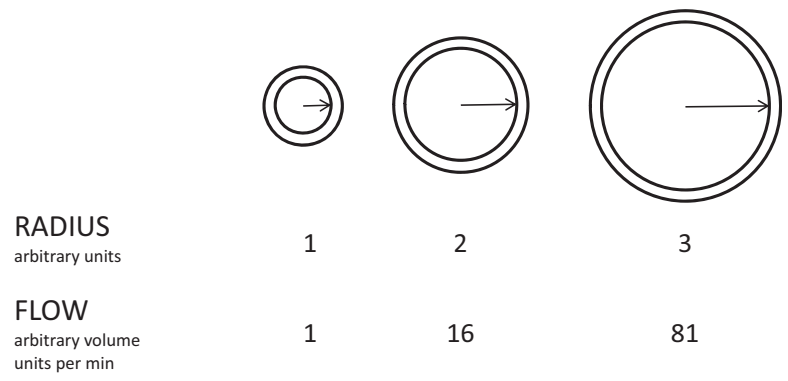

FIGURE 18.9 Effect of change in vessel radius as shown by the length of the *arrow*, on fluid flow with a constant driving pressure. Flow decreases in proportion to the fourth power of the decrease in radius. Radius dimensions and relative flow volumes are in arbitrary units.

the capillary circulation are small and α will be likewise, so application of Poiseuille's formula to this vascular bed would appear, superficially, to be most appropriate. Unfortunately, blood viscosity, which can be regarded as a constant in larger vessels, may vary unpredictably in vessels of capillary size (Section 18.4.2). Therefore, caution is the watchword when applying steady flow formulations to flow driven by an oscillating pump but, even so, pulsatile flow has a mean, steady flow component and Poiseuille's law can be applied to this component, as in calculations of total peripheral resistance (Eq. 18.4).

18.4 The vascular tree

18.4.1 Arterial system

18.4.1.1 Gross anatomy

At least six pairs of aortic arches appear in the embryos of all vertebrates, recapitulating their aquatic ancestry. In birds, not all arches are present at one time and some are extremely transitory, such as the fifth pair of aortic arches which make their appearance last. Only three arches persist in the adult, represented by the carotid artery (third arch), the aorta (fourth arch), and the pulmonary artery (sixth arch). In terrestrial vertebrates other than birds and mammals, both left and right branches of the fourth aortic arch are retained whereas only the right persists in birds and the left in mammals. In some avian species, a remnant of the left aortic arch may remain as a solid core of cells while in a few others, such as the belted kingfisher (*Ceryle alcyon*), the left arch remains patent and functional although it loses its connection with the root of the aorta (Glenny, 1940). In an interesting series of experiments, Stéphan (1949) demonstrated that ligation of the right aortic arch in the embryo causes the left to develop, as in mammals. Furthermore, wall shear stress differences in the embryonic right and left aortic arch leads to differential mechanosensitive gene expression in the two embryonic aortic arches (Karakaya et al., 2018). These findings suggest that the retention or disappearance of aortic arches is dependent upon hemodynamic conditions during development, and it may be that the persistence of the right arch simply results from the unique development of the ventricular outflow tract in birds.

The first major vascular bed supplied by the aorta is that of the heart. The coronary arteries, supplying the nutritional and respiratory circulation of heart muscle, arise from the ascending aorta close to the heart (Section 18.2.1.5). The ascending aorta then gives rise to two very large brachiocephalic trunks (Figure 18.10), supplying blood to the head, wings, and flight muscles. Each brachiocephalic vessel is usually larger in diameter than the

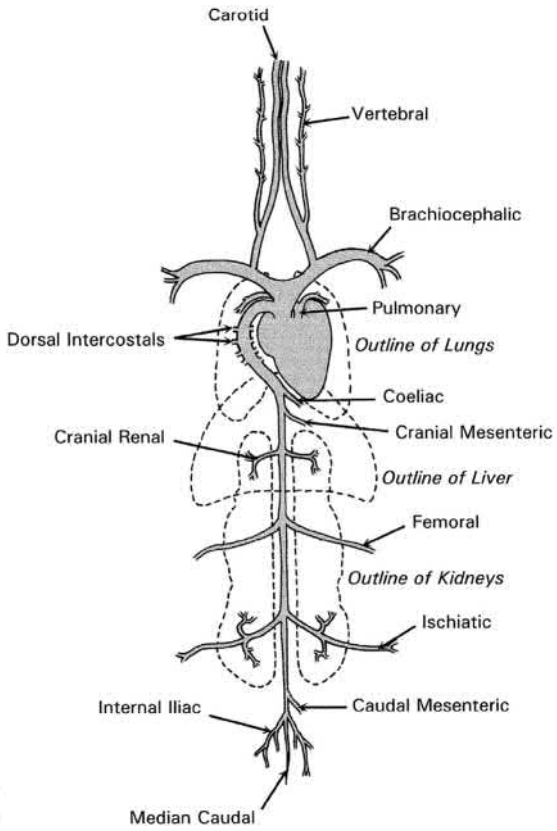

FIGURE 18.10 The major systemic arteries in the bird.

continuation of the aorta, reflecting the higher blood flow rates in the brachiocephalics.

All the arteries of the head and neck are branches of the carotid arteries. Surprising variation exists in the pattern of the carotid arteries close to the heart. The most common arrangement is two vessels of equal size running side by side (Figure 18.10). Other patterns are: (1) a single artery formed by fusion of both carotids (herons, bitterns, and kingfishers); (2) a single vessel due to loss of the right (passerines) or left (plovers) carotid; or (3) two arteries of unequal size (flamingos, sulfur-crested cockatoo).

Blood flow to the brain must not be interrupted or impairment of brain function rapidly ensues. The carotid arteries lie in a groove in the base of the neck vertebrae close to the axis of rotation and are therefore protected from possible obstruction due to compression from neck movements. Other safety measures are provided by anastomoses between the carotid and vertebral arteries and, at the base of the brain, by either an X-, I-, or H- shaped junction between the carotids. This intercarotid anastomosis has been found in all species of bird except those of the suborder Tyranni (Baumel and Gerchman, 1968). Birds do not possess a cerebral arterial circle of Willis comparable to that of

mammals but, since the intercarotid anastomosis is relatively large in many cases, it may represent a more effective collateral circulation than the mammalian arterial circle. Blood to the wings and flight muscles is supplied by the subclavian arteries. Each subclavian divides into two branches, the brachial (wing) and pectoral (flight muscles).

The descending aorta runs caudally, ventral to the vertebral column, giving off paired intercostal and lumbar arteries. Blood is supplied to organs within the abdomen and legs by the following vessels, originating from the descending aorta (see Figure 18.10):

Celiac artery	Liver, spleen, glandular stomach, gizzard, intestine, pancreas
Cranial mesenteric artery	Most of intestine, pancreas
Renal arteries	Kidneys (anterior portion), testes
Femoral arteries	Legs
Ischiatic arteries	Middle and posterior portions of kidney and legs; uterine region of oviduct
Caudal mesenteric artery	Rectum and cloaca
Internal iliac arteries	Walls of pelvis; oviduct
Caudal artery	Tail, terminal branch of aorta

There are in effect three pairs of renal arteries in birds, one pair arising from the aorta and two from the ischiatic arteries. However, in the gray heron (*Ardea cinerea)*, one pair of renal arteries arises from the femoral arteries instead of the ischiatics.

The ischiatic artery is the major vessel supplying the leg. At the level of the knee, it meets and joins the femoral artery to form the popliteal artery. This artery, passing into the lower leg, divides to form the anterior and posterior tibial arteries. In the tarsal region of the leg and in the axillary region of many birds, there are arteriovenous networks of vessels referred to as *rete mirabile*, particularly prominent in wading and aquatic birds (Midtgård, 1981). These structures serve as heat exchangers, since warm arterial blood is brought into close proximity to venous blood that has traversed the distal parts of the limbs and is therefore colder. The countercurrent arrangement of blood flow ensures that heat can be transferred from arterial to venous blood all along the length of the artery and vein apposed in the *rete*, thereby reducing heat loss to the environment by reducing the temperature of arterial blood flowing through peripheral thinner sections like the web of the foot or the wing.

18.4.1.2 Functional morphology of the arterial wall

The large arteries have two main functions. First, they serve as low-resistance conduits carrying blood to the arterioles for distribution to the peripheral vascular beds. Second, the whole arterial system serves as a pressure reservoir or *Windkessel*, accepting the volume of blood ejected by the heart and converting the highly pulsatile input into a steady flow of blood through the capillary beds. The *Windkessel* results from wall elasticity, particularly of those vessels closest to the heart.

The central arterial vessels are "elastic" while the more peripheral ones, certainly distal to the second order of branching, are "muscular." In elastic arteries, the vast majority of the wall is made up of layers of smooth muscle embedded in elastin fibers alternating with layers of collagen. One layer, composed of a combination of muscular, elastic, and collagen fibers, forms a single lamellar unit within the wall. Large numbers of concentric lamellar units make up the bulk of the wall of elastic arteries of pigeon, chicken, and the mute swan (*Cygnus olor*; Bussow, 1973). Interestingly, the lamellar units do not form complete cylinders around the vessel. This is particularly obvious in vessels very close to the heart where an individual lamella may extend around only one quarter, at most, of the vessel circumference.

Wall structure of the muscular arteries is very different. Muscular vessels consist largely of circumferentially arranged smooth muscle cells with elastic fibers distributed, either singly or in bundles, as a wide-meshed plexus between the muscle cells (Hodges, 1974). The collagenous components are transferred to the outer layer of the wall. An interesting embellishment of the normal structure of muscular arteries occurs in the cranial mesenteric artery of the chicken and turkey (Ball et al., 1963). This vessel is invested by longitudinally arranged smooth muscle fibers, the thickness of this layer being approximately the same as that of the circumferentially oriented smooth muscle within the wall proper. The functional significance of the external muscle layer is unclear, but it may serve to shorten the vessel to accommodate changes in its position brought about by gut movements.

The elastic arteries include the aortic arch and its major branches, the thoracic aorta up to about the level of the celiac artery, and the extrapulmonary portions of the pulmonary arteries, while all branches of the abdominal aorta as well as the caudal portion of the aorta itself are muscular. In most regions of the arterial tree, the change from an elastic to a muscular wall occurs rather abruptly, usually at a branch site. An exception to this is the aorta itself. In the aorta, the elastic and muscular portions are separated by a segment of the vessel extending from the celiac artery to the ischiatic arteries, whose wall structure fits neither description very well. Furthermore, in both the pigeon and turkey, the wall in this region is transversely asymmetric with a thick, muscular ventral wall, and a thin elastic dorsal wall.

The arteries *in vivo* expand and recoil with every heart beat although this behavior is seldom mimicked in *in vitro* experiments designed to study vessel mechanics. Instead,

the static rather than dynamic elastic behavior of the arterial wall is usually investigated. Essentially, a short length of excised blood vessel is inflated from a syringe and the pressure change induced by a given volume change is noted. These "pressure–volume loops" give an immediate and compelling view of how arterial elasticity changes with the degree of inflation.

Furthermore, by using blood vessels from different areas of the body, regional variations in elasticity are revealed. Pressure–volume loops are usually J-shaped, showing that the more a vessel is stretched the more resistant it becomes to further stretch (Speckmann and Ringer, 1966). The collagen fibers in the vessel wall inhibit expansion at high pressures, whereas the properties of elastin dominate at the lower pressure on the curve. It is the elastin compliance and the collagen stiffness working in concert that allows uniform and smooth expansion of the vessel wall over a range of distending pressures without formation of aneurysms. In contrast, a wall in which the properties of extension remain constant across the range of distending pressures would be prone to aneurysm formation. Rubber has a straight rather than J-shaped response to distension and aneurysms always occur in the wall of cylindrical balloons when they are inflated.

When a blood vessel is inflated, more pressure is required to expand it than is recovered during recoil of the elastic walls. The ratio between the energy recovered in deflation to that expended in inflation is a measure of the "resilience" of that vessel. Surprisingly, "resilience" is similar for both thoracic (elastic) and abdominal (muscular) aortae of the turkey. Over the range of arterial pressures encountered in turkeys, "resilience" lies between 85% and 87%, values well above those of most mammals and approaching those obtained for invertebrate blood vessels. In one sense, the higher the "resilience" the better because most of the energy cost of stretching elastic vessels with each cardiac ejection will be returned by elastic recoil on deflation. Unfortunately, if the "resilience" is too high, then the vessels may go into uncontrolled oscillations (resonance) particularly at the high repetition heart rates seen in many birds. Obviously, vascular engineering in birds is close to the edge.

Pressure–volume loops reveal characteristics specific to particular segments of whole vessels, whereas the properties of the materials making up a vessel wall are revealed by stress–strain curves (Figure 18.11A). Stress is the deforming force divided by the area of the vessel wall over which it is applied while strain is the ratio of the stretched radius to the unstretched radius of the vessel. Stress–strain curves for the ascending and descending aortae, the brachiocephalic arteries, and the thoracic aorta of the duck (*A. platyrhynchos*) are shown in Figure 18.11A. The stress–strain relationship for the abdominal aorta lies to the left of that for the other, more central, vessels indicating that, as in the turkey, the abdominal aorta is stiffer than the other vessels, a finding which would be expected given that the abdominal portions of the aortae of duck and turkey have more collagen than do more central segments of this vessel.

The slope of the line of a stress–strain curve is the elastic modulus of the material making up the blood vessel wall, but, since the slopes for blood vessels are nonlinear, the elastic modulus is continually changing. The incremental elastic modulus describes the elastic modulus for a small increment in strain (Bergel, 1961). Incremental elastic moduli for the duck aorta, which are similar to those for the turkey aorta (Speckman and Ringer, 1964), are shown in Figure 18.11B. The moduli for the abdominal aorta are well above that for the thoracic, confirming that the former is stiffer than the latter. Nevertheless, these moduli are one to two orders of magnitude below those obtained from arteries in corresponding parts of the mammalian vascular tree. In mammals, the lamellar units in the wall form complete cylinders so that those laminae containing primarily collagen must be stretched to the same extent as the more distensible muscular laminae. Consequently, such rigid laminae are more important in determining the degree of extension of the wall. However, in birds, arterial lamellar units do not form complete cylinders so there is some "series" coupling between the rigid and elastic components of the wall which allows more distensible laminae to be extended somewhat independently. Avian blood vessels have much thicker walls than mammalian vessels of the same diameter, thus compensating for their lower elastic modulus (Bussow, 1973).

18.4.1.3 Relationship between arterial pressure and flow

Each heartbeat sends a pulse through the arterial system which arrives later at sites more distal to the heart. The velocity at which the pulse wave travels is lowest in the most distensible vessels and increases in the stiffer peripheral vessels. In ducks, pulse wave velocity increases from 4.4 ± 0.8 m s^{-1} in the aortic arch to 11.7 ± 1.2 m s^{-1} in the abdominal aorta, with the major increase in velocity occurring in the thoracic aorta (Langille and Jones, 1975).

When the pulse transit time occupies a considerable proportion of each cardiac cycle, then significant phase changes occur between the pressure and flow pulses at different arterial sites. In ducks, the time taken for the pulse to travel from the heart to the distal end of the abdominal aorta is around 20 ms, which is about 5–10% of the cardiac cycle (Langille and Jones, 1975). Consequently, there are marked changes in the waveform of the systemic pressure pulse as it travels through the arterial system (Figure 18.12; Langille and Jones, 1975; Ruiz-Feria et al., 2004). Both pulse amplitude and the contour of the pulse waveform are altered, with pulse pressure increasing by about 25%. This

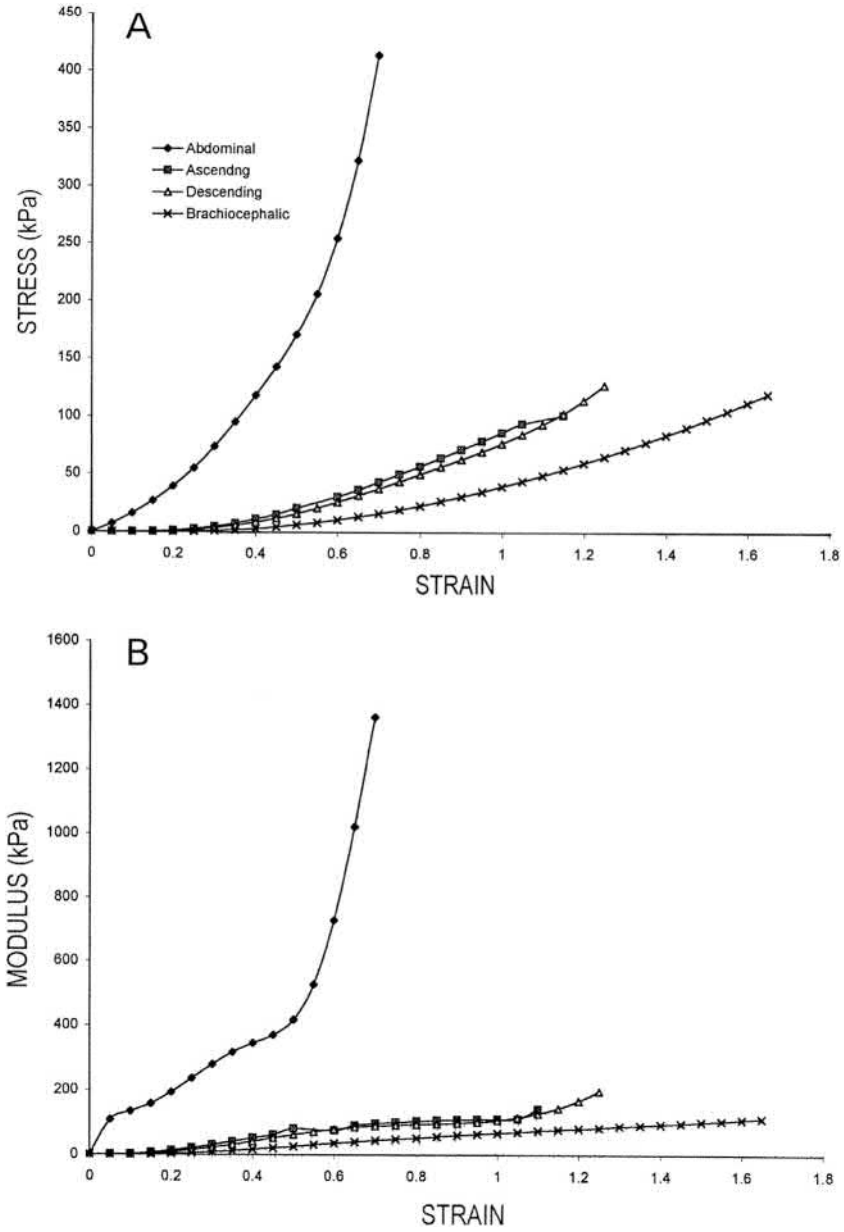

FIGURE 18.11 (A) Stress-strain curves for the blood vessel wall from four regions of the aorta in a duck (*Anas platyrhynchos*). (B) The static elastic modulus of these vessels derived from data in A. *From Braun and Jones (unpublished data).*

peaking of the pressure pulse results from a marked increase in the systolic portion with little change in the diastolic portion (Figure 18.12).

Peaking of the pressure pulse is due to wave transmission effects, primarily wave reflections. All forms of wave motion can be reflected by physical changes in the system they are traveling through. When such changes occur within the arterial system, incident pressure and flow waves will be reflected back toward the heart. These physical changes can be discrete discontinuities, such as those due to arterial branching (McDonald, 1974) or continuous variations in wall compliance due to an increase in arterial stiffening toward the periphery (Langille and Jones, 1975, 1976). However, the major reflecting site seems to be the terminal vascular bed. From this site, pressure and flow pulse waves are reflected back toward the heart to interfere, destructively or constructively, with the incident wave generated by cardiac contraction. This interference means that pressure and flow waves recorded simultaneously at any one site in the arterial system will be quite unlike those recorded at another. In a reflectionless system, pressure and flow pulses sampled at any given site should look similar to those recorded anywhere else in the system.

An essential question concerns the nature of the termination that the peripheral vascular beds present to outgoing

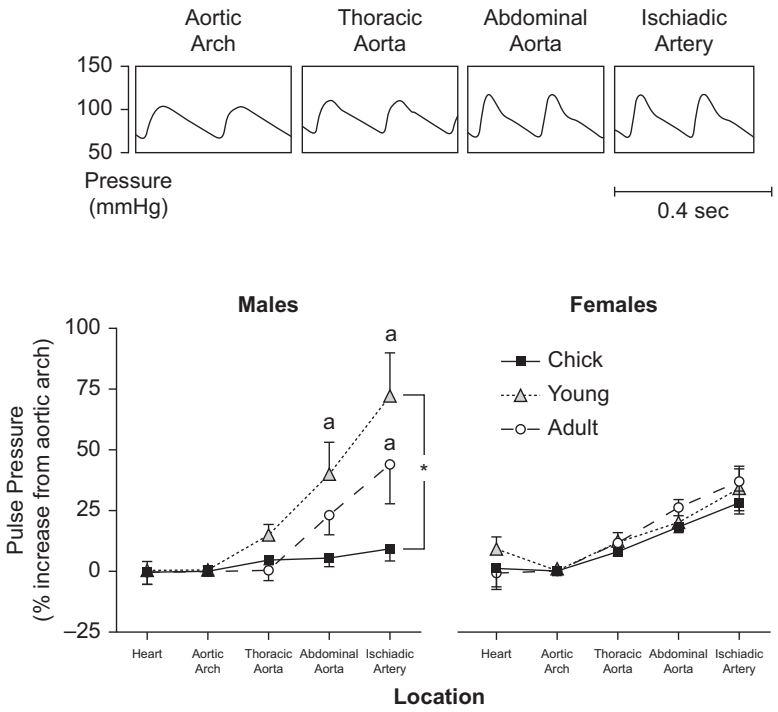

FIGURE 18.12 Pressure waves recorded simultaneous along the aortic arch, thoracic aorta, abdominal aorta, and the ischiadic artery. (A) Amplification and distortion of the pressure wave occurs during propagation along the aorta. (B) In all ages of chicken, pulse pressure increases with distance from the heart. *From Ruiz-Feria et al. (2004).*

pressure and flow waves. Peripheral beds are "closed" terminations if they present a relatively large impedance to pulsatile flow; they are "open" if they present a relatively low impedance. In higher vertebrates, reflections produce large oscillations in peripheral pressures that drive small oscillatory flows through the terminal vascular beds (Figure 18.12), indicating a high-terminal impedance; i.e., of the "closed" type. Hence, the pressure should be reflected at the closed end without a phase shift while, to satisfy the condition that high pressure oscillations are required to drive low-oscillatory flows through a high-terminal impedance, the reflected flow wave should be inverted. That is, the reflected wave should be 180 degrees out of phase with the incident wave. However, how much of the incident wave reaches the termination (because the incident pulse is attenuated, especially in the smaller vessels, as it propagates through the system) and how much of the reflected wave gets back to the heart (since its amplitude is also reduced by damping) is still a matter of speculation.

The reflection coefficient (that portion of the incident wave reflected by the terminal vascular beds) is extremely sensitive to the state of the peripheral vasculature. Under resting conditions, up to 80% of the incident wave may be reflected. Intense vasoconstriction occurring in ducks during forced diving or when voluntarily diving birds are trapped underwater and unable to surface causes 100% of the incident wave to be reflected. In contrast, vasodilatation of peripheral vascular beds, occurring during exercise or hemorrhage, may reduce the reflection coefficient to zero.

If the transit time of either pressure or flow waves through the arterial system becomes less than 5% of the cardiac cycle, then reflection effects on the shapes of these waves are not obvious. Nevertheless, reflections occur but they are diffuse, the pressure wave bouncing back and forth between the heart and periphery, until damped to extinction. In humans, atherosclerosis causes a loss of pressure pulse amplification as the pulse travels through the arterial system (O'Rourke et al., 1968); similar observations have been made in the turkey, *Meleagris* (Taylor, 1964), where atherosclerosis is very common (Ball et al., 1972; Manning and Middleton, 1972). Loss of pulse amplification in atherosclerosis results from a generalized stiffening of the major arteries, which acts to speed pulse wave propagation and thereby minimize wave transmission phenomena.

The hummingbird is among the smallest homeothermic vertebrates. Is it possible to predict the hemodynamics of the hummingbird from our knowledge of hemodynamics in the duck? Assuming pulse wave velocity is unaltered, then for similar conditions to hold in both hummingbird and duck, heart frequency rate (f_H) must increase in the same proportion as the linear dimension (L) of the animal decreases with reduction in body mass (M_b). For birds, the allometric equation relating f_H and M_b is $f_H = k_1 \bullet M_b^{-0.28}$ (Grubb, 1983; and see Section II,B), while $L = k_2 \bullet M_b^{-0.33}$ where k_1 and k_2 are constants.

According to this analysis, a hummingbird 400 times smaller than a duck will have a f_H 5.3 times higher but L will decrease nearly seven times. Even at the highest f_H

reported for the giant hummingbird (*Patagona gigas*) of 1020 beats min^{-1} (Lasiewski et al., 1967), pulse transit time as a proportion of the cardiac interval will be considerably less than that in the duck and reflection effects on pulse wave shapes will probably not be obvious (Jones, 1991).

18.4.2 Capillary beds

18.4.2.1 Gas exchange

Systemic capillaries form a vital functional interface between the blood and systemic tissues of birds. The diffusive pathway between erythrocytes in capillary blood and mitochondria in surrounding tissue represents the last in a series of resistances in the oxygen transport cascade from the lungs. Oxygen and carbon dioxide move between the systemic capillary blood and the surrounding tissue mitochondria by simple diffusion. Therefore, the diffusion distance from erythrocyte to mitochondrion and the partitioning of diffusion resistance along this route is of immense physiological interest. The concept of a capillary domain, a volume of tissue whose oxygen demands could potentially be satisfied by diffusion from one capillary, was first expounded by August Krogh in 1914 and remains a valuable concept in understanding gas exchange in muscle tissue (Krogh, 1919). A simple explanation of the factors important in capillary blood–tissue gas exchange, based on this model, is to be found in West (2008).

Studies on the systemic capillaries of birds, in particular those of flight muscle, have been dominated by two interesting themes: (1) the high workload of the avian pectoralis major muscle during flight, reflected in an increase in oxygen consumption of about five times that at rest (Butler et al., 1977), suggests that the functional anatomy of the pectoral muscle capillaries may reveal adaptations to both high tissue oxygen demand and mechanical tissue deformation during sarcomere shortening; and (2) some species fly at high altitudes (Hawkes et al., 2011; see Section 18.6). Therefore, there are specific adaptations in capillary density or geometric arrangement that facilitates the delivery of oxygen to the working pectoralis muscle in the face of a relatively low P_aO_2 (the pressure head for diffusion at the arterial end of systemic capillaries) caused by reduced atmospheric partial pressure of oxygen.

Three parameters may be considered in determining the capillarity of muscle. These are the number of capillaries per muscle fiber, the cross-sectional area of muscle fibers, and the geometrical arrangement of capillaries around each fiber (Snyder, 1990). Gray et al. (1983) found that sections of pure slow red muscle fibers from the anterior latissimus dorsi of chicken had 25% more capillaries per square millimeter than did sections of fast white fibers from the posterior part of this muscle. However, in six other species of birds ranging in mass from 11g to 6.2 kg, there was no significant correlation between fiber diameter and capillary number per fiber in slow red fibers and fast white fibers of the anterior and posterior latissimus dorsi respectively. Thus, tissue capillary density decreased in muscle with larger fibers. Snyder (1990) estimated the maximum diffusion distance from capillary to mitochondrion in slow red fibers and fast white fibers of the gastrocnemius muscle to be on average 18.4 and 36.5 μm, respectively. Torrella et al. (1999) found maximum diffusion distances ranging from 16.8 μm in the oxidative fibers of the mallard pectoralis to 34.4 μm in the glycolytic fibers of the mallard gastrocnemius. These are similar to the values obtained in mammals, suggesting that diffusion distance has been highly conserved in vertebrate evolution. Increasing the number of capillaries per fiber appears to produce diminishing returns such that beyond two capillaries per fiber there do not appear to be further measurable reductions in diffusion distance. In contrast to the situation in neonatal mammals, the capillary-to-fiber ratio in bird muscle appears to be fixed around hatching. Because the fibers hypertrophy during development, diffusion distances are shortest in newly hatched chicks—some 18 μm (Byers and Snyder, 1984).

The benefits conferred by reducing erythrocyte-to-mitochondrion diffusion distance depend on assumptions made about how the resistance to oxygen diffusion is distributed between source (blood) and sink (mitochondrion). It has been argued that the capillary-to-tissue interface represents the major resistance (Gayeski and Honig, 1986), in which case reducing the overall diffusion distance would be of limited effectiveness compared with increasing the area of this interface. However, compared with low-altitude birds, the mitochondria in flight muscle of the high-altitude flying bar-headed geese are found more toward the sarcolemma and capillaries (Scott et al., 2009).

Compared with the geometric arrangement in mammalian hindlimb muscle, there are a larger number of capillary branches running perpendicular to the long axis of muscle fibers in pigeon pectoralis muscle (Mathieu-Costello, 1991, Figure 18.13). These branch from capillaries running parallel to the long axes of the muscle fibers. The branch points move closer together as the pectoralis muscle shortens on the power stroke, but the perpendicular orientation of the branches to the long axis of the muscle fibers does not change appreciably during contraction. The short segments of capillary parallel to the muscle fiber between these branches bow as the muscle shortens, but do not become particularly tortuous. The branches perpendicular to the long axis of the muscle fibers run around the circumference of the fibers, and this arrangement together with their high density ensures that there is an effective envelope of capillary blood surrounding portions of the fibers. This results in very effective blood–tissue O_2

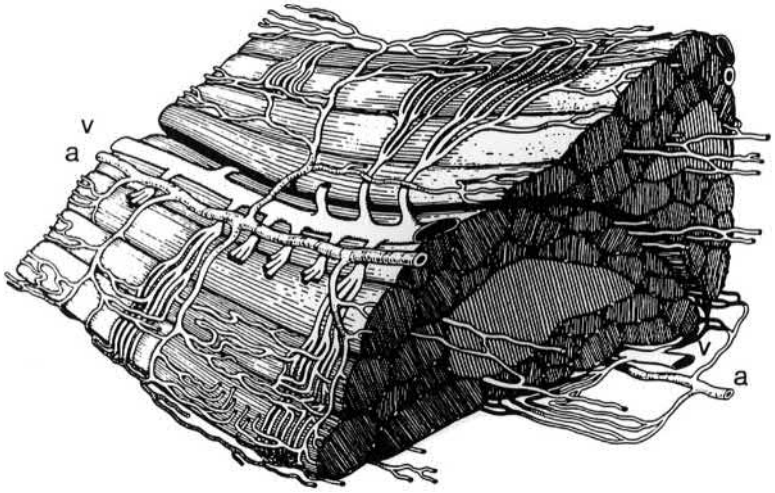

FIGURE 18.13 Schematic diagram illustrating the microvascular geometry in the pectoralis muscle of the pigeon. For clarity, the width and number of capillary branches running perpendicular to the long axis of the muscle fibers have been reduced. *a*, artery; *b*, vein. *From Mathieu-Costello et al. (1994).*

transfer (Ellis et al., 1983). Such an arrangement of capillary branches may compensate for the unfavorable rheological properties of avian blood compared with mammalian blood; these properties include relatively low-red cell deformability and a low-capillary hematocrit.

Flying hummingbirds have the highest mass-specific metabolic rate of any vertebrate, and hummingbird flight muscles have the highest oxygen demand of any vertebrate skeletal muscle. It would be expected, therefore, that the adaptations for effective gas exchange at the capillary level would be most obvious in these birds. These could include a reduced diffusion distance from the capillary to the mitochondria or possibly an increase in the capillary-to-fiber contact area. Increases in either of these factors would increase the flux of respiratory gases for a given drop in PO_2 across the capillary− mitochondrial diffusion distance. The ratio of capillary surface area to muscle fiber surface area is about twice as large in hummingbird flight muscle as in the rat soleus muscle, with similar mitochondrial density in the two muscles (Mathieu-Costello et al., 1992). Therefore, according to Fick's law, the rate of O_2 diffusion into the avian fiber would be about double that in the rat, all other factors being equal. This supports the idea that the large area of the capillary−muscle fiber interface in avian flight muscle plays an important role in enabling these muscles to maintain an extremely high-oxygen usage during flight. The respiration rates of muscle mitochondria in working hummingbird flight muscle are about double those in the locomotor muscles of mammals. Interestingly the size of this interface in the pectoralis muscle of the only actively flying mammal, the bat, is similar to that in hummingbird flight muscle.

The basic structure of the capillary network in the hummingbird is similar to that in pigeon flight muscle, although capillary density tends to be higher in the hummingbird. This results from the smaller cross-sectional area of the muscle fibers (one-half for aerobic and one 10th for glycolytic) rather than from a greater number of capillaries surrounding each fiber (Mathieu-Costello et al., 1992). The smaller cross-sectional area of fibers may be an adaptation to reduce the diffusion distance from capillary blood to the mitochondria. However, some experimental and theoretical evidence shows that the main drop in PO_2 occurs across the resistance offered by the capillary−fiber interface and PO_2 then declines more slowly, largely because of myoglobin facilitated diffusion (Honig et al., 1991). Thus, a large contact area between capillary and fiber is probably a more important factor in effective oxygen delivery than a short path between capillary and mitochondrion. This is particularly true for flight muscle in both birds and bats where fiber myoglobin content, and therefore the potential for facilitated diffusion, is high. Interestingly, a comparison of actively flying and sedentary pigeons showed little effect of flight conditioning on capillary−fiber relationships. Wild pigeons had a greater aerobic capacity than sedentary birds, achieved by a 30% greater cross-sectional area of aerobic fibers in the pectoralis together with a higher density of mitochondria. However, the capillary−fiber ratio was similar, as was capillary length−fiber volume at a given mitochondrial density (Mathieu-Costello et al., 1994). This finding is consistent with the results of Snyder and Coelho (1989), who caused hypertrophy of the right anterior latissimus dorsi of chickens by taping weights to the humerus. They found that the increased number of capillaries per fiber just matched fiber hypertrophy and concluded that muscle growth was the primary determinant of capillarity.

18.4.2.2 Microvascular fluid exchange

Capillary fluid balance is maintained by the dynamic interaction between hydrostatic and osmotic forces acting across the capillary wall, as first described by Starling over

100 years ago (Starling, 1896). Starling's original formulation has been modified and refined by Landis (1927) and Kedem and Katchalsky (1958), yielding the following equation to describe microvascular fluid exchange:

$$J_V = K_{FC}[(P_c - P_T) - \sigma_d(\pi_P - \pi_T)],$$

where J_V is net volume flow across the vascular wall, K_{FC} is capillary filtration coefficient, P_c and P_T are capillary and tissue fluid pressures, respectively, (π_P-π_T) is colloid osmotic pressure (COP) difference between plasma ($_P$) and tissue ($_T$), and σ_d is the osmotic reflection coefficient.

In the steady state, the capillary blood pressure opposes the blood COP to maintain tissue fluid balance. Blood pressure exceeds COP at the arteriolar end of the capillary and is usually below COP at the venous end. Fluids are secreted at the arteriolar and absorbed at the venous ends of the capillary. Hence, for adequate fluid exchange, COP pressure must offset capillary pressure, the latter reflecting arterial blood pressure (Landis and Pappenheimer, 1963). The value of COP is determined by the concentrations and species of blood proteins as well as by cations held in the plasma by the Donnan effect of the proteins (Guyton et al., 1975). However, it is now clear that microvascular fluid exchange is a dynamic process in which extravascular forces such as tissue fluid pressure, tissue COP, and the actual flow of lymph can influence transcapillary fluid movement (Taylor and Townsley, 1987). In addition to heterogeneity of Starling forces in different areas of the microvascular beds, there is also the possibility that heterogeneity of capillary membrane permeability will also contribute to differences between global and local values of the Starling pressures (Michel, 1997). In the light of recent knowledge, the simplistic steady state view of secretion at the arteriolar end of the capillary and absorption at the venous end of the capillary can only be regarded as a transient phenomenon at best.

Studies on avian species have contributed little to this discussion although microvascular fluid exchange in birds presents some unique and interesting features. For instance, in turkey and duck, the ratio of protein concentration in the interstitial fluid to that in the blood is much lower than the ratio in mammals (Hargens et al., 1974). Hargens et al. (1974) pointed out that the lower ratio in birds is correlated with a higher arterial blood pressure. Also, birds as a group seem to be highly resistant to hemorrhage, tolerating blood loss much better than mammals. Kovách and Balint (1969) have shown that increased hemorrhage tolerance becomes apparent only during prolonged bleeding because hemodilution continues in the pigeon through the period of blood loss, whereas in the rat no further hemodilution occurs after about 15−20 min of bleeding. Hemodilution is achieved by inflow of isotonic fluid with low-protein content.

The restoration of blood volume results from absorption of tissue fluid across the capillary walls due to reduced capillary pressure. This fall in capillary pressure could be brought about by an increase in the ratio between pre- and postcapillary resistances as well as by changes in arterial and venous pressures during hemorrhage. Resistance changes across the capillaries seem to be the most important factor in rapid restoration of blood volume in ducks. Blockade of α-adrenergic receptors eliminates vasoconstriction in the skeletal muscle, which forms the major reserve of tissue fluid and leads to a greatly retarded restoration of blood volume (Djojosugito et al., 1968). Djojosugito et al. (1968) attribute the difference in ability to restore blood volume after hemorrhage in ducks and cats to a very pronounced reflex vasoconstriction in duck skeletal musculature and to a capillary surface area in ducks three to five times that in the cat, a condition that increases the rate of absorption of fluid into the vascular system (Folkow et al., 1966).

Many birds, such as the emu and ostrich, have extremely long necks with the head being held a meter or more above the heart. Yet emu resting mean arterial blood pressure (Grubb et al., 1983) does not differ from that of a pigeon (Butler et al., 1977). An exceptionally high-blood pressure to overcome gravitational effects on circulation and to ensure flow to the head is not needed in these birds. In a fluid filled system, the gravitational pressure of blood in the veins will counterbalance the gravitational pressure in the arteries of the neck, much like the loop of a siphon. In other words, it is no more difficult for blood to flow uphill than downhill in a system of closed tubes like the circulation. Overall circulatory flow around the body occurs due to a pressure difference between the aorta and right atrium and it matters little what actual route the blood follows.

If pressure is measured in the cerebral circulation of a long-necked bird, this will be lower than that recorded in the aorta just outside the aortic valves by an amount sufficient to cause the required blood flow along the neck artery (a small difference) and by the gravitational effect due to the height the head is held above the heart. If the head is held one meter above the heart, pressure in the arteries of the head will be about 75 mmHg less than at the heart. Consequently, in the cranial capillary beds, it is now possible that the hydrostatic pressure will be lower than the COP of the blood, and fluid will be continuously removed from the interstitial spaces, with similar consequences as those following excessive alcohol consumption. As drunken ostriches are not a common sight, then countermeasures such as markedly increased arterial blood pressure, decreased arteriolar resistance, or reduced blood COP must be in effect. It is now possible to obtain a ready supply of long-necked ostriches and emus, and it is to be hoped that these countermeasures can be subjected to empirical investigation.

18.4.2.3 Distribution of blood flow at rest

The percentage of CO distributed at rest to different organs is closely related to their aerobic metabolic activity and their size. The distribution of CO is ultimately determined by the relative resistance of systemic vascular beds that are arranged in parallel throughout the body. Vascular resistance, in turn, is determined by a variety of hormonal, autoregulatory, and neural control mechanisms (see Section 18.5). Values obtained by different investigators for relative blood flow (% CO) to various organs differ widely, probably reflecting differences in experimental technique, species, and "resting" conditions. Nevertheless, it is apparent from the limited data available that the heart, liver, kidneys, and intestines receive relatively large percentages of the total CO (Figure 18.14). The avian brain appears to receive about 3% of CO, similar to the proportion of CO going to the brain in a small mammal like the rat at rest (Ollenberger and West, 1998).

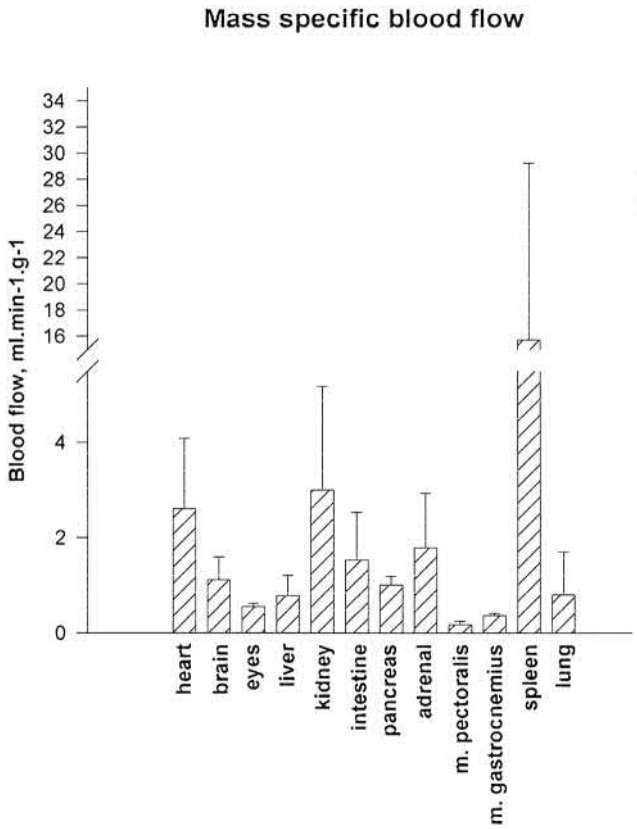

FIGURE 18.14 Mass-specific organ blood flow (mL $min^{-1}g^{-1}$) in birds at rest. Standard error bars are shown where appropriate. *Data are taken from Butler et al. (1988) (tufted duck), Duchamp and Barre (1993) (muscovy duckling), Faraci et al. (1985) (Pekin duck), Jones et al. (1979) (Pekin and mallard), Stephenson et al. (1994) (Pekin duck), and Wolfenson et al. (1978) (chicken).*

By far the highest resting blood flows thus far measured in any avian organ (about 16 mL $min^{-1}g^{-1}$ of wet tissue weight) are found in the spleen. This organ receives a disproportionately large percentage of total CO despite its small size. High-tissue flow rates also have been found in the mammalian spleen; a flow of some 12 mL $min^{-1}g^{-1}$ has been reported in conscious dogs (Grindlay et al., 1939). Such high rates are almost certainly related to the dual function of this organ: as a filter for aging erythrocytes, which are eliminated by the process of diapedesis; and as an organ of the reticuloendothelial system, in which the blood is cleaned by phagocytic reticuloendothelial cells as it passes through the splenic sinuses and pulp. Obviously, a high-flow rate is needed for this dual filtration role to be effective. In contrast to splenic blood flow, the rate of cerebral blood flow in birds is an order of magnitude less. Blood flow to the whole brain and to individual cerebral regions ranges from 0.43 to just over 2 mL min^{-1} g^{-1} under normoxic conditions, as shown in Figure 18.14 (Bickler and Julian 1992; Butler et al., 1988; Faraci and Fedde, 1986; Faraci et al., 1984; Grubb et al., 1977; Jones et al., 1979; Stephenson et al., 1994; Wolfenson et al., 1982a; Ellerby et al., 2005). Both the heart and kidneys have relatively high rates of mass-specific blood flow, reflecting the high oxygen demand of the contracting cardiac muscle and the activity of energy-dependent membrane pumps in renal tissue, respectively. Pectoral and gastrocnemius muscle, on the other hand, show relatively low-perfusion rates at rest (Figure 18.14).

18.4.3 Venous system

18.4.3.1 Functional development of venous system

The embryological development of the avian venous system follows a typical vertebrate pattern. At about the 15-somite stage of the avian embryo, paired cranial and caudal common cardinal veins develop from a vascular plexus in somatic mesoderm (Lillie, 1908; Sabin, 1917). The heart shifts caudally during embryonic development, and the cranial cardinal veins elongate to become the jugular veins. Subclavian veins, returning blood to the right side of the heart from the pectoral region and the wings, arise as tributaries of the caudal cardinal veins (Ede, 1964). The adult avian venous system cranial to the heart differs in detail from the mammalian pattern in that there are two cranial (superior) venae cavae. The right jugular vein is much larger in diameter than the left, and there is an anastomosis between the jugular veins at the base of the head, allowing some blood draining from the left side of the head and neck to return to the heart in the larger right jugular vein.

Development of the venous system caudal to the heart is primarily concerned with the formation of the physiologically important renal and hepatic portal venous circulations (see below). Subcardinal veins, which develop along with the embryonic kidney (mesonephros), initially provide renal drainage into the caudal cardinal veins. Eventually the anterior portions of the caudal cardinal veins disappear, and the subcardinals form a connection with the ductus venosus, this connection becoming the caudal vena cava. The liver develops around the ductus venosus, which subdivides into a capillary bed, forming the hepatic portal circulation. The cranial portion of the ductus venosus becomes the hepatic vein, and the caudal portion becomes the hepatic portal vein. Finally, the renal portal veins form a junction with the caudal vena cava via the common iliac veins, and the caudal subcardinal veins are replaced by the caudal renal veins.

18.4.3.2 Capacitance function

The walls of the veins in birds are, as in mammals, thinner than those of arteries so that venous distension depends on a positive transmural pressure gradient. The three basic components of blood vessel walls are present in veins: tunica intima, media, and externa. The tunica media is composed of circumferential smooth muscle fibers. In larger veins, elastic laminae appear in the tunica externa, which makes up most of the wall tissue. Veins near the heart are frequently invested with cardiac muscle fibers that are apparently functional. The caudal vena cava of the mallard can occasionally be seen to contract at the same frequency as the sinus venosus.

As in mammals, the avian venous system does not necessarily represent a passive conduit returning blood to the heart. The thin, distensible walls of veins mean that these vessels are relatively compliant compared with arteries. As applied to blood vessels, compliance is the ratio of the change in vessel volume (ΔV) resulting from a change in transmural distending pressure (ΔP):

$$\text{Compliance} = \Delta V/\Delta P.$$

In mammals, the entire vascular system has a compliance of about 3 mL blood (kg body mass mmHg)$^{-1}$. The compliance of the arterial vascular segment is only about 3% that of the venous segment (Rothe, 1983). Therefore, despite the smaller vascular pressures in the venous side of the circulation, at any one time about 60–80% of blood volume is contained in the veins. They are therefore referred to as capacitance vessels. The capacity of the venous circulation can change either passively by changes in transmural pressure or actively by changes in the contractile state of venous smooth muscle. A reduced transmural pressure and therefore a passive elastic recoil of compliant veins or a reduction in venous compliance by α-adrenergic mediated active contraction of smooth muscle in the venous walls (Section 18.5.2.4), would both serve to reduce venous capacitance. This transfers blood toward the heart. All other things being equal, this would increase atrial filling and therefore CO. The large veins of the domestic fowl are well innervated with adrenergic motor fibers (Bennett et al., 1974; Bennett and Malmfors, 1975b) and the density of this innervation suggests that there is active control of venous capacitance (Section 18.5.2.4). To date there are no physiological studies in birds analogous to those of adrenergic effects on venous capacitance function in mammals (Vanhoutte and Leusen, 1969).

18.4.3.3 Physiological role of veins in exercise and submersion

Venous pressure in pigeons flying in a low-speed wind tunnel increased to 2.5 mmHg from the resting value of 1.2 mmHg (Butler et al., 1977). CO increased 4.4 times during flight, mainly accomplished by an increase in heart rate at a constant stroke volume. In flight, the increased pressure gradient from the venous end of capillaries to the right ventricle increases venous return, right heart filling, and CO via the Frank–Starling relationship. Venous pressure is determined by the relationship between venous volume and compliance, which is reduced as venous smooth muscle contracts and the vein walls stiffen. In mammals, the venous beds of the liver, spleen, and skin act as blood reservoirs that can actively reduce capacitance during exercise, thereby increasing venous pressure and volume of venous return to the heart (Rothe, 1983). Whether these venous vascular beds also constrict during flight exercise in birds is currently unknown.

Active venoconstriction may also be important in the cardiovascular adjustments to diving in birds. Djojosugito et al. (1969) provided indirect evidence that venous pressure increased during diving in ducks and this was confirmed by Langille (1983), whose results suggested that this was due to active venoconstriction. In the latter study, cardiac stroke volume fell if central venous pressure was held constant during diving. This suggests that reduced ventricular contractility, caused by an increase in vagal motor nerve activity to the heart, is normally counteracted during diving by increased venoconstriction-induced filling via the Frank–Starling mechanism (see Section 18.5.3.2.3).

18.4.3.4 Renal portal system

In common with most other vertebrate groups, birds possess a renal portal circulation. Venous blood making its way back to the heart from the legs and the lower intestine of birds enters the kidneys through a renal portal system. Within the kidneys, this blood mixes with postglomerular

efferent arteriolar blood in peritubular sinuses that surround all nonmedullary nephron segments and eventually flows toward the renal veins. The physiological significance of the renal portal system is currently poorly understood. About 50−70% of total renal blood flow is contributed by the renal portal vein. However, this percentage is highly variable between animals and can change rapidly in the same individual for no apparent reason (Odlind, 1978). Part of the variability in flow can be attributed to the status of active, innervated renal portal valves within the iliac veins (Glahn et al., 1993). The valves receive dense reciprocal motor innervation from the parasympathetic and sympathetic divisions of the autonomic nervous system (see Section 18.5.2.3). Adrenergic stimulation produces relaxation of the smooth muscle of the valve, and cholinergic stimulation produces contraction. In contrast, smooth muscle of the renal portal vein itself shows a predominantly adrenergic contractile response typical of most vascular smooth muscle (Burrows et al., 1983). The distribution of vascular resistance within the portal system, governed by both the portal valve and the alternate, parallel venous pathways for blood returning to the heart determine the volume flow of renal portal blood.

There are several options for a "packet" of venous blood returning from the legs in the external iliac veins. (1) If the renal portal valve is open under the influence of sympathetic nervous system activation, blood can flow through the patent valve into the common iliac vein leading to the vena cava and directly back to the right side of the heart, bypassing the kidney. (2) If the valve is partially closed due to parasympathetic stimulation and resistance at the valve is high, blood can alternatively enter the renal portal system by flowing into the cranial and caudal portal veins. The portal veins are arranged functionally in parallel with the direct venous route provided by the common iliac vein and the vena cava. Blood entering the cranial and caudal portal systems eventually drains into the internal vertebral venous sinuses and caudal mesenteric veins, respectively, and makes its way back to the right side of the heart by this route. Anteriorly the caudal mesenteric vein connects with the portal system of the liver, providing another option for blood flow. The cranial and caudal portal veins are arranged in parallel with each other, and a "packet" of blood from the external iliac vein can enter one or the other, but not both. Therefore, variable fractions of venous blood derived from the legs, tail, and lower digestive tract can return directly to the right side of the heart (via the common iliac vein and vena cava) or enter the renal (cranial portal vein) or renal and hepatic portal systems (caudal portal vein). The overall pattern of venous flow will depend on the distribution of vascular resistance within the portal system.

Blood flowing from the renal glomeruli also enters the sinuses and contributes to pressure within them (Wideman et al., 1991), so any reduction in renal arterial pressure below the autoregulatory range should promote inflow to the sinuses from the portal veins. It is known that if the portal system is intact, birds can maintain total renal blood flow in the face of a fall in renal arterial pressure to 40−50 mmHg. Should arterial pressure fall, the glomerular vessels themselves can, by autoregulation, maintain glomerular filtration rate constant but only down to a minimum pressure of 70 mmHg (Wideman et al., 1992). The wider autoregulatory range for total renal blood flow may be due partially to an autoregulatory buffering effect by the portal system. Experimentally reducing portal blood flow leads to a narrowing of the range of arterial pressures over which total renal blood flow is maintained constant (Wideman et al., 1992). There are regional differences in renal blood flow, with the anterior part of the kidney apparently receiving a greater contribution from the portal veins. This suggests that renal arterial flow is normally lower in the anterior kidney.

The functional significance of the portal system in the environmental physiology of birds may be related to salt loading and dehydration. Dantzler (1989) has proposed that under these conditions, the adaptive response of the preglomerular arterial vessels of reptilian-type nephrons in the superficial renal cortex is to constrict, causing sustained cessation of filtration. Renal blood flow could be maintained under these conditions by a compensatory increase in portal flow, maintaining a nutritional blood supply to the cells of cortical nephrons (Wideman and Gregg, 1988).

18.4.4 Embryonic shunts

The circulatory system of the developing avian embryo has a number of vascular shunts found only during the embryonic stages (Dzialowski et al., 2011). These vascular shunts allow systemic venous return entering the right atria to bypass the nonventilated lungs, providing a right-to-left shunt. The first major embryonic shunt in embryonic birds is through a pair of ductus arteriosi (Dzialowski, 2018). In birds, these two embryonic vessels branch from the right and left pulmonary arteries and connect with the descending aorta (Figure 18.15). This arrangement is in contrast to the mammalian fetus that has a single ductus arteriosus connecting the pulmonary artery with the aorta in a position much closer to the heart and origin of these great vessels. During later stages of chicken embryonic development, White (1974) found that a large portion of venous return from the right anterior vena cava was shunted to the dorsal aorta through the paired ductus

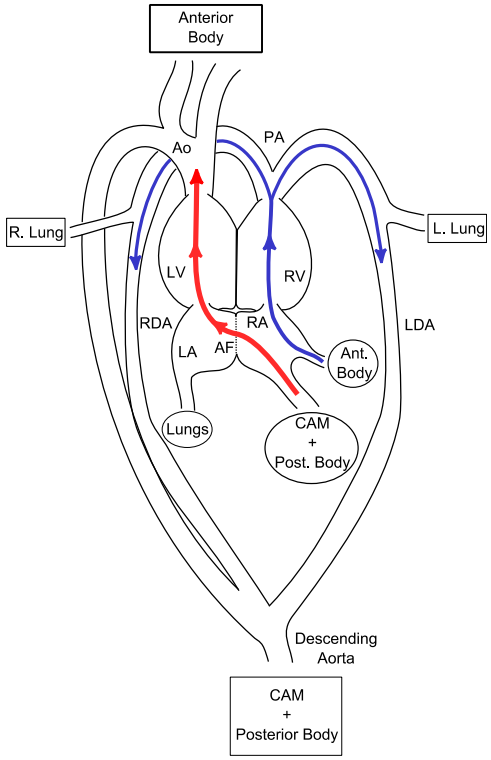

FIGURE 18.15 Embryonic circulation of a developing chicken embryo. The two right-to-left shunts are the left and right ductus arteriosi and the atrial foramina. *AF*, atrial foramina; Ao, aorta; *CAM*, chorioallantoic membrane; *LA*, left atrium; *LDA*, left ductus arteriosus; *LV*, left ventricle; *PA*, pulmonary artery; *RA*, right atrium; *RDA*, right ductus arteriosus; *RV*, right ventricle. *From Dzialowski et al. (2011).*

arteriosi. Tazawa and Takenka (1985) estimated that the ductus shunt 84% of right ventricular output to the dorsal aorta. A large fraction of dorsal aorta blood flow goes to the umbilical arteries and the embryonic gas exchanger, the chorioallantoic membrane (CAM). Patency of the mammalian ductus during the fetal stage is maintained in part by the relaxing influence of prostaglandins. Interestingly, there is no vasodilatory response to prostaglandins in the avian ductus (Dzialowski and Greyner, 2008; Greyner and Dzialowski, 2008). This difference could be due to the fact that the maternal placenta is the source of circulating prostaglandins in the mammalian fetus.

A second shunt exists between the two atria of the heart which functions like the mammalian fetal foramen ovale. The avian right and left atria are connected by perforations or foramina in the wall separating the atria. The right atrium receives posterior venous return, which includes oxygenated blood from the embryonic gas exchanger, the CAM (Figure 18.15; White, 1974). Tazawa and Takenka (1985) estimate that 60% of this posterior venous return flows through the atrial foramina resulting in a right-to-left shunt. This shunt ensures oxygenated blood flows to the anterior portion of the embryo through the carotid and subclavian arteries.

Both vascular shunts discussed above must close upon hatching to ensure adequate oxygenation of blood in the lungs. The ductus arteriosus is an oxygen sensitive blood vessel that constricts in response to increases in oxygen (Greyner and Dzialowski, 2008; Agren et al., 2007). In the embryonic chicken, the strength of oxygen-induced vasoconstriction increases during hatching. Using *in vitro* myography, the oxygen induced contractile strength of the ductus has been documented to triple between day 18 of incubation and external piping (Belanger et al., 2008). At the same time, arterial PO_2 in the hatching increases from around 30 −80 mmHg (Tazawa et al., 1983). By the time of hatching, the chicken ductus arteriosi are functionally closed (Belanger et al., 2008). Closure of the atrial foramina appears to be caused by pressure changes in the left atrium that occur with hatching (Jaffee, 1965). The perforations appear to behave in a valve-like manner, closing when the pressure in the left atrium becomes greater than the right atrium during hatching.

18.5 Control of the cardiovascular system

18.5.1 Control systems

Both the output of the heart and the resistance to blood flow in the vascular beds are subject to wide variations, depending on the activity type and intensity. CO varies in proportion to total body metabolic requirements while vascular resistance varies on a regional basis according to the blood flow requirements of different parts of the body. CO and resistance are both under the control of autoregulatory, humoral, hormonal, and neural influences. Arterial blood pressure is the product of CO and total peripheral resistance, and it is this pressure that produces the driving force to ensure adequate blood flow to the vascular beds. Blood pressure varies over a proportionally narrower range than either CO or peripheral resistance. Investigations of the regulation of cardiovascular function have been driven by the broad assumption that blood pressure is maintained within sensible limits to ensure adequate tissue perfusion in the face of the variations in CO and peripheral resistance imposed by changes in the external environment or in activity levels.

The cardiovascular system is controlled by several integrated mechanisms operating over time scales ranging from less than a second to months or longer. The most rapid adjustments in CO and peripheral resistance, which may occur within the span of a few heartbeats, are reflexogenic and primarily function to maintain short-term homeostasis and to affect rapid cardiovascular responses to changes in the internal or external environments. Autoregulatory mechanisms acting within vascular beds to modify blood flow as a result of local changes in metabolites or other

influences may operate on a time scale of seconds to minutes. Changes in humoral factors, such as levels of oxygen and carbon dioxide, pH, and metabolic products, can affect cardiovascular receptors or circulatory elements directly, producing changes in cardiac and vascular function directed toward correcting these disturbances on a time scale which may extend over long periods. An example of this is in birds undertaking extended migratory flights at high altitudes where inspired oxygen levels, and therefore blood oxygen levels, are much lower than at sea level. Circulating hormones can also affect both the peripheral circulation and the heart, and levels of many of these hormones in the blood may change depending on the activity state of the animal or on the time of year, as during molting or mating.

18.5.2 Control of peripheral blood flow

Contraction of smooth muscle in the walls of arteries provides the means for varying vessel caliber and the most effective location for altering blood flow by this means will be where the ratio of wall cross-sectional area to lumen area is maximal. The smallest arteries and arterioles possess the highest wall-to-lumen ratio, and it is here that the contraction of individual smooth muscle fibers, coordinated over the whole cross-section of the wall, will give the greatest change in resistance. The largest component of vascular resistance in the circulation is therefore set by the contractile tone of the smooth muscles in the walls of these vessels. Arterial smooth muscle tone is subject to modulation by several mechanisms: (1) intraluminal pressure changes, leading to mechanical autoregulation of blood flow; (2) humoral factors including oxygen tension, levels of local metabolites, extracellular ion concentrations, locally released vasoactive agents, and circulating hormones and vasoactive agents; as well as (3) transmitters released from autonomic nerve terminals.

Smooth muscle fibers in the walls of veins are also influenced by these factors, providing mechanisms for adjusting compliance of the venous walls and thus some control of the rate of blood return to the heart from the central venous pool. The influences of these regulatory factors on vascular function in birds are discussed in the following sections.

18.5.2.1 Mechanism of vascular reactivity

Regulation of smooth muscle contraction differs from skeletal muscle and involves activation of myosin light chain. Vascular smooth muscle contraction and relaxation are regulated by the phosphorylation and dephosphorylation state of the 20-kDa myosin light chain at Ser^{19} (MLC_{20}). In the phosphorylated state, smooth muscle contracts and produces vasoconstriction. Phosphorylation of MLC_{20} is mediated by Ca^{2+}-calmodulin-dependent MLC kinase (MLCK) that is activated by increased cytosolic Ca^{2+} due to Ca^{2+} release from sarcoplasmic reticulum stores and extracellular Ca^{2+} entry through membrane bound Ca^{2+} channels (Ganitkevich et al., 2002; Somlyo and Somlyo, 2003; Webb, 2003). Relaxation occurs when myosin light chain phosphatase (MLCP) dephosphorylates MLC_{20}. Several G-protein coupled receptor agonists inhibit MLCP leading to an increase in MLC phosphorylation and contraction without changes in cytoplasmic Ca^{2+} concentration. The result is an increase in Ca^{2+} sensitization (Ganitkevich et al., 2002; Somlyo and Somlyo, 2003; Webb, 2003).

Inhibition of MLCP involves a number of pathways in mammals. MLCP activity is inhibited by the RhoA/Rho-kinase pathway by phosphorylating the MLCP regulatory subunit, MYPT1. The second mechanism of MLCP inhibition in mammals is through phosphorylation of the smooth muscle-specific MLCP inhibitor protein CPI-17 (PKC potentiated inhibitor protein-17 kDa; Webb, 2003). Under physiological situations, Ca^{2+} release by the SR, Ca^{2+} influx, and Ca^{2+} sensitization act together to regulate vascular smooth muscle contraction. Their role in regulating avian smooth muscle contraction has only begun to be examined. The protein CPI-17 may not be involved in avian smooth muscle contraction as it was not detected in chicken smooth muscles from aorta, mesenteric artery, gizzard, or small intestine (Kitazawa et al., 2004). Additionally, there is contraction in response to PKC activation in adult chicken arteries (Kitazawa et al., 2004). In contrast, the Rho kinase inhibitors Y-27632 and hydroxyfasudil produced marked impairment of vessel contractions in femoral artery and ductus arteriosus of chicken embryos and emu (Zoer et al., 2010; Greyner and Dzialowski, 2008; Dzialowski and Greyner, 2008). The role of these pathways in avian vascular smooth muscle contraction needs further study.

18.5.2.2 Autoregulation

Vascular tone within a region of the circulation can be defined as the average level of contraction of smooth muscle fibers in the blood vessel walls within that region. At a steady intraluminal pressure and in the absence of extrinsic influences, spontaneous contractions of individual smooth muscles occur at an intrinsic rate. In resistance vessels, the smooth muscle cells are arranged at a right angle to, or on a shallow helix around, the axis of flow. The time-averaged tension generated by their contraction, in balance with the intraluminal pressure, will set vessel caliber and thus blood flow. An increase in arterial pressure will distend the vessel wall, increasing the caliber of the vessel and therefore reducing resistance to flow. As a result, blood flow through the vessel will increase. This wall distension also increases the frequency of contraction of the smooth muscles, and this increased vasomotion will

then act to reduce the caliber of the vessel, increasing its resistance and restoring blood flow toward its original level. Conversely, a reduction in pressure will reduce wall tension, resulting in a decrease in the rate of smooth muscle spontaneous activity. This leads to vasodilation and an increase in blood flow to offset the effects of reduced perfusion pressure. These myogenic changes in vascular caliber thus provide a mechanism to autoregulate blood flow around a preferred level in the face of variations in tissue perfusion pressure. In most vascular beds, autoregulatory mechanisms are probably limited to the modulation of local blood flow to ensure even blood distribution, as, for example, in the kidney where this mechanism is important in maintaining glomerular flow rate in the face of alterations in arterial blood pressure. Throughout the body local pressure-induced autoregulation will interact with locally released vasoactive agents and with neurogenically mediated vasomotion resulting from activation of autonomic reflexes to provide balanced adjustments in regional peripheral blood flow.

18.5.2.3 Humoral factors

Three broad classes of humoral factors affect blood flow in the peripheral vasculature. One class includes chemical factors such as PO_2, PCO_2, lactic acid and other metabolic byproducts, electrolyte concentrations, and pH that act directly on myocytes. The second class of factors consists of vasoactive agents typically released from local vascular endothelial cells. This group includes nitric oxide (NO), H_2S, prostaglandins, and endothelin (ET); these factors act on smooth muscle cells by receptor-mediated mechanisms. The third class includes circulating vasoactive agents, also acting via receptor-coupled mechanisms to modify smooth muscle contraction.

18.5.2.3.1 Chemical factors

If the metabolic rate of a tissue increases, for example, in skeletal muscle during exercise, regional blood flow will increase due partly to local vasodilation of resistance vessels and precapillary sphincters induced by an increase in the concentration of lactic acid and CO_2 and a fall in pH. Vasodilation under these circumstances is produced by alterations in Ca^{2+} flux and handling at the level of Ca^{2+} channels (Wray and Smith, 2004) and secondarily by direct chemical effects on the contractile apparatus of the vascular myocytes (Mellander and Johansson, 1968). Vasodilation may be further enhanced if local PO_2 falls or concentrations of extracellular ions such as K^+ increase. The resulting increase in blood flow is called functional hyperemia and serves to accelerate oxygen delivery to the muscle and to increase the clearance rate of tissue metabolites. During exercise, central arterial pressure may also rise (Butler, 1991; Saunders and Fedde, 1994) and local myogenic autoregulation would, as outlined in Section 18.5.2.2, attempt to limit the rise in blood flow; however in tissue operating at a high-metabolic rate, this mechanism is to a large extent overridden by local chemical vasodilatory influences. Vasodilation due to tissue hypoxia and buildup of metabolites also occurs during periods of ischemia, for example, when blood flow to a vascular bed is occluded as shown in Figure 18.16. Upon release of the occlusion, blood flow rises transiently to several times the preocclusion rate, with the increase in flow proportional to the duration of the occlusion. This reactive hyperemia acts to restore tissue oxygen levels and to remove metabolic products accumulating during the period of occlusion. Local hypoxia also reduces the vasoconstrictor effects of norepinephrine (NE) applied exogenously or released from sympathetic nerve terminals in avian arteries *in vitro*

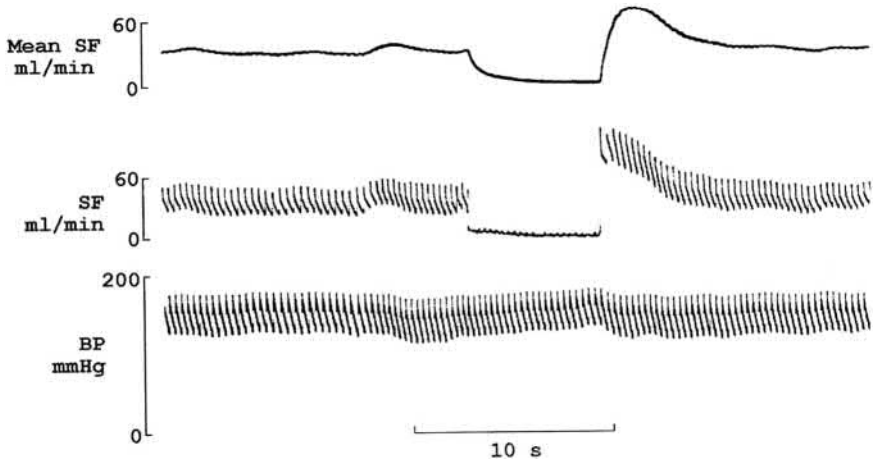

FIGURE 18.16 Change in pulsatile (SF) and mean (mean SF) blood flow in the sciatic artery of a duck in response to arterial occlusion. The period of occlusion is marked by zero flow. *BP*, arterial blood pressure. Note the hyperemia after the period of occlusion and the subsequent rapid return to the preocclusion flow rate with minimal change in pressure. *From Jones and Johansen (1972).*

(Gooden, 1980; and see Section 18.5.2.3.2), and might therefore be expected to reduce the *in vivo* effectiveness of vasoconstriction mediated neurogenically or by circulating catecholamines in support of the hyperemic response. Local hypercapnia also produces vasodilation, and in the hind limb vascular bed of the duck has an even stronger effect than hypoxia in inhibiting neurogenic or catecholamine induced vasoconstriction (Lacombe and Jones, 1990).

18.5.2.3.2 Locally released vasoactive agents

The endothelium-derived relaxing factor NO is a small, rapidly diffusible molecule released by enzymatic cleavage of L-arginine from vascular endothelial cells of vertebrates (see Donald et al., 2015 for review). In vertebrates, this molecule exerts a powerful vasodilatory effect by relaxing precontracted vascular smooth muscle. The release of NO as a result of acetylcholine (ACh) stimulation of endothelial cells provides part of the explanation for the vasodilatory effects of ACh in the circulation (Furchgott and Zawadzki, 1980). In the *in vitro* aorta and small resistance arteries, ACh acting at muscarinic receptors on endothelial cells provokes release of NO which produces local vasodilation (Hasegawa and Nishimura, 1991; Jarrett et al., 2013). NO can produce relaxation through activation of soluble guanylate cyclase which increases levels of cGMP. This activates a cGMP-dependent protein kinase that decreases intracellular Ca^{2+} levels leading to vasodilation.

Another factor provoking release of NO from avian vascular endothelial cells is angiotensin II (AII); the vasodilation produced by NO release has been proposed to cause the transient depressor effects on arterial blood pressure observed in some birds immediately after systemic injection of AII (Stallone et al., 1990; Hasegawa et al., 1993; Takei and Hasegawa, 1990). Mechanical stimuli such as flow-induced shear stress (see Section 18.5.2) can also elicit release of NO from endothelial cells in the vasculature of birds. This effect is well known in mammalian endothelial cells (Balligand et al., 2009) and, given that blood flow rates in birds are generally higher than those in mammals of comparable body size, such a mechanism could provide additional local adjustment of the degree of vasodilation within a vascular bed to match the immediate flow requirements of that bed.

Other locally released vasoactive agents, such as ET and H_2S, are important in adjusting regional blood flow in birds. ET is the most potent vasoconstrictor known in mammals (Inagami et al., 1995). In chickens, ET has been shown to produce contractions of femoral, mesenteric, and pulmonary arteries in the embryonic stages (Moonen and Villamor, 2011; Villamor et al., 2002) and pulmonary arteries from adults (Martinez-Lemus et al., 2003). In hatchling chickens, ET produced contraction at low doses and relaxation at higher doses (Moonen and Villamor, 2011). Moonen and Villamor (2011) suggest that contraction may be mediated by ET_A receptors and at higher doses ET_B receptors. Receptors for this peptide have been demonstrated on avian cardiac myocytes, and their activation causes an increase in contractile force (Kohmoto et al., 1993; Hassanpour et al., 2010). Recently, locally released H_2S has been found to be a potential important in regulating vessel tone. It has been found to produce both vasorelaxation and vasoconstriction in systemic vessels. Vasorelaxation by H_2S is proposed to act through K_{ATP} channels and cGMP levels in a fashion similar to NO (biological roles are reviewed in Kolluru et al., 2013). H_2S-mediated vasoconstriction in the mammalian aorta is mediated by downregulation of cAMP (Lim et al., 2008). In the one study looking at the pekin duck aorta, H_2S constricted the unstimulated aorta and produced a weak relaxation followed by constriction in the preconstricted vessel (Dombkowski et al., 2005). As with many of these pathways, further research is needed to determine the potential role of H_2S in regulating vessel tone in the avian system.

18.5.2.3.3 Circulating agents

Circulating catecholamines have powerful effects on all elements of the circulation in birds. The catecholamines epinephrine (EPI) and NE are released into the circulation from adrenal chromaffin cells and have direct effects on vascular smooth muscle. Significant amounts of NE are also released into the circulation by activation of the sympathetic nervous system (discussed in Section 18.5.2.4 below). A number of peptides which have vasoactive effects on mammalian vasculature are also present in avian plasma, but the specific actions of most of these peptides on the avian vasculature have not been investigated in detail. Of these peptides, the most extensively studied in birds with respect to vasomotion are AII and avian antidiuretic hormone (ADH).

Circulating NE levels in conscious ducks and fowl at rest are in the range of 3−5 nM (Lacombe and Jones, 1990; Kamimura et al., 1995), while the resting plasma level of EPI is about half the value for NE (Lacombe and Jones, 1990), as illustrated in Figure 18.17A. EPI appears to be released solely from the adrenal glands since removal of these glands eliminates EPI from the plasma (Lacombe and Jones, 1990). The loss of adrenal glands does not, however, markedly affect the resting level of circulating NE which must therefore be due to spill over into the plasma of NE released from sympathetic nerve terminals by autonomic efferent activity. Circulating levels of both EPI and NE vary under different physiological conditions. For example, plasma catecholamines can increase by factors ranging from 2 to greater than 1000 in ducks during involuntary submersion, with end dive levels being proportional to dive length as shown in Figure 18.17B (Huang et al., 1974; Hudson and Jones, 1982; Lacombe and Jones, 1990).

Both NE and EPI produce vasomotion in avian vascular smooth muscle, acting via α- and β-adrenergic receptors (Bolton and Bowman, 1969). NE, injected intravenously into conscious ducks, produces vasoconstriction throughout

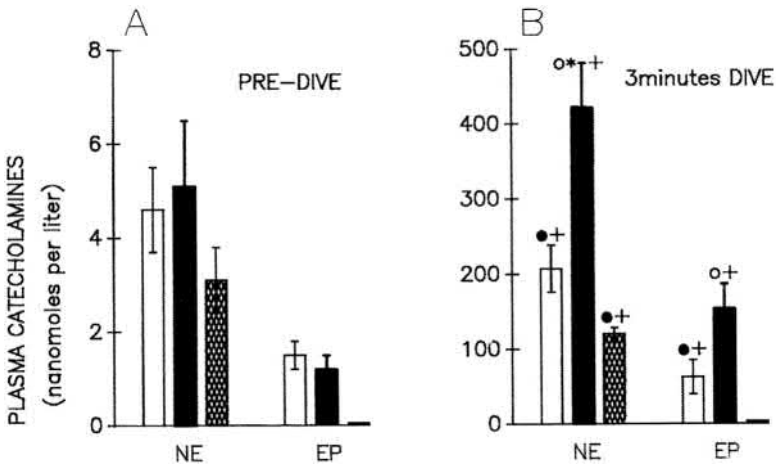

FIGURE 18.17 Plasma levels of norepinephrine (NE) and epinephrine (EPI) in intact (*open bars*), sham-operated (*filled bars*), and adrenalectomized (*cross-hatched bars*) ducks (A) before and (B) at the 3-min point during forced submergence. The *open circles* indicate significant differences from intact ducks; *closed circles*, differences from sham-operated animals; *asterisks*, differences from adrenalectomized animals; *plus signs*, differences from predive value. Adrenalectomy eliminated EPI but not NE from the plasma. Note ordinate scale change in (B). *From Lacombe and Jones (1990).*

the body. This vasoconstriction causes an increase in blood pressure produced by the collective effect of increases in resistance to flow in individual vascular beds in the body, illustrated in Figure 18.18, by increased resistance in the hind limb vascular bed. These vascular responses to NE are primarily mediated by α-adrenergic receptors (Butler et al., 1986; Wilson and West, 1986; Bolton and Bowman, 1969). Activation of α-adrenoceptors (ARs) on vascular smooth muscle acts through second-messenger systems to mobilize internal Ca^{2+}stores and to open membrane calcium channels, thus increasing intracellular Ca^{2+} concentration and activating the actin−myosin contractile apparatus (see Webb, 2003, Section 18.5.2.1). NE can also have a vasodilatory effect on the vasculature of birds, mediated through β-adrenergic receptors; however, this effect is only apparent systemically after pharmacological blockade of α-ARs (Butler et al., 1986). β-adrenergic vasodilation in the avian vasculature also works by activating intracellular second messengers, converting the actin−myosin complex to an inactive form to promote relaxation. Combined α- and β-adrenergic blockade appears to eliminate all direct effects of NE on bird vascular

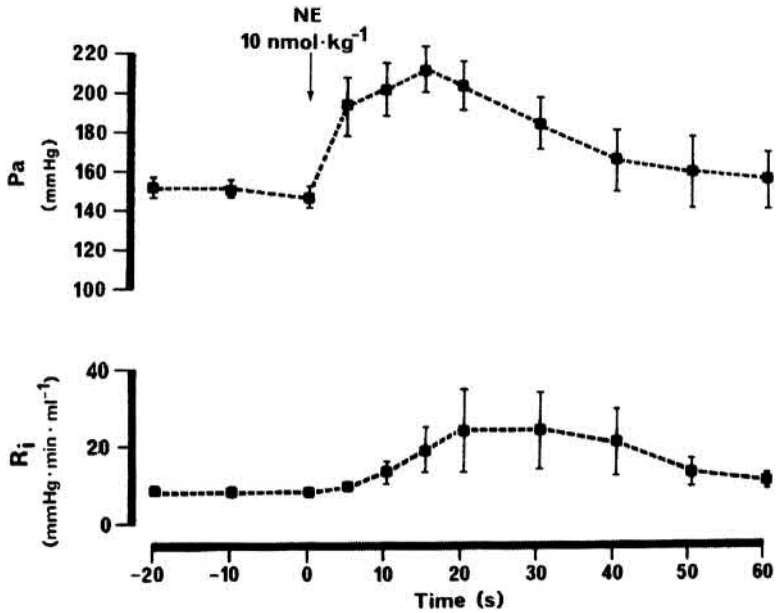

FIGURE 18.18 Responses of mean arterial blood pressure (P_a) and resistance to blood flow in the ischiatic artery (R_i) of an adult duck to a bolus intravenous injection of norepinephrine (NE, at *arrow*). The R_i values for each data point were calculated from the corresponding Pa and ischiatic blood flow values. *From Wilson and West (1986).*

smooth muscle. The overall effects of NE on peripheral resistance therefore depend on the relative abundance of α- and β-receptors in individual vascular beds. EPI also acts on ARs of vascular smooth muscle but binds to α-receptors with a higher affinity than to the β subtype, so exerts a stronger vasoconstrictive effect for the same receptor density than does NE.

Avian AII is similar to the corresponding mammalian peptide in its structure and in the biochemical pathway of its production (see reviews by Wilson, 1989; Henderson and Deacon, 1993). Renin, released from the juxtaglomerular cells lining glomerular afferent arterioles in the kidney, produces the peptide angiotensin I by hydrolysis of angiotensinogen, a plasma α-globulin. Angiotensin-converting enzyme, which has been identified in circulating plasma and fixed in the walls of blood vessels in birds (Henderson and Deacon, 1993), then cleaves angiotensin I to produce AII. A number of stimuli such as systemic hypotension, hypovolemia, decreased plasma or distal tubule ion concentrations (particularly Na^+), or the activation of juxtaglomerular β-receptors causes renin to be secreted into the plasma. This promotes an increase in circulating angiotensin I, making it available for conversion to AII. AII affects circulatory function at several levels, evoking responses in both the central nervous system and the peripheral vasculature. These responses are aimed at the conservation of water and electrolytes in order to counter the original rennin secreting stimulus.

Within the central nervous system, AII acts on receptors of some hypothalamic neurons to promote drinking behavior (Evered and Fitzsimmons, 1981). In the periphery exogenous or endogenous AII produces either an increase in systemic arterial blood pressure or a biphasic hypotensive−hypertensive response, depending on species. In ducks (Wilson and West, 1986; Butler et al., 1986) and pigeons (Evered and Fitzsimmons, 1981), systemic injections of AII produced dose-dependent increases in arterial blood pressure. Butler et al. (1986) and Wilson and West (1986) proposed that this response was due to vasoconstriction resulting from AII-mediated release of NE from sympathetic nerve terminals and enhanced EPI and NE release from the adrenal glands; in their experiments, α- and β-adrenergic blockade eliminated the pressor effects of AII injection. Indeed, Moore et al. (1981) maintained that AII has no direct vasoconstrictor effects on arterial smooth muscle in the fowl and Wilson (1989), in a review of the rennin−angiotensin system in birds, ascribes AII-induced vasoconstriction entirely to the effects of elevated catecholamine secretion.

In fowl and quail systemic circuits, AII injections produce a rapid, transient hypotension followed by a prolonged rise in arterial blood pressure (Nakamura et al., 1982; Takei and Hasegawa, 1990). The hypertensive phase of this response is mediated by adrenergic mechanisms, as in the duck and pigeon, but the transient hypotensive phase appears to be an indirect AII effect on vascular endothelial cells, working via the local release of NO from these cells as described in Section 18.5.2.3.2. *In vitro* isometric tension studies on the abdominal aorta of embryonic and adult chicken have shown AII induces a vasorelaxation that is inhibited by L-NAME and eliminated by removal of endothelium (Nishimura et al., 2003).

Arginine vasotocin (AVT), released from the posterior pituitary into the circulation under conditions of osmotic or hypovolemic challenge, is the avian homolog of the mammalian ADH arginine vasopressin. However, the effects on avian vasculature of increased endogenous AVT levels after salt loading or hemorrhage are not well understood, nor are the vasomotor effects of systemic AVT injections. In mammals, arginine vasopressin produces vasoconstriction in systemic arterioles and in glomerular afferent arterioles, both serving to facilitate antidiuresis. In birds, AVT also induces vasoconstriction of afferent glomerular arterioles (see Braun, 1982 for review), but its effects on the rest of the circulation are controversial. Several studies have reported no cardiovascular consequences of AVT injection, maintaining that the avian vasculature is not sensitive to this peptide even at doses many times greater than "physiological" levels (Simon-Oppermann et al., 1988; Robinzon et al., 1988). In contrast, Wilson and West (1986) in ducks and chickens and Brummermann and Simon (1990) in ducks found that systemic injections of AVT produced hypotension accompanied by tachycardia. The latter authors proposed that AVT directly relaxes vascular smooth muscle, producing a fall in arterial blood pressure which then evokes a baroreflex-mediated tachycardia. However, Robinzon et al. (1993) found in fowl that the direction of AVT-mediated vascular responses depended on the dose and method of application. Low doses given slowly by intravenous infusion produced hypertension similar to the mammalian response to arginine vasopressin, while bolus intravenous doses produced the hypotensive responses reported in other avian studies. Robinzon et al. (1993) therefore proposed that AVT acts primarily via modulation of vascular caliber but that the degree and direction of vasomotion was not uniform in beds throughout the body. While there appears to be consensus that AVT does have direct vascular effects in birds, the understanding of its specific actions must await further studies on isolated vascular beds *in situ* and on blood vessels *in vitro*.

18.5.2.4 Neural control

All parts of the systemic and pulmonary vascular trees, except capillary beds, are innervated by the autonomic nervous system. This innervation constitutes the final common pathway for rapid and flexible control by the

central nervous system of regional distribution of CO. Autonomic outflow to the vasculature is governed by a variety of reflexogenic inputs from visceral or somatic receptors relayed through brainstem and spinal cord pathways, and is also subject to influences originating at suprabulbar levels of the central nervous system. However, the degree of vasomotion produced in any region of the vasculature for a given intensity of autonomic drive will depend on the densities of effector terminals and postjunctional receptors in that region.

The location of autonomic terminals within the vascular wall is different in arteries and veins. Nerve fibers and terminals in the walls of arteries are, with some exceptions, limited to the tunica adventitia, extending as far as the outer elastic lamina marking the border between the adventitia and the tunica media (Bennett and Malmfors, 1970). In this respect, the innervation pattern of avian arteries is similar to that in mammals (see Hirst and Edwards, 1989 for a review of mammalian arterial innervation). In contrast to the arterial innervation pattern, nerve fibers and terminals in avian systemic veins are commonly opposed to smooth muscle in the tunica media, as well as being located in the adventitia (Bennet and Malmfors, 1970) and in this regard similar to mammals (see Shepherd and Vanhoutte, 1975 for a review of the innervation of mammalian veins).

In addition to intramural nerve fibers and terminals, large and small nerves course over the outer surfaces of both arteries and veins, and some vessels are completely surrounded by plexi of nerve fibers. Furthermore, throughout the body, nerves generally accompany blood vessels, running parallel with the vessels to form neurovascular bundles. These close associations between blood vessels and nerves have an important consequence for experimental investigations of neurogenic vasomotion. In assessing the effectiveness of neural control of vascular resistance in particular beds, electrical stimulation of autonomic nerves is commonly employed. However, some neural pathways to these beds may be interrupted if supply vessels to the beds are manipulated or sectioned (for example, to insert a blood flow probe) between the stimulus site and the expected site of vasomotion.

18.5.2.4.1 Systemic arterial innervation

The aorta from its origin to the junction with the celiac artery, the proximal brachiocephalic trunks, and the most proximal parts of the common carotid arteries are elastic vessels (see Section 18.4.1.2), having relatively little smooth muscle and thus a correspondingly sparse vasomotor innervation (Bennett and Malmfors, 1970; Bennett, 1971). The aorta, especially close to its root and adjacent to the root of the pulmonary trunk, has numerous small cells in the adventitia which contain catecholamines (Bennett, 1971). These cells occur singly or in clusters, appear to be similar to amine-containing cells of the carotid body, and are innervated by branches of the vagus nerve. While these cells may be a source of locally released catecholamines, it has also been suggested that these cells may constitute chemoreceptive "aortic bodies" (Bennett, 1971; Tcheng and Fu, 1962) similar to those found at the homologous site in mammals. In addition, the adventitia of the aortic arch is innervated by afferent vagal fibers with nerve terminals transducing wall stretch and thus signaling an index of central arterial blood pressure; these constitute the only systemic arterial baroreceptors in birds (Jones, 1973).

The transition from elastic to muscular wall structure occurs in the arterial tree distal to the branching points of major distribution arteries from the great vessels. This transition also marks an increase in the density of innervation of the arterial wall. In some arteries such as the ischiatic, varicose fibers can be seen in the media as well as at the medial−adventitial border (Bennett and Malmfors, 1970). Of the large muscular arteries, the common carotids appear to be the most heavily innervated (Bennett and Malmfors, 1970). Given that these arteries convey the majority of blood flow to the avian brain, this density of innervation possibly reflects a requirement for greater autonomic control of cephalic blood flow than in other beds. Vasomotor innervation of the smaller branches of arteries within individual vascular beds supplied by the large arteries has not been systematically described but in all beds muscular arterioles, which constitute the resistance vessels responsible for 70% to 80% of total peripheral resistance, are densely innervated (Folkow et al., 1966; Bennett and Malmfors, 1970).

The density of innervation of different regions of the arterial tree is variable among bird species, and this variation has important consequences for differences in regional neurogenic control of blood flow among species. Large arteries supplying hindlimb muscles in ducks, for instance, are more densely innervated than those in turkeys, and this difference is correlated functionally with an enhanced capability in the duck to generate and maintain neurogenically mediated intense peripheral vasoconstriction (Folkow et al., 1966). These authors proposed that this was a general physiological adaptation in diving birds, enabling the redistribution of blood flow away from those peripheral vascular beds able to withstand periods of ischemia and toward the central circulation, thus conserving blood oxygen for ischemia sensitive heart and brain tissue.

Electrical stimulation of the sympathetic innervation of a vascular bed evokes increases in vascular resistance in that bed, mimicking the effect of elevated vasoconstrictor outflow from the central nervous system. As illustrated in Figure 18.19, graded increases in stimulation frequency evoke proportionally larger increases in peripheral resistance in the hind limb vascular bed of the duck, producing a maximal increase of up to seven times the prestimulus

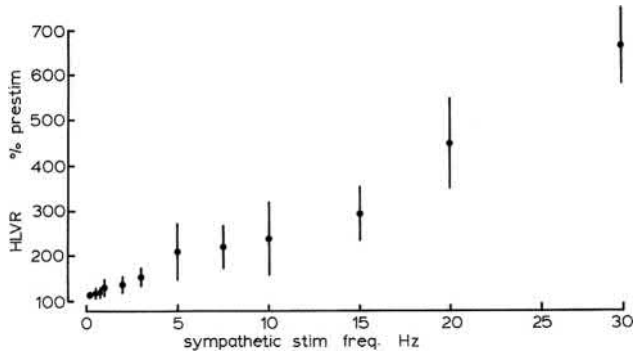

FIGURE 18.19 Relationship between frequency of electrical stimulation of the sympathetic innervation of the hind limb and vascular resistance of this bed (HLVR) in a duck. HLVR for each data point was calculated from the corresponding arterial pressure and ischiatic artery flow. Increases in HLVR are expressed in percentages relative to the prestimulus value. *From Smith (unpublished data).*

resistance value at a stimulation frequency of 30 Hz. In contrast, stimulus frequencies of less than 10 Hz are required to produce a maximal increase in resistance in the cat hind limb (Folkow, 1952). The hind limb vascular bed in the duck thus requires a greater degree of sympathetic drive than that of the cat to achieve the same order of increase in resistance to flow. This may reflect differences in the distribution of sympathetic terminals to the arteries in this bed in the two species. In support of this, Bennett and Malmfors (1970) noted that the pattern of adrenergic innervation of small intramuscular arteries in birds was not markedly different from that in mammals, but observed a higher terminal density in larger arteries of birds relative to mammals.

Some regions of the avian arterial vasculature have specialized wall structures and unusual innervation patterns, possibly reflecting enhanced capabilities for regional control of blood flow. The anterior mesenteric artery in several species of birds has, in addition to the normal circular smooth muscle in the media, an outer layer of longitudinal smooth muscle in the adventitia (Bolton, 1969; Bennett and Malmfors, 1970; Bell, 1969; Ball et al., 1963; see Section 18.4.1.2). Adrenergic fibers and varicose terminals are found at the adventitial−medial border in this as in other arteries, but these elements also extend into the longitudinal muscle itself, aligned in the direction of the muscle fibers. Longitudinal muscle of this vessel also receives cholinergic innervation (Bolton, 1967; Bell, 1969; Bennett and Malmfors, 1970), although this does not extend to the inner circular muscle (Bell, 1969). Adrenergic nerve stimulation produces contraction of the circular muscle which is mimicked and blocked by α-adrenergic agonists and antagonists, respectively (Bolton, 1969; Bell, 1969; Gooden, 1980). The longitudinal muscle is, however, relaxed by adrenergic nerve stimulation, acting through β-adrenergic receptors (Bolton, 1969; Bell, 1969). Stimulation of cholinergic nerve fibers in an *in vitro* preparation of a segment of the vessel caused the longitudinal muscle to contract, shortening the whole segment. This did not, however, markedly affect resistance to flow through the vessel but in the shortened state adrenergic vasoconstrictor responses of the circular muscle were found to be exaggerated (Bell, 1969). The cholinergic innervation of longitudinal muscle has thus been proposed to potentiate adrenergically mediated control of blood flow, possibly as an adaptation for rapid adjustment of intestinal blood flow during stress (Bell, 1969). The fact that increased sympathetic drive to this vessel has a relaxing effect on the longitudinal muscle as well as a constricting effect on the circular muscle would facilitate the effects of cholinergic input in shortening the vessel segment. Cholinergic input may also help adjust blood flow more precisely when the length of the anterior mesenteric artery changes during gross intestinal movements associated with digestion.

Coronary arteries also possess an outer coat of longitudinal muscle but adrenergic innervation of this muscle layer is very sparse. In these arteries, the majority of adrenergic nerve fibers and terminals are found at the adventitiomedial border, as in other arteries (Bennett and Malmfors, 1970). There are no reports of cholinergic innervation of the coronary arteries of birds. Cerebral arteries are, however, dually innervated by adrenergic and cholinergic fibers (Tagawa et al., 1979). Adrenergic varicosities are located in the adventitia near the border with the media throughout the cerebral circulation, in common with most other arteries of the body. Cholinergic fibers as well are located in the tunica adventitia but occur less frequently than adrenergic terminals (Tagawa et al., 1979). It is presumed that, since cerebral arteries have no smooth muscle in the adventitia, neurotransmitters released from both types of terminals diffuse into the media to act on muscle fibers there. Tagawa et al. (1979) also reported that, as in mammals, some of the cholinergic innervation of avian cerebral arteries appears to originate from central neurons, especially in the diencephalon, as well as from peripheral neurons. Studies in mammals have shown that the functional significance of reflexogenic vasomotion in overall control of cerebral blood flow is relatively minor compared with neurogenic control of blood flow in other vascular beds in the body; intracerebral blood distribution is influenced mainly by local and possibly circulating humoral factors (Kontos, 1981). This is likely to be true also in birds; Stephenson et al. (1994) estimated that neurogenic contributions to changes in cerebral blood flow in ducks during diving were minor.

18.5.2.4.2 Systemic venous innervation

Large veins in birds are more densely innervated than those in mammals. The density of noradrenergic innervation of the chicken caudal vena cava is graded, increasing in portions of the vessel more distal to the heart (Bennett, 1974; Bennett et al., 1974). The caudal vena cava has an outer coat of longitudinal muscle as well as an inner circular layer and both layers receive adrenergic innervation, with the orientation of the terminals and fibers following the direction of the muscle fibers in each layer (Bennett, 1974). There is also a sparse cholinergic innervation of this vessel. The superior venae cavae also have two muscle layers, with a similar adrenergic innervation pattern to the caudal vena cava (Bennett and Malmfors, 1970). The walls of the pectoral, subclavian, celiac, and jugular veins contain both circular and longitudinal smooth muscle. The innervation of these vessels is through a plexus of varicose fibers and terminals located primarily between the inner and outer muscle layers.

Functionally, adrenergic vasomotion appears to be preeminent in veins. Vasomotion of the caudal vena cava and other major veins is mediated primarily by α-adrenergic receptors producing vasoconstriction when activated; no functional β-adrenergic receptors are present (Bennett and Malmfors, 1974). Responses of venous smooth muscle to cholinergic nerve stimulation are weak and variable and probably do not contribute directly to neurogenic control of wall compliance; however, ACh released from cholinergic nerve terminals can modulate the release of NE from local adrenergic nerve terminals and thus may provide fine adjustments of adrenergically generated venomotor tone.

Sympathetically mediated contraction of smooth muscle in the major veins serves to decrease wall compliance and vessel diameter, thus providing a reflexogenic mechanism for reducing the volume of the central venous pool and increasing return of blood to the heart, as discussed in Section 18.4.3.2. Langille (1983) proposed that reflexogenic venoconstriction was responsible for the increased central venous pressure observed in ducks during involuntary submersion. This response may function to aid venous return to the heart to help maintain stroke volume in the face of a reduction in cardiac contractility which may develop during diving (Djojosugito et al., 1969; Langille, 1983).

The renal portal valves, located bilaterally where the external iliac veins join the junction of the caudal vena cava with the caudal renal veins, are unique to birds. These valves are in the form of sphincters of smooth muscle which can close off the direct route for blood flow from the external iliac veins to the caudal vena cava. Closure increases renal portal blood flow, venous blood from the external iliac vein being then partially redirected into the renal capillaries and thence to the caudal vena cava, as discussed in Section 18.4.3.4. The renal portal valve is heavily innervated by both adrenergic and cholinergic nerve fibers (Akester and Mann, 1969; Bennett and Malmfors, 1970) with reciprocal effects on the smooth muscle of the valve. Adrenergic nerve stimulation and sympathomimetic agents induce relaxation, mediated by β-adrenergic receptors, while cholinergic nerve stimulation and cholinomimetic agents produce contraction via muscarinic receptors (Bennett and Malmfors, 1975a; Sturkie et al., 1978). The importance of this valve in the control of venous blood distribution in the renal portal system has been the subject of some debate (Akester, 1967, Section 18.4.3.4). Functional studies of the avian kidney *in situ* by Glahn et al. (1993) have shown that the status of the renal portal valve affects total renal blood flow by altering the amount of flow in the renal portal system. In conditions of lowered arterial blood pressure in which renal arterial perfusion is below the range of autoregulation of glomerular blood flow, closure of the renal portal valve raises renal portal blood flow to compensate total renal blood flow (Glahn et al., 1993). Neural control of the renal portal valve may thus form a component of the suite of reflexogenic responses to hypotension or hypovolemia.

18.5.2.4.3 Pulmonary vessel innervation

Adrenergic innervation of the pulmonary artery in the fowl consists mostly of fibers with few varicose nerve terminals. Fibers and nerve terminals form a plexus at the adventitiomedial border of the artery, with some projections into the circular smooth muscle of the media. There is also smooth muscle oriented longitudinally in the adventitia, but innervation of this is very sparse (Bennett and Malmfors, 1970; Bennett, 1971). Some intrapulmonary arterial branches have dense adrenergic plexi occurring in short segments along their length (Bennett and Malmfors, 1970), which may help to redistribute blood flow to selected gas exchange areas within the lung to optimize local ventilation–perfusion ratios (Hebb, 1969).

The pulmonary veins proximal to the left atrium are very densely innervated with adrenergic nerve fibers and terminals, the density of this innervation being markedly greater than in the pulmonary arteries (Bennett, 1971). Abundant terminal varicosities and nerve fibers are located in a plexus at the adventitiomedial border, with some penetration into the media (Bennett, 1971; Bennett and Malmfors, 1970). There is also longitudinal smooth muscle present in the adventitia, with adrenergic terminals between the muscle fibers (Bennett, 1971; Bennett and Malmfors, 1970). The density of innervation of the longitudinal smooth muscle is reduced close to the left atrium, increasing distally along the vessel until the bifurcation to the lungs. At this junction, there is an abrupt decrease in density of innervation of the entire vessel wall, and within the lungs, the major

branches of the pulmonary veins are very sparsely innervated. Smaller branches of these vessels appear to have no innervation (Bennett, 1971).

18.5.2.4.4 Autonomic pathways

The cell bodies of adrenergic postganglionic vasoconstrictor neurons innervating the vasculature are located in paired paravertebral ganglion chains, in prevertebral ganglia and, in some cases, in small ganglia scattered throughout the viscera. Cells in the superior cervical ganglion (representing a fusion of the two most cranial cervical ganglia) innervate blood vessels of the head, including those of the salt and salivary glands, via cephalic extensions anastomosing with several cranial nerves (Bennett, 1974). In birds, pairs of sympathetic ganglia are associated with the cervical vertebrae, and cells in these ganglia innervate blood vessels of the neck. The presence of cervical paravertebral ganglia in birds constitutes a major difference in the organization of the sympathetic nervous system between this vertebrate group and mammals. In the caudal part of the neck, in the thorax, and in the wings of birds, the vasculature is innervated by neurons in the thoracic paravertebral ganglion chain. Sympathetic fibers reach wing vessels primarily through the brachial plexus. Some thoracic postganglionic neurons also contribute sympathetic fibers to the greater splanchnic nerves innervating anterior abdominal viscera via the celiac plexus (Bennet, 1971).

Vertebrae of the lumbar, sacral, and coccygeal spine are fused to form the synsacrum in birds. The paravertebral ganglion chains from each side in this region are fused in the midline at about the level of the sixth coccygeal segment in avian species so far examined, and this combined sympathetic trunk continues caudally to the pygostyle (Pick, 1970; Akester, 1979; Benzo, 1986). Axons from postganglionic neurons in this part of the sympathetic nervous system innervate abdominal and pelvic viscera via the lesser splanchnic nerves and aortic plexus, the hypogastric plexus, the pelvic plexus, and the cloacal plexus. Some sympathetic postganglionic somata are also located in prevertebral ganglia within these plexi. In addition, lumbosacral sympathetic neurons contribute vasoconstrictor axons to the hind limbs via the lumbosacral plexus (Benzo, 1986; Bennett, 1974).

Sympathetic preganglionic cell bodies that synapse on the postganglionic vasoconstrictor neurons are located in and near a bilateral column of neurons, the column of Terni, in the gray matter near the central canal of the spinal cord (see Section 18.5.3.2). All preganglionic axons innervating postganglionic neurons in the cervical sympathetic chain exit the spinal cord through ventral nerve roots of cranial thoracic segments; there are apparently no connections between the cervical spinal nerve roots and the sympathetic ganglia in the neck (Bennett, 1974; Akester, 1979; Pick, 1970). Although no detailed analysis has been done of the segmental locations of spinal preganglionic neurons projecting to postganglionic vasoconstrictor neurons innervating the thoracic, abdominal, pelvic, and limb regions, it is likely that the locations of these neurons follow the mammalian plan. That is, axons of preganglionic neurons in a particular spinal segment emerge from the cord in the ventral root of that segment to innervate postganglionic neurons in ganglia at that level or within one or two segments rostral or caudal to the exit site (see Gabella, 1976 for review).

Parasympathetic postganglionic neurons innervating the vascular smooth muscle of such organs as salt glands and salivary glands in the head of birds are located in autonomic ganglia near or embedded in the organs (Ash et al., 1969). Cell bodies of preganglionic neurons innervating parasympathetic postganglionic vasodilator neurons associated with structures in the head are located in the oculomotor, facial, glossopharyngeal, and vagal nuclei in the brainstem and course to peripheral ganglia via the respective cranial nerves associated with these nuclei (Akester, 1979). Postganglionic cholinergic nerve fibers innervating arteries and veins of the body originate from the somata of neurons located in plexuses associated with blood vessels themselves or, for vessels of the abdominal viscera, in prevertebral ganglia containing a mixture of adrenergic and cholinergic postganglionic neurons (Bennett and Malmfors, 1970; Bennett, 1974). The location of cells of origin of preganglionic axons innervating the postganglionic neurons producing vasodilation in the viscera and skeletal muscle has not been determined in detail. However, in birds, the parasympathetic outflow is organized in cranial and sacral tracts as it is in mammals. It would therefore be expected that preganglionic neuronal somata responsible for vasodilation in thoracic and anterior abdominal viscera and skeletal muscle in the upper part of the body are located in medullary vagal motor nuclei, with their axons running to postganglionic neurons via the vagus nerves. Similarly, vasodilation of posterior abdominal and pelvic viscera and skeletal muscle of the lower part of the body is likely to be mediated by preganglionic neurons with their somata located at sacral levels of the spinal cord and their axons innervating postganglionic neurons via the abdominal and pelvic autonomic nerves.

18.5.3 Control of the heart

18.5.3.1 Catecholamine effects on the heart

Both NE and EPI are present in circulating plasma of birds (see Section 18.5.2.3.3), and these amines have cardiac effects which include an increase in the rate of pacemaker depolarization (DeSantis et al., 1975; Bolton and Bowman, 1969) and augmented force of myocardial contraction (DeSantis et al., 1975; Bennett and Malmfors, 1974;

Bolton, 1967; Bolton and Bowman, 1969). In isolated heart preparations and in myocardial strips *in vitro*, NE has been found to be as effective as, or more potent than, equimolar EPI in producing inotropic and chronotropic augmentation. This is in marked contrast to the condition in the mammalian heart, in which EPI is the more potent stimulant (Gilman et al., 1990). In whole-animal experiments on birds, intravenously injected boluses of NE and EPI augment CO by transiently increasing both rate and force of contraction, contributing along with peripheral vasoconstriction to catecholamine-mediated hypertension (Wilson and Butler, 1983; Wilson and West, 1986; Bolton and Bowman, 1969; Butler et al., 1986). In the avian as in the mammalian heart, catecholamines appear to act primarily via β-adrenergic receptors on myocardial and P-cells (Bolton and Bowman, 1969; Butler et al., 1986; Bolton, 1967).

18.5.3.2 Neural control

18.5.3.2.1 Sympathetic innervation

18.5.3.2.1.1 Anatomy Postganglionic sympathetic nerve fibers arising from neuronal somata extrinsic to the heart form part of an intracardiac nerve plexus distributed throughout all four cardiac chambers. The adrenergic innervation of the proximal part of the venae cavae appears to be continuous with the intracardiac plexus associated with the right atrium (Bennett and Malmfors, 1970). Sympathetic nerve fibers form a network over the epicardial surface of the right atrium, with some fibers penetrating into the thin atrial wall to lie adjacent to bundles of myocardial cells and others passing through the wall to the subendocardium (Smith, 1971a). The overall appearance of the plexus is that of a three-dimensional latticework of fibers extending from the epicardium through the wall to the subendocardium, with varying concentrations of smooth nonvaricose and varicose nerve fibers and nerve endings in different regions of the atrial myocardium.

Bennett and Malmfors (1970) reported that the most densely innervated region of the heart was the external wall of the right atrium; furthermore, within this area the region adjacent to the confluence of the venae cavae with the wall contained the highest density of fibers and terminals. These authors referred to this area as the "sinuatrial node," presumably by analogy with the corresponding sharply defined SA node of the mammalian heart. There is, however, some evidence that the cells in the primary pacemaker site in the right atrium of the bird heart may have a functional organization different from that in the mammalian heart, in the area of the junction of the sinus venosus with the SA valves (Moore, 1965; and see Section 18.2.3.3). These valves are present in birds but are only represented by a vestigial flap in mammals. A large number of the nerve fibers in this area of the avian heart were varicose, running among the myocardial cells and aligned with the longitudinal axes of these cells. Another area with a high density of adrenergic terminals was in the right atrial wall near the AV border, an area corresponding to the AV node (Bennett and Malmfors, 1970, Section 18.2.3.3). Many nerve varicosities were also associated with blood vessels in the right atrial wall.

Bogusch (1974) reported in the fowl that the specialized cells of the pacemaker areas and conducting system in the right atrium are well innervated by nerve fibers with frequent varicosities and some bare nerve endings. In contrast, Yousuf (1965) found no investment of nerve fibers into the SA node region and few in the AV node in the sparrow heart. This disparity could be due to a species difference or to a relative lack of sensitivity of the silver stain; in any case, neither technique is neurotransmitter specific nor as sensitive as the amine fluorescence technique. Full details of the sympathetic innervation of the conducting tissues of the right atrium are still not clear.

The right AV valve has a central layer of connective tissue between two layers of cardiac muscle (Section 18.2.1.4), and nerve bundles have been observed in association with this connective tissue (Smith, 1971a). In this study, several general nerve stains as well as a cholinesterase-specific stain were used, but unfortunately no details are given regarding the specificity of staining of the valvular innervation. However, Bennett and Malmfors (1970) have shown that this valve is innervated by adrenergic nerve fibers with few terminals, arranged in a loose plexus in the leaves of the valve. These observations suggest the existence of some degree of neural control of this valve, possibly by both sympathetic and parasympathetic limbs of the autonomic nervous system.

Adrenergic innervation in the left atrium is less dense than in the right atrium, but denser than the ventricles. Adrenergic fibers and terminals of the left atrial cardiac plexus, while distributed in a three-dimensional pattern similar to that in the right atrium, appear to be more evenly spread throughout the left atrial wall with little variation in density. In addition, the interatrial septum also receives adrenergic innervation as an extension of the epicardial plexus (Akester, 1971; Akester et al., 1969). The distal portion of the left AV valve has a fibroelastic structure, while more proximally cardiac muscle is associated with the fibrous skeleton (Section 18.2.1.4). Smith (1971a) has described a fine network of nerve fibers, continuous with the left atrial subendocardial plexus, investing the fibroelastic portion of this valve; no mention of an innervation of the muscular portion of the valve was made in this study. The staining technique used was again not transmitter specific, so the left AV valve may be under sympathetic or parasympathetic influence, or both, or the

innervation observed may be afferent. However, regarding the latter possibility, Smith (1971a) states that no simple or specialized nerve endings typical of sensory receptors were observed in or near the left AV valve.

The avian ventricles are relatively sparsely innervated compared with the atria, but even so are more densely innervated than are the ventricles mammalian hearts (Smith, 1971b). Akester et al. (1969) and Akester (1971) reported adrenergic innervation of the interventricular septum, and Bennett and Malmfors (1970) observed that innervation of this region was denser than that in the rest of the ventricle walls. While these authors did not determine the intraseptal targets of innervation, it is possible that some of these axons may innervate intraseptal Purkinje cells since bare nerve endings have been observed close to these cells (Akester, 1971). Regarding the innervation of the pulmonary and aortic valves, Smith (1971a) reported that they were sparsely innervated in comparison with the left AV valve. Fibers in the pulmonary and aortic valves comprise a plexus arranged to form a widely spaced lattice in the basal parts of the valve leaflets.

In birds, the sympathetic cardiac nerves arise from the most rostral ganglia of the thorax and the most caudal cervical ganglia, but there is some variation in detail among different accounts (see Cabot and Cohen, 1980 for summary). Macdonald and Cohen (1970) and Cabot and Cohen (1980) describe the right sympathetic cardiac nerve in the pigeon as a single trunk formed by the anastomosis of postganglionic nerves arising from the three most caudal cervical ganglia. These ganglia are associated with spinal nerves contributing to the brachial plexus; the most caudal ganglion of this group is thus associated with the last spinal segment contributing to the brachial plexus. This description closely follows that of Malinovsky (1962) in the pigeon. In the chicken, however, the origin of the right cardiac sympathetic nerve is limited to the first thoracic paravertebral ganglion (as defined by its location caudal to the head of the first rib; Pick, 1970; Tummons and Sturkie, 1969).

There has been some controversy over the nomenclature of avian sympathetic ganglia. Birds have a sympathetic ganglion associated with each cervical spinal segment (Gabella, 1976; Pick, 1970) and this observation, as well as variations in opinion on numeration of the ribs in the bird, has made it difficult to be precise about the terminology for the most caudal ganglion contributing to the cardiac nerve. Malinovsky (1962) holds that this is the first thoracic ganglion, since it lies between the heads of the first and second ribs. However, Macdonald and Cohen (1970) have sided with earlier authors in noting that the first rib should not be considered to mark the first thoracic segment since this rib is reduced in size and does not form part of the ribcage proper. As Cabot and Cohen (1980) have pointed out, the issue of terminology is not critical when considering functional aspects of cardiac sympathetic outflow to the bird heart, but may become important when attempting to draw conclusions about the homology of this pathway with the sympathetic innervation of the mammalian heart. Mammals have no cervical paravertebral ganglion chain, and postganglionic neurons efferent to the heart in this vertebrate class are located in the middle cervical ganglion and the stellate ganglion, the latter being formed by the condensation of the caudal cervical and first thoracic ganglia. This arrangement has no parallel in birds.

Regardless of the number of ganglia contributing to the right cardiac sympathetic nerve, the course of this nerve to the heart appears to follow the same general pattern in all avian species so far examined. The nerve courses toward the heart in conjunction with a small vertebral vein arising from the lateral aspect of the vertebral column between the last cervical and first thoracic spinal segments. The vessel and nerve merge with the apical pleura of the lung and run together between the pleural fascia. At the ventral surface of the pleura close to the junction of the vertebral vein with the superior vena cava, the nerve turns caudally along the vena cava toward the heart, there forming two rami. The medial ramus divides further and its fascicles enter the cardiac plexus to distribute within the right atrial wall. The lateral ramus joins the right vagus nerve in the vicinity of the right pulmonary artery (Pick, 1970; Cabot and Cohen, 1977a, 1980; Tummons and Sturkie, 1969; Macdonald and Cohen, 1970; Malinovsky, 1962). The ganglionic origin of the left sympathetic cardiac nerve is similar to that of the right, arising in the chicken from paravertebral ganglion 14 (first thoracic) and in the pigeon by anastomosis of postganglionic branches from ganglia 12, 13, and 14 (Cabot and Cohen, 1980). In the pigeon, the largest branch contributing to the left sympathetic cardiac nerve arises from ganglion 14, as on the right side. In its path to the heart, the left cardiac nerve in the pigeon divides into two or more fascicles which run in parallel for a short distance then recombine before reaching the superior vena cava. This nerve ramifies again as it runs caudally along the vena cava toward the heart and the individual rami merge with the cardiac plexus of the left atrium.

The general locations of the cells of origin of the sympathetic postganglionic axons to the avian heart and the intraspinal locations of the cardiac sympathetic preganglionic neurons have been worked out in greatest detail in the pigeon by Cabot and Cohen and their coworkers. These workers used a combination of degeneration, neuroanatomical tracing, and electrophysiological stimulation and recording techniques. Macdonald and Cohen (1970) undertook a series of neuronal degeneration studies in order to determine the ganglionic distribution of the somata of postganglionic neurons supplying axons to the heart. After section of the right or left cardiac sympathetic nerve in the thorax, the greatest number of degenerating neurons was

found in ganglion 14, with lesser numbers in ganglia 12 and 13; no degenerating neurons were observed in ganglia rostral or caudal to this level. Postganglionic cells of origin of fibers in the cardiac sympathetic nerves were thus located bilaterally in the same sympathetic ganglia which give rise to the postganglionic nerves constituting the cardiac nerve. In experiments in which the ganglia themselves or the interganglionic sympathetic trunks were stimulated electrically, Macdonald and Cohen (1970) obtained positive cardiac chronotropic responses of short latency from ganglia 12 to 16, occasional longer-latency responses from ganglia 17 and 18, and none from ganglia caudal to 18. Experiments in which stimulation of ganglia was combined with sections of the sympathetic trunk above and below the stimulation site confirmed these results. These data were interpreted to mean that preganglionic axons originating in the spinal cord as caudally as the 16th segment converged on postganglionic cardiac neurons in ganglia 12 to 14. The longer latency cardiac responses to stimulation of ganglia 17 and 18 were attributed to sympathetic activation of the adrenal glands and consequent release of catecholamines into the bloodstream; nerves arising from ganglia 17 and 18 were observed to join the splanchnic nerves, branches of which innervate the adrenal medulla.

Avian sympathetic preganglionic neurons innervating the heart are located in the same area of the spinal gray matter as those innervating the blood vessels, near the midline dorsal and lateral to the central canal, and extending rostrocaudally throughout segments 14 to 21. Most of the preganglionic neurons are confined to a distinct cell column in the midline, the column of Terni, a nucleus peculiar to the avian spinal cord (Huber, 1936; Cabot and Cohen, 1980). This cell column is the probable homolog of the mammalian intermediolateral cell column. Leonard and Cohen (1975), in a study of the cytoarchitecture of the pigeon spinal gray, reported that the rostral and caudal extents of this nucleus were indistinct due to small clusters of cells which extended into the regions between segments 13 and 14 and caudal to segment 21. Neurotracer studies using retrograde transport of horseradish peroxidase have shown that spinal preganglionic neurons efferent to the postganglionic cells in ganglion 14 of the pigeon are present from the caudal portion of segment 14 to the rostral part of segment 17 (Cabot and Cohen, 1977a). This finding provides strong anatomical support for the earlier conclusion of Macdonald and Cohen (1970), reached on the basis of functional and degeneration studies, that spinal preganglionic inputs to cardiac postganglionic neurons originate from segments 14 to 16, with some inputs possibly coming from segment 17.

The protocol used by Cabot and Cohen (1977a) did not label cardiac preganglionic neurons specifically. The region of the spinal cord containing cardiac preganglionic motor neurons has been more precisely mapped by Cabot et al. (1991b). In this study, preganglionic neurons associated with ganglion 14 in the pigeon were labeled using fragment C of tetanus toxin (a nontoxic moiety which is retrogradely transported by axons), injected into sympathetic ganglion 14. These experiments confirmed the location of preganglionic neurons in the column of Terni and also demonstrated labeling of neurons lateral to this nucleus (Figure 18.20) in an area which, in the mammalian spinal cord, is occupied by sympathetic preganglionic neurons of the nucleus intercalatus spinalis (Petras and Cummings, 1972), a term that Cabot et al. (1991b) have applied to the corresponding area in the pigeon spinal cord. Their results show that cardiac neurons in the spinal cord are not confined to the column of Terni. Few studies have labeled cardiac postganglionic sympathetic neurons in the bird which innervate specific regions of the heart. This will be required to determine the intraspinal locations of groups of neurons controlling cardiac functions such as rate and contractility.

The descending projections from higher centers in the central nervous system to sympathetic preganglionic neurons controlling the heart have not in general been delineated in birds. However, Cabot et al. (1982), in a series of anatomical studies in the pigeon, determined that the overall pattern of projections to spinal preganglionic neurons is very similar to that found in mammals, and this anatomical data corroborate the results of earlier brain stimulation studies in the bird. In particular, Cabot et al. (1982) have shown anatomically that avian preganglionic

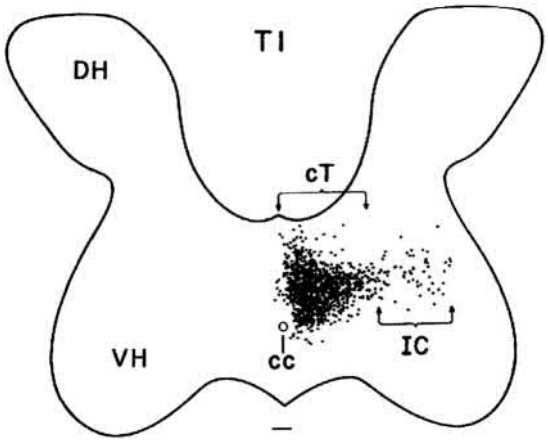

FIGURE 18.20 Mediolateral distribution of cell bodies of spinal preganglionic neurons labeled in the first thoracic segment (T1) of the spinal cord by an injection of a retrograde neurotracer (fragment C of tetanus toxin) into the right paravertebral ganglion 14 of the pigeon. The largest root of the cardiac sympathetic nerve in the pigeon arises from this ganglion. The diagram shows labeled neurons concentrated in the column of Terni [cT, large cluster of dots closest to the central canal (cc)], along with a lesser concentration of cells located more laterally in the nucleus intercalatus spinalis (IC). Although preganglionic neurons innervating the heart were not labeled specifically in this experiment, their cell bodies will be among the labeled population. *DH*, dorsal horn; *VH*, ventral horn. *Horizontal scale bar* represents 50 μm. *From Cabot et al. (1991a).*

neurons receive direct projections from diencephalic and medullary areas which, when electrically stimulated, provoke cardioaugmentation (Macdonald and Cohen, 1973; Folkow and Rubenstein, 1965; Kotilainen and Putkonen, 1974; Feigl and Folkow, 1963).

18.5.3.2.1.2 Sympathetic control Electrical activation of intramural adrenergic nerves in the avian heart produces augmented force of contraction and cardioacceleration. Bolton and Raper (1966) and Bolton (1967) first demonstrated sympathetically mediated augmentation of force of contraction of electrically paced strips of *in vitro* left ventricle from the fowl heart. In these studies, field stimulation excited both cholinergic and adrenergic nerves, and sympathetically mediated augmentatory effects were then pharmacologically isolated by the application of atropine to eliminate parasympathetic inhibitory effects. After muscarinic blockade, the increased contractile force produced by field stimulation was attributed to activation of adrenergic nerves since this effect could then be blocked by β-adrenergic antagonists. These data provided the first evidence in birds that the sympathetic nervous system can have a positive inotropic effect directly on ventricular myocardial cells.

Similar field stimulation experiments on left and right atria *in vitro* have shown that activation of intramural sympathetic nerves has powerful effects on these chambers. In the left atrium of the fowl heart, increased force of contraction of myocytes resulted from sympathetic nerve activation. These positive inotropic effects were blocked by β-adrenergic antagonists (Koch-Weser, 1971; Bennett and Malmfors, 1974, 1975b). The right atrium *in vitro* responds to field stimulation of intramural sympathetic nerves with an increase in force of contraction and rate of pacemaker discharge, with both effects mediated by β-adrenergic receptors (Pappano and Loffelholz, 1974).

In the isolated chicken heart perfused *in vitro* by Langendorff's method, stimulation of the attached right cardiac sympathetic nerve produces positive chronotropic effects (heart rate increased from 186 to 292 beats min^{-1}; Sturkie and Poorvin, 1973). The basal heart rate of this isolated preparation, supplied with adequate oxygen in the perfusate at 40°C, might be expected to be similar to that of the *in situ* chicken heart after bilateral section of the vagus and cardiac sympathetic nerves ("decentralized" state), but this was not the case. The mean rate of *in situ* decentralized hearts was in the range of 235−285 beats per min (Tummons and Sturkie, 1968, 1969). Under these conditions, stimulation of the peripheral stump of the right cardiac sympathetic nerve increased heart rate to 345 beats per min, an increase of 48%. By comparison, stimulation of the right cardiac nerve stump attached to isolated hearts *in vitro* produced a mean heart rate of 292 beats per min. That is, maximal sympathetic stimulation in this preparation could only raise heart rate to a level equivalent to the basal rate of the decentralized heart *in situ.* However, even though basal heart rate was different in these preparations, the proportional increase in rate during sympathetic stimulation was the same in both cases. Thus sympathetically mediated chronotropic effects in the isolated heart may, in relative terms, reflect the capabilities of this control system in the *in vivo* heart.

In a beating heart *in vivo*, stimulation of the cardiac sympathetic nerves produces cardioacceleration. Tummons and Sturkie (1968), in the unanesthetized chicken, showed that either cardiac sympathetic nerve could produce this effect when stimulated: activation of the right nerve increased heart rate by 48% above the prestimulation value, while activation of the nerve on the left side increased heart rate by 32%. In the pigeon, however, Macdonald and Cohen (1970) found that only the right cardiac nerve mediated cardioacceleration when stimulated (Figure 18.21, top panel) while stimulation of the left cardiac nerve altered the appearance of the T wave of the ECG without a chronotropic effect (bottom panel, Figure 18.21). Such functional asymmetry in cardiac control has also been reported for the mammalian heart (Randall, 1994).

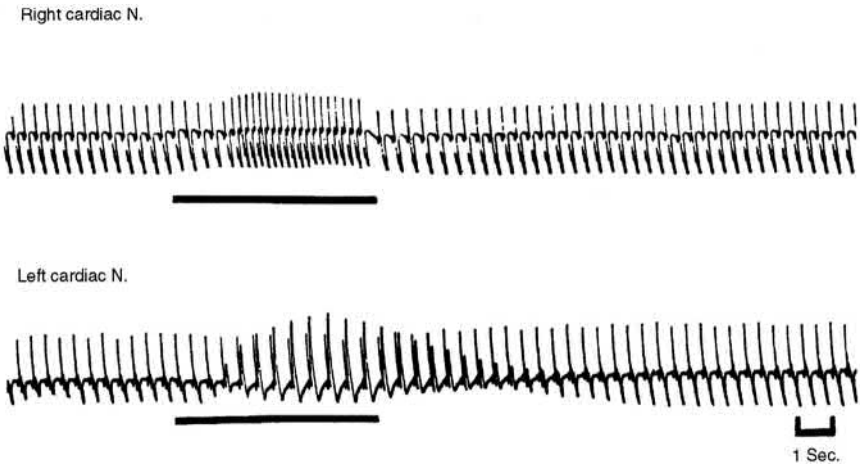

FIGURE 18.21 Electrocardiograms showing heart rate responses in the pigeon to electrical stimulation of the right (top) and left (bottom) cardiac sympathetic nerves. The duration of the stimulus train delivered to each nerve is indicated by the length of the solid bars under the traces. *From Macdonald and Cohen (1970).*

In the right atrium, the role of the dense adrenergic innervation of the SA area (see Section 18.5.3.2.1) in controlling heart rate is obvious, and a number of studies have shown that adjustments of heart rate *in vivo* are made by the sympathetic nervous system under a variety of physiological conditions. Furthermore, the anatomical evidence for widespread cardiac innervation and the data cited above for sympathetic influences on myocardial contractility in the atria and ventricles implies that the sympathetic nervous system can also produce both global and regional enhancement of contractility. Two important functional consequences of this arrangement are that (1) different patterns of sympathetic outflow from the central nervous system to individual chambers of the heart provide the means for augmenting regional contractility differentially to match the chambers' pumping actions to the hydraulic impedances into which they are working and (2) the output of each chamber can be controlled independently of pumping rate. However, to understand the function of this control system more thoroughly, it is necessary to establish whether different populations of pre- and postganglionic sympathetic neurons do in fact innervate different cardiac regions and whether such subpopulations may be differentially activated through reflexes driven by receptors in specific cardiac or vascular reflexogenic zones. Such an analysis is complicated by the location, remote from the heart, of cells of origin of the postganglionic sympathetic axons innervating the cardiac chambers, in contrast to the intracardiac locations of the postganglionic parasympathetic neurons.

Most studies of sympathetic control of cardiac function have affirmed the role of NE as the transmitter released by avian postganglionic terminals on the myocardium. However, the bird heart contains EPI as well as NE (Sturkie and Poorvin, 1973; De Santis et al., 1975; and data summarized in Holzbauer and Sharman, 1972). It has been suggested that, in other organs such as the rectum of the fowl, adrenergic terminals may release EPI (Komori et al., 1979). In the isolated chicken heart, De Santis et al. (1975) proposed that both EPI and NE may act as sympathetic neurotransmitters, on the basis of two main lines of evidence. First, sympathetic nerve stimulation, infusion of tyramine (a compound provoking the release of endogenous amines from sympathetic nerve terminals) or depolarization of intracardiac nerve terminals with a potassium-enriched perfusate all produced elevated NE and EPI efflux from the heart. Second, exogenously applied NE and EPI were equipotent in augmenting cardiac rate and strength of contraction. These authors also treated hearts with 6-hydroxydopamine to destroy sympathetic nerve endings and found that this reduced the intracardiac concentrations of both EPI and NE to very low levels. But De Santis et al. (1975) did not perform the critical experiment of determining the effect of chemical sympathectomy on release of catecholamines during cardiac nerve stimulation. Sturkie and Poorvin (1973), on the other hand, concluded that even though they and other workers had identified stores of both EPI and NE in the heart, only NE appeared to be released during sympathetic nerve stimulation. These authors concluded that EPI was sequestered in nonneuronal stores and would not, therefore, be involved in neurogenic control of the myocardium. Currently the most widely accepted view is that NE is the primary sympathetic neurotransmitter in the avian heart, as in the mammalian heart.

Autonomic tone is usually taken to mean the level of spontaneous and ongoing activity in autonomic nerves to the heart under "basal" or "resting" conditions (that is, when the animal is not actively moving or engaged in major physiological responses to its environment). Since monitoring spontaneous nerve activity is technically difficult in any preparation other than the acutely anesthetized animal instrumented for nerve recording, the level of basal heart rate is usually taken as the major indicator of cardiac autonomic tone as rate is easily measured under a variety of conditions in the whole animal. An added complication in analyzing tonic autonomic drive to the heart is that both autonomic limbs can strongly affect rate. Since rate is driven in opposite directions by parasympathetic and sympathetic inputs, the chronotropic effects of tonic activity in one limb can only be accurately assessed in the absence of influences from the other limb. Autonomic inputs to the heart can be selectively ablated by a variety of means including surgical section of the vagus or cardiac sympathetic nerves, chemical sympathectomy (by pretreatment with agents which destroy adrenergic nerve terminals or by adrenergic blockade), blockade of cardiac vagal effects with atropine, or a combination of these methods.

The level of sympathetic tone to the heart can be quantified by determining the change from basal heart rate produced by any of the above methods for functional sympathectomy after vagal influences on the heart are removed. Widely varying levels of sympathetic tone have been reported among bird species and even among different studies of the same species. A portion of this variability is likely due to the use of anesthetics. Baseline heart rate itself will change as a consequence of general anesthesia, and anesthetics will also have a blunting effect on autonomic control of the heart (Vatner and Braunwald, 1975; Brill and Jones, 1981; Lumb and Jones, 1984). Therefore the most accurate assessment of cardiac sympathetic tone would be made in awake, spontaneously breathing animals in a quiescent state after vagal influences on the heart have been eliminated.

Johansen and Reite (1964) investigated the level of autonomic tone to the heart in both awake ducks and those under general anesthesia; the authors did not differentiate between these states in reporting their data, claiming that

this made no difference to the outcome of the experiments. In vagotomized ducks in this study, β-adrenergic blockade produced a large fall in heart rate, implying the existence of strong resting sympathetic tone. Tummons and Sturkie (1969) reported that, in awake chickens at six days after recovery from surgical division of the cardiac sympathetic nerves, heart rate was about 16% less than that in intact animals. In anesthetized ducks, Kobinger and Oda (1969), using pharmacological agents to inhibit sympathetic function at central and peripheral levels of the nervous system, also found evidence for significant sympathetic tone to the heart. On the central side, they showed that clonidine mediated depression of vasopressor areas in the medulla, including the sympathetic cardiomotor area, led to a reduction in heart rate. On the peripheral side, depletion of NE from peripheral sympathetic terminals with reserpine, or prevention of NE release from these terminals, also significantly reduced cardiac rate. None of these experiments was done with accompanying vagal blockade. In contrast to the results of Kobinger and Oda (1969), Folkow et al. (1967) found no significant change in heart rate after β-adrenergic blockade in the same species. However, a complicating factor in the latter study was that the agent used (an experimental β-blocker then under development) was acknowledged by the authors to have a partial β-agonist effect which may have offset any effects of β-blockade on basal heart rate. Butler and Jones (1968; 1971) reported no significant change in heart rate in unanesthetized ducks after β-blockade with propranolol, an agent free of intrinsic β-agonist effects. In awake chickens, Butler (1967) found that β-blockade with the vagi intact produced a significant fall in heart rate to 75% of the control rate. β-blockade after vagotomy produced less of an effect, reducing heart rate to 82% of the level in animals with intact vagi. These results show that significant sympathetic tone is present in the chicken, reinforcing the contention that the level of this tone can only be accurately assessed in the absence of parasympathetic input to the heart. However, the results of Butler (1967) contrast with those of Tummons and Sturkie (1970), who found that sectioning the sympathetic nerve produced a fall of about 16% in heart rate from the level before nerve section, while vagotomy produced a rise of about the same proportion. Combined vagotomy and sympathetic nerve section resulted in a heart rate not significantly different from that in intact animals. The authors therefore concluded that, in resting intact animals, the balance between tonic sympathetic and parasympathetic inputs to the heart maintained rate at the same level as the intrinsic rate in animals after cardiac decentralization. It is clear from the foregoing discussion that further studies of tonic sympathetic drive to the heart must be rigorous in taking both the state of anesthesia and the level of concomitant parasympathetic drive into account.

An electrophysiological analysis of the compound AP of the right cardiac nerve in the pigeon has shown that axons in this nerve can be categorized into two groups separable by conduction velocity, as shown in Figure 18.22 (Cabot and Cohen, 1977a). Fibers of the more slowly conducting group (range 0.4–2 m s^{-1}) were shown to mediate sympathetic cardioacceleration. The range of conduction velocities of these axons lies within that of unmyelinated sympathetic postganglionic fibers known to innervate the viscera (Gabella, 1976), and morphological analysis of the pigeon

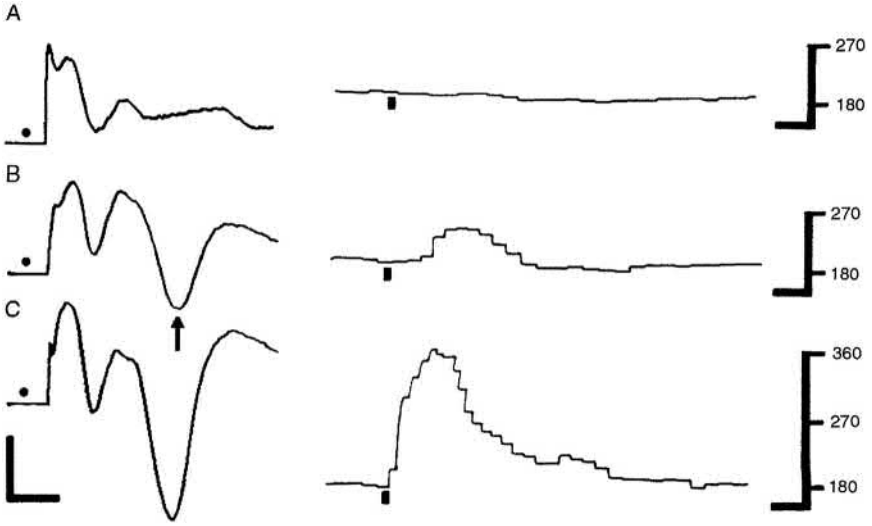

FIGURE 18.22 Correlation between components of the compound action potentials evoked by graded electrical stimulation of the right cardiac sympathetic nerve and chronotropic responses of the heart in the pigeon. The traces on the left represent the compound action potential at three intensities of stimulation increasing from A to C (*round dots* associated with each trace indicate the start of the stimulation, which consisted of a 200-ms train of 50 Hz pulses). For these traces, the vertical calibration bar represents 100 μV and the horizontal bar represents 5 ms. The traces on the right represent beat-by-beat ratemeter recordings showing heart rate responses produced by the same stimuli (*filled squares* under each trace) which evoke the nerve responses on the left. The calibration bars to the right of each trace indicate heart rate in beats min^{-1}. For these traces, the horizontal bar represents 1 s. The onset of the component of the compound action potential indicating conduction of cardioaccelerator fibers is indicated by the *arrow* in trace B; this component strengthens with increased stimulus intensity in trace C, as does the degree of cardioacceleration. *From Cabot and Cohen (1977a).*

right cardiac nerve confirms that 67% of axons in this nerve are unmyelinated (Macdonald and Cohen, 1970). The faster-conducting group of fibers in this nerve (range 2–5.6 m s^{-1}) are likely to be myelinated axons. These make up the remaining 33% of the total number of axons and probably represent so-called "sympathetic afferent" fibers (Malliani et al., 1979) with receptor endings in the heart, great vessels, or lungs. Afferent fibers in cardiac nerves have been shown to participate in cardiopressor reflexes in the pigeon (Cabot and Cohen, 1977b).

18.5.3.2.2 Parasympathetic innervation

18.5.3.2.2.1 Anatomy Efferent neurons with their cell bodies in the heart form the final common pathway for parasympathetic control of cardiac function. These postganglionic neurons receive synaptic inputs from terminals of preganglionic neurons with their somata in the brainstem and their axons coursing to the heart in the vagus nerves. It is generally accepted that parasympathetic efferent neurons in the heart are cholinergic, releasing ACh at their myocardial terminals; this neurotransmitter acts to modify myocardial function through postjunctional muscarinic receptors. Indeed, most of the anatomical studies of parasympathetic innervation of the heart have used a histochemical reaction indicating the presence of AChE as a marker to determine the distribution of cholinergic fibers and terminals of the cardiac plexus, as well as the locations of intracardiac neurons. Cabot and Cohen (1980) have extensively reviewed the cholinergic innervation of the heart, so a brief synopsis of that review and the contributions of later workers are combined below.

In all avian species so far examined, all four cardiac chambers receive AChE-positive innervation (Hirsch, 1963; Yousuf, 1965; Smith, 1971a,b; Akester and Akester, 1971; Mathur and Mathur, 1974; Rickenbacher and Müller, 1979; Kirby et al., 1987). Smith (1971a,b), in studies of the innervation pattern in the chicken heart, determined that cholinergic nerves, nerve fibers, and terminals formed a subepicardial ground plexus throughout the atria and ventricles, penetrating into the myocardium. Some fibers were observed to run all the way to the endocardial region where they contributed to a subendocardial plexus which was also distributed throughout the atria and ventricles. In many avian species, the overall intracardiac distribution of cholinergic innervation parallels the distribution of adrenergic fibers and terminals (Bennett and Malmfors, 1970). The right atrium has been a particular focus for anatomical studies of cholinergic innervation in view of the location of the primary pacemaker in this chamber and the vagally mediated inhibition of pacemaker node discharge rate. Yousuf (1965) noted in the sparrow heart that the region around the SA node was the first part of the heart to receive extrinsic cholinergic innervation during embryological development and observed that in later developmental stages this area and the right atrial wall near the AV node were heavily innervated. However, no nerve fibers were observed to enter the SA node area proper, and only a few fibers were present among the AV nodal cells. This pattern has also been observed in the pigeon heart (Mathur and Mather, 1974). However, Gossrau (as summarized in Akester, 1971) reported that in pigeon, chaffinch, and canary hearts the pacemaker region had a dense AChE-positive innervation, while in duck and chicken, this area was sparsely innervated. Differences among these studies may be partly species dependent, although the contrasting results of Mathur and Mathur (1974) and Gossrau in the pigeon heart may be due to differences in the techniques used. Bogusch (1974) observed a dense cholinergic innervation pattern around subepicardial Purkinje fibers of the fowl right atrium but noted that the density of this innervation decreased as the conducting fibers approached the AV border. In this study, multiple nerve terminals were only loosely associated with Purkinje fibers, leaving some doubt as to the nature of the neuroeffector–tissue relationship in cholinergic control of conduction in the atrium. SA valve remnants have also been reported to be the targets of cholinergic innervation in the bird heart (Akester, 1971; Mathur and Mathur, 1974).

Cholinergic innervation of the left atrium and the ventricles has been less extensively studied than that of the right atrium, but the general pattern of subepicardial and subendocardial plexi with individual nerve fibers and terminals extending into the myocardium, as described by Smith (1971b), appears to hold. Extensive cholinergic innervation has been described in the interatrial and interventricular septa (Akester, 1971), the right AV valve leaflets (Akester, 1971; Mathur and Mathur, 1974), and the left AV valve. Here the AChE-positive nerve fibers enter the basal half of the valve from the subendocardial plexus (Smith, 1971a). The cholinergic innervation of the avian chordate tendineae is controversial: Smith (1971b) reported no nerve fibers present in chordae tendineae of the chicken heart, while Mathur and Mathur (1974) found in the pigeon heart that these structures were innervated. The function of such innervation is obscure since the chordae tendineae contain no actively contracting tissue, serving only to anchor the papillary muscles to the aortic valve leaflets. It is most likely that the nerve fibers observed in these structures are efferents *en route* to either the valves or the papillary muscle, but some fibers may subserve an afferent function.

The adventitia of coronary arteries associated with all chambers of the bird heart is innervated by cholinergic nerve fibers (Hirsch, 1963; Akester, 1971; Smith, 1971a) but the origin of this innervation is not known. Cholinergic fibers innervating coronary arteries may originate from postganglionic parasympathetic neurons within the heart or

may possibly be extrinsic "sympathetic cholinergic" fibers; in either case, this innervation probably functions to increase coronary blood flow by promoting vasodilation.

In development of the chick heart, Rickenbacher and Müller (1979) determined that cell bodies of intracardiac neurons, clustered into ganglia, first developed in the left ventricle, then a large group of ganglia became evident around the coronary sulcus and the ventral surface of the ventricles and, lastly, ganglia developed in association with the dorsal atrial walls.

In the adult avian heart, ganglia are located primarily in the subepicardial plexus, usually in association with plexus nerves and frequently near the branch points of these nerves. The somata of intracardiac neurons have been characterized as multipolar (possessing more than two processes; Smith, 1971b; Yousuf, 1965), but these observations are limited to the hearts of only two species (chicken and sparrow, respectively). No morphological data exist on the variation of somatic dimensions or on the length or specific projection targets of the processes of intracardiac neurons in any avian species.

Histochemical reactions for AChE have been the primary tool used in analyzing the distribution of intracardiac neurons in the bird heart, and there seems little doubt that these techniques allow visualization of most if not all of these neurons. Such anatomical data, along with evidence from the functional studies cited below, supports the contention that the phenotype of avian intracardiac neurons is cholinergic. However, AChE has been detected in some nonneuronal elements associated with the nervous system (see review by Fibiger, 1982) and demonstration of the presence of this enzyme in neuronal somata in the heart, although necessary, may not be a sufficient criterion for designating these cells cholinergic. In the central nervous system, the most widely accepted indicator of cholinergic function is the presence of choline acetyltransferase (ChAT), an enzyme in the pathway for ACh synthesis (Fibiger, 1982). Reliable antibodies directed against ChAT are now commercially available and have begun to be applied to the mammalian peripheral autonomic nervous system. A similar application of ChAT immunohistochemical techniques to the avian heart would help verify the assumption that intracardiac neurons in this vertebrate group are in fact of cholinergic phenotype.

In their analysis of the distribution of the intracardiac ganglia during development, Rickenbacher and Müller (1979) found that the right ventricle wall contained about half of the total number of ganglia, the right atrium about one-fifth, the left ventricle about one-sixth, and the left atrium possessed the fewest ganglia. In the adult bird heart, no quantitative studies of regional neuron distribution have been done to date, so the absolute number of neurons associated with each chamber is not known. However the general pattern of distribution of intracardiac neurons in the adult heart has been established (see Cabot and Cohen, 1980 for review). Ganglia containing variable numbers of neurons are present on both dorsal and ventral aspects of the left and right atria and ventricles (Yousuf, 1965; Smith, 1971a,b; Rickenbacher and Müller, 1979; Kirby et al., 1987; reviewed by Cabot and Cohen, 1980). Smith (1971b) has reported that a larger proportion of the total number of intracardiac ganglia is found in the ventricles of bird hearts than is the case in mammalian ventricles. Ganglia have been observed near but not within the SA node region (Yousuf, 1965; Smith, 1971b). Yousuf (1965) reported that some neurons in the sulcus terminalis appeared to send projections in the direction of the nodal tissue. The AV nodal region was also reported to be devoid of ganglia (Yousuf, 1965; Smith, 1971b; Mathur and Mathur, 1974), but this region and the AV bundle appeared to be innervated by axons from ganglion neurons in the nearby AV sulcus (Yousuf, 1965). Smith (1971b) described high concentrations of ganglia within the dorsal right atrial wall near the ostia of the superior and inferior venae cavae, near the roots of the pulmonary veins on the dorsal aspect of the left atrium, within the dorsal portion of the AV groove, and clustered around the roots of the pulmonary artery and aorta. In the ventricles, neurons are located in a scattered pattern reaching from the AV groove to the apex on the ventral surface (Smith, 1971b; Rickenbacher and Müller, 1979). There are also numerous ganglia associated with nerves accompanying atrial and ventricular coronary arteries (Mathur and Mathur, 1974; Smith, 1971b).

Studies in the mammalian heart have shown that a number of neuropeptides are colocalized in axons, terminals, and somata of cholinergic intracardiac neurons, as well as in preganglionic terminals contacting these neurons (Steele et al., 1994, 1996). Peptides constitute an important class of neuromodulators in the peripheral autonomic nervous system, and their presence in specific combinations in some peripheral neurons has been proposed to chemically code subpopulations of these neurons for specific functions such as vasomotion or control of muscle cell contractility. In the bird heart, substance P and vasoactive intestinal peptide have been found in intracardiac neurons and their terminals, while somatostatin is present in intracardiac terminals but not in cell bodies (Corvetti et al., 1988). These neuropeptides have been shown to exert powerful modulatory effects on mammalian intracardiac neuronal activity and cardiodynamics (Armour et al., 1993), and their presence in the bird heart indicates that they may play a prominent role in modulation of ganglionic and neuroeffector transmission in this vertebrate group. This constitutes a promising but as yet unexplored area for the comparative study of mechanisms of neural control of the heart.

The course of the avian vagus nerve and its cardiac branches has been described for a number of species (see Pick, 1970; Jones and Johansen, 1972; Cabot and Cohen, 1980).

Cabot and Cohen (1980) points out that descriptions of the course and major branches of this nerve are consistent among species, so a general summary of the avian vagal cardiac innervation will be given here, based on the comprehensive reports of Malinovsky (1962) and Cohen et al. (1970) in the pigeon and the reviews cited above. Inside the cranium, the peripheral trunks of the vagus and glossopharyngeal nerves originate bilaterally from large ganglia composed of a fusion of the proximal ganglion of the glossopharyngeal nerve and the jugular ganglion of the vagus nerve. The trunks of these nerves emerge together from the skull through the jugular foramen, and immediately outside the foramen an anastomosis (of Staderini) connects the vagal trunk to the petrosal ganglion of the glossopharyngeal nerve. The vagal trunk continues caudad in the neck along the dorsomedial aspect of the internal jugular vein, passing over the cervical spinal nerves on their ventral sides. No major vagal branches arise from the trunk along its cervical portion, although Malinovsky (1962) described occasional small anastomoses with the nearby cervical sympathetic trunk. At the level of the thoracic inlet, the nodose (alternatively termed distal vagal) ganglia are present as spindle-shaped enlargements of the vagal trunks, as shown in Figure 18.23. Several afferent nerves carrying the axons of receptors important in the control of cardiovascular and respiratory functions arise

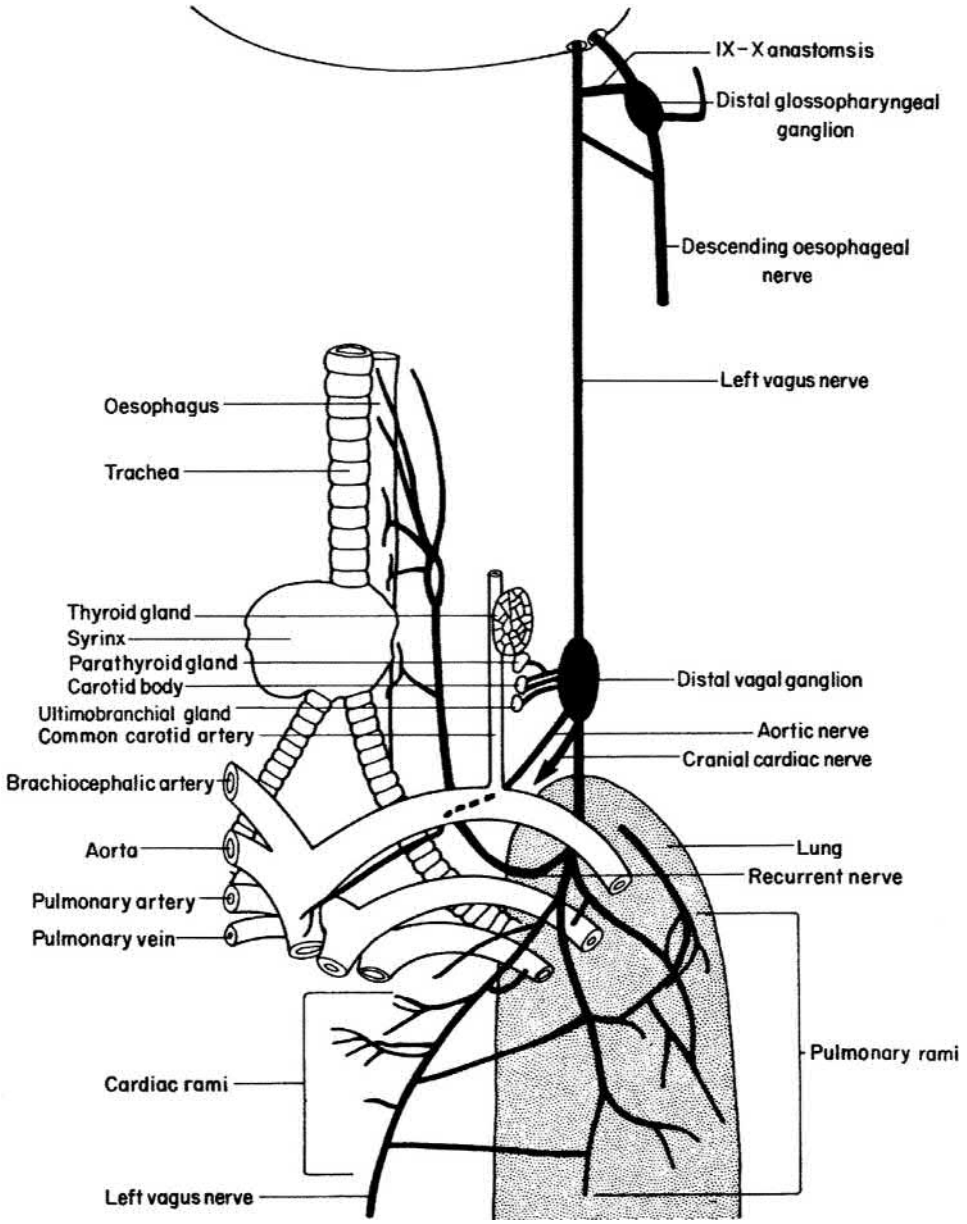

FIGURE 18.23 Schematic diagram depicting a ventral view of the pathway of the left vagus nerve in the area of the upper thorax of the duck. Details of the vagal innervation of the carotid body, ultimobranchial, thyroid, and parathyroid glands, and the aorta are illustrated. *From Jones and Johansen (1972).*

from each nodose ganglion. Along the length of this ganglion, branches arise which extend medially to innervate the thyroid, parathyroid, and ultimobranchial glands, and the carotid body (Figure 18.23).

The latter structure constitutes the primary locus for peripheral chemoreceptors sensing arterial oxygen and carbon dioxide tensions and pH in the bird (Jones and Purves, 1970; see Section 18.5.4.1). Branches exiting from the caudal portion of the nodose ganglion course to the root of the aorta. On the right side, Nonidez (1935) reported two such branches in the chick, which he designated "depressor" and "accessory depressor" nerves by analogy with the mammalian condition. Nonidez (1935) reported no equivalent nerve on the left side, but in other species, nerves from the nodose ganglion coursing to the aortic root (designated aortic nerves) have been reported to be present bilaterally (Jones and Purves, 1970; Jones, 1973; Cohen et al., 1970; Jones et al., 1983; Smith and Jones, 1990; 1992; summarized by Smith, 1994; see Figure 18.23). These nerves ramify into a plexus in the aortic wall. Jones (1973) first demonstrated that the aortic nerves carried arterial blood pressure information centripetally and that aortic baroreceptors were involved in regulating and maintaining arterial blood pressure in the duck.

A few millimeters caudal to the nodose ganglion the vagal trunk splits, as shown in Figure 18.24, to form several major divisions as it approaches the pulmonary artery. Two of these circumscribe the pulmonary artery, rejoin, and continue as the main vagal trunk *en route* to the abdominal cavity while a third forms the recurrent laryngeal nerve, coursing craniad along the trachea; no cardiac vagal branches arise from this nerve. Another major vagal branch courses to the heart to enter the dorsal cardiac plexus (Jones and Johansen, 1972; shown in Figure 18.23). The remaining vagal branches form part of the pulmonary innervation, running to the lungs along the pulmonary arteries. The main vagal trunk, after reforming caudal to the pulmonary artery, passes ventral to the ipsilateral bronchus and over the dorsal surface of the heart. From this portion of the trunk, a variable number of smaller branches arise and enter the cardiac plexus. On the right side, these branches enter the heart near the SA and AV nodes and at the caval ostia; on both the left and right sides of the heart, vagal branches also enter the cardiac plexus in the vicinity of the AV groove. That the cardiac nerves described here constitute

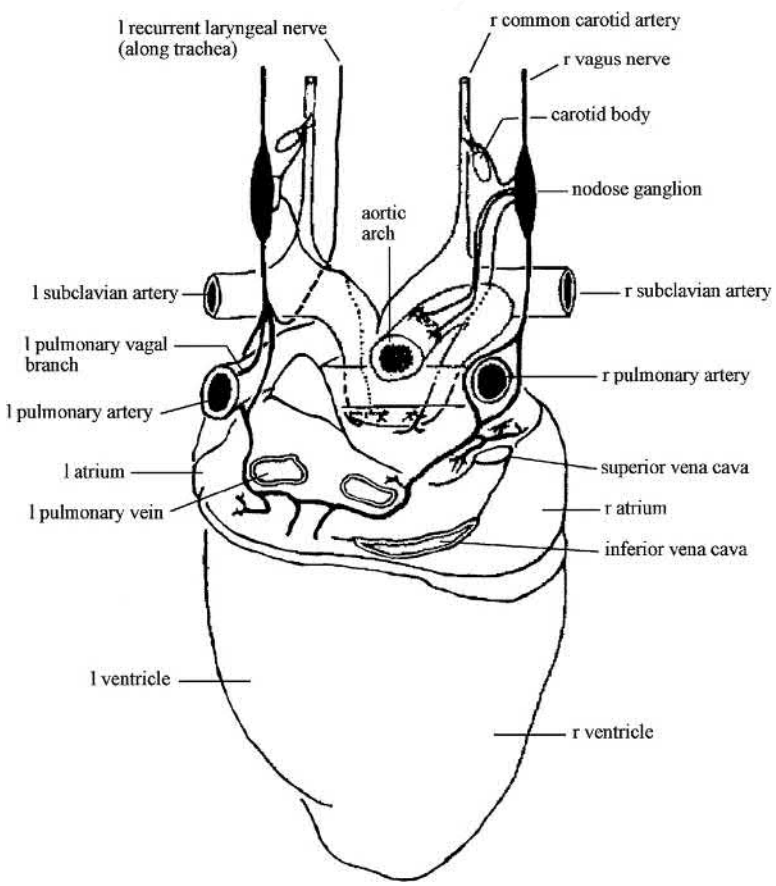

FIGURE 18.24 Schematic diagram to illustrate a dorsal view of the generalized vagal innervation of the avian heart. Note the pathways of the vagal branches as these nerves split close to the pulmonary arteries. For clarity, the right pulmonary and right recurrent laryngeal branches are not shown, and the right pulmonary vein, depicted next to the left, is not labeled (r, right; l, left). *From Cabot and Cohen (1980).*

the major efferent vagal innervation of the heart has been confirmed by functional studies in which electrical stimulation of the vagal trunk was combined with surgical section of the trunk and the various cardiac branches (Cohen et al., 1970). Caudal to the origin of the most inferior cardiac branches, the left and right vagal trunks pass ventral to the pulmonary veins where both turn medially, coming to lie in close approximation as they course to the abdominal viscera (Figure 18.24).

The location in the central nervous system of cells of origin of vagal cardioinhibitory fibers in birds has been investigated by a variety of anatomical and physiological techniques. The extent of the medullary regions containing vagal preganglionic motor neurons innervating pharyngeal structures and thoracic and abdominal viscera was originally defined anatomically by determining the extent of retrograde degeneration of neuronal somata after section of the cervical vagus nerve (Cohen et al., 1970) and by retrograde labeling of vagal neurons with neurotracers applied to the peripheral vagus nerve (Katz and Karten, 1979; 1983a,b; 1985; Cabot et al., 1991a). Cohen et al. (1970), working in the pigeon, described three major subdivisions of the dorsal motor nucleus of the vagus nerve (DMV) based on cytoarchitectonic and morphological criteria. The principal medullary location of neurons showing signs of degeneration after section of the cardiac vagal branches was in a region extending from the obex to the rostral pole of the DMV, with the highest density of degenerating cells in an area between 0.6 and 0.8 mm rostral to the obex. At this rostrocaudal level, these cells were primarily located in the most ventral region of the DMV. The results of these experiments suggested that the central arrangement of vagal cardioinhibitory neurons in birds was different than the mammalian condition; in mammals, the primary locus for these neurons is the nucleus ambiguus, ventrolateral to the DMV (reviewed by Hopkins, 1987).

In the pigeon, focal electrical stimulation of the regions of the DMV shown anatomically to contain cell bodies of putative cardioinhibitory neurons produced short-latency decreases in heart rate; this response is shown in Figure 18.25 (Cohen and Schnall, 1970). The response was rapid, occurring within one or two cardiac cycles after the start of stimulation, suggesting that cardioinhibitory preganglionic cell bodies were being directly stimulated. If stimulation was continued, complete AV blockade could be produced in some animals; a depressor response invariably occurred secondary to all negative chronotropic responses (Figure 18.25). There was no lateral asymmetry in this response: stimulating in the DMV on either side produced similar cardioinhibitory responses. The cardiac effects produced by central stimulation could be mimicked by stimulating the vagal trunks in the neck or at the thoracic inlet (Cohen and Schnall, 1970). Field potential and single-unit recordings made in the pigeon DMV during stimulation of the vagal trunk provided further confirmation that the cell bodies of a large number of cardioinhibitory neurons were located in the central zone of the DMV rostral to the obex (Schwaber and Cohen, 1978b).

Schwaber and Cohen (1978a), in an electrophysiological study of the vagus nerves, found that when the cervical vagus was stimulated at progressively greater intensities,

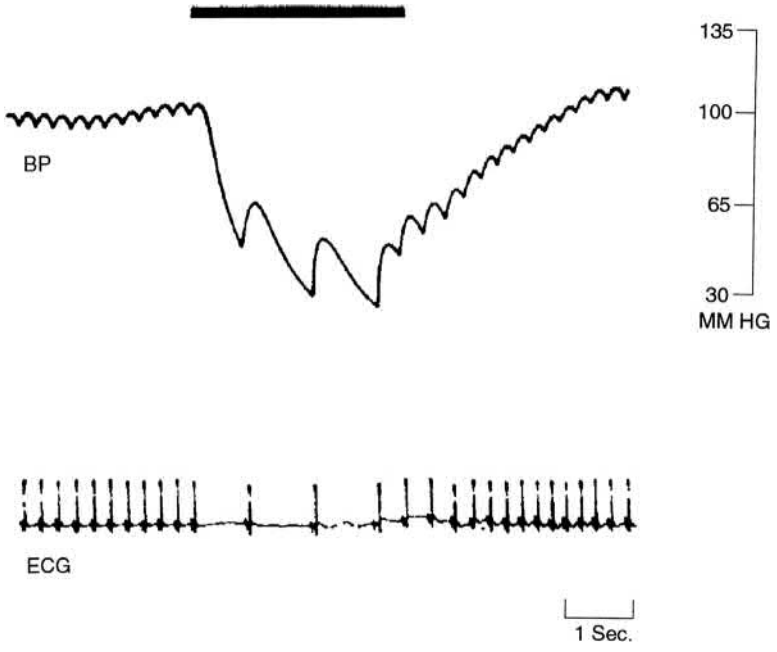

FIGURE 18.25 Arterial blood pressure (BP) and cardiac chronotropic (ECG) responses to focal electrical stimulation in the area of the dorsal motor nucleus of the vagus nerve in the pigeon. The duration of the stimulus train (50 Hz pulses) is shown by the solid horizontal bar above the traces. *From Cohen and Schnall (1970).*

the onset of bradycardia coincided with the elicitation of a specific component of the compound AP (B1 wave, Figure 18.26). This component was generated by the activation of a group of vagal axons conducting in the velocity range of 8 to 14 m s^{-1}. When the vagus nerve was stimulated with sufficient intensity to evoke both the A and B1 components (trace B of Figure 18.26) and a polarizing voltage was applied to the nerve to block the A but not the B1 component, the cardioinhibitory response was maintained. This led the authors to conclude that fibers in the vagus nerve responsible for generating the B1 component of the compound AP were responsible for cardioinhibition. This was confirmed in experiments in which field potential and single-unit activity were mapped in the DMV in correlation with synchronous compound APs recorded from the vagus nerve during stimulation of this nerve (Schwaber and Cohen, 1978b). In these experiments, stimulus-evoked activation of the B1 component in the vagus nerve produced the shortest latency, highest amplitude responses in the region of the DMV, which had been shown in previous studies to contain the somata of putative cardioinhibitory neurons. In addition to the evidence from stimulus-evoked potentials, recordings of spontaneously active single units in the DMV rostral to the obex in awake, paralyzed pigeons demonstrated rhythmic discharge patterns phase-locked to

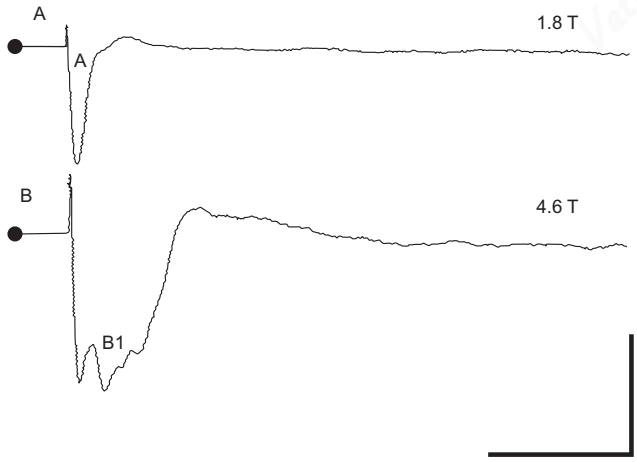

FIGURE 18.26 Compound action potentials evoked in the right vagus nerve by electrical stimulation at the midcervical level in the pigeon. Responses to stimuli of two intensities are shown. (A) Stimulation at 1.8 times the intensity which just evokes a response (threshold intensity, T) produces a short-latency component labeled the A wave, representing the fastest conducting fibers in the vagus (start of stimulus is indicated by the dot at the left side of trace). No change in heart rate is associated with the activation of this group of fibers. (B) Stimulation at 4.6 × T evokes responses in an additional, more slowly conducting group of fibers; this component of the compound action potential is labeled the B1 wave. The fibers responsible for this component conduct in the range of 8−14 m s^{-1} and when activated produce bradycardia. The vertical bar represents 250 μV; the horizontal bar represents 5 ms. *From Schwaber and Cohen (1978a)*

mechanical events in the cardiac cycle (Gold and Cohen, 1984). These authors also showed that single-unit neuronal activity in this area was decreased or eliminated by external conditioning stimuli (light flash, foot shock) which caused heart rate to increase (see Section 18.5.5).

The above anatomical and physiological evidence, taken together, indicates that in the avian brain preganglionic vagal cardioinhibitory neurons are located in the ventrolateral region of the DMV rostral to the obex. However a reexamination of the question of the location of these neurons was undertaken by Cabot et al. (1991a), using a more sensitive method for retrograde neuroanatomical tracing. These authors injected small volumes of the binding fragment of tetanus toxin into selected regions of the pigeon heart. This neurotracer was taken up by local nerve fibers and terminals at the injection site and transported retrogradely to label the somata of vagal preganglionic cardiac neurons in the medulla by two possible routes, both giving similar end results. The first of these was via direct uptake of neurotracer by fibers or terminals of the preganglionic neurons running through or close to the injection sites in the heart; in this case, the tracer would be transported directly back to the cell bodies. The second route was via transsynaptic transport. Fibers and terminals of postganglionic intracardiac neurons took up the neurotracer from the injection sites, and upon traveling to the somata and other processes of these neurons, the tracer would then cross synaptic clefts to the preganglionic terminals contacting the postganglionic cells. From these terminals, the tracer was transported to the somata of the preganglionic neurons. After intracardiac injection of the tracer, labeling of preganglionic vagal neurons was found in two locations in the medulla (Figure 18.27). The majority of label was found in neurons located ventrolateral to the DMV, in a site homologous to the nucleus ambiguus of the mammalian brainstem; these neurons were clustered within 0.5 mm of the obex as shown in the bottom panel of Figure 18.27. A smaller number of labeled neurons were found in more rostral sections in an area bordering the ventrolateral margin of the DMV (top panel of Figure 18.27), in close proximity to the region delineated in the degeneration studies of Cohen et al. (1970) and just ventral to the area described in the functional studies of Schwaber and Cohen (1978a,b). The results of Cabot et al. (1991a) have forced a reevaluation of the central organization of neurons controlling the avian heart, indicating that this organization has much more in common with the mammalian condition than was previously believed. However, these anatomical data have not been confirmed by physiological studies. In addition, it still remains for the membrane and firing properties of vagal cardioinhibitory preganglionic neurons to be investigated to determine if there are functionally discrete subpopulations within this group of neurons and, if so, whether there is any correlation

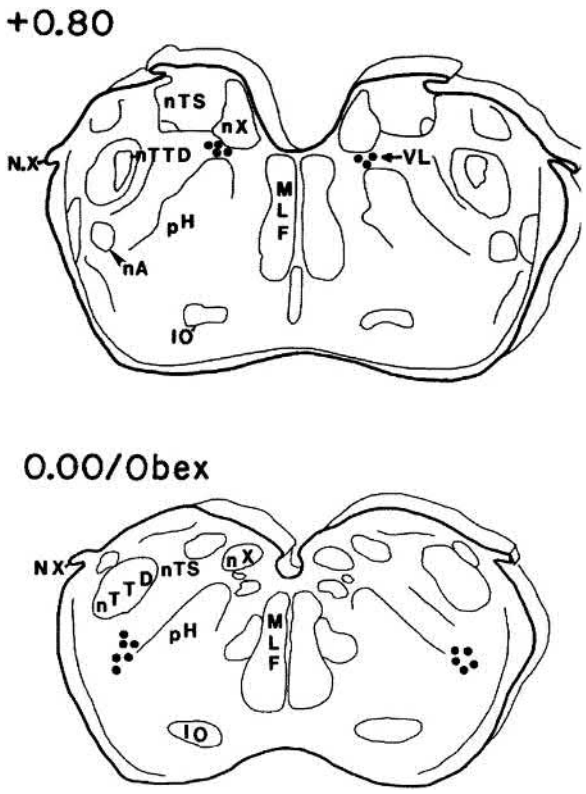

FIGURE 18.27 Outline drawings of transverse sections of the pigeon medulla in the region of the obex, depicting the location of vagal preganglionic neurons labeled by retrograde transport of tetanus toxin binding fragment C injected into the heart (see text for explanation). The top panel shows a section cut 0.8 mm rostral to the obex, with labeled neurons (*filled circles*) located just ventral to the dorsal motor nucleus of the vagus (nX) in the nucleus ventrolateralis (VL). The bottom panel, representing a section taken at the level of the obex, shows additional labeled neurons in an area of the medulla which may be the avian homolog of the mammalian nucleus ambiguus (nA), ventrolateral to nX. *IO*, inferior olivary nucleus; *MLF*, medial longitudinal fasciculus; *nTS*, nucleus and tractus solitarius; *nTTD*, nucleus and tractus trigemini descendens; *NX*, vagal nerve rootlet; *pH*, plexus of Horsley. *From Cabot et al. (1991a).*

between the functional properties of neurons and their potential roles in controlling specific aspects of cardiodynamic function.

Little is known of the nature and origins of inputs to medullary vagal cardiomotor neurons in birds. Berk and Smith (1994) have shown in the pigeon that peptide containing projections to these neurons arise from the area of the nucleus of the tractus solitarius (NTS). The NTS is one target for afferent information from visceral receptors carried in the vagus, glossopharyngeal, and other cranial nerves, and such peptidergic projections from the NTS to cardiomotor neurons may represent an important viscerovisceral reflex pathway, as has been described in mammals (Loewy and Spyer, 1990). In addition to inputs of peripheral origin, there is an extensive pattern of projections to the DMV from structures located more rostrally in the brain. Berk and Finkelstein (1983) and Berk (1987) demonstrated projections from the bed nucleus of the stria terminalis, the ventral paleostriatum, and the medial and lateral hypothalamus to the DMV. These forebrain inputs thus represent potential pathways through which central nervous control of cardiac function may be exerted in the interests of homeostasis, as well as providing pathways for neutrally mediated alterations in cardiac function which may be required during exercise, feeding, or other behaviors, or in response to changes in the external environment. In addition, Cohen and coworkers have explored the central anatomical pathways mediating conditioned responses (CRs) which target medullary cardiomotor neurons in birds (see Section 18.5.5). These cardiomotor neurons therefore integrate information from visceral and other receptors and from higher levels of the central nervous system to control cardiodynamics, but our knowledge of the integrative mechanisms involved is scant at present.

18.5.3.2.2.2 Parasympathetic control ACh acts in the bird heart to depress atrial and ventricular myocyte contractility, rate of discharge of pacemaker tissue, and rate of conduction through the specialized conductive tissues. ACh, released from preganglionic terminals, activates excitatory nicotinic receptors on the membranes of postganglionic neurons in the heart and these neurons in turn release ACh from their effector terminals to inhibit cardiac functions. Intrinsic postganglionic parasympathetic neurons release the majority of ACh which overflows from the isolated heart during vagal nerve stimulation. Only a small fraction of the total amount of ACh recovered in these experiments is released from vagal preganglionic terminals, as shown by a large reduction in vagally evoked ACh release after treatment of the isolated heart preparation to prevent release of the neurotransmitter from postganglionic terminals (Loffelholz et al., 1984).

ACh has different effects on the cell membrane conductance and thus on contractile properties of myocytes in the avian atria and ventricles. Inoue et al. (1983), using intracellular electrode techniques *in vitro*, investigated the effects of ACh on membrane ion conductance of atrial and ventricular myocytes to determine how these might differ. They found that, in ventricular muscle cells, ACh reduced the force of contraction, diminishing both amplitude and time course of the AP, but did not change either resting membrane potential or whole-cell resistance. On the other hand, in atrial myocytes, ACh hyperpolarized the membrane and reduced whole-cell resistance (implying an increase in steady-state ionic conductance) as well as causing a reduction in amplitude and time course of the AP. ACh binds to muscarinic receptors on myocyte membranes, and the authors found that this induced similar decreases in calcium-dependent sodium currents in the two types of cells. However, atrial myocytes exhibited in addition a muscarinic mediated increase in outward potassium current

which accounted for the hyperpolarization and reduction in resistance induced by ACh; this mechanism was not present in ventricular myocytes. These differences in response to ACh imply that the same neurotransmitter can differentially control atrial and ventricular contractility.

There are several subtypes of muscarinic receptor present in the mammalian heart (see Deighton et al., 1990 for review), and some of these receptor subtypes are also present in the avian heart. The majority of muscarinic receptors on mammalian myocardial cells are of the M_2 subtype (Deighton et al., 1990; Jeck et al., 1988), and this subtype is believed to mediate complex intracellular mechanisms leading to the inhibition of myocyte functions which are ultimately responsible for the parasympathetic control of the heart. In a comparison of muscarinic receptor types in the chicken and guinea pig hearts, Jeck et al. (1988) found that receptors of the M_1 subtype predominated in the myocardium of the chicken while the most prevalent type in the guinea pig heart was the M_2 subtype, as found in other studies of the mammalian heart. Detailed analyses of the muscarinic receptor subtypes present in the hearts of other avian species have not been conducted, but if the results of Jeck et al. (1988) in the chicken represent the general avian situation, there are likely to be major differences in receptor-mediated intracellular mechanisms of mucarinic inhibition of myocyte function between birds and mammals.

In avian atrial tissue *in vitro*, *in situ,* or isolated hearts, it is widely accepted that ACh has a strong negative inotropic effect (e.g., Jeck et al., 1988 and review by Sturkie, 1986), but studies of specific cholinergic effects on ventricular inotropy have been few in the bird. Avian ventricular tissue has a higher density of cholinergic innervation than does that of mammals as outlined above and a higher proportion of the total number of intracardiac neurons is associated with the ventricles of the avian than the mammalian heart (see above, and Smith, 1971b). On the basis of early anatomical evidence suggesting a high density of cholinergic innervation of the ventricular myocytes in birds, Bolton and Raper (1966) compared responses of strips of the right ventricle of fowl and guinea pig hearts *in vitro* to endogenously released and exogenously applied ACh. Field stimulation of electrically paced ventricular strips produced a strong decrease in force of contraction of fowl ventricular tissue, while guinea pig ventricular tissue responded with an increase in force. Atropine, blocking muscarinic receptors, eliminated the negative inotropic response of the fowl ventricle to stimulation, and a strongly positive response was then observed; however, atropine had no effect on the response of the guinea pig ventricle to stimulation. The authors proposed that the fowl heart has a capacity for effective parasympathetic inhibition of ventricular inotropy, mediated by intracardiac release of ACh. Furthermore, blockade of this response unmasked a stimulus-evoked increase in force of contraction which the authors determined was the result of release of NE from sympathetic nerve terminals. They concluded that, in contrast with the mammalian condition, the fowl right ventricle was innervated by both the sympathetic and parasympathetic limbs of the autonomic nervous system. Subsequent *in vitro* work has confirmed these observations (Bolton, 1967; Biegon et al., 1980; Biegon and Pappano, 1980).

The first experimental approach used to explore general questions of parasympathetic efferent control of the avian heart, dating from the early part of this century, was to examine the effects of exogenously applied ACh on the activity of P-cells in the right atrium (reviewed by Jones and Johansen, 1972; and Cabot and Cohen, 1980). More detailed characterization of this system has resulted from investigations carried out by Loffelholz and co-workers, and others. In the *in vitro* right atrium, ACh release provoked by field stimulation and by stimulation of the attached right vagus nerve produced a fall in pacemaker discharge rate (Pappano and Loffelholz, 1974; Pappano, 1976; Brehm et al., 1992). This chronotropic effect was blocked by atropine but not by the ganglionic blocker hexamethonium, so it must have been mediated by direct release of ACh from postganglionic parasympathetic neurons in the atrial wall (Pappano and Loffelholz, 1974). On the other hand, hexamethonium in the absence of atropine blocked all effects of electrical stimulation of the attached vagal stump. Vagally mediated bradycardia therefore occurred as a result of the synaptic activation of intracardiac postganglionic neurons by preganglionic terminals. As with cholinergic control of the inotropic state of the atrial and ventricular myocardium discussed above, control of pacemaker rate operates via the synaptic relay of impulses from pre- to postganglionic neurons within intracardiac ganglia.

18.5.3.2.2.2.1 Dromotropic effects. There have been no studies of the direct effects of ACh on the rate of impulse conduction through the specialized conducting cells of the avian heart and few studies of the overall parasympathetic control of this function. There are technical difficulties in identifying the locations of conducting tissues in a viable *in vitro* preparation of cardiac tissue, so work on this intriguing problem in birds has largely been conducted on hearts *in situ.* In the chicken, Goldberg et al. (1983) showed that AV conduction time could be significantly prolonged by stimulation of either vagus nerve; there was no bilateral asymmetry in this response. However, in order to unmask this dromotropic effect, the heart was paced through electrodes attached to the SA node, both to control heart rate and to prevent shifts in pacemaker position during vagal nerve stimulation. Bogusch (1974), using anatomical techniques, identified cholinergic fibers and terminals in the region of conducting cells near the AV

border and proposed a functional role for this innervation, but the study of Goldberg et al. (1983) appears to be the only physiological confirmation of this role in the bird (also see Section 18.2.3.3).

18.5.3.2.2.2.2 Chronotropic effects. The study of vagal control of heart rate in birds has a long history going back to the recognition in the last 18th century that activation of the vagus nerves could produce large reductions in heart rate and, in some cases, arrest the heart (see Cabot and Cohen, 1980 for a summary of early work). As these reviewers have pointed out, the nature of vagally mediated bradycardia has been intensively reinvestigated using recently developed techniques in a variety of avian species (Johansen and Reite, 1964; Bopelet, 1974; Peterson and Nightingale, 1976; Langille, 1983; Lindmar et al., 1983; Goldberg et al., 1983; Lang and Levy, 1989; Butler and Jones, 1968; Cohen and Schnall, 1970; Jones and Purves, 1970; and others). The negative chronotropic effects of ACh in the pharmacological studies cited above are paralleled by the effects of electrical stimulation of the vagus nerves. Several preparations have been used to assess the chronotropic consequences of vagal stimulation. These include *in vitro* atrial tissue, isolated beating hearts with attached vagal stumps, open-thorax anesthetized preparations, and anesthetized or awake animals in which only the vagi in the cervical region were exposed. Vagal control of the heart is apparently very robust in all of these preparations, and each type of preparation yields results which complement the findings obtained from the others.

Examples of stimulus-induced bradycardia obtained in pigeon are shown in Figure 18.28. The peripheral cut ends of the right (top panel) and left (bottom panel) cervical vagus nerves were stimulated with trains of pulses at a frequency of 50 Hz. In each case, the contralateral vagus nerve was intact. In these examples, the intensity of stimulation used was capable of arresting the heart. A close parallel to the negative chronotropic effect of peripheral vagal nerve stimulation can be produced by focal electrical stimulation in the medulla (Cohen and Schnall, 1970), where anatomical studies (see above) have shown that cardiac vagal preganglionic neurons are located.

The effectiveness of the left and right vagi in controlling heart rate has been shown by some workers to be equivalent, while other workers have found strong bilateral asymmetry in this system. Bopelet (1974), Peterson and Nightingale (1976), and Goldberg et al. (1983) reported no

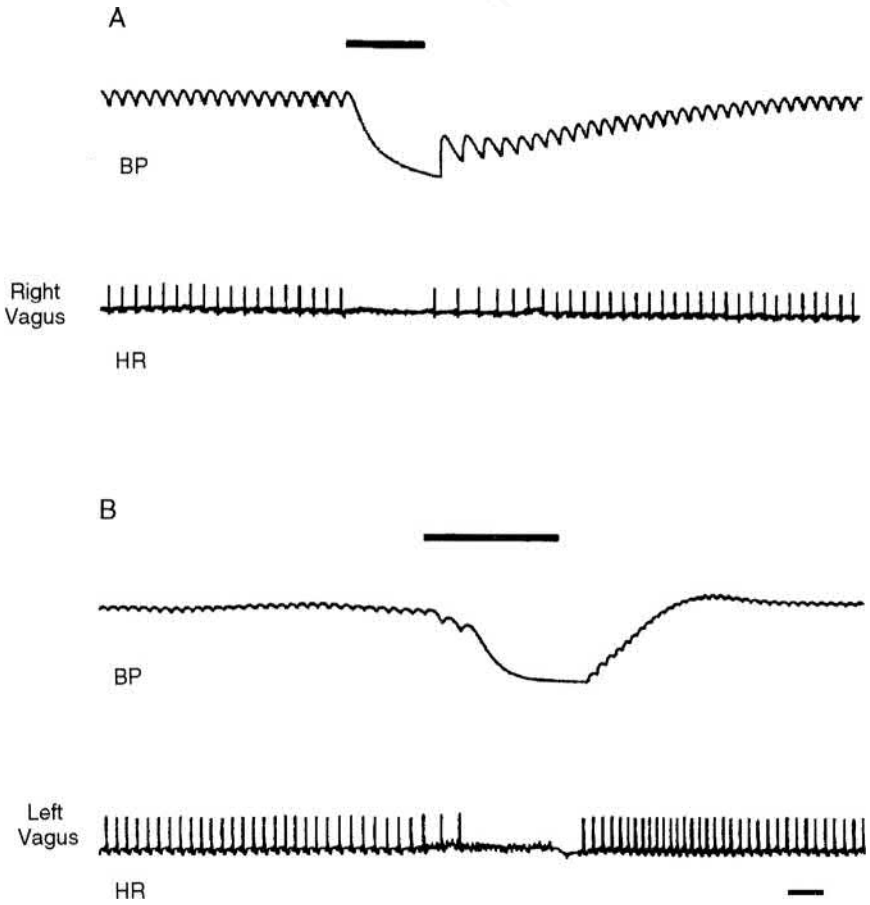

FIGURE 18.28 Effects of stimulating the right (A) and left (B) vagus nerves on heart rate (HR) and arterial blood pressure (BP) in two pigeons. The nerves were exposed in the neck and stimulated with 50 Hz trains of pulses. Stimulus duration indicated by the horizontal bars above the BP traces. Horizontal bar below the bottom trace represents 1 s. *From Cohen and Schnall (1970).*

difference in the chronotropic response of the fowl heart to electrical stimulation of left and right vagus nerves. In the same species, however, Sturkie (1986) and Lang and Levy (1989) reported that the right vagus was more effective in altering heart rate than was the left. Johansen and Reite (1964), in ducks and seagulls, Jones and Purves (1970) in ducks, and Cohen and Schnall (1970) in pigeons, all reported a similar asymmetrical response to electrical stimulation of the vagus nerves. Furthermore, in a systematic study of vagal control of heart rate in the duck, Butler and Jones (1968) showed by means of cold blockade of the vagi in the neck and by unilateral and bilateral section of these nerves that vagal dominance could change sides over time. However, the latter authors did not stimulate the peripheral cut ends of the vagi after nerve section, so it is not known whether the origin of this bilateral asymmetry was within the central nervous system or at the heart.

Lindmar et al. (1983) have quantified the amounts of ACh released in the isolated chicken heart by stimulation of the attached left and right vagal stumps in an attempt to determine if there were bilateral differences in the intracardiac connections of these nerves. If fibers from each vagus innervated approximately the same number of postganglionic intracardiac neurons, the amount of ACh released by stimulation of either nerve alone would be expected to be similar, and this was in fact found to be the case. If there were no overlap in the populations of intracardiac neurons innervated by each vagus, then the sum of ACh released by unilateral stimulation of each nerve should be the same as that released by simultaneous bilateral nerve stimulation. However, Lindmar et al. (1983) found that the sum of ACh released by separate nerve stimulation was significantly greater than that released by bilateral stimulation, indicating that a large proportion of intracardiac neurons must have been bilaterally innervated. In these experiments, it was not possible to separate the responses of postganglionic neurons innervating the pacemaker tissue from the responses of neurons subserving other functions, but if it is assumed that the overall pattern of bilateral innervation found by Lindmar et al. (1983) can be applied to the specific subpopulation of neurons controlling heart rate, then this pool of neurons may be controlled by preganglionic fibers running in either nerve. There would thus be little reason to expect that side-to-side shifts in vagal dominance result from factors acting to change the relative intracardiac influences of these nerves. This line of reasoning supports the notion that changes in the pattern of activity of vagal preganglionic neurons in the medulla may be responsible for spontaneous shifts in the dominant vagus nerve. Such central nervous factors might be investigated using the approach of Gold and Cohen (1984) to simultaneously record spontaneous activity from neurons in medullary vagal complexes on both sides.

18.5.3.2.2.2.3 Inotropic effects. Despite the evidence cited above for strong negative inotropic effects of endogenously released or exogenously applied ACh in the avian heart *in vitro*, the inotropic effects of vagal stimulation on *in situ* hearts is controversial. Folkow and Yonce (1967) unmasked a strong reduction in one index of left ventricular contractility, that of peak left ventricular chamber pressure, in the duck heart in response to vagal nerve stimulation when heart rate was kept constant by electrical pacing. These authors also found that CO declined with vagal stimulation during pacing. Since vagal stimulation was shown not to affect peripheral resistance in this study, the fall in CO must have been caused by a decrease in stroke volume. While contractile force was not measured directly, the authors attributed both the fall in left ventricular pressure and in CO to a vagally mediated decrease in ventricular contractility. That this effect was neurally mediated was demonstrated by the elimination of the effects of vagal stimulation after atropine was administered intravenously. Furnival et al. (1973), using another index of ventricular contractility, that of maximum rate of change of left ventricular pressure, reported results contrary to those of Folkow and Yonce (1967). In their comparative study of the responses of ventricular contractility to vagal stimulation in the dog, duck, and toad, Furnival et al. (1973) reported that only the amphibian heart displayed a significant reduction in contractility. These authors proposed that the ventricles of the ducks in the experiments of Folkow and Yonce (1967) had been subject to very high end-diastolic pressures as a consequence of the experimental protocol, were probably in failure as a result of this treatment, and thus responded abnormally to vagal stimulation. Yet Lang and Levy (1989), using the same index of ventricular contractility in the chicken as that employed by Furnival et al. (1973) in the duck, concluded that vagal stimulation could produce decreases of more than 50% in contractile force. Furthermore, the inotropic responses to vagal stimulation in the chicken heart reported by Lang and Levy (1989) were considerably more powerful than those that could be obtained in mammalian hearts.

The controversy surrounding this issue likely hinges on problems inherent in the methods used to evaluate ventricular contractility. Resolution of this issue will only be possible when more direct indices of contractility, such as direct attachment of Walton-Brodie type force gauges to the ventricular walls, estimation of beat-by-beat ejection fraction, or the measurement of CO in combination with ventricular and systemic pressures for calculating stroke work, are employed.

18.5.3.2.2.2.4 Tonic parasympathetic activity. Studies of tonic parasympathetic restraint of heart rate in several bird species have shown that this, like sympathetic tone, varies over a wide range. The factors discussed in Section 18.5.3.2.1, which affect the evaluation of

sympathetic tone (state of anesthesia, presence or absence of tone from the other autonomic limb), apply equally to the analysis of vagal tone, and the protocols used in studies of the extent of vagal restraint will therefore influence the way in which the results of these studies are interpreted. In a study by Johansen and Reite (1964) in awake or anesthetized ducks with intact sympathetic cardiac innervation, section of one vagus nerve (right or left) produced no change in heart rate; the chronotropic response to subsequent section of the remaining vagus was an increase in heart rate up to 65% above that in intact or unilaterally vagotomized animals. These results imply the presence of strong tonic vagal restraint of the heart; however, the authors found that after bilateral vagotomy, β-blockade revealed a high degree of sympathetic tone to the heart. Since the authors did not perform the converse experiment of β-blockade prior to bilateral vagotomy in this study, neither the balance between parasympathetic and sympathetic tone nor the actual degree of parasympathetic restraint on the heart could be ascertained. In unanesthetized ducks, Butler and Jones (1968), using a combination of cold block and section of the cervical vagi, showed that mean resting heart rate rose about 180% over the rate prior to these manipulations. In another study by the same authors, pharmacological blockade of the parasympathetic nervous system with atropine caused mean heart rate to increase to about 150% over the control value in awake ducks (Butler and Jones, 1971). In both of these studies, the sympathetic nervous system was functional during evaluations of parasympathetic tone. In chickens, Butler (1967) found that heart rate increased to 138% over the control value after bilateral vagal nerve section; in contrast to this, Bopelet (1974) reported an increase of only 8%, and Peterson and Nightingale (1976) found no change in rate in chickens after bilateral vagotomy. Sympathetic influence on the heart had not been eliminated in any of these studies. Sturkie and co-workers (reviewed by Sturkie, 1986) addressed the problem of evaluating parasympathetic tone to the heart by examining the effects of pharmacological or surgical vagotomy in the absence of sympathetic cardiac influences in the chicken using the rationale discussed in Section 18.5.3.2.1. They found that the net restraining effect of tonic parasympathetic activity on the chicken heart was the equivalent of a 20% reduction in heart rate from the rate of the completely decentralized heart. This estimate of vagal tone is substantially lower than the estimates of other workers in chickens (Butler 1967) or in ducks (Johansen and Reite, 1964; Butler and Jones, 1968, 1971) in which the sympathetic cardiac innervation was functional. The degree of parasympathetic restraint on the heart in the latter studies may have been exaggerated by the presence of ongoing sympathetic drive after the lifting of vagal influence.

18.5.3.2.3 Control of CO

The volume of blood pumped by either the left or right ventricle per unit time is termed CO. The total volume of blood pumped by the heart per unit time is therefore twice the CO, since the outputs of both sides of the heart must be exactly matched over time. CO, usually expressed in units of milliliters per minute, is the product of the rate of contraction of the heart (beats per minute) and the volume pumped during each beat, or stroke volume (mL). Rate and stroke volume are determined by factors which may be intrinsic or extrinsic to the heart. Intrinsic factors include atrial P-cell activity and contractile properties of the cardiac muscle fibers. Extrinsic factors affecting rate and stroke volume include autonomic nervous activity and levels of circulating cardiotropic hormones. CO over a given time period will thus be determined by the complex interplay of these intrinsic and extrinsic factors. Some of these have been discussed in previous sections, and references will be made to them as necessary.

18.5.3.2.3.1 Role of heart rate in control of CO The basal level of heart rate in the absence of external influences is primarily determined by the inherent membrane properties of the P-cells of the SA node (Section 18.2.3). The rate of depolarization, and thus the rate of discharge of APs in these cells, is set by the ion conductances through their membranes (particularly K^+), but this process is itself partly dependent on physical factors such as the concentrations of extracellular ions and temperature. Under most circumstances, these physical factors are kept within fairly narrow limits by homeostatic mechanisms and should therefore not affect heart rate substantially.

The interaction of the sympathetic and parasympathetic branches of the autonomic nervous system controls heart rate in a complex, nonlinear manner. Part of this complexity arises from the fact that the full chronotropic effects of vagal stimulation on heart rate occur within a few heart beats whereas it may take up to 30 s for the full expression of the cardiac response to sympathetic stimulation. Consequently, the most rapid changes in heart rate appear to be dominated by the parasympathetic system. The major reason for the nonlinearity is that the degree of parasympathetic−sympathetic interaction at the heart may be changed by increasing output of one of these limbs.

The relationship of heart rate to bilateral stimulation of the distal cut ends of the vagus and cardiac sympathetic nerves has been examined in the duck *A. platyrhynchos* (Furilla and Jones, 1987b). Increasing sympathetic activation at zero vagal activity increases heart rate by over 200 beats min^{-1} while increasing sympathetic drive at maximal vagal activation only increases heart rate by 50 beats/min. Similarly, increasing vagal activation causes heart rate to fall by more than 200 beats min^{-1} at zero sympathetic

activity and by nearly 400 beats min^{-1} at maximal sympathetic activity. Obviously, the greater the vagal drive, the more this input is able to occlude sympathetic effects on the heart, accounting for the nonlinearity in the interplay between the two branches of the autonomic nervous system at the cardiac pacemaker. This increased parasympathetic effectiveness in cardiac control is termed accentuated antagonism and may be mediated through two mechanisms. First, in response to sympathetic stimulation above a certain threshold, there is a cholinergically mediated reduction in prejunctional release of NE. Second, the magnitude of the postjunctional response to a given level of sympathetic stimulation is attenuated by ACh (Levy, 1971).

Short-term heart rate fluctuations are caused by the continued tug-of-war between the two branches of the autonomic nervous system at the pacemaker. This interplay may overlie long-term changes in heart rate caused, for instance, by changes in levels of circulating hormones. The normal homeostatic processes tend to reduce variability and maintain constancy of internal physiological functions, and short-term fluctuations in heart rate are usually seen as perturbations away from the norm. If a series of cardiac intervals is recorded from an animal, the duration of intervals within the series appears quite irregular with apparently random fluctuations occurring all the time. Whether these fluctuations are truly random or patterned, in the latter case providing evidence for chaotic control of heart rate (Denton et al., 1990; Goldberger et al., 1990), is a matter of some controversy. The strongest evidence for chaotic control of heart rate may lie in the morphology of the nerves innervating the heart. The nerves divide repeatedly, like the branching of a tree which is an intrinsically fractal structure. Hence, if the anatomy is fractal then why should the day to day workings of the system not be fractal as well? (Goldberger, cited in Pool, 1989; Goldberger, 1991).

In any event, it is clear that, rather than maintaining a homeostatic steady state, heart rate fluctuates considerably, even when recorded over short time periods (Figure 18.29A). The interbeat intervals form a time series which can be transformed into the frequency domain by Fourier analysis, revealing the presence of periodic components within the series. The square of the absolute value of the Fourier transform yields the power spectrum of the heart rate variability (PS/HRV; Kamath and Fallen, 1993).

The PS/HRV of an intact, resting, duck (*Aythya affinis*) is shown in Figure 18.29B(i). This plot reveals a respiratory sinus arrhythmia as a single major peak at the respiratory frequency. This is a manifestation of respiratory modulation of cardiac parasympathetic activity (Shah et al., 2010; the response to sympathetic heart stimulation is too slow to significantly affect heart rate at a high frequency). Blockade of the sympathetic nervous system with a β-antagonist tends to increase heart rate variability although the amplitude of the high-frequency components are reduced (Figure 18.29B(ii)), while parasympathetic blockade with atropine gives a regular, unvarying heart rate (Figure 18.29B(iii)). This confirms that short-term heart rate control is dominated by the parasympathetic nervous system in *Aythya affinis*. Similar control of heart rate variability has been found in hatchling emu (*Dromaius novaehollandiae*; Shah et al., 2010).

The PS/HRV is a quantifier of autonomic responsiveness (Saul, 1990) and allows evaluation of cardiovascular regulation in birds over long-time courses and during many types of activities. Also, the influence of other periodic functions such as arterial blood pressure and vasomotor fluctuations on PS/HRV can be evaluated using this technique. Telemetric recording of heart rate, combined with frequency analysis of cardiac function, will open new doors for studying control of physiological processes in unrestrained, active birds.

18.5.3.2.3.2 Role of stroke volume in control of CO Stroke volume, like heart rate, is dependent upon factors intrinsic and extrinsic to the heart. As all myocytes within the heart contract during each beat, the primary intrinsic factors which determine stroke volume are the inherent contractile properties of each muscle fiber and the resting lengths of all the fibers. The amount of force developed during contraction by a cardiac muscle fiber at a specified precontraction length is properly termed "contractility," but this term has also been used more loosely to describe the collective contractile properties of all muscle fibers associated with one chamber of the heart. A major problem in quantifying contractility is that the force developed by a single cardiac muscle fiber is difficult to measure in working hearts. Consequently, a number of indirect indices have been developed to estimate this variable. These include measuring cardiac outflow volume over time to calculate stroke volume; recording the ventricular peak systolic pressure developed against a fixed afterload or into a constant arterial pressure; and measuring the rate of rise of ventricular pressure during systole. The major assumption in all of these methods is that the measured variable reflects the contractility of all muscle fibers integrated over the dimensions of the whole chamber. However, the variety of indices of contractility used by investigators under different experimental conditions has made it difficult to compare estimates across studies. The direct measurement of volume flow from the ventricle would appear to give the most reliable index of cardiac contractility, being independent of the complicating effects of changing arterial or ventricular pressures. This measurement is also among the most difficult to make, requiring highly invasive procedures to place the appropriate instrumentation.

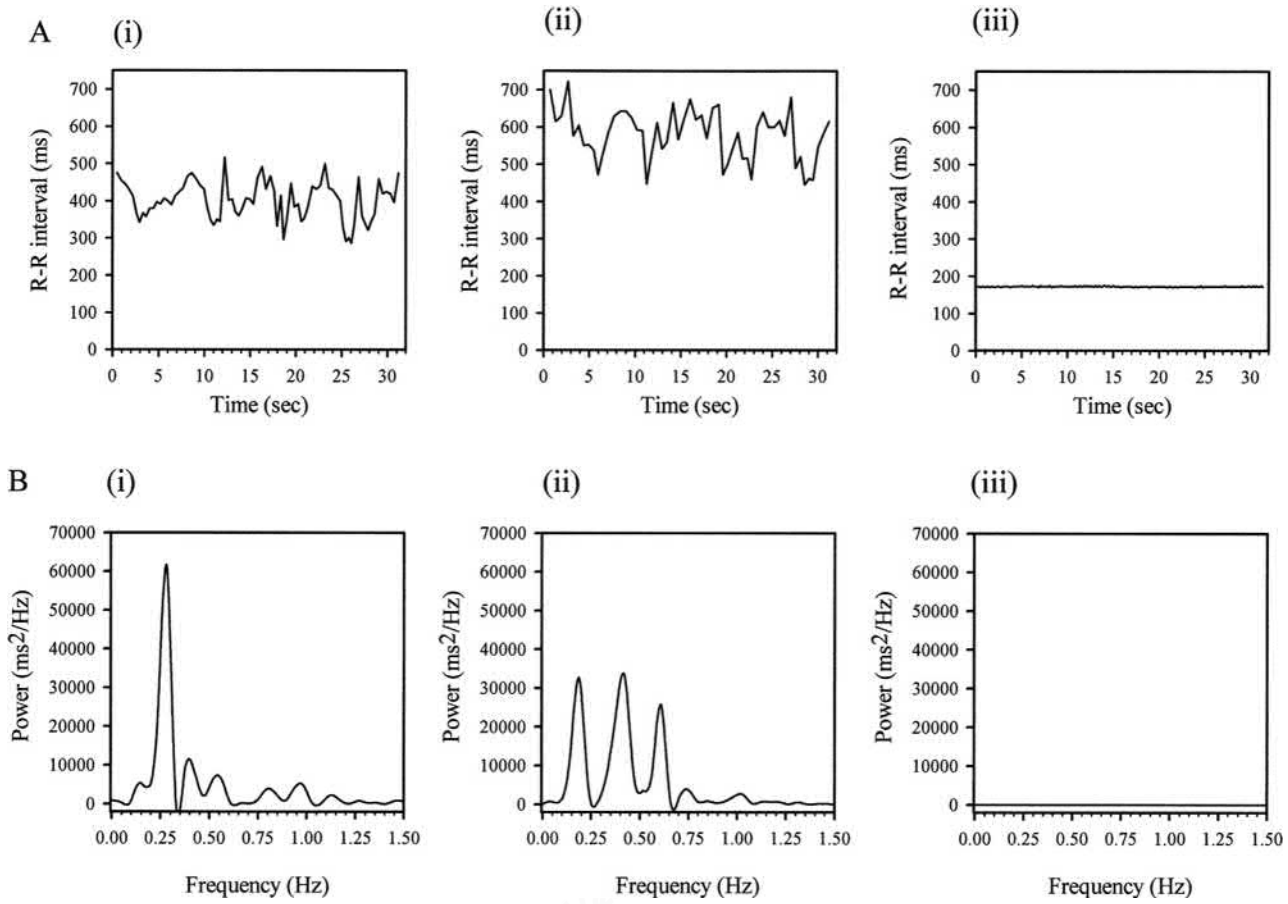

FIGURE 18.29 (A) 30-s duration time series of interbeat intervals (R−R intervals) recorded by radiotelemetry from a duck (*Aythya affinis*) while the animal was resting quietly on the water surface. (i) Control; (ii) after sympathetic nervous system blockade with Nadolol (a β-adrenergic antagonist); and (iii) after parasympathetic nervous system blockade with the muscarinic antagonist atropine. (B) Power spectra of heart rate variability derived from the time series shown in (A). (i) Control; (ii) after Nadolol blockade; and (iii) after atropine blockade. Since the time series were too short to adequately display extremely low-frequency components, these components were removed with a high-pass filter from the power spectra. *From McPhail et al. (unpublished data).*

By analogy with the contraction of skeletal muscle, the amount of force developed by a contracting cardiac muscle fiber depends upon its precontraction length ("preload"). This principle was first applied to the heart by Otto Frank (summarized in Rushmer, 1976), who showed that, within limits, the greater the preload on ventricular muscle in diastole, the more tension was developed during the next systole. This length−tension relationship was further investigated by Ernest Starling and co-workers, who demonstrated that the amount of blood ejected by the left ventricle during systole was proportional to the volume of blood in the ventricle at the end of the diastolic filling phase of the cardiac cycle. These concepts have been combined into the Frank−Starling relationship to describe the intrinsic responses of ventricular stroke volume to changes in cardiac venous return, expressed graphically in Figure 18.30. Elevated contractility of each muscle fiber in the ventricle is evoked by increasing the preload on all of the fibers by increasing the volume of blood filling the ventricle before each beat; this is reflected in an overall increase in ventricular stroke volume. The curve designated A in Figure 18.30 is termed a ventricular function curve. The relationship embodied in this curve demonstrates an autoregulatory feature of cardiac function known as heterometric regulation: a change in the resting fiber length (heterometry) results in a change in contractility in the same direction. This regulatory mechanism is an intrinsic property of cardiac muscle. The consequence of this mechanism for the overall function of the heart is that, if all other conditions remain constant, CO will be determined by venous return. An increase in venous return to the left ventricle via the left atrium will result in greater end-diastolic stretch of the ventricle walls and an increase in stroke volume at the next beat; conversely, stroke volume will be reduced if cardiac return falls. In short, the heart "pumps what it gets" if all other factors are unchanging.

Cardiac contractility is influenced by extrinsic factors in addition to the intrinsic Frank−Starling mechanism. Circulating hormones such as EPI and the autonomic

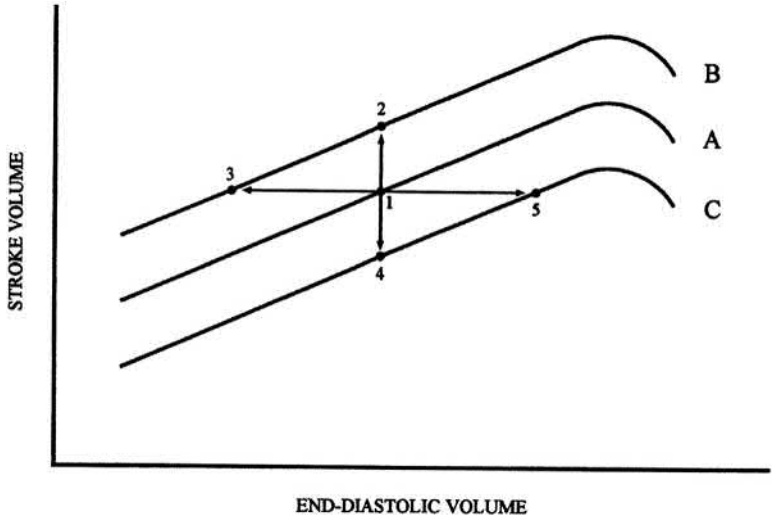

FIGURE 18.30 Idealized graphical representation of the Frank–Starling relationship for cardiac ventricular muscle. (A) Intrinsic ventricular function curve depicting the relationship between end-diastolic volume (representing degree of stretch of muscle fibers) and stroke volume (index of contractility) in the absence of extrinsic influences. The curve peaks and begins to decline at high end-diastolic volumes because resting sarcomere length is maximal here. (B and C) Factors extrinsic to the heart which alter inotropic function of cardiac muscle reset the ventricular function curve to operate over different ranges of stroke volume, independent of end-diastolic volume or initial fiber length. (B) Elevated cardiac sympathetic drive or circulating catecholamines have positive inotropic effects, resetting the curve toward higher stroke volumes. (C) Elevated vagal drive has negative inotropic effects, resetting the curve toward lower stroke volumes. Points 1 through 5 are the operating points assumed for the text discussion of the effects of extrinsic factors on ventricular function.

neurotransmitters NE and ACh (see Sections 18.5.3.1 and 18.5.3.2) directly affects the contractility of cardiac muscle fibers. These extrinsic factors are superimposed on the intrinsic autoregulatory factors governing stroke volume and can shift the whole ventricular function curve (curve A in Figure 18.30) toward higher (curve B) or lower (curve C) stroke volumes at the same resting muscle fiber length or degree of ventricular filling. This type of regulation of stroke volume is referred to as homeometric regulation to emphasize the fact that changes in contractility can occur independent of resting fiber length. An increase in sympathetic drive to the heart or an increase in the level of circulating catecholamines will increase ventricular inotropic function homeometrically; thus a greater stroke volume will result from the same degree of cardiac filling, as indicated in Figure 18.30 by the arrow from point 1 on curve A to point 2 on curve B. Another way to consider this is that after such a shift in the curve a much smaller end-diastolic volume will give the same stroke volume (arrow from point 1 to point 3). On the other hand, elevated vagal drive to the heart of birds can decrease the contractility of ventricular muscle and will shift the ventricular function curve toward a lower stroke volume (curve C in Figure 18.30). At the new operating point, the same degree of preload will result in a lower stroke volume (arrow from point 1 to point 4); alternatively, a much larger end-diastolic volume will be required to maintain the same stroke volume (arrow from point 1 to point 5).

The arterial pressure against which the ventricle pumps ("afterload") is a major extrinsic factor in determining the magnitude of stroke volume. The pressure generated during the isometric phase of ventricular contraction is a function of the contractility of the muscle fibers, and when chamber pressure exceeds that in the aorta the valves open and blood is ejected from the ventricle during the isotonic phase. If the preload on the ventricle is increased by elevating the arterial blood pressure without a change in contractility or end diastolic volume, stroke volume of subsequent beats will be reduced because more energy will be required to raise chamber pressure above the new level of arterial pressure. Initially, this will leave a larger fraction of the previous end-diastolic volume still in the chamber at the end of systole, resulting in an increased level of resting tension on the muscle fibers during the next filling phase. This increased tension, according to the Frank–Starling mechanism, will quickly result in increased contractility during subsequent beats, restoring stroke volume by heterometric regulation in the face of the increased arterial pressure.

In many species of birds, CO is adjusted to match perfusion requirements of the tissues in a variety of conditions, such as during exercise, hypoxia, or submersion (see Section 18.6). These adjustments appear to be made primarily through alterations in heart rate with stroke volume remaining relatively unchanged. Changes in CO during exercise are driven by increased heart rate in ducks (Bech and Nomoto, 1982; Kiley et al., 1985), geese (Fedde et al., 1989), and turkeys (Boulianne et al., 1993a,b). However, in the emu (Grubb et al., 1983) and the chicken (Barnas et al., 1985), stroke volume may increase by up to 100% during exercise, contributing significantly to elevated CO. Reflex changes in CO mediated by systemic arterial baroreceptor input also appear to operate via alterations in heart rate, leaving stroke volume relatively unchanged (Section 18.5.4.2). In summary, during exercise, hypoxia,

or submersion, birds display significant changes in heart rate, arterial blood pressure, and venous return from the resting condition. In the transition from the resting condition to these altered states, stroke volume also varies. However, in most of the species examined so far, stroke volume returns to values close to those at rest after a short period of initial adjustment. This indicates that intrinsic autoregulation of CO has the potential to play an important role in the maintenance of stroke volume in the face of largescale circulatory adjustments.

18.5.4 Reflexes controlling the circulation

18.5.4.1 Chemoreflexes

In birds, reflex adjustments of CO and vascular caliber are generated by chemoreflexes in response to changes in levels of oxygen, carbon dioxide, and pH in the cerebrospinal fluid and in arterial blood. Receptors sensitive to CO_2 in cerebrospinal fluid are present in the avian central nervous system (Jones et al., 1982), but no detailed studies of the location or transduction properties of these receptors have been done in birds. However, if these receptors are similar to those found in mammals, they may be located at or near the surface of the ventrolateral medulla (reviewed by Schlaefke, 1981). Arterial chemoreceptors in birds are located primarily in the carotid bodies, bilateral structures lying caudal to the thyroid gland, and close to the ultimobranchial gland and nodose ganglia of the vagus nerves and the carotid artery (from which they are supplied with blood) (Adams, 1958; Jones and Purves, 1970; Kameda, 2002). The carotid bodies are innervated by the vagus and the recurrent laryngeal nerves (Kameda, 2002). Chemoreceptors have also been reported in aortic bodies associated with the roots of the great vessels in several species of birds (Tcheng et al., 1963; Ito et al., 1999).

The discharge characteristics of arterial chemoreceptors in response to changes in arterial PCO_2 ($PaCO_2$), PO_2 (PaO_2), and arterial pH (pHa) have been studied in the duck and chicken. Receptor discharge rate increases proportionally with $PaCO_2$ and in inverse proportion to PaO_2 (Bouverot and Leitner, 1972; Bamford and Jones, 1976; Nye and Powell, 1984; Hempleman et al., 1992). Discharge sensitivities to changes in $PaCO_2$ and PaO_2 have been quantified by Hempleman et al. (1992) for carotid body chemoreceptors in the duck. When PaO_2 was maintained at a normoxic level (near 100 mmHg) mean chemoreceptor sensitivity to step changes in $PaCO_2$ (produced by changing the fraction of CO_2 in the air breathed by the bird) was +0.20 impulses s^{-1} mmHg $PaCO_2^{-1}$. Hypoxia (PaO_2 56 mmHg) potentiated chemoreceptor discharge in response to altered $PaCO_2$ (Figure 18.31). In this condition, the same step changes in $PaCO_2$ as given in normoxia resulted in a sensitivity of +0.32 impulses/s mmHg $PaCO_2$.

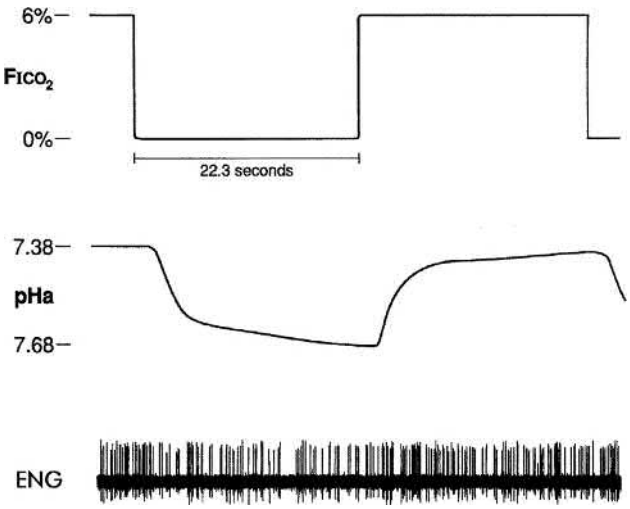

FIGURE 18.31 Single-fiber arterial chemoreceptor response recorded from vagal slip [bottom trace, electroneurogram (ENG)] to step changes in inspired CO_2 level [top trace, fraction of CO_2 in inspired gas (F_ICO_2)] during hypoxia (10% O_2 in inspired gas) in a duck. Arterial pH [middle trace (pH_a)] also changes in step with inspired CO_2. Chemoreceptor discharge is sensitive to the level of CO_2 and pH_a and to rate of change of these variables. *From Hempleman et al. (1992).*

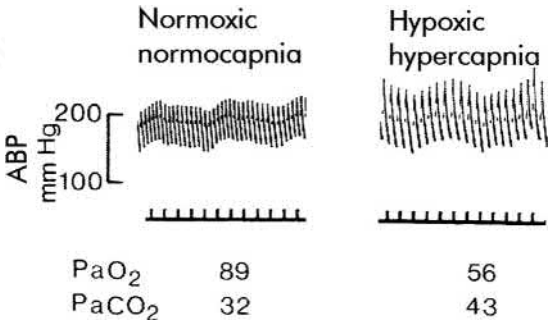

FIGURE 18.32 Effect of systemic hypoxic hypercapnia on heart rate and blood pressure in mallard duck. Animal was artificially ventilated after spontaneous respiratory movements were suppressed with intravenous pancuronium bromide. (Left panel, upper trace) Arterial blood pressure and heart rate during ventilation with air; systemic arterial blood gas values are shown at bottom. (Right panel) When blood gas values were adjusted to match those at end of 1 min submersion by altering CO_2 and O_2 levels in inspired gas, heart rate decreased as a result of arterial chemoreflex activation. In both panels the ticks on the bars under the pressure traces indicate 1-s intervals. *From Butler and Taylor (1973).*

In the absence of CO_2 in the inspired air, step changes in PaO_2 from the normoxic level to about half this level resulted in a mean sensitivity of about −0.10 impulses s^{-1} mmHg PaO_2^{-1}. Carotid body chemoreceptors are thus about twice as sensitive to changes in absolute levels of arterial CO_2 as to O_2. Some of the chemoreceptors sampled in this study were also sensitive to the rate of change of O_2 and CO_2 in the blood, indicating that proportional and rate-related information on arterial blood gas status are both transmitted to the central nervous system.

However the maximum rate of change of discharge of most rate-sensitive chemoreceptors was in the lower frequency range of physiologically occurring blood gas oscillations. Therefore, only relatively low frequencies of blood gas oscillation, such as those occurring at rest or during low-intensity activities, will be faithfully transduced. At higher oscillation frequencies, such as those occurring during panting or high-intensity exercise, chemoreceptor inputs to the central nervous system probably represent "mean" blood gas levels averaged over several oscillatory cycles (Figure 18.32).

Arterial chemoreceptors are spontaneously active at normoxic and normocapnic blood gas levels in birds, and these receptors have been proposed to play an important role in setting the level of eupneic ventilation under these conditions (Bouverot and Leitner, 1972). However, the role of arterial chemoreceptors in reflex control of the avian circulation is less clear. Analyses of the circulatory effects of chemoreceptor activation are complicated by parallel changes in ventilation. During apneic asphyxia in ducks, blood oxygen tension falls, CO_2 tension rises, and carotid body chemoreceptors become progressively more strongly stimulated; this input plays a major role in initiating and maintaining an intense bradycardia (Jones and Purves, 1970; Butler and Taylor, 1973). However, if blood gases in spontaneously breathing ducks are artificially adjusted to mimic the hypoxic and hypercapnic levels achieved during apneic asphyxia, chemoreflex drive acts to increase ventilation, leading to elevated drive from pulmonary receptors. In this state, there is little or no change in heart rate (Butler and Taylor, 1973, 1983). When the rise in ventilation (and thus the elevation in pulmonary receptor input) is prevented by controlling tidal volume and respiratory frequency during hypoxic hypercapnia in paralyzed but unanesthetized animals, heart rate falls to a level midway between that in normoxic, normocapnic animals and that obtained at end-dive (Butler and Taylor, 1973, 1983). This effect is illustrated in Figure 18.18. Subsequent cessation of respiration by stopping the ventilator pump then results in the full expression of chemoreceptor mediated bradycardia: heart rate falls to the same level as at end-dive (Butler and Taylor, 1973, 1983). These experiments show that in ducks, as in mammals, the cardiovascular responses to strong arterial chemoreceptor stimulation during spontaneous breathing are masked by elevated ventilatory drive. Butler and Taylor (1983) have suggested that pulmonary receptors activated by increased ventilation contribute to occlusion of the cardiac chemoreflex.

Input from peripheral arterial chemoreceptors can reflexively alter peripheral vascular resistance, but the general role of chemoreceptors in control of the vasculature has not been established. Indirect evidence for chemoreflex effects on the vasculature comes from a study by Bouverot et al. (1979), who showed a trend toward increased peripheral resistance in carotid body-intact ducks subjected to arterial hypoxia while breathing spontaneously. The same stimulus in animals after denervation of the carotid bodies led to a 40% fall in peripheral resistance, indicating a potential role for these chemoreceptors in generating the vascular response to hypoxia. As with cardiac responses to carotid body stimulation, elevated ventilation during hypoxia may mask the full extent of reflexogenic vasoconstriction. In the study of Bouverot et al. (1979), no attempt was made to evaluate this interaction by controlling ventilation.

It is clear that the full role of arterial chemoreflexes in circulatory control has yet to be defined in birds. Elevated carotid body input can result in both ventilatory and cardiac responses, and both of these responses are important in maintaining oxygen delivery to and CO_2 washout from working tissues. Further experiments are necessary to establish the relative importance of these limbs of the chemoreflex in matching ventilation with perfusion to cope with changes in internal and external levels of these gases.

18.5.4.2 Baroreflexes

Arterial blood pressure provides the driving force for perfusion of the systemic vascular beds and must therefore be maintained within limits that ensure optimal tissue blood flow under a variety of physiological conditions. Blood pressure in birds is maintained by the baroreflex, a mechanism employing negative feedback (see reviews by Bagshaw, 1985 and Smith, 1994). Adjustments in blood pressure produced by the baroreflex are driven by afferent signals from arterial baroreceptors. These are mechanoreceptors with their receptor endings embedded in connective tissue of the arterial wall, where they sense changes in arterial pressure as variations in wall tension. An increase in intraarterial pressure results in an increase in circumference of the vessel wall, which in turn stretches baroreceptor endings to increase their frequency of discharge of APs. Arterial baroreceptors in birds are located primarily in the walls of the aorta close to the left ventricular valves (Jones, 1973). Their axons course to the brainstem via aortic nerves which arise from the nodose ganglia of the vagus (Nonidez, 1935). In the few studies of avian baroreceptor function done to date, discharge characteristics in response to changes in blood pressure appear to be similar to those of mammalian high threshold, slowly adapting baroreceptors (Jones, 1969, 1973). Spontaneous baroreceptor impulse generation is phase locked to mechanical events in systole of the cardiac cycle. Baroreceptors are also sensitive to the rate of rise of the pressure pulse. It thus appears that baroreceptors are capable of transmitting information on cardiac rate, peak systolic pressure, and the slope of the aortic pressure waveform (which may in turn reflect cardiac contractility) to the central nervous system.

Mean arterial blood pressures of resting birds are higher than those recorded in mammals of equivalent body weight at rest; indeed, mean resting pressures may exceed 150 mmHg in some avian species (Altman and Dittmer, 1971). Avian baroreceptor discharge occurs at resting levels of blood pressure in birds (Jones, 1969, 1973), so it is likely that the baroreflex is tonically active at these pressures. Changes in blood pressure sensed at the receptors are represented to the baroreflex circuitry in the central nervous system by changes in baroreceptor afferent discharge frequency. The baroreflex acts to adjust pressure in a direction opposite to that of the initial pressure change. This reflex operates through both peripheral vascular and cardiac effectors to return blood pressure toward a set level after disturbances. Pressure is thus maintained within fairly narrow limits over time to ensure a constant pressure head for tissue perfusion. Little is known of the central nervous mechanisms involved in blood pressure regulation in birds. Inhibition of NMDA by ketamine attenuated the pressor response in the pigeon suggesting a role for the vagal nerve as in mammals (Lucitti and Hedrick, 2006). It is assumed that the basic organization of central components of the baroreflex is similar to the arrangement in mammals (Lucitti and Hedrick, 2006).

The primary cardiovascular response to changes in blood pressure is a baroreflex-mediated change in CO, seen in Figure 18.33A as a rapid fall in heart rate in response to a pharmacologically induced pressure increase. Such reflex responses are completely abolished by bilateral section of the aortic nerves (Figure 18.33B). The sensitivity of the blood pressure–heart rate relationship ranges from −0.5 to −3.13 beats min^{-1} $mmHg^{-1}$, depending on species and method of evaluation (chickens, Bagshaw and Cox, 1986; ducks, Smith and Jones, 1990; 1992; and Millard, 1980; pigeon Luctti and Hedrick, 2006; see Smith, 1994 for further discussion). The baroreflex-mediated effects of changing pressure at the receptors can be mimicked by electrical stimulation of the central cut end of an aortic nerve in an animal in which both aortic nerves are sectioned. This method was used by Smith and Jones (1992) to explore the dynamic role of baroreceptors in controlling the circulation. Stimulation of the aortic nerve in barodenervated animals evokes a decrease in arterial blood pressure in proportion to the stimulus frequency when stimulus current is set just above threshold for a response (Figure 18.34). This response works primarily through a fall in CO, mediated by decreased heart rate with no change in stroke volume (Smith and Jones, 1992). This response follows the same pattern as the baroreflex-mediated response to pharmacologically induced pressure changes in baroreceptor-intact birds; that is, in both intact and denervated animal's baroreflex activation was expressed primarily through changes in heart rate. However, the baroreflex can engage peripheral vasomotion as well as cardiac responses: in barodenervated animals, stimulation of the aortic nerve with a current intensity several times the threshold level produced decreases in peripheral resistance as well as in heart rate (Smith and Jones, 1992). These data suggest that when relatively small disturbances in pressure occur they will be compensated by

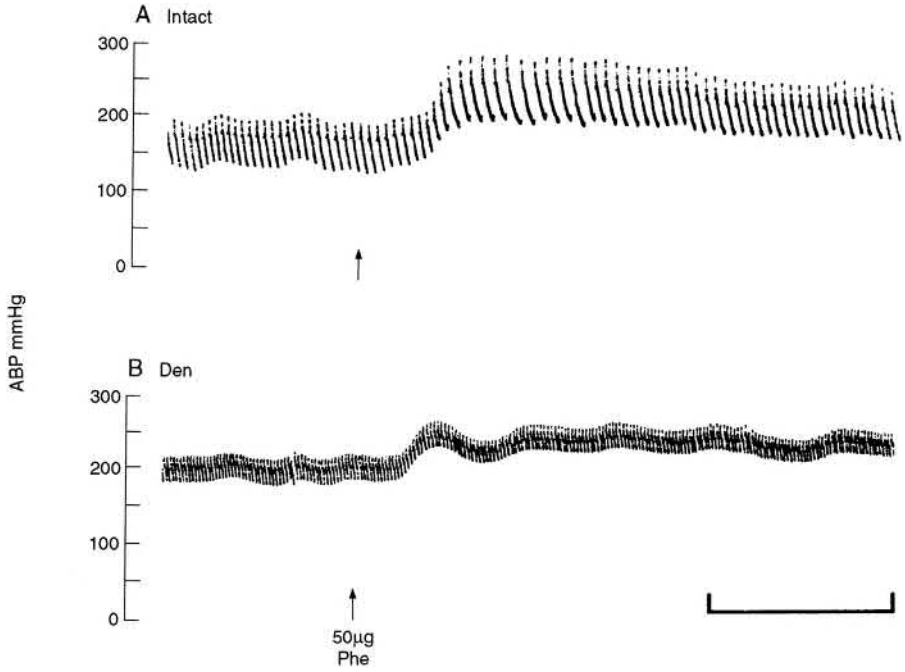

FIGURE 18.33 Heart rate responses to increased arterial blood pressure (ABP) induced by bolus i.v. doses of phenylephrine (Phe, injected at *arrows*) in the same duck (A) before and (B) after barodenervation by section of aortic nerves. Baroreflex-mediated bradycardia was eliminated by denervation of baroreceptors. Note increased preinjection blood pressure and heart rate in barodenervated animals, indicating a degree of baroreflex-mediated restraint on cardiovascular system in baroreceptor intact animal. *From Smith (unpublished data).*

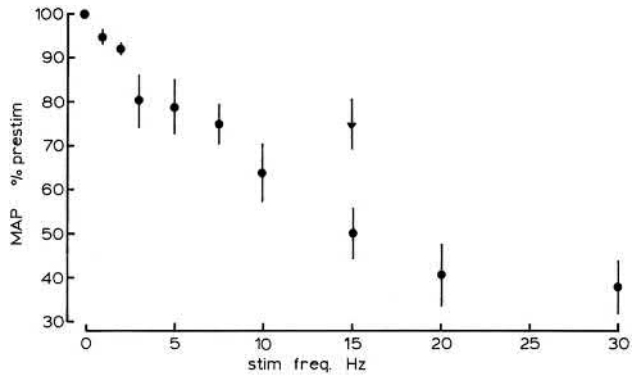

FIGURE 18.34 Normalized responses of mean arterial blood pressure (MAP) to electrical stimulation of aortic nerve in awake ducks spontaneously breathing air (P_aO_2 88 mmHg, P_aCO_2 26 mmHg; *closed circles*) or a hypoxic hypercapnic gas mixture (P_aO_2 62 mmHg, P_aCO_2 44 mmHg; *triangle*). Pressure response at each frequency of nerve stimulation is expressed as a percentage change in MAP relative to MAP just prior to stimulation. Loading the chemoreceptors attenuated the depressor effect of aortic nerve stimulation at 15 Hz. Error bars represent: S.E.M. for five trials in normoxic conditions and three trials during hypoxic hypercapnia in three animals. Stimulus pulse duration and amplitude were constant within each trial. *From Smith (unpublished data).*

adjusting CO, but larger changes in pressure will be corrected by a combination of cardiac and peripheral vascular adjustments.

The effectiveness of baroreflex control of the circulation can be modified by interaction with other reflexes, such as the chemoreflex, which may be concurrently engaged. In an effort to determine the cause of an apparent reduction in baroreflex function observed during submersion in ducks (Jones et al., 1983; Millard, 1980), Smith and Jones (1992) stimulated the aortic nerve in barodenervated ducks before and during periods of elevated chemoreceptor drive. Stimulation of chemoreceptors was accomplished by ventilating animals with a gas mixture which simulated the hypoxic and hypercapnic blood gas values observed at the end of 2 min of submersion; this significantly decreased the capability of aortic nerve stimulation to affect mean arterial pressure. This is shown in Figure 18.34 by a 50% decrease in the pressure response to aortic nerve stimulation at a frequency of 15 Hz during hypoxic hypercapnia (triangle), compared with the responses during air breathing (closed circles). That this occlusive response was due to chemoreceptor activation was further demonstrated by the attenuation of baroreflex function during perfusion of one vascularly isolated carotid body with venous blood in otherwise normoxic, normocapnic animals which were spontaneously breathing (Smith and Jones, 1992). It therefore appears that the chemoreceptor drive that develops after the first minute of submersion (Jones and Purves, 1970) is at least partly responsible for the attenuation of baroreflex control of cardiovascular variables which occurs during this period.

18.5.4.3 Reflexes from cardiac receptors

Small nerve terminals in the shape of simple knobs, plates, or rings as well as straight or spirally wound nerve endings have been observed in anatomical studies of avian atria and ventricles (Ábrahám, 1969; also see review by Jones and Milsom, 1982), but bird hearts do not appear to have the complex and highly developed sensory receptor endings present in large numbers in mammalian hearts. Few functional studies of avian cardiac receptors and their reflexogenic effects have been done. Jones (1969) established in the duck that some afferent fibers in the cervical vagus had receptor endings associated with the heart, responding to punctate stimulation near the AV junction and discharging spontaneously in patterns which were phase-locked to mechanical events in the cardiac cycle. In the chicken, Estavillo and Burger (1973a,b) found that a majority of cardiac receptors with their cell bodies in the nodose ganglia had receptive fields located in the left ventricle near the aortic valves. Discharge patterns of these receptors were either phase-locked to the cardiac cycle or were irregular and apparently unrelated to mechanical events in the cycle. The discharge of receptors of both types could be modulated by varying inspired CO_2 and pHa independently or together. In this study, the discharge rate of phasically firing cardiac receptors was proportional to arterial blood pressure over a wide pressure range, and this relationship was reset toward lower discharge rates at increased CO_2 levels. Bilateral section of the middle cardiac nerve, carrying the axons of cardiac receptors in the chicken, produced an immediate rise in arterial blood pressure (Estavillo, 1978; Estavillo et al., 1990) reminiscent of that produced in ducks after section of the aortic nerve (Figure 18.33).

Avian cardiac receptors have been proposed to contribute to blood pressure regulation and to the control of ventilation, providing sensory feedback on intracardiac pressures and volumes. Such feedback may be modulated by changes in the levels of $PaCO_2$ and pHa (Estavillo and Burger, 1973b; Estavillo et al., 1990). In the latter study, bilateral section of the middle cardiac nerve considerably blunted the increase in ventilation elicited by systemic hypercapnia, in addition to promoting elevated blood pressure.

Birds exhibit a Bezold–Jarisch reflex similar to mammals. It manifests in ducks as a fall in heart rate and arterial blood pressure when cardiac receptors are stimulated (Blix et al., 1976; Jones et al., 1980). Blix et al. (1976) proposed, on the basis of pharmacological stimulation of cardiac receptors, that this reflex contributed to the generation and maintenance of the cardiac chronotropic response to submersion. In a reexamination of this issue, Jones et al. (1980) loaded and unloaded the cardiac receptors by altering left ventricular pressure to provide more realistic physiological

stimulation of these receptors before and during submersion. The results of this study failed to confirm a link between cardiac receptor activation and diving bradycardia.

There is as yet insufficient evidence to determine the overall function of reflexes driven by inputs from cardiac receptors. While these receptors can influence blood pressure and ventilation, they do not appear to have a primary role in pressure or ventilatory regulation. However, they may mediate some of the dynamic interactions between respiratory and circulatory systems, thus helping to correct ventilation–perfusion mismatches which can develop during exercise or in adverse environmental conditions.

18.5.4.4 Reflex cardiovascular effects from skeletal muscle afferents

Reflex-mediated changes in arterial blood pressure, heart rate, and other cardiovascular variables accompany exercise, hypoxia, and hypoxic hypercapnia in birds. In several studies designed to deduce the respective roles of peripheral arterial chemoreceptors, chemosensitive areas of the central nervous system and arterial baroreceptors in these cardiovascular responses, it has been suggested that inputs from these receptor groups do not account for all of the changes observed. Thus inputs from other receptor type must also be involved. In mammals, there is a significant reflexogenic increase in mean arterial blood pressure induced by skeletal muscle activity; receptors for this response appear to be intramuscular terminals of group III afferent fibers (small myelinated fibers) and group IV fibers (unmyelinated or C-fibers) coursing in somatic nerves (see Coote, 1975 for review). Kiley et al. (1979) implicated muscle afferents in the cardiovascular responses to exercise in ducks, and Lillo and Jones (1983) proposed that somatic muscle afferents in ducks were at least partly responsible for those portions of the cardiac and vascular responses in hypoxic hypercapnia and ischemia which were independent of chemoreceptor activation. Furthermore, Solomon and Adamson (1997) demonstrated that ducks express an "exercise pressor" reflex similar to that in mammals. This effect consists of an increase in mean arterial pressure (largely due to elevation of diastolic pressure) induced by and sustained during static contraction of a large hind limb muscle, the gastrocnemius. The authors concluded that this was a reflex effect since section of the sciatic nerve carrying afferent fibers from the muscle to the spinal cord eliminated the pressor response to muscle contraction. Whether the intramuscular receptors involved in these responses were sensing mechanical events related to muscle contraction or chemical signals resulting from intramuscular metabolite buildup as the primary physiological stimulus for this reflex was not clear from this study. The authors acknowledged that receptors sensing either modality, or both, could be driving reflex changes in pressure. The studies done to date on reflex effects of activating skeletal muscle afferents suggest that direct sensory feedback from exercising or hypoxically stressed muscle to the neural circuitry controlling the circulation could be involved in initiating or intensifying cardiovascular responses to muscle activity. Such a mechanism would serve to increase the perfusion of working muscle, but the full contribution of these reflexes remains to be determined.

18.5.5 Integrative neural control

As discussed in the previous sections, the major reflexes controlling cardiovascular function are the chemoreflex, the baroreflex, and reflexes driven by receptors within the heart and skeletal muscle. Under some conditions, these reflexes may interact, as in the case of chemoreflex occlusion of the baroreflex detailed in Section 18.5.4.2. Furthermore, there are a number of other reflexes which can affect the circulation as part of more global homeostatic control systems, such as those regulating temperature and ventilation. All reflexes influencing the circulation do so through the final common pathways of the autonomic nervous system innervating the heart and vasculature, and several of these reflexes may be engaged at the same time during physiological challenges to the animal. Integrative control of the circulation by the nervous system therefore operates through complex interactions among cardiovascular and other reflexes, but the nature of these interactions is still incompletely understood in any vertebrate group. This large-scale integration makes investigation of the properties of any one reflex a considerable challenge, particularly in unanesthetized animals. One approach to this problem is to ensure that only afferents specific to the reflex in question are stimulated, while activation of afferents associated with other reflexes is prevented. However even this may not be enough to prevent complications in analysis since efferent activity associated with one reflex, and the consequences of this activity, can produce secondary activation of other reflexes. A case in point is the activation of pulmonary reflexes consequent to an increase in ventilation driven by primary stimulation of the arterial chemoreflex. The design of further studies of avian cardiovascular reflexes embedded in complex control systems must therefore take into account the integrative nature of these systems.

A single neural mediated response, such as a change in heart rate, involving the stimulation of one or more afferent or efferent pathways by a frequently induced or naturally performed behavior, may be subject to habituation or conditioning. Habitation refers to a decrement in the response (not due to sensory adaptation or motor fatigue) resulting from repeated presentations of a single triggering stimulus. In contrast, conditioning involves the animal learning a relationship between two different stimuli. In

classical conditioning, (Pavlov, 1927) a conditioned and an unconditioned stimulus are presented with little temporal dissociation between them.

The animal learns the relation between these stimuli so that after the initial trials the reflex response can then be evoked by presenting the only the conditioned stimulus. A reflex, once conditioned, will anticipate, augment, and have similar effects as the unconditioned reflex.

Cohen and his collaborators have developed a model of conditioned learning in the pigeon for exploring cellular neurophysiological mechanisms of long-term associative learning. In this model, animals are trained to respond with a transient and quantifiable increase in heart rate (the CR) to a conditioning stimulus (CS, a 6-s whole-field retinal illumination) by pairing the CS with an unconditional stimulus (US) consisting of a 0.5-s foot shock. After an initial training period of 30−50 paired-stimulus trials, further CS without US reliably evokes CRs. The properties of this CR in the pigeon are very robust, remaining stable for long periods (up to weeks) without habituating (Cohen, 1980, 1984). Such longevity facilitates electrophysiological investigations of changes in properties of neurons involved in the development of associative learning in this system. Using this model as a platform, Cohen and co-workers have anatomically and physiologically characterized the central visual pathways for the CS, the somatosensory pathways for the US, and the descending tracts converging on the autonomic motor neurons of the final common pathway efferent to the heart in the pigeon. Much of this group's work on the efferent components of this system has already been cited in the description of the neuronal circuitry controlling cardiac function appearing earlier in this chapter.

The central and peripheral nervous pathways involved in the CR have been reviewed in detail by Cohen (1980, 1984) and are briefly summarized here. Ganglion cells throughout the retina respond with a phasic burst of APs at the start of a 6-sec period of whole-field retinal illumination. This phasic wave of excitation is transmitted synchronously along multistage pathways in the central nervous system to preganglionic sympathetic and parasympathetic motor neurons in the spinal cord and brainstem, respectively. These preganglionic neurons in turn control pools of cardiac postganglionic autonomic neurons in a synergistic manner, acting to potentiate a transient sympathetic cardio acceleration and to facilitate concurrent withdrawal of parasympathetic cardio inhibition.

Studies of the development of CRs after lesioning selected components of the central visual pathways and electrophysiological studies during the conditioning process in pharmacologically immobilized pigeons have shown that the CS is conveyed in parallel through multiple pathways to the visual area of the telencephalon. These include (1) a thalamofugal pathway involving the principal optic nucleus (the avian homolog of the mammalian lateral geniculate nucleus) and (2) a tectofugal pathway projecting through the optic tectum and the nucleus rotundus (Cohen, 1980). In addition, there may be a third visual input pathway implicated in the CR, projecting through the pretectal area and the thalamus. While retinal responses to repeated CS are not modified during the development of conditioning, responses of second and higher-order neurons in the CS pathway are facilitated during this process. The time course of these changes parallels the time course of the development of the conditioned heart rate response, so neurons or their impinging synaptic fields in successive stages in the CS pathways are likely sites for modulation of cardiovascular control during associative learning.

The descending pathways involved in this conditioned cardiac response have been well established. Neurons in the medial region of the hypothalamus, along with those located in the ventral brainstem, project to preganglionic sympathetic and parasympathetic cardiomotor neurons. The medial hypothalamus in turn receives inputs from the avian homolog of the mammalian amygdala, an area which, in both groups of animals, evokes marked cardioactive effects when stimulated.

Furthermore, lesions of the avian amygdala or its hypothalamic projection either produce deficits in conditioning or can prevent development of the CR (Cohen, 1980). The telencephalic projections conveying visual information to the avian amygdala have, however, not as yet been established in detail. Convergence of the CS and US has been demonstrated at each of the established stages in the central pathway of this response. It thus appears that training-induced modification of the CS works through long-term heterosynaptic facilitation in this pathway, and such facilitation constitutes an important element in the constellation of neurophysiological mechanisms for associative learning.

The broad outlines of the central and peripheral neural pathways involved in efferent control of the circulation in birds have been established but relatively little is known about details of specific afferent and intermediary connections within the central pathways of any of the cardiovascular reflexes in birds. The working assumption guiding studies of these reflexes is that their pathways are similar to those in mammals, but given the differences in cardiovascular reflexogenic zones between birds and mammals, this is not necessarily a valid assumption. Birds have, for instance, only one major arterial baroreceptor site while mammals have two. In addition, most of the input from avian arterial chemoreceptors originates from the carotid bodies while in mammals both aortic and carotid chemoreceptors contribute to cardiovascular chemoreflexes. The organization of the neural circuitry for cardiovascular

control in birds has not been investigated in detail, so the similarity of this circuitry to that of mammals remains an open question.

18.5.6 Development of cardiovascular control

More recent advancements in general knowledge of cardiovascular control mechanisms in birds have been predominately focused on the embryonic phase of avian life history. Seminal works have extensively documented anatomical maturation of the heart and vasculature. Here we provide an overview of cardiovascular control during development in birds. It is important to recognize that the majority of studies investigating avian development have focused on the domestic chicken and the maturation of cardiovascular control is no exception.

18.5.6.1 Ontogeny of autonomic nervous system control of the heart

18.5.6.1.1 Cardiac autonomic innervation

The ontogeny of parasympathetic and sympathetic fiber innervation of the developing avian embryo heart differs. Branches of the vagus nerve (X) perforate the embryonic chicken ventricle at 15% of incubation and innervate all cardiac chambers by 35% of incubation (Pappano, 1975). Cardiac and sinal branches reach the truncus and atria around 20% of incubation (Kuratani and Tanaka, 1990). In contrast, sympathetic cardiac nerves from the sympathetic ganglia do not reach the heart until 50% of incubation (Higgins and Pappano, 1979; Kirby et al., 1980) and penetrate the myocardium at 75% of incubation (Verberne et al., 1999). The sympathetic fiber origin is either the first pair of thoracic ganglia (Kirby et al., 1980) or the cervical ganglia (Verberne et al., 1999).

Field stimulation studies have found that function lags behind the anatomical appearance of innervation. A cholinergic-dependent negative chronotropic response appeared as early as 60% of incubation in response to autonomic receptor drugs and atrial field stimulation. The negative chronotropic response appeared earlier, at 50% of incubation, when pretreated with the cholinesterase inhibitor physostigmine (Pappano and Löffelholz, 1974). In contrast, an adrenergic-dependent, positive chronotropic response to field stimulation was not observed until hatching (Pappano and Löffelholz, 1974). An adrenergic dependent response was produced as early as 50−60% of incubation by potentiating the release of catecholamines from postganglionic neurons with tyramine (Pappano, 1975; Crossley, 1999). This potentiating effect of tyramine increased with age until 90% of incubation (Crossley et al., 2003b). Collectively the data suggest functional control by the autonomic nervous system lags behind the innervation of the heart.

18.5.6.1.2 Cardiac cholinergic and adrenergic receptors

It has long been established that embryonic chicken P-cells express muscarinic cholinergic receptors as early as 10% of incubation (Cullis and Lucas, 1936; Coraboeuf et al., 1970; Pappano and Löffelholz, 1974). Stimulation of these receptors produces an ACh-dependent negative chronotropic response that is blocked by the cholinergic antagonist atropine. There are two stages to the development of ACh's negative chronotropic action (Dufour et al., 1960). Between 15% and 30% of incubation, increased ACh sensitivity is due to changes in membrane permeability. This is followed by functional parasympathetic innervation of the heart, which occurs between 40% and 55% of incubation (Pappano, 1977).

As early as 10% of incubation, P-cells exhibit β-adrenergic receptor mediated chronotropic responses with cells expressing both β_1 and β_2 receptors (Berry, 1950; Fingl et al., 1952; McCarty et al., 1960; Lenselink et al., 1994). P-cell sensitivity to EPI is constant from 60% to 85% of incubation and decreases during the later 85% to 95% of incubation (Löffelholz and Pappano, 1974). This decrease in sensitivity is associated with increased circulating catecholamine levels during the later stage of embryonic development (Crossley et al., 2003b). The embryonic chicken ventricle also possesses β-adrenergic receptors at 20% of incubation that respond to β-adrenergic stimulation with inotropic and chronotropic cardiac effects (McCarty et al., 1960; Shigenobu and Sperelakis, 1972; Frieswick et al., 1979; Higgins and Pappano, 1981). Maximal adrenergic stimulation produces a constant twitch force, but the isoproterenol ED_{50} of embryonic White Leghorn ventricular tissue increases from 75% to 90% of incubation. This is followed by a decrease prior to hatching suggesting development of a reduced adrenergic sensitivity (Higgins and Pappano, 1981). Tyramine (10 mg kg^{-1}) produces a similar inotropic and chronotropic effect on the embryonic chicken heart during this developmental period (Crossley, 1999). An age-dependent decrease in sensitivity to EPI over this incubation window has also been shown in a broiler strain of embryonic chickens due in part to internalization of β-adrenergic receptors (Lindgren and Altimiras, 2009). Overall developing chickens exhibit β-adrenergic−mediated inotropic and chronotropic cardiovascular responses early in incubation.

18.5.6.2 Ontogeny of vascular contractility

18.5.6.2.1 Vascular reactivity regulation

Embryonic circulation must meet the demands of a rapidly growing embryo while also developing into their adult phenotype. Adult vascular smooth muscle and endothelial cells must regulate vascular tone, blood pressure, and blood flow distribution. During vascular morphogenesis,

developing vascular smooth muscle and endothelial cells must proliferate, migrate, and produce the extracellular matrix, while at the same time, acquiring the physiological capacity to regulate vascular tone though smooth muscle activity (Owens et al., 2004; Rzucidlo et al., 2007).

As noted in Section 18.5.2.1, smooth muscle contraction relies on phosphorylation of MLC20 by the Ca^{2+}-dependent MLCK and the Rho-kinase pathway. The expression of MLC20, MLCK, and MLCP in chicken embryo vascular smooth muscle occurs as early as 50% of incubation (Ogut and Brozovich, 2000). The embryonic aorta tonically contracts in response to increased cytosolic Ca^{2+} as early as 40% of incubation. The levels of MLC20 phosphorylation plateau at 75% of incubation (Ogut and Brozovich, 2000). The Rho kinase pathway, providing Ca^{2+} sensitization, appears to mature during embryonic development. Contractions of the femoral artery and ductus arteriosus are inhibited by the Rho-kinase pathway inhibitors Y-27632 and hydroxyfasudil (Greyner and Dzialowski, 2008; Zoer et al., 2010). The effect of Rho Kinase inhibitors increased with incubation age, suggesting a developmental augmentation in the RhoA/Rho kinase-mediated increase in calcium sensitivity of the contractile apparatus.

18.5.6.2.2 Vascular adrenergic receptors

The vasculature expresses adrenergic receptors early in embryonic development. EPI increases arterial pressure in the embryo after 15% of incubation demonstrating that ARs are present and functional (Hoffman and VanMierop, 1971; Girard, 1973). Pharmacological manipulation to identify receptor types with specific adrenergic receptor agonists and antagonists indicate that α-adrenergic and β-adrenergic receptors are present as early as 30% of incubation (Saint-Petery and VanMierop, 1974; Koide and Tuan, 1989). Further studies to isolate differences between vascular beds of the embryo indicate that as early as 60% incubation, the mesenteric circulation expresses α-adrenergic receptors (Rouwet et al., 2000). Chicken femoral and carotid arteries increase α_1-adrenergic receptor and receptor-independent stimulation contractile reactivity from 70% to 90% incubation (Le Noble et al., 2000). In contrast, pulmonary arteries lack α-adrenergic—mediated contraction during all of embryonic development (Villamor et al., 2002). Stimulation of β-adrenergic receptors produces a relaxation in some vessels including the femoral artery. Both the sensitivity and responsiveness of the vasculature to by β-adrenergic simulation increased with incubation age.

While ARs appear functional in the arterial vasculature as early as 15% of incubation, there is a delay in sympathetic nervous control. Arterial vascular constriction to exogenous NE is present before any neurogenic responses (Le Noble et al., 2000). Sympathetic control of arterial vascular resistance seems to be restricted to the later stages of embryonic development in chickens. The femoral artery contracts to perivascular nerve stimulation late stage embryonic chicken femoral arteries. In contrast, neither the carotid nor pulmonary arteries responded to nerve stimulation. In summary, there is an increase in adrenergic control of the vasculature that initially comes from circulating catecholamines and later sympathetic nervous control.

18.5.6.2.3 Vascular cholinergic receptors and endothelial control

Cholinergic control of vessel reactivity appears early in the developing avian embryo. Muscarinic receptor stimulation relaxes the aorta, femoral artery, carotid artery, mesenteric arteries, pulmonary arteries, and ductus arteriosus of chicken embryos in a NO-mediated endothelium-dependent manner (Greyner and Dzialowski, 2008; Le Noble et al., 2000; Rouwet et al., 2000; Martinez-Lemus et al., 2003; Nishimura et al., 2003; Villamor et al., 2002). This endothelium-dependent, NO-mediated relaxation appears to be a critical for regulating embryonic circulation during early development. There is early expression of NO synthase mRNA in multiple tissues of the developing chicken cardiovascular system as early as 15% of incubation (Groenendijk et al., 2005). As early as 50% of incubation, isolated cardiomyocytes respond to sodium nitroprusside, an NO donor, and L-arginine, the NO precursor, suggesting the NO/cGMP pathway is already functional (Ungureanu-longrois et al., 1997). Isolated CAM arteries contract in respond to ACh (Lindgren et al., 2010), and NO produces increased CAM blood flow as early as 50% of incubation (Dunn et al., 2005). Early in incubation, NO donors decrease ventricular preload without changing arterial resistance, which may occur through venodilation (Bowers et al., 1996). At 45% of incubation, sodium nitroprusside produces a vasodilation, suggesting early maturation of the cellular pathway involving cGMP activation (Altimiras and Crossley, 2000). In addition, NO plays a role in maintaining systemic vascular dilation at 70% and 90% of incubation in chickens (Iversen et al., 2014). Finally, the endothelium-dependent relaxation of pulmonary and systemic arteries is constant during internal and external pipping (Villamor et al., 2002; Le Noble et al., 2000). The hatching chicken lacks depression of pulmonary endothelial function observed in neonatal mammals.

Other mediators of endothelium-dependent relaxation have received limited attention in embryonic chickens. Adenosine is involved in the CAM angiogenic response to hypoxia at 50% and 65% of incubation. Embryonic whole body vascular resistance decreases in response to adenosine at 50% to 70% of incubation (Adair et al., 1989). Adenosine receptors have been found on embryonic red blood

cells at 50% of incubation (Glombitza et al., 1996). These studies indicate that adenosine receptors are present in the developing chicken cardiovascular system.

18.5.6.3 Developmental integration of autonomic cardiovascular regulation

18.5.6.3.1 Afferent pathways

The carotid bodies and special mechanosensory nerve endings in the aorta provide the main cardiovascular reflexes in birds. The carotid bodies constitute the primary loci for peripheral chemoreceptors sensing arterial oxygen and carbon dioxide tensions and pH (Section 18.5.4.1). Initially, carotid bodies consisting of mesenchyme-like cells appear around 25% of incubation and by 40% of incubation have migrated to the adult location (Murillo-Ferrol, 1967). At 60% of incubation, the parenchyma has a large number of dispersed granule-containing cells, glomus cells or Type I cell (Kameda, 1994). The appearance of these cells coincides with peak serotonin immunoreactivity (Kameda, 1990), and appearance of long axon synaptic junctions with glomus cells (Kameda, 1994). At 70% of incubation, the developing glomus cells already express features of mature glomus cells (Kameda, 1994). Hypoxic-induced glomus cell catecholamine secretion increases after hatching and is coupled to decreased constitutive catecholamine release (Donnelly, 2005).

Refelxogenic sensory afferents of the cardiovascular system originate from the nodose ganglion. The nodose ganglion bifurcate after emerging from the cell body with one branch to the heart and viscera and the other centrally located, making connections within the central nervous system and solitary tract nucleus. The primordium of the ganglion appears at 15% of incubation and is followed by proliferation of ganglion, peaking at 30% of incubation. An apoptosis-induced decrease in cell number occurs by the time of hatching (Harrison et al., 1994). Early neuron development is independent of neurotrophins and becomes dependent on brain-derived neurotrophic factor as the neurons develop toward their target tissues. The development of the neurons is regulated by other trophic factors such as nerve growth factor during embryonic development (Hedlund and Ebendal, 1980).

Overall, the development of connection between the cardiovascular reflexogenic afferent pathways with the central nervous system occurs during the first half of incubation. The sensitivity of the carotid bodies increases when the animal hatches, however, the changes occurring in baroreceptive areas are unknown.

18.5.6.3.2 Tonic heart regulation

The role of cholinergic tonic activity does not appear to be involved in maintenance of baseline cardiovascular function during early embryonic development. The cholinergic muscarinic receptor antagonist atropine does not alter heart rate in White Leghorn chicken incubation until after hatching or just prior to (Pickering, 1895; Saint-Petery and VanMierop, 1974; Tazawa et al., 1992; Crossley and Altimiras, 2000) and has no effect on arterial pressure (Tazawa et al., 1992; Crossley and Altimiras, 2000). However this is not universal for embryonic birds, as different species differ in terms of the presence of a heart rate response to atropine administration (Crossley et al., 2003b; Swart et al., 2014). Embryonic chicken strains including broilers, black Sumatran Bantams, and red Jungle fowl vary in terms of the presence of functional cholinergic tone on heart rate, appearing as early as early as 60% to as late as 90% of incubation (Crossley et al., 2003b; Chiba et al., 2004; Crossley and Altimiras, 2012). An absence of cholinergic tone does not exclude possible recruitment and intermittent activity of the parasympathetic nervous system. Continuous recordings of instantaneous heart rate in embryonic chickens reveal heart rate decelerations likely due to transient increased parasympathetic activity (Kato et al., 2002). Although cholinergic receptors are expressed early in development and the parasympathetic efferent pathway is functional under some conditions at 60% of incubation, cardiovascular function and development continues without a tonic cholinergic stimulation throughout at least the first half of incubation.

In contrast, there is clear adrenergic tone present during the majority of embryonic bird development. α-adrenergic and β-adrenergic receptor mediated stimulatory tones on both heart rate and arterial pressure appear early in development (Saint-Petery and VanMierop, 1974; Koide and Tuan, 1989; Tazawa et al., 1992; Crossley and Altimiras, 2000). As early as 30% of incubation, a positive β-adrenergic chronotropic tone on heart rate and arterial pressure appears (Saint-Petery and VanMierop, 1974; Girard, 1973). This tone is critical to basal baseline function (Tazawa et al., 1992; Crossley, 1999; Crossley and Altimiras, 2000). In chickens, the magnitude of the β-adrenergic chronotropic tone increases in strength from 10% to 20% as the embryos progress from 40% to 95% of incubation, respectively (Crossley, 1999). Baseline heart rate is unchanged after pharmacological blockade of sympathetic nervous terminals with 6-hydroxydopamine or ganglionic blockade with (Tazawa et al., 1992; Crossley, 1999; Crossley et al., 2003b). This suggests that adrenergic heart rate tone in chicken embryos originates from circulating catecholamines. A similar change in the β-adrenergic heart rate tone during the final 30% of incubation has been observed in emus, domestic geese, and Canada geese (Crossley et al., 2003a; Swart et al., 2014).

While the direct effects of β-adrenergic inhibition on the heart is mediated through direct actions on the heart and pacemaker tissue, the mechanisms regulating the depressive actions of α-adrenergic receptor antagonists on

heart rate present from 40% of incubation through hatching is unclear (Koide and Tuan, 1989; Tazawa et al., 1992; Crossley, 1999; Crossley and Altimiras, 2000). While this tone is present and the magnitude is maximal between 60% and 95% of incubation, α-adrenergic receptors have been reported to be absent in the chicken heart (Crossley, 1999; Chess-Williams et al., 1991). Therefore, the bradycardic response to α-adrenergic receptor blockade may be secondary to the pronounced vasodilation after α-adrenergic receptor antagonist treatment (Crossley and Altimiras, 2000). Vasodilation may produce blood pooling in the CAM vasculature, reduced venous return, or decreasing heart rate and CO.

18.5.6.3.3 Tonic vasculature regulation

Total and regional vascular resistance and capacitance is regulated by the sympathetic nervous system in adult vertebrates. This vascular control is mediated by changes in catecholamine release from sympathetic nerve terminals as well as the adrenal medulla. These ligands bind to ARs types that are heterogeneously distributed with the dominant AR type dependent on the vascular bed. This allows differential hemodynamic responses to systemic catecholamine release. The vascular tone resulting from activation of different receptors is dependent on the vascular areas affected and if stimulation is arising from sympathetic nerve endings or circulating catecholamines (Guimaraes and Moura, 2001).

A strong α-AR tone maintaining vasculature constriction is active in some vascular beds and is functional from 30% to 95% of incubation (Girard, 1973; Saint-Petery and VanMierop, 1974; Koide and Tuan, 1989; Tazawa et al., 1992; Crossley, 1999; Crossley and Altimiras, 2000). A α-AR mediated vascular tone prevails in the skeletal muscles and has limited effects on the heart, intestines, and yolk sac (Mulder et al., 2001). Further α-ARs are absent from the CAM vascular tree illustrating the regionalization of AR types (Lindgren et al., 2010). While the time course has not been elucidated, a similar strong α-AR vascular tone has been observed in the Black Sumatran Bantam, Red Jungle fowl, and broiler chickens (Crossley unpublished observation, Crossley and Altimiras, 2012). In White Leghorns, the receptor subtype responsible for maintaining vascular tone in embryonic chickens is likely α_1-adrenergic receptors given similar responses following a nonspecific α-adrenergic receptor antagonist (phentolamine) and an α_1-adrenergic receptors specific antagonist (prazosin) (Crossley and Altimiras, 2000). In White Leghorn chicken embryos, there is an increase in the dependence on α-adrenergic receptor mediated vasoconstriction from a 10% contribution to resting arterial pressure to over 55% just prior to hatching (Crossley, 1999). Limited numbers of studies conducted in other species show that embryonic emus, domestic geese, and Canada geese possess a pronounced α-AR tone during the final 30% of incubation (Crossley et al., 2003a; Swart et al., 2014). Overall it is clear that embryonic chickens depend on α-mediated vasoconstriction during the majority of development, which is a feature shared by the other avian species investigated.

A β-AR vasodilator tone opposes the α-AR mediated vascular tone during embryonic development. The β-AR vasodilator tone in White Leghorn chickens appears at 30% of incubation, increases in magnitude from 35 to 60% of incubation where it stabilized until the final 5% of incubation where it disappears (Saint-Petery and VanMierop, 1974; Crossley, 1999; Girard, 1973). An active β-tone depressing arterial pressure is present in other chicken strains from 60% to 90% of incubation (Koide and Tuan, 1989; Tazawa et al., 1992; Crossley and Altimiras, 2012). This tone reaches maximal strength at 90% of incubation in other strains of embryonic chickens and in embryonic emus (Crossley et al., 2003b; Crossley and Altimiras, 2012). Unlike the chickens and emus, domestic and Canada geese embryos have a β-AR vasodilator tone at 70% of incubation that is absent at 90% (Swart et al., 2014), so clearly regulatory mechanisms may differ between species.

As with adrenergic tone on heart rate, the adrenergic vascular tone during development is due to levels of circulating plasma catecholamines. This is supported by measurements following sympathectomy with 6-hydroxydopamine or hexamethonium ganglionic blockade illustrating that resting arterial pressure in embryonic chickens in unaltered by the treatment (Crossley, 1999; Crossley and Altimiras, 2000; Crossley et al., 2003b).

18.5.6.3.4 Baroreflex regulation

Investigations of developing baroreflex function have been limited to domestic chicken breeds and have focused on characterizing reflex parameters of the cardiac limb or heart rate responses to changes in arterial pressure only (Altimiras and Crossley, 2000; Elfwing et al., 2011; Mueller et al., 2013). Two methods have been successfully utilized to quantify changes in baroreflex gain (sensitivity) and set point during chicken development; pharmacological assessment or Oxford method and spontaneous baroreflex sensitivity assessments (Altimiras and Crossley, 2000; Elfwing et al., 2011; Mueller et al., 2013). They both show baroreflex function in chickens is present as early as 80% of 21-day incubation period, dependent in part on the breed studied (Altimiras and Crossley, 2000; Elfwing et al., 2011). In addition to the timing of operation during chicken development, changes in baroreflex function have also been reported. Gain of the reflex provides an index of baroreflex maturation during chicken incubation however components

such as set point and threshold are also informative. In White Leghorns chicken embryos, the baroreflex has been reported to be functional at 85% of incubation (Altimiras and Crossley, 2000), but only 17% of the embryos showed a change in heart rate after experimental manipulation of blood pressure. This rapidly increases to 33% at 90% of incubation with a fivefold increase in baroreflex gain upon hatching (Altimiras and Crossley, 2000). Using the spontaneous assessment method in which the correlation between spontaneous fluctuations in arterial pressure and heart rate are analyzed, the reflex is functional by 80% of incubation while the gain remains constant from this point until 95% of incubation in broiler chickens (Elfwing et al., 2011). Interestingly, spontaneous gain in embryonic broiler chickens is relatively constant from 80% to 95% averaging 59.8 kPa min^{-1}. This is a higher gain than that determined with the Oxford method in the same breed, which increased progressively from 10.9 to 30 kPa min^{-1} over the same developmental period (Elfwing, 2007). Previous arguments regarding the utility of each methodological approach have been made (Di Rienzo, 2001; Elfwing et al., 2011) and may account for these reported differences in ontogeny of chicken baroreflex function. Overall while previous studies have been novel and informative about the ontogeny of avian baroreflex function, the domestic chicken has been the lone model organism. Investigations of multiple species from different avian lineages with different precocial vs. altricial developmental strategies are crucial to identify the commonalities of the ontogeny of baroreflex function in birds.

Equally informative will be investigations of the interactions between baroreflex function and other regulatory mechanisms during ontogeny, however, modulation of baroreflex of function via systemic hormones and central neuropeptides has been unexplored. Angiotensin II (AT) is an important regulatory peptide that is crucial for blood volume homeostasis in adults and is a contributor to an integrative series of signaling pathways that impacts baroreflex function. In embryonic chickens, AT modulates baroreflex function decreasing both baroreflex gain and operating point at 90% of incubation (Mueller et al., 2013). This change was attributed, in part, to a decrease in vagal inhibition that may be the result of the known elevated plasma levels of AT in embryonic chickens (Crossley et al., 2010). Thus to deepen the understanding of the development of this reflex, the ontogeny of baroreflex function must be assessed in concert with the maturation of other regulatory components of the embryonic cardiovascular system.

18.5.6.3.5 Cardiovascular response to hypoxia

The embryonic cardiovascular response to hypoxia has been as useful tool in assessing the capacity of developing regulatory mechanisms to response to an environmental insult in addition to exploring the maturation of a typical adult response to the stress. Hypoxia has been suggested to be a relevant nature occurrence during avian ontogeny (Anderwartha et al., 2011). Investigators have utilized two methods to characterize the cardiovascular response to reductions in oxygen; prolonged and acute exposures. In domestic chickens, prolonged bouts (>15 min) of hypoxic exposure results in a negligible heart rate response early embryos (15−25%), a depression in heart rate the middle of incubation (67−76%), and an increase in heart rate late (95−100%) in incubation (Khandoker et al., 2003; Andrewartha et al., 2011). Changes in arterial pressure and blood flow distributions have been yet to be investigated under prolonged periods of hypoxic exposure.

Arterial pressure responses to hypoxic exposure have been conducted primarily using acute hypoxia (<10 min). In general, hypoxia causes hypotension in embryonic chickens which is dependent on the level of hypoxia throughout embryonic development (Tazawa, 1981; Crossley et al., 2003b). Embryonic emus respond similarly at 60% of incubation, however, they transition to a hypertensive response prior to hatching (Crossley et al., 2003a). Acute hypoxia also depresses heart rate in embryonic chickens ranging from 43% to 100% of incubation with the intensity of the response dependent on the level of oxygen unlike the response seen during prolonged exposures (Tazawa, 1981; Tazawa et al., 1985; Crossley et al., 2003a). In contrast, embryonic emus either maintain or increase heart rate during hypoxic exposures during the final 30% of incubation (Crossley et al., 2003a). Blood flow measurements during hypoxic exposures beyond 30% of bird incubation in are limited. Tazawa et al. (1985) measured blood flow in the allantoic artery, the major artery supplying the CAM, of an embryonic chicken at ~70% of incubation reporting a slight decrease during hypoxia from the baseline value of 4.1−4.4 mL min^{-1} (Tazawa et al., 1985). Later work reported that severe hypoxia (0−5% O_2) reduces allantoic artery blood flow as much as 0.7 mL min^{-1} in embryonic chickens from 40% to 76% of incubation (Van Golde et al., 1997). Given that under normoxic conditions, the CAM vascular receives between 52% and 41% of CO in embryos ranging from 50% to 90% of incubation, the depression caused by hypoxia represent an important redistribution of flow (Mulder et al., 1997). The pattern of redistribution favored the increased perfusion to the heart and brain while decreasing it to the liver, yolk, and carcass (Mulder et al., 1998). Direct measures of femoral arterial blood flow also illustrate a reduction in limb perfusion during hypoxic exposures (Iversen et al., 2014). Overall the embryonic chicken response to acute hypoxic exposure is a depression of overall cardiovascular function.

The mechanisms that underlie the changes in cardiovascular function have been investigated in the embryonic chickens. In the White Leghorn, hypoxia decreases arterial

pressure in embryos from 43% to 100% of incubation (Crossley, 1999). Initially this response was partially attributed a direct effect of reduced O_2 on the vasculature inducing a relative dilation (Crossley et al., 2003b). From 70% to 90% of incubation, the hypoxic dilation is limited by an α-adrenergic and cholinergic receptor stimulation with a dilatory β-adrenergic stimulation contributing in the final ~20% of incubation (Crossley et al., 2003b). While the increased vascular cholinergic effects may result from a reflexive mechanisms, the adrenergic stimulations can be attributed to elevation in plasma catecholamines in response to hypoxic exposures in during the final 30–40% of incubation (Mulder et al., 2000; Crossley et al., 2003b). NO has been found to mediate the vasodilation at 70% and 90% of incubation as an additional contributing factor to the hypoxic hypotension in embryonic chickens (Iverson et al., 2014).

Heart rate responses to hypoxia may be partially due to the direct actions of low oxygen on cardiac muscle and pacemaker tissue of the embryo (Van Golde et al., 1997; Crossley et al., 2003b). During the final 10% of incubation, the hypoxic bradycardia may be affected by an α-adrenergic stimulation and a cholinergic inhibition induced by direct effects of low oxygen on autonomic nerve terminals as well as chromaffin tissue (Crossley et al., 2003b). It should be noted that α-adrenergic receptor mediated redistributions of CO including preferential perfusion of the heart is an important component of the embryonic chicken response and inhibition may contribute to the reported chronotropic actions of α-adrenergic during hypoxia (Mulder et al., 1998, 2001).

Clearly additional regulatory systems in multiple species must be investigated to further develop the model of how the embryonic cardiovascular system responds periods of hypoxia, however, the embryo may rely on peripheral mechanisms, such as NO, with limited action from the autonomic nervous system.

18.5.6.4 Development of humoral and local effectors of cardiovascular function

A number of hormones play an active role in cardiovascular regulation of the developing embryo. The best studied include angiotensin II (AII), ET, and natriuretic peptide (NP), and their roles in the adult have been outlined in Section 18.5.2.3. All of these hormones have been found relatively early in development of the chicken embryo.

The components of the renin-angiotensin system are present during early embryonic chicken development. The egg laying female provisions AII converting enzyme (ACE) at measurable levels in freshly laid eggs. Over the first 2 days of development, whole embryo levels of ACE-mRNA increase (Savary et al., 2005), and pathways for angiotensin synthesis and signal transduction are present. Between 15% and 20% of incubation, cardiac tissue, brachial arch tissue, and mesonephric tissue all express AII receptor mRNA (Kempf and Corvol, 2001). The CAM expresses AII receptors during at least the last half of incubation (Moellera et al., 1996) and responds to AII at 35% of incubation (Le Noble et al., 1991, 1993).

Angiotensin II appears to be a tonic regulator of cardiovascular function in the developing chicken. *In vivo* AII produces a dose-dependent increase in arterial pressure that increases in intensity from 60% of incubation until hatching (Crossley et al., 2010). In addition, embryonic chickens possess high levels of circulating AII over this same time frame and blockade of ACE results in a relative hypotension at 90% of incubation (Crossley et al., 2010; Muellar et al., 2013). While the embryonic animal responds to AT with an increase in blood pressure similar to adult birds, the embryo lacks the initial AII-induced hypotension reported in adults (Crossley et al., 2010). Embryonic chickens also do not depend entirely on α-adrenergic receptors stimulation for the AII-induced hypertension and antagonists for the AII type 1 receptor (AII1R) are ineffective in embryonic chickens until hatching (Crossley et al., 2010). The ACE is active in chicken aortas as early as 50% of incubation, and it increases in activity with development (Topouzis et al., 1992). Angiotensin also relaxes isolated aortic rings of embryonic chickens at 90% of incubation (Nishimura et al., 2003). These isolated vessels are lacking the sympathetic nerve inputs that would provide a constrictive response. Collectively the data illustrate that AII is an important component of embryonic chicken cardiovascular regulation with similarities and differences from the cardiovascular response in adult birds.

Both AII type 1 and type 2 receptors are present on the developing heart (Rabkin, 1996). Angiotensin II can act on the developing chicken heart to produce a positive inotropic effect at 85% of incubation (Freer et al., 1976). Exposure of AII during 35% to 90% of incubation produces cardiac hypertrophy through activation of the AII1R and up regulation of myosin light chain (Mathew et al., 2004; Baker and Aceto, 1990; Aceto and Baker, 1990). The observed cardiac hypertrophy may be due to direct action of AII on the heart and/or in response to changes in embryonic vasculature function. It is clear there is a role for angiotensin in chicken cardiovascular development and regulation and *in vivo* studies are necessary to further clarify the significance of the role.

The locally produced vasoconstrictor, ET, is expressed ubiquitously throughout the developing chicken cardiovascular system (Kempf et al., 1998). The myocardium and the outflow tract express ET receptor subtype mRNA transcripts as 15% of incubation (Groenendijk et al., 2008). ET converting enzyme 1 activates ET and is first detected at 20% of incubation (Ballard and Mikawa, 2002; Hall et al., 2004). ET produces changes in cardiovascular function in

both *in vivo* and *in vitro* studies. *In vivo* administration of ET antagonists at 20% of incubation resulted in reduced cardiac function (Groenendijk et al., 2008). An *in vitro* ET-mediated positive inotropic effect was observed in cultured cardiomyocytes from 50% of incubation embryos (Bézie et al., 1996). Myograph studies on isolated aorta, pulmonary arteries, and ductus arteriosus all show a vasoconstriction in response to ET (Wingard and Godt, 2002; Villamor et al., 2002, 2004; Martinez-Lemus et al., 2003; Agren et al., 2007). Active wall tension in response to ET −1 increases before hatching which could be critical for the transition to *ex ovo* life (Martinez-Lemus et al., 2003; Villamor et al., 2004).

NPs help regulate sodium and water balance and maintain cardiovascular homeostasis (Takei, 2000; Toop and Donald, 2004; Trajanovska et al., 2007). Mammals express three NP subtypes: atrial natriuretic peptide (ANP), B-type natriuretic peptide (BNP), and C-type natriuretic peptide (CNP). The subtypes ANP and BNP are produced and released from cardiac myocytes in response to increases in ventricular volume (Takei, 2000; Toop et al., 2004; Trajanovska et al., 2007). The chicken genome has four potential NP genes including BNP and CNP (Akizuki et al., 1991; Houweling et al., 2005; Trajanovska, 2007). Natriutetic peptides produce a relaxation of the vasculature that appears as early as 20% of embryonic development (Nakazawa et al., 1990). Studies on isolated cardiomyocytes found a response to NPs beginning at 50% of incubation (Bézie et al., 1996 Koide et al., 1996). These studies suggest that the receptors are present both on the heart and in the vasculature of the developing embryo. There is also some indication that ET and NP interact to regulate cardiomyocyte contractility in embryonic chickens (Bézie et al., 1996). The functional role during development remains to be fully characterized.

18.6 Environmental cardiovascular physiology

18.6.1 Flight

Avian flight requires adaptations of the respiratory and cardiovascular systems to supply sufficient O_2 to the working muscles. Given the inherent complexity of measuring these parameters in active birds, it is not surprising that few studies have examined cardiovascular adjustments that support flight. Two of the most complete studies examined cardiovascular and respiratory function in flying domestic pigeons (*Columba livia domestica*; Butler et al., 1977; Peters et al., 2005). During flight at wind tunnel speeds of 10 m s^{-1} (Butler et al., 1977) or 18.4 m s^{-1} (Peters et al., 2005), O_2 consumption increased between 10 and 17 fold. CO increased 7.4 fold and blood oxygen extraction 2.4 fold during flight, increasing convective O_2 transport to meet metabolic demands of flight muscle. During these flying bouts, heart rate which is the primary mechanism for elevating CO in these animals increased from a resting rate of 110 beats min^{-1} to flying rate of 663 beats min^{-1} (Peters et al., 2005). Interestingly the exercise induced increase in pigeon heart rate during flight is of a similar magnitude to that of flying bats and larger than those observed in running mammals (reviewed in Peters et al., 2005).

The magnitude of change in CO and O_2 consumption is flight mode dependent in birds. For example, during soaring and gliding flight, heart rate is similar to that of resting birds, while flapping flight increases heart rate 2.2 to 7.4 times with the greatest acceleration occurring during takeoff (Peters et al., 2005; Sapir et al., 2010; Sakamoto et al., 2013). There was a strong correlation between heart rate, flight mode, and time spent flapping in the brown-browed Albatross (*Thalassarche melanophrys*; Sakamoto et al., 2013). During the transition from gliding to flapping, heart rate changed almost instantaneously in the Cape gannet (*Morus capensis*; Ropert-Coudert et al., 2006). While the method of flight is correlated with changes in heart rate, flight speed does not appear to alter this cardiovascular parameter (Ward et al., 2002). At wind speeds ranging from 0 to 16 m s^{-1}, heart rate of flying cockatiels (*Nymphicus hollandicus*) is relatively constant, averaging 817 beats /min^{-1} an increase of 2.3 fold from resting levels (Ros, Guarino, and Biewener, unpublished data).

Tissue perfusion is presumably modified during flight as well with an increased distribution of CO to flight muscles during activity; however, this parameter has not been quantified to date. The data available quantify skeletal muscle perfusion during walking and running. Ellerby et al. (2005) found that during bipedal locomotion in birds, locomotory muscle perfusion increased significantly. In guinea fowl (*Numida meleagris*) as walking speed increased to 90% of VO_2 max, CO increased by 4.9 fold through increased heart rate and stroke volume (Ellerby et al., 2005). The majority of this increase in CO perfused the leg muscles, while blood flow to the brain, spleen, stomach, pancreas, intestines, and kidneys did not change. Bech and Nomoto (1982) reported that sciatic artery blood flow increased 3.7 times in Pekin ducks (*Anas domesticus*) running on a treadmill suggesting similar CO modifications occur in this species. Tissue perfusion to leg muscles in ducks increased some fivefold in ducks swimming at close to maximum sustainable rates (Butler et al., 1988). Therefore by extension one could assume that similar increases in blood perfusion to flight muscle occur during moderate to energetic flapping flight. In contrast, gliding should result in limited changes in muscle flow rates especially given the lower expected CO during these types of flying.

18.6.1.1 Altitude

Avian species, such as the bar-headed goose (*Anser indicus*), are unique in vertebrates in that they make annual migrations across mountain ranges at altitudes between 5500 and 7250 m (Hawkes et al., 2013). At these high elevations, the inspired partial pressure of oxygen (P_IO_2) falls to approximately 50 mmHg, a sea level equivalent of 7% O_2. In the O_2 cascade, maximum aerobic capacity is limited by convective movement of O_2 by the cardiovascular system (Hillman et al., 2013). Therefore, to achieve the feats of strenuous activity in a low O_2 environment at high altitudes modifications to the cardiovascular system should be anticipated, allowing for maintenance of high-aerobic activity under low-oxygen conditions. A number of studies have examined cardiovascular adjustments of high-altitude migrators (bar-headed geese, *A. indicus*; Hawkes et al., 2014; Lague et al., 2016, 2017; Meir et al., 2019), high-altitude residents (Lague et al., 2017, 2020), and low-land species to decreasing levels of O_2 both at rest and during flight. While CO increases in response to decreasing O_2 levels in both the bar-headed goose and the Barnacle goose, bar-headed geese begin to increase CO at a higher O_2 level than in Barnacle geese (Lague et al., 2016). Birds migrating at high altitude and living at high altitude are both able to increase CO in response to lowered O_2, but appear to adjust different cardiovascular responses to achieve the same elevation in CO. In response to decreased inspired O_2 levels, bar-headed geese elevate CO through increases in heart rate while Barnacle geese (*Branta leucopsis*) elevate CO through increasing stroke volume (Lague et al., 2017).

During activity, the capacity to maintain an elevated heart rate in low O_2 environments is paramount and has been investigated in bar-headed geese and Barnacle geese (Hawkes et al., 2014; Meir et al., 2019). During hypoxic exposure to 7% O_2, bar-headed geese were able to maintain running for 15 min and increase of heart rate from a normoxic running rate of 385 to 453 beats min^{-1} in hypoxia (Hawkes et al., 2014). When running at 7% O_2, Barnacle geese were unable to increase heart rate to the levels observed during normoxic running and were unable to run for more than 4 min. During normoxic flight at speeds between 45 and 54 km h^{-1}, heart rate increased roughly 2.5- to 3-fold while oxygen consumption increased 16-fold over resting values in these geese. Heart rate data for flights at 21%, 10.5%, and 7% O_2 suggest that these animals are able to maintain the elevated heart rate with the associated CO under hypoxic flight conditions that mirror the oxygen levels experienced during migratory behavior (Meir et al., 2019). Therefore, these animals are able to maintain the cardiovascular changes observed at sea level during active hypoxic flight to ensure sufficient O_2 delivery to the flight muscles.

Coronary vasodilation is critical to maintaining O_2 delivery during bouts of reduce O_2 availability or an increase in myocardial oxygen demand. Both of these factors presumably come into play during high-altitude flight in birds. In Pekin ducks and bar-headed geese, coronary perfusion has been reported to be 3.5 mL min^{-1} g^{-1} of wet heart weight at sea level when the P_IO_2 was 142 mmHg (Faraci et al., 1984). Exposure to severe hypoxia (28 mmHg P_IO_2) increases coronary blood perfusion 5.5 and 2.7 times, respectively, in ducks and geese (Faraci et al., 1984) via a hypoxic coronary vasodilation (Figure 18.35). Although bar-headed geese are accomplished high-altitude fliers, in contrast to ducks, counter intuitively these animals did not increase coronary blood perfusion to the same extent under hypoxic conditions. This may be compensated for by greater ventricle capillary density in the bar-head goose compared to other species (Scott et al., 2011).

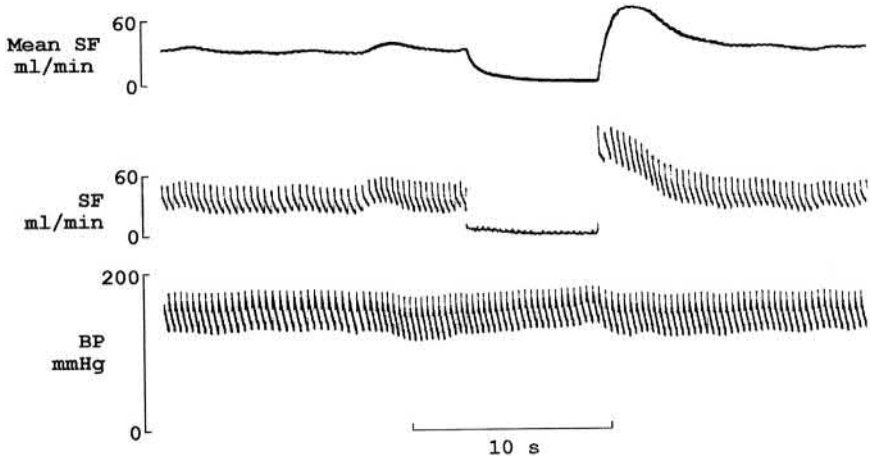

FIGURE 18.35 Responses of the coronary circulation to hypoxia in Pekin ducks and bar-headed geese. (Left) coronary blood flow (mL min^{-1} g^{-1}); (right) coronary vascular resistance (mmHg ml min^{-1} g^{-1}) as a function of the arterial O_2 partial pressure (P_aO_2). All values are means ± S.E. (n = 5) except at 25 Torr, where means for two geese were plotted. An asterisk represents significant difference from normoxia (highest P_aO_2 level) at $P \leq .05$. *From Faraci et al. (1985)*

Carbon dioxide is also a potent coronary vasodilator in mammals, coupling increased aerobic metabolism in the myocardium to an increased rate of oxygen delivery while hypocapnia increases coronary resistance and decreased coronary perfusion. This would obviously be deleterious during high-altitude migratory flight. Interestingly, the relationship between coronary blood flow and P_aCO_2 in bar-headed geese appears to be quite different than mammals. Over a range of P_aCO_2 from about 30 to 60 mmHg, there is a linear increase in coronary flow with P_aCO_2, as in the mammal. However, in the hypocapnic condition, when P_aCO_2 is 30 mmHg or lower, there appears to be no effect of P_aCO_2 on coronary resistance (Faraci and Fedde, 1986). Whether this represents a mechanism to ensure myocardial oxygen delivery during high-altitude flight remains to be determined.

Activity at high elevation subjects tissue to reduced P_IO_2 and hypocapnia. The hypocapnia and subsequent respiratory alkalosis results from increased CO_2 washout from greater hypoxemia driven ventilation (Faraci et al., 1985; Scott and Milsom, 2007). This condition could dramatically influence tissue metabolic function with the greatest impact on highly aerobic tissues of the central nervous system. In domestic geese, cerebral blood flow decreased as P_aCO_2 falls from 50 to 20 mmHg but then reached a plateau; however, PO_2 of cerebral tissue continued to fall as P_aO_2 fell below 20 mmHg, suggesting differences in cerebral vascular sensitivity to these two conditions (Bickler and Julian, 1992). Carbon dioxide is normally a potent vasodilator within the cerebral circulation (Faraci and Fedde, 1986; Grubb et al., 1977), however, the cerebral vasculature is fairly insensitive in domestic geese (*Anser anser*) and Pekin ducks while bar-headed geese are very insensitive to severe hypocapnia (Bickler and Julian, 1992; Faraci and Fedde, 1986; Grubb et al., 1977).

Given the range of altitude bird species inhabit and transiently experience during season migration differing degrees in flight muscle capillarity may also correlate with flight at high elevation. It could be predicted that high-elevation species would exhibit a relatively greater capillary density to muscle fiber density increasing the total surface area of contact between capillaries and fibers. This phenotype is evident in a number of species that fly at high elevation and that have relatively higher muscle capillarity and smaller fiber sizes. In bar-headed geese and Andean coots (*Fulica ardesiaca*) native to 4200 m the pectorals muscles, as well as some limb muscles in the coot, the number of capillaries per muscle fiber is increased compared with low-land species (Scott et al., 2009; Leon-Velarde et al., 1993). Further in the bar-headed goose, mitochondria of aerobic fibers are redistributed so they are adjacent to capillaries (Scott et al., 2009). These compensatory changes can be induced during ontogeny as evident in increased capillary-to-fiber ratio and possible changes in diffusion distances in Canada goose goslings (*Branta canadensis*) hatching from eggs raised under hypoxic conditions (Snyder et al., 1984; Snyder, 1987). In contrast, wild adult pigeons actively flying at 3800 m maintain similar capillary geometry and density compared to controls at sea level (MathieuCostello et al., 1996). Equally important are factors such as changes in P_{50}, the oxygen-carrying capacity of blood, or the myoglobin content of muscle fibers which are also significant adaptations involved in the response. Increases in carrying capacity and high levels of tissue oxygen extraction have been demonstrated in unexercised pigeons acclimatized to high altitude (Weinstein et al., 1985) and bar-headed geese (Scott, 2011). In short, while the current understanding of cardiovascular and respiratory adjustments that must accompany flight at elevation has progressed, further extensive investigations must be undertaken to explain the capacity of birds to sustain activity in low-oxygen environments.

18.6.1.2 Migration

Extensive migrations involving continuous fasting flight for long periods of time are undertaken annually by many bird species. Migrating birds exhibit extraordinary phenotypic plasticity in organs size and body mass. This organ mass plasticity manifesting as hypertrophy of the heart and other organs is akin to that observed in infrequent feeding reptiles such as snakes (Secor and Diamond, 1998; Andersen et al., 2005). For example, the barnacle goose heart hypertrophies before migration composing approximately 1.1% of body mass (Bishop et al., 1995). In contrast, the heart of a typical bird is roughly 0.8% of body mass (Section 18.2.1.2). Heart hypertrophy of the red knot (*Calidris canutus islandica*) and bar-tailed godwit (*Limosa lapponica taymyrensis*) is correlated with increased power requirements needed for migration (Piersma et al., 1999; Landys-Ciannelli et al., 2003). The garden warbler (*Sylvia borin*) migrating across the Sahara exhibited a decrease in heart mass and flight muscle mass that was restored within nine days of recovery feeding (Bauchinger et al., 2005). Few studies have examined the cardiovascular physiology associated with these long migrations and associated hypertrophy of the heart. During migration of Svalbard Barnacle geese (*Branta leucopsis*), heart rate falls on successive days from 317 to 226 beats min^{-1} (Butler et al., 1998). Butler et al. (1998) suggested that progressive bradycardia was due to decreased O_2 demand as body mass fell while heart mass remains fixed during the migration. Thus, changes in CO appear to be influenced most heavily by heart rate changes. It remains to be seen how these changes in heart mass before, during, and after migration influence cardiovascular function and performance in these species.

18.6.2 Swimming and diving

Bird species engage in surface swimming and submerged or diving swimming. In tufted ducks (*Aythya fuligula*), surface swimming at maximal sustainable speeds is associated with a 70% increase in CO from 276 to 466 mL min^{-1} (Bevan and Butler, 1992). As with flight, swimming is associated with changes in regional vascular perfusion with myocardium and active leg musculature blood flow increasing by 30% and 300%, respectively, while flow to other regions remained the same or decreased (Bevan and Butler, 1992). Similar patterns are evident in the redhead duck (*Aythya americana*) during short periods of underwater swimming which results in a 200% to 500%, increase in hind legs perfusion (Stephenson and Jones, 1992). Clearly selective perfusion takes place during swimming likely via an interaction between vasodilation in active muscle and vasoconstriction in visceral organs and inactive muscle (Figure 18.36; Butler et al., 1988; Bevan and Butler, 1992).

During a dive, animals must function with the limited O_2 stores carried within the body during the dive duration. The majority of dives are shorter than the aerobic dive limit (ADL), the length of time that a dive can be aerobic relying on the O_2 stores in the body. A large number of diving species, such as ducks and cormorants, perform multiple short dives of less than 60 s in duration. Others species, such as the emperor penguin (*Aptenodytes forsteri*), dive for longer periods of more than 20 min (Meir et al., 2008). These different diving behaviors should by necessity result in species having different physiological capacities to ensure effective O_2 transport, however, regardless of dive duration, the pattern of cardiovascular responses are similar.

The phases of the cardiovascular response to a voluntary dive include an initial tachycardia during the immediate predive followed by a diving "bradycardia." After surfacing, there is usually a postdive tachycardia. The predive and postdive tachycardia is suggested to aid in loading and replenishing of O_2 stores and elimination of CO_2 (Butler and Jones, 1997). In many species, the diving bradycardia is not a true bradycardia in that the diving heart rate remains elevated in comparison to the resting heart rate.

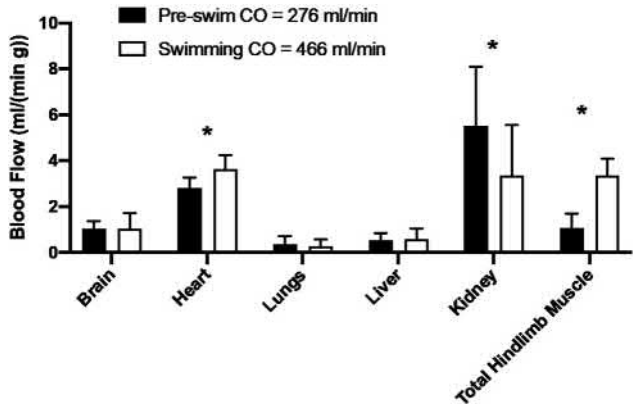

FIGURE 18.36 Mean mass-specific blood flow to selected tissues in six tufted ducks before (*shaded bars*) and during swimming at a mean velocity of 0.69 m s^{-1} (*open bars*). *Asterisks* indicate significant differences between preswimming and swimming values. *Data from Butler et al. (1988).*

In diving ducks, Jones and Holeton (1972b), Lillo and Jones (1982), Jones et al. (1983), Smith and Jones (1992), and Bevan and Butler (1992) showed that stroke volume was maintained during the large decreases in CO generated during submersion, suggesting the primary factor dictating CO during these events is heart rate. In addition, there is a negative correlation between minimum heart rate and dive duration as well as depth (Bevan et al., 1997; Meir et al., 2008). The extent of the diving bradycardia may be correlated with changes in blood oxygen levels, regulated by variation in parasympathetic output in ducks (McPhail and Jones, 1999). In diving cormorants (*Phalacrocorax auritus*), heart rate during a shallow dive was dependent upon the level of inspired oxygen (Enstipp et al., 2001). Predive inspiration of hypoxic gas resulted in a stronger bradycardia, and predive inspiration of hyperoxic gas resulted in the opposite response. Similar changes in response to inspired oxygen levels and diving has been observed in the lesser scaup duck (*Aythya affinis*; Borg et al., 2004).

Penguins have been extensively studied to understand their capacity for extended active diving bouts. During dives that are greater than the ADL, Emperor penguins become relatively bradycardic just prior to returning to the surface (Meir et al., 2008). Lesser scaup ducks decrease heart rate below resting levels during forced dives only (Borg et al., 2004). During long voluntary dives of 30 min or if this species is exposed to 9% O_2, heart rate falls below resting values during the later portions of the dive suggest that a true diving bradycardia may only occur when blood PO_2 levels become severely reduced (Borg et al., 2004). Changes in tissue perfusion have been suggested to accompany heart rate responses to diving. During long dives, Emperor penguins have blood lactate levels that suggest changes in blood flow to the skeletal muscles during the dive (Ponganis et al., 2009). The ADL is the duration at which the dive becomes anaerobic and is indicated by blood lactate levels during postdive recovery. The majority of birds carry out multiple short dives that fall within their ADL; however, blood lactate levels remain low in animals that have passed their ADL, with levels increasing during postdive period. There is also data suggesting a potential arteriovenous shunt through the extremities in the emperor penguin (Ponganis et al., 2009). Ponganis et al. (2009) propose that this shunt may be important during the initial phases of the dive by allowing enhanced transport of O_2 from the gas exchange surface to the venous system.

Regulation of the cardiovascular response to diving has been explored is some species. Baroreceptor input has been shown to have no direct role in generating or maintaining heart rate responses to voluntary submersion in diving ducks, since these animals display the same degree of bradycardia after denervation of arterial baroreceptors as before (Furilla and Jones, 1987a). However, baroreceptors may play a role in control of heart rate in dabbling ducks (*A. platyrhynchos*) which have been trained to dive voluntarily. Predive heart rate in dabblers ranged from 100 to about 500 beats min^{-1} but, regardless of the rate preceding any particular dive, rate during the dive tended to a value of approximately 250 beats min^{-1} (Furilla and Jones, 1987b). This response implies that heart rate was being regulated at a set value during voluntary dives. Removal of baroreceptor input by bilateral section of the aortic nerves eliminated the tendency of dive heart rate to approach the "set point" value, after barodenervation dive heart rate varied little from the prevailing predive rate (Furilla and Jones, 1987b). Given that the baroreflex normally regulates blood pressure by adjusting CO and vascular resistance, the physiological value of a baroreceptor-dependent "set point" for heart rate is uncertain. The behavior of arterial blood pressure during voluntary diving in dabbling ducks has not been established. However, there may be some inherent benefit to regulating heart rate under these conditions. If this is true, then strong phasic baroreceptor input to the central nervous system during systole would represent the primary afferent feedback route for heart rate–related information.

Stimulation of nasal receptors in diving ducks and chemoreceptors in dabbling ducks are the proximate causes of the development of diving bradycardia (Furilla and Jones, 1986; 1987a,b). Repeatedly submerging the head of a diving or dabbling duck in a laboratory situation causes the bradycardic response to habituate after 100 to 200 dives (Gabbott and Jones, 1987). In dabbling ducks, however, extending the period of submergence beyond 40 s virtually eliminates any attenuation of the cardiac response to submergence. Obviously, in dabbling ducks, input from the carotid body chemoreceptors is too intense for habitation after 60 s submergence. Similarly, exposing habituated animals to 10% or 15% oxygen in air before submergence causes prominent bradycardia although the very next trial, after breathing room air, evokes the habituated cardiac response. Interestingly, the heart rate response to diving after breathing air with low levels of oxygen is unaffected by training. Consequently, chemoreceptor input, which will be the same in naive and habituated ducks because blood gas levels are the same after 40 s submergence, can be habituated. Habituation of the response occurs within the central nervous system, below the thalamic level.

Even though CO is reduced during diving, the rate of perfusion of cerebral vasculature and thoracoabdominal cavity is maintained or elevated above predive levels (Heieis and Jones, 1988; Jones et al., 1979). In mallard and Pekin ducks, myocardial flow was, on average, 0.73 mL min^{-1} g^{-1} presubmersion and 0.88 mL $min^{-1}g^{-1}$ after 144–250 s of submergence. Cerebral flow increased from 0.43 to 3.68 mL min^{-1} g^{-1} over the same time period. In Pekin ducks forcibly submerged until P_aO_2 fell to 50 mmHg, cerebral blood flow increased from 1.58 to 3.2 mL min^{-1} g^{-1}. Clearly, regardless of the wide range of absolute values measured, cerebral blood flow increases in forced submersion asphyxia, maintaining oxygen delivery to brain tissue. A redistribution of blood flow away from more hypoxia tolerant regions toward more sensitive regions within the brain itself does not seem to occur in the Pekin duck (Stephenson et al., 1994). However, such heterogeneous regional changes in cerebral blood flow in response to asphyxia have been proposed to occur in neonatal mammals (Goplerud et al., 1989).

References

Ábrahám, A., 1969. Microscopic Innervation of the Heart and Blood Vessels in Vertebrates Including Man. Pergamon Press, Oxford, UK.

Aceto, J.F., Baker, K.M., 1990. [Sar1] angiotensin II receptor-mediated stimulation of protein synthesis in chick heart cells. Am. J. Physiol. 258, H806–H813.

Adair, T.H., Montani, J.P., Strick, D.M., Guyton, A.C., 1989. Vascular development in chick embryos, a possible role for adenosine. Am. J. Physiol. 2**56**, H240–H246.

Adams, W.E., 1937. A contribution to the anatomy of the avian heart as seen in the kiwi (*Apterix australis*) and the yellow-crested penguin (*Megadypte antipodum*). J. Zool. 107, 417–441.

Adams, W.E., 1958. Morphology of the Carotid Body and Carotid Sinus. Charles C. Thomas, Springfield, IL.

Agren, P., Cogolludo, A.,L., Kessels, C.G., Perez-Vizcaino, F., DeMey, J.G., Blanco, C.E., Villamor, E., 2007. Ontogeny of chicken ductus arteriosus response to oxygen and vasoconstrictors. Am. J. Physiol. 292, R485–R496.

Akester, A.R., 1967. Renal portal shunts in the kidney of the domestic fowl. J. Anat. 101, 569–594.

Akester, A.R., 1971. The heart. In: Bell, D.J., Freeman, B.M. (Eds.), Physiology and Biochemistry of the Domestic Fowl, vol. 2. Academic Press, New York, pp. 745–781.

Akester, A.R., 1979. The autonomic nervous system. In: King, A.S., McLelland, J. (Eds.), Form and Function in Birds, vol. 1. Academic Press, New York, pp. 381–441.

Akester, A.R., Akester, B., 1971. Double innervation of the avian cardiovascular system. J. Anat. 108, 618–619.

Akester, A.R., Mann, S.P., 1969. Adrenergic and cholinergic innervation of the renal portal valve in the domestic fowl. J. Anat. 104, 241–252.

Akester, A.R., Akester, B., Mann, S.P., 1969. Catecholamines in the avian heart. J. Anat. 104, 591.

Akizuki, N., Kangawa, K., Minamino, N., Matsuo, H., 1991. Cloning and sequence analysis of complementary DNA encoding a precursor for chicken natriuretic peptide. FEBS Lett. 280, 357–362.

Altimiras, J., Lindgren, I., Deck, L.M.G., Matthei, A., Garitano-Zavala, A., 2017. Aerobic performance in tinamous is limited by their small heart. A novel hypothesis in the evolution of avian flight. Sci. Rep. 7, 15964.

Altman, P.L., Dittmer, D.S., 1971. Respiration and Circulation. Federation of American Societies for Experimental Biology, Bethesda, MD.

Andersen, J.B., Rourke, B.C., Caiozzo, V.J., Bennett, A.F., Hicks, J.W., 2005. Physiology: postprandial cardiac hypertrophy in pythons. Nature 434, 37–38.

Andrewartha, S.J., Tazawa, H., Burggren, W.W., 2011. Embryonic control of heart rate: examining developmental patterns and temperature and oxygenation influences using embryonic avian models. Respir. Physiol. Neurobiol. 178, 84–95.

Armour, J.A., Huang, M.H., Smith, F.M., 1993. Peptidergic modulation of *in situ* canine intrinsic cardiac neurons. Peptides 14, 191–202.

Ash, R.W., Pearce, J.W., Silver, A., 1969. An investigation of the nerve supply to the salt gland of the duck. Q. J. Exp. Physiol. 54, 281–295.

Astrand, P.O., Rodahl, K., 1986. Textbook of Work Physiology. McGraw–Hill, New York.

Bagshaw, R.J., 1985. Evolution of cardiovascular baroreceptor control. Biol. Rev. 60, 121–162.

Bagshaw, R.J., Cox, R.H., 1986. Baroreceptor control of heart rate in chickens (*Gallus domesticus*). Am. J. Vet. Res. 47, 293–295.

Baker, K.M., Aceto, J.F., 1990. Angiotensin II stimulation of protein synthesis and cell growth in chick heart cells. Am. J. Physiol. 259, H610–H618.

Ball, R.A., Sautter, J.H., Katter, M.S., 1963. Morphological characteristics of the anterior mesenteric artery of the fowl. Anat. Rec. 146, 251–256.

Ball, R.A., Sautter, J.H., Waibel, P.E., 1972. Adaptive features in the Turkey aorta which precede plaque formation. Atherosclerosis 15, 241–247.

Ballard, V.L.T., Mikawa, T., 2002. Constitutive expression of preproendothelin in the cardiac neural crest selectively promotes expansion of the adventitia of the great vessels in vivo. Dev. Biol. 251, 167–177.

Balligand, J.L., Feron, O., Dessy, C., 2009. eNOS activation by physical forces: from short-term regulation of contraction to chronic remodeling of cardiovascular tissues. Physiol. Rev. 89, 481–534.

Berry, A., 1950. The effects of epinephrine on the myocardium of the embryonic chick. Circulation 1, 1362–1368.

Bamford, O.S., Jones, D.R., 1976. The effects of asphyxia on afferent activity recorded from the cervical vagus in the duck. Pflugers Arch. 366, 95–99.

Barnas, G.M., Gleeson, M., Rautenberg, W., 1985. Respiratoryand cardiovascular responses of the exercising chicken to spinal cord cooling at different ambient temperatures. I. Cardiovascular responses and blood gases. J. Exp. Biol. 114, 415–426.

Bauchinger, U., Wohlmann, A., Biebach, H., 2005. Flexible remodeling of organ size during spring migration of the garden warbler (*Sylvia borin*). Zoology 108, 97–106.

Baumel, J.J., 1975. *Aves* heart and blood vessels. In: Getty, R. (Ed.), Sisson and Grossman's the Anatomy of the Domestic Animals. Saunders, Philadelphia.

Baumel, J.J., Gerchman, L., 1968. The avian intercarotid anastomosis and its homologue in other vertebrates. Am. J. Anat. 122, 1–18.

Bech, C., Nomoto, S., 1982. Cardiovascular changes associated with treadmill running in the Pekin duck. J. Exp. Biol. 97, 345–358.

Belanger, C., Copeland, J., Muirhead, D., Heinz, D., Dzialowski, E.M., 2008. Morphological changes in the chicken ductus arteriosi during closure at hatching. Anat. Rec. 291, 1007–1015.

Bell, C., 1969. Indirect cholinergic vasomotor control of intestinal blood flow in the domestic chicken. J. Physiol. 205, 317–327.

Bennett, T., 1971. The adrenergic innervation of the pulmonary vasculature, the lung and the thoracic aorta, and on the presence of aortic bodies in the domestic fowl (*Gallus gallus domesticus* L.). Z. Zellforsch. 114, 117–134.

Bennett, T., 1974. Peripheral and autonomic nervous systems. In: Farner, D.S., King, J.R., Parkes, K.C. (Eds.), Avian Biology Volume 4. Academic Press, New York, pp. 1–77.

Bennett, T., Malmfors, T., 1970. The adrenergic nervous system of the domestic fowl (*Gallus domesticus* (L.)). Z. Zellforsch. 106, 22–50.

Bennett, T., Malmfors, T., 1974. Regeneration of the noradrenergic innervation of the cardiovascular system of the chick following treatment with 6-hydroxydopamine. J. Physiol. 242, 517–532.

Bennett, T., Malmfors, T., 1975a. Autonomic control of renal portal blood flow in the domestic fowl. Experientia 31, 1177–1178.

Bennett, T., Malmfors, T., 1975b. Characteristics of the noradrenergic innervation of the left atrium in the chick (*Gallus gallus domesticus*, L.). Comp. Biochem. Physiol., C 52, 47–49.

Bennett, T., Cobb, J.L.S., Malmfors, T., 1974. The vasomotor innervation of the inferior vena cava of the domestic fowl (*Gallus gallus domesticus* L.): I. Structural observations. Cell Tissue Res. 148, 521–533.

Benzo, C.A., 1986. Nervous system. In: Sturkie, P.D. (Ed.), Avian Physiology, fourth ed. Springer-Verlag, Berlin, pp. 1–36.

Bergel, D.H., 1961. The static properties of the arterial wall. J. Physiol. 156, 445–457.

Berk, M.L., 1987. Projections of the lateral hypothalamus and bed nucleus of the stria terminalis to the dorsal vagal complex in the pigeon. J. Comp. Neurol. 260, 140–156.

Berk, M.L., Finkelstein, J.A., 1983. Long descending projections of the hypothalamus in the pigeon, *Columba livia*. J. Comp. Neurol. 220, 127–136.

Berk, M.L., Smith, S.E., 1994. Local and commissural neuropeptide-containing projections of the nucleus of the solitary tract to the dorsal vagal complex in the pigeon. J. Comp. Neurol. 347, 369–396.

Bevan, R.M., Boyd, I.L., Butler, P.J., Reid, K., Woakes, A.J., Croxall, J.P., 1997. Heart rates and abdominal temperatures of free-ranging south Georgian shags, *Phalacrocorax georgianus*. J. Exp. Biol. 200, 661–675.

Bevan, R.M., Butler, P.J., 1992. Cardiac output and blood flow distribution during swimming and voluntary diving of the tufted duck (Aythya fuligula). J. Exp. Biol. 168, 199–217.

Bézie, Y., Mesnard, L., Longrois, D., Samson, F., Perret, C., Mercadier, J.J., Laurent, S., 1996. Interactions between endothelin-1 and atrial natriuretic peptide influence cultured chick cardiac myocyte contractility. Eur. J. Pharmacol. 311, 241–248.

Bezuidenhout, A.J., 1984. The coronary circulation of the heart of the ostrich. J. Anat. 138, 385–397.

Bickler, P.E., Julian, D., 1992. Regional cerebral blood flow and tissue oxygenation during hypocarbia in geese. Am. J. Physiol. 263, R221–R225.

Biegon, R.L., Epstein, P.M., Pappano, A.J., 1980. Muscarinic antagonism of the effects of phosphodiesterase inhibitor (methylisobutylxanthine) in embryonic chick ventricle. J. Pharmacol. Exp. Ther. 215, 348–356.

Biegon, R.L., Pappano, A.J., 1980. Dual mechanism for inhibition of calcium-dependent action potentials by acetylcholine in avian ventricular muscle. Relationship to cyclic AMP. Circ. Res. 46, 353–362.

Bishop, C.M., Butler, P.J., 1995. Physiological modelling of oxygen consumption in birds during flight. J. Exp. Biol. 198, 2153–2163.

Bishop, C.M., Butler, P.J., Egginton, S., el-Haj, A.J., Gabrielsen, G.W., 1995. Development of metabolic enzyme activity in locomotor and cardiac muscles in the migratory barnacle goose. Am. J. Physiol. 269, R64–R72.

Blix, A.S., Wennergren, G., Folkow, B., 1976. Cardiac receptors in ducks — a link between vasoconstriction and bradycardia during diving. Acta Physiol. Scand. 97, 13–19.

Bogusch, G., 1974. The innervation of Purkinje fibres in the atrium of the avian heart. Cell Tissue Res. 150, 57–66.

Bolton, T.B., 1967. Intramural nerves in the ventricular myocardium of the domestic fowl and other animals. Br. J. Pharmacol. Chemother. 31, 253–268.

Bolton, T.B., 1969. Spontaneous and evoked release of neurotransmitter substances in the longitudinal muscle of the anterior mesenteric artery of the domestic fowl. Br. J. Pharmacol. 35, 112–120.

Bolton, T.B., Bowman, W.C., 1969. Adrenoreceptors in the cardiovascular system of the domestic fowl. Eur. J. Pharmacol. 5, 121–132.

Bolton, T.B., Raper, C., 1966. Innervation of domestic fowl and Guinea-pig ventricles. J. Pharm. Pharmacol. 18, 192–193.

Bopelet, M., 1974. Normal electrocardiogram of the chicken: its variations during vagal stimulation and following vagotomies. Comp. Biochem. Physiol. A 47, 361–369.

Borg, K.A., Milsom, W.K., Jones, D.R., 2004. The effect of O_2 and CO_2 on the dive behavior and heart rate of lesser scaup ducks (*Aythya affinis*): quantification of the critical PaO_2 that initiates a diving bradycardia. Respir. Physiol. Neurobiol. 144, 263–279.

Bossen, E., Sommer, J.R., Waugh, R.A., 1978. Comparative stereology of the mouse and finch left ventricle. Tissue Cell 10, 773–784.

Boukens, B.J.D., Kristensen, D.L., Filogonio, R., Carreira, L.B.T., Sartori, M.R., Abe, A.S., Currie, S., Joyce, W., Conner, J., Opthof, T., Crossley, D.A., Wang, T., Jensen, B., 2019. The electrocardiogram of vertebrates: evolutionary changes from ectothermy to endothermy. Prog. Biophys. Mol. Bio. 144, 16–29.

Boulianne, M., Hunter, D.B., Julian, R.J., O'Grady, M.R., Physick Sheard, P.W., 1992. Cardiac muscle mass distribution in domestic Turkey and relationship to electrocardiogram. Avian Dis. 36, 582–589.

Boulianne, M., Hunter, D.B., Physick-Sheard, P.W., Viel, L., Julian, R.J., 1993a. Effect of exercise on cardiac output and other cardiovascular parameters of heavy turkeys and relevance to the sudden death syndrome. Avian Dis. 37, 98–106.

Boulianne, M., Hunter, D.B., Viel, L., Physick-Sheard, P.W., Julian, R.J., 1993b. Effect of exercise on the cardiovascular and respiratory systems of heavy turkeys and relevance to sudden death syndrome. Avian Dis. 37, 83–97.

Bouverot, P., Leitner, L.M., 1972. Arterial chemoreceptors in the domestic fowl. Respir. Physiol. 15, 310–320.

Bouverot, P., Douguet, D., Sébert, P., 1979. Role of the arterial chemoreceptors in ventilatory and circulatory adjustments to hypoxia in awake Pekin ducks. J. Comp. Physiol. B 133, 177–186.

Bowers, P.N., Tinney, J.P., Keller, B.B., 1996. Nitroprusside selectively reduces ventricular preload in the stage 21 chick embryo. Cardiovasc. Res. 31, E132–E138.

Braun, E.J., 1982. Glomerular filtration in birds — its control. Fed. Proc. 41, 2377–2381.

Brehm, G., Lindmar, R., Loffelholz, K., 1992. Inhibitory and excitatory muscarinic receptors modulating the release of acetylcholine from the postganglionic parasympathetic neuron of the chicken heart. Naunyn-Schmiedeberg's Arch. Pharmacol. 346, 375–382.

Brill, R.W., Jones, D.R., 1981. On the suitability of Innovar, a neuroleptic analgesic, for cardiovascular experiments. Can. J. Physiol. Pharmacol. 59, 1184–1189.

Brummermann, M., Simon, E., 1990. Arterial hypotension in ducks adapted to high salt intake. J. Comp. Physiol. B 160, 127–136.

Burrows, M.E., Braun, E.J., Duckles, S.P., 1983. Avian renal portal valve: a reexamination of its innervation. Am. J. Physiol. 245, H628–H634.

Bussow, H., 1973. Zar wandstruktur der grojen arterien der vogel. Z. Zellforsch. 142, 263–288.

Butler, D.G., Wilson, J.X., Graves, L.E., 1986. α- and β- adrenergic mechanisms mediate blood pressure control by norepinephrine and angiotensin in ducks. Gen. Comp. Endocrinol. 61, 323–329.

Butler, P.J., 1967. The effect of progressive hypoxia on the respiratory and cardiovascular systems of the chicken. J. Physiol. 191, 309–324.

Butler, P.J., 1991. Exercise in birds. J. Exp. Biol. 160, 233–262.

Butler, P.J., Jones, D.R., 1968. Onset of and recovery from diving bradycardia in ducks. J. Physiol. 196, 255–272.

Butler, P.J., Jones, D.R., 1971. The effect of variations in heart rate and regional distribution of blood flow on the normal pressor response to diving in ducks. J. Physiol. 214, 457–479.

Butler, P.J., Jones, D.R., 1997. The physiology of diving of birds and mammals. Physiol. Rev. 77, 837–899.

Butler, P.J., Taylor, E.W., 1973. The effect of hyperoxic hypoxia, accompanied by different levels of lung ventilation, on heart rate in the duck. Respir. Physiol. 19, 176–187.

Butler, P.J., Taylor, E.W., 1983. Factors affecting the respiratory and cardiovascular responses to hypercapnic hypoxia, in Mallard ducks. Respir. Physiol. 53, 109–127.

Butler, P.J., Turner, D.L., Al-Wassia, A., Bevan, R.M., 1988. Regional distribution of blood flow during swimming in the tufted duck (*Aythya fuligula*). J. Exp. Biol. 135, 461–472.

Butler, P.J., West, N.H., Jones, D.R., 1977. Respiratory and cardiovascular responses of the pigeon to sustained, level flight in a wind-tunnel. J. Exp. Biol. 71, 7–26.

Butler, P.J., Woakes, A.J., Bishop, C.M., 1998. Behaviour and physiology of *Svalbard barnacle* geese, *Branta leucopsis*, during their autumn migration. J. Avian Biol. 29, 536–545.

Byers, R.L., Snyder, G.K., 1984. Effects of maturation on tissue capillarity in chickens. Respir. Physiol. 58, 137–150.

Cabot, J.B., Cohen, D.H., 1977a. Avian sympathetic cardiac fibers and their cells of origin: anatomical and electrophysiological characteristics. Brain Res. 131, 73–87.

Cabot, J.B., Cohen, D.H., 1977b. Anatomical and physiological characterization of avian sympathetic cardiac afferents. Brain Res. 131, 89–101.

Cabot, J.B., Cohen, D.H., 1980. Neural control of the avian heart. In: Bourne, G.B. (Ed.), Hearts and Heart-like Organs, vol. 1. Academic Press, NY, pp. 199–258.

Cabot, J.B., Carroll, J., Bogan, N., 1991a. Localization of cardiac parasympathetic preganglionic neurons in the medulla oblongata of pigeon, *Columba livia*: a study using fragment C of tetanus toxin. Brain Res. 544, 162–168.

Cabot, J.B., Mennone, A., Bogan, N., Carroll, J., Evinger, C., Erichsen, J.T., 1991b. Retrograde, trans-synaptic and transneuronal transport of fragment C of tetanus toxin by sympathetic preganglionic neurons. Neuroscience 40, 805–823.

Cabot, J.B., Reiner, A., Bogan, N., 1982. Avian bulbospinal pathways: anterograde and retrograde studies of cells of origin, funicular trajectories and laminar terminations. Prog. Brain Res. 57, 79–108.

Chess-Williams, R., Austin, C.E., O'Brien, H.L., 1991. α-adrenoceptors do not contribute to the chronotropic or inotropic responses of the avian heart to noradrenaline. J. Auton. Pharmacol. 11, 27–35.

Chiba, Y., Fukuoka, S., Niiya, A., Akiyama, R., Tazawa, H., 2004. Development of cholinergic chronotropic control in chick (*Gallus gallus domesticus*) embryos. Comp. Biochem. Physiol. A. 137, 65–73.

Cinar, A., Bagci, C., Belge, F., Uzun, M., 1996. The electrocardiogram of the Pekin duck. Avian Dis. 40, 919–923.

Cohen, D.H., 1980. The functional neuroanatomy of a conditioned response. In: Thompson, R.F., Hicks, L.H., Shvyrkov, V.B. (Eds.), Neural Mechanisms of Goal-Directed Behavior and Learning. Academic Press, New York, pp. 283–302.

Cohen, D.H., 1984. Identification of vertebrate neurons modified during learning: analysis of sensory pathways. In: Alkon, D.L., Farley, J. (Eds.), Primary Neural Substrates of Learning and Behavioral Change. Cambridge Univ. Press, Cambridge, UK, pp. 129–154.

Cohen, D.H., Schnall, A.M., 1970. Medullary cells of origin of vagal cardioinhibitory fibers in the pigeon. II. Electrical stimulation of the dorsal motor nucleus. J. Comp. Neurol. 140, 321–342.

Cohen, D.H., Schnall, A.M., Macdonald, R.L., Pitts, L.H., 1970. Medullary cells of origin of vagal cardioinhibitory fibers in the pigeon. I. Anatomical studies of peripheral vagus nerve and the dorsal motor nucleus. J. Comp. Neurol. 140, 299–320.

Coote, J.H., 1975. Physiological significance of somatic afferent pathways from skeletal muscle and joints with reflex effects on the heart and circulation. Brain Res. 87, 139–144.

Coraboeuf, E., Obrecht-Coutris, G., Le-Douarin, G., 1970. Acetylcholine and the embryonic heart. Am. J. Cardiol. 25, 285–291.

Corvetti, G., Andreotti, L., Sisto-Daneo, L., 1988. Chick heart peptidergic innervation: localization and development. Basic Appl. Histochem. 32, 485–493.

Crossley, D.A., 1999. Development of Cardiovascular Regulation in Embryos of the Domestic Fowl (*Gallus gallus*) with Partial Comparison to Embryos of the Desert Tortoise (*Gopherus agassizii*) (Ph.D. dissertation). University of North Texas, Denton.

Crossley, D.A., Altimiras, J., 2000. Ontogeny of autonomic control of cardiovascular function in the domestic chicken *Gallus gallus*. Am. J. Physiol. 279, R1091–R1098.

Crossley, D.A., Altimiras, J., 2012. Effect of selection for commercially productive traits on the plasticity of cardiovascular regulation in chicken breeds during embryonic development. Poultry Sci. 91, 2628–2636.

Crossley, D.A., Bagatto, B.P., Dzialowski, E.M., Burggren, W.W., 2003a. Maturation of cardiovascular control mechanisms in the embryonic emu (*Dromiceius novaehollandiae*). J. Exp. Biol. 206, 2703–2710.

Crossley, D.A., Burggren, W.W., Altimiras, J., 2003b. Cardiovascular regulation during hypoxia in embryos of the domestic chicken *Gallus gallus*. Am. J. Physiol. 284, R219–R226.

Crossley, D.A., Jonker, S.S., Hicks, J.W., Thornburg, K.L., 2010. Maturation of the angiotensin II cardiovascular response in the embryonic White Leghorn chicken (*Gallus gallus*). J. Comp. Physiol. B. 180, 1057–1065.

Cullis, W.C., Lucas, C.L.T., 1936. Action of acetylcholine on the aneural chick heart. J. Physiol. Suppl. 86, 53–55.

Dantzler, W.H., 1989. Comparative Physiology of the Vertebrate Kidney. Springer-Verlag, New York.

Davies, F., 1930. The conducting system of the bird's heart. J. Anat. 64, 129–146.

Deighton, N.M., Motomura, S., Borquez, D., Zerkowski, H.R., Doetsch, N., Brodde, O.E., 1990. Muscarinic cholinoceptors in the human heart: demonstration, subclassification, and distribution. Naunyn-Schmiedeberg's Arch. Pharmacol. 341, 14–21.

Denton, T., Diamond, G.A., Helfant, R.H., Khan, S., Karagueuzian, H., 1990. Fascinating rhythm: a primer on chaos theory and its application to cardiology. Am. Heart J. 120, 1419–1440.

DeSantis, V.P., Lindmar, L.R., Loffelholz, K., 1975. Evidence for noradrenaline and adrenaline as sympathetic transmitters in the chicken. Br. J. Pharmacol. 55, 343–350.

Di Rienzo, M., Parati, G., Castiglioni, P., Tordi, R., Mancia, G., Pedotti, A., 2001. Baroreflex effectiveness index: an additional measure of baroreflex control of heart rate in daily life. Am. J. Physiol. 280, R744–R751.

Djojosugito, A.M., Folkow, B., Kovách, A.G.B., 1968. The mechanisms behind the rapid blood volume restoration after hemorrhage in birds. Acta Physiol. Scand. 74, 114–122.

Djojosugito, A.M., Folkow, B., Yonce, L.R., 1969. Neurogenic adjustments of muscle blood flow, cutaneous a-v shunt flow and of venous tone during "diving" in ducks. Acta Physiol. Scand. 75, 377–386.

Dombkowski, R.A., Russell, M.J., Schulman, A.A., Doellman, M.M., Olson, K.R., 2005. Vertebrate phylogeny of hydrogen sulfide vasoactivity. Am. J. Physiol. Regul. Integr. Comp. Physiol. 288, R243–R252.

Donald, J.A., Forgan, L.G., Cameron, M.S., 2015. The evolution of nitric oxide signaling in vertebrate blood vessels. J. Comp. Physiol. B. 185, 153–171.

Donnelly, D.F., 2005. Development of carotid body/petrosal ganglion response to hypoxia. Respir. Physiol. Neurobiol. 149, 191–199.

Duchamp, C., Barre, H., 1993. Skeletal muscle as the major site of nonshivering thermogenesis in cold-acclimated ducklings. Am. J. Physiol. 265, R1076–R1083.

Dufour, J.J., Posternak, J.M., 1960. Effets chronotropes de l'acetylcholine sur le coeur d'embryon de poulet. Helv. Physiol. Pharmacol. Acta 18, 563–580.

Dunn, L.K., Gruenloh, S.K., Dunn, B.E., Reddy, D.S., Falck, J.R., Jacobs, E.R., Medhora, M., 2005. Chick chorioallantoic membrane as an in vivo model to study vasoreactivity: characterization of development-dependent hyperemia induced by epoxyeicosatrienoic acids (EETs). Anat. Rec. 285, 771–780.

Dzialowski, E.M., 2018. Comparative physiology of the ductus arteriosus among vertebrates. Semin. Perinatol. 42, 203–211.

Dzialowski, E.M., Greyner, H., 2008. Maturation of the contractile response of the *Emu ductus* arteriosus. J. Comp. Physiol. B. 178, 401–412.

Dzialowski, E.M., Sirsat, T., van der Sterren, S., Villamor, E., 2011. Prenatal cardiovascular shunts in amniotic vertebrates. Respir. Physiol. Neurobiol. 178, 66–74.

Ede, D.A., 1964. Bird Structure. Hutchinson Educational, London.

Elfwing, M., 2007. The Ontogeny of the Baroreflex in Domestic Broiler Chickens (*Gallus gallus Domesticus*) (MS thesis). Linköpings Universitet, Linköping.

Elfwing, M., Lundengård, K., Altimiras, J., 2011. Fetal development of baroreflex sensitivity: the chicken embryo as a case model. Respir. Physiol. Neurobiol. 178, 75–83.

Ellerby, D.J., Henry, H.T., Carr, J.A., Buchanan, C.I., Marsh, R.L., 2005. Blood flow in Guinea fowl *Numida meleagris* as an indicator of energy expenditure by individual muscles during walking and running. J. Physiol. 564, 631–648.

Ellis, C.G., Potter, R.F., Groom, A.C., 1983. The krogh cylinder geometry is not appropriate for modelling O_2 transport in contracted skeletal muscle. Adv. Exp. Med. Biol. 159, 253–268.

Estavillo, J.A., 1978. Fiber size and sensory endings of the middle cardiac nerve of the domestic fowl (*Gallus domesticus*). Acta Anat. 101, 104–109.

Enstipp, M.R., Andrews, R.D., Jones, D.R., 2001. The effects of depth on the cardiac and behavioural responses of double-crested cormorants (*Phalacrocorax auritus*) during voluntary diving. J. Exp. Biol. 204, 4081–4092.

Estavillo, J., Burger, R.E., 1973a. Cardiac afferent activity in depressor nerve of the chicken. Am. J. Physiol. 225, 1063–1066.

Estavillo, J., Burger, R.E., 1973b. Avian cardiac receptors: activity changes by blood pressure, carbon dioxide, and pH. Am. J. Physiol. 225, 1067–1071.

Estavillo, J.A., Adamson, T.P., Burger, R.E., 1990. Middle cardiac nerve section alters ventilatory response to $PaCO_2$ in the cockerel. Respir. Physiol. 81, 349–358.

Evered, M.D., Fitzsimons, J.T., 1981. Drinking and changes in blood pressure in response to angiotensin II in the pigeon *Columba livia*. J. *Physiol*. 310, 337–352.

Faraci, F.M., Fedde, M.R., 1986. Regional circulatory responses to hypocapnia and hypercapnia in bar-headed geese. Am. J. Physiol. 250, R499–R504.

Faraci, F.M., Kilgore, D.L., Fedde, M.R., 1984. Oxygen delivery to the heart and brain during hypoxia: pekin duck vs. bar-headed goose. Am. J. Physiol. 247, R69–R75.

Faraci, F.M., Kilgore, D.L., Fedde, M.R., 1985. Blood flow distribution during hypocapnic hypoxia in Pekin ducks and bar- headed geese. Respir. Physiol. 61, 21–30.

Fedde, M.R., Orr, J.A., Shams, S., Scheid, P., 1989. Cardiopulmonary function in exercising bar-headed geese during normoxia and hypoxia. Respir. Physiol. 77, 239–252.

Feigl, E., Folkow, B., 1963. Cardiovascular responses in "diving" and during brain stimulation in ducks. Acta Physiol. Scand. 57, 99–110.

Fibiger, H.C., 1982. The organization and some projections of cholinergic neurons of the mammalian forebrain. Brain Res. Rev. 4, 327–388.

Fingl, E., Woodbury, L.A., Hecht, M.H., 1952. Effects of innervation and drugs upon direct membrane potentials of embryonic chick myocardium. J. Pharmacol. Exp. Ther. 104, 103–114.

Folkow, B., 1952. Impulse frequency in sympathetic vasomotor fibres correlated to the release and elimination of the transmitter. Acta Physiol. Scand. 25, 49–76.

Folkow, B., Rubenstein, E.H., 1965. Effect of brain stimulation on "diving" in ducks. Hvalradets Skr 48, 30–41.

Folkow, B., Yonce, L.R., 1967. The negative inotropic effect of vagal stimulation on the heart ventricles of the duck. Acta Physiol. Scand. 71, 77–84.

Folkow, B., Fuxe, K., Sonnenschein, R.R., 1966. Responses of skeletal musculature and its vasculature during "diving" in the duck: Peculiarities of the adrenergic vasoconstrictor innervation. Acta Physiol. Scand. 67, 327–342.

Folkow, B., Nilsson, N.J., Yonce, L.R., 1967. Effects of "diving" on cardiac output in ducks. Acta Physiol. Scand. 70, 347–361.

Freer, R.J., Pappano, A.J., Peach, M.J., 1976. Mechanism for the positive inotropic effect of angiotensin II on isolated cardiac mu. Circ. Res. 39, 178–183.

Frieswic, k G.M., Danielson, T., Shideman, F.E., 1979. Adrenergic inotropic responsiveness of embryonic chick and rat hearts. Dev. Neurosci. 2, 276–285.

Furchgott, R.F., Zawadzki, J.V., 1980. The obligatory role of endothelial cells in the relaxation of arterial smooth muscle by acetylcholine. Nature 288, 373–376.

Furilla, R.A., Jones, D.R., 1986. The contribution of nasal receptors to the cardiac response to diving in restrained and unrestrained redhead ducks (*Aythya americana*). J. Exp. Biol. 121, 227–238.

Furilla, R.A., Jones, D.R., 1987a. The relationship between dive and predive heart rates in restrained and free dives by diving ducks. J. Exp. Biol. 127, 333–348.

Furilla, R.A., Jones, D.R., 1987b. Cardiac responses to dabbling and diving the mallard, Anas platyrhynchos. Physiol. Zool. 60, 406–412.

Furnival, C.M., Linden, R.J., Snow, H.M., 1973. The inotropic effect on the heart of stimulating the vagus in the dog, duck and toad. J. Physiol. 230, 155–170.

Gabbott, G.R.J., Jones, D.R., 1987. Habituation of the cardiac response to involuntary diving in diving and dabbling ducks. J. Exp. Biol. 131, 403–415.

Gabella, G., 1976. Structure of the Autonomic Nervous System. J Wiley, New York.

Ganitkevich, V., Hasse, V., Pfitzer, G., 2002. Ca^{2+}-dependent and Ca^{2+}-independent regulation of smooth muscle contraction. J. Muscle Res. Cell Motil. 23, 47–52.

Gayeski, T.E.J., Honig, C.R., 1986. O_2 gradients from sarcolemma to cell interior in red muscle at maximal VO_2. Am. J. Physiol. 251, H789–H799.

Gilman, A.G., Rall, T.W., Nies, A.S., Taylor, P., 1990. The Pharmacological Basis of Therapeutics, eighth ed. Pergamon, Oxford, UK.

Girard, H., 1973. Adrenergic sensitivity of circulation in the chick embryo. Am. J. Physiol. 224, 461–469.

Glahn, R.P., Bottje, W.G., Maynard, P., Wideman, R.F., 1993. Response of the avian kidney to acute changes in arterial perfusion pressure and portal blood supply. Am. J. Physiol. 264, R428–R434.

Glenny, F.H., 1940. A systematic study of the main arteries in the region of the heart — Aves. Anat. Rec. 76, 371–380.

Glombitza, S., Dragon, S., Berghammer, M., Pannermayr, M., Baumann, R., 1996. Adenosine causes cAMP-dependent activation of

chick embryo red cell carbonic anhydrase and 2,3-DPG synthesis. Am. J. Physiol. 271, R973–R981.

Gold, M.R., Cohen, D.H., 1984. The discharge characteristics of vagal cardiac neurons during classically conditioned heart rate change. J. Neurosci. 4, 2963–2971.

Goldberg, T.M., Bolnick, D.A., 1980. Electrocardiograms from the chicken, emu, red-tailed hawk and *Chilean tinamou*. Comp. Biochem. Physiol. A 67, 15–19.

Goldberg, J.M., Johnson, M.H., Whitelaw, K.D., 1983. Effect of cervical vagal stimulation on chicken heart rate and atrioventricular conduction. Am. J. Physiol. 244, R235–R243.

Goldberger, A.L., 1991. Is the normal heartbeat chaotic or homeostatic? News Physiol. Sci. 6, 87–91.

Goldberger, A.L., Rigney, D.R., West, B.J., 1990. Chaos and fractals in human physiology. Sci. Am. 262, 42–49.

Gooden, B.A., 1980. The effect of hypoxia on vasoconstrictor responses of isolated mesenteric arterial vasculature from chicken and duckling. Comp. Biochem. Physiol. C 67, 219–222.

Goplerud, J.M., Wagerle, L.C., Delivoria-Papadopoulos, M., 1989. Regional cerebral blood flow response during and after acute asphyxia in newborn piglets. J. Appl. Physiol. 66, 2827–2832.

Gray, S.D., McDonagh, P.F., Gore, R.W., 1983. Comparison of functional and total capillary densities in fast and slow muscles of the chicken. Pflügers Arch. 397, 209–213.

Greyner, H., Dzialowski, E.M., 2008. Mechanisms mediating the oxygen-induced vasoreactivity of the ductus arteriosus in the chicken embryo. Am. J. Physiol. 295, R1647–R1659.

Grindlay, J.H., Herrick, J.F., Mann, F.C., 1939. Measurement of the blood flow of the spleen. Am. J. Physiol. 127, 106–118.

Groenendijk, B.C.W., Hierck, B.P., Vrolijk, J., Baiker, M., Pourquie, M.J.B.M., Gittenberger-de Groot, A.C., Poelmann, R.E., 2005. Changes in shear stress-related gene expression after experimentally altered venous return in the chicken embryo. Circ. Res. 96, 1291–1298.

Groenendijk, B.C.W., Stekelenburg-De Vos, S., Vennemann, P., Wladimiroff, J.W., Nieuwstadt, F.T.M., Lindken, R., Westerweel, J., Hierck, B.P., Ursem, N.T.C., Poelmann, R.E., 2008. The endothelin-1 pathway and the development of cardiovascular defects in the haemodynamically challenged chicken embryo. J. Vasc. Res. 45, 54–68.

Grubb, B.R., 1983. Allometric relations of cardiovascular function in birds. Am. J. Physiol. 245, H567–H572.

Grubb, B.R., Jorgensen, D.D., Conner, M., 1983. Cardiovascular changes in the exercising emu. J. Exp. Biol. 104, 193–201.

Grubb, B.R., Mills, C.D., Colacino, J.M., Schmidt-Neilsen, K., 1977. Effect of arterial carbon dioxide on cerebral blood flow in ducks. Am. J. Physiol. 232, H596–H601.

Guimaraes, S., Moura, D., 2001. Vascular adrenoceptors: an update. Pharmacol. Rev. 53, 319–356.

Guyton, A.C., Young, D.B., DeClue, J.W., Trippodo, N., Hall, J.E., 1975. Fluid balance, renal function and blood pressure. Clin. Nephrol. 4, 122–126.

Hall, C.E., Hurtado, R., Hewett, K.W., Shulimovich, M., Poma, C.P., Reckova, M., Justus, C., Pennisi, D.J., Tobita, K., Sedmera, D., Gourdie, R.G., Mikawa, T., 2004. Hemodynamic-dependent patterning of endothelin converting enzyme 1 expression and differentiation of impulse-conducting Purkinje fibers in the embryonic heart. Development 131, 581–592.

Hargens, A.R., Millard, R.W., Johansen, K., 1974. High capillary permeability in fishes. Comp. Biochem. Physiol. A 48, 675–680.

Harrison, T.A., Stadt, H.A., Kirby, M.L., 1994. Developmental characteristics of the chick nodose ganglion. Dev. Neurosci. 16, 67–73.

Hartman, F.A., 1961. Smithsonian Miscellaneous Collections, vol. 143, pp. 1–91.

Hasegawa, K., Nishimura, H., 1991. Humoral factor mediates acetylcholine-induced endothelium-dependent relaxation of chicken aorta. Gen. Comp. Endocrinol. 84, 164–169.

Hasegawa, K., Nishimura, H., Khosla, M.C., 1993. Angiotensin II-induced endothelium-dependent relaxation of fowl aorta. Am. J. Physiol. 264, R903–R911.

Hassanpour, H., Teshfam, M., Momtaz, H., Brujeni, G.N., Shahgholian, L., 2010. Up-regulation of Endothelin-1 and Endothelin type A receptor gene expression in the heart of broiler chickens versus layer chickens. Res. Vet. Sci. 89, 352–357.

Hawkes, L.A., Balachandan, S., Batbayar, N., Butler, P.J., Chua, B., Douglas, D.C., Frappell, P.B., Hou, Y., Milsom, M.K., Newman, S.H., Prosser, D.J., Sathiyaselvam, P., Scott, G.R., Takekawa, J.Y., Natsagdorj, T., Wikelski, M., Witt, M.J., Yan, B., Bishop, C.M., 2013. The paradox of extreme high-altitude migration in bar-headed geese *Anser indicus*. Proc. Royal Soc. B 280, 20122114.

Hawkes, L.A., Balachandran, S., Batbayar, N., Butler, P.J., Frappell, P.B., Milsom, W.K., Tseveenmyadag, N., Newman, S.H., Scott, G.R., Sathiyaselvam, P., Takekawa, J.Y., Wikelski, M., Bishop, C.M., 2011. The trans-Himalayan flights of bar-headed geese (*Anser indicus*). Proc. Natl. Acad. Sci. U.S.A. 201017295.

Hawkes, L.A., Butler, P.J., Frappell, P.B., Meir, J.U., Milsom, W.K., Scott, G.R., Bishop, C.M., 2014. Maximum running speed of captive bar-headed geese is unaffected by severe hypoxia. PLoS One 9, e94015.

Hebb, C., 1969. Motor innervation of pulmonary blood vessels. In: Fishman, A.P., Hecht, H.H. (Eds.), The Pulmonary Circulation and Interstitial Space. Univ. of Chicago Press, Chicago. Part 3.

Hedlund, K.O., Ebendal, T., 1980. The chick embryo nodose ganglion: effects of nerve growth factor in culture. J. Neurocytol. 9, 665–682.

Heieis, M., Jones, D.R., 1988. Blood flow and volume distribution during forced submergence in Pekin ducks (*Anas platyrhynchos*). Can. J. Zool. 66, 1589–1596.

Hempleman, S.C., Powell, F.L., Prisk, G.K., 1992. Avian arterial chemoreceptor responses to steps of CO_2 and O_2. Respir. Physiol. 90, 325–340.

Henderson, I.W., Deacon, C.F., 1993. Phylogeny and comparative physiology of the renin-angiotensin system. In: Robertson, J.I.S., Nicholls, M.G. (Eds.), The Renin-Angiotensin System: Biochemistry and Physiology, vol. 1. Mosby, New York, pp. 2.1–2.28.

Higgins, D., Pappano, A.J., 1979. A histochemical study of the ontogeny of catecholamine-containing axons in the chick embryo heart. J. Mol. Cell. Cardiol. 11, 661–668.

Higgins, D., Pappano, A.J., 1981. Developmental changes in the sensitivity of the chick embryo ventricle to b-adrenergic agonist during adrenergic innervation. Circ. Res. 48, 245–253.

Hill, J.R., Goldberg, J.M., 1980. P-wave morphology and atrial activation in the domestic fowl. Am. J. Physiol. 239, R483–R488.

Hillman, S.S., Hancock, T.V., Hedrick, M.S., 2013. A comparative meta-analysis of maximal aerobic metabolism of vertebrates: implications for respiratory and cardiovascular limits to gas exchange. J. Comp. Physiol. B 183, 167–179.

Hirakow, R., 1970. Ultrastructural characteristics of the mammalian and sauropsidian heart. Am. J. Cardiol. 25, 195.

Hirsch, E.F., 1963. The innervation of the human heart. V. A comparative study of the intrinsic innervation of the heart in vertebrates. Exp. Mol. Pathol. 2, 384–401.

Hirst, G.D.S., Edwards, F.R., 1989. Sympathetic neuroeffector transmission in arteries and arterioles. Physiol. Rev. 69, 546–604.

Hodges, R.D., 1974. The Histology of the Domestic Fowl. Academic Press, London.

Hoffman, L.E., Van Mierop, L.H.S., 1971. Effect of epinephrine on heart rate and arterial blood pressure of the developing chick embryo. Pediatr. Res. 5, 472–477.

Holt, J.P., Rhode, E.A., Kines, H., 1968. Ventricular volumes and body weight in mammals. Am. J. Physiol. 215, 704–715.

Holzbauer, M., Sharman, D.F., 1972. The distribution of catecholamines in vertebrates. In: Blaschko, H., Muscholl, E. (Eds.), Handbook of Experimental Pharmacology: Catecholamines, vol. 33. Springer-Verlag, Berlin, pp. 110–185.

Honig, C.R., Gayeski, T.E.J., Groebe, K., 1991. Myoglobin and oxygen gradients. In: Crystal, R.G., West, J.B., Barnes, B.J., Cherniak, N.S., Weibel, E.R. (Eds.), The Lung: Scientific Foundations. Raven, New York.

Hopkins, D.A., 1987. The dorsal motor nucleus of the vagus nerve and the nucleus ambiguus: structure and connections. In: Hainsworth, R., McWilliam, P.N., Mary, D.A.S.G. (Eds.), Cardiogenic Reflexes. Oxford Univ. Press, Oxford, UK, pp. 185–203.

Houweling, A.C., Somi, S., Massink, M.P., Groenen, M.A., Moorman, A.F., Christoffels, V.M., 2005. Comparative analysis of the natriuretic peptide precursor gene cluster in vertebrates reveals loss of ANF and retention of CNP-3 in chicken. Dev. Dyn. 233, 1076–1082.

Huang, H.C., Sung, P.K., Huang, T.F., 1974. Blood volume, lactic acid and catecholamines in diving response in ducks. *Taiwan I. Hsueh Hui Tsa Chih* 73, 203–210.

Huber, J.F., 1936. Nerve roots and nuclear groups in the spinal cord of the pigeon. J. Comp. Neurol. 65, 43–91.

Hudson, D.M., Jones, D.R., 1982. Remarkable blood catecholamine levels in forced dived ducks. J. Exp. Zool. 224, 451–456.

Inagami, R., Naruse, M., Hoover, R., 1995. Endothelium as an endocrine organ. Annu. Rev. Physiol. 57, 171–189.

Inoue, D., Hachisu, M., Pappano, A.J., 1983. Acetylcholine increases resting membrane potassium conductance in atrial but not in ventricular muscle during muscarinic inhibition of Ca^{++}- dependent action potentials in chick heart. Circ. Res. 53, 158–167.

Ito, S., Ohta, T., Nakazato, Y., 1999. Characteristics of 5-HT-containing chemoreceptor cells of the chicken aortic body. J. Physiol. 515, 49–59.

Iverson, N.K., Wang, T., Baatrup, E., Crossley, D.A., 2014. The role of nitric oxide in the cardiovascular response to chronic and acute hypoxia in White Leghorn chicken (*Gallus domesticus*). Acta Physiol. 211, 346–357.

Jaffee, O.C., 1965. Hemodynamic factors in the development of the chick embryo heart. Anat. Rec. 151, 69–76.

Jarrett, C., Lekic, M., Smith, C.L., Pusec, C.M., Sweazea, K.L., 2013. Mechanisms of acetylcholine-mediated vasodilation in systemic arteries from mourning doves (*Zenaida macroura*). J. Comp. Physiol. B. 183, 959–967.

Jeck, D., Lindmar, R., Löffelholz, K., Wanke, M., 1988. Subtypes of muscarinic receptor on cholinergic nerves and atrial cells of chicken and Guinea-pig hearts. Br. J. Pharmacol. 93, 357–366.

Johansen, K., 1964. Regional distribution of circulating blood during submersion asphyxia in the duck. Acta Physiol. Scand. 62, 1–9.

Johansen, K., Reite, O.B., 1964. Cardiovascular responses to vagal stimulation and cardioaccelerator nerve blockade in birds. Comp. Biochem. Physiol. 12, 479–487.

Jones, D.R., 1969. Avian afferent vagal activity related to respiratory and cardiac cycles. Comp. Biochem. Physiol. A 28, 961–965.

Jones, D.R., 1973. Systemic arterial baroreceptors in ducks and the consequences of their denervation on some cardiovascular responses to diving. J. Physiol. 234, 499–518.

Jones, D.R., 1991. Cardiac energetics and design of arterial systems. In: Blake, R.W. (Ed.), Efficiency and Economy in Animal Physiology. Cambridge Univ. Press, Cambridge, UK, pp. 159–168.

Jones, D.R., Holeton, G.F., 1972b. Cardiac output of ducks during diving. Comp. Biochem. Physiol. A 41, 639–645.

Jones, D.R., Johansen, K., 1972. The blood vascular system of birds. In: Farner, D.S., King, J.E. (Eds.), Avian Biology, vol. 2. Academic Press, New York, pp. 157–285.

Jones, D.R., Milsom, W.K., 1982. Peripheral receptors affecting breathing and cardiovascular function in non-mammalian vertebrates. J. Exp. Biol. 100, 59–91.

Jones, D.R., Milsom, W.K., Gabbott, G.R.J., 1982. Role of central and peripheral chemoreceptors in diving responses of ducks. Am. J. Physiol. 243, R537–R545.

Jones, D.R., Milsom, W.K., West, N.H., 1980. Cardiac receptors in ducks: the effect of their stimulation and blockade on diving bradycardia. Am. J. Physiol. 238, R50–R56.

Jones, D.R., Purves, M.J., 1970. The carotid body in the duck and the consequences of its denervation upon the cardiac responses to immersion. J. Physiol. 211, 279–294.

Jones, D.R., Bryan, R.M., West, N.H., Lord, R.H., Clark, B., 1979. Regional distribution of blood flow during diving in the duck (*Anas platyrhynchos*). Can. J. Zool. 57, 995–1002.

Jones, D.R., Milsom, W.K., Smith, F.M., West, N.H., Bamford, O.S., 1983. Diving responses in ducks after acute barodenervation. Am. J. Physiol. 245, R222–R229.

Kamath, M.V., Fallen, E.L., 1993. Power spectral analysis of heart rate variability: a noninvasive signature of cardiac autonomic function. Crit. Rev. Biomed. Eng. 21, 245–311.

Kameda, Y., 1990. Ontogeny of the carotid body and glomus cells distributed in the wall of the common carotid artery and its branches in the chicken. Cell Tissue Res. 261, 525–537.

Kameda, Y., 1994. Electron microscopic study on the development of the carotid body and glomus cell groups distributed in the wall of the common carotid artery and its branches in the chicken. J. Comp. Neurol. 348, 544–555.

Kameda, Y., 2002. Carotid body and glomus cells distributed in the wall of the common carotid artery in the bird. Microsc. Res. Techniq. 59, 196–206.

Kamimura, K., Nishimura, H., Bailey, J.R., 1995. Blockade of beta-adrenoceptor in control of blood pressure in fowl. Am. J. Physiol. 269, R914–R922.

Karakaya, C., Goktas, S., Celik, M., Kowalski, W.J., Keller, B.B., Pekkan, K., 2018. Asymmetry in mechanosensitive gene expression during aortic arch morphogenesis. Sci. Rep. 8, 16948.

Kato, K., Moriya, K., Dzialowski, E., Burggren, W.W., Tazawa, H., 2002. Cardiac rhythms in prenatal and perinatal emu embryos. Comp. Biochem. Physiol. A 131, 775–785.

Kato, M., Narematsu, M., Nakajima, Y., 2018. Anatomy of the coronary artery and cardiac vein in the quail ventricle: patterns are distinct from those in mouse and human hearts. Anat. Sci. Int. 93, 533–539.

Katz, D.M., Karten, H.J., 1979. The discrete anatomical localization of vagal aortic afferents within a catecholamine-containing cell group in the nucleus solitarius. Brain Res. 171, 187–195.

Katz, D.M., Karten, H.J., 1983a. Subnuclear organization of the dorsal motor nucleus of the vagus nerve in the pigeon, *Columba livia*. J. Comp. Neurol. 217, 31–46.

Katz, D.M., Karten, H.J., 1983b. Visceral representation within the nucleus of the tractus solitarius in the pigeon, *Columba livia*. J. Comp. Neurol. 218, 42–73.

Katz, D.M., Karten, H.J., 1985. Topographic representation of visceral target organs within the dorsal motor nucleus of the vagus nerve of the pigeon *Columba livia*. J. Comp. Neurol. 242, 397–414.

Kedem, O., Katchalsky, A., 1958. Thermodynamic analysis of the permeabililty of biological membranes to non-electrolytes. Biochim. Biophys. Acta 27, 229–246.

Kempf, H., Corvol, P., 2001. Angiotensin receptor(s) in fowl. Comp. Biochem. Physiol. A. 128, 77–88.

Kempf, H., Linares, C., Corvol, P., Gasc, J.M., 1998. Pharmacological inactivation of the endothelin type A receptor in the early chick embryo: a model of mispatterning of the branchial arch derivatives. Development 125, 4931–4941.

Kharin, S.N., 2004. Depolarisation and repolarisation sequences of ventricular epicardium in chickens (*Gallus gallus domesticus*). Comp. Biochem. Physiol. A 137, 237–244.

Khandoker, A.H., Dzialowski, E.M., Burggren, W.W., Tazawa, H., 2003. Cardiac rhythms of late pre-pipped and pipped chick embryos exposed to altered oxygen environments. Comp. Biochem. Physiol. A. 136, 289–299.

Kiley, J.P., Faraci, F.M., Fedde, M.R., 1985. Gas exchange during exercise in hypoxic ducks. Respir. Physiol. 59, 105–115.

Kiley, J.P., Kuhlmann, W.D., Fedde, M.R., 1979. Respiratory and cardiovascular responses to exercise in the duck. J. Appl. Physiol. 47, 827–833.

Kirby, M.L., Conrad, D.C., Stewart, D.E., 1987. Increase in the cholinergic cardiac plexus in sympathetically aneural chick hearts. Cell Tissue Res. 247, 489–496.

Kirby, M.L., McKenzie, J.W., Weidman, T.A., 1980. Developing innervation of the chick heart: a histoflourescence and light microscopic study of sympathetic innervation. Anat. Rec. 196, 333–340.

Kisch, B., 1951. The electrocardiogram of birds: chicken, duck, pigeon. Exp. Med. Surg. 9, 103–124.

Kitazawa, T., Polzin, A.N., Eto, M., 2004. CPI-17-deficient smooth muscle of chicken. J. Physiol. 557, 515–528.

Kobinger, W., Oda, M., 1969. Effects of sympathetic blocking substances on the diving reflex of ducks. Eur. J. Pharmacol. 7, 289–295.

Koch-Weser, J., 1971. Beta-receptor blockade and myocardial effects of cardiac glycosides. Circ. Res. 28, 109–118.

Kohmoto, O., Ikenouchi, H., Hirata, Y., Momomura, S., Serizawa, T., Barry, W.H., 1993. Variable effects of endothelin-1 on $[Ca^{2+}]$i transients, pHi, and contraction in ventricular myocytes. Am. J. Physiol. 265, H793–H800.

Koide, M., Akins, R.E., Harayama, H., Yasui, K., Yokota, M., Tuan, R.S., 1996. Atrial natriuretic peptide accelerates proliferation of chick embryonic cardiomyocytes in vitro. Differentiation 61, 1–11.

Koide, M., Tuan, R., 1989. Adrenergic regulation of calcium-deficient hypertension in chick embryos. Am. J. Physiol. 257, H1900–H1909.

Kolluru, G.K., Shen, X., Bir, S.C., Kevil, C.G., 2013. Hydrogen sulfide chemical biology: pahtophysiological roles and detection. Nitric Oxide 35, 5–20.

Komori, S., Ohashi, H., Okada, T., Takewaki, T., 1979. Evidence that adrenaline is released from adrenergic neurons in the rectum of the fowl. Br. J. Pharmacol. 65, 261–269.

Kontos, H.A., 1981. Regulation of the cerebral circulation. Annu. Rev. Physiol. 43, 397–407.

Kotilainen, P.V., Putkonen, P.T.S., 1974. Respiratory and cardiovascular responses to electrical stimulation of the avian brain with emphasis on inhibitory mechanisms. Acta Physiol. Scand. 90, 358–369.

Kovách, A.G.B., Balint, T., 1969. Comparative study of haemodilation after haemorrhage in the pigeon and the rat. Acta Physiol. Acad. Sci. Hung. 35, 231–243.

Krogh, A., 1919. The number and distribution of capillaries in muscles with calculations of the oxygen pressure head necessary for supplying the tissue. J. Physiol. 52, 409–415.

Kuratani, S., Tanaka, S., 1990. Peripheral development of the avian vagus nerve with special reference to the morphological innervation of heart and lung. Anat. Embryol. 182, 435–446.

Lacombe, A.M.A., Jones, D.R., 1990. The source of circulating catecholamines in forced dived ducks. Gen. Comp. Endocrinol. 80, 41–47.

Lague, S.L., Chua, B., Farrell, A.P., Wang, Y., Milsom, B.K., 2016. Altitude matters: differences in cardiovascular and respiratory responses to hypoxia in bar-headed geese reared at high and low altitude. J. Exp. Biol. 219, 1974–1984.

Lague, S.L., Chua, B., Alza, L., Scott, G.R., Frappell, P.B., Zhong, Y., Farrell, A.P., McCracken, K.G., Wang, Y., Milsom, W.K., 2017. Divergent respiratory and cardiovascular responses to hypoxia in bar-headed geese and Andean birds. J. Exp. Biol. 220, 4186–4194.

Lague, S.L., Ivy, C.M., York, J.M., Chua, B.A., Alza, L., Cheek, R., Dawson, N.J., Frappell, P.B., Farrell, A.P., McCracken, K.G., Scott, G.R., Milsom, W.K., 2020. Cardiovascular responses to progressive hypoxia in ducks native to high altitude in the Andes. J. Exp. Biol. 223 jeb211250.

Landis, E.M., 1927. Micro-injection studies of capillary permeability. II. The relation between capillary pressure and the rate at which fluid passes through the walls of single capillaries. Am. J. Physiol. 82, 217–238.

Landis, E.M., Pappenheimer, J.R., 1963. Exchange of substances through the capillary walls. In: Hamilton, W.F., Dow, P. (Eds.), Handbook of Physiology, Section 2: Circulation, vol. II. American Physiological Society, Washington, DC, pp. 961–1034.

Landys-Ciannelli, M.M., Piersma, T., Jukema, J., 2003. Strategic size changes of internal organs and muscle tissue in the Bar-tailed Godwit during fat storage on a spring stopover site. Funct. Ecol. 17, 151–159.

Lang, S.A., Levy, M.N., 1989. Effects of vagus nerve on heart rate and ventricular contractility in chicken. Am. J. Physiol. 256, H1295–H1302.

Langille, B.L., 1983. Role of venoconstriction in the cardiovascular responses of ducks to head immersion. Am. J. Physiol. 244, R292–R298.

Langille, B.L., Jones, D.R., 1975. Central cardiovascular dynamics of ducks. Am. J. Physiol. 228, 1856–1861.

Langille, B.L., Jones, D.R., 1976. Examination of elastic nonuniformity in the arterial system using a hydraulic model. J. Biomech. 9, 755–761.

Lasiewski, R.C., Weathers, W.W., Bernstein, M.H., 1967. Physiological responses of the giant hummingbird, *Patagona gigas*. Comp. Biochem. Physiol. 23, 797–813.

Le Noble, F.A.C., Hekking, J.W.M., Van Straaten, H.W.M., Slaaf, D.W., Boudier, H.A.J.S., 1991. Angiotensin II stimulates angiogenesis in the chorio-allantoic membrane of the chick embryo. Eur. J. Pharmacol. 195, 305–306.

Le Noble, F.A.C., Ruijtenbeek, K., Gommers, S., De Mey, J.G.R., Blanco, C.E., 2000. Contractile and relaxing reactivity in carotid and femoral arteries of chicken embryos. Am. J. Physiol. 278, H1261–H1268.

Le Noble, F.A.C., Schreurs, N.H.J.S., Van Straaten, H.W.M., Slaaf, D.W., Smits, J.F.M., Rogg, H., Struijker-Boudier, H.A.J., 1993. Evidence for a novel angiogensin II receptor involved in angiogenesis in chick embryo chorioallantoic membrane. Am. J. Physiol. 264, R460–R465.

Lenselink, D.R., Kuhlmann, R.S., Lowrence, J.M., Kolesari, G.L., 1994. Cardiovascular teratogenicity of terbutaline and ritodrine in the chick embryo. Am. J. Obstet. Gynecol. 171, 501–506.

Leon-Velarde, F., Sanchez, J., Bigard, A.X., Brunet, A., Lesty, C., Monge, C.C., 1993. High altitude tissue adaptation in *Andean coots*: capillarity, fiber area, fiber type and enzymatic activities of skeletal muscle. J. Comp. Physiol. B 163, 52–58.

Leonard, R.B., Cohen, D.H., 1975. Responses of sympathetic postganglionic neurons to peripheral nerve stimulation in the pigeon (*Columba livia*). Exp. Neurol. 49, 466–486.

Levy, M.N., 1971. Sympathetic-parasympathetic interactions in the heart. Circ. Res. 29, 437–445.

Lewis, T., 1916. The spread of the excitatory process in the vertebrate heart. V. The bird's heart. Phil. Trans. R. Soc. (Lond., Ser. B) 207, 298–311.

Lillie, F.R., 1908. Development of the Chick. Holt, New York.

Lillo, R.S., Jones, D.R., 1982. Effect of cardiovascular variables on hyperpnea during recovery from diving in ducks. J. Appl. Physiol. 52, 206–215.

Lillo, R.S., Jones, D.R., 1983. Influence of ischemia and hyperoxia on breathing in ducks. J. Appl. Physiol. 55, 400–408.

Lim, J.J., Liu, Y., Khin, E.S.W., Bian, J., 2008. Vasoconstrictive effect of hydrogen sulfide involves downregulation of cAMP in vascular smooth muscle cells. Am. J. Physiol. 295, C1261–C1270.

Lindgren, I., Altimiras, J., 2009. Chronic prenatal hypoxia sensitizes beta-adrenoceptors in the embryonic heart but causes postnatal desensitization. Am. J. Physiol. 297, R258–R264.

Lindgren, I., Zoer, B., Altimiras, J., Villamor, E., 2010. Reactivity of chicken chorioallantoic arteries, avian homologue of human fetoplacental arteries. J. Physiol. Pharmacol. 61, 619–628.

Lindmar, R., Loffelholz, K., Weide, W., Weis, S., 1983. Evidence for bilateral vagal innervation of postganglionic parasympathetic neurons in chicken heart. J. Neural. Trans. 56, 239–247.

Liu, C., Li, R., 2005. Electrocardiogram and heart rate in response to temperature acclimation in three representative vertebrates. Comp. Biochem. Physiol. A 142, 416–421.

Loewy, A.D., Spyer, K.M., 1990. Central Regulation of Autonomic Functions. Oxford Univ. Press, Oxford, UK.

Löffelholz, K., Brehm, R., Lindmar, R., 1984. Hydrolysis, synthesis, and release of acetylcholine in the isolated heart. Fed. Proc. 43, 2603–2606.

Löffelholz, K., Pappano, A.J., 1974. Increased sensitivity of sinoatrial pacemaker to acetylcholine and to catecholamines at the onset of autonomic neuroeffector transmission in chick embryo heart. J. Pharmacol. Exp. Ther. 191, 479–486.

Lu, Y., James, T.N., Bootsma, M., Terasaki, F., 1993a. Histological organization of the right and left atrioventricular valves of the chicken heart and their relationship to the atrioventricular Purkinje ring and the middle bundle branch. Anat. Rec. 235, 74–86.

Lu, Y., James, T.N., Yamamoto, S., Terasaki, F., 1993b. Cardiac conduction in the chicken: gross anatomy plus light and electron microscopy. Anat. Rec. 236, 493–510.

Lumb, W.V., Jones, E.W., 1984. Veterinary Anesthesia, second ed. Lea and Febiger, Philadelphia, PA.

Lucitti, J.L., Hedrick, M.S., 2006. Characterization of baroreflex gain in the domestic pigeon (*Columba livia*). Comp. Biochem. Physiol. A. 143, 103–111.

Macdonald, R.L., Cohen, D.H., 1970. Cells of origin of sympathetic pre- and postganglionic cardioacceleratory fibers in the pigeon. J. Comp. Neurol. 140, 343–358.

Macdonald, R.L., Cohen, D.H., 1973. Heart rate and blood pressure responses to electrical stimulation of the central nervous system in the pigeon (*Columba livia*). J. Comp. Neurol. 150, 109–136.

Malinovsky, L., 1962. Contribution to the anatomy of the vegetative nervous system in the neck and thorax of the domestic pigeon. Acta Anat. 50, 326–347.

Malliani, A., Pagani, M., Bergamaschi, M., 1979. Positive feedback sympathetic reflexes and hypertension. Am. J. Cardiol. 44, 860–865.

Mangold, E., 1919. Elektrographischel Untersuchungen del Erregungsverlaufes im Vogelherzen. Arch. Ges. Physiol. (Pflügers). 175, 327–354.

Manning, P.J., Middleton, C.C., 1972. Atherosclerosis in wild turkeys: morphological features of lesions and lipids in serum and aorta. Am. J. Vet. Res. 33, 1237–1246.

Martinez-Lemus, L.A., Hester, R.K., Becker, E.J., Ramirez, G.A., Odom, T.W., 2003. Pulmonary artery vasoactivity in broiler and leghorn chickens: an age profile. Poultry Sci. 82, 1957–1964.

Mathew, S., Mascareno, E., Siddiqui, M.A.Q., 2004. A ternary complex of transcription factors, nishéd and NFATc4, and co-activator p300 bound to an intronic xequence, intronic regulatory element, is pivotal for the up-regulation of myosin light chain-2v gene in cardiac hypertrophy. J. Biol. Chem. 279, 41018–41027.

Mathieu-Costello, O., 1991. Morphometric analysis of capillary geometry in pigeon pectoralis muscle. Am. J. Anat. 191, 74–84.

Mathieu-Costello, O., Agey, P.J., Normand, H., 1996. Fiber capillarization in flight muscle of pigeons native and flying at high altitude. Respir. Physiol. 103, 187–194.

Mathieu-Costello, O., Suarez, R.K., Hochachka, P.W., 1992. Capillary-to-fiber geometry and mitochondrial density in hummingbird flight muscle. Respir. Physiol. 89, 113–132.

Mathieu-Costello, O., Agey, P.J., Logemann, R.B., Florez-Duquett, M., Bernstein, M.H., 1994. Effect of flying activity on capillary-fiber geometry in pigeon flight muscle. Tissue Cell 26, 57–73.

Mathur, P.N., 1973. Distribution of the specialized conducting tissue in the avian heart. Indian J. Zool. 1, 17–27.

Mathur, R., Mathur, A., 1974. Nerves and nerve terminations in the heart of *Columba livia*. Anat. Anz. 136, 40–47.

McCarty, L.P., Lee, W.C., Shideman, F.E., 1960. Measurement of the inotropic effects of drugs on the innervated and noninnervated embryonic chick heart. J. Pharmacol. Exp. Ther. 129, 315–321.

McDonald, D.A., 1974. Blood Flow in Arteries. Williams and Wilkins, Baltimore, MD.

McPhail, L.T., Jones, D.R., 1999. The autonomic nervous control of heart rate in ducks during voluntary diving. Physiol. Biochem. Zool. 72, 164–169.

McKenzie, B.E., Will, J.A., Hardie, A., 1971. The electrocardiogram of the Turkey. Avian Dis. 15, 737–744.

Meir, J.U., York, J., Chua, B., Jardine, W., Hawkes, L.A., Milsom, W.K., 2019. Reduced metabolism supports hypoxic flight in the high-flying bar-headed goose (*Anser indicus*). eLife 8, e44986.

Meir, J.U., Stockard, T.K., Williams, C.L., Ponganis, K.V., Ponganis, P.J., 2008. Heart rate regulation and extreme bradycardia in diving emperor penguins. J. Exp. Biol. 211, 1169–1179.

Mellander, S., Johansson, B., 1968. Control of resistance, exchange, and capacitance functions in the peripheral circulation. Pharmacol. Rev. 20, 117–196.

Michel, C.C., 1997. Starling: the formulation of his hypothesis of microvascular fluid exchange and its significance after 100 years. Exp. Physiol. 82, 1–30.

Midtgård, U., 1981. The *Rete tibiotarsale* and arterio-venous association in the hind limb of birds: a comparative morphological study on countercurrent heat exchange systems. Acta Zool. 62, 67–87.

Millard, R.W., 1980. Depressed baroreceptor-cardiac reflex sensitivity during simulated diving in ducks. Comp. Biochem. Physiol. A 65, 247–249.

Moellera, I., Small, D.H., Reed, G., Harding, J.W., Mendelsohn, F.A.O., Chaia, S.Y., 1996. Angiotensin IV inhibits neurite outgrowth in cultured embryonic chicken sympathetic neurones. Brain Res. 725, 61–66.

Moonen, R.M., Villamor, E., 2011. Developmental changes in mesenteric artery reactivity in embryonic and newly hatched chicks. J. Comp. Physiol. B. 181, 1063–1073.

Moore, A.F., Strong, J.H., Buckley, J.P., 1981. Cardiovascular actions of angiotensin in the fowl (*Gallus domesticus*). I. Analysis. Res. Commun. Chem. Path. Pharmacol. 32, 423–445.

Moore, E.N., 1965. Experimental electrophysiological studies on avian hearts. Ann. N.Y. Acad. Sci. 127, 127–144.

Moore, E.N., 1967. Phylogenetic observations on specialized cardiac tissues. Bull. N.Y. Acad. Med. 43, 1138–1159.

Mueller, C.A., Burggren, W.W., Crossley, D.A., 2013. Angiotensin II and baroreflex control of heart rate in embryonic chickens (*Gallus gallus domesticus*). Am. J. Physiol. 305, R855–R863.

Mulder, A.L.M., van Golde, J.M.C.G., van Goor, A.A.C., Giussani, D.A., Blanco, C.E., 2000. Developmental changes in plasma catecholamine concentrations during normoxia and acute hypoxia in the chick embryo. J. Physiol. 527, 593–599.

Mulder, A.L.M., Van Goor, C.A., Giussani, D.A., Blanco, C.E., 2001. a-adrenergic contribution to the cardiovascular response to acute hypoxemia in the chick embryo. Am. J. Physiol. 281, R2004–R2010.

Mulder, T.L., van Golde, J.C., Prinzen, F.W., Blanco, C.E., 1997. Cardiac output distribution in the chick embryo from stage 36 to 45. Cardiovasc. Res. 34, 525–528.

Mulder, A.L.M., Van Golde, J.C., Prinzen, F.W., Blanco, C.E., 1998. Cardiac output distribution in response to hypoxia in the chick embryo in the second half of the incubation time. J. Physiol. 508, 281–287.

Murillo-Ferrol, N.L., 1967. The development of the carotid body in *Gallus domesticus*. Acta Anat. 68, 102–126.

Nakamura, Y., Nishimura, H., Khosla, M.C., 1982. Vasodepressor action of angiotensin in conscious chickens. Am. J. Physiol. 243, H456–H462.

Nakazawa, M., Kajio, F., Ikeda, K., Takao, A., 1990. Effect of atrial natriuretic peptide on hemodynamics of the stage 21 chick embryo. Pediatr. Res. 27, 557–560.

Nespolo, R.F., González-Lagos, C., Solano-Iguaran, J.J., Elfwing, M., Garitano-Zavala, A., Mañosa, S., Alonso, J.C., Altimiras, J., 2018. Aerobic power and flight capacity in birds: a phylogenetic test of the heart-size hypothesis. J. Exp. Biol. 221, jeb162693.

Nishimura, H., Yang, Y., Hubert, C., Gasc, J.M., Ruijtenbeek, K., DeMey, J., Struijker Boudier, H.A.J., Corvol, P., 2003. Maturation-dependent changes of angiotensis receptor expression in fowl. Am. J. Physiol. 285, R231–R242.

Nonidez, J.F., 1935. The presence of depressor nerves in the aorta and carotid of birds. Anat. Rec. 62, 47–73.

Nye, P.C.G., Powell, F.L., 1984. Steady-state discharge and bursting of arterial chemoreceptors in the duck. Respir. Physiol. 56, 369–384.

O'Rourke, M.F., Blazek, J.V., Morrells, C.L., Krovetz, L.J., 1968. Pressure wave transmission along the human aorta. Circ. Res. 23, 567–579.

Odlind, B., 1978. Blood flow distribution in the renal portal system of the intact hen: a study of a venous system using microspheres. Acta Physiol. Scand. 102, 342–356.

Ogut, O., Brozovich, F.V., 2000. Determinants of the contractile properties in the embryonic chicken gizzard and aorta. Am. J. Physiol. 279, C1722–C1732.

Ollenberger, G.P., West, N.H., 1998. Distribution of regional cerebral blood flow in voluntarily diving rats. J. Exp. Biol. 201, 549–558.

Owens, G.K., Kumar, M.S., Wamhoff, B.R., 2004. Molecular regulation of vascular smooth muscle cell differentiation in development and disease. Physiol. Rev. 84, 767–801.

Padian, K., deRicqles, A., 2009. The orgin and evolution of birds: 35 years of progress. Comptes Rendus Palevol 8, 257–280.

Pappano, A.J., 1975. Development of autonomic neuroeffector transmission in the chick embryo heart. In: Lieberman, M., Sano, T. (Eds.), Developmental and Physiological Correlates of Cardiac Muscle. Raven Press, New York, pp. 235–248.

Pappano, A.J., 1976. Onset of chronotropic effects of nicotinic drugs and tyramine on the sino-atrial pacemaker in chick embryo heart: relationship to the development of autonomic neuroeffector transmission. J. Pharmacol. Exp. Ther. 196, 676–684.

Pappano, A.J., 1977. Ontogenetic development of autonomic neuroeffector transmission and transmitter reactivity in embryonic and fetal hearts. Pharmacol. Rev. 29, 3–33.

Pappano, A.J., Loffelholz, K., 1974. Ontogenesis of adrenergic and cholinergic neuroeffector transmission in chick embryo heart. J. Pharmacol. Exp. Ther. 191, 468–478.

Pavlov, I.P., 1927. Conditioned Reflexes: An Investigation of the Physiological Activity of the Cerebral Cortex. Oxford Univ. Press, Oxford, UK. Translated by G. V. Anrep.

Perni, S., Iyer, V.R., Franzini-Armstrong, C., 2012. Ultrastructure of cardiac muscle in reptiles and birds: optimizing and/or reducing the probability of transmission between calcium release units. J. Muscle Res. Cell Motil. 33, 145–152.

Peters, G.W., Steiner, D.A., Rigoni, J.A., Mascilli, A.D., Schnepp, R.W., Thomas, S.P., 2005. Cardiorespiratory adjustments of homing pigeons to steady wind tunnel flight. J. Exp. Biol. 208, 3109–3120.

Peterson, D.F., Nightingale, T.E., 1976. Functional significance of thoracic vagal branches in the chicken. Respir. Physiol. 27, 267–275.

Petras, J.M., Cummings, J.F., 1972. Autonomic neurons in the spinal cord of the rhesus monkey: a correlation of the findings of cytoarchitectonics and sympathectomy with fiber degeneration following dorsal rhizotomy. J. Comp. Neurol. 146, 189–218.

Pick, J., 1970. The Autonomic Nervous System. Lippincott, Philadelphia, PA.

Pickering, J.W., 1895. Further experiments on the embryonic heart. J. Physiol. 18, 470–483.

Piersma, T., Gudmundsson, G.A., Lilliendahl, K., 1999. Rapid changes in the size of different functional organ and muscle groups during refueling in a long-distance migrating shorebird. Physiol. Biochem. Zool. 72, 405–415.

Ponganis, P.J., Stockard, T.K., Meir, J.U., Williams, C.L., Ponganis, K.V., Howard, R., 2009. O_2 store management in diving emperor penguins. J. Exp. Biol. 212, 21–224.

Pool, R., 1989. Is it healthy to be chaotic? Science 243, 604–607.

Price, E.R., Dzialowski, E.M., 2018. Development of endothermy in birds: patterns and mechanisms. J. Comp. Physiol. B. 188, 373–391.

Prosheva, V.I., Kaseva, N.N., 2016. Location and function characterization of the right atrioventricular pacemaker ring in the adult avian heart. J. Morph. 277, 363–369.

Prosheva, V., Dernovoj, B., Kharin, S., Kaseva, N., Shklyar, T., Blyakhman, F., 2015. Does the right muscular artrioventricular valve in the avian heart perform two functions? Comp. Biochem. Physiol. A. 184, 41–45.

Prothero, J., 1979. Heart weight as a function of body weight in mammals. Growth 43, 139–150.

Rabkin, S.W., 1996. The angiotensin II subtype 2 (AT2) receptor is linked to protein kinase C but not cAMP-dependent pathways in the cardiomyocyte. Can. J. Physiol. Pharmacol. 74, 125–131.

Randall, W.C., 1994. Efferent sympathetic innervation of the heart. In: Armour, J.A., Ardell, J.L. (Eds.), Neurocardiology. Oxford Univ. Press, Oxford, UK, pp. 77–94.

Rickenbacher, J., Müller, E., 1979. The development of cholinergic ganglia in the chick embryo heart. Anat. Embryol. 155, 253–258.

Robinzon, B., Koike, T.I., Marks, P.A., 1993. At low dose, arginine vasotocin has vasopressor rather than vosodepressor effect in chickens. Gen. Comp. Endocrinol. 91, 105–112.

Robinzon, B., Koike, T.I., Neldon, H.L., Hendry, I.R., el Halawani, M.E., 1988. Physiological effects of arginine vasotocin and mesotocin in cockerels. Br. Poultry Sci. 29, 639–652.

Ropert-Coudert, Y., Wilson, R.P., Grémillet, D., Kato, A., Lewis, S., Ryan, P.G., 2006. Electrocardiogram recordings in free-ranging gannets reveal minimum difference in heart rate during flapping versus gliding flight. Mar. Ecol. Prog. Ser. 328, 275–284.

Rothe, C.F., 1983. Venous system: physiology of the capacitance vessels. In: Shepherd, J.T., Abboud, F.M. (Eds.), Handbook of Physiology: The Cardiovascular System, Volume III. Circulation and Organ Blood Flow, Part 1. American Physiological Society, Bethesda, MD.

Rouwet, E.V., De Mey, J.G.R., Slaaf, D.W., Heineman, E., Ramsay, G., Le Noble, F.A.C., 2000. Development of vasomotor responses in fetal mesenteric arteries. Am. J. Physiol. 2**79**, H1097–H1105.

Ruiz-Feria, C.A., Zhang, D., Nishimura, H., 2004. Age- and sex-dependent changes in pulse pressure in fowl aorta. Comp. Biochem. Physiol. A. 137, **3**11–320.

Rushmer, R.F., 1976. Cardiovascular Dynamics, fourth ed. W. B. Saunders, Philadelphia.

Rzucidlo, E.M., Martin, K.A., Powell, R.J., 2007. Regulation of vascular smooth muscle cell differentiation. J. Vasc. Surg. 45 (Suppl. A), A25–A32.

Sabin, F.R., 1917. Origin and development of the primitive vessels of the chick and of the pig. Contr. Embryol. 6, 63.

Saint-Petery, L.B., Van Mierop, L.H.S., 1974. Evidence for presence of adrenergic receptors in the 6-day chick embryo. Am. J. Physiol. 227, 1406–1410.

Sakamoto, K.Q., Takahashi, A., Iwata, T., Yamamoto, T., Yamamoto, M., Trathan, P.N., 2013. Heart rate and estimated energy expenditure of flapping and gliding in black-browed albatrosses. J. Exp. Biol. 216, 3175–3182.

Sapir, N., Wikelski, M., McCue, M.D., Pinshow, B., Nathan, R., 2010. Flight modes in migrating European bee-eaters: heart rate may indicate low metabolic rate during soaring and gliding. PLoS One 5, e13956.

Saul, P.J., 1990. Beat-to-beat variations of heart rate reflect modulation of cardiac autonomic outflow. News Physiol. Sci. 5, 32–37.

Saunders, D.K., Fedde, M.R., 1994. Exercise performance of birds. In: Jones, J.H. (Ed.), Advances in Veterinary Science and Comparative Medicine: Comparative Vertebrate Exercise Physiology; Phyletic Adaptations, vol. 38B. Academic Press, New York, pp. 139–190.

Savary, K., Michaud, A., Favier, J., Larger, E., Corvol, P., Gasc, J.M., 2005. Role of the renin-angiotensin system in primitive erythropoiesis in the chick embryo. Blood 105, 103–110.

Schlaefke, M.E., 1981. Central chemosensitivity: a respiratory drive. Rev. Physiol. Biochem. Pharmacol. 90, 171–244.

Schmidt-Neilsen, K., 1984. Scaling: Why is Animal Size so Important? Cambridge Univ. Press, Cambridge, UK.

Schwaber, J.S., Cohen, D.H., 1978a. Electrophysiological and electron microscopic analysis of the vagus nerve of the pigeon, with particular reference to the cardiac innervation. Brain Res. 147, 65–78.

Schwaber, J.S., Cohen, D.H., 1978b. Field potential and single unit analyses of the avian dorsal motor nucleus of the vagus and criteria for identifying vagal cardiac cells of origin. Brain Res. 147, 79–90.

Scott, G.R., 2011. Elevated performance: the unique physiology of birds that fly at high altitudes. J. Exp. Biol. 214, 2455–2462.

Scott, G.R., Egginton, S., Richards, J.G., Milsom, W.K., 2009. Evolution of muscle phenotype for extreme high altitude flight in the bar-headed goose. Proc. Roy. Soc. Lond. B. 276, 3645–3653.

Scott, G.R., Milsom, W.K., 2007. Control of breathing and adaptation to high altitude in the bar-headed goose. Am. J. Physiol. Regul. Integr. Comp. Physiol. 293, R379–R391.

Scott, G.R., Schulte, P.M., Egginton, S., Scott, A.L.M., Richards, J.G., Milsom, W.K., 2011. Molecular evolution of cytochrome c oxidase underlies high-altitude adaptation in the bar-headed goose. Mol. Biol. Evol. 28, 351–363.

Secor, S.M., Diamond, J., 1998. A vertebrate model of extreme physiological regulation. Nature 395, 659–662.

Seymour, R.S., Blaylock, A.J., 2000. The principle of Laplace and scaling of ventricular wall stress and blood pressure in mammals and birds. Physiol. Biochem. Zool. 73, 389–405.

Shah, R., Greyner, H., Dzialowski, E.M., 2010. Autonomic control of heart rate and its variability during normoxia and hypoxia in emu (*Dromaius novaehollandiae*) hatchlings. Poultry Sci. 89, 135–144.

Sheard, T.M., Kharche, S.R., Pinali, C., Shiels, H.A., 2019. 3D ultrastructural organization of calcium release units in the avian sarcoplasmic reticulum. J. Exp. Biol. 222 jeb197640.

Shepherd, J.T., Vanhoutte, P.M., 1975. Veins and Their Control. W. B. Saunders, London.

Shiels, H.A., Galli, G.L., 2014. The sarcoplasmic reticulum and the evolution of the vertebrate heart. Physiology 29, 456–469.

Shigenobu, K., Sperelakis, N., 1972. Calcium current channels induced by catecholamines in chick embryonic potassium hearts whose fast sodium channels are blocked by tetrodotoxin or elevated potassium. Circ. Res. 31, 932–952.

Simon-Oppermann, C., Simon, E., Gray, D.A., 1988. Central and systemic antidiuretic hormone and angiotensin II in salt and fluid balance of birds as compared to mammals. Comp. Biochem. Physiol. A 90, 789–803.

Sirsat, S.K.G., Sirsat, T.S., Faber, A., Duquaine, A., Winnick, S., Sotherland, P.R., Dzialowski, E.M., 2016. Development of endothermy and concomitant increases in muscle mitochondrial respiration in the precocial Pekin Duck (*Anas platyrhynchos domestica*). J. Exp. Biol. 219, 1214–1223.

Smith, F.M., 1994. Blood pressure regulation by aortic baroreceptors in birds. Physiol. Zool. 67, 1402–1425.

Smith, F.M., Jones, D.R., 1990. Effects of acute and chronic baroreceptor denervation on diving responses in ducks. Am. J. Physiol. 258, R895–R902.

Smith, F.M., Jones, D.R., 1992. Baroreflex control of arterial blood pressure during involuntary diving in ducks (*Anas platyrhynchos* var.). Am. J. Physiol. 263, R693–R702.

Smith, R.B., 1971a. Intrinsic innervation of the avian heart. Acta Anat. 79, 112–119.

Smith, R.B., 1971b. Observations on nerve cells in human, mammalian and avian cardiac ventricles. Anat. Anz. 129, 436–444.

Snyder, G.K., 1987. Muscle capillarity in chicks following hypoxia. Comp. Biochem. Physiol. A 87, 819–822.

Snyder, G.K., 1990. Capillarity and diffusion distances in skeletal muscles in birds. J. Comp. Physiol. B 160, 583–591.

Snyder, G.K., Coelho, J.R., 1989. Microvascular development in chick anterior latissimus dorsi following hypertrophy. J. Anat. 162, 215–224.

Snyder, G.K., Byers, R.L., Kayar, S.R., 1984. Effects of hypoxia on tissue capillarity in geese. Respir. Physiol. 58, 151–160.

Solomon, I.C., Adamson, T.P., 1997. Static muscular contraction elicits a pressor reflex in the chicken. Am. J. Physiol. 272, R759–R765.

Somlyo, A.P., Somlyo, A.V., 2003. Ca^{2+} sensitivity of smooth muscle and nonmuscle myosin II: modulated by G proteins, kinases, and myosin phosphatase. Physiol. Rev. 83, 1325–1358.

Sommer, J.R., 1983. The implications of structure and geometry on cardiac electrical activity. Ann. Biomed. Eng. 11, 149–157.

Sommer, J.R., Johnson, E.A., 1969. Cardiac muscle: a comparative ultrastructural study with special reference to frog and chicken hearts. Z. Zellforsch. mikrosk. anat. 98, 437–468.

Sommer, J.R., Johnson, E.A., 1970. Comparative ultrastructure of cardiac cell membrane specialization: a review. Am. J. Cardiol. 25, 184–194.

Sommer, J.R., Bossen, E., Dalen, H., Dolber, P., High, T., Jewett, P., Johnson, E.A., Junker, J., Leonard, S., Nassar, R., Scherer, B., Spach, M., Spray, T., Taylor, I., Wallace, N.R., Waugh, R., 1991. To excite a heart: a bird's view. Acta Physiol. Scand. S599, 5–21.

Speckmann, E.W., Ringer, R.K., 1964. Static elastic modulus of the Turkey aorta. Can. J. Physiol. Pharmacol. 42, 553–561.

Speckmann, E.W., Ringer, R.K., 1966. Volume pressure relationships in the Turkey aorta. Can. J. Physiol. Pharmacol. 44, 901–907.

Stallone, J.N., Nishimura, H., Nasjletti, A., 1990. Angiotensin II binding sites in aortic endothelium of domestic fowl. Am. J. Physiol. 258, E777–E782.

Starling, E.H., 1896. On the absorption of fluids from connective tissue spaces. J. Physiol. 19, 312–326.

Steele, P.A., Gibbins, I.L., Morris, J.L., 1996. Projections of intrinsic cardiac neurons to different targets in the Guinea-pig heart. J. Auton. Nerv. Syst. 47, 177–187.

Steele, P.A., Gibbins, I.L., Morris, J.L., Mayer, B., 1994. Multiple populations of neuropoptide-containing intrinsic neurons in the Guinea-pig heart. Neuroscience 62, 241–250.

Stéphan, F., 1949. Les suppliances obtenues experimentalement dans le systeme des arcs aortiques de l'embryon d'oiseau. C. R. Soc. Anat. 36, 647.

Stephenson, R., Jones, D.R., 1992. Blood flow distribution in submerged and surface-swimming ducks. J. Exp. Biol. 166, 285–296.

Stephenson, R., Jones, D.R., Bryan, R.M., 1994. Regional cerebral blood flow during submergence asphyxia in Pekin duck. Am. J. Physiol. 266, R1162–R1168.

Sturkie, P.D., 1986. Heart: contraction, conduction, and electrocardiography. In: Sturkie, P.D. (Ed.), Avian Physiology. Springer-Verlag, Berlin, pp. 167–190.

Sturkie, P.D., Poorvin, D.W., 1973. The avian neurotransmitter. Proc. Soc. Exp. Biol. Med. 143, 644–646.

Sturkie, P.D., Dirner, G., Gister, R., 1978. Role of renal portal valve in the shunting of blood flow in renal and hepatic circulations of chickens. Comp. Biochem. Physiol., C 59, 95–96.

Swart, J., Tate, K., Crossley II., D.A., 2014. Develompetn of adrenergic and cholinergic receptor cardiovascular regulatory capacity in the Canada goose (*Branta Canadensis*) and domestic goose (*Anser anser domesticus*). Comp. Biochem. Physiol. A 167, 59–67.

Szabo, E., Viragh, S., Challice, C.E., 1986. The structure of the atrioventricular conducting system in the avian heart. Anat. Rec. 215, 1–9.

Szabuniewicz, M., McCrady, J.D., 1967. The electrocardiogram of the chicken. Southwest. Vet. 20, 287–294.

Tagawa, T., Ando, K., Wasano, T., 1979. A histochemical study of the innervation of the cerebral blood vessels in the domestic fowl. Cell Tissue Res. 198, 43–51.

Takei, Y., 2000. Structural and functional evolution of the natriuretic peptide system in vertebrates. Int. Rev. Cytol. 194, 1–66.

Takei, Y., Hasegawa, Y., 1990. Vasopressor and depressor effects of native angiotensins and inhibition of these effects in the Japanese quail. Gen. Comp. Endocrinol. 79, 12–22.

Taylor, A.E., Townsley, M.I., 1987. Evaluation of the Starling fluid flux equation. NIPS (News Physiol. Sci.) 2, 48–52.

Taylor, M.G., 1964. Wave travel in arteries and the design of the cardiovascular system. In: Attinger, E.O. (Ed.), Pulsatile Arterial Blood Flow. McGraw–Hill, New York.

Tazawa, H., 1981. Effect of O_2 and CO_2 in N_2, He, and SF6 on chick embryo blood pressure and heart rate. J. Appl. Physiol. 51, 1017–1022.

Tazawa, H., Takenaka, H., 1985. Cardiovascular shunt and model analysis in the chick embryo. In: Johansen, K., Burggren, W.W. (Eds.), Cardiovascular Shunts. Munksgaard, Copenhagen, pp. 179–194.

Tazawa, H., Hashimoto, Y., Doi, K., 1992. Blood pressure and heart rate of chick embryo (*Gallus domesticus*). within the egg: responses to autonomic drugs. In: Hill, R.B. (Ed.), Phylogenetic Models in Functional Coupling of the CNS and the Cardiovascular System. Karger, Kingston, Rhode Island, pp. 86–96.

Tazawa, H., Lomholt, J.P., Johansen, K., 1985. Direct measurement of allantoic blood flow in the chicken, *Gallus domesticus*. Responses to alteration in ambient temperature and PO_2. Comp. Biochem. Physiol. A 81, 641–642.

Tazawa, H., Visschedijk, A.H.J., Whitman, J., Piper, J., 1983. Gas exchange, blood gases and acid–base status in the chick before, during and after hatching. Respir. Physiol. 53, 173–185.

Tcheng, K.T., Fu, S.K., 1962. The structure and innervation of the aortic body of the yellow-breasted bunting. Sci. Sin. 11, 221–232.

Tcheng, K.T., Fu, S.K., Chen, T.Y., 1963. Supracardial encapsulated receptors of the aorta and the pulmonary artery in birds. Sci. Sin. 12, 73–81.

Toop, T., Donald, J.A., 2004. Comparative aspects of natriuretic peptide physiology in non-mammalian vertebrates: a review. J. Comp. Physiol. B 174, 189–204.

Topouzis, S., Catravas, J., Ryan, J., Rosenquist, T., 1992. Influence of vascular smooth muscle heterogeneity on angiotensin converting enzyme activity in chicken embryonic aorta and in endothelial cells in culture. Circ. Res. 71, 923–931.

Torrella, J.R., Fouces, V., Viscor, G., 1999. Descriptive and functional morphometry of skeletal muscle fibers in wild birds. Can. J. Zool. 77, 724–736.

Trajanovska, S., Inoue, K., Takei, Y., Donald, J.A., 2007. Genomic analyses and cloning of novel chicken natriuretic peptide genes reveal new insights into natriuretic peptide evolution. Peptides 28, 2155–2163.

Tummons, J., Sturkie, P.D., 1968. Cardio-accelerator nerve stimulation in chickens. Life Sci. 7, 377–380.

Tummons, J.L., Sturkie, P.D., 1969. Nervous control of heart rate during excitement in the adult White Leghorn cock. Am. J. Physiol. 216, 1437–1440.

Tummons, J.L., Sturkie, P.D., 1970. Beta adrenergic and cholinergic stimulants from the cardioaccelerator nerve of the domestic fowl. Z. Vergl. Physiol. 68, 268–271.

Ungureanu-longrois, D., Bezie, Y., Perret, C., Laurent, S., 1997. Effects of exogenous and endogenous nitric oxide on the contractile function of cultured chick embryo ventricular myocytes. J. Mol. Cell. Cardiol. 29, 677–687.

Van Golde, J., Mulder, T., Blanco, C.E., 1997. Changes in mean chorioallantoic artery blood flow and heart rate produced by hypoxia in the developing chick embryo. Pediatr. Res. 42, 293–298.

Vanhoutte, P.M., Leusen, I., 1969. The reactivity of isolated venous preparations to electrical stimulation. Pflügers Arch. 306, 341–353.

Vatner, S.F., Braunwald, E., 1975. Cardiovascular control mechanisms in the conscious state. New Engl. J. Med. 293, 970–976.

Verberne, M.E., Gittenberger-de Groot, A.C., Van Iperen, L., Poelmann, R.E., 1999. Contribution of the cervical sympathetic ganglia to the innervation of the pharyngeal arch arteries and the heart of in the chick embryo. Anat. Rec. 255, 407–419.

Villamor, E., Kessels, C.G.A., Ruijtenbeek, K., Van Suylen, R.J., Belik, J., De Mey, J.G.R., Blanco, C.E., 2004. Chronic *in ovo* hypoxia decreases pulmonary arterial contractile reactivity and induces biventricular cardiac enlargement in the chicken embryo. Am. J. Physiol. 287, R642–R651.

Villamor, E., Ruijtenbeek, K., Pulgar, V., DeMey, J.G., Blanco, C.E., 2002. Vascular reactivity in intrapulmonary arteries of chicken embryos during transition to ex ovo life. Am. J. Physiol. 282, R917–R927.

Ward, S., Bishop, C.M., Woakes, A.J., Butler, P.J., 2002. Heart rate and the rate of oxygen consumption of flying and walking barnacle geese (*Branta leucopsis*) and bar-headed geese (*Anser indicus*). J. Exp. Biol. 205, 3347–3356.

Webb, R.C., 2003. Smooth muscle contraction and relaxation. *Adv. Physiol. Educ*. 27, 201–206.

Weinstein, Y., Bernstein, M.H., Bickler, P.E., Gonzalez, D.V., Samaniego, F.C., Escobedo, M.A., 1985. Blood respiratory properties in pigeons at high altitudes: effects of acclimation. Am. J. Physiol. 249, R765–R775.

West, J.B., 2008. Respiratory Physiology—The Essentials, eighth ed. Lippincott, Williams and Wilkins, Baltimore, MD.

West, N.H., Langille, B.L., Jones, D.R., 1981. Cardiovascular system. In: King, A.S., McLelland, J. (Eds.), Form and Function in Birds, vol. 2. Academic Press, New York, pp. 235–339.

White, P.T., 1974. Experimental studies on the circulatory system of the late chick embryo. J. Exp. Biol. 61, 571–592.

Whittow, G.C., 2000. Avian Physiology, fifth ed. Springer-Verlag, Berlin.

Wideman, R.F., Gregg, C.M., 1988. Model for evaluating avian renal hemodynamics and glomerular filtration rate autoregulation. Am. J. Physiol. 254, R925–R932.

Wideman, R.F., Braun, E.J., Anderson, G.L., 1991. Microanatomy of the renal cortex in the domestic fowl. J. Morphol. 168, 249–267.

Wideman, R.F., Glahn, R.P., Bottje, W.G., Holmes, K.R., 1992. Use of a thermal pulse decay system to assess avian renal blood flow during reduced renal arterial perfusion pressure. Am. J. Physiol. 262, R90–R98.

Wilson, J.X., 1989. The renin-angiotensin system in birds. In: Hughes, M., Chadwick, A. (Eds.), Progress in Avian Osmoregulation. Leeds Philosophical and Literary Society, Leeds, UK, pp. 61–79.

Wilson, J.X., Butler, D.G., 1983. Catecholamine-mediated pressor responses to angiotensin II in the Pekin duck, *Anas platyrhynchos*. Gen. Comp. Endocrinol. 51, 477–489.

Wilson, J.X., West, N.H., 1986. Cardiovascular responses to neurohormones in conscious chickens and ducks. Gen. Comp. Endocrinol. 62, 268–280.

Wingard, C.J., Godt, R.E., 2002. Cardiac neural crest ablation alters aortic smooth muscle force and voltage-sensitive Ca^{2+} responses. J. Muscle Res. Cell Motil. 23, 293–303.

Wolfenson, D., Frei, Y.F., Berman, A., 1982a. Blood flow distribution during artificially induced respiratory alkalosis in the fowl. Respir. Physiol. 50, 87–92.

Wolfenson, D., Frei, Y.F., Snapir, N., Berman, A., 1978. Measurement of blood flow distribution by radioactive microspheres in the laying hen. Comp. Biochem. Physiol. A 61A, 549.

Womersley, J.R., 1957. The mathematical analysis of the arterial circulation in a state of oscillatory motion. Tech. Rep. Wright AFB Dev. Ctr. WADC-TR-56-614.

Wray, S., Smith, R.D., 2004. Mechanisms of action of pH-induced effects on vascular smooth muscle. Mol. Cell. Biochem. 263, 163–172.

Ying, L., James, T.N., Yamamoto, S., Terasaki, F., 1993. Cardiac conduction system in the chicken: gross anatomy plus light and electron microscopy. Anat. Rec. 236, 493–510.

Yousuf, N., 1965. The conducting system of the heart of the house sparrow, *Passer domesticus indicus*. Anat. Rec. 152, 235–250.

Zoer, B., Blanco, C.E., Villamor, E., 2010. Role of rho-kinase in mediating contraction of chicken embryo femoral arteries. J. Comp. Physiol. B 180, 427–435.

Chapter 19

Renal and extrarenal regulation of body fluid composition

David L. Goldstein

Department of Biological Sciences, Wright State University, Dayton, OH, United States

19.1 Introduction

Avian osmoregulation comprises a set of physiological controls that function to protect the amount and concentration of water and solutes in the intracellular and extracellular fluids (ECFs) (Table 19.1). Achieving that regulation requires balancing the input and output of water and electrolytes and involves the interacting contributions of the kidneys, intestinal tract, salt glands (when present), skin, and respiratory tracts (as routes of evaporative water loss). The integration of these organs is unique in birds among the vertebrates. Birds lack a urinary bladder, and avian urine enters the lower intestine, where it may be significantly modified in the coprodeum, colon, and ceca. Under some circumstances, in some species, the salt glands are critical for osmoregulatory balance, and the majority of total water loss may be evaporative, not excretory, with the relative roles of skin and respiration varying among species and conditions. The present chapter will focus most heavily on anatomical and functional organization of the kidneys and lower intestine, but will also examine aspects of those other organs of osmoregulation.

19.2 Intake of water and solutes

19.2.1 Drinking

Total water fluxes in free-living birds scale allometrically with an exponent of about 0.65 (Tieleman and Williams, 2000; Song and Beissinger, 2019; see Table 19.2). Some birds, especially carnivores and frugivores, acquire all needed water through their food, and a few species, particularly small, xerophilic birds, can survive on the metabolic water produced from a dry diet even in the absence of drinking water (Bartholomew, 1972). For most birds, though, drinking is an important avenue of water intake.

The rate of drinking by birds in the laboratory follows a regular relation with body mass: birds weighing 100 g or more drink approximately 5% of body mass per day, but at progressively smaller body masses drinking rates rise, to about 50% per day for birds 10−20 g (Bartholomew and Cade, 1963; Skadhauge, 1981, Cpt. 2). Birds with salt glands, drinking saline water, may drink substantially more than those without salt glands, using some of the water to excrete the ingested salt via the salt glands and thereby retaining a volume of salt-free water (Hughes et al., 1989). In nectar feeding birds, including specialists like honeyeaters, hummingbirds, and sunbirds, caloric intake comes mostly from their liquid diet. If nectars are dilute, then intake adequate to meet calorie balance may entail drinking three to five times body mass per day, similar to water influxes of aquatic amphibia (Collins, 1981; McWhorter and Martínez del Rio, 1999; Nicolson and Fleming, 2003; Nicolson and Fleming, 2014). Indeed, water fluxes in free-living nectarivores are higher than for birds generally (Song and Beissinger, 2019). The strategy for handling those high rates of fluid ingestion includes primarily modulation of intestinal water uptake in sunbirds and honeyeaters, and primarily modulation of renal water reabsorption in hummingbirds (Nicolson and Fleming, 2014).

Except for those species able to survive without any drinking water (see Krag and Skadhauge, 1972; Skadhauge and Bradshaw, 1974), minimum water requirements are typically one-third to one-half of the ad libitum drinking rate (Skadhauge, 1981).

The physiological stimuli that initiate drinking are threefold: cellular dehydration, extracellular dehydration, and angiotensin II. The osmoreceptor cells that respond to cellular dehydration (i.e., to an osmotic loss of cellular water induced by a rise in ECF osmolality) are localized in periventricular regions of the hypothalamus (Thornton, 1986a; Kanosue et al., 1990). Their response may be specific to the

Sturkie's Avian Physiology. https://doi.org/10.1016/B978-0-12-819770-7.00034-7

TABLE 19.1 Typical normal values of some regulated osmoregulatory variables in birds.[a]

Total body water	60–70 mL/100 g body mass
Extracellular fluid volume	20–25 mL/100 g body mass
Plasma volume	3.5–6.5 mL/100 g body mass
Plasma osmolality	320–370 mosmol/kg water
Plasma Na^+	150–170 meq/L
Plasma K^+	2–5 meq/L
Plasma uric acid	0.1–1 mmol/L

[a]*Values are typical for adult birds.*
Data are taken primarily from Skadhauge (1981), which should be consulted for references to original literature. The ranges presented encompass most of the variability among data compiled in that review.

TABLE 19.2 Allometric relations in avian osmoregulation, expressed in the form $Y = aM^b$, where M is mass in g.

Variable Y	Units	A	b	Reference
Field water flux	mL/d	1.41	0.66	Tieleman and Williams (2000)
Kidney volume	mm^3	8.0	1.15	Casotti et al. (1998)
Number of glomeruli	Number	3090	0.77	Yokota et al. (1985)
Glomerular filtration rate	mL/min	0.013	0.76	Bennett and Hughes (2003)
Effective renal plasma flow	mL/min	0.1	0.71	Bennett and Hughes (2003)
Salt gland dry mass, marine species	Mg	0.37	0.877	Gutiérrez et al. (2012)
Evaporative water loss, passerines at 25°C	mL/d	0.21	0.81	Gavrilov and Gavrilov (2019)
Evaporative water loss, nonpasserines at 25°C	mL/d	0.16	0.79	Gavrilov and Gavrilov (2019)

Na^+ concentration in the cerebrospinal fluid, rather than to the total osmolality (Thornton, 1986b; Kanosue et al., 1990).

Stimulation of drinking by extracellular dehydration can be demonstrated through the effects of hemorrhage or injection into various fluid compartments of a nonabsorbed, osmotically active compound such as polyethylene glycol. Both of these manipulations elicit responses consistent with the interpretation that the receptors (presumably mechanoreceptors sensitive to stretch or tension) are in the interstitial, rather than the vascular, compartment of the ECF (Kaufman and Peters, 1980; Takei et al., 1989). The dipsogenic effects of extracellular volume depletion may be mediated by angiotensin II (Takei et al., 1989).

Angiotensin II, administered either centrally (into the cerebrospinal fluid) or peripherally, elicits drinking in a wide variety of birds (Takei et al., 1989). The primary sites of action of this hormone appear to be the preoptic area and subfornical organ (Takei, 1977; Gerstberger et al., 1987; Simon et al., 1992), where TRPV1-type vanilloid receptors may contribute to osmosensing (Aman et al., 2016). In these circumventricular regions, the mRNA for AT1R-type angiotensin II receptors is upregulated in response to osmotic stress (Aman et al., 2016).

In addition to angiotensin II, other compounds within the brain may be involved in eliciting drinking. At least some pathways between dipsogenic centers in the brain (e.g., connecting preoptic area and subfornical organ) appear to use adrenergic nerve fibers (Takei et al., 1989; Denbow and Sheppard, 1993). A variety of peptides can either stimulate or inhibit drinking in birds (Takei et al., 1989), though the physiological significance of these compounds has not been defined.

When birds are dehydrated, all of the stimuli for drinking (intracellular and extracellular dehydration and angiotensin II) are elicited simultaneously. When dehydrated birds regain access to water, they may drink substantially more water than required to restore their cellular and extracellular water deficits (Takei et al., 1988; Goldstein, 1995). However, much of this water is excreted in a dilute urine or is absorbed slowly from the intestinal tract, and so aspects of fluid balance may remain in deficit despite the copious intake. In these circumstances, restoration of cellular fluid balance (osmolality) and distension of the intestinal tract with water appear to terminate drinking, even while blood volume remains depressed and angiotensin II levels remain elevated (Takei et al., 1988). With drinking as with release of antidiuretic hormone (see below), the osmolality of the ECF is a more potent stimulus (is more closely regulated) than its volume.

19.2.2 Solute intake

At least one bird, the pigeon (*Columba livia*), expresses a salt appetite in response to sodium depletion (Epstein and Massi, 1987). This response appears to depend on a synergistic action of angiotensin II and aldosterone (Massi and Epstein, 1990). In a variety of other birds, drinking rates may increase with increasing salinity of the drinking water,

with maximal drinking rates typically at 0.15−0.3 M NaCl (see review in Skadhauge, 1981, Cpt. 2). The maximum saline concentration that is drunk voluntarily is likely set by the bird's ability to extract free water, which results from the balance between renal concentrating ability and other routes of water gain and loss.

19.3 The kidneys

19.3.1 Anatomy

19.3.1.1 Gross anatomy

The avian urinary organs consist of a pair of kidneys and the ureters, which transport urine to the urodeum of the cloaca. There is no urinary bladder, though the cloaca may serve as its functional equivalent in some species and circumstances (see below).

The avian kidney lies within a cavity formed by the ventral surface of the synsacrum. The mass of the two kidneys is proportional to (body mass)$^{0.9}$, and represents approximately 0.8% of body mass in birds without salt glands, 1.4% in birds with salt glands (Hughes, 1970a; Franz et al., 2009).

The external appearance of the avian kidney is elongate and trilobed, with anterior, middle, and posterior divisions (Johnson, 1968; Michałek et al., 2016). Within each division, the kidney is divided into numerous subunits. In the cortex, nephrons are arranged around branches of the efferent venous system (central veins). These cortical units (cortical lobules) contribute nephron elements (collecting ducts and loops of Henle) to several medullary subunits; conversely, each medullary subunit receives nephron elements from several cortical units (Johnson et al., 1972). The medullary elements are wrapped in a sheath of connective tissue to form medullary cones. A kidney lobule (Figure 19.1) is defined as a medullary cone and the region of cortex that it drains. The numbers of kidney lobules, and the number per gram of kidney, vary substantially among species (Johnson and Mugaas, 1970; Goldstein and Braun, 1989, Barceló et al., 2012).

19.3.1.2 Nephron types and numbers

The structure of avian nephrons is highly heterogeneous. The smallest nephrons are located most superficially (Figure 19.1) and have simple glomeruli (Figure 19.2A). Because they resemble nephrons of reptilian kidneys, particularly in that they lack loops of Henle, these nephrons have been termed reptilian-type (RT) nephrons (Huber, 1917). Nephron size increases progressively with depth from the kidney surface. Those located most deeply have larger, more complex glomeruli (Figure 19.2B) and do possess a loop of Henle, leading to the name mammalian-type (MT) nephron. Between definitive RT and MT

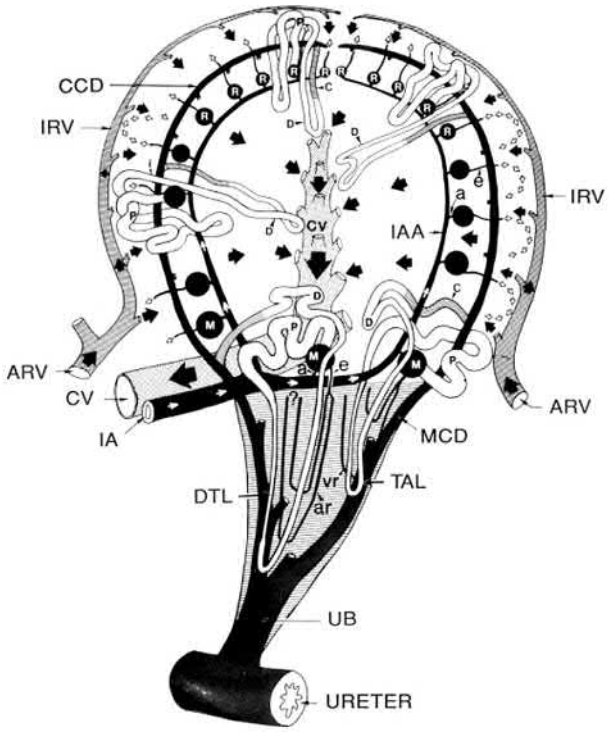

FIGURE 19.1 A typical kidney lobule from the domestic fowl. The lobule consists of a medullary cone and all cortical tissue that feeds into it. Abbreviations (in alphabetical order) are: *a*, afferent arteriole; *ar*, arteriole rectae (descending vasa recta); *ARV*, afferent renal (portal) vein; *C*, connecting tubule; *CCD*, cortical collecting duct; *CV*, central (intralobular renal) vein; *D*, distal tubule; *DTL*, descending thin limb of Henle's loop; *e*, efferent arteriole; *i*, intermediate segment; *IA*, intralobar artery; *IAA*, intralobular artery; *IRV*, interlobular renal vein; *M*, mammalian-type (MT) glomerulus; *MCD*, medullary collecting duct; *P*, proximal tubule; *R*, reptilian-type (RT) glomerulus; *TAL*, thick ascending limb of Henle's loop; *UB*, ureteral branch; *vr*, venule rectae (ascending vasa recta). *Figure is from Wideman (1988). Reprinted by permission of CRC Press, Boca Raton, Florida.*

nephrons is a continuous gradation of nephrons (Goldstein and Braun, 1989; Roush and Spotts, 1988; Mobini and Abdollahi, 2016), including those with elongated, looping intermediate segments that are not bound into the medullary cones (Boykin and Braun, 1993). The RT/MT terminology has largely been replaced with the terms loopless (LLN), transitional (TN), and looped (LN) nephrons (Braun, 1993; Boykin and Braun, 1993). Avian glomeruli may have filtration barriers that are less restrictive than those of mammalian kidneys, potentially permitting larger and more highly charged molecules to enter the urine (Casotti and Braun, 1996).

Both nephrons with and those without loops of Henle empty in a highly regular pattern into common collecting ducts (Boykin and Braun, 1993). Collecting ducts conjoin as they descend through the medullary cone, and the terminus of the medullary cone is a single large collecting duct that empties directly into the ureter. The avian kidney has no renal pelvis.

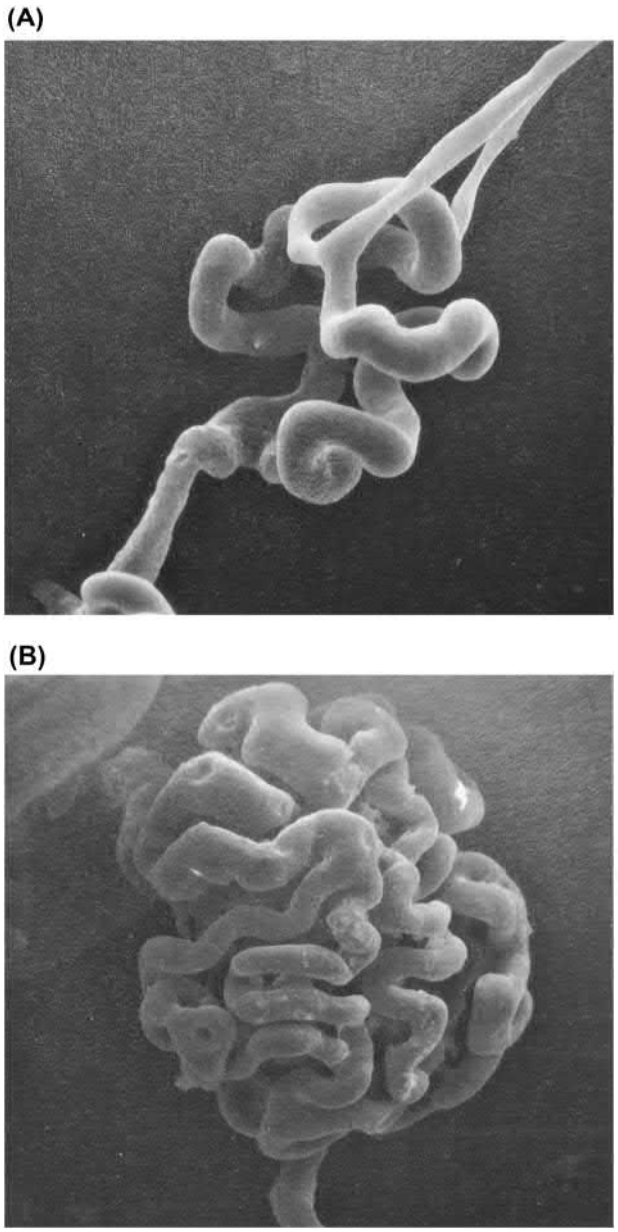

FIGURE 19.2 (A) Glomerulus from a reptilian-type nephron. Note the simple looping pattern and lack of cross-branching in these capillaries. (B) Glomerulus from a mammalian-type nephron, with a longer, more complex capillary network. *Photographs courtesy of G. Cassotti and E. J. Braun.*

Of the total nephron population, between 10 and 30% possess loops of Henle in most species examined (Goldstein and Braun, 1989). An exception is found in Anna's hummingbird, *Calypte anna*, whose kidneys, with more than 99% loopless nephrons, are capable of producing copious dilute urine in response to dilute nectar diets (Casotti et al., 1998). Several studies suggest habitat-related patterns in kidney structure, such as smaller kidneys, larger volume of medulla, or smaller volume of cortex in desert species (Thomas and Robin, 1977; Warui, 1989; Casotti and Richardson, 1992). Likewise, birds with greater osmoregulatory challenge (granivorous birds eating dry diets; passerines encountering high salt intake) may have greater percentages of medullary mass (Goldstein et al., 1990; Barceló et al., 2012; Peña-Villalobos et al., 2013). It is not yet clear how these variations relate to the different proportions of looped, transitional, and loopless nephrons.

19.3.1.3 Blood flow

The avian kidney receives both arterial and afferent venous (portal) blood supplies and is drained by efferent venous flow (Figure 19.3). The overall pattern of flow is complex; see Wideman (1988) for a detailed review.

19.3.1.3.1 Arterial supply

Each division of the kidney is supplied by a separate artery (Figure 19.3). The arteries branch upon entering the kidney

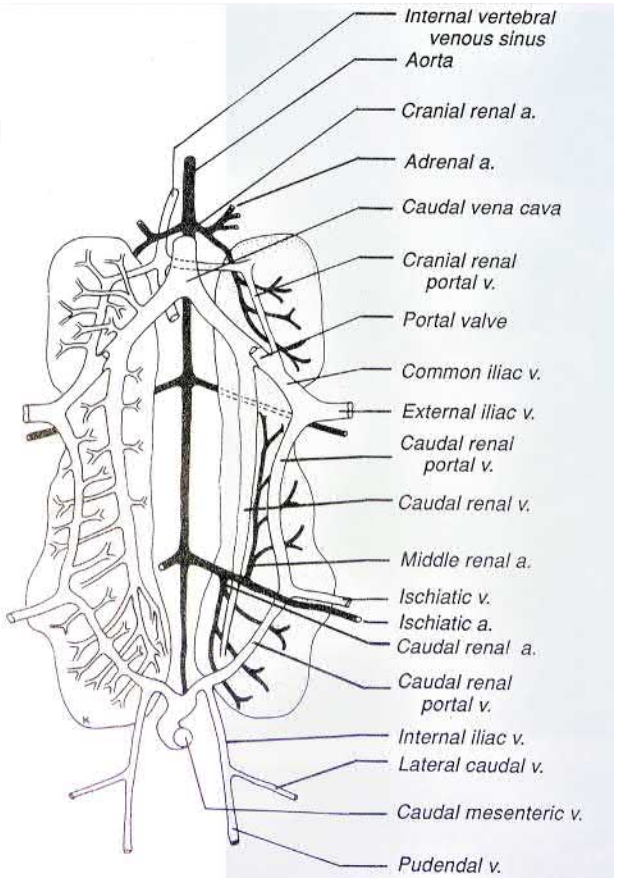

FIGURE 19.3 Major blood vessels in the avian kidney. The kidneys are drawn as though transparent, and in the left kidney only the major venous trunks are shown to permit an indication of finer levels of vessel branching. The internal vertebral venous sinus has been displaced to one side so that it can be seen. *Reproduced from King (1975) with permission.*

to form intralobar and then numerous intralobular arteries, from which arise the short afferent arterioles supplying the glomeruli.

Efferent arterioles from glomeruli of loopless nephrons empty into sinuses surrounding the cortical tubular elements, thereby forming the peritubular blood supply. In contrast, the efferent arterioles leaving glomeruli of looped (MT) nephrons enter the medullary cones to form a mesh-like network of vessels, the vasa recta (Figure 19.4). Whether the outflow from the vasa recta enters peritubular sinuses surrounding cortical components of the MT nephrons, or instead whether it enters directly into the intralobular veins, is as yet unclear (Figure 19.5).

19.3.1.3.2 Renal portal system

The second afferent blood supply to the kidney, the renal portal supply, receives blood flow from both the ischiadic and the external iliac veins. A valve, the renal portal valve, is located between the renal portal vein and the common iliac vein (Figure 19.3). This smooth muscle sphincter receives both adrenergic (stimulatory, causing valve closure) and cholinergic (inhibitory, allowing valve opening) innervation (Burrows et al., 1983). Blood from the external iliac vein may flow directly into the vena cava when the renal portal valve is open or, instead, be forced into the renal portal vein when the valve is closed.

FIGURE 19.4 The vasa recta of Gambel's quail, revealing the mesh-like, rather than simple ascending and descending, appearance of the vessel network. *Photograph courtesy of E. J. Braun.*

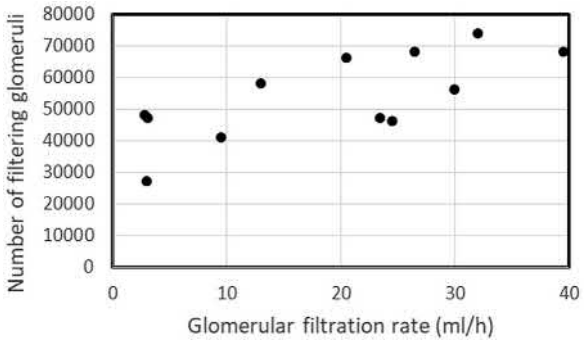

FIGURE 19.5 The number of filtering glomeruli (evaluated by infusion of the stain Alcian blue, which binds to the negatively charged filtration barrier as it is filtered) in Leach's storm petrels (*Oceanodroma leucorhoa*) whose GFR varies over a wide range in response to intravenous infusion of NaCl. *Experimental conditions are described in Goldstein (1993).*

Once in the renal portal vein, blood may enter the low-pressure peritubular sinuses formed from the efferent arterioles; the mixed portal and postglomerular blood then flows out of the kidney through efferent veins. Alternatively, blood may flow out of the kidney into vertebral sinuses or, via the caudal mesenteric vein, to the liver. The pattern of flow through these various pathways may be highly variable both among animals and within an individual animal over time (Akester, 1967; Odlind, 1978; Oelofsen, 1973; Wideman, 1988), presumably because of varying states of regulation of vascular resistances and of valve status. The functional significance of the portal system and its valve may relate in part to regulating systemic hemodynamics, particularly during times of leg muscle activity (see Wideman, 1988), and in part to regulating renal hemodynamics, particularly when arterial blood pressure or flow is reduced (Wideman, 1991; see below).

Since Sperber's (1948) convincing demonstration of portal circulation to the renal cortex, many investigators have used the so-called "Sperber technique" in studies of avian kidney function. In this approach, a compound is infused into one leg vein (and hence into the renal portal circulation), and function of the ipsilateral kidney is compared with that of the contralateral kidney that does not receive the portal infusate. Portal blood does not perfuse the glomeruli or the renal medulla, and so the Sperber technique has enabled evaluation of mechanisms and regulation of transport of organic and inorganic compounds by cortical tubular elements.

19.3.1.3.3 Venous drainage

Blood from the peritubular sinuses drains into central (intralobular) veins, which coalesce into interlobar veins. These join to form the efferent renal vein, which empties into the posterior vena cava.

19.3.2 Physiology

19.3.2.1 Overview

The primary function of the kidneys is eliminative—that is, to facilitate excretion of wastes, toxins, and excess water and solutes. To accomplish this, the kidneys receive a large fraction of the cardiac output, and from this, the entire body fluid volume is filtered through the glomeruli several times each day. Most of this volume and its solutes are then reabsorbed by the renal tubules from the urine back to the blood. Some substances, though, may additionally be secreted by the tubules into the urine. The end product of filtration, reabsorption, and secretion enters the ureters as urine.

19.3.2.2 Renal blood flow

For any substance, renal clearance is defined as the volume of blood from which that substance is removed (cleared) by the kidneys per unit time. Hence, if a substance is completely removed from the plasma (by filtration and secretion) during a single pass through the renal vasculature, renal clearance and renal plasma flow (RPF) are the same (and renal blood flow can be calculated by accounting for hematocrit). The clearance (C, mL/min) of any substance, X, is calculated from the formula: $C = U_X V/P_X$, where U_X and P_X are the urine and plasma concentrations of the substance and V is the urine flow rate (mL/min). In mammals, RPF has typically been measured as the clearance of para-amino hippuric acid (PAH), which is cleared with an efficiency of approximately 90%. This substance has been used in several studies of birds as well. However, the complexity and inaccessibility of the avian renal vasculature has made it difficult to determine the extent to which PAH is actually removed from the blood in the kidneys. Measurements in a reduced avian kidney model (with a single arterial supply and accessible renal vein) indicated PAH extraction efficiency between 50 and 75% (Wideman and Gregg, 1988), suggesting that PAH clearance is likely to underestimate RPF. Nevertheless, the values of RPF measured by Wideman (and corrected for PAH extraction) are on the lower end of values measured in other studies, which average approximately 40 mL/kg body mass min (e.g., Nechay and Nechay, 1959; Sperber, 1960; Holmes et al., 1968; Wideman, 1988; Roberts, 1992).

Measurement of RPF as C_{PAH} includes both arterial and portal contributions to RPF. Alternatively, RPF has been measured from the distribution of radioactive microspheres infused into the heart, thereby providing a measure of renal arterial blood flow, without the portal contribution. Results from these studies suggest that avian kidneys receive 10−15% of cardiac output. Along with mathematical models of avian renal blood flow (Shideman et al., 1981), these studies collectively suggest that under baseline conditions approximately 50% of avian renal blood flow might derive from the renal portal system, the remainder from arterial flow.

In the domestic fowl, renal blood flow can be autoregulated over a range of arterial pressures from about 100 to below 40 mm Hg (Wideman and Gregg, 1988). An important contributor to this autoregulation is the renal portal flow; as arterial pressure falls to the lower end of the autoregulatory range, arterial flow diminishes, but portal flow increases complementarily (Wideman, 1991). The mechanism for this coordination is unknown, but it presumably functions to maintain perfusion of the cortical tubule elements during times of reduced glomerular (and postglomerular) blood flow (see below).

Despite the ability to autoregulate, avian renal blood flow varies substantially in some circumstances. For example, in feral chickens, salt loading increased renal blood flow by more than 100% (Roberts, 1992).

19.3.2.3 Glomerular filtration

Filtration of plasma through the glomerular capillaries is the primary step in formation of avian urine. Whole kidney glomerular filtration rate (GFR) is the sum of the single nephron glomerular filtration rates (SNGFRs). SNGFR is determined by the difference between net hydrostatic pressure favoring filtration and oncotic pressure opposing it, by the hydraulic conductivity (permeability to water) of the glomerular filtration barrier, and by the surface area for filtration. Primarily because of the simplicity of avian (as compared with mammalian) glomeruli, and hence their small surface area, SNGFR in birds is low. However, because birds have more glomeruli per kidney, whole kidney GFRs are similar in birds and mammals (Yokota et al., 1985).

GFR (whole kidney or single nephron) is measured as a special case of clearance. If a substance is freely filtered and is neither secreted nor reabsorbed by the renal tubules, then the amounts filtered from the plasma and excreted in the urine are the same. The clearance of such a substance provides a measure of the GFR. Avian GFR has been measured as the clearance of inulin, polyethylene glycol, sodium ferrocyanide, iothalamate, iohexol, and others (Scope et al., 2013; Gasthuys et al., 2019).

SNGFR during mannitol diuresis has been measured in the kidneys of two species, Gambel's quail (*Callipepla gambelii*) and the European starling (*Sturnus vulgaris*), using the ferrocyanide precipitation technique (Braun and Dantzler, 1972; Braun, 1978), which permits simultaneous evaluation of filtration rates in both superficial and deep nephrons. SNGFR on average was 6−7 nL/min in loopless nephrons of both species, about 11 nL/min in "short-looped" (transitional) nephrons of the quail, and about 15 nL/min in "long-looped" nephrons. SNGFR also has

been measured in the most superficial, and hence smallest, loopless nephrons by micropuncture (Laverty and Dantzler, 1982; Roberts and Dantzler, 1990). Those values of SNGFR were much lower, from 0.25 to 0.5 nL/min. It is likely that nephrons exist with a continuum of filtration rates within that broad measured range.

Whole kidney GFR (mL/h) in normally hydrated birds varies with body mass (M, in grams) as $GFR = 1.24 \times M^{0.69}$ (Yokota et al., 1985). This equation predicts a GFR of 6 mL/h for a 10 g bird, 30 mL/h for a 100 g bird, and 145 mL/h for a 1000 g bird. Within this general relationship exists substantial variability both among and within species. For example, the GFRs of Gambel's quail and coturnix quail (*Coturnix coturnix*), both approximately 150 g, are about 15 and 36 mL/h, respectively (Braun and Dantzler, 1972; Clark and Sasayama, 1981); female Pekin ducks (*Anas platyrhynchos*) have higher GFR than males (Hughes et al., 1989), perhaps associated with different kidney sizes (Hughes et al., 1992). One might speculate that the low GFR of Gambel's quail is adaptive and provides a lesser urine flow in this desert bird. However, existing data do not support robust generalizations about habitat- or diet-related variation in GFR.

Like RPF, GFR of birds is autoregulated over a broad range of blood pressures, from 110 down to 60 mm Hg in the domestic fowl (Wideman and Gregg, 1988). This autoregulation was not affected by dietary sodium intake, as might be expected if tubuloglomerular feedback (changing renal vascular constriction in response to varying NaCl delivery to the distal tubule) were the responsible mechanism (Vena et al., 1990); these authors therefore implicated a myogenic mechanism of autoregulation, in which renal arteriolar smooth muscle responds to stretch (pressure). Despite the potential for autoregulation, GFR in birds is variable and changes in GFR contribute to regulation of urinary excretion, as discussed below.

19.3.2.4 Regulation of water excretion

The avian kidney filters a large volume of fluid, approximately 11 times the entire body water each day for a 100 g bird, and then reclaims most filtered water by tubular reabsorption. In normally hydrated birds, the percent of filtered water that is reabsorbed is typically greater than 95%. Variation from this "normal" situation can be achieved through regulation of either the rate of filtration or the rate of reabsorption, both of which may be influenced by the avian antidiuretic hormone arginine vasotocin (AVT).

19.3.2.4.1 Arginine vasotocin

AVT is a small peptide hormone released from the neurohypophysis. Circulating concentrations of AVT average about 10 pg/mL in normally hydrated birds (e.g., Möhring et al., 1980; Rice et al., 1985; Stallone and Braun, 1985; Gray and Erasmus, 1988; Gray et al., 1988; Gray et al., 2004; Aman et al., 2016). The primary stimulus for additional AVT release is a rise in ECF osmolality. In several species, the circulating concentration of AVT increases by 0.25−2 pg/mL for each mmol/kg rise in plasma osmolality (Möhring et al. et al., 1980; Arad et al., 1986; Stallone and Braun, 1986; Gray et al., 1988). A decrease in ECF volume (experimental hemorrhage) also may stimulate AVT release, but with less sensitivity than the response to osmolality (Simon-Oppermann et al., 1984; Stallone and Braun, 1986). Concentrations of AVT in dehydrated birds are typically 30−60 pg/mL (e.g., Stallone and Braun, 1986; Gray et al., 1988; Gray and Erasmus, 1988), though some higher values have been reported (Goldstein and Braun, 1988; Hughes et al., 1993). AVT receptors, possibly of the AVPR1A subtype (Wu et al., 2019), likely exist in both the vasculature and the tubules of the avian kidney (Goldstein, 2006).

19.3.2.4.2 Regulation of glomerular filtration rate

Reduction in GFR is a consistent component of the avian response to dehydration (Table 19.3) and to infusion of AVT (e.g., Ames et al., 1971; Gerstberger et al., 1985, Figure 19.6). This could reduce urine flow both directly (by a reduced throughput of water) and indirectly (by allowing enhanced tubular reabsorption and urine concentration). The diminished GFR may be brought about by an AVT-induced constriction of afferent arterioles (Braun and Dantzler, 1974), leading to a reduction or complete cessation (intermittency) of filtration in some or all nephrons (Figure 19.5). Superficial (loopless) nephrons appear most sensitive to AVT, and AVT therefore reduces the contribution of those nephrons, which lack loops of Henle and the ability to produce a concentrated urine, to urine production.

During flight, when birds risk dehydration from enhanced evaporative water loss, urine flow does diminish, but reduction of GFR appears to contribute just modestly to that antidiuresis (Giladi et al., 1997; Gerson and Guglielmo, 2013).

Birds also are able to increase GFR in response to ECF expansion induced by oral or intravenous water loading (Korr, 1939; Krag and Skadhauge, 1972; Roberts, 1992). Nevertheless, in three lineages of avian nectarivores, diuresis induced by consuming dilute liquid diets occurs by changes in tubular reabsorption, without change in GFR, despite changes in circulating AVT concentrations (Goldstein and Bradshaw, 1998; Gray et al., 2004; Hartman Bakken and Sabat, 2006; Purchase et al., 2013). Yet, GFR does vary through the day in all three nectarivore lineages, with progressive diurnal increase as dietary water is consumed and apparent nearly complete cessation at night (Hartman Bakken et al., 2004; Nicolson and Fleming,

TABLE 19.3 Representative responses of avian glomerular filtration rate to osmoregulatory challenge.

Species	Condition	Glomerular filtration rate (% of control)	Reference
House sparrow (*Passer domesticus*)	30 h dehydration	46	1
Starling (*Sturnus vulgaris*)	One d dehydration	42	2
Stubble quail (*Coturnix pectoralis*)	21–120 d dehydration	66	2
Emu (*Dromaius novaehollandiae*)	Seven d dehydration	70	2
Broad-tailed hummingbird (*Selasphorus platycercus*	Overnight fast	0	3
Swainson's thrushes (*Catharus ustulatus*)	Flight in wind tunnel	100	4
Mallard duck (*Anas platyrhynchos*)[a]	Saline acclimation	100	5
Glaucous-winged gull (*Larus glaucescens*)[a]	Saline acclimation	210	5
Canada goose (*Branta canadensis*)[a]	Saline acclimation	183	5
Starling (*Sturnus vulgaris*)	24 meq/kg NaCl infusion	200	6
Gambel's quail (*Lophortyx gambelii*)[b]	20 meq/kg NaCl infusion	90	4
Leach's storm petrel (*Oceanodroma leucorhoa*)[a]	24 meq/kg NaCl infusion	15	7
Pekin duck (*Anas platyrhynchos*)[a]	20 meq/kg NaCl infusion	100	8

References: 1. Goldstein and Braun (1988). 2. From summary table in Roberts and Dantzler (1989). 3. Hartman Bakken et al., 2004. 4. Gerson and Guglielmo (2013). 5. From summary table in Roberts et al. (1983). 6. Laverty and Wideman (1989). 7. Goldstein (1993). 8. Gerstberger et al. (1985).
[a]*Species with salt glands.*
[b]*At higher salt loads (35 - 50 meq/kg NaCl infusion), GFR decreased to ~40% of control.*

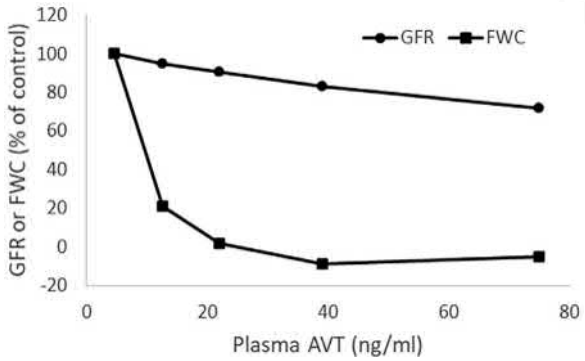

FIGURE 19.6 The effect of arginine vasotocin (AVT, the avian antidiuretic hormone) on free water clearance (FWC) and glomerular filtration rate (GFR). Note that FWC decreases markedly in response to low concentrations of AVT while GFR is essentially unchanged. *Data taken from Stallone and Braun (1985).*

2014). That nighttime reduction in GFR is seen in other small birds as well (Goldstein and Rothschild, 1993).

19.3.2.4.3 Tubular water reabsorption and the urinary concentrating mechanism

Tubular reabsorption of water in birds can range from more than 99% of the filtered volume to as low as 60% in some nectar feeders (Hartman Bakken and Sabat, 2006). As a result, the final concentration of avian urine can vary from dilute (approximately 40 mmol/kg) to hyperosmotic (2–3 times the plasma osmolality).

Both micropuncture studies of superficial proximal tubules (Laverty and Dantzler, 1982) and studies of isolated, perfused proximal tubules from deeper (transitional) nephrons (Brokl et al., 1994) suggest that, as in mammals, the avian proximal tubule reabsorbs about 70% of the filtered volume of water. That reabsorption depends on active sodium transport but not on the presence or reabsorption of bicarbonate (Brokl et al., 1994). Water reabsorption may be facilitated by the water channel protein aquaporin 1 expressed in the brush border membrane (Nishimura and Yang, 2013).

Fine tuning of water reabsorption occurs not in the proximal tubule but in more distal nephron segments. Like in mammals, birds' ability to produce a urine more concentrated than the plasma derives from the actions of a countercurrent multiplier system producing a gradient of osmolality along the depth of the renal medulla.

Earlier studies of the avian renal medulla revealed a number of the basic features associated with a countercurrent multiplier mechanism of urine concentration. Loops of Henle, providing counter-directional flow, extend into the renal medulla in parallel with collecting ducts. ^{22}Na autoradiography suggested active Na^+ reabsorption within the medullary cone (Emery et al., 1972), and this

was consistent with an osmotic gradient composed primarily of NaCl along the length of the medulla (Skadhauge and Schmidt Nielsen, 1967b; Emery et al., 1972). However, for the avian descending and ascending limbs of Henle to act as single-effect countercurrent multipliers (i.e., countercurrent multipliers whose energy source is a single active transport process, as proposed for the mammalian kidney (see, e.g., Jamison and Kriz, 1982)), they must possess two additional characteristics: (1) the ability to generate energy sufficient to develop a transverse difference in osmotic pressure and (2) differences in permeabilities. Several studies have sought to assess those characteristics.

19.3.2.4.3.1 Descending thin limb The transition from pars recta (straight descending limb of the proximal tubule) to descending thin limb (DTL) occurs with an abrupt transition in cell morphology near the base of the medullary cone (Braun and Reimer, 1988). The physiological properties of avian DTL have been studied for just the upper segment of a single species (*Coturnix coturnix*; Nishimura et al., 1989). Coturnix DTL segments fail to generate an electrical potential both when bathed in isosmotic media and when exposed to a transepithelial ion gradient; these properties derive from an absence of electrogenic ion transport, combined with high but nearly equal permeabilities to Na^+ and Cl^- (Nishimura et al., 1989). Coturnix DTL has a low permeability to water (Nishimura et al., 1989).

19.3.2.4.3.2 Thick ascending limb The avian loop of Henle makes the transition from DTL to thick ascending limb (TAL) before the hairpin turn (Figure 19.7). In cellular morphology, the avian TAL resembles other vertebrate diluting segments (Nishimura, 1993; Braun and Reimer, 1988). Functional properties include a lumen-positive voltage that requires Na^+ and Cl^- and is inhibited by the loop diuretics bumetanide and furosemide, the ability to transport NaCl against transepithelial electrochemical gradients, and low permeability to water and net water transport (Miwa and Nishimura, 1986; Nishimura et al., 1986). Ion reabsorption by the TAL is sensitive to solute delivery (enhanced either by increased flow or concentration; Osono and Nishimura, 1994), but is not affected by AVT (Miwa and Nishimura, 1986), forskolin, or isoproterenol (Osono and Nishimura, 1994). The combination of active salt reabsorption and low-water permeability implies that tubular fluid is diluted as it passes through the TAL.

19.3.2.4.3.3 Collecting duct The avian collecting duct receives dilute urine from both the TAL and from loopless nephrons, and so water reabsorption into the hyperosmotic interstitium to concentrate the urine requires that this nephron segment is, or can become, permeable to water. Indeed, infusion of AVT into the systemic circulation, at least at low doses, increases urine osmolality and reduces urine flow with little or no change in GFR (Ames et al., 1971; Stallone and Braun, 1985, Figure 19.6), suggesting enhanced permeability of the distal nephron.

Despite these findings in whole-animal studies, direct assessment of AVT's actions on isolated, perfused avian collecting ducts has failed to reveal a significant effect of the hormone (Nishimura, 1993). mRNA for AQP2, the primary ADH-responsive aquaporin (water channel

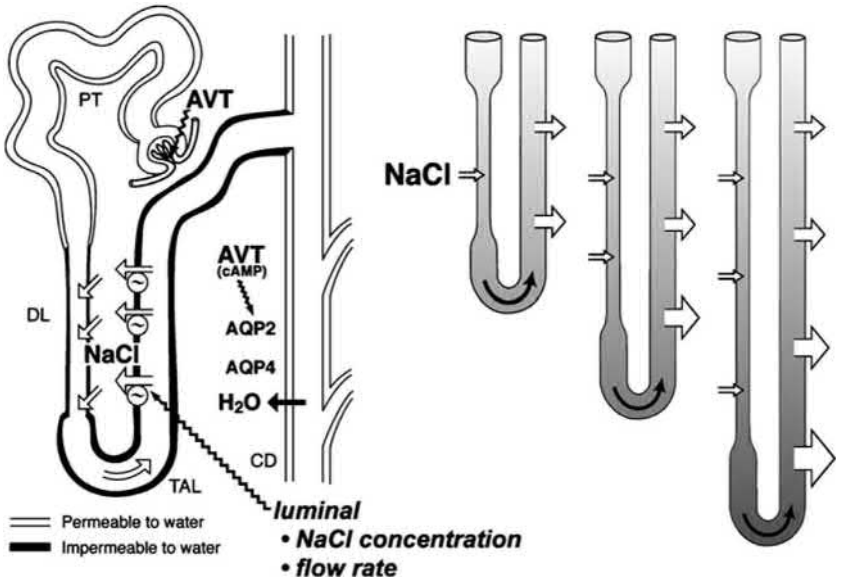

FIGURE 19.7 A proposed model for the avian urine concentrating mechanism. Tubule segments illustrated with heavy lines have low permeability to water. Possible sites of regulation include arginine vasotocin–induced reduction of the filtered load (shown), flow-sensitivity of the thick ascending limb, and cyclic adenosine monophosphate–mediated changes in water permeability of the collecting duct. To the right is pictured the hypothetical cascade effect of the concentrating mechanism that results from the presence of loops of Henle of varying length. *Figure from Nishimura (1993).* © *Cambridge University Press 1993; reprinted with the permission of Cambridge University Press.*

protein) in mammalian collecting ducts, was expressed in both medullary and superficial portions of the quail kidney, and in both regions the expression was somewhat increased by water deprivation (Nishimura and Yang, 2013). However, the coturnix quail collecting duct had a moderate baseline permeability to water even in the absence of AVT, and although forskolin (10^{-4} M), which activates cyclic adenosine monophosphate production, induced a substantial increase in permeability, AVT did so only slightly. Thus, the role of AVT-induced aquaporin expression in avian antidiuresis remains equivocal.

19.3.2.4.3.4 Urinary concentrating mechanism Nishimura (Nishimura, 1993; Osono and Nishimura, 1994) has proposed a general model of the avian urinary concentrating mechanism that incorporates the evidence described above (Figure 19.7). The single effect that drives urine concentration is active ion reabsorption by the TAL. These reabsorbed ions enter the DTL by passive diffusion without accompanying water flux. The low-water permeability of the DTL maintains volume flow through the loop, which should favor ion reabsorption by the flow-sensitive TAL. The result is that urine is concentrated as it descends through the DTL, then diluted as it ascends the TAL. The segment of thick descending limb that occurs prior to the tip of the loop should contribute to the concentrating effect (Marcano et al., 2006). Simultaneously, the interstitium surrounding the loop accumulates ions and becomes concentrated. The sensitivity of the TAL to solute delivery means that the tip of the loop (at the start of the TAL epithelium) should be the site of greatest ion reabsorption, and this should contribute to generating a concentration gradient in the medulla. These effects are amplified by the countercurrent flow, and may be further enhanced by interaction among loops of Henle which turn at different depths in the medullary cone (Layton, 1986). As the urine subsequently descends through the collecting duct, it may equilibrate osmotically with the interstitium via the baseline permeability to water of this nephron segment. Mathematical modeling of the avian kidney suggests that the effectiveness and efficiency of urine concentration can be adjusted by varying the flow and transport parameters among a population of nephrons (Marcano et al., 2006).

The exact role of AVT in this mechanism remains to be clarified. However, even if AVT acts primarily by reducing filtration rates of RT nephrons, not by an effect on tubular water permeability, then the decreased flow through the collecting ducts would permit greater equilibration of water between tubule and interstitial fluid. Other aspects of anatomical organization of the avian kidney, such as the separation of descending and ascending limbs of Henle by a ring of collecting ducts (Cassoti and Richardson, 1993), also may have (undescribed) impact on the concentrating mechanism. Lastly, it is notable that NaCl may account for just a small proportion of total osmolality (Skadhauge, 1977; Hughes et al., 1992; Goldstein, 1993b); the roles of ions other than NaCl in urine concentration deserve examination.

19.3.2.4.3.5 Net effect: avian urinary concentrating ability The net effect of the medullary concentrating mechanism is that birds typically are able to concentrate urine to an osmolality 2−3 times that of plasma. [An exception to this is a report that salt-marsh savannah sparrows, *Passerculus sandwichensis beldingi*, when drinking seawater, excreted cloacal fluid with an osmolality 4.5 times that of plasma (Poulson and Bartholomew, 1962).] The urinary concentrating ability generally varies inversely with body mass, so that small birds (10−25 g) concentrate to about 1000 mmol/kg, larger birds (>500−1000 g) mostly to about 600−700 mmol/kg (Goldstein and Braun, 1989). This pattern may result from the dependence of urine concentration on metabolically active processes (active ion reabsorption) that act at lower rates with increasing body mass (Greenwald, 1989). It remains unclear the extent to which other features of kidney anatomy, such as the proportions and number of looped and unlooped nephrons, the lengths of medullary cones, or the proportions of kidney mass composed of medullary tissue, relate to urinary concentrating ability independent of the effect of body mass (Johnson, 1974; Goldstein and Braun, 1989; Warui, 1989). At least within closely related species, urine concentration does seem to be related to the proportion of medullary tissue in the kidneys (Skadhauge, 1981).

19.3.2.5 Regulation of sodium excretion

19.3.2.5.1 Patterns of response

One of the important functions of the avian kidney is to regulate sodium excretion; sodium is the primary extracellular cation, and its content in the ECF largely determines the ECF volume and hence contributes to blood pressure regulation. Regulation of sodium excretion by the avian kidney has been examined under two general circumstances. In the first, dietary sodium intake is varied; typically these animals are able to regulate plasma sodium concentration within the normal range. In the second, birds are infused with saline, typically at a high concentration that challenges homeostasis and ultimately leads to a rise in plasma sodium concentration and osmolality.

Acclimation to increasing salt intake results, as expected, in enhanced renal salt excretion. This may involve an increase (Hughes, 1980), decrease (Hughes et al., 1989; Dawson et al., 1991), or no change (Holmes et al., 1968; Hughes, 1980; Goldstein, 1990) in GFR (Table 19.3). The renal response depends at least in part on the level of NaCl intake. For example, chukars (*Alectoris chukar*) responded to an increase from 0.25 to 2 meq Na^+/d primarily by reducing intestinal sodium absorption, with little renal

response, whereas a further increase to 10 meq/d induced a reduction in tubular sodium reabsorption (Goldstein, 1990). NaCl drinking solutions at concentrations beyond the kidneys' regulatory ability may induce dehydration and an accompanying reduction in GFR (Roberts and Hughes, 1983).

Infusion of hyperosmotic salt loads induces different responses in different species (Table 19.3). Some birds respond with large increases in GFR and reduced fractional Na^+ reabsorption (Laverty and Wideman, 1989; Roberts, 1992). In others, GFR doesn't change (Skadhauge and Schmidt-Nielsen, 1967a; Gerstberger et al., 1985; Hughes et al., 1993) or diminishes (Braun and Dantzler, 1972; Dantzler, 1966; Goldstein, 1993b). In birds with salt glands, the unchanging GFR in response to saline drinking or infusion may reflect the ability of the salt glands to excrete NaCl and thereby preserve body water. Among other species, the different responses may relate to different strategies of osmoregulation—whether to preserve extracellular volume at the expense of a rising osmolality (i.e., to retain the infused sodium, but thereby retain water), or to preserve osmolality at the expense of reduced volume (i.e., to excrete the solute load, but lose water along with it).

19.3.2.5.2 Mechanisms of regulation

A number of hormones may be involved in producing the varied patterns of sodium excretion.

19.3.2.5.2.1 Arginine vasotocin A rising extracellular osmolality would be expected to stimulate release of AVT and, indeed, saline infusion can result in elevated AVT concentrations (Koike et al., 1979; Arad et al., 1986). However, saline infusion may expand the ECF, and the consequent decrease in circulating AVT levels may allow GFR to rise. Yet other studies have measured stable or substantially increased GFR even while AVT was increased (Roberts, 1992; Hughes et al., 1993). This may reflect a countervailing effect of atrial natriuretic peptide (ANP) (see below) released in response to extracellular volume expansion.

19.3.2.5.2.2 Renin/angiotensin Birds possess a complete renin/angiotensin system: avian nephrons have a juxtaglomerular apparatus (Morild et al., 1985), and their plasma contains renin activity, angiotensin I, and angiotensin II (reviewed by Wilson, 1989). In ducks (*Anas platyrhynchos*), circulating levels of angiotensin are elevated during ECF volume contraction (Gray and Simon, 1985), as may occur when drinking high-saline concentrations (Zenteno-Savin, 1991). Seemingly in contrast with this, infusion of angiotensin II (ANGII) into ducks (Gray et al., 1986) or into the renal portal vein of chickens (Langford and Fallis, 1966; Stallone and Nishimura, 1985) stimulates natriuresis and diuresis without any change in GFR, suggesting that ANGII inhibits sodium reabsorption through a direct tubular action. Thus, the physiological effects of angiotensin vary with the osmoregulatory status of the animal. With salt and volume depletion, angiotensin stimulates reduction in GFR, urine flow, and sodium excretion (Gray and Erasmus, 1989); salt and volume loading, on the other hand, change the response so that angiotensin becomes natriuretic and diuretic. The mediator of this change has not been determined, though Gray and Erasmus (1989) suggest that prostaglandins are likely candidates.

19.3.2.5.2.3 Aldosterone Circulating concentrations of aldosterone may or may not be elevated by a diet low in NaCl or during dehydration (Skadhauge et al., 1983; Klingbeil, 1985; Árnason et al., 1986; Goldstein, 1993a). The hormone is presumed to have an action on the avian kidney similar to that seen in mammals—that is, promoting sodium conservation.

19.3.2.5.2.4 Atrial natriuretic peptide Birds, like other vertebrates, secrete a peptide hormone (29 amino acids in the chicken) from the heart atria (Toshimori et al., 1990). Infusion of chicken ANP increases renal sodium and water excretion both in the domestic duck (Gray et al., 1991; Schütz et al., 1992) and chicken (Gray, 1993), and, conversely, attenuating ANP concentrations during conditions of volume loading attenuates renal excretion (Gray et al., 1997). Although receptors for ANP have been localized on both the glomeruli and the renal tubules (Schütz et al., 1992), the mechanism of action of the hormone, including the relative contributions of glomerular versus tubular effects, remains unresolved.

19.3.2.6 Regulation of calcium and phosphate excretion

19.3.2.6.1 Calcium

Normally the avian kidney reabsorbs more than 98% of filtered calcium (Wideman, 1987) by a pathway that is apparently saturable and normally operates near its maximum capacity. Procedures that increase the filtered load of calcium, such as intravenous infusion of calcium or injection of exogenous parathyroid hormone (PTH, which increases GFR and plasma calcium levels), result in enhanced renal calcium excretion (Clark et al., 1976). On the other hand, in most birds (but not all; Clark and Mok, 1986), the normal pattern of reabsorption depends of PTH; calcium excretion is markedly increased by parathyroidectomy and is restored to control levels by PTH administration (Clark and Wideman, 1977; Clark and Sasayama, 1981). The single clearance study of the effects

of calcitonin failed to demonstrate any significant effect on renal calcium excretion (Clark and Wideman, 1980).

A cellular mechanism of calcium reabsorption and stimulation by PTH, which may occur in the TAL (Braun and Dantzler, 1987), has been proposed by Clark and Wideman (1989). Calcium likely moves across the apical cell membrane down an electrochemical gradient. Reabsorption across the basolateral membrane would then be accomplished by active transport, perhaps involving a calcium ATPase. PTH, which is known to activate cellular cyclic AMP production (e.g., Dousa, 1974; Pines et al., 1983), could promote this reabsorption via actions either on the apical permeability or the basolateral mechanism of reabsorption.

19.3.2.6.2 Phosphate

In chickens, approximately 60% of the filtered load of phosphate is excreted in the urine, a result of the simultaneous operation of a reabsorptive pathway, which reclaims about half of the filtered phosphate, and a low level of secretion (Wideman, 1987). PTH both inhibits phosphate reabsorption (Cole, 1985, in Clark and Wideman, 1989) and stimulates its secretion (Wideman and Braun, 1981). As a consequence, in the absence of PTH (i.e., following parathyroidectomy), urinary phosphate excretion falls to near zero (Clark and Wideman, 1977). In contrast, administration of PTH to intact birds can result in renal excretion of more than twice the filtered load of phosphate (Wideman and Braun, 1981). No effect of calcitonin on renal phosphate excretion has been demonstrated (Clark and Wideman, 1980).

In starlings, individual proximal tubules of superficial RT nephrons may exhibit either net secretion or net reabsorption of phosphate (Laverty and Dantzler, 1982), and this may be the site of regulation of phosphate transport. The cellular mechanism of phosphate reabsorption involves a saturable, sodium-dependent transporter located in the apical membrane (Grahn and Butterworth, 1982; Renfro and Clark, 1984). Inhibition of this transport is mediated by cyclic AMP (Cole, 1985) acting via protein kinase C and protein kinase A (Dudas et al., 2002). The mechanism of activation of phosphate secretion remains unknown. Phosphate infused only into blood supplying the renal tubules (via the renal portal vasculature) accounted for only a small fraction of net phosphate transport into the tubule lumen during times of net secretion (Wideman and Braun, 1981). The secreted phosphate may derive primarily from a pool that is sequestered within the tubule cell (Wideman, 1984).

In addition to its effects on calcium and phosphate transport, PTH may have other actions on the kidney, including most consistently increases in GFR, sodium excretion, and urine flow (Clark and Wideman, 1989).

19.3.2.7 Nitrogen excretion

The end products of nitrogen metabolism excreted by the kidneys in avian urine include urates, ammonia, urea, creatinine, amino acids, and others (Table 19.4). Urates are the predominant compounds under all circumstances, though ammonia may account for as much as 25% of total urinary nitrogen. The proportions of different nitrogenous wastes may vary with feeding cycle and age (Lyons and Goldstein, 2002). After entering the lower intestine from the ureters, modification of the urine by bacterial metabolism and intestinal transport can diminish urates in the final excreted fluid (Crouch at al., 2020) and can even

TABLE 19.4 Patterns of nitrogen excretion in avian urine.[a]

Species	Condition	Total N (g/L)	Urate (% of total)	NH_4 (% of total)	Urea (% of total)
Domestic fowl (*Gallus domesticus*)	Fed	4.4	84.1	6.8	5.2
	Fasted	2.4	57.8	23.0	2.9
	Low protein	11	54.7	17.3	7.7
	High protein	13	72.1	10.8	9.7
Turkey vulture (*Cathartes aura*)	Fed	61	87	9	4
	Fasted	13	76	17	7
American kestrel (*Falco sparverius*)	Wild nestlings, age three weeks	54.6	80.4	6.4	7.3
	Captive adult fed chicks	46.7	81.4	5.6	4.9

[a]*Data extracted from summary table in Skadhauge (1981) for fowl and turkey vulture, and from Lyons and Goldstein (2002) for kestrel. Other nitrogenous components of the urine, including creatinine, amino acids, and purines always accounted for <10% of total nitrogen.*

produce "apparent ammonotely" (Tsahar et al., 2005). The present discussion will focus on the excretion of urates by the kidneys; urinary ammonia will be discussed in the following section, as it relates to acid/base regulation.

Urate in avian plasma is thought to be all or mostly unbound to proteins and hence filterable through the glomeruli (see discussion in Dantzler, 1978). Nevertheless, with a plasma urate concentration of 0.1−0.7 mM, glomerular filtration can only account for 10−20% of the total urate excreted by the kidneys. Shannon (1938) was the first to demonstrate conclusively that the clearance of urate exceeds that of inulin, and >90% of urate in avian urine derives from tubular secretion. The source of the secreted urates is primarily the liver, though renal synthesis may account for 3−20% of the total (Martindale, 1976; Chin and Quebbemann, 1978).

Slices from avian renal cortex (Platts and Mudge, 1961; Dantzler, 1969), but not of medullary cones (Dantzler, 1969), accumulate urate in vitro, suggesting that urate secretion occurs in cortical nephron elements. Micropuncture studies of superficial proximal tubules of RT nephrons, as well as studies of urate transport by isolated proximal tubules from deeper (transitional) nephrons, have confirmed that these nephron segments secrete urate (Laverty and Dantzler, 1983; Brokl et al., 1994). Studies of isolated proximal tubules in vitro (Brokl et al., 1994) indicate that urate secretion involves transport across the basolateral membrane against an electrochemical gradient, apparently via organic anion transporters OAT and OAT3 (Dudas et al., 2005). The flux from cell to tubule lumen is down an electrochemical gradient and involves the multidrug resistance protein MRP4 (Bataille et al., 2008, Ding et al., 2009). Net urate transport in proximal tubules is always secretory, but perfused tubules show a substantial simultaneous reabsorptive flux that apparently occurs through a paracellular route. In vivo, though, there is no evidence for such a reabsorptive pathway (Nechay and Nechay, 1959).

Once secreted, the chemistry of urates in urinary solutions is complex. The acid form of urate (uric acid) has a low aqueous solubility (0.38 mmol/L), but with a pK of 5.6 and a typical urinary pH of 6 to 7, most molecules will exist as monobasic urate. Urate could form salts with a variety of cations in the urine, but sodium and potassium urate are most likely because of the abundance of these ions. The solubilities of sodium and potassium urate (6.8 and 12.1 mmol/L, respectively) substantially exceed those of uric acid; nevertheless, the high concentrations of urates in the liquid fraction of the urine exceed values accounted for by these solubilities (McNabb et al., 1973; McNabb, 1974).

Urates apparently are able to exist in solution at supersaturated concentrations because they form stable colloidal suspensions. The stability of these colloids is increased through their interaction with mucoid materials in urine (Porter, 1963). These mucopolysaccharides and glycoproteins are most abundant in distal nephron segments where the urine concentration is likely to be highest (McNabb et al., 1973; Nicholson, 1982). The concentrated aqueous colloids probably minimize formation of urate crystals and thereby facilitate passage of urates through the nephron.

Nevertheless, urates do exist in precipitated form in avian urine. This is not in the form of crystalline masses, but rather as spheres a few microns in diameter (Figure 19.8; Folk, 1969; Lonsdale and Sutor, 1971) that form as alternating layers of urate and mucoid materials with associated water (Minnich, 1976).

Anywhere from <5% to >75% of urinary Na^+ and K^+ are associated with the precipitated urate fraction of urine rather than existing in free solution (Hughes, 1972; McNabb et al., 1973; Braun, 1978; Long and Skadhauge, 1980, 1983b; Laverty and Wideman, 1989; Dawson et al., 1991). In part, the charge configuration of the water and mucopolysaccharide layers of the urate spheres may sequester cations (McNabb and McNabb, 1975). Elemental analysis of urate spheres from several avian species indicated that Na^+ and K^+ were usually the most abundant cations, with K^+ usually the more abundant ion (Casotti and Braun, 2004). The trapped ions would not contribute to urinary osmolality and may present a means of enhancing ion excretion beyond the limited concentrating ability of the avian kidney.

19.3.2.8 Renal contribution to acid/base regulation

Birds maintain an alkaline arterial pH of approximately 7.5, despite a constant metabolic production of acid. Most of this acid, resulting from hydration of CO_2, is excreted as respiratory CO_2. However, nonvolatile acids, e.g., H_2SO_4

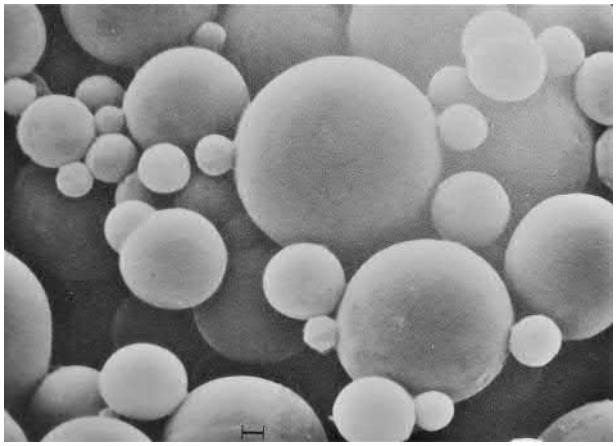

FIGURE 19.8 Scanning electron micrograph of urate spheres from the urine of Gambel's quail (*Callipepla gambelii*). The scale bar represent 1 μm. *Photograph courtesy of Giovanni Casotti and Eldon J. Braun.*

and H_3PO_4, are also a threat to acid/base homeostasis, and the kidneys must excrete the protons equivalent to these metabolic end products. Thus, while avian urine pH may range under experimental conditions from less than five to about eight (Sykes, 1971; Long and Skadhauge, 1983a), avian urine is typically acidic, with a pH in the range of 5.5−7.5. The renal defense of arterial alkaline pH is thus presumed to consist of two components, conservation of base (bicarbonate) and excretion of acid (H^+, largely buffered).

Avian renal conservation of bicarbonate is thought to be accomplished by mechanisms similar to those existing in the mammalian kidney. That is, secreted H^+ combines in the tubule lumen with filtered HCO_3^- to form CO_2 that diffuses back into the tubule cells. There, catalyzed by carbonic anhydrase, it rehydrates and dissociates into H^+ and HCO_3^-. The HCO_3^- is then reabsorbed into the blood across the basolateral membrane. Overall, birds, like mammals, can accomplish virtual complete reabsorption of filtered bicarbonate during periods of acidosis (Anderson, 1967). It is likely that bicarbonate reabsorption in the avian kidney occurs in the distal nephron, where carbonic anhydrase activity is most prominent (see Laverty, 1989; Gabrielli et al., 1998). Consistent with this, micropuncture studies of starling proximal tubules found no evidence for preferential reabsorption of bicarbonate in this nephron segment (Laverty and Alberici, 1987).

The lack of acidification of proximal tubule fluid, even in acidotic birds, suggests that H^+ secretion, too, may take place in distal nephron segments (Laverty and Alberici, 1987). The mechanism of avian renal H^+ secretion is likely to be accomplished at least in part by Na^+/H^+ exchange (Laverty, 1989). The minimum urinary pH achievable by the avian nephron is 4.5−5, and so adequate acid excretion requires that most urinary hydrogen ions be excreted in buffered form. Three compounds—ammonia, phosphate, and urate—serve as the primary urinary buffers in birds.

As noted above, ammonia may constitute up to one quarter of the total nitrogen excreted in avian urine. The urinary excretion of ammonia is inversely related to the pH of the urine (Wolbach, 1955; Long and Skadhauge, 1983a). This ammonia is presumed to derive from cellular metabolism (deamination reactions) and secretion in the distal nephron. The production of ammonia can be enhanced by infusion of the amino acids D,L-alanine, L-leucine, and glycine (Wolbach, 1955), and chronic metabolic acidosis in the chicken leads to increased activity of glutaminase in the kidney (Craan et al., 1982). Ammonia secretion is presumed to occur by nonionic diffusion. Uncharged NH_3 diffuses from the tubule cells into in the various surrounding fluid compartments. In the acidic urine of the tubule lumen, NH_3 is protonated to ammonium, NH_4^+, which permeates cell membranes more slowly than NH_3 and so is effectively trapped there for excretion.

The phosphate buffer system (HPO_4/H_2PO_4), with a pK of 6.8, also plays an important role in urinary buffering. H_2PO_4 may account for approximately 20−30% of total acid excretion at typical urinary pH, but may increase substantially when phosphate is infused during times of production of acidic urine (Wolbach, 1955; Sykes, 1971). The contribution of phosphate to acid excretion declines as urinary pH rises, perhaps because of a preferential reabsorption of the basic form of the buffer (HPO_4), which would be more abundant at the higher pH (Long and Skadhauge, 1983a).

The final major contributor to buffering of avian urine is urate/uric acid (pK 5.8). The contribution of this system to acid excretion is undoubtedly substantial (Wolbach, 1955) but is difficult to quantify accurately because of uncertainty about the chemical form of the colloidal precipitate. Calculations based on the assumptions either that all precipitated U/UA exists as UA (Lonsdale and Sutor, 1971) or that the precipitated U/UA is in equilibrium with the supernatant, suggest that U/UA constitutes 25−50% of net acid excretion (Long and Skadhauge, 1980, 1983a).

19.3.2.9 Molecular regulation: the next frontier

In recent years, understanding of normal and pathological physiology of the mammalian kidney has been advanced substantially by investigation of underlying molecular mechanisms. In particular, transcriptomic sequencing (RNA seq) has elucidated patterns of gene expression, and its responses to physiological challenge and disease, at the level of the individual renal tubule (Lee et al., 2015) and cell type (Chen et al., 2017). In birds, genome sequences now are available for diverse species (Zhang et al., 2014), and RNAseq has been applied to a number of questions related to avian physiology, development, and pathology (Jax et al., 2018). However, those approaches have been applied to avian kidneys in just a small number of studies (e.g., Hao et al., 2019; Park et al., 2017; Zeferino et al., 2017), with RNA extracted from whole kidneys or kidney regions (e.g., renal cortex). Because patterns of gene expression, and the consequent cellular mechanisms, are specific to tubule segments and cell types within the kidney (see references above), studies of whole-kidney transcriptomics in birds to date can provide just a preliminary view of physiological mechanisms.

One insight that has emerged from these molecular investigations in mammals is that, in addition to protein-based regulation, function of the kidneys is significantly influenced by expression of noncoding RNAs. That includes both short noncoding RNAs like microRNA (see Sun and Lerman, 2019; Ramanathan and Padmanabhan, 2020) and long noncoding RNAs (Ignarski et al., 2019). Such mechanisms remain unexplored in avian kidneys.

19.3.2.10 The final urine—composition and flow

One might expect that any analysis of kidney function would begin with examination of urine flow and composition. However, collection of urine from conscious birds is difficult. Urine flows from the ureters into the coprodeum, colon, and ceca, where it may be modified. A variety of approaches have been used to circumvent these difficulties. In some studies, the possibility of urine flow into the hindgut is removed, either by colostomy (in which the lower intestine is exteriorized and the ureters empty into a blind cloacal pouch; Hart and Essex, 1942; Holmes et al., 1982; Karasawa and Maeda, 1992; Belay et al., 1993) or by exteriorizing the ureters (Hart and Essex, 1942; Dicker and Haslam, 1972). Besides the potential for consequences from surgery, these techniques suffer from the possibility that urine flow is influenced by the very fact that the urine can no longer interact as normal with the lower intestine. Alternatively, urine can be collected directly from the cloaca. This may be done over an extended time via collecting devices sewn over the ureteral openings (Anderson and Braun, 1985), though again potentially disrupting normal osmotic regulation. Alternatively, a filtration marker can be infused at a constant rate, such as by an implanted micropump; urine flow rate then can be calculated based on urine collected via brief insertion of a cannula over the ureteral openings (Goldstein and Braun, 1988; Goldstein and Rothschild, 1993). This approach imposes the least interruption of normal function but provides just an "instantaneous" urine flow rate.

In unanesthetized birds with free access to water, urine flow rate is in the range of 0.5–3 mL/kg$^{.7}$h (Goldstein, 1990, using the same body mass scaling factor, kg$^{0.7}$, as pertains to GFR), and urine osmolality is typically close to isosmotic with plasma. During dehydration, urine flow diminishes and osmotic concentration increases to two to three times that of plasma. The composition of this urine has been analyzed in detail in only a small number of studies. In chickens eating grain (30 meq Na^+/kg), Na^+ and Cl^- together accounted for just over 10% of the total osmolality of 582 mM/kg (Skadhauge, 1977). The most abundant solutes were NH_4^+, phosphate, and K^+ (Table 19.5), and just 41% of the osmotic space could not be accounted for by measured solutes. In chickens eating a diet with three times the sodium content of the grain, Na^+ and Cl^- in the urine rose about threefold, NH_4^+ was substantially diminished, and other measured solutes changed by just small amounts (Table 19.4; Skadhauge, 1977). These findings—relatively high concentrations of NH_4^+, phosphate, and K^+, with Na^+ and Cl^- together accounting for less than 50% of the osmotic space—are representative of other studies as well. However, with salt loading, Na^+ concentrations can rise to as much as 30–50% of the total osmotic space in some species both with and without salt glands (Goldstein, 1990, 1993b; Bennett and Hughes, 2003).

19.3.2.11 Function of the ureters

The ureters of birds are surrounded by smooth muscle which normally possesses tone and is capable of peristalsis (Gibbs, 1929). The ureters act to "milk" the urine from the kidneys, but they also offer significant resistance to the flow of urine. Because the ureters are direct extensions of the collecting ducts, ureteral resistance may influence flow rates through the nephrons. Consistent with this, Hughes (1987) found that severing the ureter just caudal to the kidney increased urine flow and reduced urine osmolality, suggesting that a more rapid transit through the nephron impaired ion and/or water reabsorption. The state of ureteral tone and extent of peristalsis may be under the influence of the sympathetic nervous system (Gibbs, 1929).

19.4 Extrarenal organs of osmoregulation: introduction

Despite their limited urine concentrating ability, birds are as effective as mammals at water conservation. In both groups, small, desert-dwelling species are able to survive on seed diets without drinking water (Krag and Skadhauge, 1972; Skadhauge and Bradshaw, 1974); however, the

TABLE 19.5 Composition of supernatant of avian urine.[a]

Species	Condition	Na[b]	Cl	K	Mg	Ca	NH_4	PO_4	Osm[c]
Domestic fowl (*Gallus domesticus*)	Wheat and barley	41	36	73	13	7	120	130	582
	Commercial	141	121	62	11	11	50	132	594
Galah (*Cacatua roseicapilla*)	Dehydrated	78	51	30	–	–	124	118	618
Ostrich (*Struthio camelus*)	Control	85	158	266	–	1	50	3	–

[a]*Data extracted from summary table in Skadhauge (1981).*
[b]*All ion concentrations in mmol/L.*
[c]*Osmolality in mosmol/kg water.*

mechanisms responsible for those capabilities differ in the two vertebrate classes. Water conservation in birds does result at least in part from renal mechanisms, including the ability to reduce GFR and to increase tubular reabsorption of water, but desert birds lack the notable urine concentrating abilities of their mammalian counterparts. Uricotelism, too, may facilitate water conservation, as it provides a means of excreting nitrogenous waste with a minimum of water loss (because of the insolubility of the urates and hence their lack of contribution to the urinary osmotic concentration) (Smith, 1953). Beyond this, avian osmoregulation depends additionally on several other organs that regulate salt and water losses.

19.5 The lower intestine

19.5.1 Introduction

Urine leaving the avian ureters enters the urodeum of the of the lower intestine and, in most birds, flows in an orad direction, via retrograde peristalsis, from the urodeum into both coprodeum and colon (rectum) (Figure 19.9). This retrograde flow brings the urine into contact with the chyme coming from the ileum (the urine may form a coating around a central core of feces) and exposes the urine to the absorbing columnar epithelia of the coprodeum and colon (the stratified squamous epithelia of the urodeum and proctodeum are nontransporting). Retrograde flow may extend all the way to the ileo-colonic junction, and urine may enter the paired caeca in species possessing those organs. Ions, water, and organic products of bacterial fermentation [short-chain fatty acids (SCFAs)] may be absorbed in the ceca. Urinary refluxing may serve a variety of functions, including reclamation of water, electrolytes, nitrogen, or energy that would otherwise be lost.

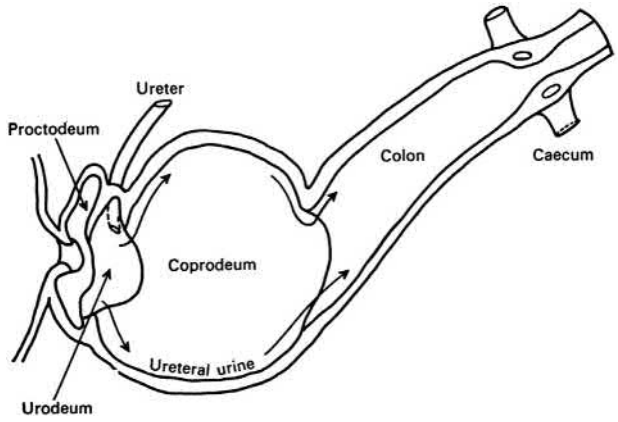

FIGURE 19.9 Lower intestine of the domestic fowl. Arrows indicate the retrograde flow of urine from urodeum to coprodeum, colon, and ceca, as well as possible directions for net fluxes of water and NaCl in coprodeum and colon. *Modified from Choshniak et al. (1977); reproduced with permission.*

19.5.2 Transport properties of coprodeum, colon, and cecum

19.5.2.1 Basic transport mechanisms in coprodeum and colon

Although coprodeum and colon, in most birds, form a common storage chamber for ureteral urine and chyme, their transport properties differ markedly.

This section is largely based on studies on the domestic fowl, as surveyed by Skadhauge (1973, 1981, 1993), Goldstein (1989), and Elbrønd et al. (1993), but the mechanisms observed in the fowl are generally observed in other avian species as different as the galah (*Cacatua roseicapilla*) and the emu (*Dromaius novaehollandiae*).

19.5.2.1.1 Transport of NaCl and water

Both coprodeum and colon have electrolyte transport properties that are regulated by, and change markedly in response to, humoral factors induced by changes in NaCl intake (Figure 19.10). Broadly speaking, the rate of Na^+ absorption is activated by NaCl depletion and suppressed by NaCl loading. The transport patterns must therefore be described and characterized in relation to the NaCl content of the diet.

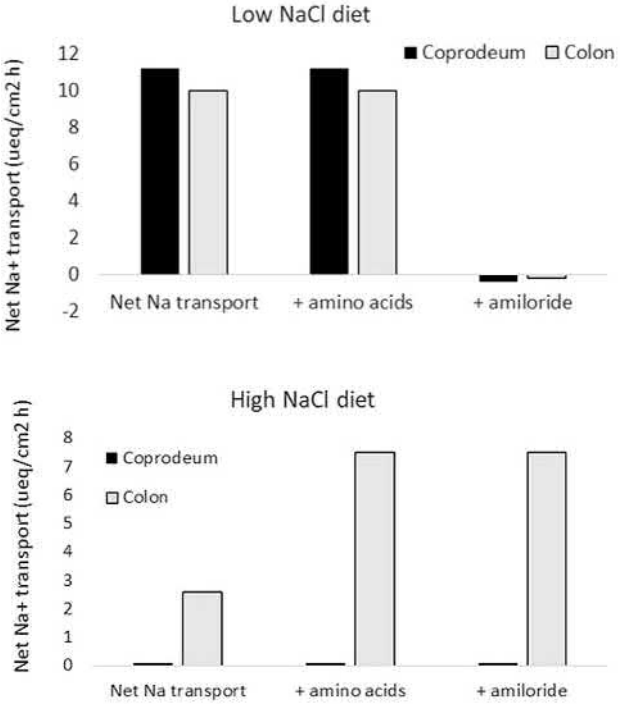

FIGURE 19.10 Effect of dietary NaCl on transport properties of coprodeum and colon in domestic fowl. Illustrated are Na^+ transport rates in the absence of luminal organic substrates (open bars), in the presence of luminal leucine and lysine (*light stippling*), and in the presence of the sodium channel blocker amiloride (*dark stippling*).

The coprodeum can be characterized as a "medium-tight" epithelium (3−500 Ω × cm^2). On a low-NaCl diet, coprodeum absorbs Na^+ at a high rate, 10−20 μeq/cm^2 hour in vitro under short-circuit conditions (Figure 19.10), and about 100 μeq/kg bodyweight × hr in vivo. Under open-circuit conditions, a transepithelial lumen-negative electrical potential difference (PD) of 40−60 mV develops in vitro, and similar differences from lumen to plasma can be measured in vivo. The PD drives passive Cl^- transport in vivo, resulting in absorption of near-neutral NaCl, whereas there is no net Cl^- transport under short-circuit conditions in vitro. Na^+ transport is completely suppressed by NaCl loading; the PD may be reversed due to a small, persisting K^+ and H^+ secretion. The cellular mechanism behind the huge change in sodium absorption is a large increase in the Na^+ permeability of the apical membrane of the enterocytes (Bindslev, 1979; Clauss et al., 1987). The Na^+ permeability is characterized by a single channel conductance of four pico-Siemens (Christensen and Bindslev, 1982). The Na^+ transport occurs through a uniform layer of cells with near-identical transport pattern (Holtug et al., 1991). There seems to be little adaptation of the Na-pump located at the basolateral membrane, as the concentration of ouabain-inhibitable Na/K-stimulated ATPase did not increase after NaCl depletion, nor did the activity or histochemical location of the K-paranitrophenylphosphatase (Mayhew et al., 1992). In coprodeum, no transport of nutrients (glucose/amino acids) is measurable, nor can solute-linked water flow be detected in vivo (Rice and Skadhauge, 1982a) or in vitro (Bindslev, 1981).

Colon from birds (domestic fowl and galah) on a low-NaCl diet has a Na-absorbing capacity and other transport characteristics similar to coprodeum, including absence of stimulation of Na^+ transport by hexoses or amino acids. The colonic epithelium is more "leaky" (80−100 Ω × cm^2) than coprodeum and consequently has a lower transmural PD, 15−20 mV in vitro and in vivo. Concomitant with this, solute-linked water absorption can be measured in colon, 16 μL/cm^2 hr in vitro (Bindslev, 1981) and 150 μL H_2O/kg bodyweight × hr in vivo (Rice and Skadhauge, 1982a).

For birds on high-NaCl intake, colonic transport parameters are markedly different from those of coprodeum (Figure 19.9). Rather than being suppressed, Na^+ absorption continues at 5−10 μeq/cm^2 hr, but only when glucose and amino acids are present on the luminal side (Lind et al., 1980a; Clauss et al., 1991; Rice and Skadhauge, 1982b). These nonelectrolytes are now co-transported with Na^+ (Lind et al., 1980b), the transport of which is not inhibited by the Na^+channel blocker amiloride (which totally suppresses Na^+ absorption in both coprodeum and colon from NaCl-depleted birds). NaCl-loading thus induces in the avian colon a switch-over from a Na^+ channel to Na^+/nutrient cotransport. The latter is half-saturated by glucose and amino acid (lysine or leucine) concentrations less than 2 mM; Na^+ absorption will therefore be activated whenever there is chyme in the colon.

19.5.2.1.2 Transport of other ions

K^+ is secreted into coprodeum and colon, as observed in the domestic fowl and the emu in vivo and in the domestic fowl in vitro (see Skadhauge, 1981). Only at high-intraluminal concentrations of K^+ this ion will be absorbed. At concentrations of K^+ typically found in ureteral urine, the net secretion of K^+ from coprodeum and colon is around 10 μmol/kg body weight x hr (Skadhauge and Thomas, 1979). As measured in the Ussing chamber (see survey by Skadhauge, 1993, p.73−74), the net secretion of K^+ in coprodeum and colon is usually around 0.5 mmol/cm^2 hr, less than 5% of the concomitant Na^+ absorption.

Both ammonium and phosphate ions are absorbed from the coprodeum and colon in vivo in the domestic fowl (Skadhauge and Thomas, 1979) and in the emu (Dawson et al., 1985). In both species, higher absorption rates were observed at higher luminal concentrations. H^+ is secreted, presumably by an apical H^+/Na^+ exchanger (see Skadhauge 1993). This secretion leads to an acid microclimate on the mucosal surface (Holtug et al., 1992), though this is also influenced by products of enterocyte metabolism (Laverty et al., 1994). The acid microclimate aids in colonic absorption of SCFA's, particularly propionate (Holtug et al., 1992).

19.5.2.1.3 Quantitative role of coprodeum versus colon

When the absorptive areas and the local transport rates of the two organs are compared, the colon has in all species examined a much higher total capacity. The colon therefore functions as the "work-horse" (Thomas, 1982) for recovery of salt and water from ureteral urine and chyme, whereas coprodeum functions as a final "tuner" of total excretion.

19.5.2.2 Dietary and hormonal regulation of coprodeal and colonic transport

Both the amount of NaCl in the diet, which induces the low/high switch-over of Na-transport, and the time-sequences of that transition have been elucidated in the domestic fowl. No other dietary components have been identified that have a measurable influence on NaCl transport.

Árnason and Skadhauge (1991) provided domestic fowls with six levels of NaCl intake ranging from 0.25 to 25 mmol/kg bodyweight day and observed plasma levels of several hormones (aldosterone, corticosterone, prolactin, and AVT) and the sodium absorption and induced chloride secretion of colon and coprodeum. The low levels of NaCl intake resulted in increasing levels of plasma aldosterone,

and colon and coprodeum absorbed sodium by an amiloride-suppressible mechanism. The highest levels of NaCl intake increased the concentration of prolactin and AVT in plasma. The intake range of 3−6 mmol NaCl/kg bodyweight day presented the least osmoregulatory stress (i.e., being sensed neither as NaCl depletion nor as a NaCl load). Aldosterone was clearly the main inducer of the high rate of Na^+ transport in coprodeum.

As Na^+ intake by chickens is depleted, Na^+ transport and aldosterone levels rise to a new steady state over a week (Thomas and Skadhauge, 1982; Árnason et al., 1986). In contrast, in the opposite protocol, acute resalination (NaCl loading), plasma aldosterone is suppressed in 8 h, and net Na^+ absorption in 24 h (Skadhauge et al., 1983; Árnason et al., 1986). The implication is that absence of aldosterone induces rapid closure of functional apical Na^+ channels.

Aldosterone supplementation during resalination maintained the low-salt pattern of colonic transport (high amiloride-sensitive short-circuit current and low glucose-stimulated short circuit) and prevented expression of sodium/glucose cotransporter (SGLT)-like protein in those tissues (Laverty et al., 2001). Thus, aldosterone suppresses both activity and protein expression of hen colonic SGLT.

Studies with external aldosterone injections reveal, however, that the hormonal (and dietary) regulation of coprodeal Na^+ transport is more complicated. Supramaximal injections of aldosterone over 24 h, the time normally needed to cause a full switch-over of an epithelium to maximal Na^+ transport rate, only induced 10−30% of the net Na^+ transport induced by full adaptation to a low-NaCl diet (Clauss et al. 1984, 1987). If instead the aldosterone was injected during the first 24 h of acute resalination, the sodium absorption was maintained at the high rate characteristic of low-NaCl adapted birds. This effect declined over 3−5 days, when the 24 h aldosterone injection was postponed later and later, to the moderate level of Na^+ transport induced by aldosterone in birds on a chronic high-NaCl intake (Clauss et al., 1984). The reason for this apparent change in sensitivity to aldosterone is a structural change induced by the hormone, entailing an increased number of both enterocytes and apical microvilli on the individual cell (see next section). This enlarges the apical area by 400%. The apparent change in aldosterone sensitivity was not caused by recruitment of aldosterone receptors (Sandor et al., 1989).

The colon of the domestic fowl does not exhibit these delayed transport changes (Clauss et al. 1984, 1991), but this organ does not change apical microvilli with diet. On the other hand, the difference in histologic appearance of colon from salt-marsh versus upland savannah sparrows (Goldstein et al., 1990) is indeed similar to that of coprodeum from high-versus low-salt chickens. The differences seen in characteristics of lower intestinal tissues from hens on low- versus high-salt diets also are largely replicated in two northern species, the rock ptarmigan (*Lagopus mutus*) and the common murre (*Uria aalge*, which possesses salt glands) that naturally ingest low- and high-salt diets, respectively (Árnason et al., 2015). Interspecific variations in colonic function, such as lack of hexose-stimulated transporter activity in *U. aalge* and amino acid cotransporter activity in proximal regions of *L. mutus* colon, may reflect natural histories and diets of the species, or could represent phylogenetic variation in gut properties.

19.5.2.3 Ultrastructural adaptation and molecular induction

Continued NaCl depletion induces in white Plymouth Rock chickens a very late effect: a structural change of the individual epithelial cells (Figure 19.11) as well as of the entire organ. This was investigated by tandem measurements of coprodeal ultrastructure and sodium transport (amiloride-suppressible short-circuit current) in vivo (Mayhew et al., 1990). The high aldosterone/low NaCl diet involves modulations of the level of mRNA that codes either for the Na-channel or a post-transcriptional regulator of the channel, since the mRNA from low-NaCl but not high-NaCl diet coprodeum expresses an amiloride-suppressible Na^+ uptake after injection into *Xenopus* oocytes (Asher et al., 1992). The microvillous surface area increased in birds chronically exposed to the low-NaCl diet, from 32 to 49 μm^2/cell without changing cell size (Figure 19.11), and the total cell number per organ increased from 270 to 420 million. The total effect was a 135% rise in apical area (Elbrønd et al., 1991; Mayhew et al., 1992). Supramaximal doses of aldosterone injected over 2−6 days also induced a substantial increase of the microvillous surface area (Elbrønd et al., 1993). This enlargement of apical area occurred more rapidly than the rate of cell turnover, and hence involved remodeling of the existing cell population (Elbrønd et al., 1993). The late effect of aldosterone to increase cell number then leads to synthesis of cells with near identical sodium transport capacity, as demonstrated by uniform histochemical localization of Na/K ATPase activity (Mayhew et al., 1992), by immunochemical localization of the amiloride-sensitive Na^+ channel (Smith et al., 1993), and by measurements of the local Na^+ transport rates by the vibrating microprobe technique (Holtug et al., 1991). The basolateral membrane area did not change significantly per individual cell following chronic NaCl depletion (Mayhew et al., 1992).

19.5.2.4 Salt and water transport in the caeca

The paired caeca are of variable size; large caeca are typically associated with herbivory and granivory (McLelland, 1989). In vivo perfusion studies in the domestic fowl demonstrate substantial absorption of NaCl and

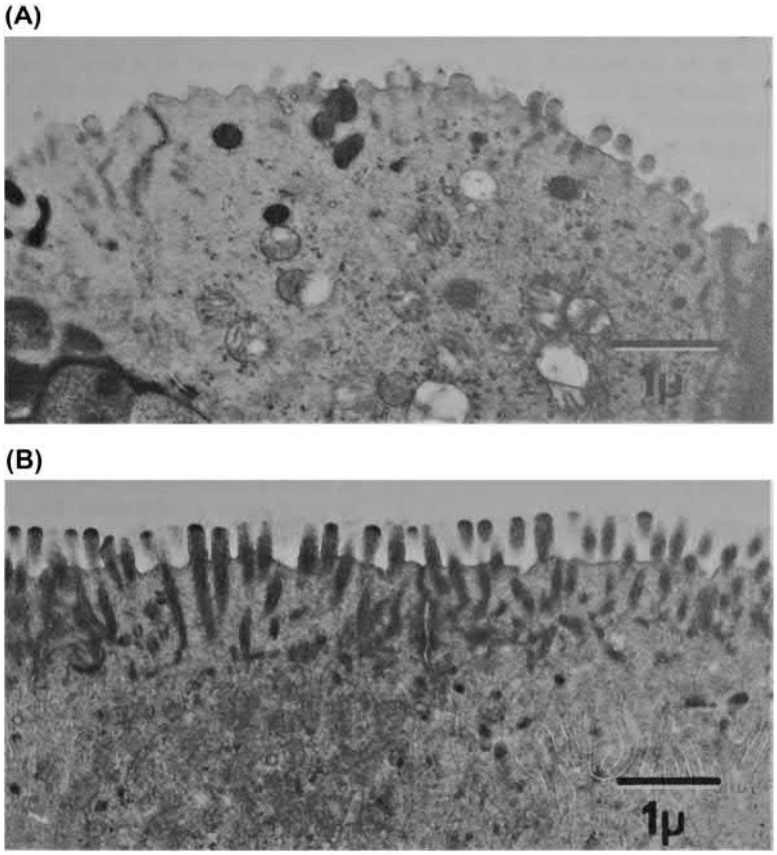

FIGURE 19.11 Transmission electron micrographs of the apical region of coprodeal epithelial cells from chickens eating either (A) a high-NaCl diet or (B) a low-NaCl diet. Note the differences in height and density of apical microvilli, providing the low-NaCl birds with a substantially enhanced absorptive surface area. *Photograph courtesy of Dr. Vibeke Elbrønd.*

water, and secretion of K^+. The Na^+ absorption is stimulated by acetate; NaCl absorption is enhanced by luminal glucose and stimulated by aldosterone (Rice and Skadhauge, 1982c; Thomas and Skadhauge, 1989a). Anatomically the caecum in the chicken has a large end (the bulbus) and a narrow neck region (see Dantzer, 1989). The bulbus had higher transport rates of both Na^+ and amino acids than the neck region (Thomas and Skadhauge, 1989b).

19.5.3 Postrenal modification of ureteral urine

19.5.3.1 Basic patterns: Hydration/NaCl loading

The interplay of kidney and cloaca depends on flow rate and ionic and osmotic concentration of ureteral urine in relation to the transport capacities of the epithelia of the lower gut. The osmotic permeability coefficient and the sodium transport rate are most important, since these parameters determine the net rates of absorption/secretion in the parts of the lower gut in which urine is stored (or flows through). One would expect the fractional effect of cloacal storage to be limited if the flow rate of ureteral urine is high. This would apply both to water reabsorption in the hydrated state and for NaCl absorption during NaCl loading. In the domestic fowl (see Skadhauge, 1973), consideration of all relevant parameters, including the resulting osmolality and Na^+ concentration of the contents of the lower gut, permits calculation that only about 2% of ureterally excreted water and NaCl will be reabsorbed in the hydrated and salt loaded state, respectively. Cloacal storage little modifies the excretory function of the kidney in these functional states. In contrast, substantial modification of urine (particularly reabsorption of NaCl) occurred in the starling even during brisk urine flow induced by mannitol diuresis (Laverty and Wideman, 1989); the transport properties of the lower intestine of this species are unstudied.

19.5.3.2 Basic patterns: Dehydration/NaCl depletion

Quantitative studies of flow rate and composition of ureteral urine of dehydrated birds, and the transport parameters of coprodeum and colon, have been carried out in three species of seed-eating land birds, the domestic fowl, the galah, and the house sparrow (*Passer domesticus*). The values obtained on the fowl and the galah have been treated by a computer simulation of the retrograde flow into the

cloaca and the integrated effect on salt and water transport (Skadhauge and Kristensen, 1972; Skadhauge, 1973). The result obtained is that 10–20% of ureterally excreted water, and 70% of Na^+, is absorbed in the cloaca of both species. This occurs in the galah despite its higher urine osmolality because of a counteracting higher rate of solute-linked water flow and lower osmotic permeability coefficient (Skadhauge, 1981). The house sparrow (Goldstein and Braun, 1988) and the budgerigar (Krag and Skadhauge, 1972) seem to have a similar interaction of cloacal recovery of NaCl and water, though in the house sparrow, the transport properties of the colon more closely parallel those of hen coprodeum (Goldstein, 1993a).

The relevance of the computer calculations has received independent support from two sources. First, slow perfusion experiments of coprodeum/colon in the domestic fowl with fluids simulating ureteral urine in the dehydrated state have demonstrated net water absorption from liquids up to 200 moM higher than plasma osmolality. Second, the computer simulation (Skadhauge, 1973) resulted in near-identical absorption rates as calculated from a detailed study with and without exteriorization of the ureters (Dicker and Haslam, 1972).

In only one study, (Skadhauge and Thomas, 1979) has the cloacal fractional absorption of K^+, NH_4^+, and PO_4 been quantitatively assessed. In the domestic fowl, it was shown that the cloaca changes the ureteral output by an additional secretion of 20% of K^+, and absorption of 8% of NH_4^+, and 2% of PO_4. Thus the cloaca seems to assist significantly in secretion of K^+, but storage in that organ has minor effect on NH_4^+ and PO_4 transport.

19.5.3.3 Special case: birds with salt glands

Schmidt-Nielsen et al. (1963) suggested that birds with salt glands might maintain high rates of intestinal salt and water reabsorption during times of substantial NaCl intake, routing the NaCl to the salt glands for excretion and thereby retrieving free water. Examinations of this problem have focused on two species, the domestic duck and the glaucous-winged gull. In both species, Na^+ uptake in the small intestine remained undiminished during saline acclimation (Hughes and Roberts, 1988). In the hindguts of the two species, the colon carries the majority of NaCl absorption and solute-linked water flow, with coprodeum being of minor size and with lower transport capacity per cm^2 serosal area. Even during salt loading, continued urine flow is necessary to maintain nitrogen excretion, and at least in ducks urine apparently continues to enter the rectum and even the ceca in saline acclimated birds (Hughes and Raveendran, 1994). Colons of both species uphold high NaCl absorption rates in the salt-loaded state (Skadhauge et al., 1984a; Goldstein et al., 1986); any NaCl that is excreted by the kidney may therefore be reabsorbed with water postrenally and finally secreted by the salt gland, thereby leaving a volume of "free water." This system operates in the duck to save approximately 0.5 mL water/kg body mass hr (Skadhauge et al., 1984a), but, because of the gull's small lower intestine and relatively low urinary NaCl concentrations, its contribution is likely minor in this species (Goldstein et al., 1986).

19.5.3.4 Special case: the ratites

In the large, flightless ratite birds, the weight of the gut and its contents is not as critical as in flying species, liberating the lower gut to take on additional functions. In the ostrich (Skadhauge et al., 1984b), the colon of the adult male is more than 10 m long and functions as a fermentation chamber, with SCFA concentrations up to 120 mmol. To a minor extent, this is paralleled by the rhea, *Rhea americana*. In both ostrich (Skadhauge et al., 1984b) and rhea (Skadhauge et al., 1993), renal concentrating ability is approximately 800 mmol/kg, but the role of the lower intestine in postrenal modification of urine appears to differ. The ostrich has a strong sphincter between coprodeum and terminal colon, and no influx of urine into colon has been observed (Skadhauge, 1983). No feces is stored in the coprodeum, which therefore functions similar to a mammalian bladder (urine storage without modification) in this species. The transport properties of the coprodeal wall have not been measured in the ostrich. The dorsal diverticulum from the proctodeum of the rhea does contain ureteral urine and is lined by a single layer of cuboidal cells with possible reabsorptive capacity (Skadhauge et al., 1993; Elbrønd et al., 2009). However, the small size of this diverticulum relegates its possible functional role to minor importance.

In contrast to these species, the emu, *Dromaius novaehollandiae*, has a conventional, small coprodeum/colon where little fermentation occurs. The dehydrated emu has a low urine-to-plasma ratio of osmolality (1.4) and a fairly high urine flow rate. To compensate, the absorption capacity of coprodeum/colon is high, resulting from extensive mucosal folding (Skadhauge et al., 1991). The cassowary (*Casuarius casuarius*) has a macroscopic anatomy of coprodeum/colon similar to that of the emu (Skadhauge et al., 1993).

19.5.3.5 Quantitative role of the caeca in osmoregulation

The main function of caeca in avian physiology is nutritional, as these organs, when present and large, take part in the digestion of fine particulate matter, food fiber, and the production of SCFA (see reviews in Braun and Duke, 1989). Furthermore, conservation of nitrogen by bacterial metabolism of uric acid of ureteral origin is possible

(Braun, 1993). Large fractions of intestinal and ureteral water and solutes move together with solids of small particle size into the caeca by peristalsis and antiperistalsis in the ileum and colon, respectively (see Skadhauge, 1981, chapter 3). Quantitative studies of caecal function (see Skadhauge, 1981), based on inflow studies of unabsorbable water markers from either ureteral urine or after oral ingestion, suggest inflow rates of about 20% from both sources. In the domestic fowl, the simple (serosal) surface area of the ceca is similar to that of coprodeum and colon, but the Na^+ and water transport rates per unit body mass are approximately threefold higher (Thomas and Skadhauge, 1989b). The transport capacity for NaCl and water reabsorption from chymus and urine is therefore large, perhaps larger than colon plus coprodeum. The quantitative rate of caecal water absorption has been estimated from 5% to 38% of body weight per day. Despite this, ligation of the ceca may have little overall effect on osmoregulation [Skadhauge, 1981 p38, and others (see Braun and Duke, 1989)], probably because of compensation by other organs (Hughes et al., 1992). The contribution of the ceca may become essential only during the combined stress of poor feeding and salt and water depletion (Thomas, 1982; Thomas and Skadhauge, 1989b).

19.5.3.6 Overall: integration of kidneys and lower intestine

The excretion of waste nitrogen as relatively nontoxic uric acid may have evolved in association with development within the closed system of the shelled egg. However, as a consequence, birds risk loss of substantial energy, protein, and nitrogen associated with urinary uric acid. Retrograde movement of urine into the lower intestine may serve a critical role in conserving those metabolites. At the same time, avian kidneys elaborate a urine that can be two or more times the concentration of the plasma, and movement of that urine into the intestinal system could undo the osmotic work of the kidneys. Nevertheless, the transport properties of the lower intestines are such that even during times of urine concentration, the gut is able to effect a net conservation of water and electrolytes. Overlain on all of these systems is the ability of birds to regulate lower intestinal motility (Brummermann and Braun, 1995) such that exposure of urine to the transporting and nontransporting regions of the lower intestine may be adjusted to meet the changing physiological demands of nutrition and osmoregulation. The mechanisms of that coupling have received just preliminary investigation (Vranish and Braun, 2011). All together, the kidneys and lower intestine constitute a system with apparent redundancies and inefficiencies but that confers homeostatic capabilities over a wide diversity of habitats and diets.

19.6 Salt glands

Although the presence of supraorbital glands in marine birds was known for many years, it was not until 1958 that their salt-secreting function was defined (Schmidt-Nielsen et al., 1958). Functional salt glands exist in approximately 10 orders of birds, including all those with marine representatives and at least two orders of terrestrial birds (several falconiformes (Cade and Greenwald, 1966) and the roadrunner [*Geococcyx californianus*, order Cuculiformes; Ohmart, 1972)]. Within related groups, glands are larger in species exposed to hypersaline food and water; thus, marine species have larger glands than coastal or terrestrial birds (Staaland, 1967; Gutiérrez et al., 2012).

19.6.1 Anatomy

The salt glands, which constitute from 0.1 to 2% of body mass, are located in depressions usually in or above the orbits (e.g., Schmidt-Nielsen, 1959; Siegel-Causey, 1990, Figure 19.12). They are distinct from lacrimal or Harderian glands. The basic structural unit of the salt gland, the lobe, consists of blind-ended secretory acini (tubules) which drain into central ducts (canals). Toward the blind end of the tubule are small, relatively undifferentiated peripheral cells, whereas most of the length of the secretory tubules is composed of principal secretory cells (Ernst and Ellis, 1969). Capillary blood flow runs counter to flow in the secretory tubules. Each gland contains numerous lobes

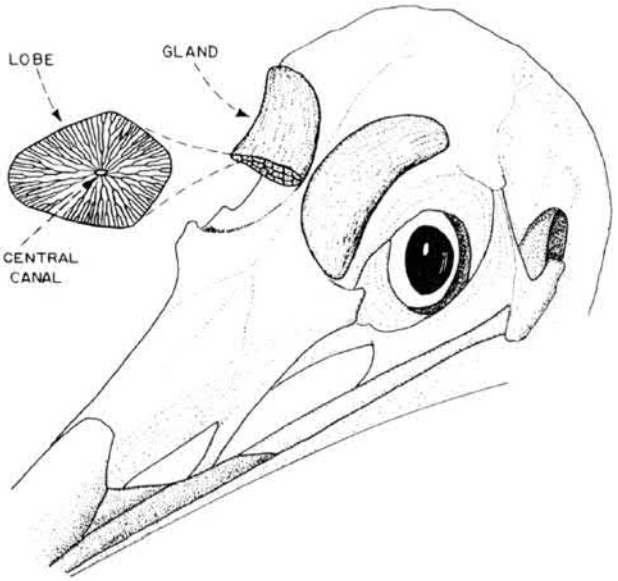

FIGURE 19.12 The supraorbital salt gland of the herring gull. Branching secretory tubules are arranged radially around the central canal. *Reproduced with permission from Schmidt-Nielsen (1960).*

whose final common ducts drain into the nasal cavity. Salt gland secretion either drips from or is shaken from the bird's beak.

Acclimation of a bird to increasing salt intake typically induces growth of the salt gland (Guttiérez et al., 2012; but see Rocha et al., 2016), accompanied by an enhanced secretory capacity. Growth of the secretory tubules includes cell hypertrophy and hyperplasia, increased membrane folding and mitochondrial density, and enhanced activity of several cellular enzymes, including Na/K ATPase, the enzyme responsible for establishing the ion gradients that drive secretion (Holmes and Phillips, 1985).

The main innervation to the salt glands is from the VIIth cranial nerve, a branch of which enters the secretory nerve ganglion near the orbit (Ash et al., 1969). Postganglionic parasympathetic fibers, which may release both acetylcholine and vasoactive intestinal peptide (VIP), then ramify through the gland, with terminals on both secretory cells and blood vessels. The blood vessels and tubules also receive adrenergic input from neurons likely running both in the walls of arteries and through the secretory nerve ganglion (Peaker and Linzell, 1975; Gerstberger, 1991).

19.6.2 Function

19.6.2.1 Stimulus for secretion

Secretion by the salt glands may be initiated by stimulation of either central or peripheral receptors. The central receptors appear to be osmoreceptors in the region of the third cerebral ventricle, with a responsiveness to the Na^+ (or other cation) concentration, not just to total osmotic concentration (Gerstberger et al., 1984).

Peripheral osmoreceptors, which are located in the vicinity of the heart and large arteries nearby, communicate with the central nervous system via the vagus nerve, the severing of which eliminates salt gland responsiveness to systemic salt loading (Hanwell et al., 1972). There are also reports of salt gland secretion during dehydration (e.g., Stewart, 1972), when ECF volume would be reduced but osmolality increased.

Numerous experiments also point to an important role for systemic volume receptors. In some species (mallard ducks, but not glaucous-winged gulls; Hughes, 1989a, b), isosmotic expansion of the ECF is sufficient to stimulate salt gland secretion. Moreover, a rise in extracellular Na^+ concentration without a rise in ECF volume may be insufficient to initiate secretion (Ruch and Hughes, 1975; Hughes, 1989b); volume and osmolality act in concert to jointly achieve a threshold for secretion (Hammel, 1989). Some evidence suggests that the ECF receptors occur not in the vasculature, but in the interstitial space (Hammel et al., 1980).

It is likely that variation in experimental results, including differing importance of volume and osmolality as stimuli for salt gland secretion, relates to variation among species. The most detailed experimental work in this field has been done using domestic ducks, descendants of wild mallards. These birds are never exposed to seawater in their natural habitat, and they are quite intolerant of saline (Schmidt-Nielsen and Kim, 1964). Studies of birds more highly adapted to saline may yield different results (Hughes, 1989b).

19.6.2.2 Secretion mechanism and fluid composition

The fluid produced by avian salt glands is typically nearly pure NaCl, with trace concentrations of K^+, HCO_3^-, Ca^{++}, and Mg^{++} (though K^+ concentrations up to 100 mM and Ca^{++} concentrations up to 50 mM may occur in some situations; Hughes, 1970b; Cade and Greenwald, 1966). The concentration of NaCl in the secretion varies among species from approximately 500 to 1000 mM (see Skadhauge, 1981, Cpt. 7), being more concentrated in species with higher salt intakes, such as those which eat marine invertebrates.

The cellular mechanism of secretion by salt gland principal cells is difficult to study in situ because of the complex anatomy of the tubules and their encasement in connective tissue. Knowledge of this process has therefore come from a variety of in vitro approaches, including studies of tissue slices, isolated dispersed cells (Shuttleworth and Thompson, 1989), and cell culture (Lowy et al., 1989). These studies collectively have suggested a model of secondary active Cl^- transport. In this model (Figure 19.13), a basolateral ouabain-sensitive Na/K ATPase establishes an inwardly directed Na^+ gradient. This gradient provides the energy for furosemide-sensitive inward transport of $Na^+/K^+/2Cl^-$, also across the basolateral membrane. Cl^- then passes down its electrochemical gradient through (putative) apical Cl^- channels into the tubule lumen. The resulting trans-tubule electrical potential (inwardly negative) provides the driving force for passive peritubular Na^+ transport. Activation of secretion also entails a brief intracellular acidification which is compensated for by a HCO_3^--dependent alkalinization as secretion is sustained (Shuttleworth and Wood, 1992). Activation of secretion can be stimulated via either of two intracellular second messenger systems, phosphatidyl inositol/Ca^+ [linked to stimulation of muscarinic acetylcholine receptors (Snider et al., 1986; Hildebrandt and Shuttleworth, 1993)] or cyclic AMP [linked to β-adrenergic stimulation or VIP (Lowy and Ernst, 1987; Lowy et al., 1987)].

These two signaling pathways apparently occur in the same cells and interact to effect appropriate responses to stimulation (Krohn and Hildebrandt, 2004).

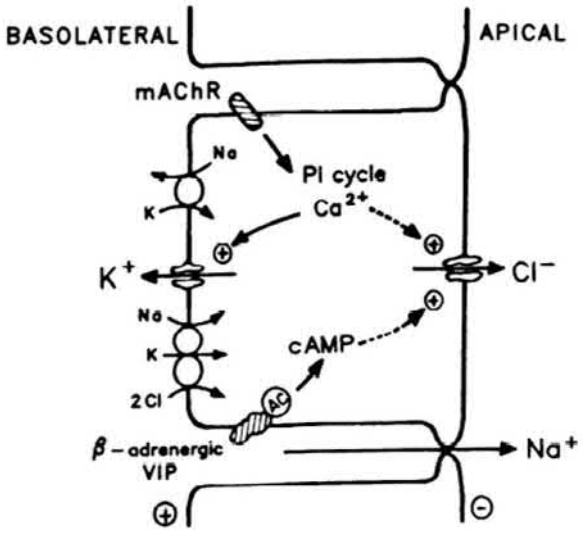

FIGURE 19.13 Proposed mechanisms of secretion by principal secretory cells in the avian salt gland. *Reproduced, with permission, from Lowy (1989).*

The concentration of the solution as elaborated by the cells lining the secretory tubules is unknown, and a variety of mechanisms have been proposed for attaining the final concentration of secreted fluid. Marshall et al. (1985) proposed that tubular cells secrete an isotonic fluid that is concentrated by the subsequent withdrawal of water along the ducts. With a final secretion rate as high as 10% of gland blood flow rate, secretion of virtually the entire plasma would be initially required. Other theories (see Holmes and Phillips, 1985; Butler et al., 1989; Gerstberger and Gray, 1993) suggest instead that the hypertonicity is generated within the tubules themselves, potentially with subsequent dilution in the ducts via osmotic water flow through aquaporins (AQP5?; Mueller et al., 2006). In various studies, the concentration of secreted fluid either increases, decreases, or does not change with the rate of secretion, and so this relationship does little to help clarify the concentrating mechanism.

Adequate secretion by the salt glands requires adequate blood flow, and this increases more than 10-fold during active secretion (Hanwell et al., 1971; Kaul et al., 1983). Over a wide range of blood flow and secretion rates, the salt glands extract a relatively constant fraction (between 15% and 20% in the Pekin duck) of the NaCl passing through the gland (Kaul et al., 1983).

19.6.2.3 Regulatory mediators

Stimulation of salt gland secretion is activated by the parasympathetic nervous system (Fänge et al., 1958) acting through muscarinic receptors for acetylcholine and independent receptors for VIP (Gerstberger, 1988). These mediators activate the principle cell secretory mechanism as well as vasodilation and enhanced blood flow (see Butler et al., 1989; Gerstberger, 1991). Secretion is inhibited by anesthesia or disturbance, at least in part via sympathetically mediated vasoconstriction.

The only hormone that directly stimulates secretion is ANP, which activates the gland via high-affinity receptors (Schütz and Gerstberger, 1990; Gerstberger, 1991). A substantial literature did suggest a role for corticosterone, but following adrenalectomy, maintenance of normal fluid balance through saline drinking water and adequate feeding restores salt gland function even in the absence of corticosterone (Butler, 1987).

Angiotensin II also may have a direct influence on salt gland secretion, though in this case inhibitory. The hormone acts by stimulating centrally mediated vasoconstriction of salt gland blood vessels (Gerstberger et al., 1984; Butler et al., 1989, 1999) and is independent of a role for catecholamines (Butler, 1999, 2007; Heinz and Gray, 2001). Peripherally produced angiotensin may be able to cross the blood brain barrier and activate these central responses.

19.6.3 Contribution of the salt glands to osmoregulation

The quantitative contribution of the salt glands relative to the kidneys has been evaluated in a few species (Skadhauge, 1981, Cpt. 7, Hughes, 2003). During conditions that stimulate the salt glands (salt loading or dehydration), typically $> 75\%$ of excreted Na^+ is lost via the salt glands. However, the division of water loss between salt glands and kidneys depends of the water load; during a copious saline load, the two organs may be equally responsible for water excretion, whereas during dehydration, the renal losses of water may be substantially reduced. The salt glands also may eliminate more than one third of excreted K^+ following a salt load, despite the relatively low concentration of K^+ in salt gland fluid. These generalizations derive from relatively few studies conducted over short experimental time spans; the relative roles of the organs under natural conditions undoubtedly reflect dietary intakes of salts and water and must vary considerably over time. For example, the spontaneous salt gland secretions of Pekin ducks varied with, and nearly matched, the NaCl concentration of their drinking water (Hughes et al., 1992).

19.7 Evaporative water loss

Evaporative losses of water from the respiratory tract and the skin constitute an important component of avian water balance. Rates of evaporation increase with body mass and with the thermoregulatory demand for evaporative heat loss (Gavrilov and Gavrilov, 2019).

Respiratory water loss is an inevitable consequence of the high rates of ventilation demanded by endothermy. It has long

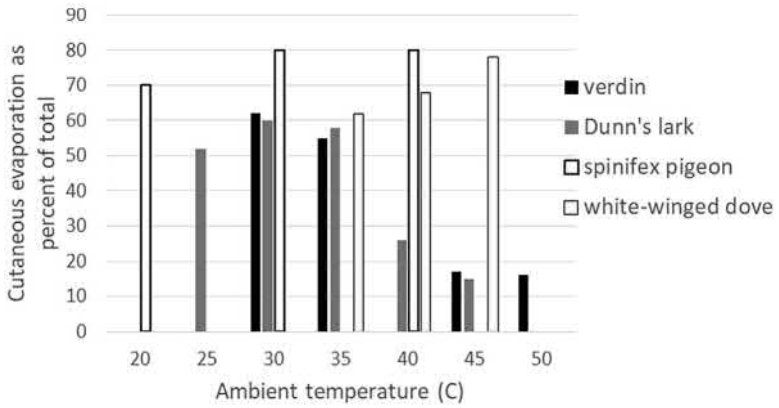

FIGURE 19.14 Relative contribution of cutaneous evaporation to total evaporative water loss in two passerine species (*darker bars*) and two columbiform species (*lighter bars*). Note that cutaneous evaporation diminishes in importance at higher temperatures in the former species but increases in the latter. *Data for verdin and spinifex pigeon from Wolf and Walsberg (1996); for Dunn's lark from Tieleman and Williams (2002); and for heat-acclimated white-winged doves from McKechnie and Wolf (2004).*

been appreciated that birds modulate respiratory evaporation, e.g., by panting or gular flutter, as a means of defending body temperature in the heat, and in many avian orders the majority of evaporative heat (and water) loss at high temperatures derives from respiratory surfaces (Dawson, 1982; Wolf and Walsberg, 1996; O'Connor et al., 2017).

In other avian groups, despite birds' lack of sweat glands, equally effective evaporative heat dissipation can be achieved across cutaneous surfaces (Wolf and Walsberg, 1996; McKechnie et al., 2016). In a number of species, the cutaneous resistance to diffusion of water vapor decreases markedly at elevated ambient temperatures, thereby enhancing evaporative heat loss (e.g., Marder and Ben-Asher, 1983; Webster and Bernstein, 1987; Withers and Williams, 1990; Wolf and Walsberg, 1996). The composition and physical state of lipids in the stratum corneum of the skin may be a major determinant of the resistance to evaporative water loss (Champagne et al., 2015) and can vary both intra- (Munoz-Garcia et al., 2008; Champagne et al., 2016) and interspecifically (Haugen et al., 2003; Ro and Williams, 2010). Thermally induced changes to those lipids might underlie increases in cutaneous evaporation. Adrenergically mediated increases to cutaneous blood flow (Marder and Raber, 1989) also may contribute to regulation of cutaneous water loss.

Evaporation typically accounts for approximately 50% of total water loss in a variety of species given unlimited water in the laboratory (summarized in Skadhauge, 1981, Chapter 4). That may rise to 80% during dehydration, when excretory water losses are minimized (Skadhauge, 1981). It does appear that the magnitude of evaporative water loss can be modulated in response to hydric conditions. For example, dehydrated birds may reduce evaporation via respiration (Crawford and Schmidt-Nielsen, 1967) or the skin (Arad et al., 1987), and budgerigars (*Melopsittacus undulatus*) can maintain constant EWL in the face of varying relative humidities (Eto et al., 2017). The mechanisms of those regulated changes are not described (Figure 19.14).

For a discussion of the role of evaporative water loss in thermoregulation, the reader should consult Chapter x (Table 19.5).

Acknowledgments

This chapter is dedicated to Erik Skadhauge, who coauthored a previous edition of this chapter and who contributed so much to the field of avian osmoregulation; to Maryanne Hughes, who took joy in unraveling the mechanisms of salt and water regulation; and to Eldon Braun, whose unending fascination with the physiology of birds has been inspiring.

References

Akester, A.R., 1967. Renal portal shunts in the kidney of the domestic fowl. J. Anat. 101, 569–594.

Aman, N.A., Nagarajan, G., Kang, S.W., Hancock, M., Kuenzel, W.J., 2016. Differential responses of the vasotocin 1a receptor (V1aR) and osmoreceptors to immobilization and osmotic stress in sensory circumventricular organs of the chicken (*Gallus gallus*) brain. Brain Res. 1649, 67–78.

Ames, E., Steven, K., Skadhauge, E., 1971. Effects of arginine vasotocin on renal excretion of Na+, K+, Cl-, and urea in the hydrated chicken. Am. J. Physiol. 221, 1223–1228.

Anderson, G.L., Braun, E.J., 1985. Postrenal modification of urine in birds. Am. J. Physiol. 248, R93–R98.

Anderson, R.S., 1967. Acid-base changes in the excreta of the laying hen. Vet. Rec. 30, 314–315.

Arad, Z., Chadwick, A., Rice, G.E., Skadhauge, E., 1986. Osmotic stimuli and NaCl-intake in the fowl; release of arginine vasotocin and prolactin. J. Comp. Physiol. B 156, 399–406.

Arad, Z., Gavrieli-Levin, I., Eylath, U., Marder, J., 1987. Effect of dehydration on cutaneous water evaporation in heat exposed pigeons *Columba livia*. Physiol. Zool. 60, 623–630.

Árnason, S.S., Elbrønd, V.S., Laverty, G., 2015. Transport characteristics and morphology of the colon and coprodeum in two wild birds of different habitats, the rock ptarmigan (Lagopus mutus) and the common murre (Uria aalge). Comp. Biochem. Physiol., A 187, 86–96.

Árnason, S.S., Skadhauge, E., 1991. Steady-state sodium absorption and chloride secretion of colon and coprodeum, and plasma levels of osmoregulatory hormones in hens in relation to sodium intake. J. Comp. Physiol. B 161, 1–14.

Árnason, S.S., Rice, G.E., Chadwick, A., Skadhauge, E., 1986. Plasma levels of arginine vasotocin, prolactin, aldosterone and corticosterone during prolonged dehydration in the domestic fowl: effect of dietary NaCl. J. Comp. Physiol. B 156, 383–397.

Ash, R.W., Pearce, J.W., Silver, A., 1969. An investigation of the nerve supply to the salt gland of the duck. Q. J. Exp. Physiol. 54, 281–295.

Asher, C., Singer, D., Eren, R., Yeger, O., Dascal, N., Garty, H., 1992. NaCl-dependent expression of amiloride-blockable Na+ channel in Xenopus oocytes. Am. J. Physiol. 262, G244–G248.

Barceló, G., Salinas, J., Sabat, P., 2012. Body mass, phylogeny and diet composition affects kidney morphology in passerine birds. J Morphol 273, 842–849.

Bartholomew, G.A., 1972. The water economy of seed-eating birds that survive without drinking. In: Proceedings of the XVth International Ornithological Congress, pp. 237–254.

Bartholomew, G.A., Cade, T.J., 1963. The water economy of land birds. Auk 80, 504–539.

Bataille, A.M., Goldmeyer, J., Renfro, J.L., 2008. Avian renal proximal tubule epithelium urate secretion is mediated by Mrp4. Am. J. Physiol. 295, R2024–R2033.

Belay, T., Bartels, K.E., Wiernusz, C.J., Teeter, R.G., 1993. A detailed colostomy procedure and its application to quantify water and nitrogen balance and urine contribution to thermobalance in broilers exposed to thermoneutral and heat-distressed environments. Poultry Sci. 72, 106–115.

Bennett, D.C., Hughes, M.R., 2003. Comparison of renal and salt gland function in three species of wild ducks. J. Exp. Biol. 206, 3273–3284.

Bindslev, N., 1979. Sodium transport in the hen lower intestine. Induction of sodium sites in the brush border by a low sodium diet. J. Physiol. 288, 449–466.

Bindslev, N., 1981. Water and NaCl transport in the hen lower intestine during dehydration. In: Ussing, H.H., Bindslev, N., Lassen, N.A., Sten-Knudsen, O. (Eds.), "Water Transport across Epithelia", Alfred Benzon Symposium 15. Munkdsgaard, Copenhagen, pp. 468–481, 1981.

Boykin, S.L.B., Braun, E.J., 1993. Entry of nephrons into the collecting duct network of the avian kidney: a comparison of chickens and desert quail. J. Morphol. 216, 259–269.

Braun, E.J., 1978. Renal response of the starling (*Sturnus vulgaris*) to an intravenous salt load. Am. J. Physiol. 231, 1111–1118.

Braun, E.J., 1993. Renal function in birds. In: Brown, J.A., Balment, R.J., Rankin, J.C. (Eds.), New Insights in Vertebrate Kidney Function. Cambridge University Press, Cambridge, United Kingdom, pp. 167–188.

Braun, E.J., Dantzler, W.H., 1972. Function of mammalian-type and reptilian type nephrons in kidney of desert quail. Am. J. Physiol. 222 (3), 617–629.

Braun, E.J., Dantzler, W.H., 1974. Effects of ADH on single nephron glomerular filtration rates in the avian kidney. Am. J. Physiol. 226, 1–12.

Braun, E.J., Dantzler, W.H., 1987. Mechanisms of hormone actions on renal function. In: Pang, P.K.T., Schreibman, M.P. (Eds.), Vertebrate Endocrinology: Fundamentals and Biomedical Implications, Regulation of Water and Electrolytes, vol. 2. Academic Press, San Diego, CA, USA, pp. 189–210.

Function of the avian cecum. In: Braun, E.J., Duke, G.E. (Eds.), J. Exp. Biol. S3 1–130.

Braun, E.J., Reimer, P.R., 1988. Structure of avian loop of Henle as related to countercurrent multiplier system. Am. J. Physiol. 255, F500–F512.

Brokl, O.H., Braun, E.J., Dantzler, W.H., 1994. Transport of PAH, urate, TEA, and fluid by isolated perfused and nonperfused avian renal proximal tubules. AJP (Am. J. Physiol.) 266, R1085–R1094.

Brummermann, M., Braun, E.J., 1995. Effect of salt and water balance on colonic motility of white leghorn roosters. Am. J. Physiol. 268, R690–R698.

Burrows, M.E., Braun, E.J., Piper Duckles, S., 1983. Avian renal portal valve: a reexamination of its innervation. AJP (Am. J. Physiol.) 245, H629–H634.

Butler, D.G., 1987. Adrenalectomy fails to block salt gland secretion in Pekin ducks (Anas playrhynchos) preadapted to 0.9% saline drinking water. Gen. Comp. Endocrinol. 16, 171–181.

Butler, D.G., 1999. Mecamylamine blocks the [Asp1,Val5] -ANG II-induced attenuation of salt gland activity in Pekin ducks. Am. J. Physiol. 277, R836–R842.

Butler, D.G., 2007. ANG II-induced attenuation of salt gland function in Pekin ducks is not catecholamine-dependent. J. Comp. Physiol. B 177, 733–742.

Butler, D.G., Siwanowicz, H., Puskas, D., 1989. In: Hughes, M.R., Chadwick, A. (Eds.), Progress in Avian Osmoregulation. Leeds Philosophical and Literary Society, Leeds, United Kingdom, pp. 127–141.

Cade, T.J., Greenwald, L., 1966. Nasal salt secretion in falconiform birds. Condor 68, 338–350.

Casotti, G., Beuchat, C.A., Braun, E.J., 1998. Morphology of the kidney in a nectarivorous bird, the Anna's hummingbird *Calypte anna*. J. Zool. 244, 175±184.

Casotti, G., Braun, E.J., 1996. Functional morphology of the glomerular filtration barrier of *Gallus gallus*. J. Morphol. 228, 327–334.

Casotti, G., Braun, E.J., 2004. Protein location and elemental composition of urine spheres in different avian species. J. Exp. Zool. 301A, 579–587.

Casotti, G., Richardson, K.C., 1992. A stereological analysis of kidney structure of honeyeater birds (Meliphagidae) inhabiting either arid or wet environments. J. Anat. 180, 281–288.

Casotti, G., Richardson, K.C., 1993. A qualitative analysis of the kidney structure of Meliphagid honeyeaters from wet and arid environments. J. Anat. 182, 239–247.

Champagne, A.M., Allen, H.C., Williams, J.B., 2015. Lipid composition and molecular interactions change with depth in the avian stratum corneum to regulate cutaneous water loss. J. Exp. Biol. 218, 3032–3041.

Champagne, A.M., Allen, H.C., Bautista-Jimenez, R.C., Williams, J.B., 2016. Organization of lipids in avian stratum corneum: changes with temperature and hydration. Chem. Phys. Lipids 195, 47–57.

Chen, L., Lee, J.W., Chou, C.L., et al., 2017. Transcriptomes of major renal collecting duct cell types in mouse identified by single-cell RNA-seq. Proc. Natl. Acad. Sci. U.S.A. 114, E9989–E9998.

Chin, T.Y., Quebbemann, A.J., 1978. Quantitation of renal uric acid synthesis in the chicken. Am. J. Physiol. 234, F446.

Choshniak, I., Munck, B.G., Skadhauge, E., 1977. Sodium chloride transport across the chicken coprodeum. Basic characteristics and dependence on sodium chloride intake. J. Physiol. 271, 489–504.

Christensen, O., Bindslev, N., 1982. Fluctuation analysis of short-circuit current in a warm-blooded sodium-retaining epithelium: site current, density, and interaction with triamterene. J. Memb.Biol. 65, 19–30.

Clark, N.B., Mok, L.L.S., 1986. Renal excretion in gull chicks: effect of parathyroid hormone and calcium loading. Am. J. Physiol. 250, R41–R50.

Clark, N.B., Sasayama, Y., 1981. The role of parathyroid hormone on renal excretion of calcium and phosphate in the Japanese quail. Gen. Comp. Endocrinol. 45, 234–241.

Clark, N.B., Wideman, R.F., 1977. Renal excretion of phosphate and calcium in parathyroidectomized starlings. Am. J. Physiol. 233, F138–F144.

Clark, N.B., Wideman Jr., R.F., 1980. Calcitonin stimulation of urine flow and sodium excretion in the starling. Am. J. Physiol. 238, R406–R412.

Clark, N.B., Wideman Jr., R.F., 1989. Actions of parathyroid hormone and calcitonin in avian osmoregulation. In: Hughes, M.R., Chadwick, A. (Eds.), Progress in Avian Osmoregulation. Leeds Philosophical and Literary Society (Scientific Section), Leeds, United Kingdom.

Clark, N.B., Braun, E.J., Wideman, R.F., 1976. Parathyroid hormone and renal excretion of phosphate and calcium in normal starlings. Am. J. Physiol. 231, 1152–1158.

Clauss, W., Árnason, S.S., Munck, B.G., Skadhauge, E., 1984. Aldosterone-induced sodium transport in lower intestine. Effects of varying Nacl intake. Pflügers Archiv 401, 354–360.

Clauss, W., Dürr, J.E., Guth, D., Skadhauge, E., 1987. Effects of adrenal steroids on Na transport in the lower intestine (coprodeum) of the hen. J. Memb. Biol. 96, 141–152.

Clauss, W., Dantzer, V., Skadhauge, E., 1991. Aldosterone modulates electrogenic Cl secretion in the colon of the hen (*Gallus domesticus*). Am. J. Physiol. 261, R1533–R1541.

Cole, J.A., 1985. The Role of Parathyroid Hormone in the Seasonal Regulation of Calcium and Phosphate Metabolism in the European Starling. *Sturnus vulgaris*. Doctoral diss. University of Connecticut.

Collins, B.G., 1981. Nectar intake and water balance for two species of Australian honeyeater, *Lichmera indistincta* and *Acanthorhynchus superciliosis*. Physiol. Zool. 54, 1–13.

Craan, A.G., Lemieux, G., Vinay, P., Gougoux, A., Quenneville, A., 1982. The kidney of chicken adapts to chronic metabolic acidosis: in vivo and in vitro studies. Kidney Int. 22, 103–111.

Crawford, E.C., Schmidt-Nielsen, K., 1967. Temperature regulation and evaportative cooling in the ostrich. Am. J. Physiol. 212, 347–353.

Crouch, N.M.A., Lynch, V.M., Clarke, J.A., 2020. A re-evaluation of the chemical composition of avian urinary excreta. J. Ornithol. 161, 17–24.

Dantzer, V., 1989. Ultrastructural differences between the two major components of chicken ceca. J. Exp. Zool. Suppl. 3, 21–31.

Dantzler, W.H., 1966. Renal response of chickens to infusion of hyperosmotic sodium chloride solution. Am. J. Physiol. 210, 640–646.

Dantzler, W.H., 1969. Effects of K, Na, and ouabain on urate and PAH uptake by snake and chicken kidney slices. Am. J. Physiol. 217, 1510.

Dantzler, W.H., 1978. Urate excretion in nonmammalian vertebrates. In: Kelley, W.N., Weiner, I.M. (Eds.), Uric Acid. Springer, Berlin Heidelberg, New York, pp. 185–210.

Dawson, T.J., Herd, R.M., Skadhauge, E., 1985. Osmotic and ionic regulation during dehydration in a large bird, the emu (*Dromaius novaehollandiae*): an important role for the cloaca-rectum. Q. J. Exp. Physiol. 70, 423–436.

Dawson, T.J., Maloney, S.K., Skadhauge, E., 1991. The role of the kidney in electrolyte and nitrogen excretion in a large flightless bird, the emu, during different osmotic regimes, including dehydration and nesting. J. Comp. Physiol.B 161, 165–171.

Dawson, W.R., 1982. Evaporative losses of water by birds. Comp. Biochem. Physiol. 71A, 495–509.

Denbow, D.M., Sheppard, B.J., 1993. Food and water intake responses of the domestic fowl to norepinephrine infusion at circumscribed neural sites. Brain Res. Bull. 31, 121–128.

Dicker, S.E., Haslam, J., 1972. Effects of exteriorization of the ureters on the water metabolism of the domestic fowl. J. Physiol. 224, 515–520.

Ding, X., Li, M., Peng, C., Wang, Z., Qian, S., Ma, Y., Fang, T., Feng, S., Li, Y., Wang, X., Li, J., Wu, J., 2019. Uric acid transporters BCRP and MRP4 involved in chickens uric acid excretion. BMC Vet. Res. 15, 180.

Dousa, T.P., 1974. Effects of hormones on cyclic AMP formation in kidneys of nonmammalian vertebrates. Am. J. Physiol. 226, 1193–1197.

Dudas, P.L., Villalobos, A.R., Gocek-Sutterlin, G., Laverty, G., Renfro, J.L., 2002. Regulation of transepithelial phosphate transport by PTH in chicken proximal tubule epithelium. Am. J. Physiol. 282, R139–R146.

Dudas, P.L., Pelis, R.M., Braun, E.J., Renfro, J.L., 2005. Transepithelial urate transport by avian renal proximal tubule epithelium in primary culture. J. Exp. Biol. 208, 4305–4315.

Elbrønd, V.S., Dantzer, V., Mayhew, T.M., Skadhauge, E., 1991. Avian lower intestine adapts to dietary salt (NaCl) depletion by increasing transepithelial sodium transport and microvillous membrane surface area. Exp. Physiol. 76, 733–744.

Elbrønd, V.S., Dantzer, V., Mayhew, T.M., Skadhauge, E., 1993. Dietary and aldosterone effects on the morphology and electrophysiology of the chicken coprodeum. In: Sharp, P.J. (Ed.), Avian Endocrinology. Journal of Endocrinology Ltd, Bristol, pp. 217–226.

Elbrønd, V.S., Laverty, G., Dantzer, V., Grøndahl, C., Skadhauge, E., 2009. Ultrastructure and electrolyte transport of the epithelium of coprodeum, colon and the proctodeal diverticulum of *Rhea americana*. Comp. Biochem. Physiol., A 152, 357–365.

Emery, N., Poulson, T.L., Kinter, W.B., 1972. Production of concentrated urine by avian kidneys. Am. J. Physiol. 223, 180–187.

Epstein, A.N., Massi, M., 1987. Salt appetite in the pigeon in response to pharmacological treatments. J. Phys. 393, 555–568.

Ernst, S.A., Ellis, R.A., 1969. The development of surface specialization in the secretory epithelium of the avian salt gland in response to osmotic stress. J. Cell Biol. 40, 305–321.

Eto, E.C., Withers, P.C., Cooper, C.E., 2017. Can birds do it too? Evidence for convergence in evaporative water loss regulation for birds and mammals. Proc. R. Soc. B 284, 20171478.

Fänge, R., Schmidt-Nielsen, K., Robinson, M., 1958. Control of secretion from the avian salt gland. Am. J. Physiol. 195, 321–326.

Folk, R.L., 1969. Spherical urine in birds: Petrography. Science 166, 1516–1518.

Franz, R., Hummel, J., Kienzle, E., Kölle, P., Gunga, H.-C., Clauss, M., 2009. Allometry of visceral organs in living amniotes and its implications for sauropod dinosaurs. Proc. R. Soc. B 276, 1731–1736.

Gabrielli, M.G., Vincenzetti, S., Vita, A., Giovanna Menghi, G., 1998. Immunohistochemical localization of carbonic anhydrase isoenzymes II and III in quail kidney. Histochem. J. 30, 489–497.

Gasthuys, E., Montesinos, A., Caekebeke, N., Devreese, M., De Baere, S., Ardiaca, M., Paepe, D., Croubels, S., Antonissen, G., 2019. Comparative physiology of glomerular filtration rate by plasma clearance of exogenous creatinine and exo-iohexol in six different avian species. Sci. Rep. 9, 19699.

Gavrilov, V.M., Gavrilov, V.V., 2019. Scaling of total evaporative water loss and evaporative heat loss in birds at different ambient temperatures and seasons. Int. J. Avian & Wildlife Biol. 4, 40–55.

Gerson, A.R., Guglielmo, C.G., 2013. Measurement of glomerular filtration rate during flight in a migratory bird using a single bolus injection of FITC-inulin. Am. J. Physiol. 305, F823–F829.

Gerstberger, R., 1988. Functional vasocative intestinal polypeptide (VIP)-system in salt gands of the Pekin Duck. Cell Tissue Res. 252, 39–48.

Gerstberger, R., 1991. Regulation of salt gland function. In: Acta XX Congressus Internationalis Ornithologici, Symposium, 38, pp. 2114–2121.

Gerstberger, R., Gray, D.A., 1993. Fine structure, innervation, and functional control of avian salt glands. Int. Rev. Cytol. 144, 129–215.

Gerstberger, R., Gray, D., Simon, E., 1984. Circulatory and osmoregulatory effects of angiostensin II perfusion of the third ventricle in a bird with salt glands. J. Physiol. 349, 167–182.

Gerstberger, R., Kaul, R., Gray, D.A., Simon, E., 1985. Arginine vasotocin and glomerular filtration rate in saltwater-acclimated ducks. Am. J. Physiol. 248, F663.

Gerstberger, R., Healy, D.P., Hammel, H.T., Simon, E., 1987. Autoradiographic localization and characterization of circumventricular angiotensin II receptors in duck brain. Brain Res. 400, 165–170.

Gibbs, O.S., 1929. The function of the fowl's ureters. Am. J. Physiol. 88, 87–100.

Giladi, I., Goldstein, D.L., Pinshow, B., Gerstberger, R., 1997. Renal function and plasma levels of arginine vasotocin during free flight in pigeons. J. Exp. Biol. 200, 3203–3211.

Goldstein, D.L., 1989. Transport of water and electrolytes by the lower intestine and its contribution to avian osmoregulation. In: Hughes, M.R., Chadwick, A. (Eds.), Progress in Avian Osmoregulation. Leeds Philosophical and Literarary Society, Leeds, United Kingdom, pp. 271–294.

Goldstein, D.L., 1990. Effects of different sodium intakes on renal and cloacal sodium excretion in Chukars (*Aves: phasianidae*). Physiol. Zool. 63 (2), 408–419.

Goldstein, D.L., 1993a. Influence of dietary sodium and other factors on plasma aldosterone concentrations and in vitro properties of the lower intestine in house sparrows (*Passer domesticus*). J. Exp. Biol. 176, 159–174.

Goldstein, D.L., 1993b. Renal response to saline infusion in chicks of Leach's storm petrel (*Oceanodroma leucorhoa*). J. Comp. Physiol. B163, 167–173.

Goldstein, D.L., 1995. Effects of water restriction during growth and adulthood on renal function in bobwhite quail. J. Comp. Physiol.B 164, 663–670.

Goldstein, D.G., 2006. Regulation of the avian kidney by arginine vasotocin. Gen. Comp. Endocrinol. 147, 78–84.

Goldstein, D.L., Bradshaw, S.D., 1998. Renal function in red wattlebirds in response to varying fluid intake. J. Comp. Physiol. B, Biochem. Syst. Environ. Physiol. 168, 265–272.

Goldstein, D.L., Braun, E.J., 1988. Contributions of the kidneys and intestines to water conservation, and plasma levels of antidiuretic hormone, during dehydration in house sparrows (*Passer domesticus*). J. Comp. Physiol. 158, 353–361.

Goldstein, D.L., Braun, E.J., 1989. Structure and concentrating ability in the avian kidney. Am. J. Physiol. 256, R501–R509.

Goldstein, D.L., Rothschild, E.L., 1993. Daily rhythms in rates of glomerular filtration and cloacal excretion in captive and wild song sparrows (*Melospiza melodia*). Physiol. Zool. 66 (5), 708–719.

Goldstein, D.L., Hughes, M.R., Braun, E.J., 1986. Role of the lower intestine in the adaptation of gulls (*Larus glaucescens*) to sea water. J. Exp. Biol. 123, 345–357.

Goldstein, D.L., Williams, J.B., Braun, E.J., 1990. Osmoregulation in the field by salt-marsh savannah sparrows Passerculus sandwichensis beldingi. Physiol. Zool. 63, 669–682.

Grahn, M.F., Butterworth, P.J., 1982. Phosphate uptake by proximal tubule cells isolated from chick kidney. Biochem. Soc. Trans. 9, 465–466.

Gray, D.A., 1993. Plasma atrial natriuretic factor concentrations and renal actions in the domestic fowl. J. Comp. Physiol. B 163, 519–523.

Gray, D.A., Erasmus, T., 1988. Plasma arginine vasotocin and angiotensin II in the water deprived kelp gull (*Larus dominicanus*), Cape gannet (Sula capensis) and jackass penguin (*Spheniscus demersus*). Comp. Biochem. Physiol. 91A, 727–732.

Gray, D.A., Erasmus, T., 1989. Control of renal and extrarenal salt and water excretion by plasma angiotensin II in the kelp gull (*Larus dominicanus*). J. Comp. Physiol. B 158, 651–660.

Gray, D.A., Fleming, P.A., Nicolson, S.W., 2004. Dietary intake effects on arginine vasotocin and aldosterone in cloacal fluid of whitebellied sunbirds (*Nectarinia talatala*). Comp. Biochem. Physiol. 138A, 441–449.

Gray, D.A., Simon, E., 1985. Control of plasma angiotensin II in a bird with salt glands (*Anas platyrhynchos*). Gen. Comp. Endocrinol. 160, 1–13.

Gray, D.A., Hammel, H.T., Simon, E., 1986. Osmoregulatory effects of angiotensin II in a bird with salt glands (*Anas platyrhynchos*). J. Comp. Physiol. B 156, 315–321.

Gray, D.A., Naude, R.J., Erasmus, T., 1988. Plasma arginine vasotocin and angiotensin II in the water deprived ostrich (*Struthio camelus*). Comp. Biochem. Physiol. 89A (2), 251–256.

Gray, D.A., Schütz, H., Gerstberger, R., 1991. Interaction of atrial natriuretic factor and osmoregulatory hormones in the Pekin duck. Gen. Comp. Endocrinol. 81, 246–255.

Gray, D.A., Downing, C., Sayed, N., 1997. Endogenous plasma atrial natriuretic peptide and the control of salt gland function in the Pekin duck. Am. J. Physiol. 273, R1080–R1085.

Greenwald, L., 1989. The Significance of renal relative medullary thickness. Physiol. Zool. 62 (5), 1005–1014.

Gutiérrez, J.S., Dietz, M.W., Masero, J.A., Gill Jr., R.E., Dekinga, A., Battley, P.F., Sánchez-Guzmán, J.M., Piersma, T., 2012. Functional ecology of saltglands in shorebirds: flexible responses to variable environmental conditions. Funct. Ecol. 26, 236–244, 2012.

Hammel, H.T., 1989. Neural control of salt gland excretion: enhanced and sustained by autofacilitation. In: Hughes, M.R., Chadwick, A. (Eds.), Progress in Avian Osmoregulation. Leeds Philosophical and Literarary Society, Leeds, United Kingdom, pp. 163–181.

Hammel, H.T., Simon-Oppermann, C., Simon, E., 1980. Properties of body fluids influencing salt gland secretion in Pekin ducks. Am. J. Physiol. 239, R489–R496.

Hanwell, A., Linzell, J.L., Peaker, M., 1971. Salt-gland secretion and blood flow in the goose. J. Physiol. (London) 213, 373–387.

Hanwell, A., Linzell, J.L., Peaker, M., 1972. Nature and location of the receptors for salt-gland secretion in the goose. J. Physiol. (London) 226, 453–472.

Hao, y., Xiong, Y., Cheng, Y., Song, G., Jia, C., Qu, Y., Lei, F., 2019. Comparative transcriptomics of 3 high-altitude passerine birds and their low-altitude relatives. Proc. Natl. Acad. Sci. U.S.A. 116, 11851–11856.

Hart, W.M., Essex, H.E., 1942. Water metabolism of the chicken (*Gallus domesticus*) with special reference to the role of the cloaca. Am. J. Physiol. 136, 657–668.

Hartman Bakken, B., Sabat, P., 2006. Gastrointestinal and renal responses to water intake in the green-backed firecrown (*Sephanoides sephanoides*), a South American hummingbird. Am. J. Physiol. 291, R830–R836.

Hartman Bakken, B., McWhorter, T.J., Tsahar, E., Martínez del Rio, C., 2004. Hummingbirds arrest their kidneys at night: diel variation in glomerular filtration rate in *Selasphorus platycercus*. J. Exp. Biol. 207, 4383–4391.

Haugen, M., Williams, J.B., Wertz, P., Tieleman, B.I., 2003. Lipids of the stratum corneum vary with cutaneous water loss among larks along a temperature- moisture gradient. Physiol. Biochem. Zool. 76, 907–917.

Heinz, M.K., Gray, D.A., 2001. Role of plasma ANG II in the excretion of acute sodium load in a bird with salt glands (*Anas platymynchos*). Am. J. Physiol. 281, R346–R351.

Hildebrandt, P., Shuttleworth, T.J., 1993. G_q-type G protein couples muscarinic receptors to inositol phosphate and calcium signaling in exocrine cells from the avian salt gland. J. Membr. Biol. 133, 183–190.

Holmes, W.N., Phillips, J.G., 1985. The avian salt gland. Biol. Rev. 60, 213–256.

Holmes, W.N., Fletcher, G.L., Stewart, D.J., 1968. The patterns of renal electrolyte excretion in the duck (*Anas platyrhynchos*) maintained on freshwater and on hypertonic saline. J. Exp. Biol. 48, 487–508.

Holmes, W.N., Gorsline, J., Wright, A., 1982. Patterns of cloacal water and electrolyte excretion in constantly-loaded intact and colostomized ducks (*Anas platyrhynchos*). Comp. Biochem. Physiol. 3A, 675–677.

Holtug, K., McEwan, G.T.A., Skadhauge, E., 1992. Effects of propionate on the acid microclimate of hen (*Gallus domesticus*) colonic mucosa. Comp. Biochem. Physiol. 103A, 649–652.

Holtug, K., Shipley, A., Dantzer, V., Sten-Knudsen, O., Skadhauge, E., 1991. Localization of sodium absorption and chloride secretion in an intestinal epithelium. J. Membr. Biol. 122, 215–229.

Huber, G.C., 1917. On the morphology of the renal tubulus of vertebrates. Anat. Res. 13, 305–339.

Hughes, M.R., 1970a. Relative kidney size in nonpasserine birds with functional salt glands. Condor 72, 164–168.

Hughes, M.R., 1970b. Flow rate and cation concentration in salt gland secretion of the glaucous-winged gull, Larus glaucescens. Comp. Biochem. Physiol. 32, 807–812.

Hughes, M.R., 1972. The effect of salt gland removal on cloacal ion and water excretion in the growing kittiwake, Rissa tridactyla. Can. J. Zool. 50, 603–610.

Hughes, M.R., 1980. Glomerular filtration rate in saline acclimated ducks, gulls, and geese. Comp. Biochem. Physiol. 65A, 211.

Hughes, M.R., 2003. Regulation of salt gland, gut and kidney interactions. Comp. Biochem. Physiol. 136A, 507–524.

Hughes, M.R., 1987. The effects of ureteral resistance on gull urine composition and flow rate. Can. J. Zool. 65, 2669–2771.

Hughes, M.R., 1989a. Extracellular fluid volume and the initiation of salt gland secretion in ducks and gulls. Can. J. Zool. 67, 194–197.

Hughes, M.R., 1989b. Stimulus for avian salt gland secretion. In: Hughes, M.R., Chadwick, A. (Eds.), Progress in Avian Osmoregulation. Leeds Philosophical and Literarary Society, Leeds, United Kingdom, pp. 143–161.

Hughes, M.R., Raveendran, L., 1994. Ion and luminal marker concentrations in the gut of saline-acclimated ducks. Condor 96, 295–299.

Hughes, M.R., Roberts, J.R., 1988. Sodium uptake from the gut of freshwater- and seawater-acclimated ducks and gulls. Can. J. Zool. 66, 1365–1370.

Hughes, M.R., Roberts, J.R., Thomas, B.R., 1989. Renal function in freshwater and chronically saline-stressed male and female Pekin ducks. Poultry Sci. 68, 408–416.

Hughes, M.R., Kojwang, D., Zenteno-Savin, T., 1992. Effects of caecal ligation and saline acclimation on plasma concentration and organ mass in male and female Pekin ducks, *Anas platyrhynchos*. J. Comp. Physiol. 162, 625–631.

Hughes, M.R., Goldstein, D.L., Raveendran, L., 1993. Osmoregulatory responses of glaucous-winged gulls (*Larus glaucescens*) to dehydration and hemorrhage. J. Comp. Physiol. B 163, 524–531.

Ignarski, M., Islam, R., Müller, R.U., 2019. Long non-coding RNAs in kidney disease. Int. J. Mol. Sci. 20, 3276.

Jamison, R.L., Kriz, W., 1982. Urinary Concentration Mechanism: Structure and Function. Oxford University Press, New York.

Jax, E., Wink, M., Kraus, R.H.S., 2018. Avian transcriptomics: opportunities and challenges. J. Ornithol. 159, 599–629.

Johnson, O.W., 1968. Some morphological features of avian kidneys. Auk 85, 216–228.

Johnson, O.W., 1974. Relative thickness of the renal medulla in birds. J. Morphol. 142 (3), 277–284.

Johnson, O.W., Mugaas, J.N., 1970. Quantitative and organizational features of the avian renal medulla. Condor 72, 288–292.

Johnson, O.W., Phipps, G.L., Mugaas, J.N., 1972. Injection studies of cortical and medullary organization in the avian kidney. J. Morphol. 136, 181–190.

Kanosue, K., Schmid, H., Simon, E., 1990. Differential osmoresponisiveness of periventricular neurons in duck hypothalamus. Am. J. Phys. 258, R973–R981.

Karasawa, Y., Maeda, M., 1992. Effect of colostomy on the utilisation of dietary nitrogen in the fowl fed on a low protein diet. Br. Poultry Sci. 33, 815–820.

Kaufman, S., Peters, G., 1980. Regulatory drinking in the pigeon, *Columba livia*. Am. J. Phys. 301, 91–99.

Kaul, R., Gerstberger, R., Meyer, U., Simon, E., 1983. Salt gland blood flow in saltwater-adapted Pekin ducks: microsphere measurement of the proportionality to secretion rate and investigation of controlling mechanisms. J. Comp. Physiol. B. 149, 457–462.

King, A.S., 1975. Aves urogenital system. In: Getty, R. (Ed.), Sisson and Grossman's The Anatomy of the Domestic Animals, 5th Ed, Vol 2.

Klingbeil, C.K., 1985. Effects of chronic changes in dietary electrolytes and acute stress on plasma levels of corticosterone and aldosterone in the duck (*Anas platyrhynchos*). Gen. Comp. Endocrinol. 58, 10–19.

Koike, T.I., Pryor, L.R., Neldon, H.L., 1979. Effect of saline infusion on plasma immunoreactive vasotocin in conscious chickens. Gen. Comp. Endocrinol. 37, 451–458.

Korr, I.M., 1939. The osmotic function of the chicken kidney. J. Cell. Comp. Physiol. 13, 175–194.

Krag, B., Skadhauge, E., 1972. Renal salt and water excretion in the budgerygah (*Melopsittacus undulatus*). Comp. Biochem. Physiol. 41A, 667–683.

Krohn, M., Hildebrandt, J.P., 2004. Cross-talk of phosphoinositide- and cyclic nucleotide-dependent signaling pathways in differentiating avian nasal gland cells. J. Comp. Physiol. B 174, 461–470.

Langford, H.G., Fallis, N., 1966. Diuretic effect of angiotensin in the chicken. Proc. Soc. Exp. Biol. Med. 123, 317–321.

Laverty, G., 1989. Renal tubular transport in the avian kidney. In: Hughes, M.R., Chadwick, A. (Eds.), Progress in Avian Osmoregulation, Leeds Philosophical and Literary Society (Scientific Section). Leeds, United Kingdom.

Laverty, G., Alberici, M., 1987. Micropuncture study of proximal tubule pH in avian kidney. Am. J. Physiol. 253, R587–R591.

Laverty, G., Bjarnadóttir, S., Elbrønd, V.S., Árnason, S.S., 2001. Aldosterone suppresses expression of an avian colonic sodium–glucose cotransporter. Am. J. Physiol. 281, R1041–R1050.

Laverty, G., Dantzler, W.H., 1982. Micropuncture of superficial nephrons in avian (*Sturnus vulgaris*) kidney. Am. J. Physiol. 243, F561.

Laverty, G., Dantzler, W.H., 1983. Micropuncture study of urate transport by superficial nephrons in avian (*Sturnus vulgaris*) kidney. Pflügers Archiv 397, 232–236.

Laverty, G., Wideman Jr., R.F., 1989. Sodium excretion rates and renal responses to acute salt loading in the European starling. J. Comp. Physiol. B 159, 401–408.

Laverty, G., Holtug, K., Elbrønd, V.S., Ridderstråle, Y., Skadhauge, E., 1994. Mucosal acidification and an acid microclimate in the hen colon in vitro. J. Comp. Physiol. B 163, 633–641.

Layton, H.E., 1986. Distribution of Henle's loops may enhance urine concentrating capability. Biophys. J. 49, 1033–1040.

Lee, J.W., Chou, C.L., Knepper, M.A., 2015. Deep sequencing in microdissected renal tubules identifies nephron segment-specific transcriptomes. J. Am. Soc. Nephrol. 26, 2669–2677.

Lind, J., Munck, B.G., Olsen, O., Skadhauge, E., 1980a. Effects of sugars, amino acids and inhibitors on electrolyte transport across hen colon at different sodium chloride intakes. J. Physiol. (London) 305, 315–325.

Lind, J., Munck, B.G., Olsen, O., 1980b. Effects of dietary intake of sodium chloride on sugar and amino acid transport across isolated hen colon. J. Physiol. (London) 305, 327–336.

Long, S., Skadhauge, E., 1980. Renal reabsorption of Na and K in Gallus: role of urinary precipitates. Acta Physiol. Scand. 109, 31A.

Long, S., Skadhauge, E., 1983a. Renal acid excretion in the domestic fowl. J. Exp. Biol. 104, 51.

Long, S., Skadhauge, E., 1983b. The role of urinary precipiates in the excretion of electrolytes and urate in the domestic fowl. J. Exp. Biol. 104, 41–50.

Lonsdale, K., Sutor, D.J., 1971. Uric acid dihydrate in bird urine. Science 172, 958–959.

Lowy, R.J., Ernst, S.A., 1987. β-adrenergic stimulation of ion transport in primary cultures of avian salt gland. Am. J. Physiol. 252, C670–C676.

Lowy, R.J., Schreiber, J.H., Ernst, S.A., 1987. Vasoactive intestinal peptide stimulates ion transport in avian salt gland. Am. J. Physiol. 253, R801–R803.

Lowy, R.J., Dawson, D.C., Ernst, S.A., 1989. Mechanism of ion transport by avian salt gland primary cell cultures. J. Gen. Physiol. 93, 1171–1194.

Lyons, M.E., Goldstein, D.L., 2002. Osmoregulation by nestling and adult American kestrels (*Falco sparverius*). Auk 119, 426–436.

Marcano, M., Layton, A.T., Layton, H.E., 2006. An optimization algorithm for a distributed-loop model of an avian urine concentrating mechanism. Bull. Math. Biol. 68, 1625–1660.

Marder, J., Ben-Asher, J., 1983. Cutaneous water evaporation –I. Its significance in heat-stressed birds. Comp. Biochem. Physiol. 75A (3), 425–431.

Marder, J., Raber, P., 1989. Beta-adrenergic control of trans-cutaneous evaporative cooling mechanisms in birds. J. Comp. Physiol. B 159, 97–103.

Marshall, A.T., Hyatt, A.D., Phillips, J.G., Condron, R.J., 1985. Isosmotic secretion in the avian nasal salt gland: X-ray microanalysis of luminal and intracellular ion distributions. J. Comp. Physiol. B. 156, 213–227.

Martindale, L., 1976. Renal urate synthesis in the fowl (*Gallus domesticus*). Comp. Biochem. Physiol. 53A, 389–391.

Massi, M., Epstein, A.N., 1990. Angiotensin/aldosterone synergy governs the salt appetite of the pigeon. Appetite 14, 181–192.

Mayhew, T.M., Dantzer, V., Elbrønd, V.S., Skadhauge, E., 1990. A sampling scheme intended for tandem measurements of sodium transport and microvillous surface area in the coprodaeal epithelium of hens on high- and low-salt diets. J. Anat. 173, 19–31.

Mayhew, T.M., Elbrønd, V.S., Dantzer, V., Skadhauge, E., Møller, O., 1992. Structural and enzymatic studies on the plasma membrane domains and sodium pump enzymes of absorptive epithelial cells in the avian lower intestine. Cell Tissue Res. 270, 577–585.

McKechnie, A.E., Wolf, B.O., 2004. Partitioning of evaporative water loss in white-winged doves: plasticity in response to short-term thermal acclimation. J. Exp. Biol. 207, 203–210.

McKechnie, A.E., Whitfield, M.C., Smit, B., Gerson, A.R., Smith, E.K., Talbot, W.A., McWhorter, T.J., Wolf, B.O., 2016. Avian thermoregulation in the heat: efficient evaporative cooling allows for extreme heat tolerance in four southern hemisphere columbids. J. Exp. Biol. 219, 2145–2155.

McLelland, J., 1989. Anatomy of the avian cecum. J. Exp. Zool. Suppl. 2–9.

McNabb, F.M.A., McNabb, R.A., Steeves, H.R., 1973. Renal mucoid materials in pigeons fed high and low protein diets. Auk 90, 14–18.

McNabb, R.A., 1974. Urate and cation interactions in the liquid and precipitated fractions of avian urine, and speculations on their physico-chemical state. Comp. Biochem. Physiol. 48A, 45–54.

McNabb, R.A., McNabb, F.M.A., 1975. Urate excretion by the avian kidney. Comp. Biochem. Physiol. 51A, 253–258.

McWhorter, T.J., Martínez del Rio, C., 1999. Food ingestion and water turnover in hummingbirds: how much dietary water is absorbed? J. Exp. Biol. 202, 2851–2858.

Michałek, K., Szczerbińska, D., Grabowska, M., Majewska, D., Laszczyńska, M., 2016. Anatomical and morphological study of the kidneys of the breeding emu (*Dromaius novaehollandiae*). Turk. J. Zool. 40, 314–319.

Minnich, J.E., 1976. Adaptations in the reptilian excretory system for excreting insoluble urates. Isr. J. Med. Sci. 12, 854–861.

Miwa, T., Nishimura, H., 1986. Diluting segment in avian kidney. II. Water and chloride transport. Am. J. Physiol. 250, R341.

Mobini, B., Abdollahi, M.H., 2016. Effect of sex on histological and histochemical structures of different parts of the kidney in Japanese quail. Poultry Sci. 95, 2145–2150.

Möhring, J., Schoun, J., Simon-Oppermann, C., Simon, E., 1980. Radioimmunossay for arginine-vasotocin (AVT) in serum of Pekin ducks: AVT concentrations after adaptation to freshwater and salt water. Pflügers Archiv 387, 91–97.

Morild, I., Monwinckel, R., Bohle, A., Christensen, J.A., 1985. The juxtaglomerular apparatus in the avian kidney. Cell Tissue Res. 240, 209–214.

Mueller, C., Sendler, M., Hildebrandt, J.-P., 2006. Downregulation of aquaporins 1 and 5 in nasal gland by osmotic stress in ducklings, Anas platyrhynchos: implications for the production of hypertonic fluid. J. Exp. Biol. 209, 4067–4076.

Muñoz-Garcia, A., Cox, R.M., Williams, J.B., 2008. Phenotypic flexibility in cutaneous water loss and lipids of the stratum corneum in house sparrows (*Passer domesticus*) following acclimation to high and low humidity. Physiol. Biochem. Zool. 81, 87–96.

Nechay, B.R., Nechay, L., 1959. Effects of probenecid sodium, salicylate, 2,4-dinitrophenol and pyrazinamide or renal secretin of uric acid in chickens. J. Pharmacol. Exp. ther. 26, 291–295.

Nicholson, J.K., 1982. The microanatomy of the distal tubules, collecting tubules and collecting ducts of the starling kidney. J. Anat. 134, 11.

Nicolson, S.W., Fleming, P.A., 2003. Energy balance in the whitebellied sunbird *Nectarinia talatala*: constraints on compensatory feeding, and consumption of supplementary water. Funct. Ecol. 17, 3–9.

Nicolson, S.W., Fleming, P.A., 2014. Drinking problems on a 'simple' diet: physiological convergence in nectar-feeding birds. J. Exp. Biol. 217, 1015–1023.

Nishimura, H., 1993. Countercurrent urine concentration in birds. In: Brown, J.A., Balment, R.J., Rankin, J.C. (Eds.), New Insights in Vertebrate Kidney Function. Cambridge University Press, Cambridge, United Kingdom, pp. 189–208.

Nishimura, H., Imai, M., Ogawa, J., 1986. Diluting segment in avian kidney. I. Characterization of trans-epithelial voltages. Am. J. Physiol. 250, R333.

Nishimura, H., Koseki, C., Imai, M., Braun, E.J., 1989. Sodium chloride and water transport in the thin descending limb of Henle of the quail. Am. J. Physiol. 257, F994–F1002.

Nishimura, H., Yang, Y., 2013. Aquaporins in avian kidneys: function and perspectives. Am. J. Physiol. 305, R1201–R1214.

O'Connor, R.S., Wolf, B.O., Brigham, R.M., McKechnie, A.E., 2017. Avian thermoregulation in the heat: efficient evaporative cooling in two southern African nightjars. J. Comp. Physiol. B 187, 477–491.

Odlind, B., 1978. Blood flow distribution in the renal portal system of the intact hen. A study of a venous system using microspheres. Acta Physiol. Scand. 102, 342.

Oelofsen, B.W., 1973. Renal function in the penguin (*Spheniscus demersus*) with special reference to the role of the renal portal valves. Zool. Afr. 8, 41.

Ohmart, R.D., 1972. Physiological and ecological observations concerning the salt-secreting nasal glands of the roadrunner. Comp. Biochem. Physiol. 43A, 311–316.

Osono, E., Nishimura, H., 1994. Control of sodium and chloride transport in the thick ascending limb in the avian nephron. Am. J. Physiol. 267, R455–R462.

Park, W., Rengaraj, D., Kil, D., Kim, H., Lee, H., Song, K., 2017. RNA-seq analysis of the kidneys of broiler chickens fed diets containing different concentrations of calcium. Sci. Rep. 7, 11740.

Peaker, M., Linzell, J.L., 1975. Salt Glands in Birds and Reptiles. Cambridge Universtiy Press, Cambridge.

Peña-Villalobos, I., Valdés-Ferranty, F., Sabat, P., 2013. Osmoregulatory and metabolic costs of salt excretion in the Rufous-collared sparrow *Zonotrichia capensis*. Comp. Biochem. Physiol. 164A, 314–318.

Pines, M., Polin, D., Hurwitz, S., 1983. Urinary cyclic AMP excretion in birds: dependence on parathyroid hormone activity. Gen. Comp. Endocrinol. 49, 90–96.

Platts, M.M., Mudge, G.H., 1961. Accumulation of uric acid by slices of kidney cortex. Am. J. Physiol. 200, 387–391.

Porter, P., 1963. Physico-chemical factors involved in urate calculus formation–II. Colloidal flocculation. Res. Vet. Sci. 4, 592–602.

Poulson, T.L., Bartholomew, G.A., 1962. Salt balance in the savannah sparrow. Physiol. Zool. 35, 109–119.

Purchase, C., Napier, K.R., Nicolson, S.W., McWhorter, T.J., Fleming, P.A., 2013. Gastrointestinal and renal responses to variable water intake in whitebellied sunbirds and New Holland honeyeaters. J. Exp. Biol. 216, 1537–1545.

Ramanathan, K., Padmanabhan, G., 2020. MiRNAs as potential biomarker of kidney diseases: a review. Cell Biochem. Funct. 2020, 1–16.

Renfro, J.L., Clark, N.B., 1984. Parathyroid hormone induced phosphate excretion following preequilibration with ^{32}P. Am. J. Physiol. 246, F373–F378.

Rice, G.E., Skadhauge, E., 1982a. The in vivo dissociation of colonic and coprodeal transepithelial transport in NaCl depleted domestic fowl. J. Comp. Physiol. 146B, 51–56.

Rice, G.E., Skadhauge, E., 1982b. Colonic and coprodeal transepithelial transport parameters in NaCl-loaded domestic fowl. J. Comp. Physiol. 147B, 65–69.

Rice, G.E., Skadhauge, E., 1982c. Caecal water and electrolyte absorption and the effects of acetate and glucose, in dehydrated, low-NaCl diet hens. J. Comp. Physiol. B 147, 61–64.

Rice, G.E., Arnason, S.S., Arad, S., Skadhauge, E., 1985. Plasma concentrations of arginine vasotocin, prolactin, aldosterone and corticosterone in relation to oviposition and dietary NaCl in the domestic fowl. Comp. Biochem. Physiol. 81A, 769–777.

Ro, J., Williams, J.B., 2010. Respiratory and cutaneous water loss of temperate-zone passerine birds. Comp. Biochem. Physiol. 156 (A), 237–246.

Roberts, J.R., 1992. Renal function and plasma arginine vasotocin during an acute salt load in feral chickens. J. Comp. Physiol. B162, 54–58.

Roberts, J.R., Dantzler, W.H., 1989. Glomerular-filtration rate in conscious unrestrained starlings under dehydration. Am. J. Physiol. 256, R836–R839.

Roberts, J.R., Dantzler, W.H., 1990. Micropuncture study of the avian kidney: infusion of mannitol or sodium chloride. Am. J. Physiol. 258, R869–R874.

Roberts, J.R., Hughes, M.R., 1983. Glomerular filtration rate and drinking rate in Japanese quail, *Coturnix coturnix* japonica, in response to acclimation to saline drinking water. Can. J. Zool. 61, 2394.

Rocha, A.R., Silva, R., Villegas, A., Sánchez-Guzmán, J.M., Ramos, J.A., Masero, J.A., 2016. Physiological, morphological and behavioural responses of self-feeding precocial chicks copying with contrasting levels of water salinity during development. PloS One 11 (10), e0165364.

Roush, W.B., Spotts, C.B., 1988. Strain differences in the number and size of glomeruli in domestic fowl. Br. Poultry Sci. 29, 113–117.

Ruch Jr., F.E., Hughes, M.R., 1975. The effects of hypertonic sodium chloride injection on body water distribution in ducks (*Anas platyrhynchos*), gulls (Larus glaucescens), and roosters (*Gallus domesticus*). Comp. Biochem. Physiol. 52A, 21–28.

Sandor, T., Skadhauge, E., Dibattista, J.A., Mehdi, A.Z., 1989. Interrelations of the intestinal glucocorticoid and mineralocorticoid receptor systems with salt homeostasis. In: Hughes, M.R., Chadwick, A. (Eds.), Progress in Avian Osmoregulation. Leeds Philosophical and Literarary Society, Leeds, United Kingdom, pp. 305–332.

Schmidt-Nielsen, K., 1960. The Salt-Secreting Gland of Marine Birds Circulation, Vol. XXI.

Schmidt-Nielsen, K., 1959. Salt glands. Sci. Am. 200, 109–116.

Schmidt-Nielsen, K., Kim, Y.T., 1964. The effect of salt intake on the size and function of the salt glands of ducks. Auk 81, 160–172.

Schmidt-Nielsen, K., Jorgensen, C.B., Osaki, H., 1958. Extrarenal salt excretion in birds. Am. J. Physiol. 193, 101–107.

Schmidt-Nielsen, K., Borut, A., Lee, P., Crawford, E., 1963. Nasal salt excretion and the possible function of the cloaca in water conservation. Science 142, 1300–1301.

Schütz, H., Gerstberger, R., 1990. Atrial natriuretic factor controls salt gland secretion in the Pekin duck (*Anas platyrhynchos*) through interaction with high affinity receptors. Endocrinology 127, 1718–1726.

Schütz, H., Gray, D.A., Gerstberger, R., 1992. Modulation of kidney function in conscious Pekin ducks by atrial natriuretic factor. Endocrin 130, 678–684.

Scope, A., Schwendenwein, I., Schauberger, G., 2013. Plasma exogenous creatinine excretion for the assessment of renal function in avian medicine—pharmacokinetic modeling in racing pigeons (*Columba livia*). J. Avian Med. Surg. 27, 173–179.

Shannon, J.A., 1938. The excretion of exogenous creatinine by the chicken. J. Cell. Comp. Physiol. 11, 123–134.

Shideman, J.R., Evans, R.L., Bierer, D.W., Quebbemann, A.J., 1981. Renal venous portal contribution to PAH and uric acid clearance in the chicken. Am. J. Physiol. 240, F46–F53.

Shuttleworth, T.J., Thompson, J.L., 1989. Intracellular [Ca^{2+}] and inositol phosphates in avian nasal gland cells. Am. J. Physiol. 257, C1020–C1029.

Shuttleworth, T.J., Wood, C.M., 1992. Changes in pH_i associated with activation of ion secretion in avian nasal salt gland cells. Am. J. Physiol. 262, C221–C228.

Siegel-Causey, D., 1990. Phylogenetic patterns of size and shape of the nasal gland depression in phalacrocoracidae. Auk 107, 110–118.

Simon, E., Gerstberger, R., Gray, D.A., 1992. Central nervous angiotensin II responsiveness in birds. Prog. Neurobiol. 39, 179–207.

Simon-Oppermann, C., Szczepanska-Sadowska, E., Gray, D.A., Simon, E., 1984. Blood volume changes and arginine vasotocin (AVT) blood concentration in conscious fresh water and salt water adapted ducks. Pflügers Archiv 400, 151–159.

Skadhauge, E., 1973. Renal and cloacal salt and water transport in the fowl (*Gallus domesticus*). Dan. Med. Bull. 20 (Suppl. 1), 1–82.

Skadhauge, E., 1977. Solute compositon of the osmotic space of ureteral urine in dehydrated chickens (*Gallus domesticus*). Comp. Biochem. Physiol. 56A, 271–274.

Skadhauge, E., 1981. Osmoregulation in Birds. Springer-Verlag, New York.

Skadhauge, E., 1983. Ionic and osmotic regulation in birds. Verh. Dtsch. Zool. Ges. 69–81.

Skadhauge, E., 1993. Basic characteristics and hormonal regulation of ion transport in avian hindguts. Adv. Comp. Environ. Physiol. 16, 67–93.

Skadhauge, E., Bradshaw, S.D., 1974. Saline drinking and cloacal excretion of salt and water in the zebra finch. Am. J. Physiol. 227, 1263–1267.

Skadhauge, E., Kristensen, K., 1972. An analogue computer simulation of cloacal resorption of salt and water from ureteral urine in birds. J. Theor. Biol. 35, 473-387.

Skadhauge, E., Schmidt-Nielsen, B., 1967a. Renal function in domestic fowl. Am. J. Physiol. 212, 793–798.

Skadhauge, E., Schmidt-Nielsen, B., 1967b. Renal medullary electrolyte and urea gradient in chickens and turkeys. Am. J. Physiol. 212, 1313–1318.

Skadhauge, E., Thomas, D.H., 1979. Transepithelial transport of K^+, NH_4^+, inorganic phosphate and water by hen (*Gallus domesticus*) lower intestine (colon and coprodeum) perfused luminally in vivo. Pflügers Archiv 379, 237–243.

Skadhauge, E., Thomas, D.H., Chadwick, A., Jallageas, M., 1983. Time course of adaptation to low and high NaCl diets in the domestic fowl: effects on electrolyte excretion and on plasma hormone levels (aldosterone, corticosterone and prolactin). Pflügers Arch. Eur. J. Physiol. 396, 301–307.

Skadhauge, E., Munck, B.G., Rice, G.E., 1984a. Regulation of NaCl and water absorption in duck intestine. In: Pequeux, A., Gilles, R., Bolis, L. (Eds.), Osmoregulation in Estuarine and Marine Animals. Lecture Notes on Coastal and Estuarine Studies. Springer, Berlin, pp. 118–133.

Skadhauge, E., Warüi, C.N., Kamau, J.M.Z., Maloiy, G.M.O., 1984b. Function of the lower intestine and osmoregulation in the ostrich: preliminary anatomical and physiological observations. Quart. J. Exp. Physiol. 69, 809–818.

Skadhauge, E., Maloney, S.K., Dawson, T.J., 1991. Osmotic adaptation of the emu (*Dromaius novaehollandiae*). J. Comp. Physiol. B 161, 173–178.

Skadhauge, E., Dantzer, V., McLean, A., Dawson, T.J., 1993. Comparative aspects of kidney-cloaca interaction in ratite birds. Proc. XXXII Cong. Int. Union. Phys. Sci. 124.

Smith, H.W., 1953. From Fish to Philosopher. Little, Brown, and Company, NY.

Smith, P.R., Bradford, A.L., Dantzer, V., Benos, D.J., Skadhauge, E., 1993. Immunocytochemical localization of amiloride-sensitive sodium channels in the lower intestine of the hen. Cell Tissue Res. 272, 129–136.

Snider, R.M., Roland, R.M., Low, R.J., Agranoff, B.A., Ernst, S.A., 1986. Muscarinic receptor-stimulated Ca^{2+} signaling and inositol lipid metabolism in avian salt gland cells. Biochim. Biophys. Acta 889, 216–224.

Song, S.R., Beissinger, S.R., 2019. Environmental and ecological correlates of avian field metabolic rate and water flux. Funct. Ecol. 34, 811–821.

Sperber, I., 1948. Investigations on the circulatory system of the avian kidney. Zool. Bidrag. 27, 429–448.

Sperber, I., 1960. Excretion. In: Marshall, A.J. (Ed.), Biology and Physiology of Birds, vol. I. Academic Press, London, New York, pp. 469–492.

Staaland, H., 1967. Anatomical and physiological adaptations of the nasal glands in charadriiformes birds. Comp. Biochem. Physiol. 23, 933–944.

Stallone, J.N., Braun, E.J., 1985. Contributions of glomerular and tubular mechanisms to antidiuresis in conscious domestic fowl. Am. J. Physiol. 249, F842.

Stallone, J.N., Braun, E.J., 1986. Regulation of plasma arginine vasotocin in conscious water-deprived domestic fowl. Am. J. Physiol. 250, R658–R664.

Stallone, J.N., Nishimura, H., 1985. Angiotensin II (AII)-induced natriuresis in anesthetized domestic fowl. Fed. Proc. 44, 1364.

Stewart, D.J., 1972. Secretion by salt gland during water deprivation in the duck. Am. J. Physiol. 223, 384–386.

Sun, O., Lerman, L.O., 2019. Urinary microRNA in kidney disease: utility and roles. Am. J. Physiol. 316, F785–F793.

Sykes, A.H., 1971. Formation and composition of urine. In: Bell, D.J., Freeman, B.M. (Eds.), Physiology and Biochemistry of the Domestic Fowl, vol. I. Academic Press, London New York, pp. 233–278. Chap. 9.

Takei, Y., 1977. The role of the subfornical organ in drinking induced by angiotensin in the Japanese quail *Coturnix coturnix* japonica. Cell Tissue Res. 185, 175–181.

Takei, Y., Okawara, Y., Kobayashi, H., 1988. Water intake induced by water deprivation in the quail, *Coturnix coturnix* japonica. J. Comp. Physiol. B 158, 519–525.

Takei, Y., Okawara, Y., Kobayashi, H., 1989. Control of drinking in birds. In: Hughes, M.R., Chadwick, A. (Eds.), Progress in Avian Osmoregulation. Leeds Philosophical and Literarary Society, Leeds, United Kingdom, pp. 1–12.

Thomas, D.H., 1982. Salt and water excretion by birds: the lower intestine as an integrator of renal and intestinal excretion. Comp. Biochem. Physiol. 71A, 527–535.

Thomas, D.H., Robin, A.P., 1977. Comparative studies of thermoregulatory and osmoregulatory behaviour and physiology of five species of sandgrouse (Aves:Pterocliidae) in Morocco. J. Zool., Lond. 183, 229–249.

Thomas, D.H., Skadhauge, E., 1982. Time course of adaptation to low and high NaCl diets in the domestic fowl: effects on electrical behaviour of isolated epithelia from the lower intestine. Pflügers Arch. Eur. J. Physiol. 395, 165–170.

Thomas, D.H., Skadhauge, E., 1989a. Water and electrolyte transport by the avian ceca. J. Exp. Zool. Suppl. 3, 95–102.

Thomas, D.H., Skadhauge, E., 1989b. Function and regulation of the avian caecal bulb: influence of dietary NaCl and aldosterone on water and electrolyte fluxes in the hen (*Gallus domesticus*) perfused in vivo. J. Comp. Physiol. B 159, 51–60.

Thornton, S.N., 1986a. Osmoreceptor localization in the brain of the pigeon (*Columba livia*). Brain Res. 377, 96–104.

Thornton, S.N., 1986b. The influence of central infusions on drinking due to peripheral osmotic stimuli in the pigeon (*Columba livia*). Physiol. Behav. 36, 229–233.

Tieleman, B.I., Williams, J.B., 2000. The adjustment of avian metabolic rates and water fluxes to desert environments. Physiol. Biochem. Zool. 73, 461–479.

Tieleman, B.I., Williams, J.B., 2002. Cutaneous and respiratory water loss in larks from arid and mesic environments. Physiol. Biochem. Zool. 75, 590–599.

Toshimori, H., Toshimori, K., Minamino, N., Kangawa, K., Oura, C., Matsukura, S., Matsuo, H., 1990. Chicken atrial natriuretic peptice (chANP) and its secretion. Cell Tissue Res. 259, 293–298.

Tsahar, E., Martínez del Rio, C., Izhaki, I., Arad, Z., 2005. Can birds be ammonotelic? Nitrogen balance and excretion in two frugivores. J. Exp. Biol. 208, 1025–1034.

Vena, V.E., Lac, T.H., Wideman, R.F., 1990. Dietary sodium, glomerular filtration rate autoregulation, and glomerular size distribution profiles in domestic fowl (Gallus gallus). J. Comp. Physiol. B 160, 7–16.

Vranish, J.R., Braun, E.J., 2011. Isolation of a putative osmoreceptor from the avian GI tract. Faseb. J. 25, 1047.3.

Warui, C.N., 1989. Light microscopic morphometry of the kidneys of fourteen avian species. J. Anat. 162, 19–31.

Webster, M.D., Bernstein, M.H., 1987. Ventilated capsule measurements of cutaneous evaporation in mourning doves. Condor 89, 863–868.

Wideman Jr., R.F., 1984. Organic phosphate probes of the avian renal phosphate secretory mechanism. Comp. Biochem. Physiol. 78B, 315.

Wideman Jr., R.F., 1987. Renal regulation of avian calcium and phosphorus metabolism. J. Nutr. 117, 808–814.

Wideman Jr., R.F., 1988. Avian kidney anatomy and physiology. In: CRC Critical Reviews in Poultry Biology, vol. 1. CRC Press, Inc, pp. 133–176. Issue 2.

Wideman Jr., R.F., 1991. Autoregulation of avian renal plasma flow: contribution of the renal portal system. J. Comp. Physiol. B 160, 663–669.

Wideman Jr., R.F., Braun, E.J., 1981. Stimulation of avian renal phosphate secretion by parathryoid hormone. Am. J. Physiol. 241, F263.

Wideman, R.F., Gregg, C.M., 1988. Model for evaluating avian hemodynamics and glomerular filtration rate autoregulation. Am. J. Physiol. 254, R925–R932.

Wilson, J.X., 1989. The renin-angiotensin system in birds. In: Hughes, M.R., Chadwick, A. (Eds.), Progress in Avian Osmoregulation. Leeds Philosophical and Literarary Society, Leeds, United Kingdom, pp. 61–79.

Withers, P.C., Williams, J.B., 1990. Metabolic and respiratory physiology of an arid-adapted Australian bird, the spinifex pigeon. Condor 92, 961–969.

Wolbach, R.A., 1955. Renal regulation of acid-base balance in the chicken. Am. J. Physiol. 181, 149–158.

Wolf, B.O., Walsberg, G.E., 1996. Respiratory and cutaneous evaporative water loss at high environmental temperatures in a small bird. J. Exp. Biol. 199, 451–457.

Wu, C., Lv, C., Wan, Y., Li, X., Zhang, J., Li, J., Wang, Y., 2019. Arginine vasotocin (AVT)/mesotocin (MT) receptors in chickens: evidence for the possible involvement of AVT-AVPR1 signaling in the regulation of oviposition and pituitary prolactin expression. Gen. Comp. Endocrinol. 281, 91–104.

Yokota, S.D., Benyajati, S., Dantzler, W.H., 1985. Comparative aspects of glomerular filtration in vertebrates. Ren. Physiol. 8, 193–221.

Zeferino, C.P., Wells, K.D., Moura, A.S.A.M.T., Rottinghaus, G.E., Ledoux, D.R., 2017. Changes in renal gene expression associated with induced ochratoxicosis in chickens: activation and deactivation of transcripts after varying durations of exposure. Poultry Sci. 96, 1855–1865.

Zenteno-Savin, 1991. Plasma Arginine Vasotocin and Angiotensin II Concentrations during Saline Acclimation in Birds with Salt Glands. M.Sc. thesis. University of British Columbia, Canada.

Zhang, G., Li, C., Li, Q., et al., 2014. Comparative genomics reveals insights into avian genome evolution and adaptation. Science 346, 1311–1320.

Chapter 20

Respiration

Frank L. Powell

Department of Medicine Division of Pulmonary, Critical Care, Sleep Medicine, University of California, San Diego La Jolla, CA, United States

20.1 Overview

The primary function of the respiratory system is *gas exchange*—delivering oxygen from the environment to the tissues and removing carbon dioxide from the tissues. Maintaining a constant body temperature in birds and mammals requires high levels of oxygen consumption and exercise in birds—namely flapping flight—creates the highest oxygen demand of any vertebrate. The structure of the avian respiratory system is very different from the mammalian lung and some of these differences support more efficient gas exchange, while others may be alternative evolutionary solutions to common problems for all air-breathing vertebrates.

Generally, the respiratory system acts as a servant to the rest of the organism by delivering enough oxygen and removing sufficient carbon dioxide for metabolic demands. As oxygen demand increases, a variety of respiratory responses insure an adequate supply of oxygen, which involve the lungs, respiratory mechanics, the pulmonary circulation, transport of oxygen and carbon dioxide in blood, pulmonary and tissue gas exchange, and the coordination of all these mechanisms by the respiratory control system. The respiratory system has a huge surface area exposing the body to the environment that requires defense mechanisms also. Individual sections in this chapter focus on each of these physiological mechanisms. References are made to mammalian respiratory physiology, so the reader can consult the extensive literature available for more details on fundamentals concepts. In birds, the respiratory system is also critical for thermoregulation (by evaporative water loss) and nonrespiratory functions such as vocalization, but these are not covered in this chapter. Current research problems and important unanswered questions are highlighted in sections labeled *Frontiers*.

20.1.1 Oxygen cascade

Figure 20.1 shows how these physiological transport steps function in series to transport oxygen from the environment to the cells. This is often referred to as the "oxygen cascade" because oxygen level (quantified as partial pressure, or P_{O_2}) decreases at each step in the model. Breathing movements bring fresh air into the lungs, and the heart pumps oxygen-poor blood to the lungs. Oxygen diffuses from gas to blood in the lungs, and this oxygen-rich blood returns to the heart via the pulmonary circulation. Arterialized blood is pumped to the various organs and tissues of the body via the systemic circulation. Finally, oxygen diffuses out of the systemic capillaries to metabolizing tissues and ultimately to the mitochondria inside cells. Carbon dioxide moves out of the cells to the environment through these same steps in the opposite direction from oxygen. Each of these steps is covered in the sections below, with an emphasis on respiratory structure function-relationships that are unique to birds, especially in comparison with mammals. Mammals are the only other vertebrates that achieve avian levels of oxygen demand during exercise.

20.1.2 Symbols and units

Table 20.1 provides a list of abbreviations used in this chapter, which are based on a few simple conventions. Primary variables are symbolized with a capital letter, and a dot over the variable indicates the first derivative with respect to time (e.g., units for inspired ventilation, $\dot{V}_I$, are L/min). Modifiers are small capitals for the gas phase and lower-case letters for liquid or tissues. Finally, a specific gas species is indicated with a subscript. Respiratory gas volumes (e.g., ventilation) are reported for physiological

Sturkie's Avian Physiology. https://doi.org/10.1016/B978-0-12-819770-7.00033-5

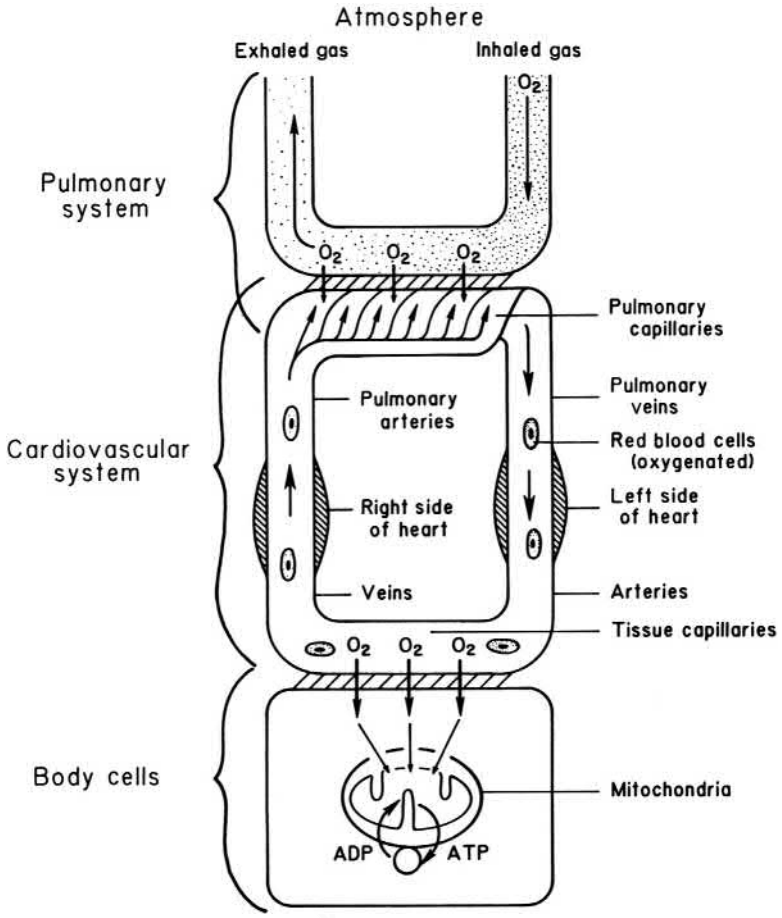

FIGURE 20.1 General model of the oxygen transport in birds. *Modified from Taylor and Weibel (1981).*

conditions (BTPS, body temperature and pressure, saturated) unless otherwise noted. Amounts of oxygen (O_2) or carbon dioxide (CO_2) are expressed in mmoles (e.g., O_2 concentration in mmol/L = mM). Pressure is expressed in Torr (7.5 Torr = 1 kPa).

20.2 Anatomy of the avian respiratory system

The structure of the avian respiratory system is unique among the vertebrates, with small lungs which do not change volume during breathing, and nine large air sacs which act as bellows to ventilate the lung but do not participate directly in gas exchange (Figure 20.2). The total volume of the respiratory system in a bird (i.e., lungs and air sacs) is larger than that in a comparably sized mammal ($\approx$15 vs. 7% of body volume), but the avian lung itself is smaller ($\approx$1%–3% of body volume). It is hypothesized that evolution of bipedal locomotion selected for a caudal expansion of the respiratory system in dinosaurs and air sacs further expanded with the evolution of flight (Farmer, 2006). Both avian and mammalian lungs evolved to support increased oxygen uptake by subdividing into smaller individual gas exchange units which increased surface area. However, the functions of ventilation and gas exchange were separated into the air sacs and parabronchial lungs in the *heterogeneous* partitioning of the avian respiratory system; in contrast, *homogenous* partitioning of the mammalian respiratory system resulted in alveolar lungs that perform both gas exchange and ventilation (Duncker, 1978) as discussed below.

Also in contrast to mammals, the avian thoracic cavity is essentially at atmospheric pressure (vs. subatmospheric), and there is no diaphragm to functionally separate it from the abdominal cavity. The parietal and visceral pleura surrounding the lungs are fused so there is no intrapleural space in birds as there is in mammals either (Maina, 2017). This section covers basic respiratory system anatomy necessary to understand respiratory function, but the reader is referred to several excellent monographs and reviews for more details (Duncker, 1971; King and Molony, 1971; Maina 2017; Mania et al., 2010; McLelland, 1989b). Terminology according to the *Nomina Anatomica Avium* is used here (King, 1979). Details of the blood-gas barrier and the anatomy of the pulmonary circulation are covered in later sections.

TABLE 20.1 Symbols in respiratory physiology.

Primary variables (and units)	
C	Concentration or content (mM = mmmol/L)
D	Diffusing capacity ($mmol_{O_2}$/(min·Torr)
P	Partial pressure or hydrostatic pressure (Torr or cm H_2O)
V	Gas volume (Liters, L, or mL)
$\dot{V}$	Ventilation (L/min)
$\dot{Q}$	Blood flow or perfusion (L/min)
$\dot{M}$	Gas flux (mmol/min)
Modifying symbols	
D	Dead space gas
E	Expired gas
$\bar{E}$	Mixed-expired gas
I	Inspired gas
T	Tidal gas
a	Arterial blood
c	Capillary blood
m	Membrane
t	Tissue
v	Venous blood
$\bar{V}$	Mixed-venous blood
Examples	
$P_{I_{O_2}}$	=Partial pressure of O_2 in inspired gas
$P_{a_{O_2}}$	Partial pressure of O_2 in arterial blood
$P_{\bar{V}_{O_2}}$	Partial pressure of O_2 in mixed-venous blood
$\dot{M}_{O_2}$	O_2 consumption per unit time
$\dot{V}_P$	Ventilation of the parabronchi per unit time

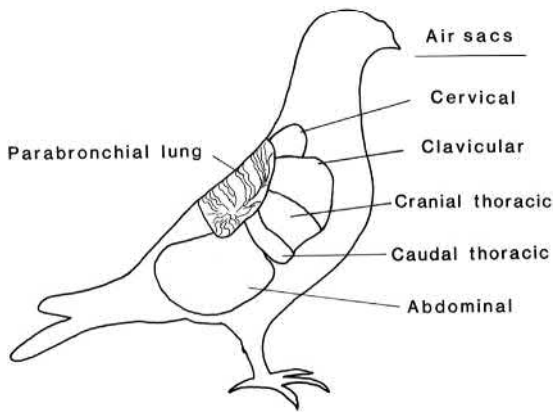

FIGURE 20.2 Respiratory system of a pigeon consisting of the parabronchial lung and air sacs.

20.2.1 Upper airways

Birds can breathe through the nares or mouth. Oronasal structures tend to heat and humidify inspired gas, and filter out large particles that could potentially damage the delicate respiratory surfaces. The oronasal cavity is separated from the trachea by the larynx, which opens into the trachea through the slit-like glottis. The laryngeal muscles contract with breathing to open the glottis during inspiration and decrease the resistance to inspiratory airflow. This rhythmic opening of the glottis is useful when attempting to intubate a bird. The trachea has complete cartilaginous rings in most avian species and plentiful smooth muscle. Interesting exceptions include the "double trachea" of penguins, with a medial septum dividing the trachea into two tubes, and the slit-like opening on the ventral surface of the trachea in emus, which is responsible for their characteristic booming call (McLelland, 1989a). The anatomy and physiology of

the larynx and trachea have been reviewed in detail (McLelland, 1989a).

Tracheal volume is an important determinant of "dead space" ventilation, and therefore gas exchange. Hinds and Calder (1971) measured tracheal volume in 27 species of birds and found in situ volume (V in ml) was related to body mass (M_B in kg) as: $V = 3.7\ M_B^{1.09}$. This equation underestimates tracheal volume in Pekin ducks (Bech et al., 1984; Hastings and Powell, 1986b) and pigeons (Powell, 1983) and overestimates the value for male chickens (Kuhlmann and Fedde, 1976), although the error is less than 25%. Tracheal volume is 4.5 times larger in birds than in comparably sized mammals (Hinds and Calder, 1971) and birds generally compensate for this increased dead space with a deep and slow breathing pattern (Bouverot, 1978). Several species of birds possess tracheal elongations, which loop inside the neck, but their function is unknown (McLelland, 1989a).

The trachea bifurcates into two primary bronchi at the syrinx, which is the vocal organ for birds (King, 1989). Like the mammalian larynx, it is a mechano-muscular valve that regulates pressure in distal airways to control airflow to the upper respiratory-vocal tract during expiration and singing. Most of the research on the syrinx has focused on vocalization and neurobiology of bird song that may have implications for the central control of breathing in birds (reviewed by Schmidt and Wild, 2014). In many species (e.g., chickens and ducks), but not all, this bifurcation occurs inside the thoracic cavity where the trachea runs through the clavicular air sac. Because of this position, the syrinx offers no protection for the lungs as the larynx does in mammals. Similar to the avian trachea, the syrinx shows considerable variation between species, and males in some species exhibit large bullae with unknown functions.

20.2.2 Lungs

The avian lung is located dorsally in the thoracoabdominal cavity of birds (Figure 20.2) and is invaginated by spinal processes anchoring the dorsal surface of the lung. Most of the volume of the lung (≈70%) is the parabronchi where gas exchange occurs (see below) and the remainder includes the pulmonary circulation and bronchi, which are illustrated in Figure 20.3 for a representative species.

20.2.2.1 Conducting airways

In most cases, the extrapulmonary primary bronchi, between the syrinx and the lungs, are relatively short. The intrapulmonary primary bronchus travels through the entire length of the lung, entering on the medioventral aspect and exiting at the caudal border of the lung into the ostium of the abdominal air sac (see below). The secondary bronchi can be considered in two functional groups based on their origin from the primary bronchus. The cranial group consists of four or five medioventral secondary bronchi, originating from the medioventral intrapulmonary primary bronchus. These cranial secondary bronchi branch further to form a fan covering the medioventral surface of the lung. The caudal group consists of 6–10 mediodorsal secondary bronchi, which also branch to form a fan over the mediodorsal surface of the lung.

A third group of secondary bronchi includes a variable number of lateroventral bronchi in most species, which also branch off caudal parts of the primary bronchus. The first or second laterobronchus forms a short connection to the posterior thoracic air sac (see below). Other lateroventral bronchi may penetrate lateroventral parts of the lung to variable degrees in different species, but they do not form a regular branching fan like the other secondary bronchi.

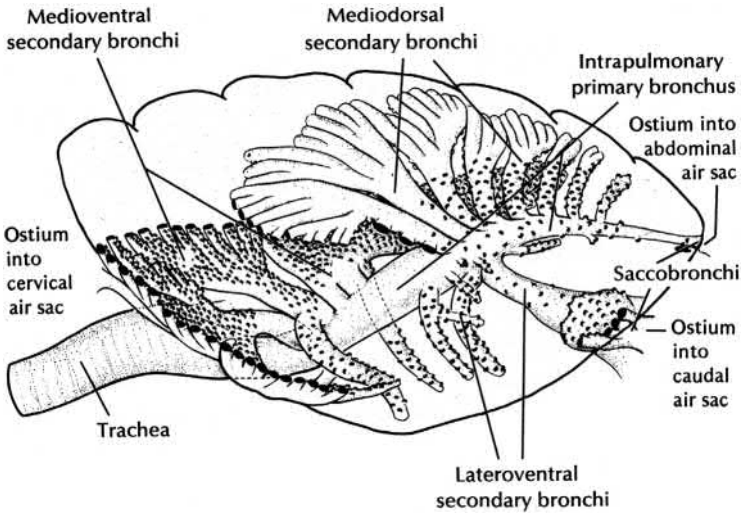

FIGURE 20.3 Bronchial arrangement in the left lung of the mute swan (*Cygnus olor*). *Modified from Duncker (1974).*

The primary and secondary bronchi are conducting airways because they do not participate in gas exchange. Cartilaginous semirings and smooth muscle support the primary bronchi, but the walls of the secondary bronchi are flaccid, and require on adhesion to the surrounding lung or pleura to remain open. The respiratory epithelium is ciliated with variable amounts of goblet cells in different species in the trachea, primary and secondary bronchi (Duncker, 1974).

20.2.2.2 Parabronchi

Parabronchi are the functional unit of gas exchange in the avian lung. They are also called "tertiary bronchi" because they can originate from the secondary bronchi, but parabronchus is the preferred terminology because they also originate from further branches of secondary bronchi (Figure 20.3). Most of the parabronchi are organized as a parallel series of several hundred tubes connecting the medioventral and mediodorsal secondary bronchi (Figure 20.3). Such parabronchi are called *paleopulmonic* parabronchi, and together with the primary and cranial and caudal groups of secondary bronchi, they comprise the simplest scheme of bronchial branching in the avian lung (Duncker, 1974).

In all birds except some penguins, there are additional parabronchi called *neopulmonic* parabronchi (Duncker, 1974). These parabronchi are not organized as regular parallel stacks of tubes but may exhibit irregular branching patterns. Neopulmonic parabronchi may connect another set of caudal laterodorsal secondary bronchi to caudal air sacs (see below) or other parabronchi. Neopulmonic parabronchi never comprise more than 25% of the parabronchi, and there are large species variations. However, it has not been possible to demonstrate any phylogenetic or evolutionary significance to neopulmonic versus paleopulmonic parabronchi, despite the implication of the terms (Maina, 1989, 2017). The functional significance of these different kinds of parabronchi is considered below.

Figure 20.4 illustrates the structure of a parabronchus and how they are organized in parallel, appearing like a honeycomb in cross-section. Gas exchange occurs in the walls of these tubes that are 0.5−2.0 mm in diameter and can be several mm long depending on the size of the bird (Duncker, 1971; Maina, 1989). The parabronchi are separated from each other along their length by a boundary of connective tissue and larger pulmonary blood vessels. The parabronchial lumen is lined by a meshwork of connective tissue and smooth muscle, which outlines the entrances to atria radiating from the parabronchial lumen. The atria lead to infundibulae and, ultimately, the air capillaries which are 2−10 μm in diameter and as long as about one-quarter of the total parabronchial diameter (Figure 20.4). The parabronchi are lined with cuboidal and squamous epithelial cells that become thinner moving into the atria and

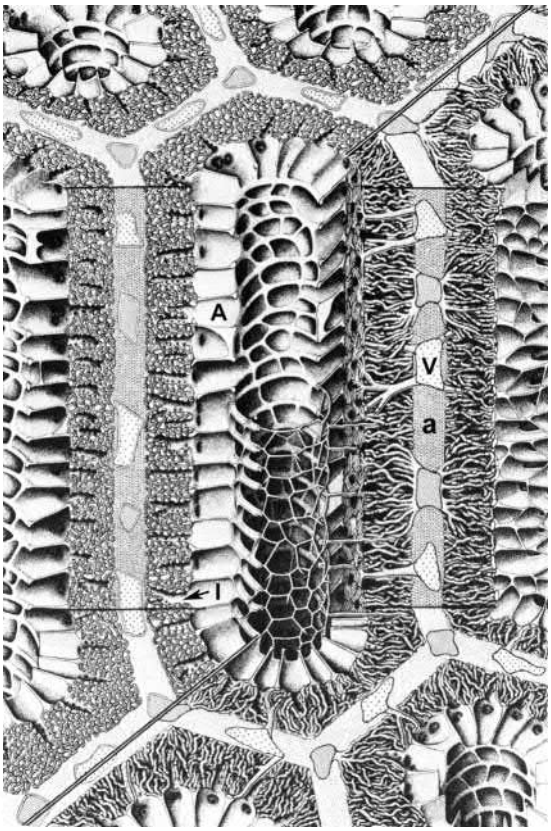

FIGURE 20.4 Cutaway drawing of a typical parabronchus (ca. 1 mm diameter). Left side shows pathway for air from parabronchial lumen into the atria (A), infundibula (I) and air capillaries. Right side shows blood flow from interparabronchial arterioles (a) into blood capillaries that collect in venules near the base of the atria and flow away from the lumen to interparabronchial venules (v). *Modified from Duncker (1974).*

exclusively squamous in the infundibulae and air capillaries (Smith et al., 1986). Air capillaries intertwine with a network of pulmonary blood capillaries in the parabronchial mantle, and the air-blood capillary interface is the site of gas exchange (see below). The gas exchange paryenchyma (air and blood capillaries and tissue) occupies 50 to 60% pf the parabronchial volume, with the balance being the lumen, atria, and large vessels in birds over a large range of sizes from hummingbirds to geese (Dubach, 1981; Powell and Mazzone, 1983).

20.2.2.3 Frontiers: *evolution of the blood-gas barrier*

The evolution of respiratory organs has been guided by at least two principles. First, the area of the blood-gas barrier has to be very large and very thin to support oxygen uptake by diffusion. Subdividing the lungs into smaller compartments increases the surface to volume ratio, so the total surface area in a bird or mammal is over 10-times that in a reptile with a simpler lung (Hsia et al., 2013). (A smaller surface area is adequate in reptiles given their lower levels

of oxygen consumption.) The second principle is keeping the blood-gas barrier extremely thin to facilitate diffusion, but this must be balanced with the need for structural integrity of the blood capillaries. This is particularly important in birds and mammals, which require high rates of blood flow to meet metabolic demands and have evolved separate pulmonary and systemic circulations allowing lower pressures in pulmonary versus systemic capillaries. Even so, pressure can increase during exercise to cause stress failure in mammalian pulmonary capillaries, but this has not been observed in bird lungs (West et al., 2006).

Birds have evolved a unique solution to these challenges that is arguably more adaptive than the mammalian solution, with the total surface area for gas exchange being about 15% greater and 2.5-times thinner in a bird than in the same-sized mammal (Maina et al., 1989; West, 2009). However, this results in air capillaries in the birds that are much smaller than alveoli in mammals. Recent detailed morphological studies reveal some of the factors providing extra strength in the dense air-blood capillary network of the parabronchial mantle, although questions remain. Figure 20.5 shows how the blood capillaries are conspicuous segments of similar dimensions while the air capillaries include larger spaces interconnected by short, narrow passages, with dimensions ranging from 3 to 20 µm in diameter (Maina, 2017). The intimate relationship between the air and blood capillaries strengthens both structures by the property of interdependence (which also is important in alveolar lungs). Further support for both kinds of capillaries is also provided by epithelial-epithelial bridges (shown separating air capillaries in Figure 20.5 upper left panel), thin collagen fibers forming a fibro-skeletal network supporting the exchange tissue, type-IV collagen in the basement membrane of the blood-gas barrier, and accumulation of trilaminar substance (surfactant) in the corners where the epithelial bridges abut blood capillaries (reviewed by Maina, 2017). The lack of volume changes in the air and blood capillaries in birds versus alveoli and capillaries in mammalian lungs must also contribute. The complete biomechanics of this system remain to be determined but the avian solution permits very high levels of oxygen uptake supporting activities such as hard exercise during flight with limited oxygen availability at high altitude (West et al., 2010).

20.2.3 Air sacs

The air sacs are thin membranous structures connected to the primary or secondary bronchi via ostia, and they comprise most of the volume of the respiratory system (Figure 20.2). Air sacs are poorly vascularized by the systemic circulation and do not directly participate in significant gas exchange but act as a bellows to ventilate the lungs. In most species, there are nine air sacs that can be considered in cranial and caudal functional groups (Duncker, 1971; Maina, 1989; McLelland, 1989b). Air sac diverticulae may also penetrate the skeleton, but there are large species differences. There is no evidence for these participating in respiration (Maina, 1989) although in an early experiment investigating the pattern of air flow in the avian respiratory system, Biggs and King (1957) showed that an anesthetized chicken could survive for several minutes breathing through the broken humerus if the trachea was blocked!

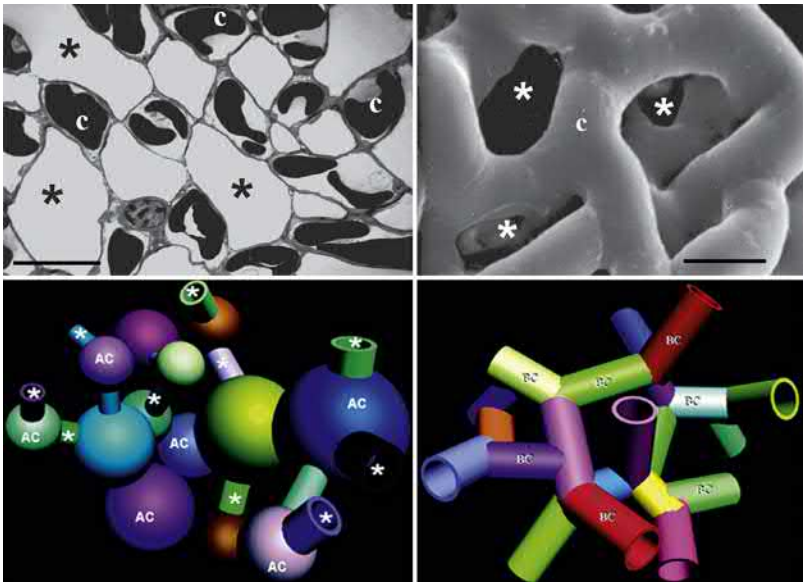

FIGURE 20.5 Top: Air (*)-blood (c) capillary network transmission electron micrograph (left) and scanning electron micrograph of case (right). Scale bar = 10 micron. Bottom: Computer-generated 3-D configuration of the air (left, AC) and blood capillaries (right, BC). AC consist of rotund spaces interconnected by short tubes (*asterisks*) while BC are short interconnected tubes of similar length and diameter. *From Maina (2007).*

The cranial group consists of the paired cervical air sacs, the unpaired clavicular air sac, and the paired cranial thoracic air sacs. The cervical sacs directly connect to the first medioventral secondary bronchus. The clavicular air sac directly connects to the third medioventral secondary bronchus and may also have indirect connections via parabronchi to other cranial (medioventral) secondary bronchi in some species, e.g., chickens. The cranial thoracic air sacs generally connect to the third medioventral secondary bronchi, and also to parabronchi originating from other cranial secondary bronchi in some species.

The caudal group consists of the paired caudal thoracic air sacs and paired abdominal air sacs. The caudal thoracic air sac is directly connected to the lateroventral secondary bronchus, and may have indirect connections to other lateroventral, or even cranial (medioventral) secondary bronchi in species with large amounts of neopulmonic parabronchi, e.g., chickens. The abdominal air sacs connect to the caudal end of the intrapulmonary primary bronchus and may have more indirect connections to parabronchi from laterodorsal secondary bronchi and the last mediodorsal secondary bronchi. Air sac connections with parabronchi are frequently grouped into a funnel-like structure called the saccobronchus.

20.2.4 Respiratory system volumes

The upper airways and bronchial branches proximal to the parabronchi comprise anatomical dead space as described above. Such conducting airways are called "dead space" because they do not participate directly in gas exchange. The intrapulmonary conducting airways make a relatively small contribution to total dead space, but total dead space volume is generally larger than most mammals, consistent with the generally long neck of birds. Physiological measures of dead space are considered below.

The actual volume of air in the avian lung directly involved in gas exchange at any moment is in the air capillaries. This averages about 30% of the lung volume in small birds (Dubach, 1981) compared to 40% in a human [considering the functional residual capacity (FRC) minus dead space]. The unique pattern of airflow in the open-ended parabronchi renews this gas exchanging volume more frequently than does tidal ventilation in dead-end alveolar lungs. This means birds experience larger variations in O_2 and CO_2 levels than mammals within the gas exchange regions of the lung during a breathing cycle.

Most of the respiratory system volume in birds is in the air sacs, and there is no comparable volume in the mammalian lung. Unlike mammalian alveoli, which change volume during ventilation, the air sacs are not important sites of gas exchange. There is tremendous variation in the volumes of air sacs reported in the literature because the value is very sensitive to the method of measurement. For example, the volume of plastic casting material that can be instilled under a pressure head into the air sacs of a dead bird may be much greater than the gas volume in live birds with muscle tone in the thorax and abdominal wall. Also, air sac volume in vivo can vary with posture, digestive, and reproductive states, as different structures in the body (e.g., eggs) displace volume. Casting under controlled pressure conditions (Duncker, 1971), gas dilution in vivo (Scheid et al., 1974) and imaging (Ponganis et al., 2015) are probably the most accurate methods available for determining air sac volume.

20.3 Ventilation and respiratory mechanics

Respiratory muscles generate pressure to move air in and out of the air sacs and through the parabronchial lung. The air sacs follow changes in body volume with respiratory muscle activity, and act as a bellows to ventilate the parabronchial lung that is essentially constant in volume (Jones et al., 1985; Macklem et al., 1979). In contrast to mammals, the avian lung volume is maintained by attachments to the body wall, and not by a subatmospheric pressure in an intrapleural space surrounding it. Also in contrast to mammals, birds have no diaphragm separating the body cavity into separate thoracic and abdominal compartments. Hence, pressures are relatively uniform in the avian thoracoabdominal cavity, which behaves mechanically as a single compartment (Scheid and Piiper, 1989).

Ventilation ($\dot{V}$) is the product of the volume per breath, or tidal volume (V_T) and the respiratory frequency (f_R), so $\dot{V}$ can be increased by breathing faster or deeper. The distribution of gas flow in the avian respiratory system depends upon the magnitude and pattern of respiratory muscle activity, as well as the mechanical properties of the body wall, lungs, and air sacs as described below.

20.3.1 Respiratory muscles

Figure 20.6 shows the changes in thoracic skeleton between normal inspiration and expiration in a bird (King and Molony, 1971; Zimmer, 1935). During inspiration, the sternum rocks cranially and ventrally with the coracoids and furcula rotating at the shoulder. Simultaneously, the vertebral ribs move cranially to expand the sternal ribs and thoracoabdominal cavity laterally.

In small birds (e.g., starlings) during flight, the furcula (wishbone) and sternum are mechanically coupled, such that the wing beat assists ventilation (Jenkins et al., 1988). However, wing movements in flight and ventilation are coordinated even in larger birds like geese so this may involve coupling of neuromuscular circuits as much as

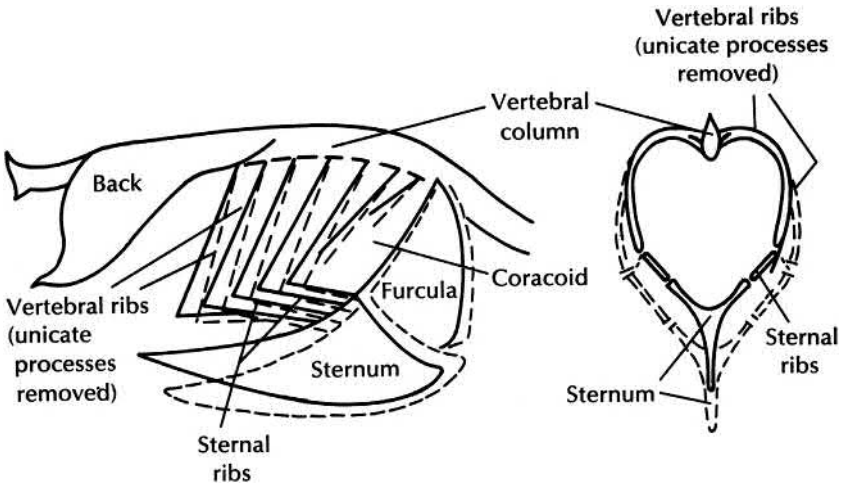

FIGURE 20.6 Changes in the position of the thoracic skeleton during breathing in a standing bird. *Solid lines* show thoracic position at the end of expiration and *dotted lines* show the end of inspiration.

respiratory mechanics (Funk et al., 1992a,b). During rest, both inspiration and expiration require active contraction of the respiratory muscles as listed in Table 20.2. The innervation for these muscles is summarized in deWet et al. (1967). Increases in ventilatory volumes are achieved by recruiting more motor units in active muscles and additional respiratory muscles, and during expiration, the opposite occurs (Fedde et al., 1963, 1964b, 1969; Kadono and Okada, 1962; Kadono et al., 1963). Therefore, the relaxed resting volume of the avian respiratory system is midway between inspiratory and expiratory volumes (Seifert, 1896), in contrast to mammals that relax to FRC at end-expiratory volume. The costoseptal muscles control the tension of the horizontal septum covering the ventral surface of the lung, but unlike the mammalian diaphragm, these are not effective at changing lung volume (Fedde et al., 1964a).

20.3.2 Mechanical properties

20.3.2.1 Compliance

Compliance (C) defines the effectiveness of small pressure changes (ΔP) at inducing volume changes (ΔV):

$$C = \Delta V/\Delta P$$

Because the pressure changes with breathing are essentially uniform throughout the coelom in birds, they can be measured as the difference between pressure in an air sac (P_{AS}) and atmospheric pressure outside the bird. Changes in respiratory system volume (V_{RS}) can be measured with a plethysmograph, which measures changes in whole body volume during breathing, or a pneumotachograph, which quantifies the amount of air inhaled or exhaled at the mouth or trachea. Compliance, measured as the slope of the steepest part of a graph plotting V_{RS} versus

TABLE 20.2 Respiratory muscles of the chicken.

Inspiratory	Expiratory
M. scalenus	Mm. intercostales externi of fifth and sixth spaces
Mm. intercostales externi (except in fifth and sixth spaces)	Mm. intercostales interni of third to sixth spaces
Intercostalis interni in second space	M. costosternalis pars minor
M. costosternalis pars major	M. obliquus externus abdominis
Mm. levatores costarum	M. obliquus internus abdominis
M. serratus profundus	M. transversus abdominis
	M. rectus abdominis
	Serratus superficialis, pars cranialis, and caudalis
	M. costoseptalis

P_{AS} in an artificially ventilated bird, ranges from 10 mL/cm H_2O in chickens (Scheid and Piiper, 1969) to 30 mL/cm H_2O in ducks (Gillespie et al., 1982b). These values are similar to compliance in mammals when correcting for body size.

Different results are obtained when compliance is measured by applying small oscillations in volume on spontaneously breathing birds. Compliance measured with this forced oscillation technique is only 7.7 mL/cm H_2O in ducks (Gillespie et al., 1982b) or much less than in mammals. In contrast, compliance measured with this technique in pigeons (2.8 mL/cm H_2O, Kampe and Crawford, 1973) is 3.7 times greater than the value predicted for a similar sized mammal (Powell, 1983). The reasons for these differences are not clear, but they suggest that compliance is exquisitely sensitivity to posture and muscular tone. Compliance primarily depends on the viscoelastic properties of the body wall and air sacs in birds, in contrast to the elastic properties of the lung in mammals (Macklem et al., 1979). Therefore, compliance in birds is high when volume changes occur by "unfolding" air sacs and stretching the abdominal wall, but it is low when volume changes are opposed by muscle tone in the body wall.

Birds native to high altitude have higher compliance than comparable species from low altitude, but this does not translate into differences in the work of breathing, which is only 1%−3% of resting metabolic rate and similar to mammals (York et al., 2017).

20.3.2.2 Resistance

Ohm's law defines the relationship between pressure, flow, and resistance (R) for the respiratory system as:

$$R = \Delta P/\dot{V}$$

where ΔP is the pressure gradient between the atmosphere and air sacs driving ventilatory airflow ($\dot{V}$). Expiration decreases air sac volume and creates a small positive pressure, which drives airflow out of the sac across small airway resistances; the opposite occurs during inspiration. Air sac pressure changes during breathing are small and similar in all of the air sacs (+1 cm H_2O), so resistance can be measured by measuring pressure and volume changes during artificial or spontaneous breathing as described above for compliance measurements (Scheid and Piiper, 1989). Airway resistance ranges from 4.8 cm H_2O/(L/s) in ducks (Gillespie et al., 1982a) to 41 cm H_2O/(L/s) in pigeons at the resonant frequency of their respiratory system (Kampe and Crawford, 1973).

Airway geometry is an important determinant of resistance. Poiseuille's law predicts resistance to laminar airflow is directly proportional to the length of an airway and inversely proportional to the fourth power of the airway radius. Therefore, resistance can vary between the different anatomical pathways possible for airflow in the avian respiratory system (see below). Different pathways presumably explain why airway resistance is generally greater during inspiration than during expiration in birds (Brackenbury, 1971, 1972; Cohn and Shannon, 1968). However, measurements using the forced oscillation technique on unanesthetized ducks find similar resistance during inspiration and expiration (Gillespie et al., 1982a). Resistance measured with this technique does not include any contributions from the body wall (Scheid and Piiper, 1989), so some differences between inspiratory and expiratory resistance may reflect muscle tone.

Physiological factors also affect airway resistance. Decreased lung P_{CO_2} increases resistance by a local effect on the openings of the mediodorsal secondary bronchi into the primary bronchus (Molony et al., 1976). However, P_{CO_2} does not affect smooth muscle contraction in the parabronchi (Barnas and Mather, 1978). Turbulent flow, which may occur in large airways at high ventilation rates or at bronchial bifurcations, can increase resistance (Brackenbury, 1972; Molony et al., 1976). Finally, resistance can change with breathing frequency. The pathway for airflow may be different with ventilation at high frequencies and small volumes (Banzett and Lehr, 1982; Hastings and Powell, 1987), and therefore affects resistance as described above. Also, the respiratory system has a resonant frequency, at which the overall impedance to breathing is minimized (e.g., 9.4 breaths/s in pigeons, Kampe and Crawford, 1973).

20.3.2.3 Air capillary surface forces

Surface tension at the gas-liquid interface of the respiratory exchange surface tends to collapse the air capillaries, and this decreases interstitial pressure between the air and blood capillaries. A decrease in interstitial pressure increases capillary filtration and can lead to edema and a thickening of the blood-gas barrier (see below). This tendency toward edema is probably a more important consequence of surface tension than airway collapse in the parabronchial lung because the air-blood capillary network tends to maintain constant volume (Maina, 2007). Similar to alveoli, air capillaries are lined by a surfactant, which lowers surface tension and counteracts these potentially deleterious effects (McLelland, 1989b). Lamellated osmophilic bodies in the parabronchial atria secrete the surfactant, which spreads as a trilaminar substance that is unique to birds over the air capillary surface (Bernhard et al., 2001; King and Molony, 1971; McLelland, 1989b; Pattle, 1978). Surface tension in avian surfactant is about threefold greater than in mammalian surfactant when subject to volume changes, but the maximum surface tension in avian surfactant is lower than in mammals (Bernhard et al., 2001). This is consistent with the chemical composition of avian versus mammalian surfactant and air capillaries not changing change volume

with ventilation, so there is no selective pressure to decrease surface tension to reduce the work of breathing in birds (Bernhard, 2016).

20.3.3 Ventilatory flow patterns

20.3.3.1 Air sac ventilation

The air sacs are ventilated roughly in proportion to their volume, such that the cranial and caudal groups (see above) each receive about 50% of the inspired volume (Scheid et al., 1974). The ventilation/volume ratio affects the O_2 and CO_2 levels in the air sacs (see below). Hence, the increase in air sac volume with changes in body wall muscle tone that may accompany anesthesia can alter air sac composition (Scheid and Piiper, 1969). There is no evidence for air flow between the sacs during normal breathing (Scheid and Piiper, 1989), although this has been postulated as a mechanism to enhance pulmonary gas exchange during breath-hold diving in birds (Boggs et al., 1996) and very complicated patterns of airflow may occur in the system during singing (Schmidt and Wild, 2014).

20.3.3.2 Pulmonary ventilation

Figure 20.7 shows the general pattern of ventilatory airflow during inspiration and expiration in the avian lung. The unidirectional flow in a caudal-to-cranial direction through the paleopulmonic parabronchi during both phases of ventilation has been established by a variety of methods (Scheid and Piiper, 1989). Early researchers noted that soot deposited primarily in the caudal regions of the lungs of pigeons collected in train stations, suggesting that inspired gas entered the lungs from a caudal direction (Dotterweich, 1930). More recently, researchers have confirmed this pattern with direct measurements of airflow (Brackenbury, 1971; Bretz and Schmidt-Nielsen, 1971; Scheid et al., 1972) and respiratory gases (Powell et al., 1981) in different parts of the lung.

Upon inspiration, about half of the tidal volume goes into the caudal air sacs and half goes into the cranial air sacs. Figure 20.7 shows how inspiratory flow bypasses the cranial secondary bronchial openings in the primary bronchus and flows directly into the caudal air sacs and caudal secondary bronchi. When gas enters the caudal secondary bronchi, it continues through the paleopulmonic parabronchi in a caudal-to-cranial direction and enters the cranial air sacs via the cranial secondary bronchi. If tidal volume is large enough, some of the inspired gas may reach the cranial air sacs via the paleopulmonic parabronchi during the same breath.

Upon expiration, the air sacs expel gas that eventually leaves the bird via the primary bronchi and trachea. Figure 20.7 shows how expiratory flow from the cranial air sacs leaves the lung via the cranial secondary bronchi emptying into the primary bronchi. Expiratory flow from the caudal air sacs is routed through the paleopulmonic parabronchi in a caudal-to-cranial direction via caudal secondary bronchi. If the expired volume is large enough, gas from the caudal air sacs will also leave the lung through the cranial secondary bronchi and mix with the gas emptying from the cranial air sacs.

Hence, airflow in the paleopulmonic parabronchi is caudal-to-cranial during both inspiration and expiration. In contrast to the paleopulmonic parabronchi, flow is bidirectional in the neopulmonic parabronchi, which are functionally in series with the caudal air sacs (Figure 20.7). Inspiratory airflow is cranial-to-caudal through neopulmonic parabronchi and into caudal air sacs, and in the caudal-to-cranial direction during expiration (Scheid and Piiper, 1989). The implications of these flow patterns for gas exchange are discussed later.

The pattern of airflow in the avian lung is determined by "aerodynamic valving." Pressure measurements show that branch points, such as the openings of the cranial secondary bronchial into the primary bronchi, are more important than distal airway resistance for determining flow patterns (Kuethe, 1988; Molony et al., 1976). There is no evidence for anatomical valves, for example, closing the primary bronchial openings of the cranial secondary bronchi during inspiration (reviewed by Scheid and Piiper, 1989 and Maina, 2017). As early as 1943, fluid dynamic models of the avian lung were used to show that these branches were critical for unidirectional caudal-to-cranial airflow in the paleopulmonic parabronchi (Hazelhoff, 1951). Modern theoretical models predict decreased effectiveness of aerodynamic valving with reduced gas

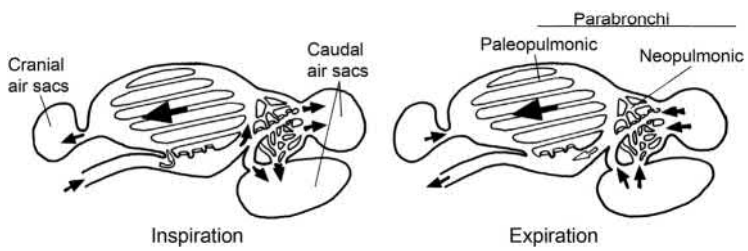

FIGURE 20.7 Pathway of airflow in the avian respiratory system during inspiration and expiration. Flow in paleopulmonic parabronchi is always caudal-to-cranial during both phases of breathing (*large solid arrows*), but neopulmonic flow is bidirectional. *Open arrows* show possible ventilatory shunts.

density, and experiments with low-density gases show valve failure and inspiratory shunts in birds (Banzett et al., 1987, 1991; Butler et al., 1988; Wang et al., 1988, 1992). In contrast, expiratory aerodynamic valving is not sensitive to gas density (Brown et al., 1995). Careful anatomical study has shown a narrowing of the primary bronchus distal to the cranial secondary bronchi that has been termed the *segmentum accelerans* (Maina, 2017). Computational fluid dynamic modeling of air flow in the ostrich lung shows a Bernoulli effect caused by flow through; this narrowing promotes flow past the cranial secondary bronchial openings to support the caudal-to-cranial flow in paleopulmonic parabronchi (Maina et al., 2009). Future experiments are necessary to determine if decreased gas density at high altitude can affect aerodynamic valving of not.

20.3.3.3 Air sac P_{O_2} and P_{CO_2}

The pattern of airflow is an important determinant of P_{O_2} and P_{CO_2} in the air sacs (Table 20.3). Cranial air sacs only receive gas from the parabronchi, so their P_{O_2} and P_{CO_2} levels are very near end-expired values. However, caudal air sacs contain a mixture of re-inhaled dead space gas (also end-expired P_{O_2} and P_{CO_2} levels) and fresh air, which raises their P_{O_2} and lowers their P_{CO_2}. Other factors that decrease P_{O_2} and increase P_{CO_2} in the air sacs include "stratification," gas exchange across the air sac wall, and gas exchange in neopulmonic parabronchi in series with the air sacs (Geiser et al., 1984).

Gas exchange across the air sac walls is less than 5% of the total respiratory gas exchange and a minor factor in determining air sac P_{O_2} and P_{CO_2} (Magnussen et al., 1976). Stratification (i.e., incomplete mixing of freshly inspired gas and resident gas in the air sacs) has been observed in ducks (Torre-Bueno et al., 1980), but its effect on air sac gas concentrations is not clear (Powell and Hempleman, 1985). Gas exchange in neopulmonic parabronchi in series with caudal air sacs seems to be the most important factor causing differences in measured P_{O_2} and P_{CO_2} values, and those predicted from re-inhaled dead space (Piiper, 1978). Bidirectional flow may also occur in a small fraction of parabronchi in the purely paleopulmonic lungs of penguins and affect P_{O_2} and P_{CO_2} in the caudal lungs of these birds too (Powell and Hempleman, 1985).

Considering the determinants of air sac P_{O_2} and P_{CO_2}, air sac sampling can offer valuable insights into respiratory function in birds under physiologically interesting conditions. For example, recent experiments sampling air sac gases in diving emperor penguins have been important for understanding how O_2 stores are utilized differently in diving birds and mammals; these differences result in similar O_2 levels in prolonged dives but the penguins

TABLE 20.3 Partial pressure of O_2 and CO_2 in air sacs and in end-expiratory gas of awake birds.

	Goose[a]	Goose[b]	Chicken[c]	Duck[d]	Pigeon[e]
Clavicular					
P_{CO_2} (Torr) P_{O_2} (Torr)	35 100	39 92	44.0 83.9	39.2 99.4	32. 109.
Cranial thoracic					
P_{CO_2} (Torr) P_{O_2} (Torr)	35 100	38 95	41.6 99.1	35.7 104.3	34. 105.
Caudal thoracic					
P_{CO_2} (Torr) P_{O_2} (Torr)	28 115	20 124	24.2 120.3	18.9 123.9	29. 111.
Abdominal					
P_{CO_2} (Torr) P_{O_2} (Torr)	28 115	18 128	14.7 130.0	17.5 126.7	27. 110.
End expiratory					
P_{CO_2} (Torr) P_{O_2} (Torr)	35 100	39 100	36.7 94.3	35.7 100.1	– –

[a] *Cohn and Shannon (1968), Figure 20.6.*
[b] *Scheid et al. (1991).*
[c] *Piiper et al. (1970).*
[d] *Vos (1935) Calculated assuming 700 Torr dry pressure.*
[e] *Scharnke (1938) Calculated assuming 700 Torr dry pressure.*

maintain normal (breathing) levels of arterial saturation during the first 7 min of a deep dive in contrast to dramatic decreases in Weddell and elephant seals (Ponganis et al., 2011).

20.3.3.4 Effective parabronchial ventilation

A quantitative description of gas exchange requires a measure of the effective ventilation of the lung. By analogy with alveolar ventilation in mammals, this is defined as parabronchial ventilation ($\dot{V}_P$) birds, and it differs from inspired ventilation ($\dot{V}_I$) because of dead space ventilation ($\dot{V}_D$). $\dot{V}_D$ in birds includes not only anatomic dead space in the upper airways but also it may result from ventilatory shunts in which airflow bypasses the parabronchi. The open arrows in Figure 20.7 show how gas might bypass the parabronchi during inspiration by directly entering the cranial secondary bronchi and air sacs, or during expiration by flowing back out the primary bronchus (Powell, 1988).

P_{CO_2} measurements in the cranial secondary bronchi show that an "inspiratory shunt", with inspired gas directly entering cranial air sacs from the primary bronchi does not occur (Powell et al., 1981). Some inspiratory flow may enter the fourth medioventral (cranial secondary) bronchus, however, and flow in a cranial-to-caudal direction through some paleopulmonic parabronchi (Powell and Hempleman, 1985), but this would not be a "shunt." In contrast, P_{CO_2} measurements indicate that an "expiratory shunt" with 10% −25% of expired gas from the caudal air sacs gas flowing out through the primary bronchus (Powell, 1988; Powell et al., 1981). Other experiments indicate that the relative proportion of expiratory flow in a mesobronchial shunt may vary from 100 to 75% at the beginning of expiration, to 0% near the midpoint of expiration (Hastings and Powell, 1986a). The magnitude of expiratory mesobronchial shunting depends on the pattern of ventilation, such as tidal volume, flow rate, and thermal panting (Bretz and Schmidt-Nielsen, 1971; Hastings and Powell, 1986a).

20.3.3.5 Artificial ventilation

The flow-through design of the rigid parabronchial lung allows a unique form of artificial ventilation, called unidirectional ventilation (Burger and Lorenz, 1960). Fresh humidified gas can be insufflated through a cannula in the trachea or an air sac, so it flows through the parabronchi before leaving the body through another cannula. This technique can be used clinically to support gas exchange during surgery which opens one of the air sacs (preventing effective spontaneous ventilation), to administer anesthetic gas or nebulized drugs (Fedde, 1978; Whittow and Ossorio, 1970), or for experimental studies (e.g., Burger et al., 1979; Fedde et al., 1974a). Artificial ventilation can also be performed manually by alternately compressing and lifting the sternum, for example, in a bird that may be anesthetized too deeply. It is also important to note that the sternum should not be compressed when holding a bird because this may lead to suffocation.

Inhalation anesthesia results in a higher mortality rate in birds (14%) compared to dogs and cats (Seamon et al., 2017) although experimental studies show that normal gas exchange can be maintained by positive pressure ventilation (e.g., Powell and Wagner, 1982). Inhalation anesthetics can inhibit intrapulmonary chemoreceptors (IPCs) in birds and inhibit CO_2-sensitive ventilatory drive (see below), which may contribute to this high mortality in birds. Further research on administering anesthetics during pressure-supported artificial ventilation in birds is warranted.

20.3.3.6 Frontiers: *lung structure-function in dinosaurs*

There is a rich literature on the evolutionary relationship between birds and dinosaurs and the progress continues in this field with modern experimental physiology. Originally, paleontology was used to generate the hypothesis that the long trachea, voluminous air sacs, and pneumatized bones found in birds evolved to enhance thermoregulation in extremely large dinosaurs (Perry et al., 2009). Subsequently, models were used to demonstrate how air sacs could facilitate the transition from quadrupedal to bipedal locomotion in dinosaurs, and this could ultimately lead to improvements in balance and agility necessary for flight (Farmer, 2006). More recently, physiological studies have demonstrated unidirectional air flow in the lungs of alligators, which have a bronchial tree similar to modern birds but no air sacs (Farmer and Sanders, 2010). This means cross-current gas exchange is possible in animals using a hepatic piston mechanism of breathing, as found in alligators and quadrupedal ancestors of birds, and costal breathing or bipedal locomotion are not prerequisites for cross-current gas exchange. The efficiency of cross-current gas exchange could have given avian ancestors a competitive advantage over synapsids when the basal archosaurs were evolving in times of low environmental oxygen. Such research demonstrates the value of comparative physiology for addressing important questions about evolution that can reach beyond what is possible with fossil skeletons.

20.4 Pulmonary circulation

The circulation is covered in another chapter, but this section highlights details of the pulmonary circulation that are relevant to understanding pulmonary gas exchange. The pulmonary circulation is unique because the lung is the only organ to receive the entire cardiac output. The "series" arrangement of the systemic and pulmonary circulations in

birds and mammals means that the lungs receive the same amount of blood flow as the whole rest of the body. However, the resistance to blood flow in the lungs is lower, and this allows lower perfusion pressure than in the systemic circulation, with the complete separation of the left and right ventricles. This section describes the structural and functional factors that determine pressures, volumes, and flows in the pulmonary capillaries, which are also important determinants of gas exchange.

20.4.1 Anatomy of the pulmonary circulation

The functional anatomy of the pulmonary circulation has been studied in detail for the domestic fowl (Abdalla and King, 1975). Interparabronchial arteries arise from main rami of the pulmonary arteries and run between the parabronchi and may perfuse more than one parabronchus. These vessels give rise to intraparabronchial arteries which perfuse the parabronchial mantle at several points along a parabronchus. The intraparabronchial arteries branch into the pulmonary blood capillaries near the outside edge of the parabronchial mantle which form a meshwork with air capillaries as described above. Pulmonary capillary blood is collected in intraparabronchial veins near the parabronchial lumen. These veins deliver blood flow to interparabronchial veins located near the outside edges of the parabronchus. The interparabronchial veins run between the parabronchi and collect blood from several points along a parabronchus and from several parabronchi. There are no anastomoses between the arterioles and veins in the lung (Abdalla, 1989).

This anatomy has two important consequences for respiratory gas exchange. First, all of the parabronchi are perfused along their entire length by mixed venous blood, and the oxygenated blood returning to the heart in the pulmonary vein (i.e., systemic arterial blood) is a mixture of blood draining the entire length of all the parabronchi. This allows cross-current gas exchange to occur, which is more efficient than alveolar gas exchange as described below. Second, it means that blood flow within the parabronchial mantle is directed from the periphery toward the lumen, which can affect the efficiency of gas exchange in the air capillaries.

20.4.2 Pulmonary capillary volume

Pulmonary capillary blood volume is similar in avian parabronchial lungs and mammalian alveolar lungs. A notable exception is the domestic fowl, which has a pulmonary blood capillary volume about threefold less than predicted for other birds that size (Maina et al., 1989). However, pulmonary blood capillary volume in birds is essentially constant under all conditions, in contrast to mammals that can increase pulmonary capillary volume by recruitment and distention when flow or pressure increases. Recruitment or distention of blood capillaries in a parabronchial lung would collapse the adjacent air capillaries and reduce gas exchange efficiency by causing a shunt (see below).

20.4.3 Pulmonary vascular pressures, resistance, and flow

20.4.3.1 Pulmonary vascular resistance and pressures

By analogy with Ohm's law:

$$PVR = \dot{Q}/\Delta P$$

where $\dot{Q}$ is cardiac output and ΔP is the difference between mean pulmonary artery and left atrial pressure. Pulmonary vascular pressures, cardiac output, and, therefore, pulmonary vascular resistances (PVRs) are similar in resting birds and mammals, but pulmonary arterial pressure changes more with cardiac output in birds. For example, doubling the blood flow through one lung of a duck almost doubles mean pulmonary artery pressure but causes no change in the resistance calculated for that lung, and no change in the capillary dimensions (Powell et al., 1985). Morphometric measurements of pulmonary blood capillaries in chickens with systematic increases in pulmonary artery pressure show no recruitment and very little distention (Watson et al., 2008). The lack of distention and recruitment of avian pulmonary capillaries also implies that the major effects of gravity and pulmonary vascular pressures on determining regional blood flow in mammalian lungs are not important in birds. The so-called Zone-1 and 2 conditions of mammalian lungs, in which alveolar pressure can collapse blood capillaries and stop or determine flow simply do not exist in birds (West et al., 2006). Hence, other mechanisms are responsible for the distribution of pulmonary blood flow in birds, as considered in the next section.

20.4.3.2 Distribution of blood flow

Local and regional changes in vascular resistance are more important than overall PVR for respiratory gas exchange. For example, regional control of blood flow between parabronchi has important effects on the efficiency of gas exchange (see below). Hypoxia has been shown to decrease local parabronchial blood flow, and gradients in P_{O_2} can explain differences in perfusion along parabronchi (Holle et al., 1978; Parry and Yates, 1979). Hypoxia and hypercapnia can also redistribute blood flow between paleopulmonic and neopulmonic parabronchi (Weidner et al., 2012). The physiological mechanism of these responses is not known. It may involve hypoxic pulmonary vasoconstriction, which is a direct effect of alveolar hypoxia on pulmonary arterioles in mammals. Smooth muscle capable of controlling local blood flow has been described for

interparabronchial arteries and veins in chickens, which could be responsible for control of blood flow between and along the lengths of parabronchi (Abdalla, 1989; Black and Tenney, 1980a; Burton et al., 1968).

20.4.3.3 Frontiers: *pulmonary vascular pressures during exercise in birds*

The lack of capillary distension and recruitment with increased cardiac output pose an interesting challenge for the avian lung during exercise. Alveolar capillary recruitment and distention is important for facilitating gas exchange during exercise by increasing the surface area for diffusion and preserving transit time for red blood cells in the capillaries to absorb oxygen by diffusion. In mammals, if pressures increase too much during exercise, for example, with extremely high cardiac outputs in elite human athletes or thoroughbred racehorses, then pulmonary capillaries suffer "stress failure" and blood to leaks into the alveoli (West, 2011). The blood-gas barrier in birds is even thinner than mammals, yet it appears to avoid stress failure on exercise. Cardiac output and therefore pulmonary blood flow increase comparably in birds and mammals, so extremely high pulmonary artery pressures are predicted with limited compliance in avian pulmonary blood capillaries. As considered above, blood capillaries may be supported better by air capillaries in birds than alveoli in mammals. However, there are no actual measurements of pulmonary circulation pressures in naturally exercising birds to date. Experiments simulating exercise, which used drug to increase metabolic rate, did not find large increases in pulmonary artery pressure as predicted for the increase in pulmonary blood flow (West et al., 2010). This is an area for future research.

20.4.4 Fluid balance

Fluid balance in the lungs, as in all organs, depends on the balance of hydrostatic and colloid osmotic pressures across the capillaries, and capillary permeability. These variables are similar in birds and mammals, although lymph drainage from avian lungs has not been measured directly (Weidner et al., 2006). Volume loading increases extravascular water in the lung interstitium, especially in the interparabronchial septum, and can lead to edema (Weidner et al., 1993; Weidner and Kinnison, 2002). The detailed anatomy of lymphatic vessels and rates pulmonary lymph drainage remains to be determined in birds.

A very important problem involving the pulmonary circulation and fluid balance in poultry husbandry is ascites in fast-growing broilers (chickens) bred for meat production (Julian, 1993). Ascites (i.e., fluid accumulation in the peritoneum) is associated with pulmonary arterial hypertension (PAH) and also occurs frequently in chickens raised at high altitude. Hence, early research on the problem focused on abnormal oxygen sensitivity, which could exaggerate increases in cardiac output with fast growth and cause hypoxic pulmonary vasoconstriction (Peacock et al., 1990). However, comparisons of PAH-susceptible and PAH-resistant broilers do not consistently reveal differences in cardiac output, although vascular capacity is limited in PAH susceptible broilers (Wideman et al., 2007). Factors that increase the PVR (e.g., hypoxia, thromboxane, endothelin-1, and serotonin) and reduce vasodilation (e.g., limited L-arginine, which is the substrate for nitric oxide) promote the onset of PAH and ascites and appear to be under genetic control (Wideman et al., 2013). Attempts to reduce deleterious effects of reactive oxygen species with antioxidative supplements to the diet have not worked consistently for ascites in very fast growing broilers. Current attempts to control the problem involve reducing the growth rate (and metabolic demand or cardiac output) and breeding resistant strains (reviewed by Kalmar et al., 2013).

20.5 Gas transport by blood

Equilibrium curves, also called dissociation curves, quantify the amount of O_2 and CO_2 in blood as functions of partial pressure. It is necessary to consider both partial pressure and concentration because partial pressure gradients drive diffusive gas transport in lungs and tissues, but concentration differences determine convective gas transport rates in lungs and the circulation. The concentration of a physically dissolved gas in a liquid is directly, and linearly, proportional to its partial pressure according to Henry's law: $C = \alpha P$, where α = solubility in mM/Torr. This means that inert gases such as nitrogen, and even anesthetic gases, increase in blood in direct proportion to their partial pressure. However, O_2 and CO_2 also enter into chemical reactions with blood. These reactions result in more complex relationships between concentration and partial pressure, but they serve to (*i*) increase O_2 and CO_2 concentrations in blood, (*ii*) allow physiological modulation of O_2 and CO_2 transport in blood, and (*iii*) make respiratory CO_2 exchange an important mechanism of acid-base balance in the body.

20.5.1 Oxygen

Oxygen concentration in normal arterial blood (Ca_{O_2}) of, for example, a pigeon is about 8.3 mM. However, the physical solubility of O_2 in blood (α_{O_2}) is only 0.00124 mM/Torr at 41°C, so only 0.117 mM of arterial O_2 content is dissolved gas with a normal arterial P_{O_2} of 95 Torr in pigeons (Powell, 1983). Most of the O_2 in blood is chemically bound to hemoglobin.

20.5.1.1 Hemoglobin

Hemoglobin is a large molecule consisting of four individual polypeptide chains, each with a heme (iron containing) protein that can bind O_2 when iron is in the *ferrous* (Fe^{2+}) form. Methemoglobin occurs when the iron is in the *ferric* form (Fe^{3+}), and it cannot bind O_2. Small amounts of methemoglobin, which occur under normal conditions, slightly reduce the amount of O_2 that can be bound to hemoglobin. One gram of pure mammalian hemoglobin can bind 0.060 mmol of O_2 when fully saturated, and this value appears similar in birds (Powell, 1983). Hemoglobin is concentrated inside red blood cells or erythrocytes. This cellular packaging is important for the biophysics of the microcirculation, and it provides physiological control of O_2 binding through cellular changes in the hemoglobin microenvironment (see below).

20.5.1.2 O_2-blood equilibrium curves

Figure 20.8 shows the O_2 equilibrium curve for duck blood as saturation (S_{O_2}) versus P_{O_2}, where S_{O_2} is defined as the percentage of the total hemoglobin sites available for binding O_2 which are occupied by O_2. Therefore, the maximum S_{O_2} is 100% and independent of hemoglobin concentration in blood. In contrast, O_2-hemoglobin equilibrium curves plotting concentration versus P_{O_2} quantify the absolute amount of O_2 in blood at a given P_{O_2}, and the maximum O_2 concentration depends on the amount of hemoglobin available. O_2 capacity defines the maximum O_2 concentration in blood when hemoglobin is 100% saturated with O_2. Total O_2 concentration in blood (C_{O_2}), including chemically bound and dissolved O_2, can be calculated as:

$$C_{O_2} = (O_2\text{capacity}[S_{O_2} / 100]) + (\alpha_{O_2} P_{O_2})$$

The sigmoidal (or "S") shape of the blood-O_2 equilibrium curve results from cooperative, *allosteric* interactions between the four subunits of hemoglobin, which determine the three-dimensional shape of the molecule. O_2 equilibrium curves for individual hemoglobin subunits are not sigmoidal, but simple convex curves like the O_2 equilibrium curve for myoglobin (see Section 20.7). The shape of the blood-O_2 hemoglobin equilibrium curve facilitates O_2 loading on blood in the lungs, and O_2 unloading from blood in the tissues.

The cooperativity between functional subunits of hemoglobin is quantified with Hill's coefficient, "n" (Powell and Scheid, 1989). High values of n, exceeding the theoretical limit of 4, have been observed in bird blood and may reflect increased cooperativity between aggregates of multiple hemoglobin molecules, or interactions between different isoforms of hemoglobin within a blood sample (Black and Tenney, 1980b; Lapennas and Reeves, 1983).

The affinity of hemoglobin for O_2 is quantified with P_{50}, which is the P_{O_2} at 50% saturation. For example, a decrease in P_{50}, or a "left shift," indicates an increase in O_2 affinity because S_{O_2} is greater for a given P_{O_2}. In general, P_{50} in avian blood is greater than in mammalian blood. Table 20.4 shows P_{50} values for several common avian species in the 40 Torr range, while P_{50} in comparably sized mammals are nearer 30 Torr. Some studies have used erythrocyte suspensions (Lutz, 1980), and this might explain the low P_{50} values they have found. However, determinations of P_{50} in avian hemoglobin solutions agree well with other published values for whole blood, for example, in pigeons (Powell, 1983). Because the efficiency of O_2 uptake in the avian lung is greater than mammals, birds may have evolved blood with low O_2 affinity to maximize O_2 delivery in tissue.

Developmental changes in hemoglobin-O_2 affinity are explained by differences in the type of hemoglobin expressed in an individual. For example, the dramatic decrease of P_{50} in chickens, from 75 Torr at 8 days to 35 Torr at 14 to 16 days of development, is explained by the replacement fetal hemoglobin with adult hemoglobin expressed in the erythrocytes (Baumann and Baumann, 1978).

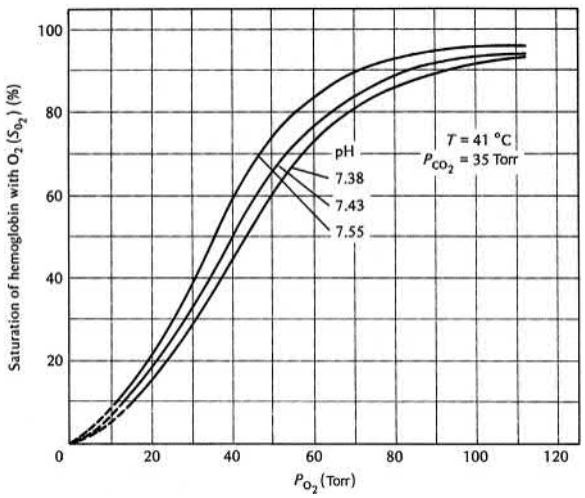

FIGURE 20.8 O_2-blood equilibrium curves for duck. Bohr effect is demonstrated by shifts of the curve as pH changes. *From Scheipers et al. (1975).*

20.5.1.3 Physiological control of O_2-hemoglobin affinity

The most important physiological factors that affect the P_{50} in a given species are (*i*) organic phosphate levels, (*ii*) pH,

TABLE 20.4 Respiratory parameters in avian whole blood.

Reference	Burrowing Owl (Athene cunicularia)[o]	Pigeon[l]	Female domestic fowl[b–d,f–j,n]	Pekin Duck[a,e]	Muscovy Duck (Cairina moschata)[h,k,m]	Bar-headed Goose (Anser indicus)[p]
Hematocrit (%)	33.7 + 2.1	48.7	26 to 30	45.4	37.3 ± 1.3	43.3 + 1.3
Hemoglobin (g%)	10.7 + 0.4	14.3	8.6 to 9.3	15.5	–	17.1 + 1.24
O_2 capacity (mmol l^{-1})	–	8.6	8.6 to 12.3	≥8.9	7.3 ± 0.51	–
P_{50} (Torr)	42.3 + 0.8	40.8 ± 1.4	47.7 ± 4.2	42.7 to 45.0	40.1 ± 3.7	31.2
Hill's n (–)	2.60 to 3.42	2.75	3.4 ± 0.1	4.3	2.9	–
Bohr coefficient (Δ log P_{50}/ΔpH)	0.42 to 0.46	0.42 to 0.53	0.50 ± 0.08	0.40 to 0.44	0.44 to 0.53	0.42 to 0.48
Temperature coefficient (Δ log P_{50}/ΔT)	–	0.015 to 0.026	0.014 to 0.015	–	–	0.024 to 0.032
Haldane effect ($\Delta C_{CO_2}/\Delta C_{O_2}$)	–	–	0.42	–	0.30	–

Where three or more measurements are available, SD is given; for less than three, the range is indicated.
[a] *Andersen and Lovo (1967).*
[b] *Bartels et al. (1966).*
[c] *Bauer et al. (1978).*
[d] *Baumann and Baumann (1977).*
[e] *Black and Tenney (1980b).*
[f] *Henning et al. (1971).*
[g] *Hirsowitz et al. (1977).*
[h] *Holle et al. (1977).*
[i] *Lapennas and Reeves (1983).*
[j] *Meyer et al. (1978).*
[k] *Morgan and Chichester (1935).*
[l] *Powell (1983).*
[m] *Scheipers et al. (1975).*
[n] *Wells (1976).*
[o] *Maginniss and Kilgore (1989).*
[p] *Meir and Milsom (2013).*

and (*iii*) temperature. These factors work by modifying the structure of the hemoglobin tetramer, so it binds O_2 more or less efficiently.

Inositol pentahosphate (IPP) is the primary organic phosphate affecting P_{50} in birds (Weber and Wells, 1989). The effect of IPP binding with hemoglobin inside erythrocytes is considerable, for example, increasing P_{50} from less than 3 Torr in stripped hemoglobin from chickens, to over 40 Torr under in vivo conditions (Weingarten et al., 1978). Physiological changes in organic phosphates have not been studied extensively in birds (Maginniss and Kilgore, 1989; Weber and Wells, 1989). In mammals, acclimatization to conditions such as altitude can modulate P_{50} by altering organic phosphates (2,3 diphosphoglycerate, or 2,3-DPG). However, it is important to note that differences in P_{50} between birds adapted over generations to low or high altitude cannot be explained by different organic phosphate concentrations. Erythrocyte inorganic phosphate levels and the effects of phosphates on P_{50} are similar in the low altitude (Canda and domestic) geese and the high altitude adapted bar-headed goose (Jendroszek et al., 2018; Petschow et al., 1977).

Figure 20.8 shows the effect of pH on the O_2 affinity, which is known as the Bohr effect. Increases in pH cause decreases in P_{50} (i.e., increase O_2-hemoglobin affinity) and vice versa. H^+ binds to histidine residues in hemoglobin, which changes the molecular conformation and ability of heme sites to bind O_2. The physiological advantage of the Bohr effect is that it facilitates O_2 loading in the lungs, where CO_2 is low and pH is high (see below). In muscles, the opposite occurs, and decreased pH facilitates O_2 unloading to the tissues. The Bohr effect is independent of saturation in most birds (Lapennas and Reeves, 1983; Maginniss, 1985; Meyer et al., 1978) and similar to values reported for mammals (Table 20.4).

In most birds, and in contrast to mammals, there is no independent effect of CO_2 on P_{50} (Meyer et al., 1978). CO_2 forms carbamino compounds with hemoglobin in mammals, and these cause small increases in P_{50}. In some birds, such as sparrows and burrowing owls, the Bohr effect is

greater when pH is changed with CO_2 compared to fixed acid (Maginniss, 1985; Maginniss and Kilgore, 1989). Therefore, carbamino formation does occur and can decrease O_2 affinity in stripped avian hemoglobin. However, strong binding of IPP to hemoglobin in most birds prevents an independent CO_2 Bohr effect (Lapennas and Reeves, 1983; Weingarten et al., 1978).

The in vivo physiological O_2 dissociation curve is steeper than the individual in vitro curves in Figure 20.8 because P_{CO_2} increases and pH decreases between arterial and venous blood. This is an advantage for gas exchange because it increases the change in O_2 concentration for a given change in P_{O_2}, thereby increasing O_2 uptake or delivery. The slope of the physiological O_2-blood equilibrium curve, in terms of O_2 concentration, is called βb_{O_2} (mM/Torr) and is used for quantitative descriptions of gas exchange (see below).

Because the combination of O_2 with hemoglobin is a chemical reaction that releases heat, increased temperature reduces the affinity of hemoglobin for O_2. This facilitates O_2 off-loading at exercising muscle with relatively high temperatures. It has also been hypothesized to facilitate O_2 loading in the lungs of birds flying at high altitude, when high rates of ventilation with extremely cold air might cool the respiratory exchange surfaces (Faraci, 1986, 1991). However, experiments to date have not been able to demonstrate decreased temperature of blood in the lungs. The effect of temperature on P_{50} in birds is generally similar to the effect in mammals (Table 20.4) except in the bar-headed goose, described next.

20.5.1.4 Frontiers: *hemoglobin adaptations to high altitude*

Hemoglobin-O_2 affinity is generally greater in birds native to high altitude compared to low altitude species, presumably as an adaptation to hypoxia (Black and Tenney, 1980b; Jessen et al., 1991; Meir and Milsom, 2013; Petschow et al., 1977). For example, P_{50} in the bar-headed goose (discussed above) is 10 Torr less than P_{50} in the closely related greylag goose, which lives on the Indian planes year-round (Petschow et al., 1977). Low P_{50} enhances pulmonary O_2 loading in extreme hypoxia (Bencowitz et al., 1982), and the trend for high O_2-affinity/low P_{50} hemoglobin in high altitude species is observed widely in both birds and mammals (Powell and Hopkins, 2010; Weber, 2007). Despite the universal nature of this adaptation, the molecular underpinnings of a low P_{50} at high altitude are diverse. In 56 pairs of avian taxa with contrasting altitudinal ranges, P_{50} was universally lower in the high altitude taxa but only a few of the amino acid substitutions explaining a low P_{50} were similar (Natarajan et al., 2016). Amino acid sequences from the bar-headed goose and greylag goose revealed a single substitution on one of the four hemoglobin subunits and genetically engineering this substitution into human hemoglobin decreases P_{50} by a similar amount to the difference between the two species of geese (Jessen et al., 1991). In general, a low P_{50} in high altitude compared to low altitude species requires only a few amino acid substitutions, and in birds these occur at contact points between subunits that stabilize hemoglobin in either low or high O_2-affinity conformations (Jendroszek et al., 2018). Effects of phosphates and H^+ on O_2-affinity are similar between low and high altitude avian hemoglobins (Weber, 2007). However, bar-headed goose hemoglobin is more sensitive to temperature than other birds (Table 20.4), and this is hypothesized to confer additional advantages. With differences in temperature and CO_2 between lungs and exercising muscle during high altitude flight, changes in P_{50} are predicted to double O_2 delivery, relative to a fixed P_{50} in bar-headed geese (Meir et al., 2013).

20.5.1.5 *Factors affecting O_2 capacity*

Changes in hemoglobin concentration [Hb] in blood will change the O_2 capacity, and therefore the O_2 concentration at any P_{O_2} as described above. [Hb] depends on both the mean corpuscular hemoglobin concentration (MCHC) and the hematocrit. Typical hematocrit and [Hb] values are given in Table 20.4; [Hb] is expressed as g/100 mL of blood instead of mM because the molecular weight was not known for all hemoglobins when they were originally measured. Typical values for MCHC in birds are 30–40 g Hb/100 mL of erythrocytes (Palomeque et al., 1979) or similar to the MCHC in mammals.

If [Hb] decreases, for example, with decreased hematocrit in anemia, then O_2 capacity and concentration decreases at any given P_{O_2}. The O_2 capacity increases when [Hb] increases, for example, by the stimulation of red blood cell production in bone marrow by the hormone erythropoietin (EPO). EPO is released from cells in the kidneys in response to decreases in arterial O_2 levels (Sturkie, 1986). Significant gender differences in [Hb], for example, in chickens, are explained by the effects of sex hormones on hematocrit (Sturkie, 1986). The functional consequences of changes in [Hb] are not always directly related to oxygen delivery (the product of blood flow and O_2 concentration) but also depend on viscosity, which increases with hematocrit and can limit tissue O_2 exchange. For example, warblers treated with anti-EPO decrease hematocrit and flight performance in a wind-tunnel at sea-level; however, their flight performance increases at 3000 m simulated altitude in a hypobaric wind tunnel (Yap et al., 2018). Optimal hematocrit depends upon the altitude at which an animal is exercising.

20.5.2 Carbon dioxide

CO_2-blood equilibrium (or dissociation) curves are nonlinear, but they have a different shape and position than O_2-blood equilibrium curves (Figure 20.9). CO_2 is carried in three forms by blood, so CO_2 concentrations in blood are generally much higher than O_2 concentrations. This results in a smaller range of P_{CO_2} values in the body, compared to the range P_{O_2} values, although the differences between arterial and venous *concentrations* are similar for CO_2 and O_2. The resulting physiological CO_2 dissociation curve between the arterial and venous points is much more linear than the physiological O_2 dissociation curve (Figure 20.9).

20.5.2.1 Forms of CO_2 in blood

CO_2 solubility in water or plasma is 0.0278 mM/Torr or about 20 times more soluble than O_2. Still, dissolved CO_2 only contributes about 5% of total CO_2 concentration in arterial blood. CO_2 can also combine with terminal amine groups in hemoglobin to form carbamino compounds. Bicarbonate ion (HCO_3^-) is the most important form of CO_2 carriage in blood. CO_2 combines with water to form carbonic acid, and this dissociates to HCO_3^- and H^+:

$$CO_2 + H_2O \; H_2CO_3 \; HCO_3^- + H^+$$

Carbonic anhydrase is the enzyme that catalyzes this reaction, and it occurs mainly in red blood cells (Maren, 1967). The reaction is almost instantaneous with carbonic anhydrase, but the uncatalyzed reaction will occur much more slowly in any aqueous medium (requiring over 4 min for equilibrium). The rapid conversion of CO_2 to bicarbonate results in about 90% of the CO_2 in arterial blood being carried in that form. The H^+ produced from CO_2 reacts with hemoglobin and affects both the O_2 dissociation curve (Bohr effect), and CO_2 dissociation curve as described next.

20.5.2.2 Factors affecting blood-CO_2 equilibrium curves

Hb-O_2 saturation is the major factor affecting the position of the CO_2 equilibrium curve. The Haldane effect increases CO_2 concentration when blood is deoxygenated, or decreases CO_2 concentration when blood is oxygenated, at any given P_{CO_2} (Figure 20.9). The Haldane effect is actually another view of the same molecular mechanism causing the Bohr effect on the O_2 equilibrium curve (see above). H^+ ions and O_2 can be thought of as competing for hemoglobin binding, so increasing O_2 decreases the affinity of hemoglobin for H^+ (Haldane effect) and increased $[H^+]$ decreases the affinity of hemoglobin for O_2 (Bohr effect).

The physiological advantages of the Haldane effect are to promote unloading of CO_2 in the lungs when blood is oxygenated, and CO_2 loading in the blood when O_2 is released to tissues. The Haldane effect also results in a steeper physiological CO_2-blood equilibrium curve (Figure 20.9), which has the physiological advantage of increasing CO_2 concentration differences for a given P_{CO_2} difference. Finally, the Haldane effect can cause apparent negative blood-gas CO_2 gradients when it is amplified by cross-current gas exchange in avian lungs (see below).

20.5.3 Acid-base

The chemical equilibrium between CO_2 and H^+/HCO_3^- ions has tremendous implications for acid-base physiology. Every mole of metabolic CO_2 produced results in 1 mole of acid, and over 95% of this acid is excreted by the lungs (Skadhauge, 1983). The ability to change blood P_{CO_2} levels rapidly by changing ventilation has a powerful effect on blood pH, so acid-base balance depends on the integrated function of respiratory and renal systems.

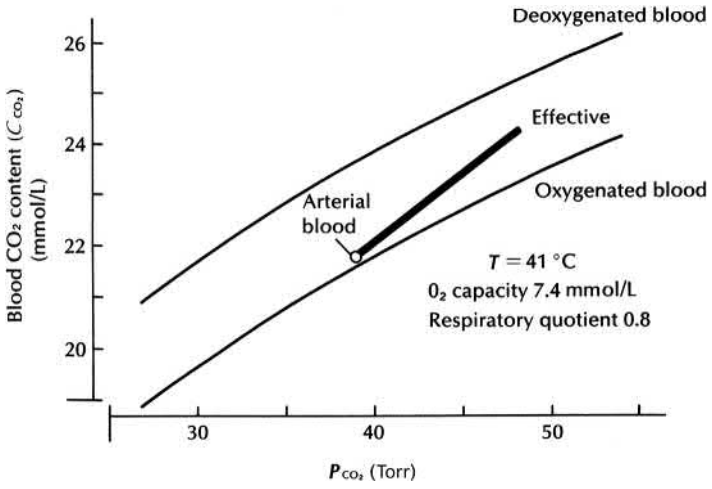

FIGURE 20.9 CO_2-blood equilibrium curves from the duck. Upper (deoxygenated blood) and lower (oxygenated blood) curves are derived from in vitro equilibration of blood samples. Heavy line is the physiological or in vivo dissociation curve from unanesthetized undisturbed birds. It illustrates the changes in CO_2 content (C_{CO_2}) in blood as it changes from arterial blood to venous blood in the tissue capillaries. *From Scheipers et al. (1975).*

20.5.3.1 Henderson-Hasselbalch equation

This equation describes the relationship between P_{CO_2}, pH, and $[HCO_3^-]$ in blood as:

$$pH = pK_a + \log\left([HCO_3^-] / \alpha P_{CO_2}\right)$$

where pK_a is $-\log_{10}$ of K_a, the dissociation constant for carbonic acid, $[HCO_3^-]$ = bicarbonate concentration in mEq/L or mM, and α is the physical solubility for CO_2 in water. A normal value for arterial pH (pHa) in chickens is 7.52 (Table 20.5), which can be calculated from $pK_a = 6.09$ and $\alpha_{CO_2} = 0.03$ mM/Torr in chicken plasma at 41°C (Helbacka et al., 1963), arterial $P_{CO_2} = 33$ Torr (Table 20.5), and arterial $[HCO_3^-] = 27.2$ mM. The buffer value for plasma in ducks is similar to the value for humans (Scheipers et al., 1975) if corrections are made for differences in [Hb]. At pH = 7.5, the $[H^+]$ is only 30 *nano*M, or significantly less than many other important ions in the body, such as Na^+, Cl_3^-, HCO_3^-, which occur in the mM range. Small changes in pH, corresponding to very small changes in $[H^+]$ can lead to dramatic changes in physiological function.

The Henderson-Hasselbalch equation shows how the physiological control of pH depends on the ratio of $[HCO_3^-]$ to $[\alpha P_{CO_2}]$. Notice, that a normal pH can occur with a variety of $[HCO_3^-]$ and P_{CO_2} values, so, for example, pH = 7.52 in a chicken does not necessarily indicate normal acid-base status. The primary cause of a chronic acid-base disturbance cannot be determined from P_{CO_2}, pH, and $[HCO_3^-]$ data alone. Other details of the disease history, pulmonary function, or blood chemistry must be obtained for a proper diagnosis.

The respiratory system controls pH primarily by changing arterial P_{CO_2} ($P_{a_{CO_2}}$). $P_{a_{CO_2}}$ is determined by parabronchial ventilation at any given metabolic rate (see below). Increasing ventilation will decrease $P_{a_{CO_2}}$ and increase pHa, while decreasing ventilation will have the opposite effects. Therefore, ventilation is an extremely effective mechanism for changing pHa quickly, and ventilatory reflex responses to pH are the most important physiological mechanisms for rapid control of pH (see below) The kidneys can also control pH by changing $[HCO_3^-]$ independent of CO_2 changes, as described in another Chapter 12, but renal changes in pH generally take longer than respiratory changes in pH.

20.5.4 Blood gas measurements

Avian blood presents special challenges to the accurate measurement of P_{O_2}, P_{CO_2}, and pH with traditional equipment designed for humans. In contrast to mammals, avian

TABLE 20.5 Gas exchange variables in awake resting birds.

Reference	Pigeon[a]	Female domestic fowl[b]	Pekin duck[c]	Pekin duck [d]	Muscovy Duck (Cairina moschata)[d]
Mb (kg)	0.38	1.6	2.37	2.4	2.16
$\dot{M}_{O_2}$ (mmol/min)	0.35	1.09	1.67	–	–
f_R (min^{-1})	27.3	23	15.6	8.2	10.5
V_T (mL)	7.5	33	58.5	98	69
$\dot{V}_E$ (L/min)	0.204	0.760	0.910	0.807	0.700
$\dot{Q}$ (L/min)	0.127	0.430	0.423	0.973	0.844
$P_{E_{O_2}}$ (Torr)	–	101.8	–	100.1	96.6
$P_{a_{O_2}}$ (Torr)	95	87	100	93.1	96.1
$P_{\bar{V}_{O_2}}$ (Torr)	50	40.8	69.6	63.3	55.9
$P_{E_{O_2}}$ (Torr)	–	33.0	–	34.2	34.2
$P_{a_{CO_2}}$ (Torr)	34	29.2	33.8	36.3	35.9
$P_{\bar{V}_{CO_2}}$ (Torr)	–	39.3	–	37.3	42.6

Data collected from birds in body plethysmographs except references b and d which used endotracheal tubes in lightly restrained upright birds. $\dot{M}_{O_2}$ not given for reference d because mixed-expired gases were not measured.
[a] *Bouverot et al. (1976).*
[b] *Piiper et al. (1970).*
[c] *Bouverot et al. (1979).*
[d] *Jones and Holeton (1972).*

erythrocytes are nucleated (as are most other vertebrates), and this may be the reason for high rates of O_2 consumption compared to mammals. Therefore, care must be taken to analyze arterial blood gases in birds as soon as possible after the sample is drawn, and to correct for any decreases in P_{O_2} with time if necessary. Storing the samples in ice water may help if immediate analysis is not possible, but the analyzed value can still differ from the in vivo value if any delay occurs, especially in normoxia where the blood-O_2 equilibrium curve is relatively flat and small O_2 content changes cause large changes in P_{O_2} (Kawashiro and Scheid, 1975). Sampling delays may also explain reports of 0 Torr P_{O_2} values in mixed venous blood from pigeons at simulated high altitude (Weinstein et al., 1985).

In addition to sampling delays, care must be taken to perform the analysis at body temperature, which is usually greater than the human value of 37°C, or to apply temperature correction values established for avian blood (Kiley et al., 1979). Also, a blood-gas correction factor needs to be established with a tonometer to account for differences in P_{O_2} measured in the liquid phase after calibrating electrodes with a gas phase (Nightingale et al., 1968). These, and other factors which may affect O_2-hemoglobin saturation measurements, have been discussed in other reviews (e.g., Powell and Scheid, 1989).

Finally, the most important determinant of arterial blood gas values is the physiological state of the bird. Table 20.5 presents arterial blood gases for several species breathing room air, but these may not be "normal" if the bird was excited by the sampling procedure. Remote-controlled sampling devices have been used for resting ducks (Scheid and Slama, 1975), and this technology is being extended to other interesting conditions such as diving penguins (Ponganis et al., 2011) and flying geese (Meir et al., 2013). Recently, a mouse pulse oximeter has been used to measure O_2-hemoglobin saturation in geese, and the results were generally as expected and the measurements are almost noninvasive (Ivy et al., 2018); however, potential errors are physiologically significant (95% confidence limits = +5% S_{O_2} in normoxia), and the device has not been calibrated against validated methods on simultaneous samples.

20.6 Pulmonary gas exchange

Theoretically, the unique anatomy of the avian respiratory system results in a more efficient model of gas exchange than the mammalian model (Piiper and Scheid, 1975). For a given level of ventilation to the gas exchange surfaces ($\dot{V}_P$), cardiac output ($\dot{Q}$), and lung diffusing capacity ($D_{L_{O_2}}$), arterial oxygenation and CO_2 elimination are predicted to be greater in a parabronchial lung, compared to an alveolar lung with the same inspired gases and metabolic demands (Powell and Scheid, 1989). This section explains the structural and functional basis for this most important function of the respiratory system and how avian gas exchange actually performs in nature under physiological conditions.

20.6.1 Basic principles of oxygen transport

20.6.1.1 Convection

Convection, or bulk flow of gas, is used to transport oxygen into the lungs by ventilation, and to the tissues by blood flow. The Fick principle, which is simply conservation of mass applied to respiratory gas transport, can be used to quantify O_2 uptake as:

$$\dot{M}_{O_2} = \dot{V}\beta_{g_{O_2}}\left(P_{I_{O_2}} - P_{\overline{E}O_2}\right)$$

where $\dot{M}_{O_2}$ is O_2 uptake, $\dot{V}$ is ventilation, $\beta_{g_{O_2}}$ is the capacitance coefficient for O_2 in the gas phase (0.512 mM/Torr at 41°C), and $(P_{I_{O_2}} - P_{\overline{E}_{O_2}})$ is the difference between inspired and mixed-expired P_{O_2} (Piiper et al., 1971; Powell and Scheid, 1989). Inspired and expired ventilation are assumed equal in this formulation of the Fick principle, so the amount of O_2 consumed is the difference between the amount of O_2 inspired and the amount expired. Mixed-expired P_{O_2} is used when total ventilation is measured or end-expired P_{O_2} is used if parabronchial ventilation ($\dot{V}_P$) is available (see above). The same principles described for O_2, also apply to CO_2 exchange.

The Fick principle can be written for the cardiovascular transport of O_2 out of the lungs and to the tissues also:

$$\dot{M}_{O_2} = \dot{Q}\beta_{b_{O_2}}\left(P_{a_{O_2}} - P_{\overline{\dot{V}}_{O_2}}\right)$$

where $\dot{Q}$ is cardiac output and $\beta_{b_{O_2}}$ is the physiological slope of the blood-O_2 equilibrium curve. Hence, the amount of O_2 taken up by blood in the lungs is the difference between the amount of O_2 leaving the lungs in arterial blood, and the amount that entered the lungs in mixed-venous blood. In a steady state, $\dot{M}_{O_2}$ is equal at each step of the O_2 cascade, so the Fick principle can be rearranged to calculate $\dot{M}_{O_2}$, $\dot{Q}$, $\dot{V}$, or P_{O_2} from measurements of other variables in the equation. Table 20.5 lists the important variables for quantifying gas exchange in several birds under resting conditions. Changes in these variables under different physiological conditions such as exercise, hypoxia, and thermal stress have been summarized in several reviews (Brackenbury, 1984; Butler, 1991; Faraci, 1991; Powell and Scheid, 1989).

20.6.1.2 Diffusion

O_2 movement over the very short distances across the blood-gas barrier occurs effectively by the "passive" mechanism of diffusion; active transport of O_2 does not occur in the body. Fick's law of diffusion describes O_2 transport from the air capillaries to the blood capillaries as:

$$\dot{M}_{O_2} = \Delta P_{O_2} \cdot D_{L_{O_2}}$$

where ΔP_{O_2} is the average P_{O_2} gradient between the air capillary and blood in the pulmonary capillary and $D_{L_{O_2}}$ is the diffusing capacity of the lung for O_2. The equation shows that a larger $D_{L_{O_2}}$ can transport more O_2 for a given P_{O_2} gradient. Determinants of $D_{L_{O_2}}$ are described in the section on lung diffusing capacity below.

20.6.2 Cross-current gas exchange

20.6.2.1 Cross-current O_2 exchange

Figure 20.10 shows how air flow and blood flow in the parabronchus can be viewed as occurring perpendicular to one another, and this is the basis for describing avian gas exchange with a "cross-current" model (Piiper and Scheid, 1972, 1975). In this idealized model of cross-current exchange, air flow is assumed continuous through the parabronchus which is uniformly perfused along its length by mixed-venous blood. At the inspiratory end of the parabronchus, there is a large P_{O_2} gradient driving diffusion of O_2 into the capillary blood, which raises capillary P_{O_2} and drops parabronchial P_{O_2}. As air flows along the parabronchus, the P_{O_2} gradient driving O_2 diffusion decreases with parabronchial P_{O_2}, while $P_{\bar{V}_{O_2}}$ is constant. At the expiratory end of the parabronchus, P_{O_2} has decreased to end-expired levels, and P_{O_2} in the capillary blood leaving this part of the parabronchus is correspondingly low. However, notice that arterialized blood returning to the heart is a mixture of capillary blood draining the entire length of the parabronchus. Therefore, arterial P_{O_2} is greater than end-expired P_{O_2} in ideal cross-current gas exchange.

A negative expired-arterial P_{O_2} difference, shown in Figure 20.10 as the overlap of P_{O_2} arrows, is not possible in alveolar gas exchange. The best situation that can be achieved in ideal alveolar gas lungs is equilibrium between expired and arterial P_{O_2}, so $(P_{E_{O_2}} - P_{a_{O_2}}) = 0$. However, negative expired-arterial P_{O_2} differences are not always observed in birds, and arterial P_{O_2} is similar in resting, normoxic birds and mammals (Table 20.5). As explained in the following sections, cross-current O_2 exchange is theoretically more efficient than alveolar exchange, but similar amounts of gas exchange limitation have a larger effect in cross-current exchange (see below).

Notice that the efficiency of cross-current exchange should not depend on the direction of ventilatory flow in the parabronchus. This is supported by experiments which reversed the direction of parabronchial flow in ducks and chickens and found no difference in the expired-arterial P_{O_2} differences for O_2 or CO_2 (Powell, 1982; Scheid and Piiper, 1972). It is physiologically significant because airflow is presumably bidirectional in neopulmonic parabronchi (see above).

20.6.2.2 Cross-current CO_2 exchange

Figure 20.10 also shows how expired P_{CO_2} can exceed arterial P_{CO_2} in a parabronchus, which is also impossible in alveolar gas exchange. This occurs similar to the "overlap" of arterial and expired P_{O_2} as explained above. However,

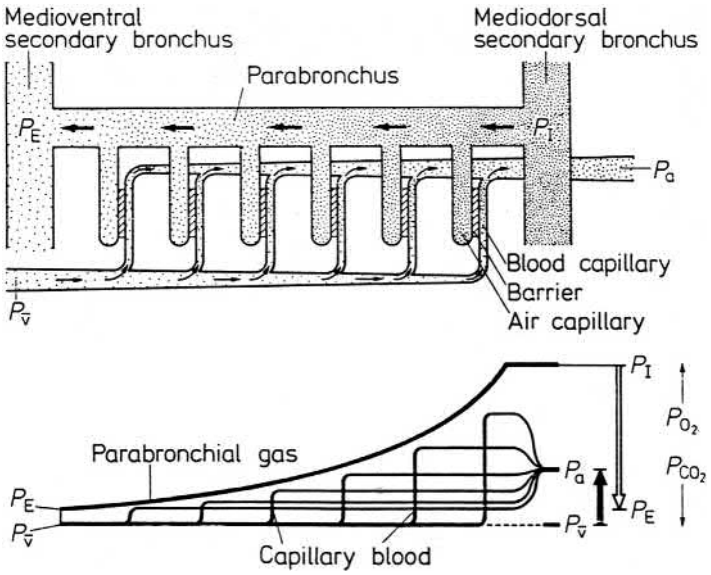

FIGURE 20.10 Cross-current model of gas exchange in the parabronchus. Lower panel shows how $P_{a_{O_2}}$ results from a mixture of blood from capillaries all along the parabronchus, where P_{O_2} ranges from P_I to P_E. Overlap of P_{O_2} in gas (*open arrows*) and blood (*filled arrows*) shows how $P_{a_{O_2}}$ can exceed $P_{E_{O_2}}$ in birds. *From Scheid (1979).*

experimental observations of expired P_{CO_2} exceeding *mixed-venous* P_{CO_2} in birds can only be explained by an interesting interaction of O_2 and CO_2 exchange in the parabronchus. Because of the shape of the O_2 and CO_2 blood equilibrium curves, the ratio of CO_2 elimination to O_2 uptake (R = respiratory exchange ratio) decreases near the expiratory ends of the parabronchus (Meyer et al., 1976). As originally postulated by Zeuthen (1942), this can lead to oxygenation of mixed-venous blood in expiratory ends of the parabronchi and increase P_{CO_2} in capillaries by the Haldane effect. Because P_{CO_2} of oxygenated mixed-venous blood is greater than $P_{\overline{V}_{O_2}}$ (Figure 20.9), P_{CO_2} in gas equilibrating with such blood at the expiratory end of the parabronchus (i.e., $P_{E_{O_2}}$) can exceed true $P_{\overline{V}_{O_2}}$.

Overlap between arterial and expired P_{CO_2} is more commonly observed than overlap for O_2 in birds (Table 20.5). This is because of differences in the O_2 and CO_2 blood equilibrium curves, and the fact that CO_2 is less sensitive than O_2 to some of the factors limiting the efficacy of cross-current gas exchange (Powell and Scheid, 1989).

CO_2 exchange can be affected by the same factors limiting O_2 exchange, which are considered in detail below. However, $P_{a_{CO_2}}$ is most sensitive to changes in ($\dot{V}_{D_{phys}}$) and effective $\dot{V}_P$. CO_2 should not be diffusion limited either because O_2 and CO_2 require similar times for diffusion equilibrium (Wagner, 1977). $\dot{V}/\dot{Q}$ mismatching and shunt increases $P_{a_{CO_2}}$ less than they decrease $P_{a_{O_2}}$ because of differences between the O_2 and CO_2-blood equilibrium curves (Powell and Scheid, 1989).

20.6.3 Lung diffusing capacity

The diffusing capacity of the lung for O_2 ($D_{L_{O_2}}$) is a complex variable that depends on several physiological processes (Powell, 1982; Powell and Scheid, 1989). These include gas-phase diffusion in the air capillaries, diffusion across the blood-gas barrier, and the chemical reaction between O_2 and hemoglobin.

20.6.3.1 Gas transport in air capillaries

Ventilatory flow in the parabronchi prevents significant P_{O_2} gradients from developing in the lumen of the parabronchus. However, the mechanism of gas transport in the air capillaries is not clear, and P_{O_2} gradients could occur between the lumen and the depths of the parabronchial mantle. Originally, it was assumed that diffusion explained gas transport over the small dimensions of the air capillary, considering the small distances involved and effectiveness of diffusive gas transport in the functional gas exchange unit of alveolar lungs. Indeed, measurements show no significant diffusive resistance to gas exchange along the air capillaries (Burger et al., 1979; Crank and Gallagher, 1978; Scheid, 1978). If diffusion is the main gas transport mechanism within air capillaries, then air-blood capillary exchange could be enhanced by an arrangement similar to counter-current exchange (Scheid, 1978). O_2 would diffuse from the lumen toward the periphery in air capillaries, which is opposite to the direction of flow in the blood capillaries (Figures 20.4 and 20.10). Therefore, blood at the end of a capillary would equilibrate with the relatively high P_{O_2} levels in air capillaries near the parabronchial lumen. However, there is no experimental evidence for this, and more recent morophometric studies of the air capillary network (Figure 20.5) shows extensive connections and branching, in contrast to the dead end tubes in Figure 20.10. This could result in convective flow instead of only diffusion in air capillaries (Maina et al., 2010).

20.6.3.2 Blood-gas barrier diffusion

The effect of the blood-gas barrier on diffusion in the lung can be evaluated by the membrane diffusing capacity ($D_{m_{O_2}}$), which can be estimated from morphometric measurements of the lung (Maina, 1989; Powell and Scheid, 1989). $D_{m_{O_2}}$ is directly proportional to the surface area and inversely proportional to the thickness of the blood-gas barrier. These variables have been measured in several species of birds now, using perfusion fixation and rapid freezing to preserve tissue for electron microscopy and stereological analysis (Dubach, 1981; Maina et al., 1982, 1989; Powell and Mazzone, 1983). The values depend on body size, which determines metabolic rate, but in general they show that $D_{m_{O_2}}$ is larger in birds than in comparably sized terrestrial mammals (Maina, 1989). For example, $D_{m_{O_2}}$ in Canada geese is 1.7-times greater than a comparably sized mammal (Powell and Mazzone, 1983). Also, the thickness of the blood-gas barrier is 2.5 times thinner, and of much more uniform thickness, than in mammals (Maina, 1989; West, 2009). Interestingly, $D_{m_{O_2}}$ is similar in birds and bats of the same body size, indicating the importance of favorable diffusion for high O_2 consumption levels during flight (Maina, 1989).

20.6.3.3 O_2-hemoglobin reaction rates

Finite reaction rates between O_2 and hemoglobin behave as an additional resistance to O_2 uptake across the blood-gas barrier. Consequently, $D_{L_{O_2}}$ increases if there is more hemoglobin available with increased capillary volume. Pulmonary capillary blood volume is similar in birds and terrestrial mammals of similar body sizes, except for chickens, which have a relatively low capillary volume (Maina, 1989). Also, estimates of the reaction rates between O_2 and avian hemoglobin in birds and mammals are similar (Phu et al., 1986). Therefore, O_2-hemoglobin reaction rates probably contribute a similar amount to

diffusion resistances in avian and mammalian lungs. In mammals, this is estimated to comprise about half of the diffusive resistance to O_2 diffusion.

20.6.3.4 Physiological estimates of $D_{L_{O_2}}$

$D_{L_{O_2}}$ can be estimated from experimental measurements on birds if certain conditions are met to satisfy the assumptions necessary for an ideal cross-current analysis of the data. For example, measurements should be made in hypoxia, where the O_2-blood equilibrium curve is linear, to satisfy the assumption of constant $\beta_{b_{O_2}}$. Physiological measurements of $D_{L_{O_2}}$ that satisfy these assumptions have been made in ducks and chickens (Burger et al., 1979; Scheid and Piiper, 1970), and they generally agree with morphometric estimates (Maina and King, 1982). Physiological $D_{L_{O_2}}$ in ducks ranges from 38 to 68 μmol/(min Torr kg) (Hempleman and Powell, 1986). Other methods for estimating potential diffusion limitations indicate complete diffusion equilibrium for O_2 in resting birds (Powell and Scheid, 1989).

Exercise and pharmacological stimulation of metabolic rate increases $D_{L_{O_2}}$ in ducks (Geiser et al., 1984; Hempleman and Powell, 1986; Kiley et al., 1985), and the change is correlated closely with increased cardiac output (Hempleman and Powell, 1986). In alveolar lungs, $D_{L_{O_2}}$ increases with cardiac output by recruitment and distention of the pulmonary capillaries, which increases surface area and capillary volume. However, these enhancements can be offset by shorter transit times in the pulmonary capillaries allowing less time for diffusion equilibrium. Recruitment and distention do not occur in avian lungs (see above), so mechanisms of increasing $D_{L_{O_2}}$ in birds during exercise are not known.

20.6.4 Heterogeneity in the lung

The avian lung is a complex structure consisting of hundreds of parabronchi. Mismatching of ventilation, blood flow, or diffusing capacity between these functional units can reduce the efficacy of gas exchange. Temporal variations in flow rates and inspired gas composition can also impair gas exchange. Under normal resting conditions at sea level, such heterogeneity in lung function is the most important factor reducing gas exchange efficacy from ideal levels in birds and in mammals.

20.6.4.1 Physiological dead space

Physiological dead space is defined as the difference between total inspired or expired ventilation ($\dot{V}_E$ or $\dot{V}_I$) and effective parabronchial ventilation ($\dot{V}_P$):

$$\dot{V}_{D_{phys}} = \dot{V}_I - \dot{V}_P$$

$\dot{V}_{D_{phys}}$ includes anatomic dead space ventilation plus any heterogeneity such as inspiratory or expiratory mesobronchial shunts (see Section 20.3.3.4) or ventilation to regions of the lung with high $\dot{V}/\dot{Q}$ ratios (see below). Therefore, $\dot{V}_{D_{phys}}$ considers ventilation "as if" total ventilation was partitioned between a single ideal parabronchus with $\dot{V}_P$ and anatomic dead space (Scheid and Piiper, 1989).

Many of the techniques used to estimate $\dot{V}_{D_{phys}}$ in alveolar lungs are not applicable to birds (Powell, 1988). However, with a computer model of O_2 and CO_2 dissociation curves and cross-current gas exchange, $\dot{V}_P$ can be calculated from measured ventilation, mixed-venous blood, and mixed-expired gas (Hastings and Powell, 1986b). $\dot{V}_{D_{phys}}$ in artificially ventilated ducks was almost 10 mL greater than anatomic plus instrument dead space, and two-thirds of the 15 mL anatomic dead space (Hastings and Powell, 1986b). This large amount of physiological dead space is consistent with relatively large amounts of total ventilation going to regions of the lung with high ventilation/perfusion ratios ($\dot{V}/\dot{Q}$, see below) and indicates that ventilatory heterogeneity within the lung has a significant impact on $\dot{V}_P$ and gas exchange.

20.6.4.2 Shunt

Shunting of pulmonary blood flow past effective gas exchange areas is very small in birds. As described above, there are no arteriovenous anastomoses in the pulmonary circulation. Shunt ranges from less than 1 to 2.7% of cardiac output in anesthetized artificially ventilated geese and ducks, respectively, using inert gas methods to quantify true intrapulmonary shunt (Burger et al., 1979; Powell and Wagner, 1982). Oxygen can be used to quantify intrapulmonary plus extra-pulmonary shunts, such as drainage of systemic venous blood from bronchial or Thebesian veins into pulmonary venous blood. Oxygen shunts average 6.3 to 8% of cardiac output in ducks, which is much greater than would be predicted given the magnitude of Thebesian and bronchial circulations in mammals (Bickler et al., 1986). One possible explanation for this large shunt is the connection between the vertebral venous and pulmonary circulations described for chickens (Burger and Estavillo, 1977), which also occur in ducks (Bickler et al., 1986). The sensitivity of extra-pulmonary shunts to various physiological conditions has not been measured, but $P_{a_{O_2}}$ is greater than predicted in hypoxia if such shunts persisted (see below).

20.6.4.3 $\dot{V}/\dot{Q}$ mismatching

Differences in the ventilation/perfusion ratio ($\dot{V}/\dot{Q}$) between individual parabronchi is the main factor reducing arterial

P_{O_2} from ideal cross-current levels in birds under resting conditions at sea level (Powell and Scheid, 1989). Ventilation and blood flow can differ between parabronchi depending on small differences in resistance or pressure gradients that can occur along the multiple parallel pathways through the lung. Physiological mechanisms, such as smooth muscle tone in the bronchi and parabronchi or interparabronchial arteries may act to reduce such heterogeneity, but matching is never perfect.

It is important to point out that the effect of such spatial $\dot{V}/\dot{Q}$ heterogeneity on gas exchange is different than the effect of changes in the *overall* $\dot{V}/\dot{Q}$ ratio. The overall $\dot{V}/\dot{Q}$ ratio can affect $P_{a_{O_2}}$, so, for example, decreases in ventilation at constant cardiac output cause decreases in $P_{a_{O_2}}$. Also, the overall ($\dot{V}/\dot{Q}$) ratio affects the magnitude of the arterial-expired P_{O_2} difference in a perfectly homogeneous cross-current gas exchanger (Powell and Scheid, 1989). However, spatial mismatching of $\dot{V}/\dot{Q}$ ratios between parabronchi will decrease $P_{a_{O_2}}$ further and make the arterial-expired P_{O_2} difference more positive than predicted for a homogeneous cross-current exchanger with the same overall $\dot{V}/\dot{Q}$ ratio; this is analogous to increasing the ideal alveolar-arterial P_{O_2} difference in mammals.

Several techniques have been used to measure distributions of $\dot{V}/\dot{Q}$ ratios in the avian lung, but they are relatively complicated and have not been applied yet to awake birds under many physiological conditions lung (Burger et al., 1979; Hempleman and Powell, 1986; Powell, 1988; Powell and Wagner, 1982). Significant amounts of ventilation go to high $\dot{V}/\dot{Q}$ regions of the lung in some cases (Powell and Wagner, 1982), and this contributes to physiological dead space. Heterogeneity in $\dot{V}/\dot{Q}$ ratios near the overall parabronchial $\dot{V}/\dot{Q}$ ratio has a large impact on O_2 exchange in birds. Compared to mammals, $\dot{V}/\dot{Q}$ heterogeneity is slightly greater (Powell and Wagner, 1982), and cross-current gas exchange is more sensitive to $\dot{V}/\dot{Q}$ mismatching than alveolar gas exchange (Powell and Hempleman, 1988; Powell and Scheid, 1989). In normoxic artificially ventilated geese, $P_{a_{O_2}}$ is 25 Torr less than the ideal level predicted for homogeneous cross-current gas exchange, which is significantly greater than the ideal-measured (alveolar-arterial) P_{O_2} difference in typical mammals (Powell and Hempleman, 1988). Hence, most of this drop in $P_{a_{O_2}}$ from ideal levels (15 Torr) is explained by $\dot{V}/\dot{Q}$ heterogeneity (Powell, 1993). The remaining 10 Torr difference between measured and ideal $P_{a_{O_2}}$ can be explained by postpulmonary shunts, which are virtually nonexistent in mammals. Pulmonary shunt is small (Bickler et al., 1986; Powell and Wagner, 1982), and there is no evidence for a diffusion limitation in normoxia at rest (Powell and Scheid, 1989).

In addition to parallel $\dot{V}/\dot{Q}$ mismatching between parabronchi, serial $\dot{V}/\dot{Q}$ mismatch can occur along a single parabronchus if the longitudinal distribution of blood flow is not even. Several studies have shown that blood flow is greater at the inspiratory ends of the parabronchi (Holle et al., 1978; Jones, 1982; Parry and Yates, 1979). However, such serial heterogeneity does not affect gas exchange unless there is a diffusion limitation (Holle et al., 1978; Powell and Scheid, 1989), and this does not occur under most conditions.

20.6.4.4 *Temporal heterogeneity*

Changes in instantaneous ventilation of the parabronchi during normal breathing could in temporal variations in the $\dot{V}/\dot{Q}$ ratio. In theory, this could significantly decrease $P_{a_{O_2}}$ relative to the ideal level predicted for continuous ventilation (Powell, 1988; Powell and Scheid, 1989). For example, a ventilatory pause could act like a breath-hold, and rapidly decrease P_{O_2} in the small gas volume of the avian lung (Powell and Scheid, 1989). However, experiments indicate that this does not occur during normal breathing because the effective parabronchial gas volume is increased by mixing with larger bronchi (Scheid et al., 1977). Temporal changes in P_{O_2} entering the parabronchi during breathing could also impact $P_{a_{O_2}}$, but the effects are predicted to be relatively small (Powell, 1988). A time-averaged $P_{I_{O_2}}$ can be calculated for the parabronchi, and it is similar to caudal air sac P_{O_2} (Scheid et al., 1978).

20.6.5 *Frontiers*: pulmonary gas exchange during high altitude flight

How birds manage high levels of O_2 consumption for flight in extreme hypoxia at very high altitudes remains a fascinating and unanswered question. Birds are generally more tolerant of hypoxia than mammals (Tucker, 1972), and radio tracking was used to confirm bar-headed geese flying over the Himalayas at altitude of 7,920 m (Hawkes et al., 2011). The first experiments actually measuring oxygen exchange during hypoxic flight took advantage of hovering flight in hummingbirds using a hypobaric chamber (Berger, 1974). $\dot{M}_{O_2}$ during hovering at sea level was 32 mmol/(kg min), which is less than the maximal $\dot{M}_{O_2}$ for a hummingbird (Wells, 1993); however, this is greater than the maximal $\dot{M}_{O_2}$ for a comparably sized mammal. Furthermore, the hummingbird was able to maintain this high level of $\dot{M}_{O_2}$ at 6,000 m simulated altitude, while maximal $\dot{M}_{O_2}$ is reduced to half the sea level value in mammals that have been studied at this altitude. Other experiments have studied $\dot{M}_{O_2}$ in hummingbirds with graded levels of exercise at different levels

of O_2 (Chai and Dudley, 1996), but maximal $\dot{M}_{O_2}$ at different altitudes has not been determined in any bird to date.

Measuring the relevant physiological variables to understand how gas exchange changes in birds flying at high altitude is a huge experimental challenge. Consequently, most of the earlier studies exposed resting or anesthetized domestic birds to hypoxia. Experiments on resting ducks and bar-headed geese show extremely high levels of ventilation at very high altitudes (Black and Tenny, 1980b; Powell et al., 2004), which are largely predicted to eliminate the advantage of cross-current gas exchange, compared to alveolar exchange (Shams and Scheid, 1989). However, these predictions are extremely sensitive to cardiac output, which varies greatly in the same species studied during hypoxic rest in different laboratories (Black and Tenney, 1980b; Shams and Scheid, 1989). Depending on the cardiac output, the advantage of cross-current compared to alveolar gas exchange could increase $P_{a_{O_2}}$ by 2 Torr in birds at 11 km altitude. But such a small change is physiologically important when the entire P_{O_2} difference between inspired gas and mixed-venous blood is only 20 Torr (Powell, 1993). Hence, cross-current gas exchange may contribute to the increases in O_2 extraction reported for birds at high altitude (reviewed by Parr et al., 2019a).

Measurements of gas exchange limitations in anesthetized ducks during hypoxia show the difference in $P_{a_{O_2}}$ predicted for an ideal cross-current lung versus the measured value is only a few Torr (Powell, 1993), which contrasts with the relatively large difference in normoxia indicating gas exchange limitations (see above). This is because the effects of $\dot{V}/\dot{Q}$ mismatching on $P_{a_{O_2}}$ are decreased in hypoxia, when exchange operates on the steep portion of the O_2-hemoglobin equilibrium curve (Powell and Scheid, 1989). $\dot{V}/\dot{Q}$ distributions do not change with hypoxia versus normoxia in anesthetized ducks (Powell and Hastings, 1983), and the increased efficiency in hypoxia may be decreased postpulmonary shunting that has been measured in normoxia (Bickler et al., 1986). Diffusion limitations are expected to be extremely small or not present in the avian lung with its extremely high-surface area and thin blood-gas barrier (Maina et al., 2017; Parr et al., 2019b; Scott and Milsom, 2006). High altitude pulmonary edema, which could impair alveolar gas exchange even at subclinical levels, does not appear to be a problem in birds apparently because of factors strengthening the blood-gas barrier discussed earlier.

Other experiments measuring all of the variables necessary for a quantitative analysis of gas exchange during exercise in hypoxia have been done in running waterfowl (Kiley et al., 1985) and emus (Schmitt et al., 2002). Such studies revealed unique features of the avian respiratory system that could provide an advantage over alveolar gas exchange, but they are limited in only increasing $\dot{M}_{O_2}$ about threefold from resting levels. Studies on the emu showed no change in $\dot{V}/\dot{Q}$ mismatching in hypoxic versus normoxia, similar to results in anesthetized ducks (Powell and Hastings, 1983). However, $\dot{V}/\dot{Q}$ mismatching did not change with exercise in the emus either, in contrast with increased $\dot{V}/\dot{Q}$ mismatching in exercising mammals and may provide an avian advantage at altitude (Powell and Hopkins, 2010).

With advances in instrumentation, it is becoming possible to measure more of the relevant gas exchange variables in flying birds. For example, hypobaric wind tunnels can be used to study birds exhibiting natural flight behavior (Yap et al., 2018). Metabolic rate measured in bar-headed geese flying in a wind tunnel show decreases in $\dot{M}_{O_2}$ when inspired O_2 is decreased to simulate altitudes of 5,500 m and 8,500 m while flight speed is maintained (Meir et al., 2019). Important for gas exchange efficiency, arterial P_{O_2} was maintained also. This indicates flight becomes more efficient in hypoxia, which might be studied with experimental approaches similar to those used to demonstrate increases in locomotor efficiency during natural diving in penguins and marine mammals (Ponganis et al., 2011). Radio-tracking has already been used to start documenting energy budgets for bar-headed geese migrating over the Himalayas (Parr et al., 2019a), but much work remains to fully investigate potential advantages of the unique structure and function of the avian respiratory system at high altitude.

20.7 Tissue gas exchange

O_2 moves out of systemic capillaries to the mitochondria in cells by diffusion. Therefore, O_2 transport in tissues is described by Fick's first law of diffusion, similar to diffusion across the blood-gas barrier in the lung:

$$\dot{M}_{O_2} = \Delta P_{O_2} \cdot D_{t_{O_2}}$$

where ΔP_{O_2} is the *average* P_{O_2} gradient between capillary blood and the mitochondria, and $D_{t_{O_2}}$ is a tissue diffusing capacity for O_2, analogous to the lung diffusing capacity (see above). The main difference between O_2 diffusion in tissue and in the lung is that diffusion pathways are much greater in tissue. Tissue capillaries may be 50 μm apart, so the distance from a capillary surface to mitochondria can be 50 times longer than the thickness of the blood-gas barrier (<0.5 μm).

20.7.1 Microcirculation

20.7.1.1 Skeletal muscle

Long diffusion distances can lead to significant P_{O_2} gradients in muscle. Also, the P_{O_2} gradient varies along the

length of a capillary as O_2 leaves the blood, and capillary P_{O_2} decreases from arterial to venous levels. However, birds have some unique structural features in the skeletal muscle microcirculation to minimize diffusion distances and enhance tissue gas exchange. For example, the number of capillaries per cross-sectional area of flight muscle fiber in hummingbirds is six times greater than the value for rat soleus muscle, and the value in pigeon flight muscle is three times greater (Mathieu-Costello, 1993; Mathieu-Costello et al., 1992). This clearly decreases radial diffusion distances for O_2 leaving capillaries in birds. This advantage is increased further in high altitude adapted species, such as bar-headed geese that have significantly higher capillary densities and higher capillary to muscle fiber ratios at the surface of flight muscles, compared to low-altitude waterfowl species (Scott et al., 2009).

In addition, skeletal muscle capillaries in birds are very tortuous and have extensive manifolds connecting capillaries running along adjacent muscle fibers (Mathieu-Costello, 1991, 1993). This geometry increases the exchange surface area, so a muscle fiber is functionally surrounded by "sheet" of capillary blood. This provides better tissue oxygenation than the traditional mammalian model of straight capillaries running along a muscle fiber (i.e., the Krogh cylinder); Krogh's model predicts that P_{O_2} at the venous end of the capillary may be zero when O_2 supply decreases or demand increases (Mathieu-Costello, 1991).

20.7.1.2 Cerebral circulation

Most evidence indicates cerebral blood flow increases with hypoxia but does not change with CO_2 in birds (Faraci, 1991). This results in significant improvements in tissue O_2 delivery during hypoxia (Faraci et al., 1984; Grubb et al., 1977). In mammals, hypoxia also increases cerebral blood flow, but this is partially offset by a vasoconstrictor effect of the decrease in $P_{a_{CO_2}}$ that accompanies the reflex increase in ventilation during hypoxia (see below). This difference in cerebral vascular control may help explain how some birds are able to tolerate severe hypoxia better than some mammals (Faraci, 1986).

20.7.2 Myoglobin

Myoglobin is an O_2-binding protein, similar to a single polypeptide chain of the hemoglobin molecule, which has an extremely high affinity for O_2. For example, the P_{50} for hummingbird's myoglobin is 2.5 Torr (Johansen et al., 1987), so myoglobin can readily accept O_2 from capillary blood. Consequently, myoglobin is thought to be important for facilitating O_2 diffusion in muscle, by shuttling O_2 to sites far away from capillaries, or toward the venous end of capillaries. High levels of myoglobin are present in the heart and skeletal muscles of diving birds (Giardina et al., 1985; Weber et al., 1974), birds native to high altitudes (Fedde, 1990), and in hummingbirds with extremely high metabolism (Johansen et al., 1987). Increases in myoglobin with physical training in birds provides further evidence for the physiological significance of myoglobin in tissue gas exchange (Butler and Turner, 1988). Mb is also a significant O_2 store in diving birds, carrying about 1/3 of the total O_2 stores while the respiratory system and blood carry similar amounts (Ponganis et al., 2011).

20.7.3 Effects of hypoxia and exercise

Generally, decreases in O_2 supply (e.g., hypoxia) or increases in O_2 demand (e.g., exercise) are satisfied at the tissue level by increased O_2 extraction from blood or increasing blood flow. This is illustrated by the Fick equation applied to the cardiovascular O_2 delivery:

$$\dot{M}_{O_2} = \dot{Q}\left(C_{a_{O_2}} - C_{\bar{v}_{O_2}}\right)$$

Increased O_2 extraction from the blood decreases $C_{\bar{v}_{O_2}}$ but $P_{\bar{v}_{O_2}}$ does not decrease much because the slope of the blood-O_2 equilibrium curve is steep around the venous point (Figure 20.8). High $P_{\bar{v}_{O_2}}$ levels are advantageous by keeping average capillary P_{O_2} levels high to drive O_2 diffusion into tissue. O_2 consumption is maintained in duck skeletal muscle during hypoxia without any change in blood flow (Grubb, 1981). During severe hypoxia in resting ducks and bar-headed geese, $C_{\bar{v}_{O_2}}$ can be less than 0.5 mM (Black and Tenney, 1980b). This suggests nearly complete O_2 extraction, although such low venous O_2 values could also result from measurement error. O_2 extraction in the cerebral and coronary circulations is not known for birds.

In exercising birds, extraction and blood flow increase to satisfy metabolic demands (Faraci, 1986; Faraci et al., 1984; Fedde, 1990). Increasing blood flow helps maintain high average capillary P_{O_2} because it raises mixed-venous O_2 concentration for any given arterial concentration and O_2 consumption (see equation above). Increases in blood flow are also observed in the ventilatory muscles of resting birds during hypoxia, which presumably reflects increased work in these muscles during increased breathing (Faraci, 1986). Under some extreme conditions of hypoxic exercise, muscle blood flow or tissue O_2 diffusion may actually limit maximal $\dot{M}_{O_2}$ in birds (Fedde et al., 1989).

Capillaries in avian skeletal muscle also show physiological plasticity and apparent genetic adaptations to hypoxia. Chronic hypoxia increases the capillary-fiber surface area contact for aerobic flight muscles in pigeons (Mathieu-Costello and Agey, 1997), and bar-headed geese have more capillaries per muscle fiber than expected for their aerobic capacity, in comparison to other geese native to lower

altitudes (Scott et al., 2009). Capillaries are also denser and more evenly spaced, and mitochondria are located closer to the capillaries in the bar-headed goose compared to other geese, but the respiratory capacities, O_2 kinetics, and phosphorylation efficiencies of isolated mitochondria were not different between species (Scott et al., 2009). Hence, acclimatization and adaptation to limited O_2 appear to involve changes in O_2 delivery versus utilization (i.e., mitochondrial respiration).

20.8 Control of breathing

Breathing originates as rhythmic motor output from the central nervous system (CNS). This basic respiratory rhythm is modulated by several reflexes, in response to changes in activity and the environment. These reflexes are examples of negative feedback control and tend to maintain normal arterial blood gases and pH homeostasis (Table 20.6). For example, if dead space increases, then

TABLE 20.6 Arterial blood gases and pH in unanesthetized birds breathing air.

Bird	P_{O_2} (Torr)	P_{CO_2} (Torr)	pH
Female black bantam chicken[a]	–	29.9	7.48
Female white leghorn chicken[d]	82	33.0	7.52
Male white rock chicken[a]	–	29.2	7.53
Mallard duck[f]	81	30.8	7.46
Muscovy duck[d]	82	38.0	7.49
Muscovy duck[e]	96.1	35.9	7.46
Pekin duck[c]	93.5	28.0	7.46
Pekin duck[g]	100	33.8	7.48
Emu[l]	99.7	33.5	7.45
Bar-headed goose[c]	92.5	31.6	7.47
Domestic goose[b]	97	32	7.52
Herring gull[a]	–	27.2	7.56
Red-tailed hawk[k]	108	27.0	7.49
Burrowing owl[m]	97.6	32.6	7.46
White pelican[a]	–	28.5	7.50
Adelie penguin[i]	83.8	36.9	7.51
Chinstrap penguin[i]	89.1	37.1	7.52
Gentoo penguin[i]	77.1	40.9	7.49
Pigeon[n]	95	30	7.503
Roadrunner[a]	–	24.5	7.58
Abdim's stork[j]	–	27.9	7.56
Mute swan[h]	91.3	27.1	7.50
Turkey vulture[a]	–	27.5	7.51

[a] *Calder and Schmidt-Nielsen (1968).*
[b] *Scheid et al. (1991).*
[c] *Black and Tenney (1980b).*
[d] *Kawashiro and Scheid (1975).*
[e] *Jones and Holeton (1972).*
[f] *Butler and Taylor (1983).*
[g] *Bouverot et al. (1979).*
[h] *Bech and Johansen (1980).*
[i] *Murrish (1982).*
[j] *Marder and Arad (1975).*
[k] *Kollias and McLeish (1978).*
[l] *Jones et al. (1983).*
[m] *Kilgore, D.L., F.M. Faraci, and M.R. Fedde (unpublished data).*
[n] *Powell (1983).*

$P_{a_{CO_2}}$ will increase if ventilation is constant. However, increased $P_{a_{CO_2}}$ stimulates an increase in tidal volume, which compensates for the increased dead space and returns $P_{a_{CO_2}}$ toward the control value. Like all reflexes, the ventilatory reflexes include (i) a sensory or afferent component, (ii) an integrating component in the CNS, and (iii) a motor or efferent component.

This topic bridges respiratory physiology and neuroscience, but the emphasis here is on respiratory aspects and ventilatory reflex responses to changes in blood gases, often called the "chemical control of ventilation." Several excellent reviews cover more details about the neuroscience of ventilatory control and control of breathing under different physiologic conditions (Bouverot, 1978; Davey and Seller, 1987; Gleeson and Molony, 1989; Jones and Milsom, 1982; Powell, 1983; Scheid and Piiper, 1986; Taylor et al., 1999).

20.8.1 Respiratory rhythm generation

The basic respiratory rhythm is generated by a "central pattern generator," composed of networks of neurons in the brainstem of the (CNS). Respiratory rhythm can be measured in neural outputs from isolated hindbrain of chicks (Fortin et al., 1994), and transecting the brainstem between the XI and XII cranial nerve roots results in apnea and eventual death in pigeons (von Saalfeld, 1936). Reciprocal inhibition between medullary inspiratory and expiratory neurons are a common feature in birds (Peek et al., 1975), but experiments in mammals show that respiratory rhythm generation can occur without inhibitory synaptic interactions, implicating pacemaker processes (Smith et al., 1991). The equivalent of the Pre-Bötzinger Complex, which is the main respiratory pattern generator in mammals (Smith et al., 1991) has not bee identified in birds yet. Other CNS structures important for sending motor outputs to ventilatory muscles in birds (Table 20.2) have been identified with stimulation experiments to study vocalization (e.g., Peek et al., 1975) and panting (e.g., Richards, 1971) in chickens or pigeons (Davey and Seller, 1987). The development of central pattern generators for bird song, which requires respiratory muscles, requires auditory feedback (Konishi, 2010), but such interactions have not been investigated for breathing.

20.8.2 Sensory inputs

20.8.2.1 Central chemoreceptors

In mammals, relatively discrete regions on the ventrolateral surface of the medulla in mammals show chemosensitivity to changes in $P_{a_{CO_2}}$ and local pH. These so-called central chemoreceptors can explain most of the reflex increase in ventilation when $P_{a_{CO_2}}$ increases in mammals (Bouverot, 1978; Guyenet et al., 2010). Central chemoreceptors have not been identified by neurophysiological or anatomic methods in birds. However, conscious ducks increase ventilation when $P_{a_{CO_2}}$ is increased in blood perfusing only the head, indicating an important physiological role for central chemoreceptors in birds (Milsom et al., 1981; Sèbert, 1979).

20.8.2.2 Arterial chemoreceptors

Arterial chemoreceptors are sensitive to changes in $P_{a_{O_2}}$, $P_{a_{CO_2}}$, and pH, and they explain all of the ventilatory response to hypoxia in birds and mammals (Bouverot, 1978). They are also important for the ventilatory response to CO_2 and pH. The carotid bodies are very small (<1 mm diameter) organs located bilaterally in the thorax between the carotid artery and the nodose ganglion of the vagus nerve (Adamson, 1958; Hempleman and Wharburton, 2013; Kameda, 2002). These organs are richly perfused by a branch of the carotid artery, and they are innervated by a branch of the vagus. Carotid bodies are near the parathyroid and ultimobranchial glands in birds and are enveloped within the parathyroid gland in some species (Kobayashi, 1969; Yamatsu and Kameda, 1995); the physiological significance of this association is unknown. Arterial chemoreceptors have also been identified in other regions of the neck, along the carotid artery and aorta by anatomical and physiological methods (reviewed by Gleeson and Molony, 1989).

Figure 20.11 shows the response of carotid body arterial chemoreceptors to changes in $P_{a_{O_2}}$ and $P_{a_{CO_2}}$ in a duck. Afferent information about hypoxia or hypercapnia is transmitted to the CNS via the vagus nerve as increased frequency of action potentials from the carotid body. The pattern of action potential firing can differ in single chemoreceptors depending on the stimulus modality (O_2 vs. CO_2), but the physiological significance of this is not known (Nye and Powell, 1984; Powell and Hempleman, 1990). Avian arterial chemoreceptors can also respond to oscillations in $P_{a_{O_2}}$, $P_{a_{CO_2}}$, and pH that can occur during breathing (Hempleman et al., 1992). The cell types and ultrastructure of the avian and mammalian carotid bodies are similar (reviewed by Gleeson and Molony, 1989), and similar chemoreceptor mechanisms on glomus cells in the carotid body probably explain P_{O_2} and P_{CO_2}/H^+ sensitivity in both classes. However, cellular mechanisms of arterial chemosensitivity are not completely understood (Kumar and Prabhakar, 2012).

20.8.2.2.1 Intrapulmonary chemoreceptors

In contrast to mammals, the lungs of birds (and reptiles) contain IPCs which respond to physiological changes in P_{CO_2} (Burger et al., 1974; Fedde et al., 1974a;

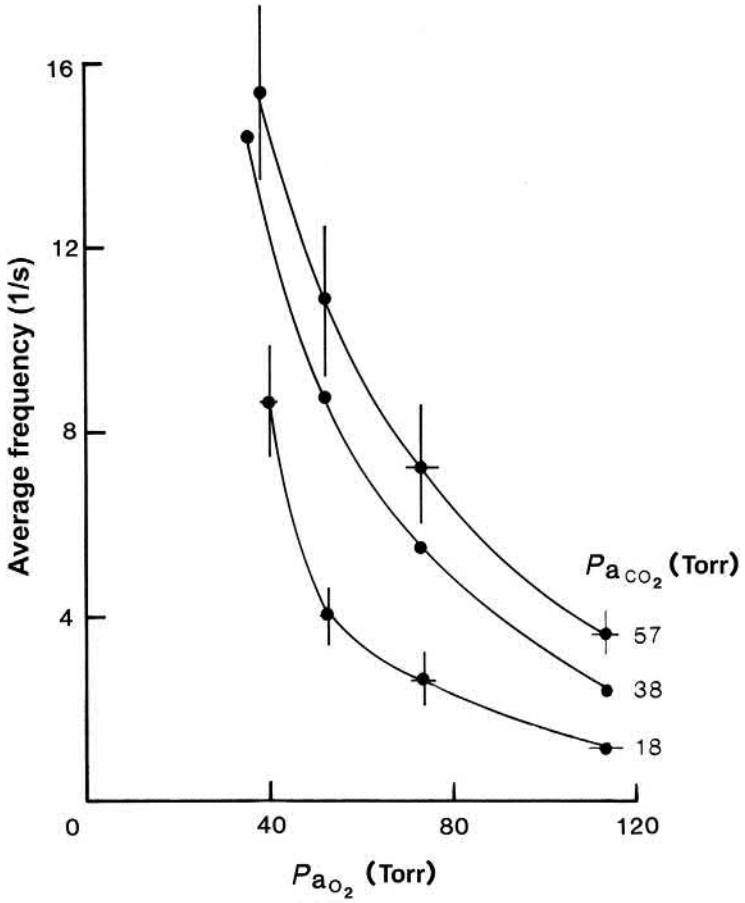

FIGURE 20.11 Average frequency of action potentials (+sem) for arterial chemoreceptors (n = 14) in domestic ducks exposed to different combinations of $P_{a_{O_2}}$ and $P_{a_{CO_2}}$. *From S.C. Hempelman and F.L. Powell, unpublished.*

Peterson and Fedde, 1968). The sensory endings of IPC have not been identified (reviewed by Gleeson and Molony, 1989), but physiological evidence indicates that these vagal afferents have multiple endings in the parabronchial mantle at several points along the length of one or more parabronchi (Hempleman and Burger, 1984). IPC can also respond to changes in CO_2 delivery to the lung by the pulmonary arteries (Banzett and Burger, 1977). Figure 20.12 shows how IPCs are stimulated by *decreases* in P_{CO_2}, in contrast to arterial chemoreceptors that are inhibited by hypocapnia. However, increases in IPC activity cause ventilation to decrease, so the reflex response to CO_2 is similar in direction for central, arterial, and IPC reflexes. The mechanism of chemoreception in IPC depends on intracellular pH (Hempleman and Posner, 2004; Scheid et al., 1978), which is regulated by Na^+/H^+ exchangers (Hempleman et al., 2003), HCO_3^-/Cl^- exchangers (Shoemaker and Hempleman, 2001), and carbonic anhydrase (Hempleman et al., 2000). Calcium and channels also modulate IPC sensitivity (Hempleman et al., 2006) and TREK potassium channels in IPC, which are inhibited by inhalation anesthetics, can explain the

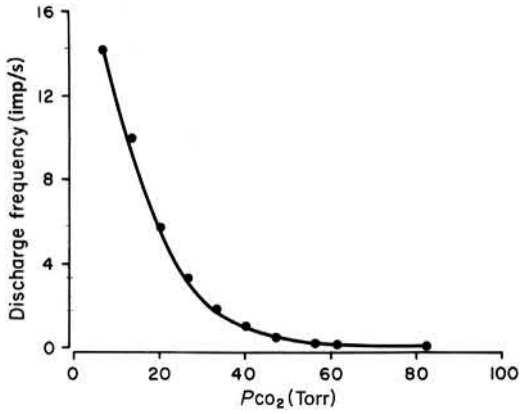

FIGURE 20.12 Average frequency of action potentials for IPC (n = 54) exposed to CO_2 levels ranging from 7 to 82 Torr. *Modified from Nye and Burger (1978).*

inhibitory effects of isoflurane and halothane on ventilation in birds (Bina and Hempleman, 2007).

IPCs are extremely sensitive to *changes* in P_{CO_2} and show large overshoots or undershoots in action potential frequency with the kinds of periodic changes in P_{CO_2} that occur in the lung during normal breathing

(Fedde and Scheid, 1976; Scheid et al., 1978). This makes IPC well suited for fine-tuning the pattern of ventilation, similar to the role of vagal pulmonary stretch receptors in mammals. However, in contrast to mammalian or reptilian pulmonary stretch receptors that are sensitive to mechanical stimuli and P_{CO_2}, avian IPCs are not sensitive to mechanical stretching of the lung (Bouverot, 1978; Fedde et al., 1974b). IPC may be important also in the respiratory transition that occurs during hatching, when gas exchange changes from the chorioallantoic membrane to the lungs (Pilarsky and Hempleman, 2007). IPC activity is not detectable prior to pipping presumably because CO_2 is relatively high. After pipping, IPC respond to CO_2 changes with breathing, but the response is more dynamic and has less sensitivity to static CO_2 levels compared to adult birds, which suggests the IPC show developmental changes similar to chemoreceptors in mammals to support the transition to air breathing.

20.8.2.3 Other receptors affecting breathing

Ventilation also responds to changes in activity from air sac mechanoreceptors, thermal receptors in the spinal cord, proprioceptors in the skin and maybe skeletal muscle, upper airway receptors sensitive to irritants, cold and water, and, perhaps, arterial baroreceptors (reviewed by Gleeson and Molony, 1989).

20.8.3 Ventilatory reflexes

20.8.3.1 CO_2 response

Most birds are not normally exposed to increases in ambient CO_2 levels, except perhaps in specialized nests or burrows. However, ventilatory responses to common stimuli, such as exercise, hot or cold temperatures, and altitude, are influenced by CO_2, so it is important to understand the response to CO_2. Figure 20.13 shows how ventilation increases with increasing inspired CO_2 in conscious ducks. Most species show increased tidal volume, but the frequency response can vary (Bouverot, 1978). At low levels of inspired CO_2, ventilation increases sufficiently to maintain $P_{a_{CO_2}}$ at normal levels (Osborne and Mitchell, 1978).

Decreases in $P_{a_{CO_2}}$ or intrapulmonary P_{CO_2} can decrease ventilation. Hence, when ventilation is increased by another stimulus, such as hypoxia or hyperthermia, the decrease in $P_{a_{CO_2}}$ will act to inhibit ventilatory drive, and ventilation will be the net result of stimulation and inhibition. The hypercapnic ventilatory response scales with size in birds, so smaller birds have reduced CO_2-sensitivity (Williams et al., 1995). It is hypothesized that this may minimize inhibition of a strong hypoxic ventilatory response in small birds, considering the inverse scaling of the hypoxic sensitivity and size in birds (Kilgore et al., 2008 and see below).

Central chemoreceptors contribute to the ventilatory response to $P_{a_{CO_2}}$ as described above. Arterial chemoreceptors play an important role in the response to dynamic changes in $P_{a_{CO_2}}$ (Fedde et al., 1982; Jones and Purves, 1970; Seifert, 1896), such as $P_{a_{CO_2}}$ oscillations which may occur during breathing, and perhaps in the response to static changes in $P_{a_{CO_2}}$ also (Gleeson and Molony, 1989). IPC may contribute to the ventilatory response to changes in $P_{a_{CO_2}}$ also, although their role in this response is controversial (Bouverot, 1978; Gleeson and Molony, 1989). Experimental

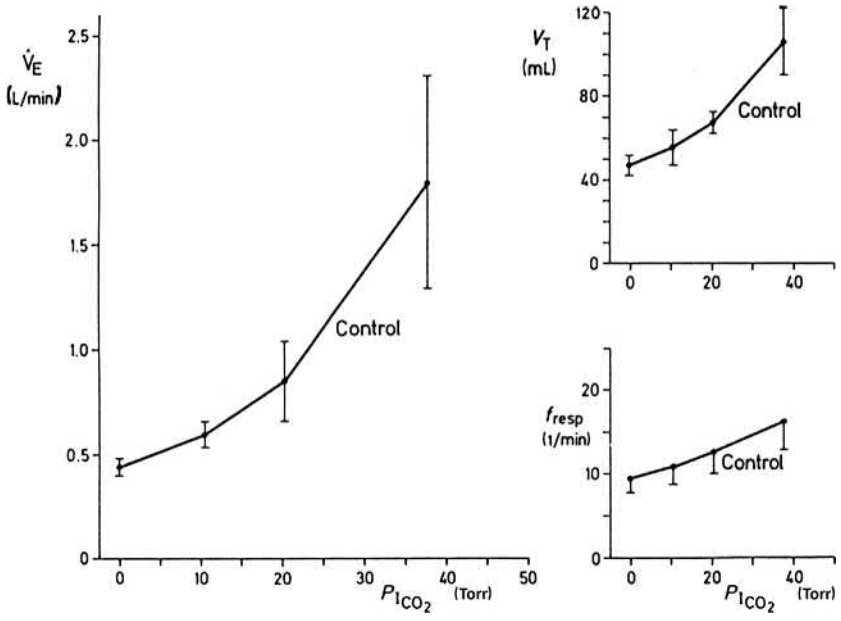

FIGURE 20.13 Ventilatory response to inhaled CO_2 in awake muscovy ducks (*Cairina moschata*), $\dot{V}_E$ = expired ventilation, V_T = tidal volume, f_{resp} = frequency. *Modified from Powell et al. (1978).*

evidence seems to favor a role for IPC in determining the pattern of breathing, but not the overall level of ventilation in conditions where $P_{a_{CO_2}}$ increases (reviewed by Gleeson and Molony, 1989). IPCs are well suited to sense breath-by-breath changes in ventilation as P_{CO_2} changes in the rigid avian lung. Therefore, IPC may play a similar role in the control of breathing to pulmonary stretch receptors in the alveolar lungs, which also sense instantaneous changes in ventilation as changes in lung volume.

20.8.3.2 Hypoxic ventilatory response

The hypoxic ventilatory response (Figure 20.14) is similar in birds and mammals (Black and Tenney, 1980b; Bouverot, 1978). Increasing $P_{a_{O_2}}$ above normal levels does not cause large decreases in ventilation, indicating that normoxic ventilatory drive from arterial chemoreceptors is relatively small (Gleeson and Molony, 1989). Also, ventilation does not change much until $P_{a_{O_2}}$ decreases below about 60 Torr in normal conditions because small increases in ventilation will decrease $P_{a_{CO_2}}$ and ventilatory drive. The hypoxic ventilatory response (Figure 20.14) has a similar shape to the arterial chemoreceptor response to $P_{a_{O_2}}$ (Figure 20.11), and arterial chemoreceptors are responsible for the hypoxic ventilatory response in birds (Jones and Purves, 1970; Seifert, 1896). However, the arterial chemoreceptor response in Figure 20.11 is measured under *isocapnic* conditions, in which $P_{a_{CO_2}}$ was held constant by manipulating CO_2 levels in gas unidirectionally ventilating the lung of anesthetized birds. The hypoxic ventilatory response can be measured under isocapnic conditions also, by manipulating inspired CO_2 in awake birds. However, in contrast to mammals, such an isocapnic hypoxic ventilatory response does not measure of the pure effects of hypoxia on ventilation (independent of CO_2 effects). Changing inspired CO_2 can affect ventilation in birds through effects on IPC independently of $P_{a_{CO_2}}$ (Powell et al., 2000; Scott and Milsom, 2007).

Plasticity is observed in the hypoxic ventilatory response of birds with chronic changes in oxygen level. Chronic sustained hypoxia, as would be experienced during residence at high altitude, causes a time-dependent increase in ventilation above the acute response level (Black and Tenney, 1980b; Bouverot, 1985; Bouverot et al, 1976, 1979; Powell et al., 2004). This is called "ventilatory acclimatization to hypoxia" in mammals and involves changes in both O_2-sensitivity of arterial chemoreceptors and plasticity in respiratory centers in the CNS, which increases respiratory motor output for a given chemoreceptor afferent input (Pamenter and Powell, 2016). In mammals, ventilatory acclimatization to hypoxia causes time-dependent increases in $P_{a_{O_2}}$, but this is not observed in all avian studies. Acclimatizing Pekin ducks to 3,800 m to 5,640 m altitude decreases $P_{a_{CO_2}} > 5$ Torr, indicating increased parabronchial ventilation, yet $P_{a_{O_2}}$ does not increase (Black and Tenny, 1980b; Powell et al., 2004). Apparently, other limitations to oxygen exchange increase during altitude acclimatization and offset the benefits of increased parabronchial ventilation for $P_{a_{O_2}}$.

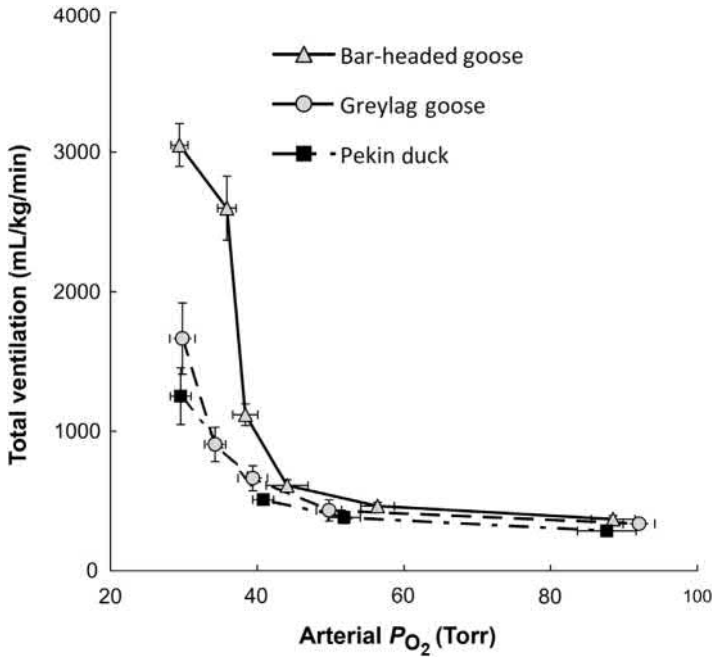

FIGURE 20.14 Hypoxic ventilatory response (isocapnic) for three species of waterfowl. *Modified from Scott and Milson (2007).*

Birds exhibit other forms of plasticity in the hypoxic ventilatory response too (Powell et al., 1998). Similar to mammals, ducks exhibit "long-term facilitation" of ventilation in which breathing remains elevated above control levels following 3−10 brief episodes of hypoxia separated by normoxia (Mitchell et al., 2001). However, inhibitory mechanisms, such as "Hypoxic Ventilatory Decline" or "roll off" are not observed in birds, in contrast to mammals and this bias toward excitatory versus inhibitory effects may provide an advantage at high altitude (Mitchell et al., 2001).

20.8.3.3 *Ventilatory response to exercise*

Exercise is the most common cause of increased ventilation, but the exact physiological mechanism for this is still unknown. The best evidence to date indicates that ventilation increases during exercise through a combination of "feed forward" mechanisms and feedback from chemoreceptors (Dempsey et al., 1995). Feed-forward mechanisms, also called central command, are neural signals from higher centers in the CNS that may stimulate respiratory centers directly. For example, neural signals to locomotor muscles may also stimulate ventilatory muscles and could contribute to some of the phase locking between wing beats and respiration (Funk et al., 1992a,b). Feedback from chemoreceptors prevents ventilation from increasing too much. $P_{a_{CO_2}}$ usually decreases in exercising birds (Kiley et al., 1979), and this hypocapnia would be even worse if ventilatory chemoreflexes did not inhibit ventilation. Other ventilatory stimuli such as body temperature and hypoxia at altitude can modify the response to exercise (reviewed by Gleeson and Molony, 1989).

20.8.3.4 Frontiers: *extreme hyperventilation at high altitude*

Birds hyperventilate more at high altitude than mammals (Powell et al., 2004). Similarly, birds adapted to high altitude, such as the bar-headed goose show a greater hypoxic ventilatory response compared to low-altitude species (Scott and Milsom, 2007). Hyperventilation in hypoxia decreases $P_{a_{CO_2}}$, which increases $P_{a_{O_2}}$ as well as exaggerating the Bohr effect to increase hemoglobin-O_2 affinity. Although $P_{a_{O_2}}$ does not increase further with ventilatory acclimatization to hypoxia in birds (see above), the time-dependent decrease in $P_{a_{CO_2}}$ will further increase arterial O_2 concentration by the Bohr effect. Hence, it appears that many of the advantages birds have at high altitude result from the extreme hyperventilation, hypocapnia, and alkalosis in response to a strong hypoxic ventilatory response. Supporting this are observations of pigeons exposed to 9,000 m simulated altitude showing only minimal stress while arterial pH is 7.85 (Lutz and Schmidt-Nielsen, 1977). Other studies show intracellular pH not changing while venous pH increases from 7.42 to 7.56 in pigeons exposed to 9,000 m (Weinstein et al., 1985). This suggests that tighter regulation of the intracellular milieu may provide an avian advantage at altitude, although the hypothesis remains to be experimentally tested. In any case, the control systems for ventilation and cerebral blood flow that permit such extreme hypocapnia and alkalosis at altitude must have evolved with, or followed from, cellular adaptations preserving function with large pH changes.

Interestingly, both humans and birds show differences in adaptations of the hypoxic ventilatory response between different high-altitude regions. The hypoxic ventilatory response is blunted in human populations in the Andes which who tend to suffer from chronic mountain sickness and other putative maladaptations to hypoxia (Simonson, 2015). In contrast, Tibetans in the Himalayan region include the Sherpa who are recognized as champions of high-altitude performance with a robust hypoxic ventilatory response and chronic mountain sickness is rare. Bird species exhibit similar differences in adaptation to high altitude with bar-headed geese from the Himalayas having a robust hypoxic ventilatory response versus Andean waterfowl having lower levels of ventilation and increased pulmonary O_2 extraction (Lague et al., 2017). Studies on several species of ducks from high altitude in the Andes and closely related species from low altitude found a greater hypoxic ventilatory response in some but not all of the high-altitude species (Ivy et al., 2019). However, increased ventilation did not translate into higher arterial O_2 saturation (as observed in Tibetan compared to Andean humans, Beall et al., 1994), except in yellow-billed pintales that also had a high O_2-hemoglobin affinity (Ivy et al., 2019). The genetic basis for these differences in humans is an intense area of research and may involve relic genes from an extinct species of Hominid (Huerta-Sánchez et al., 2014). Birds may provide an additional animal model to study such genetic adaptations to hypoxia at high altitude, which is one of the most powerful forces of natural selection described to date, at a higher phylogenetic level.

20.9 Defense systems in avian lungs

Infection and disease introduced via the respiratory system is an important problem in poultry husbandry (Maina, 2017). The unique anatomy with relatively few bronchial branches and the large air sacs means that gas exchanging regions of the system may be exposed to microbes, viruses, particulates, and other pathogens with less filtering than occurs in the mammalian respiratory system distal to the blood-gas barrier in the alveoli. Indeed, early research on the pattern of airflow in the avian respiratory system utilized deposition of coal soot in the lungs of pigeons

living in train stations (Dotterweich, 1930). Also, air sac diverticulae have been proposed as a route for infections starting under the skin to enter the respiratory system.

The effectiveness of cellular defense systems by pulmonary macrophages in birds has been questioned also. Pulmonary lavage and histological studies generally find about half the number of free surface macrophages in birds than in mammals with lungs of similar size (reviewed by Maina, 2017). However, the effectiveness of cellular defense appears just as strong in birds because the number of macrophages in pulmonary lavage increases with a challenge; additional cells may include subepithelial and intravascular macrophages, vascular polymorphonuclear neutrophils, and monocyte cells from blood and are found in air sacs as well as parabronchi (reviewed by Maina, 2017). Surfactant proteins A and D, which are important for particle opsonization in alveolar lungs, are absent in birds, which is consistent with sedimentation occurring in extrapulmonary air sacs where flow velocity is low instead of in the air capillaries (Bernhard, 2016). Hence, the most likely causes for susceptibility of poultry to aerosol borne diseases may result from husbandry practices, including overcrowding, force-feeding, and breeding for rapid weight gain and egg production.

References

Abdalla, M.A., 1989. The blood supply to the lung. In: King, A.S., McLelland, J. (Eds.), Form and Function in Birds. Academic Press, London, pp. 281–306.

Abdalla, M.A., King, A.S., 1975. The functional anatomy of the pulmonary circulation of the domestic fowl. Respir. Physiol. 23, 267–290.

Adamson, T.P., 1958. The Comparative Morphology of the Carotid Body and Carotid Sinus. Chas.C.Thomas, Springfield.

Andersen, H.T., Lövö, A., 1967. Indirect estimation of partial pressure of oxygen in arterial blood of diving ducks. Respir. Physiol. 2, 163–167.

Banzett, R.B., Burger, R.E., 1977. Response of avian intrapulmonary chemoreceptors to venous CO_2 and ventilatory gas flow. Respir. Physiol. 29, 63–72.

Banzett, R.B., Lehr, J.L., 1982. Gas exchange during high-frequency ventilation of the chicken. J. Appl. Physiol. 53 (6), 1418–1422.

Banzett, R.B., Butler, J.P., Nations, C.S., Barnas, G.M., Lehr, J.L., Jones, J.H., 1987. Inspiratory aerodynamic valving in goose lungs depends on gas density and velocity. Respir. Physiol. 70, 287–300.

Banzett, R.B., Nations, C.S., Wang, N., Fredberg, J.J., Butler, J.P., 1991. Pressure profiles show features essential to aerodynamic valving in geese. Respir. Physiol. 84, 295–309.

Barnas, G.M., Mather, F.B., 1978. Response of avian intrapulmonary smooth muscle to changes in carbon dioxide concentration. Poultry Sci. 57, 1400–1407.

Bartels, H., Hiller, G., Reinhardt, W., 1966. Oxygen affinity of chicken blood before and after hatching. Respir. Physiol. 1, 345–356.

Bauer, C., Jelkmann, W., Rollema, H.S., 1978. Mechanisms controlling the oxygen affinity of bird and reptile blood: a comparison between the functional properties of chicken and crocodile haemoglobin. In: Piiper, J. (Ed.), Respiratory Function in Birds, Adult and Embryonic. Springer-Verlag, Berlin, pp. 61–66.

Baumann, F.H., Baumann, R., 1977. A comparative study of the respiratory properties of bird blood. Respir. Physiol. 31, 333–343.

Baumann, R., Baumann, F.H., 1978. Respiratory function of embryonic chicken hemoglobin. In: Piiper, J. (Ed.), Respiratory Function in Birds, Adult and Embryonic. Springer-Verlag, Berlin, pp. 292–297.

Beall, C.M., Blangero, J., Williams-Blangero, S., Goldstein, M.C., 1994. Major gene for percent of oxygen saturation of arterial hemoglobin in Tibetan highlanders. Am. J. Phys. Anthro. 95, 271–276.

Bech, C., Johansen, K., 1980. Ventilation and gas exchange in the mute swan, Cygnus olor. Respir. Physiol. 39, 285–295.

Bech, C., Johansen, K., Brent, R., Nicol, S., 1984. Ventilatory and circulatory changes during cold exposure in the Pekin duck *Anas platyrhynchos*. Respir. Physiol. 57, 103–112.

Bencowitz, H.Z., Wagner, P.D., West, J.B., 1982. Effect of change in P50 on exercise tolerance at high altitude: a theoretical study. J. Appl. Physiol. 53, 1487–1495.

Berger, M., 1974. Energiewechsel von Kolibris beim Schwirrflug unter Höhenbedingungen. J. Ornithol. 115, 273–288.

Bernhard, W., 2016. Lung surfactant: function and composition in the context of development and respiratory physiology. Ann. Anat. 208, 146–150.

Bernhard, W., Gebert, A., Vieten, G., Rau, G.A., Hohlfeld, J.M., Postle, A.D., Freihorst, J., 2001. Pulmonary surfactant in birds: coping with surface tension in a tubular lung. Am. J. Physiol. Regul. Integr. Comp. Physiol. 281, R327–R337.

Bickler, P.E., Maginniss, L.A., Powell, F.L., 1986. Intrapulmonary and extrapulmonary shunt in ducks. Respir. Physiol. 63, 151–160.

Biggs, P., King, A.S., 1957. A new experimental approach to the problem of the air pathway within the avian lung. J. Physiol. 138, 282–289.

Bina, R.W., Hempleman, S.C., 2007. Evidence for TREK-like tandem-pore domain channels in intrapulmonary chemoreceptor chemotransduction. Respir. Physiol. Neurobiol. 156, 120–131.

Black, C.P., Tenney, S.M., 1980a. Pulmonary hemodynamic responses to acute and chronic hypoxia in two waterfowl species. Comp. Biochem. Physiol. 67A, 291–293.

Black, C.P., Tenney, S.M., 1980b. Oxygen transport during progressive hypoxia in high-altitude and sea-level waterfowl. Respir. Physiol. 39, 217–239.

Boggs, D.F., Butler, P.J., Warner, M., 1996. Fluctuations in differential pressure between the anterior and posterior air sac of Tufted ducks, *Aythya fuligula*, during breath-hold dives. Physiol. 39, A–27.

Bouverot, P., 1978. Control of breathing in birds compared with mammals. Physiol. Rev. 58 (3), 604–655.

Bouverot, P., 1985. Adaptation to Altitude-Hypoxia in Vertebrates. Springer-Verlag, Berlin.

Bouverot, P., Douguest, D., Sèbert, P., 1979. Role of the arterial chemoreceptors in ventilatory and circulatory adjustments to hypoxia in awake Pekin ducks. J. Comp. Physiol. 133, 177–186.

Bouverot, P., Hildwein, G., Oulhen, P., 1976. Ventilatory and circulatory O_2 convection at 4000 m in pigeon at neutral or cold temperature. Respir. Physiol. 28, 371–385.

Brackenbury, J., 1984. Physiological responses of birds to flight and running. Biol. Rev. 59, 559–575.

Brackenbury, J.H., 1971. Airflow dynamics in the avian lung as determined by direct and indirect methods. Respir. Physiol. 13, 319–329.

Brackenbury, J.H., 1972. Physical determinants of air flow pattern within the avian lung. Respir. Physiol. 15, 384.

Bretz, W.L., Schmidt-Nielsen, K., 1971. Bird respiration: flow patterns in the duck lung. J. Exp. Biol. 54, 103–118.

Brown, R.E., Kovacs, C.E., Butler, J.P., Wang, N., Lehr, J.L., Banzett, R.B., 1995. The avian lung: is there an aerodynamic expiratory valve? J. Exp. Biol. 198, 2349–2357.

Burger, R.E., Estavillo, J.A., 1977. Pulmonary circulation - vertebral venous interconnections in the chicken. Anat. Rec. 188 (1), 39–44.

Burger, R.E., Lorenz, F.W., 1960. Artificial respiration in birds by unidirectional air flow. Poultry Sci. 39 (1), 236–237.

Burger, R.E., Meyer, M., Graf, W., Scheid, P., 1979. Gas exchange in the parabronchial lung of birds: experiments in unidirectionally ventilated ducks. Respir. Physiol. 36, 19–37.

Burger, R.E., Osborne, J.L., Banzett, R.B., 1974. Intrapulmonary chemoreceptors in *Gallus domesticus*: adequate stimulus and functional localization. Respir. Physiol. 22, 87–97.

Burton, R.R., Besch, E.L., Smith, A.H., 1968. Effect of chronic hypoxia on the pulmonary arterial blood pressure of the chicken. Am. J. Physiol. 214 (6), 1438–1442.

Butler, J.P., Banzett, R.B., Fredberg, J.J., 1988. Inspiratory valving in avian bronchi: aerodynamic considerations. Respir. Physiol. 72, 241–256.

Butler, P.J., 1991. Exercise in birds. J. Exp. Biol. 160, 233–262.

Butler, P.J., Taylor, E.W., 1983. Factors affecting the respiratory and cardiovascular responses to hypercapnic hypoxia in mallard ducks. Respir. Physiol. 53, 109.

Butler, P.J., Turner, D.L., 1988. Effect of training on maximal oxygen uptake and aerobic capacity of locomotory muscles in tufted ducks, Aythya fuligula. J. Physiol. 401, 347–359.

Calder, W.A., Schmidt-Nielsen, K., 1968. Panting and blood carbon dioxide in birds. Am. J. Physiol. 215, 477–482.

Chai, P., Dudley, R., 1996. Limits to flight energetics of hummingbirds hovering in hypodense and hypoxic gas mixtures. J. Exp. Biol. 199, 2285–2295.

Cohn, J.E., Shannon, R., 1968. Respiration in unanesthetized geese. Respir. Physiol. 5, 259–268.

Crank, W.D., Gallagher, R.R., 1978. Theory of gas exchange in the avian parabronchus. Respir. Physiol. 35, 9–25.

Davey, N.J., Seller, T.J., 1987. Brain mechanisms for respiratory control. In: Seller, T.J. (Ed.), Bird Respiration. CRC Press, Inc., Boca Raton, pp. 169–188.

Dempsey, J.A., Forster, H.V., Ainsworth, D.M., 1995. Regulation of hyperpnea, hyperventilation, and respiratory muscle recruitment during exercise. In: Dempsey, J.A., Pack, A.I. (Eds.), Regulation of Breathing. Marcel Dekker, Inc., New York, pp. 1065–1134.

deWet, P.D., Fedde, M.R., Kitchell, R.L., 1967. Innervation of the respiratory muscles of *Gallus domesticus*. J. Morphol. 123 (1), 17–34.

Dotterweich, H., 1930. Versuche Über den weg der atemluft in der vogellunge. Z. Vergleich. Physiol. 11, 271–284.

Dubach, M., 1981. Quantitative analysis of the respiratory system of the house-sparrow, budgerigar and violet-eared hummingbird. Respir. Physiol. 46, 43–60.

Duncker, H.R., 1971. The lung air sac system of birds. Adv. Anat. Embryol. Cell Biol. 45, 7–171.

Duncker, H.R., 1974. Structure of the avian respiratory tract. Respir. Physiol. 22, 1–19.

Duncker, H.R., 1978. General morphological principles of amniotic lungs. In: Piiper, J. (Ed.), Respiratory Function in Birds, Adult and Embryonic. Springer-Verlag, Berlin, pp. 1–18.

Faraci, F.M., 1986. Circulation during hypoxia in birds. Comp. Biochem. Physiol. 85A (4), 613–620.

Faraci, F.M., 1991. Adaptations to hypoxia in birds: how to fly high. Annu. Rev. Physiol. 53, 59–70.

Faraci, F.M., Kilgore, D.L., Fedde, M.R., 1984. Oxygen delivery to the heart and brain during hypoxia: Pekin duck vs. bar-headed goose. Am. J. Physiol. 16, R69–R75.

Farmer, C.G., Sanders, K., 2010. Unidirectional airflow in the lungs of alligators. Science 327 (5963), 338–340.

Farmer, C.G., 2006. On the origin of avian air sacs. Respir. Physiol. Neurobiol. 154 (1–2), 89–106.

Fedde, M.R., 1978. Drugs used for avian anesthesia. Poultry Sci. 57, 1376–1399.

Fedde, M.R., 1990. High-altitude bird flight: exercise in a hostile environment. NIPS 5, 191–193.

Fedde, M.R., Scheid, P., 1976. Intrapulmonary CO_2 receptors in the duck: IV. Discharge pattern of the population during a respiratory cycle. Respir. Physiol. 26, 223–227.

Fedde, M.R., Burger, R.E., Kitchell, R.L., 1963. Electromyographic studies of the effects of bodily position and anesthesia on the activity of the respiratory muscles of the domestic cock. Poultry Sci. 839–846.

Fedde, M.R., Burger, R.E., Kitchell, R.L., 1964a. Anatomic and electromyographic studies of the costo-pulmonary muscles in the cock. Poultry Sci. 1177–1184.

Fedde, M.R., Burger, R.E., Kitchell, R.L., 1964b. Electromyographic studies of the effects of bilateral, cervical vagotomy on the action of the respiratory muscles of the domestic cock. Poultry Sci. 1119–1125.

Fedde, M.R., deWet, P.D., Kitchell, R.L., 1969. Motor unit recruitment pattern and tonic activity in respiratory muscles of *Gallus domesticus*. J. Neurophysiol. 32, 995–1004.

Fedde, M.R., Gatz, R.N., Slama, H., Scheid, P., 1974a. Intrapulmonary CO_2 receptors in the duck: I. Stimulus specificity. Respir. Physiol. 22, 99–114.

Fedde, M.R., Gatz, R.N., Slama, H., Scheid, P., 1974b. Intrapulmonary CO_2 receptors in the duck: II. Comparison with mechanoreceptors. Respir. Physiol. 22, 115–121.

Fedde, M.R., Kiley, J.P., Powell, F.L., Scheid, P., 1982. Intrapulmonary CO_2 receptors and control of breathing in ducks: effects of prolonged circulation time to carotid bodies and brain. Respir. Physiol. 47, 121–140.

Fedde, M.R., Orr, J.A., Shams, H., Scheid, P., 1989. Cardiopulmonary function in exercising bar-headed geese during normoxia and hypoxia. Respir. Physiol. 77, 239–262.

Fortin, G., Champagnat, J., Lumdsen, A., 1994. Onset and maturation of branchio-motor activites in the chick hindbrain. Neruoreport 5, 1149–1152.

Funk, G.D., Milsom, W.K., Steeves, J.D., 1992a. Coordination of wingbeat and respiration in the Canada goose. I. Passive wing flapping. J. Appl. Physiol. 73, 1014–1024.

Funk, G.D., Steeves, J.D., Milsom, W.K., 1992b. Coordination of wingbeat and respiration in birds. II. "Fictive" flight. J. Appl. Physiol. 73, 1025–1033.

Geiser, J., Gratz, R.K., Hiramoto, T., Scheid, P., 1984. Effects of increasing metabolism by 2,4-dinitrophenol on respiration and pulmonary gas exchange in the duck. Respir. Physiol. 57, 1–14.

Giardina, B., Corda, M., Pellegrini, M.G., Condo, S.G., Brunori, M., 1985. Functional properties of the hemoglobin system of two diving birds (*Podiceps nigricollis and Phalacrocorax carbo sinensis*). Mol. Physiol. 7, 281–292.

Gillespie, J.R., Gendner, J.P., Sagot, J.C., Bouverot, P., 1982a. Impedance of the lower respiratory system in ducks measured by forced oscillations during normal breathing. Respir. Physiol. 47, 51–68.

Gillespie, J.R., Sagot, J.C., Gendner, J.P., Bouverot, P., 1982b. Respiratory mechanics of Pekin ducks under four conditions: pressure breathing, anesthesia, paralysis or breathing CO_2-enriched gas. Respir. Physiol. 47, 177–191.

Gleeson, M., Molony, V., 1989. Control of breathing. In: King, A.S., McLelland, J. (Eds.), Form and Function in Birds. Academic Press, London, pp. 439–484.

Grubb, B.R., 1981. Blood flow and oxygen consumption in avian skeletal muscle during hypoxia. J. Appl. Physiol. 50, 450–455.

Grubb, B., Mills, C.D., Colacino, J.M., Schmidt-Nielsen, K., 1977. Effect of arterial carbon dioxide on cerebral blood flow in ducks. Am. J. Physiol. 232 (6), H596–H601.

Guyenet, P.G., Stornetta, R.L., Abbott, S.B., Depuy, S.D., Fortuna, M.G., Kanbar, R., 2010. Central CO_2 chemoreception and integrated neural mechanisms of cardiovascular and respiratory control. J. Appl. Physiol. 108, 995–1002.

Hastings, R.H., Powell, F.L., 1986a. Single breath CO_2 measurements of dead space in ducks. Respir. Physiol. 63, 139–149.

Hastings, R.H., Powell, F.L., 1986b. Physiological dead space and effective parabronchial ventilation in ducks. J. Appl. Physiol. 60 (1), 85–91.

Hastings, R.H., Powell, F.L., 1987. High-frequency ventilation of ducks and geese. J. Appl. Physiol. 63 (1), 413–417.

Hawkes, L., Balachandran, S., Batbayar, N., Butler, P.J., Frappell, P.B., Milsom, W.K., Tseveenmyadag, N., Newman, S.H., Scott, G.R., Sathiyaselvam, P., Takekawa, J.Y., Wikelski, M., Bishop, C.M., 2011. The trans-Himalayan flights of bar-headed geese (*Anser indicus*). Proc. Natl. Acad. Sci. U.S.A. 108, 9516–9519.

Hazelhoff, E.H., 1951. Structure and function of the lung of birds (reprinted from 1943). Poultry Sci. 30, 3–10.

Helbacka, N.V.L., Casterline Jr., J.L., Smith, C.J., Shaffner, C.S., 1963. Investigation of plasma carbonic acid pK' of the chicken. Poultry Sci. 138–144.

Hempleman, S.C., Warburton, S.J., 2013. Comparative embryology of the carotid body. Respir. Physiol. Neurobiol. 185, 3–8.

Hempleman, S.C., Posner, R.G., 2004. CO_2 transduction mechanisms in avian intrapulmonary chemoreceptors: experiments and models. Respir. Physiol. Neurobiol. 144, 203–214.

Hempleman, S.C., Adamson, T.P., Begay, R.S., Solomon, I.C., 2003. CO_2 transduction in avian intrapulmonary chemoreceptors is critically dependent on transmembrane Na^+/H^+ exchange. Am. J. Physiol. Regul. Integr. Comp. Physiol. 84, R1551–R1559.

Hempleman, S.C., Egan, S.X., Pilarski, J.Q., Adamson, T.P., Solomon, I.C., 2006. Calcium and avian intrapulmonary chemoreceptor response to CO_2. J. Appl. Physiol. 101, 1565–1575.

Hempleman, S.C., Rodriguez, T.A., Bhagat, Y.A., Begay, R.S., 2000. Benzolamide, acetazolamide, and signal transduction in avian intrapulmonary chemoreceptors. Am. J. Physiol. Regul. Integr. Comp. Physiol. 279, R1988–R1995.

Hempleman, S.C., Burger, R.E., 1984. Receptive fields of intrapulmonary chemoreceptors in the Pekin duck. Respir. Physiol. 57, 317–330.

Hempleman, S.C., Powell, F.L., 1986. Influence of pulmonary blood flow and O_2 flux on D_{O2} in avian lungs. Respir. Physiol. 63, 285–292.

Hempleman, S.C., Powell, F.L., Prisk, G.K., 1992. Avian arterial chemoreceptor responses to steps of CO_2 and O_2. Respir. Physiol. 90, 325–340.

Henning, B., Scheid, P., Piiper, J., 1971. Determination of the Haldane effect in chicken blood. Respir. Physiol. 11, 279–284.

Hinds, D.S., Calder, W.A., 1971. Tracheal dead space in the respiration of birds. Evolution 25, 429–440.

Hirsowitz, L.A., Fell, K., Torrance, J.D., 1977. Oxygen affinity of avian blood. Respir. Physiol. 31, 51–62.

Holle, J.P., Heisler, N., Scheid, P., 1978. Blood flow distribution in the duck lung and its control by respiratory gases. Am. J. Physiol. 234 (3), R146–R154.

Holle, J.P., Meyer, M., Scheid, P., 1977. Oxygen affinity of duck blood determined by *in vivo* and *in vitro* technique. Respir. Physiol. 29, 355–361.

Hsia, C.C.W., Schmitz, A., Lambertz, M., Perry, S.F., Maina, J.N., 2013. Evolution of air breathing: oxygen homeostasis and the transitions from water to land and sky. Compr. Physiol. 3, 849–915.

Huerta-Sánchez, E., Jin, X., Asan Bianba, Z., Peter, B.M., Vinckenbosch, N., Liang, Y., Yi, X., He, M., Somel, M., Ni, P., Wang, B., Ou, X., Huasang Luosang, J., Cuo, Z.X., Li, K., Gao, G., Yin, Y., Wang, W., Zhang, X., Xu, X., Yang, H., Li, Y., Wang, J., Wang, J., Nielsen, R., 2014. Altitude adaptation in Tibetans caused by introgression of Denisovan-like DNA. Nature 512 (7513), 194–197.

Ivy, C.M., Lague, S.L., York, J.M., Chua, B.A., Alza, L., Cheek, R., Dawson, N.J., Frappell, P.B., McCracken, K.G., Milsom, W.K., Scott, G.R., 2019. Control of breathing and respiratory gas exchange in high-altitude ducks native to the Andes. J. Exp. Biol. 222 (Pt 7), jeb198622. https://doi.org/10.1242/jeb.198622.

Ivy, C.M., York, J.M., Lague, S.L., Chua, B.A., Alza, L., McCracken, K.G., Milsom, W.K., Scott, G.R., 2018. Validation of a pulse oximetry system for high-altitude waterfowl by examining the hypoxia responses of the Andean goose (*Chloephaga melanoptera*). Physiol. Biochem. Zool. 91 (3), 859–867.

Jendroszek, A., Malte, H., Overgaard, C.B., Beedholm, K., Natarajan, C., Weber, R.E., Storz, J.F., Fago, A., 2018. Allosteric mechanisms underlying the adaptive increase in hemoglobin-oxygen affinity of the bar-headed goose. J. Exp. Biol. 221 (Pt 18), jeb185470. https://doi.org/10.1242/jeb.185470.

Jenkins, F.A., Dial, K.P., Goslow, G.E., 1988. A cineradiographic analysis of bird flight: the wishbone in starlings is a spring. Science 241, 1495–1498.

Jessen, T.H., Weber, R.E., Fermi, G., Tame, J., Braunitzer, G., 1991. Adaptation of bird hemoglobins to high altitudes: demonstration of molecular mechanism by protein engineering. Proc. Natl. Acad. Sci. U.S.A. 88, 6519–6522.

Johansen, K., Berger, M., Bicudo, J.E.P., Ruschi, A., De Almeida, P.J., 1987. Respiratory properties of blood and myoglobin in hummingbirds. Physiol. Zool. 60 (2), 269–278.

Jones, D.R., Holeton, G.F., 1972. Cardiovascular and respiratory responses of ducks to progressive hypocapnic hypoxia. J. Exp. Biol. 56, 657–666.

Jones, D.R., Milsom, W.K., 1982. Peripheral receptors affecting breathing and cardiovascular function in non-mammalian vertebrates. J. Exp. Biol. 100, 59.

Jones, D.R., Purves, M.J., 1970. The effect of carotid body denervation upon the respiratory response to hypoxia and hypercapnia in the duck. J. Physiol. 295–308.

Jones, J.H., 1982. Pulmonary blood flow distribution in panting ostriches. J. Appl. Physiol. 53, 1411–1417.

Jones, J.H., Effmann, E.L., Schmidt-Nielsen, K., 1985. Lung volume changes during respiration in ducks. Respir. Physiol. 59, 15–25.

Jones, J.H., Grubb, B., Schmidt-Nielsen, K., 1983. Panting in the emu causes arterial hypoxemia. Respir. Physiol. 54, 189.

Julian, R.J., 1993. Ascites in poultry. Avian Pathol. 23, 419–454.

Kadono, H., Okada, T., 1962. Electromyographic studies on the respiratory muscles of the domestic fowl. Jpn. J. Vet. Sci. 24 (4), 215–223.

Kadono, H., Okada, T., Ono, K., 1963. Electromyographic studies on the respiratory muscles of the chicken. Poultry Sci. 42 (1), 121–128.

Kalmar, I.D., Vanrompay, D., Janssens, G.P., 2013. Broiler ascites syndrome: collateral damage from efficient feed to meat conversion. Vet. J. 197 (2), 169–174.

Kameda, Y., 2002. Carotid body and glomus cells distributed in the wall of the common carotid artery in the bird. Microsc. Res. Tech. 59 (3), 196–206.

Kampe, G., Crawford, E.C., 1973. Oscillatory mechanics of the respiratory system of pigeons. Respir. Physiol. 18, 188–193.

Kawashiro, T., Scheid, P., 1975. Arterial blood gases in undisturbed resting birds: measurements in chicken and duck. Respir. Physiol. 23, 337–342.

Kiley, J.P., Faraci, F.M., Fedde, M.R., 1985. Gas exchange during exercise in hypoxic ducks. Respir. Physiol. 59, 105–115.

Kiley, J.P., Kuhlmann, W.D., Fedde, M.R., 1979. Respiratory and cardiovascular responses to exercise in the duck. J. Appl. Physiol. 47, 827–833.

Kilgore Jr., D.L., Boggs, D.F., Kilgore, T.J., Colby, C., Williams Jr., B.R., Bavis, R.W., 2008. Ventilatory and metabolic responses of burrowing owls, *Athene cunicularia*, tomoderate and extreme hypoxia: analysis of the hypoxic ventilatory threshold vs.hemoglobin oxygen affinity relationship in birds. Comp. Biochem. Physiol. A Mol. Integr. Physiol. 150, 247–257.

King, A.S., 1979. Systema respiratorium. In: Baumel, J.J., King, A.M., Lucas, A.M., Breazile, J.E., Evans, H.E. (Eds.), Nomina Anatomica Avium. Academic Press, London, pp. 227–265.

King, A.S., 1989. Functional anatomy of the syrinx. In: King, A.S., McLelland, J. (Eds.), Form and Function in Birds. Academic Press, London, pp. 105–192.

King, A.S., Molony, V., 1971. The anatomy of respiration. In: Bell, O.J., Freeman, B.M. (Eds.), Physiology and Biochemistry of the Domestic Fowl. Academic Press, New York, p. 227.

Kobayashi, S., 1969. Catecholamines in the avian carotid body. Specilia 25, 1075–1076.

Kollias, G.V., McLeish, I., 1978. Effects of ketamine hydrochloride in red-tailed hawks (*Buteo jamaicensis*) I. Arterial blood gas and acid base. Comp. Biochem. Physiol. 60C, 57.

Konishi, M., 2010. From central pattern generator to sensory template in the evolution of birdsong. Brain Lang. 115, 18–20.

Kuethe, D.O., 1988. Fluid mechanical valving of air flow in bird lungs. J. Exp. Biol. 136, 1–12.

Kuhlmann, W.D., Fedde, M.R., 1976. Upper respiratory dead space in the chicken: its fraction of the tidal volume. Comp. Biochem. Physiol. 54A, 409–411.

Kumar, P., Prabhakar, N.R., 2012. Peripheral chemoreceptors: function and plasticity of the carotid body. Compr. Physiol. 2 (1), 141–219.

Lague, S.L., Chua, B., Alza, L., Scot, t G.R., Frappell, P.B., Zhong, Y., Farrell, A.P., McCracken, K.G., Wang, Y., Milsom, W.K., 2017. Divergent respiratory and cardiovascular responses to hypoxia in bar-headed geese and Andean birds. J. Exp. Biol. 220 (Pt 22), 4186–4194.

Lapennas, G.N., Reeves, R.B., 1983. Oxygen affinity of blood of adult domestic chicken and red jungle fowl. Respir. Physiol. 52, 27–39.

Lutz, P.L., 1980. On the oxygen affinity of bird blood. Amer. Zool. 20, 187–198.

Lutz, P.L., Schmidt-Nielsen, K., 1977. Effect of simulated altitude on blood gas transport in the pigeon. Respir. Physiol. 30, 383–388.

Macklem, P.T., Bouverot, P., Scheid, P., 1979. Measurement of the distensibility of the parabronchi in duck lungs. Respir. Physiol. 38, 23–35.

Maginniss, L.A., 1985. Red cell organic phosphates and Bohr effects in house sparrow blood. Respir. Physiol. 59, 93–103.

Maginniss, L.A., Kilgore, D.L., 1989. Blood oxygen binding properties for the burrowing owl, *Athene cunicularia*. Respir. Physiol. 76, 205–214.

Magnussen, H., Willmer, H., Scheid, P., 1976. Gas exchange in air sacs: contribution to respiratory gas exchange in ducks. Respir. Physiol. 26, 129–146.

Maina, J.N., McCracken, K.G., Chua, B., York, J.M., Milsom, W.K., 2017. Morphological and morphometric specializations of the lung of the Andean goose, *Chloephaga melanoptera*: a lifelong high-altitude resident. PLoS One 12 (3), e0174395. https://doi.org/10.1371/journal.pone.0174395.

Maina, J.N., West, J.B., Orgeig, S., Foot, N.J., Daniels, C.B., Kiama, S.G., Gehr, P., Mühlfeld, C., Blank, F., Müller, L., Lehmann, A., Brandenberger, C., Rothen-Rutishauser, B., 2010. Recent advances into understanding some aspects of the structure and function of mammalian and avian lungs. Physiol. Biochem. Zool. 83, 792–807.

Maina, J.N., 2007. Spectacularly robust! Tensegrity principle explains the mechanical strength of the avian lung. Respir. Physiol. Neurobiol. 155, 1–10.

Maina, J.N., 2017. Pivotal debates and controversies on the structure and function of the avian respiratory system: setting the record straight. Biol. Rev. Camb. Philos. Soc. 92 (3), 1475–1504.

Maina, J.N., 1989. The morphometry of the avian lung. In: King, A.S., McLelland, J. (Eds.), Form and Function in Birds. Academic Press, London, pp. 307–368.

Maina, J.N., Abdalla, A., King, A.S., 1982. Light microscopic morphometry of the lung of 19 avian species. Acta Anat. 112, 264–270.

Maina, J.N., King, A.S., 1982. Morphometrics of the avian lung. 2. The wild mallard (*Anas platyrhynchos*) and Graying goose (*Anser anser*). Respir. Physiol. 50, 299–310.

Maina, J.N., King, A.S., Settle, G., 1989. An allometric study of pulmonary morphometric parameters in birds, with mammalian comparisons. Phil. Trans. R. Soc. Lond. B 326, 1–57.

Maina, J.N., Singh, P., Moss, E.A., 2009. Inspiratory aerodynamic valving occurs in the ostrich, *Struthio camelus* lung: computational fluid dynamics study under resting unsteady state inhalation. Res. Physiol. Neurobiol. 169, 262–270.

Marder, J., Arad, Z., 1975. The acid bas balance of abdim's stork (*Sphenorhynchus abdimii*) during thermal panting. Comp. Biochem. Physiol. 51A, 887–889.

Maren, T.H., 1967. Carbonic anhydrase: chemistry, physiology and inhibition. Physiol. Rev. 47, 595–781.

Mathieu-Costello, O., 1991. Morphometric analysis of capillary geometry in pigeon pectoralis muscle. Am. J. Anat. 191, 74–84.

Mathieu-Costello, O., 1993. Comparative aspects of muscle capillary supply. Annu. Rev. Physiol. 55, 503–525.

Mathieu-Costello, O., Agey, P.J., 1997. Chronic hypoxia affects capillary density and geometry in pigeon pectoralis muscle. Respir. Physiol. 109, 39–52.

Mathieu-Costello, O., Suarez, R.K., Hochachka, P.W., 1992. Capillary-to-fiber geometry and mitochondrial density in hummingbird flight muscle. Respir. Physiol. 89, 113–132.

McLelland, J., 1989a. Larynx and trachea. In: King, A.S., McLelland, J. (Eds.), Form and Function in Birds. Academic Press, London, pp. 69–104.

McLelland, J., 1989b. Anatomy of the lungs and air sacs. In: King, A.S., McLelland, J. (Eds.), Form and Function in Birds. Academic Press, London, pp. 221–280.

Meir, J.U., Milsom, W.K., 2013. High thermal sensitivity of blood enhances oxygen delivery in the high-flying bar-headed goose. J. Exp. Biol. 216, 2172–2175.

Meir, J.U., York, J.M., Chua, B.A., Jardine, W., Hawkes, L.A., Milsom, W.K., 2019. Reduced metabolism supports hypoxic flight in the high-flying bar-headed goose *Anser indicus*. Elife 8, e44986. https://doi.org/10.7554/eLife.44986.

Meyer, M., Holle, J.P., Scheid, P., 1978. Bohr effect induced by CO_2 and fixed acid at various levels of O_2 saturation in duck blood. Pflügers Arch. Ges. Physiol. 376, 237–240.

Meyer, M., Worth, H., Scheid, P., 1976. Gas-blood CO_2 equilibrium in parabronchial lings of birds. J. Appl. Physiol. 41, 302.

Milsom, W.K., Jones, D.R., Gabbott, G.R.J., 1981. On chemoreceptor control of ventilatory responses to CO_2 in unanesthetized ducks. J. Appl. Physiol. 50, 1121–1128.

Mitchell, G.S., Powell, F.L., Hopkins, S.R., Milsom, W.K., 2001. Time domains of the hypoxic ventilatory response in awake ducks: episodic and continuous hypoxia. Respir. Physiol. 124, 117–128.

Molony, V., Graf, W., Scheid, P., 1976. Effects of CO_2 on pulmonary air flow resistance in the duck. Respir. Physiol. 26, 333–349.

Morgan, V.E., Chichester, D.F., 1935. Properties of the blood of the domestic fowl. J. Biol. Chem. 110, 285–298.

Murrish, D.E., 1982. Acid-base balance in three species of antarctic penguins exposed to thermal stress. Physiol. Zool. 55 (2), 137–143.

Natarajan, C., Hoffmann, F.G., Weber, R.E., Fago, A., Witt, C.C., Storz, J.F., 2016. Predictable convergence in hemoglobin function has unpredictable molecular underpinnings. Science 354 (6310), 336–339.

Nightingale, T.E., Boster, R.A., Fedde, M.R., 1968. Use of the oxygen electrode in recording PO_2 in avian blood. J. Appl. Physiol. 25 (4), 371–375.

Nye, P.C.G., Burger, R.E., 1978. Chicken intrapulmonary chemoreceptors: discharge at static levels of intrapulmonary carbon dioxide and their location. Respir. Physiol. 33, 299–322.

Nye, P.C.G., Powell, F.L., 1984. Steady-state discharge and bursting of arterial chemoreceptors in the duck. Respir. Physiol. 56, 369–384.

Osborne, J.L., Mitchell, G.S., 1978. Intrapulmonary and systemic CO_2-chemoreceptor interaction in the control of avian respiration. Respir. Physiol. 33, 349–357.

Palomeque, J., Palacios, L., Planas, J., 1979. Comparative respiratory functions of blood in some passeriform birds. Comp. Biochem. Physiol. 66A, 619–624.

Pamenter, M.E., Powell, F.L., 2016. Time domains of the hypoxic ventilatory response and their molecular basis. Compr. Physiol. 6 (3), 1345–1385.

Parr, N., Bishop, C.M., Batbayar, N., Butler, P.J., Chua, B., Milsom, W.K., Scott, G.R., Hawkes, L.A., 2019a. Tackling the Tibetan Plateau in a down suit: insights into thermoregulation by bar-headed geese during migration. J. Exp. Biol. 222 (Pt 19), jeb203695. https://doi.org/10.1242/jeb.203695.

Parr, N., Wilkes, M., Hawkes, L.A., 2019b. Natural climbers: insights from avian physiology at high altitude. High Alt. Med. Biol. 20 (4), 427–437.

Parry, K., Yates, M.S., 1979. Observations on the avian pulmonary and bronchial circulation using labeled microspheres. Respir. Physiol. 38, 131–140.

Pattle, R.E., 1978. Lung surfactant and lung lining in birds. In: Piiper, J. (Ed.), Respiratory Function in Birds, Adult and Embryonic. Springer-Verlag, New York, p. 23.

Peacock, A.J., Pickett, C., Morris, K., Reeves, J.T., 1990. Spontaneous hypoxaemia and right ventricular hypertrophy in fast growing broiler chickens reared at sea level. Comp. Biochem. Physiol. 97A, 537–541.

Peek, F.W., Youngren, O.M., Phillips, R.E., 1975. Repetitive vocalizations evoked by electrical stimulation of avian brains. Brain Behav. Evol. 12, 1–41.

Perry, S.F., Christian, A., Breuer, T., Pajor, N., Codd, J.R., 2009. Implications of an avian- style respiratory system for gigantism in sauropod dinosaurs. J. Exp. Zool. A Ecol. Genet. Physiol. 311 (8), 600–610.

Peterson, D.F., Fedde, M.R., 1968. Receptors sensitive to carbon dioxide in lungs of chicken. Science 162, 1499–1501.

Petschow, D., Wurdinger, I., Baumann, R., Duhm, J., Braunitzer, G., Bauer, C., 1977. Causes of high blood O_2 affinity of animals living at high altitude. J. Appl. Physiol. 42 (2), 139–143.

Phu, D.N., Yamaguchi, K., Scheid, P., Piiper, J., 1986. Kinetics of oxygen uptake and release by red blood cells of chicken and duck. J. Exp. Biol. 125, 15–27.

Piiper, J., 1978. Origin of carbon dioxide in caudal airsacs of birds. In: Piiper, J. (Ed.), Respiratory Function in Birds, Adult and Embryonic. Springer-Verlag, Berlin, pp. 148–153.

Piiper, J., Scheid, P., 1972. Maximum gas transfer efficacy of models for fish gills, avian lungs and mammalian lungs. Respir. Physiol. 14, 115–124.

Piiper, J., Scheid, P., 1975. Gas transport efficacy of gills, lungs and skin: theory and experimental data. Respir. Physiol. 23, 209–221.

Piiper, J., Dejours, P., Haab, P., Rahn, H., 1971. Concepts and basic quantities in gas exchange physiology. Respir. Physiol. 13, 292–304.

Piiper, J., Drees, F., Scheid, P., 1970. Gas exchange in the domestic fowl during spontaneous breathing and artificial ventilation. Respir. Physiol. 9, 234–245.

Pilarski, J.Q., Hempleman, S.C., 2007. Development of avian intrapulmonary chemoreceptors. Respir. Physiol. Neurobiol. 157 (2–3), 393–402.

Ponganis, P.J., Meir, J.U., Williams, C.L., 2011. In pursuit of Irving and Scholander: a review of oxygen store management in seals and penguins. J. Exp. Biol. 214, 3325–3339.

Ponganis, P.J., St Leger, J., Scadeng, M., 2015. Penguin lungs and air sacs: for baroprotection, oxygen stores and buoyancy. J. Exp. Biol. 218 (Pt 5), 720–730.

Powell, F.L., 1982. Diffusion in avian lungs. Fed. Proc. 41, 2131–2133.

Powell, F.L., 1983. Respiration. In: Abs, M. (Ed.), Physiology and Behavior of the Pigeon. Academic Press, New York, pp. 73–95.

Powell, F.L., 1988. Lung structure and function. In: Wood, S.C. (Ed.), Comparative Pulmonary Physiology: Current Concepts. Marcel Dekker, Inc., New York, pp. 237–255.

Powell, F.L., 1993. Birds at altitude. In: Scheid, P. (Ed.), Respiration in Health and Disease. G. Fisher, Stuttgart/New York, pp. 352–358.

Powell, F.L., Hastings, R.H., 1983. Effects of hypoxia on ventilation-perfusion matching in birds. Physiol. 26, 50.

Powell, F.L., Hempleman, S.C., 1985. Sources of carbon dioxide in penguin air sacs. Am. J. Physiol. 248, R748–R752.

Powell, F.L., Hempleman, S.C., 1988. Comparative physiology of oxygen transfer in lungs. In: Gonzalez, N.C., Fedde, M.R. (Eds.), Oxygen Transfer from Atmosphere to Tissues. Plenum Press, New York, pp. 53–65.

Powell, F.L., Hempleman, S.C., 1990. Information content of artreial chemoreceptro discharge pattern. In: Eyzaguirre, C., Fidone, S.J., Fitzgerald, R.S., Lahiri, S., McDonald, D.M. (Eds.), Arterial Chemoreception. Springer-Verlag, New York, pp. 247–253.

Powell, F.L., Mazzone, R.W., 1983. Morphometrics of rapidly frozen goose lungs. Respir. Physiol. 51, 319–332.

Powell, F.L., Scheid, P., 1989. Physiology of gas exchange in the avian respiratory system. In: King, A.S., McLelland, J. (Eds.), Form and Function in Birds Volume 4. Academic Press, London, pp. 393–437.

Powell, F.L., Wagner, P.D., 1982. Ventilation-perfusion inequality in avian lungs. Respir. Physiol. 48, 233–241.

Powell, F.L., Fedde, M.R., Gratz, R.K., Scheid, P., 1978. Ventilatory responses to CO_2 in birds. I. Measurements in the unanesthetized duck. Respir. Physiol. 35, 349–359.

Powell, F.L., Geiser, J., Gratz, R.K., Scheid, P., 1981. Airflow in the avian respiratory tract: variations of O_2 and CO_2 concentrations in the bronchi of the duck. Respir. Physiol. 44, 195–213.

Powell, F.L., Hastings, R.H., Mazzone, R.W., 1985. Pulmonary vascular resistance during unilateral pulmonary arterial occlusion in ducks. Am. J. Physiol. 249 (18), R39–R43.

Powell, F.L., Dwinell, M.R., Aaron, E.A., 2000. Measuring ventilatory acclimatization to hypoxia: comparative aspects. Respir. Physiol. 122, 271–284.

Powell, F.L., Milsom, W.K., Mitchell, G.S., 1998. Time domains of the hypoxic ventilatory response. Respir. Physiol. 112, 123–134.

Powell, F.L., Hopkins, S.R., 2010. Vertebrate life at high altitude. In: Nilsson, G.E. (Ed.), Respiratory Physiology of Vertebrates: Life with and without Oxygen. Cambridge U Press, Cambridge, pp. 265–299.

Powell, F.L., Shams, H., Hempleman, S.C., Mitchell, G.S., 2004. Breathing in thin air: acclimatization to altitude in ducks. Respir. Physiol. Neurobiol. 144, 225–235.

Richards, S.A., 1971. Brain stem control of polypnoea in the chicken and pigeon. Respir. Physiol. 11, 315–326.

Scharnke, H., 1938. Experimentelle Beiträge zur Kenntnis der Vogelatmung. Z. vergl. Physiologie 25, 548–583.

Scheid, P., 1978. Analysis of gas exchange between air capillaries and blood capillaries in avian lungs. Respir. Physiol. 32, 27–49.

Scheid, P., 1979. Respiration and control of breathing in birds. Physiol. 22, 60–64.

Scheid, P., Piiper, J., 1969. Volume, ventilation and compliance of the respiratory system in the domestic fowl. Respir. Physiol. 6, 298–308.

Scheid, P., Kawashiro, T., 1975. Metabolic changes in avian blood and their effects on determination of blood gases and pH. Respir. Physiol. 23, 291–300.

Scheid, P., Piiper, J., 1970. Analysis of gas exchange in the avian lung: theory and experiments in the domestic fowl. Respir. Physiol. 9, 246–262.

Scheid, P., Piiper, J., 1972. Cross-current gas exchange in avian lungs: effects of reversed parabronchial air flow in ducks. Respir. Physiol. 16, 304–312.

Scheid, P., Piiper, J., 1986. Control of breathing in birds. In: Cherniack, N.S., Widdicombe, J.G. (Eds.), Handbook of Physiology: The Respiratory System -Control of Breathing. American Physiological Society, Bethesda, pp. 815–832.

Scheid, P., Piiper, J., 1989. Respiratory mechanics and air flow in birds. In: King, A.S., McLelland, J. (Eds.), Form and Function in Birds. Academic Press, London, pp. 369–391.

Scheid, P., Slama, H., 1975. Remote-controlled device for sampling arterial blood in unrestrained animals. Pflügers Arch 356, 373–376.

Scheid, P., Fedde, M.R., Piiper, J., 1991. Gas exchange and air-sac composition in the unanaesthetized, spontaneously breathing goose. J. Exp. Biol. 142, 373–385.

Scheid, P., Gratz, R.K., Powell, F.L., Fedde, M.R., 1978. Ventilatory response to CO_2 in birds. II. Contribution by intrapulmonary CO_2 receptors. Respir. Physiol. 35, 361–372.

Scheid, P., Slama, H., Piiper, J., 1972. Mechanisms of unidirectional flow in parabronchi of avian lungs: measurements in duck lung preparations. Respir. Physiol. 14, 83–95.

Scheid, P., Slama, H., Willmer, H., 1974. Volume and ventilation of air sacs in ducks studied by inert gas wash-out. Respir. Physiol. 21, 19–36.

Scheid, P., Worth, H., Holle, J.P., Meyer, M., 1977. Effects of oscillating and intermittent ventilatory flow on efficacy of pulmonary O_2 transfer in the duck. Respir. Physiol. 31, 251–258.

Scheipers, G., Kawashiro, T., Scheid, P., 1975. Oxygen and carbon dioxide dissociation of duck blood. Respir. Physiol. 24, 1–13.

Schmidt, M.F., Martin Wild, J., 2014. The respiratory-vocal system of songbirds: anatomy, physiology, and neural control. Prog. Brain Res. 212, 297–335.

Schmitt, P.M., Powell, F.L., Hopkins, S.R., 2002. Ventilation-perfusion inequality during normoxic and hypoxic exercise in the emu. J. Appl. Physiol. 93, 1980–1986.

Scott, G.R., Egginton, S., Richards, J.G., Milsom, W.K., 2009. Evolution of muscle phenotype for extreme high altitude flight in the bar-headed goose. Proc. Biol. Sci. B 276, 3645–3653.

Scott, G.R., Milsom, W.K., 2006. Flying high: a theoretical analysis of the factors limiting exercise performance in birds at altitude. Respir. Physiol. Neurobiol. 154, 284–301.

Scott, G.R., Milsom, W.K., 2007. Control of breathing and adaptation to high altitude in the bar-headed goose. Am. J. Physiol. Regul. Integr. Comp. Physiol. 293, R379–R391.

Seamon, A.B., Hofmeister, E.H., Divers, S.J., 2017. Outcome following inhalation anesthesia in birds at a veterinary referral hospital: 352 cases (2004-2014). J. Am. Vet. Med. Assoc. 251 (7), 814–817.

Sèbert, P., 1979. Mise en evidence de l'action centrale du stimulus $CO_2[H^+]$ de la ventilation chez le Canard Pekin. J. Physiol. Paris 75, 901–909.

Seifert, E., 1896. Über die Atmung der Reptilien und Vögel. Pflügers Arch. Ges. Physiol. 64, 321–506.

Shams, H., Scheid, P., 1989. Efficiency of parabronchial gas exchange in deep hypoxia: measurements in the resting duck. Respir. Physiol. 77, 135–146.

Shoemaker, J.M., Hempleman, S.C., 2001. Avian intrapulmonary chemoreceptor discharge rate is increased by anion exchange blocker 'DIDS'. Respir. Physiol. 128, 195–204.

Simonson, T.S., 2015. Altitude adaptation: a glimpse through various lenses. High Alt. Med. Biol. 16 (2), 125–137.

Skadhauge, E., 1983. Formation and composition of urine. In: Freeman, B.M. (Ed.), Physiology and Biochemistry of the Domestic Fowl. Academic Press, London, pp. 108–135.

Smith, J.H., Meier, J.L., Lamke, C., Neill, P.J., Box, E.D., 1986. Microscopic and submicroscopic anatomy of the parabronchi, air sacs, and respiratory space of the budgerigar (*Melopsittacus undulatus*). Am. J. Anat. 177, 221–242.

Smith, J.C., Ellenberger, H.H., Ballanyi, K., Richter, D.W., Feldman, J.L., 1991. Pre-Bötzinger complex: a Brainstem region that may generate respiratory rhythm in mammals. Science 254, 726–729.

Sturkie, P.D., 1986. Body fluids: blood. In: Sturkie, P.D. (Ed.), Avian Physiology. Springer-Verlag, New York, pp. 102–139.

Taylor, E.W., Jordan, D., Coote, J.H., 1999. Central control of the cardiovascular and respiratory systems and their interactions in vertebrates. Physiol. Rev. 79, 855–916.

Taylor, C.R., Weibel, E.R., 1981. Design of the mammalian respiratory system. I. Problem and strategy. Respir. Physiol. 44, 1–10.

Torre-Bueno, J.R., Geiser, J., Scheid, P., 1980. Incomplete gas mixing in air sacs of the duck. Respir. Physiol. 42, 109–122.

Tucker, V., 1972. Respiration during flight in birds. Respir. Physiol. 14, 75–82.

von Saalfeld, E., 1936. Untersuchungen Über das hacheln bei tauben. Z. vergl. Physiologie 23, 727–743.

Vos, H.F., 1935. Über den Weg der Atemluft in der Entenlunge. Z. vergl. Physiologie 20, 552–578.

Wagner, P.D., 1977. Diffusion and chemical reaction in pulmonary gas exchange. Physiol. Rev. 57, 257–312.

Wang, N., Banzett, R.B., Butler, J.P., Fredberg, J.J., 1988. Bird lung models show that convective inertia effects inspiratory aerodynamic valving. Respir. Physiol. 73, 111–124.

Wang, N., Banzett, R.B., Nations, C.S., Jenkins, F.A., 1992. An aerodynamic valve in the avian primary bronchus. J. Exp. Biol. 262, 441–445.

Watson, R.R., Fu, Z., West, J.B., 2008. Minimal distensibility of pulmonary capillaries in avian lungs compared with mammalian lungs. Respir. Physiol. Neurobiol. 160, 208–214.

Weber, R.E., 2007. High-altitude adaptations in vertebrate hemoglobins. Respir. Physiol. Neurobiol. 158, 132–142.

Weber, R.E., Wells, R.M.G., 1989. Hemoglobin structure and function. In: Wood, S.C. (Ed.), Comparative Pulmonary Physiology: Current Concepts. Marcel Dekker, Inc., New York, pp. 279–310.

Weber, R.E., Hemmingsen, E.A., Johansen, K., 1974. Functional and biochemical studies of penguin myoglobin. Comp. Biochem. Physiol. 49B, 197–214.

Weidner, W.J., Kinnison, J.R., 2002. Effect of extracellular fluid volume expansion on the interparabronchial septum of the avian lung. J. Comp. Pathol. 127, 219–222.

Weidner, W.J., Bradbury, C.A., Le, S.P., Wallace, S.R., 2012. Regional pulmonary blood flow in the lung of the chicken. Poult. Sci. 91, 1441–1443.

Weidner, W.J., Waddell, D.S., Furlow, J.D., 2006. Measurement of the filtration coefficient (Kfc) in the lung of *Gallus domesticus* and the effects of increased microvascular permeability. J. Comp. Physiol. B. 176, 567–574.

Weidner, W.J., Selna, L.A., McClure, D.E., DeFouw, D.O., 1993. Effect of extracellular fluid volume expansion on avian lung fluid balance. Respir. Physiol. 91, 125–136.

Weingarten, J.P., Rollema, H.S., Bauer, C., Scheid, P., 1978. Effects of inositol hexaphosphate on the Bohr effect induced by CO_2 and fixed acids in chicken hemoglobin. Pflügers Arch 377, 135–141.

Weinstein, Y., Bernstein, M.H., Bickler, P.E., Gonzales, D.V., Samaniego, F.C., Escobedo, M.A., 1985. Blood respiratory properties in pigeons at high altitudes: effects of acclimation. Am. J. Physiol. 249, R765–R775.

Wells, D.J., 1993. Ecological correlates of hovering flight of hummingbirds. J. Exp. Biol. 178, 59–70.

Wells, R.M.G., 1976. The oxygen affinity of chicken hemoglobin in whole blood and erythrocyte suspensions. Respir. Physiol. 27, 21.

West, J.B., Fu, Z., Deerinck, T.J., Mackey, M.R., Obayashi, J.T., Ellisman, M.H., 2010. Structure-function studies of blood and air capillaries in chicken lung using 3D electron microscopy. Respir. Physiol. Neurobiol. 170, 202–209.

West, J.B., Watson, R.R., Fu, Z., 2006. Major differences in the pulmonary circulation between birds and mammals. Respir. Physiol. Neurobiol. 157, 382–390.

West, J.B., 2011. Comparative physiology of the pulmonary circulation. Compr. Physiol. 1, 1525–1539.

West, J.B., 2009. Comparative physiology of the pulmonary blood-gas barrier: the unique avian solution. Am. J. Physiol. Regul. Integr. Comp. Physiol. 297, R1625–R1634.

Whittow, G.C., Ossorio, N., 1970. A new technique for anesthetizing birds. Lab. Anim. Care 20, 651–656.

Wideman, R.F., Chapman, M.E., Hamal, K.R., Bowen, O.T., Lorenzoni, A.G., Erf, G.F., Anthony, N.B., 2007. An inadequate pulmonary vascular capacity and susceptibility to pulmonary arterial hypertension in broilers. Poult. Sci. 86, 984–998.

Wideman, R.F., Rhoads, D.D., Erf, G.F., Anthony, N.B., 2013. Pulmonary arterial hypertension (ascites syndrome) in broilers: a review. Poult. Sci. 92, 64–83.

Williams Jr., B.R., Boggs, D.F., Kilgore Jr., D.L., 1995. Scaling of hypercapnic ventilatory responsiveness in birds and mammals. Respir. Physiol. 99, 313–319.

Yamatsu, Y., Kameda, Y., 1995. Accessory carotid body within the parathyroid gland III of the chicken. Histochemistry 103, 197–204.

Yap, K.N., Dick, M.F., Guglielmo, C.G., Williams, T.D., 2018. Effects of experimental manipulation of hematocrit on avian flight performance in high- and low-altitude conditions. J. Exp. Biol. 221 (Pt 22), jeb191056. https://doi.org/10.1242/jeb.191056.

York, J.M., Chua, B.A., Ivy, C.M., Alza, L., Cheek, R., Scott, G.R., McCracken, K.G., Frappell, P.B., Dawson, N.J., Laguë, S.L., Milsom, W.K., 2017. Respiratory mechanics of eleven avian species resident at high and low altitude. J. Exp. Biol. 220 (Pt 6), 1079–1089.

Zeuthen, E., 1942. The ventilation of the respiratory tract in birds. K. danske Vidensk. Selsk. Skr. 17, 1–50.

Zimmer, K., 1935. Beitrage zur Mechanik der Atmung be den Vogeln in Stand und Flug. Zoologica 33, 1.

Chapter 21

Gastrointestinal anatomy and physiology

Monika Proszkowiec-Weglarz

United States Department of Agriculture, Agricultural Research Service, Animal Biosciences and Biotechnology Laboratory, Beltsville, MD, United States

Abbreviations

A antiport
AA^0 neutral amino acids
AA^+ cationic amino acids
ACh acetylcholine;
AEC absorptive epithelial cells;
AM apical membrane
APP avian pancreatic polypeptide;
ATP2B1 (PMCA1b) plasma membrane calcium transporting ATPase 1;
ATP2B2 plasma membrane calcium transporting ATPase 2;
ATP2B4 plasma membrane calcium transporting ATPase 4;
BM basolateral membrane
BW body weight
C α-carotene
Car carotenoids
CaTN caudal thin muscle of muscular stomach
CCK cholecystokinin
CCK-4 Cholecystokinin tetrapeptide;
CCK-8 Cholecystokinin octapeptide;
CD36 cluster determinant 36;
CFU colonyforming unit;
cG chicken gastrin;
CPP cell-penetrating peptides
Cr-EDTA chromium ethylenediaminetetraacetic salt;
Cr_2O_3 chromium (III) oxide;
CrTN cranial thin muscle of muscular stomach
D duodenum
DD distal duodenum
G2 craniodorsal thin muscle
G3 caudodorsal thick muscle
GABA gamma amino butyric acid
GC goblet cell;
GI proventriculus
GIP gastric inhibitory peptide;
GIT gastrointestinal tract;
GLUT glucose transporter;
GRP gastrin-releasing peptide;
GS glandular stomach
HO-P hydroxyprolineI, intestine
I intestine
IgA immunoglobulin A;
JAM junctional adhesion molecule;
K kidney
L length
$l,25(0H)_2D_3$ 1,25-dihydroxyvitamin D_3;
Lut lutein
Lyc lycopene
L-NAME N-nitro-L-arginine methyl ester;
lSW log duration slow waves;
MCT1-4 electroneutral co-transporter 1−4;
MMC migrating motor complex;
MR mitochondria-rich cells;
MRT mean retention time;
MS muscular stomach
MUC transmembrane mucin gene;
Na/P IIb (SLC34A2) sodium-dependent P transporter;
NANC nonadrenergic, noncholinergic;
NCX1 (SLC8A) sodium/calcium exchanger 1;
nNOS neuronal nitric oxide (NO) synthase;
NO nitric oxide
NOS nitric oxide synthase
NR not reported
NPC1L1 cholesterol membrane transporter;
O ornithine
PD proximal duodenum
PP pancreatic polypeptide
PepT1 (SLC15A1) di and tripeptides transport system;
pIgR IgA receptor;
PIT1 sodium-dependent P transporter III;
PIT2 sodium-dependent P transporter III;
RBPR2 RBP4-receptor 2;
S symport
S-AA0 symport together with neutral amino acids
SCFA short chain fatty scid
SGLT-1 Na-glucose transporter;
SMCT1 or 2 sodium co-transporter;
SR-BI Scavenger Receptor class B type I;
sSW short duration slow waves;
STRA6 Stimulated by Retinoic Acid 6 protein;
T1 1% marker concentration in excreta;

Sturkie's Avian Physiology. https://doi.org/10.1016/B978-0-12-819770-7.00010-4

T50 50% marker concentration in excreta;
TK thick muscle pair
TK thick muscle pair (dorsal and ventral) of muscular stomach
TJP tight junction protein,
TN thin muscle pair
TRPC transient receptor potential cation channel subfamily C;
TRPM transient receptor potential cation channel subfamily M;
TRPV transient receptor potential cation channel;
U uniport
Ub ubiquitous.
VDR vitamin D receptor;
VFA volatile fatty acid;
Vit vitamin
VIP vasoactive intestinal peptide
WT weightα
βC β-carotene
βC β-cryptoxanthine

21.1 Anatomy of the digestive tract

The gastrointestinal tract (GIT) is not only important for nutrient digestion and absorption, but it is the largest immunological organ in the body protecting against exogenous pathogens. The digestive system (Figure 21.1) has adaptations designed to facilitate flight. The length of the intestinal tract is shorter in most birds relative to mammals (Table 21.1, McWhorter et al., 2009). To compensate for shorter digestive tract, birds generally have higher feed intakes and/or increased intestinal nutrient absorption (McWhorter et al., 2009). In contrast, nonflying birds such as ostrich have heavier organ masses including larger digestive tract (Fritz et al., 2012; Laverty and Skadhauge, 1999). Also, birds lack teeth and heavy jaw muscles, which have been replaced with a lightweight bill or beak. Food particles are swallowed whole and then reduced in size by the *ventriculus* or *gizzard* located within the body cavity.

21.1.1 Beak, mouth, and pharynx

Birds have a bill or beak. This structure shows extensive anatomical variations among species, thus allowing for adaptations for different feeding styles. The upper bill is usually covered with hard keratin. However, in some types

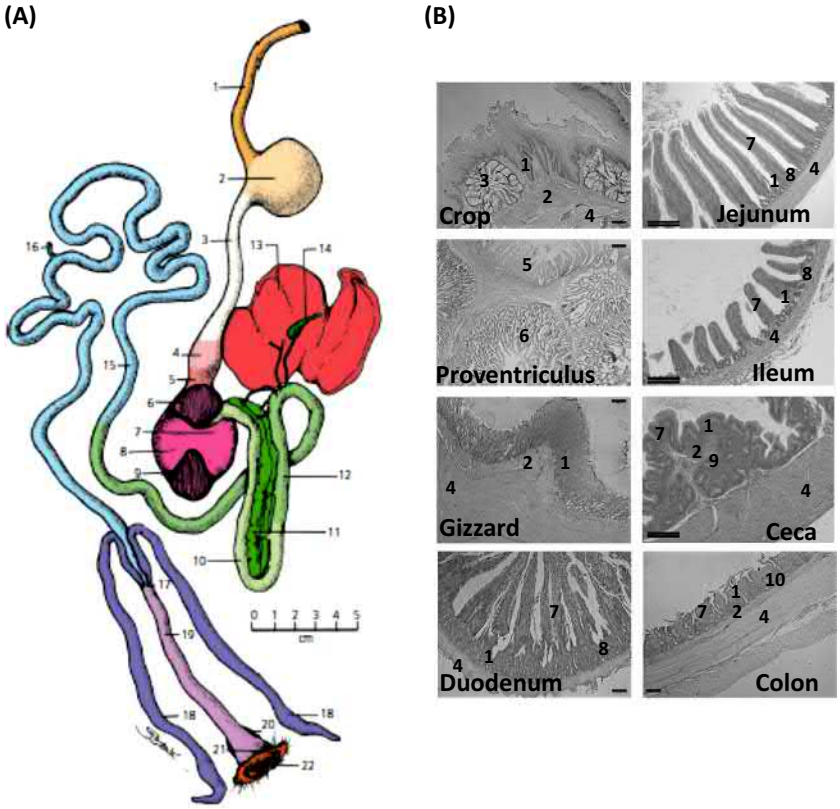

FIGURE 21.1 **Anatomical and histological structure of avian digestive tract.** (A) Digestive tract of a turkey. 1, precrop esophagus; 2, crop; 3, postcrop esophagus; 4, glandular stomach (proventriculus); 5, isthmus; 6–9, muscular stomach (gizzard); 10, proximal duodenum; 11, pancreas; 12, distal duodenum; 13, liver; 14, gallbladder; 15, jejunum; 16, Meckel's diverticulum (remnant of yolk sac); 17, ileocecocolic junction; 18, ceca; 19, colon; 20, bursa of Fabricius; 21, cloaca; 22, vent. Scale is in centimeters. (B) Histological structure of the regions of the chicken gastrointestinal tract. 1, mucus layer; 2, submucosa; 3, crop gland; 4, muscular tunic; 5, branched tubular glands; 6, deep proventricular gland, 7, villi; 8, crypt; 9, cecal gland; 10, colon gland. Single bar indicates 200 μm while double bar indicate 250 μm. *(A) Reprinted from Reece and Trampel (Reece and Trampel, 2015). Avian digestion. In: Reece, W.O. (Ed.), Duke's Physiology of Domestic Animals, 13th ed. Copyright 2015 by John Wiley & Sons, Ames, IA, p. 533. Used by permission of the publisher. Author of histology and photographs of crop, proventriculus, gizzard, duodenum and colon: A. Hrabia. Used with permission of the author.*

TABLE 21.1 Dimensions of the digestive tract of various species of birds.[a]

		Esophagus			Proventriculus and gizzard			Small intestine			Cecum		Rectum			Total	
Species	BW (kg)	L (mm)	Total %	WT (g)	L (mm)	Total %	WT (g)	L (mm)	Total %	WT (g)	L (mm)	WT (g)	L (mm)	Total (%)	WT (g)	L (mm)	L/BW
Chicken																	
Leghorn	1.2	136	9.9	8.2	86	6.3	26.7	1082	78.9	29.5	127	5.2	68	5.0	2.3	1372	1.14
Broiler	3.0	140	6.4	16.8	101	4.7	43.5	1796	82.7	73.6	188	10.7	134	6.2	5.1	2172	0.72
Turkey	3.0	123	5.7	8.5	110	5.1	52.9	1853	85.7	85.3	278	20.1	75	3.5	4.4	2161	0.72
Japanese quail		75	11.5		38	5.8		510	78.1		100		30	4.6		653	
Domestic duck	2.2	310	11.7		130	4.9		2110	79.9		140		90	3.4		2640	1.20
Emu	53.0	790	12.1		260	4.0		5200	79.4		120		300	4.6		6550	0.12
Rhea	25.0				310			1400			480		400				
Ostrich	122.0				480			6400			940		8000				
Cedar waxwing		51	16.2		36	11.4		171	54.3		0		57	18.1		315	

[a]*The length (L), body weight (BW), and weight (WT) of the gastrointestinal tract can change depending on the environment in which the birds are raised.*
Reproduced from Denbow (2015).

of birds, the whole bill is relatively soft (i.e., Charadrii or shorebirds), whereas in others, only the tip is hard (i.e., Anatidae or waterfowl). The culmen, the medial dorsal area of the upper beak, has a pointed protuberance in the embryo, the egg tooth, which drops off after hatching in most birds.

Birds, unlike mammals, do not have a sharp distinction between the pharynx and mouth. Birds lack a soft palate and a pharyngeal isthmus; the combined oral and pharyngeal cavities are referred to as the *oropharynx.* The palate contains a longitudinal fissure, the *choana,* which connects the oral and nasal cavities. Caudal to the choana is the *infundibular cleft,* which is medially located and is the common opening to the auditory tubes (Figure 21.2). The palate generally also has ridges that aid in opening the shell of seeds.

All vertebrates have a hyoid bone, which serves as an attachment site for muscles of the tongue and throat. Birds have a Y-shaped hyoid apparatus that extends to the tip of their tongue. Two long structures, the "horns" of the hyoid, protrude backwards from the fork in the Y and provide insertion sites for protractor muscles originating on the lower jaw. The hyoid horns are modified in different species and can extend to the top of the head, around the eye socket and into the nasal cavity (Short and Sandström, 1982; Wang et al., 2011). Contraction of the muscles attached to the hyoid apparatus pulls the apparatus forward and against the skull, thus thrusting the tongue outward. Lengthening of the hyoid horns and the attached muscles effectively gives the bird a tongue that is able to protrude further out the mouth.

The tongue shows adaptations for collecting, manipulating, and swallowing food (Harrison, 1964). In birds where the tongue is used for collecting food, it can be extended from the mouth during the collection process. Such tongues typically have lateral barbs and may be coated with mucous secreted by the mandibular salivary gland. The tongue may act as either a brush, a spear, or a dynamic tube (Rico-Guevara and Rubega, 2011), sometimes extending four times the length of the beak.

Tongues used to manipulate food, such as in piscivorous species, are nonprotruding and covered with stiff, sharp, caudally directed papillae. In birds of prey, the tongue is a rasp-like structure, with the rostral portion frequently being very hard and rough (McLelland, 1979). On tongues of birds that typically strain food particles (e.g., ducks), the rostral portion forms a scoop-like structure, with the lateral borders having a double row of overlapping bristles. The bristles work in conjunction with the lamellae of the bill to filter particles.

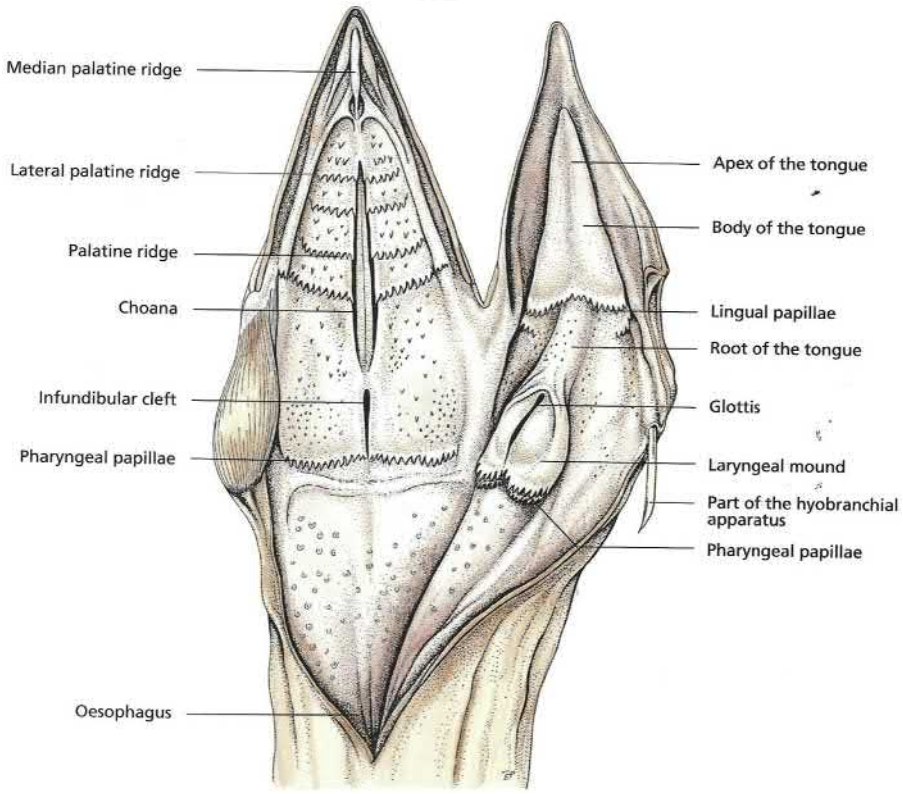

FIGURE 21.2 Oral cavity and pharynx of the chicken (opened and reflected; schematic). *Reprinted from Koenig, Liebich, Korbel and Klupiec (Koenig et al., 2016). Avian Anatomy. Copyright 2016 by HE. Koenig, R. Korbel, H-G. Liebich, p. 95. Used by permission of the copyright holders.*

In birds where the tongue is utilized to aid in swallowing food, caudally directed papillae tend to be located near the root of the tongue. These papillae function to propel food caudally. Tongues specialized for swallowing are nonprotruding.

Avian salivary glands also show considerable species variation. Although salivary glands are generally well developed in granivorous species; they are less developed in birds of prey, poorly developed in piscivores, and absent in the Anhinga and Great Cormorant (Antony, 1920). As a generalization, the *maxillary, palatine*, and *sphenopterygoid* glands are located in the roof of the mouth. The buccal gland is located in the cheeks whereas the *mandibular, lingual,* and *cricoarytenoid* glands are in the floor of the mouth. Although the salivary glands of *Gallus* and *Meleagris* are reported to secrete little amylase, the house sparrow secretes considerable amounts of amylase (Jerrett and Goodge, 1973).

Location of taste buds are variable, on the upper beak epithelium, in the anterior mandible, and the mandibular epithelium posterior to the tongue. There are also small number of taste buds located ventrolaterally on the anterior tongue. In contrast to mammals, chickens have relatively low number of taste buds (Liu et al., 2018). It is believed that chickens can have as many as 240−360 taste buds on average, with the number in broiler being higher than in layer-type chickens (Ganchrow and Ganchrow, 1985; Kudo et al., 2008). Additionally, the number of taste buds can vary among lines in the same type of chicken (Rajapaksha et al., 2016). Molecular staining of the buds showed that the number of taste buds differs between females and males and changes with age (Rajapaksha et al., 2016). In comparison to rodents, chicken taste buds develop and mature before hatch (Ganchrow et al., 1990), and the total number of taste buds is positively correlated with the sensitivity of the taste in chickens (Kudo et al., 2010). In comparison to mammals, chicken have fewer genes coding for taste receptors and are able to detect only taste of sour, umami, salt, and bitter, but not taste of sweet (Cheled-Shoval et al., 2015; Lagerstrom et al., 2006; Liu et al., 2018).

In some species of birds, the floor of the mouth contains sac-like diverticuli called *oral sacs.* These can function in carrying food or as a display apparatus during the breeding season.

Immediately behind the tongue is the *laryngeal mound.* It contains a narrow slit-like opening into the *glottis* of the larynx. The laryngeal mound generally contains rows of caudally directed cornified papillae, which aid in moving food toward the esophagus during swallowing.

21.1.2 Esophagus and crop

The esophagus is a thin-walled, distendable tube that transports food from the pharynx to the stomach, allowing birds to swallow their food whole. Thus, it contains a number of longitudinal folds that provide distensibility. The avian esophageal wall consists of four layers: mucosal, submucosal, muscle tunic, and the serosal layer; it generally contains only smooth muscle cells, with a circular muscle layer predominating (McLelland, 1979).

Unlike mammals, the avian esophagus is divided into a cervical and a thoracic region. In addition, the esophagus of birds lacks both upper and lower esophageal sphincters, which are present in mammals (Mulé, 1991).

In many, but not all (e.g., gulls, penguins, and ostriches) species of birds, the cervical esophagus is expanded to form a *crop.* The crop functions to store food and may be spindle-shaped, bilobed, or unilobed. In the chicken, the crop is a ventral diverticulum of the esophagus and contains longitudinal folds on the inner surface, thus making it distensible (Figure 21.1B). Beyond the crop, the esophagus continues as the thoracic esophagus to connect with the proventriculus.

A small number of species have a diverticulum or a bilaterally symmetrical expansion of the cervical esophagus, the *esophageal sac.* In most species that have this structure, it is present only in males and functions as a sexual display used during the breeding season, and for producing mating calls.

The esophagus and crop are lined with incompletely keratinized stratified squamous epithelia which open into numerous mucous glands. These glands are generally more numerous in the thoracic esophagus and may even be absent in the cervical region. Mucous glands are located in the crop only near its junction with the esophagus.

The cervical esophagus is innervated by parasympathetic nerves while the thoracic esophagus is innervated by the vagus and the celiac plexus. The esophagus is innervated by a few adrenergic fibers, which synapse with the myenteric plexus rather than the muscles (McLelland, 1975; Mulé, 1991).

21.1.3 Stomach

In most mammals, the stomach consists of a single chamber. However, in birds, the stomach consists of two chambers, the proventriculus and the gizzard, with the former being analogous to the mammalian stomach. The proventriculus or glandular stomach is located orad to the gizzard or muscular stomach. The proventriculus is a fusiform organ varying in size and shape among species, being relatively large and distensible in aquatic carnivores while being relatively small in granivorous species. In ostriches, which lack a crop, the proventriculus is especially large. The proventriculus secretes mucus, hydrochloric acid, and pepsinogen, whereas the gizzard functions in mechanical digestion and is the site of gastric proteolysis. The pyloric region connects the gizzard to the duodenum.

Two extremes of gastric anatomy exists in birds (McLelland, 1979). The first type, characteristic of carnivorous and piscivorous species, is adapted for storage and the digestion of a relatively soft diet. The two stomach chambers contain little separation, although one chamber may be more developed than the other, depending on the species. The second stomach type, characteristic of omnivores, insectivores, herbivores, and granivores, is adapted for very hard diets. The proventriculus and gizzard are separated by an isthmus termed the *zona intermedia gastric*. The proventriculus is relatively small, while the gizzard is large and powerful. The gizzard consists of two pairs of opposing muscles, termed thick and thin pairs (Figure 21.3), which are composed of circular muscle. These pairs of muscles are lacking in some species (e.g., herons, hawks, and owls).

The proventriculus, which generally lacks ridges except in fish- and meat-eating species, is lined with a mucous membrane. Projecting into the lumen are papillae located on the surface, from which the openings of the compound glands that secrete gastric juices can be seen. These glands generally contain only oxynticopeptic cells and secrete hydrochloric acid, pepsin, and mucous. The proventriculus contains both a myenteric and a submucosal plexus (Martínez et al., 2000).

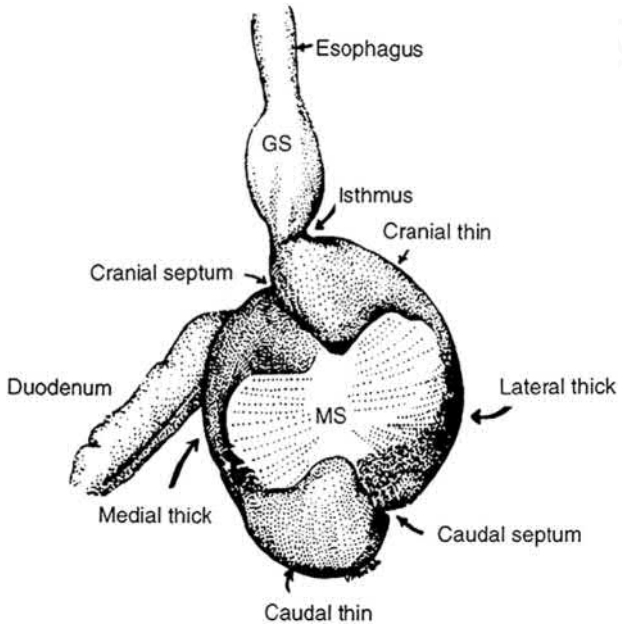

FIGURE 21.3 Anatomical features of muscular stomach of domestic turkeys. *GS*, glandular stomach; *MS*, muscular stomach. Note that cranial thin muscle of MS is continuous with lateral thick muscle and separated from caudal thin muscle at caudal septum. Similarly, the caudal thin muscle in continuous with the medial thick muscle and separated from cranial thin muscle by cranial septum. *Reprinted from Chaplin and Duke. Copyrights 1990 by American Physiological Society. Used by permission of the publisher.*

The interior surface of the gizzard is lined with a cuticle, sometimes called *koilin,* which is produced by the mucosal glands. The cuticle protects the gizzard from acid and proteolytic enzymes secreted by the proventriculus and from injury during grinding of hard food items. The greenish or brownish color of the cuticle is due to the reflux of bile pigments from the duodenum. Although in most birds the cuticle is continuously worn away and replaced, in some species, it is shed.

The pyloric portion of the stomach shows a considerable range in development. In *Gallus,* it is only 0.5 cm long. Its mucosal glands secrete mucous instead of a cuticle. In other species, the pyloric portion is enlarged and contains a cuticle. Although the function of this region is unknown, it is believed that it may slow the movement of large particles into the duodenum (Vergara et al., 1989).

The stomach is innervated by the vagus and perivascular nerve fibers from the celiac and mesenteric plexii. The muscle cells are innervated by cholinergic fibers, while noradrenergic fibers primarily innervate blood vessels. The myenteric nerve plexus lies just under the serosa, while the submucosal plexus is lacking. Because the longitudinal muscle layer is absent, the myenteric nerve plexus is normally visible through the transparent serosa.

21.1.4 Small intestine

The small intestine is divided into the duodenum, jejunum, and ileum. Although there is a distinct duodenal loop, the yolk stalk (i.e., Meckel's diverticulum) is often used as a landmark to separate the jejunum and ileum. Intestinal length varies considerably between species, being relatively shorter in frugivores, carnivores, and insectivores and long in granivores, herbivores, and piscivores. However, the length of the small intestine is relatively shorter than that of mammals in most birds.

Depending on the species, the intestinal wall can contain either folds or villi. The type of mucosal projections is not necessarily consistent between the small and large intestine. *Gallus* species have villi, which decrease in length from 1.5 mm in the duodenum to 0.4−0.6 mm in the ileum and rectum. The number of villi decreases from 1-10 days of age, but thereafter remains constant. Genetic selection for growth has altered villi morphology (Yamauchi and Isshiki, 1991). Compared to white leghorns, the villi of broilers are larger and have more epithelial cell protrusions located between the apical surface of the duodenal villi. Nevertheless, the villi of both types of chickens form a zigzag arrangement, which is thought to slow ingesta flow. Detailed description of intestinal villi and crypt organization, and function is presented in Chapter 21A.

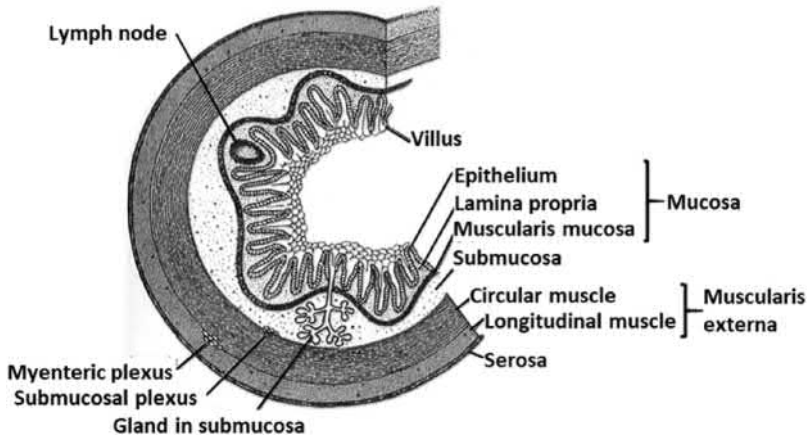

FIGURE 21.4 The general organization of layers of the gastrointestinal tract. *Reprinted from Argenzio. General function of the gastrointestinal tract and their control. In: Reece, W.O. (Ed.), Duke's Physiology of Domestic Animals, 12th ed. Copyright 2004 by Cornell University Press, Ithaca and London p. 383. Used by permission of the publisher.*

The intestinal wall contains the mucosa, submucosa, muscularis externa, and serosa layers. The mucosal layer consists of the muscularis mucosa, lamina propria, and epithelium (Figure 21.4). However, the muscularis mucosa and lamina propria are poorly developed in birds, possibly because the villi lack a central lacteal (blindly ending lymphatic capillary in the center of an intestinal villi). Although Brunner's glands, common to mammals, are absent (Calhoun, 1954), *tubular* glands (possibly homologous to Brunner's glands) are present in some species (Ziswiler and Farner, 1972). The epithelium contains chief cells, goblet cells (GCs), and endocrine cells. The crypts of Lieberkuhn are the source of epithelial cells that line the villi. The crypts contain undifferentiated cells, GCs, endocrine cells, and lymphocytes. Globular leukocytes and Paneth cells appear near the base of the crypts. The submucosa located beneath the lamina propria and muscularis mucosa, contains nerve cell bodies and blood vessels. The innercircular and longitudinal muscle layers are located underneath the submucosa. The serosa makes up the outermost layer of the intestinal wall (Argenzio, 2004).

The intestines contain extensive innervation from both the sympathetic and the parasympathetic nervous systems. As described by Bennett (1974), innervation is both cholinergic and adrenergic. The enteric nerve plexuses were described by Ali and McLelland (1978). Except in the rectum, the longitudinal muscle is sparsely innervated.

The *intestinal nerve* (nerve of Remak), which runs the length of the small and large intestine, is unique to birds. Although it has no mammalian homolog, it may be analogous to the prevertebral ganglion (Hodgkiss, 1984a). This nerve is thought to be a mixed nerve containing both sympathetic and parasympathetic autonomic fibers (Hodgkiss, 1986).

21.1.5 Ceca

Arising at the junction of the ileum and rectum are the ceca. In some species, the ceca may be absent (e.g., Psittaciformes, Apodiformes, and Piciformes) or rudimentary (e.g., Columbiformes and Piciformes). In other species, they are either paired (e.g., herbivores, most granivores, and owls), singular (Ardeidae), or consist of a double pair (secretary bird). McLelland (1979) has grouped ceca into four types based on morphology: (1) intestinal, which resemble the remainder of the intestine; (2) glandular, which are long and contain many actively secreting crypts; (3) lymphoid, which are reduced in size, containing many lymphocytes and occasional nonsecreting crypts; and (4) vestigial, which are small with a reduced lumen (Figure 21.5). A correlation between diet and cecal development, or the size of the ceca and the length and width of the rectum have not been discovered (McLelland, 1989).

In chickens, a cecum can be morphologically divided into three regions (Ferrer et al., 1991). Near the ileocecal junction is the *basis ceci,* where the villi are well developed. The medial region (*corpus ceci*) has longitudinal folds with small villi, while the distal region (*apex ceci*), similarly to *corpus ceci*, has small villi and contains both longitudinal and transverse folds. The combination of villi and musculature near the ileocecal junction effectively prevents even very small particles from entering the ceca (Ferrando et al., 1987), although fluid contents are able to enter.

The ceca are the primary fermentation site of undigested carbohydrates into short chain fatty acids (SCFAs) that serve as energy source for gut cells (Goldstein, 1989; Jamroz et al., 2002; Svihus et al., 2013). Beside its role as a fermentation chamber, the ceca is also responsible for

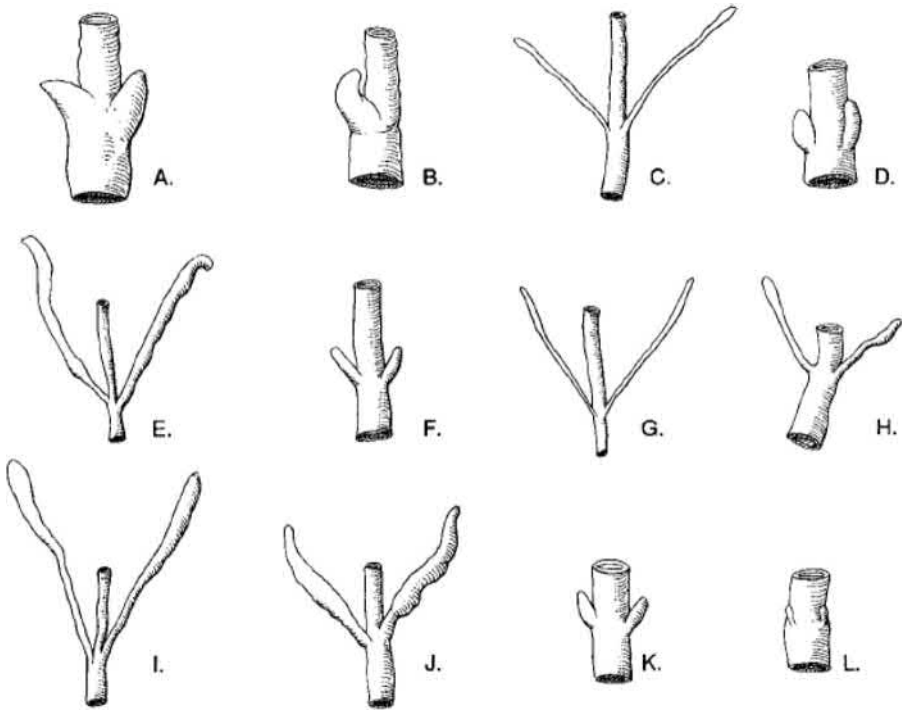

FIGURE 21.5 **Avian ceca:** (A) Little Cormorant (*Phalacrocorax niger*), (Pelecaniformes) X2.4; (B) Cattle Egret (*Bubulcus ibis*), (Ciconiiformes) X2.4; (C) Cotton Teal (*Nettapus coromandelianus*), (Anseriformes) X 1.2; (D) Crested Serpent Eagle (Spilornis cheela), (Falconiformes) X2.4; (E) Common Quail (*Coturnix coturnix*), (Galliformes) X 1.2; (F) Collared Dove (Streptopelia decaocto), (Columbiformes) X3.2; (G) Redwattled Lapwing (Vanellus indicus), (Charadriiformes) X0.8; (H) Common Koel (Eudynamys scolopacea), (Cuculiformes) X2.0; (I) Spotted Owlet (Athene brama), (Strigiformes) X 1.2; (J) Indian Roller (Coracias benghalensis), (Coraciiformes) X 1.6; (K) Oriental Skylark (Alauda gulgula), (Passeriformes) X4.0; (L) Gray Wagtail (Motacilla cinerea), (Passeriformes) X3.2. *Reprinted from Clench and Mathias. Copyrights 1995 by Wilson Ornithological Society. Used by permission of the publisher.*

partial digestion of crude fiber and proteins, microbial synthesis of vitamins, and absorption of electrolytes, sodium, and water (Jozefiak et al., 2004), monosaccharide absorption against a concentration gradient (Planas et al., 1987), cholesterol digestion and absorption (Tortuero et al., 1975), and degradation of nitrogen compounds (Goldstein, 1989).

There is growing understanding of the importance of the ceca. Cecectomy results in decrease in metabolism of food, greater loss of amino acids, and lower digestibility of crude fiber (Chaplin, 1989). The role of the ceca in absorption is discussed later in this chapter.

21.1.6 Colon (rectum) and cloaca

The colon, sometimes called the rectum, is relatively short in most birds, linking the ileum with the *coprodeal* compartment of the cloaca. In contrast, the ostrich is characterized by very long and partly sacculated colon (Skadhauge et al., 1984). Although the colon of mammals has no villi and many GCs, the colon of birds has numerous flat villi and relatively few GCs (Clauss et al., 1991). In addition, the avian rectum has relatively few crypts, which are shorter than those of mammalian species. The simple columnar epithelium lining the colon and the ceca has a well-developed brush border. As discussed in Section 21.6, the cloaca and colon have an important role in water reabsorption.

The cloaca serves as a common pathway for excretory, reproductive, and digestive wastes. It contains three chambers: *coprodeum, urodeum,* and *proctodeum.* The colon empties into coprodeum, which is the most cranial portion of the cloaca. The coprodeum lacks villi, but has mucosal folds or rugae. The urodeum is the middle and smallest compartment of the cloaca, separated from the coprodeum and proctodeum by the coprourodeal fold and the uroproctodeal fold, respectively. The urinary and reproductive tracts empty into the urodeum. The final chamber, the proctodeum, opens externally through the anus. The bursa of Fabricius, involved in immune function, projects dorsally into the proctodeum. Also, projecting into the dorsal portion of the proctodeum is the dorsal proctodeal gland, sometimes called the foam gland, which secretes a white, frothy fluid. Birds lack a urinary bladder, and it has been shown that urine enters the distal lower intestine and is forced back into the colon, ceca, and possibly the small intestine (Goldstein and Braun, 1986).

21.2 Anatomy of the accessory organs

21.2.1 Pancreas

The pancreas is a pale yellow or red organ located within the duodenal loop, although in some species, such as the budgerigar, part of it may be found outside the loop. The gland has both an endocrine function, which will be discussed later, and an exocrine function. It is relatively small in carnivores and granivores but large in piscivores and insectivores. The pancreas is generally divided into three lobes: dorsal, ventral, and splenic, but their function in unknown (Paik et al., 1974).

The exocrine pancreas consists of compound tubuloacinar glands, which are divided into lobules. The number of pancreatic ducts varies from one to three (three in the domestic fowl). The pancreatic ducts generally drain into the distal part of the ascending duodenum and rarely drain into the descending loop of the duodenum. In domestic birds, the pancreatic and bile ducts drain into the ascending loop of the duodenum by a common papilla (Figure 21.1). The pancreas secretes amylase, lipase, proteolytic enzymes, and sodium bicarbonate.

21.2.2 Liver

The liver also functions as both an endocrine and an exocrine gland. It is divided into right and left lobes, which are joined cranially at the midline. The right lobe is larger, and, in the domestic fowl and turkey, the left lobe is subdivided into the dorsal and ventral parts. The bile canaliculi drain into the interlobular ducts. The lobular ducts then combine to form the right and left hepatic ducts. In birds, unlike in mammals, bile is transported to the duodenum via two ducts. The right and left hepatic duct combine to form the common hepatoenteric duct, which then proceeds to the duodenum. However, a hepatocystic duct branches from the right hepatic duct and connects to the gallbladder which, in turn, is drained by the cysticoenteric duct into the duodenum. In species without a gallbladder (e.g., pigeons, some parrots, and ostrich), the branch of the right hepatic duct, called the right hepatoenteric duct, drains directly into the duodenum. The bile ducts generally drain into the duodenum at a site very near the pancreatic ducts. This generally occurs on the ascending loop of the duodenum. However, in some species, including the ostrich and *Columba,* the ducts empty into the descending loop of the duodenum.

21.3 Motility

As food is broken down, it not only needs to be transported along the length of the GIT (i.e., peristalsis), but there is also local, nonpropagating motility that mixes food with gastric juices and brings particles in closer proximity to the enterocytes. Motility not only occurs while an animal is eating but also while the animal is fasting (migrating motor complexes, MMCs). The latter type of motility probably helps keep the digestive tract free from indigestible particles and dead enterocytes, among others. The enteric nervous system, part of the autonomic nervous system, controls GIT function, including motility.

21.3.1 Esophagus

Deglutition (swallowing) has been studied in *Gallus* by White (1969, 1970) and Suzuki and Nomura (1975). For prehension, the head is first lowered, after which food is grasped with the beak and then moved toward the oropharynx with the tongue. The choana reflexively closes. The oral phase of swallowing involves the rapid rostrocaudal movements of the tongue for 1−3 s, which moves the food particles caudally (Suzuki and Nomura, 1975). This movement is assisted by the caudally directed papillae.

During the next phase, the pharyngeal phase, the infundibular mound and glottis close, the hyoid apparatus becomes concave, the tongue is moved backward, and the esophagus is moved forward, thus decreasing the distance between the oral cavity and the esophagus. The head is raised and further tongue movements, assisted by the rostrocaudal movements of the infundibular mound, propel the food particles from the tongue to the esophagus.

Primary peristalsis within the esophagus moves the bolus toward the stomach (esophageal phase). Contractions are more rapid in the cranial esophagus than in the thoracic esophagus. In a fasted bird, the longitudinal muscle layer obliterates the esophago-ingluvial fissura, thus preventing a bolus from entering the crop (Ashcraft, 1930). After partial gizzard filling, the esophago-ingluvial fissura is relaxed and food can either enter the crop or stomach depending on the contractile state of the gizzard. The crop acts as a temporary food storage site (Hill, 1971). The destination of food appears to be controlled by the contractile state of the gizzard, with food entering or bypassing the crop when the gizzard is contracting or relaxing, respectively. In 6- to 10-week-old turkeys fasted overnight, almost no ingested food enters the crop during the first four−six h after dawn. During each meal, the GIT fills cephalic to the upper one-third of ileum. In late afternoon meals, the crop also fills (Denbow, 2015).

Food is evacuated from the crop as a result of contractions by the crop wall. Such contractions last about 6 s with a force of approximately 20 cm H_2O (Fileccia et al., 1984). During primary peristalsis, there is a cessation of spontaneous electrical activity, which is associated with relaxation of the muscular wall. This is followed by a propagated, long-lasting spike burst of high amplitude. As the peristaltic wave moves aborad, it is preceded by inhibition of the muscles directly in front of the wave. The rate of emptying of the crop is not influenced by particle size or

whether the compounds are soluble or insoluble (Vergara et al., 1989).

Unlike mammals, spontaneous electrical activity and contractions have been recorded in the esophagi of birds (Mulé, 1991). This activity is myogenic in origin. It occurs independent of slow waves, which are absent in the esophagi of birds. Although the function of these spontaneous contractions is unknown, they may act to clear contents from the esophagus.

Primary peristalsis is mediated entirely by the extrinsic nervous system (Mulé, 1991). The enteric nervous system of birds is not responsible for propagating peristalsis, at least beyond short distances. Sectioning the glossopharyngeal or vagus nerve can disrupt peristalsis in the cervical and thoracic esophagus, respectively. Denervation of the esophagus prevents the propagation of electrical wave activity, indicating that the muscle cells act similar to multiunit smooth muscle cells.

21.3.2 Gastrointestinal cycle

Motility of the mammalian stomach is regulated by slow waves thought to arise from the interstitial cells of Cajal, which lie adjacent to the myenteric plexus (Sanders et al., 2006). These slow waves pace the "phasic muscles" increasing the probability that voltage-gated Ca^{2+} channels will open, thus exciting the muscles. Slow waves arise from distinct pacemaker regions within different parts of the GIT, thus producing regional differences in slow-wave frequency. In the stomach, the pacemaker cells reside in the greater curvature of the stomach. The slow waves do not propagate from the stomach to the small intestine, but instead the small intestine has its own pacemaker cells. The stomachs of most birds lack longitudinal smooth muscle and do not display slow waves. As a result, gastric motility is more complex in birds than in mammals (Dziuk and Duke, 1972).

During the gastrointestinal cycle of birds, the thin muscles of the muscular stomach contract and the isthmus closes, after which the pylorus opens and gastric contents flow into the duodenum (Figure 21.6). Next, the duodenum contracts, followed by relaxation of the isthmus and a contraction of the thick muscles of the muscular stomach. This precipitates a refluxing of the contents of the muscular stomach into the glandular stomach. The cycle is completed with contraction of the glandular stomach. A gastroduodenal cycle occurs with a frequency of 3.3 cycles/min in turkey (Duke, 1982). As might be expected, the largest change in intraluminal pressure is associated with contraction of the thick muscles (Figure 21.7).

As stated earlier, the pyloric region appears to control the movement of materials from the gizzard to the duodenum. Whereas soluble material is readily transported from the gizzard to the duodenum, larger particles are retained longer within the muscular stomach (Vergara et al., 1989).

Initiation of the gastrointestinal cycle is not dependent on extrinsic innervation in sated birds, suggesting that there is an intrinsic pacemaker controlling the cycle (Chaplin and Duke, 1988). Denervation of the stomach slows the rate of the gastrointestinal cycle in fasted birds and disrupts its normal synchronization (Figure 21.8), indicating that the gastrointestinal cycle is not independent of external neural input.

The pacemaker for the gastrointestinal cycle appears to reside in the isthmus (Chaplin and Duke, 1990). Destruction of the myenteric plexus in this area reduced contractions of the muscular stomach and duodenum by 50%, while simultaneously abolishing glandular stomach contractions.

The muscular stomach of raptors lacks the two pairs of opposing muscles characteristic of other types of birds; as a result, the gastroduodenal cycle is simplified. It is described as having three phases, including mechanical, chemical, and pellet formation and egestion (Kostuch and Duke, 1975). A peristaltic wave originating in the proventriculus moves aborad through the gizzard and into the small

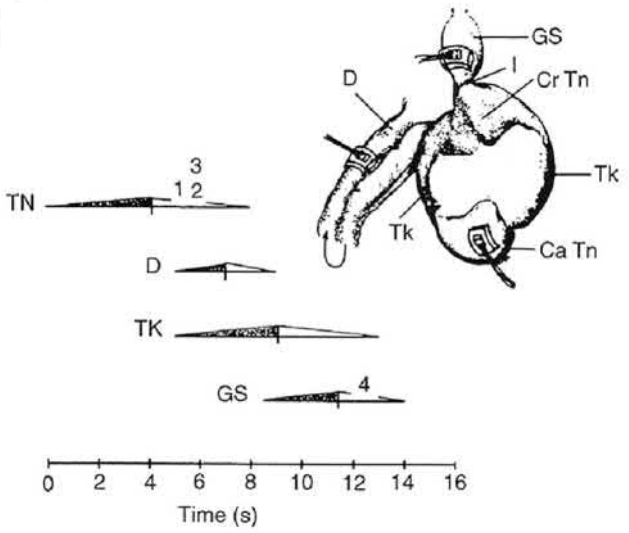

FIGURE 21.6 Top right: illustration of gastroduodenal apparatus of turkeys showing anatomical relationships of organs and placement of strain gauge transducers. Letters refer to organs as follows: *CaTN*, caudal thin muscle of muscular stomach; *CrTN*, cranial thin muscle of muscular stomach; D, duodenum; *GS*, glandular stomach; *I*, isthmus; *TK*, thick muscle pair (dorsal and ventral) of muscular stomach. Bottom left; triangles graphically represent sequence and duration of events in gastroduodenal cycle. Stippled areas indicate duration of contraction and clear areas indicate duration of relaxation of thin muscle pair (TN) and thick muscle pair (TK) of the muscular stomach, duodenum (D), and glandular stomach (GS). Numbers refer to noncontractile events in gastroduodenal cycle; 1, pylorus open; 2, isthmus open; 3, pylorus closed; 4, isthmus closed. *Reprinted from Chaplin and Duke. Copyrights 1988 by American Physiological Society. Used by permission of the publisher.*

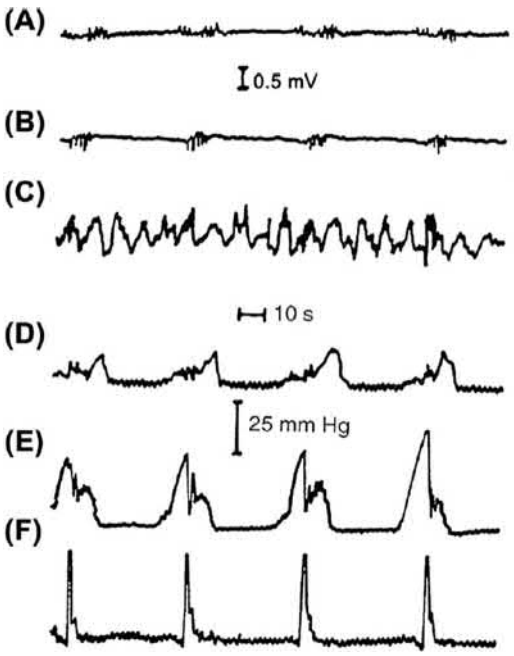

FIGURE 21.7 Tracings of typical records of electrical potential and intraluminal pressure changes from the stomach and duodenum of turkeys. (A), (B), and (C) are tracings of electrical potential changes recorded from the proventriculus, thick cranioventral muscle of the gizzard, and proximal duodenum, respectively. Slow waves with spikes are evident in the duodenum; only spikes associated with contractions are evident in the proventriculus and gizzard. (D), (E), and (F) are tracings of the corresponding intraluminal pressure changes recorded from these same organs, respectively. Time constant for electrical recordings was I.Is. *Reprinted from Duke et al. (1975) Copyrights 1975 by Springer Nature. Used by permission of the publisher.*

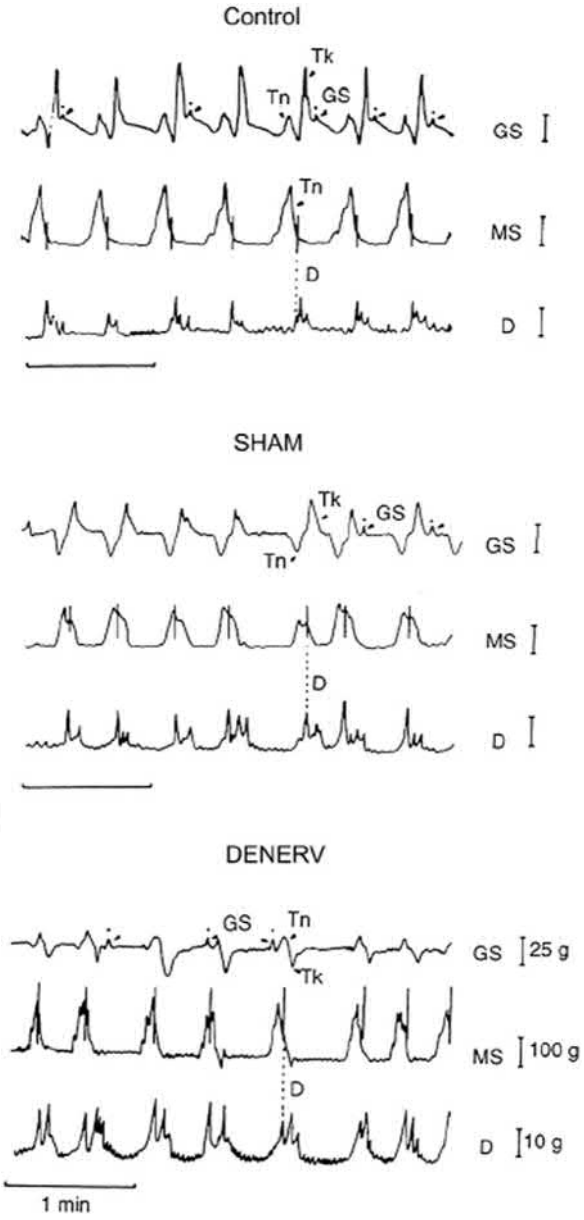

FIGURE 21.8 Tracings of recordings of glandular stomach (GS), muscular stomach (MS), and duodenal (D) contractions detected by implanted strain gauge transducers. Recordings were obtained on day 3 after surgery in three treatment groups used. Arrows and lettering identify contractions of each organ during one gastroduodenal cycle. Glandular stomach contractions are marked with an arrow and a closed circle; duodenal synchronization is identified with a dashed line. Note normal synchronization of contractions in the control tracings. *Reprinted from Chaplin and Duke. Copyrights 1988 by American Physiological Society. Used by permission of the publisher.*

intestine. Although the sequence of motility in the stomach of raptors resembles that in mammals, slow waves have not been recorded in these species.

Egestion is another gastrointestinal function unique to birds (Rea, 1973). This process, which involves the oral expulsion of nondigestible material, is more common in carnivores. Whenever bone, fur, or feathers are ingested, these materials are compacted and orally egested. This process is unlike regurgitation in ruminants or vomiting in mammals (Duke and Evanson, 1976; Duke et al., 1976a,b). Beginning approximately 12 min prior to egestion, gizzard contractions increase in frequency and amplitude. This process both compacts the material into a pellet and moves it into the lower esophagus. Beginning 8–10 s prior to egestion, the pellet is moved orad by esophageal antiperistalsis. Neither the abdominal nor duodenal muscles are involved.

Enterogastric reflexes control gastric emptying. Simply increasing intraduodenal pressure, or administering intraduodenal injections of HCl, hypertonic NaCl, or amino acid solutions, inhibits gastric motility (Duke et al., 1977, 1989; Duke and Evanson, 1972). Inhibition is related to dose and volume; it generally occurs within 3–30 s, and it persists for 2–35 min. Following an intraduodenal injection of a lipid solution, gastric motility decreases after 4–6 min and remains inhibited for 24–45 min. This latter response appears to involve hormonal regulation, presumably by an enterogastrone.

In addition, the presence of bile acids increases in the gizzard in proportion to the amount of wood shavings retained in the gizzard (Hetland et al., 2003). Because bile acids arrive in the intestine in the ascending loop of the duodenal duodenum, there is retrograde transport into the gizzard.

Reverse peristalsis occurs in three areas of the GIT, including proventriculus. The first retrograde movements occurs when digesta are moved from gizzard to proventriculus due to contraction of thick muscle of gizzard (Duke, 1994).

21.3.3 Small intestine

The MMCs are characterized by electrical potential changes known as slow waves, which travel aborad and are associated with periodic spike potentials and smooth muscle contraction (Figure 21.9). Although the MMC has not been extensively studied in birds, available data suggest that the MMC is similar in birds and mammals (Clench et al., 1989). The MMC has three phases: quiescence (phase l); irregularly spaced spike activity superimposed on slow waves (phase 2); and high-amplitude, regular spike activity superimposed on slow waves (phase 3). In chickens, the MMC has a periodicity of 77−122 min, whereas in owls it is only 21 min. The duration of phase 3 lasts approximately 5−8 min (Figure 21.10). These values are similar to those in mammals. Nevertheless, the propagation speed in birds is relatively slow, ranging from 0.48 to 0.62 cm/min. Although the MMC has been observed in the duodenum of chickens, quail, and owls, it has only been observed aborad of the duodenum in turkeys (Mueller et al., 1990).

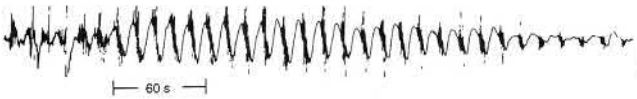

FIGURE 21.9 Myoelectric recording of action potentials on slow waves (Gallus). *Reprinted from Clench et al. Migrating myoelectric complex demonstrated in four avian species. Copyrights 1989 by American Physiological Society. Used by permission of the publisher.*

Intestinal refluxes appear unique to birds (Duke et al., 1973). Increases in intraluminal pressure of the duodenum normally follow increased pressure in the muscular stomach. However, approximately every 15−20 min in the turkey, large pressure changes are observed in the duodenum, which are associated with an inhibition of gastric motility and a reflux of intestinal contents (Figure 21.11). This has been observed in a number of other species as well, and appears more frequently as dietary fat levels increase (Duke et al., 1989).

21.3.4 Ceca

Motility in the ceca is not well understood. The ceca are filled as a result of the convergence of rectal antiperistaltic waves and ileal peristaltic waves. Due to the morphology of the ileocecal junction, only fluids or very small particles are allowed entrance to the ceca. In fact, 87−97% of cecal fluid originates from urine (Bjornhag and Sperber, 1977). The importance of the movement of urine to the ceca is discussed below.

While MMC-like bursts of electrical activity have been observed within the cecum, this activity does not migrate

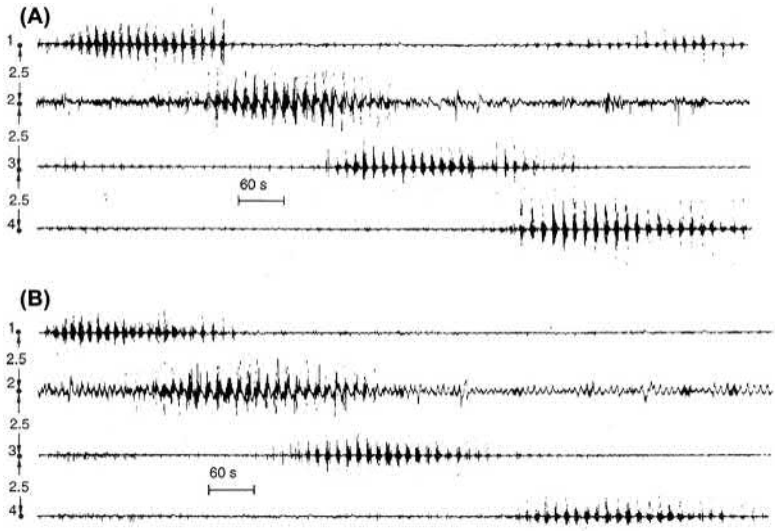

FIGURE 21.10 **Representative myoelectric recording of a migrating myoelectric complex (MMC) in strix.** The electrodes were placed on the proximal ileum 2.5 cm apart. (A): bird in fed state. (B): bird in fasted state. High frequency of MMCs in this owl species in indicated in (A), with a second regular spike activity beginning on lead one before previous complex has propagated through lead 4. *Reprinted from Clench et al. Copyrights 1989 by American Physiological Society. Used by permission of the publisher.*

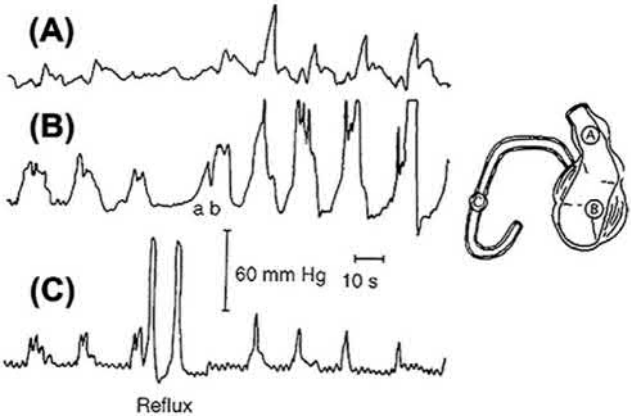

FIGURE 21.11 Tracings of typical records of pressure changes obtained from the proventriculus (A), gizzard (B), and upper proximal duodenum (C) of a turkey, showing pressure events occurring during a duodenal reflux. Positions of open-tipped tubes within gastrointestinal tract are indicated by letters (A), (B), and (C) (*circled*) on the diagram of a sagittal section of the stomach. The biphasic patter (B) of the tracing representing the contraction of the gizzard is quite variable; two phases of one cycle are (a) pressure wave due to contraction of thin muscle pair; and (b) of thick muscle pair. *Reprinted from Duke et al. (1972), Copyrights 1972 by American Physiological Society. Used by permission of the publisher.*

and thus does not constitute an MMC (Clench et al., 1989). Two types of contractions have been recorded in the ceca of turkeys (Duke et al., 1989). One type has a low amplitude, occurring at a rate of 2.6/min, while the other has a higher amplitude and occurs at a rate of 1.2/min. Low-amplitude contractions are associated with mixing, whereas high-amplitude contractions are propulsive. While aborad contractions are more common than orad contractions, the latter contractions have a greater amplitude and thus prevent the collection of digesta in the distal ceca. Peristalsis in a cecum appears to be myogenically mediated, with inhibitory neural input apparently able to suppress such contractions (Hodgkiss, 1984b). In mammals, distention causes an ascending stimulation and a descending inhibition, which is neurogenically mediated by the enteric nervous system and can be blocked by tetrodotoxin. By contrast, in birds, distention causes contraction of the circular muscle, which is unaffected by tetrodotoxin and thus apparently not controlled by the enteric nervous system.

The contents of the ceca are much different in consistency than that of the rectum and can therefore be easily distinguished from rectal feces. The ceca evacuate relatively infrequently compared to the rectum, with rectal evacuations preceding cecal evacuations (Duke et al., 1980). Cecal evacuations in young turkeys typically occur within 1−5 min of lights-on and again in late afternoon. There is an increase in the frequency of high-amplitude contractions, with four to seven such contractions occurring during the 2 min preceding cecal evacuation. These contractions are associated with high-amplitude electrical spiking. One high-amplitude contraction also occurs in the ileum and rectum at the time of cecal evacuation. The ratio of cecal to rectal evacuations is also influenced by diet, ranging from 1:7.3 when feeding barley to 1:11.5 when feeding corn (Röseler, 1929). As discussed in Section 21.6, the extended time that digesta spends in the ceca provides a unique role for this organ.

21.3.5 Colon

The rectum displays almost continuous antiperistalsis. Such motility is responsible for carrying urine from the urodeum. Contraction of the rectum appears to be mediated by noncholinergic, nonadrenergic nerves (Bartlet, 1974; Takewaki et al., 1977) into the colon and ceca (Akester et al., 1967; Goldstein and Braun, 1986; Polin et al., 1967). Two types of colonic slow waves have been recorded (Lai and Duke, 1978). These include small, short duration (sSW) and large, long duration (lSW) slow waves (Figure 21.12). The sSW are associated with small contractions and, as shown with radiography, are antiperistaltic. The lSW are associated with large contractions but, radiographically, could not be associated with movements of rectal contents.

The frequencies of sSW and lSW are shown in Table 21.2 The frequency of sSW is highest in the distal colon. In contrast, the frequency of lSW is highest in the proximal colon and cannot be recorded from the distal colon. This pattern of slow waves, when compared to the

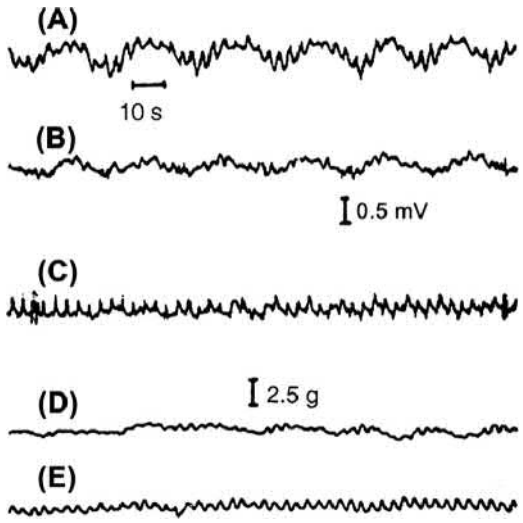

FIGURE 21.12 Electrical potential changes and contractile forces recorded from three bipolar electrodes ((A), (B), (C)) and two strain gauges ((D), (E)) in the colon of a turkey. Electrodes and strain gauges were implanted at 10, 6, and 1, and 8 and 3 cm from the cloaca, respectively. Both large and small slow waves are evident in tracings (A) and (B); only small slow waves are evident in tracing (C). Small contractions (antiperistalsis are evident in tracings (D) and (E)) but large contractions (peristalsis) can be seen only in tracings (D). *Reprinted from Lai et al. Copyrights 1978 by Springer nature. Used by permission of the publisher.*

TABLE 21.2 Mean frequency and amplitude of small and large contraction and of small and large slow waves in the rectum of Turkeys.

	Contractions				Slow waves			
	Small		Large		Small		Large	
	Frequency (cycles/min)	Amplitude (g)	Frequency (cycles/min)	Amplitude (g)	Frequency (per min)	Amplitude (mV)	Frequency (per min)	Amplitude (mV)
Proximal	14.6 ± 0.85	0.45 ± 0.24	2.66 ± 0.26	0.54 ± 0.20	15.4 ± 1.07	0.17 ± 0.08	2.83 ± 0.26	0.21 ± 0.09
Middle	–	–	–	–	15.8 ± 1.12	0.16 ± 0.09	2.76 ± 0.24	0.12 ± 0.06
Distal	15.4 ± 0.69	<0.70 ± 0.33	–	–	16.4 ± 2.16	0.25 ± 0.12	–	–

Proximal, middle, and distal refer to electrode implant sites on the colon 10, 6, and 1 cm from the cloaca, respectively, or the strain gauge transducer implants at 8 (proximal) and 3.5 (distal) cm from the cloaca. (Large contractions were not recorded from the distal strain gauge nor were large slow waves recorded from the distal electrode.)
Reproduced from Denbow (2015).

motility pattern, suggests that sSW arise at the distal colon and are responsible for antiperistaltic movement, whereas the lSW begin in the proximal colon and are responsible for peristaltic movement of rectal contents.

The nearly continuous antiperistaltic activity of the colon is interrupted only near the time of defecation (Duke, 1982). Beginning approximately 10 min prior to defecation, the amplitude of the sSW begins to decrease while the frequency gradient of lSW increases. These conditions favor inhibition of antiperistalsis and stimulation of peristalsis. Defecation is associated with a strong contraction beginning at the proximal colon, moving aborad and carrying the contents the length of the colon in less than 4 s.

21.3.6 Other influences on motility

Motility of the GIT shows diurnal variations. In turkeys, the frequency and amplitude of muscular stomach contractions increased during light periods relative to dark periods (Duke et al., 1976a,b). The increased and decreased gastric contractions coincided with just prior to "lights-on" and "lights-off," respectively. Although less pronounced, this diurnal rhythm of gastric activity continued when birds were fasted.

Birds also display cephalic, gastric, and intestinal phases of motility. In 24 h fasted great horned owls, turkeys, and red-tailed hawks, the sight of food stimulated gastric contractions (Duke et al., 1976a,b). When allowed to eat, gastric activity increased further, indicative of the gastric phase. During the intestinal phase, entrance of food into the duodenum slows the frequency of gastric contractions to allow time for digestion (Duke et al., 1973). While the cephalic phase is mediated largely by the nervous system, there appears to also be an as yet unidentified endocrine component that increases motility.

Motility is influenced by many factors. For example, anesthetics, including nembutal and methoxyflurane, reduce gastroduodenal motility as well as decrease gastric secretion (Duke et al., 1977; Kessler et al., 1972). High-environmental temperatures decrease gastrointestinal motility, whereas cold temperatures differentially affect motility in various parts of the digestive system but appear to have an overall effect of decreasing transit time (Tur and Rial, 1985).

21.4 Neural and hormonal control of motility

Extrinsic and intrinsic innervations of the avian GIT appear similar to mammals (Olsson and Holmgren, 2011). Extrinsic innervations are largely from the vagus nerve, nerve of Remak (ganglionic nerve running along the gut), and fibers from the splanchnic and pelvic nerves (Nilsson, 2011). Nitric oxide synthase (NOS) is found in many neurons associated with the gut. Many of these neurons also contain vasoactive intestinal peptide (VIP) and pituitary adenylate cyclase-activating polypeptide. In pigeons, these nerves also contain galanin. In addition, most regions of the gut have nerves containing tachykinin-immunoreactivity, and the intestines have neurons containing gamma amino butyric acid. The myenteric plexus of the gizzard has aminergic neurons, although it has been reported that catecholamines are not present in the chicken intestine (Aisa et al., 1997).

Contractions of the esophagus are increased by acetylcholine (ACh) and vagal stimulation and unaffected by sympathetic nerve stimulation (Bowman and Everett, 1964; ŌHashi and Ohga, 1967; Taneike et al., 1988). However, there is evidence for nonadrenergic, noncholinergic

TABLE 21.3 Age of chicks embryos (days of incubation) at first appearance of endocrine cells showing immunoreactivity for various regulatory peptides, chromogranin, and serotonin in the gut.

	Pyloric				Upper	Lower		Large
	Proventriculus	Gizzard	Region	Duodenum	Ileum	Ileum	Ceca	Intestine
Chromogranin	9	12	12	10.5	10.5	15.5	13.5	10
Enkephalin	21	–	–	–	–	–	–	–
Gastrin/CCK	12	–	11	11	11	17	17	17
GRP	11	21	21	–	–	–	–	–
Glucagon	13	–	14	13	14	14	–	–
Motilin	–	21	21	21	13	17	17	17
Neurotensin	12	–	12	12	13	14	14	9
PP	14	–	14	13	13	14	–	21
Peptide YY	–	12	12	18	21	21	–	–
Serotonin	8	–	12	11	11	14	14	9
Somatostatin	12	–	12	11	13	14	17	13
Substance P	–	–	–	21	11	17	17	13
VIP	21	–	–	19	12[4]	19	21	21

No cell existed that were immunoreactive with the designated compound; *CCK,* cholecystokinin; *GRP,* gastrin-releasing peptide; *PP,* pancreatic polypeptide; *VIP,* vasoactive intestinal peptide.
Reproduced from Denbow (2015).

(NANC) inhibition of esophageal smooth muscles (Postorino et al., 1985; Sato et al., 1970). Serotonin also causes contractions of the esophagus (Mule et al., 1987), and this effect appears to be mediated indirectly by activation of both cholinergic and NANC excitatory neurons (Fileccia et al., 1987). In addition, tachykinins cause contraction of the gut (Liu and Burcher, 2001). In contrast, epinephrine induces relaxation of the chicken rectum via α-adrenergic receptors (Ojewole, 1980).

The proventriculus has been shown to contain gastric inhibitory peptide, VIP, and neuronal NOS (nNOS), but not somatostatin, peptide histidine-isoleucine, peptide tyrosine-tyrosine, neuropeptide tyrosine, bombesin, met-enkephalin, serotonin, substance P, galanin, or calcitonin gene-related peptide (Martínez et al., 2000), VIP and nNOS. VIP and nitric oxide (NO) probably cause relaxation of smooth muscle. The proventricular secretions are controlled by parasympathetic nerves and a diffuse endocrine system.

As shown in Table 21.3, many peptides have been identified within the GIT of birds. The function of these peptides remains to be elucidated. Although the identity of the NANC excitatory neurotransmitter was not identified, it has been shown that neurotensin can induce contraction of crop smooth muscle (Denac and Scharrer, 1987). This latter effect is a postjunctional response not mediated by ACh, prostaglandins, or opioids.

Histamine interacts with cholinergic neurotransmission to control esophageal contractions (Taneike et al., 1988). Histamine dose-dependently induces esophageal contractions, but this effect is blocked by tetrodotoxin, suggesting that its effect is mediated by the release of ACh. Contractions induced by vagal stimulation are increased by the presence of histamine, whereas histamine-induced contractions were enhanced by acetylcholinesterase inhibitors. It appears, therefore, that histamine modulates, via H_1 receptors, the release of ACh to control the contraction of esophageal smooth muscle. As indicated in Figure 21.13, enkephalins also cause contraction of the esophagus, but their effect is mediated by serotonergic neurons.

The crop appears to be controlled similarly to the esophagus. Electrical stimulation of the crop causes contraction that is largely, but not completely, due to ACh release because it can be significantly blocked by atropine (Denac et al., 1990). While it is unclear as to which neurotransmitters are responsible for the contraction not blocked by atropine (i.e., NANC-induced), neurotensin, bombesin, and substance P have been shown to cause atropine-resistant contractions following electrical stimulation of the crop (Denac and Scharrer, 1987, 1988). Norepinephrine caused crop muscle relaxation that was mediated by B-adrenoceptors. It appears that the crop and esophagus are controlled by three types of nerves:

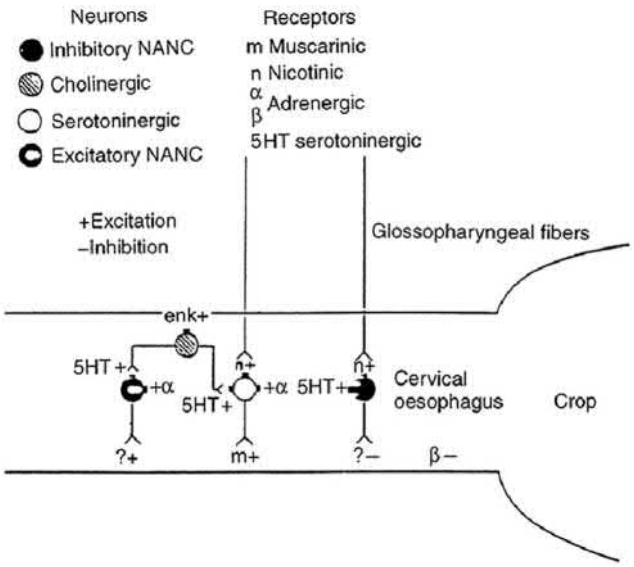

FIGURE 21.13 Schematic diagram illustrating the putative pattern of the intrinsic innervation of the pigeon cervical esophagus. Different neuron types are present in the intramural plexuses; excitatory cholinergic. excitatory NANC-, inhibitory NANC-, and serotoninergic neurons. *Reprinted from Mule. Copyrights 1991 by Elsevier.*

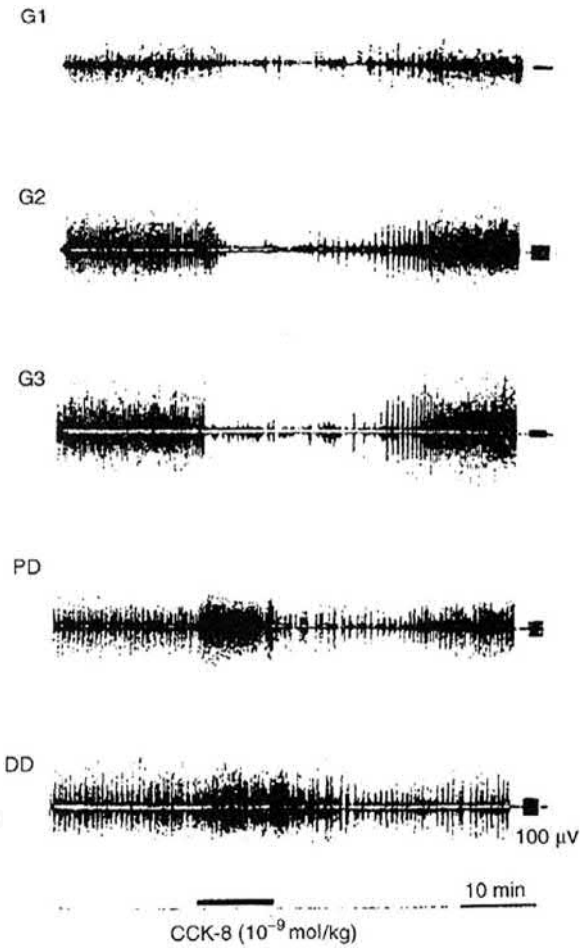

FIGURE 21.14 Recording of gastroduodenal electrical activity showing effect of cholecystokinin octapeptide (CCK-8; 10^{-9} mol/kg) infusion. Studied gastric areas are as follows: *DD*, distal duodenum; *GI*, proventriculus; *G2*, craniodorsal thin muscle; *G3*, caudodorsal thick muscle; *PD*, proximal duodenum. Similar responses were observed in all animals. *Reprinted from Martinez et al. Copyrights 1993 by American Physiological Society. Used by permission of the publisher.*

stimulatory cholinergic neurons, stimulatory NANC neurons (probably peptides), and inhibitory noradrenergic nerves.

Cholecystokinin octapeptide (CCK-8) is the most studied regulator of intestinal motility. Intravenous infusion of CCK-8 inhibited gastric and duodenal motility (Savory et al., 1981). CCK-8 and CCK-tetrapeptide (CCK-4) inhibited gastric electrical activity (Martinez et al., 1993). Whereas CCK-4 inhibited duodenal electrical activity, CCK-8 stimulated such activity (Figure 21.14]. CCK-A and CCK-B receptor antagonists were unable to block the effects of CCK. It appears that the action of CCK on gastric and duodenal motility is similar in birds and mammals. CCK inhibits stomach motility, and the increase in duodenal activity is suggested to cause segmental contractions, and, thus, also delay gastric emptying (Martinez et al., 1993).

Vagotomy and hexamethonium blocked the response to CCK-8 in the chicken stomach (i.e., proventriculus and gizzard) but had no effect on the duodenal response (Martinez et al., 1993). Furthermore, the action of CCK-8 in the duodenum was not altered by atropine or methysergide. Phentolamine and propranolol had no effect on the gastric or duodenal response to CCK-8. It appears, therefore, that the action of CCK-8 on the stomach is mediated via the vagus, whereas the action in the duodenum probably involved a direct effect on smooth muscle cells. The action of CCK-8 on the stomach was blocked by N-nitro-L-arginine methyl ester (L-NAME), suggesting that the inhibitory effect of CCK involves the release of NO. Because L-NAME did not completely block the CCK effect on the caudodorsal thick muscle, it is likely that another neurotransmitter, possibly VIP, is involved in this latter response. Interestingly, CCK-8 caused an excitatory action in the stomach of vagotomized chickens, indicating that CCK-8 may, in addition to acting via the vagus, have a direct action on gastric muscles. The increase in electrical activity caused by CCK-8 in the duodenum was enhanced by L-NAME, indicating that nitric oxide may be a tonic inhibitor of duodenal electrical activity.

Chicken gastrin (cG), which belongs to the gastrin/CCK family, has been isolated from the chicken antrum (Dimaline et al., 1986). Intravenous infusions of cG caused effects similar to CCK-4 (Martinez et al., 1993). This suggests the existence of one receptor subtype in the stomach recognizing both CCK and cG, but possibly two receptors in the duodenum, one recognizing CCK-8 and the other CCK-4 and cG.

Opioid peptides appear to be involved in the MMC. Infusion of met-enkephalin, morphine, and casomorphin (5×10^{-7} mol/kg) induced intense electrical activity, similar to phase 3 of the MMC, in the distal duodenum which migrated through the small intestine (Jiménez et al., 1992). The effect of morphine was blocked by naloxone (5×10^{-7} mol/kg), while higher doses of naloxone reduced gastroduodenal motility. Simultaneous to increasing duodenal electrical activity, activity in the stomach is inhibited.

21.4.1 Rate of passage

The rate of passage in the GIT influences the exposure time of feed to the digestion and absorption processes. The rate of passage of material through the digestive tract has been measured in many ways. Because digesta consists of both solid and liquid components, different types of markers have been used. Insoluble markers such as chromium-mordanted rice, cerium-mordanted rice, Cr_2O_3 (chromium (III) oxide), or radiopaque plastic pellets (Branch and Cummings, 1978; Ferrando et al., 1987; Udén et al., 1980) have been used as indicators of solid transit time, whereas a soluble marker such as Cr-EDTA (chromium ethylenediaminetetraacetic acid salt) (Vergara et al., 1989) or phenol red (Gonalons et al., 1982) has been used to measure liquid transit time. In general, it was found that larger particles are retained longer in the digestive tract.

The rate of passage is determined by measuring the time of 1% marker concentration in excreta (T1), time of 50% marker concentration in excreta (T50), or mean retention time (MRT) (Rochell et al., 2012). In broiler chickens, T1, T50, and MRT depends on the diet and ranges from 0.87 to 1.36 h, 4.47 to 4.97 h, and 5.13 to 5.62 h, respectively (Rochell et al., 2012). The MRT in laying hens fed corn and soybean meal diet is estimated for 5 h and 59 min (Shires et al., 1987). In Japanese quail, the T1 and T50 is lower while the MRT is higher than in broiler chickens (Nobrega et al., 2020).

Transit time of digesta is influenced by genetics. When comparing broiler and Leghorn-type chickens, the overall MRT is similar, but the time food spent in various parts of the digestive tract is different (Table 21.4).

The rate of food passage is affected by many factors. Feed transit time through the small and large intestine increases with age (Shires et al., 1987). This may account for increases in metabolizable energy values of feedstuffs noted in older birds. Adding lipid (Sell et al., 1983) or protein (Sibbald, 1979) to the diet can increase passage time. Increases in environmental temperature also slows transit time. Transit time depends also on the digestive capacity of the birds. In birds with digestive capacity, particles, regardless of the size, spent 10 times less time in gizzard in comparison to birds characterized by high-digestive capacity (Rougiere and Carre, 2010).

TABLE 21.4 Mean retention time (min) of solid phase markers in various segments of the digestive system of broilers and leghorns.

Gastrointestinal tract segments	Broilers[a]	Leghorns	Broilers[a]
Crop	31	48	41
Proventriculus and gizzard	39	71	33
Duodenum	10	7	5
Jejunum	84	85	71
Ileum	97	84	90
Ceca	119	112	–
Rectum	56	51	26

[a]*Different source of data, for details, see Denbow (2015).*
Reproduced from Denbow (2015).

21.5 Secretion and digestion

At hatch, the chick has to make a transition from dependence on a lipid-rich endogenous diet coming from the yolk to an exogenous diet rich in carbohydrate and protein (Sklan, 2001). Access to feed at hatch results in an approximately twofold increase in small intestine length of chicks, but only a 60% increase if birds remain fasted (Sklan and Noy, 2000). The increase in intestinal weight is correlated with increases in trypsin, amylase, and lipase activities, which remain unchanged in the absence of feed. Functional genomics of the digestive tract has been recently characterized in broiler chickens (Juanchich et al., 2018). Genes upregulated upstream and downstream of the gizzard junction were related to motility and trophicity, while in the gizzard and jejunum, upregulated genes were related to physical breakdown of the feed, absorption, and body defense, respectively (Juanchich et al., 2018, Figure 21.15).

21.5.1 Mouth

The salivary glands secrete mucous, and depending on the species, amylase. Although amylase is not present in the saliva of *Gallus* and *Meleagris,* it is found in the saliva of the house sparrow (Jerrett and Goodge, 1973) and other species (Bhattacharya and Ghose, 1971). The volume of daily salivary secretion in *Gallus* ranges from 7 to 25 mL (Leasure and Link, 1940).

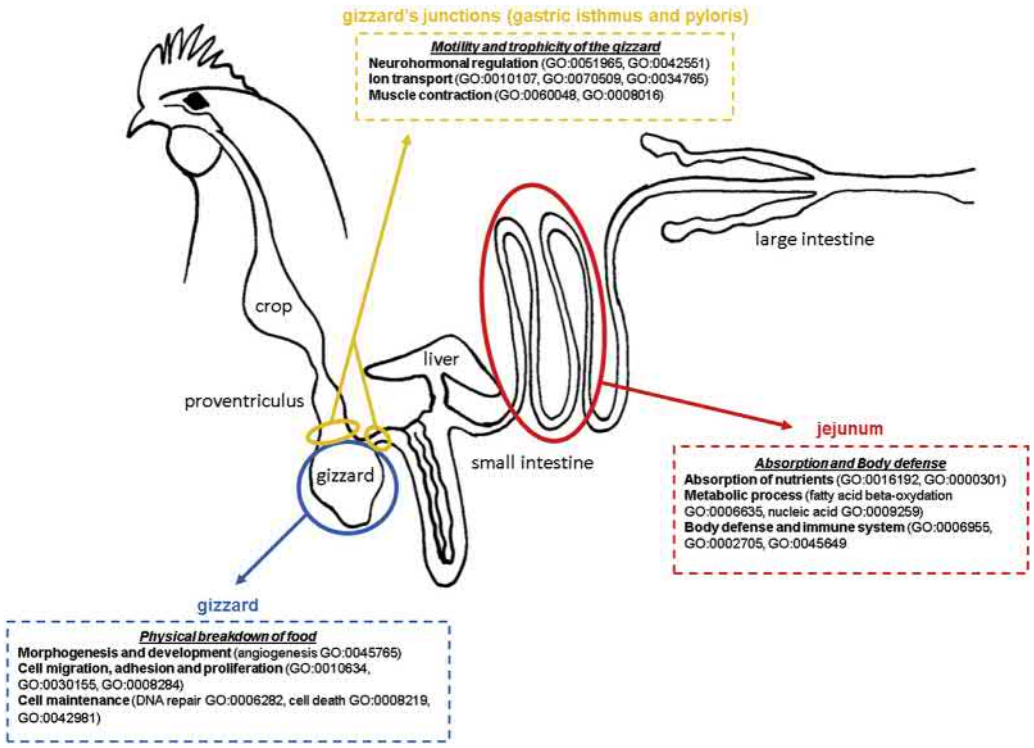

FIGURE 21.15 Representation of the molecular portrait of the digestive tract in broilers from results of this study. *Reprinted from Juanchich et al. Copyrights 2018 Springer Nature. Used under Creative Commons Attribution license (CC BY).*

Mucous functions to lubricate food and allow it to move down the esophagus. However, in some species, mucous also functions as an adhesive coating on the tongue to aid in capturing insects or as a material that cements components during the construction of nests.

21.5.2 Esophagus and crop

The esophagus is not important in chemical digestion, as its major secretion is mucous. The secretion of esophageal mucous is nevertheless important because it is necessary to supplement the limited secretion of saliva. However, in some species, including the greater flamingo and male emperor penguin, a nutritive merocrine-type secretion is produced by the wall of the esophagus, which is fed to the young.

Some carbohydrate digestion may occur in the crop due to the presence of amylase activity (Philips and Fuller, 1983). Amylase activity at this site comes from either salivary secretions, intestinal reflux, or plant and/or bacterial sources. Bolton (1965) reported that starch is hydrolyzed within the crop where it can either be absorbed; converted to either alcohol, lactic acid, or other acids; or transported down the GIT. Pinchasov and Noy (1994) showed that substantial amylolysis occurs in the crop. Sucrose is also hydrolyzed within the crop. While absorption of sugars from the crop appears possible, it is probably minimal.

The crop is not essential for normal growth when access to food is sufficient. Cropectomy has no effect on growth rate of ad libitum fed chickens, but it does decrease growth rate when food intake is limited. This supports the view that the primary function of the crop is food storage, and it is not essential for digestion.

In pigeons and doves, "crop-milk" is produced during the breeding season under the influence of prolactin. Crop milk contains 12.4% protein, 8.6% lipids, 1.37% ash, and 74% water (Vandeputte-Poma, 1968). Therefore, while rich in protein and essential fatty acids (Desmeth, 1980), it is devoid of carbohydrates and calcium.

21.5.3 Stomach

The oxynticopeptic cells found in birds secrete both HCI and pepsinogen. Pepsinogen, under the influence of acid or pepsin that is already present in the stomach, is converted to pepsin. While lipase has been found in gastric secretions, this is probably due to reflux from the duodenum. The basal gastric secretory rate is 15.4 mL/h and contains 93 mEq/L of acid and 247 Pu/mL of pepsin (Long, 1967) with a pH of 2.6 (Joyner and Kokas, 1971). The pH of gastric contents, however, is normally above 2.6 due to the presence of ingesta. The pH has been determined in several species immediately after sacrifice (Table 21.5). Higher pH values have been reported when measurements were made on live

TABLE 21.5 The pH of contents of the digestive tract of avian species.

	Chicken	Pigeon	Pheasant	Duck	Turkey
Crop	4.51	6.3	5.8	4.9	6.0
			4.28		
Proventriculus	4.8	1.4	4.7	3.4	4.7
		4.8			
Gizzard	4.74	2.0	2.0	2.3	2.2
	2.50				
Duodenum	5.7–6.0	6.4	5.6–6.0	6.0–6.2	5.8–6.5
	6.4	5.2–5.4			
Jejunum	5.8–5.9	5.3–5.9	6.2–6.8	6.1–6.7	6.7–6.9
	6.6				
Ileum	6.3–6.4	6.8	6.8	6.9	6.8
		7.2	5.6		
Ceca	5.7		5.4	5.9	5.9
	6.9				
	5.5–7.0				
Rectum	6.3	5.4	6.6	6.7	6.5
		6.6			
Bile	7.7		6.2	6.1	6.0
	6.6				
	5.9				

Reproduced from Denbow (2015).

birds. For example, Winget et al. (1962) reported the following values for chickens: mouth, 6.7; crop, 6.4; ileum, 6.7; rectum, 7.1. Age has no effect on pH of the digestive tract (Herpol, 1966). Acid secretion of chickens is high relative to mammals, possibly because of the rapid digestive transit time (Table 21.6).

While amylolysis occurs in the crop, it is not evident in the ventriculus. This is the result of the low pH of the stomach, which is unfavorable for amylase activity (Pinchasov and Noy, 1994).

There are three phases to gastric secretion: the cephalic phase, the gastric phase, and the intestinal phase. All three phases are present in birds (Burhol, 1982). The cephalic phase entails an increase in hydrogen ion (H^+) and pepsin secretion caused by the sight, smell, or expectation of food. This phase is under vagal control. As summarized by Duke (1986), vagal stimulation increases both gastric secretion rate and pepsin secretion. Vagal stimulation causes a greater increase in gastric secretion than do cholinergic agents (Gibson et al., 1974). This suggests, as discussed below, that gastric secretion is stimulated by other neurotransmitters acting together with ACh. In birds, vagal stimulation causes greater pepsin than H^+ accumulation (Burhol, 1982). In contrast, insulin injection inhibits gastric H^+ secretion without affecting pepsin secretion. Therefore, H^+ and pepsin secretion may be under different control.

Pepsin from chicken and duck has been well characterized (Bohak, 1969; Pichová and Kostka, 1990). Chicken pepsinogen and pepsin have 367 and 325 amino acids, respectively. Chicken pepsin stability is temperature dependent with stability up to pH 8 at 24°C and inactivation above pH 8.5 (Bohak, 1969). Duck pepsinogen and pepsin have 374 and 324 amino acids, respectively. Duck pepsin has a pH-optimum of 4, is stable up to pH 7.5, and is inactivated at pH 9.6 (Pichová and Kostka, 1990).

Many hormones are involved in gastric secretion (Table 21.7). Gastrin plays a role in the gastric phase of secretion. cG has been isolated from the chicken pylorus, which is equivalent to the mammalian antrum (Dimaline et al., 1986). While structurally similar to CCK, cG has markedly different secretory functions (Dimaline and Lee, 1990). Infusion of cG increases both acid and pepsin

TABLE 21.6 Basal acid secretion in various species.

	Body weight (kg)	Acid output (mEq/kg/h)	Pesin output (PU/kg/h)
Man	70	0.03	862
Dog	15	0–0.004	0–62
Rat	0.34	0.25	2230
Monkey	2.5	0.12	730
Chicken	1.75	0.78	2430

Reproduced from Denbow (2015).

TABLE 21.7 Gastrointestinal hormones in the domestic fowl.

Hormone	Site of orgin	Biological action
Gastrin	Proventriculus	Stimulates gastric acid and pepsin secretion
Cholecystokinin	Duodenum and jejunum	Stimulates gallbladder contraction and pancreatic enzyme secretion and gastric acid secretion; inhibits gastric emptying; potentiates secretin-induced stimulation of pancreatic electrolyte secretion
Secretin	Duodenum and jejunum	Stimulates bicarbonate secretion by pancreas
Vasoactive intestinal peptide	Duodenum and jejunum	May be a more potent stimulator of pancreatic electrolyte secretion than secretin; inhibit smooth muscle contraction
Pancreatic polypeptide	Pancreas, proventriculus, and duodenum	Stimulates gastric acid and pepsin secretion
Gastrin-releasing peptide (bombesin)	Proventriculus	Stimulates pancreatic enzyme secretion; stimulates crop contraction
Somatostatin	Pancreas, gizzard, proventriculus, duodenum, and ileum	Inhibits secretion of other gut hormones

Reproduced from Denbow (2015).

secretion. Unlike CCK, gastrin has no effect on gallbladder contractions or pancreatic secretion. Another peptide, GRP, also induces acid secretion, but it is not known whether it acts via gastrin release (Campbell et al., 1991).

The intestinal phase of gastric secretion is controlled by several hormones including CCK, secretin, and avian pancreatic polypeptide (APP). APP, originally discovered in chickens (Kimmel et al., 1968; Larsson et al., 1974), is released from the pancreas postprandially in response to amino acids and HCl (Duke et al., 1982; Hazelwood et al., 1973). APP does not appear to act during the cephalic phase of gastric secretion because it is not released during sham feeding (Kimmel and Pollock, 1975). APP increases gastric acid and pepsin secretion, and this effect is independent of the vagus nerve (Hazelwood et al., 1973).

CCK (Dockray, 1977) and secretin (Nilsson, 1974) have been isolated from the duodenum and jejunum of birds. CCK stimulates gastric acid secretion while having no effect on pepsin secretion. Contrary to its effects in mammals, in which secretin inhibits acid and stimulates pepsin secretion, in chickens, secretin stimulates both acid and pepsin secretion (Burhol, 1974).

As in mammals, histamine is involved in gastric acid release. Injection of cimetidine, an H_2-receptor blocker, raises the pH of the proventriculus and duodenal contents (Ward et al., 1984). The increase in gastric acid secretion induces by the intravenous injection of 2-deoxy-D-glucose is also blocked by metiamide, an H_2-receptor blocker (Nakagawa et al., 1983).

21.5.4 Intestines

Intestinal digestion includes both luminal and brush-border digestion. The brush border contains sucrase-isomaltase, peptidases, and phosphatases. Chicks can hydrolyze disaccharides beginning prehatch, and sucrase-isomaltase expression increases posthatch. Glucose is transported across the enterocyte membrane via a Na-glucose transporter (SGLT-1), which increases in expression beginning two days prehatch and involves a secondary active transport system driven by the active removal of Na from the basolateral membrane of the enterocytes. Absorptive capacity of the intestines increases proportionally to body weight, but the absorption rate for glucose is greatest during the first week and then declines, as does brush border SGLT-1 density (Barfull et al., 2002).

Amylase is produced by both the pancreas and intestine (Osman, 1982). While found in all parts of the small intestine, it is present in particularly high concentrations in the jejunum, with 80% of the activity found there. The high levels found in the jejunum are presumably due to the fact that the openings of the pancreatic ducts discharge near the anterior jejunum. Amylase is found in only trace amounts

TABLE 21.8 Enzymes secreted by the intestines.

Enzyme	Substrate	Product of function
Maltase	Maltose	Glucose
Isomaltase	Dextrins	Glucose
Sucrase	Sucrose	Glucose and fructose
Enterokinase	Trypsinogen	Trypsin
Lipase	Monoglicerides	Glycerol and fatty acids
Peptidases	Di- and tripeptides	Amino acids

Reproduced from Denbow (2015).

TABLE 21.9 Pancreatic digestive enzymes.

Enzyme	Percent of total
Trypsinogen	10
Chymotripsinogen (A, B, and C)	20
Trypsin inhibitor	11.3
Amylase	28.9
Procarboxypeptidase (A and B)	29.8

Reproduced from Denbow (2015).

in the ceca. The optimum pH of the pancreatic and intestinal amylase is 7.5 and 6.9, respectively.

Intestinal enzymes provide the last step in digestion. These secretions are responsible for digesting starch, sucrose, fats, and protein (Table 21.8). The small intestine of birds contains maltase, sucrase, palatinase, but does not trehalase (Siddons, 1969). Whether lactase is present appears to be debatable. However, it has been reported that lactase is not present in germ-free chicks, and that the rate of mortality of germ-free chicks fed lactose as the sole energy source is very high (Siddons, 1972). Enzyme activity is the highest in the jejunum and decreases both proximally and distally. These enzymes are located in the epithelial cells of the villi. The maltase, sucrase, and palatinase activity found in the large intestine comes from the small intestine, whereas the lactase activity present in the large intestine probably originates from cecal bacteria.

Relatively little is known about the control of intestinal secretions in birds. Intestinal secretion is increased by duodenal distention, vagal stimulation, and secretin. Vagal stimulation has a greater effect on stimulating mucous secretion than enzyme secretion.

21.5.5 Colon

Chloride (Cl^-) ions are secreted in the rectum, ceca, and coprodeum. This is discussed in Section 21.6.

21.5.6 Pancreas

As mentioned previously, pancreatic and bile secretions enter the GIT near the anterior jejunum. Pancreatic secretions have a pH of 6.4–6.8 in chickens (Hulan and Bird, 1972) and 7.4–7.8 in turkeys (Duke, 1986). Secretions include an aqueous phase containing water and bicarbonate ions, as well as an enzymatic phase.

Digestive enzymes found in the pancreas of broiler type chickens are listed in Table 21.9. Although not shown, the pancreas is also reported to secrete ribonuclease and deoxyribonuclease (Borgo et al., 1968). Amylase is found in the duodenum, jejunum, ileum, and colon. Both trypsin and amylase are present in highest concentrations in the jejunum (Bird, 1971; Osman, 1982), presumably because the pancreatic ducts enter near the end of the duodenum. Both pancreatic and intestinal amylase have a requirement for chloride ion. Characterization of these enzymes suggests that pancreatic amylase is similar to mammalian α-amylase, while intestinal amylase is similar to glucoamylase.

Pancreatic secretion is controlled by both nervous and hormonal mechanisms. The secretion rate is higher in birds than in mammals (Table 21.10). Secretion has both a cephalic and an intestinal phase. When fasted birds are allowed to eat, pancreatic secretion increases immediately (Kokue and Hayama, 1972). This response is blocked by vagotomy or atropine and can be augmented by cholinergic agents (Hokin and Hokin, 1953).

Secretin-like activity is released in response to diluted HCl placed in the duodenum (Nilsson, 1974). Secretin, when injected intravenously, increases the aqueous

TABLE 21.10 Pancreatic secretory rate and influence of fasting in the chicken, dog, rat, and sheep.

Species	Starvation time (h)	Pancreatic secretory volume (mL/kg/h)
Chicken	24	0.70
	48	0.68
	72	0.65
Dog	24	0.1–0.3
	48	Negligible
Rat	24	0.6–0.7
Sheep	24	0.13
	48	0.07

Reproduced from Denbow (2015).

component of pancreatic secretion. However, in contrast to mammals, VIP stimulates the secretion of pancreatic fluids more strongly (Vaillant et al., 1980). VIP is found in the neurons of both the GIT and pancreas. It is believed that VIP, rather than secretin, is the primary regulator of pancreatic juice secretion and that this response may be either neuronally or hormonally mediated (Dockray, 1988). VIP does not stimulate pancreatic enzyme secretion.

CCK is released in response to lipids and amino acids. The administration of CCK has been shown to increase pancreatic secretion in pigeons (Sahba et al., 1970) and to increase the flow rate and protein secretion rate in turkeys (Dockray, 1975). Two GRPs, which are structurally related to bombesin, have been isolated from the proventriculus (Campbell et al., 1991). These peptides are found in endocrine cells and contain either 27 or 6 amino acids. Distension of the proventriculus with peptone stimulates pancreatic juice and enzyme secretion. This effect appears to be mediated by GRP-27, with GRP-6 being ineffective. Distension with saline is less effective.

Diet can influence the secretory rate of pancreatic enzymes. Increasing the carbohydrate and fat content of the diet increases amylase and lipase activity in pancreatic secretions (Hulan and Bird, 1972).

21.5.7 Bile

Bile, produced and secreted by the liver, is essential for fat digestion. It acts to emulsify lipids so that they can be more efficiently digested by lipase. In addition, amylase begins to appear in chicken bile at four to eight weeks of age (Farner, 1943). Therefore, bile is also involved in carbohydrate digestion.

Relatively little is known about biliary secretion in birds possibly because of the complex anatomy in which bile enters the small intestine via both the hepato-enteric duct and the cysticoenteric duct. The biliary secretion rate is 24.2 μL/min in fasted broilers (Lisbona et al., 1981). Chemodeoxycholyltaurine and cholyltaurine are the predominant bile acids in chickens and turkeys, while chenodeoxycholyltaurine and phocaecholyltaurine predominate in ducks (Elkin et al., 1990). These are secreted by an active transport system.

The bile salts glycocholate and taurocholate are readily absorbed through the intestinal wall. The absorption rate is higher near the distal end of the small intestine (Lindsay and March, 1967). This allows for recirculation of bile acids, thus allowing for their reuse in lipid digestion. It is estimated that 90% of bile salts are reabsorbed in the jejunum and ileum (Hurwitz et al., 1973).

Since chickens have low levels of liver glucuronyl transferase and little or no biliverdin reductase, the secretion rate of biliverdin is high relative to that of bilirubin (14.7 vs. 0.9 μg/kg/min). The green color observed in coprodeal droppings is likely due to biliverdin. The reason for the brown color associated with cecal droppings is unknown, but it may be due to bacterial reduction of biliverdin to bilirubin and subsequent dehydrogenation (Hill, 1983).

21.6 Absorption

21.6.1 Carbohydrates

Absorption of carbohydrates in birds occurs by mechanisms similar to those found in mammals. Absorption occurs more rapidly from the small intestine compared to the cecum with carbohydrates being absorbed by both active and passive mechanisms. Absorption of sugars from the distal regions of the intestinal tract may account for as much as 5% of the total capacity. Those sugars containing a six-membered ring with a hydroxyl group in the number three position oriented similarly to glucose are actively transported. Active transport accounts for at least 80% of glucose absorption. D-Glucose and D-galactose are absorbed faster than D-xylose and D-fructose and D-arabinose. These sugars are absorbed faster than L-arabinose, L-xylose, D-ribose, D-mannose, and D-cellobiose.

Glucose is absorbed via the apically located Na-dependent SGLT-1 system found in both the small and large intestine. Fructose is transported by the apical GLUT5-type system (Garriga et al., 2004). Once inside the epithelial cells, these sugars are transported into the interstitial space by the basolateral GLUT2 transporter. Absorption rates appear greatest during the first week of life, and decline thereafter (Barfull et al., 2002). SGLT-1 expression is regulated by the rennin-antiotensin-aldosterone system (Garriga et al., 2004).

The absorption of sugars against a concentration gradient involves an apically located Na-dependent, phloridzin-sensitive transport. This system is coupled to Na^+-K^+-ATPase located on the basolateral membrane. Contrary to what is believed to occur in mammals, the active transport of one molecule of carbohydrate in birds is coupled to the movement of two molecules of Na (Kimmich and Randles, 1984). Sugars leave the enterocytes on their way to the bloodstream crossing the basolateral membrane by either simple diffusion or facilitated by a Na-independent mechanism.

Within the small intestine, the greatest absorption of glucose occurs in the duodenum (Figure 21.16). Cumulatively, up to 65, 85, and 97% of ingested starch is digested through the duodenum, jejunum, and the terminal ileum, respectively (Riesenfeld et al., 1980). Virtually all of the glucose released from starch digestion is absorbed within the small intestine.

Significant absorption of glucose also occurs in the cecum (Savory and Mitchell, 1991). While the entire cecum

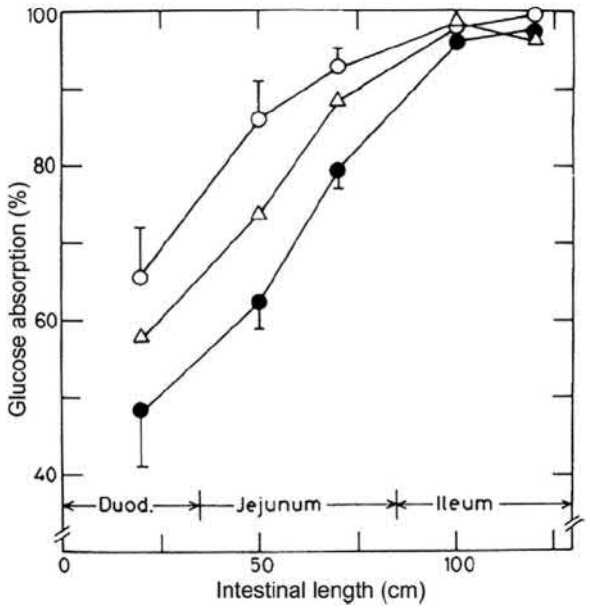

FIGURE 21.16 Cumulative percentage of glucose and starch disappearance from the intestine of seven-week-old chicks. Glucose absorption from glucose monohydrate as the sole dietary carbohydrate source (○), starch digestion (Δ), and absorption (●) in chicks fed starch as the sole dietary carbohydrate source. Values given in the figure are means of six chickens ± standard error. *Reprinted from Riesenfeld et al. Copyrights 1980 by Oxford University Press. Used by permission of the publisher.*

is able to transport sugars at hatch, this ability is soon limited to the proximal region (Planas et al., 1986). The ability of the cecum to actively absorb sugars at low concentrations appears higher than that of the jejunum (Vinardell and Lopera, 1987).

There is a greater affinity for active transport of glucose in the ileum (Levin et al., 1983). The ileum appears well suited for transporting glucose which may not be absorbed within the jejunum.

The GIT also has a role in glucose homeostasis (Riesenfeld et al., 1982). Plasma glucose levels are maintained relatively constant in chickens when fed semi-purified diets in which glucose is replaced with either fructose, soybean oil, or cellulose. While this is partially the result of varying glucose turnover rates, it is largely a result of varying rates of conversion of glucose to lactate by the intestine.

21.6.2 Amino acid and peptides

Amino acid and peptide absorption in birds (Gilbert et al., 2008) is similar to that in mammals. Amino acid transport occurs via a secondary active transport system. This process is saturable, coupled to Na + transport, and uses adenosine triphosphate for energy. The amino acid transport systems can be classified in four groups based on their ability to transport: (1) neutral amino acids; (2) proline, B-alanine, and related amino acids; (3) basic amino acids; and (4) acidic amino acids. This classification, however, is not rigid because many amino acids can be transported by more than one group of transport molecules. For example, leucine, a neutral amino acid, can inhibit the uptake of proline and arginine, a basic amino acid. Glycine transport is partially inhibited by both proline and β-alanine.

The primary site for amino acid absorption is the small intestine. It is still unclear as to which section of the small intestine has the greatest capacity for absorption because there is a lack of agreement among studies. The rectum of hens is also capable of absorbing methionine via a saturable process. As with glucose transport, the K_m for various amino acids is lower in the ileum than in the duodenum (Table 21.11).

Peptide (i.e., di- and tripeptides) absorption can occur via paracellular movement and specific transport systems (Figure 21.17). Many amino acid transporters have been characterized. These include the neutral amino acid transporters with preference for leucine and other large hydrophobic neutral amino acids (system L), system A with preference for alanine and other small and polar neutral amino acids, and system ASC with preference for alanine, serine, and cysteine (Table 21.12). In addition, separate nomenclature (x for anionic, y for cationic, z for neutral) has been applied to systems mediating transport of cationic amino acids (system y+) and anionic amino acids (system X^-_{AG}). With some exceptions (system L, system T), lowercase acronyms indicate Na^+-independent transporters, whereas uppercase acronyms are used for Na + -dependent transporters.

For the absorption of di- and tripeptides, only one transport system, designated as PepTl (SLC15Al), is known. This is a low-affinity, high-capacity transport system and handles essentially all possible protein-derived di-

TABLE 21.11 K_m (mM) and J_{max} (Pmol $Cm^{-2}d^{-1}$) for saturable amino acid absorption in the chicken small intestine.

Amino acid	Jejunum		Ileum	
	K_m	J_{max}	K_m	J_{max}
Amino-isobutyric acid	4.6 ± 0.9	46 ± 7	2.5 ± 0.2	56 ± 6
Glycine	4.2 ± 0.4	37 ± 5	2.7 ± 0.2	55 ± 6
Histidine	3.4 ± 0.7	132 ± 12	0.8 ± 0.2	129 ± 4
Methionine	4.9 ± 0.6	147 ± 14	1.9 ± 0.6	148 ± 5
Valine	3.2 ± 0.7	38 ± 7	1.5 ± 0.2	82 ± 13

Reproduced from Denbow (2015).

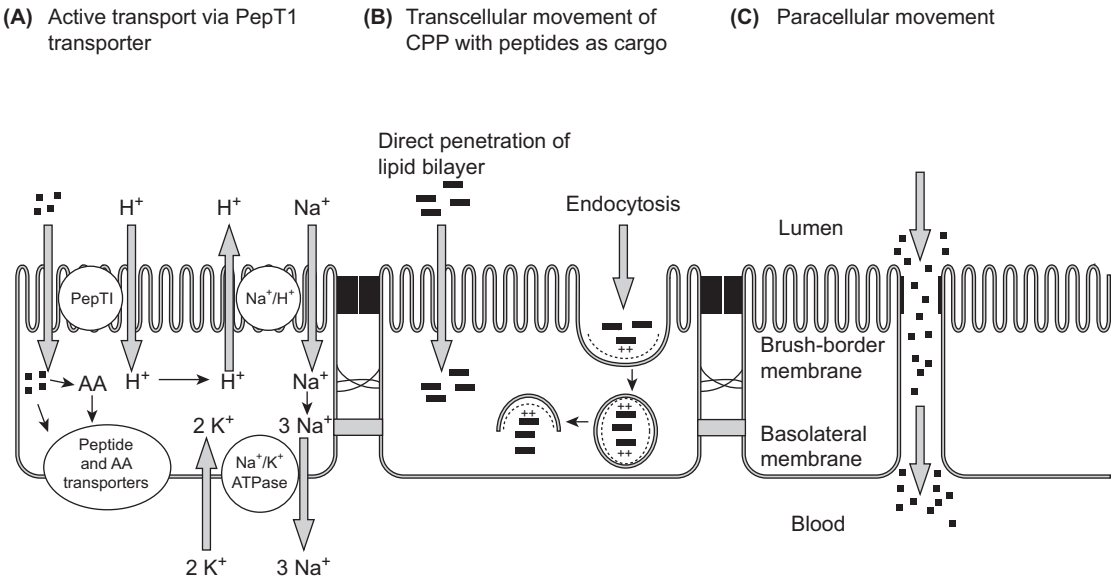

FIGURE 21.17 Potential routes of peptide uptake in enterocytes. (A) The primary route of di- and tripeptide absorption is through cotransport with H+ by the peptide transporter, PepTl. (B) Cell-penetrating peptides (CPP) are capable of carrying cargo such as peptides to the inside of cells. (C) Increased permeability of tight junctions permits uptake of peptides via the paracellular route. *Reprinted from Gilbert et al. Copyrights 2008 by Oxford University Press. Used by permission of the publisher.*

and tripeptides as well as various peptidomimetics, such as aminocephalosporins and various prodrugs. PepTl utilizes the cotransport of protons. It has been well characterized in many species, including chickens and turkeys (Gilbert et al., 2008). Peptides appear to be absorbed more rapidly than amino acids. Absorption of peptides acts to eliminate competition between amino acids for uptake and thus helps increase the speed of absorption. PepTl expression is upregulated during feed restriction. This may be a mechanism to compensate for decreased mucosal surface area caused by reduced villi height and crypt depth observed in broilers given delayed access to feed at hatch. Increased expression of PepTl may be mediated by peroxisome-proliferator-activated receptor alpha (Shimakura et al., 2006).

The ceca are also important in amino acid absorption. Proline is absorbed in the cecum via a Na-dependent carrier-mediated transport system, with transport rates being higher in the proximal than distal cecum (Obst and Diamond, 1989). In addition, leucine, phenylalanine, proline, and glycylsarcosine are absorbed against a concentration gradient (Calonge et al., 1990; Gasaway, 1976; Moreto et al., 1991). Proline and methionine have also been shown to be transported by a Na-independent system (Moreto et al., 1991).

The ceca have a greater ability to transport amino acids than sugars (Moreto et al., 1991). This may be functionally important when considering the following: (1) uric acid, which is retrogradely carried to the ceca from the coprodeum, may be microbially converted to amino acids; and (2) proteases are in high concentration within the ceca and may release amino acids from proteins. Therefore, the ceca may be important in amino acid absorption.

21.6.3 Fatty acids and bile acids

Fatty acid absorption occurs in the distal half of the jejunum and, to a lesser extent, in the ileum. Because the bile duct enters the GIT of birds near the distal duodenum, emulsification of fats is delayed in birds relative to mammals.

In mammals, fatty acids enter the enterocytes where they are esterified to triglycerides and packaged into chylomicrons which enter the lymphatic system. However, in birds, after being re-esterified, lipids are packaged into portomicrons, which pass directly into the hepatic portal blood supply.

21.6.4 Volatile fatty acids

The concentration of volatile fatty acids (VFAs), mainly acetate, but some propionate and butyrate, in the ceca is high (Table 21.13). It can reach 107 mM/kg in the chicken and 20−151 mM/kg in the goose (Goldstein, 1989). VFAs are one of the byproducts of microbial decomposition of uric acid (Braun and Campbell, 1989). Levels of VFAs are higher in the portal blood of conventionally raised compared to germ-free birds, suggesting that VFAs produced by bacteria are absorbed by the GIT. VFAs can be absorbed from both the small intestine and the ceca by passive transport (Sudo and Duke, 1980). Recently, the role

TABLE 21.12 Amino acid transporter system.

System	cDNA[a]	SLC	Amino acid substrates
A	SNAT2	SLC38A2	G,P,A,S,C,Q,N,H,M
	SNAT4	SLC38A4	G,A,S,C,Q,N,M,AA^+
ASC	ASCT1	SLC1A4	A,S,C
	ASCT2	SLC1A5	A,S,C,T,Q
Asc	4F2hc/ asc1	SLC3A2/ SLC7A10	G,A,S,C,T
B^0	B^0AT1	SLC6A19	AA^0
	B^0AT2	SLC6A15	P,L,V,I,M
$B^{0,+}$	$ATB^{0,+}$	SLC6A14	AA0,AA^+, β-Ala
$b^{0,+}$	rBAT/ $b^{0,+}$AT	SLC3A1/ SLC7A9	R,K,O, cysteine
β	TauT	SLC6A6	Tau, β-Ala
Gly	XT2	SLC6A18	G
Imino	Imino	SLC6A20	P, HO—P
L	4F2hc/ LAT1	SLC3A2/ SLC7A5	H,M,L,I,V,F,Y,W
	4F2hc/ LAT2	SLC3A2/ SLC7A8	AA^0 except P
	LAT3	SLC43A1	L,I,M,F
	LAT4	SLC43A2	L,I,M,F
N	SNAT3	SLC38A3	Q,N,H
	SNAT5	SLC38A5	Q,N,H,S,G
PAT (Imino acid)	PAT1	SLC36A1	P,G,A GABA, β-Ala
	PAT2	SLC36A2	P,G,A
T	TAT1	SLC16A10	F,Y,W
X^-_{AG}	EAAT2	SLC1A2	E,D
	EAAT3	SLC1A1	E,D
x^-_C	4F2hc/ xCT	SLC3A2/ SLC7A11	E, cysteine$^-$
y^+	Cat-1	SLC7A1	R,K,O,H
y^+L	4F2hc/ y^+LAT1	SLC3A2/ SLC7A7	K,R,Q,H,M,L
	4F2hc/ y^+LAT2	SLC3A2/ SLC7A6	K,R,Q,H,M,L,A,C

A, antiport; *AA^+*, cationic amino acids; *AA^0*, neutral amino acids; *AM*, apical membrane; *BM*, basolateral membrane; *K*, kidney; *I*, intestine; *NR*, not reported; *S-AA^0*, symport together with neutral amino acids; *U*, uniport; *S*, symport; *Ub*, ubiquitous. Amino acids are given in one-letter codes. *GABA*, gamma amino butyric acid; *HO—P*, hydroxyproline; *O*, ornithine;
Affinity: high, <100 μM; medium, 100 μM to 1 mM; low,> 1 mM.
[a]*Expression in epithelial cells of kidney and intestine.*
Reproduced from Denbow (2015).

of VFA transporters has been characterized in mammalian species. Monocarboxylates linked with H^+ can be transported by Na co-transporters (SMCT1 and 2) (Halestrap and Meredith, 2004; Poole and Halestrap, 1993) as well as electroneutral co-transporters (MCT1-4) (Halestrap, 2012; Halestrap and Meredith, 2004; Halestrap and Wilson, 2012). MCT1 is involved in SCFA transport at the brush border membrane while MCT4 functions at the basolateral membrane (Gill et al., 2005; Rajendran and Binder, 1994). Presence of mRNA level for both transporters, SMCT1 and MCT1 in ceca of chickens has been confirmed in broilers during posthatch development (Qu et al., 2021). Microbial fermentation within the ceca of birds can provide enough VFAs to meet between 8% (chicken) to 75% (ostrich) of the energy needs for basal metabolic rate (Jozefiak et al., 2004).

21.6.5 Calcium and phosphorus

The major site of calcium and phosphate absorption is the upper jejunum (Levin et al., 1983). Calcium can be transported through active, transcellular, or passive, paracellular transport mechanisms (Dimke et al., 2011).

Transcellular transport involves entry across the cell wall via transient receptor potential vanilloid (TRPV) 5 or TRPV6 transporters, diffusion through the cytoplasm by binding to Calbindin D_{28k}, and extrusion at the basolateral membrane via plasma membrane calcium ATPase 1b (PMCA1b, ATP2B1) and sodium/calcium exchanger 1 (NCX1, SLC8A) (Dimke et al., 2011; Hoenderop et al., 2005). In laying hens, new candidates have been identified for transcellular Ca transport, including TRPV2, TRPC1, and TRPM7 located on the brush border membrane, and two additional plasma membrane Ca ATPases: ATP2B2 and ATP2B4 located at the basolateral membrane (Gloux et al., 2019). The presence of TRPV6 as Ca entry point is controversial in GITs of chickens (Gloux et al., 2019; Proszkowiec-Weglarz and Angel, 2013; Rousseau et al., 2016; Yang et al., 2011).

Paracellular transport is characterized by ion movement from the intestine to the blood along the chemical gradient through tight junctions (Dimke et al., 2011). Tight junction proteins (TJP)1, 2, and 3, claudin 1, 2, 10, and 12, occludin, and junctional adhesion molecule 2 have been suggested to play a role in paracellular Ca transport in laying hens (Gloux et al., 2019).

Similarly to Ca, P transport involves uptake of the mineral through the apical brush border membrane by Na-dependent transporter, translocation across the cells and exit at the basolateral membrane (Tenenhouse et al., 1998). In contrast to the well-known Ca transporter system, little is known about P diffusion through cells and extrusion into blood (Marks et al., 2010; Tenenhouse, 2005).

TABLE 21.13 Composition of volatile fatty acids, pH, and water in cecal content of domestic and wild birds.

Species	Water (%)	pH	Lactic acid	Volatile fatty acids			
				Acetic	Propionic	Butyric	Total
Turkey	77	5.3–7.2					74 mM/kg
Goose	87	6.0–6.7	1–2 mM/L				20–151 mM/kg
Guinea fowl	76						
Chicken		6.7–7.8		56 mM/kg	29 mM/kg	10 mM/kg	107 mM/kg
Mallard		6.5–5.9		62–68 mM/L	19–22 mM/L	10–14 mM/L	116–149 mM/L
Willow ptarmigan, red grouse			4.5 mM/kg	36 mM/kg	10 mM/kg	3 mM/kg	
Rock ptarmigan	78						
Emu	69						
Ostrich	92	7.0		100 mM/L			160 mM/L

Adapted from Goldstain (1989) and Jozefiak et al. (2004).

In mammals, three classes of Na-dependent P transporters have been identified with class one (Na/PI) being predominantly expressed in the brush border membrane of kidneys, type two (Na/PII) expressed in both renal (IIa and IIc) and intestinal (IIb) epithelium, and type III (PIT1 and PIT2) expressed in most tissues in mammals with predominant presence in kidney (PIT2) and intestine (PIT1) (Marks et al., 2010; Miyamoto et al., 1997; Murer et al., 2000; Tenenhouse, 2007; Tenenhouse et al., 1998). Presence and changes in expression of Na/PIIb (SLC34A2) and PIT1 (SLC20A1) during development and in response to dietary factors in the small intestine of chickens has been characterized (Ashwell and Angel, 2010; Nie et al., 2013; Olukosi et al., 2011; Proszkowiec-Weglarz et al., 2019; Yan et al., 2007). However, the exact role of PIT1 has not been well defined in birds. A hypothetical model of transcellular and paracellular Ca and P transport in poultry is shown in Figure 21.18.

Calcium absorption is influenced by the vitamin D hormone 1,25-dihydroxyvitamin **D_3** ($1,25(0H)_2D_3$) interacting with either cytoplasmic or nuclear vitamin D receptor. It is believed that stimulation of Ca absorption requires active vitamin D synthesis, an increase in gene expression of intestinal Ca transporters, and increase in Calbindin D_{28K} synthesis. Feeding chickens a Ca− or P-deficient diet, repleting vitamin D-deficient chickens with vitamin D, or injecting $1,25(0H)_2D_3$ causes an increase in plasma membrane calcium pump mRNA in the duodenum, jejunum, ileum, and rectum (Cai et al., 1993). A study in white leghorn chicks showed that vitamin D can significantly affect P transfer in all segments of small intestine (Wasserman and Taylor, 1973).

21.6.6 Potassium and magnesium

The absorption and secretion of potassium (K) and magnesium (Mg) in the GIT of broilers has been characterized by Van Der Klis et al. (1990). K and Mg are secreted in the duodenum. In addition, there is some secretion of Mg in the ileum and rectum. The major site of absorption for these minerals is the proximal jejunum, with some absorption of Mg occurring in the gizzard. This coincides with the fact that dry matter spends approximately 25% of its time in the jejunum. There is little absorption of these minerals beyond the jejunum.

21.6.7 Water, sodium, and chloride

Water is absorbed throughout the small and large intestine and the ceca. Absorption of water occurs as a secondary response to the active absorption of other compounds such as glucose, Na, and amino acids.

Birds generally secrete a very dilute urine. Urine can travel into the coprodeum and, via antiperistalsis, continue orad into the ceca. Note that there are exceptions, such as the ostrich, which can concentrate urine and has no movement of urine back into the colon (Elbrønd et al., 2009). The excreta of cecectomized chickens are higher in water, indicating that the lower part of the intestinal tract has an important role in water and salt balance.

Sodium is secreted in the proximal portion of the intestinal tract (Van Der Klis et al., 1990). The major sites for Na absorption are the proximal jejunum followed by the colon. The ileum also has a small capacity for Na absorption.

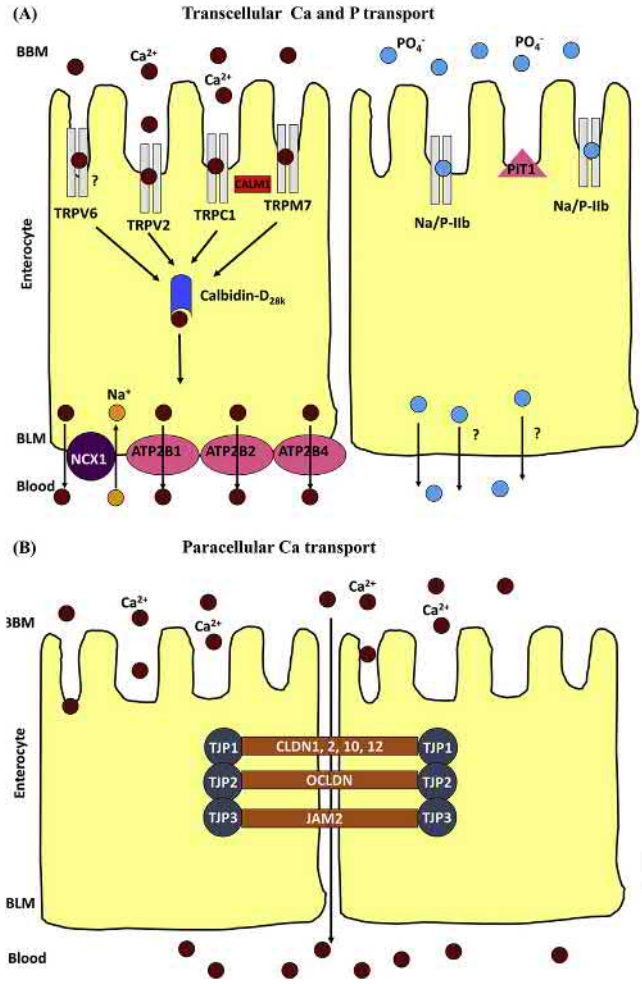

FIGURE 21.18 **Proposed model depicting transcellular (A) calcium and phosphorus transport and paracellular (B) calcium transport across the intestinal epithelial barrier in the chickens.** *ATP2B1*, ATPase plasma membrane Ca^{+2} transporting 1; *ATP2B2*, ATPase plasma membrane Ca^{+2} transporting 2; *ATP2B4*, ATPase plasma membrane Ca^{+2} transporting 4; *BBM*, brush border membrane; *BLM*, basolateral membrane; *CALM1*, Calmodulin 1; *CLDN1, 2, 10 and 12*, Claudin 1, 2, 10 and 12; *JAM2*, Junctional adhesion molecule; *Na/P-IIb*, sodium-phosphorus cotransporter IIb; *NCX1*, sodium and calcium exchanger; *OCLDN*, Occludin; *PiT1*, sodium-phosphorus cotransporter type III; *TJP1, 2 and 3*, Tight junction protein 1, 2 and 3; *TRPC1*, Transient receptor potential cation channel subfamily C member 1; *TRPM7*, Transient receptor potential cation channel subfamily M member 7; *TRPV2*, Transient receptor potential cation channel subfamily V member 2; *TRPV6*, Transient receptor potential cation channel subfamily V member 6. *Adapted from Proszkowiec-Weglarz and Angel (2013) and Gloux et al. (2019).*

The coprodeum, colon, and ceca serve an important role in Na, chloride (Cl), and water balance (Laverty et al., 2006). When birds are fed a low-NaCl diet, there is a net absorption of Na from the coprodeum, colon, and ceca. Na^+ absorption occurs by active transport mediated by apical electrogenic and amiloride-sensitive Na^+ channels and basolateral Na^+ pumps (Na^+/K^+-ATPase) (Figure 21.19). The mucosal lining of the colon and coprodeum consists of simple, columnar epithelium with absorptive epithelial cells, GCs, and mitochondria-rich cells. On a low-salt diet, there is an extensive microvillous brush border present. When fed a high-NaCl diet, absorption of Na^+ from the coprodeum nearly ceases, while in the colon absorption remains high provided a low concentration of hexoses and amino acids is maintained on the mucosal side. There is an increased expression of SGLT in the colon which is associated with increased dietary salt. This represents a dramatic change from electrogenic, channel-mediated Na + transport to organic substrate Na^+ - cotransport consistent with what is observed in the small intestine but not in the mammalian large intestine. When fed a high-salt diet, the colon morphology remains the same, but that of the coprodeum shows a decrease in density and length of microvilli. The adaptation to a low-salt diet is mediated by circulating aldosterone and maximizes Na + transport (absorption). Aldosterone suppresses SGLT expression (Laverty et al., 2001).

In addition, there is also a net secretion of Cl from the coprodeum and rectum, but the secretory ability of the coprodeum disappears in birds fed a high-NaCl diet (Skadhauge, 1989). The secretion of Cl is induced by serotonin (Hansen and Bindslev, 1989). Receptor antagonists for 5-HT_{1A}, 5-HT_{1B}, 5-HT_{1C}, 5-HT_{1D}, 5-HT_{2}, 5-HT_{3}, adrenergic, cholinergic, and histaminergic receptors were unable to block the response. However, the second messenger for serotonin-induced chloride secretion is cAMP (Hansen and Bindslev, 1989).

The absorption of Na and secretion of Cl within the lower gut is regulated by plasma aldosterone (Clauss et al., 1991). Increases in plasma aldosterone stimulate amiloride-sensitive Na uptake in the coprodeum, rectum, and ceca. Feeding high-NaCl diets causes a decrease in plasma aldosterone, and a decrease in amiloride-dependent Na absorption. Furthermore, there is a switch to amiloride-independent hexose/amino acid stimulated Na-transport within the rectum and cecum, but a cessation of Na-transport in the coprodeum. The hexose/amino acid stimulated Na-transport in the rectum functions to counteract the osmotic water loss due to feeding a high-NaCl diet (Skadhauge et al., 1985), and is stimulated by increases in plasma arginine vasotocin and/or prolactin (Arnason and Skadhauge, 1991).

21.6.8 Vitamins

Vitamin A and carotenoid metabolism in chickens is very similar to that of humans (Diaz-Gomez et al., 2017). Fat-soluble vitamin A and carotenoids follow the fate of lipids in the upper GIT, and their absorption occurs in the upper half of the small intestine (Borel, 2003). It has been long assumed that carotenoids are absorbed by a passive diffusion process while vitamin A absorption occurred via energy dependent transport (Reboul, 2013). During the

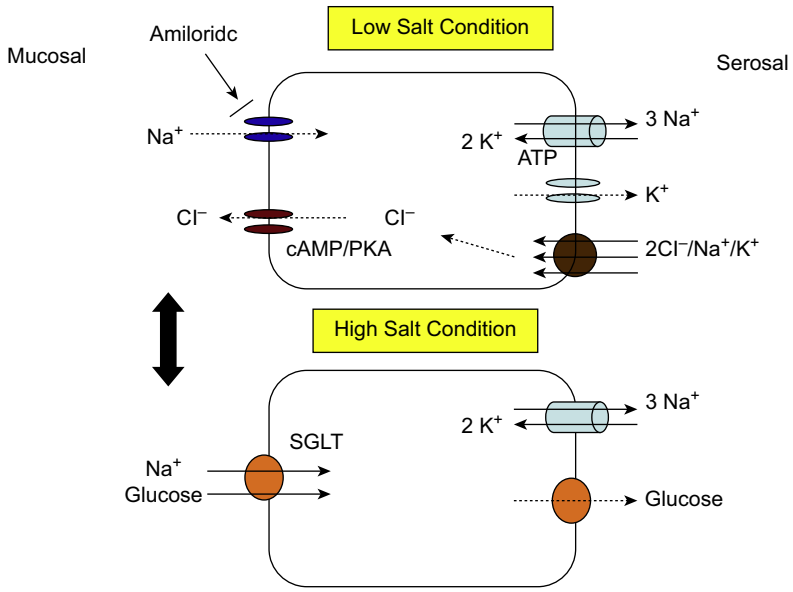

FIGURE 21.19 Working model for transport pathways in the hen lower intestine. The two panels show the different Na + absorptive pathways for tissues from low and high salt-acclimated hens. Example shown is for colon and would represent the extreme conditions of salt intake, in which there is a complete transition in transport pattern. SGLT-mediated glucose uptake and basolateral release via GLUT transporters is representative of several organic substrate cotransporter systems (amino acids and hexoses) expressed in the high salt-acclimated tissues. The diuretic amiloride blocks low salt ENaC channels at concentrations of 10^{-5} M. Potassium channels, shown on the basolateral or serosal side, may also be present on the apical surface and mediate K^+ secretion. For simplicity, the CJ-secretory pathway is shown only in the low salt condition, even though it is also observed under high salt. *Reprinted from Laverty et al. Copyrights 2006 by Elsevier.*

digestion process, carotenoids and fat-soluble vitamins are incorporated with lipids into mixed micelles (Borel, 2003). Retinol (vitamin A) is believed to be transported at the brush border membrane by stimulated by retinoic acid 6 protein and RBP4-receptor 2 while carotenoids are transported by scavenger receptor class B type I, cluster determinant 36 (CD36), and NPC1L1 (cholesterol membrane transporters) in the intestine (Figure 21.20, Reboul, 2013). In the enterocytes, transport of retinol and its metabolites involves retinoid-binding proteins while a carotenoid-binding protein has not yet been identified (Reboul, 2013). Major fractions of vitamin A and carotenoids are incorporated into chylomicrons and secreted into the lymph on the basolateral side of enterocytes.

Absorption of vitamin B-6 occurs throughout the small intestine, but primarily in the duodenum (Heard and Annison, 1986). Absorption can also occur in the crop and cecum, but this is minimal. The mechanism of absorption is passive diffusion. Although microbial synthesis of vitamin B-6 does occur, this is not important in meeting a bird's vitamin requirement.

Members of the vitamin E family, such as dietary alpha tocopherol, nonalpha-tocopherols, and tocotrienols, are absorbed by intestinal cells by passive diffusion and receptor-mediated transport, and are delivered to the lymph via chylomicrons (Schmolz et al., 2016).

Transport of folic acid in the intestine is carried out by a specific folate transporter under acidic conditions. Three major folate transporters have been identified in the intestinal cells including folate receptor, the reduced folate carrier, and the proton-coupled folate transporter (Steinberg, 1984). The reduced folate carrier and proton-coupled folate transporter are widely expressed in the small and large intestine of laying hens (Jing et al., 2009, 2010). Functional studies have shown that folic acid is absorbed in all regions of the intestine with greater transport activity in the upper half of the small intestine while transport of folic acid in the ceca is reduced, indicating the role for bacterially derived folate as an alternative source of folate (Tactacan et al., 2011).

21.7 Age-related effects on gastrointestinal function

The small intestine grows rapidly during the later days of incubation, increasing from 1% of body weight at day 17 to 3.5% at hatch (day 21), followed by a two- to four-fold increase in intestine length through 12 days posthatch (Uni, 2006). Villi grow in length near the end of incubation and increase in size and number following hatch. Duodenal villus growth is nearly complete by day seven, whereas in the jejunum and ileum, growth continues beyond 14 days of age. Unlike in mammals, in which most enterocyte proliferation occurs within the crypts, in poultry, proliferation occurs along the length of the villi. Enterocyte migration to the tip of the villi takes three days in four-day-old chicks and four days in older birds.

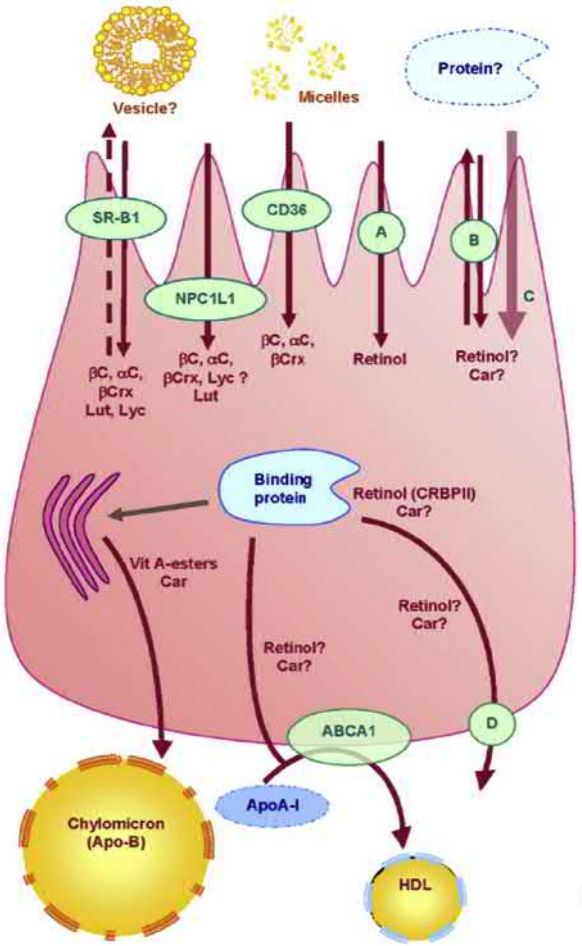

FIGURE 21.20 Proteins involved in uptake, transport, and secretion pathways of vitamin A and carotenoids across the enterocyte. *A*, retinol putative specific transporter; *B*, unidentified apical transporter; *C*, passive diffusion; *Car*, carotenoids; *D*, unidentified basolateral efflux transporter; *Lut*, lutein; *Lyc*, lycopene; *Vit*, vitamin; *αC*, α-carotene; *βC*, β-carotene; *βC*, β-cryptoxanthine; ? = putative pathway. Carotenoids are captured from mixed micelles by apical membrane transporters: SR-BI, CD36, and NPC1L1. Apical membrane proteins involved in apical uptake of retinol have not yet been identified. A fraction of vitamin A and carotenoids may then be effluxed back to the intestinal lumen via apical membrane transporters (SR-BI and possibly other transporters). Another fraction is transported to the site where they are incorporated into chylomicrons. Some proteins may be involved in intracellular transport of carotenoids, but none has been clearly identified. Conversely, CRBPII has clearly been described as involved in intracellular transport retinol. Retinyl esters and carotenoids are secreted in the lymph into chylomicrons, while a part of the more polar metabolites may be secreted by the portal route. It is suggested that free retinol can also be secreted at the basolateral side via ABCA1 (apoAI pathway). *Reprinted from Reboul et al. Copyrights 2013 by the authors. Used under Creative Commons Attribution license (CC BY).*

It was hypothesized that the postnatal growth rate is at least partially determined by the differential growth of various organs (Lilja, 1983). The intestinal tract grows rapidly following hatch, with small intestine length increasing by 2.5 cm/d in modern broilers (Schmidt et al., 2009). The most of the posthatch growth (70% of the total length) occurs between day two and seven with plateau phase between day 7 and 14, and second elongation period between day 14 and 28 in broiler chickens (Schmidt et al., 2009).

With regards to pancreatic enzyme activity within the intestines, trypsin, protease, and amylase activity increases rapidly during the first 21 days posthatch in turkey poults (Krogdahl and Sell, 1989) and during the first 14 days posthatch in broiler chickens (Nitsan et al., 1991). However, lipase activity does not begin to increase until after 21 days of age. Feeding a high-fat diet did not significantly increase lipase activity until after 21 days of age. At least during the first few weeks posthatch, it appeared that lipase activity may be a limiting factor in digestion.

Several notable changes have been found in the development of nutrient transport systems during ontogeny in broilers (Obst and Diamond, 1989). During the first week posthatch, proline uptake by the small intestine is high relative to glucose uptake. Because the relative growth rate of broilers is greatest during the first week, it appears that amino acid uptake may parallel this growth pattern. The uptake of glucose displays a transitory increase during week two. This increase is hypothesized to be a result of a switch from lipid metabolism to carbohydrate metabolism due to depletion of the yolk reserves. Because of the allometric growth of the intestine, during the second week posthatch, the intestine displays a decrease in size relative to body weight. This may be a second reason for the increase in uptake of glucose occurring at this time. There is a transitory increase in proline uptake during week six. This increase parallels the first postjuvenile molt and a rise in absolute growth rate.

Interestingly, the intestinal uptake capacity of broilers closely matches a bird's nutrient needs. This contrasts with results in mammals, where uptake far exceeds the animal's needs. It remains to be determined whether this may indicate that nutrient uptake represents a potential constraint for increased growth in broilers, or whether it means that broilers are better allocating resources.

Feeding immediately posthatch stimulates intestinal development. Delaying feed for 24–48 h decreased villi length, enterocyte migration rate (Geyra et al., 2001), and enterocyte number but increased GCs producing acid and neutral mucin (Uni et al., 2003).

21.8 Gastrointestinal microbiota

Most information about avian microbiota comes from studies using broiler chickens and to a lesser extent, laying hens. The GIT of chickens harbors complex microbial communities (bacteria, fungi, archaea, protozoa, and viruses) dominated by diverse bacterial populations (Wei et al., 2013). Due to anatomical differences between birds

and mammals (with a few exemptions, a shorter GIT and faster digesta transit), the microbiota is different in comparison to mammals (Pan and Yu, 2014). Most of the bacteria in the GIT are considered commensal with benefits but also a cost to the host (Dibner and Richards, 2005; Gaskins et al., 2002). Microbiota of the GIT plays an important role in health, nutrition, host physiology regulation, GIT development, and growth. It is also involved in competitive exclusion of pathogens and nonindigenous microbes, immune stimulation and programming, contribution to host nutrition by producing energy and nutrients such as vitamins, amino acids, SCFAs, and in metabolism of host nitrogen compounds (Clavijo and Florez, 2018; Rehman et al., 2007; Shang et al., 2018). The cost to the host of harboring commensal microbiota is related to increased mucus production and secretion, increase in epithelial cell turnover, a more developed immune system, and increased production of IgA. These processes increase the demand for energy and protein from the host (Shang et al., 2018). Chicken microbiota can also be a source of pathogens such as *Salmonella enterica*, *Campylobacter jejuni or coli*, *Escherichia coli*, and *Clostridium perfringens* that pose a threat to public health (Kumar et al., 2018; Mancabelli et al., 2016; Oakley et al., 2014).

The gastrointestinal microbiota can also be classified as the luminal microbiota residing in the lumen and the mucosal microbiota attached to the epithelial cells. The microbiota present in the lumen is influenced by available nutrients, physical properties of the digesta, presence of antimicrobial factors and feed passage rate, while mucosal microbiota is restricted by host factors, such as expression of specific adhesion sites, secretion of immunoglobulin, and mucin production rate (Borda-Molina et al., 2018; Jeurissen et al., 2002; Shang et al., 2018). Both microbiota populations influence each other and can be altered by diet (Jeurissen et al., 2002; Shang et al., 2018).

The composition of the gut microbiota can be affected by various factors such as age of birds, chicken type and breed, anatomical location, maternal factors, sex of the birds, diet and feeding regime, environment (housing, hygiene, temperature, litter quality and age, as well as climate and geographical location), stress, or medication (Clavijo and Florez, 2018; Kers et al., 2018, Figure 21.21). Moreover, the gastrointestinal microbiota can be modulated by many factors including probiotics, prebiotics, synbiotics, organic acids, phytogenics, bacteriophages, and antimicrobial peptides (Clavijo and Florez, 2018; Gadde et al., 2017; Pourabedin and Zhao, 2015, Figure 21.22). All of which are also considered as alternatives to antibiotic growth promoters (Gadde et al., 2017).

The GIT of chickens has been considered to be sterile at hatch. However, recent data indicate that one-day old chicks carry a community of microorganisms in their intestinal tract (Ballou et al., 2016; Kumar et al., 2018)

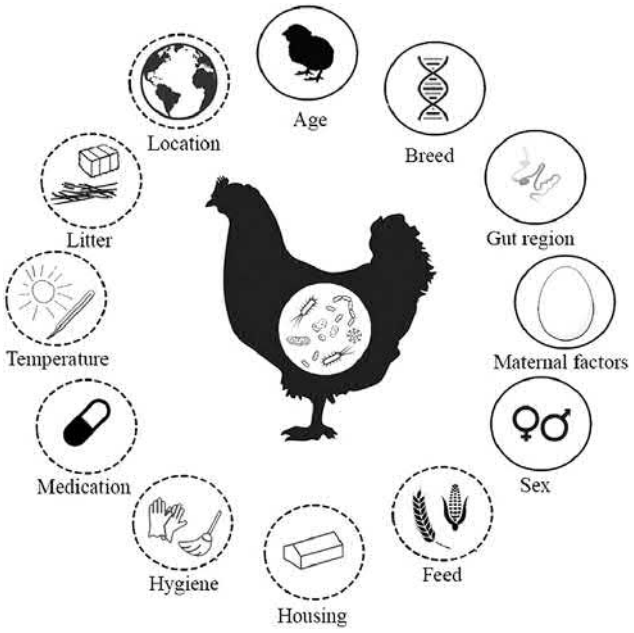

FIGURE 21.21 Factors that affect the intestinal microbiota composition of chickens. Factors found in the literature that determine the development of the intestinal microbiota in broiler chickens. *Solid line* indicates host characteristics, *dashed line* indicates environmental factors. The gut regions comprise the crop, proventriculus, gizzard, duodenum, jejunum, ileum, caeca, large intestine, and cloaca. Maternal factors include horizontal transmission, vertical transmission, and maternal antibodies. *Reprinted from Kers et al. Copyrights 2018 by the authors. Used under Creative Commons Attribution license (CC BY).*

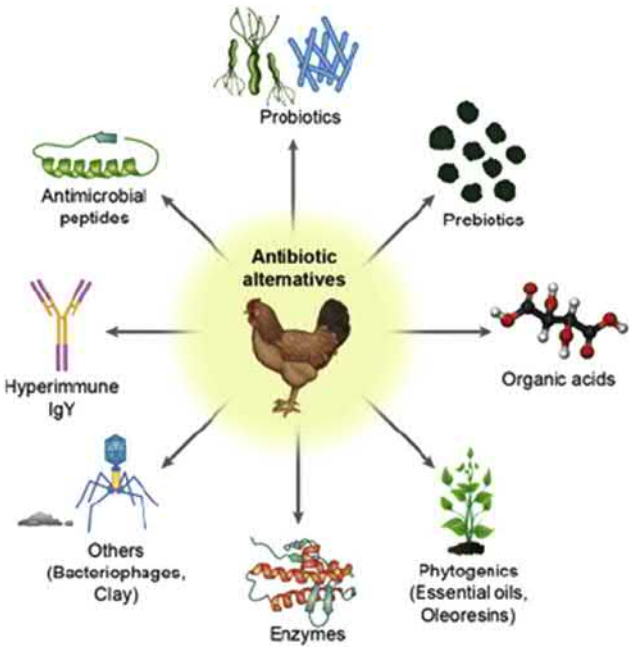

FIGURE 21.22 Various classes of antibiotic alternatives that are available for use in poultry production. *Reprinted from Gadde et al. Copyrights 2017 by Cambridge University Press. Used by permission of the publisher.*

coming directly from the oviduct of the mother or from the egg management and incubation environment, through the pores in the eggshell (Cason et al., 1994; Gantois et al., 2009; Roto et al., 2016). After hatch, colonization of the GIT evolves rapidly in a process of ecological succession. Newly hatched chicks are exposed to microbes from the hatchery environment, human handlers, transport boxes, and transport vehicles before they are exposed to farm and feed microbes (Stanley et al., 2013). In the ileum, the number of bacteria increases from 10^8 CFU per g of digesta on day one posthatch to 10^9 CFU and 10^{8-9} CFU per g of digesta 3 and 42 days after hatch, respectively (Chambers and Gong, 2011). In the ceca, the number of bacteria increases from 10^{10} to 10^{11} and 10^{10-11} CFU per g of digesta 1, 3, and 42 days after hatch, respectively (Chambers and Gong, 2011). The first 14–21 days posthatch are considered as the developmental stages of microbiota and are characterized by transient changes in bacterial composition in the GIT. The intestinal microbial richness defined as the number of different microbial taxa, increases during the first week posthatch and the individual variation in microbiota composition decreases with chicken age (Ballou et al., 2016; Crhanova et al., 2011; Danzeisen et al., 2011). Chicken intestinal microbiota colonization and maturation is influenced by diverse microbial communities carried by poultry feed (Haberecht et al., 2020). The presence of microbiota in the GIT influences the development, morphology, and the weight of the small intestine and ceca in chickens (Forder et al., 2007; Furuse and Okumura, 1994; Gabriel et al., 2006).

The GIT of chickens is composed of the crop, proventriculus, gizzard, duodenum, jejunum, ileum, ceca, large intestine, and cloaca. Each of these sections plays different metabolic function affecting their microbial community (Shang et al., 2018). The diversity of microbiota in chickens is relatively low in comparison to other animals due to the anatomical and physiological differences between birds and mammals, mentioned earlier. Bacterial communities of the small intestine and ceca differ in alpha diversity indexes such as richness, evenness, numbers of operational taxonomic units or Shannon index (Figure 21.23A). Principal coordinate analysis based on the Unweighted UniFrac (beta diversity) clearly shows separations of bacterial communities between duodenum, jejunum, ileum, and cecum and between mucosal and luminal population of bacteria in each of the gut section (Figure 21.23B author's unpublished data).

The taxonomic composition of chicken microbiota depends on the location in GIT (Table 21.14). The proximal part of the digestive tract (crop, proventriculus, and gizzard) is mainly colonized by Lactobacilli that are responsible for starch decomposition and fermentation (Rychlik, 2020; Shang et al., 2018; Wei et al., 2013). The total number of bacteria decreases from 10^{8-9} in crop to 10^{7-8} CFU per g of digesta in proventriculus and gizzard due to presence of low pH of gastric juices (Yeoman et al., 2012). The composition and complexity of the microbiota increases in distal parts of the GIT. The small intestine, with the ileum being the most studied, harbors bacterial population dominated by three main phyla, Firmicutes, Bacteroides, and Proteobacteria with smaller abundance of Actinobacteria (Shang et al., 2018). In comparison to the ileum, the cecum is populated by the most diverse, rich and stable microbial population with, Firmicutes and Bacteroidetes being the most abundant phyla followed by Proteobacteria and Actinobacteria (Shang et al., 2018; Wei et al., 2013). Cecal microbiota is responsible for digestion of feed particles rich in cellulose, starch, and polysaccharides (Clench and Mathias, 1995; Goldstein, 1989). Based on metagenomic data, cecal bacteria are characterized by high proportion of sequences encoding glycosyl hydroxylases with more than 200 genes of nonstarch polysaccharide degrading enzymes (Sergeant et al., 2014; Waite and Taylor, 2014). Excreta samples are not properly representative of the GIT microbiota due to differential mixing effects and less frequent voiding of the ceca in comparison to the rest of the GIT (Oakley et al., 2014).

Similar taxonomic composition was observed in turkey microbiota, but with different distribution of genera in comparison to chicken microbiota in the GIT (Wei et al., 2013).

The numbers of studies concerning microbiota in wild birds are limited (Grond et al., 2018; Hird, 2017). The microbiota of birds, especially wild birds, can be influenced by migratory behavior, flight capacity, diet, mating system, longevity, and birds physiology (Grond et al., 2018). It is well established that captivity alters the microbiota in mammals, fish, amphibians, as well as in birds due to the dietary, social, and environmental conditions in captivity (Hird, 2017). Excreta samples are most commonly analyzed for wild birds as this is one of the few nondestructive methods to determine avian microbiota (Borrelli et al., 2020). In general, core microbiota of wild birds is very similar to the domesticated chicken with Firmicutes, Bacteroidetes, Actinobacteria, and Proteobacteria been the predominant phyla (Grond et al., 2018). Among arctic migratory birds, Firmicutes and Bacteroidetes are dominant in snow buntings and sanderlings while pink-footed geese excreta are dominated by Proteobacteria. Moreover, bacterial diversity is much higher in buntings and sanderlings in comparison to pink-footed geese (Cho and Lee, 2020). Environmental factors such as urbanization and landscape affect the alpha and beta diversity of gut microbiota in the white-crowned sparrow. Among these birds, "urban" and "rural" microbiota differed with urban communities being driven by host morphology while rural communities were influenced more by environmental factors (Berlow et al., 2020).

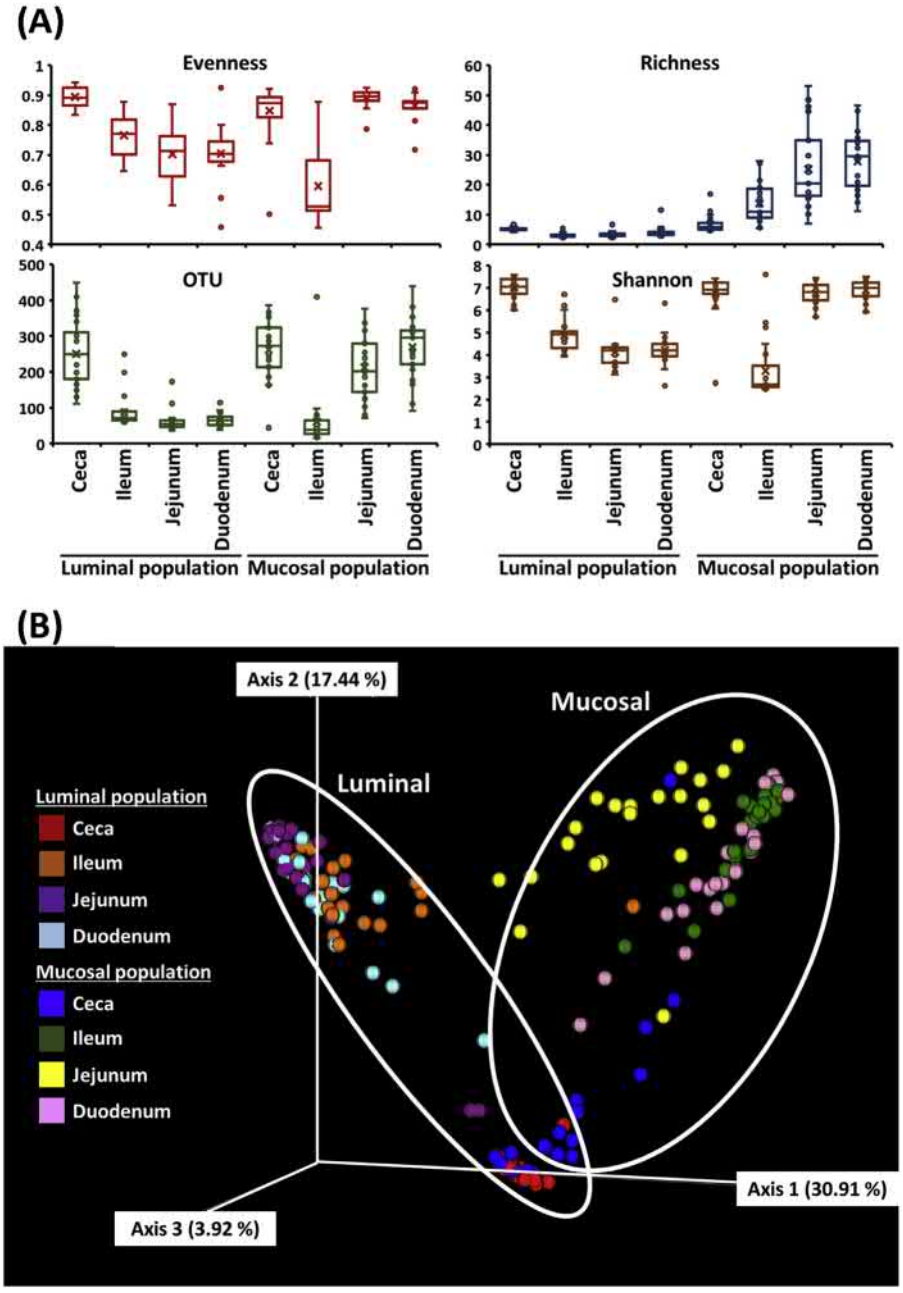

FIGURE 21.23 Alpha and beta diversities of luminal and mucosal population of bacteria in four different parts of chicken gastrointestinal tract. (A) Comparison of evenness, richness, numbers of operational taxonomic units and Shannon index between mucosal and luminal bacterial populations in ceca, ileum, jejunum, and duodenum in broiler chickens. (B) Beta diversity based on Unweighted UniFrac in luminal and mucosal population of ceca, ileum, jejunum, and duodenum in broiler chickens.

Among other wild birds, hoatzins have very well-developed foregut fermenting crop system that contains microbial population functionally analogous to the bovine rumen (Godoy-Vitorino et al., 2008, 2012). In birds, such as carnivores, piscivores, nectarivores, or frugivores, that do not have ceca, the specific function of cecal bacteria is fulfilled by other areas of GIT (Grond et al., 2018).

21.9 Intestinal barrier

In addition to their role in digestion, secretion, and absorption, intestinal cells also form a physical barrier separating the external environment from the internal environment of the host. The intestinal barrier prevents loss of water and electrolytes and entry of antigens and

TABLE 21.14 Spatial distribution of most common and abundant bacteria taxa at phylum and genus level in the gastrointestinal tract of chickens irrespectively of age, diet, or technique used to determine the taxonomy.

GIT location	CFU per g of digesta	Taxonomy level	
		Phylum	Genus
Crop	10^8–10^9	Firmicutes Actinobacteria Proteobacteria	*Lactobacillus* *Bifidobacterium* *Enterobacter*
Gizzard	10^7–10^8	Firmicutes	*Lactobacillus* *Enterococcus*
Small intestine	10^8–10^9	Firmicutes Cytophaga/Flexibacter/Bacteroides Proteobacteria Actinobacteria/Cyanobacteria	*Enterococcus, Clostricium, Lactobacillus, Candidatus Arthomitus, Weisella, Ruminococcus, Eubacterium, Bacillus, Staphylococcus, Streptococcus, Turicibacter, Methylobacteriu* *Bacteroidetes, Flavibacterium, Fusobacterium, Bifidobacterium* *Ochrobacterium, Alcaligenes, Escherichia, Campylobacter, Hafnia, Shigella* *Corynebacterium*
Ceca	10^{10}–10^{11}	Methanogenic archaea Firmicutes Bacteroides/Cytophaga/Flexibacter Actinobacteria Proteobacteria	*Methanobrevibacter, Methanobacterium, Methanothermobacter, Methanosphaera, Methanopyrus, Methanothermus, Methanococc* *Anaerotruncus, Ruminococcus, Faecallibacterium, Bacillus, Streptococcus, Clostridium, Megamonas, Lactobacillus, Enterococcus, Weisella, Eubacterium, Staphylococcus, Streptococcus* *Bacteroidetes, Alistuipes, Fusobacterium, Bifidobacterium, Flavibacterium, Odoribacter* *Corynebacterium* *Ochrobaterium, Alcaligenes, Escherichia, Campylobacter*
Large intestine		Firmicutes Proteobacteria	*Lactobacillus* *Escherichia*

Adapted from Shang et al. (2018).

microorganisms into the body, and allows exchange of molecules between the host and its environment (Brandtzaeg, 2011).

The intestinal barrier is formed by mechanical (mucus layer, glycocalyx, epithelial cells, and tight junction in the paracellular spaces), humoral [defensins and immunoglobulin A (IgA)], immunological (lymphocytes, innate immune cells), muscular, and neurological elements (Bischoff et al., 2014; Okumura and Takeda, 2017). The mucus layer is divided into an outer layer associated with bacteria and loosely attached to the epithelium while the inner layer is characterized by high concentrations of IgA and mucin, and is adherent to the epithelium. In chickens, three transmembrane mucins (MUC4, 13, and 16) and four gel-forming mucins (MUC2, 5ac, 5b, and 6) have been identified (Lang et al., 2006). In comparison to mammals, chickens lack gel-forming MUC19 and transmembrane MUC3, 12, 15, and 17 (Lang et al., 2006). Chicken mucin genes show differential expression in among the regions of the GIT suggesting that they have specific roles in maintaining mucosal integrity (Forder et al., 2012). MUC2 gene codes for the main secreted mucin in the intestine (Van Klinken et al., 1995a,b) and is exclusively expressed in the small intestine, ceca, and large intestine in birds (Woodfint et al., 2017). MUC2 mRNA expression increases during late embryonic development and early posthatch in chickens and ducks (Zhang et al., 2015) while lack of feed during first 48 h posthatch decreases MUC2 expression in chickens (Proszkowiec-Weglarz et al., 2020). Decrease in MUC2 gene expression is associated with deterioration of intestinal mucosa (Forder et al., 2012) and can lead to spontaneous inflammation of the small intestine (Van der Sluis et al., 2006). Mucus secretion from GCs is regulated by the host sensing the presence of gut microbes or their metabolites (Kim and Ho, 2010).

Mucin can be classified into neutral mucin, sialic acid containing mucin, and ester sulfate containing mucin (Deplancke and Gaskins, 2001). Before hatch, an acidic type of mucin is predominantly produced, while after hatch, neutral mucin is coproduced in GCs (Cheled-Shoval et al., 2014). The physiological relevance of the distinct mucin types is not well understood, but it has been suggested that it can influence their protective properties (Deplancke and Gaskins, 2001). Acidic mucin protects against bacterial translocation because it appears to be less degradable by bacterial enzymes and proteases than other mucin types (Deplancke and Gaskins, 2001).

Mucins provide adhesive sites for IgA, the most abundant immunoglobulin isotype at mucosal sites (Brandtzaeg, 2010) and an important factor in preventing infection and regulating the composition of microbiota (Den Hartog et al., 2016). In birds, IgA is poorly expressed during the first week of life and increases during the second week posthatch (Proszkowiec-Weglarz et al., 2020; Zhang et al., 2015). The function of IgA depends on its transport from lamina propria, where it is secreted, via IgA receptor (pIgR) located on the basolateral side of mucosal epithelial cells (Johansen et al., 1999; Kaetzel, 2005). Similarly to IgA, pIgR expression was upregulated later during posthatch development in birds (Proszkowiec-Weglarz et al., 2020; Zhang et al., 2015).

One of the major components of the intestinal barrier are tight junctions that occur between epithelial cells (Anderson and Van Itallie, 1995; Mitic et al., 2000). Tight junctions are multiprotein complexes that seal the paracellular space between adjacent epithelial cells and regulate the permeability of the intestinal barrier (Awad et al., 2017; Chen et al., 2015). They open and close when exposed to a range of stimuli including, nutrients, absorption processes, hormonal or neuronal signals, various cellular pathways, and inflammatory mediators (Barekatain et al., 2019). A tight junction consists of zona occludens-1, occludins, claudins, and actin-myosin cytoskeletal proteins (Gil-Cardoso et al., 2016). Occludins and claudins are the main transmembrane proteins that contribute to the paracellular seal while zona occludens-1 serves as cytoplasmic plaque proteins that interact with both transmembrane, and cytoskeletal proteins (Fanning et al., 1998; Yu and Turner, 2008). Expression of genes that encode tight junctions is modulated among others, by heat stress, access to feed, feed additives, stocking density, bacterial stimuli, pathogen bacteria, and LPS challenge, and can also differ between slow, moderate, and fast-growing broiler chickens (Chen et al., 2018; Goo et al., 2019; Huang et al., 2019; Li et al., 2015; Liu et al., 2018a, 2018b; Saeed et al., 2019; Shao et al., 2013; Song et al., 2014; Tabler et al., 2020; Uerlings et al., 2018; Yang et al., 2015).

Failure of the intestinal barrier in birds can be caused by oxidative stress, glucocorticoids, poorly digestible protein in the diet, or coccidiosis (Barekatain et al., 2020; Latorre et al., 2014; Tellez et al., 2014; Williams, 2005), and leads to increased intestinal permeability (Bischoff et al., 2014). Intestinal permeability can be altered by several factors including diet, intestinal microflora, stress, diseases, infections, toxins, antibiotics, and short- or long-term fasting, epithelial damage, disruption of tight junctions, and alteration of the mucosa layer (Barekatain et al., 2020; Bischoff et al., 2014; Gilani et al., 2017, 2018a, 2018b; Kansagra et al., 2003; Kuttappan et al., 2015; Schumann et al., 2005). Increased intestinal permeability in chickens is often associated with compromised health and performance, bacterial translocation, coccidiosis, immune activation, and lameness (Chapman, 2014; Chen et al., 2015; Gilani et al., 2016; Wideman et al., 2012). Modern broiler chickens are characterized by higher intestinal permeability in comparison to their ancestors, the red junglefowl (Baxter et al., 2019).

References

Aisa, J., Lahoz, M., Serrano, P.J., Junquera, C., Peg, M.T., Vera-Gil, A., 1997. Intrinsic innervation of the chicken lower digestive tract. Neurochem. Res. 22 (12), 1425–1435.

Akester, A.R., Anderson, R.S., Hill, K.J., Osbaldiston, G.W., 1967. A radiographic study of urine flow in the domestic fowl. Br. Poultry Sci. 8 (3), 209–212.

Ali, H.A., McLelland, J., 1978. Avian enteric nerve plexuses - a histochemical study. Cell Tissue Res. 189 (3), 537–548.

Anderson, J.M., Van Itallie, C.M., 1995. Tight junctions and the molecular basis for regulation of paracellular permeability. Am. J. Physiol. 269 (4 Pt 1), G467–G475.

Antony, M., 1920. Uber die Speicheldrusen der Vogel. Zool. Jahrb. - Abt. Anat. Ontog. Tiere 41, 547–660.

Argenzio, R.A., 2004. General functions of the gastrointestinal tract and their control. In: Reece, W.O. (Ed.), Duke's Physiology of Domestic Animals, twelfth ed. Cornell University Press, Ithaca and London, pp. 381–390.

Arnason, S.S., Skadhauge, E., 1991. Steady-state sodium absorption and chloride secretion of colon and coprodeum, and plasma levels of osmoregulatory hormones in hens in relation to sodium intake. J. Comp. Physiol. B 161 (1), 1–14.

Ashcraft, D.W., 1930. The correlative activities of the alimentary canal of the fowl. Am. J. Physiol. 93 (1), 105–110.

Ashwell, C.M., Angel, R., 2010. Nutritional genomics: a practical approach by early life conditioning with dietary phosphorus. Rev. Bras. Zootec. 39, 268–278.

Awad, W.A., Hess, C., Hess, M., 2017. Enteric pathogens and their toxin-induced disruption of the intestinal barrier through alteration of tight junctions in chickens. Toxins 9 (2).

Ballou, A.L., Ali, R.A., Mendoza, M.A., Ellis, J.C., Hassan, H.M., Croom, W.J., Koci, M.D., 2016. Development of the chick microbiome: how early exposure influences future microbial diversity. Front. Vet. Sci. 3, 2.

Barekatain, R., Nattrass, G., Tilbrook, A.J., Chousalkar, K., Gilani, S., 2019. Reduced protein diet and amino acid concentration alter intestinal barrier function and performance of broiler chickens with or without synthetic glucocorticoid. Poultry Sci. 98 (9), 3662–3675.

Barekatain, R., Howarth, G.S., Willson, N.L., Cadogan, D., Wilkinson, S., 2020. Excreta biomarkers in response to different gut barrier dysfunction models and probiotic supplementation in broiler chickens. PloS One 15 (8), e0237505.

Barfull, A., Garriga, C., Tauler, A., Planas, J.M., 2002. Regulation of SGLT1 expression in response to Na^+ intake. Am. J. Physiol. Regul. Integr. Comp. Physiol. 282 (3), R738–R743.

Bartlet, A.L., 1974. Actions of putative transmitters in the chicken vagus nerve/oesophagus and remak nerve/rectum preparations. Br. J. Pharmacol. 51 (4), 549–558.

Baxter, M.F.A., Dridi, S., Koltes, D.A., Latorre, J.D., Bottje, W.G., Greene, E.S., Bickler, S.W., Kim, J.H., Merino-Guzman, R., Hernandez-Velasco, X., Anthony, N.B., Hargis, B.M., Tellez-Isaias, G., 2019. Evaluation of intestinal permeability and liver bacterial translocation in two modern broilers and their jungle fowl ancestor. Front. Genet. 10, 480.

Bennett, T., 1974. Peripheral and autonomic nervous systems. In: Farner, D.S., King, J.R. (Eds.), Avian Biology. Academic Press, New York, pp. 1–77.

Berlow, M., Phillips, J.N., Derryberry, E.P., 2020. Effects of urbanization and landscape on gut microbiomes in white-crowned sparrows. Microb. Ecol. https://doi.org/10.1007/s00248-020-01569-8.

Bhattacharya, S., Ghose, K.C., 1971. Influence of food on the amylase system in birds. Comp. Biochem. Physiol. B Comp. Biochem. 40 (2), 317–320.

Bird, F.H., 1971. Distribution of trypsin and α-amylase activities in the duodenum of the domestic fowl. Br. Poultry Sci. 12 (3), 373–378.

Bischoff, S.C., Barbara, G., Buurman, W., Ockhuizen, T., Schulzke, J.D., Serino, M., Tilg, H., Watson, A., Wells, J.M., 2014. Intestinal permeability–a new target for disease prevention and therapy. BMC Gastroenterol. 14, 189.

Bjornhag, D., Sperber, I., 1977. Transport of various food components through the digestive tract of Turkeys, Geese and Guinea fowl. Swedish J. Agric. Sci. 7, 57–66.

Bohak, Z., 1969. Purification and characterization of chicken pepsinogen and chicken pepsin. J. Biol. Chem. 244 (17), 4638–4648.

Bolton, W., 1965. Digestion in the crop of the fowl. Br. Poultry Sci. 6 (2), 97–102.

Borda-Molina, D., Seifert, J., Camarinha-Silva, A., 2018. Current perspectives of the chicken gastrointestinal tract and its microbiome. Comput. Struct. Biotechnol. J. 16, 131–139.

Borel, P., 2003. Factors affecting intestinal absorption of highly lipophilic food microconstituents (fat-soluble vitamins, carotenoids and phytosterols). Clin. Chem. Lab. Med. 41 (8), 979–994.

Borgo, G.D., Salman, A., Pubols, M., McGinnis, J., 1968. Exocrine function of the chick pancreas as affected by dietary soybean meal and carbohydrate. Proc. Soc. Exp.Biol. Med. 129 (3), 877–881.

Borrelli, L., Minichino, A., Pace, A., Dipineto, L., Fioretti, A., 2020. Fecal sample collection method for wild birds-associated microbiome research: perspectives for wildlife studies. Animals 10 (8). https://doi.org/10.3390/ani10081349.

Bowman, W.C., Everett, S.D., 1964. An isolated parasympathetically-innervated oesophagus preparation from the chick. J. Pharm. Pharmacol. 16 (S1), 72T–79T.

Branch, W.J., Cummings, J.H., 1978. Comparison of radio-opaque pellets and chromium sesquioxide as inert markers in studies requiring accurate faecal collections. Gut 19 (5), 371–376.

Brandtzaeg, P., 2010. Homeostatic impact of indigenous microbiota and secretory immunity. Benef. Microbes 1 (3), 211–227.

Brandtzaeg, P., 2011. The gut as communicator between environment and host: immunological consequences. Eur. J. Pharmacol. 668 (Suppl. 1), S16–S32.

Braun, E.J., Campbell, C.E., 1989. Uric acid decomposition in the lower gastrointestinal tract. J. Exp. Zool. 252 (S3), 70–74.

Burhol, P.G., 1974. Gastric stimulation by intravenous injection of cholecystokinin and secretin in fistula chickens. Scand. J. Gastroenterol. 9 (1), 49–53.

Burhol, P.G., 1982. Regulation of gastric secretion in the chicken. Scand. J. Gastroenterol. 17, 321–323.

Cai, Q., Chandler, J.S., Wasserman, R.H., Kumar, R., Penniston, J.T., 1993. Vitamin D and adaptation to dietary calcium and phosphate deficiencies increase intestinal plasma membrane calcium pump gene expression. Proc. Natl. Acad. Sci. U. S. A. 90 (4), 1345–1349.

Calhoun, M., 1954. Microscopic Anatomy of the Digestive System. Iowa State College Press, Ames, Iowa.

Calonge, M.L., Ilundain, A., Bolufer, J., 1990. Glycylsarcosine transport by epithelial cells isolated from chicken proximal cecum and rectum. Am. J. Physiol. Gastrointest. Liver Physiol. 258 (5), G660–G664.

Campbell, B., Garner, A., Dimaline, R., Dockray, G.J., 1991. Hormonal control of avian pancreas by gastrin-releasing peptide from the proventriculus. Am. J. Physiol. Gastrointest. Liver Physiol. 261 (1 24–1), G16–G21.

Cason, J.A., Cox, N.A., Bailey, J.S., 1994. Transmission of *Salmonella typhimurium* during hatching of broiler chicks. Avian Dis. 38 (3), 583–588.

Chambers, J.R., Gong, J., 2011. The intestinal microbiota and its modulation for Salmonella control in chickens. Food Res. Int. 44, 3149–3159.

Chaplin, S.B., 1989. Effect of cecectomy on water and nutrient absorption of birds. J. Exp. Zool. 252 (S3), 81–86.

Chaplin, S.B., Duke, G.E., 1988. Effect of denervation on initiation and coordination of gastroduodenal motility in turkeys. Am. J. Physiol. 255 (1 Pt 1), G1–G6.

Chaplin, S.B., Duke, G.E., 1990. Effect of denervation of the myenteric plexus on gastroduodenal motility in turkeys. Am. J. Physiol. 259 (3 Pt 1), G481–G489.

Chapman, H.D., 2014. Milestones in avian coccidiosis research: a review. Poultry Sci. 93 (3), 501–511.

Cheled-Shoval, S.L., Gamage, N.S., Amit-Romach, E., Forder, R., Marshal, J., Van Kessel, A., Uni, Z., 2014. Differences in intestinal mucin dynamics between germ-free and conventionally reared chickens after mannan-oligosaccharide supplementation. Poultry Sci. 93 (3), 636–644.

Cheled-Shoval, S.L., Druyan, S., Uni, Z., 2015. Bitter, sweet and umami taste receptors and downstream signaling effectors: expression in embryonic and growing chicken gastrointestinal tract. Poultry Sci. 94 (8), 1928–1941.

Chen, J., Tellez, G., Richards, J.D., Escobar, J., 2015. Identification of potential biomarkers for gut barrier failure in broiler chickens. Front. Vet. Sci. 2, 14.

Chen, Y., Zhang, H., Cheng, Y., Li, Y., Wen, C., Zhou, Y., 2018. Dietary l-threonine supplementation attenuates lipopolysaccharide-induced inflammatory responses and intestinal barrier damage of broiler chickens at an early age. Br. J. Nutr. 119 (11), 1254–1262.

Cho, H., Lee, W.Y., 2020. Interspecific comparison of the fecal microbiota structure in three Arctic migratory bird species. Ecol. Evol. 10 (12), 5582–5594.

Clauss, W., Dantzer, V., Skadhauge, E., 1991. Aldosterone modulates electrogenic Cl secretion in the colon of the hen (*Gallus domesticus*). Am. J. Physiol. Regul. Integr. Comp. Physiol. 261 (6 30–6), R1533–R1541.

Clavijo, V., Florez, M.J.V., 2018. The gastrointestinal microbiome and its association with the control of pathogens in broiler chicken production: a review. Poultry Sci. 97 (3), 1006–1021.

Clench, M.H., Mathias, J.R., 1995. The avian cecum: a review. Wilson Bull. 107 (1), 93-21.

Clench, M.H., Pineiro-Carrero, V.M., Mathias, J.R., 1989. Migrating myoelectric complex demonstrated in four avian species. Am. J. Physiol. 256 (3 Pt 1), G598–G603.

Crhanova, M., Hradecka, H., Faldynova, M., Matulova, M., Havlickova, H., Sisak, F., Rychlik, I., 2011. Immune response of chicken gut to natural colonization by gut microflora and to *Salmonella enterica* serovar enteritidis infection. Infect. Immun. 79 (7), 2755–2763.

Danzeisen, J.L., Kim, H.B., Isaacson, R.E., Tu, Z.J., Johnson, T.J., 2011. Modulations of the chicken cecal microbiome and metagenome in response to anticoccidial and growth promoter treatment. PloS One 6 (11), e27949.

Den Hartog, G., De Vries-Reilingh, G., Wehrmaker, A.M., Savelkoul, H.F., Parmentier, H.K., Lammers, A., 2016. Intestinal immune maturation is accompanied by temporal changes in the composition of the microbiota. Benef. Microbes 7 (5), 677–685.

Denac, M., Scharrer, E., 1987. Effect of neurotensin on the smooth muscle of the chicken crop. Comp. Biochem. Physiol. C Comp. Pharmacol. 87 (2), 325–327.

Denac, M., Scharrer, E., 1988. Effect of bombesin and substance P on the smooth muscle of the chicken crop. Vet. Res. Commun. 12 (6), 447–452.

Denac, M., Kumin, G., Scharrer, E., 1990. Effect of electrical field stimulation on muscle strips from chicken crop. Exp. Physiol. 75 (1), 69–73.

Denbow, D.M., 2015. Gastrointestinal anathomy and physiology. In: Scanes, C.G. (Ed.), Sturkie's Avian Physiology, sixth ed. Academic Press, New York, pp. 337–366.

Deplancke, B., Gaskins, H.R., 2001. Microbial modulation of innate defense: goblet cells and the intestinal mucus layer. Am. J. Clin. Nutr. 73 (6), 1131S–1141S.

Desmeth, M., 1980. Lipid composition of pigeon cropmilk—II. Fatty acids. Comp. Biochem. Physiol. B Comp. Biochem. 66 (1), 135–138.

Diaz-Gomez, J., Moreno, J.A., Angulo, E., Sandmann, G., Zhu, C., Capell, T., Nogareda, C., 2017. Provitamin A carotenoids from an engineered high-carotenoid maize are bioavailable and zeaxanthin does not compromise beta-carotene absorption in poultry. Transgenic Res. 26 (5), 591–601.

Dibner, J.J., Richards, J.D., 2005. Antibiotic growth promoters in agriculture: history and mode of action. Poultry Sci. 84 (4), 634–643.

Dimaline, R., Lee, C.M., 1990. Chicken gastrin: a member of the gastrin/CCK family with novel structure-activity relationships. Am. J. Physiol. Gastrointest. Liver Physiol. 259 (5), G882–G888.

Dimaline, R., Young, J., Gregory, H., 1986. Isolation from chicken antrum, and primary amino acid sequence of a novel 36-residue peptide of the gastrin/CCK family. FEBS Lett. 205 (2), 318–321.

Dimke, H., Hoenderop, J.G., Bindels, R.J., 2011. Molecular basis of epithelial Ca^{2+} and Mg^{2+} transport: insights from the TRP channel family. J. Physiol. 589 (Pt 7), 1535–1542.

Dockray, G.J., 1975. Comparison of the actions of porcine secretin and extracts of chicken duodenum on pancreatic exocrine secretion in the cat and Turkey. J. Physiol. 244 (3), 625–637.

Dockray, G.J., 1977. Molecular evolution of gut hormones: application of comparative studies on the regulation of digestion. Gastroenterology 72 (2), 344–358.

Dockray, G.J., 1988. Evolutionary aspects of gastrointestinal hormones. In: Mutt, V. (Ed.), Adv. Metab. Disord. Elsevier, pp. 85–111.

Duke, G.E., 1982. Gastrointestinal motility and its regulation. Poultry Sci. 61 (7), 1245–1256.

Duke, G.E., 1986. Alimentary canal: anatomy, regulation of feeding, and motility. In: Sturkie, P.D. (Ed.), Avian Physiology. Springer New York, New York, NY, pp. 269–288.

Duke, G.E., 1994. Physiology of digestion and metabolism. In: Western Poultry Disease Conference, pp. 29–31.

Duke, G.E., Evanson, O.A., 1972. Inhibition of gastric motility by duodenal contents in Turkeys1. Poultry Sci. 51 (5), 1625–1636.

Duke, G.E., Dziuk, H.E., Evanson, O.A., 1972. Gastric pressure and smooth muscle electrical potential changes in turkeys. Am. J. Physiol. 222 (1), 167–173.

Duke, G.E., Kostuch, T.E., Evanson, O.A., 1975. Gastroduodenal electrical activity in turkeys. Am. J. Dig. Dis. 20 (11), 1047–1058.

Duke, G.E., Evanson, O.A., 1976. Diurnal cycles of gastric motility in normal and fasted Turkeys1. Poultry Sci. 55 (5), 1802–1807.

Duke, G.E., Evanson, O.A., Ciganek, J.G., Miskowiec, J.F., Kostuch, T.E., 1973. Inhibition of gastric motility in turkeys by intraduodenal injections of amino acid solutions1. Poultry Sci. 52 (5), 1749–1756.

Duke, G., Evanson, O., Redig, P., Rhoades, D., 1976a. Mechanism of pellet egestion in great-horned owls (*Bubo virginianus*). Am. J. Physiol. 231 (6), 1824–1829.

Duke, G.E., Evanson, O.A., Redig, P.T., 1976b. A cephalic influence on gastric motility upon seeing food in domestic turkeys (melagris gallopavo), great-horned owls (*Bubo virginianus*) and red-tailed hawks (*Buteo jamaicensis*)1. Poultry Sci. 55 (6), 2155–2165.

Duke, G.E., Dziuk, H.E., Evanson, O.A., Miller, J.E., 1977. Studies of methods for in situ observation of gastric motility in domestic turkeys. Poultry Sci. 56 (5), 1575–1578.

Duke, G.E., Evanson, O.A., Huberty, B.J., 1980. Electrical potential changes and contractile activity of the distal cecum of Turkeys1. Poultry Sci. 59 (8), 1925–1934.

Duke, G.E., Kimmel, J.R., Durham, K., Pollock, H.G., Bertoy, R., Rains-Epstein, D., 1982. Release of avian pancreatic polypeptide by various intraluminal contents in the stomach, duodenum, or ileum of turkeys. Dig. Dis. Sci. 27 (9), 782–788.

Duke, G.E., Place, A.R., Jones, B., 1989. Gastric emptying and gastrointestinal motility in leach's storm-petrel chicks (oceanodroma leucorhoa). Auk 106 (1), 80–85.

Dziuk, H., Duke, G., 1972. Cineradiographic studies of gastric motility in turkeys. Am. J. Physiol. 222 (1), 159–166.

Elbrønd, V.S., Laverty, G., Dantzer, V., Grøndahl, C., Skadhauge, E., 2009. Ultrastructure and electrolyte transport of the epithelium of coprodeum, colon and the proctodeal diverticulum of *Rhea americana*. Comp. Biochem Physiol. A Mol. Integr. Physiol. 152 (3), 357–365.

Elkin, R.G., Wood, K.V., Hagey, L.R., 1990. Biliary bile acid profiles of domestic fowl as determined by high performance liquid chromatography and fast atom bombardment mass spectrometry. Comp. Biochem. Physiol. B Comp. Biochem. 96 (1), 157–161.

Fanning, A.S., Jameson, B.J., Jesaitis, L.A., Anderson, J.M., 1998. The tight junction protein ZO-1 establishes a link between the transmembrane protein occludin and the actin cytoskeleton. J. Biol. Chem. 273 (45), 29745–29753.

Farner, D.S., 1943. Billary amylase in the domestic fowl. Biol. Bull. 84 (3), 240–243.

Ferrando, C., Vergara, P., Jiménez, M., Goñalons, E., 1987. Study of the rate of passage of food with chromium-mordanted plant cells in chickens (*Gallus gallus*). J. Exp. Physiol. 72 (3), 251–259.

Ferrer, R., Planas, J.M., Durfort, M., Moretó, M., 1991. Morphological study of the caecal epithelium of the chicken (Gallus *Gallus domesticus* L.). Br. Poultry Sci. 32 (4), 679–691.

Fileccia, R., Postorino, A., Serio, R., Mule, F., Urso, S.A., 1984. Primary peristalsis in pigeon cervical oesophagus: two EMG patterns. Arch. Int. Physiol. Biochim. 92 (3), 185–194.

Fileccia, R., Mule, F., Postorino, A., Serio, R., Abbadessa-Urso, S., 1987. 5-Hydroxytryptamine involvement in the intrinsic control of oesophageal EMG activity. Arch. Int. Physiol. Biochim. 95 (4), 281–288.

Forder, R.E., Howarth, G.S., Tivey, D.R., Hughes, R.J., 2007. Bacterial modulation of small intestinal goblet cells and mucin composition during early posthatch development of poultry. Poultry Sci. 86 (11), 2396–2403.

Forder, R.E., Nattrass, G.S., Geier, M.S., Hughes, R.J., Hynd, P.I., 2012. Quantitative analyses of genes associated with mucin synthesis of broiler chickens with induced necrotic enteritis. Poultry Sci. 91 (6), 1335–1341.

Fritz, J., Hammer, S., Hebel, C., Arif, A., Michalke, B., Dittmann, M.T., Muller, D.W., Clauss, M., 2012. Retention of solutes and different-sized particles in the digestive tract of the ostrich (*Struthio camelus* massaicus), and a comparison with mammals and reptiles. Comp. Biochem. Physiol. A, Mol. Integr. Physiol. 163 (1), 56–65.

Furuse, M., Okumura, J., 1994. Nutritional and physiological characteristics in germ-free chickens. Comp. Biochem. Physiol. A, Comp. Physiol. 109 (3), 547–556.

Gabriel, I., Lessire, M., Mallet, S., Guillot, J.F., 2006. Microflora of the digestive tract: critical factors and consequences for poultry. World's Poult. Sci. J. 62 (3), 499–511.

Gadde, U., Kim, W.H., Oh, S.T., Lillehoj, H.S., 2017. Alternatives to antibiotics for maximizing growth performance and feed efficiency in poultry: a review. Anim. Health Res. Rev. 18 (1), 26–45.

Ganchrow, D., Ganchrow, J.R., 1985. Number and distribution of taste buds in the oral cavity of hatchling chicks. Physiol. Behav. 34 (6), 889–894.

Ganchrow, J.R., Steiner, J.E., Bartana, A., 1990. Behavioral reactions to gustatory stimuli in young chicks (*Gallus gallus domesticus*). Dev. Psychobiol. 23 (2), 103–117.

Gantois, I., Ducatelle, R., Pasmans, F., Haesebrouck, F., Gast, R., Humphrey, T.J., Van Immerseel, F., 2009. Mechanisms of egg contamination by Salmonella Enteritidis. FEMS Microbiol. Rev. 33 (4), 718–738.

Garriga, C., Barfull, A., Planas, J.M., 2004. Kinetic characterization of apical D-fructose transport in chicken jejunum. J. Membr. Biol. 197 (1), 71–76.

Gasaway, W.C., 1976. Seasonal variation in diet, volatile fatty acid production and size of the cecum of rock ptarmigan. Comp. Biochem. Physiol. A, Physiol. 53 (1), 109–114.

Gaskins, H.R., Collier, C.T., Anderson, D.B., 2002. Antibiotics as growth promotants: mode of action. Anim. Biotechnol. 13 (1), 29–42.

Geyra, A., Uni, Z., Sklan, D., 2001. Enterocyte dynamics and mucosal development in the posthatch chick. Poultry Sci. 80 (6), 776–782.

Gibson, R.G., Colvin, H.W., Hirschowitz, B.I., 1974. Kinetics of gastric response in chickens to graded electrical vagal stimulation. Proc. Soc. Exp. Biol. Med. 145 (3), 1058–1060.

Gil-Cardoso, K., Gines, I., Pinent, M., Ardevol, A., Blay, M., Terra, X., 2016. Effects of flavonoids on intestinal inflammation, barrier integrity and changes in gut microbiota during diet-induced obesity. Nutr. Res. Rev. 29 (2), 234–248.

Gilani, S., Howarth, G., Kitessa, S., Forder, R., Tran, C., Hughes, B., 2016. New biomarkers for intestinal permeability induced by lipopolysaccharide in chickens. Anim. Prod. Sci. 56, 1984–1997.

Gilani, S., Howarth, G.S., Kitessa, S.M., Tran, C.D., Forder, R.E.A., Hughes, R.J., 2017. New biomarkers for increased intestinal permeability induced by dextran sodium sulphate and fasting in chickens. J. Anim. Physiol. Anim. Nutr. 101 (5), e237–e245.

Gilani, S., Howarth, G.S., Nattrass, G., Kitessa, S.M., Barekatain, R., Forder, R.E.A., Tran, C.D., Hughes, R.J., 2018a. Gene expression and morphological changes in the intestinal mucosa associated with increased permeability induced by short-term fasting in chickens. J. Anim. Physiol. Anim. Nutr. 102 (2), e653–e661.

Gilani, S., Howarth, G.S., Tran, C.D., Barekatain, R., Kitessa, S.M., Forder, R.E.A., Hughes, R.J., 2018b. Reduced fasting periods increase intestinal permeability in chickens. J. Anim. Physiol. Anim. Nutr. 102 (1), e486–e492.

Gilbert, E.R., Wong, E.A., Webb Jr., K.E., 2008. Peptide absorption and utilization: implications for animal nutrition and health. J. Anim. Sci. 86 (9), 2135–2155.

Gill, R.K., Saksena, S., Alrefai, W.A., Sarwar, Z., Goldstein, J.L., Carroll, R.E., Ramaswamy, K., Dudeja, P.K., 2005. Expression and membrane localization of MCT isoforms along the length of the human intestine. Am. J. Physiol. Cell Physiol. 289 (4), C846–C852.

Gloux, A., Le Roy, N., Brionne, A., Bonin, E., Juanchich, A., Benzoni, G., Piketty, M.L., Prie, D., Nys, Y., Gautron, J., Narcy, A., Duclos, M.J., 2019. Candidate genes of the transcellular and paracellular calcium absorption pathways in the small intestine of laying hens. Poultry Sci. 98 (11), 6005–6018.

Godoy-Vitorino, F., Ley, R.E., Gao, Z., Pei, Z., Ortiz-Zuazaga, H., Pericchi, L.R., Garcia-Amado, M.A., Michelangeli, F., Blaser, M.J., Gordon, J.I., Domínguez-Bello, M.G., 2008. Bacterial community in the crop of the hoatzin, a neotropical folivorous flying bird. Appl. Environ. Microbiol. 74 (19), 5905–5912.

Godoy-Vitorino, F., Goldfarb, K.C., Karaoz, U., Leal, S., Garcia-Amado, M.A., Hugenholtz, P., Tringe, S.G., Brodie, E.L., Dominguez-Bello, M.G., 2012. Comparative analyses of foregut and hindgut bacterial communities in hoatzins and cows. ISME J. 6 (3), 531–541.

Goldstein, D.L., 1989. Absorption by the cecum of wild birds: is there interspecific variation. J. Exp. Zool. Suppl. 3, 103–110.

Goldstein, D.L., Braun, E.J., 1986. Lower intestinal modification of ureteral urine in hydrated house sparrows. Am. J. Physiol. 250 (1 Pt 2), R89–R95.

Gonalons, E., Rial, R., Tur, J.A., 1982. Phenol red as indicator of the digestive tract motility in chickens. Poultry Sci. 61 (3), 581–583.

Goo, D., Kim, J.H., Choi, H.S., Park, G.H., Han, G.P., Kil, D.Y., 2019. Effect of stocking density and sex on growth performance, meat quality, and intestinal barrier function in broiler chickens. Poultry Sci. 98 (3), 1153–1160.

Grond, k., Sandercock, B.K., Jumpponen, A., Zeglin, L.H., 2018. The avian gut microbiota: community, physiology and function in wild birds. J. Avian Biol. 2018, e01788.

Haberecht, S., Bajagai, Y.S., Moore, R.J., Van, T.T.H., Stanley, D., 2020. Poultry feeds carry diverse microbial communities that influence chicken intestinal microbiota colonisation and maturation. Amb. Express 10 (1), 143.

Halestrap, A.P., 2012. The monocarboxylate transporter family–structure and functional characterization. IUBMB Life 64 (1), 1−9.

Halestrap, A.P., Meredith, D., 2004. The SLC16 gene family-from monocarboxylate transporters (MCTs) to aromatic amino acid transporters and beyond. Pflügers Archiv. 447 (5), 619−628.

Halestrap, A.P., Wilson, M.C., 2012. The monocarboxylate transporter family–role and regulation. IUBMB Life 64 (2), 109−119.

Hansen, M.B., Bindslev, N., 1989. Serotonin-induced chloride secretion in hen colon. possible second messengers. Comp Biochem. Physiol. A, Physiol. 94 (2), 315−321.

Harrison, J.G., 1964. Tongue. In: Thompson, A.L. (Ed.), A New Dictionary of Birds. Nelson, London, pp. 825−827.

Hazelwood, R.L., Turner, S.D., Kimmel, J.R., Pollock, H.G., 1973. Spectrum effects of a new polypeptide (third hormone?) isolated from the chicken pancreas. Gen. Comp. Endocrinol. 21 (3), 485−497.

Heard, G.S., Annison, E.F., 1986. Gastrointestinal absorption of vitamin B-6 in the chicken (*Gallus domesticus*). J. Nutr. 116 (1), 107−120.

Herpol, C., 1966. Influence de l'ago sur le pH dans le tube digestif de *Gallus domesticus*. Ann. Biol. Anim. Biochim. Biophys. 4, 239−244.

Hetland, H., Svihus, B., Krogdahl, Å., 2003. Effects of oat hulls and wood shavings on digestion in broilers and layers fed diets based on whole or ground wheat. Br. Poultry Sci. 44 (2), 275−282.

Hill, K., 1971. The physiology of digestion. In: Freeman, B.M. (Ed.), Physiology and Biochemistry of the Dy of the Domestic Fowl. Academic Press, London, p. 44.

Hill, K.J., 1983. Physiology of the digestive tract. In: Freeman, B.M. (Ed.), Physiology and Biochemistry of the dy of the Domestic Fowl. Academic Press, London, pp. 37−47.

Hird, S.M., 2017. Evolutionary biology needs wild microbiomes. Front. Microbiol. 8 (725).

Hodgkiss, J.P., 1984a. Evidence that enteric cholinergic neurones project orally in the intestinal nerve of the chicken. Quart. J. Exp. Physiol. 69 (4), 797−807.

Hodgkiss, J.P., 1984b. Peristalsis and antiperistalsis in the chicken ceacum are myogenic quart. J. Exp. Physiol. 69 (1), 161−170.

Hodgkiss, J.P., 1986. The unmyelinated fibre spectrum of the main trunk and side branches of the intestinal nerve in the chicken (*Gallus gallus* var. *domesticus*). J. Anat. 148, 99−110.

Hoenderop, J.G., Nilius, B., Bindels, R.J., 2005. Calcium absorption across epithelia. Physiol. Rev. 85 (1), 373−422.

Hokin, M.R., Hokin, L.E., 1953. Enzyme secretion and the incorporation of P32 into phospholipides of pancreas slices. J. Biol. Chem. 203 (2), 967−977.

Huang, L., Luo, L., Zhang, Y., Wang, Z., Xia, Z., 2019. Effects of the dietary probiotic, *Enterococcus faecium* NCIMB11181, on the intestinal barrier and system immune status in *Escherichia coli* O78-challenged broiler chickens. Prob. Antimicrob. Prot. 11 (3), 946−956.

Hulan, H.W., Bird, F.H., 1972. Effect of fat level in isonitrogenous diets on the composition of avian pancreatic juice. J. Nutr. 102 (4), 459−468.

Hurwitz, S., Bar, A., Katz, M., Sklan, D., Budowski, P., 1973. Absorption and secretion of fatty acids and bile acids in the intestine of the laying fowl. J. Nutr. 103 (4), 543−547.

Jamroz, D., Jakobsen, K., Bach Knudsen, K.E., Wiliczkiewicz, A., Orda, J., 2002. Digestibility and energy value of non-starch polysaccharides in young chickens, ducks and geese, fed diets containing high amounts of barley. Comp. Biochem. Physiol. A, Mol. Integr. Physiol. 131 (3), 657−668.

Jerrett, S.A., Goodge, W.R., 1973. Evidence for amylase in avian salivary glands. J. Morphol. 139 (1), 27−45.

Jeurissen, S.H., Lewis, F., van der Klis, J.D., Mroz, Z., Rebel, J.M., ter Huurne, A.A., 2002. Parameters and techniques to determine intestinal health of poultry as constituted by immunity, integrity, and functionality. Curr. Issues Intest. Microbiol. 3 (1), 1−14.

Jiménez, M., Martínez, V., Goñalons, E., Vergara, P., 1992. Opioid-induction of migrating motor activity in chickens. Life Sci. 50 (7), 465−472.

Jing, M., Tactacan, G.B., Rodriguez-Lecompte, J.C., Kroeker, A., House, J.D., 2009. Molecular cloning and tissue distribution of reduced folate carrier and effect of dietary folate supplementation on the expression of reduced folate carrier in laying hens. Poultry Sci. 88 (9), 1939−1947.

Jing, M., Tactacan, G.B., Rodriguez-Lecompte, J.C., Kroeker, A., House, J.D., 2010. Proton-coupled folate transporter (PCFT): molecular cloning, tissue expression patterns and the effects of dietary folate supplementation on mRNA expression in laying hens. Br. Poultry Sci. 51 (5), 635−638.

Johansen, F.E., Pekna, M., Norderhaug, I.N., Haneberg, B., Hietala, M.A., Krajci, P., Betsholtz, C., Brandtzaeg, P., 1999. Absence of epithelial immunoglobulin A transport, with increased mucosal leakiness, in polymeric immunoglobulin receptor/secretory component-deficient mice. J. Exp. Med. 190 (7), 915−922.

Joyner, W.L., Kokas, E., 1971. Action of serotonin on gastric (proventriculus) secretion in chickens. Comp. Gen. Pharmacol. 2 (6), 145−150.

Jozefiak, D., Rutkowski, A., Martin, S.A., 2004. Carbohydrate fermentation in the avian ceca: a review. Anim. Feed Sci. Technol. 113, 1−15.

Juanchich, A., Hennequet-Antier, C., Cabau, C., Le Bihan-Duval, E., Duclos, M.J., Mignon-Grasteau, S., Narcy, A., 2018. Functional genomics of the digestive tract in broilers. BMC Genom. 19 (1), 928.

Kaetzel, C.S., 2005. The polymeric immunoglobulin receptor: bridging innate and adaptive immune responses at mucosal surfaces. Immunol. Rev. 206, 83−99.

Kansagra, K., Stoll, B., Rognerud, C., Niinikoski, H., Ou, C.N., Harvey, R., Burrin, D., 2003. Total parenteral nutrition adversely affects gut barrier function in neonatal piglets. Am. J. Physiol. Gastrointest. Liver Physiol. 285 (6), G1162−G1170.

Kers, J.G., Velkers, F.C., Fischer, E.A.J., Hermes, G.D.A., Stegeman, J.A., Smidt, H., 2018. Host and environmental factors affecting the intestinal microbiota in chickens. Front. Microbiol. 9, 235.

Kessler, C.A., Hirschowitz, B.I., Burhol, P.G., Sachs, G., 1972. Methoxyflurane (penthrane) anesthesia effect on histamine stimulated gastric secretion in the chicken. Proc. Soc. Exp. Biol. Med. 139 (4), 1340−1343.

Kim, Y.S., Ho, S.B., 2010. Intestinal goblet cells and mucins in health and disease: recent insights and progress. Curr. Gastroenterol. Rep. 12 (5), 319−330.

Kimmel, J.R., Pollock, H.G., 1975. Factors affecting blood levels of avian pancreatic polypeptide (APP), a new pancreatic hormone. Fed. Proc. Fed. Am. Soc. Exp. Biol. 34 (454).

Kimmel, J.R., Pollock, H.G., Hazelwood, R.L., 1968. Isolation and characterization of chicken insulin. Endocrinology 83 (6), 1323–1330.

Kimmich, G.A., Randles, J., 1984. Sodium-sugar coupling stoichiometry in chick intestinal cells. Am. J. Physiol. Cell Physiol. 247 (1), C74–C82.

Koenig, H.E., Korbel, R., Liebich, H.-G., 2016. Avian digestion, 2008. In: Koenig, H.E., Korbel, R., Liebich, H.-G. (Eds.), Anatomie der Voegel (Avian Anathomy), second ed. 5m Publishing, Sheffield, UK, pp. 92–117. Schattaer, Stuttgard, Germany.

Kokue, E., Hayama, T., 1972. Effects of starvation and feeding on the exocrine pancreas of the Chicken1. Poultry Sci. 51 (4), 1366–1370.

Kostuch, T.E., Duke, G.E., 1975. Gastric motility in great horned owls (*Bubo virginianus*). Comp. Biochem. Physiol. A, Physiol. 51 (1), 201–205.

Krogdahl, Å., Sell, J.L., 1989. Influence of age on lipase, amylase, and protease activities in pancreatic tissue and intestinal contents of young Turkeys1. Poultry Sci. 68 (11), 1561–1568.

Kudo, K., Nishimura, S., Tabata, S., 2008. Distribution of taste buds in layer-type chickens: scanning electron microscopic observations. Anim. Sci. J. 79 (6), 680–685.

Kudo, K., Shiraishi, J., Nishimura, S., Bungo, T., Tabata, S., 2010. The number of taste buds is related to bitter taste sensitivity in layer and broiler chickens. Anim. Sci. J. 81 (2), 240–244.

Kumar, S., Chen, C., Indugu, N., Werlang, G.O., Singh, M., Kim, W.K., Thippareddi, H., 2018. Effect of antibiotic withdrawal in feed on chicken gut microbial dynamics, immunity, growth performance and prevalence of foodborne pathogens. PloS One 13 (2), e0192450.

Kuttappan, V.A., Berghman, L.R., Vicuna, E.A., Latorre, J.D., Menconi, A., Wolchok, J.D., Wolfenden, A.D., Faulkner, O.B., Tellez, G.I., Hargis, B.M., Bielke, L.R., 2015. Poultry enteric inflammation model with dextran sodium sulfate mediated chemical induction and feed restriction in broilers. Poultry Sci. 94 (6), 1220–1226.

Lagerstrom, M.C., Hellstrom, A.R., Gloriam, D.E., Larsson, T.P., Schioth, H.B., Fredriksson, R., 2006. The G protein-coupled receptor subset of the chicken genome. PLoS Comput. Biol. 2 (6), e54.

Lai, H.C., Duke, G.E., 1978. Colonic motility in domestic Turkeys. Am. J. Dig. Dis. 23 (8), 673–681.

Lang, T., Hansson, G.C., Samuelsson, T., 2006. An inventory of mucin genes in the chicken genome shows that the mucin domain of Muc13 is encoded by multiple exons and that ovomucin is part of a locus of related gel-forming mucins. BMC Genom. 7, 197.

Larsson, L.I., Sundler, F., Håkanson, R., Pollock, H.G., Kimmel, J.R., 1974. Localization of APP, a postulated new hormone, to a pancreatic endocrine cell type. Histochemistry 42 (4), 377–382.

Latorre, J.D., Hernandez-Velasco, X., Kogut, M.H., Vicente, J.L., Wolfenden, R., Wolfenden, A., Hargis, B.M., Kuttappan, V.A., Tellez, G., 2014. Role of a *Bacillus* subtilis direct-fed microbial on digesta viscosity, bacterial translocation, and bone mineralization in Turkey poults fed with a rye-based diet. Front. Vet. Sci. 1, 26.

Laverty, G., Skadhauge, E., 1999. Physiological roles and regulation of transport activities in the avian lower intestine. J. Exp. Zool. 283 (4–5), 480–494.

Laverty, G., Bjarnadóttir, S., Elbrønd, V.S., Árnason, S.S., 2001. Aldosterone suppresses expression of an avian colonic sodium-glucose cotransporter. Am. J. Physiol. Regul. Integr. Comp. Physiol. 281 (4), R1041–R1050.

Laverty, G., Elbrønd, V.S., Árnason, S.S., Skadhauge, E., 2006. Endocrine regulation of ion transport in the avian lower intestine. Gen. Comp. Endocrinol. 147 (1), 70–77.

Leasure, E.E., Link, R.P., 1940. Studies on the saliva of the hen. Poultry Sci. 19 (2), 131–134.

Levin, R.J., Mitchell, M.A., Barber, D.C., 1983. Comparison of jejunal and ileal absorptive functions for glucose and valine in vivo—a technique for estimating real Km and Jmax in the domestic fowl. Comp. Biochem. Physiol. A, Physiol. 74 (4), 961–966.

Li, Y., Zhang, H., Chen, Y.P., Yang, M.X., Zhang, L.L., Lu, Z.X., Zhou, Y.M., Wang, T., 2015. Bacillus amyloliquefaciens supplementation alleviates immunological stress and intestinal damage in lipopolysaccharide-challenged broilers. Anim. Feed Sci. Technol. 208, 119–131.

Lilja, C., 1983. A comparative study of postnatal growth and organ development in some species of birds. Growth Dev. Aging 47 (4), 317–339.

Lindsay, O.B., March, B.E., 1967. Intestinal absorption of bile salts in the cockerel. Poultry Sci. 46 (1), 164–168.

Lisbona, F., Jimenez, M., Esteller, A., Lopez, M.A., 1981. Basal biliary secretion in conscious chicken and role of enterohepatic circulation. Comp. Biochem. Physiol. A, Comp. Physiol. 69A, 341–344.

Liu, L., Burcher, E., 2001. Radioligand binding and functional characterisation of tachykinin receptors in chicken small intestine. N. Schmied. Arch. Pharmacol. 364 (4), 305–313.

Liu, H.X., Rajapaksha, P., Wang, Z., Kramer, N.E., Marshall, B.J., 2018. An update on the sense of taste in chickens: a better developed system than previously appreciated. J. Nutr. Food Sci. 8 (2).

Liu, N., Lin, L., Wang, J., Zhang, F., Wang, J.P., 2018a. Dietary cysteamine hydrochloride protects against oxidation, inflammation, and mucosal barrier disruption of broiler chickens challenged with *Clostridium perfringens*. J. Anim. Sci. 96 (10), 4339–4347.

Liu, S., Song, M., Yun, W., Lee, J., Lee, C., Kwak, W., Han, N., Kim, H., Cho, J., 2018b. Effects of oral administration of different dosages of carvacrol essential oils on intestinal barrier function in broilers. J. Anim. Physiol. Anim. Nutr. 102 (5), 1257–1265.

Long, J.F., 1967. Gastric secretion in unanesthetized chickens. Am. J. Physiol. 212 (6), 1303–1307.

Mancabelli, L., Ferrario, C., Milani, C., Mangifesta, M., Turroni, F., Duranti, S., Lugli, G.A., Viappiani, A., Ossiprandi, M.C., van Sinderen, D., Ventura, M., 2016. Insights into the biodiversity of the gut microbiota of broiler chickens. Environ. Microbiol. 18 (12), 4727–4738.

Marks, J., Debnam, E.S., Unwin, R.J., 2010. Phosphate homeostasis and the renal-gastrointestinal axis. Am. J. Physiol. Ren. Physiol. 299 (2), F285–F296.

Martinez, V., Jimenez, M., Gonalons, E., Vergara, P., 1993. Mechanism of action of CCK in avian gastroduodenal motility: evidence for nitric oxide involvement. Am. J. Physiol. Gastrointest. Liver Physiol. 265 (5 28–5), G842–G850.

Martínez, A., López, J., Sesma, P., 2000. The nervous system of the chicken proventriculus: an immunocytochemical and ultrastructural study. Histochem. J. 32 (1), 63–70.

McLelland, J., 1975. Aves digestive system. Anat. Dom. Anim. 1857–1882.

McLelland, J., 1979. Digestive system. In: King, A.S., McLelland, J. (Eds.), Form and Function in Birds. Academic Press, London, pp. 69–181.

McLelland, J., 1989. Anatomy of the avian cecum. J. Exp. Zool. 252 (S3), 2–9.

McWhorter, T.J., Caviedes-Vidal, E., Karasov, W.H., 2009. The integration of digestion and osmoregulation in the avian gut. Biol. Rev. Camb. Phil. Soc. 84 (4), 533–565.

Mitic, L.L., Van Itallie, C.M., Anderson, J.M., 2000. Molecular physiology and pathophysiology of tight junctions I. Tight junction structure and function: lessons from mutant animals and proteins. Am. J. Physiol. Gastrointest. Liver Physiol. 279 (2), G250–G254.

Miyamoto, K., Segawa, H., Morita, K., Nii, T., Tatsumi, S., Taketani, Y., Takeda, E., 1997. Relative contributions of Na+-dependent phosphate co-transporters to phosphate transport in mouse kidney: RNase H-mediated hybrid depletion analysis. Biochem. J. 327 (Pt 3), 735–739.

Moreto, M., Amat, C., Puchal, A., Buddington, R.K., Planas, J.M., 1991. Transport of L-proline and α-methyl-D-glucoside by chicken proximal cecum during development. Am. J. Physiol. Gastrointest. Liver Physiol. 260 (3 23–3), G457–G463.

Mueller, L.R., Duke, G.E., Evanson, O.A., 1990. Investigations of the migrating motor complex in domestic turkeys. Am. J. Physiol. Gastrointest. Liver Physiol. 259 (3), G329–G333.

Mulé, F., 1991. The avian oesophageal motor function and its nervous control: some physiological, pharmacological and comparative aspects. Comp. Biochem. Physiol. A, Physiol. 99 (4), 491–498.

Mule, F., Fileccia, R., Postorino, A., Serio, R., Abbadessa-Urso, S., La Grutta, G., 1987. Pigeon oesophageal EMG activity: analysis of intramural neural control. Arch. Int. Physiol. Biochim. 95 (4), 269–280.

Murer, H., Hernando, N., Forster, I., Biber, J., 2000. Proximal tubular phosphate reabsorption: molecular mechanisms. Physiol. Rev. 80 (4), 1373–1409.

Nakagawa, H., Nishimura, M., Urakawa, N., 1983. 2-Deoxy-D-Glucose stimulates acid secretion from chicken proventriculus. Jpn. J. Vet. Sci. 45 (6), 721–726.

Nie, W., Yang, Y., Yuan, J., Wang, J., Guo, Y., 2013. Effect of dietary nonphytate phosphorus on laying performance and small intestinal epithelial phosphate transporter expression in Dwarf pink-shell laying hens. J. Anim. Sci. Biotechnol. 4, 34.

Nilsson, A., 1974. Isolation, amino acid composition and terminal amino acid residues of the vasoactive octacosapeptide from chicken intestine. Partial purification of chicken secretin. FEBS Lett. 47 (2), 284–289.

Nilsson, S., 2011. Comparative anatomy of the autonomic nervous system. Auton. Neurosci. 165 (1), 3–9.

Nitsan, Z., Ben-Avraham, G., Zoref, Z., Nir, I., 1991. Growth and development of the digestive organs and some enzymes in broiler chicks after hatching. Br. Poultry Sci. 32 (3), 515–523.

Nobrega, I.P.T., Nogueira, H.S., Lima, M.B., Sakomura, N.K., Peruzzi, N.J., Artoni, S.M.B., Suzuki, R.M., Silva, E.P., 2020. Rate of feed passage in Japanese quail. Animal 14 (S2), s267–s274.

Oakley, B.B., Lillehoj, H.S., Kogut, M.H., Kim, W.K., Maurer, J.J., Pedroso, A., Lee, M.D., Collett, S.R., Johnson, T.J., Cox, N.A., 2014. The chicken gastrointestinal microbiome. FEMS Microbiol. Lett. 360 (2), 100–112.

Obst, B.S., Diamond, J.M., 1989. Interspecific variation in sugar and amino acid transport by the avian cecum. J. Exp. Zool. 252 (S3), 117–126.

Ojewole, J.A.O., 1980. Studies on the responses of the isolated rectum of domestic chick (*Gallus domesticus*) to drugs. Biochem. Exp. Biol. 16 (4), 413–420.

Okumura, R., Takeda, K., 2017. Roles of intestinal epithelial cells in the maintenance of gut homeostasis. Exp. Mol. Med. 49 (5), e338.

Olsson, C., Holmgren, S., 2011. Autonomic control of gut motility: a comparative view. Auton. Neurosci. 165 (1), 80–101.

Olukosi, O., Adedokum, S., Ajuwon, K.M., Adeola, O., 2011. Early responses of sodium-dependent phosphate transporter type IIb on broiler chicks to dietary phosphorus intervention. Br. Poultry Sci. 7 (39).

Osman, A.M., 1982. Amylase in chicken intestine and pancreas. Comp. Biochem. Physiol. B Comp. Biochem. 73 (3), 571–574.

Paik, Y., Fujioka, T., Yasuda, M., 1974. Comparative and topographical anatomy of the fowl. LXXVIII. Division of pancreatic lobes and distribution of pancreatic ducts (author's transl). Jpn. J. Vet. Sci. 36 (3), 213–229.

Pan, D., Yu, Z., 2014. Intestinal microbiome of poultry and its interaction with host and diet. Gut Microb. 5 (1), 108–119.

Philips, S.M., Fuller, R., 1983. The activities of amylase and a trypsin-like protease in the gut contents of germ-free and conventional chickens. Br. Poultry Sci. 24 (1), 115–121.

Pichová, I., Kostka, V., 1990. Molecular characteristics of pepsinogen and pepsin from duck glandular stomach. Comp. Biochem. Physiol. B Comp. Biochem. 97 (1), 89–94.

Pinchasov, Y., Noy, Y., 1994. Early postnatal amylolysis in the gastrointestinal tract of Turkey poults *Meleagris gallopavo*. Comp. Biochem. Physiol. A, Physiol. 107 (1), 221–226.

Planas, J.M., Carme Villá, M., Ferrer, R., Moretó, M., 1986. Hexose transport by chicken cecum during development. Pflügers Archiv. 407 (2), 216–220.

Planas, J.M., Ferrer, R., Moreto, M., 1987. Relation between alpha-methyl-D-glucoside influx and brush border surface area in enterocytes from chicken cecum and jejunum. Pflügers Archiv. 408 (5), 515–518.

Polin, D., Wynosky, E., Loukides, M., Porter, C., 1967. A possible urinary backflow to ceca revealed by studies on chicks with artificial anus and fed amprolium-C14 or thiamine-C14. Poultry Sci. 46 (1), 88–93.

Poole, R.C., Halestrap, A.P., 1993. Transport of lactate and other monocarboxylates across mammalian plasma membranes. Am. J. Physiol. 264 (4 Pt 1), C761–C782.

Postorino, A., Serio, R., Fileccia, R., Mule, F., Abbadessa Urso, S., 1985. Electrical stimulation of glossopharyngeal nerve and oesophageal EMG response in the pigeon. Arch. Int. Physiol. Biochim. 93 (4), 321–329.

Pourabedin, M., Zhao, X., 2015. Prebiotics and gut microbiota in chickens. FEMS Microbiol. Lett. 362 (15), fnv122.

Proszkowiec-Weglarz, M., Angel, R., 2013. Calcium and phosphorus metabolism in broilers: effect of homeostatic mechanism on calcium and phosphorus digestibility. J. Appl. Poultry Res. 22, 609–627.

Proszkowiec-Weglarz, M., Schreier, L.L., Miska, K.B., Angel, R., Kahl, S., Russell, B., 2019. Effect of early neonatal development and delayed feeding post-hatch on jejunal and ileal calcium and phosphorus transporter genes expression in broiler chickens. Poultry Sci. 98 (4), 1861–1871.

Proszkowiec-Weglarz, M., Schreier, L.L., Kahl, S., Miska, K.B., Russell, B., Elsasser, T.H., 2020. Effect of delayed feeding post-hatch on expression of tight junction- and gut barrier-related genes in small intestine of broiler chickens during neonatal development. Poultry Sci. 99, 4714–4729.

Qu, Y., Kahl, S., Miska, K., Schreier, L., Russell, B., Elsasser, T., Proszkowiec-Weglarz, M., 2021. The effect of delayed feeding post-hatch on caeca development in broiler chickens. Br. Poult. Sci. https://doi.org/10.1080/00071668.2021.1912291.

Rajapaksha, P., Wang, Z., Venkatesan, N., Tehrani, K.F., Payne, J., Swetenburg, R.L., Kawabata, F., Tabata, S., Mortensen, L.J., Stice, S.L., Beckstead, R., Liu, H.X., 2016. Labeling and analysis of chicken taste buds using molecular markers in oral epithelial sheets. Sci. Rep. 6, 37247.

Rajendran, V.M., Binder, H.J., 1994. Apical membrane Cl-butyrate exchange: mechanism of short chain fatty acid stimulation of active chloride absorption in rat distal colon. J. Membr. Biol. 141 (1), 51–58.

Rea, A.M., 1973. Turkey vultures casting pellets. Auk 90, 209–210.

Reboul, E., 2013. Absorption of vitamin A and carotenoids by the enterocyte: focus on transport proteins. Nutrients 5 (9), 3563–3581.

Reece, W.O., Trampel, D.W., 2015. Avian digestion. In: Reece, W.O. (Ed.), Dukes's Physiology of Domestic Animals, thirteenth ed. John Wiley & Sons, Ames, IA, pp. 532–540.

Rehman, H.U., Vahjen, W., Awad, W.A., Zentek, J., 2007. Indigenous bacteria and bacterial metabolic products in the gastrointestinal tract of broiler chickens. Arch. Anim. Nutr. 61 (5), 319–335.

Rico-Guevara, A., Rubega, M.A., 2011. The hummingbird tongue is a fluid trap, not a capillary tube. Proc. Natl. Acad. Sci. U. S. A. 108 (23), 9356–9360.

Riesenfeld, G., Sklan, D., Bar, A., Eisner, U., Hurwitz, S., 1980. Glucose absorption and starch digestion in the intestine of the chicken. J. Nutr. 110 (1), 117–121.

Riesenfeld, G., Geva, A., Hurwitz, S., 1982. Glucose homeostasis in the chicken. J. Nutr. 112 (12), 2261–2266.

Rochell, S.J., Applegate, T.J., Kim, E.J., Dozier 3rd, W.A., 2012. Effects of diet type and ingredient composition on rate of passage and apparent ileal amino acid digestibility in broiler chicks. Poultry Sci. 91 (7), 1647–1653.

Röseler, M., 1929. Die Bedeutung der Blinddärme des Haushuhnes für die Resorption der Nahrung und die Verdauung der Rohfaser. Zeitschrift für Tierzüchtung und Züchtungsbiologie einschließlich Tierernährung 13 (2), 281–310.

Roto, S.M., Kwon, Y.M., Ricke, S.C., 2016. Applications of in ovo technique for the optimal development of the gastrointestinal tract and the potential influence on the establishment of its microbiome in poultry. Front. Vet. Sci. 3, 63.

Rougiere, N., Carre, B., 2010. Comparison of gastrointestinal transit times between chickens from D+ and D- genetic lines selected for divergent digestion efficiency. Animal 4 (11), 1861–1872.

Rousseau, X., Valable, A.S., Letourneau-Montminy, M.P., Meme, N., Godet, E., Magnin, M., Nys, Y., Duclos, M.J., Narcy, A., 2016. Adaptive response of broilers to dietary phosphorus and calcium restrictions. Poultry Sci. 95 (12), 2849–2860.

Rychlik, I., 2020. Composition and function of chicken gut microbiota. Animals 10 (1).

Saeed, M., Yatao, X., Tiantian, Z., Qian, R., Chao, S., 2019. 16S ribosomal RNA sequencing reveals a modulation of intestinal microbiome and immune response by dietary L-theanine supplementation in broiler chickens. Poultry Sci. 98 (2), 842–854.

Sahba, M.M., Morisset, J.A., Webster, P.D., 1970. Synthetic and secretory effects of cholecystokinin-pancreozymin on the pigeon pancreas. Proc. Soc. Exp. Biol. Med. 134 (3), 728–732.

Sanders, K.M., Koh, S.D., Ward, S.M., 2006. Intestinal cells of cajal as pacemakers in the gastrointestinal tract. Annu. Rev. Physiol. 68 (1), 307–343.

Sato, H., Ohga, A., Nakazato, Y., 1970. The excitatory and inhibitory innervation of the stomachs of the domestic fowl. Jap. J. Pharmacol. 20 (3), 382–397.

Savory, C.J., Mitchell, M.A., 1991. Absorption of hexose and pentose sugars in vivo in perfused intestinal segments in the fowl. Comp Biochem. Physiol. A, Physiol. 100 (4), 969–974.

Savory, C.J., Duke, G.E., Bertoy, R.W., 1981. Influence of intravenous injections of cholecystokinin on gastrointestinal motility in turkeys and domestic fowls. Comp Biochem. Physiol. A, Physiol. 70 (2), 179–189.

Schmidt, C.J., Persia, M.E., Feierstein, E., Kingham, B., Saylor, W.W., 2009. Comparison of a modern broiler line and a heritage line unselected since the 1950s. Poultry Sci. 88 (12), 2610–2619.

Schmolz, L., Birringer, M., Lorkowski, S., Wallert, M., 2016. Complexity of vitamin E metabolism. World J. Biol. Chem. 7 (1), 14–43.

Schumann, A., Nutten, S., Donnicola, D., Comelli, E.M., Mansourian, R., Cherbut, C., Corthesy-Theulaz, I., Garcia-Rodenas, C., 2005. Neonatal antibiotic treatment alters gastrointestinal tract developmental gene expression and intestinal barrier transcriptome. Physiol. Genom. 23 (2), 235–245.

Sell, J., Eastwood, J., Mateos, G., 1983. Influence of supplemental fat on diet metabolizable energy and ingesta transit time in laying hens. Nutr. Rep. Int. 28 (3), 487–495.

Sergeant, M.J., Constantinidou, C., Cogan, T.A., Bedford, M.R., Penn, C.W., Pallen, M.J., 2014. Extensive microbial and functional diversity within the chicken cecal microbiome. PloS One 9 (3), e91941.

Shang, Y., Kumar, S., Oakley, B., Kim, W.K., 2018. Chicken gut microbiota: importance and detection technology. Front. Vet. Sci. 5, 254.

Shao, Y., Guo, Y., Wang, Z., 2013. beta-1,3/1,6-Glucan alleviated intestinal mucosal barrier impairment of broiler chickens challenged with *Salmonella enterica* serovar typhimurium. Poultry Sci. 92 (7), 1764–1773.

Shimakura, J., Terada, T., Shimada, Y., Katsura, T., Inui, K.-i., 2006. The transcription factor Cdx2 regulates the intestine-specific expression of human peptide transporter 1 through functional interaction with Sp1. Biochem. Pharmacol. 71 (11), 1581–1588.

Shires, A., Thompson, J.R., Turner, B.V., Kennedy, P.M., Goh, Y.K., 1987. Rate of passage of corn-canola meal and corn-soybean meal diets through the gastrointestinal tract of broiler and White Leghorn chickens. Poultry Sci. 66 (2), 289–298.

Short, L.L., Sandström, G.F., 1982. Woodpeckers of the World. Delaware Museum of Natural History.

Sibbald, I.R., 1979. Passage of feed through the adult Rooster1. Poultry Sci. 58 (2), 446–459.

Siddons, R.C., 1969. Intestinal disaccharidase activities in the chick. Biochem. J. 112 (1), 51–59.

Siddons, R.C., 1972. Effect of diet on disaccharidase activity in the chick. Br. J. Nutr. 27 (2), 343–352.

Skadhauge, E., 1989. Hormonal regulation of sodium absorption and chloride secretion across the lower intestines of birds. Zool. Sci. 6, 437–444.

Skadhauge, E., Warui, C.N., Kamau, J.M., Maloiy, G.M., 1984. Function of the lower intestine and osmoregulation in the ostrich: preliminary anatomical and physiological observations. Q. J. Exp. Physiol. 69 (4), 809–818.

Skadhauge, E., Clauss, W., Arnason, S.S., Thomas, D.H., 1985. Mineralocorticoid regulation of lower intestinal ion transport. In: Gilles, R., Gilles-Baillien, M. (Eds.), Transport Processes, Iono- and Osmoregulation. Springer Berlin Heidelberg, Berlin, Heidelberg, pp. 118–133.

Sklan, D., 2001. Development of the digestive tract of poultry. World'S Poult. Sci. J. 57, 415–428.

Sklan, D., Noy, Y., 2000. Hydrolysis and absorption in the small intestines of posthatch chicks. Poultry Sci. 79 (9), 1306–1310.

Song, J., Xiao, K., Ke, Y.L., Jiao, L.F., Hu, C.H., Diao, Q.Y., Shi, B., Zou, X.T., 2014. Effect of a probiotic mixture on intestinal microflora, morphology, and barrier integrity of broilers subjected to heat stress. Poultry Sci. 93 (3), 581–588.

Stanley, D., Geier, M.S., Hughes, R.J., Denman, S.E., Moore, R.J., 2013. Highly variable microbiota development in the chicken gastrointestinal tract. PloS One 8 (12), e84290.

Steinberg, S.E., 1984. Mechanisms of folate homeostasis. Am. J. Physiol. 246 (4 Pt 1), G319–G324.

Sudo, S.Z., Duke, G.E., 1980. Kinetics of absorption of volatile fatty acids from the ceca of domestic turkeys. Comp Biochem. Physiol. A, Physiol. 67 (2), 231–237.

Suzuki, M., Nomura, S., 1975. Electromyographic studies on the deglutition movement in the fowl. Jpn. J. Vet. Sci. 37 (5), 289–293.

Svihus, B., Choct, M., Classen, H.L., 2013. Function and nutritional role of the avian ceca: a review. World's Poult. Sci. J. 69, 249–264.

Tabler, T.W., Greene, E.S., Orlowski, S.K., Hiltz, J.Z., Anthony, N.B., Dridi, S., 2020. Intestinal barrier integrity in heat-stressed modern broilers and their ancestor wild jungle fowl. Front. Vet. Sci. 7, 249.

Tactacan, G.B., Rodriguez-Lecompte, J.C., Karmin, O., House, J.D., 2011. Functional characterization of folic acid transport in the intestine of the laying hen using the everted intestinal sac model. Poultry Sci. 90 (1), 83–90.

Takewaki, T., Ohashi, H., Okada, T., 1977. Non-cholinergic and non-adrenergic mechanisms in the contraction and relaxation of the chicken rectum. Jap. J. Pharmacol. 27 (1), 105–115.

Taneike, T., Miyazaki, H., Ohga, A., 1988. Histamine-induced potentiation of cholinergic transmission in chick oesophagus (*Gallus gallus*). Comp. Biochem. Physiol. C Comp. Pharmacol. 89 (2), 271–276.

Tellez, G., Latorre, J.D., Kuttappan, V.A., Kogut, M.H., Wolfenden, A., Hernandez-Velasco, X., Hargis, B.M., Bottje, W.G., Bielke, L.R., Faulkner, O.B., 2014. Utilization of rye as energy source affects bacterial translocation, intestinal viscosity, microbiota composition, and bone mineralization in broiler chickens. Front. Genet. 5, 339.

Tenenhouse, H.S., 2005. Regulation of phosphorus homeostasis by the type iia na/phosphate cotransporter. Annu. Rev. Nutr. 25, 197–214.

Tenenhouse, H.S., 2007. Phosphate transport: molecular basis, regulation and pathophysiology. J. Steroid Biochem. Mol. Biol. 103 (3–5), 572–577.

Tenenhouse, H.S., Roy, S., Martel, J., Gauthier, C., 1998. Differential expression, abundance, and regulation of Na^{+}-phosphate cotransporter genes in murine kidney. Am. J. Physiol. 275 (4 Pt 2), F527–F534.

Tortuero, F., Brenes, A., Rioperez, J., 1975. The influence of intestinal (ceca) flora on serum and egg yolk cholesterol levels in laying hens. Poultry Sci. 54 (6), 1935–1938.

Tur, J.A., Rial, R.V., 1985. The effect of temperature and relative humidity on the gastrointestinal motility of young broile. Comp Biochem. Physiol. A, Physiol. 80 (4), 481–486.

Udén, P., Colucci, P.E., Van Soest, P.J., 1980. Investigation of chromium, cerium and cobalt as markers in digesta. Rate of passage studies. J. Sci. Food Agric. 31 (7), 625–632.

Uerlings, J., Song, Z.G., Hu, X.Y., Wang, S.K., Lin, H., Buyse, J., Everaert, N., 2018. Heat exposure affects jejunal tight junction remodeling independently of adenosine monophosphate-activated protein kinase in 9-day-old broiler chicks. Poultry Sci. 97 (10), 3681–3690.

Uni, Z., 2006. Early development of small intestinal function. Avian Gut Func. Health Dis. 28, 29.

Uni, Z., Smirnov, A., Sklan, D., 2003. Pre- and posthatch development of goblet cells in the broiler small intestine: effect of delayed access to feed. Poultry Sci. 82 (2), 320–327.

Vaillant, C., Dimaline, R., Dockray, G.J., 1980. The distribution and cellular origin of vasoactive intestinal polypeptide in the avian gastrointestinal tract and pancreas. Cell Tissue Res. 211 (3), 511–521.

Van Der Klis, J.D., Verstegen, M.W.A., De Wit, W., 1990. Absorption of minerals and retention time of dry matter in the gastrointestinal tract of broilers. Poultry Sci. 69 (12), 2185–2194.

Van der Sluis, M., De Koning, B.A., De Bruijn, A.C., Velcich, A., Meijerink, J.P., Van Goudoever, J.B., Buller, H.A., Dekker, J., Van Seuningen, I., Renes, I.B., Einerhand, A.W., 2006. Muc2-deficient mice spontaneously develop colitis, indicating that MUC2 is critical for colonic protection. Gastroenterology 131 (1), 117–129.

Van Klinken, B.J., Dekker, J., Buller, H.A., Einerhand, A.W., 1995a. Mucin gene structure and expression: protection vs. adhesion. Am. J. Physiol. 269 (5 Pt 1), G613–G627.

Van Klinken, B.J., Tytgat, K.M., Buller, H.A., Einerhand, A.W., Dekker, J., 1995b. Biosynthesis of intestinal mucins: MUC1, MUC2, MUC3 and more. Biochem. Soc. Trans. 23 (4), 814–818.

Vandeputte-Poma, J., 1968. The composition of pigeon cropmilk. J. Anim. Breed. Genet. 58 (4), 356–363.

Vergara, P., Ferrando, C., Jiménez, M., Fernández, E., Goñalons, E., 1989. Factors determining gastrointestinal transit time of several markers in the domestic fowl. Quart. J. Exp. Physiol. 74 (6), 867–874.

Vinardell, M.P., Lopera, M.T., 1987. Jejunal and cecal 3-oxy-methyl-d-glucose absorption in chicken using a perfusion system in vivo. Comp Biochem. Physiol. A, Physiol. 86 (4), 625–627.

Waite, D.W., Taylor, M.W., 2014. Characterizing the avian gut microbiota: membership, driving influences, and potential function. Front. Microbiol. 5, 223.

Wang, L., Cheung, J.T.-M., Pu, F., Li, D., Zhang, M., Fan, Y., 2011. Why do woodpeckers resist head impact injury: a biomechanical investigation. PloS One 6 (10), e26490.

Ward, N., Jones, J., Maurice, D., 1984. Increase in intestinal pH of chickens due to cimetidine injection, Fed. Proc. Fed. Am. Soc. Exp. Biol. 43 (4), 856.

Wasserman, R.H., Taylor, A.N., 1973. Intestinal absorption of phosphate in the chick: effect of vitamin D and other parameters. J. Nutr. 103 (4), 586–599.

Wei, S., Morrison, M., Yu, Z., 2013. Bacterial census of poultry intestinal microbiome. Poultry Sci. 92 (3), 671–683.

White, S., 1969. Mechanisms involved in deglutition in *Gallus domesticus*. J. Anat. 104 (Pt 1), 177.

White, S.S., 1970. The Larynx of *Gallus domesticus*. University of Liverpool, Liverpool.

Wideman Jr., R.F., Hamal, K.R., Stark, J.M., Blankenship, J., Lester, H., Mitchell, K.N., Lorenzoni, G., Pevzner, I., 2012. A wire-flooring model for inducing lameness in broilers: evaluation of probiotics as a prophylactic treatment. Poultry Sci. 91 (4), 870–883.

Williams, R.B., 2005. Intercurrent coccidiosis and necrotic enteritis of chickens: rational, integrated disease management by maintenance of gut integrity. Avian Pathol. 34 (3), 159–180.

Winget, C.M., Ashton, G.C., Cawley, A.J., 1962. Changes in gastrointestinal pH associated with fasting in the laying hen. Poultry Sci. 41 (4), 1115–1120.

Woodfint, R.M., Chen, P.R., Ahn, J., Suh, Y., Hwang, S., Lee, S.S., Lee, K., 2017. Identification of the MUC2 promoter as a strong promoter for intestinal gene expression through generation of transgenic quail expressing GFP in gut epithelial cells. Int. J. Mol. Sci. 18 (1), 196.

Yamauchi, K.E., Isshiki, Y., 1991. Scanning electron microscopic observations on the intestinal villi in growing white leghorn and broiler chickens from 1 to 30 days of age. Br. Poultry Sci. 32 (1), 67–78.

Yan, F., Angel, R., Ashwell, C.M., 2007. Characterization of the chicken small intestine type IIb sodium phosphate cotransporter. Poultry Sci. 86 (1), 67–76.

Yang, J.H., Hou, J.F., Farquharson, C., Zhou, Z.L., Deng, Y.F., Wang, L., Yu, Y., 2011. Localisation and expression of TRPV6 in all intestinal segments and kidney of laying hens. Br. Poultry Sci. 52 (4), 507–516.

Yang, F., Wang, A., Zeng, X., Hou, C., Liu, H., Qiao, S., 2015. Lactobacillus reuteri I5007 modulates tight junction protein expression in IPEC-J2 cells with LPS stimulation and in newborn piglets under normal conditions. BMC Microbiol. 15, 32.

Yeoman, C.J., Chia, N., Jeraldo, P., Sipos, M., Goldenfeld, N.D., White, B.A., 2012. The microbiome of the chicken gastrointestinal tract. Anim. Health Res. Rev. 13 (1), 89–99.

Yu, D., Turner, J.R., 2008. Stimulus-induced reorganization of tight junction structure: the role of membrane traffic. Biochim. Biophys. Acta 1778 (3), 709–716.

Zhang, Q., Eicher, S.D., Applegate, T.J., 2015. Development of intestinal mucin 2, IgA, and polymeric Ig receptor expressions in broiler chickens and Pekin ducks. Poultry Sci. 94 (2), 172–180.

Ziswiler, V., Farner, D.S., 1972. Digestion and the digestive system. In: Farner, D.S., King, J.R. (Eds.), Avian Biology. Academic Press, Amsterdam, pp. 343–430.

ŌHashi, H., Ohga, A., 1967. Transmission of excitation from the parasympathetic nerve to the smooth muscle. Nature 216 (5112), 291–292.

Chapter 22

Avian bone physiology and poultry bone disorders

Narayan C. Rath[1] and Vijay Durairaj[2]

[1]USDA/Agricultural Research Service and Department of Poultry Science, University of Arkansas, Fayetteville, AR, United States; [2]Huvepharma Inc., Lincoln, NE, United States

Abbreviations

AC Articular cartilage
BCO Bacterial chondronecrosis with osteomyelitis
BMP Bone morphogenetic protein
ECO Endochondral ossification
FGF Fibroblast growth factor
FHN Femoral head necrosis
FHS Femoral head separation
GP Growth plate
HOX Homeotic gene
IGF-1 Insulin-like growth factor-1
IHH Indian hedgehog
IMO Intramembranous ossification
M-CSF Macrophage colony stimulating factor
MMP Matrix metalloproteinases
Na^+ K^+ ATPase Sodium potassium ATPase
NCC Neural crest cells
OC Osteocalcin
OP Osteopontin
PH Prehypertrophic
PTH Parathyroid hormone
PTHrP Parathyroid hormone related protein
RANK/RANKL Receptor activator of NF-kB/receptor activator of NF-kB for ligand
RUNX-2 Runt-related transcription factor 2
SHH Sonic hedgehog
SOX-9 Sry-related transcription factor
TD Tibial dyschondroplasia
TGF-β Transforming growth factor beta
TRAP Tartrate resistant acid phosphatase
VEGF Vascular endothelial growth factor
VVD Valgus-varus deformity
WNT Wingless-ints.
ZPA Zone of polarizing activity

22.1 Introduction

In vertebrates, the skeleton serves as the main structural framework of the body which supports the attachment of muscles and tendons and protects the internal organs. As the main reservoir of calcium (Ca) and phosphorus (P), the skeleton also maintains mineral homeostasis and acts as repository for different growth factors bound to its extracellular matrices (Clarke, 2008; Moreira et al., 2019). It also acts as an endocrine organ that releases fibroblast growth factor (FGF-23), a hormone that regulates P and vitamin D metabolism acting through kidney (Erben, 2018; Gonciulea and de Beur, 2015; Robling and Bonewald, 2020; Schwetz et al., 2012; Zofkova, 2018) and harbors bone marrow, the body's main site of hematopoiesis and immunity (Okamoto and Takayanagi, 2019). Thus, the skeleton contributes to a variety of physiological functions of the body. In birds, the skeleton has undergone several structural modifications and functional adaptations to support its aerial life and egg laying behavior (Canoville et al., 2019; Novitskaya et al., 2017; Sullivan et al., 2017). Rigid, yet light-weight skeleton with fused cranial, vertebral, and collar bone (wish bone), and the keel sternum attaching pectoral muscles, provide support for flying. The hollow limb bone of flying birds act as extensions of lungs providing additional oxygen and energy during flight (Costain, 2018; Dumont, 2010). On the other hand, some of those skeletal adaptations do not exist in flightless birds such as penguins where the bone are generally dense and heavier to support their diving habits and in some flightless birds the keel sternum is reduced or absent (Zheng et al., 2012).

Skeleton consists of both cartilage and bone with the later constituting the major bulk of adult skeletal tissue while cartilage persist only at some special sites such as joints and intervertebral spaces to protect against friction between adjacent bone. Nonetheless, the cartilage occur transiently in most parts of the skeleton preceding the development of bone. "Stable" or "permanent" cartilage make articular cartilage (AC) of joints and fibrocartilage of intervertebral spaces, whereas the "transient" cartilage

Sturkie's Avian Physiology. https://doi.org/10.1016/B978-0-12-819770-7.00037-2

develop temporarily during long bone formation and fracture healing (Bahney et al., 2019; Chijimatsu and Saito, 2019; Sophia Fox et al., 2009; Staines et al., 2013). Bone morphogenesis occurs in two ways: one, through "intramembranous ossification (IMO)", where the embryonic mesenchymal cells undergo direct ossification to form bone and the other, through "endochondral ossification (ECO)" where a cartilage template develops prior to bone formation (Hall and Miyake, 2000; Yang, 2009). Most flat bone such as skull, mandible, and keel sternum develop through intramembranous processes whereas, the long bone such as axial and appendicular bone develop through endochondral route (Clarke, 2008; Moreira et al., 2019).

22.2 Embryonic skeletal differentiation

Skeletal ontogenesis begins during gastrulation. Different instructive signals emanating locally from the neighboring cells, in the form of gene expression and the production of different growth and transcription factors, act in a highly orchestrated manner to guide embryonic cell migration, their survival, proliferation, and differentiation into prospective skeletal elements (Creuzet et al., 2005; Davey et al., 2018; Le Douarin, 2004; Ros et al., 2000). Both intramembranous and endochondral ossification pathways share many similar growth and signaling factors which facilitate their development and differentiation. However, the ultimate structural differentiation of presumptive skeletal elements and their three-dimensional patterning depend upon the origin and the locations of the responding cell population, the time of action of different growth factors, and the expressions of relevant genes (Kozhemyakina et al., 2015; Schneider, 2018). Some of the major signaling proteins and genes known to play critical roles in the early development of skeleton are: sonic hedgehog (SHH), fibroblast growth factors (FGF), bone morphogenetic proteins (BMP), and wingless-related (WNT) families of proteins, their respective receptors, and several transcription factors such as homeotic (HOX), Runt-related (RUNX), and Sry-related (SOX) genes and proteins (Creuzet et al., 2005; Eames and Helms, 2004; Schneider, 2018; Tickle, 2015). These growth and differentiation factors work through complex interactions involving synergistic, cooperative, and feedback loops. Besides the above-mentioned growth and transcription factors, there can be other secondary signaling factors that are produced locally or downstream; therefore, the commitment to either cartilage or bone lineage depend upon reciprocal and timely interactions between the precursor cells and different signaling proteins and genes (Schneider, 2018; Tickle, 2015).

Craniofacial skeletons develop from cephalic mesoderm that differentiate from neural crest cells (NCC) of the gastrulating embryo. The NCC migrate rostrally in the embryo to pharyngeal arches where they undergo epithelial to mesenchymal transition, a process that involves changes in their cytoskeletal organization and leads to the expression of specific adhesion molecules and glycoproteins, consequential to their subsequent developments (Abramyan and Richman, 2018; Creuzet et al., 2005; Minoux and Rijli, 2010; Olsen et al., 2000; Schneider, 2018). Cell migration and their transitions are regulated by SHH, one of the first signaling proteins of cranial skeletogenesis produced by ectodermal and neuroectodermal cells. The rostral domain of cephalic mesoderm is HOX gene negative that differentiates into parts of cranial skeleton (skull and mandible) through IMO, whereas the HOX gene positive posterior domain develops into parts of craniofacial skeleton (parietal, skull base) through endochondral route. The HOX genes specify the anteroposterior axis of the body structures and axial patterns acting as road maps and are expressed during development of different parts of the embryonic body (Iimura and Pourquié, 2007; Nolte et al., 2019). SHH along with FGF and BMP, produced by neuroectoderm, ectoderm, and pharyngeal endoderm, interact with cranial mesoderm cells and promote their survival, proliferation, condensation, and differentiation into different skeletal primordia (Eames and Helms, 2004; Minoux and Rijli, 2010; Schneider, 2018). The transcription factor RUNX-2 is the master regulator of osteoblast differentiation which helps in making the craniofacial dermal bone (Abramyan and Richman, 2018; Abzhanov et al., 2007; Komori, 2017; Schneider, 2018). WNT is another signaling factor that along with SHH helps in the differentiation of mesodermal cells to osteoblasts and specifies the axial patterning of skeletal rudiments (Day et al., 2005; Kozhemyakina et al., 2015; Rutkovskiy et al., 2016; Wu et al., 2016). Osteogenic differentiation is marked by the production of type I collagen (Col1α) and osteopontin (OP) by the osteoblasts (Abzhanov et al., 2007).

Paraxial and lateral mesoderm cells give rise to axial (vertebral) and appendicular (limb) skeletons respectively, through ECO. Paraxial mesoderm, flanking on either side of the neural tube, undergo somitogenesis and become the precursors of different organs including the axial skeletons (Gilbert and Barresi, 2016). Based on their locations, specific somites give rise to specific vertebral structures. Somites give rise to sclerotome under the influence of SHH produced by the notochord and floor plate neural tube, and differentiate into precartilage through the expression of a transcription factor PAX1 (Gilbert and Barresi, 2016). This differentiation process is supported by a combined action of SHH and the members of BMP, WNT, and FGF families of proteins produced by surface ectoderm and other neighboring cells (Pourquié, 2018; Pourquié et al., 1993). The lateral plate mesoderm, located ventral to intermediate and paraxial mesoderm, give rise to wing and limb skeletons (Creuzet et al., 2005; Eames and Helms, 2004; Gilbert and Barresi, 2016; Tickle, 2015). In chick embryo, the wing and

leg buds develop from lateral plate mesoderm in the levels of somites 15–20 and 26–31, respectively (Davey et al., 2018; Tickle, 2015). During limb bud chondrogenesis, the ectoderm covering the distal part of the limb bud, thicken to form apical ectodermal ridge (AER) and the proximal posterior part of the zone of polarizing activity (ZPA). AER produces FGF8 which instructs the production of other signaling proteins including different other members of FGF family-, BMP, and WNT proteins by the mesodermal cells. These proteins induce mesodermal cells to proliferate, condense, and differentiate into chondrocytes (Berendsen and Olsen, 2015; Davey et al., 2018; Kozhemyakina et al., 2015; Mariani and Martin, 2003; Tickle, 2015). Expression of a Sry-related transcription factor, SOX-9, by the condensing mesoderm is pivotal to chondrocyte differentiation and the establishment of cartilage anlagen. However, at later stages of development, the transcription factor RUNX-2, expressed by the hypertrophic chondrocytes, drives the mineralization of cartilage matrix and its replacement by the bone (Davey et al., 2018; Eames et al., 2003; Hallett et al., 2019; Long and Ornitz, 2013). Meanwhile, ZPA produces SHH that along with HOX gene and WNT helps axial morphing of the limb bud skeletons and determines their anteroposterior, dorsoventral, and proximodistal polarities. Interference of these crucial signaling processes can result in skeletal defects (Abramyan and Richman, 2018; Davey et al., 2018; Maas et al., 2011). Although the avian skeletal differentiation completes by the time of hatch, the post hatch bone growth continues through sexual maturity.

22.3 Cartilage

22.3.1 Cartilage of endochondral bone

During embryonic as well as post hatch development, the longitudinal growth of bone take place through endochondral ossification. In the embryo, the primary ossification begins at the center of the cartilage anlagen, formed by the differentiation of condensed mesoderm of embryonic limb bud, that attracts blood vessels along with osteoblasts to form bone and replace the cartilage. In post hatch avian growth plate (GP), a "reserve" or "resting zone" mesenchymal cells beneath AC, undergo successive transitions to proliferative, prehypertrophic (PH), hypertrophic chondrocytes, and form the cartilage that goes through mineralization and vascular invasion. The chondrocytes in the cartilage undergo chondrolysis and apoptosis while vascular invasion brings in the osteoblasts which lay down bone replacing the cartilage (Figure 22.1). Osteoclasts remodel the newly forming bone. This complex series of development is regulated by many different growth and signaling factors, similar to those involved in embryonic limb development; however, there may be other growth factors which are also participate in post hatch GP development (Eames et al., 2003; Haraguchi et al., 2019; Kozhemyakina et al., 2015; Kronenberg, 2003; Mackie et al., 2008; Samsa et al., 2017; Vortkamp et al., 1996, Table 22.1). BMP, FGF, and Indian hedgehog (IHH) interactively regulate proliferation of chondrocyte precursors and their differentiation to prehypertrophic (PH) chondrocytes through the expression of a transcription factor SOX-9. IHH is produced by PH and early hypertrophic chondrocytes and belongs to the same family of proteins as SHH (Kronenberg, 2003; Provot and Schipani, 2005). BMP helps in proliferation and condensation of prechondrocytic mesenchymal cells, while FGF signaling not only promotes chondrocyte proliferation but also induces their hypertrophy. Chondrocyte proliferation is regulated by parathyroid hormone-related protein (PTHrP) produced by the perichondrium that also helps in long bone growth (Zhao et al., 2002). IHH regulates the expression of PTHrP through a negative feedback loop and promotes chondrocyte hypertrophy (Vortkamp et al., 1996; Wu et al., 2016). Cartilage differentiation is marked by discrete morphological transition of mesenchymal cells to chondrocytes that produce type II collagen and aggrecan. The expression of RUNX-2 by the

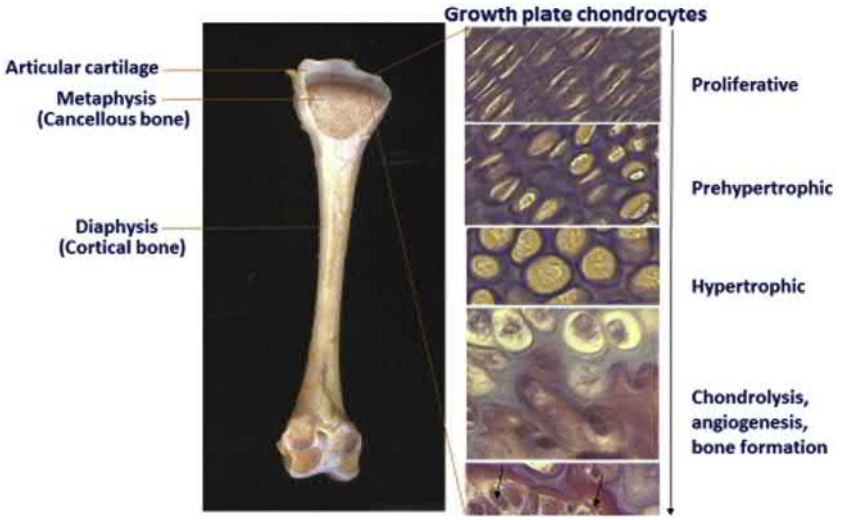

FIGURE 22.1 A two-week-old chicken tibia showing chondrocyte transitions in the growth plate. *Arrows* show newly formed osteoblasts and osteoid.

TABLE 22.1 Skeletal cell differentiation associated signaling factors and their effects.

Target cells	Signaling factors	Skeletal outcome and cells differentiated	Biomarkers	Morphogenetic processes
Neural crest cell (NCC)-derived mesodermal cells	SHH, FGF, BMP, WNT, RUNX-2↑, HOX (-ve)	Osteoblasts	Collagen I, ALP, OP, Osteocalcin	IMO: Osteogenesis
Mesenchymal stem cells	FGF, BMP, IHH, PTHrP↑, TGF-β, SOX-9 ↑	Articular chondrocytes	Collagen I, Collagen II, Aggrecan	Chondrogenesis (stable cartilage)
Mesenchymal stem cells	FGF, SHH, BMP, WNT, PTHrP ↑, SOX9 ↑	Chondrocytes	Collagen II, Aggrecan	ECO: Chondrogenesis, mesenchymal proliferation ↑, condensation, and chondrocyte differentiation
PH chondrocytes	WNT, IGF-1, FGF, IHH ↑, PTHrP ↓, SOX9 ↓, RUNX-2 ↑	Chondrocyte hypertrophy	Collagen II, MMP, OP, VEGF	ECO: Chondrocyte transition, proliferation ↓, chondrocyte hypertrophy
Hypertrophic chondrocytes	IHH, BMP, RUNX-2↑, VEGF↑	Chondrolysis/chondrocyte apoptosis	Collagen II ↓, Collagen X ↑, MMP	ECO: Matrix mineralization,
Osteoblast and angiogenic precursors	VEGF ↑, RUNX-2 WNT, IHH	Vascularization, Matrix degradation, Osteoblasts	Collagen I, ALP, OP, Osteocalcin	ECO: Matrix degradation, angiogenesis, osteogenesis
Monocytes	M-CSF, RANK/RANKL, PTH, Vitamin D, IHH	Osteoclasts	CA, cathepsin K, MMP, Na^+ K^+ ATPase, TRAP	Osteoclastogenesis, bone resorption and remodeling

ALP, Alkaline phosphatase; *BMP*, Bone morphogenetic protein; *CA*, Carbonic anhydrase II, *ECO*, Endochondral ossification; *FGF*, Fibroblast growth factor; *HOX*, Homeotic gene; *IGF-1*, Insulin-like growth factor-1; *IHH*, Indian hedgehog; *IMO*, Intramembranous ossification; *M-CSF*, Macrophage colony stimulating factor; *MMP*, Matrix metalloproteinases; *MSC*, Mesenchymal stem cells; *Na^+ K^+ ATPase*, Sodium potassium ATPase; *OP*, Osteopontin; *PH*, Prehypertrophic; *PTHrP*, Parathyroid hormone-related protein; *RANK/RANKL*, Receptor activator of NF-kB/RANK-ligand; *RUNX-2*, Runt-related transcription factor 2; *SHH*, Sonic hedgehog; *SOX-9*, Sry-related transcription factor; *TGF-β*, Transforming growth factor beta; *TRAP*, Tartrate resistant acid phosphatase; *VEGF*, Vascular endothelial growth factor; *WNT*, Wingless-ints. Upregulated ↑ and downregulated ↓.

hypertrophic chondrocytes brings about the downregulation of their type II collagen production and the onset of type X collagen production helping in the mineralization of cartilage matrix. RUNX-2 also promotes the expression of matrix-degrading enzymes that include matrix metalloproteinases (MMP) and vascular endothelial growth factors (VEGF) that help vascularization, and the infiltration of osteoblasts and osteoclasts (Kozhemyakina et al., 2015). Several other local and systemic factors including transforming growth factor β (TGF-β), growth hormone, insulin-like growth factor-1 (IGF-1), and thyroid hormones also participate in cartilage growth and development (Mackie et al., 2011; Nilsson et al., 2005; Van der Eerden et al., 2003). Although the cellular succession and their overall regulation are comparatively similar between mammalian and avian GP, the later is a relatively better vascularized organ compared with the avascular mammalian GP. The avian GP contains capillary vessels and cartilage canals penetrating deep into the chondrocyte transition zone (Figure 22.2) and the cartilage columns of avian GP are loosely organized compared with the parallel columns of mammalian GP (Blumer et al., 2004; Pines and Hurwitz, 1991). The cartilage canals serve as conduits for blood vessels and express VEGF and their corresponding receptors. Some of those structural differences likely make poultry GP vulnerable to certain bone problems such as tibial dyschondroplasia (TD), femoral head separation (FHS), and bacterial chondronecrosis with osteomyelitis (BCO), where vascular impediments can factor in their pathogenesis (Huang et al., 2018; Rath et al., 2005; Wideman, 2016). Microvascular clefts and vascular channels also account for hematogenous spread of opportunistic bacteria leading to the pathogenesis of BCO and osteomyelitis (Emslie et al., 1983; Wideman and Prisby, 2011).

22.3.2 Articular cartilage

AC belongs to "stable" cartilage group that protect bone in the joints against friction. AC remains as hyaline cartilage

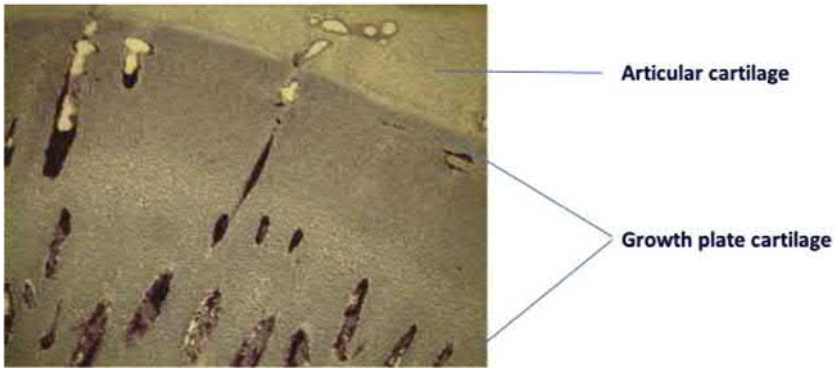

FIGURE 22.2 Growth plate of a two-week-old chicken showing the occurrence of capillary vessels and vascular clefts.

and occurs as a white translucent cap at the end of epiphysis between synovium and the GP. It is a sparsely cellular and avascular tissue rich in type II collagen and aggrecan, and contains up to 80% water. However, the avian cartilage also contains type I collagen, the proportions of which increases with the chicken's age (Eyre et al., 1978). Articular chondrocytes produce some special proteoglycans which provide lubricity to the AC. The articular chondrocytes, likely originate from a different lineage of mesenchymal cells than GP chondrocytes, following the development of joint cavity (Chijimatsu and Saito, 2019; Staines et al., 2013). The articular chondrocytes are terminally differentiated and do not undergo hypertrophy or mineralization unlike the transient cartilage of GP. Damage to AC can result in the development of degenerative joint disease such as arthritis, since this type of cartilage is difficult to heal (Li et al., 2015). There are very limited studies on the biology of avian AC.

22.4 Bone

22.4.1 Cellular components

Bone is the largest component of skeleton; it is a complex tissue consisting of cells and matrices. Osteoblasts, osteocytes, and osteoclasts are three major cell types of bone which contribute to its formation, resorption, and remodeling, therefore, responsible for maintaining the bone mass. Under normal physiology, the bone resorption and formation are coupled, and regulated by the interactions of osteoblasts and osteoclasts (Florencio-Silva et al., 2015; Moreira et al., 2019). Osteoblasts differentiate under the regulation of a transcription factor RUNX-2 and produce type I collagen, osteopontin (OP), alkaline phosphatase, and several other proteins that regulate bone mineralization (Clarke, 2008; Moreira et al., 2019; Murshed, 2018). Osteoblasts work on bone surfaces and are subject to regulation by local factors such as BMP, TGF-β, platelet-derived growth factor, FGF, and many systemic factors including growth hormone, IGF-1, thyroid hormone, calcitonin, parathyroid hormone (PTH), vitamin D3, and the sex steroids many of which support their proliferation and stimulate matrix production (Florencio-Silva et al., 2015; Rath et al., 2000; Rutkovskiy et al., 2016). Calcitonin promotes bone formation by osteoblasts and inhibits bone resorption, whereas PTH, acting through osteoblast, stimulates osteoclastic bone resorption (Goltzman, 2018; Silva and Bilezikian, 2015). Vitamin D affects bone mineralization through stimulation of osteoblast activities and its proliferation (van Driel and van Leeuwen, 2017; Zofkova, 2018).

Osteocytes are mature osteoblasts which reside in the lacunae of the Haversian system entrapped in mineralized bone matrix and communicate with other osteocytes and osteoblasts through dendritic processes extending through canaliculi (Dallas et al., 2013; Semeins et al., 2012). The actions of various growth factors, WNT, BMP, and TGF-β, are responsible for the transition of osteoblasts to osteocytes (Bonewald, 2011; Florencio-Silva et al., 2015). Osteocytes do not make bone but control the bone remodeling process through their interaction with both osteoblasts and osteoclasts, and regulate bone mass through their mechanosensory function (Bonewald and Johnson, 2008; Turner et al., 2009). Mechanical stimulation enables osteocytes to produce secondary messengers such as prostaglandin E2, nitric oxide, and several kinases which promote bone formation and improve bone strength (Turner et al., 2009; Zofkova, 2018). Osteocytes produce FGF-23 and osteocalcin (OC), the former acts through kidney to maintain phosphorus homeostasis and the latter regulates energy metabolism (Moser and van der Eerden, 2018; Robling and Bonewald, 2020; Turner et al., 2009).

Osteoclasts are multinucleate bone resorbing cells which are responsible for bone remodeling throughout life (Feng and Teitelbaum, 2013; Gay and Weber, 2000; Okamoto and Takayanagi, 2019). Osteoclasts differentiate from myeloid lineage mononuclear cells by fusion under the influence of M-colony stimulating factor (M-CSF) and through the activation of receptor activator of NF-κB (RANK) by RANK ligand (RANKL), a transmembrane

protein belonging to tumor necrosis factor (TNF) super family and produced by the osteoblasts. (Feng and Teitelbaum, 2013; Hiyama et al., 2019; Ono and Nakashima, 2018). However, there are many other factors such as interleukin-6, TGF-β, and reactive oxygen species, which also promote osteoclast activities. Osteoclasts have ruffled border through which they interact with bone surface and produce H^+, Cl^- ions, catalytic enzymes such as cathepsin K, MMP, carbonic anhydrase, and tartrate resistant acid phosphatase that hydrolyze and resorb bone matrices (Clarke, 2008). PTH, 1, 25 dihydroxy vitamin D3, calcitonin, glucocorticoid, estrogen, prostaglandins, cytokines, interleukins 1 and 6, and TNF-α are some of many factors that regulate osteoclast activities (Okamoto and Takayanagi, 2019; Ono and Nakashima, 2018). Calcitonin decreases osteoclast activity whereas PTH enhances it. Calcitonin and PTH work in a feedback loop to regulate serum calcium levels and osteoclast activity. Osteoclasts are responsible to resorb "medullary bone" which is a special bone that forms in the bone marrow cavities of hens under the regulation of estrogen and provides Ca for egg shell formation (Whitehead, 2004). Imbalance between osteoclast and osteoblast activities lead to changes in bone volume due to increased bone resorption by osteoclasts causing osteoporosis in laying hens (Jendral et al., 2008; Whitehead, 2004). Conversely, dense bone may result from low osteoclast activities leading to "osteopetrosis". Bone resorption ends with the death of osteoclasts, stimulated by calcitonin and other factors such as estrogen (Chen et al., 2018b; Ono and Nakashima, 2018).

22.4.2 Bone tissue

Bone is a dynamic tissue subject to regulation by intrinsic physiological factors and extrinsic elements such as physical activity, mechanical stress, and gravity (Setiawati and Rahardjo, 2019). Externally, bone is covered by a fibrous sheath of connective tissue called "periosteum" which contains the precursor cells of osteoblasts and blood vessels. Periosteum helps in the radial growth of bone and fracture repair. The majority mass of bone is its mineral matrix called hydroxyapatite [Ca_{10} $(PO_4)_6(OH)_2$] that makes up to 65−67% of mature bone in chickens (Rath et al., 2000). The organic matrix, called osteoid, is predominantly type I collagen that constitutes up to 85−90% of its mass and the rest consisting of several proteins that include minor collagens, proteoglycans, OP, matrix-Gla protein (MGP), and osteocalcin (OC) some of which, regulate bone mineralization (Clarke, 2008; Murshed, 2018). Collagen forms the primary scaffold of bone tissue and provides oriented support for the mineral matrix. Based on collagen orientations, the bone are termed as "woven" or "lamellar." The woven bone are immature bone with loosely organized collagen fibers and hence have lower mechanical strength and form during early stages of bone development, for instance, during intramembranous ossification and fracture healing. The "lamellar bone", on the other hand, are mature bone with collagen fibrils organized and oriented as parallel sheets or lamella. With respect to their structures, the bone are termed as "cortical" or "cancellous" bone. Cortical or "compact" bone are thick and dense bone compared to their counterpart, "cancellous" or "trabecular" bone which arrange in lattice or spongy structures. Both cortical and cancellous bone are made up of lamellar bone. The diaphyseal shafts of both tibia and femur, and the outer surface of many bone are cortical bone, whereas the metaphyseal parts of many long bone contain cancellous bone. Flat bones (skull, keel sternum) contain large amounts of cancellous bone. Compared with cortical, the cancellous bone are less calcified and contain many osteoblasts therefore, play a larger role in metabolic functions of the bone (Clarke, 2008; Florencio-Silva et al., 2015). Haversian systems are made by concentric rings of lamellar bone that run lengthwise down the axis of cortical bone and supply blood to the bone and the osteocytes residing in the Haversian system. As mentioned earlier, the birds have a type of specialized bone called "medullary bone" which exclusively form in the marrow cavities of egg laying birds (Bar, 2009; Canoville et al., 2019; Squire et al., 2017). Medullary bone are woven bone that supply calcium for egg shell formation through osteoclastic resorption (Canoville et al., 2019; Hadley et al., 2016; Whitehead, 2004). Calcification of bone takes place at discrete sites of collagen matrix initiated by the deposition of Ca^{+2} and phosphate ions on the osteoid leading to hydroxyapatite formation (Moreira et al., 2019). Membrane bound matrix vesicles, produced by osteoblasts and hypertrophic chondrocytes containing calcium mineral particles and alkaline phosphatase, facilitate the mineralization process (Kerschnitzki et al., 2016). Several other proteins in the organic matrix including MGP, OC, and OP regulate mineralization process (Murshed, 2018). Mineralization of bone is also controlled by PTH, calcitonin, and vitamin D through their effect on plasma Ca levels. PTH increases plasma Ca levels through bone resorption, whereas calcitonin decreases bone resorption and vitamin D increases intestinal absorption of Ca (Fleisch, 1997). Mineral matrix provides compressive strength and mechanical rigidity, whereas the collagen matrix provides tensile strength (Viguet-Carrin et al., 2006). The overall bone strength, however, does not depend solely upon their matrix content but also on the shapes and sizes of the bone, the distribution and the microarchitecture of their materials (Cole and van der Meulen, 2011; Fleming et al., 1998; Rath et al., 2000). Bone with similar material content but with different shapes and material structures (cortical or cancellous), and molecular properties of their constituents, for example, collagen crosslinks can differ in their strengths (Knott and Bailey, 1999). Compromised bone strength can be a

welfare issue that leads to bone deformities and breakage in both meat-type and egg layer poultry. In young broiler chickens, the leg bone deformity and lameness are thought to be related to the lack of maturity of bone making them weak to support the rapidly growing body weight, whereas in older laying hens the fractures can be due to osteoporosis (Sanchez-Rodriguez et al., 2019; Thorp, 1994; Webster, 2004). The bone of younger birds are stiff and less ductile likely, due to low content of collagen crosslinks (Rath et al., 2000). In osteoporotic hens, excessive loss of matrix increases the porosity of cortical bone and increases their vulnerability to breakage. Flying birds usually have pneumatized and high-density bone (Dumont, 2010). The hollow bone of the wing, containing struts and ridges in the medullary cavity, not only provide better buoyancy but also torsional strength for flight (Dumont, 2010; Novitskaya et al., 2017; Sullivan et al., 2017). Besides, the hollow bone are connected to air sacs which allow birds to oxygenate their blood while inhaling and exhaling and thus, provide extra energy during flight (Costain, 2018).

22.5 Poultry bone disorders

Genetics, nutrition, metabolism, infection, and housing conditions are some of the factors that underlie several poultry skeletal problems. Whereas the genetic mutations can cause structural and metabolic defects, there are several bone problems in commercial poultry that arise because of nutritional deficiencies, infection, malabsorption, physical inactivity, and poor housing and hygienic conditions (Julian, 1998; Knowles et al., 2008; Rodriguez-Navarro et al., 2018; Thorp, 1994, Figure 22.3).

In young, meat-type poultry, lameness-related leg bone problems predominate, whereas in prolific egg layers, osteoporosis and cage layer fatigue occur in older birds as a result of structural loss of bone leading to bone fragility that decreases their locomotion and increases morbidity and mortality rates. Hypoactivity increases the chances of bone weakness since mechanical loading of bone is essential for its optimal function including bone mass preservation, mineralization, and growth. Chicken embryos subjected to experimental immobilization show bone abnormalities including abnormal expressions of genes associated with bone development (Nowlan et al., 2010), whereas moderate weight loading increases mineralization and enhances vascularization of GP of young chickens (Reich et al., 2005). In young fast-growing chickens and turkeys, several leg problems appear to be associated with the proximal aspects of their leg bone which are the weight bearing ends. Cage confinement enhances bone loss in egg laying hens (Aguado et al., 2015) while increased physical activities of hens raised in aviary improve bone strength and biomechanical properties (Regmi et al., 2015; Rodriguez-Navarro et al., 2018). Thus, it posits that imposed physical inactivity due to overcrowding and cage confinement can be a major risk factors for some of the poultry leg problems.

Genetic selection of poultry for better performance with respect to growth, feed conversion, and egg production are presumed to factor in their negative impact on bone health, leading to some leg problems such as lameness in meat-type poultry and osteoporosis in laying hens (Havenstein et al., 2003; Julian, 1998; Knowles et al., 2008; Paxton et al., 2013; Weeks et al., 2002). However, genetic correlation of poultry leg problems in young chickens with better growth characteristics has not been conclusive (González-Cerón et al., 2015a,b; Sanchez-Rodriguez et al., 2019; Shim et al., 2012). The following sections describe specific poultry bone disorders/ diseases encountered in commercial, backyard, and free-range flocks.

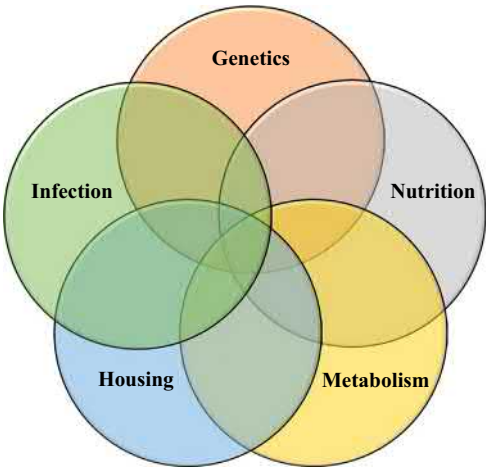

FIGURE 22.3 Poultry bone deformities and diseases are of multifactorial etiology.

22.5.1 Cage layer fatigue/osteoporosis

Cage layer fatigue/osteoporosis is a metabolic bone problem which occurs in high egg-producing layers, as a result of the loss of structural bone due to excessive osteoclast activities (Fleming, 2008; Thorp, 1994). However, osteoporosis in poultry can be related to several etiological factors. Housing system, genetics, and nutrition play major roles in the development of osteoporosis. The affected birds lose the ability to stand and resume a recumbent position. Osteoporosis manifests towards the end of laying cycle and is provoked by nutritional deficiency of Ca and P in older layers causing depletion of medullary bones. Genetics play some roles in avian osteoporosis (Fleming et al., 2006; Johnsson et al., 2015). There are several studies correlating the role of different genetic loci with bone strength of laying hens that include genes regulating bone mass, bone resorption, and metabolism (Bishop et al., 2000; Fleming et al., 2006; Johnsson et al., 2015; Raymond et al., 2018). Genetic

correlation of bone quality in older hens and the resistance to breakage with their collagen crosslink content, was reported in one study (Sparke et al., 2002). Estrogen deficiency is also implicated in avian osteoporosis, since estrogen regulates Ca absorption and its mobilization both in the uterus and the intestine (Bar, 2009; Beck and Hansen, 2004).

22.5.2 Keel bone deformity and fracture

Keel bone deformity (Figure 22.4) and fractures are prevalent in hens when they reach peak egg production which can be influenced by different management systems (Wilkins et al., 2011). Anatomical position of keel bone along with smaller breast muscle in laying hens, compounded with bone weakness due to osteoporosis, trauma, unfavorable housing conditions, and Ca deficiency contribute to keel bone problems (Fleming et al., 2004; Jung et al., 2019; Riber et al., 2018).

22.5.3 Cervical scoliosis

Poultry cervical scoliosis, characterized by an abnormal posture of neck, is a relatively new and emerging bone disease associated with excessive osteoclast activities that leads to the failure of embryo hatching (Olkowski et al., 2019). However, the inheritance of this problem or its genetic basis remains unknown.

22.5.4 Chondrodystrophy, slipped tendon/perosis, and rickets

Deficiencies of certain essential nutrients such as lysine, choline, biotin, pyridoxine, vitamin D, and trace elements including zinc and manganese contribute to chondrodystrophy, angular deformities, rickets, and osteomalacia (Fleming, 2008). Slipped tendon/perosis, indicated by enlarged tibiometatarsal joints with twisting of tibia and metatarsal bone, are common in chickens, turkeys, and ducks (Thorp, 1994). Uneven growth of long bone are also indicated in the cause of chondrodystrophy, possibly related to some metabolic disturbances that negatively impact the production of certain proteoglycans (Pines and Reshef, 2015). Failure of mineralization due to the deficiencies of vitamin D, Ca, or P and their imbalance cause rickets characterized by the thickening of GP with the accumulation of proliferative and mature chondrocytes in young and osteomalacia in older birds (Lacey and Huffer, 1982; Takechi and Itakura, 1995). Hypocalcemic chickens exhibit more proliferative and immature chondrocytes in the GP compared with hypophosphatemic birds that exhibit more hypertrophic chondrocytes.

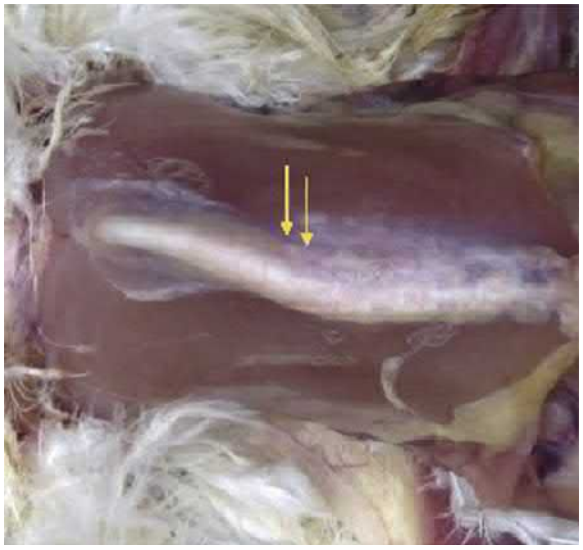

FIGURE 22.4 Keel bone deformity in chicken (*arrows* show deformed regions of keel bone).

22.5.5 Valgus-varus deformity

Valgus-varus deformity/twisted legs are caused by distortion of the long bones of legs characterized by deformed intertarsal joints. The outward angling of the leg is called valgus deformation whereas the inward bending called varus deformation (Riddell et al., 1983, Figure 22.5). Traumatic injuries to the joints are likely involved in the cause of these deformities. A recent study showed differential and abnormal expression of several bone-regulatory genes in the cartilage of chickens with VVD compared with their normal counterparts (Guo et al., 2020). It is however, not known whether the differential expression of those genes associated with bone development are the causes of VVD or they are differentially expressed as a result of to the injury induced angulation.

22.5.6 Tibial dyschondroplasia

TD is another frequently encountered poultry bone disorder that affects the proximal GP of tibia and tibiotarsal bone of fast-growing broiler chickens, turkeys, and ducks, identified

FIGURE 22.5 Valgus deformation of legs in turkeys.

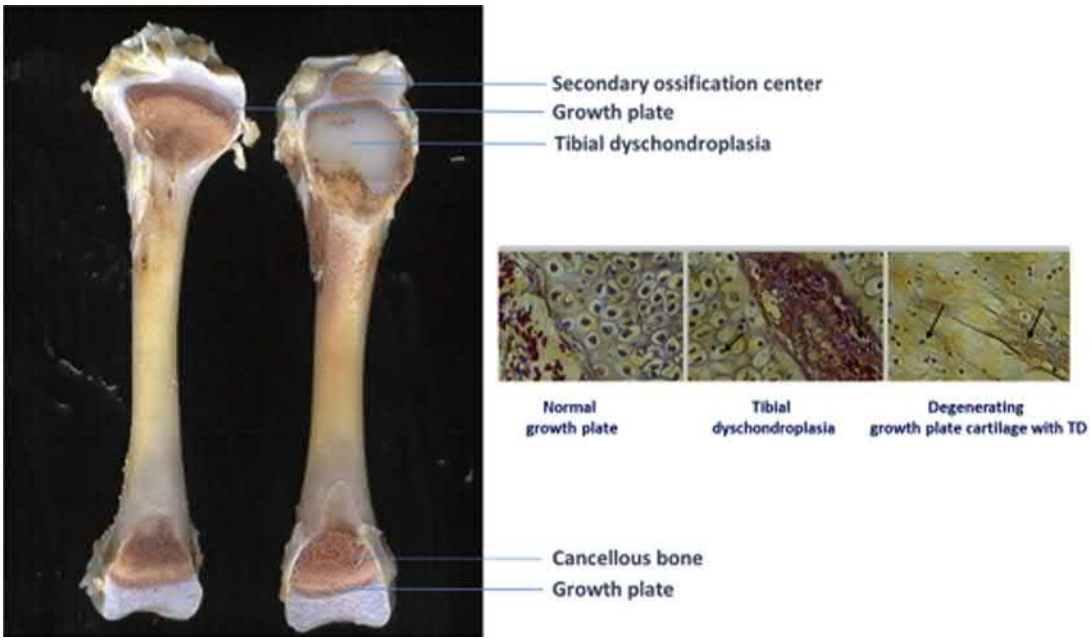

FIGURE 22.6 Tibial epiphyseal growth plates of a normal (left) and a dyschondroplasia-affected chicken bone (right) showing the histology of the hypertrophic zone of a normal and the affected growth plates with degenerating chondrocytes and blood vessels.

as a plug of opaque, nonvascularized cartilage in the GP that fails to ossify (Farquharson, 2002; Leach and Monsonego-Ornan, 2007; Lilburn and Leach, 1980; Orth and Cook, 1994; Pines et al., 2005, Figure 22.6). The presence of nonossified cartilage in the GP produces lameness and vulnerability to bone deformity and breakage. A variety of mechanisms concerning the failure of GP cartilage to form bone and the pathogenesis of TD have been proposed. These include but not limited to the deficiency of one or more critical growth factors of bone development such as, BMP, FGF, and vitamin D3 to some mineral nutrition imbalance, hypoxia, endoplasmic stress, and the factors that interfere with the GP development (Genin et al., 2008; Huang et al., 2017; Leach and Monsonego-Ornan, 2007; Pines et al., 2005; Praul et al., 2000; Rath et al., 2005; Thorp, 1994). Impaired angiogenesis and vascularization of GP has been suggested as a mechanism for the pathogenesis of TD (Huang et al., 2018). Exposure to certain dithiocarbamate pesticides, mycotoxins, copper chelators, and the vitamin D deficiency during early growth also induces TD in broiler chickens (Orth and Cook, 1994; Rath et al., 2007a; Vargas et al., 1983; Whitehead et al., 2004). Both in naturally occurring and experimentally induced TD, aberrant chondrocyte death and their accumulation in the transition zone of GP prevent ossification leading to its pathogenesis (Praul et al., 1997; Rath et al., 1998, 2005). The interesting feature of TD is that, it is primarily a proximal GP problem of tibia and tibiotarsal bone while the distal GP remain unaffected suggesting that the disease may be related to the weight bearing functions of these bone (Figure 22.6). Inclusion of vitamin D3 in the diet was shown to decrease the incidences and severity of TD induced by Ca/P deficiency (Whitehead et al., 2004). However, vitamin D3 did not have any ameliorating effect on thiram induced TD (Rath et al., 2007b).

22.5.7 Femoral head separation

FHS, also referred to as "epiphysiolysis" or "proximal femoral head degeneration," is frequently seen in heavier poultry. Loss of adhesion between AC and GP is the primary feature of FHS (Julian, 2005; Packialakshmi et al., 2015) which may be enhanced by mechanical stress on the leg bone. FHS has been linked to metabolic dyslipidemia, vascular problems of femoral epiphysis, and sporadic chondrocyte death that likely progresses to cartilage necrosis and infection (Duff and Randall, 1987; Durairaj et al., 2009; Knowles et al., 2008; Packialakshmi et al., 2015, Figure 22.7). "Proximal femoral degeneration" is another chicken femoral head problem similar to FHS that has been associated with excessive bone resorption, high MMP and altered osteoclast activities, that lead to the loss of cortical and trabecular bones (Olkowski et al., 2011). Vascular interruption is implicated as a cause of avascular necrosis of femoral head which is often the case with the mammalian disease.

22.5.8 Femoral head necrosis, osteomyelitis, bacterial chondronecrosis

Osteomyelitis, synovitis (Emslie et al., 1983; Huff et al., 2000; McNamee and Smyth, 2000; Nairn, 1973), mycoplasma chondrodystrophy (Ley et al., 2010), spondylitis

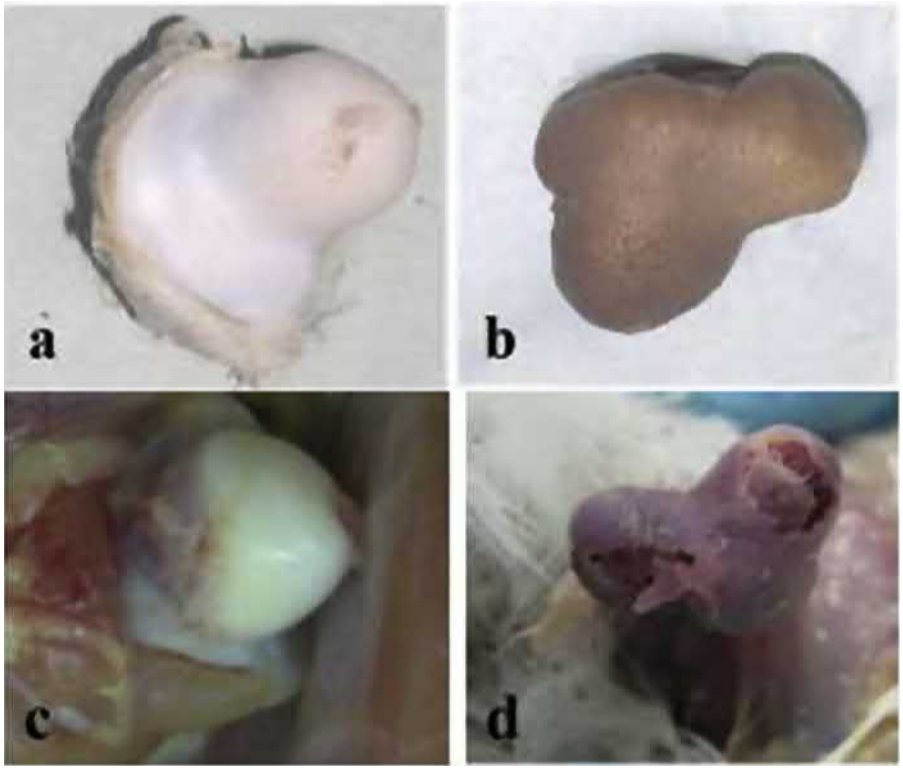

FIGURE 22.7 Healthy femoral head epiphyses with intact articular cartilage (A and C), a femoral head separated from articular cartilage without necrosis (B), and a separated femoral head with necrotic lesions (D).

(vertebral osteomyelitis) (Braga et al., 2016), and enterococcus spondylitis (Borst et al., 2017), osteochondrosis (Chen et al., 2018a), infectious synovitis, viral arthritis (Lockaby et al., 1998; Van Der Heide, 1977), and bacterial chondronecrosis with osteomyelitis (BCO) are some of the avian skeletal diseases associated with infectious agents. Infection with opportunistic pathogens induce tibial head and femoral head necrosis (THN, FHN) in chickens (Dinev, 2009; Dinev et al., 2019; Huff et al., 2000; Jiang et al., 2015; McNamee and Smyth, 2000; Mutalib et al., 1996; Nairn, 1973; Paxton et al., 2014; Wideman, 2016; Wijesurendra et al., 2017). Bacterial pathogens such as *Salmonella, Escherichia coli, Staphylococcus, Streptococcus, Ornithobacterium rhinotracheale, Mycoplasma synoviae* cause synovitis and arthritis (Clark et al., 1991; Köhler et al., 1980; Lockaby et al., 1998; Padron, 1990; Travers et al., 1996). Recently, *Staphylococcus aureus,* a bacteria involved in the pathogenesis of human osteomyelitis, was found to cause BCO in chickens and osteoblast death in culture (Greene et al., 2019). Vascular insufficiency due to inadequate blood flow into the GP because of microvasculature limitation and embolism, is implicated in the pathogenesis of BCO and GP fractures (Dinev et al., 2019; Jiang et al., 2015; Wideman, 2016; Wideman and Prisby, 2011). Mycoplasma infections cause swollen joints and vertebral chondrodystrophy (Ley et al., 2010; Morrow et al., 1997). Some bone problems in chickens have also been observed with reovirus and avian leukosis virus infections which cause FHN and brittle bone disease (van der Heide and Horzinek, 1981).

22.5.9 Amyloid arthropathy

Amyloid arthropathy in chickens is caused by the extracellular deposition of amyloid fibers in the joints that largely affect AC and synovial membranes (Landman, 1999; Peperkamp et al., 1997). The hip and tibiotarsal joints are affected more than other smaller joints. Infection-induced release of an acute phase protein serum amyloid A (SAA) from the liver and its aggregation in the joints cause inflammation and the infiltration of inflammatory cells (Zekarias, 2000). SAA has been reported in birds infected with *Enterococcus faecalis* and *Staphylococcus aureus* and show amyloid arthropathy (Blanco et al., 2016; Sevimli et al., 2013; Steentjes et al., 2002).

22.6 Conclusion

The developmental paths of both avian and mammalian skeletal elements are comparatively similar; however, the avian skeleton has evolved to support the aerial life of birds with some exceptions that occur in flightless birds, where

the skeletons show different adaptations. The lightweight bone along with fused vertebrae not only impart buoyancy and rigidity to the skeleton for flight, but also their hollow wing bone with struts and ridges support and impart high torsional strength and connection to the respiratory system, providing extra supply of oxygen to blood during flight. The keel sternum provides leverage for pectoral and wing muscles in flying birds, while it is either reduced in size or absent in flightless birds. The commercial poultry species that descended from their wild flying ancestors, have undergone rigorous genetic selections for better feed conversion, growth, and egg production, are often raised under constrained husbandry conditions forcing their adaptation to a relatively sedentary life. In the absence of adequate mechanical stimulation, the epiphyseal circulatory physiology is likely affected negatively leading to some of the degenerative joint problems. Nutritional deficiencies, poor housing, and hygienic conditions also contribute to certain skeletal problems in commercial poultry. In older laying hens, osteoporosis is a major cause of bone fracture which can be eased by proper nutrition and enhanced housing conditions that increase their physical activities. Understanding the mechanobiological basis of poultry bone diseases can improve poultry welfare.

References

Abramyan, J., Richman, J.M., 2018. Craniofacial development: discoveries made in the chicken embryo. Int. J. Dev. Biol. 62, 97–107.

Abzhanov, A., Rodda, S.J., McMahon, A.P., Tabin, C.J., 2007. Regulation of skeletogenic differentiation in cranial dermal bone. Development 134, 3133–3144.

Aguado, E., Pascaretti-Grizon, F., Goyenvalle, E., Audran, M., Chappard, D., 2015. Bone mass and bone quality are altered by hypoactivity in the chicken. PloS One 10, e0116763.

Bahney, C.S., Zondervan, R.L., Allison, P., Theologis, A., Ashley, J.W., Ahn, J., Miclau, T., Marcucio, R.S., Hankenson, K.D., 2019. Cellular biology of fracture healing. J. Orthop. Res. 37, 35–50.

Bar, A., 2009. Calcium transport in strongly calcifying laying birds: mechanisms and regulation. Comp. Biochem. Physiol. Mol. Integr. Physiol. 152, 447–469.

Beck, M.M., Hansen, K.K., 2004. Role of estrogen in avian osteoporosis. Poultry Sci. 83, 200–206.

Berendsen, A.D., Olsen, B.R., 2015. Bone development. Bone 80, 14–18.

Bishop, S., Fleming, R., McCormack, H., Flock, D., Whitehead, C., 2000. Inheritance of bone characteristics affecting osteoporosis in laying hens. Br. Poultry Sci. 41, 33–40.

Blanco, A., Barz, M., Icken, W., Cavero, D., 2016. Twenty years of amyloid arthropathy research in chickens. World's Poultry Sci. J. 72, 495–508.

Blumer, M.J., Fritsch, H., Pfaller, K., Brenner, E., 2004. Cartilage canals in the chicken embryo: ultrastructure and function. Anat. Embryol. 207, 453–462.

Bonewald, L.F., 2011. The amazing osteocyte. J. Bone Miner. Res. 26, 229–238.

Bonewald, L.F., Johnson, M.L., 2008. Osteocytes, mechanosensing and Wnt signaling. Bone 42, 606–615.

Borst, L.B., Suyemoto, M.M., Sarsour, A.H., Harris, M.C., Martin, M.P., Strickland, J.D., Oviedo, E.O., Barnes, H.J., 2017. Pathogenesis of enterococcal spondylitis caused by *Enterococcus cecorum* in broiler chickens. Vet. Pathol. 54, 61–73.

Braga, J.F., Silva, C.C., Teixeira, M.P., Martins, N.R., Ecco, R., 2016. Vertebral osteomyelitis associated with single and mixed bacterial infection in broilers. Avian Pathol. 45, 640–648.

Canoville, A., Schweitzer, M.H., Zanno, L.E., 2019. Systemic distribution of medullary bone in the avian skeleton: ground truthing criteria for the identification of reproductive tissues in extinct Avemetatarsalia. BMC Evol. Biol. 19, 71.

Chen, L.R., Suyemoto, M.M., Sarsour, A.H., Cordova, H.A., Oviedo-Rondón, E.O., Barnes, H.J., Borst, L.B., 2018a. Prevalence and severity of osteochondrosis of the free thoracic vertebra in three modern broiler strains and the Athens Canadian Random Bred control broiler. Avian Pathol. 47, 152–160.

Chen, X., Wang, Z., Duan, N., Zhu, G., Schwarz, E.M., Xie, C., 2018b. Osteoblast-osteoclast interactions. Connect. Tissue Res. 59, 99–107.

Chijimatsu, R., Saito, T., 2019. Mechanisms of synovial joint and articular cartilage development. Cell. Mol. Life Sci. 76, 3939–3952.

Clark, S.R., Barnes, H.J., Bickford, A.A., Chin, R.P., Droual, R., 1991. Relationship of osteomyelitis and associated soft-tissue lesions with green liver discoloration in tom turkeys. Avian Dis. 35, 139–146.

Clarke, B., 2008. Normal bone anatomy and physiology. Clin. J. Am. Soc. Nephrol. 3 (Suppl. 3), S131–S139.

Cole, J.H., van der Meulen, M.C., 2011. Whole bone mechanics and bone quality. Clin. Orthop. Relat. Res. 469, 2139–2149.

Costain, R., 2018. Avian Adaptation. Montana Natural History Center. https://www.montananaturalist.org/blog-post/avian-adaptations/.

Creuzet, S., Couly, G., Le Douarin, N.M., 2005. Patterning the neural crest derivatives during development of the vertebrate head: insights from avian studies. J. Anat. 207, 447–459.

Dallas, S.L., Prideaux, M., Bonewald, L.F., 2013. The osteocyte: an endocrine cell … and more. Endocr. Rev. 34, 658–690.

Davey, M.G., Towers, M., Vargesson, N., Tickle, C., 2018. The chick limb: embryology, genetics and teratology. Int. J. Dev. Biol. 62, 85–95.

Day, T.F., Guo, X., Garrett-Beal, L., Yang, Y., 2005. Wnt/beta-catenin signaling in mesenchymal progenitors controls osteoblast and chondrocyte differentiation during vertebrate skeletogenesis. Dev. Cell 8, 739–750.

Dinev, I., 2009. Clinical and morphological investigations on the prevalence of lameness associated with femoral head necrosis in broilers. Br. Poultry Sci. 50, 284–290.

Dinev, I., Kanakov, D., Kalkanov, I., Nikolov, S., Denev, S., 2019. Comparative pathomorphologic studies on the incidence of fractures associated with leg skeletal pathology in commercial broiler chickens. Avian Dis. 63, 641–650.

Duff, S.R., Randall, C.J., 1987. Observations on femoral head abnormalities in broilers. Res. Vet. Sci. 42, 17–23.

Dumont, E.R., 2010. Bone density and the lightweight skeletons of birds. Proc. Biol. Sci. 277, 2193–2198.

Durairaj, V., Okimoto, R., Rasaputra, K., Clark, F.D., Rath, N.C., 2009. Histopathology and serum clinical chemistry evaluation of broilers with femoral head separation disorder. Avian Dis. 53, 21–25.

Eames, B.F., de la Fuente, L., Helms, J.A., 2003. Molecular ontogeny of the skeleton. Birth Defects Res. C Embryo Today 69, 93–101.

Eames, B.F., Helms, J.A., 2004. Conserved molecular program regulating cranial and appendicular skeletogenesis. Dev. Dynam. 231, 4–13.

Emslie, K.R., Ozanne, N.R., Nade, S.M., 1983. Acute haematogenous osteomyelitis: an experimental model. J. Pathol. 141, 157–167.

Erben, R.G., 2018. Physiological actions of fibroblast growth factor-23. Front. Endocrinol. 9, 267.

Eyre, D.R., Brickley-Parsons, D.M., Glimcher, M.J., 1978. Predominance of type I collagen at the surface of avian articular cartilage. FEBS Lett. 85, 259–263.

Farquharson, C., 2002. Tibial Dyschondroplasia: A Growth Plate Abnormality Caused by Delayed Terminal Differentiation. IOS Press, Amsterdam.

Feng, X., Teitelbaum, S.L., 2013. Osteoclasts: new insights. Bone Res. 1, 11–26.

Fleisch, H., 1997. Bisphosphonates in Bone Disease : From the Laboratory to the Patient, third ed. Parthenon, New York ; London.

Fleming, R.H., 2008. Nutritional factors affecting poultry bone health. Proc. Nutr. Soc. 67, 177–183.

Fleming, R.H., McCormack, H.A., McTeir, L., Whitehead, C.C., 1998. Medullary bone and humeral breaking strength in laying hens. Res. Vet. Sci. 64, 63–67.

Fleming, R.H., McCormack, H.A., McTeir, L., Whitehead, C.C., 2004. Incidence, pathology and prevention of keel bone deformities in the laying hen. Br. Poultry Sci. 45, 320–330.

Fleming, R.H., McCormack, H.A., McTeir, L., Whitehead, C.C., 2006. Relationships between genetic, environmental and nutritional factors influencing osteoporosis in laying hens. Br. Poultry Sci. 47, 742–755.

Florencio-Silva, R., Sasso, G.R., Sasso-Cerri, E., Simões, M.J., Cerri, P.S., 2015. Biology of bone tissue: structure, function, and factors that influence bone cells. BioMed Res. Int. 2015, 421746.

Gay, C.V., Weber, J.A., 2000. Regulation of differentiated osteoclasts. Crit. Rev. Eukaryot. Gene Expr. 10, 213–230.

Genin, O., Hasdai, A., Shinder, D., Pines, M., 2008. Hypoxia, hypoxia-inducible factor-1alpha (HIF-1alpha), and heat-shock proteins in tibial dyschondroplasia. Poultry Sci. 87, 1556–1564.

Gilbert, S.F., Barresi, M.J.F., 2016. Developmental Biology. Sinauer Assoc. Inc., Sunderland, MA.

Goltzman, D., 2018. Physiology of parathyroid hormone. Endocrinol. Metab. Clin. N. Am. 47, 743–758.

Gonciulea, A., de Beur, S.J., 2015. The dynamic skeleton. Rev. Endocr. Metab. Disord. 16, 79–91.

González-Cerón, F., Rekaya, R., Aggrey, S.E., 2015a. Genetic relationship between leg problems and bone quality traits in a random mating broiler population. Poultry Sci. 94, 1787–1790.

González-Cerón, F., Rekaya, R., Anthony, N.B., Aggrey, S.E., 2015b. Genetic analysis of leg problems and growth in a random mating broiler population. Poultry Sci. 94, 162–168.

Greene, E., Flees, J., Dhamad, A., Alrubaye, A., Hennigan, S., Pleimann, J., Smeltzer, M., Murray, S., Kugel, J., Goodrich, J., Robertson, A., Wideman, R., Rhoads, D., Dridi, S., 2019. Double-stranded RNA is a novel molecular target in osteomyelitis pathogenesis: a translational avian model for human bacterial chondronecrosis with osteomyelitis. Am. J. Pathol. 189, 2077–2089.

Guo, Y., Tang, H., Li, Z., Zhang, Y., Li, D., Li, W., Sun, G., Kang, X., Han, R., 2020. High-throughput transcriptome analysis reveals potentially important relationships between lncRNAs and genes in broilers affected by Valgus-varus deformity (*Gallus gallus*). Gene 743, 144511.

Hadley, J.A., Horvat-Gordon, M., Kim, W.K., Praul, C.A., Burns, D., Leach, R.M., 2016. Bone sialoprotein keratan sulfate proteoglycan (BSP-KSPG) and FGF-23 are important physiological components of medullary bone. Comp. Biochem. Physiol. Mol. Integr. Physiol. 194, 1–7.

Hall, B.K., Miyake, T., 2000. All for one and one for all: condensations and the initiation of skeletal development. Bioessays 22, 138–147.

Hallett, S.A., Ono, W., Ono, N., 2019. Growth plate chondrocytes: skeletal development, growth and beyond. Int. J. Mol. Sci. 20.

Haraguchi, R., Kitazawa, R., Kohara, Y., Ikedo, A., Imai, Y., Kitazawa, S., 2019. Recent insights into long bone development: central role of hedgehog signaling pathway in regulating growth plate. Int. J. Mol. Sci. 20.

Havenstein, G.B., Ferket, P.R., Qureshi, M.A., 2003. Growth, livability, and feed conversion of 1957 versus 2001 broilers when fed representative 1957 and 2001 broiler diets. Poultry Sci. 82, 1500–1508.

Hiyama, S., Yokoi, M., Akagi, Y., Kadoyama, Y., Nakamori, K., Tsuga, K., Uchida, T., Terayama, R., 2019. Osteoclastogenesis from bone marrow cells during estrogen-induced medullary bone formation in Japanese quails. J. Mol. Histol. 50, 389–404.

Huang, S.C., Rehman, M.U., Lan, Y.F., Qiu, G., Zhang, H., Iqbal, M.K., Luo, H.Q., Mehmood, K., Zhang, L.H., Li, J.K., 2017. Tibial dyschondroplasia is highly associated with suppression of tibial angiogenesis through regulating the HIF-1α/VEGF/VEGFR signaling pathway in chickens. Sci. Rep. 7, 9089.

Huang, S.C., Zhang, L.H., Zhang, J.L., Rehman, M.U., Tong, X.L., Qiu, G., Jiang, X., Iqbal, M., Shahzad, M., Shen, Y.Q., Li, J.K., 2018. Role and regulation of growth plate vascularization during coupling with osteogenesis in tibial dyschondroplasia of chickens. Sci. Rep. 8, 3680.

Huff, G., Huff, W., Rath, N., Balog, J., 2000. Turkey osteomyelitis complex. Poultry Sci. 79, 1050–1056.

Iimura, T., Pourquié, O., 2007. Hox genes in time and space during vertebrate body formation. Dev. Growth Differ. 49, 265–275.

Jendral, M.J., Korver, D.R., Church, J.S., Feddes, J.J.R., 2008. Bone mineral density and breaking strength of white leghorns housed in conventional, modified, and commercially available colony battery cages. Poultry Sci. 87, 828–837.

Jiang, T., Mandal, R.K., Wideman, R.F., Khatiwara, A., Pevzner, I., Min Kwon, Y., 2015. Molecular survey of bacterial communities associated with bacterial chondronecrosis with osteomyelitis (BCO) in broilers. PloS One 10, e0124403.

Johnsson, M., Jonsson, K.B., Andersson, L., Jensen, P., Wright, D., 2015. Genetic regulation of bone metabolism in the chicken: similarities and differences to Mammalian systems. PloS Genet. 11, e1005250.

Julian, R.J., 1998. Rapid growth problems: ascites and skeletal deformities in broilers. Poultry Sci. 77, 1773–1780.

Julian, R.J., 2005. Production and growth related disorders and other metabolic diseases of poultry–a review. Vet. J. 169, 350–369.

Jung, L., Niebuhr, K., Hinrichsen, L.K., Gunnarsson, S., Brenninkmeyer, C., Bestman, M., Heerkens, J., Ferrari, P., Knierim, U., 2019. Possible risk factors for keel bone damage in organic laying hens. Animal 13, 2356–2364.

Kerschnitzki, M., Akiva, A., Ben Shoham, A., Asscher, Y., Wagermaier, W., Fratzl, P., Addadi, L., Weiner, S., 2016. Bone mineralization pathways during the rapid growth of embryonic chicken long bones. J. Struct. Biol. 195, 82–92.

Knott, L., Bailey, A.J., 1999. Collagen biochemistry of avian bone: comparison of bone type and skeletal site. Br. Poultry Sci. 40, 371–379.

Knowles, T.G., Kestin, S.C., Haslam, S.M., Brown, S.N., Green, L.E., Butterworth, A., Pope, S.J., Pfeiffer, D., Nicol, C.J., 2008. Leg disorders in broiler chickens: prevalence, risk factors and prevention. PloS One 3, e1545.

Komori, T., 2017. Roles of Runx2 in skeletal development. Adv. Exp. Med. Biol. 962, 83–93.

Kozhemyakina, E., Lassar, A.B., Zelzer, E., 2015. A pathway to bone: signaling molecules and transcription factors involved in chondrocyte development and maturation. Development 142, 817–831.

Kronenberg, H.M., 2003. Developmental regulation of the growth plate. Nature 423, 332–336.

Köhler, B., Nattermann, H., Witte, W., Friedrichs, F., Kunter, E., 1980. [*Staphylococcus aureus* infection in chickens in industrialized poultry units. 2. Microbiological studies: *Staphylococcus aureus* and other pathogens]. Arch. Exp. Veterinaermed. 34, 905–923.

Lacey, D.L., Huffer, W.E., 1982. Studies on the pathogenesis of avian rickets. I. Changes in epiphyseal and metaphyseal vessels in hypocalcemic and hypophosphatemic rickets. Am. J. Pathol. 109, 288–301.

Landman, W.J., 1999. Amyloid arthropathy in chickens. Vet. Q. 21, 78–82.

Le Douarin, N.M., 2004. The avian embryo as a model to study the development of the neural crest: a long and still ongoing story. Mech. Dev. 121, 1089–1102.

Leach Jr., R.M., Monsonego-Ornan, E., 2007. Tibial dyschondroplasia 40 years later. Poultry Sci. 86, 2053–2058.

Ley, D.H., Marusak, R.A., Vivas, E.J., Barnes, H.J., Fletcher, O.J., 2010. Mycoplasma iowae associated with chondrodystrophy in commercial turkeys. Avian Pathol. 39, 87–93.

Li, L., Ma, Y., Li, X., Bai, C., Ji, M., Zhang, S., Guan, W., Li, J., 2015. Isolation, culture, and characterization of chicken cartilage stem/progenitor cells. BioMed Res. Int. 2015, 586290.

Lilburn, M.S., Leach, R.M., 1980. Metabolism of abnormal cartilage cells associated with tibial dyschondroplasia. Poultry Sci. 59, 1892–1896.

Lockaby, S.B., Hoerr, F.J., Lauerman, L.H., Kleven, S.H., 1998. Pathogenicity of *Mycoplasma synoviae* in broiler chickens. Vet. Pathol. 35, 178–190.

Long, F., Ornitz, D.M., 2013. Development of the endochondral skeleton. Cold Spring Harb. Perspect. Biol. 5, a008334.

Maas, S.A., Suzuki, T., Fallon, J.F., 2011. Identification of spontaneous mutations within the long-range limb-specific Sonic hedgehog enhancer (ZRS) that alter Sonic hedgehog expression in the chicken limb mutants oligozeugodactyly and silkie breed. Dev. Dynam. 240, 1212–1222.

Mackie, E.J., Ahmed, Y.A., Tatarczuch, L., Chen, K.S., Mirams, M., 2008. Endochondral ossification: how cartilage is converted into bone in the developing skeleton. Int. J. Biochem. Cell Biol. 40, 46–62.

Mackie, E.J., Tatarczuch, L., Mirams, M., 2011. The skeleton: a multifunctional complex organ: the growth plate chondrocyte and endochondral ossification. J. Endocrinol. 211, 109–121.

Mariani, F.V., Martin, G.R., 2003. Deciphering skeletal patterning: clues from the limb. Nature 423, 319–325.

McNamee, P.T., Smyth, J.A., 2000. Bacterial chondronecrosis with osteomyelitis ('femoral head necrosis') of broiler chickens: a review. Avian Pathol. 29, 477–495.

Minoux, M., Rijli, F.M., 2010. Molecular mechanisms of cranial neural crest cell migration and patterning in craniofacial development. Development 137, 2605–2621.

Moreira, C., Dempster, D., Baron, R., 2019. Anatomy and ultrastructure of bone – histogenesis, growth and remodeling, In: Feingold, K., Anawalt, B., Boyce, A., et al., (Eds.), MDText.com, Inc., South Dartmouth (MA). www.endotext.org.

Morrow, C., Bradbury, J., Gentle, M., Thorp, B., 1997. The development of lameness and bone deformity in the broiler following experimental infection with *Mycoplasma gallisepticum* or *Mycoplasma synoviae*. Avian Pathol. 26, 169–187.

Moser, S.C., van der Eerden, B.C.J., 2018. Osteocalcin-A versatile bone-derived hormone. Front. Endocrinol. 9, 794.

Murshed, M., 2018. Mechanism of bone mineralization. Cold Spring Harb. Perspect. Med. 8.

Mutalib, A., Miguel, B., Brown, T., Maslin, W., 1996. Distribution of arthritis and osteomyelitis in turkeys with green liver discoloration. Avian Dis. 661–664.

Nairn, M.E., 1973. Bacterial osteomyelitis and synovitis of the Turkey. Avian Dis. 17, 504–517.

Nilsson, O., Marino, R., De Luca, F., Phillip, M., Baron, J., 2005. Endocrine regulation of the growth plate. Horm. Res. 64, 157–165.

Nolte, C., De Kumar, B., Krumlauf, R., 2019. Hox genes: downstream "effectors" of retinoic acid signaling in vertebrate embryogenesis. Genesis 57, e23306.

Novitskaya, E., Ruestes, C.J., Porter, M.M., Lubarda, V.A., Meyers, M.A., McKittrick, J., 2017. Reinforcements in avian wing bones: experiments, analysis, and modeling. J. Mech. Behav. Biomed. Mater. 76, 85–96.

Nowlan, N.C., Sharpe, J., Roddy, K.A., Prendergast, P.J., Murphy, P., 2010. Mechanobiology of embryonic skeletal development: insights from animal models. Birth Defects Res. C Embryo Today 90, 203–213.

Okamoto, K., Takayanagi, H., 2019. Osteoimmunology. Cold Spring Harb. Perspect. Med. 9.

Olkowski, A., Wojnarowicz, C., Olkowski, B., Laarveld, B., 2019. Cervical scoliosis and torticollis: a novel skeletal anomaly in broiler chickens. Acta Vet. Scand. 61, 47.

Olkowski, A.A., Laarveld, B., Wojnarowicz, C., Chirino-Trejo, M., Chapman, D., Wysokinski, T.W., Quaroni, L., 2011. Biochemical and physiological weaknesses associated with the pathogenesis of femoral bone degeneration in broiler chickens. Avian Pathol. 40, 639–650.

Olsen, B.R., Reginato, A.M., Wang, W., 2000. Bone development. Annu. Rev. Cell Dev. Biol. 16, 191–220.

Ono, T., Nakashima, T., 2018. Recent advances in osteoclast biology. Histochem. Cell Biol. 149, 325–341.

Orth, M.W., Cook, M.E., 1994. Avian tibial dyschondroplasia: a morphological and biochemical review of the growth plate lesion and its causes. Vet. Pathol. 31, 403–404.

Packialakshmi, B., Rath, N.C., Huff, W., Huff, G., 2015. Poultry femoral head separation and necrosis: a review. Avian Dis. 59, 349–354.

Padron, M., 1990. *Salmonella typhimurium* outbreak in broiler chicken flocks in Mexico. Avian Dis. 34, 221–223.

Paxton, H., Daley, M.A., Corr, S.A., Hutchinson, J.R., 2013. The gait dynamics of the modern broiler chicken: a cautionary tale of selective breeding. J. Exp. Biol. 216, 3237–3248.

Paxton, H., Tickle, P.G., Rankin, J.W., Codd, J.R., Hutchinson, J.R., 2014. Anatomical and biomechanical traits of broiler chickens across

ontogeny. Part II. Body segment inertial properties and muscle architecture of the pelvic limb. Peer J. 2, e473.
Peperkamp, N.H., Landman, W.J., Tooten, P.C., Ultee, A., Voorhout, W.F., Gruys, E., 1997. Light microscopic, immunohistochemical, and electron microscopic features of amyloid arthropathy in chickens. Vet. Pathol. 34, 271–278.
Pines, M., Hasdai, A., Monsonego-Ornan, E., 2005. Tibial dyschondroplasia–tools, new insights and future prospects. World Poultry Sci. J. 61, 285–297.
Pines, M., Hurwitz, S., 1991. The role of the growth plate in longitudinal bone growth. Poultry Sci. 70, 1806–1814.
Pines, M., Reshef, R., 2015. Poultry Bone Development and Bone Disorders, sixth ed. Elsevier Inc.
Pourquié, O., 2018. Somite formation in the chicken embryo. Int. J. Dev. Biol. 62, 57–62.
Pourquié, O., Coltey, M., Teillet, M.A., Ordahl, C., Le Douarin, N.M., 1993. Control of dorsoventral patterning of somitic derivatives by notochord and floor plate. Proc. Natl. Acad. Sci. U. S. A. 90, 5242–5246.
Praul, C.A., Ford, B.C., Gay, C.V., Pines, M., Leach, R.M., 2000. Gene expression and tibial dyschondroplasia. Poultry Sci. 79, 1009–1013.
Praul, C.A., Gay, C.V., Leach Jr., R.M., 1997. Chondrocytes of the tibial dyschondroplastic lesion are apoptotic. Int. J. Dev. Biol. 41, 621–626.
Provot, S., Schipani, E., 2005. Molecular mechanisms of endochondral bone development. Biochem. Biophys. Res. Commun. 328, 658–665.
Rath, N.C., Huff, G.R., Huff, W.E., Balog, J.M., 2000. Factors regulating bone maturity and strength in poultry. Poultry Sci. 79, 1024–1032.
Rath, N.C., Huff, W.E., Bayyari, G.R., Balog, J.M., 1998. Cell death in avian tibial dyschondroplasia. Avian Dis. 42, 72–79.
Rath, N.C., Huff, W.E., Huff, G.R., Kannan, L., 2007a. Induction of tibial dyschondroplasia by carbamate and thiocarbamate pesticides. Avian Dis. 51, 590–593.
Rath, N.C., Kannan, L., Pillai, P.B., Huff, W.E., Huff, G.R., Horst, R.L., Emmert, J.L., 2007b. Evaluation of the efficacy of vitamin D3 or its metabolites on thiram-induced tibial dyschondroplasia in chickens. Res. Vet. Sci. 83, 244–250.
Rath, N.C., Richards, M.P., Huff, W.E., Huff, G.R., Balog, J.M., 2005. Changes in the tibial growth plates of chickens with thiram-induced dyschondroplasia. J. Comp. Pathol. 133, 41–52.
Raymond, B., Johansson, A.M., McCormack, H.A., Fleming, R.H., Schmutz, M., Dunn, I.C., De Koning, D.J., 2018. Genome-wide association study for bone strength in laying hens. J. Anim. Sci. 96, 2525–2535.
Regmi, P., Deland, T.S., Steibel, J.P., Robison, C.I., Haut, R.C., Orth, M.W., Karcher, D.M., 2015. Effect of rearing environment on bone growth of pullets. Poultry Sci. 94, 502–511.
Reich, A., Jaffe, N., Tong, A., Lavelin, I., Genina, O., Pines, M., Sklan, D., Nussinovitch, A., Monsonego-Ornan, E., 2005. Weight loading young chicks inhibits bone elongation and promotes growth plate ossification and vascularization. J. Appl. Physiol. (1985) 98, 2381–2389.
Riber, A.B., Casey-Trott, T.M., Herskin, M.S., 2018. The influence of keel bone damage on welfare of laying hens. Front. Vet. Sci. 5, 6.
Riddell, C., King, M.W., Gunasekera, K.R., 1983. Pathology of the skeleton and tendons of broiler chickens reared to roaster weights. II. Normal chickens. Avian Dis. 27, 980–991.
Robling, A.G., Bonewald, L.F., 2020. The osteocyte: new insights. Annu. Rev. Physiol. 82, 485–506.
Rodriguez-Navarro, A.B., McCormack, H.M., Fleming, R.H., Alvarez-Lloret, P., Romero-Pastor, J., Dominguez-Gasca, N., Prozorov, T., Dunn, I.C., 2018. Influence of physical activity on tibial bone material properties in laying hens. J. Struct. Biol. 201, 36–45.
Ros, M.A., Simandl, B.K., Clark, A.W., Fallon, J.F., 2000. Methods for manipulating the chick limb bud to study gene expression, tissue interactions, and patterning. Methods Mol. Biol. 137, 245–266.
Rutkovskiy, A., Stensløkken, K.O., Vaage, I.J., 2016. Osteoblast differentiation at a glance. Med. Sci. Monit. Basic Res. 22, 95–106.
Samsa, W.E., Zhou, X., Zhou, G., 2017. Signaling pathways regulating cartilage growth plate formation and activity. Semin. Cell Dev. Biol. 62, 3–15.
Sanchez-Rodriguez, E., Benavides-Reyes, C., Torres, C., Dominguez-Gasca, N., Garcia-Ruiz, A.I., Gonzalez-Lopez, S., Rodriguez-Navarro, A.B., 2019. Changes with age (from 0 to 37 D) in tibiae bone mineralization, chemical composition and structural organization in broiler chickens. Poultry Sci. 98, 5215–5225.
Schneider, R.A., 2018. Neural crest and the origin of species-specific pattern. Genesis 56, e23219.
Schwetz, V., Pieber, T., Obermayer-Pietsch, B., 2012. The endocrine role of the skeleton: background and clinical evidence. Eur. J. Endocrinol. 166, 959–967.
Semeins, C.M., Bakker, A.D., Klein-Nulend, J., 2012. Isolation of primary avian osteocytes. Methods Mol. Biol. 816, 43–53.
Setiawati, R., Rahardjo, P., 2019. Bone development and growth. In: Yang, H. (Ed.), Osteogenesis and Bone Regeneration. IntechOpen, London, UK, pp. 1–20.
Sevimli, A., Bülbül, T., Bülbül, A., Yagci, A., 2013. Chicken amyloid arthropathy: serum amyloid A, interleukin-1beta, interleukin-6, tumour necrosis factor-alpha and nitric oxide profile in acute phase (12th hour). Pol. J. Vet. Sci. 16, 241–247.
Shim, M., Karnuah, A., Mitchell, A., Anthony, N., Pesti, G., Aggrey, S., 2012. The effects of growth rate on leg morphology and tibia breaking strength, mineral density, mineral content, and bone ash in broilers. Poultry Sci. 91, 1790–1795.
Silva, B.C., Bilezikian, J.P., 2015. Parathyroid hormone: anabolic and catabolic actions on the skeleton. Curr. Opin. Pharmacol. 22, 41–50.
Sophia Fox, A.J., Bedi, A., Rodeo, S.A., 2009. The basic science of articular cartilage: structure, composition, and function. Sport Health 1, 461–468.
Sparke, A.J., Sims, T.J., Avery, N.C., Bailey, A.J., Fleming, R.H., Whitehead, C.C., 2002. Differences in composition of avian bone collagen following genetic selection for resistance to osteoporosis. Br. Poultry Sci. 43, 127–134.
Squire, M.E., Veglia, M.K., Drucker, K.A., Brazeal, K.R., Hahn, T.P., Watts, H.E., 2017. Estrogen levels influence medullary bone quantity and density in female house finches and pine siskins. Gen. Comp. Endocrinol. 246, 249–257.
Staines, K.A., Pollard, A.S., McGonnell, I.M., Farquharson, C., Pitsillides, A.A., 2013. Cartilage to bone transitions in health and disease. J. Endocrinol. 219, R1–R12.
Steentjes, A., Veldman, K.T., Mevius, D.J., Landman, W.J., 2002. Molecular epidemiology of unilateral amyloid arthropathy in broiler breeders associated with *Enterococcus faecalis*. Avian Pathol. 31, 31–39.
Sullivan, T., Wang, B., Espinosa, H., Meyers, M., 2017. Extreme lightweight structures: avian feathers and bones. Mater. Today 20, 377–391.

Takechi, M., Itakura, C., 1995. Ultrastructural studies of the epiphyseal plate of chicks fed a vitamin D-deficient and low-calcium diet. J. Comp. Pathol. 113, 101–111.

Thorp, B.H., 1994. Skeletal disorders in the fowl: a review. Avian Pathol. 23, 203–236.

Tickle, C., 2015. How the embryo makes a limb: determination, polarity and identity. J. Anat. 227, 418–430.

Travers, A.F., Coetzee, L., Gummow, B., 1996. Pathogenicity differences between South African isolates of *Ornithobacterium rhinotracheale*. Onderstepoort J. Vet. Res. 63, 197–207.

Turner, C.H., Warden, S.J., Bellido, T., Plotkin, L.I., Kumar, N., Jasiuk, I., Danzig, J., Robling, A.G., 2009. Mechanobiology of the skeleton. Sci. Signal. 2, pt.3.

van der Heide, L.L.,D., Horzinek, M., 1981. Isolation of avian reovirus as a possible etiologic agent of osteoporosis ("brittle bone disease"; "femoral head necrosis") in broiler chickens. Avian Dis. 25, 847–856.

Van der Eerden, B., Karperien, M., Wit, J., 2003. Systemic and local regulation of the growth plate. Endocr. Rev. 24, 782–801.

Van Der Heide, L., 1977. Viral arthritis/tenosynovitis: a review. Avian Pathol. 6, 271–284.

van Driel, M., van Leeuwen, J.P.T.M., 2017. Vitamin D endocrinology of bone mineralization. Mol. Cell. Endocrinol. 453, 46–51.

Vargas, M.I., Lamas, J.M., Alvarenga, V., 1983. Tibial dyschondroplasia in growing chickens experimentally intoxicated with tetramethylthiuram disulfide. Poultry Sci. 62, 1195–1200.

Viguet-Carrin, S., Garnero, P., Delmas, P.D., 2006. The role of collagen in bone strength. Osteoporos. Int. 17, 319–336.

Vortkamp, A., Lee, K., Lanske, B., Segre, G.V., Kronenberg, H.M., Tabin, C.J., 1996. Regulation of rate of cartilage differentiation by Indian hedgehog and PTH-related protein. Science 273, 613–622.

Webster, A.B., 2004. Welfare implications of avian osteoporosis. Poultry Sci. 83, 184–192.

Weeks, C., Knowles, T., Gordon, R., Kerr, A., Peyton, S., Tilbrook, N., 2002. New method for objectively assessing lameness in broiler chickens. Vet. Rec. 151, 762–764.

Whitehead, C., McCormack, H., McTeir, L., Fleming, R., 2004. High vitamin D3 requirements in broilers for bone quality and prevention of tibial dyschondroplasia and interactions with dietary calcium, available phosphorus and vitamin A. Br. Poultry Sci. 45, 425–436.

Whitehead, C.C., 2004. Overview of bone biology in the egg-laying hen. Poultry Sci. 83, 193–199.

Wideman, R.F., 2016. Bacterial chondronecrosis with osteomyelitis and lameness in broilers: a review. Poultry Sci. 95, 325–344.

Wideman, R.F., Prisby, R.D., 2011. Bone circulatory disturbances in the development of spontaneous bacterial chondronecrosis with osteomyelitis: a translational model for the pathogenesis of femoral head necrosis. Front. Endocrinol. 3, 183-183.

Wijesurendra, D.S., Chamings, A.N., Bushell, R.N., Rourke, D.O., Stevenson, M., Marenda, M.S., Noormohammadi, A.H., Stent, A., 2017. Pathological and microbiological investigations into cases of bacterial chondronecrosis and osteomyelitis in broiler poultry. Avian Pathol. 46, 683–694.

Wilkins, L.J., McKinstry, J.L., Avery, N.C., Knowles, T.G., Brown, S.N., Tarlton, J., Nicol, C.J., 2011. Influence of housing system and design on bone strength and keel bone fractures in laying hens. Vet. Rec. 169, 414.

Wu, M., Chen, G., Li, Y.P., 2016. TGF-β and BMP signaling in osteoblast, skeletal development, and bone formation, homeostasis and disease. Bone Res. 4, 16009.

Yang, Y., 2009. Skeletal morphogenesis during embryonic development. Crit. Rev. Eukaryot. Gene Expr. 19, 197–218.

Zekarias, B, Landman, W.J., Tooten, P.C., Gruys, E, et al., 2000. Leukocyte responses in two breeds of layer chicken that differ in susceptibility to induced amyloid arthropathy. Vet. Immunol. Immunopathol. 77, 55–69.

Zhao, Q., Brauer, P.R., Xiao, L., McGuire, M.H., Yee, J.A., 2002. Expression of parathyroid hormone-related peptide (PthrP) and its receptor (PTH1R) during the histogenesis of cartilage and bone in the chicken mandibular process. J. Anat. 201, 137–151.

Zheng, X., Wang, X., O'Connor, J., Zhou, Z., 2012. Insight into the early evolution of the avian sternum from juvenile enantiornithines. Nat. Commun. 3, 1116.

Zofkova, I., 2018. Involvement of bone in systemic endocrine regulation. Physiol. Res. 67, 669–677.

Chapter 23

Skeletal muscle

Orna Halevy[1,2] and Sandra G. Velleman[1,2]
[1]The Hebrew University of Jerusalem, Rehovot, Israel; [2]The Ohio State University, Wooster, OH, United States

23.1 Introduction

Skeletal muscle is the largest tissue in the body, constituting about 40% of its mass. This chapter covers the development and growth of avian skeletal muscle, beginning with a discussion of its structural diversity in different bird species, muscle fiber types, and the mechanism of skeletal muscle contraction. An overview of embryonic and posthatch development is then provided, with a focus on satellite cells, the adult myoblast stem cells that are responsible for all posthatch muscle growth. This is followed by a description of the roles of myogenic transcriptional regulatory factors and growth factors in muscle myogenesis. New emerging areas in avian skeletal muscle biology are addressed, including satellite cell heterogeneity, myopathies in meat-type poultry, and the association of these diseases with extracellular matrix organization and regulation. New strategies to combat the myopathies are discussed.

23.2 Diversity of avian skeletal muscle

The ability to fly has allowed avian species the widespread utilization of many diverse environments and habitats. Perhaps due to this mobility, they may be the most successful terrestrial vertebrate in terms of numbers of species and body forms (Welty, 1982). There are approximately 8900 living species of birds compared to 3000 amphibians, 6000 reptiles, and 4100 mammals. The structure of the musculoskeletal system of birds varies tremendously among species depending on their flight characteristics or whether they are flightless. Most prominent on the sternum of flying birds is a large keel structure to which the powerful flight muscles are attached. Although the penguin is unable to fly, the keel serves as an anchor for muscles controlling the vestigial wings called flippers used for swimming. Flightless birds either lack a keel (ostrich) or the structure is minimal. Other skeletal structures peculiar to birds include a greatly lengthened pelvis fused with the synsacrum, covering approximately half the length of the body. Consequently, there is relatively little dorsal musculature in birds. The majority of the muscle tissue in birds is on the ventral side of the torso, but great differences exist among species. For instance, birds such as hummingbirds and swallows are highly accomplished fliers, but they are limited on the ground; approximately 25−35% of their body weight is devoted to flight musculature and only about 2% to the leg muscles. On the other hand, shore birds that rely more on running than flying have larger leg muscles than wing muscles. Additionally, raptors, which rely on strong grasping of prey, have very strong leg muscles.

The principal flight muscles are the large pectoralis and the supracoracoideus. In some birds, these two muscles may account for 25% of the total mass of the animal. In commercial poultry, genetic selection has largely focused on the size of these muscles because they are the most economically important part of the carcass. Both of these muscles arise from the keel with the supracoracoideus lying dorsal to and under the pectoralis muscle. The pectoralis attaches to the humerus and is responsible for depressing the wings. The supracoracoideus attaches to a tendon that passes dorsally through a foramen and attaches to the dorsal surface of the humerus. This “rope-and-pulley” arrangement allows for the upward movement of the wings. Additionally, there are many other smaller muscles that cause changes in the angle of the wings.

Throughout the skeletal muscular systems of birds, there are many variations in structure that allow this diverse class of vertebrates to adapt to environmental niches and feed sources. For instance, the jaw closing muscles of birds that feed on coarse seeds are stronger than those that feed on smaller grains or noncoarse materials. As will be discussed below, movement requirements of each muscle must be properly matched with the appropriate type of contractile fibers, metabolic characteristics, and neural signal.

Sturkie’s Avian Physiology. https://doi.org/10.1016/B978-0-12-819770-7.00024-4

Members of the class *Aves* are classified as either precocial or altricial in their developmental patterns. Precocial birds hatch with open eyes and a coat of down feathers; they leave the nest within 2 days. Altricial birds hatch with closed eyes, with little or no down feathers, and must be fed by parents. Included in the latter group are passerine birds, the largest order of birds. Additionally, there are birds that fall between these two classifications, which are referred to as semiprecocial or semialtricial. Among the precocial birds include aquatic species such as gulls, terns, ducks, geese, and rails. These species are able to run and swim in the first day following hatching. However, they cannot fly until fully grown (Dial and Carrier, 2012). The early maturation of the leg skeletal muscle system versus the wings allows these species to escape predators without relying on the ability to fly. Although not capable of walking following hatching, altricial birds are capable of performing alternating stepping movements following hatch, indicating that locomotor program is in place early in development (Muir, 2000). Some of the differences between precocial and altricial species are explained by the immaturity of the neurological system in the latter species (Oppenhiem, 1972). However, the sequence of movements leading to pipping and emergence from the egg remains the same in all avian species examined except for members of the family Megapodiidae (Oppenhiem, 1972).

23.3 Muscle structure and contraction

The skeletal muscles are connected to the skeleton through tendons near the joints. The entire muscle is surrounded by a connective layer, the epimysium, which consists mostly of collagen [Fig. 23.1A (old Figure 16.1)]. Within the muscle, the muscle fibers (myofibers) form bundles or fasciculi. The bundles are separated from each other by a connective tissue layer called the perimysium. Muscle bundles can vary in size from 50 to 300 myofibers per bundle, with each myofiber surrounded by the endomysial connective tissue layer. The connective tissue layers are all joined together at the myotendinous junction (the interface of the muscle–tendon connection), and thus are not independent from each other. The interconnection of the three connective tissue layers provides a strong structural framework for the muscle, with capillary beds and water-holding molecules (Koeppen and Stanton, 2018).

Mature myofibers can vary in length and diameter. They are multinucleated muscle cells with myonuclei located at their periphery, just underneath the sarcolemma. The sarcolemma is the plasma membrane of the muscle cell and contains invaginations into the myofiber called the transverse tubule (T-tubule) system. This system allows for the rapid release of calcium from the inner sarcoplasmic reticulum to the cytoplasm upon sufficient membrane depolarization (Koeppen and Stanton, 2018). Invaginations of the T-tubule system into the myofiber occur at regular intervals along the myofiber, close to the myofibrils—contractile filaments that are aligned longitudinally to the myofiber. The myofibrils have a rod-like shape and are organized as repeating units of sarcomeres (the smallest contractile unit of the muscle); each individual sarcomere is bordered by Z bands and consists of thin and thick filaments. The thin filaments are composed primarily of actin, tropomyosin, troponin complex, tropomodulin, and nebulin. The filaments are anchored to the Z band through α-actinin and CapZ. The end of the thin filament closest to the M-line is capped with tropomodulin which, in part, regulates actin filament length (Fowler et al., 1993). The troponin complex is attached to tropomyosin and contains troponin I, troponin T, and troponin C, which are involved in regulating the myosin head–actin filament interaction (Fig. 23.1C). Nebulin is an actin-binding protein. Nebulin-knockout mice have reduced actin filament length and impaired contractile properties (Bang et al., 2006). In the I zone, the actin filaments do not overlap with the myosin filaments.

The thick filaments, the myosin, in the sarcomere do not overlap with the actin filaments in the H zone, whereas the two do overlap in the A zone (Fig. 23.1B and C). Myosin is a protein dimer composed of two heavy chains and two copies of two different light chains. The N-terminus globular domain is the region that binds to actin and is attached to an α-helical myosin tail region. Located near the globular myosin head is one copy of each of the two light chains.

In a state of muscle relaxation, the troponin I–T complex causes tropomyosin to move from its natural position in the grooves of the actin helix to a position that prevents the myosin heads from binding to the actin. Muscle contraction is initiated by myosin head attachment to the actin thin filaments in the sarcomere. For a review on the muscle-contraction process, see Alberts et al. (2008). Upon motor neuron stimulation at the neuromuscular junction and generation of an action potential along the sarcolemma, calcium is released from the sarcoplasmic reticulum and binds to troponin C, causing release of the troponin I–T complex from actin. This allows tropomyosin to return to the actin groove and facilitate the binding of the myosin heads to the actin filament, leading to the latter being pushed toward the center of the sarcomere (Fig. 23.1B and C). The myosin heads need to be released from the actin filaments to prevent a constant state of contraction, and this release requires the recruitment of an adenosine triphosphate (ATP) molecule and its binding to the myosin head. The ATP is then hydrolyzed to adenosine diphosphate (ADP) by ATPase located on the myosin head, facilitating another round of myosin–actin binding (cross-bridge cycle) and further pushing of actin filaments into the

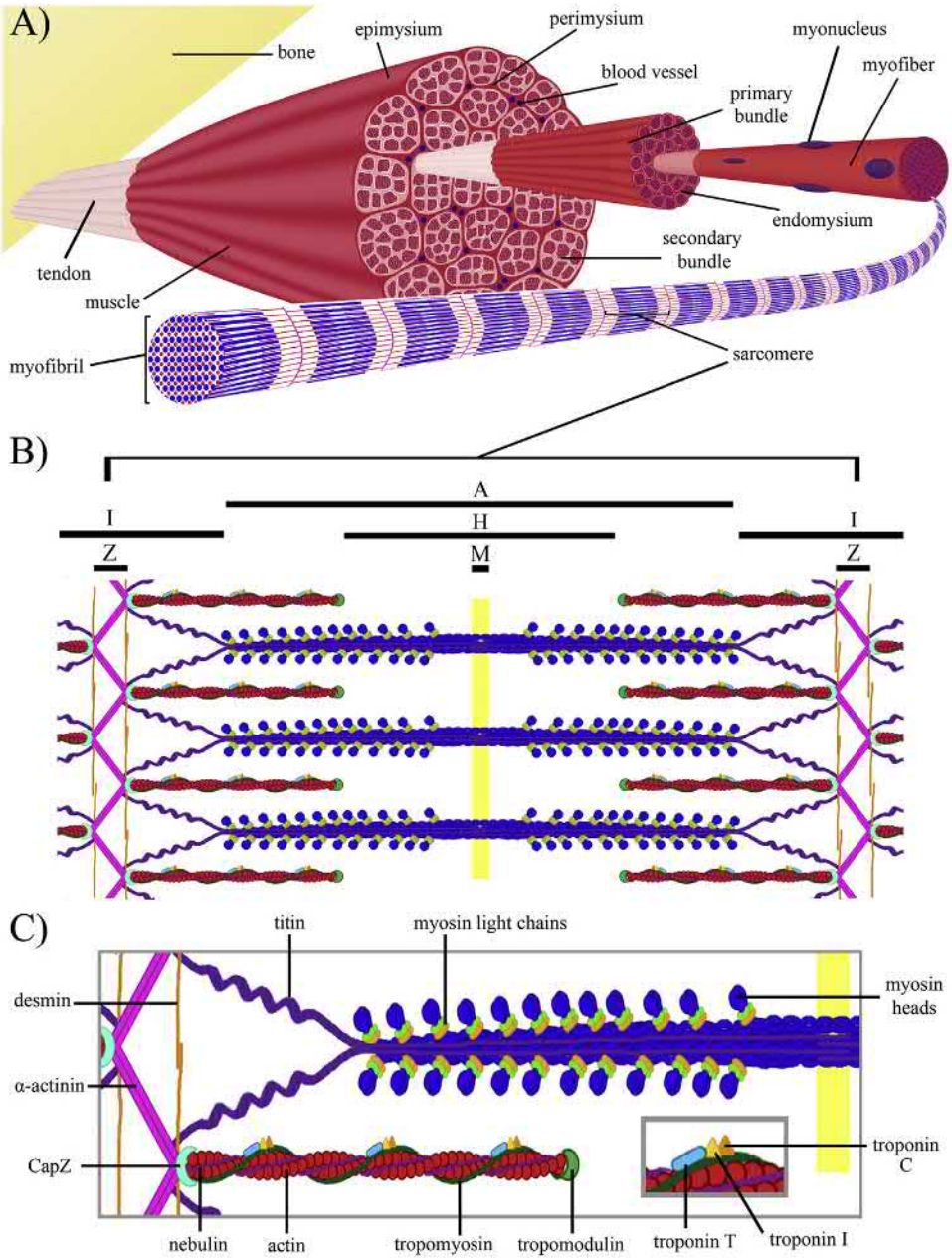

FIGURE 23.1 Schematic of muscle structure. (A) Overview of a cross-sectional area of muscle highlighting muscle fiber structure. (B) Sarcomere structure. (C) The myosin-actin overlap with the associated molecules.

sarcomere. The contraction of an entire muscle is facilitated by synchronized contractions of motor units, each unit consisting of a neural cell body residing in the dorsal root of the spinal cord and its axon, which extends to the muscle being innervated. The single axon splits into numerous branches (from a few to hundreds), each branch innervating an individual myofiber (motor unit). Motor units are interspersed throughout the muscle group regions, so individual motor units influence the contractility of a wide area (Lieber, 1992).

23.4 Skeletal muscle fiber types

Muscle fibers differ greatly in terms of contraction rate, metabolism, and function. There is generally accepted to be three muscle fiber types: (1) slow-twitch, oxidative, type I or red fiber; (2) fast-twitch glycolytic, type IIB or white myofiber; and (3) fast-twitch, oxidative/glycolytic, type IIA or intermediate fiber (Koeppen and Stanton, 2018). The myofiber types housed within muscle groups vary depending on the particular requirements for motion.

Additionally, the same anatomical muscle may differ greatly in fiber composition between species. For instance, when comparing the pectoralis major muscle of a duck and a chicken or a pheasant, it is obvious that the duck pectoralis major muscle is primarily an oxidative muscle due to its high proportion of myoglobin, giving it a red color. This powerful flight muscle ideally suits the duck for long, sustained flights of several hundred miles as required for migration. In migratory wild birds, the muscles will have a higher proportion of type I fibers compared to type IIB (Ashmore et al., 1972). The type I fibers have a higher aerobic capacity and higher blood supply necessary for sustained activity. In contrast, the pectoralis major muscle of the domestic chicken is composed of type IIB fibers and has a lower blood supply because prolonged flight activity is not necessary and the muscle will fatigue more quickly.

Aerobic muscles oxidize glycogen and glucose through glycolysis and the tricarboxylic acid cycle and oxidize fatty acids via β-oxidation. Consequently, these muscles contain greater numbers of mitochondria, smaller fiber diameter to facilitate oxygen diffusion, greater triglyceride levels, and greater capillary density. The chicken or pheasant pectoralis major muscle is primarily composed of glycolytic fast twitch muscles and myoglobin levels are much lower, giving the muscle a white color. Glycolytic muscles oxidize glycogen and glucose to lactate, and the lactate is returned to the liver for gluconeogenesis (Cori cycle). Therefore, much less energy is derived from oxidizing glucose in these muscles, so energy is expended quickly and serves to provide a rapid (but short) burst of activity. In addition to differences in energy metabolism between fiber types, contraction properties are determined by the protein isoforms contained in the contractile apparatus of the fibers. Fast-twitch fibers contain myosin isoforms with fast ATPase activity (generating energy quickly for rapid movements) and slow-twitch fibers contain myosin isoforms with slow ATPase activity (generating energy more slowly for sustained movements). Patterns of action potentials generated from nerves innervating slow muscle fibers differ from those that innervate fast muscles. The slow-switch fibers contain smaller motor units than the fast-twitch fibers. Motor units are generally recruited in order of smallest to largest, hence slow fibers will be activated before fast fibers as contraction increases. Nerve transplantation studies have revealed that the patterns of neural stimulation influence myosin isoform expression (Cerny and Bandman, 1987). When fast muscles were innervated by nerves normally innervating slow muscles, fast myosin isoforms were replaced by slow myosin isoforms. However, neural stimulation is not the only factor affecting the contractile fate of muscles. Fiber type is also influenced by the myoblast lineage that makes up the muscle fiber (Dimario and Stockdale, 1997).

Cross-sectional area of myofibers is influenced by muscle fiber type. Type I muscles have a smaller cross-sectional area than type IIB myofibers (Ashmore et al., 1972). The cross-sectional area of myofibers is not a static situation and will change based upon usage. The flight muscles of migratory birds change in myofiber diameter in anticipation of migration and during the migratory flight (Price et al., 2011). For example, during a long-migratory flight, the muscle fibers may decrease in diameter to coincide with a lighter bird weight as fat is oxidized (Lindström et al., 2000). During a stopover or rest period, the muscles may rebuild for the next flight and increase in diameter (Landys-Cianneli et al., 2003).

23.5 Embryonic development of skeletal muscle

Following gastrulation—the transformation of the spherical blastula into an elongated tubular structure, three primary germ layers are defined. The outer structure comprises the ectoderm, and the inner surface comprises the endoderm. Between these layers is the mesoderm, which is the source of cells that lead to the formation of the skeletal muscle and other internal structures. As the embryo elongates due to lengthening of a structure termed notochord, the mesoderm grows as "slabs" on both sides of the notochord, with the ectoderm above and the endoderm below (for detailed review, see Gilbert, 2019). Part of the mesoderm, called the paraxial mesoderm, will give rise to segments consisting of epithelial cells termed somites. This dynamic process, beginning at the anterior end and terminating at the posterior end of the embryo, is regulated in a well-coordinated temporal manner—"the segmentation clock" (Pourquié, 2011). The somites gradually mature and compartmentalize into different structures, depending on their location. The region of cells that flanks the notochord in the ventral half of the somite will undergo epithelial-to-mesenchymal transition and form the sclerotome, giving rise to the axial skeleton and tendons. The dorsal half of the somites will form the dermomyotome, which will further split into two layers; the dorsal layer—the dermatome—will give rise to the dermis, as well as some skeletal muscle and brown fat; the other layer—the myotome—will be created by mesenchymal cells migrating from the extreme ends of the dermomyotome to beneath the dermatome. The myotome will give rise to intrinsic back muscles and abdominal muscles. Other myogenic precursors migrate out of the dermomyotome lips to populate the body wall and limb buds, and form the limb muscles. Muscles of the head and neck do not originate from the somites but from other regions in the mesoderm.

The first myogenic precursors, the myocytes (embryonic myoblasts) are formed in the myotome. During the

first wave of myogenesis, these cells elongate along the anterior-posterior axis of the myotome and form the primary (embryonic) myofibers by fusing with cells that migrate from the dermomyotome. The primary myofibers will serve as a scaffold for the second wave of myogenesis in which the secondary (fetal) myofibers are formed. During this wave, muscle growth continues by cell fusion and the addition of myonuclei from proliferating myoblasts. In chicken, the first (embryonic) wave of myogenesis occurs between embryonic day (E) 3 and embryonic day 7 (E7) and the second (fetal) wave of myogenesis occurs from E8 until hatch.

Myofiber formation is essentially complete at the time of birth or hatch. However, a third wave of myogenesis that starts in the embryo and continues until adulthood contributes to postnatal or posthatch muscle growth. This wave consists of a specific subset of muscle precursor cells, the satellite cells, also termed "adult myoblasts" (Hartley et al., 1992). For many years, the origin of satellite cells in the embryo was unknown; however, the elegant studies of Gros et al. (2005) and Relaix et al. (2005) revealed that these cells originate from the central part of the dermomyotome in the somites. Satellite cells can be distinguished in their niche underneath the basal lamina of myofibers at later stages of embryogenesis. Whereas in the embryo they only proliferate, after birth or hatch, these muscle precursor cells undergo proliferation, terminal differentiation, and fusion into the growing myofibers.

23.6 Postnatal or posthatch skeletal muscle development

After birth or hatch, skeletal muscle growth is due to enlargement of the existing myofibers (i.e., hypertrophy). The detailed mechanism of this hypertrophy remained a mystery until the 1960s; much of what is now known about posthatch or postnatal muscle growth today was gained from studies with chickens. Smith (1963) demonstrated increases in myofiber number in chickens prior to hatch, and subsequent growth due to hypertrophy. The importance of initial myofiber number following hatch was further demonstrated by studies with different chicken lines. A growth-selected heavy strain of chickens had a greater number of myofibers that were slightly smaller in diameter at hatch than a layer strain of chickens. After 10 weeks of growth, myofiber diameters in the growth-selected line were much greater than those in the layer strain (Smith, 1963).

One of the major puzzles of muscle growth in those years was the source of the nuclei in growing and regenerating skeletal muscle. Early experiments with isolated chick embryonic myoblasts revealed that the myonuclei in the myotubes were incapable of mitotic division and that another cell was responsible for DNA accretion (Stockdale and Holtzer, 1961). While it seemed clear that embryonic myoblasts were likely responsible for the development of myofibers prenatally, the source of the cells leading to postnatal growth was unknown. The historic discovery of satellite cells by Mauro (1961), based on electron microscopic examination, paved the way to clear this enigma. Those cells, unique to skeletal muscle in all vertebrates, were termed "satellite cells" due to their peripheral location on myofibers, residing in a niche between the sarcolemma and basal lamina of the myofibers. The cell mass consisted mostly of nuclei, and there was little cytoplasm and only a few organelles, such as mitochondria or Golgi apparatus.

Early evidence of a role for satellite cells in postnatal growth was reported by Moss and Leblond (1971), where tritiated thymidine label injected into young growing rats was followed in the muscle tissue. The label was localized to the satellite cells, indicating their division in the myofibers; later, the label began to appear within myonuclei, indicating that the satellite cells had fused with the adjacent fibers. These observations established a key role for satellite cells in myofiber DNA accretion, especially in young growing animals. Moss (1968) established the idea that DNA accretion occurs only via satellite cell incorporation into the growing myofiber, and that it is based on a constant ratio of myofiber diameter to DNA content. However, recent genetic studies have challenged this idea: in mice lacking the paired box 7 (Pax7) gene (which marks only satellite cells), myofibers still retained their capacity for hypertrophy under conditions of overload (McCarthy et al., 2011). Nevertheless, it is largely accepted that satellite cells are an essential source for new myonuclei in the growing muscle and long-term hypertrophy (Wang and Rudnicki, 2011). At birth or hatch, the satellite cell population makes up about 30% of the total myonuclei; however, their proliferative capacity and numbers diminish rapidly to 1−5% toward the end of the growing period (Hawke and Garry, 2001; Halevy et al., 2004), when they become quiescent (Schultz et al., 1978) and reside in their niche. In heavy-strain chickens, satellite cell myogenic activity persists for the first 8 days posthatch and peaks on day three posthatch (Halevy et al., 2004, 2006a).

In birds, during early growth, satellite cell myogenic activity is largely influenced by nutritional and/or environmental conditions such as light or temperature, all of which affect the pool of these cells for future hypertrophy. In chicken and turkey poults, changes in nutrition (Halevy et al., 2000, 2003; Mozdziak et al., 2002; Bigot et al., 2003; Powell et al., 2014; Velleman et al., 2019) or in environmental conditions (Halevy et al., 2006b; Piestun et al., 2009a; Liu et al., 2010; Hadad et al., 2014; Patael et al., 2019) during the early posthatch period impaired or enhanced the proliferation and differentiation activity of satellite cells, resulting in changes in the cell reservoir and

long-term effects on muscle hypertrophy and growth. Recent studies have shown long-term promotive effects on satellite cells in late-term chick embryos that experienced nutritional (Kornasio et al., 2011) or environmental manipulations during the third wave of myogenesis (Halevy et al., 2006b; Piestun et al., 2009a; Zhang et al., 2012), The proportion of myofiber nuclei residing in satellite cells out of the total number myonuclei is diminished upon malnutrition in humans (Hansen-Smith et al., 1979).

Despite the inactive state of satellite cells and their diminished numbers in mature animal muscle, upon injury, excessive exercise, overload, or various types of stress, quiescent satellite cells residing in their niche do have the capacity to become active and undergo myogenesis and fusion into existing or newly formed myofibers to regenerate damaged skeletal muscle (Bischoff, 1975; Hawke and Garry, 2001). As such, satellite cells serve as a reservoir for muscle precursor cells, and are therefore considered "adult skeletal muscle stem cells" (Collins et al., 2005). They fulfill the definition of a stem cell in that they undergo asymmetric division in which one daughter cell will continue the myogenic program, and the other will replenish the muscle precursor cell reservoir. In addition, under specific external signals, satellite cells can transform from the myogenic lineage to adipogenic, chondrogenic, or fibrogenic lineages. Moreover, the small population of satellite cells can regenerate an entire muscle (reviewed in Sambasivan and Tajbakhsh, 2015).

23.7 Muscle development: function of myogenic regulatory factors

The commitment and later differentiation of muscle precursor cells during both embryonic and posthatch periods require the precise expression of myogenic regulatory factors (MRFs). The MRFs are a family of basic helix-loop-helix transcription factors that are expressed in a specific temporal order. They activate muscle-specific gene expression by heterodimerizing with E proteins and binding as heterodimers to the conserved sequence, the E-box, located on the promoters of muscle-specific genes (Olson, 1990). Myogenic determination factor 1 (MyoD) was the first identified MRF; its importance was immediately recognized because it could convert nonmyogenic cells to a skeletal muscle lineage (Davis et al., 1987). Myogenic factor 5 (Myf5) has functions that overlap with MyoD. Genetic studies on knockout mice have demonstrated that MyoD and Myf5 are functionally redundant in that disruption of either gene will allow embryonic muscle development with only minor defects (Rudnicki et al., 1992, 1993). However, the absence of both MyoD and Myf5 will result in the absence of skeletal muscle formation, suggesting their role in myogenic commitment (Rudnicki et al., 1993). Both genes are involved in early myotome formation, are expressed in two subsets of cells (Kablar et al., 1998), and are important for myoblast proliferation. Myogenin acts downstream of MyoD and Myf5 and is necessary to activate the expression of muscle-specific proteins needed for terminal differentiation with the fusion of myoblasts to form myotubes. Absence of myogenin in knockout mice results in disruption of myocyte or myoblast differentiation, with little or no muscle myofiber formation (Hasty et al., 1993). Myogenic regulatory factor 4 (MRF4, Myf6 in humans) is expressed and functions in a species-dependent manner. In mice, it is expressed in a biphasic manner: first, in the dermomyotome where it overlaps with MyoD and Myf5 in directing myogenic specification; then, in fetal myoblasts where it regulates myogenic differentiation. However, in birds, MRF4 is only expressed at later embryonic stages, in parallel to myogenin, and regulates myogenic differentiation (Mok et al., 2015). In the postnatal animal, Myf5 expression is maintained in quiescent satellite cells, while MyoD and myogenin are sequentially expressed only in activated satellite cells (Cornelison and Wold, 1997; Yablonka-Reuveni and Paterson, 2001). MRF 4 is upregulated during muscle regeneration in forming myotubes (Pavlath et al., 2003). However, in birds, it may also play a role during cell proliferation: Shin et al. (2012a) showed high MRF4 expression during turkey satellite cell proliferation. The myocyte enhancer factors (MEFs) are positive upregulators of muscle differentiation (Naya and Olson, 1999). No skeletal muscle phenotype has been attributed directly to MEFs, but they appear to function in a positive feedback manner, especially with myogenin (Ridgeway et al., 2000).

The MRFs act in concert with the paired domain and homeobox-containing transcription factors paired box 3 (Pax3) and Pax7 at different stages of myogenesis in the embryo and adult. Pax3 acts upstream of MyoD and is necessary for the delamination and migration of the muscle progenitor cells from the somites to the limb bud (Bober et al., 1994; Tajbakhsh et al., 1997). Satellite cells are formed from Pax3- and/or Pax7-expressing muscle precursor cells in the somites (Relaix et al., 2005; Schienda et al., 2006). In the postnatal or posthatch animals, Pax7 is exclusively expressed in quiescent and activated satellite cells and is required for their proliferation during muscle growth (Halevy et al., 2004), and their maintenance and self-renewal (Seale et al., 2000; Zammit et al., 2004). Pax3 expression is mostly downregulated before birth, although a subset of satellite cells expresses this gene in adult animals (Relaix et al., 2006). It has recently been shown that this subset of cells remains resistant to environmental stress, and thus may protect the muscle stem cell reservoir (Der Vartanian et al., 2019).

23.8 Growth factors affecting skeletal muscle myogenesis

Much of what has been learned about the factors regulating the proliferation and differentiation of satellite cells has been derived from cell-culture studies and the development of serum-free medium formulations for various species. Satellite cells were first isolated and cultured by Bischoff (1974) from the skeletal muscle of adult rats. The cells were capable of proliferating and differentiating into multinucleated myotubes. Since then, satellite cells have been isolated and cultured from nonmammalian and mammalian species using various approaches, among them mechanical, enzymatic, and cell sorting and fractionation by density gradient. In addition, methods to isolate and culture whole myofibers, mainly from rodent muscles, have been developed, to study the behavior of satellite cells while they are still connected to the myofiber, thus reflecting their native environment (reviewed in Yablonka-Reuveni, 2011). Notably, to date, attempts to isolate chicken myofibers have failed. Similarities have emerged between findings with avian species and with mammals. Here, we discuss the most studied growth factors—the fibroblast growth factors (FGFs), platelet-derived growth factors (PDGFs), insulin-like growth factors (IGFs), hepatocyte growth factor (HGF), transforming growth factor-beta (TGF-β), and myostatin.

The FGFs are a large group of polypeptide growth factors with diverse actions on cells and tissues. Of this group, only FGF1, FGF2, FGF4, and FGF6 are produced by, and secreted from satellite cells, and FGF1 and FGF4 are expressed in developing muscles. Satellite cells express various types of FGF receptors, mainly 1 and 4, and to a lesser extent FGF receptors 3 and 2. FGF signaling in satellite cells is regulated by a complex of cell-surface (e.g., syndecan 4) and extracellular matrix (e.g., fibronectin) molecules. The FGFs are important for self-renewal of satellite cells and proliferation of embryonic and adult myoblasts (reviewed in Pawlikowski et al., 2017). In birds, omission of FGF from serum-free media resulted in no proliferation of turkey satellite cells or embryonic myoblasts, even if other mitogens were present (McFarland et al., 1993). Some types of FGFs have more potent mitogenic activity than others: in satellite cells derived from turkey (McFarland et al., 1993) and chicken (Wilkie et al., 1995), FGF2 induced proliferation better than FGF1. While FGFs play a role as mitogens, they inhibit muscle cell differentiation in both rodents and birds. Loss of FGF receptor activity by adding an inhibitor to the receptor or expressing a dominant-negative mutant induces terminal differentiation of cultured mouse satellite cells. It is believed than by inhibiting differentiation, FGF allows the self-renewal of satellite cells (Pawlikowski et al., 2017). Addition of FGF to cultures inhibits differentiation of chicken (McFarland et al., 1997; Hodik et al., 1997) and rodent (McFarland et al., 2000) satellite cells.

The PDGF family consists of four isomers (A, B, C, and D) that can be found as homo- or heterodimers, but mainly in their BB form, in many cell types. In skeletal muscle, they are expressed in fibro—adipogenic progenitor cells/fibroblasts and pericytes that work in a paracrine manner on adjacent cells (e.g., satellite cells). The two PDGF receptors (PDGFR-α and β) transmit the PDGF signal as either homo- or heterodimers, and both are expressed in embryonic myoblasts and satellite cells. Among the four types of PDGFs, the PDGF-BB isomer is the most potent mitogen for satellite cells, and induces their migration and proliferation, as well as muscle regeneration (Yablonka-Reuveni et al., 1990; Sugg et al., 2017). Recent studies have suggested that PDGF-BB is involved in the plasticity of satellite cells, changing their fate from myogenic cells to pericytes (Gerli et al., 2019). The expression of both PDGF-AA and PDGF-BB was found to be induced in dystrophic myofibers and was assumed to contribute to their fibrotic state (Zhao et al., 2003; Piñol-Jurado et al., 2017). In birds, PDGF was shown to be a potent mitogen for embryonic chick myoblasts (Yablonka-Reuveni and Seifert, 1993). Similar findings were reported for embryonic turkey myoblasts and satellite cells (Ye et al., 1996).

IGF is a small peptide found in multiple isoforms emerging from multiple IGF mRNA transcripts that are formed by alternative splicing. These transcripts encode various precursor polypeptides that undergo post-translational modifications. The main source of circulating IGFs is the liver, but they are expressed in other tissues as well, including skeletal muscle. The two families of IGFs, IGF-I and IGF-II, share similarities with proinsulin and may elicit similar biological effects. Different forms of pro-IFG-I are expressed in resting versus exercising or regenerating muscles, pro-IGF-Ia in the former and pro-IGF-Ib/c (also termed mechano-growth factor; Yang et al., 1996) in the latter. The locally produced muscle IGF-I is crucial for myogenesis (Shavlakadze et al., 2005; Barton et al., 2012) and is involved in myoblast proliferation, terminal differentiation, and muscle hypertrophy in mammals and birds (Coleman et al., 1995; Halevy et al., 2001; Yu et al., 2015). While most of the muscle IGF-I is produced by myofibers, satellite cells also produce and secrete the peptide (Jennische et al., 1987), as do other cells residing in the muscle, all of which affect the muscle in an autocrine/paracrine manner. IGFs transduce their signal via the IGF-I tyrosine kinase receptor which shares high homology with the insulin receptor, and can therefore heterodimerize with it; both receptors are expressed in skeletal muscle, including satellite cells, and can bind either IGF-I or IGF-II. The mature IGF forms have a short half-life and are thus stabilized by either binding directly to the extracellular matrix

or forming a complex with IGF-binding proteins, which in turn may induce, or, in most cases, inhibit IGF's ability to bind to its receptor (reviewed in Vassilakos and Barton, 2018).

Both, IGF-I and IGF-II enhance proliferation, differentiation, and fusion of embryonic as well as adult myoblasts in poultry (Schmid et al., 1983; McFarland et al., 1993; Hodik et al., 1997). In addition, IGFs have insulin-like activities in both mammals and birds. For instance, IGF stimulates glucose uptake in turkey (McFarland et al., 1994) and chicken (Duclos et al., 1993a) satellite cells. In addition, IGF stimulates protein synthesis and inhibits protein degradation in myotubes derived from chick embryonic myoblasts (Janeczko and Etlinger, 1984), chick satellite cells (Duclos et al., 1993b), and turkey embryonic myoblasts and satellite cells (McFarland et al., 1994). There is recent evidence (Shinichi et al., 2012) points of an association between polymorphism of the IGF-I gene and pectoralis major muscle yield in chickens. A comparative transcriptomic analysis of breast muscle derived from three poultry strains with different growth rates revealed the expression of IGF-II transcript in all strains (Zhang et al., 2019).

Early research described mitogenic activity of a crushed muscle extract that was capable of activating quiescent satellite cells residing on isolated muscle fibers (Bischoff, 1986). One of the substances in this extract was later defined as HGF (Tatsumi et al., 1998). Using cultured quiescent satellite cells, Tatsumi et al. (2001) demonstrated that stretched cells enter the cell cycle earlier than quiescent cells cultured under static conditions. Release of HGF from the stretched satellite cells in culture was dependent on the presence of nitric oxide (Tatsumi et al., 2002). The administration of anti-HGF antibodies abolished the stretch activation of satellite cells and demonstrated that the crushed muscle mitogen was, indeed, HGF. Therefore, HGF is considered an essential factor for the activation of quiescent satellite cells during muscle regeneration postinjury.

HGF (also termed scatter factor) is a heparin-binding molecule found in the extracellular matrix; it exerts its activity via the tyrosine kinase receptor c-met. During development, HGF plays an essential role in the migration of myogenic precursor cells from the somites into the limb bud (Brand-Saberi et al., 1996). During the early growth period in mammals (Sheehan et al., 2002) and birds (Gal-Levi et al., 1998; Zeng et al., 2002), HGF induces myoblast proliferation and decreases differentiation by inhibiting the activity of MRFs and affecting cell-cycle proteins, leading to inhibition of muscle-specific protein expression (Gal-Levi et al., 1998; Leshem et al., 2000). Addition of anti-HGF antibodies to turkey satellite cells in serum-free medium decreased proliferation, supporting the role of HGF as an autocrine or paracrine factor in muscles (Zeng et al., 2002).

The transforming growth factor-β belongs to a large family of pluripotent cytokines with diverse effects during development and adulthood. It was first described as "a very potent inhibitor of myoblast differentiation" by Florini et al. (1986). To date, TGF-β is known to inhibit both muscle growth and regeneration by inhibiting the proliferative and differentiative activity of satellite cells in mammals and birds. It also promotes the pathology of muscular diseases by inducing collagen synthesis in myofibroblasts and increasing muscle fibrosis (Abrigo et al., 2018).

Myostatin is a member of the TGF-β family, believed to be an important regulator of muscle size. Defects in the myostatin gene result in dramatic increases in muscle mass seen in Belgian Blue and Piedmontese cattle breeds (McPherron and Lee, 1997). Similarly, myostatin-null mice have enhanced musculature (McPherron et al., 1997). Srinivasan et al. (2004) demonstrated elevated levels of myostatin during muscle atrophy. It is believed that elevated myostatin during muscle breakdown serves to prevent premature satellite cell activation while the degeneration is occurring. When muscle regeneration commences, myostatin levels decrease (Kirk et al., 2000). Administration of myostatin to muscle explants inhibited satellite cell activation and progression into the cell cycle (McCroskery et al., 2003). Proliferation of both turkey embryonic myoblasts and satellite cells was inhibited in serum-free medium containing myostatin (McFarland et al., 2006). Satellite cells isolated from the pectoralis major muscle of chickens were more responsive to the proliferation- and differentiation-depressing effects of myostatin compared to cells from the biceps femoris (McFarland et al., 2007).

23.9 Satellite cells and myoblast heterogeneity

There is considerable heterogeneity in myofiber structure, metabolism, and response to stimuli, depending on the specific function of the muscle. Muscles for quick short burst movement differ from muscles for sustained movement. Postural muscles also have different properties than muscles not involved in posture. Heterogeneity of satellite cells is noticed during embryogenesis; cells that reside in different muscles originate from different embryonic tissues and can be traced back to their lineage. For example, muscles in the trunk and limbs develop from the somites, whereas, most of the head muscles (apart of the tongue and some muscles of larynx and neck that originate from the paraxial mesoderm and the lateral splanchnic mesoderm). These cells maintain their signature up to adulthood as was reported in studies in which satellite cells derived from

different muscles expressed different genes and maintained the expression pattern during their proliferation and differentiation in culture (Day et al., 2007; Harel et al., 2009; reviewed in Biressi and Rando, 2010).

The heterogeneity of satellite cells was evident in clonal analyses of cultures derived from different muscles. The various clonal subpopulations expressed different myosin isoforms (Stockdale, 1990; Feldman and Stockdale, 1991; Hoh and Hughes, 1988). Based on the ability to proliferate, Schultz and Heckman-Jones (1990) demonstrated the presence of two populations of satellite cells in vivo, where one population did not appear to divide during 7 days of extensive muscle growth. Clonal analysis of chicken satellite cells by Yablonka-Reuveni et al. (1987) identified differences in colony sizes. More than 90% of the clones gave rise to large colonies, whereas 8−9% gave rise to small colonies, suggesting that satellite cells in these colonies differ in their ability to form myonuclei. The ability of these subpopulations to maintain their phenotype in culture out of their in vivo environment, suggests an intrinsic diversity of "slow" and "fast" satellite cells (Biressi and Rando, 2010). The variations in the ability satellite cells to proliferate could be explained at least in part by their different responses to growth factors, such as IGF-I, FGF-II, and PDGF (McFarland et al. 1995, 2003; Yun et al., 1997). Fast-growing clones were all more responsive to FGF2 and expressed greater levels of FGF2 and the FGF receptor-1 at the onset of proliferation than did the slow-growing clones (McFarland et al., 2003). These differences were reflected in the levels of activated intracellular signaling proteins, which were higher in the fast-growing clones (McFarland and Pesall, 2008). Satellite cells also differ in their ability to fuse. In vitro and in vivo studies on turkey satellite cells revealed that cells with high-proliferation rate fused mainly with differentiated myotubes or myofibers, cells that with slow proliferation rate mainly fused together (Rouger et al., 2004).

The heterogeneity of satellite cells in adult animals is also evident with respect to their self-renewal capacity and muscle regeneration. Genetic studies with mice have shown that of the Pax7-expressing satellite cells, the small subset that never express Myf5 contribute to the satellite cell reservoir, whereas the rest of the cells contribute to myofiber regeneration (Kuang et al., 2007). Pax3-expressing satellite cells were reported to be resistant to muscle damage followed by environmental pollutants (Der Vartanian et al., 2019). Satellite cells express a variety of cell-surface proteins (e.g., M-cadherin, CD34, syndecan 4, integrin α7), and show different engraftment and regeneration potential based on the nature of the expressed proteins (Tanaka et al., 2009; Biressi and Rando, 2010). Yet, the actual relationship between the nature of the cell-surface molecules and the ability of the satellite cells to contribute to the muscle regeneration is still unclear. Moreover, exogenous cues from the extracellular environment (e.g., acute injury) can affect satellite cells' behavior upon injury regardless their hereditary history (reviewed in Cornelison, 2018). There is considerable heterogeneity in myofiber structure, metabolism, and responses to stimuli, depending on the specific function of the muscle. Muscles for quick short burst movements differ from muscles for sustained movement. Postural muscles also have different properties than muscles that are not involved in posture. Satellite cell heterogeneity is observed during embryogenesis; cells that reside in different muscles originate from different embryonic tissues and can be traced back to their respective lineages. For example, muscles in the trunk and limbs develop from the somites, whereas most of the head muscles (apart from the tongue and some muscles of the larynx and neck that originate from the paraxial mesoderm and the lateral splanchnic mesoderm), develop from the anterior paraxial mesoderm. These cells maintain their signature into adulthood, as reported in studies in which satellite cells derived from different muscles expressed different genes, and maintained their expression patterns during their proliferation and differentiation in culture (Day et al., 2007; Harel et al., 2009; reviewed in Biressi and Rando, 2010).

The heterogeneity of satellite cells was evident in clonal analyses of cultures derived from different muscles. The various clonal subpopulations expressed different myosin isoforms (Stockdale, 1990; Feldman and Stockdale, 1991; Hoh and Hughes, 1988). Based on the ability to proliferate, Schultz and Heckman-Jones (1990) demonstrated the presence of two populations of satellite cells in vivo; one of these populations did not appear to divide during seven days of extensive muscle growth. Clonal analysis of chicken satellite cells by Yablonka-Reuveni et al. (1987) identified differences in colony sizes. More than 90% of the clones gave rise to large colonies, whereas 8−9% of them gave rise to small colonies, suggesting that satellite cells in these colonies differ in their ability to form myonuclei. The ability of these subpopulations to maintain their phenotype in culture, outside of their in-vivo environment, suggests an intrinsic diversity of "slow" and "fast" satellite cells (Biressi and Rando, 2010). The variations in the satellite cells' ability to proliferate could be explained at least in part by their different responses to growth factors, such as IGF-I, FGF2, and PDGF (McFarland et al. 1995, 2003; Yun et al., 1997). Fast-growing clones were all more responsive to FGF2, and expressed higher levels of FGF2 and FGF receptor 1 at the onset of proliferation compared to the slow-growing clones (McFarland et al., 2003). These differences were reflected in the levels of activated intracellular signaling proteins, which were higher in the fast-growing clones (McFarland and Pesall, 2008). Satellite cells also differ in their ability to fuse. In-vitro and in-vivo studies of turkey satellite cells revealed that cells with a high-proliferation rate fuse mainly with differentiated

myotubes or myofibers, and cells with a slow proliferation rate mainly fuse together (Rouger et al., 2004).

The heterogeneity of satellite cells in adult animals is also evident with respect to their self-renewal capacity and muscle regeneration. Genetic studies with mice have shown that of the Pax7-expressing satellite cells, the small subset that never expresses Myf5 contributes to the satellite cell reservoir, whereas the rest of the cells contribute to myofiber regeneration (Kuang et al., 2007). Pax3-expressing satellite cells were reported to be resistant to muscle damage from environmental pollutants (Der Vartanian et al., 2019). Satellite cells express a variety of cell-surface proteins (e.g., M-cadherin, CD34, syndecan 4, and integrin α7), and show different engraftment and regeneration potentials based on the nature of the expressed proteins (Tanaka et al., 2009; Biressi and Rando, 2010). Nevertheless, the actual relationship between the nature of the cell-surface molecules and the ability of the satellite cells to contribute to muscle regeneration is still unclear. Moreover, exogenous cues from the extracellular environment (e.g., acute injury) can affect the satellite cells' behavior upon injury, regardless of their hereditary history (Cornelison, 2018).

23.10 Novel genes involved in avian myogenesis

Avian muscle growth may involve genes that have not yet been characterized to play a role in myogenesis. A complete transcriptome analysis was performed in turkeys using a turkey skeletal muscle long oligonucleotide array constructed from the pectoralis major muscle at three developmental stages (Reed et al., 2008; Sporer et al., 2011a): E18, 1 day of age and 16 weeks of age. Of the differentially expressed genes (Sporer et al., 2011b), three were further studied for their effects on the proliferation and differentiation of satellite cells. These genes encoded versican, matrix Gla protein, and death-associated protein (DAP).

Versican is a large chondroitin sulfate proteoglycan initially reported in cultured fibroblasts (Zimmerman and Ruoslahti, 1989). By knocking down versican expression in turkey satellite cells, their proliferation increased, supporting a potential role for versican in this proliferation (Velleman et al., 2012). In addition, versican is expressed during early embryonic muscle formation and muscle regeneration; it was shown to be located in the surrounding matrix of the developing myotubes (Carrino et al., 1999). High expression of versican was found in developing synovial joint interzones, suggesting its involvement in facilitating the patterning of muscle and nerves in the developing limb (Snow et al., 2005).

Matrix Gla protein is highly expressed by vascular smooth muscle cells (Proudfoot and Shanahan, 2006), but prior to the report of Sporer et al. (2011b), it had not been identified in skeletal muscle. Knocking down only matrix Gla protein decreased proliferation in satellite cells isolated from growth-selected turkeys (Velleman et al., 2012). A later report demonstrated that matrix Gla protein binds myostatin and prevents its signaling pathway, thereby could inhibit the latter's inhibitory effect on proliferation and differentiation of satellite cells (Ahmad et al., 2017). The highly conserved proline-rich phosphoprotein DAP is a substrate of mTOR (Koren et al., 2010), which is a primary intracellular pathway controlling muscle hypertrophy (Bodine et al., 2001). In both turkey (Velleman et al., 2012) and chicken (Shin et al., 2013b) breast muscle satellite cells, knocking down DAP expression severely inhibits the formation of myotubes, suggesting DAP as a key gene in the regulation of avian myogenesis.

Other genetic factors affecting avian muscle myogenesis have been recently described, among them the microRNAs (miRNAs). These are noncoding small RNAs (i.e., 20−23 nucleotides) that regulate post-transcriptional gene expression by targeting specific sites in the 3′-untranslated region of mRNAs. The miRNAs are widely involved in biological and metabolic processes, including muscle development and growth (Hitachi and Tsuchida, 2013). Harding and Velleman (2016) found specific miRNAs that play a role in the proliferation and differentiation of turkey satellite cells; inhibition of these miRNAs led to impaired myogenesis. In addition, specific miRNAs have been reported to affect chicken growth traits, such as cell proliferation and regulation, calcium signaling, axonal guidance signaling, and oxidative stress response mediated by the nuclear factor NRF2 (Ouyang et al., 2015; Khatri et al., 2018). These miRNAs may therefore serve in future genetic strategies to manage muscle growth.

Circular RNAs (circRNAs) are noncoding closed RNA molecules derived from canonical splice sites; they are abundant in all eukaryotes, and some of them are highly conserved. Although described decades ago, their biological functions have only recently begun to be deciphered. The circRNAs may act as protein or miRNA inhibitors ("sponges or decoys"), or by regulating protein functions in biological processes in various cell systems, including epidermal, neuronal, muscular, and cancer cells (reviewed in Kristensen et al., 2019). They have been suggested to play a role in the regulation of avian myogenesis. For example, temporal expression of circRNAs was found during early and late embryonic stages of chick muscle development; of these, the circRBFOX2s were validated as promoters of myoblast proliferation by binding to and inhibiting the activity of miRNA-206 (miR-206) (Ouyang et al., 2018). In addition, circFGFR2, generated from the FGF2 receptor gene, and circHIPK3 have been reported to improve myoblast proliferation and differentiation by sponging miR-133 and miR-29 (Chen et al., 2018), and miR-30 (Chen et al., 2019), respectively. A recent study has

shown differential expression of circRNAs in breast muscle during the ontogeny of broilers versus layers (Shen et al., 2019). These studies and others suggest an additional layer of regulation which could serve as a basis for selecting specific traits in muscle growth and meat quality.

23.11 Recent emerging breast muscle necrotic and fibrotic myopathies

The poultry breeding industry has placed major emphasis in selection for increased growth rate and breast muscling. Increased growth rates in poultry have helped the poultry industry keep up with consumer demand for economical chicken and turkey products, but these increases must be accompanied by consideration of the cellular mechanisms affecting muscle growth as both the morphological structure and biochemical properties are affected. These changes in muscle, especially the breast muscle, have resulted in meat quality issues which are the end consequence of myofiber defects. Typical myofiber defects found in poultry selected for increased growth rate have included deep pectoral myopathy (Wilson et al., 1990; Sosnicki and Wilson, 1991), focal myopathy (Sosnicki, 1993), and pale, soft, and exudative (PSE) meat (Sosnicki, 1993; Pietrzak et al., 1997). Breast muscle is a fast twitch anaerobic muscle composed mainly by glycolytic myofibers. The fast growth of this muscle causes increase in the size of these myofibers leading to an increase in anaerobic capacity (Dransfield and Sosnicki, 1999; Yost et al., 2002). Being an anaerobic muscle, the breast muscle has a reduced vasculature system compared to a slow twitch aerobic muscle. Reduced capillaries have been found surrounding muscle in necrotic regions of turkey breast muscle fibers (Sosnicki and Wilson, 1991). Lactic acid is produced by anaerobic respiration, which leads to higher acid concentrations in the muscle and decreased pH. Pale soft exudative meat is characterized by low-postmortem pH. The decreased ability to remove lactic acid from breast muscles with limited circulatory supply likely contributes to the reduced pH observed in PSE meat. However, in the last decade especially in fast-growing meat-type broilers, breast muscle myopathies resulting in muscle fiber necrosis and the fibrosis or replacement of muscle fiber with connective tissue have emerged.

At the present time, white striping, wooden breast, and spaghetti breast have been phenotypically identified in the broiler breast muscle (Fig. 23.2). These myopathies have been observed globally where heavy weight fast-growing broiler lines are used. The white striping defect results in white stripes or striations following the muscle fiber orientation. It does not appear to affect the quality of the cooked breast muscle but does affect the appearance. The visual observation of white striations in the boneless skinless broiler breast muscle fillets may reduce consumer acceptance of the product and purchase intent. Almost all heavy commercial broilers marketed in the United States exhibit some degree of white striping in the breast muscle (Kuttappan et al., 2016). Since muscle fibers are surrounded by connective tissue, the white striping may arise from altered connective tissue deposition or structure. Kuttappan et al. (2013) reported that there is an increase in pathological changes in the breast muscle with white striping. White striping can vary in severity and affect the morphology of the muscle. In breast muscle samples with severe or moderate levels of white striping, there is a loss of cross striations, variable muscle fiber size, floccular or vacuolar degeneration and lysis of fibers, mild mineralization, occasional regeneration, mononuclear cell infiltration, lipidosis, and interstitial inflammation and fibrosis. In addition, the fat level is increased, and protein is decreased in white striped muscle.

Sihvo et al. (2014) first reported the wooden breast myopathy in the breast muscle of broilers. Wooden breast results in the phenotypic appearance of muscle discolorations, turbid viscous coating of the outer surface, and a palpably hard consistency (Sihvo et al., 2014; Bailey et al., 2015; Tasoniero et al., 2016). It has been estimated that 48% to 73% of commercial broilers are at least mildly affected by wooden breast (Sihvo et al., 2017). Wooden breast muscle is characterized by varying levels of myofiber necrosis, fibrosis with extensive fibrillar collagen deposition, small regenerating myofibers, hypercontracted fibers, and immune cell infiltration (Sihvo et al., 2014; Velleman and Clark, 2015). Breast muscle in wooden breast affected broilers is in oxidative stress (Abasht et al., 2016), which may result from a reduction in circulatory supply and lower mitochondrial content. Meat product downgrades or condemnation results from severe forms of wooden breast.

Spaghetti breast is a newer named breast muscle myopathy in commercial broilers. As reported by Baldi et al. (2018), spaghetti breast is characterized by the separation of muscle fiber bundles in the pectoralis major muscle. The name spaghetti breast was chosen as the muscle fiber cylindrical rods are visible and resemble pasta noodles. Similar to white striping and wooden breast, spaghetti breast muscle fibers feature large to small diameter muscle fibers along with hypercontracted fibers (Baldi et al., 2018). In contrast to wooden breast and white stripping, following processing the pectoralis major muscle can be pulled apart by hand. As described by Baldi et al. (2018), the endomysial and perimysial connective tissue layer in spaghetti breast progressively degrades. Meat quality is negatively impacted by this myopathy.

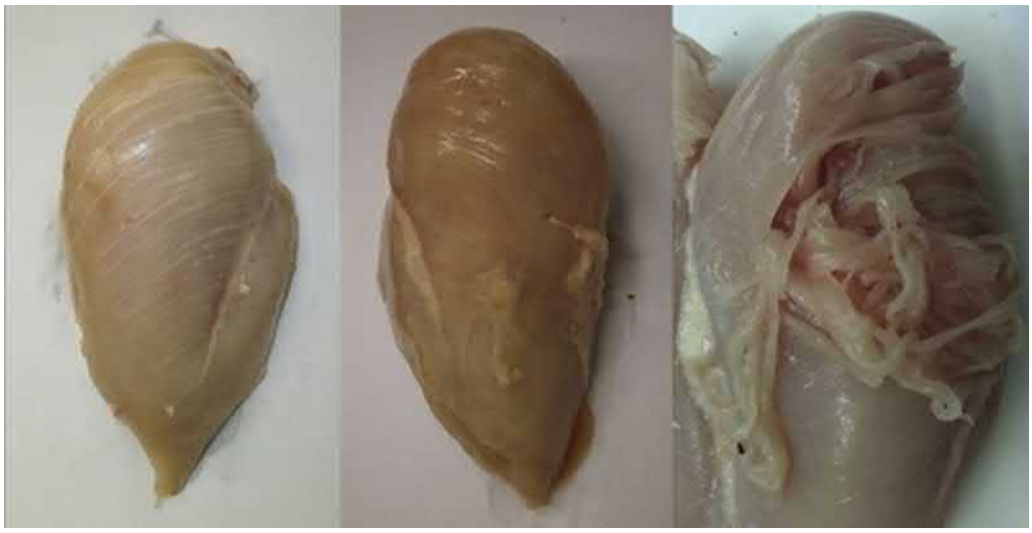

FIGURE 23.2 Breast fillets showing the novel myopathies white striping (left), wooden breast (middle), and spaghetti breast (right). *Figure reproduced with permission from Baileys et al. (2020).*

23.12 The effect of fibrillar collagen on the phnotype of necrotic breast muscle myopathies resulting in fibrosis

The skeletal muscle is surrounded by three distinct connective tissue layers: the epimysium, perimysium, and endomysium (Fig. 23.1A). The epimysium surrounds the entire muscle and is continuous with the joining of various muscle group or the tendon attaching muscle to bone. Although the epimysium is very thick, it is not a factor in meat quality as it can easily be removed. The perimysium surrounds muscle fiber bundles, and the endomysium surrounds individual muscle fibers. The connective tissue layers are responsible for many of the functional properties associated with muscle and factors affecting meat quality. Tissue structure, the elasticity of the tissue, vascular supply to the muscle tissue, and water-holding capacity are all properties linked to connective tissue primarily the perimysium which can compose up to 90% of the intramuscular connective tissue. Connective tissue is made up of cells and the extracellular matrix.

The extracellular matrix is defined to include all secreted molecules that are immobilized outside cells. Thus, the cell makes its own extracellular environment. The major macromolecular components of the extracellular matrix include collagens, proteoglycans, and noncollagenous glycoproteins. The structure of the extracellular matrix is not random as it is tissue-type and age-specific. The matrix is dynamically expressed and directly impacts muscle proliferation, adhesion, migration, and overall tissue structure including elasticity. The composition and organization are of significant with regard to the fibrotic breast muscle myopathies. The predominant extracellular matrix protein in the avian breast muscle are the fibrillar collagens especially Types I and III. Fibrosis is characterized by the excessive deposition of collagen in response to chronic cellular damage.

The fibrillar collagens are characterized by a single triple-helical domain containing three peptide chains forming a right-handed alpha helix. All collagens have the amino acid repeat in the helical domain of Gly-X-Y where X and Y can be any amino acid but are frequently proline or lysine. After the triple-helical structure is formed, collagen is secreted into the extracellular matrix space where it is aligned into a quarter stagger array leading to the formation of collagen fibrils that are stabilized by crosslinking between the collagens. Crosslinking of the fibrillar collagens is necessary for both its structural stability and functional properties and is a major determinant of meat textural properties. The covalent hydroxyl pyridinoline (HP) crosslink is a mature, nonreducible, trivalent crosslink that forms from the condensation of divalent ketoimine crosslinks (Reiser et al., 1992). The formation of HP crosslinks is progressive with age, and the toughening of meat is directly attributable to crosslink concentration. With tissue injury, the repair process results in collagen fibrils that have higher levels of HP crosslinking (Zimmerman et al., 2001). Since collagen HP crosslinking is progressive with age and increases with tissue injury, fibrotic myopathies will result in increased collagen deposition and crosslinking leading to a stiff breast muscle like what is observed in the wooden breast myopathy. The muscle necrotic and fibrotic process is characterized by both changes in tissue structure and composition of the extracellular matrix. In fibrotic tissue, there is an excessive

deposition of fibrillar collagen (Alexakis et al., 2007; Serrano et al., 2010; Velleman et al., 2017). Thus, necrotic and fibrotic conditions in skeletal muscle will result in an altered structural architecture of the extracellular matrix and function with reduced elasticity.

23.13 Relationship of fibrillar collagen organization to the phnotype of breast muscle necrotic/fibrotic myopathies

The process of fibrosis is a self-perpetuating response to muscle necrosis resulting in the progressive overproduction of fibrillar collagens Types I and III in the perimysial and endomysial connective tissue spaces. The phenotype of necrotic/fibrotic myopathies is not a direct relationship to the concentration of collagen but to the organization of collagen. Factors determining the fibrotic phenotype include, but are not limited to fibril diameter, degree of crosslinking, proteoglycan localization and type, fibril alignment, and morphometric organization of the collagen fibrils.

The three collagen polypeptide chains will wrap around each other intracellularly to form a right-handed triple helix. At this point, the collagen molecule is exocytosed into the extracellular space where fibril and fiber formation take place. The collagen fiber is the functional form impacting tissue structure, elasticity, and ultimately meat quality. After secretion, the collagen molecules will align in parallel to form a quarter staggered array which is a necessary step leading to assembly of collagen fibrils. The collagen fibrils are stabilized by the formation of reversible divalent crosslinks. The alignment of the collagen molecules is not a random process and after alignment there are gap and overlap areas within the quarter staggered array. The length of one overlap zone is 67 nm and termed a D banding-period. If the alignment of the collagen molecules is altered, the length of the D-period will be modified affecting collagen fibril function. After collagen fibril formation, the collagen fibrils will come together forming collagen fibers. With maturation, divalent ketoimine crosslinks are replaced with trivalent nonreversible HP crosslinks. The HP crosslink is a critical factor in tissue stiffening. After three collagen triple helices are linked together, additional helices are linked together increasing collagen fibril diameter and crosslinking. The formation of HP crosslinks is a progressive process with age and is likely a major factor in the phenotypic detection of wooden breast by palpation and the reduction in meat quality.

Since the wooden breast myopathy is characterized by excessive fibrotic deposition of collagen fibrils, it is of importance to understand the ultrastructural intramuscular organization of the fibrillar collagens in fast-growing meat-type broilers of differing parental lineage. A series of studies was conducting examining collagen fibril structure in three fast-growing commercial broiler lines with distinctly different levels of phenotypically detectable wooden breast (Velleman and Clark, 2015; Velleman et al., 2017; Tonniges et al., 2019). The commercial lines used in this study were referred to as A, B, and C. Line C infrequently exhibits any phenotypically detectable wooden breast whereas Line A has a high degree of affected birds, and Line B has intermediate phenotypic detection of wooden breast affected birds. Velleman and Clark (2015) and Velleman et al. (2017) using light microscopy observed that Line A with a high degree of phenotypically wooden breast affected birds, had perimysial collagen fibers characterized by parallel packing (Fig. 23.3). In contrast, Line B by palpation had a low percentage of birds categorized as wooden breast affected. Light microscopic examination revealed that the perimysial collagen was not packed but diffuse in structure. Microscopic histological examination of the muscle showed that 70% of Line B birds observable necrosis and fibrosis.

Transmission electron microscopy (TEM) analysis was used to further investigate histological differences, measure collagen D-periodicity, and collagen fiber diameter in Lines A, B, and C affected and unaffected wooden breast birds (Velleman et al., 2017). As discussed in Velleman et al. (2017), "wooden breast affected Line A muscle had overall smaller average collagen fibril diameter and longer average collagen D-period compared with unaffected Line A muscle, whereas Line B showed no such differences. Fibrotic collagen of WB-affected muscle of Line A exhibited D-period length and fibril diameter more similar to endomysial collagen of unaffected muscle of Line A. The fibrillar structure of fibrotic collagen in Line B affected with WB was more similar to perimysial collagen of Line B-unaffected muscle. The endomysial collagen of Line A was altered with WB myopathy while the endomysial collagen of Line B was not. Endomysial collagen of Line A exhibited decreased fibril diameter and increased D-period length with WB myopathy. Changes in D-period length and collagen fibril diameter are a direct consequence of the ordered arrangement of the collagen molecule within the collagen fibril. These modifications in the collagen fibril are indicative of alterations in the molecular packing of collagen monomers, which can impact collagen function by altering protein binding sites or the flexibility of the collagen fibril."

These TEM studies showed that there is different fibrotic collagen organization in the breast muscle of fast-growing meat-type broilers. These difference in fibrosis most likely represents unique uncharacterized breast muscle myopathies. Myopathies like wooden breast have increased stiffness or hardness of the breast muscle which is likely the result of high levels of collagen crosslinking.

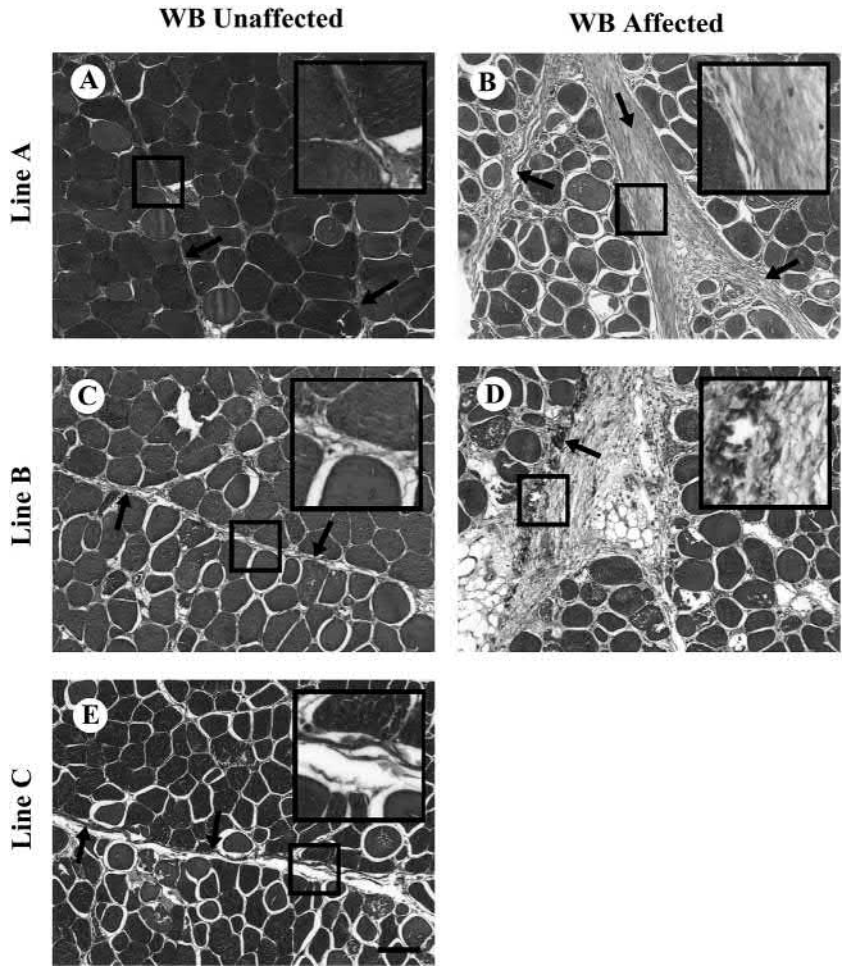

FIGURE 23.3 Masson trichrome staining of collagen organization in wooden breast (WB)-unaffected and affected pectoralis major muscle. (A), (C), and (E) are representative images of WB-unaffected pectoralis major muscle from Lines A, B, and C, respectively. (B) and (D) are representative images of WB-affected pectoralis major muscle from Lines A and B, respectively. The arrows highlight fibrillar collagen and the boxes contain enlargements of the fibrillar collagen. Scale bar = 100 μm. *Figure reproduced with permission from Velleman et al. (2017).*

Greater amounts of the HP crosslink will lead to tightly packed collagen fibrils. Fibrotic myopathies not detected by palpation is due to the collagen fibrils being diffuse with lower levels of crosslinking, and the breast will not be hard. Despite not being phenotypically detectable, the presence of necrosis and fibrosis will still alter the protein content of the breast muscle and impact meat quality.

In addition to the fibril organization differing in fast-growing broiler lines, the fibrillar collagen composition of the fibrils may also be affected by fibrosis. Skeletal muscle contains fibrillar collagens Types I and III. The expression of collagen is age-dependent. During early development, Type III collagen is the predominant collagen but with age there is a shift toward Type I collagen (Bornstein and Sage, 1980; Light and Champion, 1984; Kovanen and Suominen, 1989). With injury and inflammation as occurs in myopathies like wooden breast, the expression of collagen will shift back to an embryonic-like tissue with increased amounts of Type III collagen. With tissue repair, Type I collagen expression will increase, and Type III collagen will decrease (Bailey et al., 1975; Barnes et al., 1976; Weber et al., 1978; Merkel et al., 1988). Collagen fibrils can be homotypic composed of only a single collagen type or heterotypic containing a mixture of collagen types. Although the functional impact of collagen fibril composition is not well understood, it has been postulated that collagen fibril composition can influence muscle stiffness and meat tenderness (McCormick, 1994). Differential collagen fibril composition and its impact on broiler skeletal muscle has not been reported to date. However, in other tissue systems, heterotypic collagen fibrils containing both Types I and III collagen have reduced stiffness and collagen fibril diameter (Romanic et al., 1991; Notbohm et al., 1993; Asgari et al., 2017). When collagen Type III expression increases as observed with skeletal muscle injury (Hurme et al., 1991; Gibertini et al., 2014), Type III

collagen is localized in highly aligned and tightly packed collagen fibrils (Brisson et al., 2015; McConnell et al., 2016) as observed in wooden breast. Thus, collagen Type III expression may be associated with the fibrotic organization of collagen fibrils. Future studies will need to address the relationship of collagen fibril composition and the expression of the different fibrillar collagen types with broiler breast muscle fibrotic myopathies.

23.14 Regulation of muscle growth properties by cell-membrane associated extracellular matrix macromolecules

In addition, to the extracellular matrix having an integral function in the functional attributes and meat quality of the breast, the extracellular matrix proteoglycan component has been shown to regulate muscle growth. The cell-membrane associated proteoglycans can have extracellular, transmembrane, and cytoplasmic domains. Thus, these proteoglycans can play roles in organizing extracellular matrix structure, cytoskeletal organization, cell to cell adhesions, and cell signal transduction. The syndecans and glypicans are two families of heparan sulfate proteoglycans that are integral components in growth factor signal transduction. FGF 2 is a potent stimulator of muscle cell proliferation and a strong inhibitor of differentiation (Dollenmeier et al., 1981). In particular, the growth factor FGF2 binds with a high affinity to its tyrosine kinase receptor by binding to the heparan sulfate chains of the syndecans and glypicans (Steinfield et al., 1996).

The syndecans have four family members, syndecan-1 through -4, and all four types are found in skeletal muscle (Larraín et al., 1997, 1998; Brandan and Larraín, 1998; Fuentealba et al., 1999; Liu et al., 2006). All the syndecans are type I membrane glycoproteins (Deepa et al., 2004) and usually contain at least three heparan sulfate chains as well as N-glycosylated chains. However, the core protein can also have covalently attached dermatan and chondroitin sulfate chains. All the syndecans have extracellular, transmembrane, and cytoplasmic domains. The cytoplasmic domain for syndecan-1 through -4 have two conserved regions (C1 and C2) separated by a variable region (V). The C terminus of the cytoplasmic domain has a conserved amino acid sequence, EFYA, which allows the syndecans to function as a diverse set of cell-surface receptors (Choi et al., 2011). The following describes the known functions of each of the syndecans in skeletal muscle.

Syndecan-1 is a regulator of FGF2 signal transduction and syndecan-1 is expressed at higher levels during muscle cell proliferation than differentiation (Larraín et al., 1997; Liu et al., 2004). In growth-selected turkeys, syndecan-1 expression is higher than in turkeys without selection for growth (Liu et al., 2004). The higher expression of syndecan-1 may lead to a prolonged period of proliferation leading to a larger pool of muscle cells available to differentiate into muscle fibers.

Syndecan-2, in a manner similar to syndecan-1, is expressed at higher levels during the proliferation of avian muscle cells and expression decreases with differentiation (Liu et al., 2006). Less is known about the function of syndecan-2 in muscle than the other syndecans, but there is evidence that the cytoplasmic domain may be involved in regulating cellular responsiveness to TGF-β (Chen et al., 2004).

Recent research on syndecan-3 suggests that it may play a role in the maintenance, proliferation, and differentiation of myogenic satellite cells (Fuentealba et al., 1999; Cornelison et al., 2004; Pisconti et al., 2010). The absence of syndecan-3 leads to muscular dystrophy types of conditions characterized by impaired locomotion, fibrosis, decreased myonuclear number (Cornelison et al., 2004), and satellite cells with reduced proliferation (Pisconti et al., 2010).

Syndecan-4 is the most well studied of the syndecans in poultry muscle development. Syndecan-4 has been shown to play important roles in muscle maintenance and regeneration (Cornelison et al., 2001, 2004). In turkey satellite cells, syndecan-4 is expressed at high levels during proliferation (Velleman et al., 2007), affects satellite cell function in an age-dependent manner (Velleman et al., 2018). The primary role for syndecan-4 in muscle is in its regulation of cytoskeletal organization and muscle cell migration (Shin et al., 2012, 2013a; Song et al., 2012a,b). In the presence of phosphatidylinositol 4,5-bisphosphate (PIP_2) bound to the V region of the syndecan-4 cytoplasmic domain, syndecan-4 functions in the translocation of inactive protein kinase C α (PKCα) to the muscle cell membrane resulting in its activation (Song et al., 2012c; Shin et al., 2012). Once activated, PKCα mediates the activation of downstream RhoA signal transduction which is involved in mediating cell migration (Dovas et al., 2006; Shin et al., 2013a). Deletion of the syndecan-4 cytoplasmic domain or a knockdown of RhoA inhibits cell migration in turkey satellite cells (Shin et al., 2013a). The binding of PIP_2 also functions in the stabilization of syndecan-4 leading to the formation of syndecan-4 oligomers in turkey satellite cells (Shin et al., 2012). The oligomerization of syndecan-4 is required for the activation of syndecan-4 as syndecan-4 in the monomer form is not able to activate PKCα (Horowitz and Simons, 1998a,b).

Syndecan-4 may have varying functions with regard to FGF2 based on cell type. For example in endothelial cells, both the syndecan-4 heparan sulfate chains and the cytoplasmic domain have been shown to be necessary for syndecan-4 mediated FGF2 cell signaling (Volk et al., 1999). However, in turkey satellite cells, the heparan

sulfate chains are not required for syndecan-4 FGF2 signal transduction, but the cytoplasmic domain and cytoplasmic domain Ser^{178} in the conserved C1 region is required for modulating satellite cell responsiveness to FGF2 (Zhang et al., 2008; Song et al., 2012c,d). Horowitz and Simons (1998a,b) found that the Ser residue in the C1 domain can be phosphorylated by growth inhibitors and dephosphorylated by the addition of FGF2. The phosphorylation of the Ser in the C1 region will decrease PKCα activation. In turkey satellite cells, the Ser^{178} amino acid stimulates both PKCα activation and FGF2-induced proliferation (Song et al., 2012d).

23.15 Strategies to reduce myopathies

It has become clear that myopathies in poultry develop mainly in fast-growing meat-type chickens, with the pectoralis major muscle being more affected than the leg muscles (Powell et al., 2014; Harding et al., 2016). The genetic selection for body and breast muscle growth results in a high-metabolic rate and extensive protein accretion (Havenstein et al., 2003a,b), both of which worsen the chickens' ability to cope with stresses, such as oxidative or heat stress. This could be because the pectoralis major muscle, which is a fast glycolytic muscle with low-blood supply, has outgrown its support system (i.e., the vasculature) (Velleman and Clark, 2015; Sihvo et al., 2014, 2017), resulting in more incidences of hypoxia (Boerboom et al., 2018) and an increase in reactive oxygen species (Abasht et al., 2016). In these chickens, such stresses may lead to repetitive muscle degeneration–regeneration cycles accompanied by inflammation, fat deposition, an increase in fibrotic tissue, and depletion in the number of satellite cells (Kuttappan et al., 2016; Daughtry et al., 2017), resembling the situation in human muscular diseases. A very recent paper raised the hypothesis that deregulation of fat and glucose metabolism and chronic overload of these nutrients in the pectoralis major muscle lead to wooden breast phenotype, similar to what is observed in complications of type 2 diabetes in mammals (Lake and Abasht, 2020).

The high-metabolic rate of fast-growing meat-type chickens also leads to overproduction of body heat. Since birds are homeotherms and maintain their body temperature within a narrow range, high metabolic heat production in these chickens makes it more difficult for them to cope with environmental heat stress, even at an early age (for a comprehensive review, see Yahav, 2015). Studies on broilers have demonstrated that chronic heat exposure results in lower weight gain, coupled with a lower absolute growth of pectoralis muscle (Baziz et al., 1996) and decreased vascular support (Hadad et al., 2014; Joiner et al., 2014). Moreover, increased fat and collagen deposition was observed interstitially in pectoralis muscle; fat droplets were observed in the myofibers of chicks exposed to heat stress in the first 2 weeks posthatch (Piestun et al., 2017; Patael et al., 2019), implying a white striping myopathy in these chickens. Accumulation of fat was also observed in satellite cells derived from the heat-exposed chickens. Accumulation of fat and increased adipogenic gene expression were observed in studies using clonal satellite cells exposed to a variety of temperatures (Harding et al., 2015, 2016), suggesting transdifferentiation of satellite cells to adipogenic ones.

The full etiology of the pectoral major muscle myopathies is not fully understood, and it is not known whether onset of the diseases has a single or multiple cause. However, several strategies are being employed to ameliorate the severity of the myopathies and thereby reduce the damage to meat quality. Attempts to slow down the growth rate of fast-growing chickens, which tend to develop myopathies (Baldi et al., 2018; Petracci et al., 2019), could be made by breeding chickens that grow at a slower rate. However, even though it should still be considered, the genetic factor seems to contribute only a relatively small part to myopathy development, while the greater impact is attributed to mostly nongenetic factors (Bailey et al., 2015, 2020). Growth rate could also be reduced through feed restriction during early or later stages of growth. Factors such as the timing or duration of the feed restriction should be considered, as the first week posthatch is crucial for satellite cell myogenic activity (see Section 23.6) and for maturation of the intestinal system (Geyra et al., 2001). Feed deprivation during the first days posthatch leads to irreversible adverse effects on muscle development and growth (Halevy et al., 2001, 2003; Mozdziak et al., 2002), while feed restriction in the second week posthatch leads to compensatory growth (Plavnik and Hurwitz, 1998). Nevertheless, with regard to reducing myopathies and improving meat quality, the feed-restriction approach is still under debate. More recent studies have shown that while energy restriction negatively affects overall performance (e.g., feed conversion), the effects on breast muscle myopathies and meat quality are contradictory (Velleman al., 2014a,b; Trocino et al., 2015; Meloche et al., 2018a). However, altering the balance of dietary amino acids (e.g., D-Lysine) reduced the levels and severity of white striping and wooden breast (Meloche et al., 2018b).

Other approaches to alleviating the muscle degeneration are aimed at improving management and environmental conditions. For example, lighting with green and/or blue monochromatic light during embryonic development and early posthatch initially proved to enhance satellite cell proliferation and muscle growth (Halevy et al., 1998, 2006b; Rozenboim et al., 2004), and improve meat quality (i.e., paleness, pH, drip loss) (Karakaya et al., 2009; Zhang et al., 2012). In addition, the white striping myopathy, which has been suggested to emerge due to chronic heat

stress during the early posthatch period, may be reduced by keeping the hatching chicks under mildly colder temperatures (Patael et al., 2019). Rearing hatching chicks at a gradient of 4 to 2°C below the recommended commercial temperature for the first 2 weeks did not have any adverse effects on body growth or muscle yield, while it reduced the fat and collagen deposition in the muscle (Patael et al., 2019).

Another strategy is acclimating meat-type chickens to high temperature, enabling them to cope with heat stress. Early studies showed that thermal conditioning for 3 or 6 h on day three of age, when satellite cells are at their peak myogenic activity, promotes body weight and pectoralis muscle growth and improves thermal tolerance to heat stress (Halevy et al., 2001). Thermal manipulations in which the incubator temperature was intermittently raised during embryonic periods that are critical for the development of thermoregulation and stress systems, as well as skeletal muscle, had long-term promotive effects on muscle growth and thermotolerance (Piestun et al., 2009a, b, 2011, 2013). Loyau et al. (2013) found that intermittent thermal manipulation from E7 to E16 improves the thermotolerance of broilers exposed to heat stress on day 34 of age, without affecting meat quality of the breast muscle. A different pattern of expression of genes related to, for example, energy metabolism, vascularization, and muscle growth, was observed in a gene-array assay on pectoralis muscle derived from heat-treated embryos compared to nontreated ones (Loyau et al., 2016). These and other studies suggest that thermal manipulations during embryonic or early posthatch periods that are crucial for myogenic and thermoregulation development affect epigenetic processes, resulting in changes in the expression of specific genes and leading to long-lasting effects on thermotolerance and muscle growth (Halevy, 2020).

23.16 Summary

Muscle development involves a wide range of cellular events that have distinct embryonic and posthatch phases. Therefore, many factors can influence the development and growth of avian skeletal muscle. This chapter provides a broad overview of avian muscle structure and function, prehatch and posthatch muscle development, and the genes and factors regulating these processes. In addition, this chapter details the newly evolved muscle myopathies in meat-type chicks, the influence of the extracellular matrix on their development, and strategies to ameliorate these myopathies which have a large impact on meat quality and consequently, the poultry industry.

Acknowledgments

The authors thank Ms. Laura B. Harthan for technical graphic illustrations.

References

Abasht, B., Mutryn, M.F., Michalek, R.D., Lee, W.R., 2016. Oxidative stress and metabolic perturbations in wooden breast disorder in chickens. PLoS One 11 (4), e0153750. https://doi.org/10.1371/journal.pone.0153750.

Abrigo, J., Simon, F., Cabrera, D., Cordova, G., Trollet, C., Cabello-Verrugio, C., 2018. Central role of transforming growth factor type beta 1 in skeletal muscle dysfunctions: an update on therapeutic strategies. Curr. Protein Pept. Sci. 19, 1189–1200. https://doi.org/10.2174/1389203718666171117101916.

Ahmad, S., Jan, A.T., Baig, M.H., Lee, E.J., Choi, I., 2017. Matrix gla protein: an extracellular matrix protein regulates myostatin expression in the muscle developmental program. Life Sci. 172, 55–63. https://doi.org/10.1016/j.lfs.2016.12.011.

Alberts, B., Johnson, A., Lewis, J., Raff, M., Roberts, K., Walter, P., 2008. Molecular Biology of the Cell. Garland Science, New York.

Alexakis, C., Partridge, T., Bou-Gharios, G., 2007. Implication of the satellite cell in dystrophic muscle fibrosis: a self-perpetuating mechanism of collagen overproduction. Am. J. Physiol. 293, C661–C669.

Asgari, M., Latifi, N., Heris, H.K., Vali, H., Mongeau, L., 2017. In vitro fibrillogenesis of tropocollagen type III in collagen type I affects its relative fibrillar topology and mechanics. Sci. Rep. 7, 1392. https://doi.org/10.1038/s41598-017-01476-y.

Ashmore, C.R., Tompkins, G., Doerr, L., 1972. Postnatal development of muscle fiber type in domestic animals. J. Anim. Sci. 34, 37–41.

Bailey, A., Bazin, S., Sims, T., Le Lous, M., Nicoletis, C., Delaunay, A., 1975. Characterization of the collagen of human hypertrophic and normal scars. Biochim. Biophys. Acta 405, 412–421.

Bailey, R.A., Souza, E., Avendano, S., 2020. Characterizing the influence of genetics on breast muscle myopathies in broiler chickens. Front. Physiol. 11, 1041. https://doi.org/10.3389/fphys.2020.01041 eCollection 2020.

Bailey, R.A., Watson, K.A., Bilgili, S.F., Avendano, S., 2015. The genetic basis of pectoralis major myopathies in modern broiler chicken broiler lines. Poultry Sci. 94, 2870–2879.

Baldi, G., Soglia, F., Mazzoni, M., Sirri, F., Canonico, L., Babini, E., Laghi, L., Cavani, C., Petracci, M., 2018. Implications of white striping and spaghetti meat abnormalities on meat quality and histological features in broilers. Animal 12, 164–173.

Bang, M.-L., Li, X., Littlefield, R., Bremner, S., Thor, A., Knowlton, K.U., Lieber, R.L., Chen, J., 2006. Nebulin-deficient mice exhibit shorter thin filament lengths and reduced contractile function in skeletal muscle. J. Cell Biol. 173, 905–916.

Barnes, M., Morton, L., Bennett, R., Bailey, A., Sims, T., 1976. Presence of type III collagen in Guinea-pig dermal scar. Biochem. J. 157, 263–266.

Barton, E.R., Park, S., James, J.K., Makarewich, C.A., Philippou, A., Eletto, D., Lei, H., Brisson, B., Ostrovsky, O., Li, Z., Argon, Y., 2012. Deletion of muscle GRP94 impairs both muscle and body growth by inhibiting local IGF production. FASEB J. 26, 3691–3702.

Baziz, H.A., Geraert, P.A., Padilha, J.C.F., Guillaumin, S., 1996. Chronic heat exposure enhances fat deposition and modifies muscle and fat partition in broiler carcasses. Poultry Sci. 75, 505–513.

Bigot, K., Mignon-Grasteau, S., Picard, M., Tesseraud, S., 2003. Effects of delayed feed intake on body, intestine, and muscle development in neonate broilers. Poultry Sci. 82, 781–788.

Biressi, S., Rando, T.A., 2010. Heterogeneity in the muscle satellite cell population. Semin. Cell Dev. Biol. 21, 845–854.

Bischoff, R., 1974. Enzymatic liberation of myogenic cells from adult rat muscle. Anat. Rec. 180, 645–661.

Bischoff, R., 1975. Regeneration of single muscle fibers in vitro. Anat. Rec. 182, 215–236.

Bischoff, R., 1986. A satellite cell mitogen from crushed adult muscle. Dev. Biol. 115, 140–147.

Bodine, S.C., Stitt, T.N., Gonzalez, M., Kline, W.O., Stover, G.L., Bauerlein, R., Zlotchenko, E., Scrimgeour, A., Lawrence, J.C., Glass, D.J., Yancopoulos, G.D., 2001. Akt/mTOR pathway is a crucial regulator of skeletal muscle hypertrophy and can prevent muscle atrophy in vivo. Nat. Cell Biol. 3, 1014–1019.

Bober, E., Franz, T., Arnold, H.H., Gruss, P., Tremblay, P., 1994. Pax-3 is required for the development of limb muscles: a possible role for the migration of dermomyotomal muscle progenitor cells. Development 120, 603–612.

Boerboom, G., van Kempen, T., Navarro-Villa, A., Pèrez-Bonilla, A., 2018. Unraveling the cause of white striping in broilers using metabolomics. Poultry Sci. 97, 3977–3986. https://doi.org/10.3382/ps/pey266.

Bornstein, P., Sage, H., 1980. Structurally distinct collagen types. Annu. Rev. Biochem. 49, 957–1003.

Brandan, E., Larraín, J., 1998. Heparan sulfate proteoglycans during terminal skeletal muscle differentiation. Possible functions and regulation of their expression. Basic Appl. Myol. 8, 107–113.

Brand-Saberi, B., Muller, T.S., Wilting, J., Christ, B., Birchmeier, C., 1996. Scatter factor/hepatocyte growth factor (SF/HGF) induces emigration of myogenic cells at interlimb level in vivo. Dev. Biol. 179, 303–308.

Brisson, B.K., Mauldin, E.A., Lei, W., Vogel, L.K., Power, A., Lo, A., Dopkin, D., Khanna, C., Wells, R.G., Puré, E., Volk, S.W., 2015. Type III collagen directs stromal organization and limits metastasis in a murine model of breast cancer. Am. J. Pathol. 185, 1471–1486.

Carrino, D.A., Sorrell, J.M., Caplan, A.I., 1999. Dynamic expression of proteoglycans during chicken skeletal muscle development and maturation. Poultry Sci. 78, 769–777. https://doi.org/10.1093/ps/78.5.769.

Cerny, L.C., Bandman, E., 1987. Expression of myosin heavy chain isoforms in regenerating myotubes of innervated and denervated chicken pectoral muscle. Dev. Biol. 119, 350–362.

Chen, L., Klass, C., Woods, A., 2004. Syndecan-2 regulates transforming growth factor-beta signaling. J. Biol. Chem. 279, 15715–15718.

Chen, B., Yu, J., Guo, L., Byers, M.S., Wang, Z., Chen, X., Xu, H., Nie, Q., 2019. Circular RNA circHIPK3 promotes the proliferation and differentiation of chicken myoblast cells by sponging miR-30a-3p. Cells 8, 177. https://doi.org/10.3390/cells8020177.

Chen, X., Ouyang, H., Wang, Z., Chen, B., Nie, Q., 2018. A novel circular RNA generated by FGFR2 gene promotes myoblast proliferation and differentiation by sponging miR-133a-5p and miR-29b-1-5p. Cells 7, 199. https://doi.org/10.3390/cells7110199.

Choi, Y., Chung, H., Jung, H., Couchman, J.R., Oh, E.–S., 2011. Syndecans as cell surface receptors: unique structure equates with functional diversity. Matrix Biol. 30, 93–99.

Coleman, M.E., DeMayo, F., Yin, K.C., Lee, H.M., Geske, R., Montgomery, C., Schwartz, R.J., 1995. Myogenic vector expression of insulin-like growth factor I stimulates muscle cell differentiation and myofiber hypertrophy in transgenic mice. J. Biol. Chem. 270, 12109–12116.

Collins, C.A., Olsen, I., Zammit, P.S., Heslop, L., Petrie, A., Partridge, T.A., Morgan, J.E., 2005. Stem cell function, self-renewal, and behavioral heterogeneity of cells from the adult muscle satellite cell niche. Cell 122, 289–301.

Cornelison, D.D.W., Wold, B.J., 1997. Single-cell analysis of regulatory gene expression in quiescent and activated mouse skeletal muscle satellite cells. Dev. Biol. 191, 270–283.

Cornelison, D.D., Filla, M.S., Stanley, H.M., Rapraeger, A.C., Olwin, B.B., 2001. Syndecan-3 and syndecan-4 specifically mark skeletal muscle satellite cells and are implicated in satellite cell maintenance and muscle regeneration. Dev. Biol. 239, 79–94.

Cornelison, D.D., Wilcox-Adelman, S.A., Geotinck, P.F., Rauvala, H., Rapraeger, A.C., Olwin, B.B., 2004. Essential and separable roles for syndecan-3 and syndecan-4 in skeletal muscle development and regeneration. Genes Dev. 18, 32231–32236.

Cornelison, D., 2018. "Known unknowns": current questions in muscle satellite cell biology. Curr. Top. Dev. Biol. 126, 205–233.

Daughtry, M.R., Berio, E., Shen, Z., Suess, E.J.R., Shah, N., Geiger, A.E., Berguson, E.R., Dalloul, R.A., Persia, M.E., Shi, H., Gerrard, D.E., 2017. Satellite cell-mediated breast muscle regeneration decreases with broiler size. Poultry Sci. 96, 3457–3464. https://doi.org/10.3382/ps/pex068.

Davis, R.L., Weintruab, H., Lassar, A.B., 1987. Expression of a single transfected cDNA converts fibroblasts to myoblasts. Cell 51, 987–1000.

Day, K., Shefer, G., Richardson, J.B., Enikolopov, G., Yablonka-Reuveni, Z., 2007. Nestin-GFP reporter expression defines the quiescent state of skeletal muscle satellite cells. Dev. Biol. 304, 246–259.

Deepa, S.S., Yamada, S., Zako, M., Goldberg, O., Sughara, K., 2004. Chondroitin sulfate chains on syndecan-1 and syndecan-4 from normal murine mammary gland epithelial cells are structurally and functionally distinct and cooperate with heparan sulfate chains to bind growth factors. A novel function to control binding of midkine, pleiotrophin, and basic fibroblast growth factor. J. Biol. Chem. 279, 37368–37376.

Der Vartanian, A., Quétin, M., Michineau, S., Auradé, F., Hayashi, S., Dubois, C., Rocancourt, D., Drayton-Libotte, B., Szegedi, A., Buckingham, M., Conway, S.J., Gervais, M., Relaix, F., 2019. PAX3 confers functional heterogeneity in skeletal muscle stem cell responses to environmental stress. Cell Stem Cell 24, 958–973.e9.

Dial, T.R., Carrier, D.R., 2012. Precocial hindlimbs and altricial forelimbs: partitioning ontogenetic strategies in mallards (*Anas platyrhynchos*). J. Exp. Biol. 215, 3703–3710.

Dimario, J.X., Stockdale, F.E., 1997. Both myoblast lineage and innervation determine fiber type and are required for expression of the slow myosin heavy chain 2 gene. Dev. Biol. 188, 167–180.

Dollenmeier, P., Turner, D.C., Eppenberger, H.M., 1981. Proliferation and differentiation of chick skeletal muscle cells cultured in a chemically defined medium. Exp. Cell Res. 135, 47–61.

Dovas, A., Yoneda, A., Couchman, J.R., 2006. PKC alpha-dependent activation by syndecan-4 during focal adhesion formation. J. Cell Sci. 119, 2837–2846.

Dransfield, E., Sosnicki, A.A., 1999. Relationship between muscle growth and poultry meat quality. Poultry Sci. 78, 743–746.

Duclos, M.J., Chevalier, B., Goddard, C., Simon, J., 1993b. Regulation of amino acid transport and protein metabolism in myotubes derived from chicken muscle satellite cells by insulin-like growth factor-I. J. Cell. Physiol. 157, 650–657.

Duclos, M.J., Chevalier, B., Le Marchand-Brustel, Y., Tanti, J.F., Goddard, C., Simon, J., 1993a. Insulin-like growth factor-I stimulated glucose transport in myotubes derived from chicken muscle satellite cells. J. Endocrinol. 137, 465–472.

Feldman, J.L., Stockdale, F.E., 1991. Skeletal muscle satellite cell diversity: satellite cells form fibers of different types in cell culture. Dev. Biol. 143, 320–334.

Florini, J.R., Roberts, A.B., Ewton, D.Z., Falen, S.L., Flanders, K.C., Sporn, M.B., 1986. Transforming growth factor-β. A very potent inhibitor of myoblast differentiation, identical to the differentiation inhibitor secreted by buffalo rat liver cells. J. Biol. Chem. 261, 16509–16513.

Fowler, V.M., Sussmann, M.A., Miller, P.G., Flucher, B.E., Daniels, M.P., 1993. Tropomodulin is associated with the free (pointed) ends of the thin filaments in rat skeletal muscle. J. Cell Biol. 120, 411–420.

Fuentealba, L., Carey, D.J., Brandan, E., 1999. Antisense inhibition of syndecan-3 expression during skeletal muscle differentiation accelerates myogenesis through a basic fibroblast growth factor-dependent mechanism. J. Biol. Chem. 274, 37876–37884.

Gal-Levi, R., Leshem, Y., Aoki, S., Nakamura, T., Halevy, O., 1998. Hepatocyte growth factor plays a dual role in regulating skeletal muscle satellite cell proliferation and differentiation. Biochim. Biophys. Acta 1402, 39–51.

Gerli, M.F.M., Moyle, L.A., Benedetti, S., Ferrari, G., Ucuncu, E., Ragazzi, M., Constantinou, C., Louca, I., Sakai, H., Ala, P., De Coppi, P., Tajbakhsh, S., Cossu, G., Tedesco, F.S., 2019. Combined Notch and PDGF signaling enhances migration and expression of stem cell markers while inducing perivascular cell features in muscle satellite cells. Stem Cell Rep. 12, 461–473. https://doi.org/10.1016/j.stemcr.2019.01.007.

Geyra, A., Uni, Z., Sklan, D., 2001. Enterocyte dynamics and mucosal development in the posthatch chick. Poultry Sci. 80, 776–782. https://doi.org/10.1093/ps/80.6.776.

Gibertini, S., Zanotti, S., Savadori, P., Curcio, M., Saredi, S., Salerno, F., Andreetta, F., Bernasconi, P., Mantegazza, R., Mora, M., 2014. Cell Tissue Res 356, 427–443. https://doi.org/10.1007/s00441-014-1854-4.

Gilbert, S.F., 2019. Developmental Biology, twelfth ed. Sinauer Associates, Inc.

Gros, J., Manceau, M., Thomas, V., Marcelle, C., 2005. A common sonic origin for embryonic muscle progenitors and satellite cells. Nature 435, 654–958.

Hadad, Y., Cahaner, A., Halevy, O., 2014. Featherless and feathered broilers under control versus hot conditions. 2. Breast muscle development and growth in pre- and post-hatch periods. Poultry Sci. 93, 1076–1087.

Halevy, O., 2020. Timing is everything-the high sensitivity of avian satellite cells to thermal conditions during embryonic and posthatch periods. Front. Physiol. 11, 235. https://doi.org/10.3389/fphys.2020.00235.

Halevy, O., Biran, I., Rozenboim, I., 1998. Various light source treatments affect body and skeletal muscle growth by affecting skeletal muscle satellite cell proliferation in broilers. Comp. Biochem. Physiol. 120, 317–323.

Halevy, O., Geyra, A., Barak, M., Uni, Z., Sklan, D., 2000. Early post-hatch starvation decreases satellite cell proliferation and skeletal muscle growth in chicks. J. Nutr. 130, 858–864.

Halevy, O., Krispin, A., Leshem, Y., McMurtry, J.P., Yahav, S., 2001. Early-age heat exposure affects skeletal muscle satellite cell proliferation and differentiation in chicks. Am. J. Physiol. Regul. Integr. Comp. Physiol. 281, R302–R309.

Halevy, O., Nadel, Y., Barak, M., Rozenboim, I., Sklan, D., 2003. J. Nutr. 133, 1376–1382.

Halevy, O., Piestun, Y., Allouh, M.Z., Rosser, B.W., Rinkevich, Y., Reshef, R., Rozneboim, I., Wleklinski-Lee, M., Yablonka-Reuveni, Z., 2004. Pattern of Pax7 expression during myogenesis in the posthatch chicken establishes a model for satellite cell differentiation and renewal. Dev. Dyn. 231, 489–502.

Halevy, O., Rozenboim, I., Yahav, S., 2006a. Enhancement of meat production by environmental manipulation in embryo and young broilers. World Poult. Sci. J. 62, 485–497.

Halevy, O., Piestun, Y., Rozenboim, I., Yablonka-Reuveni, Z., 2006b. In-ovo exposure to monochromatic green light promotes skeletal muscle cell proliferation and synchronizes myofiber development in posthatch chicks. Am. J. Physiol. Regul. Integr. Comp. Physiol. 290, R1062–R1070.

Hansen-Smith, F.M., Picou, D., Golden, M.N., 1979. Muscle satellite cells in malnourished and nutritionally rehabilitated children. J. Neurol. Sci. 41, 207–221.

Harding, R.L., Velleman, S.G., 2016. MicroRNA regulation of myogenic satellite cell proliferation and differentiation. Mol. Cell. Biochem. 412, 181–195. https://doi.org/10.1007/s11010-015-2625-6.

Harding, R.L., Clark, D.L., Halevy, O., Coy, C.S., Yahav, S., Velleman, S.G., 2015. The effect of temperature on apoptosis and adipogenesis on skeletal muscle satellite cells derived from different muscle types. Physiol. Rep. 3, e12539. https://doi.org/10.14814/phy2.12539.

Harding, R.L., Halevy, O., Yahav, S., Velleman, S.G., 2016. The effect of temperature on proliferation and differentiation of skeletal muscle satellite cells isolated from different muscle types. Physiol. Rep. 4, e12539. https://doi.org/10.14814/phy2.12539.

Harel, I., Nathan, E., Tirosh-Finkel, L., Zigdon, H., Guimarães-Camboa, N., Evans, S.M., Tzahor, E., 2009. Distinct origins and genetic programs of head muscle satellite cells. Dev. Cell 16, 822–832.

Hartley, R.S., Bandman, E., Yablonka-Reuveni, Z., 1992. Skeletal muscle satellite cells appear during late chicken embryogenesis. Dev. Biol. 153, 206–216.

Hasty, P., Bradley, A., Morris, J.H., Edmondson, D.G., Venuti, J.M., Olson, E.N., Klein, W.H., 1993. Muscle deficiency and neonatal death in mice with a targeted mutation in the myogenin gene. Nature 364, 501–506.

Havenstein, G.B., Ferket, P.R., Qureshi, M.A., 2003a. Growth, livability, and feed conversion of 1957 vs. 2001 broilers when fed representative 1957 and 2001 broiler diets. Poultry Sci. 82, 1500–1508.

Havenstein, G.B., Ferket, P.R., Qureshi, M.A., 2003b. Carcass composition and yield of 1957 vs. 2001 broilers fed representative 1957 and 2001 broiler diets. Poultry Sci. 82, 1509–1518.

Hawke, T.J., Garry, D.J., 2001. Myogenic satellite cells: physiology to molecular biology. J. Appl. Physiol. 91, 534–551.

Hitachi, K., Tsuchida, K., 2013. Role of microRNAs in skeletal muscle hypertrophy. Front. Physiol. 4, 408.

Hodik, V., Mett, A., Halevy, O., 1997. Mutual effects of growth hormone and growth factors on chicken satellite cells. Gen. Comp. Endocrinol. 108, 161–170.

Hoh, J.F.Y., Hughes, S., 1988. Myogenic and neurogenic regulation of myosin gene expression in cat jaw-closing muscles regenerating in fast and slow limb muscle beds. J. Muscle Res. Cell Motil. 9, 59–72.

Horowitz, A., Simons, M., 1998a. Regulation of syndecan-4 phosphorylation in vivo. J. Biol. Chem. 273, 10914–10918.

Horowitz, A., Simons, M., 1998b. Phosphorylation of the cytoplasmic tail of syndecan-4 regulates activation of protein kinase C alpha. J. Biol. Chem. 273, 25548–25551.

Hurme, T., Kalimo, H., Sandberg, M., Lehto, M., Vuorio, E., 1991. Localization of type I and III collagen and fibronectin production in injured gastrocnemius muscle. Lab. Investig. 64, 76–81.

Janeczko, R.A., Etlinger, J.D., 1984. Inhibition of intracellular proteolysis in muscle cultures by multiplication-stimulating activity and insulin on proteolysis, protein synthesis, amino acid uptake, and sugar transport. J. Biol. Chem. 259, 6292–6297.

Jennische, E., Skottner, A., Hansson, H.A., 1987. Satellite cells express the trophic factor IGF-I in regenerating skeletal muscle. Acta Physiol. Scand. 129, 9–15.

Joiner, K.S., Hamlin, G.A., Lien, A.R., Bilgili, S.F., 2014. Evaluation of capillary and myofiber density in the pectoralis major muscles of rapidly growing, high-yield broiler chickens during increased heat stress. Avian Dis. 38, 377–382. https://doi.org/10.1637/10733-112513-Reg.1.

Kablar, B., Asakura, A., Krastel, K., Ying, C., May, L.L., Goldhamer, D.J., Rudnicki, M.A., 1998. MyoD and Myf-5 define the specification of musculature of distinct embryonic origin. Biochem. Cell. Biol. 76, 1079–1091.

Karakaya, M., Parlat, S.S., Yilmaz, M.T., Yildirim, I., Ozalp, B., 2009. Growth performance and quality properties of meat from broiler chickens reared under different monochromatic light sources. Br. Poult. Sci. 50, 76–82. https://doi.org/10.1080/00071660802629571.

Khatri, B., Seo, D., Shouse, S., Pan, J.H., Hudson, N.J., Kim, J.K., Bottje, W., Kong, B.C., 2018. MicroRNA profiling associated with muscle growth in modern broilers compared to an unselected chicken breed. BMC Genom. 19, 683. https://doi.org/10.1186/s12864-018-5061-7.

Kirk, S., Oldham, J., Kambadur, R., Sharma, M., Dobbie Bass, J., 2000. Myostatin regulation during skeletal muscle regeneration. J. Cell. Physiol. 184, 356–363.

Koeppen, B.M., Stanton, B.A., 2018. Skeletal muscle physiology. In: Koeppen, B.M., Stanton, B.A. (Eds.), Berne & Levy Physiology, seventh ed., Updated Edition. Elsevier Inc., Philadelphia, PA, pp. 242–267.

Kornasio, R., Kedar, O., Halevy, O., Uni, Z., 2011. Effect of in ovo feeding and its interaction with timing of first feed on glycogen reserves, muscle growth, and body weight. Poultry Sci. 90, 1467–1477.

Koren, I., Reem, E., Kimchi, A., 2010. DAP1, a novel substrate of mTOR, negatively regulates autophagy. Curr. Biol. 20, 1093–1098.

Kovanen, V., Suominen, H., 1989. Age- and training-related changes in collagen metabolism of rat skeletal muscle. Eur. J. Appl. Physiol. 58, 765–771.

Kristensen, L.S., Andersen, M.S., Stagsted, L.V.W., Ebbesen, K.K., Hansen, T.B., Kjems, J., 2019. The biogenesis, biology and characterization of circular RNAs. Nat. Rev. Genet. 20, 675–691. https://doi.org/10.1038/s41576-019-0158-7.

Kuang, S., Kuroda, K., Le Grand, F., Rudnicki, M.A., 2007. Asymmetric self-renewal and commitment of satellite stem cells in muscle. Cell 129, 999–1010.

Kuttappan, V.A., Hargis, B.M., Owens, C.M., 2016. White striping and woody breast myopathies in the modern poultry industry. A review. Poultry Sci. 95, 2724–2733.

Kuttappan, V.A., Shivaprasad, H.I., Shaw, B.A., Valentine, B.A., Hargis, B.M., Clark, F.D., McKee, S.R., Owens, C.M., 2013. Pathological changes associated with white striping in broiler breast muscles. Poultry Sci. 92, 331–338.

Lake, J.A., Abasht, B., 2020. Front. Physiol. https://doi.org/10.3389/fphys.2020.00169.

Landys-Cianneli, M.M., Piersma, T., Jukema, J., 2003. Strategic size changes of internal organs and muscle tissue in the bar-tailed godwit during fat storage on a spring stopover site. Funct. Ecol. 17, 151–159.

Larraín, J., Carey, D.J., Brandan, E., 1998. Syndecan-1 expression inhibits myoblast differentiation through basic fibroblast growth factor-dependent mechanisms. J. Biol. Chem. 273, 32288–32296.

Larraín, J., Cizmeci-Smith, G., Troncoso, V., Stahl, R.C., Carey, D.J., Brandan, E., 1997. Syndecan-1 expression is down-regulated during myoblast terminal differentiation. Modulation by growth factors and retinoic acid. J. Biol. Chem. 272, 18418–18424.

Leshem, Y., Spicer, D.B., Gal-Levi, R., Halevy, O., 2000. Hepatocyte growth factor (HGF) inhibits skeletal muscle cell differentiation: a role for the bHLH protein Twist and the cdk inhibitor p27. J. Cell. Physiol. 184, 101–109.

Lieber, R.L., 1992. Skeletal muscle physiology. In: Butler, J.P. (Ed.), Skeletal Muscle Structure and Function: Implications for Rehabilitation and Sports Medicine. Williams & Wilkins, Baltimore, MD, pp. 49–110 (Chapter 2).

Light, N., Champion, A.E., 1984. Characterization of muscle epimysium, perimysium, and endomysium collagens. Biochem. J. 219, 1017–1026.

Lindström, Å., Kvist, A., Piersma, T., Dekinga, T., Dietz, M.W., 2000. Avian pectoral muscle size rapidly tracks body mass changes during flight, fasting and fueling. J. Exp. Biol. 203, 913–919.

Liu, C., McFarland, D.C., Nestor, K.E., Velleman, S.G., 2006. Differential expression of membrane-associated heparan sulfate proteoglycans in the skeletal muscle of turkeys with different growth rates. Poultry Sci. 85, 422–428.

Liu, X., McFarland, D.C., Nestor, K.E., Velleman, S.G., 2004. Developmental regulated expression of syndecan-1 and glypican in pectoralis major muscle in turkeys with different growth rates. Dev. Growth Differ. 46, 37–51.

Liu, W., Wang, Z., Chen, Y., 2010. Effects of monochromatic light on developmental changes in satellite cell population of pectoral muscle in broilers during early posthatch period. Anat. Rec. 293, 1315–1324. https://doi.org/10.1002/ar.21174.

Loyau, T., Berri, C., Bedrani, L., Métayer-Coustard, S., Praud, C., Duclos, M.J., Tesseraud, S., Rideau, N., Everaert, N., Yahav, S., Mignon-Grasteau, S., Collin, A., 2013. Thermal manipulation of the embryo modifies the physiology and body composition of broiler chickens reared in floor pens without affecting breast meat processing quality. J. Anim. Sci. 91, 3674–3685. https://doi.org/10.2527/jas.2013-6445.

Loyau, T., Hennequet-Antier, C., Coustham, V., Berri, C., Leduc, M., Crochet, S., Sannier, M., Duclos, M.J., Mignon-Grasteau, S., Tesseraud, S., Brionne, A., Métayer-Coustard, S., Moroldo, M., Lecardonnel, J., Martin, P., Lagarrigue, S., Yahav, S., Collin, A., 2016. Thermal manipulation of the chicken embryo triggers differential gene expression in response to a later heat challenge. BMC Genom. 17, 329. https://doi.org/10.1186/s12864-016-2661-y.

Mauro, A., 1961. Satellite cell of skeletal muscle fibers. J. Biophys. Biochem. Cytol. 9, 493–495.

McCarthy, J.J., Mula, J., Miyazaki, M., Erfani, R., Garrison, K., Farooqui, A.B., Srikuea, R., Lawson, B.A., Grimes, B., Keller, C., Van Zant, G., Campbell, K.S., Esser, K.A., Dupont-Versteegden, E.E., Peterson, C.A., 2011. Effective fiber hypertrophy in satellite cell-depleted skeletal muscle. Development 138, 3657–3666.

McConnell, J.C., O'Connell, O.V., Brennan, K., Weiping, L., Howe, M., Joseph, L., Knight, D., O'Cualain, R., Lim, Y., Leek, A., Waddington, R., Rogan, J., Astley, S.M., Gandhi, A., Kirwan, C.C., Sherratt, M.J., Streuli, C.H., 2016. Increased peri-ductal collagen micro-organization may contribute to raise mammographic density. Breast Cancer Res. 18, 5. https://doi.org/10.1186/s13058-015-0664-218.

McCormick, R.J., 1994. The flexibility of the collagen compartment of muscle. Meat Sci. 36, 79–91.

McCroskery, S., Thomas, M., Maxwell, L., Sharma, M., Kambadur, R., 2003. Myostatin negatively regulates satellite cell activation and self-renewal. J. Cell Biol. 162, 1135–1147.

McFarland, D.C., Gilkerson, K.K., Pesall, J.E., Ferrin, N.H., Wellenreiter, R.H., 1997. In vitro characteristics of myogenic satellite cells derived from the pectoralis major and biceps femoris muscles of the chicken. Cytobios 91, 45–52.

McFarland, D.C., Gilkerson, K.K., Pesall, J.E., Walker, J.S., Yun, Y., 1995. Heterogeneity in growth characteristics of satellite cell populations. Cytobios 82, 21–27.

McFarland, D.C., Liu, X., Velleman, S.G., Zeng, C., Coy, C.S., Pesall, J.E., 2003. Variation in fibroblast growth factor response and heparan sulfate proteoglycan production in satellite cell populations. Comp. Biochem. Physiol., C 134, 341–351.

McFarland, D.C., Pesall, J.E., 2008. Phospho-MAPK as a marker of myogenic satellite cell responsiveness to growth factors. Comp. Biochem. Physiol. B 149, 463–467.

McFarland, D.C., Pesall, J.E., Gilkerson, K.K., 1993. The influence of growth factors on Turkey embryonic myoblasts and satellite cells in vitro. Gen. Comp. Endocrinol. 89, 415–424.

McFarland, D.C., Pesall, J.E., Gilkerson, K.K., Ferrin, N.H., Ye, W.V., Swenning, T.A., 1994. Comparison of protein metabolism and glucose uptake in Turkey (*Meleagris gallopavo*) satellite cells and embryonic myoblasts in vitro. Comp. Biochem. Physiol. A 107, 301–306.

McFarland, D.C., Singh, Y.N., Johnson, A.D., Pesall, J.E., Gilkerson, K.K., Vander Wal, L.S., 2000. Isolation and characterization of myogenic satellite cells from the muscular dystrophic hamster. Tissue Cell 32, 257–265.

McFarland, D.C., Velleman, S.G., Pesall, J.E., Liu, C., 2006. Effect of myostatin on Turkey myogenic satellite cells and embryonic myoblasts. Comp. Biochem. Physiol. A 144, 501–508.

McFarland, D.C., Velleman, S.G., Pesall, J.E., Liu, C., 2007. The role of myostatin in chicken (*Gallus domesticus*) myogenic satellite cell proliferation and differentiation. Gen. Comp. Endocrinol. 151, 351–357.

McPherron, A.C., Lee, S.-J., 1997. Double muscling in cattle due to mutations in the myostatin gene. Proc. Natl. Acad. Sci. U.S.A. 94, 12457–12461.

McPherron, A.C., Lawler, A.M., Lee, S.-J., 1997. Regulation of skeletal muscle mass in mice by a new TGF-β superfamily member. Nature 387, 83–90.

Meloche, K.J., Fancher, B.I., Emmerson, D.A., Bilgili, S.F., Dozier 3rd, W.A., 2018a. Effects of reduced dietary energy and amino acid density on pectoralis major myopathies in broiler chickens at 36 and 49 days of age. Poultry Sci. 97, 1794–1807. https://doi.org/10.3382/ps/pex454.

Meloche, K.J., Fancher, B.I., Emmerson, D.A., Bilgili, S.F., Dozier 3rd, W.A., 2018b. Effects of reduced digestible lysine density on myopathies of the pectoralis major muscles in broiler chickens at 48 and 62 days of age. Poultry Sci. 97, 3311–3324. https://doi.org/10.3382/ps/pey171.

Merkel, J., DiPaolo, B., Hallock, G., Rice, D., 1988. Type I and type III collagen content of healing wounds in fetal and adult rats. Proc. Soc. Exp. Biol. Med. 187, 493–497.

Mok, G.F., Mohammed, R.H., Sweetman, D., 2015. Expression of myogenic regulatory factors in chicken embryos during somite and limb development. J. Anat. 227, 352–360.

Moss, F.P., 1968. The relationship between the dimensions of the fibres and the number of nuclei during normal growth of skeletal muscle in the domestic fowl. Am. J. Anat. 122, 555–564.

Moss, F.P., Leblond, C.P., 1971. Satellite cells as the source of nuclei in muscles of growing rats. Anat. Rec. 170, 421–436.

Mozdziak, P.E., Walsh, T.J., McCoy, D.W., 2002. The effect of early posthatch nutrition on satellite cell mitotic activity. Poultry Sci. 81, 1703–1708.

Muir, G.D., 2000. Early ontogeny of locomotor behavior: a comparison between altricial and precocical animals. Brain Res. Bull. 53, 719–726.

Naya, F.J., Olson, E., 1999. MEF2: a transcriptional target for signaling pathways controlling skeletal muscle growth and differentiation. Curr. Opin. Cell Biol. 6, 683–688.

Notbohm, H., Mosler, S., Müller, P.K., Brinckmann, J., 1993. In vitro formation and aggregation of heterotypic collagen I and III fibrils. Int. J. Biol. Macromol. 15, 299–304.

Olson, E.N., 1990. MyoD family: a paradigm for development? Genes Dev. 4, 1454–1461.

Ouyang, H., He, X., Li, G., Xu, H., Jia, X., Nie, Q., Zhang, X., 2015. Deep sequencing analysis of miRNA expression in breast muscle of fast-growing and slow-growing broilers. Int. J. Mol. Sci. 16, 16242–16262. https://doi.org/10.3390/ijms160716242.

Oppenhiem, R.W., 1972. Prehatching and hatching behavior in birds: a comparative study of altricial and precocial species. Anim. Behav. 20, 644–655.

Ouyang, H., Chen, X., Wang, Z., Yu, J., Jia, X., Li, Z., Luo, W., Abdalla, A.B., Jebessa, E., Nie, Q., Zhang, X., 2018. Circular RNAs are abundant and dynamically expressed during embryonic muscle development in chickens. DNA Res. 25, 71–86. https://doi.org/10.1093/dnares/dsx039.

Pavlath, G.K., Dominov, J.A., Kegley, K.M., Miller, J.B., 2003. Regeneration of transgenic skeletal muscles with altered timing of expression of the basic helix-loop-helix muscle regulatory factor MRF4. Am. J. Pathol. 162, 1685–1691.

Patael, T., Piestun, Y., Soffer, A., Mordechay, S., Yahav, S., Velleman, S.G., Halevy, O., 2019. Early posthatch thermal stress causes long-term adverse effects on pectoralis muscle development in broilers. Poultry Sci. 93, 268–3277.

Pawlikowski, B., Vogler, T.O., Gadek, K., Olwin, B.B., 2017. Regulation of skeletal muscle stem cells by fibroblast growth factors. Dev. Dyn. 246, 359–367.

Petracci, M., Soglia, F., Madruga, M., Carvalho, L., Ida, E., Estévez, M., 2019. Wooden breast, white striping and spaghetti meat; causes, consequences and consumer perception of emerging broiler meat abnormalities. Compr. Rev. Food Sci. Food Saf. https://doi.org/10.1111/1541-4337.12431.

Pietrzak, M., Greaser, M.L., Sosnicki, A.A., 1997. Effect of rapid rigor mortis processes on protein functionality in pectoralis major muscle of domestic turkeys. J. Anim. Sci. 75, 2106–2116.

Piestun, Y., Harel, M., Barak, M., Yahav, S., Halevy, O., 2009a. Thermal manipulations in late-term chick embryos affect skeletal muscle development and promote myoblast proliferation and muscle hypertrophy. J. Appl. Physiol. 106, 233–240.

Piestun, Y., Halevy, O., Yahav, S., 2009b. Thermal manipulations of broiler embryos—the effect on thermoregulation and development during embryogenesis. Poultry Sci. 88, 2677–2688.

Piestun, Y., Druyan, S., Brake, J., Yahav, S., 2013. Thermal manipulations during broiler incubation alter performance of broilers to 70 days of age. Poultry Sci. 5, 1155–1163. https://doi.org/10.3382/ps.2012-02609.

Piestun, Y., Halevy, O., Shinder, D., Ruzal, M., Druyan, S., Yahav, S., 2011. Thermal manipulations during broiler embryogenesis improves post-hatch performance under hot conditions. J. Thermal Biol. 36, 469–474.

Piestun, Y., Patael, T., Yahav, S., Velleman, S.D., Harding, R.L., Coy, C.S., Halevy, O., 2017. Early post-hatch thermal stress affects broiler muscle development and satellite cell fate. Poultry Sci. 96, 2877–2888.

Piñol-Jurado, P., Gallardo, E., de Luna, N., Suarez-Calvet, X., Sanchez-Riera, C., Fernandez-Simon, E., Gomis, C., Illa, I., Diaz-Manera, J., 2017. Platelet-derived growth factor BB influences muscle regeneration in Duchenne muscle dystrophy. Am. J. Pathol. 187, 1814–1827.

Pisconti, A., Cornelison, D.D.W., Olguin, H.C., Antwine, T.L., Olwin, B.B., 2010. Syndecan-3 and Notch cooperate in regulating adult myogenesis. J. Cell Biol. 190, 427–441.

Plavnik, I., Hurwitz, S., 1988. Early feed restriction in chicks: effect of age, duration and sex. Poultry Sci. 76, 1407–1413.

Pourquié, O., 2011. Vertebrate segmentation: from cyclic gene networks to scoliosis. Cell 145, 650–663. https://doi.org/10.1016/j.cell.2011.05.011.

Powell, D.J., McFarland, D.C., Cowieson, A.J., Muir, W.I., Velleman, S.G., 2014. The effect of nutritional status and muscle fiber type on myogenic satellite cell fate and apoptosis. Poultry Sci. 93, 163–173.

Price, E.R., Bauchinger, U., Zajac, D.M., Cerasale, D.J., McFarlan, J.T., Gerson, A.R., McWilliams, S.R., Guglielmo, C.G., 2011. Migrationand exercise-induced changes to flight muscle size in migratory birds and association with IGF1 and myostatin mRNA expression. J. Exp. Biol. 214, 2823–2831.

Proudfoot, D., Shanahan, C.M., 2006. Molecular mechanisms mediating vascular calcification: role of matrix Gla protein. Nephrology 11, 455–461.

Reed, K.M., Mendoza, K.M., Juneja, B., Fahrenkrung, S.C., Velleman, S.G., Chiang, W., Strasburg, G.M., 2008. Characterization of expressed sequence tags from Turkey skeletal muscle. Anim. Genet. 39, 635–644.

Reiser, J.M., McCormick, R.J., Rucker, R.B., 1992. The enzymatic and non-enzymatic crosslinking of collagen and elastin. FASEB J 6, 2439–2449.

Relaix, F., Rocancourt, D., Mansouri, A., Buckingham, M., 2005. A Pax3/Pax7-dependent population of skeletal muscle progenitor cells. Nature 435, 948–953.

Relaix, F., Montarras, D., Zaffran, S., Gayraud-Morel, B., Rocancourt, D., Tajbakhsh, S., Mansouri, A., Cumano, A., Buckingham, M., 2006. Pax3 and Pax7 have distinct and overlapping functions in adult muscle progenitor cells. J. Cell Biol. 172, 91–102.

Ridgeway, A.G., Wilton, S., Sherjanc, I.S., 2000. Myocyte enhance factor 2C and myogenin up-regulate each other's expression and induce the development of skeletal muscle in P19 cells. J. Biol. Chem. 275, 41–46.

Romanic, A.M., Adachi, E., Kadler, K.E., Hojima, Y., Prockop, D.J., 1991. Copolymerization of pNcollagen III and collagen I. pNcollagen III decreases the rate of incorporation of collagen I into fibrils, the amount of collagen I incorporate, and the diameter of the fibrils formed. J. Biol. Chem. 266, 12703–12709.

Rouger, K., Brault, M., Daval, N., Leroux, I., Guigand, L., Lesoeur, J., Fernandez, B., Cherel, Y., 2004. Muscle satellite cell heterogeneity: in vitro and in vivo evidences for populations that fuse differently. Cell Tissue Res. 317, 319–326. https://doi.org/10.1007/s00441-004-0911-9.

Rozenboim, I., Biran, I., Chaiseha, Y., Yahav, S., Rosenstrauch, A., Sklan, D., Halevy, O., 2004. The effect of a green and blue monochromatic light combination on broiler growth and development. Poultry Sci. 83, 842–845. https://doi.org/10.1093/ps/83.5.842.

Rudnicki, M.A., Braun, T., Hinuman, S., Jaenisch, R., 1992. Inactivation of MyoD in mice leads to upregulation of the myogenic HLH gene Myf-5 and results in apparently normal muscle development. Cell 71, 383–390.

Rudnicki, M.A., Schnesgelsber, P.N., Stead, H., Braun, T., Arnold, H.H., Jaenisch, R., 1993. MyoD or Myof-5 is required for the formation of skeletal muscle. Cell 75, 1351–1359.

Sambasivan, R., Tajbakhsh, S., 2015. Adult skeletal muscle stem cells. Results Probl. Cell Differ. 56, 191–213.

Schienda, J., Engleka, K.A., Jun, S., Hansen, M.S., Epstein, J.A., Tabin, C.J., Kunkel, L.M., Kardon, G., 2006. Somitic origin of limb muscle satellite and side population cells. Proc. Natl. Acad. Sci. U.S.A. 103, 945–950.

Schmid, C., Steiner, T., Froesch, E.R., 1983. Preferential enhancement of myoblast differentiation by insulin-like growth factors (IGF I and IGF II). FEBS Lett. 161, 117–121.

Schultz, E., Gibson, M.C., Champion, I., 1978. Satellite cells are mitotically quiescent in mature mouse muscle: an EM and radioautographic study. J. Exp. Zool. 206, 451–456.

Schultz, E., Heckman-Jones, L., 1990. Labeling characteristics of satellite cells in vivo. J. Cell Biol. 111, 34A (Abstr.).

Seale, P., Sabourin, L.A., Girgis-Gabardo, A., Mansouri, A., Gruss, P., Rudnicki, M.A., 2000. Pax7 is required for the specification of myogenic satellite cells. Cell 102, 777–786.

Serrano, A.L., Muñoz-Cánoves, P., 2010. Regulation and dysregulation of fibrosis in skeletal muscle. Exp. Cell Res. 316, 3050–3058.

Shavlakadze, T., Winn, N., Rosenthal, N., Grounds, M.D., 2005. Reconciling data from transgenic mice that overexpress IGF-I specifically in skeletal muscle. Growth Hormone IGF Res. 15, 4–18.

Sheehan, S.M., Tatsumy, R., Temm-Grove, C.J., Allen, R.E., 2002. HGF is an autocrine growth factor for skeletal muscle satellite cells in vitro. Muscle Nerve 23, 239–245.

Shen, X., Liu, Z., Cao, X., He, H., Han, S., Chen, Y., Cui, C., Zhao, J., Li, D., Wang, Y., Zhu, Q., Yin, H., 2019. Circular RNA profiling identified an abundant circular RNA circTMTC1 that inhibits chicken skeletal muscle satellite cell differentiation by sponging miR-128-3p. Int. J. Biol. Sci. 15, 2265–2281. https://doi.org/10.7150/ijbs.36412.

Shin, J., McFarland, D.C., Strasburg, G.M., Velleman, S.G., 2013b. The function of death-associated protein 1 in proliferation, differentiation, and apoptosis of chicken satellite cells. Muscle Nerve 48 (5), 777–790.

Shin, J., McFarland, D.C., Velleman, S.G., 2013a. Migration of Turkey muscle satellite cells is enhanced by the syndecan-4 cytoplasmic domain through the activation of RhoA. Mol. Cell. Biochem. 375, 115–130.

Shin, J., Song, Y., McFarland, D.C., Velleman, S.G., 2012. Function of the syndecan-4 cytoplasmic domain in oligomerization and association with α-actinin in Turkey muscle satellite cells. Mol. Cell. Biochem. 363, 437–444.

Shinichi, S., Tsuyoshi, O., Yoshinobu, U., Yumi, O., Eiji, K., 2012. Polymorphism of insulin-like growth factor 1 gene is associated with breast muscle yields in chickens. Anim. Sci. J. 83, 1–6.

Sihvo, H.-K., Lindén, J., Airas, K., Immonen, K., Valaja, J., Puolanee, E., 2017. Wooden breast myodegeneration of pectoralis major muscle over the growth period in broilers. Vet. Pathol. 54, 119–128.

Sihvo, H.-K., Immonen, K., Puolanne, E., 2014. Myodegeneration with fibrosis and regeneration in the pectoralis major muscle of broilers. Vet. Pathol. 51, 619–623.

Smith, J.H., 1963. Relation of body size to muscle cell size and number in the chicken. Poultry Sci. 42, 283–290.

Snow, H.E., Riccio, L.M., Mjaatvedt, C.H., Hoffman, S., Capehart, A.A., 2005. Versican expression during skeletal/joint morphogenesis and patterning of muscle and nerve in the embryonic mouse limb. Anat. Rec. A Discov. Mol. Cell Evol. Biol. 282, 95–105. https://doi.org/10.1002/ar.a.20151.

Song, Y., McFarland, D.C., Velleman, S.G., 2012a. Syndecan-4 cytoplasmic domain regulation of Turkey satellite cell focal adhesions and apoptosis. Mol. Biol. Rep. 39, 8251–8264.

Song, Y., McFarland, D.C., Velleman, S.G., 2012b. Role of syndecan-4 side chains in Turkey satellite cell apoptosis and focal adhesion formation. Cell Biol. Int. 36, 433–440.

Song, Y., McFarland, D.C., Velleman, S.G., 2012c. Fibroblast growth factor 2 and protein kinase C alpha are involved in syndecan-4 cytoplasmic domain modulation of Turkey myogenic satellite cell proliferation. Comp. Biochem. Physiol. A 161, 44–52.

Song, Y., McFarland, D.C., Velleman, S.G., 2012d. Critical amino acids in syndecan-4 cytoplasmic domain modulation of Turkey satellite cell growth and development. Comp. Biochem. Physiol. A 161, 271–278.

Sosnicki, A.A., 1993. Focal myonecrosis effects in Turkey muscle tissue. Reciprocal Meat Conf. Proc 46, 97–102.

Sosnicki, A.A., Wilson, B.W., 1991. Pathology of Turkey skeletal muscle: implications for the poultry industry. Food Struct. 10, 317–326.

Sporer, K.R.B., Chiang, W., Tempelman, R.J., Ernst, C.W., Reed, K.M., Velleman, S.G., Strasburg, G.M., 2011a. Characterization of a 6K oligonucleotide Turkey skeletal muscle microarray. Anim. Genet. 42, 75–82.

Sporer, K.R.B., Tempelman, R.J., Ernst, C.W., Reed, K.M., Velleman, S.G., Strasburg, G.M., 2011b. Transcriptional profiling identifies differentially expressed genes in developing Turkey skeletal muscle. BMC Genom. 12, 143.

Srinivasan, D., Dodig, M., Muc Sean, M., Kalhan, S.C., McCullough, A.J., 2004. Skeletal muscle atrophy is associated with an increased expression of myostatin and impaired satellite cell function in the portacaval anastomosis rat. Am. J. Physiol. Gastrointest. Liver Physiol. 287, G1124–G1130.

Steinfield, R., Van Den Berghe, H., David, G., 1996. Stimulation of fibroblast growth factor receptor-1 occupancy and signaling by cell surface associated syndecans and glypican. J. Cell Biol. 133, 405–416.

Stockdale, F.E., 1990. The myogenic lineage: evidence for multiple precursors during avian limb development. Proc. Soc. Exp. Biol. Med. 194, 71–75.

Stockdale, F.E., Holtzer, H., 1961. DNA synthesis and myogenesis. Exp. Cell Res. 24, 508–520.

Sugg, K.B., Korn, M.A., Sarver, D.C., Markworth, J.F., Mendias, C.L., 2017. Inhibition of platelet-derived growth factor signaling prevents muscle fiber growth during skeletal muscle hypertrophy. FEBS Lett. 591, 801–809.

Tajbakhsh, S., Rocancourt, D., Cossu, G., Buckingham, M., 1997. Redefining the genetic hierarchies controlling skeletal myogenesis: Pax-3 and Myf-5 act upstream of MyoD. Cell 89, 127–138.

Tanaka, K.K., Hall, J.K., Troy, A.A., Cornelison, D.D., Majka, S.M., Olwin, B.B., 2009. Syndecan-4-expressing muscle progenitor cells in the SP engraft as satellite cells during muscle regeneration. Cell Stem Cell 4, 217–225.

Trocino, A., Piccirillo, A., Birolo, M., Radaelli, G., Bertotto, D., Filiou, E., Petracci, M., Xiccato, G., 2015. Effect of genotype, gender and feed restriction on growth, meat quality and the occurrence of white striping and wooden breast in broiler chickens. Poultry Sci. 94, 2996–3004. https://doi.org/10.3382/ps/pev296.

Tasoniero, G., Cullere, M., Cecchinato, M., Puolanne, E., Zotte, A.D., 2016. Technological quality, mineral profile, and sensory attributes of broiler chicken breasts affected by white striping and wooden breast myopathies. Poultry Sci. 95, 2707–2714.

Tatsumi, R., Anderson, J.E., Neveret, C.J., Halevy, O., Allen, R.E., 1998. HGF/SF is present in normal adult skeletal muscle and is capable of activating satellite cells. Dev. Biol. 194, 114–128.

Tatsumi, R., Hattori, A., Ikeuchi, Y., Anderson, J.E., Allen, R.E., 2002. Release of hepatocyte growth factor from mechanically stretched skeletal muscle satellite cells and role of pH and nitric oxide. Mol. Biol. Cell 13, 2909–2918.

Tatsumi, R., Sheehan, S.M., Iwasaki, H., Hattori, A., Allen, R.E., 2001. Mechanical stretch induces activation of skeletal muscle satellite cells in vitro. Exp. Cell Res. 267, 107–114.

Tonniges, J.R., Clark, D.L., Velleman, S.G., 2019. The effect of the wooden breast fibrotic myopathy in broilers on fibrillar collagen organization and decorin-collagen binding. Avian Dis. 63, 48–60.

Vassilakos, G., Barton, E.R., 2018. Insulin-like growth factor I regulation and its actions in skeletal muscle. Comp. Physiol. 9, 413–438. https://doi.org/10.1002/cphy.c180010.

Velleman, S.G., Coy, C.S., Emmerson, D.A., 2014a. Effect of the timing of posthatch feed restrictions on broiler breast muscle development and muscle transcriptional regulatory factor gene expression. Poultry Sci. 93, 1484–1494.

Velleman, S.G., Coy, C.S., Emmerson, D.A., 2014b. Effect of the timing of posthatch feed restrictions on the deposition of fat during broiler breast muscle development. Poultry Sci. 93, 2622–2627.

Velleman, S.G., Coy, C.S., McFarland, D.C., 2007. Effect of syndecan-1, syndecan-4, and glypican-1 on Turkey muscle satellite cell proliferation, differentiation, and responsiveness to fibroblast growth factor 2. Poultry Sci. 86, 1406–1413.

Velleman, S.G., Sporer, K.R.B., Ernst, C.W., Reed, K.M., Strasburg, G.M., 2012. Versican, matrix Gla protein, death-associated protein expression affect muscle satellite cell proliferation and differentiation. Poultry Sci. 91, 1964–1973.

Velleman, S.G., Clark, D.L., 2015. Histopathologic and myogenic gene expression changes associated with wooden breast in broiler breast muscles. Avian Dis. 59, 410–418.

Velleman, S.G., Clark, D.L., Tonniges, J.R., 2017. Fibrillar collagen organization associated with the broiler wooden breast fibrotic myopathy. Avian Dis. 61, 481–490.

Velleman, S.G., Clark, D.L., Tonniges, J.R., 2018. The effect of syndecan-4 and glypican-1 knockdown on the proliferation and differentiation of turkey satellite cells differing in age and growth rates. Comp. Biochem. Physiol. A Mol. Integr. Physiol. 223, 33–41. https://doi.org/10.1016/j.cbpa.2018.05.014.

Velleman, S.G., Clark, D.L., Tonniges, J.R., 2019. The effect of nutrient restriction and syndecan-4 or glypican-1 knockdown on the differentiation of Turkey pectoralis major satellite cells differing in age and growth selection. Poultry Sci. 98, 6078–6090.

Volk, R., Schwartz, J.J., Li, J., Rosenberg, R.D., Simons, M., 1999. The role of syndecan cytoplasmic domain in basic fibroblast growth factor dependent signal transduction. J. Biol. Chem. 274, 24417–24424.

Wang, Y.X., Rudnicki, M.A., 2011. Satellite cells, the engines of muscle repair. Nat. Rev. Mol. Cell Biol. 13, 127–133.

Weber, L., Meigel, W., Spier, W., 1978. Collagen polymorphism in pathologic human scars. Arch. Dermatol. Res. 261, 63–71.

Welty, J.C., 1982. Birds as flying machines; bones and muscles. In: The Life of Birds, third ed. Saunders College Publishing, pp. 1–8. 63-77.

Wilkie, R.S., O'Neill, I.E., Butterwith, S.C., Duclos, M.J., Goddard, C., 1995. Regulation of chick muscle satellite cells by fibroblast growth factors: interaction with insulin-like growth factor-I and heparin. Growth Regul. 5, 18–27.

Wilson, B.W., Nieberg, P.S., Buhr, R.J., 1990. Turkey muscle growth and focal myopathy. Poultry Sci. 69, 1553–1562.

Yablonka-Reuveni, Z., Quinn, L.S., Nameroff, M., 1987. Isolation and clonal analysis of satellite cells from chicken pectoralis muscle. Dev. Biol. 119, 252–259.

Yablonka-Reuveni, Z., Balestreri, T.M., Bowen-Pope, D.F., 1990. Regulation of proliferation and differentiation of myoblasts derived from adult mouse skeletal muscle by specific isoforms of PDGF. J. Cell Biol. 111, 1623–1629.

Yablonka-Reuveni, Z., 2011. The skeletal muscle satellite cell: still young and fascinating at 50. J. Histochem. Cytochem. 59, 1041–1059.

Yablonka-Reuveni, Z., Seifert, R.A., 1993. Proliferation of chicken myoblasts is regulated by specific isoforms of platelet-derived growth factor: evidence for differences between myoblasts and mid and late stages of embryogenesis. Dev. Biol. 156, 307–318.

Yablonka-Reuveni, Z., Paterson, B.M., 2001. MyoD and myogenin expression patterns in cultures of fetal and adult chicken myoblasts. J. Histochem. Cytochem. 49, 455–462.

Yahav, S., 2015. Regulation of body temperature: strategies and mechanisms. In: Scanes, C.G. (Ed.), Sturkie's Avian Physiology, sixth ed. Academic Press, pp. 869–905.

Yang, S., Alnaqeeb, M., Simpson, H., Goldspink, G., 1996. Cloning and characterization of an IGF-1 isoform expressed in skeletal muscle subjected to stretch. J. Muscle Res. Cell Motil. 17, 487–495.

Ye, W.V., McFarland, D.C., Gilkerson, K.K., Pesall, J.E., 1996. The role of platelet-derived growth factor in Turkey skeletal muscle development. Cytobios 88, 53–62.

Yu, M., Wang, H., Xu, Y., Yu, D., Li, D., Liu, X., Du, W., 2015. Insulin-like growth factor-1 (IGF-1) promotes myoblast proliferation and skeletal muscle growth of embryonic chickens via the PI3K/Akt signalling pathway. Cell Biol. Int. 39, 910–922.

Yun, Y., McFarland, D.C., Pesall, J.E., Gilkerson, K.K., Vander Wal, L.S., Ferrin, N.H., 1997. Variation in response to growth factor stimuli in satellite cell populations. Comp. Biochem. Physiol. 117A, 463–470.

Yost, J.K., Kenney, P.B., Slider, S.D., Russell, R.W., Killefer, J., 2002. Influence of selection for breast muscle mass on myosin isoform composition and metabolism of deep pectoralis muscles of male and female turkeys. Poultry Sci. 81, 911–917.

Zammit, P.S., Golding, J.P., Nagata, Y., Hudon, V., Partridge, T.A., Beauchamp, J.R., 2004. Muscle satellite cells adopt divergent fates: a mechanism for self-renewal. J. Cell Biol. 166, 347–357.

Zeng, C.Y., Pesall, J.E., Gilkerson, K.K., McFarland, D.C., 2002. The effect of hepatocyte growth factor on Turkey satellite cell proliferation and differentiation. Poultry Sci. 81, 1191–1198.

Zhang, X., Nestor, K.E., McFarland, D.C., Velleman, S.G., 2008. The role of syndecan-4 and attached glycosaminoglycan chains on myogenic satellite cell growth. Matrix Biol. 27, 619–630.

Zhang, L., Zhang, H.J., Qiao, X., Yue, H.Y., Wu, S.G., Yao, J.H., Qi, G.H., 2012. Effect of monochromatic light stimuli during embryogenesis on muscular growth, chemical composition, and meat quality of breast muscle in male broilers. Poultry Sci. 91, 1026–1031. https://doi.org/10.3382/ps.2011-01899.

Zhang, Z., Du, H., Yang, C., Li, Q., Qiu, M., Song, X., Yu, C., Jiang, X., Liu, L., Hu, C., Xia, B., Xiong, X., Yang, L., Peng, H., Jiang, X., 2019. Comparative transcriptome analysis reveals regulators mediating breast muscle growth and development in three chicken breeds. Anim. Biotechnol. 30, 233–241. https://doi.org/10.1080/10495398.2018.1476377.

Zhao, Y., Haginoya, K., Sun, G., Dai, H., Onuma, A., Iinuma, K., 2003. Platelet-derived growth factor and its receptors are related to the progression of human muscular dystrophy: an immunohistochemical study. J. Pathol. 201, 149–159.

Zimmerman, D.R., Ruoslahti, E., 1989. Multiple domains of the large fibroblast proteoglycan, versican. EMBO J. 8, 2975–2981.

Zimmerman, S.D., Thomas, D.P., Velleman, S.G., Li, X., Hansen, T.R., McCormick, R.J., 2001. Time course of collagen and decorin changes in rat cardiac and skeletal muscle post-MI. Am. J. Physiol. Heart Circ. Physiol. 281, H1816–H1822.

Further reading

Velleman, S.G., Anderson, J., Nestor, K.E., 2003a. Possible maternal inheritance of breast muscle morphology in turkeys at sixteen weeks of age. Poultry Sci. 82, 1479–1484.

Velleman, S.G., Anderson, J.W., Coy, C.S., Nestor, K.E., 2003b. Effect of selection for growth rate on muscle damage during Turkey breast muscle development. Poultry Sci. 82, 1069–1074.

Velleman, S.G., Coy, C.S., Nestor, K.E., 2010. The influence of age on maternal inheritance of breast muscle morphology in turkeys. Poultry Sci. 89, 876–882.

Velleman, S.G., Nestor, K.E., 2004. Inheritance of breast muscle morphology in turkeys at sixteen weeks of age. Poultry Sci. 83, 1060–1066.

Velleman, S.G., Nestor, K.E., 2006. Inheritance of breast muscle morphology in a line of turkeys selected for increased egg production, its random bred control line, and reciprocal crosses between them. Poultry Sci. 85, 2130–2134.

Velleman, S.G., Yeager, J.D., Krider, H., Carrino, D.A., Zimmerman, S.D., McCormick, R.J., 1996. The avian low score normal muscle weakness alters decorin expression and collagen crosslinking. Connect. Tissue Res. 34, 33–39.

Chapter 24

Immunophysiology of the avian immune system

Michael H. Kogut
Southern Plains Agricultural Research Center, USDA-ARS, College Station, TX, United States

24.1 Introduction

Like the previous edition of this book, the chicken remains the primary focus of this chapter because of its worldwide economic importance. However, since the last edition of this book, there has been a dramatic, and almost instantaneous, shift in how chickens are grown. The advent and development of ongoing social and political changes in the 21st century has resulted in consumer demands for drug-free poultry products. Consequently, avian immunology research has resulted in more applied exploration into avian immune modulation as an alternative to antibiotics, functional studies on immune mechanisms of action, regulation of host responses by the innate immune system, the impact of the intestinal microbiota on immunity, and the introduction of the area of immunometabolism. Instead of trying to summarize all components aspects of the avian immune system, repeating the anatomy of the avian immune system and describing the differences of the immune response between avians and mammals that was thoroughly covered by our late colleague, Professor Pete Kaiser, this chapter will concentrate on the physiological functions of the avian immune system.

24.2 Innate immune system recognition, sensing, and function

Innate immunity is the first line of defense against pathogens, which, consequently, has critical roles in shaping further specific adaptive immune responses. To induce host resistance against a given pathogen, the immune system must activate mechanisms that aim to overcome potential escape mechanisms induced by the pathogen. Evolution has enabled cells of the innate immune system to develop multiple pattern recognition receptors (PRRs) that sense microbial-associated molecular patterns (MAMPs). MAMPs are molecular structures shared by large groups of pathogens that are conserved products of microbial metabolism not subject to antigenic variability (Fearon and Locksley, 1996). They are required for either the survival or pathogenicity of the microbe and are distinct from any host antigens. The innate immune system can not only discriminate self from nonself via recognition of MAMPs (Janeway, 1989; Palm and Medzhitov, 2009), but it can also discriminate between live and dead microorganisms through a distinct set of MAMPs called vita-MAMPs associated uniquely with live microorganisms (Sander et al., 2011; Blander and Sander, 2012). Vita- MAMPs are detected in combination with classic MAMPs such as lipopolysaccharide (LPS) and DNA, which are shared between live and dead microorganisms (Sander et al., 2011; Blander and Sander, 2012). Detection of MAMPs in the absence of vita-PAMPs signifies a dead microbe, whereas detection of a vita-MAMP alongside a MAMP signifies live microbes and mediates a heightened immune response not warranted to dead microorganisms (Blander and Sander, 2012). The activity of virulence factors associated with live pathogens elicits a vigorous immune response, but continued expression of virulence factors becomes unnecessary once a pathogen has gained access to sterile tissues. Targeting microbial viability per se independently of virulence factors is a far better strategy for the immune system to eliminate the infectious threat and protect tissue integrity. Two vita-MAMPs, bacterial messenger RNA (mRNA) in the context of a response to live gram-negative bacteria (Sander et al., 2011; Barbet et al., 2018; Ugolini et al., 2018), and cyclic-di-adenosine monophosphate (c-di-AMP) in the context of a response to live gram-positive bacteria (Moretti et al., 2017) have been identified so far. The incorporation of a vita-MAMP into a killed or subunit vaccine could recapitulate the efficacy of a live vaccine.

Sturkie's Avian Physiology. https://doi.org/10.1016/B978-0-12-819770-7.00020-7

24.2.1 Innate cell receptors: pattern recognition receptors

The host receptors that recognize MAMPs are evolutionarily conserved proteins that are expressed on cells that first encounter infectious agents including all effector cells of innate immunity, antigen-presenting cells, and surface epithelium of the respiratory, genital, and intestinal tracts (Medzhitov and Janeway, 1997a). Functionally, PRRs induce innate effector function and alert the host to the presence of infectious agents. Furthermore, it is readily apparent that an essential function of the innate immune system appears to be to instruct the lymphocytes to develop a particular effector response to a specific pathogen (Janeway, 1989; Fearon and Locksley, 1996). Since MAMPs are produced exclusively by microbes and not by the host, recognition by host PRRs signals the presence of pathogens. MAMP recognition activates effector mechanisms of innate host defenses, including phagocytosis, the synthesis of antimicrobial peptides, and the induction of the respiratory burst and nitric oxide synthase. These endogenous signals orchestrate the recruitment of leukocytes to the site of infection and regulate the activation of the suitable effector mechanisms by controlling differentiation of T lymphocytes into effector cells of a particular type. Lastly, and most importantly, recognition of MAMPs by PRRs induces the expression of co-stimulatory molecules by antigen-presenting cells, i.e., natural adjuvant activity, and leads to the development of highly antigen-specific memory cells (Medzhitov and Janeway, 1997a, b, 2002; Kopp and Medzhitov, 1999). The ability of the lymphocytes to differentiate into effector cells is dependent upon and controlled by signals produced by the cells of the innate system (Medzhitov and Janeway, 1997a). Thus, it can be seen that adjuvants are primarily MAMPs that induce the innate immune response to produce the required co-stimulatory molecules that result in protection.

Innate immune cell activation through distinct PRRs leads to the induction of responses that are adapted to the features of the invading pathogen. The type of innate immune response executed downstream of PRRs has important implications for not only initial host resistance but also for the induction of long-lasting adaptive immunity. Recognition or sensing platforms of the innate immune system are critical for orchestrating the communication between the host and its microbial environment. Further, the genomic sequences and function of PRRs are more extensively conserved than B and T cell receptors (Temperly et al., 2008) signifying that the capability to identify MAMPs may be more essential for species survival than the acquired immune response.

Multiple recognition systems have coevolved to preserve normal interactions with the commensal flora and to initiate immune responses to invading pathogens and perturbations in tissue homeostasis. Endosomal and extracellular toll-like receptors (TLRs) recognize mainly MAMPs found in and on microbes including proteins, lipids, and nucleic acids. Meanwhile, a multitude of cytosolic receptors [nod-like receptors (NLRs)] recognize not only intracellular MAMPS but also the host-derived signals known as "damage-associated molecular patterns" (DAMPs). The cooperation between these compartmentalized surveillance systems allows organisms to sense and respond to a number of infectious and sterile insults to the host. Innate immune recognition of MAMPs initiates a signal transduction cascade that leads to the transcription of immune response genes through nuclear factor-κB (NF-κB) and the production of various effector molecules.

24.2.1.1 Toll-like receptors

TLRs consist of a leucine-rich repeat domain that specifically binds to individual MAMPs, a transmembrane region, and a cytoplasmic Toll/interleukin-1 receptor domain (Rock et al., 1998). Members of the TLR family are typically located either at the surface of eukaryotic cells or in the endolysosomal compartment. Each of the TLRs has a distinct ligand specificity; most often of microbial origin. TLR ligands are structurally conserved, absent in the host, and important, not necessarily for virulence of microbe, but for the survival of the microbe. This ensures detection by the host of a wide range of bacteria, viruses, or fungi with a minimum of TLR.

According to Keestra et al. (2013), the chicken homologs of the human TLRs are TLR1 type 1, TLR1 type 2, TLR2 type 1 and TLR2 type 2, TLR3, TLR4, TLR5, TLR7, as well two that are unique for chickens, TLR15 and TLR21 (Boyd et al., 2001; Dil and Qureshi, 2002; Yilmaz et al., 2005; Higgs et al., 2006; Keestra et al., 2007; Temperley et al., 2008). These receptors can act alone or in concert with other TLRs and adaptors including CD14 (Kogut et al., 2005a) and MD-2 (Keestra and van Patten, 2008). Chicken TLR1, 2, 3, 4, 5, and 7 are orthologous to their mammalian counterparts but chickens lack TLR8 and 9. Chickens have two TLR1s (TLR1A and B) and two TLR2s (TLR2A and B) as a result of gene duplication. These variants dimerise to form cell surface receptors which recognize the same PAMPs as human TLR2 (Higuchi et al., 2008), which can dimerise with human TLR1, 6, and 10, thus suggesting chickens recognize a similar range of MAMPs as mammals, although using a different TLR repertoire (Kaiser, 2010). Chicken TLR2 type 2 can respond to LPS suggesting that this receptor may also covers the function of TLR4 in chicken (Fukui et al., 2001). Further, chicken TLR2 isoform type 2 in conjunction with chTLR16 (putative chicken TLR with unknown function) reacts to both di- and triacylated peptides similar in function to that of mammalian TLR2/1 and TLR2/6 receptor complexes (Keestra et al., 2007).

Activation of TLRs by specific MAMP binding attracts cytoplasmic mediators that direct signal transduction through NF-κB and the mitogen-activated protein kinase (MAPK) pathways. Activation of the NF-κB transcription factor allows it to translocate from the cytosol to the nucleus where it affects expression of numerous genes involved in the immune response (Camaño and Hunter, 2002). In chickens, TLR activation is followed by increased transcription of cytokines, including IL-1β and IL-6, and chemokines, including CXCLi2, CXCLi1, and CCLi4 (Kogut et al., 2005b, 2006).

The two chicken-specific TLRs, TLR15 and TLR21, have been identified and characterized. TLR15 is activated by fungal and some bacterial proteases (De Zoete et al., 2011; Higgs et al., 2006; Oven et al., 2013; Neerukonda and Katneni, 2020). (TLR21 is the functional homolog of TLR9 in humans that recognizes bacterial CpG DNA (Brownlie et al., 2009)). TLR21 activation by CpG oligodeoxynucleotide induces heterophil degranulation in vitro (He et al., 2005) and in vivo primed heterophils degranulation and oxidative burst (He et al., 2007; MacKinnon et al., 2009). Stimulation of chicken heterophils with TLR agonists flagellin (TLR5) and LPS (TLR4) induced the activation of all three members of the MAPK family, ERK, c-Jun, and p38 that then induced the translocation and activation of the transcription factors NF-κB and AP-1 resulting in the increased expression of IL6 and CXCLi2 (Kogut et al., 2005, Kogut et al., 2006, 2008).

24.2.1.2 Nod-like receptors

The NLR family of intracellular PRRs that sense microbial products or the products of damaged host cells, such as ATP and uric acid, play a pivotal role in the initiation of antimicrobial immune responses. Despite the increased understanding of NLR function and interactions in mammals, most aspects related to mechanisms of sensing, downstream signaling, and in vivo functions in avians remain elusive (Neerukonda and Katneni, 2020). To date, there have only been four NLRs found in the chicken genome: NOD1 (Tao et al., 2015) NLRP3 (Ye et al., 2015), NLRC5 (Lian et al., 2012; Ciraci et al., 2010), and NLRC3 (Neerukonda and Katneni, 2020) with only NLRP3 and NLRP5 having been functionally characterized (Ciraci et al., 2010; Ye et al., 2015; Liu et al., 2015).

24.2.1.3 RIG-like receptors

The RIG-like receptor family are select cytosolic RNA helicases which bind nucleic acids (Loo and Gale, 2011). RLRs sense viral pathogens from non-self RNA (Magor et al., 2013; Campbell and Magor, 2020). In mammals, the RLR family contains the retinoic acid-inducible gene 1 (RIG-1), melanoma differentiation-associated protein 5 (MDA5), and laboratory of genetics and physiology 2 (LGP2) as members. However, chickens lack RIG-1 while ducks possess tissue specific RIG-1 (trachea and intestine) (Campbell and Magor, 2020) which accounts for the susceptibility of chickens to single-stranded RNA viruses such as influenza A and Newcastle disease virus and the relative resistance of ducks to both viruses (Campbell and Magor, 2020; Neerukonda and Katneni, 2020). Interestingly, the MDA5 family, present in chickens and ducks, can detect avian influenza and generates an interferon response (Karpala et al., 2011; Campbell and Magor, 2020; Neerukonda and Katneni, 2020). LGP2 lacks two N-terminal components that are involved in downstream signal transduction integration, but LGPs does appear to be a positive regulator of interferon-beta production following viral recognition by RIG-1 and MDA5 (Satoh et al., 2010).

24.2.1.4 C-type lectin receptors

Nerren and Kogut (2009) were the first to report that the C-type lectin receptor, dectin-1, primary PRR for exogenous β-glucan, a component of fungal and bacterial cell walls, respond to a Dectin-1-specific agonist by significantly increased production of an oxidative burst. Further, we have shown that administration of β-glucan as a feed additive resulted in increased phagocytosis, oxidative burst, and bactericidal capacity of chicken heterophils, resulting in significantly reduced organ invasion by *Salmonella enterica* serovar Enteritidis (Lowry et al., 2005).

Cooperation of TLR signaling with other PRRs in bacterial recognition and signal integration is indicative of the life cycle of the respective pathogen. The example of *Salmonella typhimurium* infection best illustrates this concept. As mentioned above, both TLR5 and NLRC4 recognize bacterial flagellin, but at different subcellular localizations. Both PRRs initiate distinct signaling pathways in response to *Salmonella* infection (NF-kB signaling and inflammasome, respectively), which proceed independently of one another. This strategy accounts for the hierarchy of effector mechanisms and the fitness cost that is associated with it; Extracellular *Salmonell*a is detected by surface-bound TLR5, initiating a MyD88-dependent NF-kB response and the induction of cytokines. Once *Salmonella* has invaded the cell cytoplasmic flagellin triggers the inflammasome, a pathway that causes pyroptotic cell death and the release of IL-1β, one of the most potent proinflammatory mediators and modulators of systemic organism physiology.

24.2.2 Host defense peptides

Host-defense peptides (HDPs), formerly known as antimicrobial peptides, are a diverse group of small peptides found in most species of life (Cuperus et al., 2013; Mansour

et al., 2014; Robinson et al., 2015). HDPs are 10–50 amino acids peptides that are enriched in hydrophobic and cationic amino acid residues. As part of the innate immune system, HDPs possess both antimicrobial and immunomodulatory properties. HDPs antibacterial mode of action is via a physical electrostatic interaction that disrupt the bacterial cell membrane. The majority of the HDPs are synthesized by the host's phagocytic and mucosal epithelial cells lining the urogenital, respiratory, and gastrointestinal (GI) tracts (Zasloff, 2002). Mature HDPs are active *Salmonella* and *Campylobacter* (van Dijk et al., 2012; Garcia et al., 2018, 2020) and have activity against fungi and enveloped viruses (Zhang and Sunkara, 2014; Robinson et al., 2015). There are three classes of HDPs found in chickens including 14 β-defensins (AvBD1-14), four cathelicidins (CATH1-3 and CATH-B1) (Zanetti, 2005), and liver-expressed antimicrobial peptide 2 (LEAP2) (Zhang and Sunkara, 2014). HDPs also recruit and activate immune cells, which are involved in host defense against pathogens (Cuperus et al., 2013).

Avian β-defensins (AvBDs) were the first to be discovered in chickens. Sequencing of all 14 AvBDs revealed that the N-terminal signal peptide regions are highly conserved. AvBDs are synthesized as inactive prepropeptides consisting of a short signal peptide, a propeptide and the mature peptide. Transcriptional analysis of AvBD genes have found that AvBD1, 2, and 4 to 7 are predominately expressed in the bone marrow, while AvBD3, and 8 to 14 are expressed by epithelial cells (Lee et al., 2016). However, AvBDs can be expressed in either the bone marrow or epithelial cells as well as in other tissues.

Presently, four avian cathelicidins (CATHs) have been discovered in chickens (Zanetti, 2005). CATH1 and CATH2 are predominantly expressed in the bone marrow but have been shown to be expressed in other tissues. CATH1 expressed in the gizzard, small intestine, and large intestine while CATH2 expression is highest in liver and in the cecal tonsils. CATH3 is predominately expressed in the lung bone marrow and liver (Goitsuka et al., 2007; Achonta et al., 2012). CATHB1 expression has been predominantly found in the bursa of Fabricius (Lee et al., 2016).

LEAP2 is expressed as part of the epithelial innate defense system (Lynn et al., 2007; Townes et al., 2004) and functions to prevent pathogens from interacting with epithelial surfaces and potentially invading tissues. Townes et al. (2004) found that in 4-day-old 16 chicks, which had been orally inoculated with *Salmonella*, there was a significant upregulation of LEAP2 mRNA in the small intestine and liver. It was later reported that in vitro, LEAP2 is able to affect the permeability of the bacterial outer membrane, leading to cell death (Townes et al., 2009). Host defense peptides are essential since they are the first response to pathogens as part of the innate immune system.

24.2.3 Innate immune memory: trained immunity

Recently, the concept of "trained immunity" or innate immune memory has emerged and challenged conventional paradigms of T and B cell-mediated adaptive memory (Netea et al., 2011). Essentially, trained immunity is induced after either a primary infection or innate modulation and confers protection independently of T or B cells, is mediated by innate immune cells, and increases resistance to infection by the same and other pathogens. In addition, several studies have demonstrated that priming with *Candida albicans* or the fungal cell-wall component β-glucan nonspecifically induces enhanced secondary responses. Recent studies have shown, however, that innate immune cell populations such as myeloid cells and NK cells also undergo functional adaptation after infection or vaccination, a de facto innate immune memory that is also termed trained immunity (Netea et al., 2011, 2016). In addition, several studies have demonstrated that, in mouse and human cells, priming with *Candida albicans* or the fungal cell-wall component β-glucan nonspecifically induces enhanced secondary responses. Trained immunity differs from immune priming since after recovery from infection, innate immune responses do not return to the steady-state level. This is due to the epigenetic reprogramming of innate immune cells rather than the short-lived change of state seen in immune priming. Stimulation of the innate immune response with prominent microbial components that activate PRRs offer therapeutic and adjuvant potential in poultry since they not only directly stimulate arrange of cell types but can give rise to robust adaptive responses through driving maturation of antigen-presenting cells. Recent data have provided compelling evidence that the innate immune system can be "trained" to respond more rapidly and effectively to pathogens following treatment with Dectin-1 agonists (Lowry et al., 2005; Nerren and Kogut, 2009; Kogut et al., 2010·2012, 2013). We have successfully purified multiple natural Dectin-1 ligands from yeast that change the transcriptional program of innate immune cells from poultry. Innate immune memory differs from adaptive memory in many aspects, including the lack of gene rearrangements, the epigenetic reprogramming, the type of cells involved (innate cells vs. T and B lymphocytes), and the receptors engaged in pathogen or antigen recognition (selective PRRs vs. antigen-specific T cell and B cell receptors) (Netea et al., 2011, 2016).

24.3 Acquired immune recognition and function

24.3.1 The major histocompatibility complex

The adaptive immune response is only triggered when pathogen antigens are presented to T cells in the context of molecules called the major histocompatibility complex (MHC). The region of the genome that encodes the MHC is highly polymorphic and in mammals includes approximately 300 genes. The most relevant for antigen presentation are the class I genes, which present antigens from intracellular pathogens, mainly to CD8+ T cells, and the class II genes, which present antigens from extracellular pathogens, mainly to CD4+ T cells. MHC class I proteins are expressed on most cell types, whereas MHC class II proteins are mainly expressed on antigen-presenting cells such as dendritic cells (DCs), macrophages, and B cells. In contrast to the mammalian MHC, the chicken has a minimal essential MHC (Kaufman et al., 1999). In mammals, there are several class I and class II genes; precise numbers vary from species to species and in some cases between individuals of the same species. In contrast, in the chicken, the minimal essential MHC contains only two class I genes and two class IIβ genes, with only one of each dominantly expressed (reviewed in Kaufman, 2000). This has some striking consequences, particularly for the chicken's ability to mount an immune response to a pathogen, especially a virus.

24.3.2 Th1/Th2 paradigm and T helper cell subsets

The polarization of naïve chicken CD4+ T cells into two subsets of activated CD4 T cells, Th1 and Th2 cells, which differ from each other in their pattern of cytokine production and their functions (the Th1/Th2 paradigm) was demonstrated over 15 years ago (Degen et al., 2005). Broadly, Th1 cells mediate a cellular immune response, and Th2 cells potentiate a humoral response. Specifically, Th1 cells are especially effective in protecting against intracellular infections by viruses and bacteria and microorganisms that grow in macrophages. Th2 cells are indispensable for host immunity to extracellular parasites, such as helminths (Kidd, 2003). Functional genes of signature cytokines hallmarking Th1- and Th2-type responses in mammals, particularly interleukin (IL)-4, IL-12, IL-13, IL-18, and interferon-γ (IFN-γ), have been identified in chicken (Avery et al., 2004; Balu and Kaiser, 2003; Degen et al., 2004; Kaiser, 2010). In addition, the existence of a Th1-like system was shown in vitro through IL-18-induced proliferation and IFN-γ secretion of chicken splenic $CD4^+$ T cells (Göbel et al., 2003). Another study also found Th1 and Th2-like responses in vivo, characterized by elevated expression of IFN-γ, IL-4, and IL-13 following infection of birds with a virus (Newcastle disease virus) and a helminth (*Ascaridia galli*), representing intracellular and extracellular pathogens, respectively (Degen et al., 2005; Pleidrup et al., 2019; Dalgaard et al., 2015). However, it should be noted that the avian Th1/Th2 system has some oddities, for example, during a Th2 response in chickens, IL-4 and IL-13 are expressed (Degen et al., 2005; Powell et al., 2009), but IL-5 expression is switched off. In mammals, IgE production is dependent on Il-5 expression by Th2 cells, but in chickens, IgE is not produced and there is an absence of the effector cell of IgE, functional eosinophils, which are involved in the mammalian Th2 response (Kaiser and Stäheli, 2014).

More recently, two more CD4+ subsets have been discovered in chickens. First, T regulatory (Tregs) have been identified (Shanmugasundaram and Selvaraj, 2010, 2011). Treg cells secrete IL-10 and transforming growth factor (TGF)-β that temper CD4+ T-cell activity and suppress some of their functions, inducing tolerance to antigens. More recently, a fourth subset of CD4+ cells, the Th17 cell, has been identified in the chicken (Reid et al., 2016). Th17 effector cells play a fundamental role in both tissue inflammation and activation of granulocytes to combat extracellular bacteria predominantly in the mucosal surfaces of the intestine and respiratory systems. Remarkably, the master regulators of transcription for Tregs and Th17, Forkhead box P3 (FoxP3) and the retinoic-acid-related orphan receptor gamma t, respectively, have not been identified in the chicken although a recent study has shown phylogenetic evidence of FoxP3 in birds (Denyer et al., 2016). However, all of the cytokines crucial to driving mammalian Th lineage development have now been identified in the chicken (Kaiser, 2012) including the recently identified IL-23 (Truong et al., 2017).

24.4 Gastrointestinal tract and immune system of poultry

The GI tract lumen can be considered as being part of the external environment. One of the most important roles of the gut is providing a barrier between the internal and external environment, as the GI tract is the site of colonization and invasion of many pathogenic bacteria. Through this and several other functions, the GI tract has an important role in the immune function of a bird (Patterson and Burkeholder, 2003; Beal et al., 2006). Posthatching is a vital time for the development of the gut immune system of the bird. The immune system must differentiate between food, beneficial bacteria, and harmful pathogens, so there is

a fine balance between tolerance and response to antigens. This is fundamental to gut health as a prolonged immune response can cause problems such as villus atrophy. The sequential development of various phase of intestinal immunity have been characterized in broiler chickens during the first weeks of posthatch: (a) innate development and influx of immune cells; (b) immune differentiation and specialization; and (c) maturation and immune regulation (Bar-Shira et al., 2003; Bar-Shira and Friedman, 2006; Schokker et al., 2009).

24.4.1 Mucosal lymphoid tissues and cells

The combined mucosal surfaces of the gut, respiratory, and reproductive tracts represent by far the largest surface area in contact with the external milieu. They can also be considered the largest organ system in vertebrates, with each tract involved in diverse physiological functions, such as digestion and gas exchange. These functions come along with the continuous movement of external substances—nutrients and air, respectively—and the need to transport or exchange essential molecules across the mucosal surface. Hence, there is a continual challenge from new materials and microorganisms, including pathogenic microorganisms, which pass through the system. To prevent the entry of pathogens through the mucosal tissues, a wide variety of protective mechanisms has evolved. These range from barrier functions (e.g., keratinized skin, ciliated cells in the trachea, mucus secretion) to highly specialized immune cells (e.g., Langerhans cells in the skin) and organized lymphoid structures. In particular, the mucosal immune systems of the respiratory, gut, and reproductive tracts have highly developed lymphoid tissues, such as bronchus-associated lymphoid tissues and gut-associated lymphoid tissue, along with Peyer's patches, cecal tonsils, and lymphoid follicles. In addition, the lamina propria harbors a wide range of immune cells, such as intraepithelial and lamina propria lymphocytes, macrophages, and DCs. In mammalian species, the gut contains more lymphocytes than all secondary lymphoid tissues collectively. It is likely that this is also the case in avian species (reviewed in Schat and Meyers, 1991), particularly because birds lack lymph nodes. Numerous lymphoid follicles are found throughout the gut; typically, these consist of one or more B cell follicles and a surrounding T cell zone. It is not clear if these structures represent secondary or tertiary lymphoid tissues; however, given the increasing number of different classes (Baptista et al., 2013) of similar structures that have been identified in mammals, it is likely that the lymphoid follicles of the chicken gut represent lymphoid tissues of diverse ontogenies and functions. Finally, the epithelial cells of the mucosal surfaces are able to sense pathogens and actively shape the response of the immune cells underneath.

24.4.2 Intestinal barrier system

The intestinal innate defenses are characterized by a "mucosal firewall," a system of barriers that separates the lumenal side of the intestine from the subepithelial tissues (Macpherson et al., 2009; Belkaid and Hand, 2014). The reliability of the mucosal firewall is vital for the interactions between the immune system components and the intestinal contents. The first component of the mucosal firewall is the microbiological barrier where the microbiota live in or at the upper mucus layer. These commensal bacteria function to provide colonization resistance against pathogen colonization, produce metabolites/components that modulate immune signaling, and promote immune homeostasis (Garrett et al., 2010; Belkaid and Hand, 2014; Belkaid and Harrison, 2017). The second firewall is the chemical barrier consisting of the mucus overlaying the gut epithelium. The mucus regulates contact between the commensal bacteria and the epithelial cells. This division between the epithelium and commensals is achieved by the activity of the mucus produced by goblet cells in the epithelium, antimicrobial peptides released by the epithelial cells, and mucosal IgA produced by DCs in the intestine (Vaishnava et al., 2011; Belkaid and Harrison, 2017). The third component of the firewall is the physical barrier provided by the single cell epithelial cell layer. The intestinal epithelium is a single cell layer that assists the absorption of nutrients while providing a physical barrier that prevents both pathogen invasion and extraintestinal translocation of commensal microbes. Besides being the primary barrier preventing a microbial breach of the intestine, the epithelial cells should also be considered part of the cellular component of the innate immune response possessing PRRs for sensing MAMPs, but also capable of producing cytokines and chemokines to drive an inflammatory response against pathogen infection. The final component of the mucosal firewall is the immunological barrier where the professional immune cells (macrophages, DCs, lymphocytes) reside in the lamina propria (Abraham and Medzhitov, 2011). Further innate sensing of microbes is conducted by the macrophages and DCs which can present antigens to T cells resulting in the differentiation and activation of various T cell subsets (Abraham and Medzhitov, 2011). Specialized epithelial cells of the GI tract function together with lymphoid, myeloid, and stromal cells to secrete mucus, antimicrobial peptides, IgA, and chemokines that limit direct contact between the epithelium and infectious agents and activate target cells that mediate innate defenses (Medzhitov, 2001; Akira et al., 2006; Abreu et al., 2005; Kawai and Akira, 2009; Mantis and Forbes, 2010). The importance of these epithelial defense mechanisms is highlighted by the ability of enteric pathogens to target these mechanisms to achieve invasion and

dissemination (Awad et al., 2017; Goto et al., 2017; Alemka et al., 2012).

24.4.3 Intestinal microbiota

Chickens, like all production animals, are metaorganisms that maintain a diverse population of microorganisms on their barrier surfaces, collectively named the microbiota. Since most pathogens either cross or inhabit barrier surfaces, the microbiota plays a critical and often protective role during infections, both by modulating immune system responses and by mediating colonization resistance. However, the microbiota can also act as a reservoir for opportunistic microorganisms that can "bloom," significantly complicating diseases of barrier surfaces by contributing to inflammatory immune responses. With the advent of next-generation sequencing technologies, our understanding of the complex relationship between the host and its resident microbes has been fundamentally changed. The microbes that inhabit the intestinal barrier surface are not the result of random colonization but are shaped by interactions with the host and are therefore unique to each tissue site (reviewed by Bloom and Kogut, 2018). Chickens have evolved in the context of microbial colonization; therefore, there are multiple host functions dependent upon cues derived from the microbiota (Sommer and Backhead, 2013; Bloom and Kogut, 2018). Not least of these is the immune system, which can sense the microbiota directly via its expression of microbe-associated molecular patterns, enzymatically derived metabolites, and foreign antigens (Belkaid and Hand, 2017; Bloom and Kogut, 2018). Thus, the immune system relies upon the microbiota for protection against invading pathogens, but this close relationship comes with a significant risk in that if it becomes perturbed, responses against the microbiota can contribute to disease.

Poultry are naturally adapted to hosting a complex GI microbial community with hundreds of bacterial species and up to 10^{11} CFU per gram of gut contents (Barnes, 1979). Benefits conferred by this microbial community (the GI microbiome) include promoting beneficial development of the intestinal mucus layer, epithelial monolayer, and lamina propria (Shakouri et al., 2009; McCraken and Gaskins, 1999), excluding pathogenic taxa (Nurmi et al., 1992), breaking down polysaccharides (Beckman et al., 2006), providing energy as amino acids and short chain fatty acids (Dunkley et al., 2007; van Der Wielen et al., 2000) and promoting proper development and homeostasis of the immune system (Oakley et al., 2014).

The GI tract, or "gut," regulates homeostasis of the microbiological, physiological, and physical functions that allows the host to endure infectious and noninfectious stressors that it encounters (Crhanova et al., 2011; Sansonetti, 2004; Garriga et al., 2006; Maslowski and Mackay, 2011; Quintero-Fiho et al., 2012). Because the gut has the greatest surface area separating the environmentally exposed lumen and the internal subepithelial tissue, it is constantly exposed to infectious and noninfectious stressors making it an active immune organ containing more resident immune cells than any other organ in the host. The gut mucosal immune system, a highly regulated network of innate and acquired elements, provides a remarkable ability to respond and modify to these extremely diverse encounters (Thaiss et al., 2016; Honda and Littman, 2016). The development of the different divisions of the immune response has corresponded with the acquisition and maintenance of a symbiotic microbiota. The microbiota trains, stimulates, and functionally adjusts the different features of the immune system (Hooper and Macpherson, 2010; Hooper et al., 2012).

24.4.4 Intestinal immune functionality

24.4.4.1 Gut microbiota-immunity communication

The crosstalk that occurs between the host and its gut microbiota affects host metabolism, immunity, and health mediated by dietary nutrients, host and microbiota metabolites, microbial structural components, as well as antimicrobial compounds. Microbiota growth and anatomical location are regulated by the host through production of nonspecific antimicrobial peptides such as defensins (Xiao et al., 2006; Bomnineni et al., 2014), IgA (Lammers et al., 2004; Den Hartog et al., 2016), and miRNAs that regulate bacterial transcripts and bacterial growth (Liu et al., 2016).

The commensal microbes in the intestinal tract sense the local environment to induce biochemical pathways to activate bacterial metabolism that allows them to avoid, alter, and/or survive host innate immune killing. Moreover, some microbial-based molecules can promote specific commensal processes that are beneficial to both host and microbe. Similarly, the host detects the microbes through their production of specific molecules or components with unique molecular patterns that leads to activation of innate and acquired immune responses. Thus, the adaptation of the commensal bacteria (as well as viruses and fungi) living in the intestine of a host has resulted in a mutually beneficial coexistence for both microbiota and host during homeostasis (Kogut, 2013; Kogut et al., 2017; Broom and Kogut, 2018). The interdependent relationship between host and microbiota pointedly influences the host immune response to induce an immune tolerance to commensal microbes while also maintaining responsiveness to invading pathogens (Bene et al., 2017; Guo et al., 2017; Shi et al., 2017). Altering the intestinal microbial communities disturbs this immune balance and leads to immune dysregulation and susceptibility to diseases.

24.4.4.1.1 Components of the microbiota

The microbiota is directly engaged in maintaining the functional innate immunity of the host. The host immune system consistently senses the intestinal microenvironment to determine the metabolic state and colonization status (Levy et al., 2016). In the steady state, the metabolites and/or components of the commensal microbiota are recognized by various PRRs to regulate intestinal epithelial barrier function, cellular lifespan of phagocytes, and induce secretion of antimicrobial peptides and IgA (Levy et al., 2016; Blacher et al., 2017). Further, beneficial bacteria ferment dietary fibers to produce small chain fatty acids (SCFAs) which stimulate the production of anti-inflammatory cytokines (Levy et al., 2016; Blacher et al., 2017) that drives the production of regulatory T cells (Tregs). In addition, the microbiota influences the priming signal of the inflammasome activation that leads to the transcription of IL-6, as well as pro-IL-1β and pro-IL-18.

There is growing evidence that some commensal and symbiotic bacteria have MAMPs that promote a tolerant host phenotype. *Bacteriodes fragilis* polysaccharide A, for example, interacts with TLR2 on regulatory T-cells (T_{regs}) to promote tolerance and inhibit T_{H17} responses (Round and Mazmanian, 2010; Round et al., 2011). Other bacteria, particularly *Clostridia* species, are able to stimulate the development of T_{regs} as well (Round and Mazmanian, 2010; Round et al., 2011; Atarashi et al., 2011), while attachment of segmented filamentous bacteria, notably Candidatus Savagella, in the ileum has been shown to stimulate differentiation of proinflammatory T_{H17} type cells (Ivanov et al., 2009).

24.4.4.1.2 Microbial metabolites

It has also become apparent that the intestinal immune system can also detect the metabolic state of the microbiota by recognition of microbial metabolites via their PRRs (Levy et al., 2017; Blacher et al., 2017). The microbiota, using several biochemical pathways, metabolizes both diet- and host-derived metabolites that then influence various components of the intestinal immune system. For example, the microbiota converts nondigestible fibers to SCFA that have several anti-inflammatory activities (Postler and Ghosh, 2017). Dietary tryptophan can be degraded by the microbiota into indoles which promote epithelial cell barrier function (Postler and Ghosh, 2017). Likewise, the microbiota can metabolize dietary arginine to polyamines that inhibit the production of proinflammatory cytokines by macrophages (Postler and Ghosh, 2017). The microbiota converts primary host-derived hepatic bile acids to secondary bile acids that inhibit proinflammatory cytokine secretion by DCs and macrophages (Thaiss et al., 2014). Besides having a repertoire of metabolite sensing receptors, the host has developed immune signaling pathways (inflammasomes) expressed in various intestinal cell subsets (macrophages, DCs, epithelial cells, T cells) that recognize microbial-mediated metabolic activity that can stimulate antimicrobial activity involved in stable colonization of the intestine (Levy et al., 2015; Wang et al., 2015; Birchenough et al., 2016).

24.4.4.1.3 Microbial epigenetic modifications

Epigenetics involves genomic modifications through post-translational and post-transcriptional modifications induced by environmental factors, but without modifying the nucleotide sequence of the host cell (Shenderov et al., 2012). Epigenetic mechanisms regulate transcriptional control by external environmental including host-microbe crosstalk (Woo and Alenghat, 2007; Grabiec and Potempa, 2018). Since epigenetic events do not alter the DNA, the epigenomic effects are associated with the attachment of different chemical groups to DNA, histones, and chromatin post-translationally and the epigenetic alterations can persist for several generations (Furrow et al., 2011; Shenderov et al., 2012). These epigenetic alterations affect both the chromatin structure and serve as recognition elements for proteins with motifs dedicated to binding particular modifications.

Since the gut microbiota plays such a pivotal role in poultry metabolism, microbiota-induced epigenetic alterations by dietary nutrients could be a significant environmental factor affecting poultry performance and health. Based on studies in mammals, microbiota-generated metabolites of dietary components can be epigenetic activators of gene expression that modify or inhibit enzymes involved in epigenetic pathways (Alenghat et al., 2013; Alenghat and Artis, 2014; Hullar et al., 2014, Woo and Alenghat, 2007). This can best be exemplified by the production of SCFAs (acetate, propionate, butyrate) produced by intestinal microbiota by bacterial fermentation of non-digestible carbohydrates (Guilloteau et al., 2010; Jian et al., 2015). Butyrate is best known for its beneficial effects on intestinal barrier function, anti-inflammatory activity, and as the primary source of energy to intestinal epithelial cells (Hamer et al., 2008; Guilloteau et al., 2010; Leonel and Alvarez-Leite, 2012; Huang et al., 2015). Butyrate regulates these biological activities of host gut health by functioning as a histone deacetylase inhibitor (HDAC) (Canani et al., 2012; Liu et al., 2018). Butyrate anti-inflammatory activity is mediated by HDAC suppression of NF-κB in phagocytic cells and DCs, increased production of anti-inflammatory cytokines, and the increased differentiation of naive T cells into T regulatory cells (Usami et al., 2008; Arpaia et al., 2013). Other microbial metabolites derived from dietary components, such as nicotinamide adenine dinucleotide (NAD)-dependent deacetylases called sirtuins, have been shown to mediate the regulation of epigenetic

modifications, including DNA methylation noncoding RNAs and histone modification, in the host intestinal immune-barrier function of mammals (Kobayashi et al., 2012; Ganal et al., 2012; Singh et al., 2012). Further research is needed to determine whether such gut microbiota metabolite-mediated epigenetic modifications of the immuno-barrier function occur in the poultry intestine.

24.4.5 Gut microbiota: immune homeostasis

Based on new concept brought forward by Andreas Baumler and colleagues, homeostasis of the gut microbiota-immune interactome is a "state of immune competence" (Byndloss et al., 2019; Litvak and Baumler, 2019) that involves two complimentary elements: the traditional protective *anti-infective immunity* and a distinct type of immune response called *microbiota-nourishing immunity* (Byndloss et al., 2019; Litvak and Baumler, 2019). During homeostasis or health, the microbiota can effectively inhibit colonization and overgrowth by invading microbes such as pathogens. This phenomenon is called "colonization resistance" and is associated with a stable and diverse microbiota in tandem with a controlled lack of inflammation, and involves specific interactions between the mucosal immune system and the microbiota (Lawley and Walker, 2013; Buffie and Pamer, 2013). According to Byndloss et al. (2019), the first step in intestinal immune protection against pathogens is microbiota-nourishing immunity which functions in maintaining a balanced intestinal microbiota so that colonization resistance may be initiated. Microbiota-nourishing immunity involves the activation of two components of colonization resistance: direct (microbiota origin) and indirect (host origin) activities which function to protect the "microbial organ" within the host intestinal organ. The second component of the intestinal immune response is the activation of the conventional anti-infective immunity which prevents colonization and growth of pathogens through antimicrobial peptide production, inflammasome activation, and the expression and production of IL-17, IL-10, and IL-22 (Belkaid and Hand, 2014; Sassone-Corsi and Raffatellu, 2015; Lee and Mazmanian, 2010; Round and Mazmanian, 2009; O'Mahony et al., 2008; Ivanov et al., 2009). As described above, in a healthy microbiota, the commensal microbiota provides colonization resistance against potential pathogens in the gut. However, when perturbations (antibiotics, dietary changes) disrupt the commensals, colonization resistance is compromised. Pathogens like *S. typhimurium* and *Clostridium perfringens* can exploit the ecological opportunity by the availability of resources to expand. Thus, the pathogens change the playing field by inducing inflammation and causing other physiological changes (diarrhea) that influences the intestinal environment to promote their own growth (Winter et al., 2013).

24.4.5.1 Gut microbiota: immune dysfunction—dysbiosis

The microbiota in the GI is impacted, and potentially altered, when exposed to antibiotics, infection of the host by pathogens, diet, and several other host- and environmental-dependent influences. As describe previously, during homeostasis, the bacteria work together to produce beneficial metabolites that are used by the host. Dysbiosis (dysbacteriosis) occurs when there is a perturbation in the microbiota composition and/or function that leads to an imbalance between beneficial and harmful bacteria resulting in an unwanted immune response against commensal bacteria. Dysbiosis leads to a decrease in bacterial diversity and essential functions directly affecting metabolic activity, which can then deprive the host of valuable end products leading to poor gut health and bird performance (Ducatelle et al., 2015). Based on the Baumler concept (Byndloss et al., 2019), dysbiosis is a weakening in microbiota-nourishing immunity that disrupts colonization resistance, thus, allowing pathogens a physiological "opening" to exploit for colonization. As described above, in a healthy microbiota, the commensal microbiota provides colonization resistance against potential pathogens in the gut. However, when perturbations (antibiotics, dietary changes) disrupt the commensals, colonization resistance is compromised. Pathogens like *S. typhimurium* and *Clostridium perfringens* can expand by exploiting the ecological opportunity of increased availability of nutritional and physiological resources. Thus, the pathogens change the playing field by inducing inflammation and causing other physiological changes (diarrhea) that influences the intestinal environment to promote their own growth (Strecher et al., 2007; Winter et al., 2013; Hughes et al., 2017).

Intestinal inflammation is involved in dysbiosis in poultry (Ducatelle et al., 2018; Kogut et al., 2018), but it is not clear if the inflammation is the cause or the effect of the disruption in gut homeostasis (Sommer et al., 2017; Zeng et al., 2017). However, both pathogenic (microbial infection or tissue injury) and metabolic (excess dietary nutrients) inflammation cause dysbiosis (Kogut et al., 2018). Targeted use of dietary interventions, direct-fed microbials (DFMs) including pro/prebiotics, and other bioactive compounds may constitute an effective therapeutic strategy to rebalance gut dysbiosis and restore colonization resistance. However, existing microbe-targeted therapies, including prebiotics, probiotics, enzymes, and DFM have been developed for enhancing performance (increase nutritional value of feed, improved feed conversion, breast meat yield, egg production) not for normalizing immune cell function. Nevertheless, there are a few examples of the use of commercial feed additives improving immunity or decreasing gut inflammation including β-mannanase (Arsenault et al., 2017; Scapini et al., 2019), amino acids

(Bortoluzzi et al., 2018, 2020), and butyrate (Zou et al., 2019; Song et al., 2017; Bortoluzzi et al., 2017).

24.4.5.2 Gut microbiota: immune dysfunction—inflammation

Inflammation is basic physiological function of the innate host defense system in reaction to alterations in tissue homeostasis (Medzhitov, 2008). Inflammation is elicited by PRRs that detect not only infectious agents but also host damage and danger signaling molecules (DAMPs) that activate a highly regulated network of immunological and physiological events for the purpose of maintaining homeostasis and restoring functionality (Chovatlya and Medzhitov, 2013). Activation of the innate responses directs the production of a number of cells and proinflammatory molecules crucial to controlling most infectious and noninfectious challenges (Nathan, 2002; Barton, 2008).

24.4.5.2.1 Inflammatory phenotypes

Inflammation is an adaptable physiological response that adjusts to the conditions of a particular environment such as tissue injury or malfunction, excessive nutrients and metabolites, toxins, or infection (Garret et al., 2010; Sansonetti and Medzhitov, 2009; Hotamisligil, 2017) resulting in a large range of inflammatory reactions. The animal production industries are most familiar with gut inflammation as a pathological process associated with a decrease in weight gain, feed intake, feed efficiency, survivability, and uniformity (Iseri and Klasing, 2014; Kogut, 2013; Gaskins, 2008). However, recent research has shown that inflammation, although tightly regulated, displays phenotypic plasticity that is dependent upon the "trigger" that activates the response (Medzhitov, 2008; Ashley et al., 2012). For example, even under homeostatic conditions, the gut is continually exposed to a multitude of exogenous antigenic, dietary and toxic stimuli, as well as, endogenous stimuli such as structural bacterial components [LPSs and peptidoglycans (PGNs)] and bacterial-derived metabolites from bacterial microbiota all of which induce a low-grade stimulation of the innate immune system that is continuously regulated and contained; thus preventing intestinal tissue damage. This controlled inflammatory response has been defined as "hysiological inflammation" (Smith and Nagler-Anderson, 2005; Fiocchi, 2008) and is dependent upon the balance of the innate immune response that mediates host defense and tolerance in the gut. However, the induction of an infection resulting in an increase in pathogenic microbe-specific molecules (MAMPs) and/or virulence factors or cell debris from tissue injury (DAMPs) would transform physiological inflammation to "pathological inflammation" or classical or inflammation (Medzhitov, 2008; Barton, 2008).

24.4.5.3 Induction of inflammatory phenotypes

24.4.5.3.1 Physiological inflammation

Under homeostatic conditions, the immune system in the intestine concurrently performs two different functions: (1) defense against pathogen organisms and prevention of access of the intestinal microflora and (2) maintains a state of tolerance to the commensal microbes in the gut (Medzhitov, 2008; Abraham and Medzhitov, 2011). This continuous monitoring of the microbiota involves the constitutive physical and biochemical barriers of the mucus layer, epithelial cell layer, and secreted antimicrobial peptides, as well as, the immunological barrier of the immune cells dispersed in the intestinal mucosa and secretory IgA released from plasma cells also in the intestinal mucosa (Abraham and Medzhitov, 2011). During physiological inflammation or as described by Abraham and Medzhitov (2011) immune homeostasis, the immune tolerance in the intestine to the resident microbiota and food antigens is preferential to activation of an inflammatory response.

During physiological inflammation, the intestinal microbiome and the intestinal immune system exist in a symbiotic homeostasis sharing a bidirectional relationship, with both elements influencing each other's development, composition, and functionality (Nicolson et al., 2012). The normal host immune defenses that prevent pathogen invasion of the intestine also play a functional role in tolerance. Tolerance still involves the activation of PRRs initiated by the continuous release of commensal gut bacterial-derived products (MAMPs) and bacterial metabolites, such as SCFAs and polysaccharide A which drive down inflammation (Takeuchi and Akira, 2010; Pedra et al., 2009; Abraham and Medzhitov, 2011). However, the PRRs that are activated are found on unique populations of innate immune cells that regulate the PRR-mediated signaling pathways that alter PRR responsiveness, induce the production of high levels of regulatory proteins such as IL-10 and TGF-β, and induce the differentiation of the T-regulatory cells (Abraham and Medzhitov, 2011; Kinnebrew and Pamer, 2012).

24.4.5.3.2 Pathological inflammation

When an acute microbial infection or tissue injury occurs, the host defense: tolerance balance is disturbed and physiological inflammation converts to a true inflammatory response or pathological inflammation (Medzhitov, 2008; Barton, 2008). A number of cell types in the intestinal tissue express PRRs, especially TLRs and NLRs, that recognize the various triggers of inflammation (Nathan, 2002; Medzhitov, 2007; Takeda et al., 2010; Bianchi, 2007). The primary inducers of pathological inflammation are the MAMPs found on microbial pathogens, pathogen

virulence factors, DAMPS, such as ATP and nucleic acids, normally found intracellular, but are released into the extracellular space following tissue injury and cell death, and commensal gut bacterial-derived products and bacterial metabolites (Medzhitov, 2008; Barton, 2008; Rock and Kono, 2008; Bianchi, 2007).

24.4.5.3.3 Sterile inflammation

A low-grade chronic inflammation, in the absence of an infection, in response to a chemical (oxidative stress), physical (microbiota-derived components), and metabolic (nonstarch polysaccharides [NSPs] from dietary components) stimuli is known as sterile inflammation (Rubartelli et al., 2013). With a sterile inflammatory response, the stimulus persists without being eliminated suggesting that collateral damage is the cause of the disease (Rock et al., 2010). In sterile inflammation, PRRs recognize microbiome-derived components like LPS, PGN, and bacterial DNA (CpG) following microbiome bacterial cell wall turnover or bacterial lysis, but also DAMPs released from host cells after oxidative stress induced cell death (Rock et al., 2010).

Further, certain ingredients used in commercial broiler diets contain dietary NSPs that are indigestible by poultry, but represent a potential energy source which can be utilized with the proper addition of exogenous enzymes (Meng et al., 2005). For example, soybean meal (SBM) is a primary source of vegetable protein that contains 3% soluble NSP and 16% insoluble NSP, consisting mainly of mannans and galactomannans (Slominski, 2011). β-mannan is similar in structure to surface components of multiple pathogenic microbes and is recognized by a specific PRR, the mannose receptor, that stimulates the intestinal innate immune system leading to a purposeless energy draining immune response called feed-induced immune response (FIIR) (Hsiao et al., 2006; Martinez-Cummer, 2015).

Each meal leads to postprandial (low-grade) inflammation response in the intestine, the magnitude of which is related to the caloric value, specific components. If not properly regulated, postprandial inflammation could lead to unwanted consequences such as muscle catabolism, inappetite, and predisposition to infections (Niewold, 2014; Margioris, 2009).

However, standard feed ingredients in US commercial broiler diets, such as soybean, sesame, and sunflower meal, contain the immunogenic indigestible NSPs. Dietary NSPs are indigestible by poultry but do represent a potential valuable energy source that can be utilized by the birds with the addition of enzymes to the diet (Meng et al., 2005). Unfortunately, many of these NSP can be recognized by host PRR, for example, the mannose receptor, recognizes the major NSP in SBM, β-galactomannan (Hsaio et al., 2006). Recognition of these NSP by PRRs can lead to a chronic feed-induced inflammation resulting in a nonproductive energy expenditure on immunity. The addition of exogenous enzymes to the diet, such as β-mannases, phytases, and amylases, enhance NSP-containing feed not only by increasing digestion but also by reducing the FIIR because the NSPs are no longer recognized by PRR as demonstrated recently (Ferriera et al., 2016; Arsenault et al., 2017).

Finally, the largest potential source of endogenous triggers of sterile inflammation in the intestine are the 10^7–10^{11} bacteria/g in the microbiota. For example, PGN is the foremost component of gram-positive bacterial cell walls as well as being present in gram-negative bacterial cells walls (McDonald et al., 2005). Likewise, LPS (gram-negative bacterial cell wall) and unmethylated CpG oligodeoxynucleotide of all prokaryotic DNA are all ligands of host TLR and NLRs (Keestra et al., 2013; He et al., 2011). Both PGN and LPS are shed when bacteria in the microbiota divide and all components are released upon bacterial lysis (Myhre et al., 2006). Under homeostatic conditions, these components play a role in physiological inflammation. However, under stress conditions, such as FIIR, oxidative and heat stress, or feeding diets with high levels of NSPs that increase feed passage time and or decrease intestinal motility, as well as the frequency of reverse peristalsis, results prolonging the exposure to these triggers resulting in the induction of a low-grade sterile inflammatory response (Sacranie et al., 2007).

24.4.5.3.4 Metabolic inflammation

A chronic low-grade inflammation generated by excessive nutrient intake and the metabolic surplus fosters metabolic dysfunction by activating the same signaling transduction molecules and pathways as immune responses to infections (Hotamisligil, 2006). Metabolic dysfunction appears to take center stage by integrating signals from both the immune and metabolic systems (Kogut, 2013). Further, Humphrey et al. (2014) believed that "in modern broiler breeds, the drive toward improved productivity and carcass conformity has a negative impact on immune regulation in the gut, microbiota dysbiosis, and a persistent nutrient excess (fatty acids and carbohydrates) that result in chronic systemic inflammation, poorly controlled local and systemic inflammation, and increased metabolic diseases." This metabolic or metainflammation due to modern genetic/management practices for growing broilers and turkeys are virtually identical to those characteristics that lead to metabolic diseases in humans as a result of chronic low-grade inflammation, i.e., increased muscle mass, increased fat deposition, high-metabolic rate, ingesting high-nutrient dense diets, and consume food at a high rate, just to name a few (Hotamisligil, 2006; Hotamisligil and Erbay, 2008; Gregor and Hotsamisligil, 2011).

The innate immune cell recognition system and immune cell metabolism have coevolved and share the same signal transduction pathways (Assamann and Finlay, 2016). Thus, nutrient excess from diets can result in overloads of metabolites that act as DAMPs that can be sensed by PRRs of the innate immune system (Assamann and Finlay, 2016; Land, 2015; Lackey and Olefsky, 2016); thereby, simulating a chronic inflammation. PRRs, such as TLR4 and NLRP3, act as metabolite sensors activated by different metabolite DAMPS including free fatty acids, carbohydrates, and lipids (Gregor and Hotsamisligil, 2011). Continuous activation of these PRRs through excessive nutrient intake leads to the production of proinflammatory cytokines, such as IL-1β and IL-6, which maintain the low-grade inflammatory response.

Lastly, when nutrient excess leads to activation of PRR-mediated inflammation, there is a concurrent increase in metabolic pathways in the mitochondria of activated immune cells (Tannehil et al., 2013; McGettrick and O'Neill, 2013) that results in the overproduction of various metabolites via the Krebs cycle (succinate, citrate, NAD^+) and glycolysis (lactate) (Tannehil et al., 2013; McGettrick and O'Neill, 2013; Tretter et al., 2016). All four metabolites have been shown to be signals for multiple inflammatory mediators that result in a low-grade chronic inflammation (Tannehil et al., 2013; Loftus and Finlay, 2016). Increased succinate production results in an increase in stabilization of the transcription factor hypoxia inducible fact (HIF-1α) (Tannehil et al., 2013; Pucino et al., 2017). The stabilization of HIF-α results in increased glycolysis and the persistent production of the proinflammatory cytokine IL-1β (Tannehil et al., 2013; Loftus and Finlay, 2016). Likewise, citrate is also increased via the Kreb's cycle and is a signal for the increase production of inflammatory mediators such as reactive oxygen species, nitric oxide, and prostaglandins (Infantino et al., 2011). Lactate is a waste production produced in the immune cell cytoplasm at the end of glycolysis that affects local T cell immunity by inhibiting T cell motility, inducing the change of CD4+ cells to Th17 proinflammatory T cell subset that leads to the production of IL-17, which is a hallmark of chronic inflammation (Haas et al., 2016).

24.5 Tissue immunometabolism: tissue homeostasis and tissue resident immune cells

Cellular metabolism is a collective phrase to describe how cells generate the energy and metabolites required for cell growth and maintenance. Immunometabolism refers to the central role that metabolism plays in shaping the development, differentiation, and function of immune cells (O'Neill et al., 2016; Chauhan and Saha, 2018). The foundation of immunometabolism is the assertion that the engagement of specific metabolic pathways, the production or utilization of specific metabolites, or the noncanonical functions of metabolic enzymes can be decisive in the balance between inflammation, immune tolerance, or resolution.

The interface of the immune system and metabolism is an emerging field of study. The initial impetus for researchers to consider an immune-metabolic perspective was the human health concerns related to obesity, diabetes, and metabolic disorders. Excessive fat deposition can lead to an innate immune inflammatory response (O'Neill and Hardie, 2013). This chronic low-grade inflammation was linked to resultant diseases such as type 2 diabetes, fatty liver disease, gout, and cirrhosis. It has become apparent that metabolic shifts within immune cells result in shaping the effector responses (Jha et al., 2015 ; Norata et al., 2015). The resultant shifts in energy supply and demand can lead to transcriptional and translation changes in tissue phenotype (Palsson-McDermott and O'Neill, 2020). Such phenotypic shifts can imprint fundamental changes to tissue metabolism and local inflammatory/immune cell functions. In mammals, cell intrinsic metabolic programs are orchestrated by multiple metabolic sensors, including mTOR, AMPK, PPARγ, HIF-1γ, and sirtuins, that modulate immune cell trafficking and function (Gonzales et al., 2020; Chun et al., 2017; Palsson-McDermott and O'Neill, 2020).

An intricate relationship exists between macrophage and T cell biology and host metabolism (Palsson-McDermott and O'Neill, 2020). A proinflammatory phenotype of monocytes M1 macrophages, activated B cells and Th1 and Th17 T cells is characterized by an increase in aerobic glycolysis (Jha et al., 2015; Norata et al., 2015). Alternatively, the anti-inflammatory phenotype of M2 macrophages and T regulatory cells is characterized by oxidative phosphorylation-mediated metabolism (Jha et al., 2015; Norata et al., 2015).

The metabolic phenotype of immune cells can be modulated by the tissue environment where they are present. The immediate and sustained metabolic alterations that modulate host defensive functions during infection through metabolic regulations regulated by nutrient-sensing machineries. Thus, the availability of nutrients can impact the functional activity of the immune system to control or eliminate tumors and pathogens. However, exploiting the immunometabolic mechanisms in a complex tissue microenvironment in an effort to fine-tune cellular metabolism of resident immune cells either in homeostatic or diseased settings is still being explored and characterized. Nevertheless, the immune cell mitochondria metabolism has been found to be a primary regulator of immune cell phenotype and function (Aguilar-Lopez et al., 2020; Weinberg et al., 2015). Mitochondria can rapidly switch from being catabolic organelles generating ATP to anabolic organelles that

generate both ATP and building blocks for macromolecule synthesis, enabling them to deliver suitable metabolic demands of different immune cells. Mitochondria have multiple mechanisms that allow them to activate intracellular signaling pathways that can alter AMP/ATP ratio, release ROS and TCA cycle metabolites, and localize immune regulatory proteins on the outer mitochondria membrane (Aguilar-Lopez et al., 2020; Weinberg et al., 2015).

Within poultry production, a consideration of the immunometabolic consequences would be invaluable. A focus solely on maximizing animal growth can reduce immune potential, while a strong immune response has negative consequences on growth (Humphrey and Klasing, 2014). A consideration of the integrated whole may allow one to maximize growth and animal production without having a detrimental impact on animal health and immune potential. We have shown the nearly innumerable links between cellular signaling proteins classically characterized as members of either the immune or metabolic functional groups (Arsenault et al., 2014).

A feature of avian salmonellosis is persistent intestinal infection or carrier state. Intestinal carriage may occur for several months following infection. The establishment of persistence is in the face of a substantial immune response that requires either evasion or modulation of the response by the bacteria. The fact that many *Salmonella* serovars persist within the chicken intestinal tract with little sign of GI disease despite eliciting a considerable inflammatory response, and that inflammatory responses to *Salmonella* are relatively short-lived (Withnage et al., 2005), strongly suggests there is a degree of regulation of this response. Some years ago, it was shown that the lowering of intestinal proinflammatory signals following colonization with *S. typhimurium* corresponded to increased expression of TGF-β, suggesting that regulation of inflammation was taking place (Tang et al., 2018, II 86:e00307-18). Upon infection of chickens with paratyphoid serovars of *Salmonella*, the regulation of immune and metabolic pathways are altered. Based on our findings (Kogut and Arsenault, 2017), combining Treg cell isolation and functional studies, cytokine transcriptional analysis and kinome analysis of immune and metabolic signaling pathways in the cecum of chickens during an early (4 to 48 h) and late (4 to 14 days) infection with *Salmonella* Enteritidis, we observed three separate immune-metabolic phases associated with different times postinfection. First, we observed an inflammatory phase 1 to 3 days postinfection, characterized by the up-regulation of proinflammatory cytokine mRNA transcription and the induction of mTOR-mediated anabolic metabolism (protein synthesis, glycogen synthesis, and fatty acid synthesis). The second phase appears around 4 days postinfection characterized by profound changes in cecal immunity and metabolism. In general, the local immune microenvironment changed from proinflammatory to anti-inflammatory exemplified by a decrease in proinflammatory cytokine mRNA transcription to control levels and a dramatic increase in anti-inflammatory cytokine mRNA expression accompanied by a significant increase in the number and function of Tregs in the cecum. In addition, we observed a remarkable metabolic reprogramming in the cecal tissue at this time with a shift from anabolic to catabolic reactions mediated by the significant phosphorylation of AMPK. It is during this phase that we speculate that *Salmonella* takes advantage of the lack of host response to infection to begin to establish a persistent cecal colonization. The third phase appears to begin shortly after day four postinfection with a gradual return to homeostasis. The number of Tregs in the cecum remains elevated over noninfected tissue and IL-10 and TGF-β appear to regulate a more tolerant microenvironment. Lastly, there is a final metabolic reprogramming from catabolic to homeostasis with no difference in metabolism between infected and noninfected birds. We speculate that the *Salmonella* have established itself as part of the normal microbiome of the cecum and is no longer recognized by the host immune system.

References

Abraham, C., Medzhitov, R., 2011. Interaction between the host innate immune system and microbes in inflammatory bowel disease. Gastroenterology 140, 1729–1737.

Abreu, M.T., Fukata, M., Arditi, M., 2005. TLR signaling in the gut in health and disease. J. Immunol. 174, 4453–4460.

Achanta, M., Sunkara, L.T., Dai, G., Bommineni, Y.R., Jiang, W., Zhang, G., 2012. Tissue expression and developmental regulation of chicken cathelicidin antimicrobial peptides. J. Anim. Sci. Biotechnol. 3, 15.

Aguilar-Lopez, B.A., Moreno-Altamirano, M.M.B., Dockrell, H.M., Duchen, M.R., Sanchez-Garcia, F.J., 2020. Mitochondria: an integrative hub coordinating circadian rhythms., metabolism, the microbiome, and immunity. Front. Cell Dev. Biol. 8, 51.

Akira, S., Uematsu, S., Takeuchi, O., 2006. Pathogen recognition and innate immunity. Cell 124, 783–801.

Alemka, A., Corcionivoschi, N., Bourke, B., 2012. Defense and adaptation: the complex inter-relationship between *Campylobacter jejuni* and mucus. Front. Cell. Infect. Microbiol. 2. Article 15.

Alenghat, T., Artis, D., 2014. Epigenomic regulation of host-microbe interactions. Trends Immunol. 35, 518–525.

Alenghat, T., Osborne, L.C., Saenz, S.A., Kubuley, D., Ziegler, C.G.K., et al., 2013. Histone deacetylase 3 coordinates commensal-bacteria-dependent intestinal homeostasis. Nature 504, 153–157.

Arpaia, N., Campbell, C., Fan, X., Dikly, S., van der Veeken, D., et al., 2013. Metabolites produced by commensal bacteria promote peripheral regulatory T-cell generation. Nature 504, 451–455.

Arsenault, R.J., Lee, J.T., Latham, R., Carter, B., Kogut, M.H., 2017. Changes in immune and metabolic gut response in broilers fed β-mannanase in β-mannan-containing diets. Poultry Sci. 96, 4307–4316.

Arsenault, R.J., Trost, B., Kogut, M.H., 2014. A comparison of the chicken and turkey proteomes and phosphoproteomes in the development of poultry-specific immuno- metabolism kinome peptide arrays. Front. Vet. Infect. Dis. 1, 22.

Ashley, N.T., Weil, Z.M., Nelson, R.J., 2012. Inflammation: mechanisms, costs, and natural variation. Annu. Rev. Ecol. Evol. Syst. 43, 385–406.

Assamann, N., Finlay, D.K., 2016. Metabolic regulation of immune responses: therapeutic opportunities. J. Clin. Invest. 126, 2031–2039.

Atarashi, K., Tanoue, T., Shima, T., Imaoka, A., Kuwahara, T., Momose, Y., Cheng, G., Yamasaki, S., Saito, T., Ohba, Y., Taniguchi, T., Takeda, K., Hori, S., Ivanov, I.I., Umesaki, Y., Itoh, K., Honda, K., 2011. Induction of colonic regulatory T cells by indigenous Clostridium species. Science 331, 337–341.

Avery, S., Rothwell, L., Degen, W.D.J., Schijns, V., Young, J., Kaufman, J., Kaiser, P., 2004. Characterization of the first non-mammalian T2 cytokine gene cluster: the cluster contains functional single-copy genes for IL-3, IL-4, IL-13, and GM-CSF, a gene for IL-5 that appears to be a pseudogene, and a gene encoding another cytokine-like transcript, KK34. J. IFN Cytokine. Res. 24, 600–610.

Awad, W.A., Hess, C., Hess, M., 2017. Enteric pathogens and their toxin-induced disruption of the intestinal barrier through alteration of tight junctions in chickens. Toxins 9, 60.

Balu, S., Kaiser, P., 2003. Avian interleukin-12 beta (p40): cloning and characterization of the cDNA and gene. J. IFN Cytokine Res. 23, 699–707.

Baptista, A.P., Olivier, B.J., Coverse, G., Grueter, M., Kippenberg, M., Kusser, K., Domingues, R.G., Velga-Fernandes, H., Luster, A.D., Lugering, A., Randall, T.D., Cupedo, T., Mebius, R.E., 2013. Colonic patch and colonic SILT development are independent and differentially regulated events. Mucosal Immunol. 6, 511–521.

Bar-Shira, E., Friedman, A., 2006. Development and adaptations of innate immunity in the gastrointestinal tract of the newly hatched chick. Dev. Comp. Immunol. 30, 930–941.

Bar-Shira, E., Sklan, D., Friedman, A., 2003. Establishment of immune competence in the avian GALT during the immediate post-hatch period. Dev. Comp. Immunol. 27, 147–157.

Barbet, G., Sander, L.E., Geswell, M., Leonardi, A., Cerutti, A., Iliev, I., Blander, J.M., 2018. Sensing microbial viability through bacterial RNA augments T follicular helper cell and antibody responses. Immunity 48, 584–598.

Barnes, E.M., 1979. The intestinal microflora of poultry and game birds during life and after storage. J. Appl. Bacteriol. 46, 407–419.

Barton, G.M., 2008. A calculated response: control of inflammation by the innate immune system. J. Clin. Invest. 118, 413–420.

Beal, R.K., Poupos, C.T., Davison, F., Smith, A.L., 2006. Immunological development of the avian gut. In: Perry, G.C. (Ed.), Avian Gut Function in Health and Disease. CAB International, Oxon, pp. 85–103.

Beckmann, L., Simon, O., Vahjen, W., 2006. Isolation and identification of mixed linked β-glucan degrading bacteria in the intestine of broiler chickens and partial characterization of respective 1,3-1,4-β-gluconidase activities. J. Basic Microbiol. 46, 175–185.

Belkaid, Y., Hand, T., 2014. Role of the microbiota in immunity and inflammation. Cell 157, 121–141.

Belkaid, Y., Harrison, O.J., 2017. Homeostatic immunity and the microbiota. Immunity 46, 562–576.

Bene, K., Varga, Z., Petrov, V.O., Boyko, N., Rahnavolgyi, E., 2017. Gut microbiota species can invoke both inflammatory and tolerogenic immune responses in human dendritic cells mediated by retinoic acid receptor alpha ligation. Front. Immunol. 8. Article 427.

Bianchi, M.E., 2007. DAMPS, PAMPS, and alarmins: all we need to know about danger. J. Leukoc. Biol. 81, 1–5.

Birchenough, G.M.H., Nystrom, E.E.L., Johansson, M.E.V., Hansson, G.C., 2016. A sentinel goblet cell guards the colonic crypt by triggering NLRP6-dependent Muc2 secretion. Science 352, 1535–1542.

Blacher, E., Levy, M., Tatirovsky, E., Elinov, E., 2017. Microbiome-modulated metabolites at the interface of host immunity. J. Immunol. 198, 572–580.

Blander, J.M., Sander, L.E., 2012. Beyond pattern recognition: five immune checkpoints for scaling the microbial threat. Nat. Rev. Immunol. 12, 215–225.

Bomminieni, Y.R., Pham, G.H., Sunkara, L.T., Achanta, M., Zhang, G., 2014. Immune regulatory activities of fowlcidin-1, a cathelicidin host defense peptide. Mol. Immunol. 59, 55–63.

Bortoluzzi, C., Pedroso, A.A., Mallo, J.J., Puyalto, M., Kim, W.K., Applegate, T.J., 2017. Sodium butyrate improved performance while modulating the cecal microbiota regulating the expression of intestinal immune-related genes of broiler chickens. Poultry Sci. 96, 3981–3993.

Bortoluzzi, C., Rochell, S.J., Applegate, T.J., 2018. Threonine, arginine, and glutamine: influences on intestinal physiology, immunology, and microbiology in broilers. Poultry Sci. 97, 937–945.

Bortoluzzi, C., Fernandes, I.M., Doranalli, K., Applegate, T.J., 2020. Effects of dietary amino acids in ameliorating intestinal function during enteric challenges in broiler chickens. Anim. Feed Sci. Technol. 262. Article 114383.

Boyd, Y., Goodchild, M., Morrol, S., Bumstead, N., 2001. Mapping of the chicken and mouse genes for toll-like receptor 2 (TLR2) to an evolutionarily conserved chromosome segment. Immunogenetics 52, 294–298.

Broom, L.J., Kogut, M.H., 2018. The role of the gut microbiome in shaping the immune system of chickens. Vet. Immunol. Immunopathol. 204, 44–51.

Brownlie, R., Zhu, J., Allan, B., Mutwiri, G.K., Babiuk, L.A., Potter, A., Griebel, P., 2009. Chicken TLR21 acts as a functional homologue to mammalian TLR9 in the recognition of CpG oligodeoxynucleotides. Mol. Immunol. 46, 3163–3170.

Buffie, C.G., Pamer, E.G., 2013. Microbiota-mediated colonization resistance against intestinal pathogens. Nat. Rev. Immunol. 13, 790–801.

Byndloss, M.X., Litvak, Y., Baumler, A.J., 2019. Microbiota-nourishing immunity and its relevance for ulcerative colitis. Inflamm. Bowel Dis. 25, 811–815.

Caamaño, J., Hunter, C.A., 2002. NF-κB family of transcription factors: central regulators of innate and adaptive immune functions. Clin. Microbiol. Rev. 15, 414–429.

Campbell, L.K., Magor, K.E., 2020. Pattern recognition receptor signaling and innate responses to influenza A viruses in the mallard duck, compared to humans and chickens. Front. Cell. Infect. Microbiol. 10. Article 209.

Canani, R.B., DiCostanzo, M., Leone, L., 2012. The epigenetic effects of butyrate: potential therapeutic implications for clinical practice. Clin. Epigenet. 4, 4.

Chauhan, P., Saha, B., 2018. Metabolic regulation of infection and inflammation. Cytokine 112, 1–11.

Chovatiya, R., Medzhitov, R., 2013. Stress, inflammation, and defense of homeostasis. Mol. Cell 54, 281–288.

Chun, C., Zheng, L., Colgan, S.P., 2017. Tissue metabolism and host-microbial interactions in the intestinal mucosa. Free Rad. Biol. Med. 105, 86–92.

Ciraci, C., Tuggle, C.K., Wannemuechle, M.J., Nettleton, D., Lamont, S.J., 2010. Unique genome-wide transcriptome profiles of chicken macrophages expose to *Salmonella*-derived endotoxin. BMC Genom. 9, 256.

Crhanova, M., Hradecka, H., Faldynova, M., Matulova, M., Havlickova, H., Sisak, H., Rychlik, I., 2011. Immune response of chicken gut to natural colonization by gut microflora and to *Salmonella enterica* serovar Enteritidis infection. Infect. Immun. 79, 2755–2763.

Cuperus, T., Coorens, M., van Dijk, A., Haagsman, H.P., 2013. Avian host defense peptides. Dev. Comp. Immunol. 41, 352–369.

Dalgaard, T.S., Skovgaard, K., Norup, L.R., Pleidrup, J., Permin, A., Schou, T.W., Vadekaer, D.F., Jungerson, G., Juul-Madsden, H.R., 2015. Immune gene expression in the spleen of chickens experimentally infected with *Ascaridia galli*. Vet. Immunol. Immunopathol. 164, 79–86.

Degen, W.G.J., Van Daal, N., Van Zuilekom, H.I., Burnside, J., Schijns, V., 2004. Identification and molecular cloning of functional chicken IL-12. J. Immunol. 172, 4371–4380.

Degen, W.G., Daal, N., Rothwell, L., Kaiser, P., Schijns, V.E., 2005. Th1/Th2 polarization by viral and helminth infection in birds. Vet. Microbiol. 105, 163–167.

Den Hartog, G., De Vries-Reilingh, G., Wehmaker, A.M., Savelkoul, H.F., Parmentier, H.K., Lammers, A., 2016. Intestinal immune maturation is accompanied by temporal changes in the composition of the microbiota. Benef. Microbes 7, 677–685.

Denyer, M.P., Pinheiro, D.Y., Garden, O.A., Shepard, A.J., 2016. Missed, not missing: phylogenomic evidence for the existence of avian FoxP3. PLoS One 11, e0150988.

De Zoete, M.R., Bouwman, L.I., Keestra, A.M., van Putten, J.P.M., 2011. Cleavage and activation of a Toll-like receptor by microbial proteases. Proc. Natl. Acad. Sci. U.S.A. 108, 4968–4973.

Dil, N., Qureshi, M.A., 2002. Differential expression of inducible nitric oxide synthase is associated with differential Toll-like receptor-4 expression in chicken macrophages from different genetic backgrounds. Vet. Immunol. Immunopathol. 84, 191–207.

Ducatelle, R., Eeckhaut, E.E., Haesebrouke, F., van Immerseel, F., 2015. A review on prebiotics and probiotics for the control of dysbiosis: present status and future perspectives. Animal 9, 43–48.

Ducatelle, R., Goossens, E., De Meyer, F., Eeckhaut, V., Antonissen, G., Haesebrouck, F., van Immerseel, F., 2018. Biomarkers for monitoring intestinal health in poultry: present status and future perspectives. Vet. Res. 49, 43.

Dunkley, K.D., Dunkley, C.S., Njongmeta, N.L., Calloway, T.R., Hume, M.E., Kubena, L.F., Nisbet, D.J., Ricke, S.C., 2007. Comparison of in vitro fermentation and molecular microbial profiles of high-fiber feed substrates incubated with chicken cecal inocula. Poultry Sci. 86, 801–810.

Fearon, D.T., Locksley, R.M., 1996. The instructive role of innate immunity in the acquired immune response. Science 272, 50–54.

Ferriera Jr., H.C., Hannas, M.I., Albino, F.T., Rostagno, H.S., Neme, R., Faria, D., Xavier Jr., M.L., Renn, L.N., 2016. Effect of the addition of β-mannanase on the performance, metabolizable energy, amino acid digestibility coefficients, and immune functions of broilers fed different nutritional levels. Poultry Sci. 95, 1848–1857.

Fiocchi, C., 2008. What is "physiological" intestinal inflammation and how does it differ from "pathological" inflammation? Inflamm. Bowel Dis. 14 (S2), S77–S78.

Fukui, A., Inoue, N., Matsumoto, M., Nomura, M., Yamada, K., Matsuda, Y., Toyoshima, K., Seya, T., 2001. Molecular cloning and functional characterization of chicken Toll-like receptors. A single chicken toll covers multiple molecular patterns. J. Biol. Chem. 276, 47143–47149.

Furrow, R.E., Christiansen, F.B., Feldman, M.W., 2011. Environment-sensitive epigenetics and the heritability of complex diseases. Genetics 189, 1377–1389.

Ganal, S.C., Sanos, S.L., Kalifass, C., Oberle, K., Johner, C., Kirsching, C., Linenklaus, S., Weiss, S., Staeheli, P., Aichele, P., Diefenbach, A., 2012. Priming of natural killer cells by non-mucosal mononuclear phagocytes requires instructive signals from commensal microbiota. Immunity 37, 171–186.

Garcia, J.S., Byrd, J.A., Wong, E.A., 2018. Expression of nutrient transporters and host defense peptides in *Campylobacter* challenged broilers. Poultry Sci. 97, 3671–3680.

Garcia, J.S., Byrd, J.A., Wong, E.A., 2020. Tissue-, age- and dose-dependent changes in avian β-defensin and LEAP2 mRNA abundance in the intestines of *Salmonella* Typhimurium challenged broilers. Anim. Biotechnol. https://doi.org/10.1080/10495398.2020.1738449.

Garrett, W.S., Gordon, J.I., Glimcher, L.H., 2010. Homeostasis and inflammation in the intestine. Cell 140, 859–870.

Garriga, C., Hunter, R.R., Amat, C., Planas, J.M., Mitchell, M.A., 2006. Heat stress increases apical glucose transport in the chicken jejunum. Am. J. Reg. Inter. Comp. Physiol. 290, R195–R201.

Gaskins, H.R., 2008. Host and intestinal microbiota negotiations in the context of animal growth efficiency. In: Taylor-Picard, J.A., Spring, P. (Eds.), Gut Efficiency: The Key Ingredient in Pig and Poultry Production. Wageningen Academic Publishers, Wageningen, The Netherlands, pp. 32–43.

Gobel, T.W., Schneider, K., Schaerer, B., Mejri, I., Puehler, F., Weigend, S., Stayheli, P., Kaspers, B., 2003. IL-18 stimulates the proliferation and IFN-γ release of CD4+ T cells in the chicken: conservation of a Th1-like system in a nonmammalian species. J. Immunol. 171, 1809–1815.

Goitsuka, R., Chen, C.-L.H., Benyon, L., Asano, Y., Kitamura, D., Cooper, M.D., 2007. Chicken cathelicidin-B1, an antimicrobial guardian at the mucosal M cell gateway. Proc. Natl. Acad. Sci. U.S.A. 104, 15063–15068.

Gonzales, A., Hall, M.N., Lin, S.-C., Hardie, D.G., 2020. AMPK and TOR: the yin and yang of cellular nutrient sensing and growth control. Cell Metabol. 31, 472–492.

Goto, R., Miki, T., Nakimura, N., Fujimoto, M., Okada, N., 2017. *Salmonella typhimurium* PagP- and Ugtl-dependent resistance to antimicrobial peptides contribute to gut colonization. PLoS One 12, e0190095.

Grabiec, A.M., Potempa, J., 2018. Epigenetic regulation of bacterial infections: targeting histone deacetylases. Crit. Rev. Microbiol. 44, 336–350.

Gregor, M.F., Hotamisligil, G.S., 2011. Inflammatory mechanisms in obesity. Annu. Rev. Immunol. 29, 415–445.

Guilloteau, P., Eeckhaut, M.V., Ducatelle, R., Zabielski, R., van Immerseel, F., 2010. From the gut to the peripheral tissues: the multiple effects of butyrate. Nutr. Res. Rev. 23, 366–384.

Guo, C.-J., Chang, F.-Y., Wyche, T.P., Backus, K.M., Nayfach, S., Pollard, K.S., Craik, C.S., Cravett, B.F., Clardy, J., Voigt, C.A., Fischbach, M.A., 2017. Discovery of reactive microbiota-derived metabolites that inhibit host proteases. Cell 168, 617–628.

Haas, R., Smith, J., Rocher-Ros, V., Nadkarni, S., Montero-Melendez, T., D'Acquisto, F., Bland, E.J., Bombardieri, M., Pitzalis, C., Perretti, M., Marelli-Berg, F.M., Mauro, C., 2016. Lactate regulates metabolic and pro-inflammatory circuits in control of T cell migration and effector functions. PLoS Biol. 13, e1002202.

Hamer, H.M., Jonkers, D., Venema, K., Vanhoutvin, S., Troost, F.J., Brummer, R.-J., 2008. Review article: the role of butyrate on colonic function. Aliment. Pharmacol. Therpeutics 27, 104–119.

He, H., Lowry, V.K., Ferro, P.M., Kogut, M.J., 2005. CpG-oligodeoxynucleotide- stimulated chicken heterophil degranulation is serum cofactor and cell surface receptor dependent. Dev. Comp. Immunol. 29, 255–264.

He, H., Genovese, K.J., Swaggerty, C.L., Nisbet, D.J., Kogut, M.H., 2007. In vivo priming heterophil innate immune functions and increasing resistance to *Salmonella enteritidis* infection in neonatal chickens by immune stimulatory CpG oligodeoxynucleotides. Vet. Immunol. Immunopathol. 117, 275–283.

He, H., Genovese, K.J., Swaggerty, C.L., MacKinnon, K.M., Kogut, M.H., 2011. Co-stimulation with TLR3 and TLR21 ligands synergistically up-regulates Th-1 cytokine, IFN-gamma and regulatory cytokine, IL10 expression in chicken monocytes. Dev. Comp. Immunol. 36, 756–760.

Higgs, R., Cormican, P., Cahalane, S., Allan, B., Lloyd, A.T., Meade, K., James, T., Lynn, D.J., Babiuk, L.A., O'Farrelly, C., 2006. Induction of a novel chicken Toll-like receptor following *Salmonella enterica* serovar Typhimurium infection. Infect. Immun. 74, 1692–1698.

Higuchi, M., Matsuo, A., Shingai, M., Shida, K., Ishii, A., Funami, K., Suzuki, Y., Oshiumi, H., Matsumoto, M., Seya, T., 2008. Combinational recognition of bacterial lipoproteins and peptidoglucans by chicken Toll-like receptor 2 subfamily. Dev. Comp. Immunol. 32, 147–155.

Honda, K., Litman, D.R., 2016. The microbiota in adaptive immune homeostasis and disease. Nature 535, 75–84.

Hooper, L.V., MacPherson, A.J., 2010. Immune adaptations that maintain homeostasis with the intestinal microbiota. Nat. Rev. Immunol. 10, 159–169.

Hooper, L.V., Litman, D.R., MacPherson, A.J., 2012. Interactions between the microbiota and the immune system. Science 336, 1268–1273.

Hotamisligil, G.S., 2006. Inflammation and metabolic disorders. Nature 444, 860–867.

Hotamisligil, G.S., 2017. Inflammation, metainflammation, and immunometabolic disorders. Nature 542, 177–185.

Hotamisligil, G.S., Erbay, E., 2008. Nutrient sensing and inflammation in metabolic diseases. Nat. Rev. Immunol. 8, 923–934.

Hsaio, H.Y., Anderson, D., Dale, N., 2006. Levels of β-mannan in soybean meal. Poultry Sci. 85, 1430–1432.

Huang, C., Song, P., Fan, P., Hou, C., Thacker, P., Ma, Z., 2015. Dietary sodium butyrate decreases postweaning diarrhea by modulating intestinal permeability and changing the bacterial communities in weaned piglets. J. Nutr. 145, 2774–2780.

Hughes, E.R., Winter, M.G., Duerkop, B.A., Spiga, L., Furtado de Carvalho, T., Zhu, W., Gillis, C.C., Buttner, L., Smoot, M.P., Behrendt, C.L., Cherry, S., Santos, R.L., Hooper, L.V., Winter, S.E., 2017. Microbial respiration and formate oxidation as metabolic signatures of inflammation-associated dysbiosis. Cell Host Microbe 21, 208–219.

Huller, M.A.J., Fu, B.C., 2014. Diet, the gut microbiome, and epigenetics. Cancer J. 20, 170–175.

Humphrey, S., Chaloner, G., Kemmett, K., Davidson, N., Williams, N., Kipar, A., Humphrey, T., Wigley, P., 2014. *Campylobacter jejuni* is not merely a commensal in commercial broiler chickens and affects bird welfare. mBio 5 e01384-14.

Infantino, V., Convertini, P., Cucci, L., Panaro, M.A., DiNoia, M.A., Calvello, R., Palmieri, F., Iacobazzi, V., 2011. The mitochondrial citrate carrier: a new player in inflammation. Biochem. J. 438, 433–436.

Iseri, V.J., Klasing, K.C., 2014. Changes in the amount of lysine in protective proteins and immune cells after a systemic response to dead *Escherichia coli*: implications for the nutritional costs of immunity. Integr. Comp. Biol. 54, 922–930.

Ivanov, I.I., Atarashi, K., Manel, N., Brodie, E.L., Shima, T., Karaoz, U., Wei, D., Goldfarb, K.C., Santee, C.A., Lynch, S.V., Tanoue, T., Imaoka, A., Itoh, K., Takeda, K., Umesaki, Y., Honda, K., Littman, D.R., 2009. Induction of intestinal Th17 cell by segmented filamentous bacteria. Cell 139, 485–498.

Janeway, C.A., 1989. Approaching the asymptote? Evolution and revolution in immunology. Cold Spring Harbor Symp. Quant. Biol. 54, 1–13.

Jha, A.K., Huang, S.C.-C., Sergushichev, A., Lampropoulou, V., Ivanova, Y., Loginicheva, E., Chmielewski, K., Stewart, K.M., Ashall, J., Everts, B., Pearce, E.J., Driggers, E.M., Artyomov, M.N., 2015. Network integration of parallel metabolic and transcriptional data reveals metabolic modules that regulate macrophage polarization. Immunity 42, 419–430.

Jiang, Y., Zhang, W., Gao, F., Zhou, G., 2015. Effect of sodium butyrate on intestinal inflammatory response to lipopolysaccharide in broiler chickens. Can. J. Anim. Sci. 95, 389–395.

Kaiser, P., 2010. Advances in avian immunology–prospects for disease control: a review. Avian Pathol. 39, 309–324.

Kaiser, P., 2012. The long view: a bright past, a brighter future? Forty years of chicken immunology pre- and post-genome. Avian Pathol. 41, 511–518.

Kaiser, P.,P., Staheli, P., 2014. Avian cytokines and chemokines. In: Schat, K.A., Kaspers, B., Kaiser, P. (Eds.), Avian Immunology. Elsevier, London, UK, pp. 189–204.

Karpala, A., Stewart, C., McKay, J., Lowenthal, J.W., Bean, A.G.D., 2011. Characterization of chicken MDA5 activity: regulation of IFN-β in the absence of RIG-1 functionality. J. Immunol. 186, 5397–5405.

Kaufman, J., 2000. The simple chicken major histocompatibility complex: life and death in the face of pathogens and vaccines. Phios. Trans. R. Soc. Lond. B Biol. Sci. 355, 1077–1084.

Kaufman, J., Milne, S., Gobel, T.W., Walker, B.A., Jacob, J.P., Auffray, C., Zoorob, R., Beck, S., 1999. The chicken B locus is a minimal essential major histocompatibility complex. Nature 401, 923–925.

Kawai, T., Akira, S., 2009. The roles of TLRs, RLRs and NLRs in pathogen recognition. Int. Immunol. 21, 317–327.

Keestra, A.M., van Putten, J.P.M., 2008. Unique properties of the chicken TLR4/MD-2 complex: selective lipopolysaccharide activation of the MyD88-dependent pathway. J. Immunol. 181, 4354–4362.

Keestra, A.M., de Zoete, M.R., Bouwman, l.I., Vaezirad, M.M., van Putten, J.P.M., 2013. Unique features of chicken Toll-like receptors. Dev. Comp. Immunol. 41, 316–323.

Keestra, A.M., de Zoete, M.R., van Aubel, R.A.M.H., van Putten, J.P.M., 2007. The central leucine-rich repeat region of chicken TLR16 dictates unique ligand specificity and species- interaction with TLR2. J. Immunol. 178, 7110–7119.

Kidd, P., 2003. Th1/Th2 balance: the hypothesis, its limitations, and implications for health and disease. Alternative Med. Rev. 8, 223–246.

Kinnebrew, M.A., Pamer, E.G., 2012. Innate immune signaling in defense against intestinal microbes. Immunol. Rev. 245, 113–131.

Kobayashi, T., Matsuoka, K., Shiekh, S.Z., Russo, S.M., Mishima, Y., Collins, C., deZoeten, E.F., Karp, C.L., Ting, J.P.Y., Sartor, R.B., Plevy, S.E., 2012. IL-10 regulates *Il12b* expression via histone deacetylation: implications for intestinal macrophage homeostasis. J. Immunol. 189, 1792–1799.

Kogut, M.H., 2013. The gut microbiome and host innate immunity: regulators of host metabolism and metabolic diseases in poultry? J. Appl. Poultry Res. 22, 637–646.

Kogut, M.H., 2018. The effect of microbiome modulation on the intestinal health of poultry. An. Feed Sci. Technol. 26, 605–612.

Kogut, M.H., Arsenault, R.J., 2017. Immunometabolic phenotype alterations associated with the induction of disease tolerance and persistent asymptomatic infection of *Salmonella* in the chicken intestine. Front. Immunol. 8. Article 372.

Kogut, M.H., Muhammed, I., He, H., Philbin, V., Kaiser, P., Smith, A., 2005. Expression and function of Toll-like receptors in chicken heterophils. Develop. Comp. Immunol. 29, 791–807.

Kogut, M.H., Rothwell, L., Kaiser, P., 2005a. Interferon-γ upregulates the expression of proinflammatory and Th1 cytokine mRNA in chicken heterophils during receptor-mediated phagocytosis of opsonized and nonopsonized *Salmonella enterica* serovar Enteritidis. J. IFN Cytokine Res. 25, 73–81.

Kogut, M.H., He, H., Genovese, K.J., Jiang, Y., 2010. Feeding the BT cationic peptides to chickens at hatch reduces cecal colonization by *Salmonella enterica* serovar Enteritidis and primes innate immune cell functional activity. Foodborne Path. Dis. 7, 23–30.

Kogut, M.H., He, H., Kaiser, P., 2005b. Lipopolysaccharide binding protein/CD14/TLR4-dependent recognition of *Salmonella* LPS induces the functional activation of chicken heterophils and up-regulation of pro-inflammatory cytokine and chemokine gene expression in these cells. An. Biotechnol. 16, 165–181.

Kogut, M.H., Swaggerty, C.L., He, H., Pevzner, I., Kaiser, P., 2006. Toll-like Receptor Agonists Stimulate Differential Functional Activation and Cytokine and Chemokine Gene Expression, vol. 8, pp. 1866–1874.

Kogut, M.H., Genovese, K.J., He, H., Kaiser, P., 2008. Flagellin and lipopolysaccharide up-regulation of IL-6 and CXCLi2 gene expression in chicken heterophils is mediated by ERK1/2-dependent activation of AP-1 and NF-κB signaling pathways. Innate Immun. 14, 213–221.

Kogut, M.H., Genovese, K.J., Nerren, J., He, H., 2012. Effects of avian triggering receptor expressed on myeloid cells (TREM-A1) activation on heterophil functional activities. Dev. Comp. Immunol. 36, 157–165.

Kogut, M., Yin, X., Yuan, J., Bloom, L., 2017. Gut health in poultry. CAB Rev. 12 (031).

Kopp, E.B., Medzhitov, R., 1999. The Toll0like receptor family and control of innate immunity. Curr. Opin. Immunol. 11, 13–18.

Lackey, D.E., Olefsky, J.M., 2016. Regulation of metabolism by the innate immune system. Nat. Rev. Endocrinol. 12, 15–28.

Lammers, A., Wieland, W.H., Kruijit, L., Jansma, A., Straetemans, T., Schots, A., den Hartog, G., Parmentier, H.K., 2004. Successive immunoglobulin and cytokine expression in the small intestine of juvenile chicken. Dev. Comp. Immunol. 34, 1252–1262.

Land, W.G., 2015. The role of damage-associated molecular patterns (DAMPs) in human diseases. Sultan Qaboos Univ. Med. J. 15, e157–e170.

Lawley, T.D., Walker, A.W., 2013. Intestinal colonization resistance. Immunology 138, 1–11.

Lee, M.O., Jang, H.J., Rengaraj, D., Yang, S.-Y., Han, J.Y., Lamont, S.J., Womack, J.E., 2016. Tissue expression and antibacterial activity of host defense peptides in chicken. BMC Vet. Res. 12, 231.

Lee, Y.K., Mazmanian, S.K., 2010. Has the microbiota played a critical role in the evolution of the adaptive immune system? Science 330, 1768–1773.

Leonel, A.J., Alvarez-Leite, J.I., 2012. Butyrate: implications for intestinal function. Curr. Opin. Clin. Nutr. Metab. Care 15, 474–479.

Levy, M., Thiass, C.A., Katz, M.N., Suez, J., Elinav, E., 2015. Inflammasomes and the microbiota – partners in the preservation of mucosal homeostasis. Semin. Immunopathol. 37, 39–46.

Levy, M., Blacher, E., Elinav, E., 2017. Microbiome, metabolites and host immunity. Curr. Opin. Microbiol. 35, 8–15.

Levy, M., Thiass, C.A., Elinav, E., 2016. Metabolites: messengers between the microbiota and the immune system. Genes Dev. 30, 1589–1597.

Lian, L., Ciraci, C., Chang, G., Hu, J., Lamont, S.J., 2012. NLRC5 knockdown in chicken macrophages alters response to LPS and poly (I:C) stimulation. BMC Vet. Res. 8, 23.

Litvak, Y., Baumler, A.J., 2019. Microbiota-nourishing immunity: a guide to understanding our microbial self. Immunity 51, P214–P224.

Liu, X., Ma, T., Wang, H., Sheng, Z., Dou, X., Wang, K., Li, Z., Pan, Z., Chang, G., Chen, G., 2015. Up-regulation of NLRC5 and NF-κB signaling pathway in carrier chickens challenged with *Salmonella enterica* serovar Pullorum at different persistence periods. Indian J. Biochem. Biophys. 52, 132–139.

Liu, S., da Cunha, A.P., Rezende, R.M., Cialic, R., Wei, Z., Bry, L., Comstock, L., Gandhi, R., Weiner, H.L., 2016. The host shapes the gut microbiota via fecal microRNA. Cell Host Microbe 19, 32–43.

Liu, H., He, T., Becker, S., Zhang, G., Li, D., Ma, X., 2018. Butyrate: a double-edged sword for health? Ad. Nutr. 9, 21–29.

Loftus, R.M., K Finlay, D., 2016. Immunometabolism: cellular metabolism turns immune regulator. J. Biol. Chem. 291, 1–10.

Loo, Y.-M., Gale Jr., M., 2011. Immune signaling by RIG-I-like receptors. Immunity 34, 680–692.

Lowry, V.K., Farnell, M.B., Ferro, P.J., Swaggerty, C.L., Bahl, A., Kogut, M.H., 2005. Purified beta-glucan as an abiotic feed additive up-regulates the innate immune response in immature chickens against *Salmonella enterica* serovar enteritidis. Int. J. Food Microbiol. 98, 309–318.

Lynn, D.J., Higgs, R., Loyd, A.T., O'Farrelly, C., Herve-Grepinet, V., Brinkman, F.S.L., Yu, P.-L., Soulier, A., Kaiser, P., Zhang, G., Lehrer, R.I., 2007. Avian beta-defensin nomenclature: a community proposed update. Immunol. Lett. 110, 86–89.

MacKinnon, K.M., He, H., Kogut, M.H., 2009. Expression profile of Toll-like receptors within the gastrointestinal tract of 2-day-old *Salmonella enteriditis*-infected broiler chickens. Vet. Microbiol. 137, 313–319.

Macpherson, A.J., Slack, E., Geuking, M.B., McCoy, K.D., 2009. The mucosal firewalls against commensal intestinal microbes. Semin. Immunopathol. 31, 145–149.

Magor, K.E., Navarro, D.M., Barber, M.R.W., Petkau, K., Fleming-Canepa, X., Blyth, G.A.D., Blaine, A.H., 2013. Defense genes: missing from the flight division. Dev. Comp. Immunol. 41, 377–388.

Mansour, S.C., Pena, O.M., Hancock, R.E.W., 2014. Host defense peptides: front-line immunomodulators. Trend Immunol. 35, 443–450.

Mantis, N.J., J Forbes, S., 2010. Secretory IgA: arresting microbial pathogens at epithelial borders. Immunol. Invest. 39, 383–406.

Margioris, A.N., 2009. Fatty acids and postprandial inflammation. Curr. Opin. Clin. Nutr. Metab. Care 12, 127–137.

Martinez-Cummer, M.A., 2015. Immunogenic ingredients in poultry: applications of innovative concepts leading to sustainable solutions for improved productivity. Aust. Poult. Sci. Proc. 2105, 209–212.

Maslowski, K.M., Mackay, C.R., 2011. Diet, gut microbiota, and immune responses. Nat. Immunol. 12, 5–9.

McCraken, V.J., Gaskins, H.R., 1999. Probiotics and the immune system. In: Tannock, G.W. (Ed.), Probiotics: A Critical Review. Horizon Scientific Press, Norfolk, England, pp. 85–111.

McDonald, C., Inohara, N., Nunez, G., 2005. Peptidoglycan signaling in innate immunity and inflammatory disease. J. Biol. Chem. 280, 20177–20180.

McGettrick, A.F., O'Neill, L.A., 2013. How metabolism generates signals during innate immunity and inflammation. J. Biol. Sci. 288, 22893–228898.

Medzhitov, R., 2001. Toll-like receptors and innate immunity. Nat. Rev. Immunol. 1, 135–145.

Medzhitov, R., 2007. Recognition of microorganisms and activation of the immune response. Nature 449, 819–826.

Medzhitov, R., 2008. Origin and physiological roles of inflammation. Nature 454, 428–435.

Medzhitov, R., Janeway Jr., C.A., 1997a. Innate immunity: impact of the adaptive immune response. Curr. Opin. Immunol. 9, 4–9.

Medzhitov, R., Janeway Jr., C.A., 1997b. Innate immunity: the virtues of a nonclonal system of recognition. Cell 91, 295–298.

Medzhitov, R., Janeway, C.A., 2002. Decoding the patterns of self and nonself by the innate immune response. Science 296, 298–300.

Meng, X., Slominski, B.A., Nyachoti, C.M., Campbell, L.D., Geunter, W., 2005. Degradation of cell wall polysaccharides by combinations of carboxylase enzymes and their effect on nutrient utilization and broiler chicken performance. Poultry Sci. 84, 37–47.

Moretti, J., Roy, S., Bozec, D., Martinez, J., Chapman, J.R., Ueberheide, B., Lamming, D.W., Chen, Z.J., Horng, T., Yeretssian, G., Green, D.R., Blander, J.M., 2017. STING senses microbial viability to orchestrate stress-mediated autophagy of the endoplasmic reticulum. Cell 171, 809–823.

Myhre, A.E., Aasen, A.O., Thiermann, C., Wang, J.E., 2006. Peptidoglycan- an endotoxin in its own right? Shock 25, 227–235.

Nathan, C., 2002. Points of control in inflammation. Nature 420, 846–852.

Neerukonda, S.N., Katneni, U., 2020. Avian pattern recognition sensing and signaling. Vet. Sci. 7. Article 14.

Nerren, J.R., Kogut, M.H., 2009. The selective Dectin-1 agonist, curdlan, induces an oxidative burst response in chicken heterophils and peripheral blood monocytes. Vet. Immunol. Immunopathol. 127, 162–166.

Netea, M.G., Quintin, J., van der Meer, J.W., 2011. Trained immunity: a memory for innate host defense. Cell Host Microbe 9, 355–361.

Netea, M.G., Joosten, L.A.B., Latz, E., Mills, K.H.G., Natoli, G., Stunnenberg, H.G., O'Neill, L.A.J., Xavier, R.J., 2016. Trained immunity: a program of innate immune memory in health and disease. Science 352, aaf1098.

Nicolson, J.K., Holmes, E., Kinross, J., Burcelin, R., Gibson, G., Jia, W., Pattersson, S., 2012. Host-gut microbiota metabolic interactions. Science 336, 1262–1267.

Niewold, T.A., 2014. Gut health, intestinal innate immunity, and performance. Auast. Poult. Sci. Symp. Proc. 2014, 72–77.

Norata, G.D., Caligiuri, G., Chavakis, T., Matarese, G., Netea, M.G., Nicoletti, A., O'Neill, L.A.J., Marelli-Berg, F.M., 2015. The cellular and molecular basis of translational immunometabolism. Immunity 43, 421–434.

Nurmi, E., Nuotio, L., Schneitz, C., 1992. The competitive exclusion concept: development and future. Int. J. Food Microbiol. 15, 237–240.

Oakley, B.B., Lillhoj, H.S., Kogut, M.H., Kim, W.K., Maurer, J.J., Pedroso, A., Lee, M.D., Collett, S.R., Johnson, T.J., Cox, N.A., 2014. The chicken gastrointestinal microbiome. FEMS Microbiol. Lett. 360, 100–112.

Oven, I., Rus, K.R., Dusanic, D., Bencina, D., Keeler, C.L., Narat, M., 2013. Diacylated lipoprotein from *Mycoplasma synoviae* mediated TLR15 induced innate immunity responses. Vet. Res. 44. Article 99.

O'Mahony, C., Scully, P., O'Mahony, D., Murphy, S., O'Brien, F., Lyons, A., Sherlock, G., MacSharry, J., Kiely, B., Shanahan, F., O'Mahony, L., 2008. Commensal-induced regulatory T cells mediate protection against pathogen-stimulated NF-κB activation. PLoS Pathog. 11, e100112.

O'Neill, L.A.J., Hardie, D.G., 2013. Metabolism of inflammation limited by AMPK and pseudo-starvation. Nature 493, 346–355.

O'Neill, L.A.J., Kishton, R.J., Rathmell, J., 2016. A guide to immunometabolism for immunologists. Nat. Rev. Immunol. 16, 553–565.

Pallson-McDermott, E.M., O'Neill, L.A.J., 2020. Targeting immunometabolism as an anti-inflammatory strategy. Cell Res. 30, 300–314.

Palm, N.W., Medzhitov, R., 2009. Pattern recognition receptors and control of adaptive immunity. Immunol. Rev. 227, 221–233.

Patterson, J.A., Burkholder, K.M., 2003. Application of prebiotics and probiotics in poultry production. Poultry Sci. 82, 627–631.

Pedra, J.H.F., Cassel, S.L., Sutterwala, F.S., 2009. Sensing pathogens and danger signals by the inflammasome. Curr. Opin. Immunol. 21, 10–16.

Pleidrup, A., Norup, L.R., Dalgaard, T.S., Kaiser, P., Permin, A., Schou, T.W., Vadakaer, D.F., Jungersen, G., Soresen, P., Juul-Madsen, H.R., 2019. Cytokine gene expression profiles in chicken spleen and intestinal tissues during *Ascaris galli* infection. Vet. Parasitol. 206, 317–321.

Postler, T.S., Ghosh, S., 2017. Understanding the holobiont: how microbial metabolites affect human health and shape the immune system. Cell Metabol. 26, 110–130.

Powell, F., Rothwell, L., Clarkson, M., Kaiser, P., 2009. The turkey, compared to the chicken, fails to mount an effective early immune response to *Histomonas meleagridis* in the gut; towards an understanding of the mechanisms underlying the differential survival of poultry species. Parasite Immunol. 31, 312–327.

Pucino, V., Bombardieri, M., Pitzalis, C., Mauro, C., 2017. Lactate at the crossroads of metabolism, inflammation, and autoimmunity. Eur. J. Immunol. 47, 14–21.

Quinteiro-Filho, W.M., Rodrigues, M.V., Ribeiro, A., Ferraz-de-Paula, V., Pinheiro ML, M.L., Sa, L.R.M., Ferreira, A.J.P., Palermo-Neto, J., 2012. Acute heat stress impairs performance parameters and induces mild intestinal enteritis in broiler chickens: role of acute hypothalamic-pituitary adrenal axis activation. J. Anim. Sci. 90, 1986−1994.

Reid, W.D.K., Close, A.J., Humphrey, S., Chaloner, G., Lacharme-Lora, L., Rothwell, L., Kaiser, P., Williams, N.J., Humphrey, T.J., Wigley, P., Rushton, S.P., 2016. Cytokine responses in birds challenged with the human food-borne pathogen *Campylobacter jejuni* implies a Th17 response. R. Soc. Open Sci. 3, 150541.

Robinson, K., Deng, Z., Hou, Y., Zhong, G., 2015. Regulation of the intestinal barrier function by host defense peptides. Front. Vet. Sci. 2. Article 57.

Rock, R.L., Kono, H., 2008. The inflammatory response to cell death. Annu. Rev. Pathol. 3, 99−126.

Rock, F.L., Hardiman, G., Timans, J.C., Kastelein, R.A., Bazan, J.F., 1998. A family of human receptors structurally related to *Drosophila* toll. Proc. Natl. Acad. Sci. U.S.A. 95, 588−593.

Round, J.L., Mazmanian, S.K., 2009. The gut microbiota shapes intestinal immune responses during health and disease. Nat. Rev. Immunol. 9, 313−323.

Round, J.L., Mazmanian, S.K., 2010. Inducible Foxp3+ regulatory T-cell development by a commensal bacterium of the intestinal microbiota. Proc. Natl. Acad. Sci. U.S.A. 107, 12204−12209.

Rock, R.L., Latz, E., Ontiveros, F., Kono, H., 2010. The sterile inflammatory response. Annu. Rev. Immunol. 28, 321−342.

Round, J.L., Lee, S.M., Li, J., Tran, G., Jabri, B., Chatila, T.A., Mazmanian, S.K., 2011. The Toll-like receptor 2 pathway establishes colonization by a commensal of the human microbiota. Science 332, 974−977.

Rubartelli, A., Lotze, M.T., Latz, E., Manfredi, A., 2013. The mechanisms of sterile inflammation. Front. Immunol. 4. Article 398.

Sacranie, A., Iji, P.A., Mikkelson, L.L., Choct, M., 2007. Occurrence of reverse peristalsis in broiler chickens. Aust. Poult. Sci. Proc. 2007, 161−164.

Sander, L.E., Davis, M.J., Boekschoten, M.V., Amsen, D., Dascher, C.C., Ryffel, B., Swanson, J.A., Muller, M., Blander, J.M., 2011. Detection of prokaryotic mRNA signifies microbial viability and promotes immunity. Nature 474, 385−389.

Sansonetti, P.J., 2004. War and peace at mucosal surfaces. Nat. Rev. Immunol. 4, 953−964.

Sansonetti, P.J., Medzhitov, R., 2009. Learning tolerance while fighting ignorance. Cell 138, 416−420.

Sassone-Corsi, M., Raffatellu, M., 2015. No vacancy: how beneficial microbes cooperate with immunity to provide colonization resistance to pathogens. J. Immunol. 194, 4089−4093.

Sato, T., Kato, H., Yoneyama, M., Sato, S., Matsushita, K., Tsujimura, T., Fujita, T., Akira, S., Takeuchi, O., 2010. LGP2 is a positive regulator of RIG-1 and MDA5-mediated antiviral responses. Proc. Natl. Acad. Sci. U.S.A. 107, 1512−1517.

Scapini, L.B., de Cristo, A.B., Schmidt, J.M., Buzim, R., Nogueira, L.K., Palma, S.C., Fernandes, J.I.M., 2019. Effect of β-mannanse supplementation in conventional diets on the performance, immune competence, and intestinal quality of broilers challenged with *Eimeria* sp. J. Appl. Poult. Res. 28, 1048−1057.

Schat, K.A., Myers, T.J., 1991. Avian intestinal immunity. Crit. Rev. Poult. Biol. 3, 19.

Schokker, D., Hoekman, A.J., Smits, M.A., Rebel, J.M., 2009. Gene expression patterns associated with chicken jejunal development. Dev. Comp. Immunol. 33, 1156−1164.

Shakouri, M.D., iji, p.A., Mikkelsen, L.L., Cowieson, A.J., 2009. Intestinal function and gut microflora of broiler chickens as influenced by cereal grains and microbial enzyme supplementation. J. Anim. Physiol. Anim. Nutr. 93, 647−658.

Shanmugasundaram, R., Selvaraj, R.K., 2010. In vitro human TGF-beta treatment converts $CD4^{+}CD25^{-}$ T cells into induced T regulatory like cells. Vet. Immunol. Immunopathol. 137, 161−165.

Shanmugasundaram, R., Selvaraj, R.K., 2011. Regulatory T cell properties of chicken $CD4^{+}CD25^{+}$ cells. J. Immunol. 186, 1997−2002.

Shenderov, B.A., 2012. Gut indigenous microbiota and epigenetics. Microb. Ecol. Health Dis. 2012, 23.

Shi, N., Xi, N., Duan, X., Niu, H., 2017. Interaction between the gut microbiome and mucosal immune system. Mil. Med. Res. 4, 14.

Singh, N., Shirdel, E.A., Waldron, L., Zhang, R.-H., Jurisca, I., Cornelli, E.M., 2012. The murine caecal microRNA signature depends on the presence of the endogenous microbiota. Int. J. Biol. Sci. 8, 171−186.

Slominski, B.A., 2011. Review: recent advances in research on enzymes for poultry diets. Poultry Sci. 90, 2013−2023.

Smith, D.W., Nagler-Anderson, C., 2005. Preventing intolerance: the induction of nonresponsiveness to dietary and microbial antigens in the intestinal mucosa. J. Immunol. 174, 3851−3857.

Sommer, F., Backhead, F., 2013. The gut microbiota- masters of host development and physiology. Nat. Rev. Microbiol. 11, 227−238.

Sommer, F., Anderson, J.M., Bharti, R., Raes, J., Rosenstiel, P., 2017. The resilience of the intestinal microbiota influences health and disease. Nat. Rev. Microbiol. 15, 630−638.

Song, B., Li, H., Wu, Y., Zhen, W., Wang, Z., Xia, Z., Gao, Y., 2017. Effect of microencapsulated sodium butyrate dietary supplementation on growth performance and intestinal barrier function of broiler chickens infected with necrotic enteritis. Anim. Feed Sci. Technol. 232, 6−15.

Stecher, B., Robbiani, R., Walker, A.W., Westendorf, A.M., Barthel, M., Kremer, M., Chaffron, S., MacPerson, A.J., Buer, J., Parkhill, J., Dougan, G., von Mering, C., Hardt, W.-D., 2007. *Salmonella enterica* serovars Typhimurium exploits inflammation to compete with the intestinal microbiota. PLoS Biol. 5, e244.

Takeda, K., Kaisho, T., Akira, S., 2010. Toll-like receptors. Annu. Rev. Immunol. 21, 335−376.

Takeuchi, O., Akira, S., 2010. Pattern recognition receptors and inflammation. Cell 140, 805−810.

Tang, Y., Foster, N., Jones, M.A., Barrow, P.A., 2018. Model of persistent *Salmonella* infection: *Salmonella enterica* serovar Pullorum modulates the immune response of the chicken from a Th17-type response towards a Th2-type response. Infect. Immun. 86, e000307−e000318.

Tannahil, G.M., Curtis, A.M., Adamik, J., Palsson-McDermott, E.M., McGettrick, A.E., Goel, G., Frezza, C., Bernard, N.J., Kelly, B., Foley, N.H., Zheng, L., Gardet, A., Tong, Z., Jany, S.S., Corr, S.C., Haneklaus, S.M., Caffrey, B.E., Pierce, K., Walmsley, S., Beasley, F.C., Cummins, E., Nizet, V., Whyte, M., Taylor, C.T., Lin, H., Masters, S.L., Gottlieb, E., Kelly, V.P., Clish, C., Auron, P.E., Xaviers, R.J., O'Neill, L.A., 2013. Succinate is an inflammatory signal that induces IL-1β through HIF1-α. Nature 496, 238−242.

Tao, Z.Y., Zhu, C.H., Shi, Z.H., Song, C., Xu, W.J., Song, W.T., Zou, J.M., Qin, A.T., 2015. Molecular characterization, expression, and functional analysis of NOD1 in Qingyun partridge chicken. Genet. Mol. Res. 14, 2691–2701.

Temperley, N.D., Berlin, S., Paton, I.R., Griffin, D.K., Burt, D.W., 2008. Evolution of the chicken Toll-like receptor gene family: a story of gene gain and gene loss. BMC Genom. 9, 62.

Thaiss, C.A., Levy, M., Suez, J., Elinav, E., 2014. The interplay between the innate immune system and the microbiota. Curr. Opin. Immunol. 26, 41–48.

Thaiss, C.A., Zmora, N., Levy, M., Elinav, E., 2016. The microbiome and innate immunity. Nature 535, 65–74.

Townes, C.L., Michailidis, G., Nile, C.J., Hall, J., 2004. Induction of cationic chicken liver-expressed antimicrobial peptide 2 in response to *Salmonella enterica* infection. Infect. Immun. 12, 6987–6993.

Townes, C.L., Michailidis, G., Hall, J., 2009. The interaction of the antimicrobial peptide cLEAP-2 and the bacterial membrane. Biochem. Biophys. Res. Commun. 387, 500–503.

Tretter, L., Patocs, A., Chinopoulas, C., 2016. Succinate, an intermediate in metabolism, signal transduction, ROS, hypoxia, and tumorigenesis. Biochim. Biophys. Acta 288, 22893–22898.

Truong, A.D., Hoang, C.T., Hong, Y., Lee, J., Lee, K., Lillehoj, H.S., Hong, Y.H., 2017. Functional analyses of the interaction of chicken interleukin 23 subunit p19 with IL-12 subunit p40 to form the IL-23 complex. Mol. Immunol. 92, 54–67.

Ugolini, M., Gerhard, J., Bukurth, F., Sur, S., Dittrich, N., Gaddam, S., Conrad, M.L., Benn, C.S., Blohm, U., Gruber, A.D., Hutlof, A., Hartmann, S., Boekschoten, M.V., Muller, M., Jungersen, G., Schumann, R.R., Suttorp, N., Sander, L.E., 2018. Recognition of microbial viability via TLR8 drives T_{FH} cell differentiation and vaccine responses. Nat. Immunol. 19, 386–396.

Usami, M., Kishimoto, K., Ohata, A., Miyoshi, M., Aoyama, M., Fueda, Y., Kotani, J., 2008. Butyrate and trichostatin A attenuate nuclear factor κB activation and tumor necrosis factor α secretion and increase prostaglandin E_2 secretion in human peripheral blood mononuclear cells. Nutr. Res. 28, 321–328.

Vaishnava, S., Yamamoto, M., Severson, K.M., Ruhn, K.A., Yu, X., Koren, O., Ley, R., Edward, K., 2011. The antibacterial lectin RegIIIγ promotes the spatial segregation of microbiota and host in the intestine. Science 334, 255–258.

Van der Wielen, P.W.J.J., Biesterveld, S., Notermans, S., Hofstra, H., Urlings, B.A., van Knapen, F., 2000. Role of volatile fatty acids in development of the cecal microflora in broiler chickens during growth. Appl. Environ. Microbiol. 66, 3536-2540.

van Dijk, A., Herrebout, M., Tersteeg-Zijderveld, M.H.G., Tjeerdsma-van Bokhoven, J.L.M., Bleumink-Pluym, N., Jansman, A.J.M., Veldhuizen, E.J.A., 2012. *Campylobacter jejuni* is highly susceptible to killing by chicken host defense peptide cathelicidin-2 and suppresses intestinal cathelicidin-2 expression in young broilers. Vet. Microbiol. 160, 347–354.

Wang, P., Zhu, S., Yang, L., Cui, S., Pan, W., Jackson, R., Zheng, Y., Rongvau, A., Sun, Q., Yang, G., Gan, S., Liu, R., You, F., Flavell, R., Fikrig, E., 2015. Nlrp6 regulates intestinal antiviral innate immunity. Science 350, 826–830.

Weinberg, S.E., Sena, L.A., Chandel, N.S., 2015. Mitochondria in the regulation of innate and adaptive immunity. Immunity 42, 405–417.

Winter, S.E., Winter, M.G., Xavier, M.N., Thiennimitr, P., Poon, V., Keestra, A.M., Laughlin, R.C., Gomez, G., Wu, J., Lawhon, S.D., Popova, I., Parikh, S.J., Adams, L.G., Tolis, R.M., Stewart, V.J., Baumler, A.J., 2013. Host-derived nitrate boosts growth of *E. coli* in the inflamed gut. Science 339, 708–711.

Withanage, G.S.K., Wigley, P., Kaiser, P., Mastroeni, P., Brooks, H., Powers, C., Beal, R., Barrow, P.A., Maskell, D., McConnell, I., 2005. Cytokine and chemokine responses associated with clearance of a primary *Salmonella enterica* serovar Typhimurium infection in the chicken and in protective immunity to rechallenge. Infect. Immun. 73, 5173–5182.

Woo, V., Alenghat, T., 2007. Host-microbiota interactions: epigenomic regulation. Curr. Opin. Immunol. 44, 52–60.

Xiao, Y., Cai, Y., Bommineni, Y.R., Fernando, S.C., Prakash, O., Gilliland, S.E., Zhang, G., 2006. Identification and functional characterization of three chicken cathelicidins with potent antimicrobial activity. J. Biol. Chem. 281, 2858.

Ye, J., Yu, M., Zhang, K., Liu, J., Wang, Q., Tao, P., Jia, K., Liao, M., Ning, Z., 2015. Tissue-specific expression pattern and histological distribution of NLRP3 in Chinese yellow chicken. Vet. Res. Commun. 39, 171–177.

Yilmaz, A., Shen, S., Adelson, D.L., Xavier, S., Zhu, J.J., 2005. Identification and sequence analysis of chicken Toll-like receptors. Immunogenetics 56, 743–753.

Zanetti, M., 2005. The role of cathelicidins in the innate host defenses of mammals. Curr. Issues Mol. Biol. 7, 179–196.

Zasloff, M., 2002. Antimicrobial peptides if multicellular organisms. Nature 415, 389–395.

Zeng, M.Y., Inohara, N., Nunez, G., 2017. Mechanisms of inflammation-driven bacterial dysbiosis in the gut. Mucosal Immunol. 10, 18–26.

Zhang, G., Sunkara, L.T., 2014. Avian antimicrobial host defense peptides: from biology to therapeutic applications. Pharmaceuticals 7, 220–247.

Zou, X., Ji, J., Qu, H., Wang, J., Shu, D.M., Wang, Y., Liu, T.F., Li, Y., Luo, C.L., 2019. Effects of sodium butyrate on intestinal health and gut microbiota composition during intestinal inflammation progression in broilers. Poultry Sci. 98, 4449–4456.

Chapter 25

Carbohydrate metabolism

Colin G. Scanes[1,2]

[1]Department of Biological Sciences, University of Wisconsin, Milwaukee, WI, United States; [2]Center of Excellence for Poultry Science, University of Arkansas, Fayetteville, AR, United States

Abbreviations

E. coli *Escherichia coli*
EGF epidermal growth factor
GLUT glucose transporter
LDH lactate dehydrogenase
LPS lipopolysaccharide
mM millimolar or millimoles per liter
RQ respiratory quotient
SEM standard error of mean
UTP uridine triphosphate

25.1 Overview of carbohydrate metabolism in birds

25.1.1 Introduction

Carbohydrate metabolism in birds has close similarities to that in mammals. Glucose is absorbed in the small intestine. Glucose can be used for energy via glycolysis, the citric acid cycle, or the pentose pathway. Some tissues only use glucose, being incapable of using fatty acids. Glucose can be stored as the polysaccharide glycogen in the liver, muscles, and other tissues or used as a substrate to produce fatty acids (lipogenesis). Glucose can be synthesized from lactate, amino acids, and other gluconeogenic precursors in the liver and kidneys. The differences between avian and mammalian carbohydrate metabolism include the following:

- The very high circulating concentrations of glucose in birds (discussed in more detail in Section 25.2)
- The site of lipogenesis being the liver

Several caveats need to be introduced. The energetic needs for extended flight are met using fatty acids, not glucose. Discussion of carbohydrate metabolism in birds is hampered by the preponderance of evidence coming from studies in domesticated birds, particularly from a single species, the chicken. The control of carbohydrate metabolism of (and hence circulating glucose concentrations by), the pancreatic hormones, glucagon, and insulin is addressed elsewhere in this volume.

The respiratory quotient (RQ) (carbon dioxide released divided by the oxygen consumed) informs as to the major substrate being used by an animal for energy. If the RQ is 1.0, carbohydrate (glucose) is the major substrate. If the RQ is 0.7, triglyceride (fatty acids) is the major substrate. If amino acids are being used for energy, the RQ is 0.8−0.9. Table 25.1 summarizes the RQ for a number of avian species. Birds seem to have an RQ of either 0.7 or 1.0, indicating that they are using either triglyceride/fatty acids or glucose. An RQ of 1.1 and greater, as reported in young chickens (Geelissen et al., 2006), reflects glucose utilization for energy production and fatty acid synthesis together with triglyceride deposition. When there is a shift from use of glucose to fatty acids predominantly, there is a decrease in RQ. For instance, the RQ decreases to 0.7 during fasting in the house sparrows (*Passer domesticus*), hummingbirds, and chickens during the nocturnal fast from $\sim$ 0.9 to $<$0.7 (see Table 25.1). 15.6 $\pm$ 0.24 (247)

25.2 Carbohydrate chains in glycoproteins

Sugar chains consisting of monosaccharides such as galactose and *N*-acetylneuraminic acid (sialic acid) play critical roles in the functionality of proteins. Egg albumen proteins are glycosylated in the magnum with this being employed to produce glycosylated proteins in transgenic chicken expression systems (Mizutani et al., 2011). Further examples of the functionality of the carbohydrates (sialyl-galactose) chains is in colonic epithelial cells that bind viruses (quail and chicken: Guo et al., 2007). Similarly, sialyl-galactose linkages affect binding of viruses to the chick embryo amnion and allantois (Ito et al., 1997).

Sturkie's Avian Physiology. https://doi.org/10.1016/B978-0-12-819770-7.00005-0

TABLE 25.1 Examples of respiratory quotients reported in birds.

Species	RQ	Reference
Chicken (*Gallus gallus*) fed	~1.0 or 1.1 or greater	Brackenbury and El-Sayed (1985); Geelissen et al. (2006)
Chicken exercising	0.97	Brackenbury and El-Sayed (1985)
Chicken fasted	0.7	Boshouwers and Nicaise (1981)
House sparrow (*Passer domesticus*) fed	0.9 or ~1.0	Walsberg and Wolf (1995)
House sparrow fasted	0.7	Walsberg and Wolf (1995); Khalilieh et al. (2012)
Rufous hummingbirds (*Selasphorus rufus*) or Anna's hummingbirds (*Calypte anna*) feeding on nectar	1.0	Welch et al. (2007); Suarez et al. (2011)
Rufous or Anna's hummingbirds fasted	0.7	Suarez et al. (1990, 2011); Welch et al. (2007)
Carnivorous birds: Sparrow hawks (*Falco sparverius*), long-eared owls (*Asio otus*), saw whet owl (*Aegoliusa cadicus*)	0.74–0.78	Gatehouse and Markham (1970)

25.2.1 Glucose

Glucose is a simple sugar, specifically a hexose. It is a major carbohydrate in the circulation of birds (discussed in section 25.2.1). It is transported into cells by glucose transporters (GLUTs) (see section 25.6) and after phosphorylation is metabolized by glycolysis (section 25.7.2) and then the aerobic tricarboxylic cycle pathway (see section 25.7.3). Alternatively, glucose can be converted to fatty acids (in lipogenesis predominantly in the liver) or into glycogen in the liver and muscles (see section 25.4).

25.2.1.1 Circulating concentrations of glucose across avian species

25.2.1.1.1 Introduction: circulating concentrations of glucose across avian species

The major circulating carbohydrate in birds is glucose. The mean circulating concentration of glucose in birds is 15.6 + 0.24 [standard error of mean (SEM); number of species (n) = 248; Table 25.2]. There are higher circulating concentrations of glucose in *Neognathae* than in the flightless ratites. There are marked differences between circulating concentrations of glucose between birds and mammals, with avian concentrations more than double those in mammals; for instance, plasma concentrations of glucose in fed and fasting rats were, respectively, 7.9 and 4.9 mM (Simon et al., 2011). The control of circulating concentrations of glucose by the pancreatic hormones, glucagon and insulin, is addressed elsewhere in this volume.

In mammals, there is a relationship between circulating concentration of glucose and body weight: the circulating concentration of glucose in mM = 7.6 − 0.44 log body mass in kilograms (Beuchat and Chong, 1998; Braun and Sweazea, 2008). In birds, a similar relationship was reported by Braun and Sweazea (2008): the circulating concentration of glucose in mM = 15.3−0.44 log body mass in kilograms. For birds, the y-intercept of the line at 1 kg is 15.3 mM (or 275 mg/dL) in wild birds (Braun and Sweazea, 2008). The basis for this relationship between circulating concentrations of glucose and body weight is not clearly established. No such relationship was observed by Beuchat and Chong (1998). There is frequently a dichotomy in the literature between research on wild and domesticated species. The analysis of circulating concentrations of glucose included only wild species.

25.2.1.1.2 Domestication and circulating concentrations of glucose

There is conjecture that domestication and intensive selection have influenced glucose metabolism and circulating concentrations of glucose, although there is also some against this theory. The circulating concentrations of glucose in wild turkeys (*Meleagris gallopavo*) are more than 50% greater than those in domestic turkeys (Lisano and Kennamer, 1977; Anthony et al., 1990; see Table 25.3). In contrast, the circulating concentrations of glucose were higher in domestic than wild geese (Gee et al., 1981; Sitbon and Mialhe, 1979; see Table 25.3). A small study directly compared red jungle fowl (*Gallus gallus*, from which chickens are thought to have been domesticated), Asian village fowl, and commercial broiler chickens (Soleimani and Zulkifli, 2010). No differences were found between circulating concentrations of glucose between red jungle fowl and domesticated chickens (Table 25.3). Moreover, there are no discernible differences between the circulating

TABLE 25.2 Circulating concentrations of glucose across the class aves.

Order of birds	Plasma/Serum glucose mM (mmol/L) ± SEM (number of species)
Accipitriformes	17.5 ± 0.71 (23)
Anseriformes	11.6 ± 0.60 (30)
Apodiformes	16.0 ± 0.47 (3)
Charadriiformes	16.9 ± 0.50 (27)
Ciconiiformes	14.7 ± 0.41 (11)
Columbiformes	16.3 ± 0.83 (9)
Coraciiformes	17.7 ± 0.94 (8)
Falconiformes	19.4 ± 1.24 (5)
Galliformes excluding poultry	16.8 ± 0.70 (16)
Gruiformes	14.7 ± 0.71 (14)
Passeriformes	18.0 ± 0.64 (35)
Pelecaniformes	12.0 ± 0.65 (12)
Phoenicopteriformes	11.8 ± 0.53 (4)
Procellariiformes	13.4 ± 1.55 (6)
Psittaciformes	15.0 ± 0.44 (21)
Sphenisciformes	13.3 ± 0.59 (9)
Strigiformes	18.3 ± 0.61 (11)
Trogoniformes	16.7 ± 1.20 (4)
Super-order	
Neognathae	15.7 ± 0.24 (245)
Palaeognathae	10.9 ± 0.84 (4)
Class	
Aves	15.6 ± 0.24 (249)

concentrations of glucose in wild or domestic pigeons or ducks (Table 25.3). At present, there are no comprehensive studies comparing chickens with red jungle fowl or domestic turkeys, ducks and geese with wild turkeys, ducks and geese, respectively. These should encompass multiple ages. Moreover, they should be performed in the same laboratory with circulating concentrations of glucose determined by the same methods to ensure consistency.

25.2.1.1.3 Fasting and circulating concentrations of glucose

In some species of birds, circulating concentrations of glucose are depressed by fasting, such as in chickens (Dupont et al., 2008; Christensen et al., 2013), domestic ducks (*Anas platyrhynchos*; Zhang et al., 2005), domestic geese (*Anser anser*; Sitbon and Mialhe, 1979), house sparrows (*P. domesticus*; Khalilieh et al., 2012), hummingbirds [Anna's hummingbird (*Calypte anna*)], Costa's hummingbird (*Calypte costae*), and ruby-throated hummingbirds (*Archilochus colubris*); Beuchat and Chong (1998), and yellow-legged gulls (*Larus cachinnans*; Alonso-Alvarez and Ferrer, 2001). For instance, circulating concentrations of glucose are depressed by 25.3% in adult house sparrows fasted for 24 h (Khalilieh et al., 2012). Similarly, circulating concentrations of glucose decreased by fasting in late juvenile/adult domestic geese, being decreased by 25.4% in birds fasted for 24 h and by 32.5% in geese fasted for four days (Sitbon and Mialhe, 1979). In contrast, circulating concentrations of glucose were not depressed by fasting in other species/studies, such as black vultures (*Coragyps atratus*; Migliorini et al., 1973), adult ring doves (*Streptopelia risoria*; Lea et al., 1992), Japanese quail (*Coturnix japonica*; Sartori et al., 1996), Adélie penguins (*Pygoscelis adeliae*; Vleck and Vleck, 2002), Emperor penguins (*Aptenodytes forsteri*; Groscolas and Rodriguez, 1981), Garden warbler (*Silva borin*; Totzke et al., 1998), and juvenile herring gulls (*Larus argentatus*;

TABLE 25.3 Comparison of circulating concentrations of glucose in domesticated birds and wild birds of the same species.

Species	Plasma/Serum concentration of glucose (mM)	Reference
Red jungle fowl/chicken (*Gallus gallus*)		
Red jungle fowl	13.3	Soleimani and Zulkifli (2010)
Fed chickens (15 studies)	13.1	Scanes (2008); Simon et al. (2011)
Turkey (*Meleagris gallopavo*)		
Wild Turkey	19.7	Lisano and Kennamer (1977)
Domestic Turkey refed	11.5	Anthony et al. (1990)
Duck (*Anas platyrhynchos*)		
Wild duck or mallard	11.5	Fairbrother et al. (1990)
Domestic duck	10.0	Applegate et al. (1999); Zhang et al. (2005)
Goose (*Anser anser*)		
Wild or Embden goose	12.3	Gee et al. (1981)
Domestic goose	15.6	Sitbon and Mialhe (1979)
Pigeons (*Columba livia*)		
Wild or rock pigeon	15.5	Gayathri et al. (2004)
Domestic or racing pigeon	16.1	Lumeij and de Brujne (1985)

Jeffrey et al., 1985); on the contrary, concentrations were increased in female ring doves (*Streptopelia risoria*; Lea et al., 1992).

25.2.1.1.4 Influence of feeding

As might be expected, circulating concentrations of glucose are influenced by feeding. For instance, plasma concentrations of glucose are depressed at night in chickens when feeding is not occurring (Christensen et al., 2013). Moreover, concentrations of glucose are markedly increased following eating in hummingbirds, with circulating concentrations rising from already high concentrations to >26.5 mM—levels way into the diabetic range in mammals (Fig. 25.1). This is not surprising with the consumption of nectar, which is high in both glucose and fructose. Plasma concentrations of glucose decline rapidly from 41 mM to basal (17 mM) within 1.5 h following feeding in, for instance, Anna's hummingbird (*Calypte anna*) (Beuchat and Chong, 1998). Similarly, oral loading with monosaccharides increases circulating concentrations of glucose in passerine birds (Fig. 25.1) and chickens (Fig. 25.2). Circulating concentrations of glucose return to basal within an hour (Sinsigalli et al., 1987, Fig. 25.2).

25.2.1.1.5 Shifts in circulating concentration with age, reproductive state, and migration

Circulating concentrations of glucose increase markedly during the second half of embryonic development (chickens: Lu et al., 2007; Willemsen et al., 2011) (see Table 25.4).

There is a transient decrease in circulating concentrations of glucose immediately after hatching, followed by a gradual rise over 12 h (chickens: Rinaudo et al., 1982). Circulating concentrations of glucose subsequently decline during posthatch growth and development in chickens (*Gallus gallus*; Sinsigalli et al., 1987, Fig. 25.2). The rate of clearance of glucose after a glucose challenge is slower in older but still juvenile birds, as shown in chickens by Sinsigalli et al. (1987; Fig. 25.2).

There are small sex differences in circulating concentrations of glucose in some birds. For instance, in adult sexually mature quail, there is a small but consistent sex difference in circulating concentrations of glucose, being decreased 6.7% (Itoh et al., 1998) and 17.0% (Scholtz et al., 2009) in females in different reports. In contrast, circulating concentrations of glucose were lower in male than female mallards (Fairbrother et al., 1990).

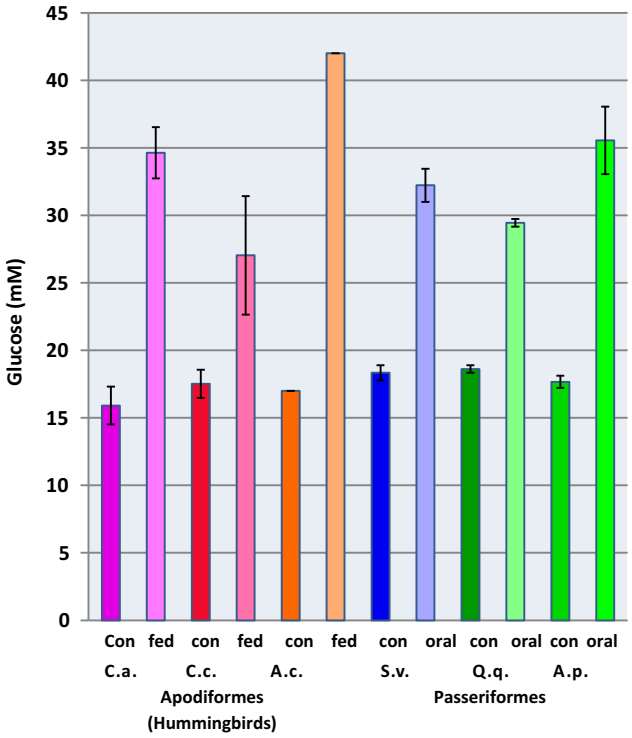

FIGURE 25.1 Effects of nectar-feeding hummingbirds and administering an oral load of 1:1 glucose: fructose (intubated) to Passeriform birds (30 min later). C.a., Anna's hummingbird (*Calypte anna*); C.c., Costa's hummingbird (*Calypte costae*); A.c., ruby-throated hummingbirds (*Archilochus colubris*); S.v., European starlings (*Sturnus vulgaris*); Q.q., common grackles (*Quiscalus quiscula*); A.p., red-winged blackbirds (*Agelaius phoeniceus*). Vertical bars: S.E.M. *Data calculated from Beuchat and Chong (1998) and Martinez del Rio et al. (1988).*

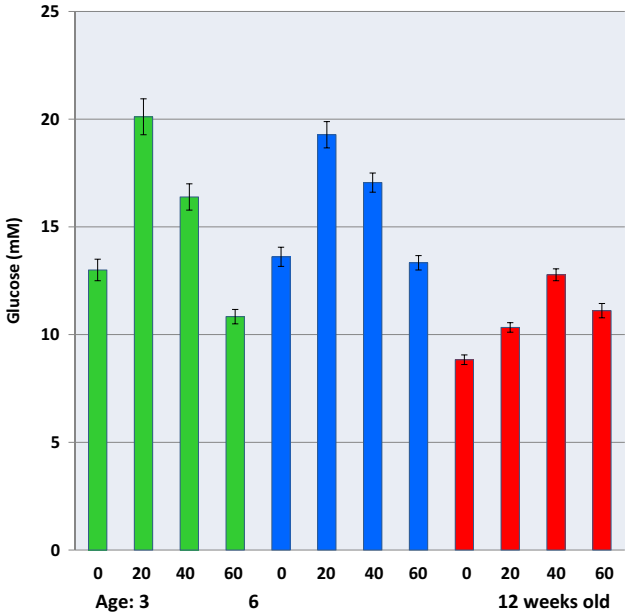

FIGURE 25.2 Effect of glucose load (2 g glucose intubated per kg or 11.1 mmol/kg) on circulating concentrations of glucose at 3, 6, and 12 weeks of age in chickens prior to (0 min) and 20, 40, and 60 min after challenge. *Data from Sinsigalli et al. (1987).*

Some changes have been reported in the circulating concentration of glucose during the breeding cycle. For instance, circulating concentrations of glucose are reduced by 53% in adult pigeons in the middle of period of incubating their eggs, but they recover late in incubation and then rise further after incubation is terminated (Gayathri et al., 2004). Similarly, in ring doves, circulating concentrations of glucose are increased after incubation and when the young squabs are receiving parental care (Lea et al., 1992). A similar reduction in circulating concentrations of glucose is reported in ducks [mallard duck (*Anas platyrhynchos*); Fairbrother et al., 1990].

Prelaying circulating concentrations of glucose correlate well with later reproductive success in raising at least one chick in the greater sage grouse (Dunbar et al., 2005). What is not clear is the physiological basis of the circulating glucose concentrations having a predictive value for reproductive success.

There was little difference in the circulating concentrations of glucose in Canada geese (*Branta canadensis interior*) irrespective of whether it was before or after the

TABLE 25.4 Changes in plasma concentrations of glucose during chick embryonic development and following hatching.

	Plasma glucose concentration Mean ± SEM mg/dL
Embryo day 10	116 ± 3
Embryo day 15	165 ± 5
Embryo day 20	198 ± 8
Day old chick	220 ± 12
Three-day-old chick	233 ± 11

Data from Lu et al. (2007).

spring migration, during the breeding season, or in the period before the fall migration (Mori and George, 1978). An increase was observed after the fall migration (Mori and George, 1978). In contrast, circulating concentrations of glucose are markedly increased in Emperor penguins undergoing both fasting and molting, increasing from a mean (SEM) of 19.7 + 2.4 mM to 28.4 + 6.5 mM (Groscolas and Rodriguez, 1981).

25.2.1.1.6 Shifts in circulating concentrations of glucose due to disease, toxicants, and husbandry practices

There are pathological changes in the circulating concentration of glucose with glucose being an indicator of health. For instance, there was a negative correlation between plasma concentrations of glucose with body condition score [pale-bellied **t**yrant-manakin (*Neopelma pallescens*) (Azeredo et al., 2016)]. Circulating concentrations of glucose are decreased with infectious disease and increased with exposure to toxicants. In the common pheasant, the circulating concentrations of glucose are depressed by severe infection with spironucleosis (Lloyd and Gibson, 2006). Similarly, in chickens with spiking mortality, there are extremely low circulating concentrations of glucose (Davis et al., 1995).

Environmental toxicants can elevate, depress, or have no effect on circulating concentrations of glucose. There is a marked increase in circulating concentrations of glucose in parakeets receiving the organophosphate insecticide quinalphos (rose-ringed parakeet, *Psittacula krameri*; Anan and Maitra, 1995). Circulating concentrations of glucose were depressed in mallard ducks exposed to the polychlorinated biphenol mixture Aroclor 1254 (Fowles et al., 1997). In contrast, there was no change in circulating concentrations of glucose in ducklings with toxicosis due to furazolidone (Webb et al., 1991).

Force feeding is used in some counties to produce *pate de fois gras* in ducks and geese. Circulating concentrations of glucose are increased by force feeding in geese (Sitbon and Mialhe, 1979) and ducks (Zhang et al., 2005).

25.2.1.1.7 Temperature and circulating concentrations of glucose

There are effects of environmental temperature on circulating concentrations of glucose. Not only does fasting for 16 h depress circulating concentrations of glucose (Boussaid-Om Ezzine et al., 2010) but also the effect is greater in birds exposed to elevated temperatures (32°C for a week in broiler chickens; Boussaid-Om Ezzine et al., 2010). Moreover, glucose plus arginine administration to birds with free access to feed evoked a larger increase in circulating concentrations of glucose in the chickens at a higher environmental temperature (Boussaid-Om Ezzine et al., 2010).

25.2.1.1.8 Issues with the circulating concentrations of glucose

Circulating concentrations of glucose are influenced by physiology but may also be influenced by sampling techniques. For instance, there was a transient increase in plasma concentrations of glucose after capture (Darwin's small ground finch: Clark et al., 2018). Unfortunately, some studies employed determination of glucose concentrations in whole blood and thus as comparison with other studies was not possible, these were not included in the analysis.

25.2.1.2 Glucose concentrations in the cerebrospinal fluid

In birds, the concentration of glucose in the cerebrospinal fluid (CSF) is 286 mg/dL (15.8 mmol/L) (Anderson and Hazelwood, 1969). This is ~20% greater than the plasma concentration of glucose. In contrast in mammals, CSF concentrations of glucose are 10−50% below circulating concentrations of glucose (rabbit 19% lower: Guerra-Romero et al., 1992; human 10−50% lower: Verbeek et al., 2016). Insulin depressed CSF concentrations of glucose (chicken: Anderson and Hazelwood, 1969).

25.2.1.3 Glucose concentrations in muscle

Muscle concentrations of glucose are influenced by physiological state being depressed by the stresses of feed withdrawal for 5 h (chicken: Savenije et al., 2002) and with 3 h of transportation (chicken: Wang et al., 2017).

25.3 Lactate and pyruvate

25.3.1 Introduction

Circulating concentrations of lactate are the result of anaerobic glycolysis (see section 25.7.2) in various tissues. Lactate is readily converted to pyruvate, e.g., in muscle (see section 25.7.2.4). Moreover, lactate is one substrate for gluconeogenesis (see section 25.8).

25.3.2 Circulating concentrations of lactate and pyruvate

Basal plasma concentrations of lactate in various avian species are summarized in Table 25.5. These avian plasma concentrations of lactate tend to be higher than those in mammals (Table 25.5). In addition, circulating concentrations of lactate are elevated by exercise or hypoxia (see Table 25.5). For instance, blood concentrations of lactate are markedly elevated during diving in Emperor penguins (*Aptenodytes forsteri*) and decline after dives returning to baseline within 10 min (Ponganis et al., 1997). Similarly, plasma concentrations of lactate are increased after a short-term flight in Northern bald ibis (*Geronticus eremite*) (Bairlein et al., 2015). While blood concentrations of

TABLE 25.5 Examples of basal and stress-induced circulating concentrations of lactate in wild and domesticated birds.

Species	Plasma lactate mmoles/L		Reference
	Basal	Stressed	
American flamingo (*Phoenicopterus ruber*)	8.57	–	Burgdorf-Moisuk et al. (2012)
Bar-headed goose (*Anser indicus*)	1.55	3.55[a] (9.5)[b]	Hawkes et al. (2014)
Boat-tailed grackles (*Quiscalus major*)	4.8[c]	5.6[d]	Harmes et al. (2016)
Budgerigar (*Melopsittacus undulatus*)	1.62[e]	4.92[f]	Balko et al. (2019)
Chicken (*Gallus gallus*)			
19 d embryo	2.0	16.0[g]	Mohammed et al. (2017)
Young chicken	4.55	–	Savenije et al. (2002); Zhang et al. (2009)
Adult female	2.0	8.4[h]	Gleeson and Brackenbury (1984)
Dalmatian Pelican (*Pelecanus crispus*)	9.3	7.45[i]	Kinney (2018)
Emperor penguin (*Aptenodytes forsteri*)	1.7	6.2[j]	Ponganis et al. (1997)
Geese (*Anser anser*)	2.5	–	Van Kha et al. (1979)
Greater rhea (*Rhea americana*)	–	24.8[a]	Bundle et al. (1999)
House sparrow (*Passer domesticus*)	3.1[c]	4.8[e]	Harmes et al. (2016)
Mourning dove (*Zenaida macroura*)	2.6[c]	7.7[e]	Harmes et al. (2016)
Pigeon (*Columba livia*)	4.48	2.75[k] (31.9[l])	Parker and George (1976); Chaplin et al. (1997)
Peking ducks (*Anas platyrhynchos*)	1.88	1,81[m]	Shimizu and Jones (1987)
Avian basal 3.75 + (12 species) SEM 0.76			
Mammals 2.17 + (20 species) 0.46			

[a]*Exercised on treadmill.*
[b]*Exercised under hypoxic conditions.*
[c]*Delayed sampling from mist nest.*
[d]*Immediate sampling from mist nest.*
[e]*Alfaxolone treated.*
[f]*Manually retained.*
[g]*Hypoxia.*
[h]*Running on a treadmill at ~ 4 kg/h*
[i]*Post-transporting.*
[j]*During diving.*
[k]*Exposure to cold.*
[l]*Exercised endurance trained pigeons.*
[m]*Simulated 4 min dive.*

lactate are depressed by fasting in chickens while those of pyruvate are increased (Table 25.6).

25.3.3 Muscle concentrations of lactate

There is considerable variation between avian species in the muscle concentrations of lactate (Table 25.7). There is limited evidence that concentrations of lactate in muscle can change. Transportation for 3 h was associated with elevated tissue concentrations of lactate (chicken: Wang et al., 2017). In contrast, there were no changes in the lactate concentration in skeletal muscle (pectoralis) in chickens subjected to feed withdrawal for 5 h (Savenije et al., 2002).

25.4 Glycerol

25.4.1 Introduction

Glycerol is produced when triglyceride is hydrolyzed. It can be phosphorylated by glycerol kinase and is then metabolized (see Fig. 25.3).

The structure of glycerol kinase has been determined from cDNA in multiple avian species, e.g., ostrich (*Struthio camelus*—Genbank XM_009683923.1), crested ibis (*Nipponia nippon*—Genbank XM_009473457.1), and burrowing owl (*Athene cunicularia*—Genbank XM_026846319.1). Glycerol kinase activity is reported in the liver (chickens: Bernardino et al., 2014) and skeletal

TABLE 25.6 Blood metabolites in chickens.

	Fed	Fasted
Lactate (mmoles/L)	5.2	3.9[a]
Pyruvate (mmoles/L)	0.22	0.34[a]
β- hydroxybutyrate (mmoles/L)	0.30	1.50[a]
Acetoacetate (μmoles/L)	74	70

[a]*Difference* $P < .05$.
Data from Belo et al. (1976).

TABLE 25.7 Comparison with the muscle concentrations of glycogen and lactate.

	Glycogen μmoles/g	Lactate μmoles/g	Reference
Birds			
Chicken breast muscle	26.8	72.6	Zhang et al. (2009); Yue et al. (2010)
Chicken thigh muscle	22.7	50.7	Zhang et al. (2009); Yue et al. (2010)
Emperor penguin	54.6	2.3	Williams et al. (2012)
Turkey pectoralis	8.9	104	Patterson et al. (2017)
Pigeon skeletal	15.6	17.6	Parker and George (1976); Ferguson (2010)

muscle of birds (pigeons, chickens, blue tits, pheasant, ducks, and robins—Newsholme and Taylor, 1969). It is assumed that glycerol kinase is not present in adipose tissue.

25.4.2 Circulating concentrations of glycerol

Circulating concentrations of glycerol exhibit marked differences across avian species (see Table 25.8). As might be expected, serum concentrations of glycerol are increased in broiler chickens fed a diet supplemented with glycerol (Romano et al., 2014). Circulating concentrations of glycerol in birds are used as an indicator of mobilization of triglyceride (e.g., Devost et al., 2014). After a migratory flight, circulating concentrations of glycerol are increased in some birds such as flycatchers (*Ficedula hypoleuca*) and garden warbler (*Silvia borin*) but not in European robins (*Erithacus rubecula*) (Jenni-Eiermann and Jenni, 1992). Similarly, plasma concentrations of glycerol are elevated during flight in red knot (*Calidris canutus*) (Jenni-Eiermann et al., 2002) and in bar-tailed godwits arriving from migration (Landys et al., 2005). The appearance rates of glycerol into the circulation per unit fat mass is greater in phase 3 than phase 2 of a fast in king penguins (*Aptenodytes patagonicus*) (Bernard et al., 2002). Circulating concentrations of glycerol are depressed in emperor penguins in phase 2 of fasting in response to glucose infusion indicating decreased lipolysis with there being a concomitant reduction in circulating concentrations of free fatty acids (Bernard et al., 2003a). Conversely, infusion of the lipolytic hormone, glucagon increased circulating concentrations of glycerol and nonesterified fatty acids (Bernard et al., 2003b).

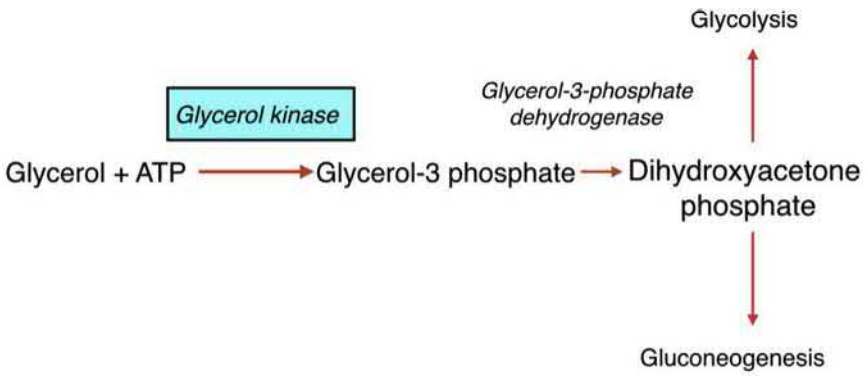

FIGURE 25.3 Glycerol metabolism in birds.

TABLE 25.8 Variation in basal circulating concentrations of glycerol across avian species.

Species	Circulating glycerol mmoles/L	Reference
Bar-tailed godwits (*Limosa lapponica*)	0.46	Landys et al. (2005)
Chicken (*Gallus gallus*)	0.25 0.11 1.44	Buyse et al. (1991) Hamano (2007); Romano et al. (2014)
European robin (*Erithacus rubecula*)	0.58	Jenni-Eiermann and Jenni (1992)
Flycatcher (*Ficedula hypoleuca*)	0.50 3.50	Jenni-Eiermann and Jenni (1992) Kern et al. (2005)
Garden warbler (*Silvia borin*)	0.64	Jenni-Eiermann and Jenni (1992)
King penguins (*Aptenodytes patagonicus*)[a]	0.065	Bernard et al. (2002)
Least flycatcher (*Empidonax minimus*)	0.67	Liu and Swanson (2014).
Ruff sandpipers (*Philomachus pugnax*)	0.37	Vaillancourt and Weber (2007)
Semipalmated sandpipers (*Calidris pusilla*)	0.42	Lyons et al. (2008)
Swainson's thrush (*Catharus ustulatus*)	0.72	Liu and Swanson (2014)
Wood thrush (*Hylocichla mustelina*)	0.45	Done et al. (2011)
Zebra finches (*Taeniopygia guttata*)	0.96	Yap et al. (2017)

[a]*Fasted—mean of phase 2 and 3.*

25.5 Glycogen

25.5.1 Introduction

Glycogen is the storage form of glucose and is broken down to glucose at times of need. It consists of a branched polymer of glucose residues with glucose residues linked predominantly by α-1,4-glycosidic bonds but with α-1,6-glycosidic bond at branching points. Granules of glycogen contain about four times as much water as carbohydrate.

In mammals, there is evidence for two types of glycogen:

- Proglycogen (acid insoluble) with a molecular weight of 400,000 and containing 10% protein
- Macro glycogen—with a molecular weight of 10,000,000 and containing 0.35% protein.

(Lomako et al., 1991). There is little information on the structure of glycogen or proglycogen and macro glycogen in avian tissues.

25.5.2 Synthesis and breakdown

Glycogen is synthesized by the enzyme, glycogen synthase (GS). In contrast, glycogen is broken down generating glucose-1-phosphate by the enzymes, glycogen phosphorylase, and glycogen debranching enzyme, working in combination. Glycogen debranching enzyme activity is reported in skeletal muscles *Musculus pectoralis superficialis* and *Musculus quadriceps femoris* (chicken: Ylä;-Ajos et al., 2006). The synthesis and degradation of glycogen is summarized in Fig. 25.6. Glycogenolysis also plays an important role in astrocyte functioning (chicken: Gibbs et al., 2006).

25.5.2.1 Glycogenesis (synthesis)

Glycogenesis is synthesis of glycogen from glucose:

Glucose 6-phosphate → Glucose 1-phosphate.

25.5.2.1.1 Phosphoglucomutase

Glucose 1-phosphate + Uridine triphosphate (UTP) → Uridine diphosphoglucose

25.5.2.1.2 Uridine triphosphate-glucose pyrophosphorylase

Glycogen (n) + Uridine diphosphoglucose → Glycogen (n + 1) + UDP.

25.5.2.1.3 Glycogen synthase

GS is expressed in pectoralis muscle (chicken: Sibut et al., 2008; Simon et al., 2012).

25.5.3 Glycogenolysis (breakdown)

Glycogenolysis is the breakdown of glycogen to glucose 1-phosphate. Glycogen phosphorylase (EC 2.4.1.1) hydrolyzes α-1,4-glycosidic bonds with glycogen debranching enzyme (EC 3.2.1.68) hydrolyzing α-1,4-glycosidic bonds:

Glycogen (n) + ATP → Glycogen (n − 1) + Glucose 1-phosphate.

25.5.3.1 Glycogen phosphorylase

Glycogen phosphorylase is expressed in pectoralis muscle (chicken: Sibut et al., 2008; Simon et al., 2012). Expression of glycogen phosphorylase in the pectoralis is increased with 3 h of transportation with accompanying feed withdrawal (chicken: Wang et al., 2017). There is also a decrease in muscle glycogen (chicken: Wang et al., 2017) presumably concomitant to increased glycogen phosphorylase activity.

25.5.3.2 Glycogenesis (breakdown)

There is little difference in hepatic phosphorylase activity between late avian embryos and newly hatched chicks (turkeys: Rosebrough et al., 1978b). As might be expected, cAMP increases phosphorylase activity in turkey liver tissue (Rosebrough and Von Vleck, 1990). There are increases in AMP-activated protein kinase (AMPK) protein, the expression of regulatory and catalytic AMPK subunits, and phosphorylation of AMPK in the liver and skeletal muscle at the end of embryonic and in early posthatch development (chicken: Walter et al., 2010). There is evidence that the rate of glycogenolysis in pectoralis muscle is increased with 3 h of transportation as evidenced by the elevated tissue concentrations of lactate (chicken: Wang et al., 2017). Glycogen debranching enzyme activity is reported in skeletal muscles *M. pectoralis superficialis* and *M. quadriceps femoris* (chicken: Ylä;-Ajos et al., 2006).

25.5.4 What is the concentration of glycogen in avian hepatocytes?

It is assumed liver is 70% hepatocytes (based on reports from the rat: Dewey, 1960; Regoeczi and Taylor, 1978), and glycogen is only present in hepatocytes (Wong and Cavey, 1992). Moreover, the volume of chicken hepatocyte is $\sim 1000\ \mu m^3$ (Wong and Cavey, 1992). Therefore, 1 gram of liver would contain 7×10^8 hepatocytes assuming the density of liver is 1.0.

The glycogen concentration in the liver has been reported as 167 µmoles glucose equivalent/g in chicks at seven days of age (see Fig. 25.4) (based on data in Zhao et al., 2017, 2018). Assuming all glycogen is proglycogen, then this can be calculated as 83.5×10^{-3} µmoles glycogen/g (83.5 nmoles glycogen/g or 83.5×10^{-9} mol glycogen/g) assuming glycogen has a molecular weight of 360,000 of glucose residues. The concentration of glycogen per hepatocyte is estimated as follows:

- 83.5×10^{-9} mol glycogen/7×10^8 hepatocytes =
  $= 11.9 \times 10^{-17}$ mol glycogen/hepatocyte
  $= 11.9 \times 10^{-17}/6.022 \times 10^{23}$(Avogadro's number).
  $= 1.98 \times 10^6$ molecules of glycogen/hepatocyte = ~2 million molecules of proglycogen per hepatocyte.

Alternatively, assuming all glycogen is *macroglycogen*, then this can be calculated as 3.34×10^{-3} µmoles glycogen/g or 80,000 molecules per cell assuming glycogen has a molecular weight of 10,000,000.

25.5.5 Hepatic concentrations of glycogen

25.5.5.1 Overview

Examples of hepatic concentrations of glycogen are shown in Table 25.9. Hepatic glycogen represents a labile storage form of glucose critically important to the maintenance of circulating concentrations of glucose and, thereby, organ functioning, particularly of the brain.

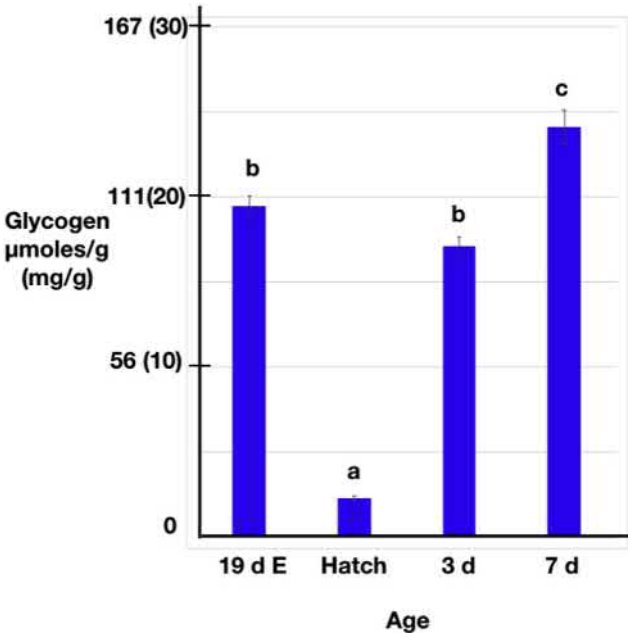

FIGURE 25.4 Changes in hepatic concentrations of glycogen in the perihatch period in chickens. *Based on data in Zhao et al. (2017, 2018).*

TABLE 25.9 Influence of feeding/fasting on muscle and liver glycogen concentrations.

Species	Glycogen concentration mg/g		Reference
	Fed	Fasted	
Liver			
Chicken (*Gallus gallus*)	7.7	3.5[a,b]	De Beer et al. (2007)
Black vulture (*Coragyps atratus*)	22	10[a]	Migliorini et al. (1973)
Muscle			
Chicken (*Gallus gallus*)	14.5	8.6[a,c]	Savenije et al. (2002)
Black vulture (*Coragyps atratus*)	6.9	2.8[a]	Migliorini et al. (1973)

[a]P < .05 compared to fed.
[b]Prior to feeding.
[c]Feed withdrawal for 5 h.

25.5.5.2 Effects of nutrition

As would be expected, hepatic concentrations of glycogen are increased following consumption of a carbohydrate meal and decreased with fasting (Tables 25.9 and 25.10).

TABLE 25.10 Effect of feeding on glycogen in liver and muscles in the newly hatched chicks.

	Glycogen content mg per organ	
Age	Liver	Pectoralis muscle
24 h	4	9
24 h, fed	26*	12*
36 h	5	6
36 h, fed	135*	18*

ED, embryonic day.
Data from Kornasio et al. (2011).
**Indicates difference with feeding* $p < 0.05$.

25.5.5.3 Developmental changes

Glycogen levels are low in the avian embryo increasing between 15 and ~19 days of embryonic development (chicken: Pulikanti et al., 2010). Large shifts in hepatic glycogen concentrations have been reported in perihatch development. There are increases between 19 days and prior to hatching (chicken: Zhai et al., 2011). There is a large decrease in the glycogen concentrations in the liver at hatching (Fig. 25.4); this reflecting mobilization of stored glycogen. Changes in hepatic glycogen during chicken embryonic development can be summarized as follows:

- Glycogen concentrations increasing threefold between 11 days of embryonic development to a maximum at day 18 (11 to 18 days: Hamer and Dickson, 1987; 16 to 18 days: Willemsen et al., 2011).
- Glycogen content increasing between 18 days of embryonic development to a maximum at day 20 (Kornasio et al., 2011).
- A decrease (58%) in the hepatic glycogen concentration between internal pipping and hatching (chicken, *Gallus gallus*: Willemsen et al., 2011)

After hatching and the onset of feeding, hepatic concentrations of glycogen rise (chickens: Zhao et al., 2017; 2018; turkey: Foye et al., 2006) (Also see Table 25.10; Fig. 25.4).

25.5.5.4 Effects of perihatch nutrition

Feeding newly hatched chicks is followed by increases in liver glycogen (Kornasio et al., 2011) (Table 25.10). It is also possible to manipulate hepatic glycogen concentrations in the embryo. Injection of dextrin and β-hydroxy-β-methylbutyrate into the amniotic fluid is followed increases in the glycogen content of liver on days 19 and 20 of embryonic development (Kornasio et al., 2011). Similarly, intra-yolk sac administration of albumen (200 mg on day eight of embryonic development) was followed by increases in the concentrations of glycogen in both the liver at hatch (Tasharofi et al., 2018).

25.5.5.5 Developmental changes in glycogenesis

The rate of hepatic glycogenesis is very low in avian embryos, but it rises immediately after hatching to achieve a plateau at approximately 2 weeks old (chicken: Goodridge, 1968a, Table 25.4). The rise in glycogenesis does not occur in newly hatched chicks until after feeding (Benzo and DeGennaro, 1974, 1981).

25.5.5.6 Other effects on hepatic glycogen

Hepatic glycogen concentrations are depressed in birds with coccidiosis (chicken: Ruff and Allen, 1982).

25.5.5.7 Muscle concentrations of glycogen

25.5.5.7.1 Overview

Table 25.7 summarizes glycogen concentration in skeletal muscle of avian species. Glycogen concentrations are influenced by physiological state being increased when glucose supplies are abundant and decreased when supplies are limited and/or muscular demand for energy is high.

25.5.5.7.2 Developmental changes

Based on studies in chickens, the glycogen concentration in skeletal muscles exhibits large changes during embryonic development. Pectoralis muscle glycogen increases in late embryo development pattern to that of liver with a 33% increase between days 18 and 20 (Kornasio et al., 2011). There is a reduction in the muscle glycogen concentration at hatching (chicken: Zhao et al., 2017, 2018) (see Fig. 25.4); this presumably reflects glucose utilization by muscles during the process of hatching.

There is a large increase in glycogen concentration in the pipping muscle between 15 and 19 days of embryonic development (chicken: Pulikanti et al., 2010). This is presumably to provide a ready source of easily mobilized glucose for the process of hatching.

25.5.5.7.3 Effects of perihatch nutrition

Pectoralis concentrations of glycogen are increased following the administration of dextrin, and β-hydroxy-β-methylbutyrate into the amniotic fluid is followed increases in the content of pectoralis muscle on days 19 and 20 of embryonic development (Kornasio et al., 2011). Moreover, intra-yolk sac administration of albumen into the yolk sac was followed by increases in the concentrations of glycogen in both muscles at hatch (Tasharofi et al., 2018). With early feeding of newly hatched chicks, muscle glycogen concentrations are increased (Kornasio et al., 2011) (Table 25.10).

25.5.6 Issues with determination of tissue concentrations of glycogen and lactate

There is considerable variation in the concentrations of glycogen and lactate in muscles in various studies (Table 25.7). The bases for these differences are unclear. One possibility is the manner of euthanizing the animals with involuntary convulsions of multiple muscle leading to increased lactate and reduced glycogen (Edwards et al., 1999). There were marked differences in muscle glycogen concentrations between birds killed by cervical dislocation and barbiturate overdose (chicken: Edwards et al., 1999). Another possibility is depletion of glycogen occurs in the times between first handling the birds, euthanasia, and taking tissue samples.

Duration and method of storage of liver affects tissue glycogen and/or glucose concentrations with storage shifts in glucose even when snap frozen and at −70°C (chicken: Cleland and Bannister, 1979). Moreover, there is marked loss of glycogen when tissue is maintained at 4°C for 3 h (chicken: Cleland and Bannister, 1979). Similarly, glucose in muscle with pectoralis muscle glucose concentrations doubles between 7 and 25 min after euthanasia in a poultry processing plant (chicken: Aliani et al., 2013); this reflecting glycogenolysis. Immediate assay after snap freezing is the ideal.

25.5.7 Glycolytic potential

The glycolytic potential can be used as an index of meat quality (e.g., broiler chicken: Berri et al., 2005; domestic turkey: Patterson et al., 2017) and is predominantly due to glycogen in the muscle.

$$\text{Glycolytic potential (expressed in uM of lactate per g of fresh muscle)} = 2[(\text{glycogen}) + (\text{glucose}) + (\text{glucose} - 6 - \text{P})] + (\text{lactate})$$

(Berri et al., 2005). *Postmortem* there is breakdown of glycogen generating lactate.

25.5.8 Glycogen body

The glycogen body is a gelatinous ovaloid organ found in dorsal area of the lumbosacral region of the spinal cord in birds (Watterson, 1949). The glycogen body is functionally separated from the circulatory system due to the blood brain barrier (Möller and Kummer, 2003). The role of the glycogen body is not well established. As its name suggests, it contains glycogen (Lee et al., 2001). Glycogen body cells incubated in vitro incorporate glucose into glycogen suggesting the presence of glycogen synthase (Lee et al., 2001).

It is composed of what was initially described as uniform glycogen body cells (Watterson, 1949). These are astroglial-like cells (Louis, 1959, 1993; De Gennaro, 1993). These cells have a high capacity to store glycogen and contain deposits of glycogen in the cytoplasm (Imagawa et al., 2006a). A second cell type has been identified based on co-incubation of glycogen body cells with cerebellar neurons. These have processes that extend and attach to neurons (Imagawa et al., 2006a). The glycogen body is derived from anterior section of the lumbosacral neural tube (De Gennaro, 1991). The lobes of Lachi have many metabolic similarities to glycogen bodies with glycogen synthase, glycogen phosphorylase, glucose6-phosphate dehydrogenases, and 6-phosphogluconate dehydrogenase together with a lack of glucose 6-phosphatase (Benzo and DeGennaro, 1981).

Glycogen bodies contain multiple metabolic enzyme activities, including the following: glycogen synthase, glycogen phosphorylase, glucose 6-phosphate dehydrogenases, and 6-phosphogluconate dehydrogenase (Benzo and DeGennaro, 1974, 1981). There is lactate dehydrogenase (LDH) activity and LDH-B expression in the glycogen body (Imagawa et al., 2006b). It is suggested that the glycogen body consumes lactate body (Imagawa et al., 2006b). The glycogen level within the glycogen body cells is refractory to both nutritional status, being unchanged by starvation, and by hormones such as insulin, glucagon, and adrenocorticotropic hormone (Imagawa et al., 2006a). There is a small effect of norepinephrine on glycogenolysis with reduced glycogen levels in the glycogen body cells in vitro (Lee et al., 2001). It is suggested that the glycogen body and the lobes of Lachi function to provide precursors via the pentose phosphate pathway for myelin synthesis (Benzo and DeGennaro, 1981).

25.6 Glucose and fructose utilization

Utilization of glucose and fructose can be very high in birds (see Table 25.11). For instance, in foraging hummingbirds, hovering flight is maintained by utilization of ingested sugars in rufous (*Selasphorus rufus*) and Anna's (*Calypte anna*) hummingbirds (Welch and Suarez, 2007). In contrast during migration, fats are employed as the energy source, with the ruby-throated hummingbird (*Archilochus colubris*) losing most of the triglyceride stored in the adipose tissue during a 20 h flight over 960 km (600 miles; Hargrove, 2005). There are very high-respiration rates of mitochondria from skeletal muscles of hummingbirds (7−10 mL O2/cc/min); the rates are twice the maximum found in mammals (Suarez et al., 1991). This may be associated with increased mitochondrial surface area (Suarez et al., 1991). There is an increase in glucose turnover with exercise in

TABLE 25.11 Glucose metabolism in chickens.

Parameter	Age	Method	Estimated glucose metabolism (μmol glucose/min/kg)	Reference
Total body glucose loss (utilization)	Eight days	Disappearance of radioactive deoxyglucose from the blood	102	Calculated from Tokushima et al. (2005)
Total body glucose utilization	Four weeks	Heat produced	174	Calculated from Buyse et al. (1993) [a]
Total body glucose utilization	Five weeks	Heat produced	112	Calculated from Buyse et al. (1993) [a]
Total body glucose disappearance	Five −Six months	Disappearance of radioactive glucose from the blood	79.4	Belo et al. (1976)
Average			116	

[a]*This assumes that the respiratory quotient (RQ) of 1.0 with glucose being utilized for energy rather than either fats or amino acids. Geelissen et al. (2006) reported RQ in similar-aged animals of 1.1 or greater. Data are calculated based on body weights of the same aged birds in the same laboratory (Buyse et al., 2004) and on catabolized energy from carbohydrate = 16.7 kJ/g substrate (3008.67 kJ per mole glucose) with RQ of 1.00 (Walsberg and Wolf, 1995).*

chickens (Brackenbury and El-Sayed, 1985). There are marked differences in glucose uptake by different organs (summarized in Table 25.12). The highest uptake is by the brain and heart. Insulin induced large increases in glucose uptake by the liver and some skeletal muscles. In contrast, glucose uptake is depressed in the brain of the chicken (Tokushima et al., 2005). There are marked changes during the day in glucose uptake by tissues in chickens on a 12 h light/12 h dark cycle (Karaganis et al., 2009).

25.6.1 Developmental changes

There is little glucose utilization for lipogenesis (fatty acid synthesis) in the liver of avian embryos and at hatching. They rise to a substantial plateau level within eight days after hatching due to feeding, as shown in chickens (Goodridge, 1968a,b; Table 25.13). Glucose oxidation in chick embryos is increased when incubated at elevated temperatures (Molenaar et al., 2013).

TABLE 25.12 Comparison of glucose uptake by different organs by chickens.

Organ	Glucose uptake (nmol/min/g)
Brain	315
Heart	223
Kidney	146
Small intestine	100
Skeletal muscle	38 (25−55)[a]
Adipose tissue	18.5
Liver	12.3

[a]*Range of different muscles.*
Data calculated From Tokushima et al. (2005) based on radioactive (3H). 2-deoxyglucose uptake in 8-day-old chickens fasted for 12 h.

25.6.2 Fasting and glucose utilization

There is reduced glucose utilization during fasting in birds. For instance, irreversible glucose turnover is depressed 32% by fasting (either associated with breeding or forced starvation) in Emperor penguins (*Aptenodytes forsteri*; Groscolas and Rodriguez, 1981):

- Fed 44.2 μmol/min/kg
- Fasted 30.1 μmol/min/kg

Similarly, there is a 57.6% decrease in glucose utilization in Japanese quail (*C. japonica*) fasted for two days (Sartori et al., 1996) and 64% in chickens fasted for one day (Belo et al., 1976). The decrease in glucose utilization is due to the following:

- Reduced glucose utilization by peripheral tissues such as skeletal muscles (Table 25.14)
- Reduced glucose utilization by the liver for:
  - Lipogenesis, with as little as 2 h fasting (Fig. 25.5). Rates of fatty acid synthesis are further decreased to 6.4% of control with one day fasting and to 0.2% of control with three days starvation [data from Yeh and Leveille (1971a, b)]. Expression of genes for enzymes in lipogenesis is depressed by fasting in chickens (Désert et al., 2008; Sherlock et al., 2012).
  - Glycolysis (Goodridge, 1968a).

TABLE 25.13 Changes in hepatic utilization of glucose for glycolysis, glycogenesis, and lipogenesis during early posthatch development in the chicken.

	Glucose utilization[a] (as percentage of plateau level)		
Age (days)	Glycolysis[b]	Glycogenesis[c]	Lipogenesis[d]
Late embryo and day 0	13.3 + 0	<0.5	<0.5
2	51.1 + 6.4	10.0 + 4.1	4.0 + 1.0
4	85.4 + 5.4	8.3 + 0	36.8 + 9.8
8	104.4 + 4.6	7.6 + 1.1	94.7 + 14.7
12	84.5 + 10.5	34.8 + 9.4	66.8 + 10.4
16	120.8 + 12.5	105.1 + 24.5	144.2 + 29.0

[a]*Determined by utilization of [U−^{14}C] glucose.*
[b]*Plateau conversion to CO_2: 1261 dpm/mg calculated from Goodridge (1968a).*
[c]*Plateau conversion to glycogen: 647 dpm/mg calculated from Goodridge (1968a).*
[d]*Plateau conversion to fatty acids: 582 dpm/mg calculated from Goodridge (1968a).*

TABLE 25.14 Glucose generation/utilization as assessed from venous-arterial differences in eight-week-old chickens either fed or starved for six days.

	Nutritional state	
Parameter and organ	Fed	Starved (6 days)
Venous-Arterial difference (nmol blood/mL)		
Liver	+940[a]	+1450
Kidney	+44	+307
Hind quarter	−792	−199
Net glucose generation		
Per unit organ weight (μmol/min/g)		
Liver[b]	1.8[a]	2.8 (gluconeogenesis)
Kidney[c]	0.4	2.8 (gluconeogenesis)
Per unit body weight (μmol/min/kg)		
Liver	34	53
Kidney	2	17
Net glucose utilization		
Per unit organ weight (nmol/min/g)		
Hind quarter/skeletal muscle[d]	40	10
Per unit body weight (μmol/min/kg)		
Skeletal muscle[e]	22	5

[a]*Includes glucose not absorbed by liver from hepatic portal venous blood.*
[b]*Liver glucose generation calculated as the product of venous arterial difference and blood flow to the liver (1.92 mL/min; Tinker et al., 1986).*
[c]*Kidney glucose generation calculated as the product of venous arterial difference and arterial blood flow to the kidneys (9 mL/min/g; Merrill et al., 1981).*
[d]*Net glucose utilization by hindquarters calculated as the product of venous arterial difference and arterial blood flow to the skeletal muscle (50 μL/min/g; Merrill et al., 1981), using skeletal muscle as a surrogate for hindquarters.*
[e]*Assumes skeletal muscle represents 55% of body weight.*
Data from Tinker et al. (1986).

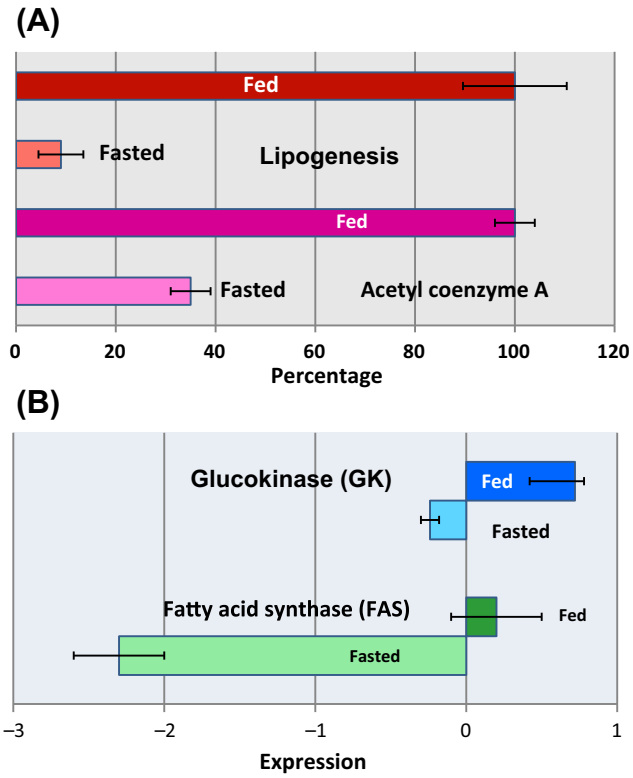

FIGURE 25.5 Effects of fasting on carbohydrate metabolism in the liver. (A) Effect of fasting (2 h) on rate of lipogenesis in the chicken liver and on the liver concentration of acetyl coenzyme A. Data are expressed as a percentage of the control (fed) Å} SEM. Calculated from Yeh and Leveille (1971a, b). (B) Effect of fasting for 5 h on the hepatic expression of key enzymes in carbohydrate metabolism in the chicken. *Based on data from Dupont et al. (2008).*

25.7 Glucose transporters

25.7.1 Introduction to avian glucose transporters

Glucose enters cells due to GLUTs. GLUTs are facilitative hexose transporters that are found in cell membranes. They have molecular weights of 45−55 KDa and have been identified across bacteria, fungi, plants, invertebrate animals, and vertebrates (Wilson-O'Brien et al., 2010). There are three classes of GLUT: 1, 2, and 3. Class 1 and 2 GLUT are distinct clades that are only found in metazoan animals (Wilson-O'Brien et al., 2010; Byers et al., 2017). In contrast, class 3 is not a distinct clade (Wilson-O'Brien et al., 2010). In mammals and birds, there are respectively 14 and 13 GLUT genes/proteins namely:

- Class 1 GLUT
  - GLUT1: Solute carrier family 2 facilitated GLUT member 1 (SLC2A1) (e.g., Anna's hummingbird: Genbank XM_008503695.1; chicken: Genbank L07300.1; house sparrow: Genbank)
  - GLUT2: SLC2A2 (e.g., Anna's hummingbird: Genbank XM_008501315.2; Bengalese finch: GenBank: 021549987.1; chicken: GenBank Z22932.1; mallard: Genbank KJ011857.1; pigeon: GenBank: JN887480.1)
  - GLUT3: SLC2A3 (e.g., Canary: Genbank XM_009102684.3; chicken: Genbank M37785.1; golden-collared manakin: Genbank XM_029 964892.1: zebra finch: Genbank XM_002190755.4)
  - GLUT4: Presumed to be absent in birds
  - GLUT14: SLC2A14 (e,g., chicken: Gene bank NM_205511.1)
- Class 2 GLUT
  - GLUT5: SLC2A5 (e,g., chicken: Gene bank CGNC ID1764; zebra finch: Genbank XM_002187376.3)
  - GLUT7: SLC2A7
  - GLUT9: SLC2A9 (e,g., Anna's hummingbird: Genbank XM_008496129.2; golden-collared manakin: Genbank XM_029958571.1)
  - GLUT11: SLC2A11 (e,g., chuck-will's-widow: Genbank XM_010162948.1); golden eagle GenBank: XM_011592834.1; golden-collared manakin: Genbank XM_018081931.3)
- Class 3 GLUT
  - GLUT6: SLC2A6 (e,g., Anna's hummingbird: Genbank XM_008497303.2)
  - GLUT8: SLC2A8 (e,g., chicken: Genbank AB083371.1)
  - GLUT10: SLC2A10 (e,g., Anna's hummingbird: Genbank XM_008498009.1)
  - GLUT12: SLC2A12 (e,g., Anna's hummingbird: Genbank XM_008494039.2; chicken: Genbank XM_419733 Coudert et al., 2015)
  - GLUT13: SLC2A13 (INT4 or H + *-myo*-inositol transporter) (e,g., Anna's hummingbird: Genbank XM_008493093.1; rifleman: Genbank: XM_009071059.1)

25.7.2 Insulin-dependent glucose transporters

There does not appear to be a homolog of the mammalian insulin-dependent GLUT4 in birds (chickens: Seki et al., 2003; house sparrows *P. domesticus*: Sweazea and Braun, 2006). There is evidence that GLUT12 expression is controlled by insulin as administration of antisera to insulin is accompanied by decrease in expression of GLUT12 in both pectoralis and thigh muscle (Coudert et al., 2015). Moreover, there are effects of both feeding and antisera against insulin of the amount of GLUT12 in cell membranes from leg muscles with more in fed than fasted consistent with elevated insulin levels and also increases with insulin administration (Coudert et al., 2015). Although GLUT1 is insulin-independent in mammals, insulin

TABLE 25.15 Comparison of citrate synthase activity between hummingbirds and chickens.

Species	Citrate synthase activity (nmol/min/g wet wt)	Reference
Hummingbird	448	Suarez et al. (2009)
Chicken	21	Azad et al. (2010)

stimulates glucose uptake along with both GLUT1 expression and protein content in avian myoblasts (chicken: Zhao et al., 2012). An insulin-dependent GLUT8 is expressed in the chicken (high: adrenal, brain, kidney, lung, pancreas, spleen, and testis; low: adipose tissue, liver, heart, and skeletal muscle; chickens: Seki et al., 2003; Kono et al., 2005) (Table 25.15).

25.7.3 Tissue expression of glucose transporters

There is high expression of GLUT1 in adipose tissue (chicken: Kono et al., 2005), brain (chicken: Kono et al., 2005), and skeletal muscle (chicken: Shimamoto et al., 2016) together with fibroblasts (Wagstaff et al., 1995). High GLUT2 expression is only found in the liver and kidneys (chicken: Kono et al., 2005; Lee et al., 2006), with low expression in the small intestine (chickens: Duarte et al., 2011). Epidermal growth factor decreases GLUT2 protein levels in chicken hepatocytes (Lee et al., 2006; Franssens et al., 2016). There is high GLUT3 expression in skeletal muscle (chicken: Shimamoto et al., 2016), brain (chicken: Kono et al., 2005) with chicken fibroblasts also expressing GLUT3 (Wagstaff et al., 1995) and all tissues expressing GLUT3 in house sparrows (Sweazea and Braun, 2006). There is also expression of GLUT8 in skeletal muscles (chicken: Shimamoto et al., 2016). GLUT9 is expressed in the liver (perihatch chickens: Franssens et al., 2016). GLUT12 expression exhibits the following pattern: skeletal muscle > heart = brain > liver = adipose tissue (Coudert et al., 2015).

25.7.4 Physiological control of glucose transporters

GLUT expression decreases during the development of the avian erythrocyte (chicken: Johnstone et al., 1998) with only 200 copies of GLUT1 per mature erythrocyte (pigeon: Diamond and Carruthers, 1993). There is high expression of GLUT2 in the liver of the young chickens, together with some expression of both GLUT1 and GLUT3 (Humphrey et al., 2004). Skeletal muscle also exhibits high expression of GLUT3, with some expression of GLUT1 but no detectable expression of GLUT2 (Humphrey et al., 2004).

25.8 Intermediary metabolism

25.8.1 Glucose phosphorylation and dephosphorylation

Glucose 6-phosphate plays a major role in the control of metabolism (Fig. 25.6). There are rapid increases in hepatic concentrations of glucose 6-phosphate after hatching (turkeys: Rosebrough et al., 1979).

25.8.1.1 Glucose phosphorylation to glucose 6-phosphate

Glucose is phosphorylated to glucose 6-phosphate catalyzed either by glucokinase or hexokinase:

$$\text{Glucose} + \text{ATP} \rightarrow \text{Glucose 6-phosphate}$$

25.8.1.1.1 Enzyme: glucokinase/hexokinase

Glucokinase has been partially characterized both from chickens and mule ducks with 99% identity (Berradi et al., 2005, 2007). There is increased expression in the liver of mule ducks with overfeeding (Berradi et al., 2004) and feeding in chickens (Berradi et al., 2007). Fasting depresses glucokinase expression by 66% in chickens (Dupont et al., 2008). Low Michaelis constant (Km) hexokinase activity is present in the chicken liver and reduced with fasting (O'Neill and Langlow, 1978; Klandorf et al., 1986). High Km hexokinase activity is found in the mitochondria of the liver (chicken: Borrebaek et al., 2007). Hexokinase is present also in the muscles of hummingbirds (Suarez et al., 1990).

25.8.1.2 Glucose 6-phosphatase

Glucose 6-phosphatase plays a critical role in glucose homeostasis:

$$\text{Glucose 6-phosphate} \rightarrow \text{Glucose} + \text{Phosphate}$$

There are markedly higher levels of glucose 6 phosphatase in the carnivorous bird, the black vultures (*C. atratus*) presumably reflecting the greater gluconeogenesis (Migliorini et al., 1973).

Glucose 6-phosphatase activity is present in the avian liver (chicken: O'Neill and Langlow, 1978). Thus, glucose 6-phosphate generated from glycogenolysis and gluconeogenesis is released from the liver into the circulation for peripheral use. There does not appear to be glucose 6-phosphatase in skeletal muscle; hence, muscle glycogen

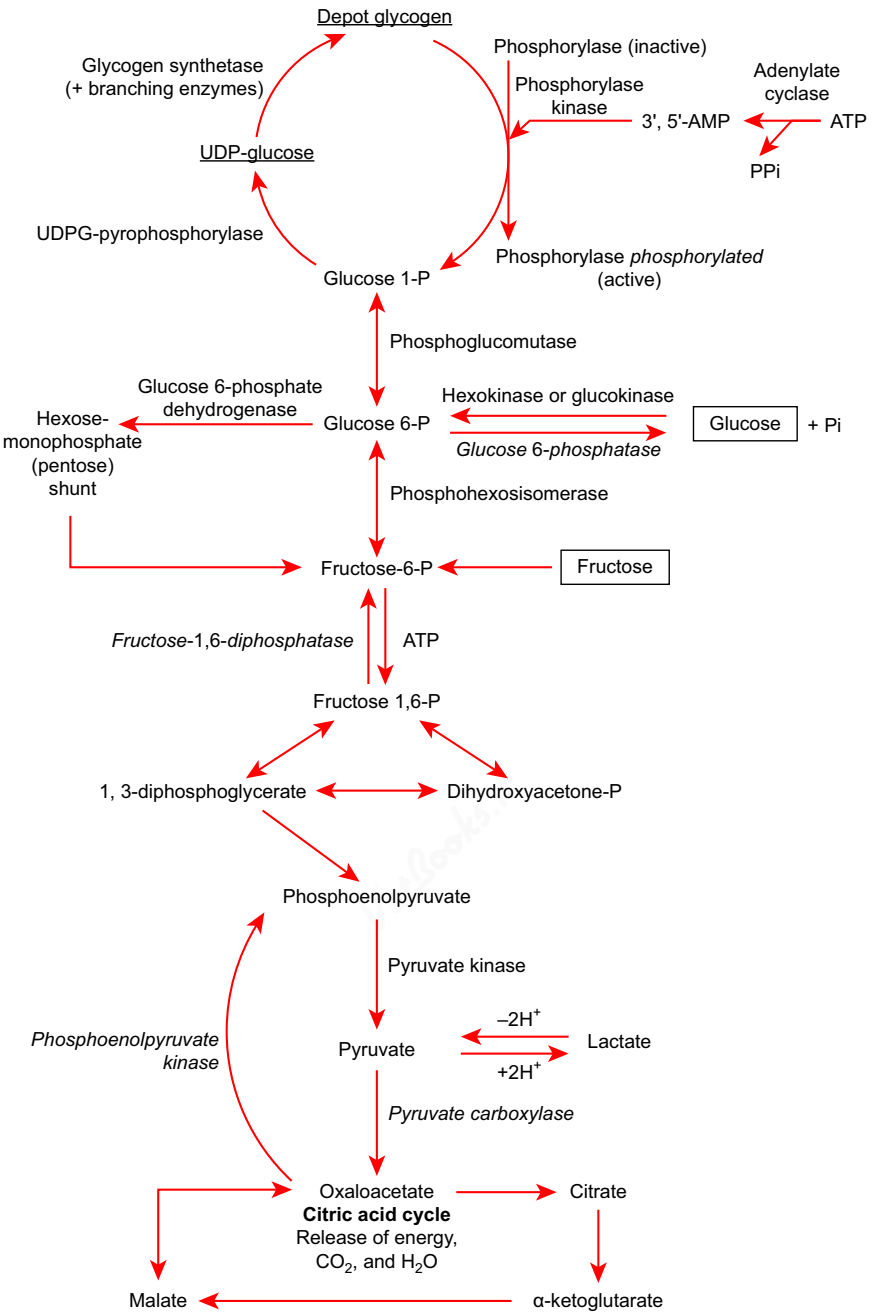

FIGURE 25.6 Overview schematic diagram of carbohydrate metabolism (glucose phosphorylation/dephosphorylation, glycolysis, glycogenesis, glycogenolysis, and pentose phosphate shunt).

is not a source of circulating glucose. Along with elevated glycogenolysis and glucogenesis with fasting, there is increased glucose 6-phosphatase activity in the liver (chicken: O'Neill and Langlow, 1978).

25.8.2 Glycolysis

Glycolysis is summarized in Fig. 25.6. The glycolytic pathway precedes carbohydrate metabolites entering the citric acid cycle and also allows the anaerobic metabolism of glucose.

25.8.2.1 Developmental changes

There are low rates of hepatic glycolysis in the liver of avian embryos, rising quickly after hatching to a plateau level achieved after about a week (chicken: Goodridge, 1968a, Table 25.13).

25.8.2.2 Physiological effects

The posthatch increase in glycolysis is induced by feeding (chicken: Goodridge, 1968b). Hepatics rates of glucose utilization for glycolysis and conversion to carbon dioxide are depressed by fasting. For instance, in young chickens, rates of glucose oxidation to carbon dioxide by liver slices are decreased by the following (Goodridge, 1968b):

- One day: 59.5% of control
- Three days: 17.5%

Expression of genes for enzymes in the glycolytic pathway is depressed by fasting in chickens (Sherlock et al., 2012). There is evidence that the rate of glycolysis in pectoralis muscle is increased with 3 h of transportation as evidenced by the elevated tissue concentrations of lactate (chicken: Wang et al., 2017).

25.8.2.3 Erythrocytes

Glycolysis and pentose phosphate shunt are the pathways to obtain energy from glucose in the erythrocyte (pigeon: Kalomenopoulou and Beis, 1990). Phosphofructokinase activity, pyruvate kinase (PK) activity, and hexokinase activity are present in the erythrocyte (pigeon: Kalomenopoulou and Beis, 1990).

25.8.2.4 Lactate dehydrogenase

LDH catalyzes the conversion of lactate to pyruvate and vice versa. Plasma/serum LDH activities are included by the biochemical reference ranges for birds [e.g., kakapo (*Strigops habroptilus*): Low et al., 2006] (see Fig. 25.7).

There are three genes for LDH in birds, respectively, ldha, ldhb, and ldhc, these encoding LDH-A, LDH-B, and LDH-C. There are tissue differences in expression of LDH such as the following:

- LDH-A expression is breast muscle = liver > kidney = heart with some expression in the brain and glycogen body (chicken: Arias et al., 2000; Imagawa et al., 2006a,b).
- LDH-B expression is kidney = heart >> breast muscle = liver with marked expression in the brain and some in the glycogen body (chicken: Arias et al., 2000; Imagawa et al., 2006a,b).

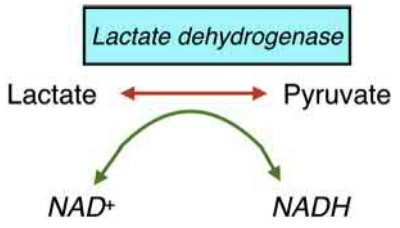

FIGURE 25.7 Conversion of lactate to pyruvate and vice versa.

- A novel LDH-B is reported in chicken testes (Arias et al., 2000).

Moreover, splice variants of LDH C chain mRNA are found in the testes (pigeon: Huang et al., 2012).

There are shifts in LDH with physiological state. Both plasma and pectoralis muscle LDH is increased after short-term transportation with consequent withholding of food (chicken: Wang et al., 2017; Xing et al., 2017). Plasma LDH activity is increased by exercise [red-tailed hawks (*Buteo jamaicensis*) Knuth and Chaplin, 1994]. There are developmental shifts in LDH enzyme activity with declines during postembryonic development (chicken: Seebacher et al., 2006). There is evidence that temperature influences LDH activity with increase in LDH concentrations in the supernatants from chicken myocardial cells exposed to elevated temperatures (Xu et al., 2017).

25.8.3 Citric acid or tricarboxylic acid cycle

25.8.3.1 Overview

Fig. 25.8 summarizes the citric acid or tricarboxylic acid cycle. There were increases in mitochondrial capacity [citrate synthase (CS) activity] at the end of embryonic and in early posthatch development (chicken: Walter et al., 2010). CS and PK activities are found in skeletal muscle from chukar, pheasant, domestic turkey, and wild turkey (Shea et al., 2007). CS activity in hummingbirds is similar to that in mammalian mitochondria (Suarez et al., 1991) but higher than that of the chicken (Table 18.9). PK has been identified by proteomics in pectoralis muscle with dietary protein deprivation (chicken: Corzo et al., 2006).

25.8.3.2 Erythrocytes

The citric acid cycle is absent in erythrocytes (pigeon: Kalomenopoulou and Beis, 1990).

25.9 Gluconeogenesis

The gluconeogenic pathway is summarized in Figs. 25.4 and 25.6. The major organs for gluconeogenesis in birds are the liver and kidneys (see below). There appears to be marked gluconeogenic potential for the yolk sac in the developing embryo, with high expression of fructose 1,6-bisphosphatase and phosphoenolpyruvate carboxykinase together with glucose 6-phosphatase (chicken: Yadgary et al., 2011). Muscle- and liver-type phosphofructokinase-1 (PFK-M and PFK-L) have been characterized in the chicken (Seki et al., 2006). There is hepatic expression of regulatory enzymes of the gluconeogenesis, specifically phosphoenolpyruvate carboxykinase 1 and 2 (PCK1 and 2)

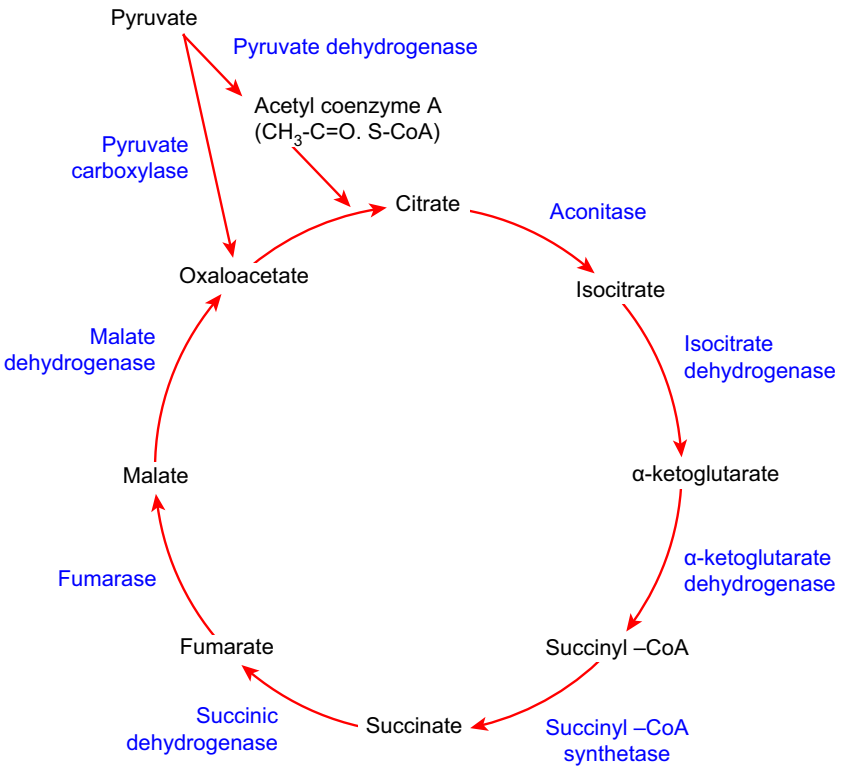

FIGURE 25.8 The citric acid or tricarboxylic acid cycle.

or fructose-1,6-biphosphatase 1 (FBP1) (perihatch chickens: Franssens et al., 2016). Chicken PFK-L is expressed at a low level in the liver, skeletal muscle, and brain (Seki et al., 2006). Chicken PFK-M is expressed in skeletal muscle (Seki et al., 2006). Basal rates of gluconeogenesis is markedly greater in carnivorous birds, black vultures (*C. atratus*) than chickens (Migliorini et al., 1973).

25.9.1 Gluconeogenesis and fasting

Fasting increases gluconeogenesis in some but not all birds. There is greatly increased net release of glucose from both the liver and kidneys (Table 25.14), together with elevated hepatic glucose 6-phosphatase, phosphoenolpyruvate carboxykinase, alanine aminotransferase, and aspartate aminotransferase activities (chickens: Veiga et al., 1978). There are marked increases in gluconeogenesis during fasting in the Japanese quail (*C. japonica*), with increases in the rate of glucose formation from ^{14}C bicarbonate in vivo (Sartori et al., 1996, 2000). Moreover, with two days fasting (phase 2), there were increases in the activity of cytoplasmic phosphoenolpyruvate carboxykinase in the kidney (Sartori et al., 2000). Similarly, fasting increases gluconeogenesis in duckling liver-based perfusion studies in which the medium contains the gluconeogenic precursor, lactate (Bedu et al., 2001). Expression of genes for enzymes in the gluconeogenic pathway is increased by fasting (chicken: Désert et al., 2008; Sherlock et al., 2012). However, gluconeogenesis is depressed in fasted carnivorous birds (black vulture *C. atratus*: Veiga et al., 1978).

25.9.2 Relative importance of the liver and the kidney

Gluconeogenesis occurs in both the liver and kidneys. The relative contribution is estimated from arteriovenous differences in fed and fasted birds, with the liver producing about 70% of the glucose and kidney about 30% in the fasted state (chicken: Tinker et al., 1986, Table 25.14). In fed carnivorous birds, there is high rates of gluconeogenesis (black vulture *C. atratus*: Veiga et al., 1978). There is likely to be some hepatic gluconeogenesis in graniferous birds. This is supported by studies of arterial-venous differences in glucose and lactate (Table 18.8). It is presumed that much of the lactate originates from gastrointestinal tract, with 37% of glucose converted to lactate in the chicken gastrointestinal tract (Riesenfeld et al., 1982).

25.10 Carbohydrate digestion and absorption

Carbohydrate digestion and absorption will be discussed in three parts: starch digestion, disaccharide digestion, and glucose absorption (Fig. 25.9).

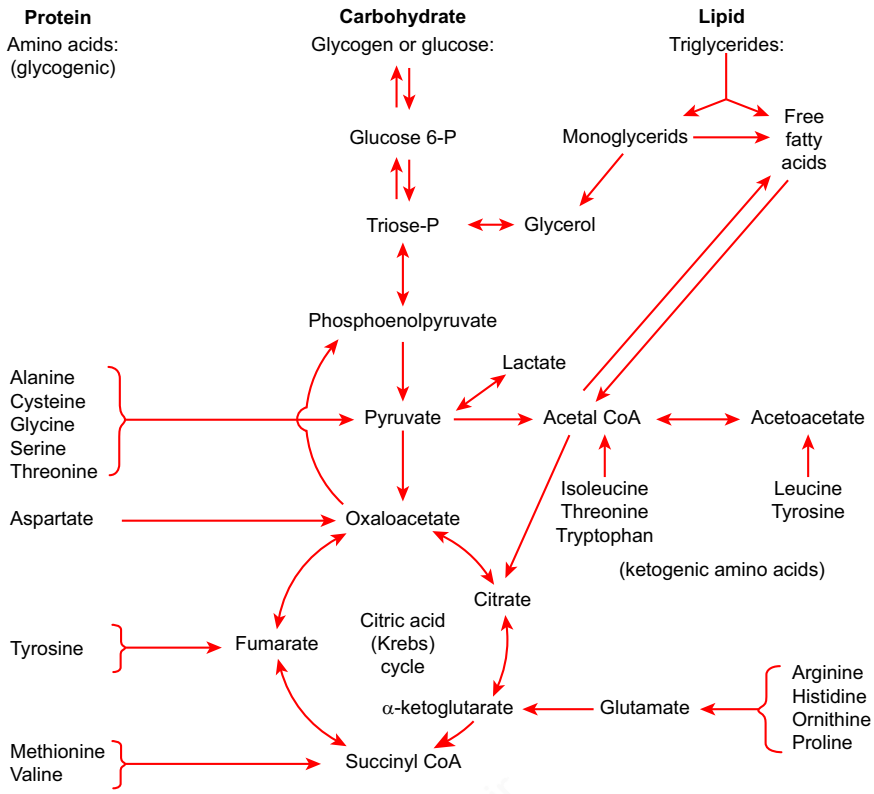

FIGURE 25.9 Overview schematic diagram of the relationships between lipid and protein metabolism with carbohydrate metabolism.

25.10.1 Starch digestion

Starch is digested by amylase, which is produced by the small intestine (see Table 25.16) and exocrine pancreas (chicken: Osman, 1982). About 97% of corn starch in the diet is digested in the chicken (Riesenfeld et al., 1980). The sites of starch digestion in the chicken small intestine are the following (calculated from Riesenfeld et al., 1980):

- Duodenum 63%
- Jejunum 19%
- Ileum 12%

However, there is markedly higher proportion of digestion of other starches, for instance from legumes, in both the duodenum and ilium of chickens (Weurding et al., 2001).

TABLE 25.16 Enzymatic activities in the chicken small intestine.

Enzyme	Duodenum	Jejunum
Amylase	13.4	19.0
Maltase	1.5	4.8
Sucrose	1.4	3.2

Based on Liu et al. (2008).

TABLE 25.17 Changes in liver glycogen with meal feeding in the chicken, allowing determination of the rate of glycogenolysis.

Time relative to feeding	Meal fed	Liver glycogen (mmole glucose equivalents)
	Once daily	3.5
+12 h following meal	Once daily	7.7
Prior to feeding	Once on alternate days	6.9
+24 h following meal	Once on alternate days	15.9

From De Beer et al. (2007).

There is secretion of amylase in the upper gastrointestinal tract and from the liver reported in some birds: from salivary glands (e.g., spotted dove (*Streptopelia chinensis*) and house crow (*Corvus splendens*)), the proventriculus [e.g., house sparrow (*P. domesticus*)] (Bhattacharya and Ghose, 1971) and from the liver in bile (chicken: Farner, 1943).

TABLE 25.18 Changes in liver glycogen with meal feeding in the chicken, allowing determination of the rate of glycogenolysis.

Time relative to feeding	Total liver glycogen (mmole glucose equivalents)	Feed as starch content in the crop (mmole glucose equivalents)
Meal fed daily		
Prior to feeding	4.0	
Immediately after feeding 0		83.1
12 h after feeding	14.1	21.5
24 h after feeding	7.8	6.5
Delta 0 to 12	*NA*	*61.6*
Delta 12 to 24	*6.3*[x]	*15.0*
Meal fed alternate days		
Prior to feeding	6.5	
0 immediately after feeding		148.1
12 h after feeding	24.2	67.1
24 h after feeding	28.7	29.9
36 h after feeding	10.7	<5
48 h after feeding	4.7	<5
Delta 0 to 12	*NA*	*81.0*
Delta 12 to 24	*−3.5*	*37.2*
Delta 24 to 36	*18.* [x]	*>24.9*
Delta 36 to 48	*6.0*[x]	*NA*

NA, not available.

25.10.2 Disaccharide digestion

25.10.2.1 Maltose

Maltase cleaves the disaccharide maltose into its two constituent glucose moieties. There is maltase activity in the duodenum and jejunum (chicken: Liu et al., 2008) but somewhat lower expression of isomaltase in the jejunum then duodenum (Liu et al., 2008). While, there are little changes in expression of isomaltase during embryonic development (Yadgary et al., 2011), both isomaltase and aminopeptidase activities increase in the brush border of the jejunum in late embryonic development (chicken: Uni et al., 2003). Moreover, there are marked increases in maltase activity in the jejunum in the first week of posthatching life (domestic ducks: Tangara et al., 2010). In contrast. there were little changes in the expression of maltase during embryonic development and posthatching development in another avian species (pigeons: Xie et al., 2020).

25.10.2.2 Sucrose

Sucrose cleaves the disaccharide sucrose into its two constituent monosaccharide moieties, glucose and galactose. There is sucrase activity in the duodenum and jejunum (chicken: Liu et al., 2008) with a similar distribution to maltose along the small intestine (Meynard et al., 1999). Similarly, there is somewhat lower expression of isomaltase in the jejunum then duodenum (Liu et al., 2008). There are marked increases in sucrase activity in the jejunum in the first week of posthatching life (domestic ducks: Tangara et al., 2010) but little changes in the expression of sucrase during embryonic development and posthatching development in another avian species (pigeons: Xie et al., 2020).

Sucrose is a major component in nectar. In ruby-throated hummingbird (*Archilochus colubris*), sucrose is digested by sucrase to fructose and glucose prior to absorption (McWhorter et al., 2006). Exogenous fructose or glucose can supply, respectively, 88 and 82% of energy needs of hovering hummingbirds (Chen and Welch, 2014).

25.10.2.3 Lactose

Lactose is poorly utilized by growing chick resulting in diarrhea (Rutter et al., 1953), presumably due to failure of lactose digestion and osmotic effects. In contrast, galactose is well utilized (Rutter et al., 1953).

25.10.3 Glucose absorption

25.10.3.1 Overview

There is active absorption of glucose in the small intestine, cecum, and colon of birds (chickens: Riley et al., 1986; Vinardell and Lopera, 1987; Moreno et al., 1996; De La Hora et al., 1998, 2001). The major site of glucose absorption is the duodenum, accounting for more than 80% of glucose absorbed in young chickens fed a diet high in glucose (Riesenfeld et al., 1980). The very high glucose absorption from the intestines of hummingbirds is due to active, mediated transport [rufous (*Selasphorus rufus*) and Anna's (*Calypte anna*) hummingbirds] (McWhorter et al., 2006). Similarly, honey eaters have a high rates of glucose absorption (Nicolson and Fleming, 2014).

Glucose absorption from the lumen of the gastrointestinal tract into enterocytes is achieved by active transport, predominantly by sodium D-glucose and galactose co-transporter 1(SGLT1). The SGLT1 protein has a high affinity for glucose (Gal-Garber et al., 2000) and is exclusively found in the brush border of enterocytes (chickens: De La Hora et al., 1998; Barfull et al., 2002). Expression of SGLT1 is high in the small intestine, being greatest in the jejunum as seen from the following values for the chicken (calculated from Gilbert et al., 2008, with expression shown as a percentage of that in the jejunum):

- Duodenum 77%
- Jejunum 100%
- Ileum 65%

Jejunal expression of sodium GLUT1 is increased in fasted chickens (Gal-Garber et al., 2000; Duarte et al., 2011) and further elevated with refeeding (Gal-Garber et al., 2000). During embryonic development, there are increases in both expression and activity of SGLT1 (chicken: Uni et al., 2003; Yadgary et al., 2011; pigeon: Dong et al., 2012). During growth, the surface area increases but expression of SGLT1 declines (Barfull et al., 2002). Aldosterone influences expression of SGLT1 (chickens: De La Hora et al., 2001). There is also expression of sodium independent glucose (galactose and fructose) transporter 2 (GLUT2) in the small intestine. Jejunal expression of GLUT2 is unaffected by either fasting or refeeding in young chickens (Duarte et al., 2011).

25.10.3.2 Noncarrier uptake of glucose

Noncarrier uptake of glucose can occur across the tight junctions between enterocytes. There is marked noncarrier uptake of glucose (occurring across tight junctions between enterocytes) during migration stop-overs in blackcaps (*Sylvia atricapilla*) (Tracy et al., 2001). Similarly, noncarrier uptake of glucose is found in nectarivorous birds such as rufous hummingbirds (*Selasphorus rufus*) and Anna's hummingbirds (*Calypte anna*) with glucose or fructose flowing down a concentration gradient from the nectar (McWhorter et al., 2006).

25.10.4 Glucose digestion in frugivorous birds

Frugivorous birds consume fruits; these having fructose and glucose. Table 25.19 summarizes the digestibility of glucose and fructose in frugivorous birds from different types of fruits. While digestibility of glucose and fructose was high (>97.5%) from *Vitis* type fruits (Witmer and Van Soest, 1998). In contrast, digestibility of fructose from *Lindera* type fruits was lower while digestibility for glucose was approximately 30% lower (Witmer and Van Soest, 1998).

TABLE 25.19 Digestive efficiencies of glucose and fructose in frugivorous birds (Witmer and Van Soest, 1998).

Type of fruit and bird species	Digestive efficiencies	
	Glucose	Fructose
***Vitis* (e.g., grapes)**		
American robin (*Turdus migratorius*)	98.1	99.2
Wood thrush (*Hylocichla mustelina*)	98.1	99.1
Cedar waxwing (*Bombycilla cedrorum*)	97.9	99.0
***Lindera* (spicewood and spicebushes)**		
American robin (*Turdus migratorius*)	24.3	52.3
Wood thrush (*Hylocichla mustelina*)	29.7	62.7
Cedar waxwing (Bombycilla cedrorum)	55.3	86.8

25.10.5 Gastrointestinal storage of ingesta

There is temporary storage of feed in the crop and gizzard of at least some graniferous birds (e.g., in the order *Galliformes*). For instance, substantial stores of feed are found in crop of in sexually immature meat-type chickens adapted to either daily or alternate day meal feeding (De Beer et al., 2008) (Fig. 25.10). In chickens, feeding is restricted to the hours of light (day). There is a marked peak in consumption prior to lights-off, with concomitant filling of both the crop and gizzard (Scanes et al., 1987; Buyse et al., 1993, Fig. 25.10). Nocturnal energy needs are accommodated by reduced metabolic rate and the release of the stored ingesta (Buyse et al., 1993, Fig. 25.11).

25.10.6 Intestinal fermentation

Limited information is available on gastrointestinal fermentation in birds.

25.10.6.1 Cellulose

25.10.6.1.1 Foregut

A neotropic bird, the hoatzin (*Opisthocomus hoazin*), is said to be unique in having foregut fermentation (Grajal et al., 1989). The microbial communities in the muscular crop have been characterized and include methanogens as in the mammalian rumen (Wright et al., 2009; Godoy-Vitorino et al., 2012).

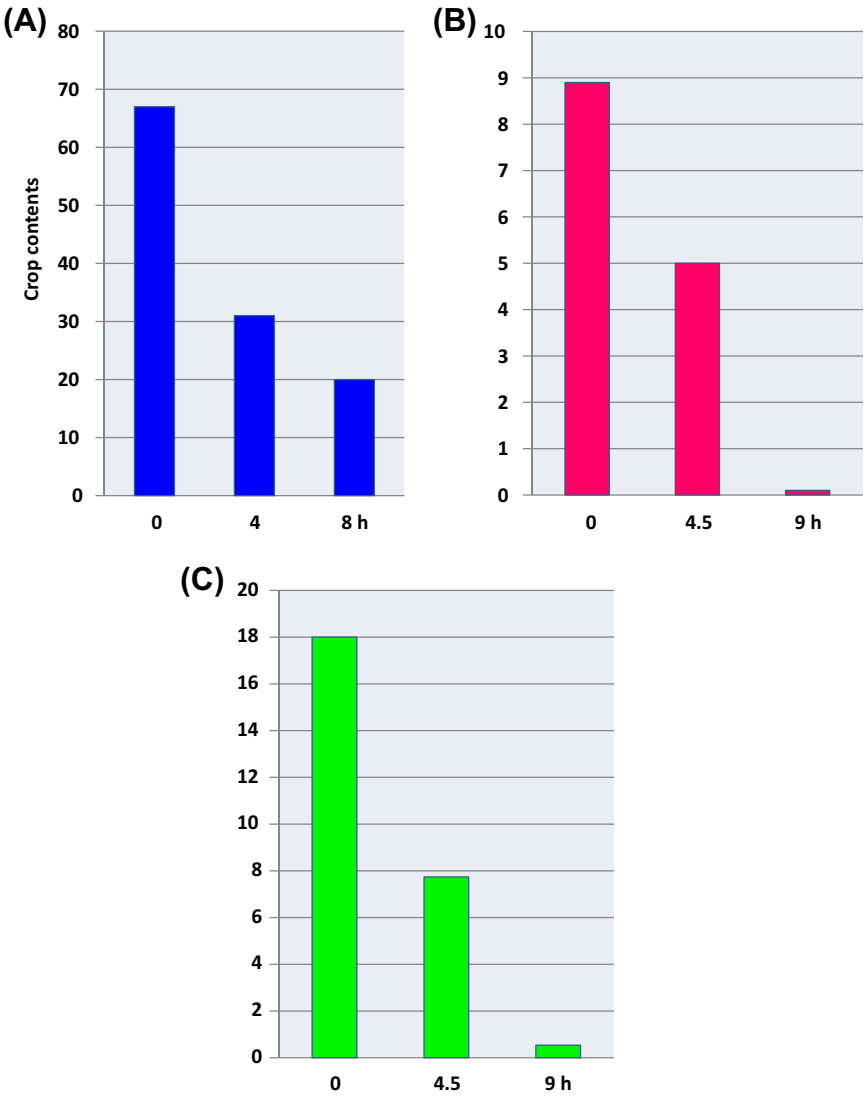

FIGURE 25.10 Mechanical storage of ingesta in the crop (g) of chickens. (A) Following meal feeding in broiler breeder pullets (sexually immature females) (De Beer et al., 2008) and (B) during the night following increased feeding prior to lights-off in young broiler chickens (Buyse et al., 1993) and during the night following increased feeding prior to lights-off in laying hens Scanes et al. (1987).

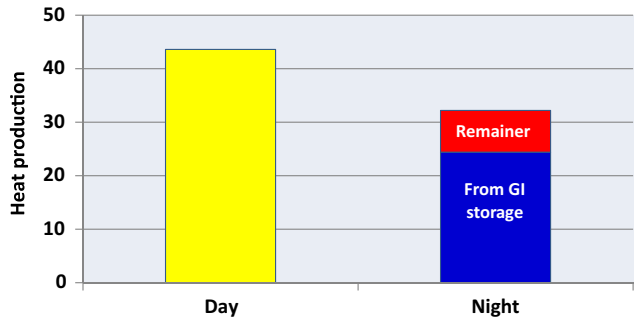

FIGURE 25.11 Comparison of heat production/energy consumption (kJ kg0.75 h) during the day and night in young chickens. Also shown are the contributions of ingesta held (short-term stored) in the crop, gizzard, and proventriculus for nocturnal needs. *Data from Buyse et al. (1993).*

25.10.6.1.2 Hindgut

Cellulose fermentation to volatile fatty acids in the ceca has been demonstrated in a galliform bird, rock ptarmigan (*Lagopus muta*) (Gasaway, 1976a, 1976b, 1976c).

25.10.6.2 Starch

There is evidence for fermentation of starch in the crop of domestic poultry. During the nocturnal storage of feed in the crop, there are marked increases in lactate acid concentrations but little increase in volatile simple fatty acids, except valeric and caproic acids (turkey: Johannsen et al., 2005). About 37% of glucose converted to lactate in the chicken gastrointestinal tract (Riesenfeld et al., 1982).

25.11 Putative roles of other monosaccharides

25.11.1 Sorbitol

The presence of sorbitol in the feed did not influence body weight gain or feed to gain ratio of broiler chickens but did depress circulating concentrations of glucose and adiposity (Furuse et al., 1991). In contrast, sorbitol prevented the reduction in growth in broiler chickens challenge with *Escherichia coli* lipopolysaccharide (LPS) endotoxin (Takahashi et al., 2001).

25.11.2 Xylitol

Feeding broiler chickens with a diet containing xylitol prevented the growth retardation following *E. coli* LPS endotoxin challenge (Takahashi et al., 2002). Moreover, the antibody response to sheep erythrocytes was increased in chicks receiving xylitol in the feed compared to glucose (Takahashi et al., 2005).

25.12 Conclusions

25.12.1 Overview

Fig. 25.12 summarizes glucose flow in the metabolism in birds. Although carbohydrate metabolism in birds is similar in mammals, there are distinct differences:

1. There are marked differences between circulating concentrations of glucose between wild birds and mammals, with avian concentrations double those in mammals.
2. Birds are very resistant to diabetes, with neither pancreatectomy nor insulin administration evoking large changes in circulating concentrations of glucose. However, chickens received passive immunization with antisera to insulin exhibit diabetic-like shifts in metabolism, with circulating concentrations of glucose of 747 mg/dL reported 5 h after antisera administration (Dupont et al., 2008; Simon et al., 2012). Identical extremely high concentrations of glucose are observed

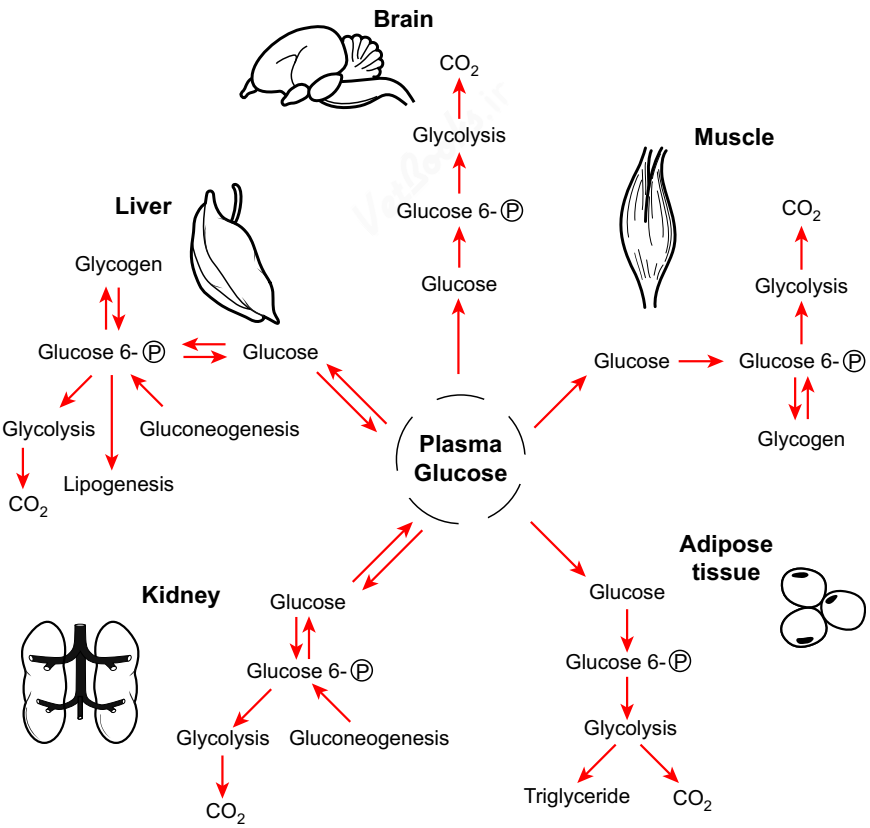

FIGURE 25.12 Overview schematic diagram summarizing the flow of glucose to and from plasma to major organs.

following feeding in hummingbirds without adverse effects (Beuchat and Chong, 1998).
3. The glucose transporter GLUT4 is missing in birds.
4. The principal site of lipogenesis is the liver (compared with adipose tissue in mammals).

25.12.2 Starvation and metabolism

It is assumed that there are four metabolic phases:

- An absorptive phase following feeding, until ingesta carbohydrates in the gastrointestinal tract are completely depleted
- A postabsorptive phase or short-term fasting
- Phase 2 starvation: protein sparing and utilization of fatty acids
- Phase 3 starvation: fatty acids depleted and a shift to amino acids.

The absorptive phase is when glucose and other simple carbohydrates are being absorbed. It encompasses both the passage of ingesta with digestion, and any storage of ingesta in the foregut (crop, gizzard, and proventriculus) prior to digestion/absorption (Fig. 25.11). In at least chickens and turkeys, there is nocturnal foregut storage of ingesta (laying hen: Scanes et al., 1987; young chicken: Buyse et al., 1993). This has been calculated to meet over 70% of energy requirements (Fig. 25.12).

It has been generally assumed that, during the postabsorptive phase, glycogen is employed as the energy source. In contrast, during phase 2 starvation, there is protein sparing and fatty acids from the breakdown of adipose triglyceride used. During phase 3 starvation, there is a shift to muscle and other protein catabolism using amino acids for gluconeogenesis as triglyceride stores are exhausted (Goodman et al., 1980; Bernard et al., 2002).

During the postabsorptive phase, together with phase 2 and 3 starvation, there is a progressive decrease utilization of glucose for glycolysis, such as by muscle (see Table 25.17) and hepatic lipogenesis (Fig. 25.5). The decrease precedes the end of absorptive phase as, for instance, the metabolic rate is decreased 26% in chickens during the nocturnal period (Fig. 25.11), when feeding has essentially stopped. Hepatic glycogenolysis only meets a small proportion of body glucose during the postabsorptive phase. Table 25.17 shows hepatic glycogen contents in meal-fed chickens; it was assumed that the hepatic glycogen contents approach maximal in chickens fed meals either daily or on alternate days. Hepatic glycogenolysis in the postabsorptive phase between meals was calculated as follows:

- 6 μmol/min/kg

This compares with

- 55 μmol/min/kg total glucose utilization (Belo et al., 1976) or 116 μmol/min/kg total glucose utilization (Table 25.18)
- Maximal rates of glucose from ingesta transiting out of the crop is 21 to 27 mmol of glucose/hour.

Thus, only about 10% of whole-body glucose utilization comes from hepatic glycogenolysis. This would indicate that hepatic gluconeogenesis is increased and hepatic glycolysis and lipogenesis are decreased during the postabsorptive phase and phase 2 starvation. Evidence for an immediate increase in gluconeogenesis and/or a decline in hepatic glycolysis comes from the observed reduction in the hepatic concentration of lactate with 2 h fasting (chicken: Yeh and Leveille, 1971b). The glycogen content in both the liver and muscle decline during fasting, being depressed by, respectively, 78 and 53% with six days of starvation in the chicken (see Table 25.13; Tinker et al., 1986).

The conceptual framework for phases 2 and 3 starvation is supported in king penguins (*Aptenodytes patagonicus),* where body fat reverses are almost exhausted with markedly decreased circulating concentrations of fatty acids (Bernard et al., 2002). Evidence for increased gluconeogenesis comes from the increase in circulating concentrations of uric acid (Bernard et al., 2002). Moreover, in chickens, starvation for six days is accompanied by increased net release of glucose into hepatic and renal veins (Tinker et al., 1986); indicating elevated gluconeogenesis (see Table 25.14). This is calculated as gluconeogenesis providing 70 μmol glucose/min/kg.

References

Aliani, M., Farmer, L.J., Kennedy, J.T., Moss, B.T., Gordon, A., 2013. Post-slaughter changes in ATP metabolites, Reducing and phosphorylated sugars in chicken meat. Meat Sci. 94, 55–62.

Alonso-Alvarez, C., Ferrer, M., 2001. A biochemical study of fasting, subfeeding, and recovery processes in yellow-legged gulls. Physiol. Biochem. Zool. 74, 703–713.

Anan, K.K., Maitra, S.K., 1995. Impact of quinalphos on blood glucose and acetyl choline activity in the brain and pancreas in a rose ringed parakeet (Psittacula mmunea borealis Newmann). Arch. Environ. Contam. Toxicol. 29, 20–23.

Anderson, D.K., Hazelwood, R.L., 1969. Chicken cerebrospinal fluid: normal composition and response to insulin. J. Physiol. 202, 83–95.

Anthony, N.B., Vasilatos-Younken, R., Bacon, W.L., Lilburn, M.S., 1990. Secretory pattern of growth hormone, insulin, and related metabolites in growing male turkeys: effects of overnight fasting and refeeding. Poultry Sci. 69, 801–811.

Applegate, T.J., Ladwig, E., Weissert, L., Lilburn, M.S., 1999. Effect of hen age on intestinal development and glucose tolerance of the Pekin duckling. Poultry Sci. 78, 1485–1492.

Arias, W.M., Mezquita, C., Mezquita, J., 2000. Expression of lactate dehydrogenases A and B Liverduring chicken spermatogenesis: characterization of testis specific transcripts. J. Cell. Biochem. 79, 15–27.

Azad, M.A., Kikusato, M., Maekawa, T., Shirakawa, H., Toyomizu, M., 2010. Metabolic characteristics and oxidative damage to skeletal muscle in broiler chickens exposed to chronic heat stress. Comp. Biochem. Physiol. Mol. Integr. Physiol. 155, 401–406.

Azeredo, L.M.M., Oliveira, T.C., Lopez, L.C.S., 2016. Blood metabolites as predictors to evaluate the body condition of *Neopelma pallescens* (Passeriformes: *pipridae*) in Northeastern Brazil. Zoologia (Curitiba) 33, e20160043.

Bairlein, F., Fritz, J., Scope, A., Schwendenwein, I., Stanclova, G., van Dijk, G., Meijer, H.A., Verhulst, S., Dittami, J., 2015. Energy expenditure and metabolic changes of free-flying migrating Northern bald ibis. PloS One 10, e0134433.

Balko, J.A., Lindemann, D.M., Allender, M.C., Chinnadurai, S.K., 2019. Evaluation of the anesthetic and cardiorespiratory effects of intramuscular alfaxalone administration and isoflurane in budgerigars (*Melopsittacus undulatus*) and comparison with manual restraint. J. Am. Vet. Med. Assoc. 254, 1427–1435.

Barfull, A., Garriga, C., Mitjans, M., Planas, J.M., 2002. Ontogenetic expression and regulation of Na (+)-D-glucose cotransporter in jejunum of domestic chicken. Am. J. Physiol. 282, G559–G564.

Bedu, E., Cohen-Adad, F., Dallevet, G., Garin, D., Barr, H., Duchamp, C., 2001. Effect of cold-acclimation on oxygen uptake and glucose production of perfused duckling liver. Comp. Biochem. Physiol. Mol. Integr. Physiol. 128, 851–861.

Belo, P.S., Romsos, D.R., Leville, G.A., 1976. Blood metabolites and glucose metabolism in the fed and fasted chicken. J. Nutr. 106, 1135–1143.

Benzo, C.A., DeGennaro, L.D., 1974. Glycogen synthetase and phosphorylase in developing chick glycogen body. J. Exp. Zool. 188, 375–380.

Benzo, C.A., DeGennaro, L.D., 1981. Glycogen metabolism in the developing accessory lobes of Lachi in the nerve cord of the chick: metabolic correlations with the avian glycogen body. J. Exp. Zool. 215, 47–52.

Bernard, S.F., Fayolle, C., Robin, J.P., Groscolas, R., 2002. Glycerol and NEFA kinetics in long-term fasting king penguins: phase II versus phase III. J. Exp. Biol. 205, 2745–2754.

Bernard, S.F., Orvoine, J., Groscolas, R., 2003a. Glucose regulates lipid metabolism in fasting king penguins. Am. J. Physiol. 285, R313–R320.

Bernard, S.F., Thil, M.A., Groscolas, R., 2003b. Lipolytic and metabolic response to glucagon in fasting king penguins: phase II vs. phase III. Am. J. Physiol 284, R444–R454.

Bernardino, V.M., Rodrigues, P.B., de Paula Naves, L., Rosa, P.V., Zangerônimo, M.G., Gomide, E.M., Saldanha, M.M., Alvarenga, R.R., 2014. Content of plasmatic glycerol and activity of hepatic glycerol kinase in broiler chickens fed diets containing different sources and concentrations of glycerine. J. Anim. Physiol. Anim. Nutr. 98, 328–337.

Berradi, H., Guy, G., Rideau, N., 2004. A glucokinase-like enzyme induced in Mule duck livers by overfeeding. Poultry Sci. 83, 161–168.

Berradi, H., Taouis, M., Cassy, S., Rideau, N., 2005. Glucokinase in chicken (*Gallus gallus*). Partial cDNA cloning, immunodetection and activity determination. Comp. Biochem. Physiol. B Biochem. Mol. Biol. 141, 129–139.

Berradi, H., Bernadet, M.D., Guy, G., Rideau, N., 2007. Expression of the glucokinase gene in mule duck liver and glucokinase activities in chicken and mule duck livers. Poultry Sci. 86, 2216–2220.

Berri, C., Debut, M., Santé-Lhoutellier, V., Arnould, C., Boutten, B., Sellier, N., Baéza, E., Jehl, N., Jégo, Y., Duclos, M.J., Le Bihan-Duval, E., 2005. Variations in chicken breast meat quality: implications of struggle and muscle glycogen content at death. Br. Poultry Sci. 46, 572–579.

Beuchat, C.A., Chong, C.R., 1998. Hyperglycemia in hummingbirds and its consequences for hemoglobin glycation. Comp. Biochem. Physiol. Mol. Integr. Physiol. 120, 409–416.

Bhattacharya, S., Ghose, K.C., 1971. Influence of food on the amylase system in birds. Comp. Biochem. Physiol. 40B, 317–320.

Boshouwers, F.M., Nicaise, E., 1981. Measurement of the respiratory metabolism of the fowl. Br. Poultry Sci. 22, 59–69.

Borrebaek, B., Christophersen, B., Tranulis, M.A., Aulie, A., 2007. Preand post-natal hepatic glucose phosphorylation in chicks (*Gallus domesticus*). Br. Poultry Sci. 48, 729–731.

Boussaid-Om Ezzine, S., Everaert, N., Métayer-Coustard, S., Rideau, N., Berri, C., Joubert, R., Temim, S., Collin, A., Tesseraud, S., 2010. Effects of heat exposure on Akt/S6K1 signaling and expression of genes related to protein and energy metabolism in chicken (Gallus gallus) pectoralis major muscle. Comp. Biochem. Physiol. B Biochem. Mol. Biol. 157, 281–287.

Brackenbury, J.H., El-Sayed, M.S., 1985. Respiratory metabolism of D[U-14C] glucose in hens and cocks during prolonged treadmill exercise. Comp. Biochem. Physiol. A Comp. Physiol. 82, 851–854.

Braun, E.J., Sweazea, K.L., 2008. Glucose regulation in birds. Comp. Biochem. Physiol. B Biochem. Mol. Biol. 151, 1–9.

Bundle, M.W., Hoppeler, H., Vock, R., Tester, J.M., Weyand, P.G., 1999. High metabolic rates in running birds. Nature 397, 31–32.

Burgdorf-Moisuk, A., Wack, R., Ziccardi, M., Larsen, R.S., Hopper, K., 2012. Validation of lactate measurement in American flamingo (*Phoenicopterus ruber*) plasma and correlation with duration and difficulty of capture. J. Zoo Wildl. Med. 43, 450–458.

Buyse, J., Decuypere, E., Huyghebaert, G., Herremans, M., 1991. The effect of clenbuterol supplementation on growth performance and on plasma hormone and metabolite levels of broilers. Poultry Sci. 70, 993–1002.

Buyse, J., Adelsohn, D.S., Decuypere, E., Scanes, C.G., 1993. Diurnal-nocturnal changes in food intake, gut storage of ingesta food transit time and metabolism in growing broiler chickens: a model for temporal control of energy balance. Br. Poultry Sci. 34, 699–709.

Buyse, J., Geypens, B., Malheiros, R.D., Moraes, V.M., Swennen, Q., Decuypere, E., 2004. Assessment of age-related glucose oxidation rates of broiler chickens by using stable isotopes. Life Sci. 75, 2245–2255.

Byers, M.S., Howard, C., Wang, X., 2017. Avian and mammalian facilitative glucose transporters. Microarrays 6, E7.

Chaplin, S.B., Munson, M.M., Knuth, S.T., 1997. The effect of exercise and restraint on pectoral muscle metabolism in pigeons. J. Comp. Physiol. B. 167, 197−203.

Chen, C.C.W., Welch, K.C., 2014. Hummingbirds can fuel expensive hovering flight completely with either exogenous glucose or fructose. Funct. Ecol. 28, 589−600.

Christensen, K., McMurtry, J.P., Thaxton, Y.V., Thaxton, J.P., Corzo, A., McDaniel, C., Scanes, C.G., 2013. Metabolic and hormonal responses of growing modern meat type chickens to fasting. Br. Poultry Sci. 54, 199−205.

Clark, T.D., Kleindorfer, S., Dudaniec, R.Y., 2018. Baseline and stress-induced blood properties of male and female Darwin's small ground finch (*Geospiza fuliginosa*) of the Galapagos Islands. Gen. Comp. Endocrinol. 259, 199−206.

Cleland, M.E., Bannister, D.W., 1979. Effects of storage conditions *in vitro* on the assay of chick liver glycogen. Br. Poultry Sci. 20, 307−310.

Corzo, A., Kidd, M.T., Dozier 3rd, W.A., Shack, L.A., Burgess, S.C., 2006. Protein expression of pectoralis major muscle in chickens in response to dietary methionine status. Br. J. Nutr. 95, 703−708.

Coudert, E., Pascal, G., Dupont, J., Simon, J., Cailleau- Audouin, E., Crochet, S., Duclos, M.J., Tesseraud, S., Metayer-Coustard, S., 2015. Phylogenesis and biological characterization of a new glucose transporter in the chicken (*Gallus gallus*), GLUT12. PloS One 10, e0139517.

Davis, J.F., Castro, A.E., de la Torre, J.C., Scanes, C.G., Radecki, S.V., Vasilatos-Younken, R., Doman, J.T., Teng, M., 1995. Hypoglycemia, enteritis, and spiking mortality in Georgia broiler chickens: experimental reproduction in broiler breeder chicks. Avian Dis. 39, 162−174.

De Beer, M., Rosebrough, R.W., Russell, B.A., Poch, S.M., Richards, M.P., Coon, C.N., 2007. An examination of the role of feeding regimens in regulating metabolism during the broiler breeder grower period. 1.Hepatic lipid metabolism. Poultry Sci. 86, 1726−1738.

De Beer, M., McMurtry, J.P., Brocht, D.M., Coon, C.N., 2008. An examination of the role of feeding regimens in regulating metabolism during the broiler breeder grower period. 2. Plasma hormones and metabolites. Poultry Sci. 87, 264−275.

De Gennaro, L.D., 1991. Origin of the avian glycogen body: I. Effects of tail bud removal in the chick embryo. Growth Dev. Aging 55, 19−26.

De Gennaro, L.D., 1993. Origin of the avian glycogen body. II. Observations in support of a glial nature in the chick embryo. Growth Dev. Aging 57, 275−281.

De La Horra, M.C., Calonge, M.L., Ilundin, A.A., 1998. Effect of dehydration on apical Na+-H+ exchange activity and Na+-dependent sugar transport in brush-border membrane vesicles isolated from chick intestine. Pflügers Archiv 436, 112−116.

De La Horra, M.C., Cano, M., Peral, M.J., Calonge, M.L., Ilundin, A.A., 2001. Hormonal regulation of chicken intestinal NHE and SGLT-1 activities. Am. J. Physiol. 280, R655−R660.

Désert, C., Duclos, M.J., Blavy, P., Lecerf, F., Moreews, F., Klopp, C., Aubry, M., Herault, F., Le Roy, P., Berri, C., Douaire, M., Diot, C., Lagarrigue, S., 2008. Transcriptome profiling of the feeding-to-fasting transition in chicken liver. BMC Genom. 9, 611.

Devost, I., Hallot, F., Milbergue, M., Petit, M., Vézina, F., 2014. Lipid metabolites as markers of fattening rate in a non-migratory passerine: effects of ambient temperature and individual variation. Comp. Biochem. Physiol. A 177, 18−26.

Dewey, W.C., 1960. Distribution and hematocrit ratios of blood in the rat. Am. J. Physiol. 198, 1011−1013.

Diamond, D.L., Carruthers, A., 1993. Metabolic control of sugar transport by derepression of cell surface glucose transporters. An insulin independent recruitment-independent mechanism of regulation. J. Biol. Chem. 268, 6437−6444.

Done, T., Gow, E.A., Stutchbury, B.J.M., 2011. Corticosterone stress response and plasma metabolite levels during breeding and molt in a free-living migratory songbird, the wood thrush (*Hylocichla mustelina*). Gen. Comp. Endocrinol. 171, 176−182.

Dong, X.Y., Wang, Y.M., Yuan, C., Zou, X.T., 2012. The ontogeny of nutrient transporter and digestive enzyme gene expression in domestic pigeon (*Columba livia*) intestine and yolk sac membrane during pre and posthatch development. Poultry Sci. 91, 1974−1982.

Duarte, C.R., Vicentini-Paulino, M.L., Buratini Jr., J., Castilho, A.C., Pinheiro, D.F., 2011. Messenger ribonucleic acid abundance of intestinal enzymes and transporters in feed-restricted and refed chickens at different ages. Poultry Sci. 90, 863−868.

Dunbar, M.R., Gregg, M.A., Giordano, M.R., Davis, D.M., Byrne, M.W., Crawford, J.A., Tornquist, S.J., 2005. Normal hematologic and biochemical values for prelaying greater sage grouse (*Centrocercus urophasianus*) and their influence on chick survival. J. Zoo Wildl. Med. 36, 422−429.

Dupont, J., Tesseraud, S., Derouet, M., Collin, A., Rideau, N., Crochet, S., Godet, E., Cailleau-Audouin, E., Métayer-Coustard, S., Duclos, M.J., Gespach, C., Porter, T.E., Cogburn, L.A., Simon, J., 2008. Insulin immune-neutralization in chicken: effects on insulin signaling and gene expression in liver and muscle. J. Endocrinol. 197, 531−542.

Edwards, M.R., McMurtry, J.P., Vasilatos-Younken, R., 1999. Relative insensitivity of avian skeletal muscle glycogen to nutritive status. Domest. Anim. Endocrinol. 16, 239−247.

Fairbrother, A., Craig, M.A., Walker, K., O'Loughlin, D., 1990. Changes in mallard (*Anas platyrhynchos*) serum chemistry due to age, sex, and reproductive condition. J. Wildl. Dis. 26, 67−77.

Farner, D.S., 1943. Biliary amylase in the domestic fowl. Biol. Bull. 84, 240−243.

Ferguson, D.C., 2010. Skeletal Muscle and Hepatic Glycogen in Birds and Mammals. Honors Thesis. University of Arizona Honors Thesis.

Fowles, J.R., Fairbrother, A., Trust, K.A., Kerkvliet, N.I., 1997. Effects of Aroclor 1254 on the thyroid gland, immune function, and hepatic cytochrome P450 activity in mallards. Environ. Res. 75, 119−129.

Foye, O.T., Uni, Z., Ferket, P.R., 2006. Effect of in ovo feeding egg white protein, beta-hydroxy-beta-methylbutyrate, and carbohydrates on glycogen status and neonatal growth of turkeys. Poultry Sci. 85, 1185−1192.

Franssens, L., Lesuisse, J., Wang, Y., Willems, E., Willemsen, H., Koppenol, A., Guo, X., Buyse, J., Decuypere, E., Everaert, N., 2016. The effect of insulin on plasma glucose concentrations, expression of hepatic glucose transporters and key gluconeogenic enzymes during the perinatal period in broiler chickens. Gen. Comp. Endocrinol. 232, 67−75.

Furuse, M., Ishii, T., Miyagawa, S., Nakagawa, J., Shimizu, T., Okumura, J.J., 1991. Effect of dietary sorbitol on the performance of broilers. Br. Poultry Sci. 32, 875–880.

Gal-Garber, O., Mabjeesh, S.J., Sklan, D., Uni, Z., 2000. Partial sequence and expression of the gene for and activity of the sodium glucose transporter in the small intestine of fed, starved and refed chickens. J. Nutr. 130, 2174–2179.

Gasaway, W.C., 1976a. Seasonal variation in diet, volatile fatty acid production and size of the cecum of rock ptarmigan. Comp. Biochem. Physiol. 53A, 109–114.

Gasaway, W.C., 1976b. Volatile fatty acids and metabolizable energy derived from cecal fermentation in the willow ptarmigan. Comp. Biochem. Physiol. 53A, 115–121.

Gasaway, W.C., 1976c. Cellulose digestion and metabolism by captive rock ptarmigan. Comp. Biochem. Physiol. 53A, 179–182.

Gatehouse, N., Markham, B.J., 1970. Respiratory metabolism in three species of raptors. Auk 87, 738–741.

Gayathri, K.L., Shenoy, K.B., Hegde, S.N., 2004. Blood profile of pigeons (*Columba livia*) during growth and breeding. Comp. Biochem. Physiol. A 138, 187–192.

Gee, C.F., Carpenter, J.W., Hensler, B.L., 1981. Species differences in hematological values of captive cranes, geese, raptors, and quail. J. Wildl. Manag. 45, 463–483.

Geelissen, S.M., Swennen, Q., Geyten, S.V., Kühn, E.R., Kaiya, H., Kangawa, K., Decuypere, E., Buyse, J., Darras, V.M., 2006. Peripheral ghrelin reduces food intake and respiratory quotient in chicken. Domest. Anim. Endocrinol. 30, 108–116.

Gibbs, M.E., Anderson, D.G., Hertz, L., 2006. Inhibition of glycogenolysis in astrocytes interrupts memory consolidation in young chickens. Glia 54, 214–222.

Gilbert, E.R., Li, H., Emmerson, D.A., Webb Jr., K.E., Wong, E.A., 2008. Dietary protein quality and feed restriction influence abundance of nutrient transporter mRNA in the small intestine of broiler chicks. J. Nutr. 138, 262–271.

Gleeson, M., Brackenbury, J.H., 1984. Effects of body temperature on ventilation, blood gases and acid-base balance in exercising fowl. Q. J. Exp. Physiol 69, 61–72.

Godoy-Vitorino, F., Goldfarb, K.C., Karaoz, U., Leal, S., Garcia-Amado, M.A., Hugenholtz, P., Tringe, S.G., Brodie, E.L., Dominguez-Bello, M.G., 2012. Comparative analyses of foregut and hindgut bacterial communities in hoatzins and cows. ISME J. 6, 531–541.

Goodman, M.N., Larsen, P.R., Kaplan, M.M., Aoki, T.T., Young, V.R., Ruderman, N.B., 1980. Starvation in the rat. II. Effect of age and obesity on protein sparing and fuel metabolism. Am. J. Physiol. Endocrinol.Metab 239, E277–E286.

Goodridge, A.G., 1968a. Conversion of [U-14C] glucose into carbon dioxide, glycogen, cholesterol and fatty acids in liver slices from embryonic and growing chicks. Biochem. J. 108, 655–661.

Goodridge, A.G., 1968b. The effect of starvation and starvation followed by feeding on enzyme activity and the metabolism of [U-14C] glucose in liver from growing chicks. Biochem. J. 108, 667–673.

Grajal, A., Strahl, S.D., Parra, R., Gloria Dominguez, M., Neher, A., 1989. Foregut fermentation in the hoatzin, a neotropical leaf-eating bird. Science 245, 1236–1238.

Groscolas, R., Rodriguez, A., 1981. Glucose metabolism in fed and fasted emperor penguins (*Aptenodytes Forsteri*). Comp. Biochem. Physiol. 70A, 191–198.

Guerra-Romero, L., Täuber, M.G., Fournier, M.A., Tureen, J.H., 1992. Lactate and glucose concentrations in brain interstitial fluid, cerebrospinal fluid, and serum during experimental pneumococcal meningitis. J. Infect. Dis. 166, 546–550.

Guo, C.-T., Takahashi, N., Yagi, H., Kato, K., Takahashi, T., Yi, S.-Q., Chen, Y., Ito, T., Otsuki, K., Kida, H., Kawaoka, Y., Hidari, K.I.-P.J., Miyamoto, D., Suzuki, T., Suzuki, Y., 2007. The quail and chicken intestine have sialyl-galactose sugar chains responsible for the binding of influenza A viruses to human type receptors. Glycobiology 17, 713–724.

Hamano, Y., 2007. Continuous infusion of lipoic acid rapidly reduces plasma beta-hydroxybutyrate with elevation of non-esterified fatty acids in broiler chickens. Br. J. Nutr. 97, 495–501.

Hamer, M.J., Dickson, A.J., 1987. Developmental changes in hepatic fructose2,6-bisphosphate content and phosphofructokinase-1 activity in the transition of chicks from embryonic to neonatal nutritional environment. Biochem. J. 245, 35–39.

Hargrove, J.L., 2005. Adipose energy stores, physical work, and the metabolic syndrome: lessons from hummingbirds. Nutr. J. 4, 36.

Harms, C.A., Jinks, M.R., Harms, R.V., 2016. Blood gas, lactate, and hematology effects of venipuncture timing and location after mist-net capture of mourning doves (*Zenaida macroura*), boat-tailed grackles (*Quiscalus major*) and house sparrows (*Passer domesticus*). J. Wildl. Dis. 52, S54–S64.

Hawkes, L.A., Butler, P.J., Frappell, P.B., Meir, J.U., Milsom, W.K., Scott, G.R., Bishop, C.M., 2014. Maximum running speed of captive bar-headed geese is unaffected by severe hypoxia. PloS One 9, e94015.

Huang, Lin, L., Jin, Y., Liu, S., Xu, W., Zheng, Y.Y., 2012. Alternative splicing of testis-specific lactate dehydrogenase C gene in mammals and pigeon. Anim. Biotechnol. 23, 114–123.

Humphrey, B.D., Stephensen, C.B., Calvert, C.C., Klasing, K.C., 2004. Glucose and cationic amino acid transporter expression in growing chickens (*Gallus gallus domesticus*). Comp. Biochem. Physiol. A 138, 515–525.

Imagawa, T., Shogaki, K., Uehara, M., 2006a. Interaction between glycogen body cell and neuron: examination in co-culture system. J. Vet. Med. Sci. 68, 1081–1087.

Imagawa, T., Yamamoto, E., Sawada, M., Okamoto, M., Uehara, M., 2006b. Expression of lactate dehydrogenase-A and -B messenger ribonucleic acids in chick glycogen body. Poultry Sci. 85, 1232–1238.

Ito, T., Suzuki, Y., Takada, A., Kawamoto, A., Otsuki, K., Masuda, H., Yamada, M., Suzuki, T., Kida, H., Kawaoka, Y., 1997. Differences in sialic acid-galactose linkages in the chicken egg amnion and allantois influence human influenza virus receptor specificity and variant selection. J. Virol. 71, 3357–3362.

Itoh, N., Makita, T., Koiwa, M., 1998. Characteristics of blood chemical parameters in male and female quails. J. Vet. Med. Sci. 60, 1035–1037.

Jeffrey, D.A., Peakall, D.B., Miller, D.S., Herzberg, G.R., 1985. Blood chemistry changes in food-deprived herring gulls. Comp. Biochem. Physiol. A 81, 911–913.

Jenni-Eiermann, S., Jenni, L., 1992. High plasma triglyceride levels in small birds during migratory flight: a new pathway for fuel supply during endurance locomotion at very high mass-specific metabolic rates? Physiol. Zool. 65, 112–123.

Jenni-Eiermann, S., Jenni, L., Kvist, A., Lindstrom, A., Piersma, T., Visser, G.H., 2002. Fuel use and metabolic response to endurance exercise: a wind tunnel study of a long-distance migrant shorebird. J. Exp. Biol. 205, 2453–2460.

Johannsen, S.A., Rasmussen, M.A., Hensley, M.J., Wilhelms, K., Griffith, R., Scanes, C.G., 2005. Effects of lactobacilli and lactose on *Salmonella typhimurium* colonisation and microbial fermentation in the crop of the young Turkey. Br. Poultry Sci. 46, 708–716.

Johnstone, R.M., Mathew, A., Setchenska, M.S., Grdisa, M., White, M.K., 1998. Loss of glucose transport in developing avian red cells. Eur. J. Cell Biol. 75, 66–77.

Kalomenopoulou, M., Beis, I., 1990. Studies on the pigeon red blood cell metabolism. Comp. Biochem. Physiol. B 95, 677–684.

Karaganis, S.P., Bartell, P.A., Shende, V.R., Moore, A.F., Cassone, V.M., 2009. Modulation of metabolic and clock gene mRNA rhythms by pineal and retinal circadian oscillators. Gen. Comp. Endocrinol. 161, 179–192.

Kern, M., Bacon, W., Long, D., Cowie, R.J., 2005. Blood metabolite and corticosterone levels in breeding adult Pied Flycatchers. Condor 107, 665–677.

Khalilieh, A., McCue, M.D., Pinshow, B., 2012. Physiological responses to food deprivation in the house sparrow, a species not adapted to prolonged fasting. Am. J. Physiol. Regul. Integr. Comp. Physiol. 303, R551–R561.

Kinney, M.E., 2018. The effects of capture, restraint, and transport on hematologic, plasma biochemical, and blood gas values in Dalmatian pelicans (*Pelecanus crispus*). J. Avian Med. Surg. 32, 95–101.

Klandorf, H., Clarke, B.L., Scheck, A.C., Brown, J., 1986. Regulation of glucokinase activity in the domestic fowl. Biochem. Biophys. Res. Commun. 139, 1086–1093.

Knuth, S.T., Chaplin, S.B., 1994. The effect of exercise on plasma activities of lactate dehydrogenase and creatine kinase in red-tailed hawks (*Buteo jamaicensis*). J. Raptor Res. 28, 27–33.

Kono, T., Nishida, M., Nishiki, Y., Seki, Y., Sato, K., Akiba, Y., 2005. Characterisation of glucose transporter (GLUT) gene expression in broiler chickens. Br. Poultry Sci. 46, 510–515.

Kornasio, R., Halevy, O., Kedar, O., Uni, Z., 2011. Effect of *in ovo* feeding and its interaction with timing of first feed on glycogen reserves, muscle growth, and body weight. Poultry Sci. 90, 1467–1477.

Landys, M.M., Piersma, T., Guglielmo, C.G., Jukema, J., Ramenofsky, M., Wingfield, J.C., 2005. Metabolic profile of long-distance migratory flight and stopover in a shorebird. Proc. Biol. Sci. 272, 295–302.

Lea, R.W., Klandorf, H., Harvey, S., Hall, T.R., 1992. Thyroid and adrenal function in the ring dove (*Streptopelia risoria*) during food deprivation and a breeding cycle. Gen. Comp. Endocrinol. 86, 138–146.

Lee, K., Makino, S., Imagawa, T., Kim, M., Uehara, M., 2001. Effects of adrenergic agonists on glycogenolysis in primary cultures of glycogen body cells and telencephalon astrocytes of the chick. Poultry Sci. 80, 1736–1742.

Lee, M.Y., Park, S.H., Lee, Y.J., Heo, J.S., Lee, J.H., Han, H.J., 2006. EGF-induced inhibition of glucose transport is mediated by PKC and MAPK signal pathways in primary cultured chicken hepatocytes. Am. J. Physiol. 291, G744–G750.

Lisano, M.E., Kennamer, J.E., 1977. Values for several blood parameters in eastern wild turkeys. Poultry Sci. 56, 157–166.

Liu, N., Ru, Y.J., Li, F.D., Cowieson, A.J., 2008. Effect of diet containing phytate and phytase on the activity and messenger ribonucleic acid expression of carbohydrase and transporter in chickens. J. Anim. Sci. 86, 3432–3439.

Liu, M., Swanson, D.L., 2014. Physiological evidence that anthropogenic woodlots can substitute for native riparian woodlands as stopover habitat for migrant birds. Physiol. Biochem. Zool. 87, 183–195.

Lloyd, S., Gibson, J.S., 2006. Haematology and biochemistry in healthy young pheasants and red-legged partridges and effects of spironucleosis on these parameters. Avian Pathol. 35, 335–340.

Lomako, J., Lomako, W.M., Whelan, W.J., 1991. Proglycogen: a low-molecular-weight form of muscle glycogen. FEBS (Fed. Eur. Biochem. Soc.) Lett. 279, 223–228.

Louis, D.D., 1959. Differentiation of the glycogen body of the chick embryo under normal and experimental conditions. Growth 23, 235–249.

Louis, D.D., 1993. Origin of the avian glycogen body II. Observations in support of a glial nature in the chick embryo. Growth Dev. Aging 57, 275–281.

Low, M., Eason, D., Elliott, G., McInnes, K., Paul-Murphy, J., 2006. Hematological and biochemical reference ranges for kakapo (*Strigops habroptilus*): generation and interpretation in a field-based wildlife recovery program. J. Avian Med. Surg. 20, 80–88.

Lu, J.W., McMurtry, J.P., Coon, C.N., 2007. Developmental changes of plasma insulin, glucagon, insulin-like growth factors, thyroid hormones, and glucose concentrations in chick embryos and hatched chicks. Poultry Sci. 86, 673–683.

Lumeij, T.J., de Brujne, J.J., 1985. Blood chemistry reference values for racing pigeons. Avian Pathol. 14, 401–408.

Lyons, J.E., Collazo, J.A., Guglielmo, C.G., 2008. Plasma metabolites and migration physiology of semipalmated sandpipers: refueling performance at five latitudes. Oecologia 155, 417–427.

Martínez del Rio, C., Stevens, B.R., Daneke, D.E., Andreadis, P.T., 1988. Physiological correlates of preference and aversion for sugars in three species of birds. Physiol. Zool. 61, 222–229.

McWhorter, T.J., Bakken, B.H., Karasov, W.H., del Rio, C.M., 2006. Hummingbirds rely on both paracellular and carrier-mediated intestinal glucose absorption to fuel high metabolism. Biol. Lett. 2, 131–134.

Meynard, C., pez-Calleja, L., Bozinovic, V., Sabat, F.P., 1999. Digestive enzymes of a small avian herbivore, the rufous-tailed plantcutter. Condor 101, 904–907.

Merrill, G.F., Russo, R.E., Halper, J.M., 1981. Cardiac output distribution before and after endotoxin challenge in the rooster. Am. J. Physiol. 241, R67–R71.

Migliorini, R.H., Linder, C., Moura, J.L., Veiga, J.A.S., 1973. Gluconeogenesis in a carnivorous bird (black vulture). Am. J. Physiol. 225, 1389–1392.

Mizutani, A., Tsunashima, H., Nishijima, K., Sasamoto, T., Yamada, Y., Kojima, Y., Makoto Motono, M., Kojima, J., Inayoshi, Y., Miyake, K., Enoch Y Park, E.Y., Iijima, S., 2011. Genetic modification of a chicken expression system for the galactosylation of therapeutic proteins produced in egg white. Transgenic Res. 21, 63–67.

Mohammed, R., Salinas, C.E., Giussani, D.A., Blanco, C.E., Cogolludo, A.L., Villamor, E., 2017. Acute hypoxia-reoxygenation and vascular oxygen sensing in the chicken embryo. Phys. Rep. 5, e13501.

Molenaar, R., van den Borne, J.J.G.C., Hazejager, E., Kristensen, N.B., Heetkamp, M.J.W., Meijerhof, R., Kim, B., van den Brand, H., 2013. High environmental temperature increases glucose requirement in the developing chicken embryo. PloS One 8, e59637.

Möller, W., Kummer, W., 2003. The blood-brain barrier of the chick glycogen body (corpus gelatinosum) and its functional implications. Cell Tissue Res. 313, 71–80.

Moreno, M., Otero, M., Tur, J.A., Planas, J.M., Esteban, S., 1996. Kinetic constants of alpha-methyl-D-glucoside transport in the chick small intestine during perinatal development. Mech. Ageing Dev. 92, 11–20.

Mori, J.C., George, J.C., 1978. Seasonal changes in serum levels of certain metabolites, uric acid and calcium in the migratory Canada goose (*Branta canadiensis interior*). Comp. Biochem. Physiol. 59B, 263–269.

Newsholme, E.A., Taylor, K., 1969. Glycerol kinase activities in muscles from vertebrates and invertebrates. Biochem. J. 112, 465–474.

Nicolson, S.W., Fleming, P.A., 2014. Drinking problems on a 'simple' diet: physiological convergence in nectar-feeding birds. J. Exp. Biol. 217, 1015–1023.

O'Neill, I.E., Langslow, D.R., 1978. Glucose phosphorylation and dephosphorylation in chicken liver. Comp. Biochem. Physiol. 59B, 317–325.

Osman, A.M., 1982. Amylase in chicken intestine and pancreas. Comp. Biochem. Physiol. 73B, 571–574.

Parker, G.H., George, J.C., 1976. Changes in blood glucose, blood and muscle lactate, and plasma lactic dehydrogenase levels in the pigeon on acute exposure to cold. Arch. Int. Physiol. Biochim. 84, 517–526.

Patterson, B.A., Matarneh, S.K., Stufft, K.M., England, E.M., Scheffler, T.L., Preisser, R.H., Shi, H., Stewart, E.C., Eilert, S., Gerrard, D.E., 2017. Pectoralis major muscle of Turkey displays divergent function as correlated with meat quality. Poultry Sci. 96, 1492–1503.

Ponganis, P.J., Kooyman, G.L., Starke, L.N., Kooyman, C.A., Kooyman, T.G., 1997. Post-dive blood lactate concentrations in emperor penguins, *Aptenodytes forsteri*. J. Exp. Biol. 200, 1623–1626.

Pulikanti, R., Peebles, E.D., Keirs, R.W., Bennett, L.W., Keralapurath, M.M., Gerard, P.D., 2010. Pipping muscle and liver metabolic profile changes and relationships in broiler embryos on days 15 and 19 of incubation. Poultry Sci. 89, 860–865.

Regoeczi, E., Taylor, P., 1978. The net weight of the rat liver. Growth 42, 451–456.

Riesenfeld, G., Sklan, D., Bar, A., Eisner, U., Hurwitz, S., 1980. Glucose absorption and starch digestion in the intestine of the chicken. J. Nutr. 110, 117–121.

Riesenfeld, G., Geva, A., Hurwitz, S., 1982. Glucose homeostasis in the chicken. J. Nutr. 112, 2261–2266.

Riley Jr., W.W., Esteve-Garcia, E., Austic, R.E., 1986. Intestinal absorption of glucose and amino acids in chickens administered monensin. Poultry Sci. 65, 2292–2298.

Rinaudo, M.T., Curto, M., Bruno, R., 1982. Blood glucose and tissue glycogen concentrations in normal and deutectomised chickens during the first twelve hours after hatching. Br. Poultry Sci. 23, 577–581.

Romano, G.G., Menten, J.F.M., Freitas, L.W., Lima, M.B., Pereira, R., Zavarize, K.C., Dias, C.T.S., 2014. Effects of glycerol on the metabolism of broilers fed increasing glycerine levels. Braz. J. Poult. Sci. 16, 97–105.

Rosebrough, R.W., Von Vleck, M.F., 1990. Glucose production and glycogen cycle enzyme activities in avian liver explants: procedural optimization. Comp. Biochem. Physiol. 96B, 163–170.

Rosebrough, R.W., Geis, E., Henderson, K., Frobish, L.T., 1978b. Glycogen metabolism in the Turkey embryo and poult. Poultry Sci. 57, 747–751.

Rosebrough, R.W., Geis, E., Henderson, K., Frobish, L.T., 1979. Control of glycogen metabolism in the developing Turkey poult. Growth 43, 188–201.

Ruff, M.D., Allen, P.C., 1982. Changes in liver glycogen of broilers during coccidiosis. Vet. Parasitol. 10, 285–295.

Rutter, W.J., Krichevsky, P., Scott, H.M., Hansen, R.G., 1953. The metabolism of lactose and galactose in the chick. Poultry Sci. 32, 706–715.

Sartori, D.R., Kettelhut, I.C., Veiga, J.A., Migliorini, R.H., 1996. Gluconeogenesis and glucose replacement rate during long-term fasting of Japanese quails. Comp. Biochem. Physiol. Physiol. 115, 121–125.

Sartori, D.R., Garofalo, M.A., Roselino, J.E., Kettelhut, I.C., Migliorini, R.H., 2000. Gluconeogenesis and P-enolpyruvate carboxykinase in liver and kidney of long-term fasted quails. J. Comp. Physiol. B. 170, 373–377.

Savenije, B., Lambooij, E., Gerritzen, M.A., Venema, K., Korf, J., 2002. Effects of feed deprivation and transport on preslaughter blood metabolites, early postmortem muscle metabolites, and meat quality. Poultry Sci. 81, 699–708.

Scanes, C.G., 2008. Perspectives on analytical techniques and standardization. Poultry Sci. 87, 2175–2177.

Scanes, C.G., Campbell, R., Grimminger, P., 1987. Control of energy balance during egg production in the laying hen. J. Nutr. 117, 605–611.

Scholtz, N., Halle, I., Flachowsky, G., Sauerwein, H., 2009. Serum chemistry reference values in adult Japanese quail (*Coturnix coturnix japonica*) including sex-related differences. Poultry Sci. 88, 1186–1190.

Seebacher, F., Schwartz, T.S., Thompson, M.B., 2006. Transition from ectothermy to endothermy: the development of metabolic capacity in a bird (*Gallus gallus*). Proc. Biol. Sci. 273, 565–570.

Seki, Y., Sato, K., Kono, T., Abe, H., Akiba, Y., 2003. Broiler chickens (Ross strain) lack insulin-responsive glucose transporter GLUT4 and have GLUT8 cDNA. Gen. Comp. Endocrinol. 133, 80–87.

Seki, Y., Sato, K., Kono, T., Akiba, Y., 2006. Two types of phosphofructokinase-1 differentially regulate the glycolytic pathway in insulin-stimulated chicken skeletal muscle. Comp. Biochem. Physiol. B Biochem. Mol. Biol. 143, 344–350.

Shea, R.E., Olson, J.M., Ricklefs, R.E., 2007. Growth rate, protein accumulation, and catabolic enzyme activity of skeletal muscles of galliform birds. Physiol. Biochem. Zool. 80, 306–316.

Shimamoto, S., Ijiri, D., Kawaguchi, M., Nakashima, K., Ohtsuka, A., 2016. Gene expression pattern of glucose transporters in the skeletal muscles of newly hatched chicks. Biosci. Biotechnol. Biochem. 80, 1382–1385.

Shimizu, M., Jones, D.R., 1987. Acid-base balance in ducks (*Anas platyrhynchos*) during involuntary submergence. Am. J. Physiol. 252, R348–R352.

Sibut, V., Le Bihan-Duval, E., Tesseraud, S., Godet, E., Bordeau, T., Cailleau- Audouin, E., Chartrin, P., Duclos, M.J., Berri, C., 2008. Adenosine monophosphate-activated protein kinase involved in variations of muscle glycogen and breast meat quality between lean and fat chickens. J. Anim. Sci. 86, 2888–2896.

Simon, J., Rideau, N., Taouis, M., Dupont, J., 2011. Plasma insulin levels are rather similar in chicken and rat. Gen. Comp. Endocrinol. 171, 267–268.

Simon, J., Milenkovic, D., Godet, E., Cabau, C., Collin, A., Métayer-Coustard, S., Rideau, N., Tesseraud, S., Derouet, M., Crochet, S., Cailleau- Audouin, E., Hennequet-Antier, C., Gespach, C., Porter, T.E., Duclos, M.J., Dupont, J., Cogburn, L.A., 2012. Insulin immune-neutralization in fed chickens: effects on liver and muscle transcriptome. Physiol. Genom. 44, 283–292.

Sinsigalli, N.A., McMurtry, J.P., Cherry, J.A., Siegel, P.B., 1987. Glucose tolerance, plasma insulin and immunoreactive glucagon in chickens selected for high and low body weight. J. Nutr. 117, 941–947.

Sitbon, G., Mialhe, P., 1979. Pancreatic hormones and plasma glucose: regulation mechanisms in the goose under physiological conditions. IV-effects of food ingestion and fasting on pancreatic hormones and gut GLI. Horm. Metab. Res. 11, 123–129.

Sherlock, L., Wathes, C.M., Cheng, Z., Wathes, D.C., 2012. Differential hepatic gene expression in the broiler chicken in response to the combined stressors of food withdrawal, catching and transport at the end of production. Stress 15, 293–305.

Soleimani, A.F., Zulkifli, I., 2010. Effects of high ambient temperature on blood parameters in red jungle fowl, village fowl and broiler chickens. J. Anim. Vet. Adv. 9, 1201–1207.

Suarez, R.K., Lighton, J.R., Moyes, C.D., Brown, G.S., Gass, C.L., Hochachka, P.W., 1990. Fuel selection in rufous hummingbirds: ecological implications of metabolic biochemistry. Proc. Natl. Acad. Sci. U.S.A 87, 9207–9210.

Suarez, R.K., Lighton, J.R., Brown, G.S., Mathieu-Costello, O., 1991. Mitochondrial respiration in hummingbird flight muscles. Proc. Natl. Acad. Sci. U.S.A 88, 4870–4873.

Suarez, R.K., Welch Jr., K.C., Hanna, S.K., Herrera, M.L.G., 2009. Flight muscle enzymes and metabolic flux rates during hovering flight of the nectar bat, *Glossophaga soricina*: further evidence of convergence with hummingbirds. Comp. Biochem. Physiol. 153A, 136–140.

Suarez, R.K., Herrera, M.L.G., Welch Jr., K.C., 2011. The sugar oxidation cascade: aerial refueling in hummingbirds and nectar bats. J. Exp. Biol. 214, 172–178.

Sweazea, K.L., Braun, E.J., 2006. Glucose transporter expression in English sparrows (*Passer domesticus*). Comp. Biochem. Physiol. 144B, 263–270.

Takahashi, K., Kawamata, K., Akiba, Y., Okada, T., 2001. Effect of dietary sorbitol on growth performance and plasma acute phase protein concentration in male broiler chickens during immunological stimulation. J. Poultry Sci. 39, 84–90.

Takahashi, K., Mashiko, T., Saito, S., Akiba, Y., 2002. Effect of dietary xylitol on growth performance and nitrogen retention in male broiler chicks during immunological stimulation. Asian Austral. J. Anim. Sci. 15, 84–88.

Takahashi, K., Kawamata, K., Akiba, Y., 2005. Effect of xylitol feeding on antibody production and inflammatory responses in broiler chicks. J. Poultry Sci. 42, 245–253.

Tangara, M., Chen, W., Xu, J., Huang, F.R., Peng, J., 2010. Effects of *in ovo* feeding of carbohydrates and arginine on hatchability, body weight, energy metabolism and perinatal growth in duck embryos and neonates. Br. Poultry Sci. 51, 602–608.

Tasharofi, S., Mohammadi, F., Amiri, N., Nazem, M.N., 2018. Effects of intra-yolk-sac injection of dextrose and albumin on performance, jejunum morphology, liver and pectoral muscle glycogen and some serum metabolites of broilers. J. Anim. Physiol. Anim. Nutr. 102, 917–923.

Tinker, D.A., Brosnan, J.T., Herzberg, G.R., 1986. Interorgan metabolism of amino acids, glucose, lactate, glycerol and uric acid in the domestic fowl (*Gallus domesticus*). Biochem. J. 240, 829–836.

Tokushima, Y., Takahashi, K., Sato, K., Akiba, Y., 2005. Glucose uptake *in vivo* in skeletal muscles of insulin-injected chicks. Comp. Biochem. Physiol. 141B, 43–48.

Totzke, U., Hübinger, A., Bairlein, F., 1998. Glucose utilization rate and pancreatic hormone response to oral glucose loads are influenced by the migratory condition and fasting in the garden warbler (*Sylvia borin*). J. Endocrinol. 158, 191–196.

Tracy, C.R., McWhorter, T.J., Wojciechowski, M.S., Pinshow, B., Karasov, W.H., 2001. Carbohydrate absorption by blackcap warblers (*Sylvia atricapill*a) changes during migratory refuelling stopovers. J. Exp. Biol. 213, 380–385.

Uni, Z., Tako, E., Gal-Garber, O., Sklan, D., 2003. Morphological, molecular, and functional changes in the chicken small intestine of the late-term embryo. Poultry Sci. 82, 1747–1754.

Vaillancourt, E., Weber, J.M., 2007. Lipid mobilization of long-distance migrant birds in vivo: the high lipolytic rate of ruff sandpipers is not stimulated during shivering. J. Exp. Biol. 210, 1161–1169.

Van Kha, H.V., Le Maho, Y., Cagnard, M., 1979. Changes in plasma levels of metabolites during long-term fasting in the goose. C. R. Seances Acad. Sci. D 289, 955–958.

Veiga, J.A., Roselino, E.S., Migliorini, R.H., 1978. Fasting, adrenalectomy, and gluconeogenesis in the chicken and a carnivorous bird. Am. J. Physiol. 234, R115–R121.

Verbeek, M.M., Leen, W.G., Willemsen, M.A., Slats, D., Claassen, J.A., 2016. Hourly analysis of cerebrospinal fluid glucose shows large diurnal fluctuations. J. Cerebr. Blood Flow Metabol. 36, 899–902.

Vinardell, M.P., Lopera, M.T., 1987. Jejunal and cecal 3-oxy-methyl-Dglucose absorption in chicken using a perfusion system in vivo. Comp. Biochem. Physiol. 86A, 625–657.

Vleck, C.M., Vleck, D., 2002. Physiological condition and reproductive consequences in Adelie penguins. Integr. Comp. Biol. 42, 76–83.

Wagstaff, P., Kang, H.Y., Mylott, D., Robbins, P.J., White, M.K., 1995. Characterization of the avian GLUT1 glucose transporter: differential regulation of GLUT1 and GLUT3 in chicken embryo fibroblasts. Mol. Biol. Cell 6, 1575–1589.

Walter, I., Hegarty, B., Seebacher, F., 2010. AMP-activated protein kinase controls metabolism and heat production during embryonic development in birds. J. Exp. Biol. 213, 3167–3176.

Walsberg, G.E., Wolf, B.O., 1995. Variation in the respiratory quotient of birds and implications for indirect calorimetry using measurements of carbon dioxide production. J. Exp. Biol. 198, 213–219.

Wang, X., Li, J., Cong, J., Chen, X., Zhu, X., Zhang, L., Gao, F., Zhou, G., 2017. Preslaughter transport effect on broiler meat quality and postmortem glycolysis metabolism of muscles with different fiber types. J. Agric. Food Chem. 65, 10310–10316.

Watterson, R.L., 1949. Development of the glycogen body of the chick spinal cord. J. Morphol. 85, 337–390.

Webb, D.M., DeNicola, D.B., Van Vleet, J.F., 1991. Serum chemistry alterations, including creatine kinase isoenzymes, in furazolidone toxicosis of ducklings: preliminary findings. Avian Dis. 35, 662–667.

Welch, K.C., Suarez, R.K., 2007. Oxidation rate and turnover of ingested sugar in hovering Anna's (*Calypte anna*) and rufous (*Selasphorus rufus*) hummingbirds. J. Exp. Biol. 210, 2154–2162.

Welch Jr., K.C., Altshuler, D.L., Suarez, R.K., 2007. Oxygen consumption rates in hovering hummingbirds reflect substrate-dependent differences in P/O ratios: carbohydrate as a 'premium fuel'. J. Exp. Biol. 210, 2146–2153.

Weurding, R.E., Veldman, A., Veen, W.A., van der Aar, P.J., Verstegen, M.W., 2001. Starch digestion rate in the small intestine of broiler chickens differs among feedstuffs. J. Nutr. 131, 2329–2335.

Willemsen, H., Li, Y., Willems, E., Franssens, L., Wang, Y., Decuypere, E., Everaert, N., 2011. Intermittent thermal manipulations of broiler embryos during late incubation and their immediate effect on the embryonic development and hatching process. Poultry Sci. 90, 1302–1312.

Williams, C.L., Sato, K., Shiomi, K., Ponganis, P.J., 2012. Muscle energy stores and stroke rates of emperor penguins: implications for muscle metabolism and dive performance. Physiol. Biochem. Zool. 85, 120–133.

Wilson-O'Brien, A.L., Patron, N., Suzanne Rogers, S., 2010. Evolutionary ancestry and novel functions of the mammalian glucose transporter (GLUT) family. BMC Evol. Biol. 10, 152.

Witmer, M.C., Van Soest, P.J., 1998. Contrasting digestive strategies of fruit-eating birds. Funct. Ecol. 12, 728–741.

Wong, G.K., Cavey, M.J., 1992. Development of the chick embryo: 1. hepatic cords and sinuses. Anat. Rec. 234, 555–567.

Wright, A.D., Northwood, K.S., Obispo, N.E., 2009. Rumen-like methanogens identified from the crop of the folivorous South American bird, the hoatzin (*Opisthocomus hoazin*). ISME J. 3, 1120–1126.

Xie, P., Wan, X.P., Yang, C.X., Zhu, J.G., Xu, Y.G., Gong, D.Q., 2020. Effects of incubation and chick rearing on intestinal morphology, digestive enzyme activities, and mRNA expression of nutrient transporter genes in the pigeon (*Columba livia*) under artificial farming conditions. Poultry Sci. 99, 2785–2797.

Xing, T., Wang, M.F., Han, M.Y., Zhu, X.S., Xu, X.L., Zhou, G.H., 2017. Expression of heat shock protein 70 in transport-stressed broiler pectoralis major muscle and its relationship with meat quality. Animal 11, 1599–1607.

Xu, J., Tang, S., Song, E., Yin, B., Wu, D., Bao, E., 2017. Hsp70 expression induced by Co-Enzyme Q10 protected chicken myocardial cells from damage and apoptosis under in vitro heat stress. Poultry Sci. 96, 1426–1437.

Yadgary, L., Yair, R., Uni, Z., 2011. The chick embryo yolk sac membrane expresses nutrient transporter and digestive enzyme genes. Poultry Sci. 90, 410–416.

Yap, K.N., Kim, O.R., Harris, K.C., Williams, T.D., 2017. Physiological effects of increased foraging effort in a small passerine. J. Exp. Biol. 220, 4282–4291.

Yeh, Y.Y., Leveille, G.A., 1971a. *In vitro* and *in vivo* restoration of hepatic lipogenesis in fasted chicks. J. Nutr. 101, 803–809.

Yeh, Y.Y., Leveille, G.A., 1971b. Studies on the relationship between lipogenesis and the level of coenzyme A derivatives, lactate and pyruvate in chick liver. J. Nutr. 101, 911–918.

YlaÄjos, M., Ruusunen, M., Puolanne, E., 2006. Glycogen debranching enzyme and some other factors relating to *post mortem* pH decrease in poultry muscles. J. Sci. Food Agric. 87, 394–398.

Yue, H.Y., Zhang, L., Wu, S.G., Xu, L., Zhang, H.J., Qi, G.H., 2010. Effects of transport stress on blood metabolism, glycolytic potential, and meat quality in meat-type yellow-feathered chickens. Poultry Sci. 89, 413–419.

Zhai, W., Bennett, L.W., Gerard, P.D., Pulikanti, R., Peebles, E.D., 2011. Effects of *in ovo* injection of carbohydrates on somatic characteristics and liver nutrient profiles of broiler embryos and hatchlings. Poultry Sci. 90, 2681–2688.

Zhang, C.L., Niu, Z.Y., Hou, S.S., Liu, F.Z., Huang, W., Xie, M., 2005. The effect of force-feeding, fasting and glucose saturated water intake on the contents of some biochemical parameters in plasma of Peking ducks. Int. J. Poultry Sci. 4, 202–205.

Zhao, J.P., Bao, J., Wang, X.J., Jiao, H.C., Song, Z.G., Lin, H., 2012. Altered gene and protein expression of glucose transporter1 underlies dexamethasone inhibition of insulin-stimulated glucose uptake in chicken muscles. J. Anim. Sci. 90, 4337–4345.

Zhao, M.M., Gao, T., Li, J.L., Lv, P.A., Yu, L.L., Gao, F., Zhou, G.H., 2017. Effects of *in ovo* feeding of creatine pyruvate on the hatchability, growth performance and energy status in embryos and broilers chicks. Animal 11, 1689–2697.

Zhao, M.M., Gong, D.Q., Gao, T., Zhang, L., Li, J.L., Lv, P.A., Yu, L.L., Gao, F., Zhou, G.H., 2018. *In ovo* feeding of creatine pyruvate modulates growth performance, energy reserves and mRNA expression levels of gluconeogenesis and glycogenesis enzymes in liver of embryos and neonatal broilers. J. Anim. Physiol. Anim. Nutr. 102, e758–e767.

Zhang, L., Yue, H.Y., Zhang, H.J., Xu, L., Wu, S.G., Yan, H.J., Gong, Y.S., Qi, G.H., 2009. Transport stress in broilers: I. Blood metabolism, glycolytic potential, and meat quality. Poultry Sci. 88, 2033–2041.

Further reading

Gao, B., Jeong, W.-I., Tian, Z., 2008. The liver: an organ with predominant innate immune. Hepatology 47, 729–736.

Hansen, B.F., Asp, S., Kiens, B., Richter, E.A., 1999. Glycogen concentration in human skeletal muscle: effect of prolonged insulin and glucose infusion. Scand. J. Med. Sci. Sports 9, 209–213.

Jensen, J., Rustad, P.I., Kolnes, A.J., Lai, Y.-C., 2011. The role of skeletal muscle glycogen breakdown for regulation of insulin sensitivity by exercise. Front. Physiol. 2, 112.

Koshoridze, N.I., Aleksidze, N.G., Surguladze, N.B., 2003. Inositol- and galactose-binding lectins of chicken brain fractions enriched with glial cells. J. Evol. Biochem. Physiol. 39, 446–450.

Leheska, J.M., Wulf, D.M., Maddock, R.J., 2003. Effects of fasting and transportation on pork quality development and extent of postmortem metabolism. J. Anim. Sci. 81, 3194–3202.

Remesar, X., Alemany, M., 1980. Changes-induced in liver and muscle glycogen and glycogen enzymes by 24-hour fasting in the rat. Horm. Metab. Res. 12, 19–22.

Rosebrough, R.W., Geis, E., Henderson, K., Frobish, L.T., 1978a. Glycogen depletion and repletion in the chick. Poultry Sci. 57, 1460–1462.

Rosenvold, K., Petersen, J.S., Lærke, H.N., Jensen, S.K., Therkildsen, M., Karlsson, A.H., Møller, H.S., Andersen, H.J., 2001. Muscle glycogen stores and meat quality as affected by strategic finishing feeding of slaughter pigs. J. Anim. Sci. 79, 382–391.

Sahlin, K., Katz, A., Henriksson, J., 1987. Redox state and lactate accumulation in human skeletal muscle during dynamic exercise. Biochem. J. 245, 551–556.

Sjøberg, K.A., Frøsig, C., Kjøbsted, R., Sylow, L., Kleinert, M., Betik, A.C., Shaw, C.S., Kiens, B., Wojtaszewski, J.F.P., Rattigan, S., Richter, E.A., McConell, G.K., 2017. Exercise increases human skeletal muscle insulin sensitivity via coordinated increases in microvascular perfusion and molecular signaling. Diabetes 66, 1501–1510.

Sterten, H., Oksbjerg, N., Frøystein, T., Ekker, A.S., Kjos, N.P., 2010. Effects of fasting prior to slaughter on pH development and energy metabolism post-mortem in *M. longissimus dorsi* of pigs. Meat Sci. 84, 93–100.

Wang, M.Y., Tsai, M.Y., Wang, C., 1994. Identification of chicken liver glucose transporter. Arch. Biochem. Biophys. 310, 172–179.

Chapter 26

Adipose tissue and lipid metabolism

Nadia Everaert[1], Eddy Decuypere[2] and Johan Buyse[2]
[1]Precision Livestock and Nutrition Unit, TERRA Teaching and Research Centre, Gembloux Agro-Bio Tech, University of Liège, Gembloux, Belgium;
[2]Laboratory of Livestock Physiology, Department of Biosystems, Faculty of Bioscience Engineering, KU Leuven, Leuven, Belgium

Abbreviations

ACC acetyl-CoA carboxylase Apo: apoprotein
C/EBP CCAAT/Enhancer binding protein FAS: fatty acid synthase
FTO Fat mass and obesity-associated (FTO) gene GH: growth hormone
HDL high-density lipoproteins IGF: insulin-like growth factor LDL: low-density lipoproteins LEPR: leptin receptor
LPL lipoprotein lipase ME: metabolizable energy
NEFA nonesterified fatty acids
PPARγ peroxisome proliferator-activated receptor γ SREBP: sterol regulatory element binding protein TAG: triacylglycerol
TNFα tumor necrosis factor-α VLDL: very low-density lipoproteins
VLDLy yolk-targeted very low-density lipoproteins

26.1 Introduction

The presumed predominant function of adipose tissue is to maintain energy homeostasis. In times of feed excess, energy is stored as hydrophobic triglyerides or triacylglycerols (TAGs) in expansive lipid droplets within the adipocytes. TAGs are very well suited for this as they contain a large amount of energy per unit of weight. In times of feed deprivation, however, adipocyte TAGs are mobilized (lipolysis), and the generated fatty acids are subsequently oxidized by various tissues to yield chemical energy. Adipose tissue is the most variable carcass component and the amount that is deposited depends on genetic as well as on exogenous factors. However, it has been become clear that adipose issue is more than only a storage buffer for energy as it also functions as an important endo- and paracrine tissue involved in many bodily processes.

26.2 Development of adipose tissue

Adipose tissue development at the cellular level consists of an increase in cell number (hyperplasia) on the one hand and of an increase in cell volume (hypertrophy) on the other hand (e.g., Wang 2019). Both adipocyte number and volume increase with age and are positively correlated with fat pad weight and with body mass (Cartwright, 1991). Hence, both hyperplasia and hypertrophy of adipose cells contribute to the accumulation of fat in the chicken. However, the magnitude of the contribution of each of these two factors to the final size and weight of the distinct fat tissues is not equal.

At younger age, increases in weight of fat depots would be mainly attributable to an increase in fat cell number whereas at later ages, lipid accumulation in fat cells would be the major determinant. Literature data are not consistent about the age at which hypertrophy becomes the most important contributor to adipose tissue growth. It was first observed that in broiler chickens of a commercial strain, the number of abdominal adipocytes increased until about 12 to 14 weeks of age whereas adipocyte volume only increased slowly. After this age, the filling of the existing adipose cells was then the predominant factor responsible for the increase in weight of the abdominal fat pad (Hood, 1982; March et al., 1984; Cartwright, 1991). In contrast, more recent studies revealed that at about seven weeks of age, increases in fat deposition were primarily due to adipocyte hypertrophy in broiler chickens (Guo et al., 2011). Still, new adipocyte formation is possible even when a positive energy balance is maintained after hypertrophy, at least in mammals and probably also in birds; then hyperplasia resumes and a greater than normal number of adipose cells is developed. Moreover, adipocytes have also been reported to dedifferentiate: mature adipocytes loose then their lipid filled morphology and assume a fibroblast-like appearance and regain preadipocyte characteristics (Kokta et al., 2004).

The modern, growth-selected meat-type chickens are proportionally fatter compared to randombred, unselected, or even growth-selected chickens of some decades ago. Therefore, it is reasonable to assume that the age at which hypertrophy becomes the major determinant for body fat accumulation is shifted to younger age and even to a lower

Sturkie's Avian Physiology. https://doi.org/10.1016/B978-0-12-819770-7.00015-3

degree of maturity. Fast-growing chickens will probably also attain their genetically determined final number of fat cells earlier than slower-growing chickens. Furthermore, sex (Hood, 1982), nutritional status (March et al., 1984; Cartwright, 1991), and surely (in)direct divergent selection for fatness (Hood and Pym, 1982; Guo et al., 2011) all affect the age- or body weight−dependent developmental pattern of adipose cellularity. As a consequence of the increase in adipocyte number and size but with a different velocity, a bimodal frequency distribution (proportional number of cells per diameter class) is present in the abdominal fat pad of broilers by seven weeks of age. With increasing age up to 22 weeks, the number of fat cells in the population of "large" cells increased slowly and the mean diameter shifted to larger values. In contrast, the number of cells in the population of "small" cells increased more rapidly but the mean cell diameter remained unchanged (March et al., 1984). A same phenomenon was observed by Merkley and Cartwright (1989) for abdominal, thigh, back, and neck fat pads. It can be concluded that differences in fatness between populations, even when considered on a same body weight basis, are attributable to both the number and size/volume of adipocytes whereas reductions in body fat content by, e.g., dietary manipulations, are mainly caused by delipidation of adipocytes (hypotrophy).

26.3 Structure, cellularity

The first step in adipogenesis is the differentiation of chicken embryonic stem cells into white preadipocytes, a process that is induced by insulin and dexamethasone (Li et al., 2011). The resulting adipocyte precursors are present in the stromal-vascular fraction of adipose tissue. These preadipocytes proliferate and then undergo differentiation to multilocular immature white adipocytes. When becoming filled with lipids, unilocular mature adipocytes appear which are characterized by distinct morphological and metabolic features (Butterwith, 1988; Evans, 1977). A mature avian fat cell (average diameter of 150 μm) is characterized by the presence of a large lipid droplet which occupies more than 80% of the total cell volume. As a consequence, all other cell organelles are displaced to the periphery where the cytoplasm appears as a narrow rim. Another morphological feature of avian adipocytes is the presence of microfilaments at the interface between cytoplasm and lipid droplet and which may provide structural support to the adipocyte (Evans, 1977; Hood, 1982).

Most of the studies concerning adipogenesis were done using cell culture systems with cell lines from mammalian and to a much lesser extent from avian (chicken and duck) origin (Wang, 2019) and were mainly focused on its endocrine regulation. It was observed that the proliferation of chicken preadipocytes grown in culture was stimulated when insulin was added to the medium. When the medium was supplemented with 10% dialyzed chicken serum or when insulin was deleted from the medium, proliferation was retarded. Moreover, it was found that chicken preadipocyte proliferation in vitro was stimulated by insulin-like growth factor (IGF)-I and −II, fibroblast growth factor-1 and -2, epidermal growth factor, transforming growth factor-α and −β, and platelet-derived growth factor (Butterwith, 1997). On the other hand, most of these growth factors also inhibit preadipocyte differentiation. These data suggest that these growth factors may be important autocrine/paracrine/endocrine regulators of preadipocyte proliferation and differentiation although species-dependent differences have to be taken into account (Wang et al., 2012a,b,c; Wang, 2019). In addition, glucose (Qi et al., 2012), dexamethasone, and insulin (Ramsay and Rosebrough, 2003) also stimulate preadipocyte differentiation. Furthermore, in a recent review, Wang (2019) summarized that exogenous fatty acids (especially oleic acid for lipid droplet deposition) are critical factors in chicken and duck preadipocyte differentiation. At the molecular level, transcription factor such as peroxisome proliferator-activated receptor-γ (PPARγ), CCAAT/enhancer binding proteins (C/EBPs), and Sterol response element-binding proteins (SREBP) are important regulators of preadipocyte differentiation through modulation of expression and activity levels of relevant genes (summarized by Wang, 2019).

26.4 Body composition

The modern meat-type chickens contain between 150 and 220 g of lipids per kg body weight at commercial slaughter age. Adipose tissue is distributed over several fat depots of which the abdominal fat pad is the largest, followed by neck, thigh, back, and gizzard fat pads. These fat depots represent about 20% of the total body fat content. The skeleton and the skin contain, respectively, 15% and 19% of the total body lipid content whereas several smaller fat depots represent about 8% of the total body fat content. The rest of the carcass contains then about one third of the total body lipid content. As avian striated muscle is characterized by only small amounts of inter- and intramuscular fat (1.5%), the remaining lipids must be located in the intestines, lungs, kidneys, glands, etc (Nir et al., 1988).

The abdominal fat pad weight is highly positively correlated with total body fat content and as it is rather easy to dissect it quantitatively, abdominal fat pad weight has been used extensively as an excellent estimator of total body fat content (Sonaiya, 1985). Indeed, selection against fatness in meat-type chickens by means of selection against abdominal fat content has been proven to be very successful (Leclercq, 1984; Baéza and Le Bihan-Duval, 2013).

The growth of higher vertebrates is not simply an increase in weight but consists also of changes in body

conformation and composition due to the differential growth rate of the constituent parts and of their functional abilities (Pálsson, 1955). The relationship between the weight of a part (Y) of the body in relation to total body weight (X) can be described by the Huxley equation:

$$Y = aX^b$$

Or after logarithmic transformation:

$$\ln Y = \ln a + b \ln X$$

The regression coefficient b is also referred to as the allometric coefficient. When $b = 1$, the weight of the dependent variable Y increases proportionally with the weight of the independent variable X (isometric). When $b \neq 1$, the proportionality of absolute weights is not maintained, but the ratio between the relative growth rates of both Y and X remains constant during the growth trajectory.

As in mammals, the allometric coefficient for the growth of body fat in relation to body weight is also greater than unity in avian species. However, not all adipose tissues, including intramuscular and physiologically necessary fat, mature at the same rate as reflected in their different allometric coefficients. Merkley and Cartwright (1989) reported greater weight gains in abdominal and back fat than neck and sartorius fat depots between 8 and 16 weeks of age of commercial female broilers. Nir et al. (1988) observed that in broiler lines selected for or against abdominal fat content, the allometric coefficients (pooled for both lines) of several fat depots increased in the following order: sartorial ≈ neck fat (0.83) < gizzard fat (1.030) < abdominal fat (1.17) < mesenteric fat (2.51). The allometric coefficients were higher for the high fat line chickens (average 1.24) compared to the low fat line chickens (average 1.02). From our studies on commercial broilers reared under continuous illumination, the following allometric coefficients were calculated: sartorial fat (1.137) ≈ scapular fat (1.171) < heart fat (1.284) < abdominal fat (1.615) ≈ stomach fat (1.623). It can also be concluded that the abdominal fat pad is relatively more affected by (non)genetic factors than other fat depots and even the fat deposited in the rest of the carcass. However, the mechanisms involved in the differential allometric growth of adipose tissues and in the regulation of the discriminative effects of genetic and exogenous factors according to their location in the body, remain to be elucidated further.

26.5 Functions of adipose tissue

26.5.1 Energy reservoir

In chickens, lipids, and especially TAGs are stored in hepatocytes, growing oocytes (for laying hens), and adipocytes (Alvarenga et al., 2011). Lipid storage in the oocytes is associated with vitellogenesis (Walzem et al., 1994), while excessive fat accumulation in the liver causes hepatic steatosis and fatty liver haemorrhagic syndrome in laying hens (Alvarenga et al., 2011). Adipose tissue (fat) is a form of loose connective tissue composed of adipocytes, able to store large quantities of excess TAGs, which can be released for oxidation (primarily by skeletal muscle) for the synthesis of ATP. Although variable between fat depots, the hydrophobic lipid content of adipocytes can mount up to 90% of the fresh tissue weight (Evans, 1977; Nir et al., 1988). Taking into account the high-energy content of lipids (±39 kJ/g) compared to protein (±23 kJ/g) and carbohydrates (±18 kJ/g), adipose tissue is indeed an appropriate reservoir of energy. In addition, fat tissue (e.g., subcutaneous fat) can play a role in insulation, is important in thermoregulation, and can act as a protective shield for internal organs. More recent studies however have revealed that adipose tissue is also involved in numerous other processes and biological functions such as appetite regulation, reproduction, angiogenesis, coagulation, fibrinolysis, vascular tone control, and immunity.

26.5.2 Adipokines

Adipose tissue is not just equal to a sum of adipose cells. In adipose tissue, 90% of adipose mass may account for roughly 25% of total cell population, the other cells being fibroblasts, blood cells, endothelial cells, pericytes, mesenchymal cells, preadipocytes, nerve tissue and immune cells, all being targets for an extensive autocrine-paracrine cross-talk with each other and involved in adipogenesis (Frühbeck and Gómez-Ambrosi, 2005). Hence adipose tissue is a multifunctional organ rather than a passive organ for the storage of excess energy in the form of fat. Indeed, fat cells are able to secrete a large number of hormones, growth factors, cytokines, and matrix proteins collectively termed adipokines or adipocytokines. At the same time, adipocytes have receptors (see Section 26.5.3) for many of these adipokines as well as for several systemic hormonal factors (e.g., pituitary and pancreatic hormones).

26.5.2.1 Leptin

The existence of avian leptin was finally confirmed by Seroussi et al. (2016). The leptin gene sequence is extremely rich in guanine-cytosine (GC) content (about 70%); there is a low sequence of conservation for both the nucleic and amino acid sequences (≤30%), and low expression level (Friedman-Einat and Seroussi, 2019). Indeed, leptin expression in adipose tissue ranges from unexpressed in wild chicken red junglefowl to low levels of expression, which is unaffected by feed deprivation (Bornelöv et al., 2018), selection for fast or slow body growth (Resnyk et al., 2017), or lean or fat genotype (Resnyk et al.,

2015). Therefore, it is assumed that adipose tissue in chicken is not signaling the amount of fat stores via leptin. Moreover, it is hypothesized that leptin requires other proteins than the leptin receptor to interact with for its functioning, that may be another role than acting as an adipostat signaling molecule (Friedman-Einat and Seroussi, 2019). To better understand the function of leptin in birds, studies at the protein level are needed.

26.5.2.2 Adiponectin

Adiponectin as well as its receptors (ADIPOR1 and ADIPOR2) are expressed in many tissues, including adipose tissue in the chicken (Hendricks et al., 2009; Ghazanfari et al., 2011; Mellouk et al., 2018a), and the expression of the adiponectin system in adipose tissue (and muscle) depends on the gender and age of the animals (Zhang et al., 2017). Plasma adiponectin, especially the plasma heavy molecular weight adiponectin isoform, and adiponectin mRNA levels in adipose tissue are inversely related to abdominal fat pad weight in chicken (Hendricks et al., 2009; Tahmoorespur et al., 2010). In adipose tissue and muscle, adiponectin seems to limit lipid deposition (Mellouk et al., 2018a), and it is suggested that it may stimulate feed intake (Sintubin et al., 2014).

26.5.2.3 Visfatin

Visfatin is another adipokine hormone involved in chickens in the regulation of muscle growth, metabolism, feed intake, and reproductive functions (Mellouk et al., 2018a). Chicken visfatin is 92−94% homologous to mammalian visfatin and mainly expressed in skeletal muscle rather than in abdominal and subcutaneous fat in chicken; therefore it is rather a myokine than an adipokine (Krzysik-Walker et al., 2008; Li et al., 2012). Nevertheless, fat-line chickens selected for high abdominal fat have a higher expression of visfatin in adipose tissue compared to their lean line counterparts (Cogburn et al., 2011). In line with these results, Li et al. (2017) showed that visfatin is more expressed in adipose tissue of a fast growing broiler line compared to a slow growing one, suggesting a potential role as a marker of fat accumulation.

26.5.2.4 Chemerin

Chemerin is an adipose cytokine that is expressed in chicken and turkeys in the liver, heart, adipose tissue, muscles, and ovarian cells (Diot et al., 2015; Mellouk et al., 2018b). In broiler hens, plasma chemerin levels are negatively correlated with the fattening state, and feed restriction decreases the mRNA levels of chemerin in liver and adipose tissue (Mellouk et al., 2018b). Further research is needed to determine the role of chemerin in metabolism and reproduction (Mellouk et al., 2018a).

26.5.2.5 Other adipokines

Tumor necrosis factor-α (TNFα), interferon-ɣ and interleukin-6, three prominent adipokines in mammals that operate in concert with leptin to control appetite, insulin resistance, and inflammation, are expressed at low levels in chicken in visceral fat (Bornelöv et al., 2018). In addition, TNFα is not affected by feed deprivation (Bornelöv et al., 2018).

As several adipokines, known in mammals to signal on energy stores in adipose tissue, do not play such role in birds, it is suggested that adipose tissue in birds may have a different endocrine role (Friedmain-Einat and Seroussi, 2019). More research is needed to determine their potential role in the endocrine control of metabolic and reproductive functions in chickens (Mellouk et al., 2018a)

26.5.3 Receptors

The chicken leptin receptor (LEPR) gene was discovered in 2000 as the first LEPR in nonmammalian vertebrates. The sequences of bird LEPRs have a normal GC content (∼45%) and a higher similarity than leptin to the corresponding mammalian orthologs (∼60%) (Friedman- Einat and Seroussi, 2019). As the expression of LEPR in the pituitary is more than 100-fold higher than in any other tissues, it may suggest that the role of leptin is rather in reproduction and stress response than on appetite (Friedman-Einat and Seroussi, 2019). In mammals, there are six different isoforms of the LEPR, the short forms of LEPR controlling clearance, transport, and stabilization of circulating leptin. In birds, the predominant form is the long form of LEPR (Seroussi et al., 2016), suggestion rather a paracrine/autocrine role (Friedman-Einat and Seroussi, 2019). There is controversy as to the leptin receptor expression in chicken adipose tissue. According to Wang et al. (2007), no leptin receptor expression in chicken adipose tissue was found, whereas Hausman et al. (2012) reported leptin receptor expression in broiler adipose tissue.

As previously mentioned, the expression of the adiponectin receptors ADIPOR1 and ADIPOR2, in adipose tissue are age and gender dependent (Zhang et al., 2017). Fasting in chicken is known to decrease adiponectin receptor expression in adipose tissue (Ghazanfari et al., 2011). For more information on adiponectin and its receptors in other tissues, we refer to the review of Mellouk et al. (2018a).

So far, no visfatin receptor has been identified in chickens (Mellouk et al., 2018a).

Three chemerin receptors are found in chickens and turkeys, i.e., chemokine-like receptor 1, G protein-coupled receptor 1, and chemokine (C−C motif) receptor-like 2, and expressed in liver, heart, adipose tissue, and ovarian cells (Diot et al., 2015; Mellouk et al., 2018b).

26.6 Lipid metabolism

26.6.1 Lipogenesis and lipolysis

Fat tissue is central in energy substrate partitioning as it acts as a reservoir, as a result from lipogenesis on the one hand and lipolysis on the other hand. In energy balance equilibrium, there is still lipogenesis and lipolysis going on continuously making fat tissue a rather dynamic tissue with a turnover rate that is relatively high [e.g., half-life of depot lipids in rodents is about eight days (Frühbeck and Gómez-Ambrosi, 2005)]. In avian species, the liver is the main tissue of de novo fatty acid synthesis, followed by adipose tissue (Leveille et al., 1975; Hermier, 1997) (Figure 26.1). The synthesis of TAGs, lipogenesis, in adipocytes requires a steady supply of free fatty acids. This supply occurs through the delivery of TAGs by lipoproteins. In chickens, fatty acids for TAG synthesis and adipose tissue expansion are acquired from plasma VLDL and portomicrons (see Section 26.6.4). There are indications that the role of the liver in lipogenesis might be overestimated and that the contribution of other tissues (e.g., bones, skin, and intestines) must also be reconsidered (Griffin and Hermier, 1988; Nir and Lin, 1982).

Acetyl-CoA, formed from pyruvate by pyruvate dehydrogenase, plays a central role in the de novo fatty acid synthesis. Nonlipid precursors are carbohydrates from dietary origin or from glycogenolysis or gluconeogenesis from glucogenic or ketogenic amino acids and metabolites such as lactate and glycerol. Acetyl-CoA is then irreversibly converted to malonyl-CoA. This reaction is catalyzed by Acetyl-CoA carboxylase (ACC), and this step is considered to be rate-limiting for fatty acid synthesis. Elongation of malonyl-CoA is catalyzed by the multienzyme complex fatty acid synthase (FAS). The newly formed fatty acids are then esterified with glycerol 3-phosphate to form TAG.

Lipolysis in chicken adipose tissue is realized by a lipase (adipose triglyceride lipase or ATGL) exclusively found in subcutaneous and abdominal fat (Lee et al., 2009), and this lipase is highly present after hatching and before feed is given. This enzyme catalyzes the first rate-limiting step of lipolysis to release a fatty acid and diacylglycerol (DAG) (Zimmerman et al., 2004). Hormone-sensitive lipase and monoglyceride lipase [catalyze fatty acid removal from DAG and monoacylglycerol, respectively (Wang et al., 2012a,b,c)]. After lipolysis in adipose tissue, the mobilized nonesterified fatty acids (NEFAs) are transported by the blood (bound to albumen), and are then taken up by diverse cell types for subsequent β-oxidation to generate ATP (Figure 26.1). In most cases, uptake of NEFA is much faster than their oxidation except during heavy and/or prolonged exercise. The NEFA used in muscle for oxidation come for 80−90% from plasma NEFA (coming from the diet and fat tissue) while only ± 10% comes from muscle lipid itself. The major proteins involved in cellular NEFA transport in mammals are CD36/FAT (fatty acid translocase), fatty acid transport proteins, and fatty acid binding proteins, which have also been described in avian adipose tissues (Wang et al., 2012a,b,c; Qi et al., 2013).

26.6.2 Lipoprotein metabolism

26.6.2.1 Portomicrons

In the digestive tract, after hydrolysis, simple sugars (hexoses and pentoses) and amino acids are transported by active or diffusion processes from the lumen of the small intestine into the blood circulation. Dietary lipids are emulsified by bile salts, hydrolyzed by lipases and the resulting free fatty acids are absorbed by the mucosal cells. Within the enterocytes, most fatty acids are re-esterified with glycerol to form new TAG. These TAG are then

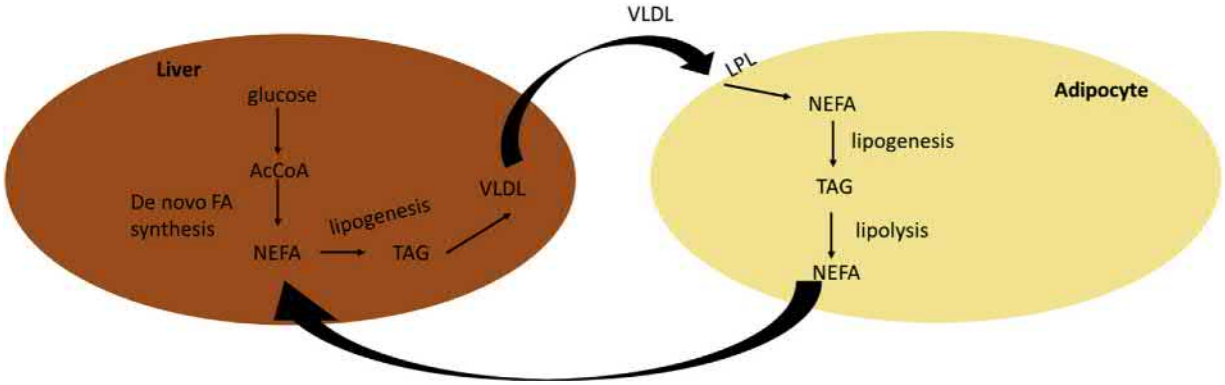

FIGURE 26.1 In the liver, de novo fatty acid (FA) synthesis starts from Acetyl-CoA to synthesize nonesterified fatty acids (NEFAs). They are esterified with glycerol during lipogenesis to form triacylglycerol (TAG). TAG are transported in very low-density lipoproteins (VLDL) that will go in the blood circulation. Activated lipoprotein lipase (LPL) at the luminal surface of the blood capillaries of adipose tissue, hydrolyzes TAG after which the NEFAs are taken up by the adipocyte. NEFAs are again incorporated in TAG during lipogenesis for storage. After lipolysis of TAG in adipose tissue, NEFA mobilization is followed up by its uptake by diverse cell types for β-oxidation.

associated with phospholipids, cholesterol (esters), and specific apolipoproteins (mainly apoB100) to form lipoproteins. In mammals, these lipoproteins are transported via the lymphatic system and are therefore termed chylomicrons. In birds however, the lymphatic system is poorly developed, and these newly formed lipoproteins are released into the portal vein. It was therefore proposed to term these lipoproteins (average diameter of 150 nm; a lipid composition of 90% TAG) from dietary origin as portomicrons (Bensadoun and Rothfeld, 1972). However, the re-esterification of the dietary free fatty acids is not complete and the NEFAs are also released to the portal system, bound to albumin, and carried to peripheral tissues. The portomicron concentration in the blood is mainly dependent on the nutritional status of the bird and of the dietary fat content (Griffin and Hermier, 1988). After the portomicrons are released into the portal vein, they are transported to the liver (Figure 26.2). However, they are not metabolized by the liver [probably because they are too large to penetrate the cellular sieve of the hepatic capillary bed (Hermier, 1997)] but pass through the liver to the extrahepatic tissues where they are partially hydrolyzed by lipoprotein lipase. The resulting portomicron-remnants are taken up by the liver, probably by an apoB100-dependent lipoprotein remnant receptor as apoE is lacking in chickens (Sato et al., 2009). The endocytosed TAG can then be used to resynthesize new TAG-rich lipoproteins (see Section 26.6.2.2).

26.6.2.2 Other lipoproteins

The TAG, from de novo fatty acid synthesis or from the portomicron-remnants, are then assembled with phospholipids, cholesterol (esters), and specific apolipoproteins (mainly apo- B100) to form very low-density lipoproteins (VLDLs). The newly synthetized VLDLs are then stored in vesicles and released into the bloodstream (Figure 26.2). VLDLs have a diameter of 30 to 90 nm and are denser than portomicrons, owing to a greater proportion of proteins. Plasma VLDL concentrations are highly positively correlated with total body fat content and can be used successfully as selection criterion for or against fat deposition in broiler lines (Whitehead, 1988; Guo et al., 2011).

As the hydrolysis of the TAG from the lipoproteins progresses (see Section 26.6.2.3), apolipoproteins are also lost and the lipoproteins decrease in size but increase in density. The partially metabolized VLDL can be recovered from chicken plasma as intermediate density lipoproteins (IDL or VLDL-remnants). The IDL is remodeled in cholesterol-rich low-density lipoproteins (LDLs). The remaining VLDL-remnants and portomicron-remnants are substrate for hepatic lipase. LDLs are taken up by receptor-mediated endocytosis in the liver and other tissues. Premature HDL probably originate in liver and intestines and receive cholesterol and phospholipids from VLDL and after interaction with LDL. As in mammals, HDLs are considered to be the main transporters of cholesterol and phospholipids in avian species. They are the smallest lipoproteins (approximately 10 nm), and comprised of 57% protein (Alvarenga et al., 2011).

As for mammals, many apolipoproteins have already been identified in birds, but there is a difference between mammals and birds in the content and function of several apoproteins (Sato et al., 2009; Alvarenga et al., 2011). VLDL mainly contains apo B-100, and HDL mainly apo A-I (Alvarenga et al., 2011). It is worthy to note that lipoproteins of birds have no apoB48 and apoE (Walzem, 1996). Moreover, chickens express an ApoVLDL-IV in liver and intestine, an apoprotein that has no mammalian counterpart, but regions of similarity with rabbit ApoC-IV (Nikolay et al., 2013). Still, many aspects regarding lipoprotein metabolism and apoproteins in birds remain unclear.

26.6.2.3 Lipoprotein lipase: a key enzyme

TAG-rich lipoproteins from the intestine (portomicrons) and from the liver (VLDL) secreted in the bloodstream are substrates for several lipase enzymes of which lipoprotein lipase (LPL) is by far the most important. LPL is synthesized by fat and by muscle cells and migrates to the luminal

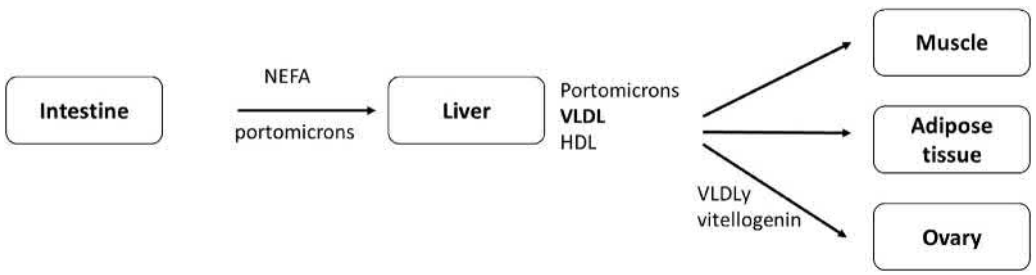

FIGURE 26.2 Nonesterified fatty acids (NEFAs) and portomicrons are released in the portal system and transported to the liver. The liver assembles very low-density lipoproteins (VLDL) and high-density lipoproteins (HDL) and releases these lipoproteins and the portomicrons into the systemic blood circulation. In laying hens, the liver synthesizes yolk-targeted VLDL (VLDLy) and vitellogenins to the ovary for yolk formation of the developing oocytes.

surface of the surrounding blood capillaries where it becomes functional after being anchored to the capillary wall by heparin and must be activated by specific apolipoproteins (apoC) on the surface coat of the lipoproteins (Butterwith, 1988; Griffin and Hermier, 1988). In mammals, apoCII is transferred from high-density lipoproteins (HDLs) to VLDL and then activates LPL. In birds, however, the equivalent activator of LPL needs to be identified (Walzem, 1996) but is present on VLDL from immature hens and portomicrons from (im)mature hens and HDL (Griffin et al., 1982). LPL hydrolyzes TAG from the core of the lipoprotein after which the liberated free fatty acids are taken up by the cells. In muscle cells, fatty acids are then oxidized to yield energy whereas in adipocytes, fatty acids are again incorporated in TAG for storage. As some of the fatty acids stored in the adipose tissue come from the diet, in nonruminant species, the fatty acid composition of the diet has a direct bearing on the fatty acid profile of lipids stored in adipose tissue. LPL activity is influenced by age and to some extent by nutritional state of the bird and is under the major stimulatory control of insulin (Griffin and Hermier, 1988).

26.6.2.4 Lipoproteins in laying hens

Plasma lipoprotein metabolism in laying hens differs substantially compared to immature hens or male chickens. As the ovary has very little capacity for lipid synthesis, all egg yolk lipids are synthesized mainly by the liver (stimulated by steroid hormones estrogens and progesterone) and transported to the ovary in special yolk-targeted TAG-rich VLDL (VLDLy) and in phospholipid-rich lipoproteins termed vitellogenins (Walzem, 1996, Figure 26.2). VLDL is the major lipoprotein responsible for the transport of lipids from the hen's liver to the oocytes and accounts for 60% of the dry yolk mass, while vitellogenin accounts for 24% (Speake et al., 1998). Compared to immature hen and normal VLDL, laying hen VLDLy are 50% smaller in size (30 nm), contain relatively more TAG and phospholipids but lower proportions of cholesterol(esters), have an unusual apoprotein composition (only apoB and apoVLDLII) and are sparely hydrolyzed by peripheral intravascular LPL (Griffin et al., 1982; Griffin and Hermier, 1988). Vitellogenin forms a very HDL and is carried to the developing oocyte, where it is broken down to form phosvitin and lipovitellin, which are proteins found in egg yolk (Hermier et al., 1989). The sequence leading to the incorporation of lipoproteins into the oocytes starts with passing through to the pores of the granulosa basal lamina (acts as a sieve to exclude larger lipoproteins) and ends with the uptake of the lipoproteins into the developing oocytes by receptor-mediated endocytosis (oocyte-specific apoB receptor in contrast to the somatic apoB receptor), followed by post-endocytotic modifications (Mann et al., 2008). Apparently, apoB acts as the ligand and not apoVLDLII (Walzem, 1996). This oocyte-specific VLDL/vitellogenin receptor or LR8 receptor was then identified as a member of the LDL receptor superfamily (Bujo et al., 1994). In this way, only lipids of hepatic origin (except for polyunsaturated fatty acids) can be deposited in the egg yolk. Besides its role in mediating the diameter of VLDLy, it has been shown that the estrogen-dependent apoVLDLII act as an inhibitor of LPL activity and in this way prevents TAG from VLDLy to be hydrolyzed by LPL (Schneider et al., 1990).

26.6.3 Endocrine control of lipid metabolism

26.6.3.1 Insulin

Adipose tissue metabolism in the chicken is regulated by energy status, and to a lesser extent by insulin. Indeed, insulin has minimal effect on glucose uptake in chicken adipose tissue, which is in contrast with mammals (Tokushima et al., 2005). In addition, insulin does not inhibit lipolysis in chicken adipose tissue, but avian pancreatic polypeptide, somatostatin (also from the pancreas), and gut glucagon-like immunoreactivity have antilipolytic effects (Dupont et al., 2012). Insulin also stimulates hepatic lipogenesis mainly by stimulating the synthesis of lipogenic enzymes, and stimulates VLDL synthesis, while thyroxine, glucagon, and epinephrine have opposite effects. In addition, insulin may increase the hydrolysis of VLDL at the adipocyte level by stimulation of LPL activity (Simon, 1989). Insulin signaling cascade in chicken adipose tissue, although similar in its downstream components (Dupont et al., 2012), is quantitatively markedly different from that operating in mammals. It has been shown that levels of insulin-receptor (IR) and IR-substrate protein (IRS-1) in chicken are lower compared to mammals (rat), contributing to a certain insulin insensitivity or refractoriness. Glucagon is the primary lipolytic hormone in birds (Scanes, 2009), in contrast to mammals where catecholamines play this role.

In addition to pancreatic hormones, two major axes can be identified: the somatotrophic axis and the thyrotrophic axis. These two axes seem to be very much interrelated in birds and especially in the determination of growth and body composition. In addition, signaling interactions between muscle and adipocytes affect relative fat and lean deposition, and the efficiency of energy utilization.

26.6.3.2 Somatotrophic hormones

The pituitary hormone, growth hormone (GH) is a potent stimulator of growth in mammals. In the young, its promotes overall body growth and in the adult, it stimulates the growth of the extremities. Therefore, it was obvious to suppose that this hormone had also a primary effect on growth in poultry (Scanes et al., 1984). The anabolic effects

of GH in relation to its pulsatile secretory pattern are discussed elsewhere (Buyse and Decuypere, 1999).

Based on these observations, it became clear that GH is not the only determinant of growth and body composition in poultry. Also, other endogenous regulatory substances such as thyroid hormones and IGF must be considered. There is ample evidence for a positive relationship between plasma GH and IGF-I levels which are known to stimulate several anabolic processes. Moreover, IGF-I stimulates adipogenesis while it inhibits the GH-induced lipolysis. Continuous administration of IGF-I reduces abdominal fat content (Buyse and Decuypere, 1999). Data on plasma IGF-II concentrations are scarce, and its biological significance is unclear, except that IGF-II administration to broilers augmented fat deposition (Buyse and Decuypere, 1999). This also holds for the role of IGF-binding proteins in avian growth, development, and body composition.

Various sources of GH have been reported to affect lipolytic activity of chicken adipose tissue explants in vitro. GH alone stimulates glycerol release but is also known to inhibit glucagon-induced lipolysis although by different cellular mechanisms (e.g., Campbell and Scanes, 1988). The physiological importance of the observed effects of GH on lipolysis in vitro can be linked with a homeostatic role of GH in nutrient metabolism.

26.6.3.3 Thyroid hormones

There is abundant evidence that thyroid hormones are not only important for embryogenesis but also for normal posthatch growth in birds. Thyroid hormones also affect body composition and fatness. A hyperthyroid status in chickens is associated with a decreased fat content while in hypothyroid chickens, fat deposition is greatly enhanced (Decuypere and Buyse, 1988). Triiodothyronine has been shown to increase basal lipolytic activity and glucagon-induced lipolysis in cultured broiler adipocytes (Harden and Oscar, 1993). In addition, triiodothyronine stimulates hepatic malic enzyme activity, and hence lipogenesis.

26.6.3.4 Other hormones

There is ample evidence that adrenal glucocorticoids (mainly corticosterone in birds) depress body weight and increase fat deposition in birds as glucocorticoids exert a direct catabolic action and stimulate lipogenic activity in avian hepatocytes.

The pituitary hormone prolactin is also known to be a lipogenic effector and a possible temporal synergistic effect between corticosterone and prolactin on fat deposition has been demonstrated in broilers and wild-type birds (Decuypere and Buyse, 1988). The role of sex steroids in the hormonal control of growth in birds is not well established except that estrogens stimulate lipogenesis whereas testosterone has the opposite effect.

Interestingly, local Agouti Signaling Peptide and Melanocortin receptor expression were found in chicken adipose tissue, as well as Pro-opiomelanocortin (Yabuuchi et al., 2010) and Neuropeptide Y (Hausman et al., 2012), indicating that hypothalamic regulatory pathways for feed intake regulation, also in birds, may also play a role, locally, in adipose tissue metabolism. In mammals, treatment with NPY leads to obesity (Kuo et al., 2007). Similarly, NPY promotes adipogenesis in chicken adipose cells in vitro, which may occur slightly differently than the mechanisms found in mammals (Zhang et al., 2015; Shipp et al., 2016).

26.6.4 Transcription factors

Several transcription factors orchestrate adipocyte development (Wang et al., 2012a,b,c). Below, we describe some studies that specifically focused on birds. For a general description of transcription factors, the reader can consult Wang et al. (2012a,b,c).

PPARγ is a central regulator of adipogenesis and is expressed in fat tissue and even more in liver but not in muscle. Its importance in birds is confirmed by a report that the suppression of PPARγ mRNA by small-interfering RNA inhibited differentiation and promoted proliferation of chicken preadipocytes (Wang et al., 2008). Moreover, a single intraperitoneal injection of troglitazone, a synthetic PPARγ ligand, to newly hatched broiler chicks resulted in a reduction of the absolute and proportional abdominal fat pad weight at 48 days of age (Sato et al., 2008). Levels of PPARγ are affected by nutrition and are also higher at the onset of egg laying in layers in liver and ovary, while it is then decreased in adipose tissue (Sato et al., 2004). Krüppel-like transcription factors (KLFs) and SREBP are other transcription factors that facilitate adipocyte maturation. In chicken preadipocytes, KLF7 was shown to enhance proliferation and suppress differentiation (Zhang et al., 2013). SREBP1 and SREBP2 chicken genes are nearly perfectly conserved compared to their mammalian homologs (Assaf et al., 2003). SREBP1 is linked to FAS protein content or activity in adipose tissue and/or liver. Therefore, SREBPs are key regulators in lipogenesis both in mammals and avian species, and their differential expression in different tissues is a major determinant for the site of fatty acid synthesis in the body (Gondret et al., 2001; Yen et al., 2005). GATA binding protein 2 is a preadipocyte-specific factor that promotes preadipocyte activity as its overexpression inhibited chicken preadipocyte differentiation (Zhang et al., 2012).

26.7 Factors affecting fat metabolism and deposition

26.7.1 Dietary factors

Nutrition has a major impact on animal performance and body composition. Nutrition is a very broad term and includes quantitative (e.g., ad libitum vs. feed restriction programs) and qualitative [e.g., metabolizable energy (ME), macro- and micronutrients, toxins] aspects as well as feeding programs (e.g., sequential feeding, "skip-a-day" feeding).

26.7.1.1 Quantitative strategies

It is common knowledge that feed deprivation/refeeding cycles are associated with fluctuations in intermediary metabolism induced by endocrine factors such as thyroid hormones, GHs, and pancreatic hormones (Buyse et al., 2001). During feed deprivation, hepatic lipogenic activity is drastically reduced, and the release of NEFA from adipose tissue is stimulated whereas the opposite is true after refeeding. The reader is referred to recent elegant studies for detailed information of feed deprivation/refeeding schedules on the dynamics of hepatic mRNA levels of lipogenic genes and transcription factors (e.g. Wang et al., 2012a,b,c; Richards et al., 2003; Saneyasu et al., 2013). In addition, such feeding schedules have also a marked effect on hypothalamic (an)orexigenic neuropeptides and lipogenic genes such as FAS and ACC (Higgins et al., 2010; Song et al., 2013). A discussion of the relevance of these findings in the framework of the control and regulation of voluntary feed intake of avian species is however beyond the scope of this chapter.

26.7.1.2 Qualitative strategies

With respect to diet quality, the impact of ME levels and macronutrient (lipids, carbohydrates, and proteins) ratio's on performance and body composition has been widely investigated mainly with broiler chickens. In general, diets with high ME levels (but normal protein levels) promote fat deposition in broiler chickens, but genetically determined body weight gain is rather maintained. This augmented fat deposition is the result of an excess in energy intake ("luxus" energy consumption) relative to the energy needed for maintenance and production. This "luxus" energy is then largely diverted to body fat deposition though also dissipated as heat to some extent (Buyse et al., 1992). Widening of the ME: protein ratio due to a reduction in protein level results in not only in a higher fat deposition but also in a reduced growth rate. The higher fat deposition is caused by an enhanced hepatic lipogenesis (demonstrated in vivo and in vitro) as reflected in the increased expression and activity of lipogenic enzymes such as malic enzyme, ACC, and FAS (e.g., Donaldson, 1985; Adams and Davis, 2001; Rosebrough et al., 2011). The reader is referred to the work of Rosebrough, Richards, and coworkers with respect to short-term adaptations in hepatic lipogenesis when switching from high to low-protein diets and vice versa (Rosebrough et al., 2011). The underlying causal mechanisms at the biochemical level of the hepatic intermediary metabolism are discussed in detail elsewhere (Swennen et al., 2007a).

Diets with a relative protein shortage also induce marked endocrine alterations (reviewed by Buyse et al., 2001; Rosebrough et al., 2011). Indeed, protein-restricted chickens are characterized by an enhanced pulsatile GH secretion, lower plasma IGF-I and thyroxine levels, but higher 3,3′,5-triiodothyronine concentrations. Feeding broilers with diets with a too high-protein content (above requirements) will result in lean broilers (decreased de novo lipogenesis and expression and activity of lipogenic enzymes). Several studies show that an increase in dietary protein decreases abdominal fat, enhances body weight gain and increases breast meat yield (Temim et al., 2000; Alleman et al., 2000; Jlali et al., 2012). Alternatively, growth could be stunted because of the energetic costs of nitrogen waste excretion. Interestingly, female broiler breeders that are fed according to their body weight curve have an increased proportional abdominal fat weight when fed a reduced protein, isoenergetic diet (Lesuisse et al., 2018). Furthermore, dietary amino acids can play a role on lipid metabolism and fat deposition (Wang et al., 2012a,b,c).

The effects of dietary fat level on body fat accretion and lipid metabolism are less unambiguous (Swennen et al., 2007a). The interpretation of studies focusing on dietary fat level is sometimes complicated by the fact that it is not clearly indicated whether the dietary fat is iso-energetically substituted with protein or carbohydrates or both. In general, an increase in dietary fat is associated with an increased abdominal fat and increasing the dietary fat level will reduce hepatic lipogenic activity probably due to the inhibitory effect of long chain acyl-CoA on ACC activity (Leveille et al., 1975). Besides the dietary fat level, the source of fat also affects body fat deposition. For example, a diet containing sunflower oil, rich in unsaturated fatty acids, decreases abdominal fat compared to animals fed tallow or lard (richer in saturated fatty acids) (Sanz, 1999), with reduced lipogenesis in the liver and an enhanced β-oxidation in the heart (Sanz et al., 2000). Both the degree of saturation and the chain length are associated with different metabolic functions of fatty acids in chickens and can regulate transcription factors (Wang et al., 2012a,b,c).

For example, conjugated linoleic acid, a mixture of mainly cis-9, trans-11 and trans-10, cis-12 fatty acid isomers reduced total body fat in chickens (Du and Ahn, 2002), increased saturated fatty acids and decreased monounsaturated fatty acids in abdominal fat of chickens (Chamruspollert and Sell, 1999), and decreased PPARɣ mRNA abundance in chicken abdominal fat (Ramiah et al., 2014).

Finally, high-carbohydrate levels in broiler diets will enhance glycolysis and hence provide plenty reducing equivalents for hepatic fatty acid production (Tanaka et al., 1983). However, these dietary fat and carbohydrate-induced changes in hepatic lipogenic activity do not necessarily result in changed body fat accretion (Swennen et al., 2007a).

26.7.2 Genetics

Intensive selection of broiler chickens for high-growth rate and feed efficiency has resulted in a tremendous progress in body weight gain and feed efficiency (direct selection response). However, several adverse indirect selection responses such as augmented fat deposition, leg problems, and metabolic diseases such as ascites and sudden death syndrome have also occurred. In addition, excessive fat is economically uninteresting, can hinder processing and is not desired by the consumers (Wang et al., 2012a,b,c). Havenstein and coworkers (Havenstein et al., 1994a,b) have elegantly assessed the differential impact of selection for growth rate and of diet regimen by comparing a typical 1957 broiler strain (Athens−Canadian randombred control strain) with a modern 1991 broiler strain (Arbor Acres) and both fed on a typical 1957 or a 1991 diet. A similar comparative study was done between the randombred 1957 strain and a commercial 2001 (Ross 308) strain and both fed on a typical 1957 or 2001 diet (Havenstein et al., 2003). These studies clearly revealed that genetics were the major contributing factor for the progress in performance and yield of carcass parts but also that carcass fat content increased due to selection for growth rate. In view of this augmented fat deposition and associated negative consequences, divergent experimental fat and lean broiler lines were established in several poultry research institutes. Different selection strategies were used: divergent selection for or against abdominal fat content (France, Israel); selection for high body weight gain (fat line) or feed efficiency (lean line) (The Netherlands, Denmark, USA); divergent selection for high (fat line) or low (lean line) plasma VLDL concentration (UK). Detailed information on heritability estimates, genotypic and phenotypic correlations as well as performance characteristics, energy, lipid, and protein metabolism, endocrine profiles and intermediary metabolism and breeder performance are provided elsewhere (Leclercq, 1988; Whitehead, 1988; Buyse et al., 1999; Baéza and Le Bihan-Duval, 2013). It is clear that either direct or indirect selection resulted in fat and lean broiler lines. With respect to lipid metabolism, all fat line broilers were characterized by a higher hepatic lipogenic capacity compared to their lean line counterparts, irrespective of the selection criteria. However, some indirect selection responses as well as the underlying endocrine mechanisms were different according to the selection strategy. Indeed, lean broilers produced by selection for feed efficiency had a higher basal as well as glucagon-stimulated lipolytic activity compared to their fat counterparts selected for high-body weight gain. Low feed efficiency-selected broilers had a higher expression of lipid synthesis genes and lower expression of triglyceride hydrolysis and cholesterol transport genes (Zhuo et al., 2015). In contrast, direct selection for high or low-abdominal fat content had apparently no effect on the lipolytic capacity of adipose tissue. Differentially expressed genes in these fat and lean chicken lines are rather associated with hemostasis, endocrine function, and metabolic syndrome in mammals (Resnyk et al., 2015). These differences in lipolytic activity, among other parameters, according to the selection strategy can be related to the differential selection-induced alterations in endocrine profile. Indeed, direct selection rather triggered the thyrotrophic axis and pancreatic hormones whereas indirect selection primarily affected the somatotrophic axis (Buyse et al., 1999). Another interesting genetic model to study the regulatory mechanisms of lipid metabolism is the selection model for high (R+: fat line) or low (R-lean line) residual feed intake of laying hens, which markedly differ in appetite, heat production including diet-induced thermogenesis, body conformation and composition, and hypothalamic transcriptome (Bordas et al., 1992; Swennen et al., 2007b; Jehl et al., 2019).

26.8 Summary and conclusions

Adipose tissue is the most variable carcass component and is traditionally being considered as a rather inert storage tissue for energy under the form of lipids. Most of the fat in chickens is located in adipose depots, which are all late maturing. At the cellular level, preadipocyte differentiation and proliferation is under the control of multiple hormones and transcription factors. The growth of fat tissue is initially due to hyperplasia followed by hypertrophy of the mature adipocytes, and the amount of fat deposited depends on genetic and nutritional factors.

Recent research has however revealed that adipose tissue must now be regarded as a dynamic tissue, which secretes a considerable number of adipokines and hence plays a role in a multitude of bodily processes.

References

Adams, K.A., Davis, J., 2001. Dietary protein concentration regulates the mRNA expression of chicken hepatic malic enzyme. J. Nutr. 131, 2269–2274.

Alleman, F., Michel, J., Chagneau, A.M., Leclerq, B., 2000. The effects of dietary protein independent of essential amino acids on growth and body composition in genetically lean and fat chickens. Br. Poultry Sci. 41, 214–218.

Alvarenga, R.R., Zangeronimo, M.G., Pereira, L.J., Rodrigues, P.B., Gomide, E.M., 2011. Lipoprotein metabolism in poultry. World's Poult. Sci. J. 67, 431–440.

Assaf, S., Hazard, D., Pitel, F., Morisson, M., Alizadeh, M., Gondret, F., Diot, C., Vignal, A., Douaire, M., Lagarrigue, S., 2003. Cloning of cDNA encoding the nuclear form of chicken sterol response element binding protein-2 (SREBP-2), chromosomal localization, and tissue expression of chicken CREBP-1 and -2 genes. Poultry Sci. 82, 54–61.

Baéza, E., Le Bihan-Duval, E., 2013. Chicken lines divergent for low or high abdominal fat deposition: a relevant model to study the regulation of energy metabolism. Animal 7, 965–973.

Bensadoun, A., Rothfeld, A., 1972. The form of absorption of lipids in the chicken, *Gallus domesticus*. Proc. Soc. Exp. Biol. Med. 141, 814–817.

Bornelöv, S., Seroussi, E., Yosefi, S., Benjamini, S., Miyara, S., Ruzal, M., Grabherr, M., Rafati, N., Molin, A.-M., Pendavis, K., Burgess, S.C., Andersson, L., Friedman-Einat, M., 2018. Comparative omics and feeding manipulations in chicken indicate a shift of the endocrine role of visceral fat towards reproduction. BMC Genom. 19, 295.

Bordas, A., Tixier-Boichard, M., Mérat, P., 1992. Direct and correlated responses to divergent selection for residual food intake in Rhode Island Red laying hens. Br. Poultry Sci. 33, 741–754.

Bujo, H., Hermann, M., Kaderli, M.O., Jacobson, L., Sugawara, S., Nimpf, J., Yamamoto, T., Schneider, W.J., 1994. Chicken oocyte growth is mediated by an eight ligand binding repeat member of the LDL receptor family. EMBO J. 13, 5165–5175.

Butterwith, S.C., 1988. Avian adipose tissue: growth and metabolism. In: Leclercq, B., Whitehead, C.C. (Eds.), Leanness in Domestic Birds. Genetic, Metabolic and Hormonal Aspects. INRA-Butterworths, London, pp. 203–222.

Butterwith, S.C., 1997. Regulators of adipocyte precursor cells. Poultry Sci. 76, 118–123.

Buyse, J., Decuypere, E., Berghman, L., Kühn, E.R., Vandesande, F., 1992. The effect of dietary protein content on episodic growth hormone secretion and on heat production of male broilers. Br. Poultry Sci. 33, 1101–1109.

Buyse, J., Decuypere, E., 1999. The role of the somatotrophic axis in the metabolism of the chicken. Domest. Anim. Endocrinol. 17, 245–255.

Buyse, J., Leenstra, F.R., Zeman, M., Rahimi, G., Decuypere, E., 1999. A comparative study of different selection strategies to breed leaner meat-type poultry. Avian Poultry Biol. Rev. 10, 121–142.

Buyse, J., Darras, V.M., Kühn, E.R., Decuypere, E., 2001. Nutritional regulation of the somatotropic axis and intermediary metabolism in the chicken. In: Dawson, A., Chaturvedi, C.M. (Eds.), Avian Endocrinology. Narosa Publishing House, New Dehli, pp. 303–313.

Campbell, R.M., Scanes, C.G., 1988. Pharmacological investigations on the lipolytic and antilipolytic effects of growth hormone (GH) in chicken adipose tissue in vitro: evidence for involvement of calcium and polyamines. Proc. Soc. Exp. Biol. Med. 188, 177–184.

Cartwright, A.L., 1991. Adipose cellularity in *Gallus domesticus*: investigations to control body composition in growing chickens. J. Nutr. 121, 1486–1497.

Chamruspollert, M., Sell, J., 1999. Transfer of dietary conjugated linoleic acid to egg yolks of chickens. Poultry Sci. 78, 1138–1150.

Cogburn, L.A., Resnyk, C., Porter, T.E., Aggrey, S.E., Le Bihan-Duval, E., Duclos, M., Simon, J., 2011. Transcriptional analysis of abdominal fat accretion in genetically fat and lean chickens: a new polygenic model of visceral obesity. FASEB. J. 25, 862–867.

Decuypere, E., Buyse, J., 1988. Thyroid hormones, corticosterone, growth hormone and somatomedins in avian species: general effects and possible implications in fattening. In: Leclercq, B., Whitehead, C.C. (Eds.), Leanness in Domestic Birds. Genetic, Metabolic and Hormonal Aspects. INRA-Butterworths, London, pp. 295–312.

Diot, M., Reverchon, M., Rame, C., Froment, P., Brillard, J.-P., Brière, S., Levêque, G., Guillaume, D., Dupont, J., 2015. Expression of adiponectin, chemerin, and visfatin in plasma and different tissues during a laying season in turkeys. Reprod. Biol. Endocrinol. 13, 81–94.

Donaldson, W.E., 1985. Lipogenesis and body fat in chicks: effects of calorie-protein ratio and dietary fat. Poultry Sci. 64, 1199–1204.

Du, M., Ahn, D., 2002. Effect of dietary conjugated linoleid acid on the growth rate of live birds and on the abdominal fat content and quality of broiler meat. Poultry Sci. 81, 428–433.

Dupont, J., Métayer-Coustard, S., Ji, B., Ramé, C., Gespach, C., Voy, B., Simon, J., 2012. Characterization of major elements of insulin signaling cascade in chicken adipose tissue: apparent insulin refractoriness. Gen. Comp. Endocrinol. 176, 86–93.

Evans, A.J., 1977. The growth of fat. In: Boorman, K.N., Wilson, B.J. (Eds.), Growth and Poultry Meat Production. Br. Poult. Sci. Ltd, Edinburgh, pp. 29–64.

Friedman-Einat, M., Seroussi, E., 2019. Avian leptin: bird's-eye view of the evolution of vertebrate energy-balance control. Trends Endocrinol. Metabol. 30, 819–832.

Frühbeck, G., Gómez-Ambrosi, J., 2005. Adipose tissue. In: Benjamin, C. (Ed.), Encyclopedia of Human Nutrition, second ed. Elsevier, Oxford, pp. 1–14.

Ghazanfari, S., Nobari, K., Yamauchi, T., 2011. Adiponectin: a novel hormone in birds. Asian J. Anim. Vet. Adv. 6, 429–439.

Gondret, F., Ferré, P., Dugail, I., 2001. ADD-1/SREBP-1 is a major determinant of tissue differential lipogenic capacity in mammalian and avian species. J. Lipid Res. 42, 106–113.

Griffin, H., Grant, G., Perry, M., 1982. Hydrolysis of plasma triacylglycerol-rich lipoproteins from immature and laying hens (*Gallus domesticus*) by lipoprotein lipase in vitro. Biochem. J. 206, 647–654.

Griffin, H., Hermier, D., 1988. Plasma lipoprotein metabolism and fattening in poultry. In: Leclercq, B., Whitehead, C.C. (Eds.), Leanness in Domestic Birds. Genetic, Metabolic and Hormonal Aspects. INRA-Butterworths, London, pp. 175–202.

Guo, L., Sun, B., Shang, Z., Leng, L., Wang, Y., Li, H., 2011. Comparison of adipose tissue cellularity in chicken lines divergently selected for fatness. Poultry Sci. 90, 2024–2034.

Harden, R.L., Oscar, T.P., 1993. Thyroid hormone and growth hormone regulation of broiler adipocyte lipolysis. Poultry Sci. 72, 669–676.

Hausman, G.J., Barb, C.R., Fairchild, B.D., Gamble, J., Lee-Rutherford, L., 2012. Expression of genes for interleukins, neuropeptides, growth hormone receptor, and leptin receptor in adipose tissue from growing broiler chickens. Domest. Anim. Endocrinol. 43, 260–263.

Havenstein, G.B., Ferket, P.R., Scheideler, S.E., Larson, B.T., 1994a. Growth, livability, and feed conversion of 1991 vs 1957 broilers when fed "typical" 1957 and 1991 diets. Poultry Sci. 73, 1785−1794.

Havenstein, G.B., Ferket, P.R., Scheideler, S.E., Larson, B.T., 1994b. Carcass composition and yield of 1991 vs 1957 broilers when fed "typical" 1957 and 1991 diets. Poultry Sci. 73, 1795−1804.

Havenstein, G.B., Ferket, P.R., Qureshi, M.A., 2003. Growth, livability, and feed conversion of 1957 versus 2001 broilers when fed representative 1957 and 2001 diets. Poultry Sci. 82, 1500−1508.

Hendricks, G.L., Hadley, J.A., Krzysik-Walker, S.M., Prabhu, K.S., Vasilatos-Younken, R., Ramachandran, R., 2009. Unique profile of chicken adiponectin, a predominantly heavy molecular weight multimer, and relationship to visceral adiposity. Endocrinology 150, 3092−3100.

Hermier, D., 1997. Lipoprotein metabolism and fattening in poultry. J. Nutr. 127, 805S−808S.

Hermier, D., Folgez, P., Williams, J., Chapman, M.J., 1989. Alterations in plasma lipoproteins and apolipoproteins associated with oestrogen-induced hyperlipidemia in the laying hen. Eur. J. Biochem. 184, 109−118.

Higgins, S.E., Ellestad, L.E., Trakooljul, N., McCarthy, F., Saliba, J., Cogburn, L.A., Porter, T.E., 2010. Transcriptional and pathway analysis in the hypothalamus of newly hatched chicks during fasting and delayed feeding. BMC Genom. 11, 162.

Hood, R.L., 1982. The cellular basis for growth of the abdominal fat pad in broiler-type chickens. Poultry Sci. 61, 117−121.

Hood, R.L., Pym, R.A.E., 1982. Correlated responses for lipogenesis and adipose tissue cellularity in chickens selected for body weight gain, food consumption, and food conversion efficiency. Poultry Sci. 61, 122−127.

Jehl, F., Désert, C., Klopp, C., Brenet, M., Rau, A., Leroux, S., Boutin, M., Lagoutte, L., Muret, K., Blum, Y., Esquerré, D., Gourichon, D., Burlot, T., Collin, A., Pitel, F., Benani, A., Zerjal, T., Lagarrigue, S., 2019. Chicken adaptive response to low energy diet: main role of the hypothalamic lipid metabolism revealed a phenotypic and multi-tissue transcriptomic approach. BMC Genom. 20, 1033.

Jlali, M., Gigaud, V., Metayer-Coustard, S., Sellier, N., Tesseraud, S., Le Bihan-Duval, E., Berri, C., 2012. Modulation of glycogen and breast meat processing ability by nutrition in chickens : effect of crude protein leel in 2 chicken genotypes. J. Anim. Sci. 90, 447−455.

Kokta, T.A., Dodson, M.V., Gertler, A., Hill, R.A., 2004. Intercellular signaling between adipose tissue and muscle tissue. Domest. Anim. Endocrinol. 27, 303−331.

Krzysik-Walker, S.M., Ocón-Grove, O.M., Maddineni, S.R., Hendricks III, G.L., Ramachandran, R., 2008. Is visfatin an adipokine or myokine? Evidence for greater visfatin expression in skeletal muscle than visceral fat in chickens. Endocrinology 194, 1543−1550.

Kuo, L.E., Kitlinska, J.B., Tilan, J.U., Li, L., Baker, S.B., Johnson, M.D., Lee, E.W., Burnette, M.S., Fricke, S.T., Kvetnansky, R., Herzog, H., Zukowska, Z., 2007. Neuropeptide Y acts directly in the periphery on fat tissue and mediates stress-induced obesity and metabolic syndrome. Nat. Med. 13, 803−811.

Leclercq, B., 1984. Adipose tissue metabolism and its control in birds. Poultry Sci. 63, 2044−2054.

Leclercq, B., 1988. Genetic selection of meat-type chickens for high or low abdominal fat content. In: Leclercq, B., Whitehead, C.C. (Eds.), Leanness in Domestic Birds. Genetic, Metabolic and Hormonal Aspects. INRA-Butterworths, London, pp. 25−40.

Lee, K., Shin, J., Latshaw, J.D., Suh, Y., Serr, J., 2009. Cloning of adipose triglyceride lipase complementary deoxyribonucleic acid in poultry and expression of adipose triglyceride lipase during development of adipose in chickens. Poultry Sci. 88, 620−630.

Lesuisse, J., Li, C., Schallier, S., Climaco, W.L.S., Bautil, A., Everaert, N., Buyse, J., 2018. Multigenerational effects of a reduced balanced protein diet during the rearing and laying period of broiler breeders. 1. Performance of the F1 breeder generation. Poultry Sci. 97, 1651−1665.

Leveille, G.A., Romsos, D.R., Yeh, Y.-Y., O'Hea, E.K., 1975. Lipid biosynthesis in the chick. A consideration of site of synthesis, influence of diet and possible regulatory mechanisms. Poultry Sci. 54, 1075−1093.

Li, B.C., Zhang, Y.I., Chen, X.N., Shi, Q.Q., Fu, D.Z., Yin, Y.H., Zhang, Z.T., Gao, B., Chen, G.H., 2011. Directional differentiation of chicken embryonic stem cells into osteoblasts, neuron-like cells and adipocytes. Afr. J. Biotechnol. 10, 7772−7779.

Li, J., Meng, F., Song, C., Wang, Y., Leung, F.C., 2012. Characterization of chicken visfatin gene: cDNA cloning, tissue distribution, and promotor analysis. Poultry Sci. 91, 2885−2894.

Li, Z., Wang, Y., Tian, X., Shang, P., Chen, H., Kang, X., Tian, Y., Han, R., 2017. Characterization of the visfatin gene and its expression pattern and effect on 3T3-L1 adipocyte differentiation in chickens. Gene 632, 16−24.

Mann, K., Olsena, V., Maceka, B., Gnada, F., Mann, M., 2008. Identification of new chicken egg proteins by mass spectrometry-based proteomic analysis. World's Poult. Sci. J. 64, 209−218.

March, B.E., MacMillan, C., Chu, S., 1984. Characteristics of adipose tissue growth in broiler-type chickens to 22 weeks of age and the effects of dietary protein and lipid. Poultry Sci. 63, 2207−2216.

Mellouk, N., Ramé, C., Barbe, A., Grandhaye, J., Froment, P., Dupont, J., 2018a. Chicken is a useful model to investigate the role of adipokines in metabolic and reproductive diseases. Internet J. Endocrinol. https://doi.org/10.1155/2018/4579734.

Mellouk, N., Ramé, C., Marchand, M., Staub, C., Touzé, J.-L., Venturi, E., Mercereand, F., Travel, A., Chartrin, P., Lecompte, F., Ma, L., Froment, P., Dupont, J., 2018b. Effect of different levels of feed restriction and fish oil fatty acid supplementation on fat deposition by using different techniques, plasma levels and mRNA expression of several adipokines in broiler breeder hens. PloS One 13. Article e0191121.

Merkley, J.W., Cartwright, A.L., 1989. Adipose tissue deposition and cellularity in cimaterol-treated female broilers. Poultry Sci. 68, 762−770.

Nikolay, B., PlieschnigSubik, J.A.D., Schneider, J.D., Schneider, W.J., Hermann, M., 2013. A novel estrogen-regulated avian apolipoprotein. Biochimie 95, 2445−2453.

Nir, I., Nitsan, Z., Keren-Zvi, S., 1988. Fat deposition in birds. In: Leclercq, B., Whitehead, C.C. (Eds.), Leanness in Domestic Birds. Genetic, Metabolic and Hormonal Aspects. INRA-Butterworths, London, pp. 141−174.

Nir, I., Lin, H., 1982. The skeleton, an important site of lipogenesis in the chick. Ann. Nutr. Metab. 26, 100−105.

Pálsson, H., 1955. Conformation and body composition. In: Hammond, J. (Ed.), Progress in the Physiology of Farm Animals, vol. 2. Butterworths, London, pp. 430−452.

Qi, R., Feng, M., Tan, X., Gan, L., Yan, G., Sun, C., 2013. FATP1 silence inhibits the differentiation and induces the apoptosis in chicken preadipocytes. Mol. Biol. Rep. 40, 2907−2914.

Qi, R.L., Sun, C., Yan, J., Yang, H.L., Zhao, T.T., Zhao, X., 2012. Effects of glucose on differentiation and fat metabolism of chicken preadipocytes. J. Anim. Vet. Adv. 11, 1223–1229.

Ramiah, S.K., Meng, G.Y., Sheau Wei, T., Swee Keong, Y., Ebrahimi, M., 2014. Dietary conjugated linoleic acid supplementation leads to downregulation of PPAR transcription in broiler chickens and reduction of adipocyte cellularity. PPAR Res. 2014.

Ramsay, T.G., Rosebrough, R.W., 2003. Hormonal regulation of postnatal chicken preadipocyte differentiation in vitro. Comp. Biochem. Physiol., B 136, 245–253.

Resnyk, C.W., Chen, C., Huang, H., Wu, C.H., Simon, J., Le Bihan-Duval, E., Duclos, M.J., Cogburn, L.A., 2015. RNA-seq analysis of abdominal fat in genetically fat and lean chickens highlights a divergence in expression of genes controlling adiposity, hemostasis, and lipid metabolism. PloS One 10, e0139549.

Resnyk, C.W., Carré, W., Wang, X., Porter, T.E., Simon, J., Le Bihan-Duval, E., Duclos, M.J., Aggrey, S.E., Cogburn, L.A., 2017. Transcriptional analysis of abdominal fat in chickens divergently selected on bodyweight at two ages reveals novel mechanisms controlling adiposity: validating visceral adipose tissue as a dynamic endocrine and metabolic organ. BMC Genom. 18, 626.

Richards, M.P., Poch, S.M., Coon, N.C., Rosebrough, R.W., Ashwell, C.M., McMurtry, J.P., 2003. Feed restriction significantly alters lipogenic gene expression in broiler breeder chickens. J. Nutr. 133, 707–715.

Rosebrough, R.W., Russell, B.A., Richards, M.P., 2011. Further studies on short-term adaptations in the expression of lipogenic genes in broilers. Comp. Biochem. Physiol. A 159, 1–6.

Saneyasu, T., Shiragaki, M., Nakanishi, K., Kamisoyama, H., Honda, K., 2013. Effects of short term fasting on the expression of genes involved in lipid metabolism in chicks. Comp. Biochem. Physiol. B 165, 114–118.

Sanz, M., 1999. Higher lipid accumulation in broilers fed on saturated fats than in those fed on unsaturated fats. Br. Poultry Sci. 40, 95–101.

Sanz, M., Lopez-Bote, C.J., Menoyo, D., Bautista, J.M., 2000. Abdominal fat deposition and fatty acid synthesis are lower and β-oxidation is higher in broiler chickens fed diets containing unsaturated rather than saturated fat. J. Nutr. 130, 3034–3037.

Sato, K., Fukao, K., Seki, Y., Akiba, Y., 2004. Expression of the chicken peroxisome proliferator-activated receptor-γ gene is influenced by aging, nutrition, and agonist administration. Poultry Sci. 83, 1342–1347.

Sato, K., Matsushita, K., Matsubara, Y., Kamada, T., Akiba, Y., 2008. Adipose tissue fat accumulation is reduced by a single intraperitoneal injection of peroxisome proliferator- activated receptor gamma agonist when given to newly hatched chicks. Poultry Sci. 87, 2281–2286.

Sato, K., Suzuki, K., Akiba, Y., 2009. Characterization of chicken portomicron remnant and very low density lipoprotein remnant. J. Poultry Sci. 46, 35–39.

Scanes, C.G., Harvey, S., Marsh, J.A., King, D.B., 1984. Hormones and growth in poultry. Poultry Sci. 63, 2062–2074.

Scanes, C.G., 2009. Perspectives on the endocrinology of poultry growth and metabolism. Gen. Comp. Endocrinol. 163, 24–32.

Schneider, W.J., Carroll, R., Severson, D.L., Nimpf, J., 1990. Apolipoprotein VLDL-II inhibits lipolysis of triglyceride-rich lipoproteins in the laying hen. J. Lipid Res. 31, 507–513.

Seroussi, E., Cinnamon, Y., Yosefi, S., Genin, O., Smith, J.G., Rafati, N., Bornelov, S., Andersson, L., Friedman-Einat, M., 2016. Identification of the long-sought leptin in chicken and duck: expression pattern of the highly GC-rich avian leptin fits an autocrine/paracrine rather than endocrine function. Endocrinology 157, 737–751.

Shipp, S.L., Cline, M.A., Gilbert, E.R., 2016. Promotion of adipogenesis by neuropeptide Y during the later stages of chicken preadipocyte differentiation. Phys. Rep. 4 https://doi.org/10.14814/phy2.13006.

Simon, J., 1989. Chicken as a useful species for the comprehension of insulin action. Crit. Rev. Poult. Biol. 2, 121–148.

Sintubin, P., Greene, E., Collin, A., Bordas, A., Zerjal, T., Tesseraud, S., Buyse, J., Dridi, S., 2014. Expression profile of hypothalamic neuropeptides in chicken lines selected for high or low residual feed intake. Neuropeptides 48, 213–220.

Sonaiya, C.J., 1985. Abdominal fat weight and thickness as predictors of total body fat in broilers. Br. Poultry Sci. 26, 453–458.

Song, Z., Everaert, N., Wang, Y., Decuypere, E., Buyse, J., 2013. The endocrine control of energy homeostasis in chicken. Gen. Comp. Endocrinol. 190, 112–117.

Speake, B.K., Noble, R.C., Murray, A.M.B., 1998. The utilization of yolk lipids by the chick embryo. Worlds Poul. Sci. J. 54, 319–334.

Swennen, Q., Decuypere, E., Buyse, J., 2007a. Implications of dietary macronutrients for growth and metabolism in broiler chickens. World's Poult. Sci. J. 63, 541–556.

Swennen, Q., Verhulst, P.-J., Collin, A., Bordas, A., Decuypere, E., Verbeke, K., Vansant, G., Buyse, J., 2007b. Further investigations on the role of diet-induced thermogenesis in the regulation of feed intake in chickens: comparison of R+ and R- cockerels. Poultry Sci. 86, 1960–1971.

Tahmoorespur, M., Ghazanfari, S., Nobari, K., 2010. Evaluation of adiponectin gene expression in the abdominal adipose tissue of broiler chickens: feed restriction, dietary energy, and protein influences adiponectin messenger ribonucleic acid expression. Poultry Sci. 89, 2092–2100.

Tanaka, K., Ohtani, S., Shigeno, K., 1983. Effect of increasing dietary energy on hepatic lipogenesis in growing chicks. I. Increasing energy by carbohydrate supplementation. Poultry Sci. 62, 445–451.

Temim, S., Chagneau, A.M., Guillaumin, S., Michel, J., Peresson, R., Tesseraud, S., 2000. Does excess dietary protein improve growth performance and carcass characteristics in heat- exposed chickens? Poultry Sci. 79, 312–317.

Walzem, R.L., Davis, P.A., Hansen, R.J., 1994. Overfeeding increases very-low-density lipoprotein diameter and causes the appearance of a unique lipoprotein particle in association with failed yolk deposition. J. Lipid Res. 35, 1354–1356.

Tokushima, Y., Takahashi, K., Sato, K., Akiba, Y., 2005. Glucose uptake in vivo in skeletal muscles of insulin-injected chicks. Comp. Biochem. Physiol. B 141, 43–48.

Walzem, R.L., 1996. Lipoproteins and the laying hen: form follows function. Avian Poultry Biol. Rev. 7, 31–64.

Wang, H.-B., Li, H., Wang, Q.-G., Zhang, X.-Y., Wang, S.-Z., Wang, Y.-X., Wang, X.-P., 2007. Profiling of chicken adipose tissue gene expression by genome array. BMC Genom. 8, 193–206.

Wang, Y., Mu, Y., Li, H., Ding, N., Wang, Q., Wang, Y., Wang, S., Wang, N., 2008. Peroxisome proliferator-activated receptor-gamma gene: a key regulator of adipocyte differentiation in chickens. Poultry Sci. 87, 226–232.

Wang, J.W., Chen, W., Kang, X.T., Huang, Y.Q., Tian, Y.D., Wang, Y.B., 2012a. Identification of differentially expressed genes induced by energy restriction using annealing control primer system from the liver and adipose tissues of broilers. Poultry Sci. 91, 972–978.

Wang, Y., Rao, K., Yuan, L., Everaert, N., Buyse, J., Grossmann, R., Zhao, R., 2012b. Chicken FTO gene: tissue-specific expression, brain distribution, breed difference and effect of fasting. Comp. Biochem. Physiol. A 163, 246–252.

Wang, Y., Zhu, Q., Yang, L., Liu, Y.-P., 2012c. Ontogenic expression pattern and genetic polymorphisms of fatty acid transport protein 4 (FABP4) gene in Chinese chicken populations. Int. J. Mol. Sci. 13, 6820–6835.

Wang, W., 2019. Research advances of adipocyte differentiation in poultry. World's Poult. Sci. J. 75, 535–545.

Whitehead, C.C., 1988. Selection for leanness in broilers using plasma lipoprotein concentration as selection criterion. In: Leclercq, B., Whitehead, C.C. (Eds.), Leanness in Domestic Birds. Genetic, Metabolic and Hormonal Aspects. INRA-Butterworths, London, pp. 41–58.

Yabuuchi, M., Bando, K., Hiramatsu, M., Takahashi, S., Takeuchi, S., 2010. Local agouti signaling protein/melanocortin signaling system that possibly regulates lipid metabolism in adipose tissues of chickens. J. Poultry Sci. 47, 176–182.

Yen, C.F., Jiang, Y.N., Shen, T.F., Wong, I.M., Chen, C.C., Chen, K.C., Chang, W.C., Tsao, Y.K., Ding, S.T., 2005. Cloning and expression of the genes associated with lipid metabolism in Tsaiya Ducks. Poultry Sci. 84, 67–74.

Zhang, Z.-W., Chen, Y.-C., Pei, W.-Y., Li, H., 2012. Overexpression of chicken GATA2 or GATA3 suppressed the transcription of PPARγ gene. Chin. J. Biochem. Mol. Biol. 28, 835–842.

Zhang, Z., Wang, H., Sun, Y., Li, H., Wang, N., 2013. Klf7 modulates the differentiation and proliferation of chicken preadipocyte. Acta Biochem. Biophys. Sin. (Shanghai) 45, 280–288.

Zhang, W., Bai, S., Liu, D., Cline, M.A., Gilbert, E.R., 2015. Neuropeptide Y promotes adipogenesis in chicken adipose cells in vitro. Comp. Biochem. Physiol. Pt. A Mol. Integr. Physoil. 181, 62–70.

Zhang, R., Lin, Y., Zhi, L., Liao, H., Zuo, L., Li, Z., Xu, Y., 2017. Expression profiles and associations of adiponectin and adiponectin receptors with intramuscular fat in Tibetan chicken. Br. Poultry Sci. 58, 151–157.

Zhuo, Z., Lamont, S.J., Lee, W.R., Abasht, B., 2015. RNA-seq analysis of abdominal fat reveals differences between modern commercial broiler chickens with high and low feed efficiencies. PloS One 10, e0135810.

Zimmerman, R., Strauss, J.G., Haemmerle, G., Schoiswohl, R., Birner-Gruenberger, R., Riederer, M., Lass, A., Neuberger, G., Eisenhaber, F., Hermetter, A., Zechner, R., 2004. Fat mobilization in adipose tissue is promoted by adipose triglyceride lipase. Science 306, 1383–1386.

Chapter 27

Protein metabolism

Colin G. Scanes[1,2] and Sami Dridi[2]

[1]Department of Biological Sciences, University of Wisconsin, Milwaukee, WI, United States; [2]Center of Excellence for Poultry Science, University of Arkansas, Fayetteville, AR, United States

27.1 Introduction

27.1.1 Protein metabolism: overview

Proteins play critical roles in birds, as in other animals, including in the following: as structural elements, such as keratin in skin and feathers; collagens in connective tissue; cellular proteins (e.g., those of the cell membrane, cytoskeleton, protein synthetic machinery); DNA-associated proteins (e.g., histones); as contractile elements in muscles (see Chapter 23); as oxygen-binding proteins, such as hemoglobin in erythrocytes and myoglobin in muscle; as receptors; as hormones, cytokines, and other messengers; as antibodies; as transporters; as nutrients for embryonic development in the yolk and egg albumin proteins (see Chapter 35); and as enzymes.

Proteins represent a major component of birds with proteins comprising the following:

- Adult verdin (*Auriparus aviceps*) with 24.5% protein
- Seven week-old domestic geese
  - Carcass 18.3% protein
  - Skin 10.6% protein
  - Feathers 54.5% protein.

Table 27.1 summarizes the composition of young chicken, adult mallards, and bald eagles as estimated by dissection and correction for muscles and associated connective tissue adhering to bone.

27.1.2 Physiological effects on protein concentrations

There are physiological effects on the protein and weights of the liver and intestine. For instance, the weights of both the liver and intestine are decreased in pied flycatchers and in willow warblers following long migrations (Schwilchet al., 2002). This is due to amino acids from protein degradation supplying some of the energy needs of flight during migration.

Diet can influence the protein metabolism of the liver and intestine. For instance, feeding a diet that is high in fiber for four weeks is followed by marked hypertrophy (2.3-fold increase) of the gizzard in Japanese quail (Starck and Rahmaan, 2003). This is explicable for the following reason: there is a marked increase in the amount of feed consumed due to its lower nutritional density compared to the high-fiber diet, and this increase results in mechanical stretching of the gizzard by the volume of ingesta.

27.1.3 Amino acids and proteins

Proteins are synthesized from amino acids. The essential or indispensable amino acids in avian diets for protein production and other functions are as follows:

- Arginine, histidine, isoleucine, lysine, methionine (with a higher requirement if cysteine is not present), threonine, tryptophan, and valine.

Other important amino acids (dispensable or in dispensable under specific conditions) for protein production are the following:

- Alanine, aspartate, asparagine, cysteine, glutamate, glutamine, glycine, leucine, proline, phenylalanine, serine, and tyrosine.

Lysine and methionine are the first limiting amino acids for growth (Bornstein and Lipstein, 1975). Amino acids are synthesized in birds, predominantly in the liver. There is interconversion of some amino acids. For instance, glutamate can be converted to glutamine, catalyzed by glutamine synthase, while glutamine can be converted to glutamate by glutaminase. There are also extranutritional effects of amino acids (see Section 27.11), with amino acids converted to glucose in gluconeogenesis (see Chapter 25), to purines, to uric acid, to neurotransmitters, and to pigment (see Section 27.10).

Sturkie's Avian Physiology. https://doi.org/10.1016/B978-0-12-819770-7.00016-5

TABLE 27.1 Importance of organs to body weight in young chickens.

Organ	% Of body weight		
	Bald eagle[a]	Chicken[b]	Mallard[c]
Skeletal muscle (and associated connective tissue)	15.8	37.7	41.2
Bone[d]	6.7	29.2	9.2
Gastrointestinal tract	3.8	13.0	14.6
Skin and feathers	25.6	12.4	18.6
Liver	1.4	3.9	2.4
Heart	1.4	1.2	0.9
Kidneys	0.61	0.8	0.7[e]
Lung	1.45	0.8	NA

NA not available.
[a]*Data from Brodkorb (1955).*
[b]*Calculated from data in Jones et al. (1986).*
[c]*Data from Janiszewski et al. (2018).*
[d]*Corrected for muscle and other soft tissues adhering to bones.*
[e]*Mean of data from Gasaway and Buss (1972); White et al. (1978); Kalisinska et al. (1998); Albers et al. (2006); Kalisinska et al. (2013); Abood et al. (2014).*

27.1.4 Posttranslational modification of amino acids

Posttranslational modification of amino acids in proteins occurs, including:

- Methylation: Histidine residues in myofibrillar proteins (e.g., actin and to a less extent myosin) are methylated (see Table 27.2).
- Phosphorylation: Phosphorylating serine, threonine, or tyrosine residues is essential for activating or deactivating enzymes.
- Glycosylation: This is to form glycoproteins.
- Acetylation with the addition of fatty acids: This results in the formation of lipoproteins.
- Sulfation.

27.2 Major proteins

27.2.1 Collagen

27.2.1.1 Overview

Collagen is major protein in the extracellular matrix of skin, tendons, and bone but is also present in other tissues including skeletal muscle. Collagen molecules are in the form of long fibrils. Collagen is said to the most abundant protein in the animal kingdom (Lodish et al., 2000). It is not readily possible to estimate the collagen content of whole bird with a degree of accuracy.

TABLE 27.2 Quantitative importance of feathers in birds.

Organ	Feathers	
	Weights as % body weight	Protein as % of body weight
Bald eagle[a]	16.6	14.1[f]
Chicken (one-week-old broiler type)[b]	1.4	1.2
Chicken (three-week-old broiler type)[c]	1.3	1.1
Chicken (10-week-old broiler type)[b]	5.5	4.7
Chicken (one-week-old layer type)[b]	2.7	2.3
Chicken (10-week-old layer type)[b]	8.3	7.1
Domestic geese (seven-week-old)[d]	8.3	4.5
Mallard ducks[e]	7.9	6.7

[a]*Data from Brodkorb (1955).*
[b]*Data from Plavnik and Hurwitz (1983).*
[c]*Urdaneta-Rincon and Leeson (2004b).*
[d]*Data from Nitsan et al. (1981).*
[e]*Data from Janiszewski et al. (2018).*
[f]*Assumes feathers are 85% protein (e.g., Peng et al., 2019).*

27.2.1.2 Quantitative aspects

The available evidence supports collagen being the predominant protein in birds. The collagen percentages have been reported for the following:

- Chicken bone is 15.7% (Kettawan et al., 2002; Cansu and Boran, 2015)
- Chicken muscle is 3.0% (Laurent et al., 1978b, 1978c); Reddy et al., 2016; Maharjan et al., 2019)

Based on these percentages and organ composition in Table 27.1, the amounts of collagen in these tissues are the following:

- Chicken bone has 5.9 g collagen per 100 g body weight
- Chicken muscle has 0.9 g collagen per 100 g body weight

What is missing is estimates of collagen in high collagen containing tissues such as the following:

- Keel cartilage—35% collagen (De Araújo Cordeiro et al., 2002)
- Feet—9.1% collagen (Liu et al., 2001)

Thus, collagen represents over 6.8 g per 100 g body weight in, at least, chickens. Is there another protein that can compete with collagen to be the most abundant in

birds? Keratin is a possible. Table 27.2 summarizes feather weights as a percentage of body weight together with protein/keratin per 100 g body weight. It is noted that estimates of the protein/keratin composition of feathers varies considerably, for instance—45% (Nitsan et al., 1981) and 85% (Peng et al., 2019). Irrespective of this, keratin is in contention for the most abundant protein in birds without including estimates of keratin in claws, beak, scales, and keratocytes.

27.2.1.3 Chemistry of collagen

The types of collagen include the following:

- Type I is found in skin, tendons, and bone consisting of three polypeptide chains (see Fig. 27.1):
  - Two α1
  - One α2
- Type II (found in cartilage) consisting of three α1 chains (see Fig. 27.1)
- Type III (found in blood vessels) consisting of three α1 chains (see Fig. 27.1).

There are three domains in procollagen, respectively, the globular N terminal, the triple helical region of collagen, and the globular C terminal (see Fig. 27.1). After trimerization including formation of disulfide bridges, procollagen is cleaved by N- and C-proteases to yield collagen. Collagen is composed of repeating amino acid residue triplets: GlycineXY with X and Y likely to be proline or possibly alanine or glycine (see Fig. 27.2). Multiple of proline residues are hydroxylated (Fig. 27.2).

27.2.1.4 Functions of collagen

Not only are collagen fibers essential to organ integrity and to movement, but also collagen has other roles. For instance, collagen fibers, in quasi-ordered parallel arrays in the dermis, are one basis for skin coloration (Prum and Torres, 2003).

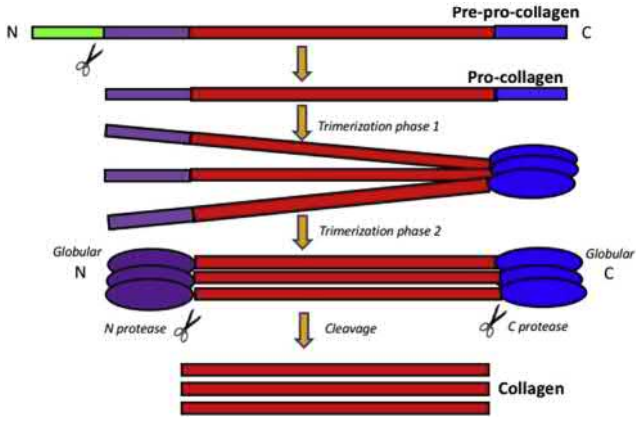

FIGURE 27.1 Processing of chicken pre-pro-collagen to procollagen and then to collagen. *Adapted from Canty and Kadler (2005).*

27.2.1.5 Control of collagen synthesis

Collagen synthesis is considered in section 26.6 below. Collagen synthesis is influenced by physiological and pathological factors. Expression of collagen in the small intestine is increased by lysolecithin (chickens: Brautigan et al., 2017). Synthesis of insoluble collagen in muscles increases during growth while that soluble collagen decreases (chicken: Maharjan et al., 2019). Collagen synthesis was reported to be increased with myopathy (chicken: Maharjan et al., 2019).

27.2.2 Keratins

27.2.2.1 Overview

Keratin is the major or sole protein in epidermal tissues and appendages including: scales, claws, and beaks (reviewed e.g., Greenwold et al., 2014). Keratins have multiple β-pleated sheets and are therefore resistant to proteolysis.

27.2.2.2 Keratin genes

Members of the α keratin gene family are found throughout the vertebrates while the β keratin gene family is only found in reptiles and birds (reviewed e.g., Greenwold et al., 2014). The keratin gene family in birds consists of the following:

1. α keratin gene family with 26 to 38 genes in birds consisting of the following:
   - Type 1 α keratin gene subfamily (10 to 18 genes in different avian species)
   - Type II α keratin gene subfamily (11 to 22 genes in different avian species)
2. The β keratin gene family (in the same 5′ to 3′ order on microchromosome 25) composed of the following gene subfamilies:
   - Feather β keratin gene subfamily (85% of β keratin genes)
   - Claw β keratin gene subfamily
   - Scale β keratin gene subfamily
   - Keratinocyte β keratin gene subfamily

(reviewed e.g., Greenwold and Sawyer, 2013; Greenwold et al., 2014). The number of β keratin genes varies from 6 in barn owls to 149 genes in zebra finch with 133 in chickens (Greenwold et al., 2014). There are also specialized forms of keratin, for instance, otokeratin (keratin, type II) in cochlea (Heller et al., 1998).

27.2.2.3 Keratin expression and protein

Both α- and β-keratin are expressed in skin appendages include beaks, feathers, scales, and claws (chicken embryo: Wu et al., 2015). However, the ratio between these varies markedly (chicken embryo: Wu et al., 2015).

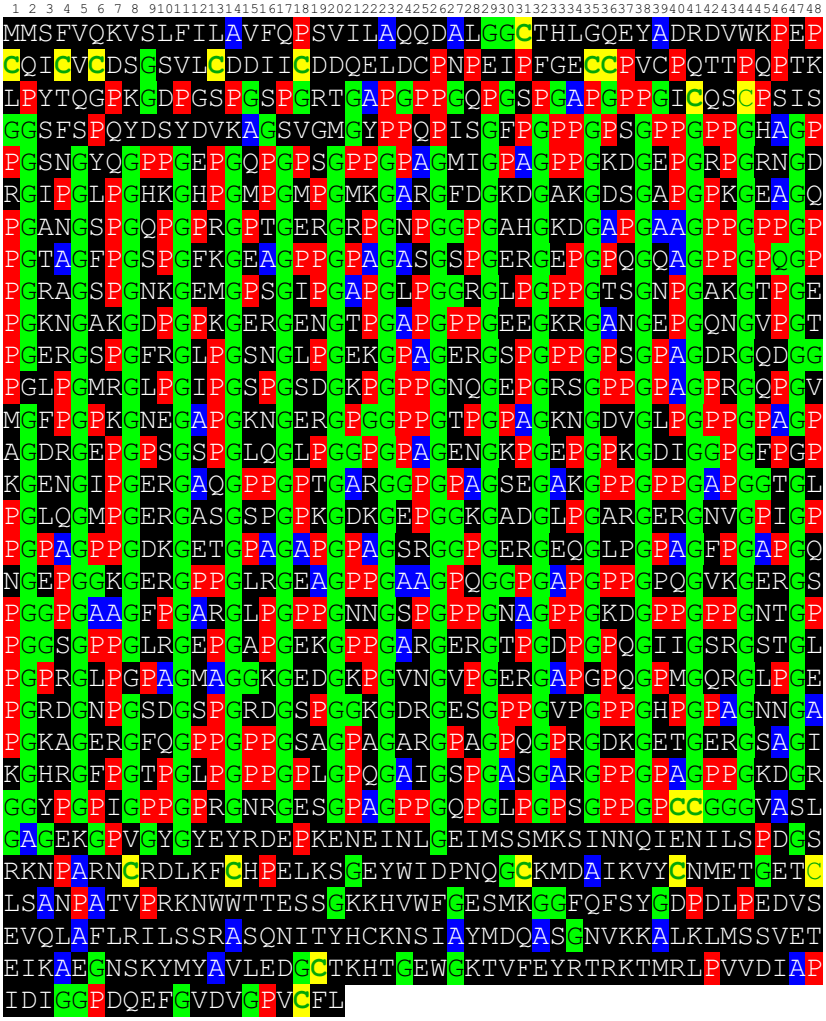

FIGURE 27.2 Structure of example of chicken pre-pro-collagen [collagen type III alpha 1 chain (COL3A1), based on cRNA (Genbank accession NM_205380 XM_421847)] showing sequences in N and C globular domains and a central collagen domain containing repeating GXY triplets.

Feathers are made of α and β-keratins. The proteins of the rachis of chicken feathers have a high content of the following four amino acids.

- Glycine: 13.5%
- Proline: 11.9%
- Cysteine: 9.7%
- Leucine: 8.3%

[In chickens, turkey, emu, white-crowned sparrow, and pygoscelid penguins (Harrap and Woods, 1967; Murphy et al., 1987; King and Murphy, 1987)]. There are differences in the relative concentrations of the amino acid residues in barbs versus rachis plus calamus (e.g., Harrap and Woods, 1967). Moreover, the proportion of barbs varies markedly between different avian species from 70% in white-crowned sparrows (*Zonotrichia leucophrys*) (King and Murphy, 1987) to 35% in penguins (calculated from Murphy et al., 1990).

A mutation in the krt75 gene (encoding an α collagen) results in defective rachis in frizzle feather chicken (Ng et al., 2012).

27.2.2.4 Feather dynamics

There are high rates of keratin synthesis. Keratin synthesis can be estimated as follows:

- Broiler chickens 1.67 g/d
- Layer type chickens 0.85 g/d
- White-crowned sparrows (*Zonotrichia leucophrys*) 75 mg/d

[Values for chickens calculated from data in the sources: chicken (7 days to 10 weeks old) Plavnik and Hurwitz (1983) using feathers as 85% protein (Peng et al., 2019)] (Murphy and Taruscio, 1995).

This replacement of feathers after losses (accidental or during molting) is critically important for flight. Rapidity of feather growth has been linked to feather abnormalities (Vágási et al., 2012). Feathers scale with the body weight of birds by 0.32 power, while feather growth rate increases across species by much less, 0.17 power of body weight (Rohwer et al., 2009).

27.2.2.5 Control of keratin synthesis

The relative weights of feathers and consequently keratin is influenced by physiological factors. There is an increase in the relative weight of feathers during growth in chickens (Plavnik and Hurwitz, 1983) (Table 27.2). Nutritional restriction decreased the overall weights of feathers from 8.45% of body weight on ad libitum feeding compared 7.74% receiving 50% feeding (chickens: Plavnik and Hurwitz, 1983).

There are shifts in feather growth in wild birds. Feather growth is followed increased in a simulated molt when feathers were removed in starlings by plucking (Romeroa et al., 2003). Hormones influence feather growth with, for instance, corticosterone depressing feather growth based on studies with implanted white-crowned sparrows (Romeroa et al., 2003).

27.3 Muscle proteins

27.3.1 Overview

Over 20% of the wet weight of skeletal muscles is protein (equivalent to 7.6% of body weight). The major proteins are myosin and actin of the thin and thick filaments, together with sarcoplasmic proteins.

Thin filaments:

- Actin
- Tropomyosin
- Troponin

Thick filaments:

- Myosin.

The physiology of myosin, actin, and other muscle proteins is considered in chapter 23. In addition to its role in muscle contract, actin has other roles. For instance, there are intracellular actin fibers (e.g., Perrin et al., 2010). Profilins (PFN) are actin binding proteins. PFN2a is expressed ubiquitously in avian tissues and plays a role in cell adhesion, spreading, and movement (chicken: Murk et al., 2009). Moreover, actin fibers are found in the avian cochlea (Tilney et al., 1992).

27.3.2 Actin and myosin genes

The distribution of actin in the body of birds can be estimated by use of 3-methyl histidine as a surrogate. About 11.8% of actin is methylated (chicken: calculated from Johnson et al., 1967) (Table 27.3). Methylated histidine residues are also found in myosin (chicken: calculated from Johnson et al., 1967) (see Table 27.3).

TABLE 27.3 Importance of various Organs to total 3-Methyl-Histidine in young chickens.

Organ	3-Methyl-Histidine as % of total body	
	Chicken	White-crowned sparrow
Skeletal muscle (and associated connective tissue)	84.0	84.1
Bone[a]	1.6	NA
Gastrointestinal tract	9.8	10.2
Skin and feathers	1.7	NA
Liver	1.0	1.0
Heart	1.4	1.3
Kidneys	0.0	0.3
Lung	0.2	0.2
Brain	0.1	NA

NA not available.
[a]*Corrected for muscle and other soft tissues adhering to bones.*
Calculated from data in Jones et al. (1986); Taruscio and Murphy (1995).

Multiple forms of myosin are expressed with differences between fiber types and during embryonic development and posthatch growth (Rosser et al., 1996, 1998). For instance, in adult chickens, pectoralis expresses fast myosin heavy chain (MyHC1), with slow myosin heavy chain (MyHC2) expressed in tonic muscles (Crew et al., 2010).

Actin genes include the following:

- α cardiac-actin (expressed in cardiac muscle)
- α skeletal-actin (expressed in skeletal muscle)
- α smooth-actin (expressed in smooth muscle)
- β cyto-actin (expressed in ubiquitously)
- γ smooth-actin (expressed in cardiac muscle)
- γ cyto-actin (expressed in ubiquitously)

(Chang et al., 1984; Perrin et al., 2010).

27.4 Other proteins

27.4.1 Blood proteins

Using data across avian species (see chapter on Blood 17), the major blood proteins are the following:

- Hemoglobin represents 1.15% of body weight
- Serum albumen represents 0.71% of body weight

27.4.2 Mucins

Another example of a family of genes/proteins are the mucin proteins. Mucin is produced by goblet cells in the gastrointestinal tract. It is a gel consisting of heavily glycolylated proteins in solution. There are multiple Muc genes in birds:

- Genes for transmembrane mucins—Muc4, Muc13, and Muc16 transmembrane mucins
- Genes for gel forming mucins—Muc2, Muc5ac, Muc5b, and Muc6

(Chicken: Lang et al., 2006). Mucin glycoproteins can be neutral or acidic sialiated or acidic sulfated (chicken: Biasato et al., 2019). Greater mucin staining is reported in both the villi and crypts in the ileum than duodenum with the jejunum being intermediate (Biasato et al., 2019).

The mucin layer is important to both gastrointestinal integrity and functioning. When young chickens receive increased dietary lysine but decreased protein, jejunal expression of MUC2 is increased (Lee et al., 2020). Moreover, jejunal expression of mucin genes is influenced by *Clostridium perfringens* with the following:

- MUC2 ↓
- MUC5AC ↑
- MUC13 ↓

(Forder et al., 2012).

27.4.3 Egg protein

Egg yolk proteins as 0.22% of body weight per day while egg white proteins as 0.23% of body weight per day (this discussed in more detail in chapter 35).

27.5 Digestion of proteins

27.5.1 Overview

Proteins, in the diet, provide animals with amino acids (both indispensable and dispensable) that a vital to maintenance, growth, feathers, and reproduction of all animals. The impact of feeding an extremely low-protein diet is shown in Table 27.4. Chicks on a very low-protein diet lost weight compared to those on a 10% protein feed demonstrating the need for protein even for maintenance. A 10% protein diet allows some growth, but this was accelerated with a 20% protein diet.

Proteins are digested in the gastrointestinal tract to amino acids and dipeptides together with some tripeptides.

TABLE 27.4 Effect of dietary protein between 7 and 17 days old in Leghorn chicks.

	Dietary protein as %			
	0	10	20	SEM
Body weight				
Change g	−16.3[a]	57.5[b]	90.8[c]	1.4
Liver				
Weight g	1.96[a]	3.61[b]	4.27[c]	0.15
DNA mg	5.3[a]	8.3[b]	8.6[b]	0.8
Protein mg	289[a]	577[b]	785[c]	33
Protein fractional synthesis rate %/d	46.8[a]	66.0[b]	91.4[c]	3.9

[a,b,c]*Different superscript letter indicates difference $P < .05$.*
Data from Kita et al. (1996).

27.5.2 Protein digestion in the gizzard and proventriculus

27.5.2.1 Overview

The digestion of proteins is initiated in the gizzard and proventriculus in birds by the following methods:

- Mechanical grinding by the gizzard
- Chemical denaturation by the low pH
- Enzymatic proteolysis by pepsin

27.5.2.2 Pepsinogen

There are multiples pepsinogen genes including the following:

- Pepsinogen A
- Progastricsin (pepsinogen C or pepsinogen II) encoded by PGC gene [e.g., chicken (Genbank accession number: NM_204877)]
- Embryonic pepsinogen [e.g., chicken Hayashi et al. (1988a); accession number: NM_204877; golden eagle (*Aquila chrysaetos*) XM_030000984; emperor penguin (*Aptenodytes forsteri*)—XM_009290607; American crow (*Corvus brachyrhynchos*)—XM_008638001].

Gastric aspartic proteinases consist of pepsin A and gastricsin (pepsinogen C or pepsinogen II) in posthatching birds. These are expressed and secreted from the mucosal cells in the chicken proventriculus (Sakamoto et al., 1998).

They are synthesized as pepsinogens with the zymogen has been activated by acid conditions (chicken: Bohak, 1969).

The embryo specific or embryonic pepsinogen exhibits homology to calf prochymosin or rennin (Foltmann, 1992). Expression of embryonic pepsinogen by endodermal tissue is a marker of differentiation of proventriculus epithelium (Hayashi et al., 1988b).

Avian pepsinogen is proteolytically activated to pepsin at low pH (Keilova et al., 1977) (Table 27.4).

27.5.3 Protein digestion in the small intestine

27.5.3.1 Overview

The predominant site of protein digestion is the small intestine (Pisano et al., 1959; Hurwitz et al., 1972) (Table 27.5). The digested protein (amino acids and dipeptides together with some tripeptides) is absorbed in the small intestine (Table 27.5). There is high digestibility/absorption of amino-acids as reflected by ileal digestibility (Table 27.6).

Proteins undergo enzymatic digestion in the small intestine by the serine proteases, trypsin, and chymotrypsin. These are produced by the pancreas as inactive zymogens (respectively, trypsinogen and chymotrypsinogen) and transported to the small intestine in the pancreatic secretions. In the small intestine, both trypsinogen and chymotrypsinogen are activated by proteolytic cleavage:

- Trypsinogen → trypsin
- Chymotrypsinogen → chymotrypsin.

In addition, there are peptidases that hydrolyze peptides generated by trypsin and chymotrypsin.

27.5.3.2 Trypsin

Trypsinogen gene family consists of the following:

- Trypsinogen I (cationic trypsin isoenzymes) subfamily six genes
- Trypsinogen II (anionic trypsin isoenzymes.) subfamily three genes

TABLE 27.5 Protein digestion and absorption in the regions of the chicken small intestine.

Protein	Digestion (%)	Protein absorption (%)
By end of duodenum	60	7
By end of jejunum	85	70
By end of ileum	93	83

Based on Hurwitz et al. (1972).

TABLE 27.6 Ileal digestibility of selected essential amino acids in chickens.

Amino acid	Mean % ileal digestibility + SEM
Cysteine	76.2 ± 1.8
Threonine	79.7 ± 1.7
Lysine	89.8 ± 0.6
Methionione	94.4 ± 0.5
Arginine	97.5 ± 4.2

Source: Fagundes et al. (2020).

(Chicken Wang et al., 1995). In addition, the structure of ostrich trypsinogen II is deduced from mRNA (Genbank accession: AY601749) (Szenthe et al., 2005).

Trypsinogen genes are expressed in the pancreas along with the liver, spleen, and thymus (Wang et al., 1995). Trypsinogen is proteolytically cleaved either by enterokinase or autocatalytically (ostrich: Szenthe et al., 2005). This proteolytic cleavage results in the formation of an active protease, trypsin. Concentrations of trypsin in the pancreas show little change during embryonic development and posthatching development [pigeon (*Columba livia*): Xie et al., 2020].

Trypsin-like activity is reported in amniotic fluid together with some in the allantoic fluid and egg albumen (chicken: Da Silva et al., 2017). There are increases in this trypsin-like activity during embryonic development (chicken: Da Silva et al., 2017).

27.5.3.3 Chymotrypsinogen

5wAvian chymotrypsinogen has been isolated from pancreas (ostrich: van der Westhuizen et al., 1989; Japanese quail: Hou et al., 1990). The structures of chymotrypsinogen have been deduced in multiple avian species from mRNA including the following: chicken (*Gallus gallus*) chymotrypsinogen A-like (Genbank XM_025154258) and B-like (NM_001277636), mallard (*Anas platyrhynchos*) (XM_027466372), tufted duck (*Aythya fuligula*) (XM_032195902), rock pigeon (*C. livia*) (XM_005504777), Anna's hummingbird (*Calypte anna*) (XM_030457979.1), peregrine falcon (*Falco peregrinus*) (XM_005233498), bald eagle (*Haliaeetus leucocephalus*) (XM_010584290), barn owl (*Tyto alba*) (XM_033001843), New Caledonian crow (*Corvus moneduloides*) (XM_032121949), zebra finch (*Taeniopygia guttata*) (XM_012570273), lance-tailed manakin (*Chiroxiphia lanceolate*) (XM_032700994), Swainson's thrush (*Catharus ustulatus*) (XM_033069904), and great tit (*Parus major*) (XM_015640042).

Chymotrypsinogen is activated to chymotrypsin in the small intestine by proteolytic cleavage, for instance by trypsin. The structure is maintained by disulfide bridges.

27.5.3.4 Aminopeptidases

27.5.3.4.1 Overview

Aminopeptidases are membrane-bound proteins in enterocytes. Most of the enzyme protein is extracellular, with a single transmembrane domain and a small intracellular domain. An avian aminopeptidase has been partially characterized (chicken: Gal-Garber and Uni, 2000), but its complete structure deduced from mRNA [e.g., chicken (*Gallus gallus*) (Y17105.1), ostrich (*Struthio camelus*) (AJ577158), turkeys (*Meleagris gallopavo*) (AJ296745.1), and zebra finch (*Taeniopygia guttata*) (XM_002194583.5)].

27.5.3.4.2 Expression of aminopeptidases

Not only is there high expression of aminopeptidase in the duodenum, jejunum, and ileum but also in the ceca (chicken: Gal-Garber and Uni, 2000; Miska et al., 2015). Aminopeptidase is also expressed in the yolk sac [e.g., rock dove (*C. livia*) (Shbailat and Aslan, 2018) and chicken: Miska et al., 2015].

Expression of aminopeptidase is influenced by physiological status. There is increased expression of aminopeptidase in the brush border of the ileum of high growth rate chickens (Miska et al., 2019). Expression of aminopeptidase is markedly depressed in young chickens challenged with *Eimeria maxima* infection (Miska and Fetterer, 2018). Administration of threonine *in ovo* was accompanied by increased ileal expression of aminopeptidase at hatching (chicken: Moreira Filho et al., 2019).

27.5.4 Amino acid absorption in the small intestine

27.5.4.1 Overview

Amino acids are absorbed in the small intestine (chicken jejunum and ileum: Tasaki and Takahashi, 1966) (discussed in detail in chapter 21). There is greater absorption of methionine in the ileum than in other regions of the small intestine (Hurwitz et al., 1972) (also see Fig. 27.3). Methionine is absorbed at the highest rate, followed by isoleucine, valine, and leucine, and glutamate is absorbed at the lowest rate, followed by aspartate, glycine, and arginine (Tasaki and Takahashi, 1966; Riley et al., 1986). There are series of amino acid transporters (10 in chickens) expressed in the enterocytes of the small intestine, with predominantly increases progressing down the small intestine from the duodenum, jejunum, and ileum (chickens: Gilbert et al., 2007). Moreover, there are increases in the expression of many amino acid transporters during the period of growth and development posthatching (chickens: Gilbert et al., 2007).

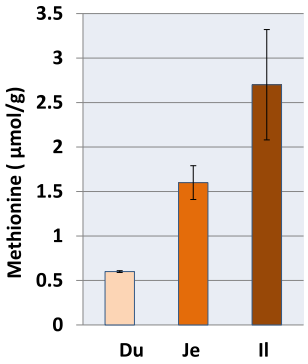

FIGURE 27.3 Absorption of methionine by different regions of the chicken intestine *in vitro*. *Du*, duodenum; *Je*, jejunum; *Il*, ileum; vertical lines, standard error of the mean. *Data from Knight and Dibner (1984).*

There is moderately high expression of the H^+-dependent peptide transporter-1 (PepT1) throughout the small intestine, with marked increases in the posthatch period (Gilbert et al., 2007). PepT1 functions to transport both dipeptides and tripeptides into the enterocyte.

27.5.4.2 Turnover times for small intestine mucosal cells

Not only are proteins in the ingesta digested with the resultant amino acids and small peptides absorbed but also mucosal intestinal cells are sloughed off and then digested. The turnover times for mucosal cells in the small intestine are estimated as the following in the chicken (calculated from data in Imondi and Bird, 1966):

- Duodenum: 111 h
- Jejunum: 55 h
- Ileum: 89 h.

27.5.5 Colon and protein digestion

There is a lack of definitive information on the roles of the colon in protein and amino acid digestion and absorption. Most of the proteins in the ingesta are digested by the time the ingesta reaches the colon (Table 20.5). There are populations of proteolytic bacteria in the colon of birds (chicken: King et al., 2009). The impact of these proteolytic bacteria is not known. Interestingly, there is absorption of the methionine analog, 2-hydroxy-4-(methylthio) butanoic acid (Alimet), in the colon as well as the small intestine (chicken: Knight and Dibner, 1984; Dibner et al., 1988).

27.5.6 Ceca and protein digestion

The ceca appear to play some role in nitrogen metabolism. Ileal protein digestibility is depressed in cecectomized

chickens (Choct et al., 1992). Moreover, there are increases in endogenous losses of nitrogen and both indispensable and dispensable amino acids in feed deprived cecectomized ducks (Ragland et al., 1999) and endogenous losses of nitrogen in chickens following cecectomy either on a low protein or on low protein plus urea diet (Kang et al., 1999). There are also decreases in uric acid excretion in cecectomized birds (duck: Ragland et al., 1999; chickens: Son et al., 1997; Kang et al., 1999). Uric acid, arginine, glycine, glutamic acid, and, to a less extent, alanine are metabolized by cecal microorganisms releasing ammonia (Karasawa et al., 1988; Karasawa, 1989). Similarly, bacterial degradation of uric acid is reported in the ceca, e.g., Gambel's quail (*Callipepla gambelii*) (Campbell and Braun, 1986).

27.6 Protein synthesis

27.6.1 Whole-body synthesis and degradation

Whole-body net protein synthesis can be estimated by nitrogen balance. For instance, Kino and Okumura (1987) estimated nitrogen balance in 14–21 day-old chickens as 0.29 g/day. Alternatively, whole-body protein net synthesis (accretion) or net degradation can be estimated by difference between determined body protein at multiple ages.

Whole-body protein synthesis can be determined by infusing a radioactive form (or equivalent stable isotopes) of a nonmetabolized amino acid such as phenylalanine or tyrosine or proline (for collagen synthesis). Combining net protein synthesis and whole-body protein synthesis allows indirect calculation of rates of protein degradation (Table 27.6).

$$\text{Whole} - \text{body protein net synthesis (accretion)} = \text{Whole} - \text{body protein synthesis} - \text{Whole} - \text{body protein degradation}$$

Where whole-body protein losses include in proteins in eggs or molted feathers. If negative, whole-body protein net synthesis is whole-body protein net degradation.

27.6.2 Fractional protein synthesis in different organs

Proteins are synthesized from the intracellular amino acid pool in the organs. There is interchange between amino acids in this pool and the plasma but markedly lower concentrations of, for instance, in the intracellular pool (Table 27.7).

The highest fractional rate of protein synthesis reported in young chickens is 172%/d for the pancreas (Muramatsu et al., 1987a). High rates are also reported in the bursa Fabricius (67%/d), spleen (46%/d), ceca (63%/d), and small intestine (see Table 27.8) (Muramatsu et al., 1987a).

TABLE 27.7 Effect of reduced dietary lysine on plasma and muscle concentrations of lysine and on muscle degradation as reflected by 3-Methyl Histidine.

	Free amino acid concentrations	
	Diet 1 (control diet meeting lysine requirement)	Diet 2 (low lysine 90% of requirement
Lysine		
Plasma (nmol/mL)	187	103[a]
Intramuscular (nmol/g)	69	42[a]
3-Methyl histidine		
Plasma (nmol/mL)	22.6	26.1[a]
Intramuscular (nmol/g)	24.2	35.5[a]

[a]*Difference with replete diet $P < .05$.*
Based on Watanabe et al. (2020).

TABLE 27.8 Comparison of fractional synthesis rates in various organs in young chicks (Muramatsu et al., 1987a; Nieto et al., 1994) with those in adult female chickens (Yuan et al., 2016; Miao et al., 2017; Vignale et al., 2015).

	Fractional synthesis rates %/d	
Organ	Young chickens	Adult female chickens
Liver	95.1	11.3
Jejunum	65.7	6.9
Skin	43.4	–
Skeletal muscle (breast/*pectoralis*)	22.2	4.7

Fractional rates of rates of protein synthesis are lower in the brain (32% of liver) (Sayegh and Lajtha, 1989) and skeletal muscle (see Table 27.8).

Protein synthesis in the liver is high (see Table 27.8), representing 11% of all protein synthesis in the bird. Similarly, gastrointestinal protein synthesis is disproportionately high compared to in other tissue. For instance, in the young chick, 18.9% of protein synthesis occurs in the small intestine plus the pancreas and ceca (calculated from Muramatsu et al., 1987a). This is in contrast to the gastrointestinal organs, which represent 5.2% of the protein in the bird or 5.9% of the body weight (Table 27.9).

TABLE 27.9 Comparison of collagen and noncollagen components in chicken muscle.

	Noncollagen	Collagen
Protein content % wet wt.		
Anterior latissimus dorsi[a]	15.6	4.0
Pectoralis major[b,c]	20.5	2.2
Posterior latissimus dorsi[a]	13.5	1.6
Synthesis % per day		
Anterior latissimus dorsi[a]	17	0.59
Pectoralis major[c]	24	0.63
Posterior latissimus dorsi[a]	6.9	0.59

[a]*Determined in adult chickens by Laurent et al. (1978b, 1978c).*
[b]*USDA Nutrient database.*
[c]*Determined in young chickens by Maharjan et al. (2019).*

27.6.3 Fractional protein synthesis in muscle

There are very similar rates of protein synthesis for sarcoplasmic and myofibrillar proteins in skeletal, heart, and smooth muscle:

- *Anterior latissimus dorsi*: 16% per day
- *Posterior latissimus dorsi*: 7% per day
- Heart: 14% per day
- Gizzard: 11% per day

(Chicken: Laurent et al., 1978a). Connective tissue makes up a significant proportion of muscle. Fractional synthesis rates for collagen are considerably lower than for myofibrillar and sarcoplasmic proteins (also see Table 27.9) (adults: Laurent et al., 1978b, 1978c; young chickens: Maharjan et al., 2020) (Table 27.11).

27.6.4 Ribosomal protein S6 and ribosomal protein S6 kinase (S6K1) and protein synthesis

Ribosomal protein S6 (RPS6) and RPS6 kinase (S6K1) play important roles in the initiation of protein synthesis (see Fig. 27.4). Protein kinase B/mechanistic (or mammalian) target of rapamycin (mTOR) pathway control activation and expression of S6K1 (see section 27.8.2 and Fig. 27.4).

Nutritional and endocrine states influence S6K1 activity (see Fig. 27.4). Phosphorylation of S6K1 in skeletal muscle is depressed with fasting in chickens (Saneyasu et al., 2019). In a reciprocal manner, arginine supplementation is followed by increases in S6K1 activity in the liver (Yuan et al., 2016) and small intestine in chickens (Miao et al., 2017). In addition, in vitro, L methionine increases phosphorylation of S6K1 (chicken myoblasts: Métayer-Coustard et al., 2010). Similarly, endocrine status influences S6K1 activity with marked increases in skeletal muscle after insulin administration (chicken: Bigot et al., 2003). Moreover, the glucocorticoid, dexamethasone, reduces both protein synthesis and phosphorylation of S6K1 (chicken: Wang et al., 2019). In addition, expression of RPS6K in breast muscle is increased following administration of 25-hydroxycholecalciferol (chickens: Vignal et al., 2015).

TABLE 27.10 Effects of age on breast muscle protein synthesis and degradation in young chickens.

Age in weeks	Fractional protein synthesis (%/d)	Fractional protein Degradation (%/d)
1	39	27
2	22	10
4	24	16
6	17	14

Means of Maruyama et al. (1978), MacDonald and Swick (1981).

TABLE 27.11 Effect of nutritional status on whole-body protein accretion (net synthesis), synthesis, and degradation in young broiler chickens.

	Whole-body protein synthesis[c]	Whole-body protein Degradation	Whole-body protein net or delta (Δ) synthesis (accretion) or, if Negative, Degradation
	g/day/kg body wt.		
Study 1[a]			
Fed	21.3[d]	11.2[d]	10.1[d]
Starved	14.7[d]	19.5[d]	−4.8[d]
Study 2[b]	%/d	%/d	g/d
Control	23[d]	18	+5[d]
Histidine-free diet	17[d]	18	−1[d]
S-amino-acid-free diet	15[d]	18	−3[d]

[a]*Muramatsu et al. (1987b).*
[b]*Kino and Okumura (1987).*
[c]*Determined using ^{3}H -phenylalanine.*
[d]*Difference $P < .05$.*

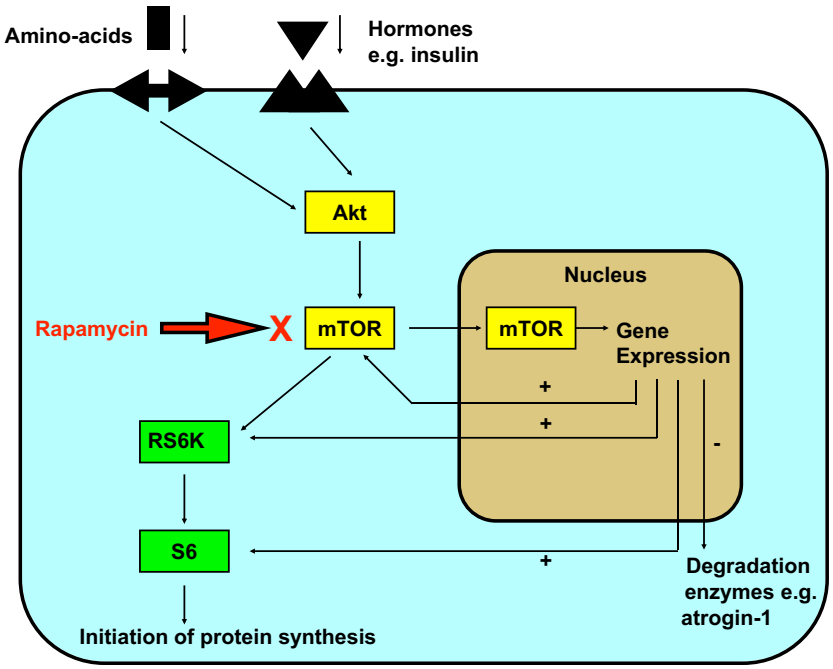

FIGURE 27.4 Schematic of the control of control of protein synthesis and degradation by amino-acids and hormones via the protein kinase B (Akt)/mechanistic (or mammalian) target of rapamycin (mTOR) pathway [Rapamycin inhibits mTOR functioning].

27.6.5 Other factors influencing protein synthesis

There is intriguing evidence that hydrogen sulfide plays a role in stimulating protein synthesis. Hydrogen sulfide is produced from cysteine and homocysteine catalyzed by cystathionine γ-lyase and cystathionine β-synthase. Phosphorylation of S6K1 in muscle is increased following injection of sodium hydrogen sulfide (chicken: Wang et al., 2019). Moreover, L-cysteine overcame the inhibitory effect of glucocorticoid on protein synthesis (chicken myoblasts: Wang et al., 2019).

27.7 Protein degradation

27.7.1 Overview

Proteins are degraded generating the amino acids in intracellular pool of the organs. There is interchange between amino acids in this pool and the plasma. Amino acids are then available for reuse. An exception is 3-methylhistidine which is excreted. As would be expected there are higher concentrations of the 3-methylhistidine in the intracellular pool than in plasma (Table 27.7).

Plasma amino acid pool ↔ Organ amino acid pool ↔ Organ protein

27.7.2 Autophagy

27.7.2.1 Overview

Autophagy ("self-eating") is the intracellular process of degradation of misfolded, unfolded, or damaged proteins together with organelles. Proteins are damaged (oxidized) by reactive oxygen species (ROS) in oxidative stress (reviewed: Bottje, 2019). Autophagy is accomplished the damaged protein associating with the autophagosome followed by fusion of autophagosomes and lysosome and subsequently proteolysis by lysosomal degradation pathway. Fusion is accomplished by soluble NSF attachment proteins (SNARE) proteins as with exocytosis.

27.7.2.2 Autophagy-related genes

There is both tissue and gender differences in the expression of autophagy-related genes with, for instance, higher expression of autophagy genes (Atg) including Atg 9 in breast muscle and brain and Atg 13 in liver and brains in females (chicken: Piekarski et al., 2014). Moreover, expression of Atg 7 and Atg16L1 in breast muscles of high than low-feed efficiency broiler type chickens (Piekarski et al., 2018a). Intracerebroventricular administration of leptin increased hypothalamic expression of autophagy-related genes including Arg 5, Atg 7, and Beclin 1

together with microtubule-associated protein 1 light chain (LC), LC3a, LC3b, and LC 3c (chicken: Piekarski et al., 2018).

27.7.3 Ubiquitin and protein degradation

27.7.3.1 Overview

There are two ubiquitin systems critical to protein degradation:

- Ubiquitin−proteasomal system
- Ubiquitin-like system.

The ubiquitin-proteosome proteolytic pathway plays a critical role in protein degradation. Proteins to be degraded undergo tagging with ubiquitin allowing recognition by autophagy receptors. Ubiquitin is small protein with 76 amino acid residues and that is ubiquitous in cells. Proteins to be degraded can be tagged by post-translational modification, specifically ubiquitination, of lysine residues. Fig. 27.5 summarizes the role of ubiquitination in autophagy (Fig. 27.6).

27.7.3.2 Atrogin-1/MAFbx and protein degradation in birds

Atrogin-1/MAFbx is a muscle-specific ubiquitin ligase. There is expression of Atrogin-1/MAFbx in skeletal, cardiac, and smooth muscle with markedly higher expression in smooth muscle (chicken: Nakashima et al., 2013). Fasting would be expected to increase catabolism with degradation of protein and, not surprisingly, expression of Atrogin-1/MAFbx is increased following fasting in skeletal muscle (chickens: Nakashima et al., 2006) and gizzards (chicken: Nakashima et al., 2013). Similarly, administration of the synthetic glucocorticoid, dexamethasone, is followed by catabolism in the skeletal muscle and increased expression of Atrogin-1/MAFbx (chickens: Nakashima et al., 2016). Moreover, expression of atrogin-1 (E3 ubiquitin ligase muscle atrophy F box) by muscle fibroblasts is depressed by insulin or the amino-acid, methionine (Japanese quail: Tesseraud et al., 2007).

Expression of Atrogin-1/MAFbx is reduced in broiler chickens compared to the red jungle fowl due to single nucleotide polymorphism (Li et al., 2019). This may be a

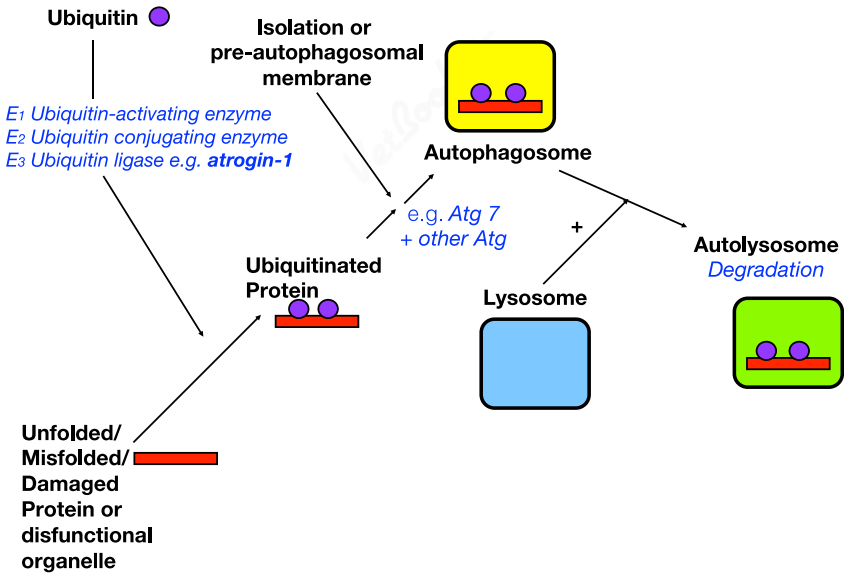

FIGURE 27.5 Simplified schematic of autophagy (degradation of damaged proteins and organelles) including ubiquitination of proteins, formation of autophagosomes, and fusion of these with lysosomes and hence enzymatic degradation.

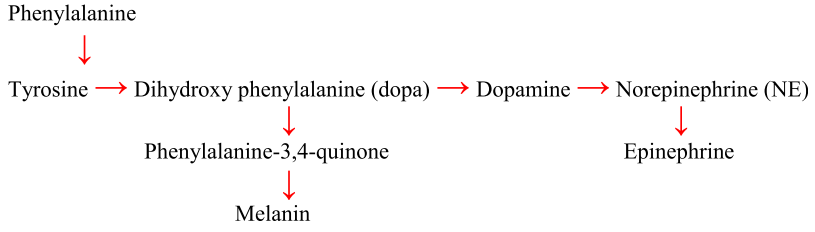

FIGURE 27.6 Synthesis of melanin, dopamine, norepinephrine, and epinephrine from phenylalanine or tyrosine.

causative factor in the lower degradation rates in broiler chickens than wild red jungle fowl.

27.7.4 Lysosomes and protein degradation

27.7.4.1 Overview

Lysosomes play a critical role in autophagy degrading unfolded, misfolded, or oxidized proteins together with damaged organelles (Fig. 27.5). Lysosomal enzymes include proteases, e.g., cathepsins (see Table 27.12) together with glycosidases, sulfatases, nucleases, and phosphatases.

27.7.4.2 Lysosomal proteases

Proteases responsible for proteolysis reported in avian tissues include the following:

- Caspases
- Cathepsins

27.7.4.2.1 Caspases

Physiological status influences expression of caspase (CASP). For instance, fasting increases the expression of the protease, CASP 3, is increased in the gizzards of fasting chickens reflecting catabolism (chicken: Nakashima et al., 2013). Moreover, administration of T2 toxin induces a series of changes in splenic cells including increases in the following: apoptosis and ROS together with expression of CASP: CASP 3 and CASP 9 (chicken: Chen et al., 2019). In contrast, dexamethasone did not influence expression of cathepsin B in muscles (chickens: Nakashima et al., 2016).

27.7.4.2.2 Cathepsins

There are multiple cathepsins in birds. Table 27.12 summarizes cathepsins in chickens. In addition to degrading damaged, misfolded, and unfolded proteins, cathepsins exert other important roles. There is evidence that cathepsin D plays a role in yolk deposition catalyzing hydrolysis of vitellogenin (VTG) in the oocyte (Ritzek et al., 1992; Sheng et al., 2013).

There is tissue-specific expression of cathepsins with expression of cathepsin E-A-like (similar to nothepsin) solely in the liver of sexually mature female birds (chickens: Bourin et al., 2012) with expression induced by estrogen and the estrogen receptor β (chicken: Zheng et al., 2018). There was markedly higher expression of cathepsin D in the uterus than magnum (chickens: Bourin et al., 2012).

27.7.5 Whole body determination of protein degradation

Degradation of muscle myofibrillar proteins can also be measured in vivo by excretion of 3-methylhistidine or in vitro by release of 3-methylhistidine (Hillgartner et al., 1981; Saunderson and Leslie, 1983). When muscle proteins are broken down, 3-methyl-histidine is released but is not reutilized. Whole-body muscle protein degradation can be measured by the excretion of 3-methyl-histidine (see Table 27.3). Rates of 3-methylhistidine excretion are increased in dystrophic chickens (Hillgartner et al., 1981). Measurement of 3-methylhistidine in avian excreta is problematic with the mixing of feces and urine and the retrograde movement of the mixture into the ceca where microbial degradation may occur.

27.8 Control of protein synthesis and degradation

27.8.1 Overview

There are high rates of both net muscle protein accretion or net protein synthesis and fractional rates of muscle protein

TABLE 27.12 Examples of cathepsins in chickens.

Cathepsin	Genbank accession number	Cathepsin	Genbank accession number
Aspartic protease		Cathepsin L-like	NM_001281488
Cathepsin D	Cathepsin O	XM_015285286.2	
Cathepsin E	Cathepsin S	XM_015280008.2	
Cathepsin E-A-like (similar to nothepsin)	Cathepsin V	NM_001168009.1	
Cysteine protease		Cathepsin Z	XM_417483.6
Cathepsin B	NM_205371.2	**Serine protease**	
Cathepsin C	NM_001321554.1	Cathepsin A	XR_003071352
Cathepsin H	JF514547	Cathepsin G	XM_423728
Cathepsin K	NM_204971.2		

synthesis in young birds with optimal nutrition (see below). Fractional rates of muscle degradation are also high in young birds but can be further increased with inadequate nutrition (see below).

27.8.2 Protein kinase B (Akt)/mechanistic (or mammalian) target of rapamycin pathway controlling protein synthesis and degradation

mTOR and the mTOR pathway plays an important role in both protein synthesis and degradation (see Fig. 27.4). Methionine depresses expression of atrogin-1 and RPS6 in muscle fibroblasts with the effects mediated by the protein kinase B (Akt)/mTOR signaling pathway being blocked by the mTOR inhibitor, rapamycin (Japanese quail: Tesseraud et al., 2007). Similarly, in the presence of both methane and rapamycin, expression of Akt is increased (Japanese quail: Tesseraud et al., 2007). Moreover, the mTOR inhibitor, rapamycin, blocks the increased activity of S6K1 induced by amino acids in insulin resistant myoblasts (chicken: Tesseraud et al., 2003).

There are physiological effects on expression of mTOR by avian tissues. For instance, 25-hydroxycholecalciferol administration increased the following breast muscle weight, muscle fractional protein synthesis rate, and muscle mTOR expression (chickens: Vignal et al., 2015). There is higher expression of mTOR in breast muscles of high than low-feed efficiency broiler type chickens (Piekarski et al., 2018a).

27.8.3 Protein synthesis and age/development

Fractional rates of rates of protein synthesis decline markedly with age with much lower rates in adult than young chickens (see Table 27.8). Moreover, there are decreases in fractional synthesis rates for protein in skeletal muscle during posthatch growth (chickens: Lauterio et al., 1986; Tesseraud et al., 2000) (also Table 27.10).

27.8.4 Effects of nutritional deficiencies on muscle protein synthesis and degradation

As might be expected, nutritional status influences the net rate of protein synthesis together both the fractional rates of protein synthesis and degradation. For instance, net protein accretion becomes negative in fasted young chickens (Table 29.11). Moreover, there is a decrease in the fractional rate of protein synthesis and an increase in the fractional rate of protein degradation (Table 29.11). Nutritional deficiencies can be accompanied by decreases in fractional rates of protein synthesis or increases in protein degradation or both. For instance, the fractional rate of protein synthesis is depressed when chicks received either a histidine or sulfur-containing deficient feeds (Table 27.10) (Kino and Okumura, 1987). In contrast, feeding a lysine deficient feed resulted in the following in leg or breast muscles of young chicks:

- Protein accretion: Falls to ~0
- Fractional rate of protein synthesis: remains unchanged
- Fractional rate of protein degradation: markedly increased

(Maruyama et al., 1978).

27.8.5 Effects of stretching on muscle protein synthesis and degradation

During hypertrophy induced by weights stretching the muscles, there are increases in the fractional rate of synthesis for both collagen and noncollagen protein (chickens: Goldspink, 1978; Laurent et al., 1978b, 1978c).

27.8.6 Hormones and muscle protein synthesis

Hormones influence muscle protein with effects on rates of both synthesis and degradation. For instance, corticosterone and other glucocorticoids suppress muscle growth (e.g., Klasing et al., 1987; Mehaisen et al., 2017). This is due to both a decrease in protein synthesis (Wang et al., 2015) and an increase in degradation (Klasing et al., 1987). Based on the limited in vitro studies with myotubes derived from chicken pectoralis satellite cells, insulin and/or insulin-like growth factor 1 (IGF1) stimulate protein synthesis and inhibit degradation (Duclos et al., 1993).

27.8.7 Microorganisms and protein synthesis in liver and gastrointestinal tract

Microorganisms influence protein status with decreases in both the weights of the liver and small intestine and in the rates of protein synthesis in these organs in chickens fed a germ-free diet (Muramatsu et al., 1987a, 1988). This would suggest that microorganisms are stimulating gastrointestinal growth.

27.8.8 Environmental temperature and protein synthesis and degradation

Prolonged high temperatures or chronic heat stress has detrimental effects on protein metabolism with, for instance, reduced breast muscle weights (young chickens: Temim et al., 2000). The adverse effect of elevated temperature is mediated, at least partially, by increase protein degradation; expression of cathepsin L2 being increased with heat stress in chicken muscle (Del Vesco et al., 2015).

27.8.9 Protein synthesis and immune functioning

As might be expected, there are high levels of protein synthesis in immune tissues. Protein synthesis in immune tissues are high (discussed above in section 27.6.3) in young growing chickens. The high rates of protein synthesis in immune tissues are disproportionate to their percentage of the body weight. There are interactions between immune functioning and amino acids with lysine increasing the proliferation of chicken thymocytes (Humphrey and Klasing, 2005).

The cationic amino acid transporter-1 through −3 (CAT1−3) is responsible for the transfer of amino acids across the cell membrane into cells. These are expressed in immune tissues—the bursa of Fabricius, the spleen, and the thymus—from seven-days-old (chicken: Humphrey et al., 2004, 2006). Expression of CAT1-3 is influenced by immune responses. Acute phase reaction, as induced by challenge with *Salmonella typhimurium* lipopolysaccharide (LPS), decreased expression of CAT1 in the bursa of Fabricius and the thymus of 11-week-old chickens (Humphrey and Klasing, 2005).

27.8.10 Other physiological effects on protein synthesis and degradation

27.8.10.1 Overview

Measurement of whole-body muscle protein degradation has not been widely employed in wild birds. An exception is the study of molting (see below).

27.8.10.2 Molt and protein synthesis

Molting influences protein metabolism in tissues not directly involved in the process. Body protein varies during the annual cycle of birds. This encompasses a progression though physiological state in female common eider (*Somateria mollissima*) with a plateau high during overwintering, prebreeding, laying, and the beginning of incubation declining to a nadir at the beginning of molting (with a loss of over 50% protein and weight) but subsequently return to the high as molt progresses (Milne, 1976).

Table 27.13 summarizes changes in protein metabolism in white-crowned sparrows (*Zonotrichia leucophrys*) (Murphy and King, 1985; Murphy and Taruscio, 1995 Taruscio and Murphy, 1995). Surprisingly, fractional rates of protein synthesis in skeletal muscle are elevated during molting (Table 27.13). There is also an increase in whole body protein synthesis (Table 27.13). On the other hand, an increase in protein degradation would be expected as this would supply amino acids for feather regrowth. This is the case with elevated excretion of 3-methyl-histidine during molting (Pearcy and Murphy, 1997).

TABLE 27.13 Effects of molting on protein metabolism synthesis in white crown sparrows.

	Nonmolting	Molting
Liver		
Weight g	0.771	1.011
Protein mg	175.8	237.4[a]
Glutathione mmoles[b]	0.576	1.757[a]
Protein fractional synthesis rate %/d	75	123[a]
Muscle		
Weight g	1.618	1.729
Protein mg	327.8	352.0
Protein fractional synthesis rate %/d	11.8	14.9[a]
Whole body		
Protein synthesis excluding integument fractional synthesis rate %/d	24.5	32.9[a]
Degradation		
3 methyl histidine excretion μmoles/d	0.79	1.23[a]

[a] *Difference with nonmolting $P < .05$.*
[b] *Early morning sampling.*
Calculated from Murphy and King (1985); Murphy and Taruscio (1995), Taruscio and Murphy (1995).

Nutrition influences protein metabolism in molting birds. There is increased excretion of 3-methyl-histidine in molting but not nonmolting white crowned sparrows fed a diet deficient in sulfur amino acids (Pearcy and Murphy, 1997). In contrast, there was decreased excretion of 3-methyl-histidine in molting white-crowned sparrows fed a protein-deficient diet (Pearcy and Murphy, 1997).

27.9 Proteins and reproduction

27.9.1 Female reproduction

There have not been definitive studies of the relative contributions of the reproductive organs to protein synthesis and degradation in birds. However, protein synthesis related to reproduction in the female is high. Birds' eggs are high in protein. For instance, the protein composition of a chicken hen's egg (assuming a 58 g egg) is the following (calculated from Belitz et al., 2009):

- Albumin: 3.6 g
- Yolk: 3.3 g
- Shell: 0.2 g

TABLE 27.14 Characteristics of sexually mature hens.

Parameter	Metric
Body weight (kg)	1.5
Carcass protein %	23.9
Carcass protein g	358
Ovary g	35.5
Oviduct g	47.1
Oviduct protein g	8.2
Liver g	24
Egg production	
Protein requirement in diet g d^{-1}	16.5
Protein taken up in yolk by developing oocyte in the ovary	3.3
Protein secreted in oviduct as egg white g d^{-1}	3.4
Protein secreted in oviduct as membranes/shell g d^{-1}	0.2
Total ***(% of protein requirement)***	7.0 (*42*)
Sexual maturation	
Increase in body weight during sexual maturation	252
Increase in body protein during sexual maturation g d^{-1}	2.2
Increase in ovarian and oviduct protein during sexual maturation g d^{-1}	0.5

From or calculated from Reid (1976), Renema et al. (2001), Belitz et al. (2009).

Egg protein contents are equivalent to 43% of the protein in the diet of the chicken (see Table 27.14). The yolk proteins are synthesized in the liver and are absorbed into the developing oocyte in the follicle (see Chapter 27).

Yolk proteins consist of the following (Moran, 1987):

- Low density (very low-density lipoproteins LDF1 and LDF2): 66%
- Granules (phosvitins and lipovitellins): 23%
- Aqueous α livetin, β livetin, and γ livetin (IgY): 11%

Both phosvitin and lipovitellin are derived from VTGs produced in the liver and secreted into the plasma. The VTG is processed to lipovitellin and phosvitin in the ovary. There are multiple VTG genes in birds (e.g., chicken VTGI, VTGII, and VTGIII: Evans et al., 1988). There is a relationship between the percentage essential amino acid in both VTGI and II with incubation time across avian species (Hughes, 2015).

Estrogens induce expression of VTGS with hepatic expression being only observed in birds either producing endogenous estrogen or receiving exogenous estrogens (chicken: Evans et al., 1988; Japanese quail: Gupta and Kanungo, 1996). Progesterone can inhibit VTGII expression (Japanese quail: Gupta and Kanungo, 1996). Interestingly, possible endocrine disrupters of chemicals such as pesticides can be evaluated using either circulating concentrations of VTG or VTG gene expression in the Japanese quail (Shibuya et al., 2005).

There is limited information on whole-body and specific-organ rates of protein synthesis and degradation in the reproductively mature female. As might be expected, protein synthesis in the oviduct is elevated when the ovulated oocyte is in the magnum (Hiramoto et al., 1990). In photostimulated sexually immature female chicken (17-week-old pullet), the development of the ovary and oviduct occurs over about 28 days (Renema et al., 2001). Oviductal growth is occurring under the influence of estrogen (estradiol) and progesterone with marked increases in protein synthesis (Muller et al., 1970).

27.9.2 Male reproduction

The importance of the male reproductive organs to overall protein metabolism has received little attention in birds. The testes of birds are considerably larger than those of mammals, as can be readily observed from the following: Sexually mature Japanese quail testes: 2.5 g or 2.5% of body weight (Vatsalya and Kashmiri, 2012), sexually mature chicken testes: 33 g (González-Moránet al., 2008).

It is likely that there are high demands for protein synthesis in spermatogenesis. However, protein requirements for seminal fluid are likely to be low as semen volume is modest, for instance, 0.4 mL, with seminal plasma protein concentrations are only 1.9% in turkeys (Kotłowska et al., 2005). There is a lack of information on the protein requirements for epididymal, ductal, phallic, and secondary sexual characteristic development and maintenance in birds.

27.10 Amino acids and metabolism

27.10.1 Amino acid transfer into muscle and other cells

There are transporters transferring amino acids into muscle cells and into the cells of other organs. Amino acid uptake by cells can be determined by uptake of [^{3}H]-amino-isobutyric acid (AIB) or ^{14}C-AIB. This approach prevents the confounding of data as AIB is not incorporated into proteins. Hormones, including IGF1 and insulin, stimulate AIB uptake by muscle cells (Duclos et al., 1993) or heart cells (Guidotti et al., 1968; Santora et al., 1979).

27.10.2 Amino acid transporters

27.10.2.1 Overview

The amino acid transporters expressed in avian skeletal muscle include the following:

- $B^{0,+}AT$ (b(0,+)-type amino acid transporter 1) [Gene—Solute carrier family 7 member A9 (SLC7A9)],
- $B^{0}AT$ (SLC6A19),
- CAT1 (SLC7A1) high affinity cationic amino acid transporters 1,
- CAT2 (SLC7A2) cationic amino acid transporters 2,
- CAT3 (SLC7A3) cationic amino acid transporters 3,
- LAT1 (SLC7A5) large neutral amino acid transporter 1
- LAT4 (SLC43A2) large neutral amino acid transporter 2
- SNAT1 (SLC38A1) sodium coupled neutral amino acid transporter 1
- SNAT2 (SLC38A2) sodium coupled neutral amino acid transporter 2
- SNAT7 (SLC38A7) sodium coupled neutral amino acid transporter 7
- TAT1 (SLC16A10) T type amino acid transporter 1 (Na^{+}-independent transporter of aromatic amino acids)

(e.g., chicken: Humphrey et al., 2004, 2006; Habashy et al., 2017).

27.10.2.2 Amino acid transporters and physiological state

Amino acid transporters are influenced by physiological state. For instance, expression of CAT1−3 is greatly decreased in birds on lysine-deficient diet (Humphrey et al., 2006). Similarly, expression of CAT 1 and 2 in *pectoralis* muscle is suppressed in newly hatched chicks when feeding is delayed (Payne et al., 2019). Acute-phase reaction as induced by challenge with *Salmonella typhimurium* LPS increased expression of CAT1−3 in the pectoralis of 11-week-old chickens (Humphrey and Klasing, 2005). Moreover, heat stress influences expression of amino acid transporters in pectoralis muscle with increases in SNAT1 and $B^{0,+}AT$ and decreases in $B^{0}AT$, SNAT7, and TAT1 (chicken: Habashy et al., 2017).

27.11 Nitrogenous waste

27.11.1 Overview

Nitrogenous waste in birds is in the form of uric acid, urea, and ammonia. The proportion of nitrogen excreted as uric acid and ammonia varies with species with, for instance, more as uric acid in Tristram's grackle (*Onychognathus tristrami*) but about equal amounts in yellow-vented bulbul (*Pycnonotus xanthopygos*) (Tsahar et al., 2005). In the hummingbird (*Archilochus alexandri*), over a quarter of nitrogenous waste is as ammonia (McWhorter et al., 2003).

The proportion of uric acid to ammonia is also influenced by protein concentration in the feed (Tsahar et al., 2005) or temperature in Anna's hummingbirds (*Calypte anna*) (Roxburgh and Pinshow, 2002). In contrast, there is no effect of dietary protein on the concentration of ammonia in pigeon excreta (*C. livia*: McNabb et al., 1972).

27.11.2 Uric acid

The major nitrogenous waste in birds is generally thought to be uric acid (Milroy, 1903) (also see above in section 27.10.1). Infusion of ammonia or glutamine increases circulating concentrations of uric acid in chickens (Karasawa, 1986). The enzymes of the uric acid cycle are found in both the liver and kidney. For instance, phosphoribosyl pyrophosphate amidotransferase and xanthine dehydrogenase activities are present in both avian liver and kidneys (chicken: McFarland and Coon, 1980, 1984). Glutamine is critically important for uric acid formation (see the below). It is not surprising that glutaminase (catalyzing glutamine to glutamate) is either not present or at very low levels in the avian liver (chicken: Wu et al., 1998).

The predominant organ responsible for uric acid formation is the liver. Chicken hepatocytes have been demonstrated to synthesize uric acid in vitro (McFarland and Coon, 1984). The kidney synthesizes only about 17% of the uric acid found in the urine of birds (chicken: Chin and Quebbemann, 1978).

Uric acid formed from the amino acids, glutamine, glycine, and aspartate by the following pathway (based on Stevens, 1996):

1. Ribose + ATP ↔ Ribose-5-phosphate + ADP
2. Ribose − 5 − phosphate + ATP ↔ 5−
   Phosphoribosyl − α − pyrophosphate (PRPP) + AMP
   Pyrophosphokinase
3. PRPP + Glutamine ↔ 5 − β−
   Phosphoribosyl amine + Glutamate
   Phosphoribosylpyrophosphate amidotransferase
   (*Aminophosphoribosyltransferase*)
4. Phosphoribosylamine +
   Glycine ↔ Glycinamide ribotide (GAR)
   [*Phosphoribosylglycineamine*]
   GAR synthetase
5. GAR + N − formyl tetrahydrofolate ↔
   Formylglyinamide ribotide (FGAR)
   [Phosphoribosyl−
   GARtransformase N − formylglycineamine] +
   Tetrahydrofolate

6. FGAR + Glutamine + ATP ↔ Formylglycineamidine ribotide (FGAM) + Glutamate + ADP
   FGAM Synthetase
7. FGAM + HCO_3^{-1} + ATP ↔ Phosphoribosyl-5-aminoimidazole-4 carboxylate + ADP
8. Phosphoribosyl − 5 − aminoimidazole−4 carboxylate + Aspartate + ATP ↔ Inosine monophosphate + Fumarate + ADP
9. Inosine monophosphate ↔ Xanthine + PRPP
   IMP dehydrogenase

PRPP is cycled back to step 3 and hence uric acid cycle or used to generate purines.

10. Xanthine ↔ Uric acid
    Xanthine dehydrogenase

Breast cancer resistance protein (BCRP) and multidrug resistance protein 4 (MRP4) are involved in uric acid excretion. Both BCRP and MRP4 are expressed in liver, kidneys, and the small intestine (chickens: Ding et al., 2019). Moreover, renal expression and concentrations of both BCRP and MRP4 are increased in chickens on a fish meal containing diet (Ding et al., 2019). Chickens on a high-protein diet have elevated serum concentrations of urate and have been proposed as a model for gout (Hong et al., 2020).

27.11.3 Urea

The existence of a urea cycle in birds has been questioned (Stevens, 1996). However, birds have both uric acid/urates as well as urea in their plasma (see Chapter 17).

The urea cycle is as follows:

1. Ornithine + Carbamyl phosphate ↔ Citrulline
2. Citrulline + Asparate + ATP ↔ Argininosuccinate + Fumarate + AMP
3. Argininosuccinate ↔ Arginine
4. Arginine ↔ Urea + Ornithine (and return to step 1)

27.11.4 Glutamine and ammonia detoxification

The primary ammonia-detoxifying enzyme in the avian liver is glutamine synthase. The gene has been characterized (Pu and Young, 1989). Glutamine synthase is expressed in the liver, brain, and retina (chicken: Satoh and Matsuno, 1983; Patejunas and Young, 1987). In contrast to the situation in mammals, there is little zonation of the enzyme in the avian liver (chicken and ducks: Smith and Campbell, 1988). Moreover, while glutamine synthase is cytosolic in mammals, the enzyme is located in the mitochondria in birds (chicken and ducks: Smith and Campbell, 1988).

27.11.5 Amino acids as energy sources

27.11.5.1 Amino acids and metabolism

Multiple amino acids can be deamidated and then be converted to glucose or readily metabolizable carbohydrates in the process of gluconeogenesis (discussed in detail in chapter 25 Carbohydrates). There is also evidence that during migration, birds use both lipid but also metabolize protein with the later catabolism providing water (Gerson and Guglielmo, 2011; Giulivia and Ramsey, 2015).

27.11.5.2 Glutamine as an energy source

Glutamine is a significant energy source for at least some tissues in birds. For instance, it is the major energy source for avian erythrocytes (chicken: Mathew et al., 1993). Glutamine is also employed as a major energy source for enterocytes (chicken: Watford et al., 1979).

27.12 Amino acid derivatives

27.12.1 Overview

There are multiple compounds in the animals that are derived from amino acids via biosynthetic pathways. These include the following:

- Neurotransmitters—dopamine, norepinephrine, and epinephrine from tyrosine (and phenylalanine)
- Epinephrine (hormone) from tyrosine (and phenylalanine)
- Glutamate (neuromodulator)
- Histamine (neurotransmitter and inflammatory response) from histidine
- Melatonin (hormone) from tryptophan
- Melanin (pigment) from tyrosine
- Nitric oxide (signal molecule) from arginine catalyzed by nitric oxide synthase
- Norepinephrine (neurotransmitter and hormone) from tyrosine (and phenylalanine)
- Nucleotides (purines, e.g., adenine, and guanine together with uric acid) from glutamine, aspartate, and glycine
- Serotonin (neurotransmitter) from tryptophan
- Thyroxine and triiodothyronine (hormone) from thyroglobulin (iodinated tyrosine residues)
- Urea from arginine

Phenylalanine and tyrosine are precursors for the synthesis of the neurotransmitters, dopamine, norepinephrine, and epinephrine and for melanin (Fig. 27.6).

27.12.2 Melanin

The melanocytes in the skin synthesize polymeric melanin which is subsequently transferred to feathers. The colors range from red due to phaeomelanin (produced from benzothiazole), black due to eumelanin (made of dihydroxyindole oligomers), and gray (produced from benzothiazine) (reviewed Galván and Solano, 2016) (also see Fig. 27.4). For instance, the orange feathers of the Eastern bluebird have high concentrations of phaeomelanin while the black feathers of penguins have high concentrations of eumelanin (McGraw et al., 2004).

27.13 Extranutritional effects of amino acids

27.13.1 Overview

There is intriguing research supporting amino acids having regulatory roles.

27.13.2 Amino acids in the control of metabolism

27.13.2.1 Glutamine and muscle growth

Glutamine has been proposed to be playing a role in the control of muscle protein synthesis (Wu et al., 1998). Either ammonia or glutamine increases myotubule diameters in vitro (Stern and Mozdziak, 2019) (Table 27.15). In addition, there are decreased levels of free glutamate and glutamine in leg but not pectoralis muscles from starved chickens along with the suppression of protein synthesis in leg but not pectoralis muscles (chicken: Watford and Wu, 2005) (see Table 27.16). Both glutamine synthase and glutaminase activities are reported in avian muscle. There is also much higher activity of glutamine synthase but not glutaminase in leg muscles than in pectoralis muscles (chicken and pigeon (*C. livia*): Watford and Wu, 2005).

TABLE 27.15 Effects of ammonia (ammonium acetate) or glutamine on growth of primary chicken myotubules in culture for 24 h.

	Myotubule diameters mean in μm + SEM	
Treatment	Breast	Thigh
Control	11.4 + 0.4[a]	11.1 + 0.4[a]
Ammonia	24.6 + 1.4[a]	24.2 + 0.6[a]
Glutamine	25.3 + 1.4[a]	19.9 + 0.6[a]

[a]*Different superscript letters indicate difference $P < .05$.*
Based on Stern and Mozdziak (2019).

TABLE 27.16 Effect of Starvation on fractional rate of protein synthesis and amino acid concentrations of different muscles in young chickens. Data shown is mean + (n = 5) SEM.

	Fed	Starved[a]
Fractional protein synthesis rate		
Pectoralis %/d	10.5 + 0.9	10.4 + 0.8
Leg muscle %/d	36.1 + 1.5	13.6 + 0.5[b]
Free glutamine		
Pectoralis μmoles/g	1.41 + 0.04	1.38 + 0.07
Leg muscle μmoles/g	9.45 + 0.64	3.02 + 0.17[b]
Plasma μmoles/mL	1.09 + 0.06	0.94 + 0.03
Free glutamate		
Pectoralis μmoles/g	0.90 + 0.06	0.89 + 0.05
Leg muscle μmoles/g	3.43 + 0.28	1.69 + 0.12[b]
Plasma (μmoles/mL)	0.26 + 0.02	0.32 + 0.01[b]
Free alanine		
Pectoralis μmoles/g	1.20 + 0.08	1.70 + 0.09[b]
Leg muscle μmoles/g	3.21 + 0.15	3.93 + 0.10[b]
Plasma (μmoles/mL)	0.51 + 0.01	0.62 + 0.01[b]

[a]*starved for 48 h.*
[b]*Difference $P < .05$ from fed.*
Based on Watford and Wu (2005).

27.13.2.2 Glutamine and intestinal growth

Supplementing a corn–soybean diet with glutamine increased both duodenal and jejunal mucosal villi height in young chickens despite not impacting growth (Bartell and Batal, 2007). For instance, duodenal villi height was reported to be increased by 41% with glutamine supplementation in the following manner (Bartell and Batal, 2007):

- Controls on corn–soybean diet: 652 μm
- Supplemented with 4% glutamine: 921 μm.

27.13.2.3 Dipeptides

Muscle contains alanine and histidine containing dipeptides:

- Carnosine—β-alanyl L-histidine
- Anserine—β-alanyl -3-methyl-L-histidine.

These are proposed to exert physiological effects. Muscle concentrations of carnosine and anserine are much greater in chickens than hummingbirds (Dolan et al., 2018). Moreover, there is markedly greater concentrations of anserine and carnosine in both breast than thigh muscle and

in slow growing than rapid growth rate young birds (chickens: Barbaresi et al., 2019). Muscle concentrations of anserine are greater than those of carnosine (chickens: Barbaresi et al., 2019).

27.14 Other uses of avian proteins

There are intriguing and, in many cases, novel applications using avian proteins:

1. Paleoproteomics can be performed on the collagens in fossil avian bones (Horn et al., 2019). This approach complements phylogenetics.
2. Recombinant chicken feather keratin is being employed to assay for keratinase activity (Jin et al., 2017).
3. Plasma concentrations of protein and of albumen are depressed with inadequate nutrition (black-necked swan: Artacho et al., 2007). Plasma concentrations of protein have been proposed as an indicator of nutritional status of wild bird populations.
4. The albumen layer of penguin eggs contains an "anti-freeze" like protein, penalbumin [Adélie penguin (*Pygoscelis adeliae*) and emperor penguin (*Aptenodytes forsteri*)] (Feeney, 1982; Osuga et al., 1983). There is a concomitant decrease in the amount of egg albumin with the presence this highly glycosylated protein (Feeney, 1982; Osuga et al., 1983).
5. Expression of actin is used in expression studies as actin is viewed as a house-keeping gene (e.g., Fagundes et al., 2020). LAT4 expression in both the ileum and kidneys is increased in methionine deficient chickens (Fagundes et al., 2020).

References

Abood, D.A., Reshag, A.F., Azhar, S.K., Ahmed, M.A., 2014. Comparative anatomical and histological features of the kidney in harrier (*Circus aueroginosus*), chicken (*Gallus domesticus*) and Mallard duck (*Anas platyrhynchos*). Iraqi J. Vet. Med. 38, 107–113.

Albers, P.H., Klein, P.N., Green, D.E., Melancon, M.J., Bradley, B.P., Noguchi, G., 2006. Chlorfenapyr and mallard ducks: overview, study design, macroscopic effects, and analytical chemistry. Environ. Toxicol. Chem. 25, 438–445.

Artacho, P., Soto-Gamboa, M., Verdugo, C., Nespolo, R.F., 2007. Blood biochemistry reveals malnutrition in black-necked swans (*Cygnus melanocoryphus*) living in a conservation priority area. Comp. Biochem. Physiol. 146A, 283–290.

Barbaresi, S., Maertens, L., Claeys, E., Derave, W., De Smet, S., 2019. Differences in muscle histidine-containing dipeptides in broilers. J. Sci. Food Agric. 99, 5680–5686.

Bartell, S.M., Batal, A.B., 2007. The effect of supplemental glutamine on growth performance, development of the gastrointestinal tract, and humoral immune response of broilers. Poultry Sci. 86, 1940–1947.

Belitz, H.-D., Grosch, W., Schieberle, P., 2009. Food Chemistry, fourth ed. Springer, Berlin, Germany.

Biasato, I., Ferrocino, I., Grego, E., Dabbou, S., Gai, F., Gasco, L., Cocolin, L., Capucchio, M.T., Schiavone, A., 2019. Gut microbiota and mucin composition in female broiler chickens fed diets including yellow mealworm (*Tenebrio molitor*, L.). Animals 9, 213.

Bigot, K., Taouis, M., Tesseraud, S., 2003. Refeeding and insulin regulate S6K1 activity in chicken skeletal muscles. J. Nutr. 133, 369–373.

Bohak, Z., 1969. Purification and characterization of chicken pepsinogen and chicken pepsin. J. Biol. Chem. 244, 4638–4648.

Bornstein, S., Lipstein, B., 1975. The replacement of some of the soybean meal by the first limiting amino acids in practical broiler diets. I. The value of special supplementation of chick diets with methionine and lysine. Br. Poultry Sci. 16, 177–188.

Bottje, W.G., 2019. Oxidative stress and efficiency: the tightrope act of mitochondria in health and disease. J. Anim. Sci. 97, 3169–3179.

Bourin, M., Gautron, J., Berges, M., Nys, Y., Rehault-Godbert, S., 2012. Sex- and tissue-specific expression of 'similar to nothepsin' and cathepsin D in relation to egg yolk formation in *Gallus gallus*. Poultry Sci. 91, 2288–2293.

Brautigan, D.L., Li, R., Kubicka, E., Turner, S.D., Garcia, J.S., Weintraut, M.L., Wong, E.A., 2017. Lysolecithin as feed additive enhances collagen expression and villus length in the jejunum of broiler chickens. Poultry Sci. 96, 2889–2898.

Brodkorb, P., 1955. Number of feathers and weights of various systems in a bald eagle. Wilson Bull. 67, 142.

Campbell, C.E., Braun, E.J., 1986. Cecal degradation of uric acid in Gambel quail. Am. J. Phys. 251, R59–R62.

Cansu, Ü., Boran, G., 2015. Optimization of a multi-step procedure for isolation of chicken bone collagen. Korean J. Food Sci. Anim. Resour. 35, 431–440.

Canty, E.G., Kadler, K.E., 2005. Procollagen trafficking, processing and fibrillogenesis. J. Cell Sci. 118, 1341–1353.

Chang, K.S., Zimmer, W.E., Bergsma, D.J., Dodgson, J.B., Schwartz, R.J., 1984. Isolation and characterization of six different chicken actin genes. Mol. Cell Biol. 4, 2498–2508.

Chen, Y., Han, S., Wang, Y., Li, D., Zhao, X., Zhu, Q., Yin, H., 2019. Oxidative stress and apoptotic changes in broiler chicken splenocytes exposed to T-2 toxin. BioMed Res. Int. 2019, 5493870.

Chin, T.Y., Quebbemann, A.J., 1978. Quantitation of renal uric acid synthesis in the chicken. Am. J. Physiol. 234, F446–F451.

Choct, M., Annison, G., Trimble, R.P., 1992. Soluble wheat pentosans exhibit different anti-nutritive activities in intact and cecectomized broiler chickens. J. Nutr. 122, 2457–2465.

Crew, J.R., Falzari, K., DiMario, J.X., 2010. Muscle fiber type specific induction of slow myosin heavy chain 2 gene expression by electrical stimulation. Exp. Cell Res. 316, 1039–1049.

Da Silva, M., Labas, V., Nys, Y., Réhault-Godbert, S., 2017. Investigating proteins and proteases composing amniotic and allantoic fluids during chicken embryonic development. Poultry Sci. 96, 2931–2941.

De Araújo Cordeiro, A.R., Alencar Bezerra, T.K., Menêses de Queiroz, A.L., De Sousa Galvão, M., Cavalcanti, M.T., Bertoldo Pacheco, M.T., Madruga, M.S., 2002. Collagen production from chicken keel bone using acid and enzymatic treatment at a temperature of 30°C. Food Sci. Technol. 40, 491–497.

Del Vesco, A.P., Gasparino, E., Grieser, D.O., Zancanela, V., Voltolini, D.M., Khatlab, A.S., Guimarães, S.E.F., Soares, M.A.M., Neto, A.R.O., 2015. Effects of methionine supplementation on the expression of protein deposition-related genes in acute heat stress-exposed broilers. PloS One 10, e0115821.

Dibner, J.J., Knight, C.D., Swick, R.A., Ivey, F.J., 1988. Absorption of 14C-2-hydroxy-4-(methylthio)butanoic acid (Alimet) from the hindgut of the broiler chick. Poultry Sci. 67, 1314–1321.

Ding, X., Li, M., Peng, C., Wang, Z., Qian, S., Ma, Y., Fang, T., Feng, S., Yu Li, Y., Wang, X., Li, J., Jinjie Wu, J., 2019. Uric acid transporters BCRP and MRP4 involved in uric acid excretion. BMC Vet. Res. 15, 80.

Dolan, E., Saunders, B., Dantas, W.S., Murai, I.H., Roschel, H., Artioli, G.G., Harris, R., Bicudo, J.E.P.W., Sale, C., Gualano, B., 2018. A comparative study of hummingbirds and chickens provides mechanistic insight on the histidine containing dipeptide role in skeletal muscle metabolism. Sci. Rep. 8, 14788.

Duclos, M.J., Chevalier, B., Goddard, C., Simon, J., 1993. Regulation of amino acid transport and protein metabolism in myotubes derived from chicken muscle satellite cells by insulin-like growth factor-I. J. Cell. Physiol. 157, 650–657.

Evans, M.I., Silva, R., Burch, J.B., 1988. Isolation of chicken vitellogenin I and III cDNAs and the developmental regulation of five estrogen responsive genes in the embryonic liver. Genes Dev. 2, 116–124.

Fagundes, N.S., Milfort, M.C., Williams, S.M., Da Costa, M.J., Fuller, A.L., Menten, J.F., Rekaya, R., Aggrey, S.E., 2020. Dietary methionine level alters growth, digestibility, and gene expression of amino acid transporters in meat-type chickens. Poultry Sci. 99, 67–75.

Feeney, R.E., 1982. Penguin egg-white and polar fish blood-serum proteins. Int. J. Pept. Protein Res. 19, 215–232.

Foltmann, B., 1992. Chymosin: a short review on foetal and neonatal gastric proteases. Scand. J. Clin. Lab. Invest. Suppl. 210, 65–79.

Forder, R.E., Nattrass, G.S., Geier, M.S., Hughes, R.J., Hynd, P.I., 2012. Quantitative analyses of genes associated with mucin synthesis of broiler chickens with induced necrotic enteritis. Poultry Sci. 91, 1335–1341.

Gal-Garber, O., Uni, Z., 2000. Chicken intestinal aminopeptidase: partial sequence of the gene, expression and activity. Poultry Sci. 79, 41–45.

Galván, I., Solano, F., 2016. Bird integumentary melanins: biosynthesis, forms, function and evolution. Int. J. Mol. Sci. 17, 520.

Gasaway, W.C., Buss, I.O., 1972. Zinc toxicity in the mallard duck. J. Wildl. Manag. 36, 1107–1117.

Gerson, A.R., Guglielmo, C.G., 2011. Flight at low ambient humidity increases protein catabolism in migratory birds. Science 333, 1434–1436.

Gilbert, E.R., Li, H., Emmerson, D.A., Webb Jr., K.E., Wong, E.A., 2007. Developmental regulation of nutrient transporter and enzyme mRNA abundance in the small intestine of broilers. Poultry Sci. 86, 1739–1753.

Giulivia, C., Ramsey, J., 2015. On fuel choice and water balance during migratory bird flights. Int. Biol. Rev 2015, 58.

Goldspink, D.F., 1978. The influence of passive stretch on the growth and protein turnover of the denervated *extensor digitorum longus* muscle. Biochem. J. 174, 595–602.

González-Morán, M.G., Guerra-Araiza, C., Campos, M.G., Camacho-Arroyo, I., 2008. Histological and sex steroid hormone receptor changes in testes of immature, mature, and aged chickens. Domest. Anim. Endocrinol. 35, 371–379.

Greenwold, M.J., Sawyer, R.H., 2013. Molecular evolution and expression of archosaurian β-keratins: diversification and expansion of archosaurian β-keratins and the origin of feather β-keratins. J. Exp. Zool. 320B, 393–405.

Greenwold, M.J., Bao, W., Jarvis, E.D., Hu, H., Li, C., Thomas, M., Gilbert, P., Zhang, G., Sawyer, R.H., 2014. Dynamic evolution of the alpha (α) and beta (β) keratins has accompanied integument diversification and the adaptation of birds into novel lifestyles. BMC Evol. Biol. 14.

Guidotti, G.G., Borghetti, A.F., Gaja, G., Lo Reti, L., Ragnotti, G., Fo, P.P., 1968. Amino acid uptake in the developing chick embryo heart. The effect of insulin on α-aminoisobutyric acid accumulation. Biochem. J. 107, 565–574.

Gupta, S., Kanungo, M.S., 1996. Modulation of vitellogenin II gene by estradiol and progesterone in the Japanese quail. Biochem. Biophys. Res. Commun. 222, 181–185.

Habashy, W.S., Milfort, M.C., Adomako, K., Attia, Y.A., Rekaya, R., Aggrey, S.E., 2017. Effect of heat stress on amino acid digestibility and transporters in meat-type chickens. Poultry Sci. 96, 2312–2319.

Harrap, B.S., Woods, E.F., 1967. Species differences in the proteins of feathers. Comp. Biochem. Physiol. 20, 449–460.

Hayashi, K., Agata, K., Mochii, M., Yasugi, S., Eguchi, G., Mizuno, T., 1988a. Molecular cloning and the nucleotide sequence of cDNA for embryonic chicken pepsinogen: phylogenetic relationship with prochymosin. J. Biochem. 103, 290–296.

Hayashi, K., Yasugi, S., Mizuno, T., 1988b. Pepsinogen gene transcription induced in heterologous epithelial-mesenchymal recombinations of chicken endoderms and glandular stomach mesenchyme. Development 103, 725–731.

Heller, S., Sheane, C.A., Javed, Z., Hudspeth, A.J., 1998. Molecular markers for cell types of the inner ear and candidate genes for hearing disorders. Proc. Natl. Acad. Sci. U.S.A. 95, 11400–11405.

Hillgartner, F.B., Williams, A.S., Flanders, J.A., Morin, D., Hansen, R.J., 1981. Myofibrillar protein degradation in the chicken. 3-Methylhistidine release *in vivo* and *in vitro* in normal and genetically muscular-dystrophic chickens. Biochem. J. 196, 591–601.

Hiramoto, K., Muramatsu, T., Okumura, J., 1990. Protein synthesis in tissues and in the whole body of laying hens during egg formation. Poultry Sci. 69, 264–269.

Hong, F., Zheng, A., Xu, P., JialinWang, J., Xue, T., Dai, S., Pan, S., Guo, Y., Xie, X., Li, L., Qiao, X., Liu, G., Yonggong Zhai, Y., 2020. High-protein diet induces hyperuricemia in a new animal model for studying human gout. Int. J. Mol. Sci. 21, 2147.

Horn, I.R., Kenens, Y., Palmblad, N.M., van der Plas-Duivesteijn, S.J., Langeveld, B.W., Meijer, H.J.M., Dalebout, H., Marissen, R.J., Fischer, A., Florens, F.B.V., Niemann, J., Rijsdijk, K.F., Schulp, A.S., Laros, J.F.J., Gravendeel, B., 2019. Palaeoproteomics of bird bones for taxonomic classification. Zool. J. Linn. Soc. 186, 650–665.

Hou, D.X., Maeda, Y., Okamoto, S., Hashiguchi, T., 1990. Purification and characterization of chymotrypsinogen from pancreas of Japanese quail (*Coturnix coturnix japonica*). Comp. Biochem. Physiol. B 97, 761–766.

Hughes, A.L., 2015. Life-history evolution at the molecular level: adaptive amino acid composition of avian vitellogenins. Proc. Biol. Sci. 282, 20151105.

Humphrey, B.D., Klasing, K.C., 2005. The acute phase response alters cationic amino acid transporter expression in growing chickens (*Gallus gallus domesticus*). Comp. Biochem. Physiol. A 142, 485–494.

Humphrey, B.D., Stephensen, C.B., Calvert, C.C., Klasing, K.C., 2004. Glucose and cationic amino acid transporter expression in growing chickens (*Gallus gallus domesticus*). Comp. Biochem. Physiol. A 138, 515–525.

Humphrey, B.D., Stephensen, C.B., Calvert, C.C., Klasing, K.C., 2006. Lysine deficiency and feed restriction independently alter cationic amino acid transporter expression in chickens (*Gallus gallus domesticus*). Comp. Biochem. Physiol. A 143, 218–227.

Hurwitz, S., Shamir, N., Bar, A., 1972. Protein digestion and absorption in the chick: effect of *Ascarida galli*. Am. J. Clin. Nutr. 25, 311–316.

Imondi, A.R., Bird, F.H., 1966. The turnover of intestinal epithelium in the chick. Poultry Sci. 45, 142–147.

Janiszewski, P., Murawska, D., Hanzal, V., Gesek, M., Michalik, D., Zawacka, M., 2018. Carcass characteristics, meat quality, and fatty acid composition of wild-living mallards (*Anas platyrhynchos* L.). Poultry Sci. 2018, 709–715.

Jin, H.-S., Park, S.Y., Kim, K., Lee, Y.-J., Nam, G.-W., Kang, N.J., Lee, D.-W., 2017. Development of a keratinase activity assay using recombinant chicken feather keratin substrates. PloS One 12, e0172712.

Johnson, P., Harris, C.I., Perry, S.V., 1967. 3-Methylhistidine in actin and other muscle proteins. Biochem. J. 105, 361–370.

Jones, S.J., Aberle, E.D., Judge, M.D., 1986. Estimation of the fractional breakdown rates of myofibrillar proteins in chickens from quantitation of 3-methylhistidine excretion. Poultry Sci. 65, 2142–2147.

Kalisińska, E., Pierko, M., Bartzyel, B., Dasńczak, A., 1998. Kidney morphometry in the mallard *Anas platyrhinchos*. Zecz. Nauk. Chów i Hod. Drobiu. 36, 13–21.

Kalisińska, E., Kosik-Bogacka, D.I., Lisowski, P., Lanocha, N., 2013. Mercury in the body of the most commonly occurring European game duck, the mallard (*Anas platyrhynchos* L. 1758), from Northwestern Poland. Arch. Environ. Contam. Toxicol. 64, 583–593.

Kang, H.S., Son, J.H., Karasawa, Y., Joen, H.Y., Kahn, K.H., 1999. Effect of cecectomy on nitrogen utilization and excretion in chickens fed a low protein diet or a low protein diet plus urea. Jpn. Poult. Sci. 36, 388–393.

Karasawa, Y., 1986. Ammonia production and its contribution to urinary nitrogenous compounds in chickens fed low or high protein diet. J. Nutr. 116, 2378–2386.

Karasawa, Y., 1989. Ammonia production from uric acid, urea, and amino acids and its absorption from the ceca of the cockerel. J. Exp. Zool. Suppl. 3, 75–80.

Karasawa, Y., Okamoto, M., Kawai, H., 1988. Ammonia production from uric acid and its absorption from the ceca of the cockerel. Br. Poultry Sci. 29, 119–124.

Keilova, H., Kostka, V., Kay, J., 1977. The first step in the activation of chicken pepsinogen is similar to that of prochymosin. Biochem. J. 167, 855–858.

Kettawan, A., Sungpuag, P., Sirichakwal, P.P., Chavasit, V., 2002. Chicken bone calcium extraction and its application as food fortificant. J. Natl. Res. Counc. Thai. 34, 163–180.

King, J.R., Murphy, M.E., 1987. Amino acid composition of the calamus, rachis, and barbs of white-crowned sparrow feathers. Condor 89, 436–439.

King, M.D., Guentzel, M.N., Arulanandam, B.P., Lupiani, B., Chambers, J.P., 2009. Proteolytic bacteria in the lower digestive tract of poultry may affect avian influenza virus pathogenicity. Poultry Sci. 88, 1388–1393.

Kino, K., Okumura, J., 1987. Whole-body protein turnover in chicks fed control, histidine, or methionine plus cystine-free diets. Poultry Sci. 66, 1392–1397.

Kita, K., Matsunami, S., Okumura, J., 1996. Relationship of protein synthesis to mRNA levels in the liver of chicks under various nutritional conditions. J. Nutr. 126, 1610–1617.

Klasing, K.C., Laurin, D.E., Peng, R.K., Fry, D.M., 1987. Immunologically mediated growth depression in chicks: influence of feed intake, corticosterone and interleukin-1. J. Nutr. 117, 1629–1637.

Knight, C.D., Dibner, J.J., 1984. Comparative absorption of 2-hydroxy-4-(methylthio)-butanoic acid and l-methionine in the broiler chick. J. Nutr. 114, 2179–2186.

Kotłowska, M., Glogowski, J., Dietrich, G.J., Kozłowski, K., Faruga, A., Jankowski, J., Ciereszko, A., 2005. Biochemical characteristics and sperm production of Turkey semen in relation to strain and age of the males. Poultry Sci. 84, 1763–1768.

Lang, T., Hansson, G.C., Samuelsson, T., 2006. An inventory of mucin genes in the chicken genome shows that the mucin domain of MUC13 is encoded by multiple exons and that ovomucin is part of a locus of related gel-forming mucins. BMC Genom. 7, 197.

Laurent, G.J., Sparrow, M.P., Bates, P.C., Millward, D.J., 1978a. Turnover of muscle protein in the fowl (*Gallus domesticus*). Rates of protein synthesis in fast and slow skeletal, cardiac and smooth muscle of the adult fowl. Biochem. J. 176, 393–401.

Laurent, G.J., Sparrow, M.P., Millward, D.J., 1978b. Turnover of muscle protein in the fowl. Changes in rates of protein synthesis and breakdown during hypertrophy of the anterior and posterior *latissimus dorsi* muscles. Biochem. J. 176, 407–417.

Laurent, G.J., Sparrow, M.P., Bates, P.C., Millward, D.J., 1978c. Turnover of muscle protein in the fowl. Collagen content and turnover in cardiac and skeletal muscles of the adult fowl and the changes during stretch induced growth. Biochem. J. 176, 419–427.

Lauterio, T.J., Decuypere, E., Scanes, C.G., 1986. Growth, protein synthesis and plasma concentrations of growth hormone, thyroxine and triiodothyronine in dwarf, control and growth selected strains of broiler-type domestic fowl. Comp. Biochem. Physiol. 83A, 627–632.

Lee, C.Y., Song, A.A.-L., Loh, T.C., Rahim, R.A., 2020. Effects of lysine and methionine in a low crude protein diet on the growth performance and gene expression of immunity genes in broilers. Poultry Sci. 99, 2916–2925.

Li, J., Hu, Y., Li, L., Wang, Y., Li, Q., Feng, C., Lan, H., Gu, X., Zhao, Y., Larsson, M., Hu, X., Li, N., 2019. A discovery of a genetic mutation causing reduction of atrogin-1 expression in broiler chicken muscle. Front. Genet. 10, 716.

Liu, D.C., Lin, Y.K., Chen, M.T., 2001. Optimum condition of extracting collagen from chicken feet and its characteristics. Asian-Australas. J. Anim. Sci. 14, 1638–1644.

Lodish, H., Berk, A., Zipursky, S.L., Matsudaira, P., Baltimore, D., James Darnell, J., 2000. Molecular Cell Biology, fourth ed. W. H. Freeman, New York.

MacDonald, M.L., Swick, R.W., 1981. The effect of protein depletion and repletion on muscle-protein turnover in the chick. Biochem. J. 194, 811–819.

Maharjan, P., Owens, C.M., Coon, C., 2019. *In-vivo* intramuscular collagen synthesis, muscle fiber growth and histomorphology of *Pectoralis major* of a fast-growing broiler strain *Gallus gallus domesticus*. Front. Vet. Sci. 6, 470.

Maruyama, K., Sunde, M.L., Swick, R.W., 1978. Growth and muscle protein turnover in the chick. Biochem. J. 176, 573–582.

Mathew, A., Grdisa, M., Johnstone, R.M., 1993. Nucleosides and glutamine are primary energy substrates for embryonic and adult chicken red cells. Biochem. Cell. Biol. 71, 288–295.

McFarland, D.C., Coon, C.N., 1980. Purine metabolism studies in the high and low uric acid containing lines of chickens: *de novo* uric acid synthesis and xanthine dehydrogenase activities. Poultry Sci. 59, 2250–2255.

McFarland, D.C., Coon, C.N., 1984. Purine metabolism in high and low uric acid lines of chickens: de novo uric acid synthesis in isolated hepatocytes and phosphoribosylpyrophosphate amidotransferase activities. Proc. Soc. Exp. Biol. Med. 177, 417–421.

McGraw, K.J., Wakamatsu, K., Ito, S., Nolan, P.M., Jouventin, P., Dobson, F.S., Austic, R.E., Safran, R.J., Siefferman, L.M., Hill, G.E., Parker, R.S., 2004. You can't judge a pigment by its color: carotenoids and melanin content of yellow and brown feathers in swallows, bluebirds, penguins, and domestic chickens. Condor 106, 390–395.

McNabb, F.M.A., McNabb, R.A., Ward Jr., J.M., 1972. The effects of dietary protein content on water requirements and ammonia excretion in pigeons, *Columbia livia*. Comp. Biochem. Physiol. A 43, 181–185.

McWhorter, T.J., Powers, D.R., Martnez Del Rio, C., 2003. Are hummingbirds facultatively ammonotelic? Nitrogen excretion and requirements as a function of body size. Physiol. Biochem. Zool. 76, 731–743.

Mehaisen, G.M.K., Eshak, M.G., Elkaiaty, A.M., Atta, A.-R., Mashaly, M.M., Abass, A.O., 2017. Comprehensive growth performance, immune function, plasma biochemistry, gene expressions and cell death morphology responses to a daily corticosterone injection course in broiler chickens. PloS One 12, e0172684.

Métayer-Coustard, S., Mameri, H., Seiliez, I., Crochet, S., Crépieux, P., Mercier, Y., Geraert, P.A., Tesseraud, S., 2010. Methionine deprivation regulates the $S6K_1$ pathway and protein synthesis in avian QM_7 myoblasts without activating the GCN_2/eIF_2 alpha cascade. J. Nutr. 140, 1539–1545.

Miao, L.P., Yuan, C., Dong, X.Y., Zhang, X.Y., Zhou, M.Y., Zou, X.T., 2017. Effects of dietary L-arginine levels on small intestine protein turnover and the expression of genes related to protein synthesis and proteolysis of layers. Poultry Sci. 96, 1800–1808.

Milne, H., 1976. Bodyweights and carcass composition of the common eider. Wildfowl 27, 115–122.

Milroy, T.H., 1903. The formation of uric acid in birds. J. Physiol. 30, 47–60.

Miska, K.B., Fetterer, R.H., 2018. The effect of *Eimeria maxima* infection on the expression of amino acid and sugar transporters aminopeptidase, as well as the di- and tri-peptide transporter PepT1, is not solely due to decreased feed intake. Poultry Sci. 97, 1712–1721.

Miska, K.B., Fetterer, R.H., 2019. Expression of amino acid and sugar transporters, aminopeptidase, and the di- and tri-peptide transporter PepT1; differences between modern fast growing broilers and broilers not selected for rapid growth. Poultry Sci. 98, 2272–2280.

Miska, K.B., Fetterer, R.H., Wong, E.A., 2015. mRNA Expression of amino acid transporters, aminopeptidase, and the di- and tri-peptide transporter pepT1 in the intestine and liver of posthatch broiler chicks. Poultry Sci. 94, 1323–1332.

Moran Jr., E.T., 1987. Protein requirement, egg formation and the hen's ovulatory cycle. J. Nutr. 117, 612–618.

Moreira Filho, A.L.B., Ferket, P.R., Malheiros, R.D., Oliveira, C.J.B., Aristimunha, P.C., Wilsmann, D.E., Givisiez, P.E.N., 2019. Enrichment of the amnion with threonine in chicken embryos affects the small intestine development, ileal gene expression and performance of broilers between 1 and 21 days of age. Poultry Sci. 98, 1363–1370.

Muller, K.R., Cox, R.F., Carey, N.H., 1970. Effects of progesterone on protein metabolism in chicken oviduct tissue pretreated with oestrogen. Biochem. J. 120, 337–344.

Muramatsu, T., Takasu, O., Furuse, M., Tasaki, I., Okumura, J., 1987a. Influence of the gut microflora on protein synthesis in tissues and in the whole body of chicks. Biochem. J. 246, 475–479.

Muramatsu, T., Aoyagi, Y., Okumura, J., Tasaki, I., 1987b. Contribution of whole-body protein synthesis to basal metabolism in layer and broiler chickens. Br. J. Nutr. 57, 269–277.

Muramatsu, T., Takasu, O., Furuse, M., Okumura, J., 1988. Effect of diet type on enhanced intestinal protein synthesis by the gut microflora in the chick. J. Nutr. 118, 1068–1074.

Murk, K., Buchmeier, S., Jockusch, B.J., Rothkegel, M., 2009. In birds, profilin-2a is ubiquitously expressed and contributes to actin-based motility. J. Cell Sci. 122, 957–964.

Murphy, M.E., King, J.R., 1985. Diurnal variation in liver and muscle glutathione pools of molting and non molting White-crowned Sparrows. Physiol. Zool. 58, 646–654.

Murphy, M.E., Taruscio, T.G., 1995. Sparrows increase their rates of tissue and whole-body protein synthesis during the annual molt. Comp. Biochem. Physiol. 111A, 385–396.

Murphy, M.E., King, J.R., Taruscio, T.G., Guepel, G.R., 1990. Amino-acid composition of feather barbs in three species of pygoscelid penguins three species of pygoscelid penguins: nutritional implications. Condor 92, 913–921.

Nakashima, K., Yakabe, Y., Yamazaki, M., Abe, H., 2006. Effects of fasting and refeeding on expression of atrogin-1 and Akt/FOXO signaling pathway in skeletal muscle of chicks. Biosci. Biotechnol. Biochem. 70, 2775–2778.

Nakashima, K., Ishida, A., Katsumata, M., 2013. Atrogin-1/MAFbx, a muscle-specific ubiquitin ligase, is highly expressed in the smooth muscle of the chicken gizzard. Biosci. Biotechnol. Biochem. 77, 1092–1095.

Nakashima, K., Ishida, A., Ijiri, D., Ohtsuka, A., 2016. Effect of dexamethasone on the expression of atrogin-1/MAFbx in chick skeletal muscle. Anim. Sci. J. 87, 405–410.

Ng, C.S., Wu, P., Foley, J., Foley, A., McDonald, M.-L., Juan, W.-J., Huang, C.-J., Lai, Y.-T., Lo, W.-S., Chen, C.-F., Leal, S.M., Zhang, H., Widelitz, R.B., Patel, P.I., Li, W.-H., Chuong, C.-M., 2012. The chicken frizzle feather is due to an α-keratin (*krt75*) mutation that causes a defective rachis. PLoS Genet. 8, e1002748.

Nieto, R., Palmer, R.M., Fernández-Fígares, I., Pérez, L., Prieto, C., 1994. Effect of dietary protein quality, feed restriction and short-term fasting on protein synthesis and turnover in tissues of the growing chicken. Br. J. Nutr. 72, 499–507.

Nitsan, Z., Dvorin, A., Nir, I., 1981. Composition and amino acid content of carcass, skin and feathers of the growing gosling. Br. Poultry Sci. 22, 79–84.

Osuga, D.T., Aminlari, M., Ho, C.Y.-K., Allison, R.G., Feeney, R.E., 1983. Sulfhydryl proteins of penguin egg white: ovalbumin and penalbumin. Comparisons with penguin serum albumin, chicken ovalbumin, and bovine serum albumin. J. Protein Chem. 2, 43–62.

Patejunas, G., Young, A.P., 1987. Tissue-specific regulation of avian glutamine synthetase expression during development and in response to glucocorticoid hormones. Mol. Cell Biol. 7, 1070–1077.

Payne, J.A., Proszkowiec-Weglarz, M., Ellestad, L.E., 2019. Delayed access to feed alters expression of genes associated with carbohydrate and amino acid utilization in newly hatched broiler chicks. Am. J. Physiol. 317, R864–R878.

Pearcy, S.D., Murphy, M.E., 1997. 3-Methylhistidine excretion as an index of muscle protein breakdown in birds in different states of malnutrition. Comp. Biochem. Physiol. A 116, 267–272.

Peng, Z., Mao, X., Zhang, J., Du, G., Jian Chen, J., 2019. Effective biodegradation of chicken feather waste by co-cultivation of keratinase producing strains. Microb. Cell Factories 18, 84.

Perrin, B.J., Ervasti, J.M., 2010. The actin gene family: function follows isoform. Cytoskeleton (Hoboken) 67, 630–634.

Piekarski, A., Khaldi, S., Greene, E., Lassiter, K., Mason, J.G., Anthony, N., Bottje, W., Dridi, S., 2014. Tissue distribution, gender- and genotype-dependent expression of autophagy-related genes in avian species. PloS One 9, e112449.

Piekarski, A., Nagarajan, G., Ishola, P., Flees, J., Greene, E.S., Kuenzel, W.J., Ohkubo, T., Maier, H., Bottje, W.G., Cline, M.A., Dridi, S., 2018. AMP-activated protein kinase mediates the effect of leptin on avian autophagy in a tissue-specific manner. Front. Physiol. 9, 541.

Piekarski-Welsher, A., Greene, E., Lassiter, K., Kong, B.C., Dridi, S., Bottje, W., 2018. Enrichment of autophagy and proteosome pathways in breast muscle of feed efficient pedigree male broilers. Front. Physiol. 9, 1342.

Pisano, J.J., Paine, C.M., Taylor, M.W., 1959. The effect of methionine deficiency on nitrogen absorption from the intestinal tract of chickens. J. Nutr. 67, 213–222.

Plavnik, I., Hurwitz, S., 1983. Organ weights and body composition in chickens as related to the energy and amino acid requirements: effects of strain, sex, and age. Poultry Sci. 62, 152–163.

Prum, R.O., Torres, R., 2003. Structural colouration of avian skin: convergent evolution of coherently scattering dermal collagen arrays. J. Exp. Biol. 206, 2409–2429.

Pu, H.F., Young, A.P., 1989. The structure of the chicken glutamine synthetase encoding gene. Gene 81, 169–175.

Ragland, D., Thomas, C.R., Elkin, R.G., Shafer, D.J., Adeola, O., 1999. The influence of cecectomy on metabolizable energy and amino acid digestibility of select feedstuffs for white Pekin ducks. Poultry Sci. 78, 707–713.

Reddy, G.V.B., Mallika, E.N., Reddy, O.B., Azad, S.A.K., Maheswara Reddy, D.M., 2016. Comparison on meat quality characteristics of spent breeder, layer and broiler birds. Int. J. Environ. Sci. Technol. 5, 2590–2595.

Reid, B.L., 1976. Estimated daily protein requirements of laying hens. Poultry Sci. 55, 1641–1645.

Renema, R.A., Robinson, F.E., Oosterhoff, H.H., Feddes, J.J., Wilson, J.L., 2001. Effects of photostimulatory light intensity on ovarian morphology and carcass traits at sexual maturity in modern and antique egg type pullets. Poultry Sci. 80, 47–56.

Riley Jr., W.W., Esteve-Garcia, E., Austic, R.E., 1986. Intestinal absorption of glucose and amino acids in chickens administered monensin. Poultry Sci. 65, 2292–2298.

Ritzek, H., Steyrer, E., Sanders, J., Nimpf, J., Schneider, W.J., 1992. Molecular cloning and functional characterization of chicken cathepsin D, a key enzyme for yolk formation. DNA Cell Biol. 11, 661–672.

Rohwer, S., Ricklefs, R.E., Rohwer, V.G., Copple, M.M., 2009. Allometry of the duration of flight feather molt in birds. PLoS Biol. 7, e1000132.

Romeroa, L.M., Strochlica, D., Wingfield, J.C., 2003. Corticosterone inhibits feather growth: potential mechanism explaining seasonal down regulation of corticosterone during molt. Comp. Biochem. Physiol. A 142, 65–73.

Rosser, B.W., Wick, M., Waldbillig, D.M., Bandman, E., 1996. Heterogeneity of myosin heavy-chain expression in fast-twitch fiber types of mature avian pectoralis muscle. Biochem. Cell. Biol. 74, 715–728.

Rosser, B.W., Wick, M., Waldbillig, D.M., Wright, D.J., Farrar, C.M., Bandman, E., 1998. Expression of myosin heavy chain isoforms during development of domestic pigeon pectoralis muscle. Int. J. Dev. Biol. 42, 653–661.

Roxburgh, L., Pinshow, B., 2002. Ammonotely in a passerine nectarivore: the influence of renal and post-renal modification on nitrogenous waste product excretion. J. Exp. Biol. 205, 1735–1745.

Sakamoto, N., Saiga, H., Yasugi, S., 1998. Analysis of temporal expression pattern and cis-regulatory sequences of chicken pepsinogen A and C. Biochem. Biophys. Res. Commun. 250, 420–424.

Saneyasu, T., Nakano, Y., Tsuchii, N., Kitashiro, A., Tsuchihashi, T., Kimura, S., Honda, K., Kamisoyama, H., 2019. Differential regulation of protein synthesis by skeletal muscle type in chickens. Gen. Comp. Endocrinol. 284, 113246.

Santora II, A.C., Wheeler, F.B., DeHaan, R.L., Elsas II, L.J., 1979. Relationship of insulin binding to amino acid transport by cultured 14-day embryonic chick heart cells. Endocrinology 104, 1059–1068.

Satoh, T., Matsuno, T., 1983. Purification and comparison of glutamine synthetase from chicken liver, brain and neural retina. Comp. Biochem. Physiol. B 75, 655–658.

Saunderson, C.L., Leslie, S., 1983. N tau-methyl histidine excretion by poultry: not all species excrete N tau-methyl histidine quantitatively. Br. J. Nutr. 50, 691–700.

Sayegh, J.F., Lajtha, A., 1989. *In vivo* rates of protein synthesis in brain, muscle, and liver of five vertebrate species. Neurochem. Res. 4, 1165–1168.

Schwilch, R., Grattarola, A., Spina, F., Jenni, L., 2002. Protein loss during long-distance migratory flight in passerine birds: adaptation and constraint. J. Exp. Biol. 205, 687–695.

Shbailat, S.J., Aslan, I.O., 2018. Fate of egg proteins during the development of *Columba livia domestica* embryo. J. Exp. Zool. B Mol. Dev. Evol. 330, 23–32.

Sheng, Q., Cao, D., Zhou, Y., Lei, Q., Han, H., Li, F., Lu, Y., Wang, C., 2013. Detection of SNPs in the cathepsin D gene and their association with yolk traits in chickens. PloS One 8, e56656.

Shibuya, K., Wada, M., Mizutani, M., Sato, K., Itabashi, M., Sakamoto, T., 2005. Vitellogenin detection and chick pathology are useful endpoints to evaluate endocrine-disrupting effects in avian one-generation reproduction study. Environ. Toxicol. Chem. 24, 1654–1666.

Smith Jr., D.D., Campbell, J.W., 1988. Distribution of glutamine synthetase and carbamoyl-phosphate synthetase I in vertebrate liver. Proc. Natl. Acad. Sci. U.S.A. 85, 160–164.

Son, J.H., Karasawa, Y., Nahm, K.H., 1997. Effect of cecectomy on nitrogen utilization and nitrogen excretion in chickens fed a low protein diet supplied with urea. Asian-Australas. J. Anim. Sci. 10, 274–276.

Starck, J.M., Rahmaan, G.H., 2003. Phenotypic flexibility of structure and function of the digestive system of Japanese quail. J. Exp. Biol. 206, 1887–1897.

Stern, R.A., Mozdziak, P.E., 2019. Glutamine synthetase in avian muscle contributes to a positive myogenic response to ammonia compared with mammalian muscle. Am. J. Physiol. 317, R214–R221.

Stevens, L., 1996. Avian Biochemistry and Molecular Biology. Cambridge University Press, Cambridge, UK.

Szenthe, B., Frost, C., Szilgyi, L., Patthy, A., Naud, R., Grf, L., 2005. Cloning and expression of ostrich trypsinogen: an avian trypsin with a highly sensitive autolysis site. Biochim. Biophys. Acta 1748, 35–42.

Taruscio, T.G., Murphy, M.E., 1995. 3-Methyl histidine excretion by molting and non-molting sparrows. Comp. Biochem. Physiol. 111A, 397–403.

Tasaki, I., Takahashi, N., 1966. Absorption of amino acids from the small intestine of domestic fowl. J. Nutr. 88, 359–364.

Temim, S., Chagneau, A.M., Guillaumin, S., Mitchel, J., Peresson, R., Tesseraud, S., 2000. Does excess dietary protein improve growth performance and carcass characteristics in heat exposed chickens? Poultry Sci. 79, 312–317.

Tesseraud, S., Chagneau, A.M., Grizard, J., 2000. Muscle protein turnover during early development in chickens divergently selected for growth rate. Poultry Sci. 79, 1465–1471.

Tesseraud, S., Bigot, K., Taouis, M., 2003. Amino acid availability regulates S6K1 and protein synthesis in avian insulin-insensitive QM7 myoblasts. FEBS Lett. 540, 176–180.

Tesseraud, S., Métayer-Coustard, S., Boussaid, S., Crochet, S., Audouin, E., Derouet, M., Seiliez, I., 2007. Insulin and amino acid availability regulate atrogin-1 in avian QT6 cells. Biochem. Biophys. Res. Commun. 357, 181–186.

Tilney, L.G., Cotanche, D.A., Tilney, M.S., 1992. Actin filaments, stereocilia and hair cells of the bird cochlea. VI. How the number and arrangement of stereocilia are determined. Development 116, 213–226.

Tsahar, E., Martínez del Rio, C., Izhaki, I., Arad, Z., 2005. Can birds be ammonotelic? Nitrogen balance and excretion in two frugivores. J. Exp. Biol. 208, 1025–1034.

Urdaneta-Rincon, M., Leeson, S., 2004b. Effect of dietary crude protein and lysine on feather growth in chicks to twenty-one days of age. Poultry Sci. 83, 1713–1717.

Vágás, C.I., Pap, P.L., Vincze, O., Benkő, Z., Marton, A., Barta, Z., 2012. Haste makes waste but condition matters: molt rate-feather quality trade-off in a sedentary songbird. PLoS Biol. 7, e40651.

van der Westhuizen, N., Naud, R.J., Oelofsen, W., 1989. The isolation and partial characterization of chymotrypsinogen from the pancreas of the ostrich (*Struthio camelus*). Int. J. Biochem. 21, 91–97.

Vatsalya, V., Kashmiri, A.L., 2012. Allometric growth of testes in relation to age, body weight and selected blood parameters in male Japanese quail (*Coturnix japonica*). Int. J. Poultry Sci. 11, 251–258.

Vignale, K., Greene, E.S., Caldas, J.V., England, J.A., Boonsinchai, N., Sodsee, P., Erik D Pollock, E.D., Dridi, S., Coon, C.N., 2015. 25-Hydroxycholecalciferol enhances male broiler breast meat yield through the mTOR pathway. J. Nutr. 145, 855–863.

Wang, K., Gan, L., Lee, I., Hood, L., 1995. Isolation and characterization of the chicken trypsinogen gene family. Biochem. J. 307, 471–479.

Wang, X., Jia, Q., Xiao, J., Jiao, H., Lin, H., 2015. Glucocorticoids retard skeletal muscle development and myoblast protein synthesis through a mechanistic target of rapamycin (mTOR)-signaling pathway in broilers (*Gallus gallus domesticus*). Stress 18, 686–698.

Wang, R., Li, K., Wang, H., Jiao, H., Wang, X., Zhao, J., Lin, H., 2019. Endogenous CSE/hydrogen sulfide system regulates the effects of glucocorticoids and insulin on muscle protein synthesis. Oxid. Med. Cell Longev. 2019, 9752698.

Watanabe, G., Kobayashi, H., Shibata, M., Kubota, M., Kadowaki, M., Fujimura, S., 2020. Reduction in dietary lysine increases muscle free amino acids through changes in protein metabolism in chickens. Poultry Sci. 99, 3102–3110.

Watford, M., Wu, G., 2005. Glutamine metabolism in uricotelic species: variation in skeletal muscle glutamine synthetase, glutaminase, glutamine levels and rates of protein synthesis. Comp. Biochem. Physiol. B 140, 607–614.

Watford, M., Lund, P., Krebs, H.A., 1979. Isolation and metabolic characteristics of rat and chicken enterocytes. Biochem. J. 178, 589–596.

White, D.H., Finley, M.T., Ferrell, J.F., 1978. Histopathologic effects of dietary cadmium on kidneys and testes of mallard ducks. J. Toxicol. Environ. Health 4, 551–558.

Wu, G., Chung-Bok, M.I., Vincent, N., Kowalski, T.J., Choi, Y.H., Watford, M., 1998. Distribution of phosphate-activated glutaminase isozymes in the chicken: absence from liver but presence of high activity in pectoralis muscle. Comp. Biochem. Physiol. B 120, 285–290.

Wu, P., Ng, C.,S., Yan, J., Lai, Y.-C., Chen, C.-K., Lai, Y.-T., Wu, S.-M., Chen, J.-J., Luo, W., Widelitz, W.R.B., Li, W.-H., Chuong, C.-M., 2015. Topographical mapping of α- and β-keratins on developing chicken skin integuments: functional interaction and evolutionary perspectives. Proc. Nat. Acad. Sci. USA 112, E6770–E6779.

Xie, P., Wan, X.P., Yang, C.X., Zhu, J.G., Xu, Y.G., Gong, D.Q., 2020. Effects of incubation and chick rearing on intestinal morphology, digestive enzyme activities, and mRNA expression of nutrient transporter genes in the pigeon (*Columba livia*) under artificial farming conditions. Poultry Sci. 99, 2785–2797.

Yuan, C., Bu, X.C., Yan, H.X., Lu, J.J., Zou, X.T., 2016. Dietary L-arginine levels affect the liver protein turnover and alter the expression of genes related to protein synthesis and proteolysis of laying hens. Poultry Sci. 95, 261–267.

Zheng, H., Li, H., Tan, W., Xu, C., Jia, L., Wang, D., Li, Z., Sun, G., Kang, X., Yan, F., Liu, X., 2018. Oestrogen regulates the expression of cathepsin E-A-like gene through ER β in liver of chicken (*Gallus gallus*). J. Genet. 97, 145–155.

Further reading

Austin, G.T., 1971. Body composition and organ weights of the Verdin (*Auriparus aviceps*). Great Basin Nat. 31, 66–68.

Barnard, E.A., Lyles, J.M., Pizzey, J.A., 1982. Fibre types in chicken skeletal muscles and their changes in muscular dystrophy. J. Physiol. 331, 333–354.

Barnes, D.M., Calvert, C.C., Klasing, K.C., 1995. Methionine deficiency decreases protein accretion and synthesis but not tRNA acylation in muscles of chicks. J. Nutr. 125, 2623–2630.

Hutt, F.B., Ball, L., 1938. Number of feathers and body size in passerine birds. Auk 55, 651.

Karasawa, Y., Tasaki, I., 1973. Effect on uric acid synthesis of the infusion of various levels of ammonium acetate or glutamine in chickens. J. Nutr. 103, 1727–1730.

Marquez, J., Sweazea, K.L., Braun, E.J., 2006. Skeletal muscle fiber composition of the English sparrow (*Passer domesticus*). Comp. Biochem. Physiol. B 143, 126–131.

O'Reilly, E.L., Burchmore, R.J., Sparks, N.H., Eckersall, P.D., 2016. The effect of microbial challenge on the intestinal proteome of broiler chickens. Proteome Sci. 15, 10.

Presland, R.B., Gregg, K., Molloy, P.L., Morris, C.P., Crocker, L.A., Rogers, G.E., 1989. Avian keratin genes. I. A molecular analysis of the structure and expression of a group of feather keratin genes. J. Mol. Biol. 209, 549–559.

Urdaneta-Rincon, M., Leeson, S., 2004a. Muscle (*pectoralis major*) protein turnover in young broiler chickens fed graded levels of lysine and crude protein. Poultry Sci. 83, 1897–1903.

Velotto, S., Crasto, A., 2004. Histochemical and morphometrical characterization and distribution of fibre types in four muscles of ostrich (*Struthio camelus*). Anat. Histol. Embryol. 33, 251–256.

Welch Jr., K.C., Altshuler, D.L., 2009. Fiber type homogeneity of the flight musculature in small birds. Comp. Biochem. Physiol. B 152, 324–331.

Zhang, S., Saremi, B., Gilbert, E.R., Wong, E.A., 2017. Physiological and biochemical aspects of methionine isomers and a methionine analogue in broilers. Poultry Sci. 96, 425–439.

Chapter 28

Food intake regulation

Mark A. Cline[1], Mike Denbow[1], Elizabeth Gilbert[1] and Sami Dridi[2]
[1]Department of Animal and Poultry Sciences, Virginia Tech, Blacksburg, VA, United States; [2]Center of Excellence for Poultry Science, University of Arkansas, Fayetteville, AR, United States

28.1 Introduction

Birds, like mammals, have complex mechanisms regulating food intake. Given a choice between more than one diet, turkeys, broilers, layers, and other avian species display the ability to self-select a diet adequate for growth or production (Denbow, 1999). Although compensation may not be complete, if exposed to severe feed restriction early in life, birds compensate by increasing their intake in order to support weight gain following the restriction. In contrast, force-feeding birds twice their ad libitum food intake causes Leghorns to stop eating for 7−10 days until their fat stores approach pre-force-feeding levels. Therefore, clearly, birds have the ability to regulate food intake.

Among the strongest evidence that food intake is regulated in birds is the temporal response to dietary amino acid imbalances. Broiler chicks decrease intake of a diet deficient in lysine, methionine, and tryptophan within 24 h posthatch (Picard et al., 1993). Preferences for certain diets are evident in as little as 7 h posthatch. The ability to discriminate among diets deficient in amino acids is dependent on the genetic background of the bird (Noble et al., 1993).

Intense genetic selection of poultry has resulted in strains optimized for either meat production or egg production. Genetic selection has resulted in broilers that are more than five times larger than layer-type chicks at 6 weeks of age (Zhao et al., 2004; Buzala and Janicki, 2016). This increased growth rate has resulted largely from increased food intake. Broiler breeders will essentially eat to gut capacity whereas layers will consume to meet an energetic need. There is evidence that broilers have more taste buds and display less contrafreeloading (choosing a food that requires more effort to select) than layer-type chickens (Buzala and Janicki, 2016).

Food intake regulation in birds has been reviewed (Kuenzel, 1994; Denbow, 2000; Furuse et al., 2007; Richards and Proszkowiec-Weglarz, 2007; Cline and Furuse, 2012; Tran et al., 2019) and involves sites both within and outside the central nervous system (CNS), and signals are integrated within the CNS. As in mammals, the CNS, and specifically the hypothalamus, has emerged as a key site in appetite control (Hussain and Bloom, 2013). Because the bulk of the research on avian food intake regulation has used poultry as a model, this chapter focuses mainly on domestic fowl species, in particular, the neonatal chick model. However, research with other avian species is reported in several tables.

28.2 Peripheral regulation of food intake

28.2.1 Gastrointestinal tract and ghrelin

Outside of the CNS, food intake is regulated by multiple organs, such as the gastrointestinal tract, liver (Denbow, 1994), and adipose tissue (Zhang et al., 2014). The crop does not appear to have a direct role in food intake regulation in that it does not appear to have receptors or release factors that modulate food intake. However, it may restrict intake physically when its capacity is reached and several studies referenced within this chapter describe appetite regulatory effects that are accompanied by changes in the rate of crop emptying. The gastrointestinal tract has osmoceptors that, when stimulated by hyperosmotic solutions, result in reduced food intake. Intraduodenal infusions of hyperosmotic solutions decrease food intake via a decrease in gastrointestinal motility (Denbow, 1994).

Ghrelin, originally identified as a growth hormone-releasing peptide, is released from the stomach of mammals. Intracerebroventricular (ICV) and intraperitoneal (IP) injections of ghrelin increase food intake in humans and rodents. In addition, its levels increase in plasma during fasting, and decrease upon refeeding. Ghrelin is also found in the proventriculus of birds. Plasma ghrelin levels increase during fasting in Japanese quail and six-day-old

Sturkie's Avian Physiology. https://doi.org/10.1016/B978-0-12-819770-7.00038-4

TABLE 28.1 Effects of compounds on food intake when infused into the hepatic portal system.[a]

Compound	Broilers	Leghorns
Glucose	→	↓
Amino acid preparation[b] FreAmineIII®	ND	→
Lysine	ND	↓
Leucine	ND	Delayed ↓
Ammonium chloride	ND	→
Epinephrine	ND	↓
Fatty acids[c] Liposyn®	→	↓

[a] *→, no effect; ↓, decrease in food intake;* ND, *not determined (Denbow, 1999).*
[b] *FreAmineIII® contains isoleucine, leucine, lysine, methionine, phenylalanine, threonine, tryptophan, valine, alanine, dl-, arginine, histidine, proline, serine, glycine, cysteine, sodium acetate, magnesium acetate, sodium chloride, potassium chloride, phosphoric acid, and potassium metabisulfite.*
[c] *Liposyn® is a commercial emulsified fat product.*

layers, but not in 3-week-old broilers (Richards and Proszkowiec-Weglarz, 2007; Richards and McMurtry, 2010). Ghrelin mRNA and peptide levels increase in the proventriculus during fasting and return to control levels after refeeding. However, brain ghrelin mRNA does not change during fasting or refeeding. While the changes in plasma ghrelin levels associated with fasting would suggest it may act as a peripheral orexigenic signal, in contrast to in rodents and humans, central administration of ghrelin decreases food intake in birds (Furuse et al., 2001). In Japanese quail, while IP injections of relatively low doses of ghrelin increase food intake, higher doses decrease food intake. Intravenous (IV) injections of ghrelin in chickens either weakly decreased food intake or had no effect.

In addition to ghrelin, cleavage of proghrelin yields a 23-amino acid amidated peptide called obestatin, which was first isolated and purified from the rat stomach. This peptide was reported to be the endogenous ligand of the GPR39 receptor (Wolfgang et al., 2006), although this has been questioned (Dong et al., 2009). The role of obestatin is unclear since it has been reported to decrease food intake and body weight, but other studies failed to show an effect on food intake in rats (Seoane et al., 2006). Xu et al. (2011a) reported that ICV injection of obestatin increased food intake in a dose-dependent manner in a high-weight selected line of chickens. However, Song et al. (2013) found that IV injection of obestatin had no effect on food intake in broilers or Leghorns. Further studies are needed to elucidate the role of obestatin in food intake in birds.

28.2.2 Liver

After absorption from the gastrointestinal tract, nutrients generally travel directly to the liver. Whereas in mammals, absorbed lipids are packaged into chylomicrons, enter the lymphatic system, and are transported to the subclavian vein; in birds, lipids are packaged into portomicrons that enter the hepatic portal vein and travel directly to the liver. Therefore, the liver is strategically located to monitor nutrient intake and control food intake in birds. Intrahepatic infusion of glucose, lysine, or lipids decreases food intake (Table 28.1), and these effects vary with the strain of bird. For example, intrahepatic infusion of glucose decreased food intake in Leghorns, but not broilers. Similarly, infusions of lipids decreased food intake in free feeding Leghorns, but not broilers. Although the liver appears able to alter food intake in response to changes in hepatic portal blood glucose concentration, there is little evidence that plasma or brain concentrations of glucose influence food intake. Savory (1987) reported no correlation between plasma glucose concentrations and food intake. Furthermore, injections of glucose, or its antimetabolites, into the lateral cerebroventricle have no effect on food intake (Denbow et al., 1982).

28.2.3 Dietary nutrients

While food intake is modified by direct injection of lipids into the liver, dietary lipids also alter food intake (Denbow, 1989). Feeding medium-chain triglycerides (glyceryl tricaprylate or glyceryl tricaprate) or corn oil-containing long-chain triglycerides to Leghorn chickens decreased food intake as soon as 30 min postfeeding. This agrees with studies showing that short- and medium-chain triacylglycerols were more effective in decreasing food intake than long-chain triacylglycerols when infused into the hepatic–portal system (Denbow, 1994). However, medium- and long-chain triacylglycerols were equally effective in decreasing food intake when administered intragastrically. Ketone bodies, acting both peripherally and centrally, also decrease food intake in chicks (Sashihara et al., 2001).

Dietary macronutrient (including lipid) composition not only influences food intake and dietary preference but also affects the food intake response to centrally injected neuropeptides. In turn, central administration of peptides may influence the preference for certain diets. Most studies that examined interactions of peptide injection and diet composition were conducted with rodent models, although within the past decade such studies have surfaced in chickens. One model was developed whereby isocaloric corn-soybean-meal-based broiler starter diets were formulated to differ in protein and fat content, resulting in a high-carbohydrate (HC), high-fat (HF), and high-protein (HP) formulation. In one study, the HF diet was formulated to have 60% of the metabolizable energy (ME) derived from lard and the HP diet to have 30% crude protein (CP) (Nelson et al., 2015). When broiler chicks were given free access to all diets and intracerebroventricularly (ICV; into the left lateral ventricle in the brain) injected with the hunger-stimulating peptide neuropeptide Y (NPY), they selected the HC or HP diets over the HF diet and chicks that were raised on the HF diet appeared to have a greater sensitivity to the orexigenic effects of centrally injected NPY (Nelson et al., 2015). In another study, prolactin-releasing peptide (PrRP), another orexigenic factor in birds, had slightly different associations with the diet; chicks that were raised on the HP diet were more sensitive to the orexigenic effects of ICV-injected PrRP and injection of the peptide in turn increased the preference of the chicks for the HP diet (Wang et al., 2015a). When dietary formulations were adjusted to reduce the amount of protein and fat in the HP (to 25% CP) and HF (15% and 30% ME from soybean oil instead of lard) diets, respectively, there were differences among diets that were magnified by fasting and refeeding, including reduced food intake in the chicks that consumed the HP and HF diets, and hypothalamic gene expression differences suggesting that corticotropin-releasing factor (CRF) and melanocortin signaling systems were involved (McConn et al., 2018c). Using these diets, the response to ICV NPY was tested in broiler chicks, and it was observed that chicks raised on the HC diet displayed the most robust NPY-induced increase in food intake while those on the HF diet had a lower threshold response to NPY (McConn et al., 2018a). Following ICV injection of NPY, chicks selected the HP and HC diet over the HF diet, with hypothalamic melanocortin receptor subtypes 4 (MC4R) and NPY receptor subtype 1 (NPYR1) mRNAs reduced in the chicks that consumed the HP and HC diets (McConn et al., 2018a). These results collectively suggest that nutrients from the diet can indirectly influence endogenous appetite regulatory systems via effects on major hypothalamic neuropeptide signaling systems, such as NPY.

28.2.4 Adipose tissue and leptin

An important physiological mechanism for regulating body weight involves bidirectional communication between the hypothalamus and adipose tissue (Zhang et al., 2014). The adipose tissue, at least in mammals, is richly vascularized and innervated by the sympathetic nervous system (SNS), the terminals of which co-store NPY and norepinephrine (NE) and project onto adipocytes. In addition to being a major stimulator of appetite, NPY stimulates adipogenesis and fat storage in adipocytes, both in mammals and in chickens (Zhang et al., 2015; Shipp et al., 2016). Thus, signals from the hypothalamus can be directed to the adipose tissue via endocrine or neurocrine mechanisms involving the SNS. The lipostatic theory of food intake proposed that the brain senses the state of fat depots and makes appropriate adjustments in food intake to maintain fat stores. In 1994, a protein coded by the Ob gene, named leptin, was cloned from the mouse (Zhang et al., 1994), and is believed to be part of a feedback system that indicates an animal's stores of white adipose tissue. As fat stores increase, circulating plasma leptin levels increase. This protein is lacking in ob/ob mice. Administering recombinant leptin to ob/ob mice reduces food intake, decreases body weight and lipid content, and increases thermogenesis. Thus, in mammals, leptin plays a critical role in maintaining energy homeostasis via signaling energy reserves to the brain and by suppressing appetite. After its discovery, attempts to identify the orthologous gene in birds yielded conflicting and controversial results.

In 1998, a group reported to have cloned the chicken leptin gene, with 97%, 96%, and 83% similarity to the mouse, rat, and human amino acid sequences, respectively (Taouis et al., 1998; Ashwell et al., 1999). The following year, another group reported that they were unable to amplify this putative chicken leptin sequence by PCR, concluding that the publication had reported a spurious sequence, likely the result of contamination with mammalian DNA (Friedman-Einat et al., 1999). During the time that the presence of leptin was still debated, the chicken leptin receptor was identified (Horev et al., 2000; Ohkubo et al., 2007). Central injection of human leptin into chickens was associated with a reduction in food intake, suggesting that receptor function is conserved in avians (Denbow et al., 2000). The existence of an endogenous and conserved receptor without a ligand seemed unlikely from an evolutionary standpoint and studies persisted until the Peregrine Falcon (*Falco peregrinus*) leptin sequence was reported (Prokop et al., 2014). Researchers attributed the difficulty in finding the falcon leptin gene to the high GC content (54.7%), and unusual tissue distribution which had led others to search for expression in tissues where it was

absent (Prokop et al., 2014). Shortly thereafter, leptin orthologues were identified for the zebra finch (*Taeniopygia guttata*) (Huang et al., 2014) and rock dove (*Columba livia*) (Friedman-Einat et al., 2014). For both species, there was little to no expression of leptin in the adipose tissue, which is in contrast to mammals where the transcript is most abundant in the adipose tissue, with a strong positive correlation between abundance and fat mass (Friedman and Halaas, 1998; Rosenbaum et al., 1996). Partial sequences from the Japanese quail (*Coturnix japonica*) (Friedman-Einat and Seroussi, 2014), and RNA-sequencing data were what led to the identification of the chicken leptin sequence (Seroussi et al., 2016). Similar to other avian species, chicken leptin bears a low homology to the mammalian sequence, and its mRNA is not highly expressed in the adipose tissue, and similarly to zebra finch, it is not expressed in the liver (Huang et al., 2014; Seroussi et al., 2016). These results imply that leptin does not function as an adipose tissue-derived signal to control energy balance in birds. With relatively low expression of leptin and its receptor in the hypothalamus, the major part of the brain thought to be responsible for modulating feeding behavior, it is unlikely that endogenous leptin plays a major role in appetite regulation in birds (Friedman-Einat et al., 2014; Huang et al., 2014). Consistent with this, ICV injections of a partial sequence corresponding to the chicken leptin identified by Seroussi et al. (2016) had no effect on food intake in broiler chicks (Sims et al., 2017).

Thus, there are some differences between birds and mammals in the roles of some hormone systems in regulating energy balance, in particular, ghrelin and leptin, which are major hunger- and satiety-associated factors in mammals, respectively, but appear to have different roles in avian species. Other hormonal systems including proteinaceous and nonproteinaceous hormones play an important role in regulating food intake and body fat mass. Many of the peptide hormones and systems will be described throughout this chapter, and it is important to bear in mind the relationship of feeding behavior to other physiological processes, such as reproduction, immune system activation, metabolic rate and growth, and stress responses, to name a few. A critical factor responsible for stress cascade activation is CRF. Release of CRF from the paraventricular nucleus (PVN) of the hypothalamus promotes the release of adrenocorticotropic hormone (ACTH) from the anterior pituitary, which then targets the adrenal cortex to stimulate the production of cortisol (Smith and Vale, 2006). Both CRF (Wang et al., 2019a, 2019c) and ACTH (Shipp et al., 2015b) are anorexigenic; ICV injection into chicks leads to reduced food intake. Central administration of ACTH was associated with activation of the lateral hypothalamic area (LHA), ventromedial hypothalamic nucleus (VMH), and infundibular nucleus (IN) the equivalent of the mammalian arcuate nucleus (ARC) and decreased hypothalamic CRF, urotensin 2 (UTS2), agouti-related peptide (AgRP), orexin, and melanocortin receptor 1 (MC1R) mRNA (Shipp et al., 2015b). While this chapter does not contain an exhaustive list of hormones and their effects on food intake in domestic fowl, it is important to note that many do indeed affect feeding behavior either directly or indirectly.

28.3 Central nervous system control of food intake

Food intake regulation is highly conserved across animals, and thus neural and endocrine networks controlling this behavior are similarly conserved. The hypothalamus has emerged as the major site of food intake regulation (Hussain and Bloom, 2013). The hypothalamus receives signals from the gut, pancreas, liver, and adipose tissue as well as other parts of the brain, and it integrates these inputs to modulate appetite and feeding behavior (Figure 28.1) (Richards and Proszkowiec-Weglarz, 2007). As in mammals, lesioning the medial hypothalamus of avian species increases food intake, whereas lesioning the LHA decreases food intake (Kuenzel et al., 1999). While these sites were traditionally considered the satiety and hunger centers, respectively, it is currently believed that they are considered to be parts of larger neural circuits involved in food intake regulation (Figure 28.2).

The neurochemical control of food intake is complex. Within the CNS, many neurochemicals have been shown to function in food intake control. As will be discussed in the "Classical Neurotransmitters" section, there are many classical neurotransmitters (Table 28.2) as well as peptides (Table 28.3) that act in the CNS to alter food intake. In general, these compounds act similarly between mammals and avian species. However, there are some notable exceptions. While peptide YY and pancreatic polypeptide decrease food intake in mammals, they stimulate food intake in birds. As discussed earlier, ghrelin is a potent orexigenic peptide in mammals but is anorexigenic in birds, and leptin acts as an important satiety factor that signals fat mass in mammals but does not appear to exert either of these functions in birds. Other peptides shown to be orexigenic in mammals, including melanin concentrating hormone (MCH), orexins (A and B) (Katayama et al., 2010a), and motilin, have no effect on food intake in chickens. Finally, PrRP stimulates food intake in chickens but inhibits it in mammals.

28.4 Classical neurotransmitters

Many classical neurotransmitters have a role in the CNS in the control of food intake in birds, and this effect can vary with the type of bird (Table 28.2). For example, ICV injection of epinephrine (E) increased food intake in broiler (meat-type) chickens (Denbow et al., 1981), but was

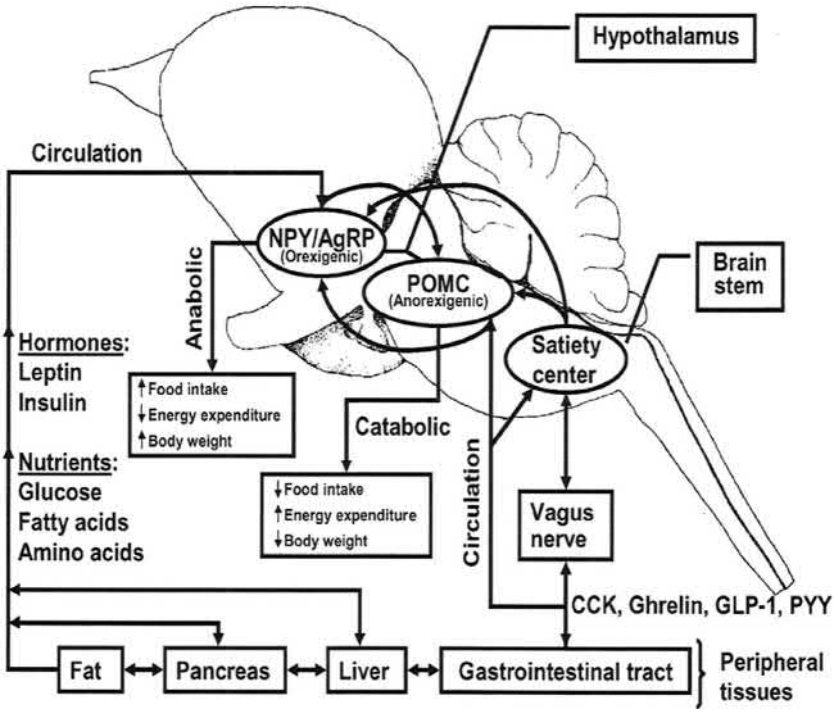

FIGURE 28.1 A proposed model describing the long-term regulation of appetite and energy balance to achieve a stable body weight in poultry that integrates peripheral tissue and central nervous system circuits regulated by hormonal, neural, neuroendocrine, and nutrient signaling mechanisms. *AgRP*, agouti-related peptide; *CCK*, cholecystokinin; *GLP-1*, glucagon-like peptide-1; *NPY*, neuropeptide Y; *POMC*, pro-opiomelanocortin; *PYY*, peptide YY.

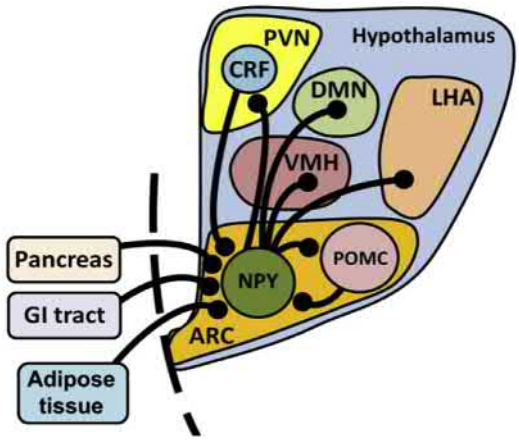

FIGURE 28.2 Based on the mammalian models, projections of NPY neurons from the ARC to other appetite-associated hypothalamic nuclei, reciprocal innervation between NPY and POMC neurons in the ARC, and reciprocal innervation between NPY and CRF in the ARC and PVN, receptively. Peripheral signals influence feed intake by affecting the ARC. *Adapted from Broberger et al. (1999); Tebbe et al. (2003); Mercer et al. (2011).*

without effect in Leghorn (egg-type) chickens (Denbow et al., 1983), and reduced food intake in turkeys (Denbow, 1983). More recently, Katayama et al. (2010b) reported that high doses of NE injected ICV reduced food intake in broiler chicks, and this effect was not associated with changes in brain NPY or pro-opiomelanocortin (POMC) concentrations. However, Bungo et al. demonstrated a stimulatory effect of ICV NE on food intake in layer chicks. Dopamine, L -DOPA, and tyrosine did not affect feeding in layer chicks (Bungo et al., 2010). Serotonin (5-hydroxytryptamine; 5-HT) decreases food intake when injected into the brain of both Leghorns and broilers (Table 28.2). When serotonin was ICV injected into broiler chicks, there was activation of the VMH and IN, implicating these hypothalamic regions in mediating the food intake-reducing effects of 5-HT (Zhang et al., 2017). Adding fenfluramine, a drug that increases the action of serotonin, to the diet of layers and broilers decreased food intake (Hocking and Bernard, 1993), supporting that endogenous serotonin acts as an appetite suppressant in chickens.

In mammals, NE, when injected into specific brain sites, both increases and decreases food intake depending on the site of injection. Injections into the VMH or PVN stimulate feeding, while injections into lateral sites including the perifornical region decrease feeding. In Leghorns, NE stimulated food intake when injected into the VMH, PVN, and medial septal sites (Denbow and Sheppard, 1993). NE inhibited food intake when injected near the lateral septal organ and the anterior portion of both the nucleus reticularis superior, pars dorsalis, and the tractus occipitomesencephalicus. Furthermore, food intake was increased in layer-type chicks after ICV injections of clonidine, an α2-adrenergic agonist acting at presynaptic sites, and this effect was attenuated by yohimbine, an α2-adrenergic antagonist (Tachibana et al., 2009b). Whereas ICV injections of 0.1 and 0.2 nmol of clonidine stimulated food

TABLE 28.2 Effects of various neurotransmitters or their agonists on food intake in poultry when injected directly into the central nervous system.[a]

Neurotransmitter	Broilers	Leghorns	Turkeys
AMPA (α-amino-3-hydroxy-5-methyl-4-isoxazole propionic acid)[b]	→		
Bicuculline[c]	↓		
Dopamine	→	→	→
Epinephrine	↑	→	↓
Glutamate[c]	↓		
Isoproterenol[d]	↓		
Kainate[b]	→		
NMDA (N-methyl-D-aspartate)[b]	↑		
Norepinephrine	↑	↑	↓
5-HT (fed birds)	↓	↓	↓
5-HT (fasted birds)	→	↓	↓
Histamine[e]	↓	↓	ND
Carbachol (cholinergic agonist)	↓	ND	ND
Methacholine (muscarinic cholinergic agonist)	→	ND	ND
Muscimol[f] (GABA agonist)	↑	↑	↑
Propranolol[d]	↑		

[a] *→, no effect; ↓, decrease in food intake; ↑, increase in food intake; ND, not determined. Data are from Denbow (1999) unless otherwise stated.*
[b] *From Bungo et al. (2011). AMPA and NMDA reduced feed intake in pigeons (Zeni et al., 2000).*
[c] *From Zendehdel et al. (2009). Glutamate also reduced feed intake in pigeons (Zeni et al., 2000).*
[d] *From Baghbanzadeh et al. (2010).*
[e] *Results for broilers are from Cline and Furuse (2012); those for Leghorns are from Meade and Denbow (2001).*
[f] *Results for broilers are from Zendehdel et al. (2009), those for Leghorns are from Bungo et al. (2003).*

TABLE 28.3 Peptides administered centrally having an orexigenic effect on food intake in various avian species.

Orexigenic peptide	Broilers	Leghorns	Other birds
Avian pancreatic peptide		Denbow (1999)	
Astressin	Emadi et al. (2011)		
Beta-cell-tropin	Shipp et al. (2015a)		
CB65 (N-cyclohexyl-7-chloro-1-[2- (4-morph-olinyl) ethyl] quinolin-4(1H)-one-3-carboxamide)	Emadi et al. (2011)		
Clonidine	Bungo et al. (1999)	Tachibana et al. (2009b)	
CNQX (6-cyano-7-nitroquinoxaline-2, 3-dione)			Pigeons: Zeni et al. (2000)
β-Endorphin	Denbow (1999)	Denbow (1999)	
Galanin		Cline and Furuse (2012)	Body weight-selected line chicks: Hagen et al. (2013)

Continued

TABLE 28.3 Peptides administered centrally having an orexigenic effect on food intake in various avian species.—cont'd

Orexigenic peptide	Broilers	Leghorns	Other birds
GnIH (gonadotropin-inhibiting hormone)	Tachibana et al. (2008)	Cline and Furuse (2012) McConn et al. (2014)	Body weight-selected line chicks: McConn et al. (2016)
Kyotorphin	Webster et al. (2013)		
(Met^5)-enkephalin	McCormack and Denbow (1989)		
MK801			Pigeons: Zeni et al. (2000)
Neuropeptide Y	Denbow (1999)	Cline and Furuse (2012)	Ring doves: Strader and Buntin (2001) White-crowned sparrows: Richardson et al. (1995) Body weight-selected line chicks: Newmyer et al. (2013) Japanese quail: McConn et al. (2018b)
Nociceptin	Cline and Furuse (2012)	Cline and Furuse (2012)	
Peptide YY	Cline and Furuse (2012)	Cline and Furuse (2012)	
Prolactin			Domestic turkey: Denbow (1999)[a] Ring doves: Foreman et al. (1990) European quail: Boswell et al. (1995) Carneau pigeons: Miller and Riddle (1943)
Prolactin-releasing peptide	Wang et al., 2015a, b	Cline and Furuse (2012)	Japanese quail: McConn et al. (2020)
Somatostatin		Cline and Furuse (2012)	
Visfatin	Cline and Furuse (2012)		
Xenopsin	McConn et al. (2015)		
26RFa (VGTALGSLAEELNGYNRKKGGFSFRFNH 2)	Cline and Furuse (2012)	Cline and Furuse (2012)	

Authors and dates denote referenced papers, and blank spaces denote no reported data.
[a]*Had an anorexic effect.*

intake in broilers (Bungo et al., 1999), 0.8 but not 0.4 nmol increased food intake in layer-type chicks. Therefore, it appears that selection for rapid growth rate in broilers results in increased sensitivity to α2-adrenergic stimulation. ICV injection of BRL37344, a β3-adrenergic receptor agonist, suppressed food intake (Tachibana et al., 2003a).

The major inhibitory neurotransmitter in the CNS is γ-aminobutyric acid (GABA). GABA increases food intake in both broilers and turkeys (see Table 28.2). This effect appears mediated by GABAA, but not GABAB (Jonaidi et al., 2002). Muscimol, a GABAA receptor agonist, was able to stimulate food intake in broilers, while baclofen, a GABAB receptors agonist, had no effect.

Histamine inhibits food intake when injected ICV into both broiler and Leghorn chicks (Meade and Denbow, 2001). Histamine can work at three receptor subtypes: H1, H2, and H3. The H3 receptor is an autoreceptor that inhibits the release of endogenous histamine from histaminergic

neurons. The anorexigenic effect of histamine was attenuated by the H1 receptor antagonist chlorpheniramine and the H2 receptor antagonist cimetidine. Taati et al. (2010) showed that injection of thioperaminde, an H3 antagonist that enhanced histamine release, decreased food intake in 3-week-old broilers. In contrast, R-α-methylhistamine, an H3 agonist, increased food intake. The H1 receptor antagonist chlorpheniramine attenuated the effect of thioperaminde, whereas famotidine, an H2 receptor antagonist, had no effect except at high doses, at which it decreased food intake. Therefore, while it appears that the H1 receptor is involved in mediating the effect of a histamine-induced decrease in food intake, the role of the H2 receptor is still unclear.

28.5 Peptides

The list of peptides known to alter food intake is large and growing (Cline and Furuse, 2012). Many of these peptides have orexigenic effects (Table 28.3), and most have anorexigenic effects (Table 28.4). In the discussions that follow note that the source of peptide is not indicated for most studies and whether an avian species-specific or mammalian sequence-specific peptide was used could influence the food intake and behavioral response to injection of the peptide, as could the route of administration. For most studies that focus on effects of central administration, peptides are injected ICV, with some involving cannulation into specific nuclei at older ages. Almost all of the studies cited herein (at least those that involve ICV injection) were conducted with chicks that were less than a week old. The reason is that the skull has not yet ossified, permitting a free-hand injection, which is also why cannulations are required at an older age.

During the last decade, there have been many reports of peptide-induced changes in feeding behavior that are accompanied by molecular studies, primarily a survey of gene expression changes at the whole hypothalamic and even nucleus-specific level. Because the understanding of appetite regulation in birds has lagged behind mammalian research, such studies have enhanced knowledge of appetite regulatory mechanisms by leaps and bounds although much remains to be elucidated, and such work is difficult due to the anatomical and functional complexities of the CNS. Punch-biopsy techniques for isolating brain nuclei and procedures facilitating the extraction of high-quality nucleic acids, as well as advents in sequencing technology have facilitated understanding the resolution of gene expression at the nucleus level. This is particularly important given the distinct functionalities of different hypothalamic nuclei. For most of the research described herein, assessments of molecular changes in response to ICV administration were carried out at 1-h postinjection, allowing for comparisons among studies. The 1-h time point is not arbitrary; it is the time at which expression of c-Fos, an indirect marker for neuronal activation, is expected to be most robust, and as such it is considered to be an optimal time to quantify it as a marker for brain nucleus activation.

28.5.1 Neuropeptide Y

First isolated from the pig brain in 1982 (Tatemoto et al., 1982), NPY is one of the most abundantly expressed peptides in the CNS. With a highly conserved sequence of 36 amino acids, the mammalian and avian amino acid sequences differ by a single residue (Blomqvist et al., 1992; Larhammar, 1996). In both mammals and avian species,

TABLE 28.4 Peptides administered centrally and peripherally having an anorexigenic effect (causing loss of appetite) on food intake in various avian species.

	Central administration			Peripheral administration		
Anorexigenic peptide	Broilers	Leghorns	Other birds	Broilers	Leghorns	Other birds
Adrenocorticotropic hormone (ACTH)	Shipp et al. (2015b)					
Adrenomedullin	Wang et al. (2014b)					
Alytesin	Cline and Furuse (2012)			Cline and Furuse (2012)		
AM251 (1-(2,4-dichlorophenyl)-5-(4-iodophenyl)-4-methyl-N-(1-piperidyl) pyrazole-3-carboxamide)				Novoseletsky et al. (2011)		

Continued

TABLE 28.4 **Peptides administered centrally and peripherally having an anorexigenic effect (causing loss of appetite) on food intake in various avian species.—cont'd**

Anorexigenic peptide	Central administration			Peripheral administration		
	Broilers	Leghorns	Other birds	Broilers	Leghorns	Other birds
Amylin	Cline et al. (2008d)			Cline et al. (2008d)		
Anserine	Cline and Furuse (2012)					
AVT (arginine vasotocin)		Cline and Furuse (2012) Masunari et al. (2016)				
Bombesin	Denbow (1999)	Meade and Denbow (2003) Tachibana et al. (2010c)	Domestic turkey: Denbow (1999)		Denbow (1999) Tachibana et al. (2010c)	Domestic turkey: Denbow (1999)
Calcitonin	Cline and Furuse (2012)		Body weight-selected line chicks: Cline et al. (2010b)			
Carnosine	Cline and Furuse (2012)					
CCK (cholecystokinin)	Denbow (1999)	Rodríguez-Sinovas et al. (1997) Tachibana et al. (2012)	Domestic turkey: Denbow (1999) White-crowned sparrows: Richardson et al. (1993)	Denbow (1999)	Denbow (1999) Tachibana et al. (2012)	
CGRP (calcitonin gene-related peptide)	Cline and Furuse (2012)		Body weight-selected line chicks: Cline et al. (2010b)	Cline et al. (2009a)		
CRF (corticotrophin releasing factor)	Cline and Furuse (2012) Wang et al. (2019c)	Cline and Furuse (2012) Ogino et al. (2014)	White-crowned sparrows: Richardson et al. (2000) Japanese quail: Wang et al. (2019a)			
Gastrin	Cline and Furuse (2012)	Denbow (1999)		Denbow (1994)		
Gastrin-releasing peptide	Bohler et al. (2019)					

Continued

TABLE 28.4 Peptides administered centrally and peripherally having an anorexigenic effect (causing loss of appetite) on food intake in various avian species.—cont'd

Anorexigenic peptide	Central administration			Peripheral administration		
	Broilers	Leghorns	Other birds	Broilers	Leghorns	Other birds
Ghrelin	Cline and Furuse (2012)	Cline and Furuse (2012)	Japanese quail: Shousha et al. (2005a)	Geelissen et al. (2006)	Kaiya et al. (2007)[a]	Japanese quail: Shousha et al. (2005a)[a,b]
GLP (glucagon-like peptide)	Cline and Furuse (2012)	Cline and Furuse (2012)	Japanese quail: Shousha et al. (2007)			Japanese quail: Shousha et al. (2007)
Glucagon		Denbow (1999)		Honda et al. (2007a)[a]		
GHRH (growth hormone-releasing hormone)	Cline and Furuse (2012)	Cline and Furuse (2012)				
Insulin	Cline and Furuse (2012)	Cline and Furuse (2012)	Body weight-selected line chicks: Smith et al. (2011)		Bermudez et al. (1983)[a]	
Leptin	Denbow et al. (2000)	Denbow et al. (2000)				
Litorin	Cline and Furuse (2012)	Cline and Furuse (2012)[a]				
LPLRF (Leu—Pro—Leu—Arg—Phe)	Cline and Furuse (2012)	Cline and Furuse (2012)[a]	Bobwhite quail: Cline et al. (2009c)			
Mesotocin	McConn et al. (2019b)	Masunari et al. (2013) Masunari et al. (2016)	Body weight-selected line chicks: McConn et al. (2019b)			
Oxytocin	McConn et al. (2019a)		Body weight-selected line chicks: McConn et al. (2019a)			
MSH (α, β, and γ) (melanocyte-stimulating hormone)	Cline and Furuse (2012)	Cline and Furuse (2012) α MSH only	Japanese quail: Lear et al. (2017)			
NAME (N-nitro-arginine methyl-ester)	Denbow (1999)	Khan et al. (2007)[c]		Khan et al. (2007)	Khan et al. (2007)	
Neuromedin (B, C, S. and U)		B and C: Cline and Furuse (2012) Tachibana et al. (2010a,b,c)	Japanese quail (NMU): Shousha et al. (2005b)		B and C: Tachibana et al. (2010c)	Japanese quail (NMU): Shousha et al. (2005b)

Continued

TABLE 28.4 **Peptides administered centrally and peripherally having an anorexigenic effect (causing loss of appetite) on food intake in various avian species.—cont'd**

	Central administration			Peripheral administration		
Anorexigenic peptide	**Broilers**	**Leghorns**	**Other birds**	**Broilers**	**Leghorns**	**Other birds**
Neuropeptide AF, FF, K, S, SF, and VF	Cline and Furuse (2012) NPK: Prall and Cline (2008)		Japanese quail (NPK): Wang et al. (2019b)			
Oxyntomodulin	Cline and Furuse (2012)					
PACAP (pituitary adenylate cyclase-activating polypeptide)		Cline and Furuse (2012)				
Stresscopin	Cline and Furuse (2012)	Cline et al. (2009d)				
Substance P	Mace et al. (2014)	Cline and Furuse (2012)	Japanese quail: Pauliukonis et al. (2020)			
Urocortin	Cline and Furuse (2012)	Ogino et al. (2014)				
Urotensin	Cline and Furuse (2012)					
VIP (vasoactive intestinal polypeptide)		Cline and Furuse (2012) Khan et al. (2013)				
Xenin	Cline and Furuse (2012) Cline et al. (2007b)			Cline et al. (2007b)		

Authors and dates denote referenced papers, and blank spaces denote no reported data.
[a]*Treatment did not affect food intake.*
[b]*At low doses, had an anorexigenic effect; at high doses, had an orexigenic effect.*
[c]*Treatment had an orexigenic effect.*

NPY is one of the most potent orexigenic regulators of food intake (Kuenzel and McMurtry, 1988). NPY stimulates food intake via NPY Y2 and Y5 receptors, but not the Y1 receptor. Whereas in mammals peptide YY and pancreatic polypeptide suppress appetite, in broiler and Leghorn chicks peptide YY increases food intake (Kuenzel et al., 1987; Denbow et al., 1988). Peptide YY was much more potent than NPY in stimulating food intake, which may

reflect a difference in the affinities of NPY and peptide YY to these NPY receptor subtypes.

In mammals, within the hypothalamus, the ARC is a major site for food intake regulation (Hussain and Bloom, 2013). This nucleus has a semipermeable blood−brain barrier allowing peripheral signals to reach the brain. There are first-order orexigenic neurons in the ARC containing NPY and co-expressing AgRP, and a second population of anorexigenic neurons containing POMC−CART (cocaine- and amphetamine-regulated transcript) neurons. These neurons then communicate with second-order neurons in other nuclei expressing such peptides as CRF, orexins, and MCH. Upon fasting, NPY mRNA levels increase in the ARC, and this coincides with an increase in NPY peptide content and release in the PVN.

The melanocortin 4 receptor (MC4R) is associated with inhibition of food intake. Release of AgRP, an endogenous MC4R antagonist, from the NPY−AgRP neurons in the ARC blocks the MC4R, causing increased food intake. In addition, α-melanocyte-stimulating hormone (α-MSH), which is cleaved from the POMC protein, is an agonist at the MC4R and causes decreased food intake. Therefore, fasting increases expression of AgRP mRNA and decreases expression of POMC mRNA.

In avian species, NPY-containing neurons are located in the IN, homologous to the ARC in mammals (Kuenzel, 1994; Wang et al., 2001), and these neurons co-express AgRP (Boswell et al., 2002). As in mammals, NPY gene expression increases in the hypothalamus in fasted and food-restricted avian species (Phillips-Singh et al., 2003; Song et al., 2012). Therefore, as in mammals, AgRP blocks the anorexigenic melanocortin pathway, while NPY mediates the orexigenic pathway.

ICV injections of NE do not alter brain NPY or POMC mRNA expression (Katayama et al., 2010b). However, the increase in food intake induced by ICV NPY is attenuated by yohimbine, an α 2-adrenergic receptor antagonist (Tachibana et al., 2009b). This suggests that NPY neurons possibly work via communication with adrenergic neurons that act at α2-adrenergic receptors. Furthermore, a GABAA antagonist is able to attenuate the response to NPY (Jonaidi and Noori, 2012). In young Japanese quail, ICV NPY was orexigenic, but only during the light cycle, and the IN was activated robustly, similar to other species (McConn et al., 2018b). Hypothalamic AgRP and NPYR1 and two mRNAs were all increased in NPY-injected quail, with increased NPYR2 mRNA also observed within the ARC (McConn et al., 2018b).

28.5.2 Melanocortins

Melanocortins are peptide hormones that are derived from POMC, including the melanocyte-stimulating hormones and ACTH, and in mammals most are released from neurons in the ARC. While these peptides can act at five different melanocortin receptor subtypes (MC1R through MC5R) distributed throughout the body, MC3R and MC4R are expressed in the mammalian brain. MC3R appears to regulate energy expenditure, while MC4R is involved with food intake. Agonists of the MC3R receptor decrease food intake.

ICV injection of α-MSH reduced food intake in fasted broiler chicks and attenuated NPY-induced food intake (Kawakami et al., 2000). Conversely, AgRP attenuated α-MSH-induced anorexia (Tachibana et al., 2001). CART, which is also found in the POMC neurons, also decreased food intake in broiler and layer chicks and attenuated NPY-induced feeding (Tachibana et al., 2003b). Broiler chicks ICV injected with α-MSH had more c-Fos expression in the IN, PVN, dorsomedial nucleus (DMN), and LHA (Delp et al., 2017). Moreover, in the IN, there was greater mRNA abundance of NPY, mesotocin (MT) receptor, and AgRP, and in the PVN reduced expression of NPYR1 and greater expression of c-Fos mRNA (Delp et al., 2017). In the DMN of α-MSH-injected chicks, there was also greater c-Fos mRNA and more L-amino acid decarboxylase (AADC) mRNA. These results collectively suggest that in broiler chicks, melanocortin signaling reduces NPY signaling in the PVN while activating NPY/AgRP neurons in the IN to reestablish basal levels of food intake. Anorexigenic effects were also observed in young Japanese quail, as well as activation of the VMH and PVN, which differed from activation patterns in broiler chicks (Lear et al., 2017). Hypothalamic (nucleus-specific samples were not collected) expression of AgRP and AADC was reduced while MC4R mRNA was increased in α-MSH-injected quail (Lear et al., 2017).

In mammals, β-MSH binds MC4R with higher affinity than α-MSH (Harrold et al., 2003), suggesting that it may be the main endogenous melanocortin receptor agonist. However, in chickens, α-MSH binds to MC4R with greater affinity than does β-MSH (Ling et al., 2004). In broiler chicks, β-MSH decreased food and water intake while increasing plasma corticosterone concentrations (Smith et al., 2008). Gamma-MSH, a selective MC3R agonist, also reduced food intake in broiler chicks, but required larger doses than α- or β-MSH (Smith et al., 2011). Hence, it appears that the melanocortin system is involved in anorexigenic pathways in birds, but the role and location of the various receptors still need further elucidation.

28.5.3 Corticotropin-releasing factor, urocortins, and urotensins

The CRF family of proteins includes CRF, sauvagine, urotensins, and urocortins in mammals. CRF acts within the brain to decrease food intake in both broilers and Leghorns (Furuse et al., 1997; Denbow et al., 1999). ICV injection of

the CRF homolog stresscopin reduced food and water intake in broiler and White Leghorn chicks (Cline et al., 2009d). This was associated with an increased number of c-Fos immunoreactive cells in the VMH, the parvicellular and magnocellular divisions of the PVN, and the posterior hypothalamic nucleus (PHN), indicating increased neuronal activity in these areas. This anorexigenic effect was mediated via CRF receptors. In broiler chicks, CRF injection was associated with activation of the IN, DMN, VMH, and PVN (Wang et al., 2019c). There was also decreased hypothalamic NPYR1 mRNA, more IN-specific CRF and CRFR2 mRNA, but less AgRP, NPY, and NPYR1 mRNA, and more CRFR2 and MT mRNA in the PVN and VMH, respectively. In the DMN, there was less NPYR1 mRNA in CRF-injected chicks (Wang et al., 2019c). Khan et al. (2008) showed that the anorexigenic effect of CRF was attenuated by blocking nitric oxide in broiler chicks. In layer chicks, CRF and urocortin-3 (UCN3) exerted similar anorexigenic effects post-ICV injection and also delayed crop emptying and increased cloacal temperatures (Ogino et al., 2014). In Japanese quail, the anorexigenic response to CRF was associated with activation of the LHA and PVN and increases in the hypothalamic mRNA abundance of POMC, MC4R, CRF, and CRFR2 (Wang et al., 2019a).

As discussed above, the site of action of ghrelin is the CNS. In mammals, ghrelin potently stimulates food intake mainly by stimulating NPY neurons located in the ARC. In contrast, an ICV injection of ghrelin inhibits food intake in broiler chicks, an effect opposite that in mammals (Furuse et al., 2007). In elucidating the mechanism of ghrelin in birds, Saito et al. (2005) showed that an ICV injection of ghrelin increased plasma corticosterone. Co-injection of the CRF receptor antagonist astressin attenuated the ghrelin-induced decrease in food intake and plasma corticosterone increase. Furthermore, co-injection of ghrelin with NPY inhibited the NPY-induced increase in food intake, and the ICV injection of ghrelin did not change NPY mRNA expression. In contrast to mammals, in which ghrelin induces the release of NPY from neurons in the ARC, in birds, ghrelin in the CNS inhibits food intake through the release of endogenous CRF. Taati et al. (2010) demonstrated that blockade of histamine H1 but not H2 receptors attenuated ghrelin's anorexigenic effect. Thus, in chicks, ghrelin, via the histaminergic system, likely causes CRF release, which is ultimately responsible for ghrelin-induced anorexia.

28.5.4 Mesotocin and arginine-vasotocin

Mesotocin (MT) and arginine-vasotocin (AVT) are both posterior pituitary-derived hormones that are homologous to mammalian oxytocin (OT) and vasopressin, respectively. ICV administration of MT to layer chicks decreased food intake, whereas IP injection had no effect (Masunari et al., 2013). Interestingly, both ICV-injected MT and AVT are anorexigenic and induce wing-flapping in chicks and effects are thought to be mediated through the vasopressin-4 receptor (Masunari et al., 2016). ICV-injected MT decreased food intake in broiler chicks and activated the PVN and LHA (McConn et al., 2019c). MT-injected chicks had greater expression of MT mRNA in the LHA and AADC in the PVN, and similar to OT, MT injection elevated cloacal temperatures (McConn et al., 2019c). Previous studies had alluded to involvement of α-adrenergic signaling in MT's effects, although ICV administration of yohimbine, an α_2-adrenergic receptor antagonist, had no effect on food intake, MT-mediated changes in food intake or hyperthermia (McConn et al., 2019c). ICV injection of OT also decreased feeding behavior in broiler chicks, which was accompanied by activation of the IN, DMN, LHA, PVN, and VMH, reduced hypothalamic CRF mRNA, and increased cloacal temperature (McConn et al., 2019a). It is interesting to note that OT and MT differ by only a single amino acid, yet they elicited slightly different effects in broiler chicks.

28.5.5 Opioids and kyotorphin

Opioids act as inhibitory neurotransmitters and are widely distributed throughout the CNS. Opioid receptors include μ, δ, or κ subtypes. The opioid antagonists naloxone and naltrexone decrease food intake in both broilers and layers (see Denbow, 1999). Met-enkephalin, also known as opioid growth factor, is an endogenous opioid peptide derived from proenkephalin that activates the opioid receptors. Opioids appear to alter food intake in birds by acting at the δ- and κ- opioid receptors (Bungo et al., 2004). Dodo et al. (2005) reported that antagonists of the μ-opioid receptor, especially the μ1-receptor, reduced NPY-induced feeding in neonatal chicks.

Nociceptin−orphanin FQ (N/OFQ) is structurally similar to opioids, and binds to the opioid-like G protein-coupled receptor 1, or nociceptin receptor (NOP). N/OFQ shows structural similarities to the classical opioid peptides, particularly dynorphin A, but N/OFQ does not interact with the dynorphin A−κ-opioid receptor system. N/OFQ stimulated food intake in rats (Polidori et al., 2000). Similar to other opioids, ICV injection of N/OFQ increased food intake and pecking frequency in broiler chicks (Abbasnejad et al., 2005). Similarly, ICV N/OFQ stimulated food intake in White Leghorn chicks, and this was associated with increased AgRP and decreased CART mRNA expression in the diencephalon (Bungo et al., 2009). N/OFQ-induced increase in food intake was blocked by α-MSH. There was no change in NPY or POMC mRNA.

Kyotorphin, (L-tyrosyl−L-arginine), a met-enkephalin-releasing dipeptide, is associated with analgesic and orexigenic effects, in association with opioid receptor signaling

(Webster et al., 2013). In broiler chicks, ICV injection of kyotorphin was orexigenic and effects were blocked when all opioid receptor subtypes were antagonized, suggesting that hunger-stimulating effects were mediated through opioid receptor signaling (Webster et al., 2013). These findings were consistent with earlier working showing that met-enkephalin administration increased food intake in chicks (McCormack and Denbow, 1989). Kyotorphin injection was also associated with increased c-Fos expression in the LHA, ARC, and nucleus of the solitary tract (NTS) in the brainstem, implicating these regions in mediating the central effects of kyotorphin (Webster et al., 2013).

28.5.6 FMRFamides

Since molluscan neuropeptide Phe−Met−Arg−Phe−NH2 (FMRFamide) was isolated from the ganglia of the clam, similar neuropeptides containing the RFamide sequence at their C-termini (RFamide peptides) have been characterized in various invertebrates. The chicken pentapeptide Leu−Pro−Leu−Arg−Phe−NH2 (LPLRFamide) cross-reacts with the FMRFamide antibody and was the first RFamide isolated from a vertebrate (Dockray et al., 1983). Several RFamides function as orexigenic factors in neonatal chicks, including PrRP and gonadotropin-inhibitory hormone (GnIH).

PrRP was originally proposed to be a stimulator of prolactin release in mammals, hence the name (Hinuma et al., 1998). PrRP in mammals consists of two versions, PrRP-20 (20 amino acids) and PrRP-31 (31 amino acids), with the shorter having the same sequence as the C-terminus of PrRP-31 (Tachibana and Sakamoto, 2014). A 31-amino acid PrRP known as PrRP2, and the C-terminal PrRP-20 were both identified in the brain of chickens, with the 31-amino acid version increasing food intake in chicks and decreasing prolactin concentrations after central administration (Tachibana et al., 2011b). Interestingly the effect on prolactin secretion in chicks differed depending on route of administration, where peripheral injection of the chicken PrRP2 (31 amino acids) increased prolactin secretion, and circulating growth hormone levels decreased in response to both central and peripheral injection (Tachibana et al., 2011b). In chickens, two PrRP receptors (cPrRPR1 and cPrRPR2) have been identified and detected in several brain regions, including the telencephalon, midbrain, cerebellum, hindbrain, and hypothalamus (Wang et al., 2012).

While central administration of PrRP decreased food intake in rats (Lawrence et al., 2000, 2002; Ellacott et al., 2002), ICV injection of PrRP increased food intake in layer chicks (Tachibana et al., 2004b), broiler chicks (Wang et al., 2015a, b), and young Japanese quail (McConn et al., 2020). In general, PrRP has a weaker orexigenic effect than NPY on an equimolar basis. The orexigenic effect of NPY was further enhanced with co-injection of PrRP, and hypothalamic NPY mRNA was increased in PrRP-injected chicks (Wang et al., 2015b). In Japanese quail, ICV PrRP was associated with activation of the DMN and ARC, with less and greater mRNA abundance of CRF in the DMN and ARC, respectively (McConn et al., 2020). Thus, PrRP and NPY may augment each other's orexigenic effects to stimulate feeding behavior in chickens.

Tsutsui et al. (2000) isolated a novel decapeptide containing the C-terminal LPLRFamide motif, SIKPSAYLPLRFamide, from the quail brain. This peptide inhibited gonadotropin-releasing factor, and it was termed GnIH. The GnIH precursor encodes one GnIH and two GnIH-related peptides (called GnIH-RP-1 and GnIH-RP-2). ICV injection of GnIH, GnIH-RP-1, and GnIH-RP-2 significantly stimulated food intake in layer chicks (Tachibana et al., 2005a). Tachibana et al. (2008) demonstrated that the effect of GnIH is likely mediated via the μ-, but not δ- or κ-opioid receptor in broiler chicks. GnIH also did not appear to work via nitric oxide since a nitric oxide synthesis inhibitor had no effect on GnIH-induced feeding. More recent studies provide insights on molecular mechanisms. McConn et al. (2014) demonstrated that increased feeding in layer chicks in response to ICV GnIH was associated with activation of the LHA and some changes in hypothalamic gene expression, including an increase in NPY and decrease in POMC mRNA in the whole hypothalamus and increase in MCH mRNA within the LHA (McConn et al., 2014).

Ukena et al. (2010) demonstrated that another RFamide, 26RFa, exists in the anterior hypothalamus of Japanese quail. Its receptor, GPR103, was detected in the cerebrum, diencephalon, mesencephalon, and cerebellum. Ukena et al. (2010) also demonstrated that central injection of 26RFa increased food intake of broiler but not layer-type chicks. Additionally, metastin, another RFamide first isolated from the placenta, increased food intake in broiler chicks, and its effects were mediated by μ-opioid receptors (Khan et al., 2009).

In contrast to PrRP, GnIH, and 26RFa, there are other members of this family associated with anorexia. Chicks that received ICV LPLRFamide ate less at 30 min postinjection, but this effect dissipated by 40 min postinjection (Cline et al., 2009c). Since LPLRFamide-treated chicks spent more time in deep rest while other behaviors were unaffected, the short-term anorexigenic effect of LPLRFamide is likely secondary to this behavior. Further evidence that LPLRFamide may not have a specific effect on food intake is a report of it having no effect on food intake in layer chicks Tachibana et al. (2005b).

Several members of the neuropeptide FF (NPFF) subfamily of the RFamide family decreased food intake in chicks (Cline and Furuse, 2012). For instance, ICV injections of NPFF dose-dependently reduced food intake in broilers (Cline et al., 2007a). The effect of NPFF is mediated through the μ and κ subtypes of opioid receptors, and NPFF attenuates NPY and β-endorphin (β-END)-induced food intake stimulation (Cline and Mathews, 2008).

28.5.7 Galanin

Galanin, a peptide found in both the CNS and intestine, is conserved across species. Tachibana et al. (2008) demonstrated that ICV galanin stimulated food but not water intake in both broiler and layer-type chicks. It appears to work via μ-opioid receptors, and α2 adrenoceptors likely mediate this response. In chicks from lines selected for low or high body weight, the IN is activated after ICV injection, suggesting that this nucleus is involved in the orexigenic effect of galanin (Hagen et al., 2013).

28.5.8 Visfatin

Visfatin, also known as pre-B cell colony-enhancing factor, is a peptide that was originally isolated from visceral fat of humans and mice, and mimics the actions of insulin (Fukuhara et al., 2005). Visfatin is associated with metabolic syndrome in humans (Filippatos et al., 2007). The effect of visfatin on food intake was first determined in broilers in which ICV injections nearly doubled food intake and pecking efficiency (Cline et al., 2008c). This was accompanied by an increase in the number of c-Fos immunoreactive cells in the LHA and a decrease in activity in the VMH. Brunetti et al. (2012) showed that in rats, visfatin injection into the ARC increased food intake and decreased CART and CRF mRNA levels, suggesting that visfatin has a similar effect in birds and mammals. More recently, another group confirmed that ICV injection of visfatin increased food intake in chicks and through transcriptomic analysis identified hypothalamic pathways that are likely involved, including POMC/CRF and NPY/AgRP (Li et al., 2018).

28.5.9 Somatostatin

Somatostatin, known for the inhibition of growth hormone release, also affects food intake. While it was shown to increase and decrease food intake in rats depending on their feeding state, ICV injections of somatostatin increased food intake in broilers and layer-type chicks (Tachibana et al., 2009a). Its effects were mediated by μ-opioid and adrenergic α2 receptors. Through ICV injections of somatostatin analogs, it was shown that somatostatin receptors SSTR2, SSTR3, and SSTR5, but not SSTR4, were associated with somatostatin-induced increased food intake (Tachibana et al., 2011a).

28.5.10 Glucagon superfamily

Glucagon-like peptide-1 (GLP1) is a member of the glucagon superfamily of peptides. Similar to mammals, ICV injection of GLP1 decreases food intake in broiler chicks (Bungo and Furuse, 2001). Growth hormone-releasing factor increases food intake in rats; however, it is a potent inhibitor of food intake in broiler chicks (Furuse et al., 2001). Similarly, other neuropeptides belonging to the glucagon superfamily, including vasoactive intestinal peptide (VIP) (Khan et al., 2013), gastric inhibitory peptide, and pituitary adenylate cyclase-activating polypeptide (PACAP), reduced food intake in layer chicks (Tachibana et al., 2004a). ICV injection of PACAP and VIP increases plasma corticosterone concentrations, and these effects are attenuated by co-injection with the CRF receptor antagonist astressin, suggesting that PACAP and VIP function through activation of CRF neurons (Tachibana et al., 2004a). Consistent with this hypothesis, ICV injection of VIP was associated with decreased diencephalic gene expression of CRF, UCN3, and CRFR2, suggesting involvement of CRF receptor signaling in mediating the anorexigenic effects of VIP (Khan et al., 2013). Similarly, glucagon (Honda et al., 2007a) and oxyntomodulin (Cline et al., 2008a) decreased food intake in chicks when injected ICV.

28.5.11 Cholecystokinin and gastrin

Cholecystokinin (CCK), originally isolated from the porcine small intestine, decreases food intake when injected peripherally or centrally into mammals. There are multiple bioactive forms of CCK, including CCK33, CCK (26−33; sulfated CCK8, CCK8S), and CCK (30−33; CCK4), with sulfated (tyrosine that is seventh amino acid from C-terminus) and unsulfated forms eliciting physiological effects. In chickens, CCK decreased food intake when centrally injected into broilers (Denbow and Myers, 1982). In layer chicks, both CCK8 and 8S reduced food intake following IP or ICV injection, however, via both routes effects of the sulfated form were of a greater magnitude than the nonsulfated form (Tachibana et al., 2012). That chicks displayed conditioned aversion with greater plasma corticosterone concentrations suggested that anorexigenic effects might be related to malaise, especially via the central route. In contrast, CCK4 had no effect on food intake via either injection route (Tachibana et al., 2012).

The structurally related peptide gastrin does not appear to decrease food intake in mammals. While the amino acid sequence of chicken CCK8 is identical to that of mammalian species, differences exist between chicken and mammalian gastrin. Furuse et al. (1999) demonstrated that ICV injection of chicken gastrin inhibits food intake and food passage in neonatal chicks. Moreover, the efficacy of these peptides depends on the length of their peptide sequence (Furuse et al., 2000).

28.5.12 Calcitonin family

Like the glucagon superfamily, members of the calcitonin gene peptide superfamily, including calcitonin, calcitonin

gene-related peptide (CGRP), adrenomedullin, and amylin, appear involved in food intake regulation. These peptides are derived via tissue-specific alternative splicing of the primary RNA transcripts of the calcitonin gene.

Amylin causes a dose-dependent decrease in food intake after ICV and IP injection in broilers (Cline et al., 2008d). This was associated with increased neuronal activity in the area postrema and the NTS, two nuclei in the brainstem. In addition, amylin caused increased alimentary canal transit time, plasma corticosterone concentration, and anxiety-related behaviors. Because amylin is co-secreted with insulin, it may be involved in terminating meals in chicks.

ICV injection of calcitonin also reduced food and water intake in broiler chicks (Layne et al., 2009). This was associated with increased activation of the ARC, DMN, and VMH, and the CRF system likely does not mediate this response. Similarly, broilers that received ICV and IP CGRP reduced both their food and water intake, but CGRP's effect on water intake appeared to be related to its effect on food intake (Cline et al., 2009a). CGRP-induced anorexia coincided with increased activation of the ARC, PVN, PHN, and VMH. Adrenomedullin, when ICV injected, produced anorexigenic effects in broiler chicks that appeared to be CRF-independent, and associated with activation of the PVN, VMH, and DMN (Wang et al., 2014a).

28.5.13 Insulin

Insulin decreases food intake when injected into the brain of mammals. Similarly, ICV injection of insulin decreased food intake in White Leghorn chicks (Honda et al., 2007b; Shiraishi et al., 2008a) while increasing expression of POMC, CART, and CRF, but not affecting NPY and AgRP mRNA in the hypothalamus (Honda et al., 2007b). Shiraishi et al. (2008a), however, reported a decrease in NPY expression after ICV insulin when including the brain stem. Blocking the melanocortin receptors prevented the anorexic effect of ICV insulin (Shiraishi et al., 2008a). Coinjection of β-END and insulin decreased central POMC expression more than insulin injection alone, while blocking μ-opioid receptors reduced the effect of insulin on food intake (Shiraishi et al., 2008b). Food intake was decreased in Leghorns by chicken and pig insulin, but not by human or bovine insulin (Shiraishi et al., 2009).

Several other appetite regulators related to insulin function have been identified. Beta-cell-tropin is derived from ACTH and is a beta-cell insulin secretagogue as the name implies. ICV injection into broiler chicks stimulated food intake, similar to rats, making it one of the relatively few endogenous factors that stimulates appetite (Shipp et al., 2015a). The drug, rosiglitazone (a thiazolidinedione and PPARγ agonist), is used to treat diabetes because of its insulin-sensitizing effects in peripheral tissues and one of the documented side effects is increased eating, which was also observed after ICV injection into broiler chicks (Matias et al., 2017).

28.5.14 Bombesin

Bombesin, a tetradecapeptide identified in amphibian skin, inhibits food intake in mammalian species. Denbow (1989) reported that both ICV and IV injection of bombesin decreased food and water intake in turkeys. ICV injection of bombesin inhibits food intake in broilers, and co-injection with NPY suppressed the orexigenic effect of NPY (Bungo et al., 2000). ICV and IP injections of bombesin analogs alytesin and litorin also decreased food intake in broiler chicks (Cline et al., 2008b, 2010a). Similar to its analogs, bombesin, when administered IP, was anorexigenic in layer chicks, and also delayed crop emptying (Tachibana et al., 2010c).

28.5.15 Neuromedin family

There are at least seven neuropeptides in the neuromedin family, including the bombesin-like peptides (B and C), tachykinin-like (K and L), neurotensin-like (N), and neuromedin U-like (U and S), most of which have been demonstrated to inhibit appetite in chicks. Several bombesin-like peptides, including gastrin-releasing peptide (GRP) and neuromedins B and C (NMB and NMC, respectively) (Tachibana et al., 2010b), as well as NMS (Tachibana et al., 2010a), exerted potent anorexigenic effects following ICV injection into layer chicks, with no effect on drinking behavior. Via the ICV route, GRP reduced food intake in broiler chicks but had no effect on alimentary canal transit rate (Bohler et al., 2019). In GRP-injected chicks, there was increased activation of the LHA, PVN, ARC, as well as the NTS (Bohler et al., 2019).

Neuromedins B and C were also anorexigenic when administered via the IP route, and reduced crop-emptying rate irrespective of route of administration, although effects were weaker than for bombesin (Tachibana et al., 2010c).

Substance P, a member of the tachykinin family, reduced food intake after ICV injection into broiler chicks (Mace et al., 2014). The PVN of substance P-injected chicks was activated, and this coincided with increased UTS2 mRNA within the PVN, suggestive of a potential hypothalamic molecular mechanism involving CRF receptor signaling. In Japanese quail, similar effects were observed after ICV injection, with activation of the PVN and LHA, and upregulation of UTS2 and CRF mRNA in the PVN (Pauliukonis et al., 2020).

Neuropeptide K (NPK), another tachykinin peptide, reduced food intake of chicks and Japanese quail after ICV

injection, and these effects in quail were associated with activation of the ARC, LHA, and PVN (Wang et al., 2019b), and in chicks only the ARC and PVN (Prall and Cline, 2008). In the ARC of NPK-injected quail, there was less NPYR1, NPY, and AgRP mRNA but more POMC, CART, and neurokinin receptor 1 mRNA. In the PVN, NPK injection was associated with increases in CRF, CRFR2, MC3R, MC4R, and UCN3 mRNA (Wang et al., 2019b). These results suggested that effects of NPK are mediated via the PVN, and indeed, when NPK was microinjected into the PVN of broilers, there was a reduction in food intake (McConn et al., 2019b). ICV injection of NPK into broiler chicks was also associated with reduced PVN-specific CRF mRNA and ARC-specific AgRP mRNA (McConn et al., 2019b).

28.6 Selection for single growth-related traits alters food intake control mechanisms

As already discussed, while broilers have been genetically selected for rapid body weight gain and feed conversion, Leghorn chickens have been selected for egg production and, thus, a smaller body mass, and differences have been identified in their feeding responses to centrally and peripherally administered neurotransmitters and peptides. Much of the work exploring how selection for growth rate has altered the mechanisms controlling food intake has been conducted using unique lines of birds divergently selected for either low (LWS) or high (HWS) body weight at 8 weeks of age (Siegel, 1962; Rubin et al., 2010; Marquez et al., 2010; Jambui et ala., 2017). Selected for more than 60 generations, these lines at selection age (56 days) have more than a 12-fold difference in body weight with correlated differences in food intake and body composition, and they are composed of anorexic and obese individuals. The LWS line exhibits natural anorexia (Zelenka et al., 1988), and delayed (Dunnington and Siegel, 1996) or prevented sexual maturity (Dunnington et al., 1983, 1984). The HWS line contains compulsive eaters (Dunnington and Siegel, 1984). Burkhart et al. (1983) reported that lesioning the VMH of LWS chickens resulted in nonhyperphagic obesity, whereas similar lesions in HWS chickens had no effect. The VMH is thought to be involved in satiety, and selection for body weight may have altered its function.

As was suggested by Bray (1991) for mammals, Denbow (1999) suggested that differences in body weight in lines of chickens may have resulted from changes in the balance between the parasympathetic nervous system and SNS. Selection for increased body weight may have augmented the actions of the parasympathetic branch of the autonomic nervous system. Support for this hypothesis was provided when it was shown that LWS birds appear to have greater SNS activity compared to the HWS line (Kuo et al., 2001). For many of the anorexigenic neuropeptides, including α-MSH, CRF, insulin (Smith et al., 2011), amylin, and neuropeptide AF, the LWS birds respond to a lower dose than the HWS birds (Cline et al., 2010b). For example, CRF decreases food intake in both the LWS and HWS lines, but the LWS line responded to a lower dose than did the HWS line (Cline et al., 2009b). However, for OT (McConn et al., 2019a), neuropeptide S, calcitonin (Cline et al., 2010c), and CGRP (Cline et al., 2010c), the HWS respond to a lower dose than the LWS. MT, which differs by OT by only a single amino acid, produced anorexigenic effects in both lines, with the HWS responding at a higher dose threshold but having a longer duration of response (McConn et al., 2019b). The HWS and LWS respond similarly to GnIH (McConn et al., 2016), ghrelin, and galanin (Hagen et al., 2013). For several peptides, one line is nonresponsive; the LWS does not respond to NPY (Newmyer et al., 2013) or AgRP, while the HWS line does not reduce food intake when administered human recombinant leptin.

The lack of response in the LWS line to NPY was of particular interest because it is such a potent orexigenic factor with effects highly conserved among species, and hypothalamic nucleus activation was similar between lines after ICV injection; the LHA and PVN displayed increases in c-Fos expression in both lines. It was later discovered that the reduced sensitivity to NPY in the LWS chicks was stress-dependent; when LWS but not HWS chicks were exposed to a combination of nutritional and thermal stressor on the day of hatch, they became resistant to food intake-stimulating effects of ICV NPY 5 days later (Yi et al., 2016). It was then confirmed that stress-induced magnification of anorexia in the LWS was CRF-signaling dependent (Wang et al., 2017). ICV injection of astressin prior to stressor exposure abolished the refractoriness to NPY in LWS chicks, and in stressed LWS chicks there was increased mRNA abundance of CRF and its receptors in the PVN and NPY in the ARC (Wang et al., 2017). This stress-induced upregulation of hypothalamic CRF involved epigenetic changes in the CRF gene. In stressed LWS chicks, there was reduced methylation of DNA at a single site in the promoter region that disrupted binding of a transcriptional repressor, methyl-domain binding-protein 2 (Xiao et al., 2020). These results coupled to the observation that LWS chicks have greater SNS tone and concentrations of circulating corticosterone than HWS chicks, suggest that this line is more sensitive to chronic activation of the stress cascade, which is accompanied by increased anorexigenic tone due to heightened hypothalamic CRF signaling.

Several other avian genetic lines have been developed and used to determine the molecular mechanisms involved in the regulation of feed intake. Clark and co-workers determined the feed intake pattern of ISA brown layer

hens selected for high or low feed conversion ratio and showed that there is an impact of daytime on energy intake (Clark et al., 2019). Specifically, they found that both groups increased their feeding rate from 0300 to 1700h. Average feed intake was greater in low-feed efficient compared to the high-feed efficient birds (Clark et al., 2019).

Two Rhode Island Red chicken lines, divergently selected (Bordas and Merat, 1981) for high (R^+) or low (R^-) residual feed consumption exhibit a significant difference in energy intake where the R^+ line consumes (~70%) more feed compared to their R^- counterparts (Sintubin et al., 2014). Several orexigenic hypothalamic neuropeptides such as NPY and AgRP were more highly expressed at the mRNA level in R^+ compared to R^- chickens, which may explain the hyperphagic phenotype of the R^+ line (Sintubin et al., 2014). The hypothalamic adiponectin system, ghrelin system, and suppressor of cytokine signaling 3 (SOCS3) were differentially expressed between R^+ and R^- chicken lines (Sintubin et al., 2014). Although there is still a paucity of information in chickens, adiponectin has been shown to maintain energy homeostasis via stimulating appetite and feed intake in mammals (Kubota et al., 2007). Interestingly, serum and cerebrospinal fluid levels of adiponectin increased during fasting and were reduced after refeeding in rodents and adiponectin-deficient mice fed a high-fat diet exhibited reduced feed intake (Kubota et al., 2007). SOCS3 mRNA is localized throughout the brain and overexpression of SOCS3 in POMC neurons caused leptin resistance and obesity in mice (Reed et al., 2010). In addition, rats with SOCS3 knockdown in the mediobasal hypothalamus showed dysregulation of NPY expression in the ARC and alterations in their meal patterns: average meal size in the light period was increased and was accompanied by a compensatory decrease in meal frequency in the dark phase (De Backer et al., 2010). However, it is still unknown if other brain areas are involved in the effects of SOCS 3 on appetite and feed intake.

The expression profiles of (an)orexigenic hypothalamic neuropeptides were also determined in quail lines divergently selected for feed efficiency. The feed efficiency phenotype was achieved by reduced feed intake in females and increased body weight gain in males, suggesting that the mechanisms involved in the feed efficiency are gender-dependent. Molecular analyses showed that the relative expression of classical hypothalamic neuropeptides such as NPY, POMC, CART, CRF, melanocortin receptors (MC1R, MC2R, MC4R, and MC5R), and orexin was decreased in the high-feed efficient compared to low-feed efficient male quail (Blankenship et al., 2016). In female quail, the above-mentioned genes did not differ between groups, however adiponectin gene expression was lower in high-feed efficient compared to low-feed efficient female quails (Blankenship et al., 2016).

In summary, several lines of chicken and quail have been developed through selection for body weight or feed intake and serve as valuable models for understanding the physiological pathways involved in regulating appetite and whole-body energy homeostasis.

28.7 Other pathways involved in central appetite regulation

28.7.1 Cannabinoids

The active ingredient in marijuana is Δ9-tetrahydrocannabinol (Δ9-THC), and it can bind to the cannabinoid receptors CB1 and CB2 found in the brain. The endogenous ligands for the cannabinoid receptors are 2-arachidonoylglycerol and anandamide, and endogenous antagonists include O-2050 and AM4113. Endogenous cannabinoids are synthesized from phospholipid precursors in the cell membrane, and are typically released post-synaptically and act in a retrograde manner at presynaptic terminals. The CB1 receptor is present in the brain, as well as peripherally, in both birds and mammals, while the CB2 receptor is found on immune and blood cells (Pagotto et al., 2006). While the effects of Δ9-THC on food intake have been mixed, it is generally believed that it causes increased food intake and that decreased food intake is a secondary effect due to sedation (Pagotto et al., 2006). Abel et al. (1972) first showed an increase in food intake in chicks in response to Δ9-THC. Giving an inverse agonist either via the feed or by IV injection attenuated food intake in broiler chicks (Novoseletsky et al., 2011), supporting an orexigenic role for cannabinoids in birds.

28.7.2 AMP-activated protein kinase

AMP-activated protein kinase (AMPK) is a heterotrimeric enzyme complex composed of one catalytic (alpha) subunit and two regulatory (beta and gamma) subunits. AMPK is activated by allosteric regulation of AMP and by phosphorylation of threonine (thr 172) on the alpha subunit by upstream kinases, including liver kinase B1, calcium/calmodulin-dependent protein kinase kinase, and TGF-beta-activated kinase-1. AMPK acts as an energy sensor. Glucose, leptin, and insulin inhibit hypothalamic AMPK activity and decrease food intake in mice, while ghrelin and adiponectin stimulate hypothalamic AMPK activity and increase food intake in rats (Xu et al., 2011a). ICV injection of ghrelin inhibited hypothalamic AMPK gene expression and phosphorylation of the alpha subunit of AMPK. Furthermore, ghrelin was more efficacious in decreasing food intake in low-weight selected birds than in high-weight selected birds, supporting the hypothesis that selection for lower body weight resulted in increased sensitivity to ghrelin and the AMPK system (Xu et al., 2011a). When an AMPK stimulator AICAR and inhibitor Compound C were ICV injected into chicks, AICAR decreased food intake in the low-weight but not high-weight chicks, whereas Compound C increased food

intake in high-weight but not low-weight chicks (Xu et al., 2011b). Further evidence that endogenous AMPK regulates appetite is that dietary supplementation of alpha-lipoic acid, an AMPK inhibitor, decreased food intake in broiler chicks, an effect that was associated with reductions in the activated form of AMPK in the hypothalamus and was not due to taste aversion (Wang et al., 2014b).

28.7.3 Mechanistic target of rapamycin

In addition to its critical role in early brain development, synaptic plasticity, learning, and memory (Hentges et al., 2001; Tang et al., 2002; Ehninger et al., 2008), the highly conserved serine/threonine kinase mechanistic target of rapamycin (mTOR; Brown et al., 1994; Sabatini et al., 1994), plays a crucial and complex role in feed intake control. In 2006, Seeley's group demonstrated that mTOR and its downstream mediators such as the P70 ribosomal S6 protein kinase 1 (S6K1) are co-localized with AgRP- and POMC-expressing neurons in the rat ARC (Cota et al., 2006). Administration of leucine or leptin activated mTOR signaling and reduced feed intake and body weight, and inhibition of mTOR blockaded leptin's anorectic effects (Cota et al., 2006). Leptin was found to increase hypothalamic mTOR activity via the signal transducer and activator of transcription 3 (Buettner et al., 2006), and STATs have been reported to regulate the expression of (an)orexigenic neuropeptides which promote changes in feeding behavior (Münzberg et al., 2003; Ladyman and Grattan, 2013). Deletion of the tumor suppressor TSC1, the major upstream inhibitory regulator of mTOR, in POMC neurons resulted in hyperphagia and an obesity phenotype in mice (Mori et al., 2009). In quail, hypothalamic mTOR mRNA was lower, but STAT1, 5, and 6 were higher in high compared to low-feed efficient males (Blankenship et al., 2016). Lee and Aggrey found that mTOR gene expression was upregulated in the duodenum of chickens divergently selected for low-residual feed intake compared to their high-residual feed intake counterparts (Lee and Aggrey, 2016). Although mechanistic and functional studies are needed, the differential expression of central and peripheral mTOR between high- and low-feed efficient avian (quails and chickens) species suggests that mTOR may play a key role in energy homeostasis regulation.

28.7.4 Autophagy

Autophagy, a cellular self-eating or self-degradative process, was first characterized by Christian De Duve in 1967 (Deter and De Duve, 1967). Originally, autophagy was generally thought of as a programmed cell death called autophagic cell death (Yu et al., 2004, 2006). In more recent years, autophagy was identified as a survival mechanism. It plays a housekeeping role in removing misfolded and aggregated proteins, eliminating intracellular pathogens, and clearing damaged organelles such as endoplasmic reticulum (reticulophagy) and mitochondria (mitophagy) (Lee et al., 2012; Kroemer et al., 2008; Youle and Narendra, 2011). Evidence has emerged to support the role of autophagy in the regulation of energy homeostasis. Firstly, autophagy is activated not only by cellular damage, but also by starvation (Lin et al., 2012). When nutrients are scarce, autophagy allows cells to reutilize their own constituents for energy. More recently, Meng and Cai showed, by using site-specific deletion of autophagy related gene (Atg7) in the mediobasal hypothalamus, that inhibition of central autophagy increased feed intake and reduced energy expenditure (Meng and Cai, 2011) and demonstrated that this effect was mediated through the NF-κB pathway. Kaushik et al. (2011) demonstrated that starvation increased hypothalamic uptake of free fatty acids (FFAs) to make triglycerides within neuronal lipid droplets. This, in turn, leads to induction of neuronal autophagy that degrades lipid droplets (lipophagy) and generates neuron-intrinsic FFA, which induce the hypothalamic expression of AgRP and promote feed intake (Kaushik et al., 2011). Blocking lipophagy in AgRP-expressing neurons upregulated the hypothalamic levels of POMC and its cleavage product α-MSH leading to decreased feed intake in response to feed deprivation (Kaushik et al., 2011). Quan et al. (2012), on the other hand, generated a mouse model with site-specific deletion of Atg7 in hypothalamic POMC neurons and identified a key role in feeding behavior and leptin signaling. In chickens, Piekarski-Welsher et al. (2018) reported that autophagy machinery was enhanced in high-feed efficient compared to low-feed efficient pedigree male broilers. ICV administration of human recombinant leptin reduced feed intake, induced autophagic machinery, and modulated the hypothalamic expression of feeding-related neuropeptides in chickens (Piekarski et al., 2018). Together these studies indicate that autophagy may regulate feeding behavior in chickens which merits further in-depth mechanistic and functional studies.

References

Abbasnejad, M., Jonaidi, H., Denbow, D.M., Pour Rahimia, A.M., 2005. Feeding and locomotion responses to centrally injected nociceptin/orphanin FQ in chicks. Physiol. Behav. 85, 383–386.

Abel, E.L., McMillan, D.E., Harris, L.S., 1972. Tolerance to the behavioral and hypothermic effects of 1-9-tetrahydrocannabinol in neonatal chicks. Experientia 28, 1188–1189.

Ashwell, C.M., Czerwinski, S.M., Brocht, D.M., McMurtry, J.P., 1999. Hormonal regulation of leptin expression in broiler chickens. Am. J. Physiol. 276, R226–R232.

Baghbanzadeh, A., Hajinezhad, M.R., Shohreh, B., Maleklou, R., 2010. Intralateral hypothalamic area injection of isoproterenol and propranolol affects food and water intake in broilers. J. Comp. Physiol. A 196, 221–226.

Bermudez, F.F., Forbes, J.M., Injidi, M.H., 1983. Involvement of melatonin and thyroid hormones in the control of sleep, food intake and energy metabolism in the domestic fowl. J. Physiol. 337, 19–27.

Blankenship, K., Gilley, A., Piekarski, A., Orlowski, S., Greene, E., Bottje, W., Anthony, N., Dridi, S., 2016. Differential expression of feeding-related hypothalamic neuropeptides in the first generation of quails divergently selected for low or high feed efficiency. Neuropeptides 58, 31–40.

Blomqvist, A.G., Soderberg, C., Lundell, I., Milner, R.J., Larhammar, D., 1992. Strong evolutionary conservation of neuropeptide Y: sequences of chicken, goldfish, and *Torpedo marmorata* DNA clones. Proc. Natl. Acad. Sci. U.S.A. 89, 2350–2354.

Bohler, M., Dougherty, C., Tachibana, T., Gilbert, E.R., Cline, M.A., 2019. Gastrin releasing peptide-induced satiety is associated with hypothalamic and brainstem changes in chicks. Neurosci. Lett. 713, 134529.

Bordas, A., Merat, P., 1981. Genetic variation and phenotypic correlations of food consumption of laying hens corrected for body weight and production. Br. Poult. Sci. 22, 25–33.

Boswell, T., Li, Q., Takeuchi, S., 2002. Neurons expressing neuropeptide Y mRNA in the infundibular hypothalamus of Japanese quail are activated by fasting and co-express agouti-related protein mRNA. Mol. Brain Res. 100, 31–42.

Boswell, T., Sharp, P.J., Hall, M.R., Goldsmith, A.R., 1995. Migratory fat deposition in European quail: a role for prolactin? J. Endocrinol. 146, 71–79.

Bray, G.A., 1991. Obesity, a disorder of nutrient partitioning: the MONA LISA hypothesis. J. Nutr. 121, 1146–1162.

Brunetti, L., Recinella, L., De Nisio, C., Chiavaroli, A., Leone, S., Ferrante, C., Orlando, G., Vacca, M., 2012. Effects of visfatin/PBEF/NAMPT on feeding behavior and hypothalamic neuromodulators in the rat. J. Biol. Reg. Homeost. Agents 26, 295–302.

Broberger, C., 1999. Hypothalamic cocaine-and amphetamine-regulated transcript (CART) neurons: histochemical relationship to thyrotropin releasing hormone, melanin-concentrating hormone, orexin/hypocretin and neuropeptide. Y. Brain Res. 848, 101–113.

Brown, E.J., Albers, M.W., Shin, T.B., Ichikawa, K., Keith, C.T., Lane, W.S., Schreiber, S.L., 1994. A mammalian protein targeted by G1-arresting rapamycin-receptor complex. Nature 369, 756–758.

Buettner, C., Pocai, A., Muse, E.D., Etgen, A.M., Myers, M.G., Rossetti, L., 2006. Critical role of STAT3 in leptin's metabolic actions. Cell Metabol. 4, 49–60.

Bungo, T., Ando, R., Kawakami, S.-I., Ohgushi, A., Shimojo, M., Masuda, Y., Furuse, M., 2000. Central bombesin inhibits food intake and the orexigenic effect of neuropeptide Y in the neonatal chick. Physiol. Behav. 70, 573–576.

Bungo, T., Furuse, M., 2001. Glucagon-like peptide-1 (7–36) amide (GLP-1) is a potent satiety agent in chickens. In: Dawson, A., Chaturvedi, C.M. (Eds.), Avian Endocrinology. Narosa Publishing House, New Delhi, India, pp. 337–348.

Bungo, T., Izumi, T., Kawamura, K., Takagi, T., Ueda, H., Furuse, M., 2003. Intracerebroventricular injection of muscimol, baclofen or nipecotic acid stimulates food intake in layer-type, but not meat-type, chicks. Brain Res. 993, 235–238.

Bungo, T., Kawamura, K., Izumi, T., Dodo, K.-I., Ueda, H., 2004. Feeding responses to μ-, δ- and κ-opioid receptor agonists in the meat-type chick. Pharmacol. Biochem. Behav. 78, 707–710.

Bungo, T., Shimojo, M., Masuda, Y., Choi, Y.-H., Denbow, D.M., Furuse, M., 1999. Induction of food intake by a noradrenergic system using clonidine and fusaric acid in the neonatal chick. Brain Res. 826, 313–316.

Bungo, T., Yanagita, K., Shiraishi, J., 2010. Feed intake after infusion of noradrenalin, dopamine or its precursor into the lateral ventricles in neonatal chicks. J. Anim. Vet. Adv. 9, 760–763.

Bungo, T., Shiraishi, J.-I., Kawakami, S.-I., 2011. Feeding responses to central glutamatergic receptor agonist administration in meat-type chicks. J. Anim. Vet. Adv. 10, 955–958.

Bungo, T., Shiraishi, J.-I., Yanagita, Y., Ohta, Y., Fujita, M., 2009. Effect of nociceptin/orphanin FQ on feeding behavior and hypothalamic neuropeptide expression in layer-type chicks. Gen. Comp. Endocrinol. 163, 47–51.

Burkhart, C.A., Cherry, J.A., Van Krey, H.P., Siegel, P.B., 1983. Genetic selection for growth rate alters hypothalamic satiety mechanism in chickens. Behav. Genet. 13, 295–300.

Buzala, M., Janicki, B., 2016. Review: effects of different growth rates in broiler breeder and layer hens on some productive traits. Poult. Sci. 95, 2151–2159.

Clark, C.E.F., Akter, Y., Hungerford, A., Thomson, P., Islam, M.R., Groves, P.J., O'Shea, C.J., 2019. The intake pattern and feed preference of layer hens selected for high or low feed conversion ratio. PLoS One 14 (9), e0222304.

Cline, M.A., Bowden, C.N., Nandar, W., Rogers, J.O., 2008a. Central oxyntomodulin causes anorexigenic effects associated with the hypothalamus and alimentary canal in chicks (*Gallus gallus*). Comp. Biochem. Physiol. A Mol. Integr. Physiol. 149, 405–410.

Cline, M.A., Fouse, D., Prall, B.C., 2008b. Central and peripheral alytesin cause short-term anorexigenic effects in neonatal chicks. Neuropeptides 42, 283–291.

Cline, M.A., Nandar, W., Prall, B.C., Bowden, C.N., Denbow, D.M., 2008c. Central visfatin causes orexigenic effects in chicks. Behav. Brain Res. 186, 293–297.

Cline, M.A., Nandar, W., Smith, M.L., Pittman, B.H., Kelly, M., Rogers, J.O., 2008d. Amylin causes anorexigenic effects via the hypothalamus and brain stem in chicks. Regul. Pept. 146, 140–146.

Cline, M.A., Calchary, W., Nandar, W., 2009a. Effect of calcitonin gene-related peptide (CGRP) on avian appetite-related processes. Behav. Brain Res. 196, 242–247.

Cline, M.A., Kuo, A., Smith, M., Nandar, W., Prall, B.C., Siegel, P.B., Denbow, D.M., 2009b. Differential food intake responses to central corticotrophin releasing factor in lines of chickens divergently selected for low or high body weight. Comp. Biochem. Physiol. A Mol. Integr. Physiol. 152, 130–134.

Cline, M.A., Layne, J.E., Calchary, W.A., Sheehy, R.S., Tachibana, T., Furuse, M., 2009c. LPLRFamide causes anorexigenic effects in broiler chicks and bobwhite quail. Gen. Comp. Endocrinol. 165, 315–320.

Cline, M.A., Prall, B., Rogers, J.O., Tachibana, T., 2009d. Satiety induced by central stresscopin is mediated by corticotrophin-releasing factor receptors and hypothalamic changes in chick. Pharmacol. Biochem. Behav. 92, 663–669.

Cline, M.A., Cofield, S.A., Tachibana, T., 2010a. Central litorin injection is associated with primary anorexigenic effects that coincide with activation of the magnocellular division of the paraventricular nucleus. Neuropeptides 44, 247–252.

Cline, M.A., Nandar, W., Bowden, C., Calchary, W., Smith, M., Prall, B., Newmyer, B., Rogers, J.O., Siegel, P.B., 2010b. The threshold of amylin-induced anorexia is lower in chicks selected for low compared to high juvenile body weight. Behav. Brain Res. 208, 650–654.

Cline, M.A., Siders, R., Newmyer, B.A., Smith, M.L., Siegel, P.B., 2010c. Both calcitonin and calcitonin gene-related peptides' thresholds of hypophagia are considerably lower in chicks selected for high rather than low juvenile body weight. Physiol. Behav. 101, 254–259.

Cline, M.A., Furuse, M., 2012. Neuropeptide regulation of food intake in chicks. In: Morrison, J.L. (Ed.), Food Intake: Regulation, Assessing and Controlling. Nova Science Publishers, Inc., NY.

Cline, M.A., Mathews, D., 2008. Anoretic effects of neuropeptide FF are mediated via central mu and kappa subtypes of opioid receptors and receptor ligands. Gen. Comp. Endocrinol. 159, 125–129.

Cline, M.A., Nandar, W., Rogers, J.O., 2007a. Central neuropeptide FF reduces feed consumption and affects hypothalamic chemistry in chicks. Neuropeptides 41, 433–439.

Cline, M.A., Nandar, W., Rogers, J.O., 2007b. Xenin reduces feed intake by activating the ventromedial hypothalamus and influences gastrointestinal transit time in chicks. Behav. Brain Res. 179, 28–32.

Cota, D., Proulx, K., Smith, K.A., Kozma, S.C., Thomas, G., Woods, S.C., Seeley, R.J., 2006. Hypothalamic mTOR signaling regulates food intake. Science 312, 927–930.

De Backer, M.W.A., Brans, M.A.D., Van Rozen, A.J., Van der Zwaal, E.M., Luijendijk, M.C.M., Garner, K.G., de Krom, M., Van Beekum, O., La Fleur, S.E., Adan, R.A.H., 2010. J. Mol. Endocrinol. 45, 341–353.

Delp, M.S., Cline, M.A., Gilbert, E.R., 2017. The central effects of alpha-melanocyte stimulating hormone (alpha-MSH) in chicks involve changes in gene expression of neuropeptide Y and other factors in distinct hypothalamic nuclei. Neurosci. Lett. 651, 52–56.

Denbow, D.M., 1983. Food intake and temperature response to injections of catecholamines into the lateral ventricle of the Turkey brain. Poult. Sci 62, 1088–1092.

Denbow, D.M., 1989. Centrally and peripherally administered bombesin decreases food intake in turkeys. Peptides 10, 275–279.

Denbow, D.M., 1994. Peripheral regulation of food intake. J. Nutr. 124, 1349S–1354S.

Denbow, D.M., 1999. Food intake regulation in birds. J. Exp. Zool. 283, 333–338.

Denbow, D.M., 2000. Gastrointestinal anatomy and physiology. In: Whittow, G.C. (Ed.), Avian Physiology, fifth ed. Academic Press, Orlando, Florida.

Denbow, D.M., Cherry, J.A., Siegel, P.B., Van Krey, H.P., 1981. Eating, drinking and temperature response of chicks to brain catecholamine injections. Physiol. Behav. 27, 265–269.

Denbow, D.M., Cherry, J.A., Van Krey, H.P., Siegel, P.B., 1982. Food and water intake following injection of glucose into the lateral ventricle of the brain of broiler-type chicks. Poult. Sci. 61, 1713–1719.

Denbow, D.M., Duke, G.E., Chaplin, S.B., 1988. Food intake, gastric secretion, and motility as affected by avian pancreatic polypeptide administered centrally in chickens. Peptides 9, 449–454.

Denbow, D.M., Meade, S., Robertson, A., McMurtry, J.P., Richards, M., Ashwell, C., 2000. Leptin induced decrease in food intake in chickens. Physiol. Behav. 69, 359–362.

Denbow, D.M., Myers, R.D., 1982. Eating, drinking, and temperature responses to intracerebroventricular cholecystokinin in the chick. Peptides 3, 739–743.

Denbow, D.M., Sheppard, B.J., 1993. Food and water intake responses of the domestic fowl to norepinephrine infusion at circumscribed neural sites. Brain Res. Bull. 31, 121–128.

Denbow, D.M., Snapir, N., Furuse, M., 1999. Inhibition of food intake by CRF in chickens. Physiol. Behav. 66, 645–649.

Denbow, D.M., Van Krey, H.P., Lacy, M.P., Dietrick, T.J., 1983. Feeding, drinking and body temperature of Leghorn chicks: effects of ICV injections of biogenic amines. Physiol. Behav. 31, 85–90.

Deter, R.L., De Duve, C., 1967. Influence of glucagon, an inducer of cellular autophagy, on some physical properties of rat liver lysosomes. J. Cell Biol. 33, 437–449.

Dockray, G.J., Reeve Jr., J.R., Shively, J., Gayton, R.J., Barnard, C.S., 1983. A novel active pentapeptide from chicken brain identified by antibodies to FMRFamide. Nature 305, 328–330.

Dodo, K.-I., Izumi, T., Ueda, H., Bungo, T., 2005. Response of neuropeptide Y-induced feeding to μ-, δ- and κ-opioid receptor antagonists in the neonatal chick. Neurosci. Lett. 373, 85–88.

Dong, X.Y., He, J.M., Tang, S.Q., Li, H.Y., Jiang, Q.Y., Zou, X.T., 2009. Is GPR39 the natural receptor of obestatin? Peptides 30, 431–438.

Dunnington, E.A., Siegel, P.B., 1984. Thermoregulation in newly hatched chicks. Poult. Sci 63, 1303–1313.

Dunnington, E.A., Siegel, P.B., 1996. Long-term divergent selection for eight-week body weight in white Plymouth Rock chickens. Poult. Sci. 75, 1168–1179.

Dunnington, E.A., Siegel, P.B., Cherry, J.A., Soller, M., 1983. Relationship of age and body weight at sexual maturity in selected lines of chickens. Arch. Geflugelk. 47, 85–89.

Dunnington, E.A., Siegel, P.B., Cherry, J.A., 1984. Delayed sexual maturity as a correlated response to selection for reduced 56-day body weight in White Plymouth Rock pullets. Arch. Geflugelk. 48, 111–113.

Ehninger, D., Han, S., Shilyansky, C., Zhou, Y., Li, W., Kwiatkowski, D.J., Ramesh, V., Silva, A.J., 2008. Reversal of learning deficits in a Tsc2+/- mouse model of tuberous sclerosis. Nat. Med. 14, 843–848.

Ellacott, K.L., Lawrence, C.B., Rothwell, N.J., Luckman, S.M., 2002. PRL-releasing peptide interacts with leptin to reduce food intake and body weight. Endocrinology 143, 368–374.

Emadi, L., Jonaidi, H., Hosseini Amir Abad, E., 2011. The role of central CB2 cannabinoid receptors on food intake in neonatal chicks. J. Comp. Physiol. A 197, 1143–1147.

Filippatos, T.D., Derdemezis, C.S., Kiortsis, D.N., Tselepis, A.D., Elisaf, M.S., 2007. Increased plasma levels of visfatin/pre-B cell colony enhancing factor in obese and overweight patients with metabolic syndrome. J. Endocrinol. Invest. 30, 323–326.

Foreman, R., Leaf, M., Buntin, J.P., 1990. Changes in feeding activity, plasma luteinizing hormone and testes weight in ring doves following hypothalamic injections of prolactin. J. Neuroendocrinol. 2, 667–673.

Friedman-Einat, M., Boswell, T., Horev, G., Girishvarma, G., Dunn, I.C., Talbot, R.T., Sharp, P.J., 1999. The chicken leptin gene: has it been cloned? Gen. Comp. Endocrinol. 115, 354–363.

Friedman-Einat, M., Cogburn, L.A., Yosefi, S., Hen, G., Shinder, D., Shirak, A., Seroussi, E., 2014. Discovery and characterization of the first genuine avian leptin gene in the rock dove (*Columba livia*). Endocrinology 155, 3376–3384.

Friedman-Einat, M., Seroussi, E., 2014. Quack leptin. BMC Genom. 15, 551.

Friedman, J.M., Halaas, J.L., 1998. Leptin and the regulation of body weight in mammals. Nature 395, 763–770.

Fukuhara, A., Matsuda, M., Nishizawa, M., Segawa, K., Tanaka, M., Kishimoto, K., Matsuki, Y., Murakami, M., Ichisaka, T., Murakami, H., Watanabe, E., Takagi, T., Akiyoshi, M., Ohtsubo, T., Kihara, S., Yamashita, S., Makishima, M., Funahashi, T., Yamanaka, S., Hiramatsu, R., Matsuzawa, Y., Shimomura, I., 2005. Visfatin: a protein secreted by visceral fat that mimics the effects of insulin. Science 307, 426–430.

Furuse, M., Ao, R., Bungo, T., Ando, R., Shimojo, M., Masuda, Y., Saito, N., 1999. Central gastrin inhibits feeding behavior and food passage in neonatal chicks. Life Sci. 65, 305–311.

Furuse, M., Bungo, T., Ao, R., Ando, R., Shimojo, M., Masuda, Y., Denbow, D.M., 2000. Involvement of central gastrin and cholecystokinin in the regulation of food intake in the neonatal chick. J. Appl. Anim. Res. 18, 129–136.

Furuse, M., Matsumoto, M., Saito, N., Sugahara, K., Hasegawa, S., 1997. The central corticotrophin-releasing factor and glucagon-like peptide-1 in food intake of the neonatal chick. Eur. J. Pharmacol. 339, 211–213.

Furuse, M., Tachibana, T., Ohgushi, A., Ando, R., Yoshimatsu, T., Denbow, D.M., 2001. Intracerebroventricular injection of ghrelin and growth hormone releasing factor inhibits food intake in neonatal chicks. Neurosci. Lett. 301, 123–126.

Furuse, M., Yamane, H., Tomonaga, S., Tsuneyoshi, Y., Denbow, D.M., 2007. Neuropeptidergic regulation of food intake in the neonatal chick: a review. Poult. Sci. 44, 349–356.

Geelissen, S.M., Swennen, Q., Geyten, S.V., Kuhn, E.R., Kaiya, H., Kangawa, K., Decuypere, E., Buyse, J., Darras, V.M., 2006. Peripheral ghrelin reduces food intake and respiratory quotient in chicken. Domest. Anim. Endocrinol. 30, 108–116.

Harrold, J.A., Widdowson, P.S., Williams, G., 2003. beta-MSH: a functional ligand that regulated energy homeostasis via hypothalamic MC4-R? Peptides 24, 397–405.

Hagen, C.J., Newmyer, B.A., Webster, R.I., Gilbert, E.R., Siegel, P.B., Tachibana, T., Cline, M.A., 2013. Stimulation of food intake after central galanin is associated with arcuate nucleus activation and does not differ between genetically selected low and high body weight lines of chickens. Neuropeptides 47, 281–285.

Hentges, K.E., Sirry, B., Gingeras, A.C., Sarbassov, D., Sonenberg, N., Sabatini, D., Peterson, A.S., 2001. FRAP/mTOR is required for proliferation and patterning during embryonic development in the mouse. Proc. Natl. Acad. Sci. U.S.A. 98, 13796–13801.

Hinuma, S., Habata, Y., Fujii, R., Kawamata, Y., Hosoya, M., Fukusumi, S., Kitada, C., Masuo, Y., Asano, T., Matsumoto, H., Sekiguchi, M., Kurokawa, T., Nishimura, O., Onda, H., Fujino, M.A., 1998. A prolactin releasing peptide in the brain. Nature 393, 272–276.

Hocking, P.M., Bernard, R., 1993. Evaluation of putative appetite suppressants in the domestic fowl (*Gallus domesticus*). Br. Poult. Sci. 34, 393–404.

Honda, K., Kamisoyama, H., Saito, N., Kurose, Y., Sugahara, K., Hasegawa, S., 2007a. Central administration of glucagon suppresses food intake in chicks. Neurosci. Lett. 416, 198–201.

Honda, K., Kamisoyama, H., Saneyasu, T., Sugahara, K., Hasegawa, S., 2007b. Central administration of insulin suppresses food intake in chicks. Neurosci. Lett. 423, 153–157.

Horev, G., Einat, P., Aharoni, T., Eshdat, Y., Friedman-Einat, M., 2000. Molecular cloning and properties of the chicken leptin-receptor (CLEPR) gene. Mol. Cell. Endocrinol. 162, 95–106.

Huang, G., Li, J., Wang, H., Lan, X., Wang, Y., 2014. Discovery of a novel functional leptin protein (LEP) in zebra finches: evidence for the existence of an authentic avian leptin gene predominantly expressed in the brain and pituitary. Endocrinology 155, 3385–3396.

Hussain, S.S., Bloom, S.R., 2013. The regulation of food intake by the gut-brain axis: implications for obesity. Int. J. Obes. 37, 625–633.

Jambui, M., Honaker, C.F., Siegel, P.B., 2017. Correlated responses to long-term divergent selection for 8-week body weight in female White Plymouth Rock chickens: sexual maturity. Poult. Sci. 96, 3844–3851.

Jonaidi, H., Babapour, V., Denbow, D.M., 2002. GABAergic control of food intake in meat-type chickens. Physiol. Behav. 76, 465–468.

Jonaidi, H., Noori, Z., 2012. Neuropeptide Y-induced feeding is dependent on GABAA receptors in neonatal chicks. J. Comp. Physiol. A 198, 827–832.

Kaiya, H., Saito, E.S., Tachibana, T., Furuse, M., Kangawa, K., 2007. Changes in ghrelin levels of plasma and proventriculus and ghrelin mRNA of proventriculus in fasted and refed layer chicks. Domest. Anim. Endocrinol. 32, 247–259.

Katayama, S., Hamasu, K., Shigemi, K., Cline, M.A., Furuse, M., 2010a. Intracerebroventricular injection of orexin-A, but not orexin-B, induces arousal of layer-type neonatal chicks. Comp. Biochem. Physiol. A Mol. Integr. Physiol. 157, 132–135.

Katayama, S., Tomonaga, S., Sato, M., Yamane, H., Tsuneyoshi, Y., Denbow, D.M., Furuse, M., 2010b. Norepinephrine does not alter NPY and POMC mRNA expression in neonatal chicks. Comp. Biochem. Physiol. A 156, 143–146.

Kaushik, S., Rodriguez-Navarro, J.A., Arias, E., Kiffin, R., Sahu, S., Schwartz, G., Guervo, A.M., Singh, R., 2011. Autophagy in hypothalamic AgRP neurons regulates food intake and energy balance. Cell. Metab. 14, 173–183.

Kawakami, S.-I., Bungo, T., Ando, R., Ohgushi, A., Shimojo, M., Masuda, Y., Furuse, M., 2000. Central administration of α-melanocyte stimulating hormone inhibits fasting- and neuropeptide Y-induced feeding in neonatal chicks. Eur. J. Pharmacol. 398, 361–364.

Khan, M.S., Cline, M.A., Aramaki, T., Ueda, H., Tachibana, T., 2013. Feeding response following central administration of chicken vasoactive intestinal peptide in chicks. Gen. Comp. Endocrinol. 184, 61–66.

Khan, M.S.I., Nakano, Y., Tachibana, T., Ueda, H., 2008. Nitric oxide synthase inhibitor attenuates the anorexigenic effect of corticotropin releasing hormone in neonatal chicks. Comp. Biochem. Physiol. A Mol. Integr. Physiol. 149, 325–329.

Khan, M.S.I., Ohkubo, T., Masuda, N., Tachibana, T., Ueda, H., 2009. Central administration of metastin increases food intake through opioid neurons in chicks. Comp. Biochem. Physiol. A Mol. Integr. Physiol. 153, 209–212.

Khan, M.S.I., Tachibana, T., Hasebe, Y., Masuda, N., Ueda, H., 2007. Peripheral or central administration of nitric oxide synthase inhibitor affects feeding behavior in chicks. Comp. Biochem. Physiol. A 148, 458–462.

Kroemer, G., Levine, B., 2008. Autophagic cell death: the story of a misnomer. Nat. Rev. Mol. Cell Biol. 9, 1004–1010.

Kubota, N., Yano, W., Kubota, T., Yamauchi, T., Itoh, S., Kumagai, H., Kozono, H., Takamoto, I., Okamoto, S., Shiuchi, T., Suzuki, R., Satoh, H., Tsuchida, A., Moroi, M., Sugi, K., Noda, T., Ebinuma, H., Ueta, Y., Kondo, T., Araki, E., Ezaki, O., Nagai, R., Tobe, K., Terauchi, Y., Ueki, K., Minokoshi, Y., Kadowaki, T., 2007. Adiponectin stimulates AMP-activated protein kinase in the hypothalamus and increases food intake. Cell Metabol. 6 (1), 55–68.

Kuenzel, W.J., 1994. Central neuroanatomical systems involved in the regulation of food intake in birds and mammals. J. Nutr. 124, 1355S–1370S.

Kuenzel, W.J., Beck, M.M., Teruyama, R., 1999. Neural sites and pathways regulating food intake in birds: a comparative analysis to mammalian systems. J. Exp. Zool. 283, 348–364.

Kuenzel, W.J., Douglass, L.W., Davison, B.A., 1987. Robust feeding following central administration of neuropeptide Y or peptide YY in chicks, *Gallus domesticus*. Peptides 8, 823–828.

Kuenzel, M.J., McMurtry, J., 1988. Neuropeptide Y: brain localization and central effects on plasma insulin levels in chicks. Physiol. Behav. 44, 669–678.

Kuo, A.Y., Lee, J.C., Siegel, P.B., Denbow, D.M., 2001. Differential cardiovascular effects of pharmacological agents in chickens selected for high and low body weight. Physiol. Behav. 74, 573–579.

Ladyman, S.R., Grattan, D.R., 2013. JAK-STAT and feeding. JAKSTAT 2, e23675.

Lawrence, C.B., Celsi, F., Brennand, J., Luckman, S.M., 2000. Alternative role for prolactin-releasing peptide in the regulation of food intake. Nat. Neurosci. 3, 645–646.

Larhammar, D., 1996. Evolution of neuropeptide Y, peptide YY and pancreatic polypeptide. Regul. Pept. 62, 1–11.

Lawrence, C.B., Ellacott, K.L., Luckman, S.M., 2002. PRL-releasing peptide reduces food intake and may mediate satiety signaling. Endocrinology 143, 360–367.

Layne, J.L., Hunt, K.E., True, T., Gill, R.S., Combos, R.E., Cline, M.A., 2009. Central calcitonin exerts anorectic effects via the hypothalamus in chicks. Pharmacol. Biochem. Behav. 92, 433–438.

Lear, T., Liu, L., O'Donnell, M., McConn, B.R., Denbow, D.M., Cline, M.A., Gilbert, E.R., 2017. Alpha-melanocyte stimulating hormone-induced anorexia in Japanese quail (*Coturnix japonica*) likely involves the ventromedial hypothalamus and paraventricular nucleus of the hypothalamus. Gen. Comp. Endocrinol. 252, 97–102.

Lee, I.H., Kawai, Y., Fergusson, M.M., Rovira, I.I., Bishop, A.J.R., Motoyama, N., Cao, L., Finkel, T., 2012. Atg7 modulates p53 activity to regulate cell cycle and survival during metabolic stress. Science 336, 225–228.

Lee, J., Aggrey, S.E., 2016. Transcriptomic differences of genes in the avian target of rapamycin (avTOR) pathway in a divergent line of meat-type chickens selected for feed efficiency. Gene. Molec. Res. 15 (2). https://doi.org/10.4238/gmr.15027120.

Li, Z., Liu, X., Zhang, P., Han, R., Sun, G., Jiang, R., Wang, Y., Liu, X., Li, W., Kang, X., Tian, Y., 2018. Comparative transcriptome analysis of hypothalamus-regulated feed intake induced by exogenous visfatin in chicks. BMC Genom. 19, 249.

Lin, L., Chen, Y., Gibson, S.B., 2012. Starvation-induced autophagy is regulated by mitochondrial reactive oxygen species leading to AMPK activation. Cell. Signal. 25, 50–65.

Ling, M.K., Hotta, E., Kilianova, Z., Haitina, T., Ringholm, A., Johansson, L., Gallo-Payet, N., Takeuchi, S., Schiöth, H.B., 2004. The melanocortin receptor subtypes in chicken have high preference to ACTH-derived peptides. Br. J. Pharmacol. 143, 626–637.

Mace, J.D., Tachibana, T., Wang, G., Newmyer, B.A., Guilliams, E., Gilbert, E.R., Cline, M.A., 2014. Substance P is associated with hypothalamic paraventricular nucleus activation that coincides with increased urotensin 2 mRNA in chicks. Neuropeptides 48, 305–311.

Marquez, G.C., Siegel, P.B., Lewis, R.M., 2010. Genetic diversity and population structure in lines of chickens divergently selected for high and low 8-week body weight. Poult. Sci. 89, 2580–2588.

Masunari, K., Cline, M.A., Khan, S.I., Tachibana, T., 2016. Feeding response following central administration of mesotocin and arginine-vasotocin receptor agonists in chicks (*Gallus gallus*). Physiol. Behav. 153, 149–154.

Masunari, K., Khan, M.S., Cline, M.A., Tachibana, T., 2013. Central administration of mesotocin inhibits feeding behavior in chicks. Regul. Pept. 187, 1–5.

Matias, J.A., Gilbert, E.R., Denbow, D.M., Cline, M.A., 2017. Effects of intracerebroventricular injection of rosiglitazone on appetite-associated parameters in chicks. Gen. Comp. Endocrinol. 246, 99–104.

McConn, B.R., Wang, G., Yi, J., Gilbert, E.R., Osugi, T., Ubuka, T., Tsutsui, K., Chowdhury, V.S., Furuse, M., Cline, M.A., 2014. Gonadotropin-inhibitory hormone-stimulation of food intake is mediated by hypothalamic effects in chicks. Neuropeptides 48, 327–334.

McConn, B.R., Cline, M.A., Gilbert, E.R., 2018a. Dietary macronutrient composition and central neuropeptide Y injection affect dietary preference and hypothalamic gene expression in chicks. Nutr. Neurosci. 21, 403–413.

McConn, B.R., Gilbert, E.R., Cline, M.A., 2018b. Appetite-associated responses to central neuropeptide Y injection in quail. Neuropeptides 69, 9–18.

McConn, B.R., Koskinen, A., Denbow, D.M., Gilbert, E.R., Siegel, P.B., Cline, M.A., 2019a. Central injection of oxytocin reduces food intake and affects hypothalamic and adipose tissue gene expression in chickens. Domest. Anim. Endocrinol. 67, 11–20.

McConn, B.R., Matias, J., Wang, G., Cline, M.A., Gilbert, E.R., 2018c. Dietary macronutrient composition affects hypothalamic appetite regulation in chicks. Nutr. Neurosci. 21, 49–58.

McConn, B.R., Newmyer, B.A., St John, N., Tachibana, T., Gilbert, E.R., Cline, M.A., 2019b. The anorexigenic effect of neuropeptide K in chicks involves the paraventricular nucleus and arcuate nucleus of the hypothalamus. Peptides 122, 170157.

McConn, B.R., Park, J., Gilbert, E.R., Cline, M.A., 2015. A novel role for xenopsin: stimulation of food intake. Behav. Brain Res. 292, 500–507.

McConn, B.R., Siegel, P.B., Cline, M.A., Gilbert, E.R., 2019c. Anorexigenic effects of mesotocin in chicks are genetic background-dependent and are associated with changes in the paraventricular nucleus and lateral hypothalamus. Comp. Biochem. Physiol. A Mol. Integr. Physiol. 232, 79–90.

McConn, B.R., Tachibana, T., Gilbert, E.R., Cline, M.A., 2020. Prolactin-releasing peptide increases food intake and affects hypothalamic physiology in Japanese quail (*Coturnix japonica*). Domest. Anim. Endocrinol. 72, 106464.

McConn, B.R., Yi, J., Gilbert, E.R., Siegel, P.B., Chowdhury, V.S., Furuse, M., Cline, M.A., 2016. Stimulation of food intake after central administration of gonadotropin-inhibitory hormone is similar in genetically selected low and high body weight lines of chickens. Gen. Comp. Endocrinol. 232, 96–100.

McCormack, J.F., Denbow, D.M., 1989. Ingestive responses to mu and delta opioid receptor agonists in the domestic fowl. Br. Poult. Sci. 30, 343–356.

Meade, S., Denbow, D.M., 2001. Feeding, drinking and temperature responses of chickens to intracerebroventricular histamine. Physiol. Behav. 73, 65–73.

Meade, S., Denbow, D.M., 2003. The interaction of bombesin and corticotropin-releasing hormone on ingestive behavior in the domestic fowl. Physiol. Behav. 78, 611–614.

Meng, Q., Cai, D., 2011. Defective hypothalamic autophagy directs the central pathogenesis of obesity via the IκB kinase β (IKKβ)/NF-κB pathway. J. Biol. Chem. 286, 32324–32332.

Mercer, R.E., Chee, M.J., Colmers, W.F., 2011. The role of NPY in hypothalamic mediated food intake. Front. Neuroendocrinol. 32, 398–415.

Miller, R.A., Riddle, O., 1943. Effects of prolactin and corticohormones on body weight and food intake on adrenalectomized pigeons. Exp. Biol. Med. 52, 231–233.

Mori, H., Inoki, K., Münzberg, H., Opland, D., Faouzi, M., Villanueva, E.C., Ikenoue, T., Kwiatkowski, D., MacDougald, O.A., Myers, M.G., Guan, K.L., 2009. Critical role for hypothalamic mTOR activity in energy balance. Cell Metabol. 9, 362–374.

Münzberg, H., Huo, L., Nillni, E.A., Hollenberg, A.N., Bjørbaek, C., 2003. Role of signal transducer and activator of transcription 3 in regulation of hypothalamic proopiomelanocortin gene expression by leptin. Endocrinology 144, 2121–2131.

Nelson, L.A., Gilbert, E.R., Cline, M.A., 2015. Effects of dietary macronutrient composition on exogenous neuropeptide Y's stimulation of food intake in chicks. Neurosci. Lett. 591, 171–175.

Newmyer, B.A., Nandar, W., Webster, R.I., Gilbert, E., Siegel, P.B., Cline, M.A., 2013. Neuropeptide Y is associated with changes in appetite-associated hypothalamic nuclei but not food intake in a hypophagic avian model. Behav. Brain Res. 236, 327–331.

Noble, D.O., Picard, M.L., Dunnington, E.A., Uzu, G., Larsen, A.S., Siegel, P.B., 1993. Food intake adjustments of chicks: short term reactions of genetic stocks to deficiencies in lysine, methionine or tryptophan. Br. Poult. Sci. 34, 725–735.

Novoseletsky, N., Nussinovitch, A., Friedman-Einat, M., 2011. Attenuation of food intake in chicks by an inverse agonist of cannabinoid receptor 1 administered by either injection or ingestion in hydrocolloid carriers. Gen. Comp. Endocrinol. 170, 522–527.

Ogino, M., Okumura, A., Khan, M.S., Cline, M.A., Tachibana, T., 2014. Comparison of brain urocortin-3 and corticotrophin-releasing factor for physiological responses in chicks. Physiol. Behav. 125, 57–61.

Ohkubo, T., Nishio, M., Tsurudome, M., Ito, M., Ito, Y., 2007. Existence of leptin receptor protein in chicken tissues: isolation of a monoclonal antibody against chicken leptin receptor. Gen. Comp. Endocrinol. 151, 269–273.

Pagotto, U., Marsicano, G., Cota, D., Lutz, B., Pasquali, R., 2006. The emerging role of the endocannabinoid system in endocrine regulation and energy balance. Endocr. Rev. 27, 73–100.

Pauliukonis, A.C., Buenaventura, C., Cline, M.A., Gilbert, E.R., 2020. Anorexigenic effects of substance P in *Coturnix japonica*. Neuropeptides 102045.

Phillips-Singh, D., Li, Q., Takeuchi, S., Ohkubo, T., Sharp, P.J., Boswell, T., 2003. Fasting differentially regulates expression of agouti-related peptide, pro-opiomelanocortin, prepro-orexin, and vasoactive intestinal polypeptide mRNAs in the hypothalamus of Japanese quail. Cell Tissue Res. 313, 217–225.

Picard, M.I., Uzu, G., Dunnington, E.A., Siegel, P.B., 1993. Food intake adjustments of chicks: short term reactions to deficiencies in lysine, methionine and tryptophan. Br. Poult. Sci. 34, 737–746.

Piekarski-Welsher, A., Greene, E., Lassiter, K., Kong, B.C., Dridi, S., Bottje, W., 2018. Enrichment of autophagy and proteosome pathways in breast muscle of feed efficient pedigree male broilers. Front. Physiol. 9, 1342.

Piekarski, A., Nagarajan, G., Ishola, P., Flees, J., Greene, E.S., Kuenzel, W.J., Ohkubo, T., Maier, H., Bottje, W.G., Cline, M.A., Dridi, S., 2018. AMP-activated protein kinase mediates the effect of leptin on avian autophagy in a tissue-specific manner. Front. Physiol. 9, 541.

Polidori, C., de Caro, G., Massi, M., 2000. The hyperphagic effect of nociceptin/orphanin FQ in rats. Peptides 21, 1051–1062.

Prall, B.C., Cline, M.A., 2008. Anorexigenic effects of central neuropeptide K are associated with hypothalamic changes in juvenile *Gallus gallus*. Gen. Comp. Endocrinol. 159, 130–135.

Prokop, J.W., Schmidt, C., Gasper, D., Duff, R.J., Milsted, A., Ohkubo, T., Ball, H.C., Shawkey, M.D., Mays, H.L., Cogburn, L.A., Londraville, R.L., 2014. Discovery of the elusive leptin in birds: identification of several 'missing links' in the evolution of leptin and its receptor. PloS One 9, e92751.

Quan, W., Kim, H.K., Moon, E.Y., Kim, S.S., Choi, C.S., Komatsu, M., Jeong, Y.T., Lee, M.K., Kim, K.W., Kim, M.S., Lee, M.S., 2012. Role of hypothalamic proopiomelanocortin neuron autophagy in the control of appetite and leptin response. Endocrinology 153, 1817–1826.

Reed, A.S., Unger, E.K., Olofsson, L.E., Piper, M.L., Myers, M.G., Xu, A.W., 2010. Functional role of suppressor of cytokine signaling 3 upregulation in hypothalamic leptin resistance and long-term energy homeostasis. Diabetes 59, 894–906.

Richards, M.P., McMurtry, J.P., 2010. The avian proghrelin system. Int. J. Pept. 2010, 1–14.

Richards, M.P., Proszkowiec-Weglarz, M., 2007. Mechanisms regulating feed intake, energy expenditure, and body weight in poultry. Poult. Sci. 86, 1478–1490.

Richardson, R.D., Boswell, T., Rafferty, B.D., Seely, R., Wingfield, J.C., Woods, C., 1995. NPY increases food intake in white-crowned sparrows: effect in short and long photoperiods. Am. J. Physiol. 268, R1418–R1422.

Richardson, R.D., Boswell, T., Weatherford, S.C., Wingfield, J.C., Woods, S.C., 1993. Cholecystokinin octapeptide decreases food intake in white-crowned sparrows. Am. J. Physiol. 264, R852–R856.

Richardson, R.D., Boswell, T., Woods, S.C., Wingfield, J.C., 2000. Intracerebroventricular corticotropin-releasing factor decreases food intake in white-crowned sparrows. Physiol. Behav. 71, 213–216.

Rodríguez-Sinovas, A., Fernández, E., Manteca, X., Fernández, A.G., Goñalons, E., 1997. CCK is involved in both peripheral and central mechanisms controlling food intake in chickens. Am. J. Physiol. 272, R334–R340.

Rosenbaum, M., Nicolson, M., Hirsch, J., Heymsfield, S.B., Gallagher, D., Chu, F., Leibel, R.L., 1996. Effects of gender, body composition, and menopause on plasma concentrations of leptin. J. Clin. Endocrinol. Metab. 81, 3424–3427.

Rubin, C.J., Zody, M.C., Eriksson, J., Meadows, J.R.S., Sherwood, E., Webster, M.T., Jiang, L., Ingman, L., Sharpe, T., Ka, S., Hallbook, F., Besnier, F., Carlborg, O., Bed'hom, B., Tixier-Boichard, B., Jensen, P., Siegel, P., Lindblad-Toh, K., Andersson, L., 2010. Whole-genome resequencing reveals loci under selection during chicken domestication. Nature 464, 587–591.

Sabatini, D.M., Erdjument-Bromage, H., Lui, M., Tempst, P., Snyder, S.H., 1994. RAFT1: a mammalian protein that binds to FKBP12 in a rapamycin-dependent fashion and is homologous to yeast TORs. Cell 78, 35–43.

Saito, E.-S., Kaiya, H., Tachibana, T., Tomonaga, S., Denbow, D.M., Kangawa, K., Furuse, M., 2005. Inhibitory effect of ghrelin on food intake is mediated by the corticotropin-releasing factor system in neonatal chicks. Regul. Pept. 125, 201–208.

Sashihara, K., Miyamoto, M., Ohgushi, A., Denbow, D.M., Furuse, M., 2001. Influence of ketone body and the inhibition of fatty acid oxidation on food intake. Br. Poult. Sci 42, 405–408.

Savory, C.J., 1987. An alternative explanation for apparent satiating properties of peripherally administered bombesin and cholecystokinin in domestic fowls. Physiol. Behav. 39, 191–202.

Seoane, L.M., Al-Massadi, O., Pazos, Y., Pagotto, U., Casanueva, F.F., 2006. Central obestatin administration does not modify either spontaneous or ghrelin-induced food intake in rats. J. Endocrinol. Invest. 29, RC13–RC15.

Seroussi, E., Cinnamon, Y., Yosefi, S., Genin, O., Smith, J.G., Rafati, N., Bornelov, S., Andersson, L., Friedman-Einat, M., 2016. Identification of the long-sought leptin in chicken and duck: expression pattern of the highly GC-rich avian leptin fits an autocrine/paracrine rather than endocrine function. Endocrinology 157, 737–751.

Shipp, S., Cline, M.A., Gilbert, E.R., 2016. Promotion of adipogenesis by neuropeptide Y during the later stages of chicken preadipocyte differentiation. Physiol. Rep. 4, 1–12.

Shipp, S.L., Smith, M.L., Gilbert, E.R., Cline, M.A., 2015a. Beta-cell-tropin is associated with short-term stimulation of food intake in chicks. Gen. Comp. Endocrinol. 224, 278–282.

Shipp, S.L., Yi, J., Dridi, S., Gilbert, E.R., Cline, M.A., 2015b. The central anorexigenic mechanism of adrenocorticotropic hormone involves the caudal hypothalamus in chicks. Neuropeptides 53, 29–35.

Shiraishi, J.I., Yanagita, K., Fujita, M., Bungo, T., 2008a. Central insulin suppresses feeding behavior via melanocortins in chicks. Domest. Anim. Endocrinol. 34, 223–228.

Shiraishi, J.I., Yanagita, K., Fujita, M., Bungo, T., 2008b. μ-Opioid receptor agonist diminishes POMC gene expression and anorexia by central insulin in neonatal chicks. Neurosci. Lett. 439, 227–229.

Shiraishi, J.I., Yanagita, K., Nishikawa, F., Tahara, Y., Fujita, M., McMurtry, J.P., Bungo, T., 2009. A comparison of the anorexic effects of chicken, porcine, human and bovine insulin on the central nervous system of chicks. Poult. Sci 46, 144–148.

Shousha, S., Nakahara, K., Kojima, M., Miyazato, M., Hosoda, H., Kangawa, K., Murakami, N., 2005a. Different effects of peripheral and central ghrelin on regulation of food intake in the Japanese quail. Gen. Comp. Endocrinol. 141, 178–183.

Shousha, S., Nakahara, K., Miyazato, M., Kangawa, K., Murakami, N., 2005b. Endogenous neuromedin U has anorectic effects in the Japanese quail. Gen. Comp. Endocrinol. 140, 156–163.

Shousha, S., Nakahara, K., Nasub, T., Sakamoto, T., Murakami, N., 2007. Effect of glucagon-like peptide-1 and -2 on regulation of food intake, body temperature and locomotor activity in the Japanese quail. Neurosci. Lett. 415, 102–107.

Siegel, P.B., 1962. Selection for body weight at eight weeks of age. Poult. Sci. 41, 954–962.

Sims, W., Yi, J., Cline, M.A., Gilbert, E.R., 2017. Central injection of a synthetic chicken partial leptin peptide does not affect food intake in chicks. Neurosci. Lett. 656, 165–168.

Sintubin, P., Greene, E., Collin, A., Bordas, A., Zerjal, T., Tesseraud, S., Buyse, J., Dridi, S., 2014. Expression profile of hypothalamic neuropeptides in chicken lines selected for high or low residual feed intake. Neuropeptides 48, 213–220.

Smith, S.M., Vale, W.W., 2006. The role of the hypothalamic-pituitary-adrenal axis in neuroendocrine responses to stress. Dialogues Clin. Neurosci. 8, 383–395.

Smith, M.L., Prall, B., Nandar, W., Cline, M.A., 2008. Beta-melanocyte stimulating hormone potently reduces appetite via the hypothalamus in chicks. J. Neuroendocrinol. 20, 220–226.

Smith, M.L., Prall, B.P., Siegel, P.B., Cline, M.A., 2011. The threshold of insulin-induced hypophagia is lower in chicks selected for low rather than high juvenile body weight. Behav. Brain Res. 216, 719–722.

Song, Z., Everaert, N., Wang, Y., Decuypere, E., Buyse, J., 2013. The endocrine control of energy homeostasis in chickens. Gen. Comp. Gen. Comp. Endocrinol. 190, 112–117.

Song, Z., Liu, L., Yue, Y., Jiao, H., Lin, H., Sheikhahmadi, A., Everaert, N., Edcuypere, E., Buyse, J., 2012. Fasting alters protein expression of AMP-activated protein kinase in the hypothalamus of broiler chicks (*Gallus gallus domesticus*). Gen. Comp. Endocrinol. 178, 546–555.

Strader, A.D., Buntin, J.D., 2001. Neuropeptide-Y: a possible mediator of prolactin-induced feeding and regulator of energy balance in the ring dove (*Streptopelia risoria*). J. Neuroendocrinol. 13, 386–392.

Taati, M., Nayebzadeh, H., Khosravinia, H., Cheraghi, J., 2010. The role of the histaminergic system on the inhibitory effect of ghrelin on feed intake in broiler chickens. Iran. J. Vet. Res. 11, 38–45.

Tachibana, T., Sakamoto, T., 2014. Functions of two distinct "prolactin-releasing peptides" evolved from a common ancestral gene. Front. Endocrinol. 5, 170.

Tachibana, T., Sugahara, K., Ohgushi, A., Ando, R., Kawakami, S.-I., Yoshimatsu, T., Furuse, M., 2001. Intracerebroventricular injection of agouti-related protein attenuates the anorexigenic effect of alphamelanocyte stimulating hormone in neonatal chicks. Neurosci. Lett. 305, 131–134.

Tachibana, T., Cline, M.A., Sakirul, M.D., Khan, I., Ueda, H., Hiramatsu, H., 2011a. Feeding responses to central administration of several somatostatin analogs in chicks. Comp. Biochem. Physiol. A Mol. Integr. Physiol. 158, 47–51.

Tachibana, T., Moriyama, S., Takahashi, A., Tsukada, A., Oda, A., Takeuchi, S., Sakamoto, T., 2011b. Isolation and characterisation of prolactin-releasing peptide in chicks and its effect on prolactin release and feeding behaviour. J. Neuroendocrinol. 23, 74–81.

Tachibana, T., Cline, M.A., Sugahara, K., Ueda, H., Hiramatsu, K., 2009a. Central administration of somatostatin stimulates feeding behavior in chicks. Gen. Comp. Endocrinol. 161, 354–359.

Tachibana, T., Sugahara, K., Ueda, H., Cline, M.A., 2009b. Role of adrenergic alpha-2-receptors on feeding behavior in layer-type chicks. Gen. Comp. Endocrinol. 161, 407–411.

Tachibana, T., Matsuda, K., Khan, M.S., Ueda, H., Cline, M.A., 2010a. Feeding and drinking response following central administration of neuromedin S in chicks. Comp. Biochem. Physiol. A Mol. Integr. Physiol. 157, 63–67.

Tachibana, T., Matsuda, K., Khan, S.I., Ueda, H., Cline, M.A., 2010b. Feeding and drinking response following central administrations of bombesin-like peptides in chicks. Comp. Biochem. Physiol. A Mol. Integr. Physiol. 156, 394–399.

Tachibana, T., Matsuda, K., Sawa, H., Mikami, A., Ueda, H., Cline, M.A., 2010c. Differential thresholds of neuromedins B-, C-, and bombesin-induced anorexia and crop-emptying rate in chicks. Gen. Comp. Endocrinol. 169, 144–150.

Tachibana, T., Matsuda, K., Kawamura, M., Ueda, H., Khan, M.S., Cline, M.A., 2012. Feeding-suppressive mechanism of sulfated cholecystokinin (26–33) in chicks. Comp. Biochem. Physiol. A Mol. Integr. Physiol. 161, 372–378.

Tachibana, T., Masuda, N., Tsutsui, K., Ukena, K., Ueda, H., 2008. The orexigenic effect of GnIH is mediated by central opioid receptors in chicks. Comp. Biochem. Physiol. A Mol. Integr. Physiol. 150, 21–25.

Tachibana, T., Saito, E.-S., Takahashi, H., Saito, S., Takagi, T., Boswell, T., Furuse, M., 2004a. Anorexigenic effect of pituitary adenylate cyclaseactivating polypeptide and vasoactive intestinal peptide in the chick brain are mediated by corticotrophin-releasing factor. Regul. Pept. 120, 99–105.

Tachibana, T., Saito, S., Tomonaga, S., Takagi, T., Saito, E.-S., Nakanishi, T., Koutoku, T., Tsukada, A., Ohkubo, T., Boswell, T., Furuse, M., 2004b. Effect of central administration of prolactin-releasing peptide on feeding in chicks. Physiol. Behav. 80, 713–719.

Tachibana, T., Sato, M., Takahashi, H., Ukena, K., Tsutsui, K., Furuse, M., 2005a. Gonadotropin-inhibiting hormone stimulates feeding behavior in chicks. Brain Res. 1050, 94–100.

Tachibana, T., Tsukada, A., Fujimoto, M., Takahashi, H., Ohkubo, T., Boswell, T., Furuse, M., 2005b. Comparison of mammalian prolactin-releasing peptide and Carassius RFamide for feeding behavior and prolactin secretion in chicks. Gen. Comp. Endocrinol. 144, 264–269.

Tachibana, T., Takagi, T., Saito, E.-S., Tomonaga, S., Zhang, R., Koga, Y., Kido, Y., Denbow, D.M., Furuse, M., 2003a. Beta 3-adrenergic receptor is involved in feeding regulation in chicks. Comp. Biochem. Physiol. A Mol. Integr. Physiol. 135A, 403–409.

Tachibana, T., Takagi, T., Tomonaga, S., Ohgushi, A., Ando, R., Denbow, D.M., Furuse, M., 2003b. Central administration of cocaine- and amphetamine-regulated transcript inhibits food intake in chicks. Neurosci. Lett. 337, 131–134.

Tang, S.J., Reis, G., Kang, H., Gingras, A.-C., Sonenberg, N., Schuman, E.M., 2002. A rapamycin-sensitive signaling pathway contributes to long-term synaptic plasticity in the hippocampus. Proc. Natl. Acad. Sci. U.S.A. 99, 467–472.

Taouis, M., Chen, J.W., Daviaud, C., Dupont, J., Derouet, M., Simon, J., 1998. Cloning the chicken leptin gene. Gene 208, 239–242.

Tatemoto, K., Carlquist, M., Mutt, V., 1982. Neuropeptide Y – a novel brain peptide with structural similarities to peptide YY and pancreatic polypeptide. Nature 296, 659–660.

Tebbe, J.J., Mronga, S., Schafer, M.K., Ruter, J., Kobelt, P., Monnikes, H., 2003. Stimulation of neurons in rat ARC inhibits gastric acid secretion via hypothalamic CRF1/2- and NPY-Y1 receptors. Am. J. Physiol. Gastr. Liver Physiol. 285, G1075–G1083.

Tran, P.V., Chowdhury, V.S., Furuse, M., 2019. Central regulation of feeding behavior through neuropeptides and amino acids in neonatal chicks. Amino Acids 51, 1129–1152.

Tsutsui, K., Saigoh, E., Ukena, K., Teranishi, H., Fujisawa, Y., Kikuchi, M., Ishii, S., Sharp, P.J., 2000. A novel avian hypothalamic peptide inhibiting gonadotropin release. Biochem. Biophys. Res. Commun. 275, 661–667.

Ukena, K., Tachibana, T., Iwakoshi-Ukena, E., Saito, Y., Minakata, H., Kawaguchi, R., Osugi, T., Tobari, Y., Leprince, J., Vaudry, H., Tsutsui, K., 2010. Identification, localization, and function of a novel avian hypothalamic neuropeptide, 26RFa, and its cognate receptor, G protein-coupled receptor-103. Endocrinology 151, 2255–2264.

Wang, G., Brumfield, B., DiCroce, M., Nelson, L., Newmyer, B.A., Flower, J., Hipskind, K., Sharma, S., Gilbert, E.R., Cline, M.A., 2014a. Anorexigenic effects of central adrenomedullin are associated with hypothalamic changes in juvenile *Gallus gallus*. Gen. Comp. Endocrinol. 204, 223–228.

Wang, G., Tachibana, T., Gilbert, E.R., Cline, M.A., 2015a. Dietary macronutrient composition affects the influence of exogenous prolactin-releasing peptide on appetite responses and hypothalamic gene expression in chickens. J. Nutr. 145, 2406–2411.

Wang, G., Tachibana, T., Gilbert, E.R., Cline, M.A., 2015b. Exogenous prolactin-releasing peptide's orexigenic effect is associated with hypothalamic neuropeptide Y in chicks. Neuropeptides 54, 79–83.

Wang, J., DePena, M., Taylor, G., Gilbert, E.R., Cline, M.A., 2019a. Hypothalamic mechanism of corticotropin-releasing factor's anorexigenic effect in Japanese quail (*Coturnix japonica*). Gen. Comp. Endocrinol. 276, 22–29.

Wang, J., Gilbert, E.R., Cline, M.A., 2019b. Hypothalamic mechanisms associated with neuropeptide K-induced anorexia in Japanese quail (*Coturnix japonica*). Comp. Biochem. Physiol. A Mol. Integr. Physiol. 237, 110539.

Wang, J., Matias, J., Gilbert, E.R., Tachibana, T., Cline, M.A., 2019c. Hypothalamic mechanisms associated with corticotropin-releasing factor-induced anorexia in chicks. Neuropeptides 74, 95–102.

Wang, J., Yi, J., Siegel, P.B., Cline, M.A., Gilbert, E.R., 2017. Stress-induced suppression of neuropeptide Y-induced hunger in anorexic chicks involves corticotrophin-releasing factor signalling and the paraventricular nucleus of the hypothalamus. J. Neuroendocrinol. 29.

Wang, X., Day, J.R., Vasilatos-Younken, R., 2001. The distribution of neuropeptide Y gene expression in the chicken brain. Mol. Cell. Endocrinol. 174, 129–136.

Wang, Y., Song, Z., Everaert, N., De Ketelaere, B., Willemsen, H., Decuypere, E., Buyse, J., 2014b. The anorectic effects of alpha-lipoic acid are mediated by central AMPK and are not due to taste aversion in chicken (*Gallus gallus*). Physiol. Behav. 132, 66–72.

Wang, Y., Wang, C.Y., Wu, Y., Huang, G., Li, J., Leung, F.C., 2012. Identification of the receptors for prolactin-releasing peptide (PrRP) and Carassius RFamide peptide (C-RFa) in chickens. Endocrinology 153, 1861–1874.

Webster, R.I., Newmyer, B.A., Furuse, M., Gilbert, E.R., Cline, M.A., 2013. The orexigenic effect of kyotorphin in chicks involves hypothalamus and brainstem activity and opioid receptors. Neuropeptides 47, 193–198.

Wolfgang, M.J., Jurama, T., Dai, Y., Suwa, A., Asaumi, M., Matsumoto, S.-I., Cha, S.H., Shimokawa, T., Lane, M.D., 2006. The brain carnitine palmitoyltranserase-1c regulates energy homeostasis. Proc. Natl. Acad. Sci. U.S.A. 103, 7282–7287.

Xiao, Y., Wang, J., Siegel, P.B., Cline, M.A., Gilbert, E.R., 2020. Early-life stress induced epigenetic changes of corticotropin-releasing factor gene in anorexic low body weight-selected chicks. Life (in press).

Xu, P., Siegel, P.B., Denbow, D.M., 2011a. Genetic selection for body weight in chickens has altered responses of the brain's AMPK system to food intake regulation effect of ghrelin, but not obestatin. Behav. Brain Res. 221, 216–226.

Xu, P., Siegel, P.B., Denbow, D.M., 2011b. AICAR and Compound C regulate food intake independently of AMP-activated protein kinase in lines of chickens selected for high or low body weight. Comp. Biochem. Physiol. A Mol. Integr. Physiol. 159, 401–412.

Yi, J., Delp, M.S., Gilbert, E.R., Siegel, P.B., Cline, M.A., 2016. Anorexia is associated with stress-dependent orexigenic responses to exogenous neuropeptide Y. J. Neuroendocrinol. 28.

Youle, R.J., Narendra, D.P., 2011. Mechanisms of mitophagy. Nat. Rev. Mol. Cell Biol. 12, 9–14.

Yu, L., Alva, A., Su, H., Dutt, P., Freundt, E., Welsh, S., Baehrecke, E.H., Lenardo, M.J., 2004. Regulation of an ATG7-beclin 1 program of autophagic cell death by caspase-8. Science 304, 1500–1502.

Yu, L., Wan, F., Dutta, S., Welsh, S., Liu, Z., Freundt, E., Baehrecke, E.H., Lenardo, M., 2006. Autophagic programmed cell death by selective catalase degradation. Proc. Natl. Acad. Sci. U.S.A. 103, 4952–4957.

Zhang, W., Bai, S., Liu, D., Cline, M.A., Gilbert, E.R., 2015. Neuropeptide Y promotes adipogenesis in chicken adipose cells in vitro. Comp. Biochem. Physiol. Mol. Integr. Physiol. 181, 62–70.

Zhang, W., Cline, M.A., Gilbert, E.R., 2014. Hypothalamus-adipose tissue crosstalk: neuropeptide Y and the regulation of energy metabolism. Nutr. Metab. 11, 27–39.

Zhang, W., Didehvar, D., Wang, G., Yi, J., Gilbert, E.R., Cline, M.A., 2017. Anorexigenic effect of serotonin is associated with changes in hypothalamic nuclei activity in an avian model. Gen. Comp. Endocrinol. 246, 81–87.

Zhang, Y., Proenca, R., Maffei, M., Barone, M., Leopold, L., Friedman, J.M., 1994. Positional cloning of the mouse obese gene and its human homologue. Nature. 372 (6505), 425–432. https://doi.org/10.1038/372425a0.

Zhao, R., Muehlbauer, E., Decuypere, E., Grossmann, R., 2004. Effect of genotype-nutrition on growth and somatotripic gene expression in the chicken. Gen. Comp. Endocrinol. 136, 2–11.

Zelenka, D.J., Dunnington, E.A., Cherry, J.A., Siegel, P.B., 1988. Anorexia and sexual maturity in female white rock chickens. I. Increasing the feed intake. Behav. Genet. 18, 383–387.

Zendehdel, M., Baghbanzadeh, A., Babapour, V., Cheraghi, J., 2009. The effects of bicuculline and muscimol on glutamate-induced feeding behavior in broiler cockerels. Comp. Physiol. A 195, 715–720.

Zeni, L.A., Seidler, H.B., De Carvalho, N.A., Freitas, C.G., Marino-Neto, J., Paschoalini, M.A., 2000. Glutamatergic control of food intake in pigeons: effects of central injections of glutamate, NMDA, and AMPA receptor agonists and antagonists. Pharmacol. Biochem. Behav. 65, 67–74.

Further reading

Chehab, F.F., Mounzih, K., Lu, R., Lim, M.E., 1997. Early onset of reproductive function in normal female mice treated with leptin. Science 275, 88–90.

Denbow, D.M., 1985. Food intake control in birds. Neurosci. Biobehav. Rev. 9, 223–232.

Denbow, D.M., Van Krey, H.P., Siegel, P.B., 1986. Selection for growth alters the feeding response to brain injections of biogenic amines. Pharmacol. Biochem. Behav. 24, 39–42.

Farooqi, I.S., 2002. Leptin and the onset of puberty: insights from rodent and human genetics. Semin. Reprod. Med. 20, 139–144.

Qiu, J., Ogus, S., Mounzih, K., Ewart-Toland, A., Chehab, F.F., 2001. Leptin-deficient mice backcrossed to the BALB/cJ genetic background have reduced adiposity, enhanced fertility, normal body temperature, and severe diabetes. Endocrinology 142, 3421–3425.

Chapter 29

Overviews of avian neuropeptides and peptides

Yajun Wang

Key Laboratory of Bio-resources and Eco-environment of Ministry of Education, College of Life Sciences, Sichuan University, Chengdu, Sichuan, PR China

29.1 Introduction

Peptides are short stretches of amino acids (aas) linked by peptide bonds. They play important roles in nearly all physiological processes such as growth and development, reproduction, stress, metabolism, calcium homeostasis, immunity, cardiovascular functions, and central nervous system (CNS) functions (e.g., food intake, memory, behavior and analgesia). Inside the cells, peptide precursors (prepropeptides) generally require proteolytic cleavage and sometimes posttranslational modification(s) (such as amidation and disulfide formation) to become the bioactive mature peptides. Most peptides act either as hormones or neurotransmitters/neuromodulators to exert their actions via membrane-spanning receptors, such as G protein-coupled receptor (GPCR) with seven transmembrane domains. Some peptides also display antimicrobial activities. According to their sources and functions, peptides can be further classified as neuropeptides, endocrine peptides (hormones), gut peptides and host defense peptides (HDPs), etc. Among these, neuropeptides are the peptides released by neurons to influence the physiological activity in the body.

Due to the availability of sequenced genomes of many birds, such as chickens, turkeys, and zebra finches, nearly all avian peptides and their receptors can be predicted through bioinformatic approach (Delfino et al., 2010; Xie et al., 2010). The recent advancement in sequencing technology also accelerates the studies on the structures and functions of avian peptides and their receptors, which will not only help to uncover the roles of these peptides in avian physiological processes, such as growth, reproduction, metabolism, and energy balance, but also facilitate our better understanding of their contributions to the unique phenotypical traits of birds (e.g., flight and migration) and domestication of avian species (e.g., chickens and ducks).

Based on the literatures and sequenced avian genomes, in this chapter, we will present an overview of the structures, expression, and major actions of 134 peptides (Table 29.1) belonging to different peptide families in birds (e.g., chickens, quails, and finches) and their differences to mammalian peptides. In addition, the cognate/predicted receptors for avian peptides are also mentioned briefly.

29.1.1 Galanin/spexin peptide family

Galanin is a neuromodulator in the brain and peripheral nervous system (PNS) of vertebrates. Several structurally related peptides, including galanin-like peptide (GALP, 60 aas) (Ohtaki et al., 1999), Spexin (SPX), and Kisspeptins (KISS 1, KISS2, KISS3, and KISS4), have later been identified, all of which are proposed to be originated from a common ancestral gene and belong to the same peptide family (Kim et al., 2014).

Galanin was isolated from the chicken intestine (Norberg et al., 1991) and quail oviduct (Li et al., 1996). It is a 29-residue peptide which contains an amidated threonine at its C-terminus, which is proteolytically cleaved from a large precursor. Interestingly, *GALP* gene is likely lost in the avian lineage (Ho et al., 2012).

SPX is a 14-residue peptide encoded by the *C12ORF30* gene (Mirabeau et al., 2007; Sonmez et al., 2009) in mammals. In chickens, two ortholog peptides of 14 aas (named SPX1 and SPX2) encoded by separate genes have been identified. Both peptides share high sequence similarity with each other and a comparatively low identity with chicken galanin (Fig. 29.1) (Kim et al., 2014; Lim et al., 2019).

Sturkie's Avian Physiology. https://doi.org/10.1016/B978-0-12-819770-7.00046-3

TABLE 29.1 Peptides/Neuropeptides in chickens.

Peptide	Gene	Accession no.	Peptide sequence
GAL	*GAL*	XM_015286791	GWTLNSAGYLLGPRRIDHLLMIKEMPIAR$_{-NH2}$
SPX1	*SPX1*	XM_015290798	NWTPQAMLYLKGAQ$_{-NH2}$
SPX2	*SPX2*	XM_025151343	NWGPQSILYLKGRY$_{-NH2}$
SP/NKA	*TAC1*	XM_025148454	RPRPQQFFGLM$_{-NH2}$/HKTDSFVGLM$_{-NH2}$
NKB	*TAC3*	XM_025145446	DMHDFFVGLM$_{-NH2}$
CT	*CACLA*	NM_001113708	CASLSTCVLGKLSQELHKLQTYPRTDVGAGTP$_{-NH2}$
CGRP	*CACLA*	NM_001271965	ACNTATCVTHRLADFLSRSGGVGKNNFVPTNVGSKAF$_{-NH2}$
IAPP	*IAPP*	NM_205397	KCNTATCVTQRLADFLVRSSSNIGAIYSPTNVGSNTY$_{-NH2}$
ADM	*ADM*	XM_015286460	YRQSVNSFPHLPTFRMGCRFGTCTVQKLAHQLYQLTDKVKDGAAPVNKISPQGY$_{-NH2}$
ADM2	*ADM2*	XM_025153017	HLGVRLRHAQPLRVGCVLGTCQVQNLSHRLWQLMGRPGRQDSSPMNPNSPHSY$_{-NH2}$
PTH	*PTH*	NM_205452	SVSEMQLMHNLGEHRHTVERQDWLQMKLQDVHSALEDARTQRPRNKEDIVLGEIRNRRLLPEHLRAAVQKKSIDL DKAYMNVLFKTKP
PTHrP/Osteostatin	*PTHrP*	NM_001174106	AVSEHQLLHDKGKSIQDLRRRIFLQNLIEGVNTAEIRATSEVSPNPKPATNTKNYPVRFGSEDEGRYLTQETNKSQTYKEQ PLKVSGKKKKAKPGKRKEQEKKKRRARSAWLNSGMYGSNVTESPVLDNSVTTHNHILRRR
PTH-L	*PTH-L*	Predicted	AVTEHQLMHDKARAFQGLKRLLWLHNALGSVHTASSRDISLSNAIWDSQKSRDPSDLYNSISRDETSNPMKQLLE LIEDEQGFPLLRKQYLLQNPKTPEGNWNPQDVFDLLQIKEFGRRRNHSNQPQNFSH
RLN3	*RLN3*	MT263682	A-chain: ESLGLAGMCCKWGCTKAEISTICRV B-chain: ALVPAGDGDGYGVKLCGREFIRAVIFTCGGSRW
INSL5	*INSL5*	MT263683	A-chain: REVAKLLTTSCCSVGCSERDISLLC/B$_{-chain}$: EGNAVKLCGRDFVRAIVFTCGGSRW
GHRL	*GHRL*	NM_001305129	GSSFLSPTYKNIQQQKDTRKPTARLH
MLN	*MLN*	NM_001001131	FVPFFTQSDIQKMQEKERNKGQ
NMU25/NMU9	*NMU*	NM_001277921	YKVDEDLQGAGGIQSRGYFFFRPRN$_{-NH2}$/GYFFFRPRN$_{-NH2}$
NURP33	*NMU*	NM_001277921	FLFHYSKTHDSGNSDVRSSVLHPLLQLVPQLNE
NMS-9	*NMS*	MF967032	PFFLFRPRN$_{-NH2}$
NPS	*NPS*	XM_025151926	SFRNGVGSGIKKTSFRRAKS
NTS/NN (LANT6)	*NTS*	NM_001277360	QLHVNKARRPYIL/KNPYIL
NPAF	*NPFF*	KF296315	SWDPPSAPFWTMATPQRF$_{-NH2}$
GnIH	*NPVF*	NM_204363	SIRPSAYLPLRF$_{-NH2}$
GnIH-RP1	*NPVF*	NM_204363	SSIQSLLNLPQRF$_{-NH2}$
GnIH-RP2	*NPVF*	NM_204363	SLNFEEMKDWGSKNFLKVNTPTVNKVPNSVANLPLRF$_{-NH2}$

PrRP	*PrRP*	EF418015	NPDIDPSWYTGRGIRPVGRF$_{-NH2}$
PrRP2$_{31}$/PrRP2$_{20}$	*C-RFa*	EU031788	SRPFKHQIDNRSPEIDPFWYVGRGVRPIGRF$_{-NH2}$/SPEIDPFWYVGRGVRPIGRF$_{-NH2}$
QFRP	*QFRP*	XM_001235088	GGGGTLGDLAEELNGYGRKKGGFAFRF-NH2
CCK8	*CCK*	NM_001001741	DYMGWMDF$_{-NH2}$
GAST53	*GAST*	NM_205400	DWPEPPSQEQQQRFISRFLPHVFAELSDRKGFVQGNGAVEALHDHFYPDWMDF$_{-NH2}$
Orexin-A	*HCRT*	NM_204185	QSLPECCRQKTCSCRIYDLLHGMGNHAAGILTL$_{-NH2}$
Orexin-B	*HCRT*	NM_204185	KSIPPAFQSRLYRLLHGSGNHAAGILTI$_{-NH2}$
MCH	*MCH*	HM853641	DFDMLRCMLGRVYRPCWQV
PROK1	*PROK1*	2373041	AVITGACERDLQCGGGTCCAVSLWLRGLRMCTPLGQEGDECHPFSHKVPFLGKRQHHTCPCLPNFSCSRFLDGRYRCSL DFKNFDF
PROK2	*PROK2*	XM_015293233	AVITGACDRDQQCGGGMCCAVSLWIRSLRMCTPMGNVGEECHPLSHRVPFPGRRMHHTCPCLPSLSCTRASPSKFRCLP DFRKEDVFF
CRH	*CRH*	NM_001123031	SEEPPISLDLTFHLLREVLEMARAEQLAQQAHSNRKLMEII-NH2
CRH2	*CRH2*	KU887752	EGKPNSLDLTFHLLREFLEMSREERLAQKALSNKLLLQSI$_{-NH2}$
UCN	*UCN*	XM_015285002	DDPPLSIDLTFHLLRHLLLLARAQSQRARADTNRRILDAV$_{-NH2}$
UCN2	*UCN2*	KX017224	VSLSLDVPTHILRILLDLAREKELQAKAAANAELMARI$_{-NH2}$
UCN3	*UCN3*	XM_001231710	TKVTLSLDVPTNIMNILFNIAKAKNLRAKAAANAHLMAQI-NH2
NPW23/NPW30	*NPW*	KU059546	WYKHVASPRYHTVGRASGLLMGV/WYKHVASPRYHTVGRASGLLMGVRRSPYLW
NPB28	*NPB*	KU059545	WYRQAAAPLSYPVGRASGLLSGLRLPYS
Enkephalins	*PENK*	2373041	YGGFM (Met-enkephalin)/YGGFL ((Leu-enkephalin)
Dynorphins	*PYDN*	2373041	YGGFMRRIRPKLKWDNQ (Dynorphin-A)/YGGFLRRQFKVTT (Dynorphin-B)
Nociceptin	*PNOC*	2373041	YGGFIGVRKSARKWNNQ
β-endorphin	*POMC*	NM_001031098	YGGFMSLEHSQTPLMTLFKNAIVKSAYKKGQ
SST14/SST28	*SST*	NM_205336	AGCKNFFWKTFTSC/ANSNPALAPRERKAGCKNFFWKTFTSC
CST14	*SS2*	NM_204455	LAQLSQRDRKAPCKNFFWKTFTSC
UTS2$_{17}$/UTS2$_{12}$	*UTS2*	AY563615	QYKKRGNLSECFWKYCV/GNLSECFWKYCV
URP	*UTS2B*	NM_206989	ACFWKYCI
GCG	*GCG*	NM_001190165	HSQGTFTSDYSKYLDSRRAQDFVQWLMST
GLP1	*GCG*	NM_001190165	HAEGTYTSDITSYLEGQAAKEFIAWLVNGR$_{-NH2}$
GLP2	*GCG*	NM_001190165	HADGTFTSDINKILDDMAAKEFLKWLINTKVTQ
GCGL	*GCGL*	EU718628	HSEGTFTSDFTRYLDKMKAKDFVHWLINT
GIP	*GIP*	NM_001080104	YSEATLASDYSRTMDNMLKKNFVEWLLARREKKSDNVIEPY

Continued

TABLE 29.1 Peptides/Neuropeptides in chickens.—cont'd

Peptide	Gene	Accession no.	Peptide sequence
$GHRH_{27}$/$GHRH_{47}$	*GHRH*	DQ465018	HADAIFTDNYRKFLGQISARKFLQTII$_{\text{-NH2}}$/HADAIFTDNYRKFLGQISARKFLQTIIGKRLRNSESSPGEGVHKLLT
VIP	*VIP*	NM_205366	HSDAVFTDNYSRFRKQMAVKKYLNSVLT$_{\text{-NH2}}$
PHI	*VIP*	NM_205366	HADGIFTSVYSHLWAKLAVKRYLHSLI
GHRH-LP	*ADCYAP1*	AY956323	HADGIFSKAYRKLLGQLSARKYLHSLMAKRVGGASSGLGDEAEPLS
$PACAP_{27}$/$PACAP_{38}$	*ADCYAP1*	AY956323	HIDGIFTDSYSRYRKQMAVKKYLAAVL$_{\text{-NH2}}$/HIDGIFTDSYSRYRKQMAVKKYLAAVLGKRYKQRVKNK$_{\text{-NH2}}$
SCT-LP	*SCT*	EU686392	HADGLFHSELSKMNDNAYVQQLVKHLVGLKERTQ
SCT	*SCT*	EU686392	HSDGLFTSEYSKMRGNAQVQKFIQNLM$_{\text{-NH2}}$
Apelin-36	*APLN*	KX017222	LVRPRGARRGNVRRPGGWRRLRRPRPRLSHKGPMPF
Elabela-32	*APELA*	KX017223	QRPANLALRRKLHRHNCSHRRCMPLHSRVPFP
NPY	*NPY*	NM_205473	YPSKPDSPGEDAPAEDMARYYSALRHYINLITRQRY$_{\text{-NH2}}$
PYY	*PYY*	KU059551	AYPPKPESPGDAASPEEIAQYFSALRHYINLVTRQRY$_{\text{-NH2}}$
PP	*PP*	NM_204786	GPSQPTYPGDDAPVEDLIRFYNDLQQYLNVVTRHRY$_{\text{-NH2}}$
BNP	*BNP*	NM_204925	MMRDSGCFGRRIDRIGSLSGMGCNGSRKN
RNP	*RNP*	NM_001198747	HFSGCFGTRMERIGAQTGLGCNHYKARFWRRRRS
CNP	*CNP*	2373041	GLGKGCFGLKLDRIGAMSGLGC
CNP1	*CNP1*	NM_001193616	ALSGDWAWKAVPRGCFGLKMDRIGAFSGLGC
CNP3	*CNP3*	NM_001111259	GLSRSCFGVKLDRIGSMSGLGC
OSTN	*OSTN*	NM_001098608	VLLAEAAPEPLEPSAALGMAAHPTASEEKSASSLAAKLLLLDELVSLENEVTETKKKRSFPGFGSPIDRISATSVDAKGKQRKVVE LPKRRFGVPLDRIGVSRLGNTKG
NPGL	*NPGL*	AB909129	HSQIDPLALGRADPQCWESSSAVLLEMRKPRISDSVSGFWDFMIFLKSSENLKHGALFWDLAQLFWDIYVD CVLSRTHGL$_{\text{-NH2}}$
NPGM	*NPGM*	XM_025148430	NLDYLKEAPASLGQIDHQCWEVSSHGLVEMKKLKVADPVIALWDFMLFLKESPKPKHNELFNDLAQNFWD-MYVDCVLSRSHGM$_{\text{-NH2}}$
Ornitho-kinin	*KNG1*	XM_422766	RPPGFTPLR
Ang II/Ang I	*AGT*	XM_004935493	DRVYVHPF/DRVYVHPFSL
EDN1	*EDN1*	MK139007	CSCSSLLDEECVYFCHLDIIW
EDN2	*EDN2*	MK139008	CSCNSWLDKECIYFCHLDIIW
EDN3	*EDN3*	MK139009	CTCYTYKDKECVYYCHLDIIW
GRP_{27}/GRP_{10}	*GRP*	NM_001277900	APLQPGGSPALTKIYPRGSHWAVGHLM$_{\text{-NH2}}$/GSHWAVGHLM$_{\text{-NH2}}$
NMB_{10}	*NMB*	NM_001079476	GNLWATGHFM$_{\text{-NH2}}$

ACTH	*POMC*	NM_001031098	SYSMEHFRWGKPVGRKRRPIKVYPNGVDEESAESYPMEF
α-MSH	*POMC*	NM_001031098	SYSMEHFRWGKPV$_{\text{-NH2}}$
β-MSH	*POMC*	NM_001031098	DGGSYRM RHFRWHAPLKD
ɣ-MSH	*POMC*	NM_001031098	YVMSHFRWNKF$_{\text{-NH2}}$
ASIP	*ASIP*	NM_001115079	HLIIEEKTECNLSKSNKTNLPDLPPISIVDLTKRSQKVSRKEAENKKSSKKNAELKAPPKPRPTPAADCVPNFKTCKPHLNSCC NYCALCKCRIFQTICQCLLLNPKC
AgRP	*AgRP*	NM_001031457	ILTSDLSHSPLQKMSAGLGEADRARYPSLLHKAKEASVELAGALPRPDLDQMALEVQEGDGNLLQKSSVLEPQALSTALQAA GREERSSPRRCVRLLESCLGHQIPCCDPCATCYCRFFNAFCYCRKISTTFPCGKN
AVT	*AVP*	NM_205185	CYIQNCPRG$_{\text{-NH2}}$
MT	*OXT*	XM_025150346	CYIQNCPIG$_{\text{-NH2}}$
CART	*CART*	KC249966	VPHYEKKFGQVPMCDAGEQCAVRKGARIGKLCDCPRGTSCNSFLLKCL
CART2	*CART2*	KC249967	PGRVPSCHLGEPCAVRVGARYGKRCSCPPGTACNLYVLRCS
LEP	*LEP*	JN120790 (zebra finch)	AAGGGRPVRLEGLRADARALTRTLSTRLQQLQLFPLTLRLSGLEGVPEGVPEGVPEGGVPPGLGWAAQRLQLFQRLLG ALPGPDPRLAQVANDLENLRSLLALLGTLLGCPPPRDPRPPPPAPLAEAPHTVAGVALARLRRCLDGVAACLEGVPACSP- PRAEKLRADARSLSRTLSARLGDVKPPPPSLRLSAPDPLPPADPPPNLGAAEQRLRRFQRLLQALPPTPLLLQLRSDLDNL CSLLQAMAVLKGCGDPPGPGPPPYEHRDPPQLEPELKELLEEAPHTVAAMALGRLRSCVEGVVVGLEGGVGC
TRH	*TRH*	NM_001030383	QHP$_{\text{-NH2}}$
Augurin	*ECRG4*	2373041	APGVPRGNKLKRMLQKREAPIATKPEVSLKEEAAKGFLRSLRRPRRQLWDRSQPDVQQWYQQFLYLGFDE AKFEDDMSYWTSLGRGGSEYYGGYYQHHYDEDSPIGPRNPHTFRHGAGVNYDDY
Chemerin	*RARRES2*	NM_001277476	GQSPLQRRVVKDVLDYFHSRSNVQFLFREQSVEGAVERVDSSGTFVQLHLNLAQTACRKQAQRKQNCRIMENRR KPVCLACYKFDSSDVPKVLDKYYNCGPSHHLAMKDIKHRDEAECRAVEEAGKMSDVLYLPGMFAFS
Vasostatin-1	*CHGA*	XM_421330	LPVTNEMNKGDTKVMKCIVEVISDTLSKPDPLPISEECLETLRGDERIISILRHQNLLKELQEIAAQGANERTQQQ
Serpinin	*CHGA*	XM_421330	TEDQELESLAAIEAELERVAHKLHEL
CgB$_{1\text{-}41}$	*CHGB*	XM_419377	VPVEKDHMEEMITQCIVEVLSNALSKPNAPPINPECKEIL
Secretolytin	*CHGB*	XM_419377	LQKIAETFNNNRR$_{\text{-NH2}}$
SN	*SCG2*	XM_015277029	TNEIVEEQYTPQSLATLESVFQELGKMAGPSNH
EM66	*SCG2*	XM_015277029	ERLDEDQKLYADDEDDVYKVNNIAYEDVVGGEDWNPIEEKVESQTQEEIKDSKEEIDKHEEEVDDEM
AvBD1	*AvBD1*	NM_204993	GRKSDCFRKSGFCAFLKCPSLTLISGKCSRFYLCCKRIW$_{\text{-NH2}}$
AvBD2	*AvBD2*	NM_001201399	RDMLFCKGGSCHFGGCPSHLIKVGSCFGFRSCCKWPWNA
AvBD3	*AvBD3*	NM_204650	TATQCRIRGGFCRVGSCRFPHIAIGKCATFISCCGRAYEVDALNSVRTSPWLLAPGNNPH
AvBD4	*AvBD4*	NM_001001610	RYHMQCGYRGTFCTPGKCPYGNAYLGLCRPKYSCCRWL
AvBD5	*AvBD5*	NM_001001608	GLPQDCERRGGFCSHKSCPPGIGRIGLCSKEDFCCRSRWYS
AvBD6	*AvBD6*	NM_001001193	QPYFSSPIHACRYQRGVCIPGPCRWPYYRVGSCGSGLKSCCVRNRWA

Continued

TABLE 29.1 Peptides/Neuropeptides in chickens.—cont'd

Peptide	Gene	Accession no.	Peptide sequence
AvBD7	*AvBD7*	NM_001001194	QPFIPRPIDTCRLRNGICFPGICRRPYYWIGTCNNGIGSCCARGWRS
AvBD8	*AvBD8*	NM_001001781	NNEAQCEQAGGICSKDHCFHLHTRAFGHCQRGVPCCRTVYD
AvBD9	*AvBD9*	NM_001001611	ADTLACRQSHGSCSFVACRAPSVDIGTCRGGKLKCCKWAPSS
AvBD10	*AvBD10*	NM_001001609	PDTVACRTQGNFCRAGACPPTFTISGQCHGGLLNCCAKIPAQ
AvBD11	*AvBD11*	NM_001001779	LPRDTSRCVGYHGYCIRSKVCPKPFAAFGTCSWRQKTCCVDTTSDFHTCQDKGGHCVSPKIRCLE EQLGLCPLKRWTCCKEI
AvBD12	*AvBD12*	NM_001001607	PDSCNHDRGLSRVGNCNPGEYLAKYCFEPVILCCKPLSPTPTKT
AvBD13	*AvBD13*	NM_001001780	SDSQLCRNNHGHCRRLCFHMESWAGSCMNGRLRCCRFSTKQPFSNPKHSVLHTAEQDPSPSLGGT
AvBD14	*AvBD14*	NM_001348511	DTVTCRKMKGKCSFLLCPFFKRSSGTCYNGLAKCCRPFW
OvoDA1	*OvoDA1*	NM_001317339	VLKYCPKIGYCSNTCSKTQIWATSHGCKMYCCLPASWKWK
OvoDA2	*OvoDA2*	NM_001317340	VLKYCPKIGYCSNTCSKTQIWATSHGCKMYCCLPASWKWK
OvoDA3	*OvoDA3*	NM_001317341	VLKYCPKIGYCSNTCSKTQIWATSHGCKMYCCLPANWKWK
OvoDB1	*OvoDB1*	NM_001317139	APGYRKRKGTCKGYCAPTCNKKDEWSFHQSCKKMYCCLLPLKKGK
OvoDBb	*OvoDBb*	MH125211	TPGKSQSKKCCGRCSSRMCTKREKEEHTEDCRGSFCCLTHRKKK
NK-lysin	*NK-lysin*	NM_001044680	GIKCRFCVSLVKKVQKIVGDDPDEDAINNALNKVCSTGRRQRSICKQLLKKLRQQLSDALQNNDDPRDVCTTLGLCKG
CATH1	*CATH1*	NM_001001605	RVKRVWPLVIRTVIAGYNLYRAIKKK
CATH2	*CATH2*	NM_001024830	LVQRGRFGRFLRKIRRFRPKVTITIQGSARFG
CATH3	*CATH3*	NM_001311177	RVKRFWPLVPVAINTVAAGINLYKAIRRK
CATHB1	*CATHB1*	NM_001271172	PIRNWWIRIWEWLNGIRKRLRQRSPFYVRGHLNVTSTPQP
LEAP2	*LEAP2*	NM_001001606	ASLHQPQPLLRLKRMTPFWRGVSLRPVGASCRDNSECITMLCRKNRCFLRTASE
Hepcidin	*HAMP*	XM_033084442	HSPHFPLCSFCCGCCANRGCGFCCRT (Swainson's thrush)

Note: Only the major chicken peptides/neuropeptides are listed here; "-NH2" means C-terminal amidation of peptide may be required for its biological activity; other modifications (e.g., disulfide bond, sulfonation, acylation, and N-terminal glutamate cyclization) of peptides are described in the main text, and not described here.

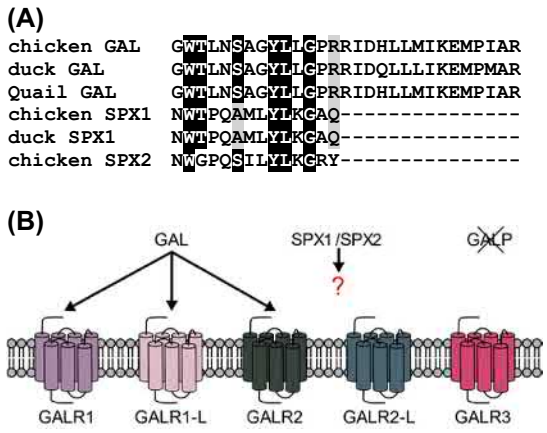

FIGURE 29.1 (A) Alignment of galanin family peptides, Galanin (GAL) and Spexin (SPX1, SPX2) in chickens, ducks, and quails. Two other galanin family members found in mammals, GALP and KISS, are likely lost in avian lineage. (B) Five receptors [GALR1 (EU647890), GALR1-like (GALR1-L, EU530818), GALR2 (EU525170), GALR2-like (GALR2-L, EU725863), and GALR3 (NP_001124057)] have been identified in birds. Among them, GALR1-L and GALR2-L exist in birds and have not been identified in mammals. GALR1, GALR1-L, and GALR2 can function as receptors for GAL. It is unknown whether they can act as receptor(s) for SPX1 and SPX2 in birds.

KISS1 has been proposed to be a key regulator of reproduction by activating gonadotropin-releasing hormone (GnRH) neurons, which can initiate the onset of puberty in mammals (Pinilla et al., 2012). However, KISS1 is possibly lost in avian genomes (Um et al., 2010). Interestingly, a KISS2-like gene was identified in ducks (HG328246), zebra finches, and rock pigeons (Pasquier et al., 2014). Nevertheless, avian KISS2 seems to be degenerated considerably in avian lineage, questioning its roles in birds.

In mammals, three GPCRs for GAL, GALP, and SPX, named GALR1, GALR2, and GALR3, have been identified. GALR1 is a high-affinity receptor for GAL. GALR2 and GALR3 are high-affinity receptors for GALP. GALR3 can function as a high-affinity receptor for SPX. In contrast, 5 GPCRs, named GALR1, GALR1-like (GALR1-L), GALR2, GALR2-like, and GALR3, have been identified in birds. GALR1, GALR1-L, and GALR2 can function as the three receptors for chicken GAL, and their activation inhibits cAMP/PKA signaling and stimulates the MAPK/ERK cascade (Ho et al., 2011, 2012). However, it is unknown whether SPX1 and SPX2 can activate the five receptors (Kim et al., 2014).

GPR54 can function as a receptor for KISS1 peptide in mammals. However, *GPR54* is likely lost in birds. The failure in identifying *KISS1* and *GPR54* does not support the role of KISS−GPR54 signaling in avian reproduction (Pasquier et al., 2014).

Galanin peptide is widely expressed in avian CNS, PNS, and other tissues, such as the intestine and oviduct (Norberg et al., 1991). In chickens, galanin is distributed in the CNS including the hypothalamus and brainstem (Jozsa and Mess, 1993; Klein et al., 2006) and is important in its regulation, such as stimulating food intake of layer and broiler chicks (Tachibana et al., 2008). In quail oviduct, galanin is expressed in the lumbosacral sympathetic ganglion neurons innervating the avian uterine muscle and thus can induce oviposition in quails (Li et al., 1996; Sakamoto et al., 2000; Ubuka et al., 2001). To date, the roles of SPXs in birds remain unclear.

29.1.2 Tachykinin peptide family

The tachykinin family neuropeptides are 10−12 aas in length and characterized by the presence of a C-terminal pentapeptide "Phe-X-Gly-Leu-Met-NH2", where X is either an aromatic aa (Phe/Tyr) or an aliphatic aa (Val or Ile) (Severini et al., 2002). Two tachykinin genes, TAC1 and TAC3, likely exist in chicken and other birds. After posttranslational processing, chicken TAC1 precursor can give rise to three bioactive peptides, substance P (SP, 11 aa), neurokinin A (NKA, 10 aa) and, neuropeptide ɣ (21 aa, an N-terminally extended form of NKA), among which SP and NKA were first purified from chicken small intestine (Conlon et al., 1988). TAC3 precursor can produce a neurokinin B (NKB, 10 aa).

In mammals, three GPCRs, named TACR1, TACR2, and TACR3, can selectively bind to SP, NKA, and NKB, respectively. Likewise, TACR1, TACR2, and TACR3 are predicted to exist in avian genomes. The pharmacological property, signaling property, and ligand selectivity of three receptors are largely unknown in birds.

In birds, SP immunoreactivity is widely distributed in neuronal cells or nerve fibers of the spinal cord (Du et al., 1987; Du and Dubois, 1988; Sakamoto and Atsumi, 1989), retina (Millar and Chubb, 1984a,b; Tahara et al., 1986), different brain regions (Reubi and Jessell, 1978) [e.g., hippocampus (Gould et al., 2001), hypothalamus (Erichsen et al., 1982), and median eminence [ME] (Ho and DePalatis, 1980)], epidermis and dermis (Sann et al., 1996), parathyroid gland (Egawa and Kameda, 1995), gut (Fontaine-Perus et al., 1981; McGregor et al., 1982; Saffrey et al., 1982; Epstein et al., 1983), and oviduct (De Saedeleer et al., 1989). In contrast to SP, the information regarding the distribution of NKA/NKB is limited. Radioisotope-binding assays or qPCR assays indicate the existence and expression of tachykinin (SP, NKA, and NKB) receptors in chicken brain (Too and Hanley, 1988), intestinal muscle (Liu and Burcher, 2001), and hypothalamic nuclei (Wang et al., 2019).

The expression of tachykinins (SP or NPK) and their receptors in the CNS and PNS suggests that as in mammals, tachykinins mainly function as neurotransmitters or neuromodulators associated with many physiological processes, such as pain transmission, inhibition of food intake

in chickens (Prall and Cline, 2008; Tachibana et al., 2010a; Mace et al., 2014; McConn et al., 2019) and quails (Wang et al., 2019; Pauliukonis et al., 2020), water intake in ducks and pigeons (de Caro et al., 1980a, 1980b; Massi et al., 1987), antidromic vasodilation (Sann et al., 1996), nasal salt gland secretion in ducks (Wilson, 1987), contraction of intestinal smooth muscle in chickens (Brodin et al., 1981), and oviductal and duodenal motility (De Saedeleer et al., 1989).

29.1.3 Calcitonin peptide family

Calcitonin (CT) peptide family includes CT, calcitonin gene-related peptide (CGRP), amylin (IAPP), and adrenomedullin (ADM) (Poyner et al., 2002). In chickens, these peptides were also found and encoded by four genes, *CACLA, IAPP, ADM*, and *ADM2*. Two *CACLA* transcripts generated by tissue-specific alternative splicing were identified: one coding for a bioactive CT peptide (32 aa) (Homma et al., 1986) and the other for a CGRP neuropeptide (37 aa) (Minvielle et al., 1986, 1987). *IAPP* encodes a bioactive IAPP of 37 aa, which shares ~80% sequence identity to human IAPP (Fan et al., 1994). *ADM* encodes a mature ADM peptide of 54 aa, which shares ~72% sequence identity to the human ortholog (Zudaire et al., 2005); *ADM2* is predicted to encode a mature ADM2 peptide of 53 aa (also named intermedin). These peptides show low aa sequence identity with each other; however, their secondary structures are conserved, including an intramolecular disulfide bond close to the N-terminus, a region of the amphipathic α-helix, and an amidated C terminus (Fig. 29.2A) (Poyner et al., 2002).

In mammals, two receptors for CT family peptides, calcitonin receptor (CTR) and calcitonin receptor-like receptor (CLR), have been identified. CTR alone can function as a CTR (Poyner et al., 2002), while CTR or CLR must heterodimerize with one of the three receptor activity–modifying proteins (RAMP1, RAMP2, and RAMP3) and give rise to the receptor(s) for CGRP (CLR–RAMP1 complex), ADM (CLR–RAMP2 complex), ADM2 (CLR–RAMP3 complex), and IAPP (three receptors, CTR–RAMP1, CTR-RAMP2, and CTR–RAMP3) (Poyner et al., 2002; Hay et al., 2018). Although the two receptors for CT family peptides (CTR and CLR) and three RAMPs have been identified in birds, the functionality of these avian receptors/receptor complexes is still unknown.

In birds (e.g., chicken), CT peptide is expressed predominantly in the C cells of ultimobranchial glands (Kameda, 1991), but also found in other tissues, such as ovarian follicles and the anterior pituitary (Krzysik-Walker et al., 2007; Maddineni et al., 2007). CGRP-ir, sometimes colocalized with SP, is widely distributed in neurons or neuronal fibers of the CNS and peripheral tissues (Lanuza et al., 2000). *IAPP* appears to be predominantly expressed

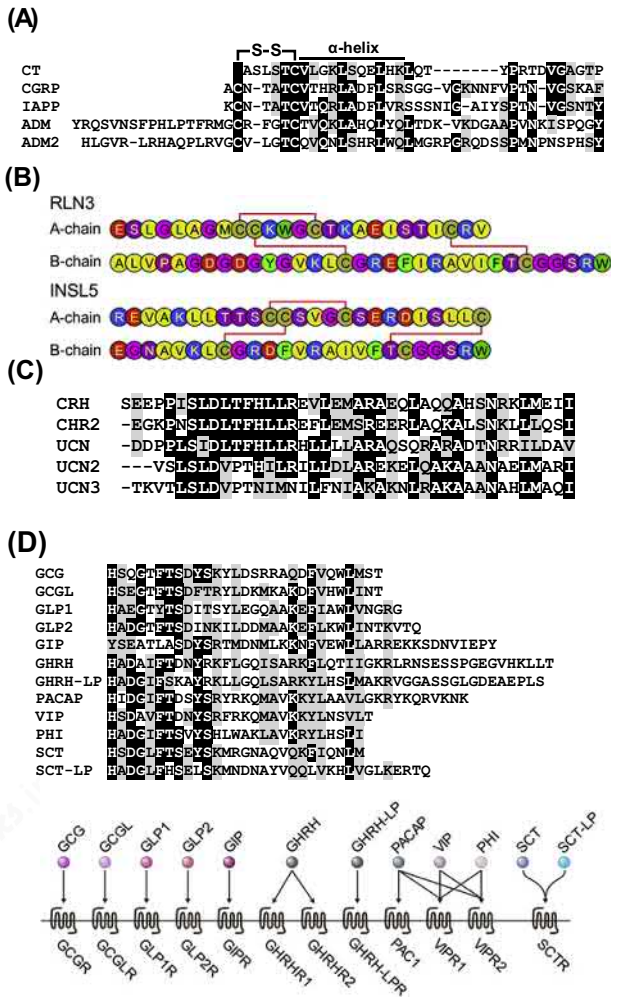

FIGURE 29.2 (A–D) Sequences of chicken calcitonin (CT) family peptides (A), relaxin family peptides (RLN3, INSL5) (B), CRH family peptides (C), and glucagon (GCG) superfamily peptides (D). *Note*: in (A), each CT family peptide contains one disulfide bond and an α-helix structure. In (D), the receptor(s) for each GCG superfamily peptide are shown at the bottom. GHRH has two GHRH receptors (GHRHR1 and GHRHR2); GCGL has a specific receptor (GCGLR); PHI and VIP share the two receptors (VIPR1, VIPR2), while PACAP has three receptors (PAC1, VIPR1, and VIPR2); SCT and SCT-LP share a common receptor (SCTR).

in the extrapancreatic tissues including the brain and intestine endocrine cells, contrasting to the abundant coexpression of IAPP with insulin in rodent islet β-cells (Fan et al., 1994; Mulder et al., 1997). Both *ADM* mRNA and ADM–ir have been detected in a variety of chicken tissues including the lung, adrenal gland, colon, small intestine, pancreas, kidneys, and pituitary, but nondetectable in the brain, suggesting that it cannot function as a neurotransmitter or neuromodulator in chicken brain, as reported in mammals (Lopez et al., 1999; Cuesta et al., 2005).

In birds, CT was originally proposed to control calcium homeostasis (Copp et al., 1967); however, its

calcium-lowering effect has yet been confirmed (Chan et al., 1969; Baimbridge and Taylor, 1980; Anderson et al., 1982; Sommerville and Fox, 1987; Hurwitz, 1996). CT also plays roles in the pituitary, hypothalamus, adrenal gland, and ovary, such as inhibition of food and water intake and stimulation of adrenocorticotropic hormone (ACTH)-induced corticosterone production in chickens (Krzysik-Walker et al., 2007; Maddineni et al., 2007; Nakagawa-Mizuyachi et al., 2009; Cline et al., 2010b). As a neuropeptide, CGRP plays a variety of roles in the CNS and peripheral tissues, such as vasodilation, intestinal smooth muscle relaxation, food and water intake, and calcium metabolism (Ancill et al., 1990; Cline et al., 2010b). IAPP has been reported to affect feeding and alimentary canal transit in chickens after central and peripheral administration (Cline et al., 2008b; Cline et al., 2010a). Interestingly, long-term subcutaneous (sc) injection of IAPP can lower the plasma calcium level and increase the thickness of eggshell (Guzel et al., 2009). Despite the diverse roles of ADM and ADM2 reported in mammals, such as vasodilation, regulation of hormone secretion, promotion of angiogenesis, cardiovascular homeostasis, and antimicrobial activity (Hinson et al., 2000; Hong et al., 2012), however, the roles of avian ADM/ADM2 remain largely unknown, except for the potential roles of ADM in food intake and pulmonary hypertension in chickens (Gomez et al., 2007; Wang et al., 2014).

29.1.4 Parathyroid hormone family

In vertebrates, the parathyroid hormone (PTH) family consists of four structurally related peptides, including PTH, parathyroid hormone−related protein (PTHrP), tuberoinfundibular peptide of 39 residues (TIP39, also known as PTH2), and PTH-like peptide (PTH-L). In birds, only PTH, PTHrP, and PTH-L have been identified, while TIP39 is likely lost in the avian lineage (Pinheiro et al., 2010). In chickens, *PTH* encodes a mature PTH hormone of 88 aa (Khosla et al., 1988; Russell and Sherwood, 1989). *PTHrP* can generate multiple spliced transcripts and thus give rise to two forms of PTHrP differing in their C-terminal tails ($PTHrP_{1\text{-}139}$, 139 aa and $PTHrP_{1\text{-}141}$, 141 aa) (Thiede and Rutledge, 1990; Pinheiro et al., 2010). In chickens and turkeys, *PTH-L* produces a mature peptide of 131 or 130 aa. Despite the length of these three hormones, the N-terminal region (34 aa) of $PTH_{1\text{-}34}$, $PTHrP_{1\text{-}34}$, and $PTH\text{-}L_{1\text{-}34}$ is highly conserved and crucial for their biological activity, while their C-terminal region is less conserved (Pinheiro et al., 2012).

Two GPCRs, named PTH1R and PTH3R, for the three hormones have been identified in chickens. Both receptors share ~52% aa identity with each other and belong to the GPCR B1 subfamily. Intriguingly, PTH1R expressed in HEK293 cells can be potently activated by $PTHrP_{1\text{-}34}$ and $PTH\text{-}L_{1\text{-}34}$ (not by $PTH_{1\text{-}34}$) and its activation increases the intracellular cAMP level and calcium concentration, whereas PTH3R can be effectively activated by $PTHrP_{1\text{-}34}$ and $PTH_{1\text{-}34}$ (not by $PTH\text{-}L_{1\text{-}34}$) and its activation stimulates cAMP accumulation (Pinheiro et al., 2012). The considerably low potency of chicken $PTH_{1\text{-}34}$ in activating PTH1R suggests that PTH1R may require accessory protein(s) (e.g., RAMPs) to fulfill its function in vivo, or PTH1R could be potently activated only by the full-length PTH peptide.

PTH2R and *TIP39* genes are lost in avian genomes, suggesting that the functions of TIP39−PTH2R may be replaced by other PTH family member(s) in birds.

In chickens, *PTH* mRNA is nearly exclusively expressed in the parathyroid gland, while *PTHrP* and *PTH-L* have similarly wide tissue expression, including the cartilage, muscle, kidney, midbrain, hindbrain, pituitary, bone, thyroid, and parathyroid gland (Pinheiro et al., 2010). In egg-laying hens, *PTHrP* is expressed in the isthmus and shell gland of oviduct, which likely acts a local modulator of vascular smooth muscle tension and shell gland motility in birds (Thiede et al., 1991; Francis et al., 2003). *PTH1R* is widely expressed in embryos and adult chicken tissues, including parathyroid gland, lung, kidneys, liver, bone, and cartilage, while *PTH3R* is weakly expressed in adult chicken tissues and embryos (Pinheiro et al., 2012; Dale et al., 2015).

In birds, PTH is released by parathyroid chief cells in response to low serum calcium levels. It acts as an endocrine hormone to control serum calcium and phosphate levels via PTH receptor expressed in the bone, kidneys, and intestine, and thus plays important roles in calcium homeostasis, endochondral bone formation, bone remodeling, and eggshell calcification (Dacke, 1976; van de Velde et al., 1984; Singh et al., 1986; Wideman, 1987; Hurwitz, 1996). Although PTHrP and PTH have similar biological actions on target tissues, it is more likely that PTHrP acts as a paracrine/autocrine regulator in avian tissues, such as controlling the pace of growth plate chondrocyte proliferation and differentiation (O'Keefe et al., 1997; Medill et al., 2001). In addition to their effects on calcium homeostasis, PTH/PTHrP have been reported to enhance the basal or ACTH-stimulated aldosterone/corticosterone secretion in chicken adrenocortical cells (Rosenberg et al., 1986, 1988, 1989; Kawashima et al., 2005), control ovarian follicle selection by stimulating proliferation, and steroidogenic capacity of follicular cells (Guo et al., 2019) and inhibit blood vessel constriction (Pang et al., 1984).

PTH-L is a novel hormone identified in birds; it is unknown whether it plays roles similar to PTHrP/PTH in birds. It was reported that as in mammals (Strewler, 2000), PTHrP precursor can produce another bioactive peptide, osteostatin ($PTH_{107\text{-}139/141}$); however, its roles remain to be clarified in birds.

29.1.5 Relaxin peptide family

Relaxin (RLN)/insulin-like peptide (INSL) family contains seven members, including three RLN-like peptides (RLN1, RLN2, and RLN3) and four INSL peptides (INSL3, INSL4, INSL5, and INSL6) in humans. These peptides are encoded by separate genes, which were predicted to be originated from a common ancestral gene (Yegorov and Good, 2012). Each bioactive peptide is composed of A-chain and B-chain linked by two intermolecular disulfide bonds. In addition, an intramolecular disulfide bond is present on the A-chain (Bathgate et al., 2013). In chickens, only *RLN3* (a paralog of human *RLN3*) and *INSL5* genes have been found in the genome (Lovell et al., 2014). Chicken RLN3 peptide is a putative heterodimer consisting of A-chain (25 aa) and B-chain (33 aa), while INSL5 is likely a heterodimer consisting of A-chain of 25aa and B-chain of 25 aa (Fig. 29.2B).

Three GPCRs (named RXFP1, RXFP2-like, and RXFP3) for RLN3 and INSL5 are predicted to exist in avian genomes (Yegorov and Good, 2012). Our preliminary data show that chicken RXFP1 and RXFP3 can function as receptors for RLN3 and their activation stimulates Gs-cAMP and Gi-cAMP signaling pathways, respectively, while RXFP2L can act as a receptor for INSL5 and its activation stimulates Gs-cAMP/PKA signaling pathway (Lv and Wang, Unpublished data).

In birds, only a few studies reported the expression of *RLN3* in the ovary, pituitary, and hypothalamus (Higgins et al., 2010). In chickens, RLN-like immunoreactive signals are localized in granulosa cells of postovulatory follicles and likely act as an ovarian hormone to inhibit uterine muscle contraction (Brackett et al., 1997). The latest findings from our laboratory show that chicken *RLN3* is abundantly expressed in the hypothalamus, pituitary gonadotrophs, and granulosa cells of developing ovarian follicles, and *INSL5* is predominantly expressed in the rectum and cecum. These findings suggest that avian RLN3 is likely a peptide hormone/neuropeptide to regulate many physiological processes, such as feeding and reproduction, as reported in mammals (Bathgate et al., 2013), while avian INSL5 is likely a novel gut hormone derived from the lower part of the gastrointestinal (GI) tract in birds.

29.1.6 Ghrelin/motilin peptide family

Ghrelin (GHRL) and motilin (MLN) peptides are two structurally related gut hormones (Asakawa et al., 2001; Peeters, 2005), which belong to the same peptide family (Hara et al., 2018). GHRL is a 26-aa peptide purified from chicken proventriculus. It is derived from a precursor of 116 aa (Kaiya et al., 2002; Richards et al., 2006). Acylation of either *n*-octanoic or n-decanoic acid at Ser-3 of this peptide is essential for ligand bioactivity and binding affinity. MLN was first isolated from acid extracts of chicken small intestine mucosa. It is a 22-aa peptide found in chickens, quails, and pheasants. It shows six residue differences when compared to the human ortholog (De Clercq et al., 1996; Huang et al., 1999; Apu et al., 2016; Zhang et al., 2020).

The specific receptor for GHRL and MLN has been cloned from chickens. GHRL receptor (GHSR1) has two isoforms (GHSR1a and GHSR1c) generated by alternative splicing. GHSR1a is a full-length receptor containing seven transmembrane domains (TM1−7), while GHSR1c lacks TM6 (Geelissen et al., 2003; Tanaka et al., 2003). Motilin receptor (MLNR) is a GPCR of 349 aa (Yamamoto et al., 2008). GHSR1a and MLNR share ∼53% aa sequence identity with each other, and their activation can increase the intracellular calcium concentration (Yamamoto et al., 2008; Kitazawa et al., 2009).

GHRL is predominantly expressed in the proventriculus and weakly in other tissues (e.g., brain and intestine) of chickens (Kaiya et al., 2002; Neglia et al., 2004; Richards et al., 2006), while GHSR is widely expressed with high expression level noted in the anterior pituitary and hypothalamus and low expression in the GI tract (Tanaka et al., 2003; Richards et al., 2006). MLN-ir is localized in the mucosal layer of small intestine (duodenum, jejunum, and ileum) in quails and chickens (Apu et al., 2016). MLNR is also widely distributed in chicken tissues, with the abundant expression in the proventriculus, duodenum, and oviduct (Yamamoto et al., 2008).

In birds, MLN and GHRL induce contraction of the GI tract in a region-dependent manner (Kitazawa and Kaiya, 2019). MLN stimulates the smooth muscle contraction of small intestine and proventriculus in quails, pheasants, and chickens (Kitazawa et al., 1995; Apu et al., 2016; Zhang et al., 2020), whereas GHRL appears to mainly regulate contractions of the upper (crop) and lower (colon) GI tract in chickens and quails (Kitazawa et al., 2007, 2009). Moreover, GHRL was reported to be associated with other physiological processes, such as regulation of feeding, growth hormone (GH) secretion, and HPA axis activity. For instance, intravenous injection of GHRL can increase plasma GH and corticosterone levels (Ahmed and Harvey, 2002; Kaiya et al., 2002); intracerebroventricular (*icv*) injection of GHRL inhibits food intake in chicks, contrary to the orexigenic action of GHRL in mammals (Furuse et al., 2001; Saito et al., 2002, 2005).

29.1.7 NMU/NMS peptide family

Neuromedin U (NMU) is a neuropeptide conserved across vertebrates (Brighton et al., 2004). In chickens, two NMU forms, named NMU-9 (9 aa) and NMU-25 (25 aa), have been purified from the intestine (O'Harte et al., 1991; Domin et al., 1992). NMU-25 is an N-terminally extended

form of NMU-9. Both NMU-25 and NMU-9 have an amidated C-terminus and are derived from the same precursor encoded by *NMU* gene, which also encodes an NMU precursor−related peptide of 33 aa (Wan et al., 2018).

In rodents, neuromedin S (NMS) is a neuropeptide of 36 aa encoded by *NMS* gene (Mori et al., 2008; Mitchell et al., 2009). In chickens, *NMS* gene encodes an NMS peptide of 9 aa with an amidated C-terminus (NMS-9) (Wan et al., 2018). The question whether the longer form of NMS exists in birds remains. Interestingly, chicken NMU-9 and NMS-9 share high structural similarity with only 2 aa difference noted at positions 1 and 4 (Wan et al., 2018).

Two receptors for NMU and NMS have been identified in chickens and named NMUR1 and NMUR2, respectively (Mitchell et al., 2009; Yamamoto et al., 2011). Both receptors are primarily coupled to Gq protein and their activation triggers intracellular calcium mobilization and enhances ERK phosphorylation (Yamamoto et al., 2011; Wan et al., 2018). Chicken NMUR1 is a receptor common for NMU-25, NMU-9, and NMS-9, while chicken NMUR2 is likely an NMS-preferring receptor (Wan et al., 2018).

In chickens, *NMU* and *NMUR1* are widely expressed in a variety of tissues with abundant expression noted in the GI tract, whereas *NMUR2* expression is mainly restricted to the brain (e.g., hypothalamus) and anterior pituitary, and *NMS* is widely expressed in many tissues including the pituitary, hypothalamus, and adrenal gland (Yamamoto et al., 2011; Wan et al., 2018).

In birds, central injection of NMU or NMS can inhibit food intake and increase locomotor activity and wing-flapping behavior in chicks (Kamisoyama et al., 2007; Tachibana et al., 2010b,c) or quails (Shousha et al., 2005, 2006). However, it is unknown whether they are involved in the regulation of smooth muscle contraction, pain, pituitary hormone secretion, blood pressure, and circadian rhythm in birds, as reported in mammals (Mori et al., 2008; Mitchell et al., 2009).

29.1.8 Neuropeptide S

In mammals, neuropeptide S (NPS) and its receptor (NPSR) have been reported to play important physiological/pathophysiological roles in the CNS, such as locomotor activity, wakefulness, panic disorder, anxiolytic behavior, sleeping disorders, food intake, memory, asthma, and drug addiction (Guerrini et al., 2010; Valsalan and Manoj, 2014). *NPS* and *NPSR* also exist in avian genome. In chickens, *NPS* is predicted to produce a bioactive peptide of 20 aa. NPSR is a seven-transmembrane GPCR of 373 aa (KX595273).

In chickens, *icv* injection of rat NPS inhibits food intake, reduces plasma corticosterone concentration, decreases exploratory pecking, jumping, and locomotion and increases time spent in deep rest (Cline et al., 2007; Cline et al., 2008c). Moreover, HWS chicken is more sensitive to NPS injection than LWS chickens (Cline et al., 2008c).

29.1.9 Neurotensin and neuromedin N

Neurotensin (NTS) is a peptide of 13 aa expressed in the CNS and GI tract in mammals and plays diverse roles in many physiological/pathological processes, such as regulation of analgesia, feeding, blood pressure, and sleep in the CNS and control of gastric acid secretin (SCT) and colonic motility in the GI tract (Mustain et al., 2011). Besides NTS, neuromedin N (NN, 6 aa) is also encoded by *NTS* gene. In chickens, both NTS (13 aa) and NN (6 aa, also called LANT6) peptides have been purified from the small intestine (Carraway and Bhatnagar, 1980; Carraway and Ferris, 1983). It is clear that both NTS and NN share structural and functional similarity, which are derived from the same NTS precursor (Carraway et al., 1993; Tanaka et al., 2013). In addition, a large LANT6 form of ~15 kDa also exists in chicken intestine. It may display the biological activity similar to NN, as in mammals (Carraway et al., 1993). The biological actions of chicken NTS and NN are likely mediated by an NTSR1, which is a member of GPCR family and its activation can increase calcium concentration (Numao et al., 2011).

In chickens, NN and NTS peptides were detected to exist in a molar ratio of ~1.2−1.7 in HCl extracts of chicken tissues, including the small intestine, cecum, colon, brain, thymus, and pancreas. Among these tissues, NTS and NN have the greatest abundance in the intestine (Carraway et al., 1993), where NTS-ir is mainly distributed in the endocrine N cells of GI epithelium layer in chickens, Japanese quails, and pigeons (Sundler et al., 1977; Atoji et al., 1994). Recently, Nishimura et al. (2017) reported the colocalization of NTS with glucagon-like peptide 1 (GLP1) in some enteroendocrine cells of distal ileum crypts (Nishimura et al., 2017). Beside the GI tract, NTS-ir is distributed in thymus endocrine cells (Atoji et al., 1996b). Moreover, NN/NTS-ir neurons/fibers are widely distributed in the CNS, including the retina (Eldred et al., 1987), various brain regions (e.g., hypothalamus and nucleus accumbens) (Atoji et al., 1996a; Masuda et al., 2014; Balint et al., 2016), and spinal cord (Atoji et al., 1996a). Like NTS, NTSR1 is also expressed in the GI tract, liver, thymus epithelial cells, and CNS (Numao et al., 2011; Tanaka et al., 2013). These findings suggest that NTS/NN may act as a circulating gut hormone, local paracrine factor, and neurotransmitter in avian CNS, GI tract, thymus, and liver.

So far, NTS has been reported to elevate the hepatic bile acid output (Gui et al., 2000), inhibit pepsin output from the proventriculus (Degolier et al., 1997), and induce motility

of the ileum and cecum (Rawson et al., 1990) in birds. The other physiological roles of avian NTS/NN in the CNS and peripheral tissues remain to be clarified.

29.1.10 RF-amide peptide family

In birds, RF-amide peptide family includes eight structurally related peptides: neuropeptide AF (NPAF), gonadotropin-inhibitory peptide (GnIH), GnIH-related peptide 1 (GnIH-RP1), GnIH-related peptide 2 (GnIH-RP2), prolactin-releasing peptide (PrRP), prolactin-releasing peptide 2 (PrRP2, also named C-RFa), and 26RFa (also called QRFP) (Osugi et al., 2006; Wang et al., 2012c; Tachibana and Sakamoto, 2014). All these peptides are characterized by the presence of a C-terminal Arg-Phe-NH2 (RF-amide) motif, which is essential for their biological activity and receptor binding. Moreover, all peptides are proteolytically cleaved from their precursors encoded by *NPFF*, *NPVF*, *PrRP*, *PrRP2*, and *QRFP* genes, respectively.

In birds, NPFF precursor can produce a single bioactive NPAF peptide of 20 aa, which can potently activate NPFF receptor 2 (NPFFR2) and inhibit cAMP/PKA signaling pathway (Chen et al., 2020). NPVF precursor is likely to generate three structurally related peptides, GnIH (12 aa), GnRH-RP1 (37 aa), and GnIH-RP2 (13 aa) (Satake et al., 2001; Ikemoto and Park, 2005; Tobari et al., 2010), all of which can bind to the same NPFF receptor 1 (NPFFR1, also called GnIH-R) with high affinity (Yin et al., 2005). Like NPFFR2, NPFFR1 activation also inhibits cAMP/PKA and activates MAPK/ERK1/2 signaling pathways in chickens (Shimizu and Bedecarrats, 2010).

PrRP precursor can produce a mature PrRP peptide of 20 aa (Wang et al., 2012c), while PrRP2 precursor generates two forms of PrRP2 peptide with an identical C-terminus: $PrRP2_{20}$ ($C\text{-}RFa_{20}$, 20 aa) and $PrRP2_{31}$ ($C\text{-}RFa_{31}$, 31 aa). $PrRP2_{31}$ is an N-terminally extended form of $PrRP2_{20}$ (Tachibana et al., 2011b; Wang et al., 2012c). Three GPCRs for PrRP and PrRP2 have been identified and named as PrRPR1, PrRPR2, and PrRP2-R (also called C-RFaR). PrRPR1 and PrRPR2 can act as the receptors common for both PrRP and PrRP2, whereas PrRP2-R can function as a PrRP2-specific receptor (Wang et al., 2012c). Three receptors are primarily coupled to Gq protein and their activation triggers intracellular calcium mobilization (Wang et al., 2012c).

QRFP precursor produces a mature 26RFa peptide of 27 aa, which can activate its receptor GPR103 (QRFPR) potently and trigger postreceptor calcium mobilization (Ukena et al., 2010).

In chickens, *NPFF* mRNA is highly expressed in the CNS, including the hypothalamus and weakly in other tissues, while its receptor *NPFFR1* is highly expressed in the anterior pituitary and hypothalamus and weakly in other tissues (Ikemoto and Park, 2005; Chen et al., 2020). *icv* injection of rat NPAF inhibits food and water intake and decreases plasma glucose concentration in chicks (Cline et al., 2009a).

In quails and zebra finches, GnIH-ir is mainly localized in the hypothalamic paraventricular nuclei (PVN) and some GnIH-ir fibers project into the external layer of ME (Tsutsui et al., 2000). A later study revealed that GnIH-ir is also localized at the dorsomedial nucleus of the hypothalamus, and GnIH-ir fibers are widely distributed in multiple brain regions, including the preoptic area (POA) rich in GnRH-I neurons in finch brain (Tobari et al., 2010). GnIH receptor (NPFFR1) is expressed in several brain regions and the anterior pituitary (Ikemoto and Park, 2005; Yin et al., 2005). In quails, GnIH can inhibit basal luteinizing hormone (LH) secretion of the anterior pituitary (Tsutsui et al., 2000). Similarly, GnIH can inhibit basal pituitary follicle-stimulating hormone (FSH) and LH release and *FSHβ* and *CGA* expression in chickens (Ciccone et al., 2004). Moreover, *icv* injection of GnIH stimulates food intake and upregulates orexigenic factor (melanin-concentrating hormone [MCH] and neuropeptide Y [NPY]) expression and downregulates proopiomelanocortin (POMC) expression (McConn et al., 2014). These findings indicate that NPAF and GnIH (or GnIH-RPs) can act as a neuromodulator or neuroendocrine hormone in birds.

In chickens, *PrRP* and *PrRP2* are widely expressed in adult tissues, including the hypothalamus, anterior pituitary, and gonads detected by RT-PCR assay, while the three receptors for PrRP and PrRP2 are widely expressed in most tissues including the anterior pituitary, hypothalamus, and gonads (Wang et al., 2012c). *icv* injection of chicken $PrRP2_{31}$ increases food intake, contrary to the anorexic action of PrRP observed in rats and goldfish (Tachibana et al., 2011b; Tachibana and Tsutsui, 2016). Moreover, central and peripheral administration of PrRP2 decreases plasma GH levels, while peripheral administration of PrRP2 can increase plasma prolactin (PRL) level, and *icv* injection of PrRP2 decrease PRL levels.

In chickens, *QRFP* (26RFa) is expressed in the anterior hypothalamus nucleus (AM) (Ukena et al., 2010). In zebra finches, QRFP is also expressed in the AM and other hypothalamus nuclei (e.g., ventromedial nucleus of hypothalamus and lateral hypothalamus) associated with feeding, while QRFPR (GPR103) is distributed throughout the brain expressed including the hypothalamus (Tobari et al., 2011). In zebra finches and broiler (not layer) chickens, *icv* injection of RF26a can increase food intake (Ukena et al., 2010; Tobari et al., 2011). This finding indicates the involvement of 26RFa in the regulation of feeding and energy balance.

29.1.11 Cholecystokinin and gastrin peptide family

Cholecystokinin (CCK) and gastrin (GAST) are two peptides encoded by separate genes and sharing the conserved C-terminal "Trp-Met-Asp-Phe-NH2" motif, which is crucial for their biological activity. In chickens, CCK precursor can produce multiple CCKs of different lengths, namely CCK70, CCK8, and CCK7, in the intestine after posttranslational processing, all of which have the identical C-terminus, but vary in the length of their N-termini (Jonson et al., 2000). As in mammals, avian CCK peptide exists in nonsulfated and sulfated forms, in which the latter has a sulfated tyrosine at position 7 counted from the C-terminus. Chicken GAST precursor can produce four forms of peptides at different lengths with an identical C-terminus: gastrin-53, gastrin-30, gastrin-21, and gastrin-7, among which gastrin-53 is the predominant form existed in antrum mucosa (Bjornskov et al., 1992; Wu et al., 1995; Jensen et al., 2001). Chicken GAST mainly exists in the sulfated form with a sulfated tyrosine at position 7 countered from the C-terminus (Bjornskov et al., 1992).

Two GPCRs, named CCK1R (CCKAR) and CCK2R (CCKBR) for CCK/GAST have been cloned from chickens (Nilsson et al., 2003). Chicken CCK2R displays high affinity for sulfated CCK8 and gastrin-17 and a lower affinity for CCK4 in vitro, thus acting as a common receptor for GAST and CCK (Nilsson et al., 2003). Nevertheless, the signaling property of avian CCK1R and CCK2R is unknown.

In chickens, GAST mRNA or peptide is exclusively expressed in gastric antrum region revealed by qPCR assay (Reid and Dunn, 2018) and immunostaining (Martinez et al., 1993), whereas CCK is highly expressed in the basal hypothalamus, moderately in the small intestine (e.g., in ileum endocrine cells), and weakly in other remaining parts of the GI tract (Reid and Dunn, 2018). Both CCK1R and CCK2R are widely, but differentially, expressed in chicken tissues. For instance, CCK2R is preferentially expressed in the brain and proventriculus (Ohkubo et al., 2007).

In birds, CCK and GAST act as the neurotransmitter or gut hormone to regulate brain and gut functions. In the GI tract, CCK increases bile outflow and pancreatic enzyme secretion and inhibits crop emptying (Furuse, 1999). In addition, central/peripheral injection of CCK reduces food intake (Savory and Gentle, 1980; Denbow and Myers, 1982; Rodriguez-Sinovas et al., 1997; Dunn et al., 2013); thus, CCK can act as a satiety signal involved in the control of feeding and growth in poultry (Rikimaru et al., 2012; Dunn et al., 2013; Reid and Dunn, 2018; Yi et al., 2018). Recently, CCK−CCK2R signaling in the nucleus intercollicularis of midbrain has been reported to be associated with chicken crowing (Shimmura et al., 2019). Unlike CCK, GAST secreted from gastric antrum can stimulate gastric acid secretion, but has no effect on pancreatic secretion and gall bladder contraction in chickens (Dimaline and Lee, 1990; Furuse, 1999).

29.1.12 Orexin peptide family

In chickens, two orexin peptides, orexin-A and orexin-B (also called hypocretins), have been identified, both of which share ~50% sequence identity and are produced by the same precursor. Chicken orexin-A is a neuropeptide of 33 aa with two intramolecular disulfide bonds (Cys6−Cys12 and Cys7−Cys14) and an amidated C-terminus, while orexin-B is a 28 aa and C-terminally amidated neuropeptide (Ohkubo et al., 2002). Only a single GPCR for orexins A and B named OX2R has been identified in chickens, which contrasts the findings in mammals, where two orexin receptors (OX1R, OX2R) have been identified (Sakurai et al., 1998; Ohkubo et al., 2003). The pharmacological and signaling property of OX2R remains unclear in birds.

In birds, orexin is predominantly expressed in the hypothalamus (Ohkubo et al., 2002). Within the hypothalamus, orexin neurons are reported to be distributed in the periventricular nucleus and lateral hypothalamic area in chickens (Ohkubo et al., 2002) and quails (Phillips-Singh et al., 2003) in earlier studies. However, recent studies show that orexin neurons are localized in the PVN in chickens and house finches (Singletary et al., 2006; Miranda et al., 2013). *OX2R* is abundantly expressed in the hypothalamus, cerebrum, and optic tectum and weakly in the pituitary gland, adrenal gland, and testis. It is clear that orexin can act as a neuropeptide functioning in chicken brain; however, more studies are required to clarify the roles of orexin in avian CNS (Furuse et al., 1999; Katayama et al., 2010; Song et al., 2012; Miranda et al., 2013).

29.1.13 Melanin-concentrating hormone peptide

MCH is a 17-aa cyclic peptide, which was originally identified in chum salmon pituitaries as a hormone that induces aggregation of melanin granules within melanophores in fish scales (Kawauchi et al., 1983). Recently, *MCH* cDNA was cloned from chicken hypothalamus (Sun et al., 2013). The mature chicken MCH is a 19-aa cyclic peptide and shares high structural similarity to fish MCH (Cui et al., 2017). Moreover, an MCH receptor (named *MCHR4*) has also been identified in chickens and ducks. Avian MCHR4 is coupled to Gq protein and its activation triggers calcium mobilization and enhances ERK phosphorylation (Cui et al., 2017).

In chickens, *MCH* mRNA is predominantly expressed in the hypothalamus (Cui et al., 2017), and MCH-ir perikarya are localized in the periventricular hypothalamic

nucleus near the paraventricular organ and in the lateral hypothalamic areas (Cardot et al., 1999). The distribution pattern of MCH in the hypothalamus suggests that MCH may play roles in avian CNS, such as regulation of feeding, similar to those described in rats (Cardot et al., 1999). qPCR assay revealed that *MCHR4* is widely expressed in chicken hypothalamus and other brain regions, further supporting the central actions of MCH in birds. Interestingly, *MCHR4* is also highly expressed in the testis (Cui et al., 2017); however, its physiological role therein is unknown.

29.1.14 Prokineticin peptide family

In mammals, prokineticin (PROK) family comprises two structurally related peptides, named PROK1 and PROK2. As in mammals, both *PROK1* and *PROK2* genes exist in chickens, quails, and other birds. Chicken *PROK1* is predicted to encode a peptide of 86 aa, while *PROK2* produces a peptide of 88 aa. Both peptides possess five intramolecular disulfide bonds and a conserved "AVITGA" motif at the N-termini essential for their biological activity (Negri et al., 2007). Interestingly, only a single PROK receptor exists in chicken genome and is designated as PKR1 (FJ61954), contrasting to the findings in mammals, where two receptors (PKR1 and PKR2) for PROK1 and PROK2 have been identified (Negri and Ferrara, 2018). Therefore, further studies are required 1) to examine the functionality of PROK1/2-PKR2 system in birds and 2) to elucidate whether as in mammals, PROK/PKR2 is involved in the regulation of GI tract motility, circadian rhythm, neurogenesis, angiogenesis, hematopoiesis, reproduction, and nociception (Negri and Ferrara, 2018).

29.1.15 Corticotropin-releasing hormone peptide family

In birds, corticotropin-releasing hormone (CRH) family consists of five peptides: CRH, urocortin (UCN), urocortin II (UCN2), urocortin III (UCN3), and corticotropin-releasing hormone 2 (CRH2) (Vandenborne et al., 2005a; Grommen et al., 2017; Bu et al., 2019). These peptides share ~23−63% aa sequence identity with each other and all are C-terminally amidated. Five peptides are derived from their respective precursors encoded by separate genes, which were originated from a common ancestral gene. In chickens, CRH is a 41-aa peptide and CRH2 is a 40-aa peptide. Both peptides share ~63% aa identity (Vandenborne et al., 2005a; Bu et al., 2019). The UCN, UCN2, and UCN3 peptides have 40, 38, and 40 aa, respectively, and share a relatively low identity with CRH/CRH2 (Fig. 29.2C). The biological actions of CRHs/UCNs are mediated by two structurally related GPCRs, named CRH receptor 1 (CRHR1) and CRH receptor 2 (CRHR2) (Yu et al., 1996; de Groef et al., 2004). Both receptors have been proven to couple to Gs-AC/cAMP signaling pathways (Mo et al., 2015). Chicken CRHR1 can be potently activated by CRH and UCN, thus acting as a receptor common for both peptides. CRHR2 can be potently activated by CRH, CRH2, UCN, UCN2, and UCN3 and is a receptor common for the five peptides (Mo et al., 2015; Bu et al., 2019) (Wan et al., unpublished data).

In birds, CRH is expressed in the hypothalamus (paraventricular, preoptic, and mammillary nuclei [MM] of the hypothalamus) and other brain regions (e.g., nuclei dorsomedialis and dorsolateralis thalami, nucleus accumbens, etc.) (Jozsa et al., 1984, 1986; Yamada and Mikami, 1985). CRH can directly stimulate pituitary ACTH and TSH secretion via CRHR1 and CRHR2, respectively (De Groef et al., 2005). In addition, central CRH also regulates other physiological processes, such as decreased food intake, retarded crop-emptying rate, and increased body temperature, voluntary activity, and numbers of vocalization (Ogino et al., 2014).

Unlike *CRH*, *CRH2* is widely expressed in chicken tissues including the CNS, GI tract, and pituitary. *In vitro* experiments show that CRH2 can stimulate pituitary *TSHβ* expression and ACTH secretion. These findings suggest that CRH2 plays roles similar, but nonidentical, to those of CRH (Bu et al., 2019).

Using in situ hybridization, *UCN3* mRNA was found to be expressed predominantly in the hypothalamus, pons, and medulla of posthatch chick brains. This finding implies the involvement of UCN3 in the regulation of feeding and the autonomic motor control of the GI tract system (Cline et al., 2009b; Ogino et al., 2014; Grommen et al., 2017). To date, information regarding the physiological roles of CRHs/UCNs remains rather limited in birds.

29.1.16 Neuropeptide W and neuropeptide B

Neuropeptide W (NPW) and neuropeptide B (NPB) are two structurally related peptides in mammals. Both peptides are reported to be involved in the central regulation of neuroendocrine axes, feeding behavior, energy homeostasis, circadian rhythm, pain sensation, and emotions (Chottova Dvorakova, 2018). In chickens, NPW, NPB, and their receptors have recently been characterized. Chicken *NPW* encodes a mature NPW peptide of 23 and 30 aa (NPW23 and NPW30), while *NPB* gene encodes a NPB peptide of 28 aa (NPB28). NPW30 and NPB28 share 57% aa sequence identity. Two GPCRs for NPW and NPB (NPBWR1 and NPBWR2) have been identified in birds. NPBWR2 is likely an NPW-specific receptor, which can also be activated by NPB at high concentrations (>100 nM). Interestingly, NPBWR1 seems nonfunctional

in chickens (Bu et al., 2016; Scanes, 2016). However, high concentration of NPW was reported to activate this receptor in geese.

In adult chickens, *NPW* is highly expressed in the hypothalamus and weakly expressed in other tissues including the anterior pituitary and other brain regions, while NPW receptor (*NPBWR2*) is predominantly expressed in the anterior pituitary. This finding suggests that NPW–NPBWR2 signaling is involved in the regulation of pituitary functions, such as inhibition of GH and PRL secretion (Bu et al., 2016). *NPB* is widely expressed in a variety of chicken tissues including the hypothalamus, and *NPBWR1* is highly expressed in the hypothalamus, telencephalon, hindbrain, and midbrain. However, the physiological relevance of *NPB*/*NPBWR1* expression is unknown in birds (Bu et al., 2016).

29.1.17 Opioid peptide family

In mammals, opioid peptide family includes several structurally related neuropeptides, including Met-enkephalin, Leu-enkephalin, β-endorphin, Met-enkephalin-Arg-Phe, dynorphin-A and dynorphin-B, neo-endorphin, Met-enkephalin-Arg-Gly-Leu, metorphamide, and nociceptin. All these peptides differ in length, but possess an identical core motif (Y/FGGF) at their N-termini. In birds, these opioid peptides are derived from four distinct precursors, i.e., proenkephalin (PENK), POMC, prodynorphin (PDYN), and pronociceptin (PNOC), which are encoded by four separate genes, namely *PENK*, *POMC*, *PDYN*, and *PNOC* (Scanes and Pierzchala-Koziec, 2018). In chickens, PENK precursor may produce four copies of Met-enkephalin (YGGFM), one Leu-enkephalin (YGGFL), one Met-enkephalin-Arg-Phe (YGGFMRF), and one octopeptide (Met-enkephalin-Arg-Ser-Val). PDYN precursor is predicted to generate dynorphin-A, dynorphin-B, and one Met-enkephalin, which is absent in other vertebrate groups. However, chicken PDYN precursor cannot produce "neo-endorphin." Chicken PNOC and POMC precursors can produce mature nociceptin (17aa) and β-endorphin (31aa), respectively (Bu et al., 2020).

Four functional receptors for opioid peptides, named DOR, MOR, KOR, and ORL1, have been characterized in chickens. DOR acts as a common receptor for Met-enkephalin and Leu-enkephalin, while KOR is a receptor common for dynorphin-A, dynorphin-B, and nociceptin. In contrast, ORL1 can only be specifically activated by nociceptin and thus is a nociceptin-specific receptor. Unlike DOR, KOR, and ORL1, MOR is moderately/weakly activated by enkephalins and other opioid peptides, including β-endorphin (Bu et al., 2020). Activation of these receptors can decrease intracellular cAMP levels and stimulate MAPK/ERK signaling pathway (Bu et al., 2020).

In chickens, *PENK* mRNA is highly expressed in the brain (including the hypothalamus, midbrain, hindbrain, and telencephalon), spinal cord and testes, and moderately in the anterior pituitary and skin. *cPOMC* mRNA is expressed predominantly in the anterior pituitary, moderately in the hypothalamus, and weakly in the spinal cord, skin, ovary, testes, and muscle. Interestingly, *cPDYN* mRNA is abundantly expressed in the hypothalamus, heart, and muscle, and weakly in other tissues including spinal cord, lung, and anterior pituitary. *cPNOC* is highly expressed in the brain (e.g., hypothalamus, hindbrain, midbrain, cerebellum, and telencephalon), spinal cord and heart, and weakly expressed in the muscle. Like the four opioid precursors, the four opioid receptors (*OPRD1, OPRM1, OPRK1,* and *OPRL1*) expression is mainly restricted to various brain regions (including the hypothalamus) and spinal cord. Only a moderate/weak expression of opioid receptor(s) was noted in several peripheral tissues, including the lung (*OPRM1*), testis (*OPRM1*), anterior pituitary (*OPRK1, OPRL1,* and *OPRM1*), and ovary (*OPRK1*) (Bu et al., 2020).

The predominant expression of opioid peptides and their receptors in chicken brain and spinal cord suggests that opioid peptides play crucial roles in avian CNS, such as addiction, analgesic action, antinociception, memory formation, reproduction, and food intake (Bungo et al., 2004, 2009; Dodo et al., 2005). The expression of β-endorphin in the pituitary, enkephalins in the pituitary and testis, nociceptin in the heart, and dynorphins in the heart and muscle hints that these opioid peptides play paracrine/autocrine or endocrine roles in avian peripheral tissues (Bu et al., 2020).

29.1.18 Somatostatin/cortistatin peptide family

In birds and mammals, SST and CST are two structurally and functionally related cyclic peptides and encoded by two separate genes, *SST* and *CST* (Gunther et al., 2018). In chickens, after proteolytic processing, SST precursor can produce a mature SST peptide of 14 aa (SST14) or 28 aa (SST28). SST28 is an N-terminally extended form of SST14. CST precursor can produce a mature CST peptide of 14 aa (CST14) or 24 aa (CST24) with an identical C-terminus (Trabucchi et al., 2003). Interestingly, SST14 shows remarkable structural conservation with CST14 with only one aa difference noted at position 2 (Gly in SST14 and Pro in CST14) (Meng et al., 2014).

Five GPCRs for SST and CST, namely SSTR1, SSTR2, SSTR3, SSTR4, and SSTR5, have been characterized in chickens (Meng et al., 2014). SSTR1 to 4 are the four receptors common for SST14, SST28, and CST14 peptides, while SSTR5 is a SST28-specific receptor. Activation of the five receptors can decrease intracellular cAMP levels (Meng et al., 2014).

In chickens, *SST* mRNA is abundantly expressed in the brain, spinal cord, and pancreas detected by Northern blot, while *CST* mRNA expression is mainly restricted to brain and spinal cord (Trabucchi et al., 2003). RT-PCR assay revealed that *SST* and *CST* are also expressed in the intestine and gonads (Meng et al., 2014). Within the brain, *SST* mRNA is distributed in the hippocampus, hyperstriatum, POA, ventricular hypothalamic nuclei, optic tectum, and several nuclei of the mesencephalon and rhombencephalon, while C*ST* is expressed in the paraolfactory lobe, the paleostriatum, and some nuclei of the mesencephalon and rhombencephalon. In addition to the above-mentioned tissues, SST-ir cells were also detected in the retina (Buckerfield et al., 1981), thyroid gland, gut, carotid body (Kameda, 1989), and pancreatic D-cells (Weir et al., 1976; Hazelwood, 1984). Like SST/CST, SSTR1-5 are widely, but differentially, expressed in chicken tissues including various brain regions, indicating that the diverse actions of SST/CST are likely mediated by the distinct SSTR(s) expressed in tissue-/cell-specific manner.

In chickens, SST and its receptors have been reported to inhibit pituitary hormone (e.g., GH and TSH) secretion (Harvey et al., 1978; Perez et al., 1987; Donoghue and Scanes, 1991; De Groef et al., 2003, 2007; Anderson and Scanes, 2012; Meng et al., 2014), pancreatic hormone (e.g., glucagon, insulin, and PP) secretion (Honey et al., 1980, 1981; Hazelwood, 1984), lipolysis (Strosser et al., 1983), thyroid function, as well as stimulate food intake (Tachibana et al., 2009; Tachibana et al., 2011a; Yousefvand et al., 2019). However, the information regarding the roles of CST is largely unknown in birds (Meng et al., 2014).

29.1.19 Urotensin II/urotensin II–related peptide family

Urotensin 2 (UTS2) and URP are cyclic peptides, which function as neuropeptides to regulate multiple physiological processes, such as sleep, food intake, cardiovascular function, locomotion, and anxiety (Vaudry et al., 2015). Both peptides share high structural similarity and contain a conserved cyclic motif (CFWKYC) crucial for their biological activity (Leprince et al., 2008; Vaudry et al., 2015). In chickens, *UTS* gene likely encodes a mature UTS2 of 12 or 17 aa (UTS2-12. UTS2-17), while *URP* encodes a URP peptide of 8 aa (Tostivint et al., 2006). Four GPCRs for UTS2/URP, namely *UTS2R1*, *UTS2R2*, *UTS2R3,* and *UTS2R5,* exist in chicken genome (Tostivint et al., 2014; Vaudry et al., 2015). However, our knowledge regarding the expression, functionality, and roles of UTS2, URP and their four receptors in birds is currently limited.

29.1.20 Glucagon peptide superfamily

In birds, glucagon (GCG) superfamily consists of 12 structurally related peptides, including GCG (29 aa), GLP1 (30 aa), glucagon-like peptide 2 (GLP2, 33 aa), glucose-dependent insulinotropic polypeptide (GIP, 41 aa), glucagon-like peptide (GCGL, 29 aa), SCT (27 aa), secretin-like peptide (SCT-LP, 34 aa), growth hormone–releasing hormone (GHRH, 27aa/47aa), GHRH-related peptide (GHRH-LP, 46 aa), pituitary adenylate cyclase–activating polypeptide (PACAP: 27 aa/38 aa), vasoactive intestinal polypeptide (VIP, 28 aa), and peptide histidine–isoleucine (PHI, 27 aa) (Fig. 29.2D). Among them, GCGL, GHRH-LP, and SCT-LP peptides are lost in mammals. These peptides are encoded by seven genes, namely *GCG*, *GIP, GCGL, GHRH, SCT, PACAP* (*ADCYAP1*), and *VIP*, which are generated by genome duplication during early vertebrate evolution (Sherwood et al., 2000; Wang et al., 2012b). In chickens, *GCG* gene encodes three bioactive peptides, i.e., GCG, GLP1, and GLP2 (Hasegawa et al., 1990; Irwin and Wong, 1995; Richards and McMurtry, 2008); *GIP*, *GCGL*, and *GHRH* genes code for GIP, GCGL, and GHRH peptides, respectively (Irwin and Zhang, 2006; Wang et al., 2007; Wang et al., 2012b); *SCT* encodes for SCT-LP and SCT peptides (Wang et al., 2012a); *PACAP* encodes two bioactive peptides, i.e., GHRH-LP and PACAP (McRory et al., 1997; Wang et al., 2006); and *VIP* codes for bioactive VIP and PHI peptides (Talbot et al., 1995).

Nearly, all the receptors for GCG family peptides (except GIP) have been functionally characterized in chickens (Fig. 29.2D). These receptors are coupled to Gs-cAMP/PKA signaling pathway. GCG, GLP1, GLP2, GCGL, GHRH, and GHRH-LP possess their specific receptor(s), named GCG receptor (GCGR) (Wang et al., 2008), GLP1 receptor (GLP1R) (Huang et al., 2012), GLP2 receptor (GLP2R) (Mo et al., 2014), GCGL receptor (GCGLR) (Wang et al., 2012), GHRH receptors (GHRHR1 and GHRHR2) (Wang et al., 2010), and GHRH-LP receptor (GHRH-LPR) (Wang et al., 2010). Interestingly, PACAP, VIP, and PHI share two common receptors, named VIPR1 and VIPR2, and PACAP also has a PACAP-specific receptor (PAC1) (Wang et al., 2010). SCT and SCT-LP share a common receptor, SCT receptor (SCTR) (Wang et al., 2012a). The functionality of GIP receptor still remains unknown in birds.

In vertebrates, GCG superfamily peptides can function as gut hormones, neuroendocrine hormones, and neurotransmitters/neuromodulators (Sherwood et al., 2000).

Specifically, in birds, *GHRH* mRNA is mainly expressed in the hypothalamus (Wang et al., 2007; Martinez-Moreno et al., 2014) and can potently stimulate pituitary GH secretion in vitro, thus being an authentic GH-releasing factor. In addition, *icv* injection of GHRH inhibits food intake in the hypothalamus (Harvey et al., 2014; Meng et al., 2014; Tachibana et al., 2015).

GCG is highly expressed in chicken pancreas and proventriculus and moderately/weakly in other tissues including the duodenum, liver, brain, heart, lung, muscle,

fat, kidney, and spleen (Richards and McMurtry, 2008). In the pancreas, GCG peptide is abundantly expressed in the islet A cells. Three receptors (GCGR, GLP1R, and GLP2R) for GCG, GLP1, and GLP2 have also been reported to be widely, but differentially, expressed in chicken tissues. The predominant expression of GCGR in liver and fat indicates that GCG can stimulate glucose output and inhibit lipogenesis in liver and promote lipolysis in adipocytes (Langslow and Hales, 1969; Langslow, 1973; Goodridge et al., 1974; Krug et al., 1976; Campbell and Scanes, 1987; Richards and McMurtry, 2008; Wang et al., 2008). The wide expression of GLP1R and GLP2R in chicken tissues including the hypothalamus and pancreas (Richards and McMurtry, 2008; Huang et al., 2012; Mo et al., 2014) suggests their possible involvement in the regulation of feeding, pancreatic functions, GI tract motility, and intestinal growth in birds (Furuse et al., 1997; Richards and McMurtry, 2008; Huang et al., 2012; Mo et al., 2014; Honda et al., 2015).

GCGL is highly expressed in the hypothalamus and *GCGLR* is predominantly expressed in the anterior pituitary thyrotropes and hypothalamus (Wang et al., 2012c; Huang et al., 2014a). Further studies revealed that GCGL can stimulate pituitary TSH expression and secretion specifically and inhibit food intake in the hypothalamus (Honda et al., 2014; Huang et al., 2014a).

SCT is predominantly expressed in the duodenum, jejunum, and ileum, while SCTR is highly expressed along the GI tract (including proventriculus, gizzard, duodenum, jejunum, ileum, and colon), liver, and testis. This finding indicates that SCT and SCT-LP peptides are mainly produced by small intestine and play important roles in GI tract activity (gastric acid and pepsin secretion) and hepatic functions (Burhol, 1974; Wang et al., 2012a).

VIP gene produces two alternative spliced transcripts: the long transcript encoding PHI and VIP peptides, while the short one encodes VIP only and is the predominant form expressed in chicken tissues (Talbot et al., 1995). VIP mRNA/peptide is abundantly expressed in the hypothalamus and has been proved to be the major PRL-releasing factor in birds (Sharp et al., 1989; Talbot et al., 1995). In addition, *VIP* mRNA is also expressed in other brain regions (cerebellum and forebrain), liver, kidneys, gut, pancreas, and pituitary. This finding, together with the wide expression of two VIP receptors in all chicken tissues, including various brain regions, GI tract, liver, pancreas, ovary, and testis, suggests that VIP can act as a neurotransmitter or local factor to regulate many physiological processes, such as pancreatic bicarbonate secretion, vasodilation, intestinal smooth muscle relaxation, and ovarian granulosa cell differentiation and steroidogenesis (Dimaline and Dockray, 1979; Johnson and Tilly, 1988; Johnson et al., 1994; Kim and Johnson, 2016). Since PHI-coding transcript is weakly expressed in avian tissues, it implies a limited role of PHI in birds.

PACAP mRNA/ir is found in the brain (e.g., hypothalamus), small intestine, testis, ovary, and heart (Sundler et al., 1992; McRory et al., 1997; Peeters et al., 1998; Wang et al., 2006; Prisco et al., 2019). These findings, together with the expression of the specific receptor for GHRH-LP (GHRH-LPR)/PACAP (PAC1) in these tissues (Wang et al., 2010), suggest that GHRH-LP and PACAP can function as a neuromodulator/neurotransmitter and play important roles in avian CNS, such as inhibition of food intake (Tachibana et al., 2015) or function as a local regulatory factor in the heart, intestine, and gonads.

To date, the expression, functionality, and role of GIP—GIPR are largely unknown in birds.

29.1.21 Apelin and elabela peptides

In mammals and teleosts, Apelin (APLN), and Elabela (ELA, also named Apela) are two peptides sharing little structural similarity; however, both peptides use the same Apelin receptor (APLNR) to exert their regulatory roles in vivo, such as the regulation of cardiovascular development and function, blood pressure, fluid homeostasis, angiogenesis, neuroendocrine activity, heart development, food intake, drinking behavior, pituitary hormone secretion, metabolism, and neuroprotection (Pitkin et al., 2010). In chickens, *APLN* gene is predicted to generate a mature APLN peptide of different lengths, such as 36 aa (APLN-36), 16 aa (APLN-16), and 13 aa (APLN-13), while *ELA* gene is predicted to generate a mature ELA peptide of different lengths, including 32 aa (ELA-32), 22 aa (ELA-22), or 11 aa (ELA-11). The shortest forms of APLN/ELA peptides (APLN-13/ELA-11) correspond to the C-terminal portion of APLN-36/ELA-32 and seem to be less bioactive than their longest forms (Zhang et al., 2018b).

Three GPCRs for APLN and ELA, namely APLNR1, APLNR2, and GPR25, have been identified in chickens. APLNR1 can be potently activated by APLN-36 ($EC_{50:}$ 0.18 nM) and ELA-32 ($EC_{50:}$ 0.87 nM) and thus is a receptor common for APLN and ELA. In contrast, APLNR2 could only be weakly activated by APLN-36/ELA-32 at a high concentration far beyond the physiological range, implying a less significant role of APLNR2 in chickens (Zhang et al., 2018b). Interestingly, GPR25, which is an orphan receptor in mammals, can be activated by chicken APLN and ELA-32, indicating that GPR25 is a novel functional receptor for APLN and ELA (Zhang et al., 2018a). Activation of APLNR1, APLNR2, and GPR25 has been shown to decrease intracellular cAMP levels (Zhang et al., 2018a, 2018b).

In chickens, *APLN* and *ELA* are widely, but differentially, expressed in various tissues. *APLN* is highly expressed in the brain, heart, and lung and moderately/weakly expressed in other tissues, while ELA is highly expressed in the kidney, liver, spleen, and pancreas and

moderately/weakly expressed other remaining tissues. This finding, together with the expression of *APLNR1/GPR25* in these tissues, suggests that APLN/ELA plays important roles in avian tissues, which requires further investigation (Zhang et al., 2018a, 2018b).

29.1.22 Neuropeptide Y family

Neuropeptide Y (NPY) family includes three structurally and functionally related peptides, NPY, peptide YY (PYY), and pancreatic polypeptide (PP) in vertebrates. These peptides are composed of 36 (or 37) aa and characterized by the presence of a PP-fold and an amidated C-terminus (Cerda-Reverter and Larhammar, 2000). In chickens, NPY, PYY, and PP peptides have 36, 37, and 36 aa (named NPY_{1-36}, PYY_{1-37}, and PP_{1-36}), respectively, all of which are cleaved from their corresponding large precursors (NPY-, PYY-, and PP-precursor) (Kimmel et al., 1975; Blomqvist et al., 1992; Conlon and O'Harte, 1992; Aoki et al., 2017; Gao et al., 2017; Reid et al., 2017). Among them, NPY_{1-36} and PYY_{1-37} show remarkable conservation between birds and mammals, whereas PP_{1-36} is less conserved.

In chickens, six GPCRs for NPY_{1-36}/PYY_{1-37}/PP_{1-36} (named Y1, Y2, Y4, Y5, Y6, and Y7) have been identified (Salaneck et al., 2000; Holmberg et al., 2002; Bromee et al., 2006b). Y2 and Y7 can function as the receptors common for NPY_{1-36} and PYY_{1-37}; Y1 can function as a common receptor for NPY_{1-36} and PYY_{1-37} with a slight selectivity toward NPY_{1-36}; Y5 is a receptor common for the three peptides with a slight selectivity toward NPY_{1-36} and PYY_{1-37}; Y4 is a PP-preferring receptor, which can also be activated by PYY_{1-37} with a low potency; and Y6 shows little response to NPY family peptides, causing one to question whether avian Y6 is functional (He et al., 2016; Gao et al., 2017).

In chickens, *NPY* mRNA is highly expressed in the hypothalamus, telencephalon, midbrain, hindbrain, and anterior pituitary and weakly in other tissues detected by qPCR assay (Gao et al., 2017). *PYY* is highly expressed in the pancreas, moderately in various brain regions (e.g., hypothalamus), and small intestine (duodenum, jejunum, and ileum) (Aoki et al., 2017; Gao et al., 2017; Reid et al., 2017). In contrast, *PP* is nearly exclusively expressed in the pancreas (Gao et al., 2017; Reid et al., 2017).

NPY family peptides are suggested to be involved in the regulation of food intake, adipogenesis, gastric acid secretion and contraction, and pancreatic functions in birds (Leclercq, 1984; Duke et al., 1985; Kuenzel et al., 1987; Denbow et al., 1988; Kuenzel, 1994; Zhang et al., 2015).

29.1.23 Natriuretic peptide family

In vertebrates, natriuretic peptide (NP) family consists of seven structurally related members, including atrial natriuretic peptide (ANP), brain natriuretic peptide (BNP), ventricular natriuretic peptide, and four C-type natriuretic peptides (CNP1, CNP2, CNP3, and CNP4) (Takei et al., 2011). These peptides are involved in the control of sodium and water balance, cardiovascular homeostasis, and skeletal development (Potter et al., 2009). All the peptides are characterized by the presence of a 17-aa cyclic ring and cleaved from their corresponding preprohormones encoded by separate genes. In chickens, the genes encoding the four natriuretic peptides (BNP, ANP-like peptide, CNP1, and CNP3) have been cloned (Akizuki et al., 1991; Trajanovska et al., 2007). The mature BNP, ANP-like peptide (also called RNP), CNP1, and CNP3 have 29, 34, 22, and 22 aa, respectively (Miyata et al., 1988; Arimura et al., 1991; Trajanovska et al., 2007). Interestingly, a novel gene orthologous to human *CNP* also exists in chicken genome (XM_015291500), which encodes a CNP peptide of 22 aa (Fig. 29.3A).

The actions of the five avian NPs are likely mediated by four NP receptors: NPR1 (XM_015298478), NPR2 (XM_003642919.4), a novel NPR1-like receptor (NPR1L, XM_025145121), and NPR3 (XM_004937172.3). The first three receptors may bind to the five NPs and increase intracellular cGMP levels, while NPR3 may

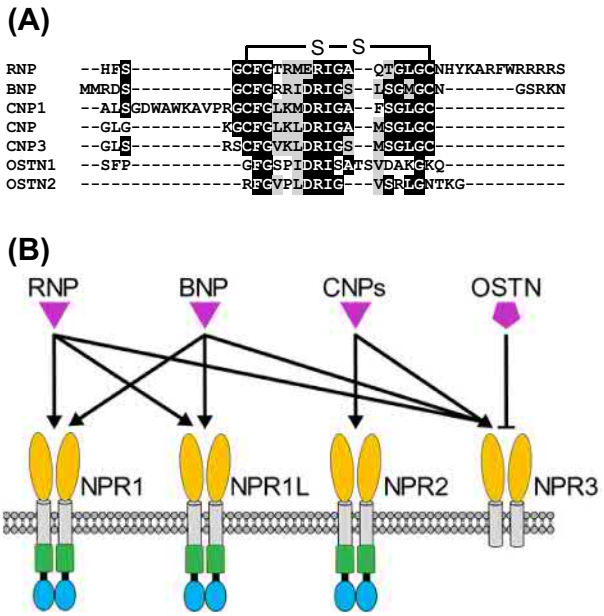

FIGURE 29.3 (A) Sequence alignment of five chicken natriuretic peptides (RNP, BNP, CNP, CNP1, and CNP3) with the two regions of OSTN peptide ($OSTN_1$/$OSTN_2$) homologous to NPs; (B) Hypothetical interaction of the five avian NPs and OSTN with the four NP receptors (NPR1, NPR1L, NPR2, and NPR3), which requires experimental validation. NPR1, NPR1L, and NPR2 may bind the five NPs and increase cGMP levels, while NPR3 may act as a clearance receptor for the five NPs. OSTN may bind to NPR3 and thus modulates the availability and action of the NPs.

function as a clearance receptor for the five NPs in birds. The ligand–receptor interaction proposed here needs further verification (Fig. 29.3B).

In chickens, *BNP* mRNA is abundantly expressed in both atria and ventricles (Toshimori et al., 1990; Trajanovska et al., 2007), but not in other tissues. ANP-like gene (*RNP*) is highly expressed in the kidney and weakly in the heart. *CNP1* is expressed in the brain, intestine, liver, and adrenal gland. *CNP3* is expressed in the brain, heart, and kidney. Moreover, four *NP* mRNAs are also expressed in chicken embryos (Houweling et al., 2005; Trajanovska et al., 2007). To date, the expression of novel *CNP* remains unknown.

In birds, NPs are likely to be involved in avian cardiovascular functions and fluid regulation and sodium excretion (Toop and Donald, 2004; Bie, 2018). In addition, NPs also regulate other physiological processes in birds. For instance, CNP3–NPR2 signaling is involved in the synthesis of glycosaminoglycans of the chondrogenic matrix and hypertrophy of differentiated chondrocytes (Kocamaz et al., 2012), while BNP–NPR1 signaling can stimulate proliferation and differentiation of preadipocytes in chicken (Huang et al., 2015).

29.1.24 Osteocrin peptide

In mammals, osteocrin (OSTN) peptide was identified as a novel bone-secreted factor modulating osteoblast phenotype, or as a muscle-derived factor (named Musclin) linked to glucose metabolism (Thomas et al., 2003; Nishizawa et al., 2004). OSTN peptide contains two regions homologous to NP, but lacks the two cysteine residues for ring structure formation of NPs (Fig. 29.3A) (Moffatt and Thomas, 2009). OSTN can bind to the clearance receptor NPR3 for NPs with high affinity (Moffatt et al., 2007; Kita et al., 2009) and thus modulate the action/availability of NPs in vivo. In chickens, *OSTN* is predicted to encode a peptide of 109 aa or a short peptide of 51 aa after proteolytic cleavage at the putative KKKR site (Thomas et al., 2003). However, the biological activity and physiological roles of OSTN are unknown in birds.

29.1.25 Neurosecretory protein GL and neurosecretory protein GM family

Neurosecretory protein GL (NPGL) and neurosecretory protein GM (NPGM) are two secretory peptides recently identified in chickens and mammals. In chickens, NPGL is a 83-aa peptide encoded by *NPGL* (*FAM237A*) gene, while NPGM is a 83-aa peptide encoded by *NPGM* (*FAM237B*) gene. Both peptides share ~54% aa identity and contain a putative intramolecular disulfide bond and an amidated C-terminus (Ukena et al., 2014; Shikano et al., 2018a). To date, the receptors for the two peptides have yet been identified in any vertebrate species.

NPGL is expressed in the infundibular nuclei (IN) and medial MM of the mediobasal hypothalamus. sc and icv infusions of NPGL can increase body mass gain and feeding in chicks (Shikano et al., 2018b; Ukena, 2018). *NPGM* is also expressed in the MM and IN. In particular, NPGM and NPGL show a degree of colocalization, especially in the MM. *icv* injection of NPGM decreases food intake, while chronic *sc* infusion of NPGM increases body mass gain in chicks (Shikano et al., 2018c).

29.1.26 Ornitho-kinin peptide

Kinin is implicated in the regulation of pain, inflammation, vasodilation, vascular permeability, and natriuresis in mammals (Marceau and Regoli, 2004). It is a 9-aa peptide, which is released from the kininogen precursor under the processing of kallikrein enzymes (Conlon, 1999). In chickens, kinin peptide contains 9 aa (Arg-Pro-Pro-Gly-Phe-Thr-Leu-Arg), which has two aa difference when compared to human kinin, thus is named as "ornitho-kinin" (Kimura et al., 1987).

Two GPCRs orthologous to human bradykinin B1 (*BDKRB1*) and B2 (*BDKRB2*) receptors exist in chicken genome (Bromee et al., 2006a). BDKRB2 can be activated by ornitho-kinin potently and stimulates intracellular Gq-phospholipase C (Gq-PLC) signaling pathway (Schroeder et al., 1997); however, the pharmacological property of avian BDKRB1 remains unclear.

The information regarding the roles and expression of ornitho-kinin and its receptors is limited in birds. In chickens, the kininogen gene (*KNG1*) encoding ornitho-kinin is reported to be expressed in the liver, while *BDKRB1* and *BDKRB2* are expressed in the liver and lung. In chickens, ornitho-kinin can induce the contraction of oviduct smooth muscle and has a strong hypotensive effect after injection via the wing vein (Kimura et al., 1987). A recent study reported that ornitho-kinin and their receptors participate in the inflammatory response of chickens (Guabiraba et al., 2017).

29.1.27 Angiotensin II peptide

In vertebrates, angiotensinogen encoded by *AGT* gene is processed by renin to produce a decapeptide angiotensin I. Angiotensin I is further cleaved by an angiotensin-converting enzyme to produce the bioactive octapeptide Angiotensin II (Ang II), which causes vasoconstriction, increased blood pressure, and stimulates adrenal aldosterone secretion in most vertebrate groups (Karnik et al., 2015). In chickens, Ang II is also an 8-aa peptide, which shows two aa difference at positions 1 (Asp^1) and 5 (Val^5) to human Ang II (Nakayama et al., 1973).

Two GPCRs for Ang II, named AT1 and AT2, exist in avian genomes. In chickens and turkeys, Ang II can activate AT1 and stimulate intracellular IP production and

calcium mobilization (Carsia et al., 1993; Murphy et al., 1993; Kempf et al., 1996); however, the signaling property of AT2 remains unclear in birds.

In chickens, *AT1* is expressed in the adrenal gland, heart, kidney, and endothelial cells (Kempf et al., 1996). Ang II can not only regulate cardiovascular development (Baker and Aceto, 1990) and arterial pressure (Crossley et al., 2010) at embryonic stage but also control cardiovascular functions and blood pressure of chickens (Nishimura et al., 1982, 2003). However, in contrast to its exclusive vasopressor action in mammals, Ang II has a dual action when administered to chickens (Nishimura et al., 1982; Kempf and Corvol, 2001). Chicken Ang II [(Asp^1, Val^5) Ang II] can produce an endothelium-dependent vasorelaxation, followed by a vasopressor action that is induced by an Ang II-dependent catecholamine release (Kempf and Corvol, 2001). The dual action of Ang II observed in birds is likely associated with the unique spatio-temporal expression patterns of AT1 and/or AT2 in target tissues (Kempf and Corvol, 2001; Nishimura et al., 2003), which requires further investigation.

29.1.28 Endothelin peptide family

In birds, three endothelin (EDN) peptides, named endothelin-1 (EDN1), endothelin-2 (EDN2), and endothelin-3 (EDN3), have been identified. Each EDN peptide is derived from a precursor of ~200 aa (named prepro-EDN) (Liu et al., 2019). This large precursor is first processed by furin endopeptidase to yield an intermediate product of 39–42 aa (known as Big-EDN, which is biologically inactive), which is further cleaved by endothelin-converting enzymes to give bioactive mature EDN peptides (Liu et al., 2019). These mature bioactive EDNs are peptides of 21 aa and characterized by the presence of two intrachain disulfide bonds at Cys3-Cys11 and Cys1-Cys15 (Davenport et al., 2016; Liu et al., 2019).

Three GPCRs for EDN1/EDN2/EDN3, named EDNRA, EDNRB, and EDNRB2, have been characterized in chickens (Liu et al., 2019). Among them, EDNRA is a receptor common for EDN1 and EDN2, while EDNRB and EDNRB2 are the two receptors common for EDN1, EDN2, and EDN3. Activation of the three receptors by EDNs stimulates intracellular Gq-PLC and Gs-AC/cAMP/PKA signaling pathways.

qPCR assays revealed that *EDNs* and *EDNRs* are widely, but differentially, expressed in chicken tissues (Liu et al., 2019). In birds, EDN–EDNR signaling has been reported to play critical roles in many physiological/pathological processes, such as cardiovascular development (Gourdie et al., 1998; Groenendijk et al., 2008), angiogenesis (Cruz et al., 2001), pulmonary arterial hypertension (Gomez et al., 2007), morphogenesis of the face and heart (Kempf et al., 1998; Nataf et al., 1998), and the proliferation, migration, and differentiation of trunk neural crest cells into the enteric nervous system (Nagy and Goldstein, 2006) or the melanocytes (Lahav et al., 1996; Pla and Larue, 2003; Harris et al., 2008) which influence skin pigmentation and plumage patterning in quails and chickens (Dorshorst et al., 2011; Shinomiya et al., 2012; Han et al., 2014; Kinoshita et al., 2014).

29.1.29 Bombesin peptide family

Gastrin-releasing peptide (GRP) and neuromedin B (NMB) are two structurally related peptides, which belong to bombesin peptide family. In chickens, two active forms of GRP with an identical C terminus, GRP_{27} (27 aas) and GRP_{10} (10 aas) (McDonald et al., 1980; Campbell et al., 1990), have been isolated from the proventriculus. Both GRP forms are released by cleavage from the same precursor encoded by *GRP* gene. NMB is a 10-aa peptide encoded by *NMB* gene and shares high aa sequence identity (60%) with GRP_{10} (Mo et al., 2017).

Three GPCRs for GRP and NMB, namely GRPR, NMBR, and Bombesin receptor subtype 3 (BRS3), have been characterized in chickens (Iwabuchi et al., 2003; Mo et al., 2017). GRPR and NMBR are GRP-specific and NMB-specific receptors, respectively. Interestingly, BRS3 can function as a common receptor for both peptides in chickens (Mo et al., 2017), contrary to mammalian finding, in which BRS3 is reported to be an orphan receptor. Activation of the three chicken receptors can stimulate calcium mobilization and enhance ERK phosphorylation.

qPCR assay revealed that GRP has the highest expression level in the anterior pituitary and a comparatively low expression level in other tissues, such as the proventriculus, hypothalamus, telencephalon, spinal cord, gizzard, ovary, and testes. Immunostaining studies showed that GRP is localized in gonadotrophs (LH cells) and endocrine cells in the proventriculus (Vaillant et al., 1979; Buffa et al., 1982; Mo et al., 2017). These findings, together with the wide expression of GRPR in chicken tissues including the hypothalamus, proventriculus, ovary and pancreas, indicate that GRP may act as an endocrine hormone or a local factor to regulate many physiological processes of birds, such as feeding, gall bladder motility, crop-emptying rate, pancreatic fluid secretion, gastric acid secretion, and reproduction (Linari et al., 1975; Linari and Linari, 1975; Tachibana et al., 2010b,c). Unlike *GRP*, *NMB* is highly expressed in the testes and moderately/weakly expressed in other tissues (including the CNS and ovary), except the kidneys, liver, lung, and muscle (Mo et al., 2017). This finding indicates that NMB is more likely a local paracrine/autocrine factor (e.g., as a neuromodulator in the CNS) to regulate avian physiological processes, such as food intake and testis development/functions (Tachibana et al., 2010b,c; Tachibana et al., 2010d; Mo et al., 2017). The predominant

expression of BRS3 in chicken telencephalon suggests a role of BRS3 signaling in avian brain (Ohki-Hamazaki et al., 2005; Mo et al., 2017), which warrants further investigation.

29.1.30 Melanocortin system peptides

In birds, melanocortin system consists of melanocortin peptides, Agouti-related peptide (AgRP), Agouti signaling protein (ASIP), melanocortin receptors, and two melanocortin receptor 2 accessory proteins (MRAP and MRAP2). In chickens, melanocortin peptides include α-melanocyte-stimulating hormone (α-MSH, 13 aa), β-MSH (18 aa), ɣ-MSH (11 aa), and adrenocorticotropin (ACTH, 39 aa) (Takeuchi et al., 1999), all of which contain a conserved "HFRW" motif essential for melanocortin receptor activation. It is clear that all melanocortin peptides are produced from the same POMC precursor after tissue-specific processing by two prohormone convertases (PC2 and PC1/3) (Dores et al., 2016; Zhang et al., 2017). Chicken AgRP and ASIP are two structurally related peptides of 137 aa and 108 aa, respectively, and both peptides contain multiple (say four−five) intramolecular disulfide bonds.

Five GPCRs, named MC1R, MC2R, MC3R, MC4R, and MC5R, have been cloned and identified as the receptors for melanocortins, AgRP, and ASIP (Fig. 29.4A) (Takeuchi et al., 1998; Takeuchi and Takahashi, 1998, 1999; Ling et al., 2003, 2004). α-MSH and ACTH can

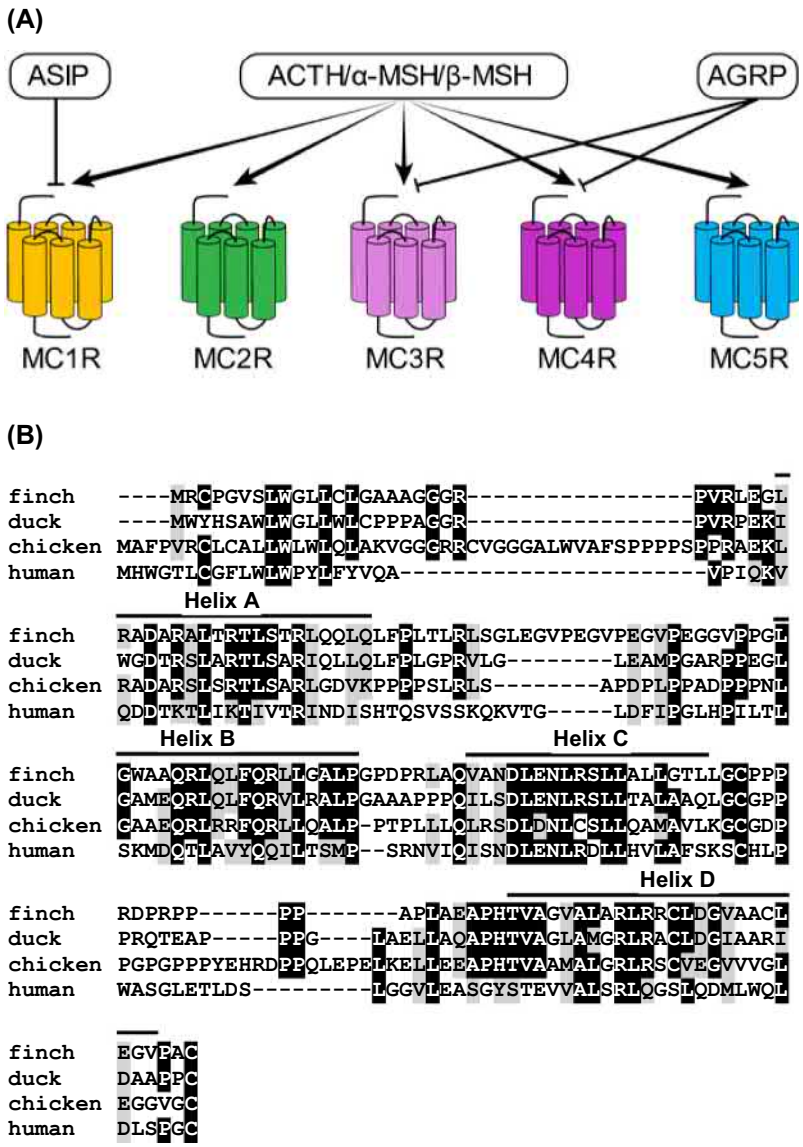

FIGURE 29.4 (A) melanocortin peptides (e.g., ACTH, α-MSH, and β-MSH) can activate the five melanocortin receptors (MC1R, MC2R, MC3R, MC4R, and MC5R) and increase cAMP levels, while AgRP or ASIP can act as either an endogenous antagonist or an inverse agonist to modulate receptor signaling. (B) Sequence alignment of zebra finch, duck, chicken, and human leptin (LEP). Only ~30% amino acid identity is observed between avian and human/mouse leptin (LEP); however, four α-helix structures also exist in avian LEP. These are marked in the figure.

function as the endogenous agonists for MC1R, while ASIP likely acts as an endogenous antagonist or reverse agonist of MC1R to modulate its signaling (Ling et al., 2003). MC2R can interact with MRAP to enhance its surface expression and ligand binding, thus enabling it to become a functional ACTH-specific receptor (Barlock et al., 2014; Zhang et al., 2017). MC3R and MC4R can act as the two receptors common for $ACTH_{1\text{-}39}$, α-MSH, β-MSH, and ɣ-MSH, in the absence of MRAP2. However, in the presence of MRAP2, both MC3R and MC4R become ACTH-preferring receptors (Zhang et al., 2017). Interestingly, AgRP has dual functions. It acts either as an endogenous antagonist or reverse agonist of MC3R and MC4R to modulate their signaling (Zhang et al., 2017). MC5R can function as a receptor for ACTH, α-MSH, and β-MSH (Ling et al., 2004). When coexpressed with MRAP, MC5R displays an increased sensitivity to ACTH (Thomas et al., 2018).

In chickens, *POMC* mRNA is expressed predominantly in the anterior pituitary, moderately in the hypothalamus, and weakly in other tissues including the skin, kidneys, adrenal gland, fat, and gonads (Takeuchi et al., 1999; Zhang et al., 2017). *AgRP* mRNA is widely expressed in chicken tissues with a high expression level noted in the hypothalamus (Takeuchi et al., 2000; Zhang et al., 2017). Interestingly, three types of *ASIP* transcripts likely driven by alternative promoter usage are reported to allow their differential expression in chicken tissues including the skin (feather follicles), hypothalamus, pituitary, heart, lung, spleen, adrenal gland, ovary, and testes (Yoshihara et al., 2012).

Five melanocortin receptors are also found to be differentially expressed in chicken tissues including the hypothalamus, adrenal gland, and skin (Takeuchi et al., 2000; Zhang et al., 2017; Thomas et al., 2018). This finding supports that the five receptors may mediate the diverse actions of melanocortins, AgRP, and ASIP in birds, such as MC1R-mediated skin melanin synthesis and plumage color formation (Kerje et al., 2003; Ling et al., 2003), MC2R-mediated adrenal steroidogenesis (Barlock et al., 2014), and MC3R/MC4R-mediated feeding, energy balance, growth, and body weight control (Boswell et al., 2002; Cline et al., 2008a; Smith et al., 2008; Shipp et al., 2015; Zhang et al., 2017). To date, the role of MC5R signaling is unknown in birds.

29.1.31 Arginine vasotocin/mesotocin peptides

In birds, arginine vasotocin (AVT) and mesotocin (MT) are two structurally related peptides and orthologous to mammalian arginine vasopressin (AVP) and oxytocin (OXT) peptides, respectively. They are also the two endocrine hormones secreted by avian posterior pituitary. Both peptides contain 9 aa and share structural conservation across vertebrates, including the presence of an intramolecular disulfide bond and an amidated C-terminus.

Four GPCRs for AVT and MT have been characterized in chickens and named AVPR1A (also called VT4, or V1a) (Selvam et al., 2013), AVPR1B (VT2 or V1b) (Cornett et al., 2003), MTR (VT3, or OXTR) (Gubrij et al., 2005), and AVPR2b (VT1) (Tan et al., 2000), respectively (Wu et al., 2019). Among them, *AVPR1A*, *AVPR1B*, and *MTR* are orthologous to human *AVPR1A*, *AVPR1B*, and *OXTR*, respectively, whereas *AVPR2b* exists in birds, but is lost in mammals (e.g., humans) (Wu et al., 2019). Avian AVPR1A, AVPR1B, AVPR2b, and MTR are the four functional receptors for AVT, while MTR functions as the sole receptor for MT. Since AVT is ∼four to eightfold more potent than MT in activating AVPR2b, thus avian AVPR2b can be viewed as an AVT-preferring receptor. All receptors are coupled to Gq (/Gs) protein and their activation triggers calcium mobilization and stimulates MAPK/ERK and cAMP/PKA signaling pathways (Wu et al., 2019).

The physiological roles of avian AVT and MT have been described in other chapters of this book, and thus not included here.

29.1.32 Cocaine- and amphetamine-regulated transcript peptides

Cocaine- and amphetamine-regulated transcript (CART) peptide is a neuropeptide of 41 or 48 aa abundantly expressed in the hypothalamic arcuate nucleus (ARC) and reported to play important roles in regulating feeding and energy balance in mammals (Rogge et al., 2008). In chickens, two *CART* genes, named *CART1* (KC249966) and *CART2* (KC249967), were identified. Chicken *CART1* is orthologous to mammalian *CART*, while *CART2* is likely lost in mammals but exists in birds and other lower vertebrates. Chicken *CART1* (also called *CART*) encodes a mature CART peptide of 41 aa ($CART_{48\text{-}89}$) or 48 aa ($CART_{42\text{-}89}$), which shows 96−98% aa identity to human CART and shares the three characteristic putative intramolecular disulfide bonds. Chicken *CART2* is predicted to produce a mature peptide of 41 aa ($CART2_{51\text{-}91}$), which shows only 59% sequence identity to human CART (Cai et al., 2015). To date, the receptor for CART peptide remains unknown in vertebrates.

In chickens, CART peptide (encoded by *CART1*) is predominantly expressed in the anterior pituitary and its expression and secretion is regulated by hypothalamic gonadotropin-releasing hormone 1(GnRH1) (Cai et al., 2015; Mo et al., 2019). This finding indicates that CART peptide is a novel pituitary hormone in chickens, which is likely associated with avian reproduction (Mo et al., 2019). Moreover, fasting downregulates and CRH upregulates pituitary *CART1* mRNA expression (Cai et al., 2015;

Mo et al., 2015). Besides the pituitary, *CART* is also expressed in the hypothalamus and fasting downregulates *CART1* expression. In zebra finches, CART-ir cells were observed in the bed nucleus of the stria terminalis, hypothalamic paraventricular, supraoptic, dorsomedial, IN, lateral hypothalamic, Edinger–Westphal, and parabrachial nuclei. Moreover, fasting reduces, and refeeding increases CART-ir fibers in the IN, where CART-ir fibers contact and interact with NPY neurons. These findings indicate that CART also plays roles in the CNS, such as the regulation of food intake and energy homeostasis in birds (Tachibana et al., 2003; Singh et al., 2016).

Unlike *CART1*, *CART2* has an extremely low expression level in chickens (Cai et al., 2015), implying a less significant role under normal physiological conditions.

29.1.33 Leptin

In mammals, leptin (LEP), an adipose-derived peptide, plays pivotal roles in the regulation of food intake, energy balance, obesity, and reproduction. Recently, an authentic LEP of ~16 kDa has been identified in avian species, including zebra finches (Huang et al., 2014b; Prokop et al., 2014), budgerigars (Huang et al., 2014b), peregrine falcons (Prokop et al., 2014), rock doves (Friedman-Einat et al., 2014), chickens, ducks (Seroussi et al., 2016), and Japanese quails (Wang et al., 2016). The full-length avian LEP only shows ~30% sequence identity to mammalian ortholog, but it contains a pair of cysteine residues and four-helix bundle structure, resembling the tertiary structure of mouse/human LEP (Fig. 29.4B) (Huang et al., 2014b; Friedman-Einat and Seroussi, 2019).

Functional assay shows that recombinant finch LEP can potently activate finch/chicken LEP receptor (LEPR) and stimulate the intracellular JAK2-STAT3 signaling pathway (Huang et al., 2014b), indicating that LEPR is a functional receptor for avian LEP.

qPCR and RNA-seq analysis reveal that *LEP* mRNA is highly expressed in the brain (e.g., cerebellum and telencephalon) and pituitary and weakly in other tissues of zebra finches and chickens, while *LEPR* is abundantly expressed in the anterior pituitary, moderately in the brain (including cerebellum), gonads, and weakly in other tissues examined (Huang et al., 2014b; Seroussi et al., 2016). The little or no expression of *LEP* in the adipose tissue and liver indicates that LEP can neither act as an adipocyte-derived signal nor as a liver-derived signal to control energy balance and food intake in birds. Meanwhile, these findings suggest that LEP acts more likely as an autocrine/paracrine factor, instead of an adipocyte-derived circulating hormone, in avian tissues, such as in the brain and anterior pituitary (Huang et al., 2014b; Seroussi et al., 2016; Friedman-Einat and Seroussi, 2019). The "nonadipokine" nature of avian LEP also urges us to find other hidden "adipostat signal(s)," which can function as the long-term peripheral metabolic signal to control avian energy balance.

29.1.34 Thyrotropin-releasing hormone

Thyrotropin-releasing hormone (TRH) is a 3-aa neuropeptide hormone secreted by the hypothalamus of vertebrates. In chickens, bioactive TRH (pyro-Glu-His-Pro-NH2) is cleaved from the TRH precursor, which contains four copies of "Gln-His-Pro-Gly" motifs flanked by the dibasic residues (Vandenborne et al., 2005b).

Two structurally related TRH receptors (TRHRs) have been characterized in chickens and named TRHR1 and TRHR3, respectively (Li et al., 2020). TRHR1 and TRHR3 are likely coupled to Gq protein, and their activation can trigger calcium mobilization and MAPK/ERK signaling cascade (Sun et al., 1998; Li et al., 2020).

In birds (e.g., chickens and ducks), TRH is predominantly expressed in the hypothalamus (e.g., in the parvocellular portion of the PVN and lateral hypothalamic area) revealed by qPCR (Li et al., 2020), in situ hybridization (Vandenborne et al., 2005b), and immunostaining (Jozsa et al., 1988). *TRHR1* is predominantly expressed in chicken anterior pituitary and weakly in other tissues including the hypothalamus (Sun et al., 1998), while *TRHR3* is widely expressed in chicken tissues (Li et al., 2020). In testes, TRH has a moderate expression level. These findings indicate that TRH can regulate the functions of the pituitary (e.g., TSH, PRL, and GH secretion) and extrapituitary tissue.

29.1.35 Esophageal cancer–related gene 4–derived peptides

Esophageal cancer–related gene 4 (*ECRG4*), also called *C2ORF40* gene, is predicted to encode a hormone-like peptide involved in the regulation of many processes, such as tumor suppression, stress, and inflammatory response in mammals (Gonzalez et al., 2011). In chickens, *ECRG4* is predicted to encode a mature augurin peptide of 124 aa ($ECRG4_{29\text{-}152}$). This augurin peptide could be further processed by furin or thrombin. Furin processing at site 71–74 may produce two fragments, $ECRG_{29\text{-}70}$ (ecilin) and $ECRG4_{75\text{-}152}$ (argilin). Thrombin processing at site 132–136 may produce $ECRG4_{29\text{-}131}$ (CΔ16-augurin), $ECRG4_{75\text{-}131}$ (CΔ16-argilin), and $ECRG4_{137\text{-}152}$ (CΔ16).

Recently, in mammals, several scavenger receptors (e.g., LOX1) were identified as the receptors for ECRG-derived peptide, CΔ16-argilin (Moriguchi et al., 2018). In addition, CΔ16 (the C-terminal ECRG4 fragment of 16 aa) was also reported to interact with toll-like receptor 4–CD14–MD2 complex (Podvin et al., 2015). However, little is known about the receptors and roles of ECRG4-derived peptides in birds.

29.1.36 Chemerin

Chemerin is a chemoattractant protein and adipokine encoded by the retinoic acid receptor responder 2 (*RARRES2*) gene, which has been reported to regulate many physiological/pathological processes in mammals, such as inflammation, adipogenesis, obesity, cardiovascular disease, reproduction, and host defense (e.g., inhibition of bacterial growth) (Kulig et al., 2011; Banas et al., 2013; Kennedy and Davenport, 2018). In chickens, *RARRES2* encodes a precursor protein of 162 aa, which contains an N-terminal signaling peptide of 17 aa and a C-terminal prochemerin (18−162 aa) containing three disulfide bonds. The circulating prochemerin has low biological activity and thus needs the removal of its short C-terminus to produce the most active chemerin of 140 aa (named chemerin$_{18\text{-}147}$).

Two putative GPCRs, named chemokine-like receptor 1 (CMKLR1) and G-protein−coupled receptor 1 (GPR1), for chemerin$_{18\text{-}147}$ exist in chicken and other birds; however, their functionality is unknown.

In turkeys, *RARRES2* was reported to be mainly expressed in the liver, while *CMKLR1* and *GPR1* ubiquitously expressed in various tissues, including ovarian follicular cells (Diot et al., 2015). In chickens, food restriction can increase plasma chemerin levels during laying periods, which is proposed to be associated with increased fertility in broiler breeder hens (Mellouk et al., 2018). These pioneering studies suggest that chemerin may regulate avian reproduction. Despite the high concentration of chemerin (∼200 ng/mL in broiler chickens) detected in avian plasma (Mellouk et al., 2018), little is known about the ratio of active versus inactive chemerin forms in vivo and the other physiological roles of chemerin in birds, such as its roles in inflammation, lipid metabolism, and host defense etc.

29.1.37 Granin-derived peptides

Chromogranin A (CgA), chromogranin B (CgB), and secretogranin II (SgII) are three members in granin family, which are expressed in the neurons and endocrine tissues. These acidic secretory proteins are not only involved in the regulation of sorting and packaging hormones inside secretory granules and secretory granule formation but also can be proteolytically processed into many biologically active peptides in mammals (Troger et al., 2017). CgA, CgB, and SgII proteins also exist in birds and are expressed in endocrine tissues (e.g., pituitary and adrenal gland) and neurons (Salvi et al., 1996; Kameda et al., 1998; Gomi et al., 2015). Although the overall aa sequence identity (∼37−57%) between avian (e.g., chicken) and human CgA, CgB, and SgII is not high (Proudman et al., 2003), avian CgA protein can produce two peptides, vasostatin I (CgA$_{1\text{-}76}$, 76 aa) and serpinin peptide (26 aa) in ostrich pituitaries (Lazure et al., 1990; Tota et al., 2012; Troger et al., 2017). Chicken CgB may produce cCgB$_{1\text{-}41}$ (41 aa) and secretolytin (cCgB$_{641\text{-}653}$; 13 aa) (Montero-Hadjadje et al., 2008), and SgII can produce secretoneurin (SN, 33 aa, SgII$_{159\text{-}191}$) (Leitner et al., 1998) and a potential "EM66 peptide" (cSgII$_{194\text{-}260}$: 67 aa). In chickens, CgB$_{1\text{-}41}$, secretolytin, SN, and EM66 peptides show high sequence identity with their corresponding mammalian counterparts (Leitner et al., 1998). In contrast, other granin-derived peptides previously reported (e.g., pancreastatin and catastatin) (Troger et al., 2017) show little or low sequence identity between birds and mammals.

Granin-derived peptides play multiple functional roles in mammals (Troger et al., 2017). For instance, vasotatin I displays antimicrobial activity and regulates cardiovascular function; Serpinins (three forms: serpinin, serpinin-RRG, and pyro-Glu-serpinin) derived from the C-terminus of CgA can modulate cardiovascular function; CgB$_{1\text{-}41}$ inhibits parathormone release and secretolytin displays antimicrobial activity; SN is involved in the regulation of neurogenesis, neuroprotection, angiogenesis, chemoattraction, and hormone secretion, while EM66 is involved in the hypothalamic regulation of feeding behavior (Trebak et al., 2017). Despite the presence of these granin-derived peptides in birds, however, their roles are unknown. Moreover, the identity of cognate receptors for these avian peptides is an open question.

Besides CgA, CgB, and SgII, four additional proteins, namely secretogranin 3 (SgIII), secretogranin 5 (SgV), VGF (SgVII), and proSAAS, belong to the granin family (Bartolomucci et al., 2011). Since SgIII, SgV, and VGF exist in chickens (/zebra finches), this supports the existence of additional granin-derived peptides in birds, which require further studies.

It was reported that in mammals (e.g., humans), proSAAS can be processed into two active peptides, named PEN (AADHDVGSELPPEGVLGALLRV) and big-LEN (LETPAPQVPARRLLPP), which can function as the endogenous ligands for GPR83 and GPR171, respectively (Gomes et al., 2013, 2016). However, *proSAAS* gene is lost in avian lineage, clearly indicating that PEN and big-LEN peptides are not the endogenous ligands for avian GPR83, GPR83-like receptor, and GPR171.

29.1.38 Antimicrobial host defense peptides

HDPs are small and cationic peptides of <50 aa, which function as an essential part of innate host defense against pathogens in vertebrates. In birds, HDPs consist of β-defensins, ovo-defensins, cathelicidins (CATH), liver-expressed antimicrobial peptide-2 (LEAP-2), NK-lysin (NK3), hepcidin, etc.

Over 25 β-defensin peptides/genes have been identified in birds (Cuperus et al., 2013). In chickens, 14 defensin

genes clustered on chromosome 3 have been identified and named *AvBD1-14*, respectively (Xiao et al., 2004; Lynn et al., 2007). In zebra finches, 22 defensin genes have been identified, and 10 of them are orthologous to chicken defensin genes (Hellgren and Ekblom, 2010). The variation in the copy number of defensin genes in birds is caused by rapid local gene duplication or gene loss during speciation. In chickens, each defensin gene encodes a precursor, which generally contains a signal peptide and C-terminal mature defensin peptide. The predicted mature defensin peptides, except AvBD11, are ~40 aa long and characterized by the presence of three disulfide bridges and the formation of three β-sheets and α-helix structure at their N termini. AvBD11 is an 82-aa peptide and contains two defensin domains, N- and C-terminal domains (Guyot et al., 2020). The N-terminal domain mediates antibacterial, antiparasitic, and antiinvasive activities, while the C-terminal domain potentiates the latter two activities. The antiviral activity in infected chicken cells, accompanied by marked cytotoxicity, requires the full-length AvBD11 peptide (Guyot et al., 2020). In addition, posttranslational modifications have been identified in some chicken AvBDs, such as the C-terminal amidation of mature AvBD1 and the N-terminal glutaminyl cyclization (pyroglutamic acid at position 1) of mature AvBD7 (Derache et al., 2009) and AvBD6.

Ovo-defensins were originally identified in avian oviducts, where they are secreted and stored in the egg white and display antibacterial activity (Gong et al., 2010). In chickens and zebra finches, five ovo-defensins, named OvoDA1, OvoDA2, OvoDA3, OvoDB1, and OvoDBb, have been identified and all of them share structural similarity to β-defensin, such as the presence of three disulfide bonds and formation of three antiparallel β-sheets (Whenham et al., 2015; Zhang et al., 2019).

Avian CATH prepropeptide contains an N-terminal signal peptide, a cathelin-like domain, and a C-terminal mature CATH peptide of 26–40 aa. In chickens, four *CATH* genes clustered on chromosome 2 have been identified, named *CATH1*, *CATH2*, *CATH3*, and *CATHB1*, respectively (Xiao et al., 2006; Goitsuka et al., 2007; van Dijk et al., 2011). They are α-helical cationic peptides and have an amphipathic structure to interact with negatively charged molecules on bacterial surface, like lipopolysaccharide or lipoteichoic acid (Bommineni et al., 2007; Cuperus et al., 2013). Thus, all four CATH peptides display potent antiantimicrobial activity. In addition, two C-terminal amidated forms of CATH2 (26 aa/31 aa) may also exist in chickens, as in mammals (van Dijk et al., 2011).

LEAP-2 peptide is a 54 aa, cationic peptide with two disulfide bridges, and is highly expressed in chicken liver and small intestine and its expression is upregulated by *Salmonella* infection (Lynn et al., 2003, 2004). *In vitro*, LEAP2 peptide shows antibacterial activity against *Salmonella typhimurium* by permeabilizing bacterial outer membrane (Townes et al., 2004, 2009).

In chickens, NK−lysin gene encodes a mature cysteine-rich NK−lysin peptide of 78 aa with five α-helical regions, which display an antibacterial activity (Hong et al., 2006; Lee et al., 2014). Interestingly, aa substitution at the position 29 (Asn^{29} to Asp^{29}) of NK−lysin in chicken strains (White leghorn vs. Cornish) affects its antimicrobial activity and anticancer activity (Lee et al., 2012).

In mammals, hepcidin was initially identified as a cationic antibacterial/fungal peptide of 20/25 aa with four disulfide bonds, which is predominantly expressed in the liver (Krause et al., 2000; Park et al., 2001). Later studies show that hepcidin is likely a hepatic peptide hormone involved in the maintenance of iron homeostasis, such as the regulation of iron storage in macrophages, and intestinal iron absorption (Pigeon et al., 2001; Wunderer et al., 2020). Interestingly, hepcidin gene likely exists in some avian species, such as Swainson's thrush (XM_033084442) (Fig. 29.5). Moreover, avian hepcidin gene can encode a mature hepcidin peptide of 25 aa, which contains four intramolecular disulfide bonds crucial for stabilizing their β-sheet structures, implying a conserved role of hepcidin in birds. However, the antimicrobial activity of hepcidin has yet been tested in avian species.

Taken together, the presence of cationicity and amphipathicity characterized in HDPs is essential for their biological activities, such as antibacterial activity, antiviral activity, antifungal activity, antiparasitic activity, immunomodulatory actions, wound healing, and induction of adaptive immunity (Mookherjee et al., 2020). Future studies on their inter-/intraspecies copy number variation, tissue-specific expression, pathogen-/hormone-regulated expression, posttranslational modifications, and unique biological activities will help to uncover the roles of avian HDPs and promote their applications in poultry industry.

FIGURE 29.5 Sequence comparison of hepcidin peptide predicted in 14 avian species, including *Catharus ustulatus* (Swainson's thrush).

29.1.39 Other peptides

In addition to the peptides mentioned above, many other peptides such as GnRH1, GnRH2, insulin, pituitary hormones [GH, PRL, FSH, LH, and thyrotropin (TSH)], cytokines, chemokines, and peptide growth factors (e.g., EGF, IGF, VEGF, and TGFβ families/superfamily), have been described in other chapters (or elsewhere), and thus, are not described here.

29.2 Summary

In this chapter, we briefly described the structure, functions, expression, and major actions of 134 peptides/neuropeptides involved in the regulation of avian growth, stress, food intake, energy balance, lipid and glucose metabolism, reproduction, water homeostasis, calcium homeostasis, cardiovascular functions, blood pressure, host defense, etc. These peptides are encoded by 111 genes. Most of these avian peptides (97) have their corresponding mammalian orthologs, and some of them play physiological roles similar to those in mammals, such as hypothalamic GHRH and SST, stimulate, and inhibit pituitary GH secretion, respectively (Meng et al., 2014). However, notable differences are present between these two animal groups:

Firstly, more than 20 unique peptides exist in birds. Most of these peptides are derived from gene duplication and are the expanded peptide family members, which are likely lost or absent in mammals. For instance, avian GCG superfamily has 12 members including GCGL, SCT-LP, GHRH-LP peptides, while mammalian GCG superfamily only has 9 bioactive members and GCGL, SCT-LP, and GHRH-LP are lost in the lineage. Similarly, unique members were also identified in the avian CRH family (CRH2), PTH family (PTH-L), RF-amide peptide family contains (PrRP2), NP family (CNP1, CNP3), and host defensin peptides (five ovo-defensins birds).

Secondly, some peptide families have fewer members in birds when compared to mammals. For example, only two members of RLN family (RLN3-like and INSL5) were identified in chickens, while seven members are present in human RLN family (RLN1, RLN2, RLN3, INSL3, INSL4, INSL5, and INSL6). Likewise, a few member(s) in the galanin peptide superfamily (GALP and KISS) and opioid peptide family (Neo-endorphin) were probably lost in avian lineage.

Thirdly, the number of receptors for most peptide families differs between birds and mammals. For instance, chicken GHRH has two GHRHRs (GHRHR1 and GHRHR2), while mammals only have one GHRH receptor (Wang et al., 2010). Similarly, PrRP has three receptors (PrRPR1, PrRPR2, and PrRP2R); in comparison, there is one PrRP receptor in mammals (Wang et al., 2012c). Mammals got an AVT receptor (AVPR2a) and a PTH receptor (PTH2R), which are likely lost in chickens (Wu et al., 2019). The difference in the repertoires of avian peptides and their receptors indicate that further studies are required to examine how avian peptide–receptor interaction differs from that of mammals.

Finally, although the names of some peptides are used across different species, it is of important to note that it should not be taken for granted that they exert the same actions as their names imply in avian species. In particular, some avian peptides may have actions and expression patterns distinct from their mammalian counterparts. For instance, avian SCT does not exert characteristic regulation on pancreatic fluid secretion (Wang et al., 2012a), and avian LEP (*ob*) is not expressed in avian adipose tissue and cannot display an "adipostat activity" to control energy balance as in mammals (Friedman-Einat and Seroussi, 2019). Thus, caution should be taken to elucidate the physiological roles of these avian peptides.

Taken together, the number, structures, function, expression, and major actions of avian peptides and their receptors likely differ from those in mammals, so we cannot simply transfer our knowledge on mammalian peptides onto avian models. Clearly, it is essential to perform further extensive in-depth studies on the functions and roles of avian peptides and their receptors. This will not only help to reveal their unique roles in avian biology, such as body composition, feathering and plumage patterning, metabolism, brooding, singing, and energy storage and utilization before and during flight, migration and seasonal breeding, etc., but also aid to uncover the "hidden" conserved roles of peptide–receptor pairs across vertebrates from the perspective of comparative endocrinology.[1]

References

Ahmed, S., Harvey, S., 2002. Ghrelin: a hypothalamic GH-releasing factor in domestic fowl (*Gallus domesticus*). J. Endocrinol. 172, 117–125.

Akizuki, N., Kangawa, K., Minamino, N., Matsuo, H., 1991. Cloning and sequence analysis of complementary DNA encoding a precursor for chicken natriuretic peptide. FEBS Lett. 280, 357–362.

Ancill, A.K., Bascal, Z.A., Whitaker, G., Dacke, C.G., 1990. Effects of rat and chicken calcitonin gene-related peptides (CGRP) upon calcium metabolism in chicks. Regul. Pept. 30, 231–238.

Anderson, L.L., Scanes, C.G., 2012. Nanobiology and physiology of growth hormone secretion. Exp. Biol. Med. 237, 126–142.

Anderson, R.E., Schraer, H., Gay, C.V., 1982. Ultrastructural immunocytochemical localization of carbonic anhydrase in normal and calcitonin-treated chick osteoclasts. Anat. Rec. 204, 9–20.

Aoki, K., Kondo, M., Okuda, M., Saneyasu, T., Honda, K., Kamisoyama, H., 2017. Identification, expression analysis, and functional characterization of peptide YY in chickens (*Gallus gallus domesticus*). Gen. Comp. Endocrinol. 242, 11–17.

1. Due to page limit, regrettably not all of the relevant literatures regarding avian peptides can be cited in this chapter.

Apu, A.S., Mondal, A., Kitazawa, T., Takemi, S., Sakai, T., Sakata, I., 2016. Molecular cloning of motilin and mechanism of motilin-induced gastrointestinal motility in Japanese quail. Gen. Comp. Endocrinol. 233, 53–62.

Arimura, J.J., Minamino, N., Kangawa, K., Matsuo, H., 1991. Isolation and identification of C-type natriuretic peptide in chicken brain. Biochem. Biophys. Res. Commun. 174, 142–148.

Asakawa, A., Inui, A., Kaga, T., Yuzuriha, H., Nagata, T., Ueno, N., Makino, S., Fujimiya, M., Niijima, A., Fujino, M.A., Kasuga, M., 2001. Ghrelin is an appetite-stimulatory signal from stomach with structural resemblance to motilin. Gastroenterology 120, 337–345.

Atoji, Y., Shibata, N., Yamamoto, Y., Suzuki, Y., 1996a. Distribution of neurotensin-containing neurons in the central nervous system of the pigeon and the chicken. J. Comp. Neurol. 375, 187–211.

Atoji, Y., Watanabe, H., Nimamoto, N., Sugiyama, M., Yamamoto, Y., Suzuki, Y., 1994. Neurotensin immunoreactive cells in the gastrointestinal epithelium of the chicken, pigeon and Japanese quail. Eur. J. Histochem. 38, 65–72.

Atoji, Y., Yamamoto, Y., Suzuki, Y., 1996b. Neurotensin-containing endocrine cells and neurotensin receptor mRNA-expressing epithelial cells in the chicken thymus. Arch. Histol. Cytol. 59, 197–203.

Baimbridge, K.G., Taylor, T.G., 1980. Role of calcitonin in calcium homoeostasis in the chick embryo. J. Endocrinol. 85, 171–185.

Baker, K.M., Aceto, J.F., 1990. Angiotensin II stimulation of protein synthesis and cell growth in chick heart cells. Am. J. Physiol. 259, H610–H618.

Balint, E., Balazsa, T., Zachar, G., Mezey, S., Csillag, A., 2016. Neurotensin: revealing a novel neuromodulator circuit in the nucleus accumbens-parabrachial nucleus projection of the domestic chick. Brain Struct. Funct. 221, 605–616.

Banas, M., Zabieglo, K., Kasetty, G., Kapinska-Mrowiecka, M., Borowczyk, J., Drukala, J., Murzyn, K., Zabel, B.A., Butcher, E.C., Schroeder, J.M., Schmidtchen, A., Cichy, J., 2013. Chemerin is an antimicrobial agent in human epidermis. PloS One 8, e58709.

Barlock, T.K., Gehr, D.T., Dores, R.M., 2014. Analysis of the pharmacological properties of chicken melanocortin-2 receptor (cMC2R) and chicken melanocortin-2 accessory protein 1 (cMRAP1). Gen. Comp. Endocrinol. 205, 260–267.

Bartolomucci, A., Possenti, R., Mahata, S.K., Fischer-Colbrie, R., Loh, Y.P., Salton, S.R., 2011. The extended granin family: structure, function, and biomedical implications. Endocr. Rev. 32, 755–797.

Bathgate, R.A., Halls, M.L., van der Westhuizen, E.T., Callander, G.E., Kocan, M., Summers, R.J., 2013. Relaxin family peptides and their receptors. Physiol. Rev. 93, 405–480.

Bie, P., 2018. Natriuretic peptides and normal body fluid regulation. Comp. Physiol. 8, 1211–1249.

Bjornskov, I., Rehfeld, J.F., Johnsen, A.H., 1992. Identification of four chicken gastrins, obtained by processing at post-Phe bonds. Peptides 13, 595–601.

Blomqvist, A.G., Soderberg, C., Lundell, I., Milner, R.J., Larhammar, D., 1992. Strong evolutionary conservation of neuropeptide Y: sequences of chicken, goldfish, and *Torpedo marmorata* DNA clones. Proc. Natl. Acad. Sci. U. S. A. 89, 2350–2354.

Bommineni, Y.R., Dai, H., Gong, Y.X., Soulages, J.L., Fernando, S.C., Desilva, U., Prakash, O., Zhang, G., 2007. Fowlicidin-3 is an alpha-helical cationic host defense peptide with potent antibacterial and lipopolysaccharide-neutralizing activities. FEBS J. 274, 418–428.

Boswell, T., Li, Q., Takeuchi, S., 2002. Neurons expressing neuropeptide Y mRNA in the infundibular hypothalamus of Japanese quail are activated by fasting and co-express agouti-related protein mRNA. Brain Res Mol Brain Res 100, 31–42.

Brackett, K.H., Fields, P.A., Dubois, W., Chang, S.M., Mather, F.B., Fields, M.J., 1997. Relaxin: an ovarian hormone in an avian species (*Gallus domesticus*). Gen. Comp. Endocrinol. 105, 155–163.

Brighton, P.J., Szekeres, P.G., Willars, G.B., 2004. Neuromedin U and its receptors: structure, function, and physiological roles. Pharmacol. Rev. 56, 231–248.

Brodin, E., Alumets, J., Hakanson, R., Leander, S., Sundler, F., 1981. Immunoreactive substance P in the chicken gut: distribution, development and possible functional significance. Cell Tissue Res. 216, 455–469.

Bromee, T., Sjodin, P., Fredriksson, R., Boswell, T., Larsson, T.A., Salaneck, E., Zoorob, R., Mohell, N., Larhammar, D., 2006a. Neuropeptide Y-family receptors Y6 and Y7 in chicken. Cloning, pharmacological characterization, tissue distribution and conserved synteny with human chromosome region. FEBS J. 273, 2048–2063.

Bromee, T., Venkatesh, B., Brenner, S., Postlethwait, J.H., Yan, Y.L., Larhammar, D., 2006b. Uneven evolutionary rates of bradykinin B1 and B2 receptors in vertebrate lineages. Gene 373, 100–108.

Bu, G., Cui, L., Lv, C., Lin, D., Huang, L., Li, Z., Li, J., Zeng, X., Wang, Y., 2020. Opioid peptides and their receptors in chickens: structure, functionality, and tissue distribution. Peptides 128, 170307.

Bu, G., Fan, J., Yang, M., Lv, C., Lin, Y., Li, J., Meng, F., Du, X., Zeng, X., Zhang, J., Li, J., Wang, Y., 2019. Identification of a novel functional corticotropin-releasing hormone (CRH2) in chickens and its roles in stimulating pituitary TSHbeta expression and ACTH secretion. Front. Endocrinol. 10, 595.

Bu, G., Lin, D., Cui, L., Huang, L., Lv, C., Huang, S., Wan, Y., Fang, C., Li, J., Wang, Y., 2016. Characterization of neuropeptide B (NPB), neuropeptide W (NPW), and their receptors in chickens: evidence for NPW being a novel inhibitor of pituitary GH and prolactin secretion. Endocrinology 157, 3562–3576.

Buckerfield, M., Oliver, J., Chubb, I.W., Morgan, I.G., 1981. Somatostatin-like immunoreactivity in amacrine cells of the chicken retina. Neuroscience 6, 689–695.

Buffa, R., Solovieva, I., Fiocca, R., Giorgino, S., Rindi, G., Solcia, E., Mochizuchi, T., Yanaihara, C., Yanaihara, N., 1982. Localization of bombesin and GRP (gastrin releasing peptide) sequences in gut nerves or endocrine cells. Histochemistry 76, 457–467.

Bungo, T., Kawamura, K., Izumi, T., Dodo, K., Ueda, H., 2004. Feeding responses to mu-, delta- and kappa-opioid receptor agonists in the meat-type chick. Pharmacol. Biochem. Behav. 78, 707–710.

Bungo, T., Shiraishi, J., Yanagita, K., Ohta, Y., Fujita, M., 2009. Effect of nociceptin/orphanin FQ on feeding behavior and hypothalamic neuropeptide expression in layer-type chicks. Gen. Comp. Endocrinol. 163, 47–51.

Burhol, P.G., 1974. Gastric stimulation by intravenous injection of cholecystokinin and secretin in fistula chickens. Scand. J. Gastroenterol. 9, 49–53.

Cai, G., Mo, C., Huang, L., Li, J., Wang, Y., 2015. Characterization of the two CART genes (CART1 and CART2) in chickens (Gallus gallus). PloS One 10, e0127107.

Campbell, B.J., Young, J., Dimaline, R., Dockray, G.J., 1990. Isolation, sequence and biosynthetic significance of a novel fragment of gastrin-

releasing peptide from chicken proventriculus. Biochim. Biophys. Acta 1048, 66–71.

Campbell, R.M., Scanes, C.G., 1987. Growth hormone inhibition of glucagon- and cAMP-induced lipolysis by chicken adipose tissue in vitro. Proc. Soc. Exp. Biol. Med. 184, 456–460.

Cardot, J., Griffond, B., Risold, P.Y., Blahser, S., Fellmann, D., 1999. Melanin-concentrating hormone-producing neurons in birds. J. Comp. Neurol. 411, 239–256.

Carraway, R., Bhatnagar, Y.M., 1980. Isolation, structure and biologic activity of chicken intestinal neurotensin. Peptides 1, 167–174.

Carraway, R.E., Ferris, C.F., 1983. Isolation, biological and chemical characterization, and synthesis of a neurotensin-related hexapeptide from chicken intestine. J. Biol. Chem. 258, 2475–2479.

Carraway, R.E., Mitra, S.P., Duke, G.E., 1993. A common precursor to neurotensin and LANT6 and its differential processing in chicken tissues. Peptides 14, 1245–1251.

Carsia, R.V., McIlroy, P.J., Kowalski, K.I., Tilly, J.L., 1993. Isolation of Turkey adrenocortical cell angiotensin II (AII) receptor partial cDNA: evidence for a single-copy gene expressed predominantly in the adrenal gland. Biochem. Biophys. Res. Commun. 191, 1073–1080.

Cerda-Reverter, J.M., Larhammar, D., 2000. Neuropeptide Y family of peptides: structure, anatomical expression, function, and molecular evolution. Biochem. Cell. Biol. 78, 371–392.

Chan, A.S., Cipera, J.D., Belanger, L.F., 1969. The ultimobranchial gland of the chick and its response to a high calcium diet. Rev. Canad. Biol. 28, 19–31.

Chen, J., Huang, S., Zhang, J., Li, J., Wang, Y., 2020. Characterization of the neuropeptide FF (NPFF) gene in chickens: evidence for a single bioactive NPAF peptide encoded by the NPFF gene in birds. Domest. Anim. Endocrinol. 72, 106435.

Chottova Dvorakova, M., 2018. Distribution and function of neuropeptides W/B signaling system. Front. Physiol. 9, 981.

Ciccone, N.A., Dunn, I.C., Boswell, T., Tsutsui, K., Ubuka, T., Ukena, K., Sharp, P.J., 2004. Gonadotrophin inhibitory hormone depresses gonadotrophin alpha and follicle-stimulating hormone beta subunit expression in the pituitary of the domestic chicken. J. Neuroendocrinol. 16, 999–1006.

Cline, M.A., Godlove, D.C., Nandar, W., Bowden, C.N., Prall, B.C., 2007. Anorexigenic effects of central neuropeptide S involve the hypothalamus in chicks (Gallus gallus). Comp. Biochem. Physiol. Mol. Integr. Physiol. 148, 657–663.

Cline, M.A., Nandar, W., Bowden, C., Calchary, W., Smith, M.L., Prall, B., Newmyer, B., Orion Rogers, J., Siegel, P.B., 2010a. The threshold of amylin-induced anorexia is lower in chicks selected for low compared to high juvenile body weight. Behav. Brain Res. 208, 650–654.

Cline, M.A., Nandar, W., Bowden, C., Hein, P.P., Denbow, D.M., Siegel, P.B., 2008a. Differential feeding responses to central alpha-melanocyte stimulating hormone in genetically low and high body weight selected lines of chickens. Life Sci. 83, 208–213.

Cline, M.A., Nandar, W., Smith, M.L., Pittman, B.H., Kelly, M., Rogers, J.O., 2008b. Amylin causes anorexigenic effects via the hypothalamus and brain stem in chicks. Regul. Pept. 146, 140–146.

Cline, M.A., Newmyer, B.A., Smith, M.L., 2009a. The anorectic effect of neuropeptide AF is associated with satiety-related hypothalamic nuclei. J. Neuroendocrinol. 21, 595–601.

Cline, M.A., Prall, B.C., Rogers, J.O., Tachibana, T., 2009b. Satiety induced by central stresscopin is mediated by corticotrophin-releasing factor receptors and hypothalamic changes in chicks. Pharmacol. Biochem. Behav. 92, 663–669.

Cline, M.A., Prall, B.C., Smith, M.L., Calchary, W.A., Siegel, P.B., 2008c. Differential appetite-related responses to central neuropeptide S in lines of chickens divergently selected for low or high body weight. J. Neuroendocrinol. 20, 904–908.

Cline, M.A., Siders, R., Newmyer, B.A., Smith, M.L., Siegel, P.B., 2010b. Both calcitonin and calcitonin gene-related peptides' thresholds of hypophagia are considerably lower in chicks selected for high rather than low juvenile body weight. Physiol. Behav. 101, 254–259.

Conlon, J.M., 1999. Bradykinin and its receptors in non-mammalian vertebrates. Regul. Pept. 79, 71–81.

Conlon, J.M., Katsoulis, S., Schmidt, W.E., Thim, L., 1988. [Arg3]substance P and neurokinin A from chicken small intestine. Regul. Pept. 20, 171–180.

Conlon, J.M., O'Harte, F., 1992. The primary structure of a PYY-related peptide from chicken intestine suggests an anomalous site of cleavage of the signal peptide in preproPYY. FEBS Lett. 313, 225–228.

Copp, D.H., Cockcroft, D.W., Kueh, Y., 1967. Calcitonin from ultimobranchial glands of dogfish and chickens. Science 158, 924–925.

Cornett, L.E., Kirby, J.D., Vizcarra, J.A., Ellison, J.C., Thrash, J., Mayeux, P.R., Crew, M.D., Jones, S.M., Ali, N., Baeyens, D.A., 2003. Molecular cloning and functional characterization of a vasotocin receptor subtype expressed in the pituitary gland of the domestic chicken (*Gallus domesticus*): avian homolog of the mammalian V1b-vasopressin receptor. Regul. Pept. 110, 231–239.

Crossley 2nd, D.A., Jonker, S.S., Hicks, J.W., Thornburg, K.L., 2010. Maturation of the angiotensin II cardiovascular response in the embryonic White Leghorn chicken (Gallus gallus). J. Comp. Physiol. B 180, 1057–1065.

Cruz, A., Parnot, C., Ribatti, D., Corvol, P., Gasc, J.M., 2001. Endothelin-1, a regulator of angiogenesis in the chick chorioallantoic membrane. J. Vasc. Res. 38, 536–545.

Cuesta, N., Martinez, A., Cuttitta, F., Zudaire, E., 2005. Identification of adrenomedullin in avian type II pneumocytes: increased expression after exposure to air pollutants. J. Histochem. Cytochem. 53, 773–780.

Cui, L., Lv, C., Zhang, J., Mo, C., Lin, D., Li, J., Wang, Y., 2017. Characterization of melanin-concentrating hormone (MCH) and its receptor in chickens: tissue expression, functional analysis, and fasting-induced up-regulation of hypothalamic MCH expression. Gene 615, 57–67.

Cuperus, T., Coorens, M., van Dijk, A., Haagsman, H.P., 2013. Avian host defense peptides. Dev. Comp. Immunol. 41, 352–369.

Dacke, C.G., 1976. Parathyroid hormone and eggshell calcification in Japanese quail. J. Endocrinol. 71, 239–243.

Dale, M.D., Mortimer, E.M., Kolli, S., Achramowicz, E., Borchert, G., Juliano, S.A., Halkyard, S., Seitz, N., Gatto, C., Hester, P.Y., Rubin, D.A., 2015. Bone-remodeling transcript levels are independent of perching in end-of-lay white leghorn chickens. Int. J. Mol. Sci. 16, 2663–2677.

Davenport, A.P., Hyndman, K.A., Dhaun, N., Southan, C., Kohan, D.E., Pollock, J.S., Pollock, D.M., Webb, D.J., Maguire, J.J., 2016. Endothelin. Pharmacol. Rev. 68, 357–418.

de Caro, G., Mariotti, M., Massi, M., Micossi, L.G., 1980a. Dipsogenic effect of angiotensin II, bombesin and tachykinins in the duck. Pharmacol. Biochem. Behav. 13, 229–233.

de Caro, G., Massi, M., Micossi, L.G., 1980b. Modifications of drinking behaviour and of arterial blood pressure induced by tachykinins in rats and pigeons. Psychopharmacology 68, 243–247.

De Clercq, P., Depoortere, I., Macielag, M., Vandermeers, A., Vandermeers-Piret, M.C., Peeters, T.L., 1996. Isolation, sequence, and bioactivity of chicken motilin. Peptides 17, 203–208.

De Groef, B., Geris, K.L., Manzano, J., Bernal, J., Millar, R.P., Abou-Samra, A.B., Porter, T.E., Iwasawa, A., Kuhn, E.R., Darras, V.M., 2003. Involvement of thyrotropin-releasing hormone receptor, somatostatin receptor subtype 2 and corticotropin-releasing hormone receptor type 1 in the control of chicken thyrotropin secretion. Mol. Cell. Endocrinol. 203, 33–39.

De Groef, B., Grommen, S.V., Darras, V.M., 2007. Feedback control of thyrotropin secretion in the chicken: thyroid hormones increase the expression of hypophyseal somatostatin receptor types 2 and 5. Gen. Comp. Endocrinol. 152, 178–182.

de Groef, B., Grommen, S.V., Mertens, I., Schoofs, L., Kuhn, E.R., Darras, V.M., 2004. Cloning and tissue distribution of the chicken type 2 corticotropin-releasing hormone receptor. Gen. Comp. Endocrinol. 138, 89–95.

De Groef, B., Vandenborne, K., Van As, P., Darras, V.M., Kuhn, E.R., Decuypere, E., Geris, K.L., 2005. Hypothalamic control of the thyroidal axis in the chicken: over the boundaries of the classical hormonal axes. Domest. Anim. Endocrinol. 29, 104–110.

De Saedeleer, V., Wechsung, E., Houvenaghel, A., 1989. The influence of substance P on oviductal, duodenal and blood pressure in the anaesthetized domestic hen. Vet. Res. Commun. 13, 183–191.

Degolier, T.F., Duke, G.E., Carraway, R.E., 1997. Neurotensin decreases pepsin output and gastrointestinal motility in chickens. Poultry Sci. 76, 1435–1439.

Delfino, K.R., Southey, B.R., Sweedler, J.V., Rodriguez-Zas, S.L., 2010. Genome-wide census and expression profiling of chicken neuropeptide and prohormone convertase genes. Neuropeptides 44, 31–44.

Denbow, D.M., Duke, G.E., Chaplin, S.B., 1988. Food intake, gastric secretion, and motility as affected by avian pancreatic polypeptide administered centrally in chickens. Peptides 9, 449–454.

Denbow, D.M., Myers, R.D., 1982. Eating, drinking and temperature responses to intracerebroventricular cholecystokinin in the chick. Peptides 3, 739–743.

Derache, C., Labas, V., Aucagne, V., Meudal, H., Landon, C., Delmas, A.F., Magallon, T., Lalmanach, A.C., 2009. Primary structure and antibacterial activity of chicken bone marrow-derived beta-defensins. Antimicrob. Agents Chemother. 53, 4647–4655.

Dimaline, R., Dockray, G.J., 1979. Potent stimulation of the avian exocrine pancreas by porcine and chicken vasoactive intestinal peptide. J. Physiol. 294, 153–163.

Dimaline, R., Lee, C.M., 1990. Chicken gastrin: a member of the gastrin/CCK family with novel structure-activity relationships. Am. J. Physiol. 259, G882–G888.

Diot, M., Reverchon, M., Rame, C., Froment, P., Brillard, J.P., Briere, S., Leveque, G., Guillaume, D., Dupont, J., 2015. Expression of adiponectin, chemerin and visfatin in plasma and different tissues during a laying season in turkeys. Reprod. Biol. Endocrinol. 13, 81.

Dodo, K., Izumi, T., Ueda, H., Bungo, T., 2005. Response of neuropeptide Y-induced feeding to mu-, delta- and kappa-opioid receptor antagonists in the neonatal chick. Neurosci. Lett. 373, 85–88.

Domin, J., Benito-Orfila, M.A., Nandha, K.A., Aitken, A., Bloom, S.R., 1992. The purification and sequence analysis of an avian neuromedin U. Regul. Pept. 41, 1–8.

Donoghue, D.J., Scanes, C.G., 1991. Possible involvement of adenylyl cyclase-cAMP-protein kinase a pathway in somatostatin inhibition of growth hormone release from chicken pituitary cells. Gen. Comp. Endocrinol. 81, 113–119.

Dores, R.M., Liang, L., Davis, P., Thomas, A.L., Petko, B., 2016. 60 years OF POMC: melanocortin receptors: evolution of ligand selectivity for melanocortin peptides. J. Mol. Endocrinol. 56, T119–T133.

Dorshorst, B., Molin, A.M., Rubin, C.J., Johansson, A.M., Stromstedt, L., Pham, M.H., Chen, C.F., Hallbook, F., Ashwell, C., Andersson, L., 2011. A complex genomic rearrangement involving the endothelin 3 locus causes dermal hyperpigmentation in the chicken. PLoS Genet. 7, e1002412.

Du, F., Charnay, Y., Dubois, P., 1987. Development and distribution of substance P in the spinal cord and ganglia of embryonic and newly hatched chick: an immunofluorescence study. J. Comp. Neurol. 263, 436–454.

Du, F., Dubois, P., 1988. Distribution of substance P and vasoactive intestinal polypeptide neurons in the chicken spinal cord, with notes on their postnatal development. J. Comp. Neurol. 278, 253–264.

Duke, G.E., Kimmel, J.R., Hunt, H., Pollock, H.G., 1985. The influence of avian pancreatic polypeptide on gastric secretion and motility in laying hens. Poultry Sci. 64, 1231–1235.

Dunn, I.C., Meddle, S.L., Wilson, P.W., Wardle, C.A., Law, A.S., Bishop, V.R., Hindar, C., Robertson, G.W., Burt, D.W., Ellison, S.J., Morrice, D.M., Hocking, P.M., 2013. Decreased expression of the satiety signal receptor CCKAR is responsible for increased growth and body weight during the domestication of chickens. Am. J. Physiol. Endocrinol. Metab. 304, E909–E921.

Egawa, C., Kameda, Y., 1995. Innervation of the chicken parathyroid glands: immunohistochemical study with the TuJ1, galanin, VIP, substance P, CGRP and tyrosine hydroxylase antibodies. Anat. Embryol. 191, 445–450.

Eldred, W.D., Li, H.B., Carraway, R.E., Dowling, J.E., 1987. Immunocytochemical localization of LANT-6-like immunoreactivity within neurons in the inner nuclear and ganglion cell layers in vertebrate retinas. Brain Res. 424, 361–370.

Epstein, M.L., Hudis, J., Dahl, J.L., 1983. The development of peptidergic neurons in the foregut of the chick. J. Neurosci. 3, 2431–2447.

Erichsen, J.T., Reiner, A., Karten, H.J., 1982. Co-occurrence of substance P-like and Leu-enkephalin-like immunoreactivities in neurones and fibres of avian nervous system. Nature 295, 407–410.

Fan, L., Westermark, G., Chan, S.J., Steiner, D.F., 1994. Altered gene structure and tissue expression of islet amyloid polypeptide in the chicken. Mol. Endocrinol. 8, 713–721.

Fontaine-Perus, J., Chanconie, M., Polak, J.M., Le Douarin, N.M., 1981. Origin and development of VIP and substance P containing neurons in the embryonic avian gut. Histochemistry 71, 313–323.

Francis, M., Arkle, M., Martin, L., Butler, T.M., Cruz, M.C., Opare-Aryee, G., Dacke, C.G., Brown, J.F., 2003. Relaxant effects of parathyroid hormone and parathyroid hormone-related peptides on oviduct motility in birds and mammals: possible role of nitric oxide. Gen. Comp. Endocrinol. 133, 243–251.

Friedman-Einat, M., Cogburn, L.A., Yosefi, S., Hen, G., Shinder, D., Shirak, A., Seroussi, E., 2014. Discovery and characterization of the first genuine avian leptin gene in the rock dove (*Columba livia*). Endocrinology 155, 3376–3384.

Friedman-Einat, M., Seroussi, E., 2019. Avian leptin: bird's-eye view of the evolution of vertebrate energy-balance control. Trends Endocrinol. Metabol. 30, 819–832.

Furuse, M., 1999. Release and endogenous actions of the gastrin/cholecystokinin (CCK) family in the chicken. J. Exp. Zool. 283, 448–454.

Furuse, M., Ando, R., Bungo, T., Ao, R., Shimojo, M., Masuda, Y., 1999. Intracerebroventricular injection of orexins does not stimulate food intake in neonatal chicks. Br. Poultry Sci. 40, 698–700.

Furuse, M., Matsumoto, M., Okumura, J., Sugahara, K., Hasegawa, S., 1997. Intracerebroventricular injection of mammalian and chicken glucagon-like peptide-1 inhibits food intake of the neonatal chick. Brain Res. 755, 167–169.

Furuse, M., Tachibana, T., Ohgushi, A., Ando, R., Yoshimatsu, T., Denbow, D.M., 2001. Intracerebroventricular injection of ghrelin and growth hormone releasing factor inhibits food intake in neonatal chicks. Neurosci. Lett. 301, 123–126.

Gao, S., Zhang, J., He, C., Meng, F., Bu, G., Zhu, G., Li, J., Wang, Y., 2017. Molecular characterization of neuropeptide Y (NPY) receptors (Y1, Y4 and Y6) and investigation of the tissue expression of their ligands (NPY, PYY and PP) in chickens. Gen. Comp. Endocrinol. 240, 46–60.

Geelissen, S.M., Beck, I.M., Darras, V.M., Kuhn, E.R., Van der Geyten, S., 2003. Distribution and regulation of chicken growth hormone secretagogue receptor isoforms. Gen. Comp. Endocrinol. 134, 167–174.

Goitsuka, R., Chen, C.L., Benyon, L., Asano, Y., Kitamura, D., Cooper, M.D., 2007. Chicken cathelicidin-B1, an antimicrobial guardian at the mucosal M cell gateway. Proc. Natl. Acad. Sci. U.S.A. 104, 15063–15068.

Gomes, I., Aryal, D.K., Wardman, J.H., Gupta, A., Gagnidze, K., Rodriguiz, R.M., Kumar, S., Wetsel, W.C., Pintar, J.E., Fricker, L.D., Devi, L.A., 2013. GPR171 is a hypothalamic G protein-coupled receptor for BigLEN, a neuropeptide involved in feeding. Proc. Natl. Acad. Sci. U.S.A. 110, 16211–16216.

Gomes, I., Bobeck, E.N., Margolis, E.B., Gupta, A., Sierra, S., Fakira, A.K., Fujita, W., Muller, T.D., Muller, A., Tschop, M.H., Kleinau, G., Fricker, L.D., Devi, L.A., 2016. Identification of GPR83 as the receptor for the neuroendocrine peptide PEN. Sci. Signal. 9, ra43.

Gomez, A.P., Moreno, M.J., Iglesias, A., Coral, P.X., Hernandez, A., 2007. Endothelin 1, its endothelin type A receptor, connective tissue growth factor, platelet-derived growth factor, and adrenomedullin expression in lungs of pulmonary hypertensive and nonhypertensive chickens. Poultry Sci. 86, 909–916.

Gomi, H., Morikawa, S., Shinmura, N., Moki, H., Yasui, T., Tsukise, A., Torii, S., Watanabe, T., Maeda, Y., Hosaka, M., 2015. Expression of secretogranin III in chicken endocrine cells: its relevance to the secretory granule properties of peptide prohormone processing and bioactive amine content. J. Histochem. Cytochem. 63, 350–366.

Gong, D., Wilson, P.W., Bain, M.M., McDade, K., Kalina, J., Herve-Grepinet, V., Nys, Y., Dunn, I.C., 2010. Gallin; an antimicrobial peptide member of a new avian defensin family, the ovodefensins, has been subject to recent gene duplication. BMC Immunol. 11, 12.

Gonzalez, A.M., Podvin, S., Lin, S.Y., Miller, M.C., Botfield, H., Leadbeater, W.E., Roberton, A., Dang, X., Knowling, S.E., Cardenas-Galindo, E., Donahue, J.E., Stopa, E.G., Johanson, C.E., Coimbra, R., Eliceiri, B.P., Baird, A., 2011. Ecrg4 expression and its product augurin in the choroid plexus: impact on fetal brain development, cerebrospinal fluid homeostasis and neuroprogenitor cell response to CNS injury. Fluids Barriers CNS 8, 6.

Goodridge, A.G., Garay, A., Silpananta, P., 1974. Regulation of lipogenesis and the total activities of lipogenic enzymes in a primary culture of hepatocytes from prenatal and early postnatal chicks. J. Biol. Chem. 249, 1469–1475.

Gould, K.L., Newman, S.W., Tricomi, E.M., DeVoogd, T.J., 2001. The distribution of substance P and neuropeptide Y in four songbird species: a comparison of food-storing and non-storing birds. Brain Res. 918, 80–95.

Gourdie, R.G., Wei, Y., Kim, D., Klatt, S.C., Mikawa, T., 1998. Endothelin-induced conversion of embryonic heart muscle cells into impulse-conducting Purkinje fibers. Proc. Natl. Acad. Sci. U.S.A. 95, 6815–6818.

Groenendijk, B.C., Stekelenburg-de Vos, S., Vennemann, P., Wladimiroff, J.W., Nieuwstadt, F.T., Lindken, R., Westerweel, J., Hierck, B.P., Ursem, N.T., Poelmann, R.E., 2008. The endothelin-1 pathway and the development of cardiovascular defects in the haemodynamically challenged chicken embryo. J. Vasc. Res. 45, 54–68.

Grommen, S.V.H., Scott, M.K., Darras, V.M., De Groef, B., 2017. Spatial and temporal expression profiles of urocortin 3 mRNA in the brain of the chicken (Gallus gallus). J. Comp. Neurol. 525, 2583–2591.

Guabiraba, R., Garrido, D., Bailleul, G., Trotereau, A., Pinaud, M., Lalmanach, A.C., Chanteloup, N.K., Schouler, C., 2017. Unveiling the participation of avian kinin ornithokinin and its receptors in the chicken inflammatory response. Vet. Immunol. Immunopathol. 188, 34–47.

Gubrij, K.I., Chaturvedi, C.M., Ali, N., Cornett, L.E., Kirby, J.D., Wilkerson, J., Mikhailova, M., Turner, M.L., Baeyens, D.A., 2005. Molecular cloning of an oxytocin-like receptor expressed in the chicken shell gland. Comp. Biochem. Physiol. B Biochem. Mol. Biol. 142, 37–45.

Guerrini, R., Salvadori, S., Rizzi, A., Regoli, D., Calo, G., 2010. Neurobiology, pharmacology, and medicinal chemistry of neuropeptide S and its receptor. Med. Res. Rev. 30, 751–777.

Gui, X., Degolier, T.F., Duke, G.E., Carraway, R.E., 2000. Neurotensin elevates hepatic bile acid secretion in chickens by a mechanism requiring an intact enterohepatic circulation. Comp. Biochem. Physiol. C Toxicol. Pharmacol. 127, 61–70.

Gunther, T., Tulipano, G., Dournaud, P., Bousquet, C., Csaba, Z., Kreienkamp, H.J., Lupp, A., Korbonits, M., Castano, J.P., Wester, H.J., Culler, M., Melmed, S., Schulz, S., 2018. International union of basic and clinical pharmacology. CV. Somatostatin receptors: structure, function, ligands, and new nomenclature. Pharmacol. Rev. 70, 763–835.

Guo, X., Wang, Y., Chen, Q., Yuan, Z., Chen, Y., Guo, M., Kang, L., Sun, Y., Jiang, Y., 2019. The role of PTHLH in ovarian follicle selection, its transcriptional regulation and genetic effects on egg laying traits in hens. Front. Genet. 10, 430.

Guyot, N., Meudal, H., Trapp, S., Iochmann, S., Silvestre, A., Jousset, G., Labas, V., Reverdiau, P., Loth, K., Herve, V., Aucagne, V., Delmas, A.F., Rehault-Godbert, S., Landon, C., 2020. Structure, function, and evolution of Gga-AvBD11, the archetype of the structural avian-double-beta-defensin family. Proc. Natl. Acad. Sci. U.S.A. 117, 337–345.

Guzel, S., Gunes, N., Yildiz, H., Yilmaz, B., 2009. Effects of amylin on bone development and egg production in hens. Poultry Sci. 88, 1719–1724.

Han, R., Yang, P., Tian, Y., Wang, D., Zhang, Z., Wang, L., Li, Z., Jiang, R., Kang, X., 2014. Identification and functional characterization of copy number variations in diverse chicken breeds. BMC Genom. 15, 934.

Hara, Y., Yamaguchi, K., Onimaru, K., Kadota, M., Koyanagi, M., Keeley, S.D., Tatsumi, K., Tanaka, K., Motone, F., Kageyama, Y., Nozu, R., Adachi, N., Nishimura, O., Nakagawa, R., Tanegashima, C., Kiyatake, I., Matsumoto, R., Murakumo, K., Nishida, K., Terakita, A., Kuratani, S., Sato, K., Hyodo, S., Kuraku, S., 2018. Shark genomes provide insights into elasmobranch evolution and the origin of vertebrates. Nat Ecol Evol 2, 1761–1771.

Harris, M.L., Hall, R., Erickson, C.A., 2008. Directing pathfinding along the dorsolateral path - the role of EDNRB2 and EphB2 in overcoming inhibition. Development 135, 4113–4122.

Harvey, S., Gineste, C., Gaylinn, B.D., 2014. Growth hormone (GH)-releasing activity of chicken GH-releasing hormone (GHRH) in chickens. Gen. Comp. Endocrinol. 204, 261–266.

Harvey, S., Scanes, C.G., Chadwick, A., Bolton, N.J., 1978. The effect of thyrotropin-releasing hormone (TRH) and somatostatin (GHRIH) on growth hormone and prolactin secretion in vitro and in vivo in the domestic fowl (*Gallus domesticus*). Neuroendocrinology 26, 249–260.

Hasegawa, S., Terazono, K., Nata, K., Takada, T., Yamamoto, H., Okamoto, H., 1990. Nucleotide sequence determination of chicken glucagon precursor cDNA. Chicken preproglucagon does not contain glucagon-like peptide II. FEBS Lett. 264, 117–120.

Hay, D.L., Garelja, M.L., Poyner, D.R., Walker, C.S., 2018. Update on the pharmacology of calcitonin/CGRP family of peptides: IUPHAR Review 25. Br. J. Pharmacol. 175, 3–17.

Hazelwood, R.L., 1984. Pancreatic hormones, insulin/glucagon molar ratios, and somatostatin as determinants of avian carbohydrate metabolism. J. Exp. Zool. 232, 647–652.

He, C., Zhang, J., Gao, S., Meng, F., Bu, G., Li, J., Wang, Y., 2016. Molecular characterization of three NPY receptors (Y2, Y5 and Y7) in chickens: gene structure, tissue expression, promoter identification, and functional analysis. Gen. Comp. Endocrinol. 236, 24–34.

Hellgren, O., Ekblom, R., 2010. Evolution of a cluster of innate immune genes (beta-defensins) along the ancestral lines of chicken and zebra finch. Immunome Res. 6, 3.

Higgins, S.E., Ellestad, L.E., Trakooljul, N., McCarthy, F., Saliba, J., Cogburn, L.A., Porter, T.E., 2010. Transcriptional and pathway analysis in the hypothalamus of newly hatched chicks during fasting and delayed feeding. BMC Genom. 11, 162.

Hinson, J.P., Kapas, S., Smith, D.M., 2000. Adrenomedullin, a multifunctional regulatory peptide. Endocr. Rev. 21, 138–167.

Ho, J.C., Jacobs, T., Wang, Y., Leung, F.C., 2012. Identification and characterization of the chicken galanin receptor GalR2 and a novel GalR2-like receptor (GalR2-L). Gen. Comp. Endocrinol. 179, 305–312.

Ho, J.C., Kwok, A.H., Zhao, D., Wang, Y., Leung, F.C., 2011. Characterization of the chicken galanin type I receptor (GalR1) and a novel GalR1-like receptor (GalR1-L). Gen. Comp. Endocrinol. 170, 391–400.

Ho, R.H., DePalatis, L.R., 1980. Substance P immunoreactivity in the median eminence of the North American opossum and domestic fowl. Brain Res. 189, 565–569.

Holmberg, S.K., Mikko, S., Boswell, T., Zoorob, R., Larhammar, D., 2002. Pharmacological characterization of cloned chicken neuropeptide Y receptors Y1 and Y5. J. Neurochem. 81, 462–471.

Homma, T., Watanabe, M., Hirose, S., Kanai, A., Kangawa, K., Matsuo, H., 1986. Isolation and determination of the amino acid sequence of chicken calcitonin I from chicken ultimobranchial glands. J. Biochem. 100, 459–467.

Honda, K., Saneyasu, T., Shimatani, T., Aoki, K., Yamaguchi, T., Nakanishi, K., Kamisoyama, H., 2015. Intracerebroventricular administration of chicken glucagon-like peptide-2 potently suppresses food intake in chicks. Anim. Sci. J. 86, 312–318.

Honda, K., Saneyasu, T., Yamaguchi, T., Shimatani, T., Aoki, K., Nakanishi, K., Kamisoyama, H., 2014. Intracerebroventricular administration of novel glucagon-like peptide suppresses food intake in chicks. Peptides 52, 98–103.

Honey, R.N., Arimura, A., Weir, G.C., 1981. Somatostatin neutralization stimulates glucagon and insulin secretion from the avian pancreas. Endocrinology 109, 1971–1974.

Honey, R.N., Fallon, M.B., Weir, G.C., 1980. Effects of exogenous insulin, glucagon, and somatostatin on islet hormone secretion in the perfused chicken pancreas. Metabolism 29, 1242–1246.

Hong, Y., Hay, D.L., Quirion, R., Poyner, D.R., 2012. The pharmacology of adrenomedullin 2/intermedin. Br. J. Pharmacol. 166, 110–120.

Hong, Y.H., Lillehoj, H.S., Dalloul, R.A., Min, W., Miska, K.B., Tuo, W., Lee, S.H., Han, J.Y., Lillehoj, E.P., 2006. Molecular cloning and characterization of chicken NK-lysin. Vet. Immunol. Immunopathol. 110, 339–347.

Houweling, A.C., Somi, S., Massink, M.P., Groenen, M.A., Moorman, A.F., Christoffels, V.M., 2005. Comparative analysis of the natriuretic peptide precursor gene cluster in vertebrates reveals loss of ANF and retention of CNP-3 in chicken. Dev. Dynam. 233, 1076–1082.

Huang, G., He, C., Meng, F., Li, J., Zhang, J., Wang, Y., 2014a. Glucagon-like peptide (GCGL) is a novel potential TSH-releasing factor (TRF) in Chickens: I) Evidence for its potent and specific action on stimulating TSH mRNA expression and secretion in the pituitary. Endocrinology 155, 4568–4580.

Huang, G., Li, J., Fu, H., Yan, Z., Bu, G., He, X., Wang, Y., 2012. Characterization of glucagon-like peptide 1 receptor (GLP1R) gene in chickens: functional analysis, tissue distribution, and identification of its transcript variants. Domest. Anim. Endocrinol. 43, 1–15.

Huang, G., Li, J., Wang, H., Lan, X., Wang, Y., 2014b. Discovery of a novel functional leptin protein (LEP) in zebra finches: evidence for the existence of an authentic avian leptin gene predominantly expressed in the brain and pituitary. Endocrinology 155, 3385–3396.

Huang, H.Y., Zhao, G.P., Liu, R.R., Li, Q.H., Zheng, M.Q., Li, S.F., Liang, Z., Zhao, Z.H., Wen, J., 2015. Brain natriuretic peptide stimulates lipid metabolism through its receptor NPR1 and the glycerolipid metabolism pathway in chicken adipocytes. Biochemistry 54, 6622–6630.

Huang, Z., Depoortere, I., De Clercq, P., Peeters, T., 1999. Sequence and characterization of cDNA encoding the motilin precursor from chicken, dog, cow and horse. Evidence of mosaic evolution in pre-promotilin. Gene 240, 217–226.

Hurwitz, S., 1996. Homeostatic control of plasma calcium concentration. Crit. Rev. Biochem. Mol. Biol. 31, 41–100.

Ikemoto, T., Park, M.K., 2005. Chicken RFamide-related peptide (GnIH) and two distinct receptor subtypes: identification, molecular characterization, and evolutionary considerations. J. Reprod. Dev. 51, 359–377.

Irwin, D.M., Wong, J., 1995. Trout and chicken proglucagon: alternative splicing generates mRNA transcripts encoding glucagon-like peptide 2. Mol. Endocrinol. 9, 267–277.

Irwin, D.M., Zhang, T., 2006. Evolution of the vertebrate glucose-dependent insulinotropic polypeptide (GIP) gene. Comp. Biochem. Physiol. Genom. Proteonomics 1, 385–395.

Iwabuchi, M., Ui-Tei, K., Yamada, K., Matsuda, Y., Sakai, Y., Tanaka, K., Ohki-Hamazaki, H., 2003. Molecular cloning and characterization of avian bombesin-like peptide receptors: new tools for investigating molecular basis for ligand selectivity. Br. J. Pharmacol. 139, 555–566.

Jensen, H., Orskov, C., Rehfeld, J.F., Johnsen, A.H., 2001. A processing enzyme cleaving avian progastrin at post-Phe bonds. Biochim. Biophys. Acta 1547, 64–71.

Johnson, A.L., Li, Z., Gibney, J.A., Malamed, S., 1994. Vasoactive intestinal peptide-induced expression of cytochrome P450 cholesterol side-chain cleavage and 17 alpha-hydroxylase enzyme activity in hen granulosa cells. Biol. Reprod. 51, 327–333.

Johnson, A.L., Tilly, J.L., 1988. Effects of vasoactive intestinal peptide on steroid secretion and plasminogen activator activity in granulosa cells of the hen. Biol. Reprod. 38, 296–303.

Jonson, L., Schoeman, N., Saayman, H., Naude, R., Jensen, H., Johnsen, A.H., 2000. Identification of ostrich and chicken cholecystokinin cDNA and intestinal peptides. Peptides 21, 1337–1344.

Jozsa, R., Korf, H.W., Csernus, V., Mess, B., 1988. Thyrotropin-releasing hormone (TRH)-immunoreactive structures in the brain of the domestic mallard. Cell Tissue Res. 251, 441–449.

Jozsa, R., Mess, B., 1993. Galanin-like immunoreactivity in the chicken brain. Cell Tissue Res. 273, 391–399.

Jozsa, R., Vigh, S., Mess, B., Schally, A.V., 1986. Ontogenetic development of corticotropin-releasing factor (CRF)-containing neural elements in the brain of the chicken during incubation and after hatching. Cell Tissue Res. 244, 681–685.

Jozsa, R., Vigh, S., Schally, A.V., Mess, B., 1984. Localization of corticotropin-releasing factor-containing neurons in the brain of the domestic fowl. An immunohistochemical study. Cell Tissue Res. 236, 245–248.

Kaiya, H., Van Der Geyten, S., Kojima, M., Hosoda, H., Kitajima, Y., Matsumoto, M., Geelissen, S., Darras, V.M., Kangawa, K., 2002. Chicken ghrelin: purification, cDNA cloning, and biological activity. Endocrinology 143, 3454–3463.

Kameda, Y., 1989. Distribution of CGRP-, somatostatin-, galanin-, VIP-, and substance P-immunoreactive nerve fibers in the chicken carotid body. Cell Tissue Res. 257, 623–629.

Kameda, Y., 1991. Immunocytochemical localization and development of multiple kinds of neuropeptides and neuroendocrine proteins in the chick ultimobranchial gland. J. Comp. Neurol. 304, 373–386.

Kameda, Y., Miura, M., Ohno, S., 1998. Localization and development of chromogranin A and luteinizing hormone immunoreactivities in the secretory-specific cells of the hypophyseal pars tuberalis of the chicken. Histochem. Cell Biol. 109, 211–222.

Kamisoyama, H., Honda, K., Saneyasu, T., Sugahara, K., Hasegawa, S., 2007. Central administration of neuromedin U suppresses food intake in chicks. Neurosci. Lett. 420, 1–5.

Karnik, S.S., Unal, H., Kemp, J.R., Tirupula, K.C., Eguchi, S., Vanderheyden, P.M., Thomas, W.G., 2015. International union of basic and clinical pharmacology. XCIX. Angiotensin receptors: interpreters of pathophysiological angiotensinergic stimuli [corrected]. Pharmacol. Rev. 67, 754–819.

Katayama, S., Shigemi, K., Cline, M.A., Furuse, M., 2010. Intracerebroventricular injection of orexin-A stimulates monoamine metabolism but not HPA axis in neonatal chicks. Neurosci. Lett. 484, 157–161.

Kawashima, M., Takahashi, T., Yanai, H., Ogawa, H., Yasuoka, T., 2005. Direct action of parathyroid hormone-related peptide to enhance corticosterone production stimulated by adrenocorticotropic hormone in adrenocortical cells of hens. Poultry Sci. 84, 1463–1469.

Kawauchi, H., Kawazoe, I., Tsubokawa, M., Kishida, M., Baker, B.I., 1983. Characterization of melanin-concentrating hormone in chum salmon pituitaries. Nature 305, 321–323.

Kempf, H., Corvol, P., 2001. Angiotensin receptor(s) in fowl. Comp. Biochem. Physiol. Mol. Integr. Physiol. 128, 77–88.

Kempf, H., le Moullec, J.M., Corvol, P., Gasc, J.M., 1996. Molecular cloning, expression and tissue distribution of a chicken angiotensin II receptor. FEBS Lett. 399, 198–202.

Kempf, H., Linares, C., Corvol, P., Gasc, J.M., 1998. Pharmacological inactivation of the endothelin type A receptor in the early chick embryo: a model of mispatterning of the branchial arch derivatives. Development 125, 4931–4941.

Kennedy, A.J., Davenport, A.P., 2018. International union of basic and clinical pharmacology CIII: chemerin receptors CMKLR1 (Chemerin1) and GPR1 (Chemerin2) nomenclature, pharmacology, and function. Pharmacol. Rev. 70, 174–196.

Kerje, S., Lind, J., Schutz, K., Jensen, P., Andersson, L., 2003. Melanocortin 1-receptor (MC1R) mutations are associated with plumage colour in chicken. Anim. Genet. 34, 241–248.

Khosla, S., Demay, M., Pines, M., Hurwitz, S., Potts Jr., J.T., Kronenberg, H.M., 1988. Nucleotide sequence of cloned cDNAs encoding chicken preproparathyroid hormone. J. Bone Miner. Res. 3, 689–698.

Kim, D., Johnson, A.L., 2016. Vasoactive intestinal peptide promotes differentiation and clock gene expression in granulosa cells from prehierarchal follicles. Mol. Reprod. Dev. 83, 455–463.

Kim, D.K., Yun, S., Son, G.H., Hwang, J.I., Park, C.R., Kim, J.I., Kim, K., Vaudry, H., Seong, J.Y., 2014. Coevolution of the spexin/galanin/kisspeptin family: Spexin activates galanin receptor type II and III. Endocrinology 155, 1864–1873.

Kimmel, J.R., Hayden, L.J., Pollock, H.G., 1975. Isolation and characterization of a new pancreatic polypeptide hormone. J. Biol. Chem. 250, 9369–9376.

Kimura, M., Sueyoshi, T., Takada, K., Tanaka, K., Morita, T., Iwanaga, S., 1987. Isolation and characterization of ornitho-kininogen. Eur. J. Biochem. 168, 493–501.

Kinoshita, K., Akiyama, T., Mizutani, M., Shinomiya, A., Ishikawa, A., Younis, H.H., Tsudzuki, M., Namikawa, T., Matsuda, Y., 2014. Endothelin receptor B2 (EDNRB2) is responsible for the tyrosinase-independent recessive white (mo(w)) and mottled (mo) plumage phenotypes in the chicken. PloS One 9, e86361.

Kita, S., Nishizawa, H., Okuno, Y., Tanaka, M., Yasui, A., Matsuda, M., Yamada, Y., Shimomura, I., 2009. Competitive binding of musclin to natriuretic peptide receptor 3 with atrial natriuretic peptide. J. Endocrinol. 201, 287–295.

Kitazawa, T., Kaiya, H., 2019. Regulation of gastrointestinal motility by motilin and ghrelin in vertebrates. Front. Endocrinol. 10, 278.

Kitazawa, T., Kaiya, H., Taneike, T., 2007. Contractile effects of ghrelin-related peptides on the chicken gastrointestinal tract in vitro. Peptides 28, 617–624.

Kitazawa, T., Maeda, Y., Kaiya, H., 2009. Molecular cloning of growth hormone secretagogue-receptor and effect of quail ghrelin on gastrointestinal motility in Japanese quail. Regul. Pept. 158, 132–142.

Kitazawa, T., Taneike, T., Ohga, A., 1995. Excitatory action of [Leu13] motilin on the gastrointestinal smooth muscle isolated from the chicken. Peptides 16, 1243–1252.

Klein, S., Jurkevich, A., Grossmann, R., 2006. Sexually dimorphic immunoreactivity of galanin and colocalization with arginine vasotocin in the chicken brain (Gallus gallus domesticus). J. Comp. Neurol. 499, 828–839.

Kocamaz, E., Gok, D., Cetinkaya, A., Tufan, A.C., 2012. Implication of C-type natriuretic peptide-3 signaling in glycosaminoglycan synthesis and chondrocyte hypertrophy during TGF-beta1 induced chondrogenic differentiation of chicken bone marrow-derived mesenchymal stem cells. J. Mol. Histol. 43, 497–508.

Krause, A., Neitz, S., Magert, H.J., Schulz, A., Forssmann, W.G., Schulz-Knappe, P., Adermann, K., 2000. LEAP-1, a novel highly disulfide-bonded human peptide, exhibits antimicrobial activity. FEBS Lett. 480, 147–150.

Krug, E., Gross, R., Mialhe, P., 1976. The contribution of the pancreas and the intestine to the regulation of lipolysis in birds. 2. Impaired lipolytic activity of pancreatic glucagon in the absence of either the pancreas or the intestine in the chicken. Horm. Metab. Res. 8, 345–350.

Krzysik-Walker, S.M., Ocon-Grove, O.M., Maddineni, S.B., Hendricks 3rd, G.L., Ramachandran, R., 2007. Identification of calcitonin expression in the chicken ovary: influence of follicular maturation and ovarian steroids. Biol. Reprod. 77, 626–635.

Kuenzel, W.J., 1994. Central neuroanatomical systems involved in the regulation of food intake in birds and mammals. J. Nutr. 124, 1355S–1370S.

Kuenzel, W.J., Douglass, L.W., Davison, B.A., 1987. Robust feeding following central administration of neuropeptide Y or peptide YY in chicks, *Gallus domesticus*. Peptides 8, 823–828.

Kulig, P., Kantyka, T., Zabel, B.A., Banas, M., Chyra, A., Stefanska, A., Tu, H., Allen, S.J., Handel, T.M., Kozik, A., Potempa, J., Butcher, E.C., Cichy, J., 2011. Regulation of chemerin chemoattractant and antibacterial activity by human cysteine cathepsins. J. Immunol. 187, 1403–1410.

Lahav, R., Ziller, C., Dupin, E., Le Douarin, N.M., 1996. Endothelin 3 promotes neural crest cell proliferation and mediates a vast increase in melanocyte number in culture. Proc. Natl. Acad. Sci. U. S. A. 93, 3892–3897.

Langslow, D.R., 1973. The action of gut glucagon-like immunoreactivity and other intestinal hormones on lipolysis in chicken adipocytes. Horm. Metab. Res. 5, 428–432.

Langslow, D.R., Hales, C.N., 1969. Lipolysis in chicken adipose tissue in vitro. J. Endocrinol. 43, 285–294.

Lanuza, E., Davies, D.C., Landete, J.M., Novejarque, A., Martinez-Garcia, F., 2000. Distribution of CGRP-like immunoreactivity in the chick and quail brain. J. Comp. Neurol. 421, 515–532.

Lazure, C., Paquet, L., Litthauer, D., Naude, R.J., Oelofsen, W., Chretien, M., 1990. The ostrich pituitary contains a major peptide homologous to mammalian chromogranin A(1-76). Peptides 11, 79–87.

Leclercq, B., 1984. Adipose tissue metabolism and its control in birds. Poultry Sci. 63, 2044–2054.

Lee, M.O., Jang, H.J., Han, J.Y., Womack, J.E., 2014. Chicken NK-lysin is an alpha-helical cationic peptide that exerts its antibacterial activity through damage of bacterial cell membranes. Poultry Sci. 93, 864–870.

Lee, M.O., Kim, E.H., Jang, H.J., Park, M.N., Woo, H.J., Han, J.Y., Womack, J.E., 2012. Effects of a single nucleotide polymorphism in the chicken NK-lysin gene on antimicrobial activity and cytotoxicity of cancer cells. Proc. Natl. Acad. Sci. U.S.A. 109, 12087–12092.

Leitner, B., Schneitler, C., Klocker, H., Volknandt, W., Zimmermann, H., Winkler, H., Fischer-Colbrie, R., 1998. Formation and sequence analysis of secretoneurin, a neuropeptide derived from secretogranin II, in mammalian, bird, reptile, amphibian and fish brains. Neurosci. Lett. 248, 105–108.

Leprince, J., Chatenet, D., Dubessy, C., Fournier, A., Pfeiffer, B., Scalbert, E., Renard, P., Pacaud, P., Oulyadi, H., Segalas-Milazzo, I., Guilhaudis, L., Davoust, D., Tonon, M.C., Vaudry, H., 2008. Structure-activity relationships of urotensin II and URP. Peptides 29, 658–673.

Li, D., Tsutsui, K., Muneoka, Y., Minakata, H., Nomoto, K., 1996. An oviposition-inducing peptide: isolation, localization, and function of avian galanin in the quail oviduct. Endocrinology 137, 1618–1626.

Li, X., Li, Z., Deng, Y., Zhang, J., Li, J., Wang, Y., 2020. Characterization of a novel thyrotropin-releasing hormone receptor, TRHR3, in chickens. Poultry Sci. 99, 1643–1654.

Lim, C.H., Lee, M.Y.M., Soga, T., Parhar, I., 2019. Evolution of structural and functional diversity of spexin in mammalian and non-mammalian vertebrate species. Front. Endocrinol. 10, 379.

Linari, G., Baldieri, M., Angelucci, L., 1975. The action of bombesin on gastric secretion of the chicken. Eur. J. Pharmacol. 34, 143–150.

Linari, G., Linari, M.B., 1975. Effect of bombesin on pancreatic secretion and gall bladder motility of the chicken. Eur. J. Pharmacol. 34, 305–310.

Ling, M.K., Hotta, E., Kilianova, Z., Haitina, T., Ringholm, A., Johansson, L., Gallo-Payet, N., Takeuchi, S., Schioth, H.B., 2004. The melanocortin receptor subtypes in chicken have high preference to ACTH-derived peptides. Br. J. Pharmacol. 143, 626–637.

Ling, M.K., Lagerstrom, M.C., Fredriksson, R., Okimoto, R., Mundy, N.I., Takeuchi, S., Schioth, H.B., 2003. Association of feather colour with constitutively active melanocortin 1 receptors in chicken. Eur. J. Biochem. 270, 1441–1449.

Liu, H., Luo, Q., Zhang, J., Mo, C., Wang, Y., Li, J., 2019. Endothelins (EDN1, EDN2, EDN3) and their receptors (EDNRA, EDNRB, EDNRB2) in chickens: functional analysis and tissue distribution. Gen. Comp. Endocrinol. 283, 113231.

Liu, L., Burcher, E., 2001. Radioligand binding and functional characterisation of tachykinin receptors in chicken small intestine. Naunyn-Schmiedeberg's Arch. Pharmacol. 364, 305–313.

Lopez, J., Cuesta, N., Cuttitta, F., Martinez, A., 1999. Adrenomedullin in nonmammalian vertebrate pancreas: an immunocytochemical study. Gen. Comp. Endocrinol. 115, 309–322.

Lovell, P.V., Wirthlin, M., Wilhelm, L., Minx, P., Lazar, N.H., Carbone, L., Warren, W.C., Mello, C.V., 2014. Conserved syntenic clusters of protein coding genes are missing in birds. Genome Biol. 15, 565.

Lynn, D.J., Higgs, R., Gaines, S., Tierney, J., James, T., Lloyd, A.T., Fares, M.A., Mulcahy, G., O'Farrelly, C., 2004. Bioinformatic discovery and initial characterisation of nine novel antimicrobial peptide genes in the chicken. Immunogenetics 56, 170–177.

Lynn, D.J., Higgs, R., Lloyd, A.T., O'Farrelly, C., Herve-Grepinet, V., Nys, Y., Brinkman, F.S., Yu, P.L., Soulier, A., Kaiser, P., Zhang, G., Lehrer, R.I., 2007. Avian beta-defensin nomenclature: a community proposed update. Immunol. Lett. 110, 86–89.

Lynn, D.J., Lloyd, A.T., O'Farrelly, C., 2003. In silico identification of components of the Toll-like receptor (TLR) signaling pathway in clustered chicken expressed sequence tags (ESTs). Vet. Immunol. Immunopathol. 93 (3–4), 177–184.

Mace, J.D., Tachibana, T., Wang, G., Newmyer, B.A., Guilliams, E., Gilbert, E.R., Cline, M.A., 2014. Substance P is associated with hypothalamic paraventricular nucleus activation that coincides with increased urotensin 2 mRNA in chicks. Neuropeptides 48, 305–311.

Maddineni, S.R., Krzysik-Walker, S.M., Ocon-Grove, O.M., Motch, S.M., Hendricks 3rd, G.L., Ramachandran, R., 2007. Calcitonin is expressed in the chicken pituitary gland: influence of gonadal steroids and sexual maturation. Cell Tissue Res. 327, 521–528.

Marceau, F., Regoli, D., 2004. Bradykinin receptor ligands: therapeutic perspectives. Nat. Rev. Drug Discov. 3, 845–852.

Martinez-Moreno, C.G., Lopez-Marin, L.M., Carranza, M., Giterman, D., Harvey, S., Aramburo, C., Luna, M., 2014. Growth hormone (GH) and GH-releasing hormone (GHRH): Co-localization and action in the chicken testis. Gen. Comp. Endocrinol. 199, 38–45.

Martinez, V., Jimenez, M., Gonalons, E., Vergara, P., 1993. Mechanism of action of CCK in avian gastroduodenal motility: evidence for nitric oxide involvement. Am. J. Physiol. 265, G842–G850.

Massi, M., Perfumi, M., Polidori, C., de Caro, G., 1987. Effect of kassinin, neurokinin A and neurokinin B on drinking behaviour in the pigeon. Regul. Pept. 17, 85–97.

Masuda, K., Iwakoshi-Ukena, E., Bessho, Y., Taniuchi, S., Maejima, S., Shikano, K., Kondo, K., Furumitsu, M., Ukena, K., 2014. Identification of neurotensin and LANT-6 and localization of mRNA encoding their precursor in the chicken brain. Zool. Sci. 31, 353–359.

McConn, B., Wang, G., Yi, J., Gilbert, E.R., Osugi, T., Ubuka, T., Tsutsui, K., Chowdhury, V.S., Furuse, M., Cline, M.A., 2014. Gonadotropin-inhibitory hormone-stimulation of food intake is mediated by hypothalamic effects in chicks. Neuropeptides 48, 327–334.

McConn, B.R., Newmyer, B.A., St John, N., Tachibana, T., Gilbert, E.R., Cline, M.A., 2019. The anorexigenic effect of neuropeptide K in chicks involves the paraventricular nucleus and arcuate nucleus of the hypothalamus. Peptides 122, 170157.

McDonald, T.J., Jornvall, H., Ghatei, M., Bloom, S.R., Mutt, V., 1980. Characterization of an avian gastric (proventricular) peptide having sequence homology with the porcine gastrin-releasing peptide and the amphibian peptides bombesin and alytesin. FEBS Lett. 122, 45–48.

McGregor, G.P., Woodhams, P.L., O'Shaughnessy, D.J., Ghatei, M.A., Polak, J.M., Bloom, S.R., 1982. Developmental changes in bombesin, substance P, somatostatin and vasoactive intestinal polypeptide in the rat brain. Neurosci. Lett. 28, 21–27.

McRory, J.E., Parker, R.L., Sherwood, N.M., 1997. Expression and alternative processing of a chicken gene encoding both growth hormone-releasing hormone and pituitary adenylate cyclase-activating polypeptide. DNA Cell Biol. 16, 95–102.

Medill, N.J., Praul, C.A., Ford, B.C., Leach, R.M., 2001. Parathyroid hormone-related peptide expression in the epiphyseal growth plate of the juvenile chicken: evidence for the origin of the parathyroid hormone-related peptide found in the epiphyseal growth plate. J. Cell. Biochem. 80, 504–511.

Mellouk, N., Rame, C., Delaveau, J., Rat, C., Marchand, M., Mercerand, F., Travel, A., Brionne, A., Chartrin, P., Ma, L., Froment, P., Dupont, J., 2018. Food restriction but not fish oil increases fertility in hens: role of RARRES2? Reproduction 155, 321–331.

Meng, F., Huang, G., Gao, S., Li, J., Yan, Z., Wang, Y., 2014. Identification of the receptors for somatostatin (SST) and cortistatin (CST) in chickens and investigation of the roles of cSST28, cSST14, and cCST14 in inhibiting cGHRH1-27NH2-induced growth hormone secretion in cultured chicken pituitary cells. Mol. Cell. Endocrinol. 384, 83–95.

Millar, T.J., Chubb, I.W., 1984a. Substance P in the chick retina: effects of light and dark. Brain Res. 307, 303–309.

Millar, T.J., Chubb, I.W., 1984b. Treatment of sections of chick retina with acetylcholinesterase increases the enkephalin and substance P immunoreactivity. Neuroscience 12, 441–451.

Minvielle, S., Cressent, M., Delehaye, M.C., Segond, N., Milhaud, G., Jullienne, A., Moukhtar, M.S., Lasmoles, F., 1987. Sequence and expression of the chicken calcitonin gene. FEBS Lett. 223, 63–68.

Minvielle, S., Cressent, M., Lasmoles, F., Jullienne, A., Milhaud, G., Moukhtar, M.S., 1986. Isolation and partial characterization of the calcitonin gene in a lower vertebrate. Predicted structure of avian calcitonin gene-related peptide. FEBS Lett. 203, 7–10.

Mirabeau, O., Perlas, E., Severini, C., Audero, E., Gascuel, O., Possenti, R., Birney, E., Rosenthal, N., Gross, C., 2007. Identification of novel peptide hormones in the human proteome by hidden Markov model screening. Genome Res. 17, 320–327.

Miranda, B., Esposito, V., de Girolamo, P., Sharp, P.J., Wilson, P.W., Dunn, I.C., 2013. Orexin in the chicken hypothalamus: immunocytochemical localisation and comparison of mRNA concentrations during the day and night, and after chronic food restriction. Brain Res. 1513, 34–40.

Mitchell, J.D., Maguire, J.J., Davenport, A.P., 2009. Emerging pharmacology and physiology of neuromedin U and the structurally related peptide neuromedin S. Br. J. Pharmacol. 158, 87–103.

Miyata, A., Minamino, N., Kangawa, K., Matsuo, H., 1988. Identification of a 29-amino acid natriuretic peptide in chicken heart. Biochem. Biophys. Res. Commun. 155, 1330–1337.

Mo, C., Cai, G., Huang, L., Deng, Q., Lin, D., Cui, L., Wang, Y., Li, J., 2015. Corticotropin-releasing hormone (CRH) stimulates cocaine- and amphetamine-regulated transcript gene (CART1) expression through CRH type 1 receptor (CRHR1) in chicken anterior pituitary. Mol. Cell. Endocrinol. 417, 166–177.

Mo, C., Huang, L., Cui, L., Lv, C., Lin, D., Song, L., Zhu, G., Li, J., Wang, Y., 2017. Characterization of NMB, GRP and their receptors (BRS3, NMBR and GRPR) in chickens. J. Mol. Endocrinol. 59, 61–79.

Mo, C., Lv, C., Huang, L., Li, Z., Zhang, J., Li, J., Wang, Y., 2019. Regulation of pituitary cocaine- and amphetamine-regulated transcript expression and secretion by hypothalamic gonadotropin-releasing hormone in chickens. Front. Physiol. 10, 882.

Mo, C., Zhong, Y., Wang, Y., Yan, Z., Li, J., 2014. Characterization of glucagon-like peptide 2 receptor (GLP2R) gene in chickens: functional analysis, tissue distribution, and developmental expression profile of GLP2R in embryonic intestine. Domest. Anim. Endocrinol. 48, 1–6.

Moffatt, P., Thomas, G., Sellin, K., Bessette, M.C., Lafreniere, F., Akhouayri, O., St-Arnaud, R., Lanctot, C., 2007. Osteocrin is a specific ligand of the natriuretic Peptide clearance receptor that modulates bone growth. J. Biol. Chem. 282, 36454–36462.

Moffatt, P., Thomas, G.P., 2009. Osteocrin–beyond just another bone protein? Cell. Mol. Life Sci. 66, 1135–1139.

Montero-Hadjadje, M., Vaingankar, S., Elias, S., Tostivint, H., Mahata, S.K., Anouar, Y., 2008. Chromogranins A and B and secretogranin II: evolutionary and functional aspects. Acta Physiol. 192, 309–324.

Mookherjee, N., Anderson, M.A., Haagsman, H.P., Davidson, D.J., 2020. Antimicrobial host defence peptides: functions and clinical potential. Nat. Rev. Drug Discov. 19, 311–332.

Mori, K., Miyazato, M., Kangawa, K., 2008. Neuromedin S: discovery and functions. Results Probl. Cell Differ. 46, 201–212.

Moriguchi, T., Takeda, S., Iwashita, S., Enomoto, K., Sawamura, T., Koshimizu, U., Kondo, T., 2018. Ecrg4 peptide is the ligand of multiple scavenger receptors. Sci. Rep. 8, 4048.

Mulder, H., Ekelund, M., Ekblad, E., Sundler, F., 1997. Islet amyloid polypeptide in the gut and pancreas: localization, ontogeny and gut motility effects. Peptides 18, 771–783.

Murphy, T.J., Nakamura, Y., Takeuchi, K., Alexander, R.W., 1993. A cloned angiotensin receptor isoform from the Turkey adrenal gland is pharmacologically distinct from mammalian angiotensin receptors. Mol. Pharmacol. 44, 1–7.

Mustain, W.C., Rychahou, P.G., Evers, B.M., 2011. The role of neurotensin in physiologic and pathologic processes. Curr. Opin. Endocrinol. Diabetes Obes. 18, 75–82.

Nagy, N., Goldstein, A.M., 2006. Endothelin-3 regulates neural crest cell proliferation and differentiation in the hindgut enteric nervous system. Dev. Biol. 293, 203–217.

Nakagawa-Mizuyachi, K., Takahashi, T., Kawashima, M., 2009. Calcitonin directly increases adrenocorticotropic hormone-stimulated corticosterone production in the hen adrenal gland. Poultry Sci. 88, 2199–2205.

Nakayama, T., Nakajima, T., Sokabe, H., 1973. Comparative studies on angiotensins. 3. Structure of fowl angiotensin and its identification by DNS-method. Chem. Pharm. Bull. (Tokyo) 21, 2085–2087.

Nataf, V., Grapin-Botton, A., Champeval, D., Amemiya, A., Yanagisawa, M., Le Douarin, N.M., 1998. The expression patterns of endothelin-A receptor and endothelin 1 in the avian embryo. Mech. Dev. 75, 145–149.

Neglia, S., Arcamone, N., Esposito, V., Gargiulo, G., 2004. Ghrelin in the gastroenteric tract of birds: immunoreactivity expression. Vet. Res. Commun. 28 (Suppl. 1), 213–215.

Negri, L., Ferrara, N., 2018. The prokineticins: neuromodulators and mediators of inflammation and myeloid cell-dependent angiogenesis. Physiol. Rev. 98, 1055–1082.

Negri, L., Lattanzi, R., Giannini, E., Melchiorri, P., 2007. Bv8/Prokineticin proteins and their receptors. Life Sci. 81, 1103–1116.

Nilsson, I.B., Svensson, S.P., Monstein, H.J., 2003. Molecular cloning of an unusual bicistronic cholecystokinin receptor mRNA expressed in chicken brain: a structural and functional expression study. Regul. Pept. 114, 37–43.

Nishimura, H., Nakamura, Y., Sumner, R.P., Khosla, M.C., 1982. Vasopressor and depressor actions of angiotensin in the anesthetized fowl. Am. J. Physiol. 242, H314–H324.

Nishimura, H., Yang, Y., Hubert, C., Gasc, J.M., Ruijtenbeek, K., De Mey, J., Boudier, H.A., Corvol, P., 2003. Maturation-dependent changes of angiotensin receptor expression in fowl. Am. J. Physiol. Regul. Integr. Comp. Physiol. 285, R231–R242.

Nishimura, K., Hiramatsu, K., Watanabe, T., Kita, K., 2017. Glucagon-like peptide-1 is co-localized with neurotensin in the chicken ileum. Cell Tissue Res. 368, 277–286.

Nishizawa, H., Matsuda, M., Yamada, Y., Kawai, K., Suzuki, E., Makishima, M., Kitamura, T., Shimomura, I., 2004. Musclin, a novel skeletal muscle-derived secretory factor. J. Biol. Chem. 279, 19391–19395.

Norberg, A., Sillard, R., Carlquist, M., Jornvall, H., Mutt, V., 1991. Chemical detection of natural peptides by specific structures. Isolation of chicken galanin by monitoring for its N-terminal dipeptide, and determination of the amino acid sequence. FEBS Lett. 288, 151–153.

Numao, M., Sudo, H., Yamamoto, I., Nakao, N., Kaiya, H., Miyazato, M., Tsushima, N., Tanaka, M., 2011. Molecular characterization of structure and tissue distribution of chicken neurotensin receptor. Gen. Comp. Endocrinol. 171, 33–38.

O'Harte, F., Bockman, C.S., Zeng, W., Abel, P.W., Harvey, S., Conlon, J.M., 1991. Primary structure and pharmacological activity of a nonapeptide related to neuromedin U isolated from chicken intestine. Peptides 12, 809–812.

O'Keefe, R.J., Loveys, L.S., Hicks, D.G., Reynolds, P.R., Crabb, I.D., Puzas, J.E., Rosier, R.N., 1997. Differential regulation of type-II and type-X collagen synthesis by parathyroid hormone-related protein in chick growth-plate chondrocytes. J. Orthop. Res. 15, 162–174.

Ogino, M., Okumura, A., Khan, M.S., Cline, M.A., Tachibana, T., 2014. Comparison of brain urocortin-3 and corticotrophin-releasing factor for physiological responses in chicks. Physiol. Behav. 125, 57–61.

Ohki-Hamazaki, H., Iwabuchi, M., Maekawa, F., 2005. Development and function of bombesin-like peptides and their receptors. Int. J. Dev. Biol. 49, 293–300.

Ohkubo, T., Boswell, T., Lumineau, S., 2002. Molecular cloning of chicken prepro-orexin cDNA and preferential expression in the chicken hypothalamus. Biochim. Biophys. Acta 1577, 476–480.

Ohkubo, T., Shamoto, K., Ogino, T., 2007. Structure and tissue distribution of cholecystokinin-1 receptor in chicken. J. Poult. Sci. 44 (1), 98−104.

Ohkubo, T., Tsukada, A., Shamoto, K., 2003. cDNA cloning of chicken orexin receptor and tissue distribution: sexually dimorphic expression in chicken gonads. J. Mol. Endocrinol. 31, 499−508.

Ohtaki, T., Kumano, S., Ishibashi, Y., Ogi, K., Matsui, H., Harada, M., Kitada, C., Kurokawa, T., Onda, H., Fujino, M., 1999. Isolation and cDNA cloning of a novel galanin-like peptide (GALP) from porcine hypothalamus. J. Biol. Chem. 274, 37041−37045.

Osugi, T., Ukena, K., Sower, S.A., Kawauchi, H., Tsutsui, K., 2006. Evolutionary origin and divergence of PQRFamide peptides and LPXRFamide peptides in the RFamide peptide family. Insights from novel lamprey RFamide peptides. FEBS J. 273, 1731−1743.

Pang, P.K., Zhang, R.H., Yang, M.C., 1984. Hypotensive action of parathyroid hormone in chicken. J. Exp. Zool. 232, 691−696.

Park, C.H., Valore, E.V., Waring, A.J., Ganz, T., 2001. Hepcidin, a urinary antimicrobial peptide synthesized in the liver. J. Biol. Chem. 276, 7806−7810.

Pasquier, J., Lafont, A.G., Rousseau, K., Querat, B., Chemineau, P., Dufour, S., 2014. Looking for the bird Kiss: evolutionary scenario in sauropsids. BMC Evol. Biol. 14, 30.

Pauliukonis, A.C., Buenaventura, C., Cline, M.A., Gilbert, E.R., 2020. Anorexigenic effects of substance P in *Coturnix japonica*. Neuropeptides 81, 102045.

Peeters, K., Berghman, L.R., Vandesande, F., 1998. Comparative distribution of pituitary adenylate cyclase-activating polypeptide and vasoactive intestinal polypeptide immunoreactivity in the chicken forebrain. Ann. N. Y. Acad. Sci. 839, 417−419.

Peeters, T.L., 2005. Ghrelin: a new player in the control of gastrointestinal functions. Gut 54, 1638−1649.

Perez, F.M., Malamed, S., Scanes, C.G., 1987. Growth hormone secretion from chicken adenohypophyseal cells in primary culture: effects of human pancreatic growth hormone-releasing factor, thyrotropin-releasing hormone, and somatostatin on growth hormone release. Gen. Comp. Endocrinol. 65, 408−414.

Phillips-Singh, D., Li, Q., Takeuchi, S., Ohkubo, T., Sharp, P.J., Boswell, T., 2003. Fasting differentially regulates expression of agouti-related peptide, pro-opiomelanocortin, prepro-orexin, and vasoactive intestinal polypeptide mRNAs in the hypothalamus of Japanese quail. Cell Tissue Res. 313, 217−225.

Pigeon, C., Ilyin, G., Courselaud, B., Leroyer, P., Turlin, B., Brissot, P., Loreal, O., 2001. A new mouse liver-specific gene, encoding a protein homologous to human antimicrobial peptide hepcidin, is overexpressed during iron overload. J. Biol. Chem. 276, 7811−7819.

Pinheiro, P.L., Cardoso, J.C., Gomes, A.S., Fuentes, J., Power, D.M., Canario, A.V., 2010. Gene structure, transcripts and calciotropic effects of the PTH family of peptides in Xenopus and chicken. BMC Evol. Biol. 10, 373.

Pinheiro, P.L., Cardoso, J.C., Power, D.M., Canario, A.V., 2012. Functional characterization and evolution of PTH/PTHrP receptors: insights from the chicken. BMC Evol. Biol. 12, 110.

Pinilla, L., Aguilar, E., Dieguez, C., Millar, R.P., Tena-Sempere, M., 2012. Kisspeptins and reproduction: physiological roles and regulatory mechanisms. Physiol. Rev. 92, 1235−1316.

Pitkin, S.L., Maguire, J.J., Bonner, T.I., Davenport, A.P., 2010. International Union of Basic and Clinical Pharmacology. LXXIV. Apelin receptor nomenclature, distribution, pharmacology, and function. Pharmacol. Rev. 62, 331−342.

Pla, P., Larue, L., 2003. Involvement of endothelin receptors in normal and pathological development of neural crest cells. Int. J. Dev. Biol. 47, 315−325.

Podvin, S., Dang, X., Meads, M., Kurabi, A., Costantini, T., Eliceiri, B.P., Baird, A., Coimbra, R., 2015. Esophageal cancer-related gene-4 (ECRG4) interactions with the innate immunity receptor complex. Inflamm. Res. 64, 107−118.

Potter, L.R., Yoder, A.R., Flora, D.R., Antos, L.K., Dickey, D.M., 2009. Natriuretic peptides: their structures, receptors, physiologic functions and therapeutic applications. Handb. Exp. Pharmacol. 341−366.

Poyner, D.R., Sexton, P.M., Marshall, I., Smith, D.M., Quirion, R., Born, W., Muff, R., Fischer, J.A., Foord, S.M., 2002. International Union of Pharmacology. XXXII. The mammalian calcitonin gene-related peptides, adrenomedullin, amylin, and calcitonin receptors. Pharmacol. Rev. 54, 233−246.

Prall, B.C., Cline, M.A., 2008. Anorexigenic effects of central neuropeptide K are associated with hypothalamic changes in juvenile Gallus gallus. Gen. Comp. Endocrinol. 159, 130−135.

Prisco, M., Rosati, L., Agnese, M., Aceto, S., Andreuccetti, P., Valiante, S., 2019. Pituitary adenylate cyclase-activating polypeptide in the testis of the quail *Coturnix coturnix*: expression, localization, and phylogenetic analysis. Evol. Dev. 21, 145−156.

Prokop, J.W., Schmidt, C., Gasper, D., Duff, R.J., Milsted, A., Ohkubo, T., Ball, H.C., Shawkey, M.D., Mays Jr., H.L., Cogburn, L.A., Londraville, R.L., 2014. Discovery of the elusive leptin in birds: identification of several 'missing links' in the evolution of leptin and its receptor. PloS One 9, e92751.

Proudman, J.A., Clerens, S., van den Bergh, G., Garrett, W.M., Verhaert, P.D., Vandesande, F., Berghman, L.R., 2003. Immunohistochemical localization of chromogranin A in gonadotrophs and somatotrophs of the Turkey and chicken pituitary. Gen. Comp. Endocrinol. 132, 293−303.

Rawson, R.E., Duke, G.E., Brown, D.R., 1990. Effect of avian neurotensin on motility of chicken (*Gallus domesticus*) lower gut in vivo and in vitro. Peptides 11, 641−645.

Reid, A.M.A., Dunn, I.C., 2018. Gastrointestinal distribution of chicken gastrin-cholecystokinin family transcript expression and response to short-term nutritive state. Gen. Comp. Endocrinol. 255, 64−70.

Reid, A.M.A., Wilson, P.W., Caughey, S.D., Dixon, L.M., D'Eath, R.B., Sandilands, V., Boswell, T., Dunn, I.C., 2017. Pancreatic PYY but not PPY expression is responsive to short-term nutritional state and the pancreas constitutes the major site of PYY mRNA expression in chickens. Gen. Comp. Endocrinol. 252, 226−235.

Reubi, J.C., Jessell, T.M., 1978. Distribution of substance P in the pigeon brain. J. Neurochem. 31, 359−361.

Richards, M.P., McMurtry, J.P., 2008. Expression of proglucagon and proglucagon-derived peptide hormone receptor genes in the chicken. Gen. Comp. Endocrinol. 156, 323−338.

Richards, M.P., Poch, S.M., McMurtry, J.P., 2006. Characterization of Turkey and chicken ghrelin genes, and regulation of ghrelin and ghrelin receptor mRNA levels in broiler chickens. Gen. Comp. Endocrinol. 145, 298−310.

Rikimaru, K., Komatsu, M., Suzuki, K., Uemoto, Y., Takeda, H., Takahashi, H., 2012. Association between cholecystokinin type A receptor haplotypes and growth traits in Japanese Hinai-dori crossbred chickens. Mol. Biol. Rep. 39, 4479−4484.

Rodriguez-Sinovas, A., Fernandez, E., Manteca, X., Fernandez, A.G., Gonalons, E., 1997. CCK is involved in both peripheral and central mechanisms controlling food intake in chickens. Am. J. Physiol. 272, R334–R340.

Rogge, G., Jones, D., Hubert, G.W., Lin, Y., Kuhar, M.J., 2008. CART peptides: regulators of body weight, reward and other functions. Nat. Rev. Neurosci. 9, 747–758.

Rosenberg, J., Pines, M., Hurwitz, S., 1986. Relationship between endogenous cyclic AMP production and steroid hormone secretion in chick adrenal cells. Comp. Biochem. Physiol. B 84, 71–75.

Rosenberg, J., Pines, M., Hurwitz, S., 1988. Stimulation of chick adrenal steroidogenesis by avian parathyroid hormone. J. Endocrinol. 116, 91–95.

Rosenberg, J., Pines, M., Levy, J.J., Nutt, R.F., Caulfield, M.P., Russell, J., Sherwood, L.M., Hurwitz, S., 1989. Renal and adrenal adenosine 3',5'-monophosphate production and corticosteroid secretion in response to synthetic chicken parathyroid hormone-(1-34). Endocrinology 125, 1082–1089.

Russell, J., Sherwood, L.M., 1989. Nucleotide sequence of the DNA complementary to avian (chicken) preproparathyroid hormone mRNA and the deduced sequence of the hormone precursor. Mol. Endocrinol. 3, 325–331.

Saffrey, M.J., Polak, J.M., Burnstock, G., 1982. Distribution of vasoactive intestinal polypeptide-, substance P-, enkephalin and neurotensin-like immunoreactive nerves in the chicken gut during development. Neuroscience 7, 279–293.

Saito, E.S., Kaiya, H., Tachibana, T., Tomonaga, S., Denbow, D.M., Kangawa, K., Furuse, M., 2005. Inhibitory effect of ghrelin on food intake is mediated by the corticotropin-releasing factor system in neonatal chicks. Regul. Pept. 125, 201–208.

Saito, E.S., Kaiya, H., Takagi, T., Yamasaki, I., Denbow, D.M., Kangawa, K., Furuse, M., 2002. Chicken ghrelin and growth hormone-releasing peptide-2 inhibit food intake of neonatal chicks. Eur. J. Pharmacol. 453, 75–79.

Sakamoto, H., Atsumi, S., 1989. Substance P-immunoreactive elements in laminae I and II of the chicken spinal cord: a light- and electron-microscopic study. Neurosci. Res. 7, 103–116.

Sakamoto, H., Ubuka, T., Kohchi, C., Li, D., Ukena, K., Tsutsui, K., 2000. Existence of galanin in lumbosacral sympathetic ganglionic neurons that project to the quail uterine oviduct. Endocrinology 141, 4402–4412.

Sakurai, T., Amemiya, A., Ishii, M., Matsuzaki, I., Chemelli, R.M., Tanaka, H., Williams, S.C., Richarson, J.A., Kozlowski, G.P., Wilson, S., Arch, J.R., Buckingham, R.E., Haynes, A.C., Carr, S.A., Annan, R.S., McNulty, D.E., Liu, W.S., Terrett, J.A., Elshourbagy, N.A., Bergsma, D.J., Yanagisawa, M., 1998. Orexins and orexin receptors: a family of hypothalamic neuropeptides and G protein-coupled receptors that regulate feeding behavior. Cell 92, 1 page following 696.

Salaneck, E., Holmberg, S.K., Berglund, M.M., Boswell, T., Larhammar, D., 2000. Chicken neuropeptide Y receptor Y2: structural and pharmacological differences to mammalian Y2(1). FEBS Lett. 484, 229–234.

Salvi, E., Buffa, R., Renda, T.G., 1996. Ontogeny, distribution and amine/peptide content of chromogranin A- and B-immunoreactive endocrine cells in the small and large intestine of the chicken. Anat. Embryol. 194, 89–98.

Sann, H., Friedrich, R., Pierau, F.K., 1996. Substance P and calcitonin gene-related peptide in the chicken skin: distribution and cardiovascular effects. Neuropeptides 30, 273–281.

Satake, H., Hisada, M., Kawada, T., Minakata, H., Ukena, K., Tsutsui, K., 2001. Characterization of a cDNA encoding a novel avian hypothalamic neuropeptide exerting an inhibitory effect on gonadotropin release. Biochem. J. 354, 379–385.

Savory, C.J., Gentle, M.J., 1980. Intravenous injections of cholecystokinin and caerulein suppress food intake in domestic fowls. Experientia 36, 1191–1192.

Scanes, C.G., 2016. Opening a new door: neuropeptide W (NPW) is a novel inhibitory secretagogue for GH and prolactin acting via the Gi protein-coupled NPBWR2. Endocrinology 157, 3394–3397.

Scanes, C.G., Pierzchala-Koziec, K., 2018. Perspectives on endogenous opioids in birds. Front. Physiol. 9, 1842.

Schroeder, C., Beug, H., Muller-Esterl, W., 1997. Cloning and functional characterization of the ornithokinin receptor. Recognition of the major kinin receptor antagonist, HOE140, as a full agonist. J. Biol. Chem. 272, 12475–12481.

Selvam, R., Jurkevich, A., Kang, S.W., Mikhailova, M.V., Cornett, L.E., Kuenzel, W.J., 2013. Distribution of the vasotocin subtype four receptor (VT4R) in the anterior pituitary gland of the chicken, Gallus gallus, and its possible role in the avian stress response. J. Neuroendocrinol. 25, 56–66.

Seroussi, E., Cinnamon, Y., Yosefi, S., Genin, O., Smith, J.G., Rafati, N., Bornelov, S., Andersson, L., Friedman-Einat, M., 2016. Identification of the long-sought leptin in chicken and duck: expression pattern of the highly GC-rich avian leptin fits an autocrine/paracrine rather than endocrine function. Endocrinology 157, 737–751.

Severini, C., Improta, G., Falconieri-Erspamer, G., Salvadori, S., Erspamer, V., 2002. The tachykinin peptide family. Pharmacol. Rev. 54, 285–322.

Sharp, P.J., Sterling, R.J., Talbot, R.T., Huskisson, N.S., 1989. The role of hypothalamic vasoactive intestinal polypeptide in the maintenance of prolactin secretion in incubating bantam hens: observations using passive immunization, radioimmunoassay and immunohistochemistry. J. Endocrinol. 122, 5–13.

Sherwood, N.M., Krueckl, S.L., McRory, J.E., 2000. The origin and function of the pituitary adenylate cyclase-activating polypeptide (PACAP)/glucagon superfamily. Endocr. Rev. 21, 619–670.

Shikano, K., Bessho, Y., Kato, M., Iwakoshi-Ukena, E., Taniuchi, S., Furumitsu, M., Tachibana, T., Bentley, G.E., Kriegsfeld, L.J., Ukena, K., 2018a. Localization and function of neurosecretory protein GM, a novel small secretory protein, in the chicken hypothalamus. Sci. Rep. 8, 704.

Shikano, K., Kato, M., Iwakoshi-Ukena, E., Furumitsu, M., Matsuura, D., Masuda, K., Tachibana, T., Bentley, G.E., Kriegsfeld, L.J., Ukena, K., 2018b. Effects of chronic intracerebroventricular infusion of neurosecretory protein GL on body mass and food and water intake in chicks. Gen. Comp. Endocrinol. 256, 37–42.

Shikano, K., Taniuchi, S., Iwakoshi-Ukena, E., Furumitsu, M., Bentley, G.E., Kriegsfeld, L.J., Ukena, K., 2018c. Chronic subcutaneous infusion of neurosecretory protein GM increases body mass gain in chicks. Gen. Comp. Endocrinol. 265, 71–76.

Shimizu, M., Bedecarrats, G.Y., 2010. Activation of the chicken gonadotropin-inhibitory hormone receptor reduces gonadotropin releasing hormone receptor signaling. Gen. Comp. Endocrinol. 167, 331–337.

Shimmura, T., Tamura, M., Ohashi, S., Sasaki, A., Yamanaka, T., Nakao, N., Ihara, K., Okamura, S., Yoshimura, T., 2019. Cholecystokinin induces crowing in chickens. Sci. Rep. 9, 3978.

Shinomiya, A., Kayashima, Y., Kinoshita, K., Mizutani, M., Namikawa, T., Matsuda, Y., Akiyama, T., 2012. Gene duplication of endothelin 3 is closely correlated with the hyperpigmentation of the internal organs (Fibromelanosis) in silky chickens. Genetics 190, 627–638.

Shipp, S.L., Yi, J., Dridi, S., Gilbert, E.R., Cline, M.A., 2015. The central anorexigenic mechanism of adrenocorticotropic hormone involves the caudal hypothalamus in chicks. Neuropeptides 53, 29–35.

Shousha, S., Nakahara, K., Miyazato, M., Kangawa, K., Murakami, N., 2005. Endogenous neuromedin U has anorectic effects in the Japanese quail. Gen. Comp. Endocrinol. 140, 156–163.

Shousha, S., Nakahara, K., Sato, M., Mori, K., Miyazato, M., Kangawa, K., Murakami, N., 2006. Effect of neuromedin S on feeding regulation in the Japanese quail. Neurosci. Lett. 391, 87–90.

Singh, O., Kumar, S., Singh, U., Kumar, V., Lechan, R.M., Singru, P.S., 2016. Cocaine- and amphetamine-regulated transcript peptide (CART) in the brain of zebra finch, *Taeniopygia guttata*: organization, interaction with neuropeptide Y, and response to changes in energy status. J. Comp. Neurol. 524, 3014–3041.

Singh, R., Joyner, C.J., Peddie, M.J., Taylor, T.G., 1986. Changes in the concentrations of parathyroid hormone and ionic calcium in the plasma of laying hens during the egg cycle in relation to dietary deficiencies of calcium and vitamin D. Gen. Comp. Endocrinol. 61, 20–28.

Singletary, K.G., Deviche, P., Strand, C., Delville, Y., 2006. Distribution of orexin/hypocretin immunoreactivity in the brain of a male songbird, the house finch, Carpodacus mexicanus. J. Chem. Neuroanat. 32, 81–89.

Smith, M.L., Prall, B., Nandar, W., Cline, M.A., 2008. Beta-melanocyte-stimulating hormone potently reduces appetite via the hypothalamus in chicks. J. Neuroendocrinol. 20, 220–226.

Sommerville, B.A., Fox, J., 1987. Changes in renal function of the chicken associated with calcitonin and parathyroid hormone. Gen. Comp. Endocrinol. 66, 381–386.

Song, Z., Liu, L., Yue, Y., Jiao, H., Lin, H., Sheikhahmadi, A., Everaert, N., Decuypere, E., Buyse, J., 2012. Fasting alters protein expression of AMP-activated protein kinase in the hypothalamus of broiler chicks (*Gallus gallus domesticus*). Gen. Comp. Endocrinol. 178, 546–555.

Sonmez, K., Zaveri, N.T., Kerman, I.A., Burke, S., Neal, C.R., Xie, X., Watson, S.J., Toll, L., 2009. Evolutionary sequence modeling for discovery of peptide hormones. PLoS Comput. Biol. 5, e1000258.

Strewler, G.J., 2000. The physiology of parathyroid hormone-related protein. N. Engl. J. Med. 342, 177–185.

Strosser, M.T., Di Scala-Guenot, D., Koch, B., Mialhe, P., 1983. Inhibitory effect and mode of action of somatostatin on lipolysis in chicken adipocytes. Biochim. Biophys. Acta 763, 191–196.

Sun, G., Li, M., Li, H., Tian, Y., Chen, Q., Bai, Y., Kang, X., 2013. Molecular cloning and SNP association analysis of chicken PMCH gene. Mol. Biol. Rep. 40, 5049–5055.

Sun, Y.M., Millar, R.P., Ho, H., Gershengorn, M.C., Illing, N., 1998. Cloning and characterization of the chicken thyrotropin-releasing hormone receptor. Endocrinology 139, 3390–3398.

Sundler, F., Ekblad, E., Absood, A., Hakanson, R., Koves, K., Arimura, A., 1992. Pituitary adenylate cyclase activating peptide: a novel vasoactive intestinal peptide-like neuropeptide in the gut. Neuroscience 46, 439–454.

Sundler, F., Hakanson, R., Hammer, R.A., Alumets, J., Carraway, R., Leeman, S.E., Zimmerman, E.A., 1977. Immunohistochemical localization of neurotensin in endocrine cells of the gut. Cell Tissue Res. 178, 313–321.

Tachibana, T., Cline, M.A., Khan, M.S., Ueda, H., Hiramatsu, K., 2011a. Feeding responses to central administration of several somatostatin analogs in chicks. Comp. Biochem. Physiol. Mol. Integr. Physiol. 158, 47–51.

Tachibana, T., Cline, M.A., Sugahara, K., Ueda, H., Hiramatsu, K., 2009. Central administration of somatostatin stimulates feeding behavior in chicks. Gen. Comp. Endocrinol. 161, 354–359.

Tachibana, T., Khan, M.S., Matsuda, K., Ueda, H., Cline, M.A., 2010a. Central administration of substance P inhibits feeding behavior in chicks. Horm. Behav. 57, 203–208.

Tachibana, T., Matsuda, K., Khan, M.S., Ueda, H., Cline, M.A., 2010b. Feeding and drinking response following central administration of neuromedin S in chicks. Comp. Biochem. Physiol. Mol. Integr. Physiol. 157, 63–67.

Tachibana, T., Matsuda, K., Khan, S.I., Ueda, H., Cline, M.A., 2010c. Feeding and drinking response following central administrations of bombesin-like peptides in chicks. Comp. Biochem. Physiol. Mol. Integr. Physiol. 156, 394–399.

Tachibana, T., Matsuda, K., Sawa, H., Mikami, A., Ueda, H., Cline, M.A., 2010d. Differential thresholds of neuromedins B-, C-, and bombesin-induced anorexia and crop-emptying rate in chicks. Gen. Comp. Endocrinol. 169, 144–150.

Tachibana, T., Mori, M., Khan, M.S., Ueda, H., Sugahara, K., Hiramatsu, K., 2008. Central administration of galanin stimulates feeding behavior in chicks. Comp. Biochem. Physiol. Mol. Integr. Physiol. 151, 637–640.

Tachibana, T., Moriyama, S., Takahashi, A., Tsukada, A., Oda, A., Takeuchi, S., Sakamoto, T., 2011b. Isolation and characterisation of prolactin-releasing peptide in chicks and its effect on prolactin release and feeding behaviour. J. Neuroendocrinol. 23, 74–81.

Tachibana, T., Sakamoto, T., 2014. Functions of two distinct "prolactin-releasing peptides" evolved from a common ancestral gene. Front. Endocrinol. 5, 170.

Tachibana, T., Sugimoto, I., Ogino, M., Khan, M.S., Masuda, K., Ukena, K., Wang, Y., 2015. Central administration of chicken growth hormone-releasing hormone decreases food intake in chicks. Physiol. Behav. 139, 195–201.

Tachibana, T., Takagi, T., Tomonaga, S., Ohgushi, A., Ando, R., Denbow, D.M., Furuse, M., 2003. Central administration of cocaine- and amphetamine-regulated transcript inhibits food intake in chicks. Neurosci. Lett. 337, 131–134.

Tachibana, T., Tsutsui, K., 2016. Neuropeptide control of feeding behavior in birds and its difference with mammals. Front. Neurosci. 10, 485.

Tahara, Y., Kumoi, Y., Kiyama, H., Tohyama, M., 1986. Ontogeny of substance P-containing structures in the chicken retina: immunohistochemical analysis. Brain Res. 395, 37–45.

Takei, Y., Inoue, K., Trajanovska, S., Donald, J.A., 2011. B-type natriuretic peptide (BNP), not ANP, is the principal cardiac natriuretic peptide in vertebrates as revealed by comparative studies. Gen. Comp. Endocrinol. 171, 258–266.

Takeuchi, S., Kudo, T., Takahashi, S., 1998. Molecular cloning of the chicken melanocortin 2 (ACTH)-receptor gene. Biochim. Biophys. Acta 1403, 102–108.

Takeuchi, S., Takahashi, S., 1998. Melanocortin receptor genes in the chicken–tissue distributions. Gen. Comp. Endocrinol. 112, 220–231.

Takeuchi, S., Takahashi, S., 1999. A possible involvement of melanocortin 3 receptor in the regulation of adrenal gland function in the chicken. Biochim. Biophys. Acta 1448, 512–518.

Takeuchi, S., Teshigawara, K., Takahashi, S., 1999. Molecular cloning and characterization of the chicken pro-opiomelanocortin (POMC) gene. Biochim. Biophys. Acta 1450, 452–459.

Takeuchi, S., Teshigawara, K., Takahashi, S., 2000. Widespread expression of Agouti-related protein (AGRP) in the chicken: a possible involvement of AGRP in regulating peripheral melanocortin systems in the chicken. Biochim. Biophys. Acta 1496, 261–269.

Talbot, R.T., Dunn, I.C., Wilson, P.W., Sang, H.M., Sharp, P.J., 1995. Evidence for alternative splicing of the chicken vasoactive intestinal polypeptide gene transcript. J. Mol. Endocrinol. 15, 81–91.

Tan, F.L., Lolait, S.J., Brownstein, M.J., Saito, N., MacLeod, V., Baeyens, D.A., Mayeux, P.R., Jones, S.M., Cornett, L.E., 2000. Molecular cloning and functional characterization of a vasotocin receptor subtype that is expressed in the shell gland and brain of the domestic chicken. Biol. Reprod. 62, 8–15.

Tanaka, M., Miyazaki, T., Yamamoto, I., Nakai, N., Ohta, Y., Tsushima, N., Wakita, M., Shimada, K., 2003. Molecular characterization of chicken growth hormone secretagogue receptor gene. Gen. Comp. Endocrinol. 134, 198–202.

Tanaka, M., Nakao, N., Yamamoto, I., Tsushima, N., Ohta, Y., 2013. Changes in expression levels of neurotensin precursor and receptor mRNA in chicken intestinal tissues and liver during late embryonic and early posthatching development. Poultry Sci. 92, 2765–2771.

Thiede, M.A., Harm, S.C., McKee, R.L., Grasser, W.A., Duong, L.T., Leach Jr., R.M., 1991. Expression of the parathyroid hormone-related protein gene in the avian oviduct: potential role as a local modulator of vascular smooth muscle tension and shell gland motility during the egg-laying cycle. Endocrinology 129, 1958–1966.

Thiede, M.A., Rutledge, S.J., 1990. Nucleotide sequence of a parathyroid hormone-related peptide expressed by the 10 day chicken embryo. Nucleic Acids Res. 18, 3062.

Thomas, A.L., Maekawa, F., Kawashima, T., Sakamoto, H., Sakamoto, T., Davis, P., Dores, R.M., 2018. Analyzing the effects of co-expression of chick (Gallus gallus) melanocortin receptors with either chick MRAP1 or MRAP2 in CHO cells on sensitivity to ACTH(1-24) or ACTH(1-13) NH2: implications for the avian HPA axis and avian melanocortin circuits in the hypothalamus. Gen. Comp. Endocrinol. 256, 50–56.

Thomas, G., Moffatt, P., Salois, P., Gaumond, M.H., Gingras, R., Godin, E., Miao, D., Goltzman, D., Lanctot, C., 2003. Osteocrin, a novel bone-specific secreted protein that modulates the osteoblast phenotype. J. Biol. Chem. 278, 50563–50571.

Tobari, Y., Iijima, N., Tsunekawa, K., Osugi, T., Haraguchi, S., Ubuka, T., Ukena, K., Okanoya, K., Tsutsui, K., Ozawa, H., 2011. Identification, localisation and functional implication of 26RFa orthologue peptide in the brain of zebra finch (*Taeniopygia guttata*). J. Neuroendocrinol. 23, 791–803.

Tobari, Y., Iijima, N., Tsunekawa, K., Osugi, T., Okanoya, K., Tsutsui, K., Ozawa, H., 2010. Identification of gonadotropin-inhibitory hormone in the zebra finch (*Taeniopygia guttata*): peptide isolation, cDNA cloning and brain distribution. Peptides 31, 816–826.

Too, H.P., Hanley, M.R., 1988. Solubilization and characterization of substance P-binding sites from chick brain membranes. Biochem. J. 252, 545–551.

Toop, T., Donald, J.A., 2004. Comparative aspects of natriuretic peptide physiology in non-mammalian vertebrates: a review. J. Comp. Physiol. B 174, 189–204.

Toshimori, H., Toshimori, K., Minamino, N., Kangawa, K., Oura, C., Matsukura, S., Matsuo, H., 1990. Chicken atrial natriuretic peptide (chANP) and its secretion. Cell Tissue Res. 259, 293–298.

Tostivint, H., Joly, L., Lihrmann, I., Parmentier, C., Lebon, A., Morisson, M., Calas, A., Ekker, M., Vaudry, H., 2006. Comparative genomics provides evidence for close evolutionary relationships between the urotensin II and somatostatin gene families. Proc. Natl. Acad. Sci. U. S. A. 103, 2237–2242.

Tostivint, H., Ocampo Daza, D., Bergqvist, C.A., Quan, F.B., Bougerol, M., Lihrmann, I., Larhammar, D., 2014. Molecular evolution of GPCRs: somatostatin/urotensin II receptors. J. Mol. Endocrinol. 52, T61–T86.

Tota, B., Gentile, S., Pasqua, T., Bassino, E., Koshimizu, H., Cawley, N.X., Cerra, M.C., Loh, Y.P., Angelone, T., 2012. The novel chromogranin A-derived serpinin and pyroglutaminated serpinin peptides are positive cardiac beta-adrenergic-like inotropes. Faseb. J. 26, 2888–2898.

Townes, C.L., Michailidis, G., Hall, J., 2009. The interaction of the antimicrobial peptide cLEAP-2 and the bacterial membrane. Biochem. Biophys. Res. Commun. 387, 500–503.

Townes, C.L., Michailidis, G., Nile, C.J., Hall, J., 2004. Induction of cationic chicken liver-expressed antimicrobial peptide 2 in response to *Salmonella enterica* infection. Infect. Immun. 72, 6987–6993.

Trabucchi, M., Tostivint, H., Lihrmann, I., Blahser, S., Vallarino, M., Vaudry, H., 2003. Characterization of the cDNA encoding a somatostatin variant in the chicken brain: comparison of the distribution of the two somatostatin precursor mRNAs. J. Comp. Neurol. 461, 441–451.

Trajanovska, S., Inoue, K., Takei, Y., Donald, J.A., 2007. Genomic analyses and cloning of novel chicken natriuretic peptide genes reveal new insights into natriuretic peptide evolution. Peptides 28, 2155–2163.

Trebak, F., Dubuc, I., Arabo, A., Alaoui, A., Boukhzar, L., Maucotel, J., Picot, M., Cherifi, S., Duparc, C., Leprince, J., Prevost, G., Anouar, Y., Magoul, R., Chartrel, N., 2017. A potential role for the secretogranin II-derived peptide EM66 in the hypothalamic regulation of feeding behaviour. J. Neuroendocrinol. 29.

Troger, J., Theurl, M., Kirchmair, R., Pasqua, T., Tota, B., Angelone, T., Cerra, M.C., Nowosielski, Y., Matzler, R., Troger, J., Gayen, J.R., Trudeau, V., Corti, A., Helle, K.B., 2017. Granin-derived peptides. Prog. Neurobiol. 154, 37–61.

Tsutsui, K., Saigoh, E., Ukena, K., Teranishi, H., Fujisawa, Y., Kikuchi, M., Ishii, S., Sharp, P.J., 2000. A novel avian hypothalamic peptide inhibiting gonadotropin release. Biochem. Biophys. Res. Commun. 275, 661–667.

Ubuka, T., Sakamoto, H., Li, D., Ukena, K., Tsutsui, K., 2001. Developmental changes in galanin in lumbosacral sympathetic ganglionic neurons innervating the avian uterine oviduct and galanin induction by sex steroids. J. Endocrinol. 170, 357–368.

Ukena, K., 2018. Avian and murine neurosecretory protein GL participates in the regulation of feeding and energy metabolism. Gen. Comp. Endocrinol. 260, 164–170.

Ukena, K., Iwakoshi-Ukena, E., Taniuchi, S., Bessho, Y., Maejima, S., Masuda, K., Shikano, K., Kondo, K., Furumitsu, M., Tachibana, T., 2014. Identification of a cDNA encoding a novel small secretory protein, neurosecretory protein GL, in the chicken hypothalamic infundibulum. Biochem. Biophys. Res. Commun. 446, 298–303.

Ukena, K., Tachibana, T., Iwakoshi-Ukena, E., Saito, Y., Minakata, H., Kawaguchi, R., Osugi, T., Tobari, Y., Leprince, J., Vaudry, H., Tsutsui, K., 2010. Identification, localization, and function of a novel avian hypothalamic neuropeptide, 26RFa, and its cognate receptor, G protein-coupled receptor-103. Endocrinology 151, 2255–2264.

Um, H.N., Han, J.M., Hwang, J.I., Hong, S.I., Vaudry, H., Seong, J.Y., 2010. Molecular coevolution of kisspeptins and their receptors from fish to mammals. Ann. N. Y. Acad. Sci. 1200, 67–74.

Vaillant, C., Dockray, G.J., Walsh, J.H., 1979. The avian proventriculus is an abundant source of endocrine cells with bombesin-like immunoreactivity. Histochemistry 64, 307–314.

Valsalan, R., Manoj, N., 2014. Evolutionary history of the neuropeptide S receptor/neuropeptide S system. Gen. Comp. Endocrinol. 209, 11–20.

van de Velde, J.P., Loveridge, N., Vermeiden, J.P., 1984. Parathyroid hormone responses to calcium stress during eggshell calcification. Endocrinology 115, 1901–1904.

van Dijk, A., Molhoek, E.M., Bikker, F.J., Yu, P.L., Veldhuizen, E.J., Haagsman, H.P., 2011. Avian cathelicidins: paradigms for the development of anti-infectives. Vet. Microbiol. 153, 27–36.

Vandenborne, K., De Groef, B., Geelissen, S.M., Boorse, G.C., Denver, R.J., Kuhn, E.R., Darras, V.M., Van der Geyten, S., 2005a. Molecular cloning and developmental expression of corticotropin-releasing factor in the chicken. Endocrinology 146, 301–308.

Vandenborne, K., Roelens, S.A., Darras, V.M., Kuhn, E.R., Van der Geyten, S., 2005b. Cloning and hypothalamic distribution of the chicken thyrotropin-releasing hormone precursor cDNA. J. Endocrinol. 186, 387–396.

Vaudry, H., Leprince, J., Chatenet, D., Fournier, A., Lambert, D.G., Le Mevel, J.C., Ohlstein, E.H., Schwertani, A., Tostivint, H., Vaudry, D., 2015. International Union of Basic and Clinical Pharmacology. XCII. Urotensin II, urotensin II-related peptide, and their receptor: from structure to function. Pharmacol. Rev. 67, 214–258.

Wan, Y., Zhang, J., Fang, C., Chen, J., Li, J., Li, J., Wu, C., Wang, Y., 2018. Characterization of neuromedin U (NMU), neuromedin S (NMS) and their receptors (NMUR1, NMUR2) in chickens. Peptides 101, 69–81.

Wang, C.Y., Wang, Y., Li, J., Leung, F.C., 2006. Expression profiles of growth hormone-releasing hormone and growth hormone-releasing hormone receptor during chicken embryonic pituitary development. Poultry Sci. 85, 569–576.

Wang, D., Xu, C., Wang, T., Li, H., Li, Y., Ren, J., Tian, Y., Li, Z., Jiao, Y., Kang, X., Liu, X., 2016. Discovery and functional characterization of leptin and its receptors in Japanese quail (*Coturnix japonica*). Gen. Comp. Endocrinol. 225, 1–12.

Wang, G., Brumfield, B., DiCroce, M., Nelson, L., Newmyer, B.A., Flower, J., Hipskind, K., Sharma, S., Gilbert, E.R., Cline, M.A., 2014. Anorexigenic effects of central adrenomedullin are associated with hypothalamic changes in juvenile Gallus gallus. Gen. Comp. Endocrinol. 204, 223–228.

Wang, J., Gilbert, E.R., Cline, M.A., 2019. Hypothalamic mechanisms associated with neuropeptide K-induced anorexia in Japanese quail (*Coturnix japonica*). Comp. Biochem. Physiol. Mol. Integr. Physiol. 237, 110539.

Wang, J., Wang, Y., Li, X., Li, J., Leung, F.C., 2008. Cloning, tissue distribution, and functional characterization of chicken glucagon receptor. Poultry Sci. 87, 2678–2688.

Wang, Y., Huang, G., Li, J., Meng, F., He, X., Leung, F.C., 2012a. Characterization of chicken secretin (SCT) and secretin receptor (SCTR) genes: a novel secretin-like peptide (SCT-LP) and secretin encoded in a single gene. Mol. Cell. Endocrinol. 348, 270–280.

Wang, Y., Li, J., Wang, C.Y., Kwok, A.H., Leung, F.C., 2007. Identification of the endogenous ligands for chicken growth hormone-releasing hormone (GHRH) receptor: evidence for a separate gene encoding GHRH in submammalian vertebrates. Endocrinology 148, 2405–2416.

Wang, Y., Li, J., Wang, C.Y., Kwok, A.Y., Zhang, X., Leung, F.C., 2010. Characterization of the receptors for chicken GHRH and GHRH-related peptides: identification of a novel receptor for GHRH and the receptor for GHRH-LP (PRP). Domest. Anim. Endocrinol. 38, 13–31.

Wang, Y., Meng, F., Zhong, Y., Huang, G., Li, J., 2012b. Discovery of a novel glucagon-like peptide (GCGL) and its receptor (GCGLR) in chickens: evidence for the existence of GCGL and GCGLR genes in nonmammalian vertebrates. Endocrinology 153, 5247–5260.

Wang, Y., Wang, C.Y., Wu, Y., Huang, G., Li, J., Leung, F.C., 2012c. Identification of the receptors for prolactin-releasing peptide (PrRP) and Carassius RFamide peptide (C-RFa) in chickens. Endocrinology 153, 1861–1874.

Weir, G.C., Goltsos, P.C., Steinberg, E.P., Patel, Y.C., 1976. High concentration of somatostatin immunoreactivity in chicken pancreas. Diabetologia 12, 129–132.

Whenham, N., Lu, T.C., Maidin, M.B., Wilson, P.W., Bain, M.M., Stevenson, M.L., Stevens, M.P., Bedford, M.R., Dunn, I.C., 2015. Ovodefensins, an oviduct-specific antimicrobial gene family, have evolved in birds and reptiles to protect the egg by both sequence and intra-six-cysteine sequence motif spacing. Biol. Reprod. 92, 154.

Wideman Jr., R.F., 1987. Renal regulation of avian calcium and phosphorus metabolism. J. Nutr. 117, 808–815.

Wilson, J.X., 1987. Reevaluation of the effect of substance P on nasal salt gland secretion in the duck (*Anas platyrhynchos*). Gen. Comp. Endocrinol. 67, 256–262.

Wu, C., Lv, C., Wan, Y., Li, X., Zhang, J., Li, J., Wang, Y., 2019. Arginine vasotocin (AVT)/mesotocin (MT) receptors in chickens: evidence for the possible involvement of AVT-AVPR1 signaling in the regulation of oviposition and pituitary prolactin expression. Gen. Comp. Endocrinol. 281, 91–104.

Wu, S.V., Walsh, J.H., Campbell, B.J., Dimaline, R., 1995. Molecular characterization and physiological regulation of a TATA-less gene encoding chicken gastrin. Eur. J. Biochem. 230, 439–446.

Wunderer, F., Traeger, L., Sigurslid, H.H., Meybohm, P., Bloch, D.B., Malhotra, R., 2020. The role of hepcidin and iron homeostasis in atherosclerosis. Pharmacol. Res. 153, 104664.

Xiao, Y., Cai, Y., Bommineni, Y.R., Fernando, S.C., Prakash, O., Gilliland, S.E., Zhang, G., 2006. Identification and functional characterization of three chicken cathelicidins with potent antimicrobial activity. J. Biol. Chem. 281, 2858–2867.

Xiao, Y., Hughes, A.L., Ando, J., Matsuda, Y., Cheng, J.F., Skinner-Noble, D., Zhang, G., 2004. A genome-wide screen identifies a single beta-defensin gene cluster in the chicken: implications for the origin and evolution of mammalian defensins. BMC Genom. 5, 56.

Xie, F., London, S.E., Southey, B.R., Annangudi, S.P., Amare, A., Rodriguez-Zas, S.L., Clayton, D.F., Sweedler, J.V., 2010. The zebra finch neuropeptidome: prediction, detection and expression. BMC Biol. 8, 28.

Yamada, S., Mikami, S., 1985. Immunohistochemical localization of corticotropin-releasing factor (CRF)-containing neurons in the hypothalamus of the Japanese quail, *Coturnix coturnix*. Cell Tissue Res. 239, 299–304.

Yamamoto, I., Kaiya, H., Tsutsui, C., Sakai, T., Tsukada, A., Miyazato, M., Tanaka, M., 2008. Primary structure, tissue distribution, and biological activity of chicken motilin receptor. Gen. Comp. Endocrinol. 156, 509–514.

Yamamoto, I., Nakao, N., Kaiya, H., Miyazato, M., Tsushima, N., Arai, T., Tanaka, M., 2011. Two chicken neuromedin U receptors: characterization of primary structure, biological activity and tissue distribution. Gen. Comp. Endocrinol. 174, 116–123.

Yegorov, S., Good, S., 2012. Using paleogenomics to study the evolution of gene families: origin and duplication history of the relaxin family hormones and their receptors. PloS One 7, e32923.

Yi, Z., Li, X., Luo, W., Xu, Z., Ji, C., Zhang, Y., Nie, Q., Zhang, D., Zhang, X., 2018. Feed conversion ratio, residual feed intake and cholecystokinin type A receptor gene polymorphisms are associated with feed intake and average daily gain in a Chinese local chicken population. J. Anim. Sci. Biotechnol. 9, 50.

Yin, H., Ukena, K., Ubuka, T., Tsutsui, K., 2005. A novel G protein-coupled receptor for gonadotropin-inhibitory hormone in the Japanese quail (*Coturnix japonica*): identification, expression and binding activity. J. Endocrinol. 184, 257–266.

Yoshihara, C., Fukao, A., Ando, K., Tashiro, Y., Taniuchi, S., Takahashi, S., Takeuchi, S., 2012. Elaborate color patterns of individual chicken feathers may be formed by the agouti signaling protein. Gen. Comp. Endocrinol. 175, 495–499.

Yousefvand, S., Hamidi, F., Zendehdel, M., Parham, A., 2019. Interaction of neuropeptide Y receptors (NPY1, NPY2 and NPY5) with somatostatin on somatostatin-induced feeding behaviour in neonatal chicken. Br. Poultry Sci. 60, 71–78.

Yu, J., Xie, L.Y., Abou-Samra, A.B., 1996. Molecular cloning of a type A chicken corticotropin-releasing factor receptor with high affinity for urotensin I. Endocrinology 137, 192–197.

Zhang, J., Li, X., Zhou, Y., Cui, L., Li, J., Wu, C., Wan, Y., Li, J., Wang, Y., 2017. The interaction of MC3R and MC4R with MRAP2, ACTH, alpha-MSH and AgRP in chickens. J. Endocrinol. 234, 155–174.

Zhang, J., Wan, Y., Fang, C., Chen, J., Ouyang, W., Li, J., Wang, Y., 2018a. The orphan G protein-coupled receptor 25 (GPR25) is activated by Apelin and Apela in non-mammalian vertebrates. Biochem. Biophys. Res. Commun. 501, 408–414.

Zhang, J., Zhou, Y., Wu, C., Wan, Y., Fang, C., Li, J., Fang, W., Yi, R., Zhu, G., Li, J., Wang, Y., 2018b. Characterization of the apelin/elabela receptors (APLNR) in chickens, turtles, and zebrafish: identification of a novel apelin-specific receptor in teleosts. Front. Endocrinol. 9, 756.

Zhang, L., Chen, D., Yu, L., Wei, Y., Li, J., Zhou, C., 2019. Genome-wide analysis of the ovodefensin gene family: monophyletic origin, independent gene duplication and presence of different selection patterns. Infect. Genet. Evol. 68, 265–272.

Zhang, S., Okuhara, Y., Iijima, M., Takemi, S., Sakata, I., Kaiya, H., Teraoka, H., Kitazawa, T., 2020. Identification of pheasant ghrelin and motilin and their actions on contractility of the isolated gastrointestinal tract. Gen. Comp. Endocrinol. 285, 113294.

Zhang, W., Bai, S., Liu, D., Cline, M.A., Gilbert, E.R., 2015. Neuropeptide Y promotes adipogenesis in chicken adipose cells in vitro. Comp. Biochem. Physiol. Mol. Integr. Physiol. 181, 62–70.

Zudaire, E., Cuesta, N., Martinez, A., Cuttitta, F., 2005. Characterization of adrenomedullin in birds. Gen. Comp. Endocrinol. 143, 10–20.

Chapter 30

Pituitary gland

Colin G. Scanes[1,2]

[1]Department of Biological Science, University of Wisconsin Milwaukee, Milwaukee, WI, United States; [2]Center of Excellence for Poultry Science, University of Arkansas, Fayetteville, AR, United States

Abbreviations

ACTH adrenocorticotropic hormone
AVT arginine vasotocin
CART cocaine- and amphetamine-regulated transcript peptides
CRH corticotropin-releasing hormone
CSF1R colony-stimulating factor 1 receptor
CYTL1 cytokine-like 1
FSH follicle-stimulating hormone
GCGL glucagon-like peptide
GH growth hormone
GHBP GH binding proteins
GHR growth hormone receptor
GHRH growth hormone—releasing hormone
GHS-R GH secretagogue receptor
GJA5 gap junction protein alpha 5
GnIH gonadotropin-inhibitory hormone
GnIH-RP gonadotropin-inhibitory hormone—related peptide
GnRH gonadotropin-releasing hormone
GRP Gastrin-releasing peptide
IGF-1 insulin-like growth factor 1
JAK janus kinase
LH luteinizing hormone
MSH melanocyte-stimulating hormone
MT mesotocin
PHI peptide HI
POMC pro-opiomelanocortin
PRL prolactin
PRL-L prolactin-like protein
PRLHR1 PrRP receptor
PrRP prolactin-releasing peptide
PTHrP parathyroid hormone—related peptide
SNP single nucleotide polymorphism
SRIH somatostatin
SS somatostatin
STAT signal transducers and activators of transcription
T_3 triiodothyronine
T_4 thyroxine
TRH thyrotropin-releasing hormone or thyroliberin
TSH thyrotropin or thyroid-stimulating hormone
VIP vasoactive intestinal peptide
β-EP β-endorphin
β-LPH β-lipotropin

30.1 Introduction

The pituitary gland (hypophysis) is intimately connected to the hypothalamus in both an anatomically and functionally close relationship. The structure of the hypothalamo-hypophyseal complex is shown in Figure 30.1. The pituitary gland consists of two distinct structures as summarized in Table 30.1:

- The anterior pituitary gland or pars distalis, which sits in a depression in the bone—sella turcica
- The posterior pituitary gland or pars nervosa, which is connected to the base of the brain by the infundibulum

30.2 Embryonic development of the pituitary gland

The pituitary gland has a complex structure and an interesting embryonic development. The anterior and posterior pituitary glands have distinctly differences in anatomy, physiology, and embryonic developments. Pituitary tissue can be classified as either adenohypophysis or neurohypophysis each with a distinct embryonic origin (see Figure 30.2). The adenohypophysis is derived from Rathke's pouch and this, in turn, derived from the medial stomodeal ectoderm (i.e., from the roof of the mouth) at the rostral border of the neural plate (chicken: Sánchez-Arrones et al., 2015). A distinct Rathke's pouch is developed during Hamburger and Hamilton stage 12 (Romanoff, 1960). It expresses transcription factor 4 (Tcf4), the paired like homodomain transcription factor (Pitx2) and sonic

Sturkie's Avian Physiology. https://doi.org/10.1016/B978-0-12-819770-7.00008-6

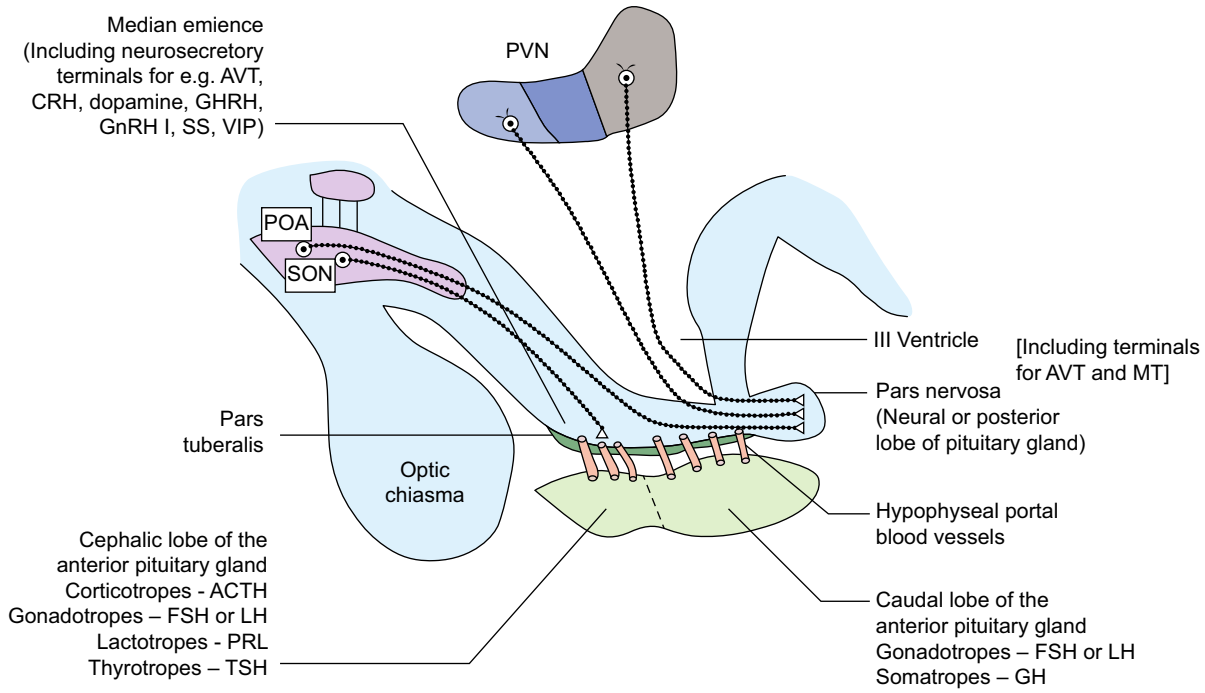

FIGURE 30.1 Schematic diagram of the structure of the avian hypothalamus and pituitary gland. Dark green: pars tuberalis; light blue: nervous tissue in the hypothalamus; light green: pars distalis or anterior pituitary gland; red: blood vessels of the hypothalamo-hypophyseal portal system bringing releasing hormones from the neurosecretory terminals in the median eminence to stimulate or inhibit hormone secretion from ells of the anterior pituitary gland; neurosecretory cells have their cell bodies in nuclei in the hypothalamus and terminate either in the median eminence or the posterior pituitary gland. *AVT*, arginine vasotocin; *MT*, mesotocin; *POA*, preoptic area; *PVN*, paraventricular nucleus; *SON*, supraoptic nucleus.

TABLE 30.1 Divisions of the pituitary gland.

Divisions of pituitary gland	Mammals	Birds
1. Adenohypophysis	✓	✓
a. Pars distalis	✓	✓
b. Pars intermedia	✓	X
c. Pars tuberalis	✓	✓
i. Anterior pituitary gland	Pars distalis + Pars intermedia	Pars distalis
2. Neurohypophysis	✓	✓
a. Pars nervosa (or posterior pituitary gland)	✓	✓
b. Infundibular stalk	✓	✓
c. Median eminence[a]	✓	✓

[a]*Frequently considered only as part of hypothalamus.*

hedgehog signally molecule (Shh) (Sánchez-Arrones et al., 2015). The lens protein, δ-crystallin, is transiently expressed in cells of the Rathke's pouch (chicken embryo: Inoue et al., 2012). Subsequently by Hamburger and Hamilton stage 18, the adenohypophysis primordium is fully formed and is moving to close by and underlying the hypothalamus (Sánchez-Arrones et al., 2015). The neurohypophysis is derived from the infundibulum (an outgrowth of the brain). In birds, the adenohypophysis goes on to form the pars distalis with some adenohypophyseal cells migrating to form the pars tuberalis below the median eminence.

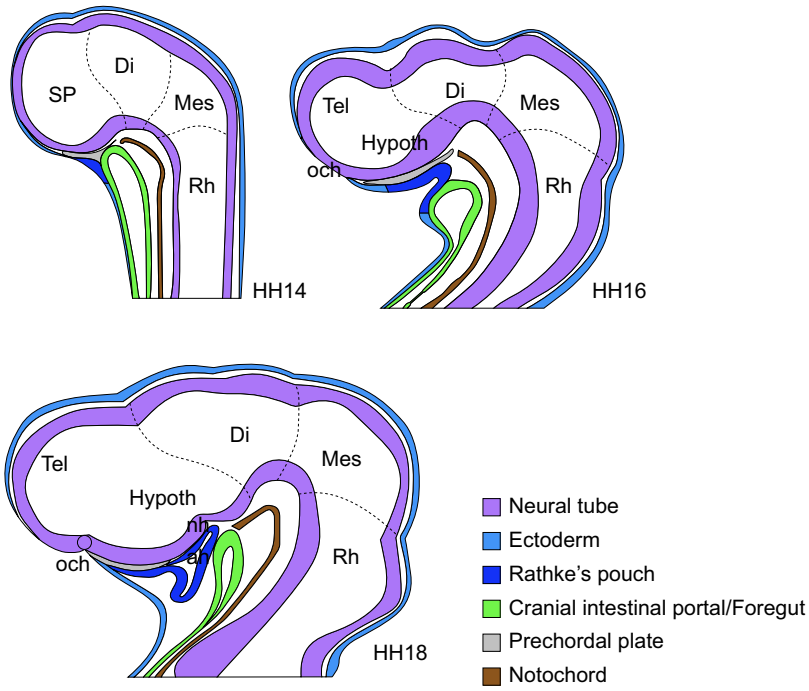

FIGURE 30.2 **Embryonic development of the pituitary gland.** Key: Neural tube—purple, ectoderm—light blue, Rathke's pouch—bright blue, endoderm green, notochord—brown, prechordal plate—gray. AH—adenohypophysis, NH—neurohypophysis, och—optic chiasm. *Based on Sánchez-Arrones, L., Ferrán, J.L., Hidalgo-Sanchez, M., Puelles, L., 2015. Origin and early development of the chicken adenohypophysis. Front. Neuroanat. 9, 7.*

30.3 Anatomy of the pituitary gland

30.3.1 Anatomy of the anterior pituitary gland (pars distalis)

The avian pars distalis consists of two distinct lobes: the cephalic and caudal lobes. The anterior pituitary gland is composed of secretory cells, folliculo-stellate cells, extracellular colloid, and connective tissues composed of fibrous materials (Mohanty, 2006) together possibly with microglial cells (discussed below).

30.3.1.1 Secretory cells

The anterior pituitary gland (pars distalis) has the full complement of secretory cells: corticotropes producing adrenocorticotropic hormone (ACTH), gonadotropes producing either luteinizing hormone (LH) or follicle-stimulating hormone (FSH), lactotropes producing prolactin (PRL), somatotropes producing growth hormone (GH), and thyrotropes producing thyrotropin/thyroid-stimulating hormone (TSH) (Table 30.2). Gastrin-releasing peptide (GRP) is expressed in LH-producing gonadotropes (Mo et al., 2017). In addition, there are somatolactotropes producing both GH and PRL (turkey: Ramesh et al., 1998, 2001) and cells that co-express pro-opiomelanocortin (POMC) and α-sub-unit of the glycoprotein hormones LH, FSH, and TSH (chickens: Pals et al., 2006).

There are changes in secretory cells with physiological state with specific secretory cells undergoing proliferation or apoptosis. For instance, there are marked changes after cessation of lay due to forced molt (chicken: Yoshimura et al., 1997; Chowdhury and Yoshimura, 2002).

The pars distalis is richly supplied with blood vessels including the hypophyseal portal vessels. These provide a route from the neurosecretory nerve terminals in the median eminence to the anterior pituitary gland (Figure 30.1). Indeed, it is by way of these portal blood vessels that the anterior pituitary gland is controlled by releasing hormones (or hypothalamic hypophysiotropic factors) (Figure 30.1; Table 30.3).

In some avian species, pituitary tumors have been identified with multiple somatotropes (budgerigar: Langohr et al., 2012).

30.3.1.2 Folliculo-stellate cells

In addition to secretory cells, there are nonendocrine cells, the folliculo-stellate cells in both the cephalic and caudal lobes of the anterior pituitary gland. Avian folliculo-stellate cells are of extrapituitary origin. These mesenchyme cells invade the anterior pituitary gland between days 15 and 18 of embryonic development in the chicken (Horiguchi et al., 2016). These cells express markers including immune-reactive S-100 proteins (quail: Harrison et al., 1982; Van

TABLE 30.2 Summary of the chemistry of the hormones of the pituitary gland.

Pituitary hormone	Alternate name (IUPAC/IUB)	Chemistry
Hormones of anterior pituitary gland		
Adrenocorticotropic hormone (ACTH)	Corticotropin	Synthesized as protein (pro-opiomelanocortin or POMC) then proteolytically cleaved to 39 amino acid residue polypeptide
Follicle-stimulating hormone (FSH)	Follitropin	Two glycoprotein subunits: * α-subunit common to FSH, LH, and TSH * β-subunit—specific to FSH
Luteinizing hormone (LH)	Lutropin	Two glycoprotein subunits: * α-subunit common to FSH, LH, and TSH * β-subunit—specific to LH
Growth hormone (GH)	Somatotropin	Protein + glycosylated variants
Prolactin (PRL)	Lactotropin	Protein + glycosylated variants
Thyroid-stimulating hormone (TSH)	Thyrotropin	Two glycoprotein subunits: * α-subunit common to FSH, LH, and TSH * β-subunit—specific to TSH
Hormones of posterior pituitary gland		
	Other names	
Arginine vasotocin (AVT)	8-arginine oxytocin	Synthesized as a protein, then proteolytically cleaved yielding peptide with 9 amino acid residues
Mesotocin (MT)	8-isoleucine oxytocin	Synthesized as a protein, then proteolytically cleaved yielding peptide with 9 amino acid residues
Putative pituitary hormones		
Melanocyte-stimulating hormone (MSH)	Melanotropin	Three distinct peptides—α-, β-, and γ-MSH
β-endorphin		Polypeptide
Lipotropic hormone	Lipotropin	Polypeptide

TABLE 30.3 Summary of stimulatory and inhibitory releasing hormones in birds.

Anterior pituitary hormone	Stimulatory-releasing hormone	Inhibitory-releasing hormone
Adrenocorticotropic hormone (ACTH)	* Corticotropin-releasing hormone (CRH) (via CRH type 1 receptor) * Arginine vasotocin (AVT)	—
Follicle-stimulating hormone (FSH)	* Gonadotropin-releasing hormone I (GnRH 1) * GnRH II * Activin	* Gonadotropin-inhibitory hormone (GnIH) * Inhibin
Luteinizing hormone (LH)	* Gonadotropin-releasing hormone I (GnRH 1) * GnRH II	* Gonadotropin-inhibitory hormone (GnIH)
Growth hormone (GH)	* Growth hormone—releasing hormone (GHRH) * Thyrotropin-releasing hormone (TRH) * Glucagon-like peptide (GCGL) * Ghrelin * Neuropeptide W * PACAP, leptin, GnRH	Somatostatin (SS or SRIF)
Prolactin (PRL)	* Vasoactive intestinal peptide (VIP) * Prolactin-releasing peptide (PrRp) * Neuropeptide W * TRH, AVT, peptide histidine isoleucine (PHI)	Dopamine
Thyroid-stimulating hormone (TSH)	* TRH * CRH (via CRH type 2 receptor)	SS

Nassauw et al., 1987; Harrison, 1989; chicken: Allaerts et al., 1999) and cytokeratin (chicken: Nishimura et al., 2017). Folliculo-stellate cells are agranular and do not express anterior pituitary hormones (chicken: Nishimura et al., 2017). Possible roles for the folliculo-stellate cells may include aiding structural integrity of the follicles and/or autocrine-paracrine regulation of adjacent secretory cells and/or immune-endocrine interaction. There is evidence that folliculo-stellate cells influence thyrotropes (quail: Harrison et al., 1982) and possibly vice versa as folliculo-stellate cells express TSH receptors (TSHRs) (chicken: Grommen et al., 2009).

30.3.1.3 Macrophage

Based on the presence of a pan-macrophage antigen, there are macrophage or macrophage-like cells in the embryonic pituitary (chicken: Allaerts et al., 1999). These are scattered and located in the connective tissue (chicken: Allaerts et al., 1999). Microglial cells are a specialized form of macrophage that are normally found in the central nervous system. There is expression of colony-stimulating factor 1 receptor (CSF1R) in avian pituitary glands indicating the presence of microglial cells (Japanese quail: Walker et al., 2019). Posthatching stressing by unpredictable feed availability depressed pituitary expression of CSF1R (Japanese quail: Walker et al., 2019). However, it is not clear whether CSF1R-expressing microglial cells are found in the anterior and/or posterior pituitary gland.

30.3.2 Pars intermedia

In mammals, the pars intermedia are formed from adenohypophyseal cells and produces α-melanocyte-stimulating hormone (α-MSH). It is generally considered that the pars intermedia is not present in birds (chicken: Rahn, 1939; other birds: Rahn and Painter, 1941). However, it is not possible to preclude migration of cells from the primordial pars intermedia to the pars distalis and/or pars tuberalis.

30.3.3 Pars tuberalis

The pars tuberalis is derived from Rathke's pouch, specifically the upper anterior portion (Sasaki et al., 2003). The pars tuberalis develops along the median eminence between days 8 and 14 of incubation in the chick embryo (Kameda et al., 2000). Many pars tuberalis cells express the α-sub-unit of glycoprotein hormones, and this is seen as early as day three of embryonic development (Inoue et al., 2013). By day 10 of embryonic development, cells within the pars tuberalis exhibit high expression of both cytokine-like 1 and gap junction protein alpha 5 genes (Aizawa et al., 2016).

The pars tuberalis consists of adenohypophyseal located along the ventral surface of the median eminence. It consists of the following cell types: (1). pars distalis secretory specific cells, (2). pars distalis cell types including corticotropes, gonadotropes, lactotropes, somatotropes, and thyrotropes (Mohanty et al., 1997), (3). follicular cells (reviewed: Yasuo and Korf, 2011), and (4). macrophage.

The pars tuberalis can communicate in a retrograde manner with the median eminence and in an anterograde manner with the pars distalis. There is high expression of the α-subunit of LH, FSH, and TSH (Kameda et al., 2000) in the pars tuberalis.

30.3.4 Posterior pituitary gland or pars nervosa

The posterior pituitary gland consists of neurosecretory terminals that release either mesotocin (MT) or arginine vasotocin (AVT) (Table 30.2). These hormones are synthesized in cell bodies in nuclei in the hypothalamus and are transported to the pars nervosa (posterior pituitary gland) through modified axons in the infundibular stalk (Figure 30.1).

30.4 Gonadotropins

30.4.1 Gonadotropin subunits, genes, mRNA, and glycoproteins

Avian LH and FSH are glycoproteins with molecular weights of 30 KDa (turkey: Burke et al., 1979a). Both LH and FSH consist of two glycoprotein subunits: an α-subunit that is common to LH, FSH, and TSH and a hormone-specific β-subunit (with different β-subunits for LH, FSH, and TSH). Both subunits are required for biological activity (turkey: Burke et al., 1979b). The α-subunit is a sequence of 96 amino acid residues with an additional signal peptide of 24 amino acids (domestic duck: Hsieh et al., 2001). The amino acid residue sequences have been deduced from the nucleotide sequences of the cDNA for the α-subunit or β-subunit. For example, FSH β subunit is a glycoprotein with 111 amino acid residues [goose: Huang et al., 2015; wild birds (FSH β-subunit: burrowing owl XM_026850847.1; emu XM_026122133.1; Saker falcon: XM_005436169.1; white-throated sparrow: XM_005492327.2; willow flycatcher: XM_027902612)]. It is synthesized with a 20 amino acid signal peptide (goose: Huang et al., 2015). FSH-β-subunit has two disulfide bonds and two asparagine-linked glycosylation sites (Shen and Yu, 2002). Shen and Yu (2002) noted the "remarkable" degree of homogeneity among FSH β-subunit across avian species (see Figure 30.3).

Plasma concentrations of LH and FSH are illustrated in Table 30.4.

30.4.1.1 Expression of pituitary glycoprotein subunits

There is independent control of the expression of α-subunit and LH, FSH, and TSH β subunits as seen from the following:

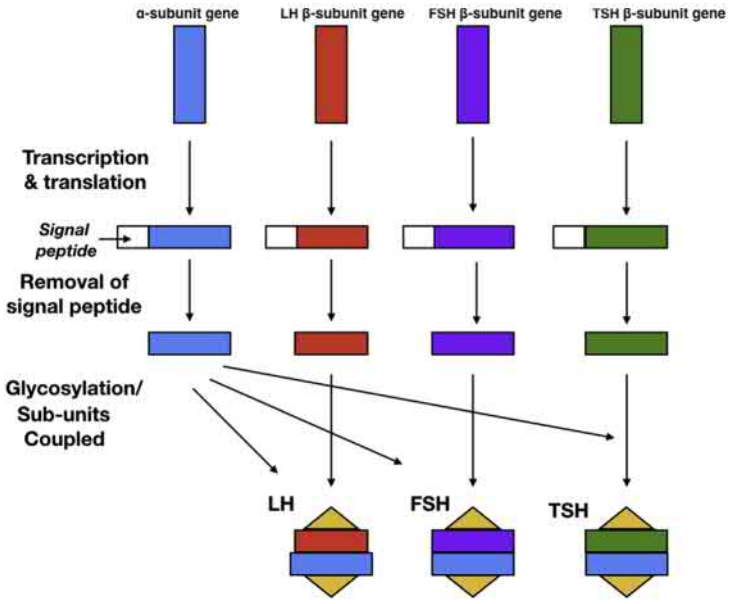

FIGURE 30.3 Synthesis of pituitary glycoprotein hormones.

TABLE 30.4 Basal plasma hormone concentrations in birds.

	Species	Plasma hormone concentration		References
		pg/mL	pmoles/L	
Follicle-stimulating hormone				
	Chicken	333	11	Han et al. (2017)
Luteinizing hormone				
	Chicken	5000	166	Dunn et al. (2017)
	Chicken	1400	47	Han et al. (2017)
Prolactin				
	Chicken	4000	200	Dunn et al. (2017)
α-melanocyte-stimulating hormone				
	Chicken	3095	1860	Shipp et al. (2017)
Adrenocorticotropic hormone				
	Chicken	104	22.9	Carsia et al. (1988)
β-endorphin				
	Domestic goose	104	30	Barna et al. (1998a)
Arginine vasotocin				
	Chicken	15[a]	14[a]	Robinzon et al. (1990)
	Domestic duck	8.4	8.0	Gray and Maloney (1998)
	Japanese quail	7.0, 2.8	6.7, 2.7	Seth et al. (2004b); Minvielle et al. (2007)
	White-bellied sunbirds	22	21	Gray et al. (2004)
Mesotocin				
	Chicken	19, 15	18, 14	Robinzon et al. (1990); Chaturvedi et al. (2001)

[a]*Other studies reported a much higher basal concentration of arginine vasotocin in chickens, e.g., 12 ng/mL (11 nmol/L) Sirotkin et al. (2017); 22 ng/mL (21 nmol/L) Takahashi et al. (2011).*

- Pituitary expression of α-subunit is stimulated in vitro by incubation with either gonadotropin-releasing hormone (GnRH) or thyrotropin-releasing hormone (TRH) (domestic duck: Hsieh et al., 2001).
- GnRH-1 increased expression of LH β subunits (turkey: You et al., 1995).
- Pituitary expression of TSH β subunits is increased by glucagon-like peptide (GCGL) (chicken: Huang et al., 2014).

30.4.2 Actions of gonadotropins

For a more detailed discussion of the control of female and male reproduction, see Chapters 34 and 35.

30.4.2.1 Actions of luteinizing hormone in the female

30.4.2.1.1 Luteinizing hormone and ovulation

A major role of LH is to induce ovulation. Premature ovulation is provoked following injection of LH (laying hen chicken: Imai, 1973; broiler breeder chicken: broiler breeders: Liu et al., 2004; Japanese quail: Onagbesan and Peddie, 1988). Moreover, there is a small increase or surge in plasma concentrations of LH 4–6 h prior to ovulation (chicken: Furr et al., 1973; turkey: Liu et al., 2001; Liu et al., 2004) (also see Figure 30.4). Administration of LH is followed by a series of events in the most mature follicle: (1). breakdown of the germinal vesicle, (2). dissociation of the junctions between the granulosa projections and the oocyte surface, (3). development of a perivitelline space, and (4). formation of the first and then second maturation spindle (Japanese quail: Yoshimura et al., 1993). There is evidence that LH surges are synchronized by societal and other cues (e.g., to alternate days in glaucous-winged gulls Henson et al., 2011).

30.4.2.1.2 Luteinizing hormone and steroidogenesis

LH increases ovarian production of progesterone and androgens by the large yolky follicles. LH increased progesterone and testosterone in both the circulation and tissue from large follicles in vivo (laying hen chickens: Shahabi et al., 1975). The effects of LH are on both granulosa and theca cells. LH stimulates the production of progesterone and androstenedione by granulosa cells in vitro from the largest yolk-filled follicles while FSH is largely without effect (Scanes and Fagioli, 1980; Tilly and Johnson, 1987, 1988a, b). LH increases also expression of steroidogenic acute regulatory protein (StAR) in granulosa cells from the largest yellow (F1) follicles (Johnson and Bridgham, 2001). However, granulosa cells from 9 to 12 mm follicles or smaller did not respond to LH (Tilly et al., 1991a).

Moreover, LH increased androstenedione release from thecal cells from F2 follicles in vitro (Tilly and Johnson, 1989b). Theca cells from 6 to 8 mm follicles respond to LH with increased steroidogenesis (Kowalski et al., 1991).

30.4.2.1.3 Luteinizing hormone and follicular development

There are effects of LH on follicular development. For instance, LH increases proliferation of granulosa cells from large yolky F1–F3 follicles (broiler breeder chickens: Onagbesan et al., 1999). In addition, LH suppressed plasminogen activator activity in granulosa cells from the largest follicles (Tilly and Johnson, 1987).

30.4.2.1.4 Luteinizing hormone and ovarian inhibin/activin receptors

There are effects of LH on ovarian activin (Act) and inhibin receptors. LH increases expression of ActRIIA and inhibin

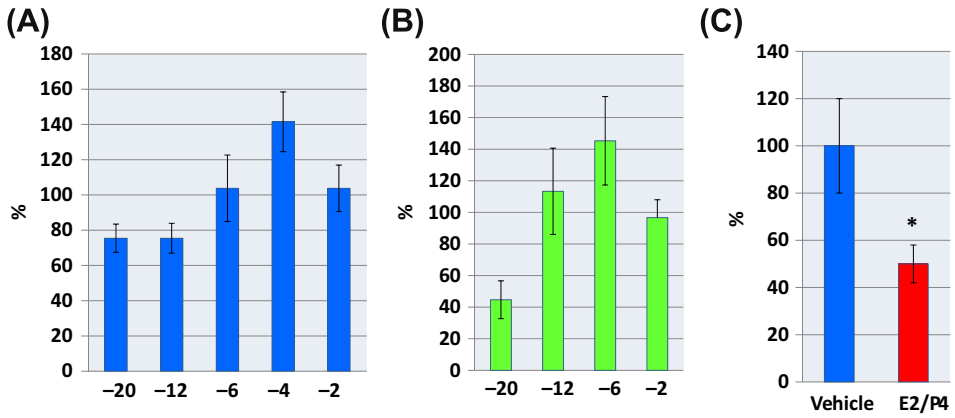

FIGURE 30.4 Changes in luteinizing hormone (LH) during the ovulatory cycle of the chicken. (A) Circulating concentrations of LH during the ovulatory cycle. (B) Pituitary gonadotropin-releasing hormone (GnRH) receptor expression during the ovulatory cycle (Data from Lovell et al. (2005)). (C) Effect of in vivo treatment with estradiol (E2) and progesterone (P4) in immature hens on pituitary expression of GnIH receptors by chicken anterior pituitary tissue (Maddineni et al., 2008).

co-receptor by theca cells from F1 follicles (chicken: Lovell et al., 2007). Expression of ActR type I, ActRIIA, ActRIIB, and inhibin co-receptor by granulosa cells from 6 to 8 mm and F1 follicles is increased by LH (chicken: Lovell et al., 2007).

30.4.2.2 Actions of follicle-stimulating hormone in the female

In vivo either FSH or equine chorionic gonadotropin (formerly pregnant mare serum gonadotropin) increases the number of large follicles but did not influence the number of 6–8 mm prerecruitment follicles (chicken: Ghanem and Johnson, 2019).

Granulosa cells from 6 to 8 mm follicles respond to FSH were reduced expression of activin receptor (ActR) (typeIIB) and ActRI but increased expression of ActRIIA and inhibin co-receptor in granulosa cells from either 6–8 mm or F1 follicles (Lovell et al., 2007). Among the downregulated differentially expressed genes after FSH treatment of granulosa cells in vitro are the following: follistatin, superoxide dismutase 1, fatty acyl-CoA reductase 1, transforming growth factor (TGF)-beta receptor-associated protein 1 (domesticated goose: Du et al., 2018).

30.4.2.2.1 Follicle-stimulating hormone and steroidogenesis

FSH increases progesterone from smaller follicles but not the largest follicles. FSH increased progesterone production by granulosa cells from 9 to 12 mm follicles (Tilly et al., 1991a). Granulosa cells from 6 to 8 mm follicles do not convert cholesterol to pregnenolone. However, after incubation with FSH, these cells can convert cholesterol to pregnenolone and there is increased expression of P450scc and StAR (Tilly et al., 1991; Li and Johnson, 1993; Johnson and Bridgham, 2001). Theca cells from 6 to 8 mm follicles respond to FSH with increased steroidogenesis (Kowalski et al., 1991).

30.4.2.2.2 Follicle-stimulating hormone and ovarian cell remodeling and proliferation

FSH increases proliferation of granulosa cells from prehierarchical follicles (6 to 8 mm in diameter) with the effect increased in the presence of activin A and transfection with FOXL2 plasmids (Qin et al., 2015). Apoptosis in prehierarcichal follicle granulosa cells is depressed in the presence of FSH (Johnson et al., 1996a). Moreover, FSH increases the expression of annexin A2 in follicular theca cells, and this may be increasing angiogenesis (chicken: Zhu et al., 2015). In addition, in a culture of embryonic ovarian cells, FSH stimulates proliferation of germ cells as indicated by counting cells with immune-reactivity to cell nuclear antigen (chicken: Xie et al., 2004; Liu et al., 2010).

30.4.2.3 Actions of luteinizing hormone in the male

In birds, as in mammals, LH stimulates both differentiation of Leydig cells and production of testosterone. The administration of chicken LH to hypophysectomized Japanese quail markedly increases the number of mature Leydig cells decreasing the number of fibroblasts and transitional cell types in the interstitium (Brown et al., 1975). In birds, testosterone production is increased by LH in vitro (Japanese quail: Maung and Follett, 1977; chicken: e.g., Opałka et al., 2004) and in vivo (Japanese quail: Maung and Follett, 1978).

30.4.2.4 Actions of follicle-stimulating hormone in the male

The major role of FSH is stimulating spermatogenesis and the supporting "nurse" cells, the Sertoli cells. When FSH is injected into hypophysectomized quail, there are increases in testicular size (8.8 fold) together with differentiation of Sertoli cells and promotion of spermatogenesis (Brown et al., 1975). In vitro, FSH increased the number of germ cells and expression of stem cell factor receptor c-kit (chicken: Mi et al., 2004). Administration of FSH elevates expression of tyrosine kinase receptor A, the receptors for nerve growth factor (chicken: Ma et al., 2015). Sertoli cells treated with FSH in vitro exhibit the following increases: proliferation, concentrations of 3β-hydroxysteroid dehydrogenase, and lactate production (chicken: Guibert et al., 2011). However, FSH had little effect on overall testosterone production by testicular cells (Maung and Follett, 1978).

30.4.2.5 Other actions of follicle-stimulating hormone

FSH increases lipid deposition into avian preadipocytes in vitro and weight of abdominal fat pad in vivo (broiler chickens: Cui et al., 2012). FSH also increases the expression of enzymes controlling lipid metabolism, namely, retinol dehydrogenase 10 (*Rdh10*), lipoprotein lipase (*Lpl*), retinoic acid receptor beta (*RarB*), and diglyceride acyltransferase (*Dgat*) genes (broiler chickens: Cui et al., 2012). FSHR is expressed by avian adipose tissue and expression is increased by FSH in vivo and in vitro (broiler chickens: Cui et al., 2012).

30.4.2.6 Luteinizing hormone receptors

The structures of avian luteinizing hormone receptor (cLH-R) have been deduced from the cDNA in initially in poultry species (chicken: Johnson et al., 1996b; turkey: You et al., 2000) and also in wild birds (e.g., emu: XM_026095388.1, rock pigeon: XM_021287698.1, hooded crow:

TABLE 30.5 Effect of growth factors on the expression of follicle-stimulating hormone receptor in granulosa cells from prehierarchal (6–8 mm diameter) follicles in chickens.

Hormone/growth factor	Direction of change	References
Follicle-stimulating hormone	↑	e.g., Haugen and Johnson (2010)
Transforming growth factor β1	↑	Woods and Johnson (2005)
Activin A	↑	Woods and Johnson (2005)
Bone morphogenetic protein (BMP) 4	↑	Kim et al. (2013)
BMP 6	↑	Ocón-Grove et al. (2012)
BMP 2	↓	Haugen and Johnson (2010)

XM_019282421.2, common starling: KM588217.1, and white-throated sparrow: XM_026796127.1).

Ovarian expression of LHR is influenced by tissue (theca vs. granulosa) and follicular development. In thecal tissue, expression of LH-R increases with follicle development to a maximum in the F2 follicle (chicken: Johnson et al., 1996). Moreover, expression of LH-R in granulosa cells is first detectible in 9–12 mm diameter follicles and progressively increases to preovulatory follicles. Expression of LHR is influenced by hormones and growth factors. For instance, expression of LHR by F1 follicle granulosa cells is increased activin, bone morphogenetic protein (BMP) 6, LH, and testosterone (chicken: Johnson et al., 2006; Al-Musawi et al., 2007; Rangel et al., 2009). Testosterone depresses testicular LH receptors based on LH binding (Ottinger et al., 2002).

The signal transduction mechanism by which LH exerts its effect in both thecal and granulosa cells is via adenylate cyclase and cAMP (chicken: e.g., Asem et al., 1987; Tilly and Johnson, 1988a, b, 1989) and calcium mobilization (chicken: Johnson and Tilly, 1988).

30.4.2.7 Follicle-stimulating hormone receptors

The structure of the FSH receptor has been deduced from cDNA in poultry (chicken: You et al., 1996; Genbank accessions duck: EU049608.1) and wild birds (e.g., brown kiwi XM_013949769.1, rock pigeon: FJ913876.1, peregrine falcon: XM_027782943, emperor penguin XM_009272697.1 and collared flycatcher XM_005042962). Variants FSH receptors transcripts have been identified in multiple species of birds of different families, orders, superorders, and infraclasses including the following: Infraclass *Palaeognathae*: Chilean tinamou; Infraclass *Neognathae*: Superorder *Galloanserae*: Order *Galliformes*: chicken, Japanese quail, helmeted guineafowl, Order *Anseriformes*: domestic duck, domestic geese; Superorder *Neoaves*: Order *Accipitriformes*: golden eagle, Order *Passeriformes*: great tit, blue tit, hooded crow, jungle crow, saffron-crested tyrant-manakin, white-throated sparrow and willow flycatcher.

In the male, FSH receptors (based on binding) are upregulated by FSH (Tsuisui and Ishii, 1980) but depressed by testosterone (Ottinger et al., 2002). In the females, expression of FSHR is influenced by stage of follicular development together with hormones and growth factors (see Table 30.5). The FSHR is expressed in the ovary with expression declining in both thecal and granulosa cells with follicular development (chicken: You et al., 1996). Expression of FSH-R is increased in granulosa cells by TGF β1, activin A, BMP6, and growth differentiation factor 9 (GDF9) and decreased by BMP2 (chicken: Woods and Johnson, 2005; Haugen and Johnson, 2010; Ocón-Grove et al., 2012; Qin et al., 2015). In granulosa cells transfected by Forkhead box L2 (FOXL2) plasmids, expression is further increased in the presence of either GDF9 or activin (Qin et al., 2015).

Signal transduction for FSH in Sertoli cells encompasses FSH binding to FSHR and activation of adenylate cyclase-cAMP-protein kinase A, phosphatidyl-inositol 3 kinase (protein kinase B), and mitogen-activated protein kinase (extracellular signal-regulated kinases, ERK1/2) pathways (chickens: Guibert et al., 2011; Faure et al., 2017).

30.4.3 Control of gonadotropin release

30.4.3.1 Introduction

In birds, release of LH and FSH is under predominantly stimulatory control by the hypothalamus based on deafferentation and lesioning studies (Japanese quail: Davies and Follett, 1980). GnRH stimulates the release of LH in birds while gonadotropin-inhibitory hormone (GnIH) inhibits LH release.

30.4.3.2 Gonadotropin hormone–releasing hormone

30.4.3.2.1 Chemistry

There are two GnRH peptides in the avian hypothalamus, each with separate genes, respectively, for prepro-GnRH 1 and prepro-GnRH-2 (Dunn et al., 1993; Ikemoto and Parks, 2006):

30.4.3.2.1.1 Chicken GnRH 1 (cGnRH1) pGlu-His-Trp-Ser-Tyr-Gly-Leu-Gln-Pro-Gly-amide [pEHWSYGLQPG-NH_2] (King and Millar, 1982).

30.4.3.2.1.2 Chicken GnRH 2 (cGnRH2) pGlu-His-Trp-Ser-His-Gly-Trp-Tyr-Pro-Gly-amide [pEHWSHG-WYPG-NH_2] (Miyamoto et al., 1984).

The structure of GnRH1 appears to be perfectly conserved across the *Aves* with identical structures in the ostrich (Powell et al., 1987), the chicken, the domestic goose (e.g., DQ023158.1), and several passerine species (zebra finch: Stevenson et al., 2009; Ubuka and Bentley, 2009; starling: Stevenson et al., 2009; Ubuka et al., 2009). There is, however, only 58% homology between the sequence of prepro-GnRH 1 in starlings and chicken (Ubaka et al., 2009).

30.4.3.2.2 Biological activity

The major secretagogue for LH is cGnRH1 with cGnRH2 having either a lesser or no role. This is supported by the presence of cGnRH1 but not cGnRH2 in the median eminence and the suppression of reproduction following immunization against cGnRH1 but not cGnRH2 (Sharp et al., 1990). Parenthetically, there is gonadal regression after active immunization against mammalian GnRH also (Quaresma et al., 2017); this being employed as an alternative to surgical castration/caponization. However, cGnRH2 is considerably more potent than cGnRH1 in stimulating LH release in vitro (chicken: Chou et., 1985; Millar et al., 1986) and in vivo (chicken: Wilson et al., 1989; Proudman et al., 2006). However, cGnRH1 is likely to be releasing hormone of LH.

The hypothalamic control of FSH release remains enigmatic. Neither cGnRH1 nor cGnRH2 appear to be physiological stimuli of FSH release as cGnRH1 or cGnRH2 either evoke only a very small increase in FSH release (Japanese quail: Hattori et al., 1986) or are completely ineffective (chicken: Krishnan et al., 1993; Dunn et al., 2003; Proudman et al., 2006).

30.4.3.2.3 Gonadotropin-releasing hormone receptors and signal transduction

There are two GnRH receptor subtypes in the chickens, namely, GnRHR1 and GnRHR3 with cGnRH2 being more potent cGnRH1 (Joseph et al., 2009). There is much higher expression of GnRHR3 than GnRHR1 in the anterior pituitary gland (chicken: Joseph et al., 2009). There is also expression of both GnRHR3 and GnRHR1 in the median eminence (chicken: Joseph et al., 2009). In the Muscovy duck, GnRHR is expressed in the pituitary gland together with the hypothalamus (Wu et al., 2015).

The actions of cGnRH1 or GnRH2 are mediated by binding to GnRHR and subsequently synthesis of cAMP and inositol phosphate (Bonney and Cunningham, 1977; Joseph et al., 2009).

30.4.3.2.4 Control of gonadotropin-releasing hormone release and synthesis

GnRH1 expression is chiefly located in cell bodies in the preoptic area (Stevenson et al., 2009). GnRH1 is released from neurosecretory terminals in the median eminence in response to stimuli. Neurotransmitters and neuropeptides stimulate or inhibit release of GnRH1 with release stimulated by norepinephrine (chicken: Knight et al., 1982) and neuropeptide Y (chicken: Fraley and Kuenzel, 1993; Contijoch et al., 1992) and inhibited by dopamine (chicken: Knight et al., 1982), β endorphin (chicken: Contijoch et al., 1993), and GnIH (see below).

GnRH-I expression is related to reproductive state being, for instance, greater in sexually mature than immature birds (zebrafinch: Ubuka and Bentley, 2009). In addition, hypothalamic expression of GnRH1 is elevated in photostimulated birds but falls to a very low level in photorefractory birds (starlings: Ubuka et al., 2009). While there is interaction between kisspeptins (Kiss) and its receptor Gpr54 and GnRH neurons in mammals, the Kiss/Gpr54 system appears to be absent in birds based on studies in the chicken and zebra finch (reviewed: Tsutsui et al., 2010; Joseph et al., 2013).

30.4.3.2.5 Changes in hypothalamic gonadotropin-releasing hormone content

The variation in hypothalamic GnRH immunoreactivity and/or expression is consistent with GnRH1 having a role in the control of reproduction in birds. Expression of GnRH in hypothalamus varies during posthatching development (chicken: Chen et al., 2019). In turkeys, hypothalamic cGnRH1 levels are higher in laying hens compared to nonphotostimulated birds (with photostimulated birds intermediate) (Rozenboim et al., 1993). Photostimulation of turkeys resulted in activation (c-fos expression) of cGnRH1 in the nucleus commissura palli and dopamine neurons in the nucleus premammillaris (Thayananuphat et al., 2007). In female chickens when incubating eggs, there is a decrease in hypothalamic expression of cGnRH1 (Dunn et al., 1996) and when young male chickens receive estradiol administration (Dunn and Sharp, 1999). The

number of neurons with cGnRH1 immunoreactivity in the nucleus commissurae pallii is lower in birds rearing chicks than those not rearing chicks (native chickens: Chaiyachet et a., 2013). There is markedly higher cGnRH1 expression in neurosecretory neurons in the preoptic area of the hypothalamus in photostimulated than nonphotostimulated birds (starling: Ukaka et al., 2009). There are effects of long- versus short-daylengths and the presence or absence of sulfamethazine in feed on expression of cGnRH1 expression in the septal–preoptic/anterior hypothalamic area and mid-hypothalamus (chicken: Kang and Kuenzel, 2015).

There are external influences on cGnRH1 expression. Both cGnRH1 and cGnRH1 gene expressions were depressed by rearing chickens in green LED lighting with the effect being lost following pinealectomy (Zhang et al., 2017). Administration of the serotonin synthesis inhibitor, parachlorophenylalanine (PCPA) to old male chickens increased expression of GnRH-I in the hypothalamus (old male chickens: Avital-Cohen et al., 2015). Administration of PRL depressed expression of GnRH-I in the hypothalamus in PCPA-treated birds (old male chickens: Avital-Cohen et al., 2015). Hypothalamic expression of GnRH-I is increased during sexual maturation (chicken: Han et al., 2017) and as birds come into lay (domestic goose: Bhattacharya et al., 2015). Hypothalamic expression of GnRH1 is influenced by exposure to long daylengths and/or treatment with sulfamethazine (2 weeks old chickens: Kang Kang and Kuenzel, 2015).

There are also changes in cGnRH2 in the hypothalamus with reproductive state. The hypothalamic contents of cGnRH2 are increased following photostimulation; they are higher in laying hens, but reduced in incubating and photorefractory birds (domestic turkey: Rozenboim et al., 1993). Similarly, there are more cGnRH2 neurons in breeding than not breeding zebra finches (Perfito et al., 2011).

30.4.3.2.6 Changes in pituitary responsiveness

There are shifts in the responsiveness of pituitary to GnRH with physiological state and due to external influences. For instance, plasma concentrations of LH but not FSH were elevated after GnRH challenge in 5 and 8 weeks old sexually immature females (chicken: Dunn et al., 2003). Moreover, the putative endocrine disruptor, phytosterol, reduced pituitary responsiveness to GnRH-1 and pituitary LH content after GnRH1 challenge (Japanese quail: Qasimi et al., 2018).

30.4.3.2.7 Extrahypothalamic production of gonadotropin-releasing hormone and gonadotropin-releasing hormone receptors

Both GnRH and GnRHR are expressed in the gonads (chicken: Sun et al., 2001). There is expression of GnRHR1 in the small intestine and testes GnRHR3 in the small intestine (chicken: Joseph et al., 2009). In the Muscovy duck, GnRHR is not only expressed in the pituitary gland but also in the ovary (Wu et al., 2015). There is higher expression of GnRH in thecal than granulosa tissue (chicken: Chen et al., 2019). There is evidence that cGnRH1 influences gonadal functioning. For instance, in the presence of cGnRH1, the LH increase in LHR expression in thecal cells is attenuated (chicken: Chen et al., 2019). GnRH immune-reactivity is reported in mast cells in the medial habenular region with the number and distribution of these cells dependent on reproductive behavior, e.g., courtship behavior (ring dove: Silver et al., 1992; Zhung et al., 1993).

30.4.3.3 Gonadotropin-inhibitory hormone

30.4.3.3.1 Chemistry and synthesis

There are three RF amide peptides derived from the GnIH precursor in birds:

1. GnIH 12 amino acids
2. GnIH-related peptide (GnIH-RP)-1
3. GnIH-RP-2

(for structures see Figure 30.5); RFamide peptides having been first identified as hormones in invertebrates. GnIH, GnIH-RP-1, and GnIH-RP2 share a C terminal LPXRF amide motif (where X = L or Q) (Kriegsfeld et al., 2015). GnIH was first isolated from quail brains (Tsutsui et al., 2000). Despite there being structural similarities between GnIH and neuropeptide NF, there are two genes. The existence of separate GnIH and NPNF genes was the result of one of the two gene duplications in early vertebrate evolution chromosome 2 (Tsutsui et al., 2018). The GnIH gene is found on chromosome 2 in chickens (Tsutsui et al., 2018).

30.4.3.3.2 Actions of gonadotropin-inhibitory hormone

GnIH decreases the release of FSH and LH from the avian anterior pituitary gland. Administration of GnIH depressed reproductive functioning in male Japanese quail with testicular atrophy, inhibition of spermatogenesis together with reductions in plasma concentrations of testosterone and LH (Ubuka et al., 2006). In vitro GnIH decreased release of both LH and FSH from pituitary tissue (chicken: Ciccone et al., 2004). GnIH-R co-locates in both gonadotropes exhibiting either LH or FSH (chicken: Maddineni et al., 2008). RNA interference of GnIH influences reproductive behavior (Japanese quail: Ubuka et al., 2013).

The number of GnIH cells in hypothalamus varies through the reproductive cycle with a peak at the beginning of incubation (European starling: Calisi et al., 2016). Hypothalamic GnIH cells are reduced by stress in the Spring but not Fall (house sparrow: Calisi et al., 2008).

FIGURE 30.5 Gonadotropin-inhibitory hormone and related peptides in avian species [Goose-domestic goose (Genbank: KC514473.1), chicken (AB120325.1), Japanese quail (AB120325.1), rock pigeon (MG589638.1), Eurasian tree sparrow (KT351598.1), white-crowned sparrow (AB128164.1), zebra finch (AB522971.1)].

GnIH decreases the synthesis of FSH and LH in the avian anterior pituitary gland. Expression of the common α subunit and LH β are reduced in Japanese quail receiving GnIH in vivo (Ukuka et al., 2006). Similarly, expression of α subunit and FSH β is depressed with GnIH treatment (chicken: Ciccone et al., 2004).

30.4.3.3.3 Gonadotropin-inhibitory hormone receptors

Two putative GnIH receptors have been characterized, albeit partially: GnIHR or RFRPR from chicken pituitary gland and NPFFR from the chicken diencephalon (Ikemoto and Park, 2005). The GnIHR is a G protein-coupled receptor (reviewed: Tsutsui et al., 2018). GnIH-R is expressed in the pituitary gland (Japanese quail and starling: Bentley et al., 2008).

30.4.3.3.4 Hypothalamic gonadotropin-inhibitory hormone content

Hypothalamic GnIH contents vary with reproductive state. Hypothalamic GnIH contents are greater in incubating than laying chickens (Ciccone et al., 2004). Pituitary expression of GnIH-R is greater in sexually immature than mature birds (chicken: Maddineni et al., 2008). Moreover, administration of estradiol and/or progesterone depresses pituitary expression of GnIH-R (see Figure 30.4) (chicken: Maddineni et al., 2008). Employing green light LEDs during growth was accompanied by increases in the number of GnIH-cells of the paraventricularis magnocellularis (chickens: Zhang et al., 2017). Expression of GnIH and GnIHR in the hypothalamus has been reported to be depressed following pinealectomy (chickens: Zhang et al., 2017).

30.4.3.3.5 Extrapituitary expression of gonadotropin-inhibitory hormone

GnIH is expressed in the brain, testes, epididymis, vas deferens, ovaries, and oviduct (Japanese quail and starling: Bentley et al., 2008). Moreover, GnIH-R is expressed in the brain, testes, epididymis, vas deferens, ovaries, and oviduct (Japanese quail and starling: Bentley et al., 2008).

30.4.4 Control of gonadotropin subunit expression

30.4.4.1 Control of common α-subunit expression

Expression of the common LH–FSH–TSH α-subunit changes with physiology: It is not clear whether these changes are isolated to specific cell types. Starvation depresses pituitary expression of the common α subunit of LH, FSH, and TSH (Japanese quail: Kobayashi et al., 2002). Increasing food intake in previously feed-restricted hens is followed by increased α-subunit expression (Ciccone et al., 2007). There appears to be a negative feedback effect on expression of the α-subunit, as this is increased following ovariectomy in chickens, and this effect is reversed by estradiol replacement therapy (Terada et al., 1997). In vivo GnIH reduces pituitary expression of the α-subunit in Japanese quail (Ubuka et al., 2006).

30.4.4.2 Control of follicle-stimulating hormone β-subunit expression

FSH β subunit is expressed in pituitary gland but also in the hypothalamus, ovary, and oviduct and in all four organs,

expression is increased as birds start egg production (domestic goose: Huang et al., 2015). Pituitary expression of FSH β-subunit changes with developmental stage by feedback from the gonadal hormones, and it seems to be affected by the hypothalamus. Chicken embryos as early as day 11 express the FSH β-subunit in their anterior pituitary glands (Grzegorzewska et al., 2009). Pituitary expression of FSH β-subunit is increased during sexual maturation (chicken: Han et al., 2017) but decreased with aging (chicken: Avital-Cohen et al., 2013). Inhibin exerts a negative feedback effect on the expression of the FSH β-subunit in birds. Turkeys immunized against inhibin show increased pituitary FSH β-subunit expression and more small yellow follicles, presumably due to elevated FSH (Ahn et al., 2001).

There is stimulatory central nervous control of FSH β-subunit expression, but the hypothalamic factors participating in birds have not been definitively identified. Evidence for the hypothalamic control comes from the following. Photostimulation is accompanied by increased FSH β-subunit expression (chickens: Li et al., 2009). Early puberty is induced by sulfamethazine with increased pituitary expression of the FSH β-subunit (chickens: Li et al., 2009). Similarly, exposure of two-week-old chickens to long daylengths is followed by increases in the expression of FSH β subunit in the pituitary gland with this effect much greater in birds receiving sulfamethazine treatment (Kang and Kuenzel, 2015). Expression of FSH β-subunits is reduced by starvation in Japanese quail (Kobayashi et al., 2002). Restraint stress is reported to be followed by reduced pituitary expression of FSH β-subunit (zebra finch: Ernst et al., 2016). Administration of the serotonin synthesis inhibitor, PCPA to old male chickens increased pituitary expression of FSH β subunit (old male chickens: Avital-Cohen et al., 2015).

30.4.4.3 Control of luteinizing hormone β subunit expression

Expression of the LH β-subunit is influenced by developmental stage and by hypothalamic and ovarian hormones. Pituitary expression of LH β-subunit is detected as early as day 11 of embryonic development (Grzegorzewska et al., 2009) and increases during sexual maturation (chicken: Han et al., 2017). There is reduced expression of LH β subunits in old versus young males (chicken: Avital-Cohen et al., 2013). GnRH1 increases in vitro pituitary expression of LH β-subunit (turkey: You et al., 1995) while GnIH exerts an inhibitory effect (Japanese quail: Ubuka et al., 2006). Expression of the LH β-subunit is also decreased, in a feedback manner, by ovarian hormones such as estradiol (Terada et al., 1997). PRL decreases expression of the LH β-subunit by turkey pituitary cells in vitro (You et al., 1995). LH β-subunit expression by anterior pituitary cells is elevated by prostaglandin D_2 (PGD2) or PGJ_2, downstream metabolites of prostaglandin-D synthase via a PPAR signaling pathway (Chen et al., 2010).

LH β-subunit expression is reduced by starvation (Japanese quail: Kobayashi et al., 2002), presumably due to decreased stimulation by GnRH1. Administration of PCPA to old male chickens increases expression of LH β subunit in the anterior pituitary gland (old male chickens: Avital-Cohen et al., 2015). Administration of PRL depressed expression of the LH β subunit in the pituitary of PCPA treated or control birds (old male chickens: Avital-Cohen et al., 2015).

30.4.5 Physiological control of gonadotropins

30.4.5.1 Episodic secretion of gonadotropins

There is episodic release of both LH and FSH with, for instance, pulse frequencies of 0.5 per hour for LH and 0.33 pulses per hour for FSH in unrestrained male broiler breeders (Vizcarra et al., 2004).

30.4.5.2 Feedback and gonadotropin release

Sex steroids influence gonadotropin release and synthesis in birds, via direct effect on the anterior pituitary gland or shifts in the release of releasing hormones from the hypothalamus. This is predominantly an inhibitory control. Gonadectomy leads to large increases in the circulating concentrations of both LH and FSH (e.g., Japanese quail: Davies et al., 1980). The inhibitory effect of androgens on LH secretion is mediated via androgen and estrogen receptors (quail: Davies et al., 1980) or predominantly estrogen receptors (chickens: Wilson et al., 1983; Fennell et al., 1990).

In females, estradiol exerts a negative feedback effect on LH secretion. Progesterone can either stimulate or inhibit LH release depending on the state of the bird, with the preovulatory LH surge in the hen induced by progesterone. In the ovariectomized domestic hen, plasma concentrations of LH are decreased by a single injection of either progesterone or estradiol (Wilson and Sharp, 1976a, b). Progesterone has a positive feedback effect on LH release in intact hens or in ovariectomized hens that have been primed with progesterone and estradiol (Wilson and Sharp, 1976a, b). Progesterone receptors are present in the chicken hypothalamus, with increases in immunoreactivity following estradiol administration (Gasc and Baulieu, 1988). Estrogens also induce the presence of progesterone receptors in gonadotropes (LH-producing cells) (Gasc and Baulieu, 1988).

Plasma concentrations of FSH are increased in broiler breeder pullets after ovariectomy (Bruggeman et al., 1998). Pituitary concentrations of both LH and FSH are depressed by estradiol in 5 and 8 weeks old sexually immature

females (chicken: Dunn et al., 2003). The ability of GnRH to elevate plasma concentrations of LH was abolished after estradiol treatment (chicken: Dunn et al., 2003).

30.4.5.3 Seasonal breeding (photoperiod, temperature, and rainfall)

It is critically important for wild birds to reproduce at a time when the offspring will have high-feed availably. Daylength is an excellent predictor of most advantageous season for breeding particularly in the temperate zone. Increasing daylengths increase LH and FSH secretion in temperate-zone birds (Japanese quail: Follett and Maung, 1978; Henare et al., 2011; starlings: Dawson et al., 1985). As little as one long day of increased daylength, there is increased release of LH and FSH (e.g., Japanese quail: Follett, 1978) together with expression of FSH β-subunit (great tit: Perfito et al., 2012). Light is detected by a photopigment, vertebrate ancient opsin, found in the avian hypothalamus (Nakane et al., 2010; Davies et al., 2012). Reproduction is induced when light coincides with the photoinducible phase; the latter being due to "clock genes." For instance, there are shifts in hypothalamic expression of PER2 gene (period circadian regulator 2) during the day (great tit: Perfito et al., 2012). The role of the pars tuberalis in photoperiodism is discussed in Section 30.9.1.

Reproduction is similarly induced by long daylengths in poultry (chickens, turkeys, and ducks). For instance, sexual development is induced by increasing photoperiod (broiler breeder chickens: Onagbesan et al., 2006). There are peaks in the plasma concentrations of LH and FSH at about 20 weeks of age, but these increases can be delayed by feed restriction (broiler breeder chickens: Onagbesan et al., 2006). There are also age-related effects with plasma concentrations of LH increased after transfer from short to long daylengths in eight weeks old but not 5 weeks old sexually immature females (chicken: Dunn et al., 2003).

Temperature is an environmental cue for timing reproduction, with low temperatures slowing the photoperiodic induction of reproduction (Wingfield et al., 2003; Visser et al., 2009). Increasing temperature accelerates the timing of reproduction (great tits: Silverin et al., 2008; Schaper et al., 2012). Conversely, very high temperatures reduce reproductive success (Cruz-McDonnell and Wolf, 2016). In arid-regions, reproduction is induced by the rainfall or, specifically, first rainfall (e.g., blue cranes: Altwegg et al., 2009; sociable weavers: Mares et al., 2017; zebra finch: Zann et al., 1995). Availability of water also increases the photoperiodic response in song sparrows (Wingfield et al., 2012). The importance of supplementary environmental cues becomes progressively more important at lower latitudes (Silverin et al., 2008).

30.4.5.4 Preovulatory luteinizing hormone surge

Plasma concentrations of LH are increased 4–6 h prior to ovulation (chicken: Furr et al., 1973; turkey: Liu et al., 2001; Liu et al., 2004) (also see Figure 30.4). The preovulatory LH surge has been related to the scotophase (e.g., turkeys: Yang et al., 2000). The preovulatory LH surge is provoked by progesterone in the presence of estrogen priming (Wilson and Sharp, 1976a, b). There are increases in the expression of GnRHR in the chicken anterior pituitary gland during the ovulatory cycle (Lovell et al., 2005) (Figure 30.4). Moreover, in immature hens treated with progesterone in the presence of estradiol, there are marked decreases in the expression of GnIH (Lovell et al., 2005). There is little change in the circulatory concentrations of FSH during the ovulatory cycle of the hen (Scanes et al., 1977; Krishnan et al., 1993; Lovell et al., 2005).

30.4.5.5 Nutrition and gonadotropin release

Nutrition influences gonadotropin release in birds. Plasma concentrations of LH but not FSH were depressed by starvation (Japanese quail: Kobayashi et al., 2002). Plasma concentrations of LH and FSH are depressed in broiler breeder pullets (16-week-old) or ovariectomized pullets subject to feed restriction (Bruggeman et al., 1998). Similarly, plasma concentrations of LH are very low in male chickens on a protein deficient diet (Buonomo et al., 1982).

30.4.6 Pituitary origin of gonadotropins

Based on studies in the chicken, avian gonadotropes seem to contain either LH or FSH (Proudman et al., 1999). The gonadotropes containing LH are considerably more numerous than the gonadotropes containing FSH (Proudman et al., 1999). Gonadotropes containing either LH or FSH are found in both the cephalic and caudal lobes of the anterior pituitary gland, particularly in the periphery (Proudman et al., 1999; McFarlane et al., 2011). Most gonadotropes producing LH also express the estrogen receptor α, while some also express the androgen receptor (Sun et al., 2012). FSH-producing gonadotropes express also betaglycan, the type 3 receptor for TGFβ and an accessory receptor for inhibin (chicken: Sweeney and Johnson, 2005).

FSH-producing gonadotropes are first observed on day seven while LH-producing gonadotropes are observed on day eight (chicken embryo: Maseki et al., 2004).

30.5 Thyrotropin

The genes for both *TSH* and the *TSHR* are located on chromosome 26 in chickens.

30.5.1 Thyrotropin subunits, genes, mRNA, and glycoproteins

Avian TSH is a heterodimer consisting of α- and β-subunits. Ostrich TSH has been purified and is a glycoprotein (Papkoff et al., 1982). The avian TSH β-subunit has been characterized based on the sequence of the cDNA (e.g., chicken: Gregory and Porter, 1997; Kato et al., 1998; domestic and mule duck: Hsieh et al., 2007; chuck-will's-widow: Genbank XM_010163622; crested ibis: AB089501.1; mallard: NM_001310425.1; yellow-throated sandgrouse: XM_010077796).

30.5.2 Actions of thyroid-stimulating hormone

30.5.2.1 Role

TSH stimulates the avian thyroid glands to increase in size (Robinson et al., 1976) and to release thyroxine (T_4). Injections of TSH are followed by increases in circulating concentrations of T_3 and T_4 (chickens: MacKenzie, 1981; Williamson and Davison, 1985; doves and Japanese quail: McNichols and McNabb, 1988) (see Figure 30.6). It is likely that TSH is directly increasing release of T_4 from the thyroid but only indirectly increasing circulating concentrations of T_3 as thyroid concentrations of T_3 are very low (McNichols and McNabb, 1988), and T_4 is readily converted to T_3 in the periphery (Decuypere et al., 1988).

30.5.2.2 Thyroid-stimulating hormone receptors

TSH acts by binding to TSHRs; these being linked to adenylate cyclase via G-proteins. The TSHR has been characterized in poultry species (e.g., chicken: Grommen et al., 2006) and wild birds (e.g., willow flycatcher: XM_027904358.1). In many birds, there are multiple TSHR transcript variants. TRHR is expressed in follicular cells of the avian thyroid and, in addition, the brain, pituitary gland, pineal, and retina (chicken: Grommen et al., 2006).

TSH increases cAMP release from thyroid tissue in vitro (chicken: Tonoue and Kitch, 1978) and elevates the thyroid cAMP content in vivo (Japanese quail: McNichols and McNabb, 1988).

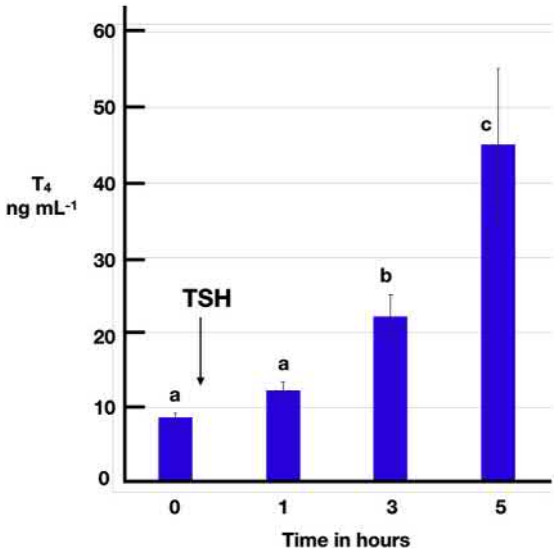

FIGURE 30.6 Effect of thyroid-stimulating hormone on the plasma concentrations of T_4 in chickens in vivo. *Data from MacKenzie, D.S., 1981. In vivo thyroxine release in day-old cockerels in response to acute stimulation by mammalian and avian pituitary hormones. Poult. Sci. 60, 2136–2143.*

30.5.3 Thyroid-stimulating hormone receptor and domestication

The TSHR has been proposed as a domestication locus with a domestic (a missense mutation from glycine to arginine) and wild-type allele (Rubin et al., 2010; Karlsson et al., 2015). The domestic allele is found in domesticated chickens (Karlsson et al., 2015). Male chickens homologous domestic allele exhibit less fear-related behaviors and reduced circulating concentrations of T_4 (Karlsson et al., 2015).

30.5.4 Control of thyroid-stimulating hormone release and subunit expression in the anterior pituitary gland

30.5.4.1 Thyrotropin-releasing hormone and thyroid-stimulating hormone release and subunit expression

The release of TSH from the anterior pituitary gland is under hypothalamic control by at least four releasing hormones or putative releasing hormones: (1). stimulators: thyrotropin-releasing hormone (TRH) or thyroliberin, corticotropin-releasing hormone (CRH), and GCGL and (2). inhibitors: somatostatin (SS or SRIH)

30.5.4.1.1 Thyrotropin-releasing hormone

The structure of TRH is the following:

Pyro-glutamyl-histidyl-proline-amide [pQHP-NH_2] (Bøler et al., 1969)

ProTRH is synthesized as prepro-TRH (see Figure 30.7). The signal peptide is then removed to form proTRH. There are five KRQHPGKR motifs in avian proTRH (e.g., chicken NM_001030383.2) together one other similar motif (KHQHPGRR). These are proteolytically cleaved to yield octapeptides (KHQHPGRR) followed by clipping off the flanking dibasic amino acid residues and then TRH-Gly is then converted to TRH (see Figure 30.7).

TRH stimulates release of TSH from avian pituitary tissue (chicken: Scanes, 1974; Huang et al., 2014) and, also, increases expression of TSH β subunits (duck: Hsieh et al.,

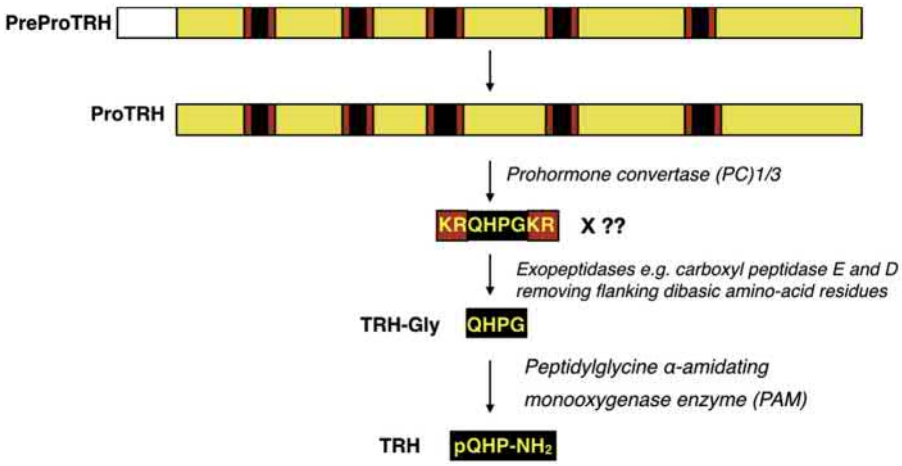

FIGURE 30.7 Synthesis of thyrotropin-releasing hormone. *Based on Nillni, E.A., 2010. Regulation of hypothalamic thyrotropin releasing hormone (TRH) neuron by neuronal and peripheral inputs. Front. Neuroendocrinol. 31, 134–156.*

2007; chicken: Huang et al., 2014). The structure of TRH receptor has been deduced from cDNA in poultry (e.g., chicken: NM_204930.1; domestic duck: XM_005022942.4) and wild birds (burrowing owl: XM_026843473.1; emperor penguin: M_009281974.1; emu: XM_026099712.1; willow flycatcher: XM_027905759.1).

TRH is expressed in the avian brain (nucleus preopticus periventicularis, nucleus preopticus medialis, regio lateralis hypothalami, paraventricular nucleus, nucleus periventricularis hypothalamic, and nucleus ventromedialis hypothalami (chicken: Aoki et al., 2007).

30.5.4.2 Corticotropin-releasing hormone and thyroid-stimulating hormone release and subunit expression

CRH induces TSH release from avian thyrotropes acting via CRH receptor type 2 (chicken: De Groef et al., 2003a; zebra finch: Watanabe et al., 2018).

30.5.4.3 Glucagon-like peptide and thyroid-stimulating hormone release and subunit expression

GCGL receptors are expressed in the cephalic lobe of the chicken anterior pituitary gland as are TSH β subunits (Huang et al., 2014). GCGL stimulates release of TSH and GH from chicken pituitary tissue together with elevating expression of GH and TSH β subunits (Huang et al., 2014).

30.5.4.4 Somatostatin and thyroid-stimulating hormone release

There is also inhibitory control of TSH release. Somatostatin depresses TSH release (chicken: Geris et al., 2003) acting via somatostatin receptors (SSTRs) type 2 and 5 (chicken: De Groef et al., 2003b; Geris et al., 2003).

30.5.4.5 Negative feedback

T_3 exerts a negative feedback effect on TSH release in birds. This is supported by the ability of goitrogens to increase thyrotrope numbers (Sharp et al., 1979). Moreover, T_3 or T_4 inhibits expression of TSH β subunit (chicken: Gregory and Porter, 1997; Gregory et al., 1998; duck: Hsieh et al., 2007).

30.5.4.6 Environmental factors and thyroid-stimulating hormone release

It is assumed that cold evokes a rapid increase in TSH release in birds. The absence of validated assays for TSH has restricted direct examination of this. However, circulating concentrations of T4 are increased with cold exposure (Japanese quail: Herbute et al., 1984). This is likely to be mediated by TRH as cold stress increases expression of prepro-TRH in the hypothalamus (chicken: Wang and Xu, 2008).

30.5.5 Control of thyroid-stimulating hormone β-subunit expression

As might be expended, releasing factors and thyroid hormones influence expression of the TSH β-subunit with pituitary expression increased by TRH in pituitary tissue in vitro (duck: Hsieh et al., 2007) (see Figure 30.8). Moreover, thyroid hormones inhibit expression of the TSH β-subunit with either T_3 or T_4 suppressing pituitary expression in vitro (chicken: Gregory and Porter, 1997; duck: Hsieh et al., 2007). Hypothyroidism increases expression of the TSH β-subunit by goitrogen-treatment (Japanese quail: Catena et al., 2003). In addition, glucocorticoids such as corticosterone depress expression of the

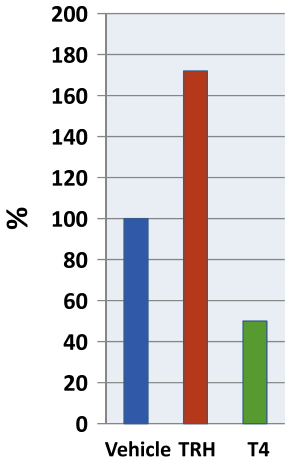

FIGURE 30.8 Effect of thyrotropin-releasing hormone and thyroxine (T_4) on the expression of thyroid-stimulating hormone β-subunit by duck anterior pituitary tissue in vitro. *Data from Hsieh, Y.L., Chowdhury, I., Chien, J.T., Chatterjee, A., Yu, J.Y., 2007. Molecular cloning and sequence analysis of the cDNA encoding thyroid-stimulating hormone beta-subunit of common duck and mule duck pituitaries: in vitro regulation of steady-state TSH beta mRNA level. Comp. Biochem. Physiol. B 146, 307–317.*

TSH β-subunit in duck pituitary tissue in vitro (Hsieh et al., 2007). There is no change in the expression of the TSH β -subunit with starvation in Japanese quail (Kobayashi et al., 2002; Kobayashi and Ishii, 2002).

Pituitary expression of TSH β subunit is increased following exposure to long daylengths in two weeks old chickens (Kang and Kuenzel, 2015). Studies in mule ducks (a hybrid of male Muscovy ducks and female domestic ducks) indicate preferential transcription of the TSH β-subunit from the maternal genome (Hsieh et al., 2007).

30.5.6 Origin of thyroid-stimulating hormone

30.5.6.1 Anterior pituitary gland

The thyrotropes, the cells producing TSH, are located almost entirely in the cephalic (or rostal) lobe of the anterior pituitary gland (Figure 30.1) based on studies immunocytochemistry with antisera to TSH β subunit (Sharp et al., 1979). Thyrotropes represent between 2% and 6% of the anterior pituitary cells (ring doves: Reichert, 1993). Some thyrotropes express androgen receptors (Sun et al., 2012), but the interactions between androgen and TSH secretion are not well-established. (Pars tuberalis TSH is discussed below).

30.5.6.2 Extrapituitary thyroid-stimulating hormone

There is evidence of extrapituitary TSH in birds with TSH β subunit immunoreactivity in various organs in the embryo. In chick embryos, TSH β subunit immunoreactivity has been reported in multiple tissues including the following: crop, diencephalon and mesencephalon, neural ganglia, trigeminal nerve, ependymal cells lining the spinal canal (and diocoele and mesocoele), hepatocytes, linings of the proventriculus, bronchial ducts, pleural and pericardial cavities, and trunk epidermal cells (Murphy and Harvey, 2001, 2002).

30.5.7 Ontogeny of thyroid-stimulating hormone

TSH and TRH are detectible in, respectively, the pituitary gland and hypothalamus by day six of embryonic

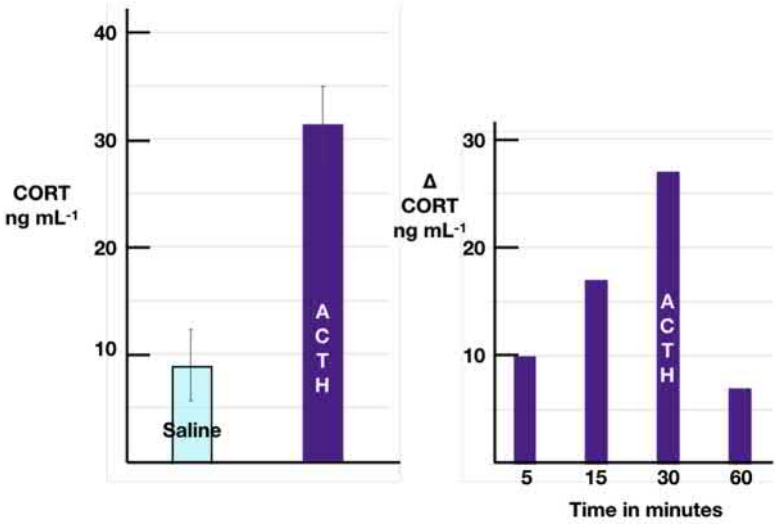

FIGURE 30.9 Effect of adrenocorticotropic hormone (ACTH) challenge on circulating concentrations of corticosterone in birds. Left: Effect of ACTH challenge or saline nestling northern mockingbirds. Right: Increase in plasma concentrations of corticosterone in young chickens after ACTH challenge. *Data from Sims, C.G., Holberton, R.L., 2000. Development of the corticosterone stress response in young northern mockingbirds (*Mimus polyglottos*). Gen. Comp. Endocrinol. 119, 193–201, Post, J., Rebel, J.M.J., ter Huurne, A.A.H.M., 2003. Physiological effects of elevated plasma corticosterone concentrations in broiler chickens. An alternative means by which to Assess the physiological effects of stress. Poult. Sci. 82, 1313–1318.*

development (chicken: Thommes et al., 1983, 1985). Expression of TSH β subunit is first reported on day 11 with marked increases in late embryonic development (chicken: Gregory et al., 1998; Ellestad et al., 2011).

30.6 Growth hormone

30.6.1 Growth hormone gene, mRNA, and protein

The chicken GH gene consists of five exons and four introns encoding a 217 amino acid residue protein (Tanaka et al., 1992b) and is located in the G-band region 1q4 of chromosome 1 (Shaw et al., 1991). The promoter region includes a binding site for the pituitary-specific transcription factor, GHF-1/Pit-1 (Tanaka et al., 1992). The GH gene encodes a 217 amino acid residue protein consisting of a signal peptide and GH (Tanaka et al., 1992a). The structure of pre-GH has been determined from multiple avian species (e.g., emu: Genbank: XM_026099439.1; mallard: NM_001310345; Anna's hummingbird: XM_008502276; Adelie penguin XM_009326511; burrowing owl: XM_026864712.1; rifleman XM_009080681.1; Zebra finch: Arai and Iigo, 2010). There are two GH genes in the order *Passeriformes*, respectively, GH1A and GH1B (Yuri et al., 2008; Arai and Iigo, 2010). These resulted from gene duplication with Yuri et al. (2008) concluding that the "*duplication occurred in the ancestral lineage of extant passerines.*" Both GH1A and GH1B are expressed in the pituitary gland with GH1A also expressed in multiple tissues while GH1B is also expressed in erythrocytes and specific brain regions (Arai and Iigo, 2010).

30.6.2 Post-translational variants of growth hormone

There are charge and size variants of GH. Unlike the situation with human GH where there is a splicing variant, variants of avian GH are post-translational modifications. There are reports of glycosylated GH (Berghman et al., 1987), phosphorylated GH (Arámburo et al., 1990, 1992), a cleaved 15 Da GH (Arámburo et al., 2001), and dimeric and other oligomeric forms (Houston and Goddard, 1988) in the chicken.

There is evidence that the release of GH variants is differentially controlled. There are shifts in the ratio of variants during growth and with growth hormone–releasing hormone (GHRH) (chicken: Arámburo et al., 2000; Martínez-Coria et al., 2002). In addition, the ratio of glycosylated to nonglycosylated GH varies during growth (chicken: Berumen et al., 2004).

30.6.3 Actions of growth hormone

Studies on the role of GH being conducted predominantly on one species—the domesticated chicken. The effects of GH have been reported on hepatocyte gene expression comprehensively (chicken Wang et al., 2014).

30.6.3.1 Growth hormone and growth

The available evidence supports GH having some role in permitting birds to achieve their optimal growth rates. Growth is reduced by ~50% following hypophysectomy in chicks (King and Scanes; Kusnik et al., 2008). In contrast, hypophysectomy was reported to either have no effect (Proudman and Opel., 1990a) or reduce growth by ~30% (Proudman et al., 1994). The effect of hypophysectomy is partially overcome by GH replacement therapy in young chickens (King and Scanes; Scanes et al., 1986) but not turkeys (Proudman et al., 1994). In young intact birds, GH does not increase growth more than transiently (chickens: Leung et al., 1986; Burke et al., 1987; Cogburn et al., 1989; turkeys: Proudman et al., 1994). In mid-growth, pulsatile administration of GH was reported to increase growth (Vasilatos-Youngen et al., 1988). In contrast, in ovo administration of GH is followed by increased body weights, skeletal growth, and adipocyte size (chicken: Hargis et al., 1989). There is some evidence that polymorphisms in GH are associated with differences in overall growth (Anh et al., 2015 but not in Yan et al., 2003) and muscle growth (Yan et al., 2003). However, there were no effects differences in plasma concentrations of GH in faster than slower growing broiler chickens (Xiao et al., 2017).

30.6.3.1.1 Growth hormone and insulin-like growth factor 1

Circulating insulin-like growth factor 1 (IGF-1) is controlled by GH. In young birds, plasma concentrations of IGF-1 are reduced following hypophysectomy and partially restored by GH treatment (chickens: Huybrechts et al., 1985; turkeys: Proudman et al., 1994). Moreover, there were elevated plasma concentrations of IGF1 in intact young chickens receiving GH treatment and exhibiting increased growth (Vasilatos-Youngen et al., 1988). Both pulsatile and continuous administration of GH increased hepatic expression of IGF-1 (young chickens: Rosselot et al., 1995). Chronic administration of GH to adult chickens is followed by increased plasma concentrations of IGF-1 (males: Radecki et al., 1997; females: Scanes et al., 1999).

In vitro, GH increases IGF-1 release from avian hepatocytes, particularly in the presence of insulin (chicken: Houston and O'Neill, 1991). Plasma concentrations of both GH and IGF-1 are elevated posthatch when eggs are incubated under monochromatic green light than in darkness (chicken: Zhang et al., 2014). Plasma concentrations of IGF-1 are higher in faster than slower growing broiler chickens (Xiao et al., 2017). Myogenic growth is positively related to expression of IGF-1 or IGF1R (chickens: Davis et al., 2015).

30.6.3.1.2 Other mechanisms controlling insulin-like growth factor 1

There are other controls on expression of IGF-1 in muscles with acute exercise increasing expression of IGF-1 (white-throated sparrows and European starlings: Price et al., 2011). Moreover, exogenous glucocorticoids reduce circulating concentrations of IGF-1 (chicken: Leili and Scanes, 1998). There are relationships between prefledging plasma concentrations of IGF-1 and feather corticosterone in decreased broods (positive) and increased broods (negative) (great tits: Lodjak et al., 2016). Circulating concentrations of IGF-1 are decreased by capture handling stress but are not influenced by corticosterone administration (bearded reedlings: Tóth et al., 2018).

30.6.3.2 Growth hormone and lipid metabolism

GH exerts effects on lipid metabolism in birds. Growth hormone receptors (GHRs) are expressed in adipose tissue (chicken: Hausman et al., 2012). Administration of GH to chickens can influence the amount of adipose tissue, with the direction of the effect influenced by the mode of administration. For instance, body fat is decreased by pulsatile administration of GH (see Table 30.6) (Vasilatos-Younken et al., 1988; Rosebrough et al., 1991). In contrast, intravenous infusion of chicken GH (either pulsatile or continuous) was followed by increased body fat in male chickens (Moellers and Cogburn, 1995) as did subcutaneous injections of GH (Cogburn et al., 1989). In some studies, there were no effects of infusions of chicken GH on abdominal fat pad weights (Cravener et al., 1989; Moellers and Cogburn, 1995; Scanes et al., 1999).

Lipolysis can be influenced by GH. Acutely in vivo, GH increases circulating concentrations of nonesterified fatty acids acutely (chickens: Hall et al., 1987; Scanes, 1992; hypophysectomized ducks: Foltzer and Mialhe, 1976) but was without an effect in intact or hypophysectomized young turkeys (Proudman et al., 1994). GH stimulates in vitro lipolysis by avian adipose explants was reported to be increased in the presence of native and biosynthetic chicken and mammalian GH (chickens, turkeys, and pigeons: Harvey et al., 1977; adult male chicken: Campbell and Scanes, 1985) but not by reptilian and fish GH (Campbell et al., 1991). The effect of GH is blocked by a GH antagonist (chicken: Campbell et al., 1993) or by inhibitors of protein or RNA synthesis (chicken: Campbell and Scanes, 1988). In addition, GH exerts an effect on avian adipose that is analogous to the insulin-like effect of GH in mammals. Glucagon or cAMP-stimulated lipolysis in vitro by chicken adipose tissue explants is reduced in the presence of GH irrespective of whether of avian, mammalian, reptilian, or piscine origins (Campbell and Scanes, 1987; Campbell et al., 1991) and of a GH antagonist. The antilipolytic effect of GH was not influenced by inhibitors of protein or RNA synthesis (Campbell and Scanes, 1988). There has been GH influences lipogenesis in birds with the predominant effect being inhibitory. GH per se increases hepatic lipid biosynthesis (Cupo and Cartwright, 1989). GH suppressed insulin-stimulated synthesis of fatty acids by chick hepatocytes in vitro (Harvey et al., 1977). Similarly, GH depressed IGF-1 stimulated lipogenesis (Cupo and Cartwright, 1989). Moreover, pulsatile GH administration to young pullets in vivo reduced hepatic lipogenesis (see Table 30.6) (Rosebrough et al., 1991). The effect of GH on lipogenesis may be direct or due to the increase in plasma concentrations of T_3 (see below GH and thyroid hormones) with elevated T_3 depressing lipogenesis (Rosebrough et al., 1992). There were marked effects of GH treatment in vitro on the expression of genes related to lipid metabolism in hepatocytes (chicken: Wang et al., 2014).

30.6.3.3 Growth hormone and carbohydrate metabolism

There is some evidence that GH influences carbohydrate metabolism. A single injection of recombinant chicken GH was followed by increased plasma concentrations of glucose (chicken: Hall et al., 1987). However, in other studies, there were no effects of GH on glucose metabolism (e.g., Scanes et al., 1999).

30.6.3.4 Growth hormone and thyroid hormones

There are marked effects of GH on circulating concentrations of the thyroid hormone, triiodothyronine (T_3). It is not established whether GH influences thyroxine (T_4) release from the avian thyroid (chicken: MacKenzie, 1981). In young chicks, GH increases the circulating concentration of T_3 (Kuhn et al., 1985). This is due to GH reducing both the activity of hepatic type 3 monodeiodinase (the catabolic

TABLE 30.6 Effect of growth hormone on lipid metabolism in chickens (data are expressed as % of control ± SEM).

Parameter	Control	Continuous growth hormone	Pulsatile growth hormone	Reference
Abdominal fat pad	100 ± 6.9^a	90.0 ± 13.8^a	67.5 ± 7.0^b	Rosebrough et al. (1991)
Hepatic lipogenesis	100 ± 11.2^a	96.9 ± 23.2^a	18.7 ± 5.2^b	Rosebrough et al. (1991)
Plasma T_3	100 ± 11.8^a	152.9 ± 17.6^b	200.0 ± 17.6^b	Rosebrough et al. (1991)

^{a,b}Different superscript letters indicate difference $P < .05$.

enzyme metabolizes T_3 to T_2; Darras et al., 1992, 1993) and the expression of this deiodinase (Van der Geyten et al., 1999). This is a physiological effect of GH as type 3 monodeiodinase is elevated following hypophysectomy and partially restored to normal by GH replacement therapy (Darras et al., 1993).

30.6.3.5 Growth hormone and immune functioning

Immune functioning is influenced by GH. This appears to be due to both pituitary derived GH and to GH synthesized in immune tissues (discussed under extrapituitary GH). Thymus weights are decreased following hypophysectomy with this being partially overcome by GH replacement therapy (chicken: King and Scanes, 1986; Johnson et al., 1993). Administration of chicken GH to hypophysectomized chicks was followed by increased percentage of CD4+ peripheral blood lymphocytes (chicken: Johnson et al., 1993). Moreover, GH increases bursa weights in hypophysectomized birds also receiving T_3 (chicken: Scanes et al., 1986). In addition, GH increases proliferation of peripheral blood T cells to a mitogenic challenge in obese chicks (Marsh et al., 1992).

30.6.3.6 Growth hormone and reproduction

There is evidence that GH influences reproduction in females with polymorphisms in GH being associated with differences in egg production (chicken: Makhsous et al., 2013; Su et al., 2014). There is both GHR expression and immune-reactive GHR along the length of the oviduct, in the magnum, isthmus, and shell gland together with some in the infundibulum (chicken: Hrabia et al., 2013). Moreover, GHR is expressed in the ovary, particularly the F4 and F5 large yellow follicles (chicken: Ahumada-Solórzano et al., 2012). Administration of GH was also associated with increases in the plasma concentrations of progesterone, testosterone, and estradiol (fasted chickens: Socha et al., 2017).

Direct effects of GH on both ovarian and oviductal functioning have been reported. There is increased production of progesterone in the presence of GH from granulosa cells (Ahumada-Solórzano et al., 2012) or large yellow follicles (Hrabia et al., 2014a) incubated in vitro. In addition, GH stimulates proliferation of granulosa cells as well as increasing IGF-1 release from these cells in the ovary (chickens: Ahumada-Solórzano et al., 2016).

There are multiple effects of GH on oviductal functioning with increased weight, reduced apoptosis, and gene expression (Table 30.7) (sexually immature chickens: Hrabia et al., 2014b). Moreover, in fasted hens, GH administration increased magnum expression of progesterone receptor, estrogen receptor α, and avidin (chickens: Socha et al., 2017). Despite GH having no effect on overall egg production, some improvements in shell-thickness were noted (chicken: Donoghue et al., 1990).

What is not clear is whether GH acting on the ovary and/or oviduct is hormonal with GH from the pituitary or locally produced GH acting in a paracrine manner with GH being expressed in the ovary, particularly the F4 and F5 large yellow follicles (chicken: Ahumada-Solórzano et al., 2012).

30.6.3.7 Growth hormone and adrenocortical hormones

There is evidence that GH can influence the avian adrenal cortex stimulating production of corticosterone. Plasma concentrations of corticosterone are acutely increased following administration of recombinant chicken GH (Cheung et al., 1988) or chronically following continuous administration of native chicken GH (Rosebrough et al., 1991). There are shifts in in vitro corticosteroidogenesis in adrenal cells from hypophysectomized chicks or hypophysectomized chicks receiving GH administration (Carsia et al., 1985).

30.6.3.8 Growth hormone and apoptosis

GH reduces apoptosis of bursal lymphocytes cells in vitro (chicken: Luna-Acosta et al., 2015) and oviductal cells in vivo (Hrabia et al., 2014b). Similarly, GH has a neuroprotective role reducing apoptosis of retinal ganglion cells induced by glutamate (Japanese quail: Martínez-Moreno et al., 2016).

30.6.3.9 Growth hormone receptors and Signal Transduction

The GHR is a member of the class I cytokine receptor superfamily. Chicken GHR cDNA has been sequenced (Burnside et al., 1991). As with the mammalian GHR, the chicken GHR consists of three domains: an extracellular domain, a single transmembrane domain, and an intracellular domain. Binding of GH leads to receptor dimerization and activation JAK-2 and then STAT1, STAT3, and STAT5 signaling. In addition, GH binding to the GHR activates Src family kinase signaling pathway independently of JAK2 (reviewed: Dehkhoda et al., 2018). The amino acid sequence of avian GHR has been deduced from cDNA in Muscovy ducks (Ji et al., 2016) and other birds (burrowing owl: XM_026865892.1; collared flycatcher: XM_005060581.2; Okarito brown kiwi: XM_XM_026062927.1; rock pigeon: U20353.1). Incubation of chicken hepatocytes with GH resulted in shifts in expression of genes are proteins in the STAT and MAPK pathways (Wang et al., 2014).

The GHR gene is expressed in multiple tissues in birds including the liver, skeletal muscle, adipose tissue, hypothalamus, extrahypothalamic brain tissues, thymus,

spleen, and bursa (chicken: Hull and Harvey, 1998; Mao et al., 1998; young Muscovy duck: Ji et al., 2016). There are shifts in hepatic expression of GHR during growth and development being high in late embryonic development, decreasing at hatch and then rising (chicken: Burnside and Cogburn, 1992; Mao et al., 1997; Wu et al., 2011). GH downregulates expression of GHR in the liver, thymus, bursa, spleen, and brain (Hull and Harvey, 1998). Similarly, GH binding to liver membranes is increased following hypophysectomy and depressed by GH replacement therapy (Vanderpooten et al., 1991). Moreover, there is high correlation between GH and GHR expression in skeletal muscles in Muscovy ducks (Ji et al., 2016). Expressions of both GHR and IGF-1 are depressed with heat stress in both liver and muscle (Japanese quail: Gasparino et al., 2013). Muscle expression of GHR is also elevated with cold stress (Japanese quail: Gasparino et al., 2013). A single nucleotide polymorphism (SNP) in the GHR gene is associated with growth and fat deposition (chicken: Ouyang et al., 2008).

Sex-linked dwarf chickens exhibit reductions in growth together elevated plasma concentrations GH together with reduction in the plasma concentrations of both T_3 (Scanes et al., 1982) and IGF-1 (Huybrechts et al., 1985). The lesion in sex linked dwarf chickens is a mutation in the GHR leading to GHR malfunctioning (Burnside et al., 1991, 1992).

30.6.3.10 Growth hormone binding protein

There are specific GH binding proteins (GHBPs) in the circulation of birds (chicken e.g., Tobar-Dupres et al., 1993). GHBP is generated by alternative splicing of the GHR gene transcript (chicken: Bingham et al., 1994; Hull et al., 1999) and/or proteolytic cleavage of GHR (Vleurick et al., 1999).

30.6.4 Control of growth hormone release

30.6.4.1 Introduction

Release of GH from the avian pituitary gland is under hypothalamic control with multiple stimulatory-releasing hormones including GHRH, ghrelin, neuropeptide W, TRH, and the inhibitory releasing hormone (SS). In addition, there are neuropeptides that stimulate GH release and/or somatotropes and that are putative releasing hormones. Examples of the later include PACAP and GCGL (Table 30. 3).

30.6.4.2 Growth hormone–releasing hormone

GHRH or somatoliberin is a peptide with 47 amino acid residues. It is synthesized as prepro-GHRH and is cleaved to pro-GHRH and then to GHRH (see Figure 30.10). The structure of GHRH is similar across avian species (see Figure 30.10).

GHRH is expressed in the avian hypothalamus and also in the small intestine, kidneys, lung, ovary, anterior pituitary gland, spleen, and testes (chicken: Wang et al., 2007). There is high expression of GHRH in the embryo day eight, but, subsequently, this declines to a low plateau level on days 12–20 (Wang et al., 2006). GHRH increases GH release in vivo and in vitro (chicken: Scanes et al., 1984). Avian somatotropes respond to GHRH with increased intracellular calcium (chicken: Scanes et al., 2007) (Table 30.7).

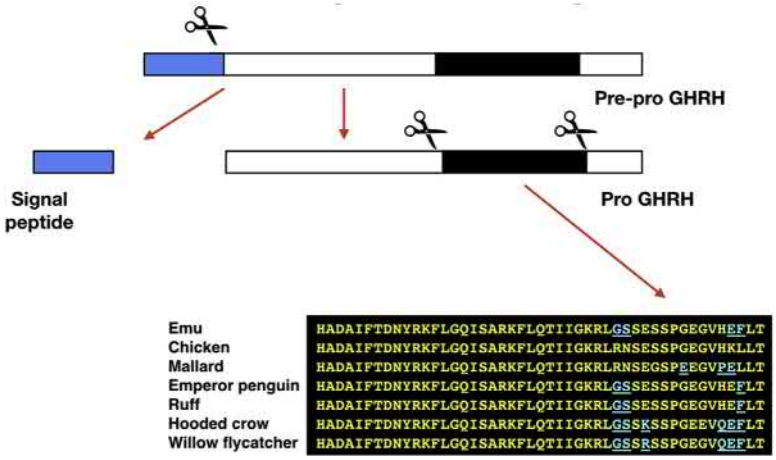

FIGURE 30.10 Processing of prepro-gonadotropin-releasing hormone to pro-gonadotropin-releasing hormone and then gonadotropin-releasing hormone. Also shown is the structures of GHRH in example avian species, namely the following: in the Infraclass *Paleognathae*: Emu (Genbank XM_026093031) and in the Infraclass *Neognathae*: Superorder *Galloanserae*: Order *Galliformes*: Chicken (NM_001040464), Order *Anseriformes*: Mallard (XM_013103655), in the Infraclass *Neoaves*: Order *Sphenisciformes*: E. penguin—Emperor penguin (XM_009275539), Order *Charadriiformes*: Ruff (XM_014941254), Order *Passeriformes*: H. crow—Hooded crow (XM_010397141) and W. flyc—Willow flycatcher (XM_027885084.1). Letters with red font indicate difference from sequence in chicken. Letters with blue font indicate difference from sequence in other birds in the Superorder *Neoaves*.

TABLE 30.7 Effect of chicken growth hormone on the oviduct in young female chickens.

	Control	Chicken growth hormone[a]
Body weight kg	1.50 ± 0.02	1.52 ± 0.02
Oviductal characteristics		
Relative oviduct weight%	0.43 ± 0.11	1.22 ± 0.27[b]
Proliferating cells as % of control	100 ± 3.2	102 ± 3.0
Apoptotic cells as % of control	100 ± 2.8	63 ± 2.3[c]
Expression of ovalbumin in magnum as % of control	100 ± 18	309 ± 68[b]
Expression of ovocalyxin-32 in shell gland as % of control	100 ± 16	703 ± 234[b]

[a]*Chicken GH (200 μg) injected 3 times per week between weeks 12 and 16.*
[b]*Different from control P < .05.*
[c]P < .001.
Calculated from Hrabia, A., Leśniak-Walentyn, A., Sechman, A., Gertler, A., 2014b. Chicken oviduct-the target tissue for growth hormone action: effect on cell proliferation and apoptosis and on the gene expression of some oviduct-specific proteins. Cell Tissue Res. 357, 363–372.

30.6.4.3 Ghrelin/growth hormone secretagogue receptor

30.6.4.3.1 Action and chemistry

Ghrelin stimulates release of GH and increases in intracellular calcium in birds acting via the GH secretagogue receptor (GHS-R) (chicken: Ahmed and Harvey, 2002; Scanes et al., 2007) (Table 30.8). Interestingly, only a minority of somatotropes (about one fifth) respond to ghrelin with increased intracellular calcium (Scanes et al., 2007).

The structure of chicken ghrelin has been deduced (Kaiya et al., 2002). The ghrelin gene is transcribed to form preproghrelin (or preproghrelin/obestatin). This is processed to the ghrelin peptide together with another peptide, obestatin (Figure 30.11). There are marked differences between the sequence of amino acid residues in human and avian ghrelin with chicken ghrelin being 46% different from human ghrelin. Moreover, there are differences between the structures of ghrelin in avian species with, for instance, 23.1%, 34.6%, and 38% differences between chicken and, respectively, ostrich, mallard, and rifleman ghrelins (Figure 30.11). The amino acid sequences of avian obestatins are markedly different from human obestatin but exhibit less amino acid substitutions within the Aves than for ghrelin (Figure 30.11). These differences emphasize the need in experimentation to employ synthesized ghrelin or obestatin identical or at least very similar to that of the species of interest. There is no information on the effects of obestatin on pituitary functioning in birds.

30.6.4.3.2 Growth hormone secretagogue receptor

Ghrelin acts via the GHS-R with avian GHS-R characterized (Japanese quail: Kitazawa et al., 2009). There are at least two forms of GHS-R in the avian anterior pituitary gland: GHS-R1a and GH-SR1c. Expression of these is depressed by ghrelin, GHRH, and corticosterone (chicken: Geelissen et al., 2003). Based on comparison of lines of chickens with three genotypes expressing GHS-R with adjacent SNPs in the GHS-R, there are physiological effects of GHS-R on both GH and growth (El-Magd et al., 2016).

TABLE 30.8 Effects of neuropeptides on the intracellular concentrations in responsive chicken somatotropes

Neuropeptide	% Of somatotropes responding	$\Delta[Ca^{2+}]_i$ Mean ± SEM
Growth hormone–releasing hormone	100	120 ± 6
Thyrotropin-releasing hormone	73	222 ± 16
Ghrelin	21	94 ± 16
PACAP	85	90 ± 14
Leptin	58	83 ± 10

Data from Scanes, C.G., Glavaski-Joksimovic, A., Johannsen, S.A., Jeftinija, S., Anderson, L.L., 2007. Subpopulations of somatotropes with differing intracellular calcium concentration responses to secretagogues. Neuroendocrinology 85, 221–231.

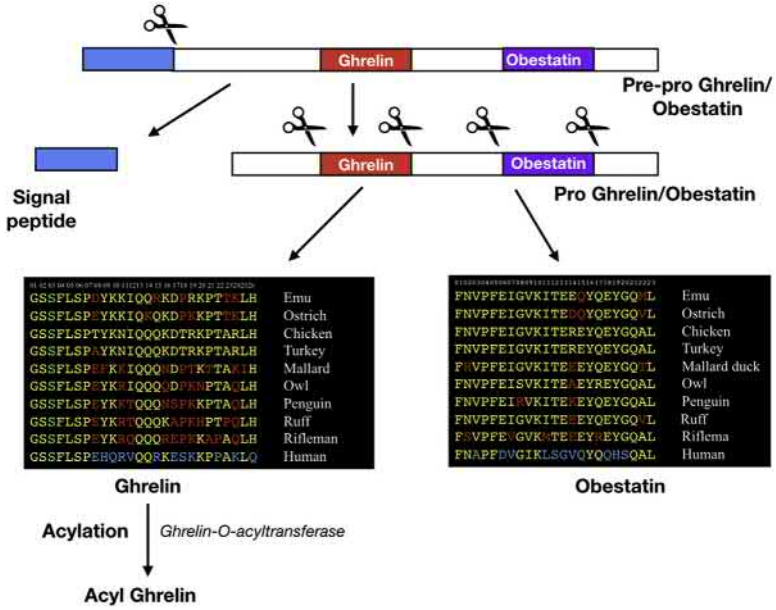

FIGURE 30.11 Synthesis of ghrelin and obestatin from preproghrelin obestatin (preproghrelin). Also shown are the structures of ghrelin and obestatin from poultry and selected wild birds. Subclass *Paleognathae*: Emu (*Dromaius novaehollandiae*) (XM_026099658.1), Ostrich (*Struthio camelus*) (XM_009681128.1), Subclass *Neognathae,* Superorder *Galloanserae*: Order *Galliformes*: chicken (*Gallus gallus*) (AB075215.1), turkey (*Meleagris gallopavo*) (AY497549.1), Order *Anseriformes*: mallard duck (*Anas platyrhynchos*) (XM_027467410.1), Superorder *Neoaves*: Order *Strigiformes*: Owl—burrowing owl (*Athene cunicularia*) (XM_026857822.1), penguin—Order *Sphenisciformes*: Adelie penguin (*Pygoscelis adeliae*) (XM_009320113.1), Order *Charadriiformes*: Ruff (*Calidris pugnax*) (XM_014946895.1), Order: *Passeriformes*: rifleman (*Acanthisitta chloris*) (XM_009082274.1), and human (AB029434.1). *Red letters* indicate difference with chicken ghrelin or obestatin, *blue letters* indicate where human ghrelin or obestatin differs from chicken ghrelin or obestatin. Light green indicates site of acylation (with octanyl) in ghrelin.

30.6.4.3.3 Extrapituitary actions of ghrelin

There is abundant evidence that ghrelin has effects on nonpituitary tissues including the gastrointestinal tract with ghrelin synthesis and demonstrated effects (duck: Shao et al., 2010; chicken: Kitazawa et al., 2017), bursa Fabricius with ghrelin, ghrelin-o-acyltransferase, and GHS-R expression (chicken: Yu et al., 2019), and central nervous system. For instance, there is evidence that ghrelin exerts effects with the hypothalamus. For instance, expression of ghrelin and GHS-R in the hypothalamus differs in lines of chickens with high or low-residual feed intake (Sintubin et al., 2014; Gastón et al., 2015).

30.6.4.4 Neuropeptide W

Chicken neuropeptide W (NPW) 23 but not NPB28 inhibits GHRH induced release of GH from chicken pituitary cells (Bu et al., 2016). There is high expression of NPW and NPBWR1 in the hypothalamus and of NPBWR1 in the pituitary gland (chicken: Bu et al., 2016). In addition, there is some expression of NPB in both the hypothalamus and pituitary gland (chicken: Bu et al., 2016).

30.6.4.5 Thyrotropin-releasing hormone

TRH stimulates release of GH from pituitary tissue (chicken: Huang et al., 2014).

30.6.4.6 Glucagon-like peptide

GCGL stimulates both release of GH from chicken pituitary tissue together with GH expression (Huang et al., 2014).

30.6.4.7 Somatostatin and cortistatin

Two genes for somatostatin are present in birds, namely the following:

1. Somatostatin 1 (SST) encoding the peptides: SST14 and SST28 (see Figure 30.12)
2. Cortistatin (CST) or SST 2 encoding the peptide, CST (see Figure 30.12).

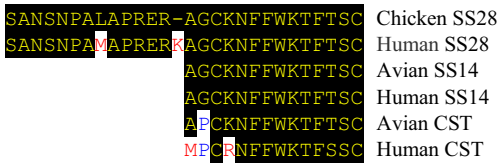

FIGURE 30.12 **Comparison of the structures of avian and human SS14, SS28, and cortistatin.** *Red letters* indicate difference between avian and human sequences, *blue letters* indicate difference between SS14 and CST] [structures of avian CST are based on deduced sequences for the following: (Bengalese finch) XM_021529840.1; chicken: NM_204455.1, duck: XM_005021277.4, emperor penguin: XM_009289625.1; emu) XM_026095553.1].

There are five avian somatostatin receptors (SSTR1-5) with SST14, SST28, and CST being equipotent for SST1R-4 (chicken: Meng et al., 2014). In contrast, SST18 is markedly more potent than CST and SST14 with SSTR5 (chicken: Meng et al., 2014).

Infusion of SS14 depresses both basal and either GHRH or TRH-stimulated GH release in vivo (chicken: Scanes and Harvey, 1989). In the presence of SS14 or SS28 or CST14, both basal and GHRH induced GH release is inhibited (chicken: Meng et al., 2014). What is not clear is the extent to which SS14 and/or SS28 and/or CST14 are physiologically controlling GH release in birds. There is little information of the effects of peptides derived from other members of the somatostatin family (urotensin II or urotensin II-related peptide) on the release GH or other pituitary hormones in birds.

30.6.5 Control of growth hormone expression

GH expression is under multiple stimulatory and inhibitory influences:

- Stimulatory:
  - GHRH ↑ GH mRNA in vivo (Vasilatos-Younken et al., 1992) and in vitro (Radecki et al., 1994) via a cAMP-dependent protein kinase pathway (Kansaku et al., 1998).
  - Other hypothalamic releasing factors/hormones: TRH ↑, PACAP ↑, and ghrelin ↑stimulates expression (Porter et al., 2006).
  - Corticosterone ↑ in embryonic pituitary cells (Bossis and Porter, 2003; Heuck et al., 2009).
- Inhibitory:
  - SRIF ↓ (chicken: Porter et al., 2006),
  - T_3 ↓ (chicken: Radecki et al., 1994), and
  - GH or IGF-1 ↓ when administered continuously in vivo (chicken: Scanes et al., 1999).

The changes in GH expression during growth are similar to those of plasma concentrations of GH (chicken: McCann-Levorse et al., 1993). The pattern of gene expression during the development of avian somatotropes can be described by self-organizing maps (Ellestad et al., 2006).

30.6.6 Environmental factors and growth hormone release

Plasma concentrations of GH are elevated in birds when receiving insufficient nutrition, for example, being increased with fasting (chicken: Harvey et al., 1978; turkey: Anthony et al., 1990), protein deficient diets (chicken: Scanes et al., 1981), and overall dietary restriction (American kestrels: Lacombe et al., 1993). There is evidence that stressors inhibit release of GH with plasma concentrations of GH depressed in chickens following anesthesia (Harvey and Scanes, 1977) and insulin-induced hypoglycemia (Harvey et al., 1978).

30.6.7 Pituitary origin of growth hormone

The somatotrophs are located in the caudal lobe of the anterior pituitary gland (chicken: Mikami, 1980; dove: Reichardt et al., 1993; zebra finches: Christensen and Vleck, 2015) (Figure 30.1). During late embryological development and early posthatch life, the number of somatotrophs increases rapidly until a plateau level is achieved (dove: Reichardt et al., 1993; chicken: Malamed et al., 1997). There are ontogenic changes in the structure of the somatotroph. The number of secretory granules per unit volume of the cell increases during late embryonic development (chicken: Malamed et al., 1993), and there are also more in the adult than the young (chicken: Malamed et al., 1985, 1988).

30.6.8 Extrapituitary expression of growth hormone

There is evidence that GH is expressed in multiple extrapituitary tissues. Posthatching, GH immunoreactivity has been observed in the following organs in chickens: lymphoid tissues (bursa Fabricius, thymus, and spleen) (Luna et al., 2005), testes (Luna et al., 2004), ovary (Hrabia, 2015), and cerebellum (Alba-Betancourt et al., 2011). GH is released from ovarian granulosa cells (chickens: Ahumada-Solórzano et al., 2016). In addition, GH stimulates proliferation of these cells as well as increasing IGF-1 release from granulosa cells (chickens: Ahumada-Solórzano et al., 2016). There is expression of GH in both breast and leg muscles in Muscovy ducks (Ji et al., 2016). In chick embryos, GH immunoreactivity has been reported in multiple tissues including the following: crop, diencephalon and mesencephalon, neural ganglia, trigeminal nerves, dorsal and ventral root ganglia, dorsal and ventral horns of the spinal cord, hepatocytes, intracostal muscles, limb bud cartilage, lungs, and Müllerian duct (Harvey et al., 2000; Murphy and Harvey, 2001; Beyea et al., 2005). In addition, GH expression is seen in embryonic lung tissue (Beyea et al., 2005).

30.6.9 Ontogeny of growth hormone

30.6.9.1 Pou 1 (Pit1)

Pituitary specific transcription factor-1 (*Pit-1* or POU class 1 homeobox 1) plays an important role in the differentiation of somatotropes and lactotropes. In birds, Pit-1 can transactivate a promoter for the GH gene (chicken: Murase et al., 2011). Avian Pou 1 (Pit 1) has been characterized (turkey:

Wong et al., 1992; chicken: Tanaka et al., 1999) and is first expressed on embryonic day five (chicken: Van As et al., 2000). Two Pou 1 (Pit 1) transcripts, Pit1α and Pit1γ, are expressed in both the cephalic and caudal lobes of the chicken pituitary gland, with expression increasing in posthatching growth in a manner parallel to that of GH (chicken: Tanaka et al., 1999). Pou 1 (Pit 1) has been demonstrated to be present in somatotrophs (turkey: Weatherley et al., 2001). While no changes in Pou 1 (Pit 1)-expressing cells occur with corticosterone (chicken: Fu and Porter, 2004), TRH increases expression of Pou 1 (Pit 1) (Van As et al., 2004).

Polymorphisms in Pit-1 gene are associated with improved growth rate and feed efficiency (chickens: Nie et al., 2008; Bhattacharya et al., 2012; Jin et al., 2018) and egg production (Muscovy duck: Xu et al., 2015).

30.6.9.2 Somatotrophs and their differentiation

Somatotropes increase in numbers of somatotrophs beginning about day 14 of incubation (chicken: Porter et al., 1995). GHRH increases the number of somatotrophs (Porter et al., 1995). This increase is due to stimulatory effects of corticosterone and probably also of GHRH and thyroid hormones (Dean and Porter, 1999; Liu and Porter, 2004). The glucocorticoid induction of somatotroph differentiation involves both type 1 (mineralocorticoid) and type 2 (glucocorticoid) receptors (Bossis et al., 2004). Corticosterone induction of the GH gene is via a cis-acting glucocorticoid responsive element (Heuck-Knubel et al., 2012). Glucocorticoids act via the ERK1/2 pathway with Ras effector downstream (Ellestad et al., 2015). It is likely that the corticosterone inducing differentiation of somatotrophs is of adrenal origin, but steroidogenic enzymes are expressed in the embryonic anterior pituitary gland (Zheng et al., 2008).

30.6.9.3 Secretion

A common pattern of circulating concentrations of GH has been observed in all species of birds examined. This consists of progressively rising circulating concentrations of GH in late embryonic development and early posthatch development, high plasma concentrations of GH during the period of rapid posthatching growth, and low GH concentrations in older and adult birds (e.g., chicken: Harvey et al., 1979a, b; American kestrel: Lacombe et al., 1993; European starlings and Japanese quail: Schew et al., 1996). The mechanistic basis for this ontogenic profile includes changes in GH synthesis, somatotroph numbers, and pituitary sensitivity to secretagogues.

30.7 Prolactin

30.7.1 Prolactin gene, mRNA, and protein

There are genes for PRL and prolactin-like protein (*PRL-L*):

- *PRL* gene is on chicken chromosome 2
- *PRL-L* gene is on chicken chromosome 1

(Wang et al., 2010). The structure of PRL from multiple avian species has been deduced from the cDNA [e.g., ostrich (XM_009688738), mallard duck (JQ677091), chicken (NM_205466), rock pigeon (XM_005506024), chimney swift (XM_010004518), Adelie penguin (*Pygoscelis adeliae*) (XM_009326511), canary (XM_009093894)].

A polymorphism of intron 1 of the PRL gene is associated with increased egg production (domestic duck: Bai et al., 2019). Plasma concentrations of PRL in birds are illustrated in Table 30.4.

30.7.2 Post-translational variants of prolactin

There are post-translational variants of PRL in birds. Two glycosylated PRL variants (one *O*- and one *N*- glycosylated) have been identified as well as a nonglycosylated form (turkeys: Corcoran and Proudman, 1991). The glycosylated PRL variants exhibit reduced radioreceptor activity (turkeys: Corcoran and Proudman, 1991). In chickens, PRL variants have been reported as either glycosylated (Berghman et al., 1992) or phosphorylated (Arámburo et al., 1992). Physiological state influences PRL variants. For instance, there are shifts in the proportion of variants in the pituitary between nonlaying, laying, and incubating hens (chicken: Hiyami et al., 2009).

30.7.3 Actions of prolactin

30.7.3.1 Prolactin and the crop sac gland

In columbiform birds, PRL stimulates the production of "crop milk" from the crop sac from both males and females. The composition of pigeon crop milk initially is the following:

- Protein 64.1%
- Lipid 29.7%
- Water 6.2%

(Hu et al., 2016). There are changes in the composition of crop milk with lipid falling from 30% of dry weight to day one of chick rearing to 5% on day 20 (Xie et al., 2017).

The milk is fed to newly hatched chicks or squabs. In both males and females, plasma concentrations of PRL

increase during the period that they are incubating eggs peaking at the time the chicks hatch (ring doves: Goldsmith et al., 1981; pigeon: Hu et al., 2016; Xie et al., 2018). PRL acts via prolactin receptor (PRLR) to induce increases in crop size; the maximal size of the crop being on day three of "lactation" in domestic pigeons (Hu et al., 2016) but at the same time as hatching in ring doves (Goldsmith et al., 1981). Expression of PRLR crop increases during incubation, remaining high during the first 7 days of chick rearing (Xie et al., 2018). Moreover, expressions of the following enzymes related to lipid metabolism are consistently elevated in crop tissue with maxima immediately prior to the chicks hatching: fatty acid translocase (FAT/CD36), fatty acid-binding protein 5 (EFABP), acyl-CoA-binding protein (ACBP), acetyl-CoA carboxylase (ACC) and fatty acid synthase (FAS) (Xie et al., 2017). In vitro, PRL increases lipid production by pigeon crop tissue (Wan et al., 2019).

Other hormones play a role in crop development and production of crop milk. Crop concentrations of EGF and IGF-1, together with EGF expression, follow the same profile as plasma concentrations of PRL (Xie et al., 2018). There is decreased expression of progesterone receptor, estrogen receptor, and GHR at hatching in the parents (Xie et al., 2018). PRL acts via binding to the PRLR and the insulin receptor substance 1(IRS1)/Protein kinase B (Akt)/TOR signaling pathway (Hu et al., 2016). The ability of PRL to stimulate the crop sac has been used as a biossay for PRL (Nicholl, 1967).

30.7.3.2 Prolactin and behavior

In different birds, PRL induces or at least influences behaviors including those related to incubation and/or broodiness (care of chicks). Administration of PRL induces broodiness (chickens: Riddle et al., 1935; turkeys: Youngren et al., 1991). Incubation behavior is completely suppressed in turkey hens actively immunized against PRL (Crióstomo et al., 1998).

There is evidence that PRL directly influences behavior as there are discrete PRL binding sites in the brain (ring doves: Buntin et al., 1993). In addition, PRL induces phosphorylation of STAT5 (Signal Transducer and Activator of Transcription 5) by JAK2 (Janus kinase 2) in specific sites in the forebrain (ring doves: Buntin and Buntin, 2014).

30.7.3.3 Prolactin and reproduction

PRL increases as the birds incubate eggs and declines during the period when the adults are caring for the chicks (zebra finch: Smiley and Adkins-Regan, 2016). Prebreeding plasma concentrations of PRL were a good predictor of numbers of offspring fledged (house sparrows: Ouyang et al., 2011). PRL can act directly on the gonadotropes that secrete LH, with PRL depressing LH release from turkey anterior pituitary cells in vitro (turkey: You et al., 1995). Prebreeding plasma concentrations of PRL were a good predictor of numbers of offspring fledged (house sparrows: Ouyang et al., 2011).

30.7.3.4 Other roles of prolactin and adrenocortical functioning

There is evidence that PRL influences adrenocortical functioning in birds. Net production of corticosterone by chicken adrenal cells in vitro is increased by PRL; the effect being due to inhibition of 5α-reductase (Carsia et al., 1984, 1987). Similarly, plasma concentrations of CORT are elevated following injection of either mammalian PRL in chickens (Decuypere and Kühn, 1985; Skwarlo-Sonta et al., 1987) or native or mono-polyethylene glycol (PEG)ylated chicken PRL (chicken: Oclon et al., 2018).

30.7.3.5 Prolactin receptor

The PRLR is a member of the class I cytokine receptor superfamily and activates the JAK-2/STAT 5 signaling pathway. The PRLR gene was first cloned from kidney tissue (chickens: Tanaka et al., 1992b). There is a duplicated PRLR gene in the late-feathering chickens carrying the K (i.e., late-feathering) locus (chickens: Bu et al., 2013b). A different mutation in the PRLR is responsible for late feathering in turkeys (Derks et al., 2018).

- Type I PRLR high expression in the kidneys and small intestine plus some in the brain and pancreas.
- Type II PRLR expression in the brain, intestine, kidneys, lung, skeletal muscle, testes, ovaries, pituitary, and pancreas plus some in the heart, liver, and spleen
- Type-v1 PRLR high expression in the brain, intestine, kidneys, and pituitary gland plus some in the heart, liver, lungs, muscle, ovary, testis, and pancreas.

(chicken: Bu et al., 2013a). PLP exhibited very limited ability to activate the PRLR (potency <0.1% that of PRL) (chicken: Bu et al., 2013a).

Expression of PRLR in the ovary differs by functional unit with highest expression in the stroma followed by small follicles and a decline with follicular growth/maturation (chicken: Hu et al., 2017). In addition, PRLR expression is markedly higher in granulosa than theca tissue in large follicles (chicken: Hu et al., 2017). Moreover, PRLR expression is increased in granulosa cells from 6 to 8 mm, F3 and F2 follicles following treatment with FSH or glycosylated or nonglycosylated PRL (chicken: Hu et al., 2017).

30.7.4 Control of prolactin release

In birds, PRL secretion is predominantly under stimulatory hypothalamic control, although there are some inhibitory influences. What is not clear is how the multiple PRL secretagogues interact physiologically and why there are so many hypothalamo-hypophysiotropic factors in birds.

30.7.4.1 Vasoactive intestinal peptide and prolactin release

30.7.4.1.1 Introduction

Vasoactive intestinal peptide is a major hypothalamo-hypophysiotropic factor acting physiologically to stimulate PRL release (Table 30.3). PRL release in birds can be stimulated by VIP in vivo (chickens: Macnamee et al., 1986; turkeys: Opel and Proudman, 1988; white-crowned sparrow: Maney et al., 1999; nonincubating zebra finch: Christensen and Vleck, 2008) and in vitro (turkeys: Proudman and Opel, 1988). VIP is found in the avian hypothalamus, particularly in the median eminence (chickens: Macnamee et al., 1986). VIP is synthesized as prepro-peptide histidine isoleucine (PHI) VIP, and this is subject to proteolytic cleavage to generate the peptides, VIP and PHI (Figure 30.13). VIP is expressed in the hypothalamus together with the pituitary gland, small intestine, and other tissues (domestic goose: Liu et al., 2014). The amino acid sequence for a VIP from several avian species is shown in Figure 30.13.

Dopamine stimulates release of VIP from the hypothalamus via D_1 dopamine receptors (turkey: Youngren et al., 1996; Chaiseha et al., 1997). In addition, serotonin increases PRL secretion via hypothalamic effects on dopaminergic neurons and, then, release of VIP (turkey: El Halawani et al., 1995; Chaiseha et al., 2010).

30.7.4.2 Arginine vasotocin

AVT has some PRL releasing activity (Table 30.3). Posterior pituitary extracts can provoke PRL release from turkey pituitary cells due to both AVT and VIP. AVT stimulates prolactin release, while antiserum to AVT partially neutralizes the PRL-releasing effects of posterior pituitary extracts (El Halawani et al., 1992).

30.7.4.3 Prolactin-releasing peptide

30.7.4.3.1 Chemistry

Prolactin-releasing peptide (PrRP)is an RF-amide peptide. The precursor (pre-proprolactin-releasing peptide) for avian PrRP has been characterized in the chicken from its cDNA; there are PrRPs with 20- and 31-amino acid residues (Tachibana et al., 2011). Moreover, PrRP20 and PrRP31 have a consistent structure across birds (Canary: Genbank XM_009086200; Rhinoceros hornbill: XM_010138474; Rifleman: XM_009079364; Saker falcon: XM_005437134):

PrRP31	SRPFKHQIDNRSPEIDPFWYVGRGVRPIGRF-NH_2
PrRP20	SPEIDPFWYVGRGVRPIGRF-NH_2

There is expression of PrRP in specific regions of the chicken brain, including the hypothalamus, hindbrain, and telencephalon together with the pituitary gland (Wang et al., 2012).

30.7.4.3.2 Actions

Avian PrRP is thought to influence PRL secretion in birds. There is a small increase in circulating concentration of PRL after peripheral administration of an intermediate dose of PrRP31 in chickens, presumably reflecting increased prolactin release (Tachibana et al., 2011) (Table 30.3). In contrast, central administration of PrRP31 into the brain consistently depresses circulating concentrations of PRL, indicating an ultrashort feedback effect (Tachibana et al., 2011).

30.7.4.3.3 Receptors

The structure of PrRP receptor (PRLHR1) and PrRP receptor like (PRLHR2) has been deduced from cDNA

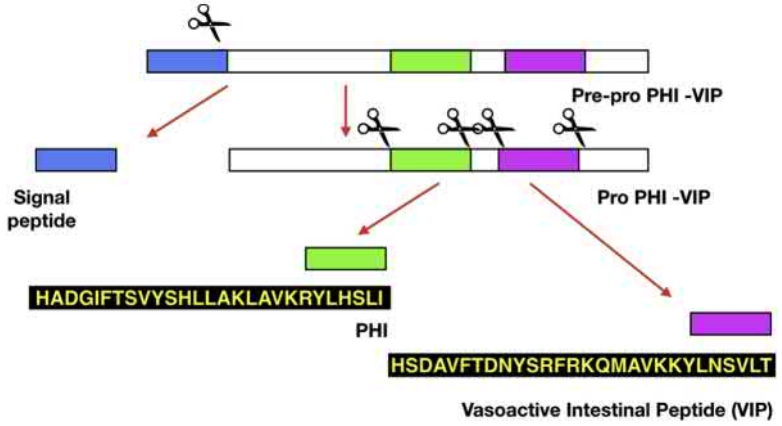

FIGURE 30.13 Synthesis of peptide histidine isoleucine (PHI) and vasoactive intestinal peptide (VIP) as prepro-PHI VIP cleaved to pro-PHI VIP and subsequent proteolytic cleavage to PHI and VIP. The structures of avian PHA [identical in chicken (Genbank U09350.1) and goose (JQ941869) and VIP [identical in chicken (Genbank U09350.1), domestic goose (JQ941869) and rock pigeon (FJ913875.1)] are shown.

from multiple avian species (e.g., PRLHR1: chicken: Genbank AY847003.1; rock pigeon: XM_005515615; starling: XM_014872461.1; PRLHR2: burrowing owl: XM_026863027; chicken: NM_001024585; Chilean tinamou: XM_026042650; emu: XM_026114221; Okarito brown kiwi: XM_026064463). These receptors exhibit homologies to the NPY receptor and are derived from redundant NPY receptors early in vertebrate evolution (Lagerstrom et al., 2005). There is expression of PRLHR1 and PRLHR2 in the pituitary gland and specific regions of the chicken brain, including the hypothalamus, hindbrain, and telencephalon (Wang et al., 2012).

30.7.4.4 Neuropeptide W

Chicken NPW23 but not NPB28 inhibits VIP induced release of PRL from chicken pituitary cells with the effect mediated by binding to the NPBWR1 (Bu et al., 2016).

30.7.4.5 Dopamine

The neurotransmitter, dopamine directly inhibits prolactin release and expression from avian lactotropes. For instance, dopamine or the dopamine D_2 agonist, quinpirole, inhibited prolactin expression by pituitary cells in vitro as induced by either VIP or forskolin (chicken: Lv et al., 2018). Dopamine acts via binding to dopamine receptors (members of the G Protein-coupled receptor). There is high expression of two dopamine receptors: DRD2 (D_2) and DRD4 (D_4) in the cephalic lobe of the anterior pituitary gland (chicken: Lv et al., 2018; domestic goose: Wang et al., 2014).

30.7.4.6 Other stimulatory factors

Other peptides stimulate PRL secretion in birds. PRL release is stimulated by TRH (turkey in vivo: Saeed and El Halawini, 1986) and PHI (turkey: Proudman and Opel, 1990b).

30.7.5 External influences on prolactin release

30.7.5.1 Photoperiod and prolactin release

Nocturnal plasma concentrations of prolactin are increased in young pullets after a single long day (chickens: Dunn et al., 2017). Moreover, expression of TSH β subunit is increased (Dunn et al., 2017).

30.7.5.2 Stress and prolactin release

Plasma concentrations of prolactin can be increased, decreased, or not affected by stress in birds. For instance, plasma concentrations of prolactin were increased by handling stress birds prior to incubation but were decreased in incubating birds (Manx shearwater: Riou et al., 2010). Similarly, plasma concentrations of prolactin were reported to the increased after capture and handling stress in failed breeders but stress decreased plasma concentrations of prolactin in breeding and incubating birds (Cape petrel: Angelier et al., 2013). In another study, plasma concentrations of prolactin are depressed after capture stress (pigeon: Angelier et al., 2016) while handling stress tended to depress plasma concentrations of prolactin (mourning doves: Miller et al., 2009). There were no effects of heat stress on plasma concentrations of prolactin (chicken: Elnagar et al., 2010). Similarly, acute restraint stress does not influence plasma concentrations of prolactin (Gambel's white-crowned sparrow: Krause et al., 2015).

30.7.6 Prolactin expression

Expression of PRL is under hypothalamic control. Photostimulation of young chickens is accompanied by increased PRL expression in the anterior pituitary gland (Li et al., 2009). Moreover, PRL expression is greatly increased during incubation (turkey: Wong et al., 1991). VIP increases PRL expression (turkey: Kang et al., 2004). Moreover, immunizing turkeys against VIP decreases pituitary PRL expression (El Halawani et al., 2000; Ahn et al., 2001). In addition, there is ultra-short loop feedback with PRL influencing PRL expression; administration of PRL increasing expression of PRL in the anterior pituitary gland in control together with either VIP or PCPA treated birds (chickens: Avital-Cohen et al., 2015). Expression of PRL in the anterior pituitary gland was depressed in old males following either PCPA or VIP treatment (chickens: Avital-Cohen et al., 2015).

30.7.7 Adenohypophyseal cells producing prolactin

Prolactin expression is limited to the cephalic lobe of the anterior pituitary gland (chicken: Lv et al., 2018) (Figure 30.1). Lactotropes are predominantly located in the ventral aspect of the cephalic lobe of the anterior pituitary gland (zebra finches: Christensen and Vleck, 2015).

30.8 Pro-opiomelanocortin-derived peptides—adrenocorticotropic hormone, lipotropic hormone, melanocyte-stimulating hormone, and β-endorphin

30.8.1 Pro-opiomelanocortin: gene, processing, and derived peptides

ACTH is synthesized as part of POMC (Table 30.1). The POMC gene is present on chromosome 3 (Rancourt et al., 2018). SNPs mutations in POMC gene are related to pelvis breadth, body weight, and chest depth (chickens: Bai et al., 2012).

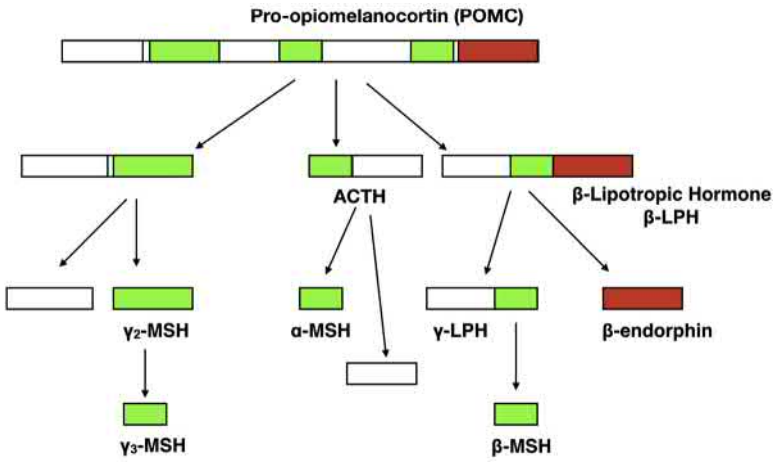

FIGURE 30.14 Post-translational changes (proteolytic cleavage) of pro-opiomelanocortin generating adrenocorticotropic hormone, melanocyte-stimulating hormone (MSH) (α-MSH, β-MSH, and γ_2 MSH) (green), β-lipotropic hormone, and β-endorphin (red).

POMC also contains the sequences of β-endorphin (β-EP), which in itself is part of β-lipotropin (β-LPH), together with α- and β-MSH. The cDNA for chicken POMC has been characterized (Takeuchi et al., 1999) (Figure 30.14). ACTH, β-EP, and β-LPH have been purified from several avian species (see Figure 30.2). Avian ACTH, like its mammalian homolog, is a simple polypeptide containing 39 amino acids (Li et al., 1978; Chang et al., 1980; Hayashi et al., 1991). Plasma concentrations of ACTH and MSH in birds are illustrated in Table 30.4.

30.8.2 Actions of adrenocorticotropic hormone

30.8.2.1 Control of adrenocorticotropic hormone release

Stress induces the release of ACTH from the anterior pituitary gland stimulated by CRH and AVT. ACTH subsequently elevates secretion of corticosterone.

There is evidence of endocannabinoid signaling in the stress response presumably acting at the hypothalamic level. Administration of the cannabinoid receptor (CB)1 antagonist, AM251, increased the increase in plasma concentrations of corticosterone in response to restraint stress (European starling: Dickens et al., 2015).

30.8.2.1.1 Corticotropin-releasing hormone

CRH stimulates ACTH secretion acting via CRH receptor type 1 (Table 30.2). Immunoreactive CRH is present in the hypothalamus, particularly the median eminence (chicken: Jozsa et al., 1984). CRH receptor type 1 is limited to the corticotropes (chicken: De Groef et al., 2003b).

The cDNAs for CRH precursors from multiple avian species have been sequenced. CRH precursor is proteolytically cleaved to generate CRH and this is identical across *Aves* including in chickens (Genbank AJ621492.3; Vandenborne et al., 2005a), ducks (XM_027452300.1), emu (XM_026115236), falcon (XM_005443202), Okarito brown kiwi (XM_026077064), rock pigeon (XM_005506466), Saker falcon (XM_005443202), willow flycatcher (XM_027894702) and zebra finch (NM_001245612) and mammals. The structure of avian CRH is the following:

SEEPPISLDLTFHLLREVLEMARAEQLAQQAHSN-RKLMEIIGK

Release of CRH is influenced by neurotransmitters/neuropeptides such as NPY. Intraventricular administration of NPY is accompanied by an increase in plasma concentrations of corticosterone (chicken: Kuenzel et al., 2016); this being presumably via increased CRH release. Similarly, central administration of ghrelin increases circulating concentrations of corticosterone in young chickens (Saito et al., 2005), presumably due to elevated CRH release.

30.8.2.1.1.1 *Other effects of corticotropin-releaseing hormone* CRH increases pituitary expression of cocaine- and amphetamine-regulated transcript (CART) 1 acting via CRHR1 (chicken: Mo et al., 2015). Moreover, administration of CRH to embryos on day 18 of incubation accelerates hatching (chicken: Watanabe et al., 2017).

30.8.2.1.2 Arginine vasotocin, mesotocin, and adrenocorticotropic hormone release

Both AVT and MT stimulate ACTH release (Castro et al., 1986) with AVT synergistically increasing CRH stimulated ACTH release (Mikhailova et al., 2007; Cornett et al., 2013). CRH and AVT are not co-localized in hypothalamic neurons (chicken: Nagarajan et al., 2014). There is evidence that the mechanism involves dimerization of the CRH-R1 and VT2R (Mikhailova et al., 2007; Cornett et al.,

2013). Acute stress reduces the number of AVT-immunoreactive neurons in specific areas within the hypothalamus (chicken: Nagarajan et al., 2014).

30.8.2.1.3 Calcium-related hormones and adrenocorticotropic hormone release

Calcium-related hormones influence ACTH release with parathyroid hormone—related peptide (PTHrP) per se increasing ACTH in vitro (chicken: Nakayama et al., 2011a) and calcitonin augmenting the effect of CRH on ACTH release in vitro (chicken: Nakayama et al., 2011b). It is not clear whether PTHrP acts via PTH1R or PTH3R (Pinheiro et al., 2012).

30.8.2.1.4 Feedback

Glucocorticoids inhibit the release of ACTH via effects at both the hypothalamic and pituitary levels. This has demonstrated in vivo (Herold et al., 1992) and in vitro (Carsia et al., 1986). Corticosterone also reduces expression of CRH in the hypothalamus (chicken: Vandenborne et al., 2005b). While corticosterone does not affect CRH-R expression in the anterior pituitary gland (chicken Vandenborne et al., 2005b), paradoxically pituitary expression of VT2R, presumably in corticotropes, is upregulated by corticosterone (Sharma et al., 2009b). Protein-deprived chicks that have elevated circulating concentrations of corticosterone also have reduced circulating concentrations of ACTH (Carsia et al., 1988), presumably due to increased glucocorticoid negative feedback.

30.8.3 Control of proopiomelanocortin expression

There are stress-related shifts in pituitary POMC expression. Anterior pituitary concentrations of POMC mRNA are paradoxically reduced 15 min after immobilization stress (chicken: Jayanthi et al., 2014). In contrast, pituitary concentrations of heteronuclear RNA are elevated by immobilization stress and in in vitro studies, by CRH, AVT, and CRH together with AVT (chicken: Jayanthi et al., 2014). Expression of POMC mRNA in the chicken anterior pituitary gland is decreased by either water deprivation (when there is elevated AVT release) or testosterone administration (Sharma and Chaturvedi, 2011). Moreover, the effect of CRH together with AVT is markedly attenuated in the presence of an antagonist of the avian vasotocin 4 receptor (chicken: Jayanthi et al., 2014). Prolonged water deprivation reduces pituitary expression of POMC (chickens: Sharma et al., 2009a). Corticosterone administration in vivo does not influence expression of POMC in the anterior pituitary gland, but corticosterone is effective in reducing anterior pituitary expression of POMC in vitro (chicken: Vandenborne et al., 2005b; Sharma et al., 2009).

Expression of POMC and PC1 lower in the pituitary of domesticated chickens than jungle fowl (Løtvedt et al., 2017). POMC expression greater in males (chickens: Rancourt et al., 2018).

30.8.4 Pituitary origin of adrenocorticotropic hormone

POMC is expressed and processed to ACTH in corticotropes. POMC is expressed and processed to ACTH in corticotropes; these being located in the cephalic lobe of the anterior pituitary gland (chicken: Gerets et al., 2000) (Figure 30.1). The chicken anterior pituitary gland has a high content of ACTH (1.6 μg) but low levels of α-MSH (10 ng) (Hayashi et al., 1991), with ACTH and α-MSH coexisting in the same cells (Iturriza et al., 1980; Hayashi et al., 1991). The number of chicken anterior pituitary cells that express POMC increases when cultured in the presence of CRH (Pals et al., 2006). VT2R is found in avian corticotropes (Jurkevich et al., 2005).

30.8.5 Extrapituitary production

POMC is expressed in multiple organs in addition to the anterior pituitary gland. Expression of POMC has been reported in the brain, kidneys, adrenal glands, adipose tissue, gonads, and uropygial gland (chicken: Takeuchi et al., 1999). There are perikarya in the infundibular nucleus and median eminence together with fibers in the preoptic area and in the medial basal hypothalamus that contain POMC (Gerets et al., 2000). In addition, immunoreactive POMC products are present in immune tissues such as both the thymus and bursa Fabricius (Franchini et al., 1999). POMC and prohormone convertase 1 and 2 (PC1 and PC2) are expressed in feather follicles (Yoshihara et al., 2011).

The MCR is expressed in multiple tissues. There is expression of MC2-R in the spleen (Takeuchi et al., 1998). There is expression of both MC4-R and MC5-R in the brain, adrenal glands, gonads, and adipose tissues of the chicken, with expression of MC4-R also in the spleen and that of MC5-R also in the kidneys and the uropygial gland (Takeuchi and Takahashi, 1998b). The roles of these POMC products are not well established. Feather follicles also express MC1-R, which binds α-MSH or ACTH and thereby changes feather coloration (Yoshihara et al., 2011).

30.8.6 Ontogeny of adrenocorticotropic hormone

Corticotropes are first observed on day seven in embryonic development (chicken: Jozsa et al., 1979). Plasma concentrations of ACTH and corticosterone increase between embryonic days 11 and 17 (Jenkins et al., 2007). The rising circulating concentrations of corticosterone during

embryonic development subsequently induce increase in somatotropes in the anterior pituitary gland (chickens: Jenkins et al., 2007; domestic goose: Yu et al., 2018).

30.8.7 Melanocyte-stimulating hormone and lipotropic hormone

Information on MSH and LPH in birds is limited. It is assumed that the MSH is of little importance due to the absence of a pars intermedia (Rahn, 1939; Rahn and Painter, 1941). However, release of pro-γ-MSH and LPH from the anterior pituitary gland has been reported (ostrich: Naudé et al., 2006). Early work demonstrated the presence of biologically active MSH in the anterior pituitary gland (chicken: Rahn and Drager, 1941). There were also increasing pituitary concentrations during embryonic development following by plateau concentrations but elevated contents in postnatal growth (chicken: Rahn and Drager, 1941). Moreover, there are relatively high concentrations of α-MSH in the circulation (Table 30.4) (chicken: Shipp et al., 2017) and anterior pituitary gland (duck: Estivariz et al., 1980). Avian corticotropes, or at least a major subset of these, contain both α-MSH and ACTH (duck: Estivariz et al., 1980b).

The physiological roles for either MSH or LPH in birds are not well-established. Although there is evidence that α-MSH has biological activity exerting marked lipolytic activity in birds (chickens: Shipp et al., 2017).

30.8.8 β-Endorphin

30.8.8.1 Chemistry of β-endorphin

POMC and a β-EP domain are found in all birds examined (reviewed: Scanes and Pierzchala-Koziec, 2018). β-EP is a peptide with 31 amino acid residues with an N terminal met-enkephalin YGGFM motif (reviewed: Scanes and Pierzchala-Koziec, 2018). There are few amino acid substitutions in the structure of β-EP across the class *Aves* except in the Passeriforms (reviewed: Scanes and Pierzchala-Koziec, 2018).

30.8.8.2 Physiology of β-endorphin release

There is limited information of the physiology of β-EP in birds. β-EP is released from the anterior pituitary gland along with ACTH, LPH, and pro-γ-MSH (ostrich: Naudé et al., 2006). Circulating concentrations of β-EP are similar to than those of ACTH (domestic geese: Barna et al., 1998a). The reason for plasma concentration of β-EP being higher than that of ACTH may reflect slower clearance of β-EP. Plasma concentrations of both ACTH and β-EP are increased following ether stress (domestic geese: Barna et al., 1998b). There is some evidence for differential release of ACTH and β-EP with either castration or endotoxin challenge increasing plasma concentrations of ACTH but not those of β-EP (domestic geese: Barna et al., 1998a; b).

30.8.8.3 Physiological role of β-endorphin

β-endorphin acts via binding to mu (μ) opioid peptide receptor. It is presumed that β-EP acts to reduce pain.

30.8.9 Extrapituitary production of proopiomelanocortin peptides

POMC is expressed by multiple tissues in birds. For instance, POMC is expressed in feather follicles (chicken: Yoshihara et al., 2011), in the hypothalamus with the POMC gene subjected to methylation (Rancourt et al., 2018), in the adrenal gland with expression increased 15 min after stressing (chicken and jungle fowl: Fallah-sharoudim et al., 2015). In addition, immunoreactive POMC peptides are observed in the thymus and bursa of Fabricius (Franchini and Ottaviani, 1999).

30.9 Other anterior pituitary gland peptides/proteins

In addition to the "classical" hormones of the anterior pituitary gland, other hormones or hormone-like proteins are expressed. Examples of these are discussed below in alphabetical order:

30.9.1 Adiponectin

Adiponectin is a 30 KDa adipose hormone and considered a member of the adipokine family of hormones. In birds and mammals, adiponectin is glycosylated and circulates in multiple forms: light, medium, and heavy (>670 kDa) (Hendricks et al., 2009). The anterior pituitary expresses the adipose hormone, adiponectin (chicken: Maddineni et al., 2005) together with its receptor (ApipoR1 and ApipoR2) (chicken: Ramachandran et al., 2007). Pituitary expression of adiponectin and its receptors are influenced by the physiological and energy status of the bird. Expression of adiponectin is increased while that ApipoR1 and ApipoR2 are decreased by 48 h of feed withdrawal (chicken: Maddineni et al., 2005; Ramachandran et al., 2007).

30.9.2 Chromogranin A

Chromogranin A is an acidic peptide that can be secreted along with protein hormones. The structure of the chromogranin A precursor protein has been deduced from the cDNA from numerous birds including the burrowing owl (*Athene cunicularia*) (XM_026849996.1), chicken (*Gallus*

gallus) (XM_025153471), emu (*Dromaius novaehollandiae*) (XM_026111552), rock pigeon (*Columba livia*) (XM_021292417), Saker falcon (*Falco cherrug*) (XM_005438875.2), and Tibetan ground-tit (*Pseudopodoces humilis*) (XM_014249753.1).

While the function of chromogranin A is not fully established, there is some information on its cellular distribution and change with physiological state. Chromogranin A immunoreactivity is found in LH containing gonadotropes from young chickens and somatotropin from adults but not in lactotropes (chickens and turkeys: Proudman et al., 2003). While this is correlated with low hormone secretion, contrary to this, pituitary chromogranin-A protein concentrations are increased as the birds come into egg production (domestic goose: Luan et al., 2014).

30.9.3 Cocaine- and amphetamine-regulated transcript peptides

Two CART genes have been identified in birds, respectively, CART1 and CART2 (chicken: Cai et al., 2015). CART1 encodes a 111 amino acid containing precursor protein. This can be proteolytically cleaved to form biologically active peptides, CART1(42−89) and CART1(49−89); these having high homology to mammalian CART peptides (Cai et al., 2015). Expression of CART1 is greatest in the anterior pituitary gland (both cephalic and caudal lobes) but with some observed in brain regions, particularly the hypothalamus (chicken: Cai et al., 2015; Mo et al., 2015). CART2 is also expressed in the anterior pituitary gland (Cai et al., 2015). Pituitary expression of CART1 is depressed by fasting (chicken: Cai et al., 2015) and elevated by CRH (via CRHR1) (chicken: Mo et al., 2015).

30.9.4 Synaptotagmin-1

Synaptotagmin-1 is a transmembrane protein. There are large increases in pituitary expression of the transmembrane protein, synaptotagmin-1, during early egg laying and further increases at peak egg laying (domestic goose: Luan et al., 2014).

30.9.5 Interleukins

There is pituitary expression of the proinflammatory cytokine, interleukin 1-beta (IL-1β), and the anti-inflammatory cytokine, IL-10 (Japanese quail: Walker et al., 2019).

30.10 Pars tuberalis

The pars tuberalis has the same embryonic origin as the anterior pituitary gland, namely the adenohypophysis. It is not surprising that pars tuberalis contain the same repertoire of hormones as the anterior pituitary gland. Immunocytochemical studies indicate the presence of LH containing cells in the pars tuberalis (chicken: Kameda et al., 1998) and Indian birds, namely the Coraciiform kingfisher (*Halcyon smyrnensis*) together with the Passeriform munia (*Lonchura striata*) and drongo (*Dicrurus adsimilis*) (Mohanty et al., 1997). Moreover, pars tuberalis cells from Indian birds exhibit reactivity with antisera to GH, PRL, POMC, and TSH (Mohanty et al., 1997).

30.10.1 Functioning of the pars tuberalis

An exciting area of pituitary research is the role of the pars tuberalis in circadian functioning and photoperiodism.

30.10.1.1 Pars tuberalis and photoperiodism

There is now abundant evidence that the pars tuberalis plays an important role in avian circadian rhythmicity and photoperiodism. In the Japanese quail, photoperiodic stimulation for 14 h increases expression of the TSH β-subunit in the pars tuberalis (Nakao et al., 2008). TSH is thought to act in a retrograde manner on ependymal cells in the hypothalamus triggering a cascade including up-regulation of type II iodothyronine deiodinase and local accumulation of T_3 and thereby inducing seasonal breeding (Yoshimura et al., 2003; Nakao et al., 2008; reviewed, e.g., Korf, 2018). Organic anion transporting polypeptides (Oatp) are expressed in the ventrolateral walls of basal tuberal hypothalamus (Nakao et al., 2006) with these Oatp transporting thyroid hormones into target cells.

30.10.2 Pineal effects on the pars tuberalis

Communication with the pineal gland and the pars tuberalis is supported by the presence of melatonin-binding sites (Japanese quail: Cozzi et al., 1993) and melatonin receptor (Mel(1c)) expression in the pars tuberalis (Kameda et al., 2002). Moreover, pars tuberalis expression of the common LH−FSH−TSH glycoprotein α-subunit is increased following pinealectomy (chicken: Kameda et al., 2002). Moreover, the diurnal changes in the expression of the pituitary glycoprotein hormone α-subunit in the pars tuberalis are controlled by pineal melatonin (chicken: Arai and Kameda, 2004).

30.10.3 Circadian rhythms and the pars tuberalis

There are diurnal changes in the expression of glycoprotein α-subunits in the pars tuberalis (chicken: Arai and Kameda, 2004). There are endogenous circadian rhythms within the pars tuberalis. Circadian genes Cry1 and BMAL1 are expressed in the pars tuberalis of the Japanese quail (Yasuo et al., 2004; Ikegami et al., 2009). BMAL1 is also

expressed in the pars distalis as well as the median eminence, infundibular nucleus, and medial suprachiasmatic nucleus (Japanese quail: Ikegami et al., 2009). There is communication between the pars tuberalis and both photoreceptors in other tissues. Neurons containing the photoreceptive protein opsin-5 extend to the outer region of the median eminence adjacent to the pars tuberalis (Halford et al., 2009; Nakane et al., 2010). Fibers from opsin 5-containing neurons extend to areas of the median eminence immediately adjacent to the pars tuberalis (chicken: Nakane et al., 2010). Expression of the pituitary glycoprotein hormone α-subunit in the pars tuberalis is decreased by continuous light regimens and increased by extended darkness irrespective of whether the birds are intact or pinealectomized (Kameda et al., 2002).

30.11 Neurohypophysis

30.11.1 Introduction

The anatomy of the hypothalamic neurosecretory tracts (neurons) leading to their secretory terminals in the pars nervosa is shown in Figure 30.1. The two hormones of the neurohypophysis are AVT and MT (Table 30.1) equivalent to, respectively, arginine vasopressin and oxytocin in mammals. There are two genes. The first is the avian OXT encoding preprooxyphysin, the proteolytic products being MT and neurophysin-1. The second is the avian AVP gene encoding the precursor protein for AVT and neurophysin-2. Both genes are located on chromosome 4 in chickens. MT and AVT are synthesized with their binding protein as, respectively, neurophysin-1 and neurophysin-2. The structure of prepro-MT—neurophysin-1 (VLDV-neurophysin) has been deduced in from cDNA (Figure 30.15) in multiple birds [chicken (XM_025,150,346.1), common cuckoo (XM_009566863.1), domestic goose (XM_013182245.1), emperor penguin (XM_009290727.1), golden eagle (XM_011588837.1), hooded crow (XM_010402115.2), kea (XM_010009290.1), little egret (XM_009639558.1), Okarito brown kiwi (XM_026072773.1), turkey (XM_010710575.2), white-throated sparrow (XM_005494991.3)]. The structure of prepro-AVT—neurophysin-2 (MSEL-neurophysin) has similarly been deduced in chickens (NM_205185.2) and golden eagle (XM_011588908.1).

AVT and MT are produced by and secreted from predominantly separate neurosecretory neurons. The cell bodies of the AVT and MT neurons are located in both separate and overlapping areas within the hypothalamus (mallard and Japanese quail: Goosens et al., 1977; Bons, 1980; Tennyson et al., 1985). The AVT- and MT-containing cell bodies and axons develop in the chicken embryo between days 6 and 17 (Tennyson et al., 1986).

The hormones of the avian neurohypophysis, AVT and MT, are shown in Figure 30.15. AVT differs from arginine

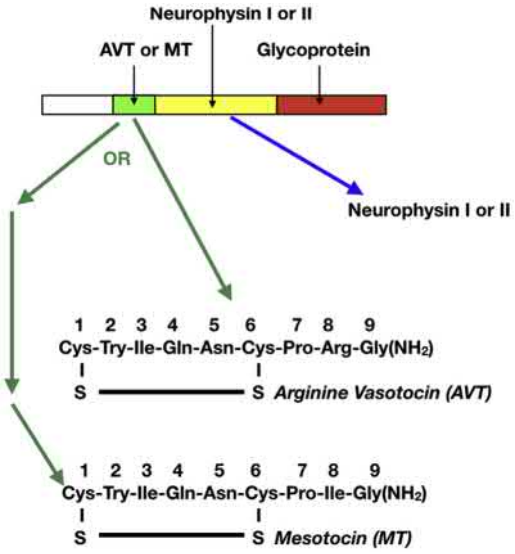

FIGURE 30.15 Synthesis of the Avian Neurohypophyseal Hormones [Mesotocin (MT) and arginine vasotocin (AVT)] with the precursor containing MT or AVT together with either neurophysin I or II. The precursors are subjected to proteolytic cleavage to generate MT or AVT. The structures of the avian nonapeptides (AVT and MT) are shown.

vasopressin, the mammalian antidiuretic hormone, by a single amino acid residue substitution (isoleucine at position three for phenylalanine). MT differs from the mammalian homolog, oxytocin, by the substitution of isoleucine for leucine (position 8). Based on the cDNA structure, MT is replaced by 8-lysine oxytocin in Anna's hummingbird (XM_008491101.1). The posterior pituitary gland contains high levels of AVT and MT (chicken: 4.0 μg AVT and 0.9 μg MT) (Robinzon et al., 1988a). Low concentrations of these neuropeptides are also found throughout the brain (Robinzon et al., 1988a) and in the ovary (Saito et al., 1990). It is presumed that the major source of circulating concentrations of AVT and MT is the posterior pituitary gland, although there is significant ovarian production (Saito et al., 1990).

The anatomy of the hypothalamic neurosecretory tracts (neurons) leading to their secretory terminals in the pars nervosa is shown in Figure 30.1. The two posterior pituitary gland hormones are the following:

- AVT
- MT

(Table 30.2). AVT is equivalent to vasopressin in mammals, and MT is the homolog of mammalian oxytocin. Plasma concentrations of AVT and MT are illustrated in Table 30.4.

30.11.2 Receptors for arginine vasotocin and mesotocin

Avian vasotocin receptors are proteins with seven transmembrane domains and members of the large rhodopsin-

TABLE 30.9 Arginine vasotocin and mesotocin receptors in birds.

Avian receptor	Mammalian homolog[a]	Location	Role	Relative activity	References
VT1R	V2R	Shell gland + brain	Induction of oviposition	AVT > MT	Tan et al. (2000)
VT2R	V1bR	Anterior pituitary gland	Control of ACTH release	AVT > MT	Cornett et al. (2003)
VT3R	OTR	Shell gland	Induction of oviposition	MT > AVT	Gubrij et al. (2005)
VT4R	V1Ar	Vascular smooth muscle, anterior pituitary gland	Control of blood pressure; control of ACTH release	AVT > MT	Baeyens and Cornett (2006); Kuenzel et al. (2016)

OTR, Oxytocin receptor; *VR*, Vasopressin receptor; *VTR*, Vasotocin receptor.
[a]*Equivalent to mammalian AVP/OT receptor.*
Based review by Cornett, L.E., Kang, S.W., Kuenzel, W.J., 2013. A possible mechanism contributing to the synergistic action of vasotocin (VT) and corticotropin-releasing hormone (CRH) receptors on corticosterone release in birds. Gen. Comp. Endocrinol. 188, 46–53.

like family of G-protein-coupled receptors. There are at least four avian vasotocin receptors (Table 30.9). Some years ago, Goldstein (2006) concluded that the "*receptors for AVT in avian kidney-either on renal vasculature or on the tubules-have yet to be localized or identified.*" There is still need to clarify the renal AVT receptor in birds.

There are physiological effects on the expression of VT receptors. For instance, prolonged water deprivation reduces pituitary expression of VT2R but increased immunereactive VT2R (chickens: Sharma et al., 2009b). Moreover, glucocorticoid administration increases VT2R expression and immunoreactive concentration in the anterior pituitary gland (Sharma et al., 2009b). Acute immobilization stress is followed by shifts in VTR expression in the anterior pituitary gland with expression of VT4R decreased and that of VT4R decreased (Selvam et al., 2013).

VT4R immune-reactivity is found in corticotropes but not other adenohypophyseal cell types (Selvam et al., 2013). In contrast, VT2R immune-reactivity is found in corticotropes together with some lactotropes (Jurkevich et al., 2008).

30.11.3 Actions of arginine vasotocin

The major roles of AVTH are in renal and cardiovascular functioning together with reproduction.

30.11.3.1 Arginine vasotocin and renal functioning

AVT is the major antidiuretic hormone in birds decreasing the following:

1. Urine flow
2. Glomerular filtration rate (GFR)

(reviewed: Goldstein, 2006). Urine volume is largely increased after surgical removal of the posterior pituitary gland and, therefore, in the absence of AVT (chicken: Shirley and Nalbandov, 1956). In intact birds, AVT reduces urine flow (Figure 30.16) (chicken: Brummermann and Braun, 1995; Takahashi et al., 1995; house sparrow: Goecke and Goldstein, 1997). The effect on urine flow is mediated via V2R (house sparrow: Goecke and Goldstein, 1997). In addition, AVT depressed GFR via a VT1R mechanism (house sparrow: Goecke and Goldstein, 1997).

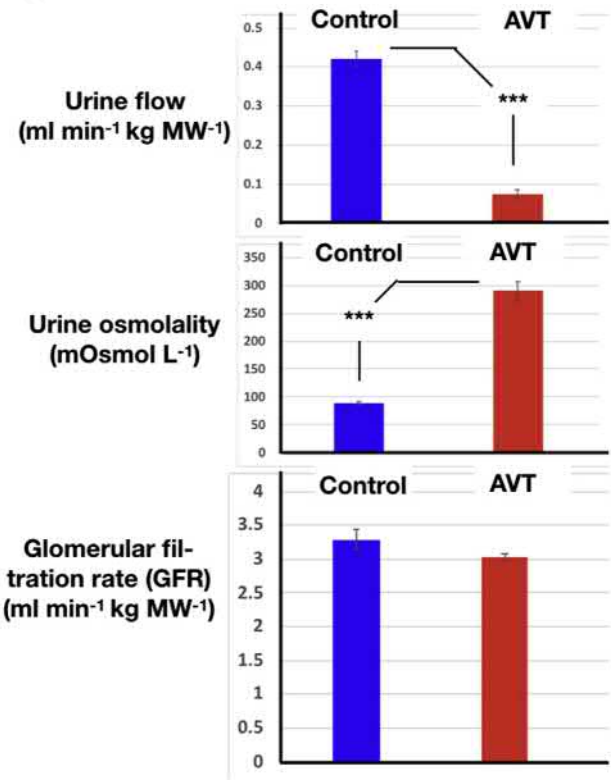

FIGURE 30.16 Effect of arginine vasotocin on urine flow with a concomitant increase in urine osmolality but no change in glomerular filtration rate in adult male chickens. *Data from Brummermann, M., Braun, E.J., 1995. Renal response of roosters with diabetes insipidus to infusions of arginine vasotocin. Am. J. Physiol. 269, R57–R63.*

There is evidence of the importance of AVT and its receptors from lines of birds with different genetic mutations. In control chickens, AVT infusion decreases urine flow (Brummermann and Braun, 1995). In birds with hereditary diabetes insipidus, AVT was without effect on urine flow but increased GFR (Brummermann and Braun, 1995). In addition, chickens with diabetes insipidus had elevated plasma concentrations of AVT (Brummermann and Braun, 1995). These observations are consistent with there being a lesion at or downstream from, the AVT receptor level. Moreover, there were no impacts on plasma concentrations of AVT in a line of Japanese quail with polyuria (increased urine volume) (Minvielle et al., 2007). This was despite the reduced renal aquaporin 2 (AQP2) expression (Japanese quail: Yang et al., 2008).

AVT influences adenylyl cyclase in regions of avian medullary nephrons:

- Thin descending limb—no effect
- Thick ascending limb—stimulated
- Collecting duct—markedly stimulated

(house sparrow: Goldstein et al., 1999). There is evidence that AVT acts by increasing expression of AQP2 and AQP3 and, hence, movement of water in the collecting ducts of both looped and loop-less nephrons (Japanese quail: Yang et al., 2004; Lau et al., 2009; reviewed: Nishimura and Yang, 2013) and, thereby, increasing water reabsorption and reducing urine volume.

30.11.3.2 Arginine vasotocin and oviposition

AVT causes oviposition, the physical process of laying eggs or expelling the egg from the vagina of the oviduct. The hen uterus contracts in response to AVT but not MT alone (chicken: Koike et al., 1988). However, the effect of AVT is potentiated by MT (Figure 30.17) (Takahashi and Kawashima, 2008a). The mechanism by which AVT provokes premature oviposition is not fully established but may involve AVT stimulating local production of prostaglandins (probably E_1) by the uterus and this in turn induces uterine contractions (chicken: Rzasa, 1978; 1984). Circulating concentrations of both AVT and MT increase at the time of oviposition (Figure 30.17) (Takahashi and Kawashima, 2008a). Both VT1R and VT3R are expressed in both the endometrium and myometrium of the shell gland (chicken: Seth et al., 2004a; Gudrij et al., 2005).

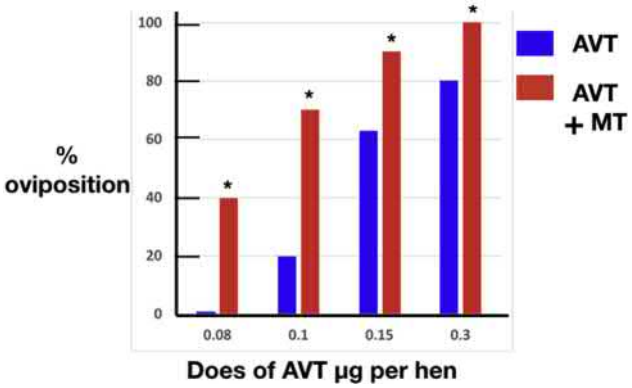

FIGURE 30.17 Arginine vasotocin and mesotocin and oviposition. (A) Ability of MT to potentiate AVT induction of oviposition in female chickens. The ability of AVT to induce oviposition in female chickens. *Data from Takahashi, T., Kawashima, M., 2008a. Mesotocin increases the sensitivity of the hen oviduct uterus to arginine vasotocin. Poult. Sci. 87, 2107–2111.*

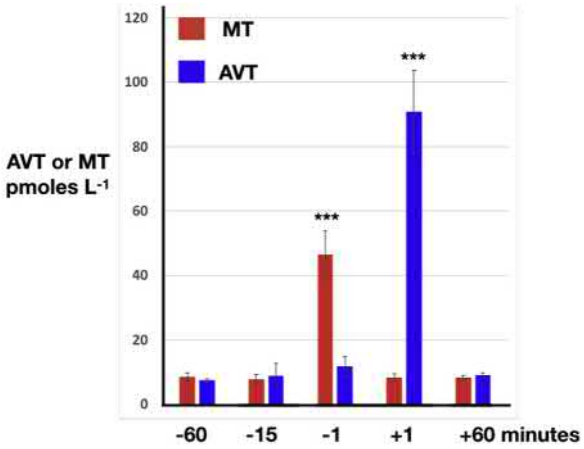

FIGURE 30.17B Plasma concentrations of mesotocin and arginine vasotocin around the time of oviposition in hens. *Data from Takahashi, T., Kawashima, M., 2008a. Mesotocin increases the sensitivity of the hen oviduct uterus to arginine vasotocin. Poult. Sci. 87, 2107–2111.*

30.11.3.3 Cardiovascular effects of arginine vasotocin

AVT can have both vasodressor and vasopressor activity in birds. Bolus injections of AVT to conscious adult chickens or either adult or young domestic ducks results in a marked drop in mean arterial pressure (Wilson and West, 1986; Robinzon et al., 1988b). In contrast, infusion of AVT can increase arterial blood pressure in conscious chickens (Robinzon et al., 1993). In an analogous manner, bolus injection of AVT elevates hear rate while infusion of AVT depresses heart frequency (Wilson and West, 1986; Robinzon et al., 1988b, 1993).

30.11.3.4 Other effects of arginine vasotocin

Infusion of AVT is followed by decreased temperature of the comb and shank but did not influence either cloacal or skin temperatures (chickens: Robinzon et al., 1988a). Infusion of AVT increased the circulating concentrations of prolactin but decreased those of aldosterone (chickens: Robinzon et al., 1988a).

30.11.4 Actions of mesotocin

30.11.4.1 Mesotocin and renal functioning

MT at low concentrations reduced urine volume but increased urine volume at high concentrations (chickens Takahashi et al., 1995). There is specific binding of MT to membrane fractions from the medulla and cortex of the kidney with binding displaced by MT but not AVT in the medulla but by both MT and AVT in the cortex (chicken: Takahashi et al., 1997).

30.11.4.2 Mesotocin and oviposition

The ability of AVT to induce oviposition is potentiated by MT (Figure 30.17A and B) (Takahashi and Kawashima, 2008a). Moreover, there is specific binding of MT (i.e., not inhibited by AVT) to uterine membranes (chickens: Takahashi and Kawashima, 2008b). There is decreased binding of MT to uterine membranes is decreased after oviposition (chickens: Takahashi and Kawashima, 2008b).

30.11.4.3 Other effects of mesotocin

Infusion of MT is followed by decreased temperature of the comb and shank but did not influence either cloacal or skin temperatures (chickens: Robinzon et al., 1988). Infusion of MT also decreased the circulating concentrations of AVT and aldosterone (chickens: Robinzon et al., 1988). There was a transient increased in respiratory rate with infusion of MT (chickens: Robinzon et al., 1988a).

30.11.5 Neurohypophyseal hormones and behavior

There is growing evidence that MT influences avian behavior in both wild Passeriform birds and in poultry species. For instance, subcutaneous administration of an oxytocin receptor antagonist reduced the time that female zebra finch (*Taeniopygia guttata*) spent with conspecifics (Goodson et al., 2009). Similarly, knock-down of MT synthesis in the paraventricular nucleus reduces gregariousness in female zebra finch (Kelly and Goodson, 2014). In addition, s.c. administration of an oxytocin receptor antagonist reduced time on the nest in female zebra finch (Klatt and Goodson, 2013a). Moreover, intraventricular administration of oxytocin receptor antagonist to socially monogamous zebra finch was followed by reduced duration of pairing in females (Klatt and Goodson, 2013b). Furthermore, intramuscular administration of an oxytocin receptor antagonist was associated with increased latency to pair bonding together with reduced pair bonding in zebra finch (Pedersen and Tomaszycki, 2012). Another effect of administration (sc) of oxytocin antagonist was reduced aggression in both male and female violet-eared waxbills (*Uraeginthus granatinus*) (Goodson et al., 2015). These reports are consistent with MT released from the posterior pituitary gland and/or locally produced MT within the CNS influencing behaviors.

In poultry species, there is evidence for behavioral effects of MT. In chicken and pigeon, AVT increases sexual behavior (Kihlstrom and Danninge, 1972). When turkey hens incubating eggs are exposed to young poults, there is induction of c-fos expression in MT-containing neurons in the nucleus paraventriculus magnocelluaris (PVN) and nucleus supraopticus paraventralis (SOv) (Thayananuphat et al., 2011). Moreover, intraventricular administration of OT receptor antagonist reduced brooding behavior when turkey hens were exposed to poults (Thayananuphat et al., 2011). Further evidence that MT is involved in female behaviors comes from the changes in the number of MT-neurons in the hypothalamus [specifically the nuclei supraopticus, pars ventralis (SOv), preopticus medialis (POM), and paraventricular (PVN)] with reproductive state:

- Nonlaying hens—low
- Laying hens—high
- Incubating hens—high
- Rearing chicks—very high
- Not-rearing chicks—low
- Incubation disrupted—low

(native chickens: Chokchaloemwong et al., 2013; Sinpru et al., 2017).

30.11.6 Control of arginine vasotocin and mesotocin release

The release of AVT and MT from the posterior pituitary gland is under independent control. For instance, heat stress increases plasma concentrations of AVT but depresses those of MT (Wang et al., 1989). Similarly, plasma concentrations of AVT were increased gradually following anesthesia and/or carotid cannulation while those of MT declined (Bottje et al., 1990). Furthermore, there are changes in the circulating concentrations of AVT and MT during the day/night in hens with peak concentrations of AVT but nadir concentrations of MT at the beginning of the scotophase (chickens: Chaturvedi et al., 2001). The diurnal shifts in neither AVT nor MT were observed in water-deprived hens (chickens: Chaturvedi et al., 2001).

30.11.6.1 Control of arginine vasotocin release

Table 30.10 summarizes the effects of physiological factors that influence circulating concentrations of AVT. Physiological factors influencing AVT release can be categorized as osmotic related, other stressors, and reproduction. Angiotensin II administration increases plasma concentrations of AVT (chicken: Takahashi et al., 2011). Plasma concentrations of AVT are increased following flight (pigeons: Giladi et al., 1997).

TABLE 30.10 Factors influencing circulating concentrations of aginine vasotocin in birds.

Physiological factor	Chicken	Other birds
Osmotic factors		
Withholding water (water deprivation)	↑↑	↑↑ (domestic ducks, house sparrow, Japanese quail)
Hemorrhage	↑↑	↑↑ (domestic ducks)
Sodium chloride loading	↑↑	↑↑ (domestic ducks)
Feeding high concentrations of sucrose	NA	↑↑ (white-bellied sunbirds)
Angiotensin II	↑↑	NA
Calcitonin	↑↑	NA
Other stresses/factors		
Anesthesia	↓	NA
Heat stress	↑↑	NA
Lipopolysaccharide (LPS)	NA	↑↑ (domestic ducks)
Flight	NA	↑↑ (pigeons)
Reproduction		
Oviposition	↑↑	NA

NA, *Information not available.*
Table is based on Scanes, C.G., 2015. Pituitary gland. In: Scanes, C.G. (ed.), Sturkie's Avian Physiology. sixth ed., Amsterdam: Elsevier. pp. 497–553 supplemented with reports discussed in the text.

30.11.6.2 Osmotic-related arginine vasotocin release

AVT is released when blood osmolality is high (see Table 30.10) in order to reduce water loss. Water deprivation is followed by large increases in plasma concentrations of AVT together with elevated hypothalamic AVT expression and number of AVT neurons (Japanese quail: Seth et al., 2004b; Minvielle et al., 2007). Similarly, plasma concentrations of AVT are increased with feeding elevated concentrations of sucrose to nectarivorous white-bellied sunbirds (*Nectarinia talatala*) (Gray et al., 2004).

30.11.6.3 Other effects on arginine vasotocin

Plasma concentrations of AVT are increased following the administration of lipopolysaccharide (domestic ducks: Gray and Maloney, 1998). There is no effect of estradiol or testosterone on plasma concentrations of AVT despite either increasing numbers of AVT neurons (Japanese quail: Seth et al., 2004b). (Japanese quail: Seth et al., 2004b). Calcitonin administration increased the plasma concentration of AVT in hens (Nakayama et al., 2010).

30.11.6.4 Arginine vasotocin and mesotocin and oviposition

AVT stimulates oviposition. Administration of AVT induced premature oviposition by induction of the contractions of the smooth muscles of the vagina but also the nervous reflex of bearing down (Takahashi and Kawashima, 2003).

30.11.7 Arginine vasotocin and mesotocin expression

MT is expressed in cell bodies in the paraventricular nucleus, specifically the parvocellular, magnocellular, and periventricular subgroups (chicken: Barth et al., 1997). Some cell bodies express both MT and AVT (Barth et al., 1997). AVT is expressed in cell bodies in the supraoptic nucleus and specifically the ventral and external subgroups (chicken: Barth et al., 1997). Expression of the AVT gene is increased both at the time of oviposition (Japanese quail: Seth et al., 2004a; chicken: Seth et al., 2004b) and with water deprivation (Japanese quail: Seth et al., 2004a; Minvielle et al., 2007). Water deprivation increases the number of neurons containing AVT immunoreactivity (Japanese quail: Seth et al., 2004a). Water restriction did not influence renal expression of AVT (Orlowski et al., 2017). There is increased expression of AVT following administration of either estradiol or testosterone (Japanese quail: Seth et al., 2004b).

30.11.8 Hormonal influences on the posterior pituitary gland

There is specific binding of a series of hormones to a membrane fraction from chicken posterior pituitary glands, and there is variation in binding with physiological state. For instance, not only is there is binding of estradiol to membrane fraction from the posterior pituitary gland but

also binding is lower in laying hens than pullets (Takahashi and Kawashima, 2009a). Moreover, binding changes during the ovulation/oviposition cycle with reduced binding between 3 h before oviposition and the time of oviposition (Takahashi and Kawashima, 2009). Moreover, there is binding of the angiotensin II (Takahashi et al., 2011), calcitonin (Nakayama et al., 2011c), and prostaglandin $F_{2\alpha}$ (Takahashi and Kawashima, 2009b). Administration of estradiol is followed by decreased binding of angiotensin II (Takahashi et al., 2011), calcitonin (Nakayama et al., 2011), estradiol (Takahashi and Kawashima, 2009a), and prostaglandin $F_{2\alpha}$ (Takahashi and Kawashima, 2009b). Interestingly, there is a marked decline in binding of both calcitonin and angiotensin II to neurohypophyseal cell membranes at the time of oviposition (Nakayama et al., 2010; Takahashi et al., 2011). In addition, binding of angiotensin II was depressed after administration of either angiotensin II (Takahashi et al., 2011). The physiological relevance of hormone binding to neurohypophyseal cell membranes is unclear.

30.11.9 Infundibular peptides

A unique neurosecretory peptide, neurosecretory protein GL (NSGL), was identified in the chicken infundibulum (Ukena et al., 2014). Growth was enhanced with intracerebroventricular infusion of NSGL (chicken: Shikano et al., 2018a). The NSGL did not influence expression of GH, PRL, POMC, or TSH beta subunit when administered peripherally (Shikano et al., 2018b).

References

Ahmed, S., Harvey, S., 2002. Ghrelin: a hypothalamic GH-releasing factor in domestic fowl (*Gallus domesticus*). J. Endocrinol. 172, 117–125.

Ahn, J., You, S., Kim, H., Chaiseha, Y., El Halawani, M., 2001. Effects of active immunization with inhibin alpha subunit on reproductive on reproductive characteristics of Turkey hens. Biol. Reprod. 65, 1594–1600.

Ahumada-Solórzano, S.M., Carranza, M.E., Pedernera, E., Rodríguez-Méndeza, J., Luna, M., Arámburo, C., 2012. Local expression and distribution of growth hormone and growth hormone receptor in the chicken ovary: effect of GH on steroidogenesis in cultured follicular granulosa cells. Gen. Comp. Endocrinol. 175, 297–310.

Ahumada-Solórzano, S.M., Martínez-Moreno, C.G., Carranza, M., Ávila-Mendoza, J., Luna-Acosta, J.L., Harvey, S., Luna, M., Arámburo, C., 2016. Autocrine/paracrine proliferative effect of ovarian GH and IGF-I in chicken granulosa cell cultures. Gen. Comp. Endocrinol. 234, 47–56.

Aizawa, S., Higaki, Y., Dudaui, A., Nagasaka, M., Takahashi, S., Sakata, I., Sakai, T., 2016. Identification of marker genes for pars tuberalis morphogenesis in chick embryo: expression of cytokine-like 1 and gap junction protein alpha 5 in pars tuberalis. Cell Tissue Res. 366, 721–731.

Alba-Betancourt, C., Arámburo, C., Avila-Mendoza, J., Ahumada-Solórzano, S.M., Carranza, M., Rodríguez-Méndez, A.J., Harvey, S., Luna, M., 2011. Expression, cellular distribution, and heterogeneity of growth hormone in the chicken cerebellum during development. Gen. Comp. Endocrinol. 170, 528–540.

Allaerts, W., Boonstra-Blom, A.G., Peeters, K., Janse, E.M., Berghman, L.R., Jeurissen, S.H., 1999. Prenatal development of hematopoietic and hormone-producing cells in the chicken adenohypophysis. Gen. Comp. Endocrinol. 114, 213–224.

Al-Musawi, S.L., Gladwell, R.T., Knight, P.G., 2007. Bone morphogenic protein-6 enhances gonadotrophin-dependent progesterone and inhibit secretion and expression of mRNA transcripts encoding gonadotrophin receptors and inhibin/activin subunits in chicken granulosa cells. Reproduction 134, 293–306.

Altwegg, R., Anderson, M.D., 2009. Rainfall in arid zones: possible effects of climate change on the population ecology of blue cranes. Funct. Ecol. 23, 1014–1021.

Angelier, F., Wingfield, J.C., Trouvé, C., de Grissac, S., Chastel, O., 2013. Modulation of the prolactin and the corticosterone stress responses: do they tell the same story in a long-lived bird, the Cape petrel? Gen. Comp. Endocrinol. 182, 7–15.

Angelier, F., Parenteau, C., Ruault, S., Angelier, N., 2016. Endocrine consequences of an acute stress under different thermal conditions: a study of corticosterone, prolactin, and thyroid hormones in the pigeon (*Columbia livia*). Comp. Biochem. Physiol. A 196, 38–45.

Anh, N.T.L., Kunhareang, S., Monchai Duangjinda, M., 2015. Association of chicken growth hormones and insulin-like growth factor gene polymorphisms with growth performance and carcass traits in Thai broilers. Asian-Australas. J. Anim. Sci. 28, 1686–1695.

Anthony, N.B., Vasilatos-Younken, R., Bacon, W.L., Lilburn, M.S., 1990. Secretory pattern of growth hormone, insulin and related metabolites in growing male turkeys: effect of overnight fasting and refeeding. Poult. Sci. 69, 801–811.

Aoki, Y., Ono, H., Yasuo, S., Masuda, T., Yoshimura, T., Ebihara, S., Iigo, M., Yanagisawa, T., 2007. Molecular evolution of prepro-thyrotropin-releasing hormone in the chicken (Gallus gallus) and its expression in the brain. Zoolog. Sci. 24, 686–692.

Arai, N., Iigo, M., 2010. Duplicated growth hormone genes in a passerine bird, the jungle crow (*Corvus macrorhynchos*). Biochem. Biophys. Res. Commun. 397, 553–558.

Arai, Y., Kameda, Y., 2004. Diurnal rhythms of common alpha-subunit mRNA expression in the pars tuberalis of hamsters and chickens. Cell Tissue Res. 317, 279–288.

Aramburo, C., Donoghue, D., Montiel, J.L., Berghman, L.R., Scanes, C.G., 1990. Phosphorylation of chicken growth hormone. Life Sci. 47, 945–952.

Arámburo, C., Montiel, J.L., Proudman, J.A., Berghman, L.R., Scanes, C.G., 1992. Phosphorylation of prolactin and growth hormone. J. Mol. Endocrinol. 8, 183–191.

Arámburo, C., Luna, M., Carranza, M., Reyes, M., Martínez-Coria, H., Scanes, C.G., 2000. Growth hormone size variants: changes in the pituitary during development of the chicken. Proc. Soc. Exp. Biol. Med 223, 67–74.

Arámburo, C., Carranza, M., Reyes, M., Luna, M., Coria, H., Berúmen, L., Scanes, C.G., 2001. Characterization of a bioactive 15 kda fragment produced by proteolytic cleavage of chicken growth hormone. Endocrine 15, 231–240.

Asem, E.K., Molnar, M., Hertelendy, F., 1987. Luteinizing hormone-induced intracellular calcium mobilization in granulosa cells: comparison with forskolin and 8-bromo-adenosine 3',5'-monophosphate. Endocrinology 120, 853–859.

Avital-Cohen, N., Heiblum, R., Argov-Argaman, N., Rosenstrauch, A., Chaiseha, Y., Mobarkey, N., Rozenboim, I., 2013. Age-related changes in gonadal and serotonergic axes of broiler breeder roosters. Domest. Anim. Endocrinol. 44, 145–150.

Avital-Cohen, N., Heiblum, R., Rosenstrauch, A., Chaiseha, Y., Mobarkey, N., Gumułka, M., Rozenboim, I., 2015. Role of the serotonergic axis in the reproductive failure associated with aging broiler breeder roosters. Dom. Anim. Endocrinol. 53, 42–51.

Baeyens, D.A., Cornett, L.E., 2006. The cloned avian neurohypophysial hormone receptors. Comp. Biochem. Physiol. B: Biochem. Mol. Biol. 143, 12–19.

Bai, Y., Sun, G., Kang, X., Han, R., Tian, Y., Li, H., Wei, Y., Zhu, S., 2012. Polymorphisms of the pro-opiomelanocortin and agouti-related protein genes and their association with chicken production traits. Mol. Biol. Rep. 39, 7533–7539.

Bai, D.-P., Hu, Y.-Q., Li, Y.-B., Huang, Z.-B., Li, A., 2019. Polymorphisms of the prolactin gene and their association with egg production traits in two Chinese domestic ducks. Br. Poult. Sci. 60, 125–129.

Barna, I., Koenig, J.I., Péczely, P., 1998a. Characteristics of the proopiomelanocortin system in the outdoor-bred domestic gander. I. ACTH and beta-endorphin levels in the brain, pituitary, and plasma. Gen. Comp. Endocrinol. 109, 44–51.

Barna, I., Koenig, J.I., Péczely, P., 1998b. Characteristics of the proopiomelanocortin system in the outdoor-bred domestic gander. II. Seasonal and circadian rhythmicity; effect of ether stress and lipopolysaccharide administration. Gen. Comp. Endocrinol. 109, 52–59.

Barth, S.W., Bathgate, R.A., Mess, A., Parry, L.J., Ivell, R., Grossmann, R., 1997. Mesotocin gene expression in the diencephalon of domestic fowl: cloning and sequencing of the MT cDNA and distribution of MT gene expressing neurons in the chicken hypothalamus. J. Neuroendocrinol. 9, 777–787.

Bentley, G.E., Ubuka, T., McGuire, N.L., Chowdhury, V.S., Morita, Y., Yano, T., Hasunuma, I., Binns, M., Wingfield, J.C., Tsutsui, K., 2008. Gonadotropin inhibitory hormone and its receptor in the avian reproductive system. Gen. Comp. Endocrinol. 156, 34–43.

Berghman, L.R., Lens, P., Decuypere, E., Kühn, E.R., Vandesande, F., 1987. Glycosylated chicken growth hormone. Gen. Comp. Endocrinol. 68, 408–414.

Berghmann, L.R., Grauwels, L., Vanhamme, L., Proudman, J.A., Foidart, A., Balthazart, J., Vandesande, F., 1992. Immunocytochemical and immunoblotting of avian prolactins using polyclonal and monoclonal antibodies towards a synthetic fragment of chicken prolactin. Gen. Comp. Endocrinol. 85, 346–357.

Berumen, L.C., Luna, M., Carranza, M., Martínez-Coria, H., Reyes, M., Cárabez, A., Arámburo, C., 2004. Chicken growth hormone: further characterization and ontogenic changes of an N-glycosylated isoform in the anterior pituitary gland. Gen. Comp. Endocrinol. 139, 113–123.

Beyea, J.A., Olson, D.M., Vandergriend, R.A., Harvey, S., 2005. Expression of growth hormone and its receptor in the lungs of embryonic chicks. Cell Tissue Res. 322, 379–392.

Bhattacharya, T.K., Chatterjee, R.N., Priyanka, M., 2012. Polymorphisms of Pit-1 gene and its association with growth traits in chicken. Poult. Sci. 91, 1057–1064.

Bhattacharya, T.K., Chatterjee, R.N., Dushyanth, K., Paswan, C., Shukla, R., Shanmugam, M., 2015. Polymorphism and expression of insulin-like growth factor 1 (IGF1) gene and its association with growth traits in chicken. Br. Poult. Sci. 56 (4), 398–407.

Bingham, B., Oldham, E.R., Baumbach, W.R., 1994. Regulation of growth hormone receptor and binding protein expression in domestic species. Proc. Soc. Exp. Biol 206, 195–199.

Bøler, J., Enzmann, F., Bower, C.Y., Schally, A.V., 1969. The identity of chemical and hormonal properties of thyrotropin releasing hormone and pyroglutamyl-histidyl-proline amide. Biochem. Biophys. Res. Commun 37, 705–710.

Bonney, R.C., Cunningham, F.J., 1977. A role of cyclic AMP as a mediator for the action of LH-RH on chicken anterior pituitary cells. Mol. Cell. Endocrinol. 7, 233–244.

Bons, N., 1980. The topography of mesotocin and vasotocin systems in the brain of the domestic mallard and Japanese quail: immunocytochemical identification. Cell Tissue Res. 213, 37–51.

Bossis, I., Porter, T.E., 2003. Evaluation of glucocorticoid-induced growth hormone gene expression in chicken embryonic pituitary cells using a novel in situ mRNA quantitation method. Mol. Cell. Endocrinol. 201, 13–23.

Bossis, I., Nishimura, S., Muchow, M., Porter, T.E., 2004. Pituitary expression of type I and type II glucocorticoid receptors during chicken embryonic development and their involvement in growth hormone cell differentiation. Endocrinology 145, 3523–3531.

Bottje, W.G., Wang, S., Kinzler, S., Neldon, H.L., Koike, T.I., 1990. Plasma concentrations of arginine vasotocin and mesotocin following pentobarbital anaesthesia and carotid cannulation in domestic fowl. Br. Poult. Sci. 31, 189–195.

Brown, N.L., Bayle, J.D., Scanes, C.G., Follett, B.K., 1975. Chicken gonadotrophins: their effects on the testes of immature and hypophysectomized Japanese quail. Cell Tiss. Res. 156, 499–520.

Bruggeman, V., Onagbesan, O., Vanmontfort, D., Berghman, L., Verhoeven, G., Decuypere, E., 1998. Effect of long-term food restriction on pituitary sensitivity to cLHRH-I in broiler breeder females. J. Reprod. Fertil. 114, 267–276.

Brummermann, M., Braun, E.J., 1995. Renal response of roosters with diabetes insipidus to infusions of arginine vasotocin. Am. J. Physiol. 269, R57–R63.

Bu, G., Ying Wang, C., Cai, G., Leung, F.C., Xu, M., Wang, H., Huang, G., Li, J., Wang, Y., 2013a. Molecular characterization of prolactin receptor (cPRLR) gene in chickens: gene structure, tissue expression, promoter analysis, and its interaction with chicken prolactin (cPRL) and prolactin-like protein (cPRL-L). Mol. Cell. Endocrinol. 370, 1491–1462.

Bu, G., Huang, G., Fu, H., Li, J., Huang, S., Wang, Y., 2013b. Characterization of the novel duplicated PRLR gene at the late-feathering K locus in Lohmann chickens. J. Mol. Endocrinol. 51, 261–276.

Bu, G., Lin, D., Cui, L., Huang, L., Lv, C., Huang, S., Wan, Y., Fang, C., Li, J., Wang, Y., 2016. Characterization of neuropeptide B (NPB), neuropeptide W (NPW), and their receptors in chickens: evidence for NPW being a novel inhibitor of pituitary GH and prolactin secretion. Endocrinology 157, 3562–3576.

Buntin, J.D., Buntin, L., 2014. Increased STAT5 signaling in the ring dove brain in response to prolactin administration and spontaneous elevations in prolactin during the breeding cycle. Gen. Comp. Endocrinol. 200, 1–9.

Buntin, J.D., Ruzychi, E., Witebsky, J., 1993. Prolactin receptors in dove brain: autoradiographic analysis of binding characteristics in discrete brain regions and accessibility to blood-borne prolactin. Neuroendocrinology 57, 738–750.

Buonomo, F.C., Griminger, P., Scanes, C.G., 1982. Effects of gradation in protein-calorie restriction on the hypothalamo-pituitary-gonadal axis in the young domestic fowl. Poult. Sci. 61, 800–803.

Burke, W.H., Licht, P., Papkoff, H., Bona Gallo, A., 1979a. Isolation and characterization of luteinizing hormone and follicle stimulating hormone from pituitary gland of the Turkey (*Meleagris gallopavo*). Gen. Comp. Endocrinol. 37, 508–520.

Burke, W.H., Papkoff, H., Licht, P., Bona Gallo, A., 1979b. Preparation of luteinizing hormone (LH) subunits from the Turkey (*Meleagris gallopavo*) and their recombination with subunits of ovine LH. Gen. Comp. Endocrinol. 37, 501–507.

Burke, W.H., Moore, J.A., Ogez, J.R., Builder, S.E., 1987. The properties of recombinant chicken growth hormone and its effect on growth, body composition, feeding efficiency and otherv factors in broiler chickens. Endocrinology 120, 651–658.

Burnside, J., Cogburn, L.A., 1992. Developmental expression of hepatic growth hormone receptor and insulin-like growth factor-I mRNA in the chicken. Mol. Cell. Endocrinol. 89, 91–96.

Burnside, J., Liou, S.S., Cogburn, L.A., 1991. Molecular cloning of the chicken growth hormone receptor complimentary DNA: mutation of the gene in sex-linked dwarf chickens. Endocrinology 128, 3183–3192.

Burnside, J., Liou, S.S., Zhong, C., Cogburn, L.A., 1992. Abnormal growth hormone receptor gene expression in the sex-linked dwarf chicken. Gen. Comp. Endocrinol. 88, 20–28.

Cai, G., Mo, C., Huang, L., Li, J., Wang, Y., 2015. Characterization of the two CART genes (CART1 and CART2) in chickens (*Gallus gallus*). PLoS One 10, e0127107.

Calisi, R.M., Rizzo, N.O., Bentley, G.E., 2008. Seasonal differences in hypothalamic EGR-1 and GnIH expression following capture-handling stress in house sparrows (*Passer domesticus*). Gen. Comp. Endocrinol. 157, 283–287.

Calisi, R.M., Geraghty, A.C., Avila, A., Kaufer, D., Bentley, G.E., Wingfield, J.C., 2016. Patterns of hypothalamic GnIH change over the reproductive period in starlings and rats. Gen. Comp. Endocrinol. 237, 140–146.

Campbell, R.M., Scanes, C.G., 1985. Lipolytic activity of purified pituitary and bacterially derived growth hormone on chicken adipose tissue in vitro. Proc. Soc. Exp. Biol. Med 180, 513–517.

Campbell, R.M., Scanes, C.G., 1987. Growth hormone inhibition of glucagon and cAMP-induced lipolysis by chicken adipose tissue in vitro. Proc. Soc. Exp. Biol. Med 184, 456–460.

Campbell, R.M., Scanes, C.G., 1988. Pharmacological investigations of the lipolytic and antilipolytic effects of growth hormone (GH) on chicken adipose tissue in vitro: evidence for involvement of calcium and polyamines. Proc. Soc. Exp. Biol. Med 188, 177–184.

Campbell, R.M., Kawauchi, H., Lewis, U.J., Papkoff, H., Scanes, C.G., 1991. Comparison of lipolytic and antilipolytic activities of lower vertebrate growth hormones on chicken adipose tissue in vitro. Proc. Soc. Exp. Biol. Med 197, 409–415.

Campbell, R.M., Chen, W.Y., Wiehl, P., Kelder, B., Kopchick, J.J., Scanes, C.G., 1993. A growth hormone (GH) analog that antagonizes the lipolytic effect but retains full insulin-like (antilipolytic) activity of GH. Proc. Soc. Exp. Biol. Med 203, 311–316.

Carsia, R.V., Scanes, C.G., Malamed, S., 1984. Self-suppression of corticosteroidogenesis: evidence for a role of adrenal 5-α reductase. Endocrinology 115, 2464–2472.

Carsia, R.V., Weber, H., King, D.B., Scanes, C.G., 1985. Adrenocortical cell function in the hypophysectomized domestic fowl: effects of growth hormone and 3,5,3'-triiodothyronine replacement. Endocrinology 117, 928–933.

Carsia, R.V., Weber, H., Perez, F.M., 1986. Corticotropin releasing factor stimulates the release of adrenocorticotropin from domestic fowl pituitary cells. Endocrinology 118, 143–148.

Carsia, R.V., Scanes, C.G., Malamed, S., 1987. Polyhormonal regulation of avian and mammalian corticosteroidogenesis in vitro. Comp. Biochem. Physiol. A 88, 131–140.

Carsia, R.V., Weber, H., Lauterio, T.J., 1988. Protein malnutrition in the domestic fowl induces alterations in adrenocortical function. Endocrinology 22, 673–680.

Castro, M.G., Estivariz, F.E., Iturriza, F.C., 1986. The regulation of the corticomelanotropic cell activity in aves. II. Effect of various peptides on the release of ACTH from dispensed, perfused duck pituitary cells. Comp. Biochem. Physiol. A 83, 71–75.

Catena, M.L., Porter, T.E., McNabb, F.M., Ottinger, M.A., 2003. Cloning of a partial cDNA for Japanese quail thyroid-stimulating hormone and effects of methimazole on the thyroid and reproductive axes. Poult. Sci. 82, 381–387.

Chaiseha, Y., Youngren, O.M., El Halawani, M.E., 1997. Dopamine receptors influence vasoactive intestinal peptide release from Turkey hypothalamic explants. Neuroendocrinology 65, 423–429.

Chaiseha, Y., Kang, S.W., Leclerc, B., Kosonsiriluk, S., Sartsoongnoen, N., El Halawani, M.E., 2010. Serotonin receptor subtypes influence prolactin secretion in the Turkey. Gen. Comp. Endocrinol. 165, 170–175.

Chang, W.-C., Chung, D., Li, C.H., 1980. isolation and characterization of β-lipotropin and adrenocorticotropin from turkey pituitary glands. Int. J. Pept. Protein Res. 15, 261–270.

Chaturvedi, C.M., Chowdhury, A., Cornet, L.E., 2001. Water deprivation and circadian changes in plasma arginine vasotocin and mesotocin in the domestic hen (*Gallus domesticus*). Chronobiol. Int. 18, 947–956.

Chaiyachet, O.A., Chokchaloemwong, D., Prakobsaeng, N., Sartsoongnoen, N., Kosonsiriluk, S., Chaiseha, Y., 2013. Gonadotropin releasing hormone and brooding behavior in the native Thai hen. Acta Histochem. 115, 626–636.

Chen, L.R., Lee, S.C., Lin, Y.P., Hsieh, Y.L., Chen, Y.L., Yang, J.R., Liou, J.F., Chen, C.F., Lee, Y.P., Shiue, Y.L., 2010. Prostaglandin-D synthetase induces transcription of the LH beta subunit in the primary culture of chicken anterior pituitary cells via the PPAR signaling pathway. Theriogenology 73, 367–382.

Chen, Q., Duan, J., Wu, H., Li, J., Jiang, Y., Tang, H., Li, X., Kang, L., 2019. Expression dynamics of gonadotropin-releasing hormone-I and its mutual regulation with luteinizing hormone in chicken ovary and follicles. Gen. Comp. Endocrinol. 270, 96–102.

Cheung, A., Hall, T.R., Harvey, S., 1988. Stimulation of corticosterone release in the fowl by recombinant DNA-derived chicken growth hormone. Gen. Comp. Endocrinol. 69, 128–132.

Chokchaloemwong, D., Prakobsaeng, N., Sartsoongnoen, N., Kosonsiriluk, S., El Halawani, M., Chaiseha, Y., 2013. Mesotocin and maternal care of chicks in native Thai hens (*Gallus domesticus*). Horm. Behav. 64, 53–69.

Chou, H.F., Johnson, A.L., Williams, J.B., 1985. Luteinizing hormone releasing activity of [Gln8]-LHRH and [His5, Trp7, Tyr8]-LHRH in the cockerel, *in vivo* and *in vitro*. Life Sci. 37, 2459–2465.

Chowdhury, V.S., Yoshimura, Y., 2002. Cell proliferation and apoptosis in the anterior pituitary of chicken during inhibition and resumption of laying. Gen. Comp. Endocrinol. 125, 132–141.

Christensen, D., Vleck, C.M., 2008. Prolactin release and response to vasoactive intestinal peptide in an opportunistic breeder, the zebra finch (*Taeniopygia guttata*). Gen. Comp. Endocrinol. 157, 91–98.

Christensen, D., Vleck, C.M., 2015. Effects of age and reproductive experience on the distribution of prolactin and growth hormone secreting cells in the anterior pituitary of a passerine. Gen. Comp. Endocrinol. 222, 54–61.

Ciccone, N.A., Dunn, I.C., Boswell, T., Tsutsui, K., Ubuka, T., Ukena, K., Sharp, P.J., 2004. Gonadotrophin inhibitory hormone depresses gonadotrophin alpha and follicle-stimulating hormone beta subunit expression in the pituitary of the domestic chicken. J. Neuroendocrinol. 16, 999–1006.

Ciccone, N.A., Dunn, I.C., Sharp, P.J., 2007. Increased food intake stimulates GnRH-I, glycoprotein hormone alpha-subunit and follistatin mRNAs, and ovarian follicular numbers in laying broiler breeder hens. Domest. Anim. Endocrinol. 33, 62–76.

Cogburn, L.A., Liou, S.S., Rand, A.L., McMurtry, J.P., 1989. Growth, metabolic and endocrine responses of broiler cockerels given a daily sub-cutaneous inject of native or biosynthetic growth hormone. J. Nutr. 119, 1213–1222.

Cornett, L.E., Kang, S.W., Kuenzel, W.J., 2013. A possible mechanism contributing to the synergistic action of vasotocin (VT) and corticotropin-releasing hormone (CRH) receptors on corticosterone release in birds. Gen. Comp. Endocrinol. 188, 46–53.

Contijoch, A.M., Gonzalez, C., Singh, H.N., Malamed, S., Troncoso, S., Advis, J.P., 1992. Dopaminergic regulation of luteinizing hormone-releasing hormone release at the median eminence level: immunocytochemical and physiological evidence in hens. Neuroendocrinology 55, 290–300.

Contijoch, A.M., Malamed, S., Sarkar, D.K., Advis, j.P., 1993. Beta-endorphin regulation of LHRH release at the median eminence level: immunocytochemical and physiological evidence in hens. Neuroendocrinology 57, 365–373.

Corcoran, D.H., Proudman, J.A., 1991. Isoforms of Turkey prolactin: evidence for differnces in glyxcosylation and in trypic-peptide mapping. Comp. Biochem. Physiol. B 99, 563–570.

Cornett, L.E., Kirby, J.D., Vizcarra, J.A., Ellison, J.C., Thrash, J., Mayeux, P.R., Crew, M.D., Jones, S.M., Ali, N., Baeyens, D.A., 2003. Molecular cloning and functional characterization of a vasotocin receptor subtype expressed in the pituitary gland of the domestic chicken (*Gallus domesticus*): avian homolog of the mammalian V1b-vasopressin receptor. Regul. Pept. 110, 231–239.

Cozzi, B., Stankov, B., Viglietti-Panzica, C., Capsoni, S., Aste, N., Lucini, V., Fraschini, F., Panzica, G.C., 1993. Distribution and characterization of melatonin receptors in the brain of the Japanese quail, *Coturnix japonica*. Neurosci. Lett. 150, 149–152.

Cravener, T.L., Vasilatos-Younken, R., Wellenreiter, R.H., 1989. Effect of subcutaneous infusion of pituitary- derived chicken growth hormone on growth performance of broiler pullets. Poult. Sci. 68, 1133–1140.

Crióstomo, S., Guémené, D., Garreau-Mills, M., Morvan, C., Zadworny, D., 1998. Prevention of incubation behavior expression in Turkey hens by active immunization against prolactin. Theriology 50, 675–690.

Cruz-McDonnell, K.K., Wolf, B.O., 2016. Rapid warming and drought negatively impact population size and reproductive dynamics of an avian predator in the arid southwest. Glob. Change Biol. 22, 237–253.

Cui, H., Zhao, G., Liu, R., Zheng, M., Chen, J., Wen, J., 2012. FSH stimulates lipid biosynthesis in chicken adipose tissue by upregulating the expression of its receptor FSHR. J. Lipid Res. 53, 909–917.

Cupo, M.A., Cartwright, A.L., 1989. Lipid synthesis and lipoprotein secretion by chick liver cells in culture: influence of growth hormone and insulin-like growth factor-I. Comp. Biochem. Physiol. B 94, 355–360.

Darras, V.M., Berghman, L.R., Vanderpooten, A., Kühn, E.R., 1992. Growth hormone acutely decreases type III iodothyronine deiodinase in chicken liver. FEBS Lett. 310, 5–8.

Darras, V.M., Rudas, P., Visser, T.J., Hall, T.R., Huybrechts, L.M., Vanderpooten, A., Berghman, R., Decuypere, E., Kühn, R., 1993. Endogenous growth hormone controls high plasma levels of 3,3′,5-triiodothyronine (T_3) in growing chickens by increasing the T_3-degrading type III deiodinase activity. Domest. Anim. Endocrinol. 10, 55–65.

Davies, D.T., Follett, B.K., 1980. Neuroendocrine regulation of gonadotrophin-releasing secretion in Japanese quail. J. Endocrinol. 40, 220–225.

Davies, D.T., Massa, R., James, R., 1980. Role of testosterone and of its metabolites in regulating gonadotrophin secretion in the Japanese quail. J. Endocrinol. 84, 211–222.

Davies, W.I., Turton, M., Peirson, S.N., Follett, B.K., Halford, S., Garcia-Fernandez, J.M., Sharp, P.J., Hankins, M.W., Foster, R.G., 2012. Vertebrate ancient opsin photopigment spectra and the avian photoperiodic response. Biol. Lett. 8, 291–294.

Davis, R.V., Lamont, S.J., Rothschild, M.F., Persia, M.E., Ashwell, C.M., Schmidt, C.J., 2015. Transcriptome analysis of post-hatch breast muscle in legacy and modern broiler chickens reveals enrichment of several regulators of myogenic growth. PLoS One 10, e0122525.

Dean, C.E., Porter, T.E., 1999. Regulation of somatotroph differentiation and growth hormone (GH) secretion by corticosterone and GH-releasing hormone during embryonic development. Endocrinology 140, 1104–1110.

Decuypere, E., Kühn, E.R., 1985. Effect of a single injection of prolactin on the serum concentration of thyroid hormones and corticosterone and liver monodeiodinase in domestic fowl before and after hatching. J. Endocrinol. 103, 363–366.

Decuypere, E., Ighal, A., Michels, H., Kühn, E.R., Schneider, R., El Azeem, A.A., 1988. Thyroid hormone response to thyrotropin releasing factor after cold treatment during pre- and post-natal development in the domestic fowl. Horm. Metab. Res. 20, 484–489.

De Groef, B., Goris, N., Arckens, L., Kühn, E.R., Darras, V.M., 2003a. Corticotropin-releasing hormone (CRH)-induced thyrotropin release is directly mediated through CRH receptor type 2 on thyrotropes. Endocrinology 144, 5537–5544.

Dawson, A., Follett, B.K., Goldsmith, A.R., Nicholls, T.J., 1985. Hypothalamic gonadotrophin-releasing hormone and pituitary and plasma FSH and prolactin during photostimulation and photorefractoriness in intact and thyroidectomized starlings (Sturnus vulgaris). J. Endocrinol. 105, 71–77.

De Groef, B., Geris, K.L., Manzano, J., Bernal, J., Millar, R.P., Abou-Samra, A.B., Porter, T.E., Iwasawa, A., Kühn, E.R., Darras, V.M., 2003b. Involvement of thyrotropin-releasing hormone receptor, somatostatin receptor subtype 2 and corticotropin-releasing hormone receptor type 1 in the control of chicken thyrotropin secretion. Mol. Cell. Endocrinol. 203, 33–39.

Dehkhoda, F., Lee, C.M.M., Medina, J., Brooks, A.J., 2018. The growth hormone receptor: mechanism of receptor activation, cell signaling, and physiological aspects. Front. Endocrinol 9, 35.

Derks, M.F.L., Herrero-Medrano, J.M., Crooijmans, R.P.M.A., Vereijken, A., Long, J.A., Megens, H.J., Groenen, M.A.M., 2018. Early and late feathering in Turkey and chicken: same gene but different mutations. Genet. Sel. Evol. 50, 7.

Dickens, M.J., Vecchiarelli, H.A., Hill, M.N., Bentley, G.E., 2015. Endocannabinoid signaling in the stress response of male and female songbirds. Endocrinology 156, 4649–4659.

Donoghue, D.J., Campbell, R.M., Scanes, C.G., 1990. Effect of biosynthetic chicken growth hormone on egg production in white leghorn hens. Poult. Sci. 69, 1818–1821.

Du, L., Zhang, Y., Huang, Z., Wu, N., Zhao, W., Chang, G., Xu, Q., Chen, G., 2018. Transcriptome profiling to identify key mediators of granulosa cell proliferation upon FSH stimulation in the goose (*Anser cygnoides*). Br. Poult. Sci. 59, 416–421.

Dunn, I.C., Sharp, P.J., 1999. Photo-induction of hypothalamic gonadotrophin hormone-I mRNA in the domestic chicken: a role for oestrogen? J. Neuroendocrinol. 11, 371–375.

Dunn, I.C., Chen, Y., Hook, Y., Sharp, P.J., Sang, H.M., 1993. Characterization of the chicken preprogonadotropin-releasing hormone-I gene. J. Mol. Endocrinol. 11, 19–29.

Dunn, I.C., Beattie, K.K., Maney, D., Sang, H.M., Talbot, R.T., Wilson, P.W., Sharp, P.J., 1996. Regulation of chicken gonadotropin-releasing hormone-I mRNA in incubating, nest deprived and laying bantam hens. Neuroendocrinology 63, 504–513.

Dunn, I.C., Lewis, P.D., Wilson, P.W., Sharp, P.J., 2003. Acceleration of maturation of FSH and LH responses to photostimulation in prepubertal domestic hens by oestrogen. Reproduction 126, 217–225.

Dunn, I.C., Wilson, P.W., Shi, Y., Burt, D.W., Loudon, A.S.I., Sharp, P.J., 2017. Diurnal and photoperiodic changes in thyrotrophin-stimulating hormone β expression and associated regulation of deiodinase enzymes (DIO2, DIO3) in the female juvenile chicken hypothalamus. J. Neuroendocrinol. 29 (12). https://doi.org/10.1111/jne.12554.

El Halawani, M.E., Silsby, J.L., Koike, T.I., Robinzon, B., 1992. Evidence of a role for the Turkey posterior pituitary in prolactin release. Gen. Comp. Endocrinol. 87, 436–442.

El Halawani, M.E., Youngren, O.M., Rozenboim, I., Pitts, G.R., Silsby, J.L., Phillips, R.E., 1995. Serotonergic stimulation of prolactin secretion is inhibited by vasoactive intestinal peptide immunoneutralization in the Turkey. Gen. Comp. Endocrinol. 99, 69–74.

El Halawani, M., Whiting, S.E., Silsby, J.L., Pitts, G.R., Chaisaha, Y., 2000. Active immunization with vasoactive intestinal peptide in Turkey hens. Poult. Sci. 79, 349–354.

Ellestad, L.E., Puckett, S.A., Porter, T.E., 2015. Mechanisms involved in glucocorticoid induction of pituitary GH expression during embryonic development. Endocrinology 156, 1066–1079.

El-Magd, M.A., Saleh, A.A., Abdel-Hamid, T.M., Saleh, R.M., Afifi, M.A., 2016. Is really endogenous ghrelin a hunger signal in chickens? Association of GHSR SNPs with increase appetite, growth traits, expression and serum level of GHRL, and GH. Gen. Comp. Endocrinol. 237, 131–139.

Ellestad, L.E., Carre, W., Muchow, M., Jenkins, S.A., Wang, X., Cogburn, L.A., Porter, T.E., 2006. Gene expression profiling during cellular differentiation in the embryonic pituitary gland using cDNA microarrays. Physiol. Genomics 25, 414–425.

Ellestad, L.E., Saliba, J., Porter, T.E., 2011. Ontogenic characterization of gene expression in the developing neuroendocrine system of the chick. Gen. Comp. Endocrinol. 171, 82–93.

Elnagar, S.A., Scheideler, S.E., Beck, M.M., 2010. Reproductive hormones, hepatic deiodinase messenger ribonucleic acid, and vasoactive intestinal polypeptide-immunoreactive cells in hypothalamus in the heat stress-induced or chemically induced hypothyroid laying hen. Poult. Sci. Sep 89, 2001–2009.

Ernst, D.K., Lynn, S.E., Bentley, G.E., 2016. Differential response of GnIH in the brain and gonads following acute stress in a songbird. Gen. Comp. Endocrinol. 227, 51–57.

Estivariz, F.E., Levitin, H.P., Iturriza, F.C., 1980. Chromatographic and electrophoretic characterization of melanocyte-stimulating substances in the duck pituitary. Gen. Comp. Endocrinol. 40, 123–127.

Fallahsharoudim, A., de Kock, N., Johnsson, M., Ubhayasekera, S.J., Bergquist, J., Wright, D., Jensen, P., 2015. Domestication effects on stress induced steroid secretion and adrenal gene expression in chickens. Sci. Rep. 5, 15345.

Faure, M., Guibert, E., Crochet, S., Chartrin, P., Brillard, J.P., Collin, A., Froment, P., 2017. Differential proliferation and metabolic activity of Sertoli cells in the testes of broiler and layer breeder chickens. Poult. Sci. 96, 2459–2470.

Fennell, M.J., Johnson, A.L., Scanes, C.G., 1990. Influence of androgens on plasma concentrations of growth hormone in growing castrated and intact chickens. Gen. Comp. Endocrinol. 77, 466–475.

Follett, B.K., 1978. The stimulation of luteinizing hormone and follicle-stimulating hormone secretion in quail with complete and skeleton photoperiods. Gen. Comp. Endocrinol. 45, 306–316.

Foltzer, C., Mialhe, P., 1976. Pituitary and adrenal control of pancreatic endocrine function in the duck. II. Plasma free fatty acids and insulin variations following hypophysectomy and replacement therapy with growth hormone and corticosterone. Diabet. Metab 2, 101–105.

Fraley, G.S., Kuenzel, W.J., 1993. Precocious puberty in chicks (Gallus domesticus) induced by central injection of neuropeptide Y. Life Sci. 52, 1649–1656.

Franchini, A., Ottaviani, E., 1999. Immunoreactive POMC-derived peptides and cytokines in the chicken thymus and bursa of Fabricius microenvironments: age-related changes. J. Neuroendocrinol. 11, 685–692.

Fu, X., Porter, T.E., 2004. Glucocorticoid induction of lactotrophs and prolactin gene expression in chicken embryonic pituitary cells: a delayed response relative to stimulated growth hormone production. Endocrinology 145, 1322–1330.

Furr, B.J.A., Bonney, R.C., England, R.J., Cunningham, F.J., 1973. Luteinizing hormone and progesterone in peripheral blood during the ovulation cycle of the hen (*Gallus domesticus*). J. Endocrinol. 57, 157–169.

Gasc, J.M., Baulieu, E.E., 1988. Regulation by estradiol of the progesterone receptor in the hypothalamus and pituitary: an immunohistochemical study in the chicken. Endocrinology 122, 1357–1365.

Gasparino, E., Voltolini, D.M., Del Vesco, A.P., S.E.G, G., Souza do Nascimento, C., Oliveira Neto, A.R.O., 2013. IGF-I, GHR and UCP mRNA expression in the liver and muscle of high- and low-feed-efficiency laying Japanese quail at different environmental temperatures. Livest. Sci. 257, 339–344.

Gastón, M.S., Schiöth, H.B., De Barioglio, S.R., Salvatierra, N.A., 2015. Gabaergic control of anxiety-like behavior, but not food intake, induced by ghrelin in the intermediate medial mesopallium of the neonatal chick. Horm. Behav. 67, 66–72.

Geelissen, S.M., Beck, I.M., Darras, V.M., Kühn, E., Van der Geyten, S., 2003. Distribution and regulation of chicken growth hormone secretagogue isoforms. Gen. Comp. Endocrinol. 134, 167–174.

Gerets, H.H., Peeters, K., Arckens, L., Vandersande, F., Berghman, L.R., 2000. Sequence and distribution of pro-opiomelanotropin in the pituitary and the brain of the chicken (*Gallus gallus*). J. Comp. Neurol. 417, 250–262.

Geris, K.L., de Groef, B., Rohrer, S.P., Geelissen, S., Kühn, E., Darras, V.M., 2003. Identification of somatostatin receptors controlling growth hormone and thyrotrophin secretion in the chicken using receptor sub-type-specific agonists. J. Endocrinol. 177, 279–286.

Ghanem, K., Johnson, A.L., 2019. Response of hen pre-recruitment ovarian follicles to follicle stimulating hormone, in vivo. Gen. Comp. Endocrinol. 270, 41–47.

Giladi, I., Goldstein, D.L., Pinshow, B., Gerstberger, R., 1997. Renal function and plasma levels of arginine vasotocin during free flight in pigeons. J. Exp. Biol. 200, 3203–3211.

Goldsmith, A.R., Edwards, C., Koprucu, M., Silver, R., 1981. Concentrations of prolactin and luteinizing hormone in plasma of doves in relation to incubation of the crop. J. Endocrinol. 90, 437–443.

Goldstein, D.L., 2006. Regulation of the avian kidney by arginine vasotocin. Gen. Comp. Endocrinol. 147, 78–84.

Goldstein, D.L., Reddy, V., Plaga, K., 1999. Second messenger production in avian medullary nephron segments in response to peptide hormones. Am. J. Physiol. 276. R847–R454.

Goecke, C.S., Goldstein, D.L., 1997. Renal glomerular and tubular effects of antidiuretic hormone and two antidiuretic hormone analogues in house sparrows (*Passer domesticus*). Physiol. Zool. 70, 283–291.

Goodson, J.L., Schrock, S.E., Klatt, J.D., Kabelik, D., Kingsbury, M.A., 2009. Mesotocin and nonapeptide receptors promote estrildid flocking behavior. Science 325, 862–826.

Goodson, J.L., Schrock, S.E., Kingsbury, M.A., 2015. Oxytocin mechanisms of stress response and aggression in a territorial finch. Physiol. Behav. 141, 154–163.

Goosens, N.S., Blahser, S., Oksche, A., Vandesande, F., Dierickx, K., 1977. Immunocytochemical investigation of the hypothalo-neurohypophyseal system in birds. Cell Tissue Res. 184, 1–13.

Gray, D.A., Maloney, S.K., 1998. Antidiuretic hormone and angiotensin II plasma concentrations in febrile Pekin ducks. J. Physiol. 511, 605–610.

Gray, D.A., Fleming, P.A., Nicolson, S.W., 2004. Dietary intake effects on arginine vasotocin and aldosterone in cloacal fluid of whitebellied sunbirds (*Nectarinia talatala*). Comp. Biochem. Physiol. A 138, 441–449.

Gregory, C.C., Porter, T.E., 1997. Cloning and sequence analysis of a cDNA for the beta sub-unit of chicken thyroid-stimulating hormone. Gen. Comp. Endocrinol. 107, 182–190.

Gregory, C.C., Dean, C.E., Porter, T.E., 1998. Expression of chicken thyroid-stimulating hormone beta-subunit messenger ribonucleic acid during embryonic and neonatal development. Endocrinology 139, 474–478.

Grommen, S.V., Taniuchi, S., Jansson, T., Schoofs, L., Takahashi, S., Takeuchi, S., Darras, V.M., De Groef, B., 2006. Molecular cloning, tissue expression, and ontogenic thyroidal expression of the chicken thyrotropin receptor. Endocrinology 147, 3943–3951.

Grommen, S.V., Geysens, S., Darras, V.M., De Groef, B., 2009. Chicken folliculo-stellate cells express thyrotropin receptor mRNA. Domest. Anim. Endocrinol. 37, 236–242.

Grzegorzewska, A.K., Sechman, A., Paczoska-Eliasiewicz, H.E., Rzasa, J., 2009. The expression of pituitary FSH beta and LH beta mRNA and gonadal FSH and LH receptor mRNA in the chicken embryo. Reprod. Biol. 9, 253–269.

Gubrij, K.I., Chaturvedi, C.M., Ali, N., Cornett, L.E., Kirby, J.D., Wilkerson, J., Mikhailova, M., Turner, M.L., Baeyens, D.A., 2005. Molecular cloning of an oxytocin-like receptor expressed in the chicken shell gland. Comp. Biochem. Physiol 142B, 37–45.

Guibert, E., Brière, S., Pelletier, R., Brillard, J.P., Froment, P., 2011. Characterization of chicken Sertoli cells in vitro. Poult. Sci. 90, 1276–1286.

Halford, S., Pires, S.S., Turton, M., Zheng, L., González-Menéndez, I., Davies, W.L., Peirson, S.N., García-Fernández, J.M., Hankins, M.W., Foster, R.G., 2009. VA opsin-based photoreceptors in the hypothalamus of birds. Curr. Biol. 19, 1396–1402.

Hall, T.R., Cheung, A., Harvey, S., 1987. Some biological activities of recombinant DNA-derived growth hormone on plasma metabolite concentrations in domestic fowl. Comp. Biochem. Physiol. A 86, 29–34.

Han, S., Wang, Y., Liu, L., Li, D., Liu, Z., Shen, X., Xu, H., Zhao, X., Zhu, Q., Yin, H., 2017. Influence of three lighting regimes during ten weeks growth phase on laying performance, plasma levels- and tissue specific gene expression- of reproductive hormones in Pengxian yellow pullets. PLoS One 12, e0177358.

Hargis, P.S., Pardue, S.L., Lee, A.M., Sandel, G.W., 1989. In ovo growth hormone alters growth and adipose tissue development of chickens. Growth Develop. Aging 53, 93–99.

Harrisson, F., 1989. Primary cilia associated with striated rootlets in granulated and folliculo-stellate cells of the avian adenohypophysis. Anat. Embryol. 180, 543–547.

Harrisson, F., Van Hoof, J., Vakaet, L., 1982. The relationship between the folliculo-stellate network and the thyrotropic cells of the avian adenohypophysis. Cell Tissue Res. 226, 97–111.

Harvey, S., Scanes, C.G., 1977. Effect of anesthesia on growth hormone secretion in the domestic fowl (*Gallus domesticus*). Experientia 33, 1242–1243.

Harvey, S., Scanes, C.G., Howe, T., 1977. Growth hormone effects on *in vitro* metabolism of avian adipose and liver tissue. Gen. Comp. Endocrinol. 33, 322–328.

Harvey, S., Scanes, C.G., Chadwick, A., Bolton, N.J., 1978. Influence of fasting, glucose and insulin on the levels in the plasma of growth hormone and prolactin of the domestic fowl. J. Endocrinol. 76, 501–506.

Harvey, S., Davison, T.F., Chadwick, A., 1979a. Ontogeny of growth hormone and prolactin secretion in the domestic fowl (*Gallus domesticus*). Gen. Comp. Endocrinol. 39, 270–273.

Harvey, S., Scanes, C.G., Chadwick, A., Bolton, N.J., 1979b. Growth hormone and prolactin secretion growing domestic fowl; influence of sex and breed. Br. Poult. Sci. 20, 9–17.

Harvey, S., Johnson, C.D., Sanders, E.J., 2000. Extra-pituitary growth hormone in peripheral tissues of early chick embryos. J. Endocrinol. 66, 489–502.

Hattori, A., Ishii, S., Wada, M., 1986. Effects of two kinds of chicken luteinizing hormone-releasing hormone (LHRH), mammalian LHRH and its analogs on the release of LH and FSH in Japanese quail and chicken. Gen. Comp. Endocrinol. 64, 446–455.

Haugen, M.J., Johnson, A.L., 2010. Bone morphogenic protein 2 inhibits FSH responsiveness in hen granulosa cells. Reproduction 140, 551–558.

Hausman, G.J., Barb, C.R., Fairchild, B.D., Gamble, J., Lee-Rutherford, L., 2012. Expression of genes for interleukins, neuropeptides, growth hormone receptor, and leptin receptor in adipose tissue from growing broiler chickens. Domest. Anim. Endocrinol. 43, 260–263.

Hayashi, H., Imai, K., Imai, K., 1991. Characterization of chicken ACTH and α-MSH: the primary sequence of chicken ACTH is more similar to xenopus ACTH than to other avian ACTH. Gen. Comp. Endocrinol. 82, 434–443.

Henare, S.J., Kikuchi, M., Talbot, R.T., Cockrem, J.F., 2011. Changes in plasma gonadotrophins, testosterone, prolactin, thyroxine and triiodothyronine concentrations in male Japanese quail (Coturnix coturnix japonica) of a heavy body weight line during photo-induced testicular growth and regression. Br. Poult. 52, 782–791.

Hendricks 3rd, G.L., Hadley, J.A., Krzysik-Walker, S.M., Prabhu, K.S., Vasilatos-Younken, R., Ramachandran, R., 2009. Unique profile of chicken adiponectin, a predominantly heavy molecular weight multimer, and relationship to visceral adiposity. Endocrinology 150, 3092–3100.

Henson, S.M., Cushing, J.M., Hayward, J.L., 2011. Socially induced ovulation synchrony and its effect on seabird population dynamics. J. Biol. Dynamics 5, 495–516.

Herbute, S., Pintat, R., Ramade, F., Bayle, J.D., 1984. Effect of short exposure to cold on plasma thyroxine in Coturnix quail: role of the infundibular complex and its neural afferents. Gen. Comp. Endocrinol. 56, 1–8.

Herold, M., Brezinschek, H.P., Gruschwitz, M., Dietrich, H., Wick, G., 1992. Investigation of ACTH responses of chickens with autoimmune disease. Gen. Comp. Endocrinol. 88, 188–198.

Heuck, K.A., Ellestad, L.E., Proudman, J.A., Porter, T.E., 2009. Somatotropin response in vitro to corticosterone and triiodothyronine during chick embryonic development: Involvement of type I and type II glucocorticoid receptors. Domest. Anim. Endocrinol. 36, 186–196.

Heuck-Knubel, K., Proszkowiec-Weglarz, M., Narayana, J., Ellestad, L.E., Prakobsaeng, N., Porter, T.E., 2012. Identification of cis elements necessary for glucocorticoid induction of growth hormone gene expression in chicken embryonic pituitary cells. Am. J. Physiol. 302, R606–R619.

Hiyami, G., Kansaku, N., Kinoshitita, M., Sasanami, T., Nakamura, A., Noda, K., Tsukada, A., Shimada, K., Zadworrny, D., 2009. Changes in post-translational modifications of prolactin during development and reproductive cycles in chicken. Gen. Comp. Endocrinol. 161, 238–245.

Houston, B., Goddard, C., 1988. Molecular forms of growth hormone in the chicken pituitary gland. J. Endocrinol. 116, 35–41.

Horiguchi, K., Yako, H., Yoshida, S., Fujiwara, K., Tsukada, T., Kanno, N., Ueharu, H., Nishihara, H., Kato, T., Yashiro, T., Kato, Y., 2016. S100β-positive cells of mesenchymal origin reside in the anterior lobe of the embryonic pituitary gland. PLoS One 11, e0163981.

Hrabia, A., Grzegorzewska, A.K., Sechman, A., 2013. Expression and localization of growth hormone receptor in the oviduct of the laying hen (*Gallus domesticus*). Folia Biol. (Krakow) 61, 271–276.

Hrabia, A., Sechman, A., Rzasa, J., 2014a. Effect of growth hormone on basal and LH-stimulated steroid secretion by chicken yellow ovarian follicles. An *in vitro* study. Folia Biol. (Krakow) 62, 313–319.

Hrabia, A., Leśniak-Walentyn, A., Sechman, A., Gertler, A., 2014b. Chicken oviduct-the target tissue for growth hormone action: effect on cell proliferation and apoptosis and on the gene expression of some oviduct-specific proteins. Cell Tissue Res. 357, 363–372.

Houston, B., O'Neill, I.E., 1991. Insulin and growth hormone act synergistically to stimulate insulin-like growth factor-I production by cultured chicken hepatocytes. J. Endocrinol. 128, 389–393.

Hrabia, A., 2015. Growth hormone production and role in the reproductive system of female chicken. Gen. Comp. Endocrinol. 220, 112–118.

Hsieh, Y.L., Chatterjee, A., Chien, J.T., Yu, J.Y., 2001. Molecular cloning of the cDNAs for pituitary glycoprotein hormone alpha subunits of two species of duck and their gene regulation. J. Mol. Endocrinol. 27, 339–347.

Hsieh, Y.L., Chowdhury, I., Chien, J.T., Chatterjee, A., Yu, J.Y., 2007. Molecular cloning and sequence analysis of the cDNA encoding thyroid-stimulating hormone beta-subunit of common duck and mule duck pituitaries: in vitro regulation of steady-state TSH beta mRNA level. Comp. Biochem. Physiol. B 146, 307–317.

Hu, S., Duggavathi, R., Zadworny, D., 2017. Regulatory mechanisms underlying the expression of prolactin receptor in chicken granulosa cells. PLoS One 12, e0170409.

Hu, X.C., Gao, C.Q., Wang, X.H., Yan, H.C., Chen, Z.S., Wang, X.Q., 2016. Crop milk protein is synthesised following activation of the IRS1/Akt/TOR signalling pathway in the domestic pigeon (*Columba livia*). Br. Poult. Sci. 57, 855–862.

Huang, G., He, C., Meng, F., Li, J., Zhang, J., Wang, Y., 2014. Glucagon-like peptide (GCGL) is a novel potential TSH-releasing factor (TRF) in Chickens: I) Evidence for its potent and specific action on stimulating TSH mRNA expression and secretion in the pituitary. Endocrinology 155, 4568–4580.

Huang, Z., Li, X., Li, Y., Liu, R., Chen, Y., Wu, N., Wang, M., Song, Y., Yuan, X., Lan, L., Xu, Q., Chen, G., Zhao, W., 2015. Molecular cloning and functional analysis of the goose FSHβ gene. Br. Poult. Sci. 56, 284–292.

Hull, K.L., Harvey, S., 1998. Autoregulation of central and peripheral growth hormone receptor mRNA in domestic fowl. J. Endocrinol. 156, 323–329.

Hull, K.L., Marsh, J.A., Harvey, S., 1999. A missense mutation in the GHR gene of Cornell sex-linked dwarf chickens does not abolish serum GH binding. J. Endocrinol. 161, 495–501.

Huybrechts, L.M., King, D.B., Lauterio, T.J., Marsh, J., Scanes, C.G., 1985. Plasma concentrations of somatomedin-C in hypophysectomized, dwarf and intact growing domestic fowl as determined by heterologous radioimmunoassay. J. Endocrinol. 104, 233–239.

Ikegami, K., Katou, Y., Higashi, K., Yoshimura, T., 2009. Localization of circadian clock protein BMAL1 in the photoperiodic signal transduction machinery in Japanese quail. J. Comp. Neurol. 517, 397–404.

Ikemoto, T., Park, M.K., 2005. Chicken RFamide-related peptide (GnIH) and two distinct receptor subtypes: identification, molecular characterization, and evolutionary considerations. J. Reprod. Dev. 51, 359–377.

Ikemoto, T., Parks, M.K., 2006. Molecular and evolutionary characterization of the GnRH-II gene in the chicken: distinctive genomic organization, expression pattern, and precursor sequence. Gene 368, 28–36.

Imai, K., 1973. Effects of avian and mammalian pituitary preparations on induction of ovulation in the domestic fowl, *Gallus domesticus*. J. Reprod. Fertil. 33, 91–98.

Inoue, M., Shiina, T., Aizawa, S., Sakata, I., Takagi, H., Sakai, T., 2012. Detailed analysis of the δ-crystallin mRNA-expressing region in early development of the chick pituitary gland. J. Mol. Histol. 43, 273–280.

Inoue, M., Aizawa, S., Higaki, Y., Kawashima, A., Koike, K., Takagi, H., Sakai, T., Sakata, I., 2013. Detailed morphogenetic analysis of the embryonic chicken pars tuberalis as glycoprotein alpha subunit positive region. J. Mol. Histol. 44, 401–409.

Iturriza, F.C., Estivariz, F.E., Levitin, H.P., 1980. Coexistence of alpha-melanocyte-stimulating hormone and adrenocorticotrophin in all cells containing either of the two hormones in the duck pituitary. Gen. Comp. Endocrinol. 42, 110–115.

Jayanthi, S., Kang, S.W., Bingham, D., Tessaro, B.A., Kumar, T.K.S., Kuenzel, W.J., 2014. Identification of antagonists to the vasotocin receptor sub-type 4 (VT4R) involved in stress by molecular modelling and verification using anterior pituitary cells. J. Biomol. Struct. Dyn. 32, 648–660.

Jenkins, S.A., Muchow, M., Richards, M.P., McMurtry, J.P., Porter, T.E., 2007. Administration of adrenocorticotropic hormone during chicken embryonic development prematurely induces pituitary growth hormone cells. Endocrinology 148, 3914.

Ji, W., Sun, G., Duan, X., Dong, B., Bian, Y., 2016. Cloning of the growth hormone receptor and its muscle-specific mRNA expression in black Muscovy duck (*Cairina moschata*). Br. Poult. Sci. 57, 211–218.

Jin, S., He, T., Yang, L., Tong, Y., Chen, X., Geng, Z., 2018. Association of polymorphisms in Pit-1 gene with growth and feed efficiency in meat-type chickens. Asian-Australas. J. Anim. Sci. 31, 1685–1690.

Johnson, A.L., Bridgham, J.T., 2001. Regulation of steroidogenic acute regulatory protein and luteinizing hormone receptor messenger ribonucleic acid in hen granulosa cells. Endocrinology 142, 3116–3124.

Johnson, A.L., Tilly, J.L., 1988. Effects of vasoactive intestinal peptide on steroid secretion and plasminogen activator activity in granulosa cells of the hen. Biol. Reprod. 38, 296–303.

Johnson, B.E., Scanes, C.G., King, D.B., Marsh, J.A., 1993. Effect of hypophysectomy and growth hormone on immune development in the domestic fowl. Dev. Comp. Immunol. 17, 331–339.

Johnson, A.L., Bridgham, J.T., Witty, J.P., Tilly, J.L., 1996a. Susceptibility of avian ovarian granulosa cells to apoptosis is dependent upon stage of follicle development and is related to endogenous levels of bcl-xlong gene expression. Endocrinology 137, 2059–2066.

Johnson, A.L., Bridgham, J.T., Wagner, B., 1996b. Characterization of a chicken luteinizing hormone receptor (cLH-R) complementary deoxyribonucleic acid, and expression of cLH-R messenger ribonucleic acid in the ovary. Biol. Reprod. 55, 304–309.

Johnson, P.A., Woodcock, J.R., Kent, T.R., 2006. Effect of activin A and inhibin A on expression of the inhibin/activin beta-B-subunit and gonadotropin receptors in granulosa cells of the hen. Gen. Comp. Endocrinol. 147, 102–107.

Joseph, N.T., Morgan, K., Sellar, R., McBride, D., Millar, R.P., Dunn, I.C., 2009. The ligand type III GnRH receptor homologue is predominantly expressed in the pituitary, and exhibits similar ligand selectivity to the type I receptor. J. Endocrinol. 202, 179–190.

Joseph, N.T., Tello, J.A., Bedecarrats, G.Y., Millar, R.P., 2013. Reproductive neuropeptides: prevalence of GnRH and KNDy neural signalling components in a model avian, gallus gallus. Gen. Comp. Endocrinol. 190, 134–143.

Jozsa, R., Scanes, C.G., Vigh, S., Mess, B., 1979. Functional differentiation of the embryonic chicken pituitary gland studied by an immunohistochemical approach. Gen. Comp. Endocrinol. 39, 158–163.

Jozsa, R., Vigh, S., Schally, A.V., Mess, B., 1984. Localization of corticotropin releasing factor- containing neurons in the brain of the domestic fowl. Cell Tiss. Res. 236, 245–248.

Jurkevich, A., Berghman, L.R., Cornett, L.E., Kuenzel, W.J., 2005. Characterization and immunohistochemical visualization of the vasotocin VT2 receptor in the pituitary gland of the chicken, *Gallus gallus*. Gen. Comp. Endocrinol. 143, 82–91.

Jurkevich, A., Berghman, L.R., Cornett, L.E., Kuenzel, W.J., 2008. Immunohistochemical characterization of chicken pituitary cells containing the vasotocin VT2 receptor. Cell Tissue Res. 333, 253–262.

Kaiya, H., Van Der Geyten, S., Kojima, M., Hosoda, H., Kitajima, Y., Matsumoto, M., Geelissen, S., Darras, V.M., Kangawa, K., 2002. Chicken ghrelin: purification, cDNA cloning, and biological activity. Endocrinology 143, 3454–3463.

Kameda, Y., Miura, M., Ohno, S., 1998. Localization and development of chromogranin A and luteinizing hormone immunoreactivities in the secretory-specific cells of the hypophyseal pars tuberalis of the chicken. Histochem. Cell Biol. 109, 211–222.

Kameda, Y., Miura, M., Ohno, S., 2000. Expression of the common alpha-subunit mRNA of glycoprotein hormones during the chick pituitary organogenesis, with special reference to the pars tuberalis. Cell Tissue Res. 299, 71–80.

Kameda, Y., Miura, M., Maruyama, S., 2002. Effect of pinealectomy on the photoperiod-dependent changes of the specific secretory cells and alpha-subunit mRNA level in the chicken pars tuberalis. Cell Tissue Res. 308, 121–130.

Kang, S.W., Kuenzel, W.J., 2015. Deep-brain photoreceptors (DBPs) involved in the photoperiodic gonadal response in an avian species, *Gallus gallus*. Gen. Comp. Endocrinol. 211, 106–113.

Kang, S.W., Gazzillo, L.C., You, S., Wong, E.A., El Halawani, M., 2004. Turkey prolactin gene regulation by VIP through 35-bp *cis*-acting element in the proximal promoter. Gen. Comp. Endocrinol. 138, 157–165.

Kansaku, N., Shimada, K., Saito, N., Hidaka, H., 1998. Effects of protein kinase A inhibitor (H-89) on VIP- and GRF-induced release and mRNA expression of prolactin and growth hormone in the chicken pituitary gland. Comp. Biochem. Physiol., C 119, 89–95.

Karlsson, A.C., Svemer, F., Eriksson, J., Darras, V.M., Andersson, L., Jensen, P., 2015. The effect of a mutation in the thyroid stimulating hormone receptor (TSHR) on development, behavior and TH levels in domesticated chickens. PLoS One 10, e0129040.

Kato, Y., Kato, T., Tomizawa, K., Kamiyoshi, M., Iwasawa, A., 1998. Complementary DNA sequence of chicken thyroid-stimulating hormone (TSH) beta subunit. Endocr. J. 45, 591–594.

Kelly, A.M., Goodson, J.L., 2014. Hypothalamic oxytocin and vasopressin neurons exert sex-specific effects on pair bonding, gregariousness, and aggression in finches. Proc. Natl. Acad. Sci. U.S.A. 111, 6069–6074.

Kihlstrom, J.E., Danninge, I., 1972. Neurohypophysial hormones and sexual behavior in males of the domestic fowl (*Gallus domesticus L.*) and the pigeon (*Columba livia Gmel*). Gen. Comp. Endocrinol. 18, 115–120.

Kim, D., Ocón-Grove, O., Johnson, A.L., 2013. Bone morphogenetic protein 4 supports the initial differentiation of hen (*Gallus gallus*) granulosa cells. Biol. Reprod. 88, 161.

King, J.A., Millar, R.P., 1982. Structure of chicken hypothalamic luteinizing hormone-releasing hormone: II. Isolation and characterization. J. Biol. Chem. 257, 10729–10732.

King, D.B., Scanes, C.G., 1986. Effects of mammalian growth hormone and prolactin on the growth of hypophysectomized chickens. Proc. Soc. Exp. Biol. Med 182, 201–207.

Kitazawa, T., Maeda, Y., Kaeya, H., 2009. Molecular cloning of growth hormone secretagogue-receptor and effect of quail ghrelin on gastro-intestinal motility in Japanese quail. Regul. Pept. 158, 132–142.

Kitazawa, T., Teraoka, H., Kaiya, H., 2017. The chicken is an interesting animal for study of the functional role of ghrelin in the gastrointestinal tract. Endocr. J. 64 (Suppl.), S5–S9.

Klatt, J.D., Goodson, J.L., 2013a. Sex-specific activity and function of hypothalamic nonapeptide neurons during nest-building in zebra finches. Horm. Behav. 64, 818–824.

Klatt, J.D., Goodson, J.L., 2013b. Oxytocin-like receptors mediate pair bonding in a socially monogamous songbird. Proc. Biol. Sci. 280, 20122396.

Kobayashi, M., Ishii, S., 2002. Effects of starvation on gonadotropin and thyrotropin subunit mRNA levels and plasma hormone levels in the male Japanese quail (*Coturnix coturnix japonica*). Zool. Sci. 19, 331–342.

Knight, P.G., Wilson, S.C., Gladwell, R.T., Cunningham, J.F., 1982. Evidence for the involvement of central catecholaminergic mechanisms in mediating the preovulatory surge of luteinizing hormone in the domestic hen. J. Endocrinol. 94, 295–304.

Kobayashi, M., Cockrem, J.F., Ishii, S., 2002. Effects of starvation and refeeding on gonadotropin and thyrotropin subunit mRNAs in male Japanese quail. Zool. Sci. 19, 449–461.

Koike, T.I., Shimada, K., Cornett, L.E., 1988. Plasma concentrations of immunoreactive mesotocin and vasotocin during oviposition in chickens: relationship to oxytocic action of the peptides in vitro and peptide interactions with myometrial binding sites. Gen. Comp. Endocrinol. 70, 119–126.

Korf, H.W., 2018. Signaling pathways to and from the hypophysial pars tuberalis, an important center for the control of seasonal rhythms. Gen. Comp. Endocrinol. 258, 236–243.

Kowalski, K.I., Tilly, J.L., Johnson, A.L., 1991. Cytochrome P450 side-chain cleavage (P450scc) in the hen ovary. I. Regulation of P450scc messenger RNA levels and steroidogenesis in theca cells of developing follicles. Biol. Reprod. 45, 955–966.

Krause, J.S., Meddle, S.L., Wingfield, J.C., 2015. The effects of acute restraint stress on plasma levels of prolactin and corticosterone across life-history stages in a short-lived bird: Gambel's white-crowned sparrow (*Zonotrichia leucophrys gambelii*). Physiol. Biochem. Zool. 88, 589–598.

Kriegsfeld, L.J., Ubuka, T., Bentley, G.E., Tsutsui, K., 2015. Seasonal control of gonadotropin-inhibitory hormone (GnIH) in birds and mammals. Front. Neuroendocrinol. 37, 65–75.

Krishnan, K.A., Proudman, J.A., Bolt, D.J., Bahr, J.M., 1993. Development of a homologous radioimmunoassay for chicken follicle stimulating hormone and measurement of plasma FSH during the ovulation cycle. Comp. Biochem. Physiol. A 105, 729–734.

Kuenzel, W.J., Hancock, M., Nagarajan, G., Aman, N.A., Kang, S.W., 2016. Central effect of vasotocin 4 receptor (VT4R/V1aR) antagonists on the stress response and food intake in chicks given neuropeptide Y (NPY). Neurosci. Lett. 620, 57–61.

Kühn, E.R., Verheyer, G., Chiasson, R.B., Huts, C., Decuypere, E., 1985. Ovine growth hormone reverses the fasting induced decrease of plasma T3 in adult chickens. IRCS Med. Sci. 13, 451–452.

Kusnik, B.I., Pateyuk, A.V., Rusaeva, N.S., 2008. Effect of tetrapeptide Lys-Glu-Asp-Gly and Ala-Glu-Asp-Gly on the structure and function of the thyroid gland in neonatally hypophysectomized chickens. Bull. Exp. Biol. Med. 145, 104–107.

Lacombe, D., Bird, D.M., Scanes, C.G., Hubbard, K.A., 1993. The effect of restricted feeding on plasma growth hormone (GH) concentrations in growing American Kestrels. Condor 98, 559–567.

Lagerstrom, M.C., Fredriksson, R., Bjarnadottir, T.K., Fridmanis, D., Holmquist, T., Andersson, J., Yan, Y.L., Raudsepp, T., Zoorob, R., Kukkonen, J.P., Lundin, L.G., Klovins, J., Chowdhary, B.P., Postlethwait, J.H., Schioth, H.B., 2005. Origin of the prolactin-releasing hormone (PRLH) receptors: evidence of coevolution between PRLH and a redundant neuropeptide Y receptor during vertebrate evolution. Genomics 85, 688–703.

Langohr, I.M., Garner, M.M., Kiupel, M., 2012. Somatotroph pituitary tumors in budgerigars (*Melopsittacus undulatus*). Vet. Pathol. 49, 503–507.

Lau, K.K., Yang, Y., Cook, G.A., Wyatt, R.J., Nishimura, H., 2009. Control of aquaporin 2 expression in collecting ducts of quail kidneys. Gen. Comp. Endocrinol. 160, 288–294.

Leili, S., Scanes, C.G., 1998. The effects of glucocorticoids (dexamethasone) on insulin-like, growth factor-I, IGF-binding proteins, and growth in chickens. Proc. Soc. Exp. Biol. Med 218, 329–333.

Leung, F.C., Taylor, J.E., Wien, S., Van Iderstine, A., 1986. Purified chicken growth hormone (GH) and a human pancreatic GH-releasing hormone increase body weight gain in chickens. Endocrinology 118, 1961–1965.

Li, H., Proudman, J., Kuenzel, W.J., 2009. Differential regulation of gene expression and release of FSH and prolactin by long day and sulfamethazine. Gen. Comp. Endocrinol. 161, 262–266.

Li, C.H., Chung, D., Oelofsen, W., Naudé, R.J., 1978. Adrenocorticotropin 53. The amino acid sequence of the hormone from the ostrich pituitary gland. Biophys. Res. Commun. 81, 900–906.

Li, Z., Johnson, A.L., 1993. Regulation of P450 cholesterol side-chain cleavage messenger ribonucleic acid expression and progesterone production in hen granulosa cells. Biol. Reprod. 49, 463–469.

Liu, H.K., Long, D.W., Bacon, W.L., 2001. Concentration changes patterns of luteinizing hormone and progesterone and distribution of hierarchical follicles in normal and arrested laying Turkey hens. Poult. Sci. 80, 1509–1518.

Liu, L., Porter, T.E., 2004. Endogenous thyroid hormones modulate pituitary somatotroph differentiation during chicken embryonic development. J. Endocrinol. 180, 45–53.

Liu, H.K., Lilburn, M.S., Koyyeri, B., Anderson, J.W., Bacon, W.L., 2004. Preovulatory surge patterns of luteinizing hormone, progesterone, and estradiol-17beta in broiler breeder hens fed ad libitum or restricted fed. Poult. Sci. 83, 823–829.

Liu, H.-Y., Zeng, W.-D., Cao, A.-L., Zhang, C.-Q., 2010. Follicle-stimulating hormone promotes proliferation of cultured chicken ovarian germ cells through protein kinases A and C activation. J. Zhejiang Univ. Sci. B 11, 952–957.

Liu, Y., Wang, C., Wang, H.Y., Wu, H.L., Chen, W.H., He, D.Q., 2014. Molecular cloning, characterisation and tissues expression analysis of the goose (*Anser cygnoides*) vasoactive intestinal peptide (VIP) gene. Br. Poult. Sci. 55, 720–727.

Lodjak, J., Tilgar, V., Mägi, M., 2016. Does the interaction between glucocorticoids and insulin-like growth factor 1 predict nestling fitness in a wild passerine? Gen. Comp. Endocrinol. 225, 149–154.

Løtvedt, P., Fallahshahroudi, A., Bektic, L., Altimiras, J., Jensen, P., 2017. Chicken domestication changes expression of stress-related genes in brain, pituitary and adrenals. Neurobiol. Stress 7, 113–121.

Lovell, T.M., Knight, P.G., Gladwell, R.T., 2005. Variation in pituitary expression of mRNAs encoding putative inhibin co-receptor (betaglycan) and type-I and type-II activin receptors during the chicken ovulatory cycle. J. Endocrinol. 186, 447–455.

Lovell, T.M., Al-Musawi, S.L., Gladwell, R.T., Knight, P.G., 2007. Gonadotrophins modulate hormone secretion and steady-state mRNA levels for activin receptors (type I, IIA, IIB) and inhibin co-receptor (betaglycan) in granulosa and theca cells from chicken prehierarchical and preovulatory follicles. Reproduction 133, 1159–1168.

Luan, X., Luo, L., Cao, Z., Li, R., Liu, D., Gao, M., Liu, M., Wang, L., 2014. Molecular cloning and expression analysis of the synaptotagmin-1 gene in the hypothalamus and pituitary of Huoyan goose during different stages of the egg-laying cycle. Reprod. Biol. Endocrinol. 12, 83.

Luna, M., Huerta, L., Berumen, L., Martínez-Coria, H., Harvey, S., Arámburo, C., 2004. Growth hormone in the male reproductive tract of the chicken: heterogeneity and changes during ontogeny and maturation. Gen. Comp. Endocrinol. 137, 37–49.

Luna, M., Barraza, N., Berumen, L., Carranza, M., Pedernera, E., Harvey, S., Arámburo, C., 2005. Heterogeneity of growth hormone immunoreactivity in lymphoid tissues and changes during ontogeny in domestic fowl. Gen. Comp. Endocrinol. 144, 28–37.

Luna-Acosta, J.L., Alba-Betancourt, C., Martínez-Moreno, C.G., Ramírez, C., Carranza, M., Luna, M., Arámburo, C., 2015. Direct antiapoptotic effects of growth hormone are mediated by PI3K/Akt pathway in the chicken bursa of Fabricius. Gen. Comp. Endocrinol. 224, 148–159.

Lv, C., Mo, C., Liu, H., Wu, C., Li, Z., Li, J., Wang, Y., 2018. Dopamine D2-like receptors (DRD2 and DRD4) in chickens: tissue distribution, functional analysis, and their involvement in dopamine inhibition of pituitary prolactin expression. Gene 651, 33–43.

Ma, W., Wang, C., Su, Y., Tian, Y., Zhu, H., 2015. Expression of nerve growth factor and its receptor, tyrosine kinase receptor A, in rooster testes. Anim. Reprod. Sci. 161, 40–46.

MacKenzie, D.S., 1981. In vivo thyroxine release in day-old cockerels in response to acute stimulation by mammalian and avian pituitary hormones. Poult. Sci. 60, 2136–2143.

Macnamee, M.C., Sharp, P.J., Lea, R.W., Sterling, R.J., Harvey, S., 1986. Evidence that vasoactive intestinal polypeptide is a physiological prolactin-releasing factor in the bantam hen. Gen. Comp. Endocrinol. 62, 470–478.

Maddineni, S., Metzger, S., Ocón, O., Hendricks, G., Ramachandran, R., 2005. Adiponectin gene is expressed in multiple tissues in the chicken.: food deprivation influences adiponectin messenger ribonucleic acid. Endocrinology 146, 4250–4256.

Maddinini, S., Ocón, O.M., Krzysik-Walker, S.M., Hendricks, G.L., Proudman, J.A., Ramachandran, R., 2008. Gonadotrophin-inhibitory hormone receptor expression in the chicken pituitary gland: potential influence of sexual maturation and ovarian steroids. J. Neuroendocrinol. 20, 1078–1088.

Makhsous, S.G., Mirhoseini, S.Z., Zamiri, M.J., Niazi, A, A., 2013. Polymorphisms of the growth hormone gene in native chicken population: association with egg production. Bull. Vet. Inst. Pulawy 57, 73–77.

Mao, J.N., Cogburn, L.A., Burnside, J., 1997. Growth hormone down-regulates growth hormone receptor mRNA in chickens but developmental increases in growth hormone receptor mRNA occur independently of growth hormone action. Mol. Cell. Endocrinol. 129, 135–143.

Malamed, S., Deaver, D., Perez, F., Radecki, S., Gibney, J., Scanes, C.G., 1997. Quantitative studies of chicken somatotrophs during growth and development by morphometry, immunocytochemistry, and flow cytometry. Gen. Comp. Endocrinol. 108, 25–34.

Malamed, S., Gibney, J.A., Cain, L.D., Perez, F.M., Scanes, C.G., 1993. Immunocytochemical studies of chicken somatotrophs and somatotroph granules before and after hatching. Cell Tiss. Res. 272, 369–374.

Malamed, S., Gibney, J.A., Loesser, K.E., Scanes, C.G., 1985. Age-related changes of the somatotrophs of the domestic fowl Gallus domesticus. Cell Tiss. Res. 239, 87–91.

Malamed, S., Gibney, J.A., Scanes, C.G., 1988. Immunogold identification of the somatotrophs of domestic fowl of different ages. Cell Tiss. Res. 251, 581–585.

Maney, D.L., Hahn, T.P., Schoech, S.J., Sharp, P.J., Morton, M.L., Wingfield, J.C., 1999. Effects of ambient temperature on photoinduced prolactin secretion in three subspecies of white-crowned sparrow, Zonotrichia leucophrys. Gen. Comp. Endocrinol. 113, 445–456.

Mao, J.N., Burnside, J., Postel-Vinay, M.C., Pesek, J.D., Chambers, J.R., Cogburn, L.A., 1998. Ontogeny of growth hormone receptor gene expression in tissue of growth-selected strains of broiler chickens. J. Endocrinol. 156, 67–75.

Mares, R., Doutrelant, C., Paquet, M., Spottiswoode, C.N., Covas, R., 2017. Breeding decisions and output are correlated with both temperature and rainfall in an arid-region passerine, the sociable weaver. R. Soc. Open Sci. 4, 170835.

Marsh, J.A., Johnson, B.E., Lillehoj, H.S., Scanes, C.G., 1992. Effect of thyroxine and chicken growth hormone on immune function in autoimmune thyroiditis (obese) strain chicks. Proc. Soc. Exp. Biol. Med. 199, 114–122.

Martínez-Coria, H., López-Rosales, L.J., Carranza, M., Berumen, L., Luna, M., Arámburo, C., 2002. Differential secretion of chicken growth hormone variants after growth hormone-releasing hormone stimulation in vitro. Endocrine 17, 91–102.

Martínez-Moreno, C.G., Ávila-Mendoza, J., Wu, Y., Arellanes-Licea, E.D.C., Louie, M., Luna, M., Arámburo, C., Harvey, S., 2016. Neuroprotection by GH against excitotoxic-induced cell death in retinal ganglion cells. Gen. Comp. Endocrinol. 234, 68–80.

Maseki, Y., Nakamura, K., Iwasawa, A., Zheng, J., Inoue, K., Sakai, T., 2004. Development of gonadotropes in the chicken embryonic pituitary gland. Zool. Sci. 21, 435–444.

Maung, Z.W., Follett, B.K., 1977. Effects of chicken and ovine luteinizing hormone on androgen release and cyclic AMP production by isolated cells from the quail testes. Gen. Comp. Endocrinol. 33, 242–253.

Maung, S.L., Follett, B.K., 1978. The endocrine control by luteinizing hormone of testosterone secretion from the testis of Japanese quail. Gen. Comp. Endocrinol. 36, 79–89.

McCann-Levorse, L.M., Radecki, S.V., Donoghue, D.J., Malamed, S., Foster, D.N., Scanes, C.G., 1993. Ontogeny of pituitary growth hormone and growth hormone mRNA in the chicken. Proc. Soc. Exp. Biol. 202, 109–113.

McFarlane, H.O., Joseph, N.T., Maddineni, S.R., Ramachandran, R., Bédécarrats, G.Y., 2011. Development, validation, and utilization of a novel antibody specific to the type III chicken gonadotropin-releasing hormone receptor. Domest. Anim. Endocrinol. 40, 110–118.

McNichols, M.J., McNabb, F.M., 1988. Development of thyroid function and its pituitary control in embryonic and hatchling precocial Japanese quail and altricial Ring doves. Gen. Comp. Endocrinol. 70, 109–118.

Meng, F., Huang, G., Gao, S., Li, J., Yan, Z., Wang, Y., 2014. Identification of the receptors for somatostatin (SST) and gene CORT cortistatin (CST) in chickens and investigation of the roles of cSST28, cSST14, and cCST14 in inhibiting cGHRH1-27NH2-induced growth hormone secretion in cultured chicken pituitary cells. Mol. Cell. Endocrinol. 384, 83–95.

Mi, Y., Zhang, C., Xie, M., Zeng, W., 2004. Effects of follicle-stimulating hormone and androgen on proliferation of cultured testicular germ cells of embryonic chickens. Gen. Comp. Endocrinol 138, 237–246.

Mikami, S., 1980. Hypothalamic control of the avian adenohypophysis. In: Tanabe, Y., Tanaka, K., Ookawa, T. (Eds.), Biological Rhythms in Birds: Neural and Endocrine Aspects. Springer-Verlag, Tokyo, pp. 17–32.

Mikhailova, M.V., Mayeux, P.R., Jurkevich, A., Kuenzel, W.J., Madison, F., Periasamy, A., Chen, Y., Cornett, L.E., 2007. Hetero-oligomerization between vasotocin and corticotropin-releasing hormone (CRH) receptors augments CRH-stimulated 3',5'-cyclic adenosine monophosphate production. Mol. Endocrinol. 21, 2178–2188.

Millar, R.B., Milton, R.C., Follett, B.K., King, J.A., 1986. Receptor binding and gonadotropin-releasing activity of a novel chicken gonadotropin-releasing hormone [His5, Trp7, Tyr8]-GnRH and a D-Arg6 analog. Endocrinology 119, 224–231.

Miller, D.A., Vleck, C.M., Otis, D.L., 2009. Individual variation in baseline and stress-induced corticosterone and prolactin levels predicts parental effort by nesting mourning doves. Horm. Behav. 56, 457–464.

Minvielle, F., Grossmann, R., Gourichon, D., 2007. Development and performances of a Japanese quail line homozygous for the diabetes insipidus (*di*) mutation. Poult. Sci. 86, 249–254.

Mo, C., Cai, G., Huang, L., Deng, Q., Lin, D., Cui, L., Wang, Y., Li, J., 2015. Corticotropin-releasing hormone (CRH) stimulates cocaine- and amphetamine-regulated transcript gene (CART1) expression through CRH type 1 receptor (CRHR1) in chicken anterior pituitary. Mol. Cell. Endocrinol. 417, 166–177.

Mo, C., Huang, L., Cui, L., Lv, C., Lin, D., Song, L., Zhu, G., Li, J., Wang, Y., 2017. Characterization of NMB, GRP and their receptors (BRS3, NMBR and GRPR) in chickens. J. Mol. Endocrinol. 59, 61–79.

Moellers, R.F., Cogburn, L.A., 1995. Chronic intravenous infusion of chicken growth hormone increases body fat content of young broiler chickens. Comp. Biochem. Physiol A 110, 47–56.

Mohanty, B., 2006. Extracellular accumulation in the avian pituitary gland: histochemical analysis in two species of Indian wild birds. Cells Tissues Organs 183, 99–106.

Mohanty, B., Das, S., Naik, D.R., 1997. Immunocytochemistry of the pars tuberalis of the pituitary gland in some Indian wild birds: a comparative study. Gen. Comp. Endocrinol. 108, 109–118.

Murphy, A.E., Harvey, S., 2001. Extrapituitary beta TSH and GH in early chick embryos. Mol. Cell. Endocrinol. 185, 161–171.

Murphy, A.E., Harvey, S., 2002. Extrapituitary TSH in early chick embryos: Pit-1 dependence? J. Mol. Neurosci. 18, 77–87.

Miyamoto, K., Hasegawa, Y., Nomara, M., Igarashi, M., Kangawa, K., Matsuo, H., 1984. Identification of the second gonadotropin releasing hormone in chicken hypothalamus: evidence that gonadotropin secretion is controlled by two distinct gonadotropin releasing hormones in avian species. Proc. Natl. Acad. Sci. U.S.A 81, 3874–3878.

Murase, D., Taniuchi, S., Takeuchi, S., Adachi, H., Kansaku, N., Okazaki, K., Ohkubo, T., 2011. Role of chicken Pit-1 isoforms in activating growth hormone gene. Gen. Comp. Endocrinol. 173, 248–252.

Nagarajan, G., Tessaro, B.A., Kang, S.W., Kuenzel, W.J., 2014. Identification of arginine vasotocin (AVT) neurons activated by acute and chronic restraint stress in the avian septum and anterior diencephalon. Gen. Comp. Endocrinol. 202, 59–68.

Nakane, Y., Ikegami, K., Ono, H., Yamamoto, N., Yoshida, S., Hirunagi, K., Ebihara, S., Kubo, Y., Yoshimura, T., 2010. A mammalian neural tissue opsin (Opsin 5) is a deep brain photoreceptor in birds. Proc. Natl. Acad. Sci. U.S.A. 107, 15264–15268.

Nakao, N., Takagi, T., Iigo, M., Tsukamoto, T., Yasuo, S., Masuda, T., Yanagisawa, T., Ebihara, S., Yoshimura, T., 2006. Possible involvement of organic anion transporting polypeptide 1c1 in the photoperiodic response of gonads in birds. Endocrinology 147, 1067–1073.

Nakao, N., Ono, H., Yamamura, T., Anraku, T., Takagi, T., Higashi, K., Yasuo, S., Katou, Y., Kageyama, S., Uno, Y., Kasukawa, T., Iigo, M., Sharp, P.J., Iwasawa, A., Suzuki, Y., Sugano, S., Niimi, T., Mizutani, M., Namikawa, T., Ebihara, S., Ueda, H.R., Yoshimura, T., 2008. Thyrotrophin in the pars tuberalis triggers photoperiodic response. Nature 452, 317–322.

Nakayama, H., Nakagawa-Mizuyachi, K., Takahashi, T., Kawashima, M., 2010. Calcitonin receptor binding in the hen neurohypophysis before and after oviposition. Poult. Sci. 89, 1473–1480.

Nakayama, H., Takahashi, T., Oomatsu, Y., Nakagawa-Mizuyachi, K., Kawashima, M., 2011a. Parathyroid hormone-related peptide directly increases adrenocorticotropic hormone secretion from the anterior pituitary in hens. Poult. Sci. 90, 175–180.

Nakayama, H., Takahashi, T., Nakagawa-Mizuyachi, K., Kawashima, M., 2011b. Effect of calcitonin on adrenocorticotropic hormone secretion stimulated by corticotropin-releasing hormone in the hen anterior pituitary. Anim. Sci. J. 82, 475–480.

Nakayama, H., Takahashi, T., Nakagawa-Mizuyachi, K., Kawashima, M., 2011c. Effect of estradiol-17β on calcitonin receptor bindings in the hen neurohypophysis. Poult. Sci. 90, 191–194.

Naudé, R., Oelofsen, W., Takahashi, A., Amano, M., Kawauchi, H., 2006. Molecular cloning and characterization of preproopiomelanocortin (prePOMC) cDNA from the ostrich (*Struthio camelus*). Gen. Comp. Endocrinol. 146, 310–317.

Nicholl, C.S., 1967. Bio-assay of prolactin. Analysis of the pigeon crop-sac response to local prolactin injection by an objective and quantitative method. Endocrinology 80, 641–655.

Nie, Q., Fang, M., Xie, L., Zhou, M., Liang, Z., Luo, Z., Wang, G., Bi, W., Liang, C., Zhang, W., Zhang, X., 2008. The PIT1 gene polymorphisms were associated with chicken growth traits. BMC Genet. 9, 20.

Nishimura, H., Yang, Y., 2013. Aquaporins in avian kidneys: function and perspectives. Am. J. Physiol. 305, R1201–R1214.

Nishimura, S., Yamashita, M., Kaneko, T., Kawabata, F., Tabata, S., 2017. Cytokeratin-positive folliculo-stellate cells in chicken adenohypophysis. Anim. Sci. J. 88, 1835–1841.

Oclon, E., Solomon, G., Hrabia, A., Druyan, S., Hayouka, Z., Gertler, A., 2018. New reagents for poultry research: preparation, purification, and in vitro evaluation of non-PEGylated and mono-PEGylated chicken prolactin. Poult. Sci. 97, 3277–3285.

Ocón-Grove, O.M., Poole, D.H., Johnson, A.L., 2012. Bone morphogenetic protein 6 promotes FSH receptor and anti-Müllerian hormone mRNA expression in granulosa cells from hen prehierarchal follicles. Reproduction 143, 825–833.

Onagbesan, O.M., Peddie, M.J., 1988. Induction of ovulation and oviposition in female quail with luteinizing hormone, luteinizing hormone releasing hormone, or progesterone. Gen. Comp. Endocrinol. 71, 124–131.

Onagbesan, O.M., Decuypere, E., Leenstra, F., Ehlhardt, D.A., 1999. Differential effects of amount of feeding on cell proliferation and progesterone production in response to gonadotrophins and insulin-like growth factor I by ovarian granulosa cells of broiler breeder chickens selected for fatness or leanness. J. Reprod. Fertil. 116, 73–85.

Onagbesan, O.M., Metayer, S., Tona, K., Williams, J., Decuypere, E., Bruggeman, V., 2006. Effects of genotype and feed allowance on plasma luteinizing hormones, follicle-stimulating hormones, progesterone, estradiol levels, follicle differentiation, and egg production rates of broiler breeder hens. Poult. Sci. 85, 1245–1258.

Opałka, M., Kamińska, B., Ciereszko, R., Dusza, L., 2004. Genistein affects testosterone secretion by Leydig cells in roosters (*Gallus gallus domesticus*). Reprod. Biol. 4, 185–193.

Opel, H., Proudman, J.A., 1988. Effects of poults on plasma concentrations of prolactin in turkey hens incubating without eggs or a nest. Br. Poult. Sci. 29, 791–800.

Orlowski, S., Flees, J., Anthony, N., Dridi, S., 2017. Differential expression of water channel- and nom-coding RNA biogenesis-related genes in three lines of chickens under a short-term water restriction. Poult. Sci. 96, 4172–4181.

Ottinger, M.A., Kubakawa, K., Kikuchi, M., Thompson, N., Ishii, S., 2002. Effects of exogenous testosterone on testicular luteinizing hormone and follicle-stimulating hormone receptors during aging. Exp. Biol. Med. 227, 830–836.

Ouyang, J.H., Xie, L., Nie, Q., Luo, C., Liang, Y., Zeng, H., Zhang, X., 2008. Single nucleotide polymorphism (SNP) at the GHR gene and its associations with chicken growth and fat deposition traits. Br. Poult. Sci. 49, 87–95.

Ouyang, J.Q., Sharp, P.J., Dawson, A., Quetting, M., Hau, M., 2011. Hormone levels predict individual differences in reproductive success in a passerine bird. Proc. R. Soc. 278, 2537–2545.

Pals, K., Boussemaere, M., Swinnen, E., Vankelecom, H., Denef, C., 2006. A Pituitary cell type coexpressing messenger ribonucleic acid of proopiomelanocortin and the glycoprotein hormone alpha-subunit in neonatal rat and chicken: rapid decline with age and reappearance in vitro under regulatory pressure of corticotropin-releasing hormone in the rat. Endocrinology 147, 4738–4752.

Papkoff, H., Licht, P., Bona-Gallo, A., MacKenzie, D.S., Oelofsen, W., Oosthuizen, M.M., 1982. Biochemical and immunological characterization of pituitary hormones from the ostrich (*Struthio camelus*). Gen. Comp. Endocrinol. 48, 181–195.

Pedersen, A., Tomaszycki, M.L., 2012. Oxytocin antagonist treatment alters the formation of pair relationships in zebra finches of both sexes. Horm. Behav. 62, 113–119.

Perfito, N., Zann, R., Ubaka, T., Bentley, G., Hau, M., 2011. Potential roles for GnIH and GnRH-II in reproductive axis regulation of an opportunist breeding songbird. Gen. Comp. Endocrinol. 173, 20–26.

Perfito, N., Jeong, S.Y., Silverin, B., Calisi, R.M., Bentley, G.E., Hau, M., 2012. Anticipating spring: wild populations of great tits (*Parus major*) differ in expression of key genes for photoperiodic time measurement. PLoS One 7, e34997.

Pinheiro, P.L., Cardoso, J.C., Power, D.M., Canario, A.V., 2012. Functional characterization and evolution of PTH/PTHrP receptors: insights from the chicken. BMC Evol. Biol. 12, 110.

Post, J., Rebel, J.M.J., ter Huurne, A.A.H.M., 2003. Physiological effects of elevated plasma corticosterone concentrations in broiler chickens. An alternative means by which to Assess the physiological effects of stress. Poult. Sci. 82, 1313–1318.

Porter, T.E., Couger, G.S., Dean, C.E., Hargis, B.M., 1995. Ontogeny of growth hormone (GH)-secreting cells during chicken embryonic development: initial somatotrophs are responsive to GH-releasing hormone. Endocrinology 136, 1850–1856.

Porter, T.E., Ellestad, L.E., Fay, A., Stewart, J.L., Bossis, I., 2006. Identification of the chicken growth hormone-releasing hormone receptor (GHRH-R) mRNA and gene: regulation of anterior pituitary GHRH-R mRNA levels by homologous and heterologous hormones. Endocrinology 147, 2535–2543.

Powell, R.C., Jach, H., Millar, R.P., King, J.A., 1987. Identification of Gln8-GnRH and His5, Trp7, Tyr8-GnRH in the hypothalamus and extrahypothalamic brain of the ostrich (*Struthio camelus*). Peptides 8, 185–190.

Price, E.R., Bauchinger, U., Zajac, D.M., Cerasale, D.J., McFarlan, J.T., Gerson, A.R., McWilliams, S.R., Guglielmo, C.G., 2011. Migration- and exercise-induced changes to flight muscle size in migratory birds and association with *IGF1* and *myostatin* mRNA expression. J. Exp. Biol. 214, 2823–2831.

Proudman, J.A., Opel, H., 1988. Stimulation of prolactin secretion from turkey anterior pituitary cells in culture. Proc. Soc. Exp. Biol. Med 187, 448–454.

Proudman, J.A., Opel, H., 1990a. Half-life and metabolic clearance rate of recombinant-derived chicken growth hormone and purified Turkey growth hormone in intact and hypophysectomized turkeys. Poult. Sci. 69, 1569–1575.

Proudman, J.A., Opel, H., 1990b. Effect of peptide histidine isoleucine on in vitro and in vivo prolactin secretion in the Turkey. Poult. Sci. 69, 1209–1214.

Proudman, J.A., McGuinness, M.C., Krishnan, K.A., Cogburn, L.A., 1994. Endocrine and metabolic responses of intact and hypophysectomized Turkey poults given a daily injection of chicken growth hormone. Comp. Biochem. Physiol., C 109, 47–56.

Proudman, J.A., Vandesande, F., Berghman, L.R., 1999. Immunohistochemical evidence that follicle-stimulating hormone and luteinizing hormone reside in separate cells in the chicken pituitary. Biol. Reprod. 60, 1324–1328.

Proudman, J.A., Clerens, S., van den Bergh, G., Garrett, W.M., Verhaert, P.D., Vandesande, F., Berghman, L.R., 2003. Immunohistochemical localization of chromogranin A in gonadotrophs and somatotrophs of the Turkey and chicken pituitary. Gen. Comp. Endocrinol. 132, 293–303.

Proudman, J.A., Scanes, C.G., Johannsen, S.A., Berghman, L.R., Camp, M.J., 2006. Comparison of the ability of the three endogenous GnRHs to stimulate release of follicle stimulating hormone and luteinizing hormone. Domest. Anim. Endocrinol. 31, 141–153.

Qin, N., Fan, X.C., Xu, X.X., Tyasi, T.L., Li, S.J., Zhang, Y.Y., Wei, M.L., Xu, R.F., 2015. Cooperative effects of FOXL2 with the members of TGF-beta superfamily on FSH Receptor mRNA expression and granulosa cell proliferation from hen prehierarchical follicles. PLoS One 10, e0141062.

Qasimi, M.I., Nagaoka, K., Watanabe, G., 2018. Feeding of phytosterols reduced testosterone production by modulating GnRH and GnIH expression in the brain and testes of male Japanese quail (*Coturnix coturnix japonica*). Poult. Sci. 97, 1066–1072.

Quaresma, M.A.G., Antunes, I.C., Ribeiro, M.F., Prazeres, S., Bessa, R.J.B., da Costa, P.M., 2017. Immunocastration as an alternative to caponization: evaluation of its effect on body and bone development and on meat color and composition. Poult. Sci. 96, 3608–3615.

Radecki, S.V., Deaver, D.R., Scanes, C.G., 1994. Triiodothyronine reduces growth hormone secretion and pituitary growth hormone mRNA in the chicken, in vivo and in vitro. Proc. Soc. Exp. Biol. Med 205, 340–346.

Radecki, S.V., McCann-Levorse, L., Agarwal, S.K., Burnside, J., Proudman, J.A., Scanes, C.G., 1997. Chronic administration of growth hormone (GH) to adult chickens exerts marked effects on circulating concentrations of insulin-like growth factor-I (IGF-I), IGF binding proteins, hepatic GH regulated gene I, and hepatic GH receptor mRNA. Endocrine 6, 117–124.

Rahn, H., 1939. The development of the chick pituitary with special reference to the cellular differentiation of the pars buccali. J. Morphol. 64, 483–517.

Rahn, H., Drager, G.A., 1941. Quantitative assay of melanophore dispersing hormone during the development of the chicken pituitary. Endocrinology 29, 725–730.

Rahn, H., Painter, B.T., 1941. The comparative histology of bird pituitary. Anat. Rec. 79, 297–311.

Ramachandran, R., Ocón-Grove, O.M., Metzger, S., 2007. Molecular cloning and tissue expression of chicken AdipoR1 and AdipoR2 complimentary deoxyribonucleic acid. Domest. Anim. Endocrinol. 33, 19–31.

Ramesh, R., Solow, R., Proudman, J.A., Kuenzel, W.J., 1998. Identification of mammosomatotrophs in the Turkey hen pituitary: increased abundance during hyperprolactinemia. Endocrinology 139, 781–786.

Ramesh, R., Kuenzel, W.J., Proudman, J.A., 2001. Increased proliferative activity and programmed cellular death in the Turkey hen pituitary gland following interruption of incubation behavior. Biol. Reprod. 64, 611–618.

Rancourt, R.C., Schellong, K., Tzschentke, B., Henrich, W., Plagemann, A., 2018. DNA methylation and expression of proopiomelanocortin (*POMC*) gene in the hypothalamus of three-week-old chickens show sex-specific differences. FEBS Open Biol. 8, 932–939.

Rangel, P.L., Rodríguez, A., Rojas, S., Sharp, P.J., Gutierrez, C.G., 2009. Testosterone stimulates progesterone production and STAR, P450 cholesterol side-chain cleavage and LH receptor mRNAs expression in hen (*Gallus domesticus*) granulosa cells. Reproduction 138, 961–969.

Reichardt, A.K., 1993. Functional differentiation of the pituitary gland during development of the domestic ring dove (*Streptopelia rose-grisea*). Gen. Comp. Endocrinol. 92, 41–53.

Riddle, O., Bates, R.W., Lahr, E.L., 1935. Prolactin induces broodiness in fowl. Am. J. Physiol. 111, 352–360.

Riou, S., Chastel, O., Lacroix, A., Hamer, K.C., 2010. Stress and parental care: prolactin responses to acute stress throughout the breeding cycle in a long-lived bird. Gen. Comp. Endocrinol. 168, 8–13.

Robinson, G.A., Wasnidge, D.C., Floto, F., Downie, S.E., 1976. Ovarian ^{125}I transference in the laying Japanese quail: apparent stimulation by FSH and lack of stimulation by TSH. Poult. Sci. 55, 1665–1671.

Robinzon, B., Koike, T.I., Neldon, H.L., Kinzler, S.L., 1988a. Distribution of immunoreactive mesotocin and vasotocin in the brain and pituitary of chickens. Peptides 9, 829–833.

Robinzon, B., Koike, T.I., Neldon, H.L., Kinzler, S.L., Henry, I.R., el Halawani, M.E., 1988b. Physiological effects of arginine vasotocin and mesotocin in cockerels. Br. Poult. Sci. 29, 639–652.

Robinzon, B., Koike, T.I., Kinzler, S.L., Neldon, H.L., 1990. Arginine vasotocin and mesotocin in the anterior hypothalamus, neurohypophysis, proventriculus and plasma of White Leghorn cockerels, during dehydration. Br. Poult. Sci. 31, 651–659.

Robinzon, B., Koike, T.I., Marks, P.A., 1993. At a low dose, arginine vasotocin has vasopressor rather than vasodepressor effect in chickens. Gen. Comp. Endocrinol. 91, 105–112.

Romanoff, A., 1960. The Avian Embryo. Structural and Functional Development. The Macmillan Co., New York.

Rosebrough, R.W., McMurtry, J.P., Vasilatos-Youngen, J., 1991. Effect of pulsatile or continuous administration of pituitary-derived chicken growth hormone (p-cGH) on lipid metabolism in broiler pullets. Comp. Biochem. Physiol. A 99, 207–214.

Rosebrough, R.W., McMurtry, J.P., Vasilatos-Younken, R., 1992. In vitro lipid metabolism, growth and metabolic hormone concentrations in hyperthyroid chickens. Br. J. Nutr. 68, 661–616.

Rosselot, G., McMurtry, J.P., Vasilatos-Younken, R., Czerwinski, S., 1995. Effect of exogenous chicken growth hormone (cGH) administration on insulin-like growth factor-I (IGF-I) gene expression in domestic fowl. Mol. Cell. Endocrinol. 114, 157–166.

Rozenboim, I., Silsby, J.L., Tabibzadeh, C., Pitts, G.R., Youngren, O.M., El Halawani, M.E., 1993. Hypothalamic and posterior pituitary content of vasoactive intestinal peptide, gonadotropin releasing hormone I and II in the Turkey hen. Biol. Reprod. 49, 622–627.

Rubin, C.-J., Zody, M.C., Eriksson, J., Meadows, J.R.S., Sherwood, E., Webster, M.T., Jiang, L., Ingman, M., Sharpe, T., Ka, S., Hallböök, F., Besnier, F., Carlborg, O., Bed'hom, B., Tixier-Boichard, M., Jensen, P., Siegel, P., Lindblad-Toh, K., Andersson, L., 2010. Whole-genome resequencing reveals loci under selection during chicken domestication. Nature 464, 587–591.

Rzasa, J., 1978. Effects of arginine vasotocin and prostaglandin E1 on the hen uterus. Prostaglandins 16, 357–372.

Rzasa, J., 1984. The effect of arginine vasotocin on prostaglandin production by the hen uterus. Gen. Comp. Endocrinol. 53, 260–263.

Saeed, W., El Halawani, M.E., 1986. Modulation of prolactin response to thyrotropin releasing hormone by ovarian steroids inovariectomized turkeys (*Meleagris gallopavo*). Gen. Comp. Endocrinol. 62, 129–136.

Saito, E.-S., Kaiya, H., Tachibana, T., Tomonaga, S., Denbow, D.M., Kangawa, K., Furuse, M., 2005. Inhibitory effect of ghrelin on food intake is mediated by the corticotropin-releasing factor system in neonatal chicks. Regul. Pept. 125, 201–208.

Saito, N., Kinzler, S., Koike, T.I., 1990. Arginine vasotocin and mesotocin levels in theca and granulosa levels of the ovary during the ovipositioncycle in hens (*Gallus domesticus*). Gen. Comp. Endocrinol. 79, 54–63.

Sasaki, F., Doshita, A., Matsumoto, Y., Kuwahara, S., Tsukamota, Y., Ogawa, K., 2003. Embryonic development of the pituitary gland in the chick. Cell Tissue Res. 173, 65–74.

Sánchez-Arrones, L., Ferrán, J.L., Hidalgo-Sanchez, M., Puelles, L., 2015. Origin and early development of the chicken adenohypophysis. Front. Neuroanat. 9, 7.

Scanes, C.G., 1974. Some in vitro effects of synthetic thyrotrophin releasing factor on the secretion of thyroid stimulating hormone from the anterior pituitary gland of the domestic fowl. Neuroendocrinology 15, 1–9.

Scanes, C.G., 1992. Lipolytic and diabetogenic effects of native and biosynthetic growth hormone. Comp. Biochem. Physiol. 101A, 871–878.

Scanes, C.G., 2015. Pituitary gland. In: Scanes, C.G. (Ed.), Sturkie's Avian Physiology, sixth ed. Elsevier, Amsterdam, pp. 497–553.

Scanes, C.G., Fagioli, J.H., 1980. Effects of mammalian and avian gonadotropins on in vitro progesterone production by avian ovarian granulosa cells. Gen. Comp. Endocrinol. 41, 1–7.

Scanes, C.G., Decuypere, E., Marsh, J., 1982. Plasma concentration of growth hormone, thyroxine and triiodothyronine during growth in dwarf strains of chickens. Poult. Sci. 61, 1539–1548.

Scanes, C.G., Harvey, S., 1989. Somatostatin inhibition of thyrotropin-releasing hormone- and growth hormone-releasing factor-induced growth hormone secretion in young and adult anesthetized chickens. Gen. Comp. Endocrinol. 75, 256–264.

Scanes, C.G., Pierzchala-Koziec, K., 2018. Perspectives on endogenous opioids in birds. Front. Physiol. 9, 1842.

Scanes, C.G., Godden, P.M.M., Sharp, P.J., 1977. A homologous radioimmunoassay for chicken FSH: observations on the ovulatory cycle. J. Endocrinol. 73, 473–482.

Scanes, C.G., Griminger, P., Buonomo, F.C., 1981. Effects of dietary protein restriction on circulating concentrations of growth hormone in growing domestic fowl (*Gallus domesticus*). Proc. Soc. Exp. Biol. Med. 168, 334–337.

Scanes, C.G., Carsia, R.V., Lauterio, T.J., Huybrechts, L., Rivier, J., Vale, W., 1984. Synthetic human pancreatic growth hormone releasing factor (GRF) stimulates growth hormone secretion in the domestic fowl (*Gallus domesticus*). Life Sci. 34, 1127–1134.

Scanes, C.G., Duyka, D.R., Lauterio, T.J., Bowen, S.J., Huybrechts, I.M., Bacon, W.L., King, D.B., 1986. Effect of chicken growth hormone, triiodothyronine and hypophysectomy in growing domestic fowl. Growth 50, 12–31.

Scanes, C.G., Proudman, J.A., Radecki, S.V., 1999. Influence of continuous growth hormone or insulin-like growth factor I administration in adult female chickens. Gen. Comp. Endocrinol. 114, 315–323.

Scanes, C.G., Glavaski-Joksimovic, A., Johannsen, S.A., Jeftinija, S., Anderson, L.L., 2007. Subpopulations of somatotropes with differing intracellular calcium concentration responses to secretagogues. Neuroendocrinology 85, 221–231.

Schaper, S.V., Dawson, A., Sharp, P.J., Gienapp, P., Caro, S.P., Visser, M.E., 2012. Increasing temperature, not mean temperature, is a cue for avian timing of reproduction. Am. Nat. 179, E55–E69.

Schew, W.A., McNabb, F.M.A., Scanes, C.G., 1996. Comparison of the ontogenesis of thyroid hormones, growth hormone, and insulin-like growth factor-I in *ad libitum* and food restricted (altricial) European starlings and (precoccial) Japanese quail. Gen. Comp. Endocrinol. 101, 304–316.

Selvam, R., Jurkevich, A., Kang, S.W., Mikhailova, M.V., Cornett, L.E., Kuenzel, W.J., 2013. Distribution of the vasotocin subtype four receptor (VT4R) in the anterior pituitary gland of the chicken, *Gallus gallus*, and its possible role in the avian stress response. J. Neuroendocrinol. 25, 56–66.

Seth, R., Xu, Y.X., Grossmann, R., Chaturvedi, C.M., 2004a. Changes in expression of AVT and AVT receptor (VT1) gene in hypothalamus and shell gland in relation to egg laying in white leghorn hen. Gen. Comp. Endocrinol. 137, 177–186.

Seth, R., Köhler, A., Grossmann, R., Chaturvedi, C.M., 2004b. Expression of hypothalamic arginine vasotocin gene in response to water deprivation and sex steroid administration in female Japanese quail. J. Exp. Biol. 207, 3025–3033.

Shahabi, N.A., Bahr, J.M., Nalbandov, A.V., 1975. Effect of LH injection on plasma concentrations and follicular steroids in the chicken. Endocrinology 96, 969–972.

Shao, Y., Liu, S., Tang, X., Gao, J., Wu, G., Li, Z., 2010. Ontogeny of ghrelin mRNA expression and identification of ghrelin-immunopositive cells in the gastrointestinal tract of the Peking duck, *Anas platyrhynchos*. Gen. Comp. Endocrinol. 166, 12–18.

Sharma, D., Chaturvedi, C.M., 2011. Testosterone modulates pituitary vasotocin receptor expression and adrenal activity in osmotically stressed chicken. Comp. Biochem. Physiol. A 158, 87–93.

Sharma, D., Cornett, L.E., Chaturvedi, C.M., 2009a. Osmotic stress induced alteration in the expression of arginine vasotocin receptor VT2 in the pituitary gland and adrenal function of domestic fowl. Gen. Comp. Endocrinol. 160, 216–222.

Sharma, D., Cornett, L.E., Chaturvedi, C.M., 2009b. Corticosterone- or metapyrone-induced alterations in adrenal function and expression of the arginine vasotocin receptor VT2 in the pituitary gland of domestic fowl, *Gallus gallus*. Gen. Comp. Endocrinol. 161, 208–215.

Sharp, P.J., Chiasson, R.B., El Tounsy, M.M., Klandorf, H., Radke, W.J., 1979. Localization of cells producing thyroid-stimulating hormone in the pituitary gland of the domestic gland of the domestic fowl. Cell Tissue Res. 198, 53–63.

Sharp, P.J., Talbot, R.T., Main, G.M., Dunn, I.C., Fraser, H.M., Huskisson, N.S., 1990. Physiological roles of chicken LHRH-I and -II in the control of gonadotrophin release in the domestic chicken. J. Endocrinol. 124, 291–299.

Shaw, E.M., Shoffner, R.N., Foster, D.N., Guise, K.S., 1991. Mapping of the growth hormone gene by in situ hybridization to chicken chromosome 1. J. Hered. 82, 505–508.

Shen, S.-T., Yu, J.Y.-L., 2002. Cloning and gene expression of a cDNA for the chicken follicle-stimulating hormone (FSH)-β-subunit. Gen. Comp. Endocrinol. 125, 375–386.

Shipp, S.L., Wang, G., Cline, M.A., Gilbert, E.R., 2017. Chick subcutaneous and abdominal adipose tissue depots respond differently in lipolytic and adipogenic activity to α-melanocyte stimulating hormone (α-MSH). Comp. Biochem. Physiol. A 209, 56–64.

Shirley, H.V., Nalbandov, A.V., 1956. Effects of neurohypophysectomy in domestic chickens. Endocrinology 58, 477–483.

Shikano, K., Taniuchi, S., Iwakoshi-Ukena, E., Furumitsu, M., Bentley, G.E., Kriegsfeld, L.J., Ukena, K., 2018a. Chronic subcutaneous infusion of neurosecretory protein GM increases body mass gain in chicks. Gen. Comp. Endocrinol. 265, 71–76.

Shikano, K., Kato, M., Iwakoshi-Ukena, E., Furumitsu, M., Matsuura, D., Masuda, K., Tachibana, T., Bentley, G.E., Kriegsfeld, L.J., Ukena, K., 2018b. Effects of chronic intracerebroventricular infusion of neurosecretory protein GL on body mass and food and water intake in chicks. Gen. Comp. Endocrinol. 256, 37–42.

Silver, R., Ramos, C.L., Silverman, A.-J., 1992. Sexual behavior triggers the appearance of non-neuronal cells containing gonadotropin-releasing-hormone-like immunoreactivity. J. Neuroendocrinol. 4, 207–210.

Silverin, B., Wingfield, J., Stokkan, K.-A., Massa, R., Järvinen, A., Andersson, N.-Å., Lambrechts, M., Sorace, A., Blomqvist, D., 2008. Ambient temperature effects on photo induced gonadal cycles and hormonal secretion patterns in Great Tits from three different breeding latitudes. Horm. Behav. 54, 60–68.

Sims, C.G., Holberton, R.L., 2000. Development of the corticosterone stress response in young northern mockingbirds (*Mimus polyglottos*). Gen. Comp. Endocrinol. 119, 193–201.

Sintubin, P., Greene, E., Collin, A., Bordas, A., Zerjal, T., Tesseraud, S., Buyse, J., Dridi, S., 2014. Expression profile of hypothalamic neuropeptides in chicken lines selected for high or low residual feed intake. Neuropeptides 48, 213–220.

Sinpru, P., Porter, T.E., El Halawani, M.E., Chaiseha, Y., 2017. Effects of nest-deprivation on hypothalamic mesotocin in incubating native Thai hens (*Gallus domesticus*). Acta Histochem. 119, 708–718.

Sirotkin, A.V., Harrath, A.H., Grossmann, R., 2017. Metabolic status and ghrelin regulate plasma levels and release of ovarian hormones in layer chicks. Physiol. Res. 66, 85–92.

Skwarlo-Sonta, K., Sotowska-Brochocka, J., Rosolowska-Huszcz, D., Pawlowska-Wojewódka, E., Gajewska, A., 1987. Effect of prolactin on the diurnal changes in immune parameters and plasma corticosterone in white leghorn chickens. Acta Endocrinol. 116, 172–178.

Smiley, K.O., Adkins-Regan, E., 2016. Relationship between prolactin, reproductive experience, and parental care in a biparental songbird, the zebra finch (*Taeniopygia guttata*). Gen. Comp. Endocrinol. 232, 17–24.

Socha, J.K., Sechman, A., Mika, M., Hrabia, A., 2017. Effect of growth hormone on steroid concentrations and mRNA expression of their receptor, and selected egg-specific protein genes in the chicken oviduct during pause in laying induced by fasting. Domest. Anim. Endocrinol. 61, 1–10.

Stevenson, T.J., Lynch, K.S., Lamba, P., Ball, G.F., Bernard, D.J., 2009. Cloning of gonadotropin-releasing hormone I complementary DNAs in songbirds facilitates dissection of mechanisms mediating seasonal changes in reproduction. Endocrinology 150, 1826–1833.

Su, Y.J., Shu, J.T., Zhang, M., Zhang, X.Y., Shan, Y.J., Li, G.H., Yin, J.M., Song, W.T., Li, H.F., Zhao, G.P., 2014. Association of chicken growth hormone polymorphisms with egg production. Genet. Mol. Res. 13, 4893–4903.

Sun, Y.M., Dunn, I.C., Baines, E., Talbot, R.T., Illing, N., Millar, R.P., Sharp, P.J., 2001. Distribution and regulation by oestrogen of fully processed and variant transcripts of gonadotropin releasing hormone I and gonadotropin releasing hormone receptor mRNAs in the male chicken. J. Neuroendocrinol. 13, 37–49.

Sun, D., Cui, T., Luo, H., Li, R., Cui, S., Liu, J., 2012. Cell-specific distribution of estrogen receptor alpha (ERα) and androgen receptor (AR) in anterior pituitary glands from adult cockerels as revealed by immunohistochemistry. Cell Tissue Res. 348, 551–558.

Sweeney, S.A., Johnson, P.A., 2005. Messenger RNA and protein expression analysis of betaglycan in the pituitary and ovary of the domestic hen. Biol. Reprod. 72, 172–178.

Tachibana, T., Moriyama, S., Takahashi, A., Tsukada, A., Oda, A., Takeuchi, S., Sakamoto, T., 2011. Isolation and characterisation of prolactin-releasing peptide in chicks and its effect on prolactin release and feeding behaviour and feeding behaviour. J. Neuroendocrinol. 23, 74–81.

Takahashi, T., Kawashima, M., 2008a. Mesotocin increases the sensitivity of the hen oviduct uterus to arginine vasotocin. Poult. Sci. 87, 2107–2111.

Takahashi, T., Kawashima, M., 2008b. Mesotocin receptor binding in oviduct uterus of the hen before and after oviposition. Poult. Sci. 87, 546–550.

Takahashi, T., Kawashima, M., 2009a. Properties of estrogen binding components in the plasma membrane of neurohypophysis in hens and changes in its binding before and after oviposition. Poult. Sci. 88, 2206–2211.

Takahashi, T., Kawashima, M., 2009b. Prostaglandin F(2alpha) receptor in the neurohypophysis of hens. Poult. Sci 88, 1712–1718.

Takahashi, T., Kawashima, M., Yasuoka, T., Kamiyoshi, M., Tanaka, K., 1995. Diuretic and antidiuretic effects of mesotocin as compared with the antidiuretic effect of arginine vasotocin in the hen. Poult. Sci. 74, 890–892.

Takahashi, T., Kawashima, M., 2003. Arginine vasotocin induces bearing down for oviposition in the hen. Poult. Sci. 82, 345–346.

Takahashi, T., Kawashima, M., Yasuoka, T., Kamiyoshi, M., Tanaka, K., 1997. Mesotocin receptor binding of cortical and medullary kidney tissues of the hen. Poult. Sci. 76, 1302–1306.

Takahashi, T., Nozaki, Y., Nakagawa-Mizuyachi, K., Nakayama, H., Kawashima, M., 2011. Changes in angiotensin II receptor bindings in the hen neurohypophysis before and after oviposition. Poult. Sci. 90, 2565–2572.

Takeuchi, S., Takahashi, S., 1998b. Melanocortin receptor genes in the chicken-tissue distributions. Gen. Comp. Endocrinol. 112, 220–231.

Takeuchi, S., Kudo, T., Takahashi, S., 1998. Molecular cloning of the chicken melanocortin 2 (ACTH)-receptor gene. Biochim. Biophys. Acta 1403, 102–108.

Takeuchi, S., Teshigawara, K., Takahashi, S., 1999. Molecular cloning and characterization of the chicken pro-opiomelanocortin (POMC) gene. Biochim. Biophys. Acta 1450, 452–459.

Tan, F.L., Lolait, S.J., Brownstein, M.J., Saito, N., MacLeod, V., Baeyens, D.A., Mayeux, P.R., Jones, S.M., Cornett, L.E., 2000. Molecular cloning and functional characterization of a vasotocin receptor subtype that is expressed in the shell gland and brain of the domestic chicken. Biol. Reprod. 62, 8–15.

Tanaka, M., Hosokawa, Y., Watahiki, M., Nakashima, K., 1992a. Structure of the chicken growth hormone-encoding gene and its promoter region. Gene 112, 235–239.

Tanaka, M., Maeda, K., Okubo, T., Nakashima, K., 1992b. Double antenna structure of chicken prolactin receptor deduced from the cDNA sequence. Biochem. Biophys. Res. Commun. 188, 490–496.

Tanaka, M., Yamamoto, I., Ohkubo, T., Wakita, M., Hoshino, S., Nakashima, K., 1999. cDNA cloning and developmental alterations in gene expression of the two Pit-1/GHF-1 transcription factors in the chicken pituitary. Gen. Comp. Endocrinol. 114, 441–448.

Tennyson, V.M., Hou-Yu, A., Nilaver, G., Zimmerman, E.A., 1985. Immunocytochemical studies of vasotocin and mesotocin in the hypothalamo-hypophysial system of the chicken. Cell Tiss. Res. 239, 279–291.

Tennyson, V.M., Nilaver, G., Hou-Yu, A., Valiquette, G., Zimmerman, E.A., 1986. Immunocytochemical study of the development of vasotocin/mesotocin in the hypothalamo-hypophysial system of the chick embryo. Cell Tissue Res. 243, 15–31.

Terada, O., Shimada, K., Saito, N., 1997. Effect of oestradiol replacement in ovariectomized chickens on pituitary LH concentrations and concentrations of mRNAs encoding LH beta and alpha subunits. J. Reprod. Fertil. 111, 59–64.

Thayananuphat, A., Kang, S.W., Bakken, T., Millam, J.R., El Halawani, M.E., 2007. Rhythmic dependent light induction of gonadotropin-releasing-hormone-I expression and activation of dopaminergic neurons within the premammillary nucleus of the Turkey hypothalamus. J. Neuroendocrinol. 19, 399–406.

Thayananuphat, A., Youngren, O.M., Kang, S.W., Bakken, T., Kosonsiriluk, S., Chaiseha, Y., El Halawani, M.E., 2011. Dopamine and mesoneurotransmission during the transition from incubation to brooding in the Turkey. Horm. Behav. 60, 327–335.

Thommes, R.C., Caliendo, J., Woods, J.E., 1985. Hypothalamo adenohypophyseal-thyroid interrelationships in the chick embryo. VI. Immunocytochemical demonstration of thyrotropin releasing hormone. Gen. Comp. Endocrinol. 57, 1–9.

Thommes, R.C., Martens, J.B., Hopkins, W.E., Caliendo, J., Sorrentino, M.J., Woods, J.E., 1983. Hypothalamo adenohypophyseal-thyroid interrelationships in the chick embryo. IV. Immunocytochemical demonstration of TSH in the hypohyseal pars distalis. Gen. Comp. Endocrinol. 51, 434–443.

Tilly, J.L., Johnson, A.L., 1987. Presence and hormonal control of plasminogen activator in granulosa cells of the domestic hen. Bill. Reprod. 37, 1156–1164.

Tilly, J.L., Johnson, A.L., 1988a. Effects of a phorbol ester, a calcium ionophore, and 3',5'-adenosine monophosphate production on hen granulosa cell plasminogen activator activity. Endocrinology 123, 1433–1441.

Tilly, J.L., Johnson, A.L., 1988b. Attenuation of hen granulosa cell steroidogenesis by a phorbol ester and 1-oleoyl-2-acetyl glycerol. Biol. Reprod. 39, 1–8.

Tilly, J.L., Johnson, A.L., 1989. Mechanisms by which a phorbol ester and a diacylglycerol analog inhibit hen granulosa cell steroidogenesis. Domest. Anim. Endocrinol. 6, 155–166.

Tilly, J.L., Johnson, A.L., 1989. Regulation of androstenedione production by adenosine 3',5'-monophosphate and phorbol myristate acetate in ovarian thecal cells of the domestic hen. Endocrinology 125, 1691–1699.

Tilly, J.L., Kowalski, K.I., Johnson, A.L., 1991. Stage of ovarian follicular development associated with the initiation of steroidogenic competence in avian granulosa cells. Biol. Reprod. 44, 305–314.

Tobar-Dupres, E.T., Froman, D.P., Davis, S.L., 1993. Factors affecting circulating growth hormone binding protein in chickens. Poult. Sci. 72, 2337–2346.

Tonoue, T., Kitch, J., 1978. Release of cyclic AMP from the chicken thyroid stimulated with TSH in vitro. Endocrinol. Jpn. 25, 105–109.

Tóth, Z., Ouyang, J.Q., Lendvai, A.Z., 2018. Exploring the mechanistic link between corticosterone and insulin- like growth factor-1 in a wild passerine bird. Peer J. 6, e5936.

Tsuisui, K., Ishii, S., 1980. Hormonal regulation of follicle-stimulating hormone receptors in the testes of Japanese quail. J. Endocrinol. 85, 511–518.

Tsutsui, K., Saigoh, E., Ukena, K., Teranishi, H., Fujisawa, Y., Kikuchi, M., Ishii, S., Sharp, P.J., 2000. A novel avian hypothalamic peptide inhibiting gonadotropin release. Biochem. Biophys. Res. Commun. 275, 661–667.

Tsutsui, K., Bentley, G.E., Kriegsfeld, L.J., Osugi, T., Seong, J.Y., Vaudry, H., 2010. Discovery and evolutionary history of gonadotrophin-inhibitory hormone and kisspeptin: new key neuropeptides controlling reproduction. J. Neuroendocrinol. 22, 716–727.

Tsutsui, K., Osugi, T., Son, Y.L., Ubuka, T., 2018. Structure, function and evolution of GnIH. Gen. Comp. Endocrinol. 264, 48–57.

Ubuka, T., Bentley, G.E., 2009. Identification, localization, and regulation of passerine GnRH-I messenger RNA. J. Endocrinol. 201, 81–87.

Ubuka, T., Ukena, K., Sharp, P.J., Bentley, G.E., Tsutsui, K., 2006. Gonadotropin-inhibitory hormone inhibits gonadal development and maintenance by decreasing gonadotropin synthesis and release in male quail. Endocrinology 147, 1187–1194.

Ubuka, T., Cadigan, P.A., Wang, A., Liu, J., Bentley, G.E., 2009. Identification of European starling GnRH-I precursor mRNA and its seasonal regulation. Gen. Comp. Endocrinol. 162, 301–306.

Ubuka, T., Mizuno, T., Fukuda, Y., Bentley, G.E., Wingfield, J.C., Tsutsui, K., 2013. RNA interference of gonadotropin-inhibitory hormone gene induces aggressive and sexual behaviors in birds. Gen. Comp. Endocrinol. 181, 179–186.

Ukena, K., Iwakoshi-Ukena, E., Taniuchi, S., Bessho, Y., Maejima, S., Masuda, K., Shikano, K., Kondo, K., Furumitsu, M., Tachibana, T., 2014. Identification of a cDNA encoding a novel small secretory protein, neurosecretory protein GL, in the chicken hypothalamic infundibulum. Biochem. Biophys. Res. Commun. 446, 298–303.

Vandenborne, K., De Groef, B., Geelissen, S.M., Boorse, G.C., Denver, R.J., Kühn, E., Darras, V.M., Van der Geyten, S., 2005a. Molecular cloning and developmental expression of corticotropin releasing factor in chicken. Endocrinology 146, 301–308.

Vandenborne, K., De Groef, B., Geelissen, S.M., Kühn, E.R., Darras, V.M., Van der Geyten, S., 2005b. Corticosterone-induced negative feedback mechanisms within the hypothalamo-pituitary-adrenal axis of the chicken. J. Endocrinol. 185, 383–391.

Van As, P., Careghi, C., Bruggeman, V., Onagbesan, O.M., Van der Geyten, S., Darras, V.M., Decuypere, E., 2004. Regulation of growth hormone expression by thyrotropin-releasing hormone through the pituitary-specific transcription factor Pit-1 in chicken pituitary. Acta Vet. Hung. 52, 389–402.

Van der Geyten, S., Buys, N., Sanders, J.P., Decuypere, E., Visser, T.J., Kühn, E.R., Darras, V.M., 1999. Acute pretranslational regulation of type III iodothyronine deiodinase by growth hormone and dexamethasone in chicken embryos. Mol. Cell. Endocrinol. 147, 49–56.

Vanderpooten, A., Darras, V.M., Huybrechts, L.M., Rudas, P., Decuypere, E., Kuhn, E.R., 1991. Effects of hypophysectomy and acute administration of growth hormone (GH) on GH- receptor binding in chick liver membranes. J. Endocrinol. 129, 275–281.

Van Nassauw, L., Harrisson, F., Cras, P., Callebaut, M., 1987. Immunohistochemical localization of S-100 protein, glial fibrillary acidic protein, and neuron-specific enolase in the pars distalis of quail, rat, and human hypophyses. Histochemistry 86, 353–358.

Van As, P., Buys, N., Onagbesan, O.M., Decuypere, E., 2000. Complementary DNA cloning and ontogenic expression of pituitary-specific transcription factor of chickens (*Gallus domesticus*) from the pituitary gland. Gen. Comp. Endocrinol. 120, 127–136.

Vasilatos-Younken, R., Gravener, T.L., Cogburn, L.A., Mast, M.G., Wellenreiter, R.H., 1988. Effect of pattern of administration on the response to exogenous pituitary-derived chicken growth hormone by broiler-strain pullets. Gen. Comp. Endocrinol. 71, 268–283.

Vasilatos-Younken, R., Tsao, P.H., Foster, D.N., Smiley, D.L., Bryant, H., Heiman, M.L., 1992. Restoration of juvenile baseline growth hormone secretion with preservation of the ultradian growth-hormone rhythm by continuous delivery of growth hormone-releasing factor. J. Endocrinol. 135, 371–382.

Visser, M.E., Holleman, L.J.M., Caro, S.P., 2009. Temperature has a causal effect on avian timing of reproduction. Proc. R. Soc. B 276, 2323–2331.

Vizcarra, J.A., Kreider, D.L., Kirby, J.D., 2004. Episodic gonadotropin secretion in the mature fowl: serial blood sampling from unrestrained male broiler breeders (*Gallus domesticus*). Biol. Reprod. 70, 1798–1805.

Vleurick, L., Kühn, E.R., Decuypere, E., Burnside, J., Pezet, A., M.Edery, M., 1999. Generation of chicken growth hormone-binding proteins by proteolysis. Gen. Comp. Endocrinol. 113, 283–289.

Walker, D.J., Zimmer, C., Larriva, M., Healy, S.D., Spencer, K.A., 2019. Early-life adversity programs long-term cytokine and microglia expression within the HPA axis in female Japanese quail. J. Exp. Biol. 222 (Pt 6). NEEDS PAGE NUMBERS).

Wan, X.P., Xie, P., Bu, Z., Zou, X.T., Gong, D.Q., 2019. Prolactin induces lipid synthesis of organ-cultured pigeon crops. Poult Sci. 98, 1842−1853.

Wang, J.T., Xu, S.W., 2008. Effects of cold stress on the messenger ribonucleic acid levels of corticotrophin-releasing hormone and thyrotrophin releasing hormone in hypothalamic of broilers. Poult. Sci. 87, 973−978.

Wang, S., Bottje, W.G., Kinzler, S., Neldon, H.L., Koike, T.L., 1989. Effect of heat stress on plasma levels of arginine vasotocin and mesotocin in domestic fowl (*Gallus domesticus*). Comp. Biochem. Physiol. A. 93, 721−724.

Wang, C.Y., Wang, Y., Li, J., Leung, F.C., 2006. Expression profiles of growth hormone-releasing hormone and growth hormone releasing hormone receptor during chicken embryonic pituitary development. Poult. Sci. 85, 569−576.

Wang, Y., Li, J., Wang, C.Y., Kwok, A.H.Y., Leung, F.C., 2007. Identification of endogenous ligands for growth hormone-releasing hormone (GHRH) receptor: evidence for a separate gene encoding GHRH in submammalian vertebrates. Gen. Comp. Endocrinol. 148, 2405−2416.

Wang, Y., Li, J., Yan Kwok, A.H., Ge, W., Leung, F.C., 2010. A novel prolactin-like protein (PRL-L) gene in chickens and zebrafish: cloning and characterization of its tissue expression. Gen. Comp. Endocrinol. 166, 200−210.

Wang, Y., Wang, C.Y., Wu, Y., Huang, G., Li, J., Leung, F.C., 2012. Identification of the receptors for prolactin-releasing peptide (PrRP) and Carassius RFamide peptide (C-RFa) in chickens. Endocrinology 153, 1861−1874.

Wang, C., Liu, Y., Wang, H., Wu, H., Gong, S., Chen, W., He, D., 2014. Molecular characterization and differential expression of multiple goose dopamine D2 receptors. Gene 535, 177−183.

Wang, X., Yang, L., Wang, H., Shao, F., Yu, J., Jiang, H., Han, Y., Gong, D., Gu, Z., 2014. Growth hormone-regulated mRNAs and miRNAs in chicken hepatocytes. PLoS One 9, e112896.

Watanabe, Y., Grommen, S.V.H., De Groef, B., 2017. Effect of *in ovo* injection of corticotropin-releasing hormone on the timing of hatching in broiler chickens. Poult. Sci. 96, 3452−3456.

Watanabe, Y., Grommen, S.V.H., De Groef, B., 2018. Thyrotropic activity of corticotropin-releasing hormone in an altricial bird species, the zebra finch (*Taeniopygia guttata*). Gen. Comp. Endocrinol. 258, 99−108.

Weatherly, K.L., Ramesh, R., Strange, H., Waite, K.L., Storrie, B., Proudman, J.A., Wong, E.A., 2001. The Turkey transcription factor Pit-1/GHF-1 can activate the Turkey prolactin and growth hormone gene promoters in vitro but is not detectable in lactotrophs in vivo. Gen. Comp. Endocrinol. 123, 244−253.

Williamson, R.A., Davison, T.F., 1985. The effects of a single injection of thyrotrophin on serum concentrations of thyroxine, triiodothyronine, and reverse triiodothyronine in the immature chicken (*Gallus domesticus*). Gen. Comp. Endocrinol. 58, 109−113.

Wilson, J.X., West, N.H., 1986. Cardiovascular responses to neurohormones in conscious chickens and ducks. Gen. Comp. Endocrinol. 62, 268−280.

Wilson, S.C., Sharp, P.J., 1976a. Induction of luteinizing hormone release by gonadal steroid in the ovariectomized domestic hen. J. Endocrinol. 71, 87−98.

Wilson, S.C., Sharp, P.J., 1976b. Effects of androgens, oestrogens and deoxycorticosterone acetate on plasma concentrations of luteinizing hormone in laying hens. J. Endocrinol. 69, 93−102.

Wilson, S.C., Knight, P.G., Cunningham, F.J., 1983. Evidence for the involvement of central conversion of testosterone to oestradiol-17 beta in the regulation of luteinizing hormone secretion in the cockerel. J. Endocrinol. 99, 301−310.

Wilson, S.C., Cunningham, F.J., Chairil, R.A., Gladwell, R.T., 1989. Maturational changes in the LH response of domestic fowl to synthetic LHRH-I and-II. J. Endocrinol. 123, 311−318.

Wingfield, J.C., Hahn, T.P., Maney, D.L., Schoech, S.J., Wada, M., Morton, M.L., 2003. Effects of temperature on photoperiodically induced reproductive development, circulating plasma luteinizing hormone and thyroid hormones, body mass, fat deposition and molt in mountain white-crowned sparrows, Zonotrichia leucophrys oriantha. Gen. Comp. Endocrinol. 131, 143−158.

Wingfield, J.C., Sullivan, K., Jaxion-Harm, J., Meddle, S.L., 2012. The presence of water influences reproductive function in the song sparrow (Melospiza melodia morphna). Gen. Comp. Endocrinol. 178, 485−493.

Wong, E.A., Ferrin, N.H., Silsby, J.L., El Halawani, M.E., 1991. Cloning of a turkey prolactin cDNA: expression of prolactin mRNA throughout the reproductive cycle of the domestic turkey (Meleagris gallopavo). Gen. Comp. Endocrinol. 83, 18−26.

Wong, E.A., Silsby, J.L., El Halawani, M.E., 1992. Complimentary DNA cloning and expression of Pit-1/GHF-1 from the domestic Turkey. DNA Cell Biol. 11, 651−660.

Woods, D.C., Johnson, A.L., 2005. Regulation of follicle-stimulating hormone-receptor messenger RNA in hen granulosa cells relative to follicle selection. Biol. Reprod. 72, 643−650.

Wu, G., Siegel, P.B., Gilbert, E.R., Yang, N., Wong, E.A., 2011. Expression profiles of somatotropic axis genes in lines of chickens divergently selected for 56-day body weight. Anim. Biotechnol. 22, 100−110.

Wu, X., Wan, X.P., Lan, J.J., Yan, M.J., Lian, S.Y., Rijal, M., Huang, Z.B., Li, A., 2015a. Cloning, expression, and polymorphism at the 5′-flanking region of the GnRH gene and their association with laying traits in Muscovy duck (*Cairina moschata*). Br. Poult. Sci. 56, 531−542.

Wu, X., Yan, M.J., Wan, X.P., Lian, S.Y., Li, A., 2015b. Cloning and tissue expression profiling of the GnRHR gene of the Muscovy duck (*Cairina moschata*): polymorphism and association with egg-laying performance. Br. Poult. Sci. 56, 164−174.

Xiao, Y., Wu, C., Li, K., Gui, G., Zhang, G., Hua Yang, H., 2017. Association of growth rate with hormone levels and myogenic gene expression profile in broilers. J. Anim. Sci. Biotechnol. 8, 43.

Xie, M., Zhang, C., Zeng, W., Mi, Y., 2004. Effects of follicle-stimulating hormone and 17beta-estradiol on proliferation of chicken embryonic ovarian germ cells in culture. Comp. Biochem. Physiol. A 139, 521−526.

Xie, P., Wang, X.-P., Bua, Z., Zou, X.-T., 2017. Differential expression of fatty acid transporters and fatty acid synthesis-related genes in crop tissues of male and female pigeons (*Columba livia domestica*) during incubation and chick rearing. Br. Poult. Sci. 58, 594−602.

Xie, P., Wan, X.P., Bu, Z., Diao, E.J., Gong, D.Q., Zou, X.T., 2018. Changes in hormone profiles, growth factors, and mRNA expression of the related receptors in crop tissue, relative organ weight, and serum biochemical parameters in the domestic pigeon (*Columba livia*) during incubation and chick-rearing periods under artificial farming conditions. Poult. Sci. 97, 2189–2202.

Xu, Z.Q., He, J., Ji, C.L., Zhang, Y., Nie, Q.H., Zhang, D.X., Zhang, X.Q., 2015. Polymorphisms in the 5'-flanking regions of the GH, PRL, and Pit-1 genes with Muscovy duck egg production. J. Anim. Sci. 93, 28–34.

Yan, B., Deng, X., Fei, J., Hu, X., Wu, C., Li, N., 2003. Single nucleotide polymorphism analysis in chicken growth hormone gene and its associations with growth and carcass traits. Chin. Sci. Bull. 48, 1561–1564.

Yang, J., Morgan, J.L.M., Kirby, J.D., Long, D.W., Bacon, W.L., 2000. Circadian rhythm of the preovulatory surge of luteinizing hormone and its relationship to rhythms of body temperature and locomotor activity in Turkey hens. Biol. Reprod. 62, 1452–1458.

Yang, Y., Cui, Y., Wang, W., Zhang, L., Bufford, L., Sasaki, S., Fan, Z., Nishimura, H., 2004. Molecular and functional characterization of a vasotocin- sensitive aquaporin water channel in quail kidney. Am. J. Physiol. 287, R915–R924.

Yang, Y., Minvielle, F., Kuykindoll, R.J., Gasc, J.M., Yamamoto, T., Nishimura, H., 2008. "Diabetes Insipidus" strain quail show poorly developed medullary cones and low aquaporin 2 water channel expression. FASEB J. 22, 934.

Yasuo, S., Watanabe, M., Tsukada, A., Takagi, T., Iigo, M., Shimada, K., Ebihara, S., Yoshimura, T., 2004. Photoinducible phase-specific light induction of Cry1 gene in the pars tuberalis of Japanese quail. Endocrinology 145, 1612–1616.

Yasuo, S., Korf, H.W., 2011. The hypophyseal pars tuberalis transduces photoperiodic signals via multiple pathways and messenger molecules. Gen. Comp. Endocrinol. 172, 15–22.

Yoshihara, C., Tashiro, Y., Taniuchi, S., Katayama, H., Takahashi, S., Takeuchi, S., 2011. Feather follicles express two classes of proopiomelanocortin (POMC) mRNA using alternative promoters in chickens. Gen. Comp. Endocrinol. 171, 46–51.

Yoshimura, Y., Okamota, T., Tamura, T., 1993. Ultrastructural changes of oocyte and follicular wall during oocyte maturation in the Japanese quail (*Coturnix coturnix japonica*). J. Reprod. Fertil. 97, 189–196.

Yoshimura, Y., Heryanto, B., Tamura, T., 1997. Changes in the population of proliferating cells in chicken anterior pituitary during induced molting: an immunocytochemical analysis for proliferating cell nuclear antigen. Poult. Sci. 76, 1569–1573.

Yoshimura, T., Yasuo, S., Watanabe, M., Iigo, M., Yamamura, T., Hirunagi, K., Ebihara, S., 2003. Light-induced hormone conversion of T_4 to T_3 regulates photoperiodic response of gonads in birds. Nature 426, 178–181.

You, S., Foster, L.K., Silsby, J.L., El Halawani, M.E., Foster, D.N., 1995. Sequence analysis of the Turkey LH beta subunit and its regulation by gonadotrophin-releasing hormone and prolactin in cultured pituitary cells. J. Mol. Endocrinol. 14, 117–129.

You, S., Bridgham, J.T., Foster, D.N., Johnson, A.L., 1996. Characterization of the chicken follicle-stimulating hormone receptor (cFSH-R) complementary deoxyribonucleic acid, and expression of cFSH-R messenger ribonucleic acid in the ovary. Biol. Reprod. 55, 1055–1062.

You, S., Kim, H., El Halawani, M.E., Foster, D.N., 2000. Three different Turkey luteinizing hormone receptor (tLH-R) isoforms II: characterization of differentially regulated tLH-R messenger ribonucleic acid isoforms in the ovary. Biol. Reprod. 62, 117–124.

Youngren, O.M., El Halawani, M.E., Silby, J.L., Phillips, R.E., 1991. Intra-cranial prolactin perfusion induced incubation behavior in Turkey hens. Biol. Reprod. 44, 425–431.

Youngren, O.M., Pitts, G.R., Phillips, R.E., El Halawani, M.E., 1996. Dopaminergic control of prolactin secretion in the Turkey. Gen. Comp. Endocrinol. 104, 225–230.

Yu, J., Yan, L., Chen, Z., Li, H., Zhu, H., Chen, R., Shi, Z., 2018. Corticosterone induces growth hormone expression in pituitary somatotrophs during goose embryonic development. J. Reprod. Dev. 64, 343–350.

Yu, Y., Zhang, Y.H., Xu, Z.Y., Liu, T.Y., Wang, Q.X., Ou, C.B., Ma, J.Y., 2019. Effects of IBDV infection on expression of ghrelin and ghrelin-related genes in chicken. Poult. Sci. 98, 119–127.

Yuri, T., Kimball, R.T., Braun, E.L., Braun, M.J., 2008. Duplication of accelerated evolution and growth hormone gene in passerine birds. Mol. Biol. Evol. 25, 352–361.

Zann, R., Morton, S., Jones, K., Burley, N., 1995. The timing of breeding by zebra finches in relation to rainfall in central Australia. Emu 95, 208–222.

Zheng, J., Takagi, H., Tsutsui, C., Adachi, A., Sakai, T., 2008. Hypophyseal corticosteroids stimulate somatotrope differentiation in the embryonic chicken pituitary gland. Histochem. Cell Biol. 129, 357–365.

Zhang, L., Wu, S., Wang, J., Qiao, X., Yue, H., Yao, J., Zhang, H., Qi, G., 2014. Changes of plasma growth hormone, insulin-like growth factors-I, thyroid hormones, and testosterone concentrations in embryos and broiler chickens incubated under monochromatic green light. Ital. J. Anim. Sci. 13, 530–535.

Zhang, L., Chen, F., Cao, J., Dong, Y., Wang, Z., Hu, M., Chen, Y., 2017. Green light inhibits GnRH-I expression by stimulating the melatonin-GnIH pathway in the chick brain. J. Neuroendocrinol. 29. https://doi.org/10.1111/jne.12468.

Zhu, G., Chen, X., Mao, Y., Kang, L., Ma, X., Jiang, Y., 2015. Characterization of annexin A2 in chicken follicle development: evidence for its involvement in angiogenesis. Anim. Reprod. Sci. 161, 104–111.

Zhuang, X., Silverman, A.J., Silver, R., 1993. Reproductive behavior, endocrine state, and distribution of GnRH-like immune-reactive mast cells in dove brain. Horm. Behav. 27, 283–295.

Further reading

Nillni, E.A., 2010. Regulation of hypothalamic thyrotropin releasing hormone (TRH) neuron by neuronal and peripheral inputs. Front. Neuroendocrinol. 31, 134–156.

Takeuchi, S., Takahashi, S., 1998a. A possible involvement of melanocortin 3 receptor in the regulation of adrenal gland function in the chicken. Biochim. Biophys. Acta 1448, 512–518.

Takeuchi, S., Suzuki, S., Hirose, S., Yabuuchi, M., Sato, C., Yamamoto, H., Takahashi, S., 1996. Molecular cloning and sequence analysis of the chick melanocortin 1-receptor gene. Biochim. Biophys. Acta 1306, 122–126.

Chapter 31

Thyroid gland

Veerle M. Darras
Department of Biology, KU Leuven, Leuven, Belgium

31.1 Introduction

Thyroid hormones (THs) are iodinated peptides produced and stored in the thyroid gland. Upon secretion, they are transported by the blood stream and taken up by cells throughout the body. THs are essential for the correct development of all tissues in the avian embryo. During posthatch life, they remain important for further development and growth, they control metabolism, and they are needed for reproduction. Many of these functions involve interactions with other hormones either in a permissive or a synergistic way.

31.2 Thyroid gland structure and development

31.2.1 Structure of the mature thyroid gland

The avian thyroid gland is a paired organ, well-vascularized, and located ventrally alongside the trachea. Each oval lobe is connected to the common carotid artery on the medial side and the jugular vein on the lateral side (Fig. 31.1A). The histology and ultrastructure of the avian thyroid gland is like that of other vertebrate classes. It consists of follicles of epithelial cells, thyrocytes that surround a colloid-filled lumen (French and Hodges, 1977; Merryman and Buckles, 1998) (Fig. 31.1B and C). The colloid contains thyroglobulin, the TH-containing protein, which provides for large extracellular stores of hormone. Such extracellular hormone storage is unique to the thyroid and is considered an adaptation to the scarcity of the trace element iodine, a key component of THs [for a review see (McNabb, 1992)]. Calcitonin cells, which are parafollicular in mammals, are lacking in the avian thyroid; they are contained in separate ultimobranchial organs (see Chapter 32).

31.2.2 Thyroid gland development

The thyroid gland arises from the ventral pharyngeal wall and appears very early in development (e.g., day two of the 21 day incubation in chicken embryos). This mass of epithelial cells is initially attached to the pharynx, but then detaches, and the thyroid lobes assume their mature positions (by day five). In precocial birds such as chicken and quail, follicle formation is initiated early and proceeds rapidly, along with functional maturation of the gland during the first half of embryonic life and establishment of hypothalamic-pituitary control in the latter half of embryonic life (McNabb, 1987; Thommes, 1987). In altricial birds such as ring doves, although some follicles appear early, most histological and functional development occurs after hatch (McNabb, 1987). Significant advances have been made in understanding both the intrinsic and extrinsic signals involved in the early steps of thyroid gland development, showing a common pattern throughout vertebrate evolution (De Felice and Di Lauro, 2011; Fernandez et al., 2015; Haerlingen et al., 2019).

31.3 Thyroid hormone synthesis and release

31.3.1 Thyroid hormone synthesis

31.3.1.1 Iodide uptake and transport

TH synthesis and release has been studied in most detail in mammals, but the mechanisms were found to be similar in other vertebrates including birds [review (McNabb, 1992; Rousset et al., 2000; Citterio et al., 2019) (Fig. 31.2)]. Essential for TH synthesis is the availability of iodine, a trace element present predominantly as iodide in food and water. Iodide is taken up from the blood at the level of the basolateral membrane of the thyrocytes by a sodium-dependent iodide (Na-I) symporter (NIS). Another transporter, pendrin, is responsible for transport of iodide into the colloid through the apical membrane [review on mammalian iodide transport (Bizhanova and Kopp, 2009)]. The avian thyroid gland contains very high iodide concentrations and has prolonged iodide retention. Although avian thyroidal iodide can be influenced by extremes of iodide availability, studies in quail showed

Sturkie's Avian Physiology. https://doi.org/10.1016/B978-0-12-819770-7.00021-9

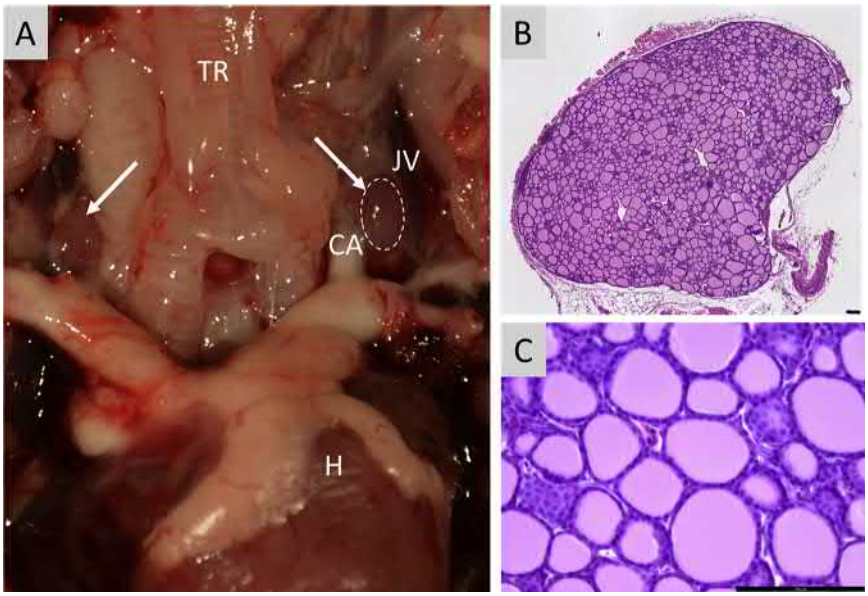

FIGURE 31.1 **Avian thyroid gland** (A) *Arrows* indicate the position of the left and right lobe of the thyroid gland in a week-old duckling. *CA*, common carotid artery; *H*, heart; *JV*, jugular vein; *TR*, trachea. (B) Hematoxylin and eosin staining of a section through a thyroid lobe of a week-old duckling containing follicles of various sizes, and (C) magnification of a few follicles showing cuboidal thyrocytes surrounding a colloid-filled lumen. Scale bar = 100 μm.

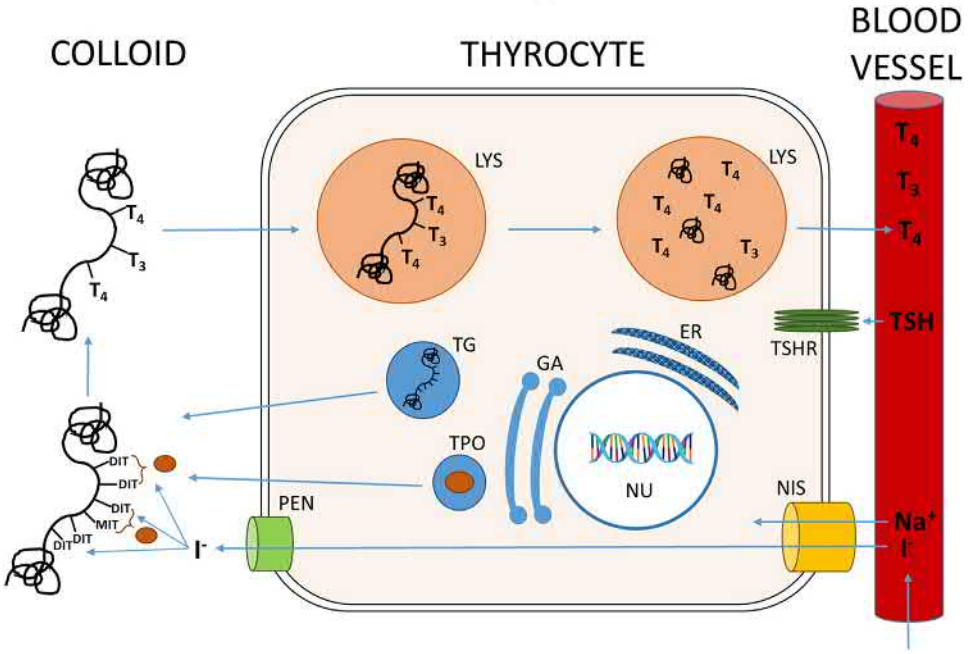

FIGURE 31.2 **Thyroid hormone synthesis.** Iodide is taken up from the blood at the level of the basolateral membrane by the sodium-dependent iodide symporter. Another transporter, pendrin, is responsible for transport of iodide into the colloid through the apical membrane. Thyroglobulin, the hormone storage protein, and thyroid peroxidase, the enzyme catalyzing hormone synthesis, are produced in the thyrocytes and extruded into the colloid by exocytosis. Thyroid peroxidase first oxidizes iodide and subsequently couples iodine atoms to the aromatic ring of the tyrosine residues present in thyroglobulin, forming monoiodotyrosine (MIT) and diiodotyrosine (DIT). What follows is the coupling of two DIT molecules to form 3,5,3′,5′-tetraiodothyronine or thyroxine, shortly called T_4. Some DIT molecules may be coupled to a MIT giving rise to 3,5,3′-triiodothyronine or T_3. Hormone release from the thyroid involves endocytosis of droplets of colloid by the follicle cells and their fusion with lysosomes. Following digestion of thyroglobulin by lysosomal enzymes, T_4 and T_3 are released into the circulation at the basolateral membrane. *ER*, endoplasmic reticulum; *GA*, Golgi apparatus; *LYS*, lysosome; *NIS*, sodium-dependent iodide symporter; *NU*, nucleus; *PEN*, pendrin; *TG*, thyroglobulin; *TPO*, thyroid peroxidase; *TSH*, thyroid stimulating hormone; *TSHR*, thyroid stimulating hormone receptor.

that circulating THs and thyroid gland hormone content are well regulated over a wide range of iodide intakes in adult animals. Embryos and chicks also show a considerable amount of iodide regulation although less than in adults (McNabb et al., 1985; McNabb et al., 1985; Stallard and McNabb, 1990).

31.3.1.2 Iodination and coupling in the colloid

TH synthesis begins with the iodination of tyrosine residues contained in thyroglobulin, the hormone storage protein of the colloid (Fig. 31.2). Thyroglobulin is produced in the thyrocytes, transported by vesicles to the apical cell border and extruded into the colloid by exocytosis (Citterio et al., 2019). Thyrocytes also produce the enzyme thyroid peroxidase which first oxidizes iodide and subsequently couples iodine atoms to the aromatic ring of the tyrosine residues present in thyroglobulin, forming monoiodotyrosine (MIT) and diiodotyrosine (DIT). What follows is the coupling of two DIT molecules to form 3,5,3′,5′-tetraiodothyronine or thyroxine, shortly called T_4. Some DIT molecules may be coupled to a MIT giving rise to 3,5,3′-triiodothyronine or T_3. However, as long as enough iodide is available, the avian thyroid gland predominantly synthesizes and secretes T_4 [review (McNabb, 1992; Rousset et al., 2000)]. In embryos, the capability for hormone synthesis precedes organization of the thyroid gland into follicles. In precocial chicken embryos, thyroidal iodide concentration and some hormone production occurs already during the first 1/4-1/3 of incubation, but in altricial ring doves, these events only start around mid-incubation (review (McNabb et al., 1998):).

31.3.1.3 Release into the circulation

Hormone release from the thyroid involves endocytosis of droplets of colloid by the follicle cells, their fusion with lysosomes, and digestion of thyroglobulin by lysosomal enzymes. While part of the amino acids and iodine are recycled within the thyrocyte, T_4 as well as a small amount of T_3 are released into the circulation at the basolateral membrane [review (McNabb, 1992; Rousset et al., 2000)]. TH secretion rates are in the range of 1−3 μg T_4/100 g of body weight per day in chickens, quails, and pigeons, but can increase or decrease due to external factors (see Section 31.6).

31.3.2 Hypothalamic-Pituitary-Thyroid Axis

31.3.2.1 Control by the pituitary

Activity of the avian thyroid gland is primarily controlled by the hypothalamic-pituitary-thyroid (HPT) axis. Thyroid stimulating hormone or thyrotropin (TSH), produced by the thyrotrophs of the anterior pituitary, is the major stimulator of TH synthesis and release. It is a glycoprotein consisting of two subunits: the α subunit, common to several pituitary hormones, and the β subunit that ensures its specificity. Binding of TSH to its receptors in the basolateral membrane of the thyrocyte stimulates the expression and synthesis of NIS and thyroglobulin, and increases TH production in the colloid. It also stimulates colloid endocytosis and subsequent hydrolysis of thyroglobulin, resulting in increased TH release into the circulation. Increased and sustained stimulation by TSH leads to both hypertrophy and hyperplasia of the thyrocytes which may result in formation of a goiter (Norris, 2007).

31.3.2.2 Control by the hypothalamus

The production and secretion of TSH is in turn regulated by three hormones from the avian hypothalamus: thyrotropin releasing hormone (TRH) and corticotropin releasing hormone (CRH) that are stimulatory and somatostatin (SRIH) that is inhibitory (De Groef et al., 2005) (Fig. 31.3). Although TRH, the major stimulator in mammals, was shown to stimulate TSH release from the chicken pituitary [review (Decuypere and Kühn, 1988)], more recent studies in birds, reptiles, amphibians, and fish have shown that CRH, rather than TRH, is often the most important hypothalamic stimulator of pituitary TSH in nonmammalian vertebrates [review (De Groef et al., 2006; Watanabe et al., 2016)]. This stimulation occurs by binding to the type 2 CRH receptor that is expressed on thyrotrophs but not on corticotrophs (De Groef et al., 2003). The most important role of TRH in influencing thyroid function in birds may be through its growth hormone (GH) releasing action, leading to inhibition of T_3 degradation by type 3 deiodinase (see Section 31.4.1). While hormones from the hypothalamus and pituitary stimulate thyroid gland activity, THs released by the gland in turn exert a negative feedback on the pituitary and hypothalamus (Fig. 31.3).

31.3.2.3 Development of the hypothalamic-pituitary-thyroid axis

During development, the establishment of HPT axis control over the thyroid gland occurs about mid-incubation (embryonic days 10.5−11.5) in precocial chickens. This was originally shown by the fact that removing the pituitary by decapitation did not alter plasma T_4 until day 11.5, but prevented the plasma T_4 increase that occurs after day 11.5 (Thommes et al., 1988). More recently, the timing was confirmed in detail by measurements of gene expression, showing a clear increase in mRNA levels of CRH, CRHR2, type 1 TRH receptor (TRHR1), and TSHβ between embryonic days 10 and 12 (Ellestad et al., 2011). Maturation

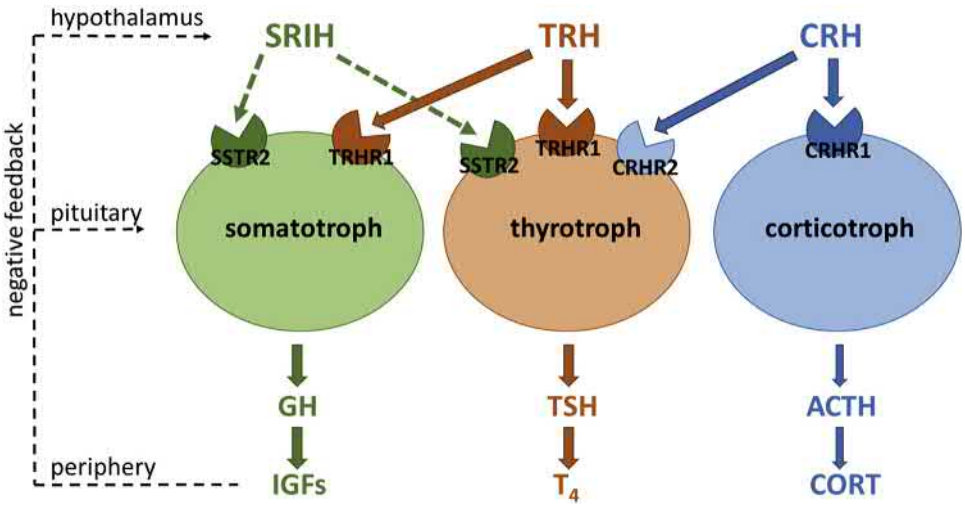

FIGURE 31.3 Avian hypothalamic-pituitary-thyroid axis. Hormone synthesis and release by the thyroid gland is stimulated by thyroid stimulating hormone or thyrotropin (TSH). The production and secretion of TSH in birds is regulated by three hypothalamic hormones: thyrotropin releasing hormone (TRH) and corticotropin releasing hormone (CRH) that are stimulatory and somatostatin (SRIH) that is inhibitory. TRH stimulation occurs by binding to the type 1 TRH receptor while the stimulatory effect of CRH occurs by binding to the type 2 CRH receptor that is expressed on thyrotrophs and not on corticotrophs. Thyroid hormones released by the gland exert a negative feedback on both the pituitary and the hypothalamus. *ACTH*, adrenocorticoptropic hormone; *CRHR1*, type 1 CRH receptor; *CRHR2*, type 2 CRH receptor; *CORT*, corticosterone; *GH*, growth hormone; *IGFs*, insulin-like growth factors; *SSTR2*, type 2 somatostatin receptor; *TRHR1*, type 1 TRH receptor.

of the feedback response of pituitary thyrotrophs has been confirmed by embryonic day 19 by demonstrating that goitrogen suppression of circulating T_4 increased TSHβ mRNA (Muchow et al., 2005). Likewise, T_4 feedback on SRIH inhibition of TSH production also matures between day 19 and hatch (De Groef et al., 2007). Studies on ring doves suggest that in altricial species, pituitary control of the thyroid is established after hatch. In this species, the thyroid is insensitive to exogenous TSH until the second day posthatch and circulating THs remain very low, then gradually increase during the first 3 weeks posthatch. Studies of the circulating TH patterns in other altricial species (red-winged blackbirds and starlings) are consistent with this developmental pattern [review (McNabb, 2007)].

31.3.3 Thyroid hormones in circulation

31.3.3.1 Avian thyroid hormone distributor proteins

Historically, circulating THs were first measured as protein-bound iodine, then by competitive binding assay, then by radioimmunoassay and enzyme-linked immunosorbent assay, and most recently by liquid chromatography and mass spectrometry. As in other vertebrates, the major THs present in avian plasma are T_4 and T_3, while concentrations of 3,3′,5′-triiodothyronine or reverse T_3 (rT_3) in posthatch birds are normally low (Hylka et al., 1986). In comparison with mammals, avian plasma contains similar concentrations of T_3 but less T_4 (i.e., often 10-fold less). The lower T_4/T_3 ratio is at least partially linked to the evolutionary difference in TH distributor proteins (formerly called TH binding proteins or TH carrier proteins) (Chang et al., 1999). Since THs are lipophilic, these proteins act to efficiently distribute them in the blood and the cerebrospinal fluid and also increase their stability. The half-life of T_4 in chicken is much shorter than in mammals and more similar to the half-life of T_3 [between 1 and 2 h for both (Bartha et al., 1994)]. The major TH distributor proteins in birds are transthyretin (TTR), which is high affinity and low capacity, and albumin, which is low affinity and high capacity. Birds lack the very high-affinity T_4-binding protein, thyroxine binding globulin (TBG), that is present in the blood of many mammals. Also, in contrast to mammals, the affinity of TTR from birds and other nonmammalian vertebrates is higher for T_3 than for T_4 [review (Richardson, 2014)]. Both albumin and TTR are produced in the avian liver, but TTR is the only TH distributor protein that is also produced in the brain in the choroid plexus. There it has a role, together with transmembrane transporters (see Section 31.4.2), in the transfer of THs between the general circulation and the cerebrospinal fluid (Richardson et al., 2015).

31.3.3.2 Factors influencing thyroid hormone levels in circulation

Adult birds of many species have plasma or serum T_4 concentrations in the range of 5−20 ng T_4/mL (6−25 pmol/mL) and T_3 concentrations in the range of 0.5−4 ng T_3/mL

(0.7−6 pmol/mL). Diurnal cycles of plasma THs have been demonstrated, with a peak of plasma T_4 during the dark period and a peak of plasma T_3 during the light period when birds are feeding (Klandorf et al., 1978; Harvey et al., 1980). Food intake is indeed a key factor influencing peripheral T_3 production and degradation and patterns of plasma THs (see Section 31.6). Temperature also may be important; cold temperatures increase and warm temperatures depress plasma T_3 within these diurnal patterns (Cogburn and Freeman, 1987).

The ontogenic profile of plasma THs differs in birds with precocial versus altricial development. In precocial species, in which thyroid gland function and its control mature before hatching, plasma T_4 rises several fold during the latter half of embryonic life while plasma T_3 remains low. Shortly before hatching, both hormones rise dramatically to reach some of the highest concentrations that have been measured in avian plasma. The perihatch peaks in THs are associated with the initiation of pulmonary respiration and thermoregulatory responses to cooling that occur in precocial species during this period. After the perihatch peak, plasma THs decrease markedly, then gradually increase again during posthatch life to reach adult concentrations (Decuypere and Kühn, 1988; McNabb, 1988). In altricial species, plasma concentrations of T_3 and T_4 are very low during embryonic life and the perihatch period, then gradually increase during the first 2−3 weeks posthatch to approach adult levels. Endothermic responses to cooling first appear several days to a week after hatching in these altricial birds, and the young are only homeothermic by the time of fledgling (McNabb and Olson, 1996; Vyboh et al., 1996).

31.4 Thyroid hormone metabolism and action

31.4.1 Thyroid hormone activation and degradation

Once secreted by the thyroid gland, THs can be metabolized in peripheral tissues by different pathways. Oxidative deamination and decarboxylation of the alanine side chain, as well as ether link cleavage, lead to irreversible TH degradation. Sulfation and glucuronidation of the phenolic hydroxyl group are reversible processes that facilitate hormone solubility and subsequent excretion. The most important pathway, however, is deiodination consisting of removal of a single iodine from the phenolic outer ring (5′D or ORD) or from the tyrosyl or inner ring (5D or IRD) (Fig. 31.4), processes catalyzed by enzymes called iodothyronine deiodinases. Next to providing most of T_3 present in circulation, stepwise deiodination is also responsible for the low levels of rT_3 as well as different forms of diiodothyronine (T_2).

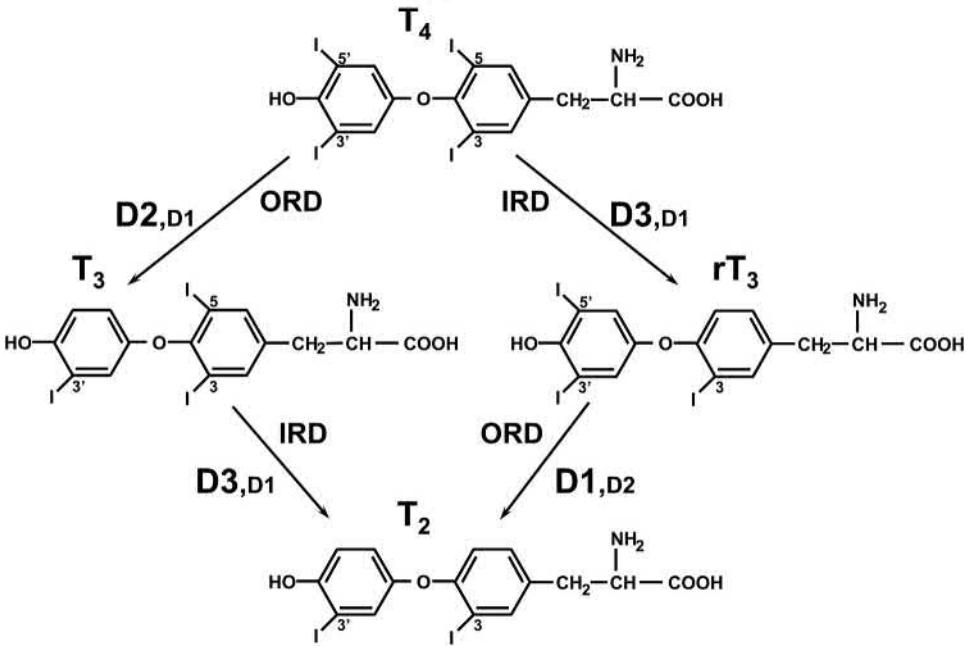

FIGURE 31.4 Thyroid hormone activation and inactivation by deiodinases. Deiodination by different types of iodothyronine deiodinases is a major mechanism regulating intracellular availability of T_3. The relative size of the symbols D1, D2, and D3 indicates their importance in the respective pathway. *T_4*, 3,5,3′,5′-tetraiodothyronine or thyroxine; *T_3*, 3,5,3′-triiodothyronine; *D1*, type 1 deiodinase; *D2*, type 2 deiodinase; *D3*, type 3 deiodinase; *IRD*, inner ring deiodination; *ORD*, outer ring deiodination; *rT_3*, 3,3′,5′-triiodothyronine; *T_2*, 3,3′-diiodothyronine.

31.4.1.1 Characterization of avian deiodinases

The first direct proof for peripheral T_4 to T_3 conversion in birds was obtained in 1978 in Peking ducks (Astier and Newcomer, 1978). As for mammals, biochemical characterizations of deiodinating activities in birds first used liver homogenates, sampled from chicken (Borges et al., 1980; Rudas, 1986), quail (McNabb et al., 1986), and ring doves (Rieman and McNabb, 1991), and this was later extended to other tissues such as kidney, intestine, and brain. The subsequent cloning of three chicken iodothyronine deiodinases: type 1 (D1 encoded by *DIO1*), type 2 (D2 encoded by *DIO2*), and type 3 (D3 encoded by *DIO3*) (Van der Geyten et al., 1997; Gereben et al., 1999) confirmed the high homology with their mammalian homologs [review (Bianco et al., 2002; Darras and Van Herck, 2012)]. By now, databases also include sequences for several other birds, including both precocial and altricial species. All avian deiodinases are selenoproteins with a selenocysteine in their catalytic site. Therefore they depend on the presence of a selenocysteine insertion sequence element in the 3′ untranslated region of their mRNA to allow selenocysteine incorporation (Bianco et al., 2002). The D1 enzyme is a nonselective enzyme catalyzing both ORD and IRD. In contrast, D2 only catalyzes ORD while D3 only catalyzes IRD and is a purely inactivating enzyme (Fig. 31.4).

31.4.1.2 Role of deiodinases

D1 is highly expressed in avian liver, kidney, and small intestine and contributes to peripheral T_3 production and degradation of rT_3. D2 is predominantly expressed in brain where it is important in the local conversion of T_4 that has entered the brain to T_3. D3 is found in variable amounts in almost all avian tissues and is believed to protect cells from overexposure to T_3 in specific situations such as early development, disease, and starvation [review (Darras et al., 2006)].

As the major secretory product of the avian thyroid gland is T_4, deiodinases in peripheral tissues are responsible for most of the T_3 found in the general circulation. This is clearly illustrated during the perihatch period in precocial birds. D3 expression is particularly high in embryonic chicken liver. The sharp decline in hepatic D3 activity occurring in the last days before hatching is the major factor contributing to the perihatch peak in circulating T_3 (Galton and Hiebert, 1987; Darras et al., 1992). At the same time, differential expression of deiodinases also allows individual tissues to adjust local T_3 concentrations dynamically according to their specific developmental or metabolic need, irrespective of circulating levels.

31.4.2 Cellular uptake of thyroid hormones

Since THs are quite lipophilic, it was originally assumed that they cross the plasma membrane simply by passive diffusion. However, studies in rat hepatocytes already showed around 1980 that T_4 and T_3 enter the cell at least partially by active transport and via separate transport systems (Krenning et al., 1981). It took 30 more years before the first TH transporter proteins were identified (Friesema et al., 2001, 2003), but we now know that several transmembrane proteins facilitate the transport of THs in and out of cells. They include proteins belonging to the families of the monocarboxylate transporters (MCTs), the Na-independent organic anion transporting polypeptides (OATPs), and the L-type amino acid transporters (LATs), as well as the Na-taurocholate cotransporting polypeptide (NTCP) [reviews (Visser et al., 2008; Schweizer et al., 2014)].

31.4.2.1 Characterization of avian thyroid hormone transporters

Based on data in chicken, the characteristics of TH transporters in birds are identical to those of their mammalian orthologs (Bourgeois et al., 2016). As in humans and rodents, OATP1C1 (encoded by *SLCO1C1*) is a high-affinity transporter for T_4 while MCT8 (encoded by *SLC16A2*) and MCT10 (encoded by *SLC16A10*) efficiently transport both T_3 and T_4. Also similar to mammals, the transporter LAT1 (encoded by *SLC7A5*) has a somewhat lower affinity for T_3 and T_4 and its preferred substrate is 3,3′-T_2. LAT2, however, appears to be missing in birds (Bourgeois et al., 2016). TH transporters are already present in the embryo where they regulate TH uptake in developing tissues, including brain [(Geysens et al., 2012; Bourgeois et al., 2016), see Section 31.5.1.2]. In the adult quail hypothalamus, OATP1C1 is believed to be involved in the TH-dependent stimulation of seasonal reproduction [(Nakao et al., 2006), see Section 31.5.3.2 and Chapter 43]. It is important to mention that TH transporters do not only facilitate cellular TH uptake but also TH export. This is important in the regulation of exchange of THs between different cell types and between cells and the general circulation.

31.4.3 Mechanism of action of thyroid hormones

In birds, as in other vertebrate classes, most TH actions are mediated through nuclear TH receptors (TRs) which are members of the nuclear receptor superfamily. TRs, also referred to as T_3 receptors because of their high affinity for T_3, are responsible for the transcriptional effects of THs (i.e., the receptors are transcription factors that act on TH-responsive genes). Since the affinity of TRs for T_4 is relatively low, with respect to transcriptional effects, T_4 is considered to be mainly a prohormone. The direct responses mediated by THs are of two types, developmental and metabolic (see Sections 31.5.1 and 31.5.2), but there are also indirect or permissive effects of THs as well as interactive effects with other hormones (see e.g., Section 31.5.1.1.2).

31.4.3.1 Genomic actions via nuclear thyroid hormone receptors

31.4.3.1.1 Characterization of thyroid hormone receptors in birds

The first steps into the identification of the molecular structure of vertebrate TRs were made in birds by the finding that the protein encoded by the previously described chicken *C-ERB-A* gene was a high affinity TH receptor (Sap et al., 1986). TRs are coded for by two genes, *THRA* and *THRB*, that generate a number of receptor isoforms. Some variation exists in the number and type of isoforms among vertebrate classes. So far, TRα is the only transcript of the *THRA* gene described in birds, and it has a structure and activity similar to the mammalian TRα1 isoform. Two isoforms have been identified for the *THRB* gene, TRβ0 and TRβ2. Their structure and function correspond to those of mammalian TRβ1 and TRβ2, respectively, with the exception that the amino-terminal domain of chicken TRβ0 is shorter than that of mammalian TRβ1 [review (Darras et al., 2011)]. Each isoform has distinct functions but in some cases functions overlap. The TRα receptor is generally expressed ubiquitously while TRβ expression is restricted to fewer tissues and characteristically varies strongly in relation to development (Darras et al., 2011). TRβ2 is also the major TR involved in TH feedback at the level of the HPT axis (Grommen et al., 2008).

31.4.3.1.2 Thyroid hormone action mechanism via nuclear Thyroid hormone receptors

The molecular mechanisms of TR-mediated TH action at the level of the nucleus have mainly been studied in mammals, but what we know from birds is very similar [reviews (Cheng et al., 2010; Darras et al., 2011)] (Fig. 31.5). TRs act as dimers that bind to TH-response elements (TREs), specific sequences in the promotor region of TH-responsive genes. The most effective dimer is a heterodimer of TR with retinoid X receptor, while TR homodimers are less effective. When no T_3 is bound to the TR, the heterodimer interacts with co-repressor proteins that inhibit/repress transcription of positively regulated genes. Upon ligand binding, co-repressors are replaced by co-activators and gene transcription is stimulated. In the case of negatively regulated genes (e.g., *TRH* and *TSHB*), ligand binding results in the opposite switch (Dupre et al., 2004). The extent of receptor binding of T_3 (i.e., binding saturation) strongly depends on local T_3 availability which is in turn largely dependent on cellular TH uptake and metabolism (see Sections 31.4.1 and 31.4.2). Other important factors regulating local TR-mediated signaling

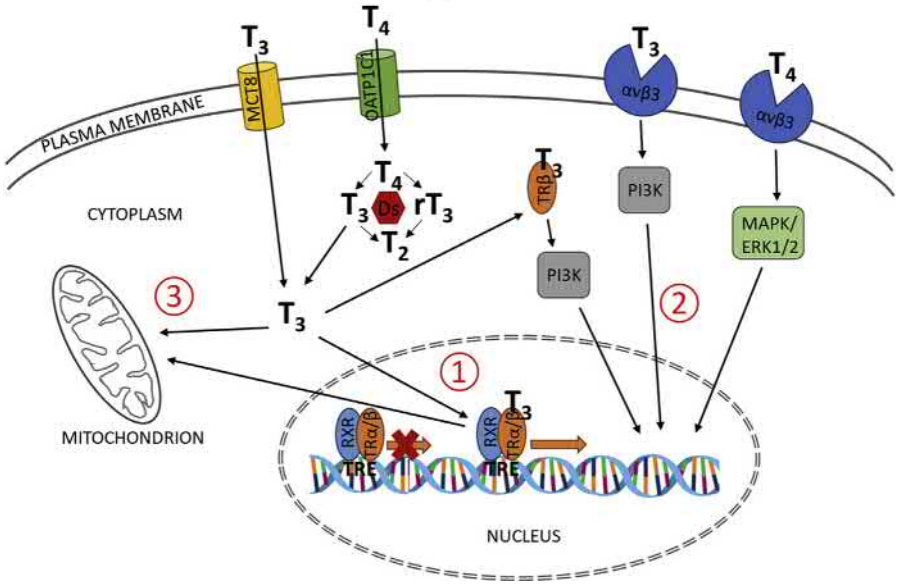

FIGURE 31.5 **T_3 and T_4 uptake, metabolism, and action mechanisms.** Thyroid hormone (TH) transporters such as MCT8 and OATP1C1 are located in the plasma membrane and facilitate T_4 and T_3 uptake. Within the cell, THs are activated/inactivated by enzymes, mainly deiodinases. Classical TH action ① occurs by binding of predominantly T_3 to TH receptors (TRs) present on TH-responsive genes in the nucleus. Hormone binding typically induces a shift from gene repression to activation of gene transcription. Nonclassical actions of THs ② that may eventually also lead to changes in gene transcription start either at the level of the plasma membrane by binding of T_4 or T_3 to integrin αvβ3 leading to activation of PI3K and/or the MAPK/ERK1/2 pathway, or in the cytoplasm where binding of T_3 to TRs residing in the cytoplasm can also activate the PI3K pathway. Finally, THs are also key regulators of mitochondrial respiration and biogenesis ③ involving both direct and indirect mechanisms. *Ds*, deiodinases; *MCT8*, monocarboxylate transporter 8; *OATP1C1*, organic anion transporting polypeptide 1C1; *RXR*, retinoid X receptor; *TR*, thyroid hormone receptor; *TRE*, thyroid hormone response element.

are the relative abundance of different TR isoforms and the presence of different co-repressors and co-activators. Differences in the regulation of the different receptor isoforms in target tissues have been demonstrated in birds, as in mammals, by altering thyroid status with a goitrogen (e.g., methimazole) combined or not with TH supplementation. Hypothyroidism, sufficient to decrease growth and several developmental markers in ducklings, did not affect mRNA levels for THRα but did result in decreased levels of transcript for TRβ0 in some but not all muscles analyzed. Hyperthyroidism also did not alter TRα mRNA but increased TRβ0 mRNA in cardiac, leg, and pectoralis muscles above that in euthyroid controls (Bishop et al., 2000).

31.4.3.2 Alternative routes of thyroid hormone action

Next to this long-known classical or "genomic" action within the nucleus, it is now clear that THs also have actions at the level of plasma membranes, in cytoplasm and in mitochondria, i.e., the so-called "nongenomic" actions. These effects too have mostly been investigated in mammals [review (Cheng et al., 2010)]. THs can bind to a recognition site on integrin αvβ3, a structural protein of the plasma membrane which is also found in birds as shown for instance in chicken ovary (Sechman, 2013). Without entering the cell, they can activate MAPK/ERK1/2 and initiate complex cellular events such as angiogenesis and tumor cell proliferation. Interestingly, T_4 binds with greater affinity than T_3 to this membrane receptor. T_3 can also activate the PI3K pathway starting either from the plasma membrane or by binding to TRβ, and possibly also TRα, residing in the cytoplasm. Data from experiments on chick embryo hepatocytes clearly indicated that T_3 and T_4, as well as the naturally occurring metabolite 3,5-diiodothyronine (3,5-T_2), can have rapid actions at the level of the cytoplasm. They can stimulate the PKC-MAPK and PI3K-AKT pathways, finally leading to stimulation of the growth process (Incerpi et al., 2002; Alisi et al., 2004; Scapin et al., 2009). Although the above-mentioned mechanisms are initially nongenomic, they potentially influence gene expression, independent of TREs, and therefore may serve as nonclassical pathways for transcriptional regulation (Moeller and Broecker-Preuss, 2011) (Fig. 31.5).

THs are also key regulators of mitochondrial respiration and biogenesis. While stimulation of mitochondrial respiration occurs via a rapid, nongenomic mechanism, increase in mitochondrial biogenesis involves both TH-responsive nuclear genes and direct action of TH at mitochondrial binding sites (Vaitkus et al., 2015). Recent data confirmed that mitochondria isolated from breast muscle indeed contain TRs, more specifically TRα, in both chicken and quail (Lassiter et al., 2018). It has been shown in rodents that next to T_3 and T_4, 3,5-T_2 is able to directly and rapidly stimulate mitochondrial activity (Vaitkus et al., 2015).

31.5 Physiological effects of thyroid hormones

31.5.1 Thyroid hormone effects on development

31.5.1.1 General development and hatching

THs influence both aspects of avian development, i.e., growth and differentiation/maturation. Growth, i.e., increase in mass, involves primarily cell proliferation (hyperplasia), but also may result from increases in cell size (hypertrophy). In general, THs appear to act permissively or indirectly, in concert with other control substances, in their stimulation of growth in birds [review (McNabb and King, 1993)]. The primary direct hormonal stimulation of body growth results from circulating growth factors [such as insulin-like growth factor-1 (IGF1)], which are primarily under the control of GH from the pituitary (see Chapter 30).

31.5.1.1.1 Precocial versus altricial birds

Differentiation and maturation of most, if not all, avian tissues is highly dependent on THs. As a matter of fact, this impact of THs on development is probably their most ancient role that is present in both vertebrate and invertebrate chordates, and has even been documented in some mollusks and flatworms (Taylor and Heyland, 2017). In birds, this has been predominantly studied in precocial species where hatching, a crucial transition in avian life span, is accompanied by a peak in circulating T_4 and T_3. Both increased T_4 production by the thyroid gland and changes in peripheral T_3 metabolism (mainly a decrease in D3 activity) contribute to this peak (Darras et al., 1992). A wide variety of studies showed that blocking this TH peak by goitrogens or other thyroid inhibiting compounds severely delayed or even completely blocked hatching. In contrast, a single injection of TH resulted in premature yolk sac retraction and pipping [reviews (Decuypere et al., 1991; De Groef et al., 2013)].

Altricial birds have no perihatch peak in circulating THs, and many aspects of tissue maturation are shifted to the first weeks posthatch, concomitant with maturation of the HPT axis. It is still unclear why altricial birds can hatch in the absence of high TH concentrations, but it is possible that the low levels that are present, mainly of maternal origin (see Section 31.5.1.3), are sufficient to allow maturation of tissues such as the lungs to a stage where pipping and transition to air breathing is possible. It has therefore been suggested that the high levels of THs occurring in

precocial birds during the perihatch peak are mainly needed for the initiation of thermogenesis (McNabb, 2006).

31.5.1.1.2 Interaction with other hormones

In many tissues, the stimulatory effect of THs on differentiation/maturation involves interaction with other hormones. In chicken embryonic gut, THs alone can stimulate cellular differentiation and induce digestive enzymes, but combination with glucocorticoids is necessary for the maturation of intestinal glucose transport [review (McNabb, 2006)]. Skeletal muscle differentiation and growth require both GH and THs. GH alone seems to be sufficient to increase muscle weight in hypothyroid chickens, but both hormones are needed to restore normal myosin development. The appearance of specific myosin isoforms critical to functional maturation during late embryonic development is also modulated by T_3 [review (McNabb, 2006)]. THs also interact with IGF1, e.g., in skeletal development. In vitro studies of pelvic cartilages from early chicken embryos have shown that THs trigger cartilage differentiation/maturation by stimulating matrix production and ossification. In this case, T_3 stimulates chondrocyte hypertrophy, but does not influence cell proliferation, which is only stimulated in the presence of IGF1 [review (McNabb, 2006)].

Lung maturation, crucial for the switch from chorioallantoic to lung respiration during pipping, is controlled by the combined action of THs and glucocorticoids. No direct effect of THs was found so far on surfactant phospholipid synthesis. They may however be important in regulating blood flow in the maturing lungs and expression of TRβ increases strongly toward the end of incubation [review (De Groef et al., 2013)].

Next to functioning in a cooperative/synergistic way with THs for tissue maturation, GH and corticosterone (CORT) also have a stimulatory impact on T_3 availability. Both hormones acutely inhibit hepatic expression of the *DIO3* gene while CORT additionally increases *DIO2* expression in developing brain [review (Darras et al., 2006)]. In turn, THs modulate somatotroph differentiation and abundance during chicken pituitary development (Liu and Porter, 2004) adding another link to the complex interplay between TH, GH, and CORT during avian development.

31.5.1.2 Development of the brain

The vertebrate organ that depends most heavily on THs for normal development is the brain. This has been known since long for the later stages of brain development, but more recently, it became clear that THs are also crucial for the early development of the central nervous system [reviews (Morreale de Escobar et al., 2004; Preau et al., 2015; Vancamp and Darras, 2017)]. TRα is expressed in chicken neuroectoderm from the start of development and receptor expression increases during neurulation (Flamant and Samarut, 1998). THs of maternal origin are present in the early embryonic brain and TTR, TH transporters, deiodinases, and TRs show a dynamic and region-specific expression pattern in brain throughout embryonic development (Forrest et al., 1991; Darras et al., 2009; Van Herck et al., 2012, 2015). THs are needed for the development of normal brain architecture and neuronal connections critical to the function of signaling networks as shown for instance in cerebellum of hypothyroid embryos and posthatch chicks (Bouvet et al., 1987; Verhoelst et al., 2004). Studies in chicken embryos have also been particularly helpful in elucidating the important role of locally expressed deiodinases and TH transporters in central nervous system development (Verhoelst et al., 2005; Van Herck et al., 2015; Delbaere et al., 2016). Site-specific knockdown of MCT8 revealed the need for facilitated transmembrane T_3 transport for normal corticogenesis in mesencephalon and cerebellum and for the formation of the retina and differentiation of the photoreceptors (Delbaere et al., 2017; Vancamp et al., 2017, 2018).

THs also are essential for early learning, both in precocial and altricial birds. It was shown in chicken that they determine the start of the sensitive period for filial imprinting shortly after hatching and may prime the brain for later learning (Yamaguchi et al., 2012). This property seems to be based on a rapid nongenomic action where binding of T_3 to a TR upregulates the phosphorylation level of nucleotide diphosphate kinase 2 (Yamaguchi et al., 2016). In zebra finch, it was found that expression of the TH-activating enzyme D2 is specifically high in the song control nuclei in male birds during the sensorimotor phase of song learning, suggesting that locally increased T_3 levels are needed for the correct development and maturation of the song control circuit (Raymaekers et al., 2017).

31.5.1.3 Role of maternal thyroid hormones

Although THs are needed from the start of development to coordinate the correct sequence of cell proliferation, differentiation, and maturation in different tissues, the embryonic thyroid gland only matures around mid-incubation in precocial birds and around hatching in altricial species. In the absence of a continuous TH supply through the placenta as in mammals, avian embryos rely on maternal THs deposited in the eggs. Iodine too is deposited and is used for embryonic TH production. The vast majority of egg TH content is present in the yolk; concentrations vary between species but the reported T_4/T_3 ratio (calculated on a molar basis) is always above two [reviews (McNabb and Wilson, 1997; Darras, 2019)]. Maternal TH deposition in general changes in line with maternal TH status but some

extent of regulation seems possible. Regulation of maternal TH availability subsequently occurs within the embryo, starting at the level of the yolk sac membrane where TH distributor proteins, transporters, and deiodinases are expressed (Too et al., 2017). The dynamic expression pattern of these regulators in the yolk sac membrane and in different embryonic tissues allows to precisely control local amounts of maternal THs at the tissue level and even to compensate to some extent for maternal hypo- or hyperthyroidism [review (Darras, 2019)].

While strong fluctuations of maternal TH deposit clearly have adverse effects on embryonic development, more subtle changes could also have an adaptive function. Both inter- and intraindividual variations have been observed in yolk content of THs, as well as CORT and androgens, in both precocial and altricial species. In an ecological context, this may be a way in which factors such as laying sequence, temperature, and food availability influence maternal hormone deposition and hence embryonic development and offspring fitness-related traits (Ruuskanen, 2015; Ruuskanen and Hsu, 2018; Della Costa et al., 2019; Hsu et al., 2019).

31.5.2 Thyroid hormone effects on metabolism and thermoregulation

31.5.2.1 Effects on intermediate metabolism

Although it has been known for long that THs are involved in the metabolism of mammals and birds, their exact role in avian lipid, carbohydrate, and protein metabolism is far from fully understood. As in mammals, hypothyroidism in poultry is associated with increased fatness, while hyperthyroidism decreases fat deposition (Decuypere et al., 1987). However, T_3 influences both hepatic lipogenesis and lipolysis and the resulting effect seems to vary according to the thyroid status of the animal (Rosebrough and McMurtry, 2003; Rosebrough et al., 2009). Moreover, in migratory birds, plasma TH levels are increased during the period preceding vernal migration and inhibition of the thyroid completely abolishes premigratory fattening and body mass gain (Perez et al., 2016). The effects of THs on avian growth and intermediate metabolism are probably mainly indirect, and the result of their impact on/interaction with other metabolic hormones such as GH, glucagon, insulin, and CORT (Raheja et al., 1980; Buyse et al., 1990; Harden and Oscar, 1993). In this regard, it is interesting to note that rT_3, which has hypometabolic properties, was found to suppress the rise in free fatty acids induced by glucocorticoids, catecholamines, and insulin, mainly by reducing lipolysis (Bobek et al., 2002; Niezgoda et al., 2005).

31.5.2.2 Effects on thermogenesis

The maintenance of a high and constant body temperature in homeothermic birds and mammals involves different forms of heat production: (1) essential heat, (2) obligatory heat production (together basal metabolic rate, within thermoneutral zone), and (3) adaptive or facultative heat production (below thermoneutrality). THs are known to directly regulate obligatory heat production in mammals while they act permissively on facultative thermogenesis by increasing the capacity to respond to sympathetic nervous system stimulation (Danforth and Burger, 1984). As in mammals, there is a clear positive association between THs and basal metabolic rate in birds. Induction of hypothyroidism reduces heat production while TH administration was found to increase heat production in several avian species [review (Ruuskanen et al., 2020)]. Studies in a number of passerine birds also indicated that increased thermogenic capacity during the cold season was always accompanied by higher plasma T_3 levels (Zheng et al., 2013; Zheng et al., 2014).

The higher endothermic heat production in homeothermic birds and mammals, compared to ectothermic lower vertebrates, involves the uncoupling of the mitochondrial electron transport chain from ATP production, a phenomenon facilitated by anion carrier proteins in the inner mitochondrial membranes. In mammals, uncoupling protein 1 (UCP1) in brown adipose tissue plays a key role in thermogenesis, but birds do not have brown adipose tissue, so this thermogenesis must occur in other tissues. The avian homolog avUCP in chicken and duckling is predominantly expressed in skeletal muscle and its expression is strongly regulated by thyroid status [review (Collin et al., 2005)]. However, its role in avian heat production has been questioned by data showing that adenine trinucleotide translocase, which is also under the control of THs, may be the key uncoupling protein in birds (Walter and Seebacher, 2009), although avUCP may still play a role through interactions involving the β-adrenergic system (Joubert et al., 2010). A few additional potential mediators for TH-induced thermogenesis in birds have been proposed, including peroxisome proliferator-activated receptor gamma coactivator 1 and ATP hydrolysis by sarco/endoplasmic reticulum Ca^{2+}-ATPase (SERCA), but their molecular regulation by THs requires further research. The presence of TRα in mitochondria of avian skeletal muscle has recently been shown (Lassiter et al., 2018), supporting the role of THs, possibly including also 3,5-T_2, in regulation of mitochondrial function which may be both genomic and nongenomic [review (Ruuskanen et al., 2020)].

31.5.3 Thyroid hormone effects on reproduction

31.5.3.1 Role in gonadal development and function

31.5.3.1.1 Impact of hypothyroidism

As in other vertebrates, THs are needed for proper development and maturation of the avian gonads. Data on early gonadal development are scarce but temporary

exposure of both female and male chicks to thyroid inhibitors for several weeks affects later reproductive development and performance [review (McNabb, 2007)]. Studies in adult birds are more abundant. Induction of hypothyroidism by methimazole in male Japanese quail decreased plasma luteinizing hormone and testosterone levels as well as testis weight, and disturbed or even completely stopped spermatogenesis (Kirby et al., 1996; Weng et al., 2007). Multiple studies have shown that egg laying is affected by thyroid status: thyroid inhibition in adult hens resulted in a decrease or even complete cessation of egg laying in galliform birds [reviews (Decuypere et al., 1991; McNabb, 2007)] although some differences were found between species. Japanese quail hens stopped laying when treated with methimazole as soon as the dose was sufficient to decrease circulating TH levels, so they did not produce eggs deficient in THs (Wilson and McNabb, 1997). In contrast, chicken hens decreased laying rate but continued to produce eggs with reduced TH content when their own circulating TH levels were decreased by long-term treatment with a moderate dose of methimazole (Van Herck et al., 2013).

31.5.3.1.2 Impact of hyperthyroidism

While severe hypothyroidism clearly is deleterious for egg production, induction of hyperthyroidism in chicken by T_3 treatment also had adverse effects and resulted in a reduction or stoppage of egg laying (Verheyen et al., 1986; Sechman, 2013), suggesting that the link between THs and ovarian function may be complex. Granulosa and theca layers of chicken ovarian follicles express TRα, TRβ0, as well as the integrin receptor αvβ3, indicating that THs may have both genomic and nongenomic actions in the ovary. In vitro studies demonstrated a direct impact of T_3 on ovarian steroidogenesis and suggested that they participate in the processes during the selection of white follicles into preovulatory hierarchy, as well as during growth, maturation, and ovulation of the yellow hierarchical follicles (Sechman, 2013). Next to T_3, also addition of 3,5-T_2 had an effect on the production of progesterone in the granulosa layer of chicken preovulatory follicles, acting either alone or in combination with LH (Sechman et al., 2011).

Although most of the laboratory studies relating to thyroid effects on reproduction have been done on precocial galliform birds, studies of neuroendocrine control of reproduction in wild birds and studies of wild birds exposed to thyroid-disrupting environmental chemicals indicate the need for adequate thyroid function in altricial or semi-altricial species as well [review (McNabb, 2007)]. However, for most of these species, the coupling of reproduction with seasonality is an important interfering factor since changes in light, temperature, food, etc., are known to influence thyroid function.

31.5.3.2 Role in seasonal reproduction and molt

31.5.3.2.1 Effects on gonadal growth and regression

In temperate and cold climate zones, many birds use photoperiodic changes to regulate their reproduction in order to match optimal environmental conditions. A model was proposed and tested in American tree sparrows, showing that THs are implicated in photoperiodic testicular growth at the start of the breeding season, in cessation of reproduction despite continuing long-day lengths (photorefractoriness) and in postnuptial molt. Although it was shown that the model applies to both males and females (Wilson and Reinert, 1996, 1999), most researchers continued to work on male birds to investigate the role of THs in seasonal reproduction.

Over the years, studies combining thyroidectomy and TH supplementation have often produced contradictory results in different species and resulted in contrasting views on the need or not of THs for testicular recrudescence and for induction of photorefractoriness [review (Dawson et al., 2001)]. Starting in 2003, a series of studies has gradually elucidated the molecular mechanism underlying the stimulatory effect of THs on photoperiodic testicular growth using Japanese quail. Transfer of birds from nonbreeding short-day conditions to breeding long-day conditions induced production and secretion of TSH in the pars tuberalis. This TSH, different from the TSH secreted by the pars distalis and with minimal bioactivity on the thyroid gland, stimulated the expression of *DIO2* while inhibiting the expression of *DIO3* in the tanycytes lining the ventrolateral walls of the third ventricle. The resulting rise in local T_3 availability induced rapid changes in the morphology of the glial endfeet surrounding the gonadotropin-releasing hormone (GnRH) nerve terminals, increasing GnRH secretion into the portal capillaries of the median eminence and hence activating the pituitary-gonadal axis [review (Nakayama and Yoshimura, 2018) and Chapter 43]. In contrast to this light-dependent central action of T_3, testicular regression at the end of the breeding season may be due to stimulation of the HPT-axis by lowering temperatures. The resulting increase in circulating T_3 may subsequently trigger apoptosis and accelerate testicular regression (Ikegami et al., 2015). Whether this combination of central and peripheral effects of TH on testis is identical in passerine birds living in the wild remains to be elucidated,

since both similarities and differences have been reported [e.g., (Bentley et al., 2013; Perez et al., 2018)].

31.5.3.2.2 Effects on molting

THs have long been known to be important in postnuptial molt in both wild and domestic birds and alterations in plasma THs occur in conjunction with natural molts [review (Kuenzel, 2003) and Chapter 46)]. Inhibition of reproductive activity (including cessation of egg laying) and molt occur concurrently in seasonally reproducing wild birds, and in commercial poultry practice THs and/or starvation have been used to induce molt. Interestingly, although T_3 had some effects, T_4 proved to be the most active hormone to speed up molting in force-molted hens in both chicken and turkey (Verheyen et al., 1986; Queen et al., 1997). This is in line with a study in thyroidectomized American tree sparrows showing that T_4 and not T_3 was able to induce photorefractoriness and postnuptial molt (Mishra et al., 2004). In contrast, both hormones restored normal patterns of prenuptial molt in thyroidectomized Gambel's white-crowned sparrows (Perez et al., 2018) suggesting that different and possibly indirect effects are involved.

31.6 Environmental influences on thyroid function

Changes in the environment have an impact on the avian thyroid and external factors such as temperature, light, and food availability are important modulators of thyroid function. Many of these changes are mediated through the HPT axis, but they may also be induced at the peripheral level, e.g., by changes in TH metabolism. Moreover, some effects may be indirect resulting from interaction with other hormones.

31.6.1 Impact of food availability

The impact of food availability is a perfect example to illustrate this complexity. Similar to other vertebrates, both food restriction and starvation reduce circulating T_3 concentrations and increase circulating rT_3 concentrations in birds (Klandorf and Harvey, 1985; Cherel et al., 1988; Abdel-Fattah et al., 1991; Totzke et al., 1999). The primary cause of the decrease in circulating T_3 is a rapid upregulation of hepatic *DIO3* expression and hence increased T_3 degradation by D3-dependent inner ring deiodination, while D1 activity is not affected (Van der Geyten et al., 1999; Gyorffy et al., 2009). The effect of energy restriction on circulating T_4 levels seems to be more variable. Partial energy restriction and complete fasting were repeatedly shown to induce a rise in plasma T_4 in chicken (Klandorf and Harvey, 1985; Van der Geyten et al., 1999; Gyorffy et al., 2009), while food restriction in quail and complete fasting in king penguin and herring gulls led to a decrease in plasma T_4 (Cherel et al., 1988; Totzke et al., 1999; Ronning et al., 2009). The rise in plasma T_4 in fasted chicken occurred in spite of a concomitant drop in plasma TSH. Further research suggested that this drop was the result of a reduced hypothalamic stimulation of the thyrotrophs due to a fasting-induced increase in circulating CORT (Geris et al., 1999). Comparison of all data available from birds as well as other vertebrates indicates that both the length and the severity of energy restriction may influence the balance between the effects on the HPT axis and peripheral TH metabolism and hence the net result on plasma T_4.

31.6.2 Impact of environmental temperature

As THs are needed for thermoregulation (see Section 31.5.2.2), changes in environmental temperature induce changes in thyroid function. Circulating levels of T_3 were found to be higher in cold than in warm conditions in many species, including quail, chicken, barn owl, and Eurasian tree sparrows (Bobek et al., 1980; Rudas and Pethes, 1986; Klein et al., 2006; Zheng et al., 2008). Again, the impact on thyroid function occurs both at the central and peripheral level. Cold stress increased pituitary cAMP-dependent protein kinase activity in cockerels (Chiasson and Carr, 1985) and thyroidal iodide uptake in goslings (Poczopko and Uliasz, 1975) while neural deafferentiation of the hypothalamus abolished the thyroidal response to cold in quail (Herbute et al., 1984) indicating that cold activates the HPT axis. Direct effects at the peripheral level were shown by experiments in thyroidectomized or hypophysectomized chickens where cold exposure directly influenced TH deiodination leading to an increase in T_3 availability (Rudas and Pethes, 1986). Overall, these changes provide increased T_3 availability in association with the metabolic increases required for homeothermy at cold ambient temperatures. Changes in plasma T_4 concentrations are often slower, more variable, and relatively mild (Kühn and Nouwen, 1978; Rudas and Pethes, 1986; Hangalapura et al., 2004; Klein et al., 2006). In general, hot temperatures have the opposite effect, i.e., they depress thyroid function [review (Sharp and Klandorf, 1985)].

31.6.3 Impact of chemical pollutants

In addition to natural environmental events, endocrine disrupting chemicals in the environment influence thyroid function of birds exposed to such chemicals. The impact of endocrine disruptors on birds is covered in more detail in Chapter 50 and only a few examples are included here.

Perchlorate compounds, which have been used as experimental goitrogens, are environmental contaminants in many regions, so they affect thyroid function in animals exposed through drinking water or food sources.

The primary effect of the perchlorate ion is to competitively inhibit thyroidal iodide uptake by NIS, creating iodine deficiency and the consequent effects on thyroid function. Most of what is known about perchlorate effects in birds comes from laboratory studies in quail, showing induction of hypothyroidism with thyroid gland hypertrophy and hyperplasia and reduced T_4 content, decreased plasma T_4 and T_3 levels and increased expression of *DIO2* in liver but not in brain (McNabb et al., 2004; Gentles et al., 2005; Chen et al., 2009).

Polychlorinated biphenyls (PCBs) are industrial chemicals that have been released in large amounts into the environment. Bioaccumulation of PCBs in fish-eating herring gulls around the contaminated Great lakes resulted in population declines and thyroid disruption [review (Fox, 1993)]. Although PCB manufacture was banned in the United States in 1977, studies of thyroid function in gull embryos collected in 1998−2000 suggested that embryonic thyroid disruption, from the persistent environmental PCBs, continued at contaminated sites (McNabb and Fox, 2003). More recent studies have explored how PCBs and their hydroxylated/sulfated metabolites affect thyroid function through multiple mechanisms. They were shown to interfere with TH synthesis [e.g., (Techer et al., 2016)], TH binding to distributor proteins [e.g, (Ucan-Marin et al., 2010)], peripheral TH metabolism and clearance [e.g., (Beck et al., 2006; Webb and McNabb, 2008)], and TH binding to TRs [e.g., (Miyazaki et al., 2004; Ren et al., 2019)].

Other categories of industrial compounds that have received attention in recent years are those used as flame retardants (e.g., polybrominated diphenyl ethers) as well as those employed as nonstick coatings for cookware (perfluoroalkyl compounds) and bisphenol A, which is used in plastics and food can liners. These materials are widespread, persistent contaminants that are present in wild birds and have been shown to alter thyroid function. Brominated and chlorinated organic flame retardants have been shown to interfere with thyroid function in a wide variety of species [review (Guigueno and Fernie, 2017)]. Similar to PCBs, interaction occurs at different levels following either environmental or experimental exposure [e.g., (Farhat et al., 2013; Jacobsen et al., 2017; Marteinson et al., 2017; Techer et al., 2018)].

Important in the context of endocrine disruptors is the fact that free living birds are continuously exposed to a mixture of contaminants and that the adverse effect of these mixtures on thyroid function may be even more detrimental than the sum of the individual compounds (Mughal et al., 2018). It is also important to take into account that most of these compounds are deposited in the eggs and as such transferred to the developing embryos, which are the most vulnerable stages.

References

Abdel-Fattah, K.I., Bobek, S., Sechman, A., 1991. Serum pattern of thyroxine (T4), 3,3',5-triiodothyronine (T3) and 3,3',5'-triiodothyronine (rT3) in fed and fasted cocks following TRH stimulation. Zentralbl Veterinarmed A 38 (6), 401−408.

Alisi, A., Spagnuolo, S., Napoletano, S., Spaziani, A., Leoni, S., 2004. Thyroid hormones regulate DNA-synthesis and cell-cycle proteins by activation of PKCalpha and p42/44 MAPK in chick embryo hepatocytes. J. Cell. Physiol. 201 (2), 259−265.

Astier, H.S., Newcomer, W.S., 1978. Extrathyroidal conversion of thyroxine to triiodothyronine in a bird: the Peking duck. Gen. Comp. Endocrinol. 35 (4), 496−499.

Bartha, T., Dewil, E., Rudas, P., Kühn, E.R., Scanes, C.G., Decuypere, E., 1994. Kinetic-parameters of plasma thyroid-hormone and thyroid-hormone receptors in a Dwarf and control line of chicken. Gen. Comp. Endocrinol. 96 (1), 140−148.

Beck, V., Roelens, S.A., Darras, V.M., 2006. Exposure to PCB 77 induces tissue-dependent changes in iodothyronine deiodinase activity patterns in the embryonic chicken. Gen. Comp. Endocrinol. 148 (3), 327−335.

Bentley, G.E., Tucker, S., Chou, H., Hau, M., Perfito, N., 2013. Testicular growth and regression are not correlated with Dio2 expression in a wild male songbird, sturnus vulgaris, exposed to natural changes in photoperiod. Endocrinology 154 (5), 1813−1819.

Bianco, A.C., Salvatore, D., Gereben, B., Berry, M.J., Larsen, P.R., 2002. Biochemistry, cellular and molecular biology, and physiological roles of the iodothyronine selenodeiodinases. Endocr. Rev. 23 (1), 38−89.

Bishop, C.M., McCabe, C.J., Gittoes, N.J., Butler, P.J., Franklyn, J.A., 2000. Tissue-specific regulation of thyroid hormone receptor mRNA isoforms and target gene proteins in domestic ducks. J. Endocrinol. 165 (3), 607−615.

Bizhanova, A., Kopp, P., 2009. Minireview: the sodium-iodide symporter NIS and pendrin in iodide homeostasis of the thyroid. Endocrinology 150 (3), 1084−1090.

Bobek, S., Niezgoda, J., Pietras, M., Kacinska, M., Ewy, Z., 1980. The effect of acute cold and warm ambient temperatures on the thyroid hormone concentration in blood plasma, blood supply, and oxygen consumption in Japanese quail. Gen. Comp. Endocrinol. 40 (2), 201−210.

Bobek, S., Sechman, A., Niezgoda, J., Jacek, T., 2002. Reverse 3,3',5'-triiodothyronine suppresses increase in free fatty acids in chickens elicited by dexamethasone or adrenaline. J. Vet. Med. A Physiol. Pathol. Clin. Med. 49 (3), 121−124.

Borges, M., LaBourene, J., Ingbar, S.H., 1980. Changes in hepatic iodothyronine metabolism during ontogeny of the chick embryo. Endocrinology 107 (6), 1751−1761.

Bourgeois, N.M., Van Herck, S.L., Vancamp, P., Delbaere, J., Zevenbergen, C., Kersseboom, S., Darras, V.M., Visser, T.J., 2016. Characterization of chicken thyroid hormone transporters. Endocrinology 157 (6), 2560−2574.

Bouvet, J., Usson, Y., Legrand, J., 1987. Morphometric analysis of the cerebellar Purkinje cell in the developing normal and hypothyroid chick. Int. J. Dev. Neurosci. 5 (4), 345−355.

Buyse, J., Decuypere, E., Simon, J., 1990. The effect of thyroid hormone status on plasma glucose-insulin interrelationship in broiler chickens. Reprod. Nutr. Dev. 30 (6), 683−692.

Chang, L., Munro, S.L., Richardson, S.J., Schreiber, G., 1999. Evolution of thyroid hormone binding by transthyretins in birds and mammals. Eur. J. Biochem. 259 (1−2), 534−542.

Chen, Y., McNabb, F.M., Sible, J.C., 2009. Perchlorate exposure induces hypothyroidism and affects thyroid-responsive genes in liver but not brain of quail chicks. Arch. Environ. Contam. Toxicol. 57 (3), 598−607.

Cheng, S.Y., Leonard, J.L., Davis, P.J., 2010. Molecular aspects of thyroid hormone actions. Endocr. Rev. 31 (2), 139−170.

Cherel, Y., Robin, J.P., Walch, O., Karmann, H., Netchitailo, P., Le Maho, Y., 1988. Fasting in king penguin. I. Hormonal and metabolic changes during breeding. Am. J. Physiol. 254 (2 Pt 2), R170−R177.

Chiasson, R.B., Carr, B.L., 1985. The effects of castration and/or methimazole feeding on the pituitary response to temperature extremes by cockerels. Gen. Comp. Endocrinol. 60 (3), 427−433.

Citterio, C.E., Targovnik, H.M., Arvan, P., 2019. The role of thyroglobulin in thyroid hormonogenesis. Nat. Rev. Endocrinol. 15 (6), 323−338.

Cogburn, L.A., Freeman, R.M., 1987. Response-surface of daily thyroid-hormone rhythms in young chickens exposed to constant ambient-temperature. Gen. Comp. Endocrinol. 68 (1), 113−123.

Collin, A., Cassy, S., Buyse, J., Decuypere, E., Damon, M., 2005. Potential involvement of mammalian and avian uncoupling proteins in the thermogenic effect of thyroid hormones. Domest. Anim. Endocrinol. 29 (1), 78−87.

Danforth, E., Burger, A., 1984. The role of thyroid-hormones in the control of energy-expenditure. Clin. Endocrinol. Metabol. 13 (3), 581−595.

Darras, V.M., 2019. The role of maternal thyroid hormones in avian embryonic development. Front. Endocrinol. 10, 66.

Darras, V.M., Van Herck, S.L., 2012. Iodothyronine deiodinase structure and function: from ascidians to humans. J. Endocrinol. 215 (2), 189−206.

Darras, V.M., Van Herck, S.L., Geysens, S., Reyns, G.E., 2009. Involvement of thyroid hormones in chicken embryonic brain development. Gen. Comp. Endocrinol. 163 (1−2), 58−62.

Darras, V.M., Van Herck, S.L., Heijlen, M., De Groef, B., 2011. Thyroid hormone receptors in two model species for vertebrate embryonic development: chicken and zebrafish. J. Thyroid Res. 2011, 402320.

Darras, V.M., Verhoelst, C.H., Reyns, G.E., Kühn, E.R., Van der Geyten, S., 2006. Thyroid hormone deiodination in birds. Thyroid 16 (1), 25−35.

Darras, V.M., Visser, T.J., Berghman, L.R., Kühn, E.R., 1992. Ontogeny of type I and type III deiodinase activities in embryonic and posthatch chicks: relationship with changes in plasma triiodothyronine and growth hormone levels. Comp. Biochem. Physiol. A Comp. Physiol. 103 (1), 131−136.

Dawson, A., King, V.M., Bentley, G.E., Ball, G.F., 2001. Photoperiodic control of seasonality in birds. J. Biol. Rhythm. 16 (4), 365−380.

De Felice, M., Di Lauro, R., 2011. Minireview: intrinsic and extrinsic factors in thyroid gland development: an update. Endocrinology 152 (8), 2948−2956.

De Groef, B., Goris, N., Arckens, L., Kühn, E.R., Darras, V.M., 2003. Corticotropin-releasing hormone (CRH)-induced thyrotropin release is directly mediated through CRH receptor type 2 on thyrotropes. Endocrinology 144 (12), 5537−5544.

De Groef, B., Grommen, S.V., Darras, V.M., 2007. Feedback control of thyrotropin secretion in the chicken: thyroid hormones increase the expression of hypophyseal somatostatin receptor types 2 and 5. Gen. Comp. Endocrinol. 152 (2−3), 178−182.

De Groef, B., Grommen, S.V., Darras, V.M., 2013. Hatching the cleidoic egg: the role of thyroid hormones. Front. Endocrinol. 4, 63.

De Groef, B., Van der Geyten, S., Darras, V.M., Kühn, E.R., 2006. Role of corticotropin-releasing hormone as a thyrotropin-releasing factor in non-mammalian vertebrates. Gen. Comp. Endocrinol. 146 (1), 62−68.

De Groef, B., Vandenborne, K., Van As, P., Darras, V.M., Kühn, E.R., Decuypere, E., Geris, K.L., 2005. Hypothalamic control of the thyroidal axis in the chicken: over the boundaries of the classical hormonal axes. Domest. Anim. Endocrinol. 29 (1), 104−110.

Decuypere, E., Buyse, J., Scanes, C.G., Huybrechts, L., Kühn, E.R., 1987. Effects of hyper- or hypothyroid status on growth, adiposity and levels of growth hormone, somatomedin C and thyroid metabolism in broiler chickens. Reprod. Nutr. Dev. 27 (2B), 555−565.

Decuypere, E., Dewil, E., Kühn, E.R., 1991. In: Tullett, S.G. (Ed.), The Hatching Process and the Role of Hormones. Avian Incubation, vol. 22. Butterworth-Heinemann, London, pp. 239−256.

Decuypere, E., Kühn, E.R., 1988. Thyroid-hormone physiology in Galliformes - age and strain related changes in physiological control. Am. Zool. 28 (2), 401−415.

Delbaere, J., Van Herck, S.L., Bourgeois, N.M., Vancamp, P., Yang, S., Wingate, R.J., Darras, V.M., 2016. Mosaic expression of thyroid hormone regulatory genes defines cell type-specific dependency in the developing chicken cerebellum. Cerebellum 15 (6), 710−725.

Delbaere, J., Vancamp, P., Van Herck, S.L., Bourgeois, N.M., Green, M.J., Wingate, R.J., Darras, V.M., 2017. MCT8 deficiency in Purkinje cells disrupts embryonic chicken cerebellar development. J. Endocrinol. 232 (2), 259−272.

Della Costa, N.S., Navarro, J.L., Bernad, L., Marin, R.H., Martella, M.B., 2019. Effect of maternal environment on yolk immunoreactive corticosterone and its influence on adrenocortical and behavioral activity in chicks of Greater Rhea (*Rhea americana*). Horm. Behav. 114, 104534.

Dupre, S.M., Guissouma, H., Flamant, F., Seugnet, I., Scanlan, T.S., Baxter, J.D., Samarut, J., Demeneix, B.A., Becker, N., 2004. Both thyroid hormone receptor (TR)beta 1 and TR beta 2 isoforms contribute to the regulation of hypothalamic thyrotropin-releasing hormone. Endocrinology 145 (5), 2337−2345.

Ellestad, L.E., Saliba, J., Porter, T.E., 2011. Ontogenic characterization of gene expression in the developing neuroendocrine system of the chick. Gen. Comp. Endocrinol. 171 (1), 82−93.

Farhat, A., Crump, D., Chiu, S., Williams, K.L., Letcher, R.J., Gauthier, L.T., Kennedy, S.W., 2013. In Ovo effects of two organophosphate flame retardants–TCPP and TDCPP–on pipping success, development, mRNA expression, and thyroid hormone levels in chicken embryos. Toxicol. Sci. 134 (1), 92−102.

Fernandez, L.P., Lopez-Marquez, A., Santisteban, P., 2015. Thyroid transcription factors in development, differentiation and disease. Nat. Rev. Endocrinol. 11 (1), 29−42.

Flamant, F., Samarut, J., 1998. Involvement of thyroid hormone and its alpha receptor in avian neurulation. Dev. Biol. 197 (1), 1−11.

Forrest, D., Hallbook, F., Persson, H., Vennstrom, B., 1991. Distinct functions for thyroid hormone receptors alpha and beta in brain development indicated by differential expression of receptor genes. EMBO J. 10 (2), 269−275.

Fox, G.A., 1993. What have biomarkers told us about the effects of contaminants on the health of fish-eating birds in the Great-lakes - the theory and a literature-review. J. Great Lake. Res. 19 (4), 722–736.

French, E.I., Hodges, R.D., 1977. Fine structural studies on the thyroid gland of the normal domestic fowl. Cell Tissue Res. 178 (3), 397–410.

Friesema, E.C., Docter, R., Moerings, E.P., Verrey, F., Krenning, E.P., Hennemann, G., Visser, T.J., 2001. Thyroid hormone transport by the heterodimeric human system L amino acid transporter. Endocrinology 142 (10), 4339–4348.

Friesema, E.C., Ganguly, S, Abdalla, A., Manning Fox, J.E., Halestrap, A.P., Visser, T.J., 2003. Identification of monocarboxylate transporter 8 as a specific thyroid hormone transporter. J. Biol. Chem. 278 (41), 40128–40135.

Galton, V.A., Hiebert, A., 1987. The ontogeny of the enzyme systems for the 5'- and 5-deiodination of thyroid hormones in chick embryo liver. Endocrinology 120 (6), 2604–2610.

Gentles, A., Surles, J., Smith, E.E., 2005. Evaluation of adult quail and egg production following exposure to perchlorate-treated water. Environ. Toxicol. Chem. 24 (8), 1930–1934.

Gereben, B., Bartha, T., Tu, H.M., Harney, J.W., Rudas, P., Larsen, P.R., 1999. Cloning and expression of the chicken type 2 iodothyronine 5'-deiodinase. J. Biol. Chem. 274 (20), 13768–13776.

Geris, K.L., Berghman, L.R., Kühn, E.R., Darras, V.M., 1999. The drop in plasma thyrotropin concentrations in fasted chickens is caused by an action at the level of the hypothalamus: role of corticosterone. Domest. Anim. Endocrinol. 16 (4), 231–237.

Geysens, S., Ferran, J.L., Van Herck, S.L., Tylzanowski, P., Puelles, L., Darras, V.M., 2012. Dynamic mRNA distribution pattern of thyroid hormone transporters and deiodinases during early embryonic chicken brain development. Neuroscience 221, 69–85.

Grommen, S.V., Arckens, L., Theuwissen, T., Darras, V.M., De Groef, B., 2008. Thyroid hormone receptor beta2 is strongly up-regulated at all levels of the hypothalamo-pituitary-thyroidal axis during late embryogenesis in chicken. J. Endocrinol. 196 (3), 519–528.

Guigueno, M.F., Fernie, K.J., 2017. Birds and flame retardants: a review of the toxic effects on birds of historical and novel flame retardants. Environ. Res. 154, 398–424.

Gyorffy, A., Sayed-Ahmed, A., Zsarnovszky, A., Frenyo, V.L., Decuypere, E., Bartha, T., 2009. Effects of energy restriction on thyroid hormone metabolism in chickens. Acta Vet. Hung. 57 (2), 319–330.

Haerlingen, B., Opitz, R., Vandernoot, I., Trubiroha, A., Gillotay, P., Giusti, N., Costagliola, S., 2019. Small-molecule screening in zebrafish embryos identifies signaling pathways regulating early thyroid development. Thyroid 29 (11), 1683–1703.

Hangalapura, B.N., Nieuwland, M.G., Buyse, J., Kemp, B., Parmentier, H.K., 2004. Effect of duration of cold stress on plasma adrenal and thyroid hormone levels and immune responses in chicken lines divergently selected for antibody responses. Poult. Sci. 83 (10), 1644–1649.

Harden, R.L., Oscar, T.P., 1993. Thyroid hormone and growth hormone regulation of broiler adipocyte lipolysis. Poult. Sci. 72 (4), 669–676.

Harvey, S., Davison, T.F., Klandorf, H., Phillips, J.G., 1980. Diurnal changes in the plasma-concentrations of thyroxine and triiodothyronine and their binding to plasma-proteins in the domestic duck (Anas-Platyrhynchos). Gen. Comp. Endocrinol. 42 (4), 500–504.

Herbute, S., Pintat, R., Ramade, F., Bayle, J.D., 1984. Effect of short exposure to cold on plasma thyroxine in *Coturnix quail*: role of the infundibular complex and its neural afferents. Gen. Comp. Endocrinol. 56 (1), 1–8.

Hsu, B.Y., Doligez, B., Gustafsson, L., Ruuskanen, S., 2019. Transient growth-enhancing effects of elevated maternal thyroid hormones at no apparent oxidative cost during early postnatal period. J. Avian Biol. 50 (1).

Hylka, V.W., Tonetta, S.A., Thommes, R.C., 1986. Plasma iodothyronines in the domestic-fowl - newly hatched to early adult stages, with special reference to reverse triiodothyronine (Rt3). Compar. Biochem. Physiol.-Physiol. 84 (2), 275–277.

Ikegami, K., Atsumi, Y., Yorinaga, E., Ono, H., Murayama, I., Nakane, Y., Ota, W., Arai, N., Tega, A., Iigo, M., Darras, V.M., Tsutsui, K., Hayashi, Y., Yoshida, S., Yoshimura, T., 2015. Low temperature-induced circulating triiodothyronine accelerates seasonal testicular regression. Endocrinology 156 (2), 647–659.

Incerpi, S., De Vito, P., Luly, P., Spagnuolo, S., Leoni, S., 2002. Short-term effects of thyroid hormones and 3,5-diiodothyronine on membrane transport systems in chick embryo hepatocytes. Endocrinology 143 (5), 1660–1668.

Jacobsen, M.L., Jaspers, V.L.B., Ciesielski, T.M., Jenssen, B.M., Loseth, M.E., Briels, N., Eulaers, I., Leifsson, P.S., Riget, F.F., Gomez-Ramirez, P., Sonne, C., 2017. Japanese quail (*Coturnix japonica*) liver and thyroid gland histopathology as a result of in ovo exposure to the flame retardants tris(1,3-dichloro-2-propyl) phosphate and Dechlorane Plus. J. Toxicol. Environ. Health 80 (9), 525–531.

Joubert, R., Metayer Coustard, S., Swennen, Q., Sibut, V., Crochet, S., Cailleau-Audouin, E., Buyse, J., Decuypere, E., Wrutniak-Cabello, C., Cabello, G., Tesseraud, S., Collin, A., 2010. The beta-adrenergic system is involved in the regulation of the expression of avian uncoupling protein in the chicken. Domest. Anim. Endocrinol. 38 (2), 115–125.

Kirby, J.D., Mankar, M.V., Hardesty, D., Kreider, D.L., 1996. Effects of transient prepubertal 6-N-propyl-2-thiouracil treatment on testis development and function in the domestic fowl. Biol. Reprod. 55 (4), 910–916.

Klandorf, H., Harvey, S., 1985. Food intake regulation of circulating thyroid hormones in domestic fowl. Gen. Comp. Endocrinol. 60 (2), 162–170.

Klandorf, H., Sharp, P.J., Duncan, I.J.H., 1978. Variations in levels of plasma thyroxine and triiodothyronine in juvenile female chickens during 24-hr and 16-hr lighting cycles. Gen. Comp. Endocrinol. 36 (2), 238–243.

Klein, A., Kulcsar, M., Krizsik, V., Matics, R., Rudas, P., Torok, J., Huszenicza, G., 2006. Effects of environmental temperature on thyroid hormones in the barn owl (*Tyto alba*). Acta Vet. Hung. 54 (3), 321–331.

Krenning, E., Docter, R., Bernard, B., Visser, T., Hennemann, G., 1981. Characteristics of active transport of thyroid hormone into rat hepatocytes. Biochim. Biophys. Acta 676 (3), 314–320.

Kuenzel, W.J., 2003. Neurobiology of molt in Avian species. Poult. Sci. 82 (6), 981–991.

Kühn, E.R., Nouwen, E.J., 1978. Serum levels of triiodothyronine and thyroxine in domestic-fowl following mild cold-exposure and injection of synthetic thyrotropin-releasing-hormone. Gen. Comp. Endocrinol. 34 (3), 336–342.

Lassiter, K., Dridi, S., Greene, E., Kong, B., Bottje, W.G., 2018. Identification of mitochondrial hormone receptors in avian muscle cells. Poult. Sci. 97 (8), 2926–2933.

Liu, L., Porter, T.E., 2004. Endogenous thyroid hormones modulate pituitary somatotroph differentiation during chicken embryonic development. J. Endocrinol. 180 (1), 45–53.

Marteinson, S.C., Palace, V., Letcher, R.J., Fernie, K.J., 2017. Disruption of thyroxine and sex hormones by 1,2-dibromo-4-(1,2-dibromoethyl)cyclohexane (DBE-DBCH) in American kestrels (*Falco sparverius*) and associations with reproductive and behavioral changes. Environ. Res. 154, 389–397.

McNabb, F.M., 1987. Comparative thyroid development in precocial Japanese quail and altricial ring doves. J. Exp. Zool. Suppl. 1, 281–290.

McNabb, F.M., 2006. Avian thyroid development and adaptive plasticity. Gen. Comp. Endocrinol. 147 (2), 93–101.

McNabb, F.M., 2007. The hypothalamic-pituitary-thyroid (HPT) axis in birds and its role in bird development and reproduction. Crit. Rev. Toxicol. 37 (1–2), 163–193.

McNabb, F.M., Fox, G.A., 2003. Avian thyroid development in chemically contaminated environments: is there evidence of alterations in thyroid function and development? Evol. Dev. 5 (1), 76–82.

McNabb, F.M., Larsen, C.T., Pooler, P.S., 2004. Ammonium perchlorate effects on thyroid function and growth in bobwhite quail chicks. Environ. Toxicol. Chem. 23 (4), 997–1003.

McNabb, F.M., Lyons, L.J., Hughes, T.E., 1986. Avian hepatic T3 generation by 5'-monodeiodination: characterization of two enzymatic pathways and the effects of goitrogens. Comp. Biochem. Physiol. A Comp. Physiol. 85 (2), 249–255.

McNabb, F.M.A., 1988. Peripheral thyroid-hormone dynamics in precocial and altricial avian development. Am. Zool. 28 (2), 427–440.

McNabb, F.M.A., 1992. Thyroid Hormones. Prentice Hall, New Jersey.

McNabb, F.M.A., Blackman, J.R., Cherry, J.A., 1985. The effects of different maternal dietary iodine concentrations on Japanese quail .1. Thyroid status of hens. Domest. Anim. Endocrinol. 2 (1), 25–34.

McNabb, F.M.A., Dicken, S.G., Cherry, J.A., 1985. The effects of different maternal dietary iodine concentrations on Japanese quail. 2. Thyroid-function in embryos and hatchlings. Domest. Anim. Endocrinol. 2 (1), 35–42.

McNabb, F.M.A., King, D.B., 1993. Thyroid hormone effects on growth, development and metabolism. In: Schreibman, M.P., Scanes, C.G., Pang, P.K.T. (Eds.), The Endocrinology of Growth, Development, and Metabolism in Vertebrates. Academic Press, New York, pp. 393–417.

McNabb, F.M.A., Olson, J.M., 1996. Development of thermoregulation and its hormonal control in precocial and altricial birds. Avian Poultry Biol. Rev. 7 (2–3), 111–125.

McNabb, F.M.A., Scanes, C.G., Zeman, M., 1998. Endocrine Control of Development. Avian Growth and Development. Evolution within the Altricial-Precocial Spectrum. Oxford University Press, New York. J. M. R. Starck, R.E.

McNabb, F.M.A., Wilson, C.M., 1997. Thyroid hormone deposition in avian eggs and effects on embryonic development. Am. Zool. 37 (6), 553–560.

Merryman, J.I., Buckles, E.L., 1998. The avian thyroid gland. Part one: a review of the anatomy and physiology. J. Avian Med. Surg. 12 (4), 234–237.

Mishra, M.K., Wilson, F.E., Scanlan, T.S., Chiellini, G., 2004. Thyroid hormone-dependent seasonality in American tree sparrows (*Spizella arborea*): effects of GC-1, a thyroid receptor beta-selective agonist, and of iopanoic acid, a deiodinase inhibitor. J. Comp. Physiol. B 174 (6), 471–479.

Miyazaki, W., Iwasaki, T., Takeshita, A., Kuroda, Y., Koibuchi, N., 2004. Polychlorinated biphenyls suppress thyroid hormone receptor-mediated transcription through a novel mechanism. J. Biol. Chem. 279 (18), 18195–18202.

Moeller, L.C., Broecker-Preuss, M., 2011. Transcriptional regulation by nonclassical action of thyroid hormone. Thyroid Res. 4 (Suppl. 1), S6.

Morreale de Escobar, G., Obregon, M.J., Escobar del Rey, F., 2004. Role of thyroid hormone during early brain development. Eur. J. Endocrinol. 151 (Suppl. 3), U25–U37.

Muchow, M., Bossis, I., Porter, T.E., 2005. Ontogeny of pituitary thyrotrophs and regulation by endogenous thyroid hormone feedback in the chick embryo. J. Endocrinol. 184 (2), 407–416.

Mughal, B.B., Fini, J.B., Demeneix, B.A., 2018. Thyroid-disrupting chemicals and brain development: an update. Endocr. Connect. 7 (4), R160–R186.

Nakao, N., Takagi, T., Iigo, M., Tsukamoto, T., Yasuo, S., Masuda, T., Yanagisawa, T., Ebihara, S., Yoshimura, T., 2006. Possible involvement of organic anion transporting polypeptide 1c1 in the photoperiodic response of gonads in birds. Endocrinology 147 (3), 1067–1073.

Nakayama, T., Yoshimura, T., 2018. Seasonal rhythms: the role of thyrotropin and thyroid hormones. Thyroid 28 (1), 4–10.

Niezgoda, J., Bobek, S., Wronska-Fortuna, D., 2005. Enhanced non-esterified fatty acids and corticosterone in blood plasma of chickens treated with insulin are significantly depleted by reverse T-3: minor changes in hypoglycaemia. J. Vet. Med. Ser. A-Physiol. Pathol. Clin. Med. 52 (9), 429–435.

Norris, D.O., 2007. Vertebrate Endocrinology. Elsevier Academic Press, Amsterdam; Boston.

Perez, J.H., Furlow, J.D., Wingfield, J.C., Ramenofsky, M., 2016. Regulation of vernal migration in Gambel's white-crowned sparrows: role of thyroxine and triiodothyronine. Horm. Behav. 84, 50–56.

Perez, J.H., Meddle, S.L., Wingfield, J.C., Ramenofsky, M., 2018. Effects of thyroid hormone manipulation on pre-nuptial molt, luteinizing hormone and testicular growth in male white-crowned sparrows (*Zonotrichia leuchophrys* gambelii). Gen. Comp. Endocrinol. 255, 12–18.

Poczopko, P., Uliasz, M., 1975. Hormonal regulation of thermogenesis in goslings. Possible role of the thyroid gland. Acta Physiol. Pol. 26 (3), 241–248.

Preau, L., Fini, J.B., Morvan-Dubois, G., Demeneix, B., 2015. Thyroid hormone signaling during early neurogenesis and its significance as a vulnerable window for endocrine disruption. Biochim. Biophys. Acta 1849 (2), 112–121.

Queen, W.H., Christensen, V.L., May, J.D., 1997. Supplemental thyroid hormones and molting in Turkey breeder hens. Poult. Sci. 76 (6), 887–893.

Raheja, K.L., Linscheer, W.G., Coulson, R., Wentworth, S., Fineberg, S.E., 1980. Elevated insulin/glucagon ratios and decreased cyclic AMP levels accompany the glycogen and triglyceride storage syndrome in the hypothyroid chick. Horm. Metab. Res. 12 (2), 51–55.

Raymaekers, S.R., Verbeure, W., Ter Haar, S.M., Cornil, C.A., Balthazart, J., Darras, V.M., 2017. A dynamic, sex-specific expression pattern of genes regulating thyroid hormone action in the developing zebra finch song control system. Gen. Comp. Endocrinol. 240, 91–102.

Ren, X.M., Li, C.H., Zhang, J.Q., Guo, L.H., 2019. Binding and activity of sulfated metabolites of lower-chlorinated polychlorinated biphenyls towards thyroid hormone receptor alpha. Ecotoxicol. Environ. Saf. 180, 686–692.

Richardson, S.J., 2014. Tweaking the structure to radically change the function: the evolution of transthyretin from 5-hydroxyisourate hydrolase to triiodothyronine distributor to thyroxine distributor. Front. Endocrinol. 5, 245.

Richardson, S.J., Wijayagunaratne, R.C., D'Souza, D.G., Darras, V.M., Van Herck, S.L., 2015. Transport of thyroid hormones via the choroid plexus into the brain: the roles of transthyretin and thyroid hormone transmembrane transporters. Front. Neurosci. 9, 66.

Rieman, J.D., McNabb, F.M., 1991. Assay validation and characterization of hepatic 5'-deiodinase activity in ring doves using reverse-T3 as substrate. Gen. Comp. Endocrinol. 82 (1), 53–59.

Ronning, B., Mortensen, A.S., Moe, B., Chastel, O., Arukwe, A., Bech, C., 2009. Food restriction in young Japanese quails: effects on growth, metabolism, plasma thyroid hormones and mRNA species in the thyroid hormone signalling pathway. J. Exp. Biol. 212 (19), 3060–3067.

Rosebrough, R.W., McMurtry, J.P., 2003. Methimazole and thyroid hormone replacement in broilers. Domest. Anim. Endocrinol. 24 (3), 231–242.

Rosebrough, R.W., Russell, B.A., Richards, M.P., 2009. Effects of short term triiodothyronine administration to broiler chickens fed methimazole. Comp. Biochem. Physiol. C Toxicol. Pharmacol. 150 (1), 72–78.

Rousset, B., Dupuy, C., Miot, F., Dumont, J., 2000. Chapter 2 Thyroid Hormone Synthesis and Secretion. Endotext. K. R. Feingold, B. Anawalt, A. Boyce et al. South Dartmouth (MA).

Rudas, P., 1986. Comparison of type I 5'-deiodination of thyroxine and of reverse-triiodothyronine in rat and chicken liver homogenates. Gen. Comp. Endocrinol. 63 (3), 400–407.

Rudas, P., Pethes, G., 1986. Acute changes of the conversion of thyroxine to triiodothyronine in hypophysectomized and thyroidectomized chickens exposed to mild cold (10 degrees). Gen. Comp. Endocrinol. 63 (3), 408–413.

Ruuskanen, S., 2015. Hormonally-mediated maternal effects in birds: lessons from the flycatcher model system. Gen. Comp. Endocrinol. 224, 283–293.

Ruuskanen, S., Hsu, B.-Y., Nord, A., 2020. Endocrinology of Thermoregulation in Birds in a Changing Climate. Available from: https://ecoevorxiv.org/jzam3/.

Ruuskanen, S., Hsu, B.Y., 2018. Maternal thyroid hormones: an unexplored mechanism underlying maternal effects in an ecological framework. Physiol. Biochem. Zool. 91 (3), 904–916.

Sap, J., Munoz, A., Damm, K., Goldberg, Y., Ghysdael, J., Leutz, A., Beug, H., Vennstrom, B., 1986. The c-erb-A protein is a high-affinity receptor for thyroid hormone. Nature 324 (6098), 635–640.

Scapin, S., Leoni, S., Spagnuolo, S., Fiore, A.M., Incerpi, S., 2009. Short-term effects of thyroid hormones on Na+-K+-ATPase activity of chick embryo hepatocytes during development: focus on signal transduction. Am. J. Physiol. Cell Physiol. 296 (1), C4–C12.

Schweizer, U., Johannes, J., Bayer, D., Braun, D., 2014. Structure and function of thyroid hormone plasma membrane transporters. Eur. Thyroid J. 3 (3), 143–153.

Sechman, A., 2013. The role of thyroid hormones in regulation of chicken ovarian steroidogenesis. Gen. Comp. Endocrinol. 190, 68–75.

Sechman, A., Pawlowska, K., Hrabia, A., 2011. Effect of 3,3',5-triiodothyronine and 3,5-diiodothyronine on progesterone production, cAMP synthesis, and mRNA expression of STAR, CYP11A1, and HSD3B genes in granulosa layer of chicken preovulatory follicles. Domest. Anim. Endocrinol. 41 (3), 137–149.

Sharp, P.J., Klandorf, H., 1985. Environmental and physiological factors controlling thyroid function. In: Follett, B.K., Ishii, S., Chandola, A. (Eds.), Galliformes. The Endocrine System and the Environment. Japan Scientific Societies Press, Tokyo and Springer-Verlag, Berlin, pp. 175–188.

Stallard, L.C., McNabb, F.M.A., 1990. The effects of different iodide availabilities on thyroid-function during development in Japanese-quail. Domest. Anim. Endocrinol. 7 (2), 239–250.

Taylor, E., Heyland, A., 2017. Evolution of thyroid hormone signaling in animals: non-genomic and genomic modes of action. Mol. Cell. Endocrinol. 459, 14–20.

Techer, R., Houde, M., Verreault, J., 2016. Associations between organohalogen concentrations and transcription of thyroid-related genes in a highly contaminated gull population. Sci. Total Environ. 545–546, 289–298.

Techer, R., Houde, M., Verreault, J., 2018. Changes in thyroid axis responses in two ring-billed gull sub-populations differentially exposed to halogenated flame retardants. Chemosphere 211, 844–854.

Thommes, R.C., 1987. Ontogenesis of thyroid function and regulation in the developing chick embryo. J. Exp. Zool. Suppl. 1, 273–279.

Thommes, R.C., Hylka, V.W., Tonetta, S.A., Griesbach, D.A., Ropka, S.L., Woods, J.E., 1988. Hypothalamic regulation of the pituitary-thyroid unit in the developing chick-embryo. Am. Zool. 28 (2), 417–426.

Too, H.C., Shibata, M., Yayota, M., Darras, V.M., Iwasawa, A., 2017. Expression of thyroid hormone regulator genes in the yolk sac membrane of the developing chicken embryo. J. Reprod. Dev. 63 (5), 463–472.

Totzke, U., Fenske, M., Huppop, O., Raabe, H., Schach, N., 1999. The influence of fasting on blood and plasma composition of herring gulls (*Larus argentatus*). Physiol. Biochem. Zool. 72 (4), 426–437.

Ucan-Marin, F., Arukwe, A., Mortensen, A.S., Gabrielsen, G.W., Letcher, R.J., 2010. Recombinant albumin and transthyretin transport proteins from two gull species and human: chlorinated and brominated contaminant binding and thyroid hormones. Environ. Sci. Technol. 44 (1), 497–504.

Vaitkus, J.A., Farrar, J.S., Celi, F.S., 2015. Thyroid hormone mediated modulation of energy expenditure. Int. J. Mol. Sci. 16 (7), 16158–16175.

Van der Geyten, S., Sanders, J.P., Kaptein, E., Darras, V.M., Kühn, E.R., Leonard, J.L., Visser, T.J., 1997. Expression of chicken hepatic type I and type III iodothyronine deiodinases during embryonic development. Endocrinology 138 (12), 5144–5152.

Van der Geyten, S., Van Rompaey, E., Sanders, J.P., Visser, T.J., Kühn, E.R., Darras, V.M., 1999. Regulation of thyroid hormone metabolism during fasting and refeeding in chicken. Gen. Comp. Endocrinol. 116 (2), 272–280.

Van Herck, S.L., Delbaere, J., Bourgeois, N.M., McAllan, B.M., Richardson, S.J., Darras, V.M., 2015. Expression of thyroid hormone transporters and deiodinases at the brain barriers in the embryonic chicken: insights into the regulation of thyroid hormone availability during neurodevelopment. Gen. Comp. Endocrinol. 214, 30–39.

Van Herck, S.L., Geysens, S., Bald, E., Chwatko, G., Delezie, E., Dianati, E., Ahmed, R.G., Darras, V.M., 2013. Maternal transfer of methimazole and effects on thyroid hormone availability in embryonic tissues. J. Endocrinol. 218 (1), 105–115.

Van Herck, S.L., Geysens, S., Delbaere, J., Tylzanowski, P., Darras, V.M., 2012. Expression profile and thyroid hormone responsiveness of transporters and deiodinases in early embryonic chicken brain development. Mol. Cell. Endocrinol. 349 (2), 289–297.

Vancamp, P., Bourgeois, N.M.A., Houbrechts, A.M., Darras, V.M., 2018. Knockdown of the thyroid hormone transporter MCT8 in chicken retinal precursor cells hampers early retinal development and results in a shift towards more UV/blue cones at the expense of green/red cones. Exp. Eye Res. 178, 135–147.

Vancamp, P., Darras, V.M., 2017. Dissecting the role of regulators of thyroid hormone availability in early brain development: merits and potential of the chicken embryo model. Mol. Cell. Endocrinol. 459, 71–78.

Vancamp, P., Deprez, M.A., Remmerie, M., Darras, V.M., 2017. Deficiency of the thyroid hormone transporter monocarboxylate transporter 8 in neural progenitors impairs cellular processes crucial for early corticogenesis. J. Neurosci. 37 (48), 11616–11631.

Verheyen, G., Decuypere, E., Kühn, E.R., Herremans, M., 1986. Dissociation of the effect of thyroxine and triiodothyronine in relation to the halt, egg-laying and molt in hens. Archiv. Exp. Vet. 40 (2), 250–259.

Verhoelst, C.H., Darras, V.M., Doulabi, B.Z., Reyns, G., Kühn, E.R., Van der Geyten, S., 2004. Type I iodothyronine deiodinase in euthyroid and hypothyroid chicken cerebellum. Mol. Cell. Endocrinol. 214 (1–2), 97–105.

Verhoelst, C.H., Roelens, S.A., Darras, V.M., 2005. Role of spatiotemporal expression of iodothyronine deiodinase proteins in cerebellar cell organization. Brain Res. Bull. 67 (3), 196–202.

Visser, W.E., Friesema, E.C., Jansen, J., Visser, T.J., 2008. Thyroid hormone transport in and out of cells. Trends Endocrinol. Metabol. 19 (2), 50–56.

Vyboh, P., Zeman, M., Jurani, M., Buyse, J., Decuypere, E., 1996. Plasma thyroid hormone and growth hormone patterns in precocial Japanese quail and altricial European starlings during postnatal development. Compar. Biochem. Physiol. C-Toxicol. Pharmacol. 114 (1), 23–27.

Walter, I., Seebacher, F., 2009. Endothermy in birds: underlying molecular mechanisms. J. Exp. Biol. 212 (15), 2328–2336.

Watanabe, Y., Grommen, S.V.H., De Groef, B., 2016. Corticotropin-releasing hormone: mediator of vertebrate life stage transitions? Gen. Comp. Endocrinol. 228, 60–68.

Webb, C.M., McNabb, F.M., 2008. Polychlorinated biphenyl effects on avian hepatic enzyme induction and thyroid function. Gen. Comp. Endocrinol. 155 (3), 650–657.

Weng, Q., Saita, E., Watanabe, G., Takahashi, S., Sedqyar, M., Suzuki, A.K., Taneda, S., Taya, K., 2007. Effect of methimazole-induced hypothyroidism on adrenal and gonadal functions in male Japanese quail (*Coturnix japonica*). J. Reprod. Dev. 53 (6), 1335–1341.

Wilson, C.M., McNabb, F.M., 1997. Maternal thyroid hormones in Japanese quail eggs and their influence on embryonic development. Gen. Comp. Endocrinol. 107 (2), 153–165.

Wilson, F.E., Reinert, B.D., 1996. The timing of thyroid-dependent programming in seasonally breeding male American tree sparrows (*Spizella arborea*). Gen. Comp. Endocrinol. 103 (1), 82–92.

Wilson, F.E., Reinert, B.D., 1999. Time of thyroidectomy variably affects seasonality in female American tree sparrows (*Spizella arborea*). Gen. Comp. Endocrinol. 114 (3), 425–430.

Yamaguchi, S., Aoki, N., Kitajima, T., Iikubo, E., Katagiri, S., Matsushima, T., Homma, K.J., 2012. Thyroid hormone determines the start of the sensitive period of imprinting and primes later learning. Nat. Commun. 3, 1081.

Yamaguchi, S., Aoki, N., Takehara, A., Mori, M., Kanai, A., Matsushima, T., Homma, K.J., 2016. Involvement of nucleotide diphosphate kinase 2 in the reopening of the sensitive period of filial imprinting of domestic chicks (*Gallus gallus* domesticus). Neurosci. Lett. 612, 32–37.

Zheng, W.H., Li, M., Liu, J.S., Shao, S.L., 2008. Seasonal acclimatization of metabolism in Eurasian tree sparrows (*Passer montanus*). Comp. Biochem. Physiol. Mol. Integr. Physiol. 151 (4), 519–525.

Zheng, W.H., Li, M., Liu, J.S., Shao, S.L., Xu, X.J., 2014. Seasonal variation of metabolic thermogenesis in Eurasian tree sparrows (*Passer montanus*) over a latitudinal gradient. Physiol. Biochem. Zool. 87 (5), 704–718.

Zheng, W.H., Lin, L., Liu, J.S., Xu, X.J., Li, M., 2013. Geographic variation in basal thermogenesis in little buntings: relationship to cellular thermogenesis and thyroid hormone concentrations. Comp. Biochem. Physiol. Mol. Integr. Physiol. 164 (3), 483–490.

Chapter 32

Mechanisms and hormonal regulation of shell formation: supply of ionic and organic precursors, shell mineralization

Yves Nys[1], Joel Gautron[1], Alejandro B. Rodriguez-Navarro[2] and Maxwell Hincke[3]

[1]*BOA, INRAE, Université de Tours, Fonction et Régulation des protéines de l'œuf, Développement de l'œuf, Valorisation, Évolution, France;* [2]*Departmento de Mineralogia y Petrologia, Universidad de Granada, Spain;* [3]*Department of Innovation in Medical Education; Department of Cellular and Molecular Medicine, Faculty of Medicine, University of Ottawa, Ottawa, ON, Canada*

Abbreviations

ACC Amorphous calcium carbonate
AFM Atomic force microscopy
Anxa 1 Annexin 1
BSP Bone sialoprotein
CA Carbonic anhydrase
Ca or Ca++ Calcium or ionic calcium
CACNA1D Voltage-dependent L-type calcium channel subunit alpha-1D
CALB1 Calbindin 28kD
cAMP Cyclic adenosine monophosphate
CaSR Ca^{2+}-sensing receptor
CGRP Calcitonin gene-related peptide
CLDN Claudins, paracellular cation channel
CREMP Cysteine-rich eggshell matrix protein
CT Calcitonin
CYP27B1 1α-hydroxylase of 25 hydroxyvitamin D_3
DBP Vitamin D binding proteins
EDIL3 EGF-like repeats and discoidin-like domains 3
EDS Energy-dispersive X-ray spectroscopic
EELS Electron energy loss spectroscopy
EPD Electrical potential difference
ER Endoplasmic reticulum
EREF Estrogen response elements
ESM Eggshell membranes
EVs Extracellular vesicles
FGF 23 Fibroblast growth factor 23, phosphatonin
FGFR1c FGF receptor-1c
ITPR1 Inositol trisphosphate receptor type 1
JAM Junctional adhesion molecule
KS Keratan sulfate
KSPG Keratan sulfate proteoglycan
LOXL2 Lysyl oxidase−like 2
M-CSF Macrophage colony-stimulating factor
MFGE8 Milk fat globule EGF-factor 8
OC Osteocalcin
OC-116 Ovocleidin-116 (MEPE)
OC-17 Ovocleidin-17
OCX 21, 32, 36 Ovocalyxins 21, 32, 36
OPG Osteoprotegerin
OPN Osteopontin (SSP1)
PLP Parathyroid-like peptide
PTGs Parathyroid glands
PMCA1 (ATP2B1) Plasma membrane calcium-transporting ATPase 1
PTH Parathyroid hormone
PTHrP Parathyroid hormone-related peptide
QTLs Quantitative trait loci
RANK Receptor-activated nuclear
RANKL Rank ligand
SNP Single nucleotide polymorphism
TEM Transmission electron microscopy
TJP Tight junction proteins
TRPM Transient receptor potential melastatin, ion channels
TRPV Transient receptor potential cation channel, Transient receptor potential cation channel, subfamily C, member 6
VAT Vacuolar (H+)-ATPase
VDR Vitamin D receptor
VDRE Vitamin D receptor element
ZO 1, 2, 3 Zonula occludens 1, 2, 3 (TJP 1, 2, 3)

Sturkie's Avian Physiology. https://doi.org/10.1016/B978-0-12-819770-7.00049-9

Gene symbol of proteins (ionic transporters, shell matrix proteins) are described in Tables 32.1 and 32.2.

1,25(OH)2D3,25-dihydroxyvitamin D_3or 25(OH)D 25 hydroxyvitamin D_3 Metabolites of vitamin D.

32.1 Introduction

Birds are oviparous and produce a cleidoic egg with its internal environment almost totally isolated from the exterior. This reproductive cell is composed of an oocyte surrounded by nutritional reserves. The unfertilized chicken egg is consumed worldwide because of its low price and high-nutritional value. It contains a large diversity of nutrients (protein, energy, vitamins, and minerals) that are largely sufficient for the human diet with the exception of calcium and vitamin C (Rehault-Godbert et al., 2019). Eggs also possess an ideal profile of balanced amino acids and contain large amounts of unsaturated fatty acids. The egg is similar between different species of birds: a yolk surrounded by an egg white, eggshell membranes (ESMs), and the eggshell. The egg is a package containing all components needed for the development of the embryo, with a variety of protective systems against physical and microbial attacks. The egg white contains numerous antimicrobial proteins and the eggshell protects the contents of the egg from mechanical insults. In addition, shell porosity regulates the exchange of water and gases during extrauterine development of the chick embryo; moreover, the eggshell is also a calcium reserve that supports embryonic bone development. The shell mineral structure is one of the most impressive terrestrial adaptations in amniotes, which allows embryonic development in the desiccating nonaquatic environment. Shell mineralization takes place in the lumen of the uterus, which secretes an acellular milieu, the uterine fluid that contains all necessary ionic and organic precursors. Its particularities, as compared to bone or teeth, are the material [calcium carbonate ($CaCO_3$) instead of calcium phosphate] and the absence of cell-directed assembly during mineralization. The ESMs play a crucial role by controlling the initial mineralization, which occurs upon organic cores on its outer surface.

In the laying chickens, eggshell formation takes place daily in the uterus and is one of the most rapid biomineralization processes known. To provide about 6 g of shell as $CaCO_3$, the hen exports each day 2.4 g of Ca corresponding to 10% of her total body calcium (Sauveur and de Reviers, 1988; Nys and Guyot, 2011) and in 1 year of egg production, the modern pedigree hen exports more than her body weight as eggshell. The intensity and discontinuity of Ca secretion challenges calcium homeostasis in hens; however, birds develop physiological adaptations in the intestine, bone, and uterus upon sexual maturity. Moreover, there is a daily cycle in these tissues during shell formation that provides the necessary Ca and bicarbonate. Two weeks before the onset of egg production, hens establish a calcium "reservoir"—the medullary bone, display a largely increased intestinal Ca retention and develop the secondary reproductive organ, the oviduct. The spatiotemporally regulated process of egg formation takes place in specialized segments of the oviduct following yolk ovulation (Figure 32.1): secretion of the vitelline membrane components in the infundibulum, secretion of albumen in the magnum, ESM deposition in the isthmus, and eggshell mineralization in the uterus (Sauveur and de Reviers, 1988; Nys and Guyot, 2011). The uterus secretes large amounts of Ca^{2+} and HCO_3^- ions to form the shell (Hurwitz, 1989a; Nys, 1993; Bar, 2009). This daily export of calcium causes a decrease in plasma calcium, which stimulates, through Ca^{2+}-sensing receptors (CaSRs), the synthesis and secretion of calcium-regulating hormones: mainly parathyroid hormone (PTH) and 1,25-dihydroxyvitamin D_3, which together influence Ca flux by acting on bone resorption and intestinal absorption (Wasserman, 2004; Christakos, 2014, 2019). Numerous classical physiological studies have explored the regulation of uterine ionic transfer, without demonstration of a direct effect of these hormones upon avian Ca metabolism (Bar, 2008, 2009; Nys and Le Roy, 2018). However, during the past 20 years, transcriptomic and proteomic in vivo analyses have provided detailed information on the proteins involved in the mechanisms of ion supply and of shell mineralization. The chicken constitutes an excellent model because the spatial and temporal sequence of egg formation is well known, and the oviduct provides experimental access to tissues that are specific to particular functions.

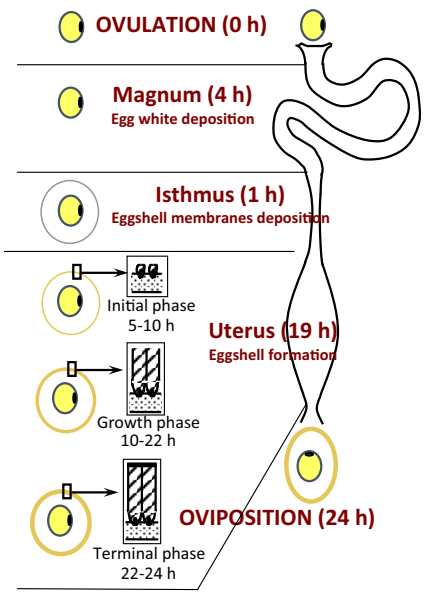

FIGURE 32.1 Spatiotemporal formation of the egg. Schematic drawing of the egg passage through the oviduct, timing and stage of shell formation.

Indeed, the components of each egg compartment are produced sequentially (Sauveur and De Reviers, 1988; Nys and Guyot, 2011). The liver synthesizes the egg yolk components that are exported to the ovary. Following ovulation, the largest ovarian follicle releases a mature ovum into the oviduct. Specialized parts of the oviduct successively synthesize and secrete: the constituents of the outer vitelline membrane which surround the yolk, the egg white, the shell membranes, and the eggshell. This temporal sequence is controlled by the daily cycle of steroid and pituitary hormones. In hens, it is possible to compare the expression of genes between specific segments of the oviduct at well-defined stages of egg formation in order to obtain insight into genes involved in specific functions associated with the formation of an egg component. Comparison of proteomic profiles of egg compartments or uterine fluid sampled at well-defined periods of egg formation also permit the identification of proteins involved in mechanisms of ionic transport, eggshell mineralization, and their regulation. These approaches have revealed in detail the mechanisms of Ca transfer at the intestinal and uterus level, identification of novel mechanisms of uterine Ca secretion (vesicular transport), as well as, identification of the matrix proteins involved in the control of eggshell mineralization. This novel information will be presented in this chapter. Transcriptomic and proteomic approaches also allow exploration of the regulation of these processes or highlight novel hormone pathways, such as fibroblast growth factor 23 (FGF23) acting on phosphate metabolism. Such studies are mainly qualitative but have allowed a myriad of protein candidates involved in ionic transport and shell mineralization to be identified. More quantitative and functional analyses are needed to hierarchize the candidates and to understand different mechanisms involved in shell formation. This chapter aims to update information in these areas and to underline the novel knowledge that has accrued on the proteins involved in providing and in building the shell material; however, there needs to be a better understanding of their physiological regulation.

32.2 Structure, composition, and formation of the eggshell

32.2.1 Structure and composition

The shell structure is similar for different species of birds and shares the same mineral component, namely the trigonal phase of $CaCO_3$ known as calcite, which is the most stable $CaCO_3$ polymorph at room temperature (Hamilton; 1986; Solomon, 1991; Nys et al., 1999; Hincke et al., 2012). In the shell ultrastructure, up to six layers can be distinguished (Figure 32.2). The inner part of the eggshell comprises two shell membranes consisting of interlacing protein fibers. The mineral portion is anchored on organic rich structures, the mammillary bodies, located at the surface of the outer shell membrane fibers. These structures have a strong calcium binding capacity and act as nucleation sites for calcite crystal formation during the initial stages of eggshell mineralization (Fernandez et al., 2001). Calcite crystals grow radiating away from mammillary bodies and forming inverted cones (mammillary layer) that fuse at their bases and continue growing outward to form a compact zone called the palisade layer. The palisades consist of juxtaposed irregular columnar units of calcite crystals that became larger toward the eggshell surface, with diameters ranging between 60 and 80 microns. The palisade layer is around 200 µm thick in chicken eggs, corresponding to about two-thirds of the eggshell thickness and has the largest contribution to eggshell mechanical properties. It is completed by a thin vertical crystal layer where the crystallites are aligned perpendicular to the shell surface which can be visualized in thin sections of eggshell viewed under an optical microscopy with crossed polarizing filters (Figures 32.3 and 32.4).

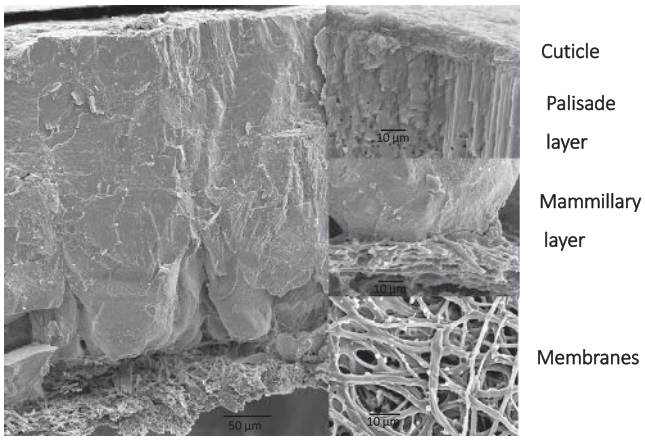

FIGURE 32.2 Left: Scanning electron micrograph (SEM) (shell thickness is 300 µm)) of a cross-fractured hen eggshell showing the different layers. Right: SEM of mammillary layer, palisade layer, and upper part of the shell (Nys et al., 2001).

The main ultrastructural characteristics (columnar structure) and mineralogical composition (calcite) of the eggshell are constant, across all avian species, but there is a notable variability in the eggshell microstructure characteristics (size, shape, and orientation of the crystals of calcite) between species and even within the same specie depending on different factors (Panheleux et al., 1999; Ahmed et al., 2005; Rodriguez-Navarro et al., 2007).

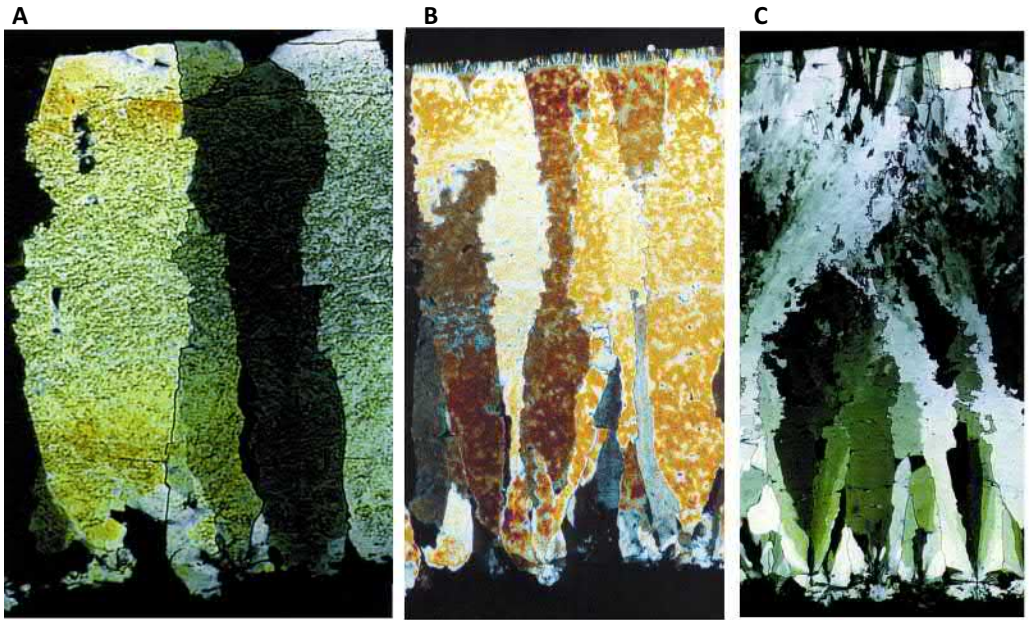

FIGURE 32.3 Cross-section of eggshell viewed in cross-polarized light photomicrographs showing the orientation of calcite crystals in the eggshells from hen (A), turkey (B), and guinea fowl (C). Note the presence of the thin vertical crystal layer at the top of the turkey shell (B) and the presence of interlaced calcite crystals in the upper palisade layer of the guinea fowl shell (C). *By courtesy of Juan Manuel Garcia-Ruiz, Laboratorio de Estudios Cristalograficos, Instituto Andaluz de Ciencias de la Tierra, Granada, Spain; Panheleux et al. (1999).*

The eggshell ultrastructure and microstructure are responsible for the exceptional mechanical properties of eggshell (in chickens, the egg breaking strength is 35N for a mean thickness of 0.33 mm). Changes in these characteristics have a strong effect on eggshell mechanical properties. A remarkable example is the Guinea fowl eggshell (Panheleux et al., 1999; Le Roy et al., 2019). Its inner part is made of calcite crystal units arranged vertically as in chickens. However, the outer zone has a more complex microstructural arrangement made of very smaller intricately interlaced calcite crystals with varying orientation (Figure 32.3). These characteristics of the Guinea fowl eggshell confer upon its superior mechanical properties compared to the eggs of other birds.

The cuticle, an organic layer, is deposited on the surface of the eggshell; it contains a large proportion (2/3) of the superficial pigments (Nys et al., 1991). The inner cuticle contains a thin layer of hydroxyapatite crystals (Dennis et al., 1996). About 10,000 respiratory pores penetrate the hen eggshell (200 pores/cm^2), which are plugged by the cuticle. They allow and control the exchange of water and metabolic gases during the extrauterine development of the chick embryo while impeding bacterial penetration through the shell and preventing contamination of the egg contents.

The ESMs are composed of disulfide-rich protein fibers (~10% cysteine) that are extensively cross-linked by irreversible lysine-derived crosslinks of desmosine and isodesmosine. Collagen was suggested to be present because of identification of hydroxylysine, the observation of digestion of ESMs by collagenase, and finally by immunochemistry using antibodies against type I, V, and X collagen (Wong et al., 1984; Arias et al., 1997; Wang et al., 2002). However, the amino acid composition of the shell membranes largely differs from that of collagenous tissues, suggesting that collagen is not predominant. In fact, a combination of proteomics and transcriptomics approaches have revealed that a major ESM component is a cysteine-rich eggshell matrix protein (abbreviated CREMP), whose sequence displays similarity to spore coat protein SP75 of cellular slime molds (Kodali et al., 2011). The structural proteins CREMP, collagen X, and fibrillin-1 are highly overexpressed in the white isthmus segment of the oviduct, which is responsible for the synthesis and secretion of the ESM constituents. CREMP contains around 14% cysteine, in contrast to collagen X (α-1) which is only 0.2% cysteine, suggesting that CREMP could account for the relatively high-cysteine content of eggshell (Du et al., 2015). Proteomics investigations suggest that the most abundant ESM proteins are CREMP, collagen X, lysyl oxidase−like 2 (LOXL2) and lysozyme, with the remaining approximately 25% constituted by more than 500 proteins (Ahmed et al., 2017, 2019a, 2019b).

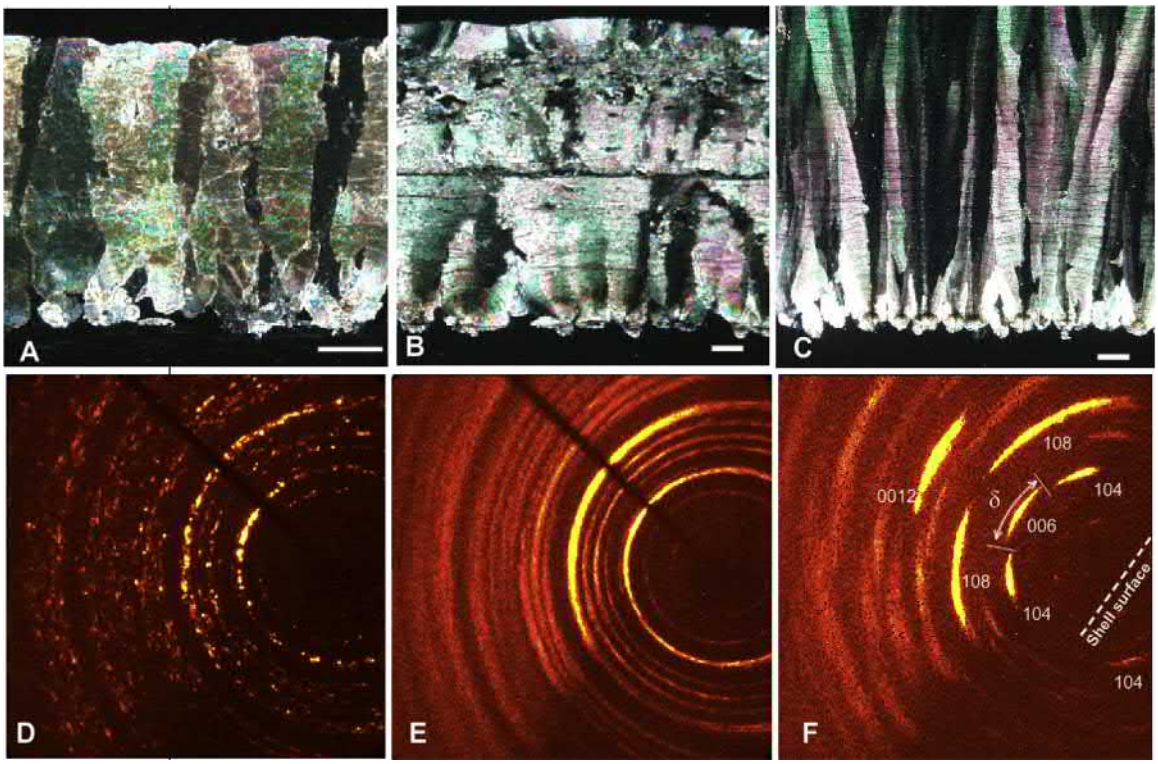

FIGURE 32.4 Upper part: Cross-section of eggshell viewed in cross-polarized light. Photomicrographs showing the orientation of calcite crystals in the eggshells from hen (A, larger randomly oriented crystals), emu (B, randomly oriented microcrystals), and ostrich (C, preferred orientation). Lower part: 2D-XRD patterns of eggshell of hen (D), emu (E), and ostrich (F) analyzing crystal orientation and size (Rodriguez-Navarro et al., 2002).

32.2.2 Kinetics and site of shell membranes and shell formation

ESM fibers are synthesized and secreted by glandular cells of the white isthmus 4 h after yolk ovulation (Nys et al., 1999, 2004). The organic components of mammillae (nucleation sites) and the first crystals are laid down on the external shell membranes in the distal red isthmus 5 h after ovulation. The progressive hydration of the egg albumen swells the forming egg, creating its ovoid shape and allowing close contact with the uterine wall about 10 h after ovulation. Active secretion of calcium, carbonate, and organic precursors over the following 12−14 h contribute to the rapid and linear deposition of the shell mineral, which ends with cuticle secretion about 1.5 h before oviposition (egg expulsion). Eggshell formation is the longest step of egg formation as it lasts about 20 h if the initial phase of shell nucleation is included; it is initiated at 4.5 h after ovulation and ends 1.5 h before oviposition. Shell formation occurs in three periods, the nucleation phase (5−10 h after ovulation), the rapid deposition of shell material (10−22 h after ovulation), and the termination of mineralization (21−23 h after ovulation).

32.3 Mineral supply: a challenge for calcium metabolism

No calcium storage occurs in the uterus before the initiation of shell formation (Sauveur and de Reviers, 1988; Nys et al., 1999). Calcium is directly provided by the ionic blood calcium. The amount needed to form a shell (2 g of Ca in chicken) is very large and the pool of blood ionic calcium in hens laying more than 320 eggs/year must be provided at a rate equivalent to its renewal every 12 min. The laying chicken exports, during 1 year of egg production, more than her body weight as eggshell. Calcium is initially provided by the hen's diet. During eggshell calcification, about two thirds of the Ca deposited in the uterus is directly supplied by the hen's diet, while one-third (30−40%) is mobilized from bone. Bone calcium mobilization is necessary because there is a desynchronization between food intake during the day and egg formation, which mainly takes place during the night. Provision of high-dietary level of Ca (3.5%), in the form of large particles of $CaCO_3$, provides sufficient intestinal Ca during the night to reduce the degree of bone mobilization for shell formation. Conversely, a hen fed a diet which is low in Ca

will mobilize up to 58% of the bone calcium. This cycle of daily resorption of bone is facilitated in hens by the presence of medullary bone. Two weeks before the onset of egg production, immature hens develop a novel and easily mobilized calcium "reservoir," the medullary bone. In addition, sexually mature laying hens largely increase their capacity to absorb Ca in the intestine under the control of the active metabolite of vitamin D (Hurwitz, 1989a; Nys, 1993; Bar, 2008; Nys and Le Roy, 2018) resulting in a threefold increase in intestinal Ca retention. The hourly kinetics of intestinal calcium absorption throughout the day is also of great importance because of the lack of overlap between the period of uterine deposition of calcium for shell during the night and the period of dietary calcium intake during the day. Hens show a specific appetite for calcium a few hours before the period of calcification, i.e., a few hours before lights off (Mongin and Sauveur, 1979). Diet and Ca-particles, when available, are stored in the crop. Dilatation of the crop elicits an increased acid secretion (Ruoff and Sewing, 1971; Lee et al., 1988). This specific appetite for calcium in hens therefore favors the storage and solubilization of the dietary calcium throughout the night especially when available as coarse particles, which partially compensates for the gap in time between dietary calcium intake and its requirement for shell formation. The timely provision of coarse calcium particles in this way also limits the hen's need to mobilize calcium from the bone reserve and therefore also decreases the associated elimination of phosphorus (Whitehead, 2004).

The shell contains 60% of carbonate originating from the blood CO_2, which penetrates the uterine glandular cells by simple diffusion through the plasma membrane (Hodges and Lörcher, 1967). Carbonic anhydrase 2 (CA2) catalyzes the reversible hydration of intracellular CO_2 to HCO_3^-. Bicarbonate is also supplied at a low level from plasma by the Na^+/HCO_3^- cotransporters (SLC4A4, A5, and A10) (Jonchère et al., 2012; Brionne et al., 2014). The carbonic anhydrase (CA) present in the uterine tubular gland cells is crucial for production of bicarbonate which is secreted into the uterine fluid through the HCO_3^-/Cl^- exchanger SLC26A9. Another less expressed CA, CA4, is also found in the uterine cells, its active site being localized in the extracellular space (Zhu and Sly, 1990). The precipitation of $CaCO_3$ in the uterine lumen provides H^+ ions, which are reabsorbed by the uterine cells. H^+ ions are exported via membrane Ca^{++} pumps, the vacuolar (H+)-ATPase (VAT) pump, and an H^+/Cl^- exchanger (Jonchère et al., 2012; Brionne et al., 2014). These pumps and exchangers control the pH balance and therefore contribute to maintenance of acid-base equilibrium in hens. The metabolic acidosis due to acidification of uterine fluid and plasma during shell formation is corrected in hens by respiratory hyperventilation and by an increased renal excretion of hydrogen (Mongin, 1978).

32.4 Hormones involved in calcium metabolism of laying hens: vitamin D, parathyroid hormone, calcitonin, and fibroblast growth factor-23

Regulation of the extracellular Ca^{2+} concentration is continuously challenged in hens by their large Ca requirement for shell formation; however, hens efficiently maintain Ca homeostasis by implementing the classical feedback mechanisms present in all vertebrates. These involve the intestines, bone, and kidney, and utilize three main calcium regulating hormones [PTH, calcitonin (CT), and 1,25-dihydroxy vitamin D3 ($1,25(OH)_2D_3$)]. FGF23 is a bone-derived hormone, which controls phosphorus homeostasis by suppressing phosphate reabsorption and vitamin D hormone synthesis in the kidney(Quarles, 2012). This mechanism has been recently revealed in birds, and the evidence demonstrating its influence on Ca metabolism are discussed in this section. These calcium-regulating hormones were initially studied in mice and human, revealing detailed information for these species. Their roles show numerous similarities with those in birds even if their actions and sensitivities are different from mammals (Dacke et al., 2015). The sex steroid hormones (estrogen and testosterone) influence Ca metabolism indirectly in hens at sexual maturity by initiating the formation of medullary bone and by increasing the appetite for Ca; however, there is no evidence of their control of Ca homeostasis. Similarly, the uterus is the major contributor to the elevated need for Ca; however, surprisingly this main organ of shell formation does not seem to be influenced by the Ca-regulating hormones even if the ionic transporters show numerous similarities at the uterine and intestinal levels (Bar, 2009; Nys and Le Roy, 2018). Other putative Ca and bone-regulating factors might influence Ca metabolism. Dacke et al. (2015) described the avian-specific actions of prostaglandins, calcitonin gene-related peptides (CGRPs), and amylin in pathways that are different from those in mammals. However, this aspect will not be discussed further in this review.

32.4.1 Regulation of vitamin D metabolites in hens

Vitamin D is essential for maintaining egg production and shell quality in hens. Its regulation in hens has been reviewed by many authors, including Hurwitz (1989), Nys (1993), Bar (2008, 2009), Christakos et al. (2014, 2019), and Nys and Le Roy (2018). One particularity of birds compared to mammals is the higher biological activity of vitamin D_3 relative to vitamin D_2 (ergocalciferol) because of the lower affinity of avian plasma vitamin D binding

proteins (DBPs) for vitamin D_2 compared to D_3 derivatives (DeLuca et al., 1988). Both vitamin D metabolism and regulation show large similarities in mammals and birds, but the magnitude of the fluctuations in hens relative to mammals is considerably larger. Vitamin D_3 is partly synthesized from 7-dehydrocholesterol in the skin in response to UV light, but is mainly provided by diet in commercial hens (Bar, 2008; Nys, 2017). The minimum daily requirement in hens was established at 7.5 µg/kg diet (corresponding to a requirement of about 1 µg/day/hen), according to earlier studies (Whitehead, 1986; Barroeta et al., 2012). The current recommendations are higher for hens producing more than 330 eggs in a laying year (50 µg/kg diet; 6 µg/bird/day) (Weber, 2009), which has a positive effect on bone strength and egg production (Barroeta et al., 2012).

Vitamin D_3 is initially hydroxylated in liver microsomes and mitochondria to form 25-hydroxyvitamin D (25(OH)D_3) (Bar, 2008; Christakos et al., 2014, 2019). This first hydroxylation is poorly regulated in contrast to the second hydroxylation step which occurs in the kidney to form the 1,25$(OH)_2D_3$ metabolite. Therefore, the plasma levels of 25(OH)D_3, which circulate as a complex with vitamin DBPs, mainly reflect the dietary supply of vitamin D_3. Its plasma level is however not directly proportional to the dietary supply of vitamin D_3 and circulating 25(OH)D_3 tends to plateau. Its biological activity is slightly higher in birds than the nonhydroxylated form, possibly as a consequence of better intestinal absorption.

A longitudinal study describing the changes in plasma DBPs and 1,25$(OH)_2D_3$ throughout embryonic development, followed by rearing of pullets (immature hens and males) until the onset of egg production at week 15−16, is shown in Figure 32.5 (Nys et al., 1986a). Vitamin 1,25$(OH)_2D_3$ is secreted first at embryonic day 13 (Moriuchi and Deluca, 1974), then its blood levels and that of DBP increase at hatching, possibly as a consequence of liver maturation. An additional increase occurs at sexual maturity under the influence of estrogens, as demonstrated by the increased 1,25$(OH)_2D_3$ induced by treatment of immature pullets with progesterone, testosterone, or estradiol (Montecuccoli et al., 1977; Baksi et Kenny, 1977; Nys et al., 1986a). The interruption of egg production induced by nutritional deficiencies is accompanied by decreases in the secretion of sex steroids and reduced concentrations of DBP and 1,25$(OH)_2D_3$. The resumption of egg production coincides with stimulation of 1,25$(OH)_2D_3$ plasma levels

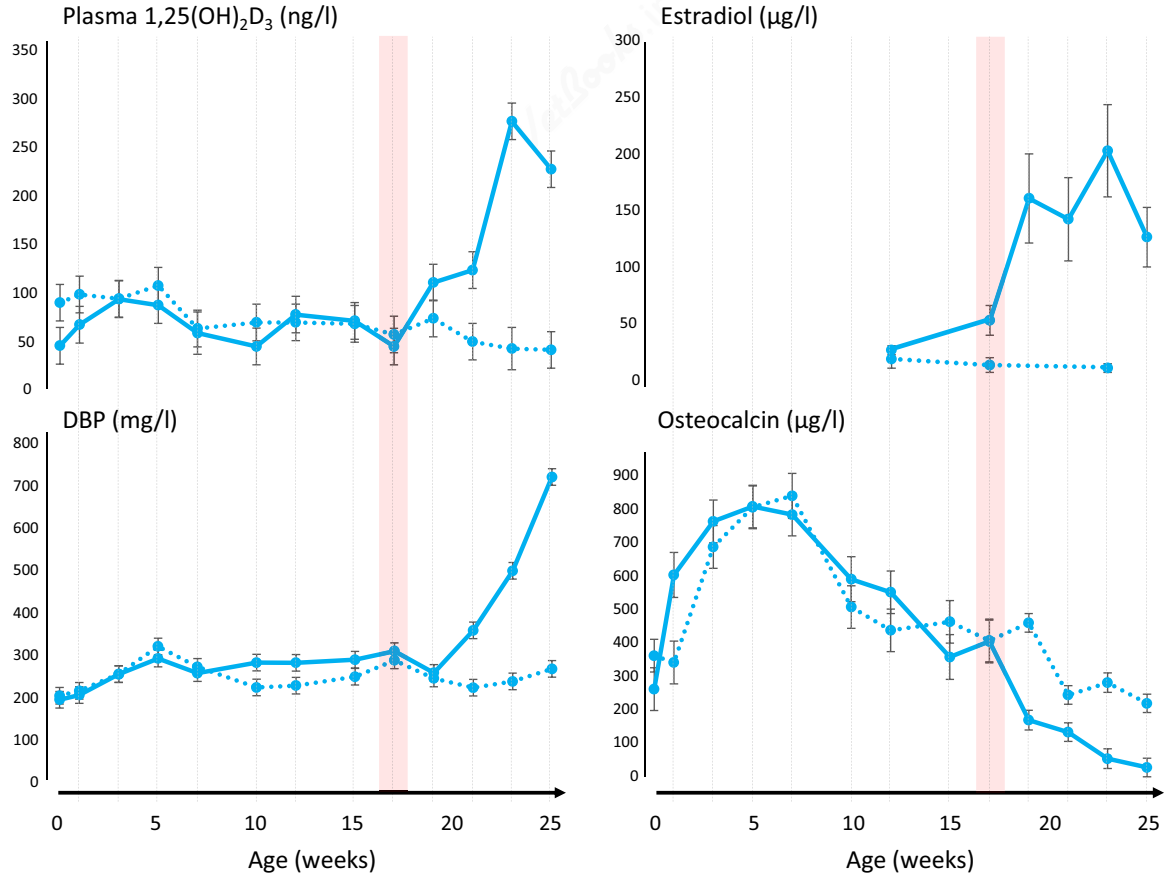

FIGURE 32.5 Evolution of plasma 1,25$(OH)_2D_3$, vitamin D-binding protein, estrogens, and osteocalcin concentrations during the growth of female (*continuous line*) and male (*dotted line*) chickens from birth to age of 25 weeks. The light orange band indicates the period of sexual maturity (Nys, 1993).

(Nys et al., 1986a, 1986b). Renal production of $24,25(OH)_2D_3$ is seven- to ninefold higher than that of $1,25(OH)_2D_3$ in immature pullets (Montecuccoli et al., 1977). However, at the onset of laying, hens activate kidney 25-hydroxycholecalciferol 1α-hydroxylase which elicits a large increase in plasma concentrations of $1,25(OH)_2D_3$ (Figure 32.5) and in intestinal $1,25(OH)_2D_3$, in contrast to $25(OH)D_3$ 24-hydroxylase (Spanos et al., 1976; Castillo et al., 1979). Daily eggshell formation coincides with slightly higher blood levels of $1,25(OH)_2D_3$. Its levels are around 100 pmol/L in immature pullets, rising to more than 200 pmol/L in hens laying shell-less eggs; however, this doubles in hens laying hard-shell eggs (Nys et al., 1986a). The stimulation of $1,25(OH)_2D_3$ depends on two types of regulation. The first is associated with sexual maturation, while the second results from changes in Ca metabolism induced by calcium exportation for eggshell formation. These observations are in agreement with numerous studies, as reviewed by many authors (Bar, 2008; Dacke et al., 2015, Nys and Le Roy, 2018). The increased $1,25(OH)_2D_3$ circulating levels in laying hens, compared to immature pullets, is due to stimulation by estrogens and, at a lower magnitude, by testosterone (Montecuccoli et al., 1977; Castillo et al., 1979; Baksi et Kenny, 1977). Estrogens act directly on the kidney production of $1,25(OH)_2D_3$ as shown in vitro (Baksi and Kenny, 1977; Tanaka et al., 1978), but with a lower magnitude than in vivo. Estrogens might act indirectly through the induced calcium deficiency (Bar and Hurwitz, 1979) due to the formation of medullary bone under the combined effect of sex steroids (Bar et al., 1978; Dacke et al., 2015). However, hens laying eggs with a soft shell due to artificial premature egg expulsion, and fed a high-dietary calcium diet, developed hypercalcemia during the entire laying cycle, while still exhibiting a relatively high level of plasma $1,25(OH)_2D_3$ (Figure 32.6). Sex steroids, therefore, can favor a high secretion of $1,25(OH)_2D_3$, even when PTH secretion is abolished and medullary bone is poorly mobilized. The largest stimulation in kidney production of $1,25(OH)_2D_3$ results from the hypocalcemia induced by shell formation at sexual maturity and to a lesser degree during the daily period of shell formation. Hypocalcemia causes increased secretion of PTH, which substantially increases the production of $1,25(OH)_2D_3$ in vivo (Garabedian et al., 1972) and in vitro (Trechsel et al., 1979). During the period of eggshell formation, the decrease in plasma ionized calcium occurs in hens laying hard-shelled eggs, but not in hens laying shell-less eggs (Figure 32.6). The hypocalcemia increases plasma PTH (van de Velde et al., 1984a; Singh et al., 1986; Yang et al., 2013; Kerschnitzki et al., 2014). Plasma hypocalcemia and PTH secretion are therefore the predominant factors stimulating $1,25(OH)_2D_3$ production, as demonstrated by the threefold increase of $1,25(OH)_2D_3$ induced in hypocalcemic hens fed a low-calcium diet (1% dietary

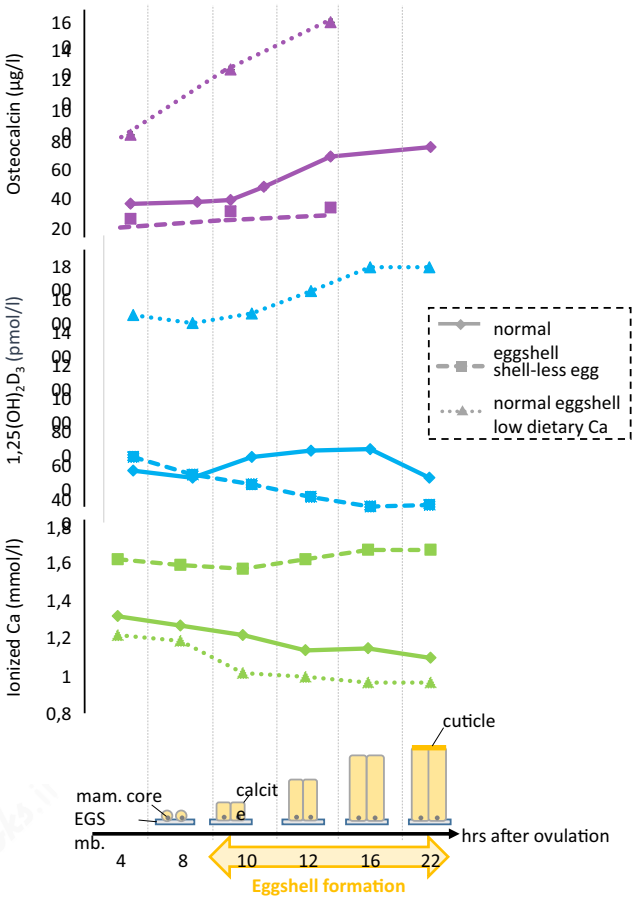

FIGURE 32.6 Plasma levels of osteocalcin, ionized calcium, and $1,25(OH)_2D_3$ throughout the ovulatory cycle. Eggshell formation takes place from 10 to 22 h after ovulation. Normal eggshell corresponds to hens laying hard-shelled eggs and fed 3.5% dietary calcium. Shell-less eggs were obtained by premature expulsion of the eggs before shell formation for a period of 4 days in hens fed 3.5% calcium. The low-dietary calcium corresponded to hens fed 1% dietary calcium and laying hard-shell eggs. EGS mb., eggshell membranes; mam. core, mammillary core (Nys, 1993; Nys and Le Roy, 2018).

calcium), compared with laying hens fed a normal calcium diet. Additional factors are thought to stimulate in vitro kidney production of $1,25(OH)_2D_3$, such as prolactin (Spanos et al., 1979), CT, and growth hormone, but are probably minor regulators of $1,25(OH)_2D_3$ in vivo in mature hens (Bar, 2008; Dacke et al., 2015).

More recently, knockout experiments in mice have revealed a novel circulating factor involved in phosphate and calcium metabolism. Fibroblast Growth Factor-23 (FGF23) is a bone-derived hormone that suppresses phosphate reabsorption and vitamin D hormone synthesis in the kidney (Quarles, 2012; Erben, 2018). Experimental approaches in mice have revealed the physiological importance of FGF23 in inhibiting renal 1α-hydroxylase (CYP27B1) transcription, which is the key enzyme for $1,25(OH)_2D_3$ synthesis (Shimada et al., 2004). FGF23 decreases serum levels of inorganic phosphate by inhibiting

renal phosphate reabsorption and calcitriol production and is suspected to have a large physiological role in phosphate homeostasis. Phosphate concentrations are less tightly regulated than serum ionized calcium levels, but are maintained in a very limited range thanks to PTH and active vitamin D. Recent evidence suggests a similar regulation of phosphate and calcium metabolism by FGF23 in laying hens.

32.4.2 Role of fibroblast growth factor-23 in regulation in calcium and phosphorus metabolism

FGF23 (phosphatonin) is a 32 kDa glycoprotein mainly produced in bone by osteoblasts and osteocytes stimulated by hyperphosphatemia, as reviewed in Erben (2018). High-dietary phosphorus stimulates FGF23 production in humans (Ferrari et al., 2005; Antoniucci et al., 2006). Its role in the control of phosphate (P) homeostasis was revealed when excessive FGF23 was discovered to be the factor responsible for inherited hypophosphatemic rickets in young children (White et al., 2000). FGF23 belongs to the family of endocrine FGFs and requires the transmembrane co-receptors α- and β-Klotho for high-affinity binding to the ubiquitously expressed FGF receptors (FGFR1-4) in target cells (Urakawa et al., 2006; Goetz et al., 2007). Among the four different FGFRs, FGF receptor-1c (FGFR1c) is probably the most important FGFR for FGF23 signaling, at least under physiological conditions (Urakawa et al., 2006). αKlotho enhances the binding affinity of FGFR1c to FGF23 by a factor of approximately 20 (Goetz et al., 2012). In humans, diseases characterized by excessive blood concentrations of intact FGF23 lead to renal phosphate wasting and inappropriately low circulating $1,25(OH)_2D_3$ levels in patients with normal kidney function (Martin et al., 2012). In the absence of FGF23 or its co-receptor α-Klotho, the endocrine control of 1α-hydroxylase transcription fails, leading to inappropriately high expression and activity of this enzyme. Hypercalcemia, hyperphosphatemia, and impaired bone mineralization are observed in α-Klotho and FGF23 deficient mice (Yoshida et al., 2002; Shimada et al., 2004). In addition, FGF23 might stimulate the expression of the 24-hydroxylase (CYP24A1) which hydrolyses $1,25(OH)_2D_3$ to the inactive 1,24, $25(OH)_2D_3$ (Liu and Quarles, 2007).

In mammals, FGF23 reduces renal phosphate reabsorption by inhibiting the activity of type IIa and type IIc phosphate transporters, which are responsible for reabsorption of phosphate from the glomerular filtrate (Gattineni et al., 2009). FGF23 promotes renal phosphate excretion by inhibiting cellular phosphate reuptake from the urine in proximal renal tubules through a cascade involving the α-Klotho/FGFR1c receptor complex. FGF23 induces the phosphorylation of the scaffolding protein Na^+/H^+ exchange regulatory cofactor (NHERF)-1 which in turn leads to degradation of the sodium-phosphate cotransporters NaPi-2a and NaPi-2c (Andrukhova et al., 2012). In addition, in distal convoluted tubules, FGF23 increases reabsorption of calcium and sodium by increasing the apical membrane abundance of the epithelial calcium channel, the transient receptor potential vanilloid-5 (TRPV5) and of the sodium-chloride cotransporter NCC (Erben, 2018). In chicken, its function on phosphate homeostasis was initially revealed by the use of antibodies against FGF23. Immunosuppression of FGF23 greatly improved phosphate utilization by young chicks, by inhibiting the stimulation of renal excretion by FGF23 (Bobbeck et al., 2012). Similarly, laying hens immunized to produce anti-FGF23 antibodies had reduced phosphate excretion (Ren et al., 2017) and improved eggshell quality (Ren et al., 2018). In hens, FGF23 expression in the liver is increased at sexual maturity (Gloux et al., 2019) and during the period of shell formation in the medullary bone (Hadley et al., 2016).

In hens and in chicken of different ages, FGF23 mRNA was expressed at higher levels in liver than other tissues evaluated, including calvaria, femur, tibia, medullary bone, brain, spleen, duodenum, jejunum, ileum, heart, and kidney; however, the highest expression of α-Klotho was found in kidney. It was also expressed in tibia but at a lower level. High-dietary phosphorus stimulates its expression in bone but not in liver (Wang et al., 2018).

Synthesis of FGF23 by medullary bone was confirmed by Gloux et al. (2019). They observed an overexpression of FGF23 in aged hens compared to young hens, which was associated with lower plasma levels of $1,25(OH)_2D_3$. In addition, FGF23 is overexpressed during the period of shell formation in younger hens when phosphoremia is elevated, in agreement with Hadley et al. (2016), but this change in FGF23 production was not observed in older hens. On the other hand, the ligands of FGF23 at the kidney level, FGFR2 and FGFR3, do not vary throughout the daily period of egg formation or with age of hens (Gloux et al., 2019). It is noteworthy that parathyroid cells in humans express both αKlotho and FGFRs, but the effect of FGF23 on the parathyroid gland (PTG) remains controversial (Goetz et al., 2012) and has not been yet explored in hens. In hens, the recommendation for dietary phosphorus has been largely decreased compared to 30 years ago because high levels negatively affect eggshell quality by an unknown process. FGF23 which is stimulated by high-dietary phosphorus and reduces the production of $1,25(OH)_2D_3$ might explain this negative impact of phosphorus on shell quality as suggested by the negative correlation between shell quality and plasma levels of phosphorus during the period of shell calcification (Sauveur and Mongin, 1983).

FGF23 might have physiologically functions on human bone mineralization, as suggested by its powerful inhibitory

effect on transcription of tissue nonspecific alkaline phosphatase (TNAP) mRNA in bone cells in a Klotho-independent manner (Murali et al., 2016). TNAP is essential for the regulation of bone mineralization by cleaving the mineralization inhibitor pyrophosphate, which is secreted by osteoblasts, to prevent premature mineralization of osteoid (Addison et al., 2007). Locally produced FGF23 may also serve as a physiological inhibitor of bone mineralization by downregulating TNAP expression. This possibility has not been yet explored in birds.

32.4.3 Parathyroid hormone and related peptides

32.4.3.1 Chemistry, secretion, and function of parathyroid hormone

The principal role of PTH is to regulate blood calcium concentration and to maintain calcium homeostasis. This system has been reviewed by many authors in humans and mice (Jüppner et al., 2000; Potts, 2005; Guerreiro et al., 2007), and in hens (Hurwitz, 1989b; Dacke, 2000; Dacke et al., 2015). Parathyroidectomy in birds leads to hypocalcemia, tetany, and death (Kenny, 1986), and reciprocally, PTH injections into birds increases plasma Ca levels (Kenny and Dacke, 1974), this effect being larger in laying birds. Changes in plasma Ca^{2+} concentrations are detected by the CaSR, which is expressed by the PTG chief cells that also store and secrete PTH (Hurwitz, 1989b). Increases in plasma Ca^{2+} levels lead to increased expression of the CaSR gene. Its expression in the PTG appears therefore to be inversely associated with changes in plasma Ca^{2+} (Yarden et al., 2000). However, it remains stable throughout the laying cycle in hens (Gloux et al., 2020a). CaSR is also expressed in bone and kidney (Courbebaisse and Soubervielle, 2011), and contributes to the physiological responses of these organs to maintain Ca homeostasis. Two (chicken) to four (Japanese quail) PTGs are present in birds, near the thyroids (Dacke et al., 2015). Sequences of mammalian forms of PTH and chicken PTH share structural homology and overlap in function (signal using the same G protein-linked receptor) (Potts, 2005). All mammalian PTH molecules consist of a single chain polypeptide with 84 amino acids and a molecular weight of approximately 9400 Da (Potts, 2005). The amino acid sequence deduced from the DNA sequence showed that chicken prepro-PTH mRNA encoded a 119 amino acid precursor and an 88 amino acid hormone (Lim et al., 1991). The sequence of chicken PTH shows significant differences in comparison with its mammalian homologs; for example, avian PTH contains two deletions in the hydrophobic middle portion of the sequence and an additional 22 amino acids near the C-terminus, which replaces the stretch of nine amino acids, residues 62 to 70, in the mammalian hormones (Potts, 2005). The amino terminal region of PTH is the minimum sequence necessary and sufficient for regulation of mineral ion homeostasis and shows high-sequence conservation among all vertebrate species (Jüppner et al., 2000). This 1−34 sequence is also present in the PTH-related peptide (PTHrP) and in a third PTH-like peptide (PTH-L) identified in chicken (Guerreiro et al., 2007; Pinheiro et al., 2010). These three peptides share the highly conserved N-terminal region, which controls Ca homeostasis and skeletal development. PTHrP and PTH-L shows a widespread and complex tissue distribution in vertebrates, which suggests their involvement in paracrine regulation (Pinheiro et al., 2010). Their role in non-mammalian vertebrates has not been fully explored.

The actions of PTH on mineral ion homeostasis in bone and kidney is mediated by a single receptor, the PTH-PTHrp receptor (PTHR1), which belongs to a distinct family of G protein-coupled receptors, as revealed by cloning in several species (Juppner et al., 2000; Potts 2005). This family of B receptors have a long amino terminal extracellular domain that is critical for binding peptide ligands such as PTH. The cloning of the receptor and studies of structure−activity relations with the PTH ligand and receptor has allowed the cellular biology of PTH action in various tissues to be explored (Jüppner et al., 2000; Potts, 2005; Courbebaisse and Soubervielle, 2011).

32.4.3.2 Regulation by parathyroid hormone of Calcium metabolism

The primary physiological role of PTH and its related proteins is to maintain in the short term the circulatory levels of ionic calcium. Hypocalcemia is detected by the PTGs and induces PTH secretion (Garabedian et al., 1972). When calcium is needed (calcium-deficient diet, vitamin D insufficiency, or eggshell formation), calcium is rapidly mobilized from bone, in particular medullary bone in laying birds, in response to increased PTH secretion. In addition, PTH stimulates calcium absorption over the longer term by increasing the synthesis of $1,25(OH)_2D$ in the kidney though activation of the 25-hydroxycholecalciferol-1−hydroxylase (Fraser and Kodicek, 1973). PTH also promotes phosphate excretion by blocking its reabsorption, leading to excretion of the phosphate excess liberated by bone resorption and reduces the excretion of urinary calcium by increasing renal calcium reabsorption at distal tubular sites in the kidney.

In bone, PTH has multiple catabolic and anabolic effects that affect the skeleton (Teitelbaum, 2000; Parra-Torres et al., 2013; Dacke et al., 2015). A number of cell lines of osteoblasts and stromal cells, utilizing specialized tissue culture systems, have evolved to study the interaction between different cell types and their role in bone formation and bone resorption (Potts, 2005). Through its abundant

receptors on osteoblasts, in contrast to osteoclasts, PTH has a variety of actions that are directly involved in promoting bone formation; however, physiologically, its most important role is to stimulate osteoclast differentiation and development and ultimately increase bone resorption. It has been shown in vitro that the maturation of macrophages into osteoclasts requires the presence of marrow stromal cells or their osteoblast progeny (Teitelbaum, 2000). Osteoclast differentiation is indirectly induced by osteoblasts that express the membrane-bound receptor for activation of nuclear factor kappa B (NF-kB) (RANK) ligand (RANKL) and macrophage colony-stimulating factor (M-CSF) (Teitelbaum, 2000). M-CSF binds to its receptor, c-Fms, on early osteoclast precursors, and provides signals required for their survival and proliferation. A direct contact between RANKL-expressing osteoblasts and RANK-possessing osteoclasts, and their progenitors, is essential for osteoclastogenesis during bone development (Yasuda et al., 1998). RANKL is also expressed in osteocytes at levels several-fold higher than in osteoblasts; therefore, osteocytes also control RANK-expressing osteoclasts during bone remodeling (Nakashima et al., 2012). This process is also regulated by a secreted decoy receptor of RANKL, osteoprotegerin (OPG), which functions as a paracrine inhibitor of osteoclast formation by competing with RANK for RANKL (Yasuda et al., 1998). Studies with avian systems confirm the critical role of RANK, RANKL, and OPG in birds (Dacke et al., 2015). Human recombinant RANKL has been shown to stimulate the resorptive activity of osteoclasts isolated from embryonic chick tibia (Boissy et al., 2001) and from bone marrow of Muscovy ducks (Gu et al., 2009). In hens, the hypercalcemic action of PTH is rapid (<30 min), firstly by inhibition of plasma Ca^{2+} clearance, followed by altering cell spread area in avian osteoclasts and by inducing the osteoclasts to form ruffled borders (Dacke et al., 2015). This effect was observed in vitro in osteoclasts located within hen medullary bone (Sugiyama and Kusuhara, 1994). Mechanisms of bone resorption by osteoclasts are similar in mammals and birds; a proton pump-ATPase and an Na^+, K^+-ATPase function in the ruffled border, and a CA and a Ca^{2+}-ATPase are located on the osteoclast plasma membrane. In laying hens, circulating PTH is implicated in the regulation of bone resorption, as evidenced by higher levels of circulating PTH during the period of shell formation, as demonstrated by a cytochemical bioassay (van de Velde et al., 1984a; Singh et al., 1986). This bioassay reflects activity of the 1−34 sequence, whatever its origin (PTH, PTHrP, or PTH-L), but was not observed in a recent study (Ren et al., 2019). However, an increased expression of PTH mRNA was also observed in the PTG during this active phase of eggshell formation (Gloux et al., 2020a). More detailed information on the role of PTH in other tissues including kidney, intestine, uterus, and smooth muscle have been reviewed by Dacke et al. (2015).

32.4.4 Calcitonin and calcitonin gene-related peptides

CT is a 32-amino acid polypeptide hormone secreted by the parafollicular cells (C-cells) of the thyroid gland in mammals and by the ultimobranchial tissue in avian and other nonmammalian species (Felsenfeld and Barton, 2015; Dacke et al., 2015; Xie et al., 2020). In humans, CT is released when plasma Ca^{2+} levels increase, and protects against the development of hypercalcemia. The secretion of CT is modified by the CaSR, as observed for PTH, but, while activation of the CaSR suppresses PTH secretion, it stimulates CT secretion. Both hormones also act on bone and kidney through receptors of the class II subclass of G-protein-coupled receptors. CTR expression is observed in the kidney, mature osteoclasts, and other tissues, and it interacts with receptor modifying proteins to form an active complex (Xie et al., 2020). CT administration decreases the magnitude of hypercalcemia during calcium loading in humans (Felsenfeld and Barton, 2015); however, birds are refractory to CT administration (Dacke et al., 2015). This hypocalcemic effect in mammals is attributed to inhibition of bone resorption by reducing osteoclast activity and to suppression of calcium release from the bone. In addition, CT increases renal production of 1,25D in the convoluted proximal tubule (Felsenfeld and Barton, 2015). Reciprocally, CT gene transcription is suppressed by $1,25(0H)_2D_3$. There is therefore evidence that CT administration in human is effective; however, since its discovery more than 50 years ago, there is no evidence that any deficiency or excess of CT observed in various human pathologies results in skeletal abnormalities. Calcium metabolism and bone mineral density are not affected in patients with medullary thyroid carcinoma with a chronically increased level of endogenous CT, or in thyroidectomized individuals with undetectable circulating CT (Xie et al., 2020). A precise role for CT remains elusive in humans and its function in nonmammalian vertebrates is even less understood (Felsenfeld and Barton., 2015). However, others still consider that under calcium stress conditions, CT might play a vital role in protecting the skeleton (Xie et al., 2020) because CT suppresses the bone disruption process in CT-deficient mice, as compared to wild-type mice. Dacke et al. (2015) reviewed some evidence in birds showing that in vitro CT can affect osteoclasts from Ca-deficient chicks. Cultured medullary bone osteoclasts from these birds respond to CT administration by a reduction in cell spread area, and by inhibiting the bone-resorptive activity or by suppressing ruffled borders. However, there is also experimental evidence that might explain why CT is not efficient in vivo to

correct hypercalcemia in birds. Dacke et al. (2015) concluded that CT plays a minor role in regulating Ca metabolism in birds. The difference between effects of CT on bone cells in vitro and in vivo in human, as well as the large variation in response between different species, brings into question the role of CT in Ca metabolism, particularly in birds.

Additional CGRPs, including CGRPs (alpha CGRP and beta CGRP), amylin, adrenomedullin, and intermedin, also contribute to bone regulation. In vitro and in vivo studies concluded that there were no inhibitory effects on osteoclasts and bone resorption and observed positive effects on osteoblasts and bone formation in mice and human. More information on their putative functions in mammals can be found in recent reviews (Naot et al., 2019; Xie et al., 2020). In birds, the roles of CGRP and amylin have been described by Dacke et al. (2015). CGRP is a 37 amino acid neuropeptide derived from the same gene as CT (amylin superfamily) and is expressed in many tissues of the central nervous system, including neurons innervating bone. CGRP might interact with osteoclastic CT receptors suggesting a paracrine role in modulation of bone turnover. A few studies show that CGRP in vivo elicits hypercalcemic and hypophosphatemic responses in chicks (Dacke et al., 2015), but very little experimental work has been carried out in birds and CGRP involvement in regulation of Ca metabolism remains hypothetical.

32.5 Intestinal absorption of calcium

32.5.1 Mechanisms of intestinal calcium absorption

Body calcium is ultimately derived from the diet, and intestinal absorption is therefore critical for calcium balance. Intestinal calcium uptake occurs in mammals through two defined mechanisms, a nonsaturable paracellular transport pathway, which results from passive diffusion and an active transcellular pathway (Courbebaisse and Soubervielle, 2011; Ghishan and Kiela, 2012; Christakos et al., 2014, 2019). High-dietary intake of calcium enables absorption by passive transport, but in humans, the dietary supply of calcium content is in the low−normal range, and the active transcellular pathway is required. This process occurs in the proximal part of the intestine (duodenum and jejunum) which shows a greater capability for calcium absorption than the distal segment. However, net calcium absorption might still be predominant in the ileal segment by passive absorption (up to 80%) due to the long-transit duration (Wasserman, 2004). Similarly, in birds, the intestinal absorption of calcium is controlled by these two distinct transport processes (Hurwitz, 1989a; Bar, 2009; Nys and Le Roy, 2018). In chicks and hens, the proximal intestine shows a high efficiency to absorb calcium, as demonstrated by direct measurement of Ca absorption using Yttrium-91 or Ca-45 (Hurwitz and Bar, 1966; Bar, 2009). The duodenum has a higher capacity for Ca absorption than the jejunum, but the transit duration is longer in the jejunum due to its greater length. In birds, most of the calcium is therefore absorbed before it reaches the lower ileum, as a result of the higher efficiency of the proximal intestine in absorbing Ca^{2+}, and of the lower ileal electrochemical potential difference (Bar, 2009). The high magnitude of calcium absorption (threefold greater in mature hens than in immature pullets), the huge increase in intestinal calbindin 28kD concentration in laying hens, the high correlation of calbindin with the capacity to absorb calcium, and the stimulation by vitamin D metabolites of key proteins involved in the transcellular pathway (Bar, 2009; Nys and Le Roy 2018), all underline the importance of the active cellular process in calcium absorption in hens. However, the paracellular pathway, which is stimulated by a favorable gradient of Ca^{2+} concentration between the intestinal and plasma compartments, might contribute to the large daily increase in Ca retention observed during the eggshell formation period (Hurwitz and Bar, 1965), as this is consistent with the higher levels of solubilized calcium in the intestinal lumen (Guinotte et al., 1995). The larger concentration of solubilized Ca in the intestinal content of the proximal intestine results firstly from the large intake of dietary calcium due to a specific appetite for calcium a few hours before shell formation (Mongin and Sauveur, 1974; Wilkinson et al., 2011), and secondly from the stimulation of acid secretion induced by dilatation of the crop a few hours before nightfall (Mongin, 1976). Inhibition of acid secretion by omeprazole (inhibitor of H^+, Na^+-ATPase) reduces net calcium intestinal retention by 20%, confirming the importance of the calcic gradient (Guinotte et al., 1995). The use of dietary calcium with a large particle size reinforces the supply of calcium for a longer period in the intestinal content, and reduced the gap between the intestinal supply of Ca and its uterine exportation for the eggshell formation, which mainly take place during the night. The use of large particles of dietary Ca is therefore very frequent in practical conditions and is well known for more than 50 years to improve shell strength (Nys, 2017). In conclusion, both passive and active processes in hens contribute to optimize the Ca retention needed for shell formation.

Both mechanisms of Ca absorption, the transcellular active transport and the paracellular nonsaturable passive pathway, are regulated by 1,25 dihydroxyvitamin D3 and have been biochemically characterized in mammals and birds (Christakos et al., 2014, 2019; Bar, 2008; Nys and Le Roy, 2018). The active transcellular calcium absorption involves the transfer of calcium across the luminal brush border membrane, through the cell interior and its extrusion from the basolateral membrane. In mammals

(Wasserman, 2004; Christakos et al., 2014, 2019), calcium entry occurs through the epithelial calcium-selective channel TRPV6 (transient receptor potential cation channel subfamily V member 6). It belongs to a super-family of cation channels (>30 different TRP subunit genes proteins in six subfamilies in mammals). TRP channels operate either as primary detectors of chemical and physical stimuli, as secondary transducers of ionotropic or metabotropic receptors, or as ion transport channels (Zheng, 2013; Alaimo and Rubert, 2019). Functional TRP channels, thought to be composed as homo- or heterotetramers, are opened or closed by conformational changes in the channel protein (Holzer, 2011). TRPV5 and TRPV6 are the most Ca^{2+}-selective members of the TRP ion channel family and play an important role in intestinal or kidney Ca^{2+} transfer in mammals (Holzer, 2011). TRPV6 is however predominantly expressed in intestinal epithelial cells while TRPV5 is more present in the kidney (Nijenhuis et al., 2005; Ko et al., 2009). TRPV6 has been identified by some authors (Yang et al., 2011; Jonchere et al., 2010, 2012; Huber et al., 2015; Li et al., 2018) in the intestine of the laying hen, but was not detected by others (Proszkowiec-Weglarz and Angel, 2013; Juanchich et al., 2018; Proszkowiec-Weglarz et al., 2019; Gloux et al., 2019). An immunoreactive TRPV6 protein was however revealed in the chicken small intestine by Western blotting (Huber et al., 2015). Additional TRPVs (TRPV2 but not TRPV5), TRPM7, and TRPC1 genes are expressed in the various part of the intestine of laying hens (Li et al., 2018; Gloux et al., 2019). A summary of ionic transporters in hen intestine is presented in Figure 32.7, and a list of putative ionic transporters in the intestine are reported in Table 32.1.

Following its entry, calcium accumulates within several minutes in the subapical brush border (Fullmer and Wasserman, 1987; Chandra et al., 1990). Cytosolic calbindin (9K in mammals, 28 kD in chicken) binds calcium with high affinity and facilitates the transcytosolic diffusion of calcium from the subapical zone to the basal membrane as reviewed by numerous authors (Wasserman, 2004; Ghishan and Kiela, 2012; Christakos et al., 2014, 2019; Hurwitz and Bar, 1989; Bar, 2009; Nys and Le Roy, 2018). Calbindins are present at high levels in all tissues that transfer large amount of Ca, including intestine and uterus (Wasserman and Taylor, 1966; Corradino et al., 1968). Its presence is considered to be a biomarker for regulated Ca transfer, since calbindin concentration is well correlated with the capacity of a tissue to transfer Ca. Ca may also be sequestered by the endoplasmic reticulum (ER) to prevent increased levels of intracellular calcium in the enterocyte (Christakos et al., 2014). Genes of the ITPR family, which are involved in Ca^{2+} extrusion from the ER, are expressed and modulated by sexual maturity in laying hens (Jonchere et al., 2012; Gloux et al., 2019). The intestinal plasma

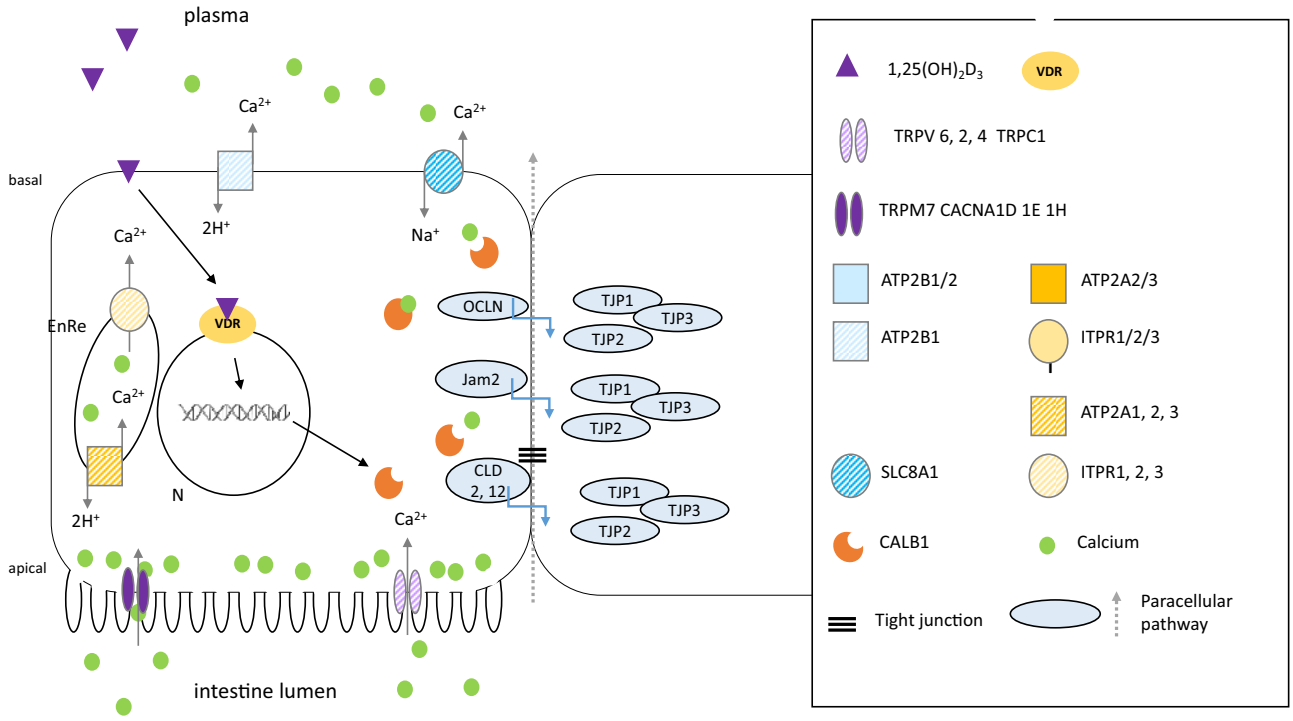

FIGURE 32.7 General model describing intestinal ion transporters acting in the enterocytes of the laying hen. All symbols are defined in the legend part (right). *EnRe*, endoplasmic reticulum; *N*, nucleus. *Data are compiled from Jonchére et al. (2012); Brionne et al. (2014); Gloux et al. (2019, 2020).*

TABLE 32.1 Major proteins involved in ionic transfer at intestinal and uterine level: description, gene expression, and presence of vitamin D response element and estrogen response element.

Gene symbol	Name	Transfer type	Cell location	Tissue expression		Presence of Gene response element	
				Uterus	Duodenum	VDR	EREF
TRPV2, 4, 6	Transient receptor potential cation channel subfamily V member2, 4, 6	Ca^{2+} channel	PM	Y	N	?	?
CALB1	Calbindin 28 K	Ca^{2+} intracellular transporter	IC	Y	Y	Y	Y
Otop2	Otopetrin	Ca^{2+} intracellular transporter?	IC	Y		?	?
ATP2A2	Endoplasmic reticulum calcium ATPase 2	Ca^{2+}ATPase	ER	Y	N	N	Y
ATP2A3	Endoplasmic reticulum calcium ATPase 3	Ca^{2+}ATPase	ER	Y	Y	Y	Y
ITPR1	IP3 receptor1	Ca^{2+} channel	ER	Y	Y	Y	N
ITPR2	IP3 receptor2	Ca^{2+} channel	ER	Y	N	Y	Y
ITPR3	IP3 receptor3	Ca^{2+} channel	ER	Y	Y	Y	Y
RYR1	Ryanodine receptor 1	Ca^{2+} channel	ER	Y	N	Y	Y
ATP2B1 PMCA1	Plasma membrane calcium-transporting ATPase 1	Ca^{2+}/H^{+} exchanger	PM	Y	Y	Y	Y
ATP2B2 PMCA2	Plasma membrane calcium-transporting ATPase 2	Ca^{2+}/H^{+} exchanger	PM	Y	Y	Y	Y
ATP2B4	Plasma membrane calcium-transporting ATPase 4 (PMCA4)	Ca^{2+}/H^{+} exchanger	PM	Y	Y	Y	Y
SLC8A1	Sodium/calcium exchanger 1	Na^{+}/Ca^{2+} exchanger	PM	Y	Y	Y	Y
SLC8A3	Sodium/calcium exchanger 3	Na^{+}/Ca^{2+} exchanger	PM	Y	Y	N	N
CACNA 1D, 1E, 1H,	Voltage-dependent L-type calcium channel subunit alpha-1D, -1E, -1H						
CA2	Carbonic anhydrase 2	Catalyze HCO_3^- formation	PM	Y	N	Y	Y
CA4	Carbonic anhydrase 4	Catalyze HCO_3^- formation	PM	Y	Y	N	Y
CA7	Carbonic anhydrase 7	Catalyze HCO_3^- formation	PM	Y	Y	Y	Y
CA9	Carbonic anhydrase 9	Catalyze HCO_3^- formation	PM	Y	N	Y	Y

TABLE 32.1 **Major proteins involved in ionic transfer at intestinal and uterine level: description, gene expression, and presence of vitamin D response element and estrogen response element.—cont'd**

Gene symbol	Name	Transfer type	Cell location	Tissue expression		Presence of Gene response element	
				Uterus	Duodenum	VDR	EREF
SLC26A9	Solute carrier family 26 member 9	HCO_3^-/Cl^- exchanger	PM	Y	Y	Y	N
SLC4A4	Solute carrier family 4 member 4	Na^+/HCO_3^- cotransporter	PM	Y	N	Y	Y
SLC4A5	Solute carrier family 4 member 5	Na^+/HCO_3^- cotransporter	PM	Y	Y	N	N
SLC4A7	Solute carrier family 4 member 7	Na^+/HCO_3^- cotransporter	PM	Y	Y	N	N
SLC4A10	Solute carrier family 4 member 10	Na^+/HCO_3^- cotransporter	PM	Y	N	Y	Y
SLC4A9	Solute carrier family 4 member 9	HCO_3^-/Cl^- exchanger	PM	Y	Y	N	N
SCNN1A	Amiloride-sensitive sodium channel subunit α	Na^+ channel	PM	Y	Y	N	N
SCNN1B	Amiloride-sensitive sodium channel subunit β	Na^+ channel	PM	Y	Y	N	N
SCNN1G	Amiloride-sensitive sodium channel subunit γ	Na^+ channel	PM	Y	Y	N	N
ATP1A1	Sodium/potassium-transporting ATPase subunit α-1	Na^+/K^+ exchanger	PM	Y	N	N	N
ATP1B1	Sodium/potassium-transporting ATPase subunit β-1	Na^+/K^+ exchanger	PM	Y	N	N	N
ATP6V1B2	Vacuolar H ATPase B subunit osteoclast isozyme	H^+ pump	Organelles and PM	Y	N	N	N
ATP6V1C2	Vacuolar H ATPase B subunit osteoclast isozyme	H^+ pump	Organelles and PM	Y	Y	N	N
Annexin-1	Vesicular calcium channels	Calcium entry in vesicles	Vesicles	Y	N	?	?
Annexin-2	Vesicular calcium channels	Calcium entry in vesicles	Vesicles	Y	Y	?	?
Annexin-8	Vesicular calcium channels	Calcium entry in vesicles	Vesicles	Y	N	?	?
Claudin 2, 10, 12	Paracellular cation channel Tight junction permeability	Paracellular pathway	Membrane protein	Y	Y	?	?
Jam	Junctional adhesion molecule	Paracellular pathway	Actin cytoskeleton.	Y	Y	?	?
TJP 1, 2, 3 ZO 1, 2, 3	Tight junction proteins 1, 2, 3 Zonula occludens 1, 2, 3	Paracellular pathway	Membrane protein	Y	Y	?	?
OCLN	Occludin	Paracellular pathway		Y	Y	?	?

ER, endoplasmic reticulum; *PM*, plasma membrane. References can be found in the text.

membrane ATPase (ATP2B1 also called PMCA1b), along with the Na^+/Ca^{2+} exchangers (SLC8A1 or NCX1), performs the final step in transcellular Ca_2 absorption, extruding Ca^{2+} from the cell interior to the interstitial space at the basolateral membrane (Stafford et al., 2017). PMCA1 (ATP2B1) is the only isoform present in enterocytes throughout the human or mouse intestine and its expression is higher proximally in the duodenum than in the jejunum or ileum (Alexander et al., 2015); expression levels are positively correlated with both intestinal Ca^{2+} absorption and bone mineral density in mice (Replogle et al., 2014). PMCA1b is also the predominant isomer expressed in the chicken intestine (Melancon and DeLuca, 1970; Bar, 2009; Jonchere et al., 2012; Brionne et al., 2014).

The Na^+/Ca^{2+} exchange mechanism (NCX, SLC8A) is the alternative transporting system involved in the "uphill" extrusion of Ca^{2+} across the basolateral membrane of the epithelial cell, toward the plasma (Bar, 2009; Liao et al., 2019). The NCX family contains three separate gene products exhibiting differential expression; NCX1 (SLC8A1) is mainly expressed in all organs of the digestive system, while NCX2 and NCX3 are expressed in the nervous system and skeletal muscle (Liao et al., 2019). Na^+/Ca^{2+} exchange activity is increased in response to calcium deficiency in chick enterocytes (Centeno et al., 2004). In laying hens, both NCX1 (SLC8A1) and NCX3 (SLC8A3) are expressed in the duodenum at a level quite similar to that of the uterus (Jonchere et al., 2012). The relative expression of both genes cannot be compared in this transcriptomic approach, but by analogy with mammals, it is likely that NCX1 predominates, and that PCMA is more active than NCX1 to extrude Ca^{2+}.

The paracellular pathway occurs between adjacent enterocytes (Figure 32.7). The most apical region of the intercellular junction is the tight junction (TJ). The barrier function and the permeability characteristics of epithelial cell sheets covering different organs are defined by the properties of the TJ and their paracellular channels (Gunzel and Yu, 2013; Alexander et al., 2014). TJs are predominantly formed by claudins, a family of four-transmembrane proteins with 27 members in human and mouse (Van Itallie and Anderson, 2014; Zeisel et al., 2019). The physiological properties of TJs allow selective transport of solutes and water between compartments, which mainly depends on the specific subtypes of claudins that they contain. These membrane proteins function as paracellular cation channels. Overexpression of claudin 2 (CLDN2) or CLDN12 enhances Ca transfer through intestinal epithelial cells in vitro (Fujita et al., 2008). TJs contain numerous additional proteins, among them transmembrane proteins including the junctional adhesion molecule (JAM), occludin (OCLN), and tricellulin. In addition, some cytoplasmic plaque proteins (Zonula occludens, ZO-1, 2, and 3, also called TJ proteins −1, 2, and 3) are framework-forming proteins that connect transmembrane proteins with the actin cytoskeleton (Van Itallie and Anderson, 2014; Zihni et al., 2016; Zeisel et al., 2019). In laying hens, expression of CLDN1, 2, 10, and 12, of TJP 1, 2, and 3, of OCLN, and of JAM2 are observed in duodenum, jejunum, and ileum (Gloux et al., 2019, 2020a). Only expression of CLDN2 and 10, OCLN, and JAM2 are affected by age or intestinal location. Expression of CLDN2 and TJP-1, 2, 3 (ZO1, 2, 3) is higher in intestine of mature hens compared to that of immature pullets (Gloux et al., 2019). Expression of CLDN2 and TJP3 is also slightly increased during the period of shell calcification (Gloux et al., 2020). Expression of both these genes and of OCLN is decreased in aged hens compared to young ones (Gloux et al., 2020). These observations confirm the relative importance of the transcellular to the paracellular Ca uptake pathway in laying hens.

32.5.2 Regulation of Calcium absorption in laying hens

Vitamin D and its metabolites, mainly $1,25(OH)_2D_3$, are the key factors regulating intestinal Ca^{2+} absorption in mammals and birds (Bouillon et al., 2003; Wasserman, 2004; Bouillon and Suda, 2014; Christakos et al., 2014, 2019; Diaz de Barbosa et al., 2015; Hurwitz, 1989a; Bar, 2008; Nys and Le Roy, 2018). In hens, sexual maturity and the egg production period coincide with a large increase in renal production and plasma $1,25(OH)_2D_3$. This large increase in levels of $1,25(OH)_2D_3$ is responsible for the large stimulation in net absorption of calcium (Bar et., 1978; Hurwitz, 1989a: Nys, 1993; Bar, 2008; Nys and Le Roy, 2018; Gloux et al., 2019). The active form of vitamin D binds to the intracellular receptor vitamin D receptor (VDR), which also interacts with retinoic X receptor (RXR), to form a VDR-RXR complex for binding with a specific vitamin D receptor element (VDRE) sequence of the targeted genes in the gene-promoter region; this stimulates the synthesis of mRNAs coding for several proteins (Schräder et 1993; Dong et al., 2010; Bar, 2008). The coupled $1,25(OH)_2D_3$ + VDR has been purified from the chicken intestine (Pike and Haussler, 1979) and is expressed in all intestinal segments (Gloux et al., 2019, 2020a), although less expressed in aged hens (Gloux et al., 2020b). This stimulates the permeation of calcium ions across the apical surface of enterocytes, as well as its cytosolic transport and extrusion from the cell (Wasserman et al., 1992). VDREs were identified in the promoters of genes encoding TRPV (Weber et al., 2001), calbindins (Christakos et al., 2014; Nys and Le Roy, 2018), and PMCAs (Glendenning et al., 2000).

TRPV6 expression is stimulated by low-dietary calcium and by $1,25(OH)_2D_3$ in mammals (Nijenhuis et al., 2005). TRPV6 is expressed at a lower level in the duodenum than in uterus (Jonchère et al., 2012). However, more recent

studies question the role of TRPV6 as they were unable to find any expression in the intestine (Gloux et al., 2019, 2020). However, changes in expression of other calcium TRP channels are observed in hens: TRPM7 and TRPC1 expression increase with age (Gloux et al., 2019), that of TRPV2 varies with intestinal localization and in response to Ca diet (Gloux et al., 2020), and expression of TRPM7 and TRPV2 is down-regulated in old hens compared to young ones (Gloux et al., 2020b); these observations suggest a possible involvement of these additional Ca channels in enterocyte Ca entry in hens.

Calbindins were intensively studied for their dependence on 1,25-$(OH)_2D_3$ (Wasserman et al., 1992; Wasserman, 2004; Christakos et al., 2014, 2019; Bar, 2009). In chickens, calbindin 28kD has been extensively investigated because of its high levels observed in epithelia transporting large amounts of calcium. The epithelial capacity to transfer calcium is highly correlated with calbindin content (Wasserman et al., 1966; Bar and Hurwitz, 1979). In vitamin D deficient chicks, CALB1 mRNA is barely detectable in the intestine (Theofan et al., 1986; Mayel-Afshar et al., 1988) and is increased approximately 10-fold after injection of $1,25(OH)_2D_3$. Calcium is rapidly (5 to 20 min) transferred from the intestinal lumen to the epithelium through the apical surface of enterocytes and accumulates at the subjacent apical zone when vitamin D is deficient. When supplied with vitamin D, calcium is transferred from the subapical region to the basal zone of the cells via calbindin (Chandra et al., 1990). Duodenal calbindin levels are correlated with changes in $1,25(OH)_2D_3$ plasma levels, whether induced by restrictions of dietary Ca^{2+} or by exogenous supply of vitamin D derivatives in young chicks (Wasserman and Taylor, 1966; Bar et al., 1990), or when egg production is induced or interrupted (Bar et al., 1978; Nys et al., 1992a; Sugiyama et al., 2007). In chickens, increased concentrations of plasma $1,25(OH)_2D_3$, increases in intestinal absorption of calcium and increases in concentration of intestinal CALB1 and its mRNA are all observed to occur at two time points: at the onset of laying after the hen becomes sexually mature, and at the time of the formation of the first eggshell (Bar et al., 1978; Nys et al., 1992a; Striem and Bar, 1991). When immature birds are not deficient in vitamin D, administration of estrogen and testosterone stimulates the synthesis of intestinal calbindin (Nys et al., 1992a; Striem and Bar, 1991). However, the largest increase in calbindin levels is associated with the onset of egg and shell formation. Induction of the production of shell-less eggs by premature expulsion of the egg for a few days decreases the intestinal level of calbindin by 50%, while resumption of shell formation stimulates levels of calbindin protein and its mRNA abundance (Nys et al., 1992a). The decreased calbindin level and mRNA expression does not occur in the few hours following egg expulsion but after a few days in the intestine in contrast to

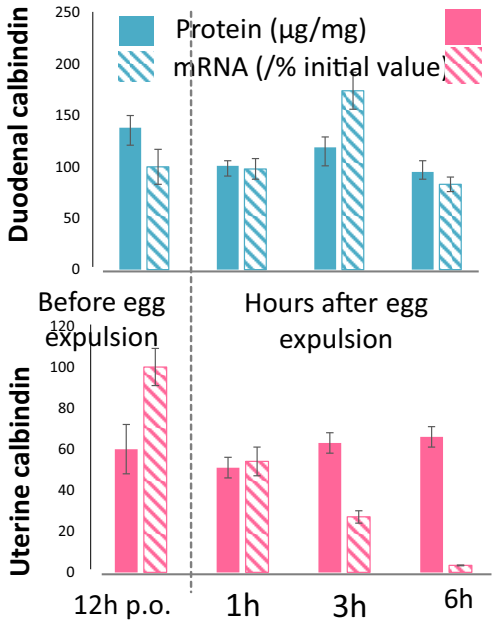

FIGURE 32.8 Level of expression and concentration of duodenal and uterine calbindin in hens during the initial phase of shell mineralization of the shell and 1, 5, and 6 h after experimental expulsion of the egg to suppress the shell formation Nys et al., 1992a.

uterus (Figure 32.8). Arrest of egg production in molted hens also reduces the intestinal concentration of calbindin (Bar et al., 1992). These changes in calbindin levels are synchronized with those of plasma $1,25(OH)_2D_3$. However, hourly changes in plasma $1,25(OH)_2D_3$ observed during the daily cycle of egg formation, or alterations induced by suppression of shell formation by egg expulsion, have no influence on mRNA expression of intestinal calbindin nor on the concentration of the protein (Nys et al., 1992a; Gloux et al., 2020a).

Extrusion of calcium from the enterocyte through the PMCA1 is also vitamin D dependent. PMCA1 (ATP2B1) expression is stimulated by the metabolite 1,25-$(OH)_2D_3$ in mice and chickens (Lee et al., 2015) or by factors influencing its metabolism in chicks (Wasserman et al., 1992). The PMCA pump (ATP2B1) is expressed at a higher level in the duodenum compared to the uterus during the active phase of calcium secretion (Jonchère et al., 2012). In hens, ATPase plasma membrane Ca^{2+} transporting 1 (ATP2B1) and ATPase plasma membrane Ca^{2+} transporting 2 (ATP2B2) are expressed in all intestinal segments at different ages; however, only ATP2B2 expression is greatly enhanced after sexual maturity in the duodenum, jejunum, and ileum (Gloux et al., 2019). PMCA1 (ATP2B1) was slightly increased during the daily period of shell formation in young hens, but not in older birds (Gloux et al., 2020a, 2020b). However, the Ca^{2+}-ATPase activity when measured globally was similar in the duodenum of hens calcifying an egg compared to hens laying shell-less eggs

(Nys and de Laage, 1984). The role of sex steroids in the regulation of duodenal PMCA1 is confirmed by stimulation of its expression by estrogens, and by the observation that ovariectomized rats and mice display reduced PMCA1 mRNA (Dong et al., 2014; Van Cromphaut et al., 2003). Moreover, an estrogen response element (EREF) is present in the ATP2B1-2 gene, in addition to a VDRE (Nys and Le Roy, 2018). No information is available on the regulation in birds of intestinal Na^{+}/Ca^{2+} exchangers (NCX1).

It has been suggested that vitamin D might also stimulate paracellular calcium absorption, as observed in mammals (Wasserman, 2004; Christakos et al., 2014). In hens, the paracellular pathway is of importance due to the large dietary consumption of Ca. Recent experimental evidence confirms this hypothesis. The expression of CLDN2 and of three TJ protein mRNAs (TJP 1,2,3 corresponding to ZO 1,2,3) in duodenum were observed to increase with age of the hen (12−23 wks) and to be highest in mature hens (Gloux et al., 2019). CLDN2 expression also increases in the jejunum between 17 and 23 wks of age and was slightly higher during the final period of shell formation (Gloux et al., 2020a). In contrast, CLDN10 decreased and exhibited a higher level of expression in ileum at sexual maturity (Gloux et al., 2019). In aged hens, the expression of CLDN2 and of the anchoring protein (TJP3) were downregulated, as was the VDR gene, suggesting a decreased efficiency in paracellular Ca transfer with increased age (Gloux et al., 2020b). Expression of other candidates involved in the paracellular pathway, claudin 1 and 12, JAM and OCLN, were not affected by sexual maturity nor by age of the hens (Gloux et al., 2020b).

In conclusion, numerous ionic transporters have been now identified in the hen intestine, but no hierarchy has yet been established on the relative roles of these candidates, within a family or between families of a particular ionic transporter (channel, pump, or exchanger). The role of vitamin D metabolites on expression of TRPV, calbindin and PMCA for the transcellular pathway and of some CLDNs and TJPs for the paracellular transfer is demonstrated in hens but remains to be characterized for additional proteins involved in calcium absorption.

32.6 Medullary bone

32.6.1 Structure and composition

One of the most relevant physiological adaptations that female birds have developed to facilitate an adequate supply of calcium for eggshell mineralization is the development of medullary bone, which can be more easily resorbed to release calcium (Dacke et al., 1993, 2015; Nys and Le Roy, 2018). Medullary bone (Figure 32.9) is a special type of bone formed within the marrow cavities of long bones of female birds during reproduction (Bloom et al., 1941, 1958; Van de Velde, 1984b, 1985; Whitehead, 2004; Kerschnitzki et al., 2014; Rodrõguez-Navarro et al., 2018). The formation of medullary bone starts about 2 weeks before laying of the first egg at sexual maturity and is associated with higher levels of plasma estrogen and vitamin D active metabolite (Figure 32.5). High-estrogen levels produce a dramatic change in bone biology, causing osteoblast function to switch from producing cortical and trabecular bone to forming medullary bone (Hudson et al., 1993; Whitehead, 2004). Medullary bone partially fills the marrow space (endosteal cavities) of long bones (tibia, humerus, femur), causing a 20% increase in skeletal weight before the commencement of egg laying. However, during the laying period, osteoclasts continue to resorb cortical and trabecular bone, resulting in a progressive reduction of the amount of structural bone and increased bone porosity (Figure 32.10). The loss of structural bone is associated with a higher accumulation of medullary bone, therefore the total amount of bone is maintained at a nearly constant level. Nevertheless, the loss of cortical bone induces a general weakening of the skeleton over the intensive laying period, causing hens to suffer a high incidence of bone deformation and fractures (especially in the keel); this is a mayor welfare problem that also has an important economic impact on egg producers (Fleming et al., 2006). The medullary bone is deposited by osteoblasts and represents about 11.7% of total bone calcium. It is a nonstructural type of woven bone consisting of a system of bone spicules that grow out from endosteal surfaces and may completely fill the marrow spaces (Dacke et al., 1993). Thus, medullary bone has no major mechanical function and is distinct from the cancelous bone, which is concentrated toward the metaphysis/epiphysis and has a mechanical functionality dependent upon the integrity of the intact long bone structure.

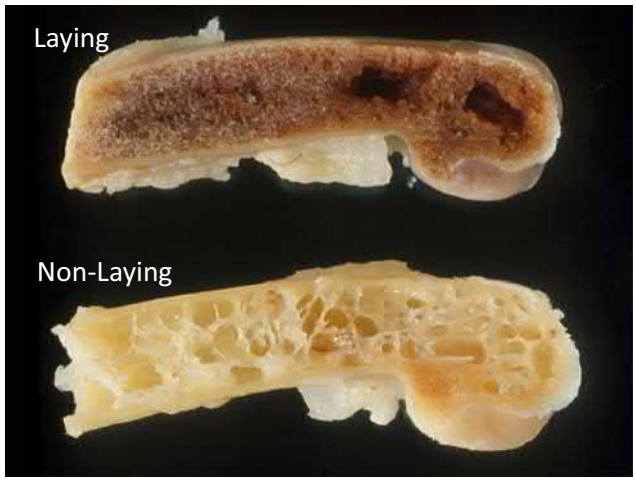

FIGURE 32.9 Images showing the presence of medullary bone in hens by comparing transverse section of the tibia of nonlaying and laying hens. *Image courtesy of the Roslin Institute & R(D)SVS, University of Edinburgh, Scotland.*

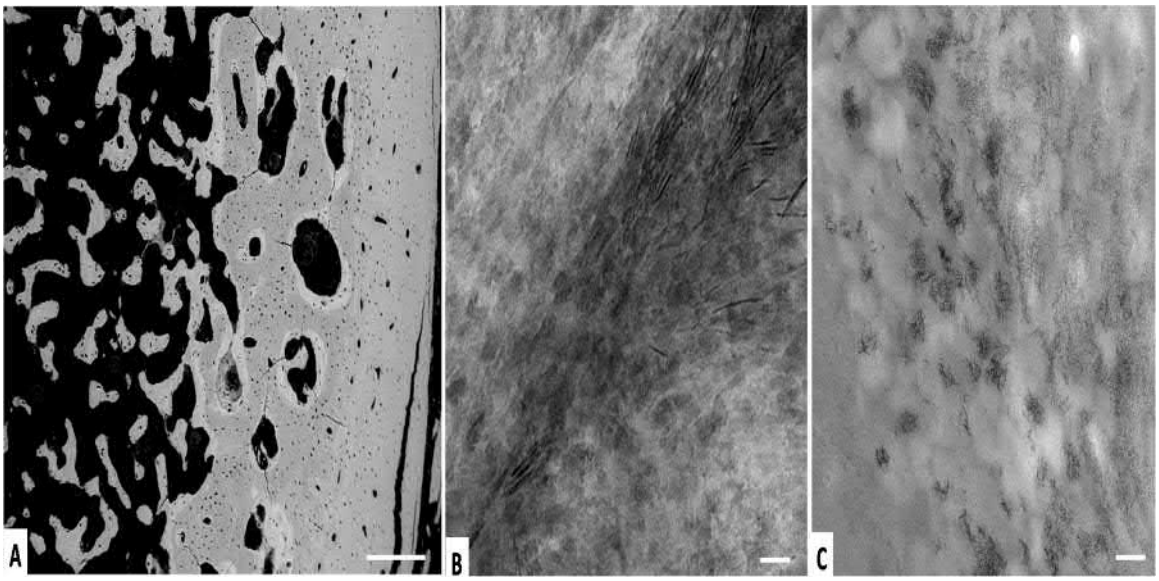

FIGURE 32.10 (A) Scanning electron microscope image of the tibia cross-section showing cortical bone (right) with large resorption centers and medullary bone (left) formed by isolated mineral trabecula. (B) Transmission electron microscopy (TEM) image of cortical bone showing oriented apatite crystals mineralizing a collagen matrix. (C) TEM image of medullary bone showing bundles of randomly oriented apatite crystals mineralizing a non-collagen matrix. Scale bars: (A) 100 μm; (B–C) 200 nm (Dominguez-Gasca et al., 2019).

Cortical bone is constituted by aligned collagen fibrils mineralized by apatite crystals oriented with their c-axis parallel to the fibrils. In contrast, medullary bone is less organized. It is formed by isolated mineral spicules or trabecula. The spicules contain osteocytes and are surrounded by a large number of osteoblasts and osteoclasts. Internally, these spicules contain collagen fibers that run in all directions. Apatite crystals of very small size cover the collagen fibrils and mineralize an extracellular organic matrix in the interfibrillar space consisting mainly of non-collagenous proteins, glycoproteins, and proteoglycans (Ascenzi et al., 1963; Bonucci and Gheraldi, 1975). This mineralization consists of ribbon-shaped apatite crystals distributed in separated bundles or foci that resemble the early stages of embryonic bone mineralization (Figure 32.10).

The mineral part of medullary bone is made of nano-crystalline carbonate-apatite (calcium phosphate), similar to cortical bone (Ascenzi et al., 1963). However, it also contains a small fraction of calcite ($CaCO_3$) as a separated mineral phase (Lörcher and Newesely, 1969). The presence of other more soluble and reactive mineral phases such as calcite and possibly noncrystalline mineral phases (amorphous $CaCO_3$ or calcium phosphate) could explain the extremely high reactivity of this form of labile bone and its main functionality as a source of calcium for the rapid calcification of the eggshell. Its solubility is at least 30-fold greater than that of cortical bone (Dominguez-Gasca et al., 2019). The high solubility of medullary bone mineral is due to its greater surface area, lower crystallinity, greater carbonate content, and organic matrix composition. The high-mineral solubility, together with its intense vascularization and spicule concentration of bone cells, explains why medullary bone can be metabolized at a much higher rate than cortical bone. While cortical bone turnover can take several months, medullary bone is turned over in only three days (Van de Velde, 1984b, 1985). Moreover, the composition of its organic matrix is believed to favor the rapid mineralization/demineralization of medullary bone.

Medullary bone cell activities are synchronized with the 24-hour egg-laying cycle (Figure 32.11). During eggshell calcification, there is an intense osteoclastic resorption of medullary bone, followed by an intense osteoblastic activity that forms new medullary bone before the beginning of the next cycle of eggshell formation (Van de Velde, 1984b, 1985). In laying hens, the medullary bone is in continuous activity throughout every stage of the egg-laying period, although osteoclast activity increases during calcification of the shell. Medullary bone serves as a calcium reservoir for eggshell calcification when calcium from the diet is exhausted (during the night) (Dacke et al., 1993; Van de Velde, 1985; Whitehead, 2004). It can be mobilized to provide 40% of the required calcium to the eggshell daily, or up to 60% when hens are fed a low-calcium diet. Taylor and Moore (1954) showed that hens on a calcium deficient diet can mobilize up to 38% of skeletal calcium before egg laying ceases. Regarding its mechanical properties, even though it is less dense and structurally weaker than cortical bone, medullary bone still contributes significantly to the overall strength of bone

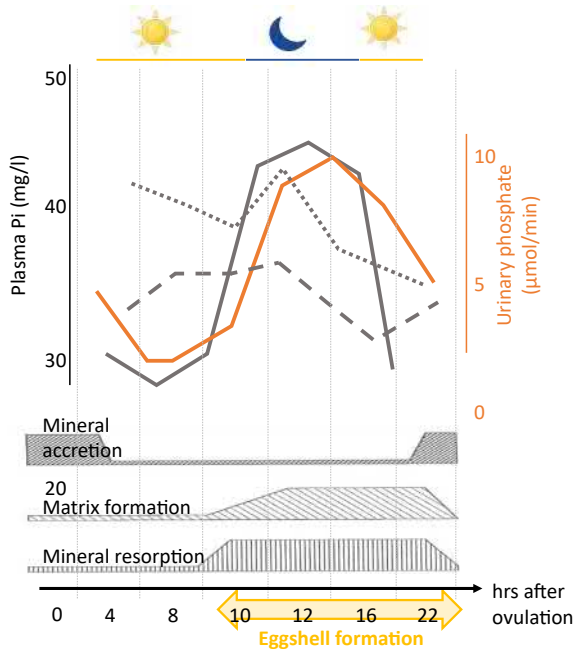

FIGURE 32.11 Plasma levels of inorganic phosphorus and urinary excretion of phosphorus during the laying cycle or in cokerel (dashes). Shell formation occurred 10–22 h after yolk ovulation in the oviduct. Laying hens were fed 3.5% dietary calcium, as fine (continuous line)or coarse particles of calcium carbonate (dotted line). Urinary calcium was sampled in hens fed fine particle calcium (3.5%). During the night (no food intake), the hen mobilize more Ca from the bone when fed fine particle compared to coarse one (Nys and Le Roy, 2018).

(Fleming et al. al., 2006; Rodrõguez-Navarro et al., 2018). In fact, the amount of medullary bone mineral has a large genetic correlation with tibia bone breaking strength (Dunn et al., in press, 2020). Additionally, the large amount of medullary bone that accumulates near the endosteal bone surfaces can also protect cortical bone against osteoclast resorption.

32.6.2 Regulation of medullary bone formation and resorption

32.6.2.1 Induction and maintenance of medullary bone by sex steroid hormones

Avian medullary bone probably represents the most estrogen-sensitive of all known vertebrate bone types, as gonadal steroids are absolutely essential for the induction and maintenance of medullary bone in egg-laying birds (Simkiss, 1967; Whitehead, 2004; 2015; Squire et al., 2017). In laying hens, the secretion of androgens and estrogens increases at sexual maturity. These gonadal hormones have a synergistic action on medullary bone formation, which can also be induced in male birds by estrogen treatment (Whitehead, 2004; Simkiss, 1967; Squire et al., 2017). Estrogens induce differentiation of endosteal cells to form osteoblasts and decrease the number of osteoclasts and their activity on the endosteal surface (Ascenzi et al., 1963; Miller and Bowman, 1981). Estrogen receptors are present in medullary bone osteoblasts (Ohashi et al., 1991) and osteoclasts (Oursler et al., 1993). In laying hens fed a calcium deficient diet, the medullary bone shows a large increase in the osteoblast population, the osteoclasts being substituted by osteoblasts on the trabecular surface (Zambonin-Zallone and Mueller, 1969). In addition, the percentage of medullary bone in the skeleton increases because of the depletion of cortical bone, which reveals the priority for medullary bone in reproductive hens (Dacke et al., 2015). However, the balance between the two types of bone and severity of bone loss depends on the duration of a calcium and vitamin D deficiency; clearly a reduction in dietary calcium and vitamin D has negative effects on bone mineralization (Dacke et al., 2015).

Bone is a metabolically active calcified tissue in a constant state of remodeling. Bone mineralization/demineralization is regulated by a complicated array of feedback processes under the control of specialized hormones related to calcium homeostasis (PTH, vitamin D). It has been well established that vitamin D contributes to bone mineralization in mammals (Pike et al., 2014; Christakos, 2014, 2019), partially by the activation of osteoblastic activity and also by the induction of bone protein synthesis. Vitamin D is clearly a key element for bone mineralization in growing chickens, but also in hens, even if medullary bone formation appears to be a priority relative to cortical bone in sexually mature hens. Vitamin D will globally contribute to the supply of calcium and phosphorus to facilitate bone mineralization, and more specifically, it will stimulate the synthesis of certain bone matrix proteins, as demonstrated for osteocalcin and osteopontin (OPN). Osteocalcin (OC) (bone γ-carboxy-glutamic acid protein) is the most abundant noncollagenous protein associated with the mineralized matrix of bone (Price, 1985). It has the ability to bind calcium, and it shows adsorption affinity for hydroxyapatite (Hauschka et al., 1989). This noncollagenous protein also plays a role in bone resorption because of its implication in the differentiation of osteoclasts (Ishida and Amano, 2004). OPN (SPP1) is a glycosylated, highly phosphorylated protein initially identified in bone and also present in eggshell (Chien et al., 2008; Hincke et al., 2008). In bone, SPP1 is considered to influence the migration and maturation of osteoclast precursors, the attachment of osteoclasts to the mineral phase of the bone, and osteoclast activity. $1,25(OH)_2D_3$ stimulates OC (Lian and Stein, 1992) and OPN (Noda et al., 1990) synthesis in osteoblast cell culture by binding to specific vitamin D-response promoter elements to enhance their gene transcription. However, OC synthesis, in contrast to calbindin, is modulated by, rather than dependent upon, vitamin D since there is substantial OC synthesis in vitamin D-deficient chicks. It has been shown that medullary bone

contains multiple isoforms of bone sialoprotein (BSP), OPN, osteonectin, OC, and dentin matrix protein-1 (Wang et al., 2005). Another particularity of medullary bone compared to cortical bone is the presence of large amounts of a keratan sulfate (KS) proteoglycan (KSPG). The core protein of KSPG is BSP (Hadley et al., 2016), which plays a key role in bone mineralization and remodeling (Staines et al., 2012). It was shown previously that KS is the major proteoglycan in medullary bone rather than chondroitin sulfate (Fisher and Schraer, 1980; Hunter and Schraer, 1983). Therefore, Hadley et al. (2016) have proposed that plasma levels of KS are a specific biomarker for medullary bone metabolism and have demonstrated that it indeed fluctuates in synchrony with the egg-laying cycle.

In hens, matrix formation within medullary bone can be induced by sex steroids regardless of the vitamin D status of chicks, but its mineralization is observed only when vitamin D3 is administered together with the gonadal steroids (Takahashi et al., 1983). It is likely that vitamin D is a key element which favors osteoblast activity in both cortical and medullary bone; however, the balance between both tissues is modulated by sex steroids, possibly indirectly, through their effects on the general parameters of bone physiology(vasculature and larger exchange surface area) (van de Velde et al., 1984b; Dacke et al., 2015). In addition, it has been demonstrated that estrogens stimulate OC secretion in response to $1,25(OH)_2D_3$ in osteoblast-like cells by increasing VDR expression, which supports the involvement of vitamin D in medullary bone formation. OC is predominantly synthesized by osteoblasts, is partially released into the circulation and has a rapid turnover (Figures 32.5 and 32.6) (Nys et al., 1986; Nys, 1993). It therefore reflects osteoblast synthesis and provides an index of bone turnover in humans (Delmas, 1992). Its plasma variation has been explored in hens in various physiological situations associated with large changes in plasma $1,25(OH)_2D_3$ (Figures 32.5 and 32.6). Unexpectedly, in immature pullets treated with gonadal steroids or in laying hens, plasma OC is lower than that of immature pullets, in contrast to the higher levels of plasma $1,25(OH)_2D_3$ (Figure 32.5). In hens, daily changes in plasma OC levels, however, parallel those in plasma $1,25(OH)_2D_3$ when inducing variation in bone activity by feeding hens with low-calcium diet or by suppressing shell formation in hens fed normal high-calcium diet (Figure 32.6). It increases during the period of shell formation in hens fed a low-calcium diet with a very high level of $1,25(OH)_2D_3$ and decreases in hens laying shell-less eggs possessing lower plasma $1,25(OH)_2D_3$ levels Nys (1993). It is further stimulated in hens fed a low-calcium diet when bone is highly implicated in shell formation. Plasma OC corresponds to the period of bone matrix synthesis, but also coincides with the period of most active bone resorption (van de Velde et al., 1984b). Therefore, hen plasma OC levels reflect osteoblastic activity only during the daily laying cycle but not during the long-term changes that occur with sexual maturity. These observations might be because of large mobilization of OC in the tissue during intensive bone formation, it being trapped in bone and no longer secreted in the plasma. It is of interest to note that estrogens stimulate OC secretion in response to $1,25(OH)_2D_3$ in osteoblast-like cells by increasing VDR expression.

32.6.2.2 Role of parathyroid hormone in daily mobilization of medullary bone

In hens, medullary bone is considered to be a labile calcium reservoir because of the daily osteoblast/osteoclast remodeling which supplies calcium for shell formation during the period when no dietary calcium is available (Hurwitz, 1965; Dacke et al., 2015; Whitehead, 2004). Eggshell formation takes place mainly during the night, when the hens have to mobilize calcium from bone since dietary calcium has been exhausted. Thus, medullary bone serves as a calcium reservoir for eggshell calcification and buffers the supply of calcium in response to its cyclical requirement. Use of large $CaCO_3$ particles, which slows down intestinal calcium solubilization and provides a higher calcium intestinal supply throughout the night, reduces bone mobilization (Figure 32.11). This nutritional approach is intensively used in practical conditions for improving eggshell quality (strength and thickness). The large resorption of medullary bone during the period of shell formation is clearly demonstrated by the huge increase in plasma phosphorus and its excretion in urine observed in hens from 10 to 22 h postovulation (Figure 32.11; Prashad and Edwards, 1973), which coincides with the period of shell deposition Wideman et al. (1987). These changes are abolished when hens are laying shell-less eggs. van de Velde et al. (1984a) reported that bone resorption was increased ninefold during shell formation due to an increase in active osteoclasts and in the resorbing surface per active osteoclast (Figure 32.11). At the same time, osteoblasts deposited some matrix protein, contributing to bone accretion that was also activated twofold to renew the medullary bone. There is a lot of evidence demonstrating that this diurnal regulation of bone resorption is under the control of PTH (van de Velde et al., 1984a; Kerschnitzki et al., 2014; Dacke et al., 2015). PTH secretion is increased during the period of shell formation (van de Velde et al., 1984a; Singh et al., 1986; Kerschnitzki et al., 2014) because of lower ionized calcium in the plasma. PTH stimulates bone resorption acutely, as described in the previous section describing the role of PTH in birds. It is noteworthy that FGF23 (phosphatonin) is expressed in medullary bone, in synchrony with the egg-laying cycle (Hadley et al., 2016; Gloux et al., 2019). This phosphatemic hormone is produced by osteocytes and plays a key

role in maintaining phosphate homeostasis, as described in the section of this review that discusses the role of hormones in Ca metabolism in hens.

32.7 Uterine secretions of Calcium

32.7.1 Mechanisms of ionic transfers

Eggshell formation takes place in the uterine segment of the oviduct (shell gland). Daily shell formation is associated with a massive transfer of calcium and bicarbonate into the lumen of the uterus during a short period (12hrs). In chickens, the mean rate of accumulation of $CaCO_3$ is 0.33 g/h between the period 10 to 22 h following ovulation and entry of the yolk into the oviduct (Eastin and Spaziani, 1978a; Nys and Guyot, 2011) this results in deposition of more than 6g of shell mineral. Calcium transfer follows a favorable positive (blood/uterine fluid) electrical potential difference (Pearson and Goldner, 1973, 1974; Bar, 2008), but is against a large and unfavorable Ca^{2+} gradient, since the level of ionized calcium in plasma (1.2 mM) is lower than its concentration in the uterine fluid (6 to 10 mM—depending on the stage of eggshell calcification) (Arad et al., 1989; Nys et al., 1991). The transcellular Ca^{2+} transport system has some similarities with mechanisms of Ca absorption in the intestine, even if the fluxes are inversed (Table 32.1). Calcium entry occurs in three steps (Figure 32.12), as reviewed by numerous authors (Hurwitz, 1989a; Nys et al., 1999; Bar, 2009): (1) passive entry of Ca^{2+} from plasma into the uterine cells via Ca channels; (2) its transfer through the cytosol bound to the Ca-binding protein, calbindin 28k; and (3) its extrusion by a calcium pump and Na/Ca exchanger. Many transcellular transporters of additional ionic species (HCO_3, Na^+, K^+, Cl^-, H^+) participate in the process of calcium secretion and in the maintenance of cellular ionic homeostasis (Eastin, W.C. and Spaziani, E., 1978a, 1978b; Jonchere et al., 2012; Brionne et al., 2014; Sah et al., 2018; Zhang et al., 2020), as observed at the intestinal level (Bar, 2009; Gloux et al., 2019). However, the additional contribution of a paracellular pathway for Ca is probably minor, even if this issue remains controversial for the uterus (Bar, 2009; Nys and Le Roy, 2018). Ca^{2+} secretion in the uterine lumen of hens shows particular features. Firstly, it has been

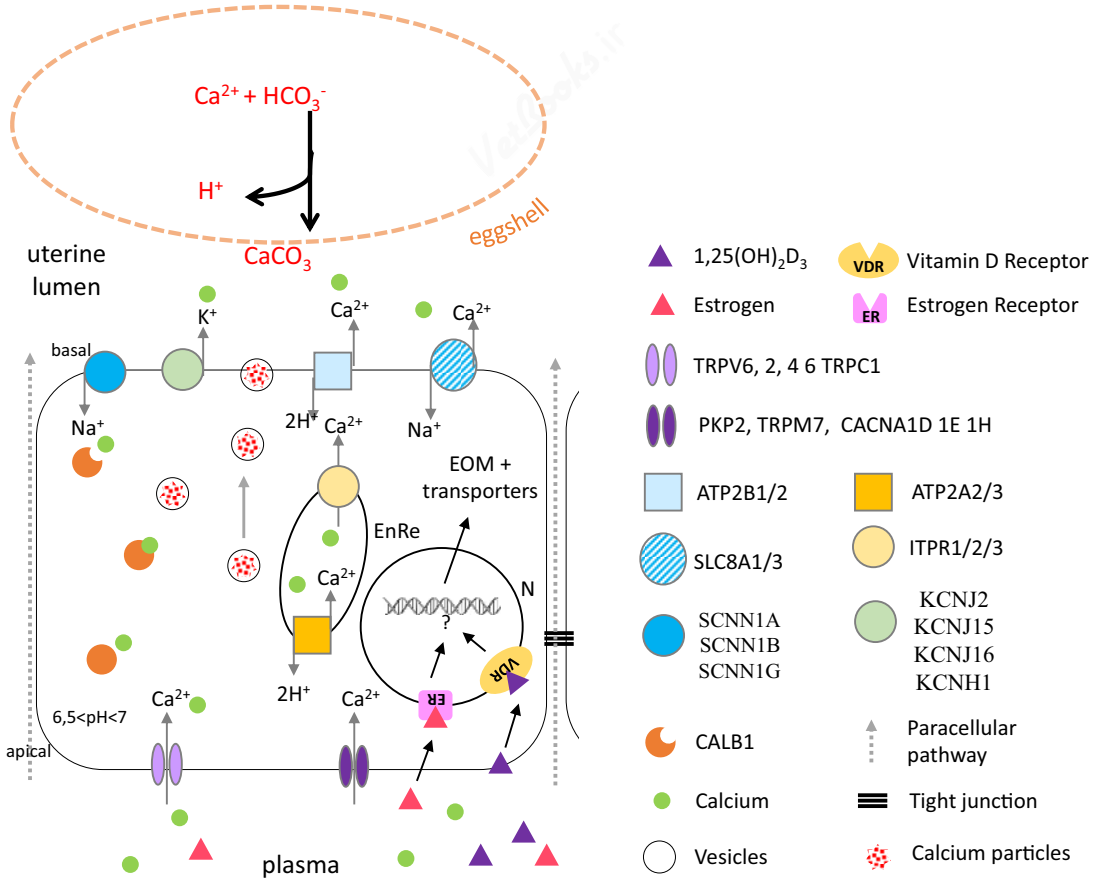

FIGURE 32.12 General model describing uterine ion transporters through the uterine cells of the laying hen. All symbols are defined in the legend part (right). *EnRe*, endoplasmic reticulum; EOM, extracellular organic matrix; *N*, nucleus. *Data are compiled from Jonchere et al. (2012); Brionne et al. (2014); Nys and Le Roy (2018).*

recently demonstrated that some of the transcellular Ca transfer into the uterine fluid occurs by secretion of extracellular vesicles (EVs) (100−400 nm) containing stabilized amorphous calcium carbonate (ACC) (Stapane et al., 2020). Secondly, the daily uterine secretion of calcium is discontinuous as the uterus expresses a high capacity to transfer Ca and bicarbonate only during the period of active shell formation (10 to 22 h postovulation, p.o. (Eastin and Spaziani, 1978a). The supply of Ca^{2+} and HCO_3^- is therefore, firstly, synchronized with the previous ovulation by unknown factors activated by the ovary or associated with ovulation, and secondly, is reinforced by the mechanical dilatation of the uterine wall elicited by the egg when it becomes fully hydrated (plumping). Mechanical stimulus is necessary, but insufficient, to elicit Ca secretion, as demonstrated by introduction of a surrogate wax egg in the oviduct. Calcification will occur only if the introduction of the artificial egg in the upper oviduct is synchronized with ovulation (Eastin, W.C. and Spaziani, E., 1978a; Nys, 1987; Nys et al., 1999).

The mineral composition of uterine fluid undergoes large changes throughout shell formation (Mongin and Sauveur, 1970; Arad et al., 1989; Nys et al., 1991). Sodium (140−80 mM) and chloride (70−45 mM) concentrations are high at the onset of shell calcification (8 h p.o.), but progressively decrease until shell calcification is complete (18 h, p.o.). The final levels of these ions are two to three folds lower than those of plasma. On the other hand, potassium levels show an inverse change, being higher at the end of calcification (12 to 60 mM). The pH decreases from 7.6 to 7.1 during shell calcification. Ca (6 to 10 mM) and bicarbonate (60 to 100 mM) levels in uterine fluid almost double during this process. Sodium is therefore reabsorbed in parallel with chloride during calcification, while the potassium flux is in the opposite direction (Sauveur and Mongin, 1971; Eastin and Spaziani, 1978b). The composition of the uterine fluid reflects absorption of sodium and chloride, while secretion of potassium, calcium, and bicarbonate occur against their electrochemical gradients. Active transport has been clearly demonstrated for Ca and Na in this process. The unidirectional fluxes of sodium are much greater than the net flux reflecting a balance between secretion of sodium linked to movement of chloride and water through the paracellular pathway. The active transport of sodium by the Na/K-ATPase, and the role of the Na/Ca exchanger have been demonstrated using specific inhibitors (Pearson and Goldner, 1974; Eastin and Spaziani, 1978b). The unfavorable gradient of Ca^{2+} concentration between plasma and uterine fluid, the discontinuity of calcium secretion and large fluctuation of the capacity of uterine Ca secretion according to the physiological stage support the predominance of an active transcellular secretion of calcium and the very limited contribution of passive Ca transport via the paracellular pathway. Bar (2009) suggested a possible contribution of the paracellular pathway due to the positive polarity of plasma with respect to mucosa, but this process contributes rather to the secretion of water, K, Na, and chloride to control osmolarity, which is stable and slightly lower than in plasma (290 vs. 320 mosm/mL in plasma) (Nys et al., 1999). The active transcellular transfer of calcium, bicarbonate, and sodium occurs mainly via the uterine glandular cells, as confirmed by the presence of calbindin 28 kD (Lippiello and Wasserman, 1975; Fullmer et al., 1976; Wasserman et al., 1991), Na/K-ATPase and CA in these cells (Pearson and Goldner, 1973; Bernstein et al., 1968); however, the vesicular secretion of ACC in the uterine fluid instead originates from the uterine epithelial cells (Stapane et al., 2020). The importance of the transcellular pathway is confirmed by the direct correlation between the calbindin mucosal concentration and the efficiency of Ca^{2+} transfer in uterus under numerous experimental conditions (Wasserman, 2004; Bar, 2009; Nys and Le Roy, 2018). This relationship is specific to the uterus and is not observed in other parts of the oviduct. Both uterine glandular and epithelial cells transfer large amounts of calcium into the uterine lumen against the concentration gradient, while preserving low-intracellular calcium levels (<2 μM). Ca^{2+} is not stored in the uterus before eggshell calcification and comes from blood plasma, the total circulating calcium being regularly renewed every 12 min. It has been demonstrated that bicarbonate is derived from CO_2 diffusion and its hydration by CA (Lörcher et al., 1970; Eastin and Spaziani, 1978a). Early physiological studies were described by an initial model of Ca secretion, with three steps: entrance into the cell by passive diffusion through Ca channels, trapping of Ca by calbindin, and then extrusion by the Ca-ATPase and Na/Ca exchange, with a role for movement of other ions (Na, K, and Cl) (Sauveur and Mongin, 1971; Nys et al., 1999). However, transcriptomic studies carried out during the past 15 years comparing various parts of the oviduct or tissues transporting large amounts of Ca (Jonchere et al., 2010, 2012; Brionne et al., 2014), or analyzing changes induced in RNA expression by physiological factors (Marie et al., 2015a, b; Sun et al., 2016; Sah et al., 2018; Khan et al., 2019; Zhang et al., 2019, 2020), have revealed upregulation and expression of a large number of ion transporters involved in uterine calcium secretion (Figure 32.12; Table 32.1), in addition to new processes such as the vesicular secretion of ACC (Stapane et al., 2020). These findings are mainly qualitative and not quantitative, but they allow hypotheses to be developed on the mechanisms of Ca secretion and other ion transfers in order to maintain cellular homeostasis. It remains, however, difficult to establish a definitive hierarchy between the putative candidates for a particular ion transfer or to evaluate the respective contribution of the different processes contributing to the supply of Ca and bicarbonate

for shell formation. All this information has been used to update the model describing the mechanisms of Ca secretion and for combined ion transport (Figure 32.12).

32.7.1.1 Transcellular transfer of Calcium and bicarbonate

The entrance of Ca into the glandular epithelial cells involves TRPV Ca^{2+} channels. In initial studies, the TRPV Ca^{2+} channel was identified as TRPV6 by microarray analysis or by Western blotting (Yang et al., 2013; Jonchere et al., 2012); however, more recent studies using RNA-seq approaches were unable to confirm TRPV6, but rather suggested TRPV2 or 3 (Brionne et al., 2014), TRPV4 (Zhang et al., 2019), the purinergic receptor P2X 7 (P2RX7), or calcium homeostasis modulator 5 (*FAM26E*) (Le Roy N., Gautron J., Nys Y., personal communication) as putative candidates. Further data are clearly needed to identify the Ca channels responsible of Ca entry into the glandular cells. In contrast, there is numerous convincing experimental evidences demonstrating that calbindin is involved in the intracellular transfer of Ca, as reviewed by Bar (2009) or Nys and Le Roy (2018). The ER also contributes to maintenance of low-intracellular calcium levels via ATP-dependent calcium pumps (ATP2A2 and 3), while and inositol trisphosphate receptors type 1, 2, and 3 (ITPR1, 2, 3) contribute to Ca release from the ER. These ER genes are over expressed during eggshell calcification (Brionne et al., 2014; Sah et al., 2018). The otopetrin gene (Otop2) is expressed in the uterus (Khan et al., 2019) and may also participate to the transepithelial transport of Ca^{2+} across the uterus by regulating intracellular calcium (Sah et al., 2018). Calcium is then extruded from the glandular cells by plasma membrane Ca^{2+} pumps (ATP2B1 and ATP2B2) and Ca^{2+}/Na^{+} exchangers (SLC8A1 and SLC8A3) (Jonchere et al., 2012; Brionne et al., 2014; Sah et al., 2018) (Figure 32.12, Table 32.1).

Blood carbon dioxide (CO_2) penetrates the uterine glandular cells by simple diffusion through the plasma membrane (Hodges and Lôrcher, 1967) and is the main source of bicarbonate. CA2 catalyzes the reversible hydration of intracellular CO_2 to HCO_3^-. However, it is also supplied at a low level from plasma by the Na^{+}/HCO_3^- cotransporters (SLC4A4, SLC4A5, and SLC4A10). Bicarbonate ions are finally secreted into the uterine fluid via the HCO_3^-/Cl^- exchanger SLC26A9 (Jonchere et al., 2012; Brionne et al., 2014). Bicarbonate from the uterine fluid can also be produced by the membrane-bound CA4, which has its active site in the extracellular space (Zhu and Sly, 1990). Expression of CA9 is also observed in the uterus, but at very low levels (Khan et al., 2019).

In parallel with the transfer of Ca and bicarbonate, cellular homeostasis is maintained by the reabsorption of sodium and chloride from the uterine fluid and secretion of potassium. Na^+ uptake from the uterine fluid is carried out by Na^{+}/Ca^{2+} exchangers (SLC8A1, 3) and by amiloride-sensitive Na^+ channels (SCNN1A, B, G) at the apical membrane. Sodium ion is extruded from the cell at the basolateral membrane against the electrochemical gradient by the Na^{+}/K^{+} ATPase, with concomitant uptake of K^+ (ATP1A1, B1) (Jonchere et al., 2012; Brionne et al., 2014). This is in addition to the $Ca^{2+/}Na^{+}$ exchangers (SLC8A1 and 3) and Na^{+}/HCO_3^- cotransporters previously described for Ca extrusion and bicarbonate entry, respectively. K entry into the cell is associated with Na (ATP1A1, B1) and associated NKAIN1, which interacts with the subunit of the Na^{+}/K^{+} ATPase (ATP1B1). The passive diffusion of K^+ into the uterine lumen through the apical membrane is facilitated by the high concentration of intracellular potassium in cells, with involvement of two voltage-dependent ion channels (KCNJ2, KCNJ16) and a large conductance calcium activated potassium channel (KCNMA1), as revealed by their high expression during eggshell calcification (Jonchere et al., 2012; Brionne et al., 2014). Chloride ions in the uterine fluid enter the cell by the HCO3-/Cl-exchanger SLC26A9 and by Cl-channels (CLCN2, CFTR), and might be extruded by the Cl-/H+ exchanger (CLCN5), in addition to the Na+ -K+ -2Cl- and K+ -Cl-cotransporters (SLC12Ax). During eggshell formation, a progressive acidification of uterine fluid and glandular cells occurs, due to production of two protons for each CO_3^{2-} (Nys et al., 1999). The V-type H^+-ATPase (VAT) (ATP6V1B2) exports protons to the plasma with hydrolysis of ATP, as suggested by its high expression during shell formation (Jonchere et al., 2012). Another VAT subunit, the H+ transporting lysosomal 42 kDa, V1 subunit C2 (ATP6V1C2) might also be involved (Brionne et al., 2014). The VAT complex is probably located in the basolateral membrane, as protons are secreted toward the plasma, which shows some acidification during the period of shell formation. This metabolic acidosis is partially compensated by hyperventilation by the hen and by an increased renal H^+ excretion (Mongin, 1978).

It is noteworthy that intestinal and uterine mechanisms of ionic transfer show some similarities, although they correspond to absorption or secretion of Ca with respect to the intestinal and uterine lumen, respectively. However, the regulation of Ca transfer largely differs between these tissues, being directly dependent upon the active metabolite of vitamin D in the intestine, in contrast to the uterus, where such regulation has not yet been demonstrated.

32.7.1.2 Vesicular secretion of calcium

Recently, uterine vesicular transport of $CaCO_3$ as ACC has been shown to deliver ACC to the site of eggshell mineralization in hens (Stapane et al., 2019, 2020). Evaluation of $CaCO_3$ vesicular transport in chicken uterus was initiated

following the observation of high levels of vesicular protein markers (EDIL3 and MFGE8) in eggshell and in uterine fluid during shell formation (Marie et al., 2015a), as inspired by the demonstration of amorphous $CaCO_3$ in invertebrates that produce a $CaCO_3$ shell (Addadi et al., 2006). ACC is a metastable polymorph of $CaCO_3$, which can deliver ions required for rapid physiological biomineralization. It was initially demonstrated in molluscan or echinoderm species that the incipient $CaCO_3$ crystal formation occurs intracellularly as a membrane-enclosed ACC phase that contributes to the calcification of $CaCO_3$ biominerals (Beniash et al., 1997; Politi et al., 2008; Addadi et al., 2003; Gomez- Morales et al., 2015). In the calcifying chicken eggshell, ACC has been demonstrated with a calcite short-range order favoring the transformation of ACC to calcite, which is the sole crystalline form of the eggshell mineral (Rodriguez-Navarro et al., 2015). ACC is a highly reactive transitional phase for the formation of $CaCO_3$ biominerals and can be stabilized by specialized molecules (Aizenberg et al., 1996). Vesicles stabilize and transport ACC to the mineralization front as shown in sea urchin (Politi et al., 2008) mollusks (Addadi et al., 2006) and corals (Bahn et al., 2017)

In hen uterus, transmission electron microscopy (TEM) observations demonstrated the presence of intracellular vesicles (100−500 nm) in the cytoplasm of the epithelial ciliated cells (Figure 32.13) (Stapane et al., 2020). Vesicles accumulate at the apical plasma membrane and bud to secrete EVs which were revealed in uterine fluid adjacent to the apical region of uterine cells (Stapane et al., 2020). The presence of $CaCO_3$ as ACC in the vesicles was confirmed by electron energy loss spectroscopy and by energy-dispersive X-ray spectroscopic. Electron diffraction on EVs extracted from uterine fluid indicated that the $CaCO_3$ inside vesicles was amorphous, similar to the ACC previously identified at the initial stage of eggshell formation (Rodriguez-Navarro et al., 2015). This observation was further explored by studying the presence of major EV proteins using transcriptomics, proteomics, and immunochemistry to decipher the origin and mechanisms of vesicle formation and function.

Three annexins (Anxa 1, 2, and 8) are expressed at high levels in the uterus at the onset of shell formation (Stapane et al., 2020), in agreement with previous proteomics studies (Mann, 2006; Jonchere et al., 2012; Marie et al., 2015b), and were revealed in the epithelium (Anxa 1, 8) and tubular glands (Anxa 8) by immunochemistry. Annexins are Ca channels proposed to contribute to uptake of Ca for intravesicular ACC formation. EDIL3 is overexpressed in the uterus and is specific to the uterine fluid EV fraction (Stapane et al., 2019, 2020). This protein possesses an EGF-like calcium-binding domain and is hypothesized to guide EVs to the mineralization front. Carbonic anhydrase 4 (CA4) is present in the epithelial cells and in EVs and is highly expressed at the early stage of shell formation. CA4 catalyzes the reversible hydration of CO_2 forming HCO_3 and might contribute to accumulation of ACC in vesicles.

A schematic representation of vesicular transport and molecular actors during eggshell mineralization is proposed (Figure 32.14). Annexins would promote calcium entry into EVs, whereas CA4 catalyzes the hydration of CO_2 into bicarbonate ions. ACC accumulates inside EVs and is stabilized by specific proteins. EDIL3 and potentially MFGE8 would serve as guidance molecules to deliver vesicular ACC to the mineralization site. The quantitative contribution of the vesicular secretion of $CaCO_3$, relative to the secretion of each ion by the transcellular pathway, remains to be explored.

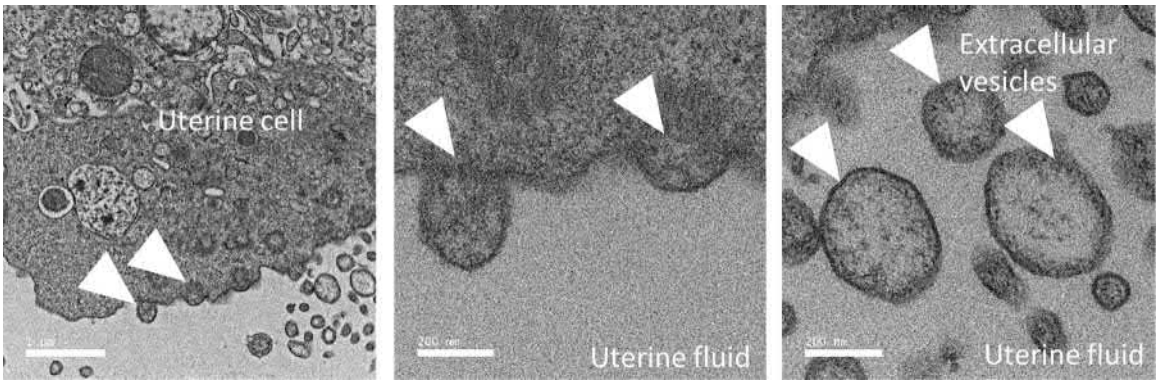

FIGURE 32.13 Transmission electron microscopy (TEM) of uterine cells. (A) TEM micrograph of uterine epithelium showing secretory activity (16 h p.o.). (B, C, D) Higher magnification TEM micrographs of uterine cells showing examples of exocytosis activity. (E, F) TEM micrographs illustrating the presence of numerous EVs in the uterine lumen (UL) at 7 h (F) and 16 h p.o. (E). Thin sections of uterus were negatively stained with 2% uranyl acetate. C: cilia, CC: ciliated cells, DG: dense granule, LG: light granule, EV: extracellular vesicle, N: nucleus, UL: uterine lumen. White ars indicate vesicle budding. Bars: A = 5 µm, B and F = 1000 nm, C = 500 nm, D and E = 200 nm. *This research was originally published in the Journal of Biological Chemistry. Stapane et al., 2020*

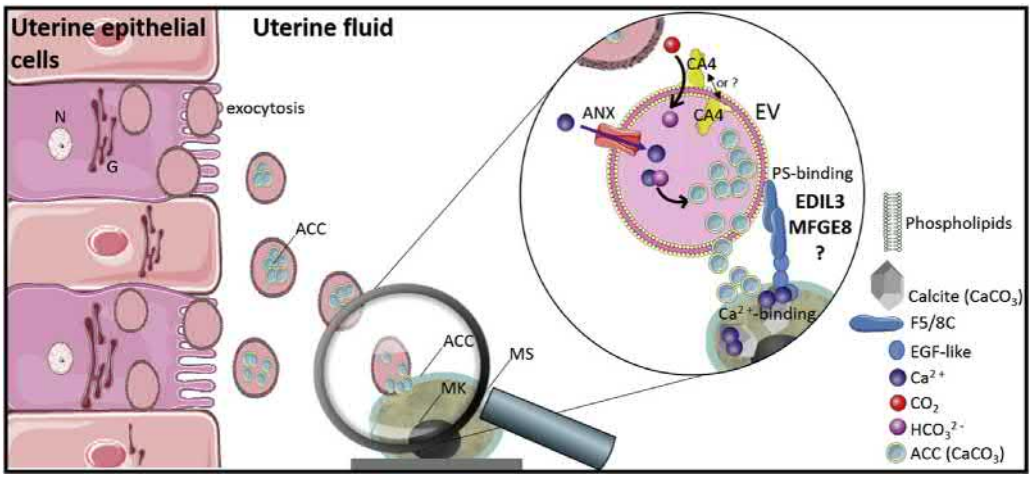

FIGURE 32.14 Comprehensive model for calcium and carbonate transport to the uterine fluid during eggshell calcification. The three potential pathways for ion transfer through uterine cells are transcellular, vesicular, and paracellular mechanisms. They could function asynchronously or in an integrated fashion. The major protein players in each pathway are indicated on the figure (left). *This research was originally published in the Journal of Biological Chemistry. Stapane et al., 2019 © the American Society for Biochemistry and Molecular Biology or © the Author(s).*

32.7.2 Regulation of uterine calcium transfer

32.7.2.1 Regulation of the timing of ion secretion

Organic and mineral precursors of eggshell are secreted daily in the uterine fluid with a specific temporal sequence. Secretion of Ca, bicarbonate, and vesicular $CaCO_3$ occurs at a low levels 6 to 10 h after ovulation in hens, and then with rapid kinetics (0.33 g/h) for the period corresponding to 10 to 22 h postovulation. During the first period, there is also a large secretion of water (plumping) which expands the egg contents within the ESMs and contributes to the ovoid shape of the egg, which generates mechanical strain upon the uterine wall at 10hrs postovulation (Sauveur and de Reviers, 1988; Nys and Guyot, 2011). This mechanical dilatation of the uterine wall is coupled to the secretion of ionic precursors of the shell mineral, as shown using in vivo perfusion of the uterus (Eastin and Spaziani, 1978a) in addition, upregulation of the Na^+/K^+-ATPase is observed. Overexpression of the calbindin (CALB1) gene is also highly synchronized with the active phase of ion secretion in the uterus, as demonstrated by upregulation of CALB1 during the eggshell formation period (Nys et al., 1989; Bar et al., 1992; Ieda et al., 1995), followed by its rapid down regulation after egg expulsion (Nys et al., 1992b). The period of shell formation and associated bicarbonate and calcium secretion is precisely synchronized with ovulation (Eastin and Spaziani, 1978a; Sauveur and de Reviers, 1988; Nys et al., 1999). Its initiation coincides with entrance of the egg into the uterus, whereas shell formation is arrested about 2 h before oviposition when the cuticle is deposited (Eastin and Spaziani, 1978a; Nys et al., 1991). An artificial intervention, either mechanical or pharmacological (using a prostaglandin inhibitor), which causes egg retention in the uterus, largely delays egg oviposition but does not elicit any additional deposition of shell (Nys, 1987; Bar et al., 1996). In addition, the combination of artificial retention with an expulsion of the egg at the expected time of oviposition shows that the eggshell was completed at 24 h. In contrast, it is possible to retain the egg in utero for 36 h by injecting progesterone 2−4 h after ovulation (Nys, 1987; Zhang et al., 2020). This treatment delays oviposition and also the arrest of shell mineralization, as shown by a 50% increase in eggshell weight; moreover, a partial shell without cuticle is formed when the retained egg is expulsed at 24 h (Nys, 1987). In addition, an artificial egg introduced in the upper part of the oviduct will be calcified only when its introduction is synchronized with the normal arrival of the yolk, 2−3 h after the natural ovulation (Nakada et al., 1976). These observations demonstrate that an active control of the timing of shell formation, initiation, and arrest of shell mineralization is associated with the process of ovulation. The largest mature follicule which is due to ovulate acquires the capacity to secrete large amount of progesterone which stimulates the hormonal secretion of luteinizing hormone by the posterior pituitary at the origin of ovulation (Johnson, 2000; Nys and Guyot, 2011). Experimental supply of progesterone will affect the interaction between pituitary gland and ovary. The putative regulator(s) of shell formation and uterine calcium secretion associated with the ovulatory cycle or follicular maturation remain to be identified.

32.7.2.2 Regulation of uterine ionic transporters

During the period of eggshell formation, hens export large amounts of calcium, bicarbonate, and carbonate into the uterine lumen, in coordination with other ions that contribute to cell homeostasis. Detailed mechanisms have been described in the previous section. Cytosolic calbindin 28k has been intensively used as a marker for Ca secretion because its epithelial levels during Ca absorption or secretion reflect their capacity to transfer Ca (Hurwitz, 1989a; Wasserman, 2004; Bar, 2008, 2009; Christakos, 2014, 2019; Nys and Le Roy, 2018). The regulation of CALB1 expression and Ca absorption in the intestine by the active metabolite of vitamin D has been clearly demonstrated; however, in contrast, numerous evidence shows that calbindin synthesis is not directly dependent on $1,25(OH)_2D_3$ levels in the hen uterus. Administration of exogenous $1,25(OH)_2D_3$ or increasing its endogenous levels by lowering dietary calcium in hens has no effect on calbindin concentration in the uterus (Bar et al., 1978, 1992; Nys and de Laage, 1984). Moreover, uterine calbindin is present in vitamin D deficient quail (Streim and Bar, 1991) and its levels increase following resumption of eggshell mineralization in parathyroidectomized hens (Nys et al., 1992). $1,25(OH)_2D_3$ might however facilitate calbindin synthesis as it stimulates calbindin production in vitro in uterine tissue from vitamin D deficient birds when added to the culture medium alone or in combination with estrogens (Corradino, 1993). The presence of the VDR in the uterus (Coty, 1980), its over expression during the period of shell calcification (Ieda et al., 1995; Bar et al., 1996), decreased expression when the egg is expelled (Bar et al., 1996) and observation of a putative VDRE in the calbindin gene (Christakos et al., 2014; Nys and Le Roy, 2018) and CA II (Quélo et al., 1994) also support a possible role for vitamin D; however, there is no evidence of a direct influence. The uterine calbindin concentration is large and CALB1 is one of the most highly expressed genes in the uterus during the process of eggshell formation (Nys et al., 1989; Striem and Bar, 1991; Bar et al., 1992); this decreases rapidly when shell formation is suppressed by artificial expulsion of the egg from the uterus (Figure 32.8). Calbindin falls to 50% and 3% of its initial expression levels at 1 and 6 h, respectively, after suppression of calcium secretion, which is in contrast to the stable level in the duodenum (Figure 32.8; Nys et al., 1992b). There is a good correlation between uterine calbindin levels and the amount of uterine calcium secreted for shell formation in mature laying hens or after arrest of egg production (Bar et al., 1984; Nys et al., 1989; Jonchere et al., 2012; Brionne et al., 2014)

The stimulation of uterine CALB1 expression occurs in two stages in mature laying hens. It is firstly stimulated by

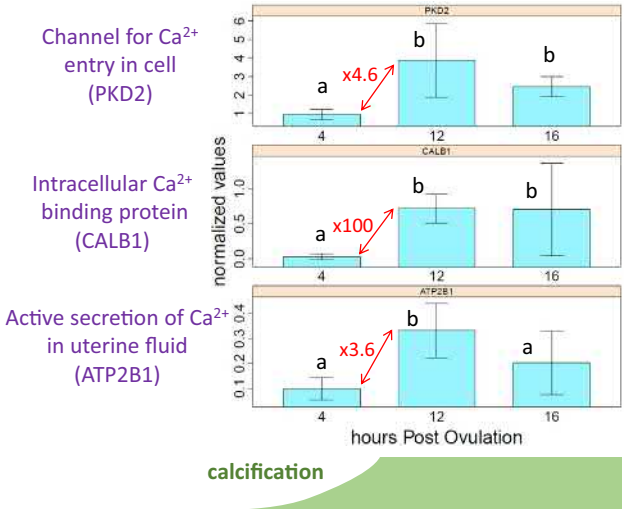

FIGURE 32.15 Overexpression of PKD2, CALB1, and ATP2B1 in hen uterus after re-induction of eggshell calcification in hens previously laying shell-less eggs due to premature expulsion Nys, Y., Gautron, J. and Brionne, A., personal communication.

sexual maturity, and secondly, during the calcification of the first shell (Figure 32.15); high calbindin levels are then maintained as long as the hen is laying. The greater estrogen secretion by the ovary at sexual maturity, and its high levels in mature hens, initially contribute to oviduct maturation and then to its maintenance in laying birds (Johnson, 2000; Nys and Guyot, 2011). Expression of CALB1 and levels of calbindin increase during sexual maturity (Wasserman and Taylor, 1968; Bar and Hurwitz, 1973; Navickis et al., 1979; Nys et al., 1989; Bar et al., 1990; 1992; Striem and Bar, 1991); this is specific to the uterus and does not occur in other segments of the oviduct (Jonchere et al., 2012). CALB1 levels are higher in laying hens, compared to immature pullets, but also compared to mature nonlaying birds (Bar et al., 1978; Striem and Bar, 1991) or in hens laying shell-less eggs with a normal ovulatory cycle (Nys et al.;, 1989; Nys et al., 1992). Uterine calbindin levels are stimulated by estrogen even if the pullets are deficient in vitamin D (Navickis et al., 1979; Bar et al., 1990; Corradino, 1993). Testosterone alone does not stimulate calbindin synthesis, but rather reinforces the estrogen effect; however, alone, it does not stimulate the increase in calbindin levels (Navickis et al., 1979). The estrogen receptor is localized in the glandular cells (Isola, 1990), as is calbindin (Jande et al., 1981).

The main increase in CALB1 expression and calbindin levels occurs during calcification of the first shell (Striem and Bar, 1991; Bar et al., 1992), or at resumption of shell formation in hens previously laying shell-less eggs (Figure 32.15; Nys et al., 1989). The high levels of calbindin in the uterus are maintained in laying hens by a daily increase in CALB1 expression during the period of shell formation (Nys et al., 1989; Bar et al., 1992; Ieda et al., 1995;

Jonchere et al., 2012; Brionne et al., 2014); however, the levels of the protein remain high in laying hens and are stable throughout the laying cycle because of its long half-live. Calbindin levels decrease after 48 h when shell formation is interrupted by egg expulsion or by an arrest of egg laying (Nys et al., 1989; Bar et al., 1992; Ieda et al., 1995) or molt (Yosefi et al., 2003). The induction of shell-less egg formation decreases expression and reduces levels of calbindin without affecting the plasma levels of sex steroids (Nys et al., 1986). We stress that $1,25(OH)_2D_3$ is not involved in the stimulation of calbindin at the uterus level in contrast to intestine. The entry of the egg into the uterus induces a mechanical stimulation to the uterus wall (distension) and has been shown to stimulate uterine calcium secretion (Eastin and Spaziani, 1978a) and expression of the Na^+/K^+-ATPase transporter (Lavelin et al., 2001), but not of CALB1 (Lavelin et al., 1998). The high synchronization between Ca entry and CALB1 upregulation in the uterus suggests that Ca might regulate CALB1 expression as has been shown in the kidney (Enomoto et al., 1992). This was experimentally confirmed in vitro (Corradino, 1993), using cultured uterus tissue from vitamin D deficient birds treated with estradiol to develop the oviduct. Administration of thapsigargin increases the entry of Ca and induces calbindin synthesis in the absence of estrogens or $1,25(OH)_2D_3$. Ca is a widely used second messenger system and fulfills numerous cell functions through complex intracellular Ca^{2+} signaling networks (Clapham, 2007; Barbado et al., 2009). The uterine effect might be mediated through the CaSR, which is expressed in calcitropic tissues such as the PTGs and kidneys in human, but also in other tissues not contributing to Ca homeostasis (Hannan et al., 2018). In hens, CaSR is found in kidney tubules and intestine, as well as in brain (Diaz et al., 1997); moreover, its expression in the parathyroid gland is stable throughout the laying cycle (Gloux et al., 2020). CaSR expression has not yet been detected in the uterus in studies exploring differential expression with physiological stimuli (Brionne et al., 2014), or associated with inferior/superior eggshell quality (Zhang et al., 2015), or correlation with hen age (Feng et al., 2020).

Regulation of other ion transporters has been less explored. Identification of the uterine ionic transporters was performed by measuring their differential expression when comparing uterus to another oviduct segment not secreting Ca, or by comparing uterine expression in the presence/absence of active calcification (Jonchére et al., 2012, Brionne et al., 2014; Sah et al., 2018; Khan et al., 2019) or different eggshell properties (Sun et al., 2016). These approaches have identified genes that are differentially expressed during Ca secretion. The ER Ca^{2+} pumps, PMCA pump (ATP2B1, 2), Na^+/Ca^{2+}/exchanger, Na channel, Na^+/K^+ exchanger, Na^+/HCO_3^- cotransporter, Na^+/K^+ ATPase, CA2, HCO_3^-/Cl^- exchanger, and vacuolar H^+ ATPase are all highly expressed in the active uterus compared to the magnum (Jonchere et al., 2012). Expression of genes involved in Ca transfer through the glandular cells of the uterus is also upregulated in hens during shell calcification compared to the hens in which shell formation has been suppressed by egg expulsion (Figure 32.15; Coty and Mc Conkey, 1982; Nys and de Laage, 1984; Jonchere et a., 2012; Brionne et al., 2014). The magnitude of the changes (two- to threefold) was however lower for the Ca channels PKD2 or TRPVs, ER pumps, PMCA (ATP2B1, Figure 32.15), Na^+/Ca^{2+}/exchanger, CA2, Na^+/HCO_3^- exchangers, Na^+/K^+ exchanger and K^+ voltage-gated channel, compared to CALB1 (16 fold). The expression of the calcium channel TRPV6 is higher during the period of calcification (Yang et al., 2013), as is that of ATP2A3 (Ca entry into the ER, CEMIP (release of Ca from the ER) and OTO2, 3 (vesicular transfer) (Khan et al., 2019). The presence of vesicular transfer of Ca has been suggested partly because of a high concentration in the eggshell of MFGE8 and EDIL3 protein (Marie et al., 2015a) and of an over expression of EDIL3 in the uterus in particular during the period of egg calcification (Stapane et al., 2019). Three Annexins (Anxa1, -2 and -3) are highly expressed in the uterus at the initial phase of shell formation (5 to 10 h postovulation) (Stepane et al., 2020). Some proteins are specific to the paracellular pathway such as claudins. However, claudins are not differentially expressed in the uterus in hens with or without a calcifying eggshell, and were not detected in transcriptomic studies (Jonchere et al., 2012; Brionne et al., 2014; Sah et al., 2018; Khan et al., 2019; Zhang et al., 2019). Therefore, shell formation clearly influences both Ca and bicarbonate transporters, but also other ionic transfers associated with regulation of cell homeostasis; however, the mechanisms of their regulation remain rather enigmatic. Mechanical dilation of the uterine wall induced by the presence of an egg can also upregulate some genes as shown for the expression of a few transporters such as Na^+/K^+-ATPase or other genes involved in shell formation (Lavelin et al., 1998, 2001). No studies have yet explored in vitro the influence of vitamin D or other hormones (steroids) on the synthesis of these ionic transporters. However, VDRE and the EREF are present in uterine transporter genes (Table 32.1, CALB1, ATP2A3, ITPR2-3, RYR2, ATP2B1-2-4, SLC8A1, SLC4A4-10, and CA2-7-9); moreover, calcium/cAMP response elements (CREB) are also observed in ATP2A2-3, ITPR1-2-3, RYR2, ATP2B1-2, SLC4A4-10, or CA2-7-9 (Nys and Le Roy, 2018). The involvement of these transporters to explain differences in shell quality due to genetic variability or the effect of hen age has been explored between groups laying eggs with different shell quality or by looking at genetic association with specific single nucleotide polymorphisms (SNPs) (Zhang et al., 2015; Feng et al., 2020). A number of genes possibly involved in Ca uterine transport (voltage-dependent L-type calcium channel subunit

alpha-1D, -1E, -1H (CACNA1D, 1E, 1H), PRKCB, and NCX1 (Na^+/Ca^{2+} exchanger, SLC8A1) were overexpressed in uterus of hens laying eggs with low-eggshell quality; in contrast, no differences were observed for the Na^+ channel (SCNN1A,1B, and 1G). Nonsynonymous SNP variations were found in the CACNA1E, CACNA1H, PRKCB, and NCX1 genes (Zhang et al., 2015). When comparing young and old hens, Feng and coworkers (Feng et al., 2020) also observed numerous differentially expressed genes among some uterine ionic transporters, including CACNA1C and CACNA1D, and SLC9A9; however, these approaches cannot reveal a change affecting numerous genes belonging to a specific process of Ca secretion.

32.8 Mineralization of the eggshell

32.8.1 Mechanisms of shell mineralization and the role of organic matrix

32.8.1.1 Eggshell temporal and spatial deposition

Avian eggshell is a porous bioceramic that is formed at body temperature in a confined and cell-free environmental space, the lumen of the uterus. Its formation is one of the fastest calcifying processes known in biology. The uterine fluid is supersaturated with respect to calcium and bicarbonate (about 70-fold relative to calcite solubility) and contains the organic precursors of the shell matrix (Gautron et al., 1997; Nys et al., 2004). The mature eggshell is made of $CaCO_3$ in the form of calcite and is formed in the absence of cell-directed assembly, in contrast to the cell-mediated mineralization of bone and teeth, which are composed of Ca phosphate. The eggshell is formed on a supporting meshwork of collagenous and noncollagenous membranes. Mineralization is initiated upon organic cores on the outer surface of the membrane fibers, which greatly influences the spacing of the mammillary cores and the subsequent mineral texture (Rodriguez-Navarro and Garcia-Ruiz, 2000; Dunn et al., 2012).

The first stage of eggshell formation is the initial phase (from 5 to 10 h after ovulation). When this phase begins, the eggshell weight is very low (0.18 g) compared to the final weight of the complete shell (about 6 g), and consists of the ESM fibers and their organic rich rounded surface structures (mammillary knobs). This corresponds to a "slow" phase, since 0.1 g of shell is deposited per hour and is divided into three events. Initially, eggshell mineralization is initiated with the deposition of flat disk-shaped ACC particles (Figure 32.16) that accumulate at specific organic-rich sites (mammillary knobs) on the ESM fibers that are rich in proteins and sulfated proteoglycans. These components are thought to promote the nucleation and stabilization of ACC with a calcite short-range order, which predetermines its conversion into calcite and the calcitic mineral composition of the mature eggshell (Figure 32.16; Rodriguez-Navarro et al., 2015). In the initial mineralization process, aggregates of calcite crystals grow radially from the nucleation sites to produce the mammillary cones. Calcite crystals from adjacent mammillary knobs continue growing until their adjacent bases merge as they compete for available space (competitive crystal growth) (Figure 32.17: Garcia-Ruiz and Rodríguez-Navarro, 1994; Rodriguez-Navarro and Garcia-Ruiz, 2000).

The second stage is the rapid-growth phase with a linear deposition of 0.33 g of calcite per hour. This phase is initiated when adjacent mammillary cones become fused (10 h postovulation), which then forms a continuous

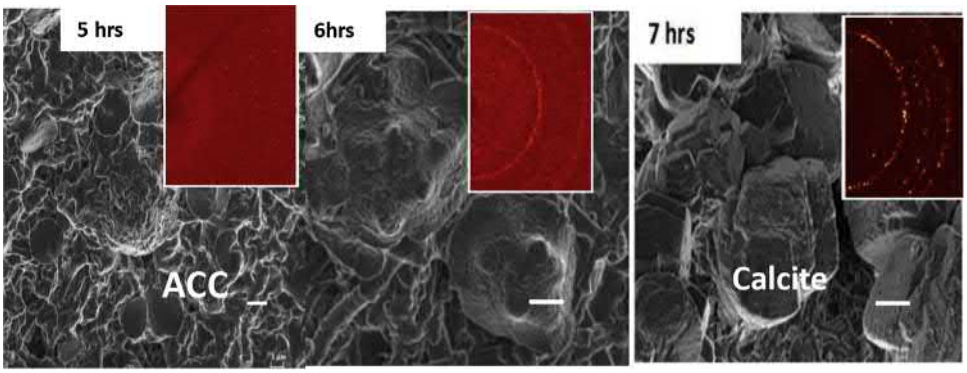

FIGURE 32.16 Scanning electron microscope microphotographs of forming eggshell collected at different stages of mineralization. At 5 h p.o., nonmineralized eggshell with organic-rich structures and appearance of mineralization by flat disk-shaped amorphous calcium carbonate particles nucleating on membrane fibers are observed. Inset: detail of a disk-shape particle showing an inner granular nanostructure. At 6 h, massive mineral deposits showing emerging calcite crystals. After 7 h, only large calcite crystals bounded by well-defined rhombohedral faces remain. Inserted in right corner: 2D-XRD patterns of eggshell membranes collected at 5 h p.o. showing no diffraction rings; at 6 h, there are weak and continuous rings produced by the incipient crystallization of nanosized calcite and at 7 h, some calcite crystals have grown and produce spotty rings whereas most of the nanocrystalline calcite has dissolved. Scale bars: (5 h) 1 μm. (6 and 7 h) 10 μm Rodríguez-Navarro et al. (2015).

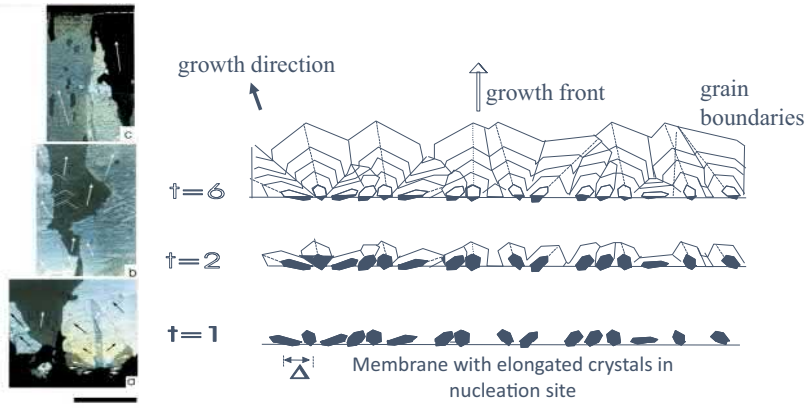

FIGURE 32.17 Left side: Cross-section of an eggshell viewed in cross-polarized light. *Arrows* indicate the orientation of the c axis of calcite crystals. Scale bar is 100 μm. (A). mammillary knobs, (B) mid palisade layer, (C) outer palisade. Right side: schematic illustration of competitive growth of crystals generating larger crystals with preferred orientation; Initially, crystals grow in all direction; eventually, only crystals growing perpendicular to the eggshell membranes will continue to grow due to competition for space between adjacent crystals Garcia-Ruiz and Rodríguez-Navarro (1994)

compact layer (palisade layer). This phase lasts 12h, corresponding to deposition of about 4 g of eggshell, which is organized as columnar calcite units with preferred orientation perpendicular to the eggshell surface. Calcite crystals with c-axis (fastest growth direction) oriented perpendicular to the shell surface continue growing outwards, blocking and burying other less favorably oriented crystals (Figure 32.17). Consequently, in the palisade layer, columnar calcite crystals increase progressively in size as they grow vertically and develop a preferred crystal orientation, with their c-axis oriented almost perpendicular to the egg surface (Sharp and Silyn-Roberts, 1984; Silyn-Robert and Sharp, 1986). This process of geometrical selection of calcite crystals is responsible for the characteristic columnar ultrastructure of avian eggshells crystal morphology and their exceptional mechanical properties, for example, the chicken eggshell (mean thickness of 0.33 mm) requires an average force of 35 N before fracture.

Finally, 2 h before oviposition, the terminal phase is characterized by the arrest of calcification and the deposition of a thin organic layer (cuticle), which constitutes a biofilm that covers the shell and plugs the respiratory pores to consequently restrict bacterial penetration through the shell.

32.8.1.2 Role of matrix proteins in the biomineralization process

Different avian species develop eggshells with specific microstructural characteristics (Figures 32.3 and 32.4; Silyn-Robert and Sharp, 1986; Panheleux et al., 1999; Dalbeck and Cusack., 2006; Rodriguez-Navarro et al., 2007). Eggshell microstructural characteristics are defined by the interaction of $CaCO_3$ with the organic matrix components during the nucleation and crystal growth phases. A particularity of the eggshell is the low amount of organic material which corresponds to 3.5% when the ESMs are included and to 2% of occluded proteins in the calcified region, in contrast to the matrix of dentin (20%), enamel (<5%), and bone (30%) (Feng, 2009; Neel et al., 2016). This organic matrix of the chicken eggshell plays a fundamental role in the manufacture of the shell and therefore in the establishment of its mechanical properties. Proteins and proteoglycans from the organic matrix stabilize the initial amorphous $CaCO_3$ and control its conversion into calcite crystals. They also inhibit the growth of the faces parallel to the c-axis of the calcite crystals that became elongated along the c-axis. This favors the growth of crystals with their c-axis that are roughly perpendicular to the egg surface during the competitive growth process (Garcia-Ruiz and Rodriguez-Navarro, 1994; Arias et al., 1993; Nys et al., 1999; 2004; Fernandez et al., 2004; Hincke et al., 2012). In vitro experiments, in situ observations and genetic association analysis has confirmed the active control of the eggshell mineralization by the organic matrix.

The first evidence implicating the matrix proteins in control of eggshell fabric/microstructure was the variation in concentration and protein species of the eggshell matrix components in the uterine fluid during the three sequential stages of shell formation, i.e., an initiation phase corresponding to the nucleation of calcite on ESMs (5 to 10 h postovulation in hens), the rapid crystal growth forming the main calcified shell (10 to 22 h postovulation) and finally, the dynamic arrest of shell calcification which occurs about 1.5 h before egg expulsion (Nys et al., 2001; Gautron et al., 1997). The composition of the uterine fluid progressively changes due to the secretion of specific proteins at different phases of eggshell formation (Figure 32.18; Gautron et al., 1997). The organic fraction contained in the shell has calcium-binding properties due to proteins (Abatangelo et al., 1978; Cortivo et al., 1982; Hincke et al., 1992), or

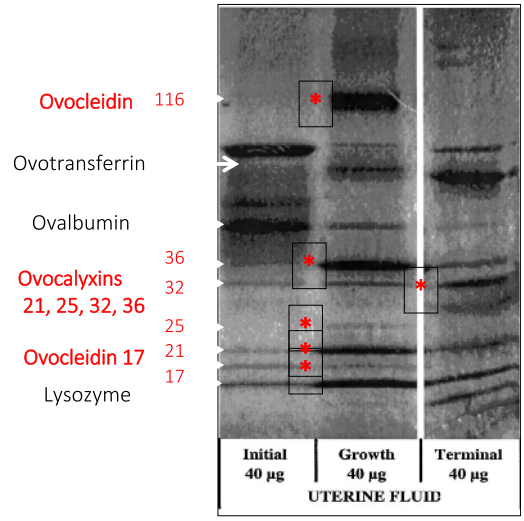

FIGURE 32.18 Electrophoretic profile (SDS-PAGE) of the uterine fluid collected at three stages of shell formation (initiation, period of rapid deposition, and termination of the hen eggshell). Molecular weights are indicated by arrows. Coomassie blue staining. Proteins involved in shell mineralization; Those in red are specific to the uterus. *Data from Gautron et al. (1997).*

proteoglycans with keratans or dermatan sulfates (Arias et al., 1992). Similarly, protein bands in uterine fluid have an affinity for calcium (Figure 32.18; Gautron et al., 1997).

In vitro experimental studies have demonstrated that components of uterine fluid favor the formation of the calcite polymorph, and influence the size, number, and morphology of crystals. The soluble organic fraction of the shell delays the precipitation of $CaCO_3$ in a dose-dependent manner (Arias et al., 1993; Gautron et al., 1996). An identical effect is observed with fractions rich in proteoglycans (Arias et al., 1992) and with macromolecules contained in the uterine fluid (Gautron et al., 1997). The synthetic crystals thus formed were collected to analyze polymorphic type and morphology. In the absence of organic constituents, the control crystals were composed of 55% calcite, and 45% of the two other polymorphs of $CaCO_3$ (vaterite and aragonite). Addition of uterine fluid increased the number of crystals produced, decreased their size, accelerated the initiation of mineralization, and favored the exclusive formation of calcite, which is the polymorphic type of $CaCO_3$ present on the shell, since the crystals formed in the presence of this fluid collected at the three stages are composed exclusively of calcite (Dominguez-Vera et al., 2000; Hernandez-Hernandez et al., 2008a). The morphology of calcite crystals was strongly modified by the presence of organic constituents extracted from the shell (Gautron et al., 1996; Hernandez-Hernandez et al., 2008b) and uterine fluid collected at the three stages of shell formation (Gautron et al., 1997; Hernandez-Hernandez et al., 2008b). The electrophoretic profile of the uterine fluid examined at the time of collection was compared with that obtained after the in vitro crystallization test (Gautron et al., 1997; Hernandez-Hernandez et al., 2008b). Numerous protein bands associated with $CaCO_3$ during precipitation and disappeared from the supernatant to be present in the precipitate containing $CaCO_3$.

The effects described above were obtained with a mixture of proteins present in the uterine fluid and shell extracts. They demonstrated that the organic matrix interacts with the mineral phase of the shell. The question quickly arose as to which constituent(s) of this matrix were involved in this mechanism of interaction between the mineral and organic phases. To answer this question, tests were conducted using proteins identified in the shell and protein fractions obtained by chromatographic separation of the organic matrix from the shell. Calcite crystals are strongly modified when formed in the presence of lysozyme, ovotransferrin, and ovocleidin-17 (Gautron et al., 2001b; Hincke et al., 2000; Jimenez-Lopez et al., 2003; Reyes-Grajeda et al., 2004; Dombre et al., 2017). Ansocalcin is a protein identified in the goose shell and is an ortholog of ovocleidin-17. It modified the crystallization of calcite crystals grown in vitro (Lakshminarayanan et al., 2002; Lakshminarayanan et al., 2003). Ovoglycan, which is a dermatan sulfate proteoglycan with ovocleidin-116 as its protein core, is polyanionic and acidic. It has a high affinity for calcium and therefore may modulate crystal growth during the formation of the palisade layer of the shell (Fernandez et al., 2001). Additional roles have been ascribed to other individual eggshell matrix proteins, such as ACC stabilization(Freeman et al., 2010). Calcium binds to ovalbumin, and this accumulation creates a nucleation center for mineralization (Schwahn et al., 2004). A schematic representation of $CaCO_3$ mineralization in the presence of ovalbumin has been proposed (Pipich et al., 2008). Calcium ions are bound to the protein by complexation through acidic groups leading to protein rearrangement. The calcium ions are the starting point for the subsequent formation of ACC nuclei, which then undergo a series of phase transitions to the stable crystalline polymorphs (Schwahn et al., 2004). The ability of ovalbumin to stabilize unstable $CaCO_3$ phases was further confirmed using in vitro experiments (Wang et al., 2009, 2010). Calcite crystals grown in vitro in the presence of lysozyme exhibited altered crystal morphology, although only at high concentrations (Hincke et al., 2000). Its role in the stabilization of ACC has been investigated but remains controversial. Lysozyme from eggshells of quail did not induced the precipitation of ACC under in vitro conditions (Lakshminarayanan et al., 2006). However, metastable ACC particles were obtained in vitro in the presence of chicken egg white lysozyme (Voinescu et al., 2007; Wang et al., 2009). Lysozyme considerably decreased the average diameter of the metastable ACC particles and promoted a network of associated particles, with the protein becoming

incorporated into the precipitate (Voinescu et al., 2007). In addition, lysozyme-ACC particles reorganized exclusively into crystalline calcite (Voinescu et al., 2007; Wang et al., 2009). Conversely, lysozyme was shown to be ineffective in the stabilization of ACC (Wolf et al., 2011). OPN is also a favorite candidate in the control of shell mineralization, since it modifies the morphology of calcite crystals and is correlated with eggshell hardness (Chien et al., 2008; Hincke et al., 2008; Freeman et al., 2010; Athanasiadou et al., 2018).

Many physical parameters (hydrophobicity, charge …) modify the adsorption or repulsion mechanisms of these proteins toward calcite and consequently alter the morphology of eggshell calcite crystals. These modifications affect the texture of the shell (size and orientation of the crystals) and therefore modify the mechanical properties of the shell. This hypothesis implies a variation in the quantity of specific proteins in the organic matrix according to the mechanical properties of the shell. The existence of this quantitative relationship between organic matrix proteins and shell strength has been demonstrated using shell samples that possess a range of mechanical properties such as breaking strength (Panheleux et al., 2000; Ahmed et al., 2005; Zhang et al., 2019).

The influence of eggshell matrix proteins on the ultrastructure of the shell and its mechanical properties is also supported by association studies between polymorphisms of genes encoding shell organic matrix proteins and different eggshell characteristics. Polymorphisms of specific shell proteins (ovalbumin, ovocleidin-116, and ovocalyxin-32) partially explain variation in specific eggshell properties (i.e., eggshell thickness, crystal size, crystal orientation, eggshell mechanical properties) (Dunn et al., 2009a, 2012; Rome and Le Roy 2016). Additionally, SNPs provide the potential to improve eggshell quality by optimizing beneficial eggshell microstructure traits through genetic assisted selection programs. These may lead to promising biological makers for genomic selection using a candidate gene approach. Indeed, a recent study recorded a total of 118 quantitative trait loci (QTLs), associated with shell strength (Rome and Le Roy, 2016). Among them, 24 are involved in fracture resistance (Sasaki et al., 2004; Dunn et al., 2009a; Jiang et al., 2010; Yao et al., 2010; Liu et al., 2011; Tuiskula-Haavisto et al., 2011) and 33 in shell stiffness (Dunn et al., 2009a; Takahashi et al., 2010; Tuiskula-Haavisto et al., 2011; Wolc et al., 2014). In addition, QTLs for characteristics such as breaking strength, shell stiffness, and shell morphological parameters were found on chromosome 2, 9, and Z of the hen (Ankra-Badu and Aggrey, 2005; Takahashi et al., 2009; Tuiskula-Haavisto et al., 2011). There are also notable changes in eggshell ultra- and microstructural properties that occur with increasing hen age (i.e., type of defects, mammillary density, size of calcite crystal units) (Rodriguez-Navarro et al., 2002; Robert et al., 2013; Park and Sohn 2018). Selection based on different haplotypes could improve the marked decrease in eggshell mechanical properties that occur in older hens. Indeed, the comparison of transcriptome of young and old hens revealed that some matrix involved in eggshell mineralization (ovalbumin, versican, and glypican 3) show differential expression (Feng et al., 2020)

The eggshell matrix proteome is currently well characterized for chicken eggs. Earlier biochemical studies, followed more recently by proteomics and transcriptomics approaches, have identified large numbers of occluded eggshell matrix proteins including those present at very low concentrations; altogether, more than 900 unique proteins have been identified in the eggshell including membranes and cuticle (Gautron et al., 2019; Gautron et al., 2020). Another integrated analysis of chicken eggshell matrix has enumerated a total of 69 phosphoproteins and 182 N-glycoproteins, for a total of 676 eggshell matrix proteins in the mineralized part (Mann et al., 2007; Yang et al., 2020). However, among Neoaves, only the zebra finch eggshell proteome has been characterized and exhibits 475 proteins (Mann, 2015). Additionally, the proteomes of a small number of closely related Neognathae species have been characterized (turkey, quail, duck, Guinea fowl), which contain 697, 622, 484, and 149 shell matrix proteins, respectively (Mann et al., 2007; Mann and Mann, 2013, 2015; Le Roy et al., 2019; Zhu et al., 2019; Marie et al., 2015a, b). These datasets must be expanded to cover a wide range of bird eggshells, with improved annotation, in order to clearly determine whether there is a minimal and essential eggshell proteome toolkit across all avian species.

As described earlier, matrix proteins play a decisive role in the establishment of the ultrastructure of the shell and its mechanical properties. In order to prioritize the most important proteins among this huge list of identified proteins, quantitative proteomics approaches have been conducted (Marie et al., 2015a, b). They have allowed characterization of the most abundant proteins at each of the crucial stages of mineralization, on the one hand, and to study their potential function by in silico approaches, on the other hand.

A first category of eggshell matrix proteins consists of proteins that direct the mineralization process through their ability to interact with the mineral (Figure 32.19). These proteins have a well-established role in the mineralization process, with functions that have been validated experimentally. Lysozyme, ovalbumin, and ovotransferrin are egg white proteins that are capable of interacting with the mineralized shell (Hincke, 1995; Hincke et al., 2000, Gautron et al., 2001; Dombre et al., 2017). OPN, ovocleidin-17, and EDIL3 are also in this category (Pines et al., 1995; Hincke et al., 1995; Hincke et al., 2008; Stapane et al., 2019, 2020).

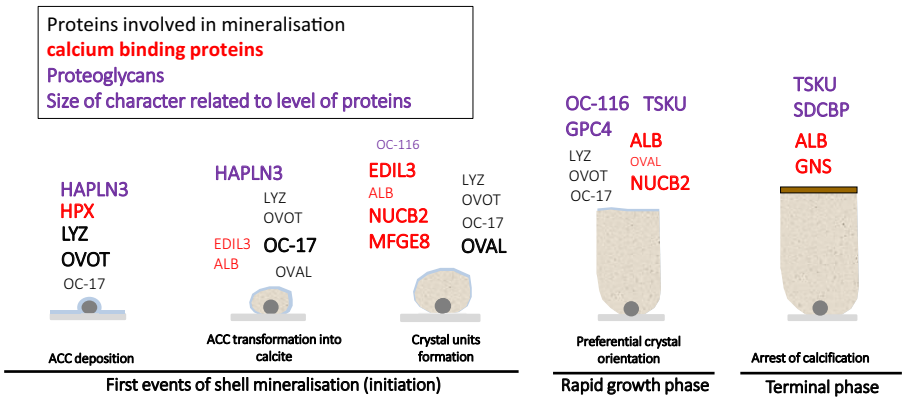

FIGURE 32.19 Schematic representation of the sequential events of mineralization and description of major matrix proteins at four time points of shell of mineralization. Size of characters is relative to their level in the eggshell extract (hierarchical ranking of the emPAI value) at individual stages. Overabundant proteins at each stage were determined using a spectral counting label free quantitative method and statistical analysis (ANOVA and HCA). *Adapted from Marie et al. (2015b).*

The second category of proteins consists of proteins regulating the activity of the proteins directing mineralization in the acellular uterine fluid. In this group, there are molecular chaperones such as clusterin that can form complexes with other proteins, and regulate their folding (Mann et al., 2003). Proteases or protease inhibitors are also identified in this group (Hincke et al., 2012; Dombre et al., 2017). They would have the role of regulating the degradation of active proteins or the activation of peptides with activity toward the mineralization process.

A great number of eggshell matrix proteins can be termed ubiquitous components, since they are also found in many other tissues and/or body fluids, and their specificity with respect to eggshell calcification is not obvious. Functionally relevant matrix constituents include OPN (SSP1) and ovocleidin-116 (OC-116, MEPE), which are phosphoglycoprotein members of the SIBLING family that are found in both bone and eggshell (Hincke et al., 2008; Hincke et al., 1999; Bardet et al., 2010). In addition, the shell matrix is constituted of proteins that originally were thought to be extremely specific to the distal oviduct of birds (isthmus and uterus) and to eggshell formation: in chicken, these have been characterized as ovocleidin 17 (OC-17), ovocalyxins 21, 25, 32, 36 (Hincke et al., 1995; Nys et al., 1999; Gautron et al., 2001; Nys et al., 2004; Gautron et al., 2007; Hincke et al., 2012). Proteomics studies of avian eggshells have identified OC-116 as the most abundant matrix protein in chicken, turkey, quail, and guinea fowl (Mann and Mann, 2013; Mann, 2015; Le Roy et al., 2019). OCX-36 is another abundant constituent of the chicken, turkey, quail, zebra finch, and Guinea fowl eggshell proteomes (Mann, 2015; Mann and Mann, 2013, 2015; Le Roy et al., 2019). OC-17 orthologs have been identified in eggshell from goose (ansocalcin), ostrich (struthiocalcin: SCA-1 and -2), emu (dromaiocalcin: DCA-1 and -2), rhea (rheacalcin: RCA-1 and -2) (Lakshminarayanan et al., 2002; Mann and Siedler, 2004; Mann and Siedler, 2006), and guinea fowl (OC-17-like and DCA-1-like) (Le Roy et al., 2019). In contrast to other eggshell matrix proteins implicated in mineralization (i.e., OCX-36, OC-116, OPN, and EDIL3), OC-17 and its orthologs appear to be both avian- and oviduct/eggshell−specific (Zhang et al., 2014). In contrast, OCX-32 protein cannot be generalized to all avian eggshells, since its absence from quail and turkey eggshell has been emphasized (Mann and Mann, 2013, 2015)

Ovocleidin 17 is the second most abundant matrix protein and modifies the morphology of calcite crystals grown in vitro (Reyes-Grajeda et al., 2004). Modeling of OC-17 suggests the involvement of this protein in the crystallization of calcite from ACC nanoparticles (Freeman et al., 2015). OPN is associated with parallel sheets of matrix in the highly mineralized palisade layer and with the {104} crystallographic faces of eggshell calcite, suggesting its role in regulating calcite crystal growth and orientation during the rapid phase of shell deposition which results in formation of the palisade layer (Chien et al., 2008). Quantitative proteomic analysis of the organic matrix proteins of the uterine fluid, where shell mineralization takes place, and of eggshell extracts, throughout the different steps of eggshell formation (ACC transformation in calcite, nucleation phase, rapid growth phase, and arrest of shell formation), reveals the presence of overabundant proteins at particular phases of the process (OC-17, OC-116, EDIL3, LOXL2, ovalbumin, ovotransferrin, lysozyme, etc …) and underlines the likely involvement of these proteins in the control of eggshell formation (Marie et al., 2015a, 2015b). In addition, significant associations between gene polymorphism and eggshell quality indicate the influence of organic matrix proteins on eggshell fabric. Ovalbumin gene polymorphism is associated with breaking strength, shell deformation, eggshell thickness, and crystal size; OC-116 with shell thickness, elastic modulus, and crystal orientation; OPN with fracture toughness; ovotransferrin

with crystal size; and OCX-32 with shell thickness and crystal orientation (Dunn et al., 2009, 2012). Nanoindentation and atomic force microscopy measurements verify OPN's influence on eggshell hardness and nanostructure, which in turn control the mechanical properties of the shell (Athanasiadou et al., 2018)

32.8.2 Regulation of eggshell matrix protein synthesis

There are numerous similarities between the regulation of ionic transporters and matrix proteins in the uterus, but specific information concerning matrix proteins remains limited. Sex steroids are implicated as shown by the increased expression of matrix proteins at hen sexual maturity of female birds compared to immature pullets (Dunn et al., 2009). Expression of OCX-21, OCX-36, OC-116 (Dunn et al., 2009), OPN (Pines et al., 1995), and OC-17 (Zhang et al., 2014) are upregulated at sexual maturity. OC-116 expression is also highly upregulated in laying compared to nonlaying hens (Brionne et al., 2014; Sah et al., 2018), and many other genes are over expressed in laying hens during the period of shell formation (Table 32.2). The upregulation of matrix proteins is associated with the development and differentiation of the oviduct induced by increased level of estrogens 2 weeks before the onset of egg production (Sauveur and de Reviers, 1988; Johnson, 2000; Nys and Guyot, 2011). The observation of an EREF family motif in some of the matrix protein genes (Table 32.2) also supports the role of estrogen in synthesis of these proteins. Secondly, a large stimulation of uterine matrix protein synthesis is linked to the process of eggshell formation, as shown by uterine expression in hens laying a hard-shelled egg compared to hens for which egg calcification has been experimentally suppressed (Jonchére et al., 2010; Brionne et al., 2014). Numerous matrix proteins (OCX-21, OCX-32, and OCX-36, OPN, OC-116, Table 32.2) are upregulated under these conditions, and the presence of a large secretion of sex steroids does not prevent the drop in matrix protein expression in hens laying a shell-less egg due to premature expulsion of the egg (Jonchere et al., 2010; Brionne et al., 2014). The induction of ovalbumin, lysozyme, and ovotransferrin expression by estrogen or progesterone has been demonstrated in the magnum (Chambon P. et al., 1984), but has not been explored in the isthmus and uterus segments. These proteins of the egg white do not seem to be upregulated by shell formation in the uterus, as their mRNAs were not differentially expressed in hens laying hard versus soft shell eggs. These changes at sexual maturity and in laying hens coincide with stimulation of $1,25(OH)_2D_3$ production and increases in its circulating plasma levels, but there is no direct evidence to implicate this metabolite in upregulation of matrix proteins, with the exception of a VDRE in certain genes (Nys and Le Roy, 2018, Table 32.2). The effect of this metabolite on expression of shell matrix proteins in vivo has not been studied yet. An exogenous supply of $1,25(OH)_2D_3$ in hens does not improve shell strength (Nys and de Laage, 1984; Bar et al., 1978; Bar et Striem, 1992). No study has yet been carried out in vitro or in vivo to explore the effect of its exogenous supply on expression of shell matrix proteins; only intracellular levels of calbindin have been assessed, which is not dependent on vitamin D in the uterus, as previously described. Another experimental approach to explore the regulation of matrix proteins is comparison of uterine gene expression between the inactive uterus (egg in magnum) with the active uterus (calcifying egg in uterus). These approaches (Jonchere et al., 2010, 2012; Brionne et al., 2014; Khan et al., 2019) reveal large differential expression in ionic transport but matrix proteins genes do not exhibit large differential gene expression between the two physiological stages (Table 32.2). Earlier studies using Western blot analysis suggested that OC-17, OC-116, OCX-32, and OPN are secreted only by the uterine segment of the oviduct, and are mainly present in the uterine fluid collected during active eggshell calcification (Hincke et al., 1995, 1999; Lavelin et al., 1998; Gautron et al., 2001). The overexpression of OPN gene (SPP1) but also that of glypican-4 were demonstrated to be induced by the mechanical strain of dilatation of the uterine wall induced by entry of the egg (Lavelin et al., 1998; Lavelin et al., 2002). However, it is not obvious to differentiate the mechanical stress from the process of eggshell mineral precursor secretion during calcification. It has been shown that Ca secretion is facilitated by dilatation but only during the period expected for shell formation (Eastin and Spaziani, 1978a). In addition, the profile of proteins in uterine fluid changes during the various phases of shell formation (Gautron et al., 1997) when the egg is present in the uterus, and this occurs without any change in mechanical stimuli. A proteomic study exploring the protein profile of uterine fluid and eggshell extract throughout the progressive mineralization of the shell, 5, 6, 7, and 19 h postovulation also revealed hourly variations in matrix protein concentrations during continuous mechanical strain associated with the presence of the egg in utero (Figure19) (Marie et al., 2015a, 2015b). This short-term temporal control of protein secretion during the phase of shell mineralization is confirmed by the observation of the specific localization of the eggshell matrix proteins in the different layers of the eggshell (Nys et al., 1999, 2004; Hincke et al., 2012). OCX-36 is upregulated during eggshell calcification and is predominantly localized in the inner part of the shell and in the inner shell membranes (Gautron et al., 2007). On the other hand, expression of OCX-32 is upregulated during the terminal phase of shell formation and is localized in the outer palisade layer, the vertical crystal layer, and the

TABLE 32.2 Major proteins involved in shell mineralization: description, gene expression, presence of vitamin D response element and estrogen response element.

	Protein			mRNA expression in chicken uterus				Gene regulation	
Gene symbol	Name	Putative role[a], functional characteristic	Stage[c] highest level (uterine fluid)	Mean expression in uterus[d]	Ratio of expression shelled eggs/ no shell	Expression in absence of mineralization (3 h p.o.)[e]	Expression during the active calcification phase in uterus	VDR	EREF
OVAL	Ovalbumin	Interact with calcite/ACC	7 h	7.29	=	nd	nd	Y	Y
TF	Ovotransferrin	Calcite crystal morphology; antimicrobial	6 h	nd	nd	nd	nd	nd	nd
SPP1	Osteopontin	Mineralization modifier	16 h	13.83***	+++	−	++	Y	Y
OC116/ MEPE	Ovocleidin 116	Mineralization modifier	16 h	15.96	+++	+	++	N	Y
OC17	Ovocleidin 17	ACC/$CaCO_3$ deposition	6 h	nd	nd	nd	nd	nd	nd
OCX36	Ovocalyxin 36	Proinflammatory mediator Antimicrobial[b]	16 h	13.48***	+++	+	+++	Y	Y
OCX32	Ovocalyxin 32	Protease inhibitor Antimicrobial	7 h		++	++	++	nd	nd
LYZ	Lysozyme	Calcite crystal morphology; antimicrobial	6 h	9.23	=	+	++	nd	nd
EDIL3	EGF-like repeats discoidin I-like domains 3	Calcium-binding Targeting of ACC in EVs	7 h	12.10	++	+	++	Y	Y
SPARC	Secreted protein acidic and cysteine rich	Calcium-binding	7 h	10.38***	=	nd	nd	Y	Y
MFGE8	Milk fat globule-EGF factor 8 protein	Calcium-binding	7 h	11.15***	+	+	+	Y	Y

Continued

TABLE 32.2 Major proteins involved in shell mineralization: description, gene expression, presence of vitamin D response element and estrogen response element.—cont'd

	Protein			mRNA expression in chicken uterus				Gene regulation	
Gene symbol	Name	Putative role[a], functional characteristic	Stage[c] highest level (uterine fluid)	Mean expression in uterus[d]	Ratio of expression shelled eggs/no shell	Expression in absence of mineralization (3 h p.o.)[e]	Expression during the active calcification phase in uterus	VDR	EREF
NUCB2	Nucleobindin 2	Calcium-binding	16 h	11.89***	+	nd	nd	nd	nd
SPINK7	Ovomucoid	Serine protease inhibitor, Kazal-like domains	5 h	10.09***	=	nd	nd	nd	nd
PPIB	Peptidylprolyl isomerase B	Accelerates protein folding	16 h	13.37	++	nd	nd	nd	nd
GPC4	Glypican 4	Heparan sulfate proteoglycan	16 h	10.98***	+	nd	nd	Y	Y
LOC 428,451	Prostatic acid phosphatase like	Protein phosphatase	7 h	12.64***	++	nd	nd	nd	nd

[a] [c]ANR-13-BSV6-0007-01, ANR-13-BSV6-0007-02 and ANR-13-BSV6-0007-05) (IMPACT Project, Gautron et al., 2013–17).
[a]*Marie et al. (2015a), Chien et al. (2008).*
[b]*Cordeiro et al. (2013).*
[c]*Marie et al. (2015a).*
[d]*Brionne et al. (2014).*
[e]*Pines et al., 1995; Gautron et al. (2007); Stapane et al. (2020).*

cuticle of the eggshell (Gautron et al., 2001). These differences clearly suggest additional regulating factors than solely mechanical strain. Moreover, a major change in crystallography of the Guinea fowl shell occurs about 12 h postovulation and is associated with changes in the matrix composition (Le Roy et al., 2019). The process of eggshell formation is therefore associated with changes in the expression of eggshell matrix genes, which occurs at a short term (hourly variation) or at longer term (daily variation); however, the mechanisms of such regulation remain to be further defined. The presence of the calcium/cAMP responsive elements (CREB) in numerous eggshell matrix protein genes (Panheleux et al., 1999; Nys and Leroy, 2018) reinforces the hypothesis of a multifactorial regulation, which might also involve some paracrine factors.

Identifying and exploring the respective roles of regulatory factors for eggshell matrix proteins is challenging in hens because of the difficulties to study uterine tissue culture in vitro and to explore individual factors in vivo when numerous physiological factors need to be preserved in order to maintain egg laying and shell formation. However, novel approaches such as CRISPR-based gene invalidation might help to decipher the mechanism of shell formation (Kuscu et al., 2017). Molecular biology (high-throughput technologies), however, has been very useful to identify the actors; emergence of more quantitative evaluation should help to establish some hierarchy between the matrix proteins and to better understand the origin of shell defects induced by physiological factors such as hen age. The comparison of gene expression in young and old hen with lower eggshell quality has revealed a large number of differentially expressed genes, among them ovalbumin, versican, and glypican 3 (Feng et al., 2020). It will be of interest to apply this approach to compare uterine expression in aged hens to the same hens after molting, as the protein profile of eggshell extracts differs between the two groups (Ahmed et al., 2005). In conclusion, biomineralization of the shell is under the control of matrix proteins, the synthesis and secretion of which is under spatiotemporal regulation. A remaining challenge is to decipher the complex interaction between sex steroids, mechanical stimulus, vitamin D, and additional unknown factors.

References

Abatangelo, G., Daga-Gordini, D., Castellani, I., Cortivo, R., 1978. Some observations on the calcium ion binding to the eggshell matrix. Calcif. Tiss. Res. 26, 247–252.

Addadi, L., Joester, D., Nudelman, F., Weiner, S., 2006. Mollusk shell formation: a source of new concepts for understanding biomineralization processes. Chem. Eur J. 12, 981–987.

Addadi, L., Raz, S., Weiner, S., 2003. Taking advantage of disorder: amorphous calcium carbonate and its roles in biomineralization. Adv. Mater. 15 (12), 959–970.

Addison, W.N., Azari, F., Sorensen, E.S., Kaartinen, M.T., McKee, M.D., 2007. Pyrophosphate inhibits mineralization of osteoblast cultures by binding to mineral up-regulating osteopontin, and inhibiting alkaline phosphatase activity. J. Biol. Chem. 282, 15872–15883.

Ahmed, T.A.E., Suso, H.P., Hincke, M.T., 2017. In-depth comparative analysis of the chicken eggshell membrane proteome. J. Proteomics 155, 49–62.

Ahmed, T.A.E., Suso, H.-P., Maqbool, A., Hincke, M.T., 2019a. Processed eggshell membrane powder: bioinspiration for an innovative wound healing product. Mater. Sci. Eng. C 95, 192–203.

Ahmed, T.A.E., Kulshreshtha, G., Hincke, M.T., 2019b. Value added uses of eggshell and eggshell membranes. Chapter 19. In: Wu, J. (Ed.), Eggs as Functional Foods and Nutraceuticals for Human Health. Royal Society of Chemistry, pp. 359–397.

Ahmed, A.M.H., Rodriguez-Navarro, A.B., Vidal, M.L., Gautron, J., Garcia-Ruiz, J.M., Nys, Y., 2005. Changes in eggshell mechanical properties,crystallographic texture and in matrix proteins induced by moult in hens. Br. Poult. Sci. 46, 268–279.

Aizenberg, J., Lambert, G., Addadi, L., Weiner, S., 1996. Stabilization of amorphous calcium carbonate by specialized macromolecules in biological and synthetic precipitates. Adv. Mater. 8, 222–226.

Alaimo, A., Rubert, J., 2019. The pivotal role of TRP channels in homeostasis and diseases throughout the gastrointestinal tract. Int. J. Mol. Sci. 20, 5277.

Alexander, R.T., Beggs, M.R., Zamani, R., Marcussen, N., Frische, S., Dimke, H., 2015. Ultrastructural and immunohistochemical localization of plasma membrane Ca2-ATPase 4 in Ca2-transporting epithelia. Am. J Physiol. Renal Physiol. 309, F604–F616.

Alexander, R.T., Rievaj, J., Dimke, H., 2014. Paracellular calcium transport across renal and intestinal epithelia. Biochem. Cell. Biol. 92, 467–480.

Ankra-Badu, G.A., Aggrey, S.E., 2005. Identification of candidate genes at quantitative trait loci on chicken Chromosome Z using orthologous comparison of chicken, mouse, and human genomes. In Silico Biol. 5 (5–6), 593–604.

Andrukhova, O., Zeitz, U., Goetz, R., Mohammadi, M., Lanske, B., Erben, R.G., 2012. FGF23 acts directly on renal proximal tubules to induce phosphaturia through activation of the ERK1/2-SGK1 signaling pathway. Bone 51, 621–628.

Antoniucci, D.M., Yamashita, T., Portale, A.A., 2006. Dietary phosphorus regulates serum fibroblast growth factor-23 concentrations in healthy men. J. Clin. Endocrinol. Metab. 91, 3144–3149.

Arad, Z., Eylath, U., Ginsbrug, M., Eyal Giladi, H., 1989. Changes in uterine fluid composition and acid base status during shell formation in the chicken. Am. J. Physiol. 257, R732–R737.

Arias, J.L., Carrino, D.A., Fernandez, M.S., Rodriguez, J.P., Dennis, J.E., Caplan, A.I., 1992. Partial biochemical and immunochemical characterization of avian eggshell extracellular matrices. Arch. Biochem. Biophys. 298, 293–302.

Arias, J.L., Fink, D.J., Xiao, S.Q., Heuer, A.H., Caplan, A.I., 1993. Biomineralization and eggshells: cell-mediated acellular compartments of mineralized extracellular matrix. Int. Rev. Cytol. 145, 217–250.

Arias, J.L., Cataldo, M., Fernandez, M.S., Kessi, E., 1997. Effect of beta-aminoproprionitrile on eggshell formation. Br. Poult. Sci. 38, 349–354.

Ascenzi, A., François, C., Steve Bocciarelli, D., 1963. On the bone induced by estrogens in birds. J. Ultrastruct. Res. 8, 491–505.

Athanasiadou, D., Jiang, W., Goldbaum, D., Saleem, A., Basu, K., Pacella, M.S., Böhm, C.F., Chromik, R.R., Hincke, M.T.,

Rodríguez-Navarro, A.B., Vali, H., Wolf, S.E., Gray, J.J., Bui, K.H., McKee, M.D., 2018. Nanostructure, osteopontin, and mechanical properties of calcitic avian eggshell. Sci. Adv. 4 (3), eaar3219.

Bahn, S.Y., Jo, B.H., Choi, Y.S., Cha, H.J., 2017. Control of nacre biomineralization by Pif80 in pearl oyster. Sci. Adv. 3 (8), e1700765.

Baksi, S.N., Kenny, A.D., 1977. Vitamin D3 metabolism in immature Japanese quail: effects of ovarian hormones. Endocrinology 101, 1216−1220.

Bar, A., 2008. Calcium homeostasis and vitamin D metabolism and expression in strongly calcifying laying birds. Comp. Biochem. Physiol. Part A Mol. Integr. Physiol. 151, 477−490.

Bar, A., 2009. Calcium transport in strongly calcifying laying birds: mechanisms and regulation. Comp. Biochem. Physiol. A Mol. Integr. Physiol. 152, 447−469.

Bar, A., Cohen, A., Edelstein, S., Shemesh, M., Montecuccoli, G., Hurwitz, S., 1978. Involvement of cholecalciferol metabolism in birds in the adaptation of calcium absorption to the needs during reproduction. Comp. Biochem. Physiol. B Comp. Biochem. 59, 245−249.

Bar, A., Hurwitz, S., 1973. Uterine calcium-binding protein in the laying fowl. Comp. Biochem. Physiol. A 45, 579−586.

Bar, A., Hurwitz, S., 1979. The interaction between dietary calcium and gonadal hormones in their effect on plasma calcium, bone, 25-hydroxycholecalciferol-1-hydroxylase, and duodenal calcium-binding protein, measured by a radioimmunoassay in chicks. Endocrinology 104, 1455−1460.

Bar, A., Rosenberg, J., Hurwitz, S., 1984. The lack of relationships between vitamin D3 metabolites and calcium-binding protein in the eggshell gland of laying birds. Comp. Biochem. Physiol. B Comp. Biochem. 78, 75−79.

Bar, A., Striem, S., Mayel Afshar, S., Lawson, D.E., 1990. Differential regulation of calbindin-D28K mRNA in the intestine and eggshell gland of the laying hen. J. Mol. Endocrinol. 4, 93−99.

Bar, A., Striem, S., Vax, E., Talpaz, H., Hurwitz, S., 1992. Regulation of calbindin mRNA and calbindin turnover in intestine and shell gland of the chicken. Am. J. Physiol. 262, R800−R805.

Bar, A., Vax, E., Hunziker, W., Halevy, O., Striem, S., 1996. The role of gonadal hormones in gene expression of calbindin (Mr 28,000) in the laying hen. Gen. Comp. Endocrinol. 103, 115−122.

Barbado, M., Fablet, K., Ronjat, M., de Waard, M., 2009. Gene regulation by voltage-dependent calcium channels. Biochim. Biophys. Acta Mol. Cell Res. 1793 (6), 1096−1104.

Bardet, C., Vincent, C., Lajarille, M.-C., Jaffredo, T., Sire, J.-Y., 2010. OC-116, the chicken ortholog of mammalian MEPE found in eggshell, is also expressed in bone cells. J. Exp. Zool. 314B.

Barroeta, A.C., Davin, R., Baucells, M.D., 2012. Optimum vitamin nutrition in laying hens. In: Optimum Vitamin Nutrition in the Production of Quality Animal Foods. 5M. Publishing Benchmark House, Sheffield, UK, pp. 89−135.

Beniash, E., Aizenberg, J., Addadi, L., Weiner, S., 1997. Amorphous calcium carbonate transforms into calcite during sea urchin larval spicule growth. P Roy. Soc. B-Biol. Sci. 264, 461−465.

Bernstein, R.S., Nevalainen, T., Schraer, R., Schraer, H., 1968. Intracellular distribution and role of carbonic anhydrase in the avian (*Gallus domesticus*) shell gland mucosa. Biochim. Biophys. Acta Enzymol. 159, 367−376.

Bobeck, E.A., Burgess, K.S., Jarmes, T.R., Piccione, M.L., Cook, M.E., 2012. Maternally-derived antibody to fibroblast growth factor-23 reduced dietary phosphate requirements in growing chicks. Biochem. Biophys. Res. Commun. 420, 666−670.

Boissy, P., Destaing, O., Jurdic, P., 2001. RANKL induces formation of avian osteoclasts from macrophages but not from macrophage polykaryons. Biochem. Biophys. Res. Commun. 288, 340−346.

Bonucci, E., Gherardi, G., 1975. Histochemical and electron microscope investigations on medullary bone. Cell Tissue Res. 163 (1), 81−97.

Brionne, A., Nys, Y., Hennequet-Antier, C., Gautron, J., 2014. Hen uterine gene expression profiling during eggshell formation reveals putative proteins involved in the supply of minerals or in the shell mineralization process. BMC Genom. 15, 220.

Castillo, L., Tanaka, Y., Wineland, M.J., Jowsey, J.O., DeLuca, H.F., 1979. Production of 1,25-dihydroxyvitamin D3 and formation of medullary bone in the egg-laying hen. Endocrinology 104, 1598−1601.

Centeno, V.A., Díaz De Barboza, G.E., Marchionatti, A.M., Alisio, A.E., Dallorso, M.E., Nasif, R., Tolosa De Talamoni, N.G., 2004. Dietary calcium deficiency increases Ca 2+ uptake and Ca 2+ extrusion mechanisms in chick enterocytes. Comp. Biochem. Physiol. A Mol. Integr. Physiol. 139, 133−141.

Chambon P., Dierich A., Gaub M.P., Jakowlev S., Jongstra J., Krust A., Lepennec J.P., Oudet P., Reudelhuber T., 1984. Promoter element of genes-coding for proteins and modulation of transcription by estrogens and progesterone. Recent Progress in Hormone Research 40, 1−42.

Chandra, S., Fullmer, C.S., Smith, C.A., Wasserman, R.H., Morrison, G.H., 1990. Ion microscopic imaging of calcium transport in the intestinal tissue of vitamin D-deficient and vitamin D-replete chickens: a 44Ca stable isotope study. Proc. Natl. Acad. Sci. U.S.A. 87, 5715−5719.

Chien, Y.C., Hincke, M.T., McKee, M.D., 2008. Avian eggshell structure and osteopontin. Cells Tissues Organs 189, 38−43.

Christakos, S., Liebsbet, L., Masuyama, R., Carmeliet, G., 2014. Vitamin D endocrine system and the intestine. ey Rep. 3, 1−7.

Christakos, S., Li, S., De La Cruz, J., Shroyer, N.F., Criss, Z.K., Verzi, M.P., Fleet, J.C., 2019. Vitamin D and the intestine: review and update. J. Steroid Biochem. Mol. Biol. https://doi.org/10.1016/j.jsbmb.2019.105501.

Clapham, D.E., 2007. Calcium Signaling Cell 131, 1047−1058.

Cordeiro, C.M.M., Esmaili, H., Ansah, G., Hincke, M.T., 2013. Ovocalyxin-36 is a pattern recognition protein in chicken eggshell membranes. PloS One 8, 1−13.

Cortivo, R., Castellani, I., Martelli, M., Michelotto, G., Abatangelo, G., 1982. Chemical characterisation of the hen eggshell matrix: isolation of an alkali-resistant peptide. J. Chromat. 237, 127−135.

Corradino, R.A., 1993. Calbindin D28K regulation in precociously matured chick egg shell gland in vitro. Gen. Comp. Endocrinol. 91, 158−166.

Corradino, R.A., Wasserman, R.H., Pubols, M.H., Chang, S.I., 1968. Vitamin D3 induction of a calcium-binding protein in the uterus of the laying hen. Arch. Biochem. Biophys. 125, 378−380.

Coty, W.A., 1980. A specific, high affinity binding protein for 1,25-dihydroxyvitamin D in the chick oviduct shell gland. Biochem. Biophys. Res. Commun. 93, 285−292.

Courbebaisse, M., Soubervbielle, J.C., 2011. Equilibre phosphocalcique : régulation et explorations. Nephrol. Ther. 7, 118−138.

Dacke, C.G., Arkle, S., Cook, D.J., Wormstone, I.M., Jones, S., Zaidi, M., Bascal, Z.A., 1993. Medullary bone and avian calcium regulation. J. Exp. Biol. 184, 63−88.

Dacke, C.G., 2000. The parathyroids, calcitonin, and vitamin D. In: Whittow, G.C. (Ed.), Avian Physiology. Academic Press, London, pp. 473–488.

Dacke, C.G., Sugiyama, T., Gay, C.V., 2015. The role of hormones in the regulation of bone turnover and eggshell calcification. In: Scanes, C.G. (Ed.), Sturkie's Avian Physiology. Academic Press, San Diego, CA, pp. 549–575.

Dalbeck, P., Cusack, M., 2006. Crystallography (electron backscatter diffraction) and chemistry (electron probe microanalysis) of the avian eggshell. Cryst. Growth Des. 6, 2558–2562.

Delmas, P.D., 1992. Clinical use of biochemical markers of bone remodeling in osteoporosis. Bone 13, S17–S21.

DeLuca, H.F., Nakada, M., Tanaka, Y., Sicinski, R., Phelps, M., 1988. The plasma binding protein for vitamin D is a site of discrimination against vitamin D-2 compounds by the chick. Biochim. Biophys. Acta 965, 16–21.

Dennis, J.E., Xiao, S.-Q., Agarwal, M., Fink, D.J., Heuer, A.H., Caplan, A.I., 1996. Microstructure of matrix and mineral components of eggshells from white leghorn chickens (*Gallus gallus*). J. Morphol. 228, 287–306.

Diaz, R., Hurwitz, S., Chattopadhyay, N., Pines, M., Yang, Y., Kifor, O., Einat, M.S., Butters, R., Hebert, S.C., Brown, E.M., 1997. Cloning, expression, and tissue localization of the calcium-sensing receptor in chicken (*Gallus domesticus*). Am. J. Physiol. 273, R1008–R1016.

Diaz de Barboza, G., Guizzardi, S., Tolosa de Talamoni, N., 2015. Molecular aspects of intestinal calcium absorption. World J. Gastroenterol. 21, 7142–7154.

Dombre, C., Guyot, N., Moreau, T., Monget, P., Da Silva, M., Gautron, J., Rehault-Godbert, S., 2017. Egg serpins: the chicken and/or the egg dilemma. Semin. Cell Dev. Biol. 62, 120–132.

Dominguez-Gasca, N., Benavides-Reyes, C., Sanchez-Rodriguez, E., Rodriguez-Navarro, A.B., 2019. Changes in avian cortical and medullary bone mineral composition and organization during acid-induced demineralization. Eur. J. Mineral 31, 209–216.

Dominguez-Vera, J.M., Gautron, J., Garcia-Ruiz, J.M., Nys, Y., 2000. The effect of avian uterine fluid on the growth behavior of calcite crystals. Poult. Sci. 79, 901–907.

Dong, P., Tao, Y., Yang, Y., Wang, W., 2010. Expression of retinoic acid receptors in intestinal mucosa and the effect of vitamin A on mucosal immunity. Nutrition 26, 740–745. Elsevier Ltd.

Dong, X.L., Zhang, Y., Wong, M.S., 2014. Estrogen deficiency-induced Ca balance impairment is associated with decrease in expression of epithelial Ca transport proteins in aged female rats. Life Sci. 96, 26–32.

Du, J., Hincke, M.T., Rose-Martel, M., Hennequet-Antier, C., Brionne, A., Cogburn, L.A., Nys, Y., Gautron, J., 2015. Identifying specific proteins involved in eggshell membrane formation using gene expression analysis and bioinformatics. BMC Genom. 16, 792.

Dunn, I.C., Joseph, N., Bain, M., Edmond, A., Wilson, P.W., Milona, P., Nys, Y., Gautron, J., Schmutz, M., Preisinger, R., Waddington, D., 2009a. Polymorphisms in eggshell organic matrix genes are associated with eggshell quality measurements in pedigree Rhode Island Red hens. Anim. Genet. 40, 110–114.

Dunn, I.C., Rodríguez-Navarro, A.B., Mcdade, K., Schmutz, M., Preisinger, R., Waddington, D., Wilson, P.W., Bain, M., 2012. Genetic variation in eggshell crystal size and orientation is large and these traits are correlated with shell thickness and are associated with eggshell matrix protein markers. Anim. Genet. 43 (4), 410–418.

Dunn, I.C., et al., 2020. Lack of genetic correlation between bone quality and egg number in the laying hen suggests increased egg production may not be responsible for reduction in bone quality. Genet. Selection Evol. (in press).

Dunn, I.C., Wilson, P.W., Lu, Z., Bain, M.M., Crossan, C.L., Talbot, R.T., Waddington, D., 2009b. New hypotheses on the function of the avian shell gland derived from microarray analysis comparing tissue from juvenile and sexually mature hens. Gen. Comp. Endocrinol. 163, 225–232.

Erben, R.G., 2018. Physiological actions of fibroblast growth factor-23. Front. Endocrinol. 9, 267.

Eastin, W.C., Spaziani, E., 1978a. On the control of calcium secretion in the avian shell gland (uterus). Biol. Reprod. 19, 493–504.

Eastin, W.C., Spaziani, E., 1978b. On the mechanism of calcium secretion in the avianshell gland (uterus). Biol. Reprod. 505–518.

Enomoto, H., Hendy, G.N., Andrews, G.K., Clemens, T.L., 1992. Regulation of avian calbindin-D28K gene expression in primary chick kidney cells: importance of posttranscriptional mechanisms and calcium ion concentration. Endocrinology 130, 3467–3474.

Felsenfeld, A.J., Barton, S.L., 2015. Calcitonin, the forgotten hormone: does it deserve to be forgotten? Clin. Kidney J. 8, 180–187.

Feng, X., 2009. Chemical and biochemical basis of cell-bone matrix interaction in health and disease. Curr. Chem. Biol. 3 (2), 189–196.

Feng, J., Zhang, H.J., Wu, S.G., Qi G., H., Wang, J., 2020. Uterine transcriptome analysis reveals mRNA expression changes associated with the ultrastructure differences of eggshell in young and aged laying hens. BMC Genomics 21 (1), 770. https://doi.org/10.1186/s12864-020-07177-7.

Fernandez, M.S., Moya, A., Lopez, L., Arias, J.L., 2001. Secretion pattern, ultrastructural localization and function of extracellular matrix molecules involved in eggshell formation. Matrix Biol. 19, 793–803.

Ferrari, S., Bonjour, J.P., Rizzoli, R., 2005. Fibroblast growth factor-23 relationship to dietary phosphate and renal handling in healthy young men. J. Clin. Endocrinol. Metab. 90, 1519–1524.

Fisher, L.W., Schraer, H., 1980. The glycosaminoglycans of estrogen-induced medullarybone in Japanese quail. Arch. Biochem. Biophys. 205, 396–403.

Fleming, R.H., McCormack, H.A., McTeir, L., Whitehead, C.C., 2006. Relationships between genetic, environmental and nutritional factors influencing osteoporosis in laying hens. Br. Poult. Sci. 47, 742–755.

Fraser, D.R., Kodicek, E., 1973. Regulation of 25-hydroxycholecalciferol-1-hydroxylase activity in kidney by parathyroid hormone. Nat. New Biol. 241 (110), 163–166.

Freeman, C.L., Harding, J.H., Quigley, D., Rodger, P.M., 2015. How does an amorphous surface influence molecular binding? Ovocleidin-17 and amorphous calcium carbonate. Phys. Chem. Chem. Phys. 17.

Fujita, H., Sugimoto, K., Inatomi, S., Maeda, T., Osanai, M., Uchiyama, Y., et al., 2008. Tight junction proteins claudin-2 and -12 are critical for vitamin D-dependent Ca2þ absorption between enterocytes. Mol. Biol. Cell 19, 1912–1921.

Fullmer, C.S., Wasserman, R.H., 1987. Chicken intestinal 28-kilodalton calbindin-D: complete amino acid sequence and structural considerations. Proc. Natl. Acad. Sci. U.S.A. 84, 4772–4776.

Garabedian, M., Holick, M.F., Deluca, H.F., Boyle, I.T., 1972. Control of 25-hydroxycholecalciferol metabolism by parathyroid glands. Proc. Natl. Acad. Sci. U.S.A. 69, 1673–1676.

Garcia-Ruiz, J., Rodríguez-Navarro, A., 1994. The mineral structure of the avian eggshell: a case of competitive crystal growth. In: Proceeding of

Fundamental of Biomineralisation. Bulletin de l'Institut Oceanographique (Monaco), pp. 85–94.

Gattineni, J., Bates, C., Twombley, K., Dwarakanath, V., Robinson, M.L., Goetz, R., et al., 2009. FGF23 decreases renal NaPi-2a and NaPi-2c expression and induces hypophosphatemia in vivo predominantly via FGF receptor 1. Am. J. Physiol. Renal. Physiol. 297, F282–F291.

Gautron, J., Bain, M., Solomon, S., Nys, Y., 1996. Soluble matrix of hen's eggshell extracts changes in vitro the rate of calcium carbonate precipitation and crystal morphology. Br. Poult. Sci. 37, 853–866.

Gautron, J., Hincke, M.T., Nys, Y., 1997. Precursor matrix proteins in the uterine fluid change with stages of eggshell formation in hens. Connect. Tissue Res. 36, 195–210.

Gautron, J., Hincke, M.T., Mann, K., Panhéleux, M., Bain, M., McKee, M.D., Solomon, S.E., Nys, Y., 2001a. Ovocalyxin-32, a novel chicken eggshell matrix protein: isolation, amino acid sequencing, cloning and immunocytochemical localization. J. Biol. Chem. 276, 39243–39252.

Gautron, J., Hincke, M.T., Panhéleux, M., Garcia-Ruiz, J.M., Boldicke, T., Nys, Y., 2001b. Ovotransferrin is a matrix protein of the hen eggshell membranes and basal calcified layer. Connect. Tissue Res. 42, 255–267.

Gautron, J., Guyot, N., Brionne, A., Réhault-Godbert, S., 2019. Bioactive egg minor proteins. In: Wu, J. (Ed.), Eggs as Functional Foods and Nutraceuticals for Human Health; Food Chemistry, Function and Analysis, Chap. 14. THE ROYAL SOCIETY OF CHEMISTRY, United Kingdom, pp. 259–284.

Gautron, J., Murayama, E., Vignal, A., Morisson, M., McKee, M.D., Rehault, S., Labas, V., Belghazi, M., Vidal, M.L., Nys, Y., Hincke, M.T., 2007. Cloning of ovocalyxin-36, a novel chicken eggshell protein related to lipopolysaccharide-binding proteins, bactericidal permeability-increasing proteins, and plunc family proteins. J. Biol. Chem. 282, 5273–5286.

Gautron, J., Stapane, L., Le Roy, N., Nys, Y., Rodriguez-Navarro, A.B., Hincke, M.T., 2020. Avian eggshell biomineralization: an update on its structure, mineralogy and protein tool kit. BMC Mater. (in revision).

Ghishan, F., Kiela, P., 2012. Small intestinal ion transport. Curr. Opin. Gastroenterol. 28, 130–134.

Glendenning, P., Ratajczak, T., Prince, R.L., Garamszegi, N., Strehler, E.E., 2000. The promoter region of the human PMCA1 Gene mediates transcriptional downregulation by 1,25-dihydroxyvitamin D3. Biochem. Biophys. Res. Commun. 277, 722–728.

Gloux, A., Le Roy, N., Brionne, A., Bonin, E., Juanchich, A., Benzoni, G., Piketty, M.L., Prié, D., Nys, Y., Gautron, J., Narcy, A., Duclos, M.J., 2019. Candidate genes of the transcellular and paracellular calcium absorption pathways in the small intestine of laying hens. Poult. Sci. 98 (11), 6005–6018.

Gloux, A., Le Roy, N., Ezagal, J., Même, N., Hennequet-Antier, C., Piketty, M.L., Prié, D., Benzoni, G., Gautron, J., Nys, Y., Narcy, A., Duclos, M.J., 2020a. Possible roles of parathyroid hormone, 1.25(OH) 2-D3 and fibroblast growth factor 23 on genes controlling calcium metabolism across different tissues of the laying hen. Domest. Anim. Endocrinol. 72, 106407.

Gloux, A., Le Roy, N., Même, N., Piketty, M.L., Prié, D., Benzoni, G., Gautron, J., Nys, Y., Narcy, A., Duclos, M.J., 2020b. Increased Expression of Fibroblast Growth Factor 23 Is the Signature of a Deteriorated Ca/P Balance in Ageing Laying Hens. Scientific Reports 10. Article number: (in press) 21124.

Goetz, R., Beenken, A., Ibrahimi, O.A., Kalinina, J., Olsen, S.K., Eliseenkova, A.V., et al., 2007. Molecular insights into the Klotho-dependent, endocrine mode of action of fibroblast growth factor 19 subfamily members. Mol. Cell Biol. 27, 3417–3428.

Goetz, R., Ohnishi, M., Ding, X., Kurosu, H., Wang, L., Akiyoshi, J., et al., 2012. Klotho coreceptors inhibit signaling by paracrine fibroblast growth factor 8 subfamily ligands. Mol. Cell Biol. 3, 1944–1954.

Gómez-Morales, J., Falini, G., Garcia-Ruiz, J.M., 2015. Biological crystallization. In: Nishinaga, T. (Ed.), Fundamentals: Thermodynamics and Kinetics, and Transport and Stability. Handbook of Crystal Growth, vol. I. Elsevier, pp. 873–913.

Gu, J.H., Liu, J.D., Shen, Y., Liu, Z.P., 2009. Effects of RANKL, osteoprotegerin, calcium and phosphorous on survival and activation of Muscovy duck osteoclasts in vitro. Vet. J. 181, 321–325.

Guerreiro, P.M., Renfro, J.L., Power, D.M., Canario, A.V., 2007. The parathyroid hormone family of peptides: structure, tissue distribution, regulation, and potential functional roles in calcium and phosphate balance in fish. Am. J. Physiol. Regul. Integr. Comp. Physiol. 292, R679–R696.

Guinotte, F., Gautron, J., Nys, Y., Soumarmon, A., 1995. Calcium solubilization and retention in the gastrointestinal tract in chicks (*Gallus domesticus*) as a function of gastric acid secretion inhibition and of calcium carbonate particle size. Br. J. Nutr. 73, 125–139.

Gunzel, D., Yu, A.S.L., 2013. Claudins and the modulation of tight junction permeability. Physiol. Rev. 93, 525–569.

Hadley, J.A., Horvat-Gordon, M., Kim, W.K., Praul, C.A., Burns, D., Leach, R.M., 2016. Bone sialoprotein keratan sulfate proteoglycan (BSPKSPG) and FGF-23 are important physiological components of medullary bone. Comp. Biochem. Physiol. A Mol. Integr. Physiol. 194, 1–7.

Hamilton, R.M.G., 1986. Food structure the microstructure of the hen' s egg shell -A short review. Food Microstruct. 5, 99–110.

Hannan, F.M., Kallay, E., Chang, W., Brandi, M.L., Thakker, R.V., 2018. Calcium-sensing receptor in physiology and in calcitropic and non-calcitropic diseases. Nat. Rev. Endocrinol. 15 (1), 33–51, 2018.

Hauschka, P.V., Lian, J.B., Cole, D.E., Gundberg, C.M., 1989. Osteocalcin and matrix Gla protein: vitamin K-dependent proteins in bone. Physiol. Rev. 69, 990–1047.

Hernández-Hernández, A., Gómez-Morales, J., Rodríguez-Navarro, A.B., Gautron, J., Nys, Y., García-Ruiz, J.M., 2008a. Identification of some active proteins in the process of hen eggshell formation. Cryst. Growth Des. 8.

Hernandez-Hernandez, A., Vidal, M.L., Gomez-Morales, J., Rodriguez-Navarro, A.B., Labas, V., Gautron, J., Nys, Y., Garcia Ruiz, J.M., 2008b. Influence of eggshell matrix proteins on the precipitation of calcium carbonate ($CaCO_3$). J. Cryst. Growth 8, 4330–4339.

Hincke, M.T., 1995. Ovalbumin is a component of the chicken eggshell matrix. Connect. Tissue Res. 31, 227–233.

Hincke, M.T., Bernard, A.M., Lee, E.R., Tsang, C.P.W., Narbaitz, R., 1992. Soluble protein constituents of the domestic fowls eggshell. Br. Poult. Sci. 33, 505–516.

Hincke, M.T., Chien, Y.C., Gerstenfeld, L.C., McKee, M.D., 2008. Colloidal-gold immunocytochemical localization of osteopontin in avian eggshell gland and eggshell. J. Histochem. Cytochem. 56, 467–476.

Hincke, M.T., Gautron, J., Tsang, C.P., McKee, M.D., Nys, Y., 1999. Molecular cloning and ultrastructural localization of the core protein

of an eggshell matrix proteoglycan, ovocleidin-116. J. Biol. Chem. 274, 32915–32923.

Hincke, M.T., Gautron, J., Panheleux, M., Garcia-Ruiz, J.M., McKee, M.D., Nys, Y., 2000. Identification and localization of lysozyme as a component of the eggshell membranes and shell matrix. Matrix Biol. 19, 443–453.

Hincke, M.T., Nys, Y., Gautron, J., Mann, K., Rodriguez-Navarro, B., McKee, M.D., 2012. The eggshell: structure, composition and mineralization. Front. Biosci. 17, 1266–1280.

Hincke, M.T., Tsang, C.P., Courtney, M., Hill, V., Narbaitz, R., 1995. Purification and immunochemistry of a soluble matrix protein of the chicken eggshell (ovocleidin 17). Calcif. Tissue Int. 56, 578–583.

Hodges, R.D., Lörcher, K., 1967. Possible sources of the carbonate fraction of egg shell calcium carbonate. Nature 216, 609–610.

Holzer, P., 2011. Transient receptor potential (TRP) channels as drug targets for diseases of the digestive system. Pharmacol. Ther. 131 (1), 142–170.

Huber, K., Zeller, E., Rodehutscord, M., 2015. Modulation of small intestinal phosphate transporter by dietary supplements of mineral phosphorus and phytase in broilers. Poult. Sci. 94, 1009–1017.

Hudson, H.A., Britton, W.M., Rowland, G.N., Buhr, R.J., 1993. Histomorphometric bone properties of sexually immature and mature White Leghorn hens with evaluation of fluorochrome injection on egg production traits. Poult. Sci. 72, 1537–1547.

Hunter, S.J., Schraer, H., 1983. In vitro synthesis of proteoglycans associated with medullary bone in Japanese quail. Arch. Biochem. Biophys. 220 (1), 272–279.

Hurwitz, S., 1989a. Calcium homeostasis in birds. Vit. Horm. 45, 173–221 (Juan).

Hurwitz, S., 1989b. Parathyroid hormone. In: Pang, P.K.T., Schreibman, M.P. (Eds.), Vertebrate Endocrinology: Fundamentals and Biomedical Implications, vol. 3. Academic Press, New York, pp. 45–77.

Hurwitz, S., Bar, A., 1965. Absorption of calcium and phosphorus along the gastrointestinal tract of the laying fowl as influenced by dietary calcium and egg shell formation. J. Nutr. 86, 433–438.

Hurwitz, S., Bar, A., 1966. Rate of passage of calcium-45 and Yttrium-91 along the intestine, and calcium absorption in the laying fowl. J. Nutr. 89, 311–316.

Ieda, T., Saito, N., Ono, T., Shimada, K., 1995. Effects of presence of an egg and calcium deposition in the shell gland on levels of messenger ribonucleic acid of CaBP-D28K and of vitamin D3 receptor in the shell gland of the laying hen. Gen. Comp. Endocrinol. 99, 145–151.

Ishida, M., Amano, S., 2004. Osteocalcin fragment in bone matrix enhances osteoclast maturation at a late stage of osteoclast differentiation. J. Bone Miner. Metab. 22, 415–429.

Isola, J.J., 1990. Distribution of estrogen and progesterone receptors and steroid-regulated gene products in the chick oviduct. Mol. Cell. Endocrinol. 69, 235–243.

Jimenez-Lopez, C., Rodriguez-Navarro, A., Dominguez-Vera, J.M., Garcia-Ruiz, J.M., 2003. Influence of lysozyme on the precipitation of calcium carbonate: a kinetic and morphologic study. Geochem. Cosmochim. Acta 67, 1667–1676.

Jande, S.S., Tolnai, S., Lawson, D.E., 1981. Immunohistochemical localization of vitamin D-dependent calcium-binding protein in duodenum, kidney, uterus and cerebellum of chickens. Histochemistry 71, 99–116.

Jiang, R.S., Xie, Z., Chen, X.Y., Geng, Z.Y., 2010. A single nucleotide polymorphism in the parathyroid hormone gene and effects on eggshell quality in chickens. Poult. Sci. 89, 2101–2105.

Johnson, A.L., Whittow, G.C., 2000. Reproduction in the Female. Sturkie's Avian Physiology, fifth ed. Academic Press, San Diego.

Jonchere, V., Rehault-Godbert, S., Hennequet-Antier, C., Cabau, C., Sibut, V., Cogburn, L.A., Nys, Y., Gautron, J., 2010. Gene expression profiling to identify eggshell proteins involved in physical defense of the chicken egg. BMC Genom. 11 (57).

Jonchère, V., Brionne, A., Gautron, J., Nys, Y., 2012. Identification of uterine ion transporters for mineralisation precursors of the avian eggshell. BMC Physiol. 12, 10.

Juanchich, A., Hennequet-Antier, C., Cabau, C., Le Bihan-Duval, E., Duclos, M.J., Mignon-Grasteau, S., Narcy, A., 2018. Functional genomics of the digestive tract in broilers. BMC Genom. 19, 1–9.

Jüppner, H.W., Gardella, T.J., Brown, E.M., et al., 2000. Parathyroid hormone and parathyroid hormone-related peptide in the regulation of calcium homeostasis and bone development. In: DeGroot, L.L., Jameson, J.L. (Eds.), Endocrinology, vol. 2. Elsevier. 4, Philadelphia, pp. 969–998.

Khan, S., Wu, S.B., Roberts, J., 2019. RNA-sequencing analysis of shell gland shows differences in gene expression profile at two time-points of eggshell formation in laying chickens. BMC Genom. 20, 89.

Kenny, A.D., 1986. Parathyroid and ultimobranchial glands. In: Sturkie, P.D. (Ed.), Avian Physiology, fourth ed. Springer-Verlag, New York, pp. 466–478.

Kenny, A.D., Dacke, C.G., 1974. The hypercalcaemic response to parathyroidhormone in Japanese quail. J. Endocrinol. 62, 15–23.

Kerschnitzki, M., Zander, T., Zaslansky, P., Fratzl, P., Shahar, R., Wagermaier, W., 2014. Rapid alterations of avian medullary bone material during the daily egg-laying cycle. Bone 69, 109–117.

Ko, S.H., Lee, G.S., Vo, T.T., Jung, E.M., Choi, K.C., Cheung, K.W., et al., 2009. Dietary calcium and 1,25-dihydroxyvitamin D3 regulate transcription of calcium transporter genes in calbindin-D9k knockout mice. J. Reprod. Dev. 55, 137–142.

Kodali, V.K., Gannon, S.A., Sivakumar, P., Sonali, R., Polenova, T., Thorpe, C., 2011. A novel disulfide-rich protein motif from avian eggshell membranes. PLoS One 6.

Kuscu, C., Parlak, M., Tufan, T., et al., 2017. CRISPR-STOP: gene silencing through base-editing-induced nonsense mutations. Nat Methods 14, 710–712.

Lakshminarayanan, R., Kini, R.M., Valiyaveettil, S., 2002. Investigation of the role of ansocalcin in the biomineralization in goose eggshell matrix. Proc. Natl. Acad. Sci. U.S.A. 99, 5155–5159.

Lakshminarayanan, R., Valiyaveetil, S., Rao, V.S., Kini, R.M., 2003. Purification, characterization, and in vitro mineralization studies of a novel goose eggshell matrix protein, ansocalcin. J. Biol. Chem. 278.

Lakshminarayanan, R., Loh, X.J., Gayathri, S., Sindhu, S., Banerjee, Y., Kini, R.M., Valiyaveettil, S., 2006. Formation of transient amorphous calcium carbonate precursor in quail eggshell mineralization: an in vitro study. Biomacromolecules 7, 3202–3209.

Le Roy, N., Combes-Soia, L., Brionne, A., Labas, V., Rodriguez-Navarro, A., Hincke, M., Nys, Y., Gautron, J., 2019. Guinea fowl eggshell quantitative proteomics yield new findings related to its unique structural characteristics and superior mechanical properties. J. Proteomics 103511.

Lavelin, I., Yarden, N., BenBassat, S., Bar, A., Pines, M., 1998. Regulation of osteopontin gene expression during egg shell formation in the laying hen by mechanical strain. Matrix Biol. 17, 615–623.

Lavelin, I., Meiri, N., Einat, M., Genina, O., Pines, M., 2002. Mechanical strain regulation of the chicken glypican-4 gene expression in the avian eggshell gland. J. Physiol. Regul. Integr. Comp. Physiol 283, R853–R861.

Lavelin, I., Meiri, N., Genina, O., Alexiev, R., Pines, M., 2001. Na+-K+-ATPase gene expression in the avian eggshell gland: distinct regulation in different cell types. Am. J. Physiol. Regul. Integr. Comp. Physiol. 281, R1169–R1176.

Lee, C.M., Dimaline, R., Moore, S., Vowles, L., Dockray, G.J., 1988. Reciprocal endocrine interactions between proventriculus and antrum in chicken. Regul. Pept. 22, 415–419.

Lee, S.M., Riley, E.M., Meyer, M.B., Benkusky, N.A, Plum, L.A., Deluca, H.F, Pike, W., 2015. 1,25-Dihydroxyvitamin D3 controls a cohort of vitamin D receptor target genes in the proximal intestine that is enriched for calcium-regulating components. JBC 290 (29), 18199–18215.

Li, Q., Zhao, X., Wang, S., Zhou, Z., 2018. Letrozole induced low estrogen levels affected the expressions of duodenal and renal calcium-processing gene in laying hens. Gen. Comp. Endocrinol. 255, 49–55.

Lian, J.B., Stein, G.S., 1992. Transcriptional control of vitamin D-regulated proteins. J. Cell. Biochem. 49, 37–45.

Liao, Q.S., Du, Q., Lou, J., Xu, J.Y., Xie, R., 2019. Roles of Na^{+}/Ca^{2+} exchanger 1 in digestive system physiology and pathophysiology. World J. Gastroenterol. 25 (3), 287–299.

Lim, S.-K., Gardella, T., Thompson, A., Rosenberg, J., Keutmann, H., Potts Jr., J., Kronenberg, H., Nussbaum, S., 1991. Full-length chicken parathyroid hormone. J. Biol. Chem. 266, 3709–3714.

Liu, S., Quarles, L.D., 2007. How fibroblast growth factor 23 works. J. Am. Soc. Nephrol. 18, 1637–1647.

Liu, W., Li, D., Liu, J., Chen, S., Qu, L., Zheng, J., Xu, G., Yang, N., 2011. A genome-wide SNP scan reveals novel loci for egg production and quality traits in white leghorn and brown-egg dwarf layers. PLoS One 6.

Lörcher, J., Newesely, H., 1969. Calcium carbonate (calcite) as a separate phase besides calcium phosphate apatite in medullary bone of laying hens. Calcif. Tissue Res. 3, 358–362.

Lörcher, K., Zscheile, C., Bronsch, K., 1970. Rate of CO2 and C14 exhalation in laying hens resting and during egg shell mineralization after a single injection of $NaHC1_4O_3$. An. Biol. Anim., Bioch., Biophys. 10, 133–139.

Mann, K., 2015. The calcified eggshell matrix proteome of a songbird, the zebra finch (*Taeniopygia guttata*). Proteome Sci. 13, 29.

Mann, K., Gautron, J., Nys, Y., McKee, M.D., Bajari, T., Schneider, W.J., Hincke, M.T., 2003. Disulfide-linked heterodimeric clusterin is a component of the chicken eggshell matrix and egg white. Matrix Biol. 22, 397–407.

Mann, K., Maček, B., Olsen, J.V., 2006. Proteomic analysis of the acid-soluble organic matrix of the chicken calcified eggshell layer. Proteomics 6, 3801–3810.

Mann, K., Mann, M., 2013. The proteome of the calcified layer organic matrix of Turkey (*Meleagris gallopavo*) eggshell. Proteome Sci. 11.

Mann, K., Mann, M., 2015. Proteomic analysis of quail calcified eggshell matrix: a comparison to chicken and Turkey eggshell proteomes. Proteome Sci. 13.

Mann, K., Siedler, F., 2004. Ostrich (*Struthio camelus*) eggshell matrix contains two different C-type lectin-like proteins. Isolation, amino acid sequence, and posttranslational modifications. Biochim. Biophys. Acta 1696, 41–50.

Mann, K., Siedler, F., 2006. Amino acid sequences and phosphorylation sites of emu and rhea eggshell C-type lectin-like proteins. Comp. Biochem. Physiol. B Biochem. Mol. Biol. 143, 160–170.

Marie, P., Labas, V., Brionne, A., Harichaux, G., Hennequet-Antier, C., Nys, Y., Gautron, J., 2015a. Quantitative proteomics and bioinformatic analysis provide new insight into protein function during avian eggshell biomineralization. J. Proteomics 113, 178–193.

Marie, P., Labas, V., Brionne, A., Harichaux, G., Hennequet-Antier, C., Rodríguez-Navarro, A.B., Nys, Y., Gautron, J., 2015b. Quantitative proteomics provides new insights into chicken eggshell matrix protein functions during the primary events of mineralisation and the active calcification phase. J. Proteomics 126, 140–154.

Martin, A., David, V., Quarles, L.D., 2012. Regulation and function of the FGF23/Klotho endocrine pathways. Physiol. Rev. 92, 131–155.

Mayel-Afshar, S., Lane, S.M., Lawson, D.E.M., 1988. Relationship between the levels of calbindin synthesis and calbindin mRNA in chick intestine. Quantitation of calbindin mRNA. J. Biol. Chem. 263, 4355–4361.

Melancon, M.J., DeLuca, H.F., 1970. Vitamin D stimulation of calcium-dependent adenosine triphosphatase in chick intestinal brush borders. Biochemistry 9, 1658–1664.

Miller, S.C., Bowman, B.M., 1981. Medullary bone osteogenesis following estrogen administration to mature male Japanese quail. Dev. Biol. 87, 52–63.

Mongin, P., 1976. Composition of crop and gizzard contents in the laying hen. Br. Poult. Sci. 17, 499–502.

Mongin, P., 1978. Acid-Base Balance during Eggshell Formation. Respiratory Function in Birds, Adult and Embryonic, pp. 247–259.

Mongin, P., Sauveur, B., 1970. Composition du fluide utérin et de l'albumen durant le séjour de l'oeuf dans l'utérus chez la poule domestique. C R Acad. Sci. (Paris), série D 270D, 1715–1718.

Mongin, P., Sauveur, B., 1974. Voluntary food and calcium intake by the laying hen. Br. Poult. Sci. 15, 349–359.

Mongin, P., Sauveur, B., 1979. The specific appetite of domestic fowl. In: Boorman, K.N., Freeman, B.M. (Eds.), Food Intake Regulation in Poutry. Br. Poult. Sci., Edinburgh, pp. 171–189.

Montecuccoli, G., Hurwitz, S., Cohen, A., Bar, A., 1977. The role of 25-hydroxycholecalciferol-1-hydroxylase in the responses of calcium absorption to the reproductive activity in birds. Comp. Biochem. Physiol. A Physiol. 57, 335–339.

Moriuchi, S., Deluca, H.F., 1974. Metabolism of vitamin D3 in the chick embryo. Arch. Biochem. Biophys. 164, 165–171.

Murali, S.K., Roschger, P., Zeitz, U., Klaushofer, K., Andrukhova, O., Erben, R.G., 2016. FGF23 regulates bone mineralization in a 1,25(OH) D and Klotho-independent manner. J. Bone Miner. Res. 31, 129–142.

Nakada, T., Koja, Z., Tokashiki, S., 1976. Influence of ovulation and gonadal hormones on shell formation in the domestic fowl. Jpn. Poult. Sci. 13, 169–174.

Nakashima, T., Hayashi, M., Takayanagi, H., 2012. New insights into osteoclastogenic mechanisms. Trends Endocrin. Met. 23, 582–590.

Naot, D., Musson, D.S., Cornish, J., 2019. The activity of peptides of the calcitonin family in bone. Physiol. Rev. 99, 781–805.

Navickis, R.J., Katzenellenbogen, B.S., Nalbandov, A.V., 1979. Effects of the sex steroid hormones and vitamin D3 on calcium-binding proteins in the chick shell gland. Biol. Reprod. 21, 1153–1162.

Neel, A.E., Aljabo, A., Strange, A., Ibrahim, S., Coathup, M., Young, A., Bozec, L., Mudera, V., 2016. Demineralization-remineralization dynamics in teeth and bone. Int. J. Nanomed. 11, 4743–4763.

Nijenhuis, T., Hoenderop, J.G.J., Bindels, R.J.M., 2005. TRPV5 and TRPV6 in Ca^{2+} (re)absorption: regulating Ca^{2+} entry at the gate. Pflugers Arch. Eur. J. Physiol. 451, 181–192.

Noda, M., Vogel, R.L., Craig, A.M., Prahl, J., DeLuca, H.F., Denhardt, D.T., 1990. Identification of a DNA sequence responsible for binding of the 1,25-dihydroxyvitamin D3 receptor and 1,25-dihydroxyvitamin D3 enhancement of mouse secreted phosphoprotein 1 (SPP-1 or osteopontin) gene expression. Proc. Natl. Acad. Sci. U.S.A. 87, 9995–9999.

Nys, Y., 1987. Progesterone and testosterone elicit increases in the duration of shell formation in domestic hens. Br. Poult. Sci. 28, 57–68.

Nys, Y., 1993. Regulation of 1,25(OH)2D3, of osteocalcin and of intestinal and uterine calbindin in hens. In: Sharp, P.J. (Ed.), Avian Endocrinology. Journal of endocrinology ltd, Bristol, UK, pp. 345–358.

Nys, Y., 2017. Laying hen nutrition: optimizing hen performance and health, bone and eggshell quality. In: Roberts, J. (Ed.), Achieving Sustainable Production of Eggs, vol. 2. Burleigh Dodds Science Publishing, pp. 29–56. Chap.2.

Nys, Y., Baker, K., Bouillon, R., Van Baelen, H., Lawson, D.E.M., 1992a. Regulation of calbindin D 28K and its mRNA in the intestine of the domestic hen. Gen. Comp. Endocrinol. 86, 460–468.

Nys, Y., Baker, K., Lawson, D.E.M., 1992b. Estrogen and a calcium flux dependent factor modulate the calbindin gene expression in the uterus of laying hens. Gen. Comp. Endocrinol. 87, 87–94.

Nys, Y., Bouillon, R., Van Baelen, H., Williams, J., 1986a. Ontogeny and oestradiol dependence of vitamin D-binding protein blood levels in chickens. J. Endocrinol. 108, 81–87.

Nys, Y., de Laage, X., 1984. Effects of suppression of eggshell calcification and of 1,25(OH)2D3 on Mg^{2+}, Ca^{2+} and $Mg^{2+}HCO^{3-}$ ATPase, alkaline phosphatase, carbonic anhydrase and CaBP levels–II. The laying hen intestine. Comp. Biochem. Physiol. A. Comp. Physiol. 78, 839–844.

Nys, Y., Gautron, J., Garcia-Ruiz, J.M., Hincke, M.T., 2004. Avian eggshell mineralization: biochemical and functional characterization of matrix proteins. CR Palevol. 3, 549–562.

Nys, Y., Gautron, J., McKee, M.D., Garcia-Ruiz, J.M., Hincke, M.T., 2001. Biochemical and functional characterization of eggshell matrix proteins in hens. Worlds Poul. Sci. J. 57, 401–413.

Nys, Y., Guyot, N., 2011. Egg formation and chemistry. In: Nys, Y., Bain, M., Van Imerseel, F. (Eds.), Improving the Safety and Quality of Egg Products. Woodhead publishing in food science, technology and nutrition, Cambridge, UK, pp. 83–132.

Nys, Y., Hincke, M.T., Arias, J.L., Garcia-Ruiz, J.M., Solomon, S.E., 1999. Avian eggshell mineralization. Poult. Avian Biol. Rev. 10, 143–166.

Nys, Y., Le Roy, N., 2018. Calcium Homeostasis and Eggshell biomineralization in female chicken. In: Feldman, D., Wesley Pike, J., Bouillon, R., Giovannucci, E., Goltzman, D., Hewison, M. (Eds.), Vitamin D, Volume 1: Biochemistry, Physiology and Diagnostics, fourth ed. Elsevier Inc, pp. 361–378.

Nys, Y., Mayel-Afshar, S., Bouillon, R., Van Baelen, H., Lawson, D.E.M., 1989. Increases in calbindin D 28K mRNA in the uterus of the domestic fowl induced by sexual maturity and shell formation. Gen. Comp. Endocrinol. 76, 322–329.

Nys, Y., N'Guyen, T.M., Williams, J., Etches, R.J., 1986b. Blood levels of ionized calcium, inorganic phosphorus, 1,25-dihydroxycholecalciferol and gonadal hormones in hens laying hard-shelled or shell-less eggs. J. Endocrinol. 111, 151–157.

Nys, Y., Zawadzki, J., Gautron, J., Mills, A., 1991. Whitening of brown-shelled eggs: mineral composition of uterine fluid and rate of protoporphyrin deposition. Poult. Sci. 70, 1236–1245.

Ohashi, T., Kusuhara, S., Ishida, K., 1991. Immunoelectron microscopic demonstration of estrogen receptors in osteogenic cells of Japanese quail. Histochemistry 96, 41–44.

Oursler, M.J., Landers, J.P., Riggs, B.J., Spelsberg, T.C., 1993. Oestrogen effects on osteoblasts and osteoclasts. Ann. Med. 25, 361–371.

Panheleux, M., Bain, M., Fernandez, M.S., Morales, I., Gautron, J., Arias, J.L., Solomon, S.E., Hincke, M., Nys, Y., 1999. Organic matrix composition and ultrastructure of eggshell: a comparative study. Br. Poult. Sci. 40, 240–252.

Panheleux, M., Nys, Y., Williams, J., Gautron, J., Boldicke, T., Hincke, M.T., 2000. Extraction and quantification by ELISA of eggshell organic matrix proteins (ovocleidin-17, ovalbumin, ovotransferrin) in shell from young and old hens. Poult. Sci. 79, 580–588.

Park, J.A., Sohn, S.H., 2018. The influence of hen aging on eggshell ultrastructure and shell mineral components. Korean J. Food Sci. Anim. Resour. 38, 1080–1091.

Parra-Torres, A.Y., Valdés-Flores, M., Orozco, L., Velázquez-Cruz, R., 2013. Molecular aspects of bone remodeling. InteckOpen. https://doi.org/10.5772/54905.

Pearson, T.W., Goldner, A.M., Calcium transport across avian uterus. I, 1973. Effects of electrolyte substitution. Am. J. Physiol. 225, 1508–1512.

Pearson, T.W., Goldner, A.M., Calcium transport across avian uterus II, 1974. Effects of inhibitors and nitrogen. Am. J. Physiol. 227, 465–468.

Pike, J.W., Haussler, M.R., 1979. Purification of chicken intestinal receptor for1,25-dihydrosyvitamin D. Proc. Natl. Acad. Sci. U.S.A. 76, 5485–5489.

Pike, J.W., Lee, S.M., Meyer, M.B., 2014. Regulation of gene expression by 1,25-dihydroxyvitamin D3 in bone cells: exploiting new approaches and defining new mechanisms. Bonekey Rep. 3, 482.

Pines, M., Knopov, V., Bar, A., 1995. Involvement of osteopontin in egg shell formation in the laying chicken. Matrix Biol. 14, 765–771.

Pinheiro, P.L., Cardoso, J.C., Gomes, A.S., Fuentes, J., Power, D.M., Canário, A.V., 2010. Gene structure, transcripts and calciotropic effects of the PTH family of peptides in Xenopus and chicken. BMC Evol. Biol. 10, 373.

Pipich, V., Balz, M., Wolf, S.E., Tremel, W., Schwahn, D., 2008. Nucleation and growth of $CaCO_3$ mediated by the egg-white protein ovalbumin: a time-resolved in situ study using small-angle neutron scattering. J. Am. Chem. Soc. 130.

Politi, Y., Metzler, R.A., Abrecht, M., Gilbert, B., Wilt, F.H., Sagi, I., Addadi, L., Weiner, S., Gilbert, P.U.P.A., 2008. Transformation mechanism of amorphous calcium carbonate into calcite in the sea urchin larval spicule. Proc. Natl. Acad. Sci. U.S.A. 105, 17362–17366.

Potts, J.T., 2005. Parathyroid hormone: past and present. J. Endocrinol. 187, 311–325.

Price, P.A., 1985. Vitamin-K-dependent formation of bone Gla protein (osteocalcin) and its function. Vit. Horm. Adv. Res. Appl. 42, 65–108.

Proszkowiec-Weglarz, M., Angel, R., 2013. Calcium and phosphorus metabolism in broilers: effect of homeostatic mechanism on calcium and phosphorus digestibility. J. Appl. Poult. Res. 22, 609–627.

Proszkowiec-Weglarz, M., Schreier, L.L., Miska, K.B., Angel, R., Kahl, S., Russell, B., 2019. Effect of early neonatal development and delayed feeding post-hatch on jejunal and ileal calcium and phosphorus transporter genes expression in broiler chickens. Poult. Sci. 1, 1–11.

Réhault-Godbert, S., Guyot, N., Nys, Y., 2019. The golden egg: nutritional value, bioactivities, and emerging benefits for human health. Nutrients 11, 684.

Ren, Z., Ebrahimi, M., Butz, D.E., Sand, J.M., Zhang, K., Cook, M.E., 2017. Antibody to fibroblast growth factor 23-peptide reduces excreta phosphorus of laying hens. Poult. Sci 96, 127–134.

Ren, Z.Z., Piepenburg, A.J., Butz, D.E., Claus, J.R., Cook, M.E., 2018. Vaccine to fibroblast growth factor 23 peptides increases eggshell strength. Poult. Sci. 97, 882–889.

Ren, Z., Sun, W., Liu, Y., Li, Z., Han, D., Cheng, X., Yan, J., Yang, X., 2019. Dynamics of serum phosphorus, calcium, and hormones during egg laying. Poult. Sci. 98, 2193–2200.

Replogle, R.A., Li, Q., Wang, L., Zhang, M., Fleet, J.C., 2014. Gene-by-diet interactions influence calcium absorption and bone density in mice. J. Bone Miner. Res. 29, 657–665.

Reyes-Grajeda, J.P., Moreno, A., Romero, A., 2004. Crystal structure of ovocleidin-17, a major protein of the calcified *Gallus gallus* eggshell - implications in the calcite mineral growth pattern. J. Biol. Chem. 279, 40876–40881.

Roberts, J.R., Chousalkar, K., Samiullah, 2013. Egg quality and age of laying hens: implications for product safety. Anim. Prod. Sci. 53, 1291–1297.

Rodriguez-Navarro, A., Kalin, O., Nys, Y., Garcia-Ruiz, J.M., 2002. Influence of the microstructure on the shell strength of eggs laid by hens of different ages. Br. Poult. Sci. 43, 395–403.

Rodríguez-Navarro, A.B., Marie, P., Nys, Y., Hincke, M.T., Gautron, J., 2015. Amorphous calcium carbonate controls avian eggshell mineralization: a new paradigm for understanding rapid eggshell calcification. J. Struct. Biol. 190, 291–303.

Rodrõguez-Navarro, A.B., McCormack, H.M., Fleming, R.H., Alvarez-Lloret, P., Romero-Pastor, J., Domõnguez Gasca, N., Prozorov, T., Dunn, I., 2018. Influence of physical activity on tibial bone material properties in laying hens. J. Struct. Biol. 201, 36–45.

Rodriguez-Navarro, A.B., Yebra, A., Nys, Y., Jimenez-Lopez, C., Garcia-Ruiz, J.M., 2007. Analysis of avian eggshell microstructure using X-ray area detectors. Eur. J. Mineral 19, 391–398.

Rome, H., Le Roy, P., 2016. Chromosomal regions influencing egg production and egg quality traits in hens. Inra Prod. Anim. 29 (2), 117–127.

Ruoff, H.J., Sewing, K.F., 1971. The role of crop in the control of gastric acid secretion in chickens. Naunyn-Schmiedeberg's Archiv. Pharm. 271, 142–148.

Sauveur, B., Reviers, M.D., 1988. Reproduction and egg production in poultry. Reproduction des volailles et production d'œufs, p. 449.

Sauveur, B., Mongin, P., 1971. Comparative study of uterine fluid and egg albumen in shell gland of hen. An. Biol. Anim. Bioch. Biophys. 11, 213–221.

Sauveur, B., Mongin, P., 1983. Plasma inorganic phosphorus concentration during eggshell formation. II. Inverse relationships with intestinal calcium content and eggshell weight. Reprod. Nutr. Dévelop. 23 (4), 755–764.

Sah, N., Lee Kuehu, D., Singh Khada, V., Deng, Y., Peplowska, K., Jha, R., Mishra, B., 2018. RNA sequencing-based analysis of the laying hen uterus revealed the novel genes and biological pathways involved in the eggshell biomineralization. Sci. Rep. 8, 16853.

Sasaki, O., Odawara, S., Takahashi, H., Nirasawa, K., Oyamada, Y., Yamamoto, R., Ishii, K., Nagamine, Y., Takeda, H., Kobayashi, E., Furukawa, T., 2004. Genetic mapping of quantitative trait loci affecting body weight, egg character and egg production in F2 intercross chickens. Anim. Genet. 35, 188–194.

Schräder, M., Bendik, I., Becker-André, M., Carlberg, C., 1993. Interaction between retinoic acid and vitamin D signaling pathways. J. Biol. Chem. 268, 17830–17836.

Schwahn, D., Balz, M., Tremel, W., 2004. Crystallization of the CaCO(3) mineral in the presence of the protein ovalbumin. Phys. B Condens. Matter 350, E947–E949.

Sharp, R.M., Silyn-Roberts, H., 1984. Development of preferred orientation in the eggshell of the domestic fowl. Biophys. J. 46, 175–179.

Shimada, T., Hasegawa, H./, Yamazaki, Y., Muto, T., Hino, R., Takeuchi, Y., et al., 2004. FGF-23 is a potent regulator of vitamin D metabolism and phosphate homeo-stasis. J. Bone Miner. Res. 19, 429–435.

Shimada, T., Kakitani, M., Yamazaki, Y., Hasegawa, H., Takeuchi, Y., Fujita, T., et al., 2004. Targeted ablation of Fgf23 demonstrates an essential physiological role of FGF23 in phosphate and vitamin D metabolism. J. Clin. Invest. 113, 561–568.

Silyn-Robert, H., Sharp, R.M., 1986. Crystal growth and the role of the organic network in eggshell biomineralization. Proceed. Royal Soc. London B227, 303–324.

Simkiss, K., 1967. Calcium in Reproductive Physiology: A Comparative Study of Vertebrates. Reinhold Pub. Corp, London: Chapman & Hall; New York.

Singh, R., Joyner, C.J., Peddie, M.J., Taylor, T.G., 1986. Changes in the concentrations of parathyroid hormone and ionic calcium in the plasma of laying hens during the egg cycle in relation to dietary deficiencies of calcium and vitamin D. Gen. Comp. Endocrinol. 61, 20–28.

Squire, M.E., Veglia, M.K., Drucker, K.A., Brazeal, K.R., Hahn, T.P., Watts, H.E., 2017. Estrogen levels influence medullary bone quantity and density in female house finches and pine siskins. Gen. Comp. Endocrinol. 246, 249–257.

Solomon, S., 1991. In Egg and Eggshell Quality. Wolfe publishing ltd, London, UK.

Spanos, E., Brown, D.J., MacIntyre, I., 1979. Regulation of 25-OHD3 metabolism by parathyroid hormone in primary chick kidney cell cultures. FEBS Lett. 105, 31–34.

Spanos, E., Pike, J.W., Haussler, M.R., Colston, K.W., Evans, I.M.A., Goldner, A.M., McCain, T.A., MacIntyre, I., 1976. Circulating 1α,25-dihydroxyvitamin D in the chicken: enhancement by injection of prolactin and during egg laying. Life Sci. 19, 1751–1756.

Stafford, N., Wilson, C., Oceand, y D., Neyses, L., Cartwright, E.J., 2017. The plasma membrane calcium ATPases and their role as major new players in human disease. Physiol. Rev. 97, 1089–1125.

Staines, K.A., MacRae, V.E., Farquharson, C., 2012. The importance of the SIBLING family of proteins on skeletal mineralisation and bone remodeling. J. Endocrinol. 214, 241l–255.

Stapane, L., Le Roy, N., Hincke, M.T., Gautron, J., 2019. The glycoproteins EDIL3 and MFGE8 regulate vesicle-mediated eggshell calcification in a new model for avian biomineralization. J. Biol. Chem. 294 (40), 14526–14545.

Stapane, L., Le Roy, N., Ezagal, J., Rodriguez-Navarro, A.B., Labas, V., Combes-Soia, L., Hincke, M.T., Gautron, J., 2020. Avian eggshell formation reveals a new paradigm for vertebrate mineralization via vesicular amorphous calcium carbonate. J. Biol. Chem. https://doi.org/10.1074/jbc.RA1120.014542. In press.

Striem, S., Bar, A., 1991. Modulation of quail intestinal and egg shell gland calbindin (Mr 28,000) gene expression by vitamin D3, 1,25-dihydroxyvitamin D3 and egg laying. Mol. Cell. Endocrinol. 75, 169–177.

Sugiyama, T., Kikuchi, H., Hiyama, S., Nishizawa, K., Kusuhara, S., 2007. Expression and localisation of calbindin D28k in all intestinal segments of the laying hen. Br. Poult. Sci. 48, 233–238.

Sugiyama, T., Kusuhara, S., 1994. Effect of parathyroid hormone on osteoclasts in organ-cultured medullary bone. Jpn. Poult. Sci. 31, 392–399.

Takahashi, K., Akiba, Y., Jensen, L., 1983. Effects of dietary-fat and cellulose on liver and plasma-lipid, and plasma estradiol in laying hens. Poult. Sci. 62, 1510.

Takahashi, H., Sasaki, O., Nirasawa, K., Furukawa, T., 2010. Association between ovocalyxin-32 gene haplotypes and eggshell quality traits in an F-2 intercross between two chicken lines divergently selected for eggshell strength. Anim. Genet. 41, 541–544.

Takahashi, N., Shinki, T., Abe, E., Horiuchi, N., Yamaguchi, A., Yoshiki, S., Suda, T., 1983. The role of vitamin D in the medullary bone formation in egg-laying Japanese quail and in immature male chicks treated with sex hormones. Calcif. Tissue Int. 35, 465–471.

Takahashi, H., Yang, D., Sasaki, O., Furukawa, T., Nirasawa, K., 2009. Mapping of quantitative trait loci affecting eggshell quality on chromosome 9 in an F-2 intercross between two chicken lines divergently selected for eggshell strength. Anim. Genet. 40 (5), 779–782.

Tanaka, Y., Castillo, L., Wineland, M.J., DeLuca, H.F., 1978. Synergistic effect of progesterone, testosterone, and estradiol in the stimulation of chick renal 25- hydroxyvitamin D3-1α-hydroxylase. Endocrinology 103, 2035–2039.

Taylor, T.G., Moore, J.H., 1954. Skeletal depletion in hens laying on a low calcium diet. Br. J. Nut. 8, 112–124.

Teitelbaum, S.L., 2000. Bone resorption by osteoclasts. Science 9 (5484), 1504–1508.

Theofan, G., Nguyen, A.P., Norman, A.W., 1986. Regulation of calbindin-D28K gene expression by 1,25-dihydroxyvitamin D3 is correlated to receptor occupancy. J. Biol. Chem. 261, 16943–1647.

Trechsel, U., Bonjour, J.P., Fleisch, H., 1979. Regulation of the metabolism of 25-hydroxyvitamin D3 in primary cultures of chick kidney cells. J. Clin. Invest. 64, 206–217.

Tuiskula-Haavisto, M., Honkatukia, M., Preisinger, R., Schmutz, M., de Koning, D.J., Wei, W.H., Vilkki, J., 2011. Quantitative trait loci affecting eggshell traits in an F-2 population. Anim. Genet. 42, 293–299.

Urakawa, I., Yamazaki, Y., Shimada, T., Iijima, K., Hasegawa, H., Okawa, K., et al., 2006. Klotho converts canonical FGF receptor into a specific receptor for FGF23. Nature 444, 770–774.

van de Velde, J.P., Loveridge, N., Vermeiden, J.P.W., 1984a. Parathyroid hormone responses to calcium stress during eggshell calcification. Endocrinology 115, 1901–1904.

van de Velde, J., Vermeiden, J.P., Touw, J.J., Veldhuijzen, J., 1984b. Changes in activity of chicken medullary bone cell populations in relation to the egg-laying cycle. Metab. Bone Dis. Relat. Res. 5, 191–193.

van de Velde, J.P., Vermeiden, J.P., Bloot, A.M., 1985. Medullary bone matrix, formation, mineralization, and remodeling related to the daily egg-laying cycle of Japanese quail: a histological and radiological study. Bone 6, 321–327.

Van Cromphaut, S.J., Rummens, K., Stockmans, I., Van Herck, E., Dijcks, F.A., Ederveen, A.G., Carmeliet, P., Verhaeghe, J., Bouillon, R., Carmeliet, G., 2003. Intestinal calcium transporter genes are upregulated by estrogens and the reproductive cycle through vitamin D receptor-independent mechanisms. J. Bone Miner. Res. 18, 1725–1736.

Van Itallie, C.M., Anderson, J.M., 2014. Architecture of tight junctions and principles of 652 molecular composition. Semin. Cell Dev. Biol. 2 (36), 157–165.

Voinescu, A.E., Touraud, D., Lecker, A., Pfitzner, A., Kunz, W., Ninham, B.W., 2007. Mineralization of $CaCO_3$ in the presence of egg white lysozyme. Langmuir 23, 12269–12274.

Wang, X., Ford, B.C., Praul, C.A., Leach, R.M., 2002. Collagen X expression in oviduct tissue during the different stages of the egg laying cycle. Poult. Sci. 81, 805–808.

Wang, X., Ford, B.C., Praul, C.A., Leach Jr., R.M., 2005. Characterization of the noncollagenous proteins in avian cortical and medullary bone. Comp. Biochem. Physiol. B Biochem. Mol. Biol. 140, 665–672.

Wang, X., Kong, R., Pan, X., Xu, H., Xia, D., Shan, H., Lu, J.R., 2009. Role of ovalbumin in the stabilization of metastable vaterite in calcium carbonate biomineralization. J. Phys. Chem. B 113, 8975–8982.

Wang, X.Q., Wu, C.M., Tao, K., Zhao, K., Wang, J.Q., Xu, H., Xia, D.H., Shan, H.H., Lu, J.R., 2010. Influence of ovalbumin on CaCO(3) precipitation during in vitro biomineralization. J. Phys. Chem. B 114, 5301–5308.

Wang, R.M., Zhao, J.P., Wang, X.J., Jiao, H.C., Wu, J.M., Lin, H., 2018. Fibroblast growth factor 23 mRNA expression profile in chickens and its response to dietary phosphorus. Poultry Sci. 97, 258–2266.

Wasserman, R.H., 2004. Vitamin D and the dual processes of intestinal calcium absorption. J. Nutr. 134, 3137–3139.

Wasserman, R.H., Chandler, J.S., Meyer, S.A., Smith, C.A., Brindak, M.E., Fullmer, C.S., Penniston, J.T., Kumar, R., 1992. Intestinal calcium transportand calcium extrusion processes at the basolateral membrane. J. Nutr. 122, 662–671.

Wasserman, R.H., Taylor, A.N., 1966. Vitamin D3-induced calcium-binding protein in chick intestinal mucosa. Science 152, 791–793.

Wasserman, R.H., Taylor, A.N., 1968. Vitamin D-dependent calcium-binding protein. Response to some physiological and nutritional variables. J. Biol. Chem. 243, 3987–3993.

Wasserman, R.H., Smith, C.A., Smith, C.M., Brindak, M.E., Fullmer, C.S., Krook, L., Penniston, J.T., Kumar, R., 1991. Immunohistochemical localization of a calcium pump and calbindin-D28k in the oviduct of the laying hen. Histochemistry 96, 413–418.

Weber, G.M., 2009. Vitamin Requirements and Economic Responses. 17th Eur Symp Poult Nutr 2009/08/23-27. WPSA, Edinburgh, UK. S3.2.

Weber, K., Erben, R.G., Rump, A., Adamski, J., 2001. Gene structure and regulation of the murine epithelial calcium channels ECaC1 and 2. Biochem. Biophys. Res. Commun. 289, 1287−1294.

White, K.E., Evans, W.E., O'Riordan, J.L.H., Speer, M.C., Econs, M.J., Lorenz-Depiereux, B., Grabowski, M., Meitinger, T., Strom, T.M., 2000. Autosomal dominant hypophosphataemic rickets is associated with mutations in FGF23. Nat. Genet. 26 (3), 345−348.

Whitehead, C.C., 2004. Overview of bone biology in the egg-laying hen. Poult. Sci. 83, 193−199.

Whitehead, C.C., 1986. Requirements for vitamins. In: Proceeding Symposium Poultry Science 19, Butterworth ed., pp. 173−189.

Wideman, R., Satnick, J., Mitsos, W., Bennett, K., Smith, S., 1987. Effect of saline adaptation and renal portal sodium infusion on glomerular size distributions and kidney function in domestic fowl. Poult. Sci. 66, 348−356.

Wolc, A., Arango, J., Jankowski, T., Dunn, I., Settar, P., Fulton, J.E., O'Sullivan, N.P., Preisinger, R., Fernando, R.L., Garrick, D.J., Dekkers, J.C., 2014. Genome-wide association study for egg production and quality in layer chickens. J. Anim. Breed. Genet. 131, 173−182.

Wolf, S., Leiterer, J., Pipich, V., Barrea, R., Emmerling, F., Tremel, W., 2011. Strong stabilization of liquid amorphous calcium carbonate by ovalbumin: gaining insight into the mechanism of 'polymer-induced liquid precursor' processes. J Am Chem Soc. 133 (32), 12642−12649. https://doi.org/10.1021/ja202622g.

Wong, M., Hendrix, M.J.C., Von der Mark, K., Little, C., Stern, R., 1984. Collagen in the egg shell membranes of the hen. Dev. Biol. 104, 28−36.

Xie, J., Guo, J., Kanwal, Z., Wu, M., Lv, X., Ibrahim, N.A., Li, P., Buabeid, M.A., Arafa, E.A., Sun, Q., 2020. Calcitonin and bone physiology: in vitro, in vivo, and clinical investigations. Hindawi Int. J. Endocrinol. 2020, 20. https://doi.org/10.1155/2020/3236828. Article ID 3236828.

Yang, R., Geng, F., Huang, X., Qiu, N., Li, S.G., Teng, H., Chen, L., Song, H.B., Huang, Q., 2020. Integrated proteomic, phosphoproteomic and N-glycoproteomic analyses of chicken eggshell matrix. Food Chem. 330.

Yang, J.H., Hou, J.F., Farquharson, C., Zhou, Z.L., Deng, Y.F., Wang, L., Yu, Y., 2011. Localisation and expression of TRPV6 in all intestinal segments and kidney of laying hens. Br. Poult. Sci. 52, 507−516.

Yang, J.H., Zhao, Z.H., Hou, J.F., Zhou, Z.L., Deng, Y.F., Dai, J.J., 2013. Expression of TRPV6 and CaBP-D28k in the egg shell gland (uterus) during the oviposition cycle of the laying hen. Br. Poult. Sci. 54, 398−406.

Yao, J.F., Chen, Z.X., Xu, G.Y., Wang, X.L., Ning, Z.H., Zheng, J.X., Qu, L.J., Yang, N., 2010. Low-density lipoprotein receptor-related protein 8 gene association with egg traits in dwarf chickens. Poult. Sci. 89, 883−886.

Yarden, N., Lavelin, I., Genina, O., Hurwitz, S., Diaz, R., Brown, E.M., Pines, M., 2000. Expression of calcium-sensing receptor gene by avian parathyroid gland in vivo: relationship to plasma calcium. Gen. Comp. Endocrinol. 117, 173−181.

Yasuda, H., Shim, a N., Nakagawa, N., Yamaguch, i K., Kinosaki, M., Mochizuki, S.I., et al., 1998. Osteoclast differentiation factor is a ligand for osteoprotegeriny osteoclastogenesis inhibitory factor and is identical to RANCE/RANKL. Proc. Natl. Acad. Sci. U.S.A. 95 (7), 3597−3602.

Yosefi, S., Braw-Tal, R., Bar, A., 2003. Intestinal and eggshell calbindin and bone ash as influenced by age of the laying hen and molting. Comp. Biochem. Physiol. A 136, 673−682.

Yoshida, T., Fujimori, T., Nabeshima, Y., 2002. Mediation of unusually high concentrations of 1,25-dihydroxyvitamin D in homozygous Klotho mutant mice by increased expression of renal 1alpha-hydroxylase gene. Endocrinology 143, 683−9.

Zambonin-Zallone, A., Mueller, W.J., 1969. Medullary bone of laying hens during calcium depletion and repletion. Calcif. Tissue Res. 4, 136−146.

Zeisel, M., Dhawan, P., Baumert, T., 2019. Tight junction proteins in gastrointestinal and liver disease. Gut 68 (3), 547−561.

Zhang, Q., Liu, L., Zhu, F., Ning, Z., Hincke, M.T., Yang, N., 2014. Integrating de novo transcriptome916 assembly and cloning to obtain chicken ovocleidin-17 full-length cDNA. PLoS One 917, 9.

Zhang, J., Wang, Y., Zhang, C., Xiong, M., Rajput, S.A., Liu, Y., Qi, D., 2019. The differences of gonadal hormones and uterine transcriptome during shell calcification of hens laying hard or weak shelled eggs. BMC Genom. 20, 707.

Zhang, J., Wang, Y., Wang, X., Sun, L., Rajput, S.A., Qi, D., 2020. The paradoxical effects of progesterone on the eggshell quality of laying hens. J. Struct. Biol. 209 (2020), 107430.

Zhang, Q., Zhu, F., Liu, L, Zheng, C.W., Wang, D.H., Hou, Z.C., et al., 2015. Integrating Transcriptome and Genome Re-Sequencing Data to Identify Key Genes and Mutations Affecting Chicken Eggshell Qualities. PLoS ONE 10(5), e0125890. https://doi.org/10.1371/.

Zheng, J., 2013. Molecular mechanism of TRP channels. Compr. Physiol. 3 (1), 221−242.

Zhu, X.L., Sly, W.S., 1990. Carbonic anhydrase IV from human lung. J. Biol. Chem. 265, 8795−8801.

Zhu, F., Zhang, F., Hincke, M., Yin, Z.-T., Chen, S.-R., Yang, N., Hou, Z.-C., 2019. iTRAQ-based quantitative proteomic analysis of duck eggshell during biomineralization. Proteomics 19.

Zihni, C., Mills, C., Matter, K., Balda, M.S., 2016. Tight junctions: from simple barriers to multifunctional molecular gates. Nat. Rev. Mol. Cell Biol. 17, 564−580.

Further reading

Bloom, M.A., Domm, L.V., Nalbandov, A.V., Bloom, W., 1958. Medullary bone of laying chickens. Am. J. Anat. 102, 411−453.

Bloom, W., Bloom, M.A., McLean, F.C., 1941. Calcification and ossification. Medullary bone changes in the reproductive cycle of female pigeons. Anat. Rec. 81, 443−475.

Bonewald, L.F., 2011. The amazing osteocyte. J. Bone Miner. Res. 6 (2), 229−238.

Bouillon, R., Van Cromphaut, S., Carmeliet, G., 2003. Intestinal calcium absorption: molecular vitamin D mediated mechanisms. J. Cell. Biochem. 88, 332−339.

Bouillon, R., Suda, T., 2014. Vitamin D: calcium and bone homeostasis during evolution. Bonekey Rep. 3, 1−10.

Chandler, M.J., Osdoby, P., Pyfferoen, J., Riggs, B.L., Spelsberg, T.C., 1991. Avian osteoclasts as estrogen target cells. Proc. Natl. Acad. Sci. U.S.A. 88, 6613−6617.

Coty, W.A., Mc Conkey, C.L., 1982. A high-affinity calcium-stimulated ATPase activity in the hen oviduct shell gland. Arch. Biochem. Biophys. 219, 444–453.

Fernandez, M.S., Passalacqua, K., Arias, J.I., Arias, J.L., 2004. Partial biomimetic reconstitution of avian eggshell formation. J. Struct. Biol. 148, 1–10.

Freeman, C.L., Harding, J.H., Quigley, D., Rodger, P.M., 2010. Structural control of crystal nuclei by an eggshell protein. Angew. Chem. Int. Ed. 49, 5135–5137.

Fullmer, C.S., Brindak, M.E., Bar, A., Wasserman, R.H., 1976. The purification of calcium-binding protein from the uterus of the laying hen. Exp. Biol. Med. 152, 237–241.

Habener, J.F., 1990. MINIREVIEW: cyclic AMP response element binding proteins: a cornucopia of transcription factors. Mol. Endocrinol. 4, 1087–1094.

Hodor, P.G., Ettensohn, C.A., 1998. The dynamics and regulation of mesenchymal cell fusion in the sea urchin embryo. Dev. Biol. 199, 111–124.

Holmes, R.S., 1977. Purification, molecular properties and ontogeny of carbonic anhydrase isozymes. Evidence for A, B and C Isozymes in avian and mammalian tissues. Eur. J. Biochem. 78, 511–520.

Khanal, R.C., Nemere, I., 2008. Regulation of intestinal calcium transport. Annu. Rev. Nutr. 28, 179–196.

Khosla, S., 2001. Minireview: the OPG/RANKL/RANK system. Endocrinology 142, 5050–5055.

Lippiello, L., Wasserman, R.H., 1975. Fluorescent antibody localization of the vitamin D-dependent calcium-binding protein in the oviduct of the laying hen. J. Histochem. Cytochem. 23, 111–116.

Mann, K., Olsen, J.V., Macek, B., Gnad, F., Mann, M., 2007. Phosphoproteins of the chicken eggshell calcified layer. Proteomics 7, 106–115.

Prashad, D., Edwards, N., 1973. Renal excretion of calcium, phosphate and magnesium in laying fowl. In: 4th European Poultry Conference. World's Poultry Science Journal, London, UK, p. 52.

Quarles, L.D., 2012. Role of FGF23 in vitamin D and phosphate metabolism: implications in chronic kidney disease. Exp. Cell Res. 318, 1040–1048.

Quélo, I., Kahlen, J.-P., Rascle, A., Jurdic, P., Carlberg, C., 1994. Identification and characterization of a vitamin D 3 response element of chicken carbonic anhydrase-II. DNA Cell Biol. 13, 1181–1187.

Rachner, T.D., Khosla, S., Hofbauer, C., 2011. Osteoporosis: now and the future. Lancet 377, 1276–1287.

Rodriguez-Navarro, A., Garcia-Ruiz, J.M., 2000. Model of textural development of layered crystal aggregates. Eur. J. Mineral 12, 609–614.

Rowe, P.S.N., 2012. The chicken or the egg: PHEX, FGF23 and SIBLINGs unscrambled. Cell Biochem. Funct. 30, 355–375.

Sun, C., Duan, Z., Qu, L., Zheng, J., Yang, N., Xu, G., 2016. Expression analysis for candidate genes associated with eggshell mechanical property. J. Integr. Agri. 15, 397–402.

Taylor, T.G., Belanger, L.F., 1969. The mechanism of bone resorption in laying hens. Calcif. Tissue Res. 4, 162–173.

Wilkinson, S.J., Selle, P.H., Bedford, M.R., Cowieso, A.J., 2011. Exploiting calcium-specific appetite in poultry nutrition. World's Poult. Sci. J. 67, 587–598.

Chapter 33

Adrenals

Rocco V. Carsia

Department of Cell Biology and Neuroscience, Rowan University School of Osteopathic Medicine, Stratford, NJ, United States

33.1 Anatomy

33.1.1 Gross anatomy, blood supply, and innervation

The paired adrenal glands are located anterior and medial to the cephalic lobes of the kidneys (Figure 33.1). They are generally flat and lie close together and are closely applied to the dorsal aorta and posterior vena cava (caudal vena cava; postcava). In the domestic chicken (*Gallus gallus*) and the African ostrich (*Struthio camelus*), the glands differ in shape in that the right gland is more triangular in shape and the left more oblong (Tang et al., 2009; Humayun et al., 2012; Moawad and Randa, 2017). The glands receive direct arterial blood supply from the cranial renal arteries and occasionally from the aorta. Each gland is drained by a single adrenal vein which enters the posterior (caudal) vena cava or its caudal bifurcation. In the chicken, each gland also receives one or two lymphatic vessels.

The gland is enclosed in a highly vascularized but extremely friable connective tissue capsule (Chester Jones and Phillips, 1986). Each gland generally has two postganglionic sympathetic ganglia (cranial and caudal), embedded within the pericapsular sheath or more deeply within the outer gland substance (discussed in Section 33.1.2.3).

33.1.2 Microanatomy

33.1.2.1 The chromaffin tissue

The adrenal gland of birds consists of what appears to be an intermingling of steroid-secreting cells (adrenocortical cells) and chromaffin (adrenomedullary) cells (Figure 33.2). The arrangement of the adrenocortical cells (Figure 33.2) is described later. The chromaffin cells are larger, polygonal cells arranged in nests or clusters surrounded by a thin basal lamina. A single nerve bundle innervates the cluster such that one neuronal terminal forms synapses with up to three chromaffin cells of the same type, i.e., norepinephrine (NE) or epinephrine (E) chromaffin cells (Unsicker, 1973). The consensus of studies suggests

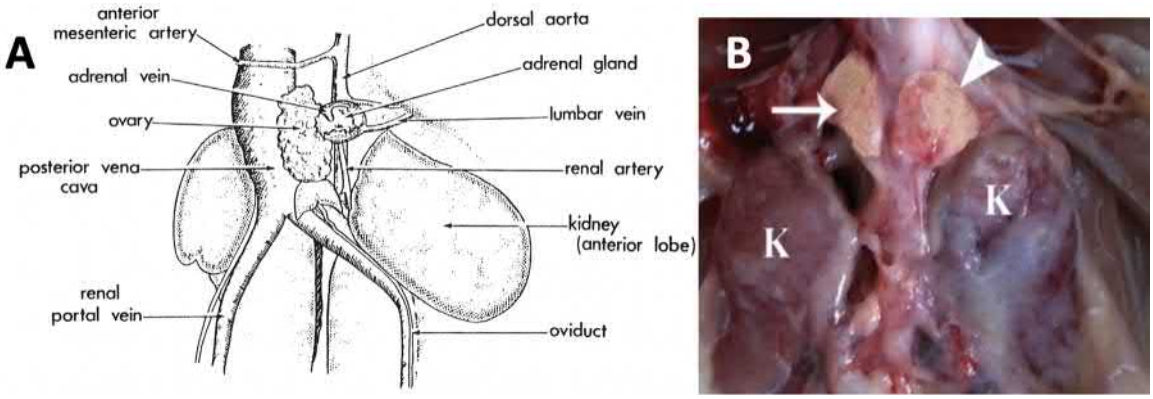

FIGURE 33.1 (A) The position of the left adrenal gland and its vascular supply in the female gull (*Larus argentatus*). (Preparation and drawing by I. Carthy and J. G. Phillips.) . (B) Ventral view of the adrenal glands of the domestic chicken (*Gallus gallus*). K, anterior lobes of the kidneys; *Arrow*, right adrenal gland; *Arrowhead*, left adrenal gland. Note the more triangular shape of the right adrenal gland. *Taken from (A) Holmes and Phillips (1976), (B) Moawad and Randa (2017).*

Sturkie's Avian Physiology. https://doi.org/10.1016/B978-0-12-819770-7.00014-1

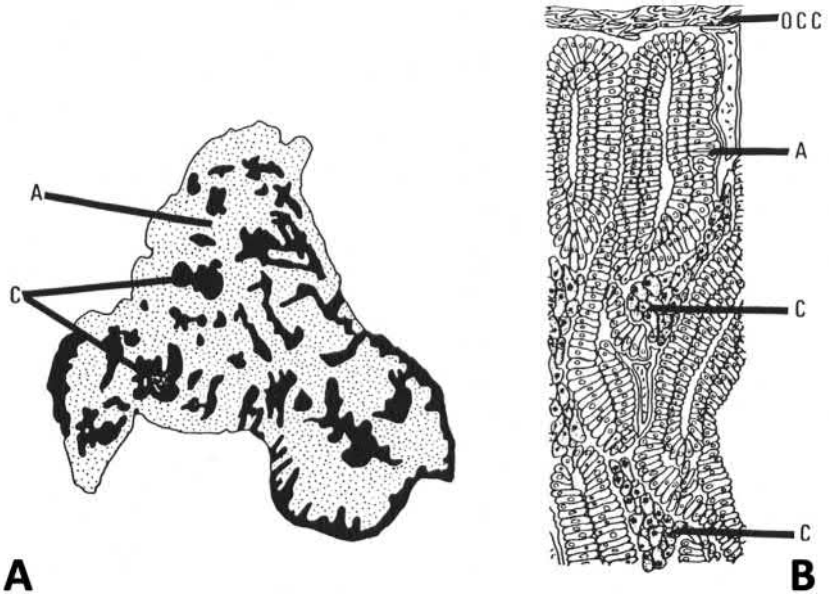

FIGURE 33.2 Microanatomy of a typical avian adrenal gland (Florida quail, *Colinus virginiatus floridanus*). (A) Distribution of chromaffin (C) and adrenocortical (A) tissues; (B) Structure of the looped cords of adrenocortical cells with intermingled chromaffin cell islets. The outer connective tissue (adrenal capsule) is also indicated (OCC). *Taken from Chester Jones and Phillips (1986).*

that the overall ratio of adrenocortical to chromaffin cells is about 1.5:1, and a similar ratio has been demonstrated in dispersed chicken adrenal cells (Carsia et al., 1985a).

The ratio of E- to NE-secreting chromaffin cells varies with species and age within a species. There is some suggestion that the ratio is smaller, i.e., greater proportion of NE cells, in orders with more primitive ancestry and greater in more recently evolved birds (Ghosh et al., 2001; Humayun et al., 2010). In the domestic chicken, about 70% of the chromaffin cells are E-secreting cells (Ohmori, 1998).

33.1.2.2 The adrenocortical tissue

The adrenocortical cells are arranged in cords consisting of a double row of adrenocortical cells oriented with their columnar axes perpendicular to the cord and with their basal side facing sinusoids (Holmes and Phillips, 1976). At the periphery of the gland, the cords form tighter loops, almost basket-like cells that in many species resemble the glomerular structure (zona glomerulosa) seen in mammals (Figure 33.2). More centrally the cords are long and interlacing.

The preponderance of histological, ultrastructural, and functional evidence indicates that birds have a modest segregation of adrenocortical cell subpopulations that resembles the zonation of the mammalian adrenal cortex (Bhattacharyya et al., 1972; Pierce et al., 1978; Holmes and Cronshaw, 1984, 1993). Histological preparations reveal at least two different zones of cells: a subcapsular zone (SCZ) and an inner zone (IZ). In the chicken, there is a fairly continuous subcapsular layer of essentially pure chromaffin cells outside the SCZ (Humayun et al., 2012; Moawad and Randa, 2017) (see Figures 33.3 and 33.4).

Adrenocortical cells of the SCZ are large and replete with lipid droplets. Like most steroid-secreting cells, they have the troika of organelles: stores of lipid, mainly in lipid droplets, varying amounts of smooth endoplasmic reticulum and mitochondria. The mitochondria bear regularly arranged tubular cristae, similar to mammalian zona glomerulosa cells. Functionally, the tissue secretes predominantly aldosterone in response to adrenocorticotropin (ACTH) and exclusively aldosterone in response to angiotensin II (Ang II) and is insensitive to ACTH withdrawal (adenohypophysectomy) (Klingbeil, 1985; Pierce et al., 1978; Holmes and Cronshaw, 1984, 1993).

Adrenocortical cells of the IZ are smaller, more elongated or columnar, contain fewer lipid droplets (Figures 33.3 and 33.4), have more abundant smooth endoplasmic reticulum and have mitochondria-bearing tubulovesicular cristae, similar to mammalian zona fasciculata cells. Functionally, the tissue secretes predominantly corticosterone in response to ACTH is refractory to Ang II and undergoes atrophy with ACTH withdrawal (adenohypophysectomy) with some cells converting to the SCZ-type (Klingbeil, 1985; Pierce et al., 1978; Holmes and Cronshaw, 1984, 1993).

The relationship of the SCZ with the IZ is not readily apparent due to the interspersed CC islets which at points "force" the IZ cords in and out of a plane of section and

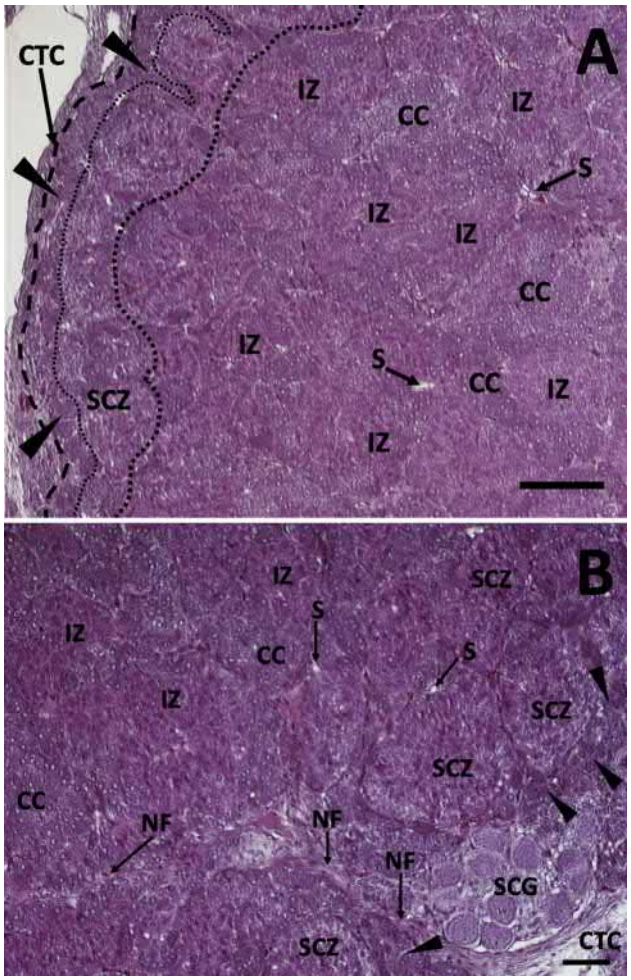

FIGURE 33.3 Light micrographs of portions of coronal sections through the right adrenal gland of the immature (2 weeks old) domestic chicken (*Gallus gallus*) (Moyer's broiler strain) (hematoxylin and eosin stain). (A) Note the zonation of the adrenal gland. There is an outer subcapsular zone (SCZ) consisting of basket-like cords of large, lipid-laden adrenocortical cells, with an outer layer of basophilic chromaffin cells (*arrowheads*) just under the connective tissue capsule (CTC). The inner zone (IZ) adrenocortical cells consists of tightly packed, eosinophilic cords with interspersed islets of lightly basophilic chromaffin-cell islets (CC). The nuclei of the chromaffin cells are conspicuously clear whereas those of the IZ cells are homogeneously granular and eosinophilic. Sinusoids (S) are seen between cords and chromaffin cell islets when cut in cross-section and also as narrow, blood-cell-containing channels squeezed between adrenocortical cords and chromaffin-cell islets. (B) Higher magnification of the SCZ and IZ adrenocortical cells and an embedded, subcapsular ganglion (SCG). The outer layer of basophilic chromaffin cells (*arrowheads*) is interrupted by the SCG and the streaming nerve fibers (NF) in relation to the SCG. Bars = 100 μM. *Histological preparations and micrographs provided by Renee M. Demarest, Ph.D., Department of Molecular Biology, Department of Cell Biology and Neuroscience, and the Histopathology Program of the Graduate School of Biomedical Sciences, Rowan University School of Osteopathic Medicine.*

disrupting a visible continuity. Nevertheless, it seems likely that the adrenocortical cords are formed by a continuously streaming lineage of cells: starting from putative capsular and/or subcapsular stem cell populations, or perhaps even within the SCZ, then moving to the more mature SCZ compartment , and then finally to the IZ. Cell-tracing and other molecular studies are currently underway to test this supposition (Chen-Che Jeff Huang, DVM, PhD; personal communication).

Additional evidence for a segregation or zonation of avian adrenocortical tissue comes from work with dispersed adrenocortical cells from the domestic turkey (*Meleagris gallopavo*) subjected to dietary Na^+ restriction and in which functionally distinct cell subpopulations were segregated based on density (Kocsis et al., 1995a). A population of high-density cells, the proportion of which was increased by the Na^+ restriction, showed a disproportionately enhanced aldosterone response to Ang II and K^+.

33.1.2.3 Extrinsic and intrinsic adrenal innervation

Preganglionic sympathetic fibers in thoracic and synsacral splanchnic nerves converge on the ganglia. However, the preponderance of the fibers (cholinergic) course through the ganglia without synapsing and penetrate the gland substance to innervate clusters of adrenal chromaffin cells. Indeed, preganglionic denervation leads to atrophy of the chromaffin tissue (Holmes and Phillips, 1976). Postganglionic sympathetic fibers emanating from the ganglia mainly innervate adrenal blood vessels (vasomotor), and the adrenergic type innervate the chromaffin cells (Ghosh et al., 2001).

The preponderance of ganglion cells is catecholaminergic, however, there appears to be noncatecholaminergic cells as well (Arcamone et al., 2006). Neuronal endings, ganglion cells, and the chromaffin cells elaborate a number of biogenic amines and neuropeptides, and the adrenal tissues exhibit a robust expression of cognate receptors. An incomplete list of biogenic amines and neuropeptides includes neuronal nitric oxide synthase (nNOS), vasoactive intestinal peptide (VIP), pituitary adenylyl cyclase-activating peptide (PACAP), neuropeptide tyrosine (NPY), galanine, atrial natriuretic peptide (ANP), substance P, and calcitonin gene-related peptide (CGRP). Moreover, the avian adrenal chromaffin cells have an intrinsic corticotropin-releasing hormone (CRH)/melanocortin system and the requisite cognate receptors (Takeuchi and Takahashi, 1998, 1999; Takeuchi et al., 1998, 1999, 2000; De Groef et al., 2004; Mirabella et al., 2004). Current thinking is that the intrinsic and extrinsic neuronal endings, the embedded ganglia, the scattered intraglandular ganglion cells, and the chromaffin cells form the intraadrenal regulation. Furthermore, this intraadrenal system is replete with neurotrophic factors and their cognate receptors (Arcamone et al., 2006). Indeed, many of the factors listed above have been shown to affect

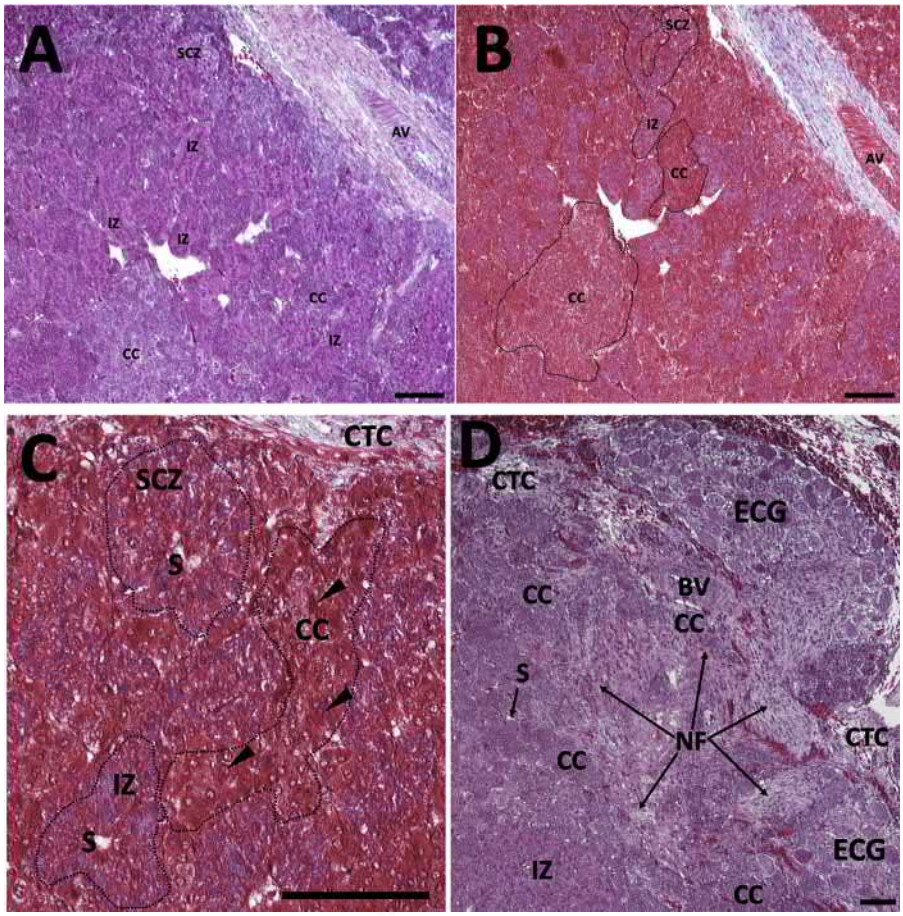

FIGURE 33.4 Light micrographs of portions of sections through the adrenal glands of the immature (2 weeks old) domestic chicken (*Gallus gallus*) (Moyer's broiler strain). (A and B) Coronal sections of the right adrenal gland to include the central adrenal vein (AV). (A) Section stained with hematoxylin and eosin and showing features mentioned in Figure 33.3; *CC*, chromaffin-cell islet; *IZ*, inner zone adrenocortical cells; *SCZ*, subcapsular zone adrenocortical cells. (B) Consecutive section prepared with Masson's trichrome stain. Adrenocortical cell cords show blueish nuclear and perinuclear staining, whereas chromaffin cells show varying intensity of reddish staining. A frequent observation is the continuity of the SCZ with the IZ (*outlined*). Note that the larger CC islet (*outlined*) has many central cells staining with less intensity compared with the CC islet (*outlined*) contiguous with surrounding IZ cords. (C) Higher power of a section demonstrating the differential staining with the Masson's trichrome stain between adrenocortical cell cords (SCZ and IZ outlined) and interspersed CC islets (*outlined*). *Arrowheads* point to some intensely staining chromaffin cells, likely epinephrine-secreting cells, whereas the paler-staining cells are likely norepinephrine-secreting cells. *CTC*, connective tissue capsule. (D) Parasagittal section through left adrenal gland stained with hematoxylin and eosin. Two extracapsular ganglia (ECG) are shown with large neurons, ~70 μM, with different staining intensities, probably a reflection of different functions. The ECG and nerve fibers (NF) coursing in relation to the interior of the ganglia and also penetrating into the gland disrupt the connective tissue capsule (CTC). Conspicuously absent in immediate relation to the ganglia are adrenocortical cell cords. CC islets are in close relationship to the ECG. *BV*, blood vessel. Note that in several sections the sinusoids (*S*) are conspicuous. Bars = 100 μM. *Histological preparations and micrographs provided by Renee M. Demarest, Ph.D., Department of Molecular Biology, Department of Cell Biology and Neuroscience, and the Histopathology Program of the Graduate School of Biomedical Sciences, Rowan University School of Osteopathic Medicine.*

steroid and catecholamine secretion in vitro. However, it is obvious that the role of this regulation appears to be modest, given the drastic effects of hypophysectomy (Carsia et al., 1985c). The main role of the intraadrenal regulation may be to remodel the adrenal tissues, that is, to alter the proportions of chromaffin and steroid-secreting cell subtypes to meet changing physiological needs dictated by life-history-cycle/stage requirements and long-term stress events. A proposed scheme of such an intra-adrenal regulation is shown in Figure 33.5.

33.2 Adrenocortical hormones

33.2.1 Corticosteroid secretory products

The glucocorticoid, corticosterone, is the principal corticosteroid released by the avian adrenal gland. The principle mineralocorticoid, aldosterone, is produced in considerably less quantity in the posthatch bird. In-vitro studies with anseriform and galliform adrenal tissues and dispersed adrenal cells indicate that the ratio of aldosterone to corticosterone production rates is about 1:19. However, based

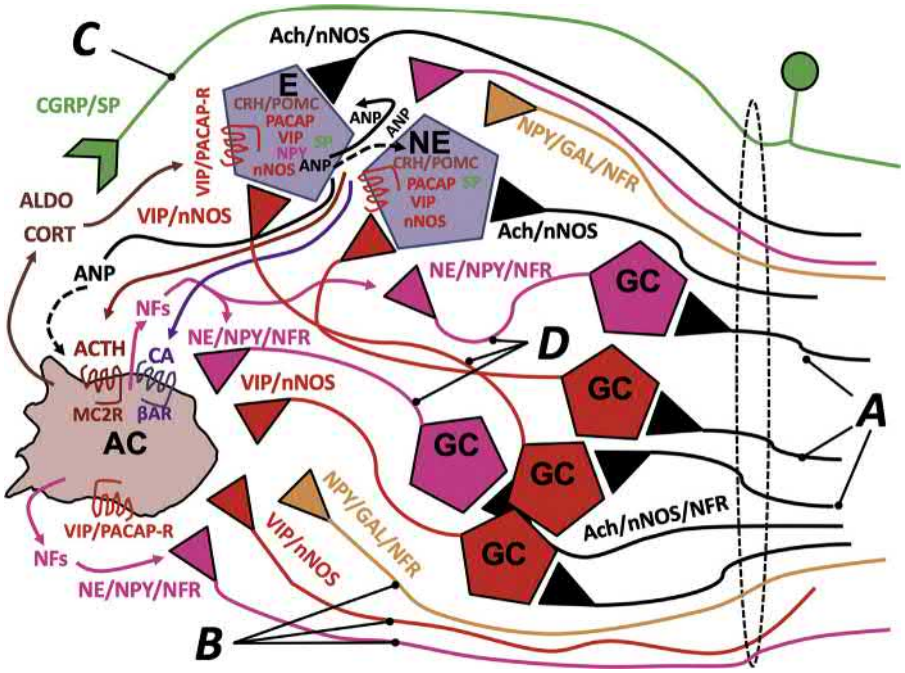

FIGURE 33.5 A proposed model for the intraadrenal neuroendocrine regulation based on comparative studies of reptiles, birds, and mammals. In birds, this model may operate with wide species differences. The neural regulation has both extrinsic and intrinsic components of the sympathetic nervous system. Its axonic terminals are represented by *black and colored triangles*. The extrinsic innervation is composed of (A), preganglionic sympathetic efferent axons containing acetylcholine (Ach) and neuronal nitric oxide synthase (nNOS) (*black*), (B), postganglionic sympathetic efferent axons containing vasoactive intestinal peptide (VIP) and nNOS (*red*), or neuropeptide tyrosine (NPY) and galanine (GAL) (*orange*), or NPY and norepinephrine (NE) (*pink*), and (C), sympathetic afferent (sensory) peripheral processes (dendrites) containing substance P (SP) and calcitonin gene-related peptide (CGRP) (*green*). *Dotted oval* represents the splanchnic nerve bundle which contains these extrinsic fibers. The intraadrenal innervation (D) is composed of the postganglionic sympathetic ganglion cells (GCs, *smaller colored pentagons*) of the cranial and caudal ganglia, embedded ganglia and the scattered GCs throughout the gland. A GC contains VIP and nNOS (*red*) or NPY and NE (*pink*). There is evidence that in some species, GCs also have phenylethanolamine N-methyltransferase for the synthesis of epinephrine (E), but it is not clear if this enzyme is active or if E is released from axonic terminals. Both preganglionic and postganglionic axons probably express neurotrophic factor receptors for axonal growth. Neurotrophic factors are probably elaborated by GCs, chromaffin cells, and adrenocortical cells and thereby in a feedback loop regulate the growth and function of presynaptic axons. For example, growth of NPY axons is stimulated by neurotrophic factors released by adrenocortical cells. Thus, many axonic terminals have cognate receptors for these neurotrophic factors (NFR). This neurotrophic loop probably remodels both the adrenocortical and chromaffin tissues during life-history cycle/stage transitions and periods of prolonged stress. The intrinsic endocrine component consists of the chromaffin cells (*larger purple pentagons*) and the adrenocortical cells (ACs). The chromaffin cells are also modifications of postganglionic sympathetic neurons and are of two functional types: E-secreting cells and NE-secreting cells. These cells also have the enzymatic machinery for an intrinsic corticotropin-releasing hormone (CRH)/adrenocorticotropin (ACTH) system in that they contain and process pro-opiomelanocortin. They also contain many neurotransmitters: pituitary adenylyl cyclase-activating peptide (PACAP), VIP, SP, and the nitric oxide-producing enzyme, nNOS. In addition, the E cells contain atrial natriuretic peptide (ANP). The intraadrenal ACTH interacts with melanocortin 2 (ACTH) receptors (MC2R) on ACs to stimulated corticosteroid [corticosterone (CORT) and aldosterone (ALDO)] synthesis and secretion (*brown arrows*). The intraadrenal CORT, in turn, stimulates E production. Whereas the intraadrenal ANP dampens corticosteroid production in ACs and inhibits NE cell function (*dotted black arrows*), it may stimulate the conversion of NE cells to E cells (*solid black curved arrow*). Both adrenocortical and chromaffin cells have VIP/PACAP receptors (VIP/PACAP-R). In general, activation of these receptors stimulates corticosteroid and catecholamine production. Furthermore, intraadrenal catecholamines interact with β-adrenergic receptors on ACs to augment corticosteroid production. SP from sensory endings stimulates ACs to produce corticosterone and aldosterone. In addition, it stimulates the release of catecholamines. CGRP and GAL also appear to be stimulatory for ACs. In this scheme, the parasympathetic components are omitted because of the absence of definitive work. See text for additional details. *Scheme drawn by R. V. Carsia.*

on studies in which both corticosteroids were measured, the average ratio of the baseline circulating concentrations of aldosterone to corticosterone is about 1:175 (Table 33.1). Younger birds tend to have higher circulating concentrations of each compared to those of adults.

The avian adrenal gland secretes additional steroids that presumably have important ontogenetic function and play a role in life-history-cycle transitions (Landys et al., 2006; Wada, 2008; Wingfield, 2013; Romero and Gormally, 2019). Cortisol is a significant secretory product during the embryonic and early posthatch period and then declines thereafter (Kalliecharan and Hall, 1974). Presumably, cortisol has a role in the development and maturation of several organ systems (see Carsia et al., 1987a). In some psittacine species, circulating cortisol is insensitive to exogenous ACTH (Lothrop et al., 1985; Walsh et al.,

TABLE 33.1 Baseline peripheral plasma concentrations of corticosterone and aldosterone in some galliform and anseriform birds in which both corticosteroids were measured in the same samples by radioimmunoassay (averages from 26 studies).

Bird order	Life-history cycle	Corticosterone (ng/mL)	Aldosterone (pg/mL)
Galliform birds[a]			
	Hatch	11	33
	Immature	11	46
	Adult	2	19
Anseriform birds[b]			
	Hatch	16	345
	Immature	8	308
	Adult	18	60

[a]*Values derived from studies using the domestic chicken* (Gallus gallus)*, the domestic turkey* (Meleagris gallopavo)*, and the Japanese quail* (Coturnix japonica)*.*
[b]*Values derived from studies using the wild mallard duck and the Pekin duck* (Anas platyrhynchos) *and the Muscovy duck* (Cairina moschata)*.*

1985). Thus, the availability and action of cortisol may be less dependent on the hypothalamic-pituitary-adrenal (HPA) axis and more dependent on the regulation at the tissue level (e.g., in (Baker, 2010) the immune system; see Section 33.3.4). Furthermore, there are other factors that segregate the tissue actions of corticosterone and cortisol: isoforms of corticosteroid-binding globulin (CBG) that preferentially bind cortisol and thus influence its half-life for delivery to sensitive tissues (Schmidt et al., 2008, 2010), and isoforms of glucocorticoid receptors (GRs) in various target tissues that selectively bind cortisol (Schmidt et al., 2010). In addition, there is interplay between systemic delivery of corticosteroids to target tissues and the intrinsic local production within tissues (Schmidt and Soma, 2008; Schmidt et al., 2008). Corticosterone may be synthesized or regenerated in the brain (Newman et al., 2008) and locally may mediate the acute effect of stress on brain aromatase activity in a sex-dependent manner (Dickens et al., 2011a). The picture is further complicated by the local expression of 11β-hydroxysteroid dehydrogenases type 2 and 1 that can degrade and regenerate active glucocorticoids, respectively, within cells. Overall, despite its relatively low-circulating concentration relative to corticosterone, cortisol produced locally throughout the posthatch life of birds, e.g., within immune tissues and possibly the brain, suggests it has unique and important functions in both an organ-specific and age-specific manner.

In addition to cortisol, the adrenal gland is an important source of sex steroids, especially testosterone (Tanabe et al., 1986; Ottinger et al., 2001) during the embryonic and perinatal period that complements the gonads for establishing adequate levels of androgens and estradiol. This "adrenal-gonadal unit" establishes the dynamic balance between systemic delivery of sex steroids to the brain and their local production within the brain, a balance which is important for sexual differentiation of the hypothalamus and the establishment of important central nervous signals that support breeding, territorial, and courtship behaviors (Soma and Wingfield, 2001; Schmidt et al., 2008; Pintér et al., 2011).

33.2.2 Other secretory products

The chicken adrenocortical tissue is a major source of inhibin during embryonic development (Rombauts et al., 1994; Decuypere et al., 1997). Dexamethasone depresses inhibin release in ovo, whereas ACTH elicits a rise in inhibin release that parallels corticosterone release in primary cultures of embryonic chick adrenal cells. Furthermore, the adrenal gland continues to be a complementary extragonadal source of inhibin in the adult (see Vanmontfort et al., 1997 and Bruggeman et al., 2003) and activin as well (Chen and Johnson, 1996).

33.2.3 Synthesis of corticosteroids

Adrenal/interrenal steroidogenesis is carried out by microsomal and mitochondrial enzymes that bear active enzymatic sites which are highly conserved among vertebrates (e.g., Nomura et al., 1999; Freking et al., 2000; Kanda et al., 2000; Kamata et al., 2004; Baker et al., 2015). StAR is the hormone-sensitive, **st**eroidogenic **a**cute **r**egulatory protein that delivers free cholesterol from the outer mitochondrial membrane to the inner mitochondrial membrane where it can access the cholesterol side-chain cleavage

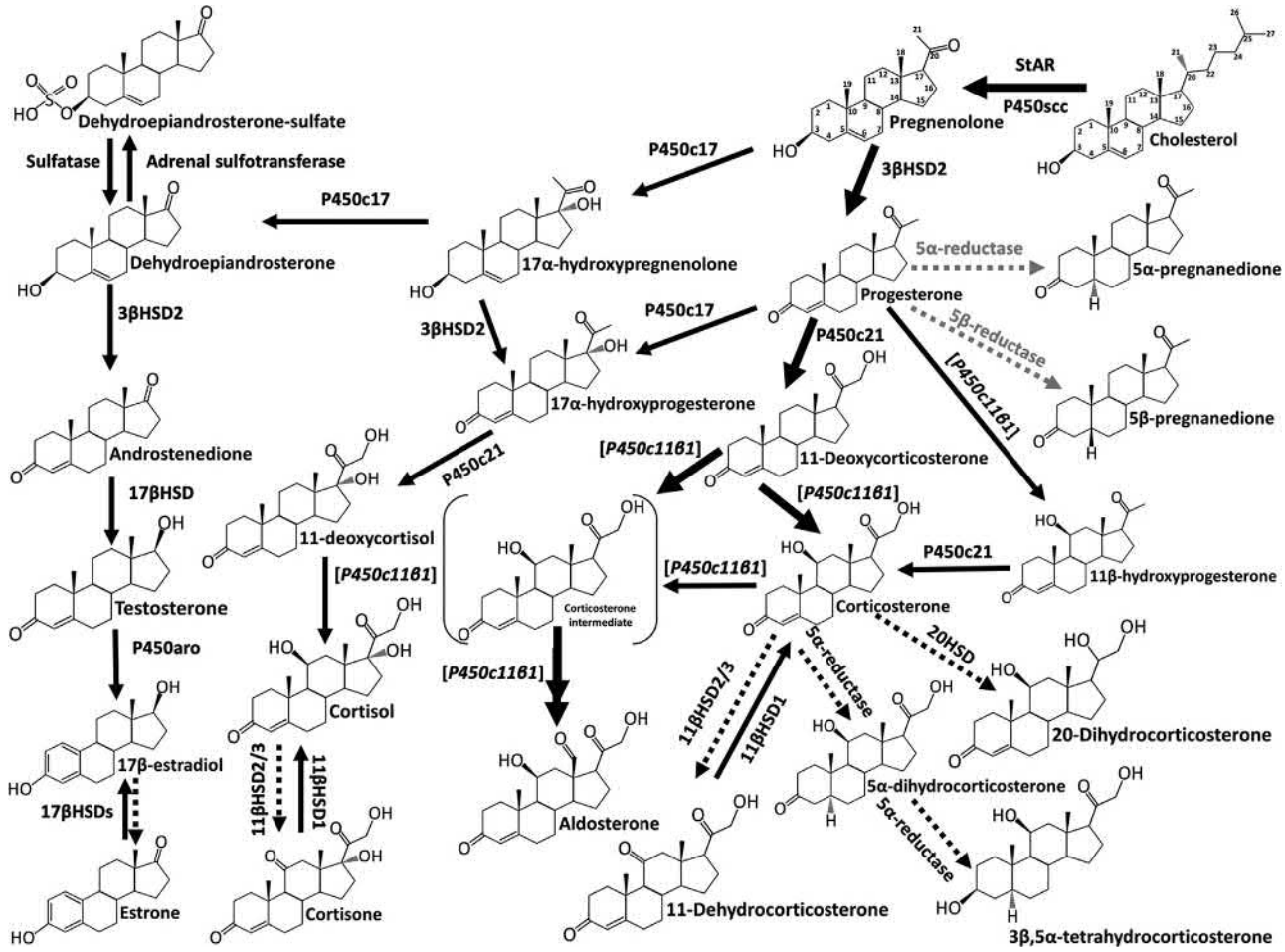

FIGURE 33.6 Steroidogenesis in the avian adrenal gland. *Thick arrows* indicate the predominant pathway of posthatch (postnatal) birds leading to corticosterone and aldosterone. *Thin arrows* indicate additional pathways that are more prominent in the embryonic and early posthatch (postnatal) periods, and during life-history-stage transitions; these are the pathways to cortisol and to the sex steroids. Also, the avian immune system may have a sufficient suite of enzymes to locally synthesize cortisol (Schmidt and Soma, 2008). *Dotted arrows* indicate steroid-inactivating or degrading pathways. Dotted *gray arrows* indicated degradative pathways of progesterone during the embryonic period. Solid *gray* and *black* bonds on steroids represent key alpha (down) and beta (up) positions, respectively, however, not all hydrogen bond positions are shown. StAR, steroidogenic acute regulatory protein; P450scc, mitochondrial cytochrome P450 cholesterol side-chain cleavage enzyme; 3βHSD2, microsomal/mitochondrial 3B-hydroxysteroid dehydrogenase/Δ5→Δ4 isomerase, type 2; P450c21, microsomal cytochrome P450 21-hydroxylase; P450c17, microsomal cytochrome P450 17α-hydroxylase/17,20-lyase; 17βHSD, microsomal 17-ketosteroid reductase; P450aro, microsomal cytochrome P450 aromatase; 17βHSDs, not fully characterized adrenal microsomal enzymes in birds; 11βHSD2/3, microsomal 11β-hydroxysteroid dehydrogenase, types 2 and 3; 11βHSD1, 11β-hydroxysteroid dehydrogenase type 1[Largely microsomal, although there is evidence for a significant cytosolic type-1 like enzyme.]; 20HSD, microsomal 20-hydroxysteroid dehydrogenase; and *P450C11β1*, mitochondrial cytochrome P450 11β-hydroxylase type 1.The last enzyme is italicized because is not clear if the avian adrenal gland expresses this or a similar enzyme. If there is just one enzyme, P450C11β1 or P450C11β1-like, it would catalyze the 11β-hydroxylation of 11-deoxycorticosterone to corticosterone and 11-deoxycortisol to cortisol. Also, under certain conditions, it would carry out (1) the 11β-hydroxylation of 11-deoxycorticosterone to a corticosterone intermediate, and then (2) an 18-hydroxylation step taking the corticosterone intermediate to 18-hydroxycorticosterone intermediate, and (3) an 18-methyl oxidase step (which is the key function of aldosterone synthase in some mammals) to aldosterone. *Double superimposed arrows* indicate steps 2 and 3. See text for additional details. *Pathway drawn by R. V. Carsia.*

enzyme, P450scc, to be converted to pregnenolone (Miller and Auchus, 2011). Not surprisingly, StAR is highly conserved in vertebrate steroidogenic tissues (Bauer et al., 2000). StAR-related-lipid-transfer-domain proteins are responsible for loading free cholesterol to the outer mitochondrial membrane to facilitate StAR activity.

The synthetic pathways of the major steroids secreted by the avian adrenal gland during the life cycle are shown in Figure 33.6. In this steroidogenic scheme, mitochondrial cytochrome P450SCC (or CYP11A1) (Nomura et al., 1997) mediates 20α-/22-hydroxylation and scission of the C20-22 carbon bond, producing pregnenolone and isocaproaldelhyde, a set of reactions traditionally called "20, 22-desmolase." Pregnenolone is converted to progesterone by 3βHSD2 (HSD3B2) (Nakabayashi et al., 1995), a non-P450 microsomal/mitochondrial dehydrogenase-isomerase

complex which mediates 3β-hydroxysteroid dehydrogenase and isomerase (Δ^5 double bond to Δ^4 double bond) activities. Microsomal P450c21 (CYP21A2) then mediates a 21-hydroxylation steps converting progesterone to 11-deoxycorticosterone. Corticosterone is the predominant corticosteroid product of the avian adrenal gland, albeit 11-deoxycorticosterone is also a significant secretory product. Corticosterone is formed from 11-deoxycorticosterone by an 11β-hydroxylation most probably via a mitochondrial enzyme.

Aldosterone is largely formed from 11-deoxycorticosterone and not from corticosterone because corticosterone is a poor substrate. Thus, 11-deoxycorticosterone undergoes an 11β-hydroxylation, converting it to enzyme-bound corticosterone which serves as an intermediate. This is followed by an 18-hydroxylation and lastly an 18-methyl oxidase step, producing the potent mineralocorticoid, aldosterone. As mentioned previously (Section 33.1.2.2), SCZ slices from the duck adrenal gland secrete predominantly aldosterone in response to ACTH and exclusively aldosterone in response to Ang II whereas the IZ tissue secretes predominantly corticosterone in response to ACTH and is refractory to Ang II (Klingbeil, 1985; Pierce et al., 1978; Holmes and Cronshaw, 1984, 1993). Dietary Na^+ restriction in the domestic turkey induces a subpopulation of adrenocortical cells that have a disproportionately enhanced aldosterone response to Ang II and K^+ (Kocsis et al., 1995a).

The current knowledge concerning the enzymes carrying out both glucocorticoid and mineralocorticoid synthesis in birds is controversial. A limited earlier analysis of avian genomes suggested that birds, just like some mammals, have just a single enzyme that carries out the steps to corticosterone and aldosterone (CYP11B1) (Baker et al., 2015). However, a more recent expanded analysis of eight diverse species from five orders indicates that except for the brown kiwi (*Apteryx australis*), which has a function CYP11B1, all others lack CYP11B1 (Nelson, 2018). The nature of an alternative enzyme(s) that carries out steps like CYP11B1 is unknown. Furthermore, how some vertebrate species with just a single enzyme, CYP11B1, selectively secrete aldosterone over corticosterone (or cortisol) from subpopulations of adrenocortical cells is an unresolved problem in steroid synthesis.

Other enzymatic activities are also apparent mainly during the embryonic and neonatal periods and at modest levels in the adult. Formation of cortisol is predominantly via 17α-hydroxylation of progesterone by a microsomal P450c17 (CYP17A1) (Ono et al., 1988) to form 17α-hydroxyprogesterone, then a 21-hydroxylation by microsomal P450c21 (CYP21A1) to form 11-deoxycortisol and finally an 11β-hydroxylation step by a mitochondrial P450c11β to form cortisol. A minor pathway is pregnenolone to 17α-hydroxypregnenolone via P450c17, and then to 17α-hydroxyprogesterone via 3βHSD2. There is some evidence that 11β-hydroxyprogesterone serves as a precursor for corticosterone (via a 21-hydroxylation step) and cortisol (via 17α- and 21-hydroxylation steps), albeit these pathways appear to be of little significance.

The main pathway for adrenal sex steroids uses a microsomal P450c17 (CYP17A1) (Ono et al., 1988) (has both 17α-hydroxylase and 17,20-lyase activities) that efficiently converts pregnenolone to 17α-hydroxypregnenolone and then to dehydroepiandrosterone (DHEA). The 3β-hydroxyl group of DHEA can be sulfated by an adrenal sulfotransferase. As mentioned previously, DHEA and DHEA-sulfate are in the avian circulation (Soma and Wingfield, 2001) and in the adrenal gland. Also, analysis of circulating steroids provides evidence for a "backdoor" pathway to androgen synthesis in birds using a group of aldo-keto reductase enzymes, but it is not clear if this pathway exists in avian adrenal/interrenal tissues (Prior et al., 2017).

Adrenal androstenedione can be converted to testosterone by a 17βHSD (Nomura et al., 1999), a microsomal, non-P450 enzyme. Indeed, androgens are detected in the avian adrenal gland (Ottinger et al., 2001; Soma and Wingfield, 2001). Furthermore, there is evidence that testosterone is aromatized to estradiol by a microsomal aromatase, P450aro (CYP19A1) (Shen et al., 1994) in that estradiol has been detected in the embryonic adrenal gland (Tanabe et al., 1979, 1986; Ottinger et al., 2001) and that it persists into the posthatch period (Ottinger et al., 2001). But this sex steroid pattern may not be uniform among the avian species in that in some species there may be an "adrenal-gonadal unit" in which the adrenals contribute precursors for gonadal steroidogenesis.

Degradation pathways exist in the avian adrenal gland during development, the posthatch period and in the adult. Metabolites of progesterone, corticosterone, cortisol, estradiol, and testosterone have been detected. It appears that the adrenal gland has the sets of enzymes to carry out both degradative and regenerative reactions. In the adult gland, a more prominent enzyme is 5α-reductase (Miller and Auchus, 2011; Langlois et al., 2010). This enzyme degrades corticosterone to 5α-dihydrocorticosterone (5α-pregnan-11β,21-diol-3,20-dione) and 5α-tetrahydrocorticosterone (5α-pregnan-3α,11β,21-triol-20-one). However, the importance of these enzyme activities in an organismal context is unclear.

33.2.4 Transport of corticosteroids

In birds, most circulating corticosterone and cortisol are transported bound in dynamic equilibrium to plasma proteins. More than 90% of circulating corticosteroids are bond to the α-2 globulin, CBG (that has a high affinity and low-binding capacity for corticosteroids). Minor amounts

are bound to low-affinity, high-capacity, nonspecific binding proteins (mostly albumin) (Wingfield et al., 1984). Complementing a previous study (Malisch and Breuner, 2009), a random survey containing more recent studies from different species suggests a fairly wide range of affinities (K_d), 1.2−8.3 nM, and capacities, 38−225 nM, for corticosterone. In chickens, corticosterone binds to CBG with an average K_d of about 2 nM and a capacity of about 50 nM (Fässler et al., 1986). In some species, cortisol binds to avian CBG with a similar affinity and capacity (Schmidt et al., 2010), however, in many species, it binds with affinities similar to the sex steroids (see Malisch and Breuner, 2009). CBG also binds progesterone with high affinity, testosterone, and dihydrotestosterone with a lower affinity but within the physiological range of these sex steroids. Binding of estrogen is negligible.

A number of factors affect the circulating concentration of CBG, and these responses vary with species and life-history stage (Malisch and Breuner, 2009) and over seasons (Romero and Gormally, 2019). Changes in CBG capacity in response to stress can be acute, occurring within 30 min (Breuner et al., 2006; Charlier et al., 2009; Malisch et al., 2010). It is also influenced by ontogenic processes, hormonal manipulations, and other physiological states (see Landys et al., 2006; Wingfield, 2013). Overall, the interaction between glucocorticoids, their cognate binding proteins, and their target tissues is complex and that the precise role played by CBGs in mediating the actions of glucocorticoids awaits further investigation.

33.2.5 Circulating concentrations of corticosterone and aldosterone

Investigations in which the circulating concentrations of corticosterone and aldosterone were measured in the same study are restricted to galliform (chicken, turkey, and Japanese quail) and anseriform (duck) species. The circulating concentration of corticosterone in unstressed birds is in the nonogram-per-milliliter range, whereas that for aldosterone is in the picogram-per-milliliter range (Table 33.1). There is a tendency for the circulating values to fall from hatch to maturity. Part of this is explained by the decrease in relative adrenal weight with age (Holmes and Phillips, 1976; Carsia and Weber, 1986). However, it also may be due to the decrease in adrenal sensitivity and maximal steroidogenic capacity with posthatch age (Carsia et al., 1985b, 1987a; Carsia and Weber, 1986).

33.2.6 Secretion, clearance, and metabolism of corticosterone and aldosterone

Not surprisingly, corticosteroid concentrations which are initially high in the adrenal gland and adrenal venous effluent (in micrograms per milliliter) and then are secreted at about a microgram per minute per kilogram (Assenmacher, 1973) are then rapidly diluted in the circulation and distributed to the extracellular fluid. Circulating concentrations of corticosteroids are maintained by the dynamic balance between metabolic clearance, adrenal secretion, and return to the general circulation by regeneration at the tissue level. Transmembrane passage of corticosteroids is rapid for all cells ($\sim 10^{-4}$ cm/s) (Giorgi and Stein, 1981) thus facilitating rapid clearance and metabolism in competent cells, particularly in the kidney and liver. Indeed, in a very limited number of studies, the average half-lives of corticosterone and aldosterone in the circulation are similar, about 8−15 min and 6−13 min, respectively, but there are differences among species, with physiological status, and after endocrine manipulations (Holmes et al., 1972, 1974; Holmes and Slikker, 1976).

The metabolic clearance rate for corticosterone is decreased with age (Holmes and Kelly, 1976) and by thyroidectomy (Kovács and Péczely, 1983). In addition, it appears to be influenced by nutritional status. In chickens subjected to dietary protein restriction, it is increased 85%, which translates to a fourfold increase in secretion rate from the adrenal gland (Carsia et al., 1988a).

Clearance from the circulation is facilitated by intracellular binding and sequestration and ultimately metabolism, primarily by the liver via hepatic 5α-reductase which converts corticosterone and aldosterone to inactive metabolites (Daniel and Assenmacher, 1971). The metabolites in urine exist as several polar and nonpolar forms including intact corticosteroids, some free and some conjugated to sulfate and glucuronide (Helton and Holmes, 1973; Holmes et al., 1974; Holmes and Slikker, 1976; Rettenbacher et al., 2004).

Glucocorticoids are the end-product signals of a system largely concerned with regulating energy flow—a system of which the HPA axis is a component. By contrast, mineralocorticoids are the end-product signals of a system largely concerned with maintaining salt and water balance—a system of which the renin-angiotensin-aldosterone system is a component. These steroid hormones work on specific effector tissues of each system. However, glucocorticoids are also essential to permit the full expression of almost all metabolic processes.

The effector molecules in the effector tissues are the GR and mineralocorticoid receptor (MR) which are ligand-inducible transcription factors. The MR binds corticosterone with an affinity that is more than 30 times that of the GR. Since the circulating concentration of corticosterone is about 20−300 times that of aldosterone, almost all of the MRs are fully occupied by corticosterone. Thus, in order for aldosterone to represent the system regulating salt and water balance, corticosterone (and cortisol) in the effector tissues needs to be either sequestered from the MR or rapidly degraded so that its intracellular concentrations exposed to the MR is extremely low.

FIGURE 33.7 Deduced amino acid sequences of adrenocorticotropin (ACTH) peptides [amino (N)-terminus to carboxyl (C)-terminus] from selected avian species based on their respective cDNAs. Green amino acids bind to the "docking" or "address" site on MC2R. In mammals, arginine $(R)^{15}$ is replaced by lysine (K); it is assumed that these amino acids are interchangeable, thus, $K^{15}/R^{15}K^{16}R^{17}R^{18}P^{19}$. Red amino acids $H^6F^7R^8W^9$ bind to the activation site of MC2R for functional binding and signal transduction (e.g., cyclic adenosine monophosphate production) and are uniformly conserved among vertebrates. Arginine $(R)^8$ is also essential for maintenance of the secondary structure of ACTH in the circulation (Ghaddhab et al., 2017). Purple amino acids are essential spacers and the proline $(P)^{12}$ (*underlined*) provides a kink inflection to properly position the activation and docking amino acids. Proline $(P)^{19}$ (*underlined*) presumably "kinks" the rest of the sequence (amino acids 20–39) out of the way for binding to the docking site. In this scenario (Liang et al., 2013), when the $R^{15}K^{16}R^{17}R^{18}P^{19}$ docking site is occupied, the $H^6F^7R^8W^9$ motif is now properly positioned for functional binding and activation of MC2R. Molecular studies have demonstrated that amino acids 20–39 are not necessary for binding and signal transduction but are important for stability in the circulation. Amino acid abbreviations: A, alanine; C, cysteine; D, aspartic acid; E, glutamic acid; F, phenylalanine; G, glycine; H, histidine; I, isoleucine; K, lysine; L, leucine; M, methionine; N, asparagine; P, proline; Q, glutamine; R, arginine; S, serine; T, threonine; V, valine; W, tryptophan; Y, tyrosine. Species names with GenBank accession numbers or reference are as follows: [a]*Struthio camelus* (Naudé et al., 2006); [b]*Anas platyrhynchos* (XM_013103743.2); [c]*Gallus gallus* (NM_001031098.1); [d]*Numida meleagris* (XM_021391833.1); [e]*Coturnix coturnix* (AB620013.1); [f]*Meleagris gallopavo* (Variants 1 and 2—XM_010708068.2 and XM_019613648.1); [g]*Columba livia* (XM_021298522.1); [h]*Opisthocomus hoazin* (XM_009942707.1); [i]*Pelecanus crispus* (XM_009480535.1); [j]*Aptenodytes forsteri* (XM_009283455.1); [k]*Haliaeetus leucocephalus* (XM_010583178.1); [l]*Corvus macrorhynchos* (AB555653.1); [m]*Taeniopygia guttata* (XM_002198019.3). *The compilation of sequences was provided by Colin G. Scanes, Ph.D., D.Sc. Color designation and description of amino-acids motifs by R. V. Carsia.*

The main enzymes that carry out the degradation of corticosterone and cortisol in target tissues are 11β-hydroxysteroid dehydrogenase 2 (11βHSD2) and 20-hydroxysteroid dehydrogenase (20HSD) (Vylitová et al., 1998; Baker, 2010; Ahmed et al., 2013) (Figure 33.6). 11βHSD2 catalyzes the oxidation of corticosterone and cortisol to the inactive metabolites, 11-dehydrocorticosterone and cortisone, respectively, and 20HSD converts corticosterone to 20-dihydrocorticosterone (see Figure 33.7). There also appears to be a second corticosterone (cortisol)-degrading enzyme, 11βHSD3, expressed in the chicken colon and to a greater extent in the kidney (Katz et al., 2008; Baker, 2010). These enzymes are obviously expressed in other avian groups. There is a robust expression of 11βHSD2 and 20HSD in the zebra finch brain and several peripheral tissues analyzed and to a lesser extent in the gonads, more so in the ovary than in the testis (Katz et al., 2010).

As mentioned previously, there are also enzymes that regenerate active glucocorticoids. In chickens is the enzyme catalyzing the reverse reactions (reductive), 11βHSD1, which regenerates corticosterone (and cortisol) (Katz et al., 2007; Baker, 2010). Thus, a balance in inactivation and reactivation of glucocorticoids provides a prereceptor modulation of corticosteroid signals in avian effector tissues (Kučka et al., 2006).

Corticosterone, along with sex steroids, does accumulate in the egg (Hahn et al., 2011) and in a species-specific manner (Quillfeldt et al., 2011). They may possibly serve as a signal from the mother to progeny concerning adverse environmental conditions (Okuliarová et al., 2010).

33.2.7 General regulation of adrenocortical function

33.2.7.1 Adrenocorticotropin

The most efficacious stimulator of avian corticosteroid secretion is corticotropin (adrenocorticotropic hormone; ACTH). ACTH is one of the several melanocortins derived from ther highly conserved protein, pro-opiomelanocortin (POMC) (Dores and Lecaude, 2005; Harris et al., 2014). The sequence of the first 19 amino acids is rigidly conserved for maintaining the functional secondary structure in the circulation (Ghaddhab et al., 2017) and most importantly, the conserved "docking" or "address" site and the binding/activation site (Liang et al., 2013; Yang and Harmon, 2020). The rest of the molecule is required for stability in circulation (see Figure 33.7 for details). Numerous studies in vivo and in vitro with isolated adrenocortical cells (Carsia, 1990) from several species demonstrate a dose-dependent and rapid (less than 5 min) corticosteroid response to ACTH. Not surprisingly, this

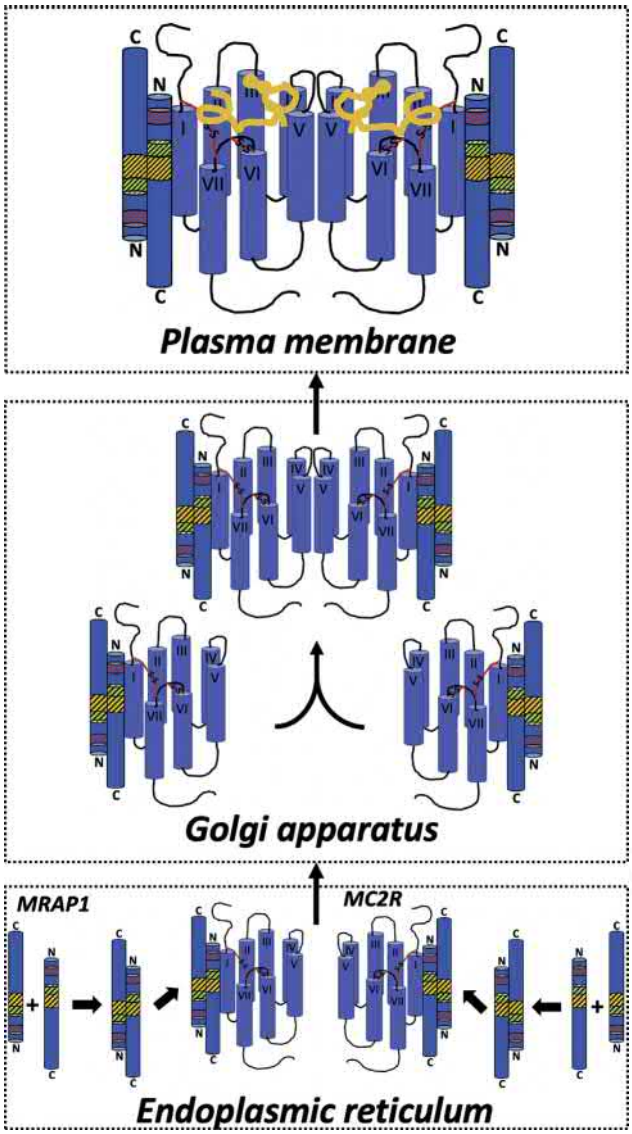

FIGURE 33.8 The functional MC2R is a heterohexameric complex formed from two MC2Rs and four MRAP1s. MRAP1 is a single-membrane spanning protein that forms an antiparallel homodimer for activity. The protomer with the extracellular amino terminus is the essential protein of the homodimeric complex (Malik et al., 2015). The blue region of MRAP1 is nonessential. The hatched orange region is the transmembrane domain. The hatched green region is essential for forming a stabile homodimer. In addition, the hatched orange and hatched green regions promote MC2R trafficking to the plasma membrane and transmembrane signaling after ACTH binding. The hatched red region is absolutely essential for functional ACTH binding to MC2R and signal transduction (i.e., G_s-protein activation and cAMP formation) (Rouault et al., 2017). In the endoplasmic reticulum, MRAP1 forms an antiparallel homodimer that couples with one MC2R. MC2R is a typical heptahelical GPCR. The MRAP1-MC2R heterotrimeric complex is transported to the Golgi apparatus where it couples with another MRAP1-MC2R heterotrimeric complex to form the functional, heterohexameric ACTH receptor complex (Fridmanis et al., 2017). It is postulated that a similar process can occur at the plasma membrane in which MRAP1 recruits and activates a pool of inactive MC2Rs (Clark and Chan, 2019). Two ACTH molecules (yellow) are bound by the functional, heterohexameric ACTH receptor complex. The ACTH molecules are depicted in their secondary structure. It is proposed that the amino-end helical region of ACTH orientates the binding amino acids to interact with transmembrane domains II, III, VI, and VII and the carboxyl-end loop of ACTH contains the "docking" amino acids that interact with transmembrane domains IV and V (Liang et al., 2013). The depicted protein interactions are purely schematic and are not to actual molecular scale nor do they reflect the actual interactions. *ACTH*, adrenocorticotropic hormone or corticotropin; *cAMP*, cyclic adenosine monophosphate; *GPCR*, G protein-coupled receptor; G_s, stimulatory G protein for cAMP formation; *MC2R*, melanocortin-2 receptor/ACTH receptor; *MRAP1*, melanocortin-2 receptor accessory protein 1. *Cartoon drawn by R.V. Carsia.*

rapid response needs to be considered when assessing corticosterone rhythms in birds (Breuner et al., 1999; de Jong et al., 2001; Romero and Reed, 2005; Romero and Gormally, 2019). In exotic avian species, ACTH stimulation test protocols result in a wide range of circulating corticosterone responses, from as little as 33−96% over baseline to as much as 2400% over baseline. This variation in maximal response is mostly due to the variation in the starting baseline level, i.e., the lower the baseline in the species, the greater the response (de Matos, 2008).

In birds, ACTH-induced corticosteroid production operates through a G-protein-coupled receptor, the melanocortin 2 receptor (MC2R) (Takeuchi et al., 1998; Boswell and Takeuchi, 2005), which is activated exclusively by ACTH (Veo et al., 2011). In addition, ACTH is a potent stimulator of the other four avian melanocortin receptors subtypes (Ling et al., 2004) and the presence of MC5R in chicken liver and adipose tissue raises intriguing questions about the possible role of ACTH in the direct regulation of avian metabolism (Thomas et al., 2018).

Comparative molecular studies (Veo et al., 2011) and numerous in-vitro studies with isolated adrenocortical cells from diverse avian species confirm that dissemination of the ACTH signal in avian adrenocortical cells is largely through the cyclic AMP (cAMP)-dependent pathway involving a stimulatory guanine nucleotide binding protein, adenylyl cyclase, cyclic adenosine monophosphate (cAMP), and cAMP-dependent protein kinase (see Carsia, 1990; McIlroy et al., 1999).

Cell-surface expression and function of the avian MC2R requires melanocortin-2 receptor accessory protein 1 (MRAP1) (Veo et al., 2011; Thomas et al., 2018). As expected, the important domains of MRAP1 are highly conserved in many vertebrates (Dores and Garcia, 2015). Chicken MRAP1 is small linear proteins of about 120 amino acids, having a single hydrophobic transmembrane domain (Barlock et al., 2014). Cytoplasmic MRAP1 forms an antiparallel homodimer that interacts with the MC2R to form a heterotrimeric complex (Rouault et al., 2017) (see Figure 33.8 for additional details). Formation of the heterotrimeric complex is essential for trafficking, eventually to the plasma membrane. The mature, functional ACTH

receptor is actually a dimer of the heterotrimeric complex, thus, a heterohexameric protein complex composed of four MRAP1s and two MC2Rs (Fridmanis et al., 2017). Stability and turnover differences between MRAP1 (shorter) and MC2R (longer) suggest that MRAP1 may recruit and activate a pool of inactive MC2Rs at the cell surface as well (Clark and Chan, 2019). This additional proposed model of recruitment of fully formed but inactive MC2Rs by MRAP1 at the plasma membrane may be advantageous in situations of significant stress.

33.2.7.2 Angiotensins

As in many vertebrates, angiotensins regulate avian adrenocortical function (reviewed in Holmes and Cronshaw, 1993). Indeed, in-vivo studies and in-vitro work with adrenal tissue and cells demonstrate that the effect is direct. This topic is discussed in detail under Section 33.2.8.

33.2.7.3 Other putative regulators

Studies indicate that avian adrenocortical function is modulated by secretory products of the immune system and other endocrine organs. Interpretations of results derived from these studies should be viewed with caution since they are restricted to anseriform and galliform species and in many instances are based on in-vitro systems that have not been substantiated in vivo. Nevertheless, these studies deserve attention. Such peripheral agents may directly stimulate or inhibit adrenocortical function or may act as positive or negative modulators of tropic-hormone-induced responses. However, a common theme with hormones not of pituitary origin that stimulate corticosteroid synthesis in vitro is the lack of organismal context, given the drastic effects of hypophysectomy on adrenocortical function.

33.2.7.3.1 Stimulators and positive modulators

33.2.7.3.1.1 Prolactin and growth hormone The pituitary secretory products, prolactin and growth hormone appear to have a positive influence on avian adrenocortical function (Figure 33.9). Both prolactin and growth hormone are increased with various stressors and growth hormone assists in the overall maintenance of the avian adrenal gland (Harvey et al., 1995; Angelier et al., 2013).

The importance of growth hormone in avian (*Gallus gallus*) adrenocortical maintenance is indicated by its restoration and augmentation of cellular steroidogenic capacity after hypophysectomy and in the absence of ACTH and other hormonal replacement (Carsia et al., 1985c). In addition, recombinant chicken growth hormone has been shown to raised circulating corticosterone (Cheung et al., 1988).

33.2.7.3.1.2 Calciotropic hormones In chicken adrenocortical cell preparations, extracts containing chicken parathyroid hormone (PTH) stimulate cAMP, corticosterone secretion and especially aldosterone secretion (Rosenberg et al., 1987, 1988a,b, 1989a). However, a more recent study with recombinant chicken PTH did not demonstrate a steroidogenic action (Lim et al., 1991). Nevertheless, avian forms of the PTH/parathyroid hormone-related peptide (PTHrP) receptor have been characterized (Pinheiro et al., 2012) and are expressed in many tissues. Furthermore, a PTH/PTHrP receptor in chicken adrenocortical cells, which is absent in chromaffin cells, has been demonstrated and PTHrP enhances ACTH-induced corticosterone production in vitro (Kawashima et al., 2005).

A similar potentiation of ACTH action is seen with chicken calcitonin, and here again, it appears to act through specific receptors on avian adrenocortical cells and not chromaffin cells (Nakagawa-Mizuyachi et al., 2009). Thus, calciotropic hormones appear to influence the action of ACTH on avian adrenocortical cells.

33.2.7.3.1.3 Humoral immune system ACTH is released from activated lymphocytes in response to CRH, and this release is inhibited by corticosterone (Hendricks et al., 1991, 1995a,b). However, it is not known whether sufficient numbers of lymphocytes populate the avian adrenal gland to influence corticosteroid secretion. In addition, the bursa of Fabricius may elaborate substances necessary for adequate corticosteroidogenic capacity during development and maturation (Pedernera et al., 1980) and for normal corticosterone response of adrenocortical cells to ACTH (El-Far et al., 1994).

33.2.7.3.2 Inhibitors and negative modulators

33.2.7.3.2.1 Thyroid hormones Evidence indicates that the thyroid hormone, 3,5,3′-triiodothyronine (T_3), is an important modulator of avian adrenocortical function (Figure 33.9). With some exceptions (Sharma and Chaturvedi, 2009), there is an inverse relationship between circulating T_3 concentrations and chicken adrenocortical function (i.e., after thyroidectomy with and without T_3 replacement) (Carsia et al., 1997). In hypophysectomized cockerels, T_3 replacement reduces corticosterone production by adrenocortical cells even more than that due to hypophysectomy, but it maintains normal cellular sensitivity to ACTH (Carsia et al., 1985c). There also may be influences at the pituitary level. In chickens, thyroid hormone status does not influence POMC mRNA levels (Sharma and Chaturvedi, 2009). However, in the rat (*Rattus norvegicus*) thyroid hormones negatively modulate POMC processing (i.e., prohormone convertase-1 expression) (Li et al., 2001). Since mRNA levels do not necessarily correlate with mature protein levels, the effect of thyroid hormones on avian POMC processing awaits investigation.

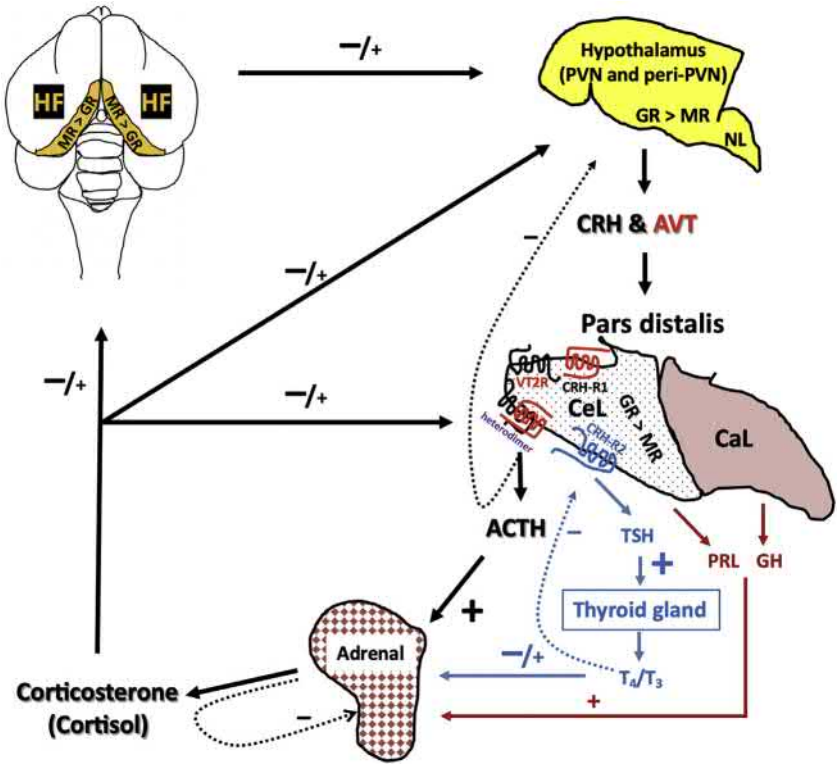

FIGURE 33.9 The hypothalamic-pituitary-adrenal (HPA) axis in birds. Negative (−) and positive characters (+) and their relative sizes when paired indicate the general consensus of the effect of a particular hormone. The hypothalamus is depicted in a sagittal view and with yellow fill. The neural lobe of the pituitary gland (NL), the paraventricular nucleus (PVN), and peri-paraventricular nuclear area (peri-PVN) are indicated. Top left is a dorsal view of the avian brain and the location of the hippocampal area (HF) is highlighted with orange fill. Relative influences or activities of the glucocorticoid receptor (GR) and mineralocorticoid receptor (MR) are indicated (GR > MR; MR > GR). The pars distalis of the pituitary gland is depicted in sagittal view with dot pattern indicating the cephalic lobe (CeL) and light brown fill indicating the caudal lobe (CaL). The adrenal gland is in brown pattern to depict the intermingling of chromaffin and adrenocortical tissues. Cartoons of structures are not drawn to actual relative size, with the pituitary disproportionately enlarged. Other abbreviations or acronyms are as follows: *ACTH*, adrenocorticotropic hormone (corticotropin); *AVT*, arginine vasotocin; *CRH*, corticotropin-releasing hormone; *CRH-R1*, type-1 corticotropin-releasing hormone receptor; *CRH-R2*, type-2 corticotropin-releasing hormone receptor; *GH*, growth hormone; *PRL*, prolactin; *VT2R*, type-2 vasotocin receptor; *T4/T3*, thyroid hormones 3,5,3′,5′-tetraiodothyronine, 3,5,3′-triiodothyronine; *TSH*, thyroid-stimulating hormone (thyrotropin). CRH and AVT (and sometimes mesotocin) interact with their respective receptors, CRH-R1 and VT2R, to stimulate the release of ACTH in a synergistic manner. Part of the synergism of CRH-R1 and VT2R is due to their separate signaling pathways, and it is also likely that part is due to their receptors undergoing heterodimerization. ACTH most likely exerts a negative short-loop feedback on CRH release. ACTH stimulates the secretion of glucocorticoids (mostly corticosterone) from adrenocortical cells of the adrenal gland. Its action is assisted by PRL, also released from the CeL, and GH, secreted from the CaL. Sufficient evidence indicates that in addition to ACTH, PRL and probably GH are released during stress. Glucocorticoids exert a negative long-loop feedback on both the pituitary gland and the hypothalamus to curtail ACTH release. However, some brain CRH neurons and pituitary VT2Rs are upregulated by glucocorticoids. Under most conditions, glucocorticoids exert a negative feedback on the HF which has indirect connections to the PVN and peri-PVN. However, under different conditions such as long-term stress, the negative feedback in the HF is reduced and stimulatory signals from the HF are relayed to the PVN for sustained CRH release and thus sustained activation of the HPA axis. Such a mechanism may explain continued glucocorticoid secretion during sustained stress and when circulating glucocorticoid levels are high. CRH also interacts with CRH-R2 to stimulate the release of TSH. TSH acts on the thyrocytes of the thyroid gland to release T4 and T3. Thyroid hormones appear to decrease VT2R expression and may also inhibit the expression of prohormone convertase-1, an enzyme that processes pro-opiomelanocortin to produce ACTH and other melanocortins. Overall, studies suggest that thyroid hormones have a negative impact on corticosteroid secretion. Finally, intraadrenal and circulating glucocorticoids exert a negative short-loop feedback on the adrenocortical cells to reduce the release glucocorticoids. See text for details of additional modulators of the HPA axis. *Cartoon drawn by R. V. Carsia.*

33.2.7.3.2.2 Androgens The effect of androgens on adrenocortical secretion appears to be variable depending on the species and type of endocrine manipulation. On the one hand, early work with orchiectomized chickens suggests that testosterone suppresses adrenocortical function (Nagra et al., 1965). More recent work with orchiectomized cockerels suggests that although androgen (testosterone and 5α-dihydrotestosterone) replacement suppresses adrenocortical cell response to ACTH, it maintains relative adrenal mass (Carsia et al., 1987b). On the other hand, exogenous testosterone in wild species seems to enhance circulating corticosterone, suggesting an increase in adrenocortical function (Ketterson et al., 1991; Schoech et al., 1999). Interestingly, orchiectomy is required to demonstrate the

effects of androgens on adrenocortical function in the domestic chicken (Nagra et al., 1965; Carsia et al., 1987b). Thus, it is quite possible that the testis elaborates both inhibitory and trophic substances that influence avian adrenocortical function.

In this connection, there are reported sex differences in adrenocortical activity and some of these are correlated to sexual maturity (see Madison et al., 2008). In addition, sex-dependent alterations in adrenocortical cellular sensitivity and maximal corticosterone response to ACTH have been reported (Carsia et al., 1987a, Carsia et al., 1988b; Kocsis and Carsia, 1989). Sex differences are also apparent at more proximal steps of the HPA axis, as for example, the axis response to CRH and arginine vasotocin (AVT) (Madison et al., 2008). However, the fact that these alterations at the cellular level are apparent during the embryonic and early posthatch period and prior to sexual maturity, (Carsia et al., 1987a; Kocsis and Carsia, 1989) argues that they may be, in part, sex-linked and separate from the greater levels of sex steroids in the circulation that accompany sexual maturity.

33.2.8 Regulation of aldosterone secretion

33.2.8.1 Role of angiotensin II

As in other vertebrates (Wilson, 1984; Holmes and Cronshaw, 1993; Kempf and Corvol, 2001; Nishimura, 2001), the avian kidney contains juxtaglomerular cells capable of producing renin. Renin cleaves fowl angiotensinogen ([Asp^1, Val^5, Ser^9]tetradecapeptide renin substrate) to form the decapeptide, angiotensin I ([Asp^1, Val^5, Ser^9]Ang I). The Ang II octapeptide produced from this decapeptide ([Val^5]Ang II; $M_r = 1031.19$) is that of most vertebrates including ovine and bovine species (thus, H-Asp^1-Arg^2-Val^3-Tyr^4-Val^5-His^6-Pro^7-Phe^8-OH), whereas other mammalian species produce [Ile^5]Ang II. In several species studied thus far (Japanese quail, duck and turkey), plasma Ang II concentrations range from 30 to 70 pg/mL (2.9×10^{-11}–6.8×10^{-11} M) but can increase to 100–400 pg/mL (9.7×10^{-11}–3.9×10^{-10} M) with perturbations to electrolyte and hemodynamic balance and with adaptation to saltwater (see Kocsis et al., 1995a).

Earlier in vivo studies demonstrated a direct regulation of aldosterone production by Ang II. Infusions of Ang II into ducks (Gray et al., 1989) showed a dose-dependent aldosterone response exclusive of alterations in circulating corticosterone increases circulating aldosterone. In addition, an exclusive, dose-dependent aldosterone response to Ang II has been demonstrated with duck adrenal tissue, specifically from the subcapsular region (Klingbeil, 1985; Holmes and Cronshaw, 1993). However, the distinction of functional zones exhibited by the duck adrenal gland may be less apparent or absent in other species. It may be that in other avian species, perturbations in electrolyte and hemodynamic homeostasis or other stressors are required to induce zona glomerulosa-like function in a subpopulation of adrenal steroidogenic cells (Kocsis et al., 1995a). Ang II does not stimulate cholesterol side-chain cleavage in turkey adrenocortical cells (Kocsis et al., 1995a). Presumably, the prevailing basal level of precursors within the cells is sufficient to support aldosterone synthesis. Thus, in vitro, a background influence of ACTH greatly enhances the efficacy of Ang II. Other evidence suggest that Ang II plays a role in remodeling of adrenocortical tissue during prolonged stress, as for example, dietary protein restriction (Carsia and Weber, 2000).

Finally, although it is fairly clear what the releasing factors for aldosterone are in birds with decreased plasma Na^+ and no cephalic (salt) glands, it is not clear what the aldosterone-releasing factors are in birds with cephalic glands and excessive Na^+ intake or when birds with cephalic glands undergo dehydration. It does not appear to be Ang II or changes in plasma K^+. Furthermore, the interaction of hormones regulating aldosterone secretion in birds that live exclusively in marine and desert environments has received much less attention (see Hughes, 2003).

33.2.8.2 Mechanism of Ang II action in avian adrenocortical cells

Studies with duck adrenal membrane preparations (Gray et al., 1989) and isolated turkey (Kocsis et al., 1994a,b, 1995a,b,c; Carsia and McIlroy, 1998) and chicken (Holmes and Cronshaw, 1993) adrenocortical cells indicate that the avian adrenal gland possesses high affinity Ang II receptors, having a K_d of 0.9–2 nM and concentration of 30,000–150,000 sites/cell. It should be pointed out that chickens are odd in that mature birds exhibit an absence of an aldosterone response to Ang II both in vivo and in vitro even though their adrenocortical cells express high affinity Ang II receptors (Holmes and Cronshaw, 1993).

Turkey (Murphy et al., 1993) and chicken (Kempf and Corvol, 2001) Ang II receptors have also been cloned. They are both 359-amino acid proteins (sharing 99.7% identity) and exhibit a 75% sequence identity with the mammalian type 1 receptor, albeit there are frank differences in pharmacological and physicochemical properties between mammalian and avian forms. Both avian forms have been shown to couple to the phosphoinositide/lipid-protein kinase C pathway (Murphy et al., 1993; Kempf and Corvol, 2001). Studies with isolated adrenocortical cells suggests that optimal signal transduction also requires calmodulin (Kocsis et al., 1995b). However, differences in tissue expression exist between turkeys and chickens. For example, the cloned turkey receptor is exclusively expressed in the adrenal gland (Carsia et al., 1993), whereas

the chicken receptor has a broader tissue expression (Kempf and Corvol, 2001). But thus far, the story is incomplete regarding the function of avian Ang II receptors at the cellular and molecular levels (Kocsis et al., 1995b; Kempf and Corvol, 2001; Nishimura, 2001).

33.2.8.3 Action of adrenocorticotropin on aldosterone secretion

Whereas an ample number of studies demonstrate the selective action of Ang II on avian aldosterone secretion, the action of ACTH is less specific, stimulating both aldosterone and corticosterone secretion. Although less potent, ACTH is 2−10-fold more efficacious than Ang II in stimulating aldosterone secretion in studies with avian adrenal tissue and avian adrenocortical cell preparations. However, the specificity and importance of Ang II reside not in its ability to greatly stimulate aldosterone secretion, but in its ability to link perturbations in electrolyte and hemodynamic balance to aldosterone secretion—a role not readily fulfilled by ACTH. As an example, stress raises both plasma corticosterone and aldosterone (Rosenberg and Hurwitz, 1987), but in response to dietary Na^+ changes, plasma aldosterone is greatly affected whereas plasma corticosterone is unaffected or modestly affected (Rosenberg and Hurwitz, 1987; Kocsis et al., 1995a). Furthermore, in vitro studies indicate that Ang II becomes equally efficacious to ACTH when some ACTH is included (Kocsis et al., 1994a).

33.2.8.4 Action of atrial natriuretic peptide on aldosterone secretion

Avian ANP was originally demonstrated as a diuretic agent in extracts from chicken hearts (Gregg and Wideman, 1986). It is a 29-amino acid peptide ($M_r = 3158.45$) that has significant structural homology to mammalian ANPs (Miyata et al., 1988). Avian ANP is stored and released from both atrial and ventricular cardiocytes (Toshimori et al., 1990), but is also produced by adrenal chromaffin cells (Wolfensberger et al., 1995). In ducks and chickens, the plasma concentration of ANP is about 70−80 pg/mL ($\sim 2.5 \times 10^{-11}$ M) and is inversely related to changes in blood volume in response to hemodynamic and electrolyte perturbations (Gray et al., 1991a; Gray, 1993). ANP receptors are found in both renal and adrenal tissue of the duck (Gray et al., 1991b). In adrenocortical cells, it is present at a concentration of ∼90,000 sites/cell (Kocsis et al., 1995c). The receptors have an apparent K_d of 1−3 nM (Gray et al., 1991b; Kocsis et al., 1995c). In the duck, infusions of avian ANP inhibit plasma aldosterone responses to Ang II without affecting circulating corticosterone (Gray et al., 1991b). In addition, in chicken adrenocortical cells, ANP is a potent (EC_{50} ∼1 nM) and efficacious inhibitor (>90%) of maximal ACTH and PTH-induced aldosterone secretion without affecting corticosterone secretion (Rosenberg et al., 1988b, 1989b). ANP appears to act at several intracellular loci (Rosenberg et al., 1989b), and cyclic GMP appears to be its second messenger (Rosenberg et al., 1988b, 1989b). Interestingly, in turkey adrenocortical cells, ANPs are as efficacious as Ang II in stimulating aldosterone production and actually augments maximal aldosterone production induced by Ang II, K^+, and ACTH (Kocsis et al., 1995c). Thus, more broadly, the actions of ANPs on adrenocortical function may be species-specific.

33.2.9 Overview of the hypothalamic-pituitary-adrenal axis

The HPA (Figure 33.9) axis is composed of (1) hypothalamic neurons in the paraventricular nucleus (PVN) which contain the releasing hormones, CRH, AVT [and sometimes mesotocin (MT)], (2) the corticotropes of the cephalic lobe of the par distalis which contain enzymes that synthesize and process (prohormone convertases) POMC to produce adrenocorticotropic hormone (corticotropin) (ACTH), and (3) the steroid-secreting cells of the adrenal gland which express the melanocortin-2 receptor (MC2R) that exclusively binds ACTH. The resultant end-product glucocorticoids facilitate the mobilization and partitioning of energy stores to meet general physiological demands, physiological adjustments during a stress response, and to assist in the recovery from periods of stress (MacDougall-Shackleton et al., 2019). Thus, the HPA axis operates within a larger regulatory system for energy flow and partitioning, especially for the central nervous system. However, the different components of the axis can have a level of independent and complex regulation: a regulation (a) suited for a life-history stage (Lattin et al., 2012a), or (b) for confronting a changing and unpredictable environment accompanying season (Dickens et al., 2011b; de Bruijn and Romero, 2018; Romero and Gormally 2019), or (c) that is altered -by genetic selection (Carsia and Weber 1986; Carsia et al., 1988b; Hazard et al., 2007).

CRH and AVT are the main stimulators of ACTH secretion from corticotropes, the ACTH-secreting cells of the cephalic lobe (Berghman et al., 1998). CRH is a 41 amino acid peptide that binds to the type 1 CRH receptor (CRH-R1) on corticotropes and activates adenylyl cyclase to elevate intracellular cAMP, resulting in the release of ACTH (Carsia et al., 1986; Kuenzel et al., 2013).

AVT is a nonapeptide that binds to the type 2 VT receptor (VT2R) (and the type 4 VT receptor) on corticotropes. VTRs activate phospholipase C, leading to the generation of inositol-1,4,5-triphosphate and diacylglycerol

for the mobilization of intracellular Ca^{2+} (see Kuenzel et al., 2013). Interestingly, AVT has role in water balance in that it recruits the HPA axis in response to osmotic stress (Sharma et al., 2009b).

Because CRH and AVT operate through different signal transduction cascades, their combined action leads to synergistic release of ACTH (Mikhailova et al., 2007). In addition, there is evidence that this synergistic effect is also due to heterodimerization of the CRH-R1 and VT2R (Mikhailova et al., 2007; Cornett et al., 2013).

It is well established that glucocorticoids exert a negative feedback on both the hypothalamus and pituitary gland to decrease CRH, and POMC in a classical negative feedback (Denver, 2009). However, this negative feedback is finely modulated by changes in the pituitary VT2R. High circulating concentrations of corticosterone increase VT2R expression and chemical adrenalectomy decreases it (Sharma et al., 2009a). Thus, the modulating effect of glucocorticoids on VT2R expression may explain the observed glucocorticoid programming of the HPA axis for enhanced stress response in zebra finches (Spencer et al., 2009).

In addition, there are two short-loop negative feedbacks operating in the HPA axis. ACTH itself appears to exert a short-loop negative feedback on the hypothalamic CRH neurons (Janowski et al., 2009), and glucocorticoids induced a short-loop negative feedback on the adrenocortical cell, probably by reducing MC2R expression and signal transduction (McIlroy et al., 1999).

Another highly important brain region in this scheme is the hippocampal (HP) formation which is highly homologous to the mammalian HP (see Smulders, 2017). Although the HP formation has indirect connections to the hypothalamus [more specifically, the PVN and periparaventricular nuclear area (peri-PVN)], it is important for glucocorticoid circadian rhythms and modulation of the HPA axis during the stress response. Under most conditions, glucocorticoids exert a negative feedback on the HF which synergizes with the negative feedback to the PVN and peri-PVN to reduced HPA activity. However, under different conditions such as long-term stress, the negative feedback in the HF is reduced and stimulatory signals from the HF are relayed to the PVN for sustained CRH release and thus sustained activation of the HPA axis (Zhu et al., 2014). This may be another mechanism that may explain continued glucocorticoid secretion during sustained stress and when circulating glucocorticoid levels are high (Romero and Gormally, 2019).

There is also considerable cross-talk between the HPA axis and other endocrine axes such as the hypothalamic-pituitary-thyroid (HPT) axis and hypothalamic-pituitary-gonadal (HPG) axis. For example, CRH also binds to the type 2 CRH receptor (CRH-R2) on thyrotropes and stimulates the secretion of thyroid-stimulating hormone (thyrotropin) (TSH) (De Groef et al., 2005, 2006). This is not surprising since thyroid hormones regulate intermediary metabolism and the HPA and HPT axes interact tightly to regulate certain developmental processes and hatching in birds. TSH acts on the thyrocytes of the thyroid gland to release T4 and T3. As mentioned previously (Section 33.2.7.3.2.1), thyroid hormones appear to decrease VT2R expression, inhibit the expression of prohormone convertase-1, an enzyme that processes POMC to produce ACTH and other melanocortins, and largely have a negative impact on corticosteroid secretion at the adrenal level. The opposite occurs with low-thyroid hormone status (Carsia et al., 1997; Sharma and Chaturvedi, 2009). Likewise, the HPG axis may interact with the HPA axis since there are sex differences in the plasma corticosterone response to CRH an AVT (Madison et al., 2008) and in AVT release and hypothalamic AVT receptor expression in response to osmotic stress (Chaturvedi et al., 2000).

Taken collectively, studies indicate that there are multiple pathways to elicit ACTH release from the cephalic lobe for optimal rhythms of corticosteroid secretion and for greater corticosteroid responses to address a variety of environmental and homeostatic stressors. The adrenal gland in turn has intrinsic mechanisms to permit the episodic release of corticosteroids of varying magnitude in responses to varying ACTH levels. This involves not only the rapid transcriptional regulation of such important proteins, MC2R, MRAP, StAR, and CYP11A but also the rapid induction of inactivation pathways (Liu et al., 2013). Finally, the resultant circadian and ultradian rhythms of free glucocorticoids are highly synchronized between the circulation, the subcutaneous tissue, and the brain (Qian et al., 2012). This underscores the precision of how glucocorticoids are distributed to different compartments for target-tissue specific functions.

33.2.10 Adrenocortical function in development, maturation, and senescence

The chicken (*Gallus gallus*) is the most studied model to describe the development of the avian adrenal gland. Thus, the pattern of development of this precocial species described herewith may be somewhat different from that of semiprecocial, semialtricial, and altricial species.

The chick adrenal begins as an adrenogenital primordium that is apparent at about 3 days of development. Development of steroidogenic cells requires the nuclear receptor, steroidogenic factor-1 (SF-1/NR5A1), which is expressed in the adrenogenital primordium (Smith et al., 1999). SF-1 promotes cell growth, limits cell death (apoptosis), and regulates the expression of genes involved in steroidogenesis, the MC2R, and StAR. In the laboratory mouse (*Mus musculus*), the MC2R is required for postnatal adrenal development and adrenal steroidogenesis (Chida

et al., 2007), and this is most likely true for avian species. Additional transcription factors are necessary for adrenocortical cell differentiation (Pihlajoki et al., 2013). At this time, the expression of key steroidogenic enzymes is detected in the chick embryo (Nomura et al., 1999) and in the developing zebra finch adrenal gland (Freking et al., 2000). However, in-situ hybridization detects these key enzymes at about five days of development (Kanda et al., 2000) and this is in agreement with a more recent gene-expression study (Kamata et al., 2004). Also, at about 5 days of development, the segregation of the adrenogenital primordium into the adrenal gland and the gonad is apparent (Smith et al., 1999) as well as the histological identification of steroid-secreting cells arranged in cords (Chimenti and Accordi, 2008). From days 7−15 of development, chromaffin cells penetrate gland and complete morphogenesis of the adrenal gland is complete by day 15.

It is thought that the adrenal gland is capable of steroidogenic function as early as day five of development, well before morphogenesis is complete. Embryonic circulating corticosterone levels slowly rise to day 15, but are independent of pituitary ACTH, even though immunoreactive ACTH is present in corticotropes at day 7 and embryonic adrenocortical cells can respond to ACTH. However, negative feedback is probably established by day 11. After day 15 to hatch, the gland is under ACTH control and CRH neurons become detectable in the hypothalamus a day earlier (see Jenkins and Porter, 2004; De Groef et al., 2008; Ellestad et al., 2011). So, there is general agreement that the adrenal gland of this precocial species is under the control of pituitary ACTH at day 15 of development. From that day to hatch, circulating corticosteroids reach their peak. This rise is matched by an abrupt increase in maximal cellular corticosteroid response and maximal cellular sensitivity to ACTH (Carsia et al., 1987a). However, 1−2 days posthatch, chicks have a stress hyporesponsive period (see Wada, 2008). This is due to a proximal HPA axial block since adrenocortical cells are fully responsive to ACTH (Carsia et al., 1987a). Interestingly, there is evidence for an age-dependent window for "imprinting" the avian adrenal gland for a long-term, enhanced setpoint of response to ACTH (Avrutina et al., 1985). In chickens, this appears to be about 2−4 weeks posthatch. For example, subjecting cockerels to transient protein restriction over this period induces long-term potentiation of adrenocortical cell function (Weber et al., 1990).

In altricial birds, the time-frame for HPA axis development is shifted later in the posthatch period. It is hypothesized that the peak corticosteroid response to a fully developed axis occurs at fledging (Wada, 2008). Here again, birds of an earlier age can respond to an ACTH challenge indicating that the reduced corticosteroid response prior to fledging is proximal to the adrenal gland. It is thought that in altricial species, this uncoupling of the hypothalamic-pituitary unit from the adrenal prevents increases in circulating corticosteroids in response to stress which could have an adverse effect on growth and immune function. In addition, body condition of nestlings, such as fat stores, impact on the HPA axis response to stress and on circulating CBG which modulates the target-tissue effects of the prevailing circulating levels of corticosterone (Müller et al., 2010).

Overall, a limited number of studies indicate a gradual decline in adrenocortical function with age (Schmeling and Nockels, 1978; Avrutina et al., 1985; Davis and Siopes, 1987) and during senescence. In chickens, this decline, in part, may be due to a decrease in adrenocortical cell sensitivity and response to ACTH (Carsia et al., 1985b, 1987a).

33.3 Physiology of adrenocortical hormones

The action of corticosteroids in birds is highly complex, sometimes quixotic and paradoxical, depending on species, gender, life-history stage, habitat, and a changing environment within a particular habitat (Romero and Gormally, 2019). This corticosteroid hormonal pleiotropy is largely due to the expression and interaction of their cognate receptors and the intracellular coactivators and transcription factors. The MR, GR, and membrane glucocorticoid receptor (mGR) have decreasing affinities to glucocorticoids [∼0.2 nM (∼69 pg/mL), ∼6 nM (∼2 ng/mL) and ∼20 nM (∼6.9 ng/mL), respectively]. Other studies use available mammalian receptor antagonists to dissect the function of these receptors, however, complete antagonists are lacking. Finally, little is known about the repertoire of intracellular coactivators and other transcription factors that mediate the activated forms of the corticosteroid receptors. Some of the factors contributing to the quixotic pleiotropic actions of corticosteroids are described in Table 33.2. Despite the complexity of corticosteroids actions, an overview of the corticosteroid receptors and the complex functions that they are thought to regulate are discussed in subsequent sections below.

33.3.1 Corticosteroid receptors and their action in target cells

The structure of avian forms of the GR (Kwok et al., 2007) and MR (Proszkowiec-Weglarz and Porter, 2010) has been determined. It is believed that there is one form of the GR (Kwok et al., 2007), albeit, it is likely that there are transcriptional isoforms and post-translational isomorphs (Table 33.2). In traditional ligand-binding and competitive-binding studies, these manifest as the low-affinity site and

TABLE 33.2 Some factors contributing to the pleiotropic effects of the glucocorticoids via the glucocorticoid receptor.

1. GR isoforms and post-translationally modified glucocorticoid receptors (GRs) (isomorphs)	a. Isoforms: alternative translation initiation sites producing GRs of different sizes b. Isomorphs: post-translational modifications (phosphorylation, acetylation, ubiquitination, SUMOylation (small ubiquitin-like modifiers)
2. Non-nuclear genomic GRs	a. GRs associated with the plasma membrane b. GRs retained within the cytoplasm c. GRs associated with mitochondrial genome (liganded are transactivators; unliganded are transrepressors)
3. Nuclear genomic GRs	a. Liganded monomers b. Unliganded monomers c. Typical liganded homodimers d. Liganded and unliganded heterodimers with other nuclear receptors or transcription factors e. Indirect interactions to DNA via tethering to transcription factors (transactivators or transrepressors)
4. Steroid receptor coactivation/corepression	GRs can interact with nuclear coactivators and corepressors, especially in the brain
5. Epigenetic mechanisms	a. GRs can recruit histone-modifying enzymes that can alter future responses to glucocorticoids by functioning as a "switch" for glucocorticoid enhancement or repression of target genes. This may be the basis for transgenerational effects of stress and glucocorticoid action. b. More broadly, other nuclear receptor response elements (e.g., androgen receptor) overlap with glucocorticoid response elements. Thus, active GRs may modify reciprocal response elements. This has clear implications for the role of GRs in modulating the transcriptional landscape of other steroid hormones. c. Some noncoding RNAs contain pseudo-glucocorticoid response elements. Thus, competent GRs are sequestered from target gene promoters.

All of these factors may have superimposed, tissue-specific characteristics. These factors may explain the lack of consistent correlation between tissue concentrations of glucocorticoid receptors and the "expected" tissue response to glucocorticoids. Note: the first category can distribute into the other categories.

high-affinity site for corticosterone binding. Both share high homology with mammalian corticosteroid receptors, and for the most part, function as homodimers after corticosteroid binding.

Localization of the unstimulated GR and MR is mainly to the cytoplasm, and there is active translocation to the nucleus with corticosteroid treatment (Proszkowiec-Weglarz and Porter, 2010). Transfection of receptors shows that aldosterone is two–three times more effective than corticosterone for receptor activation. Interestingly, like aldosterone, the glucocorticoid corticosterone is 10 times more effective in activating the MR than the GR (Proszkowiec-Weglarz and Porter, 2010). However, the mammalian GR antagonist, onapristone, only partially blocked the corticosterone-activated chicken GR, and the mammalian MR antagonist, spironolactone, was a very weak antagonist of the activated chicken MR and actually had agonistic activity. Thus, the mammalian corticosteroid receptor antagonists (Figure 33.10) do not always work with the same fidelity in avian studies.

Roughly 5–10% of classical corticosteroid receptors are associated with the plasma membrane, and there are receptors that operate within the cytoplasm as well. It is not clear whether homodimerization is a requirement but mGR do associate with other membrane proteins for signal transduction (Vernocchi et al., 2013). In general, membrane and cytoplasmic localization most often leads to pathways using extracellular signal-regulated kinases or mitogen-activated protein kinase for relatively rapid cellular responses (within seconds to a few minutes). Thus, GRs in these compartments, the plasma membrane, the cytosol and the nucleus, and also the mitochondrial compartment, contribute to the extraordinarily wide range of glucocorticoid actions (Table 33.2) (Scheschowitsch et al., 2017).

Corticosteroid nuclear signaling is also highly complex and is more than the well-characterized interaction of a homodimerized GR with glucocorticoid-response elements on DNA (e.g., Adams et al., 2003) (Table 33.2). Liganded monomers can bind and transactivate half-site regions of DNA, and unliganded monomers may repress transactivation. Liganded monomers can heterodimerize with MR monomers or monomers of other nuclear receptors, or other transcription factors and act as either transactivators or transrepressors. The picture is complicated further with

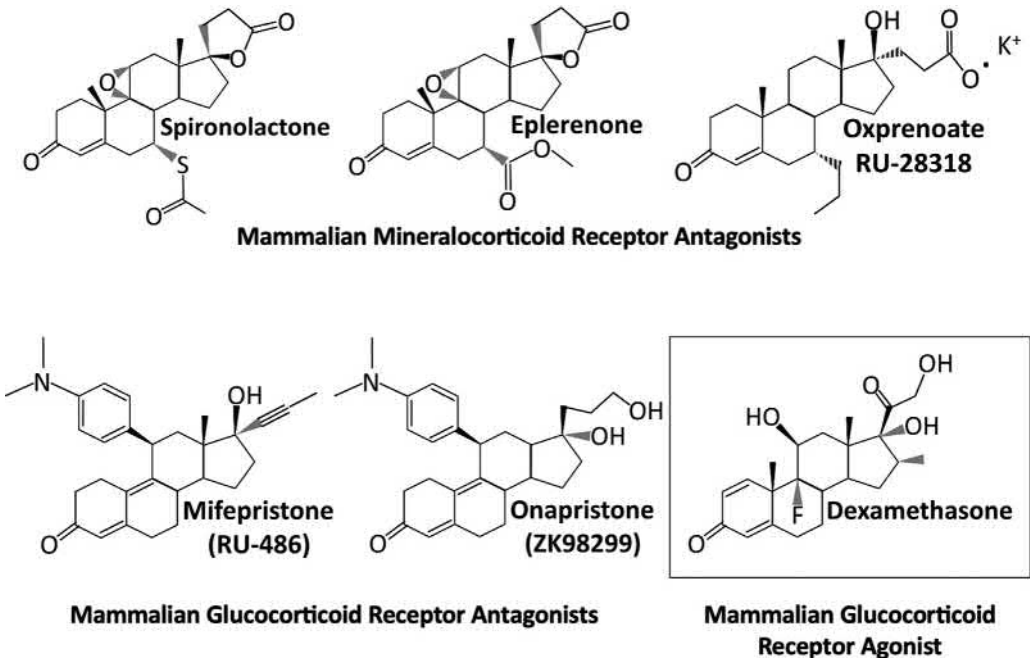

FIGURE 33.10 Chemical structure of mammalian mineralocorticoid and glucocorticoid receptor antagonists, and the potent glucocorticoid receptor agonist, dexamethasone. The use of these compounds in avian corticosteroid receptor studies has yielded mixed results, since they sometimes are only partially active or have agonist/antagonist activity opposite their usually complete action in mammalian receptor studies. *Molecules drawn by R. V. Carsia.*

competing GR isoforms (i.e., receptors of different sizes by alternative translation initiation) or post-translationally modified GRs (isomorphs) (i.e., phosphorylation, acetylation, etc.) that can compete with the function of full-sized monomers (Kadmiel and Cidlowski, 2013). For example, cytosolic and membrane-associated corticosteroid receptors differentially bind corticosterone and cortisol in a tissue-specific manner which is thought to be due to post-translational modifications (Schmidt et al., 2010). In addition, specific tissues may modulate co-activators, co-repressors, or other steroid receptor coactivators, especially the nervous system (Sun and Xu, 2020). Lastly, specific tissues may have epigenetic mechanisms (post-translational modifications of histone-modifying enzymes; noncoding RNAs) that further modify the action of GRs (Bartlett et al., 2019).

Corticosteroid receptors have been described through standard ligand- and competitive-binding studies on cytosolic and nuclear preparations of many tissues from diverse species (Breuner and Orchinik, 2001, 2009; Schmidt et al., 2010; Lattin et al., 2012b). The binding sites are sufficiently different from mammalian types in that known mammalian MR antagonists fail to displace corticosterone from the high-affinity site (MR) and similarly, the mammalian GR antagonist, mifepristone (RU-486; mifepristone) is a variable and often weak antagonist of the low-affinity site (GR). The affinities of these MRs and GRs for corticosterone are fairly consistent: K_ds of about 0.2 and 6 nM, respectively, with a membrane-binding site of about 14−30 nM. Since the affinity of avian CBG is about 2 nM, the high-affinity site (MR) can easily draw corticosterone from CBG compared to the low-affinity site (GR). Thus, corticosterone most likely activates the avian MR and only in certain tissues with high 11βHSD2 and 20HSD activity is aldosterone selectively more active. One caveat is that at the tissue level, receptor concentration may not necessarily correlate with physiological response to corticosteroids (Lattin et al., 2015).

The cloned avian GR and MR also serve as molecular tools to assess receptor expression in the avian brain (e.g., Dickens et al., 2011b). However, studies of corticosteroid receptor expression based on messenger RNA should be viewed with caution because of poor correlation with actual acceptor protein (i.e., corticosteroid receptor) levels in neuronal tissue as determined by ligand binding (Medina et al., 2013).

33.3.2 Corticosteroids and intermediary metabolism

Studies in birds indicate that glucocorticoids exert profound effects on protein, carbohydrate, and lipid metabolism (see Landys et al., 2006; Scanes, 2009). Glucocorticoids increase plasma glucose levels primarily by stimulating proteins that shuttle glucose transporters from cell membranes to the intracellular compartment (Horner et al., 1987). They also metabolize proteins when other available energy stores are inadequate. As a result, there is a tendency for prolonged elevated glucocorticoid levels to decrease body mass.

Baseline glucocorticoids are permissive for processes that maintain adequate food intake and optimal body mass, and food choice is influenced by glucocorticoids operating through an interaction between the MR and GR. Glucocorticoids also appear to work on the alimentary system by increasing transit time and the uptake of glucose, calcium, and phosphate.

Further complicating the picture is that high glucocorticoids may differentially increase oxidative stress. This appears to result in shortened telomere length and other DNA damage in tissues (Flint et al., 2007; Costantini et al., 2008; Romero and Gormally, 2019). Also, the general oxidative stress impacts on the interpretations of changes in key metabolic indicators.

Since most studies use some form of glucocorticoid depot or glucocorticoid feeding regimen, the normal rhythms of glucocorticoids and, in turn, the complementary rhythms of delivery to target tissues, and the normal responses of interacting endocrines to those rhythms are largely disrupted. Thus, it is not clear whether the responses in birds to exogenous glucocorticoids are physiological or pharmacological. Nevertheless, some conclusions as to their action can be drawn from the large number of studies conducted in diverse avian species.

33.3.2.1 Protein metabolism

The action of glucocorticoids largely results in protein catabolism (see Landys et al., 2006; Scanes, 2009). The amino acids enter the citric acid cycle as an energy source and also shunt to hepatic, renal, and possibly intestinal sites (Watford, 2005) for gluconeogenesis to maintain adequate glucose levels. Both the reduction of glucose transporters from cells and the shunting of amino acids for gluconeogenesis contribute to either raising or maintaining glucose levels. In domestic fowl, the important enzyme for gluconeogenesis is cytosolic phosphoenolpyruvate carboxykinase. In young chickens, the activity of this enzyme is localized in both the kidney and liver, whereas in the adult, it is predominantly in the kidney.

Frank changes in circulating glucose are not always apparent because of facilitated entry into cells through the action of insulin. In domestic fowl, corticosterone induces hyperinsulinemia. However, a number of molecular markers also indicate insulin resistance in the liver and muscle and an increase in muscle glycogen (Lin et al., 2007). This paradox may be due to species, dose of exogenous glucocorticoid, route of delivery, and duration of treatment.

Since one of the largest sources of protein is muscle, it is not surprising that there is muscle breakdown. Strong indicators of generalized protein catabolism and more specific muscle protein breakdown are increases in circulating uric acid and the concentration of 3-methyhistidine in muscle, respectively. In domestic fowl, both sarcoplasmic and myofibrillar protein breakdown is apparent and protein synthesis is depressed (Dong et al., 2007). However, in wild species, there is evidence for a differential effect in which sarcoplasmic reticular proteins are preferentially degraded whereas myofibrillar proteins are initially spared, presumably to preserve flight muscle. The effect of glucocorticoids on protein metabolism is clearly concentration-dependent, suggesting that these steroid hormones finely modulate protein metabolism.

33.3.2.2 Lipid metabolism

Exogenous glucocorticoids, at concentrations reflecting ranges just exceeding circulating baseline levels and probably into stress levels, do have an impact on lipid metabolism (see Landys et al., 2006; Scanes, 2009). Again, as with protein catabolism, lipid stores are accessed to preserve circulating glucose and to provide an alternate energy source. Corticosteroids play a significant role during periods of prolonged food deprivation to maintain metabolic processes and the required energy partitioning by operating in three phases: phase I, glucose metabolism; phase II, fatty acid metabolism after glucose stores are exhausted; and phase III, protein catabolism, once fatty acid stores are depleted (see de Buijn and Romero, 2018). Evidence suggests that the action of glucocorticoids on lipid metabolism is mediated through the low-affinity GR in that some actions are blocked by RU-486 (mifepristone). Thus far, only the low-affinity, GR-type receptor is detected in avian adipose tissue (Lattin, et al., 2012b).

In birds with positive energy balance, glucocorticoids also stimulate lipogenesis and fat deposition in the liver and increase abdominal fat pad size. This lipogenic effect may be driven largely by insulin. In adequately fed, growing poultry, all glucocorticoid-driven effects on lipid metabolism are seen: an increase in adiposity and hepatic lipogenesis, an increase in circulating free fatty acids, and a decrease in glucose utilization (Scanes, 2009).

33.3.3 Corticosteroids and electrolyte balance

Birds regulated both plasma electrolytes and plasma volume within fairly narrow limits. Corticosteroids are critical for maintaining electrolyte and water balance. Most of the action of corticosteroids is mediated by the high-affinity MR. Thus, prevailing glucocorticoids are sufficient to maintain this balance. However, specific detection systems of perturbations in this balance activate the MRs in the main target tissues, the kidney, intestine, and hindgut, by deploying the potent mineralocorticoid, aldosterone. Since some extreme perturbations also call in the HPA axis, it is

especially important that glucocorticoid-inactivating enzymes (11βHSD2, 20HSD) are upregulated and/or activated in these target tissues to permit aldosterone action (see Hughes, 2003; Landys et al., 2006; Laverty et al., 2006). This is especially important in birds with life-history stages between freshwater and marine habitats, or between water-replete environments and arid environments.

Interestingly, the mechanism of aldosterone action on these target tissues is similar between birds without and with cephalic (salt) glands. Birds without salt glands cannot tolerate high Na^+ intake, but they do respond to low Na^+ intake. In this situation, there is the expected increase in circulating aldosterone in order to maintain adequate plasma Na^+ concentrations. Aldosterone acts on the kidney to reabsorb Na^+ from the glomerular filtrate. In addition, it increases the Na^+ channels and their activity in the colon and coprodeum to reabsorb lost Na^+ from the ureteral fluid. Furthermore, it induces ureteral fluid reflux from the coprodeum to more orad (proximal) segments for additional cycles of Na^+ reabsorption.

In estuarian and marine birds with salt glands, aldosterone levels are maintained and elevated with high Na^+ intake through an unknown mechanism. The actions of aldosterone are for the most part the same as in birds without salt glands. Birds with salt glands tend to have larger kidneys and greater rates of glomerular filtration compared to birds without salt glands. Thus, there is an increase in Na^+ and water reabsorption at the kidney and hindgut with refluxing to augment reabsorption. However, in birds with salt glands, the resultant excess circulating Na^+ is secreted from the salt glands, which are stimulated by high-plasma osmolality and high-extracellular fluid volume but are not under the control of aldosterone. In this way, water is added to the extracellular fluid without the high concentrations of Na^+, thereby maintaining a plasma volume and osmolality compatible with life.

33.3.4 Corticosteroids and immune function

The obvious importance of corticosteroids in immune regulation is evinced by a growing body of literature indicating that the immune tissues of birds have an intrinsic system for either the local production of corticosteroids (Lechner et al., 2001) and/or the enzymes capable of reactivating circulating corticosteroid metabolites (Schmidt et al., 2008). Furthermore, it appears that avian immune tissues possess both MRs and GRs, with the suggestion that the MRs are activated preferentially by corticosterone (and aldosterone?) and the GRs by cortisol (Schmidt et al., 2010; Lattin et al., 2012b). Interestingly, the developing avian immune system appears to contain the steroidogenic enzymes necessary to locally synthesize cortisol de novo from cholesterol (Schmidt and Soma, 2008).

In general, birds have a different repertoire of immune organs, immune cells, and elaborated signaling molecules and immune-regulating genes compared to those of mammals. For example, birds lack lymph nodes for antigen presentation and rely predominantly on tissue dendritic cells. Nevertheless, the observed effects of glucocorticoids on the avian immune system appear consistent with that seen in mammalian immune system, that is, the effects are largely immunosuppressive through their cross-talk with several immune signaling pathways (see Odihambo Mumma et al., 2006; Kaiser et al., 2009; Shini et al., 2010; Petta et al., 2016). Exogenous corticosterone reduces the relative weight of the spleen and the bursa of Fabricius and stimulates heterophils and reduces leukocytes thereby increasing the heterophil/leukocyte ratio. Other research on this topic are beyond the scope of this chapter, but the overall consensus is that glucocorticoids may finely modulate immune response, and its group of cognate receptors may serve as an important avian immune rheostat to ensure optimal immune response in birds.

33.3.5 Corticosteroids and behavior

Behavior strategies used by birds, especially breeding behavior, are energy-costly. Glucocorticoids and other hormones function to partition energy flow in order to balance breeding-related activity and self-maintenance and survival-oriented activities (Landys et al., 2006; Cornelius et al., 2013a,b; Wingfield, 2013). This balance is strongly influenced by the investment in breeding for the perpetuation of the species (Cornelius et al., 2013b). Those species with a high investment in a breeding cycle because of limited opportunities for breeding or because of short life spans, employ mechanisms to dampen the HPA axis, allowing for just basic maintenance levels of corticosterone for permissive functions that support other hormones involved in energy partitioning. For those species with greater life spans that permit numerous opportunities for breeding, greater emphasis is on maintaining an active HPA axis in order to exploit those opportunities. Since many activities are associated with preparation for breeding, migration, territorial behavior, nest building, etc., it is not surprising that glucocorticoids regulate these activities.

In general, glucocorticoids affect activity patterns, cognitive and learning processes, reproductive parameters such as courtship, copulation, and parental behavior such as interaction with offspring and procurement of food for offspring (Möstl and Palme, 2002; Rubolini et al., 2005). Since glucocorticoids regulate a number of locomotory patterns of birds, it is not surprising that locomotory activity and circulating glucocorticoid levels are tightly linked (Landys et al., 2006). The effect of glucocorticoids is rapid, concentration-dependent, and is not blocked by the GR antagonist RU-486 (mifepristone). This suggests that the receptor mode employed to regulate locomotory activity is nongenomic.

Glucocorticoids are essential for processes related to migration. They regulate the replenishment of energy stores

at stopover points and at final breeding grounds by increasing brain neurotransmitters controlling the increase in food intake, by decreasing thermogenesis and by promoting fat deposition (Cornelius et al., 2013a). They also regulate the transition from migration to breeding in that high-circulating levels inhibit the progression into breeding if environmental conditions are not conducive for nesting.

Of recent interest and of great importance is the role of glucocorticoids in the behavioral responses of birds to anthropogenic stressors and the world-wide encroachment of urbanization (Bonier, 2012; Wingfield, 2013). Evidence indicates that these persistent abiotic stressors can shape endocrine traits including glucocorticoid responses. As mentioned previously, glucocorticoids can be deleterious to survival or to species propagation by disrupting breeding. The emerging picture is that due to the variations in the HPA axis plasticity among avian species, urban stressors may differentiate species into urban avoiders, urban adaptors. and urban exploiters (Bonier, 2012).

33.4 Adrenal chromaffin tissue hormones

33.4.1 Catecholamine synthesis and secretion

Catecholamines are widely synthesized throughout the postganglionic sympathetic nervous system which includes the adrenal chromaffin tissue. They are also synthesized in some tissues as, for example, the brain (Yamsaki et al., 2003), but these sites are not thought to contribute substantially to the pool in circulation.

The biosynthetic pathway for the adrenal catecholamines (Ghosh et al., 2001; Mahata et al., 2002; Trifaró, 2002) is outline in Figure 33.11. The rate limiting step in

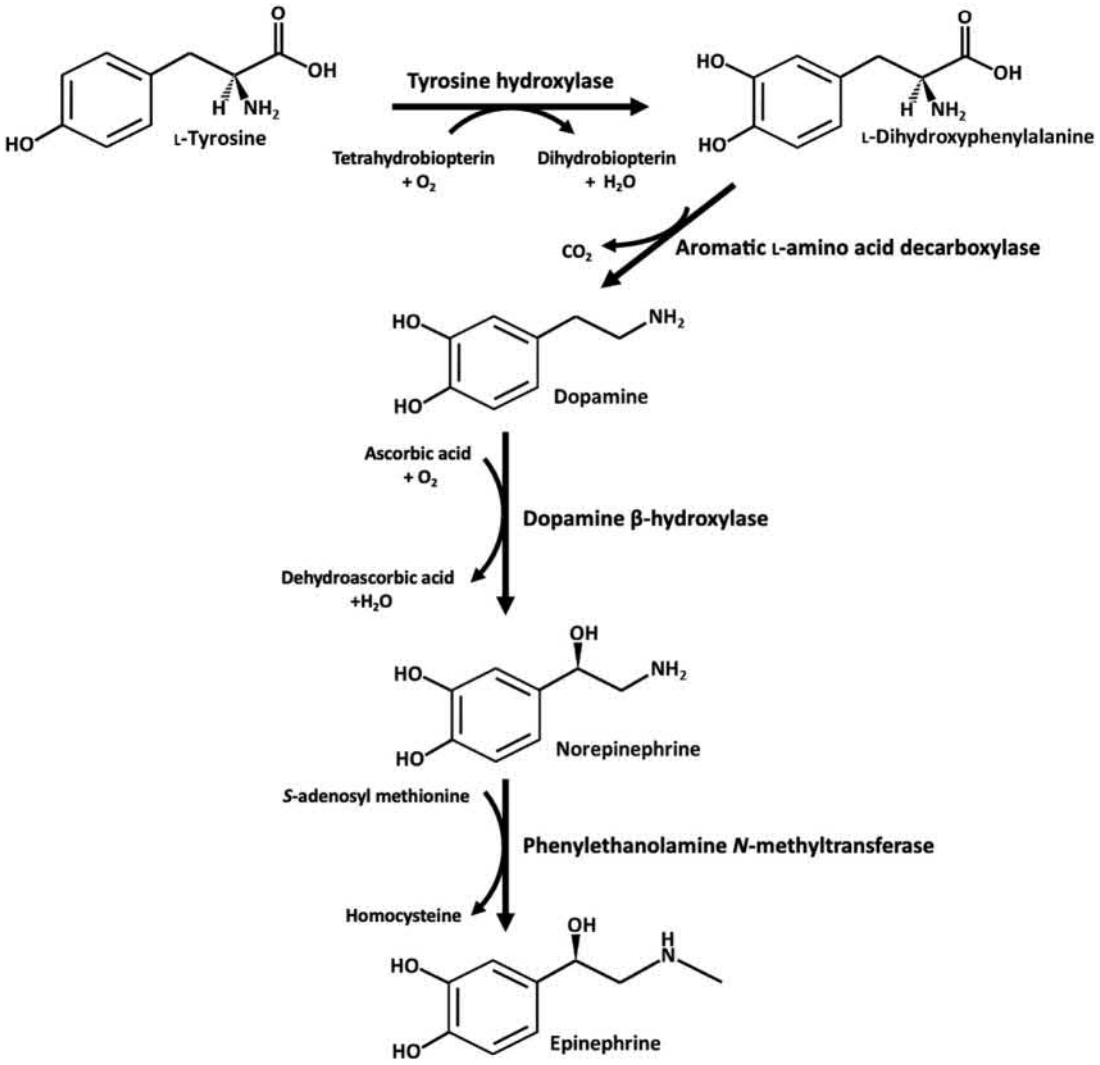

FIGURE 33.11 Biosynthesis of norepinephrine and epinephrine. Solid *black* and *hatched* bonds on molecules represent key beta (up) and alpha (down) positions, respectively, however, not all hydrogen bond positions are shown. See text for additional details. *Pathway drawn by R. V. Carsia.*

catecholamine biosynthesis is tyrosine hydroxylase. Catecholamines exert a negative feedback on tyrosine hydroxylase. Concerning the description of catecholamine release from the adrenal gland, it is best to use the framework of the catecholamine pathway in the "fight or flight" response to a particular stressor.

The perception of a stressor by the bird impacts on the proximal sympathetic nervous system that is relayed to preganglionic neurons of the spinal cord. The axons of these neurons comprise splanchnic nerves destined for the chromaffin tissue of the adrenal gland. Acetylcholine released from preganglionic sympathetic (splanchnic) nerve terminals interacts with both nicotinic and muscarinic receptors to stimulate phosphorylation of tyrosine hydroxylase, for rapid catecholamine synthesis and release, and upregulates tyrosine hydroxylase synthesis for more long-term stimulation. Phosphorylation lowers the K_m of tyrosine hydroxylase for tetrahydrobiopterin, a cofactor necessary for tyrosine hydroxylase activity. VIP and PACAP also stimulate the phosphorylation of tyrosine hydroxylase.

Tyrosine hydroxylase catalyzes the conversion of tyrosine to L-dihydrophenylalanine (L-DOPA). L-DOPA is converted to dopamine by aromatic L-amino acid decarboxylase (L-DOPA decarboxylase). Dopamine is either secreted or undergoes further conversion to NE by dopamine β-hydroxylase with ascorbic acid as a cofactor.

The final step to E is carried out by phenylethanolamine *N*-methyltransferase (PNMT) in which the *S*-methyl group of *S*-adenosyl methionine is transferred to the primary nitrogen group of NE. All of these enzymes have some requirement for innervation and are affected by numerous intra-adrenal peptides. However, PNMT is strictly GR-dependent.

The release of catecholamines into the circulation occurs by the well-studied, stimulus-secretion coupling mechanism. In addition to catecholamines, there are a number of neuropeptides that are co-released (see Section 33.1.2.3). Furthermore, chromogranins and secretogranins are also released. Chromogranins are necessary for sequestration of synthesized catecholamines in secretory granules. The peptides derived from chromogranins have autocrine and paracrine effects on catecholamine release (Trifaró, 2002; Mahata et al., 2010; Tota et al., 2012).

There is no preferential release of E or NE from isolated chicken chromaffin cells in response to acetylcholine analogs (Knight and Baker, 1986). In vivo, however, the secretion of E and NE from the avian adrenal gland is thought to be finely regulated by a number of neural-derived and blood-borne factors and hormones resulting in the differential release of catecholamines (Ghosh et al., 2001). Yet, it is not known precisely how the differential adrenal secretion of E and NE occurs in response to disparate physiological conditions and stressors. Since the preganglionic fibers of splanchnic nerves originate in the spinal cord and since chromaffin cells exert an influence on the presynaptic endings, it may be that preganglionic neurons are connected to either NE- or E-secreting chromaffin cells. What is fairly clear is that the adrenal gland is nearly the sole contributor to circulating E and most of the NE in response to acute stressors (Butler and Wilson, 1985; Lacombe and Jones, 1990).

33.4.2 Circulating catecholamines and stress response

The most recent and consistent values of circulating catecholamines in birds are obtained from studies with the domestic chicken (*Gallus gallus*) and duck (*Cairina moschata*) in which catecholamines were measured using high-pressure liquid chromatography with electrochemical detection. The plasma concentrations of NE and E in growing and mature chickens average 0.52 and 0.96 ng/mL, respectively, whereas those of the duck average 0.45 and 2.10 ng/mL, respectively. Dopamine also exists at variable but comparable concentrations (Butler and Wilson, 1985; Cheng et al., 2001; Pohle and Cheng, 2009). In the chicken, NE, but not E, shows a diurnal rhythm (de Jong et al., 2001).

Catecholamines are degraded mainly in the liver by catecholamine-O-methyltransferase and monoamine oxidase and the inactive products are removed by the kidney. Monoamine oxidases are also present in the adrenal gland and thus can modulate intra-adrenal levels of catecholamines (Ghosh et al., 2001).

Adrenal catecholamines are part of the first wave of acute stress response, i.e., the "fight-or-flight response." The E response to stress stimulates immediate hepatic glycogenolysis to provide glucose for critical tissues. In addition, catecholamines appear to interact with glucagon to regulate thermogenesis in cold stress (Abdelmelek et al., 2001; Filali-Zegzouti et al., 2005). Furthermore, catecholamines enhance the activity of the HPA axis at all levels ultimately driving more glucocorticoid release. In turn, the action of catecholamines is dependent on glucocorticoids (Sapolsky et al., 2000; Cyr et al., 2009).

Glucocorticoids enhance cardiovascular sensitivity to catecholamines. The effect of glucocorticoids occurs at multiple levels of catecholamine action. They inhibit reuptake of catecholamines by sympathetic terminals, reduce the catecholamine-degrading enzymes, catechol-O-methyltransferase and monoamine oxidase, and increase the binding parameters and transmembranous signaling of β-adrenergic receptors. Indeed, a large part of the modulation of catecholamine action occurs through the regulation of adrenergic receptor function.

In wild avian species, the adrenal catecholamine response to stress is complex (see Romero and Gormally, 2019). The highly conserved "fight or flight" response of

the catecholamine pathway is more nuanced as might be expected with the myriad life-history-cycle and life-history-stage transitions of wild birds. Within a species, aspects of the pathway and the responses of target tissues are affected by season.

33.4.3 Some physiological actions of norepinephrine and epinephrine

Catecholamines have diverse effects on immune cells. For example, continuous infusion of physiological concentrations of NE and E enhance chicken leukocyte migration and differentially affect the phytohemagglutinin wattle response (McCorkle and Taylor, 1993). In addition, NE and E, in vivo and in vitro, have contrasting effects on immunoglobulin plaque-forming cells from splenic lymphocytes, and these contrasting effects are probably mediated by α- and β-adrenergic receptors (Denno et al., 1994). Catecholamines also differentially affect macrophage effector functions, in vitro (Ali et al., 1994).

The metabolic effects of catecholamines are widespread in that they interact with other regulating hormones such as insulin, prolactin, thyroid hormones, growth hormone, and glucagon. Catecholamines influence carbohydrate and lipid metabolism. E stimulates glycogenolysis in chicken hepatocytes via β-adrenergic receptor activation and cAMP production, which, in turn, activates glycogen phosphorylase. Thus, the effect of catecholamines leads to a rapid increase in blood glucose levels (Thurston et al., 1993). Catecholamines (NE and presumably E) also stimulate gluconeogenesis via α-adrenergic receptor activation of intracellular calcium mobilization (Cramb et al., 1982). It is probable that the effects of E on glycogenolysis, gluconeogenesis, and also lipogenesis (see below) are physiological roles for adrenal E, as these metabolic parameters are influenced by concentrations of E that are found in the circulation of a stressed bird.

In chickens, during periods of behavioral inactivity, there is a positive relationship between circulating catecholamines and free fatty acids. Thus, catecholamines, at least in the liver, may be physiological regulators of lipid metabolism. The synthesis of fatty acid (lipogenesis) by liver tissue and cells is inhibited by E and to a lesser extent by NE. This effect is mediated via both α- and β-adrenergic receptors, and at least partially, by - cAMP acting as the intracellular messenger (Campbell and Scanes, 1985). Lipolysis in fat cells is stimulated by E in several species of birds and appears to be mediated via β-adrenergic receptors and - cAMP (Campbell and Scanes, 1985).

33.4.4 Changes in development, maturation, and senescence

Experiments with precocial species (again, mainly *Gallus gallus*) indicate that the adrenal chromaffin cells are derived from caudal thoracic (region of somites 18−24) populations of neural crest cells (sympathoadrenal progenitor cells) (see Shtukmaster et al., 2013; Unsicker et al., 2013). Recent evidence indicates that the adrenal chromaffin cells and postganglionic sympathetic neurons are derived from a common precursor cell population. In the chick embryo at about day two, this population delaminates from the neural tube and migrates ventrally to the area of the dorsal aorta. Under the induction of bone morphogenic proteins elaborated from the aorta, the cells acquire catecholaminergic features, as for example, the expression of tyrosine hydroxylase. Cells that reach the region of the adrenal gland at around embryonic day six gradually lose neuronal features such as the expression of neurofilament proteins and gain chromaffin cell features. This transformation from neuronal type to chromaffin type does not require the GR or even adrenocortical tissue (Gut et al., 2005; Huber, 2006). However, the differentiation to E cells and the expression of PNMT is absolutely GR dependent and is apparent in chromaffin cells at day five, albeit E cell differentiation does not require penetration into the developing adrenocortical tissue (Chimenti and Accordi, 2008). Indeed, chromaffin cell migration and penetration into the developing adrenocortical tissue does not occur until around day eight or nine and is not complete until day 15. In the chick, in addition to catecholamines, a variety of peptides are elaborated by the adrenal chromaffin cells postnatally. Some of these peptides have been described previously (see Section 33.1.2.3).

E is detected in the chick embryonic circulation somewhere between embryonic days 10−13 (see von Blumröder and Tönhardt, 2002). The importance of the adrenal gland in providing catecholamines for embryonic homeostasis is unclear since catecholamines can come from both adrenal and neuronal sources. However, a consistent observation is that circulating levels of NE predominate over those of dopamine and E. In the chick embryo, plasma catecholamines increase approaching hatch (von Blumröder and Tönhardt, 2002). NE appears to be an important catecholamine that supports the embryo for pipping and hatching, and the metabolic changes associate with the perihatch transition.

There appears to be an extreme range of variation in the adrenal NE and E content of birds of different phylogenetic groups (see Ghosh et al., 2001). Although there has been recent interest in birds as comparative models to study the mechanisms of aging (Holmes et al., 2001; Holmes and Ottinger, 2005; Ricklefs, 2010), there is little information concerning the endocrine changes associated with aging. The chromaffin catecholamine content and content response to endocrine alterations appear to vary among different species with age. However, a consistent emerging picture that is shared with the limited number of vertebrate species studied thus far is that chromaffin activity increases with age in disparate avian species (Ghosh et al., 2001).

Since there is a suggestion that glucocorticoids increase with age-related failure in adaptation to environmental and seasonal stressors (Koren et al., 2012), presumably similar changes occur with adrenal catecholamines. Clearly, more definitive studies are needed to understand the specific age-related changes in adrenocortical and adrenal chromaffin function in birds.

Acknowledgments

The author thanks Robert M. Dores, PhD, for helpful discussions on avian MC2R and MRAP1. The author is especially indebted to Colin G. Scanes, PhD, ScD, for his invitation to write and update this chapter and for his invaluable guidance throughout its revision.

References

Abdelmelek, H., Fechtali, T., Filali-Zegzouti, Y., Rouanet, J.L., Cottet-Emard, J.M., Pequignot, J.M., Barré, H., 2001. Responsiveness of plasma catecholamines to intracerebroventricular injection of glucagon in Muscovy ducklings. J. Neural. Transm. 108, 793–801. https://doi.org/10.1007/s007020170029.

Adams, M., Meijer, O.C., Wang, J., Bhargava, A., Pearce, D., 2003. Homodimerization of the glucocorticoid receptor is not essential for response element binding: activation of the phenylethanolamine *N*-methyltransferase gene by dimerization-defective mutants. Mol. Endocrinol. 17 (12), 2583–2592. https://doi.org/10.1210/me.2002-0305.

Ahmed, A.A., Ma, W., Guo, F., Ni, Y., Grossmann, R., Zhao, R., 2013. Differences in egg deposition of corticosterone and embryonic expression of corticosterone metabolic enzymes between slow and fast growing broiler chickens. Comp. Biochem. Physiol. A 164 (1), 200–206. https://doi.org/10.1016/j.cbpa.2012.09.004.

Ali, R.A., Qureshi, M.A., McCorkle, F.M., 1994. Profile of chicken macrophage functions after exposure to catecholamines in vitro. Immunopharmacol. Immunotoxicol. 16 (4), 611–625. https://doi.org/10.3109/08923979409019742.

Angelier, F., Wingfield, J.C., Trouvé, C., de Grissac, S., Chastel, O., 2013. Modulation of the prolactin and the corticosterone response: do they tell the same story in a long-lived bird, the *Cape petrel*? Gen. Comp. Endocrinol. 182, 7–15. https://doi.org/10.1016/j.ygcen.2012.10.008.

Arcamone, N., Lucini, C., Maruccio, L., Castaldo, L., Gargiulo, G., De Girolamo, P., 2006. Distribution of neurotrophin and Trk receptor-like immunoreactivity I the adrenal gland of birds. Microsc. Res. Tech. 69, 130–137. https://doi.org/10.1002/jemt.20273.

Assenmacher, I., 1973. The peripheral endocrine glands. In: Farner, D.S., King, J.R. (Eds.), Avian Biology, vol. III. Academic Press, New York, pp. 183–286.

Avrutina, A.J., Galpern, I.L., Kisljuk, S.M., 1985. Stimulation of adrenals during the critical periods of development and production in fowls. World's Poult. Sci. J. 41 (2), 108–114. https://doi.org/10.1079/WPS19850009.

Baker, M., 2010. Evolution of 11[beta]-Hydroxysteroid Dehydrogenase-Type 1 and 11[beta]-Hydroxysteroid Dehydrogenase-type 3. Nat. Prec. https://doi.org/10.1038/npre.2010.4296.1.

Baker, M.E., Nelson, D.R., Studer, R.A., 2015. Origin of the response to adrenal and sex steroids: roles of promiscuity and co-evolution of enzymes and steroid receptors. J. Steroid Biochem. Mol. Biol. 151, 12–24. https://doi.org/10.1016/j.jsbmb.2014.10.020.

Barlock, T.K., Gehr, D.T., Dores, R.M., 2014. Analysis of the pharmacological properties of chicken melanocortin-2 receptor (cMC2R) and chicken melanocortin-2 accessory protein 1 (cMRAP1). Gen. Comp. Endocrinol. 205, 260–267. https://doi.org/10.1016/j.ygcen.2014.03.045.

Bartlett, A.A., Lapp, H.E., Hunter, R.G., 2019. Epigenetic mechanisms of the glucocorticoid receptor. Trends Endocrinol. Metab. 30 (11), 807–818. https://doi.org/10.1016/j.tem.2019.07.003.

Bauer, M.P., Bridgham, J.T., Langenau, D.M., Johnson, A.L., Goetz, F.W., 2000. Conservation of steroidogenic acute regulatory (StAR) protein structure and expression in vertebrates. Mol. Cell. Endocrinol. 168 (1–2), 119–125. https://doi.org/10.1016/s0303-7207(00)00316-6.

Berghman, L.R., Devreese, B., Verhaert, P., Gerets, H., Arckens, L., Vanden Broeck, J., Van Beeumen, J., Vaudry, H., Vandesande, F., 1998. The molecular characterization of chicken N-terminal pro-opiomelanocortin (POMC). Mol. Cell. Endocrinol. 142 (1–2), 119–130. https://doi.org/10.1016/s0303-7207(98)00112-9.

Bhattacharyya, T.K., Sinha, D., Ghosh, A., 1972. A comparative histological survey of the avian adrenocortical homologue. Arch. Histol. Jpn. 34 (5), 419–432. https://doi.org/10.1679/aohc1950.34.419.

Bonier, F., 2012. Hormones in the city: endocrine ecology of urban birds. Horm. Behav. 61 (5), 763–772. https://doi.org/10.1016/j.yhbeh.2012.03.016.

Boswell, T., Takeuchi, S., 2005. Recent developments in our understanding of the avian melanocortin system: its involvement in the regulation of pigmentation and energy homeostasis. Peptides 26 (10), 1733–1743. https://doi.org/10.1016/j.peptides.2004.11.039.

Breuner, C.W., Lynn, S.E., Julian, G.E., Cornelius, J.M., Heidinger, B.J., Love, O.P., Sprague, R.S., Wada, H., Whitman, B.A., 2006. Plasma binding globulins and acute stress response. Horm. Metab. Res. 38 (4), 260–268. https://doi.org/10.1055/s-2006-925347.

Breuner, C.W., Orchinik, M., 2001. Seasonal regulation of membrane and intracellular corticosteroid receptors in the house sparrow brain. J. Neuroendocrinol. 13 (5), 412–420. https://doi.org/10.1046/j.1365-2826.2001.00646.x.

Breuner, C.W., Orchinik, M., 2009. Pharmacological characterization of intracellular, membrane, and plasma binding sites for corticosterone in house sparrows. Gen. Comp. Endocrinol. 163 (1–2), 214–224. https://doi.org/10.1016/j.ygcen.2009.01.027.

Breuner, C.W., Wingfield, J.C., Romero, L.M., 1999. Diel rhythms of basal and stress-induced corticosterone in a wild, seasonal vertebrate, Gambel's white-crowned sparrow. J. Exp. Zool. 284 (3), 334–342, 10404125.

Bruggeman, V., Room, G., Vanmontfort, D., Verhoeven, G., Decuypere, E., 2003. Effect of embryonic 19-nortestosterone treatment and surgical bursectomy on plasma concentrations of reproductive hormones, on inhibin content in adrenals and gonads and on the histological appearance of the gonads in the young chicken. Gen. Comp. Endocrinol. 131 (2), 106–116. https://doi.org/10.1016/s0016-6480(02)00576-2.

Butler, D.G., Wilson, J.X., 1985. Cardiovascular function in adrenalectomized Pekin ducks (*Anas platyrhynchos*). Comp. Biochem. Physiol. A 81 (2), 353–358. https://doi.org/10.1016/0300-9629(85)90147-1.

Campbell, R.M., Scanes, C.G., 1985. Adrenergic control of lipogenesis and lipolysis in the chicken in vitro. Comp. Biochem. Physiol., C 82 (1), 137–142. https://doi.org/10.1016/0742-8413(85)90220-8.

Carsia, R.V., 1990. Hormonal control of avian adrenocortical function: cellular and molecular aspects. In: Epple, A., Scanes, C.G., Stetson, M.H. (Eds.), Progress in Comparative Endocrinology. Wiley-Liss, Inc., Delaware, pp. 439–444.

Carsia, R.V., Lamm, E.-T., Marsh, J.A., Scanes, C.G., King, D.B., 1997. The thyroid hormone, 3,5,3′-triiodothyronine, is a negative modulator of domestic fowl (*Gallus gallus domesticus*) adrenal steroidogenic function. Gen. Comp. Endocrinol. 170 (2), 251–261. https://doi.org/10.1006/gcen.1997.6919.

Carsia, R.V., McIlroy, P.J., 1998. Dietary protein restriction stress in the domestic turkey (*Meleagris gallopavo*) induces hypofunction and remodeling of adrenal steroidogenic tissue. Gen. Comp. Endocrinol. 109 (1), 140–153. https://doi.org/10.1006/gcen.1997.7016.

Carsia, R.V., McIlroy, P.J., Kowalski, K.I., Tilly, J.L., 1993. Isolation of turkey adrenocortical cell angiotensin II (AII) receptor partial cDNA: evidence for a single-copy gene expressed predominantly in the adrenal gland. Biochem. Biophys. Res. Commun. 191 (3), 1073–1080. https://doi.org/10.1006/bbrc.1993.1326.

Carsia, R.V., Morin, M.E., Rosen, H.D., Weber, H., 1987. Ontogenic corticosteroidogenesis of the domestic fowl: response of isolated adrenocortical cells. Exp. Biol. Med. 184, 436–445. https://doi.org/10.3181/00379727-184-42498.

Carsia, R.V., Reisch, N.M., Fennell, M.J., Weber, H., 1987b. Adrenocortical function of the domestic fowl: effects of orchiectomy and androgen replacement. Exp. Biol. Med. 185 (2), 223–232. https://doi.org/10.3181/00379727-185-42539.

Carsia, R.V., Scanes, C.G., Malamed, S., 1985a. Isolated adrenocortical cells of the domestic fowl (*Gallus domesticus*): steroidogenic and ultrastructural properties. J. Steroid Biochem. 22 (2), 273–279. https://doi.org/10.1016/0022-4731(85)90124-4.

Carsia, R.V., Scanes, C.G., Malamed, S., 1985b. Loss of sensitivity to ACTH of adrenocortical cells isolated from maturing domestic fowl. Exp. Biol. Med. 179 (3), 279–282. https://doi.org/10.3181/00379727-179-42096.

Carsia, R.V., Weber, H., King, D.B., Scanes, C.G., 1985c. Adrenocortical cell function in the hypophysectomized domestic fowl: effects of growth hormone and 3,5,3'-triiodothyronine replacement. Endocrinology 117 (3), 928–933. https://doi.org/10.1210/endo-117-3-928.

Carsia, R.V., Weber, H., 1986. Genetic-dependent alterations in adrenal stress response and adrenocortical cell function of the domestic fowl (*Gallus domesticus*). Exp. Biol. Med. 183 (1), 99–105. https://doi.org/10.3181/00379727-183-42392.

Carsia, R.V., Weber, H., Perez Jr., F.M., 1986. Corticotropin-releasing factor stimulates the release of adrenocorticotropin from domestic fowl pituitary cells. Endocrinology 118 (1), 143–148. https://doi.org/10.1210/endo-118-1-143.

Carsia, R.V., Weber, H., Lauterio, T.J., 1988a. Protein malnutrition in the domestic fowl induces alterations in adrenocortical function. Endocrinology 122 (2), 673–680. https://doi.org/10.1210/endo-122-2-673.

Carsia, R.V., Weber, H., Satterlee, D.G., 1988b. Steroidogenic properties of isolated adrenocortical cells from Japanese quail selected for high serum corticosterone response to immobilization. Domest. Anim. Endocrinol. 5 (3), 231–240. https://doi.org/10.1016/0739-7240(88)90034-3.

Carsia, R.V., Weber, H., 2000. Remodeling of turkey steroidogenic tissue induced by dietary protein restriction: the potential role of cell death. Gen. Comp. Endocrinol. 118 (3), 471–479. https://doi.org/10.1006/gcen.2000.7486.

Chaturvedi, C.M., Chowdhary, A., Wall, P.T., Koike, T.I., Cornett, L.E., 2000. A sexual dimorphism in hypothalamic arginine vasotocin (AVT) gene expression and AVT plasma levels in the Japanese quail (*Coturnix coturnix japonica*) in response to water deprivation. Gen. Comp. Endocrinol. 117 (1), 129–137. https://doi.org/10.1006/gcen.1999.7400.

Charlier, T.D., Underhill, C., Hammond, G.L., Soma, K.K., 2009. Effects of aggressive encounters on plasma corticosteroid-binding globulin and its ligands in white-crowned sparrows. Horm. Behav. 56 (3), 339–347. https://doi.org/10.1016/j.yhbeh.2009.06.012.

Chen, C.-C., Johnson, P.A., 1996. Molecular cloning of inhibin/activin β_A-subunit complementary deoxyribonucleic acid and expression of inhibin/activin α- and β_A-subunits in the domestic hen. Biol. Reprod. 54 (2), 429–435. https://doi.org/10.1095/biolreprod54.2.429.

Cheng, H.W., Dillworth, G., Singleton, P., Chen, Y., Muir, W.M., 2001. Effects of group selection for productivity and longevity on blood concentrations of serotonin, catecholamines, and corticosterone of laying hens. Poult. Sci. 80 (9), 1278–1285. https://doi.org/10.1093/ps/80.9.1278.

Chester Jones, I., Phillips, J.G., 1986. The adrenal and interrenal glands. In: Pang, P.K.T., Schreibman, M.P. (Eds.), Vertebrate Endocrinology: Fundamental and Biomedical Implications, vol. 1. Academic Press, New York, pp. 319–350.

Cheung, A., Hall, T.R., Harvey, S., 1988. Stimulation of corticosterone release in the fowl by recombinant DNA-derived chicken growth hormone. Gen. Comp. Endocrinol. 69 (1), 128–132. https://doi.org/10.1016/0016-6480(88)90061-5.

Chida, D., Nakagawa, S., Nagai, S., Sagara, H., Katsumata, H., Imaki, T., Suzuki, H., Mitani, F., Ogishima, T., Shimizu, C., Kotaki, H., Kakuta, S., Sudo, K., Koike, T., Kubo, M., Iwakura, Y., 2007. Melanocortin 2 receptor is required for adrenal gland development, steroidogenesis, and neonatal gluconeogenesis. Proc. Natl. Acad. Sci. U.S.A. 104 (46), 18205–18210. https://doi.org/10.1073/pnas.0706953104.

Chimenti, C., Accordi, F., 2008. Development and evolution of the adrenal gland and its homolog in teleosts, anurans, chelonians and birds. In: Capaldo, A. (Ed.), Recent Advances in Non-mammalian Adrenal Gland Research. Research Signpost, Kerala, India, pp. 1–29.

Clark, A.J.L., Chan, L., 2019. Stability and turnover of the ACTH receptor complex. Front. Endocrinol. 10, 491. https://doi.org/10.3389/fendo.2019.00491.

Cornelius, J.M., Boswell, T., Jenni-Eiermann, S., Breuner, C.W., Ramenofsky, M., 2013a. Contributions of endocrinology to the migration life history of birds. Gen. Comp. Endocrinol. 190, 47–60. https://doi.org/10.1016/j.ygcen.2013.03.027.

Cornelius, J.M., Watts, H.E., Dingle, H., Hahn, T.P., 2013b. Obligate versus rich patch opportunism: evolution and endocrine mechanisms. Gen. Comp. Endocrinol. 190, 76–80. https://doi.org/10.1016/j.ygcen.2013.04.003.

Cornett, L.E., Kang, S.W., Kuenzel, W.J., 2013. A possible mechanism contributing to the synergistic action of vasotocin (VT) and corticotropin-releasing hormone (CRH) receptors on corticosterone release in birds. Gen. Comp. Endocrinol. 188, 46–53. https://doi.org/10.1016/j.ygcen.2013.02.032.

Costantini, D., Fanfani, A., Dell'Omo, G., 2008. Effects of corticosteroids on oxidative damage and circulating carotenoids in captive adult kestrels (*Falco tinnunculus*). J. Comp. Physiol. B 178 (7), 829–835. https://doi.org/10.1007/s00360-008-0270-z.

Cramb, G., Langslow, D.R., Phillips, J.H., 1982. Hormonal effects of cyclic nucleotides and carbohydrate and lipid metabolism in isolated chicken hepatocytes. Gen. Comp. Endocrinol. 46 (3), 310–321. https://doi.org/10.1016/0016-6480(82)90004-1.

Cyr, N.E., Romero, L.M., 2009. Identifying hormonal habituation in field studies of stress. Gen. Comp. Endocrinol. 161 (3), 295–303. https://doi.org/10.1016/j.ygcen.2009.02.001.

Daniel, J.Y., Assenmacher, I., 1971. Early appearance of metabolites after single i.v. injection of ^{3}H-corticosterone in rabbit and duck. Steroids 18 (3), 325–340. https://doi.org/10.1016/0039-128x(71)90047-x.

Davis, G.S., Siopes, T.D., 1987. Plasma corticosterone response of turkeys to adrenocorticotropic hormone: age, dose and route of administration effects. Poult. Sci. 66 (10), 1727–1732. https://doi.org/10.3382/ps.0661727.

De Bruijn, R., Romero, L.M., 2018. The role of glucocorticoids in the vertebrate response to weather. Gen. Comp. Endocrinol. 269, 11–32. https://doi.org/10.1016/j.ygcen.2018.07.007.

Decuypere, E., Rombauts, L., Vanmontfort, D., Verhoeven, G., 1997. Inhibin from the embryo to the adult hen. In: Harvey, S., Etches, R.J. (Eds.), Perspectives in Avian Endocrinology. Journal of Endocrinology Ltd., Bristol, pp. 71–80.

De Groef, B., Geris, K.L., Vandenborne, K., Darras, V.M., Kühn, E.R., 2005. CRH control of thyroid function in the chicken. In: Dawson, A., Sharp, P.J. (Eds.), Functional Avian Endocrinology. Narosa Publishing House, New Delhi, India, pp. 415–426.

De Groef, B., Grommen, S.V.H., Darras, V.M., 2008. The chicken embryo as a model for developmental endocrinology: development of the thyrotropic, corticotropic and somatotropic axes. Mol. Cell. Endocrinol. 293 (1–2), 17–24. https://doi.org/10.1016/j.mce.2008.06.002.

De Groef, B, Grommen, S.V., Mertens, I, Schoofs, L, Kühn, E.R., Darras, V.M., 2004. Cloning and tissue distribution of the chicken type 2 corticotropin-releasing hormone receptor. Gen. Comp. Endocrinol. 138 (1), 89–95. https://doi.org/10.1016/j.ygcen.2004.05.006.

De Groef, B., Van der Geyten, S., Darras, V.M., Kühn, E.R., 2006. Role of corticotropin-releasing hormone as a thyrotropin-releasing factor in non-mammalian vertebrates. Gen. Comp. Endocrinol. 146 (1), 62–68. https://doi.org/10.1016/j.ygcen.2005.10.014.

De Jong, I.C., van Voorst, A.S., Erkens, J.H., Ehlhardt, D.A., Blokhuis, H.J., 2001. Determination of the circadian rhythm in plasma corticosterone and catecholamine concentrations in growing broiler breeders using intravenous cannulation. Physiol. Behav. 74 (3), 299–304. https://doi.org/10.1016/s0031-9384(01)00562-5.

De Matos, R., 2008. Adrenal steroid metabolism in birds: anatomy, physiology, and clinical considerations. Vet. Clin. North Am. Exot. Anim. Pract. 11 (1), 35–57. https://doi.org/10.1016/j.cvex.2007.09.006.

Denno, K.M., McCorkle, F.M., Taylor Jr., R.L., 1994. Catecholamines modulate chicken immunoglobulin M and immunoglobulin G plaque-forming cells. Poult. Sci. 73 (12), 1858–1866. https://doi.org/10.3382/ps.0731858.

Denver, R.J., 2009. Structural and functional evolution of vertebrate stress systems. Ann. N.Y. Acad. Sci. 1163 (1), 1–16. https://doi.org/10.1111/j.1749-6632.2009.04433.x.

Dickens, M.J., Cornil, C.A., Balthazart, J., 2011a. Acute stress differentially affects aromatase activity in specific brain nuclei of adult male and female quail. Endocrinology 152 (11), 4242–4251. https://doi.org/10.1210/en.2011-1341.

Dickens, M.J., Meddle, S.L., Romero, L.M., 2011b. Mineralocorticoid and glucocorticoid receptor mRNA expression in the brain of translocated chukar (*Alectoris chukar*). Gen. Comp. Endocrinol. 170 (3), 569–574. https://doi.org/10.1016/j.ygcen.2010.11.018.

Dong, H., Lin, H., Jiao, H.C., Song, Z.G., Zhao, J.P., Jiang, K.J., 2007. Altered development and protein metabolism in skeletal muscles of broiler chickens (*Gallus gallus domesticus*) by corticosterone. Comp. Biochem. Physiol. A 147 (1), 189–195. https://doi.org/10.1016/j.cbpa.2006.12.034.

Dores, R.M., Garcia, Y., 2015. Views on the co-evolution of the melanocortin-2 receptor, MRAPs, and the hypothalamus/pituitary/adrenal-interrenal axis. Mol. Cell. Endocrinol. 408, 12–22. https://doi.org/10.1016/j.mce.2014.12.022.

Dores, R.M., Lecaude, S., 2005. Trends in the evolution of the proopiomelanocortin gene. Gen. Comp. Endocrinol. 142 (1–2), 81–93. https://doi.org/10.1016/j.ygcen.2005.02.003.

El-Far, A.A., Mashaly, M.M., Kamar, G.A., 1994. Bursectomy and in vitro response of adrenal gland to adrenocorticotropic hormone and testis to human chorionic gonadotropin in immature male chickens. Poult. Sci. 73 (1), 113–117. https://doi.org/10.3382/ps.0730113.

Ellestad, L.E., Saliba, J., Porter, T.E., 2011. Ontogenic characterization of gene expression in the developing neuroendocrine system of the chick. Gen. Comp. Endocrinol. 171 (1), 82–93. https://doi.org/10.1016/j.ygcen.2010.12.006.

Fässler, R., Schauenstein, K., Krömer, G., Schwarz, S., Wick, G., 1986. Elevation of corticosteroid-binding globulin in obese strain (OS) chickens: possible implications for the disturbed immunoregulation and the development of spontaneous autoimmune thyroiditis. J. Immunol. 136 (10), 3657–3661.

Filali-Zegzouti, Y., Abdelmelek, H., Rouanet, J.L., Cottet-Emard, J.M., Pequignot, J.M., Barré, H., 2005. Role of catecholamines in glucagon-induced thermogenesis. J. Neural. Transm. 112 (4), 481–489. https://doi.org/10.1007/s00702-004-0199-7.

Flint, M.S., Baum, A., Chambers, W.H., Jenkins, F.J., 2007. Induction of DNA damage, alteration of DNA repair and transcriptional activation by stress hormones. Psychoneuroendocrinology 32 (5), 470–479. https://doi.org/10.1016/j.psyneuen.2007.02.013.

Freking, F., Nazairians, T., Schlinger, B.A., 2000. The expression of the sex steroid-synthesizing enzymes CYP11A1, 3β-HSD, CYP17, and CYP19 in gonads and adrenals of adult and developing zebra finches. Gen. Comp. Endocrinol. 119 (2), 140–151. https://doi.org/10.1006/gcen.2000.7503.

Fridmanis, D., Roga, A., Klovins, J., 2017. ACTH receptor (MC2R) specificity: what do we know about underlying molecular mechanisms? Front. Endocrinol. 8, 13. https://doi.org/10.3389/fendo.2017.00013.

Ghaddhab, C., Vuissoz, J.-M., Deladoëy, J., 2017. From bioinactive ACTH to ACTH Antagonist: the clinical perspective. Front. Endocrinol. 8, 17. https://doi.org/10.3389/fendo.2017.00017.

Ghosh, A., Carmichael, S.W., Mukherjee, M., 2001. Avian adrenal medulla: cytomorphology and function. Acta Biol. Szeged. 45 (1–4), 1–11.

Giorgi, E.P., Stein, W.D., 1981. The transport of steroids into animal cells in culture. Endocrinology 108 (2), 688–697. https://doi.org/10.1210/endo-108-2-688.

Gray, D.A., Gerstberger, R., Simon, E., 1989. Role of angiotensin II in aldosterone regulation in the Pekin duck. J. Endocrinol. 123 (3), 445–452. https://doi.org/10.1677/joe.0.1230445.

Gray, D.A., 1993. Plasma atrial natriuretic factor concentrations and renal actions in the domestic fowl. J. Comp. Physiol. B 163 (6), 519–523. https://doi.org/10.1007/BF00346937.

Gray, D.A., Schütz, H., Gerstberger, R., 1991a. Interaction of atrial natriuretic factor and osmoregulatory hormones in the Pekin duck. Gen. Comp. Endocrinol. 81 (2), 246–255. https://doi.org/10.1016/0016-6480(91)90009-u.

Gray, D.A., Schütz, H., Gerstberger, R., 1991b. Plasma atrial natriuretic factor responses to blood volume changes in the Pekin duck. Endocrinology 128 (3), 1655–1660. https://doi.org/10.1210/endo-128-3-1655.

Gregg, C.M., Wideman Jr., R.F., 1986. Effect of atriopeptin and chicken heart extract in *Gallus domesticus*. Am. J. Physiol. 251 (3 Pt 2), R453–R551. https://doi.org/10.1152/ajpregu.1986.251.3.R543.

Gut, P., Huber, K., Lohr, J., Brühl, B., Oberle, S., Treier, M., Ernsberger, U., Kalcheim, C., Unsicker, K., 2005. Lack of an adrenal cortex in *Sf1* mutant mice is compatible with the generation and differentiation of chromaffin cells. Development 132 (20), 4611–4619. https://doi.org/10.1242/dev.02052.

Hahn, D.C., 2011. Patterns of maternal yolk hormones in eastern screech owl eggs (*Megascops asio*). Gen. Comp. Endocrinol. 172 (3), 423–429. https://doi.org/10.1016/j.ygcen.2011.04.001.

Harris, R.M., Dijkstra, P.D., Hofmann, H.A., 2014. Complex structural and regulatory evolution of the pro-opiomelanocortin gene family. Gen. Comp. Endocrinol. 195, 107–115. https://doi.org/10.1016/j.ygcen.2013.10.007.

Harvey, S., Scanes, C.G., Daughaday, W.H., 1995. IV. Adrenocortical hormones. In: Growth Hormone. CRC Press, Inc., Boca Raton, Florida, p. 426.

Hazard, D., Couty, M., Guémené, D., 2007. Characterization of CRF, AVT and ACTH cDNA and pituitary-adrenal axis function in Japanese quail divergently selected for tonic mobility. Am. J. Physiol. Regul. Integr. Comp. Physiol. 293 (3), R1421–R1429. https://doi.org/10.1152/ajpregu.00070.2007.

Helton, E.D., Holmes, W.N., 1973. The distribution and metabolism of labeled corticosteroids in the duck (*Anas platyrhynchos*). J. Endocrinol. 56 (3), 361–385. https://doi.org/10.1677/joe.0.0560361.

Hendricks III, G.L., Siegel, H.S., Mashaly, M.M., 1991. Ovine corticotropin-releasing factor increases endocrine and immunological activity of avian leukocytes. Exp. Biol. Med. 196 (4), 390–395. https://doi.org/10.3181/00379727-196-43204.

Hendricks III, G.L., Mashaly, M.M., Siegel, H.S., 1995a. Validation of an assay to measure adrenocorticotropin in plasma and from chicken leukocytes. Poult. Sci. 74 (2), 337–342. https://doi.org/10.3382/ps.0740337.

Hendricks III, G.L., Mashaly, M.M., Siegel, H.S., 1995b. Effects of corticosterone in vivo and in vitro on adrenocorticotropic hormone production by corticotropin releasing factor-stimulated leukocytes. Exp. Biol. Med. 209 (4), 382–386. https://doi.org/10.3181/00379727-209-43911.

Holmes, D.J., Flückiger, R., Austad, S.N., 2001. Comparative biology of aging in birds: an update. Exp. Gerontol. 36 (4–6), 869–883. https://doi.org/10.1016/s0531-5565(00)00247-3.

Holmes, D.J., Ottinger, M.A., 2005. Aging in birds. Age 27, iii–v. https://doi.org/10.1007/s11357-005-4560-z.

Holmes, W.N., Bradley, E.L., Helton, E.D., Chan, M.Y., 1972. The distribution and metabolism of corticosterone in birds. Gen. Comp. Endocrinol. 3 (Suppl.), 266–278. https://doi.org/10.1016/0016-6480(72)90156-6.

Holmes, W.N., Broock, R.L., Devlin, J.M., 1974. Tritiated corticosteroid metabolism in intact and adenohypophysectomized ducks (*Anas platyrhynchos*). Gen. Comp. Endocrinol. 22 (4), 417–427. https://doi.org/10.1016/0016-6480(74)90015-x.

Holmes, W.N., Cronshaw, J., 1984. Adrenal gland: some evidence for the structural and functional zonation of the steroidogenic tissues. J. Exp. Zool. 232 (3), 627–631. https://doi.org/10.1002/jez.1402320331.

Holmes, W.N., Cronshaw, J., 1993. Some actions of angiotensin II in gallinaceous and anseriform birds. In: Sharp, P.J. (Ed.), Avian Endocrinology. Journal of Endocrinology Ltd., Bristol, pp. 201–216.

Holmes, W.N., Kelly, M.E., 1976. The turnover and distribution of labelled corticosterone during post-natal development of the duckling (*Anas platyrhynchos*). Pflügers Arch. 365 (2–3), 145–150. https://doi.org/10.1007/BF01067011.

Holmes, W.N., Phillips, J.G., 1976. The adrenal cortex of birds. In: Chester Jones, I., Henderson, I.W. (Eds.), General, Comparative and Clinical Endocrinology of the Adrenal Cortex, vol. 1. Academic Press, New York, pp. 293–413.

Holmes, W.N., Slikker, W., 1976. Some properties of the labelled material excreted by intact and adenohypophysectomized ducks (*Anas platyrhynchos*) given single doses of labeled corticosterone. Gen. Comp. Endocrinol. 29, 128–140. https://doi.org/10.1016/0016-6480(76)90014-9.

Horner, H.C., Munck, A., Lienhard, G.E., 1987. Dexamethasone causes translocation of glucose transporters from the plasma membrane to an intracellular site in human fibroblasts. J. Biol. Chem. 262 (36), 17696–17702. https://doi.org/10.1016/S0021-9258(18)45435-X.

Huber, K., 2006. The sympathoadrenal cell lineage: specification, diversification, and new perspectives. Dev. Biol. 298 (2), 335–343. https://doi.org/10.1016/j.ydbio.2006.07.010.

Hughes, M.R., 2003. Regulation of salt gland, gut and kidney interactions. Comp. Biochem. Physiol. A 136 (3), 507–524. https://doi.org/10.1016/j.cbpb.2003.09.005.

Humayun, K.A.K.M., Aoyama, M., Sugita, S., 2010. Immunohistochemical localization of catecholamine biosynthetic enzymes in the adrenal gland of the domestic fowl (*Gallus domesticus*). Poult. Sci. 89 (8), 1709–1715. https://doi.org/10.3382/ps.2009-00588.

Humayun, K.A.K.M., Aoyama, M., Sugita, S., 2012. Morphological and histological studies on the adrenal gland of the chicken (*Gallus domesticus*). J. Poult. Sci. 49 (1), 39–45. https://doi.org/10.2141/jpsa.011038.

Jankowski, M.D., Wittwer, D.J., Heisey, D.M., Franson, J.C., Hofmeister, E.K., 2009. The adrenocortical response of greater sage grouse (*Centrocercus urophasianus*) to capture, ACTH injection, and confinement, as measured in fecal samples. Physiol. Biochem. Zool. 82 (2), 190–201. https://doi.org/10.1086/596513.

Jenkins, S.A., Porter, T.E., 2004. Ontogeny of the hypothalamo-pituitary-adrenocortical axis in the chicken embryo: a review. Domest. Anim. Endocrinol. 26 (4), 267–275. https://doi.org/10.1016/j.domaniend.2004.01.001.

Kadmiel, M., Cidlowski, J.A., 2013. Glucocorticoid receptor signaling in health and disease. Trends Pharmacol. Sci. 34 (9), 518–530. https://doi.org/10.1016/j.tips.2013.07.003.

Kaiser, P., Wu, Z., Rothwell, L., Fife, M., Gibson, M., Poh, T.-Y., Shini, A., Bryden, W., Shini, S., 2009. Prospects for understanding immune-endocrine interactions in the chicken. Gen. Comp. Endocrinol. 163 (1–2), 83–91. https://doi.org/10.1016/j.ygcen.2008.09.013.

Kalliecharan, R., Hall, B.K., 1974. A developmental study of the levels of progesterone, corticosterone, cortisol, and cortisone circulating in the plasma of chick embryos. Gen. Comp. Endocrinol. 24 (4), 364–372. https://doi.org/10.1016/0016-6480(74)90149-x.

Kamata, R., Takahashi, S., Morita, M., 2004. Gene expression of sex-determining factors and steroidogenic enzymes in the chicken embryo: influence of xenoestrogens. Gen. Comp. Endocrinol. 138 (2), 148–156. https://doi.org/10.1016/j.ygcen.2004.05.011.

Kanda, I., Akazome, Y., Ogasawara, O., Mori, T., 2000. Expression of cytochrome P450 cholesterol side chain cleavage and 3β-hydroxysteroid dehydrogenase during embryogenesis in chicken adrenal glands and gonads. Gen. Comp. Endocrinol. 118 (1), 96–104. https://doi.org/10.1006/gcen.1999.7448.

Katz, A., Heiblum, R., Meidan, R., Robinzon, B., 2007. Distinct features of dehydrocorticosterone reduction into corticosterone in the liver and duodenum of the domestic fowl (*Gallus gallus domesticus*). Gen. Comp. Endocrinol. 154 (1–3), 67–74. https://doi.org/10.1016/j.ygcen.2007.06.015.

Katz, A., Heiblum, R., Meidan, R., Robinzon, B., 2008. Corticosterone oxidative neutralization by 11-β hydroxysteroid dehydrogenases in kidney and colon of the domestic fowl. Gen. Comp. Endocrinol. 155 (3), 814–820. https://doi.org/10.1016/j.ygcen.2007.10.002.

Katz, A., Oyama, R.K., Feng, N., Chen, X., Schlinger, B.A., 2010. 11-β hydroxysteroid dehydrogenase type 2 in zebra finch brain and peripheral tissues. Gen. Comp. Endocrinol. 166 (3), 600–605. https://doi.org/10.1016/j.ygcen.2010.01.016.

Kawashima, M., Takahashi, T., Yanai, H., Ogawa, H., Yasuoka, T., 2005. Direct action of parathyroid hormone-related peptide to enhance corticosterone production stimulated by adrenocorticotropic hormone in adrenocortical cells of hens. Poult. Sci. 84 (9), 1463–1469. https://doi.org/10.1093/ps/84.9.1463.

Kempf, H., Corvol, P., 2001. Angiotensin receptor(s) in fowl. Comp. Biochem. Physiol. A 128 (1), 77–88. https://doi.org/10.1016/s1095-6433(00)00298-1.

Ketterson, E.D., Nolan Jr., V., Wolf, L., Ziegenfus, C., Dufty Jr., A.M., Ball, G.F., Johnsen, T.S., 1991. Testosterone and avian life histories: the effect of experimentally elevated testosterone on corticosterone and body mass in dark-eyed juncos. Horm. Behav. 25 (4), 489–503. https://doi.org/10.1016/0018-506X(91)90016-B.

Klingbeil, C., 1985. Corticosterone and aldosterone dose-dependent responses to ACTH and angiotensin II in the duck (*Anas platyrhynchos*). Gen. Comp. Endocrinol. 59 (3), 382–390. https://doi.org/10.1016/0016-6480(85)90395-8.

Knight, D.E., Baker, P.F., 1986. Observations on the muscarinic activation of catecholamine secretion in the chicken adrenal gland. Neuroscience 19 (1), 357–366. https://doi.org/10.1016/0306-4522(86)90027-8.

Kocsis, J.F., Carsia, R.V., 1989. Steroidogenic properties of isolated turkey adrenocortical cells. Domest. Anim. Endocrinol. 6 (2), 121–131. https://doi.org/10.1016/0739-7240(89)90041-6.

Kocsis, J.F., Boyette, M.H., McIlroy, P.J., Carsia, R.V., 1994a. Regulation of aldosteronogenesis in domestic turkey (*Meleagris gallopavo*) adrenal steroidogenic cells. Gen. Comp. Endocrinol. 96 (1), 108–121. https://doi.org/10.1006/gcen.1994.1163.

Kocsis, J.F, McIlroy, P.J., Chiu, A.T., Schimmel, R.J., Carsia, R.V., 1994b. Properties of angiotensin II receptors of domestic turkey (*Meleagris gallopavo*) adrenal steroidogenic cells. Gen. Comp. Endocrinol. 96 (1), 92–107. https://doi.org/10.1006/gcen.1994.1162.

Kocsis, J.F., Lamm, E.-T., McIlroy, P.J., Scanes, C.G., Carsia, R.V., 1995a. Evidence for functionally distinct subpopulations of steroidogenic cells in the domestic turkey (*Meleagris gallopavo*) adrenal gland. Gen. Comp. Endocrinol. 98 (1), 57–72. https://doi.org/10.1006/gcen.1995.1044.

Kocsis, J.F, Schimmel, R.J., McIlroy, P.J., Carsia, R.V., 1995b. Dissociation of increases in intracellular calcium and aldosterone production induced by angiotensin II (AII): evidence for regulation by distinct AII receptor subtypes or isomorphs. Endocrinology 136 (4), 1626–1634. https://doi.org/10.1210/endo.136.4.7895673.

Kocsis, J.F, McIlroy, P.J., Carsia, R.V., 1995c. Atrial natriuretic peptide stimulates aldosterone production by turkey (*Meleagris gallopavo*) adrenal steroidogenic cells. Gen. Comp. Endocrinol. 99 (3), 364–372. https://doi.org/10.1006/gcen.1995.1120.

Koren, L., Nakagawa, S., Burke, T., Soma, K.K., Wynne-Edwards, K.E., Geffen, E., 2012. Non-breeding feather concentrations of testosterone, corticosterone, and cortisol are associated with subsequent survival in wild house sparrows. Proc. Biol. Sci. 279 (1733), 1560–1566. https://doi.org/10.1098/rspb.2011.2062.

Kovács, K, Péczely, P, 1983. Phase shifts in circadian rhythmicity of total, free corticosterone and transcortine plasma levels in hypothyroid male Japanese quails. Gen. Comp. Endocrinol. 50 (3), 483–489. https://doi.org/10.1016/0016-6480(83)90270-8.

Kučka, M., Vagnerová, K., Klusoňová, P., Mikšík, I., Pácha, J., 2006. Corticosterone metabolism in chicken tissues: evidence for tissue-specific distribution of steroid dehydrogenases. Gen. Comp. Endocrinol. 147 (3), 377–383. https://doi.org/10.1016/j.ygcen.2006.02.007.

Kuenzel, W.J., Kang, S.W., Jurkevich, A., 2013. Neuroendocrine regulation of stress in birds with an emphasis on vasotocin receptors (VTRs). Gen. Comp. Endocrinol. 190, 18–23. https://doi.org/10.1016/j.ygcen.2013.02.029.

Kwok, A.H.Y., Wang, Y., Wang, C.Y., Leung, F.C., 2007. Cloning of chicken glucocorticoid receptor (GR) and characterization of its expression in pituitary and extrapituitary tissues. Poult. Sci. 86 (2), 423–430. https://doi.org/10.1093/ps/86.2.423.

Lacombe, A.M.A., Jones, D.R., 1990. The source of circulating catecholamines in forced dived ducks. Gen. Comp. Endocrinol. 80 (1), 41–47. https://doi.org/10.1016/0016-6480(90)90146-D.

Landys, M.M., Ramenofsky, M., Wingfield, J.C., 2006. Actions of glucocorticoids at a seasonal baseline as compared to stress-related levels in the regulation of periodic life processes. Gen. Comp. Endocrinol. 148 (2), 132–149. https://doi.org/10.1016/j.ygcen.2006.02.013.

Langlois, V.S., Zhang, D., Cooke, G.M., Trudeau, V.L., 2010. Evolution of steroid-5α-reductases and comparison of their function with 5β-reductase. Gen. Comp. Endocrinol. 166 (3), 489–497. https://doi.org/10.1016/j.ygcen.2009.08.004.

Lattin, C.R., Bauer, C.M., de Bruijn, R., Romero, L.M., 2012a. Hypothalamus-pituitary-adrenal axis activity and the subsequent response to chronic stress differ depending upon life history stage. Gen. Comp. Endocrinol. 178 (3), 494–501. https://doi.org/10.1016/j.ygcen.2012.07.013.

Lattin, C.R., Keniston, D.E., Reed, J.M., Romero, L.M., 2015. Are receptor concentrations correlated across tissues within individuals? A case study examining glucocorticoid and mineralocorticoid receptor binding. Endocrinology 156 (4), 1354–1361. https://doi.org/10.1210/en.2014-1811.

Lattin, C.R., Waldron-Francis, K., Richardson, J.W., de Bruijn, R., Bauer, C.M., Breuner, C.W., Romero, L.M., 2012b. Pharmacological characterization of intracellular glucocorticoid receptors in nine tissues from house sparrow (*Passer domesticus*). Gen. Comp. Endocrinol. 179 (2), 214–220. https://doi.org/10.1016/j.ygcen.2012.08.007.

Laverty, G., Elbrønd, V.S., Árnason, S.S., Skadhauge, E., 2006. Endocrine regulation of ion transport in the avian lower intestine. Gen. Comp. Endocrinol. 147 (1), 70–77. https://doi.org/10.1016/j.ygcen.2006.01.008.

Lechner, O., Dietrich, H., Wiegers, G.J., Vacchio, M., Wick, G., 2001. Glucocorticoid production in the chicken bursa and thymus. Int. Immunol. 13 (6), 769–776. https://doi.org/10.1093/intimm/13.6.769.

Li, Q.-L., Jansen, E., Brent, G.A., Friedman, T.C., 2001. Regulation of prohormone convertase 1 (PC1) by thyroid hormone. Am. J. Physiol. Endocrinol. Metab. 280 (1), E160–E170. https://doi.org/10.1152/ajpendo.2001.280.1.E160.

Liang, L., Angleson, J.K., Dores, R.M., 2013. Using the human melanocortin-2 receptor as a model for analyzing hormone/receptor interactions between mammalian MC2 receptor and ACTH(1-24). Gen. Comp. Endocrinol. 181, 203–210. https://doi.org/10.1016/j.ygcen.2012.11.011.

Lim, S.-K., Gardella, T., Thompson, A., Rosenberg, J., Keutmann, H., Potts Jr., J., Kronenberg, H., Nussbaum, S., 1991. Full-length chicken parathyroid hormone. Biosynthesis in *Escherichia coli* and analysis of biologic activity. J. Biol. Chem. 266 (6), 3709–3714. https://doi.org/10.1016/S0021-9258(19)67852-X.

Lin, H., Sui, S.J., Jiao, H.C., Jiang, K.J., Zhao, J.P., Dong, H., 2007. Effects of diet and stress mimicked by corticosterone administration on early postmortem muscle metabolism of broiler chicks. Poult. Sci. 86 (3), 545–554. https://doi.org/10.1093/ps/86.3.545.

Ling, M.K., Hotta, E., Kilianova, Z., Haitina, T., Ringholm, A., Johansson, L., Gallo-Payet, N., Takeuchi, S., Schiöth, H.B., 2004. The melanocortin receptor subtypes in chicken have high preference to ACTH-derived peptides. Br. J. Pharmacol. 143 (5), 626–637. https://doi.org/10.1038/sj.bjp.0705900.

Liu, Y., Smith, L.I., Huang, V., Poon, V., Coello, A., Olah, M., Spiga, F., Lightman, S.L., Aguilera, G., 2013. Transcriptional regulation of episodic glucocorticoid secretion. Mol. Cell. Endocrinol. 371 (1–2), 62–70. https://doi.org/10.1016/j.mce.2012.10.011.

Lothrop, C.D., Olsen, J.H., Loomis, M.R., Jensen, J.M., Lenhard, A., 1985. Evaluation of adrenal function in psittacine birds, using the ACTH stimulation test. J. Am. Vet. Med. Assoc. 187 (11), 1113–1115.

MacDougall-Shackleton, S.A., Bonier, F., Romero, L.M., Moore, I.T., 2019. Glucocorticoids and "stress" are not synonymous. Integr. Organ. Biol. https://doi.org/10.1093/iob/obz017.

Madison, F.N., Jurkevich, A., Kuenzel, W.J., 2008. Sex differences in plasma corticosterone release in undisturbed chickens (*Gallus gallus*) in response to arginine vasotocin and corticotropin releasing hormone. Gen. Comp. Endocrinol. 155 (3), 566–573. https://doi.org/10.1016/j.ygcen.2007.08.014.

Mahata, S.K., Mahapatra, N.R, Mahata, M., O'Connor, D.T., 2002. Neuroendocrine cell type-specific and inducible expression of chromogranin/secretogranin genes. Crucial promotor motifs. Ann. N.Y. Acad. Sci. 971, 27–38. https://doi.org/10.1111/j.1749-6632.2002.tb04429.x.

Mahata, S.K., Mahata, M., Fung, M., O'Connor, D.T., 2010. Catestatin: a multifunctional peptide from chromogranin A. Regul. Pept. 162 (1–3), 33–43. https://doi.org/10.1016/j.regpep.2010.01.006.

Malik, S., Dolan, T.M., Maben, Z.J., Hinkle, P.M., 2015. Adrenocorticotropic hormone (ACTH) responses require actions of the melanocortin-2 receptor accessory protein on the extracellular surface of the plasma membrane. J. Biol. Chem. 290 (46), 27972–27985. https://doi.org/10.1074/jbc.M115.668491.

Malisch, J.L., Breuner, C.W., 2009. Steroid-binding proteins and free steroids in birds. Mol. Cell. Endocrinol. 316 (1), 42–52. https://doi.org/10.1016/j.mce.2009.09.019.

Malisch, J.L., Satterlee, D.G., Cockrem, J.F., Wada, H., Breuner, C.W., 2010. How acute is the acute stress response? Baseline corticosterone and corticosteroid-binding globulin levels change 24 h after an acute stressor in Japanese quail. Gen. Comp. Endocrinol. 165 (2), 345–350. https://doi.org/10.1016/j.ygcen.2009.08.003.

McCorkle, F.M., Taylor Jr., R.L., 1993. Biogenic amines regulate avian immunity. Poult. Sci. 72 (7), 1285–1288. https://doi.org/10.3382/ps.0721285.

McIlroy, P.J., Kocsis, J.F., Weber, H., Carsia, R.V., 1999. Dietary protein restriction stress in the domestic fowl (*Gallus gallus domesticus*) alters adrenocorticotropin-transmembranous signaling and corticosterone negative feedback in adrenal steroidogenic cells. Gen. Comp. Endocrinol. 113 (2), 255–266. https://doi.org/10.1006/gcen.1998.7201.

Medina, C.O., Lattin, C.R., McVey, M., Romero, L.M., 2013. There is no correlation between glucocorticoid receptor mRNA expression and protein binding in the brains of house sparrows (*Passer domesticus*). Gen. Comp. Endocrinol. 193, 27–36. https://doi.org/10.1016/j.ygcen.2013.07.008.

Mikhailova, M.V., Mayeux, P.R., Jurkevich, A., Kuenzel, W.J., Madison, F., Periasamy, A., Chen, Y., Cornett, L.E., 2007. Heterooligomerization between vasotocin and corticotropin-releasing hormone (CRH) receptors augments CRH-stimulated 3′,5′-cyclic adenosine monophosphate production. Mol. Endocrinol. 21 (9), 2178–2188. https://doi.org/10.1210/ME.2007-0160.

Miller, W.L., Auchus, R.J., 2011. The molecular biology, biochemistry and physiology of human steroidogenesis and its disorders. Endocr. Rev. 32 (1), 81–151. https://doi.org/10.1210/er.2010-0013.

Mirabella, N., Esposito, V., Squillacioti, C., De Luca, A., Paino, G., 2004. Expression of agouti-related protein (AgRP) in the hypothalamus and adrenal gland of the duck (*Anas platyrhynchos*). Anat. Embryol. 209, 137–141. https://doi.org/10.1007/s00429-004-0431-0.

Miyata, A., Minamino, N., Kangawa, K., Matsuo, H., 1988. Identification of a 29-amino acid natriuretic peptide in chicken heart. Biochem. Biophys. Res. Commun. 155 (3), 1330–1337. https://doi.org/10.1016/S0006-291X(88)81287-7.

Moawad, U.K., Randa, M.H., 2017. Histocytological and histochemical features of the adrenal gland of Adult Egyptian native breeds of chickens (*Gallus gallus domesticus*). Beni-Suef Univ. J. Basic Appl. Sci. 6 (2), 199–208. https://doi.org/10.1016/j.bjbas.2017.04.001.

Möstl, E., Palme, R., 2002. Hormones as indicators of stress. Domest. Anim. Endocrinol. 23 (1–2), 67–74. https://doi.org/10.1016/S0739-7240(02)00146-7.

Müller, C., Jenni-Eiermann, S., Jenni, L., 2010. Development of the adrenocortical response to stress in Eurasian kestrel nestlings: defence ability, age, brood hierarchy and condition. Gen. Comp. Endocrinol. 168 (3), 474–483. https://doi.org/10.1016/j.ygcen.2010.06.009.

Murphy, T.J., Nakamura, Y., Takeuchi, K., Alexander, R.W., 1993. A cloned angiotensin receptor isoform from the Turkey adrenal gland is pharmacologically distinct from mammalian angiotensin II receptors. Mol. Pharmacol. 44 (1), 1–7.

Nagra, C.L., Sauers, A.K., Wittmaier, H.N., 1965. Effect of testosterone, progestagens, and metopirone on adrenal activity in cockerels. Gen. Comp. Endocrinol. 5 (1), 69–73. https://doi.org/10.1016/0016-6480(65)90070-5.

Nakagawa-Mizuyachi, K., Takahashi, T., Kawashima, M., 2009. Calcitonin directly increases adrenocorticotropic hormone-stimulated corticosterone production in the hen adrenal gland. Poult. Sci. 88 (10), 2199–2205. https://doi.org/10.3382/ps.2008-00496.

Nakabayashi, O., Nomura, O., Nishimori, K., Mizuno, S., 1995. The cDNA cloning and transient expression of a chicken gene encoding a 3 beta-hydroxysteroid dehydrogenase/delta 5 → 4 isomerase unique to major steroidogenic tissues. Gene 162 (2), 261–265. https://doi.org/10.1016/0378-1119(95)00278-e.

Naudé, R., Oelofsen, W., Takahashi, A., Amano, M., Kawauchi, H., 2006. Molecular cloning and characterization of preproopiomelanocortin (prePOMC) cDNA from the ostrich (*Struthio camelus*). Gen. Comp. Endocrinol. 146 (1), 310–317. https://doi.org/10.1016/j.ygcen.2005.11.018.

Nelson, D.R., 2018. Cytochrome P450 diversity in the tree of life. Biochim. Biophys. Acta 1886 (1), 141–154. https://doi.org/10.1016/j.bbapap.2017.05.003.

Newman, A.E.M., Chin, E.H., Schmidt, K.L., Bond, L., Wynne-Edwards, K.E., Soma, K.K., 2008. Analysis of steroids in songbird plasma and brain by coupling solid phase extraction to radioimmunoassay. Gen. Comp. Endocrinol. 155 (3), 503–510. https://doi.org/10.1016/j.ygcen.2007.08.007.

Nishimura, H., 2001. Angiotensin receptors—evolutionary overview and perspectives. Comp. Biochem. Physiol. A 128 (1), 11–30. https://doi.org/10.1016/s1095-6433(00)00294-4.

Nomura, O., Nakabayashi, O., Nishimori, K., Mizuno, S., 1997. The cDNA cloning and transient expression of a chicken gene encoding cytochrome P-450scc. Gene 185 (2), 217–222. https://doi.org/10.1016/S0378-1119(96)00645-2.

Nomura, O., Nakabayashi, O., Nishimori, K., Yasue, H., Mizuno, S., 1999. Expression of five steroidogenic genes including aromatase gene at early developmental stages of chicken male and female embryos. J. Steroid Biochem. Mol. Biol. 71 (3–4), 103–109. https://doi.org/10.1016/s0960-0760(99)00127-2.

Odihambo Mumma, J.O., Thaxton, J.P., Vizzier-Thaxton, Y., Dodson, W.L., 2006. Physiological stress in laying hens. Poult. Sci. 85 (4), 761–769. https://doi.org/10.1093/ps/85.4.761.

Ohmori, Y., 1998. Localization of biogenic amines and neuropeptides in adrenal medullary cells of birds. Horm. Metab. Res. 30 (6–7), 384–388. https://doi.org/10.1055/s-2007-978902.

Okuliarová, M., Šárniková, B., Rettenbacher, S., Škrobánek, P., Zeman, M., 2010. Yolk testosterone and corticosterone in hierarchical follicles and laid eggs of Japanese quail exposed to long-term restraint stress. Gen. Comp. Endocrinol. 165 (1), 91–96. https://doi.org/10.1016/j.ygcen.2009.06.007.

Ono, H., Iwasaki, M., Sakamoto, N., Mizuno, S., 1988. cDNA cloning and sequence analysis of a chicken gene expressed during the gonadal development and homologous to mammalian cytochrome P-450c17. Gene 66 (1), 77–85. https://doi.org/10.1016/0378-1119(88)90226-0.

Ottinger, M.A., Pitts, S., Abdelnabi, M.A., 2001. Steroid hormones during development in Japanese quail: plasma, gonadal and adrenal levels. Poult. Sci. 80 (6), 795–799. https://doi.org/10.1093/ps/80.6.795.

Pedernera, E.A., Romano, M., Besedovsky, H.O., Aguilar, M.C., 1980. The bursa of Fabricius is required for normal endocrine development in chicken. Gen. Comp. Endocrinol. 42 (3), 413–419. https://doi.org/10.1016/0016-6480(80)90172-0.

Petta, I., Dejager, L., Ballegeer, M., Lievens, S., Tavernier, J., De Bosscher, K., Libert, C., 2016. The interactome of the glucocorticoid receptor and its influence on the actions of glucocorticoids in combatting inflammatory and infectious diseases. Microbiol. Mol. Biol. Rev. 80 (2), 495–522. https://doi.org/10.1128/MMBR.00064-15.

Pierce, R.B., Cronshaw, J., Holmes, W.N., 1978. Evidence for the zonation of interrenal tissue in the adrenal gland of the duck (*Anas platyrhynchos*). Cell Tissue Res. 192 (3), 363–379. https://doi.org/10.1007/BF00212319.

Pihlajoki, M., Gretzinger, E., Cochran, R., Kyrönlahti, A., Schrade, A., Hiller, T., Sullivan, L., Shoykhet, M., Schoeller, E.L., Brooks, M.D., Heikinheimo, M., Wilson, D.B., 2013. Conditional mutagenesis of Gata6 in SF1-positive cells causes gonadal-like differentiation in the adrenal cortex of mice. Endocrinology 154 (5), 1754–1767. https://doi.org/10.1210/en.2012-1892.

Pinheiro, P.L.C., Cardoso, J.C.R., Power, D.M., Canário, A.V.M., 2012. Functional characterization and evolution of PTH/PTHrP receptors: insights from the chicken. BMC Evol. Biol. 12, 110 https://doi.org/10.1186/1471-2148-12-110.

Pintér, O., Péczely, P., Zsebők, S., Zelena, D., 2011. Seasonal changes in courtship behavior, plasma androgen levels and in hypothalamic aromatase immunoreactivity in male free-living European starlings (*Sturnus vulgaris*). Gen. Comp. Endocrinol. 172 (1), 151–157. https://doi.org/10.1016/j.ygcen.2011.02.002.

Pohle, K., Cheng, H.-W., 2009. Comparative effects of furnished and battery cages on egg production and physiological parameters in White Leghorn hens. Poult. Sci. 88 (10), 2042–2051. https://doi.org/10.3382/ps.2009-00171.

Prior, N.H., Yap, K.N., Mainwaring, M.C., Adomat, H.H., Crino, O.L., Ma, C., Guns, E.S., Griffith, S.C., Buchanan, K.L., Soma, K.K., 2017. Sex steroid profiles in zebra finches: effects of reproductive state and domestication. Gen. Comp. Endocrinol. 244, 108–117. https://doi.org/10.1016/j.ygcen.2016.02.018.

Proszkowiec-Weglarz, M., Porter, T.E., 2010. Functional characterization of chicken glucocorticoid and mineralocorticoid receptors. Am. J. Physiol. Regul. Integr. Comp. Physiol. 298 (5), R1257–R1268. https://doi.org/10.1152/ajpregu.00805.2009.

Qian, X., Droste, S.K., Lightman, S.L., Reul, J.M.H.M., Linthorst, A.C.E., 2012. Circadian and ultradian rhythms of free glucocorticoid hormone are highly synchronized between the blood, the subcutaneous tissue, and the brain. Endocrinology 153 (9), 4346–4353. https://doi.org/10.1210/en.2012-1484.

Quillfeldt, P., Poisbleau, M., Parenteau, C., Trouvé, C., Demongin, L., van Noordwijk, H.J., Möstl, E., 2011. Measuring corticosterone in seabird egg yolk and the presence of high yolk gestagen concentrations. Gen. Comp. Endocrinol. 173 (1), 11–14. https://doi.org/10.1016/j.ygcen.2011.05.005.

Rettenbacher, S.E., Möstl, E., Hackl, R., Ghareeb, K., Palme, R., 2004. Measurement of corticosterone metabolites in chicken droppings. Br. Poult. Sci. 45 (5), 704–711. https://doi.org/10.1080/00071660400006156.

Ricklefs, R.E., 2010. Insights from comparative analyses of aging in birds and mammals. Aging Cell 9 (2), 273–284. https://doi.org/10.1111/j.1474-9726.2009.00542.x.

Rombauts, L., Vanmontfort, D., Berghman, L.R., Decuypere, E., Verhoeven, G., 1994. Contribution of the fetal adrenal to circulating

immunoactive inhibin in the chicken embryo. Biol. Reprod. 51 (5), 926–933. https://doi.org/10.1095/biolreprod51.5.926.

Romero, L.M., Gormally, B.M.G., 2019. How truly conserved is the "well-conserved" vertebrate stress response? Integr. Comp. Biol. 59 (2), 273–281. https://doi.org/10.1093/icb/icz011.

Romero, L.M., Reed, J.M., 2005. Collecting baseline corticosterone samples in the field: is under 3 min good enough? Comp. Biochem. Physiol. A 140 (1), 73–79. https://doi.org/10.1016/j.cbpb.2004.11.004.

Rosenberg, J., Hurwitz, S., 1987. Concentration of adrenocortical hormones in relation to cation homeostasis in birds. Am. J. Physiol. 253 (1 Pt 2), R20–R24. https://doi.org/10.1152/ajpregu.1987.253.1.R20.

Rosenberg, J., Pines, M., Hurwitz, S., 1987. Response of adrenal cells to parathyroid hormone stimulation. J. Endocrinol. 112 (3), 431–437. https://doi.org/10.1677/joe.0.1120431.

Rosenberg, J., Pines, M., Hurwitz, S., 1988a. Stimulation of chick adrenal steroidogenesis by avian parathyroid hormone. J. Endocrinol. 116 (1), 91–95. https://doi.org/10.1677/joe.0.1160091.

Rosenberg, J., Pines, M., Hurwitz, S., 1988b. Regulation of aldosterone secretion by avian adrenocortical cells. J. Endocrinol. 118 (3), 447–453. https://doi.org/10.1677/joe.0.1180447.

Rosenberg, J., Pines, M., Levy, J.J., Nutt, R.F., Caufield, M.P., Russell, J., Sherwood, L.M., Hurwitz, S., 1989a. Renal and adrenal adenosine 3',5'-monophosphate production and corticosteroid secretion in response to synthetic chicken parathyroid hormone-(1-34). Endocrinology 125 (2), 1082–1089. https://doi.org/10.1210/endo-125-2-1082.

Rosenberg, J., Pines, M., Hurwitz, S., 1989b. Inhibition of aldosterone secretion by atrial natriuretic peptide in chicken adrenocortical cells. Biochim. Biophys. Acta 1014 (2), 189–194. https://doi.org/10.1016/0167-4889(89)90033-5.

Rosenberg, J., Pines, M., Levy, J.J., Nutt, R.F., Caulfield, M.P., Russell, J., Sherwood, L.M., Hurwitz, S., 1989a. Renal and adrenal adenosine 3′,5′-monophosphate production and corticosteroid secretion in response to synthetic chicken parathyroid hormone-(1-34). Endocrinology 125, 1082–1089.

Rosenberg, J., Pines, M., Hurwitz, S., 1989b. Inhibition of aldosterone secretion by atrial natriuretic peptide in chicken adrenocortical cells. Biochem. Biophys. Acta 1014, 189–194.

Rouault, A.A.J., Srinivasan, D.K., Yin, T.C., Lee, A.A., Sebag, J.A., 2017. Melanocortin receptor accessory proteins (MRAPs): functions in the melanocortin system and beyond. Biochim. Biophys. Acta Mol. Basis Dis. 1863 (10 Pt A), 2462–2467. https://doi.org/10.1016/j.bbadis.2017.05.008.

Rubolini, D., Romano, M., Boncoraglio, G., Ferrari, R.P., Martinelli, R., Galeotti, P., Fasola, M., Saino, N., 2005. Effects of elevated egg corticosterone levels on behavior, growth, and immunity of yellow-legged gull (*Larus michahellis*) chicks. Horm. Behav. 47 (5), 592–605. https://doi.org/10.1016/j.yhbeh.2005.01.006.

Sapolsky, R.M., Romero, L.M., Munck, A.U., 2000. How do glucocorticoids influence stress responses? Integrative, permissive, suppressive, stimulatory and preparative actions. Endocr. Rev. 21 (1), 55–89. https://doi.org/10.1210/edrv.21.1.0389.

Scanes, C.G., 2009. Perspectives on the endocrinology of poultry growth and metabolism. Gen. Comp. Endocrinol. 163 (1–2), 24–32. https://doi.org/10.1016/j.ygcen.2009.04.013.

Scheschowitsch, K., Leite, J.A., Assreuy, J., 2017. New insights in glucocorticoid receptor signaling—more than just a ligand-binding receptor. Front. Endocrinol. 8, 16. https://doi.org/10.3389/fendo.2017.00016.

Schmeling, S.K., Nockels, C.F., 1978. Effects of age, sex, and ascorbic acid ingestion on chicken plasma corticosterone levels. Poult. Sci. 57 (2), 527–533. https://doi.org/10.3382/ps.0570527.

Schmidt, K.L., Malisch, J.L., Breuner, C.W., Soma, K.K., 2010. Corticosterone and cortisol binding sites in plasma, immune organs and brain of developing zebra finches: intracellular and membrane-associated receptors. Brain Behav. Immun. 24 (6), 908–918. https://doi.org/10.1016/j.bbi.2010.02.008.

Schmidt, K.L., Pradhan, D.S., Shah, A.H., Charlier, T.D., Chin, E.H., Soma, K.K., 2008. Neurosteroids, immunosteroids, and the Balkanization of endocrinology. Gen. Comp. Endocrinol. 157 (3), 266–274. https://doi.org/10.1016/j.ygcen.2008.03.025.

Schmidt, K.L., Soma, K.K., 2008. Cortisol and corticosterone in the songbird immune and nervous systems: local vs. systemic levels during development. Am. J. Physiol. Regul. Integr. Comp. Physiol. 295 (1), R103–R110. https://doi.org/10.1152/ajpregu.00002.2008.

Schoech, S.J., Ketterson, E.D., Nolan Jr., V., 1999. Exogenous testosterone and the adrenocortical response in dark-eyed juncos. Auk 116 (1), 64–72. https://doi.org/10.2307/4089454.

Sharma, D., Chaturvedi, C.M., 2009. Effects of thyroid status on arginine vasotocin receptor VT2R expression and adrenal function in osmotically stimulated domestic fowl. J. Comp. Physiol. B 179 (7), 811–819. https://doi.org/10.1007/s00360-009-0362-4.

Sharma, D., Cornett, L.E., Chaturvedi, C.M., 2009a. Corticosterone- or metapyrone-induced alterations in adrenal function and expression of the arginine vasotocin receptor VT2 in the pituitary gland of domestic fowl, *Gallus gallus*. Gen. Comp. Endocrinol. 161 (2), 208–215. https://doi.org/10.1016/j.ygcen.2008.12.019.

Sharma, D., Cornett, L.E., Chaturvedi, C.M., 2009b. Osmotic stress induced alteration in the expression of arginine vasotocin receptor VT2 in the pituitary gland and adrenal function of domestic fowl. Gen. Comp. Endocrinol. 160 (3), 216–222. https://doi.org/10.1016/j.ygcen.2008.11.025.

Shen, P., Campagnoni, C.W., Kampf, K., Schlinger, B.A., Arnold, A.P., Campagnoni, A.T., 1994. Isolation and characterization of a zebra finch aromatase cDNA: in situ hybridization reveals high aromatase expression in the brain. Mol. Brain Res. 24 (1–4), 227–237. https://doi.org/10.1016/0169-328x(94)90136-8.

Shini, S., Huff, G.R., Shini, A., Kaiser, P., 2010. Understanding stress-induced immunosuppression: exploration of cytokine and chemokine gene profiles in chicken peripheral leukocytes. Poult. Sci. 89 (4), 841–851. https://doi.org/10.3382/ps.2009-00483.

Shtukmaster, S., Schier, M.C., Huber, K., Krispin, S., Kalcheim, C., Unsicker, K., 2013. Sympathetic neurons and chromaffin cells share a common progenitor in the neural crest in vivo. Neural Dev. 8, 12 https://doi.org/10.1186/1749-8104-8-12.

Smith, C.A., Smith, M.J., Sinclair, A.H., 1999. Expression of chicken steroidogenic factor-1 during gonadal development. Gen. Comp. Endocrinol. 113 (2), 187–196. https://doi.org/10.1006/gcen.1998.7214.

Smulders, T.V., 2017. The avian hippocampal formation and the stress response. Brain Behav. Evol. 90 (1), 81–91. https://doi.org/10.1159/000477654.

Soma, K.K., Wingfield, J.C., 2001. Dehydroepiandrosterone in songbird plasma: seasonal regulation and relationship to territorial aggression. Gen. Comp. Endocrinol. 123 (2), 144–155. https://doi.org/10.1006/gcen.2001.7657.

Spencer, K.A., Evans, N.P., Monaghan, P., 2009. Postnatal stress in birds: a novel model of glucocorticoid programming of the hypothalamic-pituitary-adrenal axis. Endocrinology 150 (4), 1931–1934. https://doi.org/10.1210/en.2008-1471.

Sun, Z., Xu, Y., 2020. Nuclear receptor coactivators (NCOAs) and co-repressors (NCORs) in the brain. Endocrinology 161 (8), 1–12. https://doi.org/10.1210/endocr/bqaa083.

Takeuchi, S., Kudo, T., Takahashi, S., 1998. Molecular cloning of the chicken melanocortin 2 (ACTH)-receptor gene. Biochim. Biophys. Acta 1403 (1), 102–108. https://doi.org/10.1016/S0167-4889(98)00022-6.

Takeuchi, S., Takahashi, S., 1998. Melanocortin receptor genes in the chicken—tissue distributions. Gen. Comp. Endocrinol. 112 (2), 220–231. https://doi.org/10.1006/gcen.1998.7167.

Takeuchi, S., Takahashi, S., 1999. A possible involvement of melanocortin 3 receptor in the regulation of adrenal gland function in the chicken. Biochim. Biophys. Acta 1448 (3), 512–518. https://doi.org/10.1016/s0167-4889(98)00165-7.

Takeuchi, S., Teshigawara, K., Takahashi, S., 1999. Molecular cloning and characterization of the chicken pro-opiomelanocortin (POMC) gene. Biochim. Biophys. Acta 1450 (3), 452–459. https://doi.org/10.1016/S0167-4889(99)00046-4.

Takeuchi, S., Teshigawara, K., Takahashi, S., 2000. Widespread expression of Agouti-related protein (AGRP) in the chicken: a possible involvement of AGRP in regulating peripheral melanocortin systems in the chicken. Biochim. Biophys. Acta 1496 (2–3), 261–269. https://doi.org/10.1016/s0167-4889(00)00022-7.

Tanabe, Y., Nakamura, T., Fujioka, K., Doi, O., 1979. Production and secretion of sex steroid hormones by the testes, the ovary, and the adrenal glands of embryonic and young chickens (*Gallus domesticus*). Gen. Comp. Endocrinol. 39 (1), 26–33. https://doi.org/10.1016/0016-6480(79)90189-8.

Tanabe, Y., Saito, N., Nakamura, T., 1986. Ontogenetic steroidogenesis by testes, ovary, and adrenals of embryonic and postembryonic chickens (*Gallus domesticus*). Gen. Comp. Endocrinol. 63 (3), 456–463. https://doi.org/10.1016/0016-6480(86)90146-2.

Tang, L., Peng, K., Wang, J., Luo, H., Cheng, J., Zhang, G., Sun, Y., Liu, H., Song, H., 2009. The morphological study on the adrenal gland of African ostrich chicks. Tissue Cell 41 (4), 231–238. https://doi.org/10.1016/j.tice.2008.11.003.

Thomas, A.L., Maekawa, F., Kawashima, T., Sakamoto, H., Sakamoto, T., Davis, P., Dores, R.M., 2018. Analyzing the effects of co-expression of chick (*Gallus gallus*) melanocortin receptors with either chick MRAP1 or MRAP2 in CHO cells on sensitivity to ACTH(1-24) or ACTH(1-13)NH_2: implications for the avian HPA axis and avian melanocortin circuits in the hypothalamus. Gen. Comp. Endocrinol. 256, 50–56. https://doi.org/10.1016/j.ygcen.2017.09.002.

Thurston, R.J., Bryant, C.C., Korn, N., 1993. The effects of corticosterone and catecholamine infusion on plasma glucose levels in chicken (*Gallus domesticus*) and turkey (*Meleagris gallopavo*). Comp. Biochem. Physiol. C 106 (1), 59–62. https://doi.org/10.1016/0742-8413(93)90254-i.

Toshimori, H., Toshimori, K., Minamino, N., Kangawa, K., Oura, C., Matsukura, S., Matsuo, H., 1990. Chicken atrial natriuretic peptide (chANP) and its secretion. Cell Tissue Res. 259, 293–298. https://doi.org/10.1007/BF00318451.

Tota, B., Gentile, S., Pasqua, T., Bassino, E., Koshimizu, H., Cawley, N.X., Cerra, M.C., Loh, Y.P., Angelone, T., 2012. The novel chromogranin A-derived serpinin and pyroglutaminated serpinin peptides are positive cardiac β-adrenergic-like inotropes. FASEB J. 26 (7), 2888–2898. https://doi.org/10.1096/fj.11-201111.

Trifaró, J.-M., 2002. Molecular biology of the chromaffin cell. Ann. N.Y. Acad. Sci. 971, 11–18. https://doi.org/10.1111/j.1749-6632.2002.tb04427.x.

Unsicker, K., 1973. Fine structure and innervation of the avian adrenal gland. II. Cholinergic innervation of adrenal chromaffin cells. Cell Tissue Res. (Z. Zellforsch. Mikrosk. Anat.) 145 (3), 417–442. https://doi.org/10.1007/BF00307165.

Unsicker, K., Huber, K., Schober, A., Kalcheim, C., 2013. Resolved and open issues in chromaffin cell development. Mech. Dev. 130 (6–8), 324–329. https://doi.org/10.1016/j.mod.2012.11.004.

Vanmontfort, D., Room, G., Bruggeman, V., Rombauts, L., Berghman, L.R., Verhoeven, G., Decuypere, E., 1997. Ovarian and extraovarian sources of immunoreactive inhibin in the chicken: effects of dexamethasone. Gen. Comp. Endocrinol. 105 (3), 333–343. https://doi.org/10.1006/gcen.1996.6834.

Veo, K., Reinick, C., Liang, L., Moser, E., Angleson, J.K., Dores, R.M., 2011. Observations on the ligand selectivity of the melanocortin 2 receptor. Gen. Comp. Endocrinol. 172 (1), 3–9. https://doi.org/10.1016/j.ygcen.2011.04.006.

Vernocchi, S., Batello, N., Schmitz, S., Revets, D., Billing, A.M., Turner, J.D., Muller, C.P., 2013. Membrane glucocorticoid receptor activation induces proteomic changes aligning with classical glucocorticoid effects. Mol. Cell. Proteomics 12 (7), 1764–1779. https://doi.org/10.1074/mcp.M112.022947.

Von Blumröder, D., Tönhardt, H., 2002. Influence of long-term changes in incubation temperature on catecholamine levels in plasma of chicken embryos (*Gallus gallus f. domestica*). Comp. Biochem. Physiol. A 131 (4), 701–711. https://doi.org/10.1016/s1095-6433(02)00008-9.

Vylitová, M., Mikšík, I., Pácha, J., 1998. Metabolism of corticosterone in mammalian and avian intestine. Gen. Comp. Endocrinol. 109 (3), 315–324. https://doi.org/10.1006/gcen.1997.7035.

Wada, H., 2008. Glucocorticoids: mediators of vertebrate ontogenetic transitions. Gen. Comp. Endocrinol. 156 (3), 441–453. https://doi.org/10.1016/j.ygcen.2008.02.004.

Walsh, M.T., Beldegreen, R.A., Clubb, S.L., Chen, C.L., 1985. Effect of exogenous ACTH on serum corticosterone and cortisol concentrations in the Moluccan cockatoo (*Cacatua moluccensis*). Am. J. Vet. Res. 46 (7), 1584–1588.

Watford, M., 2005. Is the small intestine a gluconeogenic organ? Nutr. Rev. 63 (10), 356–360. https://doi.org/10.1111/j.1753-4887.2005.tb00114.x.

Weber, H., Kocsis, J.F., Lauterio, T.J., Carsia, R.V., 1990. Dietary protein restriction stress and adrenocortical function: evidence for transient and long-term induction of enhanced cellular function. Endocrinology 127 (6), 3138–3150. https://doi.org/10.1210/endo-127-6-3138.

Wilson, J.X., 1984. The renin-angiotensin system in nonmammalian vertebrates. Endocr. Rev. 5 (1), 45–61. https://doi.org/10.1210/edrv-5-1-45.

Wingfield, J.C., 2013. Ecological processes and the ecology of stress: the impacts of abiotic environmental factors. Funct. Ecol. 27 (1), 37–44. https://doi.org/10.1111/1365-2435.12039.

Wingfield, J.C., Matt, K.S., Farner, D.S., 1984. Physiological properties of steroid hormone-binding proteins in avian blood. Gen. Comp. Endocrinol. 53 (2), 281–292. https://doi.org/10.1016/0016-6480(84)90254-5.

Wolfensberger, M., Forssmann, W.G., Reinecke, M., 1995. Localization and coexistence of atrial natriuretic peptide (ANP) and neuropeptide Y (NPY) in vertebrate adrenal chromaffin cells immunoreactive to TH, DBH and PNMT. Cell Tissue Res. 280 (2), 267–276. https://doi.org/10.1007/BF00307798.

Yamasaki, I., Takagi, T., Oikawa, D., Koutoku, T., Koga, Y., Tomonaga, S., Tachibana, T., Denbow, D.M., Furuse, M., 2003. Changes in catecholamines and dopaminergic metabolites in pigeon brain during development from the late embryonic stage toward hatch. Zool. Sci. 20 (5), 551–555. https://doi.org/10.2108/zsj.20.551.

Yang, Y., Harmon, C.M., 2020. Molecular determinants of ACTH receptor for ligand selectivity. Mol. Cell. Endocrinol. 503, 110688 https://doi.org/10.1016/j.mce.2019.110688.

Zhu, L.-J., Liu, M.-Y., Li, H., Liu, X., Chen, C., Han, Z., Wu, H.-Y., Jing, X., Zhou, H.-H., Suh, H., Zhu, D.-Y., Zhou, Q.-G., 2014. The different roles of glucocorticoids in the hippocampus and hypothalamus in chronic stress- induced HPA axis hyperactivity. PLoS One 9 (5), e97689. https://doi.org/10.1371/journal.pone.0097689.

Chapter 34

Endocrine pancreas

Joëlle Dupont[1,3], Nicole Rideau[2,4] and Jean Simon[2]

[1]PRC (UMR 6175), INRA, Nouzilly, France; [2]Recherches Avicoles, (UR 83), INRA, Nouzilly, France; [3]Unité de Physiologie de la Reproduction et des Comportements, Institut National de la Recherche Agronomique, Nouzilly, France; [4]Unité de Recherches Avicoles, Institut National de la Recherche Agronomique, Nouzilly, France

Abbreviations

2DG 2 deoxyglucose
APS Adapter protein with Pleckstrin homology and Src homology two domains
Arx X-linked gene Aristaless-related homeobox
C/EBPalpha CCAAT/Enhancer Binding Protein alpha
Cbl Proto-oncogene product
ChREBP Carbohydrate-responsive element-binding protein
CNS Central Nervous System
CRF corticotrophin-releasing factor
Crk v-crk sarcoma virus CT10 oncogene homolog (avian)
DOK Downstream of kinases
E Embryonic life
EGR1 early growth response 1
FASN Fatty acid synthase
FL, LL Fat Line and Lean Line of chickens
G6PC2 Glucose-6-phosphatase catalytic
Gab1 GRB2-associated binder 1
GABA Gamma-Aminobutyric acid
GCGLR Glucagon Receptor receptor
GHIH growth hormone-inhibiting hormone
GIPR gastric inhibitory polypeptide receptor
GK glucokinase
GLP Glucagon-Like Peptide
GLUT Glucose Transporter
HSL hormone-sensitive lipase
ICV Intracerebroventricular
IGF-1R Insulin like Growth Factor-1 Receptor
IGFBP-1 Insulin like Growth Factor Binding Protein-1
IGFs Insulin Like Growth Factors
IR Insulin Receptor
IRE insulin responsive elements
IRS Insulin Receptor Substrate
LIPE gene hormone sensitive lipase gene
LMH cells chicken hepatoma cell line
MAPK-ERK1/2 Mitogen Activated Protein Kinase-extracellular signal-regulated protein kinase
miRs microRNAs
MLXIPL gene MLX interacting protein-like
NPY neuropeptide Y
Pax4 Paired box 4
PC3/PC1 prohormone convertases 3/1
PI3K Phosphatidylinositol 3-kinase
PNPLA2 gene Human adipose triglyceride lipase gene
PP Polypeptide Pancreatic
PPAR-gamma Peroxisome proliferator-activated receptor gamma
PTEN Phosphatase and TENsin homolog deleted on chromosome 10
PYY Peptide YY
QM7 quail muscle cell line
QT6 quail muscle fibroblasts cell line
QTLs Quantitative Trait Loci
ROS Reactive Oxygen Species
Shc Src Homology Collagene protein
SLC2A4 solute carrier family 2 (facilitated glucose transporter)
SNPs Single Nucleotide Polymorphisms
SREBP1 Sterol-Regulatory Element-Binding Protein 1
SRIF Somatotropin Release-Inhibiting Factor
SST Somatostatin
STZ Streptozotocin
THRSPalpha (spot-14) Thyroid hormone responsive spot 14alpha
TOE1 Target of EGR1
UCP uncoupling protein
VIP Vasoactive Intestinal Peptide
VLDL Very-low-density lipoprotein

34.1 Introduction

The endocrine pancreas of the chicken (and of birds in general) displays several peculiarities (Hazelwood, 2000; Simon, 1989). Before discussing the current knowledge, we will recall the basics from these previous reviews. Most of these are certainly connected and interacting.

1-Birds have high-plasma uric acid and glucose levels despite normal plasma insulin levels [(Simon et al., 2011), for chicken]. Such high-plasma glucose levels (2−2.15 g/L in the fasting state) would be harmful for humans.

2-In chickens and ducks, high doses of exogenous insulin are required to induce hypoglycemia and huge doses are not lethal. The chicken features high-blood glucose,

Sturkie's Avian Physiology. https://doi.org/10.1016/B978-0-12-819770-7.00048-7

low-insulin sensitivity and as will become apparent in this chapter, the weak insulin release elicited by glucose in isolated chicken pancreas is characteristic of type 2 diabetes in human.

3-Experimental diabetes models are not available for chickens. Pancreatectomies are rarely complete; plasma glucose regulation is however impaired during refeeding. Diabetogenic drugs [alloxan or streptozotocin (STZ)] are inefficient, even when glycemia is decreased before STZ injection. Some isolated cases of diabetes have been described in pet birds, although not cited here.

4-Glucagon exerts a potent hyperglycemic effect; it is the lipolytic hormone in birds. The glucagon-induced cAMP increase is comparatively small but long-lived; the feedback decrease of cAMP by fatty acids appears inefficient in chicken adipocytes. Insulin lacks an antilipolytic effect in chicken adipocytes. Several peptides have been shown to have an antilipolytic effect in vitro: avian pancreatic polypeptide (APP), somatostatin, gastrin, and gut glucagon-like immunoactivity; however their function in chicken physiology has not been fully quantified in vivo.

5-Chicken insulin is "hyperactive" whereas duck insulin is "hypoactive." Chicken insulin has accordingly been suggested as more potent at inducing hypoglycemia in chicken than sheep or bovine insulin (in (Hazelwood, 2000)). The extent of the difference may have been overestimated: at high concentrations, similar nadir (maximal hypoglycemic effect) should be achieved irrespective of insulin type. [This is the case for insulin binding and phosphorylation of artificial substrate in solubilized chicken liver or brain insulin receptors (IRs)].

6-The importance of the insulin/glucagon ratio in the control of metabolism has been demonstrated in chickens and ducks. In vivo, this ratio is governed by opposite insulin-glucagon variations in response to nutritional status (fed vs. fasting). Glucagon-insulin interactions are however more complex. Insulin immuno-neutralization in fed chickens (i.e., a nutritional status for high-insulin demand, a protocol previously developed in ducks, [Mirsky et al., 1964, in (Dupont et al., 2008)] evokes a rapid (less than 30 min) and large rise in plasma glucose levels. Surprisingly, injection of a glucagon antagonist [des-His^1 (Glu^9) glucagon] has no effect on plasma glucose level in fed chickens in (Dupont et al., 2008); a hypoglycemic effect might be expected. This strongly suggests that in normally fed chickens, the control of plasma glucose level relies more on insulin than on glucagon in (Dupont et al., 2008, 2012). The presence of glucagon is however essential: in the pathological model of "hypoglycemia-spiking mortality syndrome" where pancreatic glucagon content is extensively depleted following a virus infection, chickens do not eat and ultimately die from starvation in a profound hypoglycemic status (Davis and Vasilatos-Younken, 1995). To inhibit pancreatic glucagon release, glucose requires the presence of insulin (Dupont et al., 2008), which confirms previous results obtained in ducks and later on in mammals [see Miahle's group references in (Simon, 1989)].

7-Chicken (and bird) metabolism is also peculiar in several ways (see other chapters in this book). In short, gluconeogenesis is active in liver and kidneys but appears able to be regulated only in kidneys. Liver is the organ for de-novo lipogenesis.

8-Insulin exerts pleiotropic effects in chickens during embryonic and posthatch development. The major typical effects on carbohydrate, lipid, and protein metabolism have been demonstrated. Insulin stimulates glucose and amino acid transport in various cells. The insulin effect on glucose transport is however limited in muscle and still doubtful in chicken adipocytes. Insulin stimulation of amino acid transport requires protein synthesis. Insulin greatly stimulates liver lipogenesis and expression of lipogenic enzymes. In contrast, insulin stimulation of lipogenesis remains marginal, if any, in chicken adipocytes. (Lipogenesis is also intrinsically low in human adipocytes). Glucagon counteracts insulin stimulation of lipogenesis in chicken liver.

9-Finally, birds have a high-body temperature (about 42°C in chickens) and a high-metabolic rate and anabolism. They are able to adapt to long catabolic states and to survive long periods without food.

This chapter offers a synthetic view of current knowledge, focusing on major aspects of glucagon and insulin control for the sake of brevity. References have been kept as few as possible; early major original contributions for chickens and birds are acknowledged and listed only by first author's name and date but not referenced, including ours, when quoted in recent publications. For evident reasons, knowledge of the role of the endocrine pancreas is far more advanced in mammals; on several occasions, it was necessary to refer to it. Again, to save space, these data are listed in the text by first author's name and date. Readers will need to connect to Pubmed to have access to full references.

34.2 Pancreas embryogenesis and development

34.2.1 Morphology of avian pancreas (Fig. 34.1)

In most birds, the pancreas is situated in the duodenal loop and consists of three lobes: the dorsal, ventral, and splenic lobes: the splenic lobe is contiguous with the rest of the pancreas, but in some birds, it can be completely separated. A fourth lobe, sometimes confusingly called the "third lobe," is a part of the ventral lobe and is distinguishable in galliform birds (which include chickens and quail).

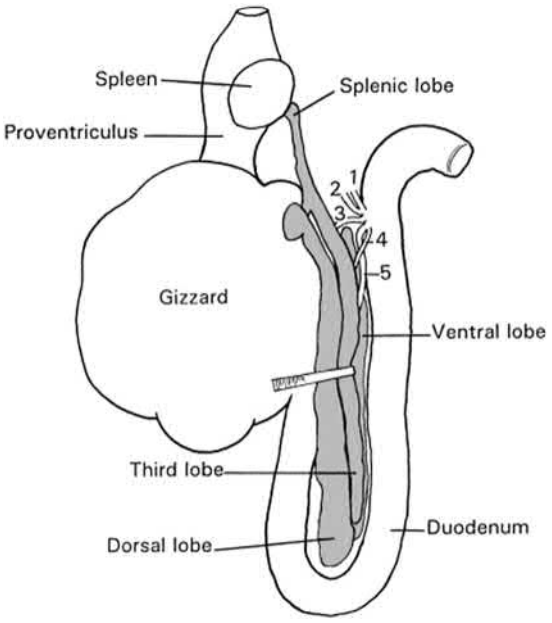

FIGURE 34.1 The anatomical relationship in the chicken of the four lobes of the pancreas (shaded) and neighboring organs (blood supply and liver not shown) viewed from the dorsal aspect. 1. cystic duct; 2. hepatic duct; 3. dorsal pancreatic duct; 4. duct of the third lobe; 5. ventral pancreatic duct. *After Mikami, S.I., Ono, K., 1962. Glucagon deficiency induced by extirpation of alpha islets of the fowl pancreas. Endocrinology 71, 464–473, The Endocrine Society.*

34.2.2 Distribution of avian pancreatic endocrine cells between the different pancreatic lobes

The endocrine pancreas contains clusters of cells called the islets of Langerhans, which are distributed throughout the exocrine parenchyma. These represent only 1%–2% of the whole gland. In contrast to mammals in which only one type of islets occurs, three types of islets are found in birds: the light, the dark, and the mixed islets. They differ in shape, size, and staining characteristics. The light islets (or B-islets) remain clear after classical staining procedures (Heidenhain's iron haematoxylin) and are essentially composed of β–and δ-cells secreting insulin and somatostatin, respectively, and occasionally very few α-cells secreting glucagon. The dark islets (or A-islets) are composed essentially of α– and δ-cells secreting glucagon and somatostatin, respectively. They are larger in size than the B-islets. The mixed islets are composed of numerous β-cells and a few α- and δ-cells. Some wild bird species have mixed islets (randomly distributed) rather than light and dark islets (Steiner et al., 2010). A fourth type of endocrine cell is found in the pancreas: the F cells. These cells synthesize and release APP; they occur as single cells or in groups disseminated in the exocrine parenchyma mainly in the dorsal and ventral lobes. Some F-cells can be found within the islets. Isolated δ-cells (as numerous as F-cells) are also found as dispersed extrainsular endocrine elements. The splenic lobe and to a lesser extent the third lobe (when present) notably contain more islet tissue per unit volume than do the dorsal and ventral lobes (Rideau, 1988).

The feature unique to the avian pancreas is the predominance of the glucagon-producing over the insulin-producing cells in the ratio of approximately 2:1 (Andrew et al., 1984 in (Manakova and Titlbach, 2007)). In addition, somatostatin-producing δ-cells are also more numerous in the avian pancreas than in that of mammals (Rideau, 1988). The existence, distribution, and relative frequency of various (neuro-)endocrine cells (biotin, serotonin, NPY, and chromogranin) have been demonstrated in the pancreas of avian species (Ku et al., 2000; Lucini et al., 2000).

The islet tissue is richly vascularized, irrigated by the pancreaticoduodenal artery and drained by the pancreaticoduodenal vein. Innervation of the pancreatic islets of birds is not as apparent as it is in mammals. Electron microscopic studies have clearly shown that the main endocrine cellular types of the pancreas of the domestic fowl are associated with nerve terminals. The nerve supply to the islets is however less abundant than that to the acinar cells; it is also less marked to the A-islets than to the B-islets. In contrast, δ cells are richly and directly innervated in chickens (Rideau, 1988).

34.2.3 Development of avian pancreas

The pancreas is of endodermal origin; it is formed from the embryonic foregut. In birds, it arises from three buds, a dorsal bud and right and left ventro-lateral buds (Rawdon, 1998) that appear at the stage of 22–31 somites (56–67 h) and begin to fuse at day seven of embryonic development (Hamburger and Hamilton stage 30, HH 30) (Matsuura et al., 2009).

The determination of endoderm to form dorsal and ventral bud derivatives occurs before formation of the buds. In mammals, the signaling pathways underlying the pancreatic development process include the Hedgehog system, the homeobox gene Pdx1, and Notch signaling. The vast majority of neurogenin-3 (ngn3)-expressing cells are committed to the endocrine lineage (Rosenberg et al., 2010). Two transcription factors, Pax4 and Arx, have competing roles in the commitment of the first of ngn3-positive cells to generate either the α/PP-cell lineage or the β/δ-cell lineage. Subsequently, within cells that are committed to the β/δ-cell lineage, persistence of pax4 expression seems to select for the β-cell lineage, whereas suppression of pax4 expression selects for the δ-cell lineage (Gittes, 2009).

Early in vitro studies by Rawdon using the dorsal pancreatic bud of five-day chick embryo established that pancreatic mesenchyme may play an instructive role with respect to the early development of the chick pancreas.

Results also suggested that the notochord plays an early role in induction of the pancreas although experimental evidence were lacking (Rawdon, 1998). Past decade studies confirmed and extended Rawdon's observations (Rawdon, 1998). Prepancreatic endoderm first receives pancreas-inducing signals from the underlying somatic mesoderm, inducing Pdx1 expression as early as 4 ss (1.5-day-old embryos) (Katsumoto et al., 2009). The regulation of pancreatic endocrine development by Notch is also found in chicken; inhibition of Notch signaling results in increased endocrine differentiation, whereas activation of the Notch1 receptor blocks endocrine development and maintains the proliferation of pancreatic progenitor cells in the embryonic chicken pancreas (Ahnfelt-Ronne et al., 2007). Neurogenin 3, which is transiently expressed in pancreatic endocrine progenitors, is responsible for the activation of a transcription factor cascade which ultimately leads to the maturation of endocrine cells in chicken endoderm (Rosenberg et al., 2010). The origin of the ventral pancreatic precursor cells has been studied less extensively; they are located at sites in which Pdx1 expression is detected by in situ hybridization (Matsuura et al., 2009).

Organization, volume, and ratio among the different endocrine cell types vary throughout embryonic development and postnatal life. The dorsal bud is the major source of insulin, glucagon, and somatostatin cells, whereas the ventral buds generate PP cells (Rawdon, 1998). In the dorsal bud, glucagon immunoreactive cells appear first at 2.25−2.5 days of incubation; then insulin cells at 3−5 days and somatostatin cells at 3.25 days (Manakova and Titlbach, 2007). Pancreatic polypeptide cells appear only later, at 7 days in the splenic lobe (Cowap, 1985). In contrast to the dorsal bud, insulin cells have not been identified in prospective ventral bud derivatives until 13 days of incubation (Manakova and Titlbach, 2007). Development of exocrine tissue is delayed in comparison to that of endocrine tissue (Manakova and Titlbach, 2007).

34.2.4 Pancreatic hormone levels during development and after hatching

Circulating concentrations of insulin and glucagon rise during development of the chicken embryo. In Cobb 500 chick embryos and hatched chicks, plasma insulin increased from 10 days of embryonic life (E) (30 pg/mL) reaching 1000 pg/mL at 17 days after hatching (Lu et al., 2007). Plasma insulin concentrations, at 3−4 ng/mL in fed growing ducks and chickens, are similar to those of mammals (Simon et al., 2011). They are low at 1 day posthatch and increase with age up to 28 d, with higher insulin sensitivity in 1-day-old chicks than in 21-day-old broiler chickens, as observed in the latest strain of broiler chickens (Shiraishi et al., 2011b) and in previous reports on egg-laying or meat-type chickens. Plasma insulin concentration decreased by 45%−50% after 6 h of fasting in 19 to 47-day-old in male and female modern meat-type chickens (Christensen et al., 2013). A low-plasma glucagon concentration (59 pg/mL) was found in embryos at 10 d of incubation, remaining low until 17 d E and then increasing approximately threefold by the time of hatching (Lu et al., 2007). Values between 152 and 450 pg/mL were measured in fed and 6h fasted modern meat-type chickens, respectively (Christensen et al., 2013). It should be noted that in some of these experiments, the feeding pattern of chickens was not always synchronized with light-dark cycles.

34.3 Factors controlling pancreatic insulin and glucagon release in birds

34.3.1 Insulin

Whereas in mammals, glucose is the primary physiological regulator of insulin secretion, the insulinotropic effect of glucose is less obvious in birds in vivo and in vitro. In vivo raising blood glucose levels in ducks and chicken only transiently increases insulin levels (Rideau, 1988). The high-basal plasma glucose concentrations found in chickens may itself contribute to the relative insensitivity of the chicken β-cell to glucose: impairment of glucose-induced insulin release has been reported in hyperglycaemic mammalian models. The mechanisms are however presently unknown in chickens. Somatostatin which is present at high concentration in the chicken pancreas (Weir et al., 1976 in (Rideau, 1988)) may also exert inhibitory paracrine effects on the β-cell and partly explain the insensitivity of the β-cell to fuel nutrients. However somatostatin immunoneutralization in isolated-perfused chicken pancreas has only transitory effects on insulin release at high-glucose concentration (42 mM) and no effect at low levels (14 mM) (Honey et al., 1981 in (Rideau, 1988)). In vitro studies provided further insight into the mechanisms responsible for the relative glucose insensitivity of chicken β−cell. Using isolated and perfused duodenum-pancreas from adult hens in (Rideau, 1988, 1998) first showed that the pancreatic β-cell is relatively insensitive to glucose as very high and nonphysiological glucose concentrations (30 to 40 mM) are required to induce a modest insulin release. This insensitivity was confirmed and extended to other fuel nutrients, which are potent insulinotropic agents in mammals, using isolated duodenum-pancreas from young chickens. D-glucose and D-Glyceraldehyde require high concentrations to evoke either very weak or delayed insulin release; leucine and its ketoacid (α-KIC) are even totally ineffective. The chicken β-cell remains however sensitive to depolarizing agents (K^+), tolbutamide (which closes K^+ATP-dependent channels), and potentiators of insulin secretion (acetylcholine or cAMP) (Rideau, 1988). Therefore, initiation of insulin

secretion by fuel nutrients, the critical and specific step of the β-cell, appears different in chickens and mammals, whereas potentiating mechanisms (arginine, acetylcholine, and cAMP in the presence of low glucose concentration) and membrane depolarization events (K^+ and arginine) are present in chickens as in mammals.

The key role of glucokinase (GK) in the regulation of insulin release and hepatic glucose utilization has been well described in mammals. Though the GK gene is not referenced in the chicken genome at Ensembl, we isolated a chicken GK cDNA and showed that GK messenger is expressed in chicken liver and pancreas (Berradi et al., 2005 in (Rideau et al., 2010) for review Panserat et al., 2014). A human GK antibody identified a GK protein in chicken liver, the amount and activity of which was insulin-dependent (Dupont et al., 2008). Furthermore, RO0281675 (a specific GK activator in mammals) caused severe hypoglycaemia in chickens but surprisingly without significantly increasing insulin levels, contrary to results obtained in mammals (Rideau et al., 2010). Thus, liver glucose utilization is substantially enhanced following liver GK activation. Though GK is present in the chicken pancreas, pancreatic GK activation may not be sufficient to cause insulin secretion, which confirms in vitro studies reported above and supports the conclusion that the coupling between intra-B-islet metabolism and insulin release is different in chicken B-islets. The lack of insulinotropic effect of leucine or α-KIC (metabolized in the mitochondria) suggests that the inefficiency is located beyond the pyruvate step in the chicken β-cell.

Isolated chicken B-islets are necessary to further understand the insensitivity of the chicken β-cell to "insulinotropic" fuel nutrients. Although functional islets were isolated in various mammalian species more than 40 years ago, isolation of avian islets of Langerhans has proven to be especially difficult due to the fact that the morphology of the isolated A- and B-islets had not been characterized. Ruffier et al. described isolation of functional A- (glucagon) chicken islets (Ruffier et al., 1998). Glucose-stimulated insulin release from B-islets isolated from the dorsal lobe of chick pancreas has been reported (Datar et al., 2006). In our opinion, however, the specificity of these preparations remains to be established as dithiocarbazone staining method stains both B- and A-islets in chickens (Ruffier et al., 1998).

Resistance to diabetogenic drugs. The extreme resistance of birds to the diabetogenic drugs alloxan and STZ was described very early. In mammals, the β-cell specificity of these drugs is mainly due to the fact that they are selectively transported by the β-cell glucose transporter, GLUT2 (Lenzen, 2008). GLUT2 expression was reported in the liver and kidney in chickens (Kono et al., 2005) but also in chick islets (Modak et al., 2007). Within the mammalian β-cell, alloxan selectively inhibits glucose-induced insulin secretion through specific inhibition of GK; in addition, it induces ROS formation, resulting in the selective necrosis of β-cells. STZ's effects are attributed to its specific alkylating potency, which modifies biological macromolecules and DNA fragments and ultimately destroys the β-cells (Lenzen, 2008). Compared with mouse islets, chicken islets generate smaller amounts of ROS under STZ. Consequently less damage to proteins, lipids and DNA can be expected in chicken than in mouse islets. These results may partly explain why STZ does not induce diabetes in chicken, even at high doses (Modak et al., 2007).

Despite the peculiarities present in chickens in the coupling between metabolism and insulin release, insulin release is under the control of multiple components in vivo and in vitro. Though glucose or a mixture of amino acids separately increases plasma insulin to a small extent, they act synergistically when combined in vivo. Refeeding with gradually increasing amounts of food results in gradual rises in plasma insulin levels, adjusting glucose to a similar level. Changes in glucose-insulin balance are observed in several experimental conditions or models, including genetically fat and lean lines of chickens, dwarf chickens (*dw/dw*), hypothyroidism, corticosterone treatment, and chronic exposure to high temperature (Rideau, 1997) (Table 34.1). The incretin effect is not documented in chickens, but a variety of other stimuli including nutrients (glucose, arginine), hormones (cholecystokinin, glucagon, corticosterone, GH) (Rideau, 1988), and neuronal stimuli (Karmann et al., 1992) increase plasma insulin levels. The effects of Ghrelin/obestatin and GLP-2 on insulin release are not known in birds. Conversely, insulin secretion is inhibited by epinephrine and somatostatin (Rideau, 1988). Though the existence of leptin in the chicken is still debated, a recombinant "chicken" leptin (or leptin analog) potently inhibits insulin secretion from the perfused chicken pancreas (Benomar et al., 2003).

34.3.2 Glucagon

Fasting markedly increases circulating concentrations of glucagon in chickens (Edwards in (Scanes, 2009). In modern meat-type chickens, plasma glucagon levels increased 3.5−3.7 fold after 6 h of fasting while plasma glucose was depressed by 11% (Christensen et al., 2013). Glucagon secretion is inhibited by glucose in vivo in domestic birds (Honey et al., 1980 in (Rideau, 1988)) and in wild species in (Scanes and Braun, 2012). Exogenous glucose (42 mM) inhibited glucagon release by 27% from isolated A-islets of Langerhans (Ruffier et al., 1998). Conversely, glucagon release is stimulated by amino acids, free fatty acids, cholecystokinin, somatostatin, and insulin in vivo (Scanes and Braun, 2012). A tonic suppression effect on glucagon by insulin is suggested in a model of insulin immune-neutralization in chickens (Dupont et al., 2008). As for

TABLE 34.1 Experimental or genetical models exhibiting changes in the plasma glucose-insulin relationship in chickens.[a]

Models	Fasting plasma levels		Glucose tolerance		Insulin sensitivity	Fattening
	Glucose	Insulin	Glucose disposal	Insulin levels		
Intermittent (IT) versus ad lib feeding (C)	IT ≥ C	IT = C	IT > C	IT < C	ND	IT ≥ C
Corticosterone (cort) treatment.	cort > C	cort > C	cort < C	cort > C	cort < C	cort > C
Fat-lean lines (FL-LL)	FL < LL	FL ≥ LL	FL > LL	FL > LL	FL ≥ LL	FL > LL
High-low glucose lines (LGl-HGl)	LGl < HGl	LGl = HGl	LGl = HGl	LGl = HGl	LGl = HGl	LGlL > HGlL
High-low growth lines (HG-LH)	HG ≤ LG	HG > LG	HG = LG	HG > LG	ND	HG > LG
Dwarf (*dw*)-Normal (N) chickens	*dw* = N	*dw* = N	*dw* = N	*dw*<N	*dw*>N	*dw* > N

[a]ND, *not determined. Refeeding experiments have been performed following a fast in several of these models. Results, not summarized in the table, can be found in Simon (1988) and in Simon et al., 2000 (LGl-HGl). Corticosterone was injected 5–6 mg doses/kg. Insulin sensitivity was evaluated through the hypoglycemic effect of exogenous insulin. Results of glucose tolerance in HG-LG chickens are unpublished data (Simon et al.).*

insulin, the effect of gastrointestinal peptides and adipose tissue hormones on glucagon secretion is unknown in birds.

The mechanisms underlying the secretion of glucagon from α-cells are largely unknown in chickens. In mammals, α-cells contain a comparable secretory "machinery" as in β-cells: a glucose transporter (in this case the ubiquitous GLUT-1), GK, K^+ATP channels, L-type voltage-gated calcium channels, and secretory granules (Le Marchand and Piston, 2010). However, α-cell secretory activity is quite different from that of β-cells. The mechanisms underlying the glucose inhibition of α-cell secretory activity are poorly understood. Two nonexclusive models have been proposed: a direct inhibition by glucose and an intraislet paracrine inhibition arising from non-α-cells. The paracrine control might involve somatostatin released from δ-cells and insulin, zinc or GABA released from β-cells. Recently Le Marchand and Piston suggested that in the absence of cell–cell contacts, isolated α-cells function similarly to β-cells, i.e., glucagon secretion increases as a function of glucose concentration. However in the islet, glucose inhibits glucagon release downstream the calcium step, presumably at the level of vesicle trafficking or exocytotic machinery (Le Marchand and Piston, 2010).

34.3.3 Somatostatin

Somatostatin (also known as growth hormone-inhibiting hormone or somatotropin release-inhibiting factor) is a 14-amino acid peptide that regulates the endocrine system. The interaction of somatostatin with thyrotropin releasing hormone signifies the physiological role of somatostatin in control of digestion, growth, and reproduction in the chicken. Chicken somatostatin is present in two forms: somatostatin-14 (SST-14) and somatostatin-28 (SST-28), which are encoded by the same gene (PSS1) as in mammals. Ontogenic expression profile of chicken SSTs is time and tissue specific (Malik et al., 2013). Chicken pancreatic A-, B-islets, and D-cells contain only SST-14 peptide form (Takayanagi et al., 1996 in (Trabucchi et al., 2003)). Another somatostatin gene variant (PSS2) exists in many species, including chickens. PSS2 messenger is expressed in chicken pancreatic islets or pancreas, and in a few specific brain structures, less numerous than structures expressing PSS1 messenger (Trabucchi et al., 2003).

34.3.4 Avian pancreatic polypeptide

APP was first isolated and characterized from chicken pancreas (Kimmel et al., 1968); it is a member of the neuropeptide Y family [PP, peptide YY (PYY) and neuropeptide Y (NPY)]. PYY and PP are gut endocrine peptides almost exclusively expressed in the digestive system, whereas NPY is expressed in the central and peripheral nervous systems at all levels of the gut–brain axis. All three peptides are 36 amino acids long and act on G-protein-coupled receptors; five receptor subtypes have been described. In mammals, PP is released from the endocrine pancreas following a meal and acts preferentially via Y4 receptors. It inhibits gastric emptying, intestinal electrolyte, water secretion intestinal motor activity, and peristalsis. PP also reduces appetite (Holzer et al., 2012). In chickens, APP is released in response to gut peptides and amino acids (Colca and Hazelwood, 1982 in (Rideau, 1988)).

Y4 receptors are expressed in a large number of peripheral tissues and in the brain (Lundell et al., 2002). APP primarily acts by inhibiting gastrointestinal tract motility and gall bladder and exocrine pancreas secretion in chickens (Hazelwood, 1993 in (Hazelwood, 2000)). It also exerts metabolic effects: liver glycogenolysis, hypoglycerolemia, lowering of plasma free fatty acids level. One study though suggests that APP increases food intake in White Leghorn chickens (Denbow et al., 1988).

34.4 Insulin and glucagon peptides

34.4.1 Insulin/preproinsulin, proinsulin, and C-peptides

The chicken insulin gene was cloned and sequenced as early as 1980 (Perler et al., in (Simon et al., 2004)); it is localized on GGA5 and exhibits the "ancestral" structure containing two introns: intron-1 interrupts the 5′ un-translated region and intron-2 [about 3.5 kb, vs. 141−786 bp in other animal species, Steiner et al., 1985, in (Simon et al., 2004)] interrupts the coding sequence. It encodes a preprohormone, i.e., preproinsulin, which contains the signal peptide (rich in hydrophobic residues), the insulin B-chain, the connecting peptide (C-peptide), and the insulin A-chain. Until now there is no evidence for the existence of a second insulin gene in birds in (Simon et al., 2004).

Insulin has been purified and sequenced in chickens, turkeys, ostriches, geese, and Pekin and Muscovy ducks in (Chevalier et al., 1996). The insulin gene has been cloned and sequenced in other bird species including humming bird and 28 other species [Fan et al., 1993, in (Simon et al., 2004)]. From deduced amino acid sequences, bird insulins appear highly conserved. As compared to human insulin, minor neutral changes on the B-chain concern few residues at both ends: B1, B2, B3, B20, B27, or B30 (out of 30 positions). On the A-chain, changes concern positions A8-10 (out of 21 positions). In our study (Simon et al., 2004), some uncertainty remains for the last six amino acids of the A-chain because the reverse primer was targeting the corresponding codons and the stop codon. Changes on the A-chain (at A8-10 positions) between bird and human insulins are not neutral. This region is the most variable and considered as the most immunogenic part. Accordingly, most antibodies prepared against mammalian insulins do not cross-react with chicken or duck insulin.

At the A8 position a histidine residue is found in most bird species, as opposed to a glutamic acid residue in six species of the Anseriform order and a threonine in human insulin. The A8 position is now thought to be involved in the insulin binding site to the IR (site 1, Sajid et al., 2009); the synthesis of human insulin analogs wearing different residues at the A8 position confirmed an early hypothesis, namely, the presence of histidine at A8 confers the properties of chicken insulin to such analogs [high-binding affinity and low-dissociation rate, Weiss et al., 2001, 2002; Wan et al., 2004 and references quoted in (Chevalier et al., 1996)]. Chicken insulin is the only natural super analog thus far described (at least twice as potent as human or pig insulins in bioassays or binding assays in many species, Kemmler et al., 1978, Schauder and Buck, 1969, Simon et al., 1974, 1977, in (Chevalier et al., 1996)).

A8 glutamic acid, as found in the Anseriform order, increases the thermodynamic stability of the molecule, which should make "duck-type" insulins even more potent than "chicken-type" insulins (Weiss et al., 2001). In fact the presence of negatively charged residues such as glutamic or aspartic acid at this position decreases the affinity of analogs for the receptor (Weiss et al., 2001). Duck insulin accordingly exhibits low affinity in rat liver membranes (Chevalier et al., 1996) and low bioactivity in rat fat cells (Moody AJ, personal communication). The fact that chicken or Pekin and Muscovy ducks IRs (IRs) do not discriminate so extensively, accordingly to potencies observed with rat IR, may be specific to bird IRs (see IR section). So, thus far, only two types of insulin have been found in 30 bird species: the hyperactive "chicken-type" insulin and the hypoactive "duck-type" insulin. From alignments of nonmammalian insulins [see references in (Simon et al., 2004)], A8 histidine was present early in the ancestor insulin molecule and disappeared in mammals (which possibly decreases the risk of hypoglycemic events and tumorigenicity). The appearance of A8 glutamic acid in anseriform birds and some snakes may have occurred independently in these species.

As in other species, bird C-peptides have been much less conserved; 14 changes out of 28 amino acid residues are found in 29 bird species (Simon et al., 2004). In other animal species, C-peptides are longer [31−38 amino acids, Gross et al., 1989 and Wahren et al., 2000, in (Simon et al., 2004)]. Whether the shortness of bird C-peptide modifies the rate and yield of insulin synthesis is unknown. C-peptide is linked to B- and A-insulin chains through two dibasic residues at both ends (RR or KR, as in other species). In mammals, proteolytic cleavage and removal of these two pairs is performed by specific endopeptidases: PC3/PC1 and PC2 prohormone convertases and carboxypeptidase E. Such endoproteases have been detected in chicken embryos using heterologous antibodies [Hernandez-Sanchez et al., 2002; Teshigawara et al., 2001, in (Simon et al., 2004)]. Though predicted to be 28 residues long in all bird species, purified duck (*Anas platyrhynchos*) C-peptide is only 26 amino acids long in (Simon et al., 2004). Such extensive cleavages are also suggested in all the birds studied (with a possible exception in *Passer*, in Simon et al., 2004). In mammalian species, at least two acidic amino acids surrounding a hydrophobic residue are present at the NH2-terminal end of C-peptide

(e.g., EAED, EVE, and EAE); such a structure has been found to be critical for a normal rate of conversion of proinsulin to insulin. A very similar structure is observed in bird species studied (DVE, DIE, or DAE, Simon et al., 2004). C-peptide has long been considered as devoid of physiological functions on its own (other than structuring the precursor during insulin biosynthesis). C-peptide is now considered to control e-NOS, Na^+, K^+-ATPase, alpha−enolase, and several transcription factors (Wahren et al., 2012; Ishii et al., 2012). The central segment (ELGGGP-GAG) or the COOH-terminal pentapeptide fragment (EGSLQ) of human C-peptide mimics the action of the entire peptide in several assays. The central part is very different in bird species and C-terminal fragments are acidic (QEEYE, HEEYQ, QEEFE, or PEEYE). The C-peptide may therefore have acquired specific biological functions only in mammals, unless the still putative receptor co-evolved in bird species.

The length of available preproinsulin gene reading frames is similar in all bird species [187 nucleotides at the 5′-end and 134 nucleotides at the 3′-end (Simon et al., 2004)]. In contrast, the size of the PCR products varies greatly [from 2.7 kb in Passeriformes (*Passer*, *Turdus* and *Pica*) to about 4.5 kb in Palaeognathae species (*Struthio*, *Rea* and *Dromiceius*)]. Phyllogenetic analyses supported the monophyletic origin of birds and identified the Palaeognathae group as an isolated group at 100%, strongly suggesting this group is basal. After the branching of Palaeognathae, a galloanserae was identified (at 63%) whereas all other Neognathae clustered at 99%. If we accept Palaeognathae, rather than Passeriformes are basal to Neornithes, intron-2 must have evolved from a very long ancient form (likely close to that found in present day Palaeognathae species) toward the shorter form found in Passeriformes.

In humans, some insulin gene polymorphisms are associated with diabetes. Some polymorphisms have been described in chicken (Bennett et al., 2006; Qiu et al., 2006) and in duck (one paper in Chinese, Kong et al., 2008) insulin genes. In the chicken, polymorphisms (mostly SNPs), thus far identified, are located in 5′-and 3′-UTR or intron. In these pioneer studies significant associations were found for body weight at hatching, 28 d or 55 w and small intestine length but not with abdominal fat weight at 13 w of age. Further studies conducted at other ages and involving other physiological parameters may reveal other associations.

34.4.2 Glucagon and glucagon-like peptides

34.4.2.1 Glucagon structure and physiological effects

Glucagon (a member of the VIP-secretin family of peptide hormones) is a 29-amino acid peptide, very similar across species. In mammals, glucagon is encoded by a single proglucagon gene, and there is a single mRNA which generates a single protein precursor that contains glucagon and two structurally related peptides at its carboxyl terminus: glucagon-like peptide 1 (GLP-1) and glucagon-like peptide 2 (GLP-2). The post-translational proteolytic processing of this unique precursor is tissue-specific. In the pancreas, glucagon is one of the major peptides released by the α cells of A-islets in response to low glucose levels, whereas GLP-1 and GLP-2, but not glucagon, are produced in intestinal L cells and central nervous system.

Chicken glucagon is also a 29-amino acids-long peptide that is derived from a single proglucagon gene, which expresses multiple mRNA transcripts with different coding potentials (Richards and McMurtry, 2008). In the case of the domestic fowl, the preproglucagon precursor is 151 amino residues long. Chicken glucagon differs from rat and human glucagon by only one amino acid (ser vs. asn at position 28) and from duck glucagon by two amino acids (ser vs. asn at position 28 and thr vs. ser at position 16). In contrast to mammals, the chicken proglucagon gene expresses two classes of proglucagon mRNA transcripts (PGA and PGB): class A mRNA (PGA) codes for glucagon and GLP-1 and resembles lower vertebrate transcripts such as those found in fish, while class B mRNA (PGB) codes for glucagon, GLP-1, and GLP-2 and is more like mammalian transcripts. Pancreas and proventriculus displayed the highest expression levels of class A and class B mRNA. Two prohormone convertases (PC) (PC2 and PC1/3) cleave the precursor into active peptides: PC2 mRNA is predominantly expressed in the pancreas and proventriculus, whereas PC1/3 mRNA is more highly expressed in the duodenum and brain. Fasting and refeeding have no effects on proglucagon mRNA expression in various chicken tissues: pancreas, proventriculus, duodenum, or whole brain. This indicates that transcriptional regulation does not account for acute changes in plasma glucagon resulting from short-term changes in energy status in birds (Richards and McMurtry, 2008, 2009). The proglucagon gene is also expressed in various neurons of the avian retina (Fischer et al., 2006) and in chicken adipose tissue (Cogburn, personal communication), where in contrast to other tissues, PGB mRNA levels appear insulin-dependent (Ji et al., 2012).

In birds, glucagon has several physiological roles and peculiarities that have been already described in Hazelwood, fifth Edition. Plasma glucagon levels are much higher in birds than in mammals. Chicken, ostrich, and pigeon glucagons were initially found to be less potent than mammalian glucagon, but this was not confirmed in a subsequent study (McCumbee and Hazelwood, 1978; Ferreira et al., 1991; Tung et al., 1977; Huang et al., 1987 in Simon, 1995). In turkeys, pig, or chicken, glucagon were found to be equally effective in promoting hyperglycemia, increase in plasma nonesterified free fatty acid levels, and a decline in

circulating levels of T_3 and T_4 (McMurtry et al., 1996). Long-term injection of glucagon has been shown to induce uncoupling protein expression in skeletal muscle of ducks consistent with the thermogenic action of this hormone in birds (Raimbault et al., 2001). Glucagon is also important in the chicken eye for regulating ocular growth (Vessey et al., 2005). Honda et al. found that central, but not peripheral, administration of glucagon suppressed food intake and induced hyperglycemia in chickens and that these effects were mediated by the downstream actions of corticotrophin-releasing factor [Honda et al. (2007) in (Honda et al., 2012)]. Thus, glucagon may serve as a neurotransmitter in the avian central nervous system as has been suggested for mammals (Mayo et al., 2003).

34.4.2.2 GLP-1

Chicken GLP-1R is expressed in pancreatic D cells that secrete somatostatin (Watanabe et al., 2014; Hiramatsu, 2020; Kolodziejski et al., 2018). Similar localization of chicken GLP-1R has been observed in the pancreatic islets of other avian species, northern bobwhites, and common ostriches (Watanabe et al., 2018). Restricted feeding increases the frequency of occurrence of GLP-1-immunoreactive cells in the chicken small intestine (Monir et al., 2014a), thereby indicating that L cells secrete GLP-1 in response to food ingestion in the chicken small intestine. Proteins and amino acids, such as lysine and methionine, are the triggers that induce GLP-1 secretion from chicken ileal L cells (Monir et al., 2014b; Nishimura et al., 2015). Significant correlation has been observed between dietary protein ingestion and frequency of occurrence of GLP-1-immunoreactive cells in the chicken ileum (Monir et al., 2014c). In addition, GLP-1 blood concentration and GLP-1 mRNA in the duodenum and GLP1-R in the pancreas are decreased in response to in ovo injection of synbiotics (Kolodziejski et al., 2018). GLP-1 slows down nutrient assimilation by inhibiting gastric emptying and acid secretion. Central but not peripheral administration of GLP-1 inhibits food intake and crop emptying in chickens and shifts fuel utilization from carbohydrates to lipids without affecting overall energy expenditure (Tachibana et al., 2007). The hypothalamus is involved in the anorexic effect of GLP-1 in chicks (Tachibana et al., 2004 in (Tachibana et al., 2007)). Moreover, the anorexigenic effect of central GLP-1 administration is mediated by the GLP-1 receptor because co-administration of a specific GLP-1 receptor antagonist (exendin 5−39) or N-terminal fragments attenuates the anorexia, while injection of the antagonist alone increases food intake in layer-type but not broiler chicks (Furuse et al., 1998). These results indicate the potential for variable responses in food intake to endogenous GLP-1 among different strains of poultry. Expression of the GLP-1 receptor mRNA in chicken pancreas is consistent with a possible incretin role for GLP-1 in birds (though not yet demonstrated in chicken, see earlier).

34.4.2.3 GLP-2

In mammals, GLP-2 plays a role in intestinal growth and nutrient absorption by maintaining the integrity of mucosal epithelial cells. Secreted by enteroendocrine L-cells in response to the presence of nutrients, GLP-2 promotes crypt cell proliferation and suppresses apoptosis in mucosal epithelial cells. Elevated expression of GLP-2 receptor mRNA in chicken duodenum is consistent with the proposed role for GLP-2 in intestinal growth and function. GLP-2 is co-stored with GLP-1 within the same secretory granule of L cells in the chicken ileum (Nishimura et al., 2013). Nevertheless, the distribution and frequency of occurrence of GLP-2-immunoreactive cells differs from those of GLP-1-immunoreactive cells in the chicken small intestine. GLP-2 immunoreactive cells are mainly located in crypts, and their frequency of occurrence is lower than that of GLP-1-immuno-reactive cells (Monir et al., 2014c). Chicken GLP-2R mRNA is widely expressed in adult chicken tissues, including pancreas and various parts of the gastrointestinal tract where it could play a role in embryonic intestine development (Mo et al., 2014). Shousha et al. reported no effect of ICV or intraperitoneal administration of GLP-2 on food intake, body temperature, or locomotor activity in Japanese quail (Shousha et al., 2007). However, these studies involved the use of rat GLP-2, which shares only 52% amino acid identity with chicken GLP-2 and may lack activity in avian species. In both broiler and layer chicks, GLP-2 functions as a potent anorexigenic peptide in the brain, as well as GLP-1 (Honda et al., 2015).

34.5 Glucagon and insulin receptors

34.5.1 Glucagon receptors

In mammals, the biological actions of glucagon are mediated by a specific glucagon receptor (GCGR; Authier and Desbuquois, 2008), a receptor belonging to G protein-coupled receptor subfamily B, which also includes the receptors for GLP-1, GLP-2, vasoactive intestinal polypeptide, growth hormone-releasing hormone, and growth hormone-releasing hormone-like peptide. Stimulation of the glucagon receptor modulates adenylate cyclase, initiates the production of cAMP, and thereby activates extracellular signal-regulated protein kinase 1/2 via cAMP-dependent protein kinase A (cAMP-PKA, Fig. 34.2). In addition, it also activates signaling pathways via cAMP-independent interactions leading to stimulation of phospholipase C and release of Ca^{2+} from IP_3-sensitive intracellular Ca^{2+} stores.

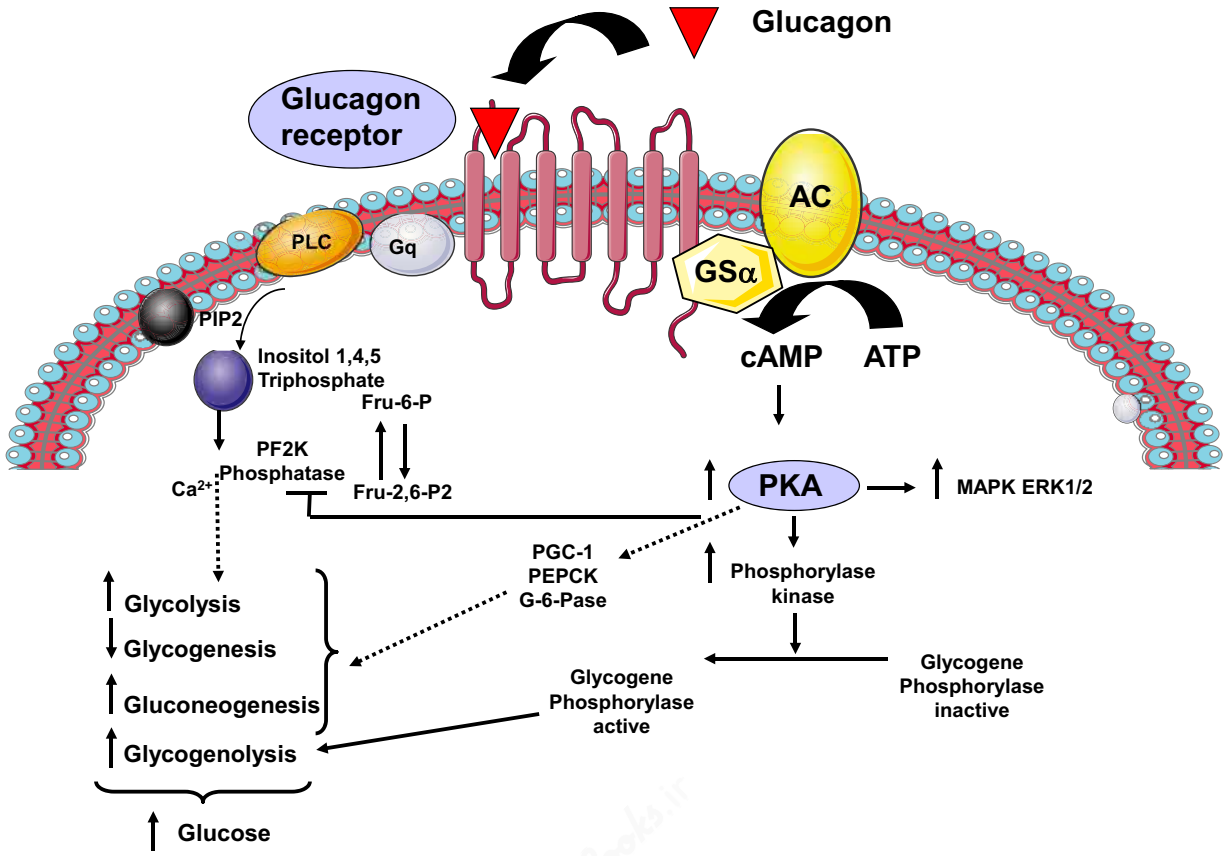

FIGURE 34.2 Glucagon receptor signaling.

The chicken glucagon receptor gene was cloned from adult brain tissue (Wang et al., 2008a, 2008b); it encodes for a short glucagon receptor of 496 AA (GCGR-s) or a long receptor variant of 554 AA, designated glucagon receptor variant 1 (GCGR-v1). The chicken GCGR-s shares high AA sequence identity with that of man (70%), rat (69%), mouse (69%), and Xenopus (64%). Functional analysis confirmed that both GCGR-s and GCGR-v1 can be activated by glucagon and are functionally coupled to the cAMP-PKA signaling pathway. The glucagon receptor is widely expressed in all tissues including the hypothalamus, with the greatest expression found in the liver, suggesting that glucagon plays a wide range of roles in both hepatic and nonhepatic chicken tissues through the two receptors, GCGR-s and GCGR-v1 (Richards and McMurtry, 2008). Recently, Wang et al. identified a novel ligand-receptor pair, named GCGL and GCGL receptor (GCGLR) from chicken brain (Wang et al., 2012) GCGL is a novel GCG-like peptide of 29 amino acids that shares high-amino acid sequence similarity with mammalian and chicken GCG (62−66%). GCGLR is a GCGL-specific receptor, which shares relatively high-amino acid sequence identity with chicken GCGR and structurally related receptors (GLP1R, GIPR, and GLP2R). GCGL mRNA expression is mainly detected in the CNS, spinal cord, and testis, whereas GCGLR is more widely expressed in chicken tissues (Wang et al., 2012).

34.5.2 Insulin receptor

Early studies on ontogeny, structure, binding affinity, binding characteristics, number, internalization, up- and down-regulation of IRs in chicken or turkey tissues have already been reviewed (Simon, 1989). Since then, changes in IR number have been described in the hypothalamus, at least at the level of IR messenger, in layer and broiler-type chicks under ad libitum conditions (Shiraishi et al., 2011a); changes in hypothalamic IR mRNA in response to photoperiodism are dependent upon gonad hormones (Anraku et al., 2007). In chicken liver plasma membranes, hepatocytes and thymocytes, insulin binding capacity (IR number) is lower than in rat or veal in (Simon, 1989), which may contribute to the low-insulin sensitivity of chickens. However, in crude liver membranes (i.e., plasma and intracellular organite membranes), the IR number is about the same in chickens and rats (Dupont et al., 2004). A high proportion of IR may therefore be internalized in chicken liver (Krup and Lane, 1981, 1982 in (Simon, 1989)).

Chicken IR shows a heterotetrameric structure (two α and two β subunits linked by disulphide bonds as described in mammals and other species [reviewed in (Simon, 1989)]. The α subunit (about 135 kDa) is entirely within the extracellular compartment and binds insulin; the β subunit (about 95 kDa) contains a large hydrophobic fragment (inserted into the membrane), crosses the cell membrane and extends into the intracellular compartment. In chickens, as in other species, the α subunit of brain or muscle receptors is smaller than that of liver receptor α subunit, in part as a result of differences in glycosylation (reviewed in Simon, 1989).

In mammals, both IR α and β chains are synthesized from a single mRNA, which is encoded by 22 exons. In mammals, exon 11 is alternatively spliced, which results in two IR isoforms (IR-A and IR-B) that differ by the absence or presence of 12 amino acids at the C-terminus of the α subunit, respectively. IR-A and IR-B isoforms display differences in ligand affinity binding, kinase activity, receptor internalization, and recycling as well as intracellular signaling capacity and tissue distribution (De Meyts, 2012). According to Hernández-Sánchez et al., the region corresponding to exon-11 is missing in chicken IR; chicken tissues would only express the "IR-A" type, i.e., the IR type showing the highest insulin affinity (Hernández-Sánchez et al., 2008). This may account for the fact that chicken IRs exhibit much higher affinity for IGFs than mammalian IR. It may also explain why chicken or duck IR do not discriminate chicken, pork, and duck insulins very well (Chevalier et al., 1996).

In its intracellular part, the IR β subunit is a tyrosine kinase activated by autophosphorylation following insulin binding to the α subunit. The chicken IR tyrosine kinase activity shows the same features as those from other species [reviewed in (Kato et al., 2000; Simon, 1989)]. Chicken liver or kidney IR tyrosine kinase activities (basal and maximal activities) are regulated, for instance, by nutritional conditions (such as fasting or refeeding), as in mammals. In contrast, muscle and adipose tissue IR kinase activity, as well as β subunit tyrosine phosphorylation, do not decrease in the fasting state or increase in refed animals, despite alterations in plasma insulin (Adamo et al., 1987; Dupont et al., 2008, 2012). Thus, for still unknown reasons, the regulation of the tyrosine phosphorylation of IR β subunit and kinase activity differs between species and tissues. As depicted in Fig. 34.3 (for chicken tissues), once

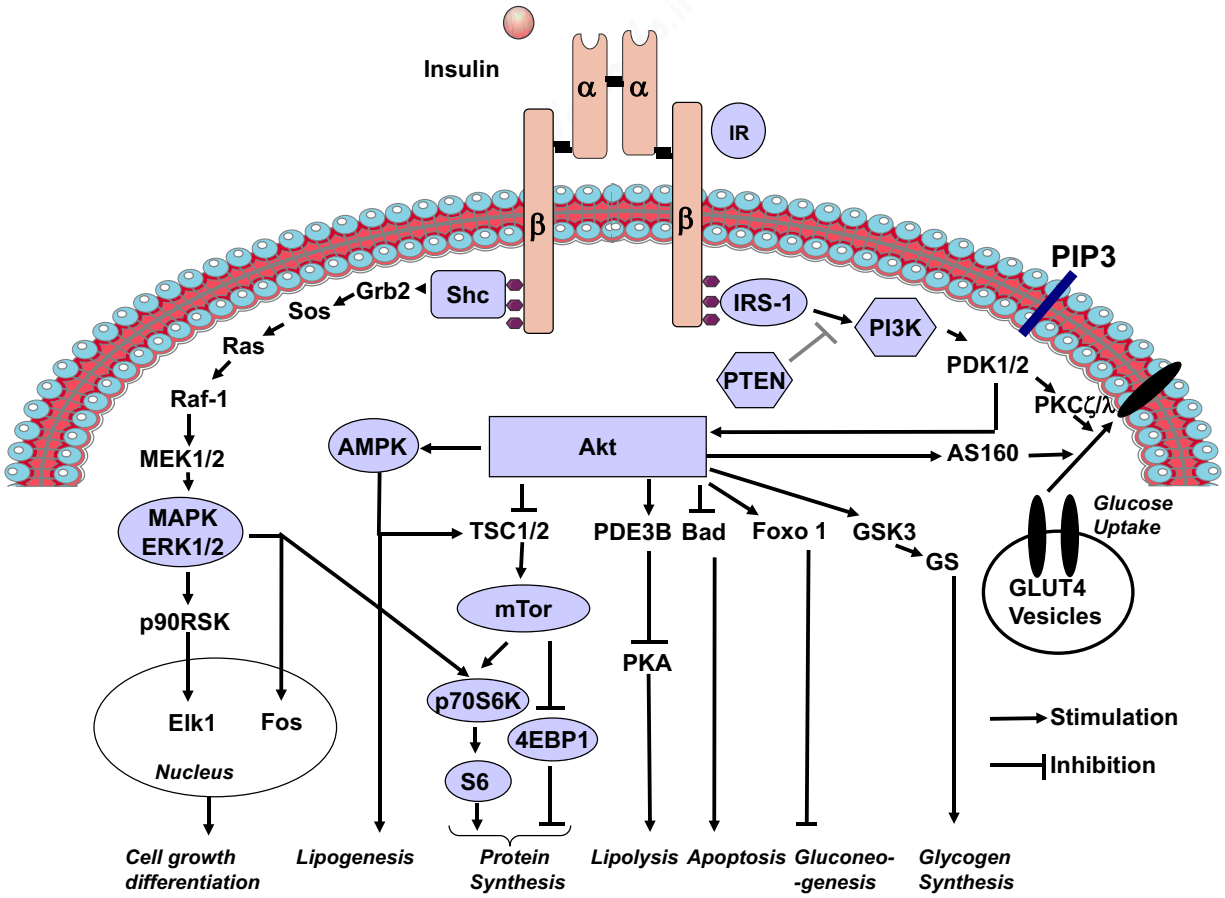

FIGURE 34.3 Insulin receptor signaling. *Adapted from mammals; only steps highlighted in blue have been characterized in chicken tissues.*

activated, the IR tyrosine kinase phosphorylates several intracellular substrates on specific tyrosine residues, which represents the proximal and early events initiating and propagating the insulin signal through a cascade of reactions leading to the multiple actions of insulin. Phosphorylated IR substrates activate directly or indirectly various protein (serine-threonine) or lipid kinases including PI3K, Akt, P70S6K, and MAPK ERK1/2. Several of these postreceptor steps also regulate insulin cell sensitivity, enabling alterations of insulin sensitivity without changes in IR number or kinase activity.

34.5.2.1 Proximal insulin receptor substrates

In mammals, at least 11 intracellular IR substrates have been identified (reviewed in Taniguchi et al., 2006; Siddle, 2012; Machado-Neto et al., 2018). These include the family of insulin receptor substrate (IRS) proteins (IRS-1−6) and Src homology collagen protein (Shc). Four different IRS proteins (IRS-1-4) have been reported in various mammals, and two additional IRS proteins have been detected in man (IRS5/DOK4 and IRS6/DOK5). These last two additional IRS proteins are involved in insulin signaling but are not involved in phosphatidylinositol 3′-kinase (PI3K) activation (the major insulin signaling step). Other IR substrates such as Gab1, Dok, APS, SH2B, Cbl, and Crk have been also described in mammalian tissues or cells (cited by Siddle, 2012).

The coding region of chicken IRS-1 gene has been cloned and sequenced (Taouis et al., 1996). The deduced chicken IRS-1 protein (cIRS-1) presents high sequence identity with its human, rat, and mouse homologs. Chicken IRS-1 is at least present in the liver, muscle, and adipose tissue and interacts with the IR [Dupont et al., 1998 in (Dupont et al., 2009, 2012), (Dupont et al., 2012)]. Interestingly or surprisingly enough, the tyrosine phosphorylation of cIRS-1 and PI3K activity (see later) is accordingly insulin-dependent upon nutritional conditions or insulin status in the liver but not in muscle or adipose tissue [Dupont et al., 1998 in (Dupont et al., 2008, 2009, 2012)], suggesting a tissue-specific regulation and a relative insulin refractoriness in chicken muscle and adipose tissue. Coding sequences have recently been described for IRS-2, IRS-4, Crk, Cbl, and APS chicken homologs (Ensemble release 71, April 2013 at http://www.ensembl.org/Gallus_gallus/index.html); they are respectively located on chromosome 1, 4, 19, 1, and 19, respectively. However, the presence of these substrates as proteins and their insulin sensitivity remains to be established in chicken tissues. Cbl and Crk, which in mammals mediate insulin signals and are associated with lipid rafts, are upregulated, at the messenger level, in chicken adipose tissue by fasting (Ji et al., 2012). In mammals, this pathway stimulates glucose uptake, in addition to and independently of PI3K activation. Whether these potential substrates contribute to the apparent refractoriness of PI3K activity to insulin that is observed in chicken skeletal muscle and adipose tissue remain unknown. It should be noticed however that insulin stimulation of glucose transport in chicken adipose tissue, if any, is very poor (see later).

In a chicken hepatoma cell line (LMH cells), cIRS-1 repression substantially increases Shc expression (Taouis et al., 1998). Shc is phosphorylated on tyrosine residues in response to insulin and therefore serves as an additional IR substrate in the absence of IRS-1. Chicken liver, muscle, and adipose tissue express homologs of the three mammalian Shc isoforms (Dupont et al., 2008, 2012). Interestingly, tyrosine phosphorylation of Shc (52 kDa) is dependent on insulin status; it increases after refeeding or insulin injection and is inhibited after insulin immunoneutralization in chicken liver but also, surprisingly, in leg muscles, in contrast to IRS-1. Also surprisingly, neither insulin privation nor fasting alter Shc tyrosine phosphorylation in adipose tissue (Dupont et al., 2009, 2012). In chicken liver, Shc, mainly the 52 kDa isoform, interacts with IR whereas the 46 kDa isoform associates with IRS-1 (Dupont et al., 1998 in (Dupont et al., 2009)). The 52 kDa Shc isoform also interacts with the p85 regulatory subunit of phosphatidylinositol 3-kinase (PI3K). Shc (52 kDa) is thus a key substrate for the IR in the chicken because, first, it is able to associate with PI3K, and second, in contrast to IRS-1, the extent of its tyrosine phosphorylation is dependent on insulin levels. Furthermore, in liver, Shc (52 kDa) phosphorylation is inhibited after insulin immuno-neutralization (Dupont et al., 2008). The possible existence of different subtypes of IR complexes signaling through IRS-1 or Shc has been investigated in the liver. The presence of a large complex involving IR, IRS-1, Shc (mainly the 52 kDa isoform), and the regulatory subunits of PI3K has been demonstrated; a third complex including IRS-1 and the 46 kDa Shc isoform is also present in chicken liver (Dupont et al., 1998 in (Dupont et al., 2009)). No such interactions have been described in mammalian tissues, and the functions of these complexes in chicken liver and their presence in other chicken tissues remain to be established.

34.5.2.2 PI3K/Akt

PI3K has been characterized in chicken liver, leg muscle, and adipose tissue [Dupont et al., 1998 in (Dupont et al., 2009, 2012)] and in LMH cells (Taouis et al., 1998 in (Dupont et al., 2009)). Liver PI3K activity depends upon the nutritional state (prolonged fasting vs. refeeding) in several experimental models (Dupont et al., 1998, 1999 in (Dupont et al., 2009)). Furthermore, PI3K activity

increases in response to insulin injection and is inhibited following insulin immunoneutralization (Dupont et al., 1998 in (Dupont et al., 2008, 2009)). This is in agreement with the changes observed for early steps of the insulin signaling cascade (tyrosine phosphorylation of IR β subunit, IRS-1, and Shc). Conversely, in muscle, the PI3K activity and, as previously mentioned, tyrosine phosphorylation of IR and IRS-1, are totally unresponsive to insulin levels in experimental models that alter insulin sensitivity, such as long-term corticosterone treatment and genetically selected fat and lean lines of chickens [Dupont et al., 1999 in (Dupont et al., 2009)]. As mentioned earlier, only the phosphorylation of the 52 kDa Shc isoform is reduced in muscle by fasting and increased by refeeding. Comparison of the responses to exogenous insulin in chickens and rats suggests that this phenomenon is specific to chicken. Furthermore, PI3K activity in leg muscle is about 30 times greater in the chicken than in the rat (Dupont et al., 2004). This "constitutive" hyperactivity of PI3K in chicken muscle may overstimulate the feedback inhibitory pathway described in mammals (see earlier), thereby desensitizing chicken muscle to insulin. The p85 regulatory subunit of PI3K itself exerts strong inhibitory control of IRS signaling in mammals (Taniguchi et al., 2006). However, lipid phosphatases such as phosphatase and TENsin homolog deleted on chromosome 10 (PTEN) may also contribute to this relative insulin insensitivity of the early steps of insulin signaling in chicken muscle. We have detected PTEN in chicken tissues, including muscle (Vaudin et al., 2006); however, the role of PTEN in the control of insulin signaling in chicken tissues remains to be determined. In adipose tissue, insulin signaling is even more peculiar; insulin privation did not alter early steps and PI3K activity, but also other downstream elements such Akt [see next paragraph (Dupont et al., 2012)].

Akt has been detected in several chicken tissues including liver, muscle (Bigot et al., 2003; Dupont et al., 2008), adipose tissue, and granulosa cells (Dupont et al., 2012; Tosca et al., 2006). The phosphorylation of Akt on Ser 473 is increased following feeding of posthatched chicks (Bigot et al., 2003); this is prevented when feeding is delayed (48 h) then rapidly restored following food intake. In fed chickens, insulin immuno-neutralization significantly decreases Akt phosphorylation in both liver and muscle, but not in adipose tissue (Dupont et al., 2008, 2012). Thus, insulin is presumably involved in Akt activation in chicken muscle, despite the fact that chickens exhibit particular features in the early steps of the insulin signaling cascade (IR, IRS-1, and PI3K). This issue remains unresolved. Potential mechanisms involved in the atypical feature found for insulin signaling in chicken muscle and adipose tissue have been discussed in (Dupont et al., 2008, 2012).

34.5.2.3 P70S6K

p70S6 kinase, a further downstream step, has been characterized in a quail muscle (QM7) cell line and in chicken skeletal muscle (Tesseraud et al., 2003, and Duchêne et al., 2008 in (Dupont et al., 2009)). p70S6K activity increases significantly in both pectoralis and gastrocnemius muscles after refeeding for 30 min following 16 h starvation, and also in fasting chickens after a single insulin injection (Bigot et al., 2003). Similarly, p70S6K activity in the muscle of neonatal chicks is correlated with the plasma insulin concentration, strongly suggesting an insulin-dependent p70S6K activation (Bigot et al., 2003). In the liver, stimulation of phosphorylation of P70S6K1 and activation of S6K (using specific artificial substrate) was not detectable (Dupont et al., 2008), though insulin stimulation of phosphorylation of S6 ribosomal protein was observed in the same conditions (Duchene et al., 2008b). Furthermore, p70S6K phosphorylation decreases in leg muscles but not in adipose tissue in response to insulin immuno-neutralization (Dupont et al., 2008, 2012). These findings and those for Akt are again surprising in view of the relative insulin refractoriness of chicken muscle to exogenous insulin (Dupont et al., 2004). However, p70S6K has been found to be involved in another feedback loop, which attenuates the ability of insulin to activate PI3K. Indeed, there is evidence in mammals that p70S6K inhibits insulin signaling by increasing the serine/threonine phosphorylation of IRS-1. In chicken muscle, refeeding and insulin injection increases the phosphorylation of both p70S6K on key residues (T389, T229, and T421/S424) and its downstream target, the ribosomal protein S6 (downstream insulin signaling steps). However, in these conditions, the phosphorylation of IRS1 on Serine 632 and Serine 635 residues is also induced (Duchene et al., 2008b). In mammals, the phosphorylation of these sites inhibits the insulin signal. Thus, the AKT/p70S6K may inhibit IRS1 tyrosine phosphorylation in chicken muscle.

34.5.2.4 mTor

The mammalian target of rapamycin (**mTor**) is an evolutionarily conservative Ser/Thr protein kinase that can perceive signals such as nutritional status, and growth factors to regulate cell growth, proliferation, apoptosis, and other physiological processes (Avruch et al., 2006). It is rapamycin-sensitive, stimulated by insulin, growth factors, energy signals, and amino acids. In mammals, amino acids, especially branched-chain amino acids (including leucine, isoleucine, and valine) or leucine alone, were reported to be important regulators of body protein turnover and translation initiation. Leucine alone can stimulate protein synthesis to the same extent as a complete amino acid

mixture by activating factors of mRNA translation initiation, primarily through mTor signaling pathway, including ribosomal protein S6 kinase (**S6K1**) and eukaryotic initiation factor 4E binding protein 1 (**4E-BP1**) in a dose-dependent fashion. In avian species, mTor signaling pathways have been described in chicks (Wang et al., 2012). In neonatal chicks, high-dietary leucine activates target of rapamycin signaling pathways in skeletal muscle, and this pathway is attenuated with aging (Deng et al., 2014). In broilers, the mTor pathway is involved in retarding muscle development and protein synthesis by glucocorticoids (Wang et al., 2015). In chicken adipocyte, mTor is also involved in the negative effect of adiponectin on the lipids deposition (Jun et al., 2014) suggesting that this pathway is an important energy sensor in avian species as in mammals.

34.5.2.5 MAPK ERK1/2 pathway

MAPK ERK has been identified in various chicken tissues (Duchene et al., 2008a). In contrast to mammals, ERK1 is not present in bird tissues; ERK2 is the only phosphorylated isoform detected (Duchene et al., 2008a). It is activated in chicken myoblasts and LMH cells in vitro by insulin (Duchene et al., 2008a). U0126, an inhibitor of the MAPK ERK pathway, completely abolishes insulin-induced S6K1 phosphorylation and activity in chicken myoblasts in vitro, implicating MAPK ERK2 in the control of S6K1 by insulin in avian cells (Duchene et al., 2008a). MAPK ERK2 phosphorylation in chicken liver muscle and adipose tissue in vivo is strongly reduced by insulin immuno-neutralization (Dupont et al., 2008, 2012). However, the role of MAPK ERK2 in insulin action in vivo in chicken has not been investigated. This signaling could be crucial to chicken growth, and this pathway may participate in the insulin-dependent regulation of p70S6K, because Shc, which is upstream, seems to be a key IR substrate in chicken muscle.

From the elements of insulin signaling thus far studied in chickens, insulin signaling appears to work in chicken liver as expected from the knowledge gained from mammals. In contrast, in muscle and adipose tissue, insulin cascade appears refractory, suggesting the presence of inhibitory counter-regulatory mechanisms in these tissues.

34.6 General effects of glucagon and insulin

34.6.1 Insulin and embryonic or posthatch development

The insulin gene is expressed early during embryonic development in extra-pancreatic tissues prior to development of the pancreas, showing specific regulations in (de la Rosa and de Pablo, 2011). Insulin accelerates growth of embryos explanted at Hamburger Hamilton stage 4, without increasing mitoses; some specific developmental genes are upregulated (Patwardhan et al., 2004). A fine tuning of insulin gene expression is required to sustain adequate morphogenesis. In chicken neurulating embryos and chicken embryo retina, proinsulin is expressed but not cleaved to insulin. Whereas this precursor is considered to exert marginal biological activity in peripheral tissues, if any, it exerts antiapoptotic effects in those tissues at this developmental stage, probably through a hybrid insulin-IGF receptor in (de la Rosa and de Pablo, 2011). Furthermore two transcription-induced chimerisms have been identified with the adjacent tyrosine hydroxylase gene [*TH*-insulin (de la Rosa and de Pablo, 2011)]. (In man, a similar mechanism has been described between the insulin gene and *IGF2*, the adjacent gene). The insulin gene is also expressed in the neural tube and somites of chicken embryos. Addition of insulin (or IGFs) to other specific factors in the incubation medium cocktail stimulates somite cell proliferation and myogenesis (Pirskanen et al., 2000). This effect is blocked by an insulin antibody and IR antibody, showing that insulin acts as a myogenic signal early in embryogenesis. Insulin also supports in vitro multiplication of one-day-old broiler muscle satellite cells and delays their differentiation (Sato et al., 2012). Surprisingly, an opposite effect is observed between insulin and IGF1 for MyoD and myogenin messengers. Insulin or tolbutamide administration to day-old broiler chicken increases Pax7 messenger (a striated cell marker) in breast muscle at 3 days of age and their body weight at 50 days, without changing their body composition (Sato et al., 2012). These interesting effects deserve further characterization. In satellite cell-derived myotubes, insulin, (at high doses though, compared with IGF1) stimulates glucose (see earlier) and amino acid transport and protein synthesis and inhibits proteolysis (Duclos et al., 1993a, 1993b).

34.6.2 Insulin-glucagon and food intake

Pioneer studies suggested that insulin contributes to the regulation of food intake [through inhibitory or stimulatory mechanisms in (Simon, 1989)]. Intracerebroventricular injection of insulin (through the melanocortin system) or glucagon inhibits food intake in young Leghorn chickens [(Honda et al., 2007; Shiraishi et al., 2011b) and quoted references]. Surprisingly insulin is inefficient in young broiler chickens in fasted or fed conditions [(Shiraishi et al., 2011b) and quoted references], suggesting a difference in their set-point or sensitivity; in broiler chickens, plasma insulin levels are higher, which appear to decrease hypothalamic IR mRNA expression (Shiraishi et al., 2011b). Insulin immuno-neutralization in fed growing chickens decreased food intake, most likely by inducing very high-plasma glucose levels (Dupont et al., 2008).

34.6.3 Insulin and the endocrine system

Insulin interacts with glucagon (see introduction) and with other endocrine systems. As early as 1hr after insulin immuno-neutralization (Dupont et al., 2008), plasma T_3 levels decreased. (No reliable measurements were obtained for T_4). After 5 h of insulin deprivation, liver D2-and D3-deiodinase messengers decreased or increased, respectively. Thus, insulin is another partner involved in bird liver T_4 metabolism [Darras et al., 2006, in (Dupont et al., 2008)]. The IGF system also appears partly insulin-dependent. Liver *IGFBP-1* messenger (microarray and qRTPCR measurements) and plasma IGFBP-1 protein levels increased after insulin immuno-neutralization. (Plasma IGF-1 was not measured). Microarrays also revealed that liver *IGFBP-2* and muscle *IGF1R* messengers increased or decreased, respectively. [Similar impairments are found in diabetic patients, Palsgaard et al., 2009, in (Simon et al., 2012)]. In another study (Nagao et al., 2001), 2d fasting decreased plasma IGF1 and increased *IGFBP-2* messenger in liver and gizzard of WL chickens (but not in brain or kidney); exogenous insulin further decreased plasma IGF1 levels and largely inhibited liver and gizzard *IGFBP-2* messenger (6h refeeding also inhibited liver and gizzard *IGFBP-2* messenger but accordingly increased plasma IGF1 levels).

34.6.4 Insulin and glucose metabolism

The severe and rapid hyperglycemia induced by insulin deprivation in fed chickens certainly depends upon multiple changes in glucose metabolism in several tissues. In liver, where glucose transport is not insulin-dependent, glucose utilization was probably greatly depressed as suggested by the drop in liver GK messenger and protein contents (see earlier discussion about the existence and the regulation of liver GK activity). In mammals, other insulin-dependent mechanisms are inhibition of liver gluconeogenesis and glucose production. Gluconeogenesis is considered to escape insulin control in chicken liver (introduction). In our transcriptome study, 27 messengers from the glycolysis/gluconeogenesis or pyruvate metabolism pathways were differentially expressed in liver following insulin deprivation, including *G6PC2* (glucose-6-phosphatase catalytic,2 messenger which increased), suggesting that liver glucose production may also be insulin-inhibitable in chicken liver. Unfortunately this was not assessed in euglycemic-hyperinsulinemic clamp experiments performed on chickens (Chou and Scanes, 1988; Hamano, 2006). Indirect evidence (prolonged fasting and corticosterone experiments) suggests that insulin also inhibits kidney gluconeogenesis by inhibiting cytosolic phosphoenolpyruvate carboxykinase activity (Bisbis et al., 1994a, 1994b and quoted references).

Insulin greatly stimulates glucose uptake in muscles and adipose tissues of mammals by recruiting insulin-sensitive Glut-4 transporters at the cell surface from an intracellular pool (Fig. 34.3). So far, no Glut-4 glucose transporter has been identified in chickens or house sparrows (*Passer domesticus*) as protein or messenger. This may be the consequence of the lack of cross-reactivity of antibodies or the absence of Glut4 in chicken or birds since no Glut-4 homolog sequence is found in the chicken Ensembl database; [an ortholog gene to human Glut-4 (*SLC2A4*) gene is however described in the Anole lizard and several fish species]. Functional and immunoreactive-Glut4 transporters have been observed in duck leg muscle [Thomas-Delloye et al., 1999, in (Dupont et al., 2009)]. Only chicken Glut-1, -2, -3, -8 have been characterized as messengers and/or proteins (Carver et al., 2001; Seki et al., 2003; Kono et al., 2005; Sweazea and Braun, 2006 in Zhao et al., 2012; Humphrey et al., 2004). It has been hypothesized that Glut-8 (encoded by *SLC2A8* gene) may act in chickens as Glut-4 does in mammals (Kono et al., 2005 in Zhao et al., 2012). In vivo, exogenous insulin increases glucose uptake moderately in some muscles but not in adipose tissue (Tokushima et al., 2005). (Surprisingly, insulin stimulated or inhibited ^{3}H-2DG uptake in liver and brain, respectively). Thus, an insulin-sensitive glucose transport is present in chicken; it however requires extensive characterization.

Currently, an increasing number of studies report QTLs as controlling growth and/or body composition and some physiological parameters in various avian species. In several cases, these QTL regions harbor glucose- and/or insulin-dependent genes. This aspect cannot be reviewed here; some references can be found in (Nadaf et al., 2009).

34.6.5 Insulin-glucagon and lipid metabolism

Several transcription factors controlling mRNA expression of lipogenic enzymes also appear insulin-sensitive in chicken liver in vivo [SREBP1, PPAR-gamma, and THRSP alpha (spot-14) and FASN messengers (Dupont et al., 2008)]. Carbohydrate-responsive element-binding protein (ChREBP, encoded by the *MLXIPL* gene) is another transcriptional factor involved in glucose metabolism, glucotoxicity and/or lipogenesis in liver, adipose tissue, and pancreas in mammals (Leclerc et al., 2012). ChREBP is also activated in parallel with lipogenesis in chicken liver (Proszkowiec-Weglarz et al., 2009). In our insulin neutralization experiment, several other enzyme messengers involved in lipogenesis or fatty acid oxidation decreased or increased, respectively, following insulin deprivation (Simon et al., 2012), extending the role of insulin in chicken liver lipid metabolism. In abdominal fat tissue, 5 h of fasting altered the level of 2016 messengers. Plasma glucagon increase certainly accounts for a major part of these changes (Ji et al., 2012). Insulin neutralization in fed chickens altered the expression of only 92 genes, 72

of which were also differentially expressed by 5 h of fasting. All genes that were affected by both treatments changed in the same direction (up- or downregulated in both groups). Most messengers that were specifically altered by insulin-neutralization (but not by fasting) were either poorly or not described; however, glucagon precursor (class B-preproglucagon) and glucagon receptor precursor were in this category and were up- and downregulated, respectively. A local insulin-dependent paracrine glucagon regulation, which needs full characterization, is suggested in chicken adipose tissue. In general, a contribution of insulin to adipose tissue development and metabolism (in addition to its control of liver lipogenesis) can be expected, despite the very atypical feature exhibited by chicken adipocytes.

Differentiation of chicken adipocyte precursors (obtained from the stromal vascular fraction of fat tissue) or trans-differentiation of fibroblasts, epithelial oviduct or primordial germ cells into adipocytes have been successfully performed using media rather similar to those used for mammalian adipocyte differentiation (Khuong and Jeong, 2011; Li et al., 2010; Liu et al., 2010; Ramsay and Rosebrough, 2003). Insulin is required but unable to support differentiation alone; IGF-1 or T3 are unable to replace insulin (Ramsay and Rosebrough, 2003). Chicken serum and dexamethasone can be deleted, provided oleic acid is introduced into the differentiation medium. Unless oleic acid exerts a specific effect, this supports the conclusion that to overcome their intrinsically low-lipogenic activity and achieve a full adipocyte phenotype, chicken adipocyte precursors need exogenous fatty acids (Liu et al., 2009; Matsubara et al., 2005, 2008). Several transcription factors are involved in adipogenesis: C/EBPalpha, PPARgamma, and SREBP1 in chicken (Liu et al., 2009, 2010; Sato et al., 2009; Wang et al., 2008a, 2008b) and duck (Xiong et al., 2010).

In adipocytes of mammals, lipolysis is under the control of several lipases, including the adipose triglyceride lipase, encoded by the *PNPLA2* gene and the hormone-sensitive lipase (HSL), encoded by the *LIPE* gene (Zechner et al., 2009). HSL (*LIPE*) disruption in normal or *ob/ob* mice leads to several changes in the endocrine pancreas and adipocytes which resemble the chicken feature (Osuga et al., 2000; Wang et al., 2001; Haemmerle et al., 2002, quoted in Zechner et al., 2009; Mulder et al., 2003; Harada et al., 2003). Though not identified in chicken, the *LIPE* gene is present in the Anole lizard and several fish. If the *LIPE* gene is really missing in chicken, some of the chicken physiological peculiarities may be due to this.

34.6.6 Insulin and protein metabolism

In addition to its general effects on protein metabolism (introduction and Tesseraud et al., 2007a), insulin acts in the ubiquitin-proteasome proteolytic pathway. It inhibits the expression of atrogin-1 messenger in quail muscle (QT6) fibroblasts (Tesseraud et al., 2007b) and in vivo in chicken muscle (Dupont et al., 2008). Following insulin immuno-neutralization, several messengers coding for enzymes of the oxidative pathway decreased. This pathway is also altered in muscle of human diabetics in (Simon et al., 2012).

34.6.7 Insulin and gene expression

In mammals, insulin stimulates the translation of pre-existing mRNA and coordinates (stimulates or inhibits) the expression of multiple genes in various tissues. Multiple insulin responsive elements (IREs) have been identified on target genes (other IREs are likely to be identified, Mounier and Posner, 2006). To our knowledge, the characterization and the functionality of IREs, as such, are still missing in chickens. The fact that several transcription factors or enzymes involved in lipid metabolism are also insulin sensitive in chickens (see earlier) suggests that major IREs have been conserved or have co-evolved in chickens. A total of 1573 and 1225 signals were altered by insulin deprivation in liver and muscle, respectively, including several transcription factors. Several messengers have been associated with energy expenditure, insulin resistance, metabolism sensing, obesity, and/or diabetes in mammals (Simon et al., 2012). The chicken elongation factor-2 (EF-2) gene, a major factor in protein synthesis in mammals, is also under the control of insulin and 8-bromo-cAMP or phorbol ester (Lim and Kim, 2007). Insulin deprivation in fed chickens (but not fasting) decreased *EGR1* (early growth response 1) messenger in liver and muscle but not in adipose tissue. However *TOE1* (target of egr 1, member 1) was also specifically decreased by insulin deprivation and not by fasting in adipose tissue (Ji et al., 2012). *EGR1* target genes are largely unknown, particularly in the field of metabolism.

Finally, microRNAs (miRs) represent another mechanism in the regulation of gene translation. At least miR-196 and −200b showed significant and opposite changes in response to insulin-neutralization (an increase in liver vs. a decrease in muscle, Bouhallier, Rouault and Simon, unpublished data). Gene targets of miR-196 and −200b need to be identified; so far miR-196 has been involved in chicken embryo development (McGlinn et al., 2009) and miR−200b in chicken liver lipid metabolism (Hu et al., 2012).

34.7 Experimental or genetical models

Table 34.1 summarizes results about fasting plasma glucose-insulin relationships, glucose tolerance, insulin sensitivity, and fattening in various experimental or genetical chicken models. Most of these results have been discussed in previous publications. (The effect of prolonged fasting has also been investigated, see above). The table is shown to support some general considerations. It should be

noted that in all these experiments, the feeding pattern of chickens has been consistently synchronized with light-dark cycles. In these conditions, as in mammals, fasting plasma glucose level appears as an indicator or a central node, which reflects or integrates general metabolism. Though the primary mechanism is unknown, changes in glucose-insulin balance and/or insulin sensitivity are associated with changes in fattening. In contrast to obese mammals, fat chickens have low-plasma glucose and do not develop insulin resistance. Conversely, chickens from a low-glucose line are fatter than their counterparts. Only the corticosterone model behaves like obese mammals (showing higher plasma glucose and impaired insulin sensitivity). As discussed earlier, changes in insulin signaling are present in the models thus far investigated. Changes in glucose tolerance are not consistently associated with changes in body composition: in a commercial broiler cross, chickens exhibiting fast or slow plasma glucose regulation at 2 and 4 weeks of age following an oral glucose load did exhibit fast or slow glucose disposal at 8 weeks of age but did not differ in fasting or glucose-induced plasma insulin levels and body composition, which remains unexplained (Simon, 1980). One can hypothesize that, as in FL chickens, enhanced glucose-induced insulin levels are required to increase fattening without necessarily leading to insulin resistance. In vitro, perfused pancreas from fat chickens released less insulin during the first phase in response to glucose or arginine or acetylcholine in the presence of glucose than pancreas from lean chickens, which remains unexplained in (Rideau, 1988). In general, chickens appear to be controlled within a much narrower range for their body composition than mammals. Whether the endocrine pancreas of birds plays a part in this remains an open question and a challenge for the future.

34.8 Conclusion

Many results highlighted in this review point out further chicken peculiarities at the level of endocrine pancreatic physiology. Chickens (and birds in general) developed several species specificities during evolution. The most original ones concern: refractoriness's of glucose-induced insulin release and insulin signaling in muscle and adipose tissue. One unidentified inefficient metabolic step makes glucose a poor insulinotropic nutrient in chickens. Though several elements of insulin signaling pathways haven't been investigated yet, several steps of the IR cascade appear insensitive in muscle; the feature is even worse in adipose tissue. In contrast, IR signaling appears "normal" in chicken liver. Unrevealing mechanisms or steps accounting for these chicken peculiarities may provide important information, including for human diabetes pathology. Glucagon physiology appears more complex in chicken than in mammals: glucagon gene encodes several transcripts; it is expressed in adipose tissue; two types of glucagon receptors are present; an insulin-dependent paracrine glucagon regulation is suggested in adipose tissue. In the fed status, insulin is coordinating the endocrine balance to permit the development or the maintenance of an active anabolism. On a practical point of view, finding the way to favor pleiotropic anabolic actions of insulin in muscle and minimize liver lipogenic and adipogenic actions of insulin would be highly profitable for human and animal nutrition. This review also pointed out many lacks or new area to explore. In short, the secretory "machinery" of A- and B-islets needs to be fully characterized. Chicken is the unique model to provide such possibility in addition, very little information is known about the physiological actions of GLP-2, oxyntomodulin, miniglucagon, glicentin, or gastrin-releasing pancreatic peptide in chicken. Full characterization of IR signaling and subsequent steps up to the control of gene expression certainly also offer large area for research in future. Finally, chicken glucose transporters (presence and functionality) need to be characterized. Though, chicken has the inconvenient to require the development of technical tools for each area to explore, it remains an almost unexplored experimental animal model of large interest for comparative endocrinology and physiology.

References

Adamo, M., Simon, J., Rosebrough, R.W., McMurtry, J.P., Steele, N.C., LeRoith, N.D., 1987. Characterization of the chicken muscle insulin receptor. Gen. Comp. Endocrinol. 68, 456–465.

Ahnfelt-Ronne, J., Hald, J., Bodker, A., Yassin, H., Serup, P., Hecksher-Sorensen, J.J., 2007. Preservation of proliferating pancreatic progenitor cells by Delta-Notch signaling in the embryonic chicken pancreas. BMC Dev. Biol. 7, 63.

Andrews, P.C., Hawke, D., Shively, J.E., Dixon, J.E., 1984. Anglerfish preprosomatostatin II is processed to somatostatin-28 and contains hydroxylysine at residue 23. J. Biol. Chem. 259 (24), 15021–15024.

Anraku, T., Takagi, T., Nakao, N., Watanabe, M., Yasuo, S., Katou, Y., Ueda, Y., Murai, A., Iigo, M., Ebihara, S., Yoshimura, T., 2007. Photoperiodic changes in hypothalamic insulin receptor gene expression are regulated by gonadal testosterone. Brain Res. 1163, 86–90.

Authier, F., Desbuquois, B., 2008. Glucagon receptors. Cell Mol. Life Sci. 65 (12), 1880–1899. https://doi.org/10.1007/s00018-008-7479-6. Review.

Avruch, J., Hara, K., Lin, Y., Liu, M., Long, X., Ortiz-Vega, S., Yonezawa, K., 2006. Insulin and amino-acid regulation of mTOR signaling and kinase activity through the Rheb GTPase. Oncogene 25, 6361–6372.

Bennett, A.K., Hester, P.Y., Spurlock, D.E., 2006. Polymorphisms in vitamin D receptor, osteopontin, insulin-like growth factor 1 and insulin, and their associations with bone, egg and growth traits in a layer–broiler cross in chickens. Anim. Genet. 37, 283–286.

Benomar, Y., Rideau, N., Crochet, S., Derouet, M., Taouis, M., 2003. Leptin fully suppresses acetylcholine-induced insulin secretion and is reversed by tolbutamide in isolated perfused chicken pancreas. Horm. Metab. Res. 35, 81–85.

Berradi, H., Taouis, M., Cassy, S., Rideau, N., 2005. Glucokinase in chicken (Gallus gallus). Partial cDNA cloning, immunodetection and activity determination. Comp. Biochem. Physiol. B Biochem. Mol. Biol. 141 (2), 129–139.

Bigot, K., Taouis, M., Tesseraud, S., 2003. Refeeding and insulin regulate S6K1 activity in chicken skeletal muscles. J. Nutr. 133, 369–373.

Bisbis, S., Derouet, M., Simon, J., 1994a. Characterization of insulin receptors in chicken kidneys: effect of nutritional status. Gen. Comp. Endocrinol. 96, 37–49.

Bisbis, S., Taouis, M., Derouet, M., Chevalier, B., Simon, J., 1994b. Corticosterone-induced insulin resistance is not associated with alterations of insulin receptor number and kinase activity in chicken kidney. Gen. Comp. Endocrinol. 96, 370–377.

Carver, F.M., Shibley Jr., I.A., Pennington, J.S., Pennington, S.N., 2001. Differential expression of glucose transporters during chick embryogenesis. Cell Mol. Life Sci. 58 (4), 645–652.

Chevalier, B., Anglade, P., Derouet, M., Mollé, D., Simon, J., 1996. Isolation and characterization of Muscovy (*Cairina moschata*) duck insulin. Comp. Biochem. Physiol. B Biochem. Mol. Biol. 114, 19–26.

Chou, H.F., Scanes, C.G., 1988. Influence of age, strain, and beta-adrenergic agonist on insulin sensitivity in chicks as determined by an adaptation of the euglycemic clamp technique. Poult. Sci. 67, 470–475.

Christensen, K., McMurtry, J.P., Thaxton, Y.V., Corzo, A., McDaniel, C., Scanes, C.G., 2013. Metabolic and hormonal responses of growing modern meat-type chickens to fasting. Br. Poult. Sci. 54, 199–205.

Colca, J.R., Hazelwood, R.L., 1982. Amino acids as in vitro secretogogues of avian pancreatic polypeptide (APP) and insulin from the chicken pancreas. Gen. Comp. Endocrinol. 47 (1), 104–110.

Cowap, J., 1985. The first appearance of endocrine cells in the splenic lobe of the embryonic chick pancreas. Gen. Comp. Endocrinol. 60, 131–137.

Darras, V.M., Verhoelst, C.H., Reyns, G.E., Kühn, E.R., Van der Geyten, S., 2006. Thyroid hormone deiodination in birds. Thyroid 16 (1), 25–35. https://doi.org/10.1089/thy.2006.16.25.

Datar, S.P., Bhonde, R.R., 2006. Chick pancreatic B islets as an alternative in vitro model for screening insulin secretagogues. Poult. Sci. 85, 2260–2264.

Davis, J.F., Vasilatos-Younken, R., 1995. Markedly reduced pancreatic glucagon levels in broiler chickens with spiking mortality syndrome. Avian Dis. 39, 417–419.

de la Rosa, E.J., de Pablo, F., 2011. Proinsulin: from hormonal precursor to neuroprotective factor. Front. Mol. Neurosci. 4, 20.

De Meyts, P., 2012. The insulin receptor isoform A: a mitogenic proinsulin receptor? Endocrinology 153, 2054–2056.

Denbow, D.M., Duke, G.E., Chaplin, S.B., 1988. Food intake, gastric secretion, and motility as affected by avian pancreatic polypeptide administered centrally in chickens. Peptides 9, 449–454.

Deng, H., Zheng, A., Liu, G., Chang, W., Zhang, S., Cai, H., 2014. Activation of mammalian target of rapamycin signaling in skeletal muscle of neonatal chicks: effects of dietary leucine and age. Poult. Sci. 93, pp114–p121.

Duchene, S., Audouin, E., Crochet, S., Duclos, M.J., Dupont, J., Tesseraud, S., 2008a. Involvement of the ERK1/2 MAPK pathway in insulin-induced S6K1 activation in avian cells. Domest. Anim. Endocrinol. 34, 63–73.

Duchene, S., Audouin, E., Berri, C., Dupont, J., Tesseraud, S., 2008b. Refeeding and insulin activate the AKT/p70S6 kinase pathway without affecting IRS1 tyrosine phosphorylation in chicken muscle. Domest. Anim. Endocrinol. 34, 1–13.

Duclos, M.J., Chevalier, B., Goddard, C., Simon, J., 1993a. Regulation of amino acid transport and protein metabolism in myotubes derived from chicken muscle satellite cells by insulin-like growth factor-I. J. Cell. Physiol. 157, 650–657.

Duclos, M.J., Chevalier, B., Le Marchand-Brustel, Y., Tanti, J.F., Goddard, C., Simon, J., 1993b. Insulin-like growth factor-I-stimulated glucose transport in myotubes derived from chicken muscle satellite cells. J. Endocrinol. 137, 465–472.

Dupont, J., Chen, J., Derouet, M., Simon, J., Leclercq, B., Taouis, M., 1999. Metabolic differences between genetically lean and fat chickens are partly attributed to the alteration of insulin signaling in liver. J. Nutr. 129 (11), 1937–1944. https://doi.org/10.1093/jn/129.11.1937.

Dupont, J., Dagou, C., Derouet, M., Simon, J., Taouis, M., 2004. Early steps of insulin receptor signaling in chicken and rat: apparent refractoriness in chicken muscle. Domest. Anim. Endocrinol. 26, 127–142.

Dupont, J., Tesseraud, S., Derouet, M., Collin, A., Rideau, N., Crochet, S., Godet, E., Cailleau-Audouin, E., Metayer-Coustard, S., Duclos, M.J., Gespach, C., Porter, T.E., Cogburn, L.A., Simon, J., 2008. Insulin immuno-neutralization in chicken: effects on insulin signaling and gene expression in liver and muscle. J. Endocrinol. 197, 531–542.

Dupont, J., Tesseraud, S., Simon, J., 2009. Insulin signaling in chicken liver and muscle. Gen. Comp. Endocrinol. 163, 52–57.

Dupont, J., Derouet, M., Simon, J., Taouis, M., 1998. Nutritional state regulates insulin receptor and IRS-1 phosphorylation and expression in chicken. Am. J. Physiol. 274 (2), E309–E316. https://doi.org/10.1152/ajpendo.1998.274.2.E309.

Dupont, J., Metayer-Coustard, S., Ji, B., Rame, C., Gespach, C., Voy, B., Simon, J., 2012. Characterization of major elements of insulin signaling cascade in chicken adipose tissue: apparent insulin refractoriness. Gen. Comp. Endocrinol. 176, 86–93.

Fan, L., Gardner, P., Chan, S.J., Steiner, D.F., 1993. Cloning and analysis of the gene encoding hummingbird proinsulin. Gen. Comp. Endocrinol. 91 (1), 25–30. https://doi.org/10.1006/gcen.1993.1100.

Ferreira, A., Litthauer, D., Saayman, H., Oelofsen, W., Crabb, J., Lazure, C., 1991. Purification and primary structure of glucagon from ostrich pancreas splenic lobes. Int. J. Pept. Protein Res. 38 (1), 90–95. https://doi.org/10.1111/j.1399-3011.1991.tb01415.x.

Fischer, A.J., Skorupa, D., Schonberg, D.L., Walton, N.A., 2006. Characterization of glucagon-expressing neurons in the chicken retina. J. Comp. Neurol. 496, 479–494.

Furuse, M., Bungo, T., Shimojo, M., Masuda, Y., Saito, N., Hasegawa, S., Sugahara, K., 1998. Effects of various N-terminal fragments of glucagon-like peptide-1(7-36) on food intake in the neonatal chick. Brain Res. 807, 214–217.

Gittes, G.K., 2009. Developmental biology of the pancreas: a comprehensive review. Dev. Biol. 326, 4–35.

Gross, D.J., Villa-Komaroff, L., Kahn, C.R., Weir, G.C., Halban, P.A., 1989. Deletion of a highly conserved tetrapeptide sequence of the proinsulin connecting peptide (C-peptide) inhibits proinsulin to insulin conversion by transfected pituitary corticotroph (AtT20) cells. J. Biol. Chem. 264 (36), 21486–21490.

Haemmerle, G., Zimmermann, R., Strauss, J.G., Kratky, D., Riederer, M., Knipping, G., Zechner, R., 2002. Hormone-sensitive lipase deficiency in mice changes the plasma lipid profile by affecting the tissue-specific expression pattern of lipoprotein lipase in adipose tissue and muscle. J. Biol. Chem. 277 (15), 12946–12952. Epub 2002 Jan 23.

Hamano, Y., 2006. Effects of dietary lipoic acid on plasma lipid, in vivo insulin sensitivity, metabolic response to corticosterone and in vitro lipolysis in broiler chickens. Br. J. Nutr. 95, 1094–1101.

Hazelwood, R.L., 1993. The pancreatic polypeptide (PP-fold) family: gastrointestinal, vascular, and feeding behavioral implications. Proc. Soc. Exp. Biol. Med. 202 (1), 44–63. https://doi.org/10.3181/00379727-202-43511g.

Hazelwood, R.L., 2000. In: Whittow, G. (Ed.), Pancreas. in Sturkie's Avian Physiology Fifth Edition. Academic Press, New York, NY, pp. 539–555.

Hernández-Sánchez, C., Mansilla, A., de Pablo, F., Zardoya, R., 2008. Evolution of the insulin receptor family and receptor isoform expression in vertebrates. Mol. Biol. Evol. 25, 1043–1053.

Hernández-Sánchez, C., Rubio, E., Serna, J., de la Rosa, E.J., de Pablo, F., 2002. Proinsulin promotes cell survival during neurulation in the chick embryo. Diabetes 51 (3), 770–777.

Hiramatsu, H., 2020. Chicken intestinal L cells and glucagon-like peptide-1 secretion. J. Poult. Sci. 57, 1–6.

Holzer, P., Reichmann, F., Farzi, A., Neuropeptide, Y., 2012. Peptide YY and pancreatic polypeptide in the gut-brain axis. Neuropeptides 46, 261–274.

Honda, K., Kamisoyama, H., Saito, N., Kurose, Y., Sugahara, K., Hasegawa, S., 2007. Central administration of glucagon suppresses food intake in chicks. Neurosci. Lett. 416, 198–201.

Honda, K., Kamisoyama, H., Uemura, T., Yanagi, T., Saito, Kurose, Y., Sugahara, K., Katoh, K., Hasegawa, S., 2012. The mechanism underlying the central glucagon-induced hyperglycemia and anorexia in chicks. Comp. Biochem. Physiol. Mol. Integr. Physiol. 163, 260–264.

Honda, K., Saneyasu, T., Shimatani, T., Aoki, K., Yamaguchi, T., Nakanishi, K., Kamisoyama, H., 2015. Intracerebroventricular administration of chicken glucagon-like peptide-2 potently suppresses food intake in chicks. Anim. Sci. J. 86, 312–318.

Honey, R.N., Arimura, A., Weir, G.C., 1981. Somatostatin neutralization stimulates glucagon and insulin secretion from the avian pancreas. Endocrinology 109 (6), 1971–1974.

Honey, R.N., Fallon, M.B., Weir, G.C., 1980. Effects of exogenous insulin, glucagon, and somatostatin on islet hormone secretion in the perfused chicken pancreas. Metabolism 29 (12), 1242–1246. https://doi.org/10.1016/0026-0495(80)90152-3.

Hu, Y., Zhang, R., Zhang, Y., Li, J., Grossmann, R., Zhao, R., 2012. In ovo leptin administration affects hepatic lipid metabolism and microRNA expression in newly hatched broiler chickens. J. Anim. Sci. Biotechnol. 3, 16.

Huang, J., Eng, J., Yalow, R.S., 1987. Chicken glucagon: sequence and potency in receptor assay. Horm. Metab. Res. 19 (11), 542–544. https://doi.org/10.1055/s-2007-1011878. PMID:2828209.

Humphrey, B.D., Stephensen, C.B., Calvert, C.C., Klasing, K.C., August 2004. Glucose and cationic amino acid transporter expression in growing chickens (*Gallus gallus domesticus*). Comp. Biochem. Physiol. Mol. Integr. Physiol. 138 (1994), 515–525.

Ishii, T., Fukano, K., Shimada, K., Kamikawa, A., Okamatsu-Ogura, Y., Terao, A., Yoshida, T., Saito, M., Kimura, K., 2012. Proinsulin C-peptide activates α-enolase: implications for C-peptide–cell membrane interaction. J. Biochem. 152 (1), 53–62. https://doi.org/10.1093/jb/mvs052. Epub 2012 May 9.

Ji, B., Ernest, B., Gooding ., J.R., Das, S., Saxton, A.M., Simon, J., Dupont, J., Metayer-Coustard, S., Campagna, S.R., Voy, B.H., 2012. Transcriptomic and metabolomic profiling of chicken adipose tissue in response to insulin neutralization and fasting. BMC Genom. 13, 441.

Jun, Y., Xiao, T., Guoyong, Y., Min, F., Haili, Y., Chao, S., 2014. Recombinant globular adiponectin inhibits lipid deposition by p38 MAPK/ATF-2 and TOR/p70 S6 kinase pathways in chicken adipocytes. Biochem. Cell. Biol. 92, 53–60.

Karmann, H., Rideau, N., Zorn, T., Malan, A., Le Maho, Y., 1992. Early insulin response after food intake in geese. Am. J. Physiol. 263, R782–R784.

Kato, H., Okubo, Y., Matsumura, Y., Roberts, C.T.J., Sugahara, K., LeRoith, D., 2000. The tyrosine kinase activity of the chicken insulin receptor is similar to that of the human insulin receptor. Biosci. Biotechnol. Biochem. 64, 903–906.

Katsumoto, K., Fukuda, K., Kimura, W., Shimamura, K., Yasugi, S., Kume, S., 2009. Origin of pancreatic precursors in the chick embryo and the mechanism of endoderm regionalization. Mech. Dev. 126, 539–551.

Kemmler, W., Renner, R., Zynamon, A., Hepp, K.D., 1978. Interactions between insulins and liver membrane receptors of guinea pig, calf and chicken. Exclusion of a species-specific insulin receptor. Biochim. Biophys. Acta. 543 (3), 349–356. https://doi.org/10.1016/0304-4165(78)90052-1.

Khuong, T.T., Jeong, D.K., 2011. Adipogenic differentiation of chicken epithelial oviduct cells using only chicken serum. In Vitro Cell. Dev. Biol. Anim. 47, 609–614.

Kimmel, J.R., Pollock, H.G., Hazelwood, R.L., 1968. Isolation and characterization of chicken insulin. Endocrinology 83, 1323–1330.

Kolodziejski, P.A., Sassek, M., Chalupka, D., Leciejewska, N., Nogowski, L., Mackowiak, P., Jozefiak, D., Stadnicka, K., Siwek, M., Bednarczyk, M., Szwaczkowski, T., Pruszynska-Oszmalek, E., 2018. GLP1 and GIP are involved in the action of synbiotics in broiler chickens. J. Anim. Sci. Biotechnol. 9, 13.

Kong, X.J., Liu, X.L., Wu, Y., Wang, J., Yi, C., 2008. Genetic variance of duck preproinsulin gene and its correlations to the traits of carcasses. Article in Chinese 30 (6), 760–764.

Kono, T., Nishida, M., Nishiki, Y., Seki, Y., Sato, K., Akiba, Y., 2005. Characterisation of glucose transporter (GLUT) gene expression in broiler chickens. Br. Poult. Sci. 46, 510–515.

Krupp, M., Lane, M.D., 1981. On the mechanism of ligand-induced down-regulation of insulin receptor level in the liver cell. J. Biol. Chem. 256 (4), 1689–1694.

Krupp, M., Lane, M.D., 1982. Evidence for different pathways for the degradation of insulin and insulin receptor in the chick liver cell. J. Biol. Chem. 257 (3), 1372–1377.

Ku, S.K., Lee, J.H., Lee, H.S., 2000. An immunohistochemical study of the insulin-, glucagon- and somatostatin-immunoreactive cells in the developing pancreas of the chicken embryo. Tissue Cell 32, 58–65.

Le Marchand, S.J., Piston, D.W., 2010. Glucose suppression of glucagon secretion: metabolic and calcium responses from alpha-cells in intact mouse pancreatic islets. J. Biol. Chem. 285, 14389–14398.

Leclerc, I., Rutter, G.A., Meur, G., Noordeen, N., 2012. Roles of Ca^{2+} ions in the control of ChREBP nuclear translocation. J. Endocrinol. 213 (2), 115–122. https://doi.org/10.1530/JOE-11-0480. Epub 2012 Mar 8. Review.

Lenzen, S., 2008. The mechanisms of alloxan- and streptozotocin-induced diabetes. Diabetologia 51, 216–226.

Li, B.C., Tian, Z.Q., Sun, M., Xu, Q., Wang, X.Y., Qin, Y.R., Xu, F., Gao, B., Wang, K.H., Sun, H.C., Chen, G.H., 2010. Directional differentiation of chicken primordial germ cells into adipocytes, neuron-like cells, and osteoblasts. Mol. Reprod. Dev. 77, 795–801.

Lim, E.J., Kim, C.W., 2007. Functional characterization of the promoter region of the chicken elongation factor-2 gene. Gene 386, 183–190.

Liu, S., Wang, L., Wang, N., Wang, Y., Shi, H., Li, H., 2009. Oleate induces transdifferentiation of chicken fibroblasts into adipocyte-like cells. Comp. Biochem. Physiol. Mol. Integr. Physiol. 154, 135–141.

Liu, S., Wang, Y., Wang, L., Wang, N., Li, Y., Li, H., 2010. Transdifferentiation of fibroblasts into adipocyte-like cells by chicken adipogenic transcription factors. Comp. Biochem. Physiol. Mol. Integr. Physiol. 156, 502–508.

Lu, J.W., McMurtry, J.P., Coon, C.N., 2007. Developmental changes of plasma insulin, glucagon, insulin-like growth factors, thyroid hormones, and glucose concentrations in chick embryos and hatched chicks. Poult. Sci. 86, 673–683.

Lucini, C., Romano, A., Castaldo, L., 2000. NPY immunoreactivity in endocrine cells of duck pancreas: an ontogenetic study. Anat. Rec. 259, 35–40.

Lundell, I., Boswell, T., Larhammar, D., 2002. Chicken neuropeptide Y-family receptor Y4: a receptor with equal affinity for pancreatic polypeptide, neuropeptide Y an:d peptide YY. J. Mol. Endocrinol. 28, 225–235.

Machado-Neto, J.A., Fenerich, B.A., Rodrigues Alves, A.P.N., Fernandes, J.C., Scopim-Ribeiro, R., Coelho-Silva, J.L., Traina, F., 2018. Insulin Substrate Receptor (IRS) proteins in normal and malignant hematopoiesis. Clinics 73 (Suppl. 1), e566s.

Manakova, E., Titlbach, M., 2007. Development of the chick pancreas with regard to estimation of the relative occurrence and growth of endocrine tissue. Anat. Histol. Embryol. 36, 127–134.

Malik, N., Moaeen-ud-Din, M., Zhao, R., 2003. Ontogeny of mRNA expression of somatostatin and its receptors in chicken embryos in association with methylation status of their promoters. Comp. Biochem. Physiol. B Biochem. Mol. Biol. 165 (4), 260–270.

Matsubara, Y., Sato, K., Ishii, H., Akiba, Y., 2005. Changes in mRNA expression of regulatory factors involved in adipocyte differentiation during fatty acid induced adipogenesis in chicken. Comp. Biochem. Physiol. Mol. Integr. Physiol. 141, 108–115.

Matsubara, Y., Endo, T., Kano, K., 2008. Fatty acids but not dexamethasone are essential inducers for chick adipocyte differentiation in vitro. Comp. Biochem. Physiol. Mol. Integr. Physiol. 151, 511–518.

Matsuura, K., Katsumoto, K., Fukuda, K., Kume, K., Kume, S., 2009. Conserved origin of the ventral pancreas in chicken. Mech. Dev. 126, 817–827.

Mayo, K.E., Miller, L.J., Bataille, D., Dalle, S., Goke, B., Thorens, B., Drucker, D.J., 2003. International Union of Pharmacology. XXXV. The glucagon receptor family. Pharmacol. Rev. 55, 167–194.

McCumbee, W.D., Hazelwood, R.L., 1978. Sensitivity of chicken and rat adiopocytes and hepatocytes to isologous and heterologous pancreatic hormones. Gen. Comp. Endocrinol. 34 (4), 421–427. https://doi.org/10.1016/0016-6480(78)90282-4.

McGlinn, E., Yekta, S., Mansfield, J.H., Soutschek, J., Bartel, D.P., Tabin, C.J., 2009. In ovo application of antagomiRs indicates a role for miR-196 in patterning the chick axial skeleton through Hox gene regulation. Proc. Natl. Acad. Sci. U.S.A. 106, 18610–18615.

McMurtry, J.P., Tsark, W., Cogburn, L., Rosebrough, R., Brocht, D., 1996. Metabolic responses of the Turkey hen (*Meleagris gallopavo*) to an intravenous injection of chicken or porcine glucagon. Comp. Biochem. Physiol. C Pharmacol. Toxicol. Endocrinol. 114, pp159–p163.

Mirsky, I.A., Jinks, R., Perisutti, G., 1964. Production of Diabetes Mellitus in the Duck by Insulin Antibodies. Am. J. Physiol. 206, 133–135.

Mo, C., Zhong, Y., Wang, Y., Yan, Z., Li, J., 2014. Characterization of glucagon-like peptide 2 receptor (GLP2R) gene in chickens: functional analysis, tissue distribution, and developmental expression profile of GLP2R in embryonic intestine. Domest. Anim. Endocrinol. 48, pp1–6.

Modak, M.A., Datar, S.P., Bhonde, R.R., Ghaskadbi, S.S., 2007. Differential susceptibility of chick and mouse islets to streptozotocin and its co-relation with islet antioxidant status. J. Comp. Physiol. B 177, 247–257.

Monir, M.M., Hiramatsu, K., Yamasaki, A., Nishimura, K., Watanabe, T., 2014. The influence of restricted feeding on glucagon-like peptide-1 (GLP-1)-containing cells in the chicken small intestine. Anat. Histol. Embryol. 43, 153–158.

Monir, M.M., Hiramatsu, K., Matsumoto, S., Nishimura, K., Takemoto, C., Shioji, T., Watanabe, T., Kita, K., Yonekura, S., Roh, S.G., 2014. Influences of protein ingestion on glucagon-like peptide (GLP)-1-immunoreactive endocrine cells in the chicken ileum. Anim. Sci. J. 85, 581–587.

Monir, M.M., Hiramatsu, K., Nishimura, K., Takemoto, C., Watanabe, T., 2014. Distribution of glucagon-like peptide (GLP)-2-immunoreactive cells in the chicken small intestine; antigen retrieval immunohistochemistry. J. Vet. Med. Sci. 76, 565–568.

Mounier, C., Posner, B.I., 2006. Transcriptional regulation by insulin: from the receptor to the gene. Can J. Physiol. Pharmacol. 84 (7), 713–724. Review.

Mulder, H., Sörhede-Winzell, M., Contreras, J.A., Fex, M., Ström, K., Ploug, T., Galbo, H., Arner, P., Lundberg, C., Sundler, F., Ahrén, B., Holm, C., 2003. Hormone-sensitive lipase null mice exhibit signs of impaired insulin sensitivity whereas insulin secretion is intact. J. Biol. Chem. 278 (38), 36380–36388.

Nadaf, J., Pitel, F., Gilbert, H., Duclos, M.J., Vignoles, F., Beaumont, C., Vignal, A., Porter, T.E., Cogburn, L.A., Aggrey, S.E., Simon, J., Le Bihan-Duval, E., 2009. QTL for several metabolic traits map to loci controlling growth and body composition in an F2 intercross between high- and low-growth chicken lines. Physiol. Genom. 38, 241–249.

Nagao, K., Aman Yaman, M., Murai, A., Sasaki, T., Saito, N., Okumura, J., Kita, K., 2001. Insulin administration suppresses an increase in insulin-like growth factor binding protein-2 gene expression stimulated by fasting in the chicken. Br. Poult. Sci. 42, 501–504.

Nishimura, K., Hiramatsu, K., Monir, M., Takemoto, C., Watanabe, T., 2013. Ultrastructural study on colocalization of glucagon-like peptide (GLP)-1 with GLP-2 in chicken intestinal L-cells. J. Vet. Med. Sci. 75, 1335–1339.

Nishimura, K., Hiramatsu, K., Watanabe, T., Makino, R., Sasaki, N., Kita, K., 2015. Amino acid supplementation to diet influences the activity of the L cells in chicken small intestine. J. Poultry Sci. 52, 221–226.

Osuga, J., Ishibashi, S., Oka, T., Yagyu, H., Tozawa, R., Fujimoto, A., Shionoiri, F., Yahagi, N., Kraemer, F.B., Tsutsumi, O., Yamada, N., 2000. Targeted disruption of hormone-sensitive lipase results in male sterility and adipocyte hypertrophy, but not in obesity. Proc. Natl. Acad. Sci. USA. 97 (2), 787–792.

Palsgaard, J., Brøns, C., Friedrichsen, M., Dominguez, H., Jensen, M., Storgaard, H., Spohr, C., Torp-Pedersen, C., Borup, R., De Meyts, P., Vaag, A., 2009. Gene expression in skeletal muscle biopsies from people with type 2 diabetes and relatives: differential regulation of insulin signaling pathways. PLoS One 4 (8), e6575.

Panserat, S., Rideau, N., Polakof, S., 2014. Nutritional regulation of glucokinase: a cross-species story. Nutr. Res. Rev. 27, 21–47.

Patwardhan, V., Gokhale, M., Ghaskadbi, S., 2004. Acceleration of early chick embryo morphogenesis by insulin is associated with altered expression of embryonic genes. Int. J. Dev. Biol. 48, 319–326.

Pirskanen, A., Kiefer, J.C., IGFs, S.D.H., insulin, S., 2000. bFGF, and TGF-beta1 interact synergistically to promote somite myogenesis in vitro. Dev. Biol. 224, 189–203.

Proszkowiec-Weglarz, M., Richards, M.P., Humphrey, B.D., Rosebrough, R.W., McMurtry, J.P., 2009. AMP-activated protein kinase and carbohydrate response element binding protein: a study of two potential regulatory factors in the hepatic lipogenic program of broiler chickens. Comp. Biochem. Physiol. B Biochem. Mol. Biol. 154, 68–79.

Qiu, F.F., Nie, Q.H., Luo, C.L., Zhang, D.X., Lin, S.M., Zhang, X.Q., 2006. Association of single nucleotide polymorphisms of the insulin gene with chicken early growth and fat deposition. Poult. Sci. 85, 980–985.

Raimbault, S., Dridi, S., Denjean, F., Lachuer, J., Couplan, E., Bouillaud, F., Bordas, A., Duchamp, C., Taouis, M., Ricquier, D., 2001. An uncoupling protein homologue putatively involved in facultative muscle thermogenesis in birds. Biochem. J. 353, 441–444.

Ramsay, T.G., Rosebrough, R.W., 2003. Hormonal regulation of postnatal chicken preadipocyte differentiation in vitro. Comp. Biochem. Physiol. B Biochem. Mol. Biol. 136, 245–253.

Rawdon, B.B., 1998. Morphogenesis and differentiation of the avian endocrine pancreas, with particular reference to experimental studies on the chick embryo. Microsc. Res. Tech. 43, 292–305.

Richards, M.P., McMurtry, J.P., 2008. Expression of proglucagon and proglucagon-derived peptide hormone receptor genes in the chicken. Gen. Comp. Endocrinol. 156, 323–338.

Richards, M.P., McMurtry, J.P., 2009. The avian proglucagon system. Gen. Comp. Endocrinol. 163, 39–46.

Rideau, N., 1988. Insulin secretion in birds Leanness in domestic birds. In: Leclercq, B., Whitehead, C.C. (Eds.), Genetic, Metabolic and Hormonal Aspects. Butterworths and Co. (Publishers) Ltd-INRA., pp. 269–294

Rideau, N., 1997. Insulin secretion. In: Haarvey, S., Etches, R.J. (Eds.), Perspectives in Avian Endocrinology. Journal of Endocrinology Ltd, Bristol, pp. 329–334.

Rideau, N., 1998. Peculiarities of insulin secretion in chickens. Ann. N.Y. Acad. Sci. 839, 162–165.

Rideau, N., Derouet, M., Grimsby, J., Simon, J., 2010. Glucokinase activation induces potent hypoglycemia without recruiting insulin and inhibits food intake in chicken. Gen. Comp. Endocrinol. 169, 276–283.

Rosenberg, L.C., Lafon, M.L., Pedersen, J.K., Yassin, H., Jensen, J.N., Serup, P., Hecksher-Sorensen, J., 2010. The transcriptional activity of Neurog3 affects migration and differentiation of ectopic endocrine cells in chicken endoderm. Dev. Dynam. 239, 1950–1966.

Ruffier, L., Simon, J., Rideau, N., 1998. Isolation of functional glucagon islets of Langerhans from the chicken pancreas. Gen. Comp. Endocrinol. 112, 153–162.

Sato, K., Yonemura, T., Ishii, H., Toyomizu, M., Kamada, T., Akiba, Y., 2009. Role of peroxisome proliferator-activated receptor beta/delta in chicken adipogenesis. Comp. Biochem. Physiol. Mol. Integr. Physiol. 154, 370–375.

Sajid, W., Holst, P.A., Kiselyov, V.V., Andersen, A.S., Conlon, J.M., Kristensen, C., Kjeldsen, T., Whittaker, J., Chan, S.J., De Meyts, P., 2009. Structural basis of the aberrant receptor binding properties of hagfish and lamprey insulins. Biochemistry 48 (47), 11283–11295. https://doi.org/10.1021/bi901269j.

Sato, K., Aoki, M., Kondo, R., Matsushita, K., Akiba, Y., Kamada, T., 2012. Administration of insulin to newly hatched chicks improves growth performance via impairment of MyoD gene expression and enhancement of cell proliferation in chicken myoblasts. Gen. Comp. Endocrinol. 175, 457–463.

Scanes, C.G., 2009. Perspectives on the endocrinology of poultry growth and metabolism. Gen. Comp. Endocrinol. 163, 24–32.

Scanes, C.G., Braun, E., 2012. Avian metabolism: its control and evolution. Front. Biol. 1–26.

Schauder, P., Buck, M.D., 1969. Differential biological activity of chick insulin in mice in vivo and in vitro. Z. Naturforsch. B Article in German 24 (11), 1424–1428.

Seki, Y., Sato, K., Kono, T., Abe, H., Akiba, Y., 2003. Broiler chickens (Ross strain) lack insulin-responsive glucose transporter GLUT4 and have GLUT8 cDNA. Gen. Comp. Endocrinol. 133 (1), 80–87.

Shiraishi, J., Tanizawa, H., Fujita, M., Kawakami, S., Bungo, T., 2011a. Localization of hypothalamic insulin receptor in neonatal chicks: evidence for insulinergic system control of feeding behavior. Neurosci. Lett. 491, 177–180.

Shiraishi, J., Yanagita, K., Fukumori, R., Sugino, T., Fujita, M., Kawakami, S., McMurtry, J.P., Bungo, T., 2011b. Comparisons of insulin related parameters in commercial-type chicks: evidence for insulin resistance in broiler chicks. Physiol. Behav. 103, 233–239.

Shousha, S., Nakahara, K., Nasu, T., Sakamoto, T., Murakami, N., 2007. Effect of glucagon-like peptide-1 and -2 on regulation of food intake, body temperature and locomotor activity in the Japanese quail. Neurosci. Lett. 415, 102–107.

Siddle, K., 2012. Molecular basis of signaling specificity of insulin and IGF receptors: neglected corners and recent advances. Front Endocrinol (Lausanne) 3 (34). https://doi.org/10.3389/fendo.2012.00034. eCollection.

Simon, J., 1980. Apparent independence of glucose tolerance and body fat content in 8-week-old broilers. Br. Poult. Sci. 21, 309–313.

Simon, J., 1988. Insulin in birds: Metabolic effects and possible implications in genetically fat and lean chickens. In: Leclercq, B., Whitehead, C.C. (Eds.), Leanness in Domestic Birds. Butterworth, London, pp. 253–268.

Simon, J., 1989. Chicken as a useful species for the comprehension of insulin action. Crit. Rev. Poult. Biol. 2, 121–148.

Simon, J., 1995. Insulin-glucagon and growth in broilers. Arch für Geflugelkunde. In: Special issue, OECD Workshop, June 7–9, 1994, Celle, Germany, pp. p14–17.

Simon, J., Freychet, P., Rosselin, G., 1974. Chicken insulin: radioimmunological characterization and enhanced activity in rat fat cells and liver plasma membranes. Endocrinology 95 (5), 1439–1449. https://doi.org/10.1210/endo-95-5-1439.

Simon, J., Freychet, P., Rosselin, G., 1977. A study of insulin binding sites in the chicken tissues. Diabetologia 13 (3), 219–228. https://doi.org/10.1007/BF01219703.

Simon, J., Guillaumin, S., Chevalier, B., Derouet, M., Guy, G., Marche, G., Ricard, F.H., Leclercq, B., 2000. Plasma glucose-insulin relationship in chicken lines selected for high or low fasting glycaemia. Br. Poult. Sci. 41, 424–429.

Simon, J., Laurent, S., Grolleau, G., Thoraval, P., Soubieux, D., Rasschaert, D., 2004. Evolution of preproinsulin gene in birds. Mol. Phylogenet. Evol. 30, 755–766.

Simon, J., Rideau, N., Taouis, M., Dupont, J., 2011. Plasma insulin levels are rather similar in chicken and rat. Gen. Comp. Endocrinol. 171, 267–268.

Simon, J., Milenkovic, D., Godet, E., Cabau, C., Collin, A., Metayer-Coustard, S., Rideau, N., Tesseraud, S., Derouet, M., Crochet, S., Cailleau-Audouin, E., Hennequet-Antier, C., Gespach, C., Porter, T.E., Duclos, M.J., Dupont, J., Cogburn, L.A., 2012. Insulin immunoneutralization in fed chickens: effects on liver and muscle transcriptome. Physiol. Genom. 44, 283–292.

Steiner, D.F., Chan, S.J., Welsh, J.M., Kwok, S.C., 1985. Structure and evolution of the insulin gene. Annu. Rev. Genet. 19, 463–484. https://doi.org/10.1146/annurev.ge.19.120185.002335.

Steiner, D.J., Kim, A., Miller, K., Hara, M., 2010. Pancreatic islet plasticity: interspecies comparison of islet architecture and composition. Islets 2, 135–145.

Sweazea, K.L., Braun, E.J., 2006. Glucose transporter expression in English sparrows (passer domesticus). Comp. Biochem. Physiol. B Biochem. Mol. Biol. 144 (3), 263–270.

Tachibana, T., Hirofuji, K., Matsumoto, M., Furuse, M., Hasegawa, S., Yoshizawa, F., Sugahara, K., 2004. The hypothalamus is involved in the anorexic effect of glucagon-like peptide-1 in chicks. Comp. Biochem. Physiol. A Mol. Integr. Physiol. 137 (1), 183–188. https://doi.org/10.1016/j.cbpb.2003.09.026.

Tachibana, T., Oikawa, D., Adachi, N., Boswell, T., Furuse, M., 2007. Central administration of alpha-melanocyte-stimulating hormone changes lipid metabolism in chicks. Comp. Biochem. Physiol. Mol. Integr. Physiol. 148, 408–412.

Taouis, M., Taylor, S.I., Reitman, M., 1996. Cloning of the chicken insulin receptor substrate 1 gene. Gene 178, 51–55.

Takayanagi, M., Okada, Y., Kita, K., Naito, J., Watanabe, T., 1996. Somatostatin-14 and somatostatin-28 in chicken pancreatic islet D-cells. Tissue Cell. 28 (4), 495–500.

Taniguchi, C.M., Emanuelli, B., Kahn, C.R., 2006. Critical nodes in signalling pathways: insights into insulin action. Nat. Rev. Mol. Cell Biol. 7 (2), 85–96. Review.

Taouis, M., Dupont, J., Gillet, A., Derouet, M., Simon, J., 1998. Insulin receptor substrate 1 antisense expression in an hepatoma cell line reduces cell proliferation and induces overexpression of the Src homology 2 domain and collagen protein (SHC). Mol. Cell. Endocrinol. 137, pp177–p186.

Teshigawara, K., Takahashi, S., Boswell, T., Li, Q., Tanaka, S., Takeuchi, S., 2001. Identification of avian alpha-melanocyte-stimulating hormone in the eye: temporal and spatial regulation of expression in the developing chicken. J. Endocrinol. 168 (3), 527–537. https://doi.org/10.1677/joe.0.1680527.

Tesseraud, S., Bigot, K., Taouis, M., 2003. Amino acid availability regulates S6K1 and protein synthesis in avian insulin-insensitive QM7 myoblasts. FEBS Lett. 540 (1–3), 176–180. https://doi.org/10.1016/s0014-5793(03)00260-6.

Tesseraud, S., Metayer, S., Duchene, S., Bigot, K., Grizard, J., Dupont, J., 2007a. Regulation of protein metabolism by insulin: value of different approaches and animal models. Domest. Anim. Endocrinol. 33, 123–142.

Tesseraud, S., Metayer-Coustard, S., Boussaid, S., Crochet, S., Audouin, Derouet, E., Seiliez, M., 2007b. I. Insulin and amino acid availability regulate atrogin-1 in avian QT6 cells. Biochem. Biophys. Res. Commun. 357, 181–186.

Thomas-Delloye, V., Marmonier, F., Duchamp, C., Pichon-Georges, B., Lachuer, J., Barré, H., Crouzoulon, G., 1999. Biochemical and functional evidences for a GLUT-4 homologous protein in avian skeletal muscle. Am. J. Physiol. 277 (6), R1733–R1740.

Tokushima, Y., Takahashi, K., Sato, K., Akiba, Y., 2005. Glucose uptake in vivo in skeletal muscles of insulin-injected chicks. Comp. Biochem. Physiol. B Biochem. Mol. Biol. 141, 43–48.

Tosca, L., Crochet, S., Ferre, P., Foufelle, F., Tesseraud, S., Dupont, J., 2006. AMP-activated protein kinase activation modulates progesterone secretion in granulosa cells from hen preovulatory follicles. J. Endocrinol. 190, 85–97.

Trabucchi, M., Tostivint, H., Lihrmann, I., Blahser, S., Vallarino, M., Vaudry, H., 2003. Characterization of the cDNA encoding a somatostatin variant in the chicken brain: comparison of the distribution of the two somatostatin precursor mRNAs. J. Comp. Neurol. 461, 441–451.

Tung, A.K., Rosenzweig, S.A., Foa, P.P., 1977. Glucagon from avian pancreatic islets: radioreceptor studies. Can. J. Biochem. 55 (8), 915–918.

Vaudin, P., Dupont, J., Duchene, S., Audouin, E., Crochet, S., Berri, C., Tesseraud, S., 2006. Phosphatase PTEN in chicken muscle is regulated during ontogenesis. Domest. Anim. Endocrinol. 31, 123–140.

Vessey, K.A., Rushforth, D.A., Stell, W.K., 2005. Glucagon- and secretin-related peptides differentially alter ocular growth and the development of form-deprivation myopia in chicks. Invest. Ophthalmol. Vis. Sci. 46, 3932–3942.

Wang, S.P., Laurin, N., Himms-Hagen, J., Rudnicki, M.A., Levy, E., Robert, M.F., Pan, L., Oligny, L., Mitchell, G.A., 2001. The adipose tissue phenotype of hormone-sensitive lipase deficiency in mice. Obes. Res. 9 (2), 119–128. https://doi.org/10.1038/oby.2001.15.

Wang, Y., Meng, F., Zhong, Y., Huang, G., Li, J., 2012. Discovery of a novel glucagon-like peptide (GCGL) and its receptor (GCGLR) in chickens: evidence for the existence of GCGL and GCGLR genes in nonmammalian vertebrates. Endocrinology 153, 5247–5260.

Wang, X.Q., Jiang, W., Tan, H.Z., Zhang, D.X., Zhang, H.J., Wei, S., Yan, H.C., 2012. Effects of breed and dietary nutrient density on the growth performance, blood metabolite, and genes expression of target of rapamycin (TOR) signalling pathway of female broiler chickens. J. Anim. Physiol. Anim. Nutr. 97, 797–806.

Wahren, J., Ekberg, K., Johansson, J., Henriksson, M., Pramanik, A., Johansson, B.L., Rigler, R., Jörnvall, H., 2000. Role of C-peptide in human physiology. Am. J. Physiol. Endocrinol. Metab. 278 (5), E759–E768. https://doi.org/10.1152/ajpendo.2000.278.5.E759.

Wahren, J., Kallas, A., Sima, A.A., 2012. The clinical potential of C-peptide replacement in type 1 diabetes. Diabetes 61 (4), 761–772. https://doi.org/10.2337/db11-1423.

Wan, Z., Xu, B., Huang, K., Chu, Y.C., Li, B., Nakagawa, S.H., Qu, Y., Hu, S.Q., Katsoyannis, P.G., Weiss, M.A., 2004. Enhancing the activity of insulin at the receptor interface: crystal structure and photo-cross-linking of A8 analogues. Biochemistry 43 (51), 16119–16133.

Wang, X., Jia, Q., Xiao, J., Jiao, H., Lin, H., 2015. Stress. Glucocorticoids retard skeletal muscle development and myoblast protein synthesis through a mechanistic target of rapamycin (mTOR)-signaling pathway in broilers (*Gallus gallus domesticus*). Stress 18, 686–698.

Wang, Y., Mu, Y., Li, H., Ding, N., Wang, Q., Wang, S., Wang, N., 2008b. Peroxisome proliferator-activated receptor-gamma gene: a key

regulator of adipocyte differentiation in chickens. Poult. Sci. 87, 226–232.

Wang, J., Wang, Y., Li, X., Li, J., Leung, F.C., 2008a. Cloning, tissue distribution, and functional characterization of chicken glucagon receptor. Poult. Sci. 87, 2678–2688.

Watanabe, T., Nishimura, K., Hosaka, Y., Shimosato, T., Yonekura, S., Suzuki, D., Takemoto, C., Monir, M., Hiramatsu, K., 2014. Histological analysis of glucagon-like peptide-1 receptor expression in chicken pancreas. Cell Tissue Res. 357, 55–61.

Hiramatsu, K., Nishimura, K., Ono, T., 2018. Glucagon-like peptide-1 receptor expression in the pancreatic D cells of three avian species; white leghorn chickens, northern bobwhites and common ostriches. J. Poult. Sci. 55, 199–203.

Weir, G.C., Goltsos, P.C., Steinberg, E.P., Patel, Y.C., 1976. High concentration of somatostatin immunoreactivity in chicken pancreas. Diabetologia 12 (2), 129–132. https://doi.org/10.1007/BF00428977.

Weiss, M.A., Hua, Q.X., Jia, W., Nakagawa, S.H., Chu, Y.C., Hu, S.Q., Katsoyannis, P.G., 2001. Activities of monomeric insulin analogs at position A8 are uncorrelated with their thermodynamic stabilities. J. Biol. Chem. 276 (43), 40018–40024. Epub 2001 Aug 21.

Weiss, M.A., Wan, Z., Zhao, M., Chu, Y.C., Nakagawa, S.H., Burke, G.T., Jia, W., Hellmich, R., Katsoyannis, P.G., 2002. Non-standard insulin design: structure-activity relationships at the periphery of the insulin receptor. J. Mol. Biol. 315 (2), 103–111.

Xiong, M., Li, S., Peng, X., Feng, Y., Yu, G., Xin, Q., Gong, Y., 2010. Adipogenesis in ducks interfered by small interfering ribonucleic acids of peroxisome proliferator-activated receptor gamma gene. Poult. Sci. 89, 88–95.

Zechner, R., Kienesberger, P.C., Haemmerle, G., Zimmermann, R., Lass, A., 2009. Adipose triglyceride lipase and the lipolytic catabolism of cellular fat stores. J. Lipid. Res. 50 (1), 3–21. https://doi.org/10.1194/jlr.R800031-JLR200. Epub 2008 Oct 23.

Zhao, J.P., Bao, J., Wang, X.J., Jiao, H.C., Song, Z.G., Lin, H., 2012. Altered gene and protein expression of glucose transporter1 underlies dexamethasone inhibition of insulin-stimulated glucose uptake in chicken muscles. J. Anim. Sci. 90 (12), 4337–4345.

Chapter 35

Reproduction in the female

Anna Hrabia

Department of Animal Physiology and Endocrinology, University of Agriculture in Krakow, Krakow, Poland

35.1 Introduction

The avian reproductive system is unique and differs from that of mammals. In majority of birds, only the left ovary and oviduct develop into the functional organs. The right primordial ovary and oviduct regress except in birds of prey. Herein the majority of information is based on studies derived from domesticated birds primarily chickens. The ovary and oviduct are dynamic organs undergoing diverse molecular, cellular, morphological, and functional changes over the course of the female reproductive cycle (development, laying, regression, and rejuvenation). Follicle development and ovulation depends on the coordinated action of hypothalamic, pituitary, and ovarian hormones and other factors. The oocyte released upon ovulation is engulfed by the oviduct where components of the laid egg are synthesized and secreted, including the egg albumen, eggshell membranes, and eggshell. In addition to the egg formation and transportation, the oviduct is the site of sperm storage and transport, fertilization, and early embryonic development. The oviduct development and function are orchestrated primarily by sex steroids. This chapter describes the current knowledge on development, morphology, and function of the female reproductive system. The cellular and molecular mechanisms underlying the regulation of follicle growth, selection, differentiation, ovulation, and regression as well as the molecular basis of egg formation are emphasized. In addition, the recent advances in molecular biology related to reproductive system development and function are included.

35.2 The ovary

In birds, gonads of ZW heterozygotes develop as asymmetric ovaries, whereas ZZ homozygotes develop as symmetric testes in processes regulated by genetic and hormonal pathways. In most female birds, only the left ovary and left Müllerian duct develop. The Müllerian duct later develops into the oviduct due to stimulatory action of estrogen and absence of anti-Müllerian factor. Those in the right side regress during embryonic life (reviewed in Shimada, 2002; Guioli et al., 2014; Kuroiwa, 2017; Hirst et al., 2018).

35.2.1 Embryonic and posthatch development of the ovary

The ovaries arise from the intermediate mesoderm, and are first evidenced at embryonic day 3−3.5, as a thickened coelomic epithelium ventral to the mesonephros. At the same time, the future ovaries are colonized by primordial germ cells (PGCs). In chickens, most of the PGCs originated from the central disc of the area pellucida (Ginsburg and Eyal-Giladi, 1987), occur in the dense accumulation in the germinal crescent at around 18−19 h of incubation, and then enter the vascular system at about 33 h of embryonic development. Thereafter, PGCs eventually migrate toward the future genital ridges. Until 72 h of incubation, most of PGCs accumulate at the genital ridges, preferentially colonize the left one, where, in female, differentiate into ova in response to different factors from surrounding somatic cells. By day five−six of incubation, PGCs are identified in higher number in the left then in the right ovary. Migration of PGCs to the genital ridge is mediated by chemokine, stromal cell-derived factor 1 and its receptor type 4 (SDF-1/CXCR4) signaling (Stebler et al., 2004) as well as stem-cell factor 1 and its receptor (Srihawong et al., 2015). As the left ovary proceeds development, the PGCs settle predominantly in the ovarian cortex and proliferate significantly, increasing in number about 25-fold between days 9 and 17 of incubation (Hughes, 1963). In the medulla of the left ovary and the right ovary, the PGCs undergo apoptosis until hatching or arrest in meiosis and do not undergo apoptosis until after hatching (Ukeshima, 1996; de Melo Bernardo et al., 2015). Meiosis is initiated by day 15.5 of incubation under influence of luteinizing hormone (LH) and retinoic acid (Smith et al., 2008a; reviewed in Tagami et al., 2017). As established in in vitro culture, PGC

Sturkie's Avian Physiology. https://doi.org/10.1016/B978-0-12-819770-7.00002-5

proliferation is regulated primarily by fibroblast growth factor 2 activating the signaling of mitogen-activated protein kinase (MAPK)/extracellular signal-regulated kinase (ERK) (Miyahara et al., 2016). Bone morphogenetic protein 4 (BMP4)- and activin-activated SMAD signaling (Whyte et al., 2015), insulin- and stem-cell factor 2-activated phosphoinositide 3 kinase/kinase Akt (protein kinase B) signaling as well as Wnt signaling via the stabilization of β-catenin and activation of its downstream genes are also proposed to be involved in enhancement of PGC proliferation (Lee et al., 2016; reviewed in Tagami et al., 2017). Recent results suggest that glycogen synthase kinase 3 is involved in cell renewal and apoptosis in chicken PGCs (Chen et al., 2020). In addition, growing evidence indicates that numerous microRNAs (miRNAs) regulate PGC biology. For example, gga-miR-181-5p, gga-miR-2127, and members of the gga-miR-302/367 cluster have a pivotal role in the regulation of avian PGC proliferation (Lázár et al., 2018).

Up to day 4.5 of incubation, the gonads are bipotential (able to differentiate into testes or ovaries) and morphologically indistinguishable until day 8−10 of incubation when are differentiated enough to be recognized upon necropsy. At this time anatomical asymmetry between the left and right ovary becomes evident due to gradual regression of the right ovary realized via apoptosis process. In contrary, the left ovary develops rapidly into a gonad with thickened an outer cortex overlying an inner medulla. The cortex differentiates into the tissue where the follicles develop, while the medulla differentiates into connective tissue, containing nerve and blood vessel systems. From day nine of embryonic development, the PGCs in the ovarian cortex begin to undergo folliculogenesis through synchronous rounds of mitosis and meiosis to form germ cell nests. Then, the germ cells are surrounded by the granulosa and thecal cells derived from somatic cells of the cortex or medulla, located just beneath the cortex. Development of the functional left ovary is completed after hatching with the formation of primordial follicles containing oocytes that are arrested in the diplotene phase of prophase I. The medullary cords, underlying the cortex of the ovary, become vacuolated and form structures called lacunae (reviewed in Cutting et al., 2012; Hirst et al., 2018).

Initial stages of gonadal differentiation is orchestrated by several genes (Guioli et al., 2014; Hirst et al., 2018). One of the earliest expressed gene is GATA4. Its expression occurs in the chicken bipotential gonad in both sexes prior gonadal differentiation at embryonic day four (Oreal et al., 2002). Steroidogenic factor-1 transcription also precedes gonadal differentiation in genetic male and female chickens and is detected at day 5.5 of incubation, then its expression increases in developing ovary (Smith et al., 1999). Differentiation of the bipotential gonad into the ovary occurs in chickens between days 6.5 and 8.5 of embryonic development and is characterized by the thickening of the outer cortex of the gonad. The proliferation and differentiation of both somatic cells and PGCs only in the cortex of the left ovary is controlled by transcription factor, paired-like homeodomain transcription factor 2, which in turn, regulates expression of the estrogen receptor α (ERα). This type of ER is predominantly involved in differentiation of the ovary and Müllerian duct/oviduct in birds (review in Guioli et al., 2014 and in Hirst et al., 2018; Mattsson and Brunström, 2017).

Although there are no ovary-determining genes linked to W sex chromosome identified, several autosomal genes were proposed to be implicated in the female sex differentiation in birds. Among them, forkhead box L2 (FOXL2) is an essential transcription factor involved in ovary development. Gene expression of FOXL2 and aromatase (CYP19A1), other critical player required for the ovary development, highly correlates in the developing gonad between days 4.7 and 12.7 of incubation (Govoroun et al., 2004). The aromatase protein (estrogen-synthesizing enzyme) is present in the medulla of female gonads from incubation day 6.5, and its expression increases during ovarian development. The proteins encoded both genes are co-expressed in the nuclei of medullar cord cells and the onset of FOXL2 expression slightly precedes aromatase expression. It is therefore thought that aromatase gene expression is under FOXL2 control (Hudson et al., 2005; reviewed in Hirst et al., 2018). R-spondin 1 (RSPO1) and wingless-type MMTV integration site family member 4 (WNT4) activation of β-catenin signaling also plays an important regulatory role in the ovary development. RSPO1 mRNA is expressed in the left and right gonads of ZW chicken embryos from day 4.5 of incubation, and increases greatly from embryonic day 8.5 onward (Smith et al., 2008b; Chue and Smith, 2011). WNT4 expression is observed in the bipotential gonads of male and female embryos at day 4.5 of incubation, and it is elevated in the left gonad of female embryo during sexual differentiation. RSPO1 and WNT4 are strongly expressed in the cortex of the developing ovary along with β-catenin (Ayers et al., 2013). Additional female-enriched candidate genes, Calpain-5 and G-protein coupled receptor 56 were recently identified in early chicken gonads, however, their precise roles in the ovary differentiation in not known yet (Ayers et al., 2015). Other studies have identified miRNAs with sexually dimorphic expression patterns in chicken embryonic gonads, implying that they are active during ovary development (review in Cutting et al., 2012; Feng et al., 2014).

35.2.2 The juvenile ovary

The age when female birds achieve sexual maturity depends on the species. For instance, quail are able to breed

within a few weeks after hatching, and domestic species within a few months. Chickens become sexually mature around 20 weeks of age. In most wild species, breeding occurs usually in the first breeding season after hatching. Larger birds may take several years to reach sexual activity (e.g., the Royal Albatross, fulmars) (Gilbert, 1979).

In period from hatching to just before the onset of egg lay, there are no key changes in the ovary. At hatching, the ovary is a small, roughly triangular in shape. During the first few weeks, the ovary grows very slowly; however, it becomes broader and more obviously triangular. Various folds develop and the cranial part is flexed laterally. The appearance of the ovary is a granular due to the numerous oocytes present. Then, a series of grooves which separate the cortical gyri develops, increase in number, and become deeper (Figure 35.1A). The medullary tissue occupies the gyri. At the time of sexual maturity, the distinction between the cortex and medulla is nearly eliminated (reviewed in Gilbert, 1979). Up to 4 week after hatching, primordial follicles in the ovary grow to the primary follicle stage (Gonzalez-Moran, 2011). During the 7 weeks preceding sexual maturity in the domestic hen, the weight of the ovary increases from about 0.34 to 35 g (Hrabia et al., 2011). Main increase in ovary weight occurs in the last week before the onset of egg lay and is due almost entirely to the growth of the yellow preovulatory follicles. Eight to five weeks before maturity, only primordial and primary follicles are seen in the ovary. White follicles appear about 4−3 weeks before the first ovulation, and 2 weeks before maturation yellowish follicles are present in the ovary (Hrabia et al., 2011; Hrabia, 2015) (Figure 35.1A−B).

The ovary lies in the cranial part of the body cavity, ventral to the aorta and the caudal vena cava, and adjacent to the cranial extremity of the left kidney and the caudal part of the left lung. It is hanged from the dorsal body wall by a peritoneal fold, the mesovarium. This fold is strengthened by connective tissue and forms the hilus containing blood vessels, nerves, and smooth muscle (Gilbert, 1979).

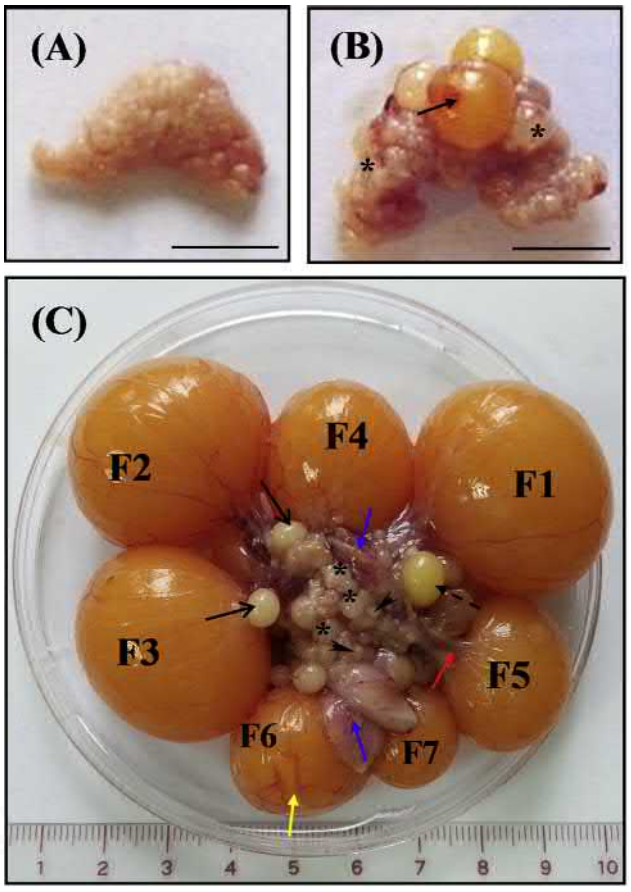

FIGURE 35.1 The hen ovary. (A) The ovary of growing chicken about 6 weeks before maturation with primordial and primary follicles. (B) The ovary of growing chickens about 2 weeks prior to the onset of egg lay, possessing white (*asterisks*) and small yellow (*arrow*) follicles. (C) The ovary of laying hen composed of prehierarchical white (*asterisks*) and yellowish (*black arrows*) follicles, small yellow follicles (*dashed arrow*), the seven largest hierarchical yellow preovulatory follicles (F7−F1), postovulatory follicles (*blue arrows*), and prehierarchical atretic follicles (*arrow heads*). *Red arrow* indicates the follicle stalk (pedicle). *Yellow arrow* indicates the follicle stigma. Bar = 1 cm.

35.2.3 The laying hen ovary

In the laying domestic hen, the ovary contains follicles of various size and stage of development (Figure 35.1C). There are numerous prehierarchical follicles (primordial and primary follicles embedded in the stroma with diameter <1 mm, white follicles >1−4 mm, and yellowish follicles >4−8 mm), the preovulatory yellow follicles (>8−36 mm; Fn-F1), which are arrange in a characteristic hierarchy (typically the largest five to eight follicles exist), and several postovulatory follicles (POFs) at different stage of regression (POF1-POFn). The largest follicle (F1) is the most developed and first to ovulate. After ovulation of the F1, less mature follicles are moved up one position in the hierarchy, and one follicle from the group of 6−8 mm follicles is recruited into the preovulatory hierarchy. Moreover, in the hen ovary several prehierarchical atretic follicles are present. The primordial follicles (up to 80 μm diameter) contain a large germinal vesicle (nucleus) and are surrounded by a single layer of flattened or cuboidal granulosa cells. Further, in primary follicles increasing in size to 1−2 mm, the basal lamina and a single layer of theca cells are addend (Figure 35.2A). These follicles exist in a quiescent phase of growth, lasting from a few weeks to several years. The next subpopulation of white follicles (numbering about 40−50 per ovary) is formed by further development of the granulosa layer into multilayer, and theca layer to the theca interna and externa layers (Figure 35.2B). Follicles become suspended from the ovarian surface by

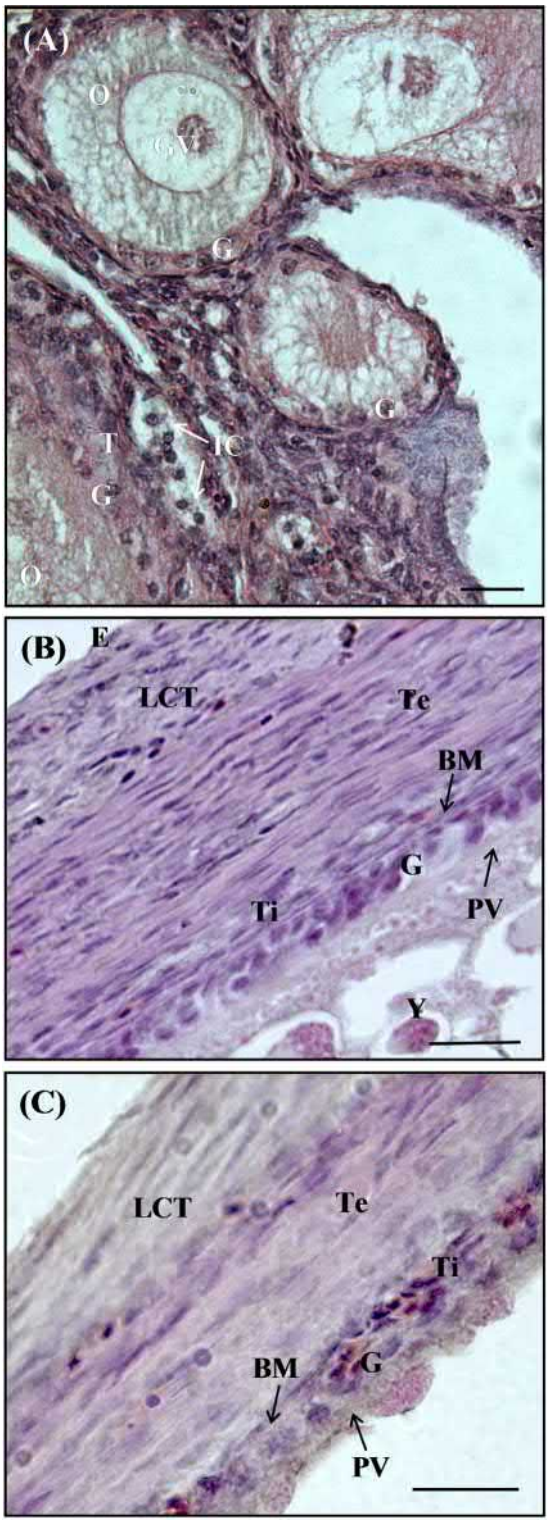

FIGURE 35.2 Histological structure of chicken ovarian follicles (hematoxylin and eosin staining). (A) Ovarian cortex with primordial and primary follicles. Primordial follicle consists of oocyte (O) with germinal vesicle (GV) and perivitelline membrane (PV) surrounded by one layer of granulosa cells (G). In further developed primary follicle, the basement membrane (BM), thin theca layer (T), and the interstitial cells (IC) in the outer area of the theca layer are additionally present. (B) The wall of prehierarchical follicles (5 mm diameter) with the multilayered granulosa. (C) The wall of the largest yellow follicle containing one layer of cuboidal granulosa cells. *E*, epithelium; *IC*, interstitial cells; *LCT*, loose connective tissue; *PV*, perivitelline layer; *Ti*, theca interna; *Te*, theca externa; *Y*, yolk. Bar = 20 μm.

a stalk. The germinal disc comprising germinal vesicle and cytoplasmic organelles is located at the animal pole of the oocyte. White follicles begin slow-growing stage, accumulate protein-rich white yolk and increase in diameter up to 4−6 mm within a few weeks. During slow-growing phase of development, the granulosa cells exhibit the highest proliferating rate, which in follicles 1−8 mm is five-, six-time greater than in the largest F3−F1 (Tilly et al., 1992). As follicle development progress through the stage of yellowish follicles (numbering 10−12 per ovary), the accumulation of lipid-rich yellow yolk starts. Approximately every 24−25 h, one 6−8 mm yellowish follicle enters into the rapid growth phase and in 5−9 days increases in size up to 36−40 mm. Fast-growing, yellow follicles contain oocyte with a large amount of yolk surrounded by the perivitelline layer, and the follicular wall including the granulosa layer, basal lamina, theca interna and externa layers, loose connective tissue, and epithelium (Figure 35.2C). Across this stage of development, there is a decrease in the rate of cell proliferation with concomitant reorganization of the granulosa layer from a multilayered to a single-cell layer, with cuboidal shape in the largest yellow follicles. In these follicles, the granulosa cells undergo intense differentiation, and their proliferation is limited to the region of the germinal disc (Tischkau et al., 1997; Yao and Bahr, 2001; Wojtysiak et al., 2011). Microvilli are well developed on lateral and apical surfaces of the granulosa cells, and they form interdigitations with adjacent cells. At the germinal disc area, the cell membrane of granulosa cells and oolemma form gap junctions (Yoshimura et al., 1993b). The basal lamina (basement membrane) separating the granulosa and theca interna layers is thick, approximately 1 μm in the largest follicle. It contains type IV collagen, noncollagenous extracellular proteins such as fibronectin, laminin, heparin sulfate proteoglycan, nidogen, and additional components that are not classified as extracellular matrix (ECM) proteins secreted by both the granulosa and theca layer cells (Asem et al., 2000). The theca interna comprises the interstitial cells, spindle-shaped fibroblasts, and relatively small amount of collagenous fibers. The interstitial (steroidogenic) cells are rich in mitochondria with tubular cristae, smooth endoplasmic reticulum, and lipid droplets. The theca externa contains fibroblast-like cells, aromatase cells, muscle fibers, and in large part is composed of ECM which contains dermatan sulfate, heparan sulfate, hyaluronic acid, and collagenous fibers. The loose connective tissue (superficial tissue) ambient the theca layers projects from the ovarian cortex and follicular stalk. Through this tissue the vascular and nervous systems enter the follicle. At the stigma region, this loose connective tissue becomes thin, while theca externa increases in thickness, and thus blood vessels except for capillaries in the theca interna are not developed here. The superficial epithelium consists of cuboidal or flattened cells (Yoshimura and Barua, 2017).

35.2.3.1 Follicle vasculature and blood flow

The blood contribution to the ovary comes through ovarian arteries originating from the left gonado-renal artery. Highly convoluted branches of the ovarian artery proceed across the medullary tissue giving off smaller branches to the cortex, and via the follicular stalk to the developing follicles. The venous efflux from the ovarian follicles collects in large veins within the medulla and leaves the organ via the cranial and caudal ovarian veins which join eventually the left suprarenal vein and the vena cava, respectively (Hodges, 1974). Prior to follicle selection, a limited number of blood vessels associated with the follicular wall is formed. The network of blood vessels increases along with the fast growth of follicle, achieving maximal development in the largest follicle (F1). The granulosa layer is lacking of vasculature, while the highly vascularized theca layer possesses an outer venous layer, a complex middle arterial and venous layers, and an inner capillary network. The progress in expansion of follicular vasculature along with follicle maturation to a final stage of development is accompanied by a gradual increase in the blood flow. Among the yellow preovulatory follicles, the blood flow is relatively constant. The five largest follicles receive about half of the ovarian blood flow (Scanes et al., 1982; Hrabia et al., 2005). Intensified angiogenesis and blood flow within the theca layer facilitate the rapid growth of preovulatory follicles by increase in incorporation of yellow yolk to the oocyte.

Increase in ovarian follicle vasculature is attributed to the enhanced level of gonadotropin-induced vascular endothelial growth factor (VEGF) expression within the granulosa cells at follicle recruitment, stimulating angiogenesis within the theca layer possessing VEGF receptors (Kim et al., 2016). Other angiogenic factor, i.e., metalloproteinase-9 (MMP-9), localized particularly around blood vessels, which expression and activity significantly increase in the theca layer of chicken preovulatory follicles, is also proposed as a regulator of ovarian vasculature development (Hrabia et al., 2019).

As an intraovarian regulator of blood flow, the most important are pituitary-derived gonadotropins and locally produced steroids, prostaglandins (PGs) or other factors such as biogenic amines. By way of example, the administration of PGF2 alpha was followed by a consistent decrease in blood flow to the largest preovulatory follicles (Scanes et al., 1982). In turn, histamine increased blood flow to chicken ovarian follicles (Hrabia et al., 2005).

35.2.3.2 Follicle innervations

The ovary possess an extrinsic and intrinsic neural system. The extrinsic innervation of the ovary consists of complex of many nerves and ganglia laying close to, or within the ovarian stalk. The intrinsic innervation of the ovarian medulla contains both large and small nerve bundles, some of which are associated with blood vessels and smooth muscles. The innervation within the ovarian cortex is predominantly associated with the follicles but also with blood vessels within stroma. With progressive growth and maturation of the follicle, the innervation increases (Gilbert, 1969). An extensive adrenergic and cholinergic innervation of the follicles is confined primarily to the theca layer. The granulosa layer possesses less than 5% of the total number of nerve fibers existing in the follicle (Gilbert, 1965, 1969). The ovarian neural system supplies numerous neurotransmitters (acetylcholine, catecholamines, serotonin, and histamine) and neuropeptides [vasoactive intestinal peptide (VIP), galanin, and brain-derived neurotropic factor] which mediate ovarian processes.

35.2.4 Follicle development, selection, and establishment of preovulatory hierarchy

Generally, in laying hen almost each day, the largest preovulatory follicle is ovulated, and the follicle number in the preovulatory hierarchy is kept essentially constant by the selection of one follicle from the pool of 6−8 mm diameter follicles. This process, occurring on a near-daily basis, is called as cyclic recruitment (Woods and Johnson, 2005) and seems to be independent of ovulation (Ghanem and Johnson, 2019a). The precise mechanisms that control a slowly growing follicle recruitment into a rapid growth phase are not fully elucidated. Nevertheless, follicle requirement is the result of well-synchronized interactions between oocyte and surrounding cells of the granulosa and theca layers, in response to a diverse endocrine, paracrine, and/or autocrine factors.

The most important event at the time of selection is that the granulosa cells becomes responsive to follicle-stimulating hormone (FSH) and VIP, which initiate G protein-coupled receptor-mediated cyclic adenosine monophosphate (cAMP) production. In turn, cAMP signaling within the granulosa cells upregulates the steroidogenic acute regulatory protein (StAR), cytochrome P450 side chain cleavage enzyme (CYP11A1), 17α-hydroxylase/17,20-lyase (CYP17A1), and LH receptor gene expression, resulting in initiation of steroidogenesis (Johnson and Bridgham, 2001; Johnson, 2015a; Ghanem and Johnson, 2018, 2019b). Prior to selection, the granulosa cells of up to 8 mm follicles remain undifferentiated and fail to initiate cAMP production in response to FSH compared to granulosa cells from the most recently recruited (9−12 mm) follicles (Tilly et al., 1991a; Johnson and Lee, 2016). Although FSH receptors (FSHR) are present at this stage of development, they fail to generate cAMP (remain in a desensitized state). Therefore, granulosa layer from follicles before selection is steroidogenically inactive. The inability of granulosa cells to generate cAMP synthesis in response to FSH is mediated through an inhibitory effect of the MAPK signaling via ESKs (ERK1,

ERK2) and/or protein kinase C pathways (Woods and Johnson, 2005; Woods et al., 2007; Johnson, 2014) as well as by β-arrestin (Kim and Johnson, 2018). There is also evidence that VIP signaling via its receptors (VPAC1 and VPAC2) in prehierarchical follicle granulosa cells is also suppressed, in vitro, by a β-arrestin-mediated event (Kim and Johnson, 2018). It was suggested that cyclic recruitment of follicle into preovulatory pool of follicles may result from a rapid decline in inhibitory cell signaling rather than the comparatively slower process of gene transcription and translation (Ghanem and Johnson, 2019b).

The FSH is a main hormone facilitating follicle selection into the preovulatory hierarchy. Treatment of hens with FSH (Palmer and Bahr, 1992) as well as with equine chorionic gonadotropin (Ghanem and Johnson, 2019b; Wolak et al., 2021), which possess mainly FSH-like properties, greatly increases the number of yellow follicles in the ovary (Figure 35.3). Even a single injection of FSH is capable of initiating FSH-responsiveness within the granulosa layer, resulting in the recruitment of multiple follicles to the preovulatory hierarchy within a single ovulatory cycle. Morphology and cellular characteristics of these follicles is the same as that following a spontaneous selection, including increased size, yellow yolk incorporation, and weight (Ghanem and Johnson, 2019b). FSHR are present in the granulosa and theca layer of growing follicles as early as 1−2 mm stage of development, and the expression of these receptors alters along follicular maturation. The highest FSHR mRNA levels noted in 6−8 and 9−12 mm follicles decrease progressively as the follicle develops to the preovulatory F1 stage (You et al., 1996; Zhang et al., 1997). An increase in FSHR expression in the granulosa cells and subsequent follicle recruitment is influenced by multiple paracrine and autocrine factors. One of them is anti-Müllerian hormone (AMH). In hens, the expression of AMH mRNA and protein, predominantly in the granulosa layer, is restricted to the growing population of follicles and is markedly decreased at around the time of follicle selection (Johnson et al., 2008; Johnson, 2012). Follicles larger than approximately 50 μm and smaller than 6 mm showed the most pronounced AMH expression, supporting the idea that the AMH signal must be reduced to promote FSH sensitivity in developing follicles (Johnson, 2012). As a regulator of AMH expression, vitamin D was proposed; it caused a decrease in the expression of AMH mRNA in the hen granulosa cells from 3−5 mm and 6−8 mm follicles concomitantly with increase in FSHR expression (Wojtusik and Johnson, 2012). Growth and differentiation factor 9 (GDF9) along with bone morphogenetic protein 15 (BMP15), oocyte-derived members of the transforming growth factor beta superfamily (TGFβ) have been identified in the ovary of hens as well, and their role was related to follicle selection (Johnson et al., 2005; Elis et al., 2007; Li et al., 2019). Expression of BMP15 receptor mRNA (BMPR1B and BMPR2) in granulosa cells increases with follicle development from 3 to 16 mm stage of development. Biological action of the GDF9 is associated with promotion of the granulosa cell proliferation (Johnson et al., 2005). BMP15 is found as a stimulator of FSHR expression and inhibitor of AMH and occludin expression in the granulosa cells from 3−5 mm and 6−8 mm follicles (Stephens and Johnson, 2016). In addition, BMP4 and BMP6 also enhance FSHR mRNA expression in granulosa cells from chicken prehierarchical follicles (Ocón-Grove et al., 2012; Kim et al., 2013). Further, Kit system containing Kit ligand (KL) and its tyrosine kinase receptor (cKit) is suggested to regulate the smaller prehierarchical follicle development and eventually recruitment. The highest KL mRNA abundances are noted in the primary <1 mm follicles and in the granulosa layer of 3 mm follicles as compared to expression in the granulosa layer of 6−12 mm follicles (Kundu et al., 2012). cKit protein is present in the theca layer and ovarian stroma but not in the granulosa cells (Kundu et al., 2012). Several potential factors involved in the regulation of KL synthesis are also proposed. For instance, treatment with heparin binding EGF-like growth factor, identified in the oocyte, resulted in a dose-dependent decrease in KL mRNA expression in the granulosa cell (Wang et al., 2007). Vitamin D3 increases, while FSH decreases expression of KL mRNA in the granulosa cells collected from 6−8 mm follicles (Kundu et al., 2012). Recently, the slit guidance ligands (SLIT1, SLIT2, and SLIT3) and their receptors

FIGURE 35.3 The hen ovary obtained after eCG treatment. Laying hens were injected subcutaneously with 75 IU eCG (PMSG)/kg of body weight for seven successive days. Treatment with eCG results in a higher number of yellowish and yellow follicles and disruption of the ovarian hierarchy.

(ROBO1, ROBO2, ROBO3, and ROBO4) have been revealed to mediate the prehierarchical follicles development in the hen ovary by an autocrine and/or paracrine fashion (Qin et al., 2015; Xu et al., 2018a, 2018b). SLIT2 and SLIT3 ligand overexpression reduces the granulosa cell proliferation as well as decreases the mRNA and protein expression levels of FSHR, GDF9, StAR protein, and CYP11A1 in the granulosa cells (Xu et al., 2018a). An inhibitory effect of SLIT ligands on granulosa cell proliferation, differentiation, and follicle selection involves primarily ROBO1 and ROBO2 receptors. In addition, SLIT2 effect in the prehierarchical follicles is mediated by the CDC42-PAKs-ERK1/2 MAPK signaling cascade (Xu et al., 2018a). Additionally, the present data based on high-throughput sequencing technology indicate that epigenetic and genetic mechanisms control ovarian follicles development and selection. Several miRNAs associated with follicle selection or growth were identified (Kang et al., 2013; Wang et al., 2018; Ocłoń and Hrabia, 2021). For example, mRNA and miRNA transcriptome profiling of the granulosa layer cells from geese ovarian follicles indicates that the genes related to junctional adhesion and lipid metabolism and interacting with the miRNAs play a key role in regulating follicle selection (Q. Li et al., 2019). Another numerous factors are identified in the prehierarchical follicles which may mediate follicle growth, differentiation, and selection by autocrine/paracrine fashion. Among them are PGs, growth factors, growth hormone (GH), inhibin, activin, and aquaporin 4.

Development of recruited follicle until ovulation is accompanied not only by enhancement of steroidogenesis process in the granulosa cells, but also by shift from FSHR-dominance to LHR-dominance, increase in the expression of antiapoptotic proteins (the follicle becomes resistant to atresia), and accumulation of huge amount of yolk in the follicle. These events are associated with morphological and functional changes attributed predominantly to the granulosa cells. Final follicle development and maturation are regulated by variety of factors such as pituitary hormones, metabolic status maintaining hormones, and locally produced growth factors (discussed in this chapter).

35.2.5 Vitellogenesis

In egg-laying hen, principal event responsible for the enormous growth of the ovarian follicle, initiated immediately after selection, involves the accumulation of hepatically derived plasma precursor yolk proteins into the oocyte. It is accomplished by increase in follicle vasculature and blood flow. In the domestic hen, within approximately nine days, the follicle weight increases from an average 0.28 g just after selection (pool of 8−12 mm follicles) to 13.5 g several hours before ovulation (34−36 mm F1).

The yolk precursor proteins such as lipoproteins, very low-density lipoprotein (VLDL), and vitellogenin (VTG) are synthesized in the liver in process of vitellogenesis, delivered to the oocyte through the vascular system, "filtered" via the basement membrane, and then moved between the granulosa cells to the perivitelline membrane to access the oocyte. Finally the yolk molecules are taken into the oocyte by receptor mediated endocytosis (Schneider, 2009, 2016) and enzymatically processed into yolk proteins that are deposited in yolk platelets or yolk spheres for future use (Ito et al., 2003). The LR8 yolk receptor, homolog of the mammalian low-density lipoprotein receptor with eight ligand binding domain repeats (Bujo et al., 1994) is an avian specific yolk receptor located on the oocyte plasma membrane. Functional absence of LR8 blocks oocytes from entering into the rapid growth phase (Schneider, 2016).

The rate of yolk molecules accumulation and thereby, facilitation of rapid growth of the preovulatory follicle is affected by communication between the oocyte and cells of the follicular wall. The size of intercellular space also selectively controls the uptake of specific plasma molecules. Prior to follicle selection, the granulosa cells lie close together and tight junctions between them prevent the smooth paracellular transport of yolk macromolecules to the oocyte. The relatively narrow intercellular space of the prehierarchical follicle allows only ferritin and other molecules of similar size to cross. At selection and through after, wide channels appear between the granulosa cells that enable dramatic increase in VTG and VLDL (containing mainly apovitellenin and apolipoprotein B) transportation to the oocyte (Ito et al., 2003). This event results, at least in part, from reduction in occludin, tight junction protein expression. In small white follicles, occludin is demonstrated at the apical region of granulosa cells, while no distinct localization of occludin is noted in larger follicles (Schuster et al., 2004). Expression of occludin mRNA is highest in small follicles, and decreases with increasing follicle size. Moreover, occludin mRNA abundance is higher in the germinal disc region of the granulosa layer than the nongerminal disc region. In granulosa cells of 3−5 mm follicles, occludin expression of ad libitum fed hens is lower compared to restricted fed broiler breeder hens concomitantly with no changes in LR8 mRNA abundance. As regulators of occludin expression, the FSH, epidermal growth factor, and activin A and B were found (Schuster et al., 2004; Stephens and Johnson, 2017).

After being taken into the oocytes, VTG and VLDL are cleaved into their constituents: lipovitellins and phosvitin, and triglycerides, cholesterol and phospholipids, respectively. This process is realized by the action of numerous proteases including cathepsin D and cathepsin E-A-like, as well as antiproteases (protease inhibitors) present in the egg yolk or the perivitelline membrane (Retzek et al., 1992;

Bourin et al., 2012; Zheng et al., 2018). In birds, three VTG genes are known: VTG1, VTG2, and VTG3, classified also as VTGAB1, VTGAB2, and VTGAB3, respectively (Finn, 2007). In the liver of the egg-laying hen, the ratio of RNA molecules per cell, encoding VTG1, VTG2, and VTG3 is 0.33:1:0.1, respectively (Evans et al., 1988).

Vitellogenesis (synthesis and deposition of the yolk precursors) is a hormone-dependent process. Of the stimulators of yolk synthesis, i.e., gonadotropins, estrogen, and androgen, the estrogen, mainly by its ERα, exerts the highest potency in transcription of egg yolk precursor genes. Other hormones may modify the response. GH is proposed as a modulator of the estrogen-potentiated vitellogenesis in the pigeon (Harvey et al., 1978) and the estrogen-induced VTG2 and very low-density apolipoprotein II (apoVLDLII) mRNA expression in the chicken liver (Socha and Hrabia, 2019). The plasma levels of VLDL and VTG increase dramatically at the onset of egg laying in hens, while decrease during a pause in laying. Examples of VTG2 and apoVLDLII mRNA expression in the laying hen liver affected by different factors are presented in Figure 35.4.

Interestingly, yolk of the large preovulatory yellow follicle of chicken contains approximately 48% of water, i.e., 9.2 g (Etches, 1996). Such huge accumulation of water requires its rapid movement. Recently, it was revealed that aquaporin 4 (integral plasma membrane protein) may facilitate water passage to the yolk in the interior of follicle (Nowak et al., 2017).

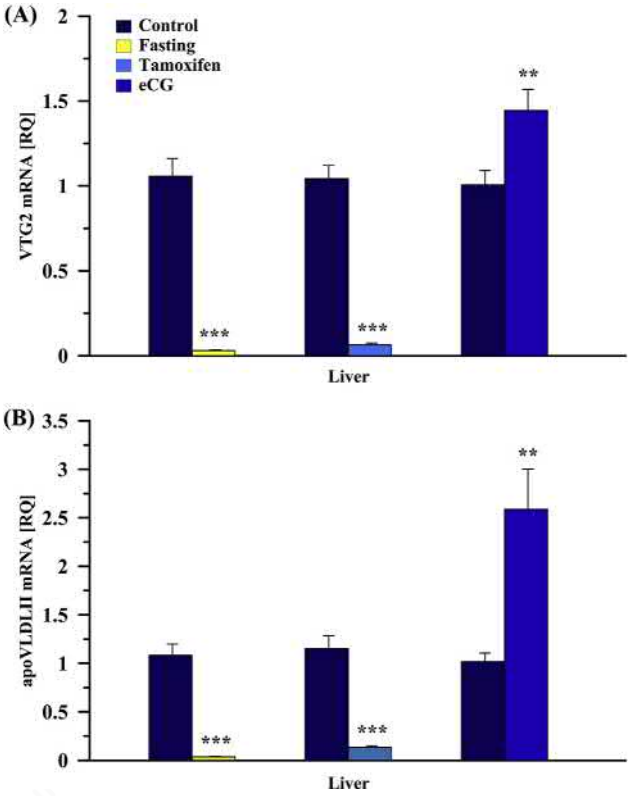

FIGURE 35.4 Expression of vitellogenin 2 (VTG2) (A) and very low-density apolipoprotein II (apoVLDLII) (B) mRNA in the chicken liver at different physiological states. The liver tissue was collected from egg laying hens and treated with a proper vehicle (Control), during a pause in laying induced by 5 days of food deprivation (Fasted), during a pause in laying induced by tamoxifen treatment for 8 days (6 mg/kg b.w.; Tamoxifen), or eCG-primed hens for 7 days (75 I.U./kg b.w.; eCG). Each value represents the mean of relative quantity (RQ) ± standard error of the mean from six or eight chickens normalized to 18S rRNA and standardized to control expression. $^{**}P < .01$, $^{***}P < .001$ - compared with the control.

35.2.6 Oocyte maturation and ovulation

The avian oocyte consists of a large amount of yolk and a structure called the germinal disc. The germinal disc is a white plaque (three to four mm in diameter) on the top of the oocyte and occupies about 1% of cell volume. It contains the nucleus and 99% of cytoplasmic organelles such as elongated membrane-bound vesicles, mitochondria, and glycogen granules. The oocyte is demarcated by the perivitelline membrane, and the overlying granulosa layer. Inside the oocyte, the perivitelline membrane is covered by extra-embryonic RNA. Several hours before ovulation, the junction between the oocyte surface and the granulosa cells projections dissociate with an accumulation of fluids in the perivitelline space. By 1 h before ovulation, the oocyte and the granulosa cells are disconnected. At this time, the oocyte maturation occurs, including the germinal vehicle break down, formation of the first and second maturation spindle just beneath the surface of the oocyte, and the release of the first polar body in the perivitelline space (Yoshimura et al., 1993b, 1993c).

The oocyte maturation is primarily under influence of LH that reaches the highest plasma concentration six–four h before ovulation. Its role has been confirmed in in vivo studies. Namely, injection of quail with LH induced the oocyte maturation (Yoshimura et al., 1993c) and premature ovulation of F1 follicle (Hrabia et al., 2003a). The preovulatory LH surge occurs coincidently with elevated secretion of progesterone mainly by F1 follicle. If the secretion of progesterone is insufficient, the LH surge with potency to induce ovulation does not occur. Participation of the maturation promoting factor and a homolog of fission yeast cdc2+ gene product (p34cdc2) was also suggested in quail oocyte maturation. Marked increase in kinase activity of p34cdc2 in the oocyte germinal disc at maturation was noted (Mori et al., 1991). More recently, overexpression of 250 genes in the germinal disc of the hen oocyte was revealed. Among them, 21 genes were suggested to be involved in different stages of final follicular maturation and eight genes (btg4, chkmos, wee, zpA, dazL, cvh, zar1, and ktfn) were indicated as a potential candidates driving maturation of the oocyte (Elis et al., 2008).

The process of ovulation includes a series of biochemical and morphological events occurring in parallel within the preovulatory F1 follicle, which lead to its rupture along stigma and release of the mature oocyte (Figure 35.5A-B). In the stigma area of follicle, the blood vessels except for capillaries are not supplied. Just before ovulation the theca externa, which comprises most of the follicular wall at the stigma region, becomes progressively thinner as a result of disintegration of the ECM elements, among others the collagenous fibers into individual fibrils and degradation of glycosaminoglycans. The granulosa layer and theca interna disappear completely in the middle part of the stigma (Yoshimura and Koga, 1982; Jackson et al., 1991). The stigma region becomes fragile and easy to be ruptured by the smooth muscle contraction of the follicle wall. The comprehensive alterations in the ECM, restricted to the stigma area, are realized by a cascade of proteolytic processes mediated by various proteases with different substrate specificities. Growing evidence has established that these events are largely controlled by the matrix metalloproteinases (MMPs). They can specifically degrade ECM components, including collagens, gelatins, elastin, laminin, and plasminogen, as well as activate other MMPs. First, Nakajo et al. (1973) suggested that proteolytic enzymes such as collagenase participate in follicular rupture in the chicken ovary. A marked increase in collagenase, acid and neutral protease activities was further observed immediately after ovulation in POF1 follicle (Tojo et al., 1982). The presence of several MMPs were demonstrated in the basal lamina of chicken preovulatory follicles indicating their involvement in the breakdown of this membrane required to release the oocyte during ovulation (Asem et al., 2000). More recently, increase in the expression of MMP-2, MMP-3, MMP-9, MMP-10, and MMP-13 mRNA and/or protein as well as increase in gelatinase (MMP-2 and MMP-9) activities in the chicken ovarian follicle along with follicular maturation has been revealed (Leśniak and Hrabia, 2012; Zhu et al., 2014; Hrabia et al., 2019; Wolak and Hrabia, 2020). Participation of gelatinases, demonstrated primarily in the theca layer of the follicular wall, in follicular rupture was further supported by the higher expression of both proteases 3 h compared to 22 h before ovulation as well as their markedly elevated activities in the F1 follicle (Hrabia et al., 2019). Plasminogen activators (PAs) have also been proposed to play an important role in the control of follicular rapture during the ovulation. An increase in PA activity and decrease in its inhibitor activity during follicular development, with the peak PA value in the largest preovulatory follicle (F1) 12−14 h before expected time of ovulation were observed (Politis et al., 1990). The dramatic increase in PA activity specifically in the stigma region of the F1 follicle, which remained high until ovulation, was additionally related to PA involvement in the ovulatory process (Jackson et al., 1993).

Ovulation is orchestrated by pituitary-derived LH and locally produced factors. It is well established that ovulation is induced by preovulatory release of LH, which achieves two−three fold increase of basal level 6−4 h before ovulation (Johnson and van Tienhoven, 1980; reviewed in Johnson, 1990; Rangel and Gutierrez, 2014). This gonadotropin might initiate follicular production of enzyme (s) capable of degrading the ECM components of the follicular wall, and that the progressive decomposition of the wall results in its rapture. Progesterone stimulates preovulatory surge of LH via positive feedback. Its increase prior to ovulation coincidently with LH peak is proceeded by plasma surges of estradiol and testosterone. Estradiol

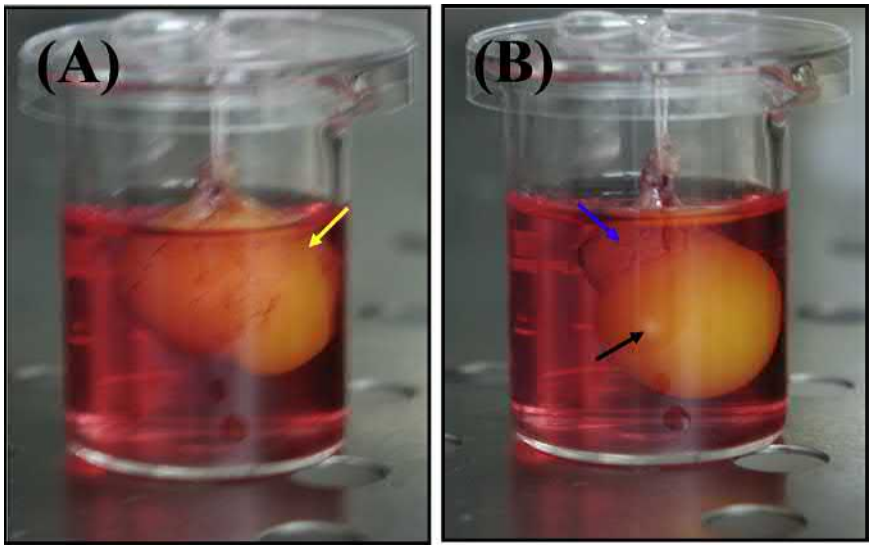

FIGURE 35.5 In vitro ovulation of F1 follicle. (A) Onset of ovulation process along stigma (*yellow arrow*). (B) Final stage of ovulation. *Blue arrow* indicates the postovulatory follicle, and *black arrow* indicates germinal disc.

"primes" the hypothalamo-pituitary axis and facilitates the progesterone-stimulated LH release. Testosterone which peak concentration occurs 10−6 h before ovulation promotes progesterone production needed for the occurrence of the preovulatory search of progesterone and LH. The stimulatory action of testosterone on progesterone synthesis by the largest preovulatory follicles is mediated by promotion of CYP11A1 and StAR mRNA expression as well as LH receptor mRNA expression (Rangel and Gutierrez, 2014). Treatment of laying hens with testosterone antagonist inhibits preovulatory surges of both progesterone and LH and ovulation (Rangel et al., 2006).

It is interesting to note that ovulation resembles the inflammatory process (Espey, 1980). Thus, inflammatory mediators such as biogenic amines and PGs also participate in the regulation of the ovulatory events. Histamine, which concentration gradually increases as follicle development progress toward ovulation (from F4 to F1), followed by a significant decrease in POF1 follicle, was suggested to play a role in the ovulatory process, as a mediator influencing the hemodynamics of blood vessels and consequently modifying blood flow through the follicle (Paczoska-Eliasiewicz and Rząsa, 1998; Hrabia et al., 2005). Moreover, histamine stimulates progesterone secretion by the granulosa cells of F1 follicle being just before ovulation (Paczoska-Eliasiewicz and Rzasa, 1999). Other biogenic amine, serotonin, exhibits similar profile of content to histamine, with the highest level 0.5 h prior to ovulation, however, it does not alter blood flow within the wall of the largest preovulatory follicle (Paczoska-Eliasiewicz and Rząsa, 1995; Rząsa et al., 2008). Catecholamines (dopamine, norepinephrine, and epinephrine) are localized primarily in the theca layer with only small amounts present in the granulosa layer. The increase in norepinephrine and epinephrine contents in the theca layer of the F1 follicle before ovulation serves them as the mediators of ovulation (Bahr et al., 1986). The granulosa cells of the largest preovulatory follicle are the major intraovarian source of PGs, and production of PGF2α is associated with the preovulatory surges of LH and steroid hormones (Etches et al., 1990). Thus, their role may be related to ovulatory processes mediation, including the increase in contraction of smooth muscles in the follicular wall to facilitate the rapture of the stigma as well as stimulation both cell-associated and secreted PA activity (Tilly and Johnson., 1987). Furthermore, PGs attract macrophages and stimulate MMP release by cells of the sow corpus luteum (Pitzel et al., 2000), therefore, similar role is plausible in the hen preovulatory follicle.

35.2.7 Postovulatory follicles

Unlike in mammals, the follicle in birds after ovulation rapidly terminates the metabolic activity and fails to form a functional corpus luteum. The structure remaining after release of the oocyte is a POF containing theca layers (internal and external) and a granulosa layer (Figure 35.6). The residual POF immediately shrinks and due to this, the wall becomes thickened, and the granulosa increases to several cells in thickness. Moreover, changes that occur in the wall of regressing POF involve cellular hypertrophy associated with accumulation of lipid, the disappearance of the basement membrane, and translocation of the theca interna and granulosa cells toward the follicle lumen. In POF3, the mass of cells contains both extra- and intracellular accumulation of lipids. During the later stages of regression, the luminal mass becomes invaded by capillaries and nerve fibers (for more details see Hodges, 1974; Gilbert, 1979; Lin et al., 2018). Regression of the granulosa layer begins immediately after F1 ovulation and is entirely completed in POF4. Degeneration of the theca layers progress slowly, and their complete resorption is observed in POF5-POF6 (Hrabia et al., 2018; Lin et al., 2018). In the chicken, the follicle undergoes tremendous regression within approximately 6−10 days after the extrusion of the oocyte.

To date it has been established that the regression of chicken POFs similarly to follicle atresia occur via the apoptotic cell death (Tilly et al., 1991b; Sundaresan et al., 2008a; Hrabia et al., 2018). Along with the progressive regression of POF, a gradual increase in the number of apoptotic cells is observed. It has been established that both the external and internal pathways of apoptosis are engaged in apoptotic cell death in POFs, involving the major mediators of these pathways, i.e., caspase 2 and 8 and caspase 9, respectively. In addition, proinflammatory caspase 1 and executive caspase 3 also mediate this process. The greatest activity of caspases is observed in POF3 (Sundaresan et al., 2008a; Hrabia et al., 2018). The intensity of cell apoptosis in POF correlated with the increase in the amount of nitric oxide (NO) and NO synthase, therefore, indicating the involvement of NO in the regulation of apoptosis (Sundaresan et al., 2007).

Recent report demonstrated that in POF regression, especially its theca cells, also autophagy is involved. A dramatic increase in the number of major autophagy markers, i.e., Beclin1 and microtubule-associated proteins 1A/1B light chain 3B (LC3B) was observed along with progressive regression of the theca layers (Lin et al., 2018).

Regression of POF tissues concerns not only changes in cell morphology and function but also turnover of the ECM architecture and components. Participation of MMPs and their tissue inhibitors (TIMPs) in this event was strongly suggested. Degree of follicle regression-dependent changes and tissue-dependent differences in the expression of selected MMPs and TIMPs, and an increase in MMP-2 and MMP-9 activity were observed concomitantly with the degeneration of POF through apoptosis (Hrabia et al., 2018).

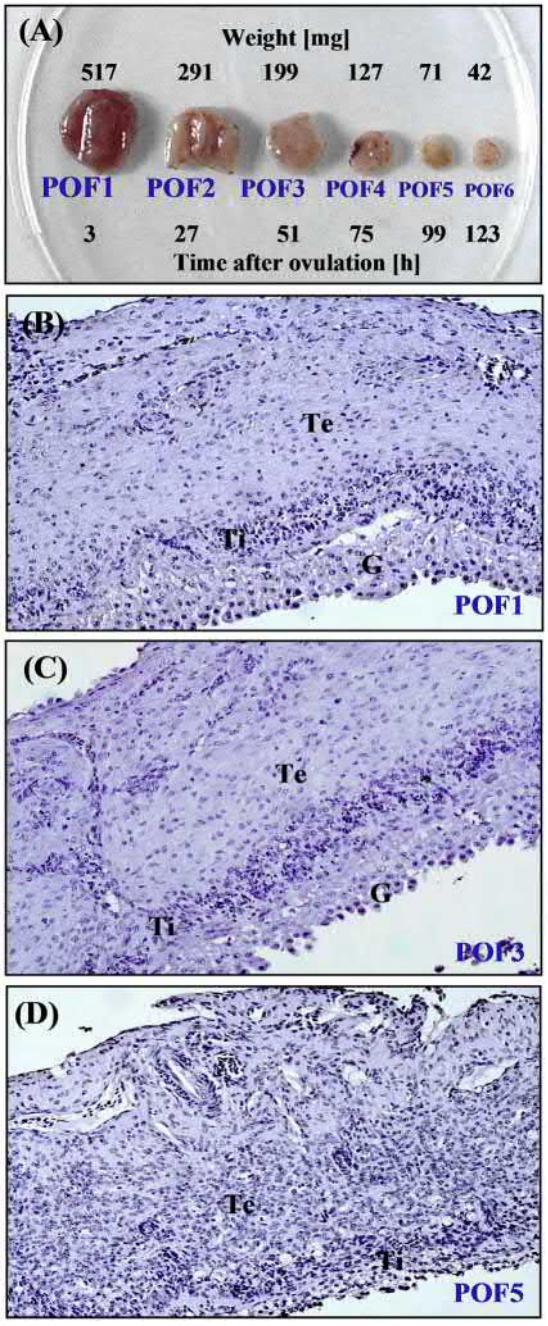

FIGURE 35.6 (A) Morphology and average weight of postovulatory follicles (POFs) in the hen ovary. (B–D) Histoarchitecture (hematoxylin staining) of the representative POFs. Note that the granulosa layer (G) in the POF1 increases to several cells in thickness due to immediate follicle wall shrink after ovulation. In the POF3, degeneration of the granulosa layer and basement membrane (BM) is advanced. In POF5, distinction among layers is very difficult due to the disappearance of the basement membrane, complete degeneration of granulosa layer, and translocation of the cells of theca interna layer toward the follicle lumen.

The contribution of the immune system to the degradation of POF is also important, as the regression of POFs resembles inflammation. POF regression is accompanied by the accumulation of macrophages, lymphocytes, and heterophiles compared to the F1 follicle (Barua et al., 1998; Sundaresan et al., 2008b). It was assumed that mainly macrophages may play a role in the POF regression by the removal of apoptotic cellular elements (Barua et al., 1998; Sundaresan et al., 2008b) and are a source of cytokines and chemokines. Increase in mRNA expression of selected cytokines (IL-1β, IL-6, IL-10, and TGF-β2) and chemokines (chCXCLi2, chCCLi2, chCCLi4, and chCCLi7) in POF as its regression progresses is observed (Sundaresan et al., 2008b). Cytokines are known activators of collagenases, gelatinase, and proteinases in various tissues. Macrophages are also a potential source of MMPs (Duncan, 2000). In turn, MMPs in addition to PG F2α may be factors enabling the influx of macrophages into POF tissues (Barua et al., 1998).

POF gradually loses steroidogenic activity. The greatest decrease in progesterone concentration in the POF is observed within the first 24 h after ovulation, which correlates with a decrease in the activity of 3β-hydroxysteroid dehydrogenase/Δ5-Δ4-isomerase (3β-HSD) (Dick et al., 1978; Lin et al., 2018). During the first 15 h after ovulation, the enzyme activity decreases drastically and then gradually. The concentration of estrogen in POF gradually decreases during its regression (Armstrong et al., 1977; Dick et al., 1978). In addition to the synthesis of steroid hormones, POFs are also a source of relaxin, whose precise role is unknown (Brackett et al., 1997), and are an important tissue for PG synthesis. The POF1 together with the F1 is the largest source of PGF2α in the chicken ovary (Saito et al., 1987; Hales et al., 2008). It has been observed that the secretory activity of POFs has an effect on egg laying time. Particularly important function was attributed to the granulosa layer of POF1. Damage or removal of this layer resulted in oviposition delay (Gilbert et al., 1978).

35.2.8 Ovarian steroidogenesis

Ovary is a main side of sex steroid synthesis (Figure 35.7). The cells involved in steroid production are the granulosa cells, thecal interstitial cells, and aromatase cells in the theca externa. The first step in steroid synthesis is transport of cholesterol from the outer to the inner mitochondrial membrane by the StAR protein, the rate-limiting factor in steroid production in all steroidogenic tissues. Expression of StAR protein in granulosa cells of prehierarchical follicles is very low. It elevates during follicular growth reaching the highest level in the F1 preovulatory follicle (Sechman et al., 2011, 2014; review in Johnson, 2015a, 2015b). Biosynthesis of steroids starts from conversion of cholesterol to pregnenolone catalyzed by the P450scc enzyme (CYP11A1) localized in the inner mitochondrial membrane. Subsequent synthesis of sex steroids can occur through two pathways: Δ4 and Δ5. In Δ4 pathway,

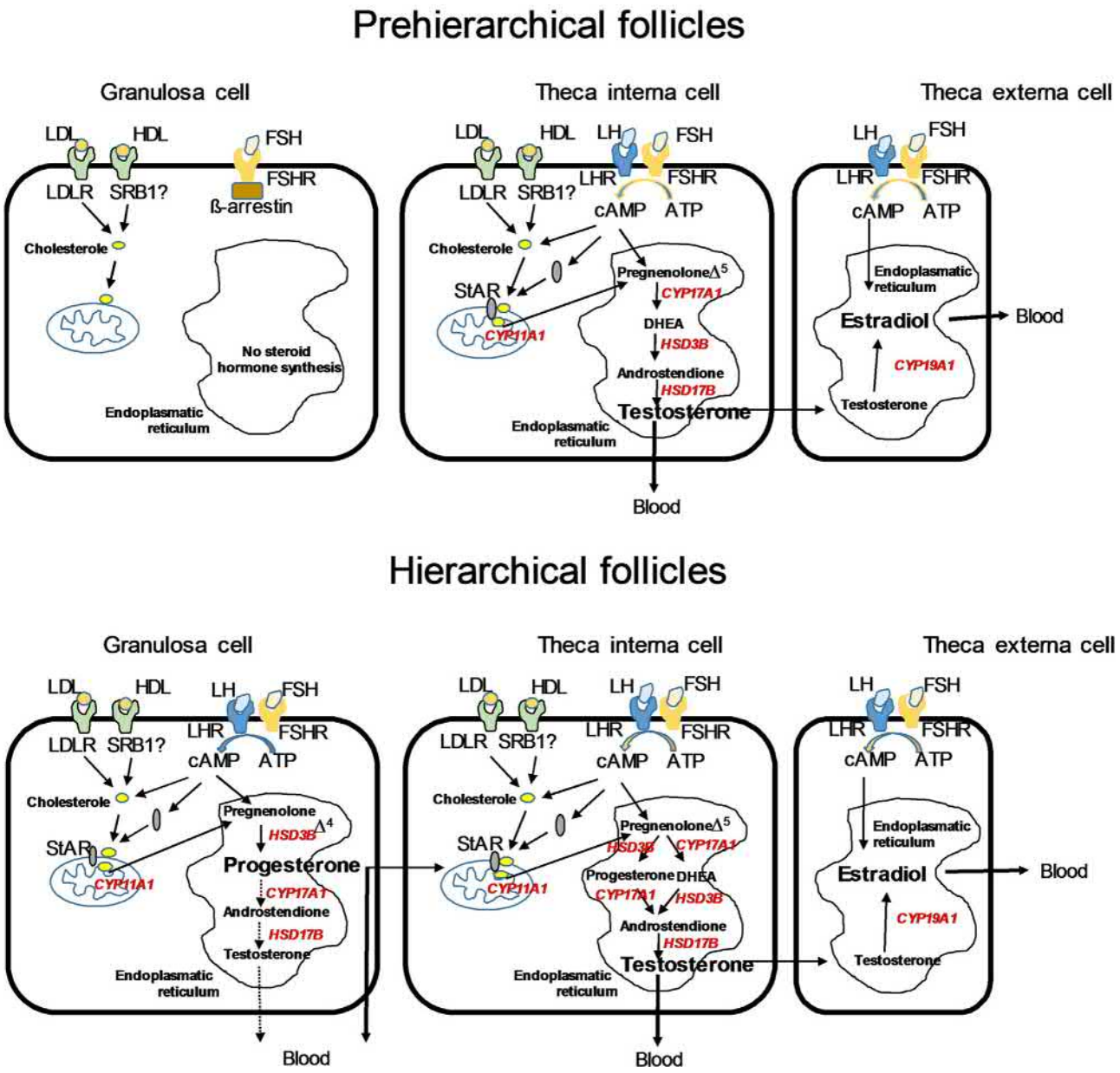

FIGURE 35.7 Diagrammatic summary of steroidogenesis in the avian ovary. Low-density lipoproteins (LDL) and high-density lipoproteins (HDL) deliver cholesterol. LDLR, LDL receptor; SRB1, receptor for HDL (it is not clear if the avian follicular cells express this receptor); StAR, steroidogenic acute regulatory protein; CYP11A1, mitochondrial cytochrome P450 cholesterol side-chain cleavage enzyme (P450scc) gene; CYP17A1, 17α-hydroxylase/17,20-lyase (P450c17) gene; HSD3β, 3β-hydroxysteroid dehydrogenase/Δ5-Δ4-isomerase (3β-HSD) gene; HSD17β, 17β-hydroxysteroid dehydrogenase (17β-HSD) gene; CYP19A1, aromatase (P450aroma) gene. LHR/FSHR, receptors for luteinizing hormone and follicular stimulating hormone, respectively. ATP, adenosine triphosphate; cAMP, cyclic adenosine monophosphate. *Thick arrow* indicates the predominant steroid released to the blood. See text for additional details. *Diagram prepared by Dr A. Sechman.*

pregnenolone is converted to progesterone and then to androstenedione. In Δ5 pathway, pregnenolone is changed to dehydroepiandrosterone (DHEA) and then to androstenedione. Androstenedione is next converted to testosterone which is aromatized to estradiol. Both pathways are functional in granulosa and theca cells of chicken ovarian follicles, but the granulosa layer preferentially metabolizes steroids by the Δ4 pathway, whereas the theca layer preferentially metabolizes steroids by the Δ5 pathway. Transformation of pregnenolone to progesterone or DHEA to androstenedione is catalyzed by 3β-hydroxysteroid dehydrogenase/Δ5-Δ4-isomerase (3β-HSD/HSD3β) bound to endoplasmic reticulum, which is the enzyme complex consisting of Δ5-3β-hydroxysteroid dehydrogenase and Δ5-3-oxosteroid isomerase. Change of pregnenolone to DHEA or progesterone to androstenedione is catalyzed

by17α-hydroxylase/17,20-lyase (P450c17/CYP17A1). In turn, conversion of androstenedione to testosterone and then testosterone to estradiol is catalyzed by 17β-hydroxysteroid dehydrogenase (17β-HSD/HSD17β) and aromatase (P450aroma/CYP19A1), respectively. Aromatase is an enzyme complex consisting of cytochrome P450 aromatase and NADPH-cytochrome P450 reductase (reviewed in Johnson, 1990, 2015b; Sechman, 2013).

Steroidogenesis in the avian ovary starts at early stage of embryogenesis. Androgens and estrogen are detected on measurable levels in undifferentiated gonads of both sexes (3−4 day of incubation). Progestins, androgens, and estrogens are further found in differentiating ovaries by days six to eight of embryogenesis. At this time of gonadal differentiation, androgen production by the right ovary is greater than that of the left ovary. By day 12 of incubation, the regressing right ovary synthesizes estradiol and testosterone in similar amounts to the left ovary, and then these steroids production decreases. Moreover, the ratio of estradiol-to-testosterone in the right ovary decreases concomitantly with its regression, while in the left ovary greatly increases throughout embryonic development. At 1 day posthatch, before the formation of primordial follicles, two types of steroidogenic cells producing testosterone and estradiol, respectively, are identified in the left ovary (reviewed in Johnson, 1990; Saito and Shimada, 2001). Steroid production occurs coincidently with gene expression of appropriate enzymes involved in synthesis of particular hormones, i.e., CYP11A1, HSD3β, CYP17A1, HSD17β, and CYP19A1. Expression of CYP17A1 mRNA in female gonad is first detected around day five of embryogenesis, CYP19A1 at day six, and CYP11A1 and HSD3β on day seven of incubation. P450c17 enzyme activity in the ovary increases from day 9 to 11 of incubation and remains unchanged between days 11 and 15 of incubation (reviewed in Saito and Shimada, 2001; Hirst et al., 2018).

Further development of the ovarian follicle is accompanied by gradual changes in their steroidogenic activity. The amount and type of steroid synthesized depends on the stage of follicle development, sensitivity to gonadotropins, and locally produced factors. In prehierarchical follicles (up to 6−8 mm), the granulosa layer cells are mitotically active, undifferentiated, and steroidogenically incompetent. In contrary, the theca of prehierarchical follicles is the source of ovarian estradiol, and in lesser extend androgen, produced predominantly by the Δ5 pathway (reviewed in Johnson, 1990, 2015b; Sechman, 2013). In hierarchical follicles, both granulosa and theca layers are steroidogenically active. At follicle selection into preovulatory hierarchy, the cells of the granulosa layer begin to express CYP11A1 mRNA and progesterone production under LH-stimulation. During preovulatory growth of the yellow follicles, the synthesis of progesterone gradually increases. The largest F1 follicle becomes the major source of progesterone in the circulation. Yellow hierarchical follicles are main source of testosterone in the avian ovary. Along with these follicles development, synthesis of testosterone in the theca interna gradually increases; the F3 follicle secretes its greatest amount, while the F1 loses ability to convert progesterone to testosterone. In contrary, the theca externa of the hierarchical follicles, due to a gradual decrease in aromatase activity, reduces estradiol synthesis and secretion (Bahr et al., 1984; Robinson and Etches, 1986; Porter et al., 1989; Kato et al., 1995; Lee et al., 1998; Sechman et al., 2014; review in Rangel and Gutierrez, 2014; Johnson, 1990, 2015b). Nevertheless, in laying hens, yellow hierarchical follicles are equally an important source of estradiol as stroma and prehierarchical follicles (Proszkowiec-Weglarz et al., 2005).

In chicken embryos, plasma testosterone and estradiol concentrations increase between days 9 and 15 of incubation. Progesterone concentration in blood plasma starts to elevate from day 10 toward the hatching (day 20) and reaches peak levels several days following hatch. Thereafter, progesterone levels decline and remain low until the prepubertal period. Plasma levels of testosterone and estradiol do not fluctuate significantly during the first month posthatch (reviewed in Johnson, 1990). During sexual maturation, a progressive increase in plasma concentrations of estradiol, produced by the ovarian stroma and the theca layer of white follicles, 3 to 1 week before puberty (onset of egg lay) is observed. Subsequently, the estradiol plasma levels decrease. Plasma testosterone concentration reaches peak at 3 week prior to puberty, and then decreases 1 week before the first oviposition, again increasing at sexual maturity. Progesterone, produced by the granulosa layer of large, yellow hierarchical follicles, increases sharply just prior to the first ovulation, afterward remains unchanged (Sechman et al., 2000; Paczoska-Eliasiewicz et al., 2006). In the laying hen, during the ovulatory cycle, lasting from 24 to 26 h in the domestic chicken, the plasma concentration of estradiol and testosterone increases between 9 and 8 h before ovulation, while the level of progesterone increases around 7 h before ovulation. Elevated levels of these hormones remain several hours (reviewed in Johnson, 1990, 2015b; Etches, 1996; Paczoska-Eliasiewicz et al., 1998; Rangel and Gutierrez, 2014).

35.2.9 Control of ovarian follicle development and functions

Ovarian development and functions are under control of coordinated actions of hypothalamic gonadotopin-releasing and -inhibiting hormones (GnRH and GnIH; Sharp et al., 1990; Tsutsui et al., 2000; Bentley et al., 2008; Maddineni et al., 2008; Bédécarrats et al., 2009, 2016), pituitary gonadotropins (LH and FSH), and other endocrine and locally

produced factors such as prolactin (PRL; Zadworny et al., 1989; Hrabia et al., 2004b; Hu and Zadworny, 2017; Hu et al., 2017a, 2017b), GH (Hrabia, 2015; Ahumada-Solórzano et al., 2016; Socha and Hrabia, 2019), thyroid hormones (Sechman, 2013), ghrelin (Sirotkin et al., 2006, 2016, 2017; Sirotkin and Grossmann, 2007a), growth factors (Onagbesan et al., 2009; Ahumada-Solórzano et al., 2016), adipokines (Ramachandran et al., 2013; Diot et al., 2015; Mellouk et al., 2018; Estienne et al., 2019; Hadley et al., 2020), calcitonin (Krzysik-Walker et al., 2007), retinoids (Pawłowska et al., 2008), leptin (Paczoska-Eliasiewicz et al., 2006; Sirotkin and Grossmann, 2007b), kisspeptin-10 (Xiao et al., 2011), PGs (Jin et al., 2006; Jia et al., 2010), parathyroid hormone-like hormone (Guo et al., 2019), and ovarian steroids (Camacho-Arroyo et al., 2007; Rząsa et al., 2009; Rangel and Gutierrez, 2014). Role of these factors is related primarily to direct or indirect regulation of ovarian cell proliferation, differentiation, apoptosis, and steroidogenesis. Some of the most important ovarian regulators are presented below.

35.2.9.1 Gonadotropin-inhibitory hormone

Gonadotropin-inhibitory hormone (GnIH) is a neuropeptide produced by and released from the hypothalamus. Its physiological effect is realized by specific receptor (GnIHR), a member of the G-protein coupled receptor family which couples to G(αi) and, upon activation inhibits adenylyl cyclase activity, consequently reducing intracellular cAMP levels. Main GnIH function is an inhibition of hypothalamic gonadotropin-releasing hormone (GnRH-I and GnRH-II) release and the synthesis and secretion of pituitary gonadotropins (Tsutsui et al., 2000; Bédécarrats et al., 2009, 2016). Presence of GnIH and its receptor in the ovary indicates that this neuropeptide influences ovarian follicle maturation, at least in part, in an autocrine/paracrine manner as well (Bentley et al., 2008). Within the chicken ovary, GnIHR mRNA is detected in both theca and granulosa cells. Greater GnIHR mRNA expression is in the theca layer of prehierarchical follicles compared with that of preovulatory follicles. GnIHR mRNA level is lower in the ovaries of sexually mature hens than in sexually immature chickens. Therefore, there is suggestion that GnIH exerts an inhibitory role in ovarian follicle development (Maddineni et al., 2008). The expression of GnIHR seems to be regulated by steroid hormones since treatment of sexually immature chickens with estradiol and/or progesterone caused a decrease in the GnIH mRNA abundance (Maddineni et al., 2008).

35.2.9.2 Gonadotropins (luteinizing hormone and follicle-stimulating hormone)

Key hormones driven ovarian follicle development and function are gonadotropins. Their release is under control of releasing and inhibitory hormones produced in the hypothalamus. The GnRH stimulates gonadotropin secretion (Sharp et al., 1990), while GnIH blocks LH an FSH release (Tsutsui et al., 2000). Both LH and FSH are responsible for follicular growth and development, while only LH induces ovulation.

In chickens, the LHβ subunit gene is expressed in the pituitary since day four of embryonic development, and LHβ immunoreactivity appears in the anterior pituitary gland on day eight of incubation (Maseki et al., 2004). In the female pituitary gland, the expression of LHβ mRNA increases on day one after hatching in comparison to embryonic day 11 or 17 (Grzegorzewska et al., 2009). The FSHβ gene is expressed in the chicken pituitary from day seven, and immunopositive reaction is detectable from day eight of incubation (Maseki et al., 2004). In the female embryo, the abundance of FSHβ transcript increases between days 11 and 17 of incubation (Grzegorzewska et al., 2009). Plasma LH in females is detected on day 10 of incubation (Tanabe et al., 1986) and increases across embryonic development reaching a plateau near hatching. Serum LH shows a maximum on day 19 of incubation (Gonzalez et al., 1987), while FSH remained low throughout the incubation period (Rombauts et al., 1993). In chickens, a prepubertal rise in plasma LH occurring 5−3 weeks prior to egg laying (Sharp, 1975; Wiliams and Sharp, 1977; Wiliams et al., 1986; Paczoska-Eliasiewicz et al., 2006) is suppressed by the increasing concentrations of estradiol 3−1 week before maturation. Then, progesterone, increasing sharply just prior to the first ovulation, triggers the preovulatory LH surge (Paczoska-Eliasiewicz et al., 2006). In addition, in immature hens, a pronounced increase in LH has been observed at the onset of darkness (Wilson et al., 1983). Comparatively less is known about circulating concentrations of FSH. In laying chickens, plasma FSH concentrations are relatively constant during ovulatory cycle, except an increase 15−12 h before ovulation (Scanes et al., 1977a; Krishnan et al., 1993). In turn, plasma LH concentrations peak 6−4 h before ovulation (Johnson and van Tienhoven, 1980; reviewed in Johnson, 1990; Rangel and Gutierrez, 2014). Role of this preovulatory LH surge is to induce ovulation (as discussed in this chapter). Less pronounced peak of LH is also noted 14−11 h prior to ovulation; however, its role is not elucidated. In addition to ovulation-related increase in LH levels, diurnal rhythm of LH secretion in the laying hen with increase in plasma concentration of LH occurring at the onset of darkness was revealed. This increase in LH may serve to time, but is not sufficient to initiate events that culminate in the preovulatory surge of LH (Wilson et al., 1983).

Gonadal expression of FSH and LH receptor mRNA (FSHR and LHR) is detected on day four of incubation in both sexes. Then, FSHR mRNA in the chicken ovary increases between days 11 and 17 of embryonic

development. There are no significant changes in LHR transcript levels in the second half of embryogenesis. Positive correlation between the ovarian FSHR mRNA expression and pituitary FSHβ transcript level indicates the crucial role of FSH in the ovarian development (Grzegorzewska et al., 2009). FSH stimulates cell proliferation and sex steroid synthesis in the left ovary (Pedernera et al., 1999; Velazquez et al., 1997) by stimulation of aromatase and 3β-HSD activity (Gómez et al., 2001). LH promotes estradiol synthesis and secretion from the left ovary in vivo (Teng et al., 1977, 1982; Woods et al., 1981) and in vitro (Gonzalez et al., 1987). LH treatment during embryonic development inhibits oogonia proliferation and induces meiotic prophase and follicle formation in the ovaries of newly hatched chicks (Gonzalez-Moran, 2007). Prepubertal changes of FSHR and LHR demonstrated in the duck ovary indicate that developing ovary is highly responsive to the FSH during the earlier stage, but when approaching the onset of sexual maturation, the ovary is likely more responsive to LH (Ni et al., 2007). The expression of FSHR and LHR genes changes according to the follicle development status. FSHR are present in both theca and granulosa layers of follicle at all developmental stages. The greatest abundance of FSHR around follicle recruitment to the preovulatory hierarchy, decreases along with follicle maturation, and is lowest in atretic follicles (You et al., 1996; Zhang et al., 1997). In contrast, LHR mRNA expression occurs in the theca cells of prehierarchical and hierarchical follicles, while within the granulosa layer is detected only after follicle selection in response to FSH and possibly VIP. Thus, revealed increase in steroid release by whole prehierarchical follicles in response to LH is attributed to the theca layer (Sechman et al., 2016, 2020). In fast growing preovulatory follicles, LHR expression in the theca layer decreases, while in the granulosa layer increases along with follicle maturation. The highest LHR expression is in the F1 follicle destined to ovulation (Zhang et al., 1997). Consequently, LHR mediates LH-stimulated progesterone, and to a lesser extent androgen, synthesis by granulosa cells in the preovulatory follicle.

35.2.9.3 Ovarian steroids

Ovarian steroids are involved in the regulation of variety of reproductive processes, including the local regulation of the ovarian development and function by autocrine/paracrine manner. Progesterone, androgen, and estrogen effects are mediated by their intracellular and membrane receptors. The first ones belong to a superfamily of ligand-activated transcription factors that control gene expression by interacting with DNA-specific sequences called hormone-responsive elements, while the latter ones are transmembrane proteins coupled to G proteins that induce changes in second messenger cascades.

35.2.9.3.1 Progesterone

Progesterone receptors (PRs) are present at all levels of the hypothalamo-pituitary-ovarian axis, in both the embryo and adult chickens. Two isoforms of nuclear PRs are expressed in birds as a product of one gene: PR-A and PR-B. They regulate different gene and exert different functions. Responsiveness to progesterone depends on the ration of PR-A and PR-B expression. Their abundance and ratio depends on the tissue and reproductive state, among others sexual maturity and ovulation-oviposition cycle (reviewed in Camacho-Arroyo et al., 2007). The role of progesterone is related primarily to ovulation process. Serum progesterone and LH preovulatory rises have a positive feedback (Lagüe et al., 1975). Progesterone stimulates preovulatory LH surge by induction of GnRH-I release from hypothalamus (Johnson, 1990, 2015b; Rangel et al., 2014). Moreover, progesterone is involved in the regulation of sexual and nesting behaviors, as well as oviduct development and its secretory activity (discussed further in this chapter).

Presence of PR protein, mainly PR-B isoform, in the female gonad is observed from day six of embryonic life. In the immature chicken ovary, PRs are detected in germinal epithelium, thecal, and stromal cells, but not in granulosa cells (Isola et al., 1987; González-Morán and Camacho-Arroyo, 2001). These results indicate that progesterone exerts its effects in the developing ovary by PR-B-mediated signaling. Differential expression of membrane PRγ was also reported in the ovaries of embryonic, newly hatched, and 1-month-old chickens suggesting participation of membrane PR in the progesterone-regulated growth and activity of the left ovary (González-Morán et al., 2013). In the laying hen ovary, PRs are localized in the granulosa layer, theca layers, and germinal epithelium including stigma region of follicles. The presence of PR in specific ovarian tissues strongly indicates that progesterone also locally regulates follicular maturation and ovulation (Yoshimura and Bahr, 1991a). Cell-specific changes in the total abundance PRs and the cellular ratio of PR-A and PR-B are under gonadotropins, estrogens, and progesterone itself control (reviewed in Camacho-Arroyo et al., 2007).

35.2.9.3.2 Androgens

Ovarian tissues are also targets for androgen actions. There is evidence that androgen by androgen receptor (AR)-mediated signaling may be involved in chicken ovarian morphogenesis (González-Morán et al., 2013). Further, AR is localized to the granulosa cells and theca cells at every stage of follicle development, except for the granulosa cells of the primordial and primary follicles (Yoshimura et al., 1993a). Testosterone plays a major role in the ovulatory process (as discussed in this chapter) and promotes progesterone production by the granulosa of the preovulatory follicles, even in absence of LH (Sasanami and Mori, 1999;

Rangel et al., 2006). As presented in vitro, the role of testosterone is related to stimulation of StAR, CYP11A1, and LHR mRNA expression when acts at physiological concentrations (Rangel et al., 2009). On the other hand, earlier results suggested that testosterone suppresses progesterone production by chicken granulosa cells of F1 follicle, acting as a competitive inhibitor of the P450scc (Johnson et al., 1988; Lee and Bahr, 1990).

35.2.9.3.3 Estrogens

The biological, multiple effects of estrogens are mediated mainly via two forms of estrogen receptors, alpha (ERα) and beta (ERβ). In birds, estrogens by ERα, but not ERβ, are thought to have a critical role in sex differentiation of gonads and development of the ovarian cortex in the left gonad. Estrogen receptor mRNA is expressed in both male and female gonads from day 4.5 of incubation; however, is more abundant in the left female gonad than in the right, from at least 7.5 day of chicken development. Moreover, ERα is present in a greater abundance in the ovarian cortex then in the medulla (Andrews et al., 1997; Guioli et al., 2014; González-Morán, 2014; Mattsson and Brunström, 2017; Hirst et al., 2018).

In the mature ovary, the roles of estrogen are related to the control of steroidogenesis, induction of PRs, cell proliferation, and protection against apoptosis. The wall of follicles at all developmental stages expresses ERα and ERβ mRNA, but in contrary to mammals, the main form of ER expressed in the avian ovary is ERα. Higher ER mRNA expression is detected in the granulosa layer then in the theca layer of preovulatory follicles (Hrabia et al., 2004a, 2008a). Immunohistochemically, ERs are localized to the interstitial cells of the theca layer of white follicles as well as to the granulosa cells and interstitial or aromatase cells in the theca layer of preovulatory follicles, suggesting involvement of estrogen in the regulation of steroidogenesis (Yoshimura et al., 1995). Such a role was evidenced. For instance, blockage of ERs by tamoxifen significantly modulates the chicken ovarian steroid production (Rząsa et al., 2009). Involvement of estradiol in mediation of LH-induced progesterone production in vitro by quail granulosa cells was also demonstrated (Sasanami and Mori, 1999). Injection of hypophysectomized birds with estrogen suppresses atresia in yellow follicles (Yoshimura and Tamura, 1986). Moreover, estradiol acts as an inducer of PRs at the hypothalamus, i.e., "primes" the hypothalamus and enhances the progesterone-stimulated LH release before ovulation (Etches, 1990).

In addition, estrogens are key hormones involved in the development of female secondary sexual characteristics, sexual differentiation of the nervous system, sexual behavior, and mobilization of calcium for eggshell formation. Synthesis of a group of egg yolk proteins, including apoVLDLII and VTG, in the liver and egg albumen proteins in the oviduct is also primarily estrogen-stimulated (as discussed in this chapter).

35.2.9.4 Growth hormone

The elevated GH concentration in chicken blood plasma at the onset of lay (Williams et al., 1986), around the time of ovulation (Harvey e al., 1979) as well as an attenuated concentrations of GH in chicken, turkey, and bantam hens with the cessation of egg laying (Scanes et al., 1979; Sharp et al., 1979; Bedrak et al., 1981) indicate the endocrine GH effects on the ovary function.

Growing evidence has demonstrated that the avian ovary is an extrapituitary site of GH synthesis and endocrine, paracrine, and/or autocrine actions. GH mRNA and protein expression occurs in the chicken ovarian follicles, with greater intensity in the granulosa layer and lower in the theca layer (Hrabia et al., 2008b; Ahumada-Solórzano et al., 2012; Luna et al., 2014). The GH receptors are also present in the chicken premature and mature ovary (Heck et al., 2003; Lebedeva et al., 2004; Hrabia et al., 2008b; Ahumada-Solórzano et al., 2012). The intraovarian role of GH is related to the regulation of steroidogenesis, cell apoptosis and proliferation, the modulation of LH action, and folliculogenesis in growing and sexually mature birds (Hrabia, 2015; Ahumada-Solórzano et al., 2016; Socha and Hrabia, 2019). The evidence of increased estradiol secretion by whole chicken prehierarchical ovarian follicles and decreased by yellow preovulatory follicles (Hrabia et al., 2012; Hrabia, 2015) as well as stimulation of progesterone production by whole (Hrabia et al., 2014a) or just the granulosa cells (Ahumada-Solórzano et al., 2012) of yellow follicles were demonstrated. The effect of recombinant chicken GH (chGH) on progesterone secretion is probably due to a direct up-regulation of CYP11A1 but not HSD3β enzyme expression (Ahumada-Solórzano et al., 2012). Moreover, an increase in both steroid contents in the ovary around the time of maturation in chickens treated with chGH during puberty as well as an increase in plasma progesterone, testosterone, and estradiol concentrations after chGH injections during a pause in laying have been reported (Hrabia et al., 2011; Socha et al., 2017).

The effects of GH observed in the avian ovary, reflect not only its direct impacts on cell functions but also indirect ones, mediated by insulin-like growth factors (IGF-1 and IGF-2). All members of the IGF system are identified in the chicken ovary, and IGFs are produced in ovarian follicles, at least in part, in response to GH (reviewed in Onagbesan et al., 1999; Hrabia, 2015). The proliferating and regulating steroidogenesis effects of the IGFs are well established (Onagbesan et al., 2009; Ahumada-Solórzano et al., 2016). In addition, an autocrine/paracrine proliferative effect of the locally

synthesized GH by granulosa cells from ovarian prehierarchical follicles, which is mediated via local IGF-1 was in vitro demonstrated (Ahumada-Solórzano et al., 2016).

35.2.9.5 Prolactin and prolactin-like protein

Apart from a fundamental role in the initiation and maintenance of incubation behavior in many species of birds (reviewed in Ohkubo, 2017), there is evidence that PRL has both pro- and antiovarian roles, acting at all levels of the hypothalamo-pituitary-ovarian axis. At the period of sexual maturation, the circulating PRL levels gradually increase at the onset of egg laying. During the ovulatory cycle of the chicken, its concentrations are highest around 10 h and lowest 6 h before ovulation (Scanes et al., 1977). An active immunization against PRL suppresses chicken egg production by reducing follicular recruitment into the hierarchy (Li et al., 2011). These observations indicate that PRL at lower concentrations appears to be progonadal. In turn, high and prolonged elevated PRL concentrations are associated with ovary regression and reduction in ovarian steroidogenesis (Hu et al., 2017a, 2017b). The direct suppression of hypothalamic GnRH levels in turkey (Rozenboim et al., 1993) and pituitary LHβ subunit mRNA expression by PRL in chicken (Kansaku et al., 1994) and turkey (You et al., 1995) is also observed.

Growing evidence has demonstrated that the avian ovary is a target site for direct PRL action. PRL gene expression occurs at very low level but PRL receptor mRNA is expressed richly in all follicle size classes, with the highest abundance found in the stroma and wall of follicles <2 mm. In the preovulatory follicles, the PRL receptor transcript is more abundant in granulosa than theca layers (Zhou et al., 1996; Hu et al., 2017a; Hrabia et al., unpublished data). It was proposed that changes in PRL receptor transcript levels during follicle development are related to changes in the process of follicular steroidogenesis and different responsiveness to gonadotropins and PRL variants (Hu et al., 2017a).

The action of PRL in the hen ovary is related to ovarian steroid synthesis. PRL suppresses both basal and gonadotropin-induced levels of progesterone and estradiol production by the ovary (Camper and Burke, 1977). In vitro, PRL inhibits both basal and LH-stimulated estrogen production by small ovarian follicles (Zadworny et al., 1989; Hrabia et al., 2004b). Effects of PRL on in vitro steroid secretion by preovulatory ovarian follicles are stimulatory or inhibitory dependant on the dose of PRL, the type of follicular wall layer, the stage of follicle maturation, and the stage of the ovulatory cycle (Hrabia et al., 2004b; Hu and Zadworny, 2017). Furthermore, glycosylation modulates the actions of PRL in basal and gonadotropin-stimulated follicular steroidogenesis depending on the concentration, the type of gonadotropin, and the stage of follicle development (Hu and Zadworny, 2017). The impact of PRL on steroid production by ovarian follicular cells of hens is mediated through modulation of the expression of steroidogenic enzyme (StAR, CYP11A1, CYP19A1, and HSD3β) expression (Tabibzadeh et al., 1995; Hu and Zadworny, 2017).

A novel prolactin-like protein (PRL-L) has been revealed in the chicken, and in contrast to PRL that is predominantly expressed in the pituitary, the PRL-L is expressed in extrapituitary tissues including the ovary, in both embryonic and adult chickens (Wang et al., 2010). Within the ovary, PRL-L mRNA levels are the highest in the wall of the smallest (<2 mm) follicles. As follicles grow and mature, the expression of PRL-L gradually declines. The transcription of PRL-L in undifferentiated granulosa cells appears to be regulated by FSH or PRL variants independently, or in combination. The stimulatory action of FSH on PRL-L expression is mediated by multiple signaling pathways including the adenylyl cyclase/cAMP/protein kinase A and the inositol phospholipid signaling pathways (Hu et al., 2017b). However, the physiological significance of PRL-L in the avian ovary remains unknown.

35.2.9.6 Ghrelin

Ghrelin is a hormone produced primarily by the proventriculus. There is also evidence for the ovarian expression of ghrelin and its receptor and involvement of ghrelin in the modulation of chicken ovarian cell proliferation, apoptosis, and hormone secretion (Sirotkin et al., 2006, 2016). Increase in testosterone secretion and decrease in estradiol release in vitro by the chicken preovulatory follicle wall in response to ghrelin was shown as well (Sirotkin and Grossmann, 2007a). Moreover, treatment of hens with ghrelin 1-18 prevents the food restriction-induced decrease in ovarian testosterone, estradiol, and arginine vasotocin (AVT), but it do not change progesterone output or egg laying (Sirotkin and Grossmann, 2015). Ghrelin can also mediate the effect of metabolic state on hormones involved in the control of reproduction (Sirotkin et al., 2017). The action of ghrelin in the ovary was proposed to be mediated by MAPK-and PKA-dependent mechanisms (Sirotkin and Grossmann, 2007a).

35.2.9.7 Thyroid hormones

It is well established that thyroid hormones, thyroxine (T4) and triiodothyronine (T3), are involved in the regulation of avian reproduction. The disturbed thyroid gland function is frequently accompanied by abnormalities in the reproductive system. In several species of birds, thyroid hormones are required for the onset of the seasonal reproductive cycle as well as for development of photorefractoriness and the

resulting cessation of reproduction, and also in the expression of incubation behavior in birds (Sharp, 2005; Nakao et al., 2008a,b; Siopes et al., 2010; reviewed in Yoshimura, 2010). They are also involved in the last phase of sexual maturation, as indicated by a negative relationship between thyroid hormones and ovarian steroids concentrations in blood plasma, during chicken sexual maturation (Peczely, 1985; Sechman et al., 2000).

Treatment of hens with single or multiple injection of T3 reduces in a dose-dependent manner the egg laying rate, ovarian weight, and decreases plasma LH and sex steroid concentrations (Sechman et al., 2009). Moreover, dose-dependent changes in the ovarian morphology, i.e., an atresia of the hierarchical follicles, are observed (Sechman, 2013). In the ovarian follicles, T3 decreases estradiol and progesterone synthesis with simultaneous reduction in CYP19A1 and HSD3β mRNA expression. These results suggest that in the laying chickens, thyroid hormone act at the hypothalamo-pituitary level, diminishing production and/or secretion of LH which in turn negatively affects ovarian steroidogenesis and/or at the ovarian level, directly influencing this process (reviewed in Sechman, 2013).

In the chicken ovarian follicles, both granulosa and theca layers express mRNA encoding the nuclear thyroid hormone receptors (TRα and TRβ0 isoforms) as well as the plasma membrane receptor, ITGAV and ITGB3 (encoding αV and β3 subunits of the integrin receptor), indicating genomic and nongenomic action of iodothyronines in the chicken ovary (Sechman et al., 2009; Sechman, 2013). In vitro studies revealed that T3 increases progesterone secretion by the granulosa layer of the largest preovulatory follicles (F3−F1), and decreases estradiol secretion by the white prehierarchical follicles and the theca layer of preovulatory F3−F1. These effects were attributed to expression of StAR protein and steroidogenic enzymes as well as to modulation of the cAMP signaling pathway in steroidogenic cells of ovarian follicles. Results to date indicate that the iodothyronines by affecting ovarian steroidogenesis may participate in the processes occurring during the recruitment of yellowish follicles into preovulatory hierarchy, and during growth and maturation of the yellow hierarchical follicles in the laying chicken (Sechman et al., 2011; Sechman, 2013).

35.2.9.8 Adipokines

Evidence is accumulating that adipokines may also play a role in the follicular development and function. In laying hens, adiponectin and two adiponectin receptor (AdipoR1 and AdipoR2) are present in both granulosa and theca cells. Systemic and/or mainly theca-derived adiponectin may affect proliferation, metabolism, and steroidogenesis in the avian ovary (Chabrolle et al., 2007; Hadley et al., 2020). Other adipokines such as chemerin and visfatin have also been identified in the avian (chicken or turkey) ovary, and their roles were related to steroid synthesis, at least in part, by influencing StAR and HSD3β expression or modulation of IGF-I effect (reviewed in Mellouk et al., 2018; Estienne et al., 2019).

35.2.10 Ovarian tissue remodeling

Follicle growth, development, ovulation, and atresia in the avian ovary are accompanied not only by changes in cell physiology but also by extensive reorganization of the ECM. The ECM components influence basic cellular processes such as proliferation, differentiation, apoptosis, and adhesion. Thus, the ECM is crucial for proper follicular development, function, and atresia/regression. The comprehensive changes in ECM across follicle development require a cascade of proteolytic processes. Former studies suggested participation of PAs that catalyze the conversion of the proenzyme plasminogen to plasmin in these events. Observed high PA activity in the nonstigma region of growing follicles or granulosa cells of the mitotically active germinal disc region of the F1 indicated possible role of PA in remodeling of the ECM of the follicular wall during follicular growth and maturation (Jackson et al., 1993). Involvement of PA in follicle cell proliferation, especially the granulosa cells, was postulated as well (Tilly et al., 1992). More recently it has been indicated that ECM turnover during follicle development/atresia is largely controlled by the MMPs (Hrabia et al., 2019; Wolak and Hrabia, 2020). Besides specific degradation of ECM constituents and activation of other MMPs, they can affect diverse signaling pathways that modulate cell biology in normal physiological and pathological processes by releasing numerous signaling proteins. Among these are growth factors, cytokines, E-cadherin, Fas ligand, and tumor necrosis factor. Recent studies have provided evidence for the hen ovary as a side of MMPs synthesis and action. The presence and changes in activity of several MMPs and alterations in expression of their tissue inhibitors in chicken ovarian follicles across the period of development, suggest that these molecules participate in the regulation of follicle growth and maturation (Leśniak and Hrabia, 2012; Zhu et al., 2014; Hrabia et al., 2019). Since localization of MMPs, mainly in the theca layers, correlated with macrophages localization and frequency (Barua et al., 1998), these cells in addition to fibroblasts were suggested to be a significant source of MMPs in the follicular wall. A role for ovarian steroids, mainly estrogen, in regulating the transcription, translation, and/or posttranslational activity of MMPs was also demonstrated (Ogawa and Goto, 1984; Zhu et al., 2014; Wolak and Hrabia, 2020).

35.2.11 Follicle atresia

Ovarian follicle atresia is a normal physiological phenomenon that eliminates unnecessary ovarian follicles by a noninflammatory process and can occur at any stage of follicular development, from primordial to ovulatory. In birds, atresia is a common destiny in the pool of small follicles that are not selected to complete follicle development (Johnson and Woods, 2007). Only 5% of white follicles reach a diameter of 6–8 mm and enter the follicular hierarchy. In normal physiological conditions, there is little atresia associated with follicles as they advance toward ovulation. In the pool of hierarchical follicles, atresia can only be induced by metabolic or environmental disturbance such decrease in gonadotropin availability, ovarian steroid imbalance, disease, fasting, or the light day shortening (Figure 35.8A). Interestingly, during the induced pause in laying the chicken hierarchical follicles undergo atresia, and the prehierarchical follicles are resistant to this event (Proszkowiec-Weglarz et al., 2005; Socha and Hrabia, 2019).

The atretic follicles differ morphologically and functionally from that of healthy, properly developing follicles. The yellow atretic follicles are shrunken and often hemorrhagic (Figure 35.8A). The wall of atretic follicle (Figure 35.8B–D) is characterized by hypertrophy of the connective tissue, loosening of the theca layers, disintegration of the granulosa layer, and displacement of the granulosa and theca cells into the lumen of the follicle (Hodges, 1974). Moreover, late atresia is associated with

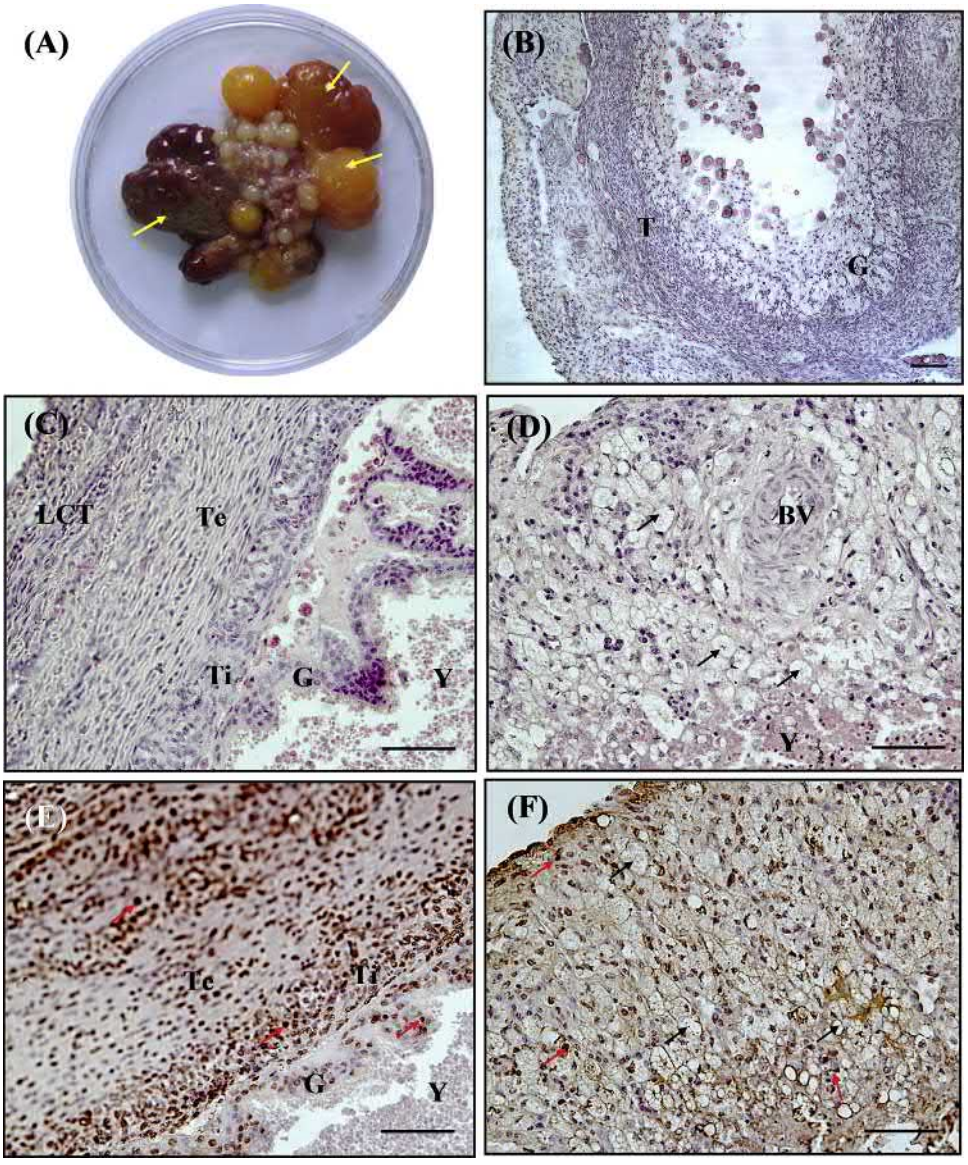

FIGURE 35.8 (A) The ovary with atretic large yellow follicles (*arrows*). The largest follicles are shrunken, grossly regressed, and often hemorrhagic. (B) Histological structure of the atretic primary follicle localized in the ovarian stroma. (C) Histological structure of the atretic yellow follicle at early stage of atresia. Detached granulosa layer (G), disappearance of the basement membrane, and disintegration of the theca interna (Ti) are observed. (D) Histological structure of the large yellow follicle at advanced stage of atresia. Disintegration of entire follicular wall and lipid accumulation (*black arrows*) are recognized. (E) and (F) Localization of apoptotic (TUNEL-positive) cells displaying brown nuclear staining (*red arrows*) in the wall of yellow follicle at early and advanced stage of atresia, respectively. *BV*, blood vessel; *LCT*, loose connective tissue; *Te*, theca externa; *Y*, yolk. Bar = 50 μm.

accumulation of huge amount of lipids. The steroidogenic activity of atretic follicles is significantly reduced. Although aromatase and 3β-HSD enzyme activities are detected at early stage of follicle atresia, the activities and accompanied estradiol and progesterone synthesis are dramatically decreased as degeneration progresses (Proszkowiec-Weglarz et al., 2005).

The follicle atresia in the avian ovary is realized mainly via apoptotic cell death initiated within the granulosa layer. As atresia continues, apoptosis progresses across the theca layers (reviewed in Johnson and Woods, 2007) (Figure 35.8E and F). Involvement of autophagy and necrosis in follicle atresia is additionally proposed (D'Herde et al., 1996). Apoptosis is a form of cell death allowing the controlled removal of unwanted, damaged, or aged cells. The control of cell death is dependent on competing pro- and antiapoptotic molecules. Among them are proteins from the B-cell lymphoma-2 (Bcl-2) family, survivin, an inhibitor of T-cell apoptosis, and the apoptosis-inducing factor FasL. In this event, two essential signaling pathways are engaged: extrinsic (initiating by the binding of a ligand to a transmembrane death receptor) and intrinsic (mediated by factors released from the mitochondria). Each of these pathways has its own initiator caspases which in turn activate effector caspases leading to the cleavage of numerous cellular proteins and finally cell death (Elmore, 2007). Most of mentioned signals are expressed in the chicken developing follicles and correspond to resistance or susceptibility of granulosa cells to apoptosis (Johnson and Woods, 2007; Socha and Hrabia, 2019).

A dramatically reduced susceptibility to atresia of the yellow preovulatory follicles is attributed to considerably increased resistance to apoptosis and elevated viability of granulosa cells after transition from a prehierarchical to preovulatory stage of development. The resistance to apoptosis is coordinated, at least in part, by numerous antiapoptotic proteins, products of genes expressed in response to cAMP signaling activation. Among them is inhibitor of apoptosis proteins, B-cell lymphoma-extra large (Bcl-xL), and Bcl-2 (Johnson, 2015a). In turn, decrease in mRNA abundance of the cell survival protein, Bcl-xL, and in addition significant reduction in expression of VEGF together with their receptors (VEGFR1 and VEGFR2) within the granulosa and theca layers, lead to follicle atresia (Kim et al., 2016). Recent study (Hrabia et al., 2019) suggests the engagement of MMPs, including MMP-2 and -9, in the atresia of chicken prehierarchical follicles. A markedly higher activity of both gelatinases in small atretic follicles in comparison with white healthy follicles was observed. This proposal may not apply to the atresia of the yellow preovulatory follicles because within them, in advanced stage of atresia, the activity or abundance of several MMPs were significantly lower than in the normal yellow hierarchical follicles (Wolak and Hrabia, 2021). Other factors such as aquaporins (AQPs) may also control follicular atresia by mediation of water loss needed for downstream apoptotic events in granulosa cells. A strong immunoreactivity for AQP4 is observed in prehierarchical atretic follicles (Nowak et al., 2017).

35.2.12 Chicken ovary as a model for human ovarian cancerogenesis

The egg production by commercial laying hens is highly efficient. They lay more than 300 eggs per year and ovulate at near 24 h intervals. As a consequence of this high-repetitive ovulation or events associated with ovulation, the development of ovarian tumors is postulated (Johnson et al., 2015). Like humans, the spontaneous occurrence of ovarian cancers in the domestic hens increases with age; up to 35% of hens develop adenocarcinoma after 2.5 year of age (Fredrickson, 1987). Repeated cycles of rupture and repair of the ovarian epithelium probably promote DNA damage and mutation of ovarian epithelium cells lading to subsequent development of an epithelial-derived cancer (Hakim et al., 2009). Oviduct may be an alternative site of ovarian tumor origin. Some oviduct-related genes including ovalbumin are identified and upregulated in hen ovarian tumors (Treviño et al., 2010). In addition, numerous proteins involved in the regulation of the oviduct function were found as a potential diagnostic biomarker of ovarian cancer in laying hens. Among them are vitelline membrane outer layer protein 1 (VMO1) (Lim and Song, 2015), apolipoprotein D (Jeong et al., 2015), alpha 2 macroglobulin (Lim et al., 2011), WNT4 (Lim et al., 2013), beta-catenin (CTNNB1) (Bae et al., 2014b), and cell cycle-related cyclins, cyclin-dependent kinases, and cyclin-dependent kinase inhibitors (Lee et al., 2012). Involvement of estrogen and specific miRNAs in these gene regulation was also indicated.

Moreover, participation of AQP3 and AQP5 in the avian ovarian tumorigenesis was suggested (Tiwari et al., 2014; Yang et al., 2016). Increased protein abundance of both AQPs was found in the chicken cancerous ovary. Similar histological subtypes and cellular marker expression (cytokeratin, proliferating cell nuclear antigen (PCNA), cyclooxygenase 1 and 2, p53 tumor suppressor gene, and HER-2/neu oncogene) in hen and human ovarian tumors, serve the avian ovary as a unique model for the human ovarian cancer investigation (Rodriguez-Burford et al., 2001; Urick and Johnson, 2006; Barua et al., 2009; Hakim et al., 2009; Treviño et al., 2012; reviewed in Johnson and Giles, 2013; Johnson et al., 2015; Yoshimura and Barua, 2017).

In addition, chicken is also an excellent model for research involving the molecular basis underlying the development of human uterine fibroid. Laying hens develop fibroids in the oviduct (magnum and shell gland)

spontaneously, with large similarities to fibroids in women. Among them is the expression of TGF, ER, PR, Bcl-2, PCNA, alpha-smooth muscle actin, and desmin (Berry et al., 2006; Machado et al., 2012).

35.3 The oviduct

The oviduct develops from the Mullerian (paramesonephric) duct, originally derived from the urogenital ridge. The tubal ridges appear on both sides on embryonic day 4 as a groove-like invagination of the coelomic epithelium at the cranial end of the mesonephros. The left Mullerian duct continues to develop, growing caudally and by day 11 it reaches the cloaca. Differentiation of the various regions of the duct becomes apparent between days 12 and 13. The right duct similarly develops for a time but its regression occurs from about embryonic day 11. It disappears completely by the time of hatching (reviewed in Gilbert, 1979).

Rapid development of the left oviduct to the fully functional organ occurs in the domestic hen during several weeks prior to the first egg lay (Figure 35.9A and B). Over a period of 7 weeks before sexual maturity, the oviduct weight increases from about 0.12 to 50.5 g and is accompanied by a remarkable capacity to secrete egg components (Hrabia et al., 2016).

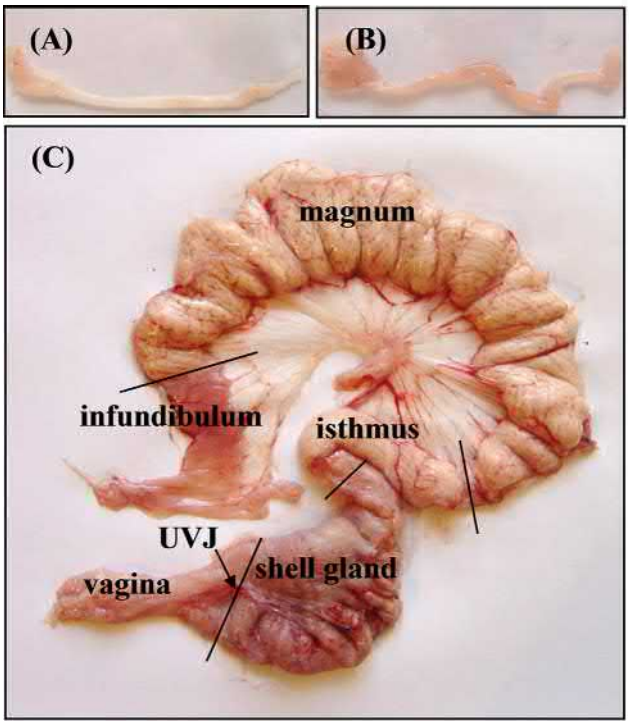

FIGURE 35.9 The hen oviduct. (A) The oviduct of growing chicken about 7 weeks before maturation. (B) The oviduct of growing chicken about 3 weeks prior to the onset of egg lay. (C) The oviduct of laying hen composed of the infundibulum, magnum, isthmus, shell gland (uterus), and vagina. *UVJ*, uterovaginal junction.

The oviduct is suspended within the abdominal cavity by dorsal and ventral ligaments, by which the blood vessels and nerves supply the particular oviductal parts. The laying hen oviduct includes five morphologically and functionally specific segments: the infundibulum, magnum, isthmus, shell gland (uterus), and vagina (Figure 35.9C).

The wall of the oviduct is composed of: (1) an outer epithelium, (2) a double layer of smooth muscles (outer longitudinal and inner circular) with an interspersed connective tissue layer in which lie blood vessels, (3) a layer of connective tissue, (4) a lamina propria including tubular glands lined by secretory cells, and (5) an inner surface (luminal) epithelium lined by ciliated nonsecretory and nonciliated secretory cells. The last two layers constitute the mucosa which possess complexity and is formed into folds. In the magnum, isthmus, and shell gland, the tubular glands are well developed to synthesize constituents of the albumen, eggshell membranes, and eggshell, respectively. The products of the tubular gland cells are delivered to the lumen via a short duct. The ultrastructural appearance and secretory activity of the mucosal cells change during the formation of the egg as it passes through the oviduct (for more details regarding oviduct histology and function see: Hodges, 1974; Etches, 1996; Chousalkar and Roberts, 2008).

The oviduct is innervated by sympathetic and parasympathetic nerves. The sympathetic innervation arises from following abdominal plexuses: the ovarian plexus innervating the infundibulum, the renal and aortic plexuses innervating the magnum, the posterior mesenteric plexus innervating the isthmus, and the hypogastric plexus innervating the shell gland and vagina. Parasympathetic pelvic plexus contains fibers from the pelvic nerve. The nerve fibers in the avian oviduct are often associated with the large blood vessels and muscle (Gilbert and Lake, 1963; Liu et al., 2007). The blood supply to the oviduct is well developed and comes from an anterior oviductal artery, middle oviductal artery, hypogastric artery, and left internal iliac artery. The venous drainage occurs through the anterior oviductal veins, middle oviductal veins, and left internal iliac vein (for more details see Hodges, 1974). Oviductal blood flow significantly changes according to oviductal activity, and 15% of cardiac output perfuses the oviduct of the laying hen, that indicates a high rate of metabolic processes in this organ (Moynihan and Edwards, 1975; Niezgoda et al., 1979). During each ovulation-oviposition cycle of 24 h, the hen lays an egg weighing 50–70 g, which is composed of 25–35 g egg white and 5–6 g eggshell produced in the oviduct. The presence of the egg in a given oviductal segment significantly (three to four times) increases blood flow to this part (Boelkins et al., 1973).

35.3.1 Infundibulum

The infundibulum consists of a thin-walled funnel and a narrow thin-walled neck (tubular region) which increases in

size and thickness to form the next oviductal segment, the magnum. Muscle fibers surrounding the infundibulum are sparse. The mucosal folds in the infundibulum are relatively thin but tall (Figure 35.10A and B). Surface epithelium in the anterior part of this segment predominantly contains ciliated cells. Cuboidal nonciliated cells are localized in groups at the base of the grooves between the epithelial ridges. The tubular glands are present in the distal parts of the infundibulum, and their function is attributed to formation of chalaze.

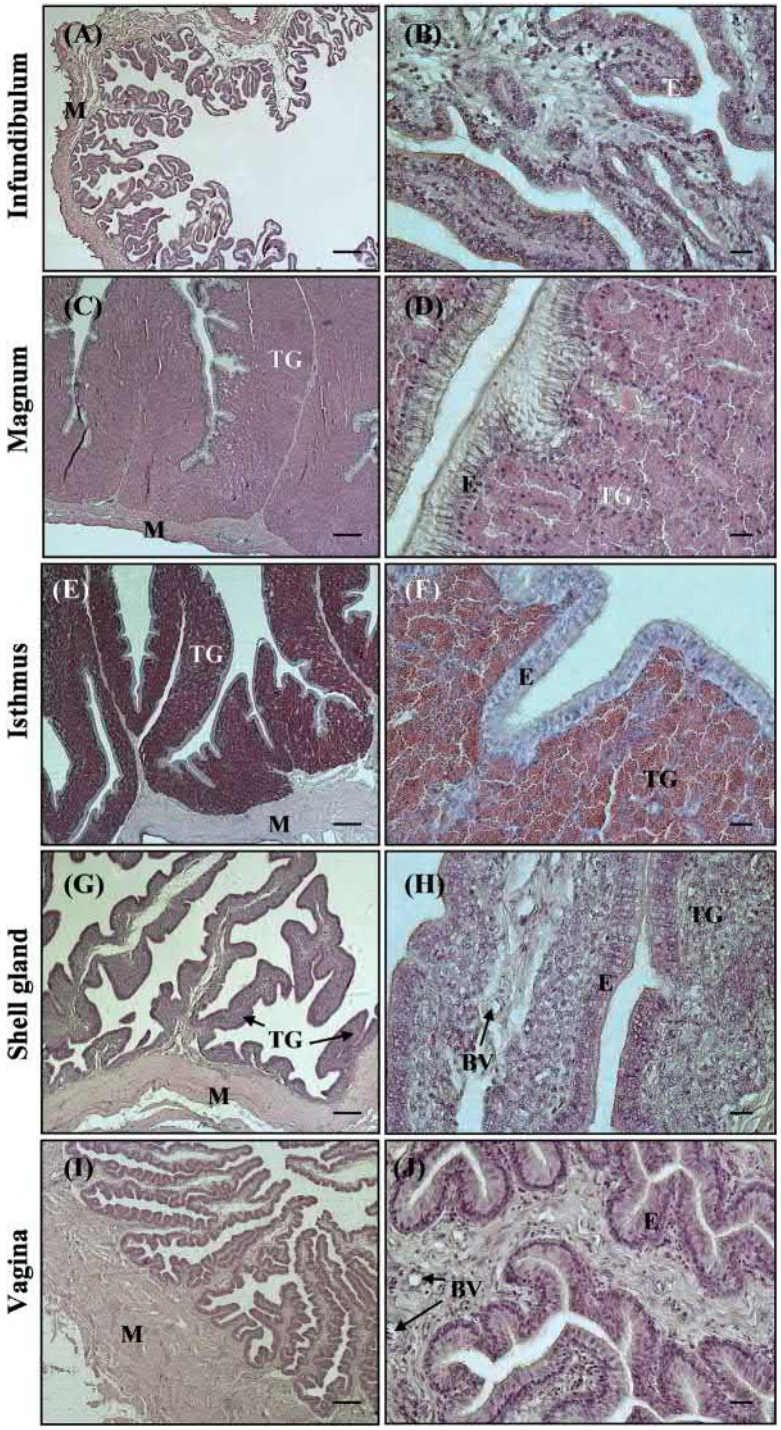

FIGURE 35.10 Histological structure of the laying hen oviduct segments (hematoxylin and eosin staining). (A) Infundibulum. (C) Magnum. (E) Isthmus. (G) Shell gland. (I) Vagina. (B, D, F, H, J) Higher magnification of mucosal tissues of a given oviduct segment. *BV*, blood vessels; *E*, surface epithelium; *M*, muscles and connective tissue; *TG*, tubular glands in the lamina propria. Bar = 200 μm (A, C, E, G, I) and 20 μm (B, D, F, H, J).

The infundibulum engulfs the ovum, which is released upon ovulation. During approximately 18 min (range: 15−30 min) of egg residence in this part, the fertilization occurs and the first layer of egg white is secreted. Fertilization must occur before the outer layer of the vitelline membrane (extravitelline layer) is laid down on the ovum since spermatozoa are not able to penetrate this layer (Bakst and Howarth, 1977; Howarth, 1984) and bind to sperm receptors in the inner perivitelline layer (Kuroki and Mori, 1997). Birds exhibit physiological polyspermy. Many sperm pass through the perivitelline layer into the germinal disc of an oocyte, where the nuclei undergo decondensation and form male pronuclei, although only one sperm successfully fertilizes the oocyte (Bakst and Howarth, 1977; Okamura and Nishiyama, 1978; Perry, 1987; Waddington et al., 1998). The supernumerary pronuclei degenerate at the very early stage of embryo development (Perry, 1987; Waddington et al., 1998), probably as a result of DNase activities (Stepińska and Olszańska, 2003). Evidence was provided that intracytoplasmic injection of a single sperm (ICSI) into quail oocyte can activate the oocyte and lead to fertilization (Hrabia et al., 2003b), although polyspermy naturally occurs in birds. However, the embryonic development after ICSI as well as after conventional in vitro fertilization (Olszańska et al., 2002) was delayed compared to that achieved naturally.

35.3.2 Magnum

The magnum is the largest region of the oviduct. Its length in the chicken is approximately 33 cm. The wall of the magnum possesses well developed muscle layers (although much less developed than in the more posterior segments of the oviduct) and the mucosa. Compared to the tubular region of the infundibulum, the mucosal ridges in the magnum increase in number, height, and thickness, mainly due to intense development of the tubular glands (Figure 35.10C and D). There are three types of tubular glands. Glands A and C are composed of one cell type but with different phases of secretory activity, whereas gland B is of a different cell type. The A cells seems to produce ovalbumin, while the C cells are assumed to be a recovery phase of the A cells. The B cells are engaged in the synthesis of lysozyme. The surface epithelium of the magnum is lined by ciliated and goblet (granular) cells.

The goblet cells synthesize avidin mainly under progesterone and its receptor control, and in less extend other steroids (Hora et al., 1986; Isola, 1990; Kunnas et al., 1992; González-Morán, 2016). Tubular gland cells are responsible for the production of ovalbumin, lysozyme, ovotranferrin, conalbumin, and antimicrobial peptides primarily under the stimulatory control of estrogen (Palmiter, 1972; Tuohimaa et al., 1989; Jung et al., 2011; Socha and Hrabia, 2018). As the ovum traverses through the magnum in approximately 2.5−3 h, most (∼15 g) of the egg white is secreted.

35.3.3 Isthmus

The isthmus is a short section of the oviduct (in chickens ∼8 cm in length), separated from the magnum by a narrow translucent line of demarcation, which is a nonglandular region. The muscular layers of the wall (especially the circular layer) are thicker than in the magnum, while tubular glands in the mucosa are less developed (Figure 35.10E and F). They contain two cell types. The surface epithelium is lined by ciliated, nonciliated, and mitochondrial (the third cell type) cells. The ridges of the isthmus are angular in a shape, and the crypts between the ridges are open.

Both inner and outer eggshell membranes, that enclose the egg albumen, are created during about 1 h and 15 min (range: 1−2 h) passage through the isthmus. There is evidence that eggshell membrane formation is accompanied by differential expression of 107 unique genes in the isthmus tissue. Highly expressed genes include membrane structural proteins such as collagens, collagen processing enzymes, and protein regulating disulfide cross-linking (Du et al., 2015). In the distal part of the isthmus, the mammillary cones of the eggshell are formed by mineralization of the outer shell membrane fibers (Hincke et al., 2012).

35.3.4 Shell gland

The shell gland is subdivided into the initial short (∼2 cm in length) tubular shell gland and the sac-like shell gland pouch (∼7 cm in length and ∼3 cm in width). The shell gland wall musculature, mainly the outer layer, is more prominently developed than in other segments of the oviduct. Mucosa is formed into numerous leaf-shaped folds, with some secondary folding on the surface and less expanded by the branched tubular gland layer (Figure 35.10G and H). The surface epithelium consists of equal numbers of apical ciliated and basal nonciliated cells. Function of the basal cells is linked to production of cuticle, and ciliated epithelial cells to calcium transport, secretion of eggshell pigment, and production of some shell matrix proteins. Tubular gland cells produce most of eggshell constituents.

During approximately 19−20 h which the egg remains in the shell gland, it takes up 15 g of fluid into albumen in process termed “plumping,” and the eggshell is deposited on the eggshell membranes. The volume of the shell gland acellular fluid significantly changes during eggshell formation. It increases during the first 6 h after entry of the egg into the shell gland, being maintained at a high level for about 6 h, and decreases during the last 6 h of eggshell

calcification. During the first 5 h of egg stay in the shell gland, 8 mL of water containing electrolytes, including Na^+, K^+, and Cl^-, accumulates in the egg. When the rate of eggshell calcification increases after this initial stage, the rate of fluid uptake decreases to 0.15 mL per 8 h or less (reviewed in Etches, 1996). The biochemical composition of the shell gland fluid also changes with stage of the shell formation (Nys et al., 2001). For instance, the K^+ and glucose concentrations increase, and Na^+ and Cl^- decrease (Etches, 1996). In addition to mentioned ions, the uterine fluid contains Ca^{2+}, Mg^{2+}, HCO_3^-, CO_2, enzymes (carbonic anhydrase, acid phosphatase, esterase, and proteases), protease inhibitors, and a variety of organic matrix protein precursors which show differential abundance according to the eggshell mineralization stage (Marie et al., 2014, 2015). These proteins are gradually incorporated into the calcifying eggshell resulting in their differential distribution throughout the eggshell regions (Hincke et al., 2012). More than 600 proteins are reported to be present in the chicken uterine fluid. Among the most abundant uterine fluid proteins are ovalbumin, ovotransferrin, ovocleidin-17, EGF-like repeats and discoidin I-like domains 3 (EDIL3), milk fat globule-EGF factor 8, and ovocalyxin-21 (Marie et al., 2015; Stapane et al., 2019). Evidence suggest that in the shell gland fluid, the elements needed for eggshell mineralization (i.e., Ca^{2+} and HCO_3^- ions) are transported in extracellular vesicles targeting the mineralization site (Stapane et al., 2019).

35.3.4.1 Eggshell calcification

The eggshell is composed of 95% calcium carbonate ($CaCO_3$), 3.5% organic matrix (proteins, polysaccharides, and proteoglycans), and 1.5% water (Hincke et al., 2012). The eggshell is formed by mineralization of ionized calcium (Ca^{2+}) and bicarbonate (HCO_3^-) in the uterine fluid. Shell formation is the fastest biomineralization process known in biology (Arias et al., 1993). The complete chicken eggshell contains about 6 g of mineral. The $CaCO_3$ precursors are supplied by the blood through transepithelial transport. As a main calcium-binding and intracellular transporting protein, calbindin D28K is accepted (Jonchčre et al., 2012). Its expression in the tubular gland cells is under the direct control of $1,25(OH)_2$ vitamin D_3 and co-regulatory action of sex steroids (Corradino, 1993). In turn Ca^{2+} pumps and Na^+/Ca^{2+} exchangers are involved in the Ca^{2+} secretion from epithelial cells into uterine fluid (Jonchčre et al., 2012). Additional several novel genes and biological pathways involved in the Ca^{2+} transportation in the shell gland of hen and their potential functions in the eggshell biomineralization have been recently proposed (Sah et al., 2018). Synthesis of HCO_3^- from CO_2 and H_2O is catalyzed by the carbonic anhydrase 2 in the tubular gland cells (Jonchčre et al., 2012). $CaCO_3$ is initially deposited as an amorphous phase, which is progressively converted into calcite. The organic components of the shell gland fluid promote the formation of calcite. In addition, the matrix-mineral interactions determine the orientation of calcite crystals, which results in the complex ultrastructure of the eggshell, its texture, and consequently its mechanical properties (Stapane et al., 2019).

Eggshell calcification occurs in three phases. The first stage lasting about 5 h corresponds to the initiation of mineralization on the surface of the outer shell membrane. This slowly occurring stage results in calcified mammillary cones formation, which then grow outwards to form the base of the palisade layer. During the second, active stage of calcification, the palisade layer formation occurs rapidly for about 10 h. During this time, about 0.33 g per hour of $CaCO_3$ is deposited. Hardness (texture) of the palisade layer as well as termination of shell calcification are, at least in part, controlled by osteopontin, a phosphoprotein secreted from nonciliated epithelial cells and deposited within the developing eggshell. The final stage of calcification lasts approximately 1.5 h and is related to termination of $CaCO_3$ deposition due to inhibitory action of inorganic phosphate and phosphoproteins (e.g., ovocalyxin-32) action; phosphate anions are able to inhibit $CaCO_3$ precipitation. For more details see Nys et al. (2001), (2004); Bar (2009); Hincke et al. (2012).

35.3.4.2 Eggshell cuticle and pigment deposition

Once calcification is completed, the cuticle is deposited on the shell surface during the final hour before oviposition. The cuticle protects avian egg from microbial invasion into the eggs. It contains proteins with antibacterial properties such as ovocalyxin-25, ovocalyxin-32, ovocalyxin-36, ovocleidin-116, ovocleidin-17, and clusterin, as well as lipids and polysaccharides related to the glycosylation of the proteins (Rose-Martel et al., 2012; Mikšik et al., 2014; Wilson et al., 2017). The hormonal factors that regulate of a given protein expression in the shell gland are unknown, although estrogen and GH involvement has been suggested, at least in regards to ovocleidin-116 and ovocalyxin-36 (Socha et al., 2017; Socha and Hrabia, 2018). In colored eggshell, pigments (porphyrin derivatives) secreted from surface epithelial cells of the shell gland are deposited during the last 3 to 0.5 h before oviposition (reviewed in Samiullah et al., 2015). Avian eggshell color is mainly determined by three kinds of pigments, i.e., protoporphyrin-IX (brown-shelled egg), biliverdin-IX (blue-shelled egg), and biliverdin zinc chelate. The molecular mechanism of pigmented eggshell formation remains still unclear. However, there is growing evidence for expression of numerous genes involved in the pathway of biliverdin (or other porphyrin derivatives) synthesis in the shell gland epithelial cells (Zhang et al., 2019).

35.3.5 Vagina

The vagina is a narrow duct (in chickens ~10 cm in length), separated from the shell gland by the uterovaginal sphincter muscle and opens at the urodeum of the cloaca. The large part of the vaginal wall is composed of the muscles. The longitudinal muscle layer consists of bundles of muscle fibers scattered within a connective tissue, and the circular one is strongly developed. The mucosa possesses numerous folds with surface epithelium thrown into many secondary folds, which are lined by ciliated and nonciliated cells. There are no tubular glands present in the lamina propria, except the sperm storage tubules (SSTs) (sperm-host glands) located in the uterovaginal junction (UVJ) (Figure 35.10I and J).

The vagina does not play any distinct roles in egg formation, but in coordination with the shell gland, takes part in the expulsion of the egg. The well-developed immune system in the vagina prevents invasion of the pathogens from the cloaca. In addition, mucin produced by epithelial cells of the lower oviductal segments (isthmus, shell gland, and vagina) provides a barrier against invasion by microbes.

35.3.6 Sperm storage in birds

In birds, the oviduct is able to store spermatozoa for a prolonged period within SSTs located in a narrow band, approximately 2−3 mm wide, at the UVJ. The UVJ is the primary site for the sperm storage, from which spermatozoa are transported to the infundibulum (site of fertilization) where additional SSTs exist (Bakst, 1981). It was estimated in turkey hens that less than 1% of the sperm inseminated into the vagina enter the SSTs (Bakst, 1994). The surface epithelium in the UVJ is lined by cells with well-developed cilia which facilitate the sperm transport to the SSTs. In addition, it is suggested that sperm motility and the seminal plasma constituents such as PGF2α, contribute to sperm entrance to the SSTs (Sasanami et al., 2015). Spermatozoa can be stored (immotile) and survive in the SSTs for a few weeks after insemination or natural mating; up to 10 days in Japanese quail, 2−3 weeks in chickens, and 10 weeks in the turkey hen. Organization of the SSTs is similar to tubular glands in other regions of the oviduct; their epithelium is a single layer of nonciliated cells with microvilli on their apical surface. There is evidence that SST cells synthesize and secrete exosomes, however their role needs to be elucidate (Huang et al., 2017).

The mechanism by which sperm can remain viable in the SSTs is not fully established, but potential roles for alkaline phosphatase (Bakst and Akuffo, 2007), carbonic anhydrase (Holm et al., 1996), avidin (Foye-Jackson et al., 2011), AQPs (Zaniboni and Bakst, 2004; Socha et al., 2018; Hrabia et al., 2020), fatty acids (Huang et al., 2016), some eggshell matrix proteins (Riou et al., 2017), albumin, and transferrin (Matsuzaki et al., 2020) in maintenance of proper microenvironment and nutrients supply for spermatozoa in SSTs are suggested. Recent report demonstrated changes in expression of numerous genes related to fatty acid metabolism, regulation of cell differentiation, regulation of transport, immune response, and pH-regulatory functions in UVJ. These alterations are attributed to sperm storage in the SSTs (Han et al., 2019). A high concentration of lactic acid in SSTs is proposed as a key factor making resident spermatozoa quiescent in the SSTs (Matsuzaki and Sasanami, 2017). Another important factor supporting spermatozoa viability in SSTs is the protection of resident spermatozoa from immune response by the TGFβ system (Das et al., 2008).

Following oviposition, spermatozoa are released from the SSTs and migrate to the infundibulum for fertilization. This event is in accordance with the ovulation timing. Progesterone which plasma concentration increases before ovulation is considered as a sperm-releasing factor. It elicits morphological changes in the SSTs, which squeeze out the stored spermatozoa. Progesterone also stimulates secretion of cuticle components from the epithelial cells of the UVJ and shell gland that support the spermatozoa migration toward the infundibulum. In addition, evidence suggests that HSP70 protein secreted from the surface epithelium of the UVJ, bound to the sperm and reactivates its motility. This help sperm movement to the fertilization site (Hiyama et al., 2013). For more details regarding unique phenomenon of sperm storage in birds, see Matsuzaki and Sasanami (2017).

35.3.7 Hormonal and physiological regulation of oviduct development and function

35.3.7.1 Ovarian steroids

The series of events related to egg formation in the avian oviduct are regulated by numerous hormones and factors, primarily by the ovarian steroids. Estrogen is the main steroid that controls the growth and function of the oviduct, but progesterone and androgens are required for development and maintenance of full secretory activity (Mika et al., 1987). Progesterone and androgens alone have little effect on the development of the oviduct (Palmiter and Wren, 1971). ERα is expressed in the avian oviduct before and after hatching, indicating participation of this form of ER in the estrogen-regulated growth of the left Müllerian duct (Kiell et al., 1982; González-Morán and Camacho-Arroyo, 1998). High abundance of ERs is also noticed in growing and laying hen oviduct, and their expression changes according to reproductive function of the oviduct (Jung et al., 2011; Hrabia et al., 2004a; Socha et al., 2017). Within the wall of the magnum and shell gland, ERs are localized in

the surface epithelium and in the tubular gland cells (Hansen et al., 2003; Jung et al., 2011). The roles of estrogen in the oviduct of growing and laying hens are attributed to growth and maintenance of mucosal cell proliferation and differentiation. Gene expression of numerous proteins related to cell functions and egg constituents is under estrogen control as well (reviewed in Dougherty and Sanders, 2005; Jung et al., 2011; Yang et al., 2016; Jeong et al., 2017a, 2018). Estrogen is also required for regulation of proteins participating in calcium metabolism for calcification of the eggshell include calbindin and epithelial calcium channels (TRPVs) (Corradino, 1993; Bar, 2009). In addition, estrogen orchestrates the remodeling of the reproductive system to increase the subsequent rate of egg production, following molting in laying hens (Socha et al., 2017; Socha and Hrabia, 2018). There is a great number of evidence regarding the response of avian oviduct to estrogen. By way of example, exposure of immature chickens to synthetic estrogen, diethylstilbestrol increases growth, development, and differentiation of the oviduct and changes expression of genes related to tubular gland formation, epithelial cell differentiation, hormone interactions, nerve development, and tissue remodeling (Song et al., 2011). In turn, treatment of chickens with estrogen receptor blocker (e.g., tamoxifen) induces regression of the oviduct via stimulation of cell apoptosis and causes decrease in expression of genes coding the egg albumen and eggshell matrix proteins (Socha and Hrabia, 2018). Similar effects are noticed in hens exhibiting low-plasma levels of estradiol and other sex steroids (progesterone and testosterone) during a pause in laying induced by fasting or high dietary Zn treatment (Heryanto et al., 1997; Anish et al., 2008; Jeong et al., 2013; Socha et al., 2017). Estrogen also induces progesterone and AR synthesis in the oviduct of immature and laying chickens (Toft and O'Malley, 1972; Hora et al., 1986; Joensuu, 1990). Co-expression of PR and ERα in all cell types of the oviductal magnum as observed in one-week and one-month-old chickens suggests that progesterone in cooperation with estradiol participates in the regulation of growth and cell differentiation at the posthatch stages of the magnum development (González-Morán, 2015). Such a role for progesterone is well established.

PRs were examined deeply in the oviductal magnum, and in a less extend, in the shell gland (Yoshimura and Bahr, 1991b; González-Morán, 2015, 2016; Socha et al., 2017). In the magnum, PRs appear at the age of one week and thereafter, concomitantly with histological changes in this oviductal segment. Within the oviductal wall of mature laying and nonlaying hens, PRs are present in the surface epithelial cells, tubular gland cells, stromal fibroblasts, and muscle cells (Yoshimura and Bahr, 1991b; González-Morán, 2016). Thus, progesterone acting through its receptor regulates the secretory activity of the surface epithelium and tubular gland cells for egg formation and the contractile activity of the myometrium. The mRNA and protein expression as well as density of PR-positive cells are greater in nonlaying hens, with atrophied oviductal tissues, than in laying hens. Therefore, it is suggested that once the cells differentiate and become responsive to progesterone, these cells maintain this responsiveness even during the nonlaying period (Yoshimura and Bahr, 1991b; Socha et al., 2017). The ratio of PR-A and PR-B changes in the oviduct according to the cell type, the age, and reproductive activity. In the laying hen oviduct, a similar expression of PR-A and PR-B is observed, but in the nonlaying or estrogen-withdrawn chickens, PR-A is a predominant isoform (Schrader and O'Malley, 1972; Syvala et al., 1997; González-Morán, 2016). It seems that in the responsiveness of the oviduct to progesterone, the ratio of PR-A and PR-B isoform abundance is important because they control expression of different genes and exert distinct functions (Tora et al., 1988).

ARs are also expressed in the avian oviduct. Androgens act synergistically with estrogen to stimulate the oviduct growth and to maintain oviductal functions (Palmiter and Haines, 1973; Kawashima et al., 1999; Socha et al., 2017).

35.3.7.2 Other factors

In recent years, an ever-increasing number of factors have been implicated in modulation of the oviduct development and function. For instance, GH is produced by oviductal tissues, and its receptors are present primarily in the mucosal cells (Ni et al., 2007; Hrabia et al., 2013, 2014b; Luna et al., 2014; Hrabia, 2015). Along with oviduct length, the GH concentration is consistent, but it progressively declines from puberty to the late laying period. The role of GH in the chicken oviduct is linked to synthesis of egg constituents. Treatment of chickens with chGH during sexual maturation results in an increase in mRNA expression of ovalbumin in the magnum as well as ovocalyxins 32 and 36 in the shell gland. Improved eggshell quality in older hens is observed after GH injections (Donoghue et al., 1990). The action of GH in the chicken oviduct is additionally related to the regulation of oviductal cell apoptosis and proliferation (Hrabia et al., 2014b). Mediation of some GH actions by IGFs in the avian oviduct is also possible since IGF-1, IGF receptor, and IGF binding protein-2 are evidenced, and paracrine and/or autocrine actions of IGF-1 in the quail oviduct during its development is suggested (Fu et al., 2001; Kida et al., 1994; Ni et al., 2007). In primary cultures of quail oviduct cells, elevation of ovalbumin synthesis by IGF-1 in cooperation with estrogen was shown (Kida et al., 1995). Ghrelin-immunopositive cells are demonstrated in the mature Japanese quail oviduct, but not in immature quail. This finding indicates that ghrelin synthesis is associated with development and differentiation of

the oviduct (Yoshimura et al., 2005). PRL protein was localized on the surface of UVJ of Japanese quail oviduct, and its role has been implicated in the maintenance of the fertilizability of the spermatozoa through the prevention of the spontaneous acrosome reaction (Hiyama et al., 2016).

To provide an appropriate environment for fertilization, early embryo development, movement of the egg during its formation, and sperm storage and transportation in the avian oviduct, the balance of water and fluid secretion is essential. In recent years, the AQPs have been implicated in regulation of the oviduct development and oviductal fluid secretion. AQP3 was proposed to be involved in the estrogen-induced development of the chicken oviduct (Yang et al., 2016). Other results provide evidence that the AQP4 mRNA and protein are present in all segments of the chicken oviduct. The expression of AQP4 depends on the segment, the cells of the wall, and reproductive activity of the oviduct. Generally, its expression is reduced during a pause in laying induced by tamoxifen treatment or starvation. The role of this channel protein is linked primarily to the regulation of water movement required for egg formation, especially for secretory processes in the infundibulum and the "plumping" of fluid into the albumen in the shell gland (Socha et al., 2018; Hrabia et al., 2020). Moreover, localization of AQP2, 3, and 9 within the apical side of the epithelial cells that form the SST in the turkey vagina implies these AQPs in water exchange that may interact with sperm residing within the SST (Zaniboni and Bakst, 2004).

It has been demonstrated that circadian clock-related genes (e.g., Bmal1, Clock, Per2, Per3, and Cry2) are expressed in four segments of the chicken oviduct (infundibulum, magnum, isthmus, and shell gland). The expression of these genes shows significant rhythmicity in a daily light-dark cycle, in the infundibulum and shell gland but not in the magnum and isthmus. These results provide evidence for a functional clock within the avian oviduct, as well as for the role of this local clock in the regulation of the infundibulum and shell gland activities related to the capture of the ovum and eggshell formation/oviposition, respectively (Zhang et al., 2016).

There is also evidence for implication of a large number of differentially expressed genes in the regulation of avian oviduct development (Dunn et al., 2009; Jung et al., 2011; Song et al., 2011; Yin et al., 2019) and function of a given oviduct segment (Lim et al., 2012; Jeong et al., 2013; Khan et al., 2019; Yin et al., 2020). In turn, gene expression can be modified by miRNAs acting at a posttranscriptional level (Lim et al., 2012; Bae et al., 2014a, 2014b; Lim and Song, 2014). There is evidence that numerous miRNAs regulate gene expression (often estrogen-induced genes) in the oviduct during developmental (Jeong et al., 2017b) and in different stage of reproductive activity (Kim et al., 2017; Jeong et al., 2013, 2018).

Changes occurring in the structural architecture of the oviductal tissues during its development, regression, and rejuvenation required the controlled turnover of the stromal ECM. This process is regulated, at least in part, by proteolytic enzymes including the MMPs and their inhibitors such as TIMPs and α2-macroglobulin, which expression is especially high in the epithelial and tubular gland cells (Lim et al., 2011). Recent studies have provided evidence for synthesis and activity of some MMPs within the domestic hen oviduct as well as changes in MMP activities in relation to oviduct development and reproductive state (Ha et al., 2004; Leśniak-Walentyn and Hrabia, 2016a, 2016b, 2017). In addition, involvement of estrogen in the regulation of MMP expression and activity was proposed (Leśniak-Walentyn and Hrabia, 2017).

35.4 The ovulatory cycle

The ovulatory cycle of the hen spans the time from one ovulation to the next ovulation. The ovulation−oviposition cycle covers the period from ovulation of an ovum to the oviposition of the fully formed egg. In the domestic hen, ovulation is followed by oviposition approximately 24−26 h later. Ovulation of the F1 (most advanced in the development) follicle occurs within 15−45 min after oviposition, or even within 5 min in commercial layer strain hens, producing more than 300 eggs per year. Ovulations happen uninterrupted for several consecutive days, after which a pause in laying, lasting one or more days, occurs. The number of eggs laid on successive days is called a sequence or clutch. The first event in a sequence is the preovulatory release of LH, second the occurrence of ovulation, and third oviposition. Laying is restricted to a 4 to 8 h period of the day, and this restriction is the result of a circardian rhythm in some components of the physiological system controlling ovulation. Each successive egg within a sequence is laid at a slightly later time each day. The differences in lag time within a sequence represent mainly variation in the amount of time between oviposition and the subsequent ovulation (reviewed in Etches, 1990; Johnson, 2015b).

Under 24 h of photoschedule cues (14 h light and 10 h dark), the preovulatory surge of LH in the domestic hen is restricted to an 4 to 11 h "open period" beginning at the onset of dark phase (the scotophase). In chickens, ovulation of the first egg of a sequence usually occurs early in the photophase. For comparison, Japanese quail ovulate the first egg of the sequence 8−9 h after the onset of the photophase. Consequently, most eggs are laid by the domestic hens in the morning, and by quail in the afternoon (Fraps, 1955; reviewed in Etches, 1990; Johnson, 2015b).

The timing of ovulation is controlled by the neuroendocrine and ovarian clock systems. At a central level, avian

circadian timing is regulated at multiple oscillatory sites, including the retina, pineal gland, and hypothalamus. A signal from the central clock is crucial for the initiation of the LH surge capable to induce ovulation. At an ovarian level, clock genes such as Bmal1, Clock, Cry1, Cry2, Per2, and Per3 are rhythmically expressed in the theca and/or granulosa layers of preovulatory F1 follicle as revealed in Japanese quail and chicken (Nakao et al., 2007; Tischkau et al., 2011; Li et al., 2014; Zhang et al., 2017). Clock gene rhythmicity is absent in the granulosa layer of prehierarchical follicles (Nakao et al., 2007) or less mature F6−F5 follicles (Zhang et al., 2017). The function of the ovarian clock is related to the timing of gene expression involved in steroidogenesis, gonadotropin responsiveness, and ovulation primarily in granulosa cells of the largest preovulatory follicle. The expression of clock genes in the ovary is regulated by the LH signaling cascades mediated by the cAMP pathway and, in lesser extent, the p38MAPK and ERK1/2 pathways (Li et al., 2014). In both theca and granulosa cells of F1 follicle, LH-regulated production of StAR changes over the course of 24 h, coincidently with changes in the abundance of the clock gene, Per2. The chicken StAR gene has the functional capacity for clock-driven expression (Nakao et al., 2007; Zhang et al., 2017). In addition, it has been evidenced that FSH provides a cue for the development of the functional cellular clock in granulosa cells of less mature hierarchical follicles, and that LH synchronizes the cellular clock of granulosa cells of the most mature follicle (Zhang et al., 2017). The data indicate that local clock system plays an important part in the regulation of ovarian follicle maturation, the timing of ovulation, and the rate of lay.

35.5 Egg transportation and oviposition

The ovum captured by the infundibulum is moved with variable speed through individual segments of the oviduct showing a different type of mobility, i.e., different frequencies and amplitude of contractions (Rząsa, 1972; Hrabia, 2000). The electrical activity and motility of the oviductal parts change during the ovulatory cycle. The highest frequency of electrical activity occurs in the shell gland at the time of oviposition (Shimada and Asai, 1978). Moreover, the ovum promotes its own transport in the oviduct, which muscles function like a stretch receptors. When the egg travels through the oviduct, the electrical activity of the musculature behind the egg is much higher than in its front. Thus, the egg stretching the wall of the oviduct, increases the contraction activity of smooth muscles, which causes the egg to move (Arjamaa and Talo, 1983).

Significant role in the egg transportation through the oviduct plays adrenergic innervation. Both adrenergic receptors (α and β) are present in the oviduct. Stimulation of α receptors contracts and stimulation of β receptors relaxes oviductal smooth muscles. In vitro and in vivo epinephrine and norepinephrine contract all oviductal segments except for the shell gland, which relax (Rząsa, 1977; Verma et al., 1977; Crossley et al., 1980). Histamine, which concentrations change throughout the length of the oviduct and depends on oviductal activity (Paczoska-Eliasiewicz et al., 1998) has also been suggested as a local regulator of the chicken oviduct contractility (Hrabia, 2000). Other results implied participation of PGs and AVT in the regulation of oviduct activity. Both PGF2α and PGE2 contract all oviductal segments except for the vagina, which is relaxed by PGE2 (Wechsung and Houvenaghel, 1976). AVT provokes a contraction of the magnum, isthmus, and shell gland, and sensitivity of the oviduct to AVT increases from infundibulum to shell gland (Rząsa, 1972).

Oviposition, i.e., expulsion of the fully formed egg from the oviduct involves the relaxation of abdominal muscles and sphincter between the shell gland and vagina as well as the vigorous contractions of smooth muscles of the shell gland. This event is controlled by AVT, PGs, acetylcholine, and galanin.

AVT is released from the posterior pituitary gland as well as is expressed in the shell gland, suggesting its paracrine effect (Srivastava et al., 2010). In laying hen, AVT plasma concentration is found to be highest at the time of oviposition (Niezgoda et al., 1973) concomitantly with the lowest plasma activity of oxytocinase (aminopeptidase), enzyme inactivating AVT (Brzezińska et al., 1967). AVT has well-documented stimulatory effects on the shell gland contractility and oviposition, acting by its receptor VT3, members of G-protein coupled receptor family. Injection of AVT or oxytocin can induce premature oviposition in laying hens (Rząsa and Ewy, 1970; reviewed in Srivastava et al., 2018). The action of AVT is mediated by locally produced PGs. Treatment with PGF2α or acetylcholine causes a marked increase in plasma AVT levels and premature oviposition (Shimada et al., 1987). Administration of indomethacin (PG synthetase inhibitor) blocks AVT-induced premature oviposition (Rząsa and Paczoska-Eliasiewicz, 1989). PGs and AVT are reported to intensify their actions. PGF2α released in the shell gland at the time of oviposition stimulates tissue contractility, which in turn increases the release of AVT (Saito et al., 1987b; Shimada et al., 1987). Moreover, AVT causes uterus contractions as well as PG release from the shell gland tissue (Rząsa, 1978, 1984; Takahashi et al., 2004). Local synthesis of AVT and the expression of its VT3 receptors in the shell gland is, at least in part, estrogen dependent (Srivastava et al., 2010).

It is well established that PGs (PGE2 and PGF2α) produced in the hen shell gland directly stimulate contractions of this oviductal segment, acting by specific receptors (Asbóth et al., 1985; Takahashi et al., 2004, 2011).

Local synthesis of PGs in the hen uterus has been confirmed recently, by presence of cyclooxygenases (COX-1 and COX-2), the rate-limiting enzymes of PG synthesis. The highest expression of COX-2 in the shell gland just prior to oviposition implies its important role in the production of PG necessary for oviposition event (Elhamouly et al., 2017). Released PGs into the blood serum are rapidly metabolized. Treatment with exogenous PGs (PGF2α or PGE1) stimulates the shell gland contractility, relaxes the vagina, and evokes premature oviposition in chickens and Japanese quail. Blocking of PG synthesis, by treatment with indomethacin, decreases the occurrence of the oviposition peak of uterine contraction and delays oviposition (Shimada and Asai, 1979; Rząsa, 1978; Rząsa and Paczoska-Eliasiewicz, 1989; Takahashi et al., 2004). There is also evidence suggesting that PGs E and F produced in the highest amount around the time of oviposition by ovarian preovulatory follicle (F1) and most recent postovulatory follicle (POF1) play an important role in the control of egg expulsion (Saito et al., 1987a; Hales et al., 2008). Removal of either the POF1 or the F1 follicle results in a 1−7 day delay in oviposition (Rothchild and Fraps, 1944).

Avian galanin is identified in the Japanese quail oviduct extract, and galanin immunoreactive fibers are localized in the muscle layers of the shell gland and vagina. The synthetic peptide enhances in vitro contractions of both the vagina and the shell gland tissues in a similar manner to the native peptide. Administration of the synthetic peptide induces quail oviposition during 5 min after injection. The direct galanin action on the oviductal shell gland and vagina is evidenced by presence of galanin binding sites. Their abundance is under combined control of estradiol and progesterone. Therefore, it is proposed that galanin may serve to evoke oviposition through mechanism of the induction of shell gland and vaginal contractions (Li et al., 1996; Tsutsui et al., 1997, 1998).

Epinephrine and norepinephrine do not play significant role in egg oviposition; however, release of epinephrine under stress causes the egg to retain in the shell gland, which is the result of the diastolic effect of catecholamines on the uterus (Rzasa, 1977; Hrabia, 2000).

35.6 The egg

The avian egg is a biological container possessing all materials and nutrients required for generating a new individual. It is composed of the yolk which accounts for 32−35% of the egg, the albumen accounts for 52−58%, and the eggshell with shell membranes accounts for 9−14%. In the yolk and albumen, the proteins, lipids, minerals, growth factors, and vitamins are stored. Eventually, proteins are used for tissue growth, while the lipids are served as a main source of energy for the developing embryo. The mineralized eggshell participates in gas and water exchange provides calcium, and protects the embryo from physical impacts and pathogens. In addition, eggs are an excellent source of protein of high-biological value that offer specific health benefits to humans. A novel functional activities of egg proteins has been identified. Among other, some egg proteins are good candidates for use as immunomodulatory agents in the food and pharmacological industries or can be used in cancer therapy (for details see Lee and Paik, 2019). Egg constituents has been well described in Gilbert (1971), Hodges (1974), Etches (1996), Solomon (2010), Nys et al. (2001, 2004), Tian et al. (2010), Hincke et al. (2010, 2012), and Ahmed et al. (2017).

35.6.1 The yolk

The ovulated oocyte filled with huge amount of yolk is enveloped with the vitelline membrane (i.e., plasma membrane, oolemma) and perivitelline layer [counterpart of mammalian zona pellucida (ZP)], which are product of the ovary. In the infundibulum, captured oocyte is further surrounded with the middle continuous layer and extravitelline layer (outer layer of the vitelline membrane), which contain proteins released from the epithelial cells of the infundibulum. These four layers together make up the yolk membrane. The vitelline membrane (8 nm thick) tightly apposed to the perivitelline layer, in some regions of the yolk is perforated. In the area of the germinal disc (blastodisc), the vitelline membrane possesses numerous microvilli that project into a perivitelline space splitting the perivitelline layer from the vitelline membrane (Etches, 1990). The perivitelline layer (egg coat; 2 to 4 μm thick) which surrounds the vitelline membrane is a unique multifunctional ECM, composed of a loosely intermeshed network of fibers, which include the ZP glycoproteins. Based on phylogenetic analyses, ZP glycoproteins are classified into six subfamilies such as ZP1, ZP2/ZPA, ZP3/ZPC, ZP4/ZPB, ZPD, and ZPAX (for more details see Okumura, 2017; Nishio et al., 2018). In birds, ZP proteins constituting the perivitelline layer are highly conserved. Among them, ZP1, ZP3, and ZPD are the predominant molecules accumulating in the matrix around the mature ovum, whereas ZP2, ZP4, and ZPAX are under detectable levels or in faint amount. These ZP proteins are secreted by granulosa cells, except for ZP1 which is liver-derived (Nishio et al., 2014, 2018). The physiological roles of ZP proteins are related to the mediation of egg−sperm interactions, induction of sperm acrosome reaction, oocyte or early embryo defense, and modification of the egg-coat architecture (Okumura, 2017; Nishio et al., 2018). In avian fertilization, the spermatozoa locally degrade and dissolve the matrix of the perivitelline layer and penetrate it through the hole made at the sperm-binding site. The sperm binds to the perivitelline layer overlying the germinal disc,

preferentially than in any other area of the egg. The middle continuous layer (50−100 nm thick) is an amorphous substance. The extravitelline layer, the thickest (6 μm) of the constituents of the yolk membrane, is composed of interwoven fibers that are deposited in concentric layers around the ovum.

The egg yolk contains approximately 48% water, 33% lipid, 17% protein, and traces of carbohydrates (∼1%; mainly oligosaccharides) and minerals (∼1%; largely phosphorus). Yolk lipids mostly include triacylglycerols, phospholipids, cholesterol, and cerebroside. The yolk provides nutrients to the growing embryo and its extraembryonic membranes during incubation.

The core of the egg is created by white yolk around which the yellow yolk, containing more protein and lipids, is deposited in concentric layers. The yolk is composed of fluid and spherical structures (∼up to 140 μm in diameter). The smaller spheres are called lipid or lipoprotein droplets. The larger spheres termed yolk spheres are enclosed by trilaminar membrane and containing subdroplets, particles, lamellar bodies (lipid-reach molecules in a membrane-like form), and aqueous phase. The subdroplets include lipids and VTG-originated proteins such as phosvitins (20 and 34 kDa of molecular weight) and lipovitellins (α- and β-lipovitellin; ∼400 kDa). The phosvitins are main proteins binding the phosphorus within the yolk (∼80%), and to a lesser extend the calcium, magnesium, and iron. The particles contain about 65% of the yolk solids and 95% of the yolk lipids. The aqueous phase contains approximately 10% of the yolk solids, majority of which are proteins, including only trace of lipids. The key proteins are serum albumin, serum α2-glycoprotein, and the immunoglobulin IgY (a counterpart of mammalian IgG). Some proteins of the aqueous phase serve as a carrier for vitamins. The yolk IgY, which concentrations range from 50 to 100 mg per egg yolk, is the avian-specific maternal immunoglobulin that protects embryos from infection before full maturation of their own adaptive immune system. It is synthesized in the B cells, secreted into the blood, delivered to the ovary, and eventually selectively incorporated into the growing oocyte in the follicle, through the Fc receptor-mediated endocytosis (Dias da Silva and Tambourgi, 2010; Murai et al., 2013). In turn, maternal IgY via yolk sac receptor FcRY (mannose receptor family member) is delivered to the prenatal chick circulation (Tesar et al., 2008).

35.6.2 The albumen

The egg albumen (egg white) secreted in the oviduct (as discussed in this chapter) is a reservoir of water, protein, and minerals for developing embryo, as well as it protects from the invasion of pathogens into the yolk. The egg albumen is composed of four layers: a chalaziferous layer closely applied around the yolk membrane, an inner thin layer, a viscous thick layer, and an outer thin layer. The layers account for about 2.7%, 17%, 57%, and 23%, respectively, of the total volume of the egg white. The chalaziferous layer contains dense albumen in which are embedded numerous mucin-like fibers. This layer forms a thin, compact structure keeping the egg yolk in the center of the egg. The inner and outer thin layers contain a higher proportion of the water-soluble proteins and these layers increase when eggs are stored. Compared with the yolk, the albumen consists largely of water (86−89%), with the remaining being solids: ∼10% proteins, ∼1% carbohydrates, traces of lipids, and minerals. Few of the vitamins are accumulated in the egg white, except the niacin and riboflavin. Minerals such as chlorine, magnesium, potassium, sodium, and sulfur are abundant in the albumen, whereas calcium, copper, iodine, iron, manganese, phosphorus, and zinc are abundant in the yolk.

Over 220 diverse proteins with the specific functions and physicochemical properties were found in the egg white (Ahmed et al., 2017). Among them, the major proteins evidenced in the egg albumen include the most abundant ovalbumin (54%), followed by ovotransferrin (12−13%; conalbumin), ovomucoid (11%), ovoglobulins G2 and G3 (8%), ovomucin (3.5%), lysozyme (3.4%), and present in lesser concentrations, ovoinhibitor (1.5%), ovoglycoprotein (1.0%), flavoprotein (0.8%), ovomacroglobulin (0.5%), avidin (0.05%), and cystatin (0.05%).

Ovalbumin is a main source of amino acids for developing embryo, and possesses antioxidant and enzyme inhibitor properties. Ovotransferrin serves as an iron chelator preventing iron utilization by microorganisms, thus exerts antibacterial effect against broad spectrum of bacteria. Ovomucoid inactivates trypsin enzyme (serine protease) and other proteases essential during bacteria growth. Similarly ovoinhibitor acts as a bacterial and fungal serine protease inhibitor. Likewise, cystatin has protease inhibitor properties and exerts both antimicrobial and antiviral activities. Ovomucin is another antimicrobial and antiviral protein. It is a highly glycosylated protein composed of α- and β-subunits differing by carbohydrate content and amino acid composition. The carbohydrate contents of α-ovomucin and β-ovomucin are approximately 15% and 60%, respectively. This insoluble fibrous protein with high-molecular weight maintains the viscosity and structure of egg albumen (mainly thick egg white) and block invasion of pathogens. Lysozyme has bacteriolytic activity, which occurs via hydrolyze of the bonds between N-acetylmuramic acid and N-acetyl-D-glucosamine residues in peptidoglycan and between N-acetyl-D-glucosamine residues in chitodextrinin of the bacterial cell wall. It is most effective against gram-positive bacteria. Avidin, also demonstrates antimicrobial activities against several bacteria due to its strong binding affinity to biotin as well as minerals, which are important for bacterial growth. It is a

glycoprotein composed of four subunits, each of them can bind a biotin molecule. Flavoprotein has ability to bind riboflavin.

35.6.3 The eggshell

The avian shell includes several layers that function together as a single unit. From the inner site, the shell layers are as follows: inner shell membrane (~15–26 μm thick), outer shell membrane (~50–70 μm), mammillary layer (~100 μm), crystal layer (palisade and vertical layers; ~200 μm), and cuticle (~5–10 μm). Chemical composition of the eggshell comprises of an inorganic material (primarily $CaCO_3$ mineral in the form of calcite; ~95% by weight) and an organic matrix (3.5%) that forms eggshell membranes, the mammillary cores, the shell matrix, and cuticle.

35.6.3.1 The shell membranes

The shell membranes are deposited around the albumen when the egg travels through the oviductal isthmus. The two membranes are tightly apposed to one other except at the blunt end of the egg where the two are separated over a small area to form the air cell (air chamber). During embryonic development, the membranes interface with the chorioallantoic membrane. Eggshell membranes are ECM, constituted by proteins (mainly fibrous, a highly cross-linked by disulfide and lysine-derived bounds), small amount of carbohydrates, and only trace of lipids. The membranes differ slightly in their chemical composition and morphology. The inner membrane is not calcified, while the fibers of the outer shell membrane are incorporated into the shell in areas termed mammillary cores that serve as center for the growth of crystals of $CaCO_3$. Recent proteomic analyses identified nearly 500 different proteins present in the shell membranes. Of these proteins, 163 are moderately and 124 are highly specified to the shell membranes. The family of proteins, recognized as shell membrane-specific, includes collagens which constitute about 10% of eggshell membrane proteins, cysteine-rich proteins (CREMPs), histones, avian β-defensins (AvBDs, formerly called gallinacins), lysyl oxidase-like 2 (an important collagen cross-linking enzyme), and ovocalyxin-36. The structural proteins such as CREMPs and collagens (types I, V, and in large part collagen X) are fundamentally associated with the formation of fibrous structure of the membranes and their subsequent physicomechanical properties that retain the egg albumen, provide structural base for biomineralization, and form the physical barrier against pathogen invasion of the egg interior. Another group of proteins, including ovocalyxin-36, AvBDs, and histones, serves as direct antimicrobial protection (Ahmad et al., 2017). In addition, other antimicrobial proteins including lysozyme and ovotransferrin have also been identified in the eggshell membranes.

35.6.3.2 The mammillary layer

The mammillary layer is a regular array of cones (mammillae, knobs) embedded in the outer shell membrane. The core of each cone is highly organic, composed largely of proteins, and in lesser abundance of mucopolysaccharides. Individual fibers of the outer shell membrane are fixed in the cores. The mammillae cores are the nucleation sites where calcification starts during the shell fabrication. The small calcite crystals in mammillary cones are deposited without particular orientation. As calcification proceeds, the calcite crystals increase their size, grow to a height of approximately 300 μm, and form the main eggshell thickness, the palisade layer. At some points, the crystals do not grow completely together, leaving pores. The roles of proteins identified as specific or highly expressed in the mammillary cones are attributed to regulation of initiation of eggshell calcification and calcium ion binding. The first group comprises ECM proteins such as ABI family member 3 (NESH) binding protein (ABI3BP), tiarin-like, hyaluronan and proteoglycan link protein 3, collagen X, collagen II, and fibronectin. The calcium-binding proteins include calumenin, EDIL3, nucleobindin-2, and SPARC (Rose-Martel et al., 2015).

The size and spacing of the mammillary cones affect the overall strength and biomechanical features of the completed eggshell. During embryo development, the mobilization of calcium, necessary for its growth, occurs from the calcium reserve body located at the base of each cone. The calcium reserve bodies contain reactive microcrystals of calcite with spherulitic texture which are more susceptible to dissolution of the mineral. Moreover, the weakened eggshell is easier to crack by developed chick during hatching (Hincke et al., 2012).

35.6.3.3 The crystal layer

The crystal layer is a continuation of the mammillary layer and constitutes the greater part of the fully formed eggshell. The lower region of the crystal layer is called palisade layer, and upper part is called vertical layer. These layers possess a specific structure composed of mineral and organic precursors that are secreted into the shell gland fluid bathed the egg during shell deposition (discussed in point 35.3.4.1). The calcified eggshell consists mostly of calcite (96%), organic matrix (2%), and remaining elements such as magnesium in the form of magnesium carbonate, phosphorus, and variety of trace elements. The palisade layer is build of groups of columns that extend outwards from the mammillary cones and are perpendicular to the eggshell surface. This layer is covered by the outer vertical

layer (3−8 μm thick) which has a crystalline structure of higher density and with greater vertical dimension to the egg surface than that of the palisade region (Nys et al., 2004; Hincke et al., 2010, 2012).

The crystal layers contain organic matrix, composed of soluble and insoluble proteins, glycoproteins, phosphoproteins, and proteoglycans rich in sulfated molecules. The elements of the organic matrix influence the texture and mechanical properties of the unique eggshell by controlling the size, shape, and orientation of the polycrystalline structure. In addition, many eggshell matrix proteins are responsible for antimicrobial defense. Matrix proteins are incorporated sequentially into the calcifying eggshell leading to their differential distribution across the mammillary and palisade layers.

The proteins in the eggshell matrix are arranged into three groups: major egg white proteins (e.g., ovalbumin, lysozyme, and ovotransferrin) localized in basal layer of the shell, ubiquitous proteins present also in other tissues (e.g., osteopontin and clusterin), and specific eggshell matrix proteins (e.g., ovocleidin-17, ovocleidin-116, ovocalyxin-21, ovocalyxin-25, ovocalyxin-32, and ovocalyxin-36). Among about 900 different proteins identified in the chicken eggshell matrix, over 700 are specific for the eggshell (Gautron, 2019). Several of these proteins are present in abundance in the eggshell matrix and plays specific role in shell mineralization and function. For instance, ovocleidin-17 is one of the most abundant chicken eggshell matrix proteins, concentrated largely in the mammillary layer. Ovocleidin-116, another prominent eggshell matrix protein is widely distributed via the palisade layer, and its role is related to eggshell thickness and shape. Ovocalyxin-32 influences the variability of crystal traits and, in turn, the thickness profile of the shell (Takahashi et al., 2010). Ovocalyxin-36 is highly expressed during the shell calcification and has antimicrobial activity, thus might play a role in the natural defense of the egg against pathogens (Gautron et al., 2011). Further details regarding the eggshell mineralization and characteristic of matrix proteins can be found in an excellent reviews of Nys et al. (2004) and Hincke et al. (2010, 2012).

35.6.3.4 The cuticle

The outermost layer of the eggshell is a noncalcified cuticle which coats the entire outer surface of the crystal layer including the mouths of the pores. It is a thin, invisible layer, varying in thickness between 5 and 10 μm in different eggs and in different regions of the eggshell, and may even be missing. The cuticle is composed of glycoprotein (90%), polysaccharides (4%), lipids (3%), and inorganic phosphorus (3%) including hydroxyapatite crystals. The function of the cuticle is to serve as a protection of the egg from water lost and against microbial invasion. Among the numerous proteins identified in the cuticle are those with known antibacterial properties (Rose-Martel et al., 2012; Mikšik et al., 2014). The cuticle and the outer region of the calcified eggshell comprise pigments responsible for shell color (described in point 35.3.4.2). The physical features and color of eggshells are rooted in the genetic factors of the species, breeds, and individuals. In addition, eggshell color is affected by feed with individual components contributing more or less (Wilson, 2017).

35.6.3.5 The respiration through the eggshell

The shell is penetrated by about 7000 to 17,000 pores, which are the areas of incomplete crystallization. They arise between the mammillae basally, traverse the shell, and are eventually open beneath the cuticle on the surface of the shell. The number of pores per unit area reduces from the blunt end of the egg toward the sharp end. The role of the pores is to permit water vapor and gas exchange between the developing embryo and the ambient air (i.e., air cell of the egg and external environment). Gas exchange occurs by diffusion via the chorioallantoic membrane and the shell membranes before lung respiration starts. The air cell of the egg, which volume increases with the egg incubation progress, enables a more effective gas diffusion (Rokitka and Rahn, 1987). The decrease in the air cell volume has a negative effect on gas exchange, embryonic development, and hatchability. The elliptical shape of the avian egg maintains the blunt end with the air chamber up after oviposition or during incubation, which favors the most effective gas exchange and high hatchability (Mao et al., 2007).

References

Ahmed, T.A., Suso, H.P., Hincke, M.T., 2017. In-depth comparative analysis of the chicken eggshell membrane proteome. J. Proteomics. 155, 49−62.

Ahumada-Solórzano, S.M., Carranza, M.E., Pedernera, E., Rodríguez-Méndez, A.J., Luna, M., Arámburo, C., 2012. Local expression and distribution of growth hormone and growth hormone receptor in the chicken ovary: effects of GH on steroidogenesis in cultured follicular granulosa cells. Gen. Comp. Endocrinol. 175 (2), 297−310.

Ahumada-Solórzano, S.M., Martínez-Moreno, C.G., Carranza, M., Ávila-Mendoza, J., Luna-Acosta, J.L., Harvey, S., Luna, M., Arámburo, C., 2016. Autocrine/paracrine proliferative effect of ovarian GH and IGF-I in chicken granulosa cell cultures. Gen. Comp. Endocrinol. 234, 47−56.

Andrews, J.E., Smith, C.A., Sinclair, A.H., 1997. Sites of estrogen receptor and aromatase expression in the chicken embryo. Gen. Comp. Endocrinol. 108 (2), 182−190.

Anish, D., Sastry, K.V., Sundaresan, N.R., Saxena, V.K., Singh, R., Mohan, J., 2008. Reproductive tissue regression: involvement of caspases, inducible nitric oxide synthase and nitric oxide during moulting in White Leghorn hens. Anim. Reprod. Sci. 104 (2−4), 329−343.

Ariamaa, O., Talo, A., 1983. Smooth muscle of the quail oviduct functions as a stretch receptor during ovum transport. Biol. Reprod. 29 (2), 472–478.

Arias, J.L., Fink, D.J., Xiao, S.Q., Heuer, A.H., Caplan, A.I., 1993. Biomineralization and eggshells: cell-mediated acellular compartments of mineralized extracellular matrix. Int. Rev. Cytol. 45, 217–250.

Armstrong, D.G., Davidson, M.F., Gilbert, A.B., Wells, J.W., 1977. Activity of 3beta-hydroxyteroid dehydrogenase in the postovulatory follicle of the domestic fowl (*Gallus domesticus*). J. Reprod. Fertil. 49 (2), 253–259.

Asbóth, G., Todd, H., Tóth, M., Hertelendy, F., 1985. PGE2 binding, synthesis, and distribution in hen oviduct. Am. J. Physiol. 248 (1 Pt 1), E80–E88.

Asem, E.K., Stingley-Salazar, S.R., Robinson, J.P., Turek, J.J., 2000. Identification of some components of basal lamina of avian ovarian follicle. Poult. Sci. 79, 589–601.

Ayers, K.L., Sinclair, A.H., Smith, C.A., 2013. The molecular genetics of ovarian differentiation in the avian model. Sex Dev. 7, 80–94.

Ayers, K.L., Lambeth, L.S., Davidson, N.M., Sinclair, A.H., Oshlack, A., Smith, C.A., 2015. Identification of candidate gonadal sex differentiation genes in the chicken embryo using RNA-seq. BMC Genom. 16, 704.

Bae, S.M., Lim, W., Jeong, W., Kim, J., Bazer, F.W., Song, G., 2014a. Expression and regulation of avian cathepsin L in the oviduct during molting. Gen. Comp. Endocrinol. 204, 88–94.

Bae, S.M., Lim, W., Jeong, W., Lee, J.Y., Kim, J., Han, J.Y., Bazer, F.W., Song, G., 2014b. Hormonal regulation of beta-catenin during development of the avian oviduct and its expression in epithelial cell-derived ovarian carcinogenesis. Mol. Cell. Endocrinol. 382 (1), 46–54.

Bahr, J.M., Johnson, A.L., 1984. Regulation of the follicular hierarchy and ovulation. J. Exp. Zool. 232, 495–500.

Bahr, J.M., Ritzhaupt, L.K., McCullough, S., Arbogast, L.A., Ben-Jonathan, N., 1986. Catecholamine content of the preovulatory follicles of the domestic hen. Biol. Reprod. 34 (3), 502–506.

Bakst, M.R., 1981. Sperm recovery from oviducts of turkeys at known intervals after insemination and oviposition. J. Reprod. Fertil. 62 (1), 159–164.

Bakst, M.R., 1994. Fate of fluorescent stained sperm following insemination: new light on oviducal sperm transport and storage in the Turkey. Biol. Reprod. 50 (5), 987–992.

Bakst, M.R., Akuffo, V., 2007. Alkaline phosphatase reactivity in the vagina and uterovaginal junction sperm-storage tubules of turkeys in egg production: implications for sperm storage. Br. Poult. Sci. 48 (4), 515–518.

Bakst, M.R., Howarth, B., 1977. Hydrolysis of the hen's perivitelline layer by cock sperm in vitro. Biol. Reprod. 17, 370–379.

Bar, A., 2009. Calcium transport in strongly calcifying laying birds: mechanisms and regulation. Comp. Biochem. Physiol. A, Mol. Integr. Physiol. 152 (4), 447–469.

Barua, A., Yoshimura, Y., Tamura, T., 1998. Localization of macrophages in the ovarian follicles during the follicular growth and postovulatory regression in chicken, Gallus domesticus. Poult. Sci. 77 (9), 1417–1421.

Barua, A., Bitterman, P., Abramowicz, J.S., Dirks, A.L., Bahr, J.M., Hales, D.B., Bradaric, M.J., Edassery, S.L., Rotmensch, J., Luborsky, J.L., 2009. Histopathology of ovarian tumors in laying hens: a preclinical model of human ovarian cancer. Int. J. Gynecol. Cancer. 19, 531–539.

Bédécarrats, G.Y., McFarlane, H., Maddineni, S.R., Ramachandran, R., 2009. Gonadotropin-inhibitory hormone receptor signaling and its impact on reproduction in chickens. Gen. Comp. Endocrinol. 163 (1–2), 7–11.

Bédécarrats, G.Y., Baxter, M., Sparling, B., 2016. An updated model to describe the neuroendocrine control of reproduction in chickens. Gen. Comp. Endocrinol. 227, 58–63.

Bedrak, E., Harvey, S., Chadwick, A., 1981. Concentrations of pituitary, gonadal and adrenal hormones in serum of laying and broody white rock hens (*Gallus domesticus*). J. Endocrinol. 89, 197–204.

Bentley, G.E., Ubuka, T., McGuire, N.L., Chowdhury, V.S., Morita, Y., Yano, T., Hasunuma, I., Binns, M., Wingfield, J.C., Tsutsui, K., 2008. Gonadotropin-inhibitory hormone and its receptor in the avian reproductive system. Gen. Comp. Endocrinol. 156 (1), 34–43.

Berry, W., Doernte, A., Conner, M., Barnes, M., Oates, S., 2006. Spontaneously occurring fibroid tumors of the laying hen oviduct. Poult. Sci. 85 (11), 1969–1974.

Boelkins, J.N., Mueller, W.J., Hall, K.L., 1973. Cardiac output distribution in the laying hen during shell formation. Comp. Biochem. Physiol. A Comp. Physiol. 46 (4), 735–743.

Bourin, M., Gautron, J., Berges, M., Hennequet-Antier, C., Cabau, C., Nys, Y., Réhault-Godbert, S., 2012. Transcriptomic profiling of proteases and antiproteases in the liver of sexually mature hens in relation to vitellogenesis. BMC Genom. 13, 457.

Brackett, K.H., Fields, P.A., Dubois, W., Chang, S.M., Mather, F.B., Fields, M.J., 1997. Relaxin: an ovarian hormone in an avian species (*Gallus domesticus*). Gen. Comp. Endocrinol. 105 (2), 155–163.

Brzezińska, E., Rzasa, J., Ewy, Z., 1967. Plasma aminopeptidase (oxytocinase) activity during oviposition in the hen. Bull. Acad. Pol. Sci. Biol. 15 (3), 143–146.

Bujo, H., Hermann, M., Kaderli, M.O., Jacobsen, L., Sugawara, S., Nimpf, J., Yamamoto, T., Schneider, W.J., 1994. Chicken oocyte growth is mediated by an eight ligand binding repeat member of the LDL receptor family. EMBO J. 13 (21), 5165–5175.

Camacho-Arroyo, I., González-Arenas, A., González-Morán, G., 2007. Ontogenic variations in the content and distribution of progesterone receptor isoforms in the reproductive tract and brain of chicks. Comp. Biochem. Physiol. A Mol. Integr. Physiol. 146 (4), 644–652.

Camper, P., Burke, W., 1977. The effects of prolactin on the gonadotropin induced rise in serum estradiol and progesterone of the laying Turkey. Gen. Comp. Endocrinol. 32, 72–77.

Chabrolle, C., Tosca, L., Crochet, S., Tesseraud, S., Dupont, J., 2007. Expression of adiponectin and its receptors (AdipoR1 and AdipoR2) in chicken ovary: potential role in ovarian steroidogenesis. Domest. Anim. Endocrinol. 33 (4), 480–487.

Chen, D., Yang, M., Xie, L., Lu, Z., Mo, L., Yang, W., Sun, J., Xu, H., Lu, K., Liao, Y., Lu, Y., 2020. GSK-3 signaling is involved in proliferation of chicken primordial germ cells. Theriogenology 141, 62–67.

Chousalkar, K.K., Roberts, J.R., 2008. Ultrastructural changes in the oviduct of the laying hen during the laying cycle. Cell Tissue Res. 332 (2), 349–358.

Chue, J., Smith, C.A., 2011. Sex determination and sexual differentiation in the avian model. FEBS J. 278, 1027–1034.

Corradino, R.A., 1993. Calbindin D28K regulation in precociously matured chick egg shell gland in vitro. Gen. Comp. Endocrinol. 91, 158–166.

Crossley, J., Ferrando, G., Eiler, H., 1980. Distribution of adrenergic receptors in the domestic fowl oviduct. Poult. Sci. 59, 2331–2335.

Cutting, A.D., Bannister, S.C., Doran, T.J., Sinclair, A.H., Tizard, M.V., Smith, C.A., 2012. The potential role of microRNAs in regulating gonadal sex differentiation in the chicken embryo. Chromosome Res. 20 (1), 201–213.

D'Herde, K., De Prest, B., Roels, F., 1996. Subtypes of active cell death in the granulosa of ovarian atretic follicles in the quail (*Coturnix coturnix* japonica). Reprod. Nutr. Dev. 36, 175–189.

Das, S.C., Isobe, N., Yoshimura, Y., December, 2008. Mechanism of prolonged sperm storage and sperm survivability in hen oviduct: a review. Am. J. Reprod. Immunol. 60 (6), 477–481.

de Melo Bernardo, A., Heeren, A.M., van Iperen, L., Fernandes, M.G., He, N., Anjie, S., Noce, T., Ramos, E.S., de Sousa Lopes, S.M., 2015. Meiotic wave adds extra asymmetry to the development of female chicken gonads. Mol. Reprod. Dev. 82 (10), 774–786.

Dias da Silva, W., Tambourgi, D.V., 2010. IgY: a promising antibody for use in immunodiagnostic and in immunotherapy. Vet. Immunol. Immunopathol. 135 (3–4), 173–180.

Dick, H.R., Culbert, J., Wells, J.W., Gilbert, A.B., Davidson, M.F., 1978. Steroid hormones in the postovulatory follicle of the domestic fowl (*Gallus domesticus*). J. Reprod. Fert. 53, 103–107.

Diot, M., Reverchon, M., Rame, C., Froment, P., Brillard, J.P., Brière, S., Levêque, G., Guillaume, D., Dupont, J., 2015. Expression of adiponectin, chemerin and visfatin in plasma and different tissues during a laying season in turkeys. Reprod. Biol. Endocrinol. 13, 81.

Donoghue, D.J., Campbell, R.M., Scanes, C.G., 1990. Effect of biosynthetic chicken growth hormone on egg production in White Leghorn hens. Poult. Sci. 69, 1818–1821.

Dougherty, D.C., Sanders, M.M., 2005. Estrogen action: revitalization of the chick oviduct model. Trends Endocrinol. Metab. 16, 414–419.

Du, J., Hincke, M.T., Rose-Martel, M., Hennequet-Antier, C., Brionne, A., Cogburn, L.A., Nys, Y., Gautron, J., 2015. Identifying specific proteins involved in eggshell membrane formation using gene expression analysis and bioinformatics. BMC Genom. 16, 792.

Duncan, W.C., 2000. The human corpus luteum: remodelling during luteolysis and maternal recognition of pregnancy. Rev. Reprod. 5 (1), 12–17.

Dunn, I.C., Wilson, P.W., Lu, Z., Bain, M.M., Crossan, C.L., Talbot, R.T., Waddington, D., 2009. New hypotheses on the function of the avian shell gland derived from microarray analysis comparing tissue from juvenile and sexually mature hens. Gen. Comp. Endocrinol. 163 (1–2), 225–232.

Elhamouly, M., Isobe, N., Yoshimura, Y., 2017. Expression and localization of cyclooxygenases in the oviduct of laying hens during the ovulatory cycle. Theriogenology 101, 1–7.

Elis, S., Dupont, J., Couty, I., Persani, L., Govoroun, M., Blesbois, E., Batellier, F., Monget, P., 2007. Expression and biological effects of bone morphogenetic protein-15 in the hen ovary. J. Endocrinol. 194, 485–497.

Elis, S., Batellier, F., Couty, I., Balzergue, S., Martin-Magniette, M.L., Monget, P., Blesbois, E., Govoroun, M.S., 2008. Search for the genes involved in oocyte maturation and early embryo development in the hen. BMC Genom. 9, 110.

Elmore, S., 2007. Apoptosis: a review of programmed cell death. Toxicol. Pathol. 35 (4), 495–516.

Espey, L.L., 1980. Ovulation as an inflammatory reaction-a hypothesis. Biol. Reprod. 22, 73–106.

Estienne, A., Bongrani, A., Reverchon, M., Ramé, C., Ducluzeau, P.H., Froment, P., Dupont, J., 2019. Involvement of novel adipokines, chemerin, visfatin, resistin and apelin in reproductive functions in normal and pathological conditions in humans and animal models. Int. J. Mol. Sci. 20 (18), E4431 pii.

Etches, R.J., 1990. The ovulatory cycle of the hen. CRC Crit. Rev. Poult. Biol. 2, 293–318.

Etches, R.J., 1996. Reproduction in Poultry. CAB international, Wallingford, UK.

Etches, R.J., Kelly, J.D., Anderson-Langmuir, C.E., Olson, D.M., 1990. Prostaglandin production by the largest preovulatory follicles in the domestic hen (*Gallus domesticus*). Biol. Reprod. 43 (3), 378–384.

Evans, M.I., Silva, R., Burch, J.B., 1988. Isolation of chicken vitellogenin I and III cDNAs and the developmental regulation of five estrogen-responsive genes in the embryonic liver. Genes Dev. 2 (1), 116–124.

Feng, Y.P., Chen, J.F., Huang, P., Wang, X., Wang, J., Peng, X.L., Gong, Y.Z., 2014. Expression analysis of differentially expressed miRNAs in male and female chicken embryos. Genet. Mol. Res. 13 (2), 3060–3068.

Finn, R.N., 2007. Vertebrate yolk complexes and the functional implications of phosvitins and other subdomains in vitellogenins. Biol. Reprod. 76 (6), 926–935.

Foye-Jackson, O.T., Long, J.A., Bakst, M.R., Blomberg, L.A., Akuffo, V.G., Silva, M.V., Guthrie, H.D., McMurtry, J.P., 2011. Oviductal expression of avidin, avidin-related protein-2, and progesterone receptor in Turkey hens in relation to sperm storage: effects of oviduct tissue type, sperm presence, and Turkey line. Poult. Sci. 90 (7), 1539–1547.

Fraps, R.M., 1955. Egg production and fertility in poultry. In: Hammond, J. (Ed.), Progress in the Physiology of Farm Animals, vol. II. Butterworth, London.

Fredrickson, T.N., 1987. Ovarian tumors of the hen. Environ. Health Perspect. 73, 35–51.

Fu, Z., Kubo, T., Noguchi, T., Kato, H., 2001. Developmental changes in the mRNA levels of IGF-I and its related genes in the reproductive organs of Japanese quail (*Coturnix coturnix* japonica). Growth Horm. IGF Res. 11, 24–33.

Gautron, J., 2019. Proteomics analysis of avian eggshell matrix proteins: toward new advances on biomineralization. Proteomics 19 (13), e1900120.

Gautron, J., Réhault-Godbert, S., Pascal, G., Nys, Y., Hincke, M.T., 2011. Ovocalyxin-36 and other LBP/BPI/PLUNC-like proteins as molecular actors of the mechanisms of the avian egg natural defenses. Biochem. Soc. Trans. 39, 971–976.

Ghanem, K., Johnson, A.L., 2018. Follicle dynamics and granulosa cell differentiation in the Turkey hen ovary. Poult. Sci. 97 (10), 3755–3761.

Ghanem, K., Johnson, A.L., 2019a. Relationship between cyclic follicle recruitment and ovulation in the hen ovary. Poult. Sci. 98 (7), 3014–3021.

Ghanem, K., Johnson, A.L., 2019b. Response of hen pre-recruitment ovarian follicles to follicle stimulating hormone, in vivo. Gen. Comp. Endocrinol. 270, 41–47.

Gilbert, A.B., 1965. Innervation of the ovarian follicle of the domestic hen. Q. J. Exp. Physiol. 50, 437.

Gilbert, A.B., 1969. Innervation of the ovary of the domestic hen. Q. J. Exp. Physiol. 54, 404–411.

Gilbert, A.B., 1971. The egg: its physical and chemical aspects. In: Bell, D.J., Freeman, B.M. (Eds.), Physiology and Biochemistry of the Domestic Fowl, vol. 3. Academic Press, London and New York, pp. 1379–1399.

Gilbert, A.B., 1979. Female genital organs. In: King, A.S., McLelland, J. (Eds.), Form and Function in Birds, vol. I. Academic Press, London and New York, pp. 258–360.

Gilbert, A.B., Lake, P.E., 1963. Terminal innervation of the uterus and vagina of the domestic hen. J. Reprod. Fertil. 5, 41–48.

Gilbert, A.B., Davidson, M.F., Wells, J.W., 1978. Role of the granulosa cells of the postovulatory follicle of the domestic fowl in oviposition. J. Reprod. Fertil. 52 (2), 227–229.

Ginsburg, M., Eyal-Giladi, H., 1987. Primordial germ cells of the young chick blastoderm originate from the central zone of the area pellucida irrespective of the embryo-forming process. Development 101 (2), 209–219.

Gomez, Y., Velazquez, P.N., Peralta-Delgado, I., Mendez, M.C., Vilchis, F., Juarez-Oropeza, M.A., Pedernera, E., 2001. Follicle-stimulating hormone regulates steroidogenic enzymes in cultured cells of the chick embryo ovary. Gen. Comp. Endocrinol. 121, 305–315.

Gonzalez, C.B., Charreau, E.H., Aragones, A., Lantos, C.P., Follett, B.K., 1987. The ontogenesis of reproductive hormones in the female embryo of the domestic fowl. Gen. Comp. Endocrinol. 68, 369–374.

González-Morán, M.G., 2007. Effects of luteinizing hormone treatment on oogenesis in ovarian germ cells of the chick (Gallus domesticus). Domest. Anim. Endocrinol. 33, 154–166.

González-Morán, M.G., 2011. Histological and stereological changes in growing and regressing chicken ovaries during development. Anat. Rec. 294 (5), 893–904.

González-Morán, M.G., 2014. Changes in the cellular localization of estrogen receptor alpha in the growing and regressing ovaries of *Gallus domesticus* during development. Biochem. Biophys. Res. Commun. 447 (1), 197–204.

González-Morán, M.G., 2015. Immunohistochemical localization of progesterone receptor isoforms and estrogen receptor alpha in the chicken oviduct magnum during development. Acta Histochem. 117 (8), 681–687.

González-Morán, M.G., 2016. Changes in progesterone receptor isoforms expression and in the morphology of the oviduct magnum of mature laying and aged nonlaying hens. Biochem. Biophys. Res. Commun. 478 (2), 999–1005.

González-Morán, G., Camacho-Arroyo, I., 1998. Histomorphometric and progesterone receptor immunohistochemical analysis in the oviduct of newly hatched chicks treated with follicle-stimulating hormone during embryonic development. Anat. Histol. Embryol. 27 (4), 277–282.

González-Morán, G., Camacho-Arroyo, I., 2001. Immunohistochemical localization of progesterone receptor isoforms in the chick prefollicular ovary. Anat. Histol. Embryol. 30 (3), 153–158.

González-Morán, M.G., González-Arenas, A., Germán-Castelán, L., Camacho-Arroyo, I., 2013. Changes in the content of sex steroid hormone receptors in the growing and regressing ovaries of *Gallus domesticus* during development. Gen. Comp. Endocrinol. 189C, 51–58.

Govoroun, M.S., Pannetier, M., Pailhoux, E., Cocquet, J., Brillard, J.P., Couty, I., Batellier, F., Cotinot, C., 2004. Isolation of chicken homolog of the FOXL2 gene and comparison of its expression patterns with those of aromatase during ovarian development. Dev. Dyn. 231, 859–870.

Grzegorzewska, A.K., Sechman, A., Paczoska-Eliasiewicz, H.E., Rzasa, J., 2009. The expression of pituitary FSHbeta and LHbeta mRNA and gonadal FSH and LH receptor mRNA in the chicken embryo. Reprod. Biol. 9 (3), 253–269.

Guioli, S., Nandi, S., Zhao, D., Burgess-Shannon, J., Lovell-Badge, R., Clinton, M., 2014. Gonadal asymmetry and sex determination in birds. Sex. Dev. 8 (5), 227–242.

Guo, X., Wang, Y., Chen, Q., Yuan, Z., Chen, Y., Guo, M., Kang, L., Sun, Y., Jiang, Y., 2019. The role of PTHLH in ovarian follicle selection, its transcriptional regulation and genetic effects on egg laying traits in hens. Front. Genet. 10, 430.

Ha, Y., Tsukada, A., Saito, N., Shimada, K., 2004. Changes in mRNA expression of MMP-2 in the Mullerian duct of chicken embryo. Gen. Comp. Endocrinol. 139, 131–136.

Hadley, J.A., Ocón-Grove, O., Ramachandran, R., 2020. Adiponectin is secreted by theca layer cells isolated from chicken ovarian follicles. Reproduction 159 (3), 275–288.

Hakim, A.A., Barry, C.P., Barnes, H.J., Anderson, K.E., Petitte, J., Whitaker, R., Lancaster, J.M., Wenham, R.M., Carver, D.K., Turbov, J., Berchuck, A., Kopelovich, L., Rodriguez, G.C., 2009. Ovarian adenocarcinomas in the laying hen and women share similar alterations in p53, ras, and HER-2/neu. Cancer Prev. Res. 2, 114–121.

Hales, D.B., Zhuge, Y., Lagman, J.A., Ansenberger, K., Mahon, C., Barua, A., Luborsky, J.L., Bahr, J.M., 2008. Cyclooxygenases expression and distribution in the normal ovary and their role in ovarian cancer in the domestic hen (*Gallus domesticus*). Endocrine 33 (3), 235–244.

Han, J., Ahmad, H.I., Jiang, X., Liu, G., 2019. Role of genome-wide mRNA-seq profiling in understanding the long-term sperm maintenance in the storage tubules of laying hens. Trop. Anim. Health Prod. 51 (6), 1441–1447.

Hansen, K.K., Kittok, R.J., Sarath, G., Toombs, C.F., Caceres, N., Beck, M.M., 2003. Estrogen receptor-alpha populations change with age in commercial laying hens. Poult. Sci. 82 (10), 1624–1629.

Harvey, S., Scanes, C.G., Chadwick, A., Knight, P.J., Callard, I.P., 1978. Effect of growth hormone and oestradiol on vitellogenesis in hypophysectomised pigeons. IRCS Med. Sci. 6, 198.

Harvey, S., Scanes, C.G., Sharp, P.J., 1979. Variations in plasma growth hormone concentrations in laying hens. Br. Poult. Sci. 20, 163–166.

Heck, A., Matayer, S., Onagbesan, O.M., Williams, J., 2003. mRNA expression of components of the IGF system and of GH and insulin receptors in ovaries of broiler breeder hens fed ad libitum or restricted from 4 to 16 weeks of age. Domest. Anim. Endocrinol. 25, 287–294.

Heryanto, B., Yoshimura, Y., Tamura, T., Okamoto, T., 1997. Involvement of apoptosis and lysosomal hydrolase activity in the oviducal regression during induced molting in chickens: a cytochemical study for end labeling of fragmented DNA and acid phosphatase. Poult. Sci. 76 (1), 67–72.

Hincke, M.T., Nys, Y., Gautron, J., 2010. The role of matrix proteins in eggshell formation. J. Poult. Sci. 47, 208–219.

Hincke, M.T., Nys, Y., Gautron, J., Mann, K., Rodriguez-Navarro, A.B., McKee, M.D., 2012. The eggshell: structure, composition and mineralization. Front. Biosci. 17, 1266–1280.

Hirst, C.E., Major, A.T., Smith, C.A., 2018. Sex determination and gonadal sex differentiation in the chicken model. Int. J. Dev. Biol. 62, 153–166.

Hiyama, G., Matsuzaki, M., Mizushima, S., Dohra, H., Ikegami, K., Yoshimura, T., Shiba, K., Inaba, K., Sasanami, T., 2013. Sperm activation by heat shock protein 70 supports migration of sperm released from sperm storage tubules in Japanese quail (Coturnix japonica). Reproduction 147 (2), 167–178.

Hiyama, G., Mizushima, S., Matsuzaki, M., Ichikawa, Y., Kansaku, N., Sasanami, T., 2016. Expression of prolactin receptor on the surface of quail spermatozoa. J. Poult. Sci. 53, 157–164.

Hodges, R.D., 1974. The Histology of the Fowl. Academic Press, New York and London.

Holm, L., RidderstrÍle, Y., Knutsson, P.G., 1996. Localisation of carbonic anhydrase in the sperm storing regions of the domestic hen oviduct. Acta Anat. 156 (4), 253–260.

Hora, J., Gosse, B., Rasmussen, K., Spelsberg, T.C., 1986. Estrogen regulation of the biological activity of the avian oviduct progesterone receptor and its ability to induce avidin. Endocrinology 119 (3), 1118–1125.

Howarth, B., 1984. Maturation of spermatozoa and mechanism of fertilization. In: Cunningham, F.J., Lake, P.E., Hewitt, D. (Eds.), Reproductive Biology of Poultry. British Poultry Science Ltd, Oxford, pp. 161–174.

Hrabia, A., 2000. Histamine in the Oviduct of the Domestic Hen (Ph.D. thesis). The Agricultural University in Cracow.

Hrabia, A., 2015. Growth hormone production and role in the reproductive system of female chicken. Gen. Comp. Endocrinol. 220, 112–118.

Hrabia, A., Takagi, S., Shimada, K., 2003a. Variable response to hormonal induction of multiple ovulation in quail. J. Poult. Sci. 40 (3), 231–238.

Hrabia, A., Takagi, S., Ono, T., Shimada, K., 2003b. Fertilization and development of quail oocytes after intracytoplasmic sperm injection. Biol. Reprod. 69 (5), 1651–1657.

Hrabia, A., Ha, Y., Shimada, K., 2004a. Expression of estrogen receptor alpha mRNA in theca and granulosa layers of the ovary in relation to follicular growth in quail. Folia Biol. (Krakow). 52 (3–4), 191–195.

Hrabia, A., Paczoska-Eliasiewicz, H., Rzasa, J., 2004b. Effect of prolactin on estradiol and progesterone secretion by isolated chicken ovarian follicles. Folia Biol. (Krakow). 52, 197–203.

Hrabia, A., Paczoska-Eliasiewicz, H., Niezgoda, J., Rząsa, J., 2005. Histamine affects blood flow through the reproductive organs of the domestic hen (*Gallus domesticus*). Folia Biol. (Krakow). 53, 209–213.

Hrabia, A., Wilk, M., Rząsa, J., 2008a. Expression of alpha and beta estrogen receptors in the chicken ovary. Folia Biol. (Krakow). 56, 187–191.

Hrabia, A., Paczoska-Eliasiewicz, H.E., Berghman, L.R., Harvey, S., Rzasa, J., 2008b. Expression and localization of growth hormone and its receptors in the chicken ovary during sexual maturation. Cell Tissue Res. 332 (2), 317–328.

Hrabia, A., Sechman, A., Gertler, A., Rząsa, J., 2011. Effect of growth hormone on steroid content, proliferation and apoptosis in the chicken ovary during sexual maturation. Cell Tissue Res. 345, 191–202.

Hrabia, A., Sechman, A., Rząsa, J., 2012. Independent, non-IGF-I mediated, GH action on estradiol secretion by prehierarchical ovarian follicles in chicken. In vitro study. Folia Biol. (Krakow). 60, 213–217.

Hrabia, A., Grzegorzewska, A.K., Sechman, A., 2013. Expression and localization of growth hormone receptor in the oviduct of the laying hen (*Gallus domesticus*). Folia Biol. (Krakow). 61, 271–276.

Hrabia, A., Sechman, A., Rząsa, J., 2014a. Effect of growth hormone on basal and LH-stimulated steroid secretion by chicken yellow ovarian follicles. An in vitro study. Folia Biol. (Krakow). 62, 313–319.

Hrabia, A., Leśniak-Walentyn, A., Sechman, A., Gertler, A., 2014b. Chicken oviduct the target tissue for growth hormone action: effect on cell proliferation and apoptosis and on the gene expression of some oviduct-specific proteins. Cell Tissue Res. 357, 363–372.

Hrabia, A., Leśniak-Walentyn, A., Ocłoń, E., Sechman, A., 2016. Changes in proliferating and apoptotic markers in the oviductal magnum of chickens during sexual maturation. Theriogenology 85 (9), 1590–1598.

Hrabia, A., Socha, J.K., Sechman, A., 2018. Involvement of matrix metalloproteinases (MMP-2, -7, -9) and their tissue inhibitors (TIMP-2, -3) in the regression of chicken postovulatory follicles. Gen. Comp. Endocrinol. 260, 32–40.

Hrabia, A., Wolak, D., Kwaśniewska, M., Kieronska, A., Socha, J.K., Sechman, A., 2019. Expression of gelatinases (MMP-2 and MMP-9) and tissue inhibitors of metalloproteinases (TIMP-2 and TIMP-3) in the chicken ovary in relation to follicle development and atresia. Theriogenology 125, 268–276.

Hrabia, A., Socha, J.K., Saito, N., Grzesiak, M., Sechman, A., 2020. Aquaporin 4 in the chicken oviduct during a pause in laying induced by food deprivation. C. R. Biol 343 (1), 89–99.

Hu, S.Q., Zadworny, D., 2017. Effects of nonglycosylated and glycosylated prolactin on basal and gonadotropin-stimulated steroidogenesis in chicken ovarian follicles. Domest. Anim. Endocrinol. 61, 27–38.

Hu, S., Duggavathi, R., Zadworny, D., 2017a. Regulatory mechanisms underlying the expression of prolactin receptor in chicken granulosa cells. PLoS One 12 (1), e0170409.

Hu, S., Duggavathi, R., Zadworny, D., 2017b. Expression and regulation of prolactin-like protein messenger RNA in undifferentiated chicken granulosa cells. Gen. Comp. Endocrinol. 240, 191–197.

Huang, A., Isobe, N., Obitsu, T., Yoshimura, Y., 2016. Expression of lipases and lipid receptors in sperm storage tubules and possible role of fatty acids in sperm survival in the hen oviduct. Theriogenology 85 (7), 1334–1342.

Huang, A., Isobe, N., Yoshimura, Y., 2017. Changes in localization and density of CD63-positive exosome-like substances in the hen oviduct with artificial insemination and their effect on sperm viability. Theriogenology 101, 135–143.

Hudson, Q.J., Smith, C.A., Sinclair, A.H., 2005. Aromatase inhibition reduces expression of FOXL2 in the embryonic chicken ovary. Dev. Dyn. 233 (3), 1052–1055.

Hughes, G.C., 1963. The population of germ cells in the developing female chick. J. Embryol. Exp. Morphol. 11 (3), 513–536.

Isola, J.J., 1990. Distribution of estrogen and progesterone receptors and steroid-regulated gene products in the chick oviduct. Mol. Cell. Endocrinol. 69 (2–3), 235–243.

Isola, J., Korte, J.M., Tuohimaa, P., 1987. Immunocytochemical localization of progesterone receptor in the chick ovary. Endocrinology 121, 1034–1040.

Ito, Y., Kihara, M., Nakamura, E., Yonezawa, S., Yoshizaki, N., 2003. Vitellogenin transport and yolk formation in the quail ovary. Zool. Sci. 20, 717–726.

Jackson, J.A., Friberg, A.C., Bahr, J.M., 1991. Preovulatory changes in glycosaminoglycans and collagen content in the stigma region of the follicle of the domestic hen. Biol. Reprod. 45, 301–307.

Jackson, J.A., Zhang, P., Bahr, J.M., 1993. Plasminogen activator activity in preovulatory follicles during the ovulatory cycle of the chicken. Biol. Reprod. 49 (5), 1141–1146.

Jeong, W., Lim, W., Ahn, S.E., Lim, C.H., Lee, J.Y., Bae, S.M., Kim, J., Bazer, F.W., Song, G., 2013. Recrudescence mechanisms and gene expression profile of the reproductive tracts from chickens during the molting period. PLoS One 8 (10), e76784.

Jeong, J., Bae, H., Lim, W., Bazer, F.W., Song, G., 2015. Diethylstilbestrol regulates expression of avian apolipoprotein D during regression and recrudescence of the oviduct and epithelial-derived ovarian carcinogenesis. Domest. Anim. Endocrinol. 52, 82–89.

Jeong, W., Bae, H., Lim, W., Bazer, F.W., Song, G., 2017a. Differential expression of neuregulin 1 (NRG1) and candidate miRNA regulating NRG1 transcription in the chicken oviduct in response to hormonal changes. J. Anim. Sci. 95 (9), 3885–3904.

Jeong, W., Bae, H., Lim, W., Song, G., 2017b. Dicer1, AGO3, and AGO4 microRNA machinery genes are differentially expressed in developing female reproductive organs and overexpressed in cancerous ovaries of chickens. J. Anim. Sci. 95 (11), 4857–4868.

Jeong, W., Bae, H., Lim, W., Bazer, F.W., Song, G., 2018. RAS-related protein 1: an estrogen-responsive gene involved in development and molting-mediated regeneration of the female reproductive tract in chickens. Animal 12 (8), 1594–1601.

Jia, Y., Lin, J., Zeng, W., Zhang, C., 2010. Effect of prostaglandin on luteinizing hormone-stimulated proliferation of theca externa cells from chicken prehierarchical follicles. Prostag. Other Lipid Mediat. 92 (1–4), 77–84.

Jin, Y., Zhang, C., Lin, X., Zeng, W., 2006. Prostaglandin involvement in follicle-stimulating hormone-induced proliferation of granulosa cells from chicken prehierarchical follicles. Prostag. Other Lipid Mediat. 81 (1–2), 45–54.

Joensuu, T.K., 1990. Chick oviduct differentiation. The effect of estrogen and progesteroneon the expression of progesterone receptor. Cell Differ. Dev. 30, 207–218.

Johnson, A.L., 1990. Steroidogenesis and actions of steroids in the hen ovary. CRC Crit. Rev. Poult. Biol. 2, 319–346.

Johnson, P.A., 2012. Follicle selection in the avian ovary. Reprod. Domest. Anim. 47 (Suppl. 4), 283–287.

Johnson, A.L., 2014. The avian ovary and follicle development: some comparative and practical insights. Turk. J. Vet. Anim. Sci. 38, 660–669.

Johnson, A.L., 2015a. Ovarian follicle selection and granulosa cell differentiation. Poult. Sci. 94 (4), 781–785.

Johnson, A.L., 2015b. Chapter 28. Reproduction in the female. In: Scanes, C.G. (Ed.), Sturkie's Avian Physiology, Sixth Ed. Academic Press, pp. 635–665.

Johnson, A.L., Bridgham, J.T., 2001. Regulation of steroidogenic acute regulatory (StAR) protein messenger RNA in hen granulosa cells. Endocrinology 142 (7), 3116–3124.

Johnson, P.A., Giles, J.R., 2013. The hen as a model of ovarian cancer. Nat. Rev. Cancer 13 (6), 432–436.

Johnson, A.L., Lee, J., 2016. Granulosa cell responsiveness to follicle stimulating hormone during early growth of hen ovarian follicles. Poult. Sci. 95 (1), 108–114.

Johnson, A.L., van Tienhoven, A., 1980. Plasma concentrations of sex steroids and LH during the ovulatory cycle of the hen, *Gallus domesticus*. Biol. Reprod. 23, 386–393.

Johnson, A.L., Woods, D.C., 2007. Chapter 6. Ovarian dynamics and follicle development. In: Jamieson, B.G.M. (Ed.), Reproductive Biology and Phylogeny of Aves. Science Publishers, Inc., pp. 243–277

Johnson, P.A., Green, C., Lee, H.T., Bahr, J.M., 1988. Inhibition of progesterone secretion from granulosa cells by estradiol and androgens in the domestic hen. Endocrinology 123 (1), 473–477.

Johnson, P.A., Dickens, M.J., Kent, T.R., Giles, J.R., 2005. Expression and function of growth differentiation factor-9 in an oviparous species, *Gallus domesticus*. Biol. Reprod. 72 (5), 1095–1100.

Johnson, P.A., Kent, T.R., Urick, M.E., Giles, J.R., 2008. Expression and regulation of anti-Mullerian hormone in an oviparous species, the hen. Biol. Reprod. 78 (1), 13–19.

Johnson, P.A., Stephens, C.S., Giles, J.R., 2015. The domestic chicken: causes and consequences of an egg a day. Poult. Sci. 94 (4), 816–820.

Jonchčre, V., Brionne, A., Gautron, J., Nys, Y., 2012. Identification of uterine ion transporters for mineralisation precursors of the avian eggshell. BMC Physiol. 12, 10.

Jung, J.G., Lim, W., Park, T.S., Kim, J.N., Han, B.K., Song, G., Han, J.Y., 2011. Structural and histological characterization of oviductal magnum and lectin-binding patterns in *Gallus domesticus*. Reprod. Biol. Endocrinol. 9, 62.

Kang, L., Cui, X., Zhang, Y., Yang, C., Jiang, Y., May 26, 2013. Identification of miRNAs associated with sexual maturity in chicken ovary by illumina small RNA deep sequencing. BMC Genom. 14 (1), 352.

Kansaku, N., Shimada, K., Terada, O., Saito, N., 1994. Prolactin, growth hormone, and luteinizing hormone-beta subunit gene expression in the cephalic and caudal lobes of the anterior pituitary gland during embryogenesis and different reproductive stages in the chicken. Gen. Comp. Endocrinol. 96 (2), 197–205.

Kato, M., Shimada, K., Saito, N., Nada, K., Ohta, M., 1995. Expression of P450 17α-hydroxylase and P450 aromatase genes in isolated granulosa, theca interna, and theca externa layers of chicken ovarian follicles during follicular growth. Biol. Reprod. 52, 405–410.

Kawashima, M., Takahashi, T., Kondo, S., Yasuoka, T., Ogawa, H., Tanaka, K., 1999. Identification of an androgen receptor within the uterus of the domestic fowl. Poult. Sci. 78 (1), 107–113.

Khan, S., Wu, S.B., Roberts, J., 2019. RNA-sequencing analysis of shell gland shows differences in gene expression profile at two time-points of eggshell formation in laying chickens. BMC Genom. 20 (1), 89.

Kida, S., Iwaki, M., Nakamura, A., Miura, Y., Takenaka, A., Takahashi, S., Noguchi, T., 1994. Insulin-like growth factor-I messenger RNA content in the oviduct of Japanese quail (*Coturnix coturnix* japonica): changes during growth and development or after estrogen administration. Comp. Biochem. Physiol. C Pharmacol. Toxicol. Endocrinol. 109, 191–204.

Kida, S., Miura, Y., Takenaka, A., Takahashi, S., Noguchi, T., 1995. Effects of insulin-like growth factor-I, estrogen, glucocorticoid, and transferrin on the mRNA contents of ovalbumin and conalbumin in primary cultures of quail (*Coturnix coturnix* japonica) oviduct cells. Comp. Biochem. Physiol. C Pharmacol. Toxicol. Endocrinol. 110, 157–164.

Kiell, C.S., Cohen, I.T., Fell, P., 1982. Development of embryonic chick oviducts in organculture under the influence of steroid hormones. J. Exp. Zool. 220, 387–390.

Kim, D., Johnson, A.L., 2018. Differentiation of the granulosa layer from hen prehierarchal follicles associated with follicle-stimulating hormone receptor signaling. Mol. Reprod. Dev. 85, 729–737.

Kim, D., Ocón-Grove, O., Johnson, A.L., 2013. Bone morphogenetic protein 4 (BMP4) supports the initial differentiation of hen (*Gallus gallus*) granulosa cells. Biol. Reprod. 88 (6), 161.

Kim, D., Lee, J., Johnson, A.L., 2016. Vascular endothelial growth factor and angiopoietins during hen ovarian follicle development. Gen. Comp. Endocrinol. 232, 25–31.

Kim, J., Lim, W., Bazer, F.W., Song, G., 2017. Rapid communication: microRNA co-expression network reveals apoptosis in the reproductive tract during molting in laying hens. J. Anim. Sci. 95 (11), 5100–5104.

Krishnan, K.A., Proudman, J.A., Bolt, D.J., Bahr, J.M., 1993. Development of an homologous radioimmunoassay for chicken follicle-stimulating hormone and measurement of plasma FSH during the ovulatory cycle. Comp. Biochem. Physiol. Comp. Physiol. 105 (4), 729–734.

Krzysik-Walker, S.M., Ocón-Grove, O.M., Maddineni, S.B., Hendricks 3rd, G.L., Ramachandran, R., 2007. Identification of calcitonin expression in the chicken ovary: influence of follicular maturation and ovarian steroids. Biol. Reprod. 77 (4), 626–635.

Kundu, M.C., Wojtusik, J., Johnson, P.A., 2012. Expression and regulation of kit ligand in the ovary of the hen. Gen. Comp. Endocrinol. 179 (1), 47–52.

Kunnas, T.A., Joensuu, T.K., Viitala, K.K., Sopanen, P., Tuohimaa, P., Kulomaa, M.S., 1992. Induction of avidin messenger ribonucleic acid in the chick oviduct by progesterone and other steroids. Endocrinology 130 (6), 3421–3426.

Kuroiwa, 2017. Sex-determining mechanism in avians. Adv. Exp. Med. Biol. 1001, 19–31.

Kuroki, M., Mori, M., 1997. Binding of spermatozoa to the perivitelline layer in the presence of a protease inhibitor. Poult. Sci. 76, 748–752.

Laguë, P.C., van Tienhoven, A., Cunningham, F.J., 1975. Concentrations of estrogens, progesterone and LH during the ovulatory cycle of the laying chicken [*Gallus domesticus*]. Biol. Reprod. 12 (5), 590–598.

Lázár, B., Anand, M., Tóth, R., Várkonyi, E.P., Liptói, K., Gócza, E., 2018. Comparison of the microRNA expression profiles of male and female avian primordial germ cell lines. Stem Cells Int. 2018, 1780679.

Lebedeva, I.Y., Lebedev, V.A., Grossmann, R., Kuzmina, T.I., Parvizi, N., 2004. Characterization of growth hormone binding sites in granulosa and theca layers at different stage of follicular maturation and ovulatory cycle in the domestic hen. Biol. Reprod. 71, 1174–1181.

Lee, H.T., Bahr, J.M., 1990. Inhibition of the activities of P450 cholesterol side-chain cleavage and 3β-hydroxysteroid dehydrogenase and the amount of P450 cholesterol side-chain cleavage by testosterone and estradiol-17β in hen granulosa cells. Endocrinology 126, 779–786.

Lee, J.H., Paik, H.D., 2019. Anticancer and immunomodulatory activity of egg proteins and peptides: a review. Poult. Sci. 98 (12), 6505–6516.

Lee, K.A., Volentine, K.K., Bahr, J.M., 1998. Two steroidogenic pathways present in the chicken ovary: theca layer prefers Δ5 pathway and granulosa layer prefers Δ4 pathway. Domest. Anim. Endocrinol. 15, 1–8.

Lee, J.Y., Jeong, W., Kim, J.H., Kim, J., Bazer, F.W., Han, J.Y., Song, G., 2012. Distinct expression pattern and post-transcriptional regulation of cell cycle genes in the glandular epithelia of avian ovarian carcinomas. PLoS One 7 (12), e51592.

Lee, H.C., Lim, S., Han, J.Y., 2016. Wnt/β-catenin signaling pathway activation is required for proliferation of chicken primordial germ cells in vitro. Sci. Rep. 6, 34510.

Leśniak, A., Hrabia, A., 2012. Expression of matrix metalloproteinase-2 mRNA in the chicken ovary in relation to follicle remodelling. Folia Biol. (Krakow). 60, 219–225.

Leśniak-Walentyn, A., Hrabia, A., 2016a. Expression and localization of matrix metalloproteinases (MMP-2, -7, -9) and their tissue inhibitors (TIMP-2, -3) in the chicken oviduct during maturation. Cell Tissue Res. 364 (1), 185–197.

Leśniak-Walentyn, A., Hrabia, A., 2016b. Involvement of matrix metalloproteinases (MMP-2, -7, -9) and their tissue inhibitors (TIMP-2, -3) in the chicken oviduct regression and recrudescence. Cell Tissue Res. 366 (2), 443–454.

Leśniak-Walentyn, A., Hrabia, A., 2017. Expression and localization of matrix metalloproteinases (MMP-2, -7, -9) and their tissue inhibitors (TIMP-2, -3) in the chicken oviduct during pause in laying induced by tamoxifen. Theriogenology 88, 50–60.

Li, D., Tsutsui, K., Muneoka, Y., Minakata, H., Nomoto, K., 1996. An oviposition-inducing peptide: isolation, localization, and function of avian galanin in the quail oviduct. Endocrinology 137 (5), 1618–1626.

Li, W.L., Liu, Y., Yu, Y.C., Huang, Y.M., Liang, S.D., Shi, Z.D., 2011. Prolactin plays a stimulatory role in ovarian follicular development and egg laying in chicken hens. Domest. Anim. Endocrinol. 41 (2), 57–66.

Li, L., Zhang, Z., Peng, J., Wang, Y., Zhu, Q., 2014. Cooperation of luteinizing hormone signaling pathways in preovulatory avian follicles regulates circadian clock expression in granulosa cell. Mol. Cell. Biochem. 394 (1–2), 31–41.

Li, J., Luo, W., Huang, T., Gong, Y., 2019. Growth differentiation factor 9 promotes follicle-stimulating hormone-induced progesterone production in chicken follicular granulosa cells. Gen. Comp. Endocrinol. 276, 69–76.

Li, Q., Hu, S., Wang, Y., Deng, Y., Yang, S., Hu, J., Li, L., Wang, J., 2019. mRNA and miRNA transcriptome profiling of granulosa and theca layers from geese ovarian follicles reveals the crucial pathways and interaction networks for regulation of follicle selection. Front. Genet. 10, 988.

Lim, W., Song, G., 2014. Identification of novel regulatory genes in development of the avian reproductive tracts. PLoS One 9 (4), e96175.

Lim, W., Song, G., 2015. Differential expression of vitelline membrane outer layer protein 1: hormonal regulation of expression in the oviduct and in ovarian carcinomas from laying hens. Mol. Cell. Endocrinol. 399, 250–258.

Lim, W., Jeong, W., Kim, J.H., Lee, J.Y., Kim, J., Bazer, F.W., Han, J.Y., Song, G., 2011. Differential expression of alpha 2 macroglobulin in response to diethylstilbestrol and in ovarian carcinomas in chickens. Reprod. Biol. Endocrinol. 9, 137.

Lim, C.H., Jeong, W., Lim, W., Kim, J., Song, G., Bazer, F.W., 2012. Differential expression of select members of the SLC family of genes and regulation of expression by microRNAs in the chicken oviduct. Biol. Reprod. 87 (6), 145.

Lim, C.H., Lim, W., Jeong, W., Lee, J.Y., Bae, S.M., Kim, J., Han, J.Y., Bazer, F.W., Song, G., 2013. Avian WNT4 in the female reproductive tracts: potential role of oviduct development and ovarian carcinogenesis. PLoS One 8 (7), e65935.

Lin, X., Liu, X., Ma, Y., Mi, Y., Zeng, W., Li, J., Zhang, C., 2018. Coherent apoptotic and autophagic activities involved in regression of chicken postovulatory follicles. Aging (Albany NY) 10 (4), 819–832.

Liu, J., Wang, W., Feng, Y., Li, M., Bao, H., Chen, Q., 2007. The sympathetic postganglionic and sensory innervation of oviducal magnum in hen: a choleratoxin subunit B-conjugated horseradish peroxidase study. J. Anat. 210 (4), 439–448.

Luna, M., Martínez-Moreno, C.G., Ahumada-Solórzano, M.S., Harvey, S., Carranza, M., Arámburo, C., 2014. Extrapituitary growth hormone in the chicken reproductive system. Gen. Comp. Endocrinol. 203, 60–68.

Machado, S.A., Bahr, J.M., Hales, D.B., Braundmeier, A.G., Quade, B.J., Nowak, R.A., 2012. Validation of the aging hen (*Gallus gallus* domesticus) as an animal model for uterine leiomyomas. Biol. Reprod. 87, 86.

Maddineni, S.R., Ocón-Grove, O.M., Krzysik-Walker, S.M., Hendricks 3rd, G.L., Ramachandran, R., 2008. Gonadotropin-inhibitory hormone (GnIH) receptor gene is expressed in the chicken ovary: potential role of GnIH in follicular maturation. Reproduction 135 (2), 267–274.

Mao, K.M., Murakami, A., Iwasawa, A., Yoshizaki, N., 2007. The asymmetry of avian egg-shape: an adaptation for reproduction on dry land. J. Anat. 210 (6), 741–748.

Marie, P., Labas, V., Brionne, A., Harichaux, G., Hennequet-Antier, C., Nys, Y., Gautron, J., 2014. Data set for the proteomic inventory and quantitative analysis of chicken uterine fluid during eggshell biomineralization. Data Brief 1, 65–69.

Marie, P., Labas, V., Brionne, A., Harichaux, G., Hennequet-Antier, C., Nys, Y., Gautron, J., 2015. Quantitative proteomics and bioinformatic analysis provide new insight into protein function during avian eggshell biomineralization. J. Proteomics. 113, 178–193.

Maseki, Y., Nakamura, K., Iwasawa, A., Zheng, J., Inoue, K., Sakai, T., 2004. Development of gonadotropes in the chicken embryonic pituitary gland. Zool. Sci. 21 (4), 435–444.

Matsuzaki, M., Sasanami, T., 2017. Sperm storage in the female reproductive tract: a conserved reproductive strategy for better fertilization success. Adv. Exp. Med. Biol. 1001, 173–186.

Matsuzaki, M., Mizushima, S., Dohra, H., Sasanami, T., 2020. Expression of transferrin and albumin in the sperm-storage tubules of Japanese quail and their possible involvement in long-term sperm storage. J. Poult. Sci. 57 (1), 88–96.

Mattsson, A., Brunström, B., 2017. Effects of selective and combined activation of estrogen receptor α and β on reproductive organ development and sexual behaviour in Japanese quail (*Coturnix japonica*). PLoS One 12 (7), e0180548.

Mellouk, N., Ramé, C., Barbe, A., Grandhaye, J., Froment, P., Dupont, J., 2018. Chicken is a useful model to investigate the role of adipokines in metabolic and reproductive diseases. Int. J. Endocrinol. 2018, 4579734.

Mika, M., Rzasa, J., Ewy, Z., 1987. Interaction of progesterone, estradiol, and testosterone in the regulation of growth and development of the chick oviduct. Folia Biol. (Krakow) 35 (1–2), 85–94.

Mikšík, I., Ergang, P., Pácha, J., 2014. Proteomic analysis of chicken eggshell cuticle membrane layer. Anal. Bioanal. Chem. 406 (29), 7633–7640.

Miyahara, D., Oishi, I., Makino, R., Kurumisawa, N., Nakaya, R., Ono, T., Kagami, H., Tagami, T., 2016. Chicken stem cell factor enhances primordial germ cell proliferation cooperatively with fibroblast growth factor 2. J. Reprod. Dev. 62 (2), 143–149.

Mori, M., Yamashita, M., Yoshikuni, M., Fukada, S., Nagahama, Y., 1991. Maturation-promoting factor and P34cdc2 kinase during oocyte maturation of the Japanese quail. Dev. Biol. 146, 246–249.

Moynihan, J.B., Edwards, N.A., 1975. Blood flow in the reproductive tract of the domestic hen. Comp. Biochem. Physiol. A, Comp. Physiol. 51 (4), 745–748.

Murai, A., Murota, R., Doi, K., Yoshida, T., Aoyama, H., Kobayashi, M., Horio, F., 2013. Avian IgY is selectively incorporated into the egg yolks of oocytes by discriminating Fc amino acid residues located on the C upsilon 3/C upsilon 4 interface. Dev. Comp. Immunol. 39, 378–387.

Nakajo, S., Zakaria, A.H., Imai, K., 1973. Effect of the local administration of proteolytic enzymes on the rupture of the ovarian follicle in the domestic fowl, *Gallus domesticus*. J. Reprod. Fertil. 34, 235e40.

Nakao, N., Yasuo, S., Nishimura, A., Yamamura, T., Watanabe, T., Anraku, T., Okano, T., Fukada, Y., Sharp, P.J., Ebihara, S., Yoshimura, T., 2007. Circadian clock gene regulation of steroidogenic acute regulatory protein gene expression in preovulatory ovarian follicles. Endocrinology 148, 3031–3038.

Nakao, N., Ono, H., Yamamura, T., Anraku, T., Takagi, T., Higashi, K., Yasuo, S., Katou, Y., Kageyama, S., Uno, Y., Kasukawa, T., Iigo, M., Sharp, P.J., Iwasawa, A., Suzuki, Y., Sugano, S., Niimi, T., Mizutani, M., Namikawa, T., Ebihara, S., Ueda, H.R., Yoshimura, T., 2008a. Thyrotropin in the pars tuberalis triggers photoperiodic response. Nature 452, 317–322.

Nakao, N., Ono, H., Yoshimura, T., 2008b. Thyroid hormones and seasonal reproductive neuroendocrine interactions. Reproduction 136 (1), 1–8.

Ni, Y., Zhu, Q., Zhou, Z., Grossmann, R., Chen, J., Zhao, R.J., 2007. Effect of dietary daidzein on egg production, shell quality, and gene expression of ER-alpha, GHR, and IGF-IR in shell glands of laying hens. J. Agric. Food Chem. 55, 6997–7001.

Niezgoda, J., Rzasa, J., Ewy, Z., 1973. Changes in blood vasotocin activity during oviposition in the hen. J. Reprod. Fertil. 35 (3), 505–509.

Niezgoda, J., Bobek, S., Kacińska, M., 1979. Blood flow in the reproductive tract of the domestic hen following treatment with a pituitary gonadotropic inhibitor. Acta Physiol. Pol. 30 (3), 393–397.

Nishio, S., Kohno, Y., Iwata, Y., Arai, M., Okumura, H., Oshima, K., Nadano, D., Matsuda, T., 2014. Glycosylated chicken ZP2 accumulates in the egg coat of immature oocytes and remains localized to the germinal disc region of mature eggs. Biol. Reprod. 91 (5), 107.

Nishio, S., Okumura, H., Matsuda, T., 2018. Egg-Coat and zona pellucida proteins of chicken as a typical species of aves. Curr. Top. Dev. Biol. 130, 307–329.

Nowak, M., Grzesiak, M., Saito, N., Kwaśniewska, M., Sechman, A., Hrabia, A., 2017. Expression of aquaporin 4 in the chicken ovary in relation to follicle development. Reprod. Domest. Anim. 52 (5), 857–864.

Nys, Y., Gautron, J., McKee, M.D., Garcia-Ruiz, J.M., Hincke, M.T., 2001. Biochemical and functional characterisation of eggshell matrix proteins in hens. World Poult. Sci. J. 57, 401–413.

Nys, Y., Gautron, J., Garcia-Ruiz, J.M., Hincke, M.T., 2004. Avian eggshell mineralization: biochemical and functional characterization of matrix proteins. C. R. Paleovol 3, 549–562.

Ocłoń, E., Hrabia, A., 2021. miRNA expression profile in chicken ovarian follicles throughout development and miRNA-mediated MMP expression. Theriogenology 160, 116–127.

Ocón-Grove, O.M., Poole, D.H., Johnson, A.L., 2012. Bone morphogenetic protein 6 promotes FSH receptor and anti-Müllerian hormone mRNA expression in granulosa cells from hen prehierarchal follicles. Reproduction 143 (6), 825–833.

Ogawa, K., Goto, K., 1984. Effects of gonadotrophins, sex steroids and adenohypophysectomy on the activities of proteolytic enzymes in the ovarian follicle wall of the domestic fowl (*Gallus domesticus*). J. Reprod. Fertil. 71 (2), 545–549.

Ohkubo, T., 2017. Neuroendocrine control of broodiness. Adv. Exp. Med. Biol. 1001, 151–171.

Okamura, F., Nishiyama, H., 1978. Penetration of spermatozoa into the ovum and transformation of the sperm nucleus into the male pronucleus in the domestic fowl, *Gallus gallus*. Cell Tissue Res. 190, 89–98.

Okumura, H., 2017. Avian egg and egg coat. Adv. Exp. Med. Biol. 1001, 75–90.

Olszańska, B., Stepińska, U., Perry, M.M., 2002. Development of embryos from in vitro ovulated and fertilized oocytes of the quail (*Coturnix coturnix* japonica). J. Exp. Zool. 292 (6), 580–586.

Onagbesan, O.M., Vleugels, B., Buys, N., Bruggeman, V., Safi, M., Decuypere, E., 1999. Insulin-like growth factors in the regulation of avian ovarian functions. Domest. Anim. Endocrinol. 17 (2–3), 299–313.

Onagbesan, O., Bruggeman, V., Decuypere, E., 2009. Intra-ovarian growth factors regulating ovarian function in avian species: a review. Anim. Reprod. Sci. 111 (2–4), 121–140.

Oréal, E., Mazaud, S., Picard, J.Y., Magre, S., Carré-Eusèbe, D., 2002. Different patterns of anti-Müllerian hormone expression, as related to DMRT1, SF-1, WT1, GATA-4, Wnt-4, and Lhx9 expression, in the chick differentiating gonads. Dev. Dyn. 225 (3), 221–232.

Paczoska-Eliasiewicz, H., Rzasa, J., 1999. Participation of histamine in avian ovarian function. Postepy Biol. Komorki 26 (12), 203–206.

Paczoska-Eliasiewicz, H., Rząsa, J., 1995. Serotonin content in the wall of preovulatory and postovulatory follicles of the domestic hen. Folia Biol. (Krakow). 53, 75–79.

Paczoska-Eliasiewicz, H., Rząsa, J., 1998. Distribution of histamine in laying hen ovary. Zentralbl. Veterinarmed. A. 45 (8), 491–497.

Paczoska-Eliasiewicz, H., Rzasa, J., Mika, M., 1998. Changes of histamine concentration in chicken oviduct during the egg-laying cycle. Zentralbl. Veterinarmed. A. 45 (2), 69–73.

Paczoska-Eliasiewicz, H.E., Proszkowiec-Weglarz, M., Proudman, J., Jacek, T., Mika, M., Sechman, A., Rzasa, J., Gertler, A., 2006. Exogenous leptin advances puberty in domestic hen. Domest. Anim. Endocrinol. 31 (3), 211–226.

Palmer, S.S., Bahr, J.M., 1992. Follicle stimulating hormone increases serum oestradiol-17 beta concentrations, number of growing follicles and yolk deposition in aging hens (*Gallus gallus* domesticus) with decreased egg production. Br. Poult. Sci. 33 (2), 403–414.

Palmiter, R.D., 1972. Regulation of protein synthesis in chick oviduct. I. Independent regulation of ovalbumin, conalbumin, ovomucoid, and lysozyme induction. J. Biol. Chem. 247 (20), 6450–6461.

Palmiter, R.D., Haines, M.E., 1973. Regulation of protein synthesis in chick oviduct. IV, Role of testosterone. J. Biol. Chem. 248 (6), 2107–2116.

Palmiter, R.D., Wrenn, J.T., 1971. Interaction of estrogen and progesterone in chick oviduct development III. Tubular gland cell cytodifferentiation. J. Cell Biol. 50, 598–615.

Pawłowska, K., Sechman, A., Suchanek, I., Grzegorzewska, A., Rzasa, J., 2008. Effect of 9-cis retinoic acid (RA) on progesterone and estradiol secretion and RA receptor expression in the chicken ovarian follicles. Folia Biol. (Krakow). 56 (1–2), 65–72.

Peczely, P., 1985. The role of thyroid and adrenal cortical hormones in the modulation of the gonadal function in birds. Acta Biol. Hung. 36, 45–70.

Pedernera, E., Solis, L., Peralta, I., Velazquez, P.N., 1999. Proliferative and steroidogenic effects of follicle-stimulating hormone during chick embryo gonadal development. Gen. Comp. Endocrinol. 116, 213–220.

Perry, M.M., 1987. Nuclear events from fertilisation to the early cleavage in the domestic fowl (*Gallus domesticus*). J. Anat. 150, 99–109.

Pitzel, L., Lüdemann, S., Wuttke, W., 2000. Secretion and gene expression of metalloproteinases and gene expression of their inhibitors in porcine corpora lutea at different stages of the luteal phase. Biol. Reprod. 62, 1121–1127.

Politis, I., Wang, L., Turner, J.D., Tsang, B.K., 1990. Changes in tissue-type plasminogen activator-like and plasminogen activator inhibitor activities in granulosa and theca layers during ovarian follicle development in the domestic hen. Biol. Reprod. 42 (5–6), 747–754.

Porter, T.E., Hargis, B.M., Silsby, J.L., El Halawani, M.E., 1989. Differential steroid production between theca interna and theca externa cells: a three cell model for follicular steroidogenesis in avian species. Endocrinology 125, 109–116.

Proszkowiec-Weglarz, M., Rząsa, J., Słomczyńska, M., Paczoska-Eliasiewicz, H., 2005. Steroidogenic activity of chicken ovary during pause in egg laying. Reprod. Biol. 5, 205–225.

Qin, N., Fan, X.C., Zhang, Y.Y., Xu, X.X., Tyasi, T.L., Jing, Y., Mu, F., Wei, M.L., Xu, R.F., 2015. New insights into implication of the SLIT/ROBO pathway in the prehierarchical follicle development of hen ovary. Poult. Sci. 94 (9), 2235–2246.

Ramachandran, R., Maddineni, S., Ocón-Grove, O., Hendricks 3rd, G., Vasilatos-Younken, R., Hadley, J.A., 2013. Expression of adiponectin and its receptors in avian species. Gen. Comp. Endocrinol. 190, 88–95.

Rangel, P.L., Gutierrez, C.G., 2014. Reproduction in hens: is testosterone necessary for the ovulatory process? Gen. Comp. Endocrinol. 203, 250–261.

Rangel, P.L., Sharp, P.J., Gutierrez, C.G., 2006. Testosterone antagonist (flutamide) blocks ovulation and preovulatory surges of progesterone, luteinizing hormone and oestradiol in laying hens. Reproduction 131 (6), 1109–1114.

Rangel, P.L., Rodríguez, A., Rojas, S., Sharp, P.J., Gutierrez, C.G., 2009. Testosterone stimulates progesterone production and STAR, P450 cholesterol side-chain cleavage and LH receptor mRNAs expression in hen (*Gallus domesticus*) granulosa cells. Reproduction 138 (6), 961–969.

Rangel, P.L., Rodríguez, A., Gutiérrez, K., Sharp, P.J., Gutierrez, C.G., 2014. Subdominant hierarchical ovarian follicles are needed for steroidogenesis and ovulation in laying hens (*Gallus domesticus*). Anim. Reprod. Sci. 147 (3–4), 144–153.

Retzek, H., Steyrer, E., Sanders, E.J., Nimpf, J., Schneider, W.J., 1992. Molecular cloning and functional characterization of chicken cathepsin D, a key enzyme for yolk formation. DNA Cell Biol. 11 (9), 661–672.

Riou, C., Cordeiro, L., Gérard, N., 2017. Eggshell matrix proteins OC-116, OC-17 and OCX36 in hen's sperm storage tubules. Anim. Reprod. Sci. 185, 28–41.

Robinson, F.E., Etches, R.J., 1986. Ovarian steroidogenesis during follicular maturation in the domestic fowl (*Gallus domesticus*). Biol. Reprod. 35 (5), 1096–1105.

Rodríguez-Burford, C., Barnes, M.N., Berry, W., Partridge, E.E., Grizzle, W.E., 2001. Immunohistochemical expression of molecular markers in an avian model: a potential model for preclinical evaluation of agents for ovarian cancer chemoprevention. Gynecol. Oncol. 81 (3), 373–379.

Rokitka, M.A., Rahn, H., 1987. Regional differences in shell conductance and pore density of avian eggs. Respir. Physiol. 68, 371–376.

Rombauts, L., Berghman, L.R., Vanmontfort, D., Decuypere, E., Verhoeven, G., 1993. Changes in immunoreactive FSH and inhibin in developing chicken embryos and the effects of estradiol and the aromatase inhibitor R76713. Biol. Reprod. 49, 549–554.

Rose-Martel, M., Du, J., Hincke, M.T., 2012. Proteomic analysis provides new insight into the chicken eggshell cuticle. J. Proteomics. 75 (9), 2697–2706.

Rose-Martel, M., Smiley, S., Hincke, M.T., 2015. Novel identification of matrix proteins involved in calcitic biomineralization. J. Proteomics. 116, 81–96.

Rothchild, I., Fraps, R.M., 1944. On the function of the ruptured ovarian follicle of the domestic fowl. Proc. Soc. Exp. Biol. Med. 56, 79–82.

Rozenboim, I., Tabibzadeh, C., Silsby, J.L., El Halawani, M.E., 1993. Effect of ovine prolactin administration on hypothalamic vasoactive intestinal peptide (VIP), gonadotropin releasing hormone I and II content, and anterior pituitary VIP receptors in laying Turkey hens. Biol. Reprod. 48, 1246–1250.

Rzasa, J., 1972. Effect of vasotocin and oxytocin on the contractility of hen's oviduct in vitro. Acta Physiol. Pol. 23 (4), 673–684 (Article in Polish).

Rzasa, J., Ewy, Z., 1970. Effect of vasotocin and oxytocin on oviposition in the hen. J. Reprod. Fertil. 21 (3), 549–550.

Rzasa, J., Paczoska-Eliasiewicz, H., 1989. Effect of indomethacin and vasotocin on oviposition in the hen (*Gallus domesticus*). Acta Physiol. Pol. 40 (1), 111–115.

Rzasa, J., Sechman, A., Paczoska-Eliasiewicz, H., Hrabia, A., 2009. Effect of tamoxifen on sex steroid concentrations in chicken ovarian follicles. Acta Vet. Hung. 57 (1), 85–97.

Rząsa, J., 1977. The effect of vasotocin and prostaglandin E1 on the oviduct contractility in birds. Zesz. Nauk. AR Krakow, Rozprawy 54, 1–44 (in Polish).

Rząsa, J., 1978. Effects of arginine vasotocin and prostaglandin E1 on the hen uterus. Prostaglandins 16 (3), 357–372.

Rząsa, J., 1984. The effect of arginine vasotocin on prostaglandin production of the hen uterus. Gen. Comp. Endocrinol. 53 (2), 260–263.

Rząsa, J., Hrabia, A., Paczoska-Eliasiewicz, H., Sechman, A., 2008. Changes of blood flow through the chicken ovary and oviduct after serotonin treatment. Bull. Vet. Inst. Pulawy 52, 241–244.

Sah, N., Kuehu, D.L., Khadka, V.S., Deng, Y., Peplowska, K., Jha, R., Mishra, B., 2018. RNA sequencing-based analysis of the laying hen uterus revealed the novel genes and biological pathways involved in the eggshell biomineralization. Sci. Rep. 8 (1), 16853.

Saito, N., Shimada, K., 2001. Sex differentiation of the gonads of birds. In: Dawson, A., Chaturvedi, C.M. (Eds.), Avian Endocrinology. Narosa Publishing House, New Dehli, pp. 155–165.

Saito, N., Sato, K., Shimada, K., 1987a. Prostaglandin levels in peripheral and follicular plasma, the isolated theca and granulosa layers of pre- and postovulatory follicles, and the myometrium and mucosa of the shell gland (uterus) during a midsequence-oviposition of the hen (*Gallus domesticus*). Biol. Reprod. 36 (1), 89–96.

Saito, N., Shimada, K., Koike, T.I., 1987b. Interrelationship between arginine vasotocin, prostaglandin, and uterine contractility in the control of oviposition in the hen (*Gallus domesticus*). Gen. Comp. Endocrinol. 67 (3), 342–347.

Samiullah, S., Roberts, J.R., Chousalkar, K., 2015. Eggshell color in brown-egg laying hens - a review. Poult. Sci. 94 (10), 2566–2575.

Sasanami, T., Mori, M., 1999. Effects of oestradiol-17α and testosterone on progesterone production in the cultured granulosa cells of Japanese quail. Br. Poult. Sci. 40, 536–540.

Sasanami, T., Izumi, S., Sakurai, N., Hirata, T., Mizushima, S., Matsuzaki, M., Hiyama, G., Yorinaga, E., Yoshimura, T., Ukena, K., Tsutsui, K., 2015. A unique mechanism of successful fertilization in a domestic bird. Sci. Rep. 5, 7700.

Scanes, C.G., Godden, P.M.M., Sharp, P.J., 1977a. An homologous radioimmunoassay for chicken follicle-stimulating hormone: observations on the ovulatory cycle. J. Endocrinol. 73, 473–481.

Scanes, C.G., Sharp, P.J., Chadwick, A., 1977b. Changes in plasma prolactin concentration during the ovulatory cycle of the chicken. J. Endocrinol. 72 (3), 401–402.

Scanes, C.G., Sharp, P.J., Harvey, S., Godden, P.M., Chadwick, A., Newcomer, W.S., 1979. Variations in plasma prolactin, thyroid hormones, gonadal steroids and growth hormone in turkeys during the induction of egg laying and moult by different photoperiods. Br. Poult. Sci. 20, 143–148.

Scanes, C.G., Mozelic, H., Kavanagh, E., Merrill, G., Rabii, J., 1982. Distribution of blood flow in the ovary of domestic fowl (*Gallus domesticus*) and changes after prostaglandin F-2alpha treatment. J. Reprod. Fertil. 64, 227–231.

Schneider, W.J., 2009. Receptor-mediated mechanisms in ovarian follicle and oocyte development. Gen. Comp. Endocrinol. 163 (1–2), 18–23.

Schneider, W.J., 2016. Lipid transport to avian oocytes and to the developing embryo. J. Biomed. Res. 30 (3), 174–180.

Schrader, W.T., O'Malley, B.W., 1972. Progesterone-binding components of chick oviduct. Characterization of purified subunits. J. Biol. Chem. 247, 51–59.

Schuster, M.K., Schmierer, B., Shkumatava, A., Kuchler, K., 2004. Activin A and follicle-stimulating hormone control tight junctions in avian granulosa cells by regulating occluding expression. Biol. Reprod. 70, 1493–1499.

Sechman, A., 2013. The role of thyroid hormones in regulation of chicken ovarian steroidogenesis. Gen. Comp. Endocrinol. 190, 68–75.

Sechman, A., Paczoska-Eliasiewicz, H., Rząsa, J., Hrabia, A., 2000. Simultaneous determination of plasma ovarian and thyroid hormones during sexual maturation of the hen (*Gallus domesticus*). Folia Biol. (Krakow). 48, 7–12.

Sechman, A., Pawłowska, K., Rząsa, J., 2009. Influence of triiodothyronine (T3) on secretion of steroids and thyroid hormone receptor expression in chicken ovarian follicles. Domest. Anim. Endocrinol. 37, 61–73.

Sechman, A., Pawłowska, K., Hrabia, A., 2011. Effect of 3,30,5-triiodothyronine and 3,5-diiodothyronine on progesterone production, cAMP synthesis and mRNA expression of STAR, CYP11A1, and HSD3B genes in granulosa layer of chicken preovulatory follicles. Domest. Anim. Endocrinol. 41, 137–149.

Sechman, A., Antos, P., Katarzyńska, D., Grzegorzewska, A., Wojtysiak, D., Hrabia, A., 2014. Effects of 2,3,7,8-tetrachlorodibenzo-p-dioxin on secretion of steroids and STAR, HSD3B and CYP19A1 mRNA expression in chicken ovarian follicles. Toxicol. Lett. 225 (2), 264–274.

Sechman, A., Batoryna, M., Antos, P.A., Hrabia, A., 2016. Effects of PCB 126 and PCB 153 on secretion of steroid hormones and mRNA expression of steroidogenic genes (STAR, HSD3B, CYP19A1) and estrogen receptors (ERα, ERβ) in prehierarchical chicken ovarian follicles. Toxicol. Lett. 264, 29–37.

Sechman, A., Grzegorzewska, A.K., Grzesiak, M., Kozubek, A., Katarzyńska-Banasik, D., Kowalik, K., Hrabia, A., 2020. Nitrophenols suppress steroidogenesis in prehierarchical chicken ovarian follicles by targeting STAR, HSD3B1, and CYP19A1 and downregulating LH and estrogen receptor expression. Domest. Anim. Endocrinol. 70, 106378.

Sharp, P.J., 1975. A comparison of variations in plasma luteinizing hormone concentrations in male and female domestic chickens (*Gallus domesticus*) from hatch to sexual maturity. J. Endocrinol. 67, 211–223.

Sharp, P.J., 2005. Photoperiodic regulation of seasonal breeding in birds. Ann. N. Y. Acad. Sci. 1040, 189–199.

Sharp, P.J., Scanes, C.G., Williams, J.B., Harvey, S., Chadwick, A., 1979. Variations in concentrations of prolactin, luteinizing hormone, growth hormone and progesterone in the plasma of broody bantams (*Gallus domesticus*). J. Endocrinol. 80, 51–57.

Sharp, P.J., Talbot, R.T., Main, G.M., Dunn, I.C., Fraser, H.M., Huskisson, N.S., 1990. Physiological roles of chicken LHRH-I and -II in the control of gonadotrophin release in the domestic chicken. J. Endocrinol. 124, 291–299.

Shimada, K., 2002. Sex determination and sex differentiation. Avian Poult. Biol. Rev. 13, 1–14.

Shimada, K., Asai, I., 1978. Uterine contraction during the ovulatory cycle of the hen. Biol. Reprod. 19, 1057–1062.

Shimada, K., Asai, I., 1979. Effects of prostaglandin F2alpha and indomethacin on uterine contraction in hens. Biol. Reprod. 21, 523–527.

Shimada, K., Saito, N., Itogawa, K., Koike, T.I., 1987. Changes in plasma concentrations of arginine vasotocin after intrauterine injections of prostaglandin F-2 alpha and acetylcholine at various times during the oviposition cycle of the domestic hen (*Gallus domesticus*). J. Reprod. Fertil. 80, 143–150.

Siopes, T.D., Millam, J.R., Steinman, M.Q., 2010. Initiating egg production in Turkey breeder hens: thyroid hormone involvement. Poult. Sci. 89, 2265–2272.

Sirotkin, A.V., Grossmann, R., 2007a. The role of ghrelin and some intracellular mechanisms in controlling the secretory activity of chicken ovarian cells. Comp. Biochem. Physiol. A Mol. Integr. Physiol. 147 (1), 239–246.

Sirotkin, A.V., Grossmann, R., 2007b. Leptin directly controls proliferation, apoptosis and secretory activity of cultured chicken ovarian cells. Comp. Biochem. Physiol. A Mol. Integr. Physiol. 148 (2), 422–429.

Sirotkin, A.V., Grossmann, R., 2015. Interrelationship between feeding level and the metabolic hormones leptin, ghrelin and obestatin in control of chicken egg laying and release of ovarian hormones. Comp. Biochem. Physiol. A Mol. Integr. Physiol. 184, 1–5.

Sirotkin, A.V., Grossmann, R., María-Peon, M.T., Roa, J., Tena-Sempere, M., Klein, S., 2006. Novel expression and functional role of ghrelin in chicken ovary. Mol. Cell. Endocrinol. 257–258, 15–25.

Sirotkin, A.V., Harrath, A.H., Grossmann, R., 2016. Comparison of the effects of human and chicken ghrelin on chicken ovarian hormone release. Comp. Biochem. Physiol. B Biochem. Mol. Biol. 201, 59–63.

Sirotkin, A.V., Harrath, A.H., Grossmann, R., 2017. Metabolic status and ghrelin regulate plasma levels and release of ovarian hormones in layer chicks. Physiol. Res. 66 (1), 85–92.

Smith, C.A., Smith, M.J., Sinclair, A.H., 1999. Expression of chicken steroidogenic factor-1 during gonadal sex differentiation. Gen. Comp. Endocrinol. 113, 187–196.

Smith, C.A., Roeszler, K.N., Bowles, J., Koopman, P., Sinclair, A.H., 2008a. Onset of meiosis in the chicken embryo; evidence of a role for retinoic acid. BMC Dev. Biol. 8, 85.

Smith, C.A., Shoemaker, C.M., Roeszler, K.N., Queen, J., Crews, D., Sinclair, A.H., 2008b. Cloning and expression of R-spondin1 in different vertebrates suggests a conserved role in ovarian development. BMC Dev. Biol. 8, 72.

Socha, J.K., Hrabia, A., 2018. Alterations in apoptotic markers and egg-specific protein gene expression in the chicken oviduct during pause in laying induced by tamoxifen. Theriogenology 105, 126–134.

Socha, J.K., Hrabia, A., 2019. Response of the chicken ovary to GH treatment during a pause in laying induced by fasting. Domest. Anim. Endocrinol. 69, 84–95.

Socha, J.K., Sechman, A., Mika, M., Hrabia, A., 2017. Effect of growth hormone on steroid concentrations and mRNA expression of their receptor, and selected egg-specific protein genes in the chicken oviduct during pause in laying induced by fasting. Domest. Anim. Endocrinol. 61, 1–10.

Socha, J.K., Saito, N., Wolak, D., Sechman, A., Hrabia, A., 2018. Expression of aquaporin 4 in the chicken oviduct following tamoxifen treatment. Reprod. Domest. Anim. 53 (6), 1339–1346.

Solomon, S.E., 2010. The eggshell: strength, structure and function. Br. Poult. Sci. 51 (Suppl. 1), 52–59.

Song, G., Seo, H.W., Choi, J.W., Rengaraj, D., Kim, T.M., Lee, B.R., Kim, Y.M., Yun, T.W., Jeong, J.W., Han, J.Y., 2011. Discovery of candidate genes and pathways regulating oviduct development in chickens. Biol. Reprod. 85 (2), 306–314.

Srihawong, T., Kuwana, T., Siripattarapravat, K., Tirawattanawanich, C., 2015. Chicken primordial germ cell motility in response to stem cell factor sensing. Int. J. Dev. Biol. 59 (10–12), 453–460.

Srivastava, R., Cornett, L.E., Chaturvedi, C.M., 2010. Age-dependent expression of AVT and its oxytocic-like receptor VT3 in the shell gland of Japanese quail, *Coturnix coturnix* japonica. Gen. Comp. Endocrinol. 165 (1), 47–52.

Srivastava, R., Cornett, L.E., Chaturvedi, C.M., 2018. Impact of estrogen and photoperiod on arginine vasotocin and VT3 receptor expression in the shell gland of quail. Front. Biosci. (Schol Ed). 10, 372–385.

Stapane, L., Le Roy, N., Hincke, M.T., Gautron, J., 2019. The glycoproteins EDIL3 and MFGE8 regulate vesicle-mediated eggshell calcification in a new model for avian biomineralization. J. Biol. Chem. 294 (40), 14526–14545.

Stebler, J., Spieler, D., Slanchev, K., Molyneaux, K.A., Richter, U., Cojocaru, V., Tarabykin, V., Wylie, C., Kessel, M., Raz, E., 2004. Primordial germ cell migration in the chick and mouse embryo: the role of the chemokine SDF-1/CXCL12. Dev. Biol. 272, 351–361.

Stephens, C.S., Johnson, P.A., 2016. Bone morphogenetic protein 15 may promote follicle selection in the hen. Gen. Comp. Endocrinol. 235, 170–176.

Stephens, C.S., Johnson, P.A., 2017. Occludin expression and regulation in small follicles of the layer and broiler breeder hen. Gen. Comp. Endocrinol. 248, 106–113.

Stepińska, U., Olszańska, B., 2003. DNase I and II present in avian oocytes: a possible involvement in sperm degradation at polyspermic fertilisation. Zygote 11 (1), 35–42.

Sundaresan, N.R., Saxena, V.K., Sastry, K.V., Anish, D., Saxena, M., Nagarajan, K., Ahmed, K.A., 2007. Nitric oxide: a possible mediator of ovulation and postovulatory follicle regression in chicken. Anim. Reprod. Sci. 101 (3–4), 351–357.

Sundaresan, N.R., Saxena, V.K., Sastry, K.V., Anish, D., Marcus Leo, M.D., Kantaraja, C., Saxena, M., Ahmed, K.A., 2008a. Caspase-mediated apoptosis in chicken postovulatory follicle regression. Vet. Res. Commun. 32 (1), 13–19.

Sundaresan, N.R., Saxena, V.K., Sastry, K.V., Nagarajan, K., Jain, P., Singh, R., Anish, D., Ravindra, P.V., Saxena, M., Ahmed, K.A., 2008b. Cytokines and chemokines in postovulatory follicle regression of domestic chicken (*Gallus gallus domesticus*). Dev. Comp. Immunol. 32 (3), 253–264.

Syvala, H., Vienonen, A., Ylikomi, T., Bläuer, M., Zhuang, Y.H., Tuohimaa, P., 1997. Expression of the chicken progesterone receptor forms A and B is differentially regulated by estrogen in vivo. Biochem. Biophys. Res. Commun. 231, 573–576.

Tabibzadeh, C., Rozenboim, I., Silsby, J.L., Pitts, G.R., Foster, D.N., El Halawani, M.E., 1995. Modulation of ovarian cytochrome P45017α-hydroxylase and cytochrome aromatase messenger ribonucleic acid by prolactin in the domestic Turkey. Biol. Reprod. 52, 600–608.

Tagami, T., Miyahara, D., Nakamura, Y., 2017. Avian primordial germ cells. Adv. Exp. Med. Biol. 1001, 1–18.

Takahashi, T., Ogawa, H., Inaba, R., Kawashima, M., 2004. Changes in prostaglandin F concentration in the uterus (shell gland) of the hen oviduct in relation to oviposition and estrogen. Poult. Sci. 83 (10), 1745–1749.

Takahashi, H., Sasaki, O., Nirasawa, K., Furukawa, T., 2010. Association between ovocalyxin-32 gene haplotypes and eggshell quality traits in an F2 intercross between two chicken lines divergently selected for eggshell strength. Anim. Genet. 41 (5), 541–544.

Takahashi, T., Tajima, H., Nakagawa-Mizuyachi, K., Nakayama, H., Kawashima, M., 2011. Changes in prostaglandin F2α receptor bindings in the hen oviduct uterus before and after oviposition. Poult. Sci. 90 (8), 1767–1773.

Tanabe, Y., Saito, N., Nakamura, T., 1986. Ontogenic steroidogenesis by testes, ovary, and adrenals of embryonic and post-embryonic chickens (*Gallus domesticus*). Gen. Comp. Endocrinol. 63, 456–463.

Teng, C.T., Teng, C.S., 1977. Studies on sex-organ development: the hormonal regulation of steroidogenesis and adenosine 3':5'-cyclic monophosphate in embryonic-chick ovaries. Biochem. J. 162, 123–134.

Teng, C.T., Teng, C.S., Bousfield, G.R., Liu, W.K., Ward, D.N., 1982. Differential response of growing and regressing chicken ovaries to gonadotropic hormones. Gen. Comp. Endocrinol. 48, 325–332.

Tesar, D.B., Cheung, E.J., Bjorkman, P.J., 2008. The chicken yolk sac IgY receptor, a mammalian mannose receptor family member, transcytoses IgY across polarized epithelial cells. Mol. Biol. Cell 19 (4), 1587–1593.

Tian, X., Gautron, J., Monget, P., Pascal, G., 2010. What makes an egg unique? Clues from evolutionary scenarios of egg-specific genes. Biol. Reprod. 83 (6), 893–900.

Tilly, J.L., Johnson, A.L., 1987. Presence and hormonal control of plasminogen activator in granulosa cells of the domestic hen. Biol. Reprod. 37 (5), 1156–1164.

Tilly, J.L., Kowalski, K.I., Johnson, A.L., 1991a. Stage of follicular development associated with the initiation of steroidogenic competence in avian granulosa cells. Biol. Reprod. 44, 305–314.

Tilly, J.L., Kowalski, K.I., Johnson, A.L., Hsueh, A.J.W., 1991b. Involvement of apoptosis in ovarian follicular atresia and postovulatory regression. Endocrinology 129, 2799–2801.

Tilly, J.L., Kowalski, K.I., Li, Z., Levorse, J.M., Johnson, A.L., 1992. Plasminogen activator activity and thymidine incorporation in avian granulosa cells during follicular development and the periovulatory period. Biol. Reprod. 46 (2), 195–200.

Tischkau, S.A., Neitzel, L.R., Walsh, J.A., Bahr, J.M., 1997. Characterization of the growth center of the avian preovulatory follicle. Biol. Reprod. 56 (2), 469–474.

Tischkau, S.A., Howell, R.E., Hickok, J.R., Krager, S.L., Bahr, J.M., 2011. The luteinizing hormone surge regulates circadian clock gene expression in the chicken ovary. Chronobiol. Int. 28 (1), 10–20.

Tiwari, A., Hadley, J.A., Ramachandran, R., 2014. Aquaporin 5 expression is altered in ovarian tumors and ascites-derived ovarian tumor cells in the chicken model of ovarian tumor. J. Ovarian Res. 7, 1–8.

Toft, D.O., OMalley, B.W., 1972. Target tissue receptors for progesterone: the influence of estrogen treatment. Endo 90, 1041–1045.

Tojo, H., Fujii, M., Ogawa, K., 1982. Proteolytic enzymes and gonadal hormones of the ovarian follicle wall during ovulation in the domestic fowl (*Gallus domesticus*). J. Reprod. Fertil. 64 (1), 73–77.

Tora, L., Gronemeyer, H., Turcotte, B., Gaub, M.P., Chambon, P., 1988. The N-terminal region ofthe chicken progesterone receptor specifies target gene activation. Nature 333, 185–188.

Treviño, L.S., Giles, J.R., Wang, W., Urick, M.E., Johnson, P.A., 2010. Gene expression profiling reveals differentially expressed genes in ovarian cancer of the hen: support for oviductal origin? Horm. Cancer. 1 (4), 177–186.

Treviño, L.S., Buckles, E.L., Johnson, P.A., 2012. Oral contraceptives decrease the prevalence of ovarian cancer in the hen. Cancer Prev. Res. (Phila). 5 (2), 343–349.

Tsutsui, K., Li, D., Azumaya, Y., Muneoka, Y., Minakata, H., Nomoto, K., 1997. Demonstration, localization, and development of galanin receptors in the quail oviduct. J. Exp. Zool. 277 (1), 57–65.

Tsutsui, K., Li, D., Ukena, K., Kikuchi, M., Ishii, S., 1998. Developmental changes in galanin receptors in the quail oviduct and the effect of ovarian sex steroids on galanin receptor induction. Endocrinology 139 (10), 4230–4236.

Tsutsui, K., Saigoh, E., Ukena, K., Teranishi, H., Fujisawa, Y., Kikuchi, M., Ishii, S., Sharp, P.J., 2000. A novel avian hypothalamic peptide inhibiting gonadotropin release. Biochem. Biophys. Res. Commun. 275, 661–667.

Tuohimaa, P., Joensuu, T., Isola, J., Keinanen, R., Kunnas, T., Niemala, A., Pekki, A., Wallen, M., Ylikomi, T., Kulomaa, M., 1989. Development of progestin-specific response in the chicken oviduct. Int. J. Dev. Biol. 33, 125–134.

Ukeshima, A., 1996. Germ cell death in the degenerating right ovary of the chick embryo. Zool. Sci. 13, 559–563.

Urick, M.E., Johnson, P.A., 2006. Cyclooxygenase 1 and 2 mRNA and protein expression in the *Gallus domesticus* model of ovarian cancer. Gynecol. Oncol. 103 (2), 673–678.

Velazquez, P.N., Peralta, I., Pedernera, E., 1997. Proliferative effect in vitro of follicle stimulating hormone on the left ovary of the chick embryo. Gen. Comp. Endocrinol. 105, 40–49.

Verma, O.P., Prasad, B.K., Yancey, A., 1977. Adrenergic activity of the oviduct of the domestic fowl. J. Reprod. Fertil. 49 (2), 195–200.

Waddington, D., Gribbin, C., Sterling, R.J., Sang, H.M., Perry, M.M., 1998. Chronology of events in the first cell cycle of the polyspermic egg of the domestic fowl (*Gallus domesticus*). Int. J. Dev. Biol. 42, 625–628.

Wang, Y., Li, J., Ying Wang, C., Yan Kwok, A.H., Leung, F.C., 2007. Epidermal growth factor (EGF) receptor ligands in the chicken ovary: I. Evidence for heparin-binding EGF-like growth factor (HB-EGF) as a potential oocyte-derived signal to control granulosa cell proliferation and HB-EGF and kit ligand expression. Endocrinology 148 (7), 3426–3440.

Wang, Y., Li, J., Yan Kwok, A.H., Ge, W., Leung, F.C., 2010. A novel prolactin-like protein (PRL-L) gene in chickens and zebrafish: cloning and characterization of its tissue expression. Gen. Comp. Endocrinol. 166, 200–210.

Wang, W., Wu, K., Jia, M., Sun, S., Kang, L., Zhang, Q., Tang, H., 2018. Dynamic changes in the global microRNAome and transcriptome identify key nodes associated with ovarian development in chickens. Front. Genet. 9, 491.

Wechsung, E., Houvenaghel, A., 1976. A possible role of prostaglandins in the regulation of ovum transport and oviposition in the domestic hen? Prostaglandins 12 (4), 599–608.

Whyte, J., Glover, J.D., Woodcock, M., Brzeszczynska, J., Taylor, L., Sherman, A., Kaiser, P., McGrew, M.J., 2015. FGF, insulin, and SMAD signaling cooperate for avian primordial germ cell self-renewal. Stem Cell Rep. 5 (6), 1171–1182.

Williams, J.B., Sharp, P.J., 1977. A comparison of plasma progesterone and luteinizing hormone in growing hens from eight weeks of age to sexual maturity. J. Endocrinol. 75, 447–448.

Williams, J., Harvey, S., Leclercq, B., 1986. Plasma levels of luteinizing hormone, growth hormone, and estradiol from six weeks of age to sexual maturity in two lines of chickens selected for low or high abdominal fat content. Poult. Sci. 65, 1782–1786.

Wilson, P.B., 2017. Recent advances in avian egg science: a review. Poult. Sci. 96 (10), 3747–3754.

Wilson, S.C., Jennings, R.C., Cunningham, F.J., 1983. An investigation of diurnal and cyclic changes in the secretion of luteinizing hormone in the domestic hen. J. Endocrinol. 98, 137–145.

Wilson, P.W., Suther, C.S., Bain, M.M., Icken, W., Jones, A., Quinlan-Pluck, F., Olori, V., Gautron, J., Dunn, I.C., 2017. Understanding avian egg cuticle formation in the oviduct: a study of its origin and deposition. Biol. Reprod. 97 (1), 39–49.

Wojtusik, J., Johnson, P.A., 2012. Vitamin D regulates anti-Mullerian hormone expression in granulosa cells of the hen. Biol. Reprod. 86 (3), 1–7.

Wojtysiak, D., Okólski, A., Sechman, A., 2011. Structure and steroidogenic activity of the granulosa layer of F1 preovulatory ovarian follicles of the hen (*Gallus domesticus*). Folia Biol. (Krakow). 59 (1–2), 59–64.

Wolak, D., Hrabia, A., 2020. Tamoxifen-induced alterations in the expression of selected matrix metalloproteinases (MMP-2, -9, -10, and -13) and their tissue inhibitors (TIMP-2 and -3) in the chicken ovary. Theriogenology 148, 208–215.

Woods, D.C., Johnson, A.L., 2005. Regulation of follicle-stimulating hormone receptor mRNA in hen granulosa cells relative to follicle selection. Biol. Reprod. 72, 643–650.

Woods, J.E., Mennella, J.A., Thommes, R.C., 1981. The hypothalamic-adenohypophysealgonadal axes in the developing chick embryo. I. LH sensitivity. Gen. Comp. Endocrinol. 45, 66–73.

Wolak, D., Hrabia., 2021. Alternations in the expression of selected matrix metalloproteinases (MMP-2, -9, -10, and -13) and their tissue inhibitors (TIMP-2 and -3) and MMP-2 and -9 activity in the chicken ovary during pause in laying induced by fasting. Theriogenology 161, 176–186.

Wolak, D., Sechman, A., Hrabia, A., 2021. Effect of eCG treatment on gene expression of selected matrix metalloproteinases (MMP-2, MMP-7, MMP-9, MMP-10, and MMP-13) and the tissue inhibitors of metalloproteinases (TIMP-2 and TIMP-3) in the chicken ovary. Anim. Reprod. Sci. 224, 106666.

Woods, D.C., Haugen, M.J., Johnson, A.L., 2007. Actions of epidermal growth factor receptor/mitogen-activated protein kinase and protein kinase C signaling in granulosa cells from *Gallus gallus* are dependent upon stage of differentiation. Biol. Reprod. 77 (1), 61–70.

Xiao, Y., Ni, Y., Huang, Y., Wu, J., Grossmann, R., Zhao, R., 2011. Effects of kisspeptin-10 on progesterone secretion in cultured chicken ovarian granulosa cells from preovulatory (F1-F3) follicles. Peptides 32 (10), 2091–2097.

Xu, R., Qin, N., Xu, X., Sun, X., Chen, X., Zhao, J., 2018a. Implication of SLIT3-ROBO1/ROBO2 in granulosa cell proliferation, differentiation and follicle selection in the prehierarchical follicles of hen ovary. Cell Biol. Int. 42 (12), 1643–1657.

Xu, R., Qin, N., Xu, X., Sun, X., Chen, X., Zhao, J., 2018b. Inhibitory effect of SLIT2 on granulosa cell proliferation mediated by the CDC42-PAKs-ERK1/2 MAPK pathway in the prehierarchical follicles of the chicken ovary. Sci. Rep. 8 (1), 9168.

Yang, C., Lim, W., Bae, H., Song, G., 2016. Aquaporin 3 is regulated by estrogen in the chicken oviduct and is involved in progression of epithelial cell-derived ovarian carcinomas. Domest. Anim. Endocrinol. 55, 97–106.

Yao, H.H., Bahr, J.M., 2001. Chicken granulosa cells show differential expression of epidermal growth factor (EGF) and luteinizing hormone (LH) receptor messenger RNA and differential responsiveness to EGF and LH dependent upon location of granulosa cells to the germinal disc. Biol. Reprod. 64, 1790–1796.

Yin, L., Yu, L., Zhang, L., Ran, J., Li, J., Yang, C., Jiang, X., Du, H., Hu, X., Liu, Y., 2019. Transcriptome analysis reveals differentially expressed genes and pathways for oviduct development and defense in prelaying and laying hens. Am. J. Reprod. Immunol. 82 (3), e13159.

Yin, Z., Lian, L., Zhu, F., Zhang, Z.H., Hincke, M., Yang, N., Hou, Z.C., 2020. The transcriptome landscapes of ovary and three oviduct segments during chicken (*Gallus gallus*) egg formation. Genomics 112 (1), 243–251.

Yoshimura, T., 2010. Neuroendocrine mechanism of seasonal reproduction in birds and mammals. Anim. Sci. J. 81, 403–410.

Yoshimura, Y., Bahr, J.M., 1991a. Localization of progesterone receptors in pre- and postovulatory follicles of the domestic hen. Endocrinology 128, 323–330.

Yoshimura, Y., Bahr, J.M., 1991b. Localization of progesterone receptors in the shell gland of laying and nonlaying chickens. Poult. Sci. 70, 1246–1251.

Yoshimura, Y., Barua, A., 2017. Female reproductive system and immunology. Adv. Exp. Med. Biol. 1001, 33–57.

Yoshimura, Y., Koga, O., 1982. Ultrastructural changes of the stigma of the follicle during the process of ovulation in the hen. Cell Tissue Res. 224 (2), 349–359.

Yoshimura, Y., Tamura, T., 1986. Effects of estradiol administration on the follicular tissue of hypophysectomized hens. Poult. Sci. 65 (9), 1808–1810.

Yoshimura, Y., Chang, C., Okamoto, T., Tamura, T., 1993a. Immunolocalization of androgen receptor in the small, preovulatory, and postovulatory follicles of laying hens. Gen. Comp. Endocrinol. 91, 81–89.

Yoshimura, Y., Okamoto, T., Tamura, T., 1993b. Ultrastructural changes of oocyte and follicular wall during oocyte maturation in the Japanese quail (*Coturnix coturnix japonica*). J. Reprod. Fertil. 97, 189–196.

Yoshimura, Y., Okamoto, T., Tamura, T., 1993c. Electron microscope observations on LH-induced oocyte maturation in Japanese quail (*Coturnix coturnix japonica*). J. Reprod. Fertil. 98, 401–407.

Yoshimura, Y., Okamoto, T., Tamura, T., 1995. Changes in localization of ovarian immunoreactive estrogen receptor during follicular development in hens. Gen. Comp. Endocrinol. 100 (3), 368–374.

Yoshimura, Y., Nagano, K., Subedi, K., Kaiya, H., 2005. Identification of immunoreactive ghrelin and its mRNA in the oviduct of laying Japanese quail, *Coturnix japonica*. J. Poult. Sci. 42, 291–300.

You, S., Foster, L.K., Silsby, J.L., El Halawani, M.E., Foster, D.N., 1995. Sequence analysis of the Turkey LH beta subunit and its regulation by gonadotrophin-releasing hormone and prolactin in cultured pituitary cells. J. Mol. Endocrinol. 14 (1), 117–129.

You, S., Bridgham, J.T., Foster, D.N., Johnson, A.L., 1996. Characterization of a chicken follicle-stimulating hormone receptor (cFSH-R) cDNA, and expression of cFSH-R mRNA in the ovary. Biol. Reprod. 55, 1055–1062.

Zadworny, D., Shimada, K., Ishida, H., Sato, K., 1989. Gonadotropin-stimulated estradiol production in small ovarian follicles of the hen is suppressed by physiological concentrations of prolactin in vitro. Gen. Comp. Endocrinol. 74, 468–473.

Zaniboni, L., Bakst, M.R., 2004. Localization of aquaporins in the sperm storage tubules in the Turkey oviduct. Poult. Sci. 83 (7), 1209–1212.

Zhang, C., Shimada, K., Saito, N., Kansaku, N., 1997. Expression of messenger ribonucleic acids of luteinizing hormone and follicle-stimulating hormone receptors in granulosa and theca layers of chicken preovulatory follicles. Gen. Comp. Endocrinol. 105 (3), 402–409.

Zhang, Z.C., Wang, Y.G., Li, L., Yin, H.D., Li, D.Y., Wang, Y., Zhao, X.L., Liu, Y.P., Zhu, Q., 2016. Circadian clock genes are rhythmically expressed in specific segments of the hen oviduct. Poult. Sci. 95 (7), 1653–1659.

Zhang, Z., Lai, S., Wang, Y., Li, L., Yin, H., Wang, Y., Zhao, X., Li, D., Yang, M., Zhu, Q., 2017. Rhythmic expression of circadian clock genes in the preovulatory ovarian follicles of the laying hen. PLoS One 12 (6), e0179019.

Zhang, T., Liu, H., Wang, J., Li, L., Han, C., Mustafa, A., Xiong, X., 2019. Evidences in duck (*Anas platyrhynchos*) by transcriptome data for supporting the biliverdin was mainly synthesized by shell gland. Poult. Sci. 98 (5), 2260–2271.

Zheng, H., Li, H., Tan, W., Xu, C., Jia, L., Wang, D., Li, Z., Sun, G., Kang, X., Yan, F., Liu, X., 2018. Oestrogen regulates the expression of cathepsin E-A-like gene through ERB in liver of chicken (*Gallus gallus*). J. Genet. 97 (1), 145–155.

Zhou, J.F., Zadworny, D., Guemene, D., Kuhnlein, U., 1996. Molecular cloning, tissue distribution, and expression of the prolactin receptor during various reproductive states in *Meleagris gallopavo*. Biol. Reprod. 55 (5), 1081–1090.

Zhu, G., Kang, L., Wei, Q., Cui, X., Wang, S., Chen, Y., Jiang, Y., 2014. Expression and regulation of MMP1, MMP3, and MMP9 in the chicken ovary in response to gonadotropins, sex hormones, and TGFB1. Biol. Reprod. 90, 1–11.

Further reading

Bellairs, R., 1965. The relationship between oocyte and follicle in the hen's ovary as shown by electron microscopy. J. Embryol. Exp. Morph. 13, 215–233.

Choi, J.W., Kim, S., Kim, T.M., Kim, Y.M., Seo, H.W., Park, T.S., Jeong, J.W., Song, G., Han, J.Y., 2010. Basic fibroblast growth factor activates MEK/ERK cell signaling pathway and stimulates the proliferation of chicken primordial germ cells. PLoS One 5 (9), e12968.

Choi, J.W., Ahn, S.E., Rengaraj, D., Seo, H.W., Lim, W., Song, G., Han, J.Y., 2011. Matrix metalloproteinase 3 is a stromal marker for chicken ovarian cancer. Oncol. Lett. 2, 1047–1051.

Etches, R.J., Williams, J.B., Rzasa, J., 1984. Effects of corticosterone and dietary changes in the hen on ovarian function, plasma LH and steroids and the response to exogenous LH-RH. J. Reprod. Fertil. 70 (1), 121–130.

Gilbert, A.B., Perry, M.M., Waddington, D., Hardie, M.A., 1983. Role of atresia in establishing the follicular hierarchy in the ovary of the domestic hen (*Gallus domesticus*). J. Reprod. Fertil. 69, 221–227.

Ishimaru, Y., Komatsu, T., Kasahara, M., Katoh-Fukui, Y., Ogawa, H., Toyama, Y., Maekawa, M., Toshimori, K., Chandraratna, R.A.S., Morohashi, K., Yoshioka, H., 2008. Mechanism of asymmetric ovarian development in chick embryos. Development 135, 677–685.

Paczoska-Eliasiewicz, H., Rząsa, J., 1988. Ovarian serotonin during oocyte development and ovulation in the domestic hen (*Gallus domesticus*). J. Vet. Med. A. 35, 617–621.

Perry, M.M., Gilbert, A.B., 1979. Yolk transport in the ovarian follicle of the hen (*Gallus domesticus*): lipoprotein-like particles at the periphery of the oocyte in the rapid growth phase. J. Cell Sci. 39, 257–272.

Rangel, P.,L., Rodríguez, A., Gutierrez, C.G., 2007. Testosterone directly induces progesterone production and interacts with physiological concentrations of LH to increase granulosa cell progesterone production in laying hens (*Gallus domesticus*). Anim. Reprod. Sci. 102 (1–2), 56–65.

Ratna, W.N., Bhatt, V.D., Chaudhary, K., Bin Ariff, A., Bavadekar, S.A., Ratna, H.N., 2016. Estrogen-responsive genes encoding egg yolk proteins vitellogenin and apolipoprotein II in chicken are differentially regulated by selective estrogen receptor modulators. Theriogenology 85 (3), 376–383.

Tanabe, Y., Ogawa, T., Nakamura, T., 1981. The effect of short-term starvation on pituitary and plasma LH, plasma estradiol and progesterone, and on pituitary response to LH-RH in the laying hen (*Gallus domesticus*). Gen. Comp. Endocrinol. 43 (3), 392–398.

Tilly, J.L., Johnson, A.L., 1990. Control of plasminogen activator activity in the thecal layer of the largest preovulatory follicle in the hen ovary. Endocrinology 126 (4), 2079–2087.

Tiwari, A., Ocón-Grove, O.M., Hadley, J.A., Giles, J.R., Johnson, P.A., Ramachandran, R., 2015. Expression of adiponectin and its receptors is altered in epithelial ovarian tumors and ascites-derived ovarian cancer cell lines. Int. J. Gynecol. Cancer. 25 (3), 399–406.

Unsicker, K., Seidel, F., Hofmann, H.D., Muller, T.H., Schmidt, R., Wilson, A., 1983. Catecholaminergic innervation of the chicken ovary. Cell Tissue Res. 230, 431–450.

van der Klein, S.A.S., Zuidhof, M.J., Bédécarrats, G.Y., 2020. Diurnal and seasonal dynamics affecting egg production in meat chickens: a review of mechanisms associated with reproductive dysregulation. Anim. Reprod. Sci. 213, 106257.

Wallace, R.A., 1985. Vitellogenesis and oocyte growth in nonmammalian vertebrates. In: Browder, W.L. (Ed.), Developmental Biology: A Comprehensive Synthesis, vol. 1. Plenum Press, New York, pp. 127–166.

Williams, J., Harvey, S., 1986. Plasma concentrations of luteinizing hormone, growth hormone, oestradiol, testosterone and androstendione in the domestic hen from 6 weeks of age to sexual maturity. Reprod. Nutr. Dev. 26, 515–522.

Woods, D.C., Johnson, A.L., 2007. Protein kinase C activity mediates LH-induced ErbB/Erk signaling in differentiated hen granulosa cells. Reproduction 133, 733–741.

Chapter 36

Reproduction in male birds

Jorge A. Vizcarra[1], Natalia Cerón-Romero[1], Nurudeen Taofeek[1] and John Kirby[2]
[1]Food and Animal Sciences, Alabama A&M University, Huntsville, AL, United States; [2]College of the Environment and Life Sciences, The University of Rhode Island, Kingston, RI, United States

36.1 Introduction

Reproduction is a process that can be organized into distinct developmental and functional phases. In the case of the male, these include fertilization, formation of a patent reproductive tract, production of sperm, manifestation of male-specific behavioral patterns, and expulsion of sperm from the body. This perspective can provide insight that may be missed if reproduction is viewed primarily as an isolated act. For example, although the reproductive tract is fully functional only in the adult, it is formed, for the most part, prior to hatching. Furthermore, while spermatogenesis is associated with puberty, spermatogenesis is not constrained by chronological age, but rather by the extent to which testicular cells proliferate and differentiate, which in turn, is coupled to the developmental limitations of gonadotropin secretion. Finally, androgens essential to the function of the reproductive tract, the appearance of secondary sexual attributes, and male behavior may have detrimental effects upon the development of immune and connective tissue if the hormonal signal appears during the period of rapid prepubertal growth and differentiation. Thus, this chapter will discuss the process of reproductive system development and function in the male bird.

36.2 Reproductive tract anatomy

36.2.1 Testis

The gross morphology and relative position of the male reproductive organs are shown in Figure 36.1. For detailed reviews see (King, 1979; Lake, 1981; Nickel et al., 1977). Paired reproductive tracts lie along the dorsal body wall. Each tract consists of a testis, an epididymis, and a highly convoluted deferent duct running alongside the ureter. The testes are connected to the body wall by a mesorchium. This peritoneal fold not only serves as an attachment for the testis but also as a conduit for nerves and blood vessels as well. Each testis is an aggregate of anastomosing seminiferous tubules with associated interstitial tissue enveloped by a connective tissue capsule. The testicular capsule is an important component of the contractile mechanism of the testes and is composed of three layers, including the tunica serosa, tunica albuginea, and tunica vasculosa. Of these three layers, the tunica albuginea represents the main tissue layer and comprises cellular elements that alternate with thick bundles of collagen fibers. The testicular capsule is, in general, thinner in birds than in mammals; however, studies in ratite birds have revealed a capsule that is considerably thicker than that of other bird species (Aire and Ozegbe, 2007; Ozegbe et al., 2008).

The testis contains two types of parenchymal tissue: the interstitial tissue and the seminiferous epithelium. The interstitial tissue contains blood and lymphatic vessels, nerves, peritubular epithelial cells, and Leydig cells; whereas thin concentric layers of myoepithelial cells, fibroblasts, and connective tissue fibrils overlie the basal lamina of the seminiferous tubule (Rothwell and Tingari, 1973). The seminiferous epithelium within the seminiferous tubules of sexually mature males is compartmentalized into basal and adluminal regions via tight junctions between adjacent Sertoli cells (Osman, 1980; Bergmann and Schindelmeiser, 1987). The seminiferous epithelium contains developing germ cells in distinct associations referred to as *stages*. The stages are arranged sequentially in a helix that extends along the length of the seminiferous tubule (Lin and Jones, 1990).

In birds, the left testis is commonly larger than the right, which may either be a byproduct of evolutionary selection for asymmetry in the female reproductive tract or an adaptation to facilitate flight (Birkhead et al., 1998; Denk and Kempenaers, 2005). The overall size of the testis scales allometrically to body mass; however, once controlled for body mass, testes size is often larger in bird species that experience a higher degree of sperm competition

Sturkie's Avian Physiology. https://doi.org/10.1016/B978-0-12-819770-7.00022-0

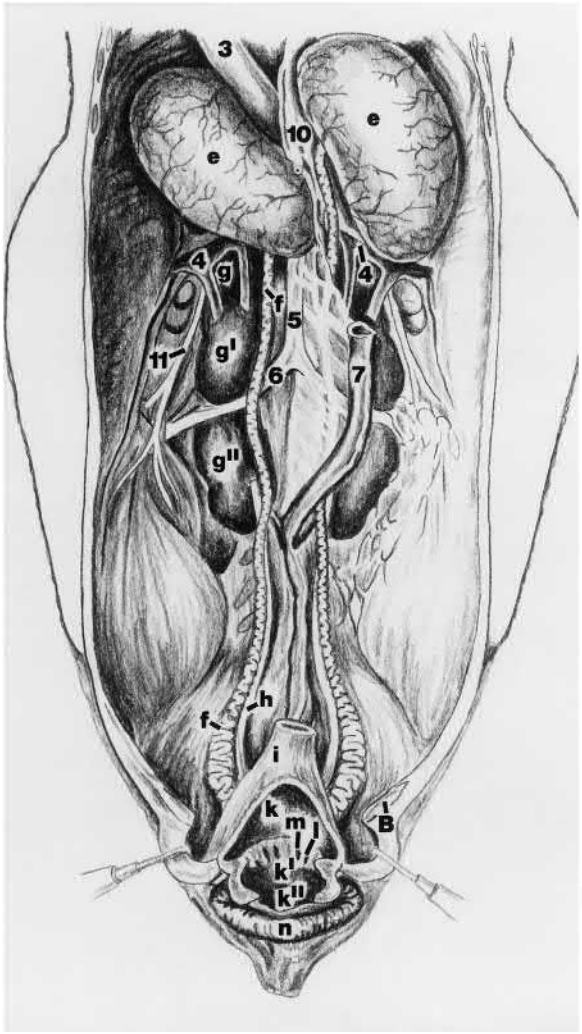

FIGURE 36.1 Topography of the dorsal body wall of the rooster. Paired testes (e) are located anterior to the cranial lobe of the kidneys (g). The deferent ducts (f) run alongside the ureters (h) towards the cloaca (k–k″), ultimately opening (l) into the urodeum (k′). Abbreviations: b, pubis; e, testis; f, ductus deferens; g, cranial; g′, middle, and g″, caudal lobes of the kidney; h, ureter; I, colon; k, coprodeum; k′, urodeum, k″, proctodeum; l, opening of left ductus deferens; m, opening of left ureter; n, anus. *Modified from Nickel et al. (1977).*

(Moller, 1991; Moller and Briskie, 1995; Pitcher et al., 2005). Sperm competition occurs when the sperm of two or more males is present in the female reproductive tract and must compete for egg fertilization. Although many bird species are socially monogamous, extra-pair copulations often occur. Species that participate in extra-pair copulations more frequently experience a more intense degree of sperm competition and have developed larger testis than species which do not frequently participate in extra-pair copulations (Moller, 1991; Moller and Briskie, 1995; Pitcher et al., 2005).

In male broiler breeders, no significant differences were observed in the weight of the right and left testis from 2 to 50 weeks of age (n = 2700; Vizcarra and Kirby, unpublished results). Testis of male broiler breeders reared under a "pedigree" breeding program had an exponential increase in weight after photostimulation (18 weeks of age; Figure 36.2). Within 10 weeks (i.e., week 18 to 28), testis weight increased from 0.4 to 28 g. However, after 28 weeks of age, testis weight was significantly decreased reaching a minimum weight of 15 g by week 42 (Figure 36.2). The reason for the testicular weight regression after 28 weeks of age is not completely clear at this time. Decreased follicle-stimulating hormone (FSH) concentrations might be responsible for testicular weight regression (Vizcarra et al., 2010). In male white Leghorns, an increase in both body and testis weight is observed as the bird ages. The growth rate reported in an 8-day-old embryo to 1-day-old chick is proportionally higher when compared to the growth rate from 1 day old to 28 weeks of age (Gonzalez-Moran and Soria-Castro, 2010). Similarly, testis weight increases but the rate of increase was much higher from 6 weeks of age to 28 weeks of age when compared to 8 days old embryo to 6 weeks of age. It can be inferred that testis growth rate increased rapidly relative to body weight (Gonzalez-Moran and Soria-Castro, 2010).

36.2.2 Excurrent ducts

The excurrent ducts or excurrent canals are ducts associated with the male reproductive tract that derive from the

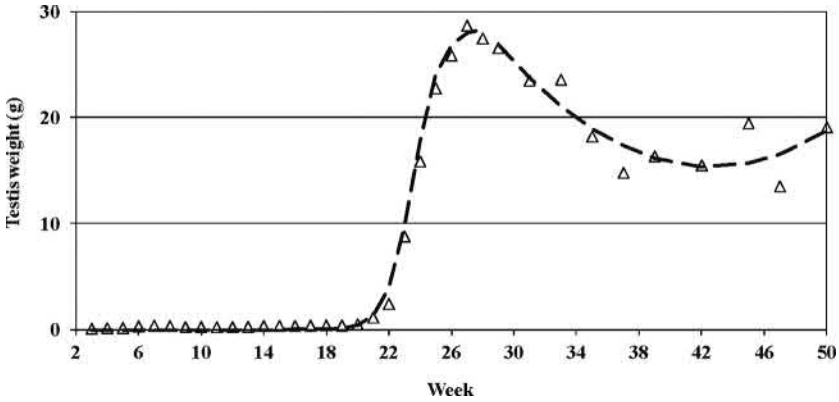

FIGURE 36.2 Least squares regression (lines) and means (symbols) for testis weight in male broiler breeders. Males on a "pedigree" breeder program were reared on a 23L:1D photoperiod and unrestricted food and water intake for 6 weeks. At 7 weeks, males were placed on a restricted diet and the photoperiod was reduced to 8L:16D. At week 18, birds were photostimulated (16L:8D) until the end of the experiment. Each symbol represents an average of 30 testes. *Modified from Vizcarra et al. (2010).*

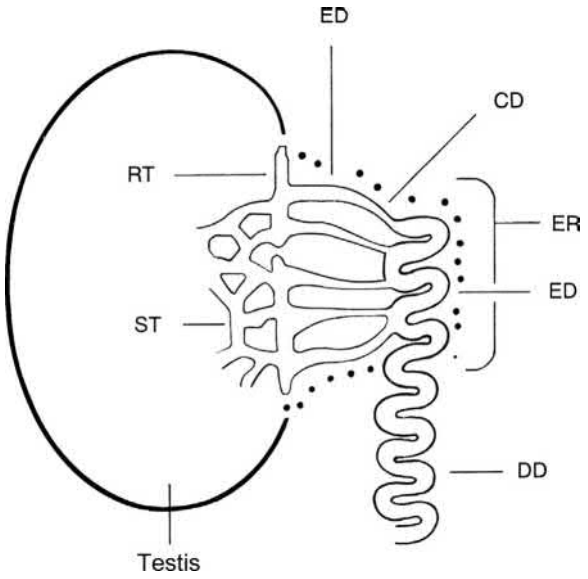

FIGURE 36.3 Schematic of the excurrent ducts of the testis. *ST*, seminiferous tubules; *RT*, rete testis; *ED*, efferent duct; *CD*, connecting duct; *ER*, epididymal region; *ED*, epididymal duct; *DD*, deferent duct. *Reproduced with permission from Academic Press, London and redrawn from Lake (1981).*

mesonephros and encompass the efferent ducts, epididymis, and deferens ducts. The epididymis is located on the dorsomedial aspect of the testis, which is referred to as the hilus (Figure 36.3). The epididymis is actually a series of ducts that ultimately empty into the deferent duct. The ducts within the epididymis include the rete testis, efferent ducts, connecting ducts, and the epididymal duct. The epididymal ducts and the deferent duct are referred to collectively as the excurrent ducts of the testis. Seminiferous tubules connect with the rete testis at discrete sites along the testis-epididymal interface (Tingari, 1971). Osman (1980), identified three distinct types of junctures between the seminiferous tubules and rete testis of the rooster: (1) a germ cell free epithelium of modified Sertoli cells that abruptly gives way to a rete-like epithelium, referred to as a terminal segment and tubulus rectus, respectively; (2) a terminal segment that connects directly to the rete testis; and (3) anastomosis of a seminiferous tubule with the rete testis. Tubuli recti have also been observed in quail testes (Aire, 1979a).

The rete testis has intratesticular, intracapsular, and extratesticular regions (Aire, 1982). As depicted in Figure 36.3, the rete testis exists as lacunae. In some avian species including domestic fowl, quail, guinea fowl, and ducks, the rete testis is lined with simple cuboidal and simple squamous epithelial cells (Aire, 1982), whereas in ratite birds, such as the ostrich, the epithelium contains cuboidal and columnar cell types (Aire and Soley, 2000, 2003). In gallinaceous birds, the rete testis exits the hilus after coursing through the testicular capsule before entering the epididymis which is in close proximity. In contrast, the rete testis of ratite birds makes up a much lower volumetric proportion of the epididymal tissue, and the rete testis travels a relatively larger distance from the testicular capsule before entering the epididymis (Ozegbe et al., 2010). Unlike the rete testis, the efferent ducts are wide at their proximal ends and narrow at their distal ends in many bird species (Aire and Soley, 2003; Simões et al., 2004); however, in ratite birds, both ducts are of similar height and diameter, which makes them less easily distinguished from one another (Aire and Soley, 2000; Ozegbe et al., 2006), whereas in emu and ostriches, the relative proportion of epididymal duct unit and the interductal connective tissue constituted a larger portion of the epididymis as compared to the rete testis and efferent ducts when combined (Ozegbe et al., 2010). On a volumetric basis (Table 36.1), the efferent ducts are the principal excurrent duct within the epididymis (Aire, 1979b; Aire and Josling, 2000). In most bird species, the efferent duct mucosa is highly folded, especially in the proximal portion (Tingari, 1971; Aire, 1979a; Bakst, 1980; Aire and Josling, 2000; Simões et al., 2004). In ratite birds, however, neither the proximal nor distal efferent ducts possess mucosal folds and they are regular in outline both internally and externally, which differs from other species (Ozegbe et al., 2006). In general, the efferent duct mucosa is characterized by a pseudostratified columnar epithelium that contains ciliated and nonciliated epithelial cells (Tingari, 1972; Budras and Sauer, 1975; Hess and Thurston, 1977; Aire, 1980; Simões

TABLE 36.1 Species Variation in Volumetric Proportions (%) of Epididymal Structures[a]

		Species	
Structures	Chicken	Japanese Quail	Guinea Fowl
Rete testis	13.3	9.9	10.7
Proximal efferent ductules	27.6	40.8	45.7
Distal efferent ductules	7.7	15.2	16.2
Connecting ducts	2.3	1.7	0.7
Epididymal duct	7.6	2.4	1.8
Connective tissue	38.7	27.3	22.6
Blood vessels	2.5	2.7	2.3
Aberrant ducts	0.3	–	–

[a]*Adapted from Aire (1979a).*

et al., 2004) as well as sparsely distributed intraepithelial lymphocytes (Aire and Malmqvist, 1979a). The epithelium of the connecting ducts is also composed of pseudostratified columnar cells (Tingari, 1971, 1972; Hess and Thurston, 1977; Aire, 1979a; Bakst, 1980; Aire and Josling, 2000). The distinguishing attributes of the connecting tubules are a narrow luminal diameter relative to that of adjacent excurrent ducts and the smooth contour of the mucosal surface (Tingari, 1971; Aire, 1979b; Bakst, 1980; Aire and Josling, 2000).

The tortuous epididymal and deferent ducts are characterized by low mucosal folds covered with nonciliated pseudostratified columnar epithelial cells (Tingari, 1971; Aire, 1979b; Bakst, 1980; Aire and Josling, 2000; Simões et al., 2004). In gallinaceous birds, the epididymal duct constitutes between 2.5% and 10% of the total epididymal volume (Aire and Josling, 2000), whereas in ratite birds, the volumetric proportion of the epididymal duct is as much as tenfold higher (Ozegbe et al., 2010). Based upon histological and morphological evidence, the deferent duct is a continuation of the epididymal duct. Luminal diameter gradually increases by threefold between the cranial epididymal duct and the distal deferent duct (Tingari, 1971). One notable difference between the epididymal duct and the deferent duct are the layers of dense connective tissue and smooth muscle surrounding the mucosa of the latter (Tingari, 1971; Aire and Josling, 2000). A dense capillary network envelope the excurrent ducts from the level of the proximal efferent ducts to the deferent duct (Nakai et al., 1988). The distal deferent duct straightens and then abruptly widens at its juncture with the cloaca. This structure, known as the receptacle of the deferent duct, has a bean-shaped appearance when it is engorged with semen. Each deferent duct terminates in the cloacal urodeum as a papilla immediately below the ostium of a ureter (Figure 36.4).

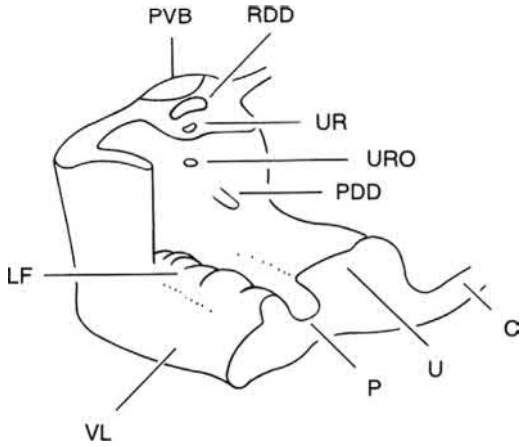

FIGURE 36.4 Schematic of the lower left quadrant of the cloaca. Before entering the cloacal wall, the deferent duct straightens then widens to form the receptacle of the deferent duct. The paracloacal body, also seen sectioned but shaded, is attached to the lateral aspect of the receptacle. The papilla of the deferent duct is within the urodeum of the cloaca. *PVB*, paracloacal vascular body; *RDD*, receptacle of the deferent duct; *C*, ventral wall of coprodeum; *U*, ventral wall of urodeum; *P*, ventral wall of proctodeum; *VL*, ventral lip of vent; *LF*, lymphatic folds. *Reproduced from King (1981), with permission from Academic Press.*

36.2.3 Accessory organs

Accessory reproductive organs include the paracloacal vascular bodies, dorsal proctodeal gland, and lymphatic folds (Fujihara, 1992). The accessory reproductive organs are either in proximity to or are an integral part of the cloaca. As shown in Figure 36.4, the paracloacal vascular body is found alongside the receptacle of the deferent duct, and lymphatic folds exist within the wall of the proctodeum. An intromittent phallus exists in only 3% of birds species (Herrera et al., 2013) including ratites and the waterfowl. In chickens, the phallus is nonintromittent and sperm is passed to the female via the "cloacal kiss" during matting (Briskie and Montgomerie, 2001). The cloacal kiss entails the union of the male and female cloacae for a few seconds. During copulation or in response to massage, a nonintromittent phallus forms a tumescent lymphatic tissue is everted through the vent immediately before ejaculation. As reviewed by Fujihara (1992), the paracloacal vascular bodies are essential for lymphatic tissue tumescence, as they are the sites where lymph is formed by ultrafiltration of blood. Thus, phallus erection in birds is lymphatic. The lymph needed for bird's lymphatic erection is produced in the paralymphatic bodies and the vascular body of the phallus, an ellipsoid spongy organ located alongside the middle of the cloaca (Brennan and Prum, 2012). In mammals, penile erection is blood-vascular and during ejaculation, semen is transported via the urethra. However, in birds semen is transported by the *sulcus spermaticus*, an external groove present in the phallus (Brennan et al., 2010).

Courtship behavior in male birds consists of searching and approaching a potential female (for an extensive review see (Ball and Balthazart, 2004)). For instance, quails display a series of sexual behaviors that include mounting and aggressive pursuit for mating (Hutchison, 1978). Most of the evidence suggests that the medial portion of the preoptic area (POA) of the brain is responsible for the control of male behavior (Adkins and Alder, 1972; Konkle and Balthazart, 2011). The POA is significantly larger in males than females, and male castration causes a reduction of the volume of this area (Panzica et al., 1987). In addition, castration reduces the normal sexual behavior in males and exogenous testosterone restores the normal behavior (Ball and Balthazart, 2004). In castrated males, estrogen can also restore normal behavior, but co-injection of testosterone and an aromatase inhibitor blocks this effect (Balthazart et al., 1997). It is now widely recognized that aromatization of testosterone in the POA is responsible for the normal

courtship behavior observed in male birds (Wade and Arnold, 1996; Cornil et al., 2011).

36.3 Ontogeny of the reproductive tract

36.3.1 Overview

The adult male reproductive tract is derived from two embryonic organs: a gonad and its associated mesonephros. However, the formation of the mesonephros precedes that of the gonad (Figure 36.5). In fact, the gonad arises from the ventromesial surface of the mesonephros (Figure 36.6). As reviewed by (Romanoff, 1960), three distinct pairs of excretory organs appear sequentially during embryonic development: the pronephros, mesonephros, and metanephros. The most anterior organ, the pronephros, disappears by day four of incubation in the chicken. Nonetheless, the pronephric duct, also known as the Wolffian duct, persists through time to (1) induce the formation of the mesonephric tubules, (2) induce the formation of the Müllerian duct, (3) temporarily link the mesonephros with the cloaca, and (4) ultimately serve as the deferent duct in males. The critical point in the ontogeny of the reproductive tract is gonadal differentiation; prior to this point in time, the embryo has bipotential gonads and the rudiments of oviducts and deferent ducts in the form of the Müllerian and Wolffian ducts, respectively.

Sex determination in mammalian species is associated with the expression of the sex-determining region Y (SRY) gene located in the Y chromosome of the heterogametic XY male. The major function of the SRY gene is to facilitate Sertoli cell differentiation via the SRY-box transcription factor 9 (Sox9) that, in turn, promotes testis development as previously reviewed (Knower et al., 2003). In contrast to mammalian species, male birds are

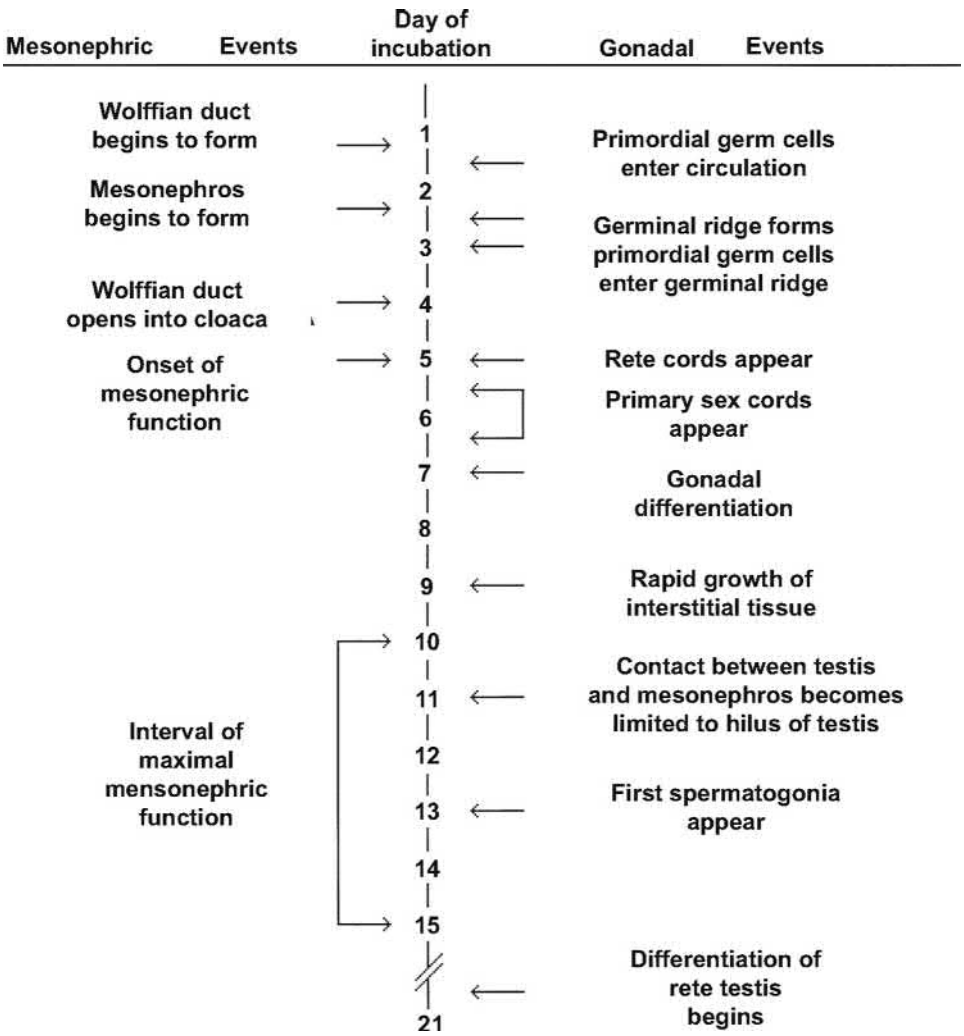

FIGURE 36.5 Chronology of developmental events in ovo associated with the formation of the male reproductive tract in Gallus domesticus. See text for details.

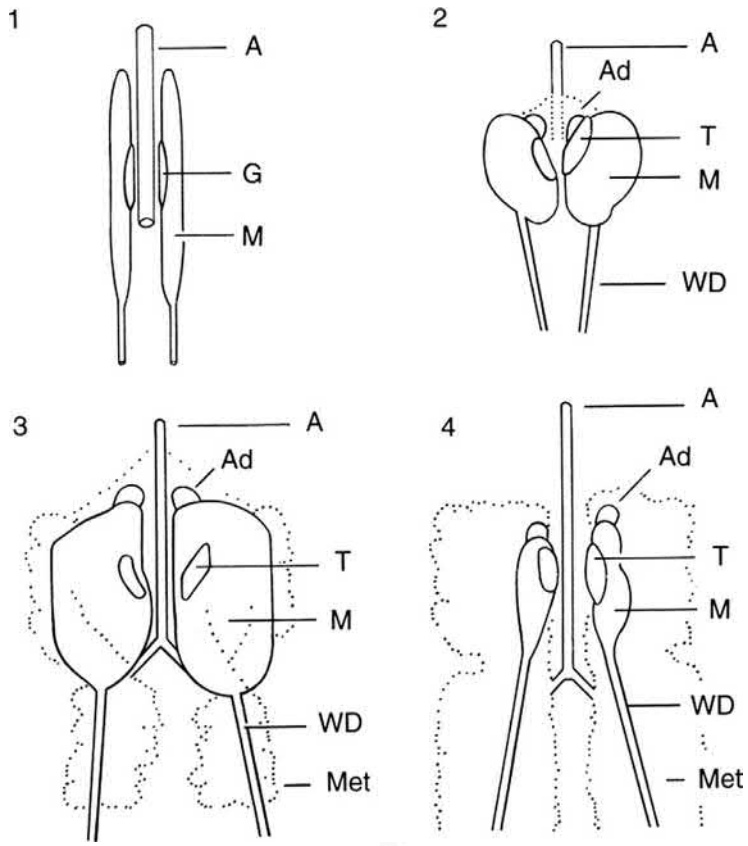

FIGURE 36.6 Stages in the development of the male urogential system. Numbers denote the first, second, third, or fourth quarter of incubation. The mesonephros forms before the differentiation of the gonad. After the metanephros becomes functional midway through incubation, mesonephric function declines and the mesonephros recedes apart from where it contacts the testis. *A*, aorta; *G*, undifferentiated gonad; *M*, mesonephros; *Ad*, adrenal gland; *T*, testis; *WD*, Wolffian duct; *Met*, metanephros. *Reproduced from Romanoff (1960), with permission from the MacMillan.*

homogametic and females are heterogametic (ZZ and ZW gonosomes, respectively). Thus, the molecular mechanism of sex determination in birds is different from mammalian species. Because females are heterogametic, one possibility is that the W chromosome is responsible for female development even when the W-linked determinant is still unidentified. Notwithstanding, the overexpression of the determinant W-linked histidine triad nucleotide binding protein in male embryos does not induce ovarian differentiation (Smith et al., 2003). In this scenario, a factor (similar to the SRY gene in male mammals) will be coupled to female differentiation. However, very few W-linked genes have been reported in the literature (Hori et al., 2000; O'Neill et al., 2000), suggesting that other mechanisms are responsible for male development. A second possibility is that a gene in the Z chromosome triggers male development when two copies of the gene are present. The Z chromosome "dosage" theory states that higher doses of a gene can initiate male differentiation if the additional copy is transcribed and translated in higher doses of the resulting protein. It has been shown that the Doublesex and Mab-3 Related Transcription factor 1, encoded by the DMRT1 gene (a zinc finger-like DNA-binding transcription factor), is a male sex determining factor in chickens (Smith et al., 2009a). In all birds studied to date, the DMRT1 gene is present in the Z chromosome and absent in the W chromosome (Chue and Smith, 2011). Reduction of DMRT1 protein expression, using RNA interference technology in early male embryos, resulted in feminization of the gonads. These data and other, supports the Z chromosome "dosage" theory in birds (Nanda et al., 1999; Chue and Smith, 2011). Similar to mammalian species, there is evidence that activation of the male determining factor in birds facilitates Sertoli cell differentiation via Sox9 or via anti-Müllerian hormone (AMH) which are upregulated in the chicken testis during gonadal development (Da Silva et al., 1996; Oreal et al., 1998; Bagheri-Fam et al., 2010). Taken together, mammals and birds use a different molecular mechanism for sex differentiation (SRY and DMRT1, respectively). After genes are expressed, a common pathway that involves a Sertoli cell differentiation factor (Sox9) promotes testicular differentiation and development (Figure 36.7).

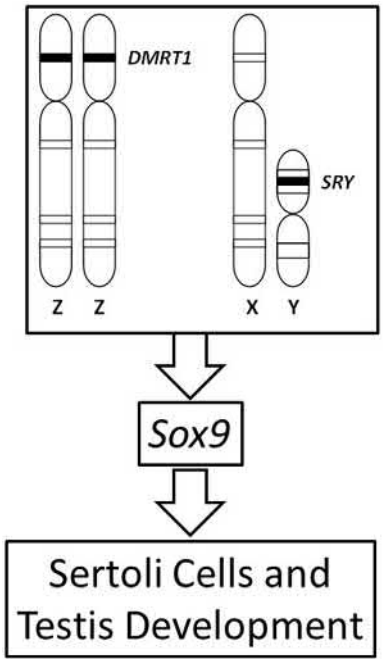

FIGURE 36.7 Differential mechanisms for sex differentiation in mammalian and avian species. In mammals, the XY male uses the SRY gene, while in birds the ZZ male uses the DMRT1 gene to facilitate Sertoli cell differentiation (via Sox9) that, in turn, promotes testis development.

36.3.2 Formation of the undifferentiated Gonad

Even though the gonad forms upon the ventromesial surface of the mesonephros, a fully differentiated mesonephros is not required for gonadal development (Merchant-Larios et al., 1984). The gonad is formed by the invasion of primordial germ cells into coelomic epithelium overlying a portion of the mesonephros (Figure 36.5), known as the germinal ridge (Romanoff, 1960; Clinton, 1998; Shimada, 2002). Primordial germ cells arise from endoderm along the anterior interface of the blastoderm's area opaca and area pellucida. After entering embryonic circulation, primordial germ cells are randomly distributed throughout the vasculature of the embryo (Meyer, 1964; Shimada, 2002; Yoshida, 2016). Subsequently, primordial germ cells colonize the germinal ridge (Fujimoto et al., 1976; Shimada, 2002). The undifferentiated gonad contains rete cords and primary sex cords in the anterior and middle regions, respectively (Romanoff, 1960).

36.3.3 Gonadal differentiation and Müllerian duct regression

Gonadal differentiation in chick embryos occurs at approximately 6.5−7 days of incubation (Figure 36.5). In comparison to the ovary, the cells of the medullary cords condense and coalesce into Sertoli cells, the cell to first emerge in the testis (Major and Smith, 2016). Embryonic testis is characterized by a germinal epithelium that recedes with time (mitotic arrest), a thicker capsule, the absence of secondary or cortical sex cords, as well as the presence of primary sex cords surrounded by stroma (Romanoff, 1960; Clinton and Haines, 1999; Shimada, 2002). Also, in the outer epithelial layer, there is no hyperproliferation (Major and Smith, 2016). The primary sex cords contain numerous primordial germ cells and are anlage of the seminiferous tubules. Biochemically, gonadal differentiation is evident in terms of increased cyclic nucleotide concentrations (Teng, 1982), increased protein synthesis (Samsel et al., 1986), and the pattern of sex steroid synthesis (Guichard et al., 1977; Imataka et al., 1988; Mizuno et al., 1993). It is noteworthy that these traits become evident prior to the development of the pituitary-gonadal axis, which appears to become functional at 13.5 days of incubation in the chick (Woods and Weeks, 1969). It must also be noted that the interval of sexual bipotentiality differs among species.

Once the testes have formed, the Müllerian ducts cease development and undergo regression in a caudocranial direction (Romanoff, 1960; Hutson et al., 1985). Müllerian duct regression is attributable to AMH, also known as Müllerian Inhibiting Substance (Bruggeman et al., 2002; Smith and Sinclair, 2004). This hormone is a 7.4 kDa gonad-specific glycoprotein (Teng et al., 1987), which, in the male, is derived from the progenitors of Sertoli cells found within the primary sex cords (Stoll and Maraud, 1973; Oreal et al., 2002). The gene encoding AMH is expressed in both males and females, but is consistently higher in males during sexual differentiation (Smith et al., 1999). Regression of the Müllerian ducts in males occurs because they contain insufficient circulating estrogen levels to counteract the effect of AMH which may be a direct result of aromatase suppression by AMH itself (MacLaughlin et al., 1983; Hutson et al., 1985; Bruggeman et al., 2002).

36.3.4 Formation of the excurrent ducts

The excurrent ducts are derived from the mesonephros. As shown in Figure 36.5 and 36.6, the mesonephros is active throughout the second and third quarters of incubation. The functional unit of the mesonephros includes a malpighian corpuscle, proximal, intermediate, and distal tubules, as well as a connecting tubule. The latter connects the series of mesonephric tubules with the Wolffian duct. The malpighian corpuscle is a capillary tuft or glomerulus within a double-walled epithelial enclosure known as Bowman's capsule. The visceral epithelial layer adheres to the glomerulus. At the pole of the corpuscle where the afferent and efferent arterioles are attached to the glomerulus within, the visceral epithelium folds back upon itself to form the parietal epithelium. As the parietal epithelium extends away from the vascular pole, it is separated from

the visceral epithelium by a lumen. After the mesonephros becomes functional, glomerular filtrate enters the lumen of the proximal tubule. After the metanephros becomes functional during mid-incubation (Romanoff, 1960), the mesonephros begins to degenerate except where there is contact with the embryonic testis. Consequently, the mesonephros undergoes a profound change in size during embryonic development (Figure 36.6).

During the last third of incubation, a subset of mesonephric tubules are converted into the excurrent ducts of the testis (Budras and Sauer, 1975) and the malpighian corpuscles in proximity to the rete cords fuse. The glomeruli undergo progressive degeneration while the simple squamous epithelial cells of the parietal epithelium differentiate into simple columnar cells. This tissue becomes the epithelium of the proximal efferent ducts. Proximal, intermediate, and distal mesonephric tubules are transformed into distal efferent ducts, connecting ductules become the connecting ducts, the Wolffian duct associated with the mesonephros becomes the epididymal duct, and the distal Wolffian duct becomes the deferent duct.

The transformation of the mesonephric ductules into the excurrent ducts of the testis is dependent on androgen production by the Leydig cells (Maraud and Stoll, 1955; Stoll and Maraud, 1974; Bruggeman et al., 2002), and is initiated shortly after the concentration of blood plasma testosterone has peaked *in ovo* (Woods et al., 1975). However, the entire process of ductule conversion in the chicken requires an interval of 8–10 weeks (Marvan, 1969; Budras and Sauer, 1975). During this time, mean plasma testosterone levels stay constant at about 12–13% of those observed in sexually mature males (Driot et al., 1979; Tanabe et al., 1979). In contrast to the mesonephric tubules, differentiation of the rete cords begins at about the time of hatching and is complete by 5 weeks of age (Budras and Sauer, 1975). The convolutions of the newly formed epididymal and deferent ducts increase until sexual maturity (Budras and Sauer, 1975). The final length of the deferent duct has been estimated to be four times greater than the linear distance between the epididymis and cloaca due to these convolutions (Marvan, 1969).

36.4 Development and growth of the testis

36.4.1 Proliferation of somatic and stem cells in the testis

The testis of the mature bird is organized into discrete, easily discernible cellular associations and functional compartments (Figure 36.8D). However, during embryonic and early posthatch development of this organization is less apparent. In white Leghorn embryos, from day 8 to day 13 of incubation, the cells of the epithelium that gives rise to

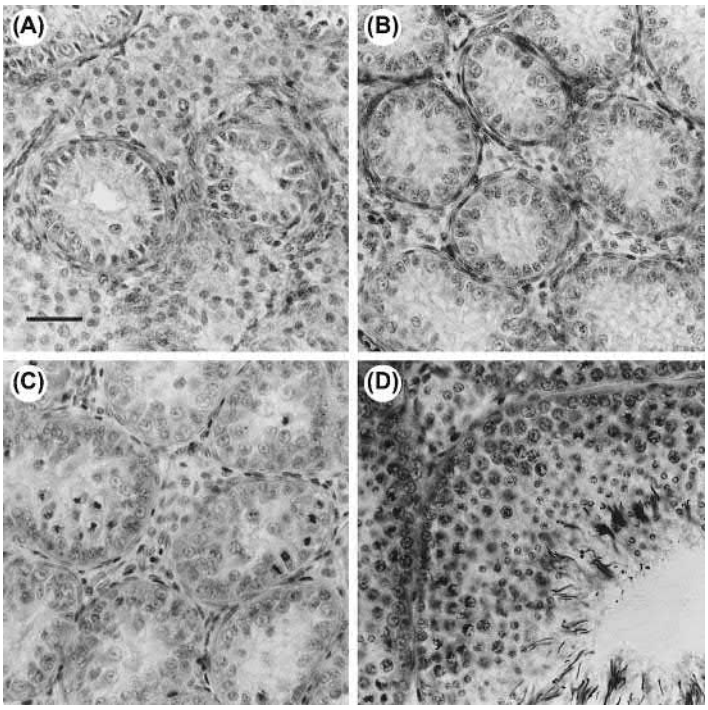

FIGURE 36.8 Cross-sections of testes of cockerels reared under 8h of light (A–C) and of an adult male on 14h of light (D). (A) Cross-section of a testis from a 14 day old male. Notice the simple single layer of spermatogonia and Sertoli cells in the tubules and the relative abundance of interstitial space. (B) Cross-section of a testis from a 56 day old cockerel. The single layer of cells within the seminiferous tubule has become taller and more complex. (C) Cross-section of a testis from a 140 day old cockerel. Notice the appearance of spermatocytes (cells with darkly stained chromatin) that have moved away from the basement membrane. (D) Cross-section of a testis from an adult male, which clearly demonstrates active spermatogenesis and the dramatic reduction in the relative area of the interstitium. The bar in (A) equals 20μm; all of the micrographs are of equivalent magnification. *Photographs by the author.*

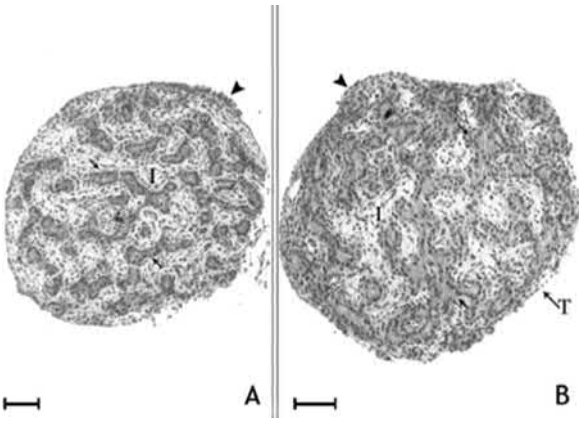

FIGURE 36.9 *Gallus domesticus* transverse histology section of testis in 8 and 13 day old embryo. Sex cords change from undulated (A) to a reticulum shape (B). interstitium (I), tunica albuginea (T). Magnification is represented by a 50-mm scale in A and B. *Microphotograph adapted from (Gonzalez-Moran and Soria-Castro, 2010).*

the tunica albuginea change from cuboidal to flatten (Figure 36.9A). The initial sex cords tend to form a reticulum that connects with the primordial tunica albuginea (Figure 36.9B). Hyperplasia of primordial germinal cells and Sertoli cells occurs proportionally as embryonic development progresses (Gonzalez-Moran and Soria-Castro, 2010). These primordial germinal cells differentiate into spermatogonia and remain arrested until 10 week of age (Oiso et al., 2013). In addition to Sertoli and primordial germinal cells, a side population (SP) of cells has been identified in the prenatal gonads. The SP cells play an important role enhancing germ cell and stem cells function in the gonad. For instance, SP cells have a particular membrane-pump system activated by Brcp1 gene. It has been suggested that BCRP seems to play an important function in genome integrity for stem cells, thereby enrichment for the niche in which stem cells colonize the male gonad (Bachelard et al., 2015).

The posthatch development of the fowl's testis can be divided into three distinct phases: (1) proliferation of spermatogonia and the somatic cells that support spermatogenesis (Sertoli, peritubular myoid, and interstitial cells); (2) differentiation and the acquisition of functional competence by somatic support cells; and (3) spermatogonial differentiation resulting in the initiation of meiosis. Although the boundaries of these phases are not clearly defined, this three-step process results in functional seminiferous tubules that can sustain spermatogenesis when the appropriate hormonal cues are present. There is some evidence that FSH may play an important role in embryonic gonad growth by stimulating cell division. Treatment with FSH increased the mitotic index in both the seminiferous tubules and peritubular cells of chicken embryo testis at around 14 days of development (Mi et al., 2004).

The testis of the young cockerel (approximately 0–6 weeks of age) is characterized by an abundance of interstitial tissue and seminiferous tubules with only a single layer of cells within the basal lamina surrounded by several layers of myoid cells (Figure 36.8A). The majority of cells located within the seminiferous tubules at this time are Sertoli cells and spermatogonia, with macrophages and mast cells observed as well (de Reviers, 1971b). The seminiferous tubules at this time are narrow (approximately 40 μm in diameter) with either a poorly formed lumen or no apparent lumen at all (seminiferous cords). This is a period of rapid cellular proliferation, as while the tubules are only slowly growing in diameter, they are growing rapidly in length (de Reviers, 1971a). Even though the somatic and stem cells are proliferating, the absolute weight and volume of the testis is increasing slowly from day eight of incubation to 6 weeks of age as the seminiferous tubules displace interstitial cells (Marvan, 1969; de Reviers, 1971a; Gonzalez-Moran and Soria-Castro, 2010). In white Leghorn, the increase in size of the seminiferous tubules is attributed to hyperplasia of the Sertoli cells. During early days of age (one to six doa), the population of Sertoli cells are dominant, whereas at 28 weeks of age the germ cells are more abundant. The growth rate of the testis from the sixth to the eighth week was greater than the rate of increase of body weight (Gonzalez-Moran and Soria-Castro, 2010).

36.4.2 Differentiation of somatic cells within the testis

Following a posthatching period of Sertoli cell proliferation, these cells become mitotically quiescent and differentiate (for a review see Russell and Griswold (1993)). In a study by (de Reviers and Williams, 1984), hemicastration was shown to result in compensatory hypertrophy of the remaining testis of males up to 8 weeks of age. As hemicastration typically results in significant hypertrophy only during the period of Sertoli cell proliferation in mammals, it is possible to postulate that Sertoli cells are proliferating in the fowl to about 8 weeks of age. A more recent study by Bozkurt et al. (2007) provides support for this hypothesis. In this study, the mitotic proliferation of Sertoli cells was observed in the testis of fowl from 1 to 10 weeks of age. Initially, the density of germ cell nuclei was less than that of Sertoli cell nuclei; however, by week six, the volume density of the two cell types had converged and remained constant until the commencement of meiosis. In addition, clear labeling of both Sertoli and germ cells was observed from weeks one through seven, but, by week eight, the only cells still labeled were germ cells. These data confirm that

the cessation of Sertoli cell proliferation occurs around eight weeks in domestic fowl.

Sertoli cells differentiate into highly polarized cells that extend from the basal lamina to the lumen of the seminiferous tubule. The mature Sertoli cell is a complex, columnar cell that contains numerous crypts into which developing sperm cells are embedded (Sertoli, 1865, 1878; Nagano, 1962). Sertoli cell functions are thought to be regulated by a myriad of endocrine and paracrine factors, although FSH and testosterone have been most thoroughly studied (Brown et al., 1975; Brown and Follett, 1977). A primary function of Sertoli cells is to provide a carefully regulated environment, including the sequestration of postmeiotic germ cells into the adluminal compartment is accomplished by the formation of tight junctions between adjacent Sertoli cells at a point basal to the maturing, meiotic, germ cell (Bergmann and Schindelmeiser, 1987; Pelletier, 1990). While tight junction formation appears to be androgen dependent in the fowl, tight junctions are maintained during periods of spermatogenic quiescence in the mallard (*Anas platyrhynchos*) (Pelletier, 1990). Another indicator of mature Sertoli cell function is the complex complement of proteins synthesized and secreted in response to androgen and/or FSH stimulation. While studied only superficially in male birds, spermatogenic stage-specific protein synthesis and secretion is well documented in other groups (see Russell and Griswold (1993)). The presence of a distinguished rough endoplasmic reticulum, lysosomes, and macrophage function in Sertoli cells has been associated to the fas-induced apoptosis mechanism that controls germinal cell population. Therefore, the number of Sertoli cells determine and regulate the development of stem primordial germinal cells into spermatogonia (Thurston and Korn, 2000).

The growth of the seminiferous tubules is associated with a reorganization and reduction of the testicular interstitium (Figure 36.8A–D). While the seminiferous tubule is the compartment where spermatogenesis will occur in the adult, Leydig cells of the interstitium are responsible for testicular androgen production. In the interstitium, there is the presence of mesenchymal cell-like Leydig cell precursors, which have vesicles of smooth endoplasmic reticulum and lipid droplets (Connell, 1972). The differentiation of these cells into their mature form is under the influence of LH (Narbaitz and Adler, 1966; Brown et al., 1975; Driot et al., 1979). Mature Leydig cells are formed following a continuum of cellular differentiation that occurs during the period of testicular growth leading to the prepubertal increases of circulating LH levels (Rothwell, 1973). While limited testosterone production is observed during embryogenesis and early development, the capacity to produce testosterone at sexually mature levels requires the presence of a fully differentiated Leydig cell population (for a review of testicular steroidogenesis see (Johnson, 1986). The mature Leydig cell of the rooster has extensive smooth endoplasmic reticulum, a prominent Golgi complex, mitochondria with tubular cristae, abundant lipid droplets, and lysosomal elements (Rothwell, 1973).

36.4.3 Initiation of meiosis

During the period of Sertoli and Leydig cell differentiation, the population of spermatogonia increases in size and complexity. As described later in the chapter, spermatogonia undergo a series of transformations prior to committing to meiosis. However, once a spermatogonium is transformed into a preleptotene spermatocyte, it separates from the basement membrane and shifts toward the adluminal compartment of the seminiferous tubule. The onset of active meiosis is marked by the presence of pachytene and zygotene spermatocytes which are easily discernible due to their highly condensed and darkly stained chromatin (Figure 36.8C). The initiation of meiosis appears to occur only after the completion of Sertoli cell proliferation, and an increase in circulating androgens is encountered (de Reviers, 1971a, b). The onset of meiosis can be significantly altered by manipulation of the photoperiod (Ingkasuwan and Ogasawara, 1966). When broiler breeders were reared on a 23L:1D photoperiod and ad libitum food and water intake for 6 weeks, males showed precocious testicular maturation with zygotene or pachytene, or both, spermatocytes visible in all seminiferous tubules at 7 weeks of age. In contrast, when broiler breeders were reared on a 15L:9D photoperiod and ad libitum food and water intake for only 2 weeks, the structures previously described were not present at seven weeks of age (Vizcarra et al., 2010).

36.4.4 Altering the pattern of testis growth and maturation

The temporal component of testicular maturation can be altered by manipulation of the endocrine milieu. Specifically, onset of meiosis and sustained spermatogenesis can be altered dramatically in the fowl by manipulating the photoperiod (Ingkasuwan and Ogasawara, 1966). Male fowl reared on a long photoperiod (14 h light or more per day) will typically have reached sexual maturity by 16–20 weeks of age (Ingkasuwan and Ogasawara, 1966; Sharp and Gow, 1983). However, as shown in Figure 36.8C, when males are reared on short days (in this case 8 h of light per day), the onset of spermatogenesis is delayed. Eventually, male fowl became refractory to short days, FSH and LH levels increase, and spermatogenesis commences. Conversely, precocious puberty and the onset of spermatogenesis can be accelerated in the fowl by chronic treatment with tamoxifen, an estrogen receptor antagonist (Rozenboim et al., 1986). Males treated with tamoxifen exhibited adult behaviors and produced viable

spermatozoa by 9 weeks of age, months ahead of their nontreated siblings (Rozenboim et al., 1986).

Testicular maturation can also be altered by exposure to estrogen and estrogen-like compounds. Rooster embryos exposed to ethinylestradiol, a synthetic form of estrogen, exhibited significant reduction in the average area of their seminiferous tubules. In addition, exposed birds had a decreased proportion of seminiferous tubules and an increase in the proportion of interstitial tissue (Blomqvist et al., 2006). In Japanese quail, male embryos exposed to ethinylestradiol became feminized and had ovary-like tissue within the testis along with persistent Müllerian ducts (Berg et al., 1999).

36.5 Hormonal control of testicular function

36.5.1 Central control of testicular function

Spermatogenesis is the process in which the division of spermatogonial stem cells ultimately yields sperm cells while a population of stems cells is maintained. This complex phenomenon occurs within the seminiferous epithelium and depends upon the availability of testosterone and FSH, the activity of Sertoli cells, as well as interactions between germ cells and Sertoli cells (Sharpe, 1994). Although spermatogenesis is controlled, in part, by cells within the testis, the process is ultimately controlled by neurons within the central nervous system (CNS; see review by (Sharp and Gow, 1983)). Neurosecretory activity, in turn, is affected by somatic and environmental stimuli. Wingfield et al. (1992) have proposed a model accounting for the central integration of environmental information that affects gonadotropin secretion on a seasonal basis. The model is based upon the interplay of endogenous "predictive" rhythms and supplementary environmental information. The duration of the period of light in a subjective day (24 h period) is the principal environmental factor that stimulates spermatogenesis in galliform birds. As reviewed by (Kuenzel, 1993), photoreceptors that affect spermatogenesis are neither found within the retina nor the pineal gland. Most of the evidence suggests that the most plausible site associated with the photoperiodic response is the medial basal hypothalamus (MBH) via direct innervations of GnRH neurons by encephalic photoreceptors (Saldanha et al., 2001) or via the pars tuberalis of the adenohypophysis (Yoshimura, 2006, 2010; Watanabe et al., 2007; Yasuo and Yoshimura, 2009). It has been reported that the pars tuberalis synthesize and secretes β-thyroid stimulating hormone (TSH) when Japanese quails are exposed to long-day stimulation (Yoshimura et al., 2003). In turn, TSH is retrogradely transported to the MBH via nonclassical mechanisms (Krieger and Liotta, 1979; Mezey et al., 1979). In the MBH, TSH regulates the expression of genes encoding type 2 (*Dio2*) and type 3 (*Dio3*) deiodinases. Thyroxine (T4) is converted (within the MBH) to the bioactive T3 (triiodothyronine) form that, subsequently, stimulates the photoperiodic response of the gonadal axis (Yoshimura et al., 2003). In photosensitive and scotorefractory quails (Figure 36.10), the mechanism by which Gonadotropin-Inhibitory Hormone (GnIH), GnRH-I and −II are regulated has been associated with the stimulation of deep brain photoreceptors and the photoreceptive neurons (psin-5 and VA-opsin) (Banerjee and Chaturvedi, 2017).

36.5.2 Control of adenohypophyseal function in males

Gonadotropin-releasing hormone (GnRH) is a decapeptide that plays a fundamental role in the release of gonadotropins from the pituitary gland, and is the primary hormone that regulates reproduction. Andrew Schally and his team isolated and synthesized for the first time the decapeptide GnRH, after the extraction of more than 250,000 pig hypothalami (Matsuo et al., 1971; Wade, 1978). In addition to GnRH, the occurrence of other two GnRH isoforms were first reported in chickens more than 10 years after of Dr. Schally's initial report. The nomenclature used to distinguish different GnRH isoforms between mammalian and nonmammalian species have been described using a variety of phylogenetic and genomic synteny analyses (Millar et al., 2004; Borosky et al., 2011; Kim et al., 2011; Tostivint, 2011). In the vertebrate classification, avian species as part of the gnathostomes have three GnRH clades (GnRH1, GnRH2, and GnRH3). Thus, cGnRH-II and −I are part of GnRH1 and GnRH2, respectively (Ubuka et al., 2013). For the purpose of this chapter, we adopted the nomenclature based on the species in which they were first discovered, depicted in Table 36.2, and described elsewhere (Millar et al., 2004).

Chicken GnRH-I (King and Millar, 1982; Miyamoto et al., 1982) differs in only one amino acid compared with the mammalian form (cGnRH-I; [Gln8]-GnRH); whereas chicken GnRH-II (Hattori et al., 1986) differs in three amino acids (cGnRH-II; [His5-Trp7-Tyr8]-GnRH). The coordination of gonadotropin secretion via cGnRH is also modulated by the interaction of the GnRH peptide with its receptors. The Gonadotropin-releasing-hormone receptors (GnRHRs) have the characteristic feature of a classical seven transmembrane, G-protein-coupled receptor (Neill, 2002; Millar, 2003, 2005). Four vertebrate GnRHR lineages have been proposed using genome synteny and phylogenetic analyses; nonmammalian type I, nonmammalian type II, nonmammalian type III/mammalian type II, and mammalian type I (Kim et al., 2011).

Two GnRHRs have been identified in chickens (Shimizu and Bédécarrats, 2006; McFarlane et al., 2011).

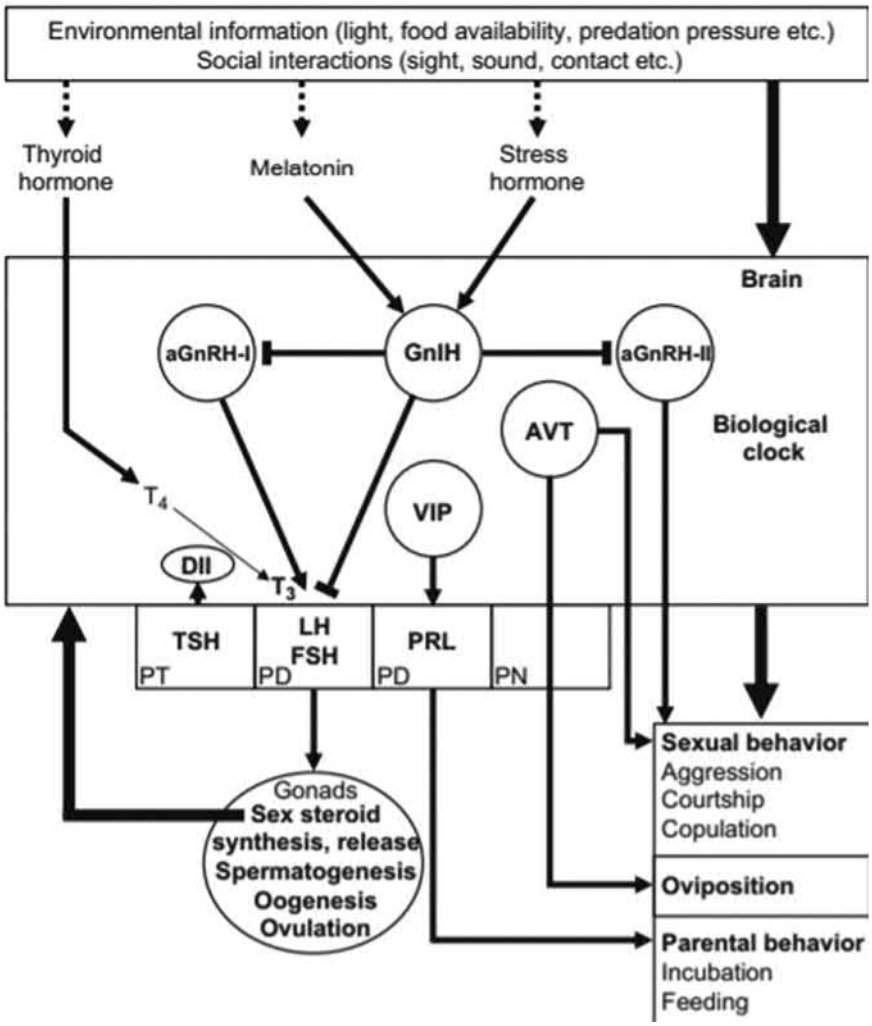

FIGURE 36.10 Neuroendocrine Control of Reproduction in Birds. *Adapted from (Ubuka and Bentley, 2011).*

TABLE 36.2 Amino Acid (AA) Sequence of GnRH Isoforms

	1 2 3 4 5 6 7 8 9 10
Mammal (mGnRH)	**pGlu-His-Trp-Ser-**Tyr-Gly-Leu-Arg**-Pro-Gly**
Chicken-I (cGnRH-I)	**pGlu-His-Trp-Ser-**Tyr-Gly-Leu-Gln**-Pro-Gly**
Chicken-II (cGnRH-II)	**pGiu-His-Trp-Ser-**His-Gly-Trp-Tyr**-Pro-Gly**

The bolded regions represent the conserved NH_3- and COOH- terminal residues. The numbers represent the relative position of each AA in the GnRH peptide (1 represents the N-terminal AA).

The nonmammalian type I receptor is predominantly expressed in the chicken pituitary gland (Shimizu and Bédécarrats, 2006; Joseph et al., 2009); whereas the nonmammalian type II receptor is not only expressed in the pituitary and the brain but also in the gonads and other tissues (Sun et al., 2001b). The nonmammalian type I receptor in chickens (NCBI accession number: NP_001012627) has been previously referred as cGnRH-R-III (McFarlane et al., 2011), GnRHR1/III (Kim et al., 2011), or GnRHR2 (Shimizu and Bédécarrats, 2006), whereas the nonmammalian type II receptor in chickens (NCBI accession number: NP_989984) has been previously

referred as cGnRH-R (Sun et al., 2001a; Kim et al., 2011) or cGnRHR 1 (Shimizu and Bédécarrats, 2006).

The affinity of the cGnRH-I peptide to the nonmammalian type II receptor is higher than the affinity of cGnRH-II peptide to the same receptor (Sun et al., 2001a). The nonmammalian type I receptor in the chicken pituitary is differentially expressed with respect to the reproductive status, and is associated with the control of gonadotropin secretion (McFarlane et al., 2011).

In the chicken, GnRHergic neurons arise within the olfactory epithelium on day 4.5 of embryonic development, reach the CNS by migrating along the olfactory nerve, and stop migrating by day 12 of embryonic development (Sullivan and Silverman, 1993). GnRHergic neurons are found within extrahypothalamic and hypothalamic sites (Kuenzel and Blahser, 1991). However, only those neurons whose axons terminate within the median eminence are believed to induce gonadotropin secretion in vivo (Mikami et al., 1988). Based upon immunocytochemical analysis, GnRH-positive axons are found within the median eminence by day 14 of embryonic development (Sullivan and Silverman, 1993). The significance of GnRHergic neurons was demonstrated well in advance of the purification of chicken GnRH with experiments that induced functional castration by either electrolytic lesions or deafferentation within the hypothalamus (Ravona et al., 1973; Davies and Follett, 1980). Axons of GnRHergic neurons terminate in proximity to capillaries within the median eminence of the hypothalamus. GnRH secreted from these axons reaches target cells within the adenohypophysis via the hypothalamo-hypophyseal portal vessels (Gilbert, 1979).

In avian species, only indirect measurements of the GnRH pulse generator is available by measuring plasma LH concentrations in frequent samples or in pituitary extracts (Wilson and Sharp, 1975; Sharp and Gow, 1983; Chou and Johnson, 1987). In addition, the episodic nature of LH and FSH was evaluated in unrestrained male broiler breeders using serial blood sampling (Vizcarra et al., 2004). Gonadotropin secretion in males is characterized by a pulsatile pattern with LH pulses being more frequent and having greater amplitude than FSH pulses (Figure 36.11). In chickens, LH- and FSH-containing gonadotrophs reside in separate cells within the pituitary gland (Proudman et al., 1999). We observed that there was a lack of synchrony between the episodic release of LH and FSH. Only 23% of the LH pulses were associated with FSH episodes, suggesting that in the adult male fowl, LH and FSH secretion are regulated independently (Vizcarra et al., 2004).

Both cGnRH-I and -II stimulates gonadotropin release in vivo and in vitro in the chicken. However, most of the evidence indicates that cGnRH-I is the prime regulator of gonadotropin release in birds (Katz et al., 1990; Sharp et al., 1990; Dawson and Sharp, 2007; Ubuka and Bentley, 2009).

Nevertheless, the relative contribution and the potency of each cGnRH isoforms on the hypothalamic–pituitary–gonadal (HPG) axis of male birds is controversial. For instance, cGnRH-II was not found in the median eminence of the male white-crowned sparrow (*Zonotrichia leucophrys gambelii*), suggesting that in these species, cGnRH-II does not regulate pituitary gonadotropin secretion (Meddle et al., 2006). On the other hand, concentrations of FSH in small cockerels were not affected by cGnRH-I challenges (Krishnan et al., 1993).

In immature cockerels (Chou et al., 1985) and male turkeys (Guemene and Williams, 1992), GnRH-II was more potent than GnRH-I in vitro and in vivo to release LH, suggesting that very small doses of GnRH-II at the pituitary level might be sufficient to induce gonadotropin release. However, no significant differences were observed between cGnRH-I and cGnRH-II, in LH releasing activity from young cockerels pituitary samples (Hattori et al., 1986). When the LH response to cGnRH-I and -II was evaluated in cockerels, both peptides were equally potent (Sharp et al., 1987). However, in a similar experiment, the response to cGnRH-II, in terms of LH release was consistently greater than the response to GnRH-I in male chickens (Wilson et al., 1989). These data suggest that there may be age differences in the LH response to both decapeptides. Whether this differential response is due to different steroid inhibitory feedback mechanism is still unknown. The negative feedback of testicular steroids on GnRH-I have been reported in starlings (*Sturnus vulgaris*). Castrated male starlings significantly increased immunoreactive GnRH-I in the rostral POA of the hypothalamus, suggesting that this may represent the neuroanatomical location that mediates steroid negative feedback (Stevenson and Ball, 2009).

Active immunization against cGnRH-I and cGnRH-II in adult broiler breeder males was associated with a differential response on the ability to produce an immune reaction (Vizcarra, 2013). Titers were increased in cGnRH-I but not in cGnRH-II treated birds compared with BSA immunized males (Figure 36.12). Concentrations of LH and FSH in frequent samples were not affected by treatment; however, testis weight was significantly decreased in cGnRH-I birds compared with the other treatments (Figure 36.13). Taken together, these data support the idea that cGnRH-I is the prime regulator of gonadotropin release in male birds.

Behavioral, visual/auditory cues, and the breeding season also regulates GnRH-I and –II in birds (Figure 36.10). In male ring doves (*Streptopelia risoria*) and male starlings (*Sturnus vulgaris*), courtship interaction increases cGnRH-I synthesis (Mantei et al., 2008; Stevenson and Ball, 2009), suggesting that sexual behavior can have a significant effect on the HPA axis. In most seasonal breeders birds, the stimulation of the gonadotropic axis is influenced by photoperiod (for review see [Dawson and Sharp, 2007]).

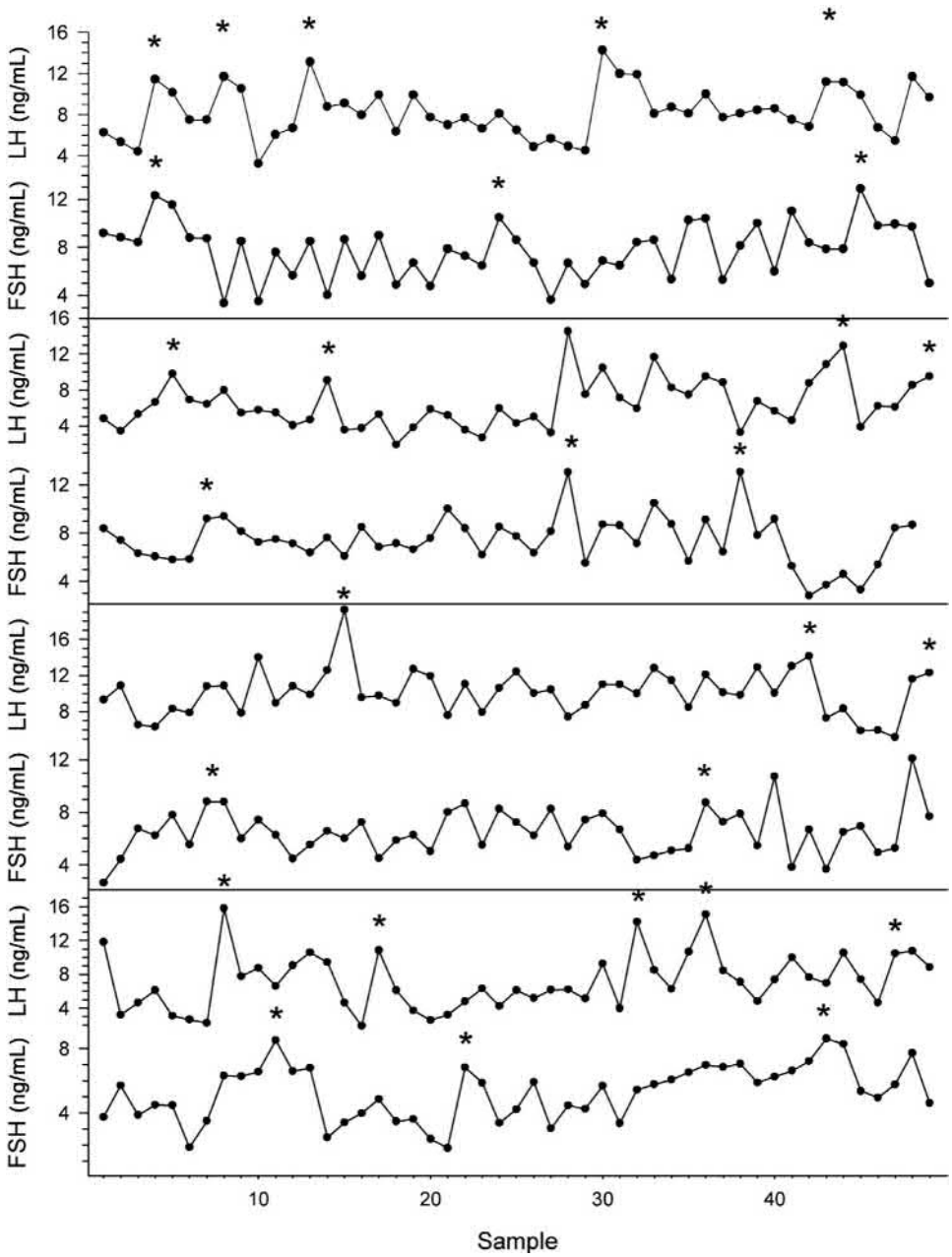

FIGURE 36.11 Pulsatile secretion of luteinizing hormone (LH) and follicle-stimulating hormone (FSH) in plasma of four birds. Blood samples were obtained every 10 min for 8 h. Asterisks indicate the presence of a pulse of LH or FSH, as determined by Pulsar. *Adapted from Vizcarra et al. (2004).*

Hypothalamic photoreceptors transduce the energy from light into a biological signal that regulates the secretion of GnRH. Encephalic photoreceptors are in close proximity with GnRH-I neurons, indicating that brain photoreceptors communicate directly with GnRH-neurons and terminals (Saldanha et al., 2001). During the breeding season, GnRH-I increases in males birds including the house finches (*Carpodacus mexicanus*), the dark-eyed juncos (*Junco hyemalis*), and the European starlings (*Sturnus vulgaris*) (Foster et al., 1987; Cho et al., 1998; Deviche et al., 2000). The contribution of GnRH-II during the breeding season is associated to the regulation of sexual behavior (Ubuka et al., 2013). In nonbreeding mature male zebra finch (*Taeniopygia guttata*), the number of cGnRH-II neurons is significantly reduced during the nonbreeding compared with the breeding season, but the area and optical density of the stained cells did not differ (Perfito et al., 2011).

Until recently, there was no known neuropeptide that directly inhibited gonadotropin secretion; however, Tsutsui et al. (2000) isolated GnIH, a hypothalamic

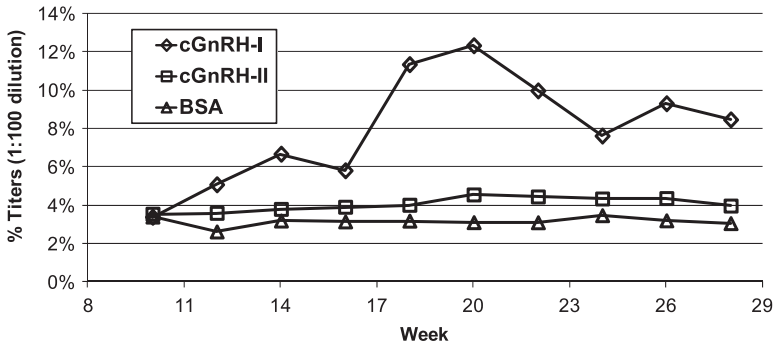

FIGURE 36.12 Antibody titers (^{125}I-cGnRH bound, %) of male broiler breeders immunized against cGnRH-I, cGnRH-II, and BSA. Titers were increased ($P<0.05$) in cGnRH-I but not in cGnRH-II treated birds compared with BSA-immunized males. *Adapted from Vizcarra (2013).*

dodecapeptide from the Japanese quail (For review see Son et al., 2019). This dodecapeptide consists of 12 amino acids in the sequence Ser(62)-Ile(252)-Lys(233)-Pro(226)-Ser(38)-Ala(194)-Tyr(173)-Leu(148)-Pro(104)-Leu(108)-Arg(45)-Phe(52) with RFamide at the C-terminus. GnIH significantly inhibits LH and FSH release in cultured quail cells (Tsutsui et al., 2000) and also inhibits circulating LH in vivo when administered continuously via osmotic pump (Ubuka et al., 2006). Interestingly, chronic GnIH treatment inhibits photoinduced testicular development, causes decreased plasma testosterone and testicular apoptosis, and results in decreased spermatogenic activity in the testis of adult quail (Ubuka et al., 2006). Similarly, testicular growth and plasma testosterone are suppressed in immature quail (Ubuka et al., 2006). Osugi et al. (2004), found that GnIH injected simultaneously with GnRH inhibited plasma LH surge in song sparrows and decreased LH concentrations in breeding free-living Gambel's white-crowned sparrows. GnIH reactive neurons were found to be localized within the paraventricular nucleus and mesencephalic regions of the hypothalamus in quail, white-crowned sparrows, and European starlings (Tsutsui et al., 2000; Bentley et al., 2003; Ubuka et al., 2003; Ukena et al., 2003). The action of GnIH is mediated by the G protein-couple receptors (GPR) GPR147 (pituitary and hypothalamus) and GPR74 (different tissues) (Aparicio et al., 2005; Osugi et al., 2012; Abdul-Rahman et al., 2016). In addition, the GnIH receptor was found to be expressed in the thecal cells, Leydig cells, germ cells, and epididymis in male quail, which suggests roles for the hormone in regulating: gonadal steroid synthesis and release, differentiation of germ cells, and sperm maturation (Bentley et al., 2003, 2008).

Melatonin and stress may be key factors involved in GnIH neural functions as the neurons of male quail have been found to contain a receptor for melatonin (Ubuka and Bentley, 2011; Osugi et al., 2012) (Figure 36.10). Administration of melatonin via implants (s.c.) stimulated the expression of GnIH in a dose-dependent way in birds that had undergone pinealectomy and orbital enucleation (Ubuka et al., 2005). In addition, hypothalamic explants from quail exposed to long-day photoperiods released greater amounts of GnIH during dark periods than during light periods in vitro. Conversely, LH concentrations decreased during dark periods. GnIH expression also increased under short-day periods when the duration of nocturnal melatonin secretion typically increases (Chowdhury et al., 2010). These results clearly indicate a role for melatonin in stimulating the release of GnIH in birds. Stimulation of GnIH, in turn, inhibits gonadal activity and sex steroid by decreasing gonadotropin synthesis and release. In Japanese quail, a prolonged photoperiod reduces the expression of GnIH and melatonin receptors (Mel_{1c}), while prolonged photoperiods increases the refractory effect and leads to desensitization of GnIH neurons (Chowdhury et al., 2010).

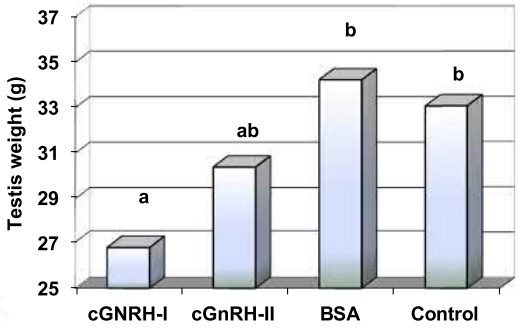

FIGURE 36.13 Testis weight of male broiler breeders immunized against cGnRH-I, cGnRH-II, BSA, and not immunized (control) birds. Different letters indicate significant differences ($P<0.05$). *Adapted from Vizcarra (2013).*

36.5.3 Effects of gonadotropins on testicular function

Gonadotropins exert their effects on the testis by binding to specific cell-surface receptors on two distinct types of testicular parenchymal cells: Leydig and Sertoli cells. These cells have been described in detail by Rothwell

(1973) and by (Cooksey and Rothwell, 1973), respectively. The principal role played by each type of cell has been determined by experiments in which one type of gonadotropin has been administered to hypophysectomized males, sexually immature males, or, in the case of Leydig cells, cells in culture (Brown et al., 1975; Ishii and Furuya, 1975; Ishii and Yamamoto, 1976). Such experiments have demonstrated that the principal effects of LH and FSH are exerted upon Leydig cells and Sertoli cells, respectively.

Leydig cells contain the steroidogenic enzymes necessary for the production of androgens [reviewed in Johnson (1986)] and respond rapidly to LH through rapid increases in the second messenger cAMP (Maung and Follett, 1977). The principal steroids secreted by Leydig cells include testosterone and androstenedione, a precursor of testosterone (Nakamura and Tanabe, 1972; Galli et al., 1973; Sharp et al., 1977). The concentration of testosterone in the general circulation is in the range of 5−15 nM, secreted as discrete pulses (Figure 36.14), which closely follow LH pulses (Driot et al., 1979; Bacon et al., 1991; Vizcarra et al., 2004), and are several times less than that in the testicular vein (Ottinger and Brinkley, 1979). The association between LH and testosterone pulses averaged 83% in unrestrained male broiler breeders fitted with jugular cannulas and free access to feed and water (Vizcarra et al., 2004). Testosterone in the adult male is essential for spermatogenesis, maintenance of the excurrent ducts and secondary sexual attributes, the expression of specific behaviors, and, as mentioned above, altering the pattern of GnRH secretion. These actions, as well as the inactivation of the hormone, depend upon transformation of testosterone by enzymes such as aromatase, 5α-reductase, and 5β-reductase (for reviews, see Ottinger (1983); Balthazart (1989)).

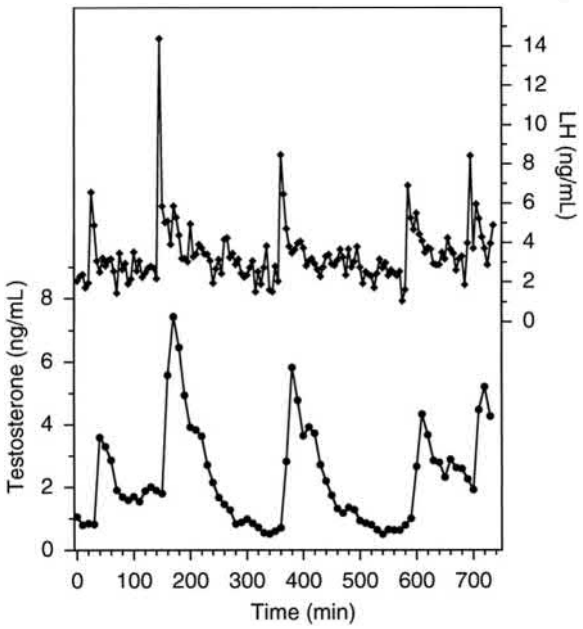

FIGURE 36.14 The pattern of pulsatile changes in circulating luteinizing hormone (LH; upper panel) and testosterone (lower panel) in an adult male domestic turkey (*Meleagris gallopavo*). The peaks of the discrete LH pulses occur prior to those of testosterone, demonstrating the close relationship between LH secretion and that of testosterone. *Figure and data kindly provided by Dr. Wayne Bacon, Ohio State University.*

Although FSH is known to affect Sertoli cells, the means by which FSH works is only poorly understood in birds. As reviewed by Walker and Cheng (2005), studies in other vertebrates have shown that the FSH receptor is a seven transmembrane G-protein, and FSH binding is known to activate at least five different signaling pathways in Sertoli cells. These pathways include the cAMP-PKA, MAP kinase, phosphatidylinositol 3-kinase, calcium, and phospholipase A2 pathways. It has been proposed that oligomerization of FSH receptors may provide a mechanism for bringing together the components of these multiple signaling pathways in order to refine and control intracellular signaling. It is well established that testosterone is absolutely essential for maintaining spermatogenesis and, unlike LH, the effect of FSH is potentiated by testosterone (Tsutsui and Ishii, 1978). As evidenced by the inability of exogenous testosterone to maintain spermatogenesis in hypophysectomized quail (Brown and Follett, 1977). LH and FSH appear to be essential for spermatogenesis in galliform birds. However, in male broiler breeders, more than 90% of the variation on testis weight was explained by changes in FSH while only 35% of the variation in testis weight was explained by changes in LH concentrations (Vizcarra et al., 2010). These results indicate that FSH is the most important regulator of Sertoli cell proliferation and differentiation. Although sperm production depends on the number of Sertoli cells (de Reviers and Williams, 1984; Sharpe, 1994), the process is ultimately controlled by the hypothalamus-pituitary-gonadal axis.

36.6 Spermatogenesis and extragonadal sperm maturation

36.6.1 Spermatogenesis

To date, spermatogenesis in galliform birds has been most fully characterized in the Japanese quail (*Coturnix coturnix japonica*). Four types of spermatogonial cells have been described in *Coturnix* (Lin and Jones, 1990, 1992). These have been designated as spermatogonia A_d, A_{p1}, A_{p2}, and B. The letter subscripts indicate intensity of staining and denote "dark" and "pale," respectively. The numerical subscripts denote ultrastructural differences (Lin and Jones, 1992). Spermatogonia A_d are stem cells. Based upon the model of stem cell renewal and spermatogonial proliferation proposed by (Lin and Jones, 1992), each division of an A_d spermatogonium yields A_d and A_{p1} daughter cells. Thus, spermatogenesis in *Coturnix* commences with the mitosis of an A_d spermatogonium. Cell types derived from each A_{p1}

spermatogonium include A_{p2} spermatogonia (n = 2), B spermatogonia (n = 4), primary spermatocytes (n = 8), secondary spermatocytes (n = 16), and spermatids (n = 32). Secondary spermatocytes and spermatids are formed by the first and second meiotic divisions, respectively.

Spermiogenesis is the transformation of spermatids into sperm cells without further cell division. Spermiogenesis in *Coturnix* entails 12 distinct morphological *steps* (Lin and Jones, 1990; Lin and Jones, 1993). In comparison, 8 to 10 steps have been reported for *Gallus* (de Reviers, 1971a; Gunawardana, 1977; Tiba et al., 1993), 10 steps for the guinea fowl (Aire, 1980), 12 steps for the turkey (Aire, 2003), 11 steps in the guinea cock (Abdul-Rahman et al., 2016) and six steps for the house sparrow (Goes and Dolder, 2002). Spermiogenesis entails formation of an acrosome and an axoneme, loss of cytoplasm, and replacement of nucleohistones with nucleoprotamine, which accompanies nuclear condensation (Nagano, 1962; Tingari, 1973; Okamura and Nishiyama, 1976; Gunawardana, 1977; Gunawardana and Scott, 1977; Oliva and Mezquita, 1986; Sprando and Russell, 1988). The reductions in cytoplasmic and nuclear volumes are striking; mature rooster sperm embody only 3% of the initial spermatid cell volume (Sprando and Russell, 1988). In summary, the seminiferous tubules contain Sertoli cells and a broad array of differentiating germinal cells including the various types of spermatogonia, spermatocytes, and spermatids.

However, germinal cells are not found in a physical continuum of differentiation within the seminiferous epithelium. Rather, they are found in distinct cellular associations. The cellular associations in *Coturnix* occupy an average of 17,902 μm^2 and contain an average of 13.5 Sertoli cells per association (Lin and Jones, 1990). There are 10 cellular associations in *Coturnix*, and each is referred to as a *stage* of the seminiferous epithelium (Figure 36.15). The seminiferous epithelium passes through each successive stage as a function of time at any fixed point. Once a complete series has been finished, a new series is initiated. Consequently, the series of stages is referred to as the cycle of the seminiferous epithelium. The duration of the cycle in *Coturnix* is 2.69 days (Lin et al., 1990). In comparison, the duration of the cycle of the seminiferous epithelium in *Gallus* has been estimated to be 3–4 days (de Reviers, 1968; Tiba et al., 1993). The time between the division of an Ad spermatogonium and spermiation, known as the duration of spermatogenesis is 12.8 days in *Coturnix* (Lin and Jones, 1990). Thus, 4.75 cycles of the seminiferous epithelium are required to produce 32 sperm cells from a single Ad spermatogonium at any fixed point within the seminiferous epithelium.

A complete series of stages in the context of a seminiferous tubule is referred to as a *spermatogenic wave*. As shown in Figure 36.16, these waves in *Coturnix* are

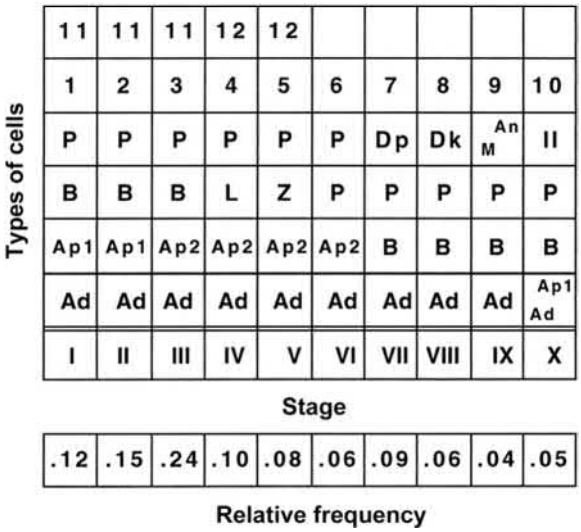

FIGURE 36.15 The cycle of the seminiferous epithelium of *Coturnix coturnix japonica*. The relative frequency of each cellular association, or stage, is shown below the stage's number. *Ad*, dark type A spermatogonia (stem cell); *Ap1 and 2*, pale type A spermatogonia; *B*, type B spermatogonia; *L*, leptotene primary spermatocytes; *Z*, zygotene primary spermatocytes; *P*, pachytene primary spermatocytes; *Dp*, diplotene primary spermatocytes; *DK*, diakinesis of primary spermatocytes; *M*, metaphase primary spermatocytes; An, anaphase primary spermatocytes; II, secondary spermatocytes; 1–12, step 1 through step 12 spermatids. *Adapted from Lin et al. (1990).*

arranged helically along the length of seminiferous tubules (Lin and Jones, 1990). It must be noted that while sequential stages may be contiguous in space (Figure 36.16), they are not observed at a common frequency (Figure 36.15) because duration of each of the stages ranges from 2.5 to 15.5 h (Lin et al., 1990). Consequently, the prevalence of any given stage is directly proportional to the stage's duration (Lin et al., 1990).

Daily sperm production may be defined as the number of sperm produced per gram of testis per day. Daily sperm production in *Coturnix* has been estimated to be 92.5×10^6 sperm per gram of testis per day (Clulow and Jones, 1982). This estimate is equivalent to the DSP of $80–120 \times 10^6$ sperm per gram of testis reported for *Gallus* (de Reviers and Williams, 1984), though the estimate was much higher for barred Plymouth Rock and Nigerian domestic fowl (*Gallus domesticus*) ($2.41 \pm 1.17 \times 10^9$ and $0.076 \pm 0.71 \times 10^9$, respectively) (Orlu and Egbunike, 2009). These values denote the number of fully formed sperm released per day from the seminiferous epithelium into the lumen of the seminiferous tubules. This phenomenon is defined as spermiation, which in *Coturnix* would be limited to the seminiferous epithelium in stage V (Figure 36.15). At the time of spermiation, superfluous cytoplasm found alongside the sperm cell's head is jettisoned as a residual body (Sprando and Russell, 1988; Lin and Jones, 1993). Sperm cells released from the seminiferous epithelium are

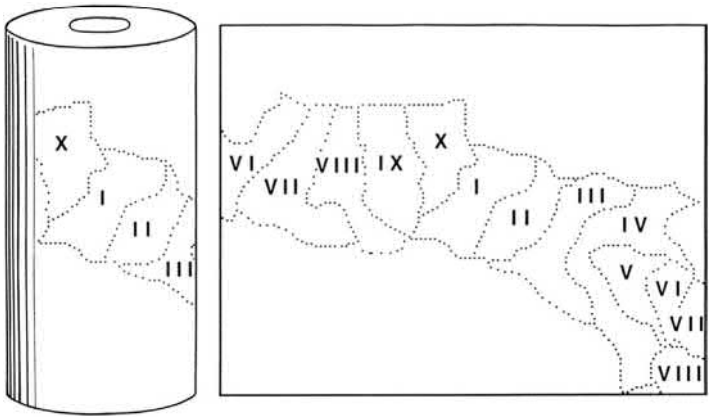

FIGURE 36.16 Spatial arrangement of the wave of spermatogenesis within a seminiferous tubule of *Coturnix coturnic japonica*. The cylinder to the right represents a section of a seminiferous tubule. The rectangle to its left denotes the two-dimensional representation of two contiguous cycles of the seminiferous epithelium. The cycle is arranged helically along the length of the tubule, Roman numerals denote stages. *Adapted from Lin and Jones (1990).*

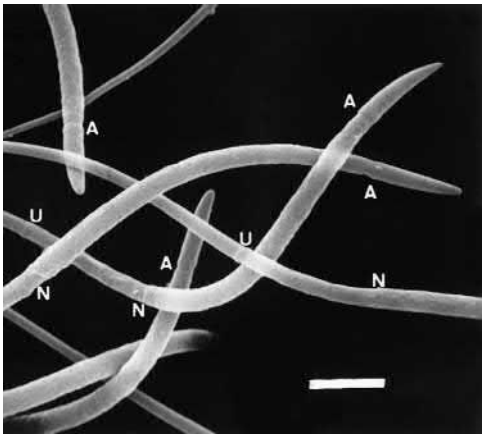

FIGURE 36.17 Scanning electron micrograph of chicken sperm cells. The constriction at the anterior end of the sperm cell (A) marks posterior boundary of the acrosome. The nucleus extends posteriorly from (A) to the neck region (N), which marks the anterior end of the midpiece. The midpiece, site of the anterior portion of the axoneme and the highly modified mitochondria, extends back to the raised annulus (U). The tail of the sperm extends from the annulus to the cell's termination. At the nucleus, chicken sperm are about 0.5 μm in diameter, with the overall length of the cell approximately 90μm. Bar = 2 μm. Adapted from Bahr and Bakst, 1987. *Reproduction in Farm Animals, fifth ed. Philadelphia, PA: © Lea & Febiger.*

immotile (Ashizawa and Sano, 1990). Galliform sperm are vermiform cells (Figure 36.17) with a maximum width of 0.5−0.7 μm and a length of 75−90 μm (Thurston and Hess, 1987). They contain a conical acrosome, a slightly bent cylindrical nucleus, and a helix of 25−30 mitochondria surrounding the proximal portion of a long flagellum, which accounts for approximately 84% of the cell's length (for review, see Thurston and Hess (1987)). The sperm of passerine birds tends to have a pointed, helical acrosome and ranges in length from 46.8−287.6 μm with the flagellum accounting for 79−95% of the total length (Helfenstein et al., 2009; Lüpold et al., 2009). One exception to this general trend is the Eurasian bullfinch, in which the sperm acrosome is rounded, not helical, and the midpiece size is extremely short (Birkhead et al., 2006). In these birds, extra-pair copulation frequency is rare in comparison to other passerines. It may be that a lack of sperm competition in this species could explain the marked difference in sperm morphology (Birkhead et al., 2006).

36.6.2 Extragonadal sperm transport and maturation

Following spermiation, sperm cells are suspended within fluid secreted by Sertoli cells. Sperm passage through the labyrinth of seminiferous tubules most likely depends upon the hydrostatic pressure of seminiferous tubule fluid and the contractility of the myoepithelial cells overlying the outer surface of the seminiferous tubule (Rothwell and Tingari, 1973). Sperm passage through the distal excurrent ducts, in particular, the deferent duct, presumably depends upon peristalsis (de Reviers, 1975). Like spermatogenesis, sperm transport through the excurrent ducts has been characterized most fully in the Japanese quail. Thus, an analysis of the phenomena and time-course of sperm transport through the excurrent ducts of *Gallus* has been estimated to take several days (Munro, 1938; de Reviers, 1975). Perhaps the most evident phenomenon that occurs during sperm transport through the excurrent ducts; as evidenced by a change in sperm concentration, is the absorption of seminiferous tubule fluid (Table 36.3). The concentration of sperm in the seminiferous tubule fluid of *Coturnix* is 3.8×10^4 sperm per μL whereas the concentration of sperm within the distal deferent duct is 2.3×10^6 per μL (Clulow and Jones, 1988). This 60-fold increase in sperm concentration is largely due to seminiferous tubule fluid absorption at the

TABLE 36.3 Estimates of Plasma Flux (Reabsorption) across the Epithelium Lining the Excurrent Ducts of Japanese Quail[a]

	Testicular Plasma	
Region	**Output (%)**	**μl/cm^2/h**
Rete testis to proximal efferent ducts	6.3	8.0
Proximal to distal efferent ducts	85.8	100.4
Distal efferent ducts to connecting ducts	6.5	21.6
Connecting ducts to epididymal duct	0.4	2.1
Epididymal duct to proximal deferent duct	0.2	0.1
Proximal to distal deferent duct	0.2	0.2

[a]*Adapted from Cluow and Jones (1988).*

level of efferent ducts. Nakai et al. (1989) demonstrated that the nonciliated epithelial cells in the proximal efferent ducts of *Gallus* incorporate fluid by pinocytosis.

The efferent ducts, which represent the principal excurrent duct within the epididymis (Figure 36.3), may be a critical site for sperm maturation. Due to extensive mucosal folding, apocrine secretion, the presence of ciliated cells, and epithelial cells with abundant microvilli, the efferent ducts appear to be a site where sperm are mixed with secretions as they are concentrated. Additional evidence of the importance of the efferent duct comes from studies of reproductive anomalies in turkeys and chickens. For instance, turkeys may ejaculate yellow rather than white semen (Thurston et al., 1982a). Epithelial cells within the efferent ducts of such turkeys have been shown to be hypertrophied, engorged with lipid droplets, and characterized by heightened phagocytosis of sperm (Hess et al., 1982). The latter phenomenon appears to be mediated by macrophages within the rete testis under normal conditions (Aire and Malmqvist, 1979b; Nakai et al., 1989), but can be mediated by epithelial cells in the excurrent ducts when the deferent duct is not patent (Tingari and Lake, 1972). Subfertile roosters with malformed proximal efferent ducts (Figure 36.18) provide a second example of the relationship between efferent duct function and reproductive performance (Kirby et al., 1990). The biochemical imbalances observed in semen from such roosters have been attributed to excurrent duct dysfunction (al-Aghbari et al., 1992).

In review, sperm are suspended in seminiferous tubule fluid prior to their passage through the excurrent ducts. The volume of this suspensory fluid and its composition (Esponda and Bedford, 1985) is altered prior to sperm entry into the epididymal duct. The resultant medium is seminal plasma. The chemical composition of seminal plasma is distinct from blood plasma as evidenced by differences in electrolyte, free amino acid, and protein composition (Lake, 1966; Lake and Hatton, 1968; Stratil, 1970; Thurston et al., 1982b; Freeman, 1984). The maintenance of these differences along the length of the excurrent ducts has been attributed to tight junctions between adjacent epithelial cells lining the ducts (Nakai and Nasu, 1991).

Apart from proteins specific to the reproductive tract (Stratil, 1970; Esponda and Bedford, 1985), the principal differences between seminal and blood plasma involve glucose, glutamate, K^+, Cl^-, and Ca^{2+} (Table 36.4). At present, it is not understood how the composition of excurrent duct fluid affects sperm motility. While Esponda and Bedford (1985) have demonstrated that sperm maturation proteins do exist in *Gallus* and while Ashizawa et al. (1988) have reported that the Na^+-to-K^+ ratio associated with the midpiece of rooster sperm increases as a function of sperm passage through the deferent duct, such changes do not induce motility; for sperm within the deferent duct are immotile (Ashizawa and Sano, 1990). Nonetheless, sperm acquire the potential for motility as they pass through the excurrent ducts (Munro, 1938; Clulow and Jones, 1982; Howarth, 1983; Ashizawa and Sano, 1990). This potential is distinct from fertilizing ability in that testicular sperm have the capacity to fertilize oocytes, providing they are placed in the oviduct above the vaginal sphincter (Howarth, 1983). As shown by Allen and Grigg (1957), sperm need not be motile to ascend the oviduct above the vaginal sphincter. Thus, the fertilizing ability of testicular sperm may not depend upon motility as much as the ability of sperm cells to undergo an acrosome reaction in response to contact with the oocyte's inner perivitelline layer (Okamura and Nishiyama, 1978).

The deferent duct, particularly the distal portion, contains the bulk of the extragonadal sperm reserve (ESR). In *Coturnix*, the number of sperm in the ESR is equivalent to the number produced daily by the testes, and 92% of these are found within the different duct (Clulow and Jones, 1982). In contrast, the ESR in *Gallus* is equivalent to $\leq$3.5 times the daily sperm production, but 95% of the ESR is found in the deferent duct (de Reviers, 1975). In either case, the duration of sperm storage within the deferent duct is relatively brief. As stated above, these sperm are immotile prior to ejaculation. While Ashizawa and Sano (1990) have proposed that a temperature change accompanying ejaculation may initiate sperm motility in *Gallus*, it is also likely that accessory reproductive fluids play a role in the initiation of sperm motility (for review, see Ashizawa et al. (2000); Fujihara (1992)). In this regard, Ca^+ and HCO^{-3} have been shown to be motility agonists in vitro (Ashizawa and Wishart, 1987; Ashizawa and Sano, 1990).

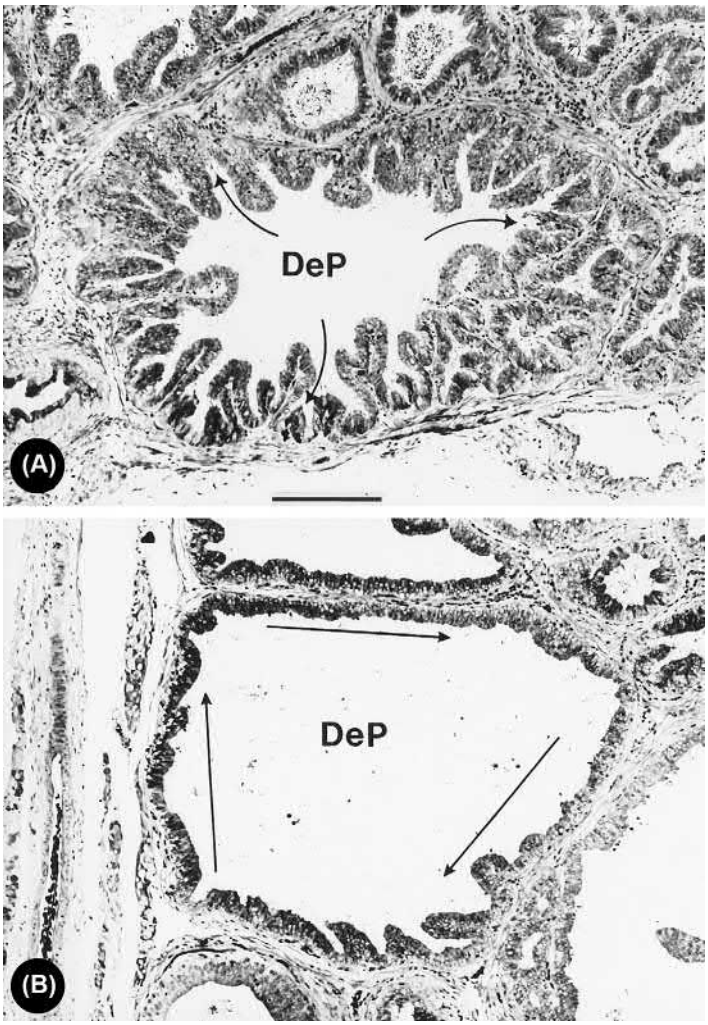

FIGURE 36.18 Cross sections through the proximal deferent ducts (DeP) of fertile (A) and subfertile (B) roosters. The presence of the sd allele in crossbred roosters (B) resulted in a twofold increase in DeP cross-sectional area and a 75% decrease in luminal surface area as compared to the wild-type (A) male. Males exhibiting this genetic defect of the DeP are characterized by poor semen quality, frequently exhibiting 30–90% dead and degenerate sperm in an ejaculate. Reproduced with permission from the Society for the Study of Reproduction. *From Kirby et al. (1990).*

TABLE 36.4 Comparison of Selected Substances in Rooster Blood Plasma and Deferent Duct Fluid[a]

Substance	Blood Plasma	Deferent Duct Fluid
Glucose (nM/L)	15	—
Glutamate (mM/L)	<1	100
Sodium (mEq/L)	160	142
Potassium (mEq/L)	5	34
Chloride (mEq/L)	115	40
Calcium (mEq/L)	5	1

[a]Adapted from appendices in "Physiology and Biochemistry of the Domestic Fowl" Vol. 5, by B. M. Freeman.

36.7 Seasonal gonadal recrudescence and regression

36.7.1 Photoperiodic control of gonadal regression and recrudescence

Environmental photoperiodism is responsible for the generation of seasonal rhythms through the induction and termination of physiological processes (Dixit and Singh, 2011). The secretion of GnRH is controlled by photo induction and is directly related to the photoperiod (Dawson, 2015). Many bird species, especially long-distance migrants, face the challenge of a narrow reproductive window because of an intense selective pressure to restrict breeding to the time of year when food is most abundant [reviewed in (Dawson, 2008, 2013)]. Typically, male birds have regressed gonads for most of the year with gonadal

recrudescence occurring only immediately prior to reproduction. Birds are generally viewed as being long-day breeders (with some exceptions) such that the HPG axis responds to increasing day lengths with a marked increase in gonadotropin secretion and gonadal growth [reviewed in Ball and Ketterson (2008)]. The exact time and rate of gonadal maturation varies between bird species; however, it has been suggested that, as photoperiod increases during the spring, a critical threshold point is reached at which gonadal recrudescence is triggered. This threshold has been termed the critical photoperiod. A study in Japanese quail provides support for this hypothesis and found that the rate of gonadal maturation was low when the photoperiod was less than 11.5 h of light per day and maturation became rapid when light exposure was increased to 12 h per day (Follett and Maung, 1978).

While gonadal maturation in the spring is in response to an increase in photoperiod, longer photoperiods at the end of the breeding season induce a condition termed photorefractoriness, which causes the gonads to regress [reviewed in Robinson and Follett (1982); Dawson (2008)]. Two forms of photorefractoriness, absolute and relative, have been identified in various bird species. In the absolute form, continued exposure to long photoperiods leads to spontaneous gonadal regression after which a further increase in photoperiod does not induce renewed gonadal maturation until the next breeding season. This state has been successfully demonstrated in species such as the European Starling, Tree Sparrow, and White-crowned Sparrow and is only dissipated when birds experience short days in autumn. Such exposure to short photoperiods is thought to induce reacquisition of photosensitivity [reviewed in Ball and Ketterson (2008)]. In contrast, relative photorefractoriness is evident when a decrease in photoperiod is necessary to induce gonadal regression, but this regression occurs under a photoperiod that is still longer than the one which induced maturation earlier in the year. In addition, exposure to long photoperiods can inhibit regression and even induce recrudescence [reviewed by Dawson (2008)]. In general, it is thought that birds with early, predictable breeding seasons tend to become absolutely photorefractory whereas those with later or less predictable breeding seasons are more likely to exhibit relative photorefractoriness.

36.7.2 Other factors affecting gonadal maturation and regression

Due to the vast variety between and within species, birds exhibit plasticity in both gonadal maturation and regression. Though photoperiod plays an important role in regulating these processes, nonphotoperiodic cues such as breeding location, temperature, rainfall, climate change, and food availability are also important in determining the rate and timing of recrudescence and regression. For example, Caro et al. (2006) observed two separate populations of Blue Tits and noticed that, not only did one population breed earlier than the other but also earlier breeding birds exhibited a faster rate of testicular development than did their later breeding counterparts. White-crowned sparrows breeding at low latitudes experienced inhibition of gonadal maturation and delayed onset of photorefractoriness at low temperatures, but the same were not true for birds of the same species breeding at mid-latitudes (Wingfield et al., 2003). Retarded rates of testicular recrudescence were also observed in Juncos subjected to low temperatures between 4 and 8°C (Engels and Jenner, 1956). In Willow Tits, high temperatures were shown to accelerate testicular maturation, but the same effect was not evident in Great Tits (Silverin and Viebke, 1994). These data may suggest that temperature is more likely to affect species with longer and more flexible breeding seasons. Climate change is another factor affecting gonadal regression. Climate change is associated with higher than normal temperature and may decrease the number of breeding attempts in multibrooded species. Therefore, birds may be constrained to a degree where they will advance breeding to compensate for food abundance (Dawson and Visser, 2010).

Interestingly, rainfall has been shown to affect gonadal maturation in several tropical bird species. For example, two populations of rufous-collared sparrows separated by only 25 km were observed to have highly asynchronous reproductive physiology based on local rainfall patterns (Moore et al., 2006). In the rufous-winged sparrow, though seasonality is known to be photoperiodically controlled, the exact time of breeding occurs in response to rainfall (Deviche et al., 2006). Darwin's finches undergo gonadal maturation at drastically different times in different years in direct response to rainfall, yet the gonads have been shown to fully regress between breeding seasons (Hau et al., 2004). Another factor which may influence seasonal recrudescence is the availability of food resources. Food availability at stopover has been directly linked to gonadal maturation during spring migration. For example, Garden Warblers experiencing limited food conditions at stopover had significantly slower testicular recrudescence and decreased testosterone in comparison to birds allowed to eat *ad libitum* (Bauchinger et al., 2009). It is clear that many factors, both intrinsic and extrinsic, have the potential to influence patterns of seasonal gonadal recrudescence and regression. The mechanisms driving such patterns are complex and likely overlap with one another. As research in this area progresses, it will be important to investigate how these mechanisms interact in order to better understand the various factors that drive reproductive success in the male bird.

References

Abdul-Rahman, I.I., Obese, F.Y., Robinson, J.E., 2016. Spermatogenesis and cellular associations in the seminiferous epithelium of Guinea cock (*Numida meleagris*). Can. J. Anim. Sci. 97 (2), 241–249.

Adkins, E.K., Alder, N.T., 1972. Hormonal control of behavior in the Japanese quail. J. Comp. Physiol. Psychol. 81 (1), 27.

Aire, T.A., 1979a. The epididymal region of the Japanese quail (*Coturnix coturnix* japonica). Acta Anat. 103 (3), 305–312.

Aire, T.A., 1979b. Micro-stereological study of the avian epididymal region. J. Anat. 129 (Pt 4), 703–706.

Aire, T.A., 1980. The ductuli efferentes of the epididymal region of birds. J. Anat. 130 (Pt 4), 707–723.

Aire, T.A., 1982. The rete testis of birds. J. Anat. 135 (Pt 1), 97–110.

Aire, T.A., 2003. Ultrastructural study of spermiogenesis in the Turkey, *Meleagris gallopavo*. Br. Poultry Sci. 44 (5), 674–682. https://doi.org/10.1080/00071660310001643651.

Aire, T.A., Josling, D., 2000. Ultrastructural study of the luminal surface of the ducts of the epididymis of gallinaceous birds. Onderstepoort J. Vet. Res. 67 (3), 191–199.

Aire, T.A., Malmqvist, M., 1979a. Intraepithelial lymphocytes in the excurrent ducts of the testis of the domestic fowl (*Gallus domesticus*). Acta Anat. 103 (2), 142–149.

Aire, T.A., Malmqvist, M., 1979b. Macrophages in the excurrent ducts of the testes of normal domestic fowl (*Gallus domesticus*). Anat. Histol. Embryol. 8 (2), 172–176.

Aire, T.A., Ozegbe, P.C., 2007. The testicular capsule and peritubular tissue of birds: morphometry, histology, ultrastructure and immunohistochemistry. J. Anat. 210 (6), 731–740. https://doi.org/10.1111/j.1469-7580.2007.00726.x.

Aire, T.A., Soley, J.T., 2000. The surface features of the epithelial lining of the ducts of the epididymis of the ostrich (*Struthio camelus*). Anat. Histol. Embryol. 29 (2), 119–126.

Aire, T.A., Soley, J.T., 2003. The morphological features of the rete testis of the ostrich (*Struthio camelus*). Anat. Embryol. 207 (4–5), 355–361. https://doi.org/10.1007/s00429-003-0347-0.

Al-Aghbari, A., Engel Jr., H.N., Froman, D.P., 1992. Analysis of seminal plasma from roosters carrying the Sd (sperm degeneration) allele. Biol. Reprod. 47 (6), 1059–1063.

Allen, T., Grigg, G., 1957. Sperm transport in the fowl. Aust. J. Agric. Res. 8 (6), 788–789. https://doi.org/10.1071/AR9570788.

Aparicio, I., Gil, M., Garcia-Herreros, M., Pena, F., Garcia-Marin, L., 2005. Inhibition of phosphatidylinositol 3-kinase modifies boar sperm motion parameters. Reproduction 129 (3), 283–289.

Ashizawa, K., Ozawa, Y., Okauchi, K., 1988. Changes of elemental concentrations around and on the surface of fowl sperm membrane during maturation in the male reproductive tract and after in vitro storage. Gamete Res. 21 (1), 23–28. https://doi.org/10.1002/mrd.1120210104.

Ashizawa, K., Sano, R., 1990. Effects of temperature on the immobilization and the initiation of motility of spermatozoa in the male reproductive tract of the domestic fowl, *Gallus domesticus*. Comp. Biochem. Physiol. A Comp. Physiol. 96 (2), 297–301.

Ashizawa, K., Wishart, G.J., 1987. Resolution of the sperm motility-stimulating principle of fowl seminal plasma into Ca^{2+} and an unidentified low molecular weight factor. J. Reprod. Fertil. 81 (2), 495–499.

Ashizawa, K., Wishart, G.J., Tsuzuki, Y., 2000. Avian sperm motility: environmental and intracellular regulation. Avian Poultry Biol. Rev. 11, 161–172.

Bachelard, E., Raucci, F., Montillet, G., Pain, B., 2015. Identification of side population cells in chicken embryonic gonads. Theriogenology 83 (3), 377–384.

Bacon, W.L., Proudman, J.A., Foster, D.N., Renner, P.A., 1991. Pattern of secretion of luteinizing hormone and testosterone in the sexually mature male Turkey. Gen. Comp. Endocrinol. 84 (3), 447–460.

Bagheri-Fam, S., Sinclair, A.H., Koopman, P., Harley, V.R., 2010. Conserved regulatory modules in the Sox9 testis-specific enhancer predict roles for SOX, TCF/LEF, Forkhead, DMRT, and GATA proteins in vertebrate sex determination. Int. J. Biochem. Cell Biol. 42 (3), 472–477.

Bakst, M.R., 1980. Luminal topography of the male chicken and Turkey excurrent duct system. Scanning Electron. Microsc. 3 (3), 419–425.

Ball, G.F., Balthazart, J., 2004. Hormonal regulation of brain circuits mediating male sexual behavior in birds. Physiol. Behav. 83 (2), 329–346.

Ball, G.F., Ketterson, E.D., 2008. Sex differences in the response to environmental cues regulating seasonal reproduction in birds. Philos. Trans. R. Soc. Lond. B Biol. Sci. 363 (1490), 231–246. https://doi.org/10.1098/rstb.2007.2137.

Balthazart, J., 1989. Steroid metabolism and the activation of social behavior. In: Advances in Comparative and Environmental Physiology, vol. 3, pp. 103–159.

Balthazart, J., Castagna, C., Ball, G.F., 1997. Aromatase inhibition blocks the activation and sexual differentiation of appetitive male sexual behavior in Japanese quail. Behav. Neurosci. 111 (2), 381.

Banerjee, S., Chaturvedi, C.M., 2017. Testicular atrophy and reproductive quiescence in photorefractory and scotosensitive quail: involvement of hypothalamic deep brain photoreceptors and GnRH-GnIH system. J. Photochem. Photobiol. B Biol. 175, 254–268.

Bauchinger, U., Van't Hof, T., Biebach, H., 2009. Food availability during migratory stopover affects testis growth and reproductive behaviour in a migratory passerine. Horm. Behav. 55 (3), 425–433. https://doi.org/10.1016/j.yhbeh.2008.12.003.

Bentley, G.E., Perfito, N., Ukena, K., Tsutsui, K., Wingfield, J.C., 2003. Gonadotropin-inhibitory peptide in song sparrows (*Melospiza melodia*) in different reproductive conditions, and in house sparrows (*Passer domesticus*) relative to chicken-gonadotropin-releasing hormone. J. Neuroendocrinol. 15 (8), 794–802.

Bentley, G.E., Ubuka, T., McGuire, N.L., Chowdhury, V.S., Morita, Y., Yano, T., Hasunuma, I., Binns, M., Wingfield, J.C., Tsutsui, K., 2008. Gonadotropin-inhibitory hormone and its receptor in the avian reproductive system. Gen. Comp. Endocrinol. 156 (1), 34–43. https://doi.org/10.1016/j.ygcen.2007.10.003.

Berg, C., Halldin, K., Fridolfsson, A.K., Brandt, I., Brunstrom, B., 1999. The avian egg as a test system for endocrine disrupters: effects of diethylstilbestrol and ethynylestradiol on sex organ development. Sci. Total Environ. 233 (1–3), 57–66.

Bergmann, M., Schindelmeiser, J., 1987. Development of the blood-testis barrier in the domestic fowl (*Gallus domesticus*). Int. J. Androl. 10 (2), 481–488.

Birkhead, T.R., Fletcher, F., Pellatt, E.J., 1998. Testes asymmetry, condition and sexual selection in birds: an experimental test. Proc. Biol. Sci. 265 (1402), 1185–1189. https://doi.org/10.1098/rspb.1998.0417.

Birkhead, T.R., Immler, S., Pellatt, E.J., Freckleton, R., 2006. Unusual sperm morphology in the Eurasian bullfinch (*Pyrrhula pyrrhula*). Auk 123 (2), 383. https://doi.org/10.1642/0004-8038(2006)123[383:usmite]2.0.co;2.

Blomqvist, A., Berg, C., Holm, L., Brandt, I., Ridderstrale, Y., Brunstrom, B., 2006. Defective reproductive organ morphology and function in domestic rooster embryonically exposed to o,p'-DDT or ethynylestradiol. Biol. Reprod. 74 (3), 481–486. https://doi.org/10.1095/biolreprod.105.045104.

Borosky, J.C., Da Rocha, M.A., Da Silva, C.A., Bridi, A.M., Monteiro, R.A., 2011. Fibra muscular, desempenho E a qualidade da carcaça de quatro grupos genéticos de suínos. Ciencia Anim. Bras. 12 (3), 427–434.

Bozkurt, H.H., Aktas, A., Ulkay, M.B., Firat, U.B., 2007. Sertoli cell proliferation during the post hatching period in domestic fowl. J. Vet. Sci. 8 (3), 219–222.

Brennan, P.L., Clark, C.J., Prum, R.O., 2010. Explosive eversion and functional morphology of the duck penis supports sexual conflict in waterfowl genitalia. Proc. Biol. Sci. 277, 1309–1314. https://doi.org/10.1098/rspb.2009.2139.

Brennan, P.L., Prum, R.O., 2012. The erection mechanism of the ratite penis. J. Zool. 286 (2), 140–144.

Briskie, J.V., Montgomerie, R., 2001. Efficient copulation and the evolutionary loss of the avian intromittent organ. J. Avian Biol. 32 (2), 184–187.

Brown, N.L., Baylé, J.D., Scanes, C.G., Follett, B.K., 1975. Chicken gonadotrophins: their effects on the testes of immature and hypophysectomized Japanese quail. Cell Tissue Res. 156 (4), 499–520. https://doi.org/10.1007/BF00225109.

Brown, N.L., Follett, B.K., 1977. Effects of androgens on the testes of intact and hypophysectomized Japanese quail. Gen. Comp. Endocrinol. 33 (2), 267–277. https://doi.org/10.1016/0016-6480(77)90251-9.

Bruggeman, V., Van As, P., Decuypere, E., 2002. Developmental endocrinology of the reproductive axis in the chicken embryo. Comp. Biochem. Physiol. Mol. Integr. Physiol. 131 (4), 839–846.

Budras, K.D., Sauer, T., 1975. Morphology of the epididymis of the cock (*Gallus domesticus*) and its effect upon the steroid sex hormone synthesis. Anat. Embryol. 148 (2), 175–196. https://doi.org/10.1007/bf00315268.

Caro, S.P., Lambrechts, M.M., Chastel, O., Sharp, P.J., Thomas, D.W., Balthazart, J., 2006. Simultaneous pituitary-gonadal recrudescence in two Corsican populations of male blue tits with asynchronous breeding dates. Horm. Behav. 50 (3), 347–360. https://doi.org/10.1016/j.yhbeh.2006.03.001.

Cho, R.N., Hahn, T.P., MacDougall-Shackleton, S., Ball, G.F., 1998. Seasonal variation in brain GnRH in free-living breeding and photorefractory house finches (*Carpodacus mexicanus*). Gen. Comp. Endocrinol. 109 (2), 244–250.

Chou, H.-F., Johnson, A.L., 1987. Luteinizing hormone secretion from anterior pituitary cells of the cockerel: evidence for an ultradian rhythm. Poultry Sci. 66 (4), 732–740.

Chou, H.-F., Johnson, A.L., Williams, J., 1985. Luteinizing hormone releasing activity of [Gln8]-LHRH and [His5, Trp7, Tyr8]-LHRH in the cockerel, in vivo and in vitro. Life Sci. 37 (26), 2459–2465.

Chowdhury, V.S., Yamamoto, K., Ubuka, T., Bentley, G.E., Hattori, A., Tsutsui, K., 2010. Melatonin stimulates the release of gonadotropin-inhibitory hormone by the avian hypothalamus. Endocrinology 151 (1), 271–280.

Chue, J., Smith, C.A., 2011. Sex determination and sexual differentiation in the avian model. FEBS J. 278 (7), 1027–1034.

Clinton, M., 1998. Sex determination and gonadal development: a bird's eye view. J. Exp. Zool. 281 (5), 457–465.

Clinton, M., Haines, L.C., 1999. An overview of factors influencing sex determination and gonadal development in birds. Cell. Mol. Life Sci. 55 (7), 876. https://doi.org/10.1007/s000180050341.

Clulow, J., Jones, R.C., 1982. Production, transport, maturation, storage and survival of spermatozoa in the male Japanese quail, *Coturnix coturnix*. J. Reprod. Fertil. 64 (2), 259–266.

Clulow, J., Jones, R.C., 1988. Studies of fluid and spermatozoal transport in the extratesticular genital ducts of the Japanese quail. J. Anat. 157, 1–11.

Connell, C., 1972. The effect of luteinizing hormone on the ultrastructure of the leydig cell of the chick. Z. für Zellforsch. Mikrosk. Anat. 128 (2), 139–151. https://doi.org/10.1007/BF00306894.

Cooksey, E.J., Rothwell, B., 1973. The ultrastructure of the Sertoli cell and its differentiation in the domestic fowl (*Gallus domesticus*). J. Anat. 114 (Pt 3), 329–345.

Cornil, C.A., Ball, G.F., Balthazart, J., Charlier, T.D., 2011. Organizing effects of sex steroids on brain aromatase activity in quail. PLoS One 6 (4), e19196.

Da Silva, S.M., Hacker, A., Harley, V., Goodfellow, P., Swain, A., Lovell-Badge, R., 1996. Sox9 expression during gonadal development implies a conserved role for the gene in testis differentiation in mammals and birds. Nat. Genet. 14 (1), 62.

Davies, D.T., Follett, B.K., 1980. Neuroendocrine regulation of gonadotrophin-releasing hormone secretion in the Japanese quail. Gen. Comp. Endocrinol. 40 (2), 220–225.

Dawson, A., 2008. Control of the annual cycle in birds: endocrine constraints and plasticity in response to ecological variability. Philos. Trans. R. Soc. Lond. B Biol. Sci. 363 (1497), 1621–1633. https://doi.org/10.1098/rstb.2007.0004.

Dawson, A., 2013. The effect of latitude on photoperiodic control of gonadal maturation, regression and molt in birds. Gen. Comp. Endocrinol. 190, 129–133.

Dawson, A., 2015. Annual gonadal cycles in birds: modeling the effects of photoperiod on seasonal changes in GnRH-1 secretion. Front. Neuroendocrinol. 37, 52–64.

Dawson, A., Sharp, P.J., 2007. Photorefractoriness in birds—photoperiodic and non-photoperiodic control. Gen. Comp. Endocrinol. 153 (1–3), 378–384.

Dawson, A., Visser, M.E., 2010. The effects of temperature on photoperiodic responses: implications for climate change. In: BOU Proceedings–Climate Change and Birds.

de Reviers, M., 1968. Determination de la duree des processus spermatogenetiques chez le coq a l'aide de thymidine tritice. 6th Int. Congr. Anim. Reprod. Paris 1, 183–185.

de Reviers, M., 1971a. Le developpement testiculaire chez le coq. I. Criissance Ponderale des testicules et devloppement des tubes seminiferes. Ann. Biol. Anim. Biochim. Biophys. 11, 519–530.

de Reviers, M., 1971b. Le developpement testiculaire chez le coq. II. Morphologie de l'epithelium seminifere et etablissement de la spermatogenese. Ann. Biol. Anim. Biochim. Biophys. 11, 531–546.

de Reviers, M., 1975. Sperm transport and survival in male birds. In: Hafez, E.S.E., Thibault, C.G. (Eds.), The Biology of Spermatozoa, pp. 10–16.

de Reviers, M., Williams, J.B., 1984. Testis development and production of spermatozoa in the cockerel (*Gallus domesticus*). In: Cunningham, F.J., Lake, P.E., Hewitt, D. (Eds.), Reproductive Biology of Poultry, pp. 183–202.

Denk, A.G., Kempenaers, B., 2005. Testosterone and testes size in mallards (*Anas platyrhynchos*). J. Ornithol. 147 (3), 436–440. https://doi.org/10.1007/s10336-005-0031-7.

Deviche, P., Saldanha, C.J., Silver, R., 2000. Changes in brain gonadotropin-releasing hormone-and vasoactive intestinal polypeptide-like immunoreactivity accompanying reestablishment of photosensitivity in male dark-eyed juncos (*Junco hyemalis*). Gen. Comp. Endocrinol. 117 (1), 8–19.

Deviche, P., Small, T., Sharp, P., Tsutsui, K., 2006. Control of luteinizing hormone and testosterone secretion in a flexibly breeding male passerine, the Rufous-winged Sparrow, *Aimophila carpalis*. Gen. Comp. Endocrinol. 149 (3), 226–235. https://doi.org/10.1016/j.ygcen.2006.06.004.

Dixit, A.S., Singh, N.S., 2011. Photoperiod as a proximate factor in control of seasonality in the subtropical male Tree Sparrow, *Passer montanus*. Front. Zool. 8 (1), 1.

Driot, F., De Reviers, M., Williams, J., 1979. Plasma testosterone levels in intact and hemicastrated growing cockerels. J. Endocrinol. 81 (2), 169–174.

Engels, W.L., Jenner, C.E., 1956. The effect of temperature on testicular recrudescense in juncos at different photoperiods. Biol. Bull. 110 (2), 129–137.

Esponda, P., Bedford, J.M., 1985. Surface of the rooster spermatozoon changes in passing through the Wolffian duct. J. Exp. Zool. 234 (3), 441–449. https://doi.org/10.1002/jez.1402340311.

Follett, B.K., Maung, S.L., 1978. Rate of testicular maturation, in relation to gonadotrophin and testosterone levels, in quail exposed to various artificial photoperiods and to natural daylengths. J. Endocrinol. 78 (2), 267–280.

Foster, R., Plowman, G., Goldsmith, A., Follett, B., 1987. Immunohistochemical demonstration of marked changes in the LHRH system of photosensitive and photorefractory European starlings (*Sturnus vulgaris*). J. Endocrinol. 115 (2), 211–NP.

Freeman, B.M., 1984. Appendix X. Reproduction: semen. In: Freeman, B.M. (Ed.), Physiology and Biochemistry of the Domestic Fowl, vol. 5, 443-424.

Fujihara, N., 1992. Accessory reproductive fludis and organs in male domestic birds. World Poultry Sci. J. 48 (1), 39–56. https://doi.org/10.1079/wps19920005.

Fujimoto, T., Ukeshima, A., Kiyofuji, R., 1976. The origin, migration and morphology of the primordial germ cells in the chick embryo. Anat. Rec. 185 (2), 139–145. https://doi.org/10.1002/ar.1091850203.

Galli, F.E., Irusta, O., Wassermann, G.F., 1973. Androgen production by testes of *Gallus domesticus* during postembryonic development. Gen. Comp. Endocrinol. 21 (2), 262–266.

Gilbert, A.B., 1979. Glandulae endocrinae. In: Baumel, J.J. (Ed.), Nomina Anatomica Avium, pp. 337–342.

Goes, R.M., Dolder, H., 2002. Cytological steps during spermiogenesis in the house sparrow (*Passer domesticus*, Linnaeus). Tissue Cell 34 (4), 273–282.

Gonzalez-Moran, M.G., Soria-Castro, E., 2010. Changes in the tubular compartment of the testis of *Gallus domesticus* during development. Br. Poultry Sci. 51 (2), 296–307. https://doi.org/10.1080/00071661003745836.

Guemene, D., Williams, J., 1992. In-vitro and in-vivo responses to chicken LHRH-I and chicken LHRH-II in male turkeys (*Meleagris gallopavo*). J. Endocrinol. 132 (3), 387–393.

Guichard, A., Cedard, L., Mignot, T.M., Scheib, D., Haffen, K., 1977. Radioimmunoassay of steroids produced by cultured chick embryonic gonads: differences according to age, sex, and side. Gen. Comp. Endocrinol. 32 (3), 255–265.

Gunawardana, V.E., 1977. Stages of spermatids in the domestic fowl: a light microscope study using Araldite sections. J. Anat. 123 (Pt 2), 351–360.

Gunawardana, V.K., Scott, M.G., 1977. Ultrastructural studies on the differentiation of spermatids in the domestic fowl. J. Anat. 124 (Pt 3), 741–755.

Hattori, A., Ishii, S., Wada, M., 1986. Effects of two kinds of chicken luteinizing hormone-releasing hormone (LH-RH), mammalian LH-RH and its analogs on the release of LH and FSH in Japanese quail and chicken. Gen. Comp. Endocrinol. 64 (3), 446–455.

Hau, M., Wikelski, M., Gwinner, H., Gwinner, E., 2004. Timing of reproduction in a Darwin's finch: temporal opportunism under spatial constraints. Oikos 106, 489–500.

Helfenstein, F., Podevin, M., Richner, H., 2009. Sperm morphology, swimming velocity, and longevity in the house sparrow *Passer domesticus*. Behav. Ecol. Sociobiol. 64 (4), 557–565. https://doi.org/10.1007/s00265-009-0871-x.

Herrera, A.M., Shuster, S.G., Perriton, C.L., Cohn, M.J., 2013. Developmental basis of phallus reduction during bird evolution. Curr. Biol. 23 (12), 1065–1074.

Hess, R.A., Thurston, R.J., 1977. Ultrastructure of epithelial cells in the epididymal region of the Turkey (*Meleagris gallopavo*). J. Anat. 124 (Pt 3), 765–778.

Hess, R.A., Thurston, R.J., Biellier, H.V., 1982. Morphology of the epididymal region of turkeys producing abnormal yellow semen. Poultry Sci. 61 (3), 531–539.

Hori, T., Asakawa, S., Itoh, Y., Shimizu, N., Mizuno, S., 2000. Wpkci, encoding an altered form of PKCI, is conserved widely on the avian W chromosome and expressed in early female embryos: implication of its role in female sex determination. Mol. Biol. Cell 11 (10), 3645–3660.

Howarth Jr., B., 1983. Fertilizing ability of cock spermatozoa from the testis epididymis and vas deferens following intramagnal insemination. Biol. Reprod. 28 (3), 586–590.

Hutchison, R., 1978. Hormonal differentiation of sexual behavior in Japanese quail. Horm. Behav. 11 (3), 363–387.

Hutson, J.M., Donahoe, P.K., MacLaughlin, D.T., 1985. Steroid modulation of Mullerian duct regression in the chick embryo. Gen. Comp. Endocrinol. 57 (1), 88–102.

Imataka, H., Suzuki, K., Inano, H., Kohmoto, K., Tamaoki, B., 1988. Sexual differences of steroidogenic enzymes in embryonic gonads of the chicken (*Gallus domesticus*). Gen. Comp. Endocrinol. 69 (2), 153–162.

Ingkasuwan, P., Ogasawara, F.X., 1966. The effect of light and temperature and their interaction on the semen production of white Leghorn males. Poultry Sci. 45 (6), 1199–1206. https://doi.org/10.3382/ps.0451199.

Ishii, S., Furuya, T., 1975. Effects of purified chicken gonadotropins on the chick testis. Gen. Comp. Endocrinol. 25 (1), 1–8.

Ishii, S., Yamamoto, K., 1976. Demonstration of follicle stimulating hormone (FSH) activity in hypophyseal extracts of various vertebrates by the response of the Sertoli cells of the chick. Gen. Comp. Endocrinol. 29 (4), 506–510.

Johnson, A.L., 1986. Reproduction in the male. In: Sturkie, P.D. (Ed.), Avian Physiology, pp. 432–451.

Joseph, N.T., Morgan, K., Sellar, R., McBride, D., Millar, R.P., Dunn, I.C., 2009. The chicken type III GnRH receptor homologue is predominantly expressed in the pituitary, and exhibits similar ligand selectivity to the type I receptor. J. Endocrinol. 202 (1), 179.

Katz, I.A., Millar, R.P., King, J.A., 1990. Differential regional distribution and release of two forms of gonadotropin-releasing hormone in the chicken brain. Peptides 11 (3), 443–450.

Kim, D.-K., Cho, E.B., Moon, M.J., Park, S., Hwang, J.-I., Kah, O., Sower, S.A., Vaudry, H., Seong, J.Y., 2011. Revisiting the evolution of gonadotropin-releasing hormones and their receptors in vertebrates: secrets hidden in genomes. Gen. Comp. Endocrinol. 170 (1), 68–78.

King, A.S., 1979. Systema urogenitale. In: Baumel, J.J. (Ed.), Nomina Anatomica Avium, pp. 289–335.

King, J.A., Millar, R.P., 1982. Structure of chicken hypothalamic luteinizing hormone-releasing hormone. I. Structural determination on partially purified material. J. Biol. Chem. 257 (18), 10722–10728.

Kirby, J.D., Froman, D.P., Engel Jr., H.N., Bernier, P.E., Hess, R.A., 1990. Decreased spermatozoal survivability associated with aberrant morphology of the ductuli efferentes proximales of the chicken (*Gallus domesticus*). Biol. Reprod. 42 (2), 383–389.

Knower, K.C., Kelly, S., Harley, V.R., 2003. Turning on the male–SRY, SOX9 and sex determination in mammals. Cytogenet. Genome Res. 101 (3–4), 185–198.

Konkle, A.T., Balthazart, J., 2011. Sex differences in the rapid control of aromatase activity in the quail preoptic area. J. Neuroendocrinol. 23 (5), 424–434.

Krieger, D.T., Liotta, A.S., 1979. Pituitary hormones in brain: where, how, and why? Science 205 (4404), 366–372.

Krishnan, K., Proudman, J., Bolt, D., Bahr, J., 1993. Development of an homologous radioimmunoassay for chicken follicle-stimulating hormone and measurement of plasma FSH during the ovulatory cycle. Comparative biochemistry and physiology. Comp. Physiol. 105 (4), 729–734.

Kuenzel, W.J., 1993. The search for deep encephalic photoreceptors within the avian brain, using gonadal development as a primary indicator. Poultry Sci. 72 (5), 959–967.

Kuenzel, W.J., Blahser, S., 1991. The distribution of gonadotropin-releasing hormone (GnRH) neurons and fibers throughout the chick brain (*Gallus domesticus*). Cell Tissue Res. 264 (3), 481–495.

Lake, P.E., 1966. Physiology and biochemistry of poultry semen. In: McLaren, A. (Ed.), Advances in Reproductive Physiology, vol. 1, pp. 93–123.

Lake, P.E., 1981. Male genital organs. In: King, A.S., McLelland, J. (Eds.), Form and Function in Birds, vol. 2, pp. 2–61.

Lake, P.E., Hatton, M., 1968. Free amino acids in the vas deferens, semen, transparent fluid and blood plasma of the domestic rooster, *Gallus domesticus*. J. Reprod. Fertil. 15 (1), 139–143.

Lin, M., Jones, R., 1992. Renewal and proliferation of spermatogonia during spermatogenesis in the Japanese quail, *Coturnix coturnix* japonica. Cell Tissue Res. 267 (3), 591–601.

Lin, M., Jones, R., Blackshaw, A., 1990. The cycle of the seminiferous epithelium in the Japanese quail (*Coturnix coturnix* japonica) and estimation of its duration. Reproduction 88 (2), 481–490.

Lin, M., Jones, R.C., 1990. Spatial arrangement of the stages of the cycle of the seminiferous epithelium in the Japanese quail, *Coturnix coturnix* japonica. J. Reprod. Fertil. 90 (2), 361–367.

Lin, M., Jones, R.C., 1993. Spermiogenesis and spermiation in the Japanese quail (*Coturnix coturnix japonica*). J. Anat. 183 (Pt 3), 525–535.

Lüpold, S., Linz, G.M., Rivers, J.W., Westneat, D.F., Birkhead, T.R., 2009. Sperm competition selects beyond relative testes size in birds. Evol. Int. J. Organ. Evol. 63 (2), 391–402.

MacLaughlin, D.T., Hutson, J.M., Donahoe, P.K., 1983. Specific estradiol binding in embryonic Mullerian ducts: a potential modulator of regression in the male and female chick. Endocrinology 113 (1), 141–145.

Major, A.T., Smith, C.A., 2016. Sex reversal in birds. Sexual Dev. 10 (5–6), 288–300.

Mantei, K.E., Ramakrishnan, S., Sharp, P.J., Buntin, J.D., 2008. Courtship interactions stimulate rapid changes in GnRH synthesis in male ring doves. Horm. Behav. 54 (5), 669–675.

Maraud, R., Stoll, R., 1955. Action de la testosterone sur la constitution de l' epididme du. Coq. C. R. Soc. Biol. 149, 704–707.

Marvan, F., 1969. Postnatal development of the male genital tract of the *Gallus domesticus*. Anat. Anzeiger 124 (4), 443–462.

Matsuo, H., Baba, Y., Nair, R.G., Arimura, A., Schally, A.V., 1971. Structure of the porcine LH-and FSH-releasing hormone. I. The proposed amino acid sequence. Biochem. Biophys. Res. Commun. 43 (6), 1334–1339.

Maung, Z.W., Follett, B., 1977. Effects of chicken and ovine luteinizing hormone on androgen release and cyclic AMP production by isolated cells from the quail testis. Gen. Comp. Endocrinol. 33 (2), 242–253.

McFarlane, H.O., Joseph, N.T., Maddineni, S.R., Ramachandran, R., Bédécarrats, G.Y., 2011. Development, validation, and utilization of a novel antibody specific to the type III chicken gonadotropin-releasing hormone receptor. Domest. Anim. Endocrinol. 40 (2), 110–118.

Meddle, S., Bush, S., Sharp, P., Millar, R., Wingfield, J., 2006. Hypothalamic pro-GnRH-GAP, GnRH-I and GnRH-II during the onset of photorefractoriness in the white-crowned sparrow (*Zonotrichia leucophrys gambelii)*. J. Neuroendocrinol. 18 (3), 217–226.

Merchant-Larios, H., Popova, L., Reyss-Brion, M., 1984. Early morphogenesis of chick gonad in the absence of mesonephros. (morphogenesis/gonad/mesonephric agenesis). Dev. Growth Differ. 26 (5), 403–417. https://doi.org/10.1111/j.1440-169X.1984.00403.x.

Meyer, D.B., 1964. The migration of primordial germ cells in the chick embryo. Dev. Biol. 10, 154–190.

Mezey, É., Kivovics, P., Palkovits, M., 1979. Pituitary-brain retrograde transport. Trends Neurosci. 2 (0), 57–60. https://doi.org/10.1016/0166-2236(79)90025-0.

Mi, Y., Zhang, C., Xie, M., Zeng, W., 2004. Effects of follicle-stimulating hormone and androgen on proliferation of cultured testicular germ cells of embryonic chickens. Gen. Comp. Endocrinol. 138 (3), 237–246. https://doi.org/10.1016/j.ygcen.2004.06.012.

Mikami, S., Yamada, S., Hasegawa, Y., Miyamoto, K., 1988. Localization of avian LHRH-immunoreactive neurons in the hypothalamus of the domestic fowl, *Gallus domesticus*, and the Japanese quail, *Coturnix coturnix*. Cell Tissue Res. 251 (1), 51–58.

Millar, R.P., 2003. GnRH II and type II GnRH receptors. Trends Endocrinol. Metabol. 14 (1), 35–43.

Millar, R.P., 2005. GnRHs and GnRH receptors. Anim. Reprod. Sci. 88 (1–2), 5–28.

Millar, R.P., Lu, Z.-L., Pawson, A.J., Flanagan, C.A., Morgan, K., Maudsley, S.R., 2004. Gonadotropin-releasing hormone receptors. Endocr. Rev. 25 (2), 235–275.

Miyamoto, K., Hasegawa, Y., Minegishi, T., Nomura, M., Takahashi, Y., Igarashi, M., Kangawa, K., Matsuo, H., 1982. Isolation and characterization of chicken hypothalamic luteinizing hormone-releasing hormone. Biochem. Biophys. Res. Commun. 107 (3), 820–827.

Mizuno, S., Saitoh, Y., Nomura, O., Kunita, R., Ohtomo, K., Nishimori, K., Ono, H., Saitoh, H., 1993. Sex-specific DNA sequences in galliformes and their application to the study of sex differentiation. In: Etches, R.J., Gibbins, A.M.V. (Eds.), Manipulation of the Avian Genome, pp. 257–274.

Moller, A.P., 1991. Sperm competition, sperm depletion, paternal care, and relative testis size in birds. Am. Nat. 137 (6), 882–906. https://doi.org/10.2307/2462406.

Moller, A.P., Briskie, J.V., 1995. Extra-pair paternity, sperm competition and the evolution of testis size in birds. Behav. Ecol. Sociobiol. 36 (5), 357–365. https://doi.org/10.1007/bf00167797.

Moore, I.T., Bentley, G.E., Wotus, C., Wingfield, J.C., 2006. Photoperiod-independent changes in immunoreactive brain gonadotropin-releasing hormone (GnRH) in a free-living, tropical bird. Brain Behav. Evol. 68 (1), 37–44. https://doi.org/10.1159/000093059.

Munro, S.S., 1938. Functional changes in fowl sperm during their passage through the excurrent ducts of the male. J. Exp. Zool. 79 (1), 71–92. https://doi.org/10.1002/jez.1400790106.

Nagano, T., 1962. Observations on the fine structure of the developing spermatid in the domestic chicken. J. Cell Biol. 14, 193–205.

Nakai, M., Hashimoto, Y., Kitagawa, H., Kon, Y., Kudo, N., 1988. Microvasculature of the epididymis and ductus deferens of domestic fowls. Nihon Juigaku Zasshi 50 (2), 371–381.

Nakai, M., Hashimoto, Y., Kitagawa, H., Kon, Y., Kudo, N., 1989. Histological study on seminal plasma absorption and spermiophagy in the epididymal region of domestic fowl. Poultry Sci. 68 (4), 582–589.

Nakai, M., Nasu, T., 1991. Ultrastructural study on junctional complexes of the excurrent duct epithelia in the epididymal region in the fowl. J. Vet. Med. Sci. 53 (4), 677–681.

Nakamura, T., Tanabe, Y., 1972. In vitro steroidogenesis by testes of the chicken (*Gallus domesticus*). Gen. Comp. Endocrinol. 19 (3), 432–440.

Nanda, I., Shan, Z., Schartl, M., Burt, D.W., Koehler, M., Nothwang, H., Grutzner, F., Paton, I.R., Windsor, D., Dunn, I., Engel, W., Staeheli, P., Mizuno, S., Haaf, T., Schmid, M., 1999. 300 million years of conserved synteny between chicken Z and human chromosome 9. Nat. Genet. 21 (3), 258–259. https://doi.org/10.1038/6769.

Narbaitz, R., Adler, R., 1966. Submicroscopic observations on the differentiation of the chick gonads. J. Embryol. Exp. Morphol. 15, 41–47.

Neill, J.D., 2002. Minireview: GnRH and GnRH receptor genes in the human genome. Endocrinology 143 (3), 737–743.

Nickel, R., Schummer, A., Seiferle, E., Siller, W.G., Wright, P.A.L., 1977. Urogenital system. In: Anatomy of the Domestic Birds, pp. 70–84.

O'Neill, M., Binder, M., Smith, C., Andrews, J., Reed, K., Smith, M., Millar, C., Lambert, D., Sinclair, A., 2000. ASW: a gene with conserved avian W-linkage and female specific expression in chick embryonic gonad. Dev. Gene. Evol. 210 (5), 243–249.

Oiso, S., Nobe, M., Yamaguchi, Y., Umemoto, S., Nakamura, K., Kariyazono, H., 2013. Establishment of a gastric cell-based assay system for exploring inhibitors of octanoylated ghrelin production. J. Biomol. Screen 18 (9), 1035–1042.

Okamura, F., Nishiyama, H., 1976. The early development of the tail and the transformation of the shape of the nucleus of the spermatid of the domestic fowl, *Gallus gallus*. Cell Tissue Res. 169 (3), 345–359.

Okamura, F., Nishiyama, H., 1978. The passage of spermatozoa through the vitelline membrane in the domestic fowl, *Gallus gallus*. Cell Tissue Res. 188 (3), 497–508.

Oliva, R., Mezquita, C., 1986. Marked differences in the ability of distinct protamines to disassemble nucleosomal core particles in vitro. Biochemistry 25 (21), 6508–6511. https://doi.org/10.1021/bi00369a025.

Oreal, E., Mazaud, S., Picard, J.Y., Magre, S., Carre-Eusebe, D., 2002. Different patterns of anti-Mullerian hormone expression, as related to DMRT1, SF-1, WT1, GATA-4, Wnt-4, and Lhx9 expression, in the chick differentiating gonads. Dev. Dynam. 225 (3), 221–232. https://doi.org/10.1002/dvdy.10153.

Oreal, E., Pieau, C., Mattei, M.G., Josso, N., Picard, J.Y., Carré-Eusèbe, D., Magre, S., 1998. Early expression of AMH in chicken embryonic gonads precedes testicular SOX9 expression. Dev. Dyn. 212, 522–532.

Orlu, E.E., Egbunike, G.N., 2009. Daily sperm production of the domestic fowl (*Gallus domesticus*) as determined by quantitative testicular histology and homogenate methods. Pakistan J. Biol. Sci. 12 (20), 1359–1364.

Osman, D.I., 1980. The connection between the seminiferous tubules and the rete testis in the domestic fowl (*Gallus domesticus*). Morphological study. Int. J. Androl. 3 (2), 177–187.

Osugi, T., Daukss, D., Gazda, K., Ubuka, T., Kosugi, T., Nozaki, M., Sower, S.A., Tsutsui, K., 2012. Evolutionary origin of the structure and function of gonadotropin-inhibitory hormone: insights from lampreys. Endocrinology 153 (5), 2362–2374.

Osugi, T., Ukena, K., Bentley, G.E., O'Brien, S., Moore, I.T., Wingfield, J.C., Tsutsui, K., 2004. Gonadotropin-inhibitory hormone in Gambel's white-crowned sparrow (*Zonotrichia leucophrys gambelii*): cDNA identification, transcript localization and functional effects in laboratory and field experiments. J. Endocrinol. 182 (1), 33–42.

Ottinger, M.A., 1983. Hormonal control of reproductive behavior in the avian male. Poultry Sci. 62 (8), 1690–1699.

Ottinger, M.A., Brinkley, H.J., 1979. Testosterone and sex related physical characteristics during the maturation of the male Japanese quail (coturnix coturnix japonica). Biol. Reprod. 20 (4), 905–909.

Ozegbe, P.C., Aire, T.A., Madekurozwa, M.C., Soley, J.T., 2008. Morphological and immunohistochemical study of testicular capsule and peritubular tissue of emu (*Dromaius novaehollandiae*) and ostrich (*Struthio camelus*). Cell Tissue Res. 332 (1), 151–158. https://doi.org/10.1007/s00441-007-0515-2.

Ozegbe, P.C., Aire, T.A., Soley, J.T., 2006. The morphology of the efferent ducts of the testis of the ostrich, a primitive bird. Anat. Embryol. 211 (5), 559–565. https://doi.org/10.1007/s00429-006-0107-z.

Ozegbe, P.C., Kimaro, W., Madekurozwa, M.C., Soley, J.T., Aire, T.A., 2010. The excurrent ducts of the testis of the emu (*Dromaius novaehollandiae*) and ostrich (*Struthio camelus*): microstereology of the epididymis and immunohistochemistry of its cytoskeletal systems. Anat. Histol. Embryol. 39 (1), 7–16. https://doi.org/10.1111/j.1439-0264.2009.00969.x.

Panzica, G.C., Viglietti-Panzica, C., Calagni, M., Anselmetti, G., Schumacher, M., Balthazart, J., 1987. Sexual differentiation and hormonal control of the sexually dimorphic medial preoptic nucleus in the quail. Brain Res. 416 (1), 59–68.

Pelletier, R.M., 1990. A novel perspective: the occluding zonule encircles the apex of the Sertoli cell as observed in birds. Am. J. Anat. 188 (1), 87–108. https://doi.org/10.1002/aja.1001880110.

Perfito, N., Zann, R., Ubuka, T., Bentley, G., Hau, M., 2011. Potential roles for GNIH and GNRH-II in reproductive axis regulation of an opportunistically breeding songbird. Gen. Comp. Endocrinol. 173 (1), 20–26.

Pitcher, T.E., Dunn, P.O., Whittingham, L.A., 2005. Sperm competition and the evolution of testes size in birds. J. Evol. Biol. 18 (3), 557–567. https://doi.org/10.1111/j.1420-9101.2004.00874.x.

Proudman, J., Vandesande, F., Berghman, L., 1999. Immunohistochemical evidence that follicle-stimulating hormone and luteinizing hormone reside in separate cells in the chicken pituitary. Biol. Reprod. 60 (6), 1324–1328.

Ravona, H., Snapir, N., Perek, M., 1973. The effect on the gonadal axis in cockerels of electrolytic lesions in various regions of the basal hypothalamus. Gen. Comp. Endocrinol. 20 (1), 112–124.

Robinson, J.E., Follett, B.K., 1982. Photoperiodism in Japanese quail: the termination of seasonal breeding by photorefractoriness. Proc. R. Soc. Lond. B Biol. Sci. 215 (1198), 95–116. https://doi.org/10.1098/rspb.1982.0030.

Romanoff, A.L., 1960. The urogenital system. In: The Avian Embryo, 783-782.

Rothwell, B., 1973. The ultrastructure of Leydig cells in the testis of the domestic fowl. J. Anat. 116 (Pt 2), 245–253.

Rothwell, B., Tingari, M.D., 1973. The ultrastructure of the boundary tissue of the seminiferous tubule in the testis of the domestic fowl (*Gallus domesticus*). J. Anat. 114 (Pt 3), 321–328.

Rozenboim, I., Gvaryahu, G., Robinzon, B., Sayag, N., Snapir, N., 1986. Induction of precocious development of reproductive function in cockerels by tamoxifen administration. Poultry Sci. 65 (10), 1980–1983.

Russell, L.D., Griswold, M.D., 1993. The Sertoli Cell. Cache River Press.

Saldanha, C.J., Silverman, A.-J., Silver, R., 2001. Direct innervation of GnRH neurons by encephalic photoreceptors in birds. J. Biol. Rhythm. 16 (1), 39–49.

Samsel, J., Lorber, B., Petit, A., Weniger, J.P., 1986. Analysis of the cytosolic proteins of chick embryo gonads by two-dimensional gel electrophoresis. J. Embryol. Exp. Morphol. 94, 221–230.

Sertoli, E., 1865. De l'esistenze di particulari cellule ramifacate nei canalicoli seminiferi dell'testicolo umano. Morgagni 7, 31–40.

Sertoli, E., 1878. Sulla sturttura dei canalicoli seminiferi dei testicolo. Arch. Sci. Med. 2 (107–146), 267–295.

Sharp, P., Dunn, I., Talbot, R., 1987. Sex differences in the LH responses to chicken LHRH-I and-II in the domestic fowl. J. Endocrinol. 115 (2), 323–331.

Sharp, P., Talbot, R., Main, G., Dunn, I., Fraser, H., Huskisson, N., 1990. Physiological roles of chicken LHRH-I and-II in the control of gonadotrophin release in the domestic chicken. J. Endocrinol. 124 (2), 291–299.

Sharp, P.J., Culbert, J., Wells, J.W., 1977. Variations in stored and plasma concentrations of androgens and luteinizing hormone during sexual development in the cockerel. J. Endocrinol. 74 (3), 467–476.

Sharp, P.J., Gow, C.B., 1983. Neuroendocrine control of reproduction in the cockerel. Poultry Sci. 62 (8), 1671–1675.

Sharpe, R.M., 1994. Regulation of spermatogenesis. In: Knobil, E., Neill, J.D. (Eds.), The Physiology of Reproduction, second ed., vol. 1, pp. 1363–1434.

Shimada, K., 2002. Sex determination and sex differentiation. Avian Poultry Biol. Rev. 13, 1–14.

Shimizu, M., Bédécarrats, G.Y., 2006. Identification of a novel pituitary-specific chicken gonadotropin-releasing hormone receptor and its splice variants. Biol. Reprod. 75 (5), 800–808.

Silverin, B., Viebke, P.A., 1994. Low temperatures affect the photoperiodically induced LH and testicular cycles differently in closely related species of tits (*Parus* spp.). Horm. Behav. 28 (3), 199–206. https://doi.org/10.1006/hbeh.1994.1017.

Simões, K., Orsi, A.M., Artoni, S.M.B., Cruz, C.d., Schimming, B.C., Pinheiro, P.F.F., 2004. Structural features of the epididymal region of the domestic duck (*Anas plathyrynchos*). Braz. J. Vet. Res. Anim. Sci. 41, 92–97.

Smith, C.A., Roeszler, K.N., Ohnesorg, T., Cummins, D.M., Farlie, P.G., Doran, T.J., Sinclair, A.H., 2009a. The avian Z-linked gene DMRT1 is required for male sex determination in the chicken. Nature 461 (7261), 267.

Smith, C.A., Roeszler, K.N., Sinclair, A.H., 2003. Genetic evidence against a role for W-linked histidine triad nucleotide binding protein (HINTW) in avian sex determination. Int. J. Dev. Biol. 53, 59–67.

Smith, C.A., Sinclair, A.H., 2004. Sex determination: insights from the chicken. Bioessays 26 (2), 120–132. https://doi.org/10.1002/bies.10400.

Smith, C.A., Smith, M.J., Sinclair, A.H., 1999. Gene expression during gonadogenesis in the chicken embryo. Gene 234 (2), 395–402.

Son, Y.L., Ubuka, T., Tsutsui, K, 2019. Molecular mechanisms of gonadotropin-inhibitory hormone (GnIH) actions in target cells and regulation of GnIH expression. Front. Endocrinol. 10, 110.

Sprando, R.L., Russell, L.D., 1988. Spermiogenesis in the red-ear turtle (Pseudemys scripta) and the domestic fowl (*Gallus domesticus*): a study of cytoplasmic events including cell volume changes and cytoplasmic elimination. J. Morphol. 198 (1), 95–118. https://doi.org/10.1002/jmor.1051980110.

Stevenson, T.J., Ball, G.F., 2009. Anatomical localization of the effects of reproductive state, castration, and social milieu on cells immunoreactive for gonadotropin-releasing hormone-I in male European starlings (*Sturnus vulgaris*). J. Comp. Neurol. 517 (2), 146–155.

Stoll, R., Maraud, R., 1974. Le role du testicule dans la differenciation sexuell des gonoductes chez l' embryon des vertebres amniotes. Bull. Assoc. Anat. 58, 699-674.

Stoll, R.L.L., Maraud, R., 1973. Sur l' origine de l'hormone testiculaire responsible de la regression des canaux de Muller de l' embryon de Poulet. C.R. Soc. Biol. 167, 1092–1096.

Stratil, A., 1970. Studies on proteins of seminal fluid from the vasa deferentia of the cock, *Gallus gallus* L. Int. J. Biochem. 1 (6), 728–734. https://doi.org/10.1016/0020-711x(70)90047-9.

Sullivan, K.A., Silverman, A.J., 1993. The ontogeny of gonadotropin-releasing hormone neurons in the chick. Neuroendocrinology 58 (6), 597–608.

Sun, Y.-M., Flanagan, C.A., Illing, N., Ott, T.R., Sellar, R., Fromme, B.J., Hapgood, J., Sharp, P., Sealfon, S.C., Millar, R.P., 2001a. A chicken gonadotropin-releasing hormone receptor that confers agonist activity to mammalian antagonists identification of d-LYS6 IN the ligand and extracellular loop two of the receptor as determinants. J. Biol. Chem. 276 (11), 7754–7761.

Sun, Y.M., Dunn, I., Baines, E., Talbot, R., Illing, N., Millar, R., Sharp, P., 2001b. Distribution and regulation by oestrogen of fully processed and variant transcripts of gonadotropin releasing hormone I and gonadotropin releasing hormone receptor mRNAs in the male chicken. J. Neuroendocrinol. 13 (1), 37–49.

Tanabe, Y., Nakamura, T., Fujioka, K., Doi, O., 1979. Production and secretion of sex steroid hormones by the testes, the ovary, and the adrenal glands of embryonic and young chickens (*Gallus domesticus*). Gen. Comp. Endocrinol. 39 (1), 26–33.

Teng, C., 1982. Ontogeny of cyclic nucleotides in embryonic chick gonads. Biol. Neonate 41 (3–4), 123–131.

Teng, C.S., Wang, J.J., Teng, J.I., 1987. Purification of chicken testicular mullerian inhibiting substance by ion exchange and high-performance liquid chromatography. Dev. Biol. 123 (1), 245–254.

Thurston, R., Korn, N., 2000. Spermiogenesis in commercial poultry species: anatomy and control. Poultry Sci. 79 (11), 1650–1668.

Thurston, R.J., Hess, R.A., 1987. Ultrastructure of spermatozoa from domesticated birds: comparative study of Turkey, chicken and Guinea fowl. Scanning Microsc. 1 (4), 1829–1838.

Thurston, R.J., Hess, R.A., Froman, D.P., Biellier, H.V., 1982a. Elevated seminal plasma protein: a characteristic of Yellow Turkey semen. Poultry Sci. 61 (9), 1905–1911.

Thurston, R.J., Hess, R.A., Hughes, B.L., Froman, D.P., 1982b. Seminal plasma free amino acids and seminal and blood plasma proteins of the Guinea fowl (*Numidia meleagris*). Poultry Sci. 61 (8), 1744–1747.

Tiba, T., Yoshida, K., Miyake, M., Tsuchiya, K., Kita, I., Tsubota, T., 1993. Regularities and irregularities in the structure of the seminiferous epithelium in the domestic fowl (*Gallus domesticus*). I. Suggestion of the presence of the seminiferous epithelial cycle. Anat. Histol. Embryol. 22 (3), 241–253.

Tingari, M.D., 1971. On the structure of the epididymal region and ductus deferens of the domestic fowl (*Gallus domesticus*). J. Anat. 109 (Pt 3), 423–435.

Tingari, M.D., 1972. The fine structure of the epithelial lining of the excurrent duct system of the testis of the domestic fowl (*Gallus domesticus*). Q. J. Exp. Physiol. Cogn. Med. Sci. 57 (3), 271–295.

Tingari, M.D., 1973. Observations on the fine structure of spermatozoa in the testis and excurrent ducts of the male fowl, *Gallus domesticus*. J. Reprod. Fertil. 34 (2), 255–265.

Tingari, M.D., Lake, P.E., 1972. Ultrastructural evidence for resorption of spermatozoa and testicular fluid in the excurrent ducts of the testis of the domestic fowl, *Gallus domesticus*. J. Reprod. Fertil. 31 (3), 373–381.

Tostivint, H., 2011. Evolution of the gonadotropin-releasing hormone (GnRH) gene family in relation to vertebrate tetraploidizations. Gen. Comp. Endocrinol. 170 (3), 575–581.

Tsutsui, K., Ishii, S., 1978. Effects of follicle-stimulating hormone and testosterone on receptors of follicle-stimulating hormone in the testis of the immature Japanese quail. Gen. Comp. Endocrinol. 36 (2), 297–305.

Tsutsui, K., Saigoh, E., Ukena, K., Teranishi, H., Fujisawa, Y., Kikuchi, M., Ishii, S., Sharp, P.J., 2000. A novel avian hypothalamic peptide inhibiting gonadotropin release. Biochem. Biophys. Res. Commun. 275 (2), 661–667. https://doi.org/10.1006/bbrc.2000.3350.

Ubuka, T., Bentley, G.E., 2009. Identification, localization, and regulation of passerine GnRH-I messenger RNA. J. Endocrinol. 201 (1), 81–87.

Ubuka, T., Bentley, G.E., 2011. Neuroendocrine control of reproduction in birds. In Hormones and Reproduction of Vertebrates. Academic Press, pp. 1–25.

Ubuka, T., Bentley, G.E., Tsutsui, K., 2013. Neuroendocrine regulation of gonadotropin secretion in seasonally breeding birds. Front. Neurosci. 7, 38.

Ubuka, T., Bentley, G.E., Ukena, K., Wingfield, J.C., Tsutsui, K., 2005. Melatonin induces the expression of gonadotropin-inhibitory hormone in the avian brain. Proc. Natl. Acad. Sci. U.S.A. 102 (8), 3052–3057. https://doi.org/10.1073/pnas.0403840102.

Ubuka, T., Ueno, M., Ukena, K., Tsutsui, K., 2003. Developmental changes in gonadotropin-inhibitory hormone in the Japanese quail (*Coturnix japonica*) hypothalamo-hypophysial system. J. Endocrinol. 178 (2), 311–318.

Ubuka, T., Ukena, K., Sharp, P.J., Bentley, G.E., Tsutsui, K., 2006. Gonadotropin-inhibitory hormone inhibits gonadal development and maintenance by decreasing gonadotropin synthesis and release in male quail. Endocrinology 147 (3), 1187–1194. https://doi.org/10.1210/en.2005-1178.

Ukena, K., Ubuka, T., Tsutsui, K., 2003. Distribution of a novel avian gonadotropin-inhibitory hormone in the quail brain. Cell Tissue Res. 312, 73–79.

Vizcarra, J.A., 2013. In: Vizcarra Dr., Jorge (Ed.), Contribution of Chicken GnRH-II and Lamprey GnRH-III on Gonadotropin Secretion, Gonadotropin. InTech. https://doi.org/10.5772/47863. ISBN: 978-953-51-1006-4.

Vizcarra, J.A., Kirby, J.D., Kreider, D.L., 2010. Testis development and gonadotropin secretion in broiler breeder males. Poultry Sci. 89 (2), 328–334.

Vizcarra, J.A., Kreider, D.L., Kirby, J.D., 2004. Episodic gonadotropin secretion in the mature fowl: serial blood sampling from unrestrained male broiler breeders (*Gallus domesticus*). Biol. Reprod. 70 (6), 1798–1805.

Wade, J., Arnold, A.P., 1996. Functional testicular tissue does not masculinize development of the zebra finch song system. Proc. Natl. Acad. Sci. U.S.A. 93 (11), 5264–5268.

Wade, N., 1978. Guillemin and Schally: The Years in the Wilderness. JSTOR.

Walker, W.H., Cheng, J., 2005. FSH and testosterone signaling in Sertoli cells. Reproduction 130 (1), 15–28. https://doi.org/10.1530/rep.1.00358.

Watanabe, T., Yamamura, T., Watanabe, M., Yasuo, S., Nakao, N., Dawson, A., Ebihara, S., Yoshimura, T., 2007. Hypothalamic expression of thyroid hormone-activating and-inactivating enzyme genes in relation to photorefractoriness in birds and mammals. Am. J. Physiol. Regul. Integr. Comp. Physiol. 292 (1), R568–R572.

Wilson, S., Cunningham, F., Chairil, R., Gladwell, R., 1989. Maturational changes in the LH response of domestic fowl to synthetic chicken LHRH-I and-II. J. Endocrinol. 123 (2), 311–318.

Wilson, S.C., Sharp, P., 1975. Episodic release of luteinizing hormone in the domestic fowl. J. Endocrinol. 64 (1), 77–86.

Wingfield, J.C., Hahn, T.P., Levin, R., Honey, P., 1992. Environmental predictability and control of gonadal cycles in birds. J. Exp. Zool. 261 (2), 214–231. https://doi.org/10.1002/jez.1402610212.

Wingfield, J.C., Hahn, T.P., Maney, D.L., Schoech, S.J., Wada, M., Morton, M.L., 2003. Effects of temperature on photoperiodically induced reproductive development, circulating plasma luteinizing hormone and thyroid hormones, body mass, fat deposition and molt in mountain white-crowned sparrows, Zonotrichia leucophrys oriantha. Gen. Comp. Endocrinol. 131 (2), 143–158.

Woods, J.E., Simpson, R.M., Moore, P.L., 1975. Plasma testosterone levels in the chick embryo. Gen. Comp. Endocrinol. 27 (4), 543–547.

Woods, J.E., Weeks, R.L., 1969. Ontogenesis of the pituitary-gonadal axis in the chick embryo. Gen. Comp. Endocrinol. 13 (2), 242–254.

Yasuo, S., Yoshimura, T., 2009. Comparative analysis of the molecular basis of photoperiodic signal transduction in vertebrates. Integr. Comp. Biol. 49 (5), 507–518. https://doi.org/10.1093/icb/icp011.

Yoshida, S., 2016. From cyst to tubule: innovations in vertebrate spermatogenesis. Wiley Interdis. Rev. Dev. Biol. 5 (1), 119–131.

Yoshimura, T., 2006. Molecular mechanism of the photoperiodic response of gonads in birds and mammals. Comp. Biochem. Physiol. Mol. Integr. Physiol. 144 (3), 345–350. https://doi.org/10.1016/j.cbpa.2005.09.009.

Yoshimura, T., 2010. Neuroendocrine mechanism of seasonal reproduction in birds and mammals. Anim. Sci. J. 81 (4), 403–410. https://doi.org/10.1111/j.1740-0929.2010.00777.x.

Yoshimura, T., Yasuo, S., Watanabe, M., Iigo, M., Yamamura, T., Hirunagi, K., Ebihara, S., 2003. Light-induced hormone conversion of T4 to T3 regulates photoperiodic response of gonads in birds. Nature 426 (6963), 178–181. https://doi.org/10.1038/nature02117.

Chapter 37

The physiology of the avian embryo

Casey A. Mueller[1], Warren W. Burggren[2] and Hiroshi Tazawa[2]
[1]Department of Biological Sciences, California State University San Marcos, San Marcos, CA, United States; [2]Developmental and Integrative Biology, Department of Biological Science, University of North Texas, Denton, TX, United States

Abbreviations

$[HCO_3^-]$ bicarbonate concentration
$[La^-]$ lactate concentration
A_p effective pore area
CAM chorioallantoic membrane
CO cardiac output
CO_2 carbon dioxide
d_{CO_2} carbon dioxide diffusion coefficient
d_{H_2O} water vapor diffusion coefficient
d_{O_2} oxygen diffusion coefficient
D_{O_2} oxygen diffusing capacity
EP external pipping
$F\bar{C}_{OX}$ mean corpuscular oxygenation velocity
G_{CO_2} carbon dioxide conductance
G_{H_2O} water vapor conductance
G_{O_2} oxygen conductance
Hb hemoglobin
Hct hematocrit
HR heart rate
I incubation period
IHR instantaneous heart rate
IP internal pipping
IRR instantaneous respiratory rate
L shell thickness
MHR mean heart rate
$\dot{M}_{CO_2}$ carbon dioxide elimination rate
$\dot{M}_{H_2O}$ rate of water loss
$\dot{M}_{O_2}$ oxygen consumption rate
O_2 oxygen
P_a arterial blood pressure
P_aCO_2 arterialized blood carbon dioxide partial pressure
$PACO_2$ air space carbon dioxide partial pressure
PAO_2 air space oxygen partial pressure
P_aO_2 arterialized blood oxygen partial pressure
P_B atmospheric pressure
$P\bar{c}O_2$ mean capillary oxygen partial pressure
P_{H_2O} water vapor pressure
$PICO_2$ effective environmental carbon dioxide partial pressure
PIO_2 effective environmental oxygen partial pressure
P_{sys} systolic blood pressure
Q_{10} temperature coefficient
Q_a allantoic blood flow
R gas constant
T_a ambient temperature
t_c contact time of erythrocytes in chorioallantoic capillary with O_2
T_{egg} egg temperature
V_c capillary volume

37.1 Introduction

The freshly laid avian egg contains most of the materials needed for embryonic growth and development, but lacks the oxygen and heat needed for successful development. Microscopic pores in the eggshell allow O_2 to diffuse into the egg from the environment and water vapor and CO_2 produced by the embryo to diffuse out. The adult bird has a key role in incubation, providing not only the heat necessary for embryonic development but also controlling the microclimate of the egg. In the poultry industry and for research purposes, the adult bird can be conveniently replaced by an incubator. The majority of research on avian incubation is undertaken using artificially incubated chicken (*Gallus gallus domesticus*) eggs. Thus, in this chapter, the chicken embryo is used to elucidate the development of physiological function during avian incubation, supplemented by additional species when data are available. Developmental physiology of the gas exchange, acid-base, cardiovascular, osmoregulatory, and thermoregulatory systems are examined. The optimal conditions for artificial incubation are outlined and embryonic responses to incubation extremes described.

37.2 The freshly laid egg

The mass of the freshly laid bird egg ranges from ~0.8 g in the bee hummingbird (*Mellisuga helenae*) to ~2 kg in the ostrich (*Struthio camelus*). The egg is composed of the eggshell and outer and inner shell membranes that

Sturkie's Avian Physiology. https://doi.org/10.1016/B978-0-12-819770-7.00030-X

encompass the albumen, which serves as a source of water and protein, and yolk, a source of necessary nutrients. The composition of the freshly laid egg is related to the maturity of the hatchling, which differs considerably between species. Hatchlings are divided into four major categories based on criteria such as mobility, amount of down, ability to feed, and locomotion. Precocial species are the most mature, and can walk, swim, or dive soon after hatching, while altricial species are the least mature and hatch naked, with eyes closed and are incapable of coordinated locomotion. Two intermediate categories, semiprecocial and semialtricial, describe species that are within these extremes. The amount of yolk in the freshly laid egg is much greater in precocial species than in altricial species (Sotherland and Rahn, 1987). The yolk is only 16% of egg mass in the altricial red-footed booby (*Sula sula*), while in the highly precocial kiwi (*Apteryx australis*), it is 69% of egg mass. As most of the energy contained in the egg is in the lipid fraction, most of which are in the yolk, the energy content of precocial eggs is higher than that of altricial eggs. Furthermore, most of the water in the egg is in the albumen, and as the yolk/albumen ratio is lower in altricial than in precocial eggs, altricial eggs have relatively higher water compared to precocial eggs (Sotherland and Rahn, 1987).

37.3 Incubation

37.3.1 Incubation period

Incubation encompasses the prenatal period, prior to "internal pipping" (IP) when the embryo penetrates its beak through the chorioallantoic and inner shell membranes into the air cell, and the perinatal or paranatal period from IP to when the embryo fractures the shell ["external pipping" (EP)] and hatches. The incubation period (I, days) increases with egg size and can be represented as follows:

$$I = 12 \cdot (\text{Egg mass})^{0.22} \tag{37.1}$$

where egg mass is in g (Rahn and Ar, 1974). In addition, as a first approximation, the product of incubation period and O_2 consumption ($\dot{M}_{O_2}$) at the stage where $\dot{M}_{O_2}$ remains unchanged (i.e., plateau) is proportional to egg mass (Rahn et al., 1974):

$$I \cdot \dot{M}_{O_2} = c \cdot (\text{Egg mass}) \tag{37.2}$$

where c is a constant. Thus, for a given egg mass, an egg which consumes less O_2 at the plateau stage needs a longer incubation period. Furthermore, because the $\dot{M}_{O_2}$ at the plateau stage is matched to the shell gas conductance, for a given egg mass, an egg with lower shell conductance requires a longer incubation period.

Apart from these general trends, eggs that are left unattended by the incubating parent for a period of time will exhibit cooling, and this results in slower embryonic growth and a longer incubation period. Some birds, notably tropical seabirds and petrels (Procellariiformes), have much longer incubation periods than that suggested by the general relationship (Whittow, 1980), even though they are incubated continuously.

37.3.2 Egg water content and shell conductance

As the embryo grows within the egg, water is lost and both the yolk and albumen diminish in mass. However, metabolic water is produced when fat in the yolk is oxidized. Part of the water is inevitably lost by diffusion through the pores in the shell to the microclimate of the egg. The rate of water loss ($\dot{M}_{H_2O}$, mg/day) is determined by two factors: the water vapor conductance of the shell and shell membranes (G_{H_2O}, mg/day/kPa) and the difference in water vapor pressure between the contents of the egg and the environment (ΔP_{H_2O}, kPa) (Rahn and Ar, 1974):

$$\dot{M}_{H_2O} = G_{H_2O} \cdot \Delta P_{H_2O} \tag{37.3}$$

G_{H_2O} is a function of the multiple factors, including: shell geometry (effective pore area, A_p, thickness of the shell combined with shell membranes, L); water vapor diffusion coefficient (d_{H_2O}); and the inverse product of the gas constant (R) and absolute temperature (T):

$$G_{H_2O} = [(A_p/L) \cdot d_{H_2O}]/RT \tag{37.4}$$

Both pore area and shell thickness increase in larger eggs (Ar et al., 1974; Birchard and Deeming, 2009). While a greater pore area increases G_{H_2O}, a thicker shell has the opposite effect because it lengthens the diffusion pathway for water vapor. The water lost from the egg is replaced by air, enlarging the air cell at the blunt pole of the egg during development. Shell thickness also decreases throughout development as the embryo absorbs calcium (Orłowski and Hałupka, 2015; Orłowski et al., 2016; Rosenberger et al., 2017). Upon IP and EP, the rate of water loss from the egg increases, as water vapor can diffuse through the cracks (pip-hole) in the shell. The water loss from the egg over the entire incubation period amounts to ~18% of the mass of the freshly laid egg.

37.3.3 Heat transfer

Many adult birds (typically but not always the female) play an important role in incubation of their eggs, by using their body and nesting material to alter the environment of the eggs. Most birds develop a seasonal bare patch of skin, the brood patch, on part of the thorax and abdomen. This directly contacts with the eggs permitting a greater rate of heat transfer than if the patch were covered with plumage. Accompanying the loss of feathers is an increase in the size and number of blood vessels in the bare skin. The adult can

adjust the rate of heat transfer to the egg by standing over or leaving the vicinity of the egg, but also by the closeness with which the bird applies its patch to the egg. The bird responds physiologically to variations in egg temperature (T_{egg}), increasing its metabolic heat production in response to cooling of the egg (Tøien et al., 1986; Rahn, 1991).

The amount of heat transferred to the eggs is directly proportional to the increase in heat production (Tøien et al., 1986). The efficiency of heat transfer to the eggs diminishes with decreasing ambient temperature and clutch size. Heat stored in the incubating bird while flying and foraging (i.e., while not incubating the eggs) can be transferred to the eggs on return to the nest (Biebach, 1986). If the egg is very cold, "cold vasodilation" occurs in the brood patch, increasing the patch blood flow and temperature and therefore heat transfer to the egg (Mitgard et al., 1985). The brood patch temperature varies from 34.9°C in the bonin petrel (*Pterodroma hypoleuca*) to 42.4°C in the dusky flycatcher (*Empidonax oberholseri*). The brood patch temperature is 1.1−5.5°C higher than the T_{egg} in numerous species (Rahn, 1991).

At the beginning of incubation, heat is transferred through the egg by conduction and the surface of egg on the opposite side to the brood patch may be 4°C or more below the brood patch temperature (Rahn, 1991). As incubation proceeds, this temperature difference diminishes as the embryo's developing circulation assists in the distribution of heat, and its increasing metabolism provides additional heat (Turner, 1987; Rahn, 1991). This effect of blood flow on heat flow is more important in large eggs than in small ones (Tazawa et al., 1988a). The main barrier to heat loss from the egg is a thin layer of air immediately adjacent to the shell, i.e., boundary layer (Sotherland et al., 1987). If the egg is in a nest, the nest itself imposes an additional resistance to heat loss.

As the embryo grows, incubation likely becomes more a matter of regulating the balance between heat gain from the mother and heat loss through radiation from the egg surfaces because the near-term embryo is producing considerable heat itself. The rate of heat loss from the egg is going to depend on many factors, though one of the more important ones may be the surface area-to-volume ratio of the egg. Thus, larger eggs (e.g., emu, ostrich) may have lower capacity for heat loss because of their smaller surface area-to-volume ratio. However, larger embryos may also show conventional metabolic scaling, with lower per gram body mass rates of temperature production than smaller embryos. Furthermore, embryos can utilize behavioral and physiological plasticity to respond to changes in their thermal environment (Du and Shine, 2015). A study that integrates egg size, embryo metabolic rate, and incubation behavior changes during embryonic development is highly warranted.

37.3.4 Energy use

As chicken embryos grow, their mass increases geometrically until growth rate slows during the last stages of development (Romanoff, 1967; Van Mierop and Bertuch, 1967; Tazawa et al., 1971a; Lemez, 1972; Clark et al., 1986; Haque et al., 1996). From the mean values of the above references, the geometrical increase in embryo wet body mass to day 16 of incubation is expressed by;

$$\text{Body mass(mg)} = 0.24 \cdot I^4 \tag{37.5}$$

Of the energy measured as oxygen uptake ($\dot{M}_{O_2}$), the majority is utilized by the embryo to synthesize new tissues for growth and to meet the physiological demands for maintenance during development. In addition, toward the end of incubation, the embryo uses energy for active control of body temperature and hatching. Prior to this, it is assumed that prenatal $\dot{M}_{O_2}$ is used for maintenance, which is proportional to body mass, and for growth, which is proportional to growth rate ($GR = \Delta Body\ mass/time$) as follows (Vleck et al., 1980; Mortola and Cooney, 2008);

$$\dot{M}_{O_2} = a \cdot (Body\ mass) + b \cdot GR \tag{37.6}$$

where coefficients a and b express the daily average cost of maintaining 1 g of tissue (mL O_2/g/day) and the cost of growing it (mL O_2/g), respectively. During days 9−18 of the ~21 day incubation period of chickens, and excluding early development when $\dot{M}_{O_2}$ of small embryos does not reflect total egg $\dot{M}_{O_2}$ because of uptake by extra-embryonic tissues, a and b are estimated as ~15 mL O_2/g/day and ~41 mL O_2/g, respectively (Mortola and Cooney, 2008). Therefore, the cost of growing 1 g of tissue averages ~3 times the cost of maintaining it. In addition, cooling due to low temperature incubation (35°C) only decreases GR with a decrease in the cost of growth, but hypoxic incubation decreases not only GR but also the cost of maintenance. That is, cold incubation decreases GR without altering the partitioning of energy expenditure while hypoxia decreases GR and alters the partitioning of the energy.

Daily energy use increases as the embryo grows and is reflected in an increase in $\dot{M}_{O_2}$. However, precocial and altricial birds show a different developmental pattern in embryonic $\dot{M}_{O_2}$ (e.g., Vleck and Vleck, 1987). In altricial species, $\dot{M}_{O_2}$ increases at an increasing rate throughout incubation, lacking a plateau. In precocial species, the rate of increase in $\dot{M}_{O_2}$ plateaus before the egg is pipped and then increases again after pipping. For a given egg size and incubation period, altricial species use less energy, so have a lower incubation energy cost to hatching than precocial species (Vleck et al., 1980). The high cost of incubation in precocial species is due to their rapid growth early in development, which results in higher maintenance costs,

i.e., there is more tissue to maintain for a longer time (Vleck et al., 1980).

Based on the assumption that both precocial and altricial species have an identical basic pattern of increase in $\dot{M}O_2$, including a plateau phase attributable to the shift of the gas exchange from the chorioallantoic membrane (CAM) to the lungs (Rahn and Ar, 1974), Prinzinger et al. (1995) defines the plateau phase as a clear interruption of the continuous exponential increase in $\dot{M}O_2$. This demonstrates no fundamental difference between both modes with respect to the presence of a plateau (Figure 37.1) (Prinzinger et al., 1995; Prinzinger and Dietz, 1995). They suggest that in small altricial species, the plateau lasts only a few hours and can be overlooked when $\dot{M}O_2$ measurement is not continuous or when many individual measurements are averaged. The extremely precocial mound-building birds (Megapodiidae) are one exception, having no plateau phase as they lack the CAM-pulmonary transition within the egg (Vleck et al., 1984).

Energy use can be reduced under hypoxic incubation conditions (Mortola et al., 2012). However, the timing of exposure is important, with $\dot{M}O_2$ reduced with hypoxia exposure during the middle period of incubation (day 6−12), but not with exposure during early (days 1−6) or late (days 12−18) incubation (Dzialowski et al., 2002).

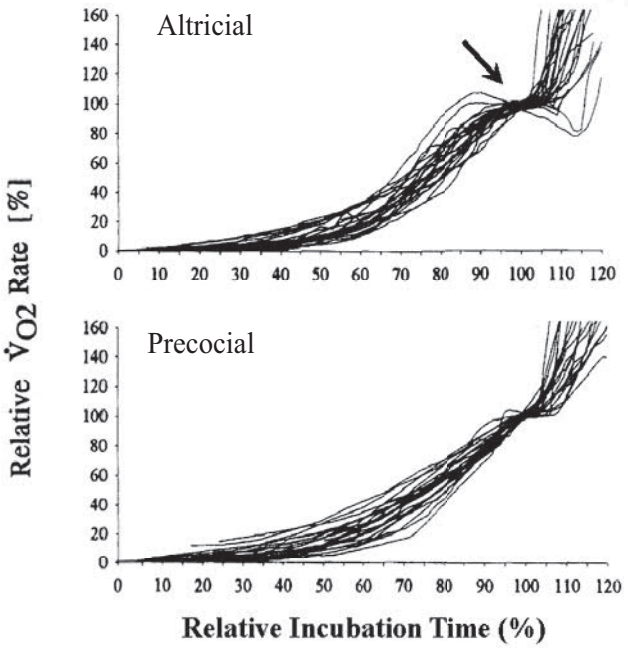

FIGURE 37.1 Developmental patterns of relative oxygen uptake ($\dot{M}O_2$, %) in precocial and semiprecocial species (N = 27) (top) and altricial and semialtricial species (N = 24) (bottom) plotted against relative incubation time (%). *Arrow* indicates the metabolic plateau characteristic of precocial and semiprecocial embryos. *Modified from Prinzinger and Dietz (1995), with permission from Elsevier.*

37.4 Development of physiological systems

37.4.1 Gas exchange

The avian embryo completely enclosed within its hard egg shell has no opportunity for ventilatory movements until the very last phase of incubation. Thus, there is no convective gas exchange per se until the embryo's lungs begin to function upon IP just before hatching. Early in incubation, prior to a formation of the heart and even initially after the forming heart beats, O_2 can be adequately supplied from the environment to the embryo through diffusion. $\dot{M}O_2$ is normally maintained without blood convection, even in chicken embryos whose main vessel from the heart is ligated or hemoglobin (*Hb*) is rendered functionless due to carbon monoxide exposure (Burggren et al., 2000, 2004; Mortola et al., 2010). As gas transport by diffusion alone become inadequate, blood convection begins to meet O_2 demand during development. Three different gas exchangers sequentially function in the egg: the area vasculosa, the chorioallantois, and the lungs. Figure 37.2 shows the growth rate of the functional surface area of the area vasculosa and the chorioallantois (Ackerman and Rahn, 1981) and the associated $\dot{M}O_2$ of the chicken embryo. The area vasculosa is a well-vascularized region of the yolk sac which fans out from the embryo and rapidly grows around the yolk during days three to five of incubation in an increasingly ordered branching manner (Guidolin et al., 2020). The blood vessels of the yolk sac connect with the dorsal aorta of the embryo by day two and blood begins to circulate through the embryo and the area vasculosa. The fine reticulation of the vitelline circulatory system plays the role of the main gas exchanger until the chorioallantois makes contact with the inner shell membrane around day six (Ackerman and Rahn, 1981). Subsequently, respiratory function transitions from the area vasculosa to the chorioallantois.

Beginning on day five of incubation, the mesenchyme covering the fundus of the allantoic sac comes into contact with the mesenchyme lining the chorion. The two membranes begin to fuse and the growing allantoic sac flattens out beneath the chorion, which lies close to the eggshell. The outer limb of the flattened allantois, composed of the cohesive chorion and allantois, is the chorioallantois. The chorioallantois grows rapidly until day 12, when it extends to envelop the contents of the whole egg, lining the entire surface of the inner shell membrane (Figure 37.2). Chorioallantoic growth is moderate between day 13 and 18, and then regresses between day 18 and 20 prior to IP (Makanya et al., 2016). Additional information on the development and growth of the CAM are provided by Nowak-Sliwinska et al. (2014), Ribatti (2017), Tufan and Satiroglu-Tufan (2017), and Burggren and Rojas Antich (2020), often in

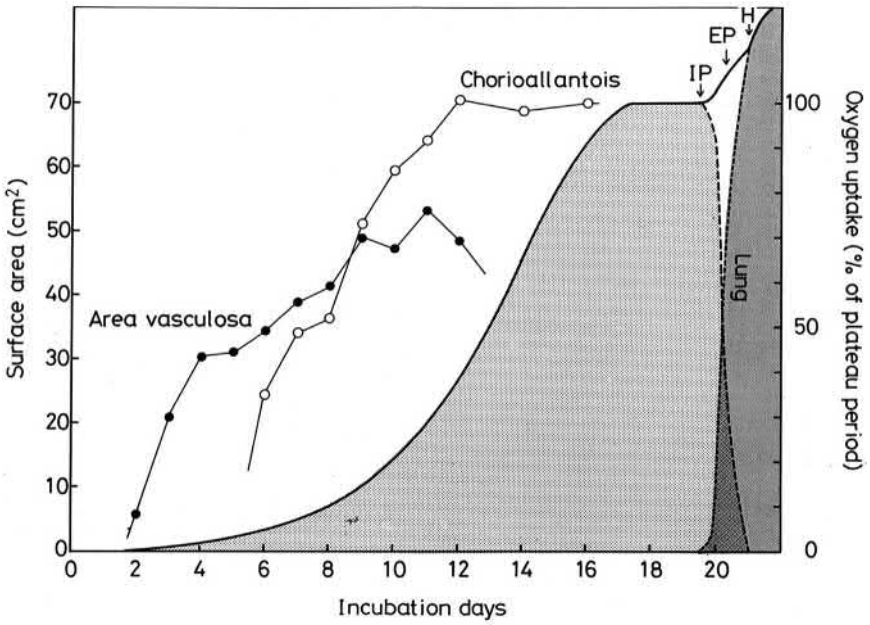

FIGURE 37.2 Daily changes in functional surface area of the area vasculosa and the chorioallantois (left ordinate), and developmental pattern of oxygen uptake ($\dot{M}_{O_2}$) during the prenatal period (until internal pipping, IP) and perinatal period (from IP to hatching, H) (right ordinate). External pipping (EP) occurs during the perinatal period. $\dot{M}_{O_2}$ is drawn diagrammatically with the plateau set at 100%. The lightly shaded area indicates $\dot{M}_{O_2}$ by diffusion through the area vasculosa/chorioallantois and the heavily shaded area $\dot{M}_{O_2}$ by the lungs. *From Ackerman and Rahn (1981) with permission from Elsevier.*

the context of using the CAM as an assay for toxicants or a model for angiogenesis.

The outer surface of the chorioallantois, i.e., CAM, is well vascularized (Wangensteen et al., 1970/71; Tazawa and Ono, 1974; Wangensteen and Weibel, 1982; Ribatti, 2017). Early in incubation, the capillaries lie on the mesenchymal surface of the CAM and vascular growth occurs through the process of "mergent angiogenesis" (Maibier et al., 2016). Capillaries begin to migrate through the ectoderm on day 10 and lie on its thin layer late in incubation. In addition, relocation of the nuclei of the CAM capillaries occurs (Mayer et al., 1995). The endothelial nuclei randomly distribute around the capillary lumen early in incubation and are located progressively on the portion of the capillaries away from the shell membrane after the chorioallantois envelops the whole contents of the egg. Together with capillary migration, the relocation of endothelial nuclei results in progressive thinning of the gas diffusion pathway between the interstices of the inner shell membrane (air space) and the capillary blood. The process of CAM angiogenesis and vascularization is influenced by ambient hypoxia. CAM growth increases under hypoxia to minimize the negative effects of reduced oxygen (Strick et al., 1991; Wagner-Amos and Seymour, 2003; Azzam and Mortola, 2007; Zhang and Burggren, 2012; Druyan and Levi 2012). Yet, various studies have demonstrated an increase, decrease, or no change in CAM vascularization under hypoxia (Burton and Palmer 1992; Wagner-Amos and Seymour, 2002, 2003; Druyan and Levi 2012). Such contradictory results may be due to differential effects caused by the timing, intensity, and duration of hypoxia (Zhang et al., 2017). CAM vasculature is also affected by toxicants such as crude oil (Burggren and Rojas Antich, 2020).

The CAM functions as a gas exchanger during prenatal development (prior to IP) until it degenerates when the embryo pips it and the inner shell membrane with the beak. The increase in $\dot{M}_{O_2}$ of the chicken embryo during the first ~16 days of incubation is enabled by the extension of the CAM (Figure 37.2). The gas exchange of embryos before IP takes place by diffusive transport across the porous shell, two shell membranes, and capillary blood of the CAM (Wangensteen and Rahn, 1970/71; Wangensteen et al., 1970/71; Wangensteen and Weibel, 1982). Then, the chick breaks the shell and breathes environmental air by lung ventilation (EP). As the near-term embryo begins ventilating the lungs, they replace the gas exchange function of the CAM.

When the CAM envelopes all contents of the egg, the gas exchange by diffusive transport is expressed by,

$$\dot{M}_{O_2} = G_{O_2} \cdot (PI_{O_2} - PA_{O_2}) \quad (37.7)$$

$$= D_{O_2} \cdot (PA_{O_2} - P\bar{c}_{O_2}) \quad (37.8)$$

where $\dot{M}_{O_2}$ is oxygen uptake (mL/min), G_{O_2} is oxygen conductance of the shell and shell membrane (mL O_2/min/kPa), D_{O_2} is the diffusing capacity of the CAM and capillary blood (mL O_2/min/kPa), PI_{O_2} is the effective

environmental oxygen partial pressure (kPa); PA_{O_2} is the air space oxygen partial pressure (kPa), and P_{CO_2} is mean capillary oxygen partial pressure (kPa).

G_{O_2} is related to G_{H_2O} by the diffusion coefficient ratio ($d_{O_2}/d_{H_2O} = 0.23/0.27$). G_{O_2} (in mL/min/kPa) is derived from G_{H_2O} (in mg/min/kPa) by multiplying by a factor of 1.06. Because G_{O_2} in air is constant during the prenatal incubation, PA_{O_2} decreases as the embryo grows and consumes more O_2 (Table 37.1). The increased difference of O_2 partial pressure between the environmental air and air space is the driving force that meets the increased O_2 demand of the developing embryo. Concurrently with the decrease in PA_{O_2}, P_{CO_2} also decreases. The O_2 flux from the air space to the *Hb* of capillary blood (inner diffusion barrier) is facilitated by an increase in D_{O_2} which is expressed by:

$$D_{O_2} = 60 \cdot V_c \cdot F\overline{C}_{OX} \cdot Hct \tag{37.9}$$

$$= \dot{Q}_a \cdot t_c \cdot F\overline{C}_{OX} \cdot Hct \tag{37.10}$$

where V_c is capillary volume of the CAM (μL), FC_{OX} is mean corpuscular oxygenation velocity during the contact time (s/kPa), *Hct* is hematocrit, $\dot{Q}_a$ is blood flow through the CAM (mL/min), and t_c is the contact time of erythrocytes with O_2 when they pass through the CAM capillaries (s) (Tazawa et al., 1976; Tazawa and Mochizuki, 1976) (Table 37.1).

D_{O_2} is increased by an increase in V_c, which depends on $\dot{Q}_a$ and t_c; $V_c = (\dot{Q}_a/60) \times t_c$ (Table 37.1). While $\dot{Q}_a$ increases about fivefold from days 10–18, the t_c halves, probably because of shortening of the blood circulation time, as cardiac output increases more rapidly than total blood volume. Consequently, V_c increases even after the CAM spreads over the whole surface of the inner shell membrane on day 12 and reaches a maximum volume on days 14 and 15. Nevertheless, D_{O_2} increases further after day 14. This is largely due to the increase in $\dot{Q}_a$ and *Hct*, as

TABLE 37.1 Gas exchange variables used to determine the diffusing capacity of the inner diffusion barrier (chorioallantoic membrane and capillary blood) in developing chicken embryos.

Age (days)	10	12	14	16	18
Body Mass	2.4	5.2	9.3	16.0	22.9
PA_{O_2}	18.5	17.2	16.3	14.7	14.4
PA_{CO_2}	1.5	2.1	3.3	3.8	4.2
P_aO_2	10.9	10.7	9.9	8.6	7.8
pH_a	7.64	7.62	7.54	7.50	7.48
S_aO_2	87.2	88.2	87.0	88.0	84.5
Pv_{O_2}	4.5	3.7	3.4	2.5	2.4
Pv_{CO_2}	2.5	3.3	4.9	5.4	5.5
S_vO_2	10.4	11.2	17.7	17.3	25.2
O_2 capacity	9.4	10.1	10.5	11.4	12.3
$\dot{M}_{O_2}$	0.08	0.15	0.25	0.36	0.42
Q_a	1.11	1.93	3.42	4.48	5.78
t_c	0.87	0.74	0.57	0.49	0.36
V_c	16.1	23.8	32.5	36.6	34.7
$F\overline{c}_{OX}$	41.9	51.0	60.8	62.3	65.3
Hct	20.5	22.6	27.6	32.8	36.5
D_{O_2}	0.83	1.65	3.27	4.49	4.96

Body mass (g); from Tazawa and Mochizuki (1976), PA_{O_2} (air space P_{O_2}, kPa), PA_{CO_2} (air space P_{CO_2}, kPa), Pv_{O_2} (mixed venous blood P_{O_2}, kPa), Pv_{CO_2} (mixed venous blood P_{CO_2}, kPa); calculated from data in Tazawa (1973) and Wangensteen and Rahn (1970/71). Note: Unit of partial pressure is converted from 'mmHg' in original sources to "kPa" in current text. P_aO_2 (arterialized P_{O_2} in the allantoic vein, kPa); from Tazawa (1973), pH_a (arterialized blood pH corresponding to the allantoic vein); from Tazawa et al. (1971), S_aO_2 (oxygen saturation of arterialized blood, %); calculated by substituting P_aO_2 and pH_a into the modified Hill's equation of the O_2 dissociation curve (Tazawa et al., 1976), S_vO_2 (oxygen saturation of mixed venous blood, %); determined by microphotometer (Tazawa and Mochizuki, 1976), O_2 capacity (vol%); determined from Tazawa (1971) and Tazawa and Mochizuki (1977), $\dot{M}_{O_2}$ (oxygen uptake, mL/min); from Tazawa (1973), Q_a (allantoic blood flow, mL/min); calculated by $\dot{M}_{O_2}/[O_2$ capacity $(S_aO_2 - S_vO_2)]$, t_c (contact time, s); determined by microphotometer (Tazawa and Mochizuki, 1976), V_c (capillary volume, 10^{-3} mL), calculated by $Q_a/60 \times t_c$, $F\overline{c}_{OX}$ (oxygenation velocity factor, s/kPa); from Tazawa et al. (1976), *Hct* (hematocrit, %); from Tazawa et al. (1971a,b), D_{O_2} (diffusing capacity of inner diffusion barrier, mL/min/kPa); calculated by $60 \cdot V_c \, F\overline{c}_{OX} \, Hct$ or $Q_a \, t_c \cdot F\overline{c}_{OX} \cdot Hct$.

both variables increase after the CAM spreads over the inner shell membrane. Toward the end of prenatal development, the increase in D_{O_2} slows down and $\dot{M}_{O_2}$ reaches a plateau. This suggests an important contribution of the inner diffusion barrier to gas exchange, which contributes, along with the outer diffusion barrier (G_{O_2}), to the plateau status of $\dot{M}_{O_2}$. This results in the developmental pattern of $\dot{M}_{O_2}$ paralleling the daily changes in D_{O_2} (Table 37.1).

In chicken eggs, the variability of shell G_{O_2} is large, higher than that of egg mass. Mass-specific $\dot{M}_{O_2}$, measured on days 16–19 of incubation, is maximal at medium G_{O_2}, decreasing at both lower and higher G_{O_2} (Visschedijk et al., 1985). The maximum $\dot{M}_{O_2}$ at medium G_{O_2} values is considered to be optimal for embryo development, and the decrease in $\dot{M}_{O_2}$ at both higher and lower G_{O_2} is a sign of compromised development. When G_{O_2} is decreased by partially covering the shell with impermeable material or increased by partially removing the shell over the air cell at the beginning of incubation, $\dot{M}_{O_2}$ of day 16 embryos increases hyperbolically with increasing G_{O_2}, reaching a maximum at the control G_{O_2} of intact eggs and decreasing with further increase in G_{O_2} (Okuda and Tazawa, 1988). A similar increase in $\dot{M}_{O_2}$ is observed when the shell is removed over the air cell immediately prior to measurement in IP embryos (Ide et al., 2017b), indicative of diffusive limitation of $\dot{M}_{O_2}$ in late embryos. When part of the shell is covered and the other is exposed to hyperoxia, $\dot{M}_{O_2}$ and growth rate do not change, indicating uniform G_{O_2}, and therefore uniform chorioallantoic perfusion, is not required to maintain $\dot{M}_{O_2}$ (Wagner-Amos and Seymour, 2002).

Because the oxygen diffusion coefficient (d_{O_2}) affects shell conductance, G_{O_2} can be changed by replacing N_2 in air with an inert background gas whose density is different from that of N_2 (e.g., He or SF_6), thus changing d_{O_2} (Erasmus and Rahn, 1976; Ar et al., 1980; Tazawa, 1981a; Tazawa et al., 1981). Accordingly, the gas exchange of the egg can be manipulated by changing G_{O_2} with He or SF_6. The d_{O_2} is also inversely related to atmospheric pressure (P_B) and thus gas exchange of the egg is increased at high altitude because the shell G_{O_2} increases inversely with P_B. The reduction of G_{O_2} in eggs laid by birds incubating at high altitude occurs as a natural adaptation to altitude (Rahn et al., 1977; Hempleman et al., 1992).

As incubation proceeds, diffusive gas exchange governed by G_{O_2} and D_{O_2} is gradually replaced by convective gas exchange through the lungs during the perinatal period, beginning at IP (Figure 37.2). Breathing movements of perinatal embryos can be recorded as pressure changes using an optical system or pressure transducer (Romijn, 1948; Vince and Salter, 1967; Dawes, 1976). Conveniently, prenatal cardiac rhythms at the onset of IP and EP and the subsequent development of respiratory rhythms until hatching can be recorded by continuous measurements of cardiogenic, ventilatory, and hatching activities in chickens

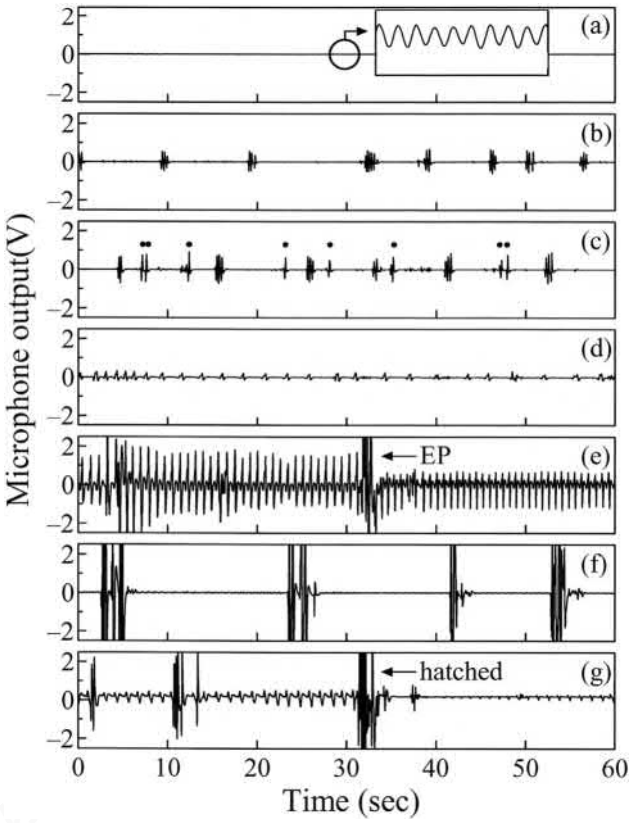

FIGURE 37.3 The cardiogenic and breathing activities of a chicken embryo from the prenatal through perinatal period to hatching, recorded by a condenser microphone attached hermetically on the shell. A 60 s recording is shown in each panel. (A) Cardiogenic signal (acousto-cardiogram, ACG) during the final stages of the prenatal period; ACG is evident in the enlarged inset. (B) Beak-clapping signals just prior to IP. (C) Onset of breathing signals occurring as single, irregular deflections (approximately once per 5 s) among beak clapping after IP (acousto-respirogram, ARG). (D) Rhythms become fast and somewhat irregular. (E) Breathing signals are more regular before and after EP. The onset of EP is evident by a sudden decrease in magnitude of ARG. (F) Approximately 1 h prior to hatching, large deflections due to hatching activities (e.g., climax) begin to occur and the breathing becomes intermittent. (G) The hatching activities continue before breathing regulates and finally the embryo hatches. Breathing signals are recorded after hatching because the microphone is located close to the beak of hatchling. *From Chiba et al. (2002), with permission from Elsevier.*

by means of a condenser-microphone measuring system (Figure 37.3) (Chiba et al., 2002; Bamelis et al., 2005). Using the breathing patterns of chickens from the onset of IP through EP to hatching, the length of the IP, EP, and whole perinatal periods are determined as 14.1 ± 2.0 (SEM) h, 13.6 ± 1.3 h and 27.6 ± 1.7 h long, respectively. The duration of the actual hatching event is 48 ± 6 min. The instantaneous respiratory rate (IRR in breaths/min) is approximately 10–15 breaths/min at the beginning of IP. IRR baseline increases up to 80–100 breaths/min with large fluctuations of IRR of 60–180 breaths/min after the onset of EP.

Pulmonary ventilation and gas exchange during the perinatal period has been quantified using a barometric plethysmograph or pneumotachograph (Pettit and Whittow, 1982a; Menna and Mortola, 2003; Sbong and Dzialowski, 2007; Szdzuy and Mortola, 2007; Ide et al., 2017a) and by measurement of gases in air cell and allantoic blood (Pettit and Whittow, 1982b; Tazawa et al., 1983b). The embryonic development of pulmonary ventilation and its regulation has been investigated and reviewed elsewhere (Mortola, 2009; Ide et al., 2017a; Whitaker-Fornek et al., 2019).

37.4.2 Acid-base regulation

Acid-base regulation in adult animals is achieved through a combination of rapidly acting molecular/biochemical changes, intermediately acting ventilatory effects, and slowly acting renal adjustments. The developmental onset and progression of these in vertebrates, including the avian embryo, has been reviewed recently (Burggren and Bautista, 2019). As the avian embryo consumes O_2, it produces CO_2, which is partially dissolved and stored in the blood and body fluids, but mostly eliminated through the eggshell. As with O_2, CO_2 elimination ($\dot{M}CO_2$) depends upon the eggshell CO_2 conductance (GCO_2) and CO_2 partial pressure difference between air cell ($PACO_2$) and atmosphere ($PICO_2$):

$$\dot{M}CO_2 = GCO_2 \cdot (PACO_2 - PICO_2) \qquad (37.11)$$

GCO_2 is a function of eggshell geometry (A_p and L), CO_2 diffusion coefficient (dCO_2), and the inverse product of R and T. $PICO_2$ is very close to zero when the egg is in air.

As embryos develop and their body mass increases, they produce more CO_2 which accumulates in the egg. $PACO_2$ increases, thus increasing arterialized blood PCO_2, P_aCO_2 (Meuer and Tietke, 1990). Consequently, arterialized blood pH is lowered (Figure 37.4) or stays relatively constant in the allantoic vein during the last half of prenatal development (Dawes and Simkiss, 1969; Girard, 1971; Erasmus et al., 1970/71; Boutilier et al., 1977; Everaert et al., 2011). The rate of decrease in pH during embryonic development slows, however, late in incubation. Although the plasma bicarbonate concentration ($[HCO_3^-]$) increases with development, the increase is more than would be expected from changes in pH and the buffer value (−16 mmol/L, Burggren et al., 2012). The pH change due to CO_2 accumulation is mitigated by an increase in non-respiratory HCO_3^- (Figure 37.4) (Tazawa, 1986, 1987). *Hb*, which serves as the noncarbonate buffer in blood, increases during the last half of incubation, and thus is partly responsible for the mitigated change in pH. Reflecting the developmental increase in *Hct* and *[Hb]*, the buffer value increases from ∼ −8 to −10 mmol/L on days 9−10 to ∼ −17 mmol/L on days 15−18 (Erasmus et al., 1970/1971; Tazawa and Piiper, 1984). In day 16 embryos, values ranging from −12.7 to −15 mmol/L are reported (Tazawa et al., 1981; Tazawa, 1980a, 1981b, 1982, 1986). Other studies have not found an increase in buffer value during development (Tazawa et al., 1983a; Andrewartha et al., 2011b; Burggren et al., 2012). The determination of the buffer value is a controversial issue, and clearly not all sources of variation have been identified. However, the value of −16 mmol/L reported by Burggren et al. (2012) is depicted in a pH-$[HCO_3^-]$ diagram (Davenport diagram, Figure 37.4) to show and estimate respiratory changes in acid-base balance.

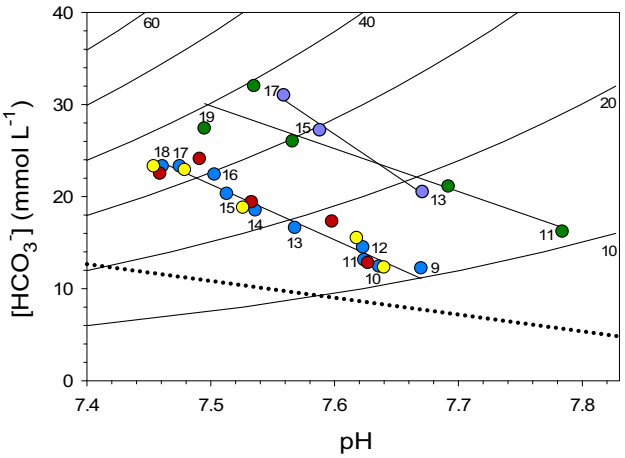

FIGURE 37.4 A Davenport diagram illustrating the daily changes in control acid-base balance of arterialized blood in chicken embryos developing in air. The dashed diagonal line is an arbitrary buffer line with the determined slope of −16 mmol/L/pH unit. Numbered curves are PCO_2 isopleths in mmHg. The numbers near the data points represent the ages of the embryos. Data are collected from the following studies; *blue circles*: Tazawa et al. (1971a), *red circles*: Tazawa et al. (1971b), *green circles*: Tazawa (1973), *purple circles*: Burggren et al. (2012), *yellow circles*: Tazawa et al. (2012). The *solid line* drawn through the data points corresponds to the following regression equation; (1) $[HCO_3^-] = -60.2$ pH + 472.6 for combined data from Tazawa et al. (1971a, 1971b) and Tazawa (1973), (2) $[HCO_3^-] = -90.9$ pH + 717.4 from Burggren et al. (2012), and (3) $[HCO_3^-] = -46.6$ pH + 379.1 from Tazawa et al. (2012).

Responses in acid-base balance to 1 day exposure to altered environmental gas mixtures differ depending on the gas mixture, age of embryos, and chicken strain (Burggren et al., 2012, 2015; Mueller et al., 2014b, 2017). One day of hypercapnic exposure (5% CO_2, 20% O_2) increases P_aCO_2 and decreases pH_a, producing respiratory acidosis that is partially (∼50%) compensated by metabolic alkalosis at all embryonic stages examined (days 13, 15, and 17). Similar patterns of partially compensated respiratory acidosis have been reported in embryos exposed to up to 10% CO_2 in air, with compensation proportional to CO_2 concentration (Dawes and Simkiss, 1969; Mueller et al., 2014b, 2017; Burggren et al., 2015). At 20% CO_2, metabolic compensation no longer increases with CO_2 concentration as observed at CO_2 levels below 10% CO_2 suggesting there is

a hypercapnic threshold for acid-base regulation >10% CO_2 (Burggren et al., 2015). Furthermore, one day of exposure to hypercapnic hypoxia (5% CO_2, 15% O_2) abolishes compensatory metabolic alkalosis in day 15 and day 17 embryos, but a metabolic compensation of ~37% still occurs in day 13 embryos. This suggests that a relatively high O_2 level is required for metabolic compensation to occur (Mueller et al., 2017). The lower $\dot{M}O_2$ and an overall higher allantoic P_aO_2 in air (Tazawa, 1971, 1980a; Tazawa et al., 1971a, b) in day 13 embryos compared with more advanced embryos preserves the metabolic compensation during hypoxia. One day of hypoxic exposure (15% O_2) creates a metabolic acidosis in day 15 and day 17 embryos, but not in day 13 embryos. Hypoxia produces hypometabolism without anaerobic energy compensation (Bjønnes et al., 1987; Mortola and Besterman, 2007; Ide et al., 2016; Haron et al., 2017). However, once a lower threshold $\dot{M}O_2$ is reached, embryos turn to anaerobic glycolysis and blood lactate concentration ($[La^-]$) increases (Grabowski, 1961, 1966; Bjønnes et al., 1987). Therefore, embryos exposed to severe hypoxia (e.g., 10% O_2) encounter metabolic acidosis caused by glycolysis (Tazawa et al., 2012). However, metabolic acidosis occurring in moderate hypoxia is attributed only slightly to glycolysis and other unverified mechanisms, such as O_2 level influencing HCO_3^- transfer across the CAM. One day exposure to hyperoxia (40% O_2) causes respiratory acidosis that varies with embryonic age. Hyperoxia causes hypermetabolism (and a consequent increase in $\dot{M}CO_2$) (Visschedijk et al., 1980; Høiby et al., 1983; Stock et al., 1985; Tazawa et al., 1992b). Increased CO_2 is accumulated in the blood and hydrated to create H^+ and HCO_3^-. Coupled with a fixed eggshell gas GCO_2, this results in respiratory acidosis. Age-specific differences in the magnitude of respiratory acidosis are due to hyperoxia causing a greater hypermetabolism in advanced embryos (Stock et al., 1985; Tazawa et al., 1992b).

Because eggshell GCO_2 is governed by dCO_2, respiratory acidosis also occurs in embryos exposed to a SF_6/O_2 gas mixture, which reduces GCO_2. Inversely, respiratory alkalosis occurs in embryos exposed to a He/O_2 atmosphere, which increases GCO_2 (Tazawa et al., 1981). Partially covering the eggshell with a gas impermeable material or by immersion in water produces respiratory acidosis while opening the eggshell over the air cell produces respiratory alkalosis (Tazawa, 1981a; Andrewartha et al., 2014). These respiratory disturbances to the acid-base balance occur rapidly and blood P_aCO_2 reaches a plateau ~10 min after changing GCO_2 (Tazawa, 1981a). Concurrently, blood pH changes to the value predicted by buffer capacity during the following 30–60 min (i.e., noncompensated respiratory acidosis/alkalosis) with a subsequent (2–6 h), but incomplete, change toward the control level, while P_aCO_2 is maintained at a constant value. Once partial metabolic compensation is achieved at ~4–6 h, the state of acid-base disturbance remains constant over the next 24 h in normoxia or hyperoxia (e.g., 5% CO_2/20% O_2 or 5% CO_2/40% O_2), but metabolic compensation is not preserved after 24 h in hypoxia (5% CO_2/15% O_2) (Mueller et al., 2013b, 2017). Therefore, preservation of metabolic compensation requires an O_2 concentration above 20%.

While partial metabolic compensation in response to hypercapnia or moderate hypoxia with hypercapnia (e.g., 15% O_2/5% CO_2) proceeds over the course of several hours in day 15 embryos, responses to severe hypoxia (10% O_2), with or without CO_2 (e.g., 5%), progress more quickly (Figure 37.5) (Tazawa et al., 2012). This is due to anaerobic glycolysis and the attendant rapid increase in $[La^-]$ that creates severe metabolic acidosis. If hypoxic embryos can preserve $[HCO_3^-]$ above ~10 mmol/L (in the case of day 15 embryos), which is generally reached beyond 2 h, embryos can survive and recover to the control state of acid-base balance in ~2 h after being returned in air (Figure 37.5) (Tazawa et al., 2012). Accordingly, hypoxia-induced acid-base disturbances are only transient and may not affect long-term survival.

Natural variations in eggshell conductance cause large differences in P_aCO_2 among eggs, but blood pH variations are minimal (Tazawa et al., 1983a). In eggs with low GCO_2, the *Hct* (and thus *Hb*) increases. In part, increased [*Hb*] may be responsible for the minimum change in pH.

The acid-base balance of chicken embryos also reacts promptly to metabolic disturbances, as shown by the time course changes in metabolic acid-base alterations created by infusion of electrolyte solution ($NaHCO_3$ and NH_4Cl) (Tazawa, 1982). For instance, the infusion of 15 μL 1 M

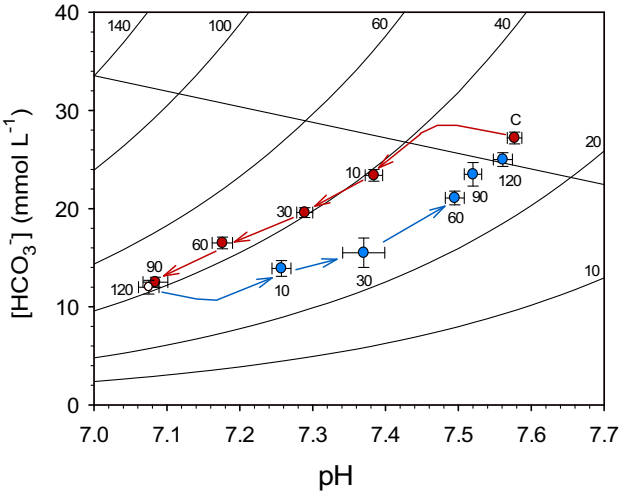

FIGURE 37.5 Time-course of acid-base disturbance in day 15 chicken embryos exposed to hypercapnic hypoxia (5% CO_2, 10% O_2) for 120 min (*red circles*) with recovery in air for 120 min (*blue circles*). Other details as in Figure 37.4. *Modified from Tazawa et al. (2012) with permission from Elsevier.*

$NaHCO_3$ increases plasma [HCO_3^-] and blood P_{CO_2}. Because the embryo has no convective ventilation, the metabolic disturbance is not subjected to respiratory compensation. The increase in P_{CO_2} 1 h after infusion indicates that the infused HCO_3^- is partly eliminated as dissolved CO_2. The acid-base status returns to control values 6 h after infusion. Besides elimination of CO_2 from the CAM, the increased fluid volume and hypertonicity of the infused $NaHCO_3$ solution may be partially responsible for the decrease in [HCO_3^-]. Additionally, penetration of HCO_3^- into the intracellular space and excretion of HCO_3^- into allantoic fluid through the CAM may contribute to the regulation (Tazawa, 1982, 1986).

In summary, acid-base regulation develops in concert with the increased CO_2 production as avian embryos grow. The ability of chicken embryos to tolerate and respond to acid-base disturbance, induced by environmental gas challenges, increases or decreases in G_{CO_2} or infusion of electrolytes, increases with development. By approximately two thirds of incubation, the chick embryo is able to mount at least partial compensatory responses to acidosis. Comparative approaches are required to examine species differences in acid-base regulation, and how tolerance to perturbations may be related to the incubation environment.

37.4.3 Cardiovascular system

37.4.3.1 Basic cardiovascular parameters

The primordial bird embryo's heart is a paired tubular structure that soon becomes a single tube. The heart begins to elongate more rapidly than the pericardial cavity containing it, and this space limitation forces the tubular heart to bend, contributing to the start of cardiac looping (Männer, 2000, 2006; Al Naieb et al., 2013). Molecular and cellular mechanisms underlying cardiac development in chicken embryos have been reviewed by Wittig and Münsterberg (2016). The impact of blood streams upon the inner surface of the contorted tube forms the external configuration and internal structure of the heart (Taber, 2001; Alford and Taber, 2003; Tobita et al., 2005) as well as contributing to blood vessel formation (le Noble et al., 2008; Burggren, 2013; Branum et al., 2013). However, the specific role of pressure and flow fluctuations to the contribution of normal and abnormal development of the heart and blood vessels remains somewhat enigmatic (Branum et al., 2013; Midgett et al., 2014, 2017).

The structural alterations that separate atrium from ventricle, ventricle from aorta, and the left from the right chambers take place during days three−eight of incubation, resulting in a four-chambered heart by days eight−nine (Pattern, 1951; Burggren and Keller, 1997; Al Naieb et al., 2013). The mass of the heart increases as a power function of incubation day (I) (Romanoff, 1967; Clark et al., 1986):

$$\text{Heart mass } (\mu g) = 12.62 \cdot I^{3.26} \qquad (37.12)$$

The growth of the heart relative to the whole body is greatest early in development and declines during incubation. The ratio of the heart mass to the whole-body mass falls from 1.8% on day 4 to 0.7% on day 18 of incubation.

The heart begins to beat at about 30 h of incubation and blood begins to circulate after about 40 h, when the connections between the dorsal aorta and the vessels of the yolk sac complete the circulation (Pattern, 1951). Despite the early generation of heartbeat and blood flow, heart rate is not initially required for convective blood flow to the tissues, but likely plays a role in angiogenesis (Burggren et al., 2000, 2004; Burggren, 2004, 2013; Branum et al., 2013).

Blood volume increases with incubation day (Figure 37.6B) (Yosphe-Purer et al., 1953; Barnes and Jensen, 1959; Lemez, 1972; Kind, 1975) and can be approximated by the following function (Tazawa and Hou, 1997):

$$\text{Blood volume } (\mu L) = 1.85 \cdot I^{2.64} \qquad (37.13)$$

The increase in blood volume during development is not as rapid as growth rate (Figure 37.6A), and therefore embryo mass-specific blood volume decreases during development from about 1 mL/g on day 4 to 0.15 mL/g on day 18.

As both the heart mass and blood volume increase, the stroke volume of the heart increases (Hughes, 1949; Faber et al., 1974; Hu and Clark, 1989; Phelan et al., 1995). During early development, prior to the left and right separation of the heart, stroke volume depends on blood volume and increases in parallel with embryonic growth (Faber et al., 1974). The relationship between stroke volume and incubation day (I, days 2−6) (Hu and Clark, 1989) can be described as:

$$\text{Stroke volume } (\mu L) = 0.002 \cdot I^{3.46} \qquad (37.14)$$

Even after the second week of incubation, stroke volume appears to increase as a power function of incubation day (Figure 37.6C) (Hughes, 1949).

For early embryos, the dorsal aortic blood flow increases as a power function of incubation day during days 2−6 (Hu and Clark, 1989). The mass (embryo)-specific value is 0.5−1 mL/min/g. The mass-specific cardiac output of days three−five embryos, determined from the stroke volume, is similar at 1 mL/min/g (Faber et al., 1974). Cardiac output calculated from the stroke volume of young embryos and that of day 16 chicken embryos estimated by model analysis and blood O_2 measurement (White, 1974; Rahn et al., 1985; Tazawa and Johansen, 1987) indicate that the mass-specific cardiac output of young/late embryos is in the narrow range of 0.5−1.5 mLmin/g. Thus, cardiac output appears to increase as a power function of incubation day (Figure 37.6D). Eventually, cardiac output may increase almost in parallel with embryonic growth. If it is assumed that the mass-specific cardiac output during the

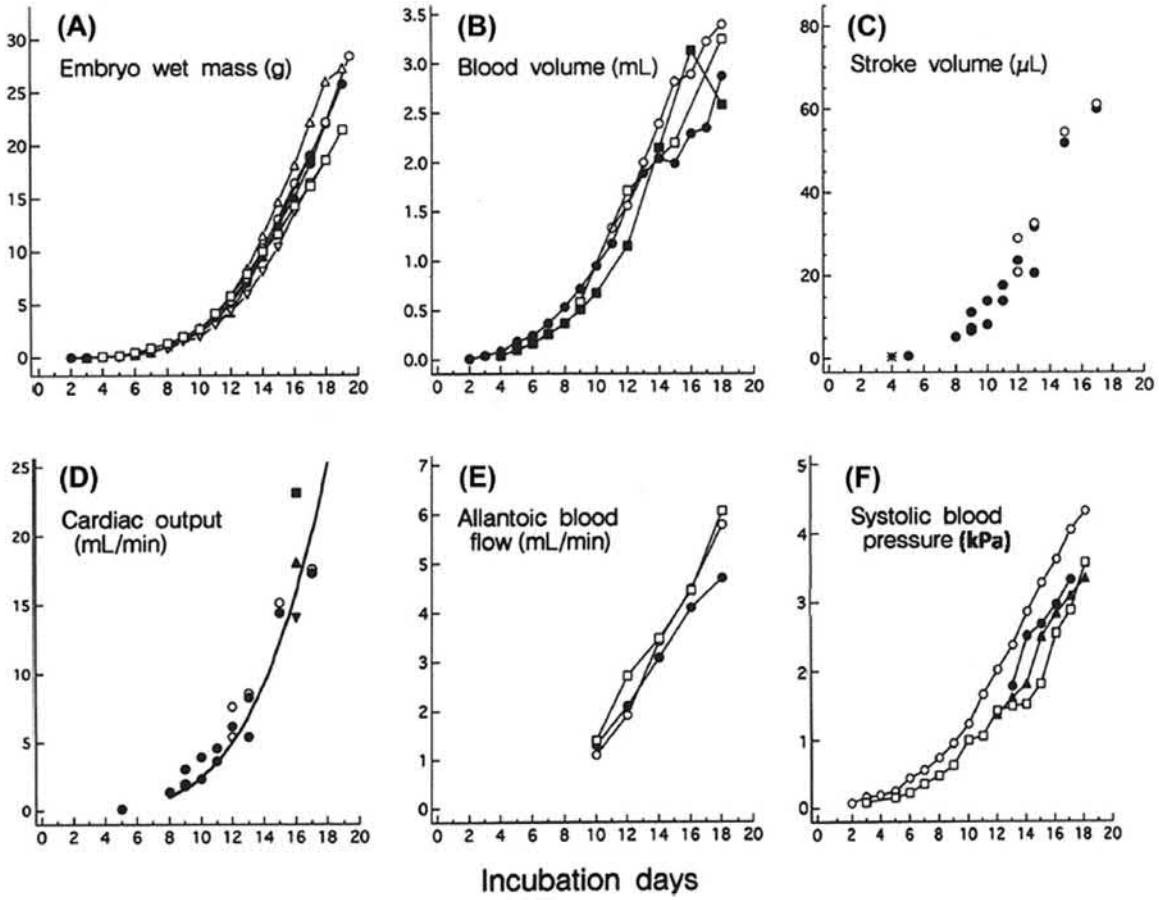

FIGURE 37.6 Developmental patterns of embryo wet mass (A), total blood volume (B), cardiac stroke volume (C), cardiac output (D), allantoic blood flow (E), and arterial systolic blood pressure (F) during the prenatal stage of chickens. Symbols connected by *solid lines* in (A, B, E, and F) indicate the developmental patterns from the papers cited in the text.

last 2 weeks of prenatal development is 1 mL/min/g, the cardiac output of young embryos is related to incubation day (I) as follows,

$$\text{Cardiac output } (\mu\text{L/min}) = 0.24 \cdot I^4 \qquad (37.15)$$

which is the same expression as that relating body mass of developing embryos to incubation day (Eq. 37.5, Figure 37.6A and D).

Blood flow through the CAM, determined from $\dot{M}_{O_2}$, blood gas analysis or via flow probe (Tazawa and Mochizuki, 1976, 1977; Bissonnette and Metcalfe, 1978; Van Golde et al., 1997), increases with embryonic growth (Figure 37.6E), but the mass-specific value decreases from ~0.5 mL/min/g on day 10 to ~0.25 mL/min/g on day 18. Although cardiac output increases in parallel with embryonic growth, its partition to the CAM decreases as the embryo grows. On days 10–13 about half of the cardiac output goes to the CAM and this decreases to ~40% on days 17–19 (Mulder et al., 1997; Dzialowski et al., 2011 for review) or to ~17–20% on days 16–18 (Tazawa and Johansen, 1987). Consequently, the percentage of cardiac output to the organs and tissues increases as development proceeds.

Arterial pressure (P_a) has been measured through several approaches. The easy access to vitelline through the shell of allows blood pressure measurement via a vitelline vessel in early embryonic chick development and an allantoic artery thereafter. Technologies that maintain normal gas exchange through the shell as blood pressure is measured have included micropipettes (Van Mierop and Bertuch, 1967; Girard, 1973), polyethylene catheters with our without needle tips (Tazawa, 1981c; Tazawa and Nakagawa, 1985) and, more recently, pressure volume catheters (Jonker et al., 2015). Arterial systolic pressure (P_{sys}), or, increases with incubation day (I) in the following manner (Figure 37.6F);

$$P_{sys}(\text{kPa}) = 0.015 \cdot I^{1.86} \qquad (37.16)$$

P_a of the vitelline artery is pulsatile by day two of chicken incubation (Van Mierop and Bertuch, 1967; Hu and Clark, 1989; Taber, 2001). While the presence of a dicrotic notch is reported in early embryos (Hu and Clark, 1989;

Yoshigi et al., 1996), a clear dicrotic notch is absent from allantoic P_a waves determined by others (Van Mierop and Bertuch, 1967; Tazawa and Nakagawa, 1985). However, the configuration of the P_a tracings and the ventricular pressure waves suggest that an arterial valve mechanism is present in early embryos which lack true cardiac valves (Van Mierop and Vertuch, 1967; Faber, 1968).

Investigations of chick embryo ventricular function, ventricular and vascular biomechanics, and hemodynamic and morphogenesis relationships, particularly in early (day two–four of incubation) development, are reviewed by Keller et al. (2020).

37.4.3.2 Mean heart rate

According to the equations expressing the relationship between incubation day and body mass (Eq. 37.5) or cardiac output (Eq. 37.15), both body mass and cardiac output in day 16 chicken embryos are ~16 g and ~16 mL/min. Assuming a mean heart rate (MHR) of 280 beat per min (bpm), the stroke volume and mass-specific stroke volume can be estimated to be ~60 μL and ~4 μL/g. The cardiac contraction generating this amount of stroke volume physically moves the body of the embryo by an almost imperceptible amount. These movements are transferred to the whole egg, producing cardiogenic ballistic movement of the egg—referred to as a "ballistocardiogram (BCG)" of the egg (Tazawa et al., 1989b). The egg movement determined by a laser displacement meter is ~1 μm (Sakamoto et al., 1995). The BCG measured by various means offers a convenient way to noninvasively determine MHR of avian embryos (Tazawa et al., 1999; Tazawa, 2005). Additionally, the heartbeat of the embryo inside the eggshell produces not only the ballistic movements of the egg but also acoustic pressure changes outside the eggshell. A conventional condenser microphone hermetically fixed on the eggshell detects the cardiogenic acoustic pressure changes, designated as an acoustocardiogram (Rahn et al., 1990), which can conveniently determine MHR of avian embryos. Use of near infrared sensing technologies provide additional methods for noninvasively measuring cardiac rhythms both in the laboratory and in the field (Lemus et al., 2009; Braune et al., 2012; Sheldon et al., 2018; Khaliduzzaman et al., 2019a,b). However, methods using infrared light have been criticized when used in small avian or reptilian eggs because the IR potentially heats up the egg shell and thus artificially increases heart rate (Sartori et al., 2015). Moreover, they may stimulate embryo movement and thus potentially interfere with detection of an accurate heart signal (Pollard et al., 2016). Most recently, a method based on photoplethysmography using a smart phone has been advanced (Phuphanin et al., 2019).

In contrast to developmental patterns of the circulatory variables that increase steadily with embryonic growth, the embryonic MHR of chickens increases rapidly after the heart commences beating and then becomes asymptotic until early in the second week of incubation (Cain et al., 1967; Van Mierop and Bertuch, 1967; Girard, 1973; Hu and Clark, 1989; Tazawa et al., 1991a; Burggren and Warburton, 1994; Howe et al., 1995). During the last half of incubation in the chicken embryo, the daily change in MHR is small with a temporal increase at 60–70% of incubation followed by a decrease toward IP and increase during hatching (Laughlin et al., 1976; Tazawa et al., 1991a). The change in MHR near the end of development in other precocial birds is shown in Table 37.2. Precocial species, from the smallest (king quail, *Coturnix chinensis*) to the largest (ostrich), show either a plateau or decrease in MHR prior to IP (Tazawa et al., 1991a, 1998a, 1998b, 2000; Pearson et al., 1998; Kato et al., 2002).

In comparison, HR increases rapidly toward hatching in small altricial embryos (Table 37.3) (Tazawa et al., 1994; Pearson et al., 1999). However, the increase in MHR during pre-pipping development slows in larger altricial eggs, e.g., MHR of crow (*Corvus corone*) and cattle egret (*Bubulcus ibis*) tends to remain unchanged during the last half of prenatal period (Pearson and Tazawa, 1999; Tazawa et al., 2001b). The trend for MHR to remain unchanged during the end of prenatal development also occurs in semiprecocial seabirds, e.g., the brown noddy (*Anous stolidus*) and laysan albatross (*Phoebastria immutabilis*) (Table 37.2) (Tazawa et al., 1991b; Tazawa and Whittow, 1994; Pearson et al., 2000). Hence, the pattern of change in MHR during development, particularly at the end of incubation, can be somewhat predicted by the degree of development at hatching. Precocial species tend to show a plateau or decrease in MHR near hatching, while MHR tends to increase in altricial species.

These determinations of embryonic MHR along with egg mass of various species (Tables 37.2 and 37.3) reveal a significant relationship between MHR at 80% of I and egg mass (Tazawa et al., 2001b). The allometric relationship derived for 20 species of altricial and semialtricial birds with egg mass ranging from 0.96 g of the zebra finch to ~41 g of the lanner falcon (*Falco biarmicus*) is:

$$\text{MHR at 80\% of } I = 371 \cdot (\text{Egg mass})^{-0.121} \quad (r = -0.846,\ P < 0.001) \tag{37.17}$$

The relationship for 13 species of precocial and semiprecocial birds with egg mass ranging from 6 g of the king quail to ~1400 g of the ostrich is:

$$\text{MHR at 80\% of } I = 433 \cdot (\text{Egg mass})^{-0.121} \quad (r = -0.963,\ P < 0.001) \tag{37.18}$$

The slopes for MHR are parallel, but MHR of semialtricial embryos is low compared to semiprecocial embryos from the same egg mass. In semialtricial embryos,

TABLE 37.2 Egg mass (g), incubation period (*I*, days), heart rate (HR, beats/min) at 80% of incubation and maximum heart rate (max HR) during prenatal development in precocial birds and heart rate prior to internal pipping (Pre-IP) and at the first star fracture of the eggshell in semiprecocial birds.

	Species	Egg mass (g)	Incubation period (*I*, days)	HR at 80% of *I* (beats/min)	Max HR (beats/min)
Precocial	[a]King quail *Coturnix chinensis*	6.0 ± 0.4	16	341 ± 8 (81%)	341 ± 8 (81%)
	[b]Japanese quail *Coturnix coturnix japonica*	10.7 ± 0.7	17	319 ± 8 (76%)	326 ± 7 (76%)
	[b]Chicken *Gallus gallus domesticus*	64.9 ± 2.5	21	287 ± 9 (81%)	287 ± 9 (81%)
	[b]Duck *Anas platyrhynchos domestica*	79.0 ± 2.5	28	247 ± 15 (82%)	258 ± 11 (61%)
	[b]Turkey *Meleagris gallopavo*	82.9 ± 2.6	28	246 ± 10 (79%)	248 ± 10 (75%)
	[b]Peafowl *Pavo cristatus*	111.3 ± 9.3	28	262 ± 12 (79%)	267 ± 9 (86%)
	[b]Goose *Anser cygnoides*	158.3 ± 11.3	30	224 ± 8 (80%)	248 ± 10 (60%)
	[c]Emu *Dromaius novaehollandiae*	634 ± 9	50	192 ± 7 (80%)	199 ± 11 (72%)
	[d]Ostrich *Struthio camelus*	1395 ± 199	42	185 ± 12 (81%)	208 ± 9 (55%)
				Pre-IP HR (beats/min)	HR at first star fracture of shell (beats/min)
Semiprecocial	[b]Brown noddy *Anous stolidus*	37.9 ± 2.2	35	298 ± 7	303 ± 13
	[e]Wedge-tailed shearwater *Puffinus pacificus*	57.2 ± 2.3	52	244 ± 10	252 ± 11
	[e]Laysan albatross *Diomedea immutabilis*	288 ± 18	65	232 ± 15	233 ± 15

Data are mean ± S.D. Values were measured at 38°C or converted to that at 38°C using (Eq. 37.2 in paper). For precocial species: if HR was not measured at 80% of *I*, the value closest to 80% of *I* was used with the % of *I* at which HR was measured shown in parentheses. The % of *I* of max HR is shown in parentheses.
Data sources:
[a]*Pearson et al. (1998)*;
[b]*Tazawa et al. (1991a)*;
[c]*Tazawa et al., (2000)*;
[d]*Tazawa et al. (1998a)*;
[e]*Tazawa and Whittow (1994)*.
Modified from Tables 37.1 and 37.2 in Tazawa et al. (2001b).

TABLE 37.3 Egg mass (g), incubation period (*I*, days), heart rate (HR, beats/min) at 80% of incubation and during internal pipping and external pipping in altricial and semialtricial birds.

Species	Egg mass (g)	Incubation period (*I*, days)	HR at 80% of *I* (beats/min)	HR during IP (beats/min)	HR during EP (beats/min)
[a]Zebra finch *Taeniopygia guttata*	0.96 ± 0.13	14	335 ± 10	376 ± 20	405 ± 12
[a]Bengalese finch *Lonchura striata* var. *domestica*	1.10 ± 0.12	15	404 ± 36	409 ± 25	448 ± 35
[a]Marsh tit *Parus palustris*	1.39 ± 0.04	14	363 ± 17	409 ± 19	–
[b]Bank swallow *Riparia riparia*	1.42 ± 0.10	14	298 ± 12	–	352 ± 16
[a]Great tit *Parus varius*	1.59 ± 0.14	14	348 ± 11	432 ± 13	495 ± 14
[a]Varied tit *Parus varius*	1.69 ± 0.01	14	356 ± 7	434 ± 11	–
[a]Tree sparrow *Passer montanus*	2.09 ± 0.07	12	335 ± 13	411 ± 32	–
[a]Budgerigar *Melopsittacus undulates*	2.19 ± 0.19	18	314 ± 14	339 ± 15	364 ± 12
[a]House martin *Delichon urbica*	2.25 ± 0.04	15	357 ± 7	369 ± 8	367 ± 11
[a]Japanese bunting *Emberiza spodocephala*	2.56 ± 0.09	13	370 ± 5	426 ± 1	–
[a]Red-cheeked starling *Sturnus philippensis*	4.14 ± 0.01	14	358 ± 1	409 ± 5	–
[a]Cockatiel *Nymphicus hollandicus*	5.08 ± 0.18	20	300 ± 8	318 ± 25	344 ± 19
[a]Brown-eared bulbul *Hypsipetes amaurotis*	6.4 ± 0.5	16	333 ± 7	402 ± 8	–
[b]Domestic pigeon *Columba domestica*	17.1 ± 1.0	18	247 ± 17	–	276 ± 13
[b]Fantail pigeon *Columba domestica*	19.7 ± 2.4	18	267 ± 10	–	293 ± 6
[b]Homing pigeon *Columba domestica*	19.8 ± 1.2	18	230 ± 16	–	273 ± 4
[c]Crow *Corvus corone*	20.5 ± 2.2	20	297 ± 11	348 ± 35	366 ± 22
[d]Barn owl *Tyto alba*	20.1 ± 0.6	30	219 ± 11	–	276 ± 13
[d]Cattle egret *Bubulcus ibis*	27.5 ± 3.3	23	251 ± 8	–	283 ± 12
[d]Lanner falcon *Falco biarmicus*	41.2 ± 0.4	33	242 ± 9	–	276 ± 6

Data are mean ± S.D. Values were measured at 38°C or converted to that at 38°C using $HR(38°C) = HR(T°C)e^{[0.0639(38-T)]}$.
Data sources:
[a]*Pearson et al. (1999)*;
[b]*Tazawa et al. (1994)*;
[c]*Pearson and Tazawa (1999)*;
[d]*Tazawa et al. (2001b)*.
Modified from Tazawa et al. (2001b).

HR becomes maximal during the pipping period, and the maximum HR is significantly related to egg mass. Consequently, the allometric relationship of maximum HR and egg mass in semialtricial and that of 80% of *I* in semiprecocial is statistically identical, expressed by a single allometric equation:

$$\mathrm{MHR} = 437 \cdot (\text{Egg mass})^{-0.123} \quad (r = -0.948,\ P < 0.001,\ N = 33) \tag{37.19}$$

In addition, determination of MHR in embryos from the same clutch (siblings) in pigeons, bank swallows, and zebra finches demonstrates that developmental patterns of MHR in siblings are more alike than those of embryos from other clutches of the same species (Burggren et al., 1994; Sheldon et al., 2018). These findings may be termed the "sibling effect" in which siblings are predisposed to show particular physiological patterns. Whether these effects are genetically based (i.e., resulting from the common genetic heritage of the F_1 offspring), due to the shared environment, or involve epigenetic influences, is uncertain. Certainly, physiological process can be transferred across generations (see Ho and Burggren, 2010; 2012; Burggren 2014; Bautista et al., 2020) through epigenetic mechanisms. However, environmental effects on the mother may also cause siblings to undergo similar patterns of physiological development through a "maternal effect" or even direct effects on the gamete cells of the mother (Burggren et al., 1994; Dzialowski and Sotherland, 2004; Ho et al., 2011; Burggren, 2014).

37.4.3.3 Instantaneous heart rate

In addition to daily changes in MHR during development, HR varies from beat to beat [(i.e., instantaneous heart rate (IHR)]. At rest, the baseline of IHR in chicken embryos is more or less constant before ~day 11, indicating that neither IHR accelerations of adrenergic origin nor IHR decelerations of cholinergic origin occurs during early development. The flat baseline of IHR begins to fluctuate with the appearance of rapid, transient decelerations on ~days 12–13, with a subsequent augmented frequency of appearance (Figure 37.7) (Höchel et al., 1998; Tazawa et al., 1999; Chiba et al., 2004). Thereafter, IHR becomes arrhythmic with the appearance of transient accelerations on ~days 15–16 and more arrhythmic with augmented decelerations and accelerations toward hatching (Höchel et al., 1998; Tazawa et al., 1999, 2002a; Moriya et al., 2000; Khandoker et al., 2003; Aubert et al., 2004). These IHR decelerations are eliminated, and baseline HR is elevated, by intravenous administration of atropine. In late embryos whose IHR fluctuations comprise of complicated decelerations and accelerations with augmented magnitude and frequency, atropine diminishes decelerations only but preserves accelerations, while the HR baseline is markedly

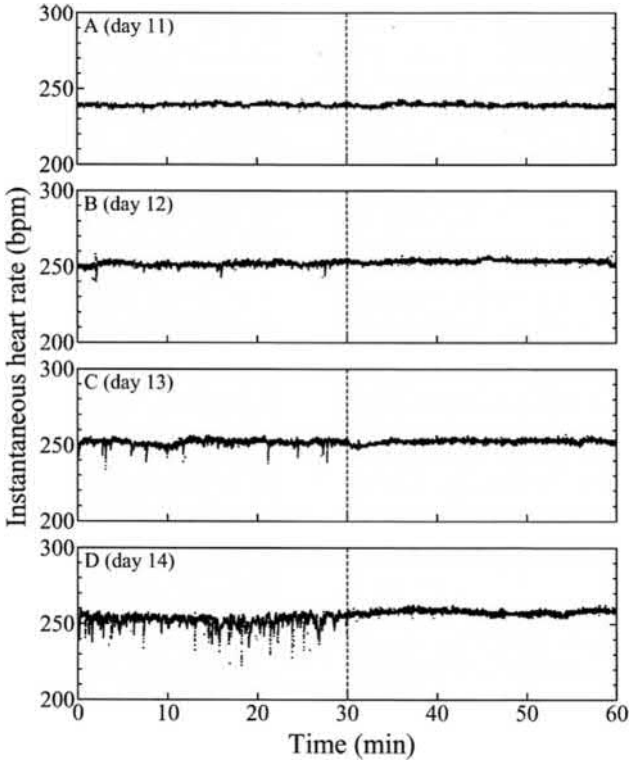

FIGURE 37.7 Instantaneous heart rate fluctuations before and after intravenous infusion of 20 μg atropine at 30 min in day 11 to day 14 chicken embryos. *From Chiba et al. (2004), with permission from Elsevier.*

elevated (Chiba et al., 2004), indicating that IHR decelerations are mediated by the vagus nerve. Accordingly, vagal tone begins to appear on ~days 12–13 of incubation in chickens, maturing with development, correcting previous reports on no vagal control of HR determined from blood pressure signals (Tazawa et al., 1992a). Furthermore, cholinergic chronotropic control of HR occurs on days 12–13 of incubation in both broiler and White Leghorn embryos (Yoneta et al., 2006c). These events coincide with the presence of a complete cholinergic effector pathway from 60% of chicken incubation (Pappano and Löffelholz, 1974).

Some controversy exists as to whether cholinergic tone is present at this developmental time point, i.e., blood pressure studies indicate no vagal tone on the heart during embryonic development of the chicken embryo (Crossley and Altimiras; 2000). Further, blood pressure studies using adrenoreceptor stimulation via pharmacological manipulation indicate that a positive β-adrenergic chronotropic tone can be induced from 60% of incubation (Crossley and Altimiras, 2000). The effect is enacted by circulating catecholamines, as ganglionic blockade with hexamethonium has no impact on HR. In contrast, pharmacological manipulation of blood pressure indicates that the emu heart is under both β-adrenergic and cholinergic control by 70%

of incubation (Crossley et al., 2003). Both cholinergic and adrenergic tone possess developmental plasticity, as evident in changes in HR and blood pressure under hypoxic incubation conditions (Mulder et al., 2002; Crossley et al., 2003; Lindgren and Altimiras, 2009).

Overall, the pattern of onset of regulatory mechanisms for blood pressure and heart rate is relatively complex, made more so by differences between species. Figure 37.8 represents an amalgam of known cardiovascular regulation in the chicken embryo.

Long-term measurement of IHR reveals the occurrence and development of various cardiac rhythms and irregularities. The developmental pattern of MHR (constructed from IHR measurement) of an embryo before and after hatching demonstrates the occurrence of infradian rhythm before and during IP, a gradual increase in HR baseline during IP, a sudden drop with a subsequent sudden increase in HR baseline during EP and the first occurrence of circadian rhythm of HR after hatching (Moriya et al., 2000). Recordings of IHR reveal respiratory arrhythmia is rare during IP (Tomi et al., 2019), but appears with EP. There are three unique patterns of IHR during the final stage of EP, i.e., relatively long-lasting cyclic small accelerations, irregular intermittent large accelerations, and short-term repeated large accelerations (Tazawa et al., 1999; Moriya et al., 2000). Short-term repeated large accelerations also occur in EP emu embryos, indicating imminent hatching (Kato et al., 2002).

After hatching, three types of IHR fluctuations (Type I, II, and III) are demonstrated in chickens (Moriya et al., 1999, 2000; Tazawa et al., 2002a). Type I is characterized as a widespread baseline HR (20−50 bpm) due to respiratory arrhythmia with a mean oscillatory frequency of ~0.7 Hz. Type II is evident by low-frequency oscillations of baseline HR at ~0.07 Hz, occurring at low T_a or when hatchlings are exposed to lowered T_a, and is thus related to thermoregulation. Type III is characterized as noncyclic irregularities, dominated by frequent transient accelerations. The image processing system developed to capture the movements of wing or whole body of the hatchling reveals that Type I and Type II HR oscillations are related to the periodic movements of the wing and Type III HR irregularities occur simultaneously with spontaneous whole body movements (Yoneta et al., 2006a). Consequently, it is likely that the chick moves the body at the same frequencies as Type I and Type II oscillations and simultaneously with Type III HR irregularities and these HR fluctuations and body movements are likely to be attributed to the same origins.

37.4.3.4 Cardiovascular regulation

The sympathetic nervous system is heavily involved in regulation of avian embryonic blood pressure (Altimiras et al., 2009; Crossley and Altimiras, 2012; Swart et al., 2014; Sirsat et al., 2018). Injection with the α-adrenoreceptor antagonist phentolamine causes hypotension from 60% of chicken incubation, indicating α-adrenergic tone on the vasculature (Girard, 1973; Saint Petery and Van Mierop, 1974; Tazawa et al., 1992a; Crossley and Altimiras 2000; Mueller et al., 2014a). Phentolamine also causes bradycardia, a likely indirect effect of vasodilation, and reduced venous return. β-adrenergic tone on the vasculature is also present from 60% of incubation, as evident by a P_a increase in response to the β-adrenereceptor antagonist propranolol (Girard, 1973; Saint Petery and Van

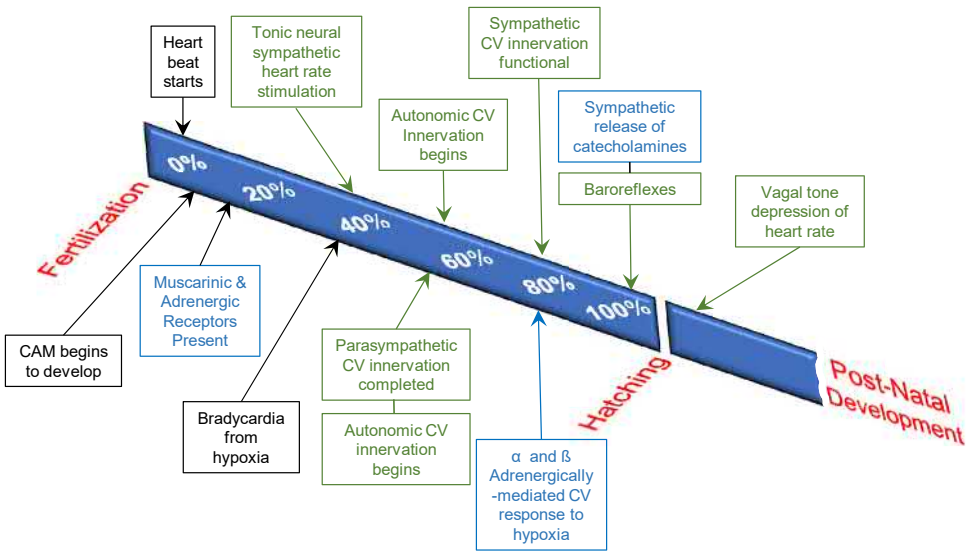

FIGURE 37.8 A proposed timeline for the onset of cardiovascular regulation in the chicken embryo. Developmental events in green relate primarily to neural components; events in blue relate primarily to hormonal components. *Modified from Burggren and Crossley (2002) with permission from Elsevier.*

Mierop, 1974; Tazawa et al., 1992a; Crossley and Altimiras 2000). The magnitude of both α- and β-adrenergic tone is maximal at 90% of incubation, just prior to IP (Crossley and Altimiras, 2000). The increase in adrenergic tone is matched to the maximal plasma catecholamine release on day 19. Catecholamine release is also elevated under hypoxic incubation of chicken embryos (Ruijtenbeek et al., 2000; Lindgren et al., 2011). Emu embryos also show signs of increasing α- and β-adrenergic tone on the vasculature matched to increasing levels of catecholamines as incubation proceeds (Crossley et al., 2003), although the onset of these responses differs from chicken embryos.

In addition to regulation via catecholamines, other hormones may also influence baseline cardiovascular function of avian embryos. The most extensively studied in chicken embryos is angiotensin II (ANG II), a strong vasoconstrictor and the active peptide of the renin-angiotensin system (RAS). Components of the RAS, including renin, angiotensin converting enzyme, ANG II, and its receptors, are present early in chicken ontogeny (Nishimura et al., 2003; Savary et al., 2005; Crossley et al., 2010). ANG II levels are elevated in embryos compared to adults, the peptide produces hypertension from at least 60% of incubation (Crossley et al., 2010), and contributes to baseline P_a at 90% of incubation (Mueller et al., 2014a). Despite an increase in P_a, ANG II does not alter MHR as it instead attenuates the embryonic cardiac baroreflex. The baroreflex is an important compensatory mechanism that buffers short-term changes in P_a and is composed of a peripheral limb adjusting vascular resistance and a cardiac limb that changes HR. A functioning baroreflex is present in chicken embryos from 80% of incubation (Altimiras and Crossley, 2000; Elfwing et al., 2011; Mueller et al., 2013a). ANG II decreases the sensitivity of the cardiac baroreflex at 90% of incubation so that reflex changes in HR in response to P_a changes are blunted (Mueller et al., 2013a). ANG II also raises the operating P_a of embryos, and it is via these short-term changes that the hormone partly enacts some of its influence on long term P_a.

Other potentially important moderators of cardiovascular function include nitric oxide (NO) and Endothelin-1 (ET-1), a potent vasodilator and vasoconstrictor, respectively, produced primarily in the endothelium, and natriuretic peptides (NPs), strong vasodilators excreted by heart muscle cells. NO tone is present from at least 70% of incubation and, unlike cholinergic and adrenergic tone, lacks plasticity as it remains unchanged under hypoxic conditions (Iversen et al., 2014). Components necessary for functional ET-1, including mRNA and converting enzymes, are found in chicken embryos from 15% of incubation (Hall et al., 2004; Groenendijk et al., 2008), and ET-1 alters chicken embryo hemodynamics (Groenendijk et al., 2008; Moonen and Villamor, 2011). Likewise, NP is present in the chicken heart and most likely contributes to hemodynamics from at least day 14 (Maksimov and Korostyshevskaya, 2013). Further research from the molecular to whole organism level is required to understand the contribution of these hormones to P_a and HR control, and therefore embryonic cardiovascular regulation.

37.4.4 Osmoregulation

During development, various avian embryos face one of two opposing osmoregulatory challenges: water loss through the pores of the eggshell in desiccating arid environments or excess water gain from the metabolic production of water as part of metabolizing the yolk stores (Ar and Rahn, 1980). Irrespective of the species-specific environmental challenge, the developing kidney and extra-embryonic structures, including the yolk, CAM and allantoic and amniotic fluids, work in concert to regulate ion and water balance. The embryonic kidney of chickens has three stages, actually comprising separate structures, the pronephros, mesonephros, and metanephros (Bolin and Burggren, 2013). The pronephros appears first and functions until day five–six of incubation (Abdel-Malek, 1950; Himura and Nakamura, 2003, Bolin and Burggren, 2013). Mesonephros function takes over from day five, is maximal on days 10–15 (Romanoff, 1960), and then degrades between days 18–19 (Atwell and Hanan, 1926). The mesonephros functions simultaneously with the metanephros, which begins developing from day four (Abdel-Malek, 1950; Klusonová and Zemanová, 2007) and continues to develop posthatching. The metanephros is the most complex of the three embryonic kidney structures, and comprises the functioning structure in adults. Figure 37.9 illustrates the developmental increase in glomerular volume of the kidney of the chicken embryo during the last third of development. The total number of nephrons grows during the middle of incubation, thereafter remaining stable until hatching. Interestingly, however, only about one-half of these nephrons are actually perfused with blood under control conditions (Bolin and Burggren, 2013). Potentially, then additional nephrons can be recruited, representing so-called "nephron-blushing," even at embryonic stages. The regulation of nephron recruitment in the avian embryo is currently unknown.

The allantoic sac first appears at ~days three–four of incubation, and acts as a repository for kidney secretions, as evident by the increase in uric acid content throughout development (Romanoff, 1967). The allantoic epithelium actively transports sodium across its membrane from days 12–19 (Stewart and Terepka, 1969; Graves et al., 1986; Gabrielli and Accili, 2010). These and other osmoregulatory mechanisms thus maintain the fluid hypo-osmotic to the blood and permitting reabsorption of water by the embryo (Hoyt, 1979; Bolin et al., 2017).

Osmoregulation is strongly tied to cardiovascular function through the synergistic maintenance of blood

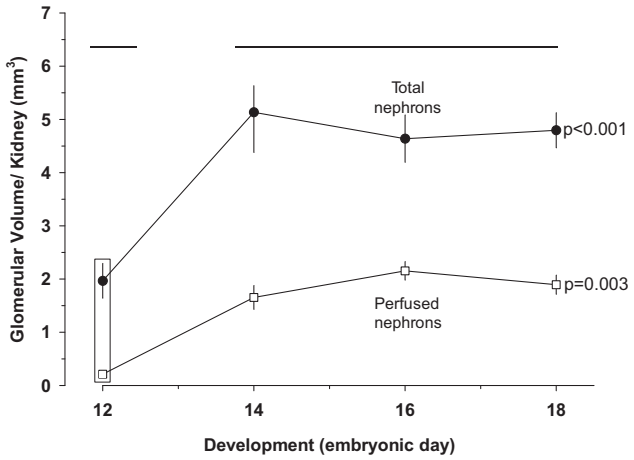

FIGURE 37.9 Total glomerular volume (*solid symbols*) and actual perfused glomerular volume (*open squares*) during days 12 through 18 of incubation in the chicken embryo. The potential exists for doubling renal function by recruiting nonperfused nephrons, though whether such control over renal function in the embryo exists is unknown. Data presented as mean values ± 1 SE and *P* values determined by one-way ANOVA for each volume across development. Mean values not significantly different from each other fall under the same *horizontal line*. Mean values within a common outlined box are not significantly different from each other. *From Bolin and Burggren (2013) with permission from Elsevier.*

pressure and osmotic homeostasis. Regulators of blood pressure, such as ANG II and NP (see above), may also contribute to ion and water balance in embryos. Chronic removal of ANG II from chicken eggs not only decreases P_a but also lowers osmolality, decreases Na^+, and increases K^+ concentration of the blood at 90% of incubation. These actions remove the osmolality gradient between the blood and allantoic fluid (Mueller et al., 2014a). Therefore, ANG II appears to influence osmotic balance and may do so by direct vasoconstrictive action or by stimulating the release of aldosterone and arginine vasotocin, which promote proximal tubular sodium reabsorption. Aldosterone is present in chicken embryo adrenal glands from day 15 (Pedernera and Lantos, 1973), and arginine vasotocin is present in the brain from day six and the plasma from day 14−16 (Klempt et al., 1992; Mühlbauer et al., 1993). Both aldosterone and arginine vasotocin alter allantoic fluid volume, allantoic salt content, and renal enzyme activity in chicken embryos (Doneen and Smith, 1982a). Prolactin and growth hormone also have osmoregulatory effects in chicken embryos (Doneen and Smith, 1982a,b; Murphy et al., 1986). The function of these hormones in osmoregulation requires further study, including how they may contribute to interactions between the developing cardiovascular and osmoregulatory systems and the maintenance of homeostasis.

37.4.5 Thermoregulation

Embryos produce metabolic heat, which increases as development progresses. Metabolic heat production of the chicken embryo increases from about 35 mW on day 12 to 130−140 mW on days 17−18 of incubation and reaches 160−170 mW at EP (Tazawa et al., 1988b). Over the same developmental range, the egg's thermal conductance is ~70 mW/°C (Tazawa et al., 2001a). This means that metabolic heat production at 38°C elevates egg temperature (T_{egg}) above ambient temperature (T_a) by ~0.5°C on day 12 and ~2.5°C in EP eggs. When eggs are cooled to 28°C, a new quasi-equilibrium state is reached in 5 h (defined as a change in T_{egg} of less than 0.2°C/h) (Tazawa and Rahn, 1987). The new difference between T_{egg} and T_a is lower so that even in EP embryos T_{egg} is only 1.2°C above T_a. In addition, during the quasi-equilibrium state at lowered T_a, embryos consume the amount of O_2 predicted by a temperature coefficient (Q_{10}) of 2 (Ide et al., 2017b). On the other hand, hatchlings, which are subjected to the same test, have body temperatures ~6°C above T_a, even right after hatching, and consume much more O_2 than that predicted by Q_{10} of 2 (Tazawa and Rahn, 1987). These observations suggest that chickens are essentially poikilothermic during embryonic stages, even at EP, and rapidly develop the capacity to maintain body temperature upon cold exposure soon after hatching.

When eggs incubated at 38°C are exposed to a T_a only 2°C lower, the heat loss from the egg is greater than the heat produced by young embryos and comparable with the heat production in late embryos. If the eggs are exposed to air 10°C cooler than the egg, the embryos would have to generate heat about 800 mW to keep T_{egg} steady (Turner, 1986). Yet, even EP embryos can generate at most 170 mW. Consequently, heat loss during cooling exceeds the embryo's maximum rate of heat production. A feeble compensatory capacity, if any, may be overwhelmed by the much larger losses of heat. The egg cools and its metabolic rate decreases as a result of the van't Hoff-Arrhenium effect. The detection of homeothermic capacity thus requires a procedure in which the heat loss from the egg does not overwhelm the heat production of the embryo. The gradual cooling test fulfills this requirement, and it shows that prenatal chicken embryos near term respond to lowered T_a by maintaining $\dot{M}O_2$ until T_a falls below 35°C (Tazawa et al., 1988b). This response in late embryos is evidently different from that in young embryos. In the prolonged cooling test, late chicken embryos are exposed to a slightly lowered T_a for a prolonged period, the $\dot{M}O_2$ is maintained at a level above that predicted by a Q_{10} of 2. This response also differs from that shown by young embryos (Tazawa et al., 1989a). Consequently, precocial chickens exhibit a feeble, incipient metabolic response to cooling, indicating endothermic homeothermy before hatching. This coincides with enhanced activity of the thyroid gland and increasing concentrations of peripheral thyroid hormones during the last stages of incubation (Decuypere et al., 1979; McNabb, 1987). In fact, while late prenatal embryos in eggs injected with saline show a feeble homeothermic metabolic response to gradual cooling, this response is absent in eggs treated with thiourea, which antagonizes the metabolic

effect of thyroid hormones (Tazawa et al., 1989c). Additionally, while the compensatory metabolic response disappears in embryos exposed to hypoxia, it is augmented in perinatal embryos in hyperoxia or following improved oxygenation by opening the shell over the air cell (Tazawa et al., 1989c; Dzialowski et al., 2007; Szdzuy et al., 2008; Ide et al., 2017b). These results indicate that the homeothermic metabolic response in precocial chickens in late development is "O_2 conductance limited" (Tazawa et al., 1988b).

The development of homeothermy in precocial and altricial birds has been modeled (Figure 37.10) and reviewed in detail (Tazawa et al., 1988b; Whittow and Tazawa, 1991; Tzschentke and Rumpf, 2011; Sirsat et al., 2016; Price and Dzialowski, 2018). The transition for a precocial bird takes place in four stages; (1) an Arrhenius-limited stage in which $\dot{M}O_2$ is directly related to the temperature with a Q_{10} value of approximately 2; (2) an O_2-conductance-limited stage in which $\dot{M}O_2$ is limited by the rate of diffusion of O_2 through the shell and CAM; (3) a power-limited stage in which the embryo has a limited capacity to generate heat in response to cooling, which is a function of the maturity of the tissues and development of thyroid activity; and (4) "full-blown" homeothermy. An altricial species does not pass through the O_2-conductance-limited stage and is subject to the Arrhenius limitation until after it hatches.

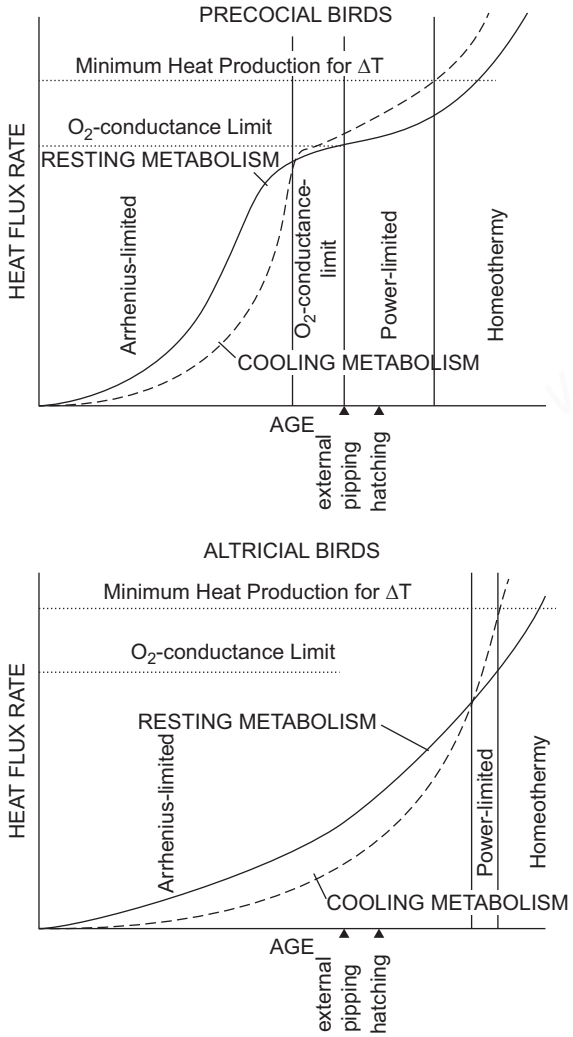

FIGURE 37.10 Models of the development of homeothermy in precocial and altricial birds. "Minimum Heat Production for ΔT" equals the amount of heat needed to keep the egg temperature warmer than ambient temperature by ΔT and homeothermy occurs when the embryo heat production reaches this level. *From Tazawa et al. (1988b), with permission from Elsevier.*

The comparative metabolic responses to prolonged cooling have been examined in the precocial duck (*Anas platyrhynchos domestica*), semi-precocial brown noddy and altricial pigeon (*Columba livia domestica*) (Matsunaga et al., 1989; Kuroda et al., 1990; Tazawa et al., 2001a; Sirsat and Dzialowski, 2016). Incipient homeothermic ability appears in the duck during prenatal development, but it is not evident in the pigeon even after emergence from the shell. The precocial chicken and semiprecocial noddy are intermediate in their metabolic response between the duck and the pigeon. Ventilatory changes, including a shift from high-breathing frequency and low-tidal volume in EP embryos to low-breathing frequency, higher tidal volume, and a ventilatory thermal sensitivity in hatchlings, that supports the endothermic metabolic phenotype (Sirsat and Dzialowski, 2016).

The development and maturation of homeothermy is expected to occur and progress even during the prenatal period in the highly precocial emu. In addition to the precocial nature of the emu, its large egg with a smaller surface area-to-volume ratio and greater contribution of blood circulation compared to smaller eggs most likely enhances thermoregulatory capacity. For emus, a more apparent metabolic response test is used in which embryos and hatchlings are exposed for a prolonged period (e.g., 1.5 h) to T_a altered sequentially by 10°C, e.g., 35-25-35°C for embryos or 25-35-25°C for hatchlings (sequential cooling-warming test, with ΔT_a of ±10°C) (Dzialowski et al., 2007). Hatchlings and EP embryos respond to ΔT_a with an endothermic change in $\dot{M}O_2$, showing an inverse metabolic response with marked increase and decrease in $\dot{M}O_2$ in response to sequential cooling and warming bouts. Late prenatal (day 45) and IP (day 49) embryos do not change $\dot{M}O_2$ in response to ΔT_a in air, but demonstrate partial (day 45) or apparent (IP) endothermic change in $\dot{M}O_2$ when the test is run in 40% O_2. This suggests that the late prenatal emu embryo already possesses homeothermic ability, but it is limited by the eggshell gas GO_2.

Changes in IHR, with apparent increases or decreases in HR baseline with oscillating pattern, in response to ΔT_a, is also effective in investigating endothermic capacity in precocial embryos and hatchlings (Tazawa et al., 2001a,

2004; Tamura et al., 2003; Khandoker et al., 2004). In the sequential cooling-warming test with ΔT_a of $\pm 10°C$, the sequence of exposure (cooling-warming and vice versa) does not affect the endothermic HR response (Yoneta et al., 2006b). In chick hatchlings, the endothermic HR response is demonstrated to be advanced by ~1 day in broiler compared with White Leghorn during 2 days of posthatch life (Yoneta et al., 2007).

In the chicken embryo, the baseline of IHR shows a thermo-conformity pattern in response to a decrease in T_a during EP (day 20), but it changes little on day 21. IHR rises accompanying HR oscillation on day 22, when the embryo stays inside the egg (Tazawa et al., 2001a; Andrewartha et al., 2011b). Although the embryo fails to hatch after EP, it matures equivalently to a hatchling on day 21 and day 22. In newly hatched chicks, HR oscillations with a period of 10–25 s occur frequently in air, reported as Type II HR fluctuation (Moriya et al., 1999, 2000). In addition, IHR oscillates with lowering T_a, resulting in Type II low frequency HR oscillation which disappears when hatchlings are transferred to high T_a (Tazawa et al., 2002b; Khandoker et al., 2004). Consequently, chicken hatchlings possess low frequency HR oscillation (Type II HR fluctuation) in relation to their thermoregulation (Tazawa, 2005 for review).

In pre-IP stage duck embryos (Figure 37.11A; day 24), the HR response during pre-IP stage indicates thermo-conformity (Andrewartha et al., 2011b). However, the recovery of HR (and T_{egg}) at T_a of 38°C is faster than chicken embryos (Tazawa et al., 2001a). By EP (C, D; day 27), duck embryos demonstrate an endothermic HR response (increase during cold exposure), larger than chicken EP embryos. Immediately after hatching, the wet duckling cannot maintain the increased HR, succumbs to the cold and HR decreases (E). However, HR of ducklings blotted dry within 2 h is maintained at similar values at T_a of 35°C (F), demonstrating incomplete endothermic capacity. By 2 and 13 h posthatching (G, H), the plumage of the ducklings has naturally dried and their HR shows an apparent endothermic response with a small decrease in body temperature, T_b ($\Delta T_b = -1.9$ and $-2.0°C$, respectively), close to full-blown homeothermy. Ducklings must attain thermoregulatory competence early (relative to the domestic chicken) during perinatal development to live in an aquatic environment soon after hatching.

In the more highly precocial emu, pre-IP and IP embryos exhibit thermoconformity and incomplete endothermic response of HR, respectively, but the apparent endothermic HR response occurs in EP embryos just like the endothermic metabolic response (Fukuoka et al., 2006; Dzialowski et al., 2007; Andrewartha et al., 2011b).

Finally, thermoregulation in chicken hatchlings has been investigated in the context of their immune responses (Amaral-Silva et al., 2020). Chicks injected with the endotoxin lipopolysaccharide showed an immune response that included transient changes in body temperature and $\dot{M}_{O_2}$, and effect that was interfered with by the common environmental pollutant TCDD (2,3,7,8-tetrachlorodibenzodioxin).

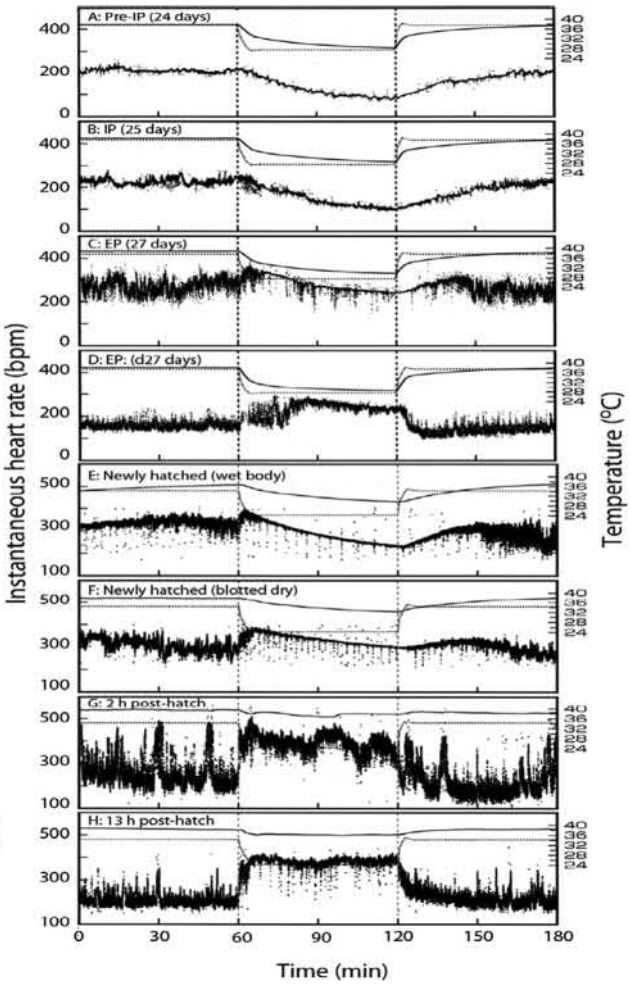

FIGURE 37.11 Responses of instantaneous heart rate (IHR) in duck embryos and hatchlings exposed sequentially to high ambient temperature ($T_a = 38°C$ for embryos and 35°C for hatchlings; *dotted line*), low-ambient temperature ($T_a = 28°C$ for embryos and 25°C for ducklings) and high temperature again for 60 min, respectively. The *solid line* represents egg temperature or body temperature. *From Andrewartha et al. (2011a), with permission from Elsevier.*

Assessments of $\dot{M}_{O_2}$ and HR responses to various tests that alter incubation temperature have been successfully utilized to assess thermoregulatory ability of avian embryos. The timing of endothermic responses differs along the precocial to altricial continuum, with precocial species generally showing thermoregulatory ability earlier than altricial species. Examination of mitochondrial, cellular, and tissue-level mechanisms is now required to further our understanding of how thermoregulatory ability develops in embryos and hatchlings.

37.5 Artificial incubation

37.5.1 Preincubation egg storage

Many precocial birds laying multiple eggs in a clutch start their incubation with the penultimate or ultimate eggs. Consequently, first laid eggs are stored in the nest until incubation starts, sometimes for many days. Egg storage is not just a phenomenon of nature, of course. Egg storage commonly occurs in commercial conditions of artificial incubation, leading to numerous studies on the effect of storage conditions on the biology of the embryos and hatchlings. If the storage temperature for freshly laid chicken eggs is kept below physiological zero (25−27°C), dormancy of the embryo is maintained and fertile eggs can be stored for several days without a major loss of hatchability (Butler, 1991; Wilson, 1991; Goliomytis et al., 2015; Branum et al., 2016). The optimal temperature for 3−7 days storage of chicken eggs is 16−17°C and it drops to 10−12°C for eggs stored for more than 7 days (Butler, 1991; Wilson, 1991). However, prolonged preincubation egg storage results in malformations and retarded growth of the embryos, decreased hatchability, increased incubation period, and it even influences hatchling growth (Arora and Kosin, 1966; Mather and Laughlin, 1979; Branum et al., 2016). Interestingly, short periods of incubation during egg storage ("SPIDES") can increase the hatchability of chicken eggs stored for more than 8 days (Dymond et al., 2013; Damaziak, 2018). The hatchability of the northern bobwhite quail (*Colinus virginianus*) remains above 70% after 14 d of preincubation storage at 20−22°C, but decreases to below 30% after 21 d of storage (Reyna, 2010). These deleterious effects are related to not only the length of storage but also the environmental and physical conditions, such as temperature, relative humidity (RH), atmospheric gas composition, orientation, and positional changes during storage (Brake et al., 1997).

Prolonged preincubation egg storage also affects the physiological function of developing chicken embryos (Haque et al., 1996; Fasenko, 2007; Goliomytis et al., 2015; Branum et al., 2016; Yalcin et al., 2017). Albumen quality, an indicator of overall egg quality, decreases with storage (Scott and Silversides, 2000; Reyna, 2010). Furthermore, while the developmental patterns of $\dot{M}_{O_2}$ are consistent among unstored (control) eggs, those stored for 20 and 30 days at 10−11°C are varied and depressed among eggs; the depression of the $\dot{M}_{O_2}$ increases in severity as the storage duration increases. The developmental trajectory of HR in stored eggs is also flattened compared with those of control eggs. As a result, the O_2 pulse (O_2 uptake every heartbeat) is markedly lowered by preincubation storage, decreasing blood O_2 transport, and retarding embryo growth in stored eggs, resulting in death during the last days of incubation (Haque et al., 1996).

37.5.2 Egg turning

In many avian species, incubating adults actively move their eggs in the nest (egg-turning). The critical period for lack of egg-turning in artificial incubation of the chicken egg ranges from day 3 to day 7 of artificial incubation (New, 1957; Deeming, 1989a). Chicken eggs should be turned minimally three times a day. Turning more than 24 times a day has long been assumed to not further enhance hatchability, although turning 96 times/day increased hatchability (Elibol and Brake, 2006). Lack of egg-turning is detrimental not only to hatchability but also can slow incubation, the development of the CAM, and embryo growth (New, 1957; Tazawa, 1980b; Deeming et al., 1987; Tullet and Deeming, 1987; Deeming, 1989a, b).

Failure to turn eggs during incubation also produces adverse effects on gas exchange through the CAM (Tazawa, 1980b). The movement of albumen into the amnion is retarded, and the unabsorbed albumen, which becomes more viscid and heavy as it loses water early in incubation, sinks toward the lower end of the egg where it remains. The chorioallantois fails to fold around the unabsorbed albumen and the interposition of the albumen between the CAM and inner shell membrane reduces gas exchange. These effects cause a pronounced fall in the arterialized blood P_{O_2} of late embryos, which is accompanied by an increase in *Hct*. The inhibition of gas exchange is reflected in the decreased $\dot{M}_{O_2}$ of unturned eggs compared to turned eggs (Pearson et al., 1996).

On an interesting comparative note, the eggs of many reptile species are killed or have greatly reduced hatchability, if they are turned during any point in incubation (Ferguson, 1985; Ruben et al., 2003), although there are species differences (Aubret et al., 2015).

37.5.3 Ambient temperature and incubation

For chickens, freshly laid eggs can be stored at a low temperature to maintain dormancy of embryos. However, once incubation starts, T_a must be kept within a certain range so that the chicken embryo temperature is maintained and cell proliferation can proceed. This differs from some other bird species. Emu eggs that are midway through their ~56 day incubation period, for example, can be cooled down to room temperature for several hours before incubation is resumed with no adverse effects (W. Burggren, pers. obs.). In artificial incubation of chicken eggs at constant T_a, hatchability decreases when T_a is lowered to 35°C or elevated to 40°C from the optimal temperature of 37.5°C. At 35°C, incubation period and embryonic development of chickens are ~3 days longer than at 38°C (Tazawa, 1973; Black and Burggren, 2004a). Survival of chicken embryos during total incubation period is reduced at 35°C (Black and Burggren, 2004a) and temperatures

below this threshold are lethal. Hypothermal incubation decreases $\dot{M}O_2$ in proportion to retarded development of embryos and preserves the relative timing of IP and EP (Tazawa, 1973; Black and Burggren, 2004a). However, at the final stages of hypothermal incubation, hematological development and blood O_2-carrying capacity are retarded (Black and Burggren, 2004b), and eventually hypothermal incubation causes a significant delay of the relative timing of the onset of thermoregulatory ability (Tzschentke et al., 2001; Nichelmann, 2004; Black and Burggren, 2004b; Mortola, 2006).

The tolerance limits of developing embryos to acutely lowered and elevated T_a have been investigated in chickens in reference to their HR (Tazawa and Rahn, 1986; Ono et al., 1994). When day 10 embryos are exposed to a T_a of 28 or 18°C, HR decreases in an exponential fashion to reach plateau values during 2–3 h of exposure. The plateau values are ~100 bpm at 28°C and ~30 bpm at 18°C, which are maintained until irreversible cardiac arrest occurs at ~100 and ~60 h after exposure to 28 and 18°C, respectively. Accordingly, day 10 embryos survive exposure to 28°C for no less than 4 days and to 18°C for about 2.5 days. Reduction of T_a to 8°C forces the heartbeat of day 10 embryos to cease after ~3 h. However, the cardiac arrest at this low T_a (8°C) does not mean the death of embryos. Ten-day embryos survive the low T_a, without a heartbeat, for 18 h more and the heart begins to beat again after rewarming at 38°C. The survival time at 8°C is reduced as the embryos grow. While the heart of day six embryos begins to beat even after 1 day exposure to 8°C, the heart of day 20 embryos fails to beat after an 8 h exposure (Tazawa and Rahn, 1986).

While chicken embryos can withstand a lowered T_a for a prolonged period without a heartbeat, at an increased T_a, the cardiac arrest following arrhythmia is irreversible and the embryos cannot withstand exposure to an increased T_a for a prolonged period (Ono et al., 1994). The HR of embryos increases in an exponential fashion at increased T_a. When T_{egg} reaches 46–47°C, regardless of the developmental stage of embryos, the HR becomes arrhythmic and irreversible cardiac arrest follows. The lethal T_a and tolerance time of chicken embryos depend upon the time T_{egg} takes to reach a lethal critical value of 46–47°C. At a T_a of 48°C, the tolerance time of day 12 embryos is ~100 min and that of day 20 embryos shortens by about half. The tolerance time to 48°C exposure is shortened as the embryos grow. This may be in part due to the higher metabolic heat which is produced by late embryos compared to earlier embryos. The HR reaches ~450 bpm at the critical T_{egg} (46–47°C) (Ono et al., 1994).

The embryos of ground nesting birds in semiarid and arid areas, in particular, experience environmental temperatures many degrees higher than typical avian incubation temperatures. For example, the northern bobwhite quail can experience nest temperatures as high as 45°C in the wild. Not surprisingly, this species shows remarkable tolerance to brief preincubation hyperthermia. Bobwhite quail embryos can survive 6 h exposure to 46°C, 3 h exposure to 49°C and, remarkably, 1 h exposure to 50°C (Reyna and Burggren, 2012, 2017). While these temperatures certainly increase mortality and decrease hatching rates, the high-temperature tolerance of the bobwhite quail highlights the importance of a comparative approach to examining temperature tolerance. Extreme temperatures in the natural environment may result in increased tolerance in avian species and warrants further investigation.

37.5.4 Humidity

Successful artificial incubation of chicken eggs occurs over an RH range of 40–70% (Robertson, 1961). Within the successful incubation range, 53% RH is optimal for embryo survival and hatchability (Bruzual et al., 2000). Either high (>85%) or low (<30%) humidity increases mortality in chicken embryos (Figure 37.12; Ar and Rahn, 1980; Bolin et al., 2017). Under low humidity, inadequate water content can result from increased water loss across the porous eggshell due to a high vapor pressure gradient between the inside of the egg and surrounding air. Under high humidity, water loss is reduced and this can exert osmotic stress on the embryo. Allantoic fluid volume, which is a balance between renal filtrate production and water reabsorption into the embryo, is reduced under high water loss conditions, and conversely increased when water loss is low (Davis et al., 1988). Under high water loss, water is reabsorbed from the allantois, uric acid levels in the allantois increase, and sodium is actively transported to maintain the allantoic fluid hypotonic to the blood and aid water reabsorption (Hoyt, 1979; Davis et al., 1988; Bolin et al., 2017). Plasma calcium, sodium, and potassium levels are elevated in late stage embryos, a sign of osmotic stress (Davis et al., 1988). After exposure to <30% RH, the kidneys of day 18 chicken embryos have additional glomeruli, more functioning glomeruli and high cloacal fluid osmolality, illustrating an increased filtering capacity (Bolin et al., 2017).

Extremes in humidity or water loss reduce hatching success (Davis et al., 1988; Bolin et al., 2017). Water balance appears to have the greatest effects on hatchability early in incubation, with hatchability related to water loss during the first half of incubation, rather than total water loss (Snyder and Birchard, 1982). Humidity extremes also affect late stage embryo wet mass, i.e., embryos from low humidity or high-water loss environments have smaller wet masses while those from high-humidity environments have higher wet masses (Bruzual et al., 2000; Bolin et al., 2017). In low-water loss environments, excess water is not always incorporated into wet mass, but is instead left behind in the albumen (Davis et al., 1988). Growth and oxygen

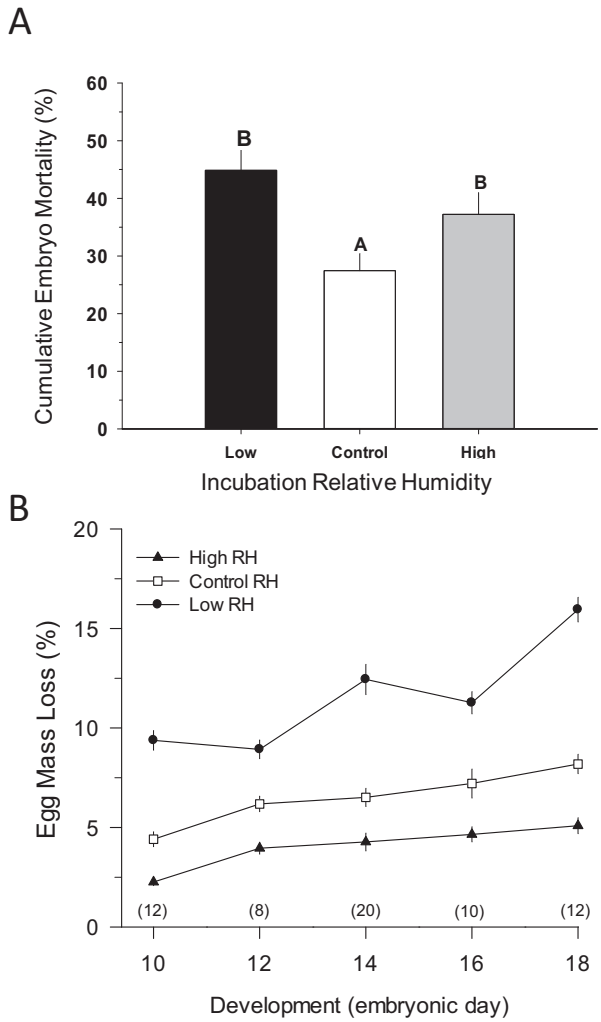

FIGURE 37.12 Effects of incubation relative humidity (RH) through the incubation period on (A) cumulative mortality and (B) body mass of chicken embryos. Low, control and high RH is 25–30%, 55–60% and 85–90%, respectively. Means ± SE shown. Letters indicated statistical comparisons of groups. N values in parentheses. *From Bolin et al. (2017) with permission from Elsevier.*

consumption can be retarded after exposure to extreme humidity (Bolin et al., 2017), but embryos that do hatch under extreme humidity reach normal weight within 7–10 days posthatch (Davis et al., 1988).

37.6 Conclusions and future directions

Incubation is the first important process experienced by the embryonic life stages of any avian species. The characteristics of the egg itself and the surrounding environment determine the success and timing of embryonic development. As we have discussed in this chapter, the study of avian embryonic physiology has provided extensive information on the complex processes that occur during avian development. A key aspect of avian development is the physical processes of incubation, including the transfer of water and heat between the egg and environment. Successful incubation outside of extremes in temperature, humidity, and other stressors enables the development of the form and function of the major physiological systems, including the gas exchange, acid-base, cardiovascular, osmoregulatory, and thermoregulatory systems.

Despite literally thousands of studies that have investigated some aspect of the physiology of the avian embryo, numerous possibilities still exist to expand our knowledge of avian development by utilizing new physiological techniques and undertaking studies using an across-discipline approach. Molecular and cellular studies will be important in revealing the mechanistic underpinnings of system and organism level observations. Furthermore, many fruitful areas of research at all levels, from genes to the whole organism, remain. These include the timing and control of important physiological events during development, how and when systems are perturbed during development and if recovery is possible, and how systems work together during development. Finally, comparative approaches are also needed to place physiological processes in an ecological and evolutionary context. The vast majority of avian developmental data have been collected in the chicken which, as a precocial bird, is not representative of all avian species. We need to find out how representative the data are from chicken embryos, especially given the venerable nature of the chicken embryo as a model for development in both basic and translational experiments (Burggren et al., 2018).

Additional research in these areas will allow us to further understand avian embryos for the complex, multisystem organisms that they are, while also contributing to the broader field of vertebrate development.

Acknowledgments

The authors thank the US National Science Foundation for ongoing financial support.

References

Abdel-Malek, E.T., 1950. Early development of the urinogenital system in the chick. J. Morphol. 86, 599–626.

Ackerman, R.A., Rahn, H., 1981. In vivo O_2 and water vapor permeability of the hen's eggshell during early development. Respir. Physiol. 45, 1–8.

Al Naieb, S., Happel, C.M., Yelbuz, T.M., 2013. A detailed atlas of chick heart development in vivo. Ann. Anat. 195, 324–341.

Alford, P.W., Taber, L.A., 2003. Regional epicardial strain in the embryonic chick heart during the early looping stages. J. Biomech. 36, 1135–1141.

Altimiras, J., Crossley II, D.A., 2000. Control of blood pressure mediated by baroreflex changes of heart rate in the chicken embryo (*Gallus gallus*). Am. J. Physiol. Reg. Int. Comp. Physiol. 278, R980–R986.

Altimiras, J., Crossley II, D.A., Villamor, E., 2009. Prenatal development of cardiovascular regulation in avian species. In: Glass, M.L., Wood, S.C. (Eds.), Cardio-Respiratory Control in Vertebrates. Springer Verlag, Berlin, pp. 397–427.

Amaral-Silva, L., Tazawa, H., Bicego, K., Burggren, W.W., 2020. Metabolic and hematological responses to endotoxin-induced inflammation in chicks experiencing embryonic 2,3,7,8-Tetrachlorodibenzodioxin exposure. Environ. Toxicol. Chem. (in press).

Andrewartha, S.J., Tazawa, H., Burggren, W.W., 2011a. Hematocrit and blood osmolality in developing chicken embryos (*Gallus gallus*): In vivo and in vitro regulation. Respir. Physiol. Neurobiol. 179, 142–150.

Andrewartha, S.J., Tazawa, H., Burggren, W.W., 2011b. Embryonic control of heart rate: examining developmental patterns and temperature and oxygenation influences using embryonic avian models. Respir. Physiol. Neurobiol. 178, 84–96.

Andrewartha, S.J., Tazawa, H., Burggren, W.W., 2014. Acute regulation of hematocrit and acid-base balance in chicken embryos in response to severe intrinsic hypercapnic hypoxia. Respir. Physiol. Neurobiol. 195, 1–10.

Ar, A., Rahn, H., 1980. Water in the avian egg overall budget of incubation. Am. Zool. 20, 373–384.

Ar, A., Paganelli, C.V., Reeves, R.B., Greene, D.G., Rahn, H., 1974. The avian egg: water vapor conductance, shell thickness, and functional pore area. Condor 76, 153–158.

Ar, A., Visschedijk, A.H.J., Rahn, H., Piiper, J., 1980. Carbon dioxide in the chick embryo towards end of development: effects of He and SF6 in breathing mixtures. Respir. Physiol. 40, 293–307.

Arora, K.L., Kosin, I.L., 1966. Changes in the gross morphological appearance of chicken and Turkey blastoderms during preincubation. Poult. Sci. 45, 819–825.

Atwell, W.J., Hanan, E.B., 1926. The time during which the mesonephros and the metanephros of the developing chick are able to store trypan blue. Anat. Rec. 32, 228.

Aubert, A.E., Beckers, F., Ramaekers, D., Verheyden, B., Leribaux, C., Aerts, J.M., Berckmans, D., 2004. Heart rate and heart rate variability in chicken embryos at the end of incubation. Exp. Physiol. 89, 199–208.

Aubret, F., Blanvillain, G., Kok, P.J., 2015. Myth busting? Effects of embryo positioning and egg turning on hatching success in the water snake *Natrix maura*. Sci. Rep. 21, 13385.

Azzam, M.A., Mortola, J.P., 2007. Organ growth in chicken embryos during hypoxia: implications on organ "sparing" and "catch-up growth". Respir. Physiol. Neurobiol. 159 (2), 155–162.

Bamelis, F., Kemps, B., Mertens, K., De Ketelaere, B., Decuypere, E., DeBaerdemaeker, J., 2005. An automatic monitoring of the hatching process based on the noise of the hatching chicks. Poult. Sci. 84, 1101–1107.

Barnes, A.E., Jensen, W.N., 1959. Blood volume and red cell concentration in the normal chick embryo. Am. J. Physiol. 197, 403–405.

Bautista, N.M., Crespel, A., Crossley, J., Padilla, P., Burggren, W.W., 2020. Parental Transgenerational epigenetic inheritance related to dietary crude oil exposure in *Danio rerio*. J. Exp. Biol. 220, jeb222224.

Biebach, H., 1986. Energetics of rewarming a clutch in starlings (*Sturnus vulgaris*). Physiol. Zool. 59, 69–75.

Birchard, G., Deeming, D., 2009. Avian eggshell thickness: scaling and maximum body mass in birds. J. Zool. 279 (1), 95–101.

Bissonnette, J.M., Metcalfe, J., 1978. Gas exchange of the fertile hen's egg: components of resistance. Respir. Physiol. 34, 209–218.

Bjønnes, P.O., Aulie, A., Høiby, M., 1987. Effects of hypoxia on the metabolism of embryos and chicks of domestic fowl. J. Exp. Zool. 1 (Suppl.), 209–212.

Black, J.L., Burggren, W.W., 2004a. Acclimation to hypothermic incubation in developing chicken embryos (*Gallus domesticus*) I. Developmental effects and chronic and acute metabolic adjustments. J. Exp. Biol. 207, 1543–1552.

Black, J.L., Burggren, W.W., 2004b. Acclimation to hypothermic incubation in developing chicken embryos (*Gallus domesticus*) II. Hematology and blood O_2 transport. J. Exp. Biol. 207, 1553–1561.

Bolin, G., Burggren, W.W., 2013. Metanephric kidney development in the chicken embryo: glomerular numbers, characteristics and perfusion. Comp. Biochem. Physiol. A 166 (2), 343–350.

Bolin, G., Dubansky, B., Burggren, W.W., 2017. Incubation relative humidity induces renal morphological and physiological remodeling in the embryo of the chicken (*Gallus gallus domesticus*). Comp. Biochem. Physiol. A 204, 185–196.

Boutilier, R.G., Gibson, M.A., Toews, D.P., Anderson, N.G., 1977. Gas exchange and acid-base regulation in the blood and extraembryonic fluids of the developing chicken embryo. Respir. Physiol. 31, 81–89.

Brake, J., Walsh, T.J., Benton Jr., C.E., Petitte, J.N., Meijerhof, R., Penalva, G., 1997. Egg handling and storage. Poult. Sci. 76, 144–151.

Branum, S.R., Tazawa, H., Burggren, W.W., 2016. Phenotypic developmental plasticity induced by preincubation egg storage in chicken embryos (*Gallus gallus domesticus*). Physiol. Rep. 4, e12712.

Branum, S.B., Yamada-Fisher, M., Burggren, W., 2013. Reduced heart rate and cardiac output differentially affect angiogenesis, growth, and development in early chick embryo (*Gallus domesticus*). Physiol. Biochem. Zool. 86, 370–382.

Braune, B., Scheuhammer, A., Crump, D., Jones, S., Porter, E., Bond, D., 2012. Toxicity of methylmercury injected into eggs of thick-billed murres and arctic terns. Ecotoxicology 21, 2143–2152.

Bruzual, J., Peak, S., Brake, J., Peebles, E., 2000. Effects of relative humidity during incubation on hatchability and body weight of broiler chicks from young breeder flocks. Poult. Sci. 79, 827–830.

Burggren, W.W., 2004. What is the purpose of the embryonic heart beat? Or how facts can ultimately prevail over physiological dogma. Physiol. Biochem. Zool. 77, 333–345.

Burggren, W.W., 2013. Cardiovascular development and angiogenesis in the early vertebrate embryo. Cardiovasc. Eng. Tech 4 (3), 234–245.

Burggren, W.W., 2014. Epigenetics as a source of variation in comparative animal physiology – or Lamarck is lookin' pretty good these days. J. Exp. Biol. In review.

Burggren, W.W., Andrewartha, S.J., Tazawa, H., 2012. Interactions of acid-base balance and hematocrit regulation during environmental respiratory gas challenges in developing chicken embryos (*Gallus gallus*). Respir. Physiol. Neurobiol. 183, 135–148.

Burggren, W., Bautista, N., 2019. Invited review: development of acid-base regulation in vertebrates. Comp. Biochem. Physiol. A Mol. Integr. Physiol. 236, 110518.

Burggren, W., Crossley II, D.A., 2002. Comparative cardiovascular development: improving the conceptual framework. Comp. Biochem. Physiol. A 132, 661–674.

Burggren, W., Flores Santin, J., Rojas Antich, M., 2018. Cardiorespiratory development in bird embryos: new insight from a venerable animal model. R. Bras. Zootec. 45, 709–728.

Burggren, W.W., Keller, B. (Eds.), 1997. Development of Cardiovascular Systems: Molecules to Organisms. Cambridge Univ. Press, New York.

Burggren, W.W., Khorrami, S., Pinder, A., Sun, T., 2004. Body, eye, and chorioallantoic vessel growth are not dependent on cardiac output level in day 3-4 chicken embryos. Am. J. Physiol. Regul. Integr. Comp. Physiol. 287, R1399–R1406.

Burggren, W.W., Mueller, C.A., Tazawa, H., 2015. Hypercapnic thresholds for embryonic acid–base metabolic compensation and hematological regulation during CO_2 challenges in layer and broiler chicken strains. Respir. Physiol. Neurobiol. 215, 1–12.

Burggren, W.W., Rojas Antich, M., 2020. Angiogenesis in the avian embryo chorioallantoic membrane: a perspective on research trends and a case study on toxic vascular effects. J. Cardiovasc. Dev. Dis. 7 (4), 56.

Burggren, W.W., Tazawa, H., Thompson, D., 1994. Genetic and maternal environmental influences on embryonic physiology: intraspecific variability in avian embryonic heart rates. Israel J. Zool. 40, 351–362.

Burggren, W.W., Warburton, S., 1994. Patterns of form and function in developing hearts: contributions from non-mammalian vertebrates. Cardioscience 5, 183–191.

Burggren, W.W., Warburton, S.J., Slivkoff, M.D., 2000. Interruption of cardiac output does not affect short-term growth and metabolic rate in day 3 and 4 chick embryos. J. Exp. Biol. 203, 3831–3838.

Burton, G., Palmer, M., 1992. Development of the chick chorioallantoic capillary plexus under normoxic and normobaric hypoxic and hyperoxic conditions: a morphometric study. J. Exp. Zool. 262 (3), 291–298.

Butler, D.E., 1991. Egg handling and storage at the farm and hatchery. In: Tullett, S.G. (Ed.), Avian Incubation. Butterworth, London, pp. 195–203.

Cain, J.R., Abbott, U.K., Rogallo, V.L., 1967. Heart rate of the developing chick embryo. Proc. Soc. Exp. Biol. Med. 126, 507–510.

Chiba, Y., Fukuoka, S., Niiya, A., Akiyama, R., Tazawa, H., 2004. Development of cholinergic chronotropic control in chick (*Gallus gallus domesticus*) embryos. Comp. Biochem. Physiol. A 137, 65–73.

Chiba, Y., Khandoker, A.H., Nobuta, M., Moriya, K., Akiyama, R., Tazawa, H., 2002. Development of respiratory rhythms in perinatal chick embryos. Comp. Biochem. Physiol. A 131, 817–824.

Clark, E.B., Hu, N., Dummett, J.L., Vandekieft, G.K., Olson, C., Tomanek, R., 1986. Ventricular function and morphology in chick embryo from stages 18 and 29. Am. J. Physiol. 250, H407–H413.

Crossley II, D., Altimiras, J., 2000. Ontogeny of cholinergic and adrenergic cardiovascular regulation in the domestic chicken (*Gallus gallus*). Am. J. Physiol. Regul. Integr. Comp. Physiol. 279, R1091–R1098.

Crossley II, D.A., Altimiras, J., 2012. Effect of selection for commercially productive traits on the plasticity of cardiovascular regulation in chicken breeds during embryonic development. Poult. Sci. 91, 2628–2636.

Crossley II, D.A., Bagatto, B.P., Dzialowski, E.M., Burggren, W.W., 2003. Maturation of cardiovascular control mechanisms in the embryonic emu (*Dromiceius novaehollandiae*). J. Exp. Biol. 206, 2703–2710.

Crossley, D., Jonker, S., Hicks, J., Thornburg, K., 2010. Maturation of the angiotensin II cardiovascular response in the embryonic White Leghorn chicken (*Gallus gallus*). J. Comp. Physiol. B. 180, 1057–1065.

Damaziak, K., Paweska, M., Gozdowski, D., Niemiec, J., 2018. Short periods of incubation, egg turning during storage and broiler breeder hens age for early development of embryos, hatching results, chick quality and juvenile growth. Poult. Sci. 97, 3264–3276.

Davis, T.A., Shen, S.S., Ackerman, R.A., 1988. Embryonic osmoregulation: consequences of high and low water loss during incubation of the chicken egg. J. Exp. Zool. 245, 144–156.

Dawes, C.M., 1976. A method for recording the respiratory and hatching movements of the chick embryo. J. Exp. Biol. 64, 379–383.

Dawes, C.M., Simkiss, K., 1969. The acid-base status of the blood of the developing chick embryo. J. Exp. Biol. 50, 79–86.

Decuypere, E., Nouwen, E.J., Kühn, E.R., Geers, R., Michels, H., 1979. Differences in serum iodohormone concentration between chick embryos with and without the bill in the air chamber at different incubation temperatures. Gen. Comp. Endocrinol. 37, 264–267.

Deeming, D.C., 1989a. Characteristics of unturned eggs: critical period, retarded embryonic growth and poor albumen utilisation. Br. Poult. Sci. 30, 239–249.

Deeming, D.C., 1989b. Importance of sub-embryonic fluid and albumen in the embryo's response to turning of the egg during incubation. Br. Poult. Sci. 30, 591–606.

Deeming, D.C., Rowlett, K., Simkiss, K., 1987. Physical influences on embryo development. J. Exp. Zool. 1 (Suppl.), 341–345.

Doneen, B.A., Smith, T.E., 1982a. Ontogeny of endocrine control of osmoregulation in chick embryo. I. Role of pituitary gland in distribution of water and ions among embryonic and extraembryonic compartments. Gen. Comp. Endocrinol. 48, 300–309.

Doneen, B.A., Smith, T.E., 1982b. Ontogeny of endocrine control of osmoregulation in chick embryo: II. Actions of prolactin, arginine vasopressin, and aldosterone. Gen. Comp. Endocrinol. 48, 310–318.

Druyan, S., Levi, E., 2012. Reduced O_2 concentration during CAM development–Its effect on angiogenesis and gene expression in the broiler embryo CAM. Gene Expr. Patterns 12 (7–8), 236–244.

Du, W., Shine, R., 2015. The behavioural and physiological strategies of bird and reptile embryos in response to unpredictable variation in nest temperature. Biol. Rev. 90, 19–30.

Dymond, J., Vinyard, B., Nicholson, A.D., French, N.A., Bakst, M.R., 2013. Short periods of incubation during egg storage increase hatchability and chick quality in long-stored broiler eggs. Poult. Sci. 92, 2977–2987.

Dzialowski, E.M., Burggren, W.W., Komoro, T., Tazawa, H., 2007. Development of endothermic metabolic response in embryos and hatchlings of the emu (*Dromaius novaehollandiae*). Respir. Physiol. Neurobiol. 155, 286–292.

Dzialowski, E.M., Sirsat, T., van der Sterren, S., Villamor, E., 2011. Prenatal cardiovascular shunts in amniotic vertebrates. Respir. Physiol. Neurobiol. 178, 66–74.

Dzialowski, E.M., Sotherland, P.R., 2004. Maternal effects of egg size on emu *Dromaius novaehollandiae* egg composition and hatchling phenotype. J. Ex. Biol. 207, 597–606.

Dzialowski, E.M., von Plettenberg, D., Elmonoufy, N.A., Burggren, W.W., 2002. Chronic hypoxia alters the physiological and morphological trajectories of developing chicken embryos. Comp. Biochem. Physiol. A 131 (4), 713–724.

Elfwing, M., Lundengård, K., Altimiras, J., 2011. Fetal development of baroreflex sensitivity: the chicken embryo as a case model. Respir. Physiol. Neurobiol. 178, 75–83.

Elibol, O., Brake, J., 2006. Effect of flock age, cessation of egg turning, and turning frequency through the second week of incubation on hatchability of broiler hatching eggs. Poult. Sci. 85, 1498–1501.

Erasmus, B. De W., Howell, B.J., Rahn, H., 1970/71. Ontogeny of acid-base balance in the bullfrog and chicken. Respir. Physiol. 11, 46–53.

Erasmus, B. De W., Rahn, H., 1976. Effects of ambient pressures, He and SF_6 on O_2 and CO_2 transport in the avian egg. Respir. Physiol. 27, 53–64.

Everaert, N., Willemsen, H., Willems, E., Franssens, L., Decuypere, E., 2011. Acid-base regulation during embryonic development in amniotes, with particular reference to birds. Respir. Physiol. Neurobiol. 178, 118–128.

Faber, J.J., 1968. Mechanical function of the separating embryonic heart. Am. J. Physiol. 214, 475–481.

Faber, J.J., Green, T.J., Thornburg, K.L., 1974. Embryonic stroke volume and cardiac output in the chick. Dev. Biol. 41, 14–21.

Fasenko, G.M., 2007. Egg storage and the embryo. Poult. Sci. 86, 1020–1204.

Fukuoka, S., Khandoker, A.H., Dzialowski, E.M., Burggren, W.W., Tazawa, H., 2006. Development of endothermic heart rate response in emu (*Dromaius novaehollandiae*) embryos. In: Yahav, S., Tzschentke, B. (Eds.), New Insights into Fundamental Physiology and Peri-natal Adaptation of Domestic Fowl. Nottingham Univ. Press, pp. 29–42.

Ferguson, M.W.J., 1985. In: Gans, C., Billett, F., Maderson, P.F.A. (Eds.), Reproductive Biology and the Embryology of the Crocodilians in Biology of the Reptilia, vol. 14. John-Wiley and Sons, pp. 330–491.

Gabrielli, M.G., Accili, D., 2010. The chick chorioallantoic membrane: a model of molecular, structural, and functional adaptation to trans-epithelial ion transport and barrier function during embryonic development. J. Biomed. Biotechnol. 2010, 12. https://doi.org/10.1155/2010/940741. ID940741.

Girard, H., 1971. Respiratory acidosis with partial metabolic compensation in chick embryo blood during normal development. Respir. Physiol. 13, 343–351.

Girard, H., 1973. Arterial pressure in the chick embryo. Am. J. Physiol. 224, 454–460.

Goliomytis, M., Tsipouzian, T., Hager-Theodorides, A.L., 2015. Effects of egg storage on hatchability, chick quality, performance and immunocompetence parameters of broiler chickens. Poult. Sci. 94, 2257–2265.

Grabowski, C.T., 1961. Lactic acid accumulation as a cause of hypoxia-induced malformations in the chick embryo. Science 134, 1359–1360.

Grabowski, C.T., 1966. Physiological changes in the bloodstream of chick embryos exposed to teratogenic doses of hypoxia. Dev. Biol. 13, 199–213.

Graves, J.S., Dunn, B.E., Brown, S.C., 1986. Embryonic chick allantois: functional isolation and development of sodium transport. Am. J. Physiol. Cell Physiol. 251, C787–C794.

Groenendijk, B.C.W., Stekelenburg-de Vos, S., Vennemann, P., Wladimiroff, J.W., Nieuwstadt, F.T.M., Lindken, R., Westerweel, J., Hierck, B.P., Ursem, N.T.C., Poelmann, R.E., 2008. The Endothelin-1 pathway and the development of cardiovascular defects in the haemodynamically challenged chicken embryo. J. Vasc. Res. 45, 54–68.

Guidolin, D., Tamma, R., Tortorella, C., Annese, T., Ruggieri, S., Marzullo, A., Ribatti, D., 2020. Morphometric analysis of the branching of the vascular tree in the chick embryo area vasculosa. Microvasc. Res. 128, 103935.

Hall, C.E., Hurtado, R., Hewett, K.W., Shulimovich, M., Poma, C.P., Reckova, M., Justus, C., Pennisi, D.J., Tobita, K., Sedmera, D., Gourdie, R.G., Mikawa, T., 2004. Hemodynamic-dependent patterning of endothelin converting enzyme 1 expression and differentiation of impulse-conducting Purkinje fibers in the embryonic heart. Development 131, 581–592.

Haque, M.A., Pearson, J.T., Hou, P.-C.,L., Tazawa, H., 1996. Effects of pre-incubation egg storage on embryonic functions and growth. Respir. Physiol. 103, 89–98.

Haron, A., Dahan, Y., Shinder, D., Druyan, S., 2017. Physiological effects of hypoxic conditions during the plateau period on the chicken embryo. Comp. Biochem. Physiol. A Mol. Integr. Physiol. 203, 32–39.

Hempleman, S.C., Powell, F.L., Adamson, T.P., Burger, R.E., 1992. CO_2 and avian eggshell formation at high altitude. Respir. Physiol. 87, 1–10.

Hiruma, T., Nakamura, H., 2003. Origin and development of the pronephros in the chick embryo. J. Anat. 203, 539–552.

Ho, D., Burggren, W.W., 2010. Epigenetics and transgenerational transfer: a physiological perspective. J. Exp. Biol. 213, 3–16.

Ho, D., Burggren, W.W., 2012. Parental hypoxic exposure confers offspring hypoxia resistance in zebrafish (*Danio rerio*). J. Exp. Biol. 215, 4208–4216.

Ho, D., Reed, W.L., Burggren, W.W., 2011. Egg yolk environment differentially influence physiological and morphological development of broiler and layer chicken embryos. J. Exp. Biol. 214, 619–628.

Höchel, J., Akiyama, R., Masuko, T., Pearson, J., Nickelmann, M., Tazawa, H., 1998. Development of heart rate irregularities in chick embryos. Am. J. Physiol. Heart Cir. Physiol. 275, H527–H533.

Høiby, M., Aulie, A., Reite, O.B., 1983. Oxygen uptake in fowl eggs incubated in air and pure oxygen. Comp. Biochem. Physiol. A 74, 315–318.

Hoyt, D.F., 1979. Osmoregulation by avian embryos: the allantois functions like a toad's bladder. Physiol. Zool. 52, 354–362.

Howe, R.S., Burggren, W.W., Warburton, S.J., 1995. Fixed patterns of bradycardia during late embryonic development in domestic fowl with C locus mutation. Am. J. Physiol. 268, H56–H60.

Hu, N., Clark, E.B., 1989. Hemodynamics of the stage 12 to stage 29 chick embryo. Cir. Res. 65, 1665–1670.

Hughes, A.F.W., 1949. The heart output of the chick embryo. J. Roy. Microsc. Soc. 69, 145–152.

Ide, R., Ide, S.T., Mortola, J.P., 2016. The hypometabolic response to repeated or prolonged hypoxic episodes in the chicken embryo. Respir. Physiol. Neurobiol. 230, 29–35.

Ide, R., Ide, S.T., Mortola, J.P., 2017a. The cessation of breathing in the chicken embryo during cold-hypometabolism. Respir. Physiol. Neurobiol. 242, 19–29.

Ide, S.T., Ide, R., Mortola, J.P., 2017b. Aerobic scope in chicken embryos. Comp. Biochem. Physiol. A 212, 81–87.

Iversen, N.K., Wang, T., Baatrup, E., Crossley, D.A., 2014. The role of nitric oxide in the cardiovascular response to chronic and acute hypoxia in White Leghorn chicken (*Gallus domesticus*). Acta Physiol. 211 (2), 346–357.

Jonker, S.S., Giraud, G.D., Espinoza, H.M., Davis, E.N., Crossley II, D.A., 2015. Effects of chronic hypoxia on cardiac function measured by pressure-volume catheter in fetal chickens. Am. J. Physiol. Regul. Integr. Comp. Physiol. 308, R680–R689.

Kato, K., Moriya, K., Dzialowski, E.M., Burggren, W.W., Tazawa, H., 2002. Cardiac rhythms in prenatal and perinatal emu embryos. Comp. Biochem. Physiol. A 131, 775–785.

Keller, B.B., Kowalski, W.J., Tinney, J.P., Tobita, K., Hu, N., 2020. Validating the paradigm that biomechanical forces regulate embryonic cardiovascular morphogenesis and are fundamental in the etiology of congenital heart disease. J. Cardiovasc. Dev. Dis. 7 (2), 23.

Khaliduzzaman, A., Fujitani, S., Kashimori, A., Suzuki, T., Ogawa, Y., Kondo, N., 2019a. A non-invasive diagnosis technique of chick embryonic cardiac arrhythmia using near infrared light. Comput. Electron. Agric. 158, 326–334.

Khaliduzzaman, A., Fujitani, S., Kondo, N., Ogawa, Y., Fujiura, T., Suzuki, T., Kashimori, A., Syduzzaman, M., Rahman, A., 2019b. Non-invasive characterization of chick embryo body and cardiac movements using near infrared light. Eng. Agric. Environ. Food 12 (1), 32–39.

Khandoker, A.H., Dzialowski, E.M., Burggren, W.W., Tazawa, H., 2003. Cardiac rhythms of late pre-pipped and pipped chick embryos exposed to altered oxygen environments. Comp. Biochem. Physiol. A 136, 289–299.

Khandoker, A.H., Fukazawa, K., Dzialowski, E.M., Burggren, W.W., Tazawa, H., 2004. Maturation of homeothermic response of heart rate to altered ambient temperature in developing chick hatchlings. Am. J. Physiol. Reg. Int. Comp. Physiol. 286, R129–R137.

Kind, C., 1975. The development of the circulating blood volume of the chick embryo. Anat. Embryol. 147, 127–132.

Klempt, M., Ellendorff, F., Grossmann, R., 1992. Functional maturation of arginine vasotocin secretory responses to osmotic stimulation in the chick embryo and the newborn chicken. J. Endocrinol. 133, 269–274.

Klusonová, P., Zemanová, Z., 2007. Characteristics of the compensatory renal growth of the remnant embryonic chick kidneys. Physiol. Res. 56, 651–654.

Kuroda, O., Matsunaga, C., Whittow, G.C., Tazawa, H., 1990. Comparative metabolic responses to prolonged cooling in precocial duck (*Anas domestica*) and altricial pigeon (*Columba domestica*) embryos. Comp. Biochem. Physiol. A 95, 407–410.

Laughlin, K.F., Lundy, H., Tait, J.A., 1976. Chick embryo heart rate during the last week of incubation: population studies. Br. Poult. Sci. 17, 293–301.

le Noble, F., Klein, C., Tintu, A., Pries, A., Buschmann, I., 2008. Neural guidance molecules, tip cells, and mechanical factors in vascular development. Cardiovasc. Res. 78, 232–241.

Lemez, L., 1972. Thrombocytes of chick embryos from the 2nd day of incubation till the 1st postembryonic day. Acta Univ. Carol. Ser. Med. Mono. 53–54, 365–371.

Lemus, J.Á., Blanco, G., Arroyo, B., Martínez, F., Grande, J., 2009. Fatal embryo chondral damage associated with fluoroquinolones in eggs of threatened avian scavengers. Environ. Pollut. 157, 2421–2427.

Lindgren, I., Altimiras, J., 2009. Chronic prenatal hypoxia sensitizes β-adrenoceptors in the embryonic heart but causes postnatal desensitization. Am. J. Physiol. Reg. Int. Comp. Physiol. 297 (2), R258–R264.

Lindgren, I., Crossley II, D., Villamor, E., Altimiras, J., 2011. Hypotension in the chronically hypoxic chicken embryo is related to the β-adrenergic response of chorioallantoic and femoral arteries and not to bradycardia. Am. J. Physiol. Reg. Int. Comp. Physiol. 301 (4), R1161–R1168.

Maibier, M., Reglin, B., Nitzsche, B., Xiang, W., Rong, W.W., Hoffmann, B., Djonov, V., Secomb, T.W., Pries, A.R., 2016. Structure and hemodynamics of vascular networks in the chorioallantoic membrane of the chicken. Am. J. Physiol. Heart Circ. Physiol. 311 (4), H913–H926.

Makanya, A.N., Dimova, I., Koller, T., Styp-Rekowska, B., Djonov, V., 2016. Dynamics of the developing chick chorioallantoic membrane assessed by stereology, allometry, immunohistochemistry and molecular analysis. PLoS One 11 (4), e0152821.

Maksimov, V.F., Korostyshevskaya, I.M., 2013. Morphogenesis and reaction to hypoxia of atrial myoendocrine cells in chick embryos (*Gallus gallus*). J. Evol. Biochem. Physiol. 49, 251–258.

Männer, J., 2000. Cardiac looping in the chick embryo: a morphological review with special reference to terminological and biomechanical aspects of the looping process. Anat. Rec. 259, 248–262.

Männer, J., 2006. Ontogenetic development of the helical heart: concepts and facts. Eur. J. Cardio. Thorac. Surg. 29 (Suppl. 1), S69–S74.

Mather, C.M., Laughlin, K.F., 1979. Storage of hatching eggs: the interaction between parental age and early embryonic development. Br. Poult. Sci. 20, 595–604.

Matsunaga, C., Mathiu, P.M., Whittow, G.C., Tazawa, H., 1989. Oxygen consumption of Brown Noddy (*Anous stolidus*) embryos in a quasiequilibrium state at lowered ambient temperatures. Comp. Biochem. Physiol. A 93, 707–710.

Mayer, A.A., Metcalfe, J., Stock, M.K., 1995. Relocation during incubation of endothelial nuclei in the chick chorioallantois. Respir. Physiol. 100, 171–176.

Menna, T.M., Mortola, J.P., 2003. Ventilatory chemosensitivity in the chick embryo. Respir. Physiol. Neurobiol. 137, 69–79.

McNabb, F.M.A., 1987. Comparative thyroid development in precocial Japanese quail and altricial ring doves. J. Exp. Zool. 1 (Suppl.), 281–290.

Meuer, H.J., Tietke, P., 1990. Changes in blood PCO_2 and acid-base status in chick embryo between day 4 and 6 of incubation. Adv. Exp. Med. Biol. 277, 751–758.

Midgett, M., Goenezen, S., Rugonyi, S., 2014. Blood flow dynamics reflect degree of outflow tract banding in Hamburger–Hamilton stage 18 chicken embryos. J. R. Soc. Interface 11 (100), 20140643.

Midgett, M., Thornburg, K., Rugonyi, S., 2017. Blood flow patterns underlie developmental heart defects. Am. J. Physiol. Heart Circ. Physiol. 312 (3), H632–H642.

Mitgard, V., Sejrsen, P., Johansen, K., 1985. Blood flow in the brood patch of Bantam hens: evidence of cold vasodilation. J. Comp. Physiol. B 155, 703–709.

Moonen, R.M., Villamor, E., 2011. Developmental changes in mesenteric artery reactivity in embryonic and newly hatched chicks. J. Comp. Physiol. B 181, 1063–1073.

Moriya, K., Höchel, J., Pearson, J., Tazawa, H., 1999. Cardiac rhythms in developing chicks. Compl. Biochem. Physiol. A 124, 461–468.

Moriya, K., Pearson, J.T., Burggren, W.W., Ar, A., Tazawa, H., 2000. Continuous measurements of instantaneous heart rate and its fluctuations before and after hatching in chickens. J. Exp. Biol. 203, 895–903.

Mortola, J.P., 2006. Metabolic response to cooling temperatures in chicken embryos and hatchlings after cold incubation. Comp. Biochem. Physiol. A 145, 441–448.

Mortola, J.P., 2009. Gas exchange in avian embryos and hatchlings. Comp. Biochem. Physiol. A 153, 359–377.

Mortola, J.P., Besterman, A.D., 2007. Gaseous metabolism of the chicken embryo and hatchling during post-hypoxic recovery. Respir. Physiol. Neurobiol. 156, 212–219.

Mortola, J.P., Cooney, E., 2008. Cost of growth and maintenance in chicken embryos during normoxic or hypoxic conditions. Respir. Physiol. Neurobiol. 162, 223–229.

Mortola, J.P., Marinescu, D.-C., Pierre, A., Artman, L., 2012. Metabolic and heart rate responses to hypoxia in early chicken embryos in the transition from diffusive to convective gas transport. Respir. Physiol. Neurobiol. 181 (2), 109–117.

Mortola, J.P., Wills, K., Trippenbach, T., Al Awam, K., 2010. Interactive effects of temperature and hypoxia on heart rate and oxygen consumption of the 3-day old chicken embryo. Comp. Biochem. Physiol. A 155, 301–308.

Mueller, C.A., Burggren, W.W., Crossley II, D.A., 2013a. Angiotensin II and baroreflex control of heart rate in embryonic chickens (*Gallus gallus domesticus*). Am. J. Physiol. Reg. Int. Comp. Physiol. 305, R855–R863.

Mueller, C.A., Tazawa, H., Burggren, W.W., 2013b. Dynamics of metabolic compensation and hematological changes in chicken (Gallus gallus) embryos exposed to hypercapnia with varying oxygen. Respir. Physiol. Neurobiol. 185, 272–280.

Mueller, C.A., Crossley II, D.A., Burggren, W.W., 2014a. The actions of the renin-angiotensin system on cardiovascular and osmoregulatory function in embryonic chickens (*Gallus gallus domesticus*). Comp. Biochem. Physiol. 178, 37–45.

Mueller, C., Tazawa, H., Burggren, W., 2014b. Dynamics of acid–base metabolic compensation and hematological regulation interactions in response to CO_2 challenges in embryos of the chicken (*Gallus gallus*). J. Comp. Physiol. B 184 (5), 641–649.

Mueller, C.A., Tazawa, H., Burggren, W.W., 2017. Dynamics of acid-base and hematological regulation in day 15 chicken embryos (*Gallus gallus domesticus*) exposed to graded hypercapnia and hypoxia. Respir. Physiol. Neurobiol. 239, 55–63.

Mühlbauer, E., Hamannt, D., Xu, B., Ivell, R., Udovic, B., Ellendorff, F., Grossmann, R., 1993. Arginine vasotocin gene expression and hormone synthesis during ontogeny of the chicken embryo and the newborn chick. J. Neuroendocrinol. 5, 281–288.

Mulder, T.L.M.,C., van Golde, J., Prinzen, F.W., Blanco, C.E., 1997. Cardiac output distribution in the chick embryo from stage 36 to 45. Cardiovasc. Res. 34, 525–528.

Mulder, A., Miedema, A., De Mey, J., Giussani, D.A., Blanco, C.E., 2002. Sympathetic control of the cardiovascular response to acute hypoxemia in the chick embryo. Am. J. Physiol. Reg. Int. Comp. Physiol. 282 (4), R1156–R1163.

Murphy, M.J., Brown, P.S., Brown, S.C., 1986. Osmoregulatory effects of prolactin and growth hormone in embryonic chicks. Gen. Comp. Endocrinol. 62, 485–492.

New, D.A.T., 1957. A critical period for the turning of hen's eggs. J. Embryol. Exp. Morphol. 5, 293–299.

Nichelmann, M., 2004. Perinatal epigenetic temperature adaptation in avian species: comparison of Turkey and Muscovy duck. J. Therm. Biol. 29, 613–619.

Nishimura, H., Yang, Y., Hubert, C., Gasc, J.-M., Ruijtenbeek, K., De Mey, J., Boudier, H.A.J.S., Corvol, P., 2003. Maturation-dependent changes of angiotensin receptor expression in fowl. Am. J. Physiol. Reg. Int. Comp. Physiol. 285, R231–R242.

Nowak-Sliwinska, P., Segura, T., Iruela-Arispe, M.L., 2014. The chicken chorioallantoic membrane model in biology, medicine and bioengineering. Angiogenesis 17, 779–804.

Okuda, A., Tazawa, H., 1988. Gas exchange and development of chicken embryos with widely altered shell conductance from the beginning of incubation. Respir. Physiol. 74, 187–198.

Ono, H., Hou, P.-C., Tazawa, H., 1994. Responses of developing chicken embryos to acute changes in ambient temperature: noninvasive study of heart rate. Israel J. Zool. 40, 467–479.

Orłowski, G., Hałupka, L., 2015. Embryonic eggshell thickness erosion: a literature survey re-assessing embryo-induced eggshell thinning in birds. Environ. Pollut. 205, 218–224.

Orłowski, G., Hałupka, L., Klimczuk, E., Sztwiertnia, H., 2016. Shell thinning due to embryo development in eggs of a small passerine bird. J. Ornithol. 157 (2), 565–572.

Pappano, A.J., Löffelholz, K., 1974. Ontogenesis of adrenergic and cholinergic neuroeffector tranmission in chick embryo heart. J. Pharmacol. Exp. Ther. 191, 468–478.

Pattern, B.M., 1951. Early Embryology of the Chick. McGraw-Hill Book Company, New York.

Pearson, J.T., Haque, M.A., Hou, P.-C.L., Tazawa, H., 1996. Developmental patterns of O_2 consumption, heart rate and O_2 pulse in unturned eggs. Respir. Physiol. 103, 83–87.

Pearson, J.T., Moriya, K., Yanone, M., Tazawa, H., 2000. Development and regulation of heart rate in embryos and hatchlings of gulls (*Larus schistisagus* and *Larus crassirostris*) in relation to growth. J. Comp. Physiol. B 170, 429–438.

Pearson, J.T., Noma, Y., Tazawa, H., 1999. Developmental patterns of heart rate in altricial avian embryos and hatchlings. J. Exp. Biol. 202, 1545–1550.

Pearson, J.T., Tazawa, H., 1999. Ontogeny of heart rate in embryonic and nestling crows (*Corvus corone* and *Corvus macrorhynchos*). J. Comp. Physiol. B 169, 256–262.

Pearson, J.T., Tsuzuki, M., Nakane, Y., Akiyama, R., Tazawa, H., 1998. Development of heart rate in the precocial king quail, *Coturnix chinensis*. J. Exp. Biol. 201, 931–941.

Pedernera, E.A., Lantos, C.P., 1973. The biosynthesis of adrenal steroids by the 15-day-old chick embryo. Gen. Comp. Endocrinol. 20, 331–341.

Pettit, T.N., Whittow, G.C., 1982a. The initiation of pulmonary respiration in a bird embryo: blood and air cell gas tension. Respir. Physiol. 48, 199–208.

Pettit, T.N., Whittow, G.C., 1982b. The initiation of pulmonary respiration in a bird embryo: tidal volume and frequency. Respir. Physiol. 48, 209–218.

Phelan, C.M., Hughes, S.F., Benson Jr., D.W., 1995. Heart rate-dependent characteristics of diastolic ventricular filling in the developing chick embryo. Pediatr. Res. 37, 289–293.

Phuphanin, A., Sampanporn, L., Sutapun, B., 2019. Smartphone-based device for non-invasive heart-rate measurement of chicken embryos. Sensors 19, 4843.

Prinzinger, R., Dietz, V., 1995. Qualitative course of embryonic O_2 consumption in altricial and precocial birds. Respir. Physiol. 100, 289–294.

Pollard, A.S., Pitsillides, A.A., Portugal, S.J., 2016. Validating a noninvasive technique for monitoring embryo movement in ovo. Physiol. Biochem. Zool. 89, 331–339.

Price, E.R., Dzialowski, E.M., 2018. Development of endothermy in birds: patterns and mechanisms. J. Comp. Physiol. B. 188, 373–391.

Prinzinger, R., Schmidt, M., Dietz, V., 1995. Embryogeny of oxygen consumption in 13 altricial and precocial birds. Respir. Physiol. 100, 283–287.

Rahn, H., 1991. Why birds lay eggs. In: Deeming, D.C., Ferguson, M.W.J. (Eds.), Egg Incubation: Its Effects on Embryonic Development in Birds and Reptiles. Cambridge Univ. Press, Cambridge, pp. 345–360.

Rahn, H., Ar, A., 1974. The avian egg: incubation time and water loss. Condor 76, 147–152.

Rahn, H., Carey, C., Balmas, K., Bhatia, B., Paganelli, C., 1977. Reduction of pore area of the avian eggshell as an adaptation to altitude. Proc. Natl. Acad. Sci. U.S.A. 74, 3095–3098.

Rahn, H., Matalon, S., Sotherland, P.R., 1985. Circulatory changes and oxygen delivery in the chick embryo prior to hatching. In: Johansen, K., Burggren, W. (Eds.), Cardiovascular Shunts: Phylogeneic, Ontogenetic and Clinical Aspects. Munksggard, Copenhagen, pp. 179–198.

Rahn, H., Paganelli, C.V., Ar, A., 1974. The avian egg: air-cell gas tension, metabolism and incubation time. Respir. Physiol. 22, 297–309.

Rahn, H., Poturalski, S.A., Paganelli, C.V., 1990. The acoustocardiogram: a non-invasive method for measuring heart rate of avian embryos in ovo. J. Appl. Physiol. 69, 1546–1548.

Reyna, K.S., 2010. Thermal Stress during Pre-incubation Induces Subsequent Developmental Plasticity in Northern Bobwhites. Doctor of Philosophy. University of North Texas.

Reyna, K.S., Burggren, W.W., 2012. Upper lethal temperatures of Northern Bobwhite embryos and the thermal properties of their eggs. Poult. Sci. 91, 41–46.

Reyna, K.S., Burggren, W.W., 2017. Altered embryonic development in northern bobwhite quail (*Colinus virginianus*) induced by pre-incubation oscillatory thermal stresses mimicking global warming predictions. PLoS One 12 (9), e0184670.

Ribatti, D., 2017. The chick embryo chorioallantoic membrane (CAM) assay. Reprod. Toxicol. 70, 97–101.

Robertson, I.S., 1961. Studies on the effect of humidity on the hatchability of hen's eggs I. The determination of optimum humidity for incubation. J. Agric. Sci. 57, 185–194.

Romanoff, A.L., 1960. The Avian Embryo. Macmillan, New York.

Romanoff, A.L., 1967. Biochemistry of the Avian Embryo. Wiley, New York.

Romijn, C., 1948. Respiratory movements of the chicken during the parafoetal period. Physiol. Comp. Oecol. 1, 24–28.

Rosenberger, J., Deeming, D.C., Łukaszewicz, E., Kowalczyk, A., 2017. Changes of eggshell characteristics during embryo development in Western Capercaillie (*Tetrao urogallus*). Avian Biol. Res. 10 (2), 92–97.

Ruben, J.A., Jones, T.D., Geist, N.R., 2003. Respiratory and reproductive paleophysiology of dinosaurs and early birds. Physiol. Biochem. Zool. 76, 141–164.

Sakamoto, Y., Haque, M.A., Ono, H., Pearson, J., Tazawa, 1995. Two-dimensional cardiogenic ballistic movements of avian eggs. Med. Biol. Eng. Comput. 33, 611–614.

Sartori, M.R., Taylor, E.W., Abe, A.S., Crossley II, D.A., 2015. An appraisal of the use of an infrared digital monitoring system for long-term measurement of heart rate in reptilian embryos. Comp. Biochem. Physiol. A Mol. Integr. Physiol. 188, 7–21.

Savary, K., Michaud, A., Favier, J., Larger, E., Corvol, P., Gasc, J., 2005. Role of the renin-angiotensin system in primitive erythropoiesis in the chick embryo. Blood 105, 103–110.

Ruijtenbeek, K, Le Noble, F.A.C., Janssen, G.M.J., Kessels, C.G.A., Fazzi, G.E., Blanco, C.E., De Mey, J. G.R., 2000. Chronic hypoxia stimulates periarterial sympathetic nerve development in chicken embryo. Circulation 102 (23), 2892–2897.

Saint Petery, L.B., Van Mierop, L.H.S., 1974. Evidence for presence of adrenergic receptors in the 6 day-old chick embryo. Am. J. Physiol. 227, 1406–1410.

Sbong, S., Dzialowski, E.M., 2007. Respiratory and cardiovascular responses to acute hypoxia and hyperoxia in internally pipped chicken embryos. Comp. Biochem. Physiol. A 148, 761–768.

Scott, T.A., Silversides, F.G., 2000. The effect of storage and strain of hen on egg quality. Poult Sci 79, 1725–1729.

Sheldon, E.L., McCowan, L.S., McDiarmid, C.S., Griffith, S.C., 2018. Measuring the embryonic heart rate of wild birds: an opportunity to take the pulse on early development. Auk 135 (1), 71–82.

Sirsat, T.S., Dzialowski, E.M., 2016. Ventilation changes associated with hatching and maturation of an endothermic phenotype in the Pekin duck (*Anas platyrhynchos domestica*). Am. J. Physiol. Regul. Integr. Comp. Physiol. 310, R766–R775.

Sirsat, S.K., Sirsat, T.S., Crossley, J.L., Sotherland, P.R., Dzialowski, E.M., 2016. The 12-day thermoregulatory metamorphosis of Red-winged Blackbirds (*Agelaius phoeniceus*). J. Comp. Physiol. B. 186, 651–663.

Sirsat, T.S., Crossley II, D.A., Crossley, J.L., Dzialowski, E.M., 2018. Thyroid hormone manipulation influences development of cardiovascular regulation in embryonic Pekin duck, *Anas platyrhynchos domestica*. J. Comp. Physiol. B. 188, 843–853.

Snyder, G.K., Birchard, G.F., 1982. Water loss and survival in embryos of the domestic chicken. J. Exp. Zool. 219, 115–117.

Sotherland, P.R., Rahn, H., 1987. On the composition of bird eggs. Condor 89, 48–65.

Sotherland, P.R., Spotila, J.R., Paganelli, C.V., 1987. Avian eggs: barriers to the exchange of heat and mass. J. Exp. Zool. 1 (Suppl.), 81–86.

Stewart, M.E., Terepka, A., 1969. Transport functions of the chick chorioallantoic membrane: I. Normal histology and evidence for active electrolyte transport from the allantoic fluid, in vivo. Exp. Cell Res. 58, 93–106.

Stock, M.K., Asson-Batres, M.A., Metcalfe, J., 1985. Stimulatory and persistent effect of acute hyperoxia on respiratory gas exchange of the chick embryo. Respir. Physiol. 62, 217–230.

Strick, D.M., Waycaster, R.L., Montani, J.-P., Gay, W.J., Adair, T.H., 1991. Morphometric measurements of chorioallantoic membrane vascularity: effects of hypoxia and hyperoxia. Am. J. Physiol. Heart Circ. Physiol. 260 (4), H1385–H1389.

Swart, J., Tate, K., Crossley II, D.A., 2014. Development of adrenergic and cholinergic receptor cardiovascular regulatory capacity in the Canada goose (*Branta canadensis*) and domestic goose (*Anser anser domesticus*). Comp. Biochem. Physiol. A Mol. Integr. Physiol. 167, 59–67.

Szdzuy, K., Fong, L.M., Mortola, J.P., 2008. Oxygenation and establishment of thermogenesis in the avian embryo. Life Sci. 82, 50–58.

Szdzuy, K., Mortola, J.P., 2007. Monitoring breathing in avian embryos and hatchlings by the barometric technique. Respir. Physiol. Neurobiol. 159, 241–244.

Taber, L.A., 2001. Biomechanics of cardiovascular development. Annu. Rev. Biomed. Eng. 3, 1–25.

Tamura, A., Akiyama, R., Chiba, Y., Moriya, K., Dzialowski, E.M., Burggren, W.W., Tazawa, H., 2003. Heart rate responses to cooling in emu hatchlings. Comp. Biochem. Physiol. A 134, 829–838.

Tazawa, H., 1971. Measurement of respiratory parameters in blood of chicken embryo. J. Appl. Physiol. 30, 17–20.

Tazawa, H., 1973. Hypothermal effect on the gas exchange in chicken embryo. Respir. Physiol. 17, 21–31.

Tazawa, H., 1980a. Oxygen and CO_2 exchange and acid-base regulation in the avian embryo. Amer. Zool. 20, 395–4004.

Tazawa, H., 1980b. Adverse effect of failure to turn the avian egg on embryo oxygen exchange. Respir. Physiol. 41, 137–142.

Tazawa, H., 1981a. Compensation of diffusive respiratory disturbances of the acid-base balance in the chick embryo. Comp. Biochem. Physiol. A 69, 333–336.

Tazawa, H., 1981b. Effect of O_2 and CO_2 in N_2, He and SF_6 on chick embryo blood pressure and heart rate. J. Appl. Physiol. 51, 1017–1022.

Tazawa, H., 1981c. Measurement of blood pressure of chick embryo with an implanted needle catheter. J. Appl. Physiol. 51, 1023–1026.

Tazawa, H., 1982. Regulatory process of metabolic and respiratory acid-base disturbances in embryos. J. Appl. Physiol. 53, 1449–1454.

Tazawa, H., 1986. Acid-base equilibrium in birds and eggs. In: Heisler, N. (Ed.), Acid-Base Regulation in Animals. Elsevier, Amsterdam, pp. 203–233.

Tazawa, H., 1987. Embryonic respiration. In: Seller, T.J. (Ed.), Bird Respiration, vol. II. CRC Press, Boca Raton, FL, pp. 3–41.

Tazawa, H., 2005. Cardiac rhythms in avian embryos and hatchlings. Avian Poult. Biol. Rev. 16, 123–150.

Tazawa, H., Akiyama, R., Moriya, K., 2002a. Development of cardiac rhythms in birds. Comp. Biochem. Physiol. A 132, 675–689.

Tazawa, H., Andrewartha, S.J., Burggren, W.W., 2012. Acute regulation of hematocrit and blood acid-base balance during severe hypoxic challenges in late chicken embryos (Gallus *gallus*). Respir. Physiol. Neurobiol. 184, 86–96.

Tazawa, H., Ar, A., Gefen, E., Moriya, K., Pearson, J.T., 1998b. Effects of incubator humidity on embryonic heart rate in the ostrich. Proc. 10th Eur. Poult. Conf. 843–847.

Tazawa, H., Ar, A., Moriya, K., Gefen, E., Pearson, J.T., 2000. Embryonic heart rate measurements during artificial incubation of emu eggs. Br. Poult. Sci. 41, 89–93.

Tazawa, H., Ar, A., Pearson, J.T., Moriya, K., Gefen, E., 1998a. Heart rate in developing ostrich embryos. Br. Poult. Sci. 39, 161–166.

Tazawa, H., Chiba, Y., Khandoker, A.H., Dzialowski, E.M., Burggren, W.W., 2004. Early development of thermoregulatory competence in chickens: responses of heart rate and oxygen uptake to altered ambient temperatures. Avian Poult. Biol. Rev. 15, 166–176.

Tazawa, H., Hashimoto, Y., Doi, K., 1992a. Blood pressure and heart rate of chick embryo (*Gallus domesticus*) within the egg: responses to autonomic drugs. In: Hill, R.B., Kuwasawa, K. (Eds.), Phylogenetic Models in Functional Coupling of the CNS and the Cardiovascular System. Karger, Amsterdam, pp. 86–96.

Tazawa, H., Hashimoto, Y., Nakazawa, S., Whittow, G.C., 1992b. Metabolic responses of chicken embryos and hatchlings to altered O_2 environments. Respir. Physiol. 88, 37–50.

Tazawa, H., Hiraguchi, T., Kuroda, O., Tullett, S.G., Deeming, O.C., 1991a. Embryonic heart rate during development of domesticated birds. Physiol. Zool. 64, 1002–1022.

Tazawa, H., Hou, P.-C.L., 1997. Avian cardiovascular development. In: Burggren, W.W., Keller, B. (Eds.), Development of Cardiovascular Systems: Molecules to Organisms. Cambridge Univ. Press, New York, pp. 193–210.

Tazawa, H., Johansen, K., 1987. Comparative model analysis of central shunts in vertebrate cardiovascular systems. Comp. Biochem. Physiol. A 86, 595–607.

Tazawa, H., Kuroda, O., Whittow, G.C., 1991b. Noninvasive determination of the embryonic heart rate during hatching in the Brown Noddy (*Anous stolidus*). Auk 108, 594–601.

Tazawa, H., Mikami, T., Yoshimoto, C., 1971a. Respiratory properties of chicken embryonic blood during development. Respir. Physiol. 13, 160–170.

Tazawa, H., Mikami, T., Yoshimoto, C., 1971b. Effect of reducing the shell area on the respiratory properties of chicken embryonic blood. Respir. Physiol. 13, 352–360.

Tazawa, H., Mitsubayashi, H., Hirata, M., Höchel, J., Pearson, J.T., 1999. Cardiac rhythms in chick embryos during hatching. Comp. Biochem. Physiol. A 124, 511–521.

Tazawa, H., Mochizuki, M., 1976. Estimation of contact time and diffusing capacity for oxygen in the chorioallantoic vascular plexus. Respir. Physiol. 28, 119–128.

Tazawa, H., Mochizuki, M., 1977. Oxygen analysis of chicken embryo blood. Respir. Physiol. 31, 203–215.

Tazawa, H., Moriya, K., Tamura, A., Akiyama, R., 2002b. Low frequency oscillation of instantaneous heart rate in newly hatched chicks. Comp. Biochem. Physiol. A 131, 797–803.

Tazawa, H., Moriya, K., Tamura, A., Komoro, T., Akiyama, R., 2001a. Ontogenetic study of thermoregulation in birds. J. Thermal Biol. 26, 281–286.

Tazawa, H., Nakagawa, S., 1985. Response of egg temperature, heart rate and blood pressure in the chick embryo to hypothermal stress. J. Comp. Physiol. B 155, 195–200.

Tazawa, H., Okuda, A., Nakazawa, S., Whittow, G.C., 1989a. Metabolic responses of chicken embryos to graded, prolonged alterations in ambient temperature. Comp. Biochem. Physiol. A 92, 613–617.

Tazawa, H., Ono, T., 1974. Microscopic observation of the chorioallantoic capillary bed of chicken embryo. Respir. Physiol. 20, 81–90.

Tazawa, H., Ono, T., Mochizuki, M., 1976. Oxygenation and deoxygenation velocity factors of chorioallantoic capillary blood. J. Appl. Physiol. 40, 399–403.

Tazawa, H., Pearson, J.T., Komoro, T., Ar, A., 2001b. Allometric relationships between embryonic heart rate and fresh egg mass in birds. J. Exp. Biol. 204, 165–174.

Tazawa, H., Piiper, J., 1984. Carbon dioxide dissociation and buffering in chicken blood during development. Respir. Physiol. 57, 123–134.

Tazawa, H., Piiper, J., Ar, A., Rahn, H., 1981. Changes in acid-base balance of chick embryos exposed to a He and SF_6 atmosphere. J. Appl. Physiol. 50, 819–823.

Tazawa, H., Rahn, H., 1986. Tolerance of chick embryos to low temperatures in reference to the heart rate. Comp. Biochem. Physiol. A 85, 531–534.

Tazawa, H., Rahn, H., 1987. Temperature and metabolism of chick embryos and hatchlings after prolonged cooling. J. Exp. Zool. 1 (Suppl.), 105–109.

Tazawa, H., Suzuki, Y., Musashi, H., 1989b. Simultaneous acquisition of ECG, BCG and blood pressure from chick embryos in the egg. J. Appl. Physiol. 67, 478–483.

Tazawa, H., Turner, J.S., Paganelli, C.V., 1988a. Cooling rates of living and killed chicken and quail eggs in air and in helium-oxygen gas mixture. Comp. Biochem. Physiol. A 90, 99–102.

Tazawa, H., Visschedijk, A.H.J., Piiper, J., 1983a. Blood gases and acid-base status in chicken embryos with naturally varying egg shell conductance. Respir. Physiol. 54, 137–144.

Tazawa, H., Visschedijk, A.H.J., Wittmann, J., Piiper, J., 1983b. Gas exchange, blood gases and acid-base status in the chick before, during and after hatching. Respir. Physiol. 53, 173–185.

Tazawa, H., Wakayama, H., Turner, J.S., Paganelli, C.V., 1988b. Metabolic compensation for gradual cooling in developing chick embryos. Comp. Biochem. Physiol. A 89, 125–129.

Tazawa, H., Watanabe, W., Burggren, W.W., 1994. Embryonic heart rate in altricial birds, the pigeon (*Columba domestica*) and the bank swallow (*Riparia riparia*). Physiol. Zool. 40, 1448–1460.

Tazawa, H., Whittow, G.C., 1994. Embryonic heart rate and oxygen pulse in two procellariiform seabirds, *Diomedea immutabilis* and *Puffinus pacificus*. J. Comp. Physiol. B 163, 642–648.

Tazawa, H., Whittow, G.C., Turner, J.S., Paganelli, C.V., 1989c. Metabolic responses to gradual cooling in chicken eggs treated with thiourea and oxygen. Comp. Biochem. Physiol. A 92, 619–622.

Tobita, K., Garrison, J.B., Liu, L.J., Tinney, J.P., Keller, B.B., 2005. Three-dimensional myofiber architecture of the embryonic left ventricle during normal development and altered mechanical loads. Anat. Rec. A Discov. Mol. Cell. Evol. Biol. 283A, 193–201.

Tøien, O., Aulie, A., Steen, J.B., 1986. Thermoregulatory responses to egg cooling in incubating bantam hens. J. Comp. Physiol. B. 156, 303–307.

Tomi, S.T., Ide, R., Mortola, J.P., 2019. Heart and breathing rate variability in the avian perinatal period: the chicken embryo as a model. Avian Biol. Res. 12 (1), 13–22.

Tufan, A.C., Satiroglu-Tufan, N.L., 2017. The chick embryo chorioallantoic membrane as a model system for the study of tumor angiogenesis, invasion and development of anti-angiogenic agents. Curr. Cancer Drug Targets 5, 249–266.

Tullett, S.G., Deeming, D.C., 1987. Failure to turn eggs during incubation: effects on embryo weight, development of the chorioallantois and absorption of albumen. Br. Poult. Sci. 28, 239–243.

Turner, J.S., 1986. Cooling rate and size of bird's eggs – a natural isomorphic body. J. Therm. Biol. 10, 101–104.

Turner, J.S., 1987. Blood circulation and the flows of heat in an incubated egg. J. Exp. Zool. 1 (Suppl.), 99–104.

Tzschentke, B., Basta, D., Nichelmann, M., 2001. Epigenetic temperature adaptation in birds: peculiarities and similarities in comparison to acclimation. News of Biomedical Science 1, 26–31.

Tzschentke, B., Rumpf, M., 2011. Embryonic development of endothermy. Respir. Physiol. Neurobiol. 178, 97–107.

Van Golde, J., Mulder, T., Blanco, C.E., 1997. Changes in mean chorioallantoic artery blood flow and heart rate produced by hypoxia in the developing chick embryo. Pediatr. Res. 42, 293–298.

Van Mierop, L.H.S., Bertuch Jr., C.J., 1967. Development of arterial blood pressure in the chick embryo. Am. J. Physiol. 212, 43–48.

Vince, M., Salter, S.H., 1967. Respiration and clicking in quail embryos. Nature 216, 582–583.

Visschedijk, A.H.J., Ar, A., Rahn, H., Piiper, J., 1980. The independent effects of atmospheric pressure and oxygen partial pressure on gas exchange of the chicken embryo. Respir. Physiol. 39, 33–44.

Visschedijk, A.H.J., Tazawa, H., Piiper, J., 1985. Variability of shell conductance and gas exchange of chicken eggs. Respir. Physiol. 59, 339–345.

Vleck, C.M., Vleck, D., 1987. Metabolism and energetic of avian embryos. J. Exp. Zool. 1 (Suppl.), 111–125.

Vleck, C.M., Vleck, D., Hoyt, D.F., 1980. Patterns of metabolism and growth in avian embryos. Am. Zool. 20, 405–416.

Vleck, D., Vleck, C.M., Seymour, R.S., 1984. Energetics of embryonic development in the megapode birds, mallee fowl *Leipoa ocellata* and brush Turkey *Alectura lathami*. Physiol. Zool. 57, 444–456.

Wagner-Amos, K., Seymour, R.S., 2002. Effect of regional changes to shell conductance on oxygen consumption and growth of chicken embryos. Resp. Physiol. 129, 385–395.

Wagner-Amos, K., Seymour, R.S., 2003. Effect of local shell conductance on the vascularisation of the chicken chorioallantoic membrane. Respir. Physiol. Neurobiol. 134, 155–167.

Wangensteen, O.D., Rahn, H., 1970/71. Respiratory gas exchange by the avian embryo. Respir. Physiol. 11, 31–45.

Wangensteen, O.D., Weibel, E.R., 1982. Morphometric evaluation of chorioallantoic oxygen transport in the chick embryo. Respir. Physiol. 47, 1–20.

Wangensteen, O.D., Wilson, D., Rahn, H., 1970/71. Diffusion of gases across the shell of the hen's egg. Respir. Physiol. 11, 16–30.

Whitaker-Fornek, J.R., Nelson, J.K., Lybbert, C.W., Pilarksi, J.Q., 2019. Development and regulation of breathing rhythms in embryonic and hatchling birds. Respir. Physiol. Neurobiol. 269, 103246.

White, P.T., 1974. Experimental studies on the circulatory system of the late chick embryo. J. Exp. Biol. 61, 571–592.

Whittow, G.C., 1980. Physiological and ecological correlates of prolonged incubation in sea birds. Am. Zool. 20, 427–436.

Whittow, G.C., Tazawa, H., 1991. The early development of thermoregulation in birds. Physiol. Zool. 64, 1371–1390.

Wilson, H.R., 1991. Physiological requirements of the developing embryo: temperature and turning. In: Tullett, S.G. (Ed.), Avian Incubation. Butterworth, London, pp. 145–156.

Wittig, J.G., Münsterberg, A., 2016. The early stages of heart development: insights from chicken embryos. J Cardiovasc. Dev. Dis. 3 (2), 12.

Yalcin, S., Gursel, I., Bilgen, G., Horuluoglu, B.H., Gucluer, G., Izzetoglu, G.T., 2017. Effect of egg storage duration and brooding temperatures on chick growth, intestine morphology and nutrient transporters. Animal 11, 1791–1797.

Yoneta, H., Akiyama, R., Nakata, W., Moriya, K., Tazawa, H., 2006a. Video analysis of body movements and their relation to the heart rate fluctuations in chicken hatchlings. In: Yahav, S., Tzschentke, B. (Eds.), New Insights into Fundamental Physiology and Peri-natal Adaptation of Domestic Fowl. Nottingham Univ. Press, pp. 57–68.

Yoneta, H., Dzialowski, E.M., Burggren, W.W., Tazawa, H., 2007. Endothermic heart rate response in broiler and White Leghorn chicks

(*Gallus gallus domesticus*) during the first two days of post hatch life. Comp. Biochem. Physiol. A 147, 529–535.

Yoneta, H., Fukazawa, K., Dzialowski, E.M., Burggren, W.W., Tazawa, H., 2006b. Does sequence of exposure to altered ambient temperature affect the endothermic heart rate response of newly hatched chicks? In: Yahav, S., Tzschentke, B. (Eds.), New Insights into Fundamental Physiology and Peri-natal Adaptation of Domestic Fowl. Nottingham Univ. Press, pp. 15–28.

Yoneta, H., Fukuoka, S., Akiyama, R., Tazawa, H., 2006c. Early development of cholinergic heart rate control in embryos of broiler and White Leghorn chickens. In: Yahav, S., Tzschentke, B. (Eds.), New Insights into Fundamental Physiology and Peri-natal Adaptation of Domestic Fowl. Nottingham Univ. Press, pp. 1–14.

Yoshigi, M., Hu, N., Keller, B.B., 1996. Dorsal aortic impedance in stage 24 chick embryo following acute changes in circulating blood volume. Am. J. Physiol. Heart Circ. Physiol. 270, H1597–H1606.

Yosphe-Purer, Y., Fendrich, J., Davies, A.M., 1953. Estimation of blood volumes of embryonated hen eggs at different ages. Am. J. Physiol. 175, 178–180.

Zhang, H., Burggren, W., 2012. Hypoxic level and duration differentially affect embryonic organ system development of the chicken (*Gallus gallus*). Poult. Sci. 91 (12), 3191–3201.

Zhang, H., Shang, P., Zhang, Y., Zhang, Y., Tian, X., Zhang, H., 2017. Angiogenesis in chicken chorioallantoic membrane under hypoxic incubations. Anim. Biol. 67 (3–4), 251–261.

Chapter 38

Stress ecophysiology

Julio Blas[1] and Graham D. Fairhurst[2]

[1]*Department of Conservation Biology, Estación Biológica de Doñana, Consejo Superior de Investigaciones Científicas (CSIC), Seville, Spain;*
[2]*School of Environment and Sustainability, University of Saskatchewan, Saskatoon, SK, Canada*

Abbreviations

ACTH Adrenocorticotropic hormone
CORT Corticosterone
DEX Dexamethasone
ELHS Emergency life history stage
GC Glucocorticoid
GCM Glucocorticoid metabolite
HPA Hypothalamic−pituitary−adrenal
LHS Life history stage
LPF Labile perturbation factor

38.1 Introduction

Birds undergo profound changes in physiology, morphology, and behavior across their lifecycles, and the endocrine system plays a fundamental role integrating external and internal signals and orchestrating adequate responses ultimately selected to maximize individual fitness. Many of these changes occur in response to predictable fluctuations in the environment, like night-day and seasons, which allow year-round anticipatory organization of major life history stages (LHSs) in cyclic patterns. However, superimposed on predictable components are unpredictable perturbations (like severe weather, loss of social rank, habitat destruction, or human disturbance) which require rapid emergency adjustments in physiology and behavior generally termed the "*stress response.*" As in other vertebrates, the avian stress response involves two major pathways (Romero and Gormally 2019): (i) the catecholamine release from the adrenal medulla, responsible for a rapid, almost instantaneous "fight-or-flight" response mediated by the autonomic nervous system, and (ii) a slower release of *glucocorticoids* (GCs) (mostly *corticosterone*, the main GC in birds) following activation of the hypothalamic−pituitary−adrenal (HPA) axis which supports longer-term responses (Figure 38.1; Chapter 33). In this chapter, we will review the latter branch, summarizing research on the adrenocortical response to stress largely performed using wild birds as study models, with the aim of linking physiological responses to ecology and life-history traits (ecophysiology).

In response to disturbance, elevated blood GC levels promote adaptive physiological and behavioral changes that redirect the individual into a survival mode while suppressing nonessential activities. GCs support mobilization of body energy, increase cardiovascular tone, regulate the immune system, and inhibit a variety of costly anabolic processes including digestion, energy storage, growth, and reproduction (Sapolsky et al., 2000; Sapolsky, 2002). However, high and prolonged elevations of GCs, like those occurring during chronic adverse conditions, exert deleterious effects on critical body systems, causing disease and eventually death (Sapolsky et al., 2000). Furthermore, low levels of blood corticosterone are fundamental for basic physiological processes regardless of exposure to stress (Landys et al., 2006). The fact that the same hormone exerts opposing ("good and bad") actions depending on its level and duration, combined with the ambiguity of the term "*stress*" (Box 38.1), has prompted the development of recent conceptual frameworks, such as the *Allostasis Model* and the *Reactive Scope Model*, aimed at promoting integrative research linking the energy requirements of birds across their lifecycles with their adrenocortical responses within a context of avian ecology and life-history. These models will be explained in Section 38.2 with an updated review of the nomenclature describing corticosterone levels and actions in birds. Why, when, and how environmental conditions promote an activation of the HPA axis will be addressed in Section 38.3, with a classification of the types of perturbations and the resulting effects of corticosterone elevations on the normal progression of individuals' lifecycles. Short-term elevations of corticosterone levels activate a facultative "emergency life history stage" (ELHS),

Sturkie's Avian Physiology. https://doi.org/10.1016/B978-0-12-819770-7.00003-7

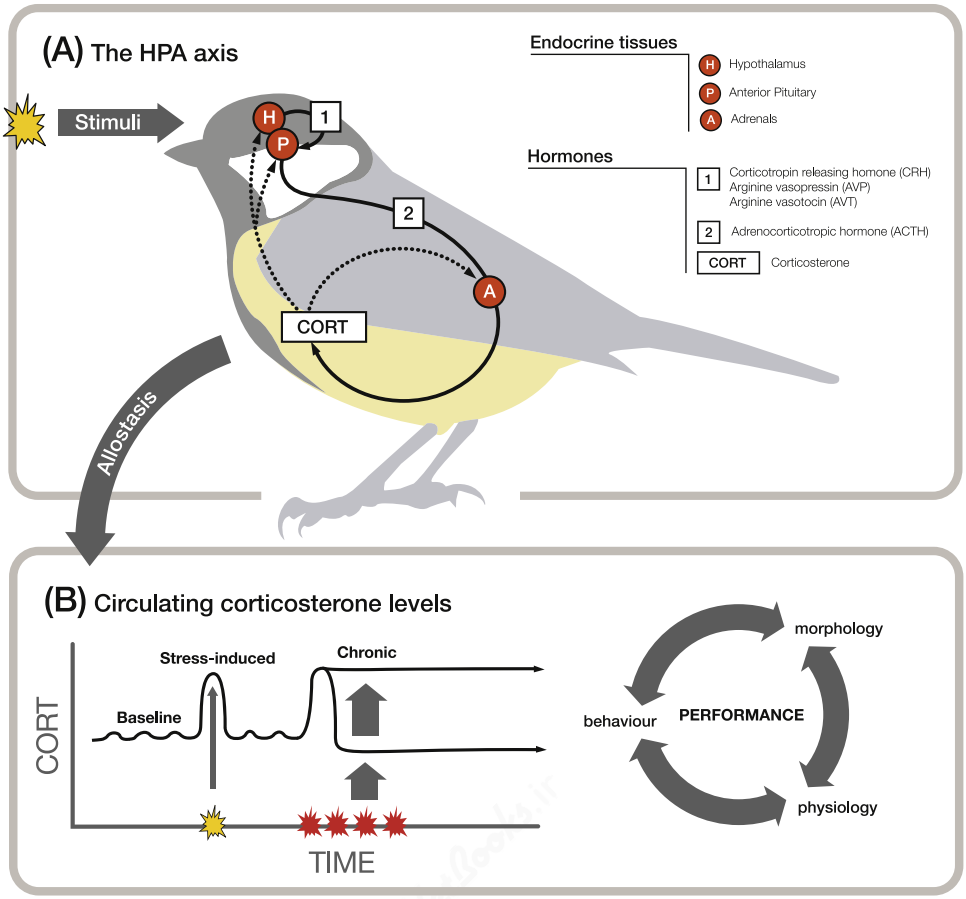

FIGURE 38.1 **The adrenocortical response to stress in birds.** (Panel 1): The hypothalamic–pituitary–adrenal (*HPA*) axis and endocrine pathway connecting the tissues (*black and white circles*) and hormones (*black and white squares*) involved in the adrenocortical response to stress. Following exposure to potentially noxious stimuli (e.g., a predator chase) the hypothalamus releases a number of hormones. These, in turn, stimulate the pituitary to secrete adrenocorticotropic hormone (*ACTH*) into circulation, which triggers the release of corticosterone (*CORT*) from the adrenal glands. Corticosterone secretion is subjected to negative feedback, as indicated with *dashed arrows*. (Panel 2): Time-related changes in circulating corticosterone levels during a stress response. Under normal (unstressed, predictable) conditions, corticosterone titers fluctuate within a narrow range of typically low levels known as "baseline" that allows a predictable adjustment of activity rhythms and metabolic functions in anticipation of change. Short-term exposure to perturbations (*black and white* star in x-axis) produces a rapid elevation of corticosterone into "stress-induced" levels, within a few minutes, which facilitate reactive changes in physiology and behavior (e.g., increased gluconeogenesis, suppression of reproductive behaviors, regulation of immune function) aimed at maximizing immediate survival. Once the perturbation has passed, corticosterone levels return to baseline range. However, prolonged or repeated exposure to perturbations (*black and white stars* in x-axis) can generate dysregulation of the HPA axis, leading to either hyper- or hyposecretion of corticosterone. In the long term, "chronic" dysregulation can jeopardize organismal performance. Ultimately, each level of corticosterone may facilitate specific changes in physiology, morphology, and behavior aimed at maintaining homeostasis through change (i.e., allostasis), and potentially affecting individual performance. *Credit: Figure modified and expanded from Blas and Baos (2008), Baos and Blas (2009), Blas et al. (2019).*

but longer-term exposure disrupts lifecycles, potentially leading to individuals' deaths and, by extension, population declines. The avian adrenocortical response shows all the features of a trait subjected to natural selection (high-individual variation, repeatability, and a genetic basis), but individuals also display a strong phenotypic plasticity. Section 38.4 reviews research on the adaptive variability of adrenocortical responses. Avian developmental modes range across a spectrum of altricial and precocial species, and the maturation of the adrenocortical response during early life varies with this gradient. This pattern has likely evolved to balance the costs and benefits of corticosterone actions with the ability of young birds to cope with perturbations without parental support. Corticosterone can be also transferred from mothers to offspring ("maternal effects"), potentially translating ecological and environmental conditions into permanent offspring responses and resulting in phenotypes that could be better adapted to cope with perturbations through "maternal programming." Adult birds of many avian species have been shown to modulate their adrenocortical response during reproduction and according to the value of their brood. Such findings suggest that modulation of corticosterone secretion allows them to trade-off energy and resources between current

BOX 38.1 The stress series, baseline, and stress-induced corticosterone.

The Stress Series: The quantification of adrenocortical responses in wild birds is traditionally accomplished through a "stress series," which involves a *standardized capture, handling, and restraint protocol* accompanied by the serial collection of blood samples at specific time intervals. Plasma corticosterone levels are subsequently determined in the laboratory. Precapture conditions (a) are supposed to reflect the true *baseline corticosterone levels* of wild, unstressed specimens. Capture (b) sets the starting time of exposure to a noxious stimuli (i.e., the experimental perturbation), and should be performed in a consistent, standardized manner (e.g., through mist netting). The relatively slow response of the HPA axis allows taking a first blood sample within 3 min postcapture (c) for subsequent quantification of baseline corticosterone levels (sampling time is generally critical). Birds are then restrained (d) in standardized conditions (e.g., inside a cloth bag), and a second blood sample collected at a specific time (e.g., 30 min postcapture) allows determination of *stress-induced corticosterone levels* (e). Additional restraint periods and blood sampling episodes at preset times (e.g., 60 min postcapture) allows further quantification of individual stress-induced corticosterone levels (f–g). Biometric measurements and bird tagging (h) are typically performed prior to release (i). Subsequent monitoring of the tagged birds (j) and determination of plasma corticosterone in the collected samples (k) allows establishing ecophysiological links.

Baseline corticosterone levels are defined here as encompassing two related concepts:

(1) the "true" circulating level associated with routine daily activities and life processes, predictable allostatic load, and seasonal variation in LHSs in wild, "unstressed" individuals (*sensu* Landys et al., 2006); and

(2) levels from blood samples taken within a short time (typically 3 min) of capture that are assumed to reflect the precapture circulating level of the hormone. These sampled levels can only be expected to "not reflect the acute stress of capture" and, as such, they are more accurately referred to as "initial" levels (Schoenemann and Bonier, 2018), particularly when taken as part of a stress-series (see above).

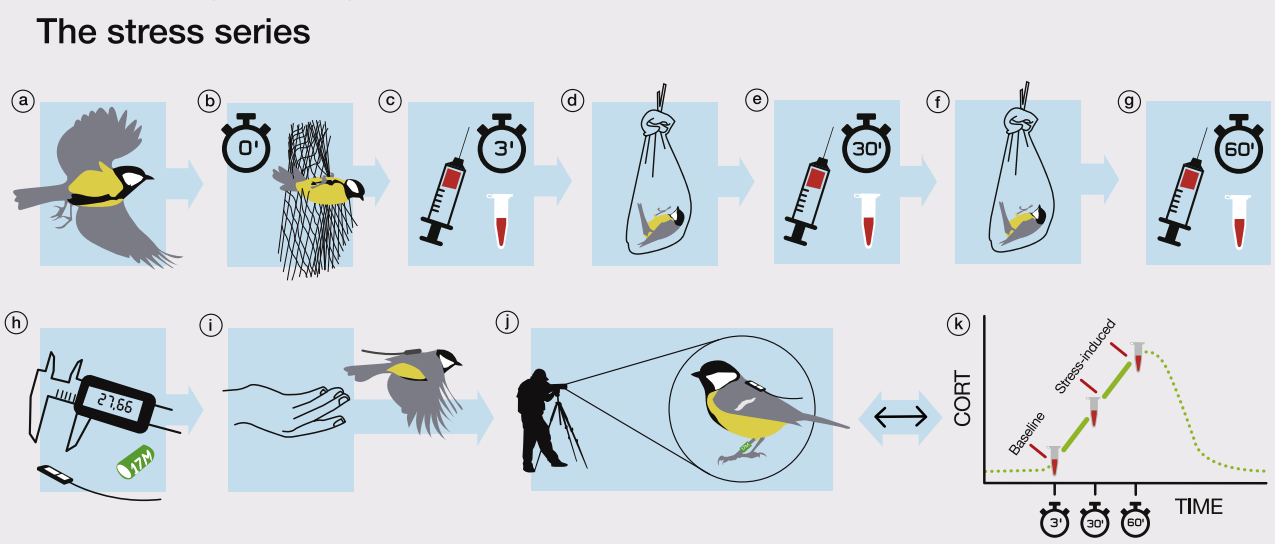

Baseline and stress-induced corticosterone: There has been debate for years about proper terminology in studies of the adrenocortical response. This debate stems in large part from the nebulous term "stress" and its frequent (mis)usage in the literature (Section 38.2; Romero 2004; Romero 2012), as well as the increasingly common misinterpretation that stress can be measured directly using levels of GCs (MacDougall-Shackleton et al., 2019). In choosing the terminology for this chapter, we were faced with balancing our desire to use the most accurate terms and contribute to efforts to improve their usage, with the reality that some of these "short-hand" terms are now used pervasively (if incorrectly) by ornithologists and behavioral endocrinologists. Thus, to maximize uptake of this chapter, and to ensure our terms match the usage in the overwhelming majority of studies, we opted to use terms that would be most broadly recognizable. We fully support efforts to improve the usage of terminology in the literature (MacDougall-Shackleton et al., 2019), including avoiding referring to GCs as "stress hormones." To that end, in our definitions below we draw readers' attention to assumptions inherent in these terms that must be considered when using them in studies of the adrenocortical response.

The majority of studies that report baseline corticosterone levels from field and laboratory settings make the assumption inherent in the second definition and, further, use the levels as a proxy of the true (seasonal) baseline. Researchers should be aware of this assumption when drawing ecophysiological inference, as a variety of factors could result in the sampled baseline value departing from the true baseline. For example, a bird could have been chased by a predator immediately prior to capture, or could be diseased, and such factors that have the potential to affect (i.e., skew) baseline corticosterone levels are often not known to the researcher.

Continued

BOX 38.1 The stress series, baseline, and stress-induced corticosterone.—cont'd

Stress-induced corticosterone levels are defined here as encompassing two related concepts:

(1) the circulating level that arises in response to life-threatening and unpredictable perturbations in wild individuals; and

(2) levels from blood samples taken after the bird has been exposed to a stressor for a specified time (typically 30 min). The capture and restraint/confinement conducted by researchers during a stress series is believed to mimic an acute natural stressor (though more naturalistic stressors can be used, e.g., Cockrem and Silverin, 2002), so is frequently used to induce stress-induced levels. Regardless of the stressor, the levels derived from this sample are assumed to reflect levels secreted by wild individuals. Birds can acclimate to stressors (see Romero, 2004), especially in captivity, so experience of the individual must be accounted for when drawing ecophysiological inference from stress-induced corticosterone levels.

Credit: The authors of this chapter.

reproductive investment and survival, providing a proximate (corticosterone-mediated) mechanism for life history evolution. Finally, field ecophysiological research conducted on wild avian models provides a richer understanding of free-living birds but imposes important challenges compared to laboratory studies, which will be addressed in Section 38.5, with a description of common methodological tools for assessing adrenocortical function in wild birds. For ease of reading, a final Section 38.6 contains a glossary of terms and abbreviations commonly used across this chapter.

38.2 Stress, energy, and glucocorticoids

The term "stress" can be misleading, and it is often misused in the ornithological literature. For example, it is relatively easy to find references to the "stress of reproduction" or the "stress of migration" in the literature, when authors are in fact referring to physiological demands of normally predictable LHSs that are not truly related to physiological stress. Prominent researchers on this topic assert that the use of this word says "virtually nothing about the underlying physiological or behavioral mechanisms" (McEwen and Wingfield, 2003b), and that "stress means whatever the author wants it to mean" (Romero, 2012). So what do we mean when using the term "stress"? As a polysemous word, depending on the context, authors may use "stress" to mean: (1) the stimulus that challenges *homeostasis* (i.e., *stressor*, *perturbation*), (2) the emergency response to perturbations (i.e., stress response), or (3) the chronic state of imbalance that follows overactivation of the adrenocortical axis (i.e., pathology, *chronic stress*). In the biomedical literature, this word remains ambiguous since it was first brought from the field of engineering by Cannon (1932) and Selye (1946). What alternative, unequivocal term could be used to avoid such confusion?

Modern ecophysiologists have made efforts to define and consolidate alternative and unequivocal terms (see Glossary in Section 38.6), leading to the recent introduction of "allostasis" and an accompanying set of terms to precisely define physiological responses to both normal life history conditions and unpredictable challenges, which are key aspects of this chapter. Allostasis is the process of maintaining homeostasis through change. This concept was introduced decades ago to redefine stress (Sterling and Eyer, 1988), but it only started to reach the ecophysiological literature after McEwen and Wingfield proposed the Allostasis Model (McEwen and Wingfield, 2003a). Through the key concepts of allostatic state, allostatic load, and allostatic overload, the model incorporates classic homeostasis in the context of an organism's lifecycle and in relation to individual experience and how the individual responds to ever-changing physical and social environments (i.e., within an ecological context; Figure 38.2; McEwen and Wingfield, 2010). This model uses the balance between energy input and energy requirements to predict when an animal should move away from the normal lifecycle into an emergency survival mode, and when a pathological imbalance would occur. The Reactive Scope Model is an offshoot of the Allostasis Model, but presents a different terminology for contextualizing the impact of stress in the body, as well as a new classification for the levels of the mediators (e.g., corticosterone in birds; see Figure 38.3) that allows the incorporation of a process known as "wear and tear." Combining traditional notions of stress and homeostasis with the more recent terminology of allostasis and allostatic load, the Reactive Scope Model addresses the mechanisms of response to perturbations and the roles of different mediators, including GCs. It is important to understand these two models and their associated terminology before we can understand the patterns of adrenocortical responses to stress and the underlying physiological mechanisms in birds, within an ecological and life history context.

- "Stress" is an unspecific term that may mean:
  (1) the stimulus that challenges homeostasis (i.e., stressor, perturbation),
  (2) the emergency response to perturbations (i.e., stress response), or

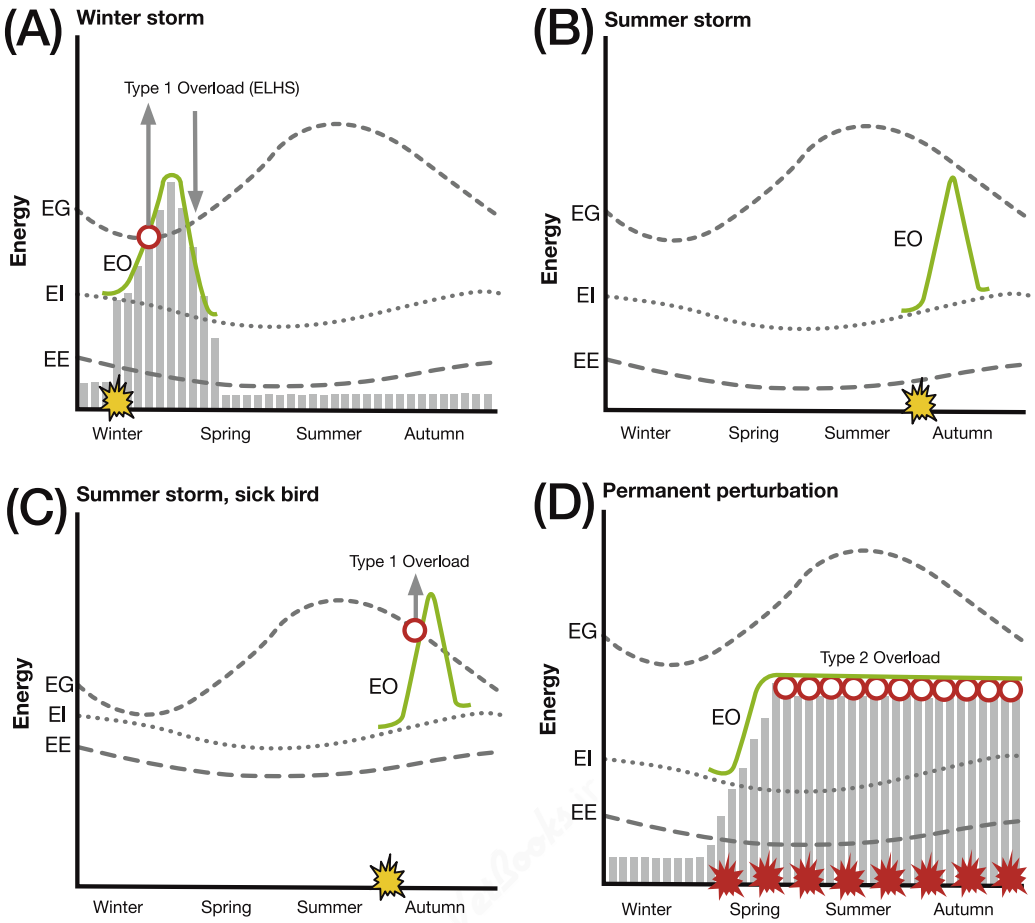

FIGURE 38.2 **The allostasis model.** The Allostasis Model provides a framework to understand the energetic requirements of organisms during their life, and predictions for when allostatic overload (*red circles*) would occur under a range of environmental, social, and individual-based scenarios. The y-axis represents potential nutritional requirements (including energy per se and nutrients) during 1 year (seasons in x-axis). The lines represent several energy components: EG (energy to be gained) represents the amount of energy in food available in the environment. In temperate areas, it is expected to rise in spring and summer and decline through autumn and winter when primary productivity is low. EE (existence energy) is the minimum existence energy (resting metabolism) required for basic homeostasis in any life history stage. It may decline in temperate spring and summer with ambient temperature. EI (ideal energy) is the extra energy required to go out, find food, process, and assimilate it under ideal conditions (when there are no perturbations) while performing seasonal routines (breeding, molting, migrating). It likely changes seasonally and for clarity we assume that it varies in parallel with EE. EO (energy following perturbation) is the additional energy required to go out, find food, process, and assimilate it under nonideal conditions. Allostatic load is the energy resulting from adding EE + EI + EO. In the figures, the *star* symbol defines when a perturbation (for example, severe weather) starts. Type 1 allostatic overload (panels A and C) occurs when allostatic load surpasses the energy available in the environment EG, promoting corticosterone elevations (*gray bars*, only shown in panels A and D for clarity) that trigger an Emergency Life History Stage (ELHS). One result is the suppression of other life history stages like migration or breeding, and bringing allostatic load below the level of EG. For example, the bird may suspend spring migration to obtain more food and only continue migrating when the perturbation ends. The bird can now survive the perturbation in positive energy balance and glucocorticoid elevations subside, avoiding pathologies associated with chronically high levels. Note that the same perturbation (for example, a severe storm) can result in Type 1 overload during winter but not in summer (compare panels A and B) when there is more food available (and EG > EE + EI + EO even during the perturbation). However, an individual heavily infected by parasites or with a permanent injury or chronic disease (panel C) would enter Type 1 allostatic overload facing the same summer storm because its intrinsic (disease-related) EE and EI levels are higher compared to a healthy bird (compare panels B and C). A second type of overload (Type 2 overload; panel D) can take place in situations where the energy available from the environment EG is not a limiting factor but a long-term perturbation (for example, climate change, captivity, permanent exposure to predators, permanent social challenge) triggers an allostatic state. The behavioral or physiological adjustments promoted by allostasis mediators (e.g., corticosterone) do not allow evading/coping with the continuing noxious stimuli (*red stars*). Corticosterone levels (*gray bars*) become chronically elevated or dysregulated, generating pathologies, and individuals would likely die early. Note that the individual must be unable to escape the perturbation in order for Type 2 allostasis overload to occur. In the figures, the levels of allostasis mediators (e.g., corticosterone) are indicated as gray bars only in the first and last panels (A and D) for simplicity, noting that their associations with energy levels (the metrics for all y-axes) are not necessarily linear. *Credit: Figures modified and expanded from McEwen and Wingfield (2003a) with permission.*

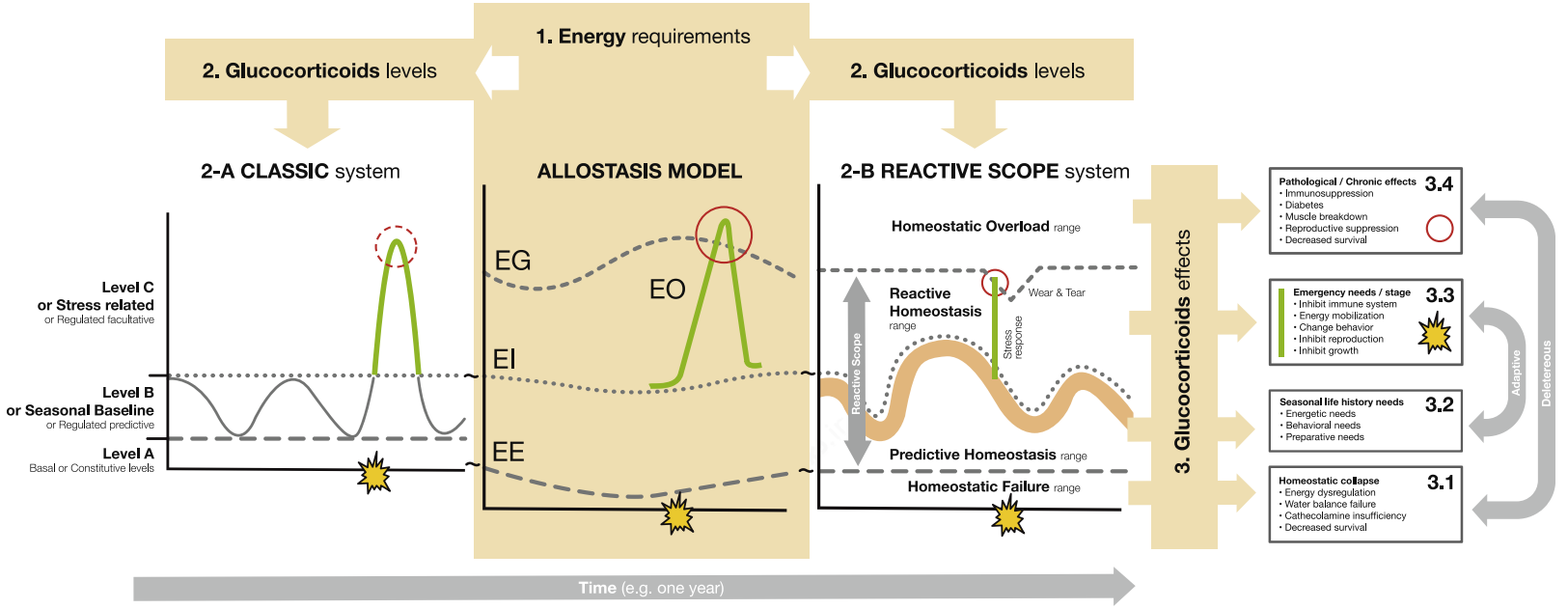

FIGURE 38.3 **Classification of corticosterone levels.** Classification of functional GC ranges according to the Classic system (panel 2A) and the Reactive Scope system (panel 2B). Both GC classification systems are presented in parallel to highlight the degree of overlapping and equivalence among system-specific terms (see main text and Section 38.6 for definitions), and in relation to the individual energy balance introduced by the Allostasis Model (panel 1). Energy requirements precede changes in GC levels, and thus the Allostasis Model is here presented as a central panel. Examples of GC effects on physiology and behavior (panel 3) are also presented in line with the corresponding GC ranges. Within any given chart, the x-axis represents the timeline (for example, 1 year), and the star symbol indicates exposure to a perturbation, which first results in increased energy demands (depicted as a *green line* in panel 1, implying increased allostatic load) and secondly in concomitant increases of GC levels reaching a range known as Level C or reactive homeostasis (*green lines* in panels 2A and 2B respectively). The perturbation may eventually bring the individual into negative energy balance (depicted as a *red circle* in panel 1, implying allostatic overload type I), and GC elevations will reach an upper range (*red circles* in panels 2A and 2B) potentially causing deleterious effects on body systems (panel 3, box 3.4). To avoid the damage associated to both the energy imbalance and the high GC levels, a facultative emergency life history stage is typically triggered (panel 3, box 3.3). If the negative energy balance subsides (because the perturbation extinguishes, or the individual relocates) GC levels return to a normal seasonal baseline known as level B or predictive homeostasis (in panels 2A and 2B, respectively) allowing resuming normal life history activities (panel 3, box 3.2). Note that the deleterious effects of GCs can occur both at very high and very low concentrations (panel 3, boxes 3.1 vs. 3.4). *Credit: Composite figure integrates graphs modified and expanded from several sources, including McEwen and Wingfield (2003a); Landys et al. (2006) and Romero et al. (2009).*

(3) the chronic state of imbalance that follows overactivation of the adrenocortical axis (i.e., pathology).

- Ecophysiologists are making ongoing efforts to define and consolidate alternative and unequivocal terms, leading to the recent introduction of the Allostasis Model and the Reactive Scope Model.

38.2.1 Allostasis: the concept and the model

Homeostasis (*sensu* Cannon, 1932) is the stability of physiological systems that are essential to life. As discussed in McEwen and Wingfield (2010), the concept of homeostasis is restricted to a few truly essential systems: pH, body temperature, glucose levels, and oxygen tension. In other words, those aspects of physiology that "keep us alive" (McEwen and Wingfield, 2003a). *Allostasis* is the process of achieving stability through change: it maintains homeostasis even though the set points and other boundaries of control may change with environmental conditions. Allostasis thus refers to those aspects of physiology that "help us adapt" (McEwen and Wingfield, 2010). Circulating GCs are major (but not the only) mediators of allostasis: additional mediators include catecholamines, cytokines, behavior, heart rate, blood pressure, and antibody titers (see Table 1 in Romero et al., 2009). GC levels can change markedly to help the body maintain homeostasis within narrow limits. To allow for this, GC levels fluctuate in daily and seasonal patterns (despite being equivocally called "stress" hormones), and also rise rapidly when a perturbation occurs. Free-living birds respond to potentially noxious stimuli (e.g., storms, social challenge, or human disturbances that reduce access to food and shelter) by increasing GC secretion, which facilitates foraging and gluconeogenesis. In addition, elevated GCs inhibit processes that are not essential to immediate survival (e.g., reproduction, migration) and increase physical activity. This allows an individual to move away from the perturbation or find shelter, as well as save energy by increasing night restfulness (Wingfield, 1994; Wingfield and Ramenofsky, 1999; Wingfield et al., 1998). When the body experiences altered and sustained activity levels of *allostasis mediators* (e.g., corticosterone), it enters an *allostatic state*, which can only be maintained for limited periods before damaging the body. The *Allostasis Model* (Figure 38.2) provides an ecological framework to understand when and how emergency responses are activated (reaching an allostatic state) through modeling the energetic requirements of organisms during their life, and in relation to the energy available in the environment. To understand the model, the following energy components need to be considered:

EG (energy to be gained): represents the amount of energy in food available in the environment. In temperate areas, it is expected to rise dramatically in spring and summer and then decline through autumn and winter when primary productivity is low.

EE (existence energy): is the minimum existence energy (resting metabolism) required for basic homeostasis in any LHS. It may decline with increasing ambient temperature (if it becomes easier to maintain body functions), e.g., in temperate spring and summer.

EI (ideal energy): is the extra energy required to go out, find food, process, and assimilate it under ideal conditions (when there are no perturbations) while performing seasonal routines (breeding, molting, migrating). It changes seasonally: it can follow EE and ambient temperature (for example, in a nonbreeding bird) or can increase during reproduction (spring-summer) and decrease during wintering. For clarity, in Figure 38.2A, it varies in parallel with EE.

EO (energy following perturbation): is the additional energy required to go out, find food, process, and assimilate it under nonideal conditions (following a perturbation). It is always higher than EE + EI. In Figure 38.2, the star symbol defines when the perturbation starts, setting the beginning point for elevations in EO energy demands.

Allostatic load can now be defined as the cumulative energetic requirements of the organism at a given time, and equals EE + EI + EO (although it is sometimes noted simply as EO). This concept relates to all the energy requirements in a broad sense (encompassing nutrients and all other potentially limiting resources), and it can be interpreted as a cost: the cumulative cost of being there, responding to the current situation whether it is predictable or not; or the "workload" of a particular moment (at certain times, an animal has to work harder—expend more energy to maintain homeostasis). A detailed definition of allostatic load in McEwen and Wingfield (2010) is "all of the energy and nutrients an organism needs to go about its daily and seasonal routines as the life cycle progresses, and to deal with unpredictable events from the physical and social environment that have the potential to be stressful." In the graphical representation, allostatic load fluctuates along a continuum with important transitional points (see red circles in Figure 38.2) that determine when the individual can cope with daily activities (seen as a cost, when is the load "affordable"?) and when it needs to trigger facultative physiological and behavioral responses evolved to reduce costs (when is the load unaffordable and becomes an overload?). In other words, transitional points determine when the individual enters overload and triggers an allostatic state.

The Allostasis Model proposes two different outcomes for *allostatic overload*. First, if energy demands exceed energy income and what can be mobilized from stores (i.e., if allostatic load surpasses EG), then Type 1 allostatic overload occurs. For example, breeding birds take

advantage of the increasing food abundance in spring to raise their broods. If inclement weather then increases the cost of maintaining homeostasis in addition to the demands of breeding, and at the same time reduces the food available to fuel this allostatic load, then a negative energy balance (overload) would result in a loss of body mass and the suppression of reproduction (see Wingfield et al., 1983 for empirical grounds). This negative energy balance is termed Type 1 allostatic overload, which leads to an allostatic state (increased levels of GCs), which then triggers physiological changes (use of lipid stores resulting in body mass loss) and behavioral changes (brood desertion). This response has been classically referred to as the ELHS and will be discussed in more detail in Section 38.3.3. Note for now, however, that short-term elevations of GCs may promote rapid physiological and behavioral changes, allowing a decrease of allostatic load below the EG level, before abandonment of the present LHS occurs. Only above a certain threshold (likely variable among individuals) would corticosterone trigger an ELHS (Wingfield and Romero, 2001). The final outcome of an allostatic state is normally survival because a positive energy balance can be reestablished: allostatic load will return to affordable levels when the individual relocates (or seeks refuge until the perturbations ends) and restores depleted condition through foraging. All of these actions are facilitated by the allostasis mediators (e.g., corticosterone levels, but also changes in behavior, hearth rate, blood pressure, cytokines, and antibody titers; see Romero et al., 2009), which are highly adaptive when elevated for a short period and then returned to normal (pre-perturbation) levels. Only in those circumstances when individuals are unable to avoid the perturbation after entering the ELHS is elevated corticosterone maintained for periods long to result in serious pathological effects and eventually death. The value of this Allostasis Model becomes more clear when we incorporate individual variation due to habitat quality, body condition, disease and parasites, reproductive state, experience, genetics, social status, and many other additional parameters. For example, because the energy available in the environment (EG) fluctuates (e.g., food is more abundant in spring than winter), a given perturbation will result in Type 1 allostatic overload faster at specific times of the year. This aspect is illustrated in Figure 38.2: the same storm (star symbol) promoting Type 1 allostatic overload in winter (panel (A)) fails to do so in summer (panel (B)) because there is sufficient energy in the environment to afford the increased allostatic load. However, an individual heavily affected by parasites or disease, or with a permanent injury (panel (C)), would enter Type 1 allostatic overload even in summer because its intrinsic (disease-related) energy requirement levels EE and EI are higher than average (in other words, its allostatic load was already elevated before the storm, and any additional EO load surpasses the energy available in the environment EG, rapidly resulting in overload). As an extreme example, habitats degraded by human transformation and climate change (Wingfield et al., 2017) often reduce food availability in the environment below the requirements for EE and EI. In the figures, the levels of allostasis mediators (for example, circulating corticosterone levels) are only indicated as gray bars in panels (A) and (D) for simplicity, but note that the metrics in the Allostasis Model refer to energy levels rather that the levels of any mediator. The relationships between energy requirement at a given moment and the level of a specific mediator are not necessarily linear because different allostasis mediators (e.g., GCs, cathecolamines, cytokines) act in concert and interact in complex physiological ways to meet allostatic demands (McEwen and Wingfield, 2010).

Second, another type of allostatic overload, qualitatively different from the Type 1 overload patterns described above, can arise in situations where energy from the environment (EG) is not limiting: then it is called Type 2 allostatic overload (see panel (D) in Figure 38.2). Here a long-term, rather than a short-term, perturbation (e.g., climate change instead of weather inclemency; captivity or permanent exposure to predators instead of a single predator chase; permanent social subordination instead of temporary social instability; see Section 38.3.3 for details) triggers an allostatic state, but concomitant elevations of GCs are unable to promote behavioral or physiological adjustments to cope with or to evade the noxious stimuli. For Type 2 allostatic overload to occur, the individual must be unable to evade the perturbation due to physical or social constraints. Corticosterone levels then become chronically elevated, generating pathologies despite adequate food resources (Type 2 overload occurs despite $EE + EI + EO < EG$; see Figure 38.2D). The effects on the body are similar to experimental exposure to high levels of exogenous corticosterone, and metabolic pathologies arise (e.g., hyperinsulinemia, hyperphagia, obesity). This situation is most likely to occur in vertebrates living in complex hierarchical systems (e.g., social primates), where subordinate (or depending on the specific system, sometimes dominant) status imposes heavy allostatic loads. However, it can also affect birds under certain conditions, such as (1) natural populations exposed to permanent habitat disturbances or climate change, (2) avian social systems where dominance structure predominates over food and shelter as a source of allostatic load (see review in Goymann and Wingfield, 2004), and (3) captive settings. The hormonal imbalances and metabolic costs imposed by Type 2 allostatic overload are high and likely result in chronic disease and premature death in the wild (e.g., birds with extreme fat stores are more likely to be depredated due to decreased maneuverability; Lind et al., 1999; Gosler et al., 2002), providing strong selection for the mechanisms limiting allostatic load.

However, in captive animals (and in human societies!), the selection pressure is not there, and pathologies can persist long-term.

In summary, the concept of allostasis (maintaining homeostasis through change) combines the energetic costs or demands associated with daily rhythms and LHSs (predictable) with those costs accompanying environmental perturbations and ecological and social challenges (unpredictable and either short- or long-term, see Section 39.3.1) into a continuum named allostatic load (see Figure 3 in Landys et al., 2006). Allostatic overload is then defined as either a short-term state in which the costs of the LHS and accompanying challenges (=allostatic load) exceeds the food resources available to provide sufficient energy (Type 1 allostatic overload), or a long-term state in which deleterious challenges are chronic and lead to a sustained allostatic state independent of seasonal changes in the environment (Type 2 allostatic overload). The terminology introduced by the Allostasis Model allows physiologists to replace the overused word "stress" by a set of distinct, unambiguous, and precisely defined terms that are being gradually incorporated into modern ecophysiological studies. However, an acknowledged weakness of the Allostasis Model is the use of energy as both the underlying mechanism and the universal metric (for a discussion of this topic see Walsberg, 2003; McEwen and Wingfield, 2003b; Romero et al., 2009; McEwen and Wingfield, 2010). This becomes a problem that is mainly a consequence of our current inability to measure individuals' energy demand (allostatic load) and environmental energy availability (EG) in free-living animals. Until we develop ways of measuring direct components of allostatic load (Porter et al., 2002; Ricklefs and Wikelski, 2002; Wilson et al., 2020), we will have to rely on the levels of allostasis mediators (e.g., circulating GCs) as best proxies to understand allostasis. Furthermore, the expected changes in corticosterone levels as a function of energy dynamics were only partially addressed in the original presentation of the Allostasis Model, and this will be the subject of the following subsection.

- Homeostasis is the stability of physiological systems that are essential to life, including pH, body temperature, glucose levels, and oxygen tension: those aspects of physiology that "keep us alive." In contrast, allostasis is the process of achieving homeostasis through change: those aspects of physiology that "help us adapt."
- The Allostasis Model provides a framework to understand the energetic requirements of organisms during their life, and in relation to the energy available. The model incorporates three concepts (allostasis, allostatic load, and allostatic overload) that allow replacing the overused and unambiguous word "stress":
  - Allostatic load is the cumulative energetic requirements of the organism in a broad sense (the "workload" in a particular moment), including predictable and unpredictable demands. Allostatic load fluctuates along a continuum, and transitional points determine when the individual can cope with daily activities and when it needs to trigger emergency responses aimed at reducing costs.
  - Type 1 allostatic overload is a short-term state of energy imbalance in which allostatic load exceeds the energy available from the environment plus the internal reserves.
  - Type 2 allostatic overload is a long-term state in which environmental or socially demanding challenges become chronic and exert deleterious effects on the individual, regardless of the energy available.
- The metric or "currency" for the Allostasis Model is energy. This represents a problem due to the difficulty of estimating energy demands and availability outside controlled conditions. However, energy management is achieved through changing levels of allostasis mediators (e.g., GCs, cathecolamines, cytokines, behavior, hearth rate, blood pressure, antibody titers) that can be measured accurately. The relationships between energy requirement at a given moment and the level of a specific mediator are not necessarily linear because different mediators act in concert and interact in complex ways.
- Corticosterone is the predominant GC in birds and a major allostasis mediator. Circulating corticosterone levels change in response to internal and external demands to manage energy balance. When the body experiences altered and sustained corticosterone elevations, it enters an allostatic state, which can only be sustained for limited periods before damaging the body.
- The Allostasis Model is a largely theoretical paradigm requiring empirical tests. However, it provides a framework for understanding when and how emergency responses are activated, and how individuals respond to changing physical and social environments.

38.2.2 Glucocorticoid levels

GCs are major allostatic mediators, meaning that they allow lifetime modulation of avian energy balance throughout changing internal and external conditions. Their role in gluconeogenesis explains much of their relevance as mediators, but they also act to facilitate morphological and behavioral changes and balance the immune system in ways that are crucial for individual fitness (see details in Chapter 33). The year-round dynamics of avian energy requirements and constraints introduced with the Allostasis Model provide a reference to describe expected changes in

GC levels (Figure 38.3). Because GCs can exert either "housekeeping" actions or devastating effects on the organism depending on their levels, it is critical to understand the range-descriptor terms and the specific terminology developed for this purpose. GCs can be "good and bad," "stress and antistress" (depending on the range), and an adequate term usage constitutes the only way to avoid confusion and to understand how opposing results regarding GC actions among studies are not necessarily contradictory. In fact, this paradox affects most allostasis mediators. The nomenclature describing GC ranges and functional thresholds differ, however, between what we will here call the *Classic System* and the *Reactive Scope System*. The two classifications are graphically presented in Figure 38.3 as two parallel panels (2A and 2B) and in relation to the Allostasis Model (but note that the latter refers to energy balance and not GC levels) for ease of comparison. As proposed by Wingfield et al. (1997) and further refined in Landys et al. (2006), the Classic System involves three hormonal thresholds (levels A, B, and C) and a set of corticosterone terms traditionally used (basal vs. baseline, constitutive vs. facultative, seasonal vs. stress related). The Reactive Scope System corresponds to a more recent classification given in the original proposal of a model (the Reactive Scope Model; Romero et al., 2009) that will be explained in the following section (Section 38.2.3). Although parallel terminologies may not help to explain the complexity of GC actions (the proposal of novel terms often generates controversy; McEwen and Wingfield, 2010), both systems ultimately agree in the following five conceptual ranges (one to five below) of increasing magnitude in circulating GC levels (Figure 38.3):

1. A pathological and physiologically unsustainable range where GC levels are too low for minimum homeostatic processes. This pathological range can be simulated by reducing levels of GCs through adrenalectomy (in mammals, Darlington et al., 1990) or chemical treatment (in birds, where adrenocortical cells are also located in the kidney tissue; see Chapter 33), and death rapidly occurs. In the Allostasis Model, this would be equivalent to an individual unable to meet the minimum energy requirements for existence (i.e., below EE level).
   a. In the Classic System, this range corresponds to GC concentrations below level A (this classification system does not have a specific place or level to represent a deadly physiological level or stage).
   b. In the Reactive Scope System, this is the GC range of *homeostatic failure.*
2. A minimum GC level allowing basic homeostatic processes (allowing meeting the existence energy demands EE in the Allostasis Model).
   a. In the Classic System, this range corresponds to GC concentrations within level (range) A, and corticosterone levels are termed basal or constitutive, (allowing "a physiological state A, representative of undisturbed animals at rest, in which hormone action maintains internal systems at a basal operating level to support the most fundamental requirements of life"; Landys et al., 2006).
   b. In the Reactive Scope System, this will be the lower end of (but already inside) the *predictive homeostasis range.*
3. A range where GC levels fluctuate according to predictable environmental changes, making it possible to cope with daily and seasonal routines of the life cycle (i.e., meeting ideal energy needs, EI, in the Allostasis Model).
   a. In the Classic System, this range corresponds to GC concentrations within levels (range) B and corticosterone levels are termed *seasonal baseline levels* or *regulated predictive level* (allowing a physiological state B where "hormone action maintains systems within a heightened operated range to support increasing demands—allostatic load, especially in association with predictable changes in the environment or life history"; Landys et al., 2006).
   b. In the Reactive Scope System, this will be the predictive homeostasis range, where GCs encompass normal circadian, daily, and seasonal changes. In the graphical representation of the Reactive Scope Model (Figure 38.3, panel 2B), the width of the orange colored area represents circadian variation (driven by predictable daily changes in light and dark; see, e.g., Dallman et al., 1987), while the convolutions of this thick line along 1 year reflect seasonal variation (predictable changes normally driven by photoperiod), which allow anticipation and progression of LHSs such as breeding (see, e.g., Romero, 2002). The thin line above the orange colored line represents corticosterone fluctuations in response to normal, and still predictable daily activities like foraging (using other terminology, "the circadian peak within the gray line corresponds to resting metabolic rate, while the thin line marks the active metabolic rate for that time of the year"; Romero et al., 2009).
4. An upper, facultative range of GC levels (superimposed above the normal circadian, daily, and seasonal fluctuations), where short-term elevations allow counteracting unpredictable changes in the environment, and either maintain or return the body to homeostasis (thus meeting the increased energy demands that follow perturbations: allostatic load EO).
   a. In the Classic System, this range corresponds to GC concentrations within level (range) C and

corticosterone levels are termed stress-induced, stress-regulated or regulated facultative (entering a physiological state C that "allow animals to survive threatening perturbations when allostatic load exceeds the immediate ability to cope, e.g., during encounters with a predator, infection, severe weather, energy storage and/or social instability"; Landys et al., 2006).

b. In the Reactive Scope System, this will be the *reactive homeostasis range*.

Both classification systems agree to term these facultative GC elevations as the "stress response," and link the physiological, morphological, and behavioral changes to a distinct ELHS (Wingfield et al., 1998), which will be presented in detail in Section 38.3.3. In panels 2A and 2B of Figure 38.3, the occurrence of a perturbation is depicted by a star symbol in the time line (x-axis), and concomitant GC elevations (the GC stress response) are represented with a thicker blue line (the same perturbation is also depicted in the central panel dedicated to the Allostasis Model with the predicted changes in energy demand EO, allostatic load, represented with a thicker green line). Note in the Reactive Scope Model (panel 2B), that the combination of predictive and reactive homeostasis ranges establishes the normal *reactive scope* for the individual, a concept that defines the upper and lower physiological constraints of a healthy animal and provides a name for the model, as we will explain shortly.

5. Finally, GC levels may reach a higher range where pathologies also develop. In the Allostasis Model, this would be equivalent to reaching Type 1 allostatic overload (when the energy demands exceed the energy available).

a. The Classic System (panel 2A) does not have a specific graphical notation for this range, likely because the development of pathology also involves a prolonged duration (time) of the GC elevations in a range that could still be indicative of typical *regulated facultative levels*. Prolonged GC elevations in this range are termed chronic GC levels. For ease of interpretation, the red circle in panel 2A depicts the highest GC concentrations that would lead to pathology if maintained for days.

b. In the Reactive Scope System, the upper GC levels would move into a homeostasis overload range (when corticosterone levels overpass the normal reactive scope above the upper end of the reactive homeostasis range). A key aspect in the Reactive Scope Model (and a conceptual novelty that was missing in both the Classic System and the Allostasis Model) is that the actual threshold for *homeostatic overload* can change within and between individuals in response to certain stimuli through a mechanism known as *wear and tear*. Therefore, the amplitude of the reactive scope is not a fixed trait in the individual. The effect of wear and tear is graphically represented in panel 2B, and its implications for reactive scope will be specifically discussed in the next section.

The absolute GC concentration defining each of these ranges varies between species (and even among populations within a given species, Wingfield and Romero, 2001), and GC actions on physiology and behavior are very different depending on the functional range (compare boxes 3.3 and 3.4 in Figure 38.3). On a more practical level, field endocrinologists typically collect blood samples from wild animals through standardized protocols such as the *stress series* (Box 38.1), which provides information about baseline and stress-induced GC levels. The simultaneous assessment of the conditions characterizing the same study subjects (e.g., health conditions, behavior, and environmental conditions) subsequently allows one to establish ecophysiological links. For simplicity, a direct association between circulating GC levels and GC actions (panel 3 in Figure 38.3) is often assumed. However, GC effects can be regulated at several levels (see Chapter 33, Wingfield, 2013b, Romero and Wingfield, 2016; Romero and Gormally, 2019), including at least (1) regulation of secretion and clearance rates, (2) regulation of transport (over 90% of circulating GCs are bound to carrier proteins, and only the remaining 10% constitute free and biological active hormone; Malisch and Breuner, 2010), (3) regulation of receptors (there are three types of receptors differing in affinities and exerting different effects on the organism), and (4) regulation of steroidogenic enzymes.

- GCs can exert housekeeping actions or devastating effects on the organism depending on what levels are involved (they can be "good and bad," "stress and antistress"). The absolute GC concentrations defining these ranges are species-specific.
- Two nomenclature systems (the Classic System and the Reactive Scope System) propose alternative terms to name GC ranges within adaptive and nonadaptive (pathological) levels.
- Healthy individuals show circulating GC levels within two narrow ranges below and above which serious pathologies occur:
  - Baseline levels fluctuate according to predictable environmental changes, allowing the individual to cope with daily and seasonal routines.
  - Stress-induced levels are facultative elevations (above seasonal baseline) that provide a means of

counteracting unpredictable changes in the environment. They are also termed the "stress response," and allow rapid physiological and behavioral changes characteristic of a distinct ELHS.

38.2.3 "Wear and tear" and the reactive scope model

Allostatic load (the "workload" to maintain homeostasis) is recognized as one the most relevant conceptual advances of the Allostasis Model (McEwen and Wingfield, 2003a). However, this concept needed to be further refined and expanded to incorporate additional body costs that were not explicitly acknowledged in the original formulation of the model. In particular, the elevation and maintenance of allostasis mediators incur a cost themselves. For example, the long-term behavioral and cardiovascular responses that characterize allostasis result in cardiovascular disease (Sapolsky, 2001), and GC elevations are known to exert a negative impact on the immune system, leading to a greater susceptibility to infections (Spencer et al., 2001). These costs are directly related to the allostasis mediators themselves and not to allostatic load per se, leading to the term "wear and tear": the cost of maintaining and using the physiological systems that mediate allostasis (Romero et al., 2009; Taff et al., 2018). The concept of wear and tear was introduced as a distinct attribute within a wider graphical interface, the *Reactive Scope Model* (Romero et al., 2009), which was proposed as a tool to characterize the physiological state of individuals across time, in response to perturbations, and according to the levels of mediators (not according to energy, which is the specific metric system of the Allostasis Model and generated ample criticism; Walsberg, 2003; Romero et al., 2009; McEwen and Wingfield, 2010). The Reactive Scope Model is therefore an extension (not a rebuttal) of the Allostasis Model and the seminal article leading to its formulation was supported by a review of the potential allostasis mediators and their effects at different ranges, including immune factors, cardiovascular responses, behavior, the central nervous system, and circulating GCs (Romero et al., 2009). For simplicity, only the later mediators (GCs; corticosterone) will be used here to explain wear and tear and the dynamics of the Reactive Scope Model across time and in response to perturbations. As we detailed in the previous section, the Reactive Scope Model also proposed a specific nomenclature to characterize the functional GC ranges (Figure 38.3, panel 2B). This new classification was justified to avoid confusion with other terms previously defined (what we called the Classic System in Figure 38.3, panel 2A), and circulating GC levels were presumed to exist in four ranges of increasing magnitude (i.e., homeostatic failure, predictive homeostasis, reactive homeostasis, and homeostatic overload). The combination of predictive and reactive homeostasis ranges establishes the normal reactive scope for the individual (which lies in between the upper and lower physiological constraints of a healthy animal, above and below which serious pathologies arise) and provides a name for the model (Figure 38.4).

In response to unpredictable perturbations, GC levels rapidly elevate outside the predictive range into the reactive homeostasis range. These elevations are graphically represented as rapid GC spikes (vertical bars in Figure 38.4), which counteract the negative effects of perturbations (depicted as numbered star symbols along the time line) through physiological and behavioral changes, and then quickly return to the predictive homeostasis range. This is the adrenocortical "stress response" aimed at maintaining homeostasis in the face of a perturbation. The sequence of perturbations experienced by a hypothetical model bird in Figure 38.4A indicates first that the magnitude of GC elevations depends on the type of perturbations. For example, the GC increase in response to perturbation 1 (e.g., a mild storm in winter) is significantly smaller than the elevations in response to perturbation 2 (a severe storm in winter). In these two examples, GC elevations remain within the reactive homeostasis range. In contrast, the same type of perturbation occurring at a different time of the year and even eliciting the exact same release of GCs can exert dramatically different effects on the individual. In Figure 38.4A, perturbations number 2 and 3 are two storms of similar quality (e.g., a severe storm occurring at the end of winter, and then again in early spring) eliciting similar GC elevations. However, only the latter causes pathology (red circle) as GC elevations reach the homeostatic overload range (GC spikes are represented now with a gray, rather than a green, bar to indicate pathological effects). A similar feature was previously suggested in the Allostasis Model with regards to an individual's likelihood of reaching states of negative energy balance at different times of the year, but some clarifications were needed. The Allostasis Model postulates that birds would be more resistant in winter because their energy requirements are lowest (winter perturbations should be stronger and demand more energy in order to reach allostatic overload Type 1; McEwen and Wingfield, 2003a), while the Reactive Scope Model postulates that birds are more resistant in winter because their GC *reactive homeostasis range* is wider (and thus reaching homeostatic overload would require a higher GC stress response, and likely a stronger perturbation; Romero et al., 2009). Energy demand (the currency of the Allostasis Model) and GC levels (the currency of the Reactive Scope Model) coincide in this example, as they both change in the same direction and result in deleterious effects, but this may not always be the case. As we pointed out, the task of maintaining GC levels in the reactive homeostasis range during a "stress response" itself incurs a cost known as wear and tear. Wear and tear can be defined

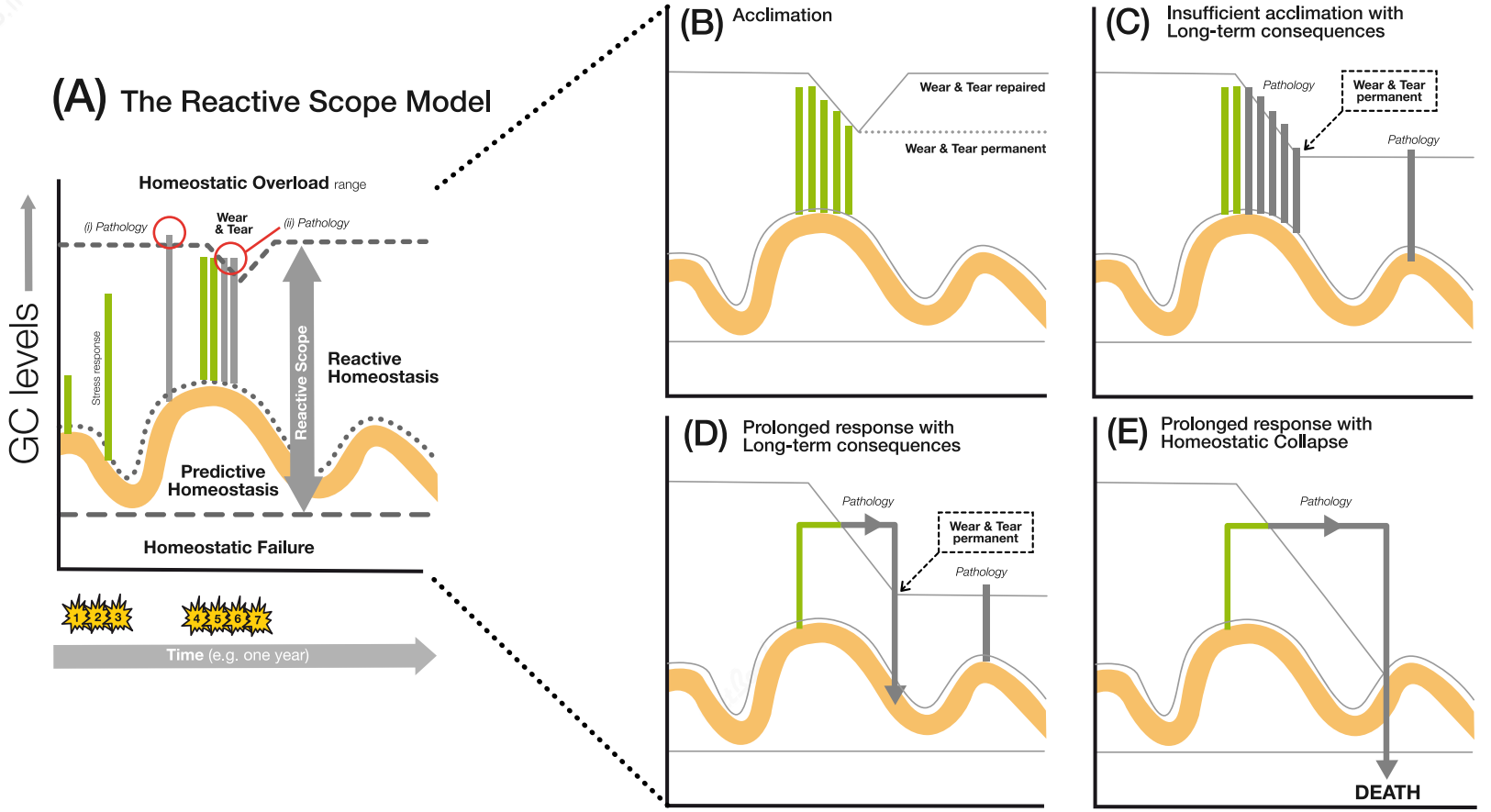

FIGURE 38.4 **The reactive scope model. Changes in circulating GC levels (y-axis) across time (x-axis) according to the reactive scope model.** Panel (A): GC levels exist in four nominal ranges: the predictive homeostasis range varies according to seasons and life history stages, and the reactive homeostasis range represents the facultative range of GC elevations in response to unpredictable perturbations. Both ranges combined define the normal reactive scope of the individual. Below and above this range, GC levels result in pathology (homeostatic failure and homeostatic overload ranges, respectively). In response to perturbations (numbered stars on x-axis), each vertical line represents both a rapid GC spike in the reactive homeostasis range and a rapid decrease when the perturbation ends. In panel (A), perturbation #2 is stronger than #1 and thus requires a stronger GC elevation to maintain homeostasis. Perturbations #2 and #3 are of similar strength, but occur at different times of year and only the latter results in GC levels extending into the homeostatic overload range (depicted as gray rather than *green bars*) and thus cause pathology. Perturbations #4 and #5 do not cause pathology, but repeated GC elevations exert "wear and tear" as depicted by a progressive decrease in the threshold between reactive homeostasis and homeostatic overload (thereby decreasing the reactive scope of the individual). Wear and tear implies that the GC response to subsequent perturbations #6 and #7 will generate pathology. In this example, wear and tear is rapidly repaired and there are no long-term consequences to the ability to respond to future perturbations (the reactive scope becomes normal after the last perturbation, #7). Panel (B) depicts acclimation. Repeated responses to stressors exert wear and tear but the animal habituates or acclimates when GC elevations decrease over time. Since GC levels never cross the threshold of homeostatic overload, pathology does not develop (note that all the bars are green). The accumulated wear and tear can be repaired once the stressor ends (*upper solid line*), or alternatively remain permanent (*lower dashed line*). Panel (C) depicts an insufficient acclimation with long-term consequences. Here the animal acclimates to a repeated perturbation but despite GC elevations progressively decrease, they enter the GC homeostatic overload range and pathology develops (denoted with *gray bars*). The threshold of reactive homeostasis could be repaired, but in this example, wear and tear exerts permanent effects, increasing susceptibility to future perturbations. As a consequence, even a moderate GC elevation elicited to face the last perturbation in this panel (C), enters the homeostatic overload range and generates pathology. Panel (D) presents an example of long-term exposure to a perturbation (e.g., chronic social stress, habitat degradation). Long-term exposure elicits prolonged GC elevations (note that the green bar now indicates extended GC secretion), which also exert wear and tear. When the sustained increase in GC levels extends above the adjusted threshold (where the green bar turns gray), pathology resulting from the elevated GCs themselves appears. Once the perturbation ends, GCs return to the predictive homeostasis range, but in this example, wear and tear becomes permanent as it likely occurs under social stress. Consequently, a later response to perturbation pushes GCs immediately into the homeostatic overload range. Panel (E) presents an extreme example of long-term exposure to perturbations. It implies that GC elevations remain in the homeostatic overload range for long periods, generating long-term pathology and accumulating continuous wear and tear. Once the threshold between GC reactive homeostasis and homeostatic overload ranges intersect with the predictive homeostasis range, GC levels collapse into the homeostatic failure range, turning pathology into death. *Credit: Figure modified and expanded from Romero et al. (2009) with permission.*

as the cumulative cost of maintaining GC levels within the reactive homeostasis range, and this cost has a consequence: a decrease in the threshold level between the reactive homeostasis range and homeostatic overload (see decreased threshold after perturbations 4 and 5 in Figure 38.4A). Note that the concept of wear and tear is different from the concept of pathology: in the latter, GCs themselves are causing damage, whereas in the former the likelihood of GCs causing damage increases. To illustrate this conceptual difference, compare the effect of perturbation 3 with the effects of perturbations number 4 and 5 in Figure 38.4A: only the former perturbation 3 positively generates pathology. Wear and tear can therefore be also interpreted as a gradual decrease in the ability to cope with perturbations. As the individual continues to respond to sequential or prolonged perturbations, GC elevations repeatedly enter the reactive homeostasis range, and the ability to counteract further stressors diminishes. At some point, the elevated GCs will cross a threshold and will start to create problems themselves. It is very important to note that, through wear and tear, GC levels can enter the homeostatic overload range even though their concentrations may not have changed. In other words the Reactive Scope Model proposes two ways of reaching homeostatic overload: either GC levels extend beyond the normal reactive scope, or GC levels remain in the reactive homeostasis range for an extended period, but wear and tear "shrinks" the reactive scope of the individual. Both scenarios are graphically depicted in Figure 38.4A. In response to perturbation 3, GC levels elevate above the normal reactive scope of the individual, entering the homeostatic overload range and generating pathology. Later that year, the same individual is exposed to perturbations number 4 and 5, which trigger GC elevations within the reactive homeostasis range. These perturbations do not cause pathology per se because concomitant GC elevations do not reach the homeostatic overload range. However, they exerted wear and tear on the individual, increasing susceptibility to enter homeostatic overload in response to subsequent perturbations (in fact, perturbations number 6 and 7 trigger GC elevations similar in magnitude to perturbations 4 and 5, but only the former cause pathology as the reactive scope range "shrunk"; see Figure 38.4A). In healthy individuals, wear and tear can be repaired after the perturbations end, but it could also remain for life, imposing a permanent decrease of the reactive scope of the individual and a permanent susceptibility to pathologies (the two options are represented within Figure 38.4B). Wear and tear and its graphical representation is an alternative way to express the concepts encompassed by allostatic load. For examples and detailed explanations of the physiological mechanisms underlying wear and tear, see Romero et al. (2009). Modeling wear and tear the way explained above illustrates why equivalent GC responses might be adaptive early, but cause problems later. It also illustrates why animals will be more resistant to stress-related pathologies during some LHSs compared to others. The model also suggests some evolutionary implications. For example, the authors propose that the slope of wear and tear in a specific individual could be determined empirically, because the threshold separating reactive homeostasis from homeostatic overload is equivalent to the maximal GC secretion of the normal reactive scope (Romero et al., 2009). Maximum GC secretion in a young, healthy, naïve bird could be determined experimentally (for example, through exogenous adrenocorticotropic hormone (ACTH) treatment; see Section 38.5.2), providing the actual limit of reactive homeostasis. Then, if a moderate perturbation is experimentally applied repeatedly to the animal for a short period, acclimation may occur (e.g., Walker et al., 2006) and the magnitude of the response will decrease (a visual example is provided as panel (B) in Figure 38.4). As long as pathological symptoms do not appear, thereby revealing that the individual has entered the homeostatic overload range, the acclimation over time will occur and the slope of wear and tear will be manifested as a time-related decrease in GC secretion. As we already mentioned, there are situations where repeated GC elevations cause permanent changes to the individual's physiology, and this can be illustrated by a permanent decrease in the reactive homeostasis range (e.g., in Figure 38.4C, the decreased reactive scope implies that this individual will have a lifelong increased susceptibility to pathologies). Also, the examples above only depict scenarios of repeated short-term perturbations followed by episodic spikes of GC into the reactive homeostasis range. These scenarios would be equivalent to Type 1 overload in the Allostasis Model (McEwen and Wingfield, 2003a,b). However, a single long-term perturbation may similarly cause prolonged GC elevations, a situation that was named Type 2 overload in the Allostasis Model and required separate conceptual explanations (McEwen and Wingfield, 2003a,b). With the graphical proposal of the Reactive Scope Model and the associated concept of wear and tear, the upper end of the reactive homeostasis range is simply expected to show a long-term (permanent) decrease in response to long-term perturbations, as depicted in panel (D). The graphical models for the response to both (1) repeated short-term perturbations (panels (A)–(C) in Figure 38.4) and (2) prolonged perturbations like subordinate social status or habitat degradation (panels (D) and (E)) are very similar under the Reactive Scope Model, and the dichotomy between Type 1 and Type 2 overloads is no longer necessary according to Romero et al. (2009). For example, low social status may impose a long-term cost to subordinate individuals compared with dominants (the reverse situation may also occur depending on the dynamics of the specific social system; Goymann and Wingfield, 2004), leading to what has been classically

termed "chronic social stress." In the Reactive Scope Model, this is depicted in Figure 38.4D (social conflict elicits a prolonged adrenocortical response, likely "shrinking" the reactive scope of individuals). In all of the examples above, we presented scenarios where the repeated/prolonged GC responses eventually end. However, the model predicts that as long as a prolonged GC response remains in the homeostatic overload range, wear and tear should continue to occur (Figure 38.4E). The threshold between *predictive homeostasis range* and homeostatic overload will decrease, until actually becoming lower than the predictive homeostasis range itself. In this situation, very low GC levels will fall into the homeostatic failure range, where normal homeostasis cannot be maintained, and death should follow. The Reactive Scope Model further provides predictions for how long GC levels can remain in the homeostatic overload range until collapse will occur. Examples of chronic malnutrition, changes in social status, and lifelong allostatic changes resulting from early life experiences are provided in the original formulation of the Reactive Scope Model (Romero et al., 2009), establishing comparisons to the Allostasis Model and highlighting the benefits of an alternative interpretation for scenarios that generate enormous interest for both biomedical researchers and ecologists. The Reactive Scope Model provides, for example, a new framework to understand the concept of eustress (Selye, 1976), and those changes that occur during development that can reset an animal's reactive scope resulting in lower (rather than higher) vulnerability to enter homeostatic overload later in life, a concept that challenges traditional models (Saino et al., 2005). Finally, note that despite the fact that considerable empirical grounds led to the formulation of both the Allostasis Model and the Reactive Scope Model, these are still today largely theoretical paradigms, requiring experimental demonstration in free-living animals under diverse ecological scenarios (Romero, 2012; DuRant et al., 2016).

- The Reactive Scope Model is an extension of the Allostasis Model and is presented as a graphical tool for characterizing the physiological state of individuals according to the levels of mediators (e.g., circulating corticosterone titers) rather than energy levels.
- The combination of the two adaptive corticosterone ranges of a healthy animal (i.e., predictive and reactive homeostasis ranges) form the normal reactive scope of the individual. Corticosterone levels above and below the reactive scope cause serious pathologies. Therefore, the reactive scope defines the upper and lower physiological constraints of a healthy individual.
- In response to unpredictable perturbations, GC levels rapidly elevate into the reactive homeostasis range during a "stress response." Even when GC elevations do not reach homeostatic overload to cause pathology, as the individual continues to respond to sequential or prolonged perturbations GC levels will exert wear and tear.
- Wear and tear is defined as the cost of maintaining and using the physiological systems that mediate allostasis and can be graphically depicted as a decreased threshold level between the reactive homeostasis range and homeostatic overload (and therefore a decreased reactive scope).
- Wear and tear implies a gradual decrease in the ability to cope with perturbations. This concept is different from pathology: GCs themselves are not causing damage, but increase the likelihood of damage due to a progressively decreased reactive scope. Wear and tear illustrates why equivalent GC responses might be adaptive early, but cause problems later.
- The Reactive Scope Model proposes two ways of reaching homeostatic overload: (1) either GC levels extend beyond the normal reactive scope and cause pathology; or (2) GC levels remain in the reactive homeostasis range for an extended period, but wear and tear "shrinks" the reactive scope of the individual, increasing the likelihood of pathology.
- The Reactive Scope Model, like the Allostatis Model, is still a largely theoretical graphical tool requiring empirical demonstrations.

38.3 Adrenocortical response to environmental change

A cornerstone question for evolutionary biologists and field endocrinologists is: How do birds respond and adapt to an ever-changing environment? There is a large amount of evidence that the mechanisms by which birds perceive potential challenges and transduce this information into neuronal and endocrine responses are fundamentally different when facing predictable versus unpredictable environmental events (Wingfield, 2013a). In this section, we will characterize the unpredictable events of the environment (the perturbations), especially those that disrupt the normal life cycle, and will summarize the adrenocortical responses that allow adaptive orchestration of facultative physiological and behavioral mechanisms aimed at maximizing fitness. The frequency and severity of disturbances is expected to increase dramatically during the coming decades through the concerted action of climate change and anthropogenic pressures, imposing severe and novel challenges for many biota through exposure to rapidly changing conditions never experienced in the preceding millennia (Sergio et al., 2018). This subject is critically relevant for basic and conservation-oriented research because human-induced perturbations can generate similar adrenocortical

responses to natural stressors and the individuals' inability to cope will likely precede many extinction processes.

38.3.1 Predictable versus unpredictable environmental change

As we have previously pointed out, some seasonality in climatic, biological, and social conditions exists to different degrees in all avian habitats, and birds have evolved mechanisms to organize their life cycles in synchrony with other individuals and the predictable environment. Internal and external (temperature, photoperiod, rainfall, social interactions) environmental cues allow anticipatory adjustments of major life history events (Wingfield, 2008). Individuals can thus prepare for energetically demanding times of year such as a cold and rainy winter or a hot and dry season, and GC levels will fluctuate within a baseline range. Regardless of how challenging local conditions may appear to the human eye, GCs do not elevate into stress-induced levels in response to the predictable environment: such conditions are not perturbations from the bird's perspective. For example, American goldfinches (*Carduelis tristis*) do not elevate GC levels in winter despite exposure to severe weather and temperatures below −20°C (Dawson et al., 1991), and adult king penguins (*Aptenodytes patagonica*) fast for weeks, relying on their fat stores during the austral winters without necessarily increasing circulating GCs (Cherel et al., 1988). Extreme cold and lack of food constitute, within certain limits, the normal environmental conditions under which these two species evolved their life cycles. However, there is no habitat subjected to perfectly foreseeable changes. Sudden severe storms outside the expected season, attacks from predators or dominant individuals, human disturbance, and parasites or disease are generally not predictable and have the potential to disrupt the life cycle of the individual, potentially causing death. Unpredictable events in the environment are generally termed perturbations or stressors. These could be characterized in the light of the Allostasis Model described earlier (Section 38.3.1), across a gradient of increased energy demands (allostatic load), and their effects (allostasis) in terms of GC secretion and subsequent adjustments of LHSs, which should depend on the energy available to each particular individual at each particular moment (see Figure 3 in Landys et al., 2006). The fact than some types of perturbations eventually bring the individual into allostatic overload makes a qualitative difference for the role of circulating GCs in behavior and physiology, as will be discussed below. A widely accepted classification for the types of perturbations is provided by Wingfield (2013a; see also Wingfield and Romero, 2001), who proposes discriminating between labile (short-term, transient) and permanent (long-term, modifying) perturbation factors. *Labile perturbation factors* (*LPFs*) are in turn roughly divided into two major groups: *indirect LPFs* (lasting seconds to a few minutes) and direct LPFs (lasting minutes to hours). The formulation for this classification takes into account the duration of the unpredictable stimuli, the actual duration of the adrenocortical response, and its resulting effects on the normal progression of the individual's life cycle (all of these factors combined). Figure 38.5 synthesizes information about these parameters and provides examples for ease of interpretation of the text below.

- The mechanisms by which birds perceive potential environmental challenges and transduce this information into endocrine responses are fundamentally different when facing predictable versus unpredictable events.
- Regardless of how challenging local conditions may appear to the human eye, birds' circulating corticosterone levels do not elevate into stress-induced levels in response to the predictable environment.
- Unpredictable and potentially noxious events in the environment are termed perturbations (or stressors), resulting in stress-induced corticosterone elevations.
- Perturbations can be classified as either (1) LPFs (short-term, transient) or (2) permanent perturbations (long-term, also called modifying factors). LPFs can in turn be classified in two major groups: indirect LPFs (lasting seconds to a few minutes) and direct LPFs (lasting minutes to hours).
- This classification takes into account the duration of the unpredictable stimuli, the duration of the associated adrenocortical response, and the resulting effects on the normal progression of the individual's life cycle.

38.3.2 Indirect, labile (short-term) perturbations

Indirect LPFs are very short-lived perturbations, lasting seconds to a few minutes and have little or no long-term effects on an individual (as long as it manages to rapidly survive the sudden exposure to noxious stimuli). Examples may include a predator chase, a conspecific agonistic interaction, the loss of nest/offspring to a short severe storm, or a brief human disturbance. Here a "flight or fight" response is typically triggered with little or no elevation of GCs into the reactive homeostasis range, and resumption of normal activities (e.g., social behavior, renesting) takes place within minutes to hours (Figure 38.5). The *flight or fight response* implies stimulation of the cholinergic sympathetic fibers that innervate the chromaffin tissue of the adrenal, causing the local release of acetylcholine, which triggers the release of predominately epinephrine in the blood. This rapid allostatic response promotes increased heart rate, vasodilation of arterioles in skeletal muscle, general venoconstriction, relaxation of bronchiolar muscles, pupilar dilation,

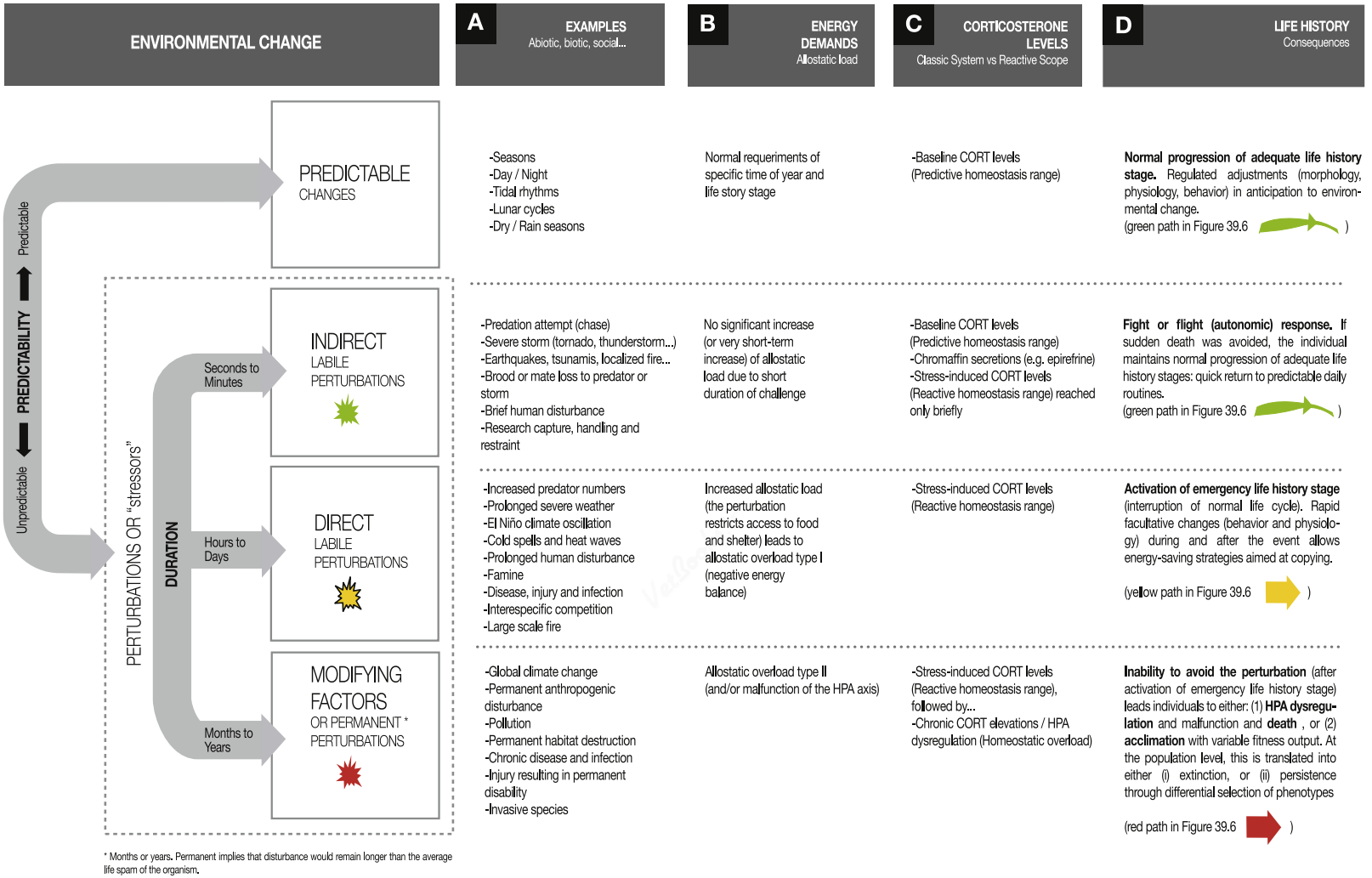

FIGURE 38.5 **Environmental change and individual responses.** Characterization of environmental change and corresponding energy, adrenocortical and life-history responses. Environmental changes can be predictable, or otherwise are termed "perturbations" or "stressors" (column A lists potential examples). Perturbations can be classified as either labile (short-term, transient) or permanent (long-term, *modifying factors*). Labile perturbation factors (LPFs) are in turn roughly divided into two major groups: indirect LPF (lasting seconds to a few minutes) and direct LPF (lasting minutes to hours). The formulation for this accepted classification takes into account not only the duration of the unpredictable noxious stimuli but also the energy demands (allostatic load) imposed on the individual (column B), the actual elevation of GC titers (column C), and the resulting effects on the normal progression of the individual's life cycle (column D). The fact that some types of perturbations may bring the individual into allostatic overload makes a qualitative difference for the actions of circulating glucocorticoid, which may trigger an emergency life history stage (adaptive response) aimed at avoiding the perturbation, or create permanent damage if the individual does not habituate to permanent stressors. *Credit: Figure created by the authors of this chapter after Wingfield (2013a), expanded to incorporate biotic and social examples from other sources and to implement concepts from the Allostatis Model and the Reactive Scope Model.*

piloerection, and (very importantly) mobilization of liver glycogen and free fatty acids (Axelrod and Reisine, 1984; Romero et al., 2009). Only if the perturbation persists beyond the first few minutes will the adrenocortical response be activated. Then an elevation of *corticotropin* (ACTH) secretion from the anterior pituitary (adenohypophysis) will trigger the increase of circulating GC levels into the reactive homeostasis range (Figure 38.1; see details for the complete cascade of hormonal secretions in Chapter 33). Sustained elevation of GCs into stress-induced levels marks the short-term response. At this point, the individual will require additional energy resources to cope with the noxious stimuli. Even though the perturbation is still short-term or labile, after a few minutes, it will only be considered indirect if the individual readily resumes its normal life cycle when the perturbation is over. For example, the experimental capture, restraint, and serial blood sampling protocol that is routinely applied to quantify adrenocortical responses in wild birds (Section 38.5.1; Box 38.1) typically lasts 30 to 60 min. Birds during this protocol elevate circulating GCs into stress-induced levels, but they typically resume normal activities (e.g., nest attendance) within minutes following release. Capture and blood sampling would not be considered an indirect LPF according to its duration and associated GC elevations (allostatic responses need to go beyond the flight or fight, autonomic response), but this event does not qualify as a direct perturbation (see below), provided a fast resumption of normal life cycle activities and no apparent energy imbalance.

- Indirect LPFs are short-lived, lasting seconds to a few minutes and have little or no long-term effects on an individual. Examples include short predator chases, agonistic interactions, the loss of nest/offspring to a short severe storm, and brief human disturbance.
- Indirect LPFs elicit a flight or fight response largely mediated by the sympathetic nervous system, with little or no elevation of GCs into stress-induced levels. Resumption of normal activities takes place within minutes to hours.

38.3.3 Direct, labile (short-term) perturbations and the "emergency life history stage"

Direct LPFs are perturbations lasting hours or days, imposing high-energetic demands and resulting in a temporary disruption of the normal life cycle (for example, resulting in brood desertion). Potential examples include exposure to prolonged severe weather, strong intra- or interspecific competition for food or shelter, increased number of predators, reduced food resources, pollution, and prolonged human disturbance (Figure 38.5A). The cumulative allostatic load brings the individual into negative energy balance (allostatic overload Type 1), and the individual redirects physiology and behavior into a facultative mode known as the *ELHS* (Wingfield et al., 1998). Figure 38.6 illustrates a sequence of life history events of a model avian species. Under normal conditions (in the absence of perturbations), the life cycle of a bird is composed of a finite number of *LHSs*: winter or nonbreeding, breeding, and moult (depending on the species there could be more, and include, for example, migration). The temporal sequence of LHSs varies from species to species and each stage is expressed at a particular time of year for which it has evolved to maximize fitness (Jacobs and Wingfield, 2000). Each LHS has a varying number of unique substages (for example, the breeding stage involves gonadal maturation, courtship, ovulation, etc.) following a specific "one-way" sequence. The development of each stage and the sequential transitions between stages are regulated by endocrine secretions, which follow predictable environmental cues such as the annual photocycle and allow adequate stage-specific changes in physiology, morphology, and behavior in anticipation of energy demands (i.e., as dictated by the predictable portion of environmental change). In contrast, exposure to a direct LPF (represented with a yellow star symbol) can occur at any time and it will trigger a facultative "emergency stage" (the ELHS) at any point of the life cycle. The substages within an ELHS are remarkably consistent in all bird species studied to date, and serve first to redirect the individual into a survival mode and then to allow it to return to the normal LHS once the perturbation passes. The behavioral and physiological components that make up the substages of an ELHS (Wingfield and Kitaysky, 2002; Wingfield and Romero, 2001) are:

1. Deactivation of territorial behavior or social hierarchies in the home range of a group.
2. Adoption of one of the following alternative strategies: (A) "leave it" strategy: movement away from the direct LPFs; (B) "take it" strategy: switch to an alternate set of energy-conserving behavioral and physiological traits; or (C) "take it at first, and then leave it" strategy: switch to energy-conserving mode first, and then move away if conditions do not improve.
3. Once a strategy has been adopted, mobilization of stored energy (fat and protein) to fuel movement away, or finding refuge and endure while sheltering.
4. Finally, once the direct LPF passes (or the individual evades), the individual must settle in an alternative habitat if an appropriate site is located or return to the original site and resume the normal sequence of LHSs (returning to the most appropriate for that time of year, whether it is the same as before the perturbation or any other; see thin green arrows in Figure 38.6).

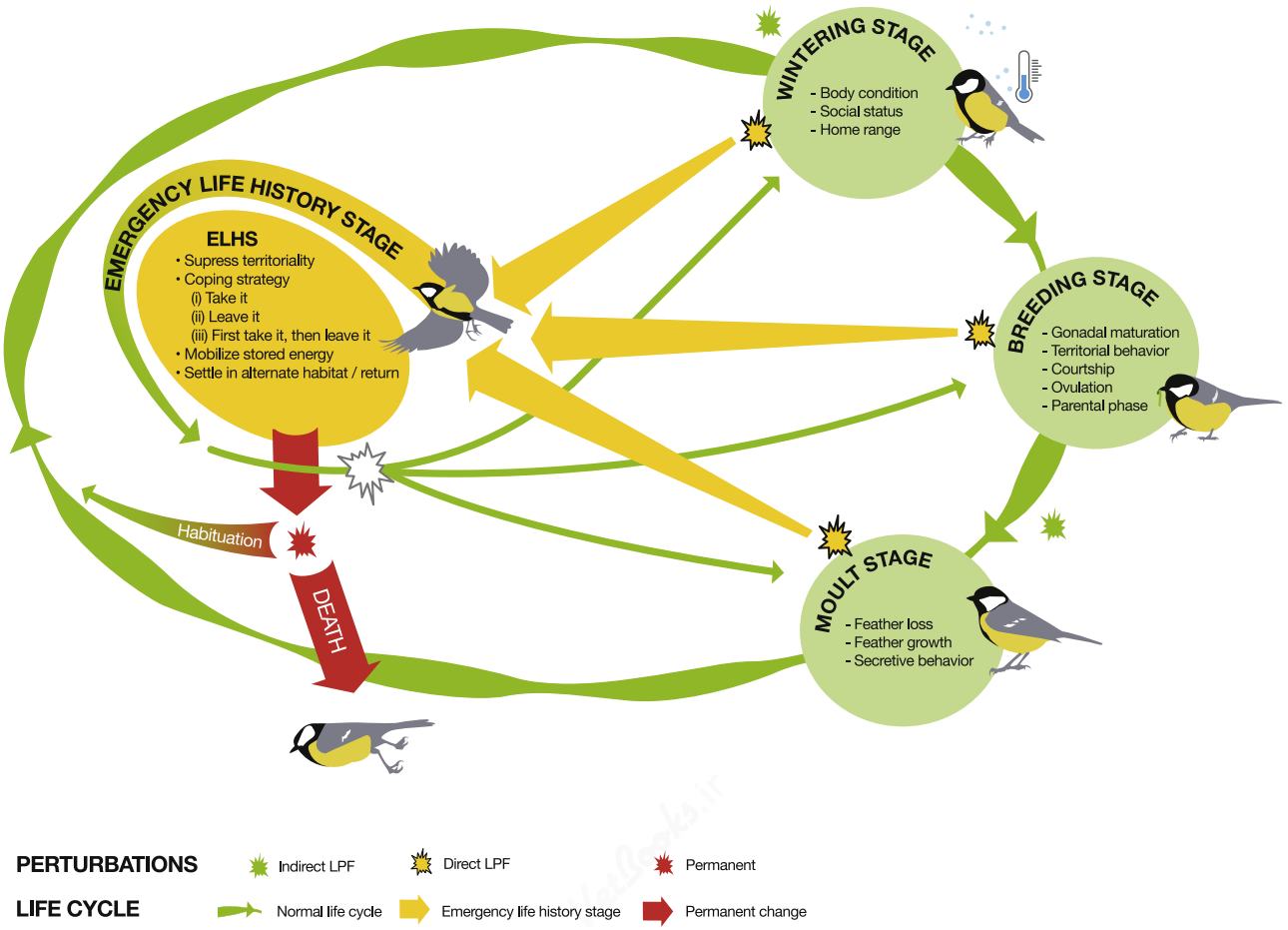

FIGURE 38.6 **The emergency life history stage.** Schematic representation of the facultative emergency life history stage (ELHS) within the life cycle of a hypothetical model avian species. The normal cycle is composed of a finite number of life history stages (LHSs) (*green boxes*) occurring in a specific, nonreversible, sequence (one-way path of *arrows*). This sequence has evolved to maximize individual fitness, and each LHS occurs at specific times of the year, when and where the environmental and social conditions are likely most adequate to use the energy available for specific life tasks. Each LHS is composed of a number of substages in a preset sequence (e.g., breeding stage: gonadal maturation, territory acquisition, etc.). Unpredictable perturbations of different magnitudes and duration (*star symbols*) may occur at any time of the year. When overcoming a perturbation requires a relatively small energy investment (e.g., response to a short predator chase), they are termed indirect labile perturbations (*green stars*), which trigger the autonomous "flight or fight" response, result in short-term or no elevations of circulating GC and allow the individual to continue its normal life cycle. However, labile perturbations may last hours or days (e.g., increased predator numbers) and demand larger energy investments for survival. They are then termed direct labile perturbations (*yellow stars*), and trigger considerable elevation of GC levels above the normal baseline into stress-induced levels. These perturbations redirect the individual's life cycle into a facultative ELHS (yellow path) aimed at coping with the increased allostatic load and survival at the expense of temporarily suppressing the normal life cycle. The marked GC elevations (see the thicker width of the *dashed yellow arrows*) promote dramatic changes in physiology and behavior, including the use of lipid and protein stores as energy to survive while sheltering or moving away (e.g., during irruptive avian migrations). Once the perturbation is over or the individual relocates, circulating GC levels return to baseline range and the individual returns to the most appropriate LHS, which may or may not be the one when the perturbation occurred (see the thinner width of the *green arrows* as they return to the *green boxes*). Perturbations, however, may not always subside (e.g., habitat destruction, climate change) eventually becoming long-term or permanent (*red stars*). If the individual cannot avoid a permanent perturbation, long-term or chronic GC elevations (*red path*) can cause deleterious effects on the organism and eventually result in death. Alternatively, individuals may habituate to the perturbation, but fitness and normal progression of LHSs would only be achieved if GC function returns to normal levels. *Credit: Figure modified and expanded after Wingfield and Kitaysky (2002).*

Such dramatic changes in behavior and physiology can occur within minutes to hours of exposure to direct LPFs, and a combination of laboratory experiments and field studies indicates that the elevation and maintenance of GC levels above seasonal baseline, and into stress-induced levels, underlies this facultative ELHS (Figure 38.6). A few examples follow (for additional examples, see Wingfield and Romero, 2001; Wingfield and Kitaysky, 2002; Wingfield et al., 2011; Wilsterman et al., 2020). Young but not adult European blackbirds (*Turdus merula*) migrated southwards when exposed to a severe weather event (direct LPF) in Germany that resulted in snow and ice covering their winter feeding grounds. The energy demanded by digging for food likely exceeded the EG, but

only among unexperienced, first year individuals. As predicted, the group of young, unexperienced birds that left the regular wintering areas showed concomitant elevations of circulating corticosterone levels compared to nonmigrating adults (Schwabl et al., 1985). There are similar studies linking unusually severe winter weather (a direct LPF) to elevated corticosterone levels and irruptive migrations (a "leave it" ELHS strategy) in ground-feeding birds because the snow covering food resources may impose an unpredictable and considerable increase to allostatic load. North America, dark-eyed juncos (*Junco hyemalis*) showed significantly higher plasma corticosterone levels during a severe snowstorm compared to before or after it; circulating GC levels were highest when home ranges were abandoned and lower when the birds found refuge after the storm (Rogers et al., 1993). In contrast, Harris's sparrows (*Zonotrichia querula*) became inactive to ride out a severe winter storm (a "take it" strategy), but also showed concomitant elevations of circulating corticosterone (Rohwer and Wingfield, 1981). Note that the influences of inclement weather on the ELHS depend upon the severity of the storm and when it occurs. Considering studies during the reproductive season, white-crowned sparrows (*Zonotrichia leucophris pugetensis*) delay the onset of breeding without elevating corticosterone levels if severe weather occurs before egg laying. This suggests that storms early in the season do not qualify as LPFs, and that they rather act as supplementary information (predictive environmental change) to fine-tune gonadal development. Alternatively, it is possible that the energy demands for that time of the year were low compared to the energy available in the environment plus the body reserves, allowing individuals to cope with a perturbation without triggering GC elevations above baseline range. However, during incubation and chick brooding, the additional energetic costs associated with these normal LHSs increase vulnerability to perturbations, and equivalent severe storms result in elevated corticosterone levels and the abandonment of nest and territory, which are typical examples of a "leave it" strategy within the ELHS (Wingfield, 1984). Because sex roles during reproduction impose different allostatic loads for males and females in many bird species, we may also expect that a given LPF should differentially trigger corticosterone elevations and an ELHS depending on the energy invested by each sex in each substage. For example, territory acquisition is largely a male role in raptors. Male black kites (*Milvus migrans*) likely face higher allostatic loads compared to females at the start of the breeding season, and they showed higher corticosterone elevations in response to the experimental LPF of capture and restraint (Blas et al., 2011). Allostatic load should be even higher among young males because they rely on the competitive displacement of an older male to initiate breeding; as expected, corticosterone levels following capture and restraint were higher in young compared to older males. This pattern was reversed among females, because young, floating individuals incur neither the allostatic loads of competition for territories nor the energy demands for egg formation: young females showed the lowest levels of corticosterone after exposure to capture, handling, and restraint and likely the lowest susceptibility to trigger an ELHS in response to perturbations (Blas et al., 2011). The effect of sex roles on the susceptibility to LPF has also been suggested in white-crowned sparrows. Severe weather may affect females more than males during the incubation period because males do not incubate, but a storm during the fledging phase would affect males more, as their parental effort is at its highest point (Wingfield, 1984; Wingfield et al., 1983). Here it is worth mentioning that although some LHSs and substages are energetically demanding (e.g., territory acquisition, incubation, and brooding), they are totally predictable and do not generate GC elevations into the reactive homeostasis range per se. However, because these life cycle activities increase allostatic load, they can generate a greater susceptibility to elevate GCs into stress-induced levels after exposure to unpredictable perturbations (and therefore a greater susceptibility to enter ELHS). The examples above indicate that stress-induced GC elevations underlie activation on the ELHS, but additional field and laboratory experiments (many of which include experimental manipulations of systemic GC titers) have allowed a more precise characterization of GC actions on the particular behavioral and physiological traits that make up the substages of an ELHS. We will briefly comment on some of these GC actions occurring within stress-induced range (i.e., those that accompany life-threatening perturbations). However, it is important to note that GC actions at the lower range that characterizes daily and seasonal life processes (that is, within baseline levels) can modify the same traits in different and even opposite ways. These aspects are thoroughly reviewed elsewhere (Landys et al., 2006; Wingfield and Romero, 2001). Major GC actions at stress-induced levels include:

1. Increased protein catabolism and gluconeogenesis: Administration of exogenous GCs to mimic stress-induced levels induces protein loss and muscle atrophy in a variety of avian species. For example, domestic fowls (*Gallus gallus*) respond to corticosterone treatment showing a rapid elevation of plasma uric acid, a byproduct of amino acid breakdown (Saadoun et al., 1987). In house sparrows (*Passer domesticus*), corticosterone implants decrease the mass of pectoralis muscles, but differentially promote catabolism of the soluble (sarcoplasmatic) protein fraction rather than contractile (myofibrilar) components, which allows maintenance of flight capabilities (Honey, 1990). By making available amino acids, reactive GC levels

support increased allostatic load through indirect provisioning of intermediates for the citric acid cycle and substrates for hepatic gluconeogenesis.

2. Increased availability of lipid energy from adipose tissue stores (Dallman et al., 1993): Stored triglycerides may be released as free fatty acids, through either an increase of triglyceride breakdown or a decrease in the rate of re-esterification. In addition, elevated GCs seem to support enzymatic mechanisms that allow delivery of fatty acids to working tissues (Mantha and Deshaies, 2000; Landys et al., 2006, and citations therein). Note that artificial elevation of GC levels may also result in increased fat depots when the experimental animals are in positive energy balance (Wingfield and Silverin, 1986).
3. Decreased body mass: Exogenous corticosterone elevations inhibit weight gain in, for example, house sparrows and rufous hummingbirds (*Selasphorus rufus*) (Honey, 1990; Hiebert et al., 2000). Mass loss might be a consequence of the two metabolic effects described above (increased energy mobilization) plus a decreased maintenance of structural tissues.
4. Modulated locomotor activity: For example, white-crowned sparrows show a rapid increase in activity after corticosterone ingestion (Breuner et al., 1998). This effect likely depends on GC concentration: while moderate elevations promote intense activity (a "leave it" ELHS strategy), very high doses may actually stimulate inactivity (a "take it" strategy; Wingfield and Ramenofsky, 1999). In addition, energy availability seems to modulate this response: while corticosterone implants increase activity in fasting birds, they decrease activity when food is ad libitum (Astheimer et al., 1992). Both the dose- and the context-dependent effects of GC elevations match the expected behavioral responses under an ELHS: when the LPF does not reduce food resources, it may be adaptive to "take it," but if the perturbation persists then a reduction of the available energy (food) would trigger higher GC elevations and a "leave it" strategy aimed at searching for energy somewhere else. GC effects on locomotor activity may be particularly relevant in avian species adapted to severe habitats such as deserts or high latitudes, which show irruptive movements in response to LPF (Wingfield and Ramenofsky, 1997). Note, however, that seasonal GC levels are typically elevated during those LHSs that demand high-physical activity such as migration and dispersal (Landys-Ciannelli et al., 2002; Belthoff and Dufty, 1998), but these effects occur within baseline range.
5. Increased food intake: Although some studies propose that GCs regulate feeding rate in a permissive capacity (Dallman et al., 1993), recent research suggest that this effect is mediated through a threshold action of GC receptors rather than by the extent of GC elevations above the seasonal baseline (see details in Landys et al., 2006). There is ample correlational evidence that foraging activities are normally highest during the times of day when baseline GC levels are maximal (e.g., López-Jiménez et al., 2016a), and that feeding intensity can be shifted by corticosterone manipulations (Dallman et al., 1993), but again, these effects occur within baseline range.
6. Suppressed territorial and reproductive behavior: For example, male song sparrows (*Melospiza melodia*) reduce territorial aggression when treated with exogenous corticosterone (Wingfield and Silverin, 1986). Similarly, free-living pied flycatchers (*Ficedula hypoleuca*) decrease the rate of feeding nestlings when treated with exogenous corticosterone (bringing a concomitant decrease in nestlings' body condition and survival), and even cease all reproductive activities (abandoning the nest and the acquired territories) when given high-dose GC implants (Silverin, 1986).
7. Increased night restfulness: Exogenous corticosterone administration in captive white-crowned sparrows and pine siskins (*Spinus spinus*) result in a uniformly low-oxygen consumption pattern, with an estimated 20% energy savings overnight compared with controls (Buttemer et al., 1991). However, similar treatment applied to other species yielded contradictory results (Palokangas and Hissa, 1971), likely because GC-induced gluconeogenesis also affects metabolic rate and thus oxygen consumption (Jimeno et al., 2018). Corticosterone administration to rufous hummingbirds results in nocturnal torpor, a form of seeking refuge ("take it") strategy that these birds acquire through decreasing body temperature (Hiebert et al., 2000).

Summarizing, GC elevations into the stress-induced range, which are typically several-fold higher than the seasonal baseline, allow critical changes in physiology and behavior aimed at coping with LPFs and thus have adaptive value in maximizing survival and lifetime reproductive success, even at the cost of a temporary suppression of the life cycle. Once the direct LPF is over or the individual relocates, circulating GC levels normally decrease back to baseline range and the individual returns to the most appropriate LHS, which may or may not be the one when the perturbation occurred. Perturbations, however, may not always subside and eventually they may become long-term or permanent (for example, habitat destruction and climate change). Then, they are termed modifying factors.

- Direct LPFs last hours or days, impose high-energetic demands (allostatic load), and result in a temporary disruption of the normal life cycle. Examples include exposure to prolonged severe weather, intraspecific

competition, increased predation pressure, reduced food resources, and prolonged human disturbance.

- The cumulative allostatic load imposed on the individual brings a negative energy balance (allostatic overload Type 1), and the individual redirects physiology and behavior into a facultative LHS known as the ELHS. Such an emergency stage is largely driven by the elevation and maintenance of GC levels above seasonal baseline and into stress-induced levels.
- Stress-induced corticosterone elevations range during an ELHS promote (1) increased protein metabolism and gluconeogenesis, (2) availability of lipid energy from adipose tissue stores, (3) decreased body mass, (4) changes in locomotor activity and foraging, (5) suppression of territorial and reproductive behavior, and (6) increased night restfulness. These corticosterone-mediated changes in physiology and behavior have adaptive value, maximizing individual fitness at the cost of a temporary suppression of the life cycle.
- Once the direct LPF is over or the individual relocates, circulating GC levels normally return to baseline range and the individual returns to normal LHSs.

38.3.4 Permanent (long-term) perturbations or "modifying factors"

Modifying factors are *permanent perturbations* lasting months to years (they are termed "permanent" because the disturbance may remain longer than the average lifespan of the organism), when they impose high-energetic demands upon the individual and result in a permanent disruption, even disintegration of the normal life cycle (Wingfield and Romero, 2001; Wingfield, 2013a). Potential examples include chronic disease and infection (e.g., high-parasite load), injury resulting in permanent disability, global climate change, and sustained anthropogenic disturbance (Figure 38.5A). The cumulative allostatic load imposed on the individual may bring a negative energy balance, leading to death if a prior activation of the ELHS did not result in evasion of the perturbation (for example, when relocation was not possible). Here the sustained long-term GC elevations into stress-induced levels exert wear and tear (see Section 38.2.3), resulting in deleterious effects on critical body systems, including inhibition of gonadotropin secretion and cessation of reproductive function (e.g., delay of puberty onset, gonadal involution), suppressed secretion of growth hormone (e.g., stress-induced dwarfism), complete breakdown of the skeletal muscle (e.g., suppressed flight and movement capabilities), suppression of T-lymphocyte response to infections (increasing susceptibility to disease), severe neuron loss in the hippocampus through impaired glutamate and calcium regulation, and decreased generation of arachidonic acid (for a review of effects, see Sapolsky, 1996; Wingfield and Romero, 2001; Romero et al., 2009). In contrast to the highly adaptive GC responses that characterize the ELHS, chronic GC elevations lack adaptive value Wingfield et al., (2017). Note also that, at a given point, chronic GC exposure will bring a disruption of the HPA axis, and the deleterious effects on the organism may occur even if the long-term perturbation subsides and the energy available in the environment becomes above the energy needs of a healthy individual (this will be equivalent to *allostatic overload Type 2*, to a critically reduced reactive scope generated by wear and tear, or to the ecological scenarios of social stress that we have already mentioned). Pollution is also considered a type of modifying factor, but its impact on avian adrenocortical function has been subjected to scarce research and there is a great need for field investigations (Baos et al., 2006; Baos and Blas, 2009; Meillère et al., 2016). A critical point regarding the effects of modifying factors is that not all the individuals within a population perceive and respond to perturbations in the same way. As a consequence, under particular scenarios (which should depend on the species and the type of perturbation), it is possible that even a drastic initial response to modifying factors (e.g., disappearance of a fraction of the population through death or emigration) is followed by a recovery through differential selection of the more tolerant phenotypes (Blas et al., 2007; Cockrem, 2007). In other words, perturbations may become selective pressures, potentially allowing adaptation. For example, burrowing owls (*Athene cunicularia*) living in urban environments showed reduced stress-induced corticosterone levels compared to rural conspecifics (Palma et al., 2020). These results suggested that only individuals expressing low HPA axis responses can thrive in cities. Population persistence could occur provided that (1) there exists some genetic variability in the response to stress, whereby specific genotypes do not activate adrenocortical responses to that specific perturbation; (2) individuals acclimate to that particular perturbation, progressively reducing their adrenocortical responses and surviving without permanent activation of the HPA axis; or (3) epigenetic effects (e.g., maternal programming) reduce the impact of the perturbation through modifying the offspring's adrenocortical responses. Unintentional artificial selection on HPA axis traits has been suggested during capture, initial acclimation, and captivity in two bird species with several invasive populations originating from the international trade in wild-caught pets: the African weavers (*Ploceus melanocephalus*) and (*Euplectes afer*) (Baños-Villalba et al., 2021). The initial acclimation and captivity that followed capture favored the differential survival of individuals with reduced feather corticosterone levels, potentially influencing the invasiveness and impact of introduced populations, and the success of biological

invasions (a global problem with large negative impacts on ecosystems and human societies).

- Permanent perturbations (also called modifying factors) last months or years, imposing high-energetic demands and resulting in a permanent disruption of life cycles. Potential examples include chronic disease and infection, global climate change, and sustained anthropogenic disturbance (e.g., urbanization and habitat destruction).
- After the initial activation of the ELHS, inability to evade the perturbation implies that the cumulated allostatic load will bring the individual into a negative energy balance, and death may follow.
- The sustained long-term GC elevations exert wear and tear, reaching the homeostatic overload range and resulting in deleterious effects on critical body systems, including (1) inhibition of gonadotropin secretion and cessation of reproductive function, (2) suppressed secretion of growth hormone, (3) complete breakdown of the skeletal muscle, (4) suppression of immune system, and (5) neuronal death.
- Modifying factors can lead to population extinctions. However, population persistence through local adaptations could also potentially occur if genetic variability and phenotypic plasticity in the response to stress allow a differential survival of stress-resistant individuals.

38.4 Phenotypic plasticity and selection on the stress response

Avian speciation has taken place under contrasting environmental scenarios (e.g., from deserts to poles), and adrenocortical responses have evolved in parallel, shaped by the prevailing perturbation factors and likely explaining the strong interspecies variability. Within a given species, different subspecies, races, morphs, and even populations have been reported to differ in the patterns of adrenocortical secretion (Wingfield and Romero, 2001). On the one hand, such variability reveals a genetic basis that controls HPA function and, for example, has allowed humans to domesticate wild animals and generate phenotypes with reduced corticosterone reactivity through artificial selection (Keith et al., 1973; Satterlee et al., 2000; Løtvedt et al., 2017). In addition to such genetically determined patterns, the adrenocortical response to stress shows a strong phenotypic plasticity. For example, the environmental conditions experienced early in life can prime lifelong differences in the patterns of adrenocortical responses, revealing epigenetic patterns that may be adaptive (Love et al., 2013; Jimeno et al., 2019). Furthermore, individuals often show the ability to modulate their adrenocortical response according to the specific requirements characterizing different LHSs, thereby maximizing the cost-benefit balance associated with the actions of corticosterone on behavior and physiology (Lendvai et al., 2007; Walker et al., 2015). Phenotypic plasticity is also manifested when repeated exposure to the same perturbations provoke gradual changes in adrenocortical function, revealing that experience-related patterns occur through acclimation, and highlighting the close connection between cognition (i.e., an individual's perception of a potential threat) and the adrenal response (Cyr and Romero, 2009). Overall, the HPA axis shows all the features of a trait subjected to natural selection (Love et al., 2013; Cockrem, 2013; Hau et al., 2016): large individual variation (Williams, 2008; Cockrem, 2013), repeatability under consistent conditions (Ouyang et al., 2011; Rensel and Schoech, 2011), heritability (comparable to that of other physiological traits; see Béziers et al., 2019 and references therein), and actual response to artificial selection (Satterlee and Johnson, 1988; Evans et al., 2006). It should be noted that the components of the HPA axis (i.e., baseline and stress-induced) may not be equally heritable, and the stress response likely shows greater adaptive potential (Jenkins et al., 2014; Homberger et al., 2015; Béziers et al., 2019).

- The HPA axis shows all the features of a trait subjected to natural selection: large individual variation, repeatability under consistent conditions, heritability, and response to artificial selection.
- Superimposed on genetically determined patterns, individuals show phenotypic plasticity in their responses to stress.

38.4.1 The stress response during development

Young birds display highly variable HPA responses during development (reviewed in Blas and Baos, 2008). On the one hand, interspecies differences reflect the wealth of variability in developmental strategies within the altricial-precocial spectrum (Figure 38.7A; Starck and Ricklefs, 1998). Although precocial species such as mallards (*Anas platyrhynchos,* which hatch with sight, covered with down, and can thermoregulate, locomote, and feed independently from parents) can elevate circulating corticosterone in response to human handling 1 day after hatching (Holmes et al., 1990), altricial species such as northern mockingbirds (*Mimus polyglottos*, which hatch blind, almost naked, and unable to thermoregulate or locomote) show little HPA response to the same stimuli during the first few days posthatch (Sims and Holberton, 2000), indicating a "*stress hyporesponsive period*." On the other hand, within a given developmental mode and species, HPA responses gradually increase as the individual grows and develops. For example, white storks (*Ciconia ciconia*), a semialtricial species, show very moderate GC responses to capture and handling until 20 days posthatching (Figure 38.7B), but the same type of experimental stimuli gradually elicit more

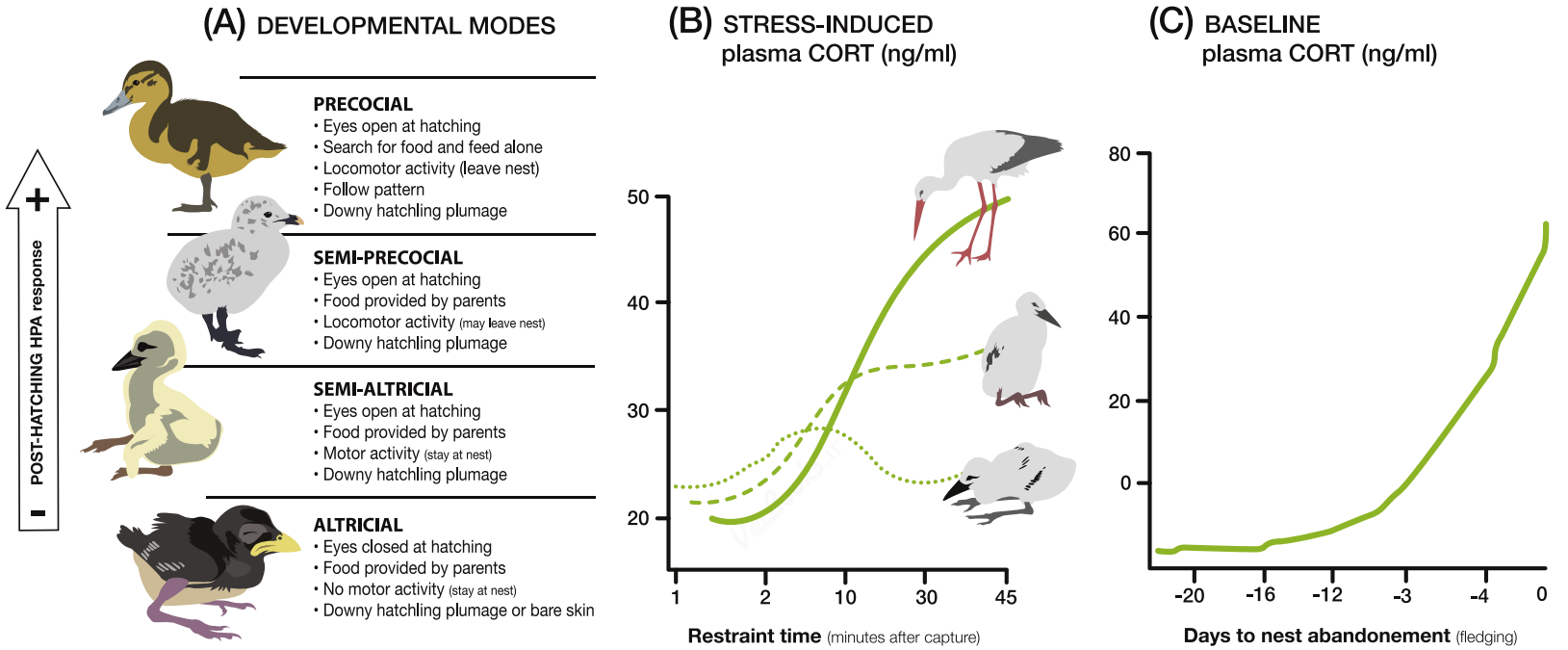

FIGURE 38.7 **The stress response during development.** Panel (A). Avian developmental modes span a gradient defined by two extremes: precocial and altricial species. Altricial species (e.g., Passeriformes, a house sparrow, *Passer domesticus*, in the drawing) hatch with closed eyes, lack of feather coat, have reduced motor capabilities, and are unable to thermoregulate or forage without parental care. Precocial species (e.g., Anseriformes; a mallard, *Anas platyrhynchos,* in the drawing) hatch in an advanced developmental stage, with open eyes, a feather coat, and independent foraging and locomotor capabilities. Intermediate developmental modes include semialtricial (e.g., a white stork, *Ciconia ciconia*) and semiprecocial species (e.g., a yellow-legged gull, *Larus michahellis*). The ability to respond to environmental and social perturbations through HPA function (e.g., ability to elevate corticosterone in response to capture and handling) increases across the developmental gradient of hatchlings: altricial species show a stress hyporesponsive period characterized by inability to show glucocorticoid elevations until days following hatching, while altricial species show robust HPA responses within 1 day posthatch. Panel (B). *Developmental changes in HPA function:* Within a given species (e.g., white storks), HPA function progressively increases during ontogenic development. The figure shows circulating corticosterone levels (*y*-axis) during the 45 min following capture and restraint (stress-induced levels) for three nestlings aged 24, 40, and 60 days old. Panel (C). *Transition from nestling to fledging stages*: Circulating baseline corticosterone levels are typically elevated shortly before hatching, fledging, and during dispersal, allowing birds to meet the increasing energy demands associated with ontogenic transitions. The figure shows baseline circulating corticosterone in thin-billed prion (*Pachyptila belcheri*) chicks, relative to the observed time of fledging ("0" on the x-axis). Note maximum corticosterone levels during the day prior to departure. *Credit: Composite figure based on Blas and Baos (2008), Blas et al. (2006a), Quillfeldt et al. (2007).*

robust corticosterone secretions as birds grow older, reaching maximal corticosterone secretion (resembling typical adult-like responses) near fledging (Blas et al., 2006a). In altricial passerines, a variety of species exhibit little or no stress-induced corticosterone response when youngest and the response gets progressively stronger throughout development (Rensel et al., 2010; Bebus et al., 2020).

The *Developmental Hypothesis* proposes that the patterns of maturation of HPA responses within and across species evolved to balance the costs and benefits of GC actions with the individual's progressive ability to overcome environmental perturbations (Blas and Baos, 2008). Two proximate hypotheses have been put forward to explain these patterns of age-related development on the ability to respond to stressors (Torres-Medina et al., 2019). On the one hand, a gradual growth and improved sensitivity of the HPA axis tissues may result in an increased ability to secrete corticosterone in response to stressors ("maturation hypothesis"). Alternatively, an age-related attenuation of the negative feedback system could gradually result in the developing bird being able to secrete increasingly more corticosterone as it grows older ("negative feedback attenuation hypothesis"). Limited experimental evidence to date supports the maturation hypothesis in semialtricial species (Torres-Medina et al., 2019), but more work is needed with species exhibiting different modes of development.

Regardless of the proximate mechanism, an inability to mount robust responses during initial developmental stages avoids exposure to high and prolonged GC levels, which reduces growth and impairs thyroid function and cognitive and competitive abilities (Schwabl, 1999; Kitaysky et al., 2003; Hayward and Wingfield, 2004). However, as the individual grows, its ability to show stress-induced responses acquires a critical adaptive value. For example, corticosterone elevations in nestling black-legged kittiwakes (*Rissa tridactyla*) at mid-developmental stages (15–20 days old) facilitate begging and aggression (Kitaysky et al., 2001, 2003), two behavioral responses highly advantageous to cope with food shortages early in life despite being still dependent on parental care.

In addition to a progressive, developmental increase in the ability to trigger robust HPA responses, baseline GC levels typically show age-related changes that serve to regulate ontogenic transitions across vertebrate taxa (reviewed in Wada, 2008). Baseline GC elevations promote maturation of critical organs and possibly control both the ability to hatch and the timing of fledging. For example, baseline corticosterone levels peaks around hatching in domestic fowls (*Gallus domesticus*; Carsia et al., 1987) and graylag geese (*Anser anser*; Frigerio et al., 2001), and exogenous corticosterone administration in turkey (*Meleagris gallopavo*) embryos two days before hatching significantly increases hatching success (Wentworth and Hussein, 1985). In white storks, baseline corticosterone levels increase prior to fledging (Corbel and Groscolas, 2008), and similar patterns have been found in American kestrels (*Falco sparverius*; Heath, 1997), pied flycatchers (Kern et al., 2001), canaries (*Serinus canaria*; Schwabl, 1999), thin-billed prions (*Pachyptila belcheri*; Quillfeldt et al., 2007), and Laysan albatross (*Phoebastria immutabilis*; Seabury and Breuner, 2005). Interestingly, baseline corticosterone elevations at the time of nest departure may be related to the species requirements to perform the first flights, and thus nest location. Avian species nesting on the ground (e.g., snowy owls, *Bubo scandiacus*) or in low brush (e.g., northern mockingbirds) do not perform their first flights until a few days following nest departure, and the later transition is not associated with baseline corticosterone elevations (Romero et al., 2006; Sims and Holberton, 2000). In contrast, avian species nesting in cavities or higher substrates (high trees, cliffs) perform their first flights as they abandon the nest, and typically show increased baseline corticosterone levels (e.g., cavity nesting American kestrels, Heath, 1997; screech-owls *Otus* sp., Belthoff and Dufty, 1998; or burrow-nestling thin-billed prions, Quillfeldt et al., 2007; see Figure 38.7C). Furthermore, corticosterone levels elevate before and during the activity periods in fledging screech-owls (Belthoff and Dufty, 1998), suggesting a role of this hormone in natal dispersal. Corticosterone elevations during avian development may thus serve to meet with the increasing energy demands *(allostatic load)* associated with ontogenic transitions including hatching, fledging, and dispersal (Wada, 2008).

- Avian developmental modes range across a gradient defined by two extremes: altricial and precocial.
- The stress response of hatchlings increases across the developmental gradient: while altricial species show a "stress hyporesponsive period" characterized by an early inability to show GC elevations, precocial species show robust HPA responses soon after hatch.
- Inability to show robust responses early during development allows avoiding exposure to high and prolonged GC levels, which reduce growth and impair thyroid function, cognitive and competitive abilities.
- The Developmental Hypothesis proposes that the patterns of maturation of HPA responses evolved to match the costs and benefits of GC actions with the individual's progressive ability to cope with perturbations (e.g., increased behavioral performance and parental independence).
- Baseline corticosterone levels increase prior to hatching, fledging, and during dispersal, making it possible to meet the increased energy demands (allostatic load) associated with ontogenic transitions.

38.4.2 Maternal effects

Studies in humans, laboratory models, and birds indicate a profound effect of the quality of parental care and the perinatal environment experienced early in life on offspring's HPA function and associated behavioral responses (McGowan and Szyf, 2010; McGowan et al., 2011; Jimeno et al., 2019). GC actions during development exert permanent organizational effects on the individual, with a stronger impact on performance (fitness: reproduction and survival), compared to reversible activational effects of the same hormones when the endocrine systems are already developed (Williams, 2008). In birds, developmental exposure to high GC levels can occur prenatally (i.e., maternally mediated changes or *in ovo* composition, e.g., Almasi et al., 2012) and also postnatally or *ex ovo* (e.g., through variation in the amount of offspring care: food provisioning, shelter, social competition; see Blas and Baos, 2008 for a review), and has the potential to translate ecological and environmental conditions into permanent offspring responses through a process termed maternal programming (Figure 38.8A and B, reviewed in Love et al., 2013). As a consequence, mothers can "prime" lifelong responses in offspring through exposure to high or low levels of GCs, resulting in a permanent modification of HPA function (Hayward and Wingfield, 2004; Love et al., 2005; Saino et al., 2005; Love and Williams, 2008; Spencer et al., 2009) that will likely affect the ability to cope with ecological perturbations. Such priming can be highly adaptive and allow animals to adjust to changing environments because exposure to a low level of perturbations early in life often result in individuals that are better able to cope with exposure to higher levels of perturbations on subsequent occasions (a process known as hormesis; Constantini et al., 2010). Note that these adaptations occur epigenetically: the genetic composition in the offspring can be the same, but the expression of different genes in response to perturbations and GCs during development will result in different phenotypes. For example, cross-fostering the biological offspring between mothers that provide high and low care can permanently reverse offspring's HPA response in laboratory animals (Francis et al., 1999).

The fitness of the phenotypes modified through maternal programming is expected to be context-specific, and determined by the environmental conditions encountered after development, and how much they resemble natal conditions (*Maternal-Match Hypothesis*; Love et al., 2013). In those situations when the early priming was a reliable predictor of the offspring's future environment, maternal programming is expected to increase offspring and even maternal fitness (Figure 38.8B). However, if maternal signaling was a poor predictor of offspring's future environment, the programming would exert negative (maladaptive) effects on the offspring ("thrifty phenotypes"; Hales and Baker, 1992). The Maternal-Match Hypothesis (Love et al., 2013) is a paradigm proposed to refine the broader Environmental-Match Hypothesis (Sheriff et al., 2009, 2010, 2011a). Although these hypotheses require testing in wild birds, there is evidence for a number of environment-maternal-offspring connections mediated through corticosterone, which constitute the pillars for maternal programming summarized in Figure 38.8:

1. *Environmental and social conditions affect GC levels in adult birds, including reproducing females.*

For example, increased risk of predation (Hawlena and Schmitz, 2010; see Clinchy et al., 2013 for a review on the "ecology of fear"), unpredictable changes in food availability (Kitaysky et al., 1999a,b, 2007; Shultz and Kitaysky, 2008), human disturbance (Thiel et al., 2008; Zhang et al., 2011), and social competition consistently promote plasma GC elevations in females that may be forming eggs, laying, or brooding offspring. Therefore, the potential for GC transfer into eggs and developing young exists. Yet, in laying hens (*Gallus gallus domesticus*), unpredictable food restriction (Janczak et al., 2007) and ACTH challenge that raised plasma levels of corticosterone (Rettenbacher et al., 2005) both failed to increase corticosterone in egg yolk. So, while it is possible that maternal stress results in a transfer of corticosterone into eggs in wild birds, more research is needed to investigate this and potential alternate mechanisms (Sheriff et al., 2011b).

2. *Environmental and social conditions affect offspring GC levels (in ovo and developing birds).*

Although the precise mechanism whereby circulating GCs are transferred from the mother to the eggs requires additional research (Groothuis et al., 2005), positive correlations between maternal (plasma) and egg (yolk) levels have been shown in European starlings (*Sturnus* vulgaris; Love et al., 2005) and barn owls (*Tyto alba*; Almasi et al., 2012). Additional studies have reported a concomitant increase in egg GC levels in response to maternal exposure to environmental challenge (barn swallows, *Hirundo rustica,* Saino et al., 2005; European starlings, *Sturnus vulgaris,* Love et al., 2008; song sparrows, *Melodia melodia,* Travers et al., 2010), including predation pressure and social conditions. For example, solitary breeding females of the semicolonial European starling deposit higher egg GC levels (Love and Williams, 2008), and reduced female condition often results in decreased food provisioning rates to nestlings, elevating posthatching GC levels (Love et al., 2004; see Angelier et al., 2007b, 2009 for seabirds). Single

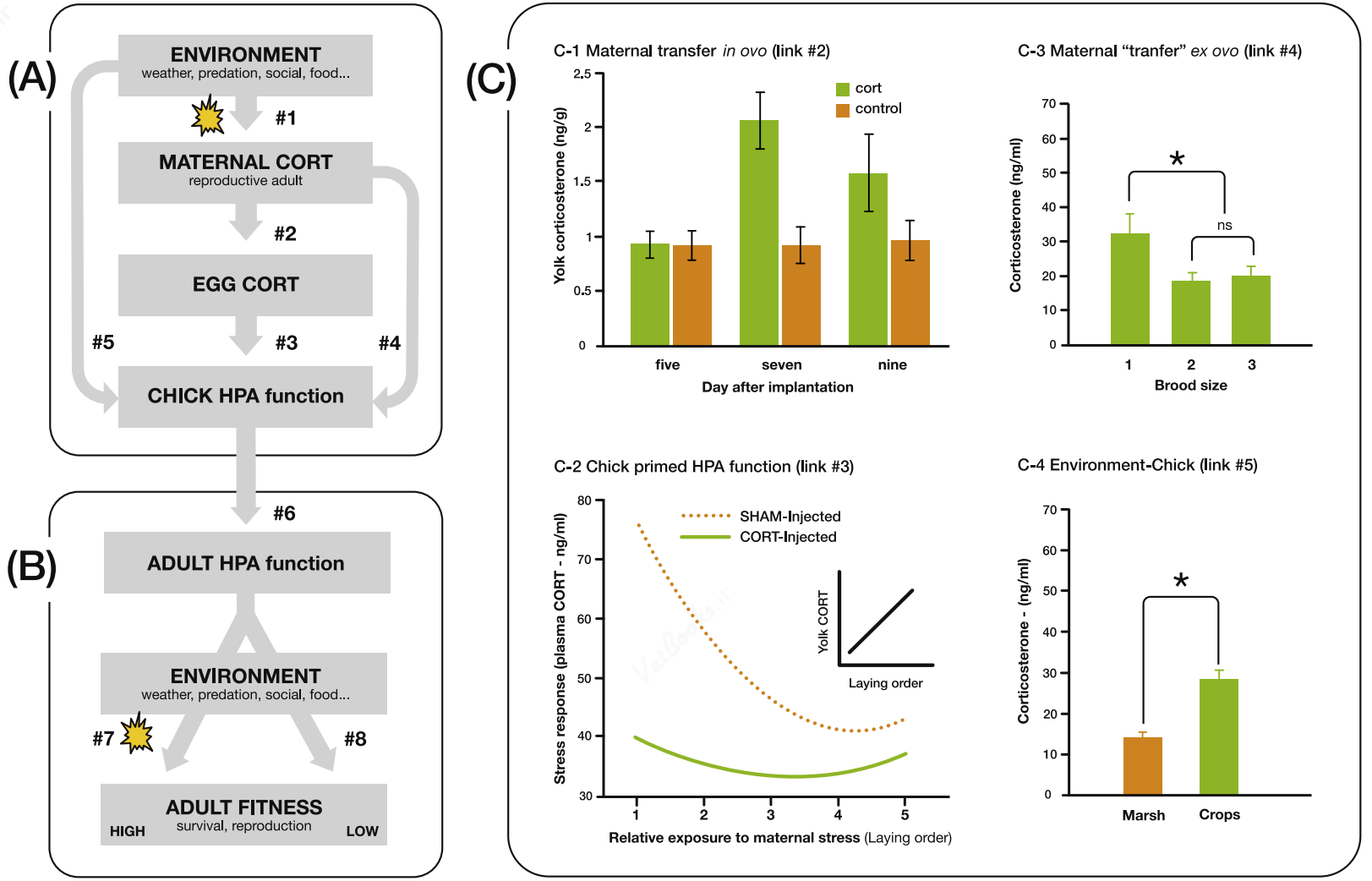

FIGURE 38.8 **Maternal effects.** Panel (A). Summary of the proposed mechanisms whereby environmental perturbations transduce into permanent changes of the hypothalamic–pituitary–adrenal (HPA) axis function in developing birds, through maternal effects (maternal programming). Environmental perturbations (star symbols) activate the HPA axis of reproducing, adult female birds (#1). Maternal stress in prelaying and laying females result in high levels of corticosterone (or other hormones) being deposited in the eggs (#2), and these will hatch nestlings developing a "primed," permanent modification of their HPA response (#3). Subsequently, variability in maternal care such as reduced attendance of nestlings and food provisioning, or increased within-brood social conflicts, can elicit further corticosterone elevations in the developing nestlings (#4). Because parental care cannot completely buffer environmental perturbations, these may also exert a direct effect on nestlings' corticosterone levels (#5) and contribute to permanent modifications of the HPA axis. The "priming" of HPA responses experienced by growing birds during development can be long-lasting, and the resulting adult phenotypes will show a permanent epigenetic modification of their response (#6). Panel (B). *The Maternal-Match Hypothesis:* Depending on the GC exposure that birds received during development (a function of maternal hormones, parental care, and natal environmental conditions; see Panel A, above), different phenotypes of HPA function will result. For example, the same pair of birds in different years could produce offspring that are high-versus low-HPA responders. Phenotypes may differ in the amount of corticosterone secreted in response to standardized perturbations, and therefore in the ability to cope with environmental challenge later in life. The maternal-match hypothesis proposes that the fitness of each phenotype will be determined by the environmental conditions encountered after development. In those situations when the early "priming" was a reliable predictor of the offspring's future environment (#7; note the same star as #1 in Panel A), offspring fitness will increase. However, if maternal signaling was a poor predictor of offspring's future environment, as may be the case with human-induced rapid environmental change, offspring fitness will be reduced (#8). Panel (C). *Examples illustrating maternal effects: C1*: Corticosterone implants in female Japanese quail (*Coturnix coturnix japonica*) significantly increased the concentrations of corticosterone in the yolk of eggs laid seven and nine days after implantation. This figure illustrates arrow #2 in panel A. *C2*: Relative responsiveness of the HPA axis (stress-induced plasma corticosterone) in fledging, free-living European starling (*Sturnus vulgaris*) in relation to natural variation in exposure to maternal stress (note that yolk corticosterone naturally increases across laying order; see insert and Love et al., 2008). The stress response of nestlings was further decreased when the eggs had been previously treated with exogenous corticosterone (*continuous line*) compared to controls (*dotted line*). This figure illustrates *arrow* #3 in panel (A). *C3*: Nestling white storks (*Ciconia ciconia*) showed higher baseline corticosterone when they were singletons, reared in nests that suffered a strong brood reduction (insufficient parental care), compared to nestlings from two- and three-chick broods. This figure illustrates *arrow* #4 in panel (A). *C4*: Baseline corticosterone in nestling white storks were higher when reared in the less productive environment (crop fields) compared to nestlings reared beside wetlands (marsh), where food availability is higher. This figure illustrates *arrow* #5 in panel (A). *Credit: Composite figure based on Hayward and Wingfield (2004); Love et al. (2013); Blas et al. (2005), and Blas and Baos (2008).*

chicks in white storks nests are the result of partial hatching failure and brood reduction (indicating insufficient parental care), and show higher circulating GC levels (baseline range) compared to nestlings from two- and three-chick broods (Figure 38.8, panel C3; Blas et al., 2005).

3. *Environmental challenge and elevated GC levels in developing offspring (in ovo, and posthatch) generate long-term differences in HPA function, behavior, and performance.*

For example, in nestling black-legged kittiwakes (*Rissa tridactyla*), experimental food restriction during development results in sustained elevations in 30-day-old chicks (Kitaysky et al., 1999a,b), and experimentally elevated corticosterone levels promote begging and aggression (Kitaysky et al., 2001) but result in long-term impairment of cognitive abilities persisting at least 8 months later (Kitaysky et al., 2003). In European starlings (*Sturnus vulgaris*), reduced maternal provisioning rates increase fledglings' adrenocortical responsiveness (Love and Williams, 2008). Within a given clutch, maternal GC levels (deposited in egg yolks) sequentially increase (Love et al., 2008), and the subsequent HPA responses of nestlings are negatively correlated with *in ovo* GC exposure (Figure 38.8, panel C2). The latter association can be further enhanced by exogenous administration of GC in the eggs, which results in fledglings showing the lowest HPA responses (Love and Williams, unpublished data in Love et al., 2013). Somehow opposing results have been reported in Japanese quail *Coturnix coturnix japonica*, where experimentally elevated plasma corticosterone in laying females is transferred to egg yolk (Figure 38.8, panel C1), but the hatched chicks (which grow at a slower rate) display higher, rather than lower responsiveness of the HPA axis as adults (Hayward and Wingfield, 2004). Unfortunately there is a lack of studies in wild birds monitoring whether such changes in HPA function, behavior, and performance persist in the phenotypes after fledging, but a negative relationship between stress-induced corticosterone levels in nestlings and survival into adulthood was found in wild, unmanipulated white storks (Blas et al., 2007). Studies that have manipulated corticosterone in early life as a proxy for environmental challenge provide additional insights into long-term effects. For example, experimental elevation of corticosterone in postnatal female zebra finches (*Taeniopygia guttata*) resulted in reduced incubation effort when they were adults (Spencer et al., 2010), and experimental dietary restriction and elevated corticosterone during development resulted in adults with significantly shorter and less complex songs (Spencer et al., 2003). In house sparrows, early-life corticosterone manipulation was associated with depressed baseline and stress-induced concentrations of corticosterone at all stages of life, through adulthood (Grace et al., 2020).

Maternal programming has been proven to be an adaptive (GC-mediated, epigenetic) mechanism bridging maternal and offspring environment to explain, for example, the cyclic population dynamics of wild mammals (see Sheriff et al., 2009, 2010, 2011a). Whether this mechanism also applies to wild birds urgently requires additional field research under contrasting environmental scenarios and in association with long-term monitoring of the individual's performance and HPA function. Human-induced rapid environmental change has a strong potential to make maternal programming maladaptive when it results in variable environmental conditions that mothers are not able to predict (Donelan et al., 2020). Thus, the likelihood that offspring are "primed" for the novel environments they are likely to face will be low, which may present a problem for all vertebrate populations, particularly of endangered species.

- Actions of GCs during development exert permanent organizational effects on individuals.
- Developmental exposure to GCs occur prehatch (*in ovo*: during egg formation), and posthatch (*ex ovo*: according to the amount of maternal and paternal care).
- GC transfer from mothers to offspring has the potential to translate ecological and environmental conditions into permanent offspring responses through a process termed "maternal programming."
- Such "priming" can be highly adaptive and allow animals to adjust to changing environments.
- The fitness of the modified phenotypes is likely context specific and determined by the environmental conditions encountered after development (Maternal-Match Hypothesis). Human-induced rapid environmental change has the potential to make maternal programming maladaptive.

38.4.3 Modulation of the stress response

The ELHS (Figure 38.6 and Section 38.3.3) redirects energy investment away from normal activities into a survival mode. Such an energy shift (mediated through corticosterone elevations) can be highly adaptive in most circumstances, but the individual also incurs important costs. In fact, life history theory postulates that organisms are continually facing trade-offs in the allocation of a limited quantity of resources/energy between competing functions (Stearns, 1992). For example, breeding birds must trade off energy and resources between current reproductive investment and survival (which determines future reproduction). Whether an individual should allocate more resources to one or the other life history trait depends on the relative importance in maximizing lifetime fitness, and natural selection has likely filtered optimal decisions. This is a core argument for widely accepted models on the cost of reproduction (Williams, 1966), leading to the

proposal of the "*Brood Value Hypothesis*" (Heidinger et al., 2006; Lendvai et al., 2007; Lendvai and Chastel, 2008; Angelier et al., 2020). The Brood Value Hypothesis proposes that the stress response should be modulated as a function of the relative importance of the current reproductive attempt; when the value of the current reproduction is relatively high, the stress response should be mitigated to ensure that the current breeding attempt is not compromised. This hypothesis has found empirical support in numerous field studies, within and across species. For example, maximum corticosterone in response to capture and restraint in red-legged partridges (*Alectoris rufa*) declines from the prelaying to the laying stage, suggesting an adaptive down-modulation of adrenocortical responses as the value of reproduction increases (Figure 38.9A; J. Blas and T. Marchant, unpublished data). The first experimental demonstration that individuals can flexibly modulate their stress response with respect to the reproductive value of their brood was performed in free-living house sparrows. By means of an experimental increase or reduction of clutch size during the nestling period, Lendvai et al. (2007) found that parents tending enlarged clutches responded less strongly to a stressor than those tending reduced clutches (Figure 38.9B). In addition, they examined whether individuals responded less strongly to a stressor as the breeding season progressed and future reproductive opportunities declined. The stress response decreased with breeding date during the birds' first breeding attempt, but it remained constant during their second breeding attempt. The same line of reasoning applies to interspecies comparisons: avian species breeding in northern latitudes have limited opportunities to renest due to a short breeding season; as predicted by the Brood Value Hypothesis, they show attenuated stress responses compared to southern populations/species, which have a longer reproductive season and thus more possibilities to breed within the same year (Silverin et al., 1997; O'Reilly and Wingfield, 2001; Breuner et al., 2003; but see Wingfield et al., 1995a). Similarly, older individuals have progressively reduced breeding opportunities, making it adaptive to increase reproductive effort as they age ("Terminal Investment Hypothesis": Clutton-Brock, 1984; Velando et al., 2006). Consistent with the Brood Value Hypothesis, older birds show attenuated secretion of GCs in response to challenges (Heidinger et al., 2006), although this pattern may not always occur (Angelier et al., 2007a). The response to stress has been shown to be reduced in the sex providing the most parental care (Wingfield et al., 1995b; O'Reilly and Wingfield, 2001; Holberton and Wingfield, 2003), during the specific breeding substages requiring higher parental investment (Meddle et al., 2003; see Figure 38.9A), and even within a given substage (e.g., brooding) as offspring quality or quantity increases (Lendvai et al., 2007; Lendvai and Chastel, 2008; Viblanc et al., 2016). A phylogenetic comparative analysis on 34 wild avian species found that those with a higher value of the current brood relative to future breeding mounted weaker corticosterone responses during acute stress (Figure 38.9C), and that females in the species with more female-biased parental care had weaker corticosterone responses (Bókony et al., 2009). Collectively, correlational, experimental, and comparative evidence suggest that modulation of the stress response

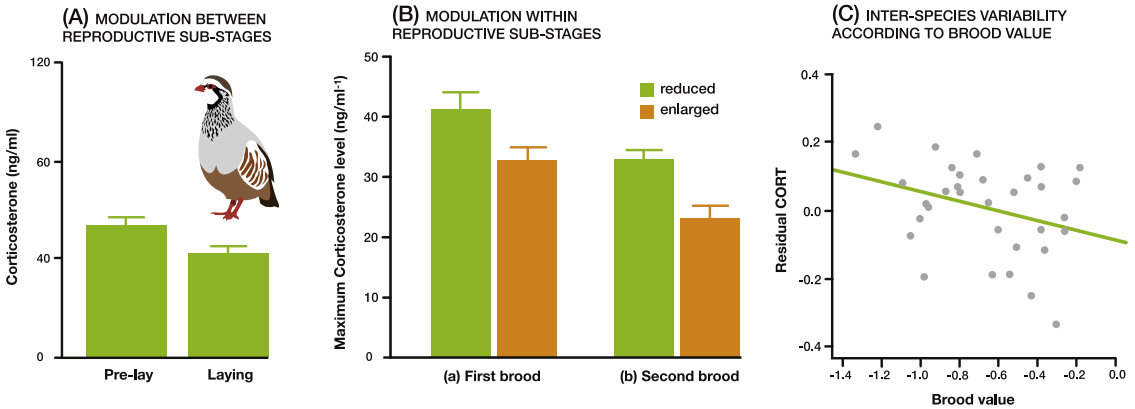

FIGURE 38.9 Modulation of the stress response during reproduction. Panel (A). Maximum corticosterone in response to capture and restraint in captive red-legged partridges (*Alectoris rufa*), across breeding substages. Stress-induced corticosterone declined as birds started laying eggs, suggesting an adaptive down-modulation of hypothalamic−pituitary−adrenal (HPA) responses as the brood value increases. Panel (B). Maximum corticosterone titers (stress-induced levels) in free-living house sparrows (*Passer domesticus*) as a function of a manipulation of brood size (number of nestlings) performed in the (a) first and (b) second breeding attempt of a year. Experimentally increased broods elevated the brood value to adult birds, which down-modulated their HPA responses. Panel (C). Residual, maximum corticosterone titers (peak plasma level controlled for baseline and breeding latitude) in relation to brood value in 34 wild avian species. Brood value expresses the putative importance of current reproduction as LOG [clutch size/(clutch size × broods per year × average reproductive life span)]. *Credit: Composite figure based on J. Blas and T.A. Marchant, unpublished data; Lendvai et al. (2007), and (2009).*

functions as a physiological mediator for the adaptive allocation of energy and resources between current and future reproduction. Importantly, these studies point to a particular hormonal mechanism, the HPA axis function, as the physiological basis for life history trade-offs, indicating that HPA function and GC secretion may be a target of selection just like other traits (Bókony et al., 2009; Hau et al., 2016; and see Bonier and Martin, 2016).

- Individuals can flexibly modulate their stress response with respect to the reproductive value of their brood (Brood Value Hypothesis).
- The intraindividual patterns of modulation are consistent with interspecies differences in stress responses, suggesting similar underlying ecological constraints. Avian species breeding in northern latitudes have limited opportunities to renest due to short breeding seasons, and show attenuated stress responses. Females in avian species showing female-biased parental care have weaker corticosterone responses.
- Modulation of corticosterone secretions makes it possible to trade off energy and resources between current reproductive investment and survival, providing a proximate mechanism for life-history evolution.

38.5 Field methods to study adrenocortical function

Our current understanding of avian adrenocortical function is to a large extent based on experimental studies performed in laboratory conditions using captive birds. This allows researchers to control a considerable number of variables known to affect *HPA* function (e.g., photoperiod, temperature, food and water, social interactions, status, age, sex, and LHS). Captive birds are easily accessible for repeated sampling and trait manipulations, and most lab facilities have readily available infrastructure to obtain, process, and store the collected samples in repeatable conditions.

However, laboratory settings impose a considerable bias when extrapolating results to the real world (Fusani et al., 2005; Calisi and Bentley, 2009). To start with, only a few avian species can be kept in captivity for experimentation, limiting research conclusions to specific species or phylogenetic groups (e.g., poultry species), and even to specific breeds whose HPA system has been voluntarily or involuntarily modified through artificial selection (Keith et al., 1973; Satterlee et al., 2000). When a wild bird is brought to captivity for experimentation, the capture and transfer to the laboratory typically exerts effects on the HPA axis (Dickens et al., 2009) which may continue throughout captivity (Fischer and Romero, 2019), and captivity-related changes in density and/or social structure can act as additional acute stressors (Dufty and Wingfield, 1986; Nephew and Romero, 2003). Furthermore, the artificial settings of captivity are unable to replicate the richness of natural stimuli and their complex interactions, and the recorded physiological and behavioral responses likely represent a minimum diversity compared to what occurs in natural habitats, when birds are exposed to real ecological scenarios (Fusani et al., 2005; Fusani, 2008). For example, wild *Passerine* species show reduced hippocampal volume, lower levels of circulating testosterone, and contrasting responses to pharmacological treatment when brought to captivity (Wingfield et al., 1990; Smulders et al., 2000; Canoine and Gwinner, 2002). Results across a range of bird (and mammal) species strongly indicate that deprivation of environmental and social cues can dramatically modify neuroendocrinological and behavioral responses and can produce contrasting information compared to studies in natural environments (Calisi and Bentley, 2009).

The past 50 years have witnessed an increasing number of behavioral endocrinologists focusing their research on wild species under natural settings, largely following the pioneering work of John Wingfield (Wingfield and Farner, 1975, 1976, 1993) who implemented methods to quantify hormones in small blood samples, avoiding the need for killing the study subjects and establishing the discipline of *Field Endocrinology*. Working in the field imposes at least five important challenges compared to laboratory settings (Fusani et al., 2005; Fusani, 2008) and has led to the use of alternative, noninvasive tools to monitor endocrine parameters (Bortolotti et al., 2008; Sheriff et al., 2011b). First, wild birds inevitably differ in nutritional condition, social status, LHS, and many other factors whose variability should be taken into account during the design of a field experiment, the collection of samples, and the subsequent statistical treatment of data. Second, catching wild birds may take a considerable amount of effort, and the trapping method should be carefully chosen to avoid additional interferences on adrenocortical function. For example, the use of visual decoys and playbacks may facilitate capture, but using social stimulation as "bait" also stimulates rapid hormone secretions (e.g., elevating testosterone levels, Wingfield and Wada, 1989), potentially effecting GC levels (Charlier et al., 2009). Even the use of passive trapping methods like mist netting should be carefully supervised because the capture event itself is a stressor, and the time elapsed until sampling need to be standardized, controlled for, or at least meticulously recorded (see Section 38.5.1 and Box 38.1). Third, sample sizes are often reduced compared to laboratory studies ($N \leq 10$ are not uncommon) due to the difficulty of capturing wild birds and also to minimize the impact on wild populations. Whenever possible, repeated measures designs are advisable to increase the statistical power, although recapturing the same individuals may not be always possible as individuals learn avoidance behaviors. Collaborative projects can overcome this issue by sharing data to increase sample sizes and

improve inferences, especially across large geographic areas (e.g., Fairhurst et al., 2015a, b; Knight et al., 2019), but strict methodological standards must be implemented. Fourth, because conditions can be primitive when working in field or remote locations, specific logistics may be required for sample processing and transportation. For example, the separation of plasma from blood samples for subsequent determination of corticosterone levels may require using a battery- or manually operated centrifuge, while plasma preservation, storage, and transport in frozen conditions may require handling dry ice or liquid nitrogen in specific containers adapted for field and travel (details in Fusani et al., 2005). The use of alternate tissues can overcome this issue but cannot replace blood sampling for studying HPA functioning or responses to acute stressors (see Section 38.5.4.1). Fifth, and finally, special care should be taken regarding the ethical and legal considerations associated with the manipulation of wild birds (Fair et al., 2010), aimed and minimizing potential impacts on the well-being of study subjects and the viability of natural populations.

All the constraints and the special considerations above imply that a first step for any field study of avian adrenocortical function requires a carefully planned experimental design. Environmental stochasticity (unpredictable events) occur frequently during field studies (Sergio et al., 2018), and this may actually result in "natural experiments" that provide unique opportunities to understand the role of adrenocortical function in birds, for example, during inclement weather (Wingfield et al., 1983), social conflict (Goymann and Wingfield, 2004), famine conditions (Kitaysky et al., 1999a,b), and pollution accidents (Baos et al., 2006; Baos and Blas, 2009). Below we will summarize common field techniques that are frequently used for assessing adrenocortical function in wild birds, some of which have been developed or largely implemented in recent years (laboratory techniques aimed at quantifying GC levels have been reviewed elsewhere; see, e.g., Sheriff et al., 2011b).

- Translocation and captivity are known to affect the HPA axis in birds. Deprivation of environmental and social cues can modify avian neuroendocrinological and behavioral responses, preventing the extrapolation of results from laboratory studies to the real world.
- Field endocrinologists focus their research on wild species under natural settings, but face important challenges during sample collection, processing, and transportation. These have led to the development of alternative and noninvasive tools to monitor endocrine function.
- Field research requires carefully planned experimental designs and special care to minimize impacts on the well-being of individuals and the viability of natural populations.
- Environmental stochasticity often results in "natural experiments" that provide unique opportunities to understand the role of the stress response in avian ecology and evolution.

38.5.1 Obtaining adequate blood samples: capture and restraint protocols and the "stress series"

Field endocrinologists face an obvious methodological difficulty when collecting samples aimed at assessing HPA function in wild animals: an adequate baseline blood sample containing GC levels truly indicative of the individual's "unstressed" conditions should not be affected by the investigator disturbance. However, the trapping and capturing activities that necessarily precede blood sampling are typically perceived by wild birds as real predation attempts (Scheuerlein et al., 2001; Canoine et al., 2002). Although many behavioral and neuroendocrine components of the "fight-or-flight" response occur within seconds (e.g., epinephrine/norepinephrine elevations accompanied by escape behaviors and alarm calls), the elevation of circulating corticosterone levels typically shows a 2–3 min delay (Romero and Reed, 2005). This short timeframe constitutes, in many field situations, a feasible period for obtaining a first blood sample in situ. This can be done through venipuncture of the wing (brachial) vein using a sterilized needle and collecting blood drops in heparinized microhematocrit tubes (e.g., one or several 50 μL tubes) or using heparinized syringes that also allow accessing the leg or jugular veins. These procedures are generally harmless provided adequate training and observing the recommended blood sampling volume limitations according to body size (Fair et al., 2010; though see Brown and Brown, 2009). Following capture and initial collection of a baseline blood sample, birds should be kept in cloth bags or immobilized with cloth corsets, allowing adequate ventilation but preventing injury if the bird struggles. Birds should also be placed in a safe place, sheltered from direct negative effects of weather, and their vision deprived (large birds may require using falconry hoods, Blas et al., 2010). It is very important to follow a strict capture, handling, and restraint protocol because subsequent collection of additional blood samples at predefined intervals of time (for example, 10, 30, and 45 min postcapture, Blas et al., 2006a) will allow the characterization of GC elevations at the individual level during a "*stress series*" (Box 38.1; Figure 38.10A). Researchers can therefore transform/adapt their normal capture and sampling activities into standardized experimental protocols that will allow establishing formal group comparisons in a repeatable manner within and across studies (for example, in relation to age, sex, and body condition). The timing and number of sampling

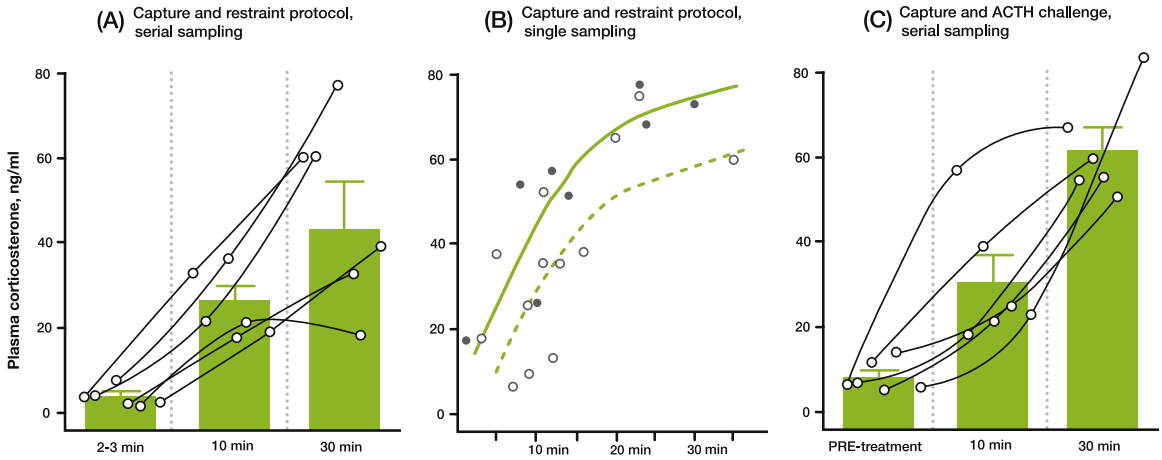

FIGURE 38.10 Protocols for assessing the "stress response". Panel (A). *Capture and restraint with repeated blood sampling*: Plasma corticosterone levels in nestling black kites (*Milvus migrans*) after standardized capture, restraint and serial bleeding of the same individuals (one line per individual, $N = 6$ birds) at three fixed times (x-axis). The green bars in the background represent mean and standard error (S.E.) per sampling episode. Panel (B). *Capture and restraint with single blood sampling*: Plasma corticosterone levels in adult male black kites after standardized capture, restraint, and collection of one single sample per individual (*single dots* are independent individuals). The *solid and dashed lines* indicate logistic regression estimates for nonbreeding (*black dots*) and adult breeding birds (*white dots*). Panel (C). *Capture and restraint with adrenocorticotropic hormone (ACTH) challenge and serial blood sampling*: Plasma corticosterone levels in nestling black kites after standardized capture, restraint and intravenous injection of ACTH. Serial blood sampling was performed before and after (10 and 30 min) treatment (one line per individual, $N = 6$ birds). ACTH injections were performed within 2 min from capture for ease of comparison with the corticosterone responses shown in Panel (A). The green bars in the background represent mean and S.E. per sampling episode. *Credit: Composite figure based on L. López et al., unpublished data; J. Blas et al., unpublished data; and Blas et al. (2011).*

intervals will depend on research objectives and logistical practicality. In some field situations, it may not be possible to obtain rapid samples from all the individuals in unstressed/baseline conditions (e.g., when the trapping method involves simultaneous capture of many birds; Blas et al., 2011) or collect repeated samples from the same individuals (e.g., in small species or during early developmental stages, when blood volume is highly limited; Fairhurst et al., 2013b). In all the cases, it is still critical to keep accurate records of the times elapsed from capture to blood sampling each individual, and GC responses can be subjected to group comparisons through regression analyses (Figure 38.10B).

- Capturing wild birds stimulates their stress response. Consequently, baseline corticosterone levels are normally assessed in blood samples obtained within 2−3 min postcapture. Additional blood samples will allow characterizing the *adrenocortical response to stress* at the individual level ("*stress series*").
- Blood sampling requires keeping meticulous records of the times elapsed from capture to blood sampling for each individual. Samples can be collected at predefined intervals of time or along a continuum, but a standardized *capture, handling, and restraint protocol* is required to establish group comparisons.

38.5.2 Quantifying the strength and sensitivity of adrenocortical responses

Although the *handling and restraint protocol* accompanied by serial collection of blood samples (Box 38.1) is a widely used method for assessing adrenocortical function in wild birds, the resulting GC elevations may be affected by perception differences among and within individuals (Romero, 2004). For example, wild penguins exposed to human presence show moderate GC elevations following the same capture and restraint protocol that triggers strong adrenocortical responses in unexposed conspecifics (Walker et al., 2006), suggesting habituation to human presence (Cyr and Romero, 2009). Similarly, acclimation was proposed to explain why parrots that were bred in captivity had attenuated corticosterone responses compared to wild-caught parrots (Cabezas et al., 2013). The reverse outcome may also occur when predator-naïve species learn that humans can be a potential danger, resulting in gradually stronger GC responses (Rödl et al., 2007). For these reasons, field studies may benefit by incorporating additional research methods to characterize adrenocortical function regardless of perceptional biases (see Canoine et al., 2002). For example, the sensitivity and the robustness of an individual's adrenocortical response can be estimated by means of administration of two commercially available

drugs followed by the collection of blood samples to monitor concomitant, short-term (e.g., within 30–90 min) changes in endogenous GC levels (Figure 38.10C).

The adrenals' *maximal ability or capacity* to secrete GC can be experimentally assessed through intravenous, intramuscular, or intraperitoneal administration of exogenous adrenocorticotropin (ACTH). Porcine ACTH is commercially available for research purposes, and it is known to elicit corticosterone release in the avian adrenals (Astheimer et al., 1994; Wasser et al., 1997; Rich and Romero, 2005). The commercial product is normally provided lyophilized, requiring suspension in an injectable isotonic solution (Ringer's solution). Dosage choice and injection volumes can be assessed according to previous references, and a pilot study using a small sample size (e.g., four to six birds) would allow selecting the minimal dose eliciting maximal response (*adrenal saturation*) and the optimal postinjection time for the subsequent collection of blood samples. Unfortunately, ACTH degrades at room temperature or following thaw–freeze cycles, requiring the preparation of aliquots maintained frozen until a few minutes before injection.

The *robustness* of an individual's adrenocortical response can be characterized through exogenous (intravenous, intramuscular, or intraperitoneal) administration of *dexamethasone* (*DEX*). DEX is a synthetic GC that competes with endogenous corticosterone for binding receptors in the brain, and artificially stimulates negative feedback (Dallman et al., 1992). Because DEX does not bind to the antibodies commonly used in radioimmunoassays (RIAs), a decrease of endogenous GC levels can be monitored by performing serial collection of blood samples within a relatively short period (e.g., 30, 60, and 90 min) after chemical challenge, allowing standardized comparisons among experimental groups (Torres-Medina et al., 2019). Negative feedback is a critical component of HPA function, as a failure in this system can lead to persistent elevated corticosterone levels that lengthen and strengthen the overall stress response (Romero, 2004), potentially resulting in stress-related disease (Sapolsky, 1992; Romero and Wikelski, 2010). Contrary to ACTH, commercial DEX solutions are generally stable at room temperature, and because it is a common anti-inflammatory drug, the product is easily accessible in veterinary clinics.

- Individual experience can affect HPA functioning (e.g., through acclimation), and methods are available to characterize adrenocortical function regardless of perceptional biases.
- The individual's *maximal capacity* to secrete GCs can be experimentally assessed through ACTH injections, followed by serial collection of blood samples and quantification of corticosterone elevations.
- The *robustness* of an individual's adrenocortical response can be characterized through exogenous administration of DEX, a synthetic GC that competes with endogenous corticosterone and stimulates negative feedback.

38.5.3 Phenotypic engineering

One of the best ways to explore whether and how traits of organisms are currently adaptive is to manipulate them experimentally and compare the relative fitness of altered and unaltered individuals. This method has been termed *phenotypic engineering*, and it is a powerful tool in field endocrinology studies (Ketterson et al., 1996; and see Bonier and Martin, 2016). For example, one could manipulate body condition and monitor the effects on circulating hormones (Figure 38.11A). More often, field endocrinologists are interested in a continuous manipulation of the individual's hormone levels (over the course of a few days or weeks) in order to assess the effects on physiology, morphology, behavior, and performance (Figure 38.11B and C). Repeated administration of a substance (e.g., daily injections) is impossible in most field conditions because focal individuals avoid being regularly recaptured. Consequently, field researchers rely on subcutaneous implant devices to deliver the target substance (e.g., corticosterone, DEX) more or less continuously. Depending on the chemical properties of the target substance and other considerations (including the researcher's budget), this can be achieved through three types of subcutaneous implant devices (described below; see also Fusani, 2008). With the required training, the associated surgical procedures are simple, fast, and minimally invasive: after applying local anesthesia (e.g., external or subcutaneous lidocaine solution between the wings, the lower neck, or the upper leg area where the implant will be placed) and superficially cleaning the area with a cotton swab impregnated in povidone-iodine solution (alcohol should be avoided), a small incision using a sterile scalpel allows subsequent insertion of the implant device with sterile forceps. The skin is subsequently closed using a small dab of tissue adhesive (for smaller incisions/birds; Fairhurst et al., 2013b) or surgical stitches (for larger ones; Blas et al., 2006b).

1. ***Silicone implants***: Silastic medical grade tubing (Dow Corning, Inc.) can be filled with crystalline hormone and the two ends closed with silicone glue. After subcutaneous insertion, the substance diffuses through the semipermeable walls for a variable period determined by the length of the tube, the thickness of the walls, the amount of drug, and its lipophilic nature. Although this inexpensive technique can be useful for highly

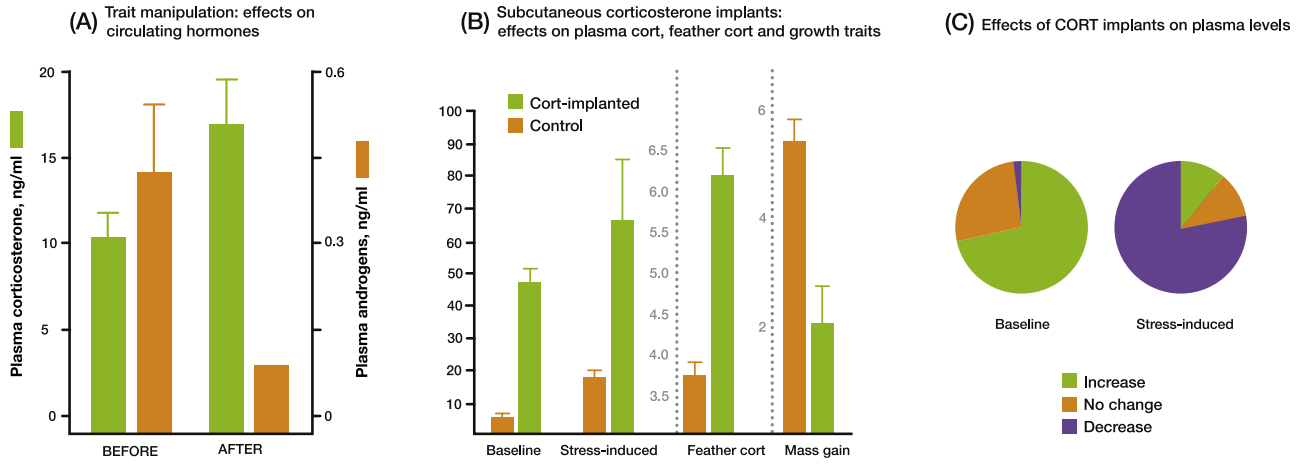

FIGURE 38.11 Phenotypic engineering influences levels of corticosterone. Panel (A). *Effects of trait manipulations on circulating hormones*: Plasma levels of baseline corticosterone ("CORT"; left axis, *green bars*) and androgens (right axis, *orange bars*) before and after an experimental food restriction that caused a decrease in the body condition of adult male red-legged partridges (*Alectoris rufa*). Bars indicate means and standard error (S.E). All plasma samples were collected 3 min postcapture. Panel (B). *Effects of sustained corticosterone manipulations on plasma CORT, feather CORT, and body mass*: Plasma corticosterone levels (ng/mL), feather corticosterone levels (pg/mm), and body mass gain (g) in nestling tree swallows (*Tachycineta bicolor*) subcutaneously implanted with time-release corticosterone pellets or drug-free control pellets (*green and orange bars* respectively) on day 7 posthatch. Baseline blood samples were collected within 2−3 min following capture, and stress-induced blood samples were collected after 30 min of restraint (all samples collected 3 d after implanting). The feathers were growing during the experimental period, and were collected on day 15 posthatch. Body mass change was estimated between days 7 and 11 posthatch. All bars indicate means and S.E. Panel (C). *Directions of the effects of CORT implants on plasma CORT levels*: A review of 50 published experiments revealed that baseline CORT levels generally increase whereas stress-induced CORT levels generally decrease following the use of subcutaneous CORT implants in birds. *Credit: Composite figure based on Pérez-Rodriguez et al. (2006); Fairhurst et al. (2013b), and Torres-Medina et al. (2018).*

lipophilic hormones such as testosterone (Blas et al., 2006b), silastic implants have low permeability for hydrophilic substances such as corticosterone (Kinel et al., 1968). In addition, *continuous* release does not mean *consistent* release (see Fusani, 2008). The choice of perforating the tube or leaving one end open causes a fast release of the hormone and thus inability to maintain a sustained elevation within or between individuals (Newman et al., 2010), which may confound experimental results. Despite such problems, this has traditionally been the most common method of manipulation in studies on wild birds, with a prevalence of 50% across the experiments performed during the last two decades (Torres-Medina et al., 2018).

2. ***Osmotic pumps***: Osmotic minipumps (Alzet, Durect Corporation, Cupertino, CA, USA) allow for up to four weeks of *continuous and consistent* hormone release independent of its solubility (e.g., Soma et al., 2000; Fusani et al., 2005). This method provides high repeatability (Fusani, 2008) but has received a rather marginal use (*ca.* 6% of avian experiments involving corticosterone implants; Torres-Medina et al., 2018), possibly because it is relatively expensive (Fusani, 2008).
3. ***Time-release pellets***: Innovative Research of America (Sarasota, Florida, USA) manufactures pellets for the most common hormones and antihormone drugs as well as placebo (vehicle only) pellets (Figure 38.11B and C). The hormone is included in a cholesterol matrix that is slowly reabsorbed when placed subcutaneously. Although commercial pellets are relatively expensive, it is not necessary to recapture the animal to remove any experimental device after the study, providing a considerable advantage compared to silicone implants and osmotic pumps. The frequency of use of this method is 44% across corticosterone implant studies on birds, with a growing tendency observed during the last two decades (Torres-Medina et al., 2018). Caution should be taken regarding dosages and expected release times (Müller et al., 2009; Fairhurst et al., 2013b); the duration of effects is typically limited to the first third of the theoretical period, making it advisable to perform pilot studies with repeated blood sampling sessions for each study model and throughout the supposedly effective (theoretical) period advertised by the manufacturer (Torres-Medina et al., 2018).

Note that the effects of corticosterone implants on baseline levels show a quadratic association with experimental dose across bird species, and decreased plasma levels may occur at both high and low-implant doses (Torres-Medina et al., 2018). Furthermore, continuing hormonal treatment for longer than a few days or 1 week can also result in endogenous readjustment of the individual's endocrine system (evolved to maintain homeostasis). Therefore, long-term administration of an exogenous hormone may result in reduced endogenous

production through negative feedback, and eventually in a regression of endocrine glands. These effects may last longer and be opposite to the intended initial manipulation (Fusani, 2008), potentially confounding the interpretation of results. Indeed, a review of 50 studies that used subcutaneous corticosterone implants found that 72% of experiments increased baseline corticosterone levels, but 78% of experiments reduced stress-induced corticosterone levels (Figure 38.11C; Torres-Medina et al., 2018). Thus, while target effects on baseline hormone levels can be expected (though by no means guaranteed), delivering the hormone using implants frequently produces stress-hyporesponsive phenotypes, which can be problematic for studies measuring downstream variation in other biological traits. Given our current gaps of knowledge regarding the effects of corticosterone implants on avian physiology, it is recommended that researchers (1) perform dose-effect pilot studies, (2) conduct a stress series to assess the consequences to both baseline and stress-induced corticosterone levels, and (3) improve the resolution and duration of blood sampling protocols aimed at assessing effective duration of implants and associated responses (Torres-Medina et al., 2018). Finally, it should be noted that experimental augmentation of GC levels generally reduces fitness across species (Bonier and Cox, 2020).

- One method to explore how endocrine traits are adaptive is to alter them experimentally and compare the fitness of altered and unaltered individuals ("phenotypic engineering").
- Field endocrinologists rely on subcutaneous implant devices to deliver the target substances (e.g., corticosterone) more or less continuously. Depending on the chemical properties of the target substance, this can be achieved through silicone implants, osmotic pumps, or time-release pellets.
- Hormonal treatment for longer than a few days, or that produce supraphysiological levels, may result in a reduced endogenous production, including hyporesponsiveness to stressors. Caution should be taken to avoid potentially confounding results, including downstream biological effects.

38.5.4 Corticosterone and its metabolites in tissues other than blood

Quantifying circulating (plasma) corticosterone levels is the best way to characterize individual adrenocortical status at a particular moment, and to understand how the HPA system works mechanistically and in relation to acute stressors. However, blood levels are instantaneous measurements, and the circulating GC titers within a given individual show dramatic temporal fluctuations according to the immediate internal and external circumstances (e.g., social, environmental, daily rhythms). Field avian researchers face a challenge when trying to establish associations between long-term metrics, such as fitness and individual adrenocortical function, because GCs at a particular instant in time (a blood sample) hardly represent the long-term allostatic responses of an individual. Likewise, studies addressing the environmental causes of individual GC physiology may find it unrealistic to expect an instantaneous GC measurement to reflect the complexity of patterns of GCs secreted in response to suites of stressors experienced over time.

Establishing robust ecophysiological associations would require repeatedly sampling the same individuals across time, space, and/or large samples sizes. Such tasks are difficult to accomplish in field scenarios, explaining, in part, why GC-fitness associations are rarely reported and remain generally elusive to ecological studies (Breuner et al., 2008; Bonier et al., 2009; Crespi et al., 2013; Dantzer et al., 2014). In addition, obtaining blood samples requires capturing live birds, which can introduce a potential artifact of the investigator disturbance on the results (Table 38.1) and raises ethical concerns related to the well-being of the individuals and the conservation of wild populations (Sheriff et al., 2011b). Studies using blood to measure ecophysiological associations over large spatial scales (e.g., effects of climate change or habitat degradation) or in relatively inaccessible species face logistical challenges. This may be solved by sampling blood during periods of the annual cycle when large numbers of individuals from across the landscape are more easily accessible (e.g., on migration), but physiological and environmental conditions at the time of sampling may bear little resemblance to the conditions relevant to fitness. For these and other methodological and logistical reasons summarized in Table 38.1, field researchers may choose alternative biological samples to study adrenocortical function in wild birds, such as feathers and excreta.

38.5.4.1 Feathers

The discovery (Bortolotti et al., 2008, 2009a) and independent confirmation (Lattin et al., 2011; Koren et al., 2012; Fairhurst et al., 2013b; Jenni-Eiermann et al., 2015) that corticosterone can be quantitatively determined in feathers has provided a minimally invasive and retrospective means of measuring avian GC physiology (Romero and Fairhurst, 2016). Outstanding methodological issues aside (reviewed in Romero and Fairhurst, 2016), the measurement of feather corticosterone can produce novel ecophysiological insights, and feathers provide excellent flexibility in the field. Not surprisingly, this technique has gained popularity in the past 10 years with behavioral ecologists and conservation physiologists. Evidence suggests that, with proper validation and careful interpretation,

TABLE 38.1 Summary of methodological advantages and disadvantages associated with the use of blood, feathers, and excreta samples for assessing adrenocortical function in wild birds.

	Blood samples (corticosterone, CORT)	Feather samples (corticosterone, CORT)	Excreta samples (glucocorticoid metabolites, GCMs)
Trapping and capture required	**Yes**	**Depends on context** Capturing is optional. Feathers can be collected after natural molt (e.g., near nest site) or from dead/museum specimens.	**Depends on context** Capturing is optional. Direct field observation may be required to collect fresh samples and assign bird identity.
Potential for researcher interference on results	**High** Blood GC levels increase 2–3 min postcapture. Variability in handling and restraint affects circulating corticosterone in the collected samples.	**Negligible** Even if capture is applied for sampling, the potential effect would only affect currently growing feathers (and even then may only be negligible on overall feather corticosterone levels). Only longer-term perturbations (such as captivity) would affect corticosterone levels in growing feathers.	**Low** If capture is applied, time until defecation may elevate excreta GCM levels (the extent of interference depends on the frequency of defecations and the species' metabolism).
Training required to obtain samples	**Yes** Proper blood sampling techniques require initial training	**Minimal** Proper collection of feathers from live birds requires minimal training. No training needed to collect feathers during natural molt in the field, or from research specimens, though collecting feathers from the latter may require following specialized (museum) protocols.	**No** Training not required. Fresh excreta can be collected in the field, or after restraining captured birds in cloth bags.
Time scale (of adrenocortical activity) reflected in samples	**Short** minutes (possibility of accurate, short-term characterization of adrenocortical responses).	**Medium-long** Days to weeks or months (depending on feather growth duration). Adult birds may have feathers grown at different times and in different locations. Feather morphology allows discrimination of different portions grown across consecutive days.	**Medium-short** Minutes to hours (timeframes depend on the actual delay between feeding and excretion in any given sample).
Logistics for sample collection and initial processing	**High** Venipuncture and blood sampling require using syringes or sterilized needles and microhematocrit tubes (preferably heparinized). Plasma should be separated from whole blood through centrifugation (field centrifuge, pipettes, tubes, etc., required).	**Low** Plastic or paper bags or envelopes. Samples should be kept as dry as possible to avoid mold.	**Medium-low** Excreta samples can be collected in vials or plastic bags.
Logistics for sample preservation, storage, and transport	**High** Coolers are required to preserve blood samples fresh until centrifugation within the same day. Storage and transport requires freezing (freezer, dry ice, or liquid nitrogen, and specific containers).	**Low** Feathers can be stored in paper envelopes or plastic bags at room temperature.	**Medium-high** Considerable microbial degradation requires freezing samples immediately. Alternatively, samples can be preserved in alcohol, dried in an oven or lyophilized.

Continued

TABLE 38.1 Summary of methodological advantages and disadvantages associated with the use of blood, feathers, and excreta samples for assessing adrenocortical function in wild birds.—cont'd

	Blood samples (corticosterone, CORT)	Feather samples (corticosterone, CORT)	Excreta samples (glucocorticoid metabolites, GCMs)
Possibility of subsampling to characterize timeframes	**No** Single samples cannot be divided temporally. Additional blood sampling is required to analyze time-related patterns (e.g., capture and restraint series).	**Yes** Feathers can be clipped and subsampled to select portions grown across different days.	**No** Subsampling should be avoided. GCMs are not uniformly distributed within a sample. Undigested materials can cause interference with final results.
Retrospective potential	**No** Circulating corticosterone reflects current adrenal activity and therefore has very little retrospective potential.	**High** GCs are incorporated in the feather structure during growth, but birds maintain the same feathers for months or years (depending on the feather tract and the species' molt patterns), allowing retrospective analyses (e.g., feathers collected this year can reflect circulating corticosterone levels of a previous year when they were grown).	**Low** Excreted CM reflects secretion, metabolism, and excretion during a variable period (minutes to hours) prior to deposition, allowing for short-term retrospective analyses (for example, researchers may decide to collect samples minutes to hours after a storm or a bout of aggressive interactions, and focal individuals can be chosen *post hoc*).
Discrimination between baseline and stress-induced GC levels	**High** Capture and restraint (and serial blood sampling) allows assessing baseline and stress-induced corticosterone levels in the individual. An evaluation of the internal (e.g., nutritional), environmental, and social conditions is required to determine whether initially collected samples represent true baseline.	**Low** Feather corticosterone integrates the amplitude and duration of circulating corticosterone levels during a growth period. Interpretation of results should take into account the potential variation in both baseline and stress-induced levels within and between feather samples.	**Low** Excreta GCMs integrate the amplitude and duration of circulating corticosterone levels between food ingestion and excreta deposition. Interpretation of results should take into account the potential variation in baseline and stress-induced levels within and between excreta samples.

Differences in laboratory assay methods required for the quantification of corticosterone or corticosterone metabolites levels in each type of sample should also be taken into account.

feather corticosterone can be a useful biomarker of allostasis, with applications to evaluate potential impacts of human activities on avian health and well-being (e.g., Fairhurst et al., 2015b; Sergio et al., 2015; Expósito-Granados et al., 2020; Baños-Villalba et al., 2021; Grunst et al., 2020).

Although the precise proximate mechanism requires additional study, there is solid evidence using radiolabeled hormone that circulating (systemic) corticosterone is gradually deposited (likely through diffusion) into the growing feather structure primarily during cell differentiation in the blood quill (Jenni-Eiermann et al., 2015). The corticosterone remains sequestered within the feather keratin structure, rather than being externally deposited (for example, through preen gland secretions; Bortolotti et al., 2008; Lattin et al., 2011; Jenni-Eiermann et al., 2015; Will et al., 2019), and can persist for at least 150 years (Fairhurst et al., 2015a). Robust experimental evidence shows that feather corticosterone reflects allostatic load (Johns et al., 2018) and can correlate with both baseline and stress-induced measurements of plasma GC levels (Figure 38.11C; Fairhurst et al., 2013b; Jenni-Eiermann et al., 2015). Moreover, feather corticosterone values mirror lifetime changes in reproductive success and survival rates (López-Jiménez et al., 2017). Collectively, this evidence supports a clear connection between energetic balance, circulating plasma levels of corticosterone, and the levels of corticosterone that are ultimately deposited in feathers. However, researchers should avoid using feather corticosterone as a proxy for plasma levels because a relationship between the two is likely to occur only when the latter reflect sustained HPA activity (Fairhurst et al., 2013b). Feather corticosterone should instead be viewed as a separate and alternate measure of GC physiology (Romero and Fairhurst, 2016).

The growth rate of feathers implies that the period over which researchers can assess an individual's GC levels is days or weeks, rather than minutes or hours. This represents a considerable methodological advantage for field studies, as feather corticosterone levels likely reflect a more representative and ecologically meaningful time scale of individual allostatic responses, including responses to the collective environmental perturbations experienced during feather growth. In the years since the technique was first described, feather corticosterone levels have been shown to correlate with individual fitness and performance (Figure 38.11B and C; Bortolotti et al., 2008; Koren et al., 2012; Fairhurst et al., 2012b, 2013a; Kouwenberg et al., 2013; Harms et al., 2015; López-Jiménez et al., 2017; Ramos et al., 2018; Monclús et al., 2020), quality-dependent traits (Bortolotti et al., 2009b; Mougeot et al., 2010; Kennedy et al., 2013; Grava et al., 2013; Fairhurst et al., 2014), and environmental conditions (Fairhurst et al., 2011, 2012a, 2013a; Carrete et al., 2013; Legagneux et al., 2013; López-Jiménez et al., 2016b; Treen et al., 2015; Messina et al., 2020). Moreover, correlations between measures of feather corticosterone in one period of the annual cycle and downstream biological traits in a subsequent period have provided insights into carry-over effects (*sensu* Harrison et al., 2011) in a variety of avian taxa, including seabirds (Crossin et al., 2013; Fairhurst et al., 2017), waterfowl (Harms et al., 2015; Hansen et al., 2016), songbirds (Boves et al., 2016; Latta et al., 2016; Imlay et al., 2019; Messina et al., 2020), and raptors (Monclús et al., 2020). Given the obvious utility of feather corticosterone for studying ecophysiology, and its flexible means of assessing GC levels retrospectively, feather corticosterone shows promise as a biomarker (Romero and Fairhurst, 2016). It is worth mentioning that the evidence for GC-fitness relationships has been mixed in birds (Bonier et al., 2009), but this is the norm in vertebrates (Dantzer et al., 2014) and is to be expected with any measure of GC physiology.

There is debate as to how best to express feather corticosterone levels, but the vast majority of studies correct corticosterone values by feather length (i.e., CORT/mm is the unit). This is because corticosterone is likely deposited in a time-dependent way and length best reflects time during feather growth (Bortolotti et al., 2008, 2009a; Bortolotti, 2010; Jenni-Eiermann et al., 2015). To account for effects of feather mass on feather corticosterone values (Romero and Fairhurst, 2016), which can be problematic in studies where poor nutritional condition and high levels of corticosterone can affect feather mass, alternate correction approaches have been proposed (Will et al., 2019). Researchers should also be aware that results from different analytical techniques are not comparable, and GC measurements derived from enzyme immunoassays (EIAs) and assay kits are overall less repeatable than those from in-house assays and RIAs (reviewed by Schoenemann and Bonier, 2018). This has important implications because EIA kits are increasingly popular for measuring feather corticosterone. As with all techniques for analyzing hormones, proper validation is paramount and reporting all appropriate QA/QC parameters is critical when publishing data (Buchanan and Goldsmith, 2004).

Feathers can be used to assess changes in HPA activity across short- or long-term scales. For example, because daily feather growth can be determined through visual examination of growth bands (one pair of dark/light bands is typically grown every 24 h; Jovani et al., 2010), by clipping and subsampling different feather portions, it is possible to assess changes in GC levels across the few days or weeks required to complete feather formation. This approach has limitations, as sectioning and analyzing small feather segments may present methodological problems (Romero and Fairhurst, 2016; Ganz et al., 2018). Alternatively, a complete feather could be used to assess GC activity over a longer period of days or weeks, depending on the total amount of time required to grow each feather type. Because birds regularly replace all body feathers in a species-specific molting sequence, different feathers from the same individuals allow assessing HPA activity at different times of the year and at different locations (Carrete et al., 2013). However, researchers should make all appropriate validations of the repeatability of feather corticosterone measures in feathers from the same or different tracts before comparing values (Harris et al., 2016), as repeatability is likely to be species- and context-dependent. Combining multiple feathers for analysis introduces additive variation that can easily obscure effects of interest, and even "symmetrically" molting feathers may grow over slightly different time periods, reflecting different ecophysiological conditions and, thus, produce different feather corticosterone values. Therefore, standardizing feather samples as best as possible can help reduce unwanted variation (see Romero and Fairhurst, 2016).

The analysis of GC levels can be combined with other intrinsic markers in the same sample to provide additional ecophysiological context. For example, combining feather corticosterone and stable isotope analysis can establish the detailed spatial-temporal dynamics of adrenocortical function (Fairhurst et al., 2013a), and contaminant levels can provide toxicological context (Meillère et al., 2016). Sample storage, transport, and preservation do not require freezing, and feathers can be stored in plastic bags or paper envelopes at room temperature. The analysis of feather hormones has the unique advantages of allowing for experimentation and sampling at any time of the year with minimal investigator-induced impacts and offering a large retrospective potential (Table 38.1). For example, molted feathers can be collected without disturbing wild birds, and

museum specimens can be used (Kennedy et al., 2013; Fairhurst et al., 2015a; reviewed in Romero and Fairhurst, 2016). Considering these benefits, feather corticosterone may well provide the ultimate noninvasive physiological measure of adrenocortical function in birds (Romero and Fairhurst, 2016). As with any biomarker, continued research and validation are essential (Madliger et al., 2018).

- Circulating corticosterone is deposited in growing feathers, remaining sequestered within the keratin structure and allowing a retrospective assessment of adrenocortical activity.
- Feather corticosterone levels are best expressed as pg/mm because length reflects time during feather growth. The slow growth rate allows inferring an individual's exposure and response to environmental perturbations across days or weeks (rather than minutes or hours).
- Feather plucking induces regrowth, allowing for experimentation with minimal investigator-induced artifacts. In addition, feathers are naturally replaced in a specific molt sequence, allowing noninvasive, long-term monitoring of adrenocortical function.
- Different feathers from a captured individual or a museum specimen allow inferring adrenocortical activity at different times of the year and at different locations.
- Depending on sampling, feather corticosterone provides a minimally- or noninvasive physiological measure of adrenocortical function. Appropriate validations and tests of repeatability are essential to interpreting and comparing feather corticosterone values.

38.5.5 Corticosterone metabolites in droppings (excreta)

Circulating corticosterone levels can be also traced using bird "droppings," the excretory products including urine and feces (both are normally mixed in the cloaca prior to excretion; Klasing, 2005). This can be done using either a homogenate of the entre dropping (Washburn et al., 2003) or collecting only the fecal portion (Hirschenhauser et al., 2005). However, it is very important to point out that there are no native GCs in excreta samples (Touma and Palme, 2005): GCs are extensively metabolized in the liver and excreted into urine (via the kidneys), or into the gut (via the bile ducts), undergoing further chemical modifications by the intestinal flora (Palme, 2005; Palme et al., 2005). This process results in complex and varied excreted *glucocorticoid metabolites* (*GCMs*) whose proportion and structure depends on the species and its metabolism at the time of dropping production (Goymann et al., 2006). Importantly, this requires a proper validation study to ensure that the final levels of the analyzed by-product (GCMs) reliably reflects the original GC levels (e.g., corticosterone) in the circulatory system of the research model (Millspaugh and Washburn, 2004; Goymann, 2005; Palme et al., 2005). Because excreta samples are also subjected to considerable microbial degradation after defecation (Möstl et al., 1999, 2005), samples should be collected fresh and preserved immediately. Samples can be frozen, which is preferable (Sherriff et al., 2011b), preserved in alcohol, or dried in an oven (Wasser et al., 1997; Khan et al., 2002; Terio et al., 2002); the choice of method will determine whether GCMs are expressed as per wet or dry mass (these two values may correlate; Wasser et al., 2000). It is also important to avoid excreta subsampling (GCM may not be uniformly distributed with a sample) and remove undigested materials if differences in diet among samples are observed, because both factors may introduce considerable interference into results.

Collecting samples of previously excreted samples in the field is noninvasive (see Table 38.1), but obtaining fresh samples implies the need to perform observations of marked/controlled individuals to monitor defecation events either visually (Wasser et al., 1997) or through remote spatial tracking (Thiel et al., 2008). Alternatively, birds can be trapped and restrained until defecation occurs (Garamszegi et al., 2012). Whether the stress caused by capture and manipulation affects excreta GCM levels depends on the frequency of defecations and the species' metabolism (Palme et al., 2005), making it advisable to keep detailed records of the times from capture to sample collection and preservation, and restrict the analyses to those samples collected within a short time after capture (for example, within 5 min: Garamszegi et al., 2012). GCM levels in droppings are assumed to reflect an integrated average of three processes: GC secretion, metabolism, and excretion. Although it is debated whether GCMs best represent baseline or stress-induced GCs, it is more likely that they reflect overall GC levels in circulation within a variable period of time (Sheriff et al., 2011b).

The noninvasive nature of excreta sampling procedures makes it a very suitable substrate for a wide array of applications in animal welfare and conservation biology (for reviews, see Millspaugh and Washburn, 2004; Busch and Hayward, 2009). For example, GCMs have been used to study avian adrenocortical function in relation to behavior (Lucas et al., 2006; Carere et al., 2003) and habitat quality (Wasser et al., 1997), to understand the effects of anthropogenic perturbations in natural environments (Thiel et al., 2008; Blickley et al., 2012), to determine responses to handling in captive endangered species (Glucs et al., 2018), and monitor responses to instrumentation for tracking movements (Latty et al., 2016).

- Adrenocortical activity can be monitored analyzing avian excretory products (bird "droppings"). However, *excreta samples do not contain native corticosterone*.

- Before excretion, circulating GCs are chemically transformed into GCMs, whose proportion and structure depends on the avian species. As a consequence, proper validation studies are required before assuming a direct association between circulating corticosterone titers and excreted GCM levels.
- Excreta sample collection is noninvasive and provides a suitable substrate for the study of avian adrenocortical activity, particularly in animal welfare and conservation contexts. Because bird "droppings" are subjected to microbial degradation, it is important to control the times from defecation to sampling.

Glossary of terms

ACTH corticotropin; adrenocorticotropic hormone.

Acute levels (of corticosterone) (also termed stress-regulated levels or regulated facultative levels). Corticosterone levels within the reactive homeostasis range.

Adrenocortical response physiological response to a stressor involving the hypothalamic–pituitary–adrenal (HPA) axis and culminating with the release of glucocorticoids (e.g., corticosterone) from the adrenal glands (Section 38.5.1) (Figure 38.1).

Allostasis mediators processes and body systems allowing allostasis (e.g., glucocorticoids, corticosterone, cytokines, cathecolamines, hearth rate, blood pressure, antibody titers) (Section 38.2.3).

Allostasis Model theoretical paradigm and framework to understand when and how animals activate emergency ("stress related") responses through modeling their energetic requirements across life and in relation to the energy available. Using energy as study metrics, the model introduces the key concepts of allostasis, allostatic state, allostatic load and allostatic overload (Section 38.2.1) (Figures 38.2 and 38.3).

Allostasis process of maintaining stability (i.e., homeostasis) through change. It refers to those aspects of physiology that "help us adapt." This concept is gradually replacing one of the meanings of the ambiguous term "stress" (Section 38.2.1) (Figures 38.1–38.3).

Allostatic load cumulative energetic requirements of the organism in a broad sense (the "workload" to maintain homeostasis in a particular moment), including predictable and unpredictable demands (Section 38.2.1) (Figures 38.2 and 38.3).

Allostatic overload type 1 short-term, deleterious state of energy imbalance in which allostatic load exceeds the energy available from the environment plus the internal energy reserves. As a response, individuals typically acquire an allostatic state (e.g., sustained corticosterone elevations) leading to the emergency life history stage ELHS (Sections 38.2.1 and 38.3.3) (Figures 38.2 and 38.3).

Allostatic overload type 2 long-term, deleterious state in which environmental or socially demanding challenges become chronic (e.g., social stress, captivity) and the sustained corticosterone elevations generate pathologies, regardless of the energy available (Sections 38.2.1 and 38.3.4) (Figure 38.2).

Allostatic state altered and sustained activity levels of allostasis mediators (e.g., elevated corticosterone), which can only be maintained for limited periods before damaging the body (Section 38.2.1) (Figure 38.2).

Basal corticosterone levels (also termed constitutive levels). Minimum levels allowing basic homeostatic processes. Minimum levels allowing a physiological "state A" representative of undisturbed animals at rest (Section 38.2.2) (Figure 38.3).

Baseline corticosterone levels (also termed seasonal baseline levels, regulated predictive levels or predictive homeostasis range). A range where corticosterone levels fluctuate according to predictable environmental changes, allowing the individual to cope with daily and seasonal routines of the life cycle but being insufficient to cope with unpredictable perturbations. Baseline levels allow a physiological "state B" where hormone actions maintain systems within a heightened operated range to support allostatic load (Section 38.2.2) (Box 38.1) (Figure 38.3).

Brood Value Hypothesis hypothesis proposing that birds can flexibly modulate their adrenocortical response according to the value of their brood (as the brood value increases, the adrenocortical response decreases) (Section 38.4.3) (Figure 38.9).

Capture, handling, and restraint protocol (also termed capture and handling) standardized method for capturing, handling, and restraining wild birds in repeatable conditions, required to establish adequate comparisons of their adrenocortical response. This protocol is frequently accompanied by the collection of a stress series (Section 38.5.1) (Box 38.1).

Chronic stress pathological state characterized by a malfunctioning of critical body systems as a consequence of prolonged or repeated exposure to perturbations. Allostatic overload type 2 (Figure 38.3).

Classic System traditional nomenclature describing corticosterone ranges and functional thresholds. This classification system combines three hormonal thresholds (levels A, B, and C) and a set of contrasting terms including basal and baseline, constitutive and facultative, seasonal and stress-related (Section 38.2.2) (Figure 38.3).

CORT corticosterone.

Corticosterone a steroid hormone and the primary avian glucocorticoid (see also "glucocorticoids").

Corticotropin (ACTH) adrenocorticotropic hormone. Hormone produced by the anterior pituitary (in response to hypothalamic signals) that stimulates the release glucocorticoids in the adrenal glands (Section 38.5.2) (Figures 38.1 and 38.10).

Developmental Hypothesis hypothesis proposing that the patterns of maturation of adrenocortical responses within and between avian species evolved to match the costs and benefits of glucocorticoid actions with the individual's progressive ability to cope with perturbations (e.g., increased behavioral performance and parental independence) (Section 38.4.1) (Figure 38.7).

DEX dexamethasone.

Dexamethasone (DEX) synthetic glucocorticoid that competes with corticosterone for binding sites and stimulates negative feedback (Section 38.5.2) (Figure 38.11).

Direct LPFs (direct labile perturbation factors) short-lived perturbations lasting hours or days, imposing high energetic demands and resulting in activation of the emergency life history stage (ELHS) temporary disrupting the normal lifecycle (Section 38.3.3) (Figures 38.5 and 38.6).

ELHS emergency life history stage.

Emergency life history stage (ELHS) facultative life stage activated in response to direct labile perturbations, and driven by the

elevation and maintenance of glucocorticoid levels above baseline titers (i.e., into the reactive homeostasis range or stress regulated levels). During an ELHS, birds change their behavior and physiology to maximize survival at the cost of temporarily suppressing their normal lifecycle (Section 38.3.3) (Figures 38.2 and 38.6).

Field Endocrinology emerging scientific discipline aimed at studying the interplay between the endocrine system and the environment, using wild animals in their natural habitats as study models (Section 38.5).

Flight or fight response physiological and behavioral responses to short-term perturbations, mediated by the sympathetic nervous system with little or no elevation of glucocorticoids (Section 38.3.2) (Figure 38.6).

GCMs glucocorticoid metabolites (Section 38.5.5) (Table 38.1).

GCs glucocorticoids (Figure 38.1).

Glucocorticoid metabolites the products of glucocorticoid metabolism; typically measured in blood, saliva, and body excretions (e.g., avian excreta, or "droppings"). (Section 38.5.5)

Glucocorticoids (GCs) (also misleadingly termed "stress hormones" for short) steroid hormones produced in the adrenals and released in response to ACTH. GCs are major allostasis mediators in vertebrates, control carbohydrate, fat and protein metabolism and their circulating levels change in response to internal and external demands to manage energy balance. The predominant GC in birds is corticosterone (Figures 38.1 and 38.3).

Homeostasis stability of the physiological systems essential to life. This concept is often restricted to a few truly essential systems such as pH, body temperature, glucose levels, and oxygen tension. Homeostasis refers to those aspects of physiology that "keep us alive" (Section 38.2.1) (Figures 38.1 and 38.4).

Homeostatic failure pathological state characterized by unsustainably low levels of corticosterone, insufficient to maintain homeostasis and resulting in death. Term associated with the Reactive Scope Model (Sections 38.2.2 and 38.2.3) (Figures 38.3 and 38.4).

Homeostatic overload pathological state characterized by abnormally elevated levels of corticosterone that disrupt normal body functions. The actual threshold for homeostatic overload can change within and between individuals in response to certain stimuli through a mechanism known as wear and tear (Sections 38.2.2 and 38.2.3) (Figures 38.2 and 38.4).

HPA axis hypothalamic−pituitary−adrenal axis (Figure 38.1).

Indirect LPFs (indirect labile perturbation factors) short-lived perturbations lasting seconds to a few minutes and inducing a flight or fight response with little or no elevation of glucocorticoids into the reactive homeostasis range (Section 38.3.2) (Figures 38.5 and 38.6).

Labile perturbation factor (LPF) short-term perturbation. According to their duration, labile perturbations can be classified as either direct (direct LPF) or indirect (indirect LPF) (Section 38.3.2) (Figure 38.5).

LHS life history stage (e.g., migration, moult, breeding) (Figure 38.6).

LPF labile perturbation factor.

Maternal Programming hypothesis proposing that the transfer of glucocorticoids from mothers to offspring is an adaptation, evolved to translate ecological and environmental conditions into permanent offspring responses (Section 38.4.2) (Figure 38.8).

Maternal-Match Hypothesis offset from the Maternal Programming Hypothesis, proposing that the fitness of the modified offspring phenotypes (through maternal programming) is context specific, and highest when the environmental conditions experienced during adulthood are similar to those experienced during development (Section 38.4.2) (Figure 38.8).

Modifying factor (also termed long-term or permanent perturbation) perturbation lasting months or years, imposing high energetic demands and resulting in a permanent disruption of lifecycles, potentially leading to populations extinction (Section 38.3.4) (Figures 38.5 and 38.6).

Permanent perturbation modifying factor.

Perturbation (also termed stressor) unpredictable and potentially noxious environmental stimulus. Perturbations can be classified as either labile (LPF; and these can be direct or indirect) or permanent (also known as modifying factors) (Section 38.3) (Figures 38.2, 38.4, and 38.5).

Phenotypic engineering experimental method consisting in altering a trait (e.g., elevating systemic hormone levels through subcutaneous implants) to explore whether and how such trait is adaptive. This method is a powerful tool in field endocrinology studies (Section 38.5.3) (Figure 38.11).

Predictive homeostasis range (corticosterone levels) intermediate levels of corticosterone allowing circadian and seasonal adjustments in response to predictable environmental changes. (Equivalent terms: baseline levels, seasonal baseline levels and regulated predictive levels) (Section 38.2.2) (Figures 38.3 and 38.4).

Reactive homeostasis range (corticosterone levels) elevated levels of corticosterone needed to reestablish homeostasis after a perturbation. Upper, facultative range of corticosterone levels required to cope with unpredictable challenges. The elevations of corticosterone levels within this range are known as the stress response, and can trigger an emergency life history stage ELHS. (Equivalent terms: acute levels, stress-regulated levels, regulated facultative levels) (Sections 38.2.2 and 38.2.3) (Figures 38.3 and 38.4).

Reactive Scope Model graphical tool for characterizing the physiological state of animals across time, in response to perturbations, and according to the levels of allostasis mediators such as circulating corticosterone. Offshoot of the Allostasis Model, presenting a different terminology for contextualizing the impact of stress in the body, a new classification of corticosterone levels (see Reactive Scope System) and introducing the concept of wear and tear (Section 38.2.3) (Figures 38.3 and 38.4).

Reactive Scope System recently proposed nomenclature describing corticosterone ranges and functional thresholds within the framework of the Reactive Scope Model. Corticosterone levels are presumed to exist in four ranges of increasing magnitude: homeostatic failure, predictive homeostasis, reactive homeostasis, and homeostatic overload (Sections 38.2.2 and 38.2.3) (Figures 38.3 and 38.4).

Reactive scope range of corticosterone levels defining the upper and lower physiological constraints of a healthy animal, according to the Reactive Scope Model. Combination of the predictive and the reactive homeostasis ranges above and below which serious pathologies arise. The amplitude of the reactive scope can be reduced through wear and tear (Section 38.2.3) (Figures 38.3 and 38.4).

Regulated facultative levels (of corticosterone) acute levels, stress regulated levels, corticosterone levels within the reactive homeostasis range.

Regulated predictive levels (of corticosterone) baseline levels, seasonal baseline levels, corticosterone levels within the predictive homeostasis range.

Seasonal baseline levels (of corticosterone) baseline levels, regulated predictive baseline levels, corticosterone levels within the predictive homeostasis range.

Stress hormones a misleading short-hand term for glucocorticoids; note that this is a misnomer, as the primary role of these hormones is the regulation of energy balance. This term should generally be avoided (Figure 38.1).

Stress hyporesponsive period temporary inability to elevate circulating glucocorticoids in response to perturbations (Section 38.4.1) (Figure 38.7).

Stress regulated levels (of corticosterone) acute levels, regulated facultative levels, corticosterone levels within the reactive homeostasis range.

Stress response facultative and short-term elevations of corticosterone levels in response to perturbations, allowing rapid physiological and behavioral changes aimed at maximizing survival (Sections 38.2.2 and 38.2.3) (Figures 38.3 and 38.4).

Stress series serial collection of blood samples at predefined intervals of time following capture, aimed at characterizing the adrenocortical response of the individual through subsequent determination of glucocorticoids levels (Section 38.5.1) (Figure 38.10) (Box 38.1)

Stress-induced corticosterone (or CORT) levels levels of corticosterone experienced after exposure to an acute stressor, including investigator handling (Box 38.1).

Stress polysemous term that depending on the context may mean: (1) the stimuli that challenges homeostasis (i.e., stressor, perturbation), (2) the emergency responses to perturbations (stress response), or (3) the chronic state of imbalance that follows overactivation of the adrenocortical axis (pathology; chronic stress). Modern field endocrinologists are making efforts to define and consolidate alternative and unequivocal terms, leading to the recent introduction of the word allostasis (Section 38.2).

Stressor perturbation.

Wear and tear the cost of maintaining corticosterone elevations during a stress response, as proposed in the Reactive Scope Model. Cost of maintaining and using the physiological systems that mediate allostasis. Wear and tear can be graphically represented as a decrease in the threshold level between the reactive homeostasis range and homeostasis overload which results in a decreased ability to cope with perturbations and increased likelihood of pathology (Section 38.2.3) (Figures 38.3 and 38.4).

Acknowledgments

The authors would like to acknowledge Dr. Tracy Marchant and Dr. Sonia Cabezas for their conversations, collaborations and support over the years, and thank Jose A. Sencianes (Casa de la Ciencia, CSIC) for the artwork and design of the revised figures.

References

Almasi, B., Rettenbacher, S., Müeller, C., Brill, S., Wagner, H., Jenni, L., 2012. Maternal corticosterone is transferred into the egg yolk. Gen. Comp. Endocrinol. 178, 139–144.

Angelier, F., Clément-Chastel, C., Welcker, J., Gabrielsen, G.W., Chastel, O., 2009. How does corticosterone affect parental behavior and reproductive success? A study of prolactin in black-legged kittiwakes. Funct. Ecol. 23, 784–793.

Angelier, F., Moe, B., Weimerskirch, H., Chastel, O., 2007a. Age-specific reproductive success in a long-lived bird: do older parents resist stress better? J. Anim. Ecol. 76, 1181–1191.

Angelier, F., Shaffer, S.A., Weimerskirch, H., Trouvé, C., Chastel, O., 2007b. Corticosterone and foraging behavior in a pelagic seabird. Physiol. Biochem. Zool. 80, 283–292.

Angelier, F., Chastel, O., Lendvai, A.Z., Parenteau, C., Weimerskirch, H., Wingfield, J.C., 2020. When do older birds better resist stress? A study of the corticosterone stress response in snow petrels. Biol. Lett. 16 (1), 20190733.

Astheimer, L.B., Buttemer, W.A., Wingfield, J.C., 1992. Interactions of corticosterone with feeding, activity and metabolism in passerine birds. Ornis Scand. 23, 355–365.

Astheimer, L.B., Buttemer, W.A., Wingfield, J.C., 1994. Gender and seasonal differences in the adrenocortical response to ACTH challenge in an arctic passerine, *Zonotrichia leucophrys gambelii*. Gen. Comp. Endocrinol. 94, 33–43.

Axelrod, J., Reisine, T.D., 1984. Stress hormones: their interaction and regulation. Science 224, 452–459.

Baos, R., Blas, J., Bortolotti, G.R., Marchant, T.A., Hiraldo, F., 2006. Adrenocortical response to stress and thyroid hormone status in free-living nestling white storks (*Ciconia ciconia*) exposed to heavy metal and arsenic contamination. Environ. Health Perspect. 114, 1497–1501.

Baños-Villalba, A., Carrete, M., Tella, J.L., Blas, J., Potti, J., Camacho, C., Diop, M.S., Marchant, T.A., Cabezas, S., Edelaar, P., 2021. Selection on individuals of introduced species starts before the actual introduction. Evol. Appl. 14 (3), 781–793.

Baos, R., Blas, J., 2009. Adrenocortical toxicology in birds: environmental contaminants and the avian response to stress. In: Harvey, P.W., Everett, D., Springall, C. (Eds.), Adrenal Toxicology, Part IV Adrenal Dysfunction in Environmental Sentinel Species. Informa Healthcare USA, Inc., New York, pp. 257–293 (Chapter 11).

Bebus, S.E., Jones, B.C., Anderson, R.C., 2020. Development of the corticosterone stress response differs among passerine species. Gen. Comp. Endocrinol. 291, 113417.

Belthoff, J.R., Dufty, J.A.M., 1998. Corticosterone, body condition and locomotor activity: a model for dispersal in screech-owls. Anim. Behav. 55, 405–415.

Béziers, P., San-Jose, L.M., Almasi, B., Jenni, L., Roulin, A., 2019. Baseline and stress-induced corticosterone levels are heritable and genetically correlated in a barn owl population. Heredity 123 (3), 337–348.

Blas, J., Baos, R., 2008. Stress in the nest: causes and consequences of adrenocortical secretion in developing birds. In: Capaldo, A. (Ed.), Recent Advances in Non-mammalian Adrenal Gland Research. Research Signpost, Kerala, pp. 89–128 (Chapter 4).

Blas, J., Baos, R., Bortolotti, G.R., Marchant, T.A., Hiraldo, F., 2005. A multi-tier approach to identifying environmental stress in altricial nestling birds. Funct. Ecol. 19, 315–322.

Blas, J., Baos, R., Bortolotti, G.R., Marchant, T.A., Hiraldo, F., 2006a. Age-related variation in the adrenocortical response to stress in nestling white storks (*Ciconia ciconia*) supports the developmental hypothesis. Gen. Comp. Endocrinol. 148, 172–180.

Blas, J., Pérez-Rodríguez, L., Bortolotti, G., Viñuela, J., Marchant, T., 2006b. Testosterone increases bioavailability of carotenoids: insights into the honesty of sexual signalling. Proc. Natl. Acad. Sci. U.S.A. 103, 18633–18637.

Blas, J., Bortolotti, G., Tella, J.L., Baos, R., Marchant, T., 2007. Stress response during development predicts fitness in a wild, long lived vertebrate. Proc. Natl. Acad. Sci. U.S.A. 104, 8080–8084.

Blas, J., López, L., Tanferna, A., Sergio, F., Hiraldo, F., 2010. Reproductive endocrinology of wild, long-lived raptors. Gen. Comp. Endocrinol. 168, 22–28.

Blas, J., Sergio, F., Wingfield, J.C., Hiraldo, F., 2011. Experimental tests of endocrine function in breeding and non-breeding raptors. Physiol. Biochem. Zool. 84, 406–416.

Blas, J., Torres-Medina, F., Cabezas, S., Sergio, F. y M., T.A., 2019. Efectos del ecoturismo sobre las respuestas fisiológicas de estrés en cigüeñas blancas del Parque Nacional de Doñana. (Effects of ecotourism on the physiological response to stress in white storks from Doñana National Park). In: Amengual, P. (Ed.), Proyectos de investigación en parques nacionales 2013–2017. Organismo Autónomo Parques Nacionales, Madrid, pp. 143–160. ISBN: 978-84-8014-924-2.

Blickley, J.L., Word, K.R., Krakauer, A.H., Phillips, J.L., Sells, S.N., Taff, C.C., Wingfield, J.C., Patricelli, G.L., 2012. Experimental chronic noise is related to elevated fecal corticosteroid metabolites in lekking male greater sage-grouse (*Centrocercus urophasianus*). PLoS One 7 (11), e50462.

Bókony, V., Lendvai, A.Z., Liker, A., Angelier, F., Wingfield, J.C., Chastel, O., 2009. Stress response and the value of reproduction: are birds prudent parents? Am. Nat. 173, 589–598.

Bonier, F., Martin, P.R., Moore, I.T., Wingfield, J.C., 2009. Do baseline glucocorticoids predict fitness? Trends Ecol. Evol. 24, 634–642.

Bonier, F., Martin, P.R., 2016. How can we estimate natural selection on endocrine traits? Lessons from evolutionary biology. Proc. Biol. Sci. 283 (1843), 20161887.

Bonier, F., Cox, R.M., 2020. Do hormone manipulations reduce fitness? A meta-analytic test of the optimal endocrine phenotype hypothesis. Mol. Cell. Endocrinol. 500, 110640.

Bortolotti, G.R., 2010. Flaws and pitfalls in the chemical analysis of feathers: bad news good news for avian chemoecology and toxicology. Ecol. Appl. 20, 1766–1774.

Bortolotti, G.R., Marchant, T.A., Blas, J., German, T., 2008. Corticosterone in feathers is a long-term, integrated measure of avian stress physiology. Funct. Ecol. 22, 494–500.

Bortolotti, G.R., Marchant, T., Blas, J., Cabezas, S., 2009a. Tracking stress: localisation, deposition and stability of corticosterone in feathers. J. Exp. Biol. 212, 1477–1482.

Bortolotti, G.R., Mougeot, F., Martinez-Padilla, J., Webster, L.M.I., Piertney, S.B., 2009b. Physiological stress mediates the honesty of social signals. PLoS One 4, e4983.

Boves, T.J., Fairhurst, G.D., Rushing, C.S., Buehler, D.A., 2016. Feather corticosterone levels are related to age and future body condition, but not to subsequent fitness, in a declining migratory songbird. Conserv. Physiol. 4 (1), cow041.

Breuner, C.W., Greenberg, A.L., Wingfield, J.C., 1998. Non-invasive corticosterone treatment rapidly increases activity in Gambel's whitecrowned sparrows (*Zonotrichia leucophrys gambelii*). Gen. Comp. Endocrinol. 111, 386–394.

Breuner, C.W., Orchinik, M., Hahn, T.P., Meddle, S.L., Moore, I.T., Owen-Ashley, N.-T., Sperry, T.S., Wingfield, J.C., 2003. Differential mechanisms for regulation of the stress response across latitudinal gradients. Am. J. Physiol. 285, R594–R600.

Breuner, C.W., Patterson, S.H., Hahn, T.P., 2008. In search of relationships between the acute adrenocortical response and fitness. Gen. Comp. Endocrinol. 157, 288–295.

Brown, M.B., Brown, C.R., 2009. Blood sampling reduces annual survival in cliff swallows (*Petrochelidon pyrrhonota*). Auk 126, 853–861.

Buchanan, K.L., Goldsmith, A.R., 2004. Noninvasive endocrine data for behavioural studies: the importance of validation. Anim. Behav. 67 (1), 183–185.

Busch, D.S., Hayward, L.S., 2009. Stress in a conservation context: a discussion of glucocorticoid actions and how levels change with conservation-relevant variables. Biol. Conserv. 142, 2844–2853.

Buttemer, W.A., Astheimer, L.B., Wingfield, J.C., 1991. The effect of corticosterone on standard metabolic rates of small passerine birds. J. Comp. Physiol. 161B, 427–431.

Cabezas, S., Carrete, M., Tella, J.L., Marchant, T.A., Bortolotti, G.R., 2013. Differences in acute stress responses between wild-caught and captive-bred birds: a physiological mechanism contributing to current avian invasions? Biol. Invasions 15 (3), 521–527.

Calisi, R.M., Bentley, G.E., 2009. Lab and field experiments: are they the same animal? Horm. Behav. 56 (1), 1–10.

Cannon, W.B., 1932. In: The Wisdom of the Body. W.W. Norton & Company Inc., New York.

Canoine, V., Gwinner, E., 2002. Seasonality in androgenic control of aggressive behavior in captive European stonechats. Horm. Behav. 41, 446.

Canoine, V., Hayden, T.J., Rowe, K., Goymann, W., 2002. The stress response of European stonechats depends on the type of stressor. Behaviour 139, 1303–1311.

Carsia, R.V., Morin, M.E., Rosen, H.D., Weber, H., 1987. Ontogenic corticosteroidogenesis of the domestic fowl response of isolated adrenocortical cells. Proc. Soc. Exp. Biol. Med. 184, 436–445.

Carere, C., Groothuis, T.G.G., Möstl, E., Daan, S., Koolhaas, J.M., 2003. Fecal corticosteroids in a territorial bird selected for different personalities: daily rhythm and the response to social stress. Horm. Behav. 43, 540–548.

Carrete, M., Bortolotti, G.R., Sánchez-Zapata, J.A., Delgado, A., Cortés-Avizanda, A., Grande, J.M., Donázar, J.A., 2013. Stressful conditions experienced by endangered Egyptian vultures on African wintering areas. Anim. Conserv. 16, 353–358.

Charlier, T.D., Underhill, C., Hammond, G.L., Soma, K., 2009. Effects of aggressive encounters on plasma corticosteroid-binding globulin and its ligands in white-crowned sparrows. Horm. Behav. 56, 339–347.

Cherel, Y., Robin, J.P., Walch, O., Karmann, H., Netchitailo, P., Le Maho, Y., 1988. Fasting in king penguin. I. Hormonal and metabolic changes during breeding. Am. J. Physiol. 254, R170–R177.

Clinchy, M., Sheriff, M.J., Zanette, L., 2013. Predator-induced stress and the ecology of fear. Funct. Ecol. 27, 56–65.

Clutton-Brock, T.H., 1984. Reproductive effort and terminal investment in iteroparous animals. Am. Nat. 123, 212–229.

Cockrem, J.F., Silverin, B., 2002. Sight of a predator can stimulate a corticosterone response in the great tit (*Parus major*). Gen. Comp. Endocrinol. 125 (2), 248–255.

Cockrem, J.F., 2007. Stress, corticosterone responses and avian personalities. J. Ornithol. 148, 169–S178.

Cockrem, J.F., 2013. Individual variation in glucocorticoid stress responses in animals. Gen. Comp. Endocrinol. 181, 45–58.

Constantini, D., Metcalfe, N.B., Monagham, P., 2010. Ecological processess in a hermetic framework. Ecol. Lett. 13, 1435–1447.

Corbel, H., Groscolas, R., 2008. A role for corticosterone and food restriction in the fledging of nestling White storks. Horm. Behav. 53, 557–566.

Crespi, E.J., Williams, T.D., Jessop, T.S., Delehanty, B., 2013. Life history and the ecology of stress: how do glucocorticoid hormones influence life-history variation in animals? Funct. Ecol. 27, 93–106.

Crossin, G.T., Phillips, R.A., Lattin, C.R., Romero, L.M., Williams, T.D., 2013. Corticosterone mediated costs of reproduction link current to future breeding. Gen. Comp. Endocrinol. 193, 112–120.

Cyr, N.E., Romero, L.M., 2009. Identifying hormonal habituation in field studies of stress. Gen. Comp. Endocrinol. 161, 295–303.

Dallman, M.F., Akana, S.F., Cascio, C.S., Darlington, D.N., Jacobson, L., Levin, N., 1987. Regulation of ACTH secretion: variations on a theme of B. Recent Prog. Horm. Res. 43, 113–173.

Dallman, M.F., Strack, A.M., Akana, S.F., Bradbury, M.J., Hanson, E.S., Scribner, K.A., Smith, M., 1993. Feast and famine: critical role of glucocorticoids with insulin in daily energy flow. Front. Neuroendocrinol. 14, 303–347.

Dantzer, B., Fletcher, Q.E., Boonstra, R., Sheriff, M.J., 2014. Measures of physiological stress: a transparent or opaque window into the status, management and conservation of species? Conserv. Physiol. 2 (1), cou023.

Darlington, D.N., Chew, G., Ha, T., Keil, L.C., Dallman, M.F., 1990. Corticosterone, but not glucose, treatment enables fasted adrenalectomized rats to survive moderate hemorrhage. Endocrinology 127, 766–772.

Dawson, W.R., Carey, C., Van't Hof, T.J., 1991. Metabolic aspects of shivering thermogenesis in passerines during winter. Proc. Symp. Hormones Physiol. Non-reprod. Behav. Birds Ornis Scand. 23, 21–23.

Dallman, M.F., Akana, S.F., Scribner, K.A., Bradbury, M.J., Walker, C.-D., Strack, A.M., Cascio, C.S., 1992. Stress, feedback and facilitation in the hypothalamo–pituitary–adrenal axis. J. Neuroendocrinol. 4, 517–526.

Dickens, M.J., Delehanty, D.J., Romero, L.M., 2009. Stress and translocation: alterations in the stress physiology of translocated birds. Proc. Biol. Sci. 276 (1664), 2051–2056.

Donelan, S.C., Hellmann, J.K., Bell, A.M., Luttbeg, B., Orrock, J.L., Sheriff, M.J., Sih, A., 2020. Transgenerational plasticity in human-altered environments. Trends Ecol. Evol. 35 (2), 115–124.

Dufty Jr., A.M., Wingfield, J.C., 1986. The influence of social cues on the reproductive endocrinology of male brown-headed cowbirds: field and laboratory studies. Horm. Behav. 20 (2), 222–234.

DuRant, S.E., Arciniega, M.L., Bauer, C.M., Romero, L.M., 2016. A test of reactive scope: reducing reactive scope causes delayed wound healing. Gen. Comp. Endocrinol. 236, 115–120.

Evans, M.R., Roberts, M.L., Buchanan, K.L., Goldsmith, A.R., 2006. Heritability of corticosterone response and changes in life history traits during selection in the zebra finch. J. Evol. Biol. 19, 343–352.

Expósito-Granados, M., Parejo, D., Chastel, O., Aviles, J.M., 2020. Physiological stress and behavioural responses of European Rollers and Eurasian Scops Owls to human disturbance differ in farming habitats in the south of Spain. Bird. Conserv. Int. 30 (2), 220–235.

Fair, J., Paul, E., Jones, J. (Eds.), 2010. Guidelines to the Use of Wild Birds in Research, third ed. The Ornithological Council, Washington, D.C. Available from: http://www.nmnh.si.edu/BIRDNET/guide/guidelines.html?Operation=ENTER+HERE+%7E+English.

Fairhurst, G.D., Frey, M.D., Reichert, J.F., Szelest, I., Kelly, D.M., Bortolotti, G.R., 2011. Does environmental enrichment reduce stress? an integrated measure of corticosterone from feathers provides a novel perspective. PLoS One 6, e17663.

Fairhurst, G.D., Treen, G.D., Clark, R.G., Bortolotti, G.R., 2012a. Nestling corticosterone response to microclimate in an altricial bird. Can. J. Zool. 90, 1422–1430.

Fairhurst, G.D., Navarro, J., González-Solís, J., Marchant, T.A., Bortolotti, G.R., 2012b. Feather corticosterone of a nestling seabird reveals consequences of sex-specific parental investment. Proc. R. Soc. B 279, 177–184.

Fairhurst, G.D., Vögeli, M., Serrano, D., Delgado, A., Tella, J.L., Bortolotti, G.R., 2013a. Can synchronizing feather-based measures of corticosterone and stable isotopes help us better understand habitat-physiology relationships? Oecologia 173, 731–743.

Fairhurst, G.D., Marchant, T.A., Soos, C., Machin, K.L., Clark, R.G., 2013b. Experimental relationships between levels of corticosterone in plasma and feathers in a free-living bird. J. Exp. Biol. 216, 4071–4081. https://doi.org/10.1242/jeb.091280.

Fairhurst, G.D., Dawson, R.D., van Oort, H., Bortolotti, G.R., 2014. Synchronizing feather-based measures of corticosterone and carotenoid-dependent signals: what relationships do we expect? Oecologia 174 (3), 689–698.

Fairhurst, G.D., Bond, A.L., Hobson, K.A., Ronconi, R.A., 2015. Feather-based measures of stable isotopes and corticosterone reveal a relationship between trophic position and physiology in a pelagic seabird over a 153-year period. Ibis 157 (2), 273–283.

Fairhurst, G.D., Berzins, L.L., Bradley, D.W., Laughlin, A.J., Romano, A., Romano, M., Scandolara, C., Ambrosini, R., Dawson, R.D., Dunn, P.O., Hobson, K.A., Liechti, F., Marchant, T.A., Norris, D.R., Rubolini, D., Saino, N., Taylor, C.M., Whittingham, L.A., Clark, R.G., 2015. Assessing costs of carrying geolocators using feather corticosterone in two species of aerial insectivore. R. Soc. Open Sci. 2 (5), 150004.

Fairhurst, G.D., Champoux, L., Hobson, K.A., Rail, J.F., Verreault, J., Guillemette, M., Montevecchi, W.A., Brousseau, P., Soos, C., 2017. Feather corticosterone during non-breeding correlates with multiple measures of physiology during subsequent breeding in a migratory seabird. Comp. Biochem. Physiol. Mol. Integr. Physiol. 208, 1–13.

Fischer, C.P., Romero, L.M., 2019. Chronic captivity stress in wild animals is highly species-specific. Conserv. Physiol. 7 (1), coz093.

Francis, D., Diorio, J., Liu, D., Meaney, M.J., 1999. Nongenomic transmission across generations of maternal behavior and stress responses in the rat. Science 286, 1155–1158.

Frigerio, D., Moestl, E., Kotrschal, K., 2001. Excreted metabolites of gonadal steroid hormones and corticosterone in greylag geese (*Anser anser*) from hatching to fledging. Gen. Comp. Endocrinol. 124, 246–255.

Fusani, L., 2008. Endocrinology in field studies: problems and solutions for the experimental design. Gen. Comp. Endocrinol. 157, 249–253.

Fusani, L., Canoine, V., Goymann, W., Wikelski, M., Hau, M., 2005. Difficulties and special issues associated with field research in behavioral neuroendocrinology. Horm. Behav. 48, 484–491.

Ganz, K., Jenny, D., Kraemer, T., Jenni, L., Jenni-Eiermann, S., 2018. Prospects and pitfalls of using feathers as a temporal archive of stress events and environmental pollutants: a review and case study. J. Ornithol. 159 (3), 771–783.

Garamszegi, L.Z., Rosivall, B., Rettenbacher, S., Markó, G., Zsebők, S., Szöllősi, E., Eens, M., Potti, J., Török, J., 2012. Corticosterone, avoidance of novelty, risk-taking and aggression in a wild bird: no evidence for pleiotropic effects. Ethology 118, 621–635.

Glucs, Z.E., Smith, D.R., Tubbs, C.W., Jones Scherbinski, J., Welch, A., Burnett, J., Clark, M., Eng, C., Finkelstein, M.E., 2018. Glucocorticoid measurement in plasma, urates, and feathers from California condors (*Gymnogyps californianus*) in response to a human-induced stressor. PLoS One 13 (10), e0205565.

Goymann, W., Wingfield, J.C., 2004. Allostatic load, social status, and stress hormones – the costs of social status matter. Anim. Behav. 67, 591–602.

Goymann, W., 2005. Noninvasive monitoring of hormones in bird droppings: physiological validation, sampling, extraction, sex differences, and the influence of diet on hormone metabolite levels. Ann. N.Y. Acad. Sci. 1046, 35–53.

Goymann, W., Trappschuh, M., Jensen, W., Schwabl, I., 2006. Low ambient temperature increases food intake and dropping production, leading to incorrect estimates of hormone metabolite concentrations in European stonechats. Horm. Behav. 49, 644–653.

Gosler, A.G., Greenwood, J.J.D., Perrins, C., 2002. Predation risk and the cost of being fat. Nature 377, 621–623.

Grace, J.K., Parenteau, C., Angelier, F., 2020. Post-natal corticosterone exposure downregulates the HPA axis through adulthood in a common passerine. Gen. Comp. Endocrinol. 292, 113421.

Grava, T., Fairhurst, G.D., Avey, M.T., Grava, A., Bradley, J., Avis, J.L., Bortolotti, G.R., Sturdy, C.B., Otter, K.A., 2013. Habitat quality affects early physiology and subsequent neuromotor development of juvenile Black-capped Chickadees. PLoS One 8 (8), e71852.

Groothuis, T.G.G., Müller, W., von Engelhardt, N., Carere, C., Eising, C., 2005. Maternal hormones as a tool to adjust offspring phenotype in avian species. Neurosci. Biobehav. Rev. 29, 329–352.

Grunst, M.L., Raap, T., Grunst, A.S., Pinxten, R., Parenteau, C., Angelier, F., Eens, M., 2020. Early-life exposure to artificial light at night elevates physiological stress in free-living songbirds. Environ. Pollut. 259, 113895.

Hales, C.N., Barker, D.J., 1992. Type 2 (non-insulin-dependent) diabetes mellitus: the thrifty phenotype hypothesis. Diabetologia 35, 595–601.

Hansen, W.K., Bate, L.J., Landry, D.W., Chastel, O., Parenteau, C., Breuner, C.W., 2016. Feather and faecal corticosterone concentrations predict future reproductive decisions in harlequin ducks (*Histrionicus histrionicus*). Conserv. Physiol. 4 (1).

Harms, N.J., Legagneux, P., Gilchrist, H.G., Bêty, J., Love, O.P., Forbes, M.R., Bortolotti, G.R., Soos, C., 2015. Feather corticosterone reveals effect of moulting conditions in the autumn on subsequent reproductive output and survival in an Arctic migratory bird. Proc. Biol. Sci. 282 (1800), 20142085.

Harris, C.M., Madliger, C.L., Love, O.P., 2016. Temporal overlap and repeatability of feather corticosterone levels: practical considerations for use as a biomarker. Conserv. Physiol. 4 (1).

Harrison, X.A., Blount, J.D., Inger, R., Norris, D.R., Bearhop, S., 2011. Carry-over effects as drivers of fitness differences in animals. J. Anim. Ecol. 80 (1), 4–18.

Hau, M., Casagrande, S., Ouyang, J.Q., Baugh, A.T., 2016. Glucocorticoid-mediated phenotypes in vertebrates: multilevel variation and evolution. Adv. Stud. Behav. 48, 41–115.

Hayward, L.S., Wingfield, J.C., 2004. Maternal corticosterone is transferred to avian yolk and may alter offspring growth and adult phenotype. Gen. Comp. Endocrinol. 135, 365–371.

Hawlena, D., Schmitz, O.J., 2010. Physiological stress as a fundamental mechanism linking predation to ecosystem functioning. Am. Nat. 175, 537–556.

Heath, J., 1997. Corticosterone levels during nest departure of juvenile American kestrels. Condor 99, 806–811.

Heidinger, B.J., Nisbet, I.C.T., Ketterson, E.D., 2006. Older parents are less responsive to a stressor in a long-lived seabird: a mechanism for increased reproductive performance with age? Proc. R. Soc. Lond. B 273, 2227–2231.

Hiebert, S.M., Salvante, K.G., Ramonofsky, M., Wingfield, J.C., 2000. Corticosterone and nocturnal torpor in the rufous hummingfbird (*Selasphorus rufus*). Gen. Comp. Endocrinol. 120, 220–234.

Hirschenhauser, K., Kotrschal, K., Möstl, E., 2005. Synthesis of measuring steroid metabolites in goose feces. Ann. N.Y. Acad. Sci. 1046, 138–153.

Holberton, R.L., Wingfield, J.C., 2003. Modulating the corticosterone stress response: a mechanism for balancing individual risk and reproductive success in arctic-breeding sparrows? Auk 120, 1140–1150.

Holmes, W.N., Crinshow, J., Redonde, J.L., 1990. The ontogeny of adrenal steroidogenic function in the mallard duck (*Anas platyrhynchos*). In: Wada, M., Ishii, S., Scanes, C.G. (Eds.), Endocrinology of Birds: Molecular to Behavioral. Jpn Sci Soc Press, Tokyo/Springer, Berlin, Heidelberg, New York, pp. 143–158.

Homberger, B., Jenni-Eiermann, S., Jenni, L., 2015. Distinct responses of baseline and stress-induced corticosterone levels to genetic and environmental factors. Gen. Comp. Endocrinol. 210, 46–54.

Honey, P.K., 1990. Avian Flight Muscle Pectoralis Major as a Reserve of Proteins and Amino Acids. M.S. thesis. University of Washington.

Imlay, T.L., Angelier, F., Hobson, K.A., Mastromonaco, G., Saldanha, S., Leonard, M.L., 2019. Multiple intrinsic markers identify carry-over effects from wintering to breeding sites for three Nearctic–Neotropical migrant swallows. Auk 136 (4), ukz053.

Jacobs, J.D., Wingfield, J.C., 2000. Endocrine control of lifecycle stages: a constraint on response to the environment? Condor 102, 35–51.

Janczak, A.M., Torjesen, P., Palme, R., Bakken, M., 2007. Effects of stress in hens on the behaviour of their offspring. Appl. Anim. Behav. Sci. 107 (1–2), 66–77.

Jenkins, B.R., Vitousek, M.N., Hubbard, J.K., Safran, R.J., 2014. An experimental analysis of the heritability of variation in glucocorticoid concentrations in a wild avian population. Proc. Biol. Sci. 281 (1790), 20141302.

Jenni-Eiermann, S., Helfenstein, F., Vallat, A., Glauser, G., Jenni, L., 2015. Corticosterone: effects on feather quality and deposition into feathers. Methods Ecol. Evol. 6, 237–246.

Jimeno, B., Hau, M., Verhulst, S., 2018. Corticosterone levels reflect variation in metabolic rate, independent of 'stress'. Sci. Rep. 8 (1), 1–8.

Jimeno, B., Hau, M., Gómez-Díaz, E., Verhulst, S., 2019. Developmental conditions modulate DNA methylation at the glucocorticoid receptor gene with cascading effects on expression and corticosterone levels in zebra finches. Sci. Rep. 9 (1), 1–11.

Johns, D.W., Marchant, T.A., Fairhurst, G.D., Speakman, J.R., Clark, R.G., 2018. Biomarker of burden: feather corticosterone reflects energetic expenditure and allostatic overload in captive waterfowl. Funct. Ecol. 32 (2), 345–357.

Jovani, R., Blas, J., Navarro, C., Mougeot, F., 2010. Feather growth bands and photoperiod. J. Avian Biol. 41, 1–5.

Keith, I., Brown, K.I., Nestor, K.E., 1973. Some physiological responses of turkeys selected for high and low adrenal response to cold stress. Poult. Sci. 52, 1948–1954.

Kennedy, E.A., Lattin, C.R., Romero, L.M., Dearborn, D.C., 2013. Feather coloration in museum specimens is related to feather corticosterone. Behav. Ecol. Sociobiol. 67, 341–348.

Kern, M., Bacon, W., Long, D., Cowie, R.J., 2001. Possible roles for corticosterone and critical size in the fledging of nestling pied flycatchers. Physiol. Biochem. Zool. 74, 651.

Ketterson, E.D., Nolan Jr., V., Cawthorn, M.J., Parker, P.G., Ziegenfus, C., 1996. Phenotypic engineering: using hormones to explore the mechanistic and functional bases of phenotypic variation in nature. Ibis 138, 70–86.

Khan, M.Z., Altmann, J., Isani, S.S., Yu, J., 2002. A matter of time: evaluating the storage of fecal samples for steroid analysis. Gen. Comp. Endocrinol. 128, 64–67.

Kinel, F.A., Benagian, G., Angee, I., 1968. Sustained release hormonal preparations I. Diffusion of various steroids through polymer membranes. Steroids 11, 673–680.

Kitaysky, A.S., Kitaiskaia, E.V., Piatt, J.F., Wingfield, J.C., 2003. Benefits and costs of increased levels of corticosterone in seabird chicks. Horm. Behav. 43, 140–149.

Kitaysky, A.S., Piatt, J.F., Wingfield, J.C., 2007. Stress hormones link food availability and population processes in seabirds. Mar. Ecol. Prog. Ser. 352, 245–258.

Kitaysky, A.S., Piatt, J.F., Wingfield, J.C., Romano, M., 1999a. The adrenocortical stress-response of black-legged kittiwake chicks in relation to dietary restrictions. J. Com. Physiol. B 169, 303–310.

Kitaysky, A.S., Wingfield, J.C., Piatt, J.F., 1999b. Food availability, body condition and physiological stress response in breeding black-legged kittiwakes. Funct. Ecol. 13, 577–584.

Kitaysky, A.S., Wingfield, J.C., Piatt, J.F., 2001. Corticosterone facilitates begging and affects resource allocation in the black-legged kittiwake. Behav. Ecol. 12, 619–625.

Klasing, K.C., 2005. Potential impact of nutritional strategy on noninvasive measurements of hormones in birds. Ann. N.Y. Acad. Sci. 1046, 5–16.

Knight, S.M., Gow, E.A., Bradley, D.W., Clark, R.G., Bélisle, M., Berzins, L.L., Blake, T., Bridge, E.S., Burke, L., Dawson, R.D., Dunn, P.O., 2019. Nonbreeding season movements of a migratory songbird are related to declines in resource availability. Auk 136 (3), ukz028.

Koren, L., Nakagawa, S., Burke, T., Soma, K.K., Wynne-Edwards, K.E., Geffen, E., 2012. Non-breeding feather concentrations of testosterone, corticosterone and cortisol are associated with subsequent survival in wild house sparrows. Proc. R. Soc. B 279, 1560–1566.

Kouwenberg, A.L., Hipfner, J.M., McKay, D.W., Storey, A.E., 2013. Corticosterone and stable isotopes in feathers predict egg size in Atlantic puffins Fratercula Arctica. Ibis 155, 413–418.

Landys, M., Ramenofsky, M., Wingfield, J.C., 2006. Actions of glucocorticoids at a seasonal baseline as compared to stress-related levels in the regulation of periodic life processes. Gen. Comp. Endocrinol. 148, 132–149.

Landys-Ciannelli, M.M., Ramenofsky, M., Piersma, T., Jukema, J., Wingfield, J.C., 2002. Baseline and stress-induced plasma corticosterone during long-distance migration in the bar-tailed godwit, Limosa lapponica. Physiol. Biochem. Zool. 75, 101–110.

Latta, S.C., Cabezas, S., Mejia, D.A., Paulino, M.M., Almonte, H., Miller-Butterworth, C.M., Bortolotti, G.R., 2016. Carry-over effects provide linkages across the annual cycle of a Neotropical migratory bird, the Louisiana Waterthrush *Parkesia motacilla*. Ibis 158 (2), 395–406.

Latty, C.J., Hollmén, T.E., Petersen, M.R., Powell, A.N., Andrews, R.D., 2016. Biochemical and clinical responses of common eiders to implanted satellite transmitters. Condor 118 (3), 489–501.

Lattin, C.R., Reed, J.M., DesRochers, D.W., Romero, L.M., 2011. Elevated corticosterone in feathers correlates with corticosteroneinduced decreased feather quality: a validation study. J. Avian Biol. 42, 247–252.

Legagneux, P., Harms, N.J., Gauthier, G., Chastel, O., Gilchrist, H.G., Bortolotti, G., Bêty, J., Soos, C., 2013. Does feather corticosterone reflect individual quality or external stress in arctic-nesting migratory birds? PLoS One 8 (12), e82644.

Lendvai, Á.Z., Chastel, O., 2008. Experimental mate-removal increases the stress response of female house sparrows: the effects of offspring value? Horm. Behav. 52, 395–401.

Lendvai, Á.Z., Giraudeau, M., Chastel, O., 2007. Reproduction and modulation of the stress response: an experimental test in the house sparrow. Proc. R. Soc. Lond. B 274, 391–397.

Lind, J., Fransson, T., Jakobson, S., Kullberg, C., 1999. Reduced takeoff ability in robins (*Erithacus rubecula*) due to migratory fuel load. Behav. Ecol. Sociobiol. 46, 65–70.

López-Jiménez, L., Blas, J., Tanferna, A., Cabezas, S., Marchant, T., Hiraldo, F., Sergio, F., 2016a. Effects of ontogeny, diel rhythms and environmental variation on the adrenocortical physiology of semi-altricial black kites (*Milvus migrans*). Physiol. Biochem. Zool. 89 (3), 213–224. https://doi.org/10.1086/684966.

López-Jiménez, L., Blas, J., Tanferna, A., Cabezas, S., Marchant, T., Hiraldo, F., Sergio, F., 2016b. Ambient temperature, body condition and sibling rivalry explain feather corticosterone levels in developing black kites. Funct. Ecol. 30 (4), 605–613.

López-Jiménez, L., Blas, J., Tanferna, A., Cabezas, S., Marchant, T., Hiraldo, F., Sergio, F., 2017. Lifetime variation in feather corticosterone levels in a long-lived raptor. Oecologia 186, 315–326.

Løtvedt, P., Fallahshahroudi, A., Bektic, L., Altimiras, J., Jensen, P., 2017. Chicken domestication changes expression of stress-related genes in brain, pituitary and adrenals. Neurobiol. Stress 7, 113–121.

Love, O.P., Breuner, C.W., Vezina, F., Williams, T.D., 2004. Mediation of a corticosterone-induced reproductive conflict. Horm. Behav. 46, 59–65.

Love, O.P., Chin, E.H., Wynne-Edwards, K.E., Williams, T.D., 2005. Stress hormones: a link between maternal condition and sex-biased reproductive investment. Am. Nat. 166, 751–766.

Love, O.P., McGowan, P.O., Sheriff, M.J., 2013. Maternal adversity and ecological stressors in natural populations: the role of stress axis programming in individuals, with implications for populations and communities. Funct. Ecol. 27, 81–92.

Love, O.P., Williams, T.D., 2008. Plasticity in the adrenocortical response of a free-living vertebrate: the role of pre- and post-natal developmental stress. Horm. Behav. 54, 496–505.

Love, O.P., Wynne-Edwards, K.E., Bond, L., Williams, T.D., 2008. Determinants of within- and among-clutch variation of yolk corticosterone in the European starling. Horm. Behav. 53, 104–111.

Lucas, J.R., Freeberg, T.M., Egbert, J., Schwabl, H., 2006. Fecal corticosterone, body mass, and caching rates of *Carolina chickadees* (*Poecile carolinensis*) from disturbed and undisturbed sites. Horm. Behav. 49, 634–643.

MacDougall-Shackleton, S.A., Bonier, F., Romero, L.M., Moore, I.T., 2019. Glucocorticoids and "stress" are not synonymous. Integr. Organismal Biol. 1 (1), obz017.

Madliger, C.L., Love, O.P., Hultine, K.R., Cooke, S.J., 2018. The conservation physiology toolbox: status and opportunities. Conserv. Physiol. 6 (1), coy029.

Malisch, J., Breuner, C., 2010. Steroid-binding proteins and free steroids in birds. Mol. Cell. Endocrinol. 316, 42–52.

Mantha, L., Deshaies, Y., 2000. Energy intake-independent modulation of triglyceride metabolism by glucocorticoids in the rat. Am. J. Physiol. Regul. Integr. Comp. Physiol. 278, R1424–R1432.

McEwen, B.S., Wingfield, J.C., 2003a. The concept of allostasis in biology and biomedicine. Horm. Behav. 43, 2–15.

McEwen, B.S., Wingfield, J.C., 2003b. Response to commentaries on the concept of allostasis. Horm. Behav. 43, 28–30.

McEwen, B.S., Wingfield, J.C., 2010. What's in a name? Integrating homeostasis, allostasis and stress. Horm. Behav. 57, 105.

McGowan, P.O., Szyf, M., 2010. The epigenetics of social adversity in early life: implications for mental health outcomes. Neurobiol. Dis. 39, 66–72.

McGowan, P.O., Suderman, M., Sasaki, A., Huang, T.C., Hallett, M., Meaney, M.J., Szyf, M., 2011. Broad epigenetic signature of maternal care in the brain of adult rats. PLoS One 6, e14739.

Meddle, S.L., Owen-Ashley, N.T., Richardson, M.I., Wingfield, J.C., 2003. Modulation of the hypothalamic-pituitary-adrenal axis of an arcticbreeding polygynandrous songbird, the Smith's longspur, *Calcarius pictus*. Proc. R. Soc. Lond. B 70, 1849–1856.

Meillère, A., Brischoux, F., Bustamante, P., Michaud, B., Parenteau, C., Marciau, C., Angelier, F., 2016. Corticosterone levels in relation to trace element contamination along an urbanization gradient in the common blackbird (*Turdus merula*). Sci. Total Environ. 566, 93–101.

Messina, S., Edwards, D.P., Marasco, V., Canoine, V., Cosset, C.C., Tomassi, S., Benedick, S., Eens, M., Costantini, D., 2020. Glucocorticoids link forest type to local abundance in tropical birds. Funct. Ecol. 34 (9), 1814–1825.

Millspaugh, J.J., Washburn, B.E., 2004. Use of fecal glucocorticoid. metabolite measures in conservation biology research: considerations for application and interpretation. Gen. Comp. Endocrinol. 138, 189–199.

Monclús, L., Tallo-Parra, O., Carbajal, A., Quevedo, M.A., Lopez-Bejar, M., 2020. Feather corticosterone in Northern Bald Ibis Geronticus eremita: a stable matrix over time able to predict reproductive success. J. Ornithol. 161, 557–567.

Möstl, E., Messman, S., Bagu, E., Robia, C., Palme, R., 1999. Measurement of glucocorticoid metabolite concentrations in faeces of domestic livestock. J. Vet. Med. A 46, 621–632.

Möstl, E., Rettenbacher, S., Palme, R., 2005. Measurement of corticosterone metabolites in birds' droppings: an analytical approach. Ann. N.Y. Acad. Sci. 1046, 17–34.

Mougeot, F., Martinez-Padilla, J., Bortolotti, G.R., Webster, L.M.I., Piertney, S.B., 2010. Physiological stress links parasites to carotenoidbased colour signals. J. Evol. Biol. 23, 643–650.

Müller, C., Almasi, B., Roulin, A., Breuner, C.W., Jenni-Eiermann, S., Jenni, L., 2009. Effects of corticosterone pellets on baseline and stress-induced corticosterone and corticosteroid-binding-globulin. Gen. Comp. Endocrinol. 160, 59–66.

Nephew, B.C., Romero, L.M., 2003. Behavioral, physiological, and endocrine responses of starlings to acute increases in density. Horm. Behav. 44 (3), 222–232.

Newman, A.E.M., MacDougall-Shackleton, S.A., An, Y.S., Kriengwatana, B., Soma, K.K., 2010. Corticosterone and dehydroepiandrosterone have opposing effects on adult neuroplasticity in the avian song control system. J. Comp. Neurol. 518, 3662–3678.

O'Reilly, K.M., Wingfield, J.C., 2001. Ecological factors underlying the adrenocortical response to capture stress in arctic-breeding shorebirds. Gen. Comp. Endocrinol. 124, 1–11.

Ouyang, J.Q., Hau, M., Bonier, F., 2011. Within seasons and among years: when are corticosterone levels repeatable? Horm. Behav. 60, 559–564.

Palma, A., Blas, J., Tella, J.L., Cabezas, S., Marchant, T.A., Carrete, M., 2020. Differences in adrenocortical responses between urban and rural burrowing owls: poorly-known underlying mechanisms and their implications for conservation. Conserv. Physiol. 8 (1), coaa054. https://doi.org/10.1093/conphys/coaa054.

Palme, R., 2005. Measuring fecal steroids: guidelines for practical application. Ann. N.Y. Acad. Sci. 1046, 75–80.

Palme, R., Rettenbacher, S., Touma, C., El-Bahr, S.M., Möstl, E., 2005. Stress hormones in mammals and birds: comparative aspects regarding metabolism, excretion, and noninvasive measurement in fecal samples. Ann. N.Y. Acad. Sci. 1040, 162–171.

Palokangas, R., Hissa, R., 1971. Thermorregulation in young blackheaded young (*Larus ribibundus* L.). Comp. Biochem. Physiol. 38A, 743–750.

Pérez-Rodríguez, L., Blas, J., Viñuela, J., Marchant, T.A., Bortolotti, G.R., 2006. Condition and androgen levels: are condition-dependent and testosterone-mediated traits two sides of the same coin? Anim. Behav. 72, 97–103.

Porter, W.P., Sabo, J.L., Tracy, C.R., Reichman, O.J., Ramankutty, N., 2002. Physiology on a landscape scale: plant animal interactions. Integr. Comp. Biol. 42, 431–453.

Quillfeldt, P., Poisbleau, M., Chastel, O., Masello, J., 2007. Corticosterone in thin-billed prion Pachyptila belcheri chicks: diel rhythm, timing of fledging and nutritional stress. Naturwissenschaften 94, 919–925.

Ramos, R., Llabrés, V., Monclús, L., López-Béjar, M., González-Solís, J., 2018. Costs of breeding are rapidly buffered and do not affect migratory behavior in a long-lived bird species. Ecology 99 (9), 2010–2024.

Rensel, M.A., Boughton, R.K., Schoech, S.J., 2010. Development of the adrenal stress response in the Florida scrub-jay (*Aphelocoma coerulescens*). Gen. Comp. Endocrinol. 165 (2), 255–261.

Rensel, M.A., Schoech, S.J., 2011. Repeatability of baseline and stress-induced corticosterone levels across early life stages in the Florida scrub-jay (*Aphelocoma coerulescens*). Horm. Behav. 59 (4), 497–502.

Rettenbacher, S., Möstl, E., Hackl, R., Palme, R., 2005. Corticosterone in chicken eggs. Ann. N. Y. Acad. Sci. 1046 (1), 193–203.

Rich, E.L., Romero, L.M., 2005. Exposure to chronic stress downregulates corticosterone responses to acute stressors. Am. J. Physiol. Regul. Integr. Comp. Physiol. 288, R1628–R1636.

Ricklefs, R.E., Wikelski, M., 2002. The physiology/life-history nexus. Trends Ecol. Evol. 17, 462–468.

Rödl, T., Berger, S., Romero, L.M., Wikelski, M., 2007. Tameness and stress physiology in a predator-naïve island species confronted with novel predation threat. Proc. R. Soc. B 274, 577–582.

Rogers, C.M., Ramenofsky, M., Ketterson, E.D., Nolan, V., Wingfield, J.C., 1993. Plasma corticosterone, adrenal mass, winter weather, and season in nonbreeding populations of dark-eyed juncos (*Junco hyemalis hyemalis*). Auk 110, 279–285.

Romero, L.M., 2002. Seasonal changes in plasma glucocorticoid concentration in free living vertebrates. Gen. Comp. Endocrinol. 128, 1–24.

Romero, L.M., 2004. Physiological stress in ecology: lessons from biomedical research. Trends Ecol. Evol. 19, 249–255.

Romero, L.M., 2012. Using the reactive scope model to understand why stress physiology predicts survival during starvation in Galápagos marine iguanas. Gen. Comp. Endocrinol. 176, 296–299.

Romero, L.M., Fairhurst, G.D., 2016. Measuring corticosterone in feathers: strengths, limitations, and suggestions for the future. Comp. Biochem. Physiol. Mol. Integr. Physiol. 202, 112–122.

Romero, L.M., Gormally, B.M., 2019. How truly conserved is the "well-conserved" vertebrate stress response? Integr. Comp. Biol. 59 (2), 273–281.

Romero, L.M., Reed, J.M., 2005. Collecting baseline corticosterone samples in the field: is under 3 min good enough? Comp. Biochem. Physiol. A Mol. Integr. Physiol. 40, 73–79.

Romero, L.M., Wikelski, M., 2010. Stress physiology as a predictor of survival in *Galapagos marine iguanas*. Proc. R. Soc. Lond. B 277, 3157–3162.

Romero, L.M., Wingfield, J.C., 2016. Tempests, Poxes, Predators, and People: Stress in Wild Animals and How They Cope. Oxford University Press, New York (NY).

Romero, L.M., Dickens, M.J., Cyr, N.E., 2009. The reactive scope model –a new model integrating homeostasis, allostasis and stress. Horm. Behav. 55, 375–389.

Romero, L.M., Holt, D.W., Maples, M., Wingfield, J.C., 2006. Corticosterone is not correlated with nest departure in snowy owl chicks (*Nyctea scandiaca*). Gen. Comp. Endocrinol. 149, 119–123.

Rohwer, S., Wingfield, J.C., 1981. A field study of social dominance, plasma levels of luteinizing hormone and steroid hormones in wintering Harris' sparrows. Z. Tierpsychol. 57, 173–183.

Saadoun, A., Simon, J., Leclercq, B., 1987. Effects of exogenous corticosterone in genetically fat and lean chickens. Br. Poult. Sci. 28, 519–528.

Saino, N., Romano, M., Ferrari, R.P., Martinelli, R., Møller, A.P., 2005. Stressed mothers lay eggs with high corticosterone levels which produce low-quality offspring. J. Exp. Zool. 303A, 998–1006.

Sapolsky, R.M., 1992. Cortisol concentrations and the social significance of rank instability among wild baboons. Psychoneuroendocrinology 17, 701–709.

Sapolsky, R.M., 1996. Why stress is bad for your brain. Science 273, 749–750.

Sapolsky, R.M., 2001. Physiological and pathophysiological implications of social stress in mammals. In: McEwen, B.S., Goodman, H.M. (Eds.), Handbook of Physiology, Section 7: The Endocrine System. Coping with the Environment: Neural and Endocrine Mechanisms, vol. IV. Oxford University Press, New York, pp. 517–532.

Sapolsky, R.M., 2002. Endocrinology of the stress response. In: Becker, J.B., Breedlove, S.M., Crews, D., McCarthy, M. (Eds.), Behavioral Endocrinology, second ed. MIT Press, Cambridge, Massachusetts, pp. 409–450.

Sapolsky, R.M., Romero, L.M., Munck, A.U., 2000. How do glucocorticosteroids influence stress responses? Integrating permissive, suppressive, stimulatory, and preparative actions. Endocr. Rev. 21, 55–89.

Satterlee, D.G., Cadd, G.G., Jones, R.B., 2000. Developmental instability in Japanese quail genetically selected for contrasting adrenocortical responsiveness. Poult. Sci. 79, 1710–1714.

Satterlee, D.G., Johnson, W.A., 1988. Selection of Japanese quail for contrasting blood corticosterone response to immobilization. Poult. Sci. 67, 25–32.

Scheuerlein, A., Van't Hof, T.J., Gwinner, E., 2001. Predators as stressors? Physiological and reproductive consequences of predation risk in tropical stonechats (*Saxicola torquata axillaris*). Proc. R. Soc. Lond. B 268, 1575–1582.

Schoenemann, K.L., Bonier, F., 2018. Repeatability of glucocorticoid hormones in vertebrates: a meta-analysis. PeerJ 6, e4398.

Schwabl, H., 1999. Developmental changes and among-sibling variation of corticosterone levels in an altricial avian species. Gen. Comp. Endocrinol. 116, 403–408.

Schwabl, H., Wingfield, J.C., Farner, D.S., 1985. Influence of winter on endocrine state and behavior in European blackbirds (*Turdus merula*). Z. Tierpsychol. 68, 244–252.

Seabury, S.R., Breuner, C.W., 2005. Timing of fledging, body condition, and corticosteroid binding globulin in Laysan Albatross. Integr. Comp. Biol. 45, 1070.

Selye, H., 1946. The general adaptation syndrome and the diseases of adaptation. J. Clin. Endocrinol. 6, 117–230.

Selye, H., 1976. The Stress of Life. McGraw-Hill, New York.

Sergio, F., Tavecchia, G., Tanferna, A., López, L., Blas, J., De Stephanis, R., Marchant, T.M., Hiraldo, F., 2015. No effect of satellite tagging on a raptor survival, recruitment, longevity, productivity, social dominance, and its offspring provisioning and condition. J. Appl. Ecol. 52, 1665–1675.

Sergio, F., Blas, J., Hiraldo, F., 2018. Animal responses to disturbance and climate extremes: coping mechanisms in the new millennium. Global Planet. Change 161, 28–40.

Sheriff, M.J., Dantzer, B., Delehanty, B., Palme, R., Boonstra, R., 2011b. Measuring stress in wildlife: techniques for quantifying glucocorticoids. Oecologia 166, 869–887.

Sheriff, M.J., Krebs, C.J., Boonstra, R., 2009. The sensitive hare: sublethal effects of predator stress on reproduction in snowshoe hares. J. Anim. Ecol. 78, 1249–1258.

Sheriff, M.J., Krebs, C.J., Boonstra, R., 2010. The ghosts of predators past: population cycles and the role of maternal effects under fluctuating predation risk. Ecology 91, 2983–2994.

Sheriff, M.J., Krebs, C.J., Boonstra, R., 2011a. From process to pattern: how fluctuating predation risk impacts the stress axis of snowshoe hares during the 10-year cycle. Oecologia 166, 593–605.

Shultz, M.T., Kitaysky, A.S., 2008. Spatial and temporal dynamics of corticosterone and corticosterone binding globulin are driven by environmental heterogeneity. Gen. Comp. Endocrinol. 155, 717–728.

Silverin, B., 1986. Corticosterone binding proteins and behavioral effects of high plasma levels of corticosterone during the breeding period in the pied flycatcher. Gen. Comp. Endocrinol. 64, 67–74.

Silverin, B., Arvidsson, B., Wingfield, J.C., 1997. The adrenocortical response to stress in breeding willow warblers Phylloscopus trochilus in Sweden: effects of latitude and gender. Funct. Ecol. 11, 376–384.

Sims, C.G., Holberton, R.L., 2000. Development of the corticosterone stress response in young northern mockingbirds (*Mimus polyglottos*). Gen. Comp. Endocrinol. 119, 193–201.

Smulders, T.V., Casto, J.M., Nolan, V., Ketterson, E.D., DeVoogd, T.J., 2000. Effects of captivity and testosterone on the volumes of four brain regions in the dark-eyed junco (*Junco hyemalis*). J. Neurobiol. 43, 244–253.

Soma, K.K., Tramontin, A.D., Wingfield, J.C., 2000. Oestrogen regulates male aggression in the non-breeding season. Proc. R. Soc. Lond. B 267, 1089–1096.

Spencer, R.L., Kalman, B.A., Dhabhar, F.S., 2001. Role of endogenous glucocorticoids in immune system function: regulation and counter-regulation. In: McEwen, B., Goodman, H.M. (Eds.), Handbook of Physiology, Section 7: The Endocrine System. Coping with the Environment: Neural and Endocrine Mechanisms, vol. IV. Oxford University Press, New York, pp. 381–423.

Spencer, K.A., Buchanan, K.L., Goldsmith, A.R., Catchpole, C.K., 2003. Song as an honest signal of developmental stress in the zebra finch (*Taeniopygia guttata*). Horm. Behav. 44 (2), 132–139.

Spencer, K.A., Evans, N.P., Monaghan, P., 2009. Postnatal stress in birds: a novel model of glucocorticoid programming of the hypothalamic-pituitary-adrenal axis. Endocrinology 150 (4), 1931–1934.

Spencer, K.A., Heidinger, B.J., D'Alba, L.B., Evans, N.P., Monaghan, P., 2010. Then versus now: effect of developmental and current environmental conditions on incubation effort in birds. Behav. Ecol. 21 (5), 999–1004.

Starck, J.M., Ricklefs, R.E., 1998. Avian Growth and Development: Evolution within the Altricial-Precocial Spectrum. Oxfod University, New York.

Stearns, S.C., 1992. The Evolution of Life History. Academic Press, London.

Sterling, P., Eyer, J., 1988. Allostasis a new paradigm to explain arousal pathology. In: Fisher, S., Reason, J. (Eds.), Handbook of Life Stress Cognition and Health. John Wiley and Sons, Inc., New York, pp. 629–650.

Taff, C.C., Zimmer, C., Vitousek, M.N., 2018. Efficacy of negative feedback in the HPA axis predicts recovery from acute challenges. Biol. Lett. 14 (7), 20180131.

Terio, K.A., Brown, J.L., Moreland, R., Munson, L., 2002. Comparison of different drying and storage methods on quantifiable concentrations of fecal steroids in the cheetah. Zoo Biol. 21, 119–134.

Thiel, D., Jenni-Eiermann, S., Braunisch, V., Palme, R., Jenni, L., 2008. Ski tourism affects habitat use and evokes a physiological stress response in capercaillie *Tetrao urogallus*: a new methodological approach. J. Appl. Ecol. 45, 845–853.

Torres-Medina, F., Cabezas, S., Marchant, T.A., Wikelski, M., Romero, L.M., Hau, M., Carrete, M., Tella, J.L., Blas, J., 2018. Corticosterone implants produce stress-hyporesponsive birds. J. Exp. Biol. 221 (19), jeb173864.

Torres-Medina, F., Cabezas, S., Marchant, T.A., Blas, J., 2019. Dexamethasone treatment supports age-related maturation of the stress response in altricial nestling birds. J. Avian Biol. 50 (10), e02091.

Touma, C., Palme, R., 2005. Measuring fecal glucocorticoid metabolites in mammals and birds: the importance of validation. Ann. N.Y. Acad. Sci. 1046, 54–74.

Treen, G.D., Hobson, K.A., Marchant, T.A., Bortolotti, G.R., 2015. Large-scale spatial variation in feather corticosterone in invasive house sparrows (*Passer domesticus*) in Mexico is related to climate. Ecology and Evolution 5 (17), 3808–3817.

Travers, M., Clinchy, M., Zanette, L., Boonstra, R., Williams, T., 2010. Indirect predator effects on clutch size and the cost of egg production. Ecol. Lett. 13, 980–988.

Velando, A., Drummond, H., Torres, R., 2006. Senescent birds redouble reproductive effort when ill: confirmation of the terminal investment hypothesis. Proc. Biol. Sci. 273, 1443–1448.

Viblanc, V.A., Gineste, B., Robin, J.P., Groscolas, R., 2016. Breeding status affects the hormonal and metabolic response to acute stress in a long-lived seabird, the king penguin. Gen. Comp. Endocrinol. 236, 139–145.

Wada, H., 2008. Glucocorticoids: mediators of vertebrate ontogenetic transitions. Gen. Comp. Endocrinol. 156, 441–453.

Walker, B.G., Boersma, P.D., Wingfield, J.C., 2006. Habituation of adult Magellanic penguins to human visitation as expressed through behavior and corticosterone secretion. Conserv. Biol. 20, 146–154.

Walker, B.G., Meddle, S.L., Romero, L.M., Landys, M.M., Reneerkens, J., Wingfield, J.C., 2015. Breeding on the extreme edge: modulation of the adrenocortical response to acute stress in two High Arctic passerines. J. Exp. Zool. A Ecol. Genet. Physiol. 323 (4), 266–275.

Walsberg, G.E., 2003. How useful is energy balance as an overall index of stress in animals? Horm. Behav. 43, 16–17.

Washburn, B.E., Millspaugh, J.J., Schulz, J.H., Jones, S.B., Mong, T., 2003. Using fecal glucocorticoids for stress assessment in mourning doves. Condor 105, 696–706.

Wasser, S.K., Bevis, K., King, G., Hanson, E., 1997. Noninvasive physiological measures of disturbance in the northern spotted owl. Conserv. Biol. 11, 1019–1022.

Wasser, S.K., Hunt, K.E., Brown, J.L., Cooper, K., Crockett, C.M., Bechert, U., Millspaugh, J.J., Larson, S., Monfort, S.L., 2000. A generalized fecal glucocorticoid assay for use in a diverse assay of non-domestic mammalian and avian species. Gen. Comp. Endocrinol. 120, 260–275.

Wentworth, B.C., Hussein, M.O., 1985. Serum corticosterone levels in embryos newly hatched and young Turkey poults. Poult. Sci. 64, 2195–2201.

Will, A., Wynne-Edwards, K., Zhou, R., Kitaysky, A., 2019. Of 11 candidate steroids, corticosterone concentration standardized for mass is the most reliable steroid biomarker of nutritional stress across different feather types. Ecol. Evol. 9 (20), 11930–11943.

Williams, G.C., 1966. Natural selection, the costs of reproduction and a refinement of Lack's principle. Am. Nat. 100, 687–690.

Williams, T.D., 2008. Individual variation in endocrine systems: moving beyond the 'tyranny of the Golden Mean'. Philos. Trans. R. Soc. Lond. B 363, 1687–1698.

Wilson, R.P., Börger, L., Holton, M.D., Scantlebury, D.M., Gómez-Laich, A., Quintana, F., Rosell, F., Graf, P.M., Williams, H., Gunner, R., Hopkins, L., Marks, N., Geraldi, N.R., Duarte, C.M., Scott, R., Strano, M.S., Robotka, H., Eizaguirre, C., Fahlman, A., Hopkins, L., 2020. Estimates for energy expenditure in free-living animals using acceleration proxies: a reappraisal. J. Anim. Ecol. 89 (1), 161–172.

Wilsterman, K., Alonge, M.M., Ernst, D.K., Limber, C., Treidel, L.A., Bentley, G.E., 2020. Flexibility in an emergency life-history stage: acute food deprivation prevents sickness behaviour but not the immune response. Proc. R. Soc. B 287 (1929), 20200842.

Wingfield, J.C., 1984. Influence of weather on reproduction. J. Exp. Biol. 232, 589–594.

Wingfield, J.C., 1994. Modulation of the adrenocortical response to stress in birds. In: Davey, K.G., Peter, R.E., Tobe, S.S. (Eds.), Perspectives in Comparative Endocrinology. National Research Council, Canada, Ottawa, pp. 520–528.

Wingfield, J.C., 2008. Organization of vertebrate annual cycles: implications for control mechanisms. Philos. Trans. R. Soc. Lond. B 363, 425–441.

Wingfield, J.C., 2013a. Ecological processess and the ecology of stress: the impacts of abiotic environmental factors. Funct. Ecol. 27, 37–44.

Wingfield, J.C., 2013b. The comparative biology of environmental stress: behavioural endocrinology and variation in ability to cope with novel, changing environments. Anim. Behav. 85, 1127–1133.

Wingfield, J.C., Farner, D.S., 1975. The determination of five steroids in avian plasma by radioimmunoassay and competitive protein-binding. Steroids 26, 311–327.

Wingfield, J.C., Farner, D.S., 1976. Avian endocrinology: field investigations and methods. Condor 78 (4), 570–573.

Wingfield, J.C., Farner, D.S., 1993. Endocrinology of reproduction in wild species. In: Farner, D.S., et al. (Eds.), Avian Biology. Academic Press, San Diego, pp. 163–327.

Wingfield, J.C., Wada, M., 1989. Changes in plasma levels of testosterone during male–male interactions in the song sparrow, Melospiza melodia: time course and specificity of response. J. Comp. Physiol. A 166, 189–194.

Wingfield, J.C., Breuner, C.W., Jacobs, J., 1997. Corticosterone and behavioral responses to unpredictable events. In: Harvey, S., Etches, R.J. (Eds.), Perspectives in Avian Endocrinology. J. Endocrinology Press, Bristol, pp. 267–278.

Wingfield, J.C., Breuner, C., Jacobs, J., Lynn, S., Maney, D., Ramenofsky, M., Richardson, R., 1998. Ecological bases of hormone-behavior interactions: the "emergency life history stage". Am. Zool. 38, 191–206.

Wingfield, J.C., Hegner, R.E., Dufty, A.M., Ball, G.F., 1990. The "challenge hypothesis": theoretical implications for patterns of testosterone secretion, mating systems, and breeding strategies. Am. Nat. 136, 829–846.

Wingfield, J.C., Kelley, J.P., Angelier, F., Chastel, O., Lei, F., Lynn, S.E., Miner, B., Davis, J.S., Li, D., Wang, G., 2011. Organism-environment interactions in a changing world: a mechanistic approach. J. Ornithol. 152 (Suppl. 1), S279–S288.

Wingfield, J.C., Kitaysky, A.S., 2002. Endocrine responses to unpredictable environmental events: stress or anti-stress hormones. Integ.Comp. Biol. 42, 600–609.

Wingfield, J.C., Kubokawa, K., Ishida, K., Ishii, S., Wada, M., 1995a. The adrenocortical response to stress in male bush warblers, Cettia diphone: a comparison of breeding populations in Honshu and Hokkaido, Japan. Zool. Sci. 12, 615–621.

Wingfield, J.C., Moore, M.C., Farner, D.S., 1983. Endocrine responses to inclement weather in naturally breeding populations of white-crowned sparrows (*Zonotrichia leucophrys pugetensis*). Auk 100, 56–62.

Wingfield, J.C., O'Reilly, K.M., Astheimer, L.B., 1995b. Modulation of the adrenocortical responses to acute stress in arctic birds: a possible ecological basis. Am. Zool. 35, 285–294.

Wingfield, J.C., Pérez, J.H., Krause, J.S., Word, K.R., González-Gómez, P.L., Lisovski, S., Chmura, H.E., 2017. How birds cope physiologically and behaviourally with extreme climatic events. Phil. Trans. Biol. Sci. 372 (1723), 20160140.

Wingfield, J.C., Ramenofsky, R., 1999. Hormones and the behavioral ecology of stress. In: Balm, P.H.M. (Ed.), Stress Physiology in Animals. CRC Press, Boca Raton, pp. 1–51.

Wingfield, J.C., Ramenofsky, R., 1997. Corticosterone and facultative dispersal in response to unpredictable events. Ardea 85, 155–166.

Wingfield, J.C., Romero, L.M., 2001. Adrenocortical responses to stress and their modulation in free-living vertebrates. In: McEwen, B.S. (Ed.), Handbook of Physiology, Section 7: The Endocrine System. Coping with the Environment: Neural and Endocrine Mechanisms, vol. IV. Oxford University Press, Oxford, pp. 211–236.

Wingfield, J.C., Silverin, B., 1986. Effects of corticosterone on territorial behavior of free-living male song sparrows Melospiza melodia. Horm. Behav. 20, 405–417.

Zhang, S., Lei, F., Liu, S., Li, D., Chen, C., Wang, P., 2011. Variation in baseline corticosterone levels of tree sparrow (*Passer montanus*) populations along an urban gradient in Beijing, China. J. Ornithol. 152, 801–806.

Chapter 39

Avian welfare: fundamental concepts and scientific assessment

N.J. Beausoleil[1], D.E.F. McKeegan[2] and J.E. Martin[3]

[1]*Animal Welfare Science and Bioethics Centre, School of Veterinary Science, Massey University, Palmerston North, Manawatū, New Zealand;* [2]*Institute of Biodiversity, Animal Health and Comparative Medicine, University of Glasgow, Glasgow, Scotland;* [3]*Royal (Dick) School of Veterinary Studies and the Roslin Institute, University of Edinburgh, Edinburgh, Scotland*

39.1 Introduction

Around the world, there is increasing public, industry, and scientific interest in the welfare of nonhuman animals (European Commission, 2007; Coleman, 2018). Despite this interest, avian welfare has received relatively little attention. Notable exceptions include research on the welfare impacts of various aspects of poultry production systems and some aspects of management and veterinary care for companion and threatened wild bird species. However, our fundamental understanding of avian biology relevant to welfare assessment, even for these species and in these contexts, still lags behind that of mammals.

The lack of general attention to avian welfare may be partly because fewer people have direct experience of, or close contact with, birds, because there are fewer commercially important avian taxa, because we humans value birds less than other kinds of animals and are therefore less disposed to be empathetic toward them, or simply due to our less well-developed understanding of their biology and behavior (Arluke and Sanders, 1996; Hawkins, 2006; Olsson et al., 2012; Paul-Murphy and Hawkins, 2015). However, understanding animal welfare is important for ethical and reputational reasons and because welfare state often influences the survival, fitness, and productivity of animals (Virden and Kidd, 2009; Von Keyserlingk et al., 2009; Coleman and Hemsworth, 2014; Beausoleil et al., 2018; Coleman, 2018; Williams et al., 2019). Thus, there is a need to improve our understanding of relevant features of avian biology, and in doing so, our ability to assess and respond to potential bird welfare issues.

The purposes of this chapter are to introduce animal welfare as a subject available for scientific exploration and to illustrate how we can undertake such explorations. In the following sections, we describe animal welfare as it is currently understood and demonstrate that birds meet the prerequisites for welfare consideration: sentience and consciousness. We then explain how our current characterization of welfare influences its scientific assessment in birds. Key to this is the use of observable indicators to infer subjective mental experiences that matter to the animal. The Five Domains Model is introduced as a method for systematically exploring the negative and positive experiences that might influence a bird's welfare in a specific situation. However, before applying the Model to assess the impacts of events or conditions on bird welfare, evidence is needed to support the capacity of the taxon of interest to have the specific mental experiences proposed, e.g., pain or fear. We outline evidence that can be compiled for this purpose and illustrate the process by evaluating the capacity of domestic chickens (*Gallus gallus domesticus*) to experience negative states such as anxiety/fear and breathlessness during preslaughter stunning using carbon dioxide.

39.2 What is animal welfare?

Animal welfare is now generally considered to represent a dynamic state within the animal itself. This state reflects the various mental experiences, both positive and negative, the animal is having at a particular point in time. In other words, an animal's welfare state is a reflection of how it is experiencing its own life at that time (Fraser and Duncan, 1998; Harvey et al., 2020). Mental experiences arise due to processing of sensory information by the animal's nervous system. Sensory receptors gather information about the outside environment (e.g., visual or auditory signals about a predator or conspecific, mechanical information about substrate hardness, chemical information about the

Sturkie's Avian Physiology. https://doi.org/10.1016/B978-0-12-819770-7.00013-X

atmosphere being breathed) and about the animal's internal physical state (e.g., body water or glucose levels, tissue damage or inflammation, appropriateness of respiration) (Denton et al., 2009). Detection, processing, integration, and interpretation of this kind of sensory information occurs at many levels of the nervous system, in a way that is specific to the species, reflecting its natural ecology, and to the individual, influenced by its genetics and previous experiences (Mellor et al., 2009; Hemsworth et al., 2015).

In vertebrates, this processing and interpretation culminates in regions of the forebrain, leading to generation of mental experiences, some of which matter to the animal (Feinberg and Mallatt, 2013; Mellor, 2019). Such experiences have valence or affective quality, i.e., they are experienced as either negative or positive, and their valence influences behavioral and physiological responses in predictable ways (Mendl et al., 2009, 2010; Paul et al., 2018). Negative or unpleasant mental experiences such as thirst, hunger, pain, breathlessness, and fear often act as signals to the animal to respond in a specific way to try to alleviate or rectify the underlying problem and/or to reduce the risk of future reoccurrence (Denton et al., 2009; Elwood, 2011; Williams et al., 2019). Positive or pleasant experiences are proposed to act as rewards to ensure that the animal behaves in ways to achieve the same outcome again in the future (Fraser and Duncan, 1998; Boissy et al., 2007; Mellor, 2015). Negative experiences are detrimental to an animal's current state of welfare (although they may have survival benefits), while positive experiences can have both short- and longer-term enhancing effects.

In addition to valence, the specific quality of experience (e.g., pain vs. breathlessness vs. thirst) and its intensity and duration will determine its influence on welfare state (Banzett et al., 2008; Beausoleil, 2017). Importantly, unpleasant experiences that cannot be effectively rectified through behavioral and physiological responses, and so persist (e.g., chronic pain), will have a greater detrimental impact on welfare state than short-lived experiences (Fraser and Duncan, 1998; Dawkins, 2015). It is also important to note that the absence of negative experiences alone is not sufficient to achieve good welfare. If welfare state is considered as a point on a continuum from poor to good, preventing or mitigating negative experiences can only ever achieve, at best, a neutral state. To ensure "good" or "acceptable" welfare, animals also need to have some positive experiences, and welfare assessments should include evaluation of both (Boissy et al., 2007; Mellor, 2015; Mellor and Beausoleil, 2015).

This focus on mental experiences in the characterization of animal welfare has not always been widely accepted (Fraser, 2008; Dawkins, 2015). Historically, animal scientists aligned to one of three main orientations to understanding and assessing welfare: biological function, affective state, or naturalness/natural living (Fraser et al., 1997; Fraser, 2003; Broom, 2007; Korte et al., 2007; Hemsworth et al., 2015; Learmonth, 2019). These orientations emphasize the physical functioning of the animal, the mental or affective experiences the animal might perceive, or the degree to which the animal is able to live a life to which it is naturally adapted, respectively. Accordingly, an animal with good welfare would function well (including being productive for many domestic animals), feel well (be largely free of unpleasant experiences and have some pleasant ones), or live a life that allowed it to express its *telos* (naturally designed purpose or function) (Fraser et al., 1997; Rollin, 2013).

While each orientation reflects a key component of animal welfare, it is now generally acknowledged that an animal's biological function and mental experiences are intrinsically linked and that both must be considered in holistic assessments of welfare (Fraser et al., 1997; Hemsworth et al., 2015; Mellor, 2017). In particular, imbalance or dysfunction within the animal's physiological systems leads to the generation of some mental experiences and these can, in turn, influence biological function. For example, the mental experience of thirst arises due to detection of an imbalance in the amount of water and solutes in body fluids (e.g., dehydration) by the animal's nervous system (Denton et al., 2009). On the other hand, being unable to escape prolonged or regular threats such as rough human handling may lead to chronic fear, which has been shown to suppress immune function, growth and productivity in pigs, poultry, and dairy cows (Barnett et al., 1992; Hemsworth et al., 1994; Coleman and Hemsworth, 2014). However, it is important to note that the relationships between biological function and welfare state are complex, and proposed associations between observable indicators of function and welfare state should be carefully scrutinized (Beausoleil and Mellor, 2017; Veasey, 2017). To illustrate, while animals selected for high productivity such as fast growth or milk yield are biologically functional in that specific regard, such selection can predispose them to other physical impairments that compromise their welfare (see Section 39.5.1).

Naturalness reflects the species' evolutionary history in terms of the physical, sensory, and social environment for which the animal is adapted. Considering naturalness in the links between physical states and mental experiences *may* allow us to determine which environmental and social features are important for good biological function and for preventing unpleasant experiences and promoting positive ones (Veasey et al., 1996; Spinka, 2006; Rushen and de Passille, 2009). For example, knowledge of the normal social structure, sensory capabilities, and home range of wild species may inform the design of captive environments, group management, or cognitive enrichment activities (but consider Veasey et al., 1996; Learmonth, 2019). However, naturalness is problematic as a conceptual

approach to understanding and assessing the welfare of domestic animals, which have co-evolved with humans and in the environments they provide (Learmonth, 2019). Thus, both biological function and naturalness can be integrated into a characterization of animal welfare that focuses on the animal's mental experiences but only with careful consideration of the caveats outlined above.

39.3 Birds are sentient and their welfare should be considered

Animals capable of having at least some affective experiences are referred to as "sentient", and sentience is considered by most to be a prerequisite for attention to welfare state (Duncan, 2006; Dawkins, 2015; Mellor, 2019). Sentience requires a nervous system sophisticated enough to generate subjective experiences from sensory information, accompanied by behavioral responses indicative of the animal's emotional capabilities (Dawkins, 2006; Elwood, 2011). Sentient animals must also have the *capacity* to be conscious, in other words they must be capable of expressing and sustaining a state in which they are *aware* of their own sensations and affective experiences (Feinberg and Mallatt, 2013; Mellor, 2019). The capacity for consciousness and thus sentience can be inferred when animals exhibit neural complexity and behavioral flexibility, including the ability to direct attention to relevant stimuli, to determine appropriate responses in novel situations (problem solving) and to engage in volitional, goal-directed behavior (Mashour and Alkire, 2013; Dawkins, 2015; Weary et al., 2017; Paul et al., 2018; Pennartz et al., 2019). Finally, sentient animals exhibit different states of consciousness at different times and only experience affective states during times that they are consciously aware (Mellor, 2019). This is important to understand when considering the relevance to welfare of sensory events occurring when animals are not conscious, e.g., when sleeping, under general anesthetic or following effective stunning before slaughter.

39.3.1 Birds are sentient and different states of consciousness can be recognized

On the basis of their neural anatomy and physiology and their behavior, birds are regarded as sentient and conscious in ways relevant to welfare (e.g., Edelman et al., 2005; Butler and Cotterill, 2006; Panksepp et al., 2012; Feinberg and Mallatt, 2013; Mellor, 2019; Pennartz et al., 2019). Briefly, the avian brain and particularly the forebrain or pallium, which is involved in many higher-level cognitive functions, is now considered to be equivalent in complexity, connectivity, and function to the cerebral cortex of mammals (Butler and Cotterill, 2006; Rattenborg et al., 2009). Specifically, neural networks considered analogous or functionally homologous to mammalian networks involved in sensory integration, long-term memory, associative learning, and emotion have been identified in birds (e.g., The Avian Brain Nomenclature Consortium, 2005; Güntürkün, 2012; Marzluff et al., 2012; Shanahan et al., 2013; Clayton and Emery, 2015).

Birds also show complex and flexible behavioral responses, reflecting high-level cognitive processes such as sophisticated problem solving, long-term memory, learning, theory of mind, social reasoning, and emotion generation (reviewed by Butler and Cotterill, 2006; Mashour and Alkire, 2013; Clayton and Emery, 2015; Pennartz et al., 2019), including in domestic chickens (e.g., Nicol and Pope, 1994; Hogue et al., 1996; Gyger and Marler, 1998; Vallortigara et al., 1998; D'eath and Stone, 1999; Abeyesinghe et al., 2005; Nicol et al., 2009; Zimmerman et al., 2011; McCabe, 2019). Some of these cognitive skills rival or even exceed those demonstrated by nonhuman primates, such as the creation and application of tools by New Caledonia crows (*Corvus moneduloides*), use and comprehension of human language by African gray parrots (*Psittacus erithacus*), and self-recognition by magpies (*Pica pica*) (e.g., Pepperberg, 2007; Prior et al., 2008; von Bayern et al., 2018).

Thus, despite 300 million years of independent evolution, it appears that similar selective pressures have resulted in the development of similar neural and cognitive functions that support complex behavior and conscious awareness in mammals and birds (Butler and Cotterill, 2006; Rattenborg et al., 2009). This understanding is reflected in the animal welfare legislation of many jurisdictions, which state or imply that birds are sentient (e.g., European Council, 2010; New Zealand Government, 2015; McCulloch, 2018; Australian Capital Territory, 2019). In addition, birds, along with all other vertebrates, are noted as sentient in the proposed Universal Declaration on Animal Welfare (Anonymous, 2014) and the World Organisation for Animal Health's Global Animal Welfare Strategy, adopted by 180 member countries (2017).

As in humans and other mammals, different states of consciousness can be recognized in birds. For example, Sandercock et al. (2014) demonstrated differences in quantitative variables derived from the electroencephalogram (EEG), reflecting changes in electrical brain activity, in five states of consciousness in chickens and turkeys. Reliable changes in both EEG and behavior were detected when birds went from being fully awake to semiconscious (sedated), unconscious (general anesthesia), or irreversibly unconscious (after killing). McIlhone et al. (2018) observed similar changes in EEG variables with deepening general anesthesia. Finally, birds, like mammals demonstrate two different types of sleep [rapid eye movement (REM) and non-REM] which are distinguishable from each other and

from the state of wakefulness using EEG, electromyography, and behavior (reviewed by Rattenborg et al., 2009; Rattenborg et al., 2019). Thus, it is possible to assess the impacts of sensory events on the welfare of birds when they are in states of conscious awareness.

39.4 How can bird welfare be scientifically assessed?

Our current characterization of welfare means that assessing birds' welfare states hinges on our ability to recognize their mental experiences. However, mental experiences and thus welfare state are subjective and internal. That is, they are not directly observable or measurable and thus are not available for scientific scrutiny in the strictest (positivist) sense (Fraser, 1999; Dawkins, 2015). Rather, observable indicators of biological function and of behavior are used to cautiously *infer* the associated mental experiences a bird might be having. This approach is supported by the reciprocal interaction between biological function and affective experiences noted above and is reflected in the framework for welfare assessment presented below.

39.4.1 The Five Domains model for welfare assessment

The Five Domains model is a framework that has proven useful for guiding scientific investigations of animal welfare. It allows systematic organization of the observable evidence and requires interpretation of that evidence in terms of the animal's likely mental experiences (Mellor and Beausoleil, 2015; Mellor, 2017). Fig. 39.1 shows the general structure of the model and provides some examples of how physical/functional impacts on the animal may relate to specific negative and positive mental experiences. As shown in the figure, specific qualities of unpleasant experience might include breathlessness, pain, thirst, hunger, and fear while pleasant ones might include feelings of

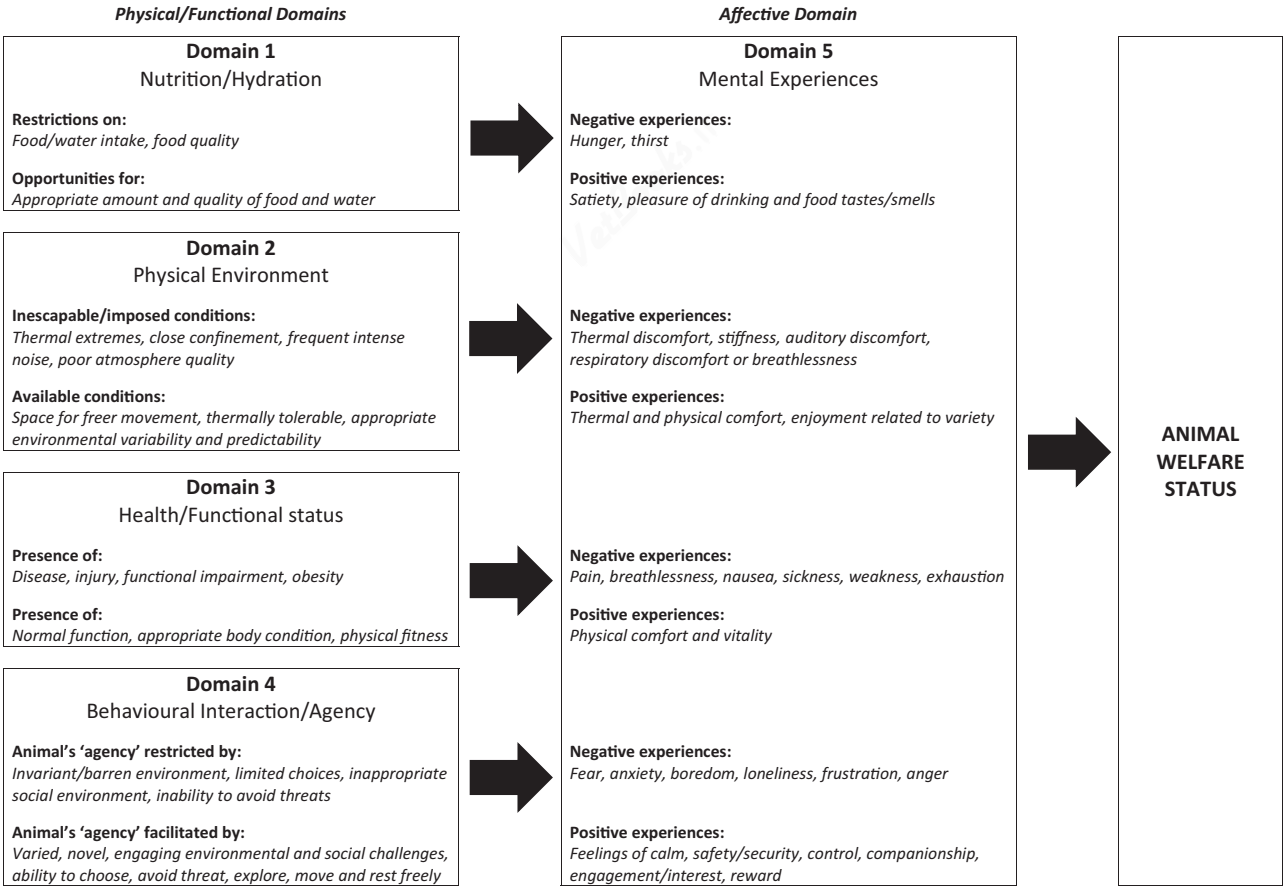

FIGURE 39.1 The Five Domains model for welfare assessment. Impacts/restrictions and opportunities in the four physical/functional domains lead to negative (unpleasant) and positive (pleasant) mental or affective experiences which are placed in Domain 5. The integrated mental/affective experiences in Domain 5 determine the welfare status of the animal. Generic examples of conditions or events that influence the animal's physical/functional state (Domains 1–4) and the associated inferred affective experiences are presented. In Domain 4, "agency" refers to animals' volitional, goal-directed behavior. Observable evidence (indicators) of physical/functional state should be collated in Domains 1–4. For more detail of the model and its application, see Mellor and Beausoleil (2015).

satiety, comfort, and companionship. Observable evidence of physical/functional states (welfare indicators) should be collated in Domains 1 to 4 and the associated mental experiences inferred in Domain 5.

Potential welfare indicators include measures of physical health and condition and behavioral, physiological and neurophysiological responses. They can be used to infer not only the occurrence but also the intensity and duration of specific affective experiences that contribute to the animal's overall welfare state. However, the onus is on the user to scientifically justify the inclusion of specific experiences for the taxon being assessed, as well as demonstrate the validity of the observed indicators considered to reflect those experiences (Beausoleil and Mellor, 2017). To ensure that the model is applied appropriately for the birds under investigation, a multidisciplinary, collaborative approach involving those with expertise in avian neuroscience, behavioral ecology, and animal welfare science is recommended (Beausoleil and Mellor, 2017; Harvey et al., 2020).

39.4.2 Hierarchy of evidence to support specific affective experiences in birds

Acknowledgment of sentience in birds means that we recognize their capacity to consciously perceive at least *some* negative and positive mental experiences that matter to them (Mellor, 2019). However, this does not mean that birds are capable of all mental experiences reported by humans, nor that we have the capacity for all of their experiences (Elwood, 2011). For example, some birds are capable of flight or of detecting polarized light or magnetic fields, things we cannot do (Freire et al., 2011; Wiltschko and Wiltschko, 2013); it seems plausible that birds might experience pleasant and unpleasant feelings associated with these kinds of sensory information that we cannot imagine (Nicol et al., 2020). In addition, the class *Aves* represents 10,000 species that are diverse in neuroanatomy, sensory physiology, behavior, and lifestyle (Martin, 2017). Thus, specific evidence is needed to support the capacity of birds, and perhaps even species of birds, for particular qualities of mental experience, to inform application of the Five Domains model for assessing the impacts of events or conditions on bird welfare.

The kinds of evidence that can be used to support the inference of a specific affective experience are: 1. Human report of experiences during exposure to similar situations or stimuli; 2. Homologous or analogous anatomical, physiological, and neural pathways and mechanisms in the taxon of interest; 3. Expression of specific protective behavioral and/or physiological responses by the animal during or after exposure; and 4. Effects of applying strategies known to circumvent or mitigate human experiences on the expression of protective responses in the taxon of interest (Dawkins, 2006; Elwood, 2011; Martin et al., 2016; Beausoleil, 2017). Note that there is also a hierarchy for the kinds of behavioral and physiological evidence that provide support for affective experiences (Dawkins, 2015; Weary et al., 2017). Following this structure, the case for birds' capacity to experience pain is outlined in Chapter 14 of this volume. While birds may not be capable of all the same experiences of humans in comparable situations, considering human experiences informs the specific affective states (and thus observed responses) that should be purposefully investigated (Steiner et al., 2019). For suspected affective experiences associated with sensory modalities humans do not have, researchers should focus on understanding the neural pathways underpinning sensory and affective processing, as well as the specific behavioral and physiological responses expressed by the animals and their mitigation.

39.5 Avian welfare research to date

While much of the research on avian neuroanatomy, sensory physiology, and high-level cognitive capabilities has been undertaken using species such as domestic pigeons, starlings, zebra finches, psittacines, and corvids (reviewed by, for example, Butler and Cotterill, 2006; Rattenborg and Martinez-Gonzalez, 2011; Shanahan et al., 2013; Güntürkün et al., 2014; Clayton and Emery, 2015; Pennartz et al., 2019), most welfare-specific research has been done on poultry, because of the very large numbers of birds commercially raised and the multiple sources of welfare compromise in these industries (see below). In addition, specific research has been done on pain and analgesia in birds kept as pets or treated in veterinary clinics (see Chapter 14, this volume), and there is increasing consideration of some aspects of welfare in free-living birds, particularly as they relate to the success of conservation activities (e.g., Sorace et al., 2001; Casper, 2009; Dickens et al., 2009; Marzluff et al., 2012; Jerem et al., 2018; Maggini et al., 2018). Because of the greater body of relevant information available, we will focus on poultry welfare here. We first briefly summarize key welfare issues relating to commercial poultry production then use one specific aspect (preslaughter stunning with carbon dioxide) to illustrate how the capacity of birds for welfare-relevant mental experiences can be scientifically evaluated.

39.5.1 Key welfare issues in commercial poultry production

Three bird species account for the majority of commercial poultry production globally: chickens (*Gallus gallus*), ducks (Pekin breed of *Anas platyrhyncos*), and turkeys (*Meleagris gallopavo*). Chickens have diverged into two types, selected specifically for meat (broilers) or egg production (layer hens). Most commercial birds are managed

indoors in closely regulated physical, thermal, atmospheric, and light environments. These factors, coupled with genetic selection for specific production traits, specialized nutrition and prevention and treatment of many infectious diseases, are tailored to maximize productivity. Some aspects of management are beneficial for welfare (e.g., supportive nutrition, disease prevention) while others present welfare risks. The selected traits, housing and management systems are generally similar for broilers, turkeys, and ducks, all of which are raised for meat, and similar welfare concerns arise for each species. Layer hens are managed differently and in more variable housing systems (e.g., caged vs. free range). Due to this, and the different physiological demands of egg production, they are predisposed to different welfare problems (reviewed by Karcher and Mench, 2018).

Broiler chickens and turkeys reach slaughter weight or conformation between five and nine weeks of age and 12 and 20 weeks, respectively (Karcher and Mench, 2018). Genetic selection for these very fast growth rates and for large breast size has numerous welfare-relevant consequences. Key problems include musculoskeletal disorders, particularly inflammatory osteoarthritis of the legs causing lameness, cardiovascular pathologies, poor thermoregulatory capacity, and poor fitness leading to limited ability to perform normal behaviors, such as walking, dust-bathing, flapping, and foraging even when opportunities exist to do so (Julian, 2005; Knowles et al., 2008; de Jong et al., 2012; Hassanzadeh et al., 2013; Norring et al., 2018; Dixon, 2020). In addition, breeding birds, which are kept into adulthood have to be severely food restricted during the rearing phase and moderately restricted during the laying phase to be reproductively competent and avoid obesity (Mench, 2002); this restriction leads to chronic hunger which is intense in the rearing phase (De Jong et al., 2002; Sandilands et al., 2006).

Layer hens are kept for much longer and are predisposed to abnormalities and fractures of the long bones and keel. This is a consequence of genetic selection for egg production, which results in osteoporosis despite adequate nutrition because calcium is preferentially deposited in eggs rather than bones (Sandilands, 2011; Wilkins et al., 2011; Tarlton et al., 2013). For both meat and egg-producing birds, welfare concerns related to housing environment and management also include respiratory and eye irritation due to poor air quality, thermal discomfort, foot problems due to poorly managed or inappropriate substrate, thwarting of strongly motivated behaviors, and the occurrence of social aggression and associated injuries and/or preventative tissue removals (i.e., beak and toe trimming in layers, turkeys, and ducks) due to limited space, high-stocking densities, and environmental barrenness (Appleby and Hughes, 1991; Rodenburg et al., 2008; de Jong et al., 2012; Widowski et al., 2016). In addition, interactions with humans, handling, and transport can induce fear and injury, especially in metabolically exhausted layer hens at the end of production (Kettlewell and Mitchell, 1994; Weeks and Nicol, 2000). Finally, the methods of bringing about unconsciousness of poultry (stunning) either prior to slaughter or during mass depopulation on farm at the end of lay or for emergency management of disease has the potential to compromise welfare before death (Steiner et al., 2019).

39.6 Case study—evaluation of the potential for chickens to experience negative states due to carbon dioxide stunning

Every year, billions of chickens are killed and some of those are first rendered unconscious by exposing them to atmospheres containing carbon dioxide (CO_2; hypercapnic atmospheres) (Nielsen et al., 2019; FAO, 2020). Here we apply the four criteria outlined above to investigate whether these birds are likely to have unpleasant experiences associated with inhaling hypercapnic gas mixtures: Human report, neural mechanisms for detection and generation of affective experiences, protective behavioral and physiological responses, and the effects of applying proposed mitigation strategies on those responses.

Normal air has less than 1% CO_2, and while CO_2 is an anesthetic gas, unconsciousness occurs only at concentrations of 15−40%, depending on the rate at which the concentration rises, the other gases in the atmosphere and the type and age of the birds (Raj et al., 1992; Gerritzen et al., 2004, 2013; Coenen et al., 2009). Inhaling CO_2 leads to higher blood CO_2 level, which strongly stimulates the rate and depth of respiration in all vertebrates (Milsom et al., 2004). Higher levels suppress neural activity, leading to loss of consciousness and death if maintained long enough (Terlouw et al., 2016). Carbon dioxide stunning is a reliable method and has welfare benefits over electrical water-bath stunning in that birds do not have to be shackled and can therefore be left in groups in their transport crates or treated in their normal housing environment with no further handling or restraint (Shields and Raj, 2010; Nielsen et al., 2019). However, breathing hypercapnic gas mixtures is known to be strongly aversive to humans and other mammals (Banzett et al., 2008). The specific unpleasant mental experiences reported by humans breathing as little as 7% CO_2 are predominantly a sense of breathlessness (air hunger) and fear/anxiety/panic, both of which intensify with rising CO_2 concentration (reviewed by Parshall et al., 2012; Améndola and Weary, 2020). In mammals, breathing CO_2 concentrations greater than about 40% also causes

painful irritation of the mucosa of the eyes, nose, and throat by activating nociceptors (Anton et al., 1991; Shusterman and Balmes, 1997). Thus, CO_2 stunning of poultry may lead to welfare impacts through at least three different unpleasant experiences: pain, air hunger, and/or anxiety.

For commercially slaughtered chickens, the most common form of CO_2 stunning involves a multiphase process, in which birds are exposed to progressively increasing concentrations of CO_2 in stages. After birds lose consciousness at around 15−30% (Raj et al., 1992; Gerritzen et al., 2004, 2013), final phases expose them to 60−80% CO_2 which is maintained until a state of nonrecovery is reached, followed by exsanguination. Although birds have CO_2-responsive nociceptors in the oral and nasal mucosa (McKeegan, 2004), most birds lose consciousness before the concentration reaches receptor activation threshold, so mucosal pain is not expected. However, on the basis of human reports and the behavioral responses of various mammals, birds might be expected to experience unpleasant breathlessness and fear before loss of consciousness if they have the capacity for sensory detection and generation of these affects.

Chickens are able to detect elevated CO_2 at concentrations much lower than those used for stunning. Unlike mammals, birds have intrapulmonary chemoreceptors that respond to small changes in inhaled CO_2, stimulating deeper, slower breathing (Milsom et al., 2004; Fedde, 2012). Other behavioral evidence also supports sensitivity to subnociceptive concentrations of CO_2 in birds. Hens spent less time feeding in a chamber containing 7.5% or 10% CO_2 than in one containing normal air (Raj and Gregory, 1991). Likewise, at 10% CO_2 and above, layer hens changed their previous behavior, began manipulations ("tasting" movements of the bill) and noticed the end of exposure (McKeegan et al., 2005, 2006).

However, detection of a hypercapnic atmosphere doesn't necessarily lead to generation of unpleasant experiences such as the breathlessness and anxiety/fear reported by humans. Since birds have a unique respiratory system (see Chapter 20 this volume), extrapolation of respiratory sensations from mammals may not be valid. For example, birds have fixed lung volume, unidirectional airflow, and higher dead space (due to air sacs), all of which may influence the adaptive value of the sensation of air hunger, which arises in mammals due to a mismatch between ventilatory drive and lung inflation (Banzett et al., 2008). Although the neurological bases of feelings of breathlessness are understood in humans and other mammals (Parshall et al., 2012; Beausoleil and Mellor, 2015), these have not been specifically explored in birds. Similarly, the neural circuitry for fear in birds is well characterized (reviewed by Papini et al., 2019) but whether it is activated by exposure to hypercapnic gases has not been investigated (Steiner et al., 2019).

Thus, the most compelling available evidence is the protective behavioral responses demonstrated by chickens exposed to hypercapnic environments. Most studies report that 30% CO_2 or higher elicits a suite of behaviors such as head shaking, mandibulation, wing flapping, and abnormal respiratory patterns, including open-bill, labored or difficult breathing with a prolonged inspiratory phase; these behaviors begin before loss of consciousness (reviewed Steiner et al., 2019). While these responses could represent unpleasant experiences ("distress"), they may be automatically generated, and their significance to welfare is difficult to interpret without additional information.

In an attempt to better access birds' affective experiences, several studies have allowed chickens to choose between remaining in a hypercapnic environment to access a food reward and withdrawing from the atmosphere but forfeiting the reward. These kinds of tests provide stronger evidence of any unpleasant experience because the animal has to cognitively compare and decide between different priorities (Weary et al., 2017). McKeegan et al. (2006) showed that broilers continued to feed in the presence of subnociceptive hypercapnic gas while hyperventilating, suggesting that respiratory disruption does not necessarily reflect an unpleasant experience in birds. Collectively, the outcomes of this and other studies suggest that atmospheres containing 10−70% CO_2 are only mildly to moderately aversive to chickens (Raj and Gregory, 1991; Gerritzen et al., 2000; Webster and Fletcher, 2004; McKeegan et al., 2006).

However, the results of some of these studies may have been confounded by the research design, e.g., requiring slaughter-weight broilers to walk up a 5 m inclined ramp to get out of the CO_2 atmosphere (Webster and Fletcher, 2004). Additionally, it has been suggested that failure to leave an area where potentially sedative or narcotic gases have been introduced may reflect the subject's physical inability to do so or reduced cognitive capacity, rather than a lack of aversion per se (Gerritzen et al., 2000; Leach et al., 2002; Wong et al., 2014). In support of this, chickens exposed to CO_2 gas mixtures exhibit sitting down in an upright posture much earlier than do birds exposed to air, which may reflect their inability to remain standing due to the anesthetic effect of the gas (Gerritzen et al., 2000). Conditioned place aversion tests may help address such limitations by asking birds to display any learned aversion after, not during, exposure to CO_2. As yet, such tests have not been undertaken.

Nor have mitigation studies been undertaken for CO_2 stunning of birds. Treating humans and rats with antianxiety drugs has demonstrated the contribution of fear/anxiety/panic to human reports of unpleasantness and animals' behavioral responses indicative of aversion (Améndola and Weary, 2020). Likewise, the effects of treatment with drugs such as inhaled furosemide, known to relieve

breathlessness in humans, on chickens' responses to CO_2 have not been explored. Overall, and despite the equivocal evidence, the general view is still that CO_2 stunning is likely to cause unpleasant experiences in poultry, although the character of those experiences is not yet clearly understood, and more specific research is needed (Steiner et al., 2019). As gaseous methods of stunning poultry are becoming more widespread (due to welfare and other advantages over electrical water-bath stunning), understanding the associated affective experiences and welfare impacts becomes all the more pressing.

39.7 General conclusions

Birds are undeniably sentient and thus capable of at least some negative and positive mental experiences that matter to them. The impacts, both negative and positive, of events and conditions on bird welfare should be systematically evaluated using a structured, evidence-based framework such as the Five Domains model. However, our current understanding of the specific affective experiences of birds is relatively limited, partly because of the strong focus of animal welfare scientists on commercial poultry species. There is a need for research to translate avian neuroscience, behavioral ecology, and cognitive sciences knowledge to better understand birds' affective experiences and welfare states, including in a wider range of avian species. This is particularly important as the effects of human activities on wild animal species is ever expanding. While productive interaction among scientific fields is growing, it is anticipated that greater cross-disciplinary discussion involving avian neuroscientists, behavioral ecologists, psychologists, and animal welfare scientists will rapidly advance our understanding of bird welfare.

References

Abeyesinghe, S.M., Nicol, C.J., Hartnell, S.J., Wathes, C.M., 2005. Can domestic fowl, *Gallus gallus domesticus*, show self control? Anim. Behav. 70, 1–11.

Améndola, L., Weary, D.M., 2020. Understanding rat emotional responses to CO_2. Transl. Psychiatry 10.

Anonymous, 2014. Universal Declaration on Animal Welfare [Online]. Available: https://en.wikipedia.org/wiki/Universal_Declaration_on_Animal_Welfare. (Accessed 20 July 2020).

Anton, F., Peppel, P., Euchner, I., Handwerker, H.O., 1991. Controlled noxious chemical stimulation: responses of rat trigeminal brainstem neurones to CO_2 pulses applied to the nasal mucosa. Neurosci. Lett. 123, 208–211.

Appleby, M.C., Hughes, B.O., 1991. Welfare of laying hens in cages and alternative systems: environmental, physical and behavioural aspects. World Poultry Sci. J. 47, 109–128.

Arluke, A., Sanders, C.R., 1996. Regarding Animals. Temple University Press, Philadelphia, USA.

Australian Capital Territory, 2019. Animal Welfare Legislation Amendment Bill 2019. Canberra, ACT, Australia.

Banzett, R.B., Pedersen, S.H., Swartzstein, R.M., Lansing, R.W., 2008. The affective dimension of laboratory dyspnoea: air hunger is more unpleasant than work/effort. Am. J. Respir. Crit. Care Med. 177, 1384–1390.

Barnett, J.L., Hemsworth, P.H., Newman, E.A., 1992. Fear of humans and its relationships with productivity in laying hens at commercial farms. Br. Poultry Sci. 33, 699–710.

Beausoleil, N.J., 2017. Dissecting Distress: What Is a Humane Death and How Can We Assess the Humaneness of Death? Australia New Zealand Council for the Care of Animals in Research and Teaching, Queenstown, NZ, pp. 113–114.

Beausoleil, N.J., Mellor, D.J., 2015. Introducing breathlessness as a significant animal welfare issue. N. Z. Vet. J. 63, 44–51.

Beausoleil, N.J., Mellor, D.J., 2017. Validating indicators of sheep welfare. In: Greyling, J. (Ed.), Achieving Sustainable Production of Sheep. Burleigh Dodds Publishing, Cambridge, U.K., pp. 327–343

Beausoleil, N.J., Mellor, D.J., Baker, L., Baker, S.E., Bellio, M., Clarke, A.S., Dale, A., Garlick, S., Jones, B., Harvey, A., Pitcher, B.J., Sherwen, S., Stockin, K.A., Zito, S., 2018. "Feelings and fitness" not "feelings or fitness"—the raison d'être of conservation welfare, which aligns conservation and animal welfare objectives. Front. Vet. Sci. 5.

Boissy, A., Manteuffel, G., Jensen, M.B., Moe, R.O., Spruijt, B., Keeling, L., Winckler, C., Forkman, B., Dimitrov, I., Langbein, J., Bakken, M., Veissier, I., Aubert, A., 2007. Assessment of positive emotions in animals to improve their welfare. Physiol. Behav. 92, 375–397.

Broom, D.M., 2007. Quality of life means welfare: how is it related to other concepts and assessed? Anim. Welf. 16, 45–53.

Butler, A.B., Cotterill, R.M., 2006. Mammalian and avian neuroanatomy and the question of consciousness in birds. Biol. Bull. 211, 106–127.

Casper, R.M., 2009. Guidelines for the instrumentation of wild birds and mammals. Anim. Behav. 78, 1477–1483.

Clayton, N.S., Emery, N.J., 2015. Avian models for human cognitive neuroscience: a proposal. Neuron 86, 1330–1342.

Coenen, A.M.L., Lankhaar, J., Lowe, J.C., McKeegan, D.E.F., 2009. Remote monitoring of electroencephalogram, electrocardiogram, and behavior during controlled atmosphere stunning in broilers: implications for welfare. Poultry Sci. 88, 10–19.

Coleman, G., 2018. Public animal welfare discussions and outlooks in Australia. Anim. Front. 8, 14–19.

Coleman, G.J., Hemsworth, P.H., 2014. Training to improve stockperson beliefs and behaviour towards livestock enhances welfare and productivity. Rev. Sci. Tech. 33, 131–137. OIE.

D'eath, R.B., Stone, R.J., 1999. Chickens use visual cues in social discrimination: an experiment with coloured light. Anim. Behav. 62, 233–242.

Dawkins, M., 2015. Animal welfare and the paradox of animal consciousness. Adv. Stud. Behav. 47, 5–38.

Dawkins, M.S., 2006. Through animal eyes: what behaviour tells us. Appl. Anim. Behav. Sci. 100, 4–10.

de Jong, I., Berg, C., Butterworth, A., Estevéz, I., 2012. Scientific Report Updating the EFSA Opinions on the Welfare of Broilers and Broiler Breeders. Supporting Publications. EN-295. Available: www.efsa.europa.eu/publications. (Accessed 1 August 2020).

de Jong, I.C., Voorst, S.V., Ehlhardt, D.A., 2002. Effects of restricted feeding on physiological stress parameters in growing broiler breeders. Br. Poultry Sci. 43, 157–168.

Denton, D.A., McKinley, M.J., Farrell, M., Egan, G.F., 2009. The role of primordial emotions in the evolutionary origins of consciousness. Conscious. Cognit. 18, 500–514.

Dickens, M.J., Delehanty, D.J., Romero, L.M., 2009. Stress and translocation: alterations in the stress physiology of translocated birds. Proc. R. Soc. Lond. Ser. B Biol. Sci. 276, 2051–2056.

Dixon, L.M., 2020. Slow and steady wins the race: the behaviour and welfare of commercial faster growing broiler breeds compared to a commercial slower growing breed. PloS One 15, e0231006.

Duncan, I.J.H., 2006. The changing concept of animal sentience. Appl. Anim. Behav. Sci. 100, 11–19.

Edelman, D.B., Baars, B.J., Seth, A.K., 2005. Identifying hallmarks of consciousness in non-mammalian species. Conscious. Cognit. 14, 169–187.

Elwood, R.W., 2011. Pain and suffering in invertebrates? ILAR J. 52, 175–184.

European Commission, 2007. Attitudes of EU Citizens towards Animal Welfare. Special Eurobarometer 270th Report. Brussels: EC. Available: http://ec.europa.eu/public_opinion/archives/ebs/ebs_270_en.pdf. (Accessed 30 July 2020).

European Council, 2010. Directive 2010/63 of the European Parliament and of the Council on the Protection of Animals Used for Scientific Purposes, 2010 O.J (L 276) 33.

FAO, 2020. Livestock Primary, Producing Animals/slaughtered. FAO STATtat [Online]. Food and Agriculture Organization of the United Nations. Available: http://www.fao.org/faostat/en/#data/QL. (Accessed 10 August 2020).

Fedde, M., 2012. Respiration. In: Sturkie, P. (Ed.), Avian Physiology, fourth ed. Springer-Verlag, New York, US, pp. 191–221.

Feinberg, T., Mallatt, J., 2013. The evolutionary and genetic origins of consciousness in the Cambrian period over 500 million years ago. Front. Psychol. 4.

Fraser, D., 1999. Animal ethics and animal welfare science: bridging the two cultures. Appl. Anim. Behav. Sci. 65, 171–189.

Fraser, D., 2003. Assessing animal welfare at the farm and group level: the interplay of science and values. Anim. Welf. 12, 433–443.

Fraser, D., 2008. Understanding animal welfare. Acta Vet. Scand. 50.

Fraser, D., Duncan, I.J.H., 1998. 'Pleasures','pains' and animal welfare: toward a natural history of affect. Anim. Welf. 7, 383–396.

Fraser, D., Weary, D.M., Pajor, E.A., Milligan, B.N., 1997. A scientific conception of animal welfare that reflects ethical concerns. Anim. Welf. 6, 187–205.

Freire, R., Eastwood, M.A., Joyce, M., 2011. Minor beak trimming in chickens leads to loss of mechanoreception and magnetoreception. J. Anim. Sci. 89, 1201–1206.

Gerritzen, M.A., Lambooij, B., Reimert, H., Stegeman, A., Spruijt, B., 2004. On farm euthanasia of broiler chickens: effects of different gas mixtures on behavior and brain activity. Poultry Sci. 83, 1294–1301.

Gerritzen, M.A., Lambooij, E., Hillebrand, S.J.W., Lankhaar, J.A.C., Pieterse, C., 2000. Behavioral responses of broilers to different gaseous atmospheres. Poultry Sci. 79, 928–933.

Gerritzen, M.A., Reimert, H.G.M., Hindle, V.A., Verhoeven, M.T.W., Veerkamp, W.B., 2013. Multistage carbon dioxide gas stunning of broilers. Poultry Sci. 92, 41–50.

Güntürkün, O., 2012. The convergent evolution of neural substrates for cognition. Psychol. Res. 76, 212–219.

Güntürkün, O., Stüttgen, M.C., Manns, M., 2014. Pigeons as a model species for cognitive neuroscience. E-Neuroforum 1–7.

Gyger, M., Marler, P., 1998. Food calling in the domestic fowl, *Gallus gallus*: the role of external referents and deception. Anim. Behav. 36, 358–365.

Harvey, A.M., Beausoleil, N.J., Ramp, D., Mellor, D.J., 2020. A ten-stage protocol for assessing the welfare of individual non-captive wild animals: free-roaming horses (*Equus ferus caballus*) as an example. Animals 19.

Hassanzadeh, M., Buyse, J., Toloei, T., Decuypere, E., 2013. Ascites syndrome in broiler chickens: a review on the aspect of endogenous and exogenous factors interactions. J. Poultry Sci. 51, 229–241.

Hawkins, M.G., 2006. The use of analgesics in birds, reptiles, and small exotic mammals. J. Exot. Pet Med. 15, 177–192.

Hemsworth, P.H., Coleman, G.J., Barnett, J.L., Jones, R.B., 1994. Behavioural responses to humans and the productivity of commercial broiler chickens. Appl. Anim. Behav. Sci. 41, 101–114.

Hemsworth, P.H., Mellor, D.J., Cronin, G.M., Tilbrook, A.J., 2015. Scientific assessment of animal welfare. N. Z. Vet. J. 63, 24–30.

Hogue, M.E., Beaugrand, J.P., Lague, P.C., 1996. Coherent use of information by hens observing their former dominant defeating or being defeated by a stranger. Behav. Process. 38, 241–252.

Jerem, P., Jenni-Eiermann, S., Herborn, K., McKeegan, D.E.F., McCafferty, D.J., Nager, R.G., 2018. Eye region surface temperature reflects both energy reserves and circulating glucocorticoids in a wild bird. Sci. Rep. 8.

Julian, R.J., 2005. Production and growth related disorders and other metabolic diseases of poultry – a review. Vet. J. 169, 350–369.

Karcher, D.M., Mench, J.A., 2018. Overview of commercial poultry production systems and their main welfare challenges. In: Mench, J.A. (Ed.), Advances in Poultry Welfare. Elsevier Ltd., Duxford, UK, pp. 3–25.

Kettlewell, P.J., Mitchell, M.A., 1994. Catching, handling and loading of poultry for road transportation. World Poultry Sci. J. 50, 54–56.

Knowles, T.G., Kestin, S.C., Haslma, S.M., Brown, S.N., Green, L.E., Butterworth, A., Pope, S.J., Pfeiffer, D., Nicol, C.J., 2008. Leg disorders in broiler chickens: prevalence, risk factors and prevention. PloS One 3, e1545.

Korte, S.M., Olivier, B., Koolhaas, J.M., 2007. A new animal welfare concept based on allostasis. Physiol. Behav. 92, 422–428.

Leach, M.C., Bowell, V.A., Allan, T.F., Morton, D.B., 2002. Aversion to gaseous euthanasia agents in rats and mice. Comp. Med. 52, 249–257.

Learmonth, M.J., 2019. Dilemmas for natural living concepts of zoo animal welfare. Animals 9, 318.

Maggini, I., Tahamtani, F.M., Cardinale, M., Fusani, L., Carere, C., 2018. Body temperature upon mist-netting procedures in three species of migratory songbirds at a stopover site: implications for welfare. Anim. Welf. 27, 93–101.

Martin, G.R., 2017. The Sensory Ecology of Birds. Oxford University Press, Oxford, UK.

Martin, J., Christensen, K., Vizzier-Thaxton, Y., McKeegan, D.E.F., 2016. Effects of analgesic intervention on behavioural responses to low atmospheric pressure stunning. Appl. Anim. Behav. Sci. 180, 157–165.

Marzluff, J.M., Miyaoka, R., Minoshima, S., Cross, D.J., 2012. Whole brain response of birds to human faces. Proc. Natl. Acad. Sci. U.S.A. 109, 15912–15917.

Mashour, G.A., Alkire, M.T., 2013. Evolution of consciousness. Proc. Natl. Acad. Sci. U.S.A. 110, 10357–10364.

McCabe, B.J., 2019. Visual imprinting in birds: behavior, models, and neural mechanisms. Front. Physiol. 10.

McCulloch, S.P., 2018. Brexit and animal protection: legal and political context and a framework to assess impacts on animal welfare. Animals 8, 213.

McIlhone, A.E., Beausoleil, N.J., Kells, N.J., Mellor, D.J., Johnson, C.B., 2018. Effects of noxious stimuli on the electroencephalogram of anaesthetised chickens (*Gallus gallus domesticus*). PloS One 13, e0196454.

McKeegan, D.E., 2004. Mechano-chemical nociceptors in the avian trigeminal mucosa. Brain Res. Rev. 46, 146–154.

McKeegan, D.E.F., McIntyre, J., Demmers, T.G.M., Wathes, C.M., Jones, R.B., 2006. Behavioural responses of broiler chickens during acute exposure to gaseous stimulation. Appl. Anim. Behav. Sci. 99, 271–286.

McKeegan, D.E.F., Smith, F.S., Demmers, T.G., Wathes, C.M., Jones, R.B., 2005. Behavioral correlates of olfactory and trigeminal gaseous stimulation in chickens, *Gallus domesticus*. Physiol. Behav. 84, 761–768.

Mellor, D.J., 2015. Enhancing animal welfare by creating opportunities for positive affective engagement. N. Z. Vet. J. 63, 3–8.

Mellor, D.J., 2017. Operational details of the five domains model and its key applications to the assessment and management of animal welfare. Animals 7.

Mellor, D.J., 2019. Welfare-aligned sentience: enhanced capacities to experience, interact, anticipate, choose and survive. Animals 9.

Mellor, D.J., Beausoleil, N.J., 2015. Extending the 'Five Domains' model for animal welfare assessment to incorporate positive welfare states. Anim. Welf. 24, 241–253.

Mellor, D.J., Patterson-Kane, E., Stafford, K.J., 2009. The Sciences of Animal Welfare. Wiley Blackwell, New Jersey, USA.

Mench, J.A., 2002. Broiler breeders: feed restriction and welfare. World Poultry Sci. J. 58, 23–29.

Mendl, M., Burman, O.H.P., Parker, R.M.A., Paul, E.S., 2009. Cognitive bias as an indicator of animal emotion and welfare: emerging evidence and underlying mechanisms. Appl. Anim. Behav. Sci. 118, 161–181.

Mendl, M., Burman, O.H.P., Paul, E.S., 2010. An integrative and functional framework for the study of animal emotion and mood. Proc. R. Soc. Lond. Ser. B Biol. Sci. 277, 2895–2904.

Milsom, W.K., Abe, A.S., Andradeb, D.V., Tattersall, G.J., 2004. Evolutionary trends in airway CO_2/H^+ chemoreception. Respir. Physiol. Neurobiol. 144, 191–202.

New Zealand Government, 2015. Animal Welfare Amendment Act (No 2). Wellington, New Zealand.

Nicol, C.J., Bejder, L., Green, L., Johnson, C.B., Keeling, L., Noren, D., Van der Hoop, J., Simmonds, M., 2020. Anthropogenic threats to wild cetacean welfare and a tool to inform policy in this area. Front. Vet. Sci. 7.

Nicol, C.J., Caplen, G., Statham, P., Browning, W.J., 2009. Decisions about foraging and risk trade-offs in chickens are associated with individual somatic response profiles. Anim. Behav. 78, 413–424.

Nicol, C.J., Pope, S.J., 1994. Social learning in small flocks of laying hens. Anim. Behav. 47, 1289–1296.

Nielsen, S.S., Alvarez, J., Bicout, D.J., Calistri, P., Depner, K., Drewe, J.A., Garin-Bastuji, B., Gonzales Rojas, J.L., Gortázar Schmidt, C., Miranda Chueca, M.Á., Roberts, H.C., Sihvonen, L.H., Spoolder, H., Stahl, K., Velarde Calvo, A., Viltrop, A., Winckler, C., Candiani, D., Fabris, C., Van der Stede, Y., Michel, V., 2019. Slaughter of animals: poultry. EFSA J. 17.

Norring, M., Valros, A., Valaja, J., Sihvo, H.K., Immonen, K., Puolanne, E., 2018. Wooden breast myopathy links with poorer gait in broiler chickens. Animal 1–6.

Olsson, I.A.S., Franco, N.H., Weary, D.M., Sandoe, P., 2012. The 3Rs principle - mind the ethical gap. ALTEX 1.

Panksepp, J., Reiss, D., Edelman, D., Van Swinderen, B., Low, P., Koch, C., 2012. The Cambridge Declaration on Consciousness [Online]. Available: http://fcmconference.org/img/CambridgeDeclarationOnConsciousness.pdf. (Accessed 20 July 2020).

Papini, M.R., Penagos-Corzo, J.C., Pérez-Acosta, A.M., 2019. Avian emotions: comparative perspectives on fear and frustration. Front. Psychol. 9.

Parshall, M.B., Schwartzstein, R.M., Adams, L., Banzett, R.B., Manning, H.L., Bourbeau, J., Calverley, P.M., Gift, A.G., Harver, A., Lareau, S., Mahler, D.A., Meek, P.M., O'Donnell, D.E., 2012. An official American thoracic society statement: update on the mechanisms, assessment, and management of dyspnea. Am. J. Respir. Crit. Care Med. 185, 435–452.

Paul-Murphy, J., Hawkins, M.G., 2015. Bird-specific considerations: recognizing pain behavior in pet birds. In: Handbook of Veterinary Pain Management, third ed., pp. 536–554.

Paul, E.S., Edgar, J.L., Caplen, G., Nicol, C.J., 2018. Examining affective structure in chickens: valence, intensity, persistence and generalization measured using a Conditioned Place Preference Test. Appl. Anim. Behav. Sci. 207, 39–48.

Pennartz, C.M.A., Farisco, M., Evers, K., 2019. Indicators and criteria of consciousness in animals and intelligent machines: an inside-out approach. Front. Syst. Neurosci. 13.

Pepperberg, I.M., 2007. Grey parrots do not always 'parrot': the roles of imitation and phonological awareness in the creation of new labels from existing vocalizations. Lang. Sci. 29, 1–13.

Prior, H., Schwarz, A., Güntürkün, O., 2008. Mirror-induced behavior in the magpie (*Pica pica*): evidence of self-recognition. PloS Biol. 6, e202.

Raj, A.M., Wotton, S.B., Gregory, N.G., 1992. Changes in the somatosensory evoked potentials and spontaneous electroencephalogram of hens during stunning with a carbon dioxide and argon mixture. Br. Vet. J. 148, 147–156.

Raj, M., Gregory, N.G., 1991. Preferential feeding behaviour of hens in different gaseous atmospheres. Br. Poultry Sci. 32, 57–65.

Rattenborg, N.C., Martinez-Gonzalez, D., 2011. A bird-brain view of episodic memory. Behav. Brain Res. 222, 236–245.

Rattenborg, N.C., Martinez-Gonzalez, D., Lesku, J.A., 2009. Avian sleep homeostasis: convergent evolution of complex brains, cognition and sleep functions in mammals and birds. Neurosci. Biobehav. Rev. 33, 253–270.

Rattenborg, N.C., van der Meij, J., Beckers, G.J.L., Lesku, J.A., 2019. Local aspects of avian non-REM and REM sleep. Front. Neurosci. 13.

Rodenburg, T.B., Komen, H., Ellen, E.D., Uitdehaag, K.A., van Arendonk, J.A., 2008. Selection method and early-life history affect behavioural development, feather pecking and cannibalism in laying hens: a review. Appl. Anim. Behav. Sci. 110, 217–228.

Rollin, B.E., 2013. Telos. In: Wathes, C.M., Corr, S.A., May, S.A., McCulloch, S.P., Whiting, M.C. (Eds.), Veterinary & Animal Ethics: Proceedings of the First International Conference on Veterinary and Animal Ethics, September 2011. Blackwell Publishing Ltd, Oxford, UK, pp. 75–83.

Rushen, J., de Passille, A.M., 2009. The scientific basis of animal welfare indicators. In: Smulders, F.J.M., Algers, B. (Eds.), The Assessment and Management of Risks for the Welfare of Production Animals. Wageningen Academic Press, Amsterdam, The Netherlands, pp. 1–26.

Sandercock, D.A., Auckburally, A., Flaherty, D., Sandilands, V., McKeegan, D.E.F., 2014. Avian reflex and electroencephalogram responses in different states of consciousness. Physiol. Behav. 133, 252–259.

Sandilands, V., 2011. The laying hen and bone fractures. Vet. Rec. 169, 411–412.

Sandilands, V., Tolkamp, B.J., Savory, C.J., Kyriazakis, I., 2006. Behaviour and welfare of broiler breeders fed qualitatively restricted diets during rearing: are there viable alternatives to quantitative restriction? Appl. Anim. Behav. Sci. 96, 53–67.

Shanahan, M., Bingman, V.P., Shimizu, T., Wild, M., Güntürkün, O., 2013. Large-scale network organization in the avian forebrain: a connectivity matrix and theoretical analysis. Front. Comput. Neurosci. 7, 1–17.

Shields, S., Raj, M., 2010. A critical review of electrical water-bath stun systems for poultry slaughter and recent developments in alternative technologies. J. Appl. Anim. Welfare Sci. 13, 281–299.

Shusterman, D., Balmes, J., 1997. Measurement of nasal irritant sensitivity to pulsed carbon dioxide: a pilot study. Arch. Environ. Health 52, 334–340.

Sorace, A., Gustin, M., Landucci, G., 2001. Evening mist-net closure: implications for data collection and bird welfare. Ring. Migr. 20, 371–376.

Spinka, M., 2006. How important is natural behaviour in animal farming systems? Appl. Anim. Behav. Sci. 100, 117–128.

Steiner, A.R., Axiak Flammer, S., Beausoleil, N.J., Berg, C., Bettschart-Wolfensberger, R., García Pinillos, R., Golledge, H.D., Marahrens, M., Meyer, R., Schnitzer, T., Toscano, M.J., Turner, P.V., Weary, D.M., Gent, T.C., 2019. Humanely ending the life of animals: research priorities to identify alternatives to carbon dioxide. Animals 9.

Tarlton, J.F., Wilkins, L.J., Toscano, M.J., Avery, N.C., Knott, L., 2013. Reduced bone breakage and increased bone strength in free range laying hens fed omega-3 polyunsaturated fatty acid supplemented diets. Bone 52, 578–586.

Terlouw, C., Bourguet, C., Deiss, V., 2016. Consciousness, unconsciousness and death in the context of slaughter. Part I. Neurobiological mechanisms underlying stunning and killing. Meat Sci. 118, 133–146.

The Avian Brain Nomenclature Consortium, 2005. Avian brains and a new understanding of vertebrate brain evolution. Nat. Rev. Neurosci. 6, 151–159.

Vallortigara, G., Regolin, L., Rigoni, M., Zanforlin, M., 1998. Delayed search for a concealed imprinted object in the domestic chick. Anim. Cognit. 1, 17–24.

Veasey, J.S., 2017. In pursuit of peak animal welfare; the need to prioritize the meaningful over the measurable. Zoo Biol. 1–3.

Veasey, J.S., Waran, N.K., Young, R.J., 1996. On comparing the behaviour of zoo housed animals with wild conspecifics as a welfare indicator. Anim. Welf. 5, 13–24.

Virden, W.S., Kidd, M.T., 2009. Physiological stress in broilers: ramifications on nutrient digestibility and responses. J. Appl. Poultry Res. 18, 338–347.

von Bayern, A.M.P., Danel, S., Auersperg, A.M.I., Mioduszewska, B., Kacelnik, A., 2018. Compound tool construction by New Caledonian crows. Sci. Rep. 8.

Von Keyserlingk, M.A.G., Rushen, J., de Passille, A.M., Weary, D.M., 2009. Invited review: the welfare of dairy cattle - key concepts and the role of science. J. Dairy Sci. 92, 4101–4111.

Weary, D.M., Droege, P., Braithwaite, V.A., 2017. Behavioral evidence of felt emotions: approaches, inferences, and refinements. Adv. Stud. Behav. 49, 27–48.

Webster, A.B., Fletcher, D.L., 2004. Assessment of the aversion of hens to different gas atmospheres using an approach-avoidance test. Appl. Anim. Behav. Sci. 88, 275–287.

Weeks, C.A., Nicol, C., 2000. Poultry handling and transport. In: Grandin, T. (Ed.), Livestock Handling and Transport, second ed. CAB International, Wallingford, UK, pp. 363–384.

Widowski, T.M., Hemsworth, P.H., Barnett, J.L., Rault, J.L., 2016. Laying hen welfare I. Social environment and space. World Poultry Sci. J. 72, 333–342.

Wilkins, L.J., McKinstry, J.L., Avery, N.C., Knowles, T.G., Brown, S.N., Tarlton, J., Nicol, C.J., 2011. Influence of housing system and design on bone strength and keel bone fractures in laying hens. Vet. Rec. 169.

Williams, C.J.A., James, L.E., Bertelsen, M.F., Wang, T., 2019. Analgesia for non-mammalian vertebrates. Curr. Opin. Physiol. 11, 75–84.

Wiltschko, R., Wiltschko, W., 2013. The magnetite-based receptors in the beak of birds and their role in avian navigation. J. Comp. Physiol. A Neuroethol. Sens. Neural Behav. Physiol. 199, 89–98.

Wong, D., von Keyserlingk, M.A.G., Richards, J.G., Weary, D.M., 2014. Conditioned place avoidance of Zebrafish (*Danio rerio*) to three chemicals used for euthanasia and anaesthesia. PloS One 9, e88030.

World Organisation for Animal Health, 2017. OIE Global Animal Welfare Strategy [Online]. Paris, France. Available: http://www.oie.int/fileadmin/Home/eng/Animal_Welfare/docs/pdf/Others/EN_OIE_AW_Strategy.pdf. (Accessed 19 July 2020).

Zimmerman, P.H., Buijs, S.A.F., Bolhuis, J.E., Keeling, L.J., 2011. Behavior of domestic fowl in anticipation of positive and negative stimuli. Anim. Behav. 81, 569–577.

Chapter 40

Reproductive behavior

Elizabeth S. Greene[1], Pierre Deviche[2] and Sami Dridi[1]

[1]Center of Excellence for Poultry Science, University of Arkansas, Fayetteville, AR, United States; [2]School of Life Sciences, Arizona State University, Tempe, AZ, United States

Abbreviations

ACTH Adrenocorticotropic hormone
AVT Arginine vasotocin
cGnRH-I Chicken gonadotropin-releasing hormone-I
CORT Corticosterone
DHT 5α-dihydrotestosterone
FSH Follicle-stimulating hormone
GnIH Gonadotropin-inhibitory hormone
GnRH Gonadotropin-releasing hormone
HPA Hypothalamo−pituitary−adrenal axis
HPG Hypothalamo−pituitary−gonadal axis
LH Luteinizing hormone
MHC: Major histocompatibility complex
POA Preoptic area
PRL Prolactin
T Testosterone

40.1 Introduction

For a species to persist, reproduction is arguably the most important life history stage. In most species, reproduction is associated with the expression of some type of reproductive behavior, an orderly sequence of behavioral events that can include visual and auditory displays, copulation, nest building, oviposition, incubation, and care (including food provisioning) of young. Reproductive behavior is a crucial target of selection, and understanding its proximate bases can therefore help us address issues related to the persistence and evolution of organisms. Within vertebrates, reproductive behavior is widespread and exhibited by representatives of all classes, and it is thought to have evolved well before the emergence of birds. Indeed, similar to modern birds, nonavian maniraptoran dinosaurs probably exhibited a daily oviposition pattern, produced eggs with a complex shell microstructure, and protected their clutch (Zheng et al., 2013). Based on correlative analysis of clutch size and adult bone morphology, Varricchio et al. (2008) conclude that some Cretaceous dinosaurs exhibited paternal care and possibly had a polygamous mating system (Varricchio et al., 2008). More recently, ancestral phoenicopterids from the early Miocene are thought to have built floating nests, as do some of their extant relatives (grebes: Grellet-Tinner et al., 2012).

Given its distant origin, it is not surprising that within each vertebrate class, reproductive behavior varies enormously with respect to complexity, seasonal timing, duration, and control mechanisms. Birds have long been considered to be choice models to investigate the mechanisms that control the expression of reproductive behavior. Being endotherms, they thrive in diverse environments ranging from cold and hot deserts across a wide range of latitudes and altitudes to tropical and equatorial forests, as well as oceanic islands. Many species are, therefore, readily accessible to researchers. In addition, all aspects of avian reproductive behavior, as well as avian social systems, which range from social monogamy to polygyny and polyandry (dunnock, *Prunella modularis*: Langmore et al., 2002; Owens, 2002; spotted sandpiper, *Actitis macularius*: Rissman and Wingfield, 1984), are extremely diverse, and this diversity presents boundless opportunities for comparative work. Furthermore, many species are diurnal and colorful, and they sport a sexually dimorphic adult plumage. Their reproductive behavior often includes conspicuous visual (e.g., social displays, copulation, and parental feeding) and auditory (e.g., song) signals that are relatively easy to observe and quantify. Also of note, the expression of avian reproductive behavior is in many species seasonal and generally restricted to the time of year when environmental resources, in particular food, that are necessary for the optimal development of the offspring are most abundant and accessible. This expression is often regulated by hormones whose secretion likewise fluctuates seasonally. Not unexpectedly, therefore, birds have long been used as primary model organisms for correlative studies on hormones and reproductive behavior, and for mechanistic research aimed at identifying the hormonal and neural bases of this behavior during ontogeny and in adulthood. Finally, several species (chicken, *Gallus*

Sturkie's Avian Physiology. https://doi.org/10.1016/B978-0-12-819770-7.00052-9

domesticus; Japanese quail, *Coturnix coturnix japonica*; domesticated turkey, *Meleagris gallopavo*; ring dove, *Streptopelia risoria*; domesticated canary, *Serinus canaria*; and zebra finch, *Taeniopygia guttata*) have long been domesticated, and many aspects of their reproductive behavior and physiology have been studied extensively (see Sections 40.4.1, 40.6.2, and 40.6.5). This knowledge gained from these studies, along with ready access, presents unsurpassed opportunities for in-depth mechanistic investigations (Ball and Balthazart, 2004; Balthazart et al., 2003).

40.2 Regulation of reproductive behavior

The expression of reproductive behavior at maturity is regulated by a multitude of external factors—environmental and social—as well as internal factors, the nature and relative importance of which often vary interspecifically, between sexes, during ontogeny, as a function of adult age and experience, and according to the reproductive stage. A comprehensive review of the vast literature related to this regulation well exceeds the scope of the present chapter. Thus, we focus on a limited number of representative topics based on their potential interest to readers, progress made in the recent past, and the generality of conclusions that can be reached based on the available information. We begin with an analysis of environmental factors and then social factors with well-documented effects on the reproductive system and behavior. Age and breeding experience can profoundly impact the adult reproductive system and the expression of reproductive behavior, and so we address the respective roles of these factors. Many studies have investigated the mechanisms by which peripheral hormones and neurohormones regulate reproductive behavior. We follow those sections with an analysis of this regulation, with particular attention paid to the role of gonadotropin-releasing hormone (GnRH), gonadotropin-inhibitory hormone (GnIH), arginine vasotocin (AVT), prolactin (PRL), gonadal steroids, and neurosteroids.

Three underlying themes run through the present chapter. First, we emphasize that gonadal hormones play an overwhelming role in the control of avian reproductive behavior. Any analysis of the mechanisms that regulate this behavior must, therefore, necessarily encompass a discussion of the mechanisms that control the activity of the reproductive system itself. For this reason, we provide examples drawn not only from the behavioral literature but also from the endocrine literature. Second, when addressing the (neuro)endocrine mechanisms that regulate reproductive behavior, one needs to take into account that this regulation is frequently reciprocal. For example, gonadal steroids profoundly influence the expression of reproductive behavior, but social and perhaps chemical signals from conspecifics can markedly affect the secretion of gonadal hormones. In some cases, even an individual's own behavior causes marked endocrine changes within this individual. Third, at the individual level, most endocrine systems do not operate independently but are functionally interrelated. Illustrating this point, gonadal steroids can markedly influence the production and secretion of behaviorally active neuropeptides such as adrenocorticotropic hormone and AVT. Furthermore, during stress, elevated secretion of hypothalamo–pituitary–adrenal (HPA) axis hormones can negatively affect aspects of reproductive physiology and behavior.

40.3 Environmental factors

Many environmental factors have the potential to influence the reproductive physiology and behavior of birds. These factors include weather-related events such as droughts (Reichert et al., 2012) and storms (Astheimer et al., 1995; Bolger et al., 2005), temperature (Ardia et al., 2009), and humidity (Cynx, 2001). Understanding the effects of these factors and how they affect reproduction is of considerable importance given the potential outcome of global climate change on biological systems (Beale et al., 2006; Senapathi et al., 2011; Shine and Brown, 2008; Moller, 2013), but this understanding is complicated by several factors. For example, weather-related events such as storms are generally perceived as stressful and often have negative reproductive consequences (e.g., they delay the onset of breeding and incubation behavior), but whether this is the case can be reproductive stage dependent (Wingfield, 1984). In addition, the effects of weather- or climate-related factors on the reproductive system can be direct (temperature: Ardia et al., 2009; Visser et al., 2009) but, alternatively or in addition, be indirect and result from changes, such as in food resources (drought: Bolger et al., 2005). Here we consider the direct and indirect roles of weather and climate, as well as other important environmental factors including light and urbanization.

40.3.1 Temperature and climate change

Global temperatures have increased over the last century, a trend that is predicted to continue at an even greater rate over the coming decades (Stillman, 2019), with a concurrent increase in number and duration of extreme weather events such as storms, floods, droughts, and heat and cold waves similarly predicted (Rahmstorf and Coumou, 2011; Coumou and Robinson, 2013). There is already an abundance of evidence for changes to physiology and behavior of a multitude of organisms due to climactic changes. These long and short-term events have the potential to impact bird populations on both a sudden and dramatic scale (i.e., mass mortality events associated with extreme events), as well as more subtle changes that may be revealed across

generations, leading to birds being considered one of the most at-risk animal groups (Foden et al., 2013). To mitigate the risk of overheating in high temperatures, birds use physiological and behavioral responses including shade-seeking behaviors, resting, changes to wing posture, and panting (Fedde, 1998; Dawson, 1982; Pattinson et al., 2020). Some species can also tolerate a controlled increase in body temperature in order to reduce the temperature gradient between their body and the environment (Gerson et al., 2019). All of these mechanisms promote survival of the individual, but often at the cost of other physiological demands, including reproductive behaviors, which can be energetically expensive. For example, the little bustard (*Tetrax tetrax*), uses "snort-calling" to signal to females, a behavior which is reduced in increased temperatures (Gudka et al., 2019), and negatively impacts breeding success. More directly, in both domestic chickens (*Gallus gallus*, Karaca et al., 2002) and zebra finch (*Taeniopygia guttata*, Hurley, et al., 2018), heat stress (where temperature and intensity are manipulated to mimic a heat wave) decreases sperm concentration and viability. Most of what is known about the effects of increasing temperature on reproduction come from studies on birds already living in tropical and other warm climates, and comparatively little research has studied the effect of climate change on those adapted to more temperate climates. This is a notable oversight, as the higher latitudes are expected to warm at an increased rate (IPCC, 2014). Photoperiod and circadian rhythms control the initiation of changes to physiology and behavior in seasonal breeders (Farner, 1964; Dawson et al., 2001); however other cues, such as temperature, can regulate gonadal growth and other reproductive behaviors due to direct and indirect effects (for review, see Chmura et al., 2020). For example, a 2017 meta-analysis showed that, over the last 45 years, the length of the breeding season has changed differentially based on the birds' brooding habits, where single-brooded species have shortened their season by two days per decade and multibrooded species have prolonged their season by four days (Figure 40.1, Halupka and Halupka, 2017a). Indirectly, changing temperature patterns can affect the availability of food sources and therefore energy available for reproduction. Foraging behaviors and successes are decreased with increasing temperatures for various species (Conradie et al., 2019). Global climate change may further complicate reproductive cues, as the timing between temperature changes and photoperiod cues (a topic addressed in Section 40.3.2) will become mismatched (Walker et al., 2019).

40.3.2 Light

In most avian species studied to date, exposure to sufficiently long days (i.e., above a minimum, species-specific threshold) stimulates a cascade of physiological events, including synthesis and secretion of chicken gonadotropin-releasing hormone-I (cGnRH-I). This stimulation ultimately causes gonadal development and increases the secretion of gonadal steroids (Dawson, 1999; Dawson et al., 2001; Stevenson et al., 2013), which play a primary role in the control of reproductive behavior (see Section 40.6.4). It is notable that even species such as the opportunistic zebra finch, which has traditionally been considered to be nonphotoperiodic, respond to very long days by activating their reproductive system (Bentley et al., 2000b). Due to its effects on the hypothalamo−pituitary−gonadal (HPG) axis, photostimulation in many cases exert effects that are indirect and mediated by elevated circulating concentrations of gonadal hormones. Limited evidence, however, suggests in some conditions that photoperiod influences avian reproductive behavior independent of its effects of the HPG axis. For example, castrated, androgen-treated ring doves exposed to long photoperiods exhibit higher levels of nest-building activity than short-photoperiod-exposed birds (McDonald and Liley, 1978). The mechanism mediating this effect remains unclear and may be related to changes in body condition. Indeed, birds exposed to long days have more time to feed and gain energy daily than short-day-exposed birds, and they may consequently be able to devote more resources to energy-consuming activities such as those associated with breeding (Perfito et al., 2008). Stimulatory effects of artificial urban lights on the timing of the dawn chorus of songbirds, as well as on their laying dates and male pairing success (Kempenaers et al., 2010; Longcore, 2010), may likewise result from extension of the daily feeding time and access to more food resources. Exposure to artificial light at night, mimicking urban light pollution, advanced gonadal development in male European blackbirds (*Turdus merula*) (Dominoni et al., 2013), and great tits (*Parus major*) (Dominoni et al., 2018). In free-ranging birds, separating behavioral effects of photoperiod that are mediated by changes in energy intake from those that are secondary to elevated HPG hormone secretion has proved challenging, and additional work on this subject is clearly warranted.

40.3.3 Food resources

Resource availability has long been thought to exert a critical influence on the timing of reproduction, including the expression of reproductive behavior, with parents generally raising young when food is seasonally most abundant. This view is supported by correlative and manipulative studies. For example, crossbills (*Loxia* spp.) feed primarily on conifer seeds, the abundance of which varies greatly and often unpredictably in time and space (Benkman, 1992). In these birds, food availability (along with day length and social factors) plays a determining

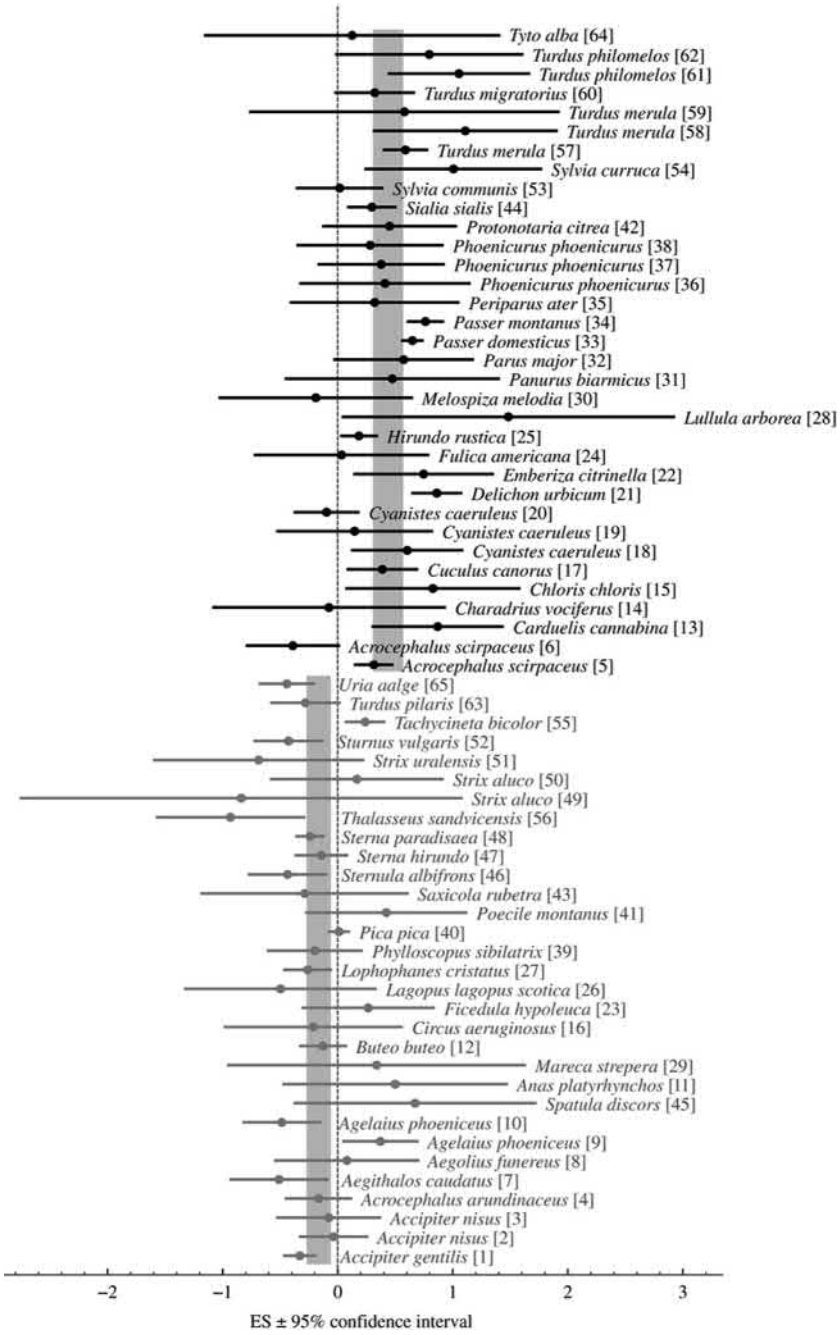

FIGURE 40.1 The rate of change of breeding season length for 65 studies of 34 multibrooded (black) and 31 single-brooded (gray) species. Numbers in brackets refer to population IDs in Haulpka and Halupka (2017a). *Reprinted from Haulpka and Halupka (2017b) with permission.*

role in the timing of reproduction (Benkman, 1990; Hahn, 1995; Deviche and Sharp, 2001). Another illustration is provided by research on blue tits (*Cyanistes caeruleus*). Blue tits preferentially feed their young noctuid lepidopteran caterpillars, but will also feed them less preferred tortricid lepidopteran caterpillars, which are smaller but easier to obtain and have a different phenology than noctuids. In this species, an adjustment of the timing of reproduction that is associated with an increased proportion of noctuids fed to young results in heavier nestlings (Garcia-Navas and Sanz, 2011).

Food resource manipulations—supplementation or restriction—are commonly used to investigate the role of these resources. With some exceptions (Harrison et al., 2010), food supplementation generally promotes the activity of the reproductive system as assessed by gonadal development, plasma levels of reproductive hormones, laying date, and expression of reproductive behavior

(Hahn, 1995; Brommer et al., 2004; Schoech et al., 2004; Watts and Hahn, 2012). It is noted that these effects are, however, susceptible to modulation by various factors, including photoperiod and social interactions (Hahn, 1995) and predation pressure (Zanette et al., 2003). In addition, the interpretation of the findings from food manipulation studies needs to consider that short-term reproductive effects of food supplementation may differ from long-term effects. For example, food supplementation to song sparrow (*Melospiza melodia*) parents has transgenerational behavioral effects, causing these parents to produce more offspring than control parents. However, this apparent advantage is mitigated by the fact that food-supplemented parents produce smaller eggs and nestlings than control birds and that their male offspring have a smaller song repertoire—and are thus presumably less fit—than the offspring of control parents (Zanette et al., 2009, Figure 40.2).

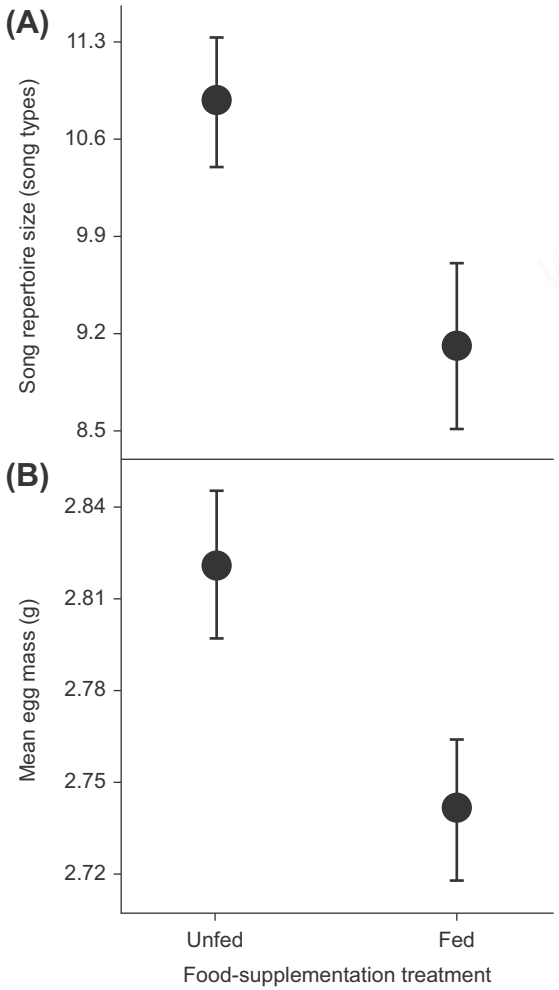

FIGURE 40.2 Food supplementation to song sparrow parents decreases (A) the song repertoire size of their sons ($P = .030$) and (B) the mean egg mass ($P = .017$). *Reprinted from Zanette et al. (2009) with permission.*

Food restriction generally results in effects in the opposite direction compared to those of food supplementation (Bauchinger et al., 2009). In the hen, this manipulation leads to lower plasma luteinizing hormone (LH) and gonadal steroids, as well as decreased mass of reproductive organs, and these changes are reversed in response to refeeding (Richard-Yris et al., 1987). Endocrine effects of food restriction in hens are reproductive stage specific, however, with plasma follicle-stimulating hormone being lower in food-restricted than *ad libitum*—fed birds prior to sexual maturity, but not in egg-laying birds (Bruggeman et al., 1998). Similar to the situation in females, food restriction in males leads to reproductive deficits such as reduced sperm quality and semen volume (Cerolini et al., 1995). In the male zebra finch, no testicular development occurs following transfer from short to long day length in food-restricted males, but this transfer stimulates testicular recrudescence in *ad libitum*—fed birds (Perfito et al., 2008). In this opportunistic breeder, food availability, therefore, apparently plays a more important role than day length in the control of HPG axis activity.

40.3.4 Case study: urbanization

The diversity of environmental factors to which birds can respond and of the effects of these factors (e.g., migration: Tryjanowski et al., 2013; reproduction: Partecke and Gwinner, 2007; Davies et al., 2013; community structure: Gagne and Fahrig, 2011; Schlesinger et al., 2008; parasite infection: Sitko and Zalesny, 2012) is well illustrated by research on the effects of urbanization. Urbanization is associated with massive and in most cases largely irreversible environmental changes, including an increase in ambient noise, temperature heat island effect: Zhang et al., 2010b, and nocturnal illumination, and differences in plant community composition and phenology (Mimet et al., 2009) that can in turn drive alterations in the food resources that are available to herbivores and carnivores. These changes, acting separately and/or cumulatively, and directly and/or indirectly, have the potential to profoundly affect the reproductive physiology and behavior of urban birds. The net consequences of urbanization on fitness remain, however, debated and poorly understood. On the one hand, urban birds frequently have an advanced reproductive phenology compared to corresponding nonurban birds (Davies et al., 2013; Davies et al., 2015; Dominoni et al., 2013), and this advancement has the potential to increase their reproductive output and fitness by increasing the duration of the annual breeding period. On the other hand, urban birds are exposed to physical factors that can be perceived as stressful and that adversely affect physiological and behavioral processes. One such factor is anthropogenic noise (noise pollution). Correlative evidence strongly suggests that noise pollution has a detrimental

influence on breeding success and individual fitness (eastern bluebird, *Sialia sialis*: Kight et al., 2012; house sparrow, *Passer domesticus*: Schroeder et al., 2012). This conclusion is supported by experimental studies. For example, greater sage grouse (*Centrocercus urophasianus*) that are experimentally exposed to chronic noise show elevated excretion of glucocorticoid metabolites, suggesting enhanced stress levels, and decreased lek attendance (Blickley et al., 2012). The reproductive effects of noise pollution are, however, often species specific and can be complex. Illustrating this, exposure to elevated ambient noise level does not substantially affect plasma corticosterone (CORT) or reproductive behavior in the Australian black swan (*Cygnus atratus*) (Payne et al., 2012). In addition, by disrupting predator–prey interactions, ambient noise can in some situations in fact *increase* breeding success (Francis et al., 2009). A few studies have examined the relationships in birds between urbanization and the acute stress response (increased plasma glucocorticoids in response to capture and restraint: Fokidis et al., 2009; Partecke et al., 2006). Urban European blackbirds (*Turdus merula*) show a lower response to acute stress than forest conspecifics (Partecke et al., 2006). For the most part, however, the physiological (including endocrine) bases of differences between urban and corresponding nonurban birds remain poorly understood, and this research topic is ripe for new correlative and manipulative investigations.

40.4 Social factors

Studies over many years, using a variety of experimental models and carried out in field and laboratory settings, consistently demonstrate that social interactions between conspecifics can influence all aspects of their reproductive behavior. Research on this subject also shows that an individual's own behavior can influence its physiology, including the production and secretion of behaviorally active hormones and neurochemicals, and this influence can in turn lead to behavioral modifications. The modulation of reproductive behavior by social factors is often complex, and with a few exceptions (e.g., the ring dove; see Section 40.4.1) the proximate underlying mechanisms—including the sensory modalities involved and the pathways that underlie sensory information processing—remain poorly understood. This topic provides rich opportunities for new and exciting research.

40.4.1 Effects of males on conspecific females

Intraspecific social interactions can profoundly affect the behavior and physiology of individuals of the opposite sex. In the female Japanese quail, plasma CORT increases as a result of mating (Rutkowska et al., 2011). This increase is not seen in females that interact with a male without opportunity for mating, but it is observed in females that interact socially with other females. Thus, direct social interactions rather than the act of mating per se apparently elevate plasma CORT in these birds. The role of social interactions is shown also by work on Gouldian finches (*Erythrura gouldiae*), in which females that are experimentally paired with a nonpreferred, poor-quality male have chronically higher plasma CORT than females paired with a preferred male (Griffith et al., 2011, Figure 40.3). Across species, lower stress levels in females that are paired with attractive mates may contribute to these females investing more in reproduction, as measured by egg size and food-provisioning behavior (Horvathova et al., 2012). In another type of investigation, exposure of females to conspecific song was found to induce behavioral and neural effects. For example, in several species, this exposure enhances female sexual responsiveness (song sparrow: Searcy and Marler, 1981; Pasteau et al., 2012; brown-headed cowbird, *Molothrus ater*: Freed-Brown and White, 2009) and activity level (European starling, *Sturnus vulgaris*: Riters and Teague, 2003). Exposing females to male songs also has physiological consequences that may influence fitness, as shown in canaries by the fact that females exposed to attractive male song repertoires deposit more testosterone (T) in their eggs than females exposed to unattractive male song repertoires (Gil et al., 2004).

The role of social interactions on the female reproductive system is further exemplified by work on captive willow tits (*Poecile montanus*), in which ovarian development is advanced in females paired with a male compared to females held in isolation (Silverin and Westin, 1995).

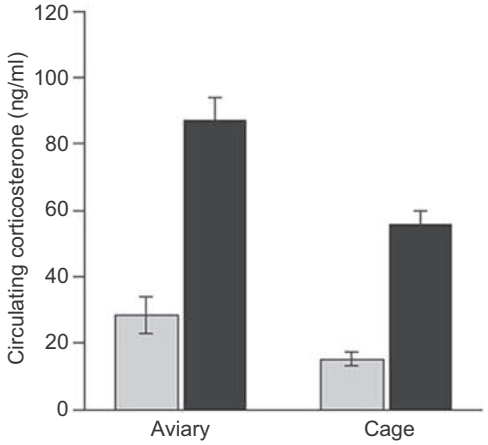

FIGURE 40.3 Baseline plasma corticosterone (CORT) during the egg-laying period in female Gouldian finches paired either with a genetically compatible (gray bars) or with a genetically incompatible (black bars) conspecific male. During breeding, birds were held either in a group aviary (aviary) or in cages containing one pair of birds (cage). Irrespective of the setting, females paired with an incompatible male have higher plasma CORT than females paired with a compatible male. *Reprinted from Griffith et al. (2011) with permission.*

This study did not isolate the factors that promote ovarian development, but other studies have addressed this question and demonstrate an important role for acoustic signals. For example, in song sparrows and domesticated canaries, exposure to conspecific song stimulates follicular development (Bentley et al., 2000a). The neuroendocrine mechanism mediating this stimulation is explored in the white-throated sparrow (*Zonotrichia albicollis*). In this species, male song rapidly (within 1 h) increases the secretion of LH and the expression of the immediate early gene, early growth response-1, in the mediobasal hypothalamus, but not in GnRH-producing neurons, suggesting behaviorally induced secretion of the peptide (Maney et al., 2007).

The most detailed investigations on the neural pathways that mediate reproductive effects of conspecific vocalizations in females have been conducted in the ring dove, a domesticated species that has long been used as an excellent model to unravel interactions between hormones and reproductive behavior (Lehrman, 1964; Lehrman and Friedman, 1969; McDonald and Liley, 1978; White, 1975). In the female ring dove, visual and auditory (but not physical) contact with a male stimulates the expression of courtship vocalizations (nest-coos) and ovarian development, and this effect is more pronounced after exposure to intact than castrated males (e.g., Lott et al., 1967). Females whose hypoglossal nerves (which innervate the vocal organ or syrinx) are sectioned show a reduction in their expression of nest-coos and, concurrently, in male courtship–induced ovarian development (Cohen and Cheng, 1979), leading to the remarkable hypothesis that a female's vocal behavior promotes her own ovarian development. The selectivity of this activation is demonstrated by the observation that plasma LH increases more in female doves that are exposed to female than male nest-coos (Cheng, 2008; Cheng et al., 1998). As neuronal track-tracing studies demonstrate, the self-stimulation of ovarian development involves the relay of auditory information to the midbrain nucleus intercollicularis (ICo). This brain region in turn communicates with the anterior hypothalamus, where some neurons themselves respond to auditory stimulation, through enkephalinergic projections (Cheng and Zuo, 1994). When stimulated, some hypothalamic neurons increase their secretion of GnRH, and this increase is in turn responsible for elevated gonadotropin secretion and ovarian development.

40.4.2 Effects of females on conspecific males

The above studies conclusively show effects of males on the reproductive system of conspecific females, but there is also strong experimental evidence that females can in some cases influence the reproductive system of conspecific males. In the domesticated Japanese quail, the reproductive maturation rate of photostimulated males that are held with females is faster than in isolated males; paired males also have higher plasma LH and T than isolated males (Delville et al., 1984). In experimental aviaries, the presence of a female increased singing and plasma T of male European starlings (*Sturnus vulgaris;* Pinxten et al., 2003). Parallel findings are reported in free-ranging birds: treatment of free-ranging female song sparrows with estradiol at the beginning of the breeding season increases their sexual behavior, and this increase correlates with elevated plasma T and territorial behavior in males residing in the same area (Wingfield and Monk, 1994). Similarly, estradiol administration to free-ranging female pied flycatchers (*Ficedula hypoleuca*) in breeding condition stimulates the aggressive behavior of their mates (Silverin, 1991). It must, however, be pointed out that the presence of females does not necessarily have stimulatory effects on the male reproductive system, and so great care must be exercised when trying to generalize findings across species. Illustrating this, in captive male willow tits exposed to long photoperiods, testicular maturation is *delayed* and birds regress their testes *earlier* when kept in the presence of a female than when in isolation (Silverin and Westin, 1995). It also needs to be stressed that experiments using estrogen-treated versus control females or comparing paired versus isolated males to study the role of social factors do not, by themselves, inform about the specific factors (e.g., visual and auditory) to which males respond behaviorally and physiologically. Even though most birds have a relatively poor sense of olfaction relative to many other vertebrates, olfaction may play a role to regulate the behavioral response of males to conspecific females. Supporting this conclusion, the courtship behavior of male chickens is apparently influenced by olfactory signals emanating from the female uropygial gland, a structure that has long been considered to be a potential source of pheromones (Zhang et al., 2010a; Hirao et al., 2009). Consistent with these findings, spotless starlings (*Sturnus unicolor*) can recognize the sex of conspecific individuals based on chemical olfactory cues that may be released by the uropygial gland (Amo et al., 2012). The crested auklet (*Aethis cristatella*) also exhibits an attraction to a feather-derived odor, which is heightened during the breeding season and is implicated in courtship displays (Hagelin et al., 2003). Interestingly, many species of vertebrate can detect differences in major histocompatibility complex (MHC) characteristics through olfactory means, allowing for mate selection to enhance genetic heterozygosity (Penn, 2002; Tregenza and Wedell, 2000). This MHC choice has been observed in several species of birds (Bonneaud et al., 2006; Juola and Dearborn, 2012; Strandh et al., 2012), and although the mechanism is unclear, there is evidence that odor can correlate with MHC make up in birds (Leclaire et al., 2012), highlighting a hypothesis for further study.

40.4.3 Effects of males on conspecific males

A great deal of research has investigated the effect of male behavior on the reproductive physiology and behavior of conspecific males, with particular attention given to the role of visual and auditory stimuli. Long-term (several weeks) studies find stimulating effects of hearing conspecific song on the HPG axis. For example, in the male rufous-winged sparrow (*Peucaea carpalis*), plasma LH is higher and testes develop faster in response to photostimulation for several weeks when birds are exposed daily to conspecific song than in control males not hearing this song (Small et al., 2008, Figure 40.4). Social stimulation can also induce short-term effects on the reproductive endocrine system. These effects are often assessed experimentally by presenting males with prerecorded conspecific vocalizations combined with a decoy bird (Balthazart et al., 2009; Wingfield, 1994b; Silverin et al., 2004). This situation, generally referred to as simulated territorial intrusion (STI), often provokes a strong aggressive response on the part of the challenged male (Wingfield, 1994a), and this response is in some cases associated with a rapid (within minutes) increase in plasma T (Wingfield and Hahn, 1994). T can exert rapid (within minutes to hours) physiological (Sachs and Leipheimer, 1988) and behavioral (Wright et al., 2009) effects, and it can enhance attention to novel conspecifics and other relevant stimuli (Archer, 1977). According to the Challenge Hypothesis (Wingfield et al., 1987; Wingfield and Goldsmith, 1990), elevated plasma T in response to social challenge may, therefore, function to enhance the persistence of a challenged individual's behavioral response even after the end of the challenge (Oyegbile and Marler, 2005; Wingfield, 1994b; Lynn et al., 2005). It should be pointed out that a social challenge of the above-described type often either fails to detectably increase (Addis et al., 2010; Deviche et al., 2012) or even decreases plasma androgens (Landys et al., 2007; for a review, see Goymann, 2009). This variability suggests a modulation of the response to STI by other factors. Indeed, it has been proposed that this response is contingent upon the mating system (Wingfield and Goldsmith, 1990; single vs. multiple broodedness: Landys et al., 2007), the contribution of males to incubation (Hirschenhauser et al., 2003), and the duration of the breeding season and the breeding state (Goymann, 2009).

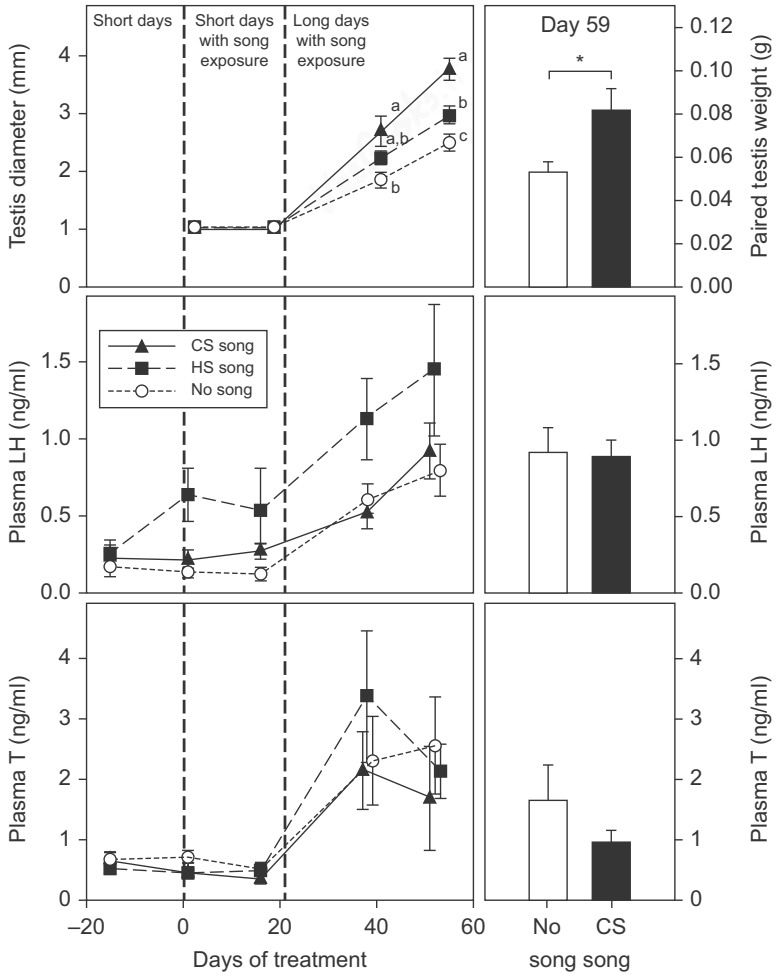

FIGURE 40.4 Left panels: Testis diameter (top left) and plasma luteinizing hormone (LH) and testosterone (T) in captive adult male rufous-winged sparrows exposed daily to conspecific song (CS Song), to heterospecific song (HS Song), or to no song (No Song). Birds were exposed to short days followed with exposure to a stimulating long photoperiod. On the same sampling day, different letters indicate significant differences between corresponding groups. Right panels: Testis mass and plasma LH and T measured at the time of euthanasia in the same birds as shown on the left panels. *Reprinted from Small et al. (2008) with permission.*

40.4.4 Effects of females on conspecific females

Though comparatively less studied than male–male interactions, female–female conspecific interactions occur in similar situations to that of males. Female birds express a variety of competitive traits that can provide a reproductive advantage including ornamentation, vocalization, and aggression. In an experimental model using the ring dove (*Streptopelia risoria*), devocalized females showed decreased follicular development, and, conversely, upon hearing other female coos, follicular growth increased (Cheng, 1986). Studies of this nature are limited, however, and most of the literature focus on female aggression. The advantages of aggressive or dominant behavior may include acquisition of breeding sites, maintenance of monogamy (Guo et al., 2020), and overall higher reproductive success. In the dark-eyed junco (*Junco hyemalis*), dominant females are more likely to breed and have a greater reproductive success (Jawor et al., 2006; Cain and Ketterson, 2012). The tree swallow (*Tachycineta bicolor*) requires a cavity for nesting, but does not make their own (Winkler et al., 2011); therefore females must compete for nesting sites. The more aggressive females out-compete those that are less aggressive (Rosvall, 2008), a behavior which may be partially mediated by T (Rosvall, 2013). The female–female aggressive behavior may come at a cost, however, as it can increase the risk of oxidative stress and injury (Silva et al., 2018), as well as place demands on time and energy at the expense of maternal care behaviors (Cain and Rosvall, 2014).

40.5 Age and experience

Ample evidence exists in birds that breeding performance is age-related (Forslund and Part, 1995). For example, the reproductive output of stitchbirds (*Notiomystis cincta*) increases during the first years of life and then declines as birds become senescent (Low et al., 2007). As discussed by Forslund and Part (1995), age-related differences in breeding performance may result from many nonexclusive factors that include age per se but also breeding experience, foraging success, and reproductive effort. Disentangling the respective contribution of these factors has been a major impetus of numerous studies. Research on free-ranging birds clearly indicates in some species that breeding experience gained during previous breeding attempts influences the reproductive output positively and independently of age. Using sophisticated statistical approaches, these studies show that breeding experience per se increases the probability of breeding and/or the reproductive output in birds belonging to various families (greater flamingo, *Phoenicopterus roseus*: Pradel et al., 2012; black-legged kittiwake, *Rissa tridactyla*: Desprez et al., 2011; snail kite, *Rostrhamus sociabilis*: Reichert et al., 2012). The interplay of age and experience is illustrated by research on free-ranging lance-tailed manakins (*Chiroxiphia lanceolata*; DuVal, 2012). In this species, males begin to breed when they reach high (alpha) social status and at an age that varies individually. The reproductive success of these males increases as a function of age and breeding experience. However, as birds get older, senescence negatively affects their breeding success, but this effect is compensated by the positive influence of social experience. Manipulative studies likewise support the idea of age-independent effects of breeding experience. For example, inexperienced male ring doves display less courtship behavior than age-matched experienced males (Cheng et al., 1986). This difference is specific to this behavior, as indicated by the observation that the two groups of males show similar levels of agonistic behavior. In another study, Cichon (2003) compared the reproductive output of inexperienced and experienced female collared flycatchers (*Ficedula albicollis*) (Figure 40.5). These two groups of birds had similar breeding success, but broods from experienced females were heavier and larger than those of inexperienced females, suggesting a positive effect of experience on fitness.

An insight into the mechanisms by which experience proximately influences reproductive behavior is provided by research on Japanese quail (Cornil and Ball, 2010). In this species, the probability of copulation is higher in sexually experienced than naïve males. However, visual (without physical) contact with a female (vs. a male or no bird) also enhances the occurrence of subsequent precopulatory behavior (latency to mate), indicating that male sexual performance is stimulated by sensory cues from females without actual sexual encounter taking place. Importantly, this study used castrated, T-treated birds, and behavioral effects of social experience were, therefore, not related to plasma T. Similarly, behavioral effects of social experience in the male ring dove (Cheng et al., 1986) do not result from differences in plasma T between naïve and experienced males. That the influence of a bird's social experience on its behavior can be modulated by sensory cues provided by another bird is demonstrated by other type of work (Michel, 1976). In the ring dove, birds with previous nest-building breeding experience are more likely to initiate incubation in response to progesterone treatment than inexperienced birds. However, the propensity of a bird to enter the nest area and stand on the nest also depends on the breeding experience of its mate.

40.6 Endocrine and neuroendocrine regulation of reproductive behavior

Based on the observation of changes in aggressive and mating behavior resulting from castration or castration

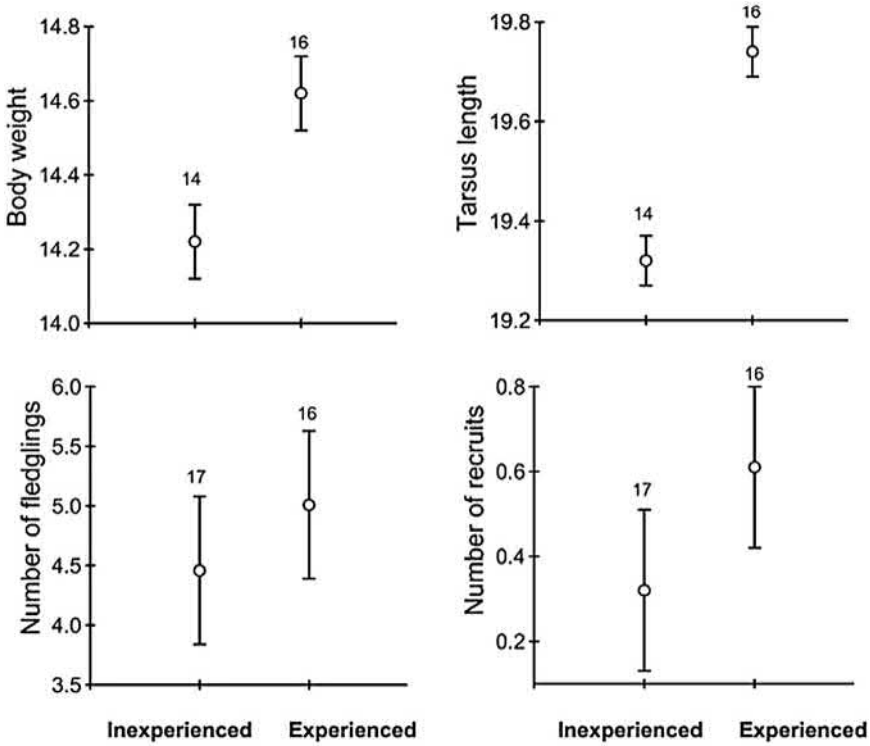

FIGURE 40.5 Breeding performance of two-year-old female collared flycatchers with (experienced) or without (inexperienced) previous breeding experience. Nestlings produced by inexperienced females were lighter (body mass on day 12 after hatching: $P = .006$) and smaller (tarsus length: $P < .001$) than those produced by experienced females, but there was no difference in the number of fledglings produced or subsequently recruited. Numbers above symbols refer to the number of nests studied. *Reprinted from Cichon (2003) with permission.*

followed with testis reinsertion into the abdominal cavity of roosters, Berthold was among the first to postulate that the reproductive behavior of birds is influenced by internally produced substances (Quiring, 1944). Since then, this behavior has been shown to be regulated by a great variety of hormones and neuropeptides. This section presents an overview of the influence of the best-studied endocrine and neuroendocrine factors on specific aspects of reproductive behavior. However, the reader should be aware that other factors that are not discussed here due to space limitations play an influential role as well. These factors include opioid peptides and corticotropin-releasing hormone, which can inhibit copulation solicitation in females (Maney and Wingfield, 1998) and sexual behavior (opioids: Kotegawa et al., 1997), and catecholamines (Barclay et al., 1992; Rauceo et al., 2008).

40.6.1 Gonadal steroids

Gonadal steroids (androgens, estrogens, and progestagens) have been the subject of most attention by far in terms of endocrine regulation of avian reproductive behavior. Their action mechanisms and behavioral effects are summarized in several reviews (Ball and Balthazart, 2010; Balthazart et al., 2010; Fusani, 2008), and the reader is referred to these publications for detailed information on this subject. Traditionally, steroid function is examined from the perspective of long-term changes to concentrations in the blood stream. Many studies on this topic are correlative and take advantage of the fact that most birds are photoperiodic (see Section 40.3.1). In these species, day length plays a critical role in the regulation of seasonal cycles, including gonadal development and the secretion of gonadal hormones, this secretion being dramatically higher during (compared to outside of) the breeding season. The seasonality of the reproductive system activity offers excellent opportunities to relate cyclic (neuro)endocrine changes (e.g., in plasma steroid concentrations) (Osorno et al., 2010; Landys et al., 2010) and the brain expression of steroid-metabolizing enzymes (Soma et al., 2003) or steroid receptors (Fraley et al., 2010), with the occurrence of reproductive behavior. Numerous studies on the behavioral role of gonadal steroids have also been manipulative. Commonly used approaches in these studies include gonadectomy (El Halawani et al., 1986; Hagelin, 2001), peripheral or central administration of hormones (Seredynski et al., 2013; Hunt and Wingfield, 2004; Komisaruk, 1967; also see Sections 40.6.4 and 40.6.6), and treatment with pharmacological agents. Some such agents serve as specific agonists or antagonists for steroid hormone receptors (Delville and Balthazart, 1987), whereas others affect the production or metabolism of steroid hormones (Belle et al., 2005; Schlinger and Callard, 1990). Investigations on the centrally mediated effects of gonadal steroids also take

advantage of the coupling of hormonal manipulations with localized brain lesions (Bailhache et al., 1993; Del Negro et al., 1998) or electrophysiological approaches (Meitzen et al., 2007).

Gonadal steroids influence aspects of reproductive behavior at all life stages, including during sexual differentiation (Adkins-Regan, 2009; Banerjee et al., 2012) and in adulthood, when they impact courtship (Fusani, 2008), singing (see Section 40.6.6), sexual receptivity, copulation, incubation, and parental behavior (O'Neal et al., 2008; Van Roo, 2004). Gonadal steroids also play important roles in the regulation of life history stages outside of the reproductive period, such as during preparation for migration (Tonra et al., 2011). They additionally influence metabolic processes and body condition (Deviche, 1992; Buchanan et al., 2001; Jaccoby et al., 1995) and immunity (Deviche and Cortez, 2005; Selvaraj and Pitchappan, 1985), although the pathways (direct vs. indirect and mediated, e.g., by glucocorticoids) involved in this influence remain poorly understood (Buttemer et al., 2008; Owen-Ashley et al., 2004). We discussed relationships between gonadal steroids and aspects of social behavior in Section 40.4. The remainder of this section further exemplifies the importance of gonadal steroids in the control of reproductive behavior, in particular, their relationships with the AVT system (see Section 40.6.4) and their critical influence on brain regions that are responsible for song production in oscine passerines (see Section 40.6.6).

40.6.2 Neurosteroids

It has become clear in the past few decades that the vertebrate (including avian) brain is capable of neurosteroidogenesis, either from de novo synthesis from cholesterol or from precursors from the periphery (Schlinger and Remage-Healey, 2012; Ubuka et al., 2009). Steroids produced in the brain can have highly localized paracrine functions, which allows for fine-tuning of its function, without effects on the general responses of physiology and behavior that are seen when steroids are in circulation (Cornil and de Bournonville, 2018; Wingfield, 2017; Wingfield et al., 2018). In bids, it has been shown that the brain expresses enzymes that are involved in the synthesis of steroids, including pregnenolone, progesterone, T, and estradiol, and this expression is region and developmental stage specific (London et al., 2006). The roles of these enzymes and their products in songbirds are well illustrated by research on brain aromatase, the enzyme that converts androgens to estrogens. Aromatase in the songbird brain is widely distributed and present, among others, in areas that are involved in the control of song production (e.g., the medial border of the HVC and robust nucleus of the arcopallium (RA); see Section 40.6.6) and auditory information processing (e.g., the caudal medial nidopallium (NCM); Schlinger and Balthazart, 2012). Physiological and behavioral studies reveal that rapid changes in the brain production of estrogen result in behavioral changes. For example, local pharmacological inhibition of estrogen production within the left NCM of male zebra finches rapidly disrupts their ability to preferentially respond behaviorally to their own song versus conspecific song (Remage-Healey et al., 2010, Figure 40.6). Reciprocally, a bird's own behavior, as well as relevant external stimuli, can rapidly modify the brain production of estrogen. Indeed, in the male zebra finch forebrain, the expression of aromatase rapidly increases in response to the act of singing (but not to hearing song; Remage-Healey et al., 2009), and the forebrain concentration of estradiol rapidly increases during social interactions with females (Remage-Healey et al., 2008). In the male white-crowned sparrow (*Zonotrichia leucophrys*), a social challenge (STI) rapidly decreases the local concentration of estrogen in several brain regions (Charlier et al., 2011). Rapid, steroid hormone—mediated, and centrally mediated changes in behavior suggest that these hormones act via nonclassic (i.e., nongenomic) mechanisms (discussed further in this section). This proposition is supported by the fact that steroids can bind to cell membrane receptors and induce rapid nongenomic cellular effects (Heimovics et al., 2012).

The Japanese quail has proved to be a particularly profitable experimental model in which to investigate the rapid behavioral effects of neurosteroids and in particularly neuroestrogens. As anatomical and functional studies demonstrate, the quail preoptic area (POA) plays a critical role in the regulation of male sexual behavior (Balthazart et al., 1992; for reviews, see Balthazart et al., 2006; Panzica et al., 1996). This brain region is sexually dimorphic (it is larger in males than females, which do not show masculine

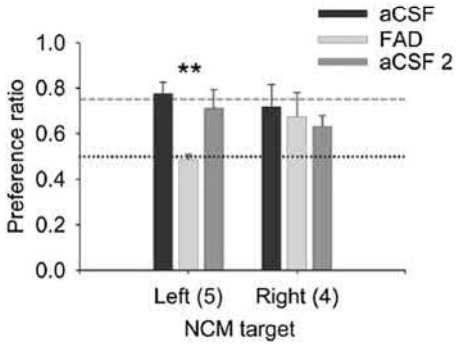

FIGURE 40.6 Influence of the aromatase inhibitor fadrozole (FAD) administered by in vivo retrodialysis into the auditory region caudal medial nidopallium (NCM) of the male zebra finch brain on behavioral preference for the bird's own song versus conspecific song. Control vehicle injections consisted of artificial cerebrospinal fluid. Song preference was abolished by FAD administration into the left but not right NCM. *Reprinted from Remage-Healey et al. (2010) with permission.*

sexual behavior) and is a target region for sex steroids: it contains androgen and estrogen receptors, and its volume decreases after castration and is restored following T treatment (Seredynski et al., 2011). The POA contains aromatase, and estrogen in the quail plays a critical role in the control of sexual behavior (Balthazart et al., 2009). Brain aromatase and, therefore, the local production of estrogens in the POA are regulated not only by slow-acting steroid-mediated genomic mechanisms that involve changes in transcription (Voigt et al., 2011) but also by nongenomic mechanisms that can rapidly (within minutes) enhance the local availability of estrogen (Balthazart et al., 2004). This stimulation can in turn stimulate a short-term increase in expression of some aspects of sexual behavior (Cornil et al., 2006a,b; Seredynski et al., 2011), particularly sexual motivation, but not copulatory behavior (Seredynski et al., 2013, 2015). Collectively, research on Japanese quail and the studies described here on songbirds firmly establish neurosteroids as important modulators of reproductive behavior (Schlinger and Remage-Healey, 2012).

40.6.3 Gonadotropin-releasing and gonadotropin-inhibitory hormones

GnRH in vertebrates plays an essential stimulatory role in the regulation of anterior pituitary gland gonadotropins. In mammals, GnRH also acts as a neurotransmitter and/or in a paracrine fashion to modulate sexual behavior, an effect that is presumably mediated by central GnRH receptors (Hsueh and Schaeffer, 1985). Limited evidence supports the view that GnRH has centrally mediated behavioral actions also in birds. Some of the original work on this subject was conducted in ring doves, in which synthetic GnRH administration stimulates courtship behavior, and this effect is apparently not mediated by LH or progesterone (Cheng, 1977). The brain of many vertebrates expresses at least two forms of GnRH: GnRH-I (cGnRH-I), which is released into the median eminence and stimulates the pituitary gland, and GnRH-II, which is normally not released into the median eminence but into extrahypothalamic brain regions. Central injection of GnRH-II to female white-crowned sparrows rapidly increases their expression of courtship behavior in response to hearing conspecific male song, and this effect is specific to GnRH-II, as it is not induced by cGnRH-I administration (Maney et al., 1997b). Thus, consistent with the situation in mammals (Hsueh and Schaeffer, 1985), GnRH in birds may act centrally to influence reproductive behavior. It should also be pointed out that, at least in some avian species, the brain contains a non-neuronal source of GnRH. This conclusion is drawn from studies on ring doves, in which the medial habenula contains immune (mast) cells that synthesize GnRH as well as other neurochemicals (Wilhelm, 2011). The activity of these cells is regulated by the endocrine (gonadal steroid) environment, and their number increases within hours in response to courtship (Zhuang et al., 1993), suggesting that their secretory products and in particular GnRH are involved in the control of reproductive behavior.

The discovery of GnIH, a neuropeptide with inhibitory effects on gonadotropin secretion and with fibers extending to a large number of brain areas (Tsutsui et al., 2000; Ukena et al., 2003), has prompted considerable research into its endocrine and behavioral functions. GnIH has been found in a multitude of avian species, including quail, chicken, sparrows, zebra finches, and starlings (for review, see Tsutsui et al., 2015). GnIH in birds is primarily localized in the paraventricular nucleus, with projections to the median eminence (Bentley et al., 2003). Centrally mediated roles for GnIH are suggested by the widespread brain distribution of immunostained GnIH fibers (Ubuka et al., 2008). In the female white-crowned sparrow, central treatment with GnIH inhibits courtship behavior (Bentley et al., 2006), thereby exerting effects that are opposite of those induced by GnRH-II treatment (Maney et al., 1997b; and discussed in this chapter). This behavioral inhibition may result from negative effects on GnRH function because midbrain regions where GnRH-II is produced contain GnIH fibers, and in the European starling, cGnRH-I- and GnRH-II–producing neurons express GnIH receptor mRNA (Bentley et al., 2008). Recent work using RNA interference of the GnIH gene in the Japanese quail provides further support for a centrally mediated behavioral role of this neuropeptide. Here, brain injection of small interfering RNA (siRNA) against GnIH precursor mRNA (GnIH siRNA) stimulated sexual behavior, and this stimulation was blocked by GnIH treatment (Ubuka et al., 2013). An emergent conclusion from studies on the behavioral role of GnIH is that it may function as an important inhibitory modulator of social interactions, including reproductive behavior (Calisi et al., 2011). In particular, GnIH administration increased the neurosynthesis of estrogen in male Japanese quail, and concurrently decreased aggressiveness, an effect which is likely mediated by GnIH effects on aromatase (Ubuka et al., 2014).

40.6.4 Arginine vasotocin

A peptide whose behavioral role in birds has received considerable attention is AVT, the avian homolog of vasopressin. Given peripherally to zebra finches, AVT decreases courtship behavior, and this decrease is attenuated by T administration (Harding and Rowe, 2003). Zebra finches are opportunistic breeders whose reproduction is induced by water availability. AVT plays a major role in the control of water balance (Sharma et al., 2009). Thus, it is postulated in these finches that drought conditions stimulate AVT secretion and the peptide in turn inhibits the reproductive system, including T secretion, thereby

preventing reproduction during periods of unfavorable environmental conditions. Contrasting with its suppressive action after peripheral administration, AVT exerts centrally mediated stimulatory behavioral effects, as shown by studies reporting that brain injection of the neuropeptide stimulates singing (Voorhuis et al., 1991a; de Kloet et al., 1993; Maney et al., 1997a). AVT is synthesized in several brain regions, including the paraventricular and supraoptic nuclei and the nucleus of the stria terminalis (Panzica et al., 1999b), and AVT-immunostained fibers extend to a large number of brain areas, some of which are involved in the control of vocal behavior (the RA and mesencephalic nucleus ICo: Kiss et al., 1987; Panzica et al., 1999b; Voorhuis and de Kloet, 1992). Binding sites for AVT in the avian brain are similarly widespread (Leung et al., 2009, 2011), and regions containing these sites are innervated by AVT fibers and terminals (Voorhuis et al., 1988b). Collectively, the neuroanatomical distribution of AVT and its receptors suggests that the peptide is involved in the control of multiple functions, including sexual behavior and GnRH secretion (Panzica et al., 2001).

As shown by a number of investigations, the central AVT system and the behavioral effects of the neuropeptide are steroid hormone sensitive. This conclusion is supported by work on canaries showing a sex difference in brain AVT immunostaining (Voorhuis et al., 1988a) and showing, in males of this species, that seasonal changes in AVT immunostaining parallel changes in plasma T (Voorhuis et al., 1991b). Manipulative studies, including gonadectomy and hormone replacement experiments, confirm an important, region-specific stimulatory role for gonadal steroids in the brain expression of AVT (Kimura et al., 1999; Plumari et al., 2004; Viglietti-Panzica et al., 1994) and AVT mRNA (Panzica et al., 1999a). In castrated male Japanese quail, the effects of T administration on the brain expression of AVT are mimicked by treatment with estradiol but not the nonaromatizable T metabolite 5α-dihydrotestosterone (5α-DHT) (Viglietti-Panzica et al., 2001). Effects of T on brain AVT in this species may, therefore, require aromatization of this steroid. Similarly, when given to female quail, estradiol but not 5α-DHT mimics the stimulatory influence of T on the brain expression of AVT mRNA (Aste et al., 2013, Figure 40.6).

It should be noted that while estradiol influences the central AVT system, there is also evidence that AVT may modulate the brain production of estrogen. Indeed, in the Japanese quail, aromatase-containing cells in brain regions that control reproductive behavior (e.g., the medial POA; see Section 40.6.2) apparently receive AVT innervation (Balthazart et al., 1997). Acute stress in quail rapidly (within minutes) upregulates their medial POA aromatase activity (Dickens et al., 2011), and there are indications that AVT contributes to mediating this effect (Dickens et al., 2013). AVT may accordingly be an important component of the neural system that controls rapid stress-induced changes in reproductive behavior, as AVT is involved in both the central and peripheral stress response (Kuenzel et al., 2020). New research is clearly warranted to confirm this hypothesis and elucidate the precise nature of this behavioral regulation.

40.6.5 Prolactin

The secretion of PRL in birds is under complex regulation by environmental and physical factors. The main environmental factor that controls PRL secretion in many species is day length, with long days stimulating this secretion (Dawson et al., 2001; Sharp et al., 1998). Plasma PRL in these species is accordingly elevated in spring and summer (i.e., during the breeding period) (Gahali et al., 2001; Sharp et al., 1998), and then declines. Elevated plasma PRL toward the end of the breeding period is believed to contribute to, but not be responsible for, the seasonal gonadal regression that signals the end of the reproductive season (Dawson et al., 2001). On a shorter term basis, the secretion of PRL is influenced by factors associated with incubation. For example, the introduction of an artificial egg into the nest of yellow-eyed penguins (*Megadyptes antipodes*), before birds normally start laying, stimulates PRL secretion in females (but has the opposite effect in males; Massaro et al., 2007). Inversely, plasma PRL rapidly decreases in captive female common eiders (*Somateria mollissima*) that are deprived of their eggs (Criscuolo et al., 2002). And in the chicken hen, a precocial species, physical contact with chicks stimulates brooding behavior and precipitates a decrease in plasma PRL, suggesting a role for the hormone in the transition from incubation to brooding (Richard-Yris et al., 1998). Consistent with this conclusion, plasma PRL in this species is high during incubation and then rapidly decreases after hatching (Kuwayama et al., 1992). In the altricial canary, however, plasma PRL remains elevated in females after hatching and decreases gradually during rearing of the young (Goldsmith et al., 1981). In over 25 species of birds, PRL shows some relationship with paternal care, with elevated levels associated with the transition from sexual to paternal activities such as incubation and male feeding behavior (Schradin and Anzenberger, 1999). However, this is not the case for all species. In male canaries, which do not incubate or feed young, plasma PRL increases only slightly during the parental phase of the reproductive cycle (Goldsmith et al., 1981). Regardless of the direction of the association, together these studies support the hypothesis that PRL is involved in the control of parental behavior. It should be noted in some species (Adélie penguin, *Pygoscelis adeliae*; and emperor penguin, *Aptenodytes forsteri*) that the increase in plasma PRL that occurs during reproduction is apparently controlled endogenously rather than by day

length or tactile stimulation (Lormee et al., 1999; Vleck et al., 2000). Sustained plasma PRL in the absence of tactile input in these species is thought to be necessary for breeding birds to maintain parental behavior despite the fact that they are absent from their nest for prolonged periods while foraging at sea.

The ring dove has proved to be a particularly informative model to study the involvement of PRL in the control of parental behavior. In contrast to the situation in many species, PRL secretion in doves does not change seasonally and is not photoperiod regulated, and these birds can breed year-round (Lea et al., 1986a). A role for nest-associated stimuli in the control of PRL secretion in this species is indicated by the observation that plasma PRL increases during incubation, but nest deprivation causes a rapid decline in hormone level (Lea et al., 1986b). Furthermore, injections of PRL enhance the persistence of incubation behavior (Janik and Buntin, 1985) and stimulate food provisioning to squabs (Buntin et al., 1991). Stimulatory effects on parental behavior (including feeding squabs) are also observed after intracerebroventricular administration of the hormone at doses that do not stimulate PRL-sensitive peripheral tissues such as the crop sac, indicating that these effects are mediated centrally (Buntin et al., 1991, Figure 40.8). Consistent with this proposition, the ring dove brain contains PRL-binding sites (Buntin and Ruzycki, 1987), and chemical lesion of the POA produces a deficit in parental behavior in response to PRL administration (Slawski and Buntin, 1995). Centrally acting PRL may be of peripheral (pituitary gland) origin. However, the dove brain contains PRL-immunopositive cells and fibers that project to several hypothalamic regions (Ramesh et al., 2000). Thus, in this species, centrally produced PRL binding to local receptors, perhaps in addition to PRL reaching the brain through systemic circulation, may activate parental behavior.

All living beings are, at times, faced with stress in the form of unpredictable stimuli, leading to the activation of the HPA axis and secretion of CORT. This elevation of CORT can, in turn, negatively influence reproductive and

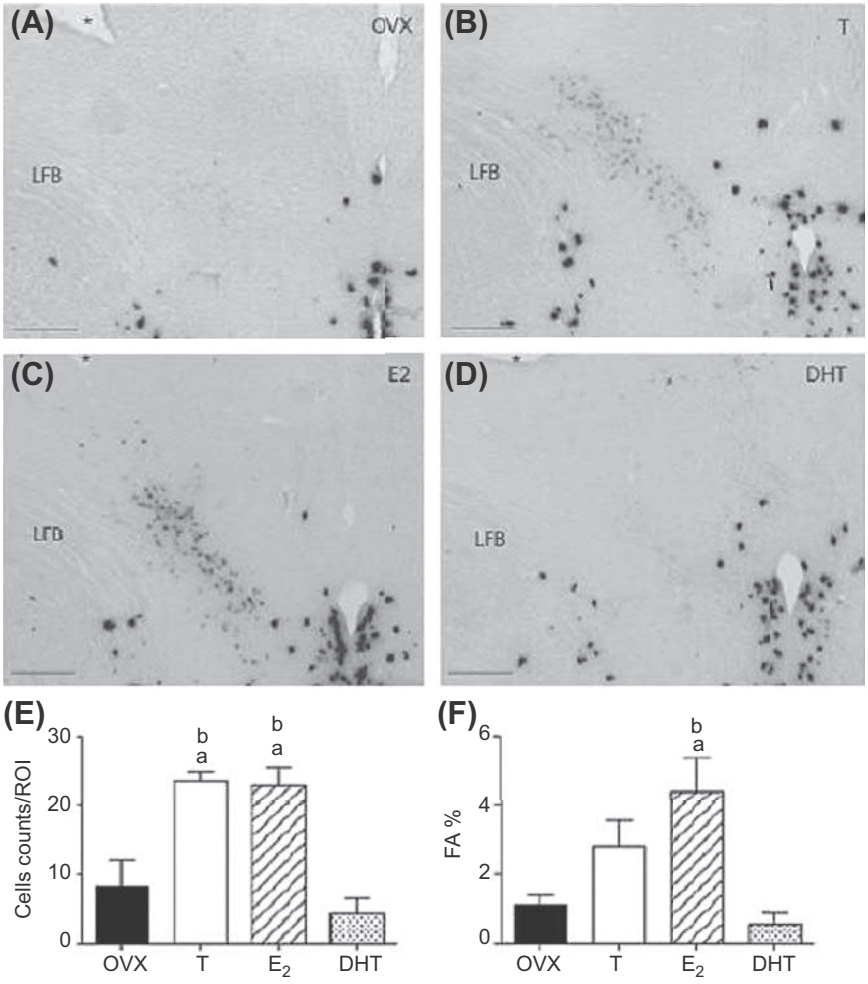

FIGURE 40.7 Regulation of arginine vasotocin (AVT) mRNA expression by gonadal steroids in the female Japanese quail brain. (A–D): Photomicrographs showing the distribution of AVT mRNA-expressing neurons in the caudomedial part of the bed nucleus of the stria terminalis after ovariectomy and one systemic injection of vehicle solution (OVX), testosterone (T), estradiol (E2), or 5α-dihydrotestosterone (5α-DHT). (E): Number of AVT mRNA-containing cells in the region of interest (ROI). This number is increased by T or E2, but not 5α-DHT, treatment. (F): Fractional area (FA) covered by mRNA hybridization signal in the same region. The FA is increased only after E2 administration. *Reprinted from Aste et al. (2013) with permission.*

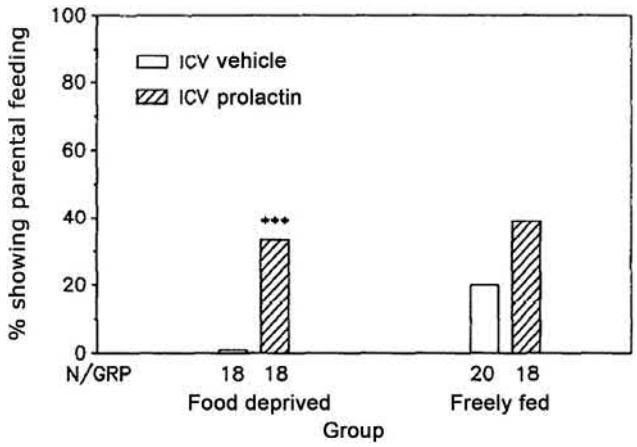

FIGURE 40.8 Stimulation of parental feeding behavior in nonbreeding ring doves by daily intracerebroventricular injection of prolactin or vehicle solution. Birds were either fed ad libitum or food deprived for 16 h before behavioral testing. N/GRP refers to the number of birds in each experimental group. *** Denotes a significant difference with the vehicle-treated group. *Reprinted from Buntin et al. (1991) with permission.*

parental behavior (Wingfield et al., 1998). Exposure to stressful conditions also often depresses plasma PRL (Angelier et al., 2013). These observations have led researchers to ask whether CORT and PRL normally exert opposite actions on parental behavior, and whether stress-related changes in plasma CORT and PRL are mechanistically related. These questions have been studied extensively in some seabirds. Correlative evidence is provided by work on black-legged kittiwakes (Chastel et al., 2005). In this species, acute stress decreases PRL more in failed breeders than in breeding birds, suggesting that maintaining sufficiently high-plasma PRL during stress may result in birds continuing to breed rather than abandoning their nest. Supporting this proposition, plasma PRL in Adélie penguins is low in birds that abandon their nest compared to birds that do not do so (Spee et al., 2010). However, pharmacological blockade of PRL secretion in this species does not cause nest desertion Thierry et al. (2013), suggesting the involvement of additional factors. One such factor may be CORT because male penguins that abandon their nest have high-plasma CORT (Spee et al., 2010), and CORT administration leads to nest desertion (Kleven et al., 2009). Thus, nest abandonment in this species may require high-plasma CORT combined with low-plasma PRL. In a more general sense, the above studies suggest in breeding birds that during periods of stress the parental decision to continue to breed can be at the expense of their own condition and survival, and this decision is critically influenced by baseline (prestress) and stress-induced plasma CORT and PRL (Angelier et al., 2009). The extent to which the PRL (decrease) and CORT (increase) stress responses are mechanistically related, however, remains largely conjectural (Angelier et al., 2013).

40.6.6 Case study: the oscine vocal control system

Acoustic signaling in some species is mediated by nonvocal signals such as those produced by wings (e.g., manakins: Schlinger et al., 2008) and tail feathers (e.g., some hummingbirds: Clark and Feo, 2008), but in many species, this signaling is mediated primarily by vocalizations. The neural circuit that controls the perception and expression of vocal behavior in passerines has been the object of enormous attention. This circuit provides an exquisite model in which to investigate how hormones regulate reproductive behavior, the central mechanisms that mediate this regulation, and the reciprocal interactions between behavior and the (neuro)endocrine system. The control of vocal perception and output has been particularly well studied in oscine passerines. Many oscines produce complex, learned vocalizations (songs), the learning and production of which are controlled by a network of discrete and interconnected brain regions called the vocal control system (Nottebohm et al., 1976, 1982, Figure 40.7). Many suboscine passerines also produce complex songs, but in contrast to oscines, vocalizations in these species are generally thought to be innate rather than learned (but see Saranathan et al., 2007), and suboscine song control regions are correspondingly absent or rudimentary (Liu et al., 2013). In oscines, song control regions are typically larger in males than females in species in which males do most of the singing (Tobari et al., 2005; Tramontin et al., 1998), and this morphological difference is associated with cytoarchitectural (Del Negro and Edeline, 2002; Nealen, 2005), biochemical (Charlier et al., 2003; Riters and Ball, 2002; Sakaguchi et al., 2000), and physiological (Adret and Margoliash, 2002; Del Negro and Edeline, 2001) differences between sexes. The exact role of song control regions in females that do not normally sing remains incompletely understood. Some of these regions serve an auditory as well as motor function (Figure 40.9), and in females they may, therefore, regulate vocal behavior perception rather than output (Hamilton et al., 1997).

A remarkable feature of the adult oscine vocal control system is its neuroplasticity. In seasonal breeders, the size of song control regions such as the HVC and RA changes seasonally. These regions are larger during the breeding season, when birds are exposed to long photoperiods, gonads are developed and release large amounts of steroid hormones, and birds sing at a high frequency, than outside this season (Meitzen and Thompson, 2008; Nottebohm, 1981; Smith et al., 1997). The basis of these changes has been researched in particular detail for the HVC, a telencephalic region that plays a major role in song production. Seasonal changes in HVC volume are associated with cytoarchitectural changes, including neuron number, density, and life span (Bowers et al., 2011; Meitzen and Thompson, 2008; Nottebohm et al., 1994). Some vocal

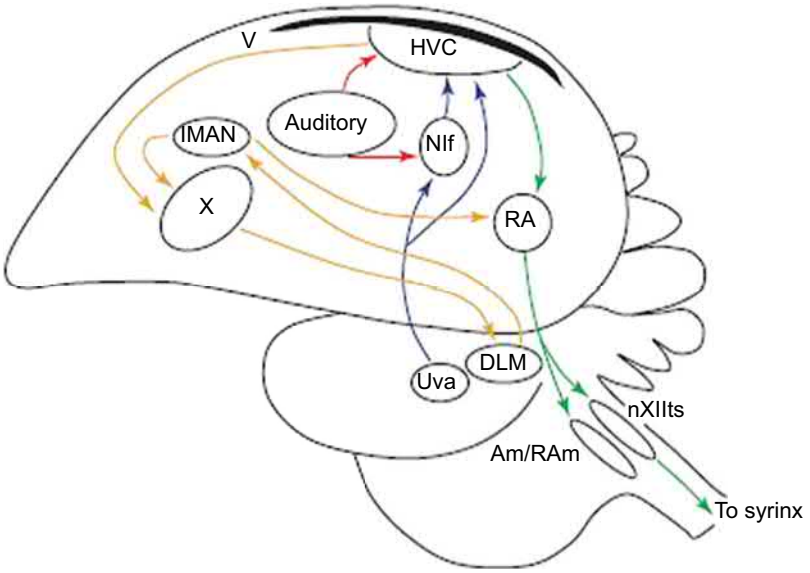

FIGURE 40.9 Projections of the major regions of the oscine brain vocal control system. The system consists of a motor pathway (green) that controls vocal output and includes projections from the HVC (correct full name; not an abbreviation) to the robust nucleus of the arcopallium (RA). A second pathway (orange) is essential for song learning and perception, and includes the medial portion of dorsolateral thalamus, the lateral magnocellular nucleus of the anterior neostriatum, area X, HVC, and RA. *Reprinted from Brenowitz and Beecher (2005) with permission.*

control regions including the HVC contain sex steroid receptors (Fraley et al., 2010; Gahr et al., 1987, 1993; Nordeen et al., 1987) whose density is regulated seasonally (Fusani et al., 2000; Soma et al., 1999), suggesting locally mediated roles for these hormones. Consistent with this view, considerable evidence indicates that gonadal steroids play many-faceted roles in the control of the vocal control system's plasticity in adulthood (Bottjer et al., 1986; Ball et al., 2003). These roles include regulation of the size of song control regions (Thompson et al., 2007; Tramontin et al., 2003), newborn neuron migration into the HVC, and the density and survival of existing neurons (Hall and MacDougall-Shackleton, 2012). Considerable attention has been devoted to the cellular and molecular mechanisms of action of steroids in song control regions (Thompson et al., 2012), and these studies have identified an important role for brain-derived neurotrophic factor (BDNF). In concert with T, BDNF is thought to promote the proliferation and survival of HVC neurons (Brenowitz, 2013; Alvarez-Borda et al., 2004; Rasika et al., 1999) and also to contribute to seasonal plasticity in the RA (Wissman and Brenowitz, 2009; Li et al., 2000). Furthermore, in the vocal control system, the expression of numerous genes that are involved with diverse functions such as neurogenesis, apoptosis, and axonal growth changes seasonally (Thompson et al., 2012). A major challenge in the future is to identify the role of these genes' products and to determine whether and how steroids regulate the activity of these genes. Adding to this complexity, factors such as photoperiod (Dloniak and Deviche, 2001; Gulledge and Deviche, 1998) and social factors (Boseret et al., 2006) influence the size and cytoarchitectural characteristics of song control regions, and this influence is in some situations independent of gonadal steroids. Finally, while this chapter's discussion makes it clear that song control regions play an important role in the expression of vocal behavior, some of these regions are also influenced by sensory (acoustic) stimulation. For example, T administration to female canaries increases their HVC volume, but this increase is attenuated after deafening (i.e., in the absence of auditory stimulation) (Bottjer et al., 1986). The mechanism mediating this difference is not fully understood, and it may involve a role for the auditory stimulus-regulated production of neurosteroids (see Section 40.6.2), in particular estradiol (Hall and MacDougall-Shackleton, 2012; Remage-Healey et al., 2012; Soma et al., 2004).

References

Addis, E.A., Busch, D.S., Clark, A.D., Wingfield, J.C., 2010. Seasonal and social modulation of testosterone in Costa Rican rufous-collared sparrows (*Zonotrichia capensis costaricensis*). Gen. Comp. Endocrinol. 166, 581–589.

Adkins-Regan, E., 2009. Hormones and sexual differentiation of avian social behavior. Dev. Neurosci. 31, 342–350.

Adret, P., Margoliash, D., 2002. Metabolic and neural activity in the song system nucleus robustus archistriatalis: effect of age and gender. J. Comp. Neurol. 454, 409–423.

Alvarez-Borda, B., Haripal, B., Nottebohm, F., 2004. Timing of brain-derived neurotrophic factor exposure affects life expectancy of new neurons. Proc. Natl. Acad. Sci. U. S. A. 101, 3957–3961.

Amo, L., Aviles, J.M., Parejo, D., Pena, A., Rodriguez, J., Tomas, G., 2012. Sex recognition by odour and variation in the uropygial gland secretion in starlings. J. Anim. Ecol. 81, 605–613.

Angelier, F., Moe, B., Blanc, S., Chastel, O., 2009. What factors drive prolactin and corticosterone responses to stress in a long-lived bird species (snow petrel *Pagodroma nivea*)? Physiol. Biochem. Zool. 82, 590–602.

Angelier, F., Wingfield, J.C., Trouve, C., de Grissac, G.S., Chastel, O., 2013. Modulation of the prolactin and the corticosterone stress responses: do they tell the same story in a long-lived bird, the cape petrel? Gen. Comp. Endocrinol. 182, 7–15.

Archer, J., 1977. Testosterone and persistence in mice. Anim. Behav. 25, 479–488.

Ardia, D.R., Perez, J.H., Chad, E.K., Voss, M.A., Clotfelter, E.D., 2009. Temperature and life history: experimental heating leads female tree swallows to modulate egg temperature and incubation behaviour. J. Anim. Ecol. 78, 4–13.

Aste, N., Sakamoto, E., Kagami, M., Saito, N., 2013. Vasotocin mRNA expression is sensitive to testosterone and oestradiol in the bed nucleus of the stria terminalis in female Japanese quail. J. Neuroendocrinol. 25, 811–825.

Astheimer, L.B., Buttemer, W.A., Wingfield, J.C., 1995. Seasonal and acute changes in adrenocortical responsiveness in an arctic-breeding bird. Horm. Behav. 29, 442–457.

Bailhache, T., Surlemont, C., Balthazart, J., 1993. Effects of neurochemical lesions of the preoptic area on male sexual behavior in the Japanese quail. Brain Res. Bull. 32, 273–283.

Ball, G.F., Balthazart, J., 2004. Hormonal regulation of brain circuits mediating male sexual behavior in birds. Physiol. Behav. 83, 329–346.

Ball, G.F., Balthazart, J., 2010. Japanese quail as a model system for studying the neuroendocrine control of reproductive and social behaviors. ILAR J. 51, 310–325.

Ball, G.F., Castelino, C.B., Maney, D.L., Appeltants, D., Balthazart, J., 2003. The activation of birdsong by testosterone: multiple sites of action and role of ascending catecholamine projections. Ann. N. Y. Acad. Sci. 1007, 211–231.

Balthazart, J., Surlemont, C., Harada, N., 1992. Aromatase as a cellular marker of testosterone action in the preoptic area. Physiol. Behav. 51, 395–409.

Balthazart, J., Absil, P., Viglietti-Panzica, C., Panzica, G.C., 1997. Vasotocinergic innervation of areas containing aromatase-immunoreactive cells in the quail forebrain. J. Neurobiol. 33, 45–60.

Balthazart, J., Baillien, M., Charlier, T.D., Cornil, C.A., Ball, G.F., 2003. The neuroendocrinology of reproductive behavior in Japanese quail. Domest. Anim. Endocrinol. 25, 69–82.

Balthazart, J., Baillien, M., Cornil, C.A., Ball, G.F., 2004. Preoptic aromatase modulates male sexual behavior: slow and fast mechanisms of action. Physiol. Behav. 83, 247–270.

Balthazart, J., Cornil, C.A., Taziaux, M., Charlier, T.D., Baillien, M., Ball, G.F., 2006. Rapid changes in production and behavioral action of estrogens. Neuroscience 138, 783–791.

Balthazart, J., Cornil, C.A., Charlier, T.D., Taziaux, M., Ball, G.F., 2009. Estradiol, a key endocrine signal in the sexual differentiation and activation of reproductive behavior in quail. J. Exp. Zool. A Ecol. Genet. Physiol. 311, 323–345.

Balthazart, J., Charlier, T.D., Barker, J.M., Yamamura, T., Ball, G.F., 2010. Sex steroid-induced neuroplasticity and behavioral activation in birds. Eur. J. Neurosci. 32, 2116–2132.

Banerjee, S.B., Arterbery, A.S., Fergus, D.J., Adkins-Regan, E., 2012. Deprivation of maternal care has long-lasting consequences for the hypothalamic-pituitary-adrenal axis of zebra finches. Proc. Biol. Sci. 279, 759–766.

Barclay, S.R., Harding, C.F., Waterman, S.A., 1992. Correlations between catecholamine levels and sexual behavior in male zebra finches. Pharmacol. Biochem. Behav. 41, 195–201.

Bauchinger, U., Van't Hof, T., Biebach, H., 2009. Food availability during migratory stopover affects testis growth and reproductive behaviour in a migratory passerine. Horm. Behav. 55, 425–433.

Beale, C.M., Burfield, I.J., Sim, I.M., Rebecca, G.W., Pearce-Higgins, J.W., Grant, M.C., 2006. Climate change may account for the decline in British ring ouzels *Turdus torquatus*. J. Anim. Ecol. 75, 826–835.

Belle, M.D., Sharp, P.J., Lea, R.W., 2005. Aromatase inhibition abolishes courtship behaviours in the ring dove (*Streptopelia risoria*) and reduces androgen and progesterone receptors in the hypothalamus and anterior pituitary gland. Mol. Cell. Biochem. 276, 193–204.

Benkman, C.W., 1990. Intake rates and the timing of crossbill reproduction. Auk 107, 376–386.

Benkman, C.W., 1992. White-winged crossbill. No. 27. In: Poole, A., Gill, F. (Eds.), The Birds of North America. Academy of Natural Sciences, Philadelphia.

Bentley, G.E., Wingfield, J.C., Morton, M.L., Ball, G.F., 2000a. Stimulatory effects on the reproductive axis in female songbirds by conspecific and heterospecific male song. Horm. Behav. 37, 179–189.

Bentley, G.E., Spar, B.D., Macdougall-Shackleton, S.A., Hahn, T.P., Ball, G.F., 2000b. Photoperiodic regulation of the reproductive axis in male zebra finches, *Taeniopygia guttata*. Gen. Comp. Endocrinol. 117, 449–455.

Bentley, G.E., Perfito, N., Ukena, K., Tsutsui, K., Wingfield, J.C., 2003. Gonadotropin-inhibitory peptide in song sparrows (*Melospiza melodia*) in different reproductive conditions, and in house sparrows (*Passer domesticus*) relative to chicken-gonadotropin-releasing hormone. J. Neuroendocrinol. 15, 794–802.

Bentley, G.E., Jensen, J.P., Kaur, G.J., Wacker, D.W., Tsutsui, K., Wingfield, J.C., 2006. Rapid inhibition of female sexual behavior by gonadotropin-inhibitory hormone (GnIH). Horm. Behav. 49, 550–555.

Bentley, G.E., Ubuka, T., McGuire, N.L., Chowdhury, V.S., Morita, Y., Yano, T., Hasunuma, I., Binns, M., Wingfield, J.C., Tsutsui, K., 2008. Gonadotropin-inhibitory hormone and its receptor in the avian reproductive system. Gen. Comp. Endocrinol. 156, 34–43.

Blickley, J.L., Word, K.R., Krakauer, A.H., Phillips, J.L., Sells, S.N., Taff, C.C., Wingfield, J.C., Patricelli, G.L., 2012. Experimental chronic noise is related to elevated fecal corticosteroid metabolites in lekking male greater sage grouse (*Centrocercus urophasianus*). PloS One 7, e50462.

Bolger, D.T., Patten, M.A., Bostock, D.C., 2005. Avian reproductive failure in response to an extreme climatic event. Oecologia 142, 398–406.

Bonneaud, C., Chastel, O., Federici, P., Westerdahl, H., Sorci, G., 2006. Complex Mhc-based mate choice in a wild passerine. Proc.R. Soc. B. 273, 1111–1116.

Boseret, G., Carere, C., Ball, G.F., Balthazart, J., 2006. Social context affects testosterone-induced singing and the volume of song control nuclei in male canaries (*Serinus canaria*). J. Neurobiol. 66, 1044–1060.

Bottjer, S.W., Schoonmaker, J.N., Arnold, A.P., 1986. Auditory and hormonal stimulation interact to produce neural growth in adult canaries. J. Neurobiol. 17, 605–612.

Bowers, E.K., Sakaluk, S.K., Thompson, C.F., 2011. Adaptive sex allocation in relation to hatching synchrony and offspring quality in house wrens. Am. Nat. 177, 617–629.

Brenowitz, E.A., 2013. Testosterone and brain-derived neurotrophic factor interactions in the avian song control system. Neuroscience 239, 115–123.

Brenowitz, E.A., Beecher, M.D., 2005. Song learning in birds: diversity and plasticity, opportunities and challenges. Trends Neurosci. 28, 127–132.

Brommer, J.E., Karell, P., Pietiainen, H., 2004. Supplementary fed Ural owls increase their reproductive output with a one year time lag. Oecologia 139, 354–358.

Bruggeman, V., Onagbesan, O., Vanmontfort, D., Berghman, L., Verhoeven, G., Decuypere, E., 1998. Effect of long-term food restriction on pituitary sensitivity to cLHRH-I in broiler breeder females. J. Reprod. Fertil. 114, 267–276.

Buchanan, K.L., Evans, M.R., Goldsmith, A.R., Bryant, D.M., Rowe, L.V., 2001. Testosterone influences basal metabolic rate in male house sparrows: a new cost of dominance signalling? Proc. Biol. Sci. 268, 1337–1344.

Buntin, J.D., Ruzycki, E., 1987. Characteristics of prolactin binding sites in the brain of the ring dove (*Streptopelia risoria*). Gen. Comp. Endocrinol. 65, 243–253.

Buntin, J.D., Becker, G.M., Ruzycki, E., 1991. Facilitation of parental behavior in ring doves by systemic or intracranial injections of prolactin. Horm. Behav. 25, 424–444.

Buttemer, W.A., Warne, S., Bech, C., Astheimer, L.B., 2008. Testosterone effects on avian basal metabolic rate and aerobic performance: facts and artefacts. Comp. Biochem. Physiol. Mol. Integr. Physiol. 150, 204–210.

Cain, K.E., Ketterson, E.D., 2012. Competitive females are successful females; phenotype, mechanism, and selection in a common songbird. Behav. Ecol. Sociobiol. 66, 241–252.

Cain, K.E., Rosvall, K.A., 2014. Next steps for understanding the selective relevance of female-female competition. Front. Ecol. Evol. 2, 32.

Calisi, R.M., Diaz-Munoz, S.L., Wingfield, J.C., Bentley, G.E., 2011. Social and breeding status are associated with the expression of GnIH. Gene Brain Behav. 10, 557–564.

Cerolini, S., Mantovani, C., Bellagamba, F., Mangiagalli, M.G., Cavalchini, L.G., Reniero, R., 1995. Effect of restricted and *ad libitum* feeding on semen production and fertility in broiler breeder males. Br. Poultry Sci. 36, 677–682.

Charlier, T.D., Balthazart, J., Ball, G.F., 2003. Sex differences in the distribution of the steroid receptor coactivator SRC-1 in the song control nuclei of male and female canaries. Brain Res. 959, 263–274.

Charlier, T.D., Newman, A.E., Heimovics, S.A., Po, K.W., Saldanha, C.J., Soma, K.K., 2011. Rapid effects of aggressive interactions on aromatase activity and oestradiol in discrete brain regions of wild male white-crowned sparrows. J. Neuroendocrinol. 23, 742–753.

Chastel, O., Lacroix, A., Weimerskirch, H., Gabrielsen, G.W., 2005. Modulation of prolactin but not corticosterone responses to stress in relation to parental effort in a long-lived bird. Horm. Behav. 47, 459–466.

Cheng, M.F., 1977. Role of gonadotrophin releasing hormones in the reproductive behaviour of female ring doves (*Streptopelia risoria*). J. Endocrinol. 74, 37–45.

Cheng, M.F., 1986. Female cooing promotes ovarian development in ring doves. Physiol. Behav. 37, 371–374.

Cheng, M.F., 2008. The role of vocal self-stimulation in female responses to males: implications for state-reading. Horm. Behav. 53, 1–10.

Cheng, M.F., Zuo, M., 1994. Proposed pathways for vocal self-stimulation: met-enkephalinergic projections linking the midbrain vocal nucleus, auditory-responsive thalamic regions and neurosecretory hypothalamus. J. Neurobiol. 25, 361–379.

Cheng, M.F., Klint, T., Johnson, A.L., 1986. Breeding experience modulating androgen dependent courtship behavior in male ring doves (*Streptopelia risoria*). Physiol. Behav. 36, 625–630.

Cheng, M.F., Peng, J.P., Johnson, P., 1998. Hypothalamic neurons preferentially respond to female nest coo stimulation: demonstration of direct acoustic stimulation of luteinizing hormone release. J. Neurosci. 18, 5477–5489.

Chmura, H.E., Wingfield, J.C., Hahn, T.P., 2020. Non-photic environmental cues and avian reproduction in an era of global change. J. Avian Biol. 51 (3).

Cichon, M., 2003. Does prior breeding experience improve reproductive success in collared flycatcher females? Oecologia 134, 78–81.

Clark, C.J., Feo, T.J., 2008. The Anna's hummingbird chirps with its tail: a new mechanism of sonation in birds. Proc. Biol. Sci. 275, 955–962.

Cohen, J., Cheng, M.F., 1979. Role of vocalizations in the reproductive cycle of ring doves (*Streptopelia risoria*): effects of hypoglossal nerve section on the reproductive behavior and physiology of the female. Horm. Behav. 13, 113–127.

Conradie, S.R., Woodborne, S.M., Cunningham, S.J., McKechnie, A.E., 2019. Chronic, sublethal effects of high temperatures will cause severe declines in southern African arid-zone birds during the 21st century. Proc. Natl. Acad. Sci. U. S. A. 116, 14065–14070.

Cornil, C.A., Ball, G.F., 2010. Effects of social experience on subsequent sexual performance in naive male Japanese quail (*Coturnix japonica*). Horm. Behav. 57, 515–522.

Cornil, C.A., Dalla, C., Papadopoulou-Daifoti, Z., Baillien, M., Balthazart, J., 2006a. Estradiol rapidly activates male sexual behavior and affects brain monoamine levels in the quail brain. Behav. Brain Res. 166, 110–123.

Cornil, C.A., Taziaux, M., Baillien, M., Ball, G.F., Balthazart, J., 2006b. Rapid effects of aromatase inhibition on male reproductive behaviors in Japanese quail. Horm. Behav. 49, 45–67.

Coumou, D., Robinson, A., 2013. Historic and future increase in the global land area affected by monthly heat extremes. Environ. Res. Lett. 8, 034018.

Cornil, C.A., de Bournonville, C., 2018. Dual action of neuro-estrogens in the regulation of male sexual behavior. Gen. Comp. Endocrinol. 256, 57–62.

Criscuolo, F., Chastel, O., Gabrielsen, G.W., Lacroix, A., Le, M.Y., 2002. Factors affecting plasma concentrations of prolactin in the common eider *Somateria mollissima*. Gen. Comp. Endocrinol. 125, 399–409.

Cynx, J., 2001. Effects of humidity on reproductive behavior in male and female zebra finches (*Taeniopygia guttata*). J. Comp. Psychol. 115, 196–200.

Davies, S., Rodriguez, N.S., Sweazea, K.L., Deviche, P., 2013. The effect of acute stress and long-term corticosteroid administration on plasma metabolites in an urban and desert songbird. Physiol. Biochem. Zool. 86, 47–60.

Davies, S., Behbahaninia, H., Giraudeau, M., Meddle, S.L., Waites, K., Deviche, P., 2015. Advanced seasonal reproductive development in a male urban bird is reflected in earlier plasma luteinizing hormone rise but not energetic status. Gen. Comp. Endocrinol. 222, 1–10.

Dawson, A., 1999. Photoperiodic control of gonadotropin-releasing hormone secretion in seasonally breeding birds. In: Rao, P., Kluwer, P. (Eds.), Neural Regulation in the Vertebrate Endocrine System. Academic/Plenum Pub, New York, pp. 141–159.

Dawson, A., King, V.M., Bentley, G.E., Ball, G.F., 2001. Photoperiodic control of seasonality in birds. J. Biol. Rhythm. 16, 365–380.

Dawson, W.R., 1982. Evaporative losses of water by birds. Comp. Biochem. Physiol. A 71, 495–509.

de Kloet, E.R., Elands, J., Voorhuis, D.A., 1993. Implication of central neurohypophyseal hormone receptor-mediated action in timing of reproductive events: evidence from novel observations on the effect of a vasotocin analogue on singing behaviour of the canary. Regul. Pept. 45, 85–89.

Del Negro, N.C., Edeline, J.M., 2001. Differences in auditory and physiological properties of HVc neurons between reproductively active male and female canaries (*Serinus canaria*). Eur. J. Neurosci. 14, 1377–1389.

Del Negro, N.C., Edeline, J.M., 2002. Sex and season influence the proportion of thin spike cells in the canary HVc. Neuroreport 13, 2005–2009.

Del Negro, C., Gahr, M., Leboucher, G., Kreutzer, M., 1998. The selectivity of sexual responses to song displays: effects of partial chemical lesion of the HVC in female canaries. Behav. Brain Res. 96, 151–159.

Delville, Y., Balthazart, J., 1987. Hormonal control of female sexual behavior in the Japanese quail. Horm. Behav. 21, 288–309.

Delville, Y., Sulon, J., Hendrick, J.C., Balthazart, J., 1984. Effect of the presence of females on the pituitary-testicular activity in male Japanese quail (*Coturnix coturnix japonica*). Gen. Comp. Endocrinol. 55, 295–305.

Desprez, M., Pradel, R., Cam, E., Monnat, J.Y., Gimenez, O., 2011. Now you see him, now you don't: experience, not age, is related to reproduction in kittiwakes. Proc. Biol. Sci. 278, 3060–3066.

Deviche, P., 1992. Testosterone and opioids interact to regulate feeding in a male migratory songbird. Horm. Behav. 26, 394–405.

Deviche, P., Sharp, P.J., 2001. Reproductive endocrinology of a free-living, opportunistically breeding passerine (white-winged crossbill, *Loxia leucoptera*). Gen. Comp. Endocrinol. 123, 268–279.

Deviche, P., Cortez, L., 2005. Androgen control of immunocompetence in the male house finch, *Carpodacus mexicanus* Muller. J. Exp. Biol. 208, 1287–1295.

Deviche, P., Sharp, P.J., Dawson, A., Sabo, J., Fokidis, B., Davies, S., Hurley, L., 2012. Up to the challenge? Hormonal and behavioral responses of free-ranging male Cassin's sparrows, *Peucaea cassinii*, to conspecific song playback. Horm. Behav. 61, 741–749.

Dickens, M.J., Cornil, C.A., Balthazart, J., 2011. Acute stress differentially affects aromatase activity in specific brain nuclei of adult male and female quail. Endocrinology 152, 4242–4251.

Dickens, M.J., Cornil, C.A., Balthazart, J., 2013. Neurochemical control of rapid stress-induced changes in brain aromatase activity. J. Neuroendocrinol. 25, 329–339.

Dloniak, S.M., Deviche, P., 2001. Effects of testosterone and photoperiodic condition on song production and vocal control region volumes in adult male dark-eyed juncos (*Junco hyemalis*). Horm. Behav. 39, 95–105.

Dominoni, D., Quetting, M., Partecke, J., 2013. Artificial light at night advances avian reproductive physiology. Proc. Biol. Sci. 280, 20123017.

Dominoni, D.M., de Jong, M., Bellingham, M., O'Shaughnessy, P., van Oers, K., Robinson, J., Smith, B., Visser, M.E., Helm, B., 2018. Dose-response effects of light at night on the reproductive physiology of great tits (*Parus major*): integrating morphological analyses with candidate gene expression. J. Exp. Zoo. A. Ecological Integ. Physiol. 329, 473–487.

DuVal, E.H., 2012. Variation in annual and lifetime reproductive success of lance-tailed manakins: alpha experience mitigates effects of senescence on siring success. Proc. Biol. Sci. 279, 1551–1559.

El Halawani, M.E., Silsby, J.L., Behnke, E.J., Fehrer, S.C., 1986. Hormonal induction of incubation behavior in ovariectomized female turkeys (*Meleagris gallopavo*). Biol. Reprod. 35, 59–67.

Farner, D.S., 1964. The photoperiodic control of reproductive cycles in birds. Am. Sci. 52, 137–156.

Fedde, M.R., 1998. Relationship of structure and function of the avian respiratory system to disease susceptibility. Poultry Sci. 77, 1130–1138.

Foden, W.B., Butchart, S.H.M., Stuart, S.N., Vié, J.-C., Akçakaya, H.R., Angulo, A., DeVantier, L.M., Gutsche, A., Turak, E., Cao, L., 2013. Identifying the world's most climate change vulnerable species: a systematic trait-based assessment of all birds, amphibians and corals. PloS One 8, e65427.

Fokidis, H.B., Orchinik, M., Deviche, P., 2009. Corticosterone and corticosteroid binding globulin in birds: relation to urbanization in a desert city. Gen. Comp. Endocrinol. 160, 259–270.

Forslund, P., Part, T., 1995. Age and reproduction in birds—hypotheses and tests. Trends Ecol. Evol. 10, 374–378.

Fraley, G.S., Steiner, R.A., Lent, K.L., Brenowitz, E.A., 2010. Seasonal changes in androgen receptor mRNA in the brain of the white-crowned sparrow. Gen. Comp. Endocrinol. 166, 66–71.

Francis, C.D., Ortega, C.P., Cruz, A., 2009. Noise pollution changes avian communities and species interactions. Curr. Biol. 19, 1415–1419.

Freed-Brown, G., White, D.J., 2009. Acoustic mate copying: female cowbirds attend to other females' vocalizations to modify their song preferences. Proc. Biol. Sci. 276, 3319–3325.

Fusani, L., 2008. Testosterone control of male courtship in birds. Horm. Behav. 54, 227–233.

Fusani, L., Van't Hof, T., Hutchison, J.B., Gahr, M., 2000. Seasonal expression of androgen receptors, estrogen receptors, and aromatase in the canary brain in relation to circulating androgens and estrogens. J. Neurobiol. 43, 254–268.

Gagne, S.A., Fahrig, L., 2011. Do birds and beetles show similar responses to urbanization? Ecol. Appl. 21, 2297–2312.

Gahali, K., El Halawani, M.E., Rozenboim, I., 2001. Photostimulated prolactin release in the Turkey hen: effect of ovariectomy and environmental temperature. Gen. Comp. Endocrinol. 124, 166–172.

Gahr, M., Flugge, G., Guttinger, H.R., 1987. Immunocytochemical localization of estrogen-binding neurons in the songbird brain. Brain Res. 402, 173–177.

Gahr, M., Guttinger, H.R., Kroodsma, D.E., 1993. Estrogen receptors in the avian brain: survey reveals general distribution and forebrain areas unique to songbirds. J. Comp. Neurol. 327, 112–122.

Garcia-Navas, V., Sanz, J.J., 2011. The importance of a main dish: nestling diet and foraging behaviour in Mediterranean blue tits in relation to prey phenology. Oecologia 165, 639–649.

Gerson, A.R., McKechnie, A.E., Smit, B., Whitfield, M.C., Smith, E.K., Talbot, W.A., McWhorter, T.J., Wolf, B.O., 2019. The functional significance of facultative hyperthermia varies with body size and phylogeny in birds. Funct. Ecol. 33, 597–607.

Gil, D., Leboucher, G., Lacroix, A., Cue, R., Kreutzer, M., 2004. Female canaries produce eggs with greater amounts of testosterone when exposed to preferred male song. Horm. Behav. 45, 64–70.

Goldsmith, A.R., Edwards, C., Koprucu, M., Silver, R., 1981. Concentrations of prolactin and luteinizing hormone in plasma of doves in relation to incubation and development of the crop gland. J. Endocrinol. 90, 437–443.

Goymann, W., 2009. Social modulation of androgens in male birds. Gen. Comp. Endocrinol. 163, 149–157.

Grellet-Tinner, G., Murelaga, X., Larrasoana, J.C., Silveira, L.F., Olivares, M., Ortega, L.A., Trimby, P.W., Pascual, A., 2012. The first occurrence in the fossil record of an aquatic avian twig-nest with phoenicopteriformes eggs: evolutionary implications. PloS One 7, e46972.

Griffith, S.C., Pryke, S.R., Buttemer, W.A., 2011. Constrained mate choice in social monogamy and the stress of having an unattractive partner. Proc. Biol. Sci. 278, 2798–2805.

Gudka, M., Santos, C.D., Dolman, P.M., Abad-Gómez, J.M., Silva, J.P., 2019. Feeling the heat: elevated temperature affects male display activity of a lekking grassland bird. PloS One 14, e0221999.

Gulledge, C.C., Deviche, P., 1998. Photoperiod and testosterone independently affect vocal control region volumes in adolescent male songbirds. J. Neurobiol. 36, 550–558.

Guo, W., Li, Z., Wei, S., Pan, W., Lu, X., 2020. Female-female aggression in a cooperatively breeding bird during the non-breeding period: the behavioral strategy to maintain long-term partnerships. J. Avian Biol. 51. https://doi.org/10.1111/jav.02514.

Hagelin, J.C., 2001. Castration in Gambel's and Scaled quail: ornate plumage and dominance persist, but courtship and threat behaviors do not. Horm. Behav. 39, 1–10.

Hagelin, J.C., Jones, I.L., Rasmussen, L.E.L., 2003. A tangerine-scented social odour in a monogamous seabird. Proc. R. Soc. B. 270, 1323–1329.

Hahn, T.P., 1995. Integration of photoperiodic and food cues to time changes in reproductive physiology by an opportunistic breeder, the red crossbill, *Loxia curvirostra* (Aves: carduelinae). J. Exp. Zool. 272, 213–226.

Hall, Z.J., MacDougall-Shackleton, S.A., 2012. Influence of testosterone metabolites on song-control system neuroplasticity during photostimulation in adult European starlings (*Sturnus vulgaris*). PloS One 7, e40060.

Halupka, L., Halupka, K., 2017a. The effect of climate change on the duration of avian breeding seasons: a meta-analysis. Proc. R. Soc. B. 284, 20171710.

Halupka, L., Halupka, K., 2017b. Electronic Supplementary: Table S1 & Table S2. Figshare. Dataset. https://doi.org/10.6084/m9.figshare.5249107.v1.

Hamilton, K.S., King, A.P., Sengelaub, D.R., West, M.J., 1997. A brain of her own: a neural correlate of song assessment in a female songbird. Neurobiol. Learn. Mem. 68, 325–332.

Harding, C.F., Rowe, S.A., 2003. Vasotocin treatment inhibits courtship in male zebra finches; concomitant androgen treatment inhibits this effect. Horm. Behav. 44, 413–418.

Harrison, T.J., Smith, J.A., Martin, G.R., Chamberlain, D.E., Bearhop, S., Robb, G.N., Reynolds, S.J., 2010. Does food supplementation really enhance productivity of breeding birds? Oecologia 64, 311–320.

Heimovics, S.A., Prior, N.H., Maddison, C.J., Soma, K.K., 2012. Rapid and widespread effects of 17beta-estradiol on intracellular signaling in the male songbird brain: a seasonal comparison. Endocrinology 153, 1364–1376.

Hirao, A., Aoyama, M., Sugita, S., 2009. The role of uropygial gland on sexual behavior in domestic chicken *Gallus gallus domesticus*. Behav. Process. 80, 115–120.

Hirschenhauser, K., Winkler, H., Oliveira, R.F., 2003. Comparative analysis of male androgen responsiveness to social environment in birds: the effects of mating system and paternal incubation. Horm. Behav. 43, 508–519.

Horvathova, T., Nakagawa, S., Uller, T., 2012. Strategic female reproductive investment in response to male attractiveness in birds. Proc. Biol. Sci. 279, 163–170.

Hsueh, A.J., Schaeffer, J.M., 1985. Gonadotropin-releasing hormone as a paracrine hormone and neurotransmitter in extra-pituitary sites. J. Steroid Biochem. 23, 757–764.

Hunt, K.E., Wingfield, J.C., 2004. Effect of estradiol implants on reproductive behavior of female Lapland longspurs (*Calcarius lapponicus*). Gen. Comp. Endocrinol. 137, 248–262.

Hurley, L.L., McDiarmid, C.S., Friesen, C.R., Griffith, S.C., Rowe, M., 2018. Experimental heatwaves negatively impact sperm quality in the zebra finch. Proc. R. Soc. B. 285, 20172547.

IPCC, 2014. Climate change 2014: synthesis report. In: Contribution of Working Groups I, II and III to the Fifth Assessment Report of the Intergovernmental Panel on Climate Change. Geneva, Switzerland.

Jaccoby, S., Arnon, E., Snapir, N., Robinzon, B., 1995. Effects of estradiol and tamoxifen on feeding, fattiness, and some endocrine criteria in hypothalamic obese hens. Pharmacol. Biochem. Behav. 50, 55–63.

Janik, D.S., Buntin, J.D., 1985. Behavioural and physiological effects of prolactin in incubating ring doves. J. Endocrinol. 105, 201–209.

Jawor, J.M., Young, R., Ketterson, E.D., 2006. Females competing to reproduce: dominance matters but testosterone may not. Horm. Behav. 49, 362–368.

Juola, F.A., Dearborn, D.C., 2012. Sequence-based evidence for major histocompatibility complex-disassortative mating in a colonial seabird. Proc. R. Soc. B. 279, 153–162.

Karaca, A.G., Parker, H.M., Yeatman, J.B., McDaniel, C.D., 2002. The effects of heat stress and sperm quality classification on broiler breeder male fertility and semen ion concentrations. Br. Poultry Sci. 43, 621–628.

Kempenaers, B., Borgstrom, P., Loes, P., Schlicht, E., Valcu, M., 2010. Artificial night lighting affects dawn song, extra-pair siring success, and lay date in songbirds. Curr. Biol. 20, 1735–1739.

Kight, C.R., Saha, M.S., Swaddle, J.P., 2012. Anthropogenic noise is associated with reductions in the productivity of breeding Eastern bluebirds (*Sialia sialis*). Ecol. Appl. 22, 1989–1996.

Kimura, T., Okanoya, K., Wada, M., 1999. Effect of testosterone on the distribution of vasotocin immunoreactivity in the brain of the zebra finch, *Taeniopygia guttata castanotis*. Life Sci. 65, 1663–1670.

Kiss, J.Z., Voorhuis, T.A., van Eekelen, J.A., de Kloet, E.R., De, W.D., 1987. Organization of vasotocin-immunoreactive cells and fibers in the canary brain. J. Comp. Neurol. 263, 347–364.

Kleven, O., Fossoy, F., Laskemoen, T., Robertson, R.J., Rudolfsen, G., Lifjeld, J.T., 2009. Comparative evidence for the evolution of sperm swimming speed by sperm competition and female sperm storage duration in passerine birds. Evolution 63, 2466–2473.

Komisaruk, B.R., 1967. Effects of local brain implants of progesterone on reproductive behavior in ring doves. J. Comp. Physiol. Psychol. 64, 219–224.

Kotegawa, T., Abe, T., Tsutsui, K., 1997. Inhibitory role of opioid peptides in the regulation of aggressive and sexual behaviors in male Japanese quails. J. Exp. Zool. 277, 146–154.

Kuenzel, W.J., Kang, S.W., Jurkevich, A., 2020. Chapter Seven - the vasotocinergic system and its role in the regulation of stress in birds. In: Litwack, G. (Ed.), Vitamins and Hormones. Academic Press, pp. 183–216.

Kuwayama, T., Shimada, K., Saito, N., Ohkubo, T., Sato, K., Wada, M., Ichinoe, K., 1992. Effects of removal of chicks from hens on concentrations of prolactin, luteinizing hormone and oestradiol in plasma of brooding Gifujidori hens. J. Reprod. Fertil. 95, 617–622.

Landys, M.M., Goymann, W., Raess, M., Slagsvold, T., 2007. Hormonal responses to male-male social challenge in the blue tit *Cyanistes caeruleus*: single-broodedness as an explanatory variable. Physiol. Biochem. Zool. 80, 228–240.

Landys, M.M., Goymann, W., Schwabl, I., Trapschuh, M., Slagsvold, T., 2010. Impact of season and social challenge on testosterone and corticosterone levels in a year-round territorial bird. Horm. Behav. 58, 317–325.

Langmore, N.E., Cockrem, J.F., Candy, E.J., 2002. Competition for male reproductive investment elevates testosterone levels in female dunnocks, *Prunella modularis*. Proc. Biol. Sci. 269, 2473–2478.

Lea, R.W., Vowles, D.M., Dick, H.R., 1986a. Factors affecting prolactin secretion during the breeding cycle of the ring dove (*Streptopelia risoria*) and its possible role in incubation. J. Endocrinol. 110, 447–458.

Lea, R.W., Sharp, P.J., Klandorf, H., Harvey, S., Dunn, I.C., Vowles, D.M., 1986b. Seasonal changes in concentrations of plasma hormones in the male ring dove (*Streptopelia risoria*). J. Endocrinol. 108, 385–391.

Leclaire, S., Merkling, T., Raynaud, C., Mulard, H., Bessière, J.-M., Lhuillier, E., Hatch, S.A., Danchin, E., 2012. Semiochemical compounds of preen secretion reflect genetic make-up in a seabird species. Proc. R. Soc. B. 279, 1185–1193.

Lehrman, D.S., 1964. The reproductive behavior of ring doves. Sci. Am. 211, 48–54.

Lehrman, D.S., Friedman, M., 1969. Auditory stimulation of ovarian activity in the ring dove (*Streptopelia risoria*). Anim. Behav. 17, 494–497.

Leung, C.H., Goode, C.T., Young, L.J., Maney, D.L., 2009. Neural distribution of nonapeptide binding sites in two species of songbird. J. Comp. Neurol. 51, 197–208.

Leung, C.H., Abebe, D.F., Earp, S.E., Goode, C.T., Grozhik, A.V., Mididoddi, P., Maney, D.L., 2011. Neural distribution of vasotocin receptor mRNA in two species of songbird. Endocrinology 152, 4865–4881.

Li, X.C., Jarvis, E.D., Alvarez-Borda, B., Lim, D.A., Nottebohm, F., 2000. A relationship between behavior, neurotrophin expression, and new neuron survival. Proc. Natl. Acad. Sci. U. S. A. 97, 8584–8589.

Liu, W.C., Wada, K., Jarvis, E., Nottebohm, F., 2013. Rudimentary substrates for vocal learning in a suboscine. Nat. Commun. 4, 2082.

London, S.E., Monks, D.A., Wade, J., Schlinger, B.A., 2006. Widespread capacity for steroid synthesis in the avian brain and song system. Endocrinology 147, 5975–5987.

Longcore, T., 2010. Sensory ecology: night lights alter reproductive behavior of blue tits. Curr. Biol. 20, R893–R895.

Lormee, H., Jouventin, P., Chastel, O., Mauget, R., 1999. Endocrine correlates of parental care in an Antarctic winter breeding seabird, the emperor penguin, Aptenodytes Forsteri. Horm. Behav. 35, 9–17.

Lott, D., Scholz, S.D., Lehrman, D.S., 1967. Exteroceptive stimulation of the reproductive system of the female ring dove (*Streptopella risoria*) by the mate and by the colony milieu. Anim. Behav. 15, 433–437.

Low, M., Part, T., Forslund, P., 2007. Age-specific variation in reproduction is largely explained by the timing of territory establishment in the New Zealand stitchbird *Notiomystis cincta*. J. Anim. Ecol. 76, 459–470.

Lynn, S.E., Walker, B.G., Wingfield, J.C., 2005. A phylogenetically controlled test of hypotheses for behavioral insensitivity to testosterone in birds. Horm. Behav. 47, 170–177.

Maney, D.L., Wingfield, J.C., 1998. Neuroendocrine suppression of female courtship in a wild passerine: corticotropin-releasing factor and endogenous opioids. J. Neuroendocrinol. 10, 593–599.

Maney, D.L., Goode, C.T., Wingfield, J.C., 1997a. Intraventricular infusion of arginine vasotocin induces singing in a female songbird. J. Neuroendocrinol. 9, 487–491.

Maney, D.L., Richardson, R.D., Wingfield, J.C., 1997b. Central administration of chicken gonadotropin-releasing hormone-II enhances courtship behavior in a female sparrow. Horm. Behav. 32, 11–18.

Maney, D.L., Goode, C.T., Lake, J.I., Lange, H.S., O'Brien, S., 2007. Rapid neuroendocrine responses to auditory courtship signals. Endocrinology 148, 5614–5623.

Massaro, M., Setiawan, A.N., Davis, L.S., 2007. Effects of artificial eggs on prolactin secretion, steroid levels, brood patch development, incubation onset and clutch size in the yellow-eyed penguin (*Megadyptes antipodes*). Gen. Comp. Endocrinol. 151, 220–229.

McDonald, P.A., Liley, N.R., 1978. The effects of photoperiod on androgen-induced reproductive behavior in male ring doves, *Streptopelia risoria*. Horm. Behav. 10, 85–96.

Meitzen, J., Moore, I.T., Lent, K., Brenowitz, E.A., Perkel, D.J., 2007. Steroid hormones act transsynaptically within the forebrain to regulate neuronal phenotype and song stereotypy. J. Neurosci. 27, 12045–12057.

Meitzen, J., Thompson, C.K., 2008. Seasonal-like growth and regression of the avian song control system: neural and behavioral plasticity in adult male Gambel's white-crowned sparrows. Gen. Comp. Endocrinol. 157, 259–265.

Michel, G.F., 1976. Role of mate's previous experience in ring dove hormone-induced incubation. J. Comp. Physiol. Psychol. 90, 468–472.

Mimet, A., Pellissier, V., Quenol, H., Aguejdad, R., Dubreuil, V., Roze, F., 2009. Urbanisation induces early flowering: evidence from *Platanus acerifolia* and *Prunus cerasus*. Int. J. Biometeorol. 53, 287–298.

Moller, A.P., 2013. Biological consequences of global change for birds. Integr. Zool. 8, 136–144.

Nealen, P.M., 2005. An interspecific comparison using immunofluorescence reveals that synapse density in the avian song system is related to sex but not to male song repertoire size. Brain Res. 1032, 50–62.

Nordeen, K.W., Nordeen, E.J., Arnold, A.P., 1987. Estrogen accumulation in zebra finch song control nuclei: implications for sexual differentiation and adult activation of song behavior. J. Neurobiol. 18, 569–582.

Nottebohm, F., 1981. A brain for all seasons: cyclical anatomical changes in song control nuclei of the canary brain. Science 214, 1368–1370.

Nottebohm, F., Stokes, T.M., Leonard, C.M., 1976. Central control of song in the canary, *Serinus canarius*. J. Comp. Neurol. 165, 457–486.

Nottebohm, F., Kelley, D.B., Paton, J.A., 1982. Connections of vocal control nuclei in the canary telencephalon. J. Comp. Neurol. 207, 344–357.

Nottebohm, F., O'Loughlin, B., Gould, K., Yohay, K., Alvarez-Buylla, A., 1994. The life span of new neurons in a song control nucleus of the adult canary brain depends on time of year when these cells are born. Proc. Natl. Acad. Sci. U. S. A. 91, 7849–7853.

O'Neal, D.M., Reichard, D.G., Pavilis, K., Ketterson, E.D., 2008. Experimentally-elevated testosterone, female parental care, and reproductive success in a songbird, the dark-eyed junco (*Junco hyemalis*). Horm. Behav. 54, 571–578.

Osorno, J.L., Nunez-de la-Mora, A., D'Alba, L., Wingfield, J.C., 2010. Hormonal correlates of breeding behavior and pouch color in the magnificent frigatebird, *Fregata magnificens*. Gen. Comp. Endocrinol. 169, 18–22.

Owen-Ashley, N.T., Hasselquist, D., Wingfield, J.C., 2004. Androgens and the immunocompetence handicap hypothesis: unraveling direct and indirect pathways of immunosuppression in song sparrows. Am. Nat. 164, 490–505.

Owens, I.P., 2002. Male-only care and classical polyandry in birds: phylogeny, ecology and sex differences in remating opportunities. Philos. Trans. R. Soc. Lond. B Biol. Sci. 357, 283–293.

Oyegbile, T.O., Marler, C.A., 2005. Winning fights elevates testosterone levels in California mice and enhances future ability to win fights. Horm. Behav. 48, 259–267.

Panzica, G.C., Viglietti-Panzica, C., Balthazart, J., 1996. The sexually dimorphic medial preoptic nucleus of quail: a key brain area mediating steroid action on male sexual behavior. Front. Neuroendocrinol. 17, 51–125.

Panzica, G., Pessatti, M., Viglietti-Panzica, C., Grossmann, R., Balthazart, J., 1999a. Effects of testosterone on sexually dimorphic parvocellular neurons expressing vasotocin mRNA in the male quail brain. Brain Res. 850, 55–62.

Panzica, G.C., Plumari, L., Garcia-Ojeda, E., Deviche, P., 1999b. Central vasotocin-immunoreactive system in a male passerine bird (*Junco hyemalis*). J. Comp. Neurol. 409, 105–117.

Panzica, G.C., Aste, N., Castagna, C., Viglietti-Panzica, C., Balthazart, J., 2001. Steroid-induced plasticity in the sexually dimorphic vasotocinergic innervation of the avian brain: behavioral implications. Brain Res. Brain Res. Rev. 37, 178–200.

Partecke, J., Gwinner, E., 2007. Increased sedentariness in European blackbirds following urbanization: a consequence of local adaptation? Ecology 88, 882–890.

Partecke, J., Schwabl, I., Gwinner, E., 2006. Stress and the city: urbanization and its effects on the stress physiology in European blackbirds. Ecology 87, 1945–1952.

Pasteau, M., Ung, D., Kreutzer, M., Aubin, T., 2012. Amplitude modulation of sexy phrases is salient for song attractiveness in female canaries (*Serinus canaria*). Anim. Cognit. 15, 639–645.

Pattinson, N.B., Thompson, M.L., Griego, M., Russell, G., Mitchell, N.J., Martin, R.O., Wolf, B.O., Smit, B., Cunningham, S.J., McKechnie, A.E., Hockey, P.A.R., 2020. Heat dissipation behaviour of birds in seasonally hot arid-zones: are there global patterns? J. Avian Biol. 51.

Payne, C.J., Jessop, T.S., Guay, P.J., Johnstone, M., Feore, M., Mulder, R.A., 2012. Population, behavioural and physiological responses of an urban population of black swans to an intense annual noise event. PloS One 7, e45014.

Penn, D.J., 2002. The scent of genetic compatibility: sexual selection and the major histocompatibility complex. Ethology 108, 1–21.

Perfito, N., Kwong, J.M., Bentley, G.E., Hau, M., 2008. Cue hierarchies and testicular development: is food a more potent stimulus than day length in an opportunistic breeder (*Taeniopygia g. guttata*)? Horm. Behav. 53, 567–572.

Pinxten, R., de Ridder, E., Eens, M., 2003. Female presence affects male behavior and testosterone levels in the European starling (*Sturnus vulgaris*). Horm. Behav. 44, 103–109.

Plumari, L., Plateroti, S., Deviche, P., Panzica, G.C., 2004. Region-specific testosterone modulation of the vasotocin-immunoreactive system in male dark-eyed junco, *Junco hyemalis*. Brain Res. 999, 1–8.

Pradel, R., Choquet, R., Bechet, A., 2012. Breeding experience might be a major determinant of breeding probability in long-lived species: the case of the greater flamingo. PloS One 7, e51016.

Quiring, D.P., 1944. Transplantation of testes (by A.A. Berthold). Bull. Hist. Med. 16, 399–401.

Rahmstorf, S., Coumou, D., 2011. Increase of extreme events in a warming world. Proc. Natl. Acad. Sci. U. S. A. 108, 17905.

Ramesh, R., Kuenzel, W.J., Buntin, J.D., Proudman, J.A., 2000. Identification of growth-hormone- and prolactin-containing neurons within the avian brain. Cell Tissue Res. 299, 371–383.

Rasika, S., Alvarez-Buylla, A., Nottebohm, F., 1999. BDNF mediates the effects of testosterone on the survival of new neurons in an adult brain. Neuron 22, 53–62.

Rauceo, S., Harding, C.F., Maldonado, A., Gaysinkaya, L., Tulloch, I., Rodriguez, E., 2008. Dopaminergic modulation of reproductive behavior and activity in male zebra finches. Behav. Brain Res. 187, 133–139.

Reichert, B.E., Cattau, C.E., Fletcher Jr., R.J., Kendall, W.L., Kitchens, W.M., 2012. Extreme weather and experience influence reproduction in an endangered bird. Ecology 93, 2580–2589.

Remage-Healey, L., Maidment, N.T., Schlinger, B.A., 2008. Forebrain steroid levels fluctuate rapidly during social interactions. Nat. Neurosci. 11, 1327–1334.

Remage-Healey, L., Oyama, R.K., Schlinger, B.A., 2009. Elevated aromatase activity in forebrain synaptic terminals during song. J. Neuroendocrinol. 21, 191–199.

Remage-Healey, L., Coleman, M.J., Oyama, R.K., Schlinger, B.A., 2010. Brain estrogens rapidly strengthen auditory encoding and guide song preference in a songbird. Proc. Natl. Acad. Sci. U. S. A. 107, 3852–3857.

Remage-Healey, L., Dong, S.M., Chao, A., Schlinger, B.A., 2012. Sex-specific, rapid neuroestrogen fluctuations and neurophysiological actions in the songbird auditory forebrain. J. Neurophysiol. 107, 1621–1631.

Richard-Yris, M.A., Leboucher, G., Williams, J., Garnier, D.H., 1987. Influence of food restriction and of the presence of chicks on the reproductive system of the domestic hen. Br. Poultry Sci. 28, 251–260.

Richard-Yris, M.A., Sharp, P.J., Wauters, A.M., Guemene, D., Richard, J.P., Foraste, M., 1998. Influence of stimuli from chicks on behavior and concentrations of plasma prolactin and luteinizing hormone in incubating hens. Horm. Behav. 33, 139–148.

Rissman, E.F., Wingfield, J.C., 1984. Hormonal correlates of polyandry in the spotted sandpiper, *Actitis Macularia*. Gen. Comp. Endocrinol. 56, 401–405.

Riters, L.V., Ball, G.F., 2002. Sex differences in the densities of alpha 2-adrenergic receptors in the song control system, but not the medial preoptic nucleus in zebra finches. J. Chem. Neuroanat. 23, 269–277.

Riters, L.V., Teague, D.P., 2003. The volumes of song control nuclei, HVC and lMAN, relate to differential behavioral responses of female European starlings to male songs produced within and outside of the breeding season. Brain Res. 978, 91–98.

Rosvall, K.A., 2008. Sexual selection on aggressiveness in females: evidence from an experimental test with tree swallows. Anim. Behav. 75, 1603–1610.

Rosvall, K.A., 2013. Life history trade-offs and behavioral sensitivity to testosterone: an experimental test when female aggression and maternal care co-occur. PloS One 8, e54120.

Rutkowska, J., Place, N.J., Vincent, S., Adkins-Regan, E., 2011. Adrenocortical response to mating, social interaction and restraint in the female Japanese quail. Physiol. Behav. 104, 1037–1040.

Sachs, B.D., Leipheimer, R.E., 1988. Rapid effect of testosterone on striated muscle activity in rats. Neuroendocrinology 48, 453–458.

Sakaguchi, H., Li, R., Taniguchi, I., 2000. Sex differences in the ventral paleostriatum of the zebra finch: origin of the cholinergic innervation of the song control nuclei. Neuroreport 11, 2727–2731.

Saranathan, V., Hamilton, D., Powell, G.V., Kroodsma, D.E., Prum, R.O., 2007. Genetic evidence supports song learning in the three-wattled bellbird *Procnias tricarunculata* (Cotingidae). Mol. Ecol. 16, 3689–3702.

Schlesinger, M.D., Manley, P.N., Holyoak, M., 2008. Distinguishing stressors acting on land bird communities in an urbanizing environment. Ecology 89, 2302–2314.

Schlinger, B.A., Callard, G.V., 1990. Aromatization mediates aggressive behavior in quail. Gen. Comp. Endocrinol. 79, 39–53.

Schlinger, B.A., Balthazart, J., 2012. Aromatase and behavior: concepts gained from studies of aromatase in the avian brain. In: Balthazart, J., Ball, G. (Eds.), Brain Aromatase, Estrogens, and Behavior. Oxford Scholarship Online.

Schlinger, B.A., Remage-Healey, L., 2012. Neurosteroidogenesis: insights from studies of songbirds. J. Neuroendocrinol. 24, 16–21.

Schlinger, B.A., Day, L.B., Fusani, L., 2008. Behavior, natural history and neuroendocrinology of a tropical bird. Gen. Comp. Endocrinol. 157, 254–258.

Schoech, S.J., Bowman, R., Reynolds, S.J., 2004. Food supplementation and possible mechanisms underlying early breeding in the Florida Scrub-Jay (*Aphelocoma coerulescens*). Horm. Behav. 46, 565–573.

Schradin, C., Anzenberger, G., 1999. Prolactin, the hormone of paternity. Physiology 14, 223–231.

Schroeder, J., Nakagawa, S., Cleasby, I.R., Burke, T., 2012. Passerine birds breeding under chronic noise experience reduced fitness. PloS One 7, e39200.

Searcy, W.A., Marler, P., 1981. A test for responsiveness to song structure and programming in female sparrows. Science 213, 926–928.

Selvaraj, P., Pitchappan, R.M., 1985. Effect of oestradiol dipropionate on the immune system of the pigeon, *Columba livia*. Dev. Comp. Immunol. 9, 669–677.

Senapathi, D., Nicoll, M.A., Teplitsky, C., Jones, C.G., Norris, K., 2011. Climate change and the risks associated with delayed breeding in a tropical wild bird population. Proc. Biol. Sci. 278, 3184–3190.

Seredynski, A.L., Ball, G.F., Balthazart, J., Charlier, T.D., 2011. Specific activation of estrogen receptor alpha and beta enhances male sexual behavior and neuroplasticity in male Japanese quail. PloS One 6, e18627.

Seredynski, A.L., Balthazart, J., Christophe, V.J., Ball, G.F., Cornil, C.A., 2013. Neuroestrogens rapidly regulate sexual motivation but not performance. J. Neurosci. 33, 164–174.

Seredynski, A.L., Balthazart, J., Ball, G.F., Cornil, C.A., 2015. Estrogen receptor β activation rapidly modulates male sexual motivation through the transactivation of metabotropic glutamate receptor 1a. J. Neurosci. 35, 13110–13123.

Sharma, D., Cornett, L.E., Chaturvedi, C.M., 2009. Osmotic stress induced alteration in the expression of arginine vasotocin receptor VT2 in the pituitary gland and adrenal function of domestic fowl. Gen. Comp. Endocrinol. 160, 216–222.

Sharp, P.J., Dawson, A., Lea, R.W., 1998. Control of luteinizing hormone and prolactin secretion in birds. Comp. Biochem. Physiol. C Pharmacol. Toxicol. Endocrinol. 119, 275–282.

Shine, R., Brown, G.P., 2008. Adapting to the unpredictable: reproductive biology of vertebrates in the Australian wet-dry tropics. Philos. Trans. R. Soc. Lond. B Biol. Sci. 363, 363–373.

Silva, L.R., Lardy, S., Ferreira, A.C., Rey, B., Doutrelant, C., Covas, R., 2018. Females pay the oxidative cost of dominance in a highly social bird. Anim. Behav. 144, 135–146.

Silverin, B., 1991. Behavioral, hormonal, and morphological responses of free-living male pied flycatchers to estradiol treatment of their mates. Horm. Behav. 25, 38–56.

Silverin, B., Baillien, M., Balthazart, J., 2004. Territorial aggression, circulating levels of testosterone, and brain aromatase activity in free-living pied flycatchers. Horm. Behav. 45, 225–234.

Silverin, B., Westin, J., 1995. Influence of the opposite sex on photoperiodically induced LH and gonadal cycles in willow tit (*Parus montanus*). Horm. Behav. 29, 207–215.

Sitko, J., Zalesny, G., 2012. The effect of urbanization on helminth communities in the Eurasian blackbird (*Turdus merula* L.) from the eastern part of the Czech Republic. J. Helminthol. 88, 97–104.

Slawski, B.A., Buntin, J.D., 1995. Preoptic area lesions disrupt prolactin-induced parental feeding behavior in ring doves. Horm. Behav. 29, 248–266.

Small, T.W., Sharp, P.J., Bentley, G.E., Millar, R.P., Tsutsui, K., Strand, C., Deviche, P., 2008. Auditory stimulation of reproductive function in male rufous-winged sparrows, *Aimophila carpalis*. Horm. Behav. 53, 28–39.

Smith, G.T., Brenowitz, E.A., Wingfield, J.C., 1997. Seasonal changes in the size of the avian song control nucleus HVC defined by multiple histological markers. J. Comp. Neurol. 381, 253–261.

Soma, K.K., Hartman, V.N., Wingfield, J.C., Brenowitz, E.A., 1999. Seasonal changes in androgen receptor immunoreactivity in the song nucleus HVc of a wild bird. J. Comp. Neurol. 409, 224–236.

Soma, K.K., Schlinger, B.A., Wingfield, J.C., Saldanha, C.J., 2003. Brain aromatase, 5 alpha-reductase, and 5 beta-reductase change seasonally in wild male song sparrows: relationship to aggressive and sexual behavior. J. Neurobiol. 56, 209–221.

Soma, K.K., Tramontin, A.D., Featherstone, J., Brenowitz, E.A., 2004. Estrogen contributes to seasonal plasticity of the adult avian song control system. J. Neurobiol. 58, 413–422.

Spee, M., Beaulieu, M., Dervaux, A., Chastel, O., Le, M.Y., Raclot, T., 2010. Should I stay or should I go? Hormonal control of nest abandonment in a long-lived bird, the Adélie penguin. Horm. Behav. 58, 762–768.

Stevenson, T.J., Bernard, D.J., McCarthy, M.M., Ball, G.F., 2013. Photoperiod-dependent regulation of gonadotropin-releasing hormone 1 messenger ribonucleic acid levels in the songbird brain. Gen. Comp. Endocrinol. 190, 81–87.

Stillman, J.H., 2019. Heat waves, the new normal: summertime temperature extremes will impact animals, ecosystems, and human communities. Physiol. 34, 86–100.

Strandh, M., Westerdahl, H., Pontarp, M., Canbäck, B., Dubois, M.-P., Miquel, C., Taberlet, P., Bonadonna, F., 2012. Major histocompatibility complex class II compatibility, but not class I, predicts mate choice in a bird with highly developed olfaction. Proc. R. Soc. B. 279, 4457–4463.

Thierry, A.M., Brajon, S., Massemin, S., Handrich, Y., Chastel, O., Raclot, T., 2013. Decreased prolactin levels reduce parental commitment, egg temperatures, and breeding success of incubating male Adelie penguins. Horm. Behav. 64, 737–747.

Thompson, C.K., Bentley, G.E., Brenowitz, E.A., 2007. Rapid seasonal-like regression of the adult avian song control system. Proc. Natl. Acad. Sci. U. S. A. 104, 15520–15525.

Thompson, C.K., Meitzen, J., Replogle, K., Drnevich, J., Lent, K.L., Wissman, A.M., Farin, F.M., Bammler, T.K., Beyer, R.P., Clayton, D.F., Perkel, D.J., Brenowitz, E.A., 2012. Seasonal changes in patterns of gene expression in avian song control brain regions. PloS One 7, e35119.

Tobari, Y., Nakamura, K.Z., Okanoya, K., 2005. Sex differences in the telencephalic song control circuitry in Bengalese finches (*Lonchura striata var. domestica*). Zool. Sci. 22, 1089–1094.

Tonra, C.M., Marra, P.P., Holberton, R.L., 2011. Early elevation of testosterone advances migratory preparation in a songbird. J. Exp. Biol. 214, 2761–2767.

Tramontin, A.D., Smith, G.T., Breuner, C.W., Brenowitz, E.A., 1998. Seasonal plasticity and sexual dimorphism in the avian song control system: stereological measurement of neuron density and number. J. Comp. Neurol. 396, 186–192.

Tramontin, A.D., Wingfield, J.C., Brenowitz, E.A., 2003. Androgens and estrogens induce seasonal-like growth of song nuclei in the adult songbird brain. J. Neurobiol. 57, 130–140.

Tregenza, T., Wedell, N., 2000. Genetic compatibility, mate choice and patterns of parentage: invited review. Mol. Ecol. 9, 1013–1027.

Tryjanowski, P., Sparks, T.H., Kuzniak, S., Czechowski, P., Jerzak, L., 2013. Bird migration advances more strongly in urban environments. PloS One 8, e63482.

Tsutsui, K., Saigoh, E., Ukena, K., Teranishi, H., Fujisawa, Y., Kikuchi, M., Ishii, S., Sharp, P.J., 2000. A novel avian hypothalamic peptide inhibiting gonadotropin release. Biochem. Biophys. Res. Commun. 275, 661–667.

Tsutsui, K., Ubuka, T., Son, Y.L., Bentley, G.E., Kriegsfeld, L.J., 2015. Contribution of GnIH research to the progress of reproductive neuroendocrinology. Front. Endocrinol. 6, 179.

Ubuka, T., McGuire, N.L., Calisi, R.M., Perfito, N., Bentley, G.E., 2008. The control of reproductive physiology and behavior by gonadotropin-inhibitory hormone. Integr. Comp. Biol. 48, 560–569.

Ubuka, T., Lai, H., Kitani, M., Suzuuchi, A., Pham, V., Cadigan, P.A., Wang, A., Chowdhury, V.S., Tsutsui, K., Bentley, G.E., 2009. Gonadotropin-inhibitory hormone identification, cDNA cloning, and distribution in rhesus macaque brain. J. Comp. Neurol. 517, 841–855.

Ubuka, T., Mizuno, T., Fukuda, Y., Bentley, G.E., Wingfield, J.C., Tsutsui, K., 2013. RNA interference of gonadotropin-inhibitory hormone gene induces aggressive and sexual behaviors in birds. Gen. Comp. Endocrinol. 181, 179–186.

Ubuka, T., Haraguchi, S., Tobari, Y., Narihiro, M., Ishikawa, K., Hayashi, T., Harada, N., Tsutsui, K., 2014. Hypothalamic inhibition of socio-sexual behaviour by increasing neuroestrogen synthesis. Nat. Commun. 5, 3061.

Ukena, K., Ubuka, T., Tsutsui, K., 2003. Distribution of a novel avian gonadotropin-inhibitory hormone in the quail brain. Cell Tissue Res. 312, 73–79.

Van Roo, B.L., 2004. Exogenous testosterone inhibits several forms of male parental behavior and stimulates song in a monogamous songbird: the blue-headed vireo (*Vireo solitarius*). Horm. Behav. 46, 678–683.

Varricchio, D.J., Moore, J.R., Erickson, G.M., Norell, M.A., Jackson, F.D., Borkowski, J.J., 2008. Avian paternal care had dinosaur origin. Science 322, 1826–1828.

Viglietti-Panzica, C., Aste, N., Balthazart, J., Panzica, G.C., 1994. Vasotocinergic innervation of sexually dimorphic medial preoptic nucleus of the male Japanese quail: influence of testosterone. Brain Res. 657, 171–184.

Viglietti-Panzica, C., Balthazart, J., Plumari, L., Fratesi, S., Absil, P., Panzica, G.C., 2001. Estradiol mediates effects of testosterone on vasotocin immunoreactivity in the adult quail brain. Horm. Behav. 40, 445–461.

Visser, M.E., Holleman, L.J., Caro, S.P., 2009. Temperature has a causal effect on avian timing of reproduction. Proc. Biol. Sci. 276, 2323–2331.

Vleck, C.M., Ross, L.L., Vleck, D., Bucher, T.L., 2000. Prolactin and parental behavior in Adélie penguins: effects of absence from nest, incubation length, and nest failure. Horm. Behav. 38, 149–158.

Voigt, C., Ball, G.F., Balthazart, J., 2011. Effects of sex steroids on aromatase mRNA expression in the male and female quail brain. Gen. Comp. Endocrinol. 170, 180–188.

Voorhuis, T.A., Kiss, J.Z., de Kloet, E.R., De Wied, W.D., 1988a. Testosterone-sensitive vasotocin-immunoreactive cells and fibers in the canary brain. Brain Res. 442, 139–146.

Voorhuis, T.A., de Kloet, E.R., De Wied, W.D., 1988b. The distribution and plasticity of [3H]vasopressin-labelled specific binding sites in the canary brain. Brain Res. 457, 148–153.

Voorhuis, T.A., de Kloet, E.R., De Wied, W.D., 1991a. Effect of a vasotocin analog on singing behavior in the canary. Horm. Behav. 25, 549–559.

Voorhuis, T.A., de Kloet, E.R., De Wied, W.D., 1991b. Ontogenetic and seasonal changes in immunoreactive vasotocin in the canary brain. Brain Res. Dev. Brain Res. 61, 23–31.

Voorhuis, T.A., de Kloet, E.R., 1992. Immunoreactive vasotocin in the zebra finch brain (*Taeniopygia guttata*). Brain Res. Dev. Brain Res. 69, 1–10.

Walker, W.H., Meléndez-Fernández, O.H., Nelson, R.J., Reiter, R.J., 2019. Global climate change and invariable photoperiods: a mismatch that jeopardizes animal fitness. Ecol. Evol. 9, 10044–10054.

Watts, H.E., Hahn, T.P., 2012. Non-photoperiodic regulation of reproductive physiology in the flexibly breeding pine siskin (*Spinus pinus*). Gen. Comp. Endocrinol. 178, 259–264.

White, S.J., 1975. Effects of stimuli emanating from the nest on the reproductive cycle in the ring dove. I: pre-laying behaviour. Anim. Behav. 23, 854–868.

Wilhelm, M., 2011. Neuro-immune interactions in the dove brain. Gen. Comp. Endocrinol. 172, 173–180.

Wingfield, J.C., 1984. Influence of weather on reproduction. J. Exp. Zool. 232, 589–594.

Wingfield, J.C., 1994a. Control of territorial aggression in a changing environment. Psychoneuroendocrinology 19, 709–721.

Wingfield, J.C., 1994b. Regulation of territorial behavior in the sedentary song sparrow, *Melospiza melodia morphna*. Horm. Behav. 28, 1–15.

Wingfield, J.C., 2017. Ecophysiological studies of hormone–behavior relations in birds: future challenges in a changing world. In: Pfaff, D.W., Joëls, M. (Eds.), Hormones, Brain and Behavior, third ed. Academic Press, Oxford, pp. 321–345.

Wingfield, J.C., Goldsmith, A.R., 1990. Plasma levels of prolactin and gonadal steroids in relation to multiple-brooding and renesting in free-living populations of the song sparrow, *Melospiza melodia*. Horm. Behav. 24, 89–103.

Wingfield, J.C., Hahn, T.P., 1994. Testosterone and territorial behaviour in sedentary and migratory sparrows. Anim. Behav. 47, 77–89.

Wingfield, J.C., Monk, D., 1994. Behavioral and hormonal responses of male song sparrows to estradiol-treated females during the non-breeding season. Horm. Behav. 28, 146–154.

Wingfield, J., Ball, G.F., Dufty, A.M., Hegner, R.E., Ramenofsky, M., 1987. Testosterone and aggression in birds. Am. Sci. 75, 602–608.

Wingfield, J.C., Donna, L.M., Creagh, W.B., Jacobs, J.D., Sharon, L., Ramenofsky, M., Ralph, D.R., 1998. Ecological bases of hormone-interactions: the "emergency life history stage". Am. Zool. 38, 191–206.

Wingfield, J.C., Wacker, D.W., Bentley, G.E., Tsutsui, K., 2018. Brain-derived steroids, behavior and endocrine conflicts across life history stages in birds: a perspective. Front. Endocrinol. 9, 270.

Winkler, D., Hallinger, K., Ardia, D., Robertson, R., Stutchbury, B., Cohen, R., 2011. Tree Swallow (Tachycineta bicolor). The Birds of North America. Cornell Lab of Ornithology, Ithaca, NY.

Wissman, A.M., Brenowitz, E.A., 2009. The role of neurotrophins in the seasonal-like growth of the avian song control system. J. Neurosci. 29, 6461–6471.

Wright, L.J., Hoblyn, R.A., Green, R.E., Bowden, C.G., Mallord, J.W., Sutherland, W.J., Dolman, P.M., 2009. Importance of climatic and environmental change in the demography of a multi-brooded passerine, the woodlark *Lullula arborea*. J. Anim. Ecol. 78, 1191–1202.

Zanette, L., Smith, J.N., van, O.H., Clinchy, M., 2003. Synergistic effects of food and predators on annual reproductive success in song sparrows. Proc. Biol. Sci. 270, 799–803.

Zanette, L., Clinchy, M., Sung, H.C., 2009. Food-supplementing parents reduces their sons' song repertoire size. Proc. Biol. Sci. 276, 2855–2860.

Zhang, J.X., Wei, W., Zhang, J.H., Yang, W.H., 2010a. Uropygial gland-secreted alkanols contribute to olfactory sex signals in budgerigars. Chem. Senses 35, 375–382.

Zhang, K., Wang, R., Shen, C., Da, L., 2010b. Temporal and spatial characteristics of the urban heat island during rapid urbanization in Shanghai, China. Environ. Monit. Assess. 169, 101–112.

Zheng, X., O'Connor, J., Huchzermeyer, F., Wang, X., Wang, Y., Wang, M., Zhou, Z., 2013. Preservation of ovarian follicles reveals early evolution of avian reproductive behaviour. Nature 495, 507–511.

Zhuang, X., Silverman, A.J., Silver, R., 1993. Reproductive behavior, endocrine state, and the distribution of GnRH-like immunoreactive mast cells in dove brain. Horm. Behav. 27, 283–295.

Chapter 41

Growth

Colin G. Scanes, Nima K. Emami and Sami Dridi
Center of Excellence for Poultry Science, University of Arkansas, Fayetteville, AR, United States

Abbreviations

ACTH Adrenocorticotropic hormone
ADG Average daily gain
BMP Bone morphogenic protein
CORT Corticosterone
EGF Epidermal growth factor
EGFR Epidermal growth factor receptor
F:G Feed to gain
GH Growth hormone
IGF Insulin-like growth factor
IGFBP Insulin-like growth factor binding protein
mTOR Mechanistic (or mammalian) target of rapamycin
NFκB Nuclear factor kappa B
Pit-1 Pituitary -specific positive transcription factor 1 also known as POU domain, class 1, transcription factor 1
TGF Transforming growth factor
TNF-α Tumor necrosis factor-α

41.1 Introduction

41.1.1 Overview

This chapter will review the current knowledge of the biology of growth in birds focusing on posthatch growth. Growth is a complex process involving tissue-specific gene expression, paracrine, autocrine, and intracrine controls, the endocrine regulatory systems, and other contributing factors including nutrition and environment. Particular attention will be placed on hormonal regulation of growth and development.

Discussion will consider growth of wild birds and poultry species. Where there is either little information on one grouping or disparate information, this will be noted. It is recognized that there is selection pressure in wild birds including the ancestors of poultry including the following:

- Optimal adult mass and organ weights for the niche and to withstand the rigors of flight and migration,
- Optimal size for flight and in preparation for egg production,
- Maximal utilization of nutrients, and
- Maximal growth rate during the period of parental care and after to increase chances for survival.

There is intensive selection by breeding companies for poultry species with the following traits being among the most important:

- Growth rate
- Feed to gain ratio (F:G) or feed efficiency
- Increased proportion of marketed meat (skeletal muscle).

41.1.2 Growth curves

Growth in poultry and wild birds can be described by a sigmoidal growth curve (Figure 41.1). This is irrespective of whether the metric for growth is body weight, skeletal length parameter, or organ weight.

41.1.2.1 Logistic equation

The growth rate can be estimated by the following logistic equation:

$$W_t = A/(1 + \exp[-k(t - t_0])$$

where W_t is the weight at time t,
t_o is the initial time,
A is the asymptote or plateau, and
k is the growth rate constant (Ricklefs, 1979). The growth rate is maximal at half A (Ricklefs, 1979). However, the early hatched chick exhibits the maximal posthatch percentage growth rate, and this will subsequently decline.

41.1.2.2 Gompertz model

An alternative and frequently used mathematical expression for growth is the Gompertz model (see below).

Sturkie's Avian Physiology. https://doi.org/10.1016/B978-0-12-819770-7.00019-0

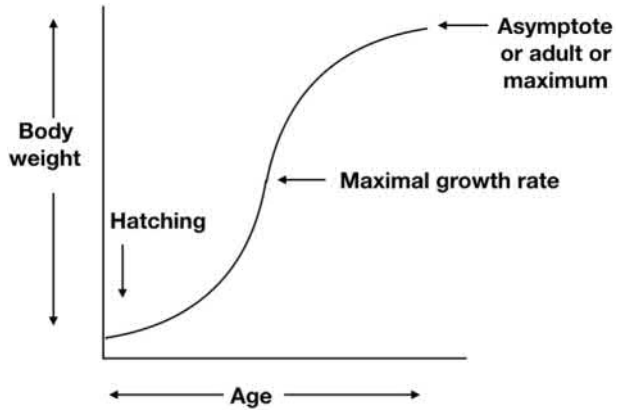

FIGURE 41.1 A generalized growth curve in birds. The sigmoidal S-shaped curve describes the accelerating growth rate in young birds (late embryonic/early post hatch) to a maximal growth rate following by decelerating growth and finally the end of growth.

Gompertz's growth model

$$W_t = A \cdot e^{-be^{-kt}}$$

where W_t is the weight at time t,
t_o is the initial time,
A is the asymptote or plateau,
B is a constant
e is the mathematical constant, and
k is the growth rate constant.

Examples of growth rate constants for three similarly sized birds are shown in Table 41.1. Growth rates were approximately fourfold greater in the altricial starling compared to the precocial Japanese quail.

An alternative approach to growth rate is average daily gain (ADG). This is equivalent to delta body weight. An example of the changes in ADG in chickens is shown in Figure 41.2.

41.1.3 Growth of different organs

In wild birds, relative organ weights exhibit marked shifts during growth with the relative organ weight for pectoralis skeletal muscle increasing ~10-fold in starlings, terns, and Japanese quail (Table 41.1). In contrast, the relative weight of the heart is consistent between young chicks and adult birds (Table 41.1). Body composition changes during growth with increases in the proportion of solids and lipids (Table 41.1). Similarly, in poultry, there is disproportional growth of organs (Table 41.2).

41.2 Evolutionary perspectives of avian growth

Growth is continuous, rapid, and without interruption in Neornithine avian species (all extant birds). In contrast, growth in preavian theropods was intermittent (Chinsamy and Elzanowski, 2001). One of the characteristics of birds is their fast growth rate.

Tables 41.3 and 41.4 compare growth rates in vertebrate taxa. Altricial land birds exhibit faster growth rates than precocial birds (Case, 1978). Modern birds (Neornithes) exhibit high growth rates and markedly greater growth rates than nonavian dinosaurs (Erickson and Tumanova, 2001; Werner and Griebeler, 2014). In contrast, based on fossil evidence from the Upper Jurassic Epoch (~150 million years ago), the growth rate of the primitive bird, *Archaeopteryx*, was slow (see Figure 41.3) (Erickson et al., 2009) and similar to that of nonavian dinosaurs (Werner and Griebeler, 2014). There appears to have been parallel evolution of high growth rates in mammals and modern birds (Neornithes).

41.3 Altricial versus precocial birds

Growth rates are markedly greater in altricial than precocial birds (Case, 1978) (Table 41.3.). This is explicable by the diversion of energy and other nutrients for development in precocial birds and altricial species requiring considerably more parental care. Interestingly, there appears to be acceleration of the posthatch development of the profile of circulating concentrations of growth hormone (GH) and insulin like growth factor (IGF) 1 in altricial species. Peaks in plasma concentrations of both GH and IGF1 during posthatch growth occur earlier in altricial (European starlings) than precocial birds (Japanese quail) (Schew et al., 1996).

41.4 Sexual dimorphism in growth

41.4.1 Overview

There is sexual dimorphism in adult body weight in birds and, hence, in growth rate. This is according to Angel and colleagues (2015); they employed the following as an index of size dimorphism:

$$\text{Size dimorphism index(SDI)} = \left[\frac{\text{Mean male}}{\text{Mean female}} - 1\right] \times 100$$

where males are larger than females, the SDI is positive, and when females are larger than males, the SDI is negative.

TABLE 41.1 Growths rates in three avian species.

	Starling (*Sturnus vulgaris*) Altricial	Common tern (*Sterna hirundo*) Semialtricial	Japanese quail (*Coturnix japonica*) Precocial
Body weight in g			
Newly hatched chick	5.23	13.5	6.5
Adult	79	110	113
Age at maximal growth rate in days	6.4	7.9	28.9
Growth rate k	0.405	0.267	0.106
Body composition			
% solid			
Chick	13.2	21.3	24.1
Adult	35.6	40.1	35.8
% lipid			
Chick	1.6	1.9	6.4
Adult	4.4	6.0	9.0
Organ weights at % of body weight			
Heart			
Chick	1.0	1.3	1.5
Adult	1.4	1.6	1.3
Liver			
Chick	3.9	4.8	2.6
Adult	5.3	6.3	3.9
Pectoralis			
Chick	2.4	1.3	1.7
Adult	20.2	16.3	19.4

Data from or calculated from Ricklefs (1979).

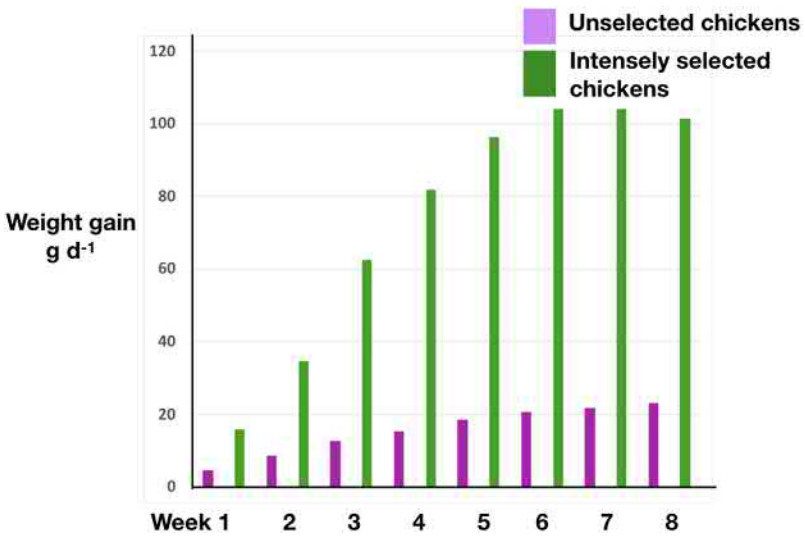

FIGURE 41.2 Changes in growth rate expressed as average daily gain in unselected meat-type chickens and highly genetically selected broiler chickens. *Data from Zuidhof et al. (2014).*

TABLE 41.2 Effect of intensive genetic selection of relative organ weights in 6-weeks-old chickens.

Genetic stock	Relative weights as %		
	Breast muscle e.g., pectoralis	Heart	Abdominal fat pad
Females			
Unselected meat-type chickens	11.9 + 0.44	0.556 + 0.030	0.50 + 0.10
Highly selected 2001 broiler chickens	20.5 + 0.44	0.484 + 0.030	1.50 + 0.10
Males			
Unselected meat-type chickens	11.2 + 0.44	0.591 + 0.030	0.75 + 0.10
Highly selected 2001 broiler chickens	19.5 + 0.44	0.535 + 0.030	1.29 + 0.10

Data shown as mean + SEM from Havenstein et al. (2003a).

TABLE 41.3 Comparison of growth rates in extant altricial with extant precocial land birds and *Archaeopteryx* and extant reptiles.

	Growth rates g/day
Extant altricial land birds	28.6
Extant precocial land birds	5.7
Archaeopteryx	1.9
Extant reptiles	0.46

Data from Case (1978).

TABLE 41.4 Differences in growth characteristics (regressions of $\log_{10}$ maximal growth rate per day versus $\log_{10}$ body weight at maximal body weight) between modern birds and other vertebrate groups.

Vertebrate taxa	Intercept [95% confidence limits]
Modern birds	
Altricial birds	−0.61 [−0.50 to −0.72]
Precocial birds	−0.83 [−0.61 to −1.05]
Eutherian mammals	−1.05 [−0.88 to −1.23]
Nonavian dinosaurs	−1.95 [−1.43 to −2.46]
Reptiles	−2.14 [−1.64 to −2.65]
Fish	−2.80 [−2.34 to −3.26]

Adapted from Werner and Griebeler (2014).

41.4.2 Sexual dimorphism in domesticated birds

There is some sexual dimorphism in growth rate in chickens, turkeys (Table 41.5), Muscovy ducks, and domestic ducks (Figure 41.4.) with size dimorphism indices (SDIs) of, respectively, 30%, 16%, 47%, and 6.5% (Tai and Rouvier, 1998; Werner and Griebeler, 2014). Interspecies hybrids between Muscovy ducks and domestic ducks exhibit either SDIs similar to those in Muscovy ducks (offspring of female Muscovy ducks and male domestic ducks) or domestic ducks (offspring of male Muscovy ducks and female domestic ducks) (Figure 41.4). The growth rate of males of interspecies hybrid males between Muscovy ducks and domestic ducks is between those in Muscovy ducks and domestic ducks. This is consistent with dosing of growth-related genes on the WW chromosomes or codominant genes. Similarly, in male offspring of male Muscovy ducks and female domestic ducks, growth rates are below that of either Muscovy ducks or domestic ducks

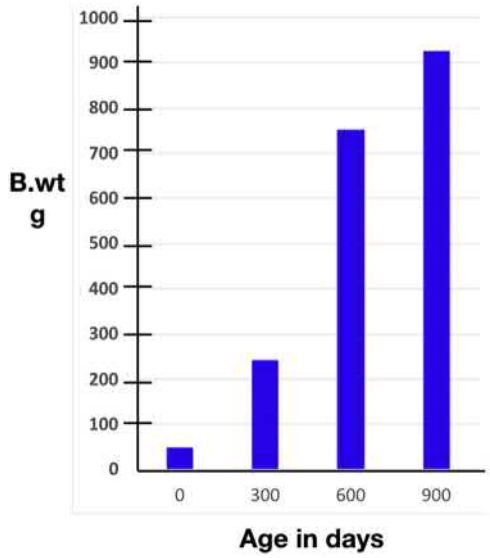

FIGURE 41.3 Slow growth of an early bird, *Archaeopteryx*. *Adapted from data in Erickson et al. (2009).*

In contrast, in female offspring of female Muscovy ducks and male domestic ducks, growth rates are below that of either Muscovy ducks or domestic ducks. This is consistent with low growth rate of this hybrid being due to the Z chromosome for the domestic duck.

Concomitant with sexual dimorphism in Muscovy ducks (Figure 41.4), there is analogous and marked sexual dimorphism in circulating concentrations of IGF1 in (Baéza et al., 2001). There was no sexual dimorphism in body weights (at either hatching or at 6 weeks posthatching) in ZW females subjected to sex reversal *in ovo* following administration of an aromatase inhibitor compared to ZZ males (Mohammadrezaei et al., 2014). In addition, there were marked increases in the growth rate of ZW genetic females subjected to sex reversal following IGF1 administration *in ovo* (Mohammadrezaei et al., 2014).

41.4.3 Sexual dimorphism in wild birds

Table 41.6 provides examples of avian species where the male is larger, the female is larger, and where there is little difference. Similarly, among seabirds, there are species where the male is larger and others where the female is larger (Fairbairn and Shine, 1993). In contrast, in 26 passeriform species, the male is larger than the female (Mills, 2008).

41.5 Growth hormone

41.5.1 Overview

GH is one of a series of hormones that influence growth rate. GH acts by binding to the growth hormone receptor (GHR). This is followed by dimerization of two GHR molecules and activation of JAK2 and ultimately synthesis and release of IGF1 (see Figure 41.5); IGF1 mediating the effects of GH on growth (Figure 41.5).

41.5.2 Chemistry and evolution of GH

There is marked conservatism in GH in nonpasserine birds (see Figure 41.6). This conservatism argues for the importance of GH in birds. Passerine birds exhibit an unusual feature with duplication of the GH gene (Yuri et al., 2008; Arai and Iigo, 2010). Along with the gene duplication of GH in passeriform birds, there is 10-fold acceleration in the rates of amino acid substitution, particularly in GH-B (Yuri et al., 2008) (see Figure 41.6). This may be due to relaxed selection pressure.

41.5.3 GH and growth

Growth of chickens was reduced by about 40% in hypophysectomized chickens (King, 1969; King and Scanes, 1986) (see Figure 41.7). Hypophysectomy not only removes GH but also depresses thyroid activity due to the absence of thyrotropin. Replacement therapy with GH improves growth rate (see Figure 41.7). In dw chickens, growth is depressed reflecting the decreases in circulating concentrations of triiodothyronine (T_3) and IGF1 (Tixier-Boichard et al., 1992) (see Figure 41.7). About 60% of growth is independent of pituitary hormones and 70% is independent of GH.

TABLE 41.5 Sexual dimorphism in growth rate in poultry science.

Species and age	Weight in kg		SDI	References
	Female	Male		
Chickens (8 weeks old)				
Nonselected	0.76	1.01	32.9%	Havenstein et al. (2003b)
Selected	3.49	4.40	26.1%	Havenstein et al. (2003b)
Turkeys (12 weeks old)				
Intensive production	5.94	6.92	16.1%	Sogut et al. (2016)
Free range	3.76	4.04	16.4%	Sogut et al. (2016)

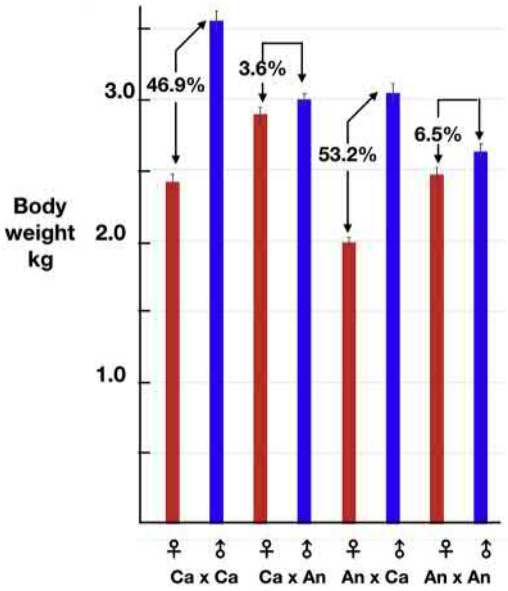

FIGURE 41.4 Sexual dimorphism in body weight at 10 weeks old in Muscovy and domestic ducks and intergeneric hybrids. [Ca - *Cairina moschata* (Muscovy ducks); An - *Anas platyrhynchos* (domestic duck and mallard)]. *Data from Tai and Rouvier (1998).*

In hypophysectomized turkeys, growth is depressed, but GH replacement has no discernible effect on growth rate of young turkeys (Proudman et al., 1994). Young rapidly growing broiler chickens (7 weeks of age) do not respond to exogenous GH (Burke et al., 1987), while older chickens appear to be GH responsive (VasilatosYounken et al., 1988), presumably due to greater abundance of the hepatic GHR (Burnside and Cogburn, 1992). There is a strong synergism between exogenous GH and dietary T_3 in reducing body fat deposition in young broiler chickens (Cogburn, 1991). In 8-week-old female chickens, pulsatile, but not continuous, GH infusion stimulated growth (Vasilatos-Younken et al., 1988), while in 12-week-old male chickens, continuous administration of GH increases growth rate (Scanes et al., 1990).

41.5.4 GH receptors

There is evidence that GHR is downregulated by GH; hepatic GH binding in chickens being increased following hypophysectomy and return to control levels with GH

TABLE 41.6 Examples of sexual dimorphism of adult body weight of birds.

	Female	Male	Reference
Body weight g			
Larger males			
Pheasant (*Phasianus colchicus*)	1,222	1,576	Whiteside et al. (2018)
Adélie Penguin (*Pygoscelis adeliae*)	4,600	5,000	Jennings et al. (2016)
Wandering albatross (*Diomedea exulans*)	7,840	9,440	Shaffer et al. (2001)
Larger females			
Australian brown falcon (*Falco berigora*)	658	486	McDonald et al. (2005)
Australasian gannet (Morus serrator)	2,705	2,570	Angel et al. (2015)
Emu (*Dromaius novaehollandiae*)	45,400	38,600	Maloney and Dawson (1993).
Wing length cm			
Larger males			
Australian brown falcon (*Falco berigora*)	36.1	33.1	McDonald et al. (2005)
Larger females			
Wandering albatross (*Diomedea exulans*)	299	331	Shaffer et al. (2001)
Flipper length cm			
Larger males			
Adélie Penguin (*Pygoscelis adeliae*)	20	21	Jennings et al. (2016)

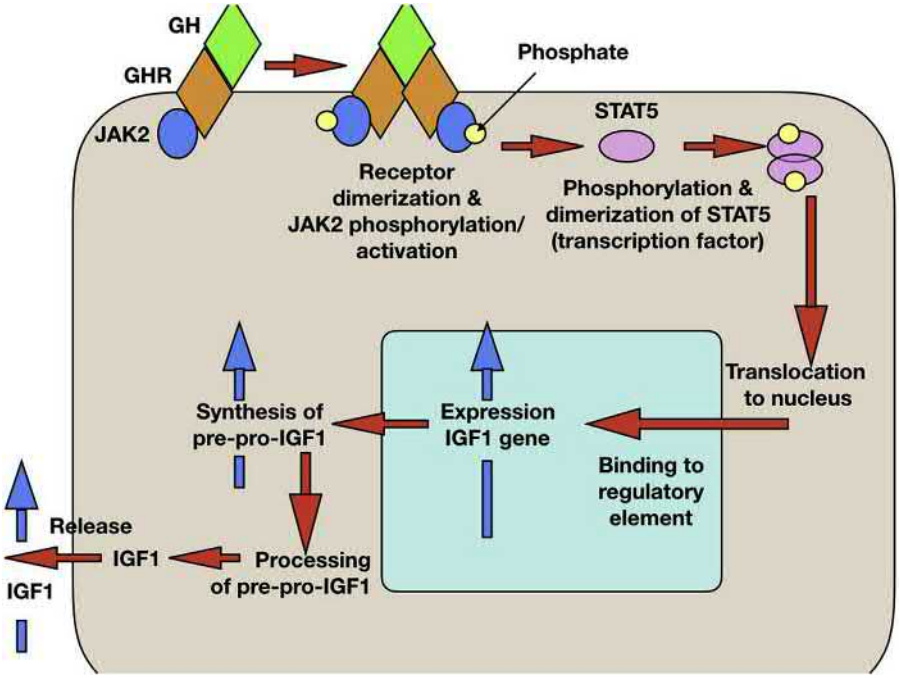

FIGURE 41.5 Mechanism of action of GH.

injections (Vanderpooten et al., 1991a). Moreover, high hepatic GH binding declines as plasma concentrations of GH rise late in embryonic development and are increased in adults that have low circulating concentrations of GH (chicken: Vanderpooten et al., 1991b).

41.5.5 Sex-linked dwarf chickens as a model for growth hormone action

The sex-linked dwarf chicken (gene symbol, dw) (Hutt, 1959; Guillaume, 1976) is an interesting model for understanding the role of GH in growth and development as dw chickens have a defect in the GHR (Burnside et al., 1991; Huang et al., 1993). Obviously, the dw chickens exhibit both reduced growth and adult size (Hutt, 1959; Guillaume, 1976; Tixier-Boichard et al., 1992). There is some, albeit very low, GH-binding activity in the liver of dw chickens (Leung et al., 1987; Vanderpooten et al., 1991b).

As might be expected, dw chickens have shifts in circulating concentrations of hormones, plasma levels of GH and thyroxine (T_4) being elevated, while those of T_3 and IGF1 levels are depressed (Scanes et al., 1983; Huybrechts et al., 1985). The depression in circulating concentrations of IGF1 would be anticipated due to the impairment of GH action. Another consequence of the GHR lesion is that metabolism of T_4 to the active thyroid hormone, T_3, is impaired (Scanes et al., 1983; Kuhn et al., 1990). This is consistent with deiodination being regulated by GH (Kuhn et al., 1987; Darras et al., 1990). The hypothyroid state of dw chickens contributes to lowered basal metabolism (Guillaume, 1976). Continuous treatment of dw chicks with both T_3 and IGF1 partially restores growth rate (see Figure 41.7) (Tixier-Boichard et al., 1992).

41.6 Insulin-like growth factors

41.6.1 Overview

As in mammals, birds have two IGFs (IGF1 and IGF2) that exert insulin-like effects on metabolism and are important regulators of cellular differentiation, proliferation, and growth of tissue. The liver is the major source of IGFs (e.g., Giachetto et al., 2004). There is also expression of both IGF1 and 2 in multiple tissues. For instance, there is marked expression of IGF1, IGF2, and IGF1 receptor (IGF1R) by both proliferative and hypertrophic chondrocytes (Leach et al., 2007) in the epiphyseal cartilage (Lu et al., 2010).

41.6.2 Chemistry and evolution of IGF1 and IGF2

IGF1 consists of a sequence of 70 amino acids. IGF1 has an identical structure across avian species, while there was a single substitution in IGF2 (see Figures 41.8 and 41.9). This remarkable conservatism argues for the very high selective value of IGF1 and IGF2. Similarly, there are very few differences (~3) between sequences of IGF1 across the eutherian mammals (Rotwein, 2017).

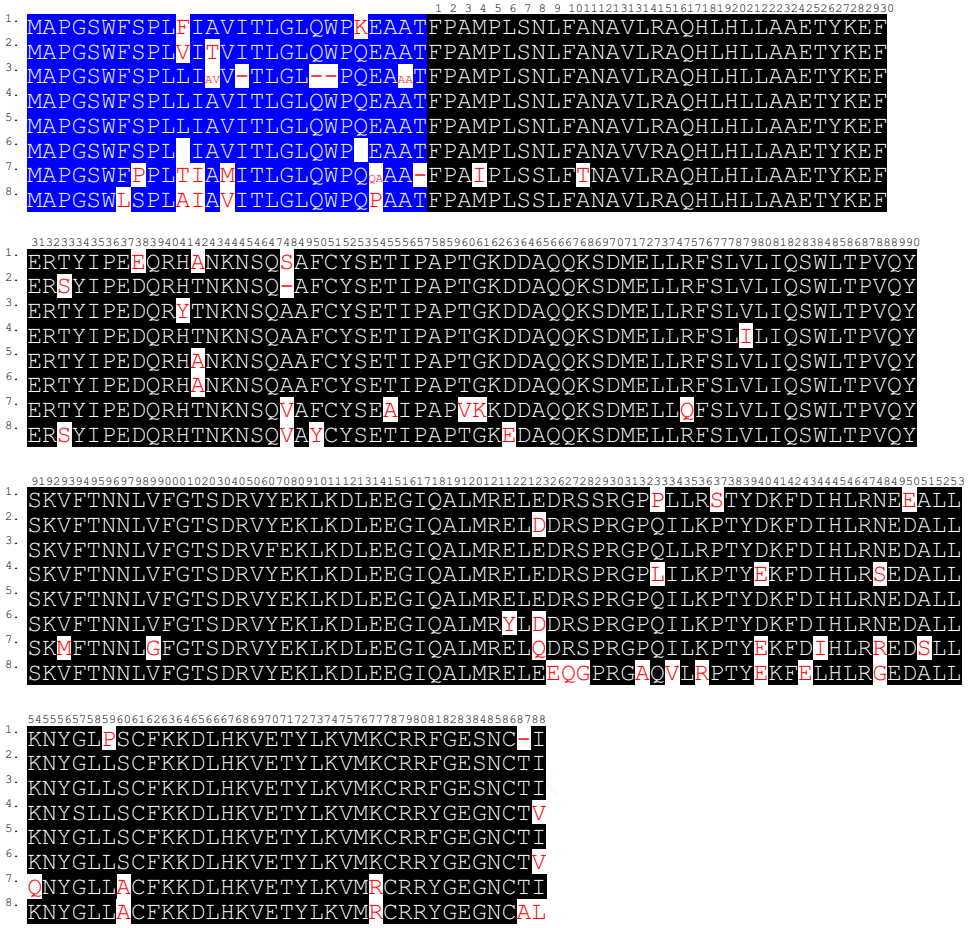

Sub-class Paleognathae
1. African ostrich (*Struthio camelus*) (JN559394.1)
Sub-class Neognathae
Super-order Galloanserae
Order Anseriformes
2. Domestic goose (*Anser anser*) (AY149895),
Order Galliformes
3. Chicken (*Gallus gallus*) (NM_204359)
Super-order Neoaves
4. Anna's hummingbird (*Calypte anna*) (XM_008502621.1)
Order Sphenisciformes
5. Emperor penguin (*Aptenodytes forsteri*) (XM_009287870.1)
Order Strigiformes
6. Barn owl (*Tyto alba*) (XM_009972035.1)
Order Passeriformes
7. GH-A American crow (*Corvus macrorhynchos*) (AB560855.1)
8. GH-B American crow (*Corvus macrorhynchos*) (AB560856.1)

FIGURE 41.6 Comparison of pro-GH structures in selected avian species. Black background indicates mature GH and blue background indicates signal peptide.

41.6.3 IGFs and growth

There is strong evidence that IGF1, and probably IGF2, plays a role in growth. Circulating concentrations of IGF1 are decreased in growth depressed young chickens whether hypophysectomized or dwarf (Huybrecht et al., 1985) (Tixier-Boichard et al., 1992). Administration of IGF1, together with T_3, partially restored growth in dw chickens to those in nondw birds (Tixier-Boichard et al., 1992) (Figure 41.7). Administration of IGF1 *in ovo* increased

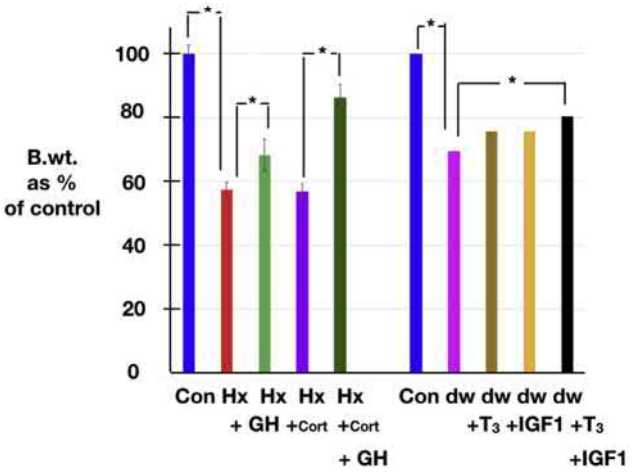

FIGURE 41.7 GH and growth in young chickens. Left: Effect of hypophysectomy (Hx) with or without GH replacement therapy (King and Scanes, 1986). Right: Difference in growth rate in dw and nondw chicks together with the effect of T_3 and/or IGF1 on growth in dw chicks (Tixier-Boichard et al., 1992).

body weights in male chickens at either hatching or at 6 weeks posthatching, thus increasing the SDI (Mohammadrezaei et al., 2014).

41.6.4 IGF1 and muscle and adipose growth

IGF1 stimulates growth of skeletal muscle There is increased proliferation of muscle satellite cells in the presence of IGF1 or IGF2 in vitro (chicken: Duclos et al., 1991). Moreover, IGF1 stimulates the proliferation of myoblast cells (Yu et al., 2015). Infusion of IGF1 increased the fractional rate protein synthesis in pectoralis muscle of fasted but not fed young chickens; fasting having depressed the fractional rate protein synthesis (Kita et al., 2002a). Moreover, a single injection of IGF1 induced an increase in the fractional rate of muscle protein synthesis (Conlon and Kita, 2002).

IGF1 also influences growth of adipose tissue with IGF1 or IGF2 stimulating proliferation of preadipocyte but

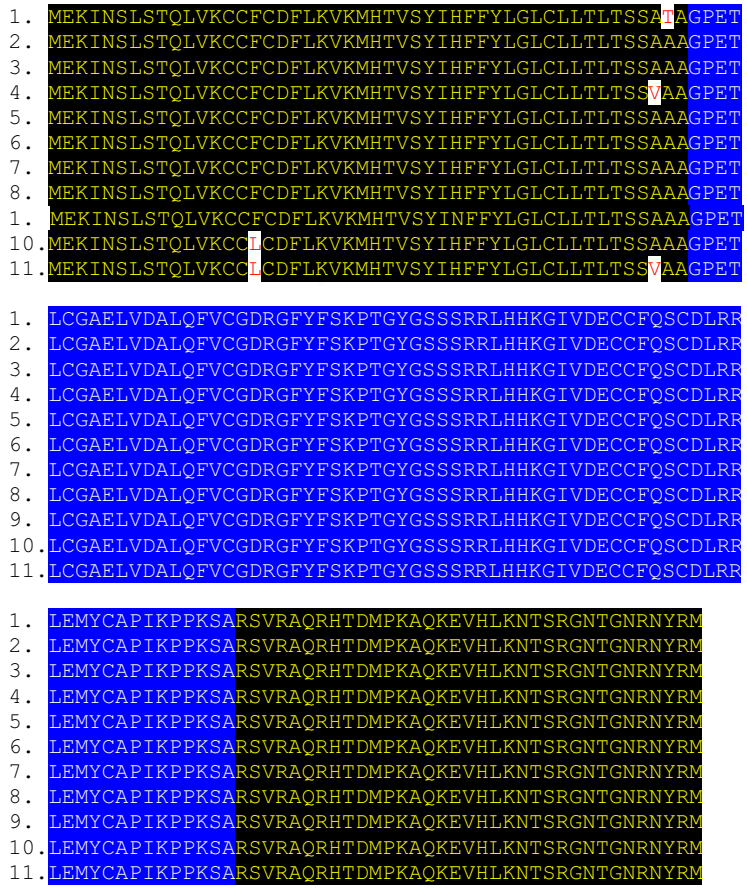

1. Emu (*Dromaius novaehollandiae*) XM_026117890
2. Okarito brown kiwi (*Apteryx rowi*) XM_026083913
3. Chicken (*Gallus gallus*) NM_001004384
4. Black swan (*Cygnus atratus*) XM_035562724
5. Rock pigeon (*Columba livia*) XM_005500280
6. Adelie penguin (*Pygoscelis adeliae*) XM_009332952
7. Little egret (*Egretta garzetta*) (XM_009649249
8. Saker falcon (*Falco cherrug*) XM_005435048
9. Barn owl (*Tyto alba*) XM_009962820
10. Kakapo (*Strigops habroptila*) XM_030480499
11. Zebra finch (*Taeniopygia guttata*) XM_002199813

FIGURE 41.8 Structure of prepro-IGF1 in birds. Blue indicates IGF1. Red indicates difference.

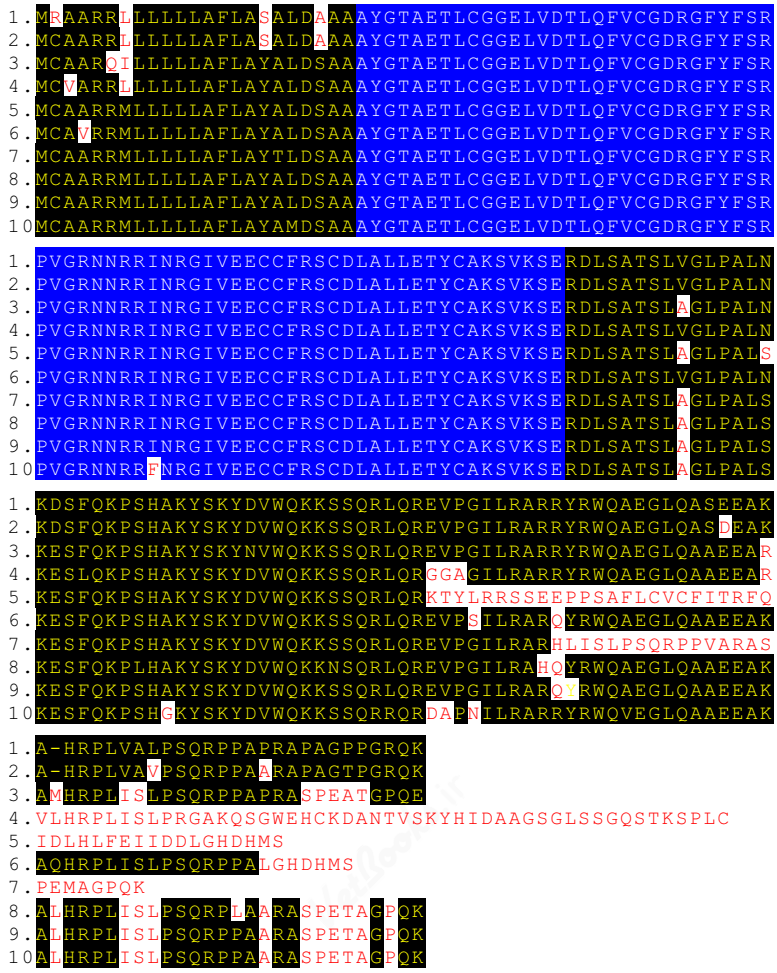

1. Emu (Dromaius novaehollandiae) Genbank XM_026092723
2. Okarito brown kiwi (*Apteryx rowi*) XM_02607899
3. Chicken (*Gallus gallus*) NM_001030342
4. Goose (*Anser cygnoides*) XM_013191560
5. Rock pigeon (Columba livia) XM_021299122
6. Adelie penguin (*Pygoscelis adeliae*) XM_009328596
7. East African grey crowned-crane (Balearica regulorum gibbericeps) XM_010301245
8. Peregrine falcon (*Falco peregrinus*) XM_005237318
9. Bald eagle (*Haliaeetus leucocephalus*) XM_010563896
10 Zebra finch (*Taeniopygia guttata*) NM_001122966.1

FIGURE 41.9 Structure of prepro-IGF2 in birds. Blue indicates IGF2. Red indicates difference.

inhibiting differentiation (chicken: Butterwith and Gilroy, 1991; Butterwith and Goddard, 1991).

41.6.5 IGF receptors

IGF1Rs are tyrosine kinases as are insulin receptors. Both IGF1 and IGF2 bind to the IGF1R in birds (chicken: Duclos et al., 1991). The structure of avian IGF1R has been deduced in the chicken (*Gallus gallus*) (Genbank accession NM_205032). The actions of IGF1 are mediated by the PI3K/Akt signalling pathway based on effects on myoblast cells (Yu et al., 2015).

41.6.6 Nutrition and IGF1

Adverse nutritional status depresses the IGF1 system. For instance, fasting is followed by decreases in circulating concentrations of IGF1 and hepatic IGF1 expression (young chickens: Kita et al., 1998; Kita et al., 2002b). Similarly, feed-restricted chickens have reduced plasma concentrations of IGF1 and IGF2 (Leili et al., 1997). Moreover, chickens fed a very low protein diet have reduced plasma concentrations of IGF1 and IGF2 (Lauterio and Scanes, 1987; Leili, and Scanes, 1998; Kita et al., 2002b). In contrast, fasted young chickens were reported to

have elevated plasma concentrations of IGF2 (McMurtry, 1998) (Figure 41.10).

41.6.7 IGF1 and IGF2 in wild birds

The selective value of IGF1 and IGF2 is supported by the unexpectedly high identity between the sequences of IGF1 or IGF2 across avian species (Figures 41.8 and 41.9). There is evidence that IGF1 plays an important role in growth and/or adult size. Plasma concentrations of IGF1 are positively associated with body weight/body size in adult passerine birds (Lodjak et al., 2018). Plasma concentrations of IGF1 were associated with tail length and UV coloration in plumage in a songbird, male-bearded reedling (*Panurus biarmicus*). There are also short-term effects on circulating concentrations of IGF1. For instance, handling stress depressed plasma concentrations of IGF1 in the bearded reedling (Tóth et al., 2018). Based on studies in European starlings (*Sturnus vulgaris*) and Japanese quail (*Coturnix japonica*), wild birds exhibit the same pattern of circulating concentrations of IGF1 as poultry with a posthatch peak and a subsequently decline (Schew et al., 1996). Nutritional restriction depressed plasma concentrations of IGF1 in European starlings and Japanese quail (Schew et al., 1996).

There is further evidence that IGF1 plays a role in muscle development in wild birds. Muscle IGF1 expression is increased following flight captive European starlings (*S. vulgaris*) and in white-throated sparrows (*Zonotrichia albicollis*) exposed to a long photoperiod that would induce migratory behavior (Price et al., 2011).

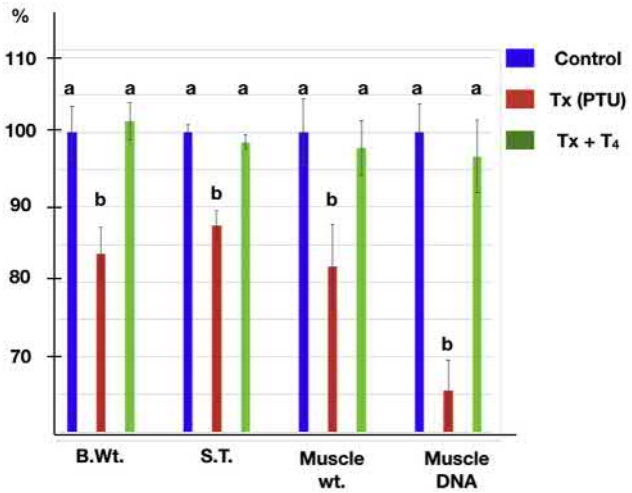

FIGURE 41.10 Effect of chemical thyroidectomy (Tx) by propylthiouracil treatment (PTU) and thyroxine (T_4) replacement therapy (by daily injections). *Using data from King and King (1973).*

41.6.8 Insulin-like growth factor–binding proteins

41.6.8.1 Overview

Both IGF1 and IGF2 circulate bound to carrier proteins known as the IGF-binding proteins (IGFBPs). Multiple tissues express IGFBPs. For instance, the proliferative and hypertrophic chondrocytes in the epiphyseal cartilage express IGFBP2, IGFBP3, IGFBP5, and IGFBP7 (Leach et al., 2007; Lu et al., 2010). Binding of IGF1 or IGF2 to IGFBPs can either increase or decrease the biological activities of the growth factors (Butterworth, 1997). Multiple IGFBPs have been reported in chickens with the sequences deduced

- IGFBP-1 Genbank Accession NM_001001294.1
- IGFBP-2 - NM_205359.1
- IGFBP-3 - NM_001101034.1
- IGFBP-4 - NM_204353.1
- IGFBP-5 - XM_422069.6
- IGFBP-7 - XM_420577.6.

41.6.8.2 Nutrition and IGFBPs

Nutritional status influences IGFBPs. There are marked changes in the expression of IGFBP2 with nutritional status in young chickens. Expression of IGFBP2 is increased in the liver and gizzard of fasted birds but decreased in the brain (Kita et al., 2002b). In contrast, hepatic expression of IGFBP2 is depressed in chicks fed a fat-free diet or an extremely low protein diet (Kita et al., 2002b). Refeeding reverses the effect of fasting in the liver and gizzard (Kita et al., 2002b). Moreover, expression of IGFBP2 and IGFBP3 is increased in the liver but not brain of fasted chickens (Fujita et al., 2018).

41.6.9 Insulin-like growth factor 2–binding proteins

There are also binding proteins that bind IGF2 mRNA. Examples include the following: IGF2I mRNA–binding protein 1 binds single-stranded RNA (Chen et al., 2019). Chickens on a high fat diet exhibit increased the weights of abdominal fat pad due to adipocytes hypertrophy together with increased expression of IGF2BP in liver and adipose tissue (Chen et al., 2019). Moreover, transfection of avian cells with IGF2BP increased expression of fatty acid metabolism (Chen et al., 2019). Another IGF2 RNA–binding protein is IGF2BP3. This translational activator of IGF2 is GH dependent; expression of IGFBP3 is being depressed in skeletal muscle of dw chickens (Lin et al., 2017).

41.7 Thyroid hormones (hypothalamo–pituitary–thyroid axis)

41.7.1 Overview

The physiology of thyroid hormones is considered elsewhere (Chapter 31); however, the role of thyroid hormones in regulation of growth and development is discussed here. In birds and mammals, the predominant iodothyronine secreted by the thyroid glands is T_4, a prohormone which is converted to the active form T_3 or catabolized to metabolically inactive reverse T_3.

41.7.2 Thyroid hormones and growth

In birds, the thyroid hormones are required for normal growth (Figure 41.10), since thyroidectomy results in a reduction in growth rate in young chickens (Raheja and Snedecor, 1970; King and King, 1973, 1976; Moore et al., 1984) or in the chick embryo (McNabb et al., 1984). In young chickens, the decrease in growth results in reductions in skeletal and bone masses (King and King, 1973, 1976; Moore et al., 1984). These effects of thyroidectomy can be overcome partially by T_3 or T_4 replacement therapy (King and King, 1973). Similarly, growth can be stimulated by T_3 or T_4 administration in hypophysectomized chicks (King, 1969; Scanes et al., 1986) and in sex-linked dw chickens, which are T_3 deficient (Scanes et al., 1983; Marsh et al., 1984; Leung et al., 1984). The stimulatory effect of thyroid hormones in growing chicks can be mediated either by increases in the circulating concentrations of IGF1 and/or by direct effects of T_3 on the growing tissues. There is, indeed, evidence that T_3 can stimulate the growth of chick embryo cartilage in vitro (Burch and Lebovitz, 1982; Burch and Van Wyk, 1987).

While T_3 is required for the full manifestation of growth, dietary T_3 depresses growth rate when continuously administered to growing chickens (May, 1980; Decuypere et al., 1987). This could be due to the inhibitory effects of T_3 on GH release in chickens.

Not only do thyroid hormones appear to be required for growth in the avian embryo but also they influence differentiation and the acquisition of full functioning by embryonic organs prior to hatching (see Chapter 15 for details). Effects of T3 in the late-stage embryo are not surprising in view of the increases in circulating concentrations observed before hatching (McNabb and Hughes, 1983). However, the reduction in growth rate in chick embryos receiving goitrogen treatment is perhaps surprising since circulating T_3 concentrations are low, although T_4 levels are high at mid-stage (days 9–11) (McNabb et al., 1984). There could be significant monodeiodination of T_4 to T_3 in the peripheral tissues or high levels of T_4 could exert effects by binding to the avian thyroid hormone receptor. The latter is unlikely based on the chicken hepatic nuclear binding studies (Bellabarba and Lehoux, 1981). Further evidence that the thyroid hormones are exerting a role in the middle of development of chick embryos comes from the reports of high levels of thyroid hormone receptor in the brain and liver (Bellabarba and Lehoux, 1981; Bellabarba et al., 1983). The thyroid hormone receptors are considered elsewhere in this volume (Chapter 15).

41.7.3 Thyroid hormones and wild birds

Circulating concentrations of the active thyroid hormone, T_3, are related to basal metabolic rate (Welcker et al., 2013).

41.8 Sex steroid hormones

41.8.1 Overview

In many mammals, growth can be stimulated by androgens and/or estrogens. These effects are exerted either directly at the tissue level or mediated by the hypothalamo–pituitary axis. In either case, estrogen acts via binding to nuclear receptors, while androgens can evoke their effect via either the nuclear androgen receptor or the estrogen receptor following aromatization to estrogen.

Sex steroids have been observed to influence growth but with remarkably large differences between species in the magnitude and even direction of the effects in avian species.

41.8.2 Sex steroids and poultry

In the chicken, the marked sexual dimorphism in growth rate does not appear to be related to either androgens or estrogens. The administration of androgens (either aromatizable (e.g., testosterone or 19-nortestosterone) or nonaromatizable (e.g., 5α-dihydrotestosterone)), at physiological concentrations, to male, female, or castrated male chicks does not stimulate growth (Fennell and Scanes, 1992a). Instead, skeletal growth, particularly of the long bones, is considerably reduced (Fennell and Scanes, 1992a). In contrast, in the domestic turkey, administration of androgens is followed by considerable increases in growth (Fennell and Scanes, 1992b). In view of the ability of either aromatizable or nonaromatizable androgens to enhance growth of the turkey,

it is probable that the effect is mediated by androgen receptors in the muscle and bone.

41.8.3 Sex steroids and wild birds

Androgens have been reported to exert either positive or negative effects on growth of wild birds. This comes predominantly from studies in which androgens were administered into eggs or comparing endogenous androgen concentrations. For instance, posthatching growth is increased after testosterone administration into the egg of male great tits (*Parus major*) (Tschirren, 2015) and canaries (*Serinus canaria*). Conversely, *in ovo* administration of androgens depressed posthatching growth of nestling American kestrels (Sockman et al., 2008) and male canaries (*S. canaria*) (Müller et al., 2008). However, a stimulatory effect of in *ovo* testosterone was reported (Schwabl, 1996). In addition, administration of testosterone to canary chicks was followed by elevated rates of growth and skeletal growth (Schwabl, 1996).

The response, posthatching growth, to androgens in eggs exhibits sexual dimorphism in birds. For instance, there was a positive relationship between egg concentrations of androgens in male barn swallows (*Hirundo rustica*) but a negative relationship in females (Saino et al., 2006). Posthatching growth is increased after *in ovo* administration in male but not female great tits (*P. major*) (Tschirren, 2015).

41.9 Adrenocorticotropin and glucocorticoids (hypothalamo–pituitary–adrenocortical axis)

41.9.1 Overview

The hypothalamo–pituitary–adrenocortical axis plays a critical role in the response to stress. The pituitary hormone, adrenocorticotropic hormone (ACTH), stimulates the release of glucocorticoids from the adrenocortical cells. It is assumed corticosterone (CORT) is the major glucocorticoids in birds. Tables P and Q summarize effects of glucocorticoids in wild birds and poultry species. Much of the research on effects of ACTH or glucocorticoids on growth in birds is on chickens. There are potentially differences between chickens and wild birds due to the effect of domestication and genetic selection and that chickens exhibit precocial development, while many wild birds are altricial. It should be noted that studies predominantly employ exogenous CORT or the synthetic glucocorticoid, dexamethasone.

41.9.2 Are glucocorticoids required for development and growth?

Activation of the hypothalamic pituitary adrenocortical axis, with increased circulating concentrations of ACTH and CORT during embryonic development, induces key features of development. For instance, the glucocorticoid, dexamethasone, stimulates secretion of phosphatidylcholine (surfactant) from type II lung cells of embryonic chickens (Sullivan and Orgeig, 2001). Moreover, pituitary grafts *in ovo* or glucocorticoids in vitro induce increased UDP glucuronyltransferase activity in the embryonic liver (Wishart and Dutton, 1974; Burchell et al., 1983). Similarly, dexamethasone induces steroid hydroxylation in the liver (Kimmett et al., 1996). In addition, *in ovo* administration of CORT induces development of somatotrophs (Dean et al., 1999).

Glucocorticoids play important roles in the control of metabolism (see Chapter 17). It is reasonable to infer that maximal growth rates require normal metabolism and, hence, adequate circulating concentrations of glucocorticoids. There is little evidence that insufficient levels of glucocorticoids adversely affect growth in birds. For instance, administration of CORT to hypophysectomized chicks failed to stimulate growth (King and Scanes, 1986).

41.9.3 Glucocorticoid depression of growth

Exogenous glucocorticoids depress or even completely suppress growth in young chickens (see Table 41.7 for examples of studies in which glucocorticoids depressed growth) and chick embryos (see Table 41.8 for examples of studies in which glucocorticoids depressed growth in avian embryos). There is evidence that the genetics and/or growth rate of chickens can influence their responsiveness to glucocorticoids. CORT exerts a greater growth suppressing effect in heavy fast-growing meat type than layer (white Leghorn) chickens (Siegel et al., 1989). Administration of CORT into the yolk of Japanese quail (*C. japonica*) was accompanied by decreased posthatching growth in males but not females (Hayward et al., 2006).

Treatment of growing chickens with CORT increases abdominal fat weight (Buyse et al., 1987; Siegel et al., 1989; Taouis et al., 1993). Similarly, injection of glucocorticoids into growing Japanese quail reduces fat-free body weight (Bray, 1993), while in adults, CORT depresses nitrogen detention and increases nitrogen excretion (De La Cruz et al., 1981). It may well be that glucocorticoids released during stress exert an inhibitory effect on growth but further research in needed particularly determining their effects on posthatching growth of altricial species. Interestingly, CORT administration depressed growth even in hypophysectomized chicks (King and Scanes, 1986). Similarly, CORT exerts a transient suppression of bone growth; for instance, preventing increases in tarsus length (canaries: Müller et al., 2009).

The inhibitory effects of glucocorticoids on muscle growth (Dong et al., 2007) are mediated at least in part by mechanistic target of rapamycin (Wang et al., 2015). Moreover, there is evidence that glucocorticoids increase muscle protein degradation (Klasing et al., 1987). In

TABLE 41.7 Effects of glucocorticoids on growth of birds.

Species and age when treatment initiated	Duration of treatment	ACTH or CORT effect	Reference
Chickens (*Gallus domesticus*)[a]			
ACTH infusion			
3 weeks ♂	14 days	↓ 11.0%	Virden et al. (2007a)
5 weeks old ♂ and ♀	8 days	↓ 81.7%	Puvadolpirod and Thaxton (2000)
6 weeks old ♂ and ♀	7 days	↓ 86.8%	Puvadolpirod and Thaxton (2000)
CORT in feed			
1 day	7 days	↓ 19%	Siegel et al. (1989)
1 day	21 days	↓ 54%	Siegel et al. (1989)
1 week	13 days	↓ 7.7%	Virden et al. (2007a)
3 weeks ♂	10 days	↓ 30.1%	Virden et al. (2007b)
3 weeks ♂	14 days	↓ 45.0%	Virden et al. (2007a)
CORT injected			
3 days ♂ high energy feed	7 days	↓ 1.9%	Yang et al. (2015)
3 days ♂ high energy feed	7 days	↓ 17.5%	Yang et al. (2015)
3 weeks old ♂ and ♀	12 days	↓ 29.7%	Buyse et al. (1987)
Dexamethasone in feed			
1 week old ♂ and ♀	7 days	↓ 39.5%	Du et al. (2019)
3 weeks old ♂ and ♀	21day	↓ 41.0%	Aengwanich (2007)
Dexamethasone injected			
1 week old ♂ and ♀	3 days	↓ 37.5%	Song et al. (2011)
1 week old ♂ and ♀	7 days	↓ 61.1%	Song et al. (2011)
5 weeks old ♂ and ♀	3 days	↓ >100%	Song et al. (2011)
38 day old ♂ and ♀	3 days	↓ 100%	Gao et al. (2010)
Japanese quail (*Coturnix japonica*)			
Dexamethasone injected			
7 week old	7 days	↓ 4.4%	Bray (1993)
Yellow-legged gull (*Larus michahellis*)			
Implanted with CORT 1 day	8 days	↓ 12.6%	Noguera et al. (2018)
Song sparrow (*Melospiza melodia*)			
Oral dosing daily			
Male	7–19 days	↑ 10.2%	Schmidt et al. (2012)
Female		↓ 9.3%	Schmidt et al. (2012)
Barn owl (*Tyto alba*)			
CORT implant		→	Almasi et al. (2012)
Eurasian kestrels (*Falco tinnunculus*)			
Pellets implanted days 10–13	Days 13–16	↓ ~100%	Müller et al. (2009)

[a]*Chickens studies employed meat-type chickens.*

TABLE 41.8 Effects of glucocorticoids administered during embryonic growth on growth of birds.

Species and day of incubation (ED)	Parameter determined	Glucocorticoid effect	Reference
Chicken (*Gallus gallus*)			
CORT			
Day 7 ED	8 weeks posthatch	↓ 21%	Heiblum et al. (2001)
Day 3 ED	Day 19 ED	↓ 26%	Mashaly (1991)
Cortisol			
Day 7 ED	8 weeks posthatch	↓ 21%	Heiblum et al. (2001)
Japanese quail (*Coturnix japonica*)			
Maternal CORT	7 days posthatch	↓ 12.6%	Hayward & Wingfield (2004)
House wrens (*Troglodytes aedon*)			
Day 1 ED	11 days posthatch	↑ 17%	Strange et al. (2016)
Yellow-legged gull (*Larus michahellis*)			
Day 1 ED	1–20 days posthatch	→	Rubolinia et al. (2005)

ED, embryonic day.

addition, there is cross-talk between the adrenocortical axis and the GH–IGF1 axis and growth factors. Dexamethasone depresses expression of IGF1 and IGF1R together with that of MYOD (myoblast determination protein 1), MSTN (myostatin) and MYF5 (Myogenic factor 5) in the *M. biceps femoris* (Song et al., 2011). In addition, effects of CORT may be mediated in part by shifts in the intestinal microbiome (Noguera et al., 2018).

41.10 Insulin

While insulin plays a major role in the control of metabolism (see Chapter 34), there is evidence from older studies that insulin is also involved in the control of growth of at least early avian embryos. Growth of chicken embryos, between days 2 and 5 of development, is increased by administration of low doses of insulin (De Pablo et al., 1985a; Girbau et al., 1987). Conversely, chick embryos treated with antisera to insulin either die or show marked growth retardation (De Pablo et al., 1985b). These reports coupled with the definitive observations of the presence of insulin in early chick embryos argue that insulin is involved in the control of early chick embryo development. Insulin can compete for binding to type-I IGF receptors, albeit to a less extent than IGF1. Thus, the effects of insulin on chicken embryo growth are probably mediated by insulin receptors because insulin is more potent than IGF in stimulating embryo growth (Girbau et al., 1987), and there is evidence from binding studies for specific insulin receptors in chick embryos (Bassas et al., 1987). Moreover, the administration of antisera against the insulin receptor to chick embryos results in reduced growth (body weight, DNA, RNA, and protein) (Girbau et al., 1988). However, the effects of insulin on muscle differentiation are probably mediated via type-I IGF receptors as antisera against the insulin receptor failed to influence embryo creatine–kinase MB isozyme (Girbau et al., 1988).

41.11 Growth factors

41.11.1 Overview

In addition to IGF1 and IGF2, multiple growth factors have been identified. These act by stimulating (or inhibiting) cell proliferation and/or differentiation. Large numbers of genes, involved in regulation of embryogenesis and development, have been studied in the chicken. During early embryogenesis, left/right asymmetry and anterior/posterior and dorsal/ventral axes are formed. Later in development, structures like the limbs and other major structures are formed. For instance, fibroblast growth factors (FGFs) and transforming growth factor β (TGF-β) play an important role in the development of the jaw (Woronowicz et al., 2018). While FGF signalling inhibits primitive hematopoeisis (Nakazawa et al., 2006).

The identification of tissue growth factors and their actions in birds will be briefly considered below.

41.12 Epidermal growth factor and transforming growth factor-α

41.12.1 Chemistry of EGF and TGF-α

The sequence of chicken EGF can be extrapolated based on the sequence of chicken preproEGF together with the

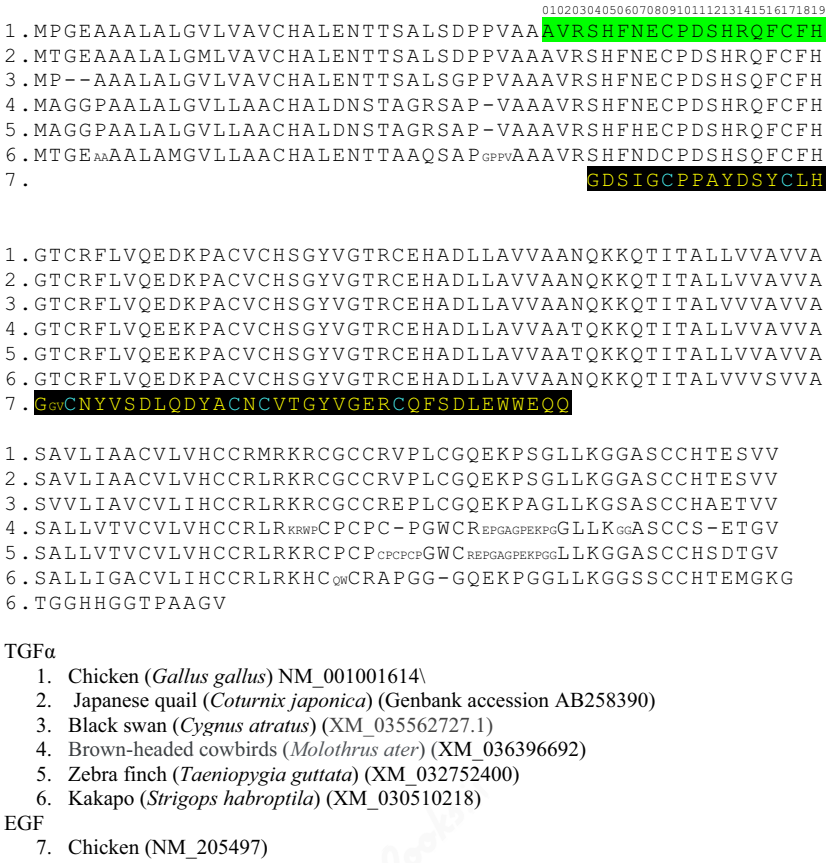

TGFα

1. Chicken (*Gallus gallus*) NM_001001614\
2. Japanese quail (*Coturnix japonica*) (Genbank accession AB258390)
3. Black swan (*Cygnus atratus*) (XM_035562727.1)
4. Brown-headed cowbirds (*Molothrus ater*) (XM_036396692)
5. Zebra finch (*Taeniopygia guttata*) (XM_032752400)
6. Kakapo (*Strigops habroptila*) (XM_030510218)

EGF

7. Chicken (NM_205497)

FIGURE 41.11 Comparison of the structures of avian TGF-α and the homologies shown TGF-α and EGF (alignments based on Marquardt et al., 1983). The amino acid sequence for avian EGF is based on the deduced structure of prepro-EGF and comparison to human EGF (Savage et al., 1972).

homology to human EGF. The sequence of chicken EGF can be extrapolated transforming growth factor-α (TGF-α) (Figure 41.11). EGF is a polypeptide with 53 amino acid residues with marked homologies with avian TGF-α (Figure 41.11).

41.12.2 EGFR receptor

Epidermal growth factor receptor (EGFR) (erbB1) is a type 1 tyrosine kinase. Other members of the family are erbB2, erbB3, and erbB4. Binding of EGF or TGF-α to the EGFR facilitates receptor dimerization and thereby activation.

41.12.3 Actions of EGF and TGF-α

In birds, EGF stimulates the proliferation of heart mesenchymal cells; this effect is potentiated by IGF1 (Balk et al., 1984). Either TGF-α or EGF can stimulate proliferation of adipocyte precursor cells but inhibit their differentiation (chicken: Butterwith et al., 1992).

41.13 Transforming growth factor-β

Functionally and structurally, avian TGF-βs are homodimers. These are formed with the concave aspect of monomer one binds to the convex aspect of monomer two. As would be expected, TGF-β 1, TGF-β 2, and TGF-β 3 are members of the TGF-β superfamily. Other members of the TGF-β superfamily include the following:

- Bone morphogenic proteins (BMPs)
- Müllerian inhibitory substance
- Activin
- Inhibin
- Growth and differentiation factors (GDF) e.g., GDF8 - myostatin (Hinck, 2012). Binding of TGF-β to its receptor activates R-Smads 2 and 3 (Hinck, 2012).

41.13.1 Structure of avian TGF-βs

The three TGF-βs are TGF-β1, TGF-β2, and TGF-β3. These have been characterized in chickens in birds (see

TABLE 41.9 Examples of TGF-α and TGF-β in birds together with related growth factors.

Growth factor	Gene	Species	GenBank accession number
EGF	EGF	Chicken/jungle fowl (*Gallus gallus*)	NM_205497
TGF-α	TGFA	Chicken/jungle fowl (*Gallus gallus*)[a]	AY605246
TGF-β 1	TGFB1	Chicken/jungle fowl (*Gallus gallus*)	NM_001318456
TGF-β 1	TGFB1	Domestic duck/mallard (*Anas platyrhynchos*)	EU661773.1
TGF-β 2	TGFB2	Chicken/jungle fowl (*Gallus gallus*)	NM_001031045
TGF-β 3	TGFB3	Chicken/jungle fowl (*Gallus gallus*)	NM_205454
TGF-β RI (TGF-β R1)	TGFBR1	Chicken/jungle fowl (*Gallus gallus*)	NM_205428
TGF-β RII (TGF-β R2)	TGFBR1	Chicken/jungle fowl (*Gallus gallus*)	NM_204339.1
TGF-β RIII (TGF-β R3)	TGFBR1	Chicken/jungle fowl (*Gallus gallus*)	NM_204339.1
BMP1	BMP1	Chicken/jungle fowl (*Gallus gallus*)	U75331
BMP2	BMP2	Chicken/jungle fowl (*Gallus gallus*)	NM_204358.1
BMP3	BMP3	Chicken/jungle fowl (*Gallus gallus*)	NM_001034819
BMP4	BMP4	Chicken/jungle fowl (*Gallus gallus*)	NM_205237
BMP4	BMP4	Kakapo (*Strigops habroptila*)	XM_030484625
BMP4	BMP4	Great Tit (*Parus major*)	XM_015629595

[a]*Partial sequence only.*

Table 41.9). TGF-β isoforms show 75−80% homology to each other in their amino acid sequence. Moreover, the TGF-β isoforms have the same overall structure as homodimers of 114-amino acid residue−containing subunits.

There is widespread expression of TGF-β in chick embryos with TGF-β1 expressed in some mesodermal and ectodermal cells, TGF-β2 in the precardiac mesoderm, in the optic vesicles, notochord, and neural tube floor plate and TGF-β3 in the lateral embryonic and extraembryonic mesoderm including the blood islands and myocardium (Cooley et al., 2014). TGF-β isoforms are known to be produced by many cell types.

41.13.2 Physiology of avian TGF-βs

TGF-β2 is expressed by muscle satellite cells (chicken: Kocamis et al., 2001), while preadipocytes express TGF-β2, TGF-β3, and TGF-β 4 (Burt et al., 1992). TGF-β1 increases preadipocyte proliferation (chicken: Butterwith and Goddard, 1991). TGF-β bind to type II transmembrane receptor serine/threonine kinase, TGF-βR2, and two type I receptors, TGF-βR1, forming a tetra-heteromeric receptor complex.

41.13.3 Myostatin

41.13.3.1 Myostatin poultry

MSTN plays an important role in muscle growth. MSTN is expressed by muscle satellite cells (chicken: Kocamis et al., 2001).

41.13.3.2 Myostatin in wild birds

There is limited information on MSTN in wild birds. However, multiple spice variation of MSTN has been identified in white-throated sparrows (*Z. albicollis*) and European starlings (*S. vulgaris*) (Price et al., 2011). Expression of MSTN is increased in white-throated sparrows (*Z. albicollis*) in which migratory behavior is induced by exposure to a long daylength (Price et al., 2011).

41.14 Bone morphogenetic protein

41.14.1 Overview

BMPs 1−4 are homodimers (Reynolds et al., 2000). The sequences of BMP1−4 have been reported in multiple birds

(see Table 41.9 for examples). Signal transduction for BMPs following receptor binding includes SMAD transcription factors.

41.14.2 Bone morphogenetic protein 1 and tolloid

BMP1 and tolloid play a role in the production of the matrix in skeletal development. BMP1 is an approximately 700 amino acid−containing protein. Two BMP1 like proteins are similar, respectively, BMP1 and a larger form, tolloid (Reynolds et al., 2000). The N terminal of the BMP1 is homologous with zinc metalloproteinases (Reynolds et al., 2000). Both BMP1 and tolloid are expressed by osteoblasts, for instance, in embryonic chick calvarial osteoblasts together with embryonic chondrocytes (Reynolds et al., 2000).

41.14.3 Bone morphogenetic protein 2

Based on studies comparing intestinal development in chicken and zebra finches, BMP2 plays an important role in the development of the intestine (Nerurkar et al., 2017).

41.14.4 Bone morphogenetic protein 3

BMP3 plays an important role in the limb development. BMP3 does not follow classic TGF-β−like signaling system (Gamer et al., 2008).

41.14.5 Bone morphogenetic protein 4

BMP4 is involved in the development and growth of adipose tissue in birds. There is high expression of BMP4 in abdominal, mesentery, and subcutaneous adipose tissue with moderate expression in the liver and spleen (7-week-old chickens: Cheng et al., 2016). Serum concentrations of BMP4 are markedly lower in chickens selected for fat content than lean birds (7-week-old chickens: Cheng et al., 2016).

41.15 Fibroblast growth factors

41.15.1 Overview

FGFs are found throughout metazoa (Itoh et al., 2015). FGFs are classified as follows:

- Intracrine
- Paracrine (requiring heparin sulfate as a cofactor)
- Endocrine

In most vertebrates, there are three endocrine FGFs: respectively, FGF19, FGF21, and FGF23. In birds, FGF21 is not found (Itoh et al., 2015).

41.15.2 Endocrine FGFs, FGF receptors, and signal transduction

Binding of the endocrine FGFs to FGF receptors 1−4 requires the presence of the coreceptor factors, α-Klotho or β-Klotho (Itoh et al., 2015).

41.15.3 Fibroblast growth factors 19

The structure of FGF23 has been deduced from cDNA from multiple avian species including the following:

- Chicken (*G. gallus*) NM_204674
- Swan goose (*Anser cygnoides*) XM_013189044.1
- Chuck-will's-widow (*Antrostomus carolinensis*) XM_010171990
- Burrowing owl (*Athene cunicularia*) XM_026850698

41.15.4 FGF23

41.15.4.1 Overview

The structure of avian FGF23 has been deduced from cDNA from multiple birds including the following:

- Chicken (*G. gallus*) M95707.1
- Budgerigar (*Melopsittacus undulatus*) XM_005147966.2
- Great Tit (*P. major*) XM_015626966

FGF23 is produced by bone with expression and presumably release influenced by phosphate status (adult female chicken: Ren et al.). Bone calvaria from hens on a phosphate restricted diet have reduced expression of FGF23 (adult female chicken: Ren et al.).

41.15.4.2 FGF23 actions

FGF23 is one of the hormones controlling mineral and bone metabolism, inhibiting phosphate reabsorption and consequently increasing phosphate excretion. Hens immunized against a FGF23 peptide exhibited a decrease in phosphate excretion together with shifts in circulating concentrations of 1, 25 dihydroxy vitamin D (increased) and parathyroid hormone (reduced) (Ren et al., 2017c).

Maternal antibodies against FGF23 influence the physiology of the progeny. Chicks from eggs produced by laying hens immunized against a FGF23 peptide and subjected to a low-phosphate diet had increases in the following: plasma concentrations of phosphate, bone mineralization, and growth rate (Ren et al., 2017a, b). In contrast, young chickens fed a low-phosphate diet exhibit reduced bone growth and mineralization but without effect on circulating concentrations of FGF23 (Horvat-Gordon et al., 2019).

41.15.5 Other FGFs

Examples of paracrine FGFs are FGF1 (acidic FGF) and FGF2 (basic FGF).

41.15.6 FGF receptors

There are four FGFRs in birds each having tyrosine kinase activity. There is expression of FGFR1, FGFR2, FGFR3, and FGFR4 together with Klotho in the small intestine, bone calvaria, liver, and kidneys (adult female chicken: Ren et al.). Moreover, there is decreased expression of FGFR1 and FGFR4 in the kidney of laying hens on a phosphate-restricted diet (Ren et al.).

41.16 Neurotrophins

Neurotrophin family includes the following: nerve growth factor (NGF), brain-derived neurotrophic factor, and neurotrophin-3 (Kullander et al., 1997). The structure of avian NGF has been deduced in the following:

- Chicken (*G. gallus*) (NM_001293108)
- Zebra finch (*Taeniopygia guttata*) (DQ377326)

NGF plays a role in early development of the chick embryo regulating axial rotation (Manca et al., 2012) and in song control (e.g., Kim and Arnold, 2006).

41.17 Cytokines

41.17.1 Cytokines

Cytokines can be members of either the growth factor or GH gene families and/or exert there effects their effect by receptors in the same families to those receptors to growth factors or GH. Moreover, their signal transduction mechanism can identical. An example of a cytokine is discussed briefly below. Cytokines are considered in detail elsewhere is the volume (chapter).

41.17.2 Tumor necrosis factor-α (TNF-α)

The structure of tumor necrosis factor-α (TNF-α) has been deduced in multiple avian species including in ostrich, brown kiwi, mallard, chickens, turkeys, rock pigeon, house finches, white-crowned sparrows, crows, and great tits (Rohde et al., 2018). The delay in characterizing avian TNF-α is due to the gene being with a high GC region. TNF-α acts via classical nuclear factor kappa B pathway (Rohde et al., 2018).

41.18 Genetics and growth

There is considerable evidence that the genetics of poultry influence their growth rate. For instance, single nucleotide polymorphism (SNP) analysis has revealed associations between growth (body weight gain) in poultry and the following hormones, binding proteins, receptors, and signal transducers in the hypothalamic–pituitary–GH–IGF1 axis.

- Pit-1 gene (Jin et al., 2018)
- GH (Anh et al., 2015)
- IGF1 (Anh et al., 2015; Hosnedlova et al., 2020)
- IGFBP1 (Ou et al., 2009)
- IGFBP2 (Hosnedlova et al., 2020)
- IGFBP3 (Ou et al., 2009)
- STAT5B (Ou et al., 2009; Zhao et al., 2012);

for breast muscle weight with the following:

- GHSR (Demeure et al., 2013);

for abdominal fat pad with the following:

- GH (Zhang et al., 2007); and

for feed to gain ratio with the following:

- GHSR
- IGF1R (Jin et al., 2014).

Moreover, SNPs have been associated with growth with candidate genes that are part of the insulin and T_3 signal mechanisms (chicken: Abdalhag et al., 2015). SNPs associated with growth have also been identified with Myf5 (chicken: Tang et al., 2014) and TGF-β2 (Hosnedlova et al., 2020).

41.19 Nutrition and growth

Maximal growth requires optimal nutrition. Growth can be in the form of skeletal, fat, or muscle accretion, and the effect of nutrition on growth is confounded with other factors such as environmental (extrinsic) and physiological (intrinsic, exp., and GIT development) factors. Diets should be balanced for all the nutrients, including amino acids, minerals, carbohydrates, fatty acids, and fiber, and excess or deficit of a nutrient could lead to retarded growth. According to Liebig's law of the minimum (Liebig's barrel), growth is dictated by the scarcest nutrient (limiting factor) which is especially pertinent to the level of amino acids in the diet (Cant et al., 2003). For commercial poultry, nutritional requirements of meat and egg-type poultry are well identified and based on the production goal (highest body weight, lowest F:G, highest egg number, or egg mass). Recommendations are available for each type and breed (Cobb, Aviagen, and NRC nutrient recommendations). The effect of physiological stage (age) should also be considered regarding nutrition and growth. As an example, the GIT and its microbiome is underdeveloped in young poultry (Lesson and Summers, 2001; Kers et al., 2018), and thus is not capable of fully digesting fats and

fibers at young age (less than 3 weeks), which stipulates that during this period carbohydrates will be a better energy source for maximal growth. In addition, environmental factors such as temperature affect feed intake and growth (Rajaei-Sharifabadi et al., 2017); therefore, nutrient requirements of poultry for maximum growth differ based on the environmental conditions and poultry need a denser diet to compensate for lower feed intake during heat stress (Saeed et al., 2019). Nutrition could affect circulating IGF1 and 2 and hepatic mRNA levels, thus affecting growth in chickens (Beccavin et al., 2001; Giachetto et al., 2003). Nutritional restriction (energy or protein) leads to reductions in circulating concentrations of both IGF1 and T_3 with increased GH secretion due removal of negative feedback (Scanes et al., 2009). There are reports showing diets deficient in amino acids decrease plasma levels of IGF1 and IGF2 (Carew et al., 2003, 2005).

41.20 Environment and growth

41.20.1 Light and growth

There are reports that the wavelength of light influences the growth of broiler chickens being greater when the birds were raised under 440 and 560 nm light (respectively, blue and green light) compared to either 650 nm (red light) or white light (Rozenboim et al., 2013). Light spectrum influences the hypothalamo−pituitary−GH−IGF1 axis. There was greater expression of GHR in muscle satellite cells from birds raised under green and blue light than red or white light (Halevy et al., 1998; Rozenboim et al., 2013). Moreover, there were more satellite cells per muscle raised under green than red or white light (Halevy et al., 1998).

Moreover, embryonic growth, and particularly weights of the pectoralis, was enhanced under green light than darkness (Halevy et al., 2006; Rozenboim et al., 2013).

References

Abdalhag, M.A., Zhang, T., Fan, Q.C., Zhang, X.Q., Zhang, G.X., Wang, J.Y., Wei, Y., Wang, Y.J., 2015. Single nucleotide polymorphisms associated with growth traits in Jinghai yellow chickens. Genet. Mol. Res. 14, 16169−16177.

Aengwanich, W., 2007. Effects of dexamethasone on physiological changes and productive performance in broilers. Asian J. Anim. Vet. Adv. 2, 157−161.

Almasi, B., Roulin, A., Korner-Nievergely, F., Jenni-Eiermann, S., Jenni, L., 2012. Coloration signals the ability to cope with elevated stress hormones: effects of corticosterone on growth of barn owls are associated with melanism. J. Evol. Biol. 12, 1189−1199.

Angel, L.P., Wells, M.R., Rodríguez-Malagón, M.A., Tew, E., Speakman, J.R., Arnould, J.P.Y., 2015. Sexual size dimorphism and body condition in the Australasian gannet. PLoS One 10, e0142653.

Anh, N.T.L., Kunhareang, S., Duangjinda, M., 2015. Association of chicken growth hormones and insulin-like growth factor gene polymorphisms with growth performance and carcass traits in Thai broilers. Asian-Australas. J. Anim. Sci. 28, 1686−1695.

Arai, N., Iigo, M., 2010. Duplicated growth hormone genes in a passerine bird, the jungle crow crow (*Corvus macrorhynchos*). Biochem. Biophys. Res. Commun. 397, 553-553.

Baéza, E., Williams, J., Guémené, D., Duclos, M.J., 2001. Sexual dimorphism for growth in Muscovy ducks and changes in insulin-like growth factor I (IGF-I), growth hormone (GH) and triiodothyronine (T_3) plasma levels. Reprod. Nutr. Dev. 41, 173−179.

Balk, S.D., Morisi, A., Gunther, H.S., Svoboda, M.F., van Wyk, J.J., Nissley, S.P., Scanes, C.G., 1984. Somatomedins (insulin-like growth factors), but not growth hormone, are mitogenic for chicken heart mesenchymal cells and act synergistically with epidermal growth factor and brain fibroblast growth factor. Life Sci. 35, 335−346.

Bassas, L., De Pablo, F., Lesniak, M.A., Roth, J., 1987. The insulin receptors of chick embryo show tissue-specific structural differences which parallel those of the insulin-like growth factor I receptors. Endocrinology 121, 1468−1476.

Beccavin, C., Chevalier, B., Cogburn, L.A., Simon, J., Duclos, M.J., 2001. Insulin-like growth factors and body growth in chickens divergently selected for high or low growth rate. J. Endocrinol. 168, 297−306.

Bellabarba, D., Beaudry, C., Lehoux, J.G., 1983. Corticosteroid receptors in the kidney of chick embryo. II. Ontogeny of corticosterone receptor and cellular development. Gen. Comp. Endocrinol. 50, 305−312.

Bellabarba, D., Lehoux, J.G., 1981. Triiodothyronine nuclear receptor in chick embryo: nature and properties of hepatic receptor. J. Endocrinol. 109, 1017−1025.

Bray, M.M., 1993. Effect of ACTH and glucocorticoids on lipid metabolism in the Japanese quail, *Coturnix coturnix japonica*. Comp. Biochem. Physiol. A 105, 689−696.

Burch, W.M., Lebovitz, H.E., 1982. Triiodothyronine stimulation of in vitrogrowth and maturation of embryonic chick cartilage. J. Endocrinol. 111, 462−468.

Burch, W.M., Van Wyk, J.J., 1987. Triiodothyronine stimulates cartilage growth and maturation by different mechanisms. Am. J. Physiol. 252, E176−182.

Burchell, B., Pratt, G.J., Duffy, I., West, L., 1983. Identification of increased amounts of UDP-glucuronyl transferase protein in phenobarbital-treated chick embryo liver cells. Biochem. J. 214, 517−523.

Burke, W.H., Moore, J.A., Ogez, J.R., Builder, S.E., 1987. The properties of recombinant chicken growth hormone and its effects on growth, body composition, feed efficiency, and other factors in broiler chickens. Endocrinology 120, 651−658.

Burnside, J., Cogburn, L.A., 1992. Developmental expression of hepatic growth hormone receptor and insulin-like growth factor-I mRNA in the chicken. Mol. Cell. Endocrinol. 89, 91−96.

Burnside, J., Liou, S.S., Cogburn, L.A., 1991. Molecular cloning of the chicken growth hormone receptor complementary DNA: mutation of the gene in sex-linked dwarf chickens. Endocrinology 128, 3183−3192.

Burt, D.W., Boswell, J.M., Paton, I.R., Butterwith, S.C., 1992. Multiple growth factor messenger RNAs are ex pressed in chicken adipocyte precursor cells. Biochem. Biophys. Res. Commun. 187, 1298−1305.

Butterworth, S.C., 1997. Regulators of adipocyte precursor cells. Poultry Sci. 76, 118−123.

Butterwith, S.C., Gilroy, M., 1991. Effects of transforming growth factor-β1 and basic fibroblast growth factor on lipoprotein lipase activity in

primary cultures of chicken (*Gallus domesticus*) adipocyte precursors. Comp. Biochem. Physiol. A 100, 473–476.

Butterwith, S.C., Goddard, C., 1991. Regulation of DNA synthesis in chicken adipocyte precursor cells by insulin-like growth factors, platelet-derived growth factor and transforming growth factor- β. J. Endocrinol. 131, 203–209.

Butterwith, S.C., Peddie, C.D., Goddard, C.J., 1992. Effects of transforming growth factor-alpha on chicken adipocyte precursor cells in vitro. Endocrinology 134, 163–168.

Buyse, J., Decuypere, E., Sharp, P.J., Huybrechts, L.M., Kuhn, E.R., Whitehead, C., 1987. Effect of corticosterone on circulating concentrations of corticosterone, prolactin, thyroid hormones and somatomedin C and on fattening in broilers selected for high or low fat content. J. Endocrinol. 112, 229–237.

Cant, J.P., Berthiaume, R., Lapierre, H., Luimes, P.H., McBride, B.W., Pacheco, D., 2003. Responses of the bovine mammary glands to absorptive supply of single amino acids. Can. J. Anim. Sci. 83, 341–355.

Carew, L.B., McMurtry, J.P., Alster, F.A., 2003. Effects of methionine deficiencies on plasma levels of thyroid hormones, insulin-like growth factors-I and -II, liver and body weights, and feed intake in growing chickens. Poultry Sci. 82, 1932–1938.

Carew, L.B., McMurtry, J.P., Alster, F.A., 2005. Effects of lysine deficiencies on plasma levels of thyroid hormones, insulin-like growth factors I and II, liver and body weights,and feed intake in growing chickens. Poultry Sci. 84, 1045–1050.

Case, T.J., 1978. On the evolution and adaptive significance of postnatal growth rates in the terrestrial vertebrates. Q. Rev. Biol. 53, 243–282.

Chen, J., Ren, X., Li, L., Lu, S., Chen, T., Tan, L., Liu, M., Luo, Q., Liang, S., Nie, Q., Zhang, X., Luo, W., 2019. Integrative analyses of mRNA expression profile reveal the involvement of *igf2bp1* in chicken adipogenesis. Int. J. Mol. Sci. 20, 2923.

Cheng, B.H., Leng, L., Wu, M.Q., Zhang, Q., Zhang, X.Y., Xu, S.S., Cao, Z.P., Li, Y.M., Luan, P., Li, H., 2016. Expression analysis of bone morphogenetic protein 4 between fat and lean birds in adipose tissue and serum. Domest. Anim. Endocrinol. 56, 13–19.

Chinsamy, A., Elzanowski, A., 2001. Evolution of growth pattern in birds. Nature 412, 402–403.

Cogburn, L.A., 1991. Endocrine manipulation of body composition in broiler chickens. Crit. Rev. Poult. Biol. 3, 283–305.

Conlon, M.A., Kita, K., 2002. Muscle protein synthesis rate is altered in response to a single injection of insulin-like growth factor-I in seven-day-old leghorn chicks. Poultry Sci. 81, 1543–1547.

Cooley, J.R., Yatskievych, T.A., Antin, P.B., 2014. Embryonic expression of the transforming growth factor beta ligand and receptor genes in chicken. Dev. Dynam. 243, 497–508.

Darras, V.M., Huybrechts, L.M., Berghman, L., Kuhn, E.R., Decuypere, E., 1990. Ontogeny of the effect of purified chicken growth hormone on the liver 5' monodeiodination activity in the chicken: reversal of the activity after hatching. Gen. Comp. Endocrinol. 77, 212–220.

Dean, C.E., Benjamin Morpurgo, B., Porter, T.E., 1999. Induction of somatotroph differentiation *in vivo* by corticosterone administration during chicken embryonic development. Endocrine 11, 151–156.

De La Cruz, L.F., Mataix, F.J., Illera, M., 1981. Effects of glucocorticoids on protein metabolism in laying quail (*Coturnix coturnix japonica*). Comp. Biochem. Physiol. A 70, 649–652.

Decuypere, E., Buyse, J., Scanes, C.G., Huybrechts, L., Kühn, E.R., 1987. Effects of hyper- or hypothyroid status on growth, adiposity and levels of growth hormone, somatomedin C and thyroid metabolism in broiler chickens Reprod. Nutr. Dev. 27, 555–565.

Demeure, O., Duclos, M.J., Bacciu, N., Le Mignon, G., Filangi, O., Pitel, F., Boland, A., Lagarrigue, S., Cogburn, L.A., Simon, J., Le Roy, P., Le Bihan-Duval, E., 2013. Genome-wide interval mapping using SNPs identifies new QTL for growth, body composition and several physiological variables in an F2 intercross between fat and lean chicken lines. Genet. Sel. Evol. 45, 36.

De Pablo, F., Girbau, M., Gomez, J.A., Hernandez, E., Roth, J., 1985a. Insulin antibodies retard and insulin accelerates growth and differentiation in early embryos. Diabetes 34, 1063.

De Pablo, F., Hernandez, E., Collia, F., Gomez, J.A., 1985b. Untoward effects of pharmacological doses of insulin in early chick embryos: through which receptor are they mediated? Diabetologia 28, 308–313.

Dong, H., Lin, H., Jiao, H.C., Song, Z.G., Zhao, J.P., Jiang, K.J., 2007. Altered development and protein metabolism in skeletal muscle of broiler chickens (*Gallus gallus domesticus*) by corticosterone. Comp. Biochem. Physiol. A 147, 189–195.

Du, A.F., Baxter, M.F.A., Graham, B.D., Hargis, B.M., Bielke, L.R., 2019. Mode of action of dietary dexamethasone may not be dependent upon microbial mechanisms in broilers. Microorganisms 7, 346.

Duclos, M.J., Wilkie, R.S., Goddard, C., 1991. Stimulation of DNA synthesis in chicken muscle satellite cells by insulin and insulin-like growth factors: evidence for exclusive mediation by a type-I insulin-like growth factor receptor. J. Endocrinol. 128, 35–42.

Erickson, G.M., Tumanova, T.A., 2001. Growth curve of *Psittacosaurus mongoliensis* Osborn (Ceratopsia: *Psittacosauridae*) inferred from long bone histology. Zool. J. Linn. Soc. 130, 551–566.

Erickson, G.M., Rauhut, O.W.M., Zhou, Z., Turner, A.H., Inouye, B.D., Hu, D., Norell, M.A., 2009. Was dinosaurian physiology inherited by birds? Reconciling slow growth in *Archaeopteryx*. PLoS One 4, e7390.

Fairbairn, J., Shine, R., 1993. Patterns of sexual size dimorphism in seabirds of the Southern Hemisphere. Oikos 68, 139–145.

Fennell, M.J., Scanes, C.G., 1992a. Effects of androgen (testosterone, 5a-dihydrotestosterone, and 19-nortestosterone in turkeys. Poultry Sci. 71, 539–549.

Fennell, M.J., Scanes, C.G., 1992b. Inhibition of growth in chickens by testosterone, 5a-dihydrotestosterone, and 19-nortestosterone. Poultry Sci. 71, 357–366.

Fujita, S., Yamaguchi, M., Hiramoto, D., Saneyasu, T., Honda, K., Kamisoyama, H., 2018. Effects of fasting and refeeding on the mRNA levels of insulin-like growth factor-binding proteins in chick liver and brain. J. Poult. Sci. 55, 269–273.

Gao, J., Lin, H., Wang, X.J., Song, Z.G., Jiao, H.C., 2010. Vitamin E supplementation alleviates the oxidative stress induced by dexamethasone treatment and improves meat quality in broiler chickens. Poultry Sci. 89, 318–327.

Gamer, L.W., Ho, V., Cox, K., Rosen, V., 2008. Expression and function of BMP3 during chick limb development. Dev. Dynam. 237, 1691–1698.

Giachetto, P.F., Guerreiro, E.N., Ferro, J.A., Ferro, M.I.T., Furlan, R.L., Macari, M., 2003. Performance and hormonal profile in broiler chickens fed with different energy levels during post restriction period. Pesq. Agropec. Bras., Brasília. 38, 697–702.

Giachetto, P.F., Riedel, E.C., Gabriel, J.E., Ferro, M.E.T., Di Mauro, S.M.Z., Macari, M., Ferro, J.A., 2004. Hepatic mRNA expression and plasma levels of insulin-like growth factor-I (IGF-I) in broiler chickens selected for different growth rates. Genet. Mol. Biol. 27, 39–44.

Girbau, M., Gomez, J.A., Lesniak, M.A., De Pablo, F., 1987. Insulin and insulin-like growth factor I both stimulate metabolism, growth, and differentiation in the postneurula chick embryo. Endocrinology 121, 1477–1482.

Girbau, M., Lesniak, M.A., Gomez, J.A., De Pablo, F., 1988. Insulin action in early embryonic life: anti-insulin receptor antibodies retard chicken embryo growth and not muscle differentiation *in vivo*. Biochem. Biophys. Res. Commun. 153, 142–148.

Guillaume, J., 1976. The dwarfing gene dw: its effects on anatomy, physiology, nutrition, management. World's Poult. Sci. J. 32, 285–304.

Halevy, O., Biran, I., Rozenboim, I., 1998. Various light source treatments affect body and skeletal muscle growth by affecting skeletal muscle satellite cell proliferation in broilers. Comp. Biochem. Physiol. 120A, 317–323.

Halevy, O., Piestun, Y., Rozenboim, I., Yablonka-Reuveni, Z., 2006. *In ovo* exposure to monochromatic green light promotes skeletal muscle cell proliferation and affects myofiber growth in posthatch chicks. Am. J. Physiol. 290, R1062–R1070.

Havenstein, G.B., Ferket, P.R., Qureshi, M.A., 2003a. Carcass composition and yield of 1957 versus 2001 broilers when fed representative 1957 and 2001 broiler diets. Poultry Sci. 82, 1509–1518.

Havenstein, G.B., Ferket, P.R., Qureshi, M.A., 2003b. Growth, livability, and feed conversion of 1957 versus 2001 broilers when fed representative 1957 and 2001 broiler diets. Poultry Sci. 82, 1500–1508.

Hayward, L.S., Wingfield, J.C., 2004. Maternal corticosterone is transferred to avian yolk and may alter offspring growth and adult phenotype. Gen. Comp. Endocrinol. 135, 365-317.

Hayward, L.S., Richardson, J.B., Grogan, M.N., Wingfield, J.C., 2006. Sex differences in the organizational effects of corticosterone in the egg yolk of quail. Gen. Comp. Endocrinol. 146, 144–148.

Heiblum, R., Arnon, E., Chazan, G., Robinzon, B., Gvaryahu, G., Snapir, N., 2001. Glucocorticoid administration during incubation: embryo mortality and posthatch growth in chickens. Poultry Sci. 80, 1357–1363.

Hinck, A.P., 2012. Structural studies of the TGF-βs and their receptors – insights into evolution of the TGF-β superfamily. FEBS Lett. 586, 1860–1870.

Horvat-Gordon, M., Hadley, J.A., Ghanem, K., Leach, R.M., 2019. Lack of a relationship between plasma fibroblast growth factor-23 and phosphate utilization in young chicks. Poultry Sci. 98, 1762–1765.

Hosnedlova, B., Vernerova, K., Kizek, R., Bozzi, R., Kadlec, J., Curn, V., Kouba, F., Fernandez, C., Machander, V., Horna, H., 2020. Associations between *IGF1, IGFBP2* and *TGFβ3* genes polymorphisms and growth performance of broiler chicken lines. Animals (Basel) 10, 800.

Huang, N., Cogburn, L.A., Agarwal, S.K., Marks, H.L., Burnside, J., 1993. Over-expression of a truncated growth hormone receptor in the sex-linked dwarf chicken: evidence for a splice mutation. Mol. Endocrinol. 7, 1391–1398.

Hutt, F.B., 1959. Sex-linked dwarfism in the fowl. J. Hered. 15, 97–110.

Huybrechts, L.M., King, D.B., Lauterio, T.J., Marsh, J., Scanes, C.G., 1985. Plasma concentrations of somatomedin-C in hypophysectomized, dwarf and intact growing domestic fowl as determined by heterologous radioimmunoassay. J. Endocrinol. 104, 233–239.

Itoh, N., Ohta, H., Konishi, M., 2015. Endocrine FGFs: evolution, physiology, pathophysiology, and pharmacotherapy. Front. Endocrinol. 6, 154.

Jennings, S., Varsani, A., Dugger, K.M., Ballard, G., Ainley, D.G., 2016. Sex-based differences in Adélie penguin (*Pygoscelis adeliae*) chick growth rates and diet. PLoS One 11, e0149090.

Jin, S., Chen, S., Li, H., Lu, Y., Xu, G., Yang, N., 2014. Associations of polymorphisms in GHRL, GHSR, and IGF1R genes with feed efficiency in chickens. Mol. Biol. Rep. 41, 3973–3979.

Jin, S., He, T., Yang, L., Tong, Y., Chen, X., Geng, Z., 2018. Association of polymorphisms in *Pit-1* gene with growth and feed efficiency in meat-type chickens. Asian-Australas. J. Anim. Sci. 31, 1685–1690.

Kers, J.G., Velkers, F.C., Fischer, E.A.J., Hermes, G.D.A., Stegeman, J.A., Smidt, H., 2018. Host and environmental factors affecting the intestinal microbiota in chickens. Front. Microbiol. 9, 235.

Kim, Y.H., Arnold, A.P., 2006. Expression of NGF and trkA mRNA in song control and other regions of the zebra finch brain. Neurosci. Lett. 409, 151–156.

Kimmett, S.M., McNamee, J.P., Marks, G.S., 1996. Chick embryo liver microsomal steroid hydroxylations: induction by dexamethasone, phenobarbital, and glutethimide and inactivation following the *in ovo* administration of porphyrinogenic compounds. Can. J. Physiol. Pharmacol. 74, 97–103.

King, D.B., 1969. Effect of hypophysectomy of young cockerels, with particular reference to body growth, liver weight, and liver glycogen level. Gen. Comp. Endocrinol. 12, 242–255.

King, D.B., King, C.R., 1973. Thyroidal influence on early muscle growth of chickens. Gen. Comp. Endocrinol. 21, 517–529.

King, D.B., King, C.R., 1976. Thyroidal influence on gastrocnemius and sartorius muscle growth in young White Leghorn cockerels. Gen. Comp. Endocrinol. 29, 473–479.

King, D.B., Scanes, C.G., 1986. Effects of mammalian growth hormone and prolactin on the growth of hypophysectomized chickens. Proc. Soc. Exp. Biol. Med. 182, 201–207.

Kita, K., Hangsanet, K., Shibata, T., Conlon, M.A., Sasaki, T., Saito, N., Okumura, J., 1998. Refeeding increases hepatic insulin-like growth factor-I (IGF-I) gene expression and plasma IGF-I concentration in fasted chicks. Br. Poultry Sci. 39, 679–682.

Kita, K., Shibata, T., Yaman, A., Nagao, K., Okumura, J., 2002a. Response of muscle protein synthesis to the infusion of insulin-like growth factor-1 and fasting in young chickens. Asian Austral. J. Anim. Sci. 15, 1653–1658.

Kita, K., Nagao, K., Taneda, N., Inagaki, Y., Hirano, K., Shibata, T., Yaman, M.A., Conlon, M.A., Okumura, J., 2002b. Insulin-like growth factor binding protein-2 gene expression can be regulated by diet manipulation in several tissues of young chickens. J. Nutr. 132, 145–151.

Klasing, K.C., Laurin, D.E., Peng, R.K., Fry, D.M., 1987. Immunologically mediated growth depression in chicks: influence of feed intake, corticosterone and interleukin-1. J. Nutr. 117, 1629–1637.

Kocamis, H., McFarland, D.C., Killefer, J., 2001. Temporal expression of growth factor genes during myogenesis of satellite cells derived from the biceps femoris and pectoralis major muscles of the chicken. J. Cell. Physiol. 186, 146–152.

Kuhn, E.R., Huybrechts, L.M., Darras, V.M., Meeuwis, R., Decuypere, E., 1990. Impaired peripheral T_3 production but normal induced thyroid hormone secretion in the sex-linked dwarf- chick embryo. Reprod. Nutr. Dev. 30, 193–201.

Kühn, E.R., Verheyen, G., Chiasson, R.B., Huts, C., Huybrechts, L., Van den Steen, P., Decuypere, E., 1987. Growth hormone stimulates the peripheral conversion of thyroxine into triiodothyronine by increasing the liver 5'-monodeiodinase activity in the fasted and normal fed chicken. Horm. Metab. Res. 19, 304–308.

Kullander, K., Carlson, B., Hallböök, F., 1997. Molecular phylogeny and evolution of the neurotrophins from monotremes and marsupials. J. Mol. Evol. 45, 311–321.

Lauterio, T.J., Scanes, C.G., 1987. Time course of changes in plasma concentrations of growth related hormones during protein restriction in the domestic fowl (*Gallus domesticus*). Proc. Soc. Exp. Biol. Med. l85, 420–426.

Leach Jr., R.M., Richards, M.P., Praul, C.A., Ford, B.C., McMurtry, J.P., 2007. Investigation of the insulin-like growth factor system in the avian epiphyseal growth plate. Domest. Anim. Endocrinol. 33, 143–153.

Leeson, S., Summers, J.D., 2001. Scott's Nutrition of the Chicken, fourth ed.

Leili, S., Buonomo, F.C., Scanes, C.G., 1997. The effects of dietary restriction on insulin-like growth factor (IGF)-I and II, and IGF-binding proteins in chickens. Proc. Soc. Exp. Biol. Med. 104–111.

Leili, S., Scanes, C.G., 1998. The effects of protein restriction on insulin-like growth factor I and IGF-binding proteins in chickens. Proc. Soc. Exp. Biol. Med. 218, 322–328.

Leung, F.C., Styles, W.J., Rosenblum, C.I., Lilburn, M.S., Marsh, J.A., 1987. Diminished hepatic growth hormone receptor binding in sex-linked dwarf broiler and Leghorn chickens. Proc. Soc. Exp. Biol. Med. 184, 234–238.

Leung, F.C., Taylor, J.E., Van Iderstine, A., 1984. Effects of dietary thyroid hormones on growth and serum T_3, T_4, and growth hormone in sex-linked dwarf chickens. Proc. Soc. Exp. Biol. Med. 177, 77–81.

Lin, S., Luo, W., Ye, Y., Bekele, E.J., Nie, Q., Li, Y., Zhang, X., 2017. Let-7b regulates myoblast proliferation by inhibiting IGF2BP3 expression in dwarf and normal chicken. Front. Physiol. 8, 477.

Lodjak, J., Raivo Mänd, R., Mägi, M., 2018. Insulin-like growth factor 1 and life-history evolution of passerine birds. Funct. Ecol. 32, 313–323.

Lu, F.Z., Jiang, Z.Y., Wang, X.X., Luo, Y.H., Li, X.F., Liu, H.L., 2010. Role of the insulin-like growth factor system in epiphyseal cartilage on the development of Langshan and Arbor Acres chickens, *Gallus domesticus*. Poultry Sci. 89, 956–965.

Maloney, S.K., Dawson, T.J., 1993. Sexual dimorphism in basal metabolism and body temperature of a large bird, the emu. Condor 95, 1034–1037.

Manca, A., Capsoni, S., Di Luzio, A., Vignone, D., Malerba, F., Paoletti, F., Brandi, R., Arisi, I., Cattaneo, A., Levi-Montalcini, R., 2012. Nerve growth factor regulates axial rotation during early stages of chick embryo development. Proc. Natl. Acad. Sci. U.S.A. 109, 2009–2014.

Marquardt, H., Hunkapiller, M.W., Hood, L.E., Twardzik, D.R., De Larco, J.E., Stephenson, J.R., Todaro, G.J., 1983. Transforming growth factors produced by retrovirus-transformed rodent fibroblasts and human melanoma cells: amino acid sequence homology with epidermal growth factor. Proc. Natl. Acad. Sci. U.S.A. 80, 4684–4688.

Marsh, J.A., Lauterio, T.J., Scanes, C.G., 1984. Effects of triiodothyronine treatments on body and organ growth and the development of immune function in dwarf chickens. Proc. Soc. Exp. Biol. Med. 177, 82–91.

Mashaly, M.M., 1991. Effect of exogenous corticosterone on chicken embryonic development. Poultry Sci. 70, 371–374.

May, J.D., 1980. Effect of dietary thyroid hormone on growth and feed efficiency of broilers. Poultry Sci. 59, 888–892.

McDonald, P.G., Olsen, P.D., Cockburn, A., 2005. Selection on body size in a raptor with pronounced reversed sexual size dimorphism: are bigger females better? Behav. Ecol. 16, 48–56.

McMurtry, J.P., 1998. Nutritional and developmental roles of insulin-like growth factors in poultry. J. Nutr. 128, 302S–305S.

McNabb, F.M.A., Hughes, T.E., 1983. The role of serum binding proteins in determining free thyroid hormone concentrations during development in quail. J. Endocrinol. 113, 957–963.

McNabb, F.M., Stanton, F.W., Weirich, R.T., Hughes, T.E., 1984. Responses to thyrotropin during development in Japanese quail. J. Endocrinol. 114, 1238–1244.

Mills, A.M., 2008. Passerines are sexually dimorphic in shape as well as size. Condor 110, 354–358.

Mohammadrezaei, M., Toghyani, M., Gheisari, A., Toghyani, M., Eghbalsaied, S., 2014. Synergistic effect of fadrozole and insulin-like growth factor-I on female-to-male sex reversal and body weight of broiler chicks. PLoS One 9, e103570.

Moore, G.E., Harvey, S., Klandorf, H., Goldspink, G., 1984. Muscle development in thyroidectomized chickens (*Gallus domesticus*). Gen. Comp. Endocrinol. 55, 195–199.

Müller, W., Vergauwen, J., Eens, M., 2008. Yolk testosterone, postnatal growth and song in male canaries. Horm. Behav. 54, 125–133.

Müller, C., Jenni-Eiermann, S., Jenni, L., 2009. Effects of a short period of elevated circulating corticosterone on postnatal growth in free-living Eurasian kestrels *Falco tinnunculus*. J. Exp. Biol. 212, 1405–1412.

Nakazawa, F., Nagai, H., Shin, M., Sheng, G., 2006. Negative regulation of primitive hematopoiesis by the FGF signaling pathway. Blood 108, 3335–3343.

Nerurkar, N.L., Mahadevan, L., Tabin, C.J., 2017. BMP signaling controls buckling forces to modulate looping morphogenesis of the gut. Proc. Natl. Acad. Sci. U.S.A. 114, 2277–2282.

Noguera, J.C., Aira, M., Pérez-Losada, M., Domínguez, J., Velando, A., 2018. Glucocorticoids modulate gastrointestinal microbiome in a wild bird. R. Soc. Open Sci. 5, 171743.

Ou, J.T., Tang, S.Q., Sun, D.X., Zhang, Y., 2009. Polymorphisms of three neuroendocrine-correlated genes associated with growth and reproductive traits in the chicken. Poultry Sci. 88, 722–727.

Price, E.R., Bauchinger, U., Zajac, D.M., Cerasale, D.J., McFarlan, J.T., Gerson, A.R., McWilliams, S.R., Guglielmo, C.G., 2011. Migration- and exercise-induced changes to flight muscle size in migratory birds and association with IGF1 and myostatin mRNA expression. J. Exp. Biol. 214, 2823–2831.

Proudman, J.A., McGuinness, M.C., Krishnan, K.A., Cogburn, L.A., 1994. Endocrine and metabolic responses of intact and hypophysectomized Turkey poults given a daily injection of chicken growth hormone. Comp. Biochem. Physiol. C 109, 47–56.

Puvadolpirod, S., Thaxton, J.P., 2000a. Model of physiological stress in chickens 1. Response parameters. Poultry Sci. 79, 363–369.

Raheja, K.L., Snedecor, J.G., 1970. Comparison of subnormal multiple doses of l-thyroxine and l-triiodothyronine in thyroidectomized chickens (*Gallus domesticus*). Gen. Comp. Endocrinol. 55, 195–199.

Rajaei-Sharifabadi, H., Ellestad, L., Porter, T., Donoghue, A., Bottje, W.G., Dridi, S., 2017. Noni (*Morinda citrifolia*) modulates the hypothalamic expression of stress- and metabolic-related genes in broilers exposed to acute heat stress. Front. Genet. 8, 192.

Ren, Z., Bütz, D.E., Sand, J.M., Cook, M.E., 2017a. Maternally-derived anti-fibroblast growth factor 23 antibody as new tool to reduce phosphorus requirement of chicks. Poultry Sci. 96, 878–885.

Ren, Z., Bütz, D.E., Wahhab, A.N., Piepenburg, A.J., Cook, M.E., 2017b. Additive effects of fibroblast growth factor 23 neutralization and dietary phytase on chick calcium and phosphorus metabolism. Poultry Sci. 96, 1167–1173.

Ren, Z.Z., Ebrahimi, M., Butz, D.E., Sand, J.M., Zhang, K.Y., Cook, M.E., 2017c. Antibody to fibroblast growth factor 23-peptide reduces excreta phosphorus of laying hens. Poultry Sci. 96, 127–134.

Ren, Z., Yan, J., Hu, Q., Liu, X., Pan, C., Liu, Y., Zhang, X., Yang, X., Yang, X., February 14, 2020. Phosphorus restriction changes the expression of fibroblast growth factor 23 and its receptors in laying hens. Front. Physiol. 11, 85.

Reynolds, S.D., Zhang, D., Puzas, J.E., O'Keefe, R.J., Rosier, R.N., Reynolds, P.R., 2000. Cloning of the chick BMP1/Tolloid cDNA and expression in skeletal tissues. Gene 248, 233–243.

Rohde, F., Schusser, B., Hron, T., Farkašová, H., Plachý, J., Härtle, S., Hejnar, J., Elleder, D., Kaspers, B., 2018. Characterization of chicken tumor necrosis factor-α, a long missed cytokine in birds. Front. Immunol. 9, 605.

Ricklefs, R., 1979. Patterns of growth in birds .5. Comparative-study of development in the starling, common tern, and Japanese quail. Auk 96, 10–30.

Rotwein, P., 2017. Diversification of the insulin-like growth factor 1 gene in mammals. PLoS One 12, e0189642.

Rozenboim, I., El Halawani, M.E., Kashash, Y., Piestun, Y., Halevy, O., 2013. The effect of monochromatic photostimulation on growth and development of broiler birds. Gen. Comp. Endocrinol. 190, 214–219.

Rubolinia, D., Romano, M., Boncoraglio, G., Ferrari, R.P., Martinelli, R., Galeotti, P., Fasola, M., Saino, N., 2005. Effects of elevated egg corticosterone levels on behavior, growth, and immunity of yellow-legged gull (*Larus michahellis*) chicks. Horm. Behav. 47, 592–605.

Saeed, M., Abbas, G., Alagawany, M., Kamboh, A.A., Abd El-Hack, M.E., Khafaga, A.F., Chao, S., 2019. Heat stress management in poultry farms: a comprehensive overview. J. Therm. Biol. 84, 414–425.

Saino, N., Ferrari, R.P., Romano, M., Martinelli, R., Lacroix, A., Gil, D., Anders Pape Møller, A.P., 2006. Maternal allocation of androgens and antagonistic effects of yolk androgens on sons and daughters. Behav. Ecol. 7, 172–181.

Savage, C.R., Inagami, T., Cohen, S., 1972. The primary structure of epidermal growth factor. J. Biol. Chem. 247, 7612–7621.

Scanes, C.G., Marsh, J., Decuypere, E., Rudas, P., 1983. Abnormalities in the plasma concentrations of thyroxine, triiodothyronine and growth hormone in sex-linked dwarf and autosomal dwarf White Leghorn domestic fowl (*Gallus domesticus*). J. Endocrinol. 97, 127–135.

Scanes, C.G., Duyka, D.R., Lauterio, T.J., Bowen, S.J., Huybrechts, I.M., Bacon, W.L., King, D.B., 1986. Effect of chicken growth hormone, triiodothyronine and hypophysectomy in growing domestic fowl. Growth 50, 12–31.

Scanes, C.G., 2009. Perspectives on the endocrinology of poultry growth and metabolism. Gen. Comp. Endocrinol. 163, 24–32.

Schmidt, K.L., MacDougall-Shackleton, E.A., MacDougall-Shackleton, S.A., 2012. Developmental stress has sex-specific effects on nestling growth and adult metabolic rates but no effect on adult body size or body composition in song sparrows. J. Exp. Biol. 215, 3207–3217.

Schwabl, H., 1996. Maternal testosterone in the avian egg enhances postnatal growth. Comp. Biochem. Physiol. A 114, 271–276.

Shaffer, S.A., Weimerskirch, H., Costa, D.P., 2001. Functional significance of sexual dimorphism in Wandering Albatrosses, *Diomedea exulans*. Funct. Ecol. 15, 203–210.

Scanes, C.G., Peterla, T.A., Kantor, S., Ricks, C.A., 1990. In vivoeffects of biosynthetic chicken growth hormone on broiler-strain chickens. Growth, Dev. Aging. 54, 95–106.

Schew, W.A., McNabb, F.M.A., Scanes, C.G., 1996. Comparison of the ontogenesis of thyroid hormones, growth hormone, and insulin-like growth factor-I in *ad libitum* and food restricted (altricial) European starlings and (precoccial) Japanese quail. Gen. Comp. Endocrinol. 101, 304–316.

Siegel, P.B., Gross, W.B., Dunnington, E.A., 1989. Effects of dietary corticosterone in young Leghorn and meat-type cockerels. Br. Poultry Sci. 30, 185–192.

Sogut, B., Celik, S., Ayasan, T., Inci, H., 2016. Analyzing growth curves of turkeys reared in different breeding systems (intensive and free-range) with some nonlinear models. Braz. J. Poult. Sci. 18, 619–628.

Song, Z.G., Zhang, X.H., Zhu, L.X., Jiao, H.C., Lin, H., 2011. Dexamethasone alters the expression of genes related to the growth of skeletal muscle in chickens (*Gallus gallus domesticus*). J. Mol. Endocrinol. 46, 217–222.

Sockman, K.W., Weiss, J., Webster, M.S., Talbott, V., Schwabl, H., 2008. Sex-specific effects of yolk-androgens on growth of nestling American kestrels. Behav. Ecol. Sociobiol. 62, 617–625.

Strange, M.S., Bowden, R.M., Thompson, C.F., Sakaluk, S.K., 2016. Pre- and post-natal effects of corticosterone on fitness-related traits and the timing of endogenous corticosterone production in a songbirds. J. Exp. Zool. A 325, 347–359.

Sullivan, L.C., Orgeig, S., 2001. Dexamethasone and epinephrine stimulate surfactant secretion in type II cells of embryonic chickens. Am. J. Physiol. 281, R770–R777.

Tai, C., Rouvier, R., 1998. Crossbreeding effect on sexual dimorphism of body weightin intergeneric hybrids obtained between Muscovy and Pekin duck. Genet. Sel. Evol. 30, 163–170.

Tang, Y., Zhang, T., Zhang, G., Wang, J., Fan, Q., Chen, X., Wei, Y., Han, K., Wang, Y., 2014. Eight SNPs of the Myf5 gene and diplotypes associated with growth and reproductive traits in Jinghai yellow chicken. Mol. Biol. Rep. 41, 6837–6844.

Taouis, M., Derouet, M., Chevalier, B., Simon, J., 1993. Corticosterone effect on insulin receptor number and kinase activity in chicken muscle and liver. Gen. Comp. Endocrinol. 89, 167–175.

Tixier-Boichard, M., Huybrechts, L.M., Decuypere, E., Kuhn, E.R., Monovoisin, J.-L., Coquerelle, G., Charrier, J., Simon, J., 1992. Effects of insulin-like growth factor-I (IGF-I) infusion and dietary triiodothyronine (T_3) supplementation on growth, body composition and plasma hormone levels in sex-linked dwarf mutant and normal chickens. J. Endocrinol. 133, 101–110.

Tóth, Z., Ouyang, J.Q., Lendvai, A.Z., 2018. Exploring the mechanistic link between corticosterone and insulin-like growth factor-1 in a wild passerine bird. PeerJ 6, e5936.

Tschirren, B., 2015. Differential effects of maternal yolk androgens on male and female offspring: a role for sex-specific selection? PLoS One 10, e0133673.

Vanderpooten, A., Darras, V.M., Huybrechts, L.M., Rudas, P., Decuypere, E., Kuhn, E.R., 1991a. Effect of hypophysectomy and acute administration of growth hormone (GH) on GH-receptor binding in chick liver membranes. J. Endocrinol. 129, 275–281.

Vanderpooten, A., Huybrechts, L.M., Decuypere, E., Kuhn, E.R., 1991b. Differences in hepatic growth hormone receptor binding during development of normal and dwarf chickens. Reprod. Nutr. Dev. 31, 47–55.

Vasilatos-Younken, R., Cravener, T.L., Cogburn, L.A., Mast, M.G., Wellenreiter, R.H., 1988. Effect of pattern of administration on the response to exogenous, pituitary-derived chicken growth hormone by broiler-strain pullets. Gen. Comp. Endocrinol. 71, 268–283.

Virden, W.S., Lilburn, M.S., Thaxton, J.P., Corzo, A., Hoehler, D., Kidd, M.T., 2007b. The effect of corticosterone-induced stress on amino acid digestibility in Ross broilers. Poultry Sci. 86, 338–342.

Virden, W.S., Thaxton, J.P., Corzo, A., Dozier III, W.A., Kidd, M.T., 2007a. Evaluation of models using corticosterone and adrenocorticotropin to induce conditions mimicking physiological stress in commercial broilers. Poultry Sci. 86, 2485–2491.

Wang, X., Jia, Q., Xiao, J., Jiao, H., Lin, H., 2015. Glucocorticoids retard skeletal muscle development and myoblast protein synthesis through a mechanistic target of rapamycin (mTOR)-signaling pathway in broilers (Gallus gallus domesticus). Stress 18, 686–698.

Welcker, J., Chastel, O., Gabrielsen, G.W., Guillaumin, J., Kitaysky, A.S., Speakman, J.R., Tremlay, Y., Bech, C., 2013. Thyroid hormones correlate with basal metabolic rate but not field metabolic rate in a wild bird species. PLoS One 8, e56229.

Werner, J., Griebeler, E.M., 2014. Allometries of maximum growth rate versus body mass at maximum growth indicate that non-avian dinosaurs had growth rates typical of fast growing ectothermic sauropsids. PLoS One 9, e88834.

Whiteside, M.A., van Horik, J.O., Langley, E.J.G., Beardsworth, C.E., Madden, J.R., 2018. Size dimorphism and sexual segregation in pheasants: tests of three competing hypotheses. Peer J 6, e5674.

Wishart, G.J., Dutton, G.J., 1974. Precocious development of detoxicating enzymes following pituitary graft. Nature 252, 408–410.

Woronowicz, K.C., Gline, S.E., Herfat, S.T., Fields, A.J., Schneider, R.A., 2018. FGF and TGFβ signaling link form and function during jaw development and evolution. Dev. Biol. 444 (Suppl. 1), S219–S236.

Yang, J., Liu, L., Sheikhahmadi, A., Wang, Y., Li, C., Jiao, H., Lin, H., Song, Z., 2015. Effects of corticosterone and dietary energy on immune function of broiler Chickens. PLoS One 10, e0119750.

Yu, M., Wang, H., Xu, Y., Yu, D., Li, D., Xiuhong Liu, X., Du, W., 2015. Insulin-like growth factor-1 (IGF-1) promotes myoblast proliferation and skeletal muscle growth of embryonic chickens via the PI3K/Akt signalling pathway. Cell Biol. Int. 39, 910–922.

Yuri, T., Kimball, R., Braun, E., Braun, M., 2008. Duplication of accelerated evolution and growth hormone gene in passerine birds. Mol. Biol. Evol. 25, 352–361.

Zhang, X.L., Jiang, X., Liu, Y.P., Du, H.R., Zhu, Q., 2007. Identification of Avai polymorphisms in the third intron of GH gene and their associations with abdominal fat in chickens. Poultry Sci. 86, 1079–1083.

Zhao, X.H., Wang, J.Y., Zhang, G.X., Wei, Y., Gu, Y.P., Yu, Y.B., 2012. Single nucleotide polymorphism in the STAT5b gene is associated with body weight and reproductive traits of the Jinghai Yellow chicken. Mol. Biol. Rep. 39, 4177–4183.

Zuidhof, M.J., Schneider, B.L., Carney, V.L., Korver, D.R., Robinson, F.E., 2014. Growth, efficiency, and yield of commercial broilers from 1957, 1978, and 2005. Poultry Sci. 93, 2970–2982.

Further reading

Ballard, F.J., Johnson, R.J., Owens, P.C., Francis, G.L., Upton, F.M., McMurtry, J.P., Wallace, J.C., 1990. Chicken insulin- like growth factor-I: amino acid sequence, radioimmunoassay, and plasma levels between strains and during growth. Gen. Comp. Endocrinol. 79, 459–468.

Darling, D.C., Brickell, P.M., 1996. Nucleotide sequence and genomic structure of the chicken insulin-like growth factor-II (IGF-II) coding region. Gen. Comp. Endocrinol. 102, 283–287.

Kajimoto, Y., Rotwein, P., 1989. Structure and expression of a chicken insulin-like growth factor I precursor. J. Mol. Endocrinol. 3, 1907–1913.

Kallincos, N.C., Wallace, J.C., Francis, G.L., Ballard, F.J., 1990. Chemical and biological characterization of chicken insulin-like growth factor-II. J. Endocrinol. 124, 89–97.

Mahr, K., Vincze, O., Tóth, Z., Hoi, H., Lendvai, Á.Z., 2020. Insulin-like growth factor 1 is related to the expression of plumage traits in a passerine species. Behav. Ecol. Sociobiol. 74, 39.

Chapter 42

Circadian rhythms

Vincent M. Cassone[1] and Vinod Kumar[2]
[1]Department of Biology, University of Kentucky, Lexington, KY, United States; [2]Department of Zoology, University of Delhi, Delhi, India

Biological circadian rhythms and the clocks that control them are fundamental properties of all freely living organisms studied in any detail. These are expressed by organisms ranging from cyanobacteria to humans with highly conserved formal properties. Among animals, the molecular details of biological clocks are highly conserved as well. The conserved nature of these rhythms and clocks likely derives from the fact that they are all adaptations to a single selective pressure—the daily change from night to day and the abiotic and biotic rhythms that accompany it. Biological clock function is particularly apparent in birds, partly due to the fact that they share with us a diurnal lifestyle, but also because time of day and time of year as we will see in the next chapter pervades all aspects of avian physiology.

42.1 Environmental cycles

42.1.1 Light cycles

Although we all know that the cycle of day to night derives from the rotation of the Earth on its axis approximately every 24 h, we experience this process through the apparent rise of the sun on the eastern horizon (dawn), its traverse across the sky, its setting in the west (dusk), and subsequent night. The most salient feature of the *solar day* is the dramatic change in visible and invisible light intensity, polarization, and wavelength spectra. Daylight intensity can be measured in a variety of radiometric and photometric ways, extending beyond the scope of this chapter. One can gather the scale of daily change in *lux* (*lx*), the International System of Units (SI) measure of *illuminance*, or the intensity of white light as perceived by the human eye. These values range from 120,000 lx in the brightest sunlight to 400 lx at dusk or dawn on a clear day to 0.0001 lx under overcast, moonless night sky. This vast range in intensity may go unperceived consciously, because our and birds' visual systems adapt to changes in intensity. However, as we shall see below, changes in absolute intensity and timing of illumination are detected and processed by the circadian clock. In addition to intensity, the wavelength of ambient light changes due to diffraction of shorter wavelengths at dawn and dusk, resulting in the perception of reddish hues at sunrise and sunset.

42.1.2 Temperature

Due to the daily changes in solar illumination, the atmosphere and surface of the Earth undergo daily changes in temperature that generally rise as the day progresses but vary dramatically due to latitude, season, and local conditions such as urban growth, proximity to bodies of water, desertification, and variations in land use (Geerts, 2002). The daily temperature range (DTR) is highly variable at different latitudes. For example, at the Equator, the DTR is 8°C in the summer and 9°C in the winter. In contrast, at 40° latitude in North America, the DTR in summer is 18°C in the summer and only 10°C in the winter. Proximity of oceans also ameliorates DTRs. For example, in July in Australia, the DTR increases from 6°C on the coast to 17°C 150 km inland. These changes are clearly important for natural ecosystems as well as agricultural activity, perhaps as important as the mean temperature itself. There is increasing evidence that, in addition to the gradual increase in mean global temperatures, the DTRs have changed as well, decreasing the daily range 0.4°C from 1950 to 1993.

42.1.3 Other physical cycles

Other physical characteristics vary over the day as a derivative of the diurnal solar cycle. These include daily changes in barometric pressure, characteristics of the magnetic field, and, in many locations, precipitation. Pressure variations derive from the thermal energy arising from the heating of the upper atmosphere that moves in a westward wave at the speed of the Earth's rotation (Hardy et al., 1998). These variations depend upon latitude, altitude, and season. Aspects of the Earth's magnetic field also vary in intensity and inclination depending on the time of day, as the solar wind emanating from the sun interacts with the magnetosphere on a regular 24 h cycle.

Sturkie's Avian Physiology. https://doi.org/10.1016/B978-0-12-819770-7.00050-5

42.1.4 Rhythms in the biotic environment

Since daily cycles in many aspects of the physical, abiotic environment are so pervasive, it should not be surprising that nearly all free-living organisms have evolved adaptations to the changing environment. Thus, in addition to daily changes in abiotic factors, birds' biotic environment is also changing on a daily basis. The presence of food, competitors, predators, parasites, and potential mates may be present at one time of day and absent in another (Bradshaw and Holzapfel, 2010). Hence, birds, like nearly all organisms on Earth, have evolved an internal biological clock that synchronizes patterns of many aspects of behavior, physiology, biochemistry, and molecular biology to external time (Pittendrigh, 1993) and coordinate internal processes to temporally maximize efficient processes within (Navarra and Nelson, 2007).

42.2 Circadian rhythms

42.2.1 Formal properties

The internal biological clock shares fundamental formal properties among most living organisms through the expression of endogenously generated circadian (*circa* = *approximately*; *dian* = *a day*) oscillations that entrain to local time through the process of *entrainment.* Rhythmic processes cannot be identified as *circadian* unless they are experimentally observed to persist when the organism in question is placed in constant environmental conditions of either constant darkness (DD) or constant dim light (dimLL) (Constant high light, LL, may have other effects, frequently abolishing circadian rhythms altogether and/or damaging photoreceptive elements in the system; Aschoff, 1979).

To study circadian rhythms in behavior or physiology, birds are isolated in light-tight, temperature-controlled chambers in which light: dark cycles (LD) can be programmed to period, T, of an LD cycle. It is important to acclimate the birds to the chambers by maintaining them in LD for several days before commencing with research. Food and water must also be available within the cage, since the repeated disturbance of feeding and changing water can affect the data. Behavior is continuously monitored using a remote sensing device, such as microswitches mounted on perches, infrared beams, telemeters, or other sensors, so that the birds are not disturbed by visual inspection. Under these constant conditions, birds will repeatedly express patterns of behavior, physiology, or biochemical processes with an endogenous period, τ, of close to but rarely exactly 24 h (Figure 42.1). These endogenously driven rhythms must then be *entrained* to the relevant environmental cycle, typically the LD cycle of day and night, such that the internal phase, ϕ_i, of the organism's clock corresponds appropriately to the external phase, ϕ_e, of the LD cycle. Thus, a diurnal bird's locomotor activity pattern entrains to the LD cycle so that activity onset ϕ_i corresponds approximately to dawn ϕ_e, maintaining a stable phase relationship, ψ_{ie}. Conversely, a nocturnal bird's ψ_{ie} would be approximately 12 h later than that of a diurnal bird.

42.2.2 Stability and lability of circadian rhythms

In DD, the circadian τ of diurnal birds is generally longer than 24 h, while τ in owls and nightjars tends to be shorter than 24 h (Aschoff, 1979). However, there is quite a bit of

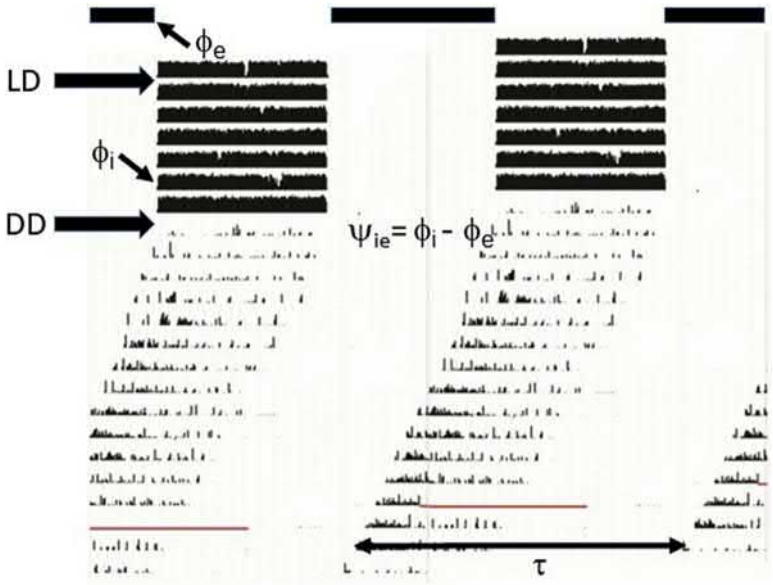

FIGURE 42.1 Actogram of locomotor activity from a single zebra finch, *Taeniopygia guttata.* The top bars indicate the times during which lights are off (black) versus on (white). These are plotted in a 48-h timespan in order to "double-plot" the data. The time of lights on, ϕ_e, indicated by the arrow, is a phase reference determined by the investigator. The internal phase, ϕ_i, is determined to be the activity onset. The relationship between ϕ_i and ϕ_e is called ψ_{ie}. This relationship may change depending on the time of year and physiological condition of the bird. The internal period, τ, is indicated here as the average interval between activity onsets.

inter- and intraspecific variability in τ and even consistent changes within an individual. For example, many house sparrows, *Passer domesticus*, will express a τ of less than 24 h upon transfer from an LD cycle to DD (see Figure 42.1). However, birds' τ gradually lengthens over several days to weeks, depending on the individual, eventually stabilizing with a τ of approximately 25 h. This is a phenomenon known as "Eskin's knee" as the actogram, described by Dr. Arnold Eskin in late 1970s (cf Menaker et al., 1978), appears bent as a knee. Once stabilized, the τ remains stable until environmental factors change.

The major environmental factor affecting τ in birds is ambient light. If diurnal birds are experimentally maintained in dim LL rather than DD, birds' τ will shorten, and as illuminance is increased, τ decreases until at constant illuminances of approximately 50−100 lx circadian patterns of locomotor activity are lost (Aschoff 1979); birds are arrhythmic. Nocturnal birds such as owls and nightjars are more highly variable than are diurnal birds. On average, however, their τs lengthen (increase) with increasing illuminance. Other environmental factors have not been studied in as much detail as has light, although birds' circadian patterns appear to be relatively insensitive to altered constant temperatures, as circadian patterns in all organisms tend to be temperature compensated with a Q_{10} of 0.8−1.1 (Pittendrigh, 1993).

42.2.3 Entrainment

A biological clock with a τ that is different from 24 h would not be a particularly useful clock if it could not confer a sense of internal time relative to external, sidereal time, or the time it takes the Earth to rotate relative to the vernal equinox, the solar day. Thus, organisms sense environmental cues called Zeitgebers (German for "time givers"), interpret them, and then adjust their internal time to external time through the process of *entrainment.* The formal properties of entrainment vary, depending on the Zeitgeber and on the process being measured.

Photic entrainment: The major Zeitgeber for nearly all organisms is the daily change in light intensity, and light affects circadian rhythms in birds profoundly. *Photic entrainment* in birds comes in two flavors: (1) *Nonparametric entrainment* entails the process by which the internal clock is differentially sensitive to the Zeitgeber depending on the time of day rather than the amount (the *parameter*) of the Zeitgeber present (Aschoff and Pohl, 1978). This process is similar to other organisms in that their circadian system is relatively insensitive to light during the subjective day. If a house sparrow is free-running in DD and she is illuminated for 15−30 min during her subjectively diurnal activity (subjective day), no or little effect on her ϕ_i will occur. However, if she is illuminated in the beginning of her *subjective night*, when she is inactive, light will change her ϕ_I ($\Delta\phi$) by delaying her activity onset ($-\Delta\phi$). If she is illuminated during the late subjective night, her subsequent activity onset will be advanced ($+\Delta\phi$). Through this process, birds' ϕ_I is maintained in a ψ_{ie} with external time (ϕ_e). This relationship between the timing of the light pulse and the amplitude and direction of the $\Delta\phi$ is referred to as the *phase response curve* (PRC), whose amplitude varies among species. (2) In diurnal birds, however, since they are active during times of great illumination, *parametric entrainment* can also contribute to the maintenance of an advantageous ψ_{ie}. Since diurnal birds tend to express a τ greater than 24 h and illumination shortens τ, illumination of increasing intensity (a *parameter*) during the day under natural conditions decreases the amplitude of $\Delta\phi$ required to maintain a stable ψ_{ie}. This is an underappreciated process that may even be relevant to human circadian organization (Roenneberg et al., 2010).

Circadian rhythms of many organisms can be entrained to LD cycles whose periods (T) do not necessarily equal 24 h within limits (Pittendrigh, 1993; Daan, 2000), including birds (Aschoff and Pohl, 1978; Zivkovic et al., 1999). T-cycles ranging in period from 22 (11 h light; 11 h dark) to 28 (14 h light; 14 h dark) can typically entrain circadian patterns of activity and other physiological functions. However, as the period of the T-cycle further strays from 24 h, the circadian system becomes less able to entrain to the T-cycle. This is largely due to the species-specific amplitude of the PRC. The T-cycles to which organisms are no longer capable of entraining are their *limits of entrainment* (Aschoff and Pohl, 1978).

It is interesting to note that birds may be unique among extant vertebrates in that they must necessarily deposit a large portion of calcium carbonate on the exterior of their eggs in order to produce the hard shell required for efficient incubation (Chapter 28). During the process of ovulation and oviposition, eggs must reside within the shell gland for a finite amount of time in order to produce a shell hard enough to withstand the pressures of incubation. In chickens, *Gallus domestica*, this period is approximately 26 h, even if the bird is entrained to a 24-h T-cycle (Fraps, 1955; Morris, 1973). Thus, as hens lay eggs in a 24-h T-cycle, the timing of oviposition drifts later and later during the day until the dark phase, at which point hens typically do not lay. This results in a 10−15 h delay in egg production (Morris, 1973). In Japanese quail, *Coturnix japonica*, the mechanism for this rhythm is only partially dependent on the circadian system itself (Underwood et al., 1997; Zivkovic et al., 1999), since removal of the eyes, which are critical for circadian rhythms in quail (see below), does not affect the oviposition rhythm (Zivkovic et al., 1999; 2000). Rather, it is more likely the result of a relaxation oscillator in the shell gland itself.

Knowledge of this oviposition cycle has been known for some time, even before the tenets of circadian organization were formulated (Byerly and Moore, 1941).

Nonphotic entrainment: Several nonphotic factors entrain birds' circadian clocks. Homoeothermic animals such as the vast majority of birds do not synchronize to daily patterns of ambient temperature, although tissue cultures from avian tissues entrain to cycles of high and low temperature (Barrett and Takahashi, 1995; Csernus et al., 2005). Further, ambient temperature can affect the rate by which birds entrain to novel light cycles (Rensing and Ruoff, 2002).

The presentation of food at a particular time of day can synchronize locomotor rhythms in many species of birds, and the data have suggested that birds, as in mammals, possess both light-entrainable oscillators and experimentally separable food-entrainable oscillators underlying food-seeking behavior. House sparrows maintained in dimLL entrain both locomotor and feeding patterns to the period of the feeding cycle, such that locomotor behavior occurs prior to the time of day at which food is presented (Hau and Gwinner, 1992). In domestic pigeons, *Columba livia,* presentation of food every 23.5 h to birds on a 24 h LD cycle results in an uncoupling of food-associated anticipatory changes in body temperature (Tb) and O_2 consumption with activity associated with LD (Rashotte and Stephan, 1996). Similarly, Svalbard ptarmigan, *Lagopus mutus hyperboreus*, and Indian weaver birds', *Ploceus philipinus*, food entrainment is coupled to birds' entrainment to the light cycle, suggesting in both species the food-entrainable oscillator is coupled to the light-entrainable pacemaker (Reierth and Stokkan, 1998; Rani et al., 2009).

Although birds are well known for their capacity to synchronize vocalization and other social cues (Benichov et al., 2016), there is a very little evidence for social cues influencing circadian patterns in birds. Daily presentation of taped sounds recorded from an aviary entrains circadian locomotor rhythms of house sparrows maintained in dimLL (Menaker and Eskin, 1966). These data suggest that birdsong and/or calls may influence the circadian clock. This may be a fruitful area for future research.

42.2.4 Masking

Photic masking: While light cycles are the major Zeitgeber involved in entraining avian circadian rhythms, light per se may not always affect the endogenous clock. Under some circumstances, exposure to light may alter the behavioral output of the clock as opposed to the clock itself. This is referred to as *masking* (Aschoff and von Goetz, 1989). As an example, Aschoff and von Goetz (1989) maintained canaries (*Serinus canaria*) in LD cycles of low intensity light. They then subjected birds to 1 h dim light pulses during the D phase and dark pulses during the dim light phase. Birds increased activity during the light pulses (positive masking), and decreased their activity during the dark pulses (negative masking). However, no long-term effect on circadian ϕ of these interventions could be discerned. The pulses did not affect the clock itself, just its output.

Artificial Light at Night: The difference between entrainment and masking may seem arcane, but the growing interest in the impacts of urban lighting and/or light pollution on avian behavior and health may require understanding of these differences. It is widely understood that artificial light is a worldwide human-caused alteration of our environment (Falchi et al., 2016), and that radiance and extent of artificial light at night (ALAN) continues to increase (Kyba et al., 2017). Since light has profound effects on avian circadian systems, many researchers have asked whether ALAN affects daily and circadian patterns of behavior. Using radio-telemetric analyses, Dominoni et al. (2013a) found that urban European blackbirds (*Turdus merula*) were more active earlier during the day than forest dwelling blackbirds. They also showed that urban blackbirds expressed lower levels of the pineal hormone melatonin (see below) than did rural birds (Dominoni et al., 2013b). Similarly, Amichai and Kronfeld-Schor (2019) found that common swifts (*Apus apus*) outfitted with acoustic loggers exhibited increased nocturnal activity under the bright lights of Jerusalem's western wall. However, it is important to point out that, although the authors indicated the data pointed to an effect on the circadian clock, laboratory analyses would be required to establish this notion.

Laboratory studies of ALAN on birds generally corroborate the idea that ALAN affects the daily distribution of behavior and can have profound effects on avian health. Zebra finches (*Taeniopygia guttata*) exposed to dim light during the night exhibit increased nocturnal locomotor behavior (Batra et al., 2019; Moaraf et al., 2020). Similarly, great tits (*Parus major*) exposed to different wavelengths of light during the night were more active during the night, with white light being more efficacious than was red or green light (Ouyang et al., 2018). There is some indication that ALAN has other deleterious effects on these birds, since great tits and house sparrows (*P. domesticus*) exposed to ALAN are also more susceptible to malaria and West Nile virus, respectively (Ouyang et al., 2018; Kernbach et al. 2018, 2020). However, it is not clear if the effects of ALAN on daily distribution of activity and disease states are causally related or just correlative.

Having said this, it's also important to point out that the effects of ALAN may not necessarily reflect an effect on the circadian clock. For example, Spoelstra et al. (2018) exposed great tits to ALAN, which advanced the ϕ of locomotor activity as in previous studies. However, to determine whether the ALAN also advanced the ϕ_i, the

authors transferred the birds into DD and revealed that the ϕ_i was not affected by the ALAN (Figure 42.2). Their activity onsets were fixed to the onset of the light cycle and not the activity onset in ALAN. Thus, these birds, at least, exhibited masking in ALAN. Of course, this does not diminish the importance and impact of ALAN on avian physiology (Schoech et al., 2013).

42.3 Photoreceptors

Since light is the major Zeitgeber involved in circadian entrainment to LD, masking, and an environmental factor that strongly influences τ under constant environmental conditions, the pathways by which light influences clocks and their outputs provide profound clues to the mechanisms underlying biological clocks. Intuitively, we might think that these photoreceptive processes are the exclusive domain of retinal photoreceptors, but this would be the furthest from the truth. While the retinae participate in photic entrainment and/or parametric responses to light, they are minor participants.

42.3.1 Encephalic photoreceptors

In addition to photoreceptors in the lateral eyes shared by all vertebrate classes, it has been known for some time that nonmammalian vertebrates express functional photopigments within the brain that are critical for entrainment of both circadian rhythms and circannual cycles (Okano and Fukada 2000). Early studies by Benoit in the 1930s showed that domestic ducks, *Anas platyrhynchos*, which had been blinded (enucleated) continued to exhibit reproductive responses to changing photoperiod (cf. Benoit and Assenmacher 1954). Work by Menaker and colleagues in the 1960s and 70s in passerine birds clearly showed that the eyes are not necessary for circadian entrainment (Menaker, 1968; Menaker and Underwood, 1976). In a classic series of experiments, Menaker's group demonstrated that enucleated house sparrows could entrain to a series of LD cycles of dimmer and dimmer illuminances, showing definitively that the eyes were not necessary for circadian entrainment. Under very dim LD cycles, birds no longer entrained and free-ran with a circadian period. They showed that the photoreceptors responsible for entrainment reside within the head by simply plucking feathers on the scalp, increasing the amount of light able to penetrate the cranium, and entrainment was reinstated. They then blocked entrainment by injecting India ink beneath the scalp (Menaker and Underwood, 1976).

Subsequent research has now identified at least four distinct structures within the brain that are functionally photoreceptive, containing several opsin-based photopigments and photoisomerases (Nakane and Yoshimura, 2010; Peirson et al., 2009; Bailey and Cassone, 2004) (Figure 42.3). These include the pineal gland, which expresses a pineal-specific opsin, pinopsin (Bailey et al., 2003;

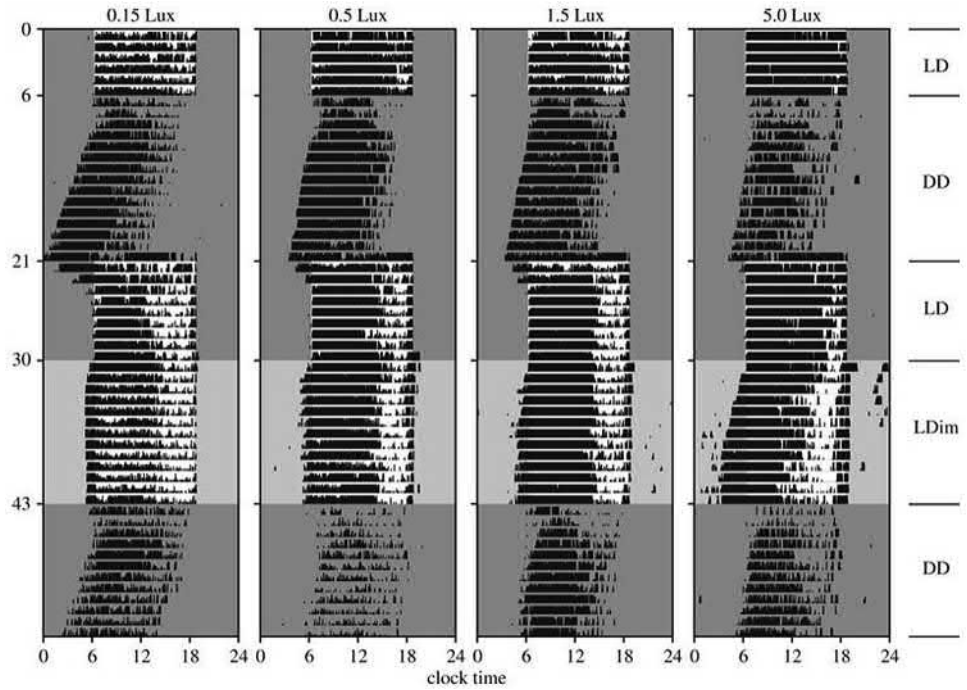

FIGURE 42.2 Example actograms of four great tits that were exposed to ALAN of different intensities from days 31–43 of these records. Note that activity onset was advanced during the ALAN, but, when birds were placed in constant darkness (DD), onsets reverted to the time of lights on (ϕ_e) demonstrated that ALAN did not entrain birds' clocks. This is an example of masking. *From Spoelstra et al. (2018).*

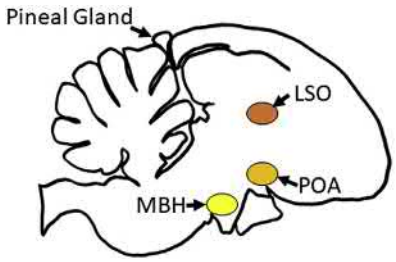

FIGURE 42.3 Schematic representation of a sagittal view of an avian brain. The general locations of extraocular photoreceptors are delineated in the pineal gland, the lateral septal organ (LSO), preoptic area (POA), and mediobasal hypothalamus (MBH).

Okano et al., 1994; Max et al., 1995), as well as melanopsin (OPN4) (Bailey and Cassone, 2005; Bailey et al., 2003; Chaurasia et al., 2005) and iodopsin (OPN1) (Masuda et al., 1994; Natesan et al., 2002) and whose photoreceptive function will be discussed further below. In addition, neurons within the preoptic area express VA (vertebrate ancient) opsin (Halford et al., 2009; Davies et al., 2010, 2012), and project to the tuberal hypothalamus, while the tuberal hypothalamus itself expresses a plethora of photoreceptive cells that appear to be divergent among avian species. In Japanese quail, *C. japonica*, CSF-contacting neurons in the mediobasal hypothalamus express both OPN4 and neuropsin (OPN5) (Nakane et al., 2010). In house sparrows, neurons within the arcuate nucleus express rhodopsin (OPN2) itself, in addition to OPN4 and OPN5 (Wang and Wingfield, 2011). Finally, the lateral septal organ expresses rhodopsin-like immunoreactivity (Wada et al., 1998). It is not clear whether each of these photoreceptive organs and/or their photopigments subserves mutually exclusive physiological processes or whether these overlap in their functions.

In addition to opsin-based photopigments, birds express flavin-based cryptochromes (Bailey et al., 2005; Chaurasia et al., 2005; Kubo et al., 2006). While cryptochrome is the major photopigment responsible for photoentrainment in *Drosophila* (Emery et al., 1998), the multiple cryptochromes expressed by vertebrates have not been established as photoresponsive molecules. Interestingly, cryptochromes have been implicated in the remarkable capacity of birds to detect and navigate by changes in the Earth's magnetic field (Wiltscko and Wilschko, 2019), and this capacity is dependent on photic conditions, such that exposure to short wavelengths of light (373−424 nm) sensitizes cryptochromes residing in cone photoreceptors to changes in magnetic inclination (Günther et al., 2018; Nießner et al., 2018). Bioinformatic (Bailey et al., 2005), chemical, and structural (Zoltowski et al., 2019) analyses of avian cryptochromes also point to a photoreceptive capacity for these proteins. However, they have as yet not been directly linked to entrainment of circadian clocks.

42.3.2 Pineal gland

The avian pineal gland emerges from the epithalamus of the diencephalon and extends to the dorsal surface of the brain, where it resides nestled between the two cerebral hemispheres and the cerebellum (Figure 42.3). There, the gland's narrow stalk extends to the skull itself, enlarges in its distal aspects, and attaches to the dura mater. There is considerable variability in pineal structure among birds (Quay, 1965; Menaker and Oksche, 1974). For example, nocturnal owls, shearwaters, and petrels exhibit only a vestigial or rudimentary pineal complex (Quay, 1965), while diurnal birds express well-developed pineal glands of differing overt anatomy. According to Menaker and Oksche (1974), avian pineal glands can be categorized as (1) saccular (passerine birds), (2) tubulofollicular (columbiform and anseriform birds), and (3) lobular (galliform birds). At the cellular level, pineal glands comprise at least four classes of cell types. The photoreceptor-like pinealocytes express outer segments reminiscent of retinal photoreceptors of a sensory ciliated type with a characteristic 7:0 microtubule configuration, although these are reduced in size and frequently coiled (Oksche et al., 1972; Menaker and Oksche 1974). These cells, as stated above, express several opsin-based photopigments, flavin-based cryptochromes, and phototransduction signaling molecules (Masuda et al., 1994; Bailey et al., 2003; Bailey and Cassone, 2004), clearly indicating that pinealocytes are directly photosensitive. This will be discussed further below. In addition, pineal glands contain "interstitial cells" that include ependymal and astrocytic neuroglia as well as leukocytes and leukoblasts (Oksche et al., 1972), and, in some species, neurons that project to the epithalamic habenular complex (Sato and Ebisawa, 1988). Finally, the pineal gland is vascularized and contains endothelial capillary cells (Oksche et al., 1972).

42.3.3 Retina

It is axiomatic that the retinae are photoreceptive, but their role as photoreceptors in avian circadian entrainment is less clear. In mammals, which do not possess extraocular photoreceptors (cf. Doyle and Menaker, 2007), circadian entrainment is predominantly mediated by intrinsically photoreceptive retinal ganglion cells, expressing melanopsin (OPN4; cf. Panda, 2007). These cells project directly to circadian pacemakers in the hypothalamic suprachiasmatic nuclei (SCN). In birds, as stated above, the eyes are not necessary for circadian entrainment to LD cycles, since enucleated house sparrows and several other species entrain to LD cycles. However, that is not to say that the eyes are not involved. Multiple layers of the retinae of domestic chicks, *Gallus gallus domesticus*,

express OPN4, including retinal ganglion cells (Bailey and Cassone, 2005; Chaurasia et al., 2005), similar to the situation in mammals.

Employing a retinal degenerate chick model developed by Semple-Rowland (Semple-Rowland and Cheng, 1999; Guido et al., 2010), Guido and colleagues have shown that the chicks possessing only inner retinal photoreceptors are capable of entraining feeding rhythms to an LD cycle (Valdez et al. 2009, 2013). When encephalic photoreceptors are covered with a blackened hood, the chicks expressed a free-running rhythm with a 24.5 h τ. When the birds were enucleated, hooded birds free-ran, but illumination of the skull reestablished entrainment. The picture that emerges is that multiple photoreceptors in the brain, the pineal gland, and the retina redundantly contribute to photic entrainment in birds (Doyle and Menaker, 2007; Guido et al., 2010; Rios et al., 2019).

42.4 Pacemakers

As we will see below, the capacity to express circadian rhythms is widely distributed among tissues and cells in multicellular organisms (Bell-Pedersen et al., 2005). However, certain tissues have been designated "pacemakers" because of their capacity for sustained circadian rhythmicity and their importance for *circadian organization.* In birds, these structures are the pineal gland, the retinae, and the hypothalamic SCN, whose mutual interactions are critical for overt circadian organization.

42.4.1 Pineal gland and melatonin

Searching for the location of the intracranial, extraretinal photoreceptors, Gaston and Menaker (1968) surgically removed the pineal gland (PINX) from house sparrows (Figure 42.4). While the birds retained their ability to entrain to LD, they became arrhythmic when placed in DD, demonstrating that the pineal gland is necessary for self-sustained circadian rhythmicity. However, the data also showed that the pineal gland is part of a system of circadian clock components, since PINX sparrows could anticipate the time of lights on in an LD cycle and because birds only gradually became arrhythmic over 5−15 days following transfer from LD to DD (Gaston and Menaker, 1968; Binkley et al., 1971; Ebihara and Kawamura, 1981; Janik et al., 1992; Lu and Cassone, 1993a; Wang et al., 2012). Further, the effect of PINX is not universal among avian species. PINX of European starlings, *Sturnus vulgaris,* results in a range of behavioral changes ranging from arrhythmicity akin to those seen in house sparrows to slight disruption of behavioral locomotor rhythmicity (Gwinner, 1978; Gwinner et al., 1987). Circadian rhythms of locomotor behavior in columbiform and galliform birds are little or not affected at all by PINX (Ebihara et al., 1984; Underwood and Siopes, 1984).

Even so, the pineal gland represents both the capacity for rhythmicity and time of day. In an elegant experiment, Zimmerman and Menaker (1979) transplanted pineal glands from two groups of house sparrows into the anterior chambers of the eye of PINX, arrhythmic sparrows

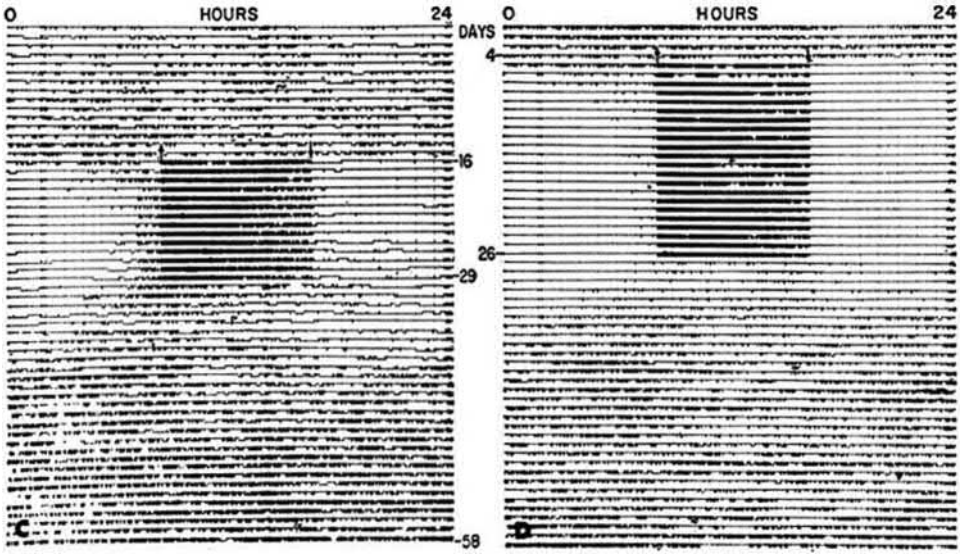

FIGURE 42.4 Effects of pinealectomy on locomotor activity rhythms in house sparrows. Birds are arrhythmic in constant darkness (DD) but are able to entrain to light:dark (LD) cycles (*small arrows up and down*, respectively). When birds are released into DD again, they take 5−15 days to become arrhythmic again. *From Gaston and Menaker (1968).*

maintained in DD. The first group of donor birds were entrained to an early LD cycle, with lights on at midnight, while the second set of donors were entrained to a late LD cycle, with lights on at 11 a.m. Transplantation restored circadian rhythms to both groups of recipients within 1 day. Moreover, birds that received pineal glands from early donors exhibited an early ϕ_i, while the recipients of late donor pineal glands exhibited a late ϕ_i. Thus, the pineal gland is not only necessary for circadian rhythmicity in these birds, but it contains a correlate that confers time of day to recipient birds.

That hormone was known even then to be the indoleamine melatonin from earlier work of Lerner and later of Axelrod, Klein, and their coworkers (cf. Klein et al., 1997), who explored the biochemical basis for melatonin biosynthesis in the pineal gland of the chick, *G. gallus domesticus* (Figure 42.5). Research from a large number of investigators has shown that pinealocytes, the photoreceptive, secretory cells of the avian pineal gland, take up the amino acid tryptophan, which is converted to 5-hydroxytryptophan by tryptophan hydroxylase (TrH; EC 1.14.16.4; Chong et al., 1998) and then decarboxylated to produce serotonin (5HT) by aromatic L-amino acid decarboxylase (AAADC; EC 4.1.1.28). During the night in LD and subjective night in DD, 5HT is converted to N-acetylserotonin (NAS) by arylalkylamine (or 5HT)-N-acetyltransferase (AANAT; EC 2.3.1.87; Bernard et al., 1997). NAS is then converted to melatonin by hydroxyindole-O-methyltransferase (HIOMT; EC 2.1.1.4; Bernard et al., 1991), alternatively named acetylserotonin methyltransferase. The genes encoding each of these enzymes have been isolated, cloned, and sequenced in several avian species. In chick, at least, TrH, AANAT, and HIOMT are regulated by both the molecular clockworks within the pinealocytes and directly by light at the transcriptional, translational, and posttranslational levels, so that the enzymatic regulation of pineal melatonin is a dynamic, rhythmic process (Klein et al., 1997).

Rhythmic administration of melatonin to PINX house sparrows, European starlings, and zebra finches, *T. guttata*, or to EX/PINX pigeons (Chabot and Menaker, 1992, Lu and Cassone, 1993b; Gwinner et al., 1997; Heigl and Gwinner 1995; Cassone et al. 1992, 2008; Wang et al., 2012) restores a daily pattern of locomotor behavior (Figure 42.6). Activity typically decreases following melatonin administration, and rebounds following the daily

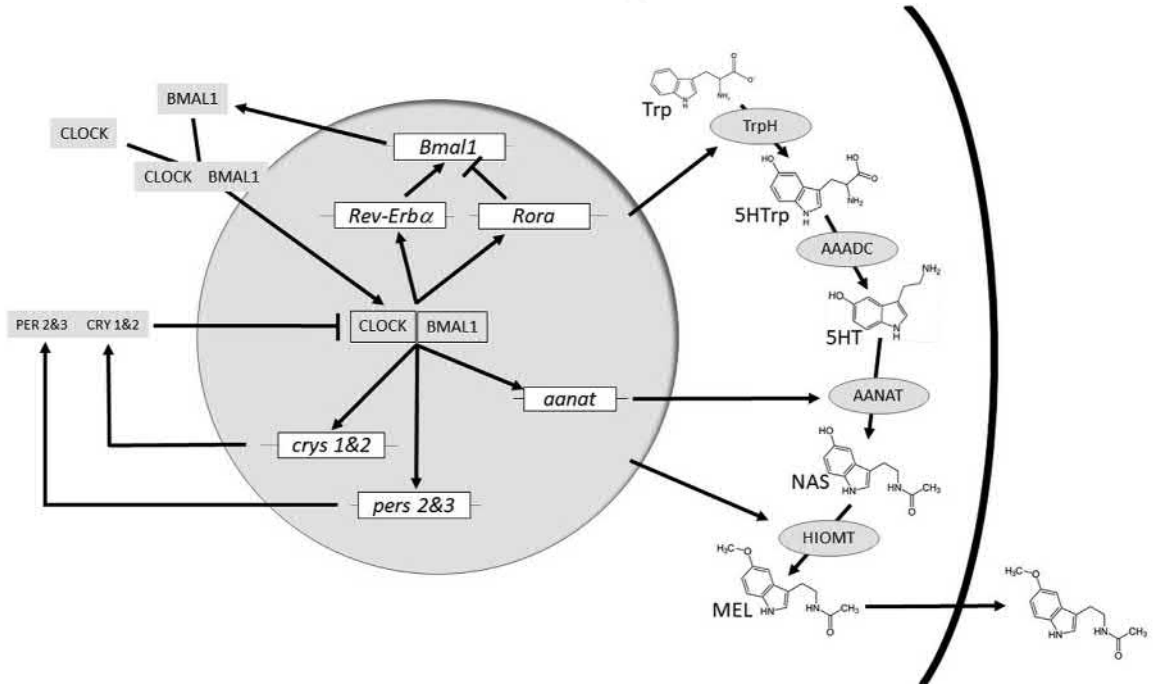

FIGURE 42.5 Schematic representation of the molecular clockworks regulating circadian patterns of melatonin biosynthesis in a pinealocytes or retinal photoreceptor. Positive elements CLOCK and BMAL1 enter the nucleus and activate expression of genes whose promoters contain an E-Box. Among these are the negative elements *period 2 and 3 (pers 2 and 3)* and *cryptochromes 1 and 2 (crys 1 and 2)*, *Rev-Erbα* and *Rora*, which form a secondary loop regulating *Bmal1* transcription, and output, clock-controlled genes such as arylalkylamine-N-actyltransferase (*aanat*). The *pers* and *crys* are translated, form heterodimers with other components, such as the casein kinases, and reenter the nucleus to interfere with CLOCK/BMAL1 activation. Melatonin biosynthesis pathways are indicated on the right. Amino acid tryptophan is converted to 5-hydroxytryptophan (Trp) by tryptophan hydroxylase (TrpH). AAADC then converts 5-hydroxytryptophan (5HTrp) to 5-hydroxytryptamine (5HT; serotonin). Then, during the night, AANAT converts 5HT to N-acetylserotonin (NAS), a substrate for hydroxyindole-O-methyltransferase (HIOMT), which produces melatonin (MEL) itself. Presumably, melatonin diffuses out of the cell at this time, although a release mechanism may exist.

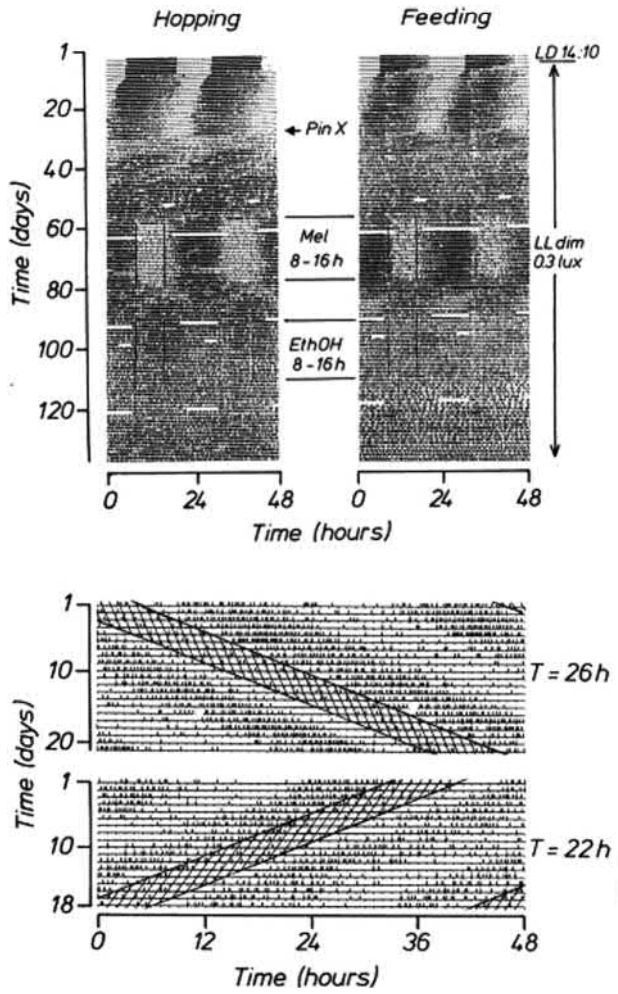

FIGURE 42.6 Effects of rhythmic administration of melatonin to house sparrows. Top. Actograms of perch-hopping and feeding behavior of house sparrows maintained in DD. Birds become arrhythmic in both behaviors following pinealectomy (PINX) and daily rhythms of behavior are reestablished with melatonin administration. Bottom. This synchronization is entrainment rather masking, because locomotor activity maintains a systematic phase relationship with the administration of the hormone. When melatonin is presented every 26 h, activity occurs after the administration, while a melatonin cycle every 22 h results in behavior that anticipates the melatonin. *From Gwinner et al. (1997).*

dosage, suggesting that melatonin induces a soporific state and/or sleep, which it may well do. In addition, however, the synchronization of locomotor behavior by rhythmic melatonin administration represents entrainment of circadian clockworks in the PINX bird, since melatonin administration in a T-cycle different from 24 h results in systematic changes in the phase relationship (ψ) of melatonin to the onset of locomotor activity (Figure 42.6; Chabot and Menaker, 1992; Gwinner et al., 1997). Further, administration of three different behaviors, locomotor behavior, call, and song, by a single melatonin regime results in entrainment at differential rates (Wang et al., 2012).

Further, constant administration of melatonin has profound effects on overt rhythmicity (Gwinner and Brandstatter, 2001). Subcutaneous implants of beeswax (Turek et al., 1976) or Silastic (Hau and Gwinner, 1995; Abraham et al., 2000) containing crystalline melatonin change τ at low concentrations and abolishe rhythmicity altogether at higher dosages. Interestingly, constant melatonin decreases the times taken to reentrain to food cycles (Hau and Gwinner, 1995) or LD cycles (Abraham et al., 2000). This is similar to the effect of PINX itself (Kumar and Gwinner, 2005), punctuating the view that it is the rhythm of endogenous melatonin that preeminently affects circadian organization and that this effect acts through the entrainment of downstream oscillators (Cassone and Westneat, 2012).

Avian pineal glands contain the circadian clockworks and photoreceptors to generate circadian patterns of melatonin biosynthesis in vitro as well as in vivo, which can be entrained to LD cycles directly (Binkley et al., 1978; Brandstatter et al., 2000; Robertson and Takahashi, 1988b; Natesan et al., 2002). Pineal tissue and pinealocyte cultures express circadian patterns of AANAT activity (Binkley et al., 1977; Deguchi, 1979), gene expression (Karaganis et al., 2008), and melatonin efflux (Figure 42.7; Takahashi et al., 1980; Robertson and Takahashi, 1988a; Li and Cassone, 2015) such that levels are high during the night and low during the day in LD. These rhythms persist for 4–10 days in DD before damping to arrhythmicity (Li and Cassone, 2015). Exposure to light has three effects on cultured pineal rhythms: (1) Light inhibits melatonin biosynthesis. (2) Light increases amplitude and decreases damping, and (3) light phase-shifts the clock within pineal cells (Zatz et al., 1988).

42.4.2 Retinae

Interestingly, the photoreceptors in the retinae of the lateral eyes also synthesize and release melatonin in many vertebrate species (Underwood et al., 1984; Iuvone et al., 1997). In fact, in Japanese quail and domestic pigeon, *C. livia*, the retinae release almost as much melatonin into the systemic circulation as does the pineal gland, and removal of this source by enucleation or retinectomy in addition to PINX results in arrhythmic circadian locomotor behavior, similar to the effects of PINX alone in passerine birds (Ebihara et al. 1984, 1997; Underwood and Siopes, 1984). Thus, the variability of the effects of PINX among birds may in part be due to this retinal component in some species and that it is not the pineal per se but rhythmic melatonin that is important for circadian locomotor behavior.

42.4.3 Suprachiasmatic nuclei

In birds, two sets of structures have been associated with SCN function: the medial suprachiasmatic nuclei (mSCN)

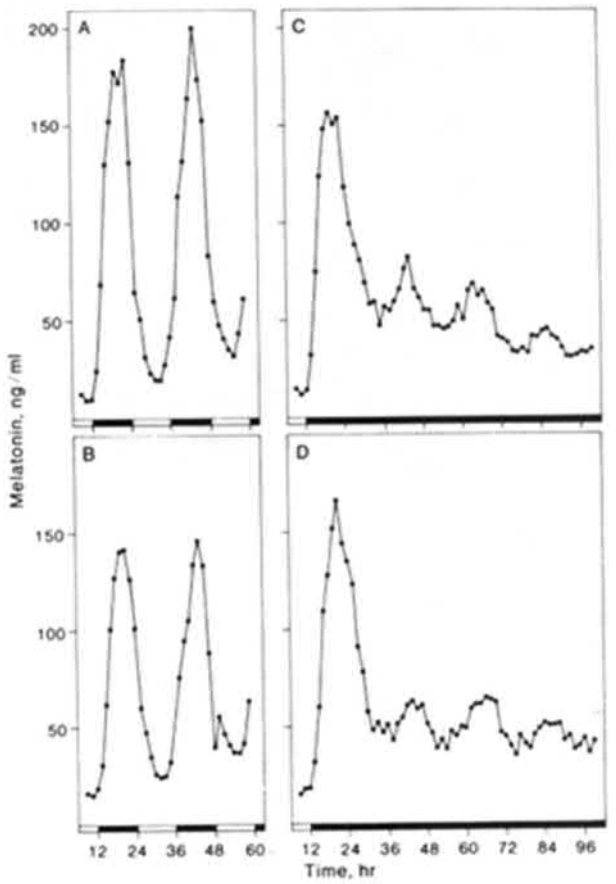

FIGURE 42.7 Melatonin rhythms from cultured chick pineal glands. Melatonin is released during the dark phase in glands maintained in LD in vitro (left). These rhythms continue in DD for several days at a lower amplitude but eventually damp out. *From Takahashi et al. (1980).*

and the visual suprachiasmatic nuclei (vSCN) (Cassone and Moore, 1987; Cantwell and Cassone, 2006a,b). These structures are connected via neuronal projections and are contiguous in terms of their cellular populations, especially in the distribution of astrocytes. The vSCN, but not the mSCN, expresses metabolic rhythmicity and electrical activity such that levels are high during the day and low during the night (Cassone, 1988; Lu and Cassone, 1993a,b; Juss et al., 1994; Cantwell and Cassone, 2002). Further, the vSCN, but not the mSCN, receives retinohypothalamic (RHT) input (Cassone and Moore, 1987; Cassone 1988, Cantwell and Cassone, 2002; 2006a,b), and the vSCN, but not the mSCN, contains melatonin receptor binding (Rivkees et al., 1989; Cassone et al., 1995). Administration of melatonin to chicks and house sparrows decreases glucose utilization within the vSCN (Lu and Cassone 1993b; Cantwell and Cassone, 2002). Finally, light activates *c*-fos expression in the vSCN, but not in the mSCN (King and Follett, 1997). In quail, only the mSCN expresses clock gene rhythmicity (Yoshimura et al., 2001; Yasuo et al., 2002), while in the house sparrow, both structures rhythmically express the expression of the "clock gene" *per2* (Abraham et al. 2002, 2003). Importantly, lesions directed at the mSCN in Java sparrows, *Padda oryzivora*, and house sparrows result in arrhythmicity similar to that observed following PINX (Ebihara and Kawamura, 1981; Takahashi and Menaker 1982). However, it is not clear whether these lesions also affected vSCN integrity.

42.5 Sites of melatonin action

42.5.1 Melatonin receptors

In the 1980s and 90s, high-affinity melatonin receptor binding using the radiolabeled agonist 2[^{125}I]-iodomelatonin (IMEL) revealed high densities of IMEL binding in retinal, retinorecipient structures, and visual integrative structures in the avian brain as well as peripheral tissues (Figure 42.8; Dubocovich and Takahashi, 1987; Rivkees et al., 1989; Cassone et al., 1995). Binding affinity studies indicated kD's in the pM range with high specificity for melatonin itself. Brain structures that bind IMEL included retinorecipient structures in the SCN of the circadian system, the ventrolateral, and dorsal geniculate nuclei of the thalamofugal visual pathway, the optic tectum of the tectofugal pathway, and the nucleus of the basal optic root or the accessory optic pathway. In all species, integrative structures of the tectofugal pathway such as nucleus rotundus and the ectopallium also bind IMEL (Rivkees et al., 1989; Cassone et al., 1995). In some but not all species, hyperpallial structures, including the visual Wulst, are sites of IMEL binding. In male passerine birds but not females, structures associated with bird song learning and control also revealed high affinity IMEL binding (Gahr and Kosar, 1996; Whitfield-Rucker and Cassone, 1996).

Reppert and colleagues were able to isolate and clone genes encoding two high affinity melatonin receptors; these were designated the Mel_{1A} and Mel_{1C} receptors (Reppert et al., 1995). Independent work isolated partial sequences encoding an ortholog of the Mel_{1B} receptor in the same year (Liu et al., 1995). Subsequent work has confirmed in birds that there are at least three melatonin receptors, the Mel_{1A}, Mel_{1B}, and the Mel_{1C} receptors (Reppert, 1997). All three melatonin receptor subtypes represent 7-transmembrane domain, GTP-binding protein structures, and all three are in the G_i GTP-binding protein category, although some cross-talk with G_q has been documented (Reppert, 1997). The distributions of these three receptor subtypes are not uniform in chicks, zebra finches, and house sparrows. The Mel_{1A} receptor predominates in central nervous neurons and peripheral tissues (Natesan and Cassone, 2002; Karaganis et al., 2009), while the Mel_{1B} receptor is expressed in inner retinal neurons and photoreceptors as well as other central nervous neurons (Natesan and Cassone, 2002). In passerines,

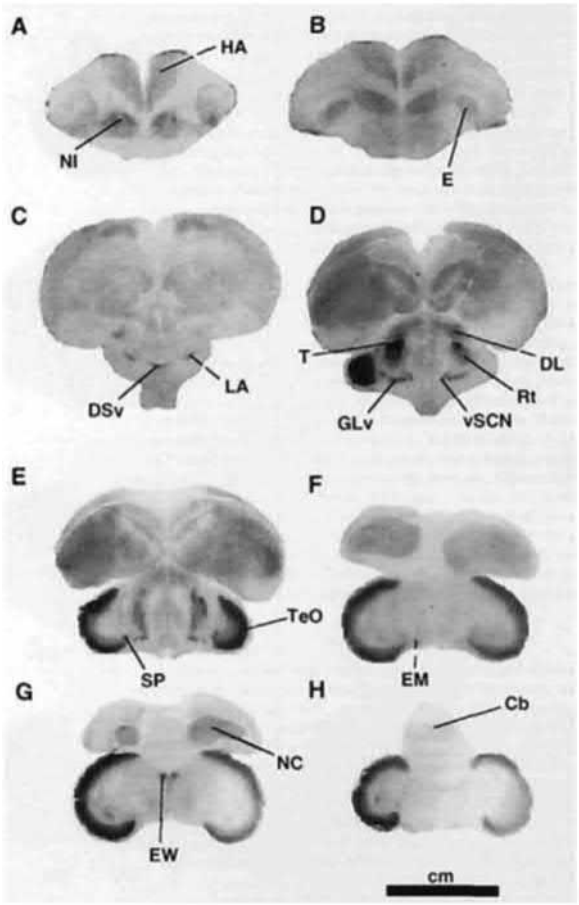

FIGURE 42.8 Melatonin receptor binding in the brain of the ring-necked pheasant, *Phasianus colchicus*. Video-digitized images of autoradiographs depicting 2[^{125}I]iodomelatonin binding (IMEL) at 50 pM from the rostral (A) to caudal (H) extents. Densest binding is present in retinorecipient and integrative structures of the circadian (vSCN), tectofugal (optic tectum (TeO), *nucleus rotundus* (Rt), and ectopallium (E)), thalamofugal (lateral anterior nucleus (LA) and dorsolateral nucleus (DL) in the thalamus and the hyperpallium anterior (HA)), and accessory optic (ectomammillary (EM; also called nucleus of the basal optic root) and nucleus of Edinger–Westphal (EW)) visual pathways. *From Cassone et al. (1995).*

the Mel_{1B} receptor is the major receptor subtype in song control nuclei, but the other two are expressed as well (Jansen et al., 2005; Bentley et al., 2013). The Mel_{1C} receptor, on the other hand, predominates in nonneuronal elements of the central nervous system (Reppert et al., 1995; Adachi et al., 2002). Culture studies with chick astrocytes (Adachi et al., 2002) show 95–100% diencephalic astrocytes express the Mel_{1C} receptor, while an overlapping 5–10% expresses Mel_{1A}. Astrocytes do not appear to express Mel_{1B}.

42.5.2 Mechanisms of action

Melatonin receptors, like all 7-transmembrane domain receptor proteins in the Gi GTP-binding protein group, act via inhibition of adenylyl cyclase activity in cells that express these receptors. There is some evidence for downstream cross-talk with other signaling pathways, however. For example, calcium signaling among chick astrocytes is mediated by a Mel_{1C} melatonin receptor through IP3-depending processes (Peters et al., 2005). In addition, there is evidence that melatonin may act via a receptor-independent and/or by receptor molecules as yet undiscovered. However, these have not been described in birds.

42.6 Avian circadian organization

Overt circadian rhythms in birds are controlled by multiple circadian pacemakers that are entrained by multiple photoreceptive elements in the central nervous system. The relative importance of these pacemakers varies among the few species studied, but in each, the core of the circadian system can be identified as the pineal gland, the retinae, and the SCN (mSCN and vSCN). Early analyses of the interactions of circadian pacemakers and photoreceptors suggested a hierarchical relationship in which the pineal gland imposes and/or entrains rhythmicity and phase on downstream processes or oscillators, respectively. The discovery of SCN and retinal pacemaker activity suggested a more complex relationship (Figure 42.9).

There is little doubt that the pineal gland and melatonin are important for circadian organization, but it is also clear that they are only part of a more complex system of structures and processes we shall call *avian circadian organization* or the *avian circadian system.* Although PINX indeed does abolish circadian locomotor, Tb, brain

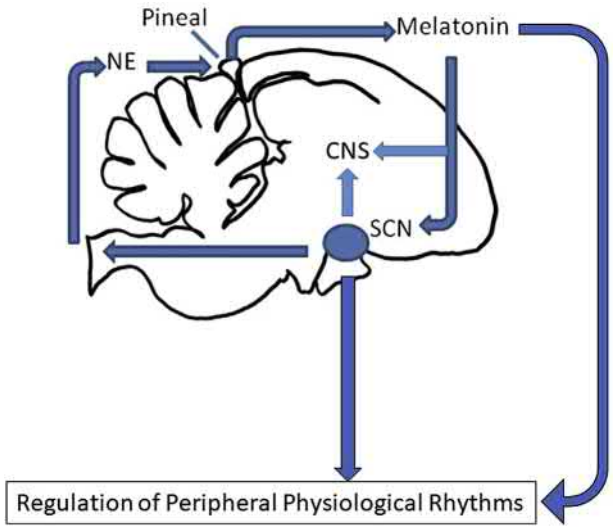

FIGURE 42.9 Neuroendocrine loop model for avian circadian organization. Pacemakers in the pineal gland and SCN interact via mutual inhibition to maintain a stable antiphase relationship. Each pacemaker can affect downstream oscillators and processes independently or in concert in the CNS and periphery. *Modified from Cassone and Westneat (2012).*

metabolism, and singing behavior rhythms in oscine passeriform birds, there is compelling evidence for other pacemakers in the system delineated above. Firstly, PINX birds entrain to LD cycles and typically commence locomotor and singing behavior before dawn (Gaston and Menaker, 1968; Menaker et al., 1978; Wang et al., 2012), indicating some capacity for time-keeping. Secondly, when PINX house sparrows, zebra finches, and other passerine birds (sparrows and finches) are transferred from LD to DD or dimLL, they express 5−10 days of damped activity that gradually descends into arrhythmicity (Figure 42.4), suggesting a remnant pacemaker underlying rhythmic behavior. Thirdly, sturnid passerines, such as starlings, and columbiform birds, such as pigeons, express a variable response to PINX, with some birds becoming arrhythmic, others disrupted, and still others unaffected (Gwinner 1978; Ebihara et al., 1984; Gwinner et al., 1994, 1997). Finally, as stated above, timed melatonin administration differentially entrains different behaviors in zebra finches (Wang et al., 2012; Prabhat et al., 2019).

At least one of the sites of melatonin action in synchronizing circadian locomotor rhythms is the vSCN. The vSCN express melatonin receptors (Rivkees et al., 1989; Reppert et al., 1995), and melatonin affects the vSCN physiologically. When intact house sparrows are placed in DD and injected with 2DG at different times during the subjective day to map metabolic activity, the vSCN expresses a rhythm in 2DG uptake for at least 10 days in DD (Lu and Cassone 1993a). However, when PINX birds are similarly placed in DD, 2DG uptake rhythms in the vSCN decline in amplitude and damp to arrhythmicity at the same rate as does locomotor activity (Lu and Cassone, 1993a). When PINX birds are administered melatonin on a daily basis, locomotor activity and vSCN 2DG uptake rhythms are both reestablished (Lu and Cassone, 1993b). Further, injection of melatonin during the late subjective day acutely decreases vSCN 2DG uptake (Cantwell and Cassone, 2002).

Conversely, while it is certain the avian pineal gland contains patent circadian oscillators and photoreceptors to establish overt circadian rhythms in melatonin secretion in vivo and in vitro (Binkley et al., 1977; Deguchi, 1979; Takahashi et al., 1980; Kumar and Follett, 1993; Csernus et al., 2005; Karaganis et al., 2008), these rhythms are not self-sustained in vitro in DD (Figure 42.7). Cultured pineal glands express rhythms of melatonin biosynthesis and secretion such that melatonin levels are high during the night and low during the day in LD, but the amplitude of this rhythm declines in DD, such that the rhythm damps to arrhythmicity in 2−8 days (cf. Cassone and Menaker, 1984; Csernus et al., 2005; Li and Cassone, 2015).

In vivo, the avian pineal gland is innervated by postganglionic sympathetic nerves (Ueck, 1979) and receives daily and circadian input through release of norepinephrine (NE) during the day and subjective day (Cassone et al., 1986). This rhythm of NE turnover is dependent on the vSCN, since surgical destruction of the vSCN, but not the mSCN, abolishes the circadian NE turnover rhythms (Cassone et al., 1990). When the pineal gland of domestic hens is denervated of its sympathetic innervation in vivo, plasma melatonin rhythms damp within 4 days (Cassone and Menaker 1983), similar to the situation of pineal glands in vitro. Administration of NE to chick pineal glands in vivo and in vitro has two effects on pineal melatonin rhythms: (1) NE inhibits melatonin biosynthesis and (2) NE increases amplitude and decreases damping, but does *not* phase-shift the pineal circadian clock (Cassone and Menaker, 1983; Zatz and Mullen, 1988; Li and Cassone, 2015).

To account for these observations in house sparrows, at least, Cassone and Menaker (1984); Cassone (1990) proposed the "neuroendocrine loop model" for avian circadian organization (Figure 42.9). In this scenario, pineal and SCN pacemakers are damped circadian oscillators. We do not know whether this damping is due to individual cells within these structures themselves damp or whether these cells are self-sustained oscillators that drift out of phase from one another. Light inhibits the output of the pineal gland oscillators through photoreceptors within the gland themselves, and light activates SCN output as well as possessing the capacity to phase-shift the clocks within each. During the night and subjective night in DD, pineal oscillators secrete melatonin and influence a wide array of downstream processes and structures. Among these are the vSCN, which are inhibited by melatonin. However, because the pineal is an endogenous oscillator, its output declines as dawn and subjective dawn in DD approach, disinhibiting SCN (vSCN and mSCN) output. The SCN in turn are active during the day and subjective day in DD, affecting a wide array of downstream processes and structures. Among these are the circadian rhythm in sympathetic outflow in NE turnover in the pineal gland at least, which are high during the day and low during the night. There, NE inhibits the biosynthesis and release of melatonin until, since the SCN are circadian oscillators, their output diminishes, and pineal oscillators are disinhibited. This mutually inhibitory relationship of SCN and pineal oscillators maintains stable phase relationships and enable each pacemaker to affect downstream processes singularly or in concert. Gwinner (1989) suggested that the relationship between pineal and SCN oscillators conveyed an "internal resonance" in which each oscillator increased the amplitude of its partner. This idea is not mutually exclusive from the neuroendocrine loop model. Indeed, it is clear that application of NE to chick pineal glands increases the amplitude of melatonin output in vivo (Cassone and Menaker, 1983) and in vitro (Zatz and Mullen, 1988) even as it inhibits melatonin output. The pineal gland releases rebounding high levels of

melatonin release following cessation of the NE administration. This effect is phase specific, since the effect of NE on in vitro melatonin releases during the subjective night as opposed to the subjective day (Li and Cassone, 2015), suggesting the pineal clock gates its sensitivity to sympathetic input.

Where do the retinae fit into this scheme? For columbiform and galliform species, whose retinae secrete melatonin rhythmically, at least part of their role is to serve as a "second (and third) pineal gland" (Menaker, 1985), secreting melatonin during the night, presumably influencing SCN and other downstream oscillators in parallel with pineal output. In addition, inner retinal photoreceptors and circadian oscillators may directly influence circadian patterns of visual perception and activity through RHT and other visual pathways (Guido et al., 2010.). It is clear however, that the retinae are the predominant pacemakers in galliform birds, but the nature of this function is not apparent at this stage (Steele et al., 2006).

The mechanism by which this system influences downstream processes is not at all clear at this stage. However, new and exciting data pointing to distributed capacities for rhythmicity are becoming available, and these are described below. First, however, we must explore the molecular aspects of avian circadian clocks.

42.7 Molecular biology

The idea that behavior and other complex processes derive from genes and their expression arises from early mutational analyses in search of mutants and the identification of the genes underlying the process. Among the early entrants in this study was the analysis of mutations affecting circadian rhythms in *Drosophila* (Konopka and Benzer, 1971; Rosbash et al., 2007).

42.7.1 Identification, characterization, and localization of molecular clockworks in birds

Circadian rhythms are regulated by a highly conserved set of genes, collectively called "clock genes," whose products are believed to dynamically interact to elicit rhythmic patterns of transcription, translation, biochemical and physiological processes, and behavior (Reppert and Weaver, 2002; Bell-Pedersen et al., 2005; Rosbash et al., 2007). In animals ranging from *Drosophila* to humans, the central core of this gene network can be broadly characterized as "positive elements" *clock* and *bmal1* and "negative elements" *period 1 (per1), period 2 (per2), period 3 (per3)*, and the cryptochromes *cryptochrome 1 (cry1)* and *cryptochrome 2 (cry2)*. In contrast to mammals, birds do not express a *per1* and have been shown to only express only *per2* and *per3* (Figure 42.10; Yoshimura et al., 2000; Yasuo et al., 2002; Bailey et al., 2003, 2004). *Clock* and *bmal1* are transcribed and then translated in the cytoplasm, where they dimerize and reenter the nucleus and activate transcription of the negative elements through the activation of E-box promoter elements (Figure 42.5; Haque et al., 2010). The *pers* and *crys* in turn are transcribed and translated in the cytoplasm, where the PER proteins are targeted for proteosomal proteolysis by a series of protein kinases, most notably casein kinase 1ε (CK1ε) and CK1δ. This process slows the accumulation of the cytoplasmic PER and thereby increases the period of the molecular cycle. In the cytoplasm, PER and CRY proteins form oligomers that reenter the nucleus and interfere with the CLOCK/BMAL1-mediated activation. A secondary cycle involving two genes containing E-box promoters, *Reverbα*, and *rorA*, amplify the cycle by activating and inhibiting *bmal1* transcription, respectively. Disruption or knockout of these genes' action has profound effects on the expression of circadian rhythms in animals in which these technologies are possible (i.e., mice and *Drosophila*) ranging from changes in period to arrhythmicity.

42.7.2 Peripheral oscillators in avian circadian clocks

While clock genes are expressed by cells within pacemaker tissues (Yoshimura et al., 2000; Yasuo et al., 2002; Bailey et al., 2002, 2003, 2004), it was surprising to find rhythmic expression of clock genes in other parts of the brain as well as in peripheral tissues, such as heart, liver, lungs, and gonads (Chong et al., 2003; Helfer et al., 2006; Karaganis et al., 2009; Zeman et al., 2009). To determine whether pacemakers in the pineal and eyes were responsible for peripheral clock gene rhythms, Karaganis et al. (2009) showed that PINX or EX of chicks decreased the amplitudes of clock gene expression and changed the ϕ_i of rhythms in *cry1*, *per3*, and *bmal1* rhythms but did not abolish them. At this stage, it is not clear whether combined PINX and EX would abolish these rhythms, but at this stage, one must conclude the peripheral oscillations persist and are only modulated by the pineal and retinae.

42.7.3 Prospects for transgenesis and molecular manipulation of avian clocks

At this stage, no stably transformed birds are available for circadian biology. However, there are now many reports of development of transgenic reporter and knock-out lines of chickens (cf. Poynter and Lansford, 2008; Nishijima and Iijima, 2013). Clearly, this is the line of future research in this field. Even so, some progress has been made with viral transductions in avian retina models (Semple-Rowland et al., 2010). Further, application of microRNA vectors associated with CLOCK and BMAL1 expression affects AANAT expression in chick retina (Haque et al., 2010).

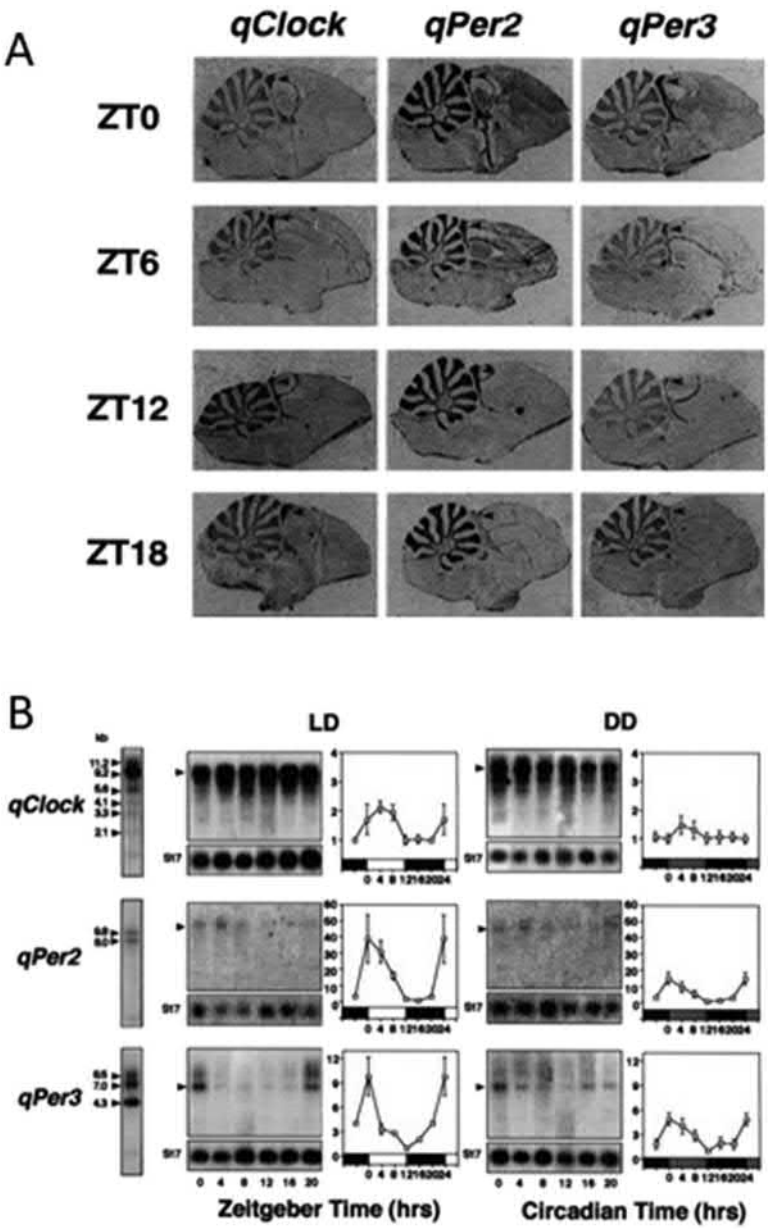

FIGURE 42.10 Circadian expression of clock genes in the (A) pineal gland by in situ hybridization and (B) retinae by northern blot analysis in the Japanese quail. In both tissues, *clock* is expressed during the day, while *per2* and *per3* are expressed in the late night. *From Yoshimura et al. (2000).*

Thus, it is possible to manipulate the avian circadian clock at the molecular level. The proof now will be in the pudding.

42.8 Conclusion and perspective

Biological clocks in birds are critical components of their physiology and behavior (Cassone 1990; Gwinner and Brandstatter, 2001). Early research studying avian circadian organization was critical in the understanding of structure–function relationships in the central nervous system. Indeed, the identification of the pineal gland as a "master pacemaker" conveyed a sense that the system was hierarchically organized. However, as the properties of the pineal gland's function became clearer and the identification of new pacemakers in the hypothalamus and retinae made the system appear more complex, it became clear that the avian circadian clock is a system of multiple circadian pacemakers in the SCN, the pineal gland, and in at least some species the retinae. Each of these was entrained to environmental light cycles by photoreceptors in the retinae, the pineal gland, and the brain. These were in turn thought to interact to accomplish a self-sustained oscillation that drove rhythmic processes downstream. The advent of molecular biological techniques revealed that even this distributed system of pacemakers acts via entrainment of

downstream oscillators rather than via direct action. It remains to be seen how molecular oscillations in the brain and peripheral tissues are coupled to physiological output, but this is the physiology of circadian clocks in the future.

References

Abraham, U., Gwinner, E., Van't Hof, T.J., 2000. Exogenous melatonin reduces the resynchronization time after phase shifts of a nonphotic zeitgeber in the house sparrow (*Passer domesticus*). J. Biol. Rhythms 15 (1), 48–56.

Abraham, U., Albrecht, U., Gwinner, E., Brandstätter, R., 2002. Spatial and temporal variation of passer Per2 gene expression in two distinct cell groups of the suprachiasmatic hypothalamus in the house sparrow (*Passer domesticus*). Eur. J. Neurosci. 16 (3), 429–436.

Abraham, U., Albrecht, U., Brandstätter, R., 2003. Hypothalamic circadian organization in birds. II. Clock gene expression. Chronobiol. Int. 20 (4), 657–669.

Adachi, A., Natesan, A.K., Whitfield-Rucker, M.G., Weigum, S.E., Cassone, V.M., 2002. Functional melatonin receptors and metabolic coupling in cultured chick astrocytes. Glia 39 (3), 268–278.

Amichai, E., Kronfeld-Schor, N., 2019. Artificial light at night promotes activity throughout the night in nesting common swifts (*Apus apus*). Sci. Rep. 9 (1), 11052. https://doi.org/10.1038/s41598-019-47544-3.

Aschoff, J., 1979. Circadian rhythms: influences of internal and external factors on the period measured in constant conditions. Z. Tierpsychol. 49 (3), 225–249.

Aschoff, J., Pohl, H., 1978. Phase relations between a circadian rhythm and its zeitgeber within the range of entrainment. Naturwissenschaften 65 (2), 80–84.

Aschoff, J., von Goetz, C., 1989. Masking of circadian activity rhythms in canaries by light and dark. J. Biol. Rhythms 4 (1), 29–38.

Bailey, M.J., Cassone, V.M., 2004. Opsin photoisomerases in the chick retina and pineal gland: characterization, localization, and circadian regulation. Invest. Ophthalmol. Vis. Sci. 45 (3), 769–775.

Bailey, M.J., Cassone, V.M., 2005. Melanopsin expression in the chick retina and pineal gland. Brain Res. Mol. Brain Res. 134 (2), 345–348.

Bailey, M.J., Chong, N.W., Xiong, J., Cassone, V.M., 2002. Chickens' Cry2: molecular analysis of an avian cryptochrome in retinal and pineal photoreceptors. FEBS Lett. 513 (2–3), 169–174.

Bailey, M.J., Beremand, P.D., Hammer, R., Bell-Pedersen, D., Thomas, T.L., Cassone, V.M., 2003. Transcriptional profiling of the chick pineal gland, a photoreceptive circadian oscillator and pacemaker. Mol. Endocrinol. 17 (10), 2084–2095.

Bailey, M.J., Beremand, P.D., Hammer, R., Reidel, E., Thomas, T.L., Cassone, V.M., 2004. Transcriptional profiling of circadian patterns of mRNA expression in the chick retina. J. Biol. Chem. 279 (50), 52247–52254.

Batra, T., Malik, I., Kumar, V., 2019. Illuminated night alters behaviour and negatively affects physiology and metabolism in diurnal zebra finches. Environ. Pollut. 254 (Pt A), 112916.

Bell-Pedersen, D., Cassone, V.M., Earnest, D.J., Golden, S.S., Hardin, P.E., Thomas, T.L., Zoran, M.J., 2005. Circadian rhythms from multiple oscillators: lessons from diverse organisms. Nat. Rev. Genet. 6 (7), 544–556.

Barrett, R.K., Takahashi, J.S., 1995. Temperature compensation and temperature entrainment of the chick pineal cell circadian clock. J. Neurosci. 15 (8), 5681–5692.

Benichov, J.I., Benezra, S.E., Vallentin, D., Globerson, E., Long, M.A., Tchernichovski, O., 2016. The forebrain song system mediates predictive call timing in female and male zebra finches. Curr. Biol. 26 (3), 309–318.

Benoit, J., Assenmacher, I., 1954. Comparative sensitivity of superficial and deep receptors in photosexual reflex in duck. C. R. Hebd. Seances Acad. Sci. 239 (1), 105–107.

Bernard, M., Voisin, P., Guerlotté, J., Collin, J.P., 1991. Molecular and cellular aspects of hydroxyindole-O-methyltransferase expression in the developing chick pineal gland. Brain Res. Dev. Brain Res. 59 (1), 75–81.

Bentley, G.E., Perfito, N., Calisi, R.M., 2013. Season- and context-dependent sex differences in melatonin receptor activity in a forebrain song control nucleus. S0018-506X(12)00287-5 Horm. Behav. 63 (5), 829–835. https://doi.org/10.1016/j.yhbeh.2012.11.015. Epub 2012 Nov 29. PMID: 23201178.

Bernard, M., Iuvone, P.M., Cassone, V.M., Roseboom, P.H., Coon, S.L., Klein, D.C., 1997. Avian melatonin synthesis: photic and circadian regulation of serotonin N-acetyltransferase mRNA in the chicken pineal gland and retina. J. Neurochem. 68 (1), 213–224.

Binkley, S., Kluth, E., Menaker, M., 1971. Pineal function in sparrows: circadian rhythms and body temperature. Science 174 (4006), 311–314.

Binkley, S., Stephens, J.L., Riebman, J.B., Reilly, K.B., 1977. Regulation of pineal rhythms in chickens: photoperiod and dark-time sensitivity. Gen. Comp. Endocrinol. 32 (4), 411–416.

Binkley, S.A., Riebman, J.B., Reilly, K.B., 1978. The pineal gland: a biological clock in vitro. Science 202 (4373), 1198–1220.

Bradshaw, W.E., Holzapfel, C.M., 2010. What season is it anyway? Circadian tracking vs. photoperiodic anticipation in insects. J. Biol. Rhythms 25 (3), 155–165.

Brandstätter, R., Kumar, V., Abraham, U., Gwinner, E., 2000. Photoperiodic information acquired and stored in vivo is retained in vitro by a circadian oscillator, the avian pineal gland. Proc. Natl. Acad. Sci. U.S.A. 97 (22), 12324–12328.

Byerly, T.C., Moore, O.K., 1941. Clutch length in relation to period of illumination in the domestic fowl. Poult. Sci. J. 20, 387–390.

Cantwell, E.L., Cassone, V.M., 2002. Daily and circadian fluctuation in 2-deoxy[(14)C]-glucose uptake in circadian and visual system structures of the chick brain: effects of exogenous melatonin. Brain Res. Bull. 57 (5), 603–611.

Cantwell, E.L., Cassone, V.M., 2006a. Chicken suprachiasmatic nuclei: I. Efferent and afferent connections. J. Comp. Neurol. 496 (1), 97–120.

Cantwell, E.L., Cassone, V.M., 2006b. Chicken suprachiasmatic nuclei: II. Autoradiographic and immunohistochemical analysis. J. Comp. Neurol. 499 (3), 442–457.

Cassone, V.M., 1988. Circadian variation of [14C]2-deoxyglucose uptake within the suprachiasmatic nucleus of the house sparrow, *Passer domesticus*. Brain Res. 459 (1), 178–182.

Cassone, V.M., 1990. Melatonin: time in a bottle. Oxf. Rev. Reprod. Biol. 12, 319–367.

Cassone, V.M., Menaker, M., 1983. Sympathetic regulation of chicken pineal rhythms. Brain Res. 272 (2), 311–317.

Cassone, V.M., Menaker, M., 1984. Is the avian circadian system a neuroendocrine loop? J. Exp. Zool. 232 (3), 539–549.

Cassone, V.M., Moore, R.Y., 1987. Retinohypothalamic projection and suprachiasmatic nucleus of the house sparrow, *Passer domesticus*. J. Comp. Neurol. 266 (2), 171–182.

Cassone, V.M., Westneat, D.F., 2012. The bird of time: cognition and the avian biological clock. Front. Mol. Neurosci. 5, 32.

Cassone, V.M., Takahashi, J.S., Blaha, C.D., Lane, R.F., Menaker, M., 1986. Dynamics of noradrenergic circadian input to the chicken pineal gland. Brain Res. 384 (2), 334–341.

Cassone, V.M., Forsyth, A.M., Woodlee, G.L., 1990. Hypothalamic regulation of circadian noradrenergic input to the chick pineal gland. J. Comp. Physiol. 167 (2), 187–192.

Cassone, V.M., Brooks, D.S., Hodges, D.B., Kelm, T.S., Lu, J., Warren, W.S., 1992. Integration of circadian and visual function in mammals and birds: brain imaging and the role of melatonin in biological clock regulation. In: Gonzalez-Lima, F., Finkenstaedt, T., Scheich, H. (Eds.), Advances in Metabolic Mapping Techniques for Brain Imaging of Behavioral and Learning Functions. Kluwer Academic Publishers, Dordrecht/Boston/London, pp. 299–318.

Cassone, V.M., Brooks, D.S., Kelm, T.A., 1995. Comparative distribution of 2[125I]iodomelatonin binding in the brains of diurnal birds: outgroup analysis with turtles. Brain Behav. Evol. 45 (5), 241–256.

Cassone, V.M., Bartell, P.A., Earnest, B.J., Kumar, V., 2008. Duration of melatonin regulates seasonal changes in song control nuclei of the house sparrow, *Passer domesticus*: independence from gonads and circadian entrainment. J. Biol. Rhythms 23 (1), 49–58.

Chabot, C.C., Menaker, M., 1992. Effects of physiological cycles of infused melatonin on circadian rhythmicity in pigeons. J. Comp. Physiol. 170 (5), 615–622.

Chaurasia, S.S., Rollag, M.D., Jiang, G., Hayes, W.P., Haque, R., Natesan, A., Zatz, M., Tosini, G., Liu, C., Korf, H.W., Iuvone, P.M., Provencio, I., 2005. Molecular cloning, localization and circadian expression of chicken melanopsin (Opn4): differential regulation of expression in pineal and retinal cell types. J. Neurochem. 92 (1), 158–170.

Chong, N.W., Cassone, V.M., Bernard, M., Klein, D.C., Iuvone, P.M., 1998. Circadian expression of tryptophan hydroxylase mRNA in the chicken retina. Brain Res. Mol. Brain Res. 61 (1–2), 243–250.

Chong, N.W., Chaurasia, S.S., Haque, R., Klein, D.C., Iuvone, P.M., 2003. Temporal-spatial characterization of chicken clock genes: circadian expression in retina, pineal gland, and peripheral tissues. J. Neurochem. 85 (4), 851–860.

Csernus, V., Faluhelyi, N., Nagy, A.D., 2005. Features of the circadian clock in the avian pineal gland. Ann. N. Y. Acad. Sci. 1040, 281–287.

Daan, S., 2000. The Colin S. Pittendrigh Lecture. Colin Pittendrigh, Jürgen Aschoff, and the natural entrainment of circadian systems. J. Biol. Rhythms 15 (3), 195–207.

Davies, W.I., Turton, M., Peirson, S.N., Follett, B.K., Halford, S., Garcia-Fernandez, J.M., Sharp, P.J., Hankins, M.W., Foster, R.G., 2012. Vertebrate ancient opsin photopigment spectra and the avian photoperiodic response. Biol. Lett. 8 (2), 291–294.

Davies, W.L., Hankins, M.W., Foster, R.G., 2010. Vertebrate ancient opsin and melanopsin: divergent irradiance detectors. Photochem. Photobiol. Sci. 9 (11), 1444–1457.

Deguchi, T., 1979. Circadian rhythm of serotonin N-acetyltransferase activity in organ culture of chicken pineal gland. Science 203 (4386), 1245–1247.

Dominoni, D.M., Helm, B., Lehmann, M., Dowse, H.B., Partecke, J., 2013a. Clocks for the city: circadian differences between forest and city songbirds. Proc. Biol. Sci. 280 (1763), 20130593.

Dominoni, D.M., Goymann, W., Helm, B., Partecke, J., 2013b. Urban-like night illumination reduces melatonin release in European blackbirds (*Turdus merula*): implications of city life for biological time-keeping of songbirds. Front. Zool. 10 (1), 60.

Doyle, S., Menaker, M., 2007. Circadian photoreception in vertebrates. Cold Spring Harbor Symp. Quant. Biol. 72, 499–508.

Dubocovich, M.L., Takahashi, J.S., 1987. Use of 2-[125I]iodomelatonin to characterize melatonin binding sites in chicken retina. Proc. Natl. Acad. Sci. U.S.A. 84 (11), 3916–3920.

Ebihara, S., Kawamura, H., 1981. The role of the pineal organ and the suprachiasmatic nucleus in the control of circadian locomotor rhythms in the Java sparrow, *Padda oryzivora*. J. Comp. Physiol. 141, 207–214.

Ebihara, S., Uchiyama, K., Oshima, I., 1984. Circadian organization in the pigeon, *Columba livia:* the role of the pineal organ and the eye. J. Comp. Physiol. A. 154, 59–69.

Ebihara, S., Adachi, A., Hasegawa, M., Nogi, T., Yoshimura, T., Hirunagi, K., 1997. In vivo microdialysis studies of pineal and ocular melatonin rhythms in birds. Biol. Signals 6 (4–6), 233–240.

Emery, P., So, W.V., Kaneko, M., Hall, J.C., Rosbash, M., 1998. CRY, a *Drosophila* clock and light-regulated cryptochrome, is a major contributor to circadian rhythm resetting and photosensitivity. Cell 95 (5), 669–679.

Falchi, F., Cinzano, P., Duriscoe, D., Kyba, C.C., Elvidge, C.D., Baugh, K., Portnov, B.A., Rybnikova, N.A., Furgoni, R., 2016. The new world atlas of artificial night sky brightness. Sci. Adv. 2 (6), e1600377. https://doi.org/10.1126/sciadv.1600377.

Fraps, R.M., Fevold, H.L., 1955. Delaying action of gonadotrophins on ovulation in the hen. Exp. Biol. Med. 90 (2), 440–446. https://doi.org/10.3181/00379727-90-22059.

Gahr, M., Kosar, E., 1996. Identification, distribution, and developmental changes of a melatonin binding site in the song control system of the zebra finch. J. Comp. Neurol. 367 (2), 308–318.

Gaston, S., Menaker, M., June 7, 1968. Pineal function: the biological clock in the sparrow? Science 160 (3832), 1125–1127.

Geerts, B., 2002. Empirical estimation of the monthly-mean daily temperature range. Theor. Appl. Climatol. 000, 1–20.

Guido, M.E., Garbarino-Pico, E., Contin, M.A., Valdez, D.J., Nieto, P.S., Verra, D.M., Acosta-Rodriguez, V.A., de Zavalía, N., Rosenstein, R.E., 2010. Inner retinal circadian clocks and non-visual photoreceptors: novel players in the circadian system. Prog. Neurobiol. 92 (4), 484–504.

Günther, A., Einwich, A., Sjulstok, E., Feederle, R., Bolte, P., Koch, K.W., Solov'yov, I.A., Mouritsen, H., 2018. Double-cone localization and seasonal expression pattern suggest a role in magnetoreception for European Robin cryptochrome 4. Curr. Biol. 28 (2), 211–223.

Gwinner, E., 1978. Effects of pinealectomy on circadian locomotor activity rhythms in European starlings, *Sturnus vulgaris*. J. Comp. Physiol. 126, 123–129.

Gwinner, E., 1989. Melatonin and the circadian system of birds: model of internal resonance. In: Hiroshige, T., Honma, K. (Eds.), Circadian Clocks and Ecology. Hokkado Univ Press, Sapporo, pp. 127–145.

Gwinner, E., Brandstätter, R., 2001. Complex bird clocks. Philos. Trans. R. Soc. Lond. B Biol. Sci. 356 (1415), 1801–1810.

Gwinner, E., Subbaraj, R., Bluhm, C.K., Gerkema, M., 1987. Differential effects of pinealectomy on circadian rhythms of feeding and perch hopping in the European starling. J. Biol. Rhythms 2 (2), 109–120.

Gwinner, E., Hau, M., Heigl, S., 1997. Melatonin: generation and modulation of avian circadian rhythms. Brain Res. Bull. 44 (4), 439–444.

Halford, S., Pires, S.S., Turton, M., Zheng, L., González-Menéndez, I., Davies, W.L., Peirson, S.N., García-Fernández, J.M., Hankins, M.W., Foster, R.G., 2009. VA opsin-based photoreceptors in the hypothalamus of birds. Curr. Biol. 19 (16), 1396–1402.

Haque, R., Ali, F.G., Biscoglia, R., Abey, J., Weller, J., Klein, D., Iuvone, P.M., 2010. CLOCK and NPAS2 have overlapping roles in the circadian oscillation of arylalkylamine N-acetyltransferase mRNA in chicken cone photoreceptors. J. Neurochem. 113 (5), 1296–1306.

Hardy, D.R., Vuille, M., Braun, C., Kemig, F., Bradley, R.S., 1998. Annual and daily meteorological cycles at high altitude on a tropical mountain. Bull. Am. Meteorol. Soc. 79, 1899–1913.

Hau, M., Gwinner, E., 1992. Circadian entrainment by feeding cycles in house sparrows, *Passer domesticus*. J. Comp. Physiol. 170 (4), 403–409.

Hau, M., Gwinner, E., 1995. Continuous melatonin administration accelerates resynchronization following phase shifts of a light-dark cycle. Physiol. Behav. 58 (1), 89–95.

Heigl, S., Gwinner, E., 1995. Synchronization of circadian rhythms of house sparrows by oral melatonin: effects of changing period. J. Biol. Rhythms 10 (3), 225–233.

Helfer, G., Fidler, A.E., Vallone, D., Foulkes, N.S., Brandstaetter, R., 2006. Molecular analysis of clock gene expression in the avian brain. Chronobiol. Int. 23 (1–2), 113–127.

Iuvone, P.M., Bernard, M., Alonso-Gomez, A., Greve, P., Cassone, V.M., Klein, D.C., 1997. Cellular and molecular regulation of serotonin N-acetyltransferase activity in chicken retinal photoreceptors. Biol. Signals 6 (4–6), 217–224.

Janik, D., Dittami, J., Gwinner, E., 1992. The effect of pinealectomy on circadian plasma melatonin levels in house sparrows and European starlings. J. Biol. Rhythms 7 (4), 277–286.

Jansen, R., Metzdorf, R., van der Roest, M., Fusani, L., ter Maat, A., Gahr, M., 2005. Melatonin affects the temporal organization of the song of the zebra finch. FASEB J. 19 (7), 848–850.

Juss, T.S., Davies, I.R., Follett, B.K., Mason, R., 1994. Circadian rhythm in neuronal discharge activity in the quail lateral hypothalamic retinorecipient nucleus (LHRN) recorded in vitro. J. Physiol. 475, 132.

Karaganis, S.P., Kumar, V., Beremand, P.D., Bailey, M.J., Thomas, T.L., Cassone, V.M., 2008. Circadian genomics of the chick pineal gland in vitro. BMC Genom. 9, 206. https://doi.org/10.1186/1471-2164-9-206.

Karaganis, S.P., Bartell, P.A., Shende, V.R., Moore, A.F., Cassone, V.M., 2009. Modulation of metabolic and clock gene mRNA rhythms by pineal and retinal circadian oscillators. Gen. Comp. Endocrinol. 161 (2), 179–192.

Kernbach, M.E., Hall, R.J., Burkett-Cadena, N.D., Unnasch, T.R., Martin, L.B., 2018. Dim light at night: physiological effects and ecological consequences for infectious disease. Integr. Comp. Biol. 58 (5), 995–1007.

Kernbach, M.E., Cassone, V.M., Unmasch, T.R., Martin, L.B., 2020. Spectral characteristics of light pollution have distinct effects on melatonin and songbird responses to West Nile virus. Condor 122, 1–13.

King, V.M., Follett, B.K., 1997. c-fos expression in the putative avian suprachiasmatic nucleus. J. Comp. Physiol. 180 (5), 541–551.

Klein, D.C., Coon, S.L., Roseboom, P.H., Weller, J.L., Bernard, M., Gastel, J.A., Zatz, M., Iuvone, P.M., Rodriguez, I.R., Bégay, V., Falcón, J., Cahill, G.M., Cassone, V.M., Baler, R., 1997. The melatonin rhythm-generating enzyme: molecular regulation of serotonin N-acetyltransferase in the pineal gland. Recent Prog. Horm. Res. 52, 307–357.

Konopka, R.J., Benzer, S., 1971. Clock mutants of *Drosophila melanogaster*. Proc. Natl. Acad. Sci. U.S.A. 68 (9), 2112–2116.

Kubo, Y., Akiyama, M., Fukada, Y., Okano, T., 2006. Molecular cloning, mRNA expression, and immunocytochemical localization of a putative blue-light photoreceptor CRY4 in the chicken pineal gland. J. Neurochem. 97 (4), 1155–1165.

Kumar, V., Follett, B.K., 1993. The circadian nature of melatonin secretion in Japanese quail (*Coturnix coturnix japonica*). J. Pineal Res. 14 (4), 192–200.

Kumar, V., Gwinner, E., 2005. Pinealectomy shortens resynchronisation times of house sparrow (*Passer domesticus*) circadian rhythms. Naturwissenschaften 92 (9), 419–422.

Kyba, C.C.M., Kuester, T., Sánchez de Miguel, A., Baugh, K., Jechow, A., Hölker, F., Bennie, J., Elvidge, C.D., Gaston, K.J., Guanter, L., 2017. Artificially lit surface of Earth at night increasing in radiance and extent. Sci Adv 3 (11), e1701528.

Li, Y., Cassone, V.M., 2015. Clock-controlled regulation of the acute effects of norepinephrine on chick pineal melatonin rhythms. J. Biol. Rhythms 30 (6), 519–532.

Liu, F., Yuan, H., Sugamori, K.S., Hamadanizadeh, A., Lee, F.J., Pang, S.F., Brown, G.M., Pristupa, Z.B., Niznik, H.B., 1995. Molecular and functional characterization of a partial cDNA encoding a novel chicken brain melatonin receptor. FEBS Lett. 374 (2), 273–278.

Lu, J., Cassone, V.M., 1993a. Pineal regulation of circadian rhythms of 2-deoxy[^{14}C]glucose uptake and 2[^{125}I]iodomelatonin binding in the visual system of the house sparrow, *Passer domesticus*. J. Comp. Physiol. A 173, 765–774.

Lu, J., Cassone, V.M., 1993b. Daily melatonin administration synchronizes circadian patterns of brain metabolism and behavior in pinealectomized house sparrows, *Passer domesticus*. J. Comp. Physiol. A 173, 775–782.

Masuda, H., Oishi, T., Ohtani, M., Michinomae, M., Fukada, Y., Shichida, Y., Yoshizawa, T., 1994. Visual pigments in the pineal complex of the Japanese quail, Japanese grass lizard and bullfrog: immunocytochemistry and HPLC analysis. Tissue Cell 26 (1), 101–113.

Max, M., McKinnon, P.J., Seidenman, K.J., Barrett, R.K., Applebury, M.L., Takahashi, J.S., Margolskee, R.F., 1995. Pineal opsin: a nonvisual opsin expressed in chick pineal. Science 267 (5203), 1502–1506.

Menaker, M., 1968. Extraretinal light perception in the sparrow. I. Entrainment of the biological clock. Proc. Natl. Acad. Sci. U.S.A. 59 (2), 414–421.

Menaker, M., 1985. Eyes–the second (and third) pineal glands? Ciba Found. Symp. 117, 78–92.

Menaker, M., Eskin, A., 1966. Entrainment of circadian rhythms by sound in *Passer domesticus*. Science 154 (3756), 1579–1581.

Menaker, M., Oksche, A., 1974. The avian pineal. In: Avian Biology, vol. IV. Academic Press, NY, pp. 80–114.

Menaker, M., Underwood, H., 1976. Extraretinal photoreception in birds. Photophysiology 23 (4), 299–306.

Menaker, M., Takahashi, J.S., Eskin, A., 1978. The physiology of circadian pacemakers. Annu. Rev. Physiol. 40, 501–526.

Moaraf, S., Vistoropsky, Y., Pozner, T., Heiblum, R., Okuliarová, M., Zeman, M., Barnea, A., 2020. Artificial light at night affects brain plasticity and melatonin in birds. Neurosci. Lett. 716, 134639.

Morris, T.R., 1973. The effects of ahemeral light and dark cycles on egg production in the fowl. Poult. Sci. 52 (2), 423–445.

Nakane, Y., Yoshimura, T., 2010. Deep brain photoreceptors and a seasonal signal transduction cascade in birds. Cell Tissue Res. 342 (3), 341–344.

Nakane, Y., Ikegami, K., Ono, H., Yamamoto, N., Yoshida, S., Hirunagi, K., Ebihara, S., Kubo, Y., Yoshimura, T., 2010. A mammalian neural tissue opsin (Opsin 5) is a deep in birds. Proc. Natl. Acad. Sci. U.S.A. 107 (34), 15264–15268.

Natesan, A.K., Cassone, V.M., 2002. Melatonin receptor mRNA localization and rhythmicity in the retina of the domestic chick, *Gallus domesticus*. Vis. Neurosci. 19 (3), 265–274.

Natesan, A., Geetha, L., Zatz, M., 2002. Rhythm and soul in the avian pineal. Cell Tissue Res. 309 (1), 35–45.

Navara, K.J., Nelson, R.J., 2007. The dark side of light at night: physiological, epidemiological, and ecological consequences. J. Pineal Res. 43 (3), 215–224.

Nießner, C., Denzau, S., Peichl, L., Wiltschko, W., Wiltschko, R., December 2018. Magnetoreception: activation of avian cryptochrome 1a in various light conditions. J. Comp. Physiol. A Neuroethol. Sens. Neural Behav. Physiol. 204 (12), 977–984.

Nishijima, K., Iijima, S., January 2013. Transgenic chickens. Dev. Growth Differ. 55 (1), 207–216. https://doi.org/10.1111/dgd.12032. Epub 2012 Dec 26.

Okano, T., Fukada, Y., 2000. Photoreceptors in pineal gland and brain: cloning, localization, and overexpression. Methods Enzymol. 316, 278–291.

Okano, T., Yoshizawa, T., Fukada, Y., 1994. Pinopsin is a chicken pineal photoreceptive molecule. Nature 372 (6501), 94–97.

Oksche, A., Kirschstein, H., Kobayashi, H., Farner, D.S., 1972. Electron microscopic and experimental studies of the pineal organ in the white-crowned sparrow, *Zonotrichia leucophrys gambelii*. Z. Zellforsch. Mikrosk. Anat. 124 (2), 247–274.

Ouyang, J.Q., Davies, S., Dominoni, D., 2018. Hormonally mediated effects of artificial light at night on behavior and fitness: linking endocrine mechanisms with function. J. Exp. Biol. 221 (Pt 6) jeb156893.

Panda, S., 2007. Multiple photopigments entrain the Mammalian circadian oscillator. Neuron 53 (5), 619–621.

Peirson, S.N., Halford, S., Foster, R.G., 2009. The evolution of irradiance detection: melanopsin and the non-visual opsins. Philos. Trans. R. Soc. Lond. B Biol. Sci. 364 (1531), 2849–2865.

Peters, J.L., Cassone, V.M., Zoran, M.J., 2005. Melatonin modulates intercellular communication among cultured chick astrocytes. Brain Res. 1031 (1), 10–19.

Pittendrigh, C.S., 1993. Temporal organization: reflections of a Darwinian clock-watcher. Annu. Rev. Physiol. 55, 16–54.

Poynter, G., Lansford, R., 2008. Generating transgenic quail using lentiviruses. Methods Cell Biol. 87, 281–293.

Prabhat, A., Jha, N.A., Taufique, S.K.T., Kumar, V., 2019. Dissociation of circadian activity and singing behavior from gene expression rhythms in the hypothalamus, song control nuclei and cerebellum in diurnal zebra finches. Chronobiol. Int. 36 (9), 1268–1284.

Quay, W.B., 1965. Histological structure and cytology of the pineal gland in birds and mammals. Prog. Brain Res. 10, 49–86.

Rani, S., Singh, S., Malik, S., Singh, J., Kumar, V., 2009. Synchronization of Indian weaver bird circadian rhythms to food and light zeitgebers: role of pineal. Chronobiol. Int. 26 (4), 653–665.

Rashotte, M.E., Stephan, F.K., 1996. Coupling between light- and food-entrainable circadian oscillators in pigeons. Physiol. Behav. 59 (4–5), 1005–1010.

Reierth, E., Stokkan, K.A., 1998. Dual entrainment by light and food in the *Svalbard ptarmigan* (*Lagopus mutus hyperboreus*). J. Biol. Rhythms 13 (5), 393–402.

Rensing, L., Ruoff, P., 2002. Temperature effect on entrainment, phase shifting, and amplitude of circadian clocks and its molecular bases. Chronobiol. Int. 19 (5), 807–864.

Reppert, S.M., 1997. Melatonin receptors: molecular biology of a new family of G protein-coupled receptors. J. Biol. Rhythms 12 (6), 528–531.

Reppert, S.M., Weaver, D.R., 2002. Coordination of circadian timing in mammals. Nature 418 (6901), 935–941.

Reppert, S.M., Weaver, D.R., Cassone, V.M., Godson, C., Kolakowski Jr., L.F., 1995. Melatonin receptors are for the birds: molecular analysis of two receptor subtypes differentially expressed in chick brain. Neuron 15 (5), 1003–1015.

Rios, M.N., Marchese, N.A., Guido, M.E., August 16, 2019. Expression of non-visual opsins Opn3 and Opn5 in the developing inner retinal cells of birds. Light-responses in müller glial cells. Front. Cell. Neurosci. 13, 376.

Rivkees, S.A., Cassone, V.M., Weaver, D.R., Reppert, S.M., 1989. Melatonin receptors in chick brain: characterization and localization. Endocrinology 125 (1), 363–368.

Robertson, L.M., Takahashi, J.S., 1988a. Circadian clock in cell culture: I. Oscillation of melatonin release from dissociated chick pineal cells in flow-through microcarrier culture. J. Neurosci. 8 (1), 12–21.

Robertson, L.M., Takahashi, J.S., 1988b. Circadian clock in cell culture: II. In vitro photic entrainment of melatonin oscillation from dissociated chick pineal cells. J. Neurosci. 8 (1), 22–30.

Roenneberg, T., Hut, R., Daan, S., Merrow, M., 2010. Entrainment concepts revisited. J. Biol. Rhythms 25 (5), 329–339.

Rosbash, M., Bradley, S., Kadener, S., Li, Y., Luo, W., Menet, J.S., Nagoshi, E., Palm, K., Schoer, R., Shang, Y., Tang, C.H., 2007. Transcriptional feedback and definition of the circadian pacemaker in Drosophila and animals. Cold Spring Harbor Symp. Quant. Biol. 72, 75–83.

Sato, T., Ebisawa, S., 1988. A pineal ganglion associated with the pineal tract in the domestic fowl. Cell Tissue Res. 252 (2), 287–292.

Schoech, S.J., Bowman, R., Hahn, T.P., Goymann, W., Schwabl, I., Bridge, E.S., 2013. The effects of low levels of light at night upon the endocrine physiology of western scrub-jays (*Aphelocoma californica*). J. Exp. Zool. A Ecol. Genet. Physiol. 319 (9), 527–538.

Semple-Rowland, S.L., Cheng, K.M., 1999. Rd and rc chickens carry the same GC1 null allele (GUCY1*). Exp. Eye Res. 69 (5), 579–581.

Semple-Rowland, S.L., Coggin, W.E., Geesey, M., Eccles, K.S., Abraham, L., Pachigar, K., Ludlow, R., Khani, S.C., Smith, W.C., 2010. Expression characteristics of dual-promoter lentiviral vectors targeting retinal photoreceptors and Müller cells. Mol. Vis. 16, 916–934.

Spoelstra, K., Verhagen, I., Meijer, D., Visser, M.E., 2018. Artificial light at night shifts daily activity patterns but not the internal clock in the great tit (*Parus major*). Proc. Biol. Sci. 285 (1875), 20172751.

Steele, C.T., Tosini, G., Siopes, T., Underwood, H., 2006. Time keeping by the quail's eye: circadian regulation of melatonin production. Gen. Comp. Endocrinol. 145 (3), 232–236.

Takahashi, J.S., Menaker, M., 1982. Role of the suprachiasmatic nuclei in the circadian system of the house sparrow, *Passer domesticus*. J. Neurosci. 2 (6), 815–828.

Takahashi, J.S., Hamm, H., Menaker, M., 1980. Circadian rhythms of melatonin release from individual superfused chicken pineal glands in vitro. Proc. Natl. Acad. Sci. U.S.A. 77 (4), 2319–2322.

Turek, F.W., McMillan, J.P., Menaker, M., 1976. Melatonin: effects on the circadian locomotor rhythm of sparrows. Science 194 (4272), 1441–1443.

Ueck, M., 1979. Innervation of the vertebrate pineal. Prog. Brain Res. 52, 45–88.

Underwood, H., Siopes, T., 1984. Circadian organization in Japanese quail. J. Exp. Zool. 232, 557–566.

Underwood, H., Binkley, S., Siopes, T., Mosher, K., 1984. Melatonin rhythms in the eyes, pineal bodies, and blood of Japanese quail (*Coturnix coturnix* japonica). Gen. Comp. Endocrinol. 56 (1), 70–81.

Underwood, H., Siopes, T., Edmonds, K., 1997. Eye and gonad: role in the dual-oscillator circadian system of female Japanese quail. Am. J. Physiol. 272 (1 Pt 2), R172–R182.

Valdez, D.J., Nieto, P.S., Garbarino-Pico, E., Avalle, L.B., Díaz-Fajreldines, H., Schurrer, C., Cheng, K.M., Guido, M.E., 2009. A nonmammalian vertebrate model of blindness reveals functional photoreceptors in the inner retina. FASEB J. 23 (4), 1186–1195.

Valdez, D.J., Nieto, P.S., Díaz, N.M., Garbarino-Pico, E., Guido, M.E., 2013. Differential regulation of feeding rhythms through a multiple-photoreceptor system in an avian model of blindness. FASEB J. 27 (7), 2702–2712.

Wada, Y., Okano, T., Adachi, A., Ebihara, S., Fukada, Y., March 6, 1998. Identification of rhodopsin in the pigeon deep brain. FEBS Lett. 424 (1–2), 53–56.

Wang, G., Wingfield, J.C., 2011. Immunocytochemical study of rhodopsin-containing putative encephalic photoreceptors in house sparrow, *Passer domesticus*. Gen. Comp. Endocrinol. 170 (3), 589–596.

Wang, G., Harpole, C.E., Trivedi, A.K., Cassone, V.M., 2012. Circadian regulation of bird song call, and locomotor behavior by pineal melatonin in the zebra finch. J. Biol. Rhythms 27 (2), 145–155.

Whitfield-Rucker, M.G., Cassone, V.M., 1996. Melatonin binding in the house sparrow song control system: sexual dimorphism and the effect of photoperiod. Horm. Behav. 30 (4), 528–537.

Wiltschko, R., Wiltschko, W., 2019. Magnetoreception in birds. J. R. Soc. Interface 16 (158). https://doi.org/10.1098/rsif.2019.0295, 20190295.

Yasuo, S., Yoshimura, T., Bartell, P.A., Iigo, M., Makino, E., Okabayashi, N., Ebihara, S., 2002. Effect of melatonin administration on qPer2, qPer3, and qClock gene expression in the suprachiasmatic nucleus of Japanese quail. Eur. J. Neurosci. 16 (8), 1541–1546.

Yoshimura, T., Yasuo, S., Suzuki, Y., Makino, E., Yokota, Y., Ebihara, S., 2001. Identification of the suprachiasmatic nucleus in birds. Am. J. Physiol. Regul. Integr. Comp. Physiol. 280 (4), R1185–R1189.

Yoshimura, T., Suzuki, Y., Makino, E., Suzuki, T., Kuroiwa, A., Matsuda, Y., Namikawa, T., Ebihara, S., 2000. Molecular analysis of avian circadian clock genes. Brain Res. Mol. Brain Res. 78 (1–2), 207–215.

Zatz, M., Mullen, D.A., 1988. Norepinephrine, acting via adenylate cyclase, inhibits melatonin output but does not phase-shift the pacemaker in cultured chick pineal cells. Brain Res. 450 (1–2), 137–143.

Zatz, M., Mullen, D.A., Moskal, J.R., 1988. Photoendocrine transduction in cultured chick pineal cells: effects of light, dark, and potassium on the melatonin rhythm. Brain Res. 438 (1–2), 199–215.

Zeman, M., Szántóová, K., Herichová, I., 2009. Ontogeny of circadian oscillations in the heart and liver in chicken. Comp. Biochem. Physiol. Mol. Integr. Physiol. 154 (1), 78–83.

Zivkovic, B.D., Underwood, H., Steele, C.T., Edmonds, K., 1999. Formal properties of the circadian and photoperiodic systems of Japanese quail: phase response curve and effects of T-cycles. J. Biol. Rhythms 14 (5), 378–390.

Zivkovic, B.D., Underwood, H., Siopes, T., 2000. Circadian ovulatory rhythms in Japanese quail: role of ocular and extraocular pacemakers. J. Biol. Rhythms 15 (2), 172–183.

Zimmerman, N.H., Menaker, M., 1979. The pineal gland: a pacemaker within the circadian system of the house sparrow. Proc. Natl. Acad. Sci. U.S.A. 76 (2), 999–1003.

Zoltowski, B.D., Chelliah, Y., Wickramaratne, A., Jarocha, L., Karki, N., Xu, W., Mouritsen, H., Hore, P.J., Hibbs, R.E., Green, C.B., Takahashi, J.S., 2019. Chemical and structural analysis of a photoactive vertebrate cryptochrome from pigeon. Proc. Natl. Acad. Sci. U.S.A. 116 (39), 19449–19457.

Further reading

Kumar, V., Gwinner, E., Van't Hof, T.J., 2000. Circadian rhythms of melatonin in European starlings exposed to different lighting conditions: relationship with locomotor and feeding rhythms. J. Comp. Physiol. A 186 (2), 205–215.

Torii, M., Kojima, D., Okano, T., Nakamura, A., Terakita, A., Shichida, Y., Wada, A., Fukada, Y., November 13, 2007. Two isoforms of chicken melanopsins show blue light sensitivity. FEBS Lett. 581 (27), 5327–5331.

Zatz, M., Lange, G.D., Rollag, M.D., 1994. What does changing the temperature do to the melatonin rhythm in cultured chick pineal cells? Am. J. Physiol. 266 (1 Pt 2), R50–R58.

Chapter 43

Circannual cycles and photoperiodism

Vincent M. Cassone[1] and Takashi Yoshimura[2]

[1]Department of Biology, University of Kentucky, Lexington, KY, United States; [2]Laboratory of Animal Integrative Physiology, Graduate School of Bioagricultural Sciences, Institute of Transformative Bio-Molecules, Nagoya University, Nagoya, Aichi Prefecture, Japan

As with daily patterns' effects on physiology and behavior, birds are also very sensitive to annual patterns in the abiotic and biotic environments. This is particularly true for species of birds in circumpolar and temperate zones, but annual cycles of avian physiology are also evident in subtropical and tropical zones of the Earth. In all cases, these annual cycles derive primarily from annual changes in solar irradiance due to the axial tilt of the Earth's rotation and the elliptical orbit of the Earth around the sun, resulting in *seasons* (Pianka, 1978). In addition, long-term trends in climate, such as global climate change, whether human-derived or astronomical, may have significant effects on avian physiology (Lockwood, 2010).

43.1 Annual cycles

43.1.1 Abiotic

43.1.1.1 Photoperiod

Seasons result from the annual revolution of the Earth around the sun and its axial tilt (Figure 43.1). When the Earth's axial tilt is *parallel* with the trajectory of the Earth's movement relative to the sun, all surfaces receive equal amounts of solar irradiance such that they receive 12 h of light and 12 h of darkness/24 h day (LD 12:12); these days are the *equinoxes*, occurring on March 20 and September 22. The duration of the day phase is the *photoperiod*, while the duration of the night phase is the *scotoperiod.* In the northern hemisphere, March 20 is the *vernal equinox,* or the beginning of *spring,* while in the southern hemisphere, it is the *autumnal equinox,* or the beginning of autumn. Conversely, September 22 is the autumnal equinox in northern hemisphere and the vernal equinox in the south.

As the Earth progresses in its orbit from March to June, the axial tilt exposes the northern hemisphere to more direct and longer durations (photoperiod) of solar illumination. Conversely, the southern hemisphere undergoes less direct and shorter photoperiods until June 21 of each year, when the Earth's axial tilt points the northern hemisphere toward the sun, perpendicular to its orbit. This is the *solstice*. In the northern hemisphere, it is the longest day, while in the southern, it is the shortest, corresponding to the beginning of *summer* and *winter*, respectively. As the Earth then progresses from June to September, the seasons progress to the autumnal equinox in the north and the vernal equinox in the south on September 22. As the Earth progresses from September to December, the Earth's axial tilt once again becomes perpendicular to the Earth's orbit, but this time, the axial tilt exposes the southern hemisphere to direct light and longer photoperiods, creating the southern summer solstice and conversely plunging the northern hemisphere into the winter solstice.

On Earth, a major result of these astronomical progressions is the annual change in photoperiod, which is in turn dependent on *latitude* (Figure 43.2). In contrast to the situation in the laboratory in which lights are turned on and off in a timed square-wave, described below, natural photoperiod depends on the definition of global illuminance one defines as *twilight*, in which the zenith angle of the sun ranges from 85° as in *civil twilight* (the sun is just below the horizon) to 105° as in *astronomical twilight* (the sun is 12° below the horizon). At the *Equator*, photoperiod at civil twilight remains static at LD 12:12 throughout the year, but as latitude increases toward the poles, the annual change in photoperiod increases in amplitude. At the Tropics of Cancer and Capricorn (23.4378°), the photoperiod at summer solstice is approximately LD 14:10, while the winter solstice is LD 10:14. At more temperate New York, NY, USA (43.5°), the photoperiod at summer solstice is approximately LD 15:9 with a winter solstice of LD 9:15, while the range of photoperiods above the Arctic Circle (66.6°) is from LD 24:0 to LD 0:24. Thus, as latitude increases from the Equator to the poles, the range of photoperiod dramatically increases over the year.

43.1.1.2 Temperature

One of the major consequences of changing photoperiod as seasons progress is a parallel change in ambient

Sturkie's Avian Physiology. https://doi.org/10.1016/B978-0-12-819770-7.00045-1

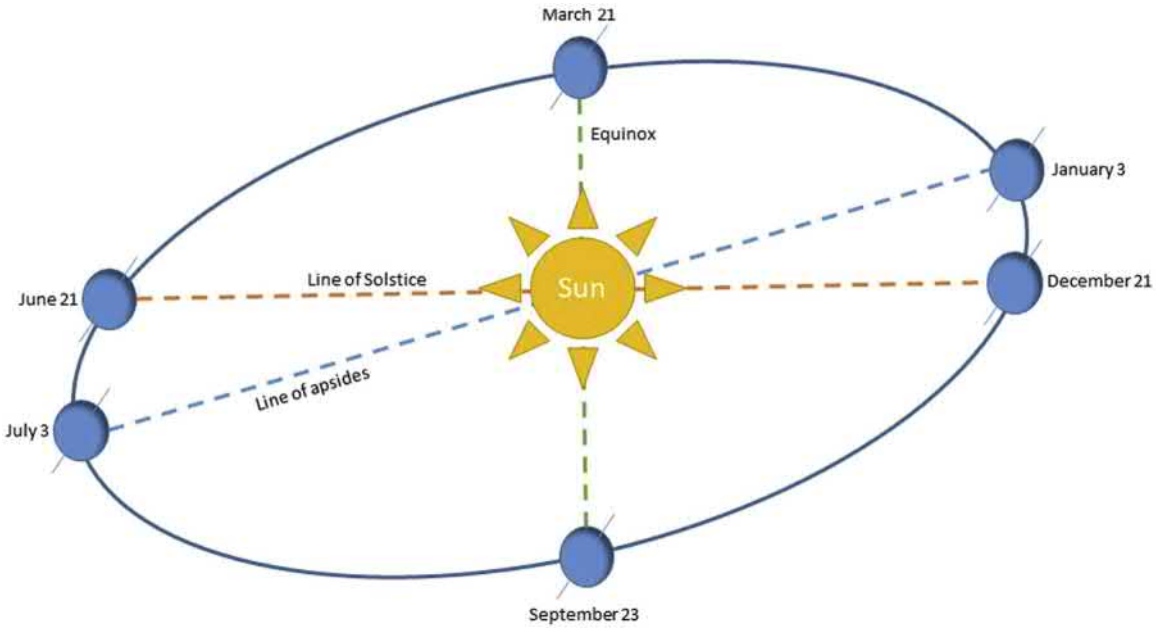

FIGURE 43.1 The astronomical basis for the seasons on Earth. Earth's rotation on its axis orients the poles asymmetrically toward or away from the sun depending on the time of year.

temperature (T_A). Average annual ranges in T_A (ΔT_A), the differences between the coldest month from the hottest month of the year (Glickman, 2000), increase with increases in latitude such that ΔT_A is 0 at the Equator to 40°C at 90° latitude in the northern hemisphere and 31°C in the south (Figure 43.5). The principal cause of the asymmetry in ΔT_A between north and south is that a higher percentage of Earth's surface is covered by ocean in the south, absorbing much of the heat. Earth's elliptical orbit in part moderates this difference because the Earth is closest to the sun in January (Figure 43.1) during the southern summer and northern winter.

In addition to latitude, altitude can dramatically affect T_A as well as ΔT_A. T_A decreases on average 6.4°C/km altitude, a phenomenon defined as the *lapse rate* (Glickman, 2000). The lapse rate depends on several variables, however, especially *humidity,* which decreases lapse rate. For example, an average *dry lapse rate* is 10°/km altitude, while wet lapse rates average 5.5 C/km altitude. Other abiotic factors that affect T_A and ΔT_A include urbanization, proximity to coasts (continentality), and precipitation.

43.1.1.3 Precipitation and wind

In addition to annual cycles of photoperiod and temperature, precipitation patterns can also provide temporal cues to birds and other organisms (Pianka, 1978; Glickman, 2000). This is especially the case in subtropical and tropical zones, which experience predictable wet and dry seasons. The *intertropical convergence zone* results from the Coriolis Effect from the Earth's rotation as well as the evaporation of oceanic water in equatorial areas. Variation in the intertropical convergence zone affects rainfall in many

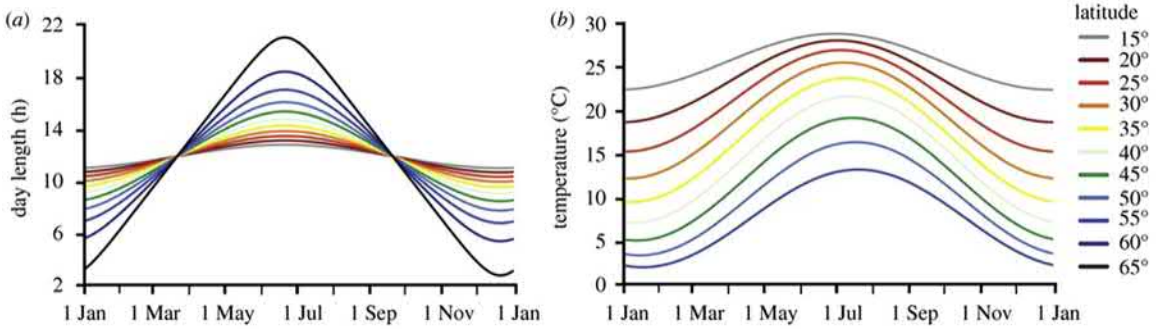

FIGURE 43.2 Annual changes in photoperiod depend upon the latitude (A) in which the amplitude of photoperiodic change is greatest at higher latitudes. Similarly, the seasonal changes in ambient temperature are also dependent on latitude (B). However, the average temperature at lower latitudes is higher than at higher latitudes. *From Wiltczek et al. (2010).*

equatorial regions, resulting in predictable wet seasons and dry seasons in subtropical and tropical zones as opposed to the cold and warm seasons at higher latitudes. For example, in tropical Queensland, Australia, precipitation ranges from 65% humidity and 400 mm rain/month the wet season (December to March) to only 17% humidity and 25 mm rain/month in the dry season (June to October). In West Africa, the rainy season extends from April to July, while the dry season falls between October and March. The absolute times of wet and dry seasons are not as predictable globally as is photoperiod because other factors such as wind direction, mountains, and other physical barriers affect them. However, they tend to be locally predictable, such that many organisms' reproductive processes are synchronized to these abiotic factors.

43.1.2 Biotic

Due to the fact that many abiotic factors vary depending on time of year, it is not surprising that aspects of birds' biotic environment are equally variable. These factors include, but are not limited to, presence and absence of food, competitors, predators, and mates. As a consequence, selective pressures for systems to tune physiological processes accurately to the timing of these biotic factors is very high (Pianka, 1978).

43.2 Annual cycles of birds

Birds' life history strategies must adapt to and predict these changing environmental factors. These life history strategies can be complex and species-specific, and the timing of the processes will determine birds' survival and fitness, perhaps more than any other vertebrate taxon. For an individual and species to survive, time must be allocated to each essential process such as reproduction, migration, molt, and other processes that may interfere with each other (King, 1974; Mewaldt and King, 1977). These processes are coordinated such that life history stages are timed to an appropriate time of year relative both to the external environmental conditions described above and among the diverse processes that are coordinated. For example, annual patterns of breeding, migration, body mass, and multiple molt patterns in long-distance migratory birds such as red knots, *Calidris canutus,* and ruffs, *Philomachus pugnax*, are orchestrated such that each stage of the species' annual cycle occurs at the appropriate time (Helm et al., 2012, Figure 43.3). Thus, birds exhibit hyperphagia and fatten up in anticipation of the vernal migration from southern hemisphere wintering grounds to northern hemisphere breeding grounds, where courtship, sexual behavior, and reproduction occur. Multiple molts occur to replace flight feathers following migratory stints, while breast molt occurs as incubation pads are prepared for incubation of young. *Phenological analyses* ["the study of the temporal aspects of recurrent natural phenomena and their relation to weather and climate of annual cycles" (Lincoln et al., 1998)], of multiple species of birds indicate similarly complex life history cycles. Obviously, transequatorial migrants such as ruffs and red knots exhibit more complex cycles, but these temporal programs are common among avian species.

43.3 Circannual rhythms

43.3.1 Circannual rhythms in the lab

How do birds synchronize their internal biological processes to prevailing environmental cycles? As with *circadian rhythms* described in Chapter 42, many physiological and behavioral rhythms in birds exhibit *circannual rhythms* (Gwinner, 2003). Circannual rhythms can only be demonstrated in the laboratory, but studies of circannual cycles in the laboratory likely reflect processes occurring in the field. Typically, birds are maintained continuously in equatorial photoperiods (LD 12:12) for several years. Under these conditions, many birds will express a "free-running" rhythm of approximately one year (hence, *circannual*), with periods of slightly less than or more than 365 days. As an example, circannual rhythms of testicular activity and molt in a single African stonechat, *Saxicola torquata axillaris*, maintained in captivity for up to 12 years in LD 12: 12 persisted with a period, τ, of approximately nine months until the bird died, presumably of old age (Figure 43.4; Gwinner, 2003). The expression of circannual rhythms is a widespread phenomenon among avian species, especially among species that experience transequatorial migration (Rani and Kumar, 2013), but circannual patterns are highly variable among species and among individuals within species (Hazlerigg and Loudon, 2008).

The mechanisms by which circannual rhythms are generated, however, are not known. System-level and molecular aspects of *circadian clocks* (Chapter 34) appear to interact with the expression of circannual rhythms, but they do not appear to be necessary. For example, pinealectomy (PINX) or constant light (LL), which abolishes circadian patterns of perch-hopping in the spotted munia, *Lonchura punctulata,* as well as other species of oscine passerine birds (Chapter 34) does not affect circannual patterns of testicular growth and regression, or premigratory fattening (Pant and Chandola-Saklani, 1992).

43.3.2 Synchronization of circannual rhythms to environmental cues

The expression of circannual patterns whose τ are different from 365 days in laboratory conditions but exactly 365 days under natural conditions suggests that, like

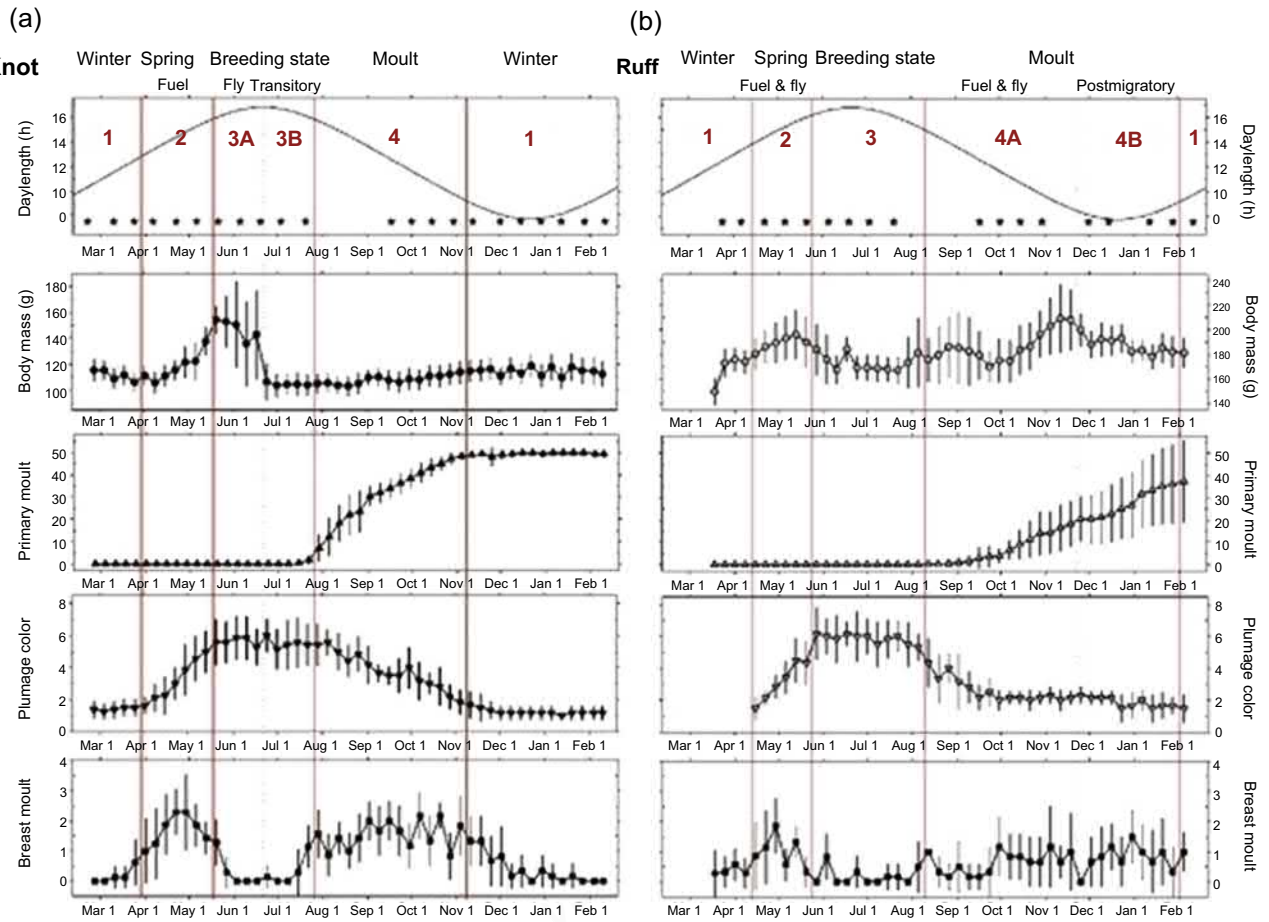

FIGURE 43.3 The complex annual life histories of two species of wading birds, the knot, *Calidris canutus*, (A) and the ruff, *Philomachus pugnax*, (B). Annual changes in body mass, vernal and autumnal molt, and plumage coloration occur in coordinated fashion in species-specific fashion. *From Helm et al. (2012).*

circadian rhythms (Chapter 34), circannual rhythms must be synchronized or entrained to prevailing environmental cues (Gwinner, 2003; Rani and Kumar, 2013). In most cases, alternating cycles of increasing and decreasing photoperiod synchronizes or entrains circannual rhythms of birds within a limit of entrainment. For example, exposure of European stonechats, *Saxicola torquata rubicola,* to alternating photoperiods of high amplitude (LD 16:6 to LD 10:14) entrain circannual patterns of testicular width and molt to 12 and 6 months in duration, respectively, but lower amplitude cycles of LD 13:11 to LD 11:13 were unable to entrain these processes to the six month cycle. There is little evidence of other zeitgebers entraining circannual rhythms in birds, although periodic presentation of novel food has transitory effects on circannual cycles in African stonechats (Gwinner and Scheuerlein, 1998; Scheuerlein and Gwinner, 2002).

43.4 Photoperiodism

43.4.1 Effects of photoperiod on avian physiological function

Aside from the entraining effects of photoperiod on circannual cycles, changes in photoperiod have direct effects on many annual cycles in birds, although it is not clear that these are necessarily mutually exclusive. In fact, it has been known for some time that seasonally breeding, temperate zone birds time reproduction and migration in a clock-like fashion in response to changing photoperiod (Rowan, 1926). Birds living in temperate zone latitudes generally restrict breeding to the spring and summer, maximizing the likelihood that young will be hatched during times at which food is plentiful (Gwinner, 1989, 2003; Hut et al., 2013).

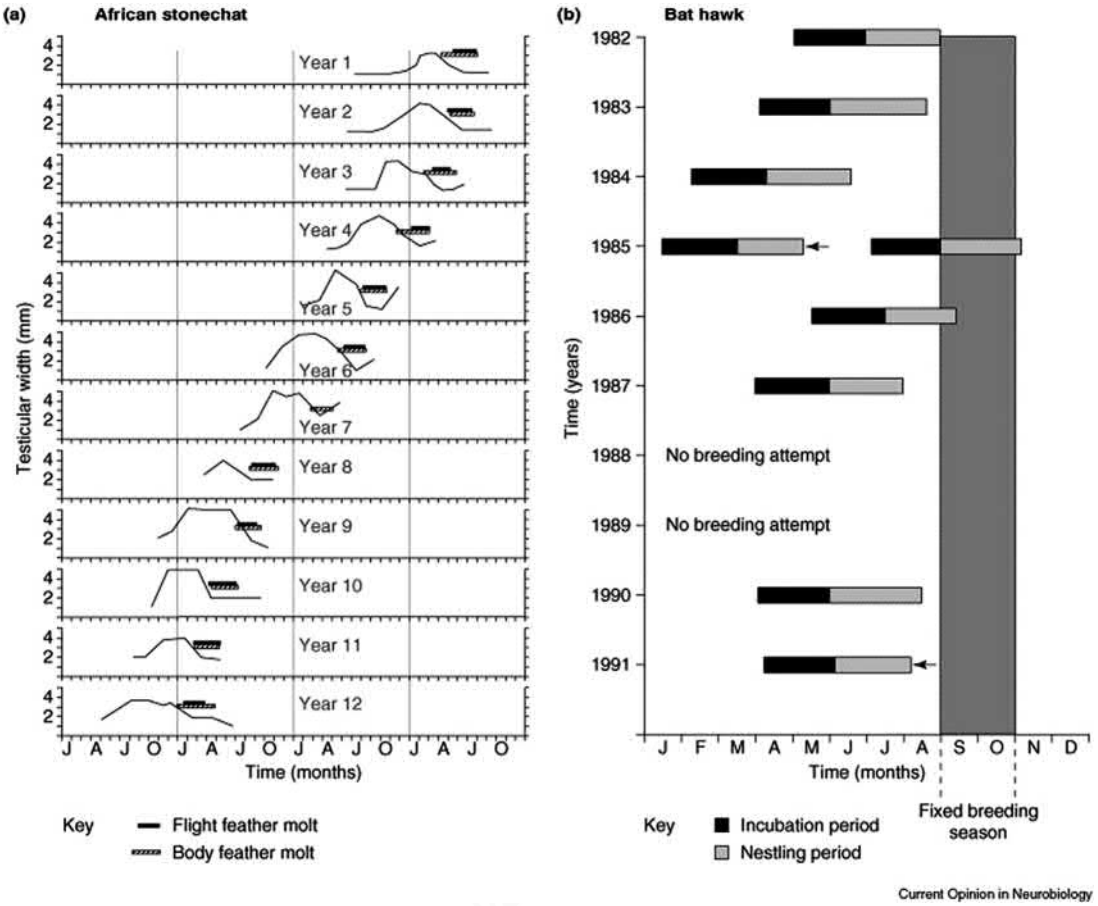

FIGURE 43.4 Circannual cycles of a single African stonechat, *Saxicola torquata axillaris*, of testicular size and molt through 12 consecutive years maintained in constant LD 12:12. *From Gwinner (2003).*

The vast majority of seasonally breeding birds are *long-day breeders*, that is, they begin sexual maturation, courtship, and mating as the photoperiod transitions from the winter solstice to longer and longer days. There is one well-documented *short-day breeding* species—the emu, *Dromaius novaehollandiae*, which breeds as the photoperiod shortens (Blache et al., 2001).

The exact photoperiod that induces or suppresses a particular function in birds is species-, latitude-, and function-specific, called the *critical photoperiod* (Siopes, 1994; Brandstatter, 2003; Hazlerigg and Loudon, 2008). This is the minimum photoperiod that induces or suppresses a seasonally regulated process (Figure 43.5). For example, annual testicular growth is induced earlier and by shorter photoperiods in the temperate zone European starling than in the Nearctic-breeding white-crowned sparrow (cf. Dawson, 2008). This corresponds to the likelihood of food availability occurring later in the season at higher versus lower latitudes at a species level. Similarly, within species, especially those that are widely distributed, critical photoperiod tends to be longer in individuals of the same species residing at higher latitudes than at lower latitudes (Dawson, 2013; Hut et al., 2013). Thirdly, the critical photoperiod that induces or suppresses different functions, such as reproduction, molt, metabolism, and migration usually differ among these processes. Obviously, molt during migration would be disadvantageous for any bird.

In seasonally reproducing, long-day birds, gonadal activity and gonad size regress (Wilson, 1986; Wilson and Reinert, 1993) and become inactive as the photoperiod decreases, while gonads recrudesce, becoming more active, in response to increased photoperiod (Figure 43.5A). If birds are maintained in long photoperiod for long periods of time, their reproductive systems become insensitive to the

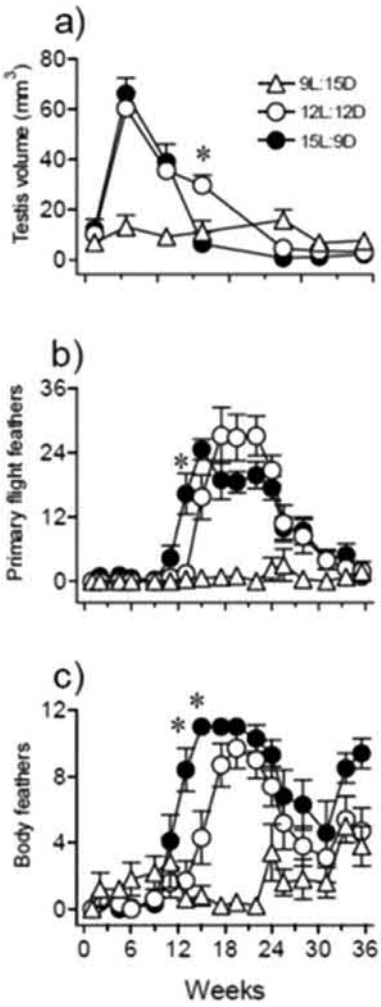

FIGURE 43.5 The effect of differing photoperiods on testes volume, primary and body molt in captive spotted munia, *Lonchura punctulata*. *From Rani and Kumar (2013).*

photostimulatory effects of long photoperiod and spontaneous regress (Figure 43.5A). This process is called *photorefractoriness*, and birds remain photorefractory until they are placed in short days for some time to make them photosensitive again (Dawson et al., 2001; Proudman and Siopes, 2002). Similarly, other photoperiodically regulated processes wax and wane depending on the photoperiod, although the absolute time at which they occur may differ from gonadal function (Figure 43.5B and C).

Subtropical and tropical birds are not immune to these changes, as the breeding seasons of these species are commonly timed as well (Scheuerlein and Gwinner, 2002; Rani and Kumar, 2013). Although the amplitude of photoperiodic change is much reduced at these latitudes (Figure 43.2), there are nonetheless many seasonal signals to which birds can synchronize reproductive and other processes. For example, the spotted antbird, *Hylophylax naevioides*, lives in Panamanian rainforests around 9°N, experiencing a very low-amplitude photoperiodic change. These birds breed in the rainy season (May−December), when insect prey are abundant (Wikelski et al., 2000). Although the rainy season occurs regularly from year to year, there is significant variation in its inception and duration (Hau et al., 2000). When male antbirds are experimentally transferred from LD 12:12 to LD 13:11, testes volume increases dramatically, while birds maintained in LD 12:12 do not, demonstrating these birds do respond to photoperiodic changes. Conversely, birds maintained in the equinoctial photoperiod stimulated with an additional dietary supplement of live crickets exhibit larger testes than birds maintained on the standard insectivorous diet of mealworms only (Hau et al., 2000). The scenario suggests that slight changes in photoperiod "primes" the birds' reproductive system to respond to the increase in diet necessary to raise young (Hau, 2001).

Similarly, in some desert species in which water may be a limiting commodity, photoperiodic control of reproduction may be triggered by access to water. Zebra finches, *Taeniopygia guttata,* are usually considered non-photoperiodic, opportunistic breeders, since these Australian desert birds breed rapidly following rainstorms (Bentley et al., 2000). Prior et al. (2013) found that severe water restriction of male zebra finches had no effect of testes size but did decrease plasma testosterone, while in females, the ovaries, oviduct size, and egg-laying was reduced by water restriction in female zebra finches. Water restriction further affects these birds' song control system (see below), since the acoustic structure of song syllables and calls of both male and female birds are decreased (Prior et al., 2019). However, these birds do respond to changes in photoperiod, since transfer of male zebra finches from short photoperiods to long photoperiods of increases plasma luteinizing hormone (LH), testicular volume, and body mass (Bentley et al., 2000). This is just one example of what is likely a wide array of adaptations to temporal changes in the subtropics and tropics, and since avian biodiversity is five times the level in the tropics than in Nearctic regions, the variability in these adaptations is likely just as diverse.

43.4.2 Role of photoreceptors

As described in detail in Chapter 34, multiple photoreceptors are involved in circadian entrainment, and these photoreceptors reside in the retinae, pineal gland, and at least three encephalic sites: lateral septal organ (LSO), preoptic area (POA), and tuberal hypothalamus/mediobasal hypothalamus (MBH) Foster and Hankins (2002). As with circadian entrainment, the retinae are not necessary for photoperiodic responses (Benoit and Assenmacher, 1954; Menaker, 1968; Menaker and Keatts, 1968; Menaker and Underwood, 1976), although there is some species

variability. In the house sparrow, *Passer domesticus,* and American tree sparrow, *Spizella arborea,* removal of the eyes, the pineal gland, or both has no effect on gonadal responses to increases or decreases in photoperiod (Menaker et al., 1970; Wilson, 1990). Enucleated Japanese quail, *Coturnix japonica*, exhibit normal photoperiodic responses to increases in photoperiod in egg-laying in females and enlargement of the cloacal gland in males, similar to the situation in sparrows. Still, termination of reproductive activity by exposure to short photoperiods requires that birds experience long days at or before the time of blinding (Homma et al., 1972). Since Japanese quail and house sparrows also differ in the role played by retinal melatonin in circadian organization (Chapter 34; Cassone and Menaker, 1984; Underwood and Siopes, 1984), it is not clear if this difference is due to differences in photoreceptors per se or due to differences in circadian organization.

Local illumination of the MBH or LSO leads to gonadal growth (Benoit, 1935; Benoit and Assenmacher, 1954; Homma et al., 1979). Nomographic analyses of the action spectra for photoperiodic responses suggest a rhodopsin-like photopigment with a peak sensitivity of 480 nm to ultraviolet wavelengths (Foster et al., 1985; Nakane et al., 2019). More recently, several genes encoding rhodopsin superfamily photopigments have been identified in the brains of several avian species, corroborating this view (Chapter 34). These include melanopsin (OPN4), vertebrate ancient opsin, neuropsin (OPN5), and rhodopsin itself (OPN2) (Silver et al., 1988; Bailey and Cassone, 2005; Chaurasia et al., 2005; Halford et al., 2009; Nakane et al., 2010; Kang et al., 2010; Davies et al., 2012; Wang et al., 2012). OPN5 is expressed in cerebrospinal fluid (CSF)-contacting neurons within the periventricular organ (PVO) of the Japanese quail (Figure 43.6; Nakane et al., 2010). OPN4-immunoreactivity and mRNA is widely expressed in the brain of the turkey, *Meleagris gallopavo*, including the POA, suprachiasmatic region [medial suprachiasmatic nucleus (mSCN) and visual suprachiasmatic nucleus (vSCN)] of the hypothalamus, lateral septal region, *pars distalis* of the *adenohypophysis*, and the premammillary nucleus (PMM) just dorsal of the PVO (Kang et al., 2010).

43.4.3 Role of circadian clocks in photoperiodic time measurement

The role of the circadian clock in annual cycles has been known for some time (Bünning, 1969; Follett et al., 1992; Menaker and Eskin, 1967). Although there are differences among species of birds and between birds and other taxa, neither the absolute length of the photoperiod, length of the scotoperiod (the duration of the dark phase) nor their ratio is the proximal causes of gonadal induction. Rather, it is the circadian phase (ϕ) at which light impinges on photoreceptive elements that causes reproductive changes. For example, male Japanese quail, *Coturnix japonica,* and white-crowned sparrows, *Zonotrichia leucophrys,* which are maintained in LD 6:18 will exhibit regressed testes. However, if the last hr. of the 6 h photoperiod is extended each long night to a specific "photoinducible phase," ϕ_{pi}, usually 11−12 h following the onset of the short photoperiod, reproductive activity is commenced. Thus, birds exposed to LD 6:18 or L5: D1: L1: D17 (a single 1 h light pulse interrupting the night) will retain regressed gonads, but if the 1 h pulse occurs 5 h later (L5:D6:L1:D12), gonads will recrudesce (Menaker and Eskin, 1967; Follett et al., 1974; Sharp, 2005). The same total amount of light (and dark) is present for each 24 h, but the effect is dramatically different. It is the *timing* of light coinciding with an internal process that induces or prevents

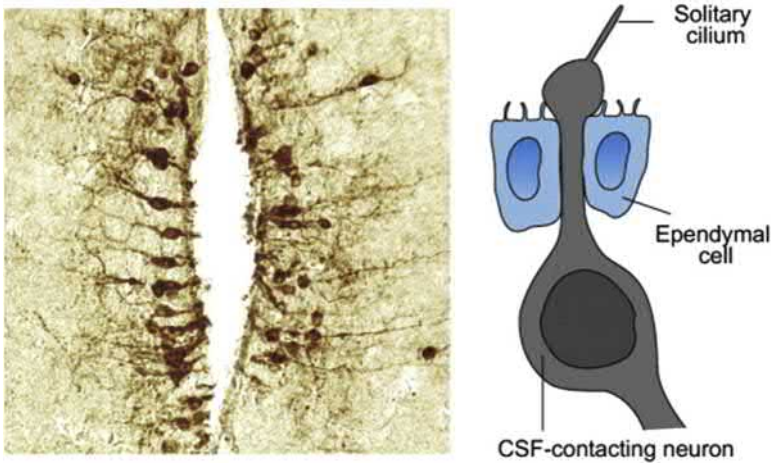

FIGURE 43.6 Expression of neuropsin (OPN5) in the periventricular organ of the mediobasal hypothalamus in the Japanese quail, *Coturnix japonica*. *From Yoshimura (2013).*

reproductive activity, suggesting a circadian clock underlies photoperiodic time measurement. Nanda and Hamner (1958) had shown this to be the case in plants through an elegant series of experiments in which soy bean plants exposed to a 6 h photoperiod coupled with scotoperiods of varying lengths that were multiples of a 24 h cycle (e.g., LD6:18; LD6:42 or LD6:66) did not flower. However, when plants were exposed to 6 h photoperiods followed by scotoperiods of lengths that did not resonate with 24 h (e.g., LD6:6; LD6:30 or LD6:54) flowering was observed. Similar studies in several species of birds showed that seasonal changes in both gonadal recrudescence and regression are regulated by a circadian clock (Follett et al., 1974, 1991; Kumar et al., 1996).

These and other observations have led to two competing models for a role of circadian clocks in photoperiodic time measurement (Figure 43.7). In one, the "external coincidence model" suggests that light has two complementary roles. First, light entrains the circadian clock with a stable ψ_{ie} such that the photoinducible phase, ϕ_{pi}, is also maintained with a stable ψ approximately 11.5 h following the beginning of the photoperiod (lights on). When light coincides with the ϕ_{pi} either because the photoperiod is long under natural conditions or through exposure to an experimental light pulse, the reproductive axis is induced (Pittendrigh, 1972, 1993). The competing notion (the "internal coincidence model") stems from the observation that many circadian systems behave as if they are composed of at least two oscillators, one entrained to dawn and the other to dusk. In the internal coincidence model, the phase relationship between the dawn oscillator and the dusk oscillator, $\psi_{dawndusk}$, induces seasonal changes in reproduction (Pittendrigh, 1972, 1993). Each of these models has support from different experimental systems in birds. However, until specific structures and/or molecules become associated with these models, they are essentially untestable at the physiological level.

43.4.4 Role of circadian system structures

As stated in Chapter 34, the avian circadian system comprises the pineal gland, the suprachiasmatic nuclei, the retinae and photoreceptors in the retinae, pineal, and brain (Cassone and Menaker, 1984). These structures mutually interact to elicit circadian patterns of a broad array of processes and to entrain them to LD cycles. In view of the fact that photoperiodic time measurement relies on circadian rhythmicity, one might expect that these structures are critical for photoperiodism as well. Intriguingly, in spite of the fact that the rhythmic production of melatonin is critical for the expression of circadian locomotor rhythms in birds, melatonin does not affect seasonal changes in primary reproductive function in these species. As in mammals, pineal melatonin levels faithfully reflect the length of the scotoperiod both in vivo and in vitro (Binkley et al., 1977; Brandstätter et al., 2000). However, PINX and/or EX of several species of birds has little effect on seasonal changes in gonad size or activity (Siopes, 1983; Bentley, 2001; Kumar et al., 2002). Moreover, administration of exogenous melatonin of different durations has little effect on primary reproductive function (Cassone et al., 2008). This corresponds to the relative absence of melatonin receptor activity in the tuberal hypothalamus and hypophysis (Cassone et al., 1995), in stark contrast to the situation in seasonally reproducing mammals, where 2[^{125}I]iodomelatonin (IMEL) binding and melatonin receptor expression in *pars tuberalis* is a major site of melatonin action (Goldman, 2001).

Circadian clock function has been localized within the MBH itself of Japanese quail controlling photoperiodic

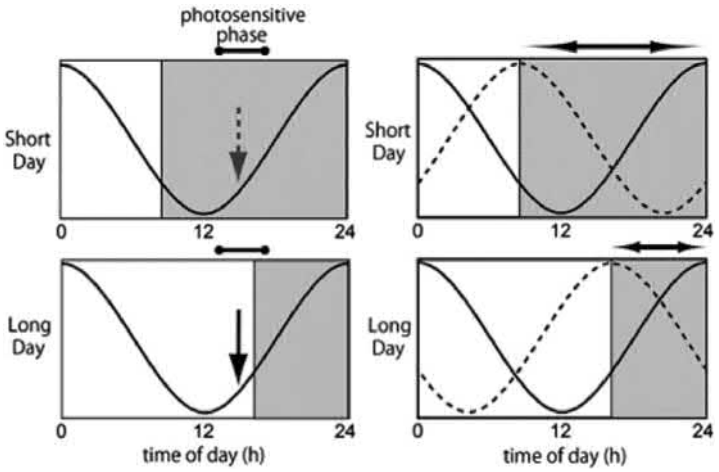

FIGURE 43.7 The difference between the external coincidence (left) and the internal coincidence (right) models for photoperiodic induction. In the case of external coincidence, light (1) entrains the circadian system to a stable phase relationship to the photoperiod and (2) stimulates or inhibits a process such as gonadal induction at a particular photoinducible phase. In the internal coincidence model, at least two circadian oscillators entrain to the photoperiod, and the phase relationship between these two oscillators induces or suppresses the seasonally controlled process. *From Yoshimura (2013).*

time measurement for reproductive function (Yoshimura, 2010, 2013). Earlier studies had shown that lesion of the MBH blocked testicular recrudescence in response to lengthening photoperiods (Sharp, 2005) and illumination of this area had resulted in excitation of the tuberal hypothalamus and testicular growth (Foster et al., 1985; Meddle and Follett, 1997). As stated above, the MBH of quail and the PMM of turkeys have been shown to express both OPN4 and OPN5 in CSF-contacting neurons (Kang et al., 2010; Nakane and Yoshimura, 2010; Nakane et al., 2010). Noting that PINX or EX or even SCN lesion had little effect on photoperiodic regulation of gonadal function, rhythmic expression of the clock genes *per2, per3, clock,* and *Bmal1* (Chapter 34) were identified in the MBH suggesting this structure contains the circadian pacemaker associated with photoperiodic time measurement (Yoshimura, 2010, 2013). Intriguingly, it has been reported that the PMM of turkeys also express the enzymes necessary for the biosynthesis in melatonin as well (Kang et al., 2007; El Halawani et al., 2009), although the significance of this observation is at this point unknown. Surgical destruction of the turkey PMM has no effect on photoperiodic control of reproduction (Moore et al., 2018).

43.5 Neuroendocrine regulation of photoperiodic time measurement

43.5.1 Photoperiodic control of gonadotropins and prolactin in seasonal reproduction

The circadian pacemaker presumably residing in the MBH controls seasonal changes in the release of *gonadotropin-releasing hormone* (GnRH) and *vasoactive intestinal polypeptide* (VIP) via the hypothalamohypophysial portal system (HHPS), which in turn regulate the synthesis and release the gonadotropin LH and *prolactin* (PRL), respectively (Sharp et al., 1998; Chapter 23). GnRH neurons predominate in the POA and anterior hypothalamus and project to the median eminence (Saldanha et al., 2001; Teruyama and Beck, 2001), while the VIP neurons are found throughout the basal hypothalamus. The GnRH cells, at least, are in direct contact with terminals arising from rhodopsin-immunoreactive cells, presumably extraocular photoreceptors in the LSO (Saldanha et al., 2001). The VIP cells project throughout the hypothalamus but also innervate the capillaries in the median eminence (Teruyama and Beck, 2001). GnRH- and VIP-immunoreactive terminals are more dense and in closer proximity to the median eminence during long-photostimulatory photoperiods than in short-photoinhibitory photoperiods.

In long-day breeding birds, lengthening photoperiods induce an increase in the release of GnRH from terminals in the median eminence into the HHPS. *Ex vivo* hypothalamic explants from male Japanese quail release GnRH in culture in response to long photoperiods (Perera and Follett, 1992). GnRH in turn induces the synthesis and release of LH, which remains high during the breeding season. However, when photoperiod decreases, LH levels also decrease. In addition, in long-day breeders, continued exposure to long days induces *photorefractoriness*, in which birds fail to respond to photostimulatory photoperiods, and LH levels decline (Sharp, 2005).

Lengthening photoperiod also presumably increases the release of VIP from median eminence terminals into the HHPS, although this has not been demonstrated directly. Even so, administration of VIP potently induces the synthesis and release of PRL by the adenohypophysis in several species of passerine, galliform, and columbiform species (Maney et al., 1999; Kosonsiriluk et al., 2008; Sharp and Blache, 2003). The rise in PRL is typically delayed relative to LH, declining only after LH declines. Immunization of European starlings, *Sturnus vulgaris,* against VIP delays and attenuates the decline in LH levels during photorefractoriness (Dawson and Sharp, 1998; Maney et al., 1999).

43.5.2 Role of the thyroid hormone in avian photoperiodism

Thyroidectomy induces gonadal recrudescence in starlings and Japanese quail (Follett and Nicholls, 1985; Dawson et al., 1986), and injection of T3 into the MBH induces quail gonadal growth (Follett and Nicholls, 1985; Yoshimura et al., 2003). Using differential subtractive hybridization, Yoshimura's group found type 2 iodothyronine deiodinase (*Dio2*) was induced in the MBH by a light pulse associated with long-day induction. *Dio2* encodes an enzyme that catalyzes the conversion of inactive thyroxine (T4) to active triiodothyroxine (T3) (Nakao et al., 2008 a,b). Later, they showed that type 3 iodothyronine deiodinase (*Dio3*), which inactivates T3, was induced in the MBH by exposure to short days. The scenario they envision is that photoperiod is perceived by photopigments in the MBH that entrain a circadian oscillator within the MBH. In long days, the circadian clock induces *Dio2*, while short days induce *Dio3*. These two gene-switches fine tune local thyroid hormone concentration within the MBH. Although precise mechanisms of thyroid hormone action remains unclear, it is proposed that locally activated thyroid hormone causes morphological changes in neuroglial interaction between GnRH nerve terminals and the endfeet of the glial processes in the median eminence that regulates or modulates the seasonal GnRH secretion (Figure 43.8; Yamamura et al., 2004).

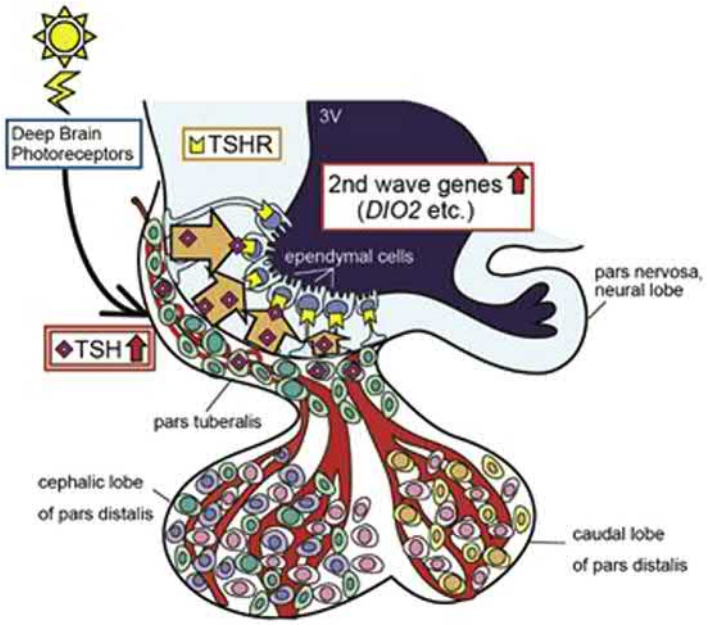

FIGURE 43.8 Schematic of the quail tuberal hypothalamus. Extraocular photoreceptors induce an increase in thyroid-stimulating hormone signaling in the *pars tuberalis* which in turn induce changes in ependymal cells or tanycytes. These cells affect the ability of neuroendocrine signals entering the hypothalamohypophysial portal system. *From Yoshimura (2013).*

43.5.3 Role of gonadal and neural steroids

As stated above, the reproductive systems of long-day breeders recrudesce as the photoperiod lengthens in response to gonadotropin activation. The exact timing of these is species- and gender-specific. For example in European starlings, seasonal testes growth begins more than a month earlier than does female follicle formation (Williams, 2012). As testes recrudesce, Sertoli cells synthesize and secrete *estrogens*, such as *estradiol,* while Leydig cells synthesize and secrete *androgens* such as *testosterone, androstenedione*, and *dehydroepiandrosterone* (Chapter 29). Ovarian granulosa cells begin to synthesize and secrete estrogens from androgens generated by adjacent thecal cells (Chapter 28). These gonadal steroids induce gender-appropriate seasonal growth and maturation of primary and secondary sexual characteristics (Adkins-Regan, 2012). In males, many of the genomic effects of testosterone are mediated by estrogens generated by local conversion by *aromatase.* When photoperiod decreases, LH also decreases, and the steroidogenic capacity of the gonads decline in parallel.

Among structures that annually recrudesce and regress are brain structures associated with reproductive behavior (Figure 43.9; Balthazart et al., 2009, 2010). The medial preoptic nucleus (POM) within the POA of Japanese quail has been well established as a structure involved in male sexual behavior (Ball and Balthazart, 2004; Balthazart and Ball, 2007), in which the size of the POM is greater in males than in females (Viglietti-Panzica et al., 1986; Ball and Ketterson, 2008). In male quail, the POM increases in volume during the spring and decreases in the fall

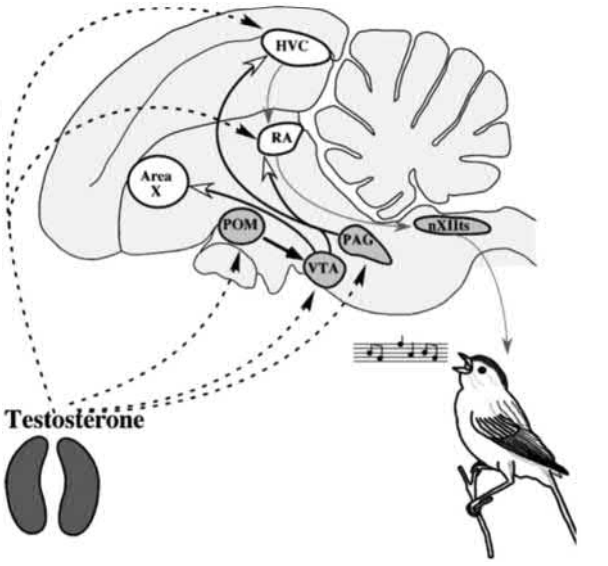

FIGURE 43.9 Schematic of the effects of testosterone on brain structures associated with reproduction and song. Steroid receptors residing in preoptic, brainstem, and forebrain structures mediate primary reproductive behavior as well as bird song. *From Ball and Balthazart (2004).*

(Thompson and Adkins-Regan, 1994). Castration of these birds abolishes this pattern, and administration of testosterone, mediated by aromatase-induced estrogens, increases POM volume through increases in cell size and dendritic branching within two weeks of administration. In contrast to the situation involving song control (see below), there is no evidence that POM growth involves de novo neurogenesis.

However, the gonads and adrenal glands are not the only sources of biologically active steroid hormone (Tsutsui et al., 1999; Schlinger and Remage-Healey, 2012). The brains of many species of birds express the enzymes capable of *neurosteroidogenesis,* biosynthesis of biologically active steroid hormones by the brain (Tsutsui et al., 1999). In the Lapland longspur, (*Calcarius lapponicus),* and song sparrow, *Melospiza melodia,* for example, the hypothalamus, hippocampus, and ventral telencephalon express aromatase, which converts androgens to estrogens, and 5-β-reductase, which deactivates testosterone (Soma et al., 1999, 2003). This suggests that the avian brain can convert circulating gonadal steroids into biologically active estrogens. Further, there is growing evidence that the brain can also synthesize steroids from circulating cholesterol (Schlinger et al., 2008; Schlinger and Remage-Healey, 2012).

The role(s) played by neurosteroids may be diverse. For example, there is evidence that estrogens synthesized by glial astrocytes may provide neuroprotection in response to traumatic brain injury, ischemia or anoxia (Pedersen et al., 2018). Steroids produced locally may enable rapid responses to local environmental changes within involving systemic responses that may have pleiotropic effects (Calisi and Saldanha, 2015).

43.5.4 Mechanisms of photoperiodic regulation of bird song

The song control system of oscine passeriform birds is a specialized network of brain nuclei involved in singing and song learning (Nottebohm, 1981; Mooney, 2009). This system receives auditory input from ascending, primary auditory pathways beginning in the cochlear nuclei, which project to the lateral dorsal mesencephalic nuclei (MLd). MLd in turn projects to the thalamic *nucleus ovoidalis*, which in turn projects to Field L in the forebrain. Song processing begins in secondary auditory areas in the caudal mesopallium and caudomedial nidopallium, which interact with the anterior forebrain pathway for song plasticity and learning. This pathway includes the HVC in the dorsal forebrain, which projects to Area X, whose projections form a loop between the dorsolateral thalamus and the lateral magnocellular nucleus of the anterior nidopallium (LMAN). Then, both HVC and LMAN project to the robust nucleus of the archipallium (RA), which forms the song motor output pathway.

This system enables birds to process a complex species-specific identification of both self and con-specifics as well as other dynamics in birds' acoustic environments (competitors, prey, predators, etc.) (Mooney, 2009). These acoustic environments as well as their reproductive and survival relevance are not constant. Territories change hands and the available range of mates fluctuates. In order to effectively interpret the acoustic features in song, the auditory system must structure its representation in such a way that allows for dynamic behavioral goals of the organism. At the same time, the structure and behavior of song itself must be tuned to reproductively appropriate situations.

Both the probability of a male bird to sing in response to a given stimulus as well as the size and complexity of the song control nuclei within its brain vary depending upon the time of year (Nottebohm, 1981). Photosensitive birds in the short days of winter possess small HVC, RA, and depending on the species other structures in the system. When birds are photostimulated as photoperiod increases, the song control nuclei grow in parallel with the growth of the testes, and, as they become photorefractory, these structures regress in both size and complexity. Some of the growth in these structures, especially in HVC, is due to de novo neurogenesis from neural stem cells residing in periventricular areas of the lateral ventricle (Alvarez-Buyla et al., 1988). These cells are born predominantly during the fall and migrate into the HVC over the course of the winter, where they differentiate and extend axonal projections to RA and other structures. In addition, increases in neuropil and glia contribute to this growth. Regression of these structures is characterized by programmed cell death as well as retraction of neuropil.

Seasonal fluctuations in androgens and estrogens appear to be critical for changes in song control (Figure 43.9). Song control nuclei contain both androgen receptors and both estrogen receptor subtypes (ERα and ERβ), as well as aromatase, capable of converting androgens into biologically active estrogens (Ball et al., 1997; Ball and Balthazart, 2010). Further, the rate of male song in several songbird species increases when testosterone levels are high, castration decreases this rate, and hormone replacement reestablishes vernal song patterns (Fusani, 2008; Balthazart et al., 2010).

Even so, a few studies have indicated gonad-independent regulation of song control nuclei under different photoperiods. In both American tree sparrows (Bernard et al., 1997) and house sparrows (Whitfield-Rucker and Cassone, 2000), HVC and RA increase in size in response to a change in photoperiod from a short day to long day (Figure 43.10). Castrated birds in these studies also exhibited photostimulated song control nuclei, although the level of induction was not as great as in the sham-operated birds. Thus, while the song system certainly responds to the seasonal changes in gonadal steroids, regulation of song control nuclei comprises a gonad-independent as well as a gonad-dependent aspect. As stated above, several studies have implicated neurosteroids in this supplemental signal to the song system (Soma et al., 1999, 2003).

Alternatively, studies employing in vitro receptor binding and IMEL in the 1980 and 1990s demonstrated high-affinity melatonin receptor binding and the identity of

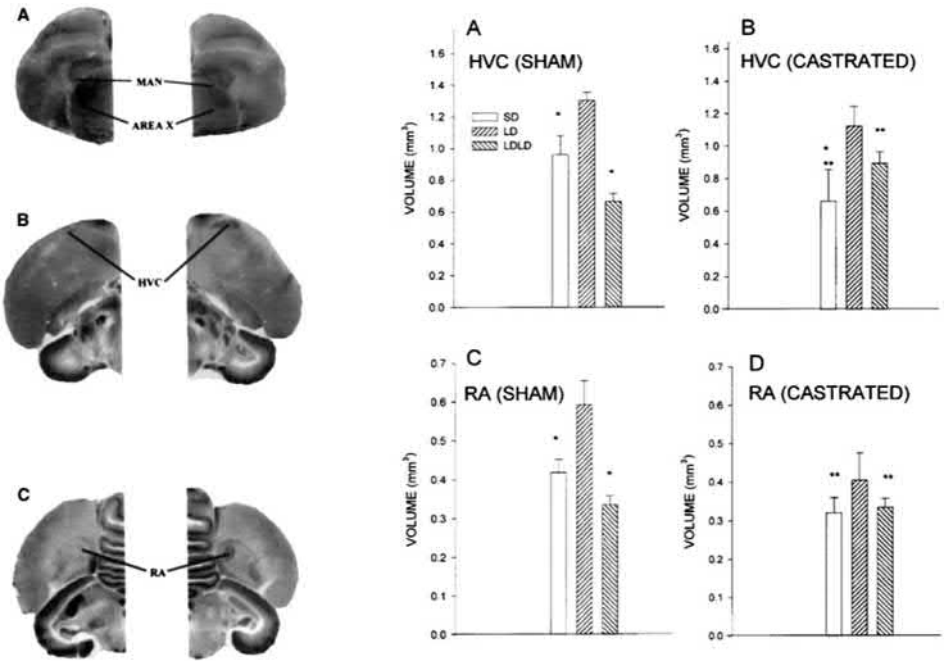

FIGURE 43.10 Bird song structures such as HVC and the nucleus robustus of the archipallium (RA) change in size and complexity depending on the photoperiod. HVC and RA are small in short days (left) and large in long days (right). Castration attenuates but does not abolish these seasonal cycles. *From Whitfield-Rucker and Cassone (2000).*

three receptor subtypes, Mel_{1A}, Mel_{1B}, and Mel_{1C} melatonin receptors, in a variety of vertebrates (Reppert et al., 1995, 1996). In birds and reptiles, IMEL binding predominates in retinorecipient and integrative structures within the visual system (Cassone et al., 1995), which has led to the view that visual sensitivity and contrast detection, are under circadian control. In male house sparrows (Whitfield-Rucker and Cassone, 1996) (Gahr and Kosar, 1996) and European starlings (Bentley and Ball, 2000) but not female birds, high-affinity IMEL binding was present in song control nuclei HVC, RA, LMAN and, to a lesser extent, Area X. Both HVC and RA express the Mel_{1B} melatonin receptor (Figure 43.11; Jansen et al., 2005).

These observations point to a role for melatonin in song behavior and in the growth and regression of song control nuclei. Bentley et al. (1999) have shown that continuous administration exogenous melatonin attenuated the long-day-induced volumetric increase in HVC and also decreased the volume of another song-control nucleus, area X, in European starlings. This effect was independent of the birds' reproductive state. House sparrows exposed to constant light (LL), which abolishes circadian patterns of behavior, and subsequent rhythmic administration of summer-like (short duration) or winter-like (long duration) melatonin, which entrains their behavior, also affects the volumes of song control nuclei HVC and RA (Cassone et al., 2008) and the distribution of song behavior (Harpole et al., 2020). Birds that received no melatonin or the short-duration melatonin cycle (who entrained to the regime) exhibited large HVC and RA, but birds that received the long duration melatonin entrained to the melatonin regime but showed regressed HVC and RA. This showed that melatonin affects song control nuclei independently of gonadal state.

43.5.5 Mechanisms of photoperiodic regulation of migration

One of the most iconic aspects of avian physiology and behavior is the biannual migration of birds from arctic and temperate zones to subtropical and tropical regions on a seasonal basis (Gwinner, 1967; Berthold, 1973) and/or from higher to lower altitudes and back (Rowan, 1926). Avian migration is an integrative process that involves circadian, circannual, and photoperiodic regulation at the genetic, epigenetic, and neuroendocrine levels, in which the timing of migration and directional navigation during migration are coordinated (Wiltschko and Wiltschko, 2012; Stevenson and Kumar, 2017; Merlin and Liedvogel, 2019). Further, it is embedded in a complex phenological pattern of integrated processes that must be coordinated precisely (Figure 43.3). These processes include hyperphagia in preparation for migration, migration itself, molt, and reproduction at appropriate times of year (Gwinner, 1989; Rattenborg et al., 2004).

The genetic bases for migratory behavior has been known for some time, due largely to the work of Berthold and colleagues (Berthold and Querner, 1981; Berthold, 1995). European blackcaps, *Sylvia atricapilla,* were selectively bred for strains that preferred a southwest autumnal

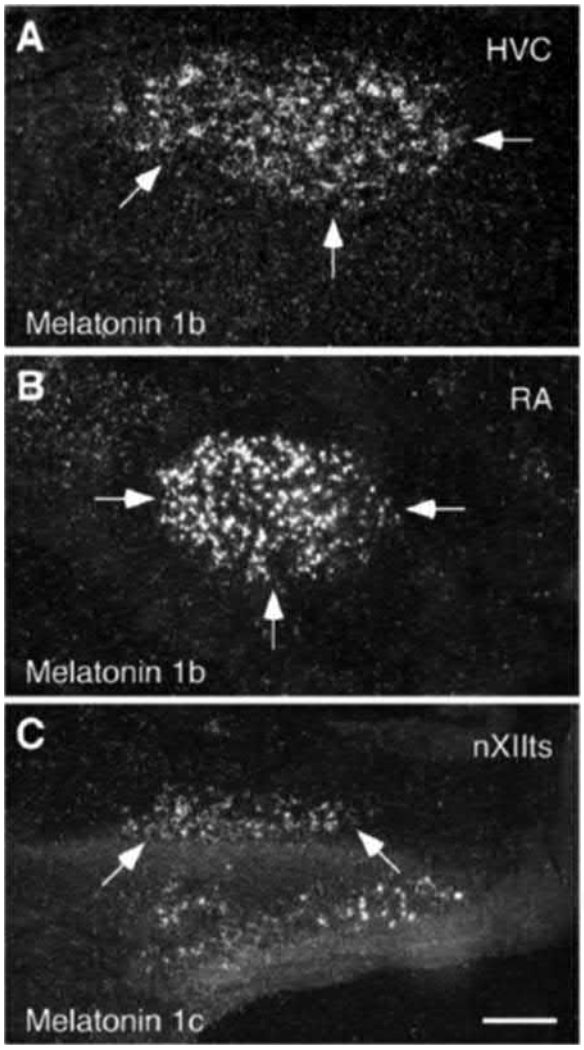

FIGURE 43.11 In situ hybridization of melatonin receptors in HVC, robust nucleus of the archipallium, and the nucleus tractus solitarius (nXIIts) of the zebra finch. *From Jansen et al. (2005).*

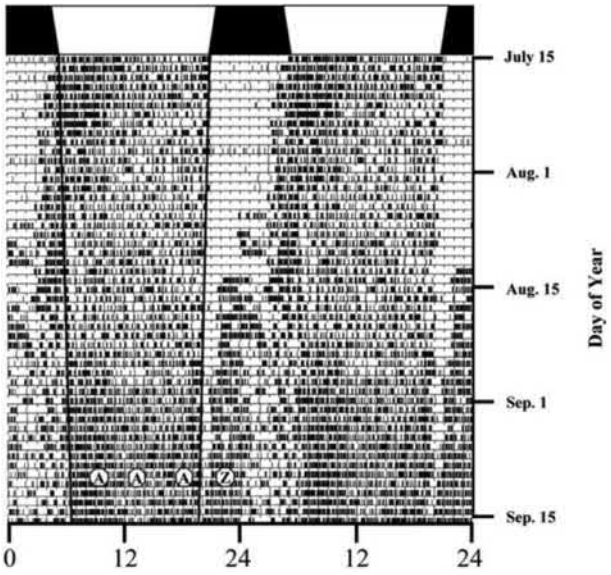

FIGURE 43.12 A double-plotted actogram of the activity patterns of a garden warbler exposed to gradually decreasing photoperiod. As photoperiod declines, nocturnal activity (*Zugunruhe)* emerges from August 5 until the end of the experiment. *From Bartell and Gwinner (2005).*

migratory direction and a southeastern autumnal migratory direction in the laboratory. When these strains were crossbred, the migratory vectors of the F1 hybrids were due south (Berthold and Querner, 1981; Berthold et al., 1992). These data strongly support the notion that migration and navigational vectors are genetically determined, but they have no bearing on the timing of migratory behavior nor do they identify candidate genes.

Many species of passerine birds migrate during the night and exhibit vernal and autumnal migrations on a semiannual basis (Rattenborg et al., 2004; Wiltschko and Wiltschko, 2012). These patterns of nocturnal behavior are expressed in the laboratory as nocturnal migratory restlessness or *Zugunruhe*, in addition to the daily diurnal pattern of activity (Figure 43.12; Gwinner, 1989; Stevenson and Kumar, 2017). *Zugunruhe* is controlled on a circadian basis in that it represents an increase in nocturnal activity that free-runs with a circadian period in constant dim light, which can be entrained to a light: dark (LD) cycle (DmDm; Bartell and Gwinner, 2005; Rani et al., 2006). Interestingly, under these conditions, the expression of the diurnal activity pattern and of *Zugunruhe* follows different circadian periods, suggesting that they are governed by separable circadian oscillators.

Zugunruhe is also governed by a circannual clock (Gwinner, 1967, 1989). For example, when willow warblers, *Phylloscopus trochilis*, were maintained in an equinoctial photoperiod for 28 months, the birds continued to display both vernal and autumnal bouts of *Zugunruhe* with periods of approximately 150 days (Gwinner, 1967). More recently, Helm et al. (2009) have established that stonechats also express circannual cycles of *Zugunruhe* under constant equinoctial photoperiods.

The annual change in photoperiod is likely to entrain circannual cycles of migratory behavior. In the laboratory, the experimental lengthening and shortening of photoperiod synchronizes the timing of vernal and autumnal bouts of *Zugunruhe* of many species, including willow warblers, garden warblers, stonechats, and other species (Gwinner, 1989; Bartell and Gwinner, 2005; Rattenborg et al., 2004). However, neither the mechanisms for the circannual clock guiding migration nor the pathways by which they entrain to time of year are well understood (Stevenson and Kumar, 2017).

Neural substrates for the expression and entrainment of migratory patterns are not completely understood either. Because the circadian clock is intimately associated with

migratory behaviors, several studies have asked whether the pineal gland in involved in the timing of *Zugunruhe*. McMillan (1970) showed that PINX of migratory white-crowned sparrows, *Zonotrichia leuchophrys*, abolishes both circadian patterns of perch-hopping behavior and circannual patterns of *Zugunruhe*. Fusani et al. (2011) found that the presence of food increases *Zugunruhe* in garden warblers even as it increases blood melatonin content, and suggested that food, rather than pineal melatonin increases or decreases the expression of migratory behavior. However, in a later paper, these authors showed that melatonin decreased the expression of *Zugunruhe* (Fusani et al., 2013). It is clear that the circadian pattern of melatonin influences the expression of *Zugunruhe*, but it is not at all clear that it affects the timing of the behavior.

Other neuronal substrates for migratory behavior have been suggested based upon neuronal activity. Black-headed buntings maintained in long days (LD 16:8) exhibited either nonmigratory behavior, when only diurnal activity was present, or migratory behavior, when *Zugunruhe* was expressed (Rastogi et al., 2011). Birds were sacrificed and processed for *c-fos* immunoreactivity (fos-lir) at midday and at midnight. Nonmigratory birds exhibited fos-lir in olfactory and visual system structures that were higher during the day than at night. In migratory birds, fos-lir in olfactory and visual system structures were higher at night. In a subsequent study, these authors (Rastogi et al., 2013, 2016) found that fos-lir was dramatically increased in the hypothalamic dorsomedial nucleus during *Zugunruhe*. Interestingly, there was no evidence for *Zugunruhe*-associated fos-lir in either circadian system pacemakers such as the mSCN or vSCN (see Chapter 34).

43.6 Molecular mechanisms of photoperiodism

Yoshimura and coworkers envision an external coincidence model in which circadian oscillators within the MBH are entrained by photoperiod co-localized in that structure (Nakao et al., 2007). When the length of the photoperiod coincides with a ϕ_{pi}, *Dio2* is induced, enabling a metabolic cascade in response to T3 hormone, and gonadal induction occurs. It is not clear, at this stage, what molecular components link the circadian clock to *Dio2* or *Dio3*. The MBH of quail and the PMM of turkeys rhythmically express clock genes (Ikegami et al., 2009; Ikegami and Yoshimura, 2012; Leclerc et al., 2010). The availability of chicken genome sequences has permitted the expansion of studies from single-gene to genome-wide transcriptome analyses in avian species. Microarray analysis of photoperiodism have identified waves of genes that were induced or reduced by long day stimulus, and long day-induced thyrotropin [thyroid-stimulating hormone (TSH)] in the pars tuberalis of the pituitary gland induces *DIO2* expression and reduces *DIO3* expression through the TSH receptor (TSHR)-Gαs-cAMP signaling pathway (Nakao et al., 2008b). Since chronic administration of TSH into the hypothalamus causes full testicular development, it is suggested that the thyrotropin secreted from the *pars tuberalis* is the master factor regulating seasonal reproduction. This result was unexpected because of the well-known function of thyrotropin in stimulation of thyroid gland.

Attempts to identify molecular components timing annual migratory patterns have been mixed. Studies focusing on allelic differences in C-terminal polyglutamine repeats in the circadian CLOCK protein in breeding and migratory patterns of barn swallows, *Hirundo rustica*, suggest a negative selection on "deviant" genotypes (Caprioli et al., 2012; Saino et al., 2013). However, other studies in several different swallow species in the genus *Tachycineta* failed to show similar associations (Dor et al., 2012).

Singh and Kumar (2017) have asked whether daily rhythms in expression of canonical circadian clock genes in the brain of black-headed buntings are altered by *Zugunruhe*. These authors measured mRNA expression of *per2, cry1, Bmal1,* and *Clock* in buntings maintained in short days (LD 8:16), when birds were nonmigratory, and in long days (LD 16:8) in both nonmigratory and migratory states. They found that daily *per2* expression patterns in the telencephalon, optic tectum, and cerebellum were unaffected by photoperiod or migratory state. In the optic tectum and cerebellum, the amplitude and phase of *cry1* and *Bmal1* rhythms were increased in *Zugunruhe*. The data show that clock gene expression in extra-hypothalamic areas of the brain is expressed rhythmically and that they are affected by photoperiod and migratory state, but they fail to provide causal clues to the mechanisms of seasonal migration.

43.7 Comparison to other vertebrate taxa

In marked contrast to nonmammalian vertebrates (Figure 43.13), the eyes are the only photoreceptor organs in mammals. Light information received by the eye is transmitted to the pineal gland through the suprachiasmatic nucleus. Melatonin is secreted during the night as in the case of birds, but the mode of melatonin action on seasonal reproduction had been unclear until recently. It has been demonstrated that melatonin receptors are expressed in the *pars tuberalis* of mammals and that melatonin suppresses TSH expression in the *pars tuberalis* via the MT1 melatonin receptor (Ono et al., 2008; Hanon et al., 2008; Yasuo et al., 2009).

Most fish living in temperate zones also exhibit a photoperiodic response and the involvement of thyroid

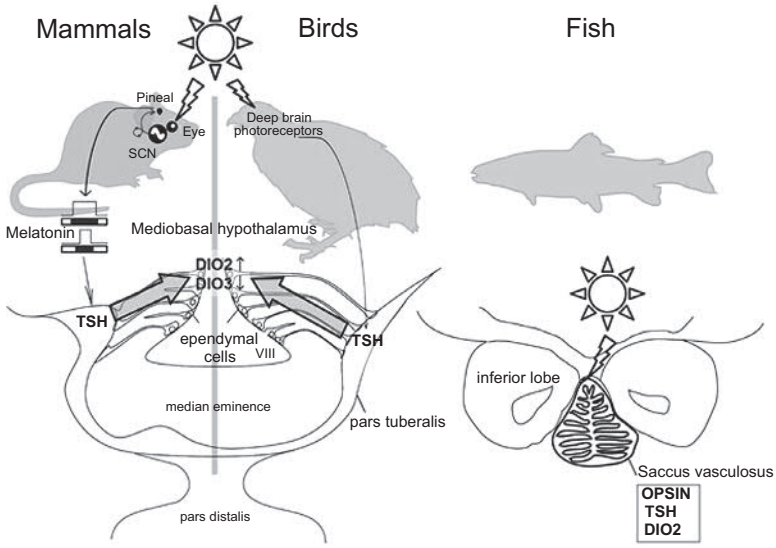

FIGURE 43.13 Vertebrates share common pathways for reproductive seasonality, but vary in several aspects. In mammals, light information arrives in the tuberal hypothalamus via transduction of the pineal hormone melatonin within the *pars tuberalis*, while in birds and fish, tuberal hypothalamic structures are directly light sensitive. The signal converge, however, through a common regulation of DIO2 and DIO3.

hormone in seasonal reproduction has been reported extensively. However, fish do not possess anatomically distinct *pars tuberalis*. Recent work has demonstrated that the *saccus vasculosus* (SV) of fish acts as a sensor of seasonal reproduction (Nakane et al., 2013). All the photoperiodic signaling pathways from photoreceptors (opsins) to neuroendocrine output (thyrotropin and DIO2) are localized in the coronet cells of the SV, and isolated SV responds to photoperiodic changes in vitro. Thus, the coronet cells of the SV may be the ancestral seasonal sensor in vertebrates.

43.8 Conclusion

The selective pressures to breed and reproduce at the most advantageous times of year, when food is most likely to be present for the provision of young are particularly strong in the many species of birds that express seasonal rhythms. This is largely due to the relatively large effort birds expend raising their young. In addition, birds' complex life cycles require a concerted orchestration of seasonal events, ranging from migration to molt to courtship to reproduction and so on. This complex phenology shares a variety of mechanisms, but these are not completely known. In oscine passeriforms, for example, the mechanisms by which primary reproductive function, which appear to be regulated by oscillators within the tuberal hypothalamus, are regulated appear to have been functionally separated from those associated with courtship and song, which in part involve pineal melatonin. Future research focused the coordination of other processes such as migration, molt, and female reproduction will go a long way toward fully understanding the complex seasonality of birds.

References

Adkins-Regan, E., 2012. Hormonal organization and activation: evolutionary implications and questions. Gen. Comp. Endocrinol. 176 (3), 279–285.

Alvarez-Buyla, A., Theelen, M., Nottebohm, F., 1988. Birth of projection neurons in the higher vocal center of the carary forebrain before, during and after song learning. Proc. Natl. Acad. Sci. U. S. A. 85, 8722–8726.

Bailey, M.J., Cassone, V.M., 2005. Melanopsin expression in the chick retina and pineal gland. Brain Res. Mol. Brain Res. 134 (2), 345–348.

Ball, G.F., Balthazart, J., 2004. Hormonal regulation of brain circuits mediating male sexual behavior in birds. Physiol. Behav. 83 (2), 329–346.

Ball, G.F., Ketterson, E.D., 2008. Sex differences in the response to environmental cues regulating seasonal reproduction in birds. Philos. Trans. R. Soc. Lond. B Biol. Sci. 363 (1490), 231–246, 27.

Ball, G.F., Riters, L.V., Balthazart, J., 1997. Neuroendocrinology of song behavior and avian brain plasticity: multiple sites of action of sex steroid hormones. Front. Neuroendocrinol. 23 (2), 137–178.

Ball, G.F., Balthazart, J., 2010. Seasonal and hormonal modulation of neurotransmitter systems in the song control circuit. J. Chem. Neuroanat. 39 (2), 82–95. https://doi.org/10.1016/j.jchemneu.2009.08.005.

Balthazart, J., Ball, G.F., 2007. Topography in the preoptic region: differential regulation of appetitive and consummatory male sexual behaviors. Front. Neuroendocrinol. 28 (4), 161–178.

Balthazart, J., Cornil, C.A., Charlier, T.D., Taziaux, M., Ball, G.F., 2009. Estradiol, a key endocrine signal in the sexual differentiation and activation of reproductive behavior in quail. J. Exp. Zool. A Ecol. Genet. Physiol. 311 (5), 323–345.

Balthazart, J., Charlier, T.D., Barker, J.M., Yamamura, T., Ball, G.F., 2010. Sex steroid-induced neuroplasticity and behavioral activation in birds. Eur. J. Neurosci. 32 (12), 2116–2132.

Bartell, P.A., Gwinner, E., 2005. A separate circadian oscillator controls nocturnal migratory restlessness in the songbird *Sylvia borin*. J. Biol. Rhythm. 20 (6), 538–549.

Benoit, J., 1935. Le role des yeux dans l'action stimulante de la lumiere sure le developpement testiculaire chez le canard. C.R. Soc. Biol. (Paris) 118, 669–671.

Benoit, J., Assenmacher, I., 1954. Comparative sensitivity of superficial and deep receptors in photosexual reflex in duck. C. R. Hebd. Seances Acad. Sci. 239 (1), 105–107.

Bentley, G.E., 2001. Unraveling the enigma: the role of melatonin in seasonal processes in birds. Microsc. Res. Tech. 53 (1), 63–71.

Bentley, G.E., Ball, G.F., 2000. Photoperiod-dependent and -independent regulation of melatonin receptors in the forebrain of songbirds. J. Neuroendocrinol. 12 (8), 745–752.

Bentley, G.E., Van't Hof, T.J., Ball, G.F., April 13, 1999. Seasonal neuroplasticity in the songbird telencephalon: a role for melatonin. Proc. Natl. Acad. Sci. U. S. A. 96 (8), 4674–4679.

Bentley, G.E., Spar, B.D., MacDougall-Shackleton, S.A., Hahn, T.P., Ball, G.F., 2000. Photoperiodic regulation of the reproductive axis in male zebra finches, *Taeniopygia guttata*. Gen. Comp. Endocrinol. 117 (3), 449–455.

Bernard, D.J., Wilson, F.E., Ball, G.F., 1997. Testis-dependent and -independent effects of photoperiod on volumes of song control nuclei in American tree sparrows (*Spizella arborea*). Brain Res. 760 (1–2), 163–169.

Berthold, P., 1973. Relationships between migratory restlessness and migratory distance. Ibis 115, 594–599.

Berthold, P., 1995. Control of Bird Migration. Springer, Berlin, Germany, ISBN 978-0-412-36380-1.

Berthold, P., Querner, U., 1981. Genetic basis of migratory behavior in European warblers. Science 212, 77–79.

Berthold, P., Helbig, A.J., Mohr, G., Querner, U., 1992. Rapid microevolution of migratory behavior in a wild bird species. Nature 360, 668–670.

Binkley, S., Stephens, J.L., Riebman, J.B., Reilly, K.B., 1977. Regulation of pineal rhythms in chickens: photoperiod and dark-time sensitivity. Gen. Comp. Endocrinol. 32 (4), 411–416.

Blache, D., Talbot, R.T., Blackberry, M.A., Williams, K.M., Martin, G.B., Sharp, P.J., 2001. Photoperiodic control of the concentration of luteinizing hormone, prolactin and testosterone in the male emu (*Dromaius novaehollandiae*), a bird that breeds on short days. J. Neuroendocrinol. 13 (11), 998–1006.

Brandstätter, R., 2003. Encoding time of day and time of year by the avian circadian system. J. Neuroendocrinol. 15 (4), 398–404.

Brandstätter, R., Kumar, V., Abraham, U., Gwinner, E., 2000. Photoperiodic information acquired and stored in vivo is retained in vitro by a circadian oscillator, the avian pineal gland. Proc. Natl. Acad. Sci. U. S. A. 97 (22), 12324–12328.

Bünning, E., 1969. Common features of photoperiodism in plants and animals. Photochem. Photobiol. 9 (3), 219–228.

Calisi, R.M., Saldanha, C.J., 2015. Neurohormones, brain, and behavior: a comparative approach to understanding rapid neuroendocrine action. Integr. Comp. Biol. 55 (2), 264–267. https://doi.org/10.1093/icb/icv007.

Caprioli, M., Ambrosini, R., Boncoraglio, G., Gatti, E., Romano, A., Romano, M., Rubolini, D., Gianfranceschi, L., Saino, N., 2012. Clock gene variation is associated with breeding phenology and maybe under directional selection in the migratory barn swallow. PloS One 7 (4), e35140. https://doi.org/10.1371/journal.pone.0035140.

Cassone, V.M., Menaker, M., 1984. Is the avian circadian system a neuroendocrine loop? J. Exp. Zool. 232 (3), 539–549.

Cassone, V.M., Brooks, D.S., Kelm, T.A., 1995. Comparative distribution of 2[^{125}I]iodomelatonin binding in the brains of diurnal birds: out-group analysis with turtles. Brain Behav. Evol. 45 (5), 241–256.

Cassone, V.M., Bartell, P.A., Earnest, B.J., Kumar, V., 2008. Duration of melatonin regulates seasonal changes in song control nuclei of the house sparrow, *Passer domesticus*: independence from gonads and circadian entrainment. J. Biol. Rhythm. 23 (1), 49–58.

Chaurasia, S.S., Rollag, M.D., Jiang, G., Hayes, W.P., Haque, R., Natesan, A., Zatz, M., Tosini, G., Liu, C., Korf, H.W., Iuvone, P.M., Provencio, I., 2005. Molecular cloning, localization and circadian expression of chicken melanopsin (Opn4): differential regulation of expression in pineal and retinal cell types. J. Neurochem. 92 (1), 158–170.

Davies, W.I., Turton, M., Peirson, S.N., Follett, B.K., Halford, S., Garcia-Fernandez, J.M., Sharp, P.J., Hankins, M.W., Foster, R.G., 2012. Vertebrate ancient opsin photopigment spectra and the avian photoperiodic response. Biol. Lett. 8 (2), 291–294.

Dawson, A., 2008. Control of the annual cycle in birds: endocrine constraints and plasticity in response to ecological variability. Philos. Trans. R. Soc. Lond. B Biol. Sci. 363 (1497), 1621–1633.

Dawson, A., 2013. The effect of latitude on photoperiodic control of gonadal maturation, regression and molt in birds. Gen. Comp. Endocrinol. 190, 129–133.

Dawson, A., Sharp, P.J., 1998. The role of prolactin in the development of photorefractoriness and postnuptial molt in the European starling (*Sturnus vulgaris*). J. Endocrinol. 139, 485–490.

Dawson, A., Goldsmith, A.R., Nicholls, T.J., Follett, B.K., 1986. Endocrine changes associated with the termination of photorefractoriness by short daylengths and thyroidectomy in starlings (*Sturnus vulgaris*). J. Endocrinol. 110 (1), 73–79.

Dawson, A., King, V.M., Bentley, G.E., Ball, G.F., 2001. Photoperiodic control of seasonality in birds. J. Biol. Rhythm. 16 (4), 365–380.

Dor, R., Cooper, C.B., Lovette, I.J., Massoni, V., Bulit, F., Liljesthrom, M., Winkler, D.W., 2012. Clock gene variation in *Tachycineta swallows*. Ecol. Evol. 2 (1), 95–105.

El Halawani, M.E., Kang, S.W., Leclerc, B., Kosonsiriluk, S., Chaiseha, Y., 2009. Dopamine-melatonin neurons in the avian hypothalamus and their role as photoperiodic clocks. Gen. Comp. Endocrinol. 163 (1–2), 123–127.

Follett, B.K., Mattocks Jr., P.W., Farner, D.S., May 1974. Circadian function in the photoperiodic induction of gonadotropin secretion in the white-crowned sparrow, Zonotrichia leucophrys gambelii. Proc. Natl. Acad. Sci. U. S. A. 71 (5), 1666–1669.

Follett, B.K., Nicholls, T.J., 1985. Influences of thyroidectomy and thyroxine replacement on photoperiodically controlled reproduction in quail. J. Endocrinol. 107 (2), 211–221.

Follett, B.K., Pearce-Kelly, A.S., 1991. Photoperiodic induction in quail as a function of the period of the light-dark cycle: implications for models of time measurement. J. Biol. Rhythm. 6 (4), 331–341.

Follett, B.K., Kumar, V., Juss, T.S., 1992. Circadian nature of the photoperiodic clock in Japanese quail. J. Comp. Physiol. 171 (4), 533–540.

Foster, R.G., Hankins, M.W., 2002. Non-rod, non-cone photoreception in the vertebrates. Prog. Retin. Eye Res. 21 (6), 507–527.

Foster, R.G., Follett, B.K., Lythgoe, J.N., 1985. Rhodopsin-like sensitivity of extra-retinal photoreceptors mediating the photoperiodic response in quail. Nature 313 (5997), 50–52.

Fusani, L., 2008. Testosterone control of male courtship in birds. Horm. Behav. 54 (2), 227–233.

Fusani, L., Cardinale, M., Schwabl, I., Goymann, W., 2011. Food availability but not melatonin affect nocturnal restlessness in a wild migrating passerine. Horm. Behav. 59 (1), 187–192.

Fusani, L., Coccon, F., Rojas Mora, A., Goymann, W., 2013. Melatonin reduces migratory restlessness in Sylvia warblers during autumnal migration. Front. Zool. 10 (1), 79. https://doi.org/10.1186/1742-9994-10-79.

Gahr, M., Kosar, E., 1996. Identification, distribution, and developmental changes of a melatonin binding site in the song control system of the zebra finch. J. Comp. Neurol. 367 (2), 308–318.

Glickman, T., 2000. Glossary of Meteorology, second ed. Am. Meteor. Soc., Boston.

Goldman, B.D., 2001. Mammalian photoperiodic system: formal properties and neuroendocrine mechanisms of photoperiodic time measurement. J. Biol. Rhythm. 16 (4), 283–301.

Gwinner, E., 1967. Circannuale periodic der mauser und der Zugunruhe bei einem Vogel. Natuwissenschaften 54, 447.

Gwinner, E., 1989. Photoperiod as a modifying and limiting factor in the expression of avian circannual rhythms. J. Biol. Rhythm. 4 (2), 237–250.

Gwinner, E., 2003. Circannual rhythms in birds. Curr. Opin. Neurobiol. 13 (6), 770–778.

Gwinner, E., Scheuerlein, A., 1998. Seasonal changes in day-light intensity as a potential Zeitgeber of circannual rhythms in equatorial Stonechats. J. Ornithol. 139, 407–412.

Halford, S., Pires, S.S., Turton, M., Zheng, L., González-Menéndez, I., Davies, W.L., Peirson, S.N., García-Fernández, J.M., Hankins, M.W., Foster, R.G., 2009. VA opsin-based photoreceptors in the hypothalamus of birds. Curr. Biol. 19 (16), 1396–1402.

Hanon, E.A., Lincoln, G.A., Fustin, J.M., Dardante, H., Masson-Pevet, M., Morgan, P.J., Hazlerigg, D.G., 2008. Ancestral TSH mechanism signals summer in a photoperiodic mammal. Curr. Biol. 18, 1147–1152.

Harpole, C.E., Miles, M.D., Cassone, V.M., 2020. Melatonin duration gates photoperiodic vocal state change in a songbird. J. Pineal Res. 68 (2), e12625. https://doi.org/10.1111/jpi.12625.

Hau, M., 2001. Timing of breeding in variable environments: tropical birds as model systems. Horm. Behav. 40 (2), 281–290. https://doi.org/10.1006/hbeh.2001.1673.

Hau, M., Wikelski, M., Wingfield, J.C., 2000. Visual and nutritional food cues fine-tune timing of reproduction in a neotropical rainforest bird. J. Exp. Zool. 286 (5), 494–504.

Hazlerigg, D., Loudon, A., 2008. New insights into ancient seasonal life timers. Curr. Biol. 18 (17), R795–R804.

Helm, B., Schwabl, I., Gwinner, E., 2009. Circannual basis of geographically distinct bird schedules. J. Exp. Biol. 212, 1259–1269.

Helm, B., Gwinner, E., Koolhaas, A., Battley, P., Schwabl, I., Dekinga, A., Piersma, T., 2012. Avian migration: temporal multitasking and a case study of melatonin cycles in waders. Prog. Brain Res. 199, 457–479.

Homma, K., Wilson, W.O., Siopes, T.D., October 27, 1972. Eyes have a role in photoperiodic control of sexual activity of coturnix. Science 178 (4059), 421–423.

Homma, K., Ohta, M., Sakakibara, Y., 1979. Photoinducible phase of the Japanese quail detected by direct stimulation of the brain. In: Suda, M., Hayaishi, O., Nakagawa, H. (Eds.), Biological Thythms and Their Central Mechanism. Elsevier, Amsterdam, pp. 85–94.

Hut, R.A., Paolucci, S., Dor, R., Kyriacou, C.P., Daan, S., July 3, 2013. Latitudinal clines: an evolutionary view on biological rhythms. Proc. Biol. Sci. 280 (1765), 20130433. https://doi.org/10.1098/rspb.2013.0433.

Ikegami, K., Yoshimura, T., 2012. Circadian clocks and the measurement of daylength in seasonal reproduction. Mol. Cell. Endocrinol. 349, 76–81.

Ikegami, K., Katou, Y., Higashi, K., Yoshimura, T., 2009. Localization of circadian clock protein BMAL1 in the photoperiodic signal transduction machinery in Japanese quail. J. Comp. Neurol. 517 (3), 397–404.

Jansen, R., Metzdorf, R., van der Roest, M., Fusani, L., ter Maat, A., Gahr, M., 2005. Melatonin affects the temporal organization of the song of the zebra finch. FASEB J 19 (7), 848–850. https://doi.org/10.1096/fj.04-2874fje.

Kang, S.W., Thayananuphat, A., Bakken, T., El Halawani, M.E., 2007. Dopamine-melatonin neurons in the avian hypothalamus controlling seasonal reproduction. Neuroscience 150 (1), 223–233.

Kang, S.W., Leclerc, B., Kosonsiriluk, S., Mauro, L.J., Iwasawa, A., El Halawani, M.E., 2010. Melanopsin expression in dopamine-melatonin neurons of the premammillary nucleus of the hypothalamus and seasonal reproduction in birds. Neuroscience 170 (1), 200–213.

King, J.R., 1974. Seasonal allocation of time and energy resources. In: Paynter, R.A. (Ed.), Avian Energetics. Publ. Nuttall Ornith. Club, Cambridge, pp. 4–70.

Kosonsiriluk, S., Sartsoongnoen, N., Chaiyachet, O.A., Prakobsaeng, N., Songserm, T., Rozenboim, I., El Halawani, M., Chaiseha, Y., 2008. Vasoactive intestinal peptide and its role in continuous and seasonal reproduction in birds. Gen. Comp. Endocrinol. 159 (1), 88–97.

Kumar, V., Jain, N., Follett, B.K., 1996. The photoperiodic clock in blackheaded buntings (*Emberiza melanocephala*) is mediated by a self-sustaining circadian system. J. Comp. Physiol. 179 (1), 59–64.

Kumar, V., Singh, S., Misra, M., Malik, S., Rani, S., 2002. Role of melatonin in photoperiodic time measurement in the migratory redheaded bunting (Emberizabruniceps) and the nonmigratory Indian weaver bird (Ploceusphilippinus). J. Exp. Zool. 292 (3), 277–286.

Leclerc, B., Kang, S.W., Mauro, L.J., Kosonsiriluk, S., Chaiseha, Y., El Halawani, M.E., 2010. Photoperiodic modulation of clock gene expression in the avian premammillary nucleus. J. Neuroendocrinol. 22 (2), 119–128.

Lincoln, R.J., Boxshall, G.A., Clark, P.F., 1998. A Dictionary of Ecology, Evolution and Systematics.

Lockwood, M., 2010. Solar change and climate: an update in the light of the current exceptional minimum. Proc. Roy. Soc. A 466, 303–329.

Maney, D.L., Schoech, S.J., Sharp, P.J., Wingfield, J.C., 1999. Effects of vasoactive intestinal peptide on plasma prolactin in passerines. Gen. Comp. Endocrinol. 113 (3), 323–330.

McMillan, J.P., 1970. Pinealectomy abolishes circadian rhythm of migratory restlessness. J. Comp. Physiol. 79, 105–110.

Meddle, S.L., Follett, B.K., 1997. Photoperiodically driven changes in Fos expression within the basal tuberal hypothalamus and median eminence of Japanese quail. J. Neurosci. 17 (22), 8909–8918.

Menaker, M., 1968. Extraretinal light perception in the sparrow. I. Entrainment of the biological clock. Proc. Natl. Acad. Sci. U. S. A. 59 (2), 414–421.

Menaker, M., Eskin, A., 1967. Circadian clock in photoperiodic time measurement: a test of the Bünning hypothesis. Science 157 (3793), 1182–1185.

Menaker, M., Keatts, H., 1968. Extraretinal light perception in the sparrow. II. Photoperiodic stimulation of testis growth. Proc. Natl. Acad. Sci. U. S. A. 60 (1), 146–151.

Menaker, M., Underwood, H., 1976. Extraretinal photoreception in birds. Photophysiology 23 (4), 299–306.

Menaker, M., Roberts, R., Elliott, J., Underwood, H., 1970. Extraretinal light perception in the sparrow. 3. The eyes do not participate in photoperiodic photoreception. Proc. Natl. Acad. Sci. U. S. A. 67 (1), 320–325.

Merlin, C., Liedvogel, M., 2019. The genetics and epigenetics of animal migration and orientation: birds, butterflies and beyond. J. Exp. Biol. 222 (Pt Suppl. 1), jeb191890.

Mewaldt, L.R., King, J.R., 1977. The annual cycle of white-crowned sparrows (Zonotrichia leuchophrys nuttalli) in coastal California. Condor 79, 445–455.

Mooney, R., 2009. Neurobiology of song learning. Curr. Opin. Neuobiol. 19, 654-650.

Moore, A.F., Cassone, V.M., Alloway, K.D., Bartell, P.A., 2018. The premammillary nucleus of the hypothalamus is not necessary for photoperiodic timekeeping in female turkeys (*Meleagris gallopavo*). PloS One 13 (2), e0190274. https://doi.org/10.1371/journal.pone.0190274.

Nakane, Y., Yoshimura, T., 2010. Deep brain photoreceptors and a seasonal signal transduction cascade in birds. Cell Tissue Res. 342 (3), 341–344.

Nakane, Y., Ikegami, K., Ono, H., Yamamoto, N., Yoshida, S., Hirunagi, K., Ebihara, S., Kubo, Y., Yoshimura, T., 2010. A mammalian neural tissue opsin (Opsin 5) is a deep brain photoreceptor in birds. Proc. Natl. Acad. Sci. U. S. A. 107 (34), 15264–15268.

Nakane, Y., Ikegami, K., Iigo, M., Ono, H., Takeda, K., Takahashi, D., Uesaka, M., Kimijima, M., Hashimoto, R., Arai, N., Suga, T., Kosuge, K., Abe, T., Maeda, R., Senga, T., Amiya, N., Azuma, T., Amano, M., Abe, H., Yamamoto, N., Yoshimura, T., 2013. The saccus vasculosus of fish is a sensor of seasonal changes in day length. Nat. Commun. 4, 2108.

Nakane, Y., Shinomiya, A., Ota, W., Ikegami, K., Shimmura, T., Higashi, S., Kamei, Y., Yoshimura, T., September 11, 2019. Action spectrum for photoperiodic control of thyroid-stimulating hormone in Japanese quail (*Coturnix japonica*). PloS One 14 (9), e0222106. https://doi.org/10.1371/journal.pone.0222106.

Nakao, N., Yasuo, S., Nishimura, A., Yamamura, T., Watanabe, T., Anraku, T., Okano, T., Fukada, Y., Sharp, P.J., Ebihara, S., Yoshimura, T., 2007. Circadian clock gene regulation of steroidogenic acute regulatory protein gene expression in preovulatory ovarian follicles. Endocrinology 148 (7), 3031–3038.

Nakao, N., Ono, H., Yoshimura, T., 2008a. Thyroid hormones and seasonal reproductive neuroendocrine interactions. Reproduction 136 (1), 1–8.

Nakao, N., Ono, H., Yamamura, T., Anraku, T., Takagi, T., Higashi, K., Yasuo, S., Katou, Y., Kageyama, S., Uno, Y., Kasukawa, T., Iigo, M., Sharp, P.J., Iwasawa, A., Suzuki, Y., Sugano, S., Niimi, T., Mizutani, M., Namikawa, T., Ebihara, S., Ueda, H.R., Yoshimura, T., 2008b. Thyrotrophin in the pars tuberalis triggers photoperiodic response. Nature 452 (7185), 317–322.

Nanda, K.K., Hamner, K.C., 1958. Studies on the nature of the endogenous rhythm affecting photoperiodic response in the Biloxi soy bean. Bot. Gaz. 120, 14–25.

Nottebohm, F., 1981. A brain for all seasons: cyclical anatomical changes in song control nuclei of the canary brain. Science 214, 1368–1370.

Ono, H., Hoshino, Y., Yasuo, S., Watanabe, M., Nakane, Y., Murai, A., Ebihara, S., Korf, H.W., Yoshimura, T., 2008. Involvement of thyrotropin in photoperiodic signal transduction in mice. Proc. Natl. Acad. Sci. U. S. A. 105, 18238–18242.

Pant, K., Chandola-Saklani, A., 1992. Pinealectomy and LL abolished circadian perching rhythms but did not alter circannual reproductive or fattening rhythms in finches. Chronobiol. Int. 9 (6), 413–420.

Perera, A.D., Follett, B., 1992. Photoperiodic induction in vitro: dynamics of gonadotrophin releasing hormone release from hypothalamic explants of the Japanese quail. Endocrinology 131, 2898–2908.

Pedersen, A.L., Brownrout, J.L., Saldanha, C.J., 2018. Neuroinflammation and neurosteroidogenesis: reciprocal modulation during injury to the adult zebra finch brain. Physiol. Behav. 187, 51–56. https://doi.org/10.1016/j.physbeh.2017.10.013.

Pianka, E.R., 1978. Evolutionary Ecology, second ed. Harper and Row, New York. 397 pp.

Pittendrigh, C.S., 1972. Circadian surfaces and diversity of possible roles of circadian organization in photoperiodic induction. Proc. Natl. Acad. Sci. U. S. A. 69, 2734–2737.

Pittendrigh, C.S., 1993. Temporal organization: reflections of a Darwinian clock-watcher. Annu. Rev. Physiol. 55, 16–54.

Prior, N.H., Heimovics, S.A., Soma, K.K., 2013. Effects of water restriction on reproductive physiology and affiliative behavior in an opportunistically-breeding and monogamous songbird, the zebra finch. Horm. Behav. 63 (3), 462–474.

Prior, N.H., Fernandez, M.S.A., Soula, H.A., Vignal, C., 2019. Water restriction influences intra-pair vocal behavior and the acoustic structure of vocalisations in the opportunistically breeding zebra finch (*Taeniopygia guttata*). Behav. Process. 162, 147–156.

Proudman, J.A., Siopes, T.D., 2002. Relative and absolute photorefractoriness in Turkey hens: profiles of prolactin, thyroxine, and triiodothyronine early in the reproductive cycle. Poultry Sci. 81 (8), 1218–1223.

Rani, S., Kumar, V., 2013. Avian circannual systems: persistence and sex differences. Gen. Comp. Endocrinol. 190, 61–67.

Rani, S., Malik, S., Trivedi, A., Singh, S., Kumar, V., 2006. A circadian clock regulates migratory restlessness in the black-headed bunting, *Emberiza melanocephala*. Curr. Sci. 91, 1093–1099.

Rastogi, A., Kumari, Y., Rani, S., Kumar, V., October 21, 2013. Neural correlates of migration: activation of hypothalamic clock(s) in and out of migratory state in the blackheaded bunting (*Emberiza melanocephala*). PloS One 8 (10), e70065. https://doi.org/10.1371/journal.pone.0070065.

Rastogi, A., Kumari, Y., Rani, S., Kumar, V., 2011. Phase inversion of neural activity in the olfactory and visual systems of a night-migratory bird during migration. Eur. J. Neurosci. 34 (1), 99–109. https://doi.org/10.1111/j.1460-9568.2011.07737.x.

Rastogi, A., Surbhi, M.S., Rani, S., Kumar, V., 2016. Annual life-history dependent seasonal differences in neural activity of the olfactory system between non-migratory and migratory songbirds. Behav. Brain Res. 296, 233–239. https://doi.org/10.1016/j.bbr.2015.09.019.

Rattenborg, N., Mandt, B.H., Obermeyer, W.H., Winsauer, P.J., Huber, R., Wilkelski, M., Benca, R.M., 2004. PloS Biol. 2, e70065.

Reppert, S.M., Weaver, D.R., Cassone, V.M., Godson, C., Kolakowski Jr., L.F., 1995. Melatonin receptors are for the birds: molecular analysis of two receptor subtypes differentially expressed in chick brain. Neuron 15 (5), 1003–1015.

Reppert, S.M., Weaver, D.R., Godson, C., 1996. Melatonin receptors step into the light: cloning and classification of subtypes. Trends Pharmacol. Sci. 17 (3), 100–102.

Rowan, W., 1926. On photoperiodism, reproductive periodicity, and the annual migrations of certain birds and fishes. Proc. Boston Soc. Nat. Hist. 38, 147–189.

Saino, N., Romano, M., Caprioli, M., Fasola, M., Lardelli, R., Micheloni, P., Scandolara, C., Rubolini, D., Gianfranceschi, L., 2013. Timing of molt of barn swallows is delayed in a rare clock genotype. Peer J 1, e17. https://doi.org/10.7717/peerj.17.

Saldanha, C.J., Silverman, A.J., Rilver, R., 2001. Direct innervation of GnRH neurons by encephalic photoreceptors in birds. J. Biol. Rhythm. 16, 39–49.

Scheuerlein, A., Gwinner, E., 2002. Is food availability a circannual zeitgeber in tropical birds? A field experiment on stonechats in tropical Africa. J. Biol. Rhythm. 17 (2), 171–180.

Schlinger, B.A., Remage-Healey, L., 2012. Neurosteroidogenesis: insights from studies of songbirds. J. Neuroendocrinol. 24 (1), 16–21.

Schlinger, B.A., Pradhan, D.S., Soma, K.K., 2008. 3beta-HSD activates DHEA in the songbird brain. Neurochem. Int. 52 (4–5), 611–620.

Sharp, P.J., 2005. Photoperiodic regulation of seasonal breeding in birds. Ann. N. Y. Acad. Sci. 1040, 189–199.

Sharp, P.J., Blache, D., 2003. A neuroendocrine model for prolactin as the key mediator of seasonal breeding in birds under long- and short-day photoperiods. Can. J. Phys. 81, 350–358.

Sharp, P.J., Dawson, A., Lea, R.W., 1998. Control of luteinizing hormone and prolactin secretion in birds. Comp. Biochem. Physiol. 119, 275–282.

Silver, R., Witkovsky, P., Horvath, P., Alones, V., Barnstable, C.J., Lehman, M.N., 1988. Coexpression of opsin- and VIP-like-immunoreactivity in CSF-contacting neurons of the avian brain. Cell Tissue Res. 253 (1), 189–198.

Siopes, T.D., 1983. Effect of pinealectomy on broodiness of Turkey hens. Poultry Sci. 62 (11), 2245–2248. https://doi.org/10.3382/ps.0622245.

Siopes, T.D., 1994. Critical day lengths for egg production and photorefractoriness in the domestic Turkey. Poultry Sci. 73 (12), 1906–1913.

Soma, K.K., Bindra, R.K., Gee, J., Wingfield, J.C., Schlinger, B.A., 1999. Androgen-metabolizing enzymes show region-specific changes across the breeding season in the brain of a wild songbird. J. Neurobiol. 41 (2), 176–188.

Soma, K.K., Schlinger, B.A., Wingfield, J.C., Saldanha, C.J., 2003. Brain aromatase, 5alpha-reductase, and 5 beta-reductase change seasonally in wild male song sparrows: relationship to aggressive and sexual behavior. J. Neurobiol. 56 (3), 209–221.

Stevenson, T.J., Kumar, V., 2017. Neural control of daily and seasonal timing of songbird migration. J. Comp. Physiol. A Neuroethol. Sens. Neural. Behav. Physiol. 203 (6–7), 399–409.

Singh, D., Kumar, V., 2017. Extra-hypothalamic brain clocks in songbirds: photoperiodic state dependent clock gene oscillations in night-migratory blackheaded buntings, *Emberiza melanocephala*. J. Photochem. Photobiol., B 169, 13–20. https://doi.org/10.1016/j.jphotobiol.2017.02.016.

Teruyama, R., Beck, M.M., 2001. Double immunocytochemistry of vasoactive intestinal peptide and GnRH-l in male quail: photoperiodic effects. Cell Tissue Res. 303, 403–414.

Thompson, R.R., Adkins-Regan, E., 1994. Photoperiod affects the morphology of a sexually dimorphic nucleus within the preoptic area of male Japanese quail. Brain Res. 667, 201–208.

Tramontin, A.D., Brenowitz, E.A., 2000. Seasonal plasticity in the adult brain. Trends Neurosci. 23 (6), 251–258.

Tsutsui, K., Ukena, K., Takase, M., Kohchi, C., Lea, R.W., 1999. Neurosteroid biosynthesis in vertebrate brains. Comp. Biochem. Physiol. C Pharmacol. Toxicol. Endocrinol. 124 (2), 121–129.

Underwood, H., Siopes, T., 1984. Circadian organization in Japanese quail. J. Exp. Zool. 232, 557–566.

Viglietti-Panzica, C., Panzica, G.C., Fiori, M.G., Calcagni, M., Anselmetti, G.C., Balthazart, J., 1986. A sexually dimorphic nucleus in the quail preoptic area. Neurosci. Ltrs 64, 129–134.

Wang, G., Harpole, C.E., Trivedi, A.K., Cassone, V.M., 2012. Circadian regulation of bird song call, and locomotor behavior by pineal melatonin in the zebra finch. J. Biol. Rhythm. 27 (2), 145–155.

Whitfield-Rucker, M.G., Cassone, V.M., 1996. Melatonin binding in the house sparrow song control system: sexual dimorphism and the effect of photoperiod. Horm. Behav. 30 (4), 528–537.

Whitfield-Rucker, M.G., Cassone, V.M., 2000. Photoperiodic regulation of the male house sparrow song control system: gonadal dependent and independent mechanisms. Gen. Comp. Endocrinol. 118, 173–183.

Wikelski, M., Hau, M., Wingfield, J.C., 2000. Seasonality of reproduction in a neotropical rainforest bird. Ecology 81, 2458–2472.

Wilczek, A.M., Burghardt, L.T., Cobb, A.R., Cooper, M.D., Welch, S.M., Schmitt, J., 2010. Genetic and physiological bases for phenological responses to current and predicted climates. Philos. Trans. R. Soc. Lond., B, Biol. Sci. 365 (1555), 3129–3147. https://doi.org/10.1098/rstb.2010.0128.

Williams, T.D., 2012. Hormones, life-history, and phenotypic variation: opportunities in evolutionary avian endocrinology. Gen. Comp. Endocrinol. 176 (3), 286–295.

Wilson, F.E., 1986. A testosterone-independent reduction in net photoperiodic drive triggers photorefractoriness in male tree sparrows (*Spizella arborea*). J. Endocrinol. 109 (1), 133–137.

Wilson, F.E., March 1990. Extraocular control of seasonal reproduction in female tree sparrows (*Spizella arborea*). Gen. Comp. Endocrinol. 77 (3), 397–402.

Wilson, F.E., Reinert, B.D., 1993. The thyroid and photoperiodic control of seasonal reproduction in American tree sparrows (*Spizella arborea*). J. Comp. Physiol. B 163 (7), 563–573.

Wiltschko, W., Wiltschko, R., 2012. Global navigation in migratory birds: tracks, strategies, and interactions between mechanisms. Curr. Opin. Neurobiol. 22 (2), 328–335.

Yamamura, T., Hirunagi, K., Ebihara, S., Yoshimura, T., 2004. Seasonal morphological changes in the neuro-glial interaction between gonadotropin-releasing hormone nerve terminals and glial endfeet in Japanese quail. Endocrinology 145, 4264–4267.

Yasuo, S., Yoshimura, T., Ebihara, S., Korf, H.W., 2009. Melatonin transmits photoperiodic signals through the MT1 melatonin receptor. J. Neurosci. 29, 2885–2889.

Yoshimura, T., 2010. Neuroendocrine mechanism of seasonal reproduction in birds and mammals. Anim. Sci. J. 81 (4), 403–410.

Yoshimura, T., 2013. Thyroid hormone and seasonal regulation of reproduction. Front. Neuroendocrinol. 34 (3), 157–166.

Yoshimura, T., Yasuo, S., Watanabe, M., Iigo, M., Yamamura, T., Hirunagi, K., Ebihara, S., 2003. Light-induced hormone conversion of T4 to T3 regulates photoperiodic response of gonads in birds. Nature 426 (6963), 178–181.

Chapter 44

Annual schedules

Helen E. Chmura[1], Elizabeth M. Schultz[2], Kathleen R. Brazeal[3], Heather E. Watts[4], Scott A. MacDougall-Shackleton[5], Thomas P. Hahn[6] and Jamie M. Cornelius[7]

[1]*Institute of Arctic Biology, University of Fairbanks, Fairbanks, AK, United States;* [2]*Department of Biology, Wittenberg University, Springfield, OH, United States;* [3]*School of Biological Sciences, University of Nebraska-Lincoln, Lincoln, NE, United States;* [4]*School of Biological Sciences, Washington State University, Pullman, WA, United States;* [5]*Departments of Psychology and Biology, University of Western, London, ON, Canada;* [6]*Department of Neurobiology, Physiology and Behavior, University of California, Davis, CA, United States;* [7]*Department of Integrative Biology, Oregon State University, Corvallis, OR, United States*

44.1 Introduction

Research into the mechanisms underlying the annual cycles of birds began in the 1920s with the pioneering work of Rowan (1925, 1926) exploring effects of changing photoperiod on migratory and reproductive physiology and behavior. Subsequent studies have progressed toward a deep understanding of these mechanisms at the organismal, cellular, and molecular levels. In recent decades, there has been a push to move beyond the breeding and migration stages and study the entire annual schedule, as well as seasonal changes in important processes such as immune function, stress responsivity, and metabolic restructuring. Climate change is leading many researchers to ask how timing mechanisms may influence the response of avian taxa to a rapidly changing environment. This chapter will focus on the current state of research on avian annual schedules, highlighting these areas of recent progress and interest. Birds continue to be exciting and productive models for understanding the basic mechanisms by which organisms respond to the environment and for revealing the importance of these proximate mechanisms in evolution.

44.2 Background: patterns of environmental variation and avian annual schedules

Long-term changes in physiology, behavior, and morphology, orchestrated by the neuroendocrine and endocrine systems, are prominent in most species of birds. In many cases, these changes create consistent annual schedules. This is typically the case for animals that experience predictable seasonal changes in environmental conditions that can exert selective pressures on timing (the "Ultimate Factors" of Baker, 1938), such as species that spend all or part of the year at mid to high latitudes (Figure 44.1A and B) or those in tropical areas with regular seasonal patterns of rainfall (Figure 44.1C). Less consistent long-term changes in physiology, behavior, and morphology prevail in species occupying environments where conditions change more erratically, such as certain deserts where rainfall is unpredictable (see Perfito et al., 2007 and also Figure 44.1D) or even in otherwise seasonal environments where variation in the food supply is not regularly seasonal (see Hahn et al., 1997, 2008). In at least some of these species (e.g., crossbills; *Loxia* spp.), temporally flexible changes in physiology, behavior, and morphology are superimposed on underlying seasonal cycles (Hahn, 1995, 1998; Hahn et al., 1997, 2008; Cornelius and Hahn, 2012; Cornelius et al., 2021). In others (e.g., Darwin's finches), it remains unclear to what extent changes in reproductive physiology are entirely opportunistic versus based in part on an underlying seasonal program (Hau et al., 2004; Hahn et al., 2008).

Whether regularly seasonal, flexible, or erratic, all annual schedules must coordinate reproduction and plumage molt, and many incorporate migrations and a nonbreeding "overwintering" stage (Wingfield, 2008). Timing and coordination of these processes is crucial to fitness and the regulatory mechanisms responsible for this can respond to selection (Bradshaw and Holzapfel, 2007, 2010; Helm et al., 2019). The timing mechanisms that evolve are based on cue response systems that link neuroendocrine and endocrine regulatory mechanisms to "Proximate Factors" (c.f. Baker, 1938)—cues such as daylength, temperature, food supply, and social interactions—that provide predictive information either in the short- or long-term regarding fluctuating Ultimate Factors in the surrounding environment. These cue response systems generally include a long-term component that sets the time

Sturkie's Avian Physiology. https://doi.org/10.1016/B978-0-12-819770-7.00039-6

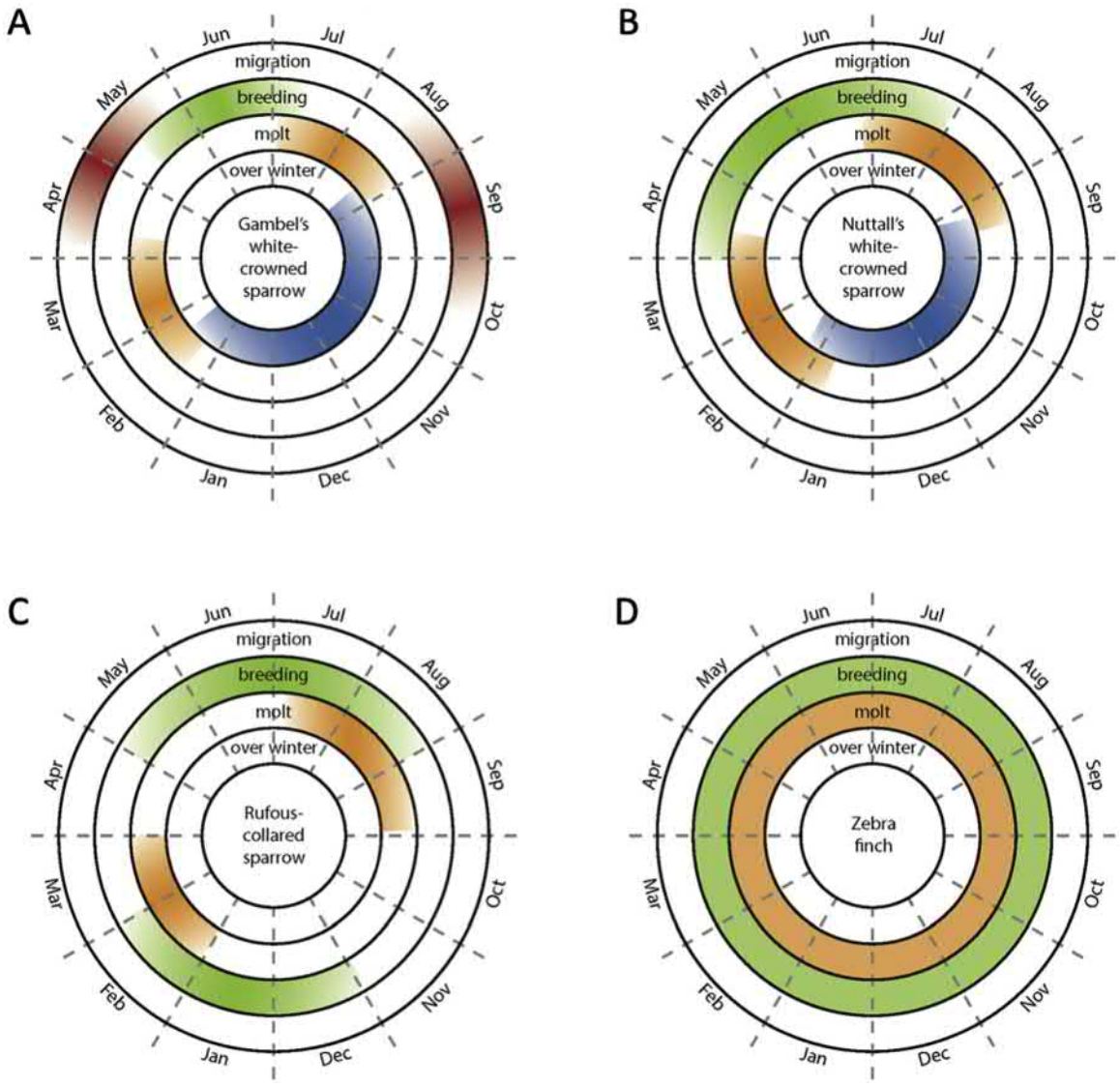

FIGURE 44.1 Diagrammatic representation of the annual schedule of the Gambel's white-crowned sparrow (A), Nuttall's white-crowned sparrow (B), Rufous-collared sparrow (C), and Zebra finch (D). Each concentric ring represents a life history stage: migration, breeding, molt, and overwintering (from outer ring to inner ring). The shading of life history stage represents the relative occurrence of that life history stage at the population level (higher intensity shading represents more birds in the population exhibiting that stage). Gambel's white-crowned sparrows are long-distance migrants and exhibit a constrained breeding season in northwestern North America. Nuttall's white-crowned sparrows also live in temperate climates but lack migration and exhibit greater flexibility in timing of breeding. The rufous-collared sparrow exhibits two defined breeding periods per year, both following seasonal rains. In contrast, zebra finches in arid Australia breed rapidly after unpredictable rain events, and therefore could be found breeding throughout the year depending upon local conditions.

windows when particular cycle stages can occur, and that dictates general features of physiological preparation for and termination of the stages. This long-term component is based on some combination of response to changing photoperiod and an endogenous program (so-called Initial Predictive cues of Wingfield, 1980, 1985; Gwinner, 1986; Wingfield and Kenagy, 1991; Wingfield and Farner, 1993; Dawson, 2002; Bradshaw and Holzapfel, 2007; Wikelski et al., 2008; Helm et al., 2013). Long-term timing is refined by responses to more immediate cues that provide accurate short-term information about local conditions, such as changing temperature, weather, food supply itself, and behavioral cues from other individuals (Wingfield, 1980, 1985 and below in Section 44.3).

Annual schedules of different species vary in their complexity and therefore potentially in the mechanisms required to orchestrate them. As shown in Figure 44.1, different species may exhibit one or more stages of migration, reproduction, or molt over the course of the year. The different components can theoretically overlap

temporally (within an individual or across the population) or occur in distinct time periods (Jacobs and Wingfield, 2000; Wingfield, 2008). Certain activities simply cannot overlap (e.g., egg-laying, incubation, and care of nestlings are incompatible with migration), but many components of "breeding," such as the gonadal maturation process (Wingfield et al., 1992; Bauchinger et al., 2007, 2008, 2009), pair formation (Ganter et al., 2005), and extended parental care of fully mobile youngsters can be compatible with migration, and plumage molt need not be incompatible with any stage of reproduction (Bond et al., 2013) or migration (Yuri and Rohwer, 1997; Voelker and Rohwer, 1998). The degree of overlap between reproduction, migration, and molt can be viewed as a continuum, from near-complete temporal separation at one extreme to near-complete temporal overlap (within constraints noted above) at the other. This variation in overlap of seasonal stages represents a critical trade-off between temporal flexibility and tolerance for environmental variation. Two relatively extreme examples illustrate this concept (Wingfield, 2008, Figure 44.1A and D). A regular seasonal migrant, the Gambel's white-crowned sparrow (*Zonotrichia leucophrys gambelii*) displays a six-part annual schedule consisting of separate and minimally overlapping stages of overwintering, partial prealternate molt, vernal migration, breeding, complete prebasic molt, and autumnal migration (Figure 44.1A). The phenotypic traits expressed during each of these stages broaden the scope of environmental variation the birds can tolerate (e.g., temperatures that can be endured, foods that are acceptable) across the entire year as compared to tolerances within any one stage. This benefit comes at a cost of temporal flexibility; however, breaking the year into multiple stages, each with unique phenotypic characteristics requiring time and energy to initiate and terminate, reduces how nimbly the animal can adjust to any environmental changes that deviate from the normal routine it has evolved to track. In contrast, certain desert-dwelling reproductive opportunists such as zebra finches (*Taeniopygia guttata*) in parts of the arid interior of Australia display such extensive overlap between stages that no truly separate stages exist (Figure 44.1D). Although the birds do not breed continuously, they can maintain near-readiness to breed for long periods of time and they display a low-intensity but essentially continuous plumage molt that may overlap with both breeding and any short-distance nonmigratory movements that do occur (Cornelius et al., 2011). Expression of this single chimaera stage confers high-temporal flexibility, since any activity is possible at any time, but at the cost of scope for tolerating environmental extremes. This strategy is an example of the jack-of-all-trades being master of none (Huey and Hertz, 1984).

The capacity to express these different patterns depends on coordination mechanisms. Specifically, separation of the annual schedule into distinct stages requires synchronization mechanisms that align the cycle and environment, as well as coordination mechanisms that limit overlap between stages, maintain stages in an adaptive sequence, and orchestrate transitions from stage to stage so that processes involved in termination of one do not interfere with processes involved in development and onset of the next (Wingfield, 2008). In contrast, if components are to overlap partially or completely, mechanisms that facilitate this overlap must be present. The next section will address recent advances in understanding the mechanisms by which diverse annual schedules are generated. We will return below to the question of whether these diverse patterns reflect adaptively specialized mechanisms or plastic outputs of common mechanistic underpinnings.

44.3 Effects of environmental cues on annual scheduling and underlying mechanisms

44.3.1 Photoperiodic response

Annual schedules that track consistent seasonal changes in the environment depend on proximate responses to changing photoperiod (Rowan, 1925, 1926; Dawson et al., 2001; Dawson, 2002; Dawson and Sharp, 2007; Bradshaw and Holzapfel, 2007). A system that uses photoperiod as a proximate cue for regulation of annual schedules (either as a driver or as an entrainer of an endogenous program, see Chapter 43) requires: a mechanism for detecting light (photoreceptors); a mechanism for determining the length of the day (known in birds to depend on a circadian clock) and; a mechanism for transducing the photoperiod information into neuroendocrine and endocrine signals that regulate the different components of the schedule, such as the septo-infundibular gonadotropin-releasing hormone (GnRH) system that regulates reproduction (see Follett, 1984).

Most birds breed seasonally on long days, and their annual reproductive cycle breaks naturally into three stages: (1) sensitivity, (2) stimulation, and (3) refractoriness (Ball, 1993; Dawson et al., 2001; Goodson et al., 2005). The transition from being *sensitive* to long days, but reproductively inactive, to *stimulated* by long days depends on responding to increasing daylength as an activational cue. Birds possess a circadian cycle of photoinducibility, whereby light occurring during a window of circadian time acts as a stimulatory long day, and activation of the hypothalamo–pituitary–gonad (HPG) axis results (Hamner, 1963, 1964; Follett et al., 1974, Figure 44.2).

Early studies demonstrated that detection of the light cue regulating seasonal cycles of birds is not retinal (Benoit, 1935) or pineal (Wilson, 1991). For example, all key

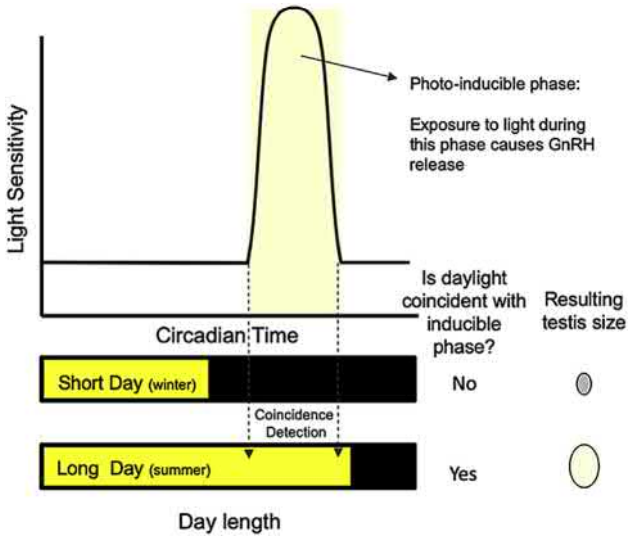

FIGURE 44.2 Illustration of the 24 h circadian cycle of photoinducibility displayed by photoperiodic birds. The reproductive system is responsive to the stimulatory effects of light during a particular phase of the circadian cycle, represented by the peak between about circadian hours 12 and 20 in the top panel. On short days, the light period always ends before this inducible phase begins; hypothalamo-pituitary activity remains minimal and gonads remain small (middle panel). On long days, the light period extends beyond the beginning of the inducible phase; hypothalamo-pituitary activity increases, and the gonads grow (bottom panel). Experiments manipulating the circadian time when short pulses of light (8 h or less) occur demonstrate that it is not light duration, but light exposure relative to circadian time that determines whether the bird activates the reproductive axis (e.g., Hamner, 1963, 1964; Follett et al., 1974).

components of avian photoperiodism—photostimulation and photorefractoriness in response to long days, and dissipation of the refractory state in response to short days—are expressed normally in pinealectomized/enucleated American tree sparrows (*Spizella arborea*; Wilson, 1991). Deep brain photoreceptors are responsible for photodetection regulating seasonality in birds and other nonmammalian vertebrates (Silver et al., 1988, see reviews in Foster et al., 1994; Foster and Soni, 1998). These cerebrospinal fluid (CSF) contacting neurons are thought to reside in the mediobasal hypothalamus (MBH) and/or lateral septum (LS); recent studies increasingly point to the cells in the LS as the key photodetectors in the avian photoneuroendocrine system (Li et al., 2004). Details of how the long day cue is transduced are emerging, although virtually all of the work to date is restricted to Japanese quail (Figure 44.3). In quail, these photoreceptors (Opsin 5-positive CSF-contacting neurons) detect light (Nakane et al., 2014). When light occurs during the inducible phase of the circadian cycle of photoinducibility (Figure 44.2), this long day signal is transmitted to thyroid-stimulating hormone (TSHB)-producing cells in the pars tuberalis (PT). TSH from these cells putatively acts on the nearby ependymal cells lining the third ventricle, inducing transcription of the iodothyronine deiodinase 2 (*Dio2*) gene, and downregulating the iodothyronine deiodinase 3 (*Dio3*) gene. These genes code for Type 2 and Type 3 deiodinase enzymes which regulate the availability of T3 (3,5,3′-triiodothyronine), the physiologically active form of thyroid hormone (Figure 44.3). Under short-day conditions (low-*Dio2* expression, high-*Dio3* expression), T3 is low and glial endfeet appear to ensheath axon terminals of GnRH cells, separating them physically from the basal lamina in the median eminence (ME) and presumably obstructing GnRH secretion into the hypothalamo-hypophysial portal blood. As a result, gonadotropin release from the anterior pituitary remains low under short days. In contrast, under long days, *Dio2* expression in the ependymal cells is enhanced (and *Dio3* expression is reduced). Thus T3 release is high under long days, and this may cause retraction of the glial endfeet sheathes so that GnRH axon terminals are closely apposed to basal lamina and GnRH release is high, leading to high-gonadotropin secretion and gonadal growth (see Ikegami and Yoshimura, 2012 for review). More recent studies have reported the existence of another neuropeptide involved in regulating reproduction (gonadotropin-inhibiting hormone), which inhibits GnRH, and research on its role in seasonal timing is ongoing (reviewed in Tsutsui et al., 2013; Kriegsfeld et al., 2018).

Whether the scenario outlined above applies generally to photoperiodic regulation of avian seasonality or only to Japanese quail exposed to abrupt changes in photoperiod remains unclear. Recent studies using quantitative PCR of whole hypothalamic punches in red-headed buntings (*Emberiza bruniceps*) report results comparable to those found in Japanese quail (Trivedi et al., 2019), with an increase in TSHB and a reciprocal switch in *Dio2* and *Dio3*

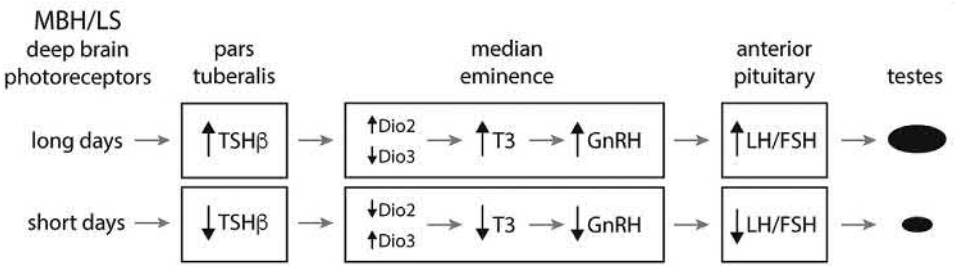

FIGURE 44.3 Illustration of the key components of the photoneuroendocrine system of the Japanese quail (*Coturnix japonica*). Full explanation in text.

expression upon exposure to an LD photoperiod. However, seasonal changes in *Dio2* and GnRH expression in European starlings (*Sturnus vulgaris*) allowed to breed in outdoor aviaries on naturally changing photoperiod are not consistent with the quail-based model (Bentley et al., 2013). Specifically, breeding males with maximal testis volume and GnRH expression did not have significantly higher *Dio2* expression in the MBH than did refractory individuals on declining photoperiod. Further, photosensitive individuals with small gonads on still-declining photoperiod in autumn had higher *Dio2* expression than did photostimulated individuals in spring. It is not known whether the distinct patterns in quail and starlings result from phylogenetic differences, differences in photoperiodic characteristics (starlings becoming absolutely refractory, whereas quail become only relatively refractory-see discussion below), or differences in the experimental conditions used (naturally changing photocycles for starlings, stepwise changes in photoperiod for quail). Regardless of the explanation, it is clear that more work testing the effects of different photoperiod conditions on a wider range of species is needed to identify robust general features of the neural mechanisms underlying photoperiodic regulation of annual schedules in birds (Bentley et al., 2013).

In the last decade, several studies have sought to further refine our understanding of the connection between a circadian cycle of photoinducibility and the decision of the photoneuroendocrine system to increase TSHB within the PT. EYA transcriptional coactivator and phosphatase 3 (EYA3; a molecule in the "eyes absent" family of proteins that may function in transcription activation) is one potential link between photoperiodic time measurement and TSHB expression under preliminary investigation (Nakao et al., 2008; Majumdar et al., 2014; Trivedi et al., 2019). While the exact link is still under study, it is clear that circadian systems and the photoneuroendocrine system are closely connected. Cells within the MBH maintain steady expression profiles of key clock genes under different photoregimes, consistent with the possibility that they are fundamentally responsible for maintaining the temporal phasing of photoinducibility (Yasuo et al., 2003, see also Ikegami and Yoshimura, 2012). These details apply to the process of photostimulation, which leads to development of the reproductive axis as well as preparations for spring migration. However, there may be critical differences in how photic induction of reproduction and migration are controlled as one recent study suggests that photoperiodically induced migratory development can be dissociated from gonadal development under different wavelengths of light (Wang et al., 2013).

At the end of the reproductive season, gonads regress and lose reproductive functionality in seasonal breeders. The transition out of the reproductive state generally depends on the development of photorefractoriness (Nicholls et al., 1988; Hahn et al., 1997; Hahn and MacDougall-Shackleton, 2008). In birds, photorefractoriness is a physiological state in which the reproductive axis is unresponsive to the stimulatory effects of long-day photoperiods (Nicholls et al., 1988). The extent to which different species become refractory is variable. In absolute refractoriness, even stimulation with constant light cannot cause gonads to grow or be maintained, while in relative refractoriness, unseasonably long photoperiods and sometimes stimulatory nonphotoperiodic cues (e.g., food) may cause gonadal maintenance or recrudescence (reviewed in Nicholls et al., 1988; Hahn and MacDougall-Shackleton, 2008).

Expression of absolute photorefractoriness is a two-stage process involving cessation of release of GnRH at the ME followed by a dramatic decline in the presence of the GnRH peptide and reduction in transcription of the GnRH gene (Ubuka et al., 2009; Stevenson and Ball, 2009; Stevenson et al., 2012a; see Stevenson et al., 2012b for review). Return of photosensitivity is associated with reappearance of the GnRH-I peptide first in the preoptic area, and then in the ME in European starlings (Dawson and Goldsmith, 1997); as refractoriness dissipates, birds become progressively more responsive to long days (Hamner, 1968). Species vary in the extent to which steroid feedback during fall and winter helps to keep gonadotropin secretion of photosensitive individuals in check until days increase sufficiently for photostimulation (Cockrem, 1995). Importantly, development of photorefractoriness of the reproductive axis does not necessarily mean that photoperiod is unimportant in the postbreeding season. The decrease in daylength can impact autumnal migration, including in first-year birds: migratory juvenile long-tailed tits exposed to an accelerated decline in photoperiod during their autumn migration increased their diurnal migratory activity relative to those on a normal photoperiod (Bojarinova and Babushkina, 2015). Similarly, daylength appears to influence food-storing behavior outside the breeding season in chickadees and titmice (e.g., Clayton and Cristol, 1996; MacDougall-Shackleton et al., 2003).

44.3.2 Processing of nonphotic cues

Overwhelmingly, research into the effects of nonphotic cues on annual schedules focuses on the initiation and termination of breeding. Here we review that literature, while also calling attention to an important body of work evaluating how nonphotic cues affect molt and migration. Such cues are also sometimes called supplementary and synchronizing cues, to differentiate them from the photoperiodic cues that initiate life history stage transitions (Wingfield 1980, 1985 and see Section 44.3.3). In general, there is much more information on the phenomenology and physiological consequences of nonphotic cues than there is

on the mechanisms by which these cues are processed. We highlight work on the effects of temperature, food, and social information on the annual schedule, which have been investigated in detail. Importantly, these are not the only nonphotic cues that regulate timing decisions; water (Perfito et al., 2006; Wingfield et al., 2012; Prior et al., 2013; Quispe et al., 2018), cues from predators (Monkkonen et al., 2009), and interactions with nesting material (Slater, 1969; Gwinner et al., 1987) also affect the annual cycle.

44.3.2.1 Effects of temperature

In many mid and high-latitude ecosystems, ambient temperature is correlated with local variation in vegetation and food phenology and is a reliable proximate cue that can be used to fine-tune timing of transitions between life cycle stages. Experimental studies in photoperiodic species suggest that while temperature manipulations can have variable effects on gonadal development and initiation of egg laying, high temperatures fairly consistently advance the onset of gonadal regression (reviewed in Chmura et al., 2020) and prebasic molt (Blackmore, 1969; Wingfield et al., 2003; Dawson, 2005). Fewer experimental studies have investigated effects of temperature on the timing of migration, but a growing body of descriptive work using tracking technologies suggests that temperature is important for at least some substages of migration.

The effects of temperature on reproductive development appear to be locally adapted as a function of breeding latitude (Wingfield et al., 1996, 1997, 2003; Silverin et al., 2008, Figure 44.4) elevation (Perfito et al., 2005), and status as a migrant or resident (Meijer et al., 1999; Dawson, 2005). These findings support theoretical predictions that populations inhabiting more predictable environments will be less responsive to supplementary environmental cues than those inhabiting less predictable environments (Wingfield et al., 1992, 1993). Response to temperature cues may be sex-specific. A few studies suggest that the annual schedule of males and females responds differently to temperature cues. High temperature advanced brood patch and follicular development in female Puget Sound white-crowned sparrows, while testis development in males was unaffected (Wingfield et al., 1997). This supports theoretical predictions that female reproductive development will be more responsive to nonphotic cues than male reproductive development (Ball and Ketterson, 2008). Birds appear to be more responsive to temperature increases across the season than to average daily temperature or daily temperature fluctuations (Schaper et al., 2012). It is important to note that different results have been obtained when using different artificial fixed photoperiods (Silverin and Viebke, 1994; Silverin et al., 2008), or using naturally changing photoperiods versus artificially long or short days (Dawson, 2005).

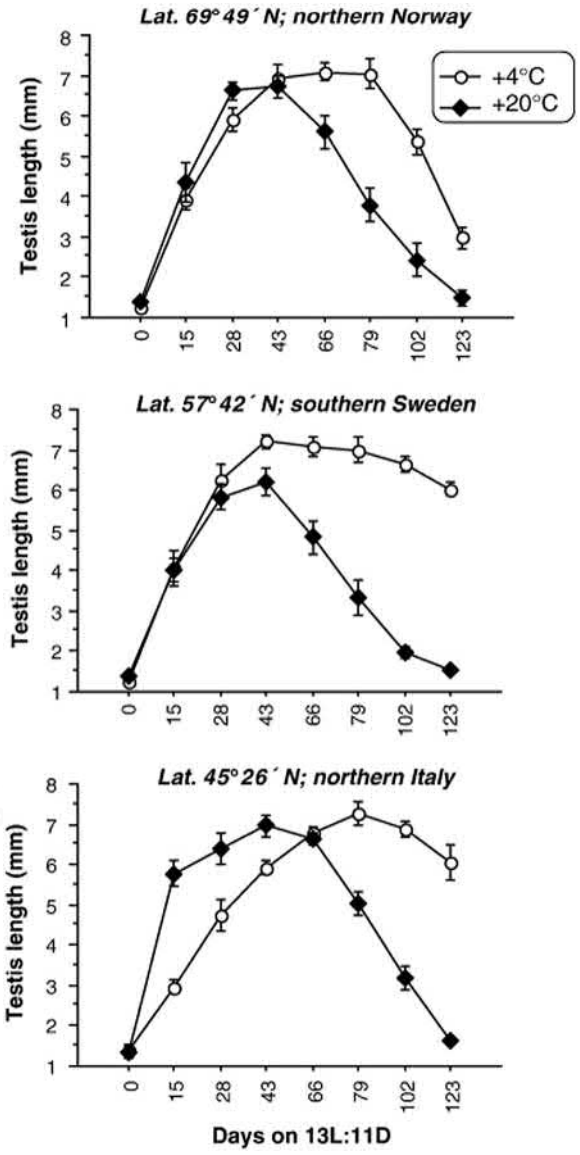

FIGURE 44.4 Effects of different temperature treatments on photoinduced gonadal development in male great tits (*Parus major*) from populations living at three different latitudes. Low temperature delayed termination of reproductive competence in all three populations but only affected rate of gonadal development in the lowest latitude population. *From Silverin et al. (2008).*

Typically, ambient temperature is detected by thermoreceptors in the periphery and while these receptors may detect seasonal changes in temperature, this has not been tested (Caro et al., 2013). Most research on supplementary cues has examined the effect of temperature on the HPG axis and other hormonal mediators associated with reproduction. Only a few studies look at hypothalamic regulators of temperature responsiveness; however, a recent study in

red-headed buntings found that a high-temperature manipulation increased expression of TSHB, *Dio2*, and GnRH in whole hypothalamic punches relative to controls (Trivedi et al., 2019). Findings in circulating hormones, for example, the effect of temperature manipulations on luteinizing hormone (LH) secretion (Wingfield et al., 1996, 1997, 2003; Silverin et al., 2008) and prolactin secretion (Maney et al., 1999; Perfito et al., 2005; Dawson and Sharp, 2010), are inconclusive. Thyroid hormones are also likely candidates for mediating temperature effects (Caro et al., 2013). In one strain of domesticated Japanese quail, the transition to refractoriness appears to require temperature-dependent conversion of T4 to T3 (Wada et al., 1990; Wada, 1993). It would be particularly interesting to explore the temperature dependence of local production of T3 in the MBH of this strain of quail in light of recent discoveries regarding this process in quail photoperiodism (see Section 44.3.1).

Additional studies propose that thyroid hormones, as mediators of metabolism, may play a role in reproductive timing through changes in energy balance. One model proposes that low temperatures, and associated thermoregulatory costs, constrain the resources available to modify aspects of physiology needed for transitions between cycle stages (Meijer et al., 1999). Though this is an intriguing possibility, this hypothesis has not been rigorously tested and the mechanisms by which physiological decisions about energy allocation are made remain largely unknown. Great tits exposed to high and low-temperature treatments did differ in oxygen consumption, but without coincident differences in testis growth rate (Caro and Visser, 2009). This implies no significant energetic constraint of temperature on gonadal growth in males, but an impact of temperature on female reproductive investment may be more relevant given the high-energy cost of yolk deposition. Further, other trade-offs may have buffered the impact in males (e.g., a decrease in immune function). In house sparrows, basal metabolic rate (BMR) and thyroid hormone levels were positively associated, and early breeding birds had an earlier peak in thyroid hormone than late breeding birds (Chastel et al., 2003). Perhaps late breeders face a metabolic constraint that prevents them from breeding early, and thyroid hormones play a role in mediating this relationship (Chastel et al., 2003). Further studies, especially investigations including females who face greater energy demands during follicle maturation, are needed.

A growing body of research indicates that temperature impacts migratory arrival in the north-temperate zone. While timing of departure is thought to be largely influenced by circannual rhythms in concert with stimulatory photoperiods and permissive flight conditions, the progression along the migratory route and arrival at remote breeding grounds is more influenced by local supplementary cues. Timing of arrival of migrant shorebirds at arctic breeding grounds, for example, is tightly correlated with snow-cover, which is in turn closely related to temperature. Ely et al. (2018) argues that temperature is the most likely cue inducing the final stage of migration from the staging grounds. Interestingly, the order of arrival remains species specific even across years that vary in absolute arrival dates—suggesting that different species have different thresholds to supplementary cues like temperature and/or that they may be using different supplementary cues (e.g., interspecific social cues) to fine-tune arrival. Migratory geese similarly use local temperature cues to infer information about the advancement of spring and to make departure decisions from stopover locations while en route (Bauer et al., 2008). Songbirds breeding at north-temperate latitudes also appear responsive to climate and temperature. Many studies have argued that arrival of migrant birds at breeding sites in Europe and North America correlates with large-scale climatic events like North Atlantic Oscillations (Forchhammer et al., 2002; MacMynowski et al., 2007), but a recent meta-analysis casts substantial doubt on that theory and instead argues that finer-scale differences in local weather conditions may be more important for predicting arrival of migrant species (Haest et al., 2018). Indeed, local temperature outperforms large-scale climate cues as the best predictor of arrival in several studies utilizing data from long-term ringing of passerines (Marra et al., 2005; Tøttrup et al., 2010).

Studies of free-living birds, however, are correlational, and it is unclear if these results are due to direct responses to temperature or indirect responses linked to changes in other cues, such as food availability. Experimental studies concerning effects of temperature on development of migratory behavior in captivity are fewer in number and somewhat equivocal in result. Some experimental investigations find that warmer temperatures advance the onset or intensity of nocturnal migratory activity in captive birds (Lewis and Farner, 1973; Nakamura and Kitahara, 1983; Metcalfe et al., 2013) and others that warmer temperatures attenuate migratory behavior and reduce premigratory fattening (Singh et al., 2012; Berchtold et al., 2017). In some of these studies, very high or very low temperatures completely suppress migratory activity (Eyster, 1954; Lewis and Farner, 1973). Thus, temperature appears to be permissive, allowing for fine-tuning of progression along the migratory route following induction by photoperiod and circannual rhythms.

The effects of temperature on the termination of reproduction and onset of prebasic molt are more consistent across species studied to date. Exposure to biologically relevant, warmer temperatures advances gonadal regression

and onset of prebasic molt in multiple studies (Storey and Nicholls, 1982; Wingfield et al., 2003; Dawson, 2005; Visser et al., 2011; Watts et al., 2018). The adjustment of molt timing in response to temperature is probably closely tied to changes in the timing of reproduction. Many field studies document advanced onset of prebasic molt that is coincident with advanced termination of breeding (Dawson, 2005; Barshep et al., 2011; Jukema and Wiersma, 2014). Similarly, delayed onset of molt is associated with delayed termination of reproduction (Barshep et al., 2011; Morrison et al., 2015) and with faster, more intense molt schedules (Morrison et al., 2015). Scheduling of breeding thus influences molt schedules, with later onset leading to more rapid molt schedules as the autumnal migration approaches.

44.3.2.2 Effects of food

The entire photoneuroendocrine timing system in birds has presumably evolved as a consequence of selection for tracking seasonal changes in food supply. However food itself is also a potent supplementary proximate factor (Hahn et al., 2005) that can assist in fine-tuning transitions of the annual schedule to local conditions. Studies of the proximate effects of food on annual schedules include correlative field studies, experimental field studies, and experimental studies with captive birds.

There is some evidence that natural changes in food supply affect migration schedule. For instance, free-living American redstarts (*Setophaga ruticilla*) alter spring departure date across years as a function of variation in rainfall and arthropod abundance (Studds and Marra, 2011). Likewise, redstarts wintering in higher quality (wetter, better food supply) habitats arrive on the breeding grounds earlier than those from lower quality wintering habitat (Marra et al., 1998; Tonra et al., 2011) and experimental reduction of food on wintering territories delays onset of migration (Cooper et al., 2015). Drought in stopover areas has been implicated in dramatic delays in arrival on breeding grounds by trans-Saharan migrants, probably because of reduced refueling rates owing to poor food supplies (Tøttrup et al., 2012). Some experimental evidence also supports the interpretation that food supply can affect timing of migration. Free-living American redstarts that are experimentally "upgraded" from low-quality winter habitat by creating vacancies for them in nearby high-quality habitat show earlier spring migration departure (Studds and Marra, 2005). Likewise, dark-eyed juncos brought temporarily into captivity and subjected to experimental diets (restricted vs. copious) vary in migration departure date (inferred from resighting surveys after release), with individuals displaying higher body condition indices departing earlier (Bridge et al., 2010). Together these data are consistent with the idea that food supply can act as a supplementary cue, influencing details of migration timing under major control by photoperiod and/or an endogenous program perhaps through changes in body condition. The mechanisms whereby food supply and body condition impact decisions are still being worked out. Recent work suggests a role for the hormone ghrelin, which relates to fat stores (a strong predictor of migratory condition) and can enhance migratory restlessness in captive birds when given exogenously (Goymann et al., 2017), but a field study in migratory blackbirds did not find correlations between ghrelin and either fat levels or departure time (Eikenaar et al., 2018b). Corticosterone has also been implicated in departure decisions (Cornelius et al., 2013), and several studies link plasma concentrations to timing of departure (Eikenaar et al., 2017, 2018a, 2020). The migratory behavior of some irruptive species, such as red crossbills, may be tied even more closely to food supply as they appear to cease breeding and initiate long-distance movements in direct response to declines in food supply (Benkman, 1990; Hahn, 1998). Experimental studies with captive crossbills indicate that these birds are very sensitive to changes in food supply, modifying activity, fat deposition, and circulating corticosterone levels in ways consistent with the hypothesis that they use food availability as a cue to regulate timing of migratory movements (Cornelius et al., 2010).

Numerous studies in the field, and a few in captivity, have manipulated aspects of food supply to determine how responsive the reproductive axis is to food as a proximate cue. Food supplementation of free-living birds generally advances timing of egg-laying (Arcese and Smith, 1988; Meijer et al., 1990; Nager and van Noordwijk, 1995; Schoech, 1996; Ruffino et al., 2014). Availability of calories is not all that matters. For instance, in calcium-poor environments, calcium supplementation can significantly advance egg-laying date (Mand et al., 2000). Even in captive birds fed ad libitum, the presence of preferred foods can modulate reproductive physiology (e.g., Furlonger et al., 2012). Some elegant field experiments have provided groups of free-living Florida scrub jays with isocaloric food supplementation that differs in protein content. Although food supplementation with either high protein or low-protein pellets advances egg-laying date compared with unsupplemented controls, the high-protein supplement advances lay date significantly more than the low-protein supplement (Schoech et al., 2004). More recent studies have examined the effects of antioxidants on reproductive timing and gonadal development and report mixed results (Costantini et al., 2016; Carbeck et al., 2018). Meta-analyses of the results of field experiments reveal a latitude effect on responsiveness to food supplementation; high-latitude populations are less responsive to the advancing effects of food supplementation than low-latitude populations (Schoech and Hahn, 2007; Ruffino et al., 2014). However, the

representation of low-latitude populations in both analyses is very small. Further, one study suggests that the apparent latitude effect could be the consequence of whether populations are single or multiple brooded (Dhondt, 2010), although this result was not duplicated in a recent meta-analysis (Ruffino et al., 2014). In any case, these analyses are consistent with the interpretation that populations vary locally in responsiveness to supplementary cues fine-tuning reproductive timing.

Captive studies suggest that the effects of food on reproductive development, in the absence of concomitant photostimulation, are subtle. This is the case even in flexible breeders such as crossbills (Hahn et al., 2005). However, effects of food manipulations in photostimulated birds can be quite dramatic. For instance, pine siskins (*Spinus pinus*) living on modestly stimulatory photoperiod and provided seeds in addition to commercial pellets show dramatically advanced gonadal development compared with those lacking seeds, and this effect occurs irrespective of social environment (Watts and Hahn, 2012, Figure 44.5). In tropical spotted antbirds (*Hylophylax naevioides*), food cues can have dramatic effects on timing of reproductive development (Hau et al., 2000; O'Brien and Hau, 2005), and at least part of this effect appears to be via non-nutritional pathways; exposure to live insect food, even if it cannot be eaten, has a pronounced positive effect on singing behavior (Hau et al., 2000). This is similar to some flexibly breeding temperate zone species, such as pinyon jays, which can show late summer reproductive development if allowed to handle as well as consume seeds from fresh developing pinyon pine cones (Ligon, 1974). However some work in canaries (*Serinus canaria*) indicates that multimodal presentations of food are a more potent stimulus of reproductive development than unimodal presentations of food cues (Voigt et al., 2011). It is important to note that effects of long days on reproductive development could potentially be explained in part by increases in food intake under longer days; however, experimental restriction of time available to feed or amount of food provided to short-day levels reveal only modest effects of food as compared with photoperiod, even in the very flexible crossbills (Dawson, 1986, 2018; Hahn, 1995; Hahn et al., 2005). Davies and Deviche (2014) provide an exhaustive review detailing how hormonal mechanisms may connect food cues to reproductive timing.

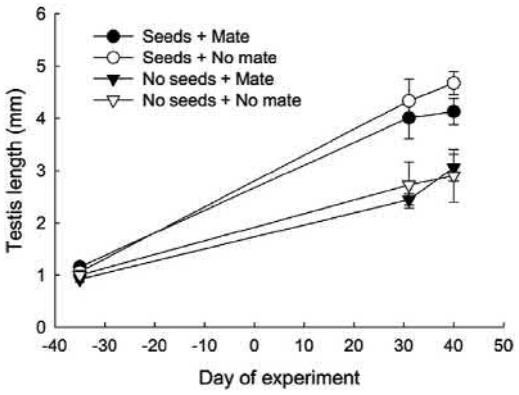

FIGURE 44.5 Effect of provisioning with sunflower and thistle seeds in addition to commercial pellet diet, as compared with pellet diet alone, in pine siskins (*Spinus pinus*). Access to seeds accelerated photoinduced gonadal development comparably whether or not the males were housed with a conspecific female. *From Watts and Hahn (2012).*

It remains important to consider the extent to which effects of food are direct ("income" effects) or operate indirectly through effects on body condition and reserves ("capital" effects; Drent and Daan, 1980; Meijer and Drent, 1999). At least part of the effect of elevated protein on laying date in scrub jays is likely to be through improved condition and protein reserves in females (i.e., may be a capital effect; see Schoech et al., 2004). Capital effects on reproductive output are well-known in large birds (e.g., snow geese; Ankney and MacInnes, 1978), but some of the effects in food supplementation experiments are consistent with nutrient reserves (capital effects) influencing reproductive timing of small passerines (see Arcese and Smith, 1988).

Food availability in north-temperate species may similarly impact molt, either through the rate of individual feather growth (Murphy et al., 1988; Swaddle and Witter, 1997) or through impacts on timing of molt onset or duration (Murphy et al., 1988; Meijer, 1991; Swaddle and Witter, 1997; Freed and Cann, 2012; Class and Moore, 2013; Danner et al., 2015; Faccio et al., 2018). However, the effects of food cues on timing of molt have not received a lot of attention.

44.3.2.3 Effects of behavioral factors

Behavioral interactions between conspecifics can provide valuable information for fine-tuning timing of transitions of physiology, behavior, and morphology, and are essential for coordination of pair, family, and group activities (Wingfield and Marler, 1988). Migration, for example, can occur in groups and many studies have found evidence of social cues permitting the synchronization of migratory timing and route selection among group members (reviewed in Helm et al., 2006). Less research examines the mechanisms by which social cues impact migratory behavior, but social cues about food can impact activity levels, corticosterone levels, and expression of corticosterone receptors in the brain in a facultative migrant (Cornelius et al., 2010, 2018). Perhaps because of the interest in the avian song system, and the use of birds as a model in studies of sexual selection, there is an especially robust body of literature examining the role of social cues

on reproductive scheduling (reviewed in Bentley et al., 2000; Helm et al., 2006; Chmura et al., 2020).

Although there are multiple sensory modalities through which behavioral interactions might influence individual schedules, acoustic stimuli from conspecifics have received the most attention. Male song has potent effects on female reproductive development (see Bentley et al., 2000 for a review), and these effects can be very rapid. For instance, female white-throated sparrows (*Zonotrichia albicollis*) exposed to male song show rapid (within 1 h) elevation of circulating LH and enhanced early growth response protein1 (Egr-1 or ZENK) immediate early gene expression in the mediobasal hypothalamus (Maney et al., 2007a,b). Other studies have investigated the effects of social cues by manipulating the presence of a prospective mate, the mate's reproductive status, visual cues provided by a mate, the presence of a social group, and the status of a mate within a social group, among other factors (reviewed in Chmura et al., 2020). Several of these studies also provide evidence for a rapid effect of social cues on reproductive preparation. Work in European starlings suggests that the presence of a male can affect the expression of *Dio2* and *Dio3* in the hypothalamus of females, which is novel in that it was previously thought that only photoperiod influenced this aspect of the HPG axis (Perfito et al., 2015). Note, however, that social cue manipulation did not affect *Dio2* or *Dio3* after a brief period of social exposure in zebra finches (Ernst and Bentley, 2016). In general, presence of a positive social stimulus enhances reproductive development and onset of laying in females, while more variable results have been reported in males. The few studies that have produced negative social environments, for example, by separating social partners ("divorce studies") (Adkins-Regan and Tomaszycki, 2007; Crino et al., 2017) or creating forced pairings with a nonpreferred partner, report retarded gonadal growth and egg laying (Bluhm et al., 1984).

Two excellent examples of the influence of social factors on annual scheduling come from experimental studies of the transition from reproduction to molt in songbirds. Photostimulated captive male European starlings delay gonadal collapse and onset of molt when housed with females (Schwab and Lott, 1969). Co-habiting with photostimulated females is now known to affect GnRH gene transcription in the septo-infundibular GnRH system of male starlings (Stevenson and Ball, 2009), supporting a centrally mediated signalized mechanism for the delaying effects of females on males' transition out of the breeding state to refractoriness and molt. Likewise, free-living male song sparrows (*Melospiza melodia melodia*) delay gonadal collapse and molt when paired to females whose reproductive competence is experimentally prolonged with exogenous estradiol (Runfeldt and Wingfield, 1985). This effect is unique to males: female song sparrows paired with testosterone-implanted males show no such socially mediated delay of the breeding-molt transition, despite their mates remaining reproductively active, territorial, and delaying molt themselves (Runfeldt and Wingfield, 1985). Prealternate molt is studied infrequently; however, a recent study suggests that auditory social cues may affect the timing of prealternate molt in Gambel's white-crowned sparrows (Chmura et al., 2017).

44.3.3 Integration of multiple cue types: parallel or serial processing?

One fundamental question about how different kinds of cues are processed and integrated relates to whether there is a hierarchy of cues, one or more of which must be stimulatory or at least permissive before others can have their effects (i.e., cues acting in series), or whether different cues can substitute for one another (i.e., cues acting in parallel). As noted above, at least for many species, the general role of endogenous mechanisms combined with seasonal changes in photoperiod take a primary role in a hierarchy of cue processing; days must first be above a certain threshold in length and/or the bird must be at the correct phase of an annual program before other cues can have an influence. This fits well with the general paradigm envisioned by Wingfield (1980, 1985) in which Supplementary Cues and Synchronizing and Integrating Cues serve to fine tune the development of a life cycle stage that has been initiated by Initial Predictive Cues. Few studies permit evaluation of whether this cue hierarchy exists, but female white-crowned sparrows (*Z. l. gambelii*) only show enhanced reproductive development with exposure to male song if they are also photostimulated (Morton et al., 1985). Similarly, high temperature only increases testis growth in photostimulated black-capped chickadees (Martin et al., 2020). It is possible, however, for cues to operate in parallel. That is, the same outcome of initiation of a life cycle stage might be achieved either through stimulation with one type of cue or with another, but both are not necessary, and neither takes hierarchical priority. Red crossbills (*Loxia curvirostra*) provide a possible example of this type of processing. These birds can be in full reproductive condition and breed in the wild on both the shortest and longest days of the year—despite a cessation of breeding in the autumn (Berthold and Gwinner, 1978; Hahn, 1998). In outdoor aviaries, they can come into full breeding condition in January, when days have barely begun to increase in length and when temperatures are low, as long as they have unlimited food and a mate (Hahn, 1995). They also come into near-full breeding condition under long-day stimulation even if they do not have mates (Hahn, 1995). These findings are consistent with the interpretation that long days and some combination of abundant food and mates can essentially substitute for one another in terms of stimulating the reproductive system in some species.

Classic models of serial processing often suggest that photoperiod is the critical initial cue; however, this may not be the case in all species exhibiting serial processing. An experimental study of zebra finches showed that enhanced food alone or in combination with long days could accelerate reproductive development, whereas long days were not stimulatory if food supply was mildly restricted (Perfito et al., 2008). These data are consistent with the interpretation that changes in food may actually act as the initial predictive cues for certain opportunists (Hahn et al., 1997), and any effects of photoperiod may either be permissive or mediated through time available to eat, unlike in many temperate zone photoperiodic species. Recent findings that social cues (Perfito et al., 2015) and temperature (Trivedi et al., 2019) can influence the activity of thyroid hormone pathways known to activate reproduction suggest that there may be some commonalities in how photoperiodic and nonphotoperiodic cues are integrated in the reproductive axis, but much more work remains to be done in this area.

It is unclear whether it is more productive to think of endogenous programs and photoperiod—both considered to be forms of Initial Predictive Cues by Wingfield (1980, 1985)—as interacting in a hierarchical fashion, or simply as complementary components of the annual scheduling process. The phase of the annual cycle (e.g., whether refractory or not) definitely determines the nature of the response to photoperiod, but photoperiodic history also has dramatic effects on whether and when transitions between stages of the annual schedule occur (Gwinner, 1986). However, the fact that annual schedules of many species persist in the absence of clear timing cues from the environment seems consistent with the idea that it may be most appropriate to consider the endogenous component as primary, and the modulatory effects of the environment as secondary, at least for some species.

44.4 Adaptive variation in cue processing mechanisms as it relates to life in different environments

There is abundant evidence of adaptive variation in life cycle scheduling in different environments, and some evidence of adaptive variation in underlying mechanisms. Many studies have examined variation in photoperiodic regulation of reproductive development (Lofts and Murton, 1968; Lambrechts et al., 1996, 1997; Lambrechts and Perret, 2000; Liedvogel et al., 2009; Hahn et al., 2009; Helm, 2009; Caprioli et al., 2012), photorefractoriness (Lofts and Murton, 1968; Nicholls et al., 1988; Hahn and MacDougall-Shackleton, 2008; Hahn et al., 2009), and timing of molt and migratory restlessness (see Gwinner, 1986 for a review).

One of the key distinctions that must be established in order to assess whether adaptive variation exists is whether interpopulation variation in annual schedules is the consequence of evolved differences in endogenous timing mechanisms and responsiveness to environmental cues or simply a result of populations experiencing different environmental conditions. This problem can be addressed in several different ways. Examination of the phylogenetic distribution of reproductive photorefractoriness is consistent with the interpretation that failure to demonstrate refractoriness is a derived trait associated specifically with the most flexible or opportunistic annual schedules (Hahn and MacDougall-Shackleton, 2008). Thus, birds such as crossbills, zebra finches, and some tropical taxa with particularly flexible annual schedules fail to develop absolute photorefractoriness when exposed to extended periods of constant long days. Such taxa wait for input from the environment before making the transition from reproduction to molt and reproductive quiescence. In contrast, most temperate zone seasonal breeders spontaneously enter molt and collapse the reproductive system after some period of reproductive activity, even if the environment provides no direct information about impending deterioration of environmental conditions (Nicholls et al., 1988). Evolutionary loss of absolute photorefractoriness can, then, be interpreted as adaptive specialization in these highly flexible taxa (Hahn and MacDougall-Shackleton, 2008)—although additional information from tropical species, which are largely untested in this regard—could change this framework.

Another way to investigate whether intertaxon variation in schedules represents adaptation to different environments is to look for evidence of a genetic basis for the observed variation. This has been reviewed copiously in the context of avian circannual rhythms by Gwinner (1986); a number of species of migratory songbirds display good evidence of robust differences in timing of diverse elements of their annual schedules (e.g., molt, migratory restlessness, body mass, reproductive condition) that persist in the absence of changing environmental conditions (Gwinner, 1986). In addition, many studies demonstrate persistent interpopulation differences in scheduling under common garden constant conditions, and intermediate phenotypes in F1 hybrids of different populations (see Gwinner, 1986 for a review). Some more recent studies look specifically at heritability (a prerequisite for adaptive change in response to selection) as well as population-level response to artificially applied selection. For instance, variation in timing of onset of autumn migratory activity of blackcaps (*Sylvia atricapilla*) is heritable, and two generations of directional selection for later migration onset led to a 10 day shift in mean date of onset of autumn migratory restlessness (Pulido et al., 2001). Recent selection line studies in great tits have shown that it is possible to select for shifts in

breeding timing (Verhagen et al., 2019). While research into how genetic variation creates variation in seasonal timing (Liedvogel et al., 2009; Saino et al., 2013; Bazzi et al., 2017) is just beginning, results from these common garden studies support the interpretation that at least some populations contain heritable variation in scheduling traits that is responsive to selection.

A recent elegant demonstration of adaptive variation in annual scheduling combined common garden manipulations of photoperiod with studies of hybrids between two subspecies of stonechats (*Saxicola torquata*) that differ in natural annual schedules (Helm et al., 2009, Figure 44.6). European stonechats undergo earlier reproductive development, remain in reproductive condition longer, and show a more protracted postbreeding plumage molt than do Siberian stonechats. In theory, these differences could result from environmental condition-dependent plasticity. However, birds from the two different populations show persistent differences in schedules when held under identical constant photoperiod, and F1 hybrids between the two display intermediate scheduling characteristics. Further, exposure to the subtly different photocycles that the two subspecies experience on their distinct wintering grounds and migratory paths produces different scheduling outcomes in the two subspecies. European stonechats exposed to seasonal photoregimes typical of Siberian stonechats shift onset of reproductive development even earlier than European stonechats on a typical photocycle and retain their prolonged period of reproductive competence and protracted molt. In contrast, Siberian stonechats exposed to the European stonechat seasonal photoregime only slightly advance onset of reproductive development, and retain their brief periods of reproduction and molt (Helm et al., 2009). This study shows that the specific annual schedules of these two subspecies differ due to subspecific variation in mechanism (both in endogenous programming and in the phase-dependent response of the system to environmental inputs) as well as differences in the experienced environment.

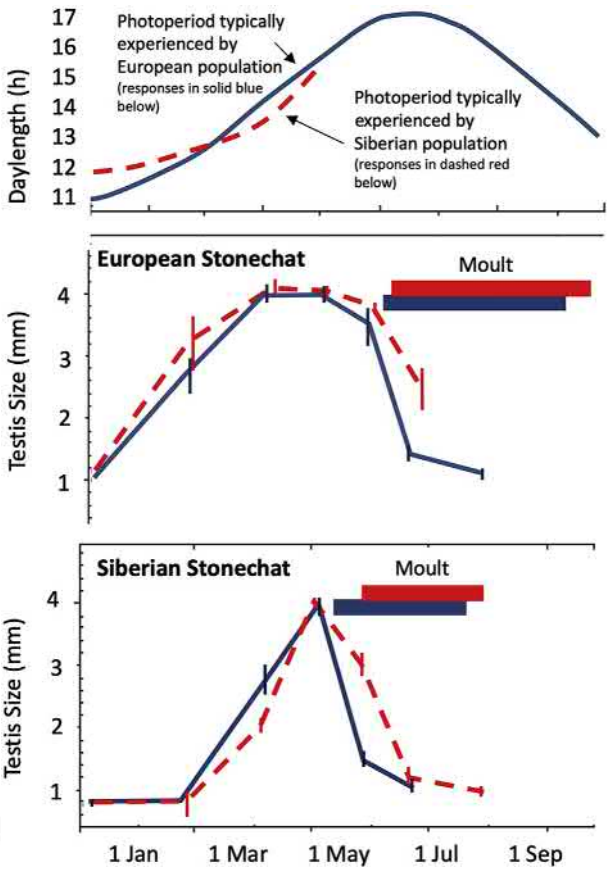

FIGURE 44.6 Comparison of gonadal development and plumage molt from a full factorial experiment conducted in European and Siberian stonechats (*Saxicola torquata*) under two different photoperiodic regimes. The top panel illustrates the daylength conditions used in the experiment: the *dashed red line* indicates the photocycle experienced by free-living birds in the Siberian population and the *solid blue line* represents the photocycle typically experienced by free-living birds from the European population. The middle panel illustrates the gonadal development (*red dashed and blue solid lines*) and molt progression (*red and blue solid bars*) of European stonechats under the two photoregimes. The bottom panel depicts the gonadal development and molt progression of Siberian stonechats under the two treatments. A detailed description of this study can be found in text. *Modified from Helm et al. (2009).*

44.5 Integrated coordination of stages and carryover effects

As noted above, stages of the annual cycle do not exist as separate entities but are intricately linked with the stages preceding and following them. Transitions between stages involve termination of one stage and development of the next (Wingfield, 2008), each of which requires mechanistic control. This may involve one mechanism controlling both termination of one stage and development of the next, or separate mechanisms. This first scenario could ensure that stages follow in the correct sequence throughout the year. For instance, in the transition from breeding to prebasic molt, the inactivation of the HPG axis as photorefractoriness develops leads to a precipitous decline in circulating sex steroids. This decline results in regression of secondary sex characteristics (e.g., cloacal protuberance, beak color, and brood patch) and declines in song and courtship as well as facilitating the final stages of parental care in males (Nicholls et al., 1988; Hahn et al., 1997; Hahn and MacDougall-Shackleton, 2008). Since sex steroids inhibit molt, the decline in their levels allows molt to proceed (Schleussner et al., 1985; Nolan et al., 1992; Dawson, 1994, 2004). However, stages occurring in the correct sequence could also result from two separate

mechanisms controlling termination and development phases of adjacent stages. This is possible if one mechanism provides a trigger for the next. As with the breeding-molt transition example above, while photorefractoriness and the resulting decline in sex steroids is important for terminating breeding and the onset of molt, other physiological changes are occurring. Changes in prolactin and thyroid hormones have long been thought to be necessary for molt, but whether these are simply correlated events or play causal roles remains unresolved (Mishra et al., 2004; Dawson, 2006,2008).

How transitions between stages are coordinated—e.g., whether stages overlap or remain distinct—has important consequences. One major source of these consequences is a phenomenon called **carry-over effects**, which occur when processes or conditions in one stage affect timing or performance in subsequent stages (Norris and Marra, 2007; Harrison et al., 2011). Most studies of carry-over effects examine individuals, but population-level consequences also may occur (Norris and Marra, 2007; McKellar et al., 2013). At the individual level, carry-over effects often result from the constraint that transitional stage overlap can place on energy or resource allocation. For example, many physiological changes take place during the transition between migration and breeding, including changes in musculature, nutrient and energy reserves, fat deposition, organ size and functioning associated with gonadal development and migration termination, as well as hormone and yolk precursor level changes (e.g., Arizmendi-Mejía et al., 2013). Female Macaroni penguins (*Eudyptes chrysolophus*) initiate vitellogenesis (yolk production) while they are still at sea migrating to the breeding territory (Crossin et al., 2010). With greater overlap of breeding preparation during migration, Macaroni penguins are able to start laying eggs sooner upon arrival. However, simultaneous expression of these functions constrains the rate of egg formation, as evidenced by lower vitellogenin (VTG) levels, and therefore lower reproductive readiness, upon arrival in late-arriving females.

Similarly, the transition from migration to breeding stages in female black-browed albatrosses (*Thalassarche melanophrys*) involves a carry-over effect on the breeding stage as a result of processes occurring during migration. Postmigratory condition (weight and hematocrit) and reproductive readiness [progesterone (P4), testosterone (T), and VTG levels] were lower in females that ended up deferring breeding compared with those who did lay eggs. This suggests a resource or condition-based allocation trade-off underlying this carry-over effect in which returning females in better condition (i.e., those that cope more effectively with the metabolic demands of migration) are more likely to initiate breeding. Furthermore, of the birds that attempted breeding, success was associated with low T and high-VTG levels, compared with failed breeders whose eggs did not hatch. This finding suggests another possible mechanism underlying carry-over effects: conflicting physiological processes. The differences in T and VTG levels between successful and failed breeders indicates a potential difference in the levels of aromatization from T to estradiol (E2), a necessary step in the process of vitellogensis (E2 stimulates vitellogenesis in the liver). The inhibition of aromatization, possibly by a stress-related mechanism (Dickens et al., 2011, 2013), may be influencing the migration-breeding transition and its resulting carry-over effects.

Reproductive decisions and outcomes are influenced by processes occurring during the migration stage that immediately precedes reproduction. However, processes even earlier, such as during the wintering stage, can have carry-over effects on migration and breeding (Marra et al., 1998; Norris et al., 2004; Studds and Marra, 2005; Reudink et al., 2009; McKellar et al., 2013). For example, American redstarts wintering in low quality, drier scrub habitats are in poorer body condition and have higher corticosterone levels than those in wetter habitats (Marra et al., 1998). Both males and females wintering in drier areas, as well as those in poorer physical condition in general, tend to depart for migration later (Marra et al., 1998). This effect was shown experimentally in two studies. Birds that were upgraded from low to high-quality winter habitats had higher body mass and departed earlier than controls (Studds and Marra, 2005) and experimental reduction of food on territories delayed migratory departure by one week (Cooper et al., 2015). High-quality wintering grounds translate into earlier arrival on breeding grounds and higher reproductive success (Norris et al., 2004; Reudink et al., 2009). Males arriving earlier from better wintering grounds sired more offspring, both within-pair and extra-pair, and had greater fledging success (Norris et al., 2004; Reudink et al., 2009). Male redstarts are predicted to decrease their chances of successful reproduction by as much as 11% with every day migration is delayed (Tonra et al., 2011). Early arriving females started laying and fledging young earlier; high-quality winter habitat predicted production of at least two more young than poor quality wintering grounds (Norris et al., 2004). These findings are complemented by similar results in other species (see above Section 44.3.2.2 on food supplementation and Arcese and Smith, 1988; Meijer et al., 1988; Schoech, 1996).

Carry-over effects such as these often are presumed to result from resource allocation trade-offs. However, studies documenting such tradeoffs often lack direct evidence to support this underlying mechanism (Harrison et al., 2011). An exception is work in Cassin's auklets (*Ptychoramphus*

aleuticus), which indicates a resource allocation trade-off, based on quality of prebreeding diet, influences laying date (Sorensen et al., 2009). Female auklets that consumed more energy-rich copepods during the period prior to breeding began laying earlier and laid larger eggs than those that consumed more energy-poor juvenile rockfish (Sorensen et al., 2009). While studies like these help to illuminate the potential mechanisms responsible for carry-over effects (and also provide additional examples of responses of annual schedule timing to food cues), much more research is needed (Norris and Marra, 2007; Harrison et al., 2011). Most studies involve observational field work, but experimental manipulations are necessary to learn more about the physiological mechanisms (Harrison et al., 2011).

Breeding can also have carry-over effects on subsequent stages. For example, late breeding can lead to delayed molt or increased overlap of breeding with prebasic molt (Morton and Morton, 1990; Sanz, 1999; Stutchbury et al., 2011). As tracking technology has improved, many new studies are investigating carry-over effects across the whole annual cycle, sometimes across multiple years. Late reproduction in savannah sparrows (*Passerculus sandwichensis*) (Mitchell et al., 2012) and delayed molt in wood thrushes (*Hylocichla mustelina*) (Stutchbury et al., 2011) can carry-over to result in later migratory departure. The extent to which these differences persist across fall migration and into arrival on the nonbreeding grounds may vary. Late departing wood thrushes did not arrive late to wintering grounds (Stutchbury et al., 2011). In contrast, Hudsonian godwits (*Limosa haemastica*) that departed late from the breeding grounds arrived late to stopover sites along their southbound migration and the wintering grounds, but this effect did not carry-over to affect timing of northbound migration in the spring (Senner et al., 2014). A study of tree swallows investigating annual scheduling in multiple populations across the species' range suggests that while timing of breeding influences timing of fall migration and arrival on the wintering grounds, the timing of departure from the wintering grounds is not influenced by timing during the preceding life cycle stages (Gow et al., 2019).

A similar pattern of "resetting" the annual cycle of activities has been found in a few experiments studying carry-over effects in free-living populations. Clutch manipulation studies in pied flycatchers suggest that birds with larger clutches delayed fall migration and had a shorter overwintering period, but did not delay the subsequent spring migration (Briedis et al., 2018). A similar pattern of carry-over effects was seen in Manx shearwater (*Puffinus puffinus*) with experimentally extended periods of parental care (Fayet et al., 2016, Figure 44.7). However clutch removal in Cory's shearwaters (*Calonectris diomedea*) led not only to earlier fall migration, but also earlier spring migration the following year (Catry et al., 2013). (Note this species does not renest).

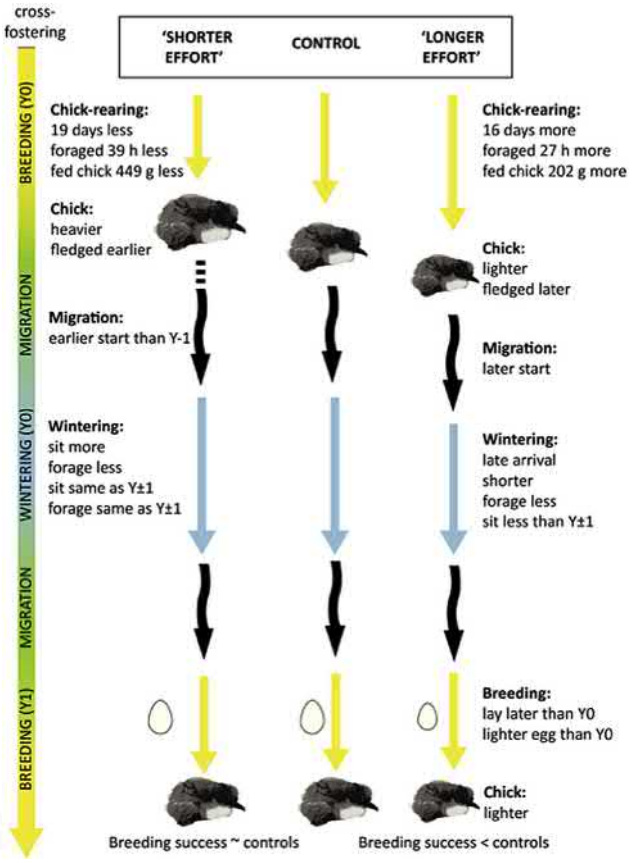

FIGURE 44.7 Infographic of results from a study investigating carry-over effects in Manx shearwater (*Puffinus puffinus*) using an experimental clutch manipulation. Cross-fostering nestlings extended or reduced the length of parental care by about 25% in manipulated nests compared to controls. *From Fayet et al. (2016).*

44.6 Variation in scheduling mechanisms and responses to rapid environmental change

Changes in phenology, or the timing of key events in the annual cycle, are one of the most commonly documented responses to climate change in both birds and other taxonomic groups (Crick et al., 1997; Parmesan, 2007; Usui et al., 2017). This has led to a plethora of studies seeking to document shifts in phenological timing with global climate change in diverse avian taxa and a smaller but strong body of recent literature examining different timing mechanisms that could affect the ability of birds to respond to climate change either through phenotypic plasticity or evolutionary change.

There are several proximate causal mechanisms that are hypothesized to influence the capacity of animals to adjust seasonal timing with climate change using existing phenotypic plasticity—either in the form of developmental plasticity or plasticity in adulthood, hereafter referred to as

flexibility (Piersma and Drent, 2003). Many studies hypothesize that because photoperiod is not shifting with climate change, birds that rely heavily on photoperiod or an endogenous rhythm to time seasonal transitions may be constrained in their ability to adjust (Both and Visser, 2001). Accordingly, flexible responses to nonphotic cues (such as temperature or food availability) that closely track climatic change are expected to facilitate adjustment of the annual cycle (Charmantier et al., 2008). Even in cases where birds have the capacity to respond to nonphotic cues, the inherent time-lag between physiological preparation for a stage and initiation of that stage complicates predictions about how birds will respond to climate change. Research suggests that climate change is heterogeneous across the year (Easterling et al., 1997), so for phenotypic plasticity and/or flexibility to provide effective routes by which birds can adjust seasonal timing, nonphotic cues must change similarly across an annual cycle stage. Similarly, spatial variation in climate change can complicate the responses of migratory birds. If climate change is not experienced similarly on breeding and wintering grounds, as well as along the migratory route, plastic changes occurring in one stage may not be adaptive for the environment that birds encounter during the next phase of the annual schedule (Knudsen et al., 2011).

The importance of studies integrating multiple annual cycle stages to accurately assess the response of birds to climate change is made clear by pioneering work by Both and Visser (2001) whose studies in pied flycatchers suggest that adjustment of breeding timing with climate change was constrained by the absence of a change in spring migratory timing (Ouwehand and Both, 2017). As our discussion on nonphotic cues illustrates, different stages may show different kinds of responses to photic and nonphotic cues. Indeed another recent analysis of long-term phenology data from pied flycatchers suggests that molt has shifted more than breeding, and that spring migratory arrival has not changed at all (Tomotani et al., 2018). Researchers attribute these differences to different responses to temperature. On nonevolutionary time-scales, asymmetric phenological shifts across the annual cycle may limit the ability of birds, particularly migrants, to respond to climate change. Hatching environment could have a developmental influence on the timing of subsequent spring migration, and this could be a transgenerational developmental mechanism by which shifts in reproductive timing with climate change could also influence timing of migration and mitigate other mechanistic constraints on migration timing (Gill et al., 2014). However, experimental hatch delays in pied flycatchers do not reliably lead to changes in spring migration and reproduction, casting doubt on this hypothesis in at least one species (Ouwehand et al., 2017).

Timing adjustments to the annual cycle, or lack thereof, with climate change become especially important when they influence individual survival and offspring recruitment into the breeding population. One of the primary ways in which phenological shifts may influence recruitment is via trophic mismatch, a hypothesis that proposes that if birds shift phenology at a different rate than the primary food source for young, young may have insufficient resources to survive and recruit into the breeding population. This may be especially likely when the two interacting trophic levels rely upon different cues to time life history stages. Over 23 years of spring temperature increase in the Netherlands, great tit egg-laying dates did not shift as much as the peak in abundance of caterpillars that they use to provision young (Visser et al., 1998). The extent to which this is the case for many or most avian species is under study (Knudsen et al., 2011), and some studies suggest that trophic mismatch is not occurring in other systems (Dunn et al., 2011; Dunn and Møller, 2014). For example, different degrees of dietary specialization may affect whether a system is likely to be affected by trophic mismatch, and different environments may exhibit different seasonal patterns in resource abundance. Additionally, most avian species must contend not only with seasonal fluctuations in resource availability, but also with fluctuations of predator abundance. While most climate change studies assume trophic match is the evolutionary default and that trophic mismatch is necessarily maladaptive, some researchers assert that mismatch may actually be advantageous in some predator-prey environments (Visser et al., 2012). Thus, a sufficiently long time series of data is important to assess the impact of trophic mismatch on birds. This is made especially clear by recent work suggesting that changes in trophic level asynchrony in 21 species of British birds over the past 30 years did not explain long-term population declines (Franks et al., 2018) despite the finding that species that had shifted their arrival earlier in Britain had more positive population growth (see also Newson et al., 2016). Clearly, this will remain an active area of research in coming years.

Seasonal timing in birds may evolve in response to climate change. However, there is strong support for evolutionary adjustments in only a few systems; this is likely due in part to the challenges associated with gathering the evidence that is required to demonstrate an evolutionary response to climate change (Charmantier and Gienapp, 2014). Nussey et al. (2005) report evidence that climate change is causing increased selection for flexibility in breeding timing in a population of great tits. Similarly, a common garden experiment in pied flycatchers conducted first in 1981 and repeated 21 years later, finds that breeding timing had advanced by nine days, which researchers

propose is evidence for evolutionary change in the endogenous circannual clock (Helm et al., 2019).

As we come to understand the mechanisms by which species are altering the annual schedule of behaviors with climate change and the implications this has for local populations, we will better be able to predict how avian populations will respond to ongoing climate change.

44.7 Effects of seasonality on constitutive processes

Although annual schedules often consist of several distinct life cycle stages, birds also adjust investment in processes that span multiple stages. These processes may be maintained during every stage, yet the appropriate level of investment may vary as a function of resource availability, environmental conditions, individual age or condition, and so forth. In this section, we will briefly discuss how birds vary investment in immune function, responses to stressors, and metabolism seasonally.

44.7.1 Seasonal modulation of immune function

Across the annual cycle, dynamic environments expose organisms to extensive seasonal variation in weather, resource availability, and disease potential (King, 1974). Natural selection dictates that longer-lived organisms, such as birds, should time costly energetic processes to maximize fitness by balancing seasonal allocation to both reproduction and survival-related processes such as immune function. Immune function contributes to survival by detecting pathogens and limiting infection, but because maintenance of immunity can be costly (e.g., Sheldon and Verhulst, 1996; Schmid-Hempel and Ebert, 2003; Klasing, 2004; Nelson, 2004), especially if immune activation is overused (Lochmiller and Deerenberg, 2000) or not sufficient to clear an infection (Nelson et al., 2002), investment in immunity is often variable (Martin et al., 2008). Many environmental and physiological variables can play a proximate role in regulating these changes in investment patterns in immunity (Nelson, 2004; Martin et al., 2008; Buehler et al., 2008a,b). Examples of these contributing environmental factors include endogenous and/or photoperiodically regulated annual cycles, changes in disease threat or parasite pressure, food availability, and weather and temperature conditions (Nelson and Demas, 1996; Nelson et al., 2002; Hasselquist, 2007; Martin et al., 2008; Adelman et al., 2013). Other factors that contribute to changes in immune function include competing physiological processes such as reproduction (Sheldon and Verhulst, 1996; Lochmiller and Deerenberg, 2000) and other survival-related processes such as plumage molt (Buehler et al., 2008b; Moreno-Rueda, 2010) growth (Prendergast et al., 2004) or migration (Nebel et al., 2012, 2013).

While studies on seasonality of immune function have been conducted in mammals, particularly small rodents (Demas and Nelson, 1998; Bilbo and Nelson, 2004; Zysling et al., 2009), the literature on seasonality in avian immunity has been growing rapidly over the last decade. Most published studies focus on single components of the annual cycle, such as breeding compared to nonbreeding, or breeding compared to molting (reviewed in Martin et al., 2008). This review will focus on studies that have been sampled more holistically across the annual cycle. Most research on seasonality in immunity has been conducted in captivity and these studies report variable findings: some have shown that cellular immunity is higher during the winter months while others report no difference across sampled timepoints (Lee, 2006; Martin et al., 2008). In a study of red knot (*Calidris canutus*) immunity sampled over the annual cycle (Buehler et al., 2008b), both higher energetic cost phagocyte-based (cellular) immunity and lower-cost lymphocyte-based (antibody) immunity were higher during periods of mass change (i.e., during fattening and spring migration in wild birds), but there was a clear shift toward lower-cost lymphocyte-based immunity during peak molt. Due to the high costs associated with synthesizing feathers (Haake and Sawyer, 1986), it is preferable for birds to use a lower cost, less phagocytic-based immune strategy, during molt. A recent study showed that lipopolysacharide (LPS which induces a "sickness response") injected house sparrows grew lower quality feathers than control birds, which supports the idea that investment in molt and immunity may trade-off against each other (Ben-Hamo et al., 2017). In a subsequent experiment in red knots using low, high, and variable temperatures, there was little effect of temperature on annual variation in immune function (Buehler et al., 2009), perhaps due to the presence of ad libitum food. However, when food levels were restricted without temperature manipulation in a follow-up experiment, no change in constitutive immunity (natural antibody and complement levels) was observed, although food restriction did diminish investment in the acute phase or induced immune response that is substantially more energetically demanding (Buehler et al., 2009). A study in red crossbills found that long days increased white blood cell counts and bacterial killing ability but did not find an effect of food restriction on constitutive immunity (Schultz et al., 2017). Conversely, a captive study of white-crowned sparrows found that seasonal changes in the acute phase response were not driven by photoperiod per se, but seemed to be associated with sex and changes in body condition (Owen-Ashley et al., 2006).

Because captivity can reduce both inflammatory and phagocytic (cellular)-based immunity (either by reducing

the pathogen pressures or due to the increased stress associated with being held in captivity; Buehler et al., 2008a), it is important to study immunity both in the wild and captivity, however few studies do so (Adelman et al., 2013). In free-living birds, few studies have looked at multiple immune indices over several components of the entire annual cycle. One study on nonmigratory great tits (*Parus major*) (Pap et al., 2010) found significant seasonal changes in immunity. Specifically, total immunoglobulin and heterophil levels were highest during the summer breeding months and continued to increase until September when the birds began molting and then decreased until the following spring. Lymphocyte levels, however, were higher in the winter than in the summer. Some immune parameters can vary quite rapidly during a season; song sparrows shift from innate defenses immediately following spring migration to acquired defenses with increasing time at the breeding grounds (Kelly et al., 2017). Few published studies to date look at multiple immune indices over several years in free-living birds. In skylarks (*Alauda arvensis*), metrics of constitutive innate immunity (complement, natural antibody, and haptoglobin levels) varied interannually but were consistently lower during fall migration than during the breeding season (Hegemann et al., 2012). However in purple-crowned fairy wrens (*Malurus coronatus coronatus*), researchers found no differences in immune parameters (haptoglobin, complement, natural antibodies, heterophil:lymphocyte ratio) between wet and dry seasons (Roast et al., 2019). The effects of precipitation on immune measures is variable across studies: precipitation and ambient temp do not predict haptoglobin, complement, or natural antibodies in red-capped larks (*Calandrella cinerea*) (Ndithia et al., 2017) but led to higher microbial killing ability in neotropical house wrens (*Troglodytes aedon*) (Tieleman et al., 2019) and lower haptoglobin, ovotransferrin, complement, and natural antibodies in common bulbuls (*Pycnonotus barbatus*) (Nwaogu et al., 2019).

Migration is an important and energetically demanding component of a bird's life history (Wikelski et al., 2003). Thus, energetic trade-offs with immune function often occur, as has been documented in several studies. For example, studies in thrushes (Owen and Moore, 2008) and Bewick's swans (*Cygnus bewickii*) (Gills et al., 2007) found that migratory activity can be immunosuppressive. Similarly, a field study of six migratory species found that long-distance migrants had a lower measure of complement immunity than short-distance migrants and the authors suggest that long-distance migrants may suppress immunity in favor of preserving energy for migration (Hegemann et al., 2018). Another recent study reports that microbial killing ability and haptoglobin levels are lower in migrant common blackbirds than residents (Eikenaar and Hegemann, 2016). Correlations between individual variation in migration distance (and stopover duration) and immune function have yielded mixed results (Kelly et al., 2016, 2017; Hegemann et al., 2018).

Correlational field studies are limited in testing whether immune function and migration trade-off because flight can affect immune function and infection can affect migratory flight. Two recent studies using a flight chamber found that simulated migration depresses several aspects of immunity. The first study on European Starlings (*Sturnus vulgaris*) found that three of four immune measures (haptoglobin, natural antibody, and complement levels) decreased after the birds were placed in the wind tunnel for 1−4 h of continuous flight (Nebel et al., 2012). Another related study on long-distance migrant western sandpipers (*Calidris mauri*) found that flight performance (flight duration of 3 h) was not diminished by a previous immune challenge of LPS, but flight while mounting a sickness response negatively affected other aspects of immune function including bacterial killing ability and natural antibody levels (Nebel et al., 2013). In addition to experimental flights affecting immune function, experimental infection with avian malaria has effects on migratory preparation and migratory restlessness (Kelly et al., 2018, 2020).

Mechanistically, these effects have been attributed to changes in seasonal hormone profiles, such as glucocorticoids (GCs), androgens, and estrogens (reviewed in Martin et al., 2008). These hormones, which can affect timing of territory establishment, reproduction, parental care, and molt, can also affect immune function (reviewed in Martin et al., 2008; Koustos and Klasing, 2013). For example, both GCs and androgens can depress immunity, but their effect on the immune system is highly dependent on the overall level and duration of increase, as well as what immune component is measured (reviewed in Koustos and Klasing, 2013). In general, acute stress or quick elevations of GCs increase levels of immunity, while chronic or persisting levels of stress dampen immune responses. For testosterone and other androgens, it is difficult to disentangle the direct effects from the indirect effects of GCs, i.e., elevated levels of testosterone may depress immunity by elevating levels of GCs (Koustos and Klasing, 2013).

As the field of avian ecoimmunology continues to grow, scientists can test hypotheses about how diversity in annual schedules is related to diversity in immune investment. A recent review proposes that seasonal variation in microbial risk varies as a function of a bird's annual schedule of activities and the environments that it encounters over the course of the year (Evans et al., 2017). Specifically authors propose that resident tropical species will exhibit a relatively high and constant investment in immune defenses year-round, while migrants and seasonal breeders will vary investment over the year (Evans et al., 2017). While data are currently insufficient to test these expectations, this is a promising area for continued work.

44.7.2 Seasonal modulation of responses to stressors

As covered in Chapter 38, birds have multiple ways to cope with environmental stressors. Here, we will focus on seasonal variation in activity along the hypothalamic–pituitary–adrenal (HPA) axis in response to stress, as it is well represented in the literature. Most studies of vertebrates, including birds, find that at least one of the two sexes shows seasonal variation in GC secretion (Romero, 2002; Romero et al., 2017 but see González-Gómez et al., 2013; Deviche et al., 2014). Seasonal variation is seen both in baseline GC secretion (i.e., samples uninfluenced by the stress induced by handling and sampling) as well as "stress-induced" GC levels (i.e., those taken after an animal experiences a standardized stressor such as handling and restraint, thought to indicate the response the HPA axis may mount in response to a natural stressor). While seasonal variation in GC secretion is a common finding, elements of seasonal variation in GC secretion can vary even among closely related species. However, in birds, most studies find that both baseline and stress-induced levels of GCs are depressed during molt (Romero, 2002), any studies find that GCs are elevated during breeding (Romero, 2002) although there is an ongoing discussion in the field as to exactly how GCs are regulated on fine temporal scales within the breeding period [e.g., between territorial establishment, egg-lay, incubation, and onset of parental care (Krause et al., 2016)].

While total circulating GC levels are studied commonly, a growing body of literature suggests that other points along the HPA axis may be regulated seasonally. A collection of studies in house sparrows indicates that there is seasonal variation in corticosteroid-binding globulins in plasma (Breuner and Orchinik, 2001) as well as seasonal variation in mineralocorticoid (MR) and glucocorticoid (GR) receptor distribution, which differ by tissue type (skin and spleen Lattin et al., 2013, brain and gonads Lattin and Romero, 2013, metabolic tissues Lattin and Romero, 2015).

There are numerous hypotheses as to why HPA activity should be modulated seasonally (Harris, 2020). Many of these hypotheses focus on the unique demands created by reproduction and the needs of parents to balance their own survival against successfully raising young. For example, the Parental Care Hypothesis (Wingfield et al., 1995) proposes that parents suppress stress-induced GC levels during periods of offspring dependence to facilitate parental care and minimize the risk of abandoning a nest. A study of an opportunistic breeder has found that reproductive suppression of the HPA axis can itself vary across seasons, with greater suppression occurring in harsher conditions (Cornelius et al., 2011). Other hypotheses focus broadly on seasonal changes in energetic demands caused by both internal processes and factors in the surrounding environment. The Energy Mobilization Hypothesis (Romero, 2002) proposes that since GCs are involved in energy mobilization, they should be highest at the most energetically demanding time of year. A related hypothesis, the Preparative Hypothesis, suggests that GC levels are modulated in anticipation of adverse changes in environmental conditions (Sapolsky et al., 2000; Romero, 2002). Given the interconnectedness of the HPA axis with many physiological systems, it seems likely that there is not a single universal explanation for temporal changes in HPA activity and that multiple mechanisms may be at play within and across avian taxa.

44.7.3 Seasonal modulation of metabolic machinery

Birds must meet daily energy demand to survive and reproduce in dynamic and seasonal environments, but there may also be costs to maintaining expensive metabolic machinery. Although the underlying mechanisms are incompletely understood, phenotypic flexibility in various metabolic traits has been documented in a wide variety of temperate and tropical species (Swanson, 2010; Pollock et al., 2019). Seasonal variation in metabolic traits is thought to largely reflect variability in energy demand of different stages and variability in environmental conditions. For example, the high cost associated with breeding or migration may be partially offset by the more benign conditions in which those events typically occur (Masman et al., 1986). Indeed, while some studies have found that birds may have similar daily energy costs during summer breeding as when overwintering, others have found that birds in the temperate zone may have much higher costs in winter—and particularly smaller birds that have lower thermal inertia (reviewed in Swanson, 2010; McKechnie et al., 2015). This may hold true even for those wintering in relatively benign locations (Weathers et al., 1999), although the seasonal changes in metabolic traits in the tropics are much more variable in direction and confer some uncertainty on how the environment and organism are interacting to influence metabolic capacity (McKechnie et al., 2015).

The Climatic Variability Hypothesis predicts that the larger the variation in temperature in a species range the more seasonally flexible metabolic traits will be (Bozinovic et al., 2011). These traits include BMR, breadth of the thermoneutral zone, and peak metabolic performance—as measured by either maximum thermogenic capacity during cold challenge (M_{sum}) or by the maximum metabolic rate (MMR) achieved during intensive exercise. Alternatively, the Cold Adaptation Hypothesis predicts the minimum temperature experienced within a species range drives the evolution of peak thermogenic rates and metabolic flexibility (Swanson and Garland, 2009). Although metabolic traits like BMR and M_{sum} can change in similar directions and degree across seasons, they may also be somewhat independent of each other: BMR is thought to reflect nonskeletal organ structure and function whereas M_{sum} and MMR are thought to reflect changes in skeletal muscle structure and function (i.e., through shivering

thermogenesis and muscle performance, respectively) (Petit et al., 2013; Dubois et al., 2016; Barceló et al., 2017). Indeed, BMR and M_{sum} do not always agree with respect to tests of the Climatic Variability and Cold Adaptation Hypotheses. Whereas variability in M_{sum} correlates with temperature variability in and across many species (Swanson and Garland, 2009; McKechnie et al., 2015)—thus supporting the Climatic Variability Hypothesis—BMR does not (McKechnie et al., 2015). Similarly, while M_{sum} predicts the minimum temperature exposure in a comparison of 40 bird species—thus supporting the Cold Adaptation Hypothesis—BMR does not (Stager et al., 2016). Therefore, flexibility in M_{sum} is thought to be the main way that metabolic scope might be increased (Swanson, 2010; Stager et al., 2016) in turn allowing birds the ability to cope with a wider array of environmental conditions (Piersma and Drent, 2003).

Metabolic traits can change in direct response to immediate energy demand, such as occurs when birds are exposed to cold winter temperatures (Swanson and Olmstead, 1999; Swanson and Vézina, 2015), or in response to photoperiodic or endogenous circannual cues in preparation for winter (Petit et al., 2013). Other local, supplementary cues that impact thermogenesis such as rainfall can also impact metabolic traits (Maldonado et al., 2012). Therefore, species may incorporate metabolic restructuring into their annual schedule in the autumn or early winter, but also show significant flexibility in response to local conditions that allow for adjustment to changing conditions. The preparative processes in anticipation of winter are not well described, but the high-energy costs observed during the autumn molt may in part be due to such processes—particularly given that feather growth cannot account for a large portion of the costs (Buttemer et al., 2019). More research concerning the timing and mechanistic processes underlying seasonal metabolic restructuring (Laplante et al., 2019; Vézina et al., 2019) would contribute important information to the understanding of annual schedules in birds, particularly as it relates to constraints or trade-offs with other processes or annual cycle stages.

References

Adelman, J.S., Ardia, D.R., Schat, K.A., 2013. Chapter 22. Ecoimmunology. In: Avian Immunology. Elsevier Ltd., pp. 1–23

Adkins-Regan, E., Tomaszycki, M., 2007. Monogamy on the fast track. Biol. Lett. 3, 617–619.

Ankney, C.D., MacInnes, C.D., 1978. Nutrient reserves and reproductive performance of female lesser snow geese. Auk 95, 459–471.

Arcese, P., Smith, J.N.M., 1988. Effects of population density and supplemental food on reproduction in song sparrows. J. Anim. Ecol. 57, 119–136.

Arizmendi-Mejía, R., Militão, T., Viscor, G., González-Solís, J., 2013. Pre-breeding ecophysiology of a long-distance migratory seabird. J. Exp. Mar. Biol. Ecol. 443, 162–168.

Baker, J.R., 1938. The evolution of breeding seasons. In: De Beer, G. (Ed.), Evolution: Essays on Aspects of Evolutionary Biology. Clarendon Press, pp. 161–177.

Ball, G.F., 1993. The neural integration of environmental information by seasonally breeding birds. Am. Zool. 33, 185–199.

Ball, G.F., Ketterson, E.D., 2008. Sex differences in the response to environmental cues regulating seasonal reproduction in birds. Philos. Trans. R. Soc. B-Biol. Sci. 363, 231–246.

Barceló, G., Love, O.P., Vézina, F., 2017. Uncoupling basal and summit metabolic rates in white-throated sparrows: digestive demand drives maintenance costs, but changes in muscle mass are not needed to improve thermogenic capacity. Physiol. Biochem. Zool. PBZ 90, 153—165.

Barshep, Y., Minton, C.D.T., Underhill, L.G., Remisiewicz, M., 2011. The primary moult of curlew sandpipers *Calidris ferruginea* in North-Western Australia shifts according to breeding success. Ardea 99, 43–51.

Bauchinger, U., Hof, T.V., Biebach, H., 2007. Testicular development during long-distance spring migration. Horm. Behav. 51, 295–305.

Bauchinger, U., Van't Hof, T., Biebach, H., 2008. Migratory stopover conditions affect the developmental state of male gonads in garden warblers (*Sylvia borin*). Horm. Behav. 54, 312–318.

Bauchinger, U., Van't Hof, T., Biebach, H., 2009. Food availability during migratory stopover affects testis growth and reproductive behaviour in a migratory passerine. Horm. Behav. 55, 425–433.

Bauer, S., Gienapp, P., Madsen, J., 2008. The relevance of environmental conditions for departure decision changes en route in migrating geese. Ecology 89, 1953–1960.

Bazzi, G., Podofillini, S., Gatti, E., Gianfranceschi, L., Cecere, J.G., Spina, F., Saino, N., Rubolini, D., 2017. Candidate genes have sex-specific effects on timing of spring migration and moult speed in a long-distance migratory bird. Curr. Zool. 63, 479–486.

Ben-Hamo, M., Downs, C.J., Burns, D.J., Pinshow, B., 2017. House sparrows offset the physiological trade-off between immune response and feather growth by adjusting foraging behavior. J. Avian Biol. 48, 837–845.

Benkman, C.W., 1990. Intake rates and the timing of crossbill reproduction. Auk 107, 376–386.

Benoit, J., 1935. Stimulation par la lumiere artificielle du developpement testiculaire chez des canards aveugles par enucleation des globes oculaires. C. R. Soc. Biol. (Paris) 120, 136–139.

Bentley, G.E., Wingfield, J.C., Morton, M.L., Ball, G.F., 2000. Stimulatory effects on the reproductive axis in female songbirds by conspecific and heterospecific male song. Horm. Behav. 37, 179–189.

Bentley, G.E., Tucker, S., Chou, H., Hau, M., Perfito, N., 2013. Testicular growth and regression are not correlated with Dio2 expression in a wild male songbird, *Sturnus vulgaris*, exposed to natural changes in photoperiod. Endocrinology 154, 1813–1819.

Berchtold, A., Nightingale, I., Vandermeer, C., MacDougall-Shackleton, S.A., 2017. Experimental temperature manipulations alter songbird autumnal nocturnal migratory restlessness. Anim. Migrat. 4, 1–7.

Berthold, P., Gwinner, E., 1978. Jahresperiodik der Gonadengröße beim Fichtenkreuzschnabel (*Loxia curvirostra*). J. Ornithol. 119, 338–339.

Bilbo, S.D., Nelson, R.J., 2004. Photoperiod influences the effects of exercise and food restriction on an antigen-specific immune response in Siberian hamsters. Endocrinology 145, 556–564.

Blackmore, F.H., 1969. The effect of temperature, photoperiod and molt on the energy requirements of the house sparrow, Passer domesticus. Comp. Biochem. Physiol. 30, 433–444.

Bluhm, C.K., Phillips, R.E., Burke, W.H., Gupta, G.N., 1984. Effects of male courtship and gonadal-steroids on pair formation, egg-laying, and serum LH in Canvasback ducks (*Aythya-valisineria*). J. Zool. 204, 185–200.

Bojarinova, J., Babushkina, O., 2015. Photoperiodic conditions affect the level of locomotory activity during autumn migration in the Long-tailed Tit (*Aegithalos c. caudatus*). Auk 132, 370–379.

Bond, A.L., Konyukhov, N.B., Jones, I.L., 2013. Variation in primary molt in the least auklet: variation de la muda las primarias en aethia pusilla. Condor 115, 348–355.

Both, C., Visser, M.E., 2001. Adjustment to climate change is constrained by arrival date in a long-distance migrant bird. Nature 411, 296–298.

Bozinovic, F., Bastias, D.A., Boher, F., Clavijo-Baquet, S., Estay, S.A., Angilletta Jr., M.J., 2011. The mean and variance of environmental temperature interact to determine physiological tolerance and fitness. Physiol. Biochem. Zool. 84, 543–552.

Bradshaw, W.E., Holzapfel, C.M., 2007. Evolution of animal photoperiodism. Annu. Rev. Ecol. Evol. Syst. 38, 1–25.

Bradshaw, W.E., Holzapfel, C.M., 2010. Light, time, and the physiology of biotic response to rapid climate change in animals. In: Annual Review of Physiology, pp. 147–166.

Breuner, C.W., Orchinik, M., 2001. Seasonal regulation of membrane and intracellular corticosteroid receptors in the house sparrow brain. J. Neuroendocrinol. 13, 412–420.

Bridge, E.S., Kelly, J.F., Bjornen, P.E., Curry, C.M., Crawford, P.H.C., Paritte, J.M., 2010. Effects of nutritional condition on spring migration: do migrants use resource availability to keep pace with a changing world? J. Exp. Biol. 213, 2424–2429.

Briedis, M., Krist, M., Kral, M., Voigt, C.C., Adamik, P., 2018. Linking events throughout the annual cycle in a migratory bird-non-breeding period buffers accumulation of carry-over effects. Behav. Ecol. Sociobiol. 72, 93.

Buehler, D.M., Piersma, T., Tieleman, B.I., 2008a. Captive and free-living red knots *Calidris canutus* exhibit differences in non-induced immunity that suggest different immune strategies in different environments. J. Avian Biol. 39, 560–566.

Buehler, D.M., Piersma, T., Matson, K., Tieleman, B.I., 2008b. Seasonal redistribution of immune function in a migrant shorebird: annual-cycle effects override adjustments to thermal regime. Am. Nat. 172, 783–796.

Buehler, D.M., Encinas-Viso, F., Petit, M., Vézina, F., Tieleman, B.I., Piersma, T., 2009. Limited access to food and physiological trade-offs in a long-distance migrant shorebird. II. Constitutive immune function and the acute-phase response. Physiol. Biochem. Zool. 82, 561–571.

Buttemer, W.A., Addison, B.A., Klasing, K.C., 2019. The energy cost of feather replacement is not intrinsically inefficient. Can. J. Zool. 98, 142–148.

Caprioli, M., Ambrosini, R., Boncoraglio, G., Gatti, E., Romano, A., Romano, M., Rubolini, D., Gianfranceschi, L., Saino, N., 2012. Clock gene variation is associated with breeding phenology and maybe under directional selection in the migratory barn swallow. PLoS One 7 (4), e35140.

Carbeck, K.M., DeMoranville, K.J., D'Amelio, P.B., Goymann, W., Trost, L., Pierce, B., Bryła, A., Dzialo, M., Bauchinger, U., McWilliams, S.R., 2018. Environmental cues and dietary antioxidants affect breeding behavior and testosterone of male European starlings (*Sturnus vulgaris*). Horm. Behav. 103, 36–44.

Caro, S.P., Visser, M.E., 2009. Temperature-induced elevation of basal metabolic rate does not affect testis growth in great tits. J. Exp. Biol. 212, 1994–1998.

Caro, S.P., Schaper, S.V., Hut, R.A., Ball, G.F., Visser, M.E., 2013. The case of the missing mechanism: how does temperature influence seasonal timing in endotherms? -. PLoS Biol. 11, e1001517.

Catry, P., Dias, M.P., Phillips, R.A., Granadeiro, J.P., 2013. Carry-over effects from breeding modulate the annual cycle of a long-distance migrant: an experimental demonstration. Ecology 94, 1230–1235.

Charmantier, A., Gienapp, P., 2014. Climate change and timing of avian breeding and migration: evolutionary versus plastic changes. Evol. Appl. 7, 15–28.

Charmantier, A., McCleery, R.H., Cole, L.R., Perrins, C., Kruuk, L.E.B., Sheldon, B.C., 2008. Adaptive phenotypic plasticity in response to climate change in a wild bird population. Science 320, 800–803.

Chastel, O., Lacroix, A., Kersten, M., 2003. Pre-breeding energy requirements: thyroid hormone, metabolism and the timing of reproduction in house sparrows *Passer domesticus*. J. Avian Biol. 34, 298–306.

Chmura, H.E., Meddle, S.L., Wingfield, J.C., Hahn, T.P., 2017. Effects of a social cue on reproductive development and pre-alternate molt in seasonally breeding migrant and resident female songbirds (*Zonotrichia leucophrys*). J. Exp. Biol. 220, 2947–2956.

Chmura, H.E., Wingfield, J.C., Hahn, T.P., 2020. Non-photic environmental cues and avian reproduction in an era of global change. J. Avian Biol. 51 https://doi.org/10.1111/jav.02243.

Class, A.M., Moore, I.T., 2013. Effects of food supplementation on a tropical bird. Oecologia 173, 355–362.

Clayton, N.S., Cristol, D.A., 1996. Effects of photoperiod on memory and food storing in captive marsh tits, Parus palustris. Anim. Behav. 52, 715–726.

Cockrem, J., 1995. Timing of seasonal breeding in birds, with particular reference to New Zealand birds. Reprod. Fertil. Dev. 7, 1–19.

Cooper, N.W., Sherry, T.W., Marra, P.P., 2015. Experimental reduction of winter food decreases body condition and delays migration in a long-distance migratory bird. Ecology 96, 1933–1942.

Cornelius, J.M., Hahn, T.P., 2012. Seasonal pre-migratory fattening and increased activity in a nomadic and irruptive migrant, the Red Crossbill *Loxia curvirostra*. Ibis 154, 693–702.

Cornelius, J.M., Breuner, C.W., Hahn, T.P., 2010. Under a neighbour's influence: public information affects stress hormones and behaviour of a songbird. Proc. R. Soc. B. 277, 2399–2404.

Cornelius, J.M., Hahn, T.P., Robart, A.R., Vernasco, B.J., Zahor, D.L., Glynn, K.J., ... & Watts, H.E., 2021. Seasonal patterns of fat deposits in relation to migratory strategy in facultative migrants. Front. Ecol. Evol. 9, 419. https://doi.org/10.3389/fevo.2021.691808.

Cornelius, J.M., Perfito, N., Zann, R., Breuner, C.W., Hahn, T.P., 2011. Physiological trade-offs in self-maintenance: plumage molt and stress physiology in birds. J. Exp. Biol. 214, 2768.

Cornelius, J.M., Boswell, T., Jenni-Eiermann, S., Breuner, C.W., Ramenofsky, M., 2013. Contributions of endocrinology to the migration life history of birds. Gen. Comp. Endocrinol. 190, 47–60.

Cornelius, J.M., Perreau, G., Bishop, V.R., Krause, J.S., Smith, R., Hahn, T.P., Meddle, S.L., 2018. Social information changes stress hormone receptor expression in the songbird brain. Horm. Behav. 97, 31–38.

Costantini, D., Casasole, G., AbdElgawad, H., Asard, H., Eens, M., 2016. Experimental evidence that oxidative stress influences reproductive decisions. Funct. Ecol. 30, 1169–1174.

Crick, H.Q.P., Dudley, C., Glue, D.E., Thomson, D.L., 1997. UK birds are laying eggs earlier. Nature 388, 526–526.

Crino, O.L., Buchanan, K.L., Fanson, B.G., Hurley, L.L., Smiley, K.O., Griffith, S.C., 2017. Divorce in the socially monogamous zebra finch: hormonal mechanisms and reproductive consequences. Horm. Behav. 87, 155–163.

Crossin, G.T., Trathan, P.N., Phillips, R.A., Dawson, A., Le Bouard, F., Williams, T.D., 2010. A carryover effect of migration underlies individual variation in reproductive readiness and extreme egg size dimorphism in macaroni penguins. Am. Nat. 176, 357–366.

Danner, R.M., Greenberg, R.S., Danner, J.E., Walters, J.R., 2015. Winter food limits timing of pre-alternate moult in a short-distance migratory bird. Funct. Ecol. 29, 259–267.

Davies, S., Deviche, P., 2014. At the crossroads of physiology and ecology: food supply and the timing of avian reproduction. Horm. Behav. 66, 41–55.

Dawson, A., 1986. The effect of restricting the daily period of food availability on testicular growth of starlings *Sturnus-vulgaris*. Ibis 128, 572–575.

Dawson, A., 1994. The effects of daylength and testosterone on the initiation and progress of moult in Starlings *Sturnus vulgaris*. Ibis 136, 335–340.

Dawson, A., 2002. Photoperiodic control of the annual cycle in birds and comparison with mammals. In: Both, C., Piersma, T. (Eds.), The Avian Calendar: Exploring the Biological Hurdles in the Annual Cycle: 355–367 (Special Issue).

Dawson, A., 2004. The effects of delaying the start of moult on the duration of moult, primary feather growth rates and feather mass in Common Starlings *Sturnus vulgaris*. Ibis 146, 493–500.

Dawson, A., 2005. The effect of temperature on photoperiodically regulated gonadal maturation, regression and moult in starlings - potential consequences of climate change. Funct. Ecol. 19, 995–1000.

Dawson, A., 2006. Control of molt in birds: association with prolactin and gonadal regression in starlings. Gen. Comp. Endocrinol. 147, 314–322.

Dawson, A., 2008. Control of the annual cycle in birds: endocrine constraints and plasticity in response to ecological variability. Philos. Trans. R. Soc. B. 363, 1621–1633.

Dawson, A., 2018. Both low temperature and shorter duration of food availability delay testicular regression and affect the daily cycle in body temperature in a songbird. Physiol. Biochem. Zool. 91, 917–924.

Dawson, A., Goldsmith, A.R., 1997. Changes in gonadotrophin-releasing hormone (GnRH-I) in the pre-optic area and median eminence of starlings (*Sturnus vulgaris*) during the recovery of photosensitivity and during photostimulation. Reproduction 111, 1–6.

Dawson, A., Sharp, P.J., 2007. Photorefractoriness in birds—photoperiodic and non-photoperiodic control. Gen. Comp. Endocrinol. 153, 378–384.

Dawson, A., Sharp, P.J., 2010. Seasonal changes in concentrations of plasma LH and prolactin associated with the advance in the development of photorefractoriness and molt by high temperature in the starling. Gen. Comp. Endocrinol. 167, 122–127.

Dawson, A., King, V.M., Bentley, G.E., Ball, G.F., 2001. Photoperiodic control of seasonality in birds. J. Biol. Rhythm. 16, 365–380.

Demas, G.E., Nelson, R.J., 1998. Photoperiod, ambient temperature, and food availability interact to affect reproductive and immune function in adult male deer mice (*Peromyscus maniculatus*). J. Biol. Rhythm. 13, 253–262.

Deviche, P., Beouche-Helias, B., Davies, S., Gao, S., Lane, S., Valle, S., 2014. Regulation of plasma testosterone, corticosterone, and metabolites in response to stress, reproductive stage, and social challenges in a desert male songbird. Gen. Comp. Endocrinol. 203, 120–131.

Dhondt, A.A., 2010. Broodedness, not latitude, affects the response of reproductive timing of birds to food supplementation. J. Ornithol. 151, 955–957.

Dickens, M.J., Cornil, C.A., Balthazart, J., 2011. Acute stress differentially affects aromatase activity in specific brain nuclei of adult male and female quail. Endocrinology 152, 4242–4251.

Dickens, M.J., Cornil, C.A., Balthazart, J., 2013. Neurochemical control of rapid stress-induced changes in brain aromatase activity. J. Neuroendocrinol. 25, 329–339.

Drent, R.H., Daan, S., 1980. The prudent parent: energetic adjustments in avian breeding 1). Ardea 55, 225–252.

Dubois, K., Hallot, F., Vézina, F., 2016. Basal and maximal metabolic rates differ in their response to rapid temperature change among avian species. J. Comp. Physiol. B 186, 919–935.

Dunn, P.O., Møller, A.P., 2014. Changes in breeding phenology and population size of birds. J. Anim. Ecol. 83, 729–739.

Dunn, P.O., Winkler, D.W., Whittingham, L.A., Hannon, S.J., Robertson, R.J., 2011. A test of the mismatch hypothesis: how is timing of reproduction related to food abundance in an aerial insectivore? Ecology 92, 450–461.

Easterling, D.R., Horton, B., Jones, P.D., Peterson, T.C., Karl, T.R., Parker, D.E., Salinger, M.J., Razuvayev, V., Plummer, N., Jamason, P., Folland, C.K., 1997. Maximum and minimum temperature trends for the globe. Science 277, 364–367.

Eikenaar, C., Hegemann, A., 2016. Migratory common blackbirds have lower innate immune function during autumn migration than resident conspecifics. Biol. Lett. 12, 20160078.

Eikenaar, C., Müller, F., Leutgeb, C., Hessler, S., Lebus, K., Taylor, P.D., Schmaljohann, H., 2017. Corticosterone and timing of migratory departure in a songbird. Proc. R. Soc. B. 284, 20162300.

Eikenaar, C., Ballstaedt, E., Hessler, S., Klinner, T., Müller, F., Schmaljohann, H., 2018a. Cues, corticosterone and departure decisions in a partial migrant. Gen. Comp. Endocrinol. 261, 59–66.

Eikenaar, C., Hessler, S., Ballstaedt, E., Schmaljohann, H., Kaiya, H., 2018b. Ghrelin, corticosterone and the resumption of migration from stopover, an automated telemetry study. Physiol. Behav. 194, 450–455.

Eikenaar, C., Schäfer, J., Hessler, S., Packmor, F., Schmaljohann, H., 2020. Diel variation in corticosterone and departure decision making in migrating birds. Horm. Behav. 122, 104746.

Ely, C.R., McCaffery, B., Gill Jr., R.E., 2018. Shorebirds adjust spring arrival schedules with variable environmental conditions: four decades of assessment on the Yukon−Kuskokwim Delta, Alaska. In: David Shuford, W., et al. (Eds.), Trends and Traditions: Avifaunal Change in Western North America: Studies of Western Birds 3. Western Field Ornithologists, pp. 296−311.

Ernst, D.K., Bentley, G.E., 2016. Neural and neuroendocrine processing of a non-photic cue in an opportunistically breeding songbird. J. Exp. Biol. 219, 783−789.

Evans, J.K., Buchanan, K.L., Griffith, S.C., Klasing, K.C., Addison, B., 2017. Ecoimmunology and microbial ecology: contributions to avian behavior, physiology, and life history. Horm. Behav. 88, 112−121.

Eyster, M.B., 1954. Quantitative measurement of the influence of photoperiod, temperature, and season on the activity of captive songbirds. Ecol. Monogr. 24, 1−28.

Faccio, M.S., Gabriel, V.A., Pizo, M.A., 2018. Tropical frugivorous birds molt and breed in relation to the availability of food resources. Ornitol. Neotrop. (29), S11−S18.

Fayet, A.L., Freeman, R., Shoji, A., Kirk, H.L., Padget, O., Perrins, C.M., Guilford, T., 2016. Carry-over effects on the annual cycle of a migratory seabird: an experimental study. J. Anim. Ecol. 85, 1516−1527.

Follett, B.K., 1984. Birds. In: Lamming, G.E. (Ed.), Marshall's Physiology of Reproduction. Longman Green, pp. 283−350.

Follett, B.K., Mattocks, P.W., Farner, D.S., 1974. Circadian function in the photoperiodic induction of gonadotropin secretion in the white-crowned sparrow, *Zonotrichia leucophrys gambelii*. PNA 71, 1666.

Forchhammer, M.C., Post, E., Stenseth, N.C.H.R., 2002. North Atlantic Oscillation timing of long- and short-distance migration. J. Anim. Ecol. 71, 1002−1014.

Foster, R.G., Soni, B.G., 1998. Extraretinal photoreceptors and their regulation of temporal physiology. Rev. Reprod. 3, 145−150.

Foster, R.G., Grace, M.S., Provencio, I., Degrip, W.J., Garcia-Fernandez, J.M., 1994. Identification of vertebrate deep brain photoreceptors. Neurosci. Biobehav. Rev. 18, 541−546.

Franks, S.E., Pearce-Higgins, J.W., Atkinson, S., Bell, J.R., Botham, M.S., Brereton, T.M., Harrington, R., Leech, D.I., 2018. The sensitivity of breeding songbirds to changes in seasonal timing is linked to population change but cannot be directly attributed to the effects of trophic asynchrony on productivity. Glob. Chang. Biol. 24, 957−971.

Freed, L.A., Cann, R.L., 2012. Changes in timing, duration, and symmetry of molt of Hawaiian forest birds. PloS One 7 e29834−e29834.

Furlonger, A.A., Huynh, L., Luloff, T.W., Schmidt, K.L., MacDougall-Shackleton, S.A., 2012. Effects of supplementation with preferred foods on the reproductive axis of American Goldfinches (*Spinus tristis*). Can. J. Zool. 90, 203−209.

Ganter, B., Sean Boyd, W., Baranyuk, V.V., Cooke, F., 2005. First pairing in Snow Geese *Anser caerulescens*: at what age and at what time of year does it occur? Ibis 147, 57−66.

Gill, J.A., Alves, J.A., Sutherland, W.J., Appleton, G.F., Potts, P.M., Gunnarsson, T.G., 2014. Why is timing of bird migration advancing when individuals are not? -. Proc. R. Soc. B. 281, 6.

Gills, J.A., Munster, V.J., Radersma, R., Liefhebber, D., Fouchier, R.A.M., Klaassen, M., 2007. Hampered foraging and migratory performance in swans infected with low-pathogenic avian influenza A virus. PloS One 2, e184.

González-Gómez, P.L., Merrill, L., Ellis, V.A., Venegas, C., Pantoja, J.I., Vasquez, R.A., Wingfield, J.C., 2013. Breaking down seasonality: androgen modulation and stress response in a highly stable environment. Gen. Comp. Endocrinol. 191, 1−12.

Goodson, J.L., Saldanha, C.J., Hahn, T.P., Soma, K.K., 2005. Recent advances in behavioral neuroendocrinology: insights from studies on birds. Horm. Behav. 48, 461−473.

Gow, E.A., Burke, L., Winkler, D.W., Knight, S.M., Bradley, D.W., Clark, R.G., Bélisle, M., Berzins, L.L., Blake, T., Bridge, E.S., Dawson, R.D., Dunn, P.O., Garant, D., Holroyd, G., Horn, A.G., Hussell, D.J.T., Lansdorp, O., Laughlin, A.J., Leonard, M.L., Pelletier, F., Shutler, D., Siefferman, L., Taylor, C.M., Trefry, H., Vleck, C.M., Vleck, D., Whittingham, L.A., Norris, D.R., 2019. A range-wide domino effect and resetting of the annual cycle in a migratory songbird. Proc. R. Soc. B. 286, 20181916.

Goymann, W., Lupi, S., Kaiya, H., Cardinale, M., Fusani, L., 2017. Ghrelin affects stopover decisions and food intake in a long-distance migrant. Proc. R. Soc. B-Biol. Sci. 114, 1946−1951.

Gwinner, E., 1986. Circannual Rhythms. Springer-Verlag.

Gwinner, H., Gwinner, E., Dittami, J., 1987. Effects of nestboxes on LH, testosterone, testicular size, and the reproductive behavior of male European starlings in spring. Beyond Behav. 103, 68−82.

Haake, A.R., Sawyer, R.H., 1986. Differences in the histogenesis and keratin expression of avian extraembryonic ectoderm and endoderm recombined with dermis. Dev. Biol. 113, 295−304.

Haest, B., Hüppop, O., Bairlein, F., 2018. Challenging a 15-year-old claim: the North Atlantic Oscillation index as a predictor of spring migration phenology of birds. Glob. Chang. Biol. 24, 1523−1537.

Hahn, T.P., 1995. Integration of photoperiodic and food cues to time changes in reproductive physiology by an opportunistic breeder, the Red Crossbill, *Loxia-curvirostra* (Aves, Carduelinae). J. Exp. Zool. 272, 213−226.

Hahn, T.P., 1998. Reproductive seasonality in an opportunistic breeder, the red crossbill, *Loxia curvirostra*. Ecology 79, 2365−2375.

Hahn, T.P., MacDougall-Shackleton, S.A., 2008. Adaptive specialization, conditional plasticity and phylogenetic history in the reproductive cue response systems of birds. Philos. Trans. R. Soc. B. 363, 267−286.

Hahn, T., Boswell, T., Wingfield, J., Ball, G., 1997. Temporal flexibility in avian reproduction. In: Nolan, V., et al. (Eds.), Current Ornithology. Springer US, pp. 39−80.

Hahn, T.P., Pereyra, M.E., Katti, M., Ward, G.M., MacDougall-Shackleton, S.A., 2005. Effects of food availability on the reproductive system. In: Dawson, A., Sharp, P.J. (Eds.), Functional Avian Endocrinology. Narosa Publishing House, pp. 167−180.

Hahn, T.P., Cornelius, J.M., Sewall, K.B., Kelsey, T.R., Hau, M., Perfito, N., 2008. Environmental regulation of annual schedules in opportunistically-breeding songbirds: adaptive specializations or variations on a theme of white-crowned sparrow? -. Gen. Comp. Endocrinol. 157, 217−226.

Hahn, T.P., Watts, H.E., Cornelius, J.M., Brazeal, K.R., MacDougall-Shackleton, S.A., 2009. Evolution of environmental cue response mechanisms: adaptive variation in photorefractoriness. Gen. Comp. Endocrinol. 163, 193−200.

Hamner, W.M., 1963. Diurnal rhythm and photoperiodism in testicular recrudescence of the house finch. Science 142, 1294.

Hamner, W.M., 1964. Circadian control of photoperiodism in the house finch demonstrated by interrupted-night experiments. Nature 203, 1400–1401.

Hamner, W.M., 1968. The photorefractory period of the house finch. Ecology 49, 211–227.

Harris, B.N., 2020. Stress hypothesis overload: 131 hypotheses exploring the role of stress in tradeoffs, transitions, and health. Gen. Comp. Endocrinol. 288, 113355.

Harrison, X.A., Blount, J.D., Inger, R., Norris, D.R., Bearhop, S., 2011. Carry-over effects as drivers of fitness differences in animals. J. Anim. Ecol. 80, 4–18.

Hasselquist, D., 2007. Comparative immunoecology in birds: hypotheses and tests. J. Ornithol. 148, 571–582.

Hau, M., Wikelski, M., Wingfield, J.C., 2000. Visual and nutritional food cues fine-tune timing of reproduction in a neotropical rainforest bird. J. Exp. Zool. 286, 494–504.

Hau, M., Wikelski, M., Gwinner, H., Gwinner, E., 2004. Timing of reproduction in a Darwin's finch: temporal opportunism under spatial constraints. Oikos 106, 489–500.

Hegemann, A., Matson, K.D., Both, C., Tieleman, B.I., 2012. Immune function in a free-living bird varies over the annual cycle, but seasonal patterns differ between years. Oecologia 170, 605–618.

Hegemann, A., Alcalde Abril, P., Muheim, R., Sjöberg, S., Alerstam, T., Nilsson, J.-Å., Hasselquist, D., 2018. Immune function and blood parasite infections impact stopover ecology in passerine birds. Oecologia 188, 1011–1024.

Helm, B., 2009. Geographically distinct reproductive schedules in a changing world: costly implications in captive Stonechats. Integr. Comp. Biol. 49, 563–579.

Helm, B., Piersma, T., Van der Jeugd, H., 2006. Sociable schedules: interplay between avian seasonal and social behaviour. Anim. Behav. 72, 245–262.

Helm, B., Schwabl, I., Gwinner, E., 2009. Circannual basis of geographically distinct bird schedules. J. Exp. Biol. 212, 1259.

Helm, B., Ben-Shlomo, R., Sheriff, M.J., Hut, R.A., Foster, R., Barnes, B.M., Dominoni, D., 2013. Annual rhythms that underlie phenology: biological time-keeping meets environmental change. Proc. R. Soc. B. 280, 20130016.

Helm, B., Van Doren, B.M., Hoffmann, D., Hoffmann, U., 2019. Evolutionary response to climate change in migratory pied flycatchers. Curr. Biol. 29, 3714–3719.e4.

Huey, R.B., Hertz, P.E., 1984. Is a jack-of-all-temperatures a master of none. Evolution 38, 441–444.

Ikegami, K., Yoshimura, T., 2012. Circadian clocks and the measurement of daylength in seasonal reproduction. Mol. Cell. Endocrinol. 349, 76–81.

Jacobs, J.D., Wingfield, J.C., 2000. Endocrine control of life-cycle stages: a constraint on response to the environment? Condor 102, 35–51.

Jukema, J., Wiersma, P., 2014. Climate change and advanced primary moult in Eurasian golden plovers *Pluvialis apricaria*. Ardea 102, 153–160.

Kelly, T.R., MacGillivray, H.L., Sarquis-Adamson, Y., Watson, M.J., Hobson, K.A., MacDougall-Shackleton, E.A., 2016. Seasonal migration distance varies with natal dispersal and predicts parasitic infection in song sparrows. Behav. Ecol. Sociobiol. 70, 1857–1866.

Kelly, T.R., MacGillivray, H.L., Hobson, K.A., MacDougall-Shackleton, S.A., MacDougall-Shackleton, E.A., 2017. Immune profiles vary seasonally, but are not significantly related to migration distance or natal dispersal, in a migratory songbird. J. Exp. Zool. Part A: Ecol. & Integr. Physiol. 327, 284–292.

Kelly, T.R., Bonner, S.J., MacDougall-Shackleton, S.A., MacDougall-Shackleton, E.A., 2018. Exposing migratory sparrows to Plasmodium suggests costs of resistance, not necessarily of infection itself. J. Exp. Zool. Part A: Ecol. & Integr. Physiol. 329, 5–14.

Kelly, T.R., Rubin, B.D., MacDougall-Shackleton, S.A., MacDougall-Shackleton, E.A., 2020. Experimental malaria infection affects songbirds' nocturnal migratory activity. Physiol. Biochem. Zool. 93, 97–110.

King, J.R., 1974. Seasonal allocation of time and energy resources in birds. In: Paynter, R.A.J. (Ed.), Avian Energetics. Nuttall Ornithological Club, pp. 4–85.

Klasing, K.C., 2004. The costs of immunity. Acta Zool. Sin. 50, 961–969.

Knudsen, E., Linden, A., Both, C., Jonzen, N., Pulido, F., Saino, N., Sutherland, W.J., Bach, L.A., Coppack, T., Ergon, T., Gienapp, P., Gill, J.A., Gordo, O., Hedenstroom, A., Lehikoinen, E., Marra, P.P., Moller, A.P., Nilsson, A.L.K., Peron, G., Ranta, E., Rubolini, D., Sparks, T.H., Spina, F., Studds, C.E., Saether, S.A., Tryjanowski, P., Stenseth, N.C., 2011. Challenging claims in the study of migratory birds and climate change. Biol. Rev. 86, 928–946.

Koustos, E.A., Klasing, K.C., 2013. Factors modulating the avian immune system. In: Avian Immunology. Elsevier Ltd., pp. 1–17

Krause, J.S., Pérez, J.H., Chmura, H.E., Meddle, S.L., Hunt, K.E., Gough, L., Boelman, N., Wingfield, J.C., 2016. The stress response is attenuated during inclement weather in parental, but not in pre-parental, Lapland longspurs (*Calcarius lapponicus*) breeding in the Low Arctic. Horm. Behav. 83, 68–74.

Kriegsfeld, L.J., Jennings, K.J., Bentley, G.E., Tsutsui, K., 2018. Gonadotrophin-inhibitory hormone and its mammalian orthologue RFamide-related peptide-3: discovery and functional implications for reproduction and stress. J. Neuroendocrinol. 30, e12597.

Lambrechts, M.M., Perret, P., 2000. A long photoperiod overrides non-photoperiodic factors in blue tits' timing of reproduction. Proc. R. Soc. B. 267, 585–588.

Lambrechts, M.M., Perret, P., Blondel, J., 1996. Adaptive differences in the timing of egg laying between different populations of birds result from variation in photoresponsiveness. Proc. R. Soc. B. 263, 19–22.

Lambrechts, M.M., Blondel, J., Maistre, M., Perret, P., 1997. A single response mechanism is responsible for evolutionary adaptive variation in a bird's laying date. Proc. Natl. Acad. Sci. U. S. A. 94, 5153.

Laplante, M.-P., McKinnon, E.A., Love, O.P., Vézina, F., 2019. Flexible response to short-term weather in a cold-adapted songbird. J. Avian Biol. 50 https://doi.org/10.1111/jav.01766.

Lattin, C.R., Romero, L.M., 2013. Seasonal variation in corticosterone receptor binding in brain, hippocampus, and gonads in house sparrows (*Passer domesticus*). Auk 130, 591–598.

Lattin, C.R., Romero, L.M., 2015. Seasonal variation in glucocorticoid and mineralocorticoid receptors in metabolic tissues of the house sparrow (*Passer domesticus*). Gen. Comp. Endocrinol. 214, 95–102.

Lattin, C.R., Waldron-Francis, K., Romero, L.M., 2013. Intracellular glucocorticoid receptors in spleen, but not skin, vary seasonally in wild house sparrows (*Passer domesticus*). Proc. R. Soc. B. 280, 20123033.

Lee, K.A., 2006. Linking immune defenses and life history at the levels of the individual and the species. Integr. Comp. Biol. 46, 1000–1015.

Lewis, R.A., Farner, D.S., 1973. Temperature modulation of photoperiodically induced vernal phenomena in White-crowned sparrows (*Zonotrichia-leucophrys*). Condor 75, 279–286.

Li, H., Ferrari, M.B., Kuenzel, W.J., 2004. Light-induced reduction of cytoplasmic free calcium in neurons proposed to be encephalic photoreceptors in chick brain. Dev. Brain Res. 153, 153–161.

Liedvogel, M., Szulkin, M., Knowles, S.C.L., Wood, M.J., Sheldon, B.C., 2009. Phenotypic correlates of Clock gene variation in a wild blue tit population: evidence for a role in seasonal timing of reproduction. Mol. Ecol. 18, 2444–2456.

Ligon, J.D., 1974. Green cones of piñon pine stimulate late summer breeding in Piñon jay. Nature 250, 80–82.

Lochmiller, R.L., Deerenberg, C., 2000. Trade-offs in evolutionary immunology: just what is the cost of immunity? Oikos 88, 87–98.

Lofts, B., Murton, R.K., 1968. Photoperiodic and physiological adaptations regulating avian breeding cycles and their ecological significance. J. Zool. 155, 327–394.

MacDougall-Shackleton, S.A., Sherry, D.F., Clark, A.P., Pinkus, R., Hernandez, A.M., 2003. Photoperiodic regulation of food storing and hippocampus volume in black-capped chickadees, *Poecile atricapillus*. Anim. Behav. 65, 805–812.

MacMynowski, D.P., Root, T.L., Ballard, G., Geupel, G.R., 2007. Changes in spring arrival of Nearctic-Neotropical migrants attributed to multiscalar climate. Glob. Chang. Biol. 13, 2239–2251.

Majumdar, G., Yadav, G., Rani, S., Kumar, V., 2014. A photoperiodic molecular response in migratory redheaded bunting exposed to a single long day. Gen. Comp. Endocrinol. 204, 104–113.

Maldonado, K., Bozinovic, F., Cavieres, G., Fuentes, C.A., Cortés, A., Sabat, P., 2012. Phenotypic flexibility in basal metabolic rate is associated with rainfall variability among populations of rufous-collared sparrow. Zool. 115, 128–133.

Mand, R., Tilgar, V., Leivits, A., 2000. Reproductive response of Great Tits, *Parus major*, in a naturally base-poor forest habitat to calcium supplementation. Can. J. Zool. 78, 689–695.

Maney, D.L., Hahn, T.P., Schoech, S.J., Sharp, P.J., Morton, M.L., Wingfield, J.C., 1999. Effects of ambient temperature on photo-induced prolactin secretion in three subspecies of white-crowned sparrow, Zonotrichia leucophrys. Gen. Comp. Endocrinol. 113, 445–456.

Maney, D.L., Goode, C.T., Ball, G.F., 2007a. Transduction of a non-photic cue: from the auditory system to a neuroendocrine response? -. J. Ornithol. 148, S527–S538.

Maney, D.L., Goode, C.T., Lake, J.I., Lange, H.S., O'Brien, S., 2007b. Rapid neuroendocrine responses to auditory courtship signals. Endocrinology 148, 5614–5623.

Marra, P.P., Hobson, K.A., Holmes, R.T., 1998. Linking winter and summer events in a migratory bird by using stable-carbon isotopes. Science 282, 1884–1886.

Marra, P.P., Francis, C.M., Mulvihill, R.S., Moore, F.R., 2005. The influence of climate on the timing and rate of spring bird migration. Oecologia 142, 307–315.

Martin, L.B., Weil, Z.M., Nelson, R.J., 2008. Seasonal changes in vertebrate immune activity: mediation by physiological trade-offs. Philos. Trans. R. Soc. B. 363, 321–339.

Martin, R.J., Kruger, M.C., MacDougall-Shackleton, S.A., Sherry, D.F., 2020. Black-capped chickadees (*Poecile atricapillus*) use temperature as a cue for reproductive timing. Gen. Comp. Endocrinol. 287, 113348.

Masman, D., Gordijn, M., Daan, S., Dijkstra, C., 1986. Ecological energetics of the kestrel- field estimates of energy-intake throughout the year. Ardea 74, 24–39.

McKechnie, A.E., Noakes, M.J., Smit, B., 2015. Global patterns of seasonal acclimatization in avian resting metabolic rates. J. Ornithol. 156, 367–376.

McKellar, A.E., Marra, P.P., Hannon, S.J., Studds, C.E., Ratcliffe, L.M., 2013. Winter rainfall predicts phenology in widely separated populations of a migrant songbird. Oecologia 172, 595–605.

Meijer, T., 1991. The effect of a period of food restriction on gonad size and molt of male and female starlings *Sturnus-vulgaris* under constant photoperiod. Ibis 133, 80–84.

Meijer, T., Drent, R., 1999. Re-examination of the capital and income dichotomy in breeding birds. Ibis 141, 399–414.

Meijer, T., Daan, S., Dijkstra, C., 1988. Female condition and reproduction- Effects of food manipulation in free-living and captive kestrels. Ardea 76, 141–154.

Meijer, T., Daan, S., Hall, M.R., 1990. Family planning in the kestrel (*Falco tinnunculus*): the proximate control of covariation of laying date and clutch size. Behaviour 114, 1–4.

Meijer, T., Nienaber, U., Langer, U., Trillmich, F., 1999. Temperature and timing of egg-laying of European starlings. Condor 101, 124–132.

Metcalfe, J., Schmidt, K.L., Bezner Kerr, W., Guglielmo, C.G., MacDougall-Shackleton, S.A., 2013. White-throated sparrows adjust behaviour in response to manipulations of barometric pressure and temperature. Anim. Behav. 86 (6), 1285–1290.

Mishra, M.K., Wilson, F.E., Scanlan, T.S., Chiellini, G., 2004. Thyroid hormone-dependent seasonality in American tree sparrows (*Spizella arborea*): effects of GC-1, a thyroid receptor β-selective agonist, and of iopanoic acid, a deiodinase inhibitor. J. Comp. Physiol. B. 174, 471–479.

Mitchell, G.W., Newman, A.E.M., Wikelski, M., Norris, D.R., 2012. Timing of breeding carries over to influence migratory departure in a songbird: an automated radiotracking study. J. Anim. Ecol. 81, 1024–1033.

Monkkonen, M., Forsman, J.T., Kananoja, T., Ylonen, H., 2009. Indirect cues of nest predation risk and avian reproductive decisions. Biol. Lett. 5, 176–178.

Moreno-Rueda, G., 2010. Experimental test of a trade-off between moult and immune response in house sparrows *Passer domesticus*. J. Evol. Biol. 23, 2229–2237.

Morrison, C.A., Baillie, S.R., Clark, J.A., Johnston, A., Leech, D.I., Robinson, R.A., 2015. Flexibility in the timing of post-breeding moult in passerines in the UK. Ibis 157, 340–350.

Morton, G.A., Morton, M.L., 1990. Dynamics of posnuptial molt in free-living mountain white-crowned sparrows. Condor 92, 813–828.

Morton, M.L., Pereyra, M.E., Baptista, L.F., 1985. Photoperiodically induced ovarian growth in the white-crowned sparrow (*Zonotrichia leucophrys gambelii*) and its augmentation by song. Comp. Biochem. Physiol. A-Physiol. 80, 93–97.

Murphy, M.E., King, J.R., Lu, J., 1988. Malnutrition during the post-nuptial molt of White-crowned Sparrows: feather growth and quality. Can. J. Zool. 66, 1403–1413.

Nager, R.G., van Noordwijk, A.J., 1995. Proximate and ultimate aspects of phenotypic plasticity in timing of great tit breeding in a heterogeneous environment. Am. Nat. 146, 454–474.

Nakamura, T., Kitahara, M., 1983. Migratory activities in caged *Emberiza rustica* exposed to different artificial lights and temperatures. J. Yamashina Inst. Ornithol. 15, 141–155.

Nakane, Y., Shimmura, T., Abe, H., Yoshimura, T., 2014. Intrinsic photosensitivity of a deep brain photoreceptor. Curr. Biol. 24, R596–R597.

Nakao, N., Ono, H., Yamamura, T., Anraku, T., Takagi, T., Higashi, K., Yasuo, S., Katou, Y., Kageyama, S., Uno, Y., Kasukawa, T., Iigo, M., Sharp, P.J., Iwasawa, A., Suzuki, Y., Sugano, S., Niimi, T., Mizutani, M., Namikawa, T., Ebihara, S., 2008. Thyrotrophin in the pars tuberalis triggers photoperiodic response. Nature 452, 317–322.

Ndithia, H.K., Bakari, S.N., Matson, K.D., Muchai, M., Tieleman, B.I., 2017. Geographical and temporal variation in environmental conditions affects nestling growth but not immune function in a year-round breeding equatorial lark. Front. Zool. 14, 28.

Nebel, S., Bauchinger, U., Buehler, D.M., Langlois, L.A., Boyles, M., Gerson, A.R., Price, E.R., McWilliams, S.R., Guglielmo, C.G., 2012. Constitutive immune function in European starlings, *Sturnus vulgaris*, is decreased immediately after an endurance flight in a wind tunnel. J. Exp. Biol. 215, 272.

Nebel, S., Buehler, D.M., MacMillan, A., Guglielmo, C.G., 2013. Flight performance of western sandpipers, *Calidris mauri*, remains uncompromised when mounting an acute phase immune response. J. Exp. Biol. 216, 2752.

Nelson, R.J., 2004. Seasonal immune function and sickness responses. Trends Immunol. 25, 187–192.

Nelson, R.J., Demas, G.E., 1996. Seasonal changes in immune function. Q. Rev. Biol. 71, 511–548.

Nelson, R.J., Demas, G.E., Klein, S.L., Kriegsfeld, L.J., 2002. Seasonal Patterns of Stress, Immune Function and Disease. Cambridge University Press.

Newson, S.E., Moran, N.J., Musgrove, A.J., Pearce-Higgins, J.W., Gillings, S., Atkinson, P.W., Miller, R., Grantham, M.J., Baillie, S.R., 2016. Long-term changes in the migration phenology of UK breeding birds detected by large-scale citizen science recording schemes. Ibis 158, 481–495.

Nicholls, T.J., Goldsmith, A.R., Dawson, A., 1988. Photorefractoriness in birds and comparison with mammals. Physiol. Rev. 68, 133–176.

Nolan, V., Ketterson, E.D., Ziegenfus, C., Cullen, D.P., Chandler, C.R., 1992. Testosterone and avian life histories: effects of experimentally elevated testosterone on prebasic molt and survival in male dark-eyed juncos. Condor 94, 364–370.

Norris, D.R., Marra, P.P., 2007. Seasonal interactions, populations dynamics in migratory birds. Condor 109, 535–547.

Norris, D.R., Marra, P.P., Kyser, T.K., Sherry, T.W., Ratcliffe, L.M., 2004. Tropical winter habitat limits reproductive success on the temperate breeding grounds in a migratory bird. Proc. R. Soc. B 271 (1534), 59–64.

Nussey, D.H., Postma, E., Gienapp, P., Visser, M.E., 2005. Selection on heritable phenotypic plasticity in a wild bird population. Science 310, 304–306.

Nwaogu, C.J., Cresswell, W., Versteegh, M.A., Tieleman, B.I., 2019. Seasonal differences in baseline innate immune function are better explained by environment than annual cycle stage in a year-round breeding tropical songbird. J. Anim. Ecol. 88, 537–553.

O'Brien, S., Hau, M., 2005. Food cues and gonadal development in neotropical spotted antbirds (*Hylophylax naevioides*). J. Ornithol. 146, 332–337.

Ouwehand, J., Both, C., 2017. African departure rather than migration speed determines variation in spring arrival in pied flycatchers. J. Anim. Ecol. 86, 88–97.

Ouwehand, J., Burger, C., Both, C., 2017. Shifts in hatch dates do not provide pied flycatchers with a rapid ontogenetic route to adjust offspring time schedules to climate change. Funct. Ecol. 31, 2087–2097.

Owen, J.C., Moore, F.R., 2008. Swainson's thrushes in migratory disposition exhibit reduced immune function. J. Ethol. 26, 383–388.

Owen-Ashley, N.T., Turner, M., Hahn, T.P., Wingfield, J.C., 2006. Hormonal, behavioral, and thermoregulatory responses to bacterial lipopolysaccharide in captive and free-living white-crowned sparrows (Zonotrichia leucophrys gambelii). Horm. Behav. 49, 15–29.

Pap, P.L., Vágási, C.I., Tökölyi, J., Czirják, G.Á., Barta, Z., 2010. Variation in haematological indices and immune function during the annual cycle in the great tit *Parus major*. Ardea 98, 105–112.

Parmesan, C., 2007. Influences of species, latitudes and methodologies on estimates of phenological response to global warming. Glob. Chang. Biol. 13, 1860–1872.

Perfito, N., Meddle, S.L., Tramontin, A.D., Sharp, P.J., Wingfield, J.C., 2005. Seasonal gonadal recrudescence in song sparrows: response to temperature cues. Gen. Comp. Endocrinol. 143, 121–128.

Perfito, N., Bentley, G., Hau, M., 2006. Tonic activation of brain GnRH immunoreactivity despite reduction of peripheral reproductive parameters in opportunistically breeding zebra finches. - brain. Behav. Evolution 67, 123–134.

Perfito, N., Zann, R.A., Bentley, G.E., Hau, M., 2007. Opportunism at work: habitat predictability affects reproductive readiness in free-living zebra finches. Funct. Ecol. 21, 291–301.

Perfito, N., Kwong, J.M.Y., Bentley, G.E., Hau, M., 2008. Cue hierarchies and testicular development: is food a more potent stimulus than day length in an opportunistic breeder (*Taeniopygia g. guttata*)? Horm. Behav. 53, 567–572.

Perfito, N., Guardado, D., Williams, T.D., Bentley, G.E., 2015. Social cues regulate reciprocal switching of hypothalamic Dio2/Dio3 and the transition into final follicle maturation in European starlings (*Sturnus vulgaris*). Endocrinology 156, 694–706.

Petit, M., Lewden, A., Vézina, F., 2013. Intra-seasonal flexibility in avian metabolic performance highlights the uncoupling of basal metabolic rate and thermogenic capacity. PloS One 8, e68292.

Piersma, T., Drent, J., 2003. Phenotypic flexibility and the evolution of organismal design. TREE 18 (5), 228–233.

Pollock, H.S., Brawn, J.D., Agin, T.J., Cheviron, Z.A., 2019. Differences between temperate and tropical birds in seasonal acclimatization of thermoregulatory traits. J. Avian Biol. 50 https://doi.org/10.1111/jav.02067.

Prendergast, B.J., Hotchkiss, A.K., Bilbo, S.D., Nelson, R.J., 2004. Peripubertal immune challenges attenuate reproductive development in male Siberian hamsters (*Phodopus sungorus*). Biol. Reprod. 70, 813–820.

Prior, N.H., Heimovics, S.A., Soma, K.K., 2013. Effects of water restriction on reproductive physiology and affiliative behavior in an opportunistically-breeding and monogamous songbird, the zebra finch. Horm. Behav. 63, 462–474.

Pulido, F., Berthold, P., Mohr, G., Querner, U., 2001. Heritability of the timing of autumn migration in a natural bird population. Proc. R. Soc. B. 268, 953–959.

Quispe, R., Yohannes, E., Gahr, M., 2018. Seasonality at the equator: isotope signatures and hormonal correlates of molt phenology in a non-migratory Amazonian songbird. Front. Zool. 15, 39.

Reudink, M.W., Marra, P.P., Kyser, T.K., Boag, P.T., Langin, K.M., Ratcliffe, L.M., 2009. Non-breeding season events influence sexual selection in a long-distance migratory bird. Proc. R. Soc. B. 276, 1619–1626.

Roast, M.J., Aulsebrook, A.E., Fan, M., Hidalgo Aranzamendi, N., Teunissen, N., Peters, A., 2019. Short-term climate variation drives baseline innate immune function and stress in a tropical bird: a reactive scope perspective. Physiol. Biochem. Zool. 92, 140–151.

Romero, L.M., 2002. Seasonal changes in plasma glucocorticoid concentrations in free-living vertebrates. Gen. Comp. Endocrinol. 128, 1–24.

Romero, L.M., Bauer, C.M., de Bruijn, R., Lattin, C.R., 2017. Seasonal rhythms. In: Fink, G. (Ed.), Stress: Neuroendocrinology and Neurobiology. Academic Press, pp. 421–427.

Rowan, W., 1925. Relation of light to bird migration and developmental changes. Nature 115, 494–495.

Rowan, W., 1926. On photoperiodism, reproductive periodicity, and the annual migrations of birds and certain fishes. Proc. Boston Soc. Nat. Hist. 38, 147–189.

Ruffino, L., Salo, P., Koivisto, E., Banks, P.B., Korpimäki, E., 2014. Reproductive responses of birds to experimental food supplementation: a meta-analysis. Front. Zool. 11, 80.

Runfeldt, S., Wingfield, J.C., 1985. Experimentally prolonged sexual activity in female sparrows delays termination of reproductive activity in their untreated mates. Anim. Behav. 33, 403–410.

Saino, N., Romano, M., Caprioli, M., Fasola, M., Lardelli, R., Micheloni, P., Scandolara, C., Rubolini, D., Gianfranceschi, L., 2013. Timing of molt of barn swallows is delayed in a rare Clock genotype. Peer J 1 e17–e17.

Sanz, J.J., 1999. Seasonal variation in reproductive success and postnuptial moult of blue tits in southern Europe: an experimental study. Oecologia 121, 377–382.

Sapolsky, R.M., Romero, L.M., Munck, A.U., 2000. How do glucocorticoids influence stress responses? Integrating permissive, suppressive, stimulatory, and preparative actions. Endocr. Rev. 21, 55–89.

Schaper, S.V., Dawson, A., Sharp, P.J., Gienapp, P., Caro, S.P., Visser, M.E., 2012. Increasing temperature, not mean temperature, is a cue for avian timing of reproduction. Am. Nat. 179, E55–E69.

Schleussner, G., Dittami, J.P., Gwinner, E., 1985. Testosterone implants affect molt in male European starlings, *Sturnus vulgaris*. Physiol. Zool. 58, 597–604.

Schmid-Hempel, P., Ebert, D., 2003. On the evolutionary ecology of specific immune defence. TREE 18, 27–32.

Schoech, S.J., 1996. The effect of supplemental food on body condition and the timing of reproduction in a cooperative breeder, the Florida scrub-jay. Condor 98, 234–244.

Schoech, S.J., Hahn, T.P., 2007. Food supplementation and timing of reproduction: does the responsiveness to supplementary information vary with latitude? -. J. Ornithol. 148, S625–S632.

Schoech, S.J., Bowman, R., Reynolds, S.J., 2004. Food supplementation and possible mechanisms underlying early breeding in the Florida scrub-jay (*Aphelocoma coerulescens*). Horm. Behav. 46, 565–573.

Schultz, E.M., Hahn, T.P., Klasing, K.C., 2017. Photoperiod but not food restriction modulates innate immunity in an opportunistic breeder, *Loxia curvirostra*. J. Exp. Biol. 220, 722.

Schwab, R.G., Lott, D.F., 1969. Testis growth and regression in starlings (*Sturnus vulgaris*) as a function of presence of females. J. Exp. Zool. 171, 39.

Senner, N.R., Hochachka, W.M., Fox, J.W., Afanasyev, V., 2014. An exception to the rule: carry-over effects do not accumulate in a long-distance migratory bird. PloS One 9, e86588.

Sheldon, B.C., Verhulst, S., 1996. Ecological immunology: costly parasite defences and trade-offs in evolutionary ecology. TREE 11, 317–321.

Silver, R., Witkovsky, P., Horvath, P., Alones, V., Barnstable, C.J., Lehman, M.N., 1988. Coexpression of opsin- and VIP-like-immunoreactivity in CSF-contacting neurons of the avian brain. Cell Tissue Res. 253, 189–198.

Silverin, B., Viebke, P.A., 1994. Low-temperatures affect the photoperiodically inducted LH and testicular cycles differently in closely-related species of tits (*Parus spp*). Horm. Behav. 28, 199–206.

Silverin, B., Wingfield, J., Stokkan, K.A., Massa, R., Jarvinen, A., Andersson, N.A., Lambrechts, M., Sorace, A., Blomqvist, D., 2008. Ambient temperature effects on photo induced gonadal cycles and hormonal secretion patterns in great yits from three different breeding latitudes. Horm. Behav. 54, 60–68.

Singh, J., Budki, P., Rani, S., Kumar, V., 2012. Temperature alters the photoperiodically controlled phenologies linked with migration and reproduction in a night-migratory songbird. Proc. R. Soc. B. 279, 509–515.

Slater, P., 1969. Stimulus to egglaying in Bengalese finch. J. Zool. 158, 427.

Sorensen, M.C., Hipfner, J.M., Kyser, T.K., Norris, D.R., 2009. Carry-over effects in a Pacific seabird: stable isotope evidence that pre-breeding diet quality influences reproductive success. J. Anim. Ecol. 78, 460–467.

Stager, M., Pollock, H.S., Benham, P.M., Sly, N.D., Brawn, J.D., Cheviron, Z.A., 2016. Disentangling environmental drivers of metabolic flexibility in birds: the importance of temperature extremes versus temperature variability. Ecography 39, 787–795.

Stevenson, T.J., Ball, G.F., 2009. Anatomical localization of the effects of reproductive state, castration, and social milieu on cells immunoreactive for gonadotropin-releasing hormone-I in male European starlings (*Sturnus vulgaris*). J. Comp. Neurol. 517, 146–155.

Stevenson, T.J., Hahn, T.P., Ball, G.F., 2012a. Variation in gonadotrophin-releasing hormone-1 gene expression in the preoptic area predicts transitions in seasonal reproductive state. J. Neuroendocrinol. 24, 267–274.

Stevenson, T.J., Hahn, T.P., MacDougall-Shackleton, S.A., Ball, G.F., 2012b. Gonadotropin-releasing hormone plasticity: a comparative perspective. Front. Neuroendocrinol. 33, 287–300.

Storey, C., Nicholls, T., 1982. Low environmental temperature delays photoperiodic induction of avian testicular maturation and the onset of post-nuptial photorefractoriness. Ibis 124, 172–174.

Studds, C.E., Marra, P.P., 2005. Nonbreeding habitat occupancy and population processes: an upgrade experiment with a migratory bird. Ecology 86, 2380–2385.

Studds, C.E., Marra, P.P., 2011. Rainfall-induced changes in food availability modify the spring departure programme of a migratory bird. Proc. R. Soc. B. 278, 3437–3443.

Stutchbury, B.J.M., Gow, E.A., Done, T., MacPherson, M., Fox, J.W., Afanasyev, V., 2011. Effects of post-breeding moult and energetic condition on timing of songbird migration into the tropics. Proc. R. Soc. B. 278, 131–137.

Swaddle, J.P., Witter, M.S., 1997. The effect of molt on the flight performance, body mass, and behavior of European starlings (*Sturnus vulgaris*): an experimental approach. Can. J. Zool. 75, 1135–1146.

Swanson, D.L., 2010. Seasonal metabolic variation in birds: functional and mechanistic correlates. In: Thompson, C.F. (Ed.), Current Ornithology, vol. 17. Springer, New York, pp. 75–129.

Swanson, D.L., Olmstead, K.L., 1999. Evidence for a proximate influence of winter temperature on metabolism in passerine birds. Physiol. Biochem. Zool. 72, 566–575.

Swanson, D.L., Garland Jr., T., 2009. The evolution of high summit metabolism and cold tolerance in birds and its impact on present-day distributions. Evolution 63, 184–194.

Swanson, D.L., Vézina, F., 2015. Environmental, ecological and mechanistic drivers of avian seasonal metabolic flexibility in response to cold winters. J. Ornithol. 156, 377–388.

Tieleman, B.I., Versteegh, M.A., Klasing, K.C., Williams, J.B., 2019. Constitutive innate immunity of tropical House Wrens varies with season and reproductive activity. The Auk 1573, 1715–1720.

Tomotani, B.M., van der Jeugd, H., Gienapp, P., de la Hera, I., Pilzecker, J., Teichmann, C., Visser, M.E., 2018. Climate change leads to differential shifts in the timing of annual cycle stages in a migratory bird. Glob. Chang. Biol. 24, 823–835.

Tonra, C.M., Marra, P.P., Holberton, R.L., 2011. Migration phenology and winter habitat quality are related to circulating androgen in a long-distance migratory bird. J. Avian Biol. 42, 397–404.

Tøttrup, A.P., Rainio, K., Coppack, T., Lehikoinen, E., Rahbek, C., Thorup, K., 2010. Local temperature fine-tunes the timing of spring migration in birds. Integr. Comp. Biol. 50, 293–304.

Tøttrup, A.P., Klaassen, R.H.G., Kristensen, M.W., Strandberg, R., Vardanis, Y., Lindstrom, A., Rahbek, C., Alerstam, T., Thorup, K., 2012. Drought in Africa caused delayed arrival of European songbirds. Science 338, 1307–1307.

Trivedi, A.K., Sur, S., Sharma, A., Taufique, S.T., Gupta, N.J., Kumar, V., 2019. Temperature alters the hypothalamic transcription of photoperiod responsive genes in induction of seasonal response in migratory redheaded buntings. Mol. Cell. Endocrinol. 493, 110454.

Tsutsui, K., Ubuka, T., Bentley, G.E., Kriegsfeld, L.J., 2013. Review: regulatory mechanisms of gonadotropin-inhibitory hormone (GnIH) synthesis and release in photoperiodic animals. Front. Neurosci. 7, 11.

Ubuka, T., Cadigan, P.A., Wang, A., Liu, J., Bentley, G.E., 2009. Identification of European starling GnRH-I precursor mRNA and its seasonal regulation. Gen. Comp. Endocrinol. 162, 301–306.

Usui, T., Butchart, S.H.M., Phillimore, A.B., 2017. Temporal shifts and temperature sensitivity of avian spring migratory phenology: a phylogenetic meta-analysis. J. Anim. Ecol. 86, 250–261.

Verhagen, I., Gienapp, P., Laine, V.N., van Grevenhof, E.M., Mateman, A.C., van Oers, K., Visser, M.E., 2019. Genetic and phenotypic responses to genomic selection for timing of breeding in a wild songbird. Funct. Ecol. 33, 1708–1721.

Vézina, F., Cornelius Ruhs, E., O'Connor, E.S., Le Pogam, A., Régimbald, L., Love, O.P., Jimenez, A.G., 2019. Consequences of being phenotypically mismatched with the environment: rapid muscle ultrastructural changes in cold-shocked black-capped chickadees (*Poecile atricapillus*). Am. J. Physiol. Regul. Integr. Comp. Physiol. 318, R274–R283.

Visser, M.E., van Noordwijk, A.J., Tinbergen, J.M., Lessells, C.M., 1998. Warmer springs lead to mistimed reproduction in great tits *(Parus major)*. Proc. R. Soc. B. 265, 1867–1870.

Visser, M.E., Schaper, S.V., Holleman, L.J.M., Dawson, A., Sharp, P., Gienapp, P., Caro, S.P., 2011. Genetic variation in cue sensitivity involved in avian timing of reproduction. Funct. Ecol. 25, 868–877.

Visser, M.E., te Marvelde, L., Lof, M.E., 2012. Adaptive phenological mismatches of birds and their food in a warming world. J. Ornithol. 153, S75–S84.

Voelker, G., Rohwer, S., 1998. Contrasts in scheduling of molt and migration in Eastern and Western warbling-vireos. Auk 115, 142–155.

Voigt, C., Meiners, T., Ter Maat, A., Leitner, S., 2011. Multisensory non-photoperiodic cue advances the onset of seasonal breeding in island canaries (*Serinus canaria*). J. Biol. Rhythm. 26, 434–440.

Wada, M., 1993. Low temperature and short days together induce thyroid activation and suppression of LH release in Japanese quail. Gen. Comp. Endocrinol. 90, 355–363.

Wada, M., Hatanaka, F., Tsuyoshi, H., Sonoda, Y., 1990. Temperature modulation of photoperiodically induced LH-secretion and its termination in Japanese-quail (Coturnix-coturnix-japonica). Gen. Comp. Endocrinol. 80, 465–472.

Wang, G., Ramenofsky, M., Wingfield, J.C., 2013. Apparent dissociation of photoperiodic time measurement between vernal migration and breeding under dim green light conditions in Gambel's white-crowned sparrow *Zonotrichia leucophrys gambelii*. Curr. Zool. 59, 349–359.

Watts, H.E., Hahn, T.P., 2012. Non-photoperiodic regulation of reproductive physiology in the flexibly breeding pine siskin (*Spinus pinus*). Gen. Comp. Endocrinol. 178, 259–264.

Watts, H.E., Jimenez, D., Pacheco, V., Vilgalys, T.P., 2018. Effects of temperature on the timing of breeding and molt transitions in house finches. J. Exp. Biol. 221, jeb185058.

Weathers, W., Olson, C., Siegel, R., Davidson, C., Famula, T., 1999. Winter and breeding-season energetics of nonmigratory White-crowned Sparrows. Auk 116, 842–847.

Wikelski, M., Tarlow, E.M., Raim, A., Diehl, R.H., Larkin, R.P., Visser, G.H., 2003. Costs of migration in free-flying songbirds. Nature 423, 704.

Wikelski, M., Martin, L.B., Scheuerlein, A., Robinsoni, M.T., Robinson, N.D., Heim, B., Hau, M., Gwinner, E., 2008. Avian circannual clocks: adaptive significance and possible involvement of energy turnover in their proximate control. Philos. Trans. R. Soc. B-Biol. Sci. 363, 411–423.

Wilson, F.E., 1991. Neither retinal nor pineal photoreceptors mediate photoperiodic control of seasonal reproduction in American tree sparrows (*Spizella arborea*). J. Exp. Zool. 259, 117–127.

Wingfield, J.C., 1980. Fine temporal adjustment of reproductive function. In: Epple, A.S. (Ed.), Avian Endocrinology. Academic Press, pp. 367–389.

Wingfield, J.C., 1985. Environmental factors influencing the termination of reproduction in finches. In: Ilyichev, V.D., Gavrilov, V.M. (Eds.), Acta XVII Congressus Internationalis Ornithologici, pp. 478–487.

Wingfield, J.C., 2008. Organization of vertebrate annual cycles: implications for control mechanisms. Philos. Trans. R. Soc. B. 363, 425–441.

Wingfield, J.C., Marler, P., 1988. Endocrine basis of communication in reproduction and aggression. In: Knobil, E., Neill, J. (Eds.), The Physiology of Reproduction. Raven Press Ltd., pp. 1657–1677

Wingfield, J.C., Kenagy, G.J., 1991. Natural control of reproduction. In: Pang, P.K.T., Schreibman, M.P. (Eds.), Handbook of Comparative Endocrinology. Academic Press, pp. 181–241.

Wingfield, J.C., Farner, D.S., 1993. Endocrinology of reproduction in wild species. Avian Biol. 9, 163–327.

Wingfield, J.C., Hahn, T.P., Levin, R., Honey, P., 1992. Environmental predictability and control of gonadal cycles in birds. J. Exp. Zool. 261, 214–231.

Wingfield, J.C., Hahn, T.P., Doak, D., 1993. Integration of environmental-factors regulating transitions of physiological state, morphology and behavior. Avian Endocrinol. J. Endocrinol. 111–112.

Wingfield, J.C., O'Reilly, K.M., Astheimer, L.B., 1995. Modulation of the adrenocortical responses to acute stress in arctic birds: a possible ecological basis. Am. Zool. 35, 285–294.

Wingfield, J.C., Hahn, T.P., Wada, M., Astheimer, L.B., Schoech, S., 1996. Interrelationship of day length and temperature on the control of gonadal development, body mass, and fat score in white-crowned sparrows, Zonotrichia leucophrys gambelii. Gen. Comp. Endocrinol. 101, 242–255.

Wingfield, J.C., Hahn, T.P., Wada, M., Schoech, S.J., 1997. Effects of day length and temperature on gonadal development, body mass, and fat depots in white-crowned sparrows, Zonotrichia leucophrys pugetensis. Gen. Comp. Endocrinol. 107, 44–62.

Wingfield, J.C., Hahn, T.P., Maney, D.L., Schoech, S.J., Wada, M., Morton, M.L., 2003. Effects of temperature on photoperiodically induced reproductive development, circulating plasma luteinizing hormone and thyroid hormones, body mass, fat deposition and molt in mountain white-crowned sparrows, Zonotrichia leucophrys oriantha. Gen. Comp. Endocrinol. 131, 143–158.

Wingfield, J.C., Sullivan, K., Jaxion-Harm, J., Meddle, S.L., 2012. The presence of water influences reproductive function in the song sparrow (*Melospiza melodia morphna*). Gen. Comp. Endocrinol. 178, 485–493.

Yasuo, S., Watanabe, M., Okabayashi, N., Ebihara, S., Yoshimura, T., 2003. Circadian clock genes and photoperiodism: comprehensive analysis of clock gene expression in the mediobasal hypothalamus, the suprachiasmatic nucleus, and the pineal gland of Japanese quail under various light schedules. Endocrinology 144, 3742–3748.

Yuri, T., Rohwer, S., 1997. Molt and migration in the northern rough-winged swallow. Auk 114, 249–262.

Zysling, D.A., Garst, A.D., Demas, G.E., 2009. Photoperiod and food restriction differentially affect reproductive and immune responses in Siberian hamsters *Phodopus sungorus*. Funct. Ecol. 23, 979–988.

Chapter 45

Regulation of body temperature: patterns and processes

Andrew E. McKechnie[1,2]

[1]South African Research Chair in Conservation Physiology, South African National Biodiversity Institute, Pretoria, Gauteng, South Africa; [2]DSI-NRF Centre of Excellence at the FitzPatrick Institute, Department of Zoology and Entomology, University of Pretoria, Hatfield, Pretoria, Gauteng, South Africa

Abbreviations

A_b surface area
AVA arteriovenous anastomoses
BMR basal metabolic rate
C dry heat transfer coefficient
CEWL cutaneous evaporative water loss
C_{total} total thermal conductance
C_{wet} wet thermal conductance
EHL evaporative heat loss
EWL evaporative water loss
f_{resp} respiratory frequency
HIF heat increment of feeding
HTPA hypothalamus–thyroid–pituitary–adrenal
M_b body mass
ME Metabolic expansibility
MHP metabolic heat production
MMR maximal exercise-induced metabolic rate
M_{sum} summit metabolism
NST nonshivering thermogenesis
POAH preoptic anterior hypothalamus
Q_{cond} conductive heat flux
Q_{conv} convective heat flux
Q_{evap} evaporative heat loss
Q_{evap_c} cutaneous evaporative heat loss
Q_{evap_r} respiratory evaporative heat loss
Q_{metab} metabolic heat production
Q_{rad} radiative heat flux
REWL respiratory evaporative water loss
RMR resting metabolic rate
R_T amplitude of circadian rhythm of T_b
SCN suprachiasmatic nuclei
SERCA sarcoplasmic reticulum Ca^{2+}-ATPase
T_{air} air temperature
T_b body temperature
T_{brain} brain temperature
T_e operative temperature
TEWL total evaporative water loss
T_{inc} incubation temperature
T_{lc} lower critical limit of thermoneutrality
TNZ thermoneutral zone
T_s surface temperature
T_{skin} skin temperature
T_{uc} upper critical limit of thermoneutrality
UCP uncoupling protein
$\dot{V}_{O_2}$ oxygen consumption
V_T tidal volume
ZLTE zone of least thermoregulatory effort

45.1 Introduction

Birds maintain some of the highest body temperatures (T_b) of any animals, using internal metabolic heat production (MHP) to balance heat loss to the environment under cold conditions and multiple avenues of heat dissipation under hot conditions. The range of environmental temperatures over which birds can defend an approximately constant T_b is wide, with the cold extreme involving values more than 100°C below T_b in penguins resident year round in Antarctica. At the opposite extreme, nightjars and shorebirds incubating eggs in exposed nest sites in Earth's hottest deserts may defend T_b more than 20°C below environmental temperature via rapid evaporative heat dissipation (Grant, 1982; O'Connor et al., 2018).

That the capacity for endothermic homeothermy evolved in birds (and independently in mammals) is remarkable when one considers the energetic cost of this mode of thermoregulation. Compared to similarly sized reptiles, the daily energy requirements of birds may be 30- to 40-fold higher in very small species (Nagy, 2005). These substantial costs of endothermic homeothermy in comparison to the ectothermic thermoregulation that characterizes the vast majority of animals reiterate the fundamental

Sturkie's Avian Physiology. https://doi.org/10.1016/B978-0-12-819770-7.00025-6

benefits conferred by the capacity to regulate T_b independently of environmental temperature, thereby maintaining a constant thermal milieu for the biochemical processes that determine physiological performance.

The study of avian thermoregulation and the underlying physiological and behavioral mechanisms is essential for understanding the ecology and evolution of the planet's ~10,000 extant bird species. This field of enquiry has taken on increased urgency in the face of rapid global heating associated with anthropogenic climate change (see Section 45.9). This chapter explores the physiological and behavioral mechanisms involved in the regulation of avian T_b, the diversity of patterns of thermoregulation among extant birds, and the multitude of ways in which thermoregulation interacts with diverse aspects of avian ecology and evolution. I start by considering the sequence of evolutionary events spanning 250 million years that gave rise to the patterns of T_b regulation in extant birds.

45.2 The evolution of avian endothermy

The major models for the evolution of avian endothermy have focused on aerobic capacity (Bennett and Ruben, 1979) or parental care (Farmer, 2000; Koteja, 2000), with additional models based on niche expansion (Crompton et al., 1978) and body mass (M_b) miniaturization (McNab, 1978) also proposed for mammalian endothermy. A new model integrating the above single-cause models has recently been developed by Lovegrove (2017, 2019), who took advantage of the dramatic recent expansion of the fossil record and new methods for inferring morphology and physiology of extinct species to develop a detailed phenology of the major evolutionary events involved. Lovegrove's three-phase iterative model argues that major developments and transitions occurred in parallel in the sauropsid and synapsid lineages leading to birds and mammals, respectively, beginning around 250 MYA at the Permian–Triassic boundary.

According to this model (Figure 45.1), the first phase of the evolution of avian endothermy involved selection for constant T_b and bipedal locomotion in large-bodied archosaurs around 250–230 MYA in the early Triassic. The highly efficient avian respiratory system characterized by continuous ventilation of parabronchi appears to have its evolutionary origins at around the same time, likely conferring significant benefits to sauropsids during the extremely hot, hypoxic and hypercapnic conditions of the early Triassic. The second phase involved rapid miniaturization of body size, increases in relative brain size, and the development of insulation during the late Triassic and Jurassic. Over the course of 50 million years commencing at the start of the Jurassic, the average M_b of the avian lineage plummeted from 163 kg in early theropod dinosaurs to < 1 kg in the earliest birds capable of powered flight (Lee et al., 2014). The Jurassic also saw several pulses of increasing brain size (encephalization), likely requiring elevated resting metabolic rates (RMR) to meet the energy requirements of neuronal tissue. Another key late-Jurassic innovation was feathers, whose initial purpose was likely insulation.

The third phase, spanning the Cretaceous and Cenozoic, involved diversification of avian locomotion subsequent to the evolution of powered flight, likely associated with strong selection for enhanced aerobic capacity of pectoral muscles as well as stable muscle temperatures (Lovegrove, 2017). A second major event driving the evolution of homeothermic endothermy during this phase was climate adaptation during the second half of Cenozoic, when high-latitude cold habitats appeared within the last ~33 million years (Zachos et al., 2001). Another aspect of Lovegrove's model that has considerable relevance for understanding

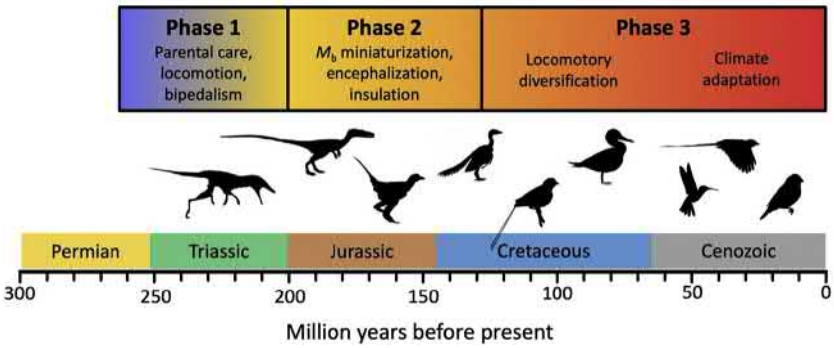

FIGURE 45.1 Summary of Lovegrove's three-phase iterative model for the evolution of avian endothermy, redrawn from Lovegrove (2017), with most of the same silhouettes of taxa representative of the various phases. The silhouettes were obtained from http://phylopic.org/, and from left to right are *Scleromochlus* (Jaime Headden, modified by T. Michael Keesey), *Coelophysis* (Emily Willoughby), *Aurornis* (Gareth Monger), *Archaeopteryx* (Dann Pigdon), *Protopteryx* (Matt Martyniuk), *Ichthyornis* (Matt Martyniuk), hummingbird (Ferran Sayol), *Urocolius* (Enoch Wetsy et al.) *Taeniopygia* (Jim Bendon and T. Michael Keesey). They are reproduced here under a Creative Commons License (https://creativecommons.org/licenses/by/3.0/).

contemporary avian thermoregulation is the notion that the pronounced reductions in T_b of which some groups are capable (see Section 45.4.4) represent a plesiomorphic (i.e., ancestral) trait. According to this argument, the facultative reductions in metabolic rate and consequent low T_{bs} that occur during hibernation and torpor represent a temporary abandonment of the maintenance of high, constant T_b and amount to a physiological reversion toward the ancestral ectothermic state.

45.3 Models of avian thermoregulation

45.3.1 Overall heat balance

Transfers of thermal energy between a bird and its environment occur via four physical processes: radiation, convection, conduction, and evaporation, and the total heat content (Q) of a bird depends on the sum of heat gain and heat loss, such that

$$\frac{dQ}{dt} = Q_{rad} + Q_{conv} + Q_{cond} + Q_{evap} + Q_{metab}$$

where Q_{rad} is radiative heat flux, Q_{conv} is convective heat flux, Q_{cond} is conductive heat flux, Q_{evap} is evaporative heat loss, and Q_{metab} is metabolic heat production. The radiative, convective, and conductive terms can each be positive or negative (i.e., comprise net heat gain or loss), whereas evaporation always involves heat loss and MHP always involves heat gain. The factors determining each term and the ways in which birds can modify these heat fluxes via behavioral adjustments are considered in more detail in Sections 45.5 and 45.6 below.

45.3.2 Avian endothermic homeothermy

Our current understanding of avian thermoregulation largely has its roots in work undertaken by Per Scholander, Laurence Irving, and their collaborators in the late 1940s, who proposed a model for the relationships between T_b, RMR, insulation, and air temperature (T_{air}) that became known as the Scholander–Irving model. The original formulation of the model (Scholander et al., 1950) did not explicitly include an upper limit to resting MHP (i.e., summit metabolism) nor thermoregulation at T_{air} above the thermoneutral zone (TNZ) (Figure 45.2), but these aspects became clear during subsequent work, such as Dawson's (1954) study of thermoregulation in towhees at high T_{air}. The Scholander–Irving model referred to T_{air} because it was developed for metabolic rates of animals placed in darkened chambers; applying this model to free-ranging birds under natural conditions requires replacing T_{air} with an integrated measure of environmental temperature, such as operative temperature (T_e) (Bakken, 1976; Robinson et al., 1976).

In the Scholander–Irving model (Figure 45.2), RMR (i.e., metabolic rate of a resting bird, in the absence of heat produced as a by-product of activity or digestion) is minimal within the TNZ, the range of T_{air} over which heat production associated with baseline metabolic costs of body maintenance is adequate to balance heat lost to a bird's surroundings. The metabolic rate in the TNZ is referred to as basal metabolic rate (BMR) if measured during the rest phase of the circadian cycle (see Section 45.6.1). The lower boundary of the TNZ is the lower critical limit of thermoneutrality (T_{lc}), and at $T_{air} < T_{lc}$, MHP increases approximately linearly to balance heat loss to the environment, providing the basis for the regulation of a stable T_b even at low T_{air}. Avian T_{lc} varies from 30 to 35°C in small species in tropical habitats down to $T_{air} \approx 0$°C in larger, high-latitude species such as glaucous gulls (*Larus hyperboreus*; Scholander et al., 1950) and snowy owls (*Bubo scandiacus*; Gessaman, 1972).

Below the T_{lc}, the relationship between metabolic rate and T_{air} is described by a linear function $RMR = C_{total} \cdot A_b(T_b - T_{air})$, where RMR = resting metabolic rate (Watts, W) and C_{total} = total thermal conductance in W/m^2°C and A_b is surface area in m^2 (although conductance is frequently expressed as whole-animal values in W/°C or similar units). The original formulation of the Scholander–Irving model implicitly assumed that conductance is minimized (and hence, insulation is maximized) at all $T_{air} < T_{lc}$, yielding the prediction of a linear increase in RMR with decreasing T_{air}. Any postural adjustments such as ptiloerection that occur at lower T_{air} may thus result in changes to the slope of RMR versus T_{air}. A key prediction of the Scholander–Irving model, arising from the assumption that conductance is minimized at all $T_{air} < T_{lc}$, is that extrapolating the RMR versus T_{air} line will see RMR reaching zero at a T_{air} value identical to normothermic T_b. The upper limit to increases in resting MHP and hence cold tolerance is determined by summit metabolism, the maximum RMR achievable via shivering and nonshivering pathways.

The upper boundary of the TNZ is the upper critical limit of thermoneutrality (T_{uc}). Although characterized by RMR remaining at a constant, minimal value from the T_{lc} up to the T_{uc}, and often seen as a sort of physiological steady state, the TNZ is in fact a range of T_{air} values over which many physiological changes are occurring. Thermal conductance, which is theoretically minimal at the T_{lc}, increases with T_{air} within the TNZ. T_b typically begins to increase at some T_{air} within the TNZ, and the same is usually true for evaporative water loss (EWL). The latter point has long been recognized, primarily in the poultry science literature, in the concept of the zone of least thermoregulatory effort, defined as the range of T_{air} bounded at the lower end by the T_{lc} and at the upper end by the inflection T_{air} at which EWL starts to increase (Etches et al., 2008, Figure 45.2).

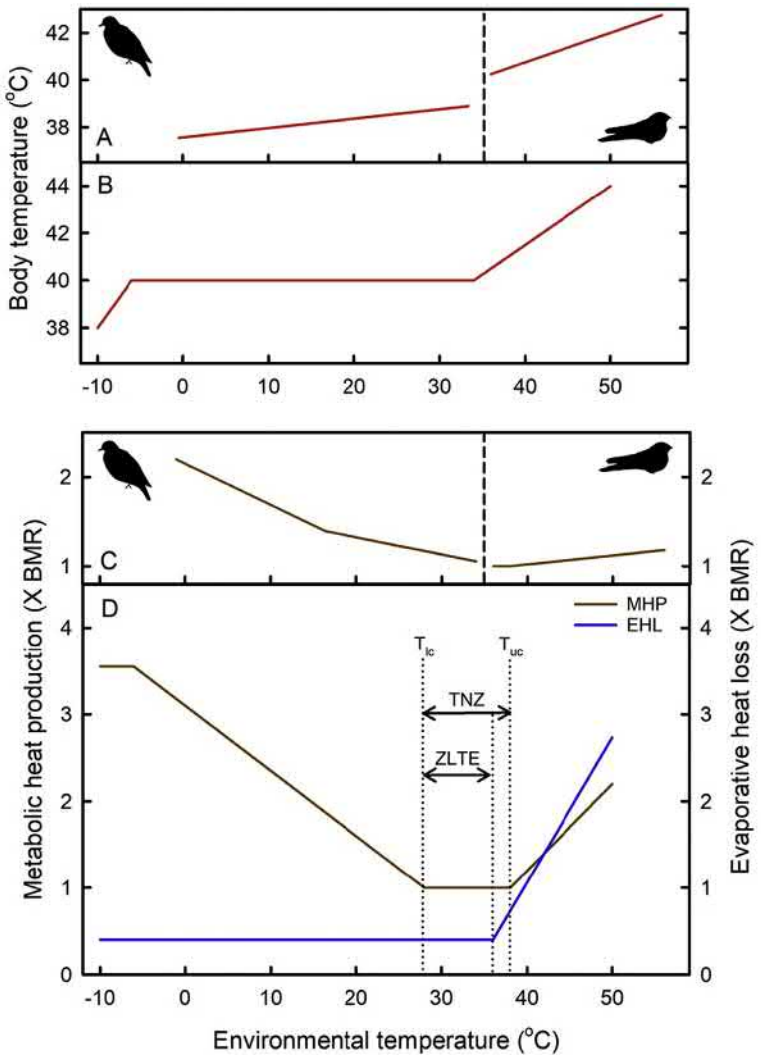

FIGURE 45.2 A general model of the relationships between body temperature (T_b; red lines in panels A and B) and resting metabolic rate and evaporative heat dissipation (panel C and D) in birds. The model, based largely on the Scholander–Irving model, is illustrated in panels (B) and (D), with both metabolic heat production (MHP) and evaporative heat loss (EHL) expressed as multiples of basal metabolic rate (BMR). In panel (D), the lower and upper critical limits of thermoneutrality (T_{lc} and T_{uc}, respectively) that bound the thermoneutral zone (TNZ) are shown by *vertical dotted lines*. Also shown is the zone of least thermoregulatory effort (ZLTE), a concept often used in poultry science literature but rarely in comparative physiology literature. Panels (A) and (C) illustrate deviations from the general model, as reported in African green pigeons (*Treron calvus*, data from Noakes et al., 2013; left of the *vertical dashed line*) and a nightjar (right of the *vertical dashed line*). The silhouettes were obtained from http://phylopic.org/: fruit-dove (L. Shyamal) and nightjar (Ferran Sayol). They are reproduced here under a Creative Commons License (https://creativecommons.org/licenses/by/3.0/).

The T_{uc} is the T_{air} above which the energetic cost of heat dissipation pathways such as panting results in an approximately linear increase in RMR (Figure 45.2D). At $T_{air} > T_{uc}$, the primary physiological process is an increase in evaporative heat dissipation to balance environmental heat gains and MHP, thereby maintaining T_b below lethal limits. Because heat dissipation increases more rapidly with T_{air} than does MHP, ratios of evaporative heat loss (EHL) to MHP increase from EHL/MHP < 1 when $T_b > T_{air}$ to EHL/MHP $= 1$ when $T_b = T_{air}$ and EHL/MHP > 1 at higher T_{air}, providing the physical basis for maintaining T_b below T_{air}.

45.3.3 Deviations from the Scholander–Irving model

Although thermoregulation in most birds investigated to date generally conforms to this model (Figure 45.2), this is not always the case. An example is provided by the African green pigeon (*Treron calvus*), in which normothermic T_b

was atypically variable for a 220-g bird, no TNZ was evident, and T_b gradually decreased with T_{air} (Noakes et al., 2013, Figure 45.2A). In addition, recent work on evaporative cooling in nightjars reveals that some species apparently lack a T_{uc} entirely, with negligible metabolic costs of gular flutter (see Section 45.6.3) resulting in RMR remaining close to minimal levels even at $T_{air} = 50–55°C$ (O'Connor et al., 2017, Figure 45.2C). In highly social taxa, patterns of thermoregulation may depend on the number of individuals roosting communally. In white-backed mousebirds (*Colius colius*), T_b decreased during the course of a night, with the cooling rate negatively related to the number of individuals in a group (McKechnie and Lovegrove, 2001a). In this species, communal roosting is apparently a prerequisite for the defense of an approximately constant rest-phase T_b.

45.3.4 Thermal conductance

Thermal conductance is the rate of total heat transfer between an object and its immediate surroundings per unit surface area per 1°C difference in temperature (IUPS, 2001). Under typical laboratory conditions, total thermal conductance of a bird (C_{total}, W/m^2°C) is quantified as follows:

$$C_{total} = \frac{RMR}{(T_b - T_{air})A_b}$$

where RMR is resting metabolic rate in W, T_b and T_{air} are in °C, and A_b is surface area in m^2. In the absence of empirical measurements of A_b, this variable can be predicted allometrically (Walsberg and King, 1978). Because C_{total} includes EHL, it is sometimes referred to as wet thermal conductance (C_{wet}) (e.g., Schleucher and Withers, 2001). It is also often expressed in the literature as total rather than surface area–specific values. To evaluate the heat transfer properties of birds without the evaporative component, the dry heat transfer coefficient (C, W/m^2°C) is calculated as follows:

$$C = \frac{RMR - EHL}{(T_b - T_{air})A_b}$$

where EHL is evaporative heat loss (W). In general, C is minimal at $T_{air} < T_{lc}$ (although postural adjustments at low T_{air} may reduce it further), increases in the TNZ, and appears to continue increasing at $T_{air} > T_b$ (Tieleman and Williams, 1999).

Within an individual bird, C_{total} and C are ~40% higher during the active phase compared to when roosting (Aschoff, 1981; Schleucher and Withers, 2001). The rest-phase reduction is achieved by increasing plumage depth by ptiloerection and postural changes. Birds roosting in cold environments typically adopt postures as close as possible to that of a sphere by hunching the neck, tucking the beak or head under scapular feathers, and squatting so that the unfeathered legs and feet are drawn into the feather layer. Roosting toucans, for instance, tuck their huge beaks into the feathers between their wings while orientating their tail feathers vertically above their backs, a posture thought to minimize heat loss while roosting (Tattersall et al., 2009).

At an interspecific level, C_{total} and C scale with M_b. Schleucher and Withers (2001) compiled rest-phase conductance data for 257 species and reported a scaling relationship for C_{wet} expressed as mass-specific oxygen consumption ($\dot{V}_{O_2}$ in mL O_2 g^{-1} h^{-1}°C^{-1}) as a function of M_b (g):

$$\log_{10} C_{wet} = -0.477 \log_{10} M_b - 0.163$$

45.4 Body temperature

Although birds are considered endothermic homeotherms that regulate an approximately constant T_b, the known range of avian T_b spans more than 40°C, from values below 5°C during torpor or hibernation to values above 45°C during heat exposure (Table 45.1). This section synthesizes the available information on avian T_b; for convenience, patterns of T_b are treated in a trichotomous fashion as normothermic, hyperthermic (increases above normothermic values), or hypothermic (decreases below normothermic values).

45.4.1 Measurement of body temperature

Historically, most T_b measurements involved thermocouple probes inserted cloacally, subcutaneously, or into tissues such as breast muscles (Dawson, 1954; Randall, 1943). Thermocouples have also been widely used for skin temperature (T_{skin}) measurements or inserted into structures such as the cornea (Pinshow et al., 1982). Cloacal thermocouple measurements remain widely used in laboratory studies of both nondomesticated (e.g., Smit and McKechnie, 2010; Tieleman et al., 2002) and domesticated birds (Arad and Marder, 1982; Marder, 1973).

Remote measurement of T_{skin} via temperature-sensitive VHF transmitters has proven invaluable for studies of thermoregulation in free-ranging birds (Brigham, 1992; Romano et al., 2019; Smit et al., 2011). However, T_{skin} can differ from core T_b by several degrees, particularly during cold weather, and even transmitters in close contact with birds' skin are affected by factors such as solar radiation. Thus, T_{skin} measurements are generally feasible only in studies where comparatively large changes in T_b are anticipated, such as during torpor, and where gradients between skin and core T_b can be experimentally determined (e.g., Brigham, 1992; McKechnie et al., 2007a).

TABLE 45.1 Body temperature (T_b) variation among avian orders in minimum hypothermic values (Min. T_b) during heterothermy, normothermic rest- and active-phase values, and maximum hyperthermic (Max. T_b) values during acute heat exposure. The latter are not lethal values but rather maximum values recorded in individuals exposed to high T_{air} and which fully recovered. Normothermic values followed by ranges in parentheses are rest- or active-phase means reported by Prinzinger et al. (1991). Other sources are listed below the table.

Order	Min. T_b (°C)	Normothermic T_b (°C)		Max. T_b (°C)
		Rest-phase	Active-phase	
Struthioniformes		38.3 (38.0–38.7)	39.3 (38.7–40.1)	
Apterygiformes		38.2 (37.4–39.0)	38.3 (38.1–39.0)	
Casuariiformes		38.6 (37.7–38.9)	38.8 (37.9–39.2)	
Tinamiformes		39.2	40.5	
Galliformes	36.5	38.9 (37.5–40.5)	41.4 (38.2–42.5)	43.6
Domestic fowl		40.5	41.5	45.5–46.2
Anseriformes	35.1	39.0 (38.3–39.5)	41.3 (39.8–43.0)	
Caprimulgiformes	4.3–18.5	37.9 (35.0–39.5)	39.7 (37.0–42.4)	40.7–43.7
Apodiformes				
Apodidae	10.7–20.1	38.6	40.0 (38.6–41.8)	44.7
Trochilidae	3.3–32	38.1 (35.2–39.5)	40.3 (35.6–44.6)	
Cuculiformes	<25–33		41.3 (39.9–42.3)	43.9
Columbiformes	24.8–35	38.6 (37.7–39.9)	40.9 (38.3–43.3)	41.9–44.7
Pterocliformes			39.0–39.4	43.2–43.6
Gruiformes		37.5	40.4 (39.1–41.4)	
Podicipediformes		38.9 (38.5–39.3)	39.5 (38.5–40.2)	
Charadriiformes		38.5 (35.2–39.5)	40.9 (38.3–42.4)	44.3
Gaviiformes		39.2 (35.0–39.5)	39.3 (39.0–39.6)	
Sphenisciformes		37.8 (35.0–39.0)	38.2 (37.0–39.0)	
Procellariiformes		38.3 (37.0–39.6)	39.4 (37.5–41.0)	
Ciconiiformes		39.3 (38.7–39.6)	40.5 (39.5–42.3)	
Pelecaniformes		37.9 (37.1–38.9)	40.6 (39.0–42.7)	
Cathartiformes	34			
Accipitriformes	35.3			
Strigiformes	29–35.5	38.7 (38.0–39.8)	40.2 (38.6–41.2)	42.9–44.2
Coliiformes	18.2–26	38.2 (35.6–39.0)	39.5 (38.0–41.5)	44.1
Coraciiformes	26–28.6	39.2	40.0 (40.0–40.7)	43.5
Piciformes		37.9–39.1	41.8 (39.0–43.0)	44.4
Falconiformes	31–38.3	39.0 (37.9–40.3)		44
Psittaciformes		37.9 (37.7–38.1)	41.3 (41.0–41.5)	43.4–44.1
Passeriformes	24–37.6	38.5 (36–40.8)	41.0 (39–44.1)	43–48.0

Minimum T_b: Brigham (1992), Butler and Woakes (2001), Hohtola et al. (1991), Koskimies (1948), Lane et al. (2004), Morrison (1962), Ramsey (1970), Wolf et al. (2020), Ohmart and Lasiewski (1971), B. Smit et al. (unpublished data), Bahat et al. (1998), Cheke (1971), Clemens (1989), Cooper et al. (2008), Graf et al. (1989), Heath (1962), McKechnie and Lovegrove (2001a), McKechnie and Lovegrove (2001b), Merola-Zwartjes and Ligon (2000), Sapsford (1986), Schleucher (2001), Shapiro and Weathers (1981), Smit and McKechnie (2010), Thouzeau et al. (1999), McKechnie and Lovegrove (2001a,b). Normothermic rest-phase T_b: Kemp et al. (2017), Lund et al. (2020), Prinzinger et al. (1991). Normothermic active-phase T_b: Prinzinger et al. (1991), Smit et al. (2008), McKechnie et al. (2016), Czenze et al. (2020). Maximum T_b: Czenze et al. (2020), Freeman et al. (2020), Kemp and McKechnie (2019), McKechnie et al. (2017), McKechnie et al. (2016), McWhorter et al. (2018), O'Connor et al. (2018), O'Connor et al. (2017), Smit et al. (2008), Smith et al. (2015), Smith et al. (2017), Talbot et al. (2018), Talbot et al. (2017), Weathers (1997), Whitfield et al. (2015), Arad and Marder (1982), Randall (1943), Czenze et al. (2020).

Devices surgically implanted into the abdominal cavities of birds are often the most feasible option for monitoring T_b, with transponders, transmitters, and data loggers all routinely used in avian thermoregulation studies. Remote measurement of the T_b of small birds using implanted temperature-sensitive transmitters dates back at least 50 years (Coulombe, 1970; Southwick, 1973), and subsequent technological advances resulting in smaller, more powerful transmitters have ensured that this approach remains widely used (e.g., Thompson et al., 2018). Constraints of this technique include the attenuation of transmitted signals by using helical rather than whip antennae, the fact that the implanted transmitter is surrounded by avian tissues, and the signal drift that has been reported for some transmitters (Cunningham et al., 2017; Williams et al., 2009).

A similar approach involves implanted data loggers that record T_b at user-specified intervals, and such devices have yielded valuable insights into avian thermoregulation in free-ranging individuals of species ranging from migratory geese to small desert passerines (Butler and Woakes, 2001; Smit et al., 2013). A nascent technology that holds much promise is loggers that can download data to a nearby base station (e.g., Tattersall et al., 2016), or use Bluetooth technology to connect to nearby devices such as smartphones (e.g., HOBO TidbiT MX loggers, Onset Computer Corporation, Bourne, MA).

Infrared thermography is another extremely useful tool for studying heat exchange between birds and their environments [see McCafferty (2013) and Yahav and Giloh (2012) for reviews of applications]. Over the last decade, this technique has provided novel insights into the role of the avian beak as a controllable heat radiator (Tattersall et al., 2009, 2018). Infrared thermography also has considerable potential for monitoring animal welfare, including remote detection of chronic inflammation and stress-induced hyperthermia in poultry (McCafferty, 2013).

45.4.2 Normothermic body temperature

Avian resting T_b is characterized by a circadian rhythm, whereby T_b during the rest phase (i.e., the period of inactivity) is lower than T_b during the active phase (daytime for diurnal species). This circadian rhythm is entrained to photoperiod and regulated by inputs from the eyes and pineal body to the suprachiasmatic nuclei (SCN) of the hypothalamus, with the hormone melatonin being the major signaling molecule involved (see Section 45.7.3). The mean ± SD rest-phase T_b for 202 species spanning most avian orders is 38.5 ± 1.0°C and the mean active-phase T_b for 724 species is 41.0 ± 1.3°C (Prinzinger et al., 1991). However, the amplitude of circadian rhythms of T_b (R_T) decreases with increasing M_b. Aschoff (1982) analyzed the scaling of circadian cycles of avian T_b and found that the amplitude is best described as $R_T = 10.856M_b^{-0.396}$ for nonpasserines and $R_T = 4.182M_b^{-0.125}$ for passerines. The data analyzed by Aschoff (1982) primarily involved species from north-temperate latitudes and more recent studies suggest that R_T for species from subtropical latitudes may be higher (Kemp et al., 2017; McKechnie and Smit, 2010).

Whether avian normothermic T_b scales with M_b is less clear. Prinzinger et al. (1991) concluded that T_b decreases with increasing M_b, particularly during the active phase, and that there is no phylogenetic variation after M_b is taken into account. A more recent analysis that did not distinguish between active- and rest-phase T_b values, but which controlled for phylogenetic relatedness, reported a marginally nonsignificant negative relationship between avian T_b and M_b, but also found evidence that the scaling of T_b may vary among orders (Clarke and Rothery, 2008). One group of birds well known for low T_b is the ratites (kiwis, emus, ostriches, and rheas), which typically have T_b equivalent to ~ 3°C below typical avian values (Clarke and Rothery, 2008; McNab, 1966).

Like many physiological traits, avian T_b exhibits phenotypic flexibility, and can be adjusted as a component of acclimation or acclimatization. Active- or rest-phase T_b varies seasonally in some species (Rintamaki et al., 1983; Swanson and Weinacht, 1997), but may also change over even shorter time scales. Studies of white-browed sparrow-weavers (*Plocepasser mahali*) in the Kalahari Desert of southern Africa have revealed that active-phase T_b (and hence R_T) can vary between conspecific populations in a manner correlated with small differences in climate and moreover can also change within a population between dry and wetter periods (Smit et al., 2013).

45.4.3 Hyperthermic body temperature

Avian T_b may increase far above normothermic levels under conditions of heat exposure or intense exercise. For instance, seven of nine species held during midsummer in large outdoor flight aviaries in the Kalahari Desert exhibited maximum $T_b > 44$°C (and in three species, > 45°C, Thompson et al., 2018), and the T_b of breeding marsh tits (*Poecile palustris*) provisioning nests in southern Sweden sometimes exceeded 45°C during warm weather (Nilsson and Nord, 2018). Under resting conditions, avian T_b typically starts increasing above the normothermic setpoint at T_{air} between 35 and 40°C, above which it increases linearly to maximum values that are usually 2−5°C above normothermic values.

Lethal avian T_b values, typically between 46 and 47°C, have been reported for both domesticated and nondomesticated species (Arad and Marder, 1982; Dawson, 1954; Randall, 1943). Avian maximum T_b values equivalent to the critical thermal maximum (CT_{max}), usually taken as the T_b at which the capacity for coordinated locomotion

ceases, typically fall between 44 and 45°C among desert passerines (McKechnie et al., 2017; Smith et al., 2017; Whitfield et al., 2015). A mean value of 45.7°C and individual T_b values as high as 47.0°C have been reported in the variable seedeater (*Sporophila aurita*), a small passerine inhabiting humid tropical lowlands (Weathers, 1997). Recently, a new upper limit for avian T_b was documented in red-billed queleas (*Quelea quelea*); the mean maximum T_b for 20 birds was 48.0°C, with a highest individual value of 49.1°C (Freeman et al., 2020). Among poultry, maximum T_b values from which most individuals recovered fully have been reported as 45.5−46.2°C (Arad and Marder, 1982; Randall, 1943). The extent to which T_b increases above normothermic values varies across taxa, with passerines exhibiting more pronounced facultative hyperthermia than other orders (Gerson et al., 2019).

Whereas maximum T_b for most taxa is restricted to a relatively narrow range of values in the mid-40s, the maximum T_{air} values birds can tolerate vary widely. Passerines from the arid zones of the American southwest, southern Africa, and the interior of Australia tolerated T_{air} of 46−54°C before T_b reached CT_{max} (McKechnie et al., 2017; Smith et al., 2017; Whitfield et al., 2015), but columbids and caprimulgids tolerated T_{air} approaching and sometimes exceeding 60°C (McKechnie et al., 2016; O'Connor et al., 2017; Smith et al., 2015; Talbot et al., 2017). The large variation among taxa in heat tolerance limits appears to arise from differences in the relative efficiency of the major avenues whereby birds dissipate heat evaporatively (see Section 45.5.4).

Like normothermic values, avian heat tolerance and T_b during acute heat exposure may vary within species and exhibit phenotypic plasticity. Heat-acclimated rock doves (*Columba livia*) maintained lower T_b during acute heat exposure compared to individuals acclimated to room temperature (Marder and Arieli, 1988), and a similar result was reported for white-winged doves (*Zenaida asiatica*; McKechnie and Wolf, 2004b). In some cases, intraspecific variation in heat tolerance is correlated with climate: a population of white-browed sparrow-weavers (*P. mahali*) inhabiting a hot, arid site tolerated significantly higher T_{air} during summer than conspecifics from cooler, mesic sites (Noakes et al., 2016).

Avian thermoregulation is characterized by the maintenance of brain temperature (T_{brain}) below core T_b, reflecting the high thermal sensitivity of brain tissue. Gradients between T_b and T_{brain} range from 0.1 to >2.0°C (Bech and Midtgård, 1981; Kilgore et al., 1976), and may reach values as high as 3.5°C in flying pigeons (Pinshow et al., 1982). The major mechanism involved in avian brain cooling is the rete opthalmicum, a network of blood vessels providing a countercurrent heat exchanger that cools arterial blood before reaching the brain (Midtgård, 1983; Porter and Witmer, 2016). The presence of a rete opthalmicum does not, however, appear to be prerequisite for brain cooling; T_b−T_{brain} gradients averaging 0.73°C occur in the calliope hummingbird (*Selasphorus calliope*) even though it lacks this structure (Burgoon et al., 1987).

45.4.3.1 Fever

Regulated hyperthermic responses associated with the activation of the innate immune system are widespread among vertebrates. Avian febrile responses have typically been investigated using lipopolysaccharide (a cellular component of gram-negative bacteria that mimics bacterial infection) to experimentally induce an immune response, with both the peak T_b and duration of fever being dose-dependent (Gray et al., 2013). Muramyl dipeptide, a cellular component of gram-positive bacteria, appears not to trigger avian febrile responses (Koutsos and Klasing, 2001; Marais et al., 2011), whereas the viral mimic polyinosinic:polycytidylic acid triggers fever in some species (Marais et al., 2011) but not others (Coon et al., 2011). The magnitude of hyperthermia during avian febrile responses is typically 1−2°C (occasionally as high as ~3°C) and varies with factors such as environmental temperature and prior exposure to pathogens (Gray et al., 2013). Fever magnitude tends to be greater when environmental temperature is above the TNZ, suggesting that fever-inducing infections could contribute substantially to avian mortality during heat waves (Gray et al., 2013).

Avian toll-like receptors (TLRs), found on the cell membranes of immune cells and which recognize pathogen cell surface molecules, differ to those of mammals. Whereas seven avian TLR genes are shared with mammals and/or fish, there are an additional three TLR genes apparently unique to birds (Temperley et al., 2008). The molecules that mediate the febrile response following TLR recognition of pathogens appear to be broadly comparable among birds and mammals, with prostaglandins, nitric oxide, and cytokines including interleukin-1β (IL-1β) and interleukin-6 (IL-6) involved. However, there are several key differences. First, the roles of IL-1β and IL-6 seem to differ in birds compared to mammals. Second, whereas prostaglandin E_2 is the major mediator of mammalian febrile responses, another prostaglandin appears to play the equivalent role in birds (Gray et al., 2013). As is the case in mammals, glucocorticoids appear to play an important role in modulating avian fever (Gray et al., 2013).

45.4.4 Hypothermic body temperature

The costs of endothermic homeothermy rapidly increase at low environmental temperatures. Some birds do indeed defend T_b at normothermic levels even at extremely low T_{air}, often relying on behaviors such as communal roosting, constructing insulated roost nests, or caching of food to avoid mismatches between energy supply and demand.

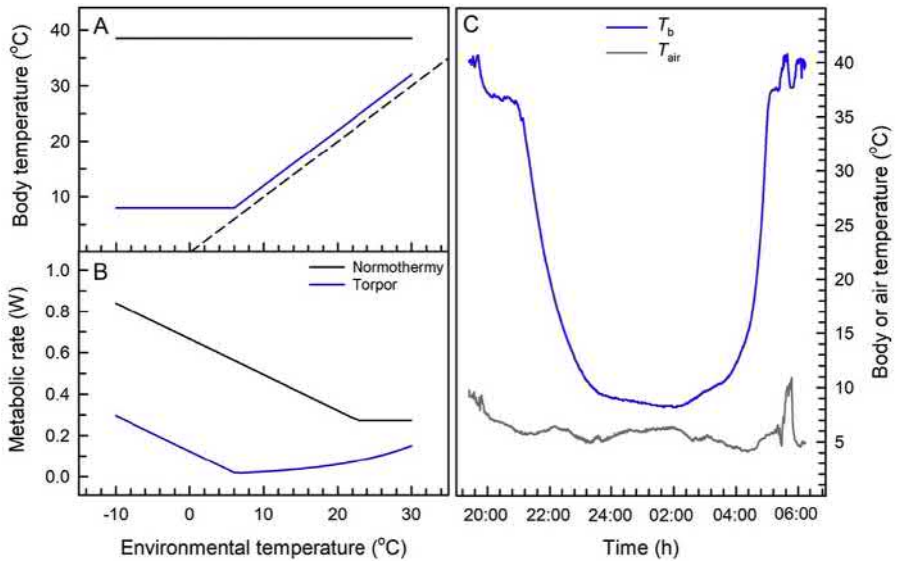

FIGURE 45.3 Avian torpor involves large reductions in metabolic rate and the resetting of body temperature (T_b) to a reduced setpoint. Panels (A) and (B) show the relationships between air temperature (T_{air}) and T_b (A) and metabolic rate (B) during normothermy (*black line*) and torpor (*blue line*) in a hypothetical 22-g bird with normothermic $T_b = 38.5°C$ and torpor setpoint $T_b = 8°C$. Note that at $T_{air} > 6°C$, thermoregulation is essentially ectothermic, with T_b remaining slightly above T_{air} (*dashed line* in panel A indicates equality) and metabolic rate decreasing in a temperature-dependent manner ($Q_{10} = 2.5$ assumed). At $T_{air} < 6°C$, thermoregulation follows the same pattern as during normothermy, with a setpoint T_b defended by linear increases in metabolic rate (panel B). Panel C is an overnight trace of T_b (blue line) and T_{air} (grey line) during a torpor bout in a giant hummingbird (*Patagona gigas*) held in captivity overnight in March 2015 at an elevation of 3800 m above sea level in the Peruvian Andes (Wolf et al., 2020).

Many others, however, show heterothermy involving regulated, reversible reductions in metabolic rate during which T_b may decrease far below normothermic levels (Figure 45.3). Distinguishing between normothermic circadian rhythms of avian T_b and facultative hypothermia is often not straightforward. Several approaches to distinguishing hypothermic T_b from normothermic T_b have been proposed, including the use of threshold T_b values (Barclay et al., 2001; Brigham et al., 2011), statistical approaches based on an assumption that normothermic T_b is normally distributed (McKechnie et al., 2007a), and, increasingly, arguments that avian T_b should be seen as a continuum between normothermy and hypothermia rather than viewed as discrete categories (Boyles et al., 2011a,b). One counterargument to the latter view concerns the fact that some studies have revealed that small differences in T_b can be associated with very different physiological states (Merola-Zwartjes and Ligon, 2000).

Facultative reductions in T_b vary in magnitude from 1-2°C below normothermic values to deep torpor with T_b reductions of >30°C, resulting in minimum $T_b \leq 5°C$. Shallow reductions in rest-phase T_b to 30°C or higher are typical of many passerines overwintering at high latitudes (Andreasson et al., 2019; Chaplin, 1976; Reinertsen and Haftorn, 1986) and are also often reported in response to food deprivation in laboratory studies (McKechnie and Lovegrove, 2003; Noakes et al., 2013; Rashotte et al., 1995). Reductions in T_b to 20−30°C are also taxonomically widespread, with minimum T_b in this range reported for columbids, coraciiformes, and a number of passerine families (Table 45.1). In contrast, the capacity to enter deep torpor and reduce T_b by > 20°C below normothermic levels appears to be restricted to a number of nonpasserine taxa, most notably hummingbirds, swifts, mousebirds, and nightjars and allies (McKechnie and Lovegrove, 2002; Schleucher, 2004).

The most pronounced reductions in avian T_b, to values $\leq 5°C$, occur in the common poorwill (*Phalaenoptilus nuttallii*), the only known avian hibernator (Jaeger, 1948; Woods et al., 2019) and in hummingbirds that inhabit high elevations (Calder and Booser, 1973; Carpenter, 1974; Pearson, 1953). Recently, a minimal cloacal T_b of just 3.3°C has been documented in a black metaltail (*Metallura phoebe*) at 3800 m above sea level in the Peruvian Andes (Wolf et al., 2020).

45.5 Avenues of heat transfer and behavioral modifications

45.5.1 Radiation

Radiative heat fluxes can vary from substantial heat losses (e.g., when roosting under a clear sky on a winter's night) to very rapid heat gains (e.g., foraging from an exposed

perch on a cloudless summer's day). Radiative heat transfer is estimated as follows:

$$Q_{rad} = \varepsilon\sigma A_b\left(T_s^4 - T_a^4\right)$$

where ε is combined emissivity, σ is the Stephan–Boltzmann constant, A_b is surface area in m^2, and T_s and T_a are surface and ambient temperatures in °K. The major avenue of radiative heat gain for free-ranging birds is solar irradiance, which at lower latitudes can exceed 1100 W/m^2 at midday when the sun is directly overhead. Approximately 42% of solar irradiance occurs in visible wavelengths (400–700 nm) and 49% as infrared (>700 nm).

Rates of solar heat gain depend on posture and surface area exposed to the sun, as well as plumage color. In still air or at low wind speeds, 10–40% of solar irradiance striking the outer surface of the plumage is absorbed across the skin as heat depending on irradiance levels (e.g., Wolf and Walsberg, 1996; Wolf et al., 2000). Interactions between pelage color and absorption of solar irradiance in visible wavelengths are not always intuitive, and at higher wind speeds, the solar heat gain associated with dark, heavily pigmented plumage can be lower than that of white plumage because of the interception of photons closer to the outside surface of heavily pigmented plumages (Wolf and Walsberg, 2000). Evidence has recently emerged for adaptive variation in plumage reflectance in near-infrared wavelengths (Medina et al., 2018).

The effect of solar radiation on environmental temperature experienced by a bird can be substantial. At midday in the Sonoran Desert when $T_{air} = 40°C$, an 11-g verdin (*Auriparus flaviceps*) shifting from a shaded site to a sunlit one experiences $T_e = 52°C$ (Wolf and Walsberg, 1996). Average midday T_e experienced by hoopoe larks (*Alaemon alaudipes*) and a female rufous-cheeked nightjar (*Caprimulgus rufigena*) nesting in exposed sites were 50.8 and 51.4°C, respectively (O'Connor et al., 2018; Tieleman et al., 2008). Under cool conditions, sun-basking can greatly enhance solar heat gain and reduce MHP requirements for thermoregulation. Greater roadrunners (*Geococcyx californianus*) and mousebirds (Coliiformes) substantially reduce metabolic costs of thermoregulation by orientating their dorsal or ventral surfaces, respectively, toward the sun and ptiloerecting their feathers so that solar irradiance is absorbed directly by their dark, heavily melanized skin (Dean and Williams, 1999; Ohmart and Lasiewski, 1971).

Under hot conditions, behavioral alterations of solar heat loads primarily involve retreating to shaded microsites to minimize heat gain. A recent comparative study of heat dissipation behavior in arid-zone bird communities on three continents revealed that T_{air} values at which 50% of observed individuals occupy shaded microsites average 30.2–31.4°C across species (Pattinson et al., 2020). There is also considerable interspecific variation, with more active species (e.g., gleaners) retreating to shade at lower T_{air} compared to less active species (e.g., sit-and-wait foragers; Pattinson et al., 2020). Many desert birds nest in sites completely exposed to the sun, apparently to avoid higher predation risk in shaded sites under vegetation (Tieleman et al., 2008), and shade their eggs by crouching above the nest with their backs orientated toward the sun and partially ptiloerecting their dorsal feathers to reduce solar heat gain and enhance convective heat loss and EHL (Grant, 1982). Birds may also seek shelter in burrows. In the Arabian Desert, several species of larks use burrows excavated by a large lizard (*Uromastyx aegypticus,* Williams et al., 1999) and in the Kalahari Desert, southern pied babblers (*Turdoides bicolor*) sometimes use the entrances of aardvark (*Orycteropus afer*) burrows as thermal refugia on very hot days (A.R. Bourne, personal observation).

45.5.2 Convection

Convective heat transfer occurs via free (or natural) convection driven by temperature and density gradients or forced convection driven by movement of air or water. Heat loss by forced convection increases linearly with wind speed or, in some cases, the square root of wind speed (Goldstein, 1983; Wolf and Walsberg, 1996; Wolf et al., 2000), with the slope of this relationship depending on both M_b and the gradient between T_b and T_{air}. Goldstein (1983) found that the slope (in $W/\sqrt{m/s}$) of avian RMR as a function of wind speed at any T_{air} below thermoneutrality can be estimated as follows:

$$\text{Slope} = 0.0092 M_b^{0.66} \Delta T^{0.32}$$

where M_b is body mass in g and $\Delta T = T_{lc} - T_{air}$ in °C.

The ~24-fold higher thermal conductivity of water compared to air means that convective heat loss occurs much more rapidly in aquatic and marine birds. For species that dive below the surface to forage [Emperor penguins (*Aptenodytes forsteri*) may dive to depths > 500 m], convective heat loss is further increased through plumage compression by hydrostatic pressure. In a heat balance model that assumed heat produced as a by-product of activity substitutes for thermoregulatory thermogenesis, depth had the greatest effect on heat loss, with net heat flux in Magellanic penguins (*Spheniscus magellanicus*) swimming at 2.1 m/s in 11°C water varying from ~0 W at the surface to a loss of ~80 W at depths of 40–50 m (Ciancio et al., 2016). Penguins respond to these rapid rates of heat loss when diving by means of peripheral vasoconstriction as well as regional heterothermy; lower abdominal temperatures of king penguins (*Aptenodytes patagonicus*) may be as low as 11°C during sustained deep diving (Handrich et al., 1997).

Roosting birds that remain normothermic employ a number of behavioral pathways to reduce nocturnal heat loss, including seeking protected microsites and postural adjustments such as facing into the wind to minimize disruption of the boundary layer provided by the plumage. Roosting in tree cavities is one way to substantially reduce nocturnal energy demands; the temperatures inside cavities occupied by acorn woodpeckers (*Melanerpes formicivorus*) were sometimes ~10°C above outside T_{air} (Weathers et al., 1990). Many species construct insulated nests and/or use the nests of other species for roosting. In the arid zone of southern Africa, sociable weavers (*Philetairus socius*) construct huge nests containing dozens of individual chambers, the internal temperatures of which may be as much as 23°C above outside T_a when occupied (White et al., 1975).

Another behavior many birds use to reduce overnight energy requirements is communal roosting, which has evolved in several avian lineages (Beauchamp, 1999) and may involve linear roosting huddles with a row of individuals tightly pressed against each other along the length of branch (e.g., long-tailed tit *Aegithalos caudatus*, Hatchwell et al., 2009) or approximately spherical clusters (e.g., mousebirds). The energy savings achieved in this way can be as high as 20–50% (Chaplin, 1982; McKechnie and Lovegrove, 2001b). Some species roost communally within insulated nests resulting in even more greater energy savings; chestnut-crowned babblers (*Pomatostomus ruficeps*) roosting in groups of seven or more individuals did not increase RMR above basal levels even when outside $T_{air} = 5$°C (Chappell et al., 2016).

45.5.3 Conduction

Conductive heat loss can be important for thermoregulation in very hot weather; Bedouin fowls respond to very high T_{air} by moving to shaded microsites, scratching away the top layer of sand, and lying prone with the ventral surfaces and legs in contact with the cooler, subsurface soil (Marder, 1973). Similar behavior occurs in desert birds such as the red lark (*Calendulauda burra*), a nondrinking species inhabiting hot, arid habitats; as T_{air} approaches T_b, the larks retreat to shaded microsites under shrubs and rest with their bellies in contact with cool sand below the surface layer (Kemp and McKechnie, 2019).

For emperor penguins breeding in the Antarctic winter, uninsulated feet are potentially a source of rapid heat loss. In addition to having the smallest feet relative to M_b of any penguin, pronounced vasoconstriction and a countercurrent heat exchanger that allows birds to maintain tissue temperatures in the distal part of the foot at ~0°C, and a characteristic resting posture with the distal parts of the feet lifted off the surface is thought to reduce conductive heat loss to the frozen substrate (Goldsmith and Sladen, 1961; Le Maho, 1977).

45.5.4 Evaporation

The evaporation of water is an endothermic reaction which, at a temperature of 40°C, uses 2.406 kJ/g H_2O (Tracy et al., 2010). EHL is thus an inevitable component of avian heat balance, but also provides the only mechanism whereby a bird can defend T_b below environmental temperature in hot environments. Although rates of EWL from a bird are primarily determined by physical factors, specifically the vapor pressure deficit arising from the temperature and humidity of surrounding air, both baseline ("insensible") evaporation (Eto et al., 2017) and thermoregulatory increases in total evaporative water loss (TEWL) (see below), are under physiological control.

TEWL (i.e., the sum of respiratory and cutaneous evaporation) measured under laboratory conditions is approximately constant at T_{air} below thermoneutrality. Baseline TEWL at thermoneutral or lower T_{air} scales allometrically with M_b, and is consistently lower in birds inhabiting arid habitats. William's (1996) analysis of TEWL at $T_{air} = 25$°C among 89 species indicated that in arid-zone birds TEWL (mL/day) $= 0.176M_b^{0.750}$, whereas in species from mesic habitats TEWL (mL/day) $= 0.365M_b^{0.661}$, equivalent to a difference of 56% for 25-g birds and 38% for 100-g birds.

When environmental temperature approaches or exceeds T_b, TEWL increases above baseline levels, with the resultant increases in Q_{evap} providing the basis for maintaining T_b below lethal limits. Under very hot conditions, most birds can increase TEWL to rates equivalent to 5–15 × baseline values, with the ratio of maximum TEWL during acute heat exposure to minimum thermoneutral TEWL referred to as evaporative scope. Authors have variously modeled the relationship between T_{air} and TEWL at $T_{air} > T_{uc}$ as an exponential curve, second-order polynomial curve, or as a segmented linear model (i.e., a "broken-stick" relationship characterized by two different linear relationships either side of an inflection T_{air}; Figure 45.2).

Heat tolerance limits, the maximum T_{air} values birds can tolerate during acute heat exposure, depend on both evaporative scope and the increase in Q_{metab} at $T_{air} > T_{uc}$. Heat tolerance limits of passerines are typically 48–52°C (McKechnie et al., 2017; Smith et al., 2017; Whitfield et al., 2015), whereas some desert doves and nightjars can tolerate $T_a \geq 60$°C using cutaneous evaporation or gular flutter (see Section 45.5.4). Recently, variation in evaporative scope among desert passerines was shown to be functionally linked to drinking behavior, with regularly drinking species capable of larger increases in Q_{evap} than nondrinkers (Czenze et al., 2020).

45.5.4.1 Respiratory evaporative water loss

The rate of EHL via respiration (Q_{evap_r}) is determined by the volume of air exhaled per unit time, the temperature of

exhaled air (generally assumed to be fully saturated with water vapor, but see Withers et al., 1981), the humidity of inhaled air, and the latent heat of vaporization in the expired air, such that Q_{evap_r} (W) is calculated as follows:

$$Q_{evap\_r} = \left[\dot{V}\left(\rho_{ex} - \frac{\Phi_a \rho_{in}}{100}\right)\lambda\right]/60$$

where $\dot{V}$ is respiratory minute volume (L/min), ρ_{ex} and ρ_{in} are the saturated water contents (g H_2O L^{-1}) of exhaled and inhaled air at their respective temperatures, Φ_a is the relative humidity (%) of inhaled air, and λ is the latent heat of vaporization for exhaled air (J/g).

The nasal cavities of birds, like those of mammals, have cartilaginous projections known as respiratory turbinates, which potentially act as countercurrent heat exchangers that raise the temperature of inhaled air to near T_b and saturate it with water vapor. On exhalation, the turbinates cool air exhaled through the nasal cavity to well below T_b, resulting in water recovery via condensation and greatly reducing EWL (Schmidt-Nielsen et al., 1970). Early and some, but not all, recent investigations support the notion of countercurrent heat exchange being the primary determinant of the temperature of exhaled air (e.g., Berger et al., 1971; Geist, 2000; Murrish, 1973). However, two species of larks showed reductions in respiratory evaporative water loss (REWL) much smaller than expected, leading the authors to suggest an alternate hypothesis, that the temperature of exhaled air is determined instead by the temperature of the uninsulated bill and surrounding tissue (Tieleman et al., 1999).

In most avian taxa investigated to date, increases in REWL provide the major avenue for evaporative cooling under hot conditions or during activity. The two major avenues of avian respiratory evaporative cooling are gular flutter and panting, with the relative importance of these two mechanisms varying among taxa. Many nonpasserines use a combination of panting and gular flutter, but gular flutter appears to be absent in some orders, including parrots and passerines.

45.5.4.1.1 Panting

Panting (or thermal tachypnea) occurs in response to increasing T_b and involves changes in respiratory frequency (f_{resp}), tidal volume (V_T), and thus respiratory minute volume (total volume of air passing through respiratory system per minute). Panting responses are broadly divisible into Type I and Type II (Figure 45.4). Type I panting is the primary mode of panting induced by small increases in T_b and involves increases in f_{resp} accompanied by decreases in V_T, which result in three- to sixfold increases in respiratory

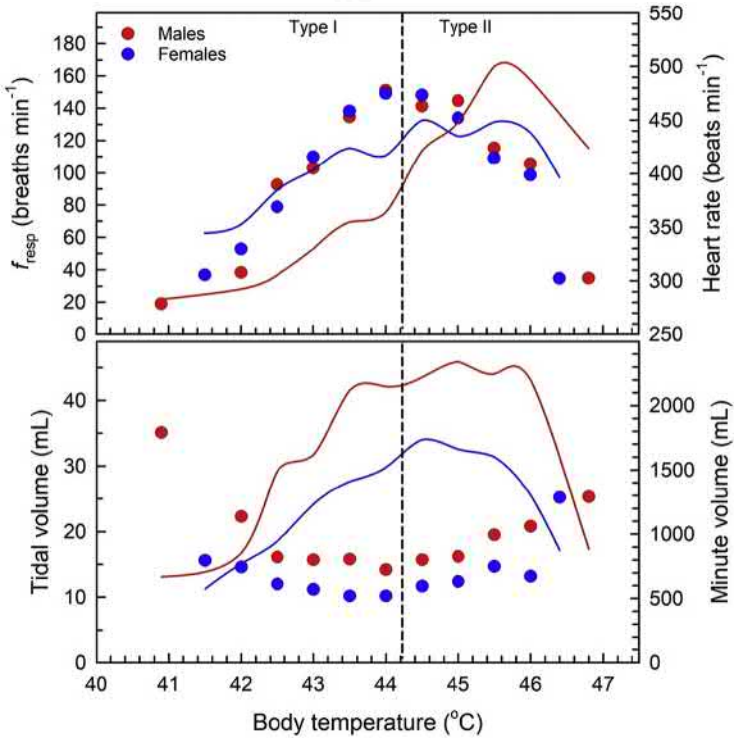

FIGURE 45.4 Relationships between body temperature (T_b) and respiratory frequency (f_{resp}; *filled circles*, upper panel), heart rate (*lines*, upper panel), tidal volume (*filled circles*, lower panel), and respiratory minute volume (*lines*, lower panel) in heat-stressed white leghorn chickens (data from Frankel et al., 1962). The *dashed vertical line* shows the approximate transition from Type I panting characterized by increases in f_{resp} and decreases in tidal volume to Type II panting associated with severe hyperthermia approaching lethal T_b during which f_{resp} decreases.

minute volume (Richards, 1970). Type II panting, on the other hand, is associated with severe heat exposure and T_b approaching lethal levels. Type II panting occurs after maximum f_{resp} of Type I panting has been reached, and involves decreases in f_{resp} and increases in V_T. Respiratory minute volume during Type II panting may increase slightly above the maximum reached during Type I panting.

Type I panting can involve gradual increases in f_{resp} with increasing T_b, the pattern that predominates in passerines, some quail, cormorants, and mousebirds (Lasiewski, 1972). In other taxa, including ostriches, roadrunners, columbids, guineafowl and pelicans, f_{resp} increases in an abrupt, step-wise fashion (Lasiewski, 1972; Nassar et al., 2001). Both resting f_{resp} and maximum f_{resp} during panting show negative scaling with M_b, with exponents varying among taxa between -0.25 and -0.35 and f_{resp} typically increasing to $\sim 16 \times$ resting levels during panting (Calder and King, 1974).

The large increases in respiratory minute volume that occur during panting have the potential to affect blood CO_2 and acid–base balance by leading to hypocapnia and alkalosis. Significant reductions in blood CO_2 and increases in pH have been reported in several studies, but are often attributable to stress associated with experimental conditions or the induction of Type II panting (Bech and Johansen, 1980; Marder and Arad, 1989). In general, birds can avoid alkalosis during Type I panting because reductions in V_T often result in increased ventilation largely confined to the respiratory dead space, whereas there is little change to ventilation of the parabronchi (Bech and Johansen, 1980). These authors argued for three general categories of avian panting response. The first is the aforementioned confinement of increased ventilation to the respiratory dead space, the second is the compound ventilation described in pigeons by Ramirez and Bernstein (1976) involving the superimposition of rapid, shallow panting on slower, deeper parabronchial ventilation, and the third is a pattern described in flamingos where bouts of panting are interspersed by brief, deeper "flush-out" breathing (Bech et al., 1979).

A long-standing question concerning respiratory evaporative cooling in species where f_{resp} during Type I panting shows a step-wise increase above resting levels is whether panting f_{resp} matches the resonant frequencies of respiratory systems, which would minimize the metabolic costs of panting (Bartholomew et al., 1968; Crawford and Kampe, 1971; Weathers, 1972). Although panting in several species, including ostriches, apparently does not occur at resonant frequencies (Schmidt-Nielsen et al., 1969), it does appear to do so in helmeted guineafowl *Numida meleagris* (Nassar et al., 2001). The authors of the latter study showed that panting f_{resp} during rest (6.67 Hz) as well as both step frequency (6.73 Hz) and f_{resp} (6.71 Hz) during treadmill locomotion did not differ significantly from the resonant frequency of the respiratory system (7.12 Hz), and argued that locomotory/respiratory entrainment at resonant frequencies of respiratory systems has evolved in both birds and mammals.

During panting, the majority of evaporation occurs in the upper respiratory tract (Lasiewski and Snyder, 1969; Menuam and Richards, 1975). In domestic fowls, surface temperatures (T_s) of the abdominal, thoracic, and clavicular air sacs did not differ from cloacal T_b, whereas those throughout the trachea and nasal and buccal regions were significantly (up to 2.3°C) lower than cloacal T_b, confirming that evaporation was largely confined to these regions (Menuam and Richards, 1975). There is, however, evidence for significant evaporation in the postthoracic and interclavicular air sacs of ostriches (Schmidt-Nielsen et al., 1969).

45.5.4.1.2 Gular flutter

Gular flutter involves rapid pulsation of the hyoid apparatus and thus the gular membranes at frequencies varying from 176 to >1000 cycles min^{-1} and may accompany panting either at frequencies synchronized with panting or independent of panting frequency (Lasiewski, 1972). The frequency of gular flutter tends to be synchronized with that of panting in quails, roadrunners, columbids, and owls, but is independent of panting in groups including pelicans, cormorants, mousebirds, and nightjars (Lasiewski, 1972). In birds belonging to the latter category, gular flutter frequencies may greatly exceed those of panting. In double-crested cormorants (*Phalacrocorax auritus*), for example, maximum panting f_{resp} was ~ 60 breaths min^{-1} when T_b exceeded 44°C, whereas the corresponding rate of gular flutter was ~ 700 min^{-1} (Bartholomew et al., 1968).

Early arguments that gular flutter provides the basis for extremely efficient evaporative cooling among caprimulgids (Dawson and Fisher, 1969; Lasiewski, 1969) have been confirmed by more recent studies, with rufous-cheeked nightjars (*C. rufigena*) achieving ratios of evaporative heat loss to metabolic heat production (EHL/MHP) > 5 (O'Connor et al., 2017). Unlike panting, gular flutter is sometimes associated with no discernible increase in MHP and some caprimulgids show virtually no evidence of an upper boundary to their TNZ (Figure 45.5).

The absence of gular flutter, most notably among passerines, constrains evaporative cooling capacity to levels well below those achievable by some nonpasserine taxa. Maximum EHL/MHP among passerines varies from 1.2–2.4 (Czenze et al., 2020; McKechnie et al., 2017), whereas several caprimulgids achieve EHL/MHP > 4 (O'Connor et al., 2017; Talbot et al., 2017). Parrots, which also lack gular flutter, augment REWL using lingual flutter,

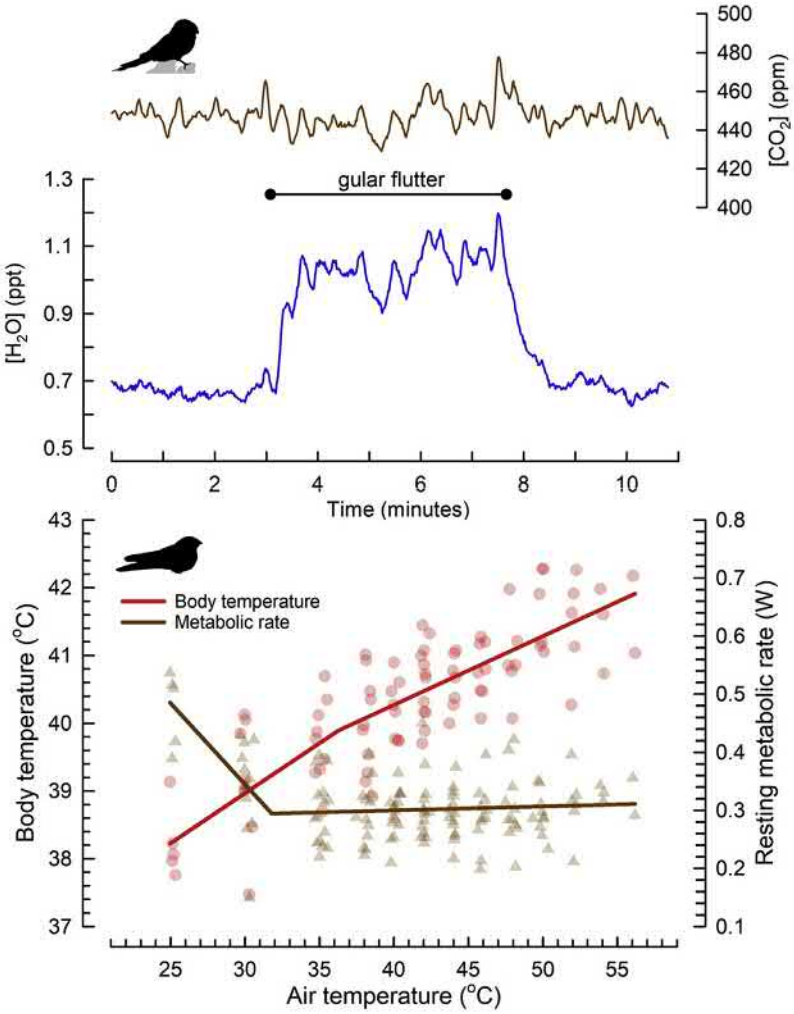

FIGURE 45.5 In nightjars and allies, gular flutter provides the basis for extremely efficient evaporative cooling at little metabolic cost. The upper panel shows a ~10-minute trace of the concentrations of H_2O vapor (*blue line*) and CO_2 (*brown line*) during measurements of evaporative water loss (EWL) and resting metabolic rate (RMR) in an Australian owlet-nightjar (*Aegotheles cristatus*) before, during, and after a bout of gular flutter (redrawn from Talbot et al., 2017). Note the large increase in EWL associated with gular flutter but lack of any discernible concomitant increase in RMR. The lower panel shows the relationships between air temperature (T_{air}) and body temperature (T_b) and RMR in a rufous-cheeked nightjar (*Caprimulgus rufigena*; data from O'Connor et al., 2017). Whereas T_b increases by 2.2°C between $T_{air} = 35$°C and $T_{air} = 55$°C, there is virtually no associated increase in RMR. The silhouettes were obtained from http://phylopic.org/: *Aegotheles* (Christopher Watson and T. Michael Keesey) and nightjar (Ferran Sayol). They are reproduced here under a Creative Commons License (https://creativecommons.org/licenses/by/3.0/).

vertical movements of the tongue at frequencies synchronized with panting (Weathers and Caccamise, 1975, 1978). In galahs (*Eolophus roseicapilla*) and mulga parrots (*Psephotellus varius*), the onset of panting is not necessarily associated with significant increases in RMR, likely reflecting the contribution of lingual flutter to enhancing evaporative cooling efficiency (McWhorter et al., 2018).

45.5.4.2 Cutaneous evaporative water loss

The rate at which birds lose water via evaporation across the skin is a function of the temperature and humidity of surrounding air, as well as the skin's resistance to water vapor diffusion, with cutaneous EHL (Q_{evap_c}) in W/m^2 calculated as follows:

$$Q_{evap\_c} = h_e\left(\frac{\Phi_{skin}}{100}P_{ws} - \frac{\Phi_a}{100}P_{wa}\right)\lambda$$

where h_e is the evaporative heat transfer coefficient (g/s m^2 kPa), Φ_{skin} and Φ_a are the relative humidities at the skin surface and of the air (%), and P_{ws} and P_{wa} are the saturation vapor pressures (kPa) at T_{skin} and T_{air}, respectively, and λ is the latent heat of vaporization at T_{skin} (J/g). If measurements of CEWL are available, whole-body skin resistance to vapor diffusion (r_v, in s/m) can be calculated as follows:

$$r_v = \frac{\rho'_{vs} - \rho_{va}}{\dot{E}}$$

where ρ'_{vs} is saturation vapor density at T_{skin} (g/m^3), ρ_{va} is vapor density of air (g/m^3), and $\dot{E}$ is CEWL in g/m^2 s (Webster et al., 1985).

The extent to which the skin acts as a barrier to EWL is primarily determined by the ultrastructure and lipid composition of the stratum corneum (Menon et al., 1988, 1989, 1996). The avian stratum corneum differs from that of mammals by containing substantial quantities of cerebrosides, although evidence has recently emerged for convergent evolution whereby the skin of bats' wings also has large cerebroside content (Ben-Hamo et al., 2016).

One of the factors contributing to reduced TEWL in desert birds (Tieleman and Williams, 2000; Tieleman et al., 2003a; Williams, 1996) appears to be reduced permeability of the skin to water vapor, and recent work by J.B. Williams and colleagues has revealed how the lipid composition of lamellar layers in the extracellular matrix of the avian stratum corneum is correlated with adaptive variation in CEWL. The stratum corneum of larks from desert habitats contains higher proportions of ceramides and lower proportions of free fatty acids (Haugen et al., 2003), and CEWL is negatively correlated with percentage cerebroside and ceramide I content and positively correlated with triacylglyceride content (Champagne et al., 2012).

Habitat-correlated differences in CEWL at moderate T_{air} may also occur at an intraspecific level. House sparrows (*Passer domesticus*) inhabiting a desert habitat had CEWL ~26% lower than conspecifics in a mesic environment (Muñoz-Garcia and Williams, 2005). Although stratum corneum lipid composition differed substantially between the two populations, rates of CEWL across nonliving skin did not differ, leading these authors to argue that skin water proofing interacts with biological control processes. Several studies have demonstrated phenotypic flexibility in CEWL, including short-term thermal acclimation in hoopoe larks (Tieleman and Williams, 2002) and acclimation to ambient humidity in house sparrows (Muñoz-Garcia et al., 2008). In these studies, the direction of changes in CEWL was consistent with the hypothesis that the function of these adjustments is water conservation in warm, dry conditions.

The skin also plays an important role in evaporative cooling during heat exposure. Avian skin lacks sweat glands and many early workers considered CEWL to contribute little to evaporative cooling, panting thought to be the major pathway for elevated TEWL at T_{air} approaching or exceeding T_b (Dawson, 1954; Dawson and Schmidt-Nielsen, 1964). By the 1970s, however, there was evidence that CEWL is important for thermoregulation in some taxa (Bernstein, 1971; Lasiewski et al., 1971), and subsequent work revealed large cutaneous components to evaporative cooling in columbids (Marder and Arieli, 1988; Webster and Bernstein, 1987; Webster and King, 1987; Withers and Williams, 1990). Rapid cutaneous evaporative heat dissipation among Columbiformes appears to provide the basis for heat tolerance exceeding that of most taxa (McKechnie et al., 2016; Smith et al., 2015).

The partitioning of columbids' EHL into respiratory and cutaneous avenues also exhibits phenotypic flexibility, with evidence for increases in CEWL over time scales of minutes in response to experimentally reduced REWL (Hoffman and Walsberg, 1999) and weeks as a component of thermal acclimation to hot environments (McKechnie and Wolf, 2004b). Increases in CEWL as a component of thermal acclimation in columbids arise from both ultrastructural changes in the skin (Peltonen et al., 1998) and microvascular adjustments (Ophir et al., 2003). Experimental inhibition or stimulation of adrenergic receptors altered arterial and venous blood flow in heat-acclimated rock doves, leading to increases in capillary hydrostatic pressure thought to cause elevated water outflow from skin capillary beds and concomitant increases in CEWL (Ophir et al., 2003).

45.5.4.3 Other avenues of evaporative cooling

EHL from the corneas contributes to the maintenance of T_{brain} below core T_b (Bernstein et al., 1979; Pinshow et al., 1982). The ocular circulation appears to represent a second source of cooled venous blood to the rete opthalmicum, augmenting cooler blood flowing from capillaries adjacent to the moist membranes of the buccopharyngeal cavity (Pinshow et al., 1982). Another site proposed to represent a significant component of avian TEWL is the cloaca. Cloacal evaporation was estimated to represent 21% of TEWL at $T_{air} = 42°C$ in Inca doves (*Columbina inca*) but just 6.4% in common quail (*Coturnix coturnix*), raising the possibility that, in some birds, regulated cloacal cooling is an important component of thermoregulation during heat exposure (Hoffman et al., 2007). Finally, in southern ground-hornbills (*Bucorvus leadbeateri*) experiencing high T_{air}, dilute fluid originating from the nares runs in grooves along the length of the beak (Kemp and Kemp, 1980). Recently, ground-hornbills were observed wiping their beaks on their dorsal feathers in an apparent effort to spread this fluid over a larger area, and thermal images suggest that the consequent evaporative cooling may contribute significantly to heat loss from the beak's surface (Janse van Vuuren et al., 2020).

45.5.5 Heat dissipation challenges in commercial poultry production

Domesticated birds, most notably chickens (*Gallus domesticus*) and turkeys (*Meleagris gallopavo*), have experienced strong artificial selection for rapid growth and

minimization of the time required to reach slaughter M_b (in the case of broilers) or high egg production (laying hens). The time required for chicken broilers to reach a slaughter M_b of 1.8 kg decreased from 90 days in the 1940s to <40 days by the end of the 20th century (Konarzewski et al., 2000). The active- and rest-phase normothermic T_b of chickens are typically 41.5 and 40.5°C, respectively (Etches et al., 2008), whereas the T_{uc} is 24−27°C (Czarick and Fairchild, 2008).

For poultry raised in large-scale commercial facilities, thermoregulatory challenges primarily relate to the dissipation of metabolic heat loads associated with rapid tissue synthesis. Panting is the primary avenue of EHL in poultry, with REWL accounting for 75% of TEWL at $T_{air} = 40$°C in chickens (Richards, 1976). The T_{air} associated with the onset of panting in poultry varies with humidity and may be as low as $T_{air} = 29$°C (reviewed by Etches et al., 2008). In contrast to the limited evidence for significant respiratory alkalosis during Type I panting in nondomesticated birds, some authors have reported increases in blood pH in poultry (e.g., Kohne and Jones, 1975; Raup and Bottje, 1990; Teeter et al., 1985). A widely used management strategy to counteract respiratory alkalosis in poultry involves dietary supplements such as sodium bicarbonate, ammonium chloride (Teeter et al., 1985), or potassium chloride (Ahmad et al., 2008).

The value of using poultry breeds from hot, arid climates to understand the upper limits to heat tolerance and evaporative cooling capacity has been demonstrated by the work of J. Marder and colleagues on Bedouin fowls, in which T_b increases from normothermic values of ~41°C at $T_{air} = 25$−30°C to hyperthermic values of ~43°C at $T_{air} = 48$°C (Marder, 1973). Rates of EWL at $T_{air} = 48$°C are equivalent to ~525% of corresponding values at $T_{air} = 30$°C. Modest increases of only ~9% in RMR over this increase in T_{air}, accompanied by no significant changes in heart rate (Marder, 1973), reveal efficient evaporative cooling in this breed which is significantly more heat resistant than commercial breeds (Arad and Marder, 1982).

Poultry species exhibit phenotypic plasticity in heat tolerance. Most work in this field has focused on developmental plasticity in response to heat exposure by embryos or hatchlings (see Section 45.8.2). However, responses to heat also involve short-term acclimation of older birds. Lott (1991), for example, showed that broilers exposed to $T_{air} = 35$°C at 30−40 days of age drank significantly more water and maintained lower T_b during acute heat exposure compared to nonacclimated individuals. A key aspect of thermoregulation in the heat for commercial poultry is heat produced via the heat increment of feeding (HIF), with removal of feed prior to heat exposure increasing survival (McCormick et al., 1979).

Heat dissipation by commercial poultry is typically enhanced by designing houses for enhanced natural ventilation or power ventilation to augment heat loss via forced convection, typically with wind speeds of 2−3 m/s (reviewed by Czarick and Fairchild, 2008). In addition to increasing convective heat loss, evaporative cooling can be enhanced via the use of fogging systems, sprinkler systems, or evaporative cooling pads that reduce incurrent T_{air} to a house by forcing air over wet surfaces (Czarick and Fairchild, 2008). The efficacy of evaporative cooling systems is strongly dependent on prevailing relative humidity. Another approach to artificially enhancing heat dissipation involves cool roosts, where birds have access to perches consisting of metal pipes within which chilled water is circulated (Okelo et al., 2003).

45.6 Metabolic heat production

The capacity of birds to produce heat through endogenous metabolic thermogenesis in the absence of activity provides the basis for avian homeothermic endothermy. For a resting, inactive bird defending a normothermic setpoint T_b, the lower and upper boundaries of metabolic thermogenesis are BMR and summit metabolism, respectively. This section provides an overview of basal and cold-induced thermoregulatory metabolism in the context of their contributions to avian heat balance. First, however, it is worth considering how metabolic heat generated during activity and feeding interacts with endogenous thermoregulatory MHP.

During activity at environmental temperatures below thermoneutrality, heat produced as a by-product of activity may contribute to heat balance, although the extent to which it does so depends on taxonomy, M_b, and environmental temperature (Humphries and Careau, 2011). In a metaanalysis of 51 studies, 28 of 32 species showed evidence for activity-thermoregulatory heat substitution, with an average magnitude of substitution of 57% (Humphries and Careau, 2011). These authors demonstrated that substitution is more likely in larger birds at T_e approaching T_{lc}, although some studies of small passerines found the extent of substitution increased with decreasing T_{air} (Paladino and King, 1984; Pohl and West, 1973).

Another source of MHP is the HIF (or specific dynamic action) associated with the digestion and absorption of ingested food. Evidence for substitution of HIF for thermoregulatory metabolic thermogenesis has been variable among studies (reviewed by Marsh and Dawson, 1989a). A series of experimental investigations of rock doves revealed a major thermoregulatory role for HIF in species that store food in their crops, and which can hence temporally separate HIF from ingestion (Geran and Rashotte, 1997; Hohtola et al., 1998; Rashotte et al., 1997). Pigeons fasted before the onset of the rest phase relied almost entirely on shivering for nocturnal thermoregulation, whereas individuals fed various quantities of food late in the active

phase maintained higher rest-phase T_b but reduced shivering, indicating that HIF contributed substantially to rest-phase thermogenic defense of T_b (Rashotte et al., 1999). In other cases, however, HIF appears to be of minimal thermoregulatory importance, particularly if the temperature of prey is far below T_b (Lovvorn, 2007).

45.6.1 Basal metabolic rate

Basal metabolic rate is the minimal normothermic rate of MHP measured under conditions that avoid any increments associated with digestion, activity, thermoregulation, growth, or reproduction. Caution is needed in evaluating published avian BMR measurements, for several reasons. First, some reported BMR measurements were (a) not conducted under the conditions required to elicit BMR or (b) conducted under unspecified conditions (McKechnie and Wolf, 2004a). Second, steady-state measurements lasting >6 h are typically required for RMR to reach minimum levels, i.e., BMR (Page et al., 2011). Third, there is evidence from domestic fowl (Misson, 1974) and budgerigars (Jacobs and McKechnie, 2014) that birds may require habituation to metabolic chambers before minimal metabolic rates are achieved.

This variable has a long history of use in comparative analyses of avian energetics (Lasiewski and Dawson, 1967; Londoño et al., 2015; Riddle et al., 1932), and BMR remains widely used for testing hypotheses concerning physiological adaptation to biotic and abiotic factors (Londoño et al., 2015; Noakes et al., 2013; Tieleman and Williams, 2000; White et al., 2007). The approximate range of avian BMR is from 0.07 W in 3-g hummingbirds to 63 W in the 93-kg common ostrich (*Struthio camelus*; Londoño et al., 2015; Withers, 1983). The number of species for which BMR measurements exist, particularly in the tropics, has increased substantially in the last decade, thanks in large measure to two studies that contributed data for 66 species in Vietnam (Bushuev et al., 2017) and a remarkable 253 species in Peru (Londoño et al., 2015).

A bird's BMR represents the sum of maintenance energy requirements of its organs and tissues, with the largest component comprising the metabolic costs of the liver, brain, kidneys, heart, and other organs (Daan et al., 1990; Suarez and Darveau, 2005; Wang et al., 2001). At the interspecific level, residual BMR was predicted by the residual combined mass of the heart and kidneys (Daan et al., 1990) and by the gut, liver, kidney, and breast muscle (Chappell et al., 1999). Lower BMR among tropical species compared to their higher-latitude counterparts has also been ascribed to proportionately smaller organs, including heart, liver, pancreas, kidneys, flight muscles, ovaries, and testes (Wiersma et al., 2012).

The largest component of variation in avian BMR is attributable to M_b. A phylogenetically corrected analysis of BMR in 488 species, with a balanced representation of tropical and temperate-latitude species, yielded the following equations predicting BMR (W) from M_b in g (Londoño et al., 2015):

$$\text{Non-passerines (excluding Apodiformes): BMR} = 0.021M_b^{0.724}$$

$$\text{Apodiformes: BMR} = 0.067M_b^{0.450}$$

$$\text{Passeriformes: BMR} = 0.045M_b^{0.627}$$

The processes underlying patterns of metabolic scaling are the subject of long-standing and ongoing debate (Darveau et al., 2002; Kleiber, 1932; Rubner, 1883; West et al., 1999). The scaling of avian BMR shows variability at both interspecific and intraspecific levels. Scaling exponents differ between wild-caught and captive-raised birds (McKechnie et al., 2006). A number of studies have revealed intraspecific slopes steeper than interspecific slopes; for instance, Kvist and Lindström (2001) reported interspecific slopes of 0.62−0.74, but intraspecific slopes of 0.93−4.21 for migratory waders.

Prior to the 1990s, it was widely accepted that passerine BMR is significantly higher than that of nonpasserines (e.g., Lasiewski and Dawson, 1967; Zar, 1968, but see also Prinzinger and Hänssler, 1980). The development of comparative methods that accounted for phylogenetic nonindependence of physiological traits (Felsenstein, 1985), however, led to the view that the higher BMR of extant passerines did not arise from selection for elevated BMR, but simply represented phylogenetic inertia and descent from a common ancestor (McKechnie and Wolf, 2004a; Reynolds and Lee, 1996). Londoño et al.'s (2015) analysis, based on a recent and well-supported avian phylogeny (Hackett et al., 2008), revealed that the BMR of passerines is indeed significantly higher than that of nonpasserines by ~12%.

After M_b and phylogenetic inertia have been taken into account, BMR is correlated with several environmental variables, in particular temperature. Among 90 species from absolute latitudes ranging from 60 degrees to the equator, BMR increased with decreasing average T_{air}, but was not related to primary productivity (White et al., 2007). Avian BMR has also been linked to diet type (McNab, 1988), although a more recent analysis of BMR in 19 neotropical passerines revealed no direct effects of diet composition on M_b-independent BMR (Sabat et al., 2010). In black-faced sheathbills (*Chionis minor*) on the subantarctic Marion Island, BMR was 35% higher in a population

with year-round access to resource-rich foraging areas compared to a population that foraged in areas poorer in resources (McClennand et al., 2016). Another broad factor affecting avian BMR is insularity; several studies have reported that the BMR of columbids whose distribution is restricted to islands is lower than that of continental species (McNab, 2000; Noakes et al., 2013).

Although sometimes viewed as a static, species-specific trait, BMR shows considerable phenotypic flexibility. Reversible, within-individual adjustments in BMR typically occur in one of three contexts: seasonal acclimatization, short-term thermal acclimation, and migration (reviewed by McKechnie, 2008; McKechnie and Swanson, 2010). Seasonal changes have long been recognized as an important component of acclimatization, particularly among nonmigratory species in temperate latitudes with long, cold winters (Pohl and West, 1973; Swanson, 2010; Weathers and Caccamise, 1978). Species occupying latitudes >35 degrees generally increase BMR in winter, sometimes by as much as 60%, whereas species from lower latitudes may exhibit winter increases or decreases (McKechnie et al., 2015). Studies tracking metabolic patterns over time have revealed that BMR is adjusted over periods of days to weeks in response to environmental temperature (Swanson and Olmstead, 1999). Moreover, acclimatization may vary substantially in direction and magnitude across years; in a desert population of white-browed sparrow-weavers (*P. mahali*), over a 4-year period BMR in winter varied from 20% lower to 68% higher than summer values (Noakes and McKechnie, 2020).

During acclimation of captive populations, BMR typically increases with decreasing T_{air} (Gelineo, 1964; McKechnie et al., 2007b). However, the magnitude of increases may vary substantially; among four species of lark, differences in BMR between conspecifics acclimated to $T_{air} = 15°C$ or $T_{air} = 35°C$ ranged from 5 to 29% (Tieleman et al., 2003b). Large changes in BMR may be associated with cyclical changes in body composition and physiology during migration. The BMR of great knots (*Calidris tenuirostris*) decreased by 42−46% during the course of migration between northwestern Australia and southern China (Battley et al., 2001), and Swanson and Dean (1999) found that BMR of yellow-rumped warblers (*Dendroica coronata*) was 31% higher during the northward spring migration compared to southward autumn migration. These changes can be very rapid; several studies have reported changes in BMR of >20% within 2−6 days (Klaassen and Biebach, 1994; Lindström et al., 1999).

The processes underlying phenotypic flexibility in BMR primarily involve changes in organ mass and/or metabolic intensity (Swanson, 2010). Changes in the masses of the digestive tract appear to be one major source of variation, with increases in BMR in cold-acclimated and -acclimatized birds thought to reflect the greater support costs of the larger digestive tracts required to process greater quantities of food during periods of elevated energy requirements (Vézina et al., 2006; Williams and Tieleman, 2000), as well as larger pectoral muscles for shivering thermogenesis (Vézina et al., 2017). In addition, the metabolic intensity of tissues is up or downregulated via changes in several key enzymes involved in aerobic metabolism (Swanson, 2010; Vézina et al., 2017).

45.6.2 Resting metabolic thermogenesis and cold tolerance

The capacity of avian tissues to produce heat in the absence of activity provides the basis for remarkable feats of cold tolerance; winter-acclimatized snowy owls can briefly tolerate T_{air} as low as −93°C (Gessaman, 1972). In a resting bird, MHP for thermoregulation primarily arises from shivering (Hohtola, 1982; Marsh and Dawson, 1989b) fueled by lipids (McWilliams et al., 2004). The large pectoral muscles often represent the primary source of shivering thermogenesis but leg muscles may also contribute substantially, particularly in young birds (Carey et al., 1989; Dietz et al., 1997).

Nonshivering thermogenesis (NST) also contributes to avian MHP (Barre et al., 1985; Bicudo et al., 2002), although birds lack brown adipose tissue and associated uncoupling protein 1(UCP1)−mediated NST similar to that of mammals (Emre et al., 2007). Avian NST primarily involves the 1a isoform of sarcoplasmic reticulum Ca^{2+}-ATPase (SERCA1a) in fast-twitch muscle fibers (Dumonteil et al., 1993). Upregulated SERCA1a expression and ryanodine receptors (Ca^{2+} channels on the sarcoplasmic reticulum) have been documented in cold-acclimated birds (e.g., Dumonteil et al., 1995). The extent to which sarcolipin, a key peptide involved in mammalian muscle NST, contributes to avian muscle NST remains unclear (Cheviron and Swanson, 2017; Nowack et al., 2017), with some recent evidence suggesting that sarcolipin-mediated NST could in fact hinder avian thermoregulation at very low T_a (Stager and Cheviron, 2020). In addition to SERCA, the existence of avian homologs to UCP1, including HmUCP, a homolog identified in the pectoral muscles of hummingbirds, suggests a second source of avian NST (Bicudo et al., 2002; Vianna et al., 2001). A UCP homolog (avUCP) identified in the skeletal muscle of chickens (Raimbault et al., 2001) has been implicated in thermogenesis, a notion supported by positive associations between avUCP mRNA expression and the HIF in domestic fowls and increases in its expression following cold acclimation or glucagon treatment (Li et al., 2013; Raimbault et al., 2001). However, the presumed mitochondrial uncoupling role of avUCP remains controversial (Walter and Seebacher, 2009).

Avian M_{sum} (also sometimes referred to as peak cold-induced metabolic rate) represents maximal thermogenic capacity and is typically measured in a helox (21% O_2, 79% He) atmosphere. The use of helox greatly increases rates of heat loss compared to those in air, obviating the need to expose birds to very low T_{air} values with the attendant risks of freezing injury. Among birds investigated to date, ratios of M_{sum}/BMR (metabolic expansibility, ME) are typically 3–9 (Noakes and McKechnie, 2020; Swanson, 2010), and M_{sum} is well below maximal exercise-induced metabolic rate (MMR). In birds from tropical Central America, M_{sum} averaged 4.52 × BMR and MMR averaged 6.44 × BMR (Wiersma et al., 2007). An analysis of data for 44 predominantly north-temperate species (Swanson and Garland, 2009) revealed a best-fit model for M_{sum} (expressed in mL O_2 min^{-1}) as a function of M_b (g) of:

$$\log_{10} M_{sum} = 0.626 \log_{10} M_b - 0.080$$

There is considerable phylogenetic variation in M_{sum} (Swanson and Garland, 2009), including ~74% higher M_{sum} in oscine passerines compared to suboscines. Swanson and Bozinovic (2011) argued this greater metabolic capacity of oscines has contributed to the dominance of this clade on all continents except South America. These two studies also revealed M_{sum} is correlated with the average winter T_{air} experienced by a species, confirming the functional link between maximum resting MHP and cold tolerance. Observations that low-latitude species have lower M_{sum} than their temperate-zone counterparts are consistent with the notion of a functional link with cold tolerance. Wiersma et al. (2007) reported M_{sum} 34% lower among tropical compared to temperate-latitude species and presented the following scaling relationships for M_{sum} (W) as a function of M_b (g):

$$\text{Tropical (19 species)}: \log_{10} M_{sum} = 0.814 \log_{10} M_b - 0.975$$

$$\text{Temperate (21 summer - acclimatized species)}: \log_{10} M_{sum} = 0.699 \log_{10} M_b - 0.654$$

Like BMR, M_{sum} exhibits considerable phenotypic flexibility, with seasonal acclimatization typically associated with increases of 25–50% among species from temperate latitudes (Swanson, 2010). Adjustments occur over shorter time scales in response to changing thermoregulatory demands. In black-capped chickadees (*Poecile atricapillus*) and dark-eyed juncos (*Junco hyemalis*), average T_{air} during 14–30 days preceding measurements was the strongest predictor of M_{sum}, whereas in American tree sparrows (*Spizelloides arborea*), average T_{air} over the preceding 0–5 days emerged as the best predictor (Swanson and Olmstead, 1999). The mechanisms underlying short-term within-individual variation in M_{sum} include changes in flight muscle size and hematocrit. An experimental manipulation of pectoral muscle size achieved by clipping half the flight feathers of black-capped chickadees revealed, upon subsequent recapture, increases in pectoral muscle size, hematocrit, and M_{sum} (Petit and Vézina, 2014). In addition to metabolic capacity responding to short-term fluctuations in winter temperature, fuel stores are also modulated: the fat reserves of snow buntings (*Plectrophenax nivalis*) respond to daily changes in T_{air} and snowfall (Laplante et al., 2019).

Seasonal adjustments in M_{sum} are not restricted to species from highly seasonal environments at high latitudes. In seven Central American species, M_{sum} was 13–35% lower in winter compared to summer (Wells and Schaeffer, 2012). In white-browed sparrow-weavers in an arid habitat at a latitude of 27°S, seasonal patterns varied from no significant change to M_{sum} 38% lower in winter, whereas cooccurring scaly feathered weavers (*Sporopipes squamifrons*) showed no seasonal changes (Noakes and McKechnie, 2020). In these species, BMR and M_{sum} were related to food availability but not minimum T_{air}, results supporting the idea that global patterns of seasonal metabolic adjustments represent a continuum driven by trade-offs between energy conservation and cold tolerance (Smit and McKechnie, 2010).

45.6.3 Metabolic costs of evaporative cooling

Another source of metabolic heat with profound thermoregulatory implications is increases in RMR during evaporative heat dissipation. The metabolic costs of evaporative cooling are highest among taxa that rely on panting, most notably passerines, in which gular flutter seems to be absent entirely. Above the TNZ, RMR increases 5- to 10-fold more rapidly in passerines than in similarly sized columbids, reflecting the latter's efficient cutaneous cooling (McKechnie et al., 2021). These authors found, based on analysis of data for 30 arid-zone passerines and six columbids, that RMR slopes at $T_{air} > T_{uc}$ (W/°C) for these two groups can be predicted from M_b (g) as follows:

$$\text{Passerines}: \log_{10}\text{Slope} = 0.856 \log_{10} M_b - 2.897$$

$$\text{Columbids}: \log_{10}\text{Slope} = 1.379 \log_{10} M_b - 4.446$$

The most exceptional taxon in terms of efficient evaporative cooling is the nightjars and allies. Because many members of this nocturnal taxon roost in exposed, sunlit microsites during the day, early workers realized they must possess an extremely effective cooling mechanism (Cowles and Dawson, 1951), and subsequent work reinforced this conclusion (Dawson and Fisher, 1969; Lasiewski, 1969). More recently, data for several species have revealed very small increases in RMR with T_{air} over the 45–60°C range (O'Connor et al., 2017; Talbot et al., 2017).

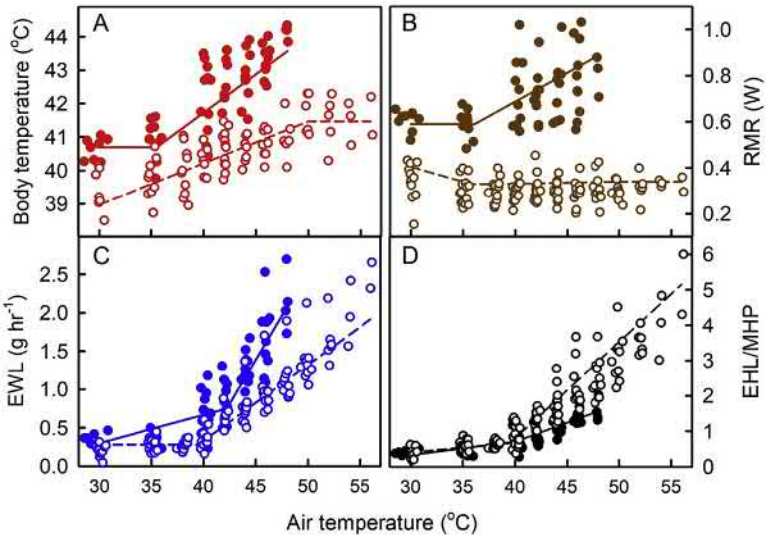

FIGURE 45.6 Interactions between body temperature (A), resting metabolic rate (RMR, B), evaporative water loss (EWL, C), and the ratio of evaporative heat loss to metabolic heat production (EHL/MHP, D) differ substantially among similarly sized (~53g) birds depending on the primary mode of evaporative cooling. Australian chestnut-crowned babblers (*Pomatostomus ruficeps*; filled symbols, solid regression lines) are passerines and rely on panting. They exhibit rapid increases in RMR (B) above an obvious upper critical limit of thermoneutrality (T_{uc}), with their body temperature (T_b) approaching 44°C (A) at a maximum tolerable air temperature (T_{air}) of 48°C and a maximum EHL/MHP of 1.6 (D). Rufous-cheeked nightjars (*Caprimulgus rufigena*; clear symbols, dashed regression lines) from southern Africa achieve similar maximum EWL (C) but make extensive use of gular flutter. In the nightjars, no T_{uc} is evident (B) and RMR remains at minimal levels even at T_{air} in the mid-50s, providing the basis for EHL/MHP > 5 (D) and T_b generally remaining below 42°C (A). Data for babblers and nightjars are from McKechnie et al. (2017) and O'Connor et al. (2017), respectively.

In rufous-cheeked nightjars, RMR at $T_{air} = 55°C$ was just 5% higher than minimum values at $T_{air} = 35°C$ (Figure 45.6).

The relationship between RMR and T_{air} in rufous-cheeked nightjars is all the more remarkable for the concomitant 2.2°C increase in T_b. This increase in T_b would be expected to cause a 17−28% increase in RMR on account of the temperature dependence of biological processes, for which Q_{10} is typically 2−3. The absence of temperature effects on avian RMR during heat exposure was reported by Weathers (1981), who noted $Q_{10} \approx 1$ in several species where T_b increased within the TNZ and temperature effects on RMR could thus be evaluated. The possibility that metabolic suppression (i.e., facultative hypometabolism) may be a component of avian thermoregulation in the heat is deserving of further investigation, and is receiving attention in small tropical mammals (Lovegrove et al., 2014; Reher et al., 2018).

45.7 Physiological control of thermoregulation

Our understanding of the neuronal thermostat underlying endothermic homeothermy in birds and mammals is rooted in the model for setpoint thermoregulation proposed by Hammel (1965). Defense of a T_b setpoint is achieved by the integration in the hypothalamus of afferent inputs from diverse thermoreceptors in the central and peripheral nervous systems and an array of efferent neuronal and endocrine responses that modulate physiological and behavioral pathways of heat gain or loss. The integration center resides primarily in the preoptic anterior hypothalamus (POAH), although an additional integration site involved in thermoregulatory responses to heat is a panting center located in the dorsal midbrain, electrical stimulation of which results in the increases in f_{resp} and decreases in V_T characteristic of Type I panting (Richards, 1971).

45.7.1 Thermoception

The network of neuronal cells providing inputs to the POAH includes thermoreceptors in the brain, spinal cord, deep tissues, and the peripheral regions spanning the skin, beak, and tongue. Unlike the case in mammals, the spinal cord is the most important site for avian thermoception. In most, but not all, species investigated to date, the spinal cord is a region of high thermosensitivity and localized heating induces rapid panting responses in species including domestic fowl (Avery and Richards, 1983). The thoracic region of the spinal cord typically exhibits greater thermosensitivity than the cervical region (Østnes and Bech, 1992; Rautenberg, 1969). Temperature transduction

also appears to involve molecular-level processes in neurons that lack thermosensory function (Simon, 2000).

A number of studies quantifying cold sensitivity in response to experimental manipulation of temperature in different regions of the central nervous system (CNS) have revealed that inputs from thermoreceptors outside the CNS comprise a major component of afferent input to the avian POAH (Mercer and Simon, 1984; Simon et al., 1981). Peripheral thermoreceptors in the skin and other tissues also play a significant role, with localized heating or cooling of feathered skin regions resulting in thermoregulatory responses (Necker, 1977). During acute cold exposure, the role of inputs from skin thermoreceptors of pigeons appears to exceed that of internal thermoreceptors (Østnes and Bech, 1998). In pigeons trained to wear masks so that inspired T_{air} could be varied without changing T_{air} of the birds' surroundings, changes in MHP suggested peripheral thermoception in the head (Bech et al., 1988). Skin thermoreceptors in regions such as the brood patch are thought to be vital for the regulation of egg temperature during incubation (Rautenberg, 1986).

A key group of molecules involved in transducing information about the temperature of a bird's surroundings are temperature-sensitive transient receptor potential (thermoTRP) channels, which are involved in both nociception and thermoception (Patapoutian et al., 2003). ThermoTRP channels are phylogenetically widespread among animals but show substantial functional diversity. For instance, TRPA1 channels appear to be heat sensitive in amphibians, reptiles, and birds, but cold sensitive or nontemperature sensitive in mammals (Yamamoto et al., 2016). An investigation of the role of TRPM8 channels in cold sensitivity in chicken dorsal root ganglion neurons suggested considerable functional overlap with mammalian TRPM8 channels, but also revealed large populations of TRPM8-independent cold-sensitive neurons (Yamamoto et al., 2016).

45.7.2 Neuronal integration

The basis for regulation of avian T_b around a setpoint involves proportional responses triggered by the firing rates of populations of warm-sensitive (i.e., firing rate positively related to T_b), cold-sensitive (i.e., firing rate negatively related to T_b), and temperature-insensitive neurons (reviewed by Boulant, 2006), with greater proportions of warm-sensitive neurons compared to cold-sensitive ones (Boulant and Dean, 1986; Simon, 2000). These neurons provide the basis for fine control of T_b, with even small deviations from the setpoint resulting in adjustments of heat loss or heat gain. Thermal control appears to involve at least two levels of regulation. One involves fine control based on differences in firing rates between cold- and warm-sensitive neurons. A second, less graded level of regulation arises from temperature guardian neurons, first described in the POAH of Muscovy ducklings (*Cairina moschata*) and which alter firing rates when T_b crosses specific lower and upper thresholds of 36.1 and 42.3°C, respectively (Basta et al., 1997).

In addition to integrating thermoreceptor inputs, the POAH also processes neuronal input related to osmotic variables. Damage to the POAH causes disruptions to both thermoregulation and osmoregulation and water balance (e.g., Kuznetsov and Kazakov, 2000). Numerous neuroactive molecules are involved in integration in the POAH and thermoregulatory effector responses are altered by a variety of experimental manipulations. Injections of norepinephrine, 5-hydroxytryptamine, or acetylcholine result in suppression of shivering thermogenesis in pigeons and domestic fowl (Hillman et al., 1980; Hohtola et al., 1989) and often result in hypothermia in the former species (Hissa, 1988). Other neuroactive molecules that play a role in thermoregulatory integration in the POAH include prostaglandins (Hissa et al., 1980; Nistico and Marley, 1976), arginine vasotocin and angiotensin II (Hassinen et al., 1994).

45.7.3 Efferent outputs

Outputs from the POAH effect an array of physiological and behavioral responses, modulated by neuronal or endocrine signaling. These include behavioral responses such as wing-drooping in domestic fowl (Lepkovsky et al., 1968). Elevated MHP primarily involves increases in thyroxine secretion by the thyroid gland and the subsequent synthesis of triiodothyronin (T_3), the primary thermogenesis-stimulating hormone, via deiodinase enzymes in tissues (Silvestri et al., 2005). The major effect of elevated T_3 is to stimulate metabolism in muscle and major organs including the kidney and liver. In addition to being the main stimulus for shivering and probably NST, T_3 also influences BMR. In black-legged kittiwakes (*Rissa tridactyla*), plasma T_3 concentrations were correlated with both whole-animal and mass-specific BMR (Welcker et al., 2013).

Another key neuroendocrine process involved in avian thermoregulation is the secretion of melatonin, which occurs in response to photoreceptor inputs integrated in pacemakers that include the hypothalamic SCN, pineal gland, and the retinae. The entrainment of avian circadian rhythms, with light levels representing the primary *Zeitgeber*, is functionally linked to elevated melatonin secretion during the rest phase. Melatonin synthesis by gastrointestinal cells has been suggested to be involved in adjusting T_b in response of restricted food availability (Saarela et al., 1999).

45.7.4 Circulatory adjustments of heat transfer

Regulation of blood flow to and from specific tissues is a critical component of avian thermoregulation. Reductions in heat loss across the skin occur through vasoconstriction of cutaneous capillary beds and directing blood flow through venae comitantes and retia, circulatory structures that promote heat transfer from warm arterial blood to cooler venous blood (Midtgård, 1989a). Arteriovenous anastomoses (AVAs) consist of low-resistance circuits that facilitate increases in peripheral blood flow and permit rapid heat loss. In domestic fowl, AVA blood flow occurs mainly in unfeathered skin and increases from 17% of total blood flow under cold conditions to 83% under hot conditions (Wolfenson, 1983). The density of AVA is a phenotypically flexible trait, with significantly higher AVA density in the nasal mucosa of heat-acclimated chickens compared to controls (Midtgård, 1989b).

Vasodilation is usually a component of circulatory responses to high T_e, serving to increase rates of heat loss, but may also be important in the prevention of freezing injury for species in which peripheral tissues are maintained at temperatures just above freezing. In swimming mallard ducks, metabolic rate increased rapidly when water temperature decreased below 0°C, reflecting vasodilation in the ducks' feet and associated increases in heat loss (Kilgore and Schmidt-Nielsen, 1975).

Birds can dissipate significant quantities of heat via vasodilation of the microvasculature of the beak (Hagan and Heath, 1980) and changes in the beak T_s of Toco toucans (*Ramphastos toco*) revealed this species' massive beak functions as a controllable heat radiator that can account for up to 100% of total heat loss (Tattersall et al., 2009). Finely controlled heat loss arising from adjustments to blood flow to the beak has been demonstrated in taxa including Darwin's finches (Tattersall et al., 2018), hornbills (van de Ven et al., 2016), and ground-hornbills (Janse van Vuuren et al., 2020), as well as the casques of cassowaries (Eastick et al., 2019).

Heat dissipation via the beak typically involves T_s increasing abruptly above some threshold T_{air}, creating a gradient for heat loss that diminishes as T_{air} approaches T_b. In southern ground-hornbills, the threshold T_{air} is approximately 20°C (Figure 45.7). Modulation of heat loss across the beak surface also appears to be a component of avian responses to perceived food scarcity. Great tits (*Parus major*) habituated to a feeder during winter immediately reduced beak T_s in response to food restriction, evidently as a preemptive measure to reduce the probability of a mismatch between energy supply and demand (Winder et al., 2020).

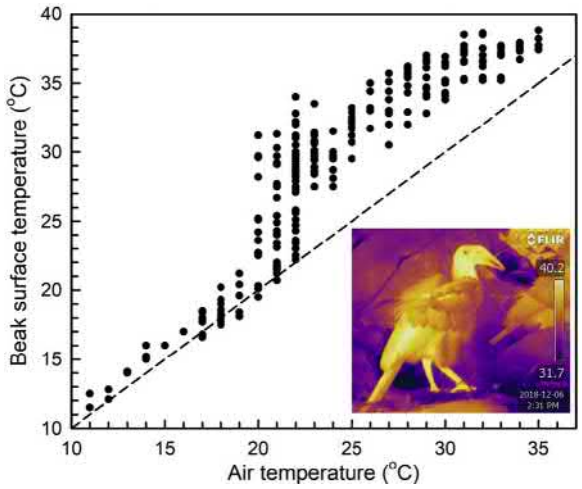

FIGURE 45.7 Beak surface temperature in southern ground-hornbills (*Bucorvus leadbeateri*) tracks air temperature (T_{air}) when $T_{air} < 20°C$, but then rapidly increases to values 6–10°C above T_{air} under warmer conditions, creating a gradient for nonevaporative heat loss. *Redrawn from Janse van Vuuren et al. (2020).*

45.8 Development of thermoregulation

Avian embryos make the transition to endothermy either before or after hatching, with the ontogenetic trajectory of endothermy involving many of the same fundamental steps that occurred during the evolution of endothermy: the acquisition of metabolic machinery to produce heat on demand, the development of a neuronal thermostat enabling the defense of a T_b setpoint, and the development of circulatory and respiratory systems suitable for transporting oxygen and nutrients to cells at the rates required to sustain metabolic rates substantially higher than those of ectotherms (Price and Dzialowski, 2018).

45.8.1 The altricial–precocial spectrum

The thermoregulatory status of hatchlings varies greatly depending on where they fall along the continuum from altriciality to precociality (Figure 45.8). The hatchlings of precocial taxa, such as Galliformes (including the domestic fowl), Anseriformes, Charadriiformes, Otidiformes, and Pteroclidiformes, hatch with down and are capable of maintaining an approximately constant T_b over a range of T_e. At the opposite end of the continuum, altricial hatchlings of orders such as Columbiformes, Cuculiformes, and Passeriformes lack any meaningful capacity for thermoregulatory heat production and are wholly dependent on external heat sources, typically the incubating parent.

As soon as the constraints on ventilation imposed by the eggshell are removed by hatching (Sirsat and

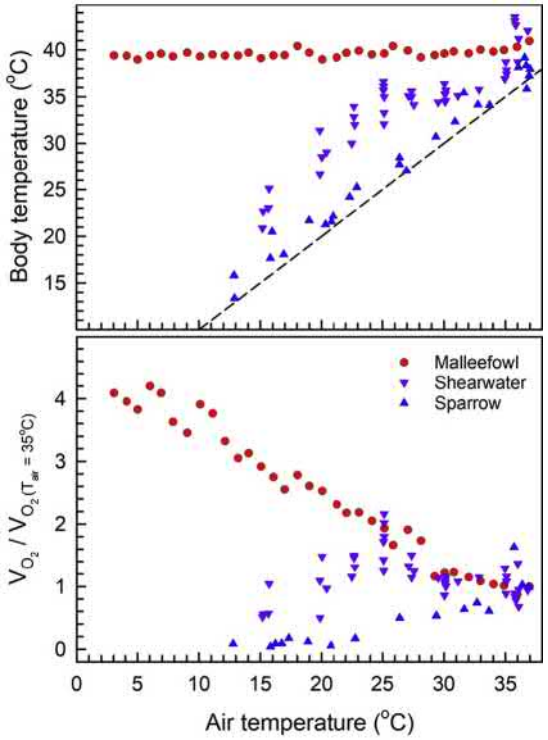

FIGURE 45.8 Thermoregulation in avian neonates represents a continuum from ectothermy in altricial species to endothermic homeothermy in precocial species, illustrated here by relationships between air temperature (T_{air}) and body temperature (T_b, upper panel) and oxygen consumption ($\dot{V}_{O_2}$, lower panel) for altricial vesper sparrows (*Pooecetes gramineus*), semiprecocial wedge-tailed shearwaters (*Ardenna pacifica*) and precocial malleefowl (*Leipoa ocellata*). In the shearwater neonates, T_b is regulated at a setpoint of ~35°C when T_{air} is between approximately 25°C and 35°C by means of increasing MHP, but declines at lower T_{air}. To account for interspecific differences in body mass, oxygen consumption (V_{O_2}) for each species is expressed as a fraction of average $\dot{V}_{O_2}$ calculated over $T_{air} = 32.5–37.5$°C. Data for sparrows, shearwaters, and malleefowl are from Dawson and Evans (1960), Mathiu et al. (1992) and Booth (1984), respectively.

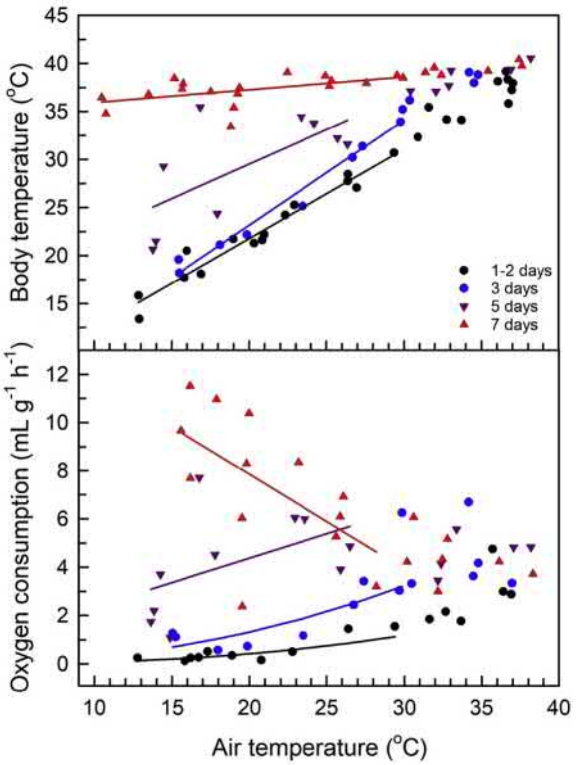

FIGURE 45.9 Development of endothermy in the altricial nestlings of vesper sparrows (*Pooecetes gramineus*), showing how the relationships between air temperature (T_{air}) and oxygen consumption (lower panel) and body temperature (upper panel) change within 7 days of hatching. The *solid lines* are regressions fitted to data at $T_{air} < 30$°C to illustrate the progressive development of endothermic homeothermy. *Data from Dawson and Evans (1960).*

Dzialowski, 2016), the neonates of precocial species show similar patterns of thermoregulation as adults, with thermogenesis compensating for heat loss at T_e below the TNZ. The thigh muscles appear to provide the major source of metabolic thermogenesis early in development, and the percentage of total M_b they represent increases rapidly immediately prior to hatching in Pekin ducks (*Anas platyrhynchos domestica*), whereas the relative mass of the heart increases more gradually (Price and Dzialowski, 2018). The metabolic intensity of cardiac and skeletal muscles also peaks at the time of hatching.

In contrast, the neonates of altricial species are fully ectothermic and develop endothermy posthatching, a process requiring from a few days up to 3 weeks (Figure 45.9). The pectoral muscles are the major sites for shivering thermogenesis and grow rapidly. In red-winged blackbirds (*Agelaius phoeniceus*), complete endothermy is attained around day 10 posthatching, associated with rapid increases in the relative mass of pectoral muscles (Olson, 2001; Sirsat et al., 2016). The growth of the pectoral muscles is accompanied by increases in activities of enzymes such as citrate synthase and pyruvate kinase and the rate of mitochondrial oxidative phosphorylation (Choi et al., 1993; Sirsat et al., 2016). The attainment of endothermy is also influenced by the number of nestlings and their collective thermal inertia; endothermy occurred earlier in blue tit (*Cyanistes caeruleus*) nestlings in experimentally reduced broods compared to control and enlarged broods (Andreasson et al., 2016).

Another functional difference between altricial and precocial species concerns the timing of the development of the thermostat provided by the neuronal integration center in the POAH. Functioning warm- and cold-sensitive neurons are evident up to a week before hatching in Muscovy duck embryos (Tzschentke and Basta, 2000) and thermoregulatory increases in MHP in malleefowl embryos 3 days before hatching imply a fully functional POAH (Booth, 1987). The neonates of many species solicit brooding behavior by means of vocalizations, which may be distinct

from food-soliciting calls. In American white pelicans (*Pelecanus erythrorhynchos*), both embryos and neonates use specific calls to solicit parental brooding (Evans, 1992), with the temperature dependence of these vocalizations shifting in parallel with the progressive development of the capacity for shivering thermogenesis during the first 2 weeks of posthatching development (Evans, 1994).

Thermoregulation during breeding may also involve heterothermy by adults or endothermic nestlings. Incubating female broad-tailed hummingbirds (*Selasphorus platycercus*) occasionally enter deep torpor while incubating eggs, with egg temperature as low as 6.5°C (Calder and Booser, 1973). After attaining endothermy at 5 days posthatching, fork-tailed storm petrel (*Oceanodroma furcata*) chicks in nesting burrows on Alaska's Barren Islands respond to extended periods without food provisioning by entering torpor, during which T_b was as low as 10.6°C (Boersma, 1986).

45.8.2 Developmental plasticity of thermoregulation

The thermal environment experienced by avian embryos can have profound effects on thermoregulation later in life. Not surprisingly, the species in which developmental plasticity of thermoregulation has received most attention is the domestic fowl, with a variety of egg thermal manipulations used to maximize commercial production. These manipulations, which typically involve exposing embryos to repeated transient increases or decreases in incubation temperature (T_{inc}), largely mimic the changes in temperature experienced by the embryos of wild species in which parental nest attendance is intermittent.

Most thermal manipulations employed in poultry production focus on the period during the middle third of incubation when the hypothalamus–thyroid–pituitary–adrenal (HTPA) axis is formed and thermal conditions are most likely to influence the development of thermoregulatory function (Yahav et al., 2009). For example, broiler embryos exposed to $T_{inc} = 39.5$°C and 65% relative humidity for 12 h/day between embryonic days E7 and E16 exhibited significantly lower eggshell temperatures, heart rates, and $\dot{V}_{O_2}$ after E18 compared to embryos incubated under control conditions of constant $T_{inc} = 37.8$°C and 56% relative humidity (Piestun et al., 2009). Posthatching, chicks from the experimental treatment had significantly lower T_b and levels of circulating thyroid hormones (Piestun et al., 2008). Responses to thermal manipulation during the period of hypothalamic development often differ from those associated with continuous thermal manipulation throughout incubation.

Changes in embryo thermal physiology induced by thermal manipulation may involve trade-offs between growth and heat production. Zebra finch embryos regularly cooled to 20°C showed lower mass and yolk reserves on E12, as well as higher mass-specific metabolic rates compared to embryos incubated at constant $T_{inc} = 37.5$°C, revealing that the efficiency of converting macronutrients contained in the egg into embryo tissue was reduced (Olson et al., 2006). The effects of periodic cooling on embryo growth appeared to be stronger in tissues such as muscles and organs compared to the skeleton (Olson et al., 2008).

An intriguing new mechanism for developmental plasticity in avian heat tolerance was reported by Mariette and Buchanan (2016). Incubating female zebra finches were observed vocalizing during periods of $T_{air} > 26$°C within 5 days of hatching and experimental playback of these heat-associated calls to eggs in artificial incubators resulted in long-term phenotypic effects. Finches exposed to the heat-associated call as embryos showed differences in begging and growth trajectories as nestlings, as well as in reproductive success and thermal preferences as adults, compared to individuals exposed to control playback of adult contact calls (Mariette and Buchanan, 2016).

Thermal acclimation soon after hatching can also significantly affect thermoregulatory performance in adults. Heat or cold acclimation during the first week posthatching significantly affects subsequent tolerance of high or low T_{air} at 6–7 weeks in chickens (Shinder et al., 2002; Yahav and Hurwitz, 1996). Far less is known about developmental plasticity in response to posthatching thermal acclimation among nestlings of wild birds, but Andreasson et al. (2018) found evidence for fitness benefits of exposure of 8- to 12-day old blue tit nestlings to high nest temperatures. Nestlings were able to maintain T_b below lethal levels even when nest temperature exceeded 50°C, and nestlings from heated nest boxes appeared to show higher annual survival and recruitment into the breeding population as adults compared to control nestlings from unheated nest boxes (Andreasson et al., 2018). Much remains to be learned about developmental plasticity in thermoregulation among wild birds. Nord and Giroud (2020) raise the interesting possibility that in altricial species, in which formation of the HTPA axis occurs during the week following hatching, posthatching thermal conditions may exert a greater influence on developmental plasticity than prehatching conditions, and vice versa for precocial species in which HTPA axis formation occurs earlier in development.

45.9 Avian thermoregulation and global heating

The thermal landscapes in which birds regulate their T_b are rapidly changing as a consequence of anthropogenic greenhouse gas emissions. In the absence of meaningful emission reductions, global average T_s is projected to

increase by ~4°C over the course of the 21st century (IPCC, 2014). The frequency, intensity, and duration of heatwaves are anticipated to increase, and some hot, arid regions are already showing more rapid heating than anticipated (van Wilgen et al., 2016). Climate change affects birds in a multitude of ways, and this section considers only direct impacts on thermoregulation.

The most obvious direct impacts of higher T_{air} are apparent in birds inhabiting hot, arid regions, where extreme heat events have occasionally caused catastrophic mortality involving vast numbers of individuals (e.g., Finlayson, 1932). More recently, smaller-scale mortality events have revealed the potential for heatwaves to rapidly cause severe declines in populations of threatened species (Saunders et al., 2011). Avian mortality by lethal hyperthermia (T_{air} exceeding species-specific heat tolerance limits) or lethal dehydration (cumulative TEWL exceeding dehydration tolerance) is predicted to occur more frequently and over larger areas under future climates, particularly in the arid zones of North America and Australia (Albright et al., 2017; Conradie et al., 2020).

Physiological constraints on maintaining T_b at sublethal levels during hot weather also create a host of trade-offs involving foraging and thermoregulatory behaviors. High T_{air} may result in reduced foraging efficiency by forcing birds to spend more time in shaded microsites or engaged in panting, with progressive loss of M_b during periods of sustained hot weather (du Plessis et al., 2012; van de Ven et al., 2019). Temperature-driven reductions in adult foraging efficiency during the nesting period may have severe negative impacts for breeding success through increased likelihood of nest abandonment, decreases in fledgling size and M_b, or increases in nest predation risk by extending the nestling period (Cunningham et al., 2013; Sharpe et al., 2019; van de Ven et al., 2019). Such trade-offs are not, however, limited to hot desert habitats; seabirds breeding at high latitudes can experience greater nestling mortality on days when $T_{air} > 14$°C forces adults to leave nests to engage in thermoregulatory behaviors such as bathing (Oswald et al., 2008).

Higher average air temperatures and more frequent and extreme heatwaves also have far-reaching impacts for domesticated birds and food production. In addition to compounding heat management challenges for commercial production, climate change is emerging as a significant threat to small-scale, subsistence poultry production systems and thus to food security and human well-being in low-income countries where rural communities rely heavily on poultry as a source of protein (Nyoni et al., 2018). In developing African countries, for example, free-ranging village chickens experience natural temperature cycles and depend on foraging to meet the nutritional requirements for survival, growth, and reproduction (Sonaiya, 2007; Yusuf et al., 2014). Domestic fowls in rural subsistence production systems in hot regions may be expected to be subject to fitness costs of hot weather similar to those observed in nondomesticated birds, and thus global heating has the potential to severely impact production and food security.

References

Ahmad, T., Khalid, T., Mushtaq, T., Mirza, M., Nadeem, A., Babar, M., Ahmad, G., 2008. Effect of potassium chloride supplementation in drinking water on broiler performance under heat stress conditions. Poultry Sci. 87, 1276–1280.

Albright, T.P., Mutiibwa, D., Gerson, A.R., Smith, E.K., Talbot, W.A., McKechnie, A.E., Wolf, B.O., 2017. Mapping evaporative water loss in desert passerines reveals an expanding threat of lethal dehydration. Proc. Natl. Acad. Sci. U. S. A. 114, 2283–2288.

Andreasson, F., Nord, A., Nilsson, J.-Å., 2016. Brood size constrains the development of endothermy in blue tits. J. Exp. Biol. 219, 2212–2219.

Andreasson, F., Nord, A., Nilsson, J.-Å., 2018. Experimentally increased nest temperature affects body temperature, growth and apparent survival in blue tit nestlings. J. Avian Biol. 49 jav-01620.

Andreasson, F., Nord, A., Nilsson, J.-Å., 2019. Age-dependent effects of predation risk on night-time hypothermia in two wintering passerine species. Oecologia 189, 329–337.

Arad, Z., Marder, J., 1982. Strain differences in heat resistance to acute heat stress, between the bedouin desert fowl, the white leghorn and their crossbreeds. Comp. Biochem. Physiol. A 72, 191–193.

Aschoff, J., 1981. Thermal conductance in mammals and birds: its dependence on body size and circadian phase. Comp. Biochem. Physiol. 69A, 611–619.

Aschoff, J., 1982. The circadian rhythm of body temperature as a function of body size. In: Taylor, C.R., Johansen, R., Bolis, L. (Eds.), A Companion to Animal Physiology. Cambridge University Press, Cambridge, pp. 173–188.

Avery, P., Richards, S., 1983. Thermosensitivity of the hypothalamus and spinal cord in the domestic fowl. J. Therm. Biol. 8, 237–239.

Bahat, O., Choshniak, I., Houston, D.C., 1998. Nocturnal variation in body temperature of Griffon vultures. Condor 100, 168–171.

Bakken, G.S., 1976. A heat transfer analysis of animals: unifying concepts and the application of metabolism chamber data to field ecology. J. Theor. Biol. 60, 337–384.

Barclay, R.M.R., Lausen, C.L., Hollis, L., 2001. What's hot and what's not: defining torpor in free-ranging birds and mammals. Can. J. Zool. 79, 1885–1890.

Barre, H., Geloen, A., Chatonnet, J., Dittmar, A., Rouanet, J.-L., 1985. Potentiated muscular thermogenesis in cold-acclimated muscovy duckling. Am. J. Physiol. Regul. Integr. Comp. Physiol. 249, R533–R538.

Bartholomew, G.A., Lasiewski, R.C., Crawford, E.C., 1968. Patterns of panting and gular flutter in cormorants, pelicans, owls, and doves. Condor 70, 31–34.

Basta, D., Tzschentke, B., Nichelmann, M., 1997. Temperature guardian neurons in the preoptic area of the hypothalamus. Brain Res. 767, 361–362.

Battley, P.F., Dekinga, A., Dietz, M.W., Piersma, T., Tang, S., Hulsman, K., 2001. Basal metabolic rate declines during long-distance migratory flight in great knots. Condor 103, 838–845.

Beauchamp, G., 1999. The evolution of communal roosting in birds: origin and secondary losses. Behav. Ecol. 10, 675–687.

Bech, C., Johansen, K., 1980. Ventilatory and circulatory responses to hyperthermia in the mute swan (*Cygnus olor*). J. Exp. Biol. 88, 195–204.

Bech, C., Johansen, K., Maloiy, G., 1979. Ventilation and expired gas composition in the flamingo, *Phoenicopterus ruber*, during normal respiration and panting. Physiol. Zool. 52, 313–328.

Bech, C., Midtgård, U., 1981. Brain temperature and the rete mirabile opthalmicum in the Zebra Finch (*Poephila guttata*). J. Comp. Physiol. B 145, 89–93.

Bech, C., Rautenberg, W., May-Rautenberg, B., 1988. Thermoregulatory responses of the pigeon (*Columba livia*) to selective changes in the inspired air temperature. J. Comp. Physiol. B 157, 747–752.

Ben-Hamo, M., Muñoz-Garcia, A., Larrain, P., Pinshow, B., Korine, C., Williams, J.B., 2016. The cutaneous lipid composition of bat wing and tail membranes: a case of convergent evolution with birds. Proc. R. Soc. B 283, 20160636.

Bennett, A.F., Ruben, J.A., 1979. Endothermy and activity in vertebrates. Science 206, 649–654.

Berger, M., Hart, J., Roy, O., 1971. Respiratory water and heat loss of the black duck during flight at different ambient temperatures. Can. J. Zool. 49, 767–774.

Bernstein, M.H., 1971. Cutaneous water loss in small birds. Condor 73, 468–469.

Bernstein, M.H., Sandoval, I., Curtis, M.B., Hudson, D.M., 1979. Brain temperature in pigeons: effects of anterior respiratory bypass. J. Comp. Physiol. 129, 115–118.

Bicudo, J.E.P.W., Bianco, A.C., Vianna, C.R., 2002. Adaptive thermogenesis in hummingbirds. J. Exp. Biol. 205, 2267–2273.

Boersma, P.D., 1986. Body temperatures, torpor, and growth in chicks of fork-tailed storm-petrels (*Oceanodroma furcata*). Physiol. Zool. 59, 10–19.

Booth, D.T., 1984. Thermoregulation in neonate mallee fowl *Leipoa ocellata*. Physiol. Zool. 57, 251–260.

Booth, D.T., 1987. Metabolic response of mallee fowl *Leipoa ocellata* embryos to cooling and heating. Physiol. Zool. 60, 446–453.

Boulant, J.A., 2006. Neuronal basis of Hammel's model for set-point thermoregulation. J. Appl. Physiol. 100, 1347–1354.

Boulant, J.A., Dean, J.B., 1986. Temperature receptors in the central nervous system. Annu. Rev. Physiol. 48, 639–654.

Boyles, J.G., Smit, B., McKechnie, A.E., 2011a. Does use of the torpor cut-off method to analyze variation in body temperature cause more problems than it solves? J. Therm. Biol. 36, 373–375.

Boyles, J.G., Smit, B., McKechnie, A.E., 2011b. A new comparative metric for estimating heterothermy in endotherms. Physiol. Biochem. Zool. 84, 115–123.

Brigham, R.M., 1992. Daily torpor in a free-ranging goatsucker, the common poorwill (*Phalaenoptilus nuttallii*). Physiol. Zool. 65, 457–472.

Brigham, R.M., Willis, C.K.R., Geiser, F., Mzilikazi, N., 2011. Baby in the bathwater: should we abandon the use of body temperature thresholds to quantify expression of torpor? J. Therm. Biol. 84, 375–379.

Burgoon, D.A., Kilgore, D.L., Motta, P.J., 1987. Body temperature in the calliope hummingbird (*Stellula calliope*): a speces lacking a *rete mirabile ophthalmicum*. J. Comp. Physiol. B 157, 583–588.

Bushuev, A., Tolstenkov, O., Zubkova, E., Solovyeva, E., Kerimov, A., 2017. Basal metabolic rate in free-living tropical birds: the influence of phylogenetic, behavioral, and ecological factors. Curr. Zool. 64, 33–43.

Butler, P.J., Woakes, A.J., 2001. Seasonal hypothermia in a large migrating bird: saving energy or fat deposition? J. Exp. Biol. 204, 1361–1367.

Calder, W., King, J., 1974. Thermal and caloric relations of birds. In: Farner, D.S., King, J.R. (Eds.), Avian Biology. Academic, New York.

Calder, W.A., Booser, J., 1973. Hypothermia of broad-tailed hummingbirds during incubation in nature with ecological correlations. Science 180, 751–753.

Carey, C., Marsh, R.L., Bekoff, A., Johnston, R.M., Olin, A.M., 1989. Enzyme activities in muscles of seasonally acclimatized House Finches. In: Bech, C., Reinertsen, R.E. (Eds.), Physiology of Cold Adaptation in birds. Springer, New York, pp. 95–104.

Carpenter, F.L., 1974. Torpor in an Andean hummingbird: its ecological significance. Science 183, 545–547.

Champagne, A.M., Muñoz-Garcia, A., Shtayyeh, T., Tieleman, B.I., Hegemann, A., Clement, M.E., Williams, J.B., 2012. Lipid composition of the stratum corneum and cutaneous water loss in birds along an aridity gradient. J. Exp. Biol. 215, 4299–4307.

Chaplin, S.B., 1976. The physiology of hypothermia in the black-capped chickadee (*Parus atricapillus*). J. Comp. Physiol. B 112, 335–344.

Chaplin, S.B., 1982. The energetic significance of huddling in common bushtits (*Psaltriparus minimus*). Auk 99, 424–430.

Chappell, M.A., Bech, C., Buttemer, W.A., 1999. The relationship of central and peripheral organ masses to aerobic performance variation in house sparrows. J. Exp. Biol. 202, 2269–2279.

Chappell, M.A., Buttemer, W.A., Russell, A.F., 2016. Energetics of communal roosting in chestnut-crowned babblers: implications for group dynamics and breeding phenology. J. Exp. Biol. 219, 3321–3328.

Cheke, R.A., 1971. Temperature rhythms in African montane sunbirds. Ibis 113, 500–506.

Cheviron, Z., Swanson, D., 2017. Comparative transcriptomics of seasonal phenotypic flexibility in two North American songbirds. Integr. Comp. Biol. 57, 1040–1054.

Choi, I.-H., Ricklefs, R.E., Shea, R.E., 1993. Skeletal muscle growth, enzyme activities, and the development of thermogenesis: a comparison between altricial and precocial birds. Physiol. Zool. 66, 455–473.

Ciancio, J.E., Quintana, F., Sala, J.E., Wilson, R.P., 2016. Cold birds under pressure: can thermal substitution ease heat loss in diving penguins? Mar. Biol. 163, 43.

Clarke, A., Rothery, P., 2008. Scaling of body temperature in mammals and birds. Funct. Ecol. 22, 58–67.

Clemens, D.T., 1989. Nocturnal hypothermia in rosy finches. Condor 91, 739–741.

Conradie, S.R., Woodborne, S., Wolf, B.O., Pessato, A., Mariette, M.M., McKechnie, A.E., 2020. Avian mortality risk during heat waves will increase greatly in arid Australia during the 21st Century. Conserv. Physiol. 8, coaa048.

Coon, C.A., Warne, R.W., Martin, L.B., 2011. Acute-phase responses vary with pathogen identity in house sparrows (*Passer domesticus*). Am. J. Physiol. Regul. Integr. Comp. Physiol. 300, R1418–R1425.

Cooper, C.E., Körtner, G., Brigham, R.M., Geiser, F., 2008. Body temperature and activity patterns of free-living laughing kookaburras: the largest kingfisher is heterothermic. Condor 110, 110–115.

Coulombe, H.N., 1970. Physiological and physical aspects of temperature regulation in the burrowing owl *Speotyto cunicularia*. Comp. Biochem. Physiol. 35, 307–337.

Cowles, R.B., Dawson, W.R., 1951. A cooling mechanism of the Texas nighthawk. Condor 53, 19–22.

Crawford Jr., E.C., Kampe, G., 1971. Resonant panting in pigeons. Comp. Biochem. Physiol. Physiol. 40, 549–552.

Crompton, A., Taylor, C.R., Jagger, J.A., 1978. Evolution of homeothermy in mammals. Nature 272, 333–336.

Cunningham, S.J., Martin, R.O., Hojem, C.L., Hockey, P.A.R., 2013. Temperatures in excess of critical thresholds threaten nestling growth and survival in a rapidly-warming arid savanna: a study of common fiscals. PLoS One 8, e74613.

Cunningham, S.J., Thompson, M.L., McKechnie, A.E., 2017. It's cool to be dominant: social status alters short-term risks of heat stress. J. Exp. Biol. 220, 1558–1562.

Czarick, M., Fairchild, B.D., 2008. Poultry housing for hot climates. In: Daghir, N.J. (Ed.), Poultry Production in Hot Climates, second ed. CAB International, Wallingford, pp. 80–132.

Czenze, Z.J., Kemp, R., van Jaarsveld, B, Freeman, M.T., Smit, B, Wolf, B.O., McKechnie, A.E., 2020. Regularly-drinking desert birds have greater evaporative cooling capacity and higher heat tolerance limits than non-drinking species. Funct. Ecol. 34 (8), 1589–1600.

Daan, S., Masman, D., Groenewold, A., 1990. Avian basal metabolic rates: their association with body compostition and energy expenditure in nature. Am. J. Physiol. 259, R333–R340.

Darveau, C.-A., Suarez, R.K., Andrews, R.D., Hochachka, P.W., 2002. Allometric cascade as a unifying principle of body mass effects on metabolism. Nature 417, 166–170.

Dawson, W.R., 1954. Temperature Regulation and Water Requirements of the Brown and Abert Towhees, *Pipilo Fuscus* and *Pipilo Aberti*. In: Bartholomew, G.A., Crescitelli, F., Bullock, T.H., Furgason, W.H., Schechtman, A.M. (Eds.), University of California Publications in Zoology. University of California Publications in Zoology. University of California Press, Berkeley, pp. 81–123.

Dawson, W.R., Evans, F.C., 1960. Relation of growth and development to temperature regulation in nestling Vesper Sparrows. Condor 62, 329–340.

Dawson, W.R., Fisher, C.D., 1969. Responses to temperature by the spotted nightjar (*Eurostopodus guttatus*). Condor 71, 49–53.

Dawson, W.R., Schmidt-Nielsen, K., 1964. Terrestrial animals in dry heat: desert birds. In: Dill, D.B. (Ed.), Handbook of Physiology: Adaptation to the Environment. American Physiological Society, Washington, D.C., pp. 481–492

Dean, W.R.J., Williams, J.B., 1999. Sunning behaviour and its possible influence on digestion in the white-backed mousebird *Colius colius*. Ostrich 70, 239–241.

Dietz, M.W., van Mourik, S., Tøien, Ø., Koolmees, P.A., Tersteeg-Zijderveld, M.H., 1997. Participation of breast and leg muscles in shivering thermogenesis in young turkeys and Guinea fowl. J. Comp. Physiol. B 167, 451–460.

du Plessis, K.L., Martin, R.O., Hockey, P.A.R., Cunningham, S.J., Ridley, A.R., 2012. The costs of keeping cool in a warming world: implications of high temperatures for foraging, thermoregulation and body condition of an arid-zone bird. Glob. Chang. Biol. 18, 3063–3070.

Dumonteil, E., Barre, H., Meissner, G., 1993. Sarcoplasmic reticulum Ca^{2+}-ATPase and ryanodine receptor in cold-acclimated ducklings and thermogenesis. Am. J. Physiol. Cell Physiol. 265, C507–C513.

Dumonteil, E., Barre, H., Meissner, G., 1995. Expression of sarcoplasmic reticulum Ca^{2+} transport proteins in cold-acclimating ducklings. Am. J. Physiol. Cell Physiol. 269, C955–C960.

Eastick, D.L., Tattersall, G.J., Watson, S.J., Lesku, J.A., Robert, K.A., 2019. Cassowary casques act as thermal windows. Sci. Rep. 9, 1966.

Emre, Y., Hurtaud, C., Ricquier, D., Bouillaud, F., Hughes, J., Criscuolo, F., 2007. Avian UCP: the killjoy in the evolution of the mitochondrial uncoupling proteins. J. Mol. Evol. 65, 392–402.

Etches, R.J., John, T.M., Verrinder Gibbins, A.M., 2008. Behavioural, physiological, neuroendocrine and molecular responses to heat stress. In: Daghir, N.J. (Ed.), Poultry Production in Hot Climates, second ed. CAB International, Wallingford, pp. 48–79.

Eto, E., Withers, P., Cooper, C., 2017. Can Birds Do it Too? Evidence for Convergence in Evaporative Water Loss Regulation for Birds and Mammals. Proc. R. Soc. B. The Royal Society, 20171478.

Evans, R.M., 1992. Embryonic and neonatal vocal elicitation of parental brooding and feeding responses in American white pelicans. Anim. Behav. 44, 667–675.

Evans, R.M., 1994. Cold-induced calling and shivering in young American white pelicans: honest signalling of offspring need for warmth in a functionally integrated thermoregulatory system. Behaviour 129, 13–34.

Farmer, C.G., 2000. Parental care: the key to understanding endothermy and other convergent features in birds and mammals. Am. Nat. 155, 326–334.

Felsenstein, J., 1985. Phylogenies and the comparative method. Am. Nat. 125, 1–15.

Finlayson, H.H., 1932. Heat in the interior of South Australia – holocaust of bird-life. South Aust. Ornithol. 11, 158–160.

Frankel, H., Hollands, K.G., Weiss, H.S., 1962. Respiratory and circulatory responses of hyperthermic chickens. Arch. Int. Physiol. Biochim. 70, 555–563.

Freeman, M.T., Czenze, Z.J., Schoeman, K., McKechnie, A.E., 2020. Extreme hyperthermia tolerance in the world's most abundant wild bird. Sci. Rep. 10, 13098.

Geist, N.R., 2000. Nasal respiratory turbinate function in birds. Physiol. Biochem. Zool. 73, 581–589.

Gelineo, S., 1964. Organ systems in adaptation: the temperature regulating system. In: Dill, D.B. (Ed.), Handbook of Physiology, Section 4, Adaptation to the Environment. American Physiological Society, Washington, DC.

Geran, L.C., Rashotte, M.E., 1997. Participation of gastrointestinal-load volume in "setting" the pigeon's nocturnal body temperature. Naturwissenschaften 84, 350–353.

Gerson, A.R., McKechnie, A.E., Smit, B., Whitfield, M.C., Smith, E.K., Talbot, W.A., Wolf, B.O., 2019. The functional significance of facultative hyperthermia varies with body size and phylogeny. Funct. Ecol. 33, 597–607.

Gessaman, J.A., 1972. Bioenergetics of the snowy owl (*Nyctea scandiaca*). Arct. Alp. Res. 4, 223–238.

Goldsmith, R., Sladen, W., 1961. Temperature regulation of some antarctic penguins. J. Physiol. 157, 251–262.

Goldstein, D.L., 1983. Effect of wind on avian metabolic rate with particular reference to Gambel's quail. Physiol. Zool. 56, 485–492.

Graf, R., Krishna, S., Heppner, F., 1989. Regulated nocturnal hypothermia induced in pigeons by food deprivation. Am. J. Physiol. 256, R733–R738.

Grant, G.S., 1982. Avian incubation: egg temperature, nest humidity, and behavioral thermoregulation in a hot environment. Ornithol. Monogr. 30, 1–100.

Gray, D.A., Marais, M., Maloney, S.K., 2013. A review of the physiology of fever in birds. J. Comp. Physiol. B 183, 297–312.

Hackett, S.J., Kimball, R.T., Reddy, S., Bowie, R.C.K., Braun, E.L., Braun, M.J., Chojnowski, J.L., Cox, W.A., Han, K.-L., Harshman, J., Huddleston, C.J., Marks, B.D., Miglia, K.J., Moore, W.S., Sheldon, F.H., Steadman, D.W., Witt, C.C., Yuri, T., 2008. A phylogenomic study of birds reveals their evolutionary history. Science 320, 1763–1768.

Hagan, A.A., Heath, J.E., 1980. Regulation of heat loss in the duck by vasomotion in the bill. J. Therm. Biol. 5, 95–101.

Hammel, H.T., 1965. Neurons and temperature regulation. In: Yamamoto, W.S., Brobeck, J.R. (Eds.), Physiological Controls and Regulations. Saunders, Philadelphia, PA, pp. 71–97.

Handrich, Y., Bevan, R., Charrassin, J.-B., Butler, P., Ptz, K., Woakes, A., Lage, J., Le Maho, Y., 1997. Hypothermia in foraging king penguins. Nature 388, 64–67.

Hassinen, E., Pyörnilä, A., Hissa, R., 1994. Vasotocin and angiotensin II affect thermoregulation in the pigeon, *Columba livia*. Comp. Biochem. Physiol. Physiol. 107, 545–551.

Hatchwell, B.J., Sharp, S.P., Simeoni, M., McGowan, A., 2009. Factors influencing overnight loss of body mass in the communal roosts of a social bird. Funct. Ecol. 23, 367–372.

Haugen, M.J., Williams, J.B., Wertz, P., Tieleman, B.I., 2003. Lipids of the stratum corneum vary with cutaneous water loss among larks along a temperature-moisture gradient. Physiol. Biochem. Zool. 76, 907–917.

Heath, J.E., 1962. Temperature fluctuation in the turkey vulture. Condor 64, 234–235.

Hillman, P.E., Scott, N., Van Tienhoven, A., 1980. Effect of 5-hydroxytryptamine and acetylcholine on the energy budget of chickens. Am. J. Physiol. Regul. Integr. Comp. Physiol. 239, R57–R61.

Hissa, R., 1988. Controlling mechanisms in avian temperature regulation: a review. Acta Physiol. Scand. Suppl. 132.

Hissa, R., Pyörnilä, A., George, J., 1980. The influence of intra-hypothalamic injections of prostaglandins E1 and F2α and ambient temperature on thermoregulation in the pigeon. J. Therm. Biol. 5, 163–167.

Hoffman, T.C.M., Walsberg, G.E., 1999. Inhibiting ventilatory evaporation produces an adaptive increase in cutaneous evaporation in mourning doves *Zenaida macroura*. J. Exp. Biol. 202, 3021–3028.

Hoffman, T.C.M., Walsberg, G.E., DeNardo, D.F., 2007. Cloacal evaporation: an important and previously undescribed mechanism for avian thermoregulation. J. Exp. Biol. 210, 741–749.

Hohtola, E., 1982. Thermal and electromyographic correlates of shivering thermogenesis in the pigeon. Comp. Biochem. & Physiol. Comp. Physiol. 73, 159–166.

Hohtola, E., Henderson, R.P., Rashotte, M.E., 1998. Shivering thermogenesis in the pigeon: the effects of activity, diurnal factors, and feeding state. Am. J. Physiol. 275, R1553–R1562.

Hohtola, E., Hissa, R., Pyörnilä, A., Rintamäki, H., Saarela, S., 1991. Nocturnal hypothermia in fasting Japanese quail: the effect of ambient temperature. Physiol. Behav. 49, 563–567.

Hohtola, E., Saarela, S., Harjula, R., Hissa, R., 1989. Cardiovascular and thermoregulatory responses to intrahypothalamically injected neurotransmitters in the pigeon. J. Therm. Biol. 14, 41–45.

Humphries, M.M., Careau, V., 2011. Heat for nothing or activity for free? Evidence and implications of activity-thermoregulatory heat substitution. Integr. Comp. Biol. 51, 419–431.

IPCC, 2014. In: Team, C.W., Pachauri, R.K., Meyer, L.A. (Eds.), Climate Change 2014: Synthesis Report. Contribution of Working Groups I, II and III to the Fifth Assessment Report of the Intergovernmental Panel on Climate Change (Geneva).

IUPS, 2001. Glossary of terms for thermal physiology. Jpn. J. Physiol. 51, 245–280.

Jacobs, P.J., McKechnie, A.E., 2014. Experimental sources of variation in avian energetics: estimated basal metabolic rate decreases with successive measurements. Physiol. Biochem. Zool. 87, 762–769.

Jaeger, E.C., 1948. Does the poor-will hibernate? Condor 50, 45–46.

Janse van Vuuren, A.K., Kemp, L.V., McKechnie, A.E., 2020. The beak and unfeathered skin as heat radiators in the Southern Ground-hornbill. J. Avian Biol. 51.

Kemp, A.C., Kemp, M., 1980. The biology of the southern ground hornbill *Bucorvus leadbeateri* (Vigors)(Aves: Bucerotidae). Ann. Transvaal Mus. 32, 65–100.

Kemp, R., McKechnie, A.E., 2019. Thermal physiology of a range-restricted desert lark. J. Comp. Physiol. B 189, 131–141.

Kemp, R., Noakes, M.J., McKechnie, A.E., 2017. Thermoregulation in free-ranging ground woodpeckers *Geocolaptes olivaceus*: no evidence of torpor. J. Avian Biol. 48, 1287–1294.

Kilgore, D.L., Bernstein, M.H., Hudson, D.M., 1976. Brain temperatures in birds. J. Comp. Physiol. 110, 209–215.

Kilgore, D.L., Schmidt-Nielsen, K., 1975. Heat loss from ducks' feet immersed in cold water. Condor 77, 475–478.

Klaassen, M., Biebach, H., 1994. Energetics of fattening and starvation in the long-distance migratory garden warbler, *Sylvia borin*, during the migratory phase. J. Comp. Physiol. B 164, 362–371.

Kleiber, M., 1932. Body size and metabolism. Hilgardia 6, 315–353.

Kohne, H., Jones, J., 1975. Changes in plasma electrolytes, acid-base balance and other physiological parameters of adult female turkeys under conditions of acute hyperthermia. Poultry Sci. 54, 2034–2038.

Konarzewski, M., Gavin, A., McDevitt, R., Wallis, I.R., 2000. Metabolic and organ mass responses to selection for high growth rates in the domestic chicken (*Gallus domesticus*). Physiol. Biochem. Zool. 73, 237–248.

Koskimies, J., 1948. On temperature regulation and metabolism in the swift, *Micropus a. apus* L. during fasting. Experimentia 4, 274–276.

Koteja, P., 2000. Energy assimilation, parental care and the evolution of endothermy. Proc. R. Soc. Lond. B Biol. Sci. 267, 479–484.

Koutsos, E.A., Klasing, K.C., 2001. The acute phase response in Japanese quail (*Coturnix coturnix japonica*). Comp. Biochem. Physiol. C Toxicol. Pharmacol. 128, 255–263.

Kuznetsov, I., Kazakov, V., 2000. Integration of thermal and osmotic afferent signals in the preoptic/anterior hypothalamic neurons. Neuroscience 99, 363–371.

Kvist, A., Lindström, Å., 2001. Basal metabolic rate in migratory waders: intra-individual, intraspecific, interspecific and seasonal variation. Funct. Ecol. 15, 465–473.

Lane, J.E., Swanson, D.L., Brigham, R.M., McKechnie, A.E., 2004. Physiological responses to temperature by Whip-poor-wills: more evidence for the evolution of low metabolic rates in caprimulgiformes. Condor 106, 921–925.

Laplante, M.P., McKinnon, E.A., Love, O.P., Vézina, F., 2019. Flexible response to short-term weather in a cold-adapted songbird. J. Avian Biol. 50.

Lasiewski, R.C., 1969. Physiological responses to heat stress in the poorwill. Am. J. Physiol. 217, 1504–1509.

Lasiewski, R.C., 1972. Respiratory function in birds. In: Farner, D.S., King, J.R. (Eds.), Avian Biology, vol. II, pp. 287–342.

Lasiewski, R.C., Bernstein, M.H., Ohmart, R.D., 1971. Cutaneous water loss in the roadrunner and poor-will. Condor 73, 470–472.

Lasiewski, R.C., Dawson, W.R., 1967. A re-examination of the relation between standard metabolic rate and body weight in birds. Condor 69, 13–23.

Lasiewski, R.C., Snyder, G.K., 1969. Responses to high temperature in nestling double-crested and pelagic cormorants. Auk 86, 529–540.

Le Maho, Y., 1977. The emperor penguin: a strategy to live and breed in the cold. Am. Sci. 65, 680–693.

Lee, M.S., Cau, A., Naish, D., Dyke, G.J., 2014. Sustained miniaturization and anatomical innovation in the dinosaurian ancestors of birds. Science 345, 562–566.

Lepkovsky, S., Snapir, N., Furuta, F., 1968. Temperature regulation and appetitive behavior in chickens with hypothalamic lesions. Physiol. Behav. 3, 911–915.

Li, Q., Xu, Z., Liu, L., Yu, H., Rong, H., Tao, L., Zhang, X., Chen, X., Gu, D., Fan, Y., 2013. Effects of breeds and dietary protein levels on the growth performance, energy expenditure and expression of avUCP mRNA in chickens. Mol. Biol. Rep. 40, 2769–2779.

Lindström, Å., Klaassen, M., Kvist, A., 1999. Variation in energy intake and basal metabolic rate of a bird migrating in a wind tunnel. Funct. Ecol. 13, 352–359.

Londoño, G.A., Chappell, M.A., del Rosario Castañeda, M., Jankowski, J.E., Robinson, S.K., 2015. Basal metabolism in tropical birds: latitude, altitude, and the "pace of life". Funct. Ecol. 29, 338–346.

Lott, B., 1991. The effect of feed intake on body temperature and water consumption of male broilers during heat exposure. Poultry Sci. 70, 756–759.

Lovegrove, B.G., 2017. A phenology of the evolution of endothermy in birds and mammals. Biol. Rev. 92, 1213–1240.

Lovegrove, B.G., 2019. Fires of Life: Endothermy in Birds and Mammals. Yale University Press.

Lovegrove, B.G., Canale, C.I., Levesque, D., Fluch, G., Řeháková-Petrů, M., Ruf, T., 2014. Are tropical small mammals physiologically vulnerable to Arrhenius effects and climate change? Physiol. Biochem. Zool. 87, 30–45.

Lovvorn, J., 2007. Thermal substitution and aerobic efficiency: measuring and predicting effects of heat balance on endotherm diving energetics. Phil. Trans. R. Soc. B: Biol. Sci. 362, 2079–2093.

Lund, J., Bolopo, D., Thomson, R.L., Elliott, D.L., Arnot, L.F., Kemp, R., Lowney, A.M., McKechnie, A.E., 2020. Winter thermoregulation in free-ranging pygmy falcons in the Kalahari Desert. J. Ornithol. 161, 549–555.

Marais, M., Gugushe, N., Maloney, S., Gray, D., 2011. Body temperature responses of Pekin ducks (*Anas platyrhynchos* domesticus) exposed to different pathogens. Poultry Sci. 90, 1234–1238.

Marder, J., 1973. Temperature regulation in the Bedouin fowl (*Gallus domesticus*). Physiol. Zool. 46, 208–217.

Marder, J., Arad, Z., 1989. Panting and acid-base regulation in heat stressed birds. Comp. Biochem. Physiol. A 94, 395–400.

Marder, J., Arieli, U., 1988. Heat balance of acclimated pigeons *Columba livia* exposed to temperatures of up to 60°C T_a. Comp. Biochem. Physiol. 91A, 165–170.

Mariette, M.M., Buchanan, K.L., 2016. Prenatal acoustic communication programs offspring for high posthatching temperatures in a songbird. Science 353, 812–814.

Marsh, R., Dawson, W., 1989a. Avian adjustments to cold. In: Wang, L.C.H. (Ed.), Advances in Comparative and Environmental Physiology. Springer-Verlag, Berlin, Germany, pp. 205–253.

Marsh, R.L., Dawson, W.R., 1989b. Avian adjustments to cold. In: Wang, L.C.H. (Ed.), Advances in Comparative and Environmental Physiology 4: Animal Adaptation to Cold. Springer-Verlag, Berlin, pp. 206–253.

Mathiu, P.M., Whittow, G.C., Dawson, W.R., 1992. Hatching and the establishment of thermoregulation in the wedge-tailed shearwater (*Puffinus pacificus*). Physiol. Zool. 65, 583–603.

McCafferty, D.J., 2013. Applications of thermal imaging in avian science. Ibis 155, 4–15.

McClennand, G.T.W., McKechnie, A.E., Chown, S.L., 2016. Basal metabolic rate of the black-faced sheathbill (*Chionis minor*): intraspecific variation in a phylogenetically distinct, island endemic. Physiol. Biochem. Zool. 89, 141–150.

McCormick, C.C., Garlich, J., Edens, F.W., 1979. Fasting and diet affect the tolerance of young chickens exposed to acute heat stress. J. Nutr. 109, 1797–1809.

McKechnie, A.E., 2008. Phenotypic flexibility in basal metabolic rate and the changing view of avian physiological diversity: a review. J. Comp. Physiol. B 178, 235–247.

McKechnie, A.E., Ashdown, R.A.M., Christian, M.B., Brigham, R.M., 2007a. Torpor in an afrotropical caprimulgid, the freckled nightjar (*Caprimulgus tristigma*). J. Avian Biol. 38, 261–266.

McKechnie, A.E., Chetty, K., Lovegrove, B.G., 2007b. Phenotypic flexibility in basal metabolic rate in Laughing Doves: responses to short-term thermal acclimation. J. Exp. Biol. 210, 97–106.

McKechnie, A.E., Freckleton, R.P., Jetz, W., 2006. Phenotypic plasticity in the scaling of avian basal metabolic rate. Proc. Roy. Soc. Lond. B 273, 931–937.

McKechnie, A.E., Gerson, A.R., McWhorter, T.J., Smith, E.K., Talbot, W.A., Wolf, B.O., 2017. Avian thermoregulation in the heat: evaporative cooling in five Australian passerines reveals within-order biogeographic variation in heat tolerance. J. Exp. Biol. 220, 2436–2444.

McKechnie, A.E., Gerson, A.R., Wolf, B.O., 2021. Thermoregulation in desert birds: scaling and phylogenetic variation in heat tolerance and evaporative cooling. J. Exp. Biol. 224, jeb229211.

McKechnie, A.E., Lovegrove, B.G., 2001a. Heterothermic responses in the speckled mousebird (*Colius striatus*). J. Comp. Physiol. B 171, 507–518.

McKechnie, A.E., Lovegrove, B.G., 2001b. Thermoregulation and the energetic significance of clustering behavior in the white-backed mousebird (*Colius colius*). Physiol. Biochem. Zool. 74, 238–249.

McKechnie, A.E., Lovegrove, B.G., 2002. Avian facultative hypothermic responses: a review. Condor 104, 705–724.

McKechnie, A.E., Lovegrove, B.G., 2003. Facultative hypothermic responses in an Afrotropical arid-zone passerine, the red-headed finch (*Amadina erythrocephala*). J. Comp. Physiol. B 173, 339–346.

McKechnie, A.E., Noakes, M.J., Smit, B., 2015. Global patterns of seasonal acclimatization in avian resting metabolic rates. J. Ornithol. 156, S367–S376.

McKechnie, A.E., Smit, B., 2010. Thermoregulation under seminatural conditions in two species of African barbets (Piciformes: Lybiidae). Ostrich 81, 97–102.

McKechnie, A.E., Swanson, D.L., 2010. Sources and significance of variation in basal, summit and maximal metabolic rates in birds. Curr. Zool. 56, 741–758.

McKechnie, A.E., Whitfield, M.C., Smit, B., Gerson, A.R., Smith, E.K., Talbot, W.A., McWhorter, T.J., Wolf, B.O., 2016. Avian thermoregulation in the heat: efficient evaporative cooling allows for extreme heat tolerance in four southern hemisphere columbids. J. Exp. Biol. 219, 2145–2155.

McKechnie, A.E., Wolf, B.O., 2004a. The allometry of avian basal metabolic rate: good predictions need good data. Physiol. Biochem. Zool. 77, 502–521.

McKechnie, A.E., Wolf, B.O., 2004b. Partitioning of evaporative water loss in white-winged doves: plasticity in response to short-term thermal acclimation. J. Exp. Biol. 207, 203–210.

McNab, B.K., 1966. An analysis of the body temperature of birds. Condor 68, 47–55.

McNab, B.K., 1978. The evolution of endothermy in the phylogeny of mammals. Am. Nat. 112, 1–21.

McNab, B.K., 1988. Food habits and the basal rate of metabolism in birds. Oecologia 77, 343–349.

McNab, B.K., 2000. The influence of body mass, climate, and distribution on the energetics of South Pacific pigeons. Comp. Biochem. Physiol. A 127, 309–329.

McWhorter, T.J., Gerson, A.R., Talbot, W.A., Smith, E.K., McKechnie, A.E., Wolf, B.O., 2018. Avian thermoregulation in the heat: evaporative cooling capacity and thermal tolerance in two Australian parrots. J. Exp. Biol. 221, jeb168930.

McWilliams, S.R., Guglielmo, C.G., Pierce, B., Klaassen, M., 2004. Flying, fasting, and feeding in birds during migration: a nutritional and physiological ecology perspective. J. Avian Biol. 35, 377–393.

Medina, I., Newton, E., Kearney, M.R., Mulder, R.A., Porter, W.P., Stuart-Fox, D., 2018. Reflection of near-infrared light confers thermal protection in birds. Nat. Commun. 9, 3610.

Menon, G.K., Baptista, L.F., Brown, B.E., Elias, P.M., 1989. Avian epidermal differentiation. II. Adaptive response of permeability barrier to water deprivation and replenishment. Tissue Cell 21, 83–92.

Menon, G.K., Baptista, L.F., Elias, P.M., Bouvier, M., 1988. Fine structural basis of the cutaneous water barrier in nestling zebra finches *Poephila guttata*. Ibis 130, 503–511.

Menon, G.K., Maderson, P.F.A., Drewes, R.C., Baptista, L.F., Price, L.F., Elias, P.M., 1996. Ultrastructural organization of avian stratum corneum lipids as the basis for facultative cutaneous waterproofing. J. Morphol. 227, 1–13.

Menuam, B., Richards, S., 1975. Observations on the sites of respiratory evaporation in the fowl during thermal panting. Respir. Physiol. 25, 39–52.

Mercer, J.B., Simon, E., 1984. A comparison between total body thermosensitivity and local thermosensitivity in mammals and birds. Pflügers Archiv. 400, 228–234.

Merola-Zwartjes, M., Ligon, J.D., 2000. Ecological energetics of the Puerto Rican tody: heterothermy, torpor and intra-island variation. Ecology 81, 990–1002.

Midtgård, U., 1983. Scaling of the brain and the eye cooling system in birds: a morphometric analysis of the rete ophthalmicum. J. Exp. Zool. 225, 197–207.

Midtgård, U., 1989a. Circulatory adaptations to cold in birds. In: Bech, C., Reinertsen, R.E. (Eds.), Physiology of Cold Adaptation in Birds. Springer, pp. 211–222.

Midtgård, U., 1989b. The effect of heat and cold on the density of arteriovenous anastomoses and tissue composition in the avian nasal mucosa. J. Therm. Biol. 14, 99–102.

Misson, B., 1974. An open circuit respirometer for metabolic studies on the domestic fowl: establishment of standard operating conditions. Br. Poultry Sci. 15, 287–297.

Morrison, P., 1962. Modification of body temperature by activity in Brazilian hummingbirds. Condor 64, 315–323.

Muñoz-Garcia, A., Cox, R.M., Williams, J.B., 2008. Phenotypic flexibility in cutaneous water loss and lipids of the stratum corneum in house sparrows (*Passer domesticus*) following acclimation to high and low humidity. Physiol. Biochem. Zool. 81, 87–96.

Muñoz-Garcia, A., Williams, J.B., 2005. Cutaneous water loss and lipids of the stratum corneum in house sparrows *Passer domesticus* from arid and mesic environments. J. Exp. Biol. 208, 3689–3700.

Murrish, D.E., 1973. Respiratory heat and water exchange in penguins. Respir. Physiol. 19, 262–270.

Nagy, K.A., 2005. Field metabolic rate and body size. J. Exp. Biol. 208, 1621–1625.

Nassar, P.N., Jackson, A.C., Carrier, D.R., 2001. Entraining the natural frequencies of running and breathing in Guinea fowl (*Numida meleagris*). J. Exp. Biol. 204, 1641–1651.

Necker, R., 1977. Thermal sensitivity of different skin areas in pigeons. J. Comp. Physiol. 116, 239–246.

Nilsson, J.-Å., Nord, A., 2018. Testing the heat dissipation limit theory in a breeding passerine. Proc. Biol. Sci. 285, 20180652.

Nistico, G., Marley, E., 1976. Central effects of prostaglandins E2, A1 and F2α in adult fowls. Neuropharmacology 15, 737–741.

Noakes, M.J., McKechnie, A.E., 2020. Seasonal metabolic acclimatization varies in direction and magnitude among years in two arid-zone passerines. Physiol. Biochem. Zool. 93, 140–152.

Noakes, M.J., Smit, B., Wolf, B.O., McKechnie, A.E., 2013. Thermoregulation in African Green Pigeons (*Treron calvus*) and a re-analysis of insular effects on basal metabolic rate and heterothermy in columbid birds. J. Comp. Physiol. B 183, 969–982.

Noakes, M.J., Wolf, B.O., McKechnie, A.E., 2016. Seasonal and geographical variation in heat tolerance and evaporative cooling capacity in a passerine bird. J. Exp. Biol. 219, 859–869.

Nord, A., Giroud, S., 2020. Lifelong effects of thermal challenges during development in birds and mammals. Front. Physiol. 11.

Nowack, J., Giroud, S., Arnold, W., Ruf, T., 2017. Muscle non-shivering thermogenesis and its role in the evolution of endothermy. Front. Physiol. 8, 889.

Nyoni, N.M.B., Grab, S., Archer, E.R.M., 2018. Heat stress and chickens: climate risk effects on rural poultry farming in low-income countries. Clim. Dev. 11, 83–90.

O'Connor, R.S., Brigham, R.M., McKechnie, A.E., 2018. Roosting in exposed microsites by a nocturnal bird, the rufous-cheeked nightjar: implications for water balance under current and future climate conditions. Can. J. Zool. 96, 1122–1129.

O'Connor, R.S., Wolf, B.O., Brigham, R.M., McKechnie, A.E., 2017. Avian thermoregulation in the heat: efficient evaporative cooling in two southern African nightjars. J. Comp. Physiol. B 187, 477–491.

Ohmart, R.D., Lasiewski, R.C., 1971. Roadrunners: energy conservation by hypothermia and absorption of sunlight. Science 172, 67–69.

Okelo, P., Carr, L., Harrison, P., Douglass, L., Byrd, V., Wabeck, C., Schreuders, P., Wheaton, F., Zimmermann, N., 2003. Effectiveness of a novel method to reduce heat stress in broilers: a cool roost system. Trans. ASAE 46, 1675.

Olson, C.R., Vleck, C.M., Adams, D.C., 2008. Decoupling morphological development from growth in periodically cooled zebra finch embryos. J. Morphol. 269, 875–883.

Olson, C.R., Vleck, C.M., Vleck, D., 2006. Periodic cooling of bird eggs reduces embryonic growth efficiency. Physiol. Biochem. Zool. 79, 927–936.

Olson, J.M., 2001. Ontogeny of catabolic and morphological properties of skeletal muscle of the red-winged blackbird (*Agelaius phoeniceus*). J. Comp. Physiol. B 171, 527–542.

Ophir, E., Peltonen, L., Arieli, Y., 2003. Cutaneous water evaporation in the heat-acclimated rock pigeon (*Columba livia*) - physiological and biochemical aspects. Isr. J. Zool. 49, 131–148.

Østnes, J.E., Bech, C., 1992. Thermosensitivity of different parts of the spinal cord of the pigeon (*Columba livia*). J. Exp. Biol. 162, 185–196.

Østnes, J.E., Bech, C., 1998. Thermal control of metabolic cold defence in pigeons *Columba livia*. J. Exp. Biol. 201, 793–803.

Oswald, S.A., Bearhop, S., Furness, R.W., Huntley, B., Hamer, K.C., 2008. Heat stress in a high-latitude seabird: effects of temperature and food supply on bathing and nest attendance of great skuas *Catharacta skua*. J. Avian Biol. 39, 163–169.

Page, A.J., Cooper, C.E., Withers, P.C., 2011. Effects of experiment start time and duration on measurement of standard physiological variables. J. Comp. Physiol. B 181, 657–665.

Paladino, F.V., King, J.R., 1984. Thermoregulation and oxygen consumption during terrestrial locomotion by white-crowned sparrows *Zonotrichia leucophrys* gambelii. Physiol. Zool. 57, 226–236.

Patapoutian, A., Peier, A.M., Story, G.M., Viswanath, V., 2003. ThermoTRP channels and beyond: mechanisms of temperature sensation. Nat. Rev. Neurosci. 4, 529–539.

Pattinson, N.B., Thompson, M.L., Griego, M., Russell, G., Mitchell, N.J., Martin, R.O., Wolf, B.O., Smit, B., Cunningham, S.J., McKechnie, A.E., Hockey, P.A.R., 2020. Heat dissipation behaviour of birds in seasonally hot arid-zones: are there global patterns? J. Avian Biol. 51.

Pearson, O.P., 1953. Use of caves by hummingbirds and other species at high altitude in Peru. Condor 55, 17–20.

Peltonen, L., Arieli, U., Pyörnila, A., Marder, J., 1998. Adaptive changes in the epidermal structure of the heat-acclimated rock pigeon (*Columba livia*): a comparative electron microscope study. J. Morphol. 235, 17–29.

Petit, M., Vézina, F., 2014. Phenotype manipulations confirm the role of pectoral muscles and haematocrit in avian maximal thermogenic capacity. J. Exp. Biol. 217, 824–830.

Piestun, Y., Halevy, O., Yahav, S., 2009. Thermal manipulations of broiler embryos—the effect on thermoregulation and development during embryogenesis. Poultry Sci. 88, 2677–2688.

Piestun, Y., Shinder, D., Ruzal, M., Halevy, O., Yahav, S., 2008. The effect of thermal manipulations during the development of the thyroid and adrenal axes on in-hatch and post-hatch thermoregulation. J. Therm. Biol. 33, 413–418.

Pinshow, B., Bernstein, M.H., Lopez, G.E., Kleinhaus, S., 1982. Regulation of brain temperature in pigeons: effects of corneal convection. Am. J. Physiol. 242, R577–R581.

Pohl, H., West, G.C., 1973. Daily and seasonal variation in metabolic response to cold during rest and exercise in the common redpoll. Comp. Biochem. Physiol. 45A, 851–867.

Porter, W.R., Witmer, L.M., 2016. Avian cephalic vascular anatomy, sites of thermal exchange, and the rete ophthalmicum. Anat. Rec. 299, 1461–1486.

Price, E.R., Dzialowski, E.M., 2018. Development of endothermy in birds: patterns and mechanisms. J. Comp. Physiol. B 188, 373–391.

Prinzinger, R., Hänssler, I., 1980. Metabolism-weight relationship in some small nonpasserine birds. Experientia 36, 1299–1300.

Prinzinger, R., Preßmar, A., Schleucher, E., 1991. Body temperature in birds. Comp. Biochem. Physiol. 99A, 499–506.

Raimbault, S., Dridi, S., Denjean, F., Lachuer, J., Couplan, E., Bouillaud, F., Bordas, A., Duchamp, C., Taouis, M., Ricquier, D., 2001. An uncoupling protein homologue putatively involved in facultative muscle thermogenesis in birds. Biochem. J. 353, 441–444.

Ramirez, J.M., Bernstein, M.H., 1976. Compound ventilation during thermal panting in pigeons: a possible mechanism for minimizing hypocapnic alkalosis. Fed. Proc. 35, 2562–2565.

Ramsey, J.J., 1970. Temperature changes in Chimney Swifts (*Chaetura pelagica*) at lowered environmental temperatures. Condor 72, 225–229.

Randall, W.C., 1943. Factors influencing the temperature regulation of birds. Am. J. Physiol. 139, 56–63.

Rashotte, M.E., Basco, P.S., Henderson, R.P., 1995. Daily cycles in body temperature, metabolic rate, and substrate utilisation in pigeons: influence of amount and timing of food consumption. Physiol. Behav. 57, 731–746.

Rashotte, M.E., Phillips, D.L., Henderson, R.P., 1997. Nocturnal digestion, cloacal excretion, and digestion-related thermogenesis in pigeons (*Columba livia*). Physiol. Behav. 61, 83–92.

Rashotte, M.E., Saarela, S., Henderson, R.P., Hohtola, E., 1999. Shivering and digestion-related thermogenesis in pigeons during dark phase. Am. J. Physiol. 277, R1579–R1587.

Raup, T., Bottje, W., 1990. Effect of carbonated water on arterial pH, PCO_2 and plasma lactate in heat-stressed broilers. Br. Poultry Sci. 31, 377–384.

Rautenberg, W., 1969. Die Bedeutung der zentralnervösen Thermosensitivität für die Temperaturregulation der Taube. Z. für Vgl. Politikwiss. (ZfVP) 62, 235–266.

Rautenberg, W., 1986. Neural control of cold defence mechanisms in the avian thermoregulatory system. In: Heller, H.C., Musacchia, X.J., Wang, L.C.H. (Eds.), Living in the Cold: Physiological and Biochemical Adaptations. Elsevier, New York, pp. 151–166.

Reher, S., Ehlers, J., Rabarison, H., Dausmann, K.H., 2018. Short and hyperthermic torpor responses in the Malagasy bat *Macronycteris commersoni* reveal a broader hypometabolic scope in heterotherms. J. Comp. Physiol. B 188, 1015–1027.

Reinertsen, R.E., Haftorn, S., 1986. Different metabolic strategies of northern birds for nocturnal survival. J. Comp. Physiol. 156, 655–663.

Reynolds, P.S., Lee, R.M., 1996. Phylogenetic analysis of avian energetics: passerines and non-passerines do not differ. Am. Nat. 147, 735–759.

Richards, S., 1971. Brain stem control of polypnoea in the chicken and pigeon. Respir. Physiol. 11, 315–326.

Richards, S., 1976. Evaporative water loss in domestic fowls and its partition in relation to ambient temperature. J. Agric. Sci. 87, 527–532.

Richards, S.A., 1970. Physiology of thermal panting in birds. Ann. Biol. Anim. Biochim. Biophys. 10, 151–168.

Riddle, O., Smith, G.C., Benedict, F.G., 1932. The basal metabolism of the mourning dove and some of its hybrids. Am. J. Physiol. 101, 206–267.

Rintamaki, H., Saarela, S., Marjakangas, A., Hissa, R., 1983. Summer and winter temperature regulation in the black grouse *Lyrurus tetrix*. Physiol. Zool. 56, 152–159.

Robinson, D.E., Campbell, G.S., King, J.R., 1976. An evaluation of heat exchange in small birds. J. Comp. Physiol. B 105, 153–166.

Romano, A.B., Hunt, A., Welbergen, J.A., Turbill, C., 2019. Nocturnal torpor by superb fairy-wrens: a key mechanism for reducing winter daily energy expenditure. Biol. Lett. 15, 20190211.

Rubner, M., 1883. Über den einfluss der körpergrösse auf stoffund kraftwechsel. Zeitschrift fur Biologie 19, 535–562.

Saarela, S., Vuori, M., Eloranta, E., Vakkuri, O., 1999. Melatonin, a candidate signalling molecule for energy sparing. Ornis Fenn. 76, 231–235.

Sabat, P., Ramirez-Otarola, N., Barceló, G., Salinas, J., Bozinovic, F., 2010. Comparative basal metabolic rate among passerines and the food habit hypothesis. Comp. Biochem. Physiol. Mol. Integr. Physiol. 157, 35–40.

Sapsford, C.W., 1986. Bioenergetics and hypothermia of pygmy falcons on the Kalahari Gemsbok National Park. Gabar 1, 20–21.

Saunders, D.A., Mawson, P., Dawson, R., 2011. The impact of two extreme weather events and other causes of death on Carnaby's Black Cockatoo: a promise of things to come for a threatened species? Pac. Conserv. Biol. 17, 141–148.

Schleucher, E., 2004. Torpor in birds: taxonomy, energetics and ecology. Physiol. Biochem. Zool. 77, 942–949.

Schleucher, E., Withers, P.C., 2001. Re-evaluation of the allometry of wet thermal conductance for birds. Comp. Biochem. Physiol. A 129, 821–827.

Schmidt-Nielsen, K., Hainsworth, F.R., Murrish, D.E., 1970. Countercurrent heat exchange in the respiratory passages: effect on water and heat balance. Respir. Physiol. 9, 263–276.

Schmidt-Nielsen, K., Kanwisher, J., Lasiewski, R.C., Cohn, J.E., Bretz, W.L., 1969. Temperature regulation and respiration in the ostrich. Condor 71, 341–352.

Scholander, P.F., Hock, R., Walters, V., Johnson, F., Irving, L., 1950. Heat regulation in some arctic and tropical mammals and birds. Biol. Bull. 99, 237–258.

Shapiro, C.J., Weathers, W.W., 1981. Metabolic and behavioural responses of American kestrels to food deprivation. Comp. Biochem. Physiol. 68A, 111–114.

Sharpe, L., Cale, B., Gardner, J.L., 2019. Weighing the cost: the impact of serial heatwaves on body mass in a small Australian passerine. J. Avian Biol. 50, e02355.

Shinder, D., Luger, D., Rusal, M., Rzepakovsky, V., Bresler, V., Yahav, S., 2002. Early age cold conditioning in broiler chickens (*Gallus domesticus*): thermotolerance and growth responses. J. Therm. Biol. 27, 517–523.

Silvestri, E., Schiavo, L., Lombardi, A., Goglia, F., 2005. Thyroid hormones as molecular determinants of thermogenesis. Acta Physiol. Scand. 184, 265–283.

Simon, E., 2000. The enigma of deep-body thermosensory specificity. Int. J. Biometeorol. 44, 105–120.

Simon, E., Martin, R., Simon-Oppermann, C., 1981. Central nervous versus total body thermosensitivity of the duck. Int. J. Biometeorol. 25, 249–256.

Sirsat, S.K.G., Sirsat, T.S., Crossley, J.L., Sotherland, P.R., Dzialowski, E.M., 2016. The 12-day thermoregulatory metamorphosis of Red-winged Blackbirds (*Agelaius phoeniceus*). J. Comp. Physiol. B 186, 651–663.

Sirsat, T.S., Dzialowski, E.M., 2016. Ventilation changes associated with hatching and maturation of an endothermic phenotype in the Pekin duck, *Anas platyrhynchos* domestica. Am. J. Physiol. Regul. Integr. Comp. Physiol. 310, R766–R775.

Smit, B., Boyles, J.G., Brigham, R.M., McKechnie, A.E., 2011. Torpor in dark times: patterns of heterothermy are associated with the lunar cycle in a nocturnal bird. J. Biol. Rhythm. 26, 241–248.

Smit, B., Brown, M., Downs, C.T., 2008. Thermoregulatory responses in seasonally acclimatized captive Southern White-faced Scops-owls. J. Therm. Biol. 33, 76–86.

Smit, B., Harding, C.T., Hockey, P.A.R., McKechnie, A.E., 2013. Adaptive thermoregulation during summer in two populations of an arid-zone passerine. Ecology 94, 1142–1154.

Smit, B., McKechnie, A.E., 2010. Avian seasonal metabolic variation in a subtropical desert: basal metabolic rates are lower in winter than in summer. Funct. Ecol. 24, 330–339.

Smith, E.K., O'Neill, J., Gerson, A.R., Wolf, B.O., 2015. Avian thermoregulation in the heat: resting metabolism, evaporative cooling and heat tolerance in Sonoran Desert doves and quail. J. Exp. Biol. 218, 3636–3646.

Smith, E.K., O'Neill, J.J., Gerson, A.R., McKechnie, A.E., Wolf, B.O., 2017. Avian thermoregulation in the heat: resting metabolism, evaporative cooling and heat tolerance in Sonoran Desert songbirds. J. Exp. Biol. 220, 3290–3300.

Sonaiya, E., 2007. Family poultry, food security and the impact of HPAI. World Poultry Sci. J. 63, 132–138.

Southwick, E.E., 1973. Remote sensing of body temperature in a captive 25-g bird. Condor 75, 464–466.

Stager, M., Cheviron, Z.A., 2020. Is there a role for sarcolipin in avian facultative thermogenesis in extreme cold? Biol. Lett. 16, 20200078.

Suarez, R.K., Darveau, C.-A., 2005. Multi-level regulation and metabolic scaling. J. Exp. Biol. 208, 1627–1634.

Swanson, D.L., 2010. Seasonal metabolic variation in birds: functional and mechanistic correlates. Curr. Ornithol. 75–129.

Swanson, D.L., Bozinovic, F., 2011. Metabolic capacity and the evolution of biogeographic patterns in oscine and suboscine passerine birds. Physiol. Biochem. Zool. 84, 185–194.

Swanson, D.L., Dean, K.L., 1999. Migration-induced variation in thermogenic capacity in migratory passerines. J. Avian Biol. 30, 245–254.

Swanson, D.L., Garland, T., 2009. The evolution of high summit metabolism and cold tolerance in birds and its impact on present-day distributions. Evolution 63, 184–194.

Swanson, D.L., Olmstead, K.L., 1999. Evidence for a proximate influence of winter temperatures on metabolism in passerine birds. Physiol. Biochem. Zool. 72, 566–575.

Swanson, D.L., Weinacht, D.P., 1997. Seasonal effects on metabolism and thermoregulation in northern bobwhite. Condor 99, 478–489.

Talbot, W.A., Gerson, A.R., Smith, E.K., McKechnie, A.E., Wolf, B.O., 2018. Avian thermoregulation in the heat: metabolism, evaporative cooling and gular flutter in two small owls. J. Exp. Biol. 221, jeb171108.

Talbot, W.A., McWhorter, T.J., Gerson, A.R., McKechnie, A.E., Wolf, B.O., 2017. Avian thermoregulation in the heat: evaporative cooling capacity of arid-zone Caprimulgiformes from two continents. J. Exp. Biol. 220, 3488–3498.

Tattersall, G.J., Andrade, D.V., Abe, A.S., 2009. Heat exchange from the toucan bill reveals a controllable vascular thermal radiator. Science 325, 468–470.

Tattersall, G.J., Chaves, J.A., Danner, R.M., 2018. Thermoregulatory windows in Darwin's finches. Funct. Ecol. 32, 358–368.

Tattersall, G.J., Roussel, D., Voituron, Y., Teulier, L., 2016. Novel energy-saving strategies to multiple stressors in birds: the ultradian regulation of body temperature. Proc. Biol. Sci. 283, 20161551.

Teeter, R., Smith, M., Owens, F., Arp, S., Sangiah, S., Breazile, J., 1985. Chronic heat stress and respiratory alkalosis: occurrence and treatment in broiler chicks. Poultry Sci. 64, 1060–1064.

Temperley, N.D., Berlin, S., Paton, I.R., Griffin, D.K., Burt, D.W., 2008. Evolution of the chicken Toll-like receptor gene family: a story of gene gain and gene loss. BMC Genomics 9, 62.

Thompson, M.L., Cunningham, S.J., McKechnie, A.E., 2018. Interspecific variation in avian thermoregulatory patterns and heat dissipation behaviours in a subtropical desert. Physiol. Behav. 188, 311–323.

Thouzeau, C., Duchamp, C., Handrich, Y., 1999. Energy metabolism and body temperature of barn owls fasting in the cold. Physiol. Biochem. Zool. 72, 170–178.

Tieleman, B.I., van Noordwijk, H.J., Williams, J.B., 2008. Nest site selection in a hot desert: trade-off between microclimate and predation risk? Condor 110, 116–124.

Tieleman, B.I., Williams, J.B., 1999. The role of hyperthermia in the water economy of desert birds. Physiol. Biochem. Zool. 72, 87–100.

Tieleman, B.I., Williams, J.B., 2000. The adjustment of avian metabolic rates and water fluxes to desert environments. Physiol. Biochem. Zool. 73, 461–479.

Tieleman, B.I., Williams, J.B., 2002. Cutaneous and respiratory water loss in larks from arid and mesic environments. Physiol. Biochem. Zool. 75, 590–599.

Tieleman, B.I., Williams, J.B., Bloomer, P., 2003a. Adaptation of metabolic rate and evaporative water loss along an aridity gradient. Proc. Roy. Soc. Lond. 270, 207–214.

Tieleman, B.I., Williams, J.B., Buschur, M.E., Brown, C.R., 2003b. Phenotypic variation of larks along an aridity gradient: are desert birds more flexible? Ecology 84, 1800–1815.

Tieleman, B.I., Williams, J.B., LaCroix, F., Paillat, P., 2002. Physiological responses of Houbara bustards to high ambient temperatures. J. Exp. Biol. 205, 503–511.

Tieleman, B.I., Williams, J.B., Michaeli, G., Pinshow, B., 1999. The role of nasal passages in the water economy of crested larks and desert larks. Physiol. Zool. 72, 219–226.

Tracy, C.R., Welch, W.R., Pinshow, B., Porter, W.P., 2010. Properties of Air: A Manual for Use in Biophysical Ecology, fourth ed. The University of Wisconsin Laboratory for Biophysical Ecology: Technical Report.

Tzschentke, B., Basta, D., 2000. Development of hypothalamic neuronal thermosensitivity in birds during the perinatal period. J. Therm. Biol. 25, 119–123.

van de Ven, T., McKechnie, A., Cunningham, S., 2019. The costs of keeping cool: behavioural trade-offs between foraging and thermoregulation are associated with significant mass losses in an arid-zone bird. Oecologia 191, 205–215.

van de Ven, T.M.F.N., Martin, R.O., Vink, T.J.F., McKechnie, A.E., Cunningham, S.J., 2016. Regulation of heat exchange across the hornbill beak: functional similarities with toucans? PloS One 11, e0154768.

van Wilgen, N.J., Goodall, V., Holness, S., Chown, S.L., McGeoch, M.A., 2016. Rising temperatures and changing rainfall patterns in South Africa's National Parks. Int. J. Climatol. 36, 706–721.

Vézina, F., Gerson, A.R., Guglielmo, C.G., Piersma, T., 2017. The performing animal: causes and consequences of body remodeling and metabolic adjustments in red knots facing contrasting thermal environments. Am. J. Physiol. Regul. Integr. Comp. Physiol. 313, R120–R131.

Vézina, F., Jalvingh, K., Dekinga, A., Piersma, T., 2006. Acclimation to different thermal conditions in a northerly wintering shorebird is driven by body mass-related changes in organ size. J. Exp. Biol. 209, 3141–3154.

Vianna, C.R., Hagen, T., Zhang, C.-Y., Bachman, E., Boss, O., Gereben, B., Moriscot, A.S., Lowell, B.B., Bicudo, J.E.P.W., Bianco, A.C., 2001. Cloning and functional characterization of an uncoupling protein homolog in hummingbirds. Physiol. Genom. 5, 137–145.

Walsberg, G.E., King, J.R., 1978. The relationship of the external surface area of birds to skin surface area and body mass. J. Exp. Biol. 76, 185–189.

Walter, I., Seebacher, F., 2009. Endothermy in birds: underlying molecular mechanisms. J. Exp. Biol. 212, 2328–2336.

Wang, Z., O'Connor, T.P., Heshka, S., Heymsfield, S.B., 2001. The reconstruction of Kleiber's law at the organ-tissue level. J. Nutr. 131, 2967–2970.

Weathers, W.W., 1972. Thermal panting in domestic pigeons, *Columba livia*, and the barn owl, *Tyto alba*. J. Comp. Physiol. 79, 79–84.

Weathers, W.W., 1981. Physiological thermoregulation in heat-stressed birds: consequences of body size. Physiol. Zool. 54, 345–361.

Weathers, W.W., 1997. Energetics and thermoregulation by small passerines of the humid, lowland tropics. Auk 114, 341–353.

Weathers, W.W., Caccamise, D.F., 1975. Temperature regulation and water requirements of the monk parakeet, *Myiopsitta monachus*. Oecologia 18, 329–342.

Weathers, W.W., Caccamise, D.F., 1978. Seasonal acclimatization to temperature in monk parakeets. Oecologia 35, 173–183.

Weathers, W.W., Koenig, W.D., Stanback, M.T., 1990. Breeding energetics and thermal ecology of the acorn woodpecker in central coastal California. Condor 92, 341–359.

Webster, M.D., Bernstein, M.H., 1987. Ventilated capsule measurements of cutaneous evaporation in Mourning Doves. Condor 89, 863–868.

Webster, M.D., Campbell, G.S., King, J.R., 1985. Cutaneous resistance to water-vapor diffusion in pigeons and the role of the plumage. Physiol. Zool. 58, 58–70.

Webster, M.D., King, J.R., 1987. Temperature and humidity dynamics of cutaneous and respiratory evaporation in pigeons (*Columba livia*). J. Comp. Physiol. B 157, 253–260.

Welcker, J., Chastel, O., Gabrielsen, G.W., Guillaumin, J., Kitaysky, A.S., Speakman, J.R., Tremblay, Y., Bech, C., 2013. Thyroid hormones correlate with basal metabolic rate but not field metabolic rate in a wild bird species. PLoS One 8, e56229.

Wells, M.E., Schaeffer, P.J., 2012. Seasonality of peak metabolic rate in non-migrant tropical birds. J. Avian Biol. 43, 481–485.

West, G.B., Brown, J.H., Enquist, B., 1999. The fourth dimension of life: fractal geometry and allometric scaling of organisms. Science 284, 1677–1679.

White, C.R., Blackburn, T.M., Martin, G.R., Butler, P.J., 2007. The basal metabolic rate of birds is associated with habitat temperature and precipitation, not productivity. Proc. R. Soc. B 274, 287–293.

White, F.N., Bartholomew, G.A., Howell, T.R., 1975. The thermal significance of the nest of the Sociable Weaver *Philetairus socius*: winter observations. Ibis 117, 171–179.

Whitfield, M.C., Smit, B., McKechnie, A.E., Wolf, B.O., 2015. Avian thermoregulation in the heat: scaling of heat tolerance and evaporative cooling capacity in three Southern African arid-zone passerines. J. Exp. Biol. 218, 1705–1714.

Wiersma, P., Chappell, M.A., Williams, J.B., 2007. Cold- and exercise-induced peak metabolic rates in tropical birds. Proc. Natl. Acad. Sci. U. S. A. 104, 20866–20871.

Wiersma, P., Nowak, B., Williams, J.B., 2012. Small organ size contributes to the slow pace of life in tropical birds. J. Exp. Biol. 215, 1662–1669.

Williams, J.B., 1996. A phylogenetic perspective of evaporative water loss in birds. Auk 113, 457–472.

Williams, J.B., Tieleman, B.I., 2000. Flexibility in basal metabolic rate and evaporative water loss among hoopoe larks exposed to different environmental temperatures. J. Exp. Biol. 203, 3153–3159.

Williams, J.B., Tieleman, B.I., Shobrak, M., 1999. Lizard burrows provide thermal refugia for larks in the Arabian desert. Condor 101, 714–717.

Williams, J.B., Tieleman, B.I., Shobrak, M., 2009. Validation of temperature-sensitive radio transmitters for measurement of body temperature in small animals. Ardea 97, 120–124.

Winder, L.A., White, S.A., Nord, A., Helm, B., McCafferty, D.J., 2020. Body surface temperature responses to food restriction in wild and captive great tits. J. Exp. Biol. 223.

Withers, P., Siegfried, W., Louw, G., 1981. Desert ostrich exhales unsaturated air. South Afr. J. Sci. 77, 569–570.

Withers, P.C., 1983. Energy, water, and solute balance of the ostrich *Struthio camelus*. Physiol. Zool. 56, 568–579.

Withers, P.C., Williams, J.B., 1990. Metabolic and respiratory physiology of an arid-adapted Australasian bird, the Spinifex pigeon. Condor 92, 961–969.

Wolf, B.O., Walsberg, G.E., 1996. Thermal effects of radiation and wind on a small bird and implications for microsite selection. Ecology 77, 2228–2236.

Wolf, B.O., Walsberg, G.E., 2000. The role of plumage in heat transfer processes of birds. Am. Zool. 40, 575–584.

Wolf, B.O., Wooden, K.M., Walsberg, G.E., 2000. Effects of complex radiative and convective environments on the thermal biology of the white-crowned sparrow (*Zonotrichia leucophrys gambelii*). J. Exp. Biol. 203, 803–811.

Wolf, B.O., McKechnie, A.E., Schmitt, J., Czenze, Z.J., Johnson, A.B., Witt, C.C., 2020. Extreme and variable torpor among high-elevation Andean hummingbird species. Biol. Lett. 16, 20200428.

Wolfenson, D., 1983. Blood flow through arteriovenous anastomoses and its thermal function in the laying hen. J. Physiol. 334, 395–407.

Woods, C.P., Czenze, Z.J., Brigham, R.M., 2019. The avian "hibernation" enigma: thermoregulatory patterns and roost choice of the common poorwill. Oecologia 189, 47–53.

Yahav, S., Giloh, M., 2012. Infrared Thermography–Applications in Poultry Biological Research. In: Prakash, R.V. (Ed.), Infrared Thermography. InTech, Rijeka, Croatia, pp. 93–116.

Yahav, S., Hurwitz, S., 1996. Induction of thermotolerance in male broiler chickens by temperature conditioning at an early age. Poultry Sci. 75, 402–406.

Yahav, S., Shinder, D., Ruzal, M., Giloh, M., Piestun, Y., 2009. Controlling body temperature—the opportunities for highly productive domestic fowl. In: Cisneros, A.B., Goins, B.L. (Eds.), Body Temperature Regulation. Nova Science Publishers, Hauppauge NY, pp. 65–98.

Yamamoto, A., Takahashi, K., Saito, S., Tominaga, M., Ohta, T., 2016. Two different avian cold-sensitive sensory neurons: transient receptor potential melastatin 8 (TRPM8)-dependent and-independent activation mechanisms. Neuropharmacology 111, 130–141.

Yusuf, S., Lategan, F., Masika, P., 2014. Characterization of indigenous poultry production systems in the Nkonkobe Municipality, Eastern Cape Province South Africa. J. Agric. Sci. 5, 31–44.

Zachos, J., Pagani, M., Sloan, L., Thomas, E., Billups, K., 2001. Trends, rhythms, and aberrations in global climate 65 Ma to present. Science 292, 686–693.

Zar, J.H., 1968. Standard metabolism comparisons between orders of birds. Condor 70, 278.

Chapter 46

Flight

Charles M. Bishop[1] and Christopher G. Guglielmo[2]

[1]School of Natural Sciences, Bangor University, Bangor, Gwynedd, United Kingdom; [2]Department of Biology, Advanced Facility for Avian Research, Western University, London, ON, Canada

46.1 Introduction

Birds typically fly between 29 and 83 km/h, with larger species generally flying faster than smaller ones (Alerstam et al., 2007). Although flapping flight is the most energy-intensive form of vertebrate locomotion, these high air speeds result in a lower cost of transport per unit distance than for terrestrial travel (Tucker, 1970; Schmidt-Nielsen, 1972; Butler, 1991), which enables birds to undertake large foraging trips (Jouventin and Weimerskirch, 1990) and long-distance seasonal migrations (Gill et al., 2009; Klaassen et al., 2011), more easily than any other group of animals. Thus, around 20% of the approximately 10,000 avian species are migratory (Sekercioglu, 2007; Kirby et al., 2008), although this is strongly influenced by breeding latitude. Almost all polar species move to lower altitudes during their winter periods, while the majority of tropical species are resident all year round. In more temperate latitudes, this is closer to 50%, despite the added problem of the birds initially carrying a relatively large amount of fuel (Alerstam and Lindström, 1990; Hedenström and Alerstam, 1992; Witter and Cuthill, 1993).

The critical factor for flight is to obtain sufficient airflow around the wings (to generate lift and thrust) and this is most challenging during take-off and slow flight. Hence, the general relationship between flight cost and speed is a U shape, with the cost of developing lift dominating at slow speeds and that of fighting drag forces dominating at high speeds (Pennycuick, 1968; Rayner, 1993; Alexander, 1997; Klein Heerenbrink et al., 2015). The large forces required from the avian flight muscles under powered take-off are relatively brief and much of it can be developed utilizing anaerobic muscle metabolism (George and Berger, 1966; Bishop and Butler, 1995). At one end of the spectrum, a few species and families of birds have evolved flight musculature that is specialized for these "burst" episodes of wing flapping, such as a number of species of Galliformes (Pheasants and Quail) and Tinamiformes (Tinamou), which they utilize to escape terrestrial predators, or to roost in trees. However, these birds are unable to sustain such activity for more than a few tens of seconds, and may be rendered incapable of flying at all after repeated bursts of activity (Marden, 1994). At the other end of the spectrum, the most aerial avian species may not touch down on land for many days, e.g., Godwits (Gill et al., 2009), or even for many months in the case of Swifts (Liechti et al., 2013; Hedenström et al., 2016).

In between these two extremes of aerial ability are birds that exhibit a range of different body masses (M_b) , adaptive wing morphology, and flight styles, which relate to the aeroecology of the species (Kunz et al., 2008). Relatively large-winged birds, like Condors (Williams et al., 2020), Frigatebirds (Weimerskirch et al., 2016), and Albatrosses (Sato et al., 2009; Richardson, 2011), may not flap their wings for many minutes at a time but remain airborne by soaring in thermals or through wind shear; or gliding over waves and mountain ridges; or other deflecting surfaces. Such behavior may reduce the cost of flight to a small fraction of the energy required for flapping flight, during both foraging and migratory journeys (Bevan et al., 1995a; Sakamoto et al., 2013; Duriez et al., 2014). Some intermediate-sized seabirds (e.g., Manx Shearwater, *Puffinus puffinus*) may regularly oscillate between flapping and gliding, with relatively short duty cycles of typically less than 5 s duration (Spivey et al., 2014). The flap-to-glide ratio of the Shearwater varies with the prevailing wind conditions, and largely determines the aerodynamic power output (P_o) of the bird. A variety of other species also display flap-gliding behavior, while generally smaller terrestrial passerines (from Woodpeckers and to Finches) employ the more extreme flight "gait" of flap-bounding (Tobalske and Dial, 1994; Tobalske et al., 2009). A number of hypotheses have been postulated to explain the possible advantages of these flapping gaits. Ideas vary from those that focus on aerodynamic consequences, e.g., that bounding may assist in generating higher horizonal velocities (Wang et al., 2018), to those that consider

Sturkie's Avian Physiology. https://doi.org/10.1016/B978-0-12-819770-7.00012-8

it primarily as a physiological constraint related to flight muscle activation and the optimal cost of producing work efficiently (Rayner, 1985a; Usherwood, 2016).

Efficient "oxidative" or "aerobic" muscle metabolism of fuel substrates is a prerequisite for sustained powered flapping flight, and results in adaptive selection on respiratory and cardiovascular functional capacity, and the fiber composition of the flight muscles. Relative heart size typically varies twofold among avian families and up to 10-fold between Hummingbirds and Tinamous (Hartman, 1961), which reflects the evolutionary selection for aerobic flight power (Bishop, 1997; Nespolo et al., 2018). Relative aerobic capacity also scales negatively with M_b, resulting in larger birds investing in anaerobic muscle fibers (George and Berger, 1966) primarily for use during take-off. Consequently, this most likely accounts for a restricted range of sustainable speeds in larger birds, reflecting the U-shaped power/velocity relationship (Bishop and Butler, 1995; Bishop, 1997). At the same time, individual birds have to regulate body temperature (T_b) during exercise to within an acceptable range (Parr et al., 2019a,b) while also controlling evaporative water loss in the face of the large amount of heat that is generated by the intense muscular activity (Torre-Bueno, 1978b; Engel et al., 2006b).

The energy cost of spring migration may be so high as to influence the subsequent energy dynamics of reproduction (Bromley and Jarvis, 1993). The postbreeding autumn migration follows a period of relatively sedentary behaviors such as incubation, brooding, and molt for the adults, during which there is evidence, for some species at least, that the main flight muscles atrophy (Mainguy and Thomas, 1985; Piersma, 1988; Bishop et al., 1996; Portugal et al., 2009). In addition, the energy and time taken for birds to molt and replace their flight feathers may be a major consideration in regulating the length of the breeding season and, even, the maximum size of flying birds (Rohwer et al., 2009). Thus, for postbreeding and postmolting adults, as well as for the season's fledglings, the flight muscles and supporting systems have to achieve an adequate level of aerobic fitness and functionality in preparation for the forthcoming migratory flights (Bishop et al., 1995, 1996). Some long flights may force birds to tackle a variety of different environmental challenges, such as crossing featureless deserts (Schmaljohann et al., 2007) and oceans (Butler et al., 1998; Shaffer et al., 2006; Gill et al., 2009), negotiating high mountains (Hawkes et al., 2011) and dealing with changes in weather conditions (Safi et al., 2013). All such challenges may affect a bird's overall energy budget and require individuals to make strategic decisions that could trade off considerations of time versus energy optimization (Efrat et al., 2019). Those species of birds that occasionally fly at high altitudes during their migration also have the combined problems of engaging in this energetically costly activity in a severely hypoxic and cold environment and at a reduced air density (Liechti and Schaller, 1999; Bishop et al., 2015).

This chapter will focus primarily on the following: the energetics of bird flight, including long distance migration; the function, physiology, and biochemistry of the flight muscles, including physical fitness in preparation for migration; deposition of fuel stores in preparation for migration and fuel use during migratory flight; respiratory and cardiovascular adjustments associated with flight, including temperature control and water loss; and the special case of flight at high altitudes. To begin with, however, there is a short introduction to the significance of animal size and scale.

46.2 Scaling effects of body size

It is important to be able to assess the significance of a particular characteristic, or adaptation, and compare it with those of other individuals and/or species, even though these other animals may vary greatly in size. The study of the consequences of changes morphological design or physiological and behavioral functions in relation to M_b is called scaling (Schmidt Nielsen, 1984), and it is frequently used in comparative biology. If two bodies are the same shape, or "geometrically similar," but of different volume (V) and mass (assuming constant tissue density, so that V and M_b are mathematically interchangeable), then their various body characteristics, such as lengths and areas, are directly proportional to their difference in M_b, and these individuals are said to scale isometrically with regard to each other. Thus, if we consider two cubes of different size, then each side will have a length (L), and the area (A) will be proportional to the length squared ($A \propto L^2$), while the mass will be proportional to the length cubed ($M \propto L^3$). From the perspective of mass, we can show that area will be proportional to mass to the two-thirds power ($A \propto M^{2/3}$ or $M_b^{0.67}$) and length will be proportional to mass to the one-third power ($L \propto M^{1/3}$ or $M_b^{0.33}$). Because M_b is a relatively easy variable to measure in most animals and one which represents the large size range seen in animals, it is most frequently used as the independent variable in scaling.

Pennycuick (1982) studied the flight and morphometric parameters of 11 species of Procellariiformes (e.g., petrels and albatrosses), ranging from 0.03 to 9 kg, and found that wing span (b) scaled in proportion to $M_b^{0.37}$ (Figure 46.1A) and wing area (S) in proportion to $M_b^{0.627}$ (Figure 46.1B). These results indicate that there is a slight tendency for larger birds to have relatively longer wings and smaller wing areas. This change of shape can be more easily demonstrated if the two measurements are combined by calculating the dimensionless variable called aspect ratio (Λ), which is the wing span divided by the mean wing width (or chord) and is equivalent to b^2/S. Figure 46.1C shows that Λ scales in proportion to $M_b^{0.116}$ and is highly significantly

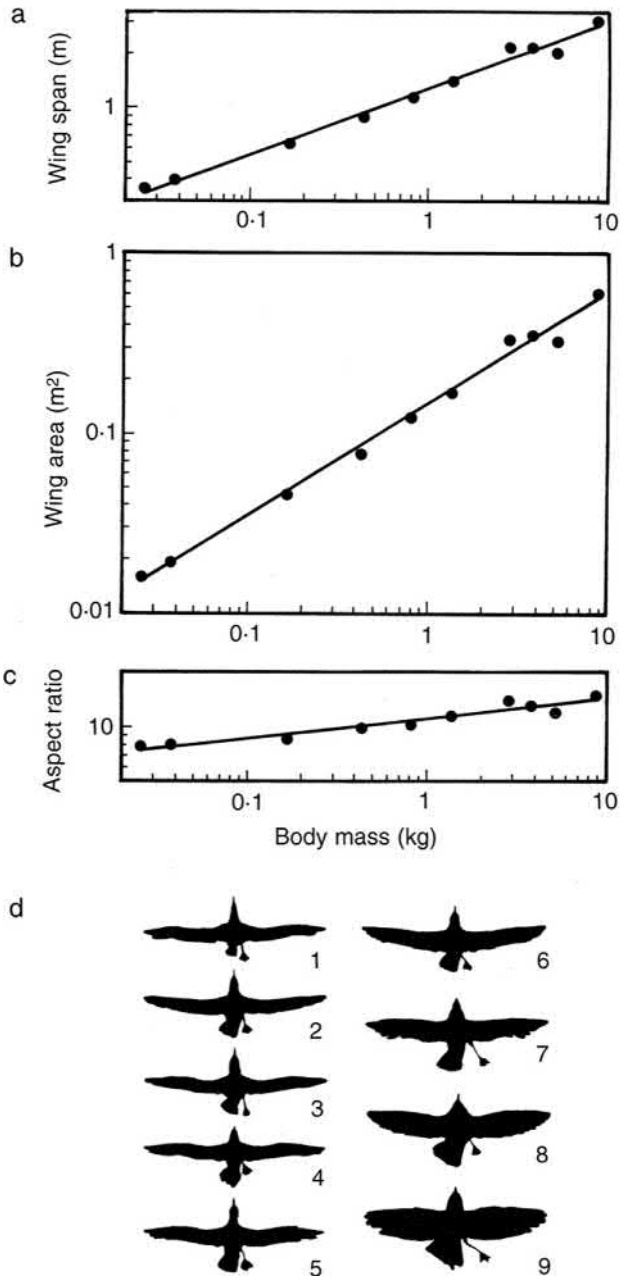

FIGURE 46.1 (A) Wing span, *S;* (B) Wing area, *A;* (C) Aspect ratio of 11 species of Procellariiform birds, plotted against body mass. (D) Wing tracings from nine of these species, with the smaller species enlarged such that all have the same wing span. 1, wandering albatross *Diomedea exulans*; 2, black-browed albatross *Diomedea melanophris*; 3, grey-headed albatross *Diomedea chysostoma*; 4, light-mantled sooty albatross *Phoebetria palpebrata*; 5, giant petrel *Macronectes* sp.; 6, white-chinned petrel *Procellaria aequinoctialis*; 7, cape pigeon *Daption capensis*; 8, dove prion *Pachyptila desolata*; 9,Wilson's storm petrel *Oceanites oceanicus*. The wing span of the largest species, *Diomedea exulans*, is 3.03 m and that of the smallest, *Oceanites oceanicus*, is 0.393 m. *(C) From C. J. Pennycuick (1992). (D) From Pennycuick (1982).*

different from the expected isometric value of $M_b^{0.0}$. Thus, this feature of birds scales allometrically with M_b. Similarly, we can easily visualize this change (Figure 46.1D) if the outlines of each species are displayed so that they all have the same wing span (Pennycuick, 1992).

Such analyses can also be used to test predictions regarding the scaling of animal energetics. Thus, the surface area of endothermic vertebrates should reflect the rate at which heat will be lost to the environment and, consequently, the metabolic rate (MR) required to replace this lost heat. Until recently, most studies of vertebrates had shown that basal metabolic rate (BMR) actually scales allometrically, at around $M_b^{0.72-0.75}$, i.e., slightly greater than predicted from the surface area law. However, at least with respect to the analysis of MR in birds and mammals, the scaling exponent has become quite a controversial subject, with some authors suggesting that there is no rigid scaling exponent and that it varies with a number of counfounding variables, such as relative exercise intensity (Koteja, 1987; Bishop, 1999; Glazier, 2008; White et al., 2009) or T_b (White et al., 2007; Gillooly and Allen, 2007). Other studies have suggested that it may also vary between taxonomic groupings or with ecological adaptations (White et al., 2007).

Despite these difficulties, scaling analysis has been used to address a wide variety of issues in biology (Schmidt-Nielsen, 1984), and the scaling of metabolic and biomechanical parameters associated with bird flight will be considered throughout this chapter.

46.3 Energetics of bird flight

One of the most useful physiological variables is the rate at which a bird expends chemical energy (i.e., power input (*P*i)) during flight. The *P*i of both resting and exercising animals are important considerations in many ecological and physiological studies of animal behavior and evolution, particularly as the metabolic power consumed by an organism is ultimately what determines how much food must be obtained from the environment. During locomotion, the chemical energy available from the catabolism of the various fuel molecules must be transformed by the myofibrillar proteins of the flight muscles into the mechanical *P*o required to fly, while the remainder is released as heat. The exact quantity of *P*o produced from a given *P*i will depend on the efficiency with which the muscles can convert the chemical energy into mechanical power. Some of the "waste" heat produced may be used to regulate T_b, but much is almost invariably "lost" to the environment.

The SI unit of mechanical *P*o is the watt (W) which is equivalent to 1 J per second. An estimate of metabolic *P*i can be obtained by converting the rate of oxygen consumption ($\dot{V}_{O_2}$, mL/s) to W. However, this conversion of $\dot{V}_{O_2}$ to *P*i depends on the metabolic substrate; for metabolism of pure carbohydrate, with a respiratory

quotient (RQ) of 1, 1 mL O_2/s = 21.1 W, whereas for pure fat metabolism (with an RQ of 0.71), 1 mL O_2/s = 19.6 W (Lusk, 1919; Brobeck and Dubois, 1980). Pure protein metabolism in birds would yield an RQ of 0.74 and 1 mL O_2/s = 18.4 W Schmidt-Nielsen, 1997. During short-duration exercise, it is likely that carbohydrate oxidation will be favored; for example, short hovering flights during foraging in hummingbirds (Suarez et al., 1990) and soon after take-off in pigeons (Butler et al., 1977), but during longer bouts of exercise, it is likely that fat oxidation will become dominant (Rothe et al., 1987). However, this may be influenced by the feeding regime and by the season well-fed and summer birds start at a higher RQ and take longer to reach an RQ of approximately 0.7 (Nachtigall, 1995). Thus, if RQ is unknown, a compromise for an RQ of 0.8 of 1 mL O_2/s = 20.1 W is often used for calculations of *P*i during aerobic activity (Schmidt- Nielsen, 1997).

In practice, it is not easy to obtain accurate experimental data from a bird during flight, either in a wind tunnel or the wild, and no single experimental method can adequately give all of the necessary information required for a full analysis of the physiological responses to flight. Thus, various techniques are used to study the biology of flight, some of which are discussed below, primarily with respect to the estimation of *P*i and *P*o during flight.

46.3.1 Techniques used to study the mechanical power output required for flight

46.3.1.1 Aerodynamic and biomechanical models

The use of aerodynamic and biomechanical models provides a theoretical framework for understanding the physiological adaptations and energetics of birds and the likely constraints acting on different species. It is theoretically possible to estimate the *P*i of a particular bird, using estimates for *P*o based on aerodynamic models (Rayner, 1979; Pennycuick, 1989; Klein Heerenbrink et al., 2015; Chin and Lentink, 2016; Deetjen et al., 2020), provided the efficiency by which the flight muscles are able to transduce chemical energy into mechanical energy is known or can be estimated. However, while Pennycuick (2008) has assumed that flight muscle efficiency is around 23% for all bird species, other authors have pointed out that the overall efficiency appears to scale positively with increasing M_b for many types of invertebrate and vertebrate locomotion, including flight (Alexander, 2005; Bishop, 2005; Askew et al., 2010). Under ideal uniform conditions, the *P*o required for different modes of flight is primarily determined by the overall mass, wing kinematics, and detailed morphology of the bird under investigation (Pennycuick, 1968). The actual energetic costs incurred in the wild are influenced by many additional effects induced by the prevailing environmental conditions, such as wind strength and direction, local air thermals and deflected currents from nearby surfaces, or air density, humidity, and temperature (Pennycuick, 1989, 2008).

As aerodynamic theory predicts that *P*o and, therefore, *P*i should vary with flight speed in a U-shaped fashion (Figure 46.2), then there is an intermediate speed at which *P*o and *P*i should be at a minimum (U_{min}) and at which the bird should fly in order to maximize its flying time. However, this is not the speed at which the bird should fly in order to maximize the distance flown for a given amount of fuel consumption (i.e., the speed at which the energy cost of transport is lowest). This is the maximum range speed (U_{mr}, Figure 46.2) and the speed at which a long-distance migrant might be expected to fly to optimize fuel use (Pennycuick, 1969; Alerstam and Lindström, 1990). Thus, Hedenström and Alerstam (1995) contend that birds should adapt their flight speed differently when migrating, or transporting food, compared with when they are foraging, and this will depend on whether the bird is time or energy limited (Hedenström, 2008).

The interspecies scaling of the biomechanical power required to hold the wings out and to support the mass of the body during gliding flight is discussed by Pennycuick (1989). Given the limited amount of data available, he tentatively concludes that the power required should scale with respect to Mb between $M_b^{0.67}$ and $M_b^{0.83}$, i.e., that the power required is approximately a fixed multiple of the aerobic BMR in birds of different mass. This is consistent with the limited amount of data on the cost of gliding in birds (see below).

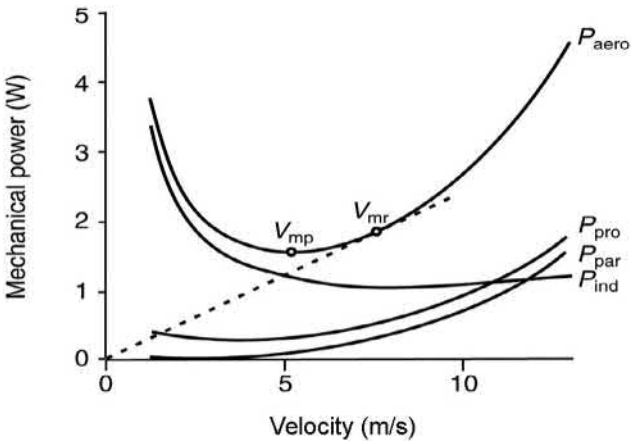

FIGURE 46.2 Calculated mechanical power output (*Paero* or *Ptot*) and its separate components (induced power, *P*ind; parasite power, *P*par; profile power, *P*pro) for the European kestrel *Falco tinnunculus* (mass 0.21 kg) flying at different speeds. Also shown are the minimum power speed (*U*min) and maximum range speed (*U*mr). *Based on Rayner (1999).*

Pennycuick (1968, 1969, 1989) has also discussed the factors which may limit the flapping flight performance of different species of birds. He hypothesizes that, for geometrically similar birds, the *P*o required for flight should scale proportional to $M_b^{1.17}$ and predicts that the *P*o available from the flight muscles should scale proportional to $M_b^{0.67}$. As the mass of the flight muscles appears to scale in direct proportion to M_b (Greenewalt, 1962; Marden, 1987; Rayner, 1988; Bishop and Butler, 1995), this results in larger birds exhibiting a reduced flight performance in terms of rate of climb, speed of take-off, ability to hover, and so on. In addition, as the maximum heart rate of both birds and mammals scale negatively with M_b, maximum sustained flight performance will also be limited by the negative scaling of maximum cardiac output (Bishop and Butler (1995); Bishop, 1997; Bishop and Spivey, 2013). Given that the M_b scaling exponents for the aerodynamic *P*o required and the sustainable metabolic *P*i available appear to be so different, there should be a clear upper limit to the size of birds which can perform flapping flight, and this would appear to be at approximately 12–20 kg (Pennycuick, 1968; Sato et al., 2009). The range of flight performance of any particular bird will depend on the detailed relationship between the U-shaped power/velocity curve and the maximum *P*o available from the flight muscles and cardiovascular system (Bishop and Butler, 1995). Thus, two categories of maximum power (P_{max}) are distinguished by Pennycuick (1968): (1) absolute P_{max}, which recruits the combined aerobic (sustained) and anaerobic (burst) capacity of the flight muscles, and (2) maximum sustainable power (P_{ms}), which only includes the aerobic capacity of the muscles and is ultimately limited by the rate of delivery of oxygen and related metabolites through the cardiorespiratory system (Figure 46.3). In the most aerobic species, e.g., hummingbirds, both P_{ms} and P_{max} may lie above the power required for hovering (Figure 46.3B), so that these birds can hover aerobically (Chai and Dudley, 1995). At the other end of the spectrum, Tinamous and many species of Pheasant have such small hearts that they cannot truly sustain any form flight (Bishop, 1997). Larger soaring specialists, such as Vultures and Condors (Figure 46.3C and D), appear to have a threshold for both P_{ms} and P_{max} that lies fairly close to the minimum power required for flapping flight, thus providing only very limited support for take-off and sustained powered performance (Duriez et al., 2014; Williams et al., 2020). The majority of bird species lie between these two extremes, with birds such as pigeons (Figure 46.3A), possessing a P_{max} sufficient to hover for brief periods using anaerobic metabolism and a P_{ms} sufficient for fast forward flight. More recent aerodynamic modeling (Klein Heerenbrink et al., 2015) suggests that the U-shaped relationship may be more skewed toward the slower speeds, so that sustaining slower speeds may be energetically more demanding than higher speeds when plotted symmetrically around the U_{min}, although ultimately drag at sufficiently high speeds will predominate.

46.3.1.2 Air flow visualization and direct force measurements

Although the mathematical models for estimating aerodynamic *P*o have been available for many years, it is only very recently that developments in technology have enabled

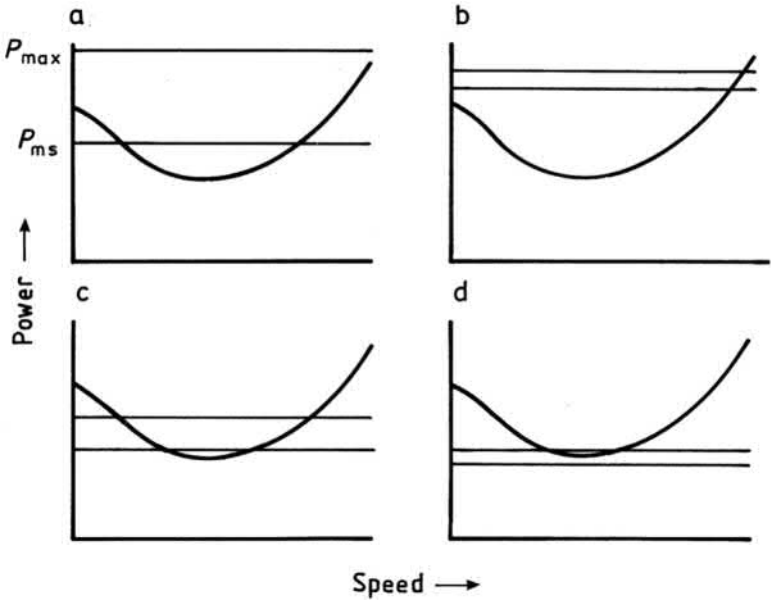

FIGURE 46.3 Power curves (see Figure 1) for (A) pigeon, *Columba livia*, (B) humming bird, *spp*., (C) white-backed vulture, *Gyps africanus*, and (D) California condor, *Gymnogyps californianus* (not to scale). The upper horizontal line represents maximum power available (*P*max), the lower line represents the maximum sustainable power (*P*ms). *Based on Pennycuick (1968).*

measurements to be made that could attempt to test the accuracy of the models by obtaining measurements of the aerodynamic forces produced by the wings. Some ingenious early experiments enabled the wake of a pigeon (*Columba livia*), jackdaw (*Corvus monedula*), and European kestrel (*Falco tinnunculus*) to be visualized, as they flew slowly during short indoor flights through a cloud of neutrally buoyant helium bubbles (Spedding, 1986; Spedding et al., 1984, 1987). The data obtained generally supported the hypothesis (Rayner, 1979) that the wake is composed of a chain of small vortex rings during slow flights (indicating that the upstroke is aerodynamically relatively inactive), but consisted of a pair of continuous, undulating trailing vortices during slightly faster speeds (indicating that the upstroke of the wing was aerodynamically active). Using wingbeat kinematics to infer lift production, Tobalske and Dial (1996) concluded that black-billed magpies (*Pica pica*) use a vortex-ring gait at all speeds, whereas pigeons use a vortex-ring gait at 6–8 m/s, a transitional gait at 10 m/s, and a continuous-vortex gait at higher speeds.

More recent work, utilizing sophisticated particle image velocimetry (PIV) equipment to monitor the wake of birds flying in wind tunnels (e.g., Thrush Nightingales *Luscinia luscinia*, Spedding et al., 2003), has indicated that, in reality, the results for most flight speeds indicate a more complex and somewhat intermediate set of wakes, with strong and continuous wing tip vortices and, at least in the case of swifts (*Apus apus*), additional vortices shed at the root (or base) of the wing (Henningsson et al., 2011). Once again, hummingbirds demonstrate their unusual aerodynamic approach, with a bound circulation that is not shed as a vortex at the end of the wingbeat but persists, so that there is a near-continuous production of lift throughout the wing cycle (Warrick et al., 2009). As a result, some 25% of the weight support is generated by the aerodynamically "active" upstroke of the wing during hovering (Warrick et al., 2012, Figure 46.4). While some other birds may hover for very limited periods, they retract the wing on the upstroke so that it almost folds up while sweeping close to the body and is, therefore, aerodynamically "inactive." To compensate for this, the pied flycatcher (*Ficedula hypoleuca*) can produce 23% of its weight support from a combination of its body and tail surfaces (Muijres et al., 2012a). An important new technique developed for bats (von Busse et al., 2014) and birds (Johansson et al., 2018) uses PIV to estimate the rate of kinetic energy imparted to the wake as a direct measurement of *P*o. Provided the cross-section of the wake can be accurately captured, this method allows measurements of *P*o across a range of speeds for the generation of power curves (Hedh et al., 2020). Comparisons of the wake structures of birds and bats (Figure 46.5) show that birds have a higher aerodynamic efficiency (including a high lift-to-drag ratio) than bats and this might contribute to the observation that birds tend to migrate more frequently and over longer distances than bats (Muijres et al., 2012b).

The first empirical attempt to measure directly the biomechanical force produced by the muscles of a bird during flight used a calibrated strain gauge, recording from the humerus of a starling (*Sturnus vulgaris*) and a pigeon (*C. livia*), and yielded estimates for the biomechanical *P*o generated by the pectoralis muscle (Biewener et al., 1992; Dial and Biewener, 1993). A more complete series of measurements were achieved with black-billed magpies (*Pica hudsonia*), with flight speeds ranging from 0 to 14 m/s (Dial et al., 1997), followed by further studies on cockatiels (*Nymphicus hollandicus*) and turtle doves (*Streptopelia risoria*) over the next few years (Tobalske et al., 2003) and finally hummingbirds (Warrick et al., 2012). For the magpie,

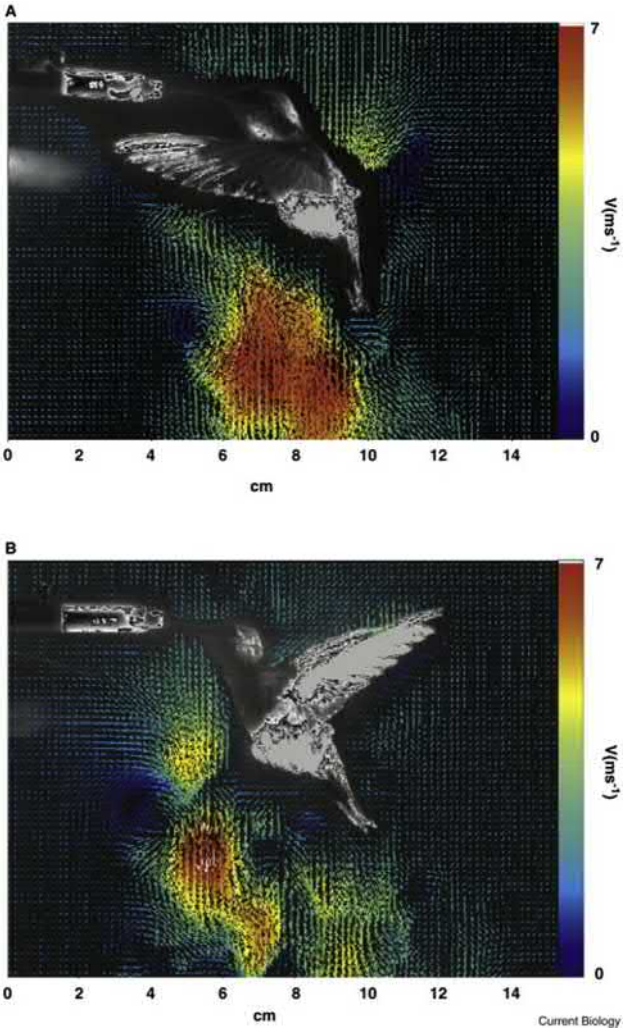

FIGURE 46.4 Flow field beneath a hovering hummingbird at the end of downstroke (A) and the end of upstroke (B) illustrating the relative strengths of the momentum jet at the end of each half-cycle. The momentum jet produced by the downstroke is normally two or more times that produced by the upstroke. *From Warrick et al. (2012).*

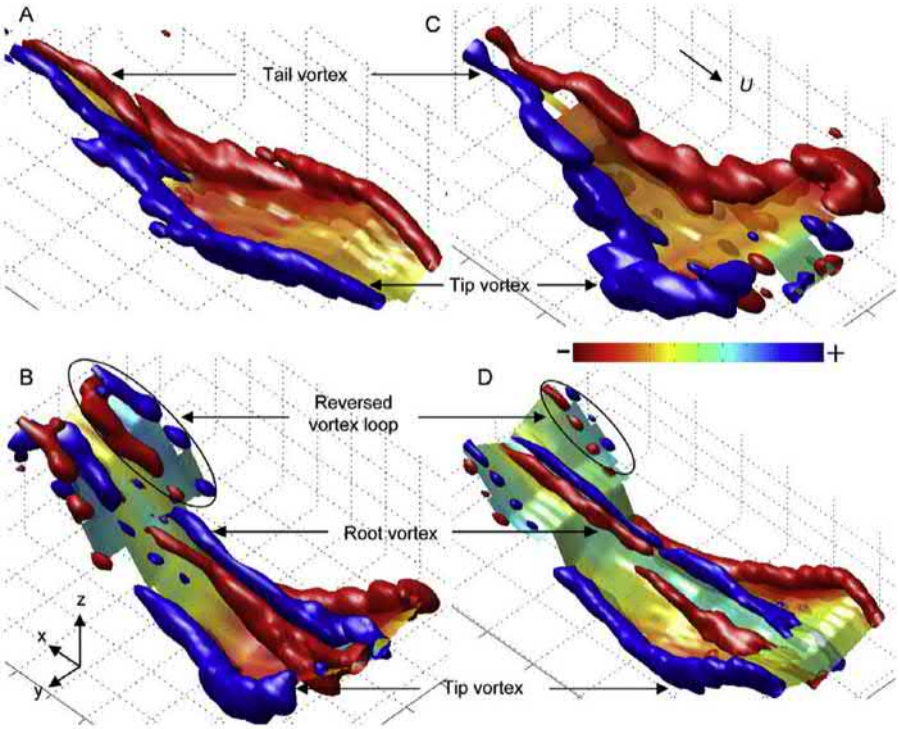

FIGURE 46.5 Reconstruction of the wake topology of a single flap cycle of two species of bird (A and C) and two species of bat (B and D) flying at 7 m/s. (A) pied flycatcher *Ficedula hypoleuca*, (B) Pallas' long-tongued bat, *Glossophaga soricina*, (C) blackcap *Sylvia atricapilla*, and (D) lesser long-nosed bat *Leptonycteris yerbabuenae*. The color-coded surface shows downwash (see color bar) as the animals fly from right to left. Bats produce root vortex at the base of the wing during the downstroke but have a slightly active upstroke that produces a reversed vortex loop due to generating thrust but negative lift. Birds have a largely inactive upstroke by retracting the wings toward the body and leaving a visible tail vortex. *From Muijres et al. (2012b).*

only hovering resulted in a significantly higher value of *P*o, compared with speeds of 2−14 m/s, yielding a so-called L-shaped curve. However, for the cockatiel, dove, and hummingbirds, changes in biomechanical *P*o during flight showed the occurrence of significant U-shaped power curves with a change in velocity, with pectoralis mass-specific *P*o ranging from 74 to 231 W/kg for the cockatiel (Figure 46.6). These authors point out that considerable flexibility in the precise shape and positioning of the power curve probably exist between avian species, which may have different flight styles and can functionally morph their wings and tail profiles during flight and, thus, affect their relative *P*o (Dial et al., 1997; Tobalske et al., 2003). This is a complex technique and the authors acknowledge that there may have been some limitations in the calibration of the strain gauges, which would have led to an underestimation of the maximal force and *P*o.

Usherwood placed differential pressure sensors along and across the wings of Canada geese, *Branta canadensis*, and pigeons (Usherwood et al., 2003, 2005), in order to measure the net aerodynamic forces acting on the wings of birds during take-off and slow forward flight. This technique was used to determine the lift and drag values for the wings and revealed a muscle mass-specific *P*o of 273 W/kg for the pigeon. This value is much higher than that determined by Tobalske et al. (2003) for cockatiels and doves flying at a similar speed (80 and 150 W/kg muscle) but

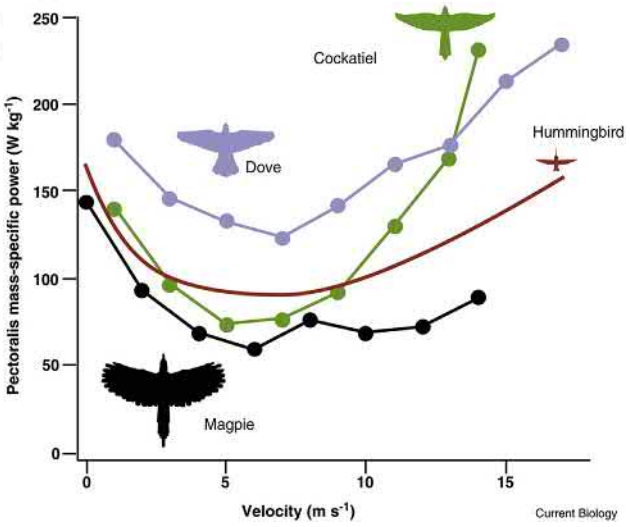

FIGURE 46.6 Comparative mean mass-specific pectoralis muscle power output as a function of flight velocity in cockatiels (*Nymphicus hollandicus*), doves (*Streptopelia risoria*), Black-billed Magpies (*Pica hudsonia*), and combined and smoothed data from Anna's Hummingbird (*Calypte anna*) and Allen's Hummingbird (*Selasphorus sasin*). *From Warrick et al. (2012).*

similar to those recorded during maximum fast flights in the wind tunnel and from the similarly sized American crow (*Corvus brachyrhynchos*) during vertical flight (Jackson and Dial, 2011). Askew and Marsh (2001) developed an in vitro method for measuring muscle force production in the blue-breasted quail (*Coturnix chinensis*), using typical

in vivo length and activity patterns, to record average *P*o of 350 W/kg. Of course, these higher values for in vitro *P*o may not accurately represent sustainable aerobic performance in vivo. A similar approach was taken by Askew and Ellerby (2007) to show that in vitro *P*o from budgerigars (*Melopsittacus undulatus*) and zebra finches (*Taeniopygia guttata*) do follow a classical U-shape.

46.3.2 Techniques used to measure the power input required for flight

46.3.2.1 Mass loss

Some of the earliest measurements of *P*i were estimated from the mass loss recorded during a long, nonstop flight, with the assumption that fat constituted by far, the major part of this loss and that the net loss of water, was negligible (Nisbet et al., 1963). Berger and Hart (1974) criticized this method, as they believed that total water loss may exceed the production of metabolic water, particularly at high environmental temperatures (cf. Nachtigall, 1995), leading to significant dehydration. Another problem with this method is that there is evidence to indicate that migrating birds also catabolize protein (e.g., muscle and intestine) during flight (Piersma and Jukema, 1990; Jenni-Eiermann and Jenni, 1991; Jenni and Jenni-Eiermann, 1998; Battley et al., 2000), and whereas fat has an energy density of 39.3 kJ/g, the value for muscle (which is composed of approximately 70% water) is only 5.4 kJ/g (cf. Schmidt-Nielsen, 1997).

Masman and Klaassen (1987) developed a more complex method of using changes in M_b to estimate flight costs. They studied the energy budgets of trained kestrels (*F. tinnunculus*) performing directional flights in the laboratory. Energy expenditure during flight was calculated by monitoring daily metabolizable energy intake, oxygen consumption and carbon dioxide production during rest, and time spent flying per day. A similar approach was applied to the study of a thrush nightingale (*L. luscinia*) flying for very long periods (seven different 12 h flight sessions) in a wind tunnel (Kvist et al., 1998).

Recently, the mass loss technique has been refined by using quantitative magnetic resonance (QMR) analysis of body composition changes during flight (Guglielmo et al., 2011, 2017; Gerson and Guglielmo, 2011a). In this technique, QMR measurements lasting a few minutes are taken immediately before and after flight, and decreases in fat, lean, and water masses are used to calculate *P*i, the relative contribution of protein to energy, and aspects of water balance. Estimates of *P*i using the QMR method are comparable to those obtained by respirometry and isotopic methods.

46.3.2.2 Doubly labeled water

The most commonly used method to determine the field metabolic rate (FMR) of air-breathing vertebrates is the doubly labeled water (DLW) method, and it has been used extensively with free-ranging birds (Hails, 1979; Ellis, 1984; Tatner and Bryant, 1989). This method was first proposed as a means of determining CO_2 production by Lifson and his coworkers over 40 years ago (Lifson et al., 1949, 1955). It involves the injection of a mixture of ^2H_2O (or ^3H_2O) and $H_2^{18}O$ into the animal, allowing these isotopes to equilibrate with the body water pool(s), taking a body fluid sample after injection and releasing the animal into the field. After a number of days, the animal is recaptured and another body fluid sample is taken. The difference between the rate of loss of the different isotopes is assumed to be equivalent to the rate of CO_2 production ($\dot{V}_{CO_2}$), from which the MR and *P*i of the animal can be estimated. The many assumptions that are made when using this technique have been thoroughly discussed by Nagy (1980), Speakman (1990, 1998).

Although DLW is a relatively simple method to use in the field, it has three major limitations. Perhaps most importantly for field work is the fact that the duration of an experiment is limited by the turnover rate of the ^{18}O; thus, it is necessary to recapture the animal after a sufficient delay following injection of the isotopes to enable a reasonable decline in the enrichment of ^{18}O, but before the enrichment is too low (Nagy, 1983). The second problem is that the technique only gives an average value for energy expenditure between the two sampling points and this is usually over a 24-h daily cycle of activity (Speakman and Racey, 1988). When DLW is used to determine the metabolic cost of a specific activity (e.g., flying), then, as with the M_b method, it is necessary to have accurate information on the duration of the flying period(s). Ideally, the RQ also needs to be known to convert the calculated $\dot{V}_{CO_2}$ to an estimate of $\dot{V}_{O_2}$ and/or *P*i (see above).

Recent validation studies with captive birds exercising at different levels of activity (but not flying) over a period of 72 h have indicated that, provided mean data are used from a number of birds, the DLW method can give estimates of MR that are within a few percent of those measured by respirometry (Nolet et al., 1992; Bevan et al., 1994, 1995a), although they do show a greater variance. The only validation study on a flying bird was that of Ward et al. (2004), in which they used three independent techniques, DLW, mask respirometry, and heat transfer modeling to measure the *P*i of the European starling (*S. vulgaris*) flying in a wind tunnel between 6 and 14 m/s. Heat transfer modeling and mask respirometry yielded

comparable results and a linear increase in *P*i with increasing velocity, but the DLW results had a greatly increased scatter and variance between individual flight measurements. DLW has been used to measure *P*i in other wind tunnel experiments where flight durations were sufficiently long (Kvist et al., 2001; Engel et al., 2006b). The advent of laser spectrometers that measure hydrogen and oxygen isotope ratios in near real time in exhaled breath water makes the DLW more practical for flight and other energetic studies (Mitchell et al., 2015).

46.3.2.3 ^{13}C sodium bicarbonate

Carbon dioxide produced by aerobic metabolism enters the bicarbonate pool until it is reconverted to CO_2 and exhaled at the lungs. Turnover of the bicarbonate pool is rapid, and the flux of CO_2 can be measured by labeling the bicarbonate pool with ^{13}C sodium bicarbonate (NaBi) and measuring the kinetics of $^{13}CO_2$ in exhaled breath. The NaBi method was first developed and applied to birds by Hambly et al. (2002) to measure *P*i of zebra finches (*T. guttata*) flying between perches for 2 min. It was similarly used in a study of European Starlings (*S. vulgaris*) and Palestine Sunbirds (*Nectarinia osea*) (Hambly et al., 2004). The bird is injected with a calibrated ^{13}C NaBi solution and placed in a respirometry chamber with a constant flow of CO_2 free air. Peak enrichment of the bicarbonate pool is reached in a few minutes after which ^{13}C enrichment of the breath CO_2 declines in a log-linear fashion at a rate that is proportional to the rate of CO_2 production at rest, which can be measured simultaneously from excurrent CO_2 concentration and the air flow rate through the chamber. The bird is then quickly removed from the chamber, flown for 1−2 min, and returned to the chamber to measure the postflight ^{13}C enrichment. The rate of CO_2 production in flight is calculated from the rate of decline in ^{13}C enrichment during the flight period, using the calibration obtained during the preflight resting period. The advantage of this technique is that it allows measurements of uninstrumented birds flying for short periods, even at uncomfortable speeds. Recently, the NaBi method was used to measure *P*i of Blackcaps (*Sylvia atricapilla*) flying at speeds between 4 and 12 m/s in a wind tunnel (Hedh et al., 2020).

46.3.2.4 Telemetry and data logging

Much progress has been made in the use of biotelemetry and data logging devices for studying the physiology of free-ranging animals (Cooke et al., 2004; Ropert-Coudert and Wilson, 2005). Any externally mounted object is likely to influence the flight performance of a bird, not only as a result of the added mass but also by increasing the aerodynamic drag of the body (Bowlin et al., 2010). These effects may be minimal for a relatively small transmitter that the bird can preen under its contour feathers (Obrecht et al., 1988). However, in some circumstances, the effects can be quite substantial, particularly for high-performance birds like homing pigeons (Gessaman and Nagy, 1988). Butler and Woakes (1980) overcame the problem of increasing body drag by implanting relatively small (<10 g) radio-transmitters into the abdominal cavity of barnacle geese (*Branta leucopsis*) and were able to record heart rate (mean, 512 beats/min) and respiratory frequency (mean, 99 breaths/min) from two birds (mean mass, 1.6 kg) flying behind an open-topped vehicle. It is now possible to implant data loggers (weighing less than 30 g) that will store basic physiological information (heart rate, T_b, etc.) over periods of many days. The data can then be downloaded after the animal is recaptured (Woakes et al., 1995; Bevan et al., 1995b; Wascher et al., 2009; Bishop et al., 2015).

46.3.2.4.1 Heart rate

Heartbeat frequency (f_H) can be accurately measured and used as a proxy for metabolic energy consumption. Thus, if properly calibrated and validated, and if mean data are used from a number of animals, f_H may be used as an indicator of the rate of oxygen uptake in free-living birds (Butler et al., 2004; Green, 2011). However, the relationships between f_H and $\dot{V}_{O_2}$ that are obtained during walking and running, or during swimming, may not be identical to those obtained when the birds are flying (Gessaman, 1980; Nolet et al., 1992; Ward et al., 2002; Bishop and Spivey, 2013). The study by Ward et al. (2002) is the only report of a direct calibration of heart rate against mask respirometry of a bird flying in a wind tunnel, in which there is a reasonable variation in both the measures of heart rate and the rate of oxygen consumption (Figure 46.7). These results indicate that f_H verses $\dot{V}_{O_2}$ relationships during flight are well described by power equations, with barnacle geese $\dot{V}_{O_2} = 0.0019 f_H^{1.98}$ and bar-headed geese $\dot{V}_{O_2} = 0.0013 f_H^{2.08}$. Thus, the $\dot{V}_{O_2}$ approximates to a quadratic or square law relationship, i.e., $\dot{V}_{O_2} = m\, f_H^{2.0}$ for these birds during flight (their "primary mode" of locomotion—defined as the mode that typically induces maximum $\dot{V}_{O_2}$ for a specific species), while it is closer to a direct linear relationship $\dot{V}_{O_2} = m\, f_H^{1.0}$ during running (i.e., nonprimary mode). The constant (m) is likely a function of both M_b and heart mass (M_h). Thus, it is likely that it is the running relationship that is unusual in these normally volant species, given that geese are not thought to be particularly reliant on running in the wild. This simple square law relationship for geese in flight can be generalized to an interspecies comparison of 24 species of endothermic vertebrates (12 birds and 12 mammals) during their appropriate "primary modes" of locomotion (Bishop and Spivey, 2013), when differences in M_b and M_h are taken

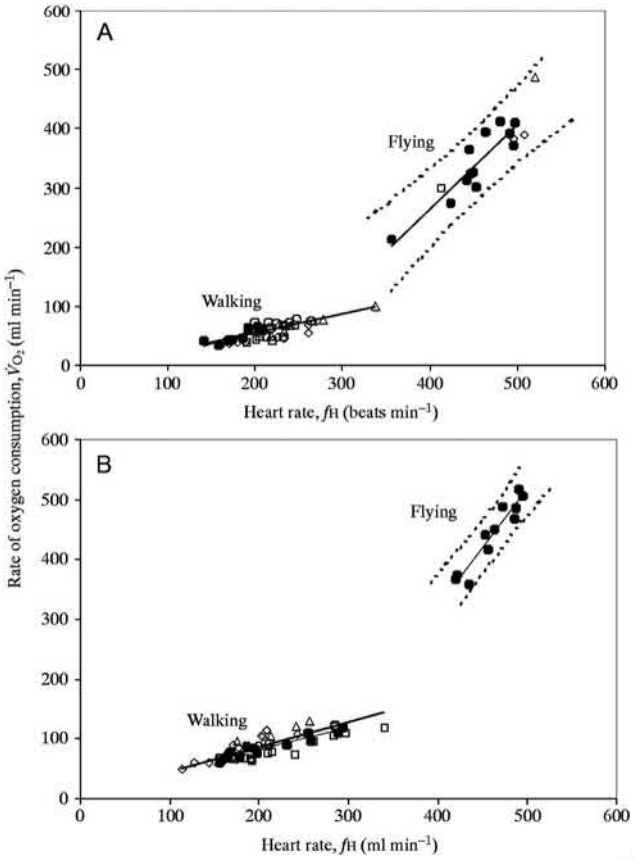

FIGURE 46.7 Linear relationships between mean rate of oxygen consumption *V*o2 and mean heart rate (f_H) of (A) barnacle geese, *Branta leucopsis*, and (B) bar-headed geese, *Anser indicus*, walking on a treadmill and flying in a wind tunnel. The filled circles show data from a single bird of each species from which most data on the relationships between f_H and *V*o2 were obtained during flight (N = 12 flights by barnacle goose B−B and 11 flights by bar-headed goose BH−O). The open symbols show data from other birds. The solid lines show the relationships between f_H and *V*o2 during walking and flight by barnacle goose B−B [walking, $Vo2 = 0.47\,f_H$ - 35.9, $r2 = 0.78$; flight, $Vo2 = 1.42\,f_H$ - 304, $r2 = 0.82$] and bar-headed goose BH−O [walking, $Vo2 = 0.35\,f_H + 12$, $r2 = 0.88$; flight, $Vo2 = 1.97\,f_H - 467.5$, $r2 = 0.90$]. The broken lines show the 95% prediction intervals. *Based on Ward et al. (2002).*

into account. Thus, while some small regulation of cardiac output may be achieved by changes in stroke volume, between rest and exercise modes, for primary modes of locomotion, such changes are relatively small compared to changes in f_H, which range from around 4- to 10-fold (Butler, 1991; Bishop and Butler, 1995).

46.3.2.4.2 Accelerometry

Accelerometers have been mounted on the body of animals to provide high-resolution measures of acceleration (or changes in velocity). During steady-state locomotion, the average acceleration, taken over a sufficient number of limb cycles (or flapping in the case of flight), is equivalent to the "static" component of acceleration due to gravity. The modulus of individual raw acceleration data points minus the mean static acceleration for a given time period gives a measure of the "Dynamic Body Acceleration" or DBA (Qasem et al., 2012). Strictly speaking, DBA should be considered a potential proxy for biomechanical *P*o in the previous section, but it is usually correlated against measures of metabolic *P*i. In multidimensional acceleration studies, summing the data taken from the different axes is called Overall Dynamic Body Acceleration (ODBA), and calculating the vectoral length is termed VeDBA (Wilson et al., 2006; Qasem et al., 2012). Both these measures have been shown to be well correlated with rates of oxygen consumption in human subjects and a number of other mammal and bird species while running on treadmills (Halsey et al., 2011; Wilson et al., 2019).

While no detailed and direct correlation of DBA and rate of oxygen consumption have been conducted on birds during flight, ODBA was shown to increase during ascending and decrease during descending flights by a captive Griffon vulture *Gyps fulvus* (Halsey et al., 2009). Elliott et al., (2013) showed that VeDBA was quite well correlated with the average daily energy expenditure (DEE) of breeding thick-billed murres (*Uria lomvia*), as determined by measurements of DLW. Mean values of DBA are correlated with heart rate for free-flying captive Griffon Vultures (*G. fulvus* and *Gyps himalayensis*) (Duriez et al., 2014) and wild living bar-headed geese (*Anser indicus*) (Bishop et al., 2015) and Great Frigatebird (*Fregata minor*) (Weimerskirch et al., 2016). In addition, Spivey and Bishop (2013) describe a mathematical model to help to interpret data collected by accelerometers mounted on the body of birds during flight. By assuming that the body motion of the bird during steady forward flight approximates to a sinusoidal waveform, they showed that the root mean square of acceleration (aRMS), another form of time averaged DBA (which is closely related to VeDBA), can be naturally derived from the mathematics. The biomechanical power visible to the body-mounted accelerometer can be interpreted in the SI units for mass-specific power ($W = m^2 \times s^{-3}$) by a number of possible terms, including the following:

$$P_{body} \text{ is proportional to } (\text{aRMS})^2 / f_w$$

where f_w is wingbeat frequency (Hz). However, this modeling approach was developed around horizontal flight and only partially accounted for climb power performance in captive Harris's Hawks (*Parabuteo unicinctus*) trained to fly at different flight angles (Van Walsum et al., 2020). Uncertainties regarding the use of accelerometry center around the alignment of the sensor with the axis of movement of the body, variation in the position of the sensor on the body, the fact that the cost of limb movements may be partially "hidden" from a body-mounted sensor, as may

changes in M_b itself, and that rotations of the body not directly linked to movement costs may exaggerate the apparent energy required. However, analysis of body movement and acceleration is already an important technique in assessing animal locomotion and energetics (Wilson et al., 2019).

Measurements of acceleration (especially in conjunction with angular velocity and/or orientation in the Earth's magnetic field) can also be used to determine relative body orientation and kinematics (Wilson et al., 2019). For example, changes in wingbeat frequency (f_w) of foraging European shags (*Phalacrocorax aristotelis*) returning to the nest to feed their chicks were reliably correlated to relative changes in M_b (Sato et al., 2008). f_w was determined for five species of Procellariiformes during take-off and during forward flight Sato et al. (2009). They showed that during take-off the wingbeat frequency was higher and scaled with $M_b^{-0.3}$, while during forward flight it scaled as $M_b^{-0.18}$. By extrapolating these two relationships until they intercepted, it was suggested that the maximum limits to practical soaring flight might be around 41 kg for a bird or pterosaur with a wingspan of around 5.1 m (Figure 46.8).

46.3.2.5 Respirometry

*P*i is most easily estimated by indirect calorimetry, and under laboratory conditions, by directly measuring the $\dot{V}_{O_2}$ of birds flying in a wind tunnel and then converting that to *P*i (see above). The increased use of wind tunnels during the past 50 years has greatly added to our knowledge and understanding of the physiology of birds during flight (Butler and Woakes, 1990; Norberg, 1990). Perhaps the main advantage of being able to use a wind tunnel is that it is possible to make physiological measurements that would be virtually impossible by other means (e.g., repeated blood samples, blood pressure and flow measurements, direct measurements of force production, etc.). However, it must also be borne in mind that, as with almost any other method for studying a living animal, the wind tunnel itself and the measuring equipment required can influence the behavior of the animal flying in it and hence affect the data obtained when compared with those from free flying birds (Butler et al., 1977; Rayner, 1994). For example, gas exchange ($\dot{V}_{O_2}$ and $\dot{V}_{CO_2}$) is usually determined by means of a lightweight mask which covers the beak and nose and through which air is drawn via an attached tube (Tucker, 1968b, 1972; Bernstein et al., 1973; Butler et al., 1977; Gessaman, 1980; Hudson and Bernstein, 1983; Rothe et al., 1987; Ward et al., 2001, 2002; Peters et al., 2005). The mask and tubing will influence the recorded data because of their mass, but more so because of the extra drag that they impose. $\dot{V}_{O_2}$ can also be measured in a similar way for hummingbirds while feeding at artificial flower heads (Wells, 1993a,b; Clark and Dudley, 2010). The only studies

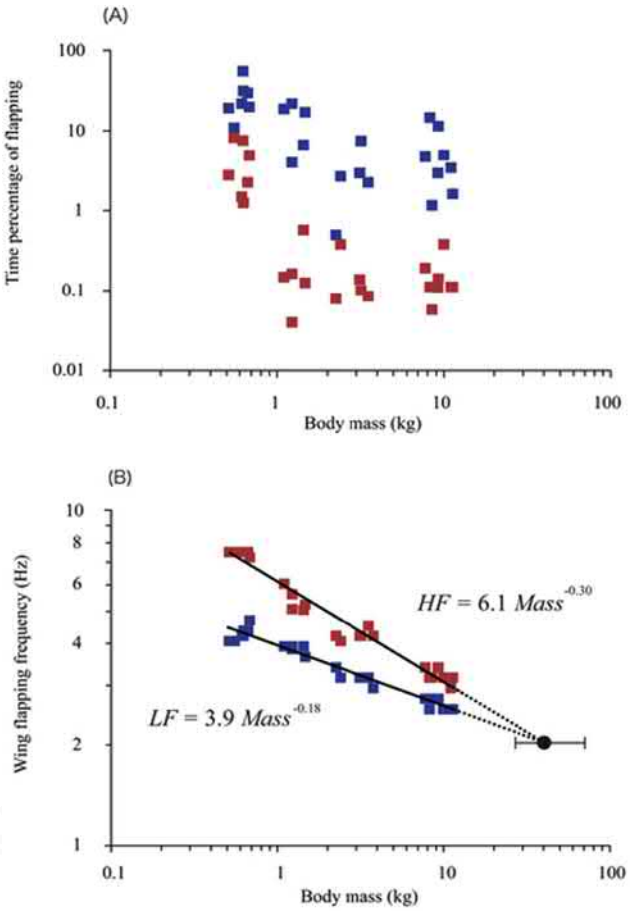

FIGURE 46.8 (A) The relationship between body mass and the percentage of time spent flapping relatively slowly (*blue squares*) and relatively quickly (*red squares*) during the foraging flights of five species of albatrosses and petrels. (B) The relationship between body mass and wingbeat frequency for the same species. Regression lines were calculated for high (*red squares*) and low (*blue squares*) frequencies and extrapolated for larger animals (*dashed lines*). The two lines intersect at a body mass of 41 kg (5.1 m wingspan), with a 95% CI (26–75 kg). *From Sato et al. (2009).*

in which gas exchange has been determined in a wind tunnel without the use of a mask are those by Tucker (1966) and Torre-Bueno and Larochelle (1978), using airtight, closed-circuit wind tunnels and measured the changing concentration of gases in the atmosphere. An aerodynamic analysis by Rayner (1994) suggested that, in closed wind tunnels, the *P*o versus speed curve (see above) will be flatter than that for free flying birds.

46.3.2.6 Modeling of cardiovascular function

Some of the shortcomings of using the aerodynamic models to estimate *P*o and then, subsequently, converting them to estimates of *P*i (by assuming a value for efficiency) could possibly be reduced by devising a model to estimate total *P*i directly. This was highlighted by the studies of Ward et al.

(2001, 2004) who pointed out starlings may not have a constant value of muscle efficiency throughout their speed range and that conversion of *P*o to *P*i was sensitive to the value of efficiency. Bishop and Butler (1995) attempted a modeling approach to estimating *P*i by assuming that the mass of an animal's heart could be used as a basis for estimating cardiac stroke volume and calculating the animal's aerobic capacity. The role of the various components of the cardiovascular system in presenting O_2 to (and removing CO_2 from) the exercising muscles can best be described by a form of Fick's formula for convection:

$$\dot{V}o_2 = f_H \times V_S \times \left(C_aO_2 - C_{\bar{v}}O_2\right)$$

where f_H is heart beat frequency (beats/min); V_S is cardiac stroke volume (mL); and $\left(C_aO_2 - C_{\bar{v}}O_2\right)$ is the difference between the oxygen content in arterial and mixed venous blood (mL of O_2 per mL of blood). In theory, each of these variables can scale independently with respect to M_b such that

$$\left(\dot{V}o_2\right)M_b^{Z} = (f_H)M_b^{w} \times (Vs)M_b^{X} \times \left(C_aO_2 - C_{\bar{v}}O_2\right)M_b^{Y}.$$

There have only been two studies in which all four variables of the Fick equation have been measured in a bird during forward flapping flight (Butler et al., 1977; Peters et al., 2005). Bishop and Butler (1995) substituted each of the values from the Butler et al. (1977) study into the above equation, based on a series of general allometric equations ($y = a.x^b$) for the scaling of f_H, Vs, and $\left(C_aO_2 - C_{\bar{v}}O_2\right)$, respectively. For birds flying close to their minimum power speeds, the individual components of the Fick equation were estimated to scale as follows: $f_H = 574\ M_b^{-0.19}$, $Vs = 3.48\ M_b^{0.96}$, and $\left(C_aO_2 - C_{\bar{v}}O_2\right) = 0.083\ M_b^{0.00}$. The estimated scaling of V_S during flight was based on the assumption that *V*s should be almost directly proportional to the M_h, or $Vs = 0.3\ M_h^{1.05}$, while f_H during flight and M_h may be readily determined experimentally.

Bishop and Butler (1995) concluded that, for birds with a high aerobic capacity (such as pigeons), $\dot{V}_{O_2}$ (mL/min) = $166M_b^{0.77}$, for birds flying close to their minimum power speeds. This compares favorably with the relationship ($\dot{V}_{O_2} = 160\ M_b^{0.74}$) calculated by Butler (1991) and reanalyzed using RMA for seven species of birds during forward flapping flight in a wind tunnel. Bishop (1997) used a similar approach to estimate the maximum $\dot{V}_{O_2}$ of birds during flight, again using M_h as the basis of the calculation, and it would appear that the use of M_h to predict the aerobic capacity of different species of birds may have more general applicability than the use of a general allometric relationship. Bishop and Spivey (2013) did a metaanalysis of data from 12 species of birds and 12 species of mammals that were said to be performing their "primary" modes of locomotion (i.e., running, swimming, or flying, respectively) and concluded that there was an overall allometric trend across all species for $\dot{V}_{O_2}$ to be approximately proportional to heart rate squared (f_H^2). Individuals and different species may vary in how closely they followed this quadratic heart rate exponent, but knowledge of both M_h and M_b gave the best predictive relationship for rate of oxygen consumption (Figure 46.9).

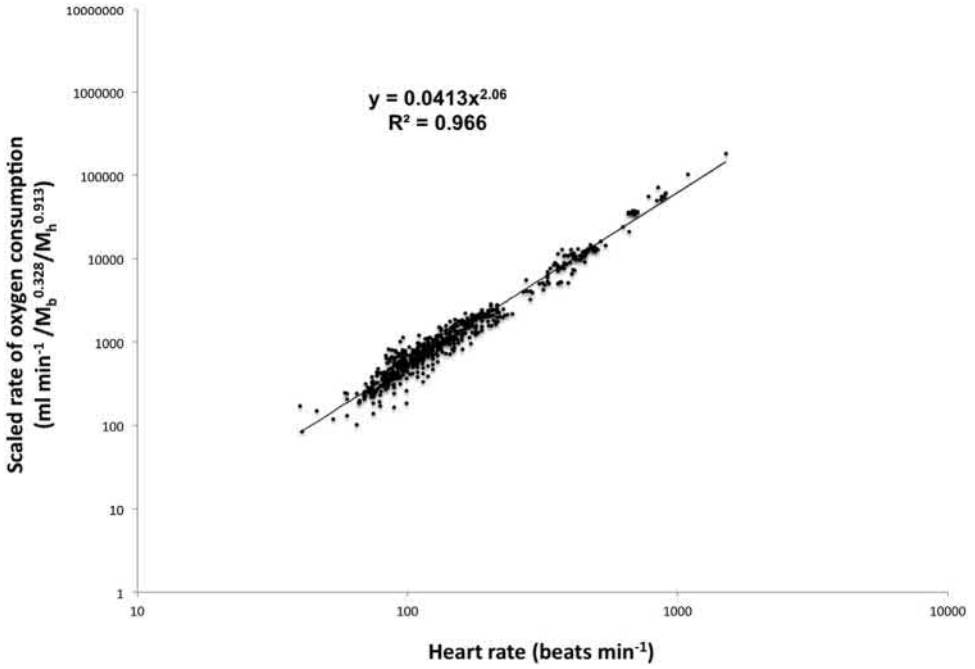

FIGURE 46.9 The relationship between heart rate (beats/min) and the rate of "rescaled" oxygen consumption (mL/min/*M*b0.328/*M*h0.913) for 12 species of birds and 12 species of mammals, after taking into account differences in body mass (*M*b) and heart mass (*M*h) between species. Each species was flying, running, or swimming, depending on what was considered their "primary mode" of locomotion, i.e., the form of locomotion that would yield the highest rate of oxygen consumption. *From Bishop and Spivey (2013).*

46.3.3 Empirical data concerning the power input during flight

An individual flight by a free-ranging bird will include at least one take-off and a period of climbing, probably several maneuvers (turns, short periods of "burst" flying, and changes of gait) as well as various periods of gliding, soaring, bounding, and flapping flight. The power requirements associated with all of these various types of flight will be different and may be provided by either anaerobic or aerobic metabolic pathways or by a combination of the two.

Species belonging to the Galliformes (e.g., pheasants, grouse, and quail) routinely engage in a powerful "burst" type of flight during take-off and short-duration flights. Their muscles use predominantly anaerobic metabolism of intracellular stores of glycogen which leads to the accumulation of lactic acid and a metabolic acidosis, followed rapidly by fatigue. Thus, a large proportion of the total cost of these explosive flights is "repaid" while the bird is resting following the flight (Bishop and Butler, 1995), and an assessment of the true cost of such explosive flights, if based on $\dot{V}_{O_2}$, would have to include the postflight period of recovery. In other words, measurements of $\dot{V}_{O_2}$ can only be used for accurate estimates of Pi if the activity is sustainable for relatively long periods of time (i.e., if the bird is metabolizing aerobically, usually for at least a few minutes).

46.3.3.1 Gliding and soaring flight

In general, BMR decreases as body size increases, while at the same time the speed of flight increases, so it would be expected that larger birds should benefit more than smaller species from the strategic use of gliding. Of course, it should be remembered that, even when gliding, birds can actively adjust the shape and span of their wings, including the sweep angle that they make to the body, in order to adjust air speed and the aerodynamic efficiency of the wing (Rosén and Hedenström, 2001; Lentink et al., 2007). Pennycuick (1997) hypothesized that the cost of holding the wings outstretched when gliding and soaring should scale at around 1.5 times the BMR. In reality, most empirical studies have recorded slightly higher costs for gliding. For herring gulls (*Larus argentatus*) gliding in a wind tunnel, Pi (calculated from measured $\dot{V}_{O_2}$) was 15.3 W/kg, or 2.1x the resting value (Baudinette and Schmidt-Nielsen, 1974).

In the wild, birds such as albatrosses try to maximize the use of soaring and gliding flight, and even in near calm conditions, they only beat their wings occasionally (Alerstam et al., 1993). In a study on black-browed albatrosses (*Diomedea melanophris*), Bevan et al. (1995b) used the f_H method to determine the FMR and salt water switches to determine when the birds were on the water. Interestingly, the average metabolic cost of flying was 6.2 W/kg, which was similar to the cost of birds when resting on the water (5.8 W/kg), approximately 2.0x the predicted BMR but around 2.2x the estimated costs duration incubation. However, the study by Bevan et al. (1995b) illustrates the importance of accurately determining the behavior of the animals under study and the advantages of using methods, such as measuring f_H and/or acceleration, for estimating the metabolic cost of the separate behaviors in combination with the satellite position data. During Section 46.2 of the trip, the albatross covered a distance of 80.1 km in 1.7 h, a mean ground speed of 13.1 m/s. This is very similar to the mean speed of 12.9 m/s that Alerstam et al. (1993) report for a visually tracked black-browed albatross. MR was remarkably low during this period (2.4 W/kg), which is likely to be dominated by soaring and gliding flight, and barely greater than that during incubation (2.2 W/kg). On the other hand, during Section 46.4 of the trip, the straight-line distance traveled was only 6.3 km at a mean ground speed of 1.6 m/s, but the bird exhibited a high MR of 8.8 W/kg. This suggests that the bird was likely foraging within a restricted area and was engaged in some form of relatively strenuous activity.

Similar to the large Procellariiformes, Frigatebirds are renowned for being one of the most aerial of avian species, spending the majority of their time in slow soaring flight, often up to a week without landing (Weimerskirch et al., 2016) while sleeping on the wing, although apparently much less than on land (Rattenborg et al., 2016). They constantly ascend and descend on thermals during the day and night, while looking for infrequent opportunities to feed on flying fish, off the sea surface without landing, or by pursuing other bird species and kleptoparasitizing their prey (Weimerskirch et al., 2003). During their long trips circumnavigating the doldrums of the Indian ocean (Figure 46.10A), the Great Frigatebird (*F. minor*) regularly soars like a vulture, typically circulating up to around 400 m, or occasionally obtaining lift inside the strong updrafts provided by cumulus clouds where they can reach up to 4000 m (Weimerskirch et al., 2016). They then glide slowly down over many kilometers before picking up another thermal and repeating the process for many hours. This rollercoaster flight pattern is achieved with only occasional bouts of wing flapping while soaring and gliding >100 m above sea level and with no access to feeding opportunities, but is then interrupted by periods of flight near the sea surface which consist of a more active and vigorous flight performance. Figure 46.10B shows a 12-h period of tracking of a Great Frigatebird during which the first 3 h are spent low over the sea and these events coincide with heart rates of over 400 beats/min and intense periods of acceleration (Weimerskirch et al., 2016). Interestingly, f_w is very focused around 2.5 Hz, but the DBA is highly variable (indicating strong amplitude modulation of

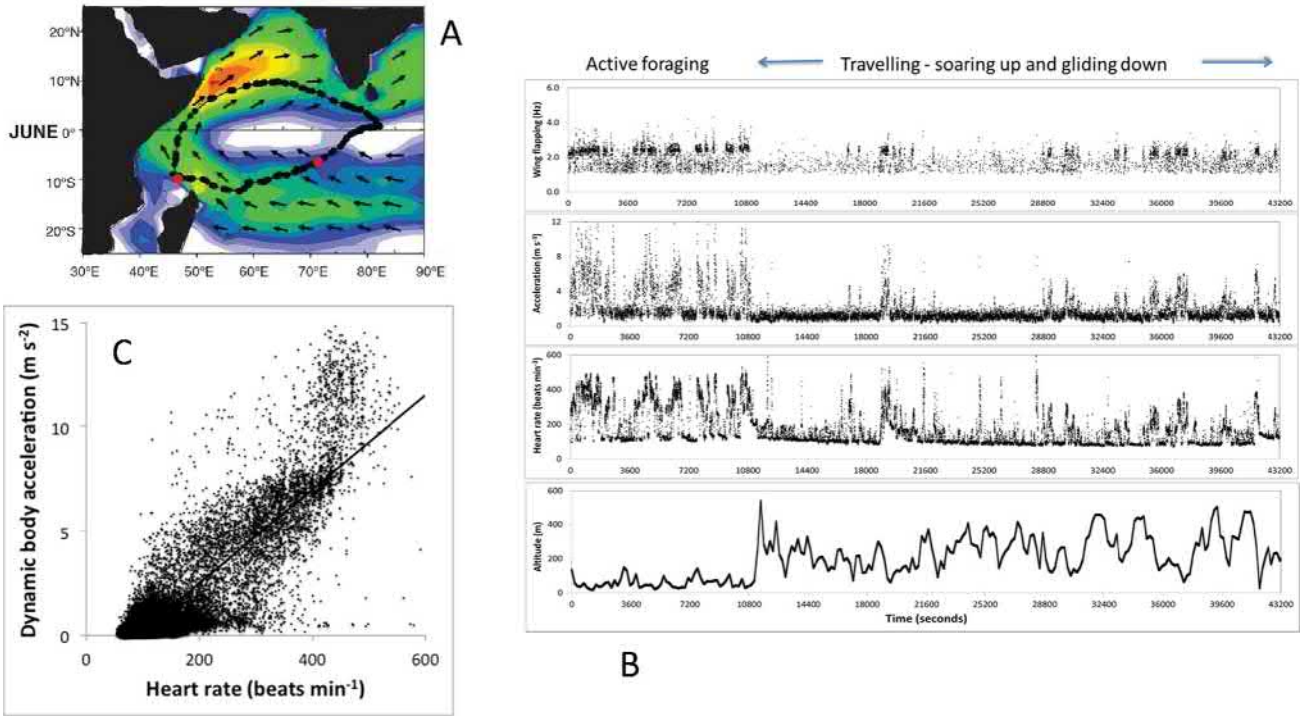

FIGURE 46.10 Tagging data from adult male Frigatebirds: (A) A 24-day clockwise foraging trip from Aldabra Island (Seychelles) in relation to wind strength (color scale – white zero to red >16 m/s) and direction (*arrows*), with a 1 h stop in the Chagos Islands. (B) Changes in wingbeat frequency, dynamic body acceleration, heart rate, and altitude over a 12 h period. (C) Root mean square DBA plotted against heart rate from a single Frigatebird over a 72 h flight. *Modified from Weimerskirch et al. (2016).*

flap effort), while the highest values for DBA (>4 m/s/s) are associated with heart rates of over 400 beats/min but are not well correlated (Figure 46.10C). These appear to represent brief but powerful bouts of flapping where the cardiovascular response is either near its maximum, or the cardiovascular response is too slow, so that the biomechanical effort involved is not reflected by the aerobic capability and where the flight muscle may be recruiting anaerobic fibers for a quick burst of extra flight performance. The final 9 h are spent routinely spiraling and soaring up to between 300 and 600 m, followed by long and shallow gliding descents. Heart rates, values of DBA, and f_w are generally very low throughout this time, even during the ascending flights. Thus, it is only the active feeding phases that are energetically costly and not the long periods of oceanic circumnavigation.

As gliding is thought to be more common in larger species of birds, it has seldom been quantified in smaller species, although some small species of birds, such as the Hirundines (martins and swallows) and the Apodidae (swifts), regularly glide. However, Sapir et al. (2010) showed that, like in the study of Black-browed albatrosses (Bevan et al., 1995b), the heart rate of resting European bee-eaters was similar to that recorded while gliding and soaring, either on migration or at stop-over sites (Figure 46.11). Surprisingly, they suggest that not only was gliding MR only 1.9 times BMR but that the air speed of soaring was sufficiently fast (10.6 m/s) as to make gliding very economic. Assuming that the rate of oxygen consumption is proportional to f_H^2 (Bishop and Spivey, 2013; Figure 46.9), provides a determination that the energy consumed during gliding flight is at least 5 times lower than during flapping flight for the bee-eaters. Swifts (*A. apus*) have been predicted to glide most efficiently at velocities of 8–10 m/s (Lentink et al., 2007), which fits nicely with their behavior of climbing high above the ground and gliding slowly at around 10 m/s while probably sleeping on the wing (Hedenström et al., 2016).

During gliding flight, it is important to minimize body (or parasite) drag and to maintain a high lift-to-drag ratio. Even turning the head from side to side can significantly increase the effective body drag. Indeed, because birds usually have laterally placed eyes with relatively low stereoscopic fields of view, they often prefer to see things either in one eye or the other. In the case of a fast diving peregrine falcon (*Falco peregrinus*), it approaches its prey

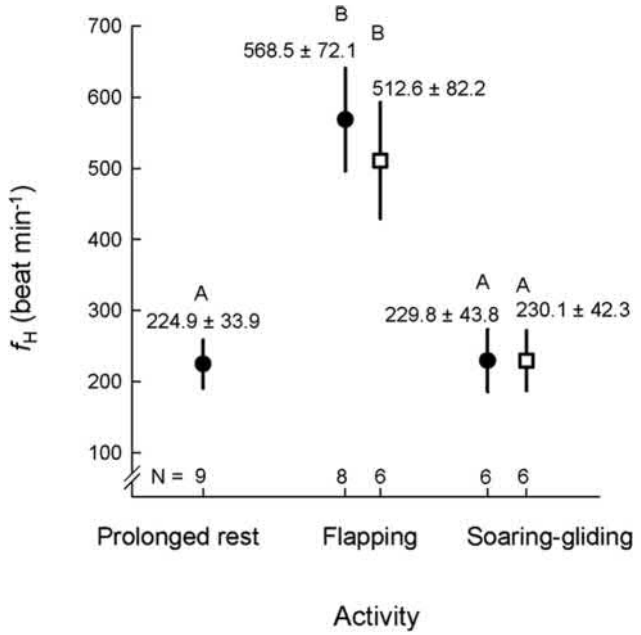

FIGURE 46.11 Heart beat frequency (f_H) of European bee-eaters, *Merops apiaster*, measured in the field in relation to their behavior. The data are presented as the mean ± standard deviation of f_H for bee-eaters resting for prolonged duration or in different flight modes recorded, during stopovers (*filled circles*) and migratory cross-country flights (*open squares*). Different letters above the bars indicate groups that differed statistically. N = number of birds whose f_H was recorded during each activity. *From Sapir et al. (2010).*

by flying along a spiral path so that it can keep its head facing forward on its body (Tucker et al., 2000). Moving the head to one side or the other can increase parasite drag by around 50%.

46.3.3.2 Forward flapping flight

Some of the most comprehensive data we have on the overall energy consumed by the body (*P*i) and the biomechanical power output by the muscles (*P*o) during forward flapping flight are those obtained from birds flying in wind tunnels. In theory, the use of wind tunnels makes it possible to estimate both *P*o and *P*i at different flight speeds, although few studies have done this simultaneously and the details of these relationships appear to vary among species. The majority of studies of *P*i were determined by measuring the rate of oxygen consumption while the birds wore a plastic respirometry mask (Figure 46.12). Results from the laughing gulls, fish crows, and white-necked ravens have shown a J-shaped curve against flight velocity (Tucker, 1972; Bernstein et al., 1973; Hudson and Bernstein, 1983), while the starling, barnacle, and bar-headed goose have a relatively flat "curve" (Ward et al., 2001, 2002). Only the budgerigar (*M. undulatus*), cockatiel, pigeon, and hummingbirds have showed an obvious U-shaped curve for *P*i (Tucker, 1966; Rothe et al., 1987; Bundle et al., 2007; Clark and Dudley, 2010), similar to that predicted by aerodynamic theory for mechanical *P*o (Pennycuick, 1969; Tucker, 1973; Greenewalt, 1975; Rayner, 1979). Arguably, the J-shaped *P*i curves may not be so different from a U-shaped curve, but very low air velocities were not obtained with these species, presumably because the birds were not able/willing to sustain flight for long enough at such speeds. Both budgerigars (Tucker, 1966; Bundle et al., 2007) and cockatiels (Bundle et al., 2007; Morris et al., 2010) show distinct U-shaped *P*i curves, but the slowest speed that they were willing to fly at while wearing a face mask was 5 m/s. However, it seems certain that slower velocities, including hovering, would have increased their aerodynamic flight costs even further. A study of Anna's and Allen's hummingbirds (*Calypte anna* and *Selasphorus sasin*, respectively), flying between 0 and 14 m/s, showed that there was a distinct *P*i minimum at intermediate speeds. Energetic costs during hovering and faster speeds were increased by around 30–40% (Clark and Dudley, 2010), while even relatively slow but backward flights showed a reduction of around 20% over that of hovering (Sapir and Dudley, 2012). The depth of the curve appeared to be slightly increased in birds with higher wing loadings, which was also more typical of males.

Figure 46.13 illustrates an allometric plot of the available data for the minimum *P*i of seven species of birds during forward flapping flight in wind tunnels (Tucker, 1968b, 1972; Bernstein et al., 1973; Butler et al., 1977; Torre Bueno and Larochelle, 1978; Gessaman, 1980; Hudson and Bernstein, 1983) and it demonstrates two interesting features. First, on average, the minimum *P*i (after adjusting for the drag of the mask and tubing, where necessary) of the seven species (mass range, 35–480 g) is 9.2 times the BMR calculated for nonpasserine birds (Prinzinger and Hänssler, 1980), and second, it is 2.2 times greater than the *P*i of mammals of similar mass (up to 900 g) running at their maximum sustainable speed (Pasquis et al., 1970). It can be seen from Figure 46.13 that the minimum MR during flight of the hummingbird, *Colibri coruscans* (Berger, 1985), is close (within 20%) to that predicted from the extrapolated regression line for the other seven species of birds. If the value from the hummingbird data is included in the regression analysis, the equation becomes $48.5M_b^{0.69}$, $r^2 = 0.98$, using least-squares regression analysis. The mean *P*i of a 1.8 kg barnacle goose (*B. leucopsis*) flying in a wind tunnel was 102 W, while that of a 2.8 kg bar-headed goose (*A. indicus*) was 135 W (Ward et al., 2002). These results are reasonably similar to the values of 81 and 113 W obtained for the predicted minimum *P*i, determined from an extrapolation of the allometric equation, $\dot{V}_{O_2} = 160M_b^{0.74}$, derived from the

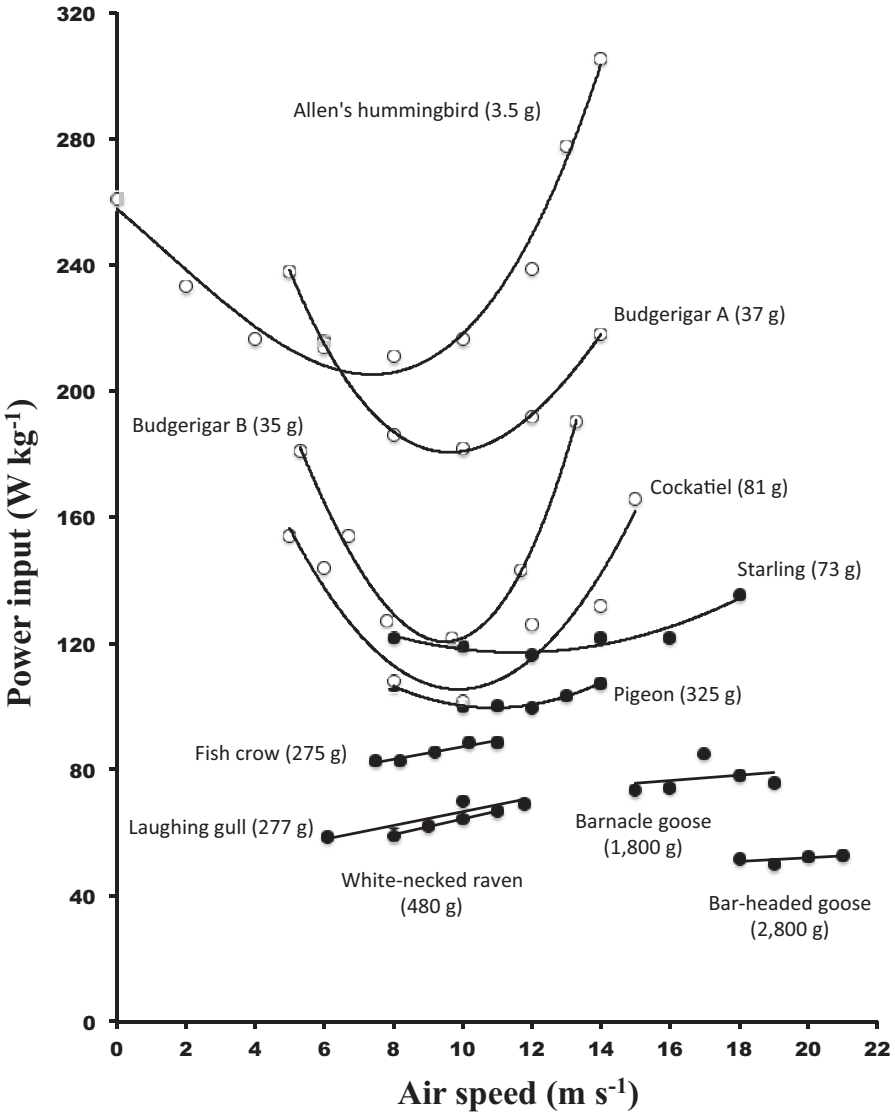

FIGURE 46.12 Power input (W/kg), converted from measurements of rates of oxygen consumption, measured at different air speeds for 10 species of birds during horizontal flapping flight in a wind tunnel. Data taken from: Allen's hummingbird, *Selasphorus sasin* (Clark and Dudley, 2010); cockatiel, *Nymphicus hollandicus*, and budgerigar, *Melopsittacus undulatus* A (Bundle et al., 2007); budgerigar B (Tucker, 1968a,b); European starling, *Sturnus vulgaris* (Ward et al., 2001); pigeon, *Columba livia* (Rothe et al., 1987); fish crow, *Corvus ossifragus* (Berstein et al., 1973); laughing gull, *Leucophaeus atricilla* (Tucker, 1972); white-necked raven, *Corvus albicollis* (Hudson and Bernstein, 1983); barnacle goose, *Branta leucopsis*; and bar-headed goose, *Anser indicus* (Ward et al., 2002).

seven species of birds flying in a wind tunnel (Butler, 1991), recalculated using RMA regression (see above). In addition, using the cardiovascular modeling approach of Bishop and Butler (1995), Butler et al. (1998) estimated the minimum $\dot{V}_{O_2}$ of premigratory barnacle geese (average $M_b = 2.3$ kg) to be around 99 W. The relatively small errors between experimental measurements and these various predictions for flight costs, whether extrapolated toward smaller or larger species using allometric equations, or applying cardiovascular modeling approaches (Bishop and Butler, 1995; Bishop, 1997), suggest that the measurement of *P*i is reasonably reliable across different studies.

46.3.3.3 To flap or not to flap: that is the question

The nature of flapping flight itself, or whether to utilize a specific type of "gait" (flap-glide or flap-bound), or to specialize in soaring and gliding for as long as possible,

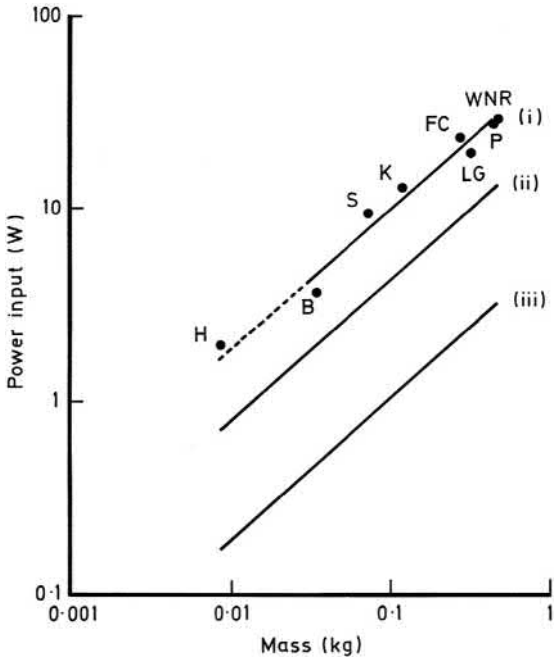

FIGURE 46.13 The relationships between power input (*P*i) and body mass, M_b, using least-squares regression analysis for (i) seven species of birds during forward flapping flight in a wind tunnel; *B*, budgerigar *Melopsittacus undulatus*; *FC*, fish crow *Corvus ossifragus*; *K*, American kestrel *Falco sparverius*; *LG*, laughing gull *Larus atricilla*; *P*, pigeon *Columba livia*; *S*, starling *Sturnus vulgaris*; *WNR*, white-necked raven *Corvus cryptoleucus*. Minimum values of power input (*P*im) were used to construct this curve and $Pim = 50.7M_b0.72$; (ii) small mammals during maximum sustainable exercise where $Pi = 22.6\ M_b0.73$ (data from Pasquis et al., 1970); and (iii) resting nonpasserine birds where $Pi = 5.5\ M_b0.73$ (data from Prinzinger and Hanssler, 1980). *From P. J. Butler and A. J. Woakes, (1985). Also included in (i), the minimum* Pi *of the hummingbird* Colibri coruscans *during forward flapping flight in a wind tunnel (H) From Berger (1985).*

has been covered to various degrees in the previous sections. However, a number of birds, especially seabirds, have a more variable strategy in which they constantly vary the ratio (flapping burst duty cycle) between relatively short periods of flapping and short periods of gliding within a limited period of time (the duty cycle). Of course, an individual bird can also vary the frequency and amount of effort exerted (amplitude) in each flap, in order to modulate the wing kinematics and, thereby, the aerodynamic *P*o.

One of the best examples of the complex temporal variations seen in the flapping patterns of birds, along with the detailed fine tuning of specific wing kinematics, is exhibited during the foraging flights of the Manx Shearwater (*P. puffinus*) in the Irish Sea (Spivey et al., 2014). This species has a characteristic pattern of alterations between time spent flapping and time spent gliding, which is frequently changing within a fairly short period of time (the duty cycle). The duty cycle length typically varied between 0.5 and 6 s (median 2.55 s), with the proportion of time spent actively flapping ranging from 20 to 80% of the time. When experiencing moderately strong cross-winds of greater than 8 m/s (Gibb et al., 2017) that were optimal for slope soaring and wing sailing close to the waves, the Shearwaters tend to increase the length of their duty cycle time while also decreasing the flap ratio down to as low as 7%. Very high flap duty cycles were only seen during ascending flights when birds visited their nesting island, or when they were exposed to strong headwinds. Notably, higher flap duty cycles correlated with decreased duty cycle lengths, but f_w and body amplitude movements were only moderately elevated. Hence, more than a threefold moderation of biomechanical *P*o could be achieved by adjusting the flap duty cycle (Spivey et al., 2014), with only a small potential contribution from changes to flap frequency (between 6 and 6.5 Hz) and wing amplitude (as indicated by DBA varying between 7 and 9 m/s/s) (Figure 46.14A), which are only weakly correlated with each other. This may be a general characteristic of the flight of the larger Procellariiformes (Shearwater and Albatross) species that are optimized for utilizing energy available from their windscape environment. Although Black-browed Albatrosses only flapped for around 4.6% of the time in flight, with a typical f_w of 3.5 Hz, heart rate was linearly correlated with the number of wing flaps per minute during cruising flight (Sakamoto et al., 2013).

Like the Manx Shearwater, the Great Frigatebird also had a very constrained f_w (between 2.2 and 2.8 Hz), when it was not soaring and gliding (Weimerskirch et al., 2016). However, in contrast to the Shearwater, DBA varied over a much larger range (typically between 2 and 8 m/s/s), with no correlation with the flap frequency, indicating that amplitude modulation was the main contributor to biomechanical *P*o when flapping, rather than fine tuning of the flap duty cycle ratio (Figure 46.14B). In further contrast with both of these species is the flight of the bar-headed goose which, like most members of the Anseriformes (swans, geese, and duck), fly with almost continuous flapping behavior in the wild. This species demonstrates a third pattern of wing kinematics (Bishop et al., 2015), as it varies *P*o through a combination of both frequency (3.5−4.5 Hz) and amplitude (DBA varying between 4 and 8 m/s/s) modulation and these two variables are very tightly correlated (Figure 46.14C). As might be expected, heart rate is also highly correlated with both f_w and DBA, thus confirming their regulation of both biomechanical *P*o and metabolic *P*i (Bishop et al., 2015).

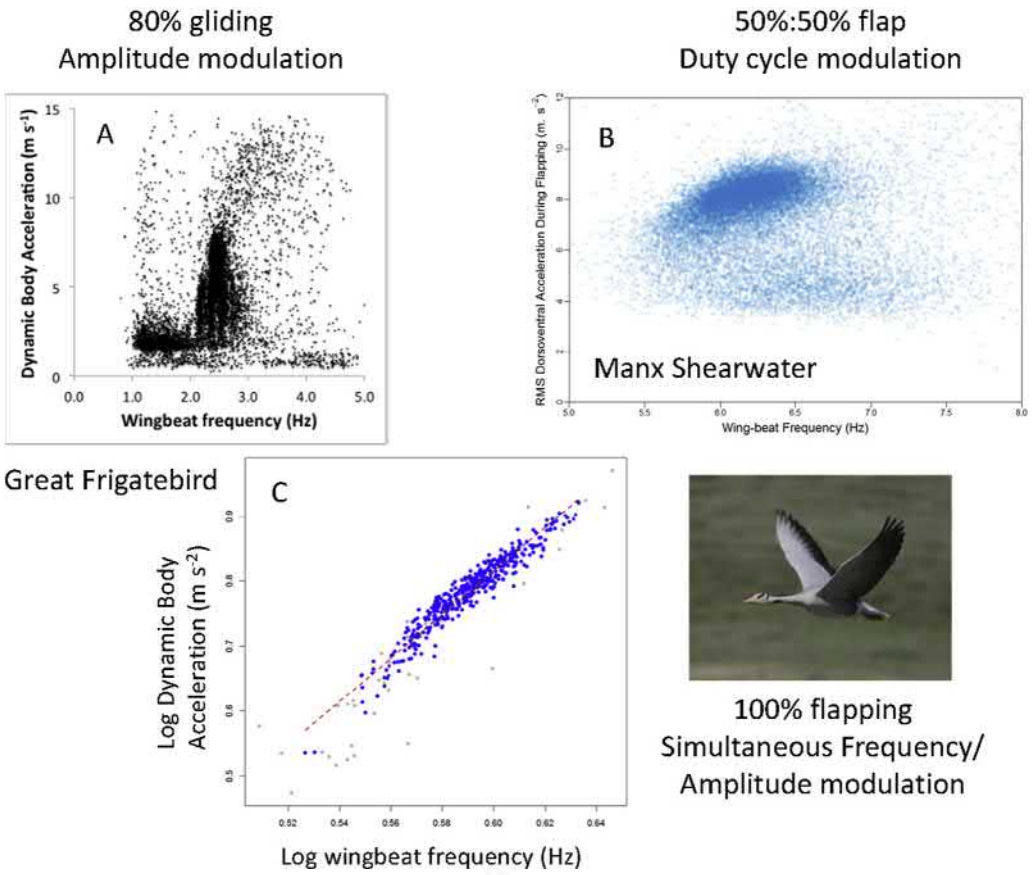

FIGURE 46.14 Wingbeat frequency plotted against Dynamic Body Acceleration for (A) Great Frigatebird, (B) Manx Shearwater, and (C) Bar-headed geese. *Modified from Weimerskirch et al. (2016), Spivey et al. (2014) and Bishop et al. (2015).*

46.3.3.4 Hovering flight and hummingbirds

As discussed above, hovering flight should be relatively costly, at least compared to intermediate air speeds. While this is the case for muscle *P*o, very few species of birds can sustain hovering in still air for long enough so that *P*i can be accurately determined (usually by measuring the rate of oxygen consumption). Only hummingbirds have been studied in which $\dot{V}_{O_2}$ for both hovering and forward flapping flight has been determined for the same bird (Berger, 1985; Clark and Dudley, 2010; Sapir and Dudley, 2012). These studies show that there was a reasonably small, but significant, difference in *P*i between the two forms of flight (Figure 46.12).

The relationship describing the interspecies allometry of hummingbird flight performance, with their unique wing kinematics, has generally been considered to be different from that calculated for all other volant species of bird, with their more conventional flapping motion (Butler, 1991). The DEE of 17 species of hummingbirds was measured with DLW and shown to scale as $\text{DEE} = 115M_b^{0.98}$ ($\text{DEE} = 110M_b^{0.96}$ when accounting for phylogenetic relatedness), while that for all other bird species scaled as $\text{DEE} = 224M_b^{0.68}$ (Shankar et al., 2020). Similarly, for nine species of hummingbirds (Butler, 1991; Wolf and Hainsworth, 1971; Wells, 1993a), hovering $\dot{V}_{O_2} = 449M_b^{0.90}$, $r^2 = 0.94$, and appeared to be similar to the estimates for the minimum oxygen consumption required for the forward flapping flight of hummingbirds, $\dot{V}_{O_2} = 314M_b^{0.90}$ (Bishop and Butler, 1995), but with a smaller intercept. These relationships compare to the scaling for nonhummingbird species during forward flight in a wind tunnel, $\dot{V}_{O_2} = 160M_b^{0.74}$ (Butler, 1991). Interestingly, these two allometric trends for hummingbirds and all other avian species cross over at approximately 15g M_b, which is very close to the size of the largest hummingbird species (*Patagona gigas*). Thus, below this body size, the mass-specific cost of forward flight is estimated to be less for hummingbirds using their unique wing kinematics than for conventional flapping fliers, while above this weight, conventional wing kinematics appear to have the advantage. However, a recent paper by Groom et al. (2018), which also accounts for phylogenetic relatedness, suggests that the energetic scaling relationship during hovering for 25 species of hummingbird is only $\dot{V}_{O_2} = 175M_b^{0.76}$, which is rather similar to forward

flight for birds in general and is difficult to reconcile with the above hypothesis. This study also makes the interesting observation that f_w was the primary scaling variable that was linked to hovering costs ($\dot{V}_{O_2} = c\, f_w^{-1.05}$, $r^2 = 0.76$), with energy cost per wingbeat scaling with M_b as $\dot{V}_{O_2} = c\, M_b^{1.4}$ ($r^2 = 0.94$), while wing loading was not significant (Groom et al., 2018).

The classic work of Chai and Dudley (1995, 1996) showed the remarkable performance of hovering hummingbirds when challenged with hypodense heliox, helium, and normal air atmosphere mixtures. Their results from 1995 show that hummingbirds gradually reduced their hover feeding time from around 25s down to 10s, when air density went from sea level to a simulated height of some 6000 m. Surprisingly, their $\dot{V}_{O_2}$ only appeared to increase between 15 and 36% between the four individual birds (although this was difficult to measure), while wingbeat amplitude increased by 20–24% and f_w by only 4–10%. Under these conditions of a normoxic but hypodense atmosphere, failure to hover was ultimately determined by a biomechanical limitation (although flight times had also significantly reduced) as the wing stroke amplitude approached 180 degrees. The subsequent work, showed that under hypoxic and hypodense conditions, failure could be induced at a higher air density (63% of sea level), with lower stroke amplitude (around 168 degrees), but with oxygen availability at only 12%, indicating insufficient oxygen supply as the cause at an equivalent altitude of around 4500 m or 15,000ft.

46.3.3.5 Scaling of flight muscle efficiency and elastic energy storage

The efficiency with which the flight muscles can produce mechanical power from chemical energy is of great physiological significance as it determines the overall energy required by the animal during exercise. Any excess heat must be lost to the environment in order to prevent hyperthermia. However, in order to estimate efficiency, it is necessary to measure both the *P*i and the *P*o of the flight muscle. As pointed out by Alexander (2005), determination of *P*o generally involves calculations which add a good deal of uncertainty, particularly for flying organisms. Thus, it seems sensible when reporting on the mechanochemical conversion efficiency of flight muscles, to refer to their "apparent" efficiency calculated when specifically combining particular values for aerobic *P*i and *P*o (Bishop, 2005). Pennycuick (1975) recommended that the value of the mechanochemical conversion efficiency of avian flight muscles should be around 0.23 (or 23%) and treated as a constant. This was based on the determination of partial efficiency (i.e., the change in *P*o/change in *P*i) during the flight of budgerigars, laughing gulls, and fish crow (Tucker, 1972; Bernstein et al., 1973), in which partial efficiency ranged from 19 to 30%. However, this runs counter to the more general observation that locomotory muscles for various vertebrate (Alexander, 2005) and invertebrate (Askew et al., 2010) groups exhibit muscle conversion efficiencies that scale positively with M_b and negatively with respect to contraction frequency. Theoretically, it should not be possible for muscle fibers to operate with an overall -efficiency greater than 28% (Rall, 1985) and, in practice, muscle fibers of larger mammals appear to operate with maximal efficiencies of between 20 and 25% (Taylor, 1994).

By using detailed kinematic and morphological analyses, Wells (1993a) calculated an estimate for *P*o (100 W/kg) during normal hovering of the broad-tailed hummingbird (*Selasphorus platycercus*) based on the aerodynamic model of Ellington (1984). $\dot{V}_{O_2}$ was measured as 50 mL/g h, which gave an estimated efficiency of 9–11% (assuming perfect elastic storage of energy). By adding weights to the birds, Wells (1993b) determined that maximum *P*o of the pectoral muscles for this species during hovering was around 117 W/kg and that the efficiency remained approximately 10%. Using the novel and elegant method of flying ruby-throated hummingbirds (*Archilochus colubris*) in an increasing atmosphere of He/O_2, Chai and Dudley (1995) estimated maximum *P*o to be 133 W/kg, with $\dot{V}_{O_2}$ measured as 62 mL/g h, and efficiency of around 10% regardless of the intensity of the flight "effort." The above calculations include an allowance of 10% for the cost of cardiorespiratory function (Tucker, 1973; Pennycuick, 1989), but there is no allowance for BMR. However, taking this into account (Krüger et al., 1982) only increases efficiency by approximately 1% in both studies. They also only studied very small species of hummingbirds with M_b of around 4 g. The recent study by Groom et al. (2018) extended the size range and included 12 species of hummingbird (4 taken from the literature). They calculated a phylogenetically adjusted positive scaling with M_b of Efficiency $= 7.6\% M_b^{0.38}$, with estimates ranging from 10 to 19%, which were inversely related to f_w. It should be noted that if we extrapolate this relationship to that of the largest species of hummingbird at 17.5 g, *P. gigas*, it would have predicted an efficiency of 22.5% at a f_w of 15 Hz, which is similar to that of elite humans cycling (Carlsson et al., 2020) with a cadence of typically around 1.5 Hz. The median mass for all birds is 38.6g (Blackburn and Gaston, 1994) which would predict an efficiency of 30% using this equation, so we would expect that efficiency might scale differently for birds with more conventional wing kinematics.

Biewener et al. (1992) used calibrated strain recordings from the humerus of flying birds to measure the force and estimate the power generated by the pectoralis muscles. Mean *P*o for three starlings (*S. vulgaris*), flying in a wind

tunnel (for unstated duration), was 1.12 W at an estimated speed of 13.7 m/s and M_b 70−73 g. Torre-Bueno and Larochelle (1978) reported mean *P*i to be 8.9 W for three starlings of mean mass 73 g and flying in a wind tunnel for 30 min over a range of speeds from 8 to 18 m/s. Thus, after subtracting BMR (Prinzinger and Hanssler, 1980) and allowing 10% for the cost of cardiorespiratory function, the estimated efficiency of the flight muscles for this species is 15.4%. Ward et al. (2001) estimated that flight muscle efficiency in two starlings flying in a wind tunnel varied between 13 and 23% depending on the bird, the flight speed, and the aerodynamic model used to calculate *P*o. This introduces the hypothesis that efficiency may not be a constant and could vary depending on specific kinematics and *P*o. In a second study using strain gauges (Dial and Biewener, 1993), mean *P*o for four pigeons was 10.5 W/kg, with M_b 301−314 g and flying at approximately 8 m/s along a 47 m long corridor. They used a *P*i value of 106 W/kg (cf. Rothe et al., 1987) to estimate flight muscle efficiency as 11.2%. However, Rothe et al. (1987) estimated that their measurements of *P*i were elevated by between 15 and 30% by the presence of the mask and tubing. If a mean overestimate of 22% is assumed, the actual value of *P*i would be 87 W/kg, which would give an efficiency of 13.8%. If the value of *P*i, after adjustment for the drag on the mask and tube, is taken from Butler et al. (1977) for pigeons of mean mass 442 g and flying at 10 m/s (61 W/kg), a flight muscle efficiency power of 19.9% is obtained. The latter estimate would appear more credible, given the M_b of the pigeons and their relatively lower f_w. Hedh et al. (2020) used PIV to measure *P*o and ^{13}C NaBi to measure *P*i in blackcaps weighing 17−22 g and found an overall efficiency of 21%, which was equivalent to a muscle conversion efficiency of 30% after accounting for BMR and cardiorespiratory costs. We can see that measuring, or estimating, flight muscle efficiency often involves a number of data uncertainties and assumptions.

Bishop (2005) attempted to estimate the maximum $\dot{V}_{O_2}$ and, ultimately, flight efficiency for 15 species of birds studied during migratory climbing flights by Hedenstrom and Alerstam (1992). The estimated *P*i was based on the cardiovascular modeling approach (Bishop and Butler, 1995; Bishop, 1997) and was then compared to the estimated aerodynamic *P*o based on the model of Pennycuick (1989). This analysis suggested that the "apparent" mechanochemical efficiency of the avian flight muscles scaled allometrically with M_b, as $30\%M_b^{0.14}$ (M_b in Kg) (Figure 46.15), or $11.6\%M_b^{0.14}$ (M_b in g). Applied to hummingbirds of 4 and 17.5 g (see above) would give predictions of 13.8 and 17%, respectively. Applied to median mass for all birds of 38.6 g and to 70 g European Starlings yields 19 and 21.7%, respectively. Thus, these various studies support the hypothesis that there is an increase in overall flight efficiency with an increase in M_b and a decrease in f_w or strain rate (cf. Rayner, 1990). A phylogenetically controlled metaanalysis of the metabolic flight costs of both birds and bats (Guigueno et al., 2019) also concluded that overall flight efficiency increased with increasing M_b, but also decreased with flight speed (counter to the conclusions of Ward et al., 2001). However, the details of these relationships are a slightly controversial subject due to the potential errors in measuring and calculating *P*i and *P*o. In particular, the fact that the larger species of birds (e.g., great than approximately 1 kg) appear to have efficiencies of over 30% is a significant issue. Of course, it is possible that the muscle efficiencies of larger species of birds do eventually reach a plateau and this would provide a further limitation to the evolution and

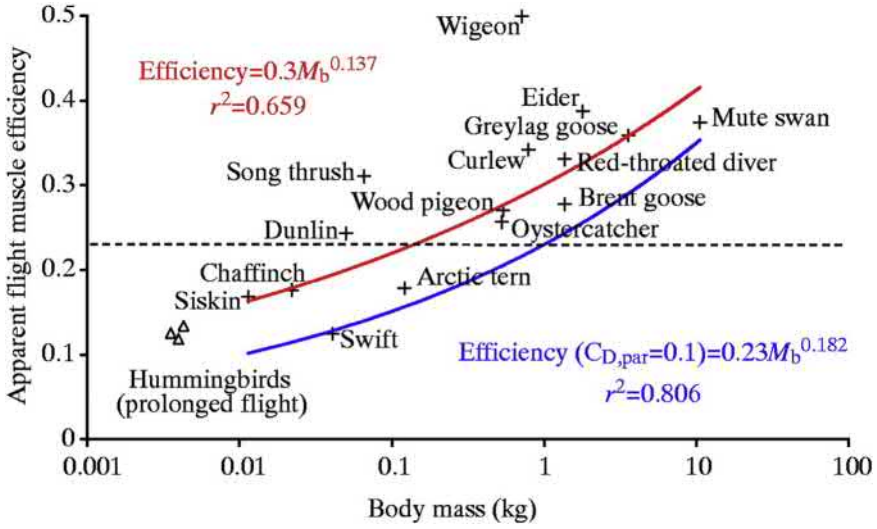

FIGURE 46.15 Estimated "apparent" flight muscle mechanochemical efficiency plotted against body mass (kg) for 15 bird species during migratory climbing flights over Sweden (see Hedenström and Alerstam, 1992). The wigeon, *Anas penelope*, is left out of the analysis as an outlier. The red regression line is based on the estimated sustainable biomechanical power output continuously available, calculated using default values for the parasite body drag coefficient (**C**D,par) ranging from 0.25 to 0.4 (Pennycuick, 1989). The blue regression line is based on a value for CD,par of 0.1. Estimates of efficiency for three species of hummingbirds (**Δ**) are also plotted. *Based on Bishop (2005).*

functional ecology of flapping flight performance. However, the uncertainties in the various calculations of aerodynamic and biomechanical *P*o are likely to be a significant confounding factor.

Typically, aerodynamic models such as those of Pennycuick (1975, 1989) and Rayner (1979) do not include the costs of accelerating and decelerating the wing during each cycle. It is argued that the inertial costs are recovered aerodynamically by assuming that the energy used to accelerate the wing can be recovered by doing either useful aerodynamic work at the end of the wing stroke or by using elastic storage of wing kinetic energy to reaccelerate the wing in the following beat. Additionally, it may be that the inertial costs are relatively small during forward flight at medium to fast speeds. Thus, Wells (1993a), Chai and Dudley (1995), and Groom et al. (2018) tend to favor calculations that hummingbirds are able to store the "inertial energy" and interpret *P*o assuming "perfect elastic storage" following each downward beat. This assumption reduces the value for the calculation of the power required to fly, especially for small species of birds that have high f_w. Bird flight muscles lack any associated specialized elastic components, such as long tendons, so any elastic component is likely to be a property of the cross-bridges and connective tissue of the muscle (Alexander and Bennett-Clark 1977). Dial et al. (1987) measured the electrical activity of the pectoralis muscles of the pigeon during flight and demonstrated that the pectoralis muscles are active before the end of the upstroke of the wings and could act like an elastic spring (Goslow and Dial, 1990).

Van den Berg and Rayner (1995) suggest that it may be necessary to consider the inertial cost. They estimated that the inertial power requirement should scale as approximately 5.8 $M_b^{0.80}$ (allowing for a 25% reduction due to wing flexion on the upstroke). Whatever the merits of each side of the debate, it seems possible that perfect elastic storage may prove to be unrealistic. Thus, any increment of the inertial costs that must be met by the flight muscles will increase the estimate of the "apparent" efficiency of the flight muscles. If "near" zero elastic storage is correct, then the inertial costs would dominate the total cost of hovering flight in hummingbirds (Spedding, 1994).

46.4 The flight muscles of birds

46.4.1 Flight muscle morphology and fiber types

The flight muscles of birds are structurally similar to the striated muscles of other vertebrates and consist of large numbers of long fibers, or cells, aligned essentially in parallel (Figure 46.16A). Each fiber can have a distinct biochemical character. At its simplest, each fiber can be specialized either for aerobic or anaerobic energy consumption, they can vary in diameter and cross-sectional area, and are supplied with various metabolites and oxygen via a network of capillaries (Figure 46.16B). Different species of birds have different amounts of flight muscle with respect to M_b (Hartman, 1961), termed the flight muscle: mass ratio by Marden (1987), and these muscles are composed of four main cell or fiber types (cf. Rosser and George, 1986a), so called slow oxidative fibers (SO, Type I), fast oxidative glycolytic fibers (FOG, Type IIa), fast glycolytic fibers (FG, Type IIb), and fibers which are intermediate (I, Type IIab) in their oxidative ability between the FOG and FG fibers.

Table 46.1 lists the major characteristics of these different fiber types. Essentially, the SO fibers have relatively slow rates of shortening, but are relatively efficient in producing force during isometric contractions, utilize oxidative metabolic pathways in the biosynthesis of energy-rich adenosine triphosphate (ATP), and are resistant to fatigue. FOG fibers are also capable of oxidative metabolism and resistance to fatigue, but can also use carbohydrates as a fuel during anaerobic metabolism, have relatively faster rates of shortening, and are relatively efficient in producing force while shortening in length. FG fibers are susceptible to fatigue and are restricted to anaerobic metabolism of carbohydrates, but produce more power per unit mass of muscle than SO and FOG fibers. One reason for the latter is that they contain a lower volume fraction of mitochondria and associated structures and, therefore, have room for more myofibrillar proteins.

The function of SO fibers is considered primarily to be of advantage in postural muscles (e.g., in the back and neck muscles) and also in the legs during rest, due to their economic production of force during isometric contractions. In birds, SO fibers have only been found in the deep layers of the pectoralis muscles and a few small muscles of the wing (coracobrachialis, triceps, and extensor metacarpi radialis) of a limited number of species (Talesara and Goldspink, 1978). The latter are generally adapted for gliding and soaring modes of flight, that is, species belonging to the avian orders of the Procellariiformes, Pelecaniformes, Ciconiiformes, Accipitriformes, Pelecaniformes, and the Gruiformes (Rosser and George, 1986a; Meyers, 1993; Rosser et al., 1994; Meyers and Mathias, 1997). Thus, Rosser et al. (1994) found that the deep "belly" of the pectoralis muscle of the American White Pelican (*Pelecanus erythrorhynchos*) is composed exclusively of SO fibers. Other authors have also reported SO fibers in the deep layers of the pectoralis muscles of the turkey vulture *Cathartes aura* (Rosser and George, 1986b) and red-tailed hawk *Buteo jamaicensis* (Rosser and George, 1986a) and associated with their soaring behavior. The SO fibers detected in various muscles of the double-crested cormorant, *Phalacrocorax auritus*, were considered to function during their wing-spreading posture frequently

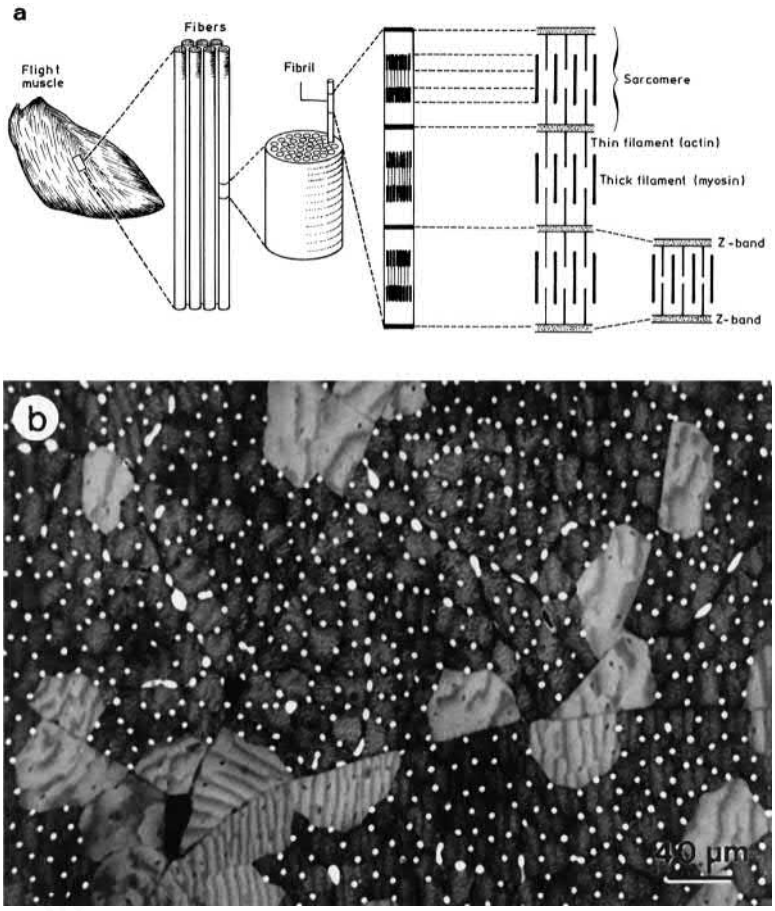

FIGURE 46.16 (A) Schematic illustration of the structure of a bird's pectoral muscle. The whole muscle is composed of many different fibers or cells, each of which consists of many fibrils and each fibril contains many thin actin filaments interspersed between thick myosin filaments. These filaments are organized into sarcomeres, which shorten during contraction as the actin and myosin filaments slide past each other. (B) Light micrograph of a 1 µm thick transverse section of pectoralis muscle of the pigeon *Columba livia*. Fast oxidative glycolytic fibers (dark and small) and fast glycolytic fibers (pale and large) can be clearly identified. Capillaries are empty following vascular perfusion fixation. Bar = 40 µm. *(A) Modified from K. Schmidt–Nielsen (1997). (B) From Mathieu-Costello (1991).*

TABLE 46.1 Simplified characteristics of muscle fiber types.

Property	Slow Oxidative SO (Type I)	Fast Oxidative Glycolytic FOG (Type IIA)	Fast Glycolytic FG (Type IIB)
Speed of contraction	Slow	Medium-fast	Medium-very fast
Aerobic capacity	High	High	Low
Anaerobic capacity	Low	Moderate	High
Capillary supply	Good	Good	Poor
Triglyceride stores	High	Medium-high	Low
Glycogen stores	Medium	Medium-high	Medium-high
Fatigue resistance	High	High	Low
Cross-sectional area	Small	Small-medium	Medium-large

adopted on land following diving (Meyers, 1997). Similar to the White Pelican, the deep layer of the pectoralis in both the Laysan and Black-footed Albatross (*Diomedea immutabilis* and *Diomedea nigripes*, respectively) consisted of 100% SO fibers, with significant contributions also found in the coracobrachialis cranialis and the extensor metacarpi radialis muscles. This fits with the extreme gliding performance of these species and supports the idea of a tendinous mechanism (the shoulder lock) that limits wing elevation above the horizontal and reduces the energetic cost during long foraging journeys (Pennycuick, 1982; Meyers and Stakebake, 2005). However, it is not always the case that

birds that regularly use soaring and gliding modes, as part of their flight performance repertoire, have specialized in SO fibers to this extent. A study of the histochemistry of the California gull (*Larus californicus*) showed that only relatively low percentages of SO fibers were present in their wing muscles and they completely lacked the deep layer to the pectoralis major muscle typically found in gliding specialists (Meyers and Mathias, 1997).

The most abundant type of fiber to be found in the flight muscles of birds capable of prolonged flapping flight is the FOG (George and Berger, 1966; Rosser and George, 1986a). In general, the flight muscles of small birds are entirely composed of FOG fibers, while larger birds have a mixture of different fiber types. However, there is a large degree of interspecies variation. George and Berger (1966) classified the pectoralis muscle of birds into six groups, with each fiber type listed in order of relative numerical abundance: (1) fowl type (FG, I, FOG); (2) duck type (FOG, FG, I); (3) pigeon type (FOG, FG); (4) kite type (mainly I); (5) starling type (FOG, I); and (6) sparrow type (FOG). While most species can be broadly assigned to one of these groups, there are many exceptions. Clearly, each individual species is adapted to cope with its own unique requirements based on its behavioral ecology, its detailed morphology, and the environmental conditions in which it lives.

Even more importantly, the histochemical classification of muscle fiber types can be misleading from a functional perspective. In reality, the fast-twitch fiber types are arbitrary classifications within a continuum of oxidative to glycolytic potentials, which may also be affected by amount of use (or training). In addition, the term "fast" is also slightly arbitrary, as there is likely to be a continuum for the rates at which the flight muscles are optimized to contract, due to the scaling of f_w with M_b (Pennycuick, 1990, 1996). A small hummingbird may beat its wings at up to 50 Hz, while a large swan may only have a wingbeat of around 2.4 Hz. Therefore, there are likely to be many associated differences in the molecular characteristics of the contractile proteins from different species of birds. As a consequence, the FOG fibers of a hummingbird are not biochemically identical to the FOG fibers of a swan. It is probable that, even within the muscle of an individual bird, the FOG fibers of the deep layers may have slightly different characteristics to the FOG fibers from the more peripheral layers. Rosser and George (1986a) suggest that, given sufficient detailed knowledge about the protein isoforms of muscle, it is conceivable that almost all muscle fibers could be described as a unique subtype.

Despite the difficulties outlined above, it is still possible to draw some interesting conclusions about the functioning of avian flight muscles by quantifying their fiber type compositions. The Galliformes, such as the domestic chicken and the ruffed grouse (*Bonasa umbellus*), have a majority of FG fibers in their pectoralis muscles (Rosser and George, 1986a). This is matched by their relatively small M_h and a low capacity to supply the muscles with oxygen (Bishop and Butler, 1995; Bishop, 1997). These birds are restricted to anaerobic flights of short duration. Typically, Galliformes birds live close to the edges of forests, have relatively short wings and relatively large flight muscles, and escape predation by being adapted for rapid take-off followed by short flights into dense vegetation or into the branches of trees. The South American ecological equivalent of the Old World Galliformes, the Tinamous, also has very small hearts and large flight muscles (Hartman, 1961) and lives on the forest floor.

The Galliformes contrast with their closest relatives, the Anseriformes (the ducks, geese, and swans) (Prum et al., 2015). Although of similar body size, the Anseriformes have relatively longer wings and live in open, uncluttered habitats. Their pectoralis muscles contain a higher proportion of FOG fibers interspersed among the FG fibers, and their relative M_h is also much larger (Magnan, 1922; Hartman, 1961). Thus, their wing morphology determines that they are slightly faster (Rayner, 1988; Pennycuick, 1989), and their muscle physiology and cardiovascular adaptations determine that they are able to prolong these flights over relatively long distances.

The aerobic nature of the flight muscles of some relatively large species of birds, such as the bustards and swans, has an important consequence for the interpretation of the size limitations to flight performance in birds. It is necessary to distinguish between "burst" flight performance and "prolonged" or aerobic flight performance (Marden, 1994) and to compare flight muscles which are adapted for similar types of flight. The data of Marden (1987) and Pennycuick et al. (1989) on the maximum lifting ability of flying animals during take-off refer only to "burst" flight performance, and bird species that have predominantly anaerobic FG flight muscle fibers will be at an advantage during take-off compared to species that have predominantly aerobic FOG muscle fibers.

Caldow and Furness (1993) studied the histochemical adaptations of two ecologically similar seabirds, the great skua (*Catharacta skua*) and the herring gull (*L. argentatus*). They found that both species had FOG fibers exclusively in their pectoralis and supracoracoideus flight muscles, but that the mass-specific activity of both the oxidative and glycolytic enzymes (see below) were higher in the muscles of the great skua and concluded that this adaptation enabled the skua (Stercorariidae) to be a more effective aerial kleptoparasite than the herring gull (Laridae). The mass of the pectoralis muscles is relatively small in the herring gull (12% of M_b), but it has a moderately large M_h (0.9% of M_b), which is consistent with the fact that its flight muscles consist entirely of FOG fibers (Bishop and Butler, 1995).

Hummingbirds are considered the most aerobic of all avian species, with 100% FOG in their pectoralis muscles

and the largest hearts of any species (Bishop, 1997; Welch and Altshuler, 2009). Assessments of their "anaerobic" burst flight performance have been assessed during loading-lifting studies during take-off (Chai and Millard, 1997; Altshuler et al., 2010) and shown that even large species can lift extra weight for a few seconds but that they tend to show a negative scaling of maximum muscle-specific *P*o with M_b. However, very brief bursts of power are also required for foraging and evasive maneuvers during flight and, for hummingbirds, it has been shown that the best predictor of the ability to perform complex turns and maneuvers was load-lifting ability and burst muscle capacity (Dakin et al., 2018). The other key variable was the relative surface area of the bird's wing and, therefore, wing loading.

46.4.2 Biochemistry of the flight muscles

As discussed by Marsh (1981), the sustained, long distance flights performed by many migrating birds require two interacting adaptions: the ability to store sufficient fuel reserves for the flight and the ability to maintain supplies of oxygen and fuel to the working tissues. Due to the very high energy density of lipids (39.3 kJ/g), compared to pure carbohydrates (17.6 kJ/g) and proteins (17.8 kJ/g), the energy for migratory flights is predominantly stored as fat in adipocytes. Thus, adaptations for the efficient oxidation of fatty acids and the potential for a high aerobic capacity are some of the most important features of most avian flight muscles. The relatively high mass-specific energy output required from the flight muscles necessitates high capillary and mitochondrial densities and high levels of mass-specific activities for the associated mitochondrial enzymes (Mathieu-Costello et al., 1992).

Hummingbirds are able to sustain the highest mass specific MRs of any vertebrate (Lasiewski, 1963), and Table 46.2 shows data from Suarez et al. (1986) for the maximum activities of various catabolic enzymes in hummingbird flight muscle. The following enzymes are of particular interest: citrate synthase (CS), as an indicator of general aerobic capacity; 3-hydroxyacyl- CoA dehydrogenase (HAD) and carnitine palmitoyl transferase, as indicators of fatty acid utilization; phosphofructokinase, as an indicator of general glycolytic flux; pyruvate kinase (PK), as an indicator of anaerobic glycolysis; and hexokinase (HEX) and glycogen phosphorylase (GPHOS), as indicators of plasma glucose and intracellular glycogen utilization, respectively. As expected, the flight muscles of hummingbirds have some of the highest catabolic enzyme activities ever measured. In particular, mass-specific CS and the HEX activities are even higher (at 448.4 and 18.4 μmol/g min, respectively) in a subsequent study with a modified extraction procedure (Suarez et al., 1990).

Various studies (Suarez et al., 1986, 1990) indicate that while it is possible for hummingbirds to meet almost all their flight requirements by oxidizing lipid fuel, it is also possible for them to meet the requirements of hovering flight utilizing carbohydrate fuels, and they oxidize glucose and fructose equally well (reviewed by Suarez and Welch, 2017). The latter possibility makes sense given that hummingbirds feed mainly on sucrose-rich nectar

TABLE 46.2 Maximum enzyme activities in the flight muscle and heart of the rufous hummingbird *selophorus rufus*[1].

Enzyme	Flight Muscle	n	Heart	n
Glygogen phosphorylase	31.22±2.5	6		
Hexokinase	9.18±0.31	4	10.08±1.9	4
Phosphofructoknase	109.8±13	6	unstable	
Pyruvate kinase	672.4±27	6	507.3±25	6
Lactate dehydrogenase	230.3±23	6	357.3±30	6
Carnitine palmitoyl transferase	4.42±0.46	6	2.83±0.72	4
3-Hydroxyacyl CoA	97.10±13	6	68.51±10	4
Glutamate-Oxaloacetate Transaminase	1388±70	5	576.4±29	5
Glutamate-pyruvate Transaminase	75.97±6.0	5	16.31±2.2	5
Citrate synthase	343.3±8.8	6	190.3±4.8	4
Creatine kinase	2848±337	5	348.9±59	5
Malate dehydrogenase	3525±331	6	2024±191	6
α-Glycerophosphate dehydrogenase	9.37±2.1	6	8.10±2.2	6

[1]*Values are expressed in μmol/min g wet wt and presented as means±SE; n, number of birds (from Suarez et al., 1986).*

(a disaccharide made of glucose and fructose) and so during the day they would have a good supply of pure carbohydrate direct from the environment. Indeed, the majority of floral nectars are dominated by sucrose, with additional amounts of fructose and glucose, to encourage both bird and bat pollinators (Wolff, 2006). However, for long-term storage, carbohydrates are stored as glycogen (a polysaccharide of glucose) which consists of at least 75% water, thus giving it a relatively poor energy density (4.4 kJ/g). It would not be possible, therefore, to store enough carbohydrates to fuel long-distance flight. In fact, it is unlikely that stored carbohydrate could support hovering flight for around 5 min (Suarez et al., 1990). However, in the short term, it is more efficient to oxidize plasma glucose directly to support flight, due to the 16% lower net yield for ATP resulting from the cost of synthesizing fatty acids from glucose for long-term storage. Indeed, this led these authors to suggest that premigratory hummingbirds should behave as "carbohydrate maximizers" by keeping their foraging flights well under 5 min duration. This would provide efficient foraging while allowing excess glucose to be stored as fat. However, while the availability of plasma glucose may not be limiting for hummingbirds, the majority of bird species may place a higher emphasis on carbohydrate "sparing." Bishop et al. (1995) found that HEX activity was relatively low in the pectoralis muscles of adult premigratory barnacle geese, and similar results have been reported for the pigeon and domestic chicken (Crabtree and Newsholme, 1972) and for the migratory semipalmated sandpiper, *Calidris pusilla* (Driedzic et al., 1993).

Many studies have shown that prior to long-distance flights, such as those performed during seasonal migrations, birds increase in M_b primarily due to the laying down of fat stores (Blem, 1976). This is usually correlated with hypertrophy of the pectoralis muscle in order to increase the power available for take-off and forward flapping flight and species-specific changes in catabolic enzyme activities. While Marsh (1981) found no change in the premigratory activity of CS in the pectoralis muscle of the catbird (*Dumetella carolinensis*), he reported a significant increase in the level of HAD (indicating an increase in the potential for fatty acid oxidation). A similar increase in the ability to oxidize fatty acids was found in the semipalmated and western sandpipers, but the level of CS did not change or decrease (Driedzic et al., 1993; Guglielmo et al., 2002). However, some species of small migratory passerine birds do appear to show an increase in the premigratory activity of both CS and HAD (Lundgren and Kiessling, 1985, 1986; McFarlan et al., 2009), while CS activity in the premigratory barnacle goose was around 30% greater than that of postmolting birds approximately 4 weeks earlier in the season (Bishop et al., 1995).

Avian muscle capillarity and diffusion distances have been studied in a variety of different tissues, but no significant allometric trends with respect to different M_b were found for any of the variables measured (Snyder, 1990). However, Snyder (1990) did find a small but significant difference in the capillary to fiber ratio (C/F) between the aerobic fiber types (1.8 caps/fiber) and the glycolytic fibers (1.4 caps/fiber). Capillary density and diffusion distances are primarily determined by the cross-sectional area of the individual fibers, and the author argues that there may be little selective advantage in having a C/F greater than 2.0. Studies on avian pectoralis muscles have generally resulted in similar conclusions. Mathieu-Costello et al. (1992) found that the C/F of the rufous hummingbird (*Selasphorus rufus*) is only 1.55 caps/fiber compared to that of the pigeon, which is 2.0 caps/fiber (Mathieu-Costello, 1991). However, fiber diameter and the cross-sectional area are much smaller in the hummingbirds than in pigeons and, therefore, the capillary density per unit area is much higher in hummingbirds. Mathieu-Costello et al. (1992) consider that one of the most important determinants of the rate of oxygen flux in aerobic fibers is the size of the capillary-to-fiber interface (i.e., the capillary-surface-per-fiber-surface area). However, in order to measure this feature accurately, it is necessary to standardize with respect to both the sarcomere length and the degree of tortuosity of the capillaries.

46.4.3 Neurophysiology and muscle function

Birds are capable of synchronizing the extension of the elbow and wrist joints of the wing during flapping flight, using automated coordinating mechanisms involving skeletal and muscular adaptations (Vazquez, 1994). However, the power and thrust generated during the wingbeat cycle, and the complex kinematics of the wing during the flapping flight of different species, require an active neuromuscular control mechanism and specialized adaptations of the flight muscles.

The detailed movements of the wing during flight actually involve a large number of different muscles (Dial et al., 1991; Dial, 1992a) and their differential (Dial, 1992a; Tobalske and Dial, 1994; Tobalske, 1995; Tobalske et al., 1997) or regional (Boggs and Dial, 1993) activation. For most studies, however, it is sufficient to focus on the functioning of the largest flight muscles, pectoralis and supracoracoideus. Dial (1992b) showed that birds were unable to take-off or perform controlled landings without the use of the muscles of the forearm, but they could sustain level flapping flight following an assisted take-off.

The largest flight muscle, the pectoralis major, can be divided into two anatomical parts (Figure 46.17), the sternobrachialis (SB: which is superficial and lies along the sternum) and the thoracobrachialis (TB: which forms a deep layer lying along the sternum), and these are separated by the membrana intermuscularis (Dial et al., 1987). The

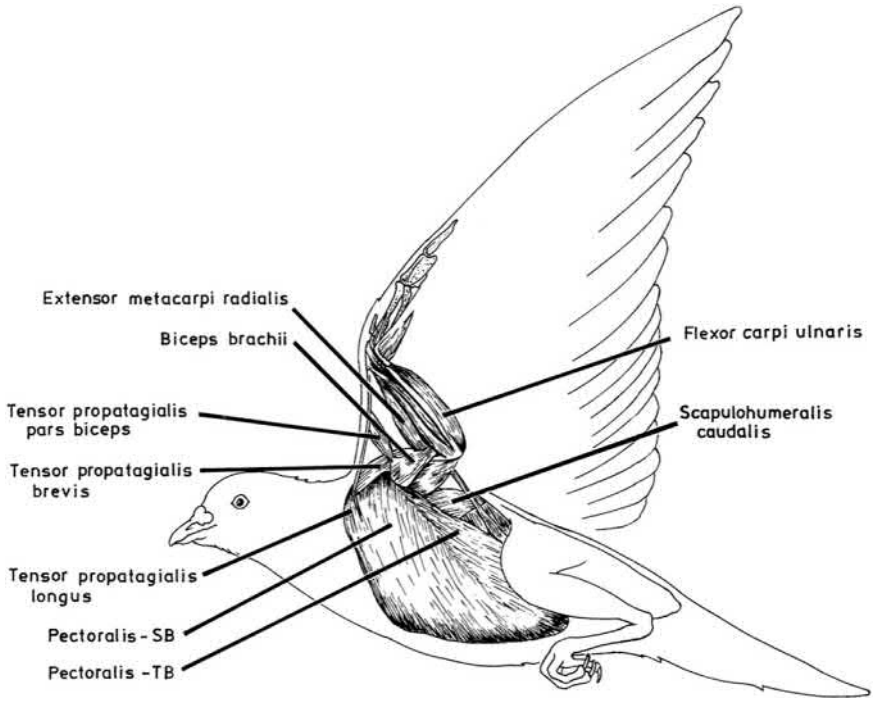

FIGURE 46.17 Illustration of the superficial flight muscles of the wings of a pigeon, *Columba livia*. The supracoracoideus muscles (not shown) are primarily used to power the upstroke and lie directly under the larger pectoralis muscles, which primarily power the downstroke. *Modified from Dial (2003).*

SB is primarily innervated by the rostral nerve branch and the TB by the caudal nerve branch of the brachial ventral cord. In the pigeon, the fibers within the SB and TB have different orientations (Dial et al., 1987), while the SB has a lower percentage of FOG fibers and relatively more FG fibers, and the TB is primarily made up of FOG fibers (Kaplan and Goslow, 1989). Thus, the histochemical analysis and the neuroanatomy support the view that the pectoralis major is made up of at least two functional subunits, each with a potential for independent action on the wing during flight (Dial et al., 1987, 1988; Kaplan and Goslow, 1989; Goslow and Dial, 1990). Dial et al. (1987) showed that both the SB and TB muscles of the pigeon were maximally activated during take-off or during large-amplitude wingbeats. However, during slow flight, the SB was relatively more important and during low-amplitude wingbeats, the activity of the TB could be almost zero. Interestingly, Dial et al. (1987) also indicate that there is a gradual reduction of large-amplitude electromyogram (EMG) spikes during the transition from take-off to level flight and that they reappear during landing. This supports the hypothesis that FG fibers are derecruited during level flight.

Tobalske et al. (1997) studied the neuromuscular control and wing kinematics of the black-billed magpie, both in the wild and while flying in a wind tunnel, and showed that this species has a particularly complex flight style, consisting of alternating high- and low-amplitude wingbeats, and occasional brief glides. This wide study found that the pectoralis consisted of FOG and I fiber types, as in the woodpecker (see below), and that the I fiber types were probably only recruited during the high-amplitude wingbeats. EMG recordings were made from six different wing muscles, and all showed that the relative intensity of the EMG signal exhibited a U-shaped output with respect to flight speed. Minimum intensity was recorded around 4.4 m/s and the highest was recorded during hovering and the top speed of 13.4 m/s. The pectoralis and the biceps brachii muscles showed strong activity during the end of the upstroke and the beginning of the downstroke, while the supracoracoideus, the humerotriceps, the scapulotriceps, and the scapulohumeralis caudalis were important during the end of the downstroke and the beginning of the upstroke.

A more detailed study of the EMG activity of 17 different muscles in the shoulder and forelimb of the pigeon during 5 different modes of flight was conducted by Dial (1992a). He concluded that the temporal pattern of activity did not vary much between different modes of flight, but that the intensity of the EMG signal was very important in determining the role of the different muscles during different modes of flight (Figure 46.18).

Tobalske (1996) studied the muscle composition and wing morphology of six different species of woodpecker, ranging in mass from 27 to 263 g, and related morphology to the scaling of intermittent flight behavior. Intermittent flight consists of regular alternation between periods of flapping and nonflapping. During the nonflapping phases,

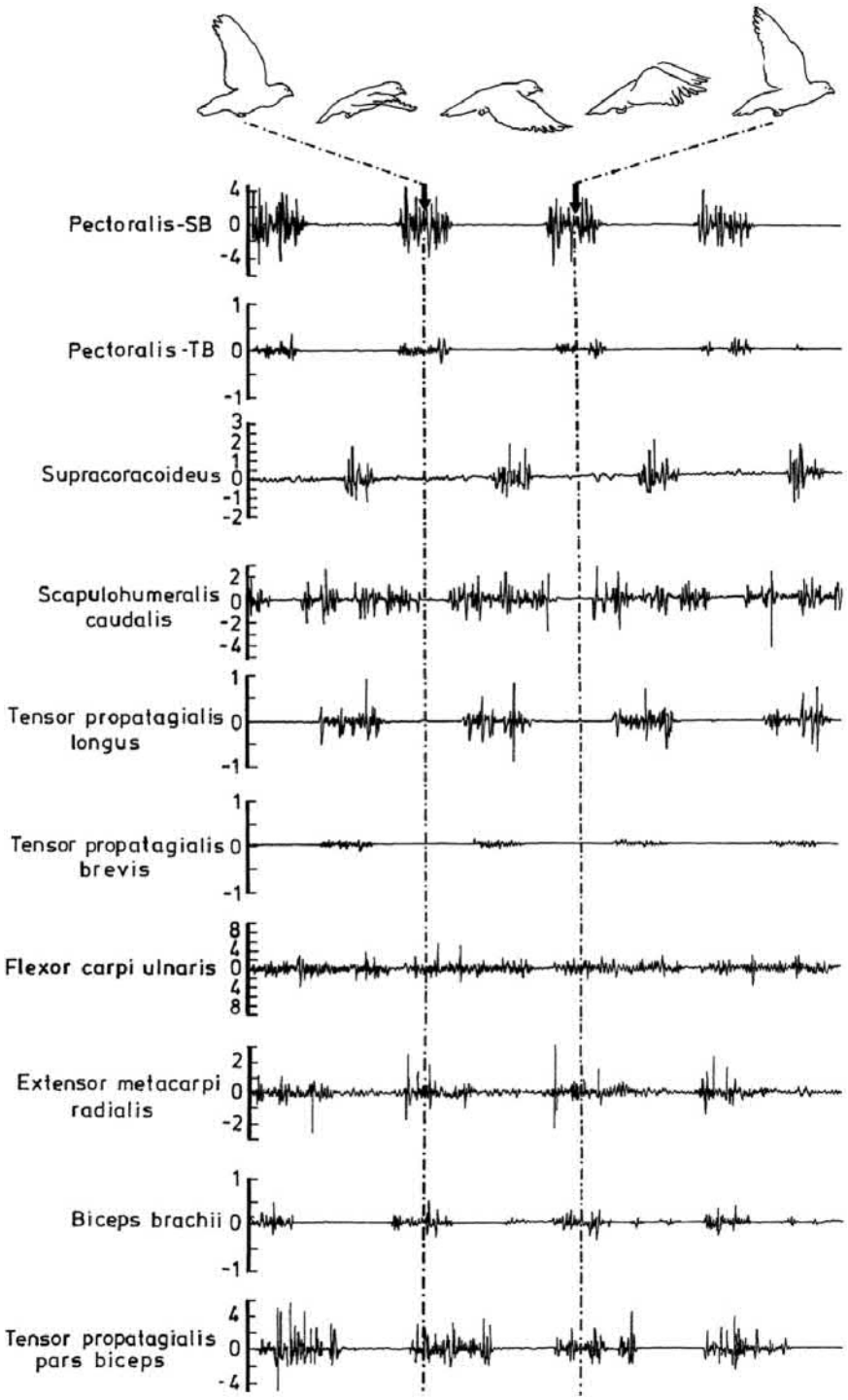

FIGURE 46.18 Electromyogram (EMG) signals recorded during level flapping flight from the various muscles of a pigeon, *Columba livia,* illustrated in Figure 13. EMG activity is presented with reference to the phase of the wingbeat cycle, with each downstroke indicated by the *vertical dashed line*. *Modified from Dial (2003).*

the bird's wings are either held folded at its side (flap-bounding flight) or held fully extended (flap-gliding flight). Biomechanical and physiological analyses suggest that intermittent flight is energetically efficient relative to continuous flapping (Rayner, 1985a), particularly for small species that have high f_w which are relatively "fixed" (Rayner, 1985a). Only FOG and I fiber types were found in these six species of woodpecker, with small species having almost exclusively FOG fibers in their pectoralis muscles, while species >100 g tended to have significant amounts of

I fibers. All six species were capable of exhibiting flap-bounding behavior, although the percentage of time spent flapping increased with increasing M_b. The empirical observations of Tobalske (1996) greatly exceed the theoretical considerations (Rayner, 1985a) that the upper limit for flap-bounding flight should be around 100 g of M_b.

However, the heterogeneous scaling of the fiber type composition of the pectoralis is likely to be one reason why the theoretical figures underestimate bird flight performance (Tobalske, 1996). FG and I fibers have the potential to produce more force per unit area than FOG fibers and, therefore, can produce more power for a given degree of fiber shortening and frequency. Thus, Tobalske (1996) argued that the positive scaling of the percentage and cross-sectional diameter of I fibers in the pectoralis of woodpeckers may be a direct result of the positive scaling of the power required for flight compared to the power available from the flight muscles (cf. Pennycuick, 1989; Marden, 1987; Ellington, 1991). Interestingly, among woodpeckers, the scaling of relative heart muscle mass is negative relative to increasing M_b (Hartman, 1961), which matches the decline in FOG content of the flight muscles. Thus, while large woodpecker species may be able to meet the power required to perform flap-bounding flight, it is likely that they will not be able to prolong these types of flight as easily as the smaller species or, perhaps, that they might utilize a higher fraction of gliding flight.

Lewis' woodpecker (*Melanerpes lewis*) was found to be able to perform both flap-bounding and flap-gliding flight, contrary to theoretical predictions that it should not perform the former (Tobalske, 1996), and this behavior was not well correlated with the morphology of the wing. In addition, Tobalske and Dial (1994) found that the 35-g budgerigar was also capable of performing flap-gliding behavior when flying slowly, but switched to flap-bounding behavior during fast flight, despite the observation that they only have a single fiber type (FOG) in their pectoralis muscles (Rosser and George, 1986a). Thus, the hypothesis that the FOG fibers of small birds should not be used for gliding as it is inefficient appears to be undermined by the budgerigars, with the pectoralis being active during the gliding phases, but inactive during the bound. Tobalske and Dial (1994) predicted that all other species that show intermittent flight should also be facultative flap-gliders and flap-bounders and that the choice of flight mode is simply dependent on flight speed.

46.5 Development of locomotor muscles and preparation for flight

Choi et al. (1993) studied the skeletal muscle growth and development of thermogenesis in European starlings (*S. vulgaris*), the northern bobwhite (*Colinus virginianus*), and Japanese quails (*Coturnix japonica*). The M_b of the altricial starling developed more rapidly than that of the precocial quail species, although the percentage of the M_b that was accounted for by muscle mass was quite similar. The main difference between these groups was in the expression of muscle mass-specific enzyme activities. In particular, the activity of CS did not exceed 50 and 30 μmol/min g in the pectoralis muscles of *Coturnix* and *Colinus* quail, respectively, throughout development. In the starling pectoralis muscle, CS activity increased rapidly, and linearly, during development and reached 142 μmol/min g around fledging at the age of 16 and approximately 230 μmol/min g in adult starlings. In bank swallows (*Riparia riparia*), CS activity increased from around 20 μmol/min g at 2 days of age and reached around 150 μmol/min g after 10 days (Marsh and Wickler, 1982).

A similar study of the barnacle goose found an even more exaggerated developmental pattern (Bishop et al., 1995), with CS expression showing almost no change in activity from hatch (12 μmol/min g) to 5 weeks of age (20 μmol/min g). Subsequently, the activity increased rapidly to 75 μmol/min g at 30 μmol/min g in the pectoralis muscles of *Coturnix* at 7 weeks of age and reached around 100 μmol/min g in the premigratory goslings and adults (see Figure 46.35). The mass-specific activity of four different mitochondrial enzymes showed broadly similar patterns of activity to each other during development (Bishop et al., 1995) and are typified by the results obtained for HAD activity in pectoralis, cardiac, and semimembranosus leg muscle (Figure 46.19A). Throughout most of development, the cardiac muscle had the highest relative capacity for aerobic metabolic flux and fatty acid oxidation. HAD activity in the semimembranosus leg muscle was intermediate in value prior to fledging at 7 weeks (when the birds first begin to fly), but subsequently declined, while CS activity in the pectoralis flight muscle was initially very low, but reached a peak in the premigratory birds (see Figure 46.35). The developmental profiles of various glycolytic enzymes, lactate dehydrogenase (LDH, Figure 46.19B), HEX (Figure 46.19C), and GPHOS (Figure 46.19D), were more tissue specific compared to those of the mitochondrial enzymes. Development of LDH and GPHOS activities in the pectoralis muscle shows a similar exponential increase as that for CS, but values for HEX remain very low at all ages.

Overall, the results suggest that the relative use of circulating plasma glucose by the pectoralis muscle during flight is low, while intramuscular stores of glycogen are of primary importance during short-burst activity and of intermediate importance during longer-term activity and that fatty acid oxidation is the main fuel during long-distance flight (Bishop et al., 1995). In general, moderate activity levels were detected in the semimembranosus muscle for all the enzymes that were measured, suggesting that the leg muscles are capable of utilizing all fuel types in almost equal amounts. However, the cardiac muscle had extremely low levels of GPHOS, indicating that it can only utilize aerobic pathways and that metabolic fuel must be

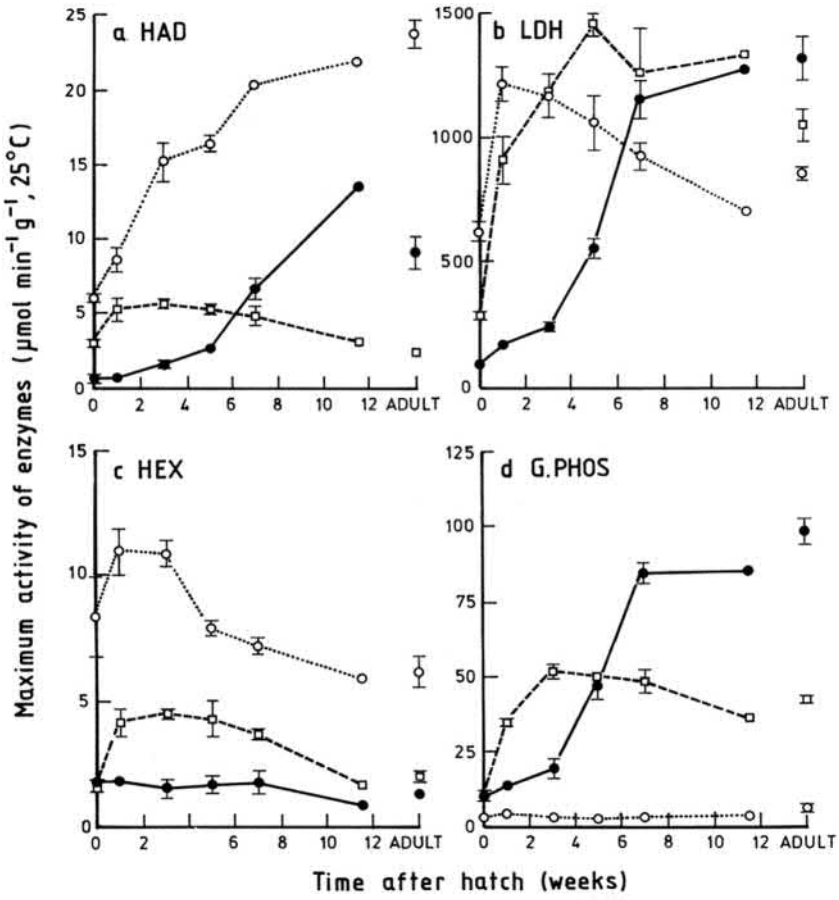

FIGURE 46.19 Mean ± SE of maximum activities of catabolic enzymes (mol/min g wet/wt at 25°C) in pectoral muscle (●——●), heart muscle (○ … ….○) and semimembranosus muscle (□————□) plotted against age of wild barnacle geese, *Branta leucopsis*. (A) 3-hydroxyacyl-CoA dehydrogenase (HAD), (B) lactate dehydrogenase (LDH), (C) hexokinase (HEX), and (D) glycogen phosphorylase (G.PHOS). N = 2−8, except for a single individual at 11.5 weeks of age. Adult geese and 11.5-week-old gosling are premigratory (see text). *Modified from Bishop et al. (1995).*

primarily supplied by blood. LDH values were relatively high in the heart, while PK levels were very low (data not shown), indicating that the heart is capable of oxidizing circulating lactate as a fuel.

The development of the locomotor and cardiac muscles, together with other morphological features, has been studied in a Svalbard population of migratory barnacle geese, from hatch until migration to the wintering grounds in southern Scotland at the age of approximately 12 weeks (Bishop et al., 1996). Up until the age of 7 weeks, the goslings are unable to fly and spend their time walking and foraging. At the age of 5 weeks, the relative mass of the leg muscles is approximately 13% of M_b, while that of the pectoral muscles is only 3.5% of M_b. During the first 5 weeks of their life, there is a strong relationship between mass of the ventricles and mass of the leg muscles. During the following 2 weeks, the flight muscles continue to grow in an exponential manner and by the time the goslings are 7 weeks old, these muscles are an impressive 14% of M_b, whereas the relative mass of the leg muscles has declined to approximately 9% of M_b. From the age of 7 weeks, the mass of the ventricles is proportional to the mass of the pectoral muscles. At 5 weeks of age, ventricular mass is 5.2% of total mass of the leg muscles, and at 7 weeks of age, it is 5.5% of mass of the pectoral muscles. Thus, as might be expected, the output capacity of the heart is closely matched to the oxygen requirements of the dominant set of locomotory muscles.

The challenge for juvenile birds undertaking their first migration may lead to increased mortality compared with mature adults, even in species such as geese and storks where the adults "guide" the youngsters on their journey. Juvenile White Storks (*Ciconia ciconia*) flap their wings 23% more than adults, had higher initial values for DBA, and are estimated to consume 14% more energy during the Autumn migration (Rotics et al., 2016). These flight inefficiencies could be a proximate cause of extra mortality, with juvenile birds that separated from the flock being left behind and with no evidence that they could compensate for the increased cost of transport by increased amounts of resting or refueling. Similarly, failure to maintain body condition can be linked to increased mortality in migrants such as the Red Knot (*Calidris canutus rufa*), in which individuals with lower body condition arrived later to the breeding grounds and appeared to experience decreased breeding success and higher seasonal mortality (Duijins et al., 2017).

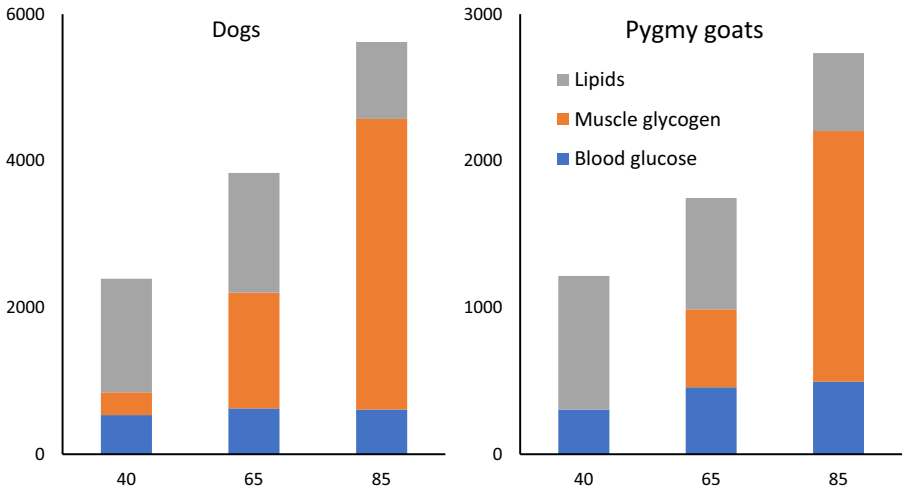

FIGURE 46.20 Substrate oxidation rates at different intensities of exercise in two species of mammals with different aerobic capacities. The large difference in the maximum rates of oxygen consumption of these two species is mainly the result of the larger rate at which glycogen is supplied from stores within the locomotor muscles themselves. *Redrawn from Weber et al. (1996), J. Exp. Biol. 199.*

46.6 Metabolic substrates for endurance flight

The use of fatty acids as the primary fuel during long-distance flights is an important adaptation, as the energy density of fat is much greater than that of other stored fuels. As pointed out earlier, the energy density of dry carbohydrate is 17.6 kJ/g; however, the storage of glycogen in cells involves between 3 and 5 g of water for each gram of glycogen, giving an effective energy density of approximately 4.4 kJ/g compared with that for lipids of 39.3 kJ/g (Schmidt-Nielsen, 1997). Protein may also be used to provide energy, but tissues such as muscle also consist of 70–80% water, so that the energy density of stored protein in vivo is around 5.4 kJ/g. Thus, during a long flight, the majority of energy is provided by fatty acids. However, fatty acid transport in the plasma (from the adipocytes to the working muscles or the liver) may be a rate-limiting step during intense exercise (Newsholme and Leech, 1983; Butler, 1991) as it is insoluble in water and is transported by a carrier protein, albumin. In fact, mammals do not increase the rate of fatty acid metabolism as the intensity of exercise increases. This is achieved predominantly by an increase in carbohydrate metabolism (see Figure 46.20), mainly by the utilization of glycogen stored in the muscles. The rate of fatty acid metabolism may actually decrease with increased intensity of exercise. However, as migrating birds use predominantly fatty acids as their energy source and as their rate of aerobic MR is at least twice that of running mammals of similar size, the rate at which migrating birds need to transport fatty acids may be up to 20 times greater than that of running mammals (Guglielmo, 2010, Figure 46.21).

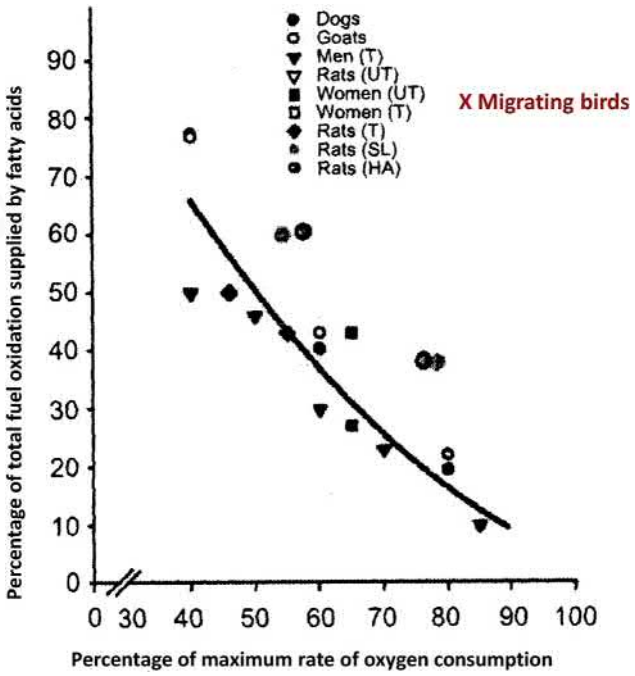

FIGURE 46.21 Percentage supply of fatty acid substrate to the muscles of mammals during increasing exercise intensity. X indicates an estimated value for migrating birds. *From McCLelland (2004).*

A mechanism has been proposed for how small birds could deliver the high rates of fatty acid required by the flight muscles without increasing the concentration of albumin in the blood. Jenni-Eiermann and Jenni (1992) measured various metabolite concentrations in the plasma of three species of small night-migrating passerines (Figure 46.22A), the robin (*Erithacus rubecula*), garden warbler (*Sylvia borin*), and pied flycatcher (*F. hypoleuca*).

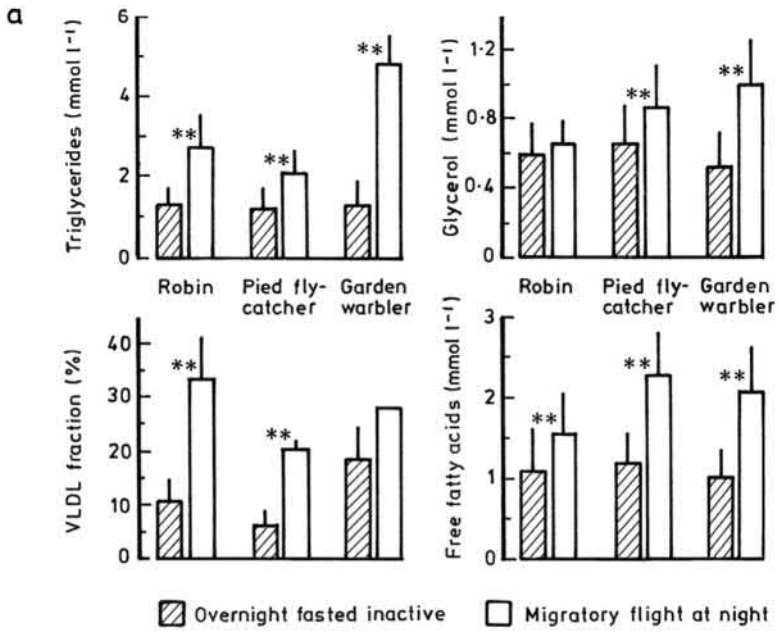

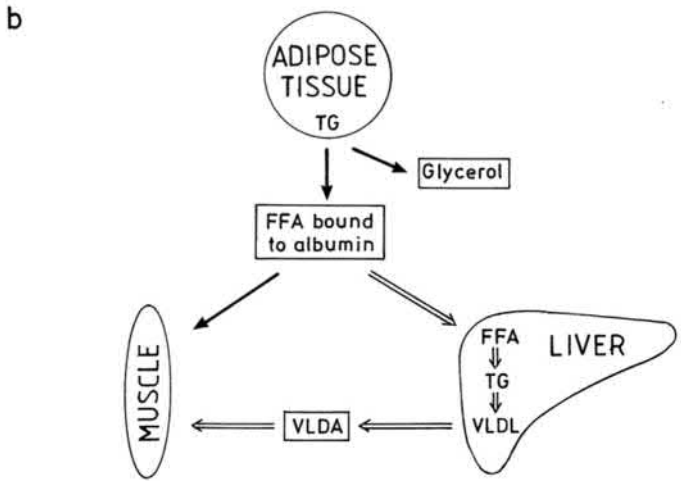

FIGURE 46.22 (A) Means SD of various fat metabolite concentrations and very low-density lipoproteins (VLDL) in the plasma of three species of birds during overnight fasting (crosshatched) or during night time migratory flights (clear). $^{**}P < .01$, Mann–Whitney *U*-test. (B) Diagram illustrating the proposed pathway for fatty acid transport to the flight muscles of small birds. FFA are released from the triglyceride (TG) stores of the adipose tissue and either taken up directly by the muscles or converted to TG by the liver and transported to the muscles as VLDL. The activity of the latter pathway (*double arrows*) is suggested to increase in small birds during flight. *Modified from Jenni-Eiermann and Jenni (1992).*

Their results indicated that during long-distance flights, plasma levels of triglyceride, glycerol, free fatty acids (FFAs), and very low-density lipoproteins (VLDLs) all increased significantly above values at rest.

The rise in triglycerides and VLDL was unexpected, but could provide a mechanism for increasing the FFA supply to the flight muscles. FFA can be reesterified to triglyceride in the liver and subsequently delivered to the blood as VLDL. Thus, the removal of FFA from the blood stream by the liver as well as by the flight muscles will increase the rate at which albumin is able to transport FFA from the adipocytes. Secondly, the VLDL can be hydrolyzed by lipoprotein lipase in the endothelium of the flight muscle capillaries, thus allowing the targeted uptake of the released FFA (Figure 46.22B). Apart from increasing the availability of FFA to the flight muscles, this mechanism has the additional advantage that the overall protein (albumin) concentration of the blood is kept relatively low and prevents unacceptable increase in colloid osmotic pressure. Also, since the proportion of fatty acids in VLDL is 60–70% (compared to only 3% in albumin), there would be a dramatic increase in the rate of fatty acid transport by the circulatory system of these birds. Wind tunnel experiments have failed to replicate the elevated triglycerides observed in field studies, and more investigation of this intriguing mechanism of fatty acid supply is needed (Guglielmo et al., 2017; Guglielmo, 2018).

Transport in the blood is not the only problem; FFAs also have to cross the plasma membrane of the muscle cells, move rapidly through the cytosol, and cross the outer and inner membranes of the mitochondria. Up until the early 1980s, it was thought that the uptake of long chain fatty acids into cells was by passive diffusion. However, evidence now suggests that the bulk of fatty acid transport is mediated by a variety of proteins both in the cell membrane and cytosol of cells. Figure 46.23 shows how the fatty acids are thought to cross the plasma membrane in mammals. Fatty acids cross the plasma membrane by passive diffusion and/or membrane-bound fatty acid binding ($FABP_{pm}$) and fatty acid translocase (FAT or CD36). Once in the cytosol, the fatty acids bind to cytosolic fatty acid binding proteins ($FABP_c$), and are converted to fatty acyl-CoA esters by acyl-CoA synthetase (ACS). They are then bound to acyl-CoA binding protein (ACBP) and translocated to sites of usage within the cell. Alternatively, fatty acid transport protein (FATP), which is also located in the plasma membrane, may transport the fatty acids into the cytosol, but, as FATP is linked to ACS, the fatty acids are immediately converted to fatty acyl-CoA esters and bound to ACBP. Recent evidence suggests that the membrane-bound transport proteins play the major role in fatty acid transport across the plasma membrane (Bonen et al., 2007; Schwenk et al., 2010). $FABP_c$ acts as a "sink" for fatty acids, thereby increasing their solubility in the cytosol, their rate of removal from the inner surface of the plasma membrane, and their rate of intracellular diffusion.

Figure 46.24 shows how the FFAs enter the mitochondria. Firstly, they are converted to their acyl carnitine esters by the enzyme carnitine acyl transferase-1 (CAT 1) which is present on the outer mitochondrial membrane. The acyl carnitine then crosses the inner mitochondrial membrane by the acyl carnitine/carnitine translocase system. Once inside the mitochondria, carnitine acyl transferase-2, which is located on the inner membrane, regenerates acyl-CoA and free carnitine. This transport process could be a major rate-limiting step in the use of fatty acids by active muscles, with either carnitine or CAT 1 being the important factors.

Studies on the flight muscles of birds indicate that they have greater concentrations of these fatty acid transporters than mammalian muscles. For example, the flight muscles of migratory western sandpipers (*Calidris mauri*) have approximately 10 times greater concentrations of $FABP_c$ than a typical mammalian muscle and approximately 14% of total cytosolic protein is $FABP_c$ in sandpipers. This is the highest value reported for any vertebrate skeletal muscle (Guglielmo et al., 1998). Also, the concentration of $FABP_c$ is 70% greater during the migratory period than during winter (Guglielmo et al., 2002). The presence of FAT/CD36 and $FABP_{pm}$ has been demonstrated in the flight muscle of white-throated sparrows (*Zonotrichia albicollis*) and the genes for these are strongly upregulated during the migratory season (McFarlan et al., 2009). These data

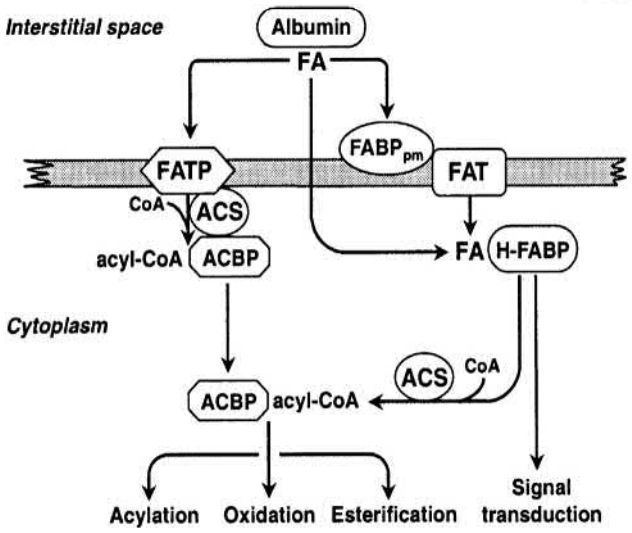

FIGURE 46.23 Long chain fatty acids (FAs) are transported in the plasma of mammals bound to albumin. Following their dissociation from the albumin, their movement across a cell membrane into the cytoplasm is either (i) by passive diffusion, or by membrane-bound fatty acid binding proteins (FABPpm) and fatty acid translocase (FAT/CD36), or by a combination of the two; (ii) by fatty acid transport protein (FATP), which is also located in the plasma membrane. Once inside the cytoplasm, the fatty acids are converted to fatty acyl-CoA esters by acyl-CoA synthetase (ACS), either via binding to a binding protein called heart-type fatty acid binding protein (H-FABP), or directly. Finally, they bind to acyl-CoA binding protein (ACBP). *From Glatz et al. (2003).*

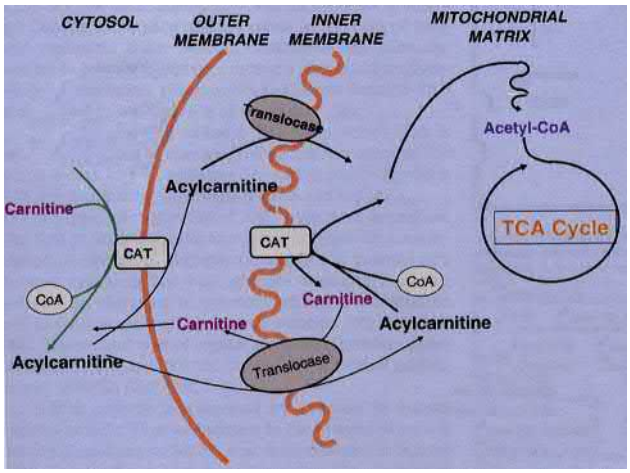

FIGURE 46.24 Transport of long-chain fatty acids (FA) into mitochondria of mammals. Acyl-CoA esters are unable to cross the inner membrane of the mitochondria so they are firstly converted to their acyl-carnitine esters by carnitine acyl transferase-1 (CAT 1) which is present on the outer membrane. Acylcarnitine crosses the inner membrane via the translocase system and, once inside the mitochondrion, acyl-CoA and free carnitine are reformed by CAT 2, which is located on the inner membrane. *From Kiens (2006).*

indicate that at least three of the muscle FATPs are important in the transport of fatty acids during bird migration.

There has been much attention on the possible significance of a number of polyunsaturated fatty acids (PUFAs) in the diet of migratory birds as natural doping agents (Maillet and Weber, 2007; Weber, 2009), although the evidence for PUFAs having an influence on flight performance is somewhat inconclusive (Guglielmo, 2018). Proposed mechanisms for the benefit of PUFAs for flight include the fuel hypothesis, the phospholipid hypothesis, and the signaling hypothesis (Weber, 2009; Price, 2010; Guglielmo, 2018). The fuel hypothesis is based on the fact that for the same carbon chain length unsaturated fatty acids are more soluble, leading them to be preferentially mobilized from adipocytes and used by key muscle enzymes involved in fatty acid oxidation. The phospholipid hypothesis proposes that greater PUFA abundance in membranes of cells and mitochondria enhances their function and increases performance of the whole organism. The signaling hypothesis is based on the fact that PUFAs are ligands for peroxisome proliferator–activated receptors (PPARs) which regulate a variety of lipid metabolism pathways, and thus may improve fatty acid oxidation capacity. European starlings (*Sturnus vulgaris*) expended 11% less energy in 6 hour flights when fed a diet high in 18:2n-6 compared to a diet high in 18:1 monounsaturated fatty acids (McWilliams et al., 2020). Other experimental studies of migratory yellow-rumped warblers (*Setophaga coronata*) found no benefits of high PUFA diets on endurance performance, muscle fatty acid oxidation capacity, or muscle oxidative damage (Dick and Guglielmo, 2019a,b). However, PPARs, fatty acid transporters, and oxidative enzymes of cultured myocytes from a shorebird (sanderling, *Calidris alba*) responded differently to PUFA supplementation than myocytes from yellow-rumped warblers, and PUFAs positively affected mitochondrial metabolism of the sanderling myocytes (Young et al., 2020). It has been hypothesized that marine-associated birds that eat diets high in long-chain PUFAs may rely more on dietary inputs of PUFAs (Guglielmo, 2018). Experimental testing of natural doping on muscle fatty acid oxidation capacity and endurance flight performance in these species would be informative.

Although protein stores are less energy dense than fat stores (see above), it may not be possible entirely to exclude their use during prolonged periods of flight without feeding. The brain and other nervous tissues are extremely dependent on glucose metabolism for the provision of energy (Newsholme and Leech, 1983). As carbohydrate stores are very limited in most animals, during starvation, the major source of glucose is via protein (amino acid) degradation to various metabolic intermediates (called oxoacids), most of which can then enter the gluconeogenesis pathway in the liver. In addition, glycerol that is produced following the hydrolysis of triglycerides can also be converted to glucose. A small number of amino acids (leucine and lysine) are degraded directly to acetyl-CoA and so can contribute to ATP synthesis via the citric acid cycle (CAC) or be converted to fat, as acetyl-CoA cannot enter the gluconeogenesis pathway. Alternatively, excess amino acid production can provide intermediates (e.g., 2-oxaloglutarate, succinyl-CoA, fumarate, and oxaloacetate) for the CAC if these should be in short supply or be converted to pyruvate and then to acetyl-CoA either to contribute to ATP synthesis or to be converted to fat. Certainly, there are a number of studies which show that protein, in the form of muscle and the intestinal tract, is catabolized during long periods of flight (Jehl, 1997) or during "simulated" flights by starvation (Biebach, 1998).

Protein catabolism during migratory flight may not always be for the reasons discussed above. When catabolized, proteins produce more water per unit of energy released (0.155 g H_2O/kJ) than fats (0.029 g H_2O/kJ). Gerson and Guglielmo (2011b) have demonstrated that when flying for durations up to 5 h in conditions of low relative humidity (13%), Swainson's thrushes (*Catharus ustulatus*) have a lean mass (protein) loss of 3.55 ± 0.91 mg/min, whereas when flying in high relative humidity (80%) air, there was no relationship between lean mass loss and flight duration. The greater rate of loss of lean mass when flying in relatively dry conditions led to a $21.7 \pm 4.9\%$ increase in endogenous water production. These data demonstrate that when flying in dry conditions, the rate of water loss induces greater metabolic water production by increasing protein catabolism. However, for those species that do not complete their migration in one nonstop flight, relatively high rates of reductions in flight muscle and the digestive system may result in reduced ability to fly and to process food after arrival at a stopover.

46.7 The cardiovascular system

A major role of the cardiovascular system is to deliver metabolic substrates and oxygen to the tissues undergoing aerobic metabolism and to remove the waste products of that metabolism. Thus, the cardiovascular system in general, and the heart in particular, must be capable of meeting the demands of the flight muscles during sustained, flapping flight. Such aerial ability has only arisen four times during the evolution of multicellular life, including the insects, Pterosaurs, birds, and bats. Dudley (1998) discussed the importance of significant historic variations in the oxygen concentration of the atmosphere of the Earth over the past 600 million years to the evolution of animal flight. During the late Carboniferous and early Permian periods, oxygen levels in the air peaked at 35%, compared to only

20.9% today. As the amount of oxygen is additional to the constant amount of nitrogen, the atmosphere also became denser, thus, making it easier to generate aerodynamic force as well as obtain oxygen for respiration. These two changes clearly stimulated a period of gigantism among flying insects of that time and may have more generally encouraged the evolution of flying invertebrates. While the first feathered dinosaurs did not evolve within a raised oxygen environment compared to the present, the majority of avian dinosaurs and early birds diversified under hyperoxic conditions, while one of the largest birds to ever fly (*Pelagornis sandersi*) with a wingspan of over 6 m (Ksepka, 2014), lived 25 million years ago when oxygen levels were around 25%.

46.7.1 The cardiac muscles

In general, birds have larger hearts and lower resting heart rates than those of mammals of similar M_b (Lasiewski and Calder, 1971; Grubb, 1983). The increased cardiac mass and, therefore, larger V_b in birds is an important factor in attaining a higher maximum $\dot{V}_{O_2}$ ($\dot{V}_{O_2,max}$) during flight than similar-sized mammals do when running. Bats have larger hearts and a higher blood oxygen–carrying capacity than other mammals of similar size (Jurgens et al., 1981), and their $\dot{V}_{O_2}$ during flight is similar to that of birds of similar mass (Butler, 1991). Among birds, those that are not capable of sustained flight, such as Galliformes, tend also to have slightly lower red blood cell concentration or hematocrit (Hct, packed cell volume) and/or hemoglobin concentration ([Hb]) than good fliers (Balasch et al., 1973), and weaker fliers have a slightly lower Hct than stronger fliers (Carpenter, 1975). Studies of exercising animals have indicated that both the locomotor and cardiac musculature, along with associated variables such as Hct, are dynamic structures that can vary in mass seasonally and/or in direct response to demand. When additional energetic "costs" occur seasonally (e.g., due to migratory fattening or the development of secondary sexual characteristics), then the relevant cardiac and locomotor musculature tend also be regulated seasonally (Hickson et al., 1983; Marsh, 1984; Driedzic et al., 1993). For example, Bishop et al. (1996) showed that both cardiac and pectoralis muscles hypertrophy during the premigratory fattening period of the barnacle goose.

Bishop and Butler (1995) suggest that M_h can be used to model the availability of oxygen to the flight muscles of birds. Assuming that the adaptations of the flight muscles are appropriately matched to the cardiovascular system, then the relative M_h of birds of a similar M_b should be a good indicator of the relative aerobic Pi available to the flight muscles. Subsequently, Bishop (1997) calculated that the $\dot{V}_{O_2,max}$ of birds should scale with respect to M_b as 230 $M_b^{0.82}$ (mL/min), while the maximum aerobic power input (aerobic $P_{i,max}$) with respect to M_h should scale as 11 $M_h^{0.88}$ (W). Thus, for studies of the prolonged aerobic flight performance of birds, the estimates of $\dot{V}_{O_2,max}$ or $P_{i,max}$ based on relative M_h should be of more practical value than the use of general scaling equations based on M_b alone.

A detailed phylogenetic analysis of differences in M_h for 915 avian species (Nespolo et al., 2018) showed that relative heart size was consistently associated with four categories of flight capability across the evolutionary spectrum for birds: short or no flight, hovering, flapping flight, gliding, and soaring (Figure 46.25). They argue that their analysis confirms that heart size has a strong constraint on flight capacity and is ultimately the result of evolutionary selection. In particular, they suggest that hovering specialists, such as Trochilidae, exhibit strong selection pressure for large hearts; that the transition of birds from ancestral short flights to prolonged flapping flight positively promoted heart size increases; and that species secondarily evolving as specialist gliders and soaring birds did not necessarily lead to a significant reduction in M_h. The latter, presumably because these species would still have to rely on flapping flight during periods of time when environmental conditions did not promote nonflapping flight modes. The mean values for M_h from selected avian families are plotted in Figure 46.26A (data from Hartman, 1961) and Figure 46.26B (data from Magnan, 1922) and indicate the interfamily adaptive diversity in aerobic capacity. The very small M_h of all three species of the ground

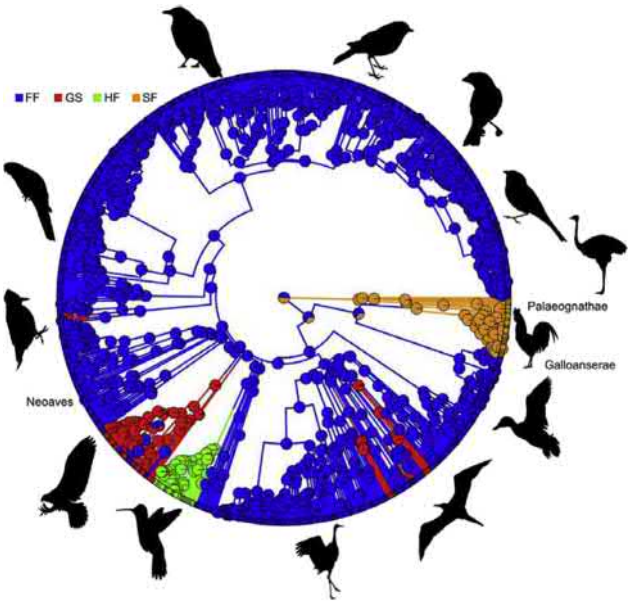

FIGURE 46.25 A summary of the flight mode classification of birds is depicted as a stochastic character map. Each circle at each node represents the most likely flight mode of the common ancestor. They estimate that the common ancestor of all birds had a ¾ probability of having been a short flyer. *FF*, flapping flight; *GS*, gliding and soaring; *HF*, hovering flight; and *SF*, short flight. *From Nespolo et al. (2018).*

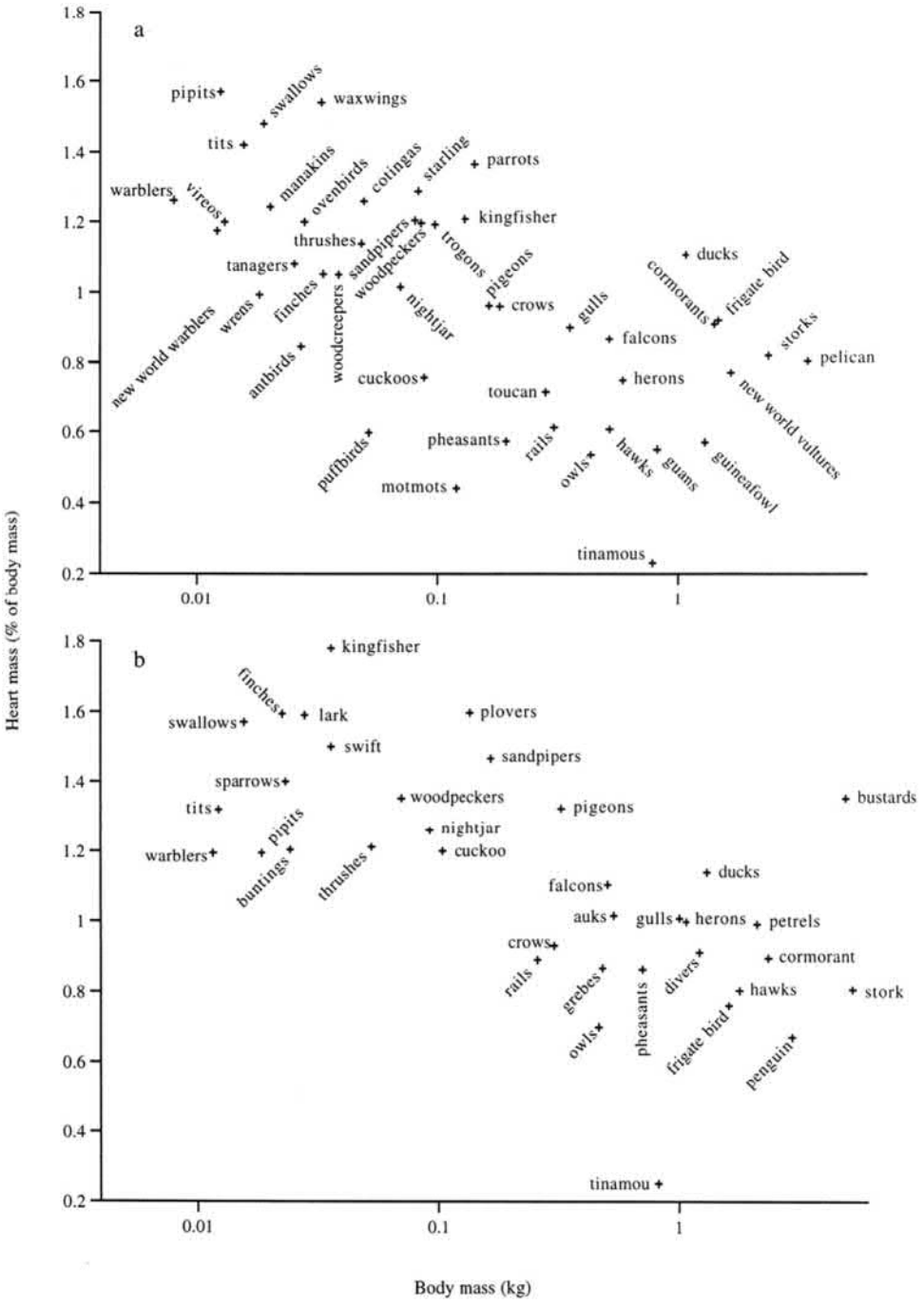

FIGURE 46.26 Mean values for cardiac muscle mass as a percentage of body mass (%), plotted against body mass (kg) for different families of birds. *(A) Data from Hartman (1961) and (B) data from Magnan (1922).*

dwelling South American Tinamidae indicate that the members of this family have the lowest aerobic ability of all bird species. As mentioned above, transitioning from weak to sustained flapping flight would have required the coevolution of a larger M_h, which is discussed by Altimiras et al. (2017) in their study of the aerobic and thermoregulatory performance of two species of Tinamou. Other relatively sedentary forest birds with small M_h include the guans, motmots, puffbirds, and antbirds. This contrasts with the relatively large M_h of other bird families that live predominantly in forest, such as the parrots, trogons, kingfishers, and hummingbirds. Interestingly, Figure 46.26B shows that the M_h values of the bustard family (Otidae), which consists of many partial migrant species (Villers et al., 2010; Kessler et al., 2013), range above the general allometric trend. The relative M_h values

of the 0.83 kg Little Bustard and the 8.95 kg Great Bustard are 1.8 and 1.4%, respectively. These relative M_h values are even larger than those of the mainly migrant species of Anatidae, which typically range from 0.8 to 1.1%. Two other observations appear to substantiate this finding for the Otidae as a group. Crile and Quiring (1940) gave the following values for the relative M_h of the sedentary and mostly terrestrial African Kori bustard: a 5.54 kg female Kori bustard (1.1%) and a 10 kg male Kori bustard (1.0%). In addition, Stickland (1977) shows that while 82% of the area between the pectoralis muscle of the white-bellied bustard is made up of "red" aerobic fibers (i.e., FOG fibers), 100% of the area of the pectoralis muscle of the similarly sized African helmeted guineafowl is made up of "white" anaerobic muscle fibers (i.e., FG fibers).

There are also some other rather interesting intrafamily differences in aerobic capacity indicated in the M_h data of Hartman (1961) and Magnan (1922). The different genera of the Columbidae (pigeons and doves) have relative M_h means ranging from 1.29 to 0.57%, while among the genera of the Falconidae (falcons), these range from 1.14 to 0.6%. In both these families, the genera with the comparatively smaller hearts occur predominantly in tropical forests and are likely to be relatively sedentary. As intrafamily pectoralis muscle mass is fairly constant in these examples, it is reasonable to assume that the relatively sedentary species are more dependent on anaerobic metabolism to support their flight activity, particularly during take-off, and that their flight muscles consist of a relatively greater proportion of FG fiber types. Thus, their flight over short distances is likely to be even more powerful than that for species of Falcons and Pigeons that are specialized for longer distances.

46.7.2 Cardiovascular adjustments during flight

The pigeon (*C. livia*) is the only species in which all but one of the variables of Fick equation (see above) have been determined during flight (Butler et al., 1977; Peters et al., 2005). In the study of Butler et al. (1977), $\dot{V}_{O_2}$ in the pigeons was 10 times the resting value (Table 46.3) when flying in a wind tunnel at 10 m/s. The respiratory system maintained CaO_2 at slightly below the resting value, but $C_{\bar{v}}O_2$ was halved, giving a 1.8-fold increase in $\left(C_aO_2 - C_{\bar{v}}O_2\right)$. There was no significant change in V_S, so the major factor in transporting the extra oxygen to the muscles was the sixfold increase in f_H. Not all of these variables were measured simultaneously on the same birds, which might introduce a small level of uncertainty in the exact relationship between variables. Similarly, measurement of $\left(C_aO_2 - C_{\bar{v}}O_2\right)$ involves cannulation of the blood vessels, which is highly invasive, and could have an effect on cardiovascular responses. Interestingly, as mean arterial blood pressure did not change, total peripheral resistance must have declined by the same proportion as cardiac output (V_b, which is $f_H \times V_S$) increased.

Many more detailed studies on cardiovascular adjustments to exercise have been conducted on mammals than birds. Early research culminated in the hypothesis of symmorphosis, in which it was postulated that all parts of a linked chain of structural variables, should have similar maximum functional capacities (Weibel et al., 1991). In particular, they studied the cardiovascular system, with its role to acquire oxygen from the atmosphere and transport it to the mitochondria of the muscles and nervous tissue. In this regard, it might be expected that the rate of change in oxygen delivery, via the blood to the muscle capillaries,

TABLE 46.3 Mean values of oxygen uptake and cardiovascular variables measured in the pigeon *columba livia* and *emu dromaius novaehollandiae*[1].

	Pigeon	(0.442kg)	Emu	(37.5kg)
	Rest	Flying	Rest	Running
Oxygen uptake (mL/min STPD)[2]	9.0	88.4	156.7	1807
Heart rate (beats/min)	115	670	45.8	180
Cardiac stroke volume (mL)	1.44 (1.14)	1.58	57	102.7
Oxygen content of arterial blood (vol%)	15.1	13.7	15.2	15.2
Oxygen content of mixed venous blood (vol%)	10.5	5.4	9.0	4.6

[1]*Measurements taken at rest and after 6min of steady level flight in a wind tunnel at a speed of 10m/s for the Pigeon and after 20min running on a treadmill at a 6-degree incline and a speed of 1.33m/s for the Emu (from Butler, 1991). Value for cardiac stroke volume in parentheses is recalculated from Butler et al. (1977), as discussed by Bishop and Butler (1995).*
[2]*STPD, Standard temperature and pressure, dry.*

should be matched by the rate of change in oxygen uptake to the cells. Thus, if stroke volume does not change very much between exercise levels, it would be hypothesized that oxygen extraction should match increases in heart rate or cardiac output. Therefore, oxygen consumption should be proportional to f_H^2. While this relationship is generally supported in an interspecies comparison of birds and mammals covering a wide size range (Bishop and Spivey, 2013), results from within-species studies vary considerably and may be subject to a number of experimental influences and confounding variables. Nevertheless, the average exponent for 24 species was close to 2 (Bishop and Spivey, 2013). Maintenance of blood pressure within tight limits between rest and exercise is a general feature seen among vertebrate groups, and supports the hypothesis that there must be a functional link between blood flow delivery, peripheral vasodilation, and an increase in rates of oxygen extraction (Joyce et al., 2019; Wang et al., 2019).

46.8 The respiratory system

The respiratory system is primarily concerned with gas exchange (i.e., the supply of oxygen to and the removal of carbon dioxide from the circulatory system and the metabolizing tissues), but it is also important for the regulation of evaporative water loss and the control of T_b. The issue of T_b regulation, in particular, has received much recent attention in association with the Heat Dissipation Limitation model (reviewed by Speakman and Król, 2010).

46.8.1 Ventilatory adjustments during flight and ventilatory/locomotor coupling

As for the cardiovascular system, there is a variation of Fick's formula for convection that describes the relationship between $\dot{V}_{O_2}$ and the various components of the respiratory system:

$$\dot{V}_{O_2} = f_{resp} \times V_T \times (C_IO_2 - C_EO_2),$$

where f_{resp} is respiratory frequency (breaths/min), V_T is respiratory tidal volume (mL), and ($C_IO_2 - C_EO_2$) is the difference in the oxygen content in the inspired and expired gas (milliliter of O_2 per mL of gas). Data on ventilation are given in Table 46.4 for five species of birds at rest and during forward flapping flight in a wind tunnel. At relatively low ambient temperatures (<23°C), minute ventilation volume $\dot{V}_I$ ($= f_{resp} \times V_T$) increases by a similar proportion as $\dot{V}_{O_2}$ and the proportion of oxygen extracted from the inspired gas ($O_{2,ext}$ effectively equal to $C_IO_2 - C_EO_2/C_IO_2$) during flight is similar to that in resting birds. The relative contributions of f_{resp} and V_T to the increase in V_I during flight vary between species. In White-necked Ravens (*Corvus cryptoleucus*), V_T does not change at all, whereas in the Fish Crow (*Corvus ossifragus*) and black-billed magpies, it doubles, and in starlings there is a fourfold increase. Thus, in the first three species, f_{resp} makes the greater contribution, but in the fourth, volume predominates. Respiratory frequency and V_T in the fish crow (Bernstein, 1976) and f_{resp} in the barnacle goose (Butler and Woakes, 1980) are independent of flight speed. This could mean that, like the starling and the fish crow, $\dot{V}_{O_2}$ of the barnacle goose is also largely independent of flight speed. However, in the budgerigar, both $\dot{V}_{O_2}$ and f_{resp} change with speed in a U-shaped fashion (Tucker, 1968b).

Despite the apparent matching between the increases in V_I and $\dot{V}_{O_2}$ during flight, in the four species listed in Table 46.4, there does appear to be an increase in effective lung ventilation above that required by MR (hyperventilation) during flight in starlings, as indicated by a decrease in the partial pressure of CO_2 (PCO_2, hypocapnia) in the anterior and posterior air sacs (Torre Bueno, 1978a). It can also be seen from Table 46.4 that $O_{2,ext}$ for the hovering hummingbird, *C. coruscans*, is similar to those of the four birds during forward flapping flight, whereas that for *Amazilia fimbriata fluviatilis* it is 50% or less. In mammals, in their investigation of how well the structural design of the respiratory and cardiovascular cascade fitted with the concept of symmorphosis, Weibel et al. (1991) concluded that while most structural variables had similar functional maxima, lung capacity appeared not to be rate limiting within the cascade. This may be similar for birds and, at least during submaximal performance, it may be possible to trade-off small changes in V_T against apposing changes in f_{resp} function. Similarly, we may expect f_H to be able to compensate for changes in cardiac stroke volume to some degree, or f_w to be able to adjust for variation in wing stroke amplitude. Of course, respiratory design and function is not limited solely to the transport of oxygen, but it is important for the removal of carbon dioxide and the rate of transfer of heat and water loss with the atmosphere.

Ever since Marey's (1890) pioneering studies on bird flight, it has been known that f_{resp} may be coordinated with the beating of the wings. Marey himself suggested that the flapping of the wings during flight might have some impact on the air sacs. In crows (*C. brachyrhynchos*) and pigeons, there is a 1:1 correspondence between f_{resp} and the frequency of wingbeating (f_{wb}), whereas ratios as high as 5:1 (f_{wb}:f_{resp}) have been reported for the black duck *Anas rubripes,* quail *C. coturnix,* and ring-necked pheasant *Phasianus colchicus* (Hart and Roy, 1966; Berger et al., 1970). However, the

TABLE 46.4 Mean values of respiratory frequency, tidal volume, minute ventilation volume, oxygen extraction, and oxygen uptake[1].

				Rest					Flight		
	Mass (kg)	f_{resp}	V_T	$\dot{V}_I$	O_{2ext}	$\dot{V}o_2$	f_{resp}	V_T	$\dot{V}_I$	O_{2ext}	$\dot{V}o_2$
Hummingbird (>20°C) (*Amazilla fimbriata fluviatilis*)[2]	0.006	-	-	-	-	-	280	0.63	0.18	0.135	4.1
Hummingbird (36°C) (Colubri *coruscans*)[3]	0.008	-	-	-	-	-	330	0.38	0.12	0.24	5.0
Budgerigar (18-20°C) (*Melopsittacus undulatus*)[4]	0.035	-	-	0.047	0.27	2.62	199	1.15	0.232	0.26	10.9
Starling (10-14°C) (*Sturnus vulgaris*)[4]	0.073	92	0.67	0.061	0.28	3.16	180	2.8	0.504	0.31	28.1
Black-billed magpie (*Pica pica*)[5]	0.165	52.4	2.95	0.154	-	-	162	6.1	0.953	-	-
Fish Crow (12-22°C) (*Corvus ossifragus*)[4]	0.275	27.3	8.2	0.223	0.19	8.5	120	14.9	1.79	0.19	68
White-necked Raven (14-22°C) (Corvus cryptoleucus)[4]	0.48	32.5	32.5	0.34	0.24	17.0	140	10.7	1.40	0.29	84.9

[1]*Abbreviations: fresp respiratory frequency (/min); V_T, tidal volume (mL); $\dot{V}_I$, minute ventilation volume L/min BTPS, except for Fish Crow where it is L/min STPD); O_{2ext}, oxygen extraction; $\dot{V}o_2$, rate of oxygen uptake (mL O_2/min STPD) during rest and while hovering in two species of hummingbirds and while flying in a wind tunnel for five other species of birds. The values for $\dot{V}o_2$ during flight are the minima that have been recorded and have been corrected for the drag and mass of mask, etc., where necessary (see Butler et al. (1977) for further details); BTPS, body temperature and pressure, saturated; STPD, standard temperature and pressure, dry.*
[2]*Berger and Hart (1972).*
[3]*Berger (1978).*
[4]*Butler and Woakes (1990).*
[5]*Boggs et al. (1997a).*

flights reported by these authors were of only a few seconds duration and it was concluded that coordination was not obligatory. During flights of up to 10-min duration, pigeons in a wind tunnel showed a very close relationship between these two activities. Wingbeats occurred in bursts and, although f_{resp} was often either slower or faster than the f_{wb} between bursts of wingbeating, there was always close coordination between the two when the wings were flapping (Figure 46.27A). Almost immediately upon landing, the pigeons panted at a frequency identical to the mean resonant frequency of the respiratory system (i.e., 10 Hz, Kampe and Crawford, 1973). During flapping flight, however, f_{resp} was slower, at approximately 7 Hz (i.e., the same as f_{wb}).

Studies with decerebrate Canada geese (Funk et al., 1992a,b) indicate that, in the absence of peripheral feedback from the flapping wings, there is predominantly a 1:1 ratio between f_{resp} and f_{wb} and that peripheral feedback is required to create the patterns of coordination seen in free-flying birds. With a 1:1 correspondence, it is possible to imagine how contractions of the flight muscles could assist respiratory air flow, but with higher ratios, this is not always so obvious. Nevertheless, a correspondence of 3:1 has been found in starlings Banzett et al. (1992) and in free-flying barnacle (1.6 kg) and Canada (3.8 kg) geese (Butler and Woakes, 1980; Funk et al., 1993), and it is clear that the wingbeat is tightly locked to fixed phases of the respiratory cycle during flights of relatively long duration (Figure 46.27B). As Tucker (1968b) comments, "It is hard to believe that the contractions of the flight muscles have no influence in ventilation…," more recent studies have attempted to investigate this intriguing possibility.

Jenkins et al. (1988) took high-speed X-ray cine films of starlings flying in a wind tunnel and suggested that the lateral movement of the furcula during the downstroke of the wing and the recoil during the upstroke may facilitate inflation and deflation, respectively, of the clavicular air sac. They also found that the sternum is moved in an expiratory direction during the downstroke and in an inspiratory direction during the upstroke. As the action of the sternum will influence the more posterior air sacs, these authors proposed that the combined action of the movements of the furcula and of the sternum, which are caused by the beating wings, is to produce a secondary respiratory cycling mechanism between the air sacs and the lungs that performs independently of (the slower) inhalation and exhalation.

Boggs et al. (1997a,b) recorded pressures and simultaneous cine radiographic images of the anterior and posterior air sacs, airflow in the trachea, and EMGs of the pectoral muscles in black-billed magpies during short (10–20s) flights in a wind tunnel (Figure 46.28A). Although they found similar patterns of movements of the furcula and sternum in the magpie during flight as Jenkins et al. (1988) described for the starling, they did not find

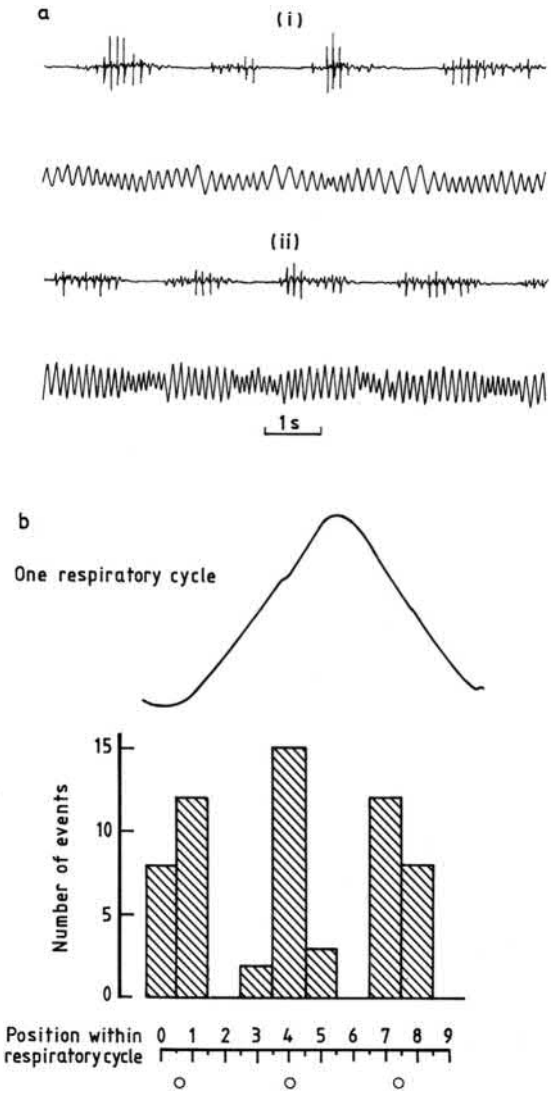

FIGURE 46.27 (A) Traces from a pigeon, *Columba livia* (0.45 kg), flying at a speed of 10 m/s in a wind tunnel, showing changes in respiratory frequency associated with periods of wingbeating and with periods of gliding (i) at the beginning of a flight (1 min after take-off) when respiratory frequency decreased during the gliding period and (ii) later in the flight (6 min after take-off) when respiratory frequency increased during the gliding period. In each series, the traces from top to bottom are electromyogram from the pectoralis muscle and respiratory movements (up to trace, inspiration). (B) Histogram showing the positions during the respiratory cycle at which the wings were fully elevated (called "events") during the flight of a barnacle goose, *Branta leucopsis,* trained to fly behind a truck. Data are from 20 respiratory cycles, which were divided into 10 equal parts. Below the histogram is plotted the mean position of each group of events (○). Above the histogram is a trace of one of *f*resp the respiratory cycles (inspiration, up). *(A) From Butler et al. (1977). (B) From Butler and Woakes (1980).*

that the pressure changes in the anterior and posterior air sacs are consistent with the internal, secondary cycling between the air sacs and the lungs, as postulated by Jenkins et al. (1988). However, the downstrokes and

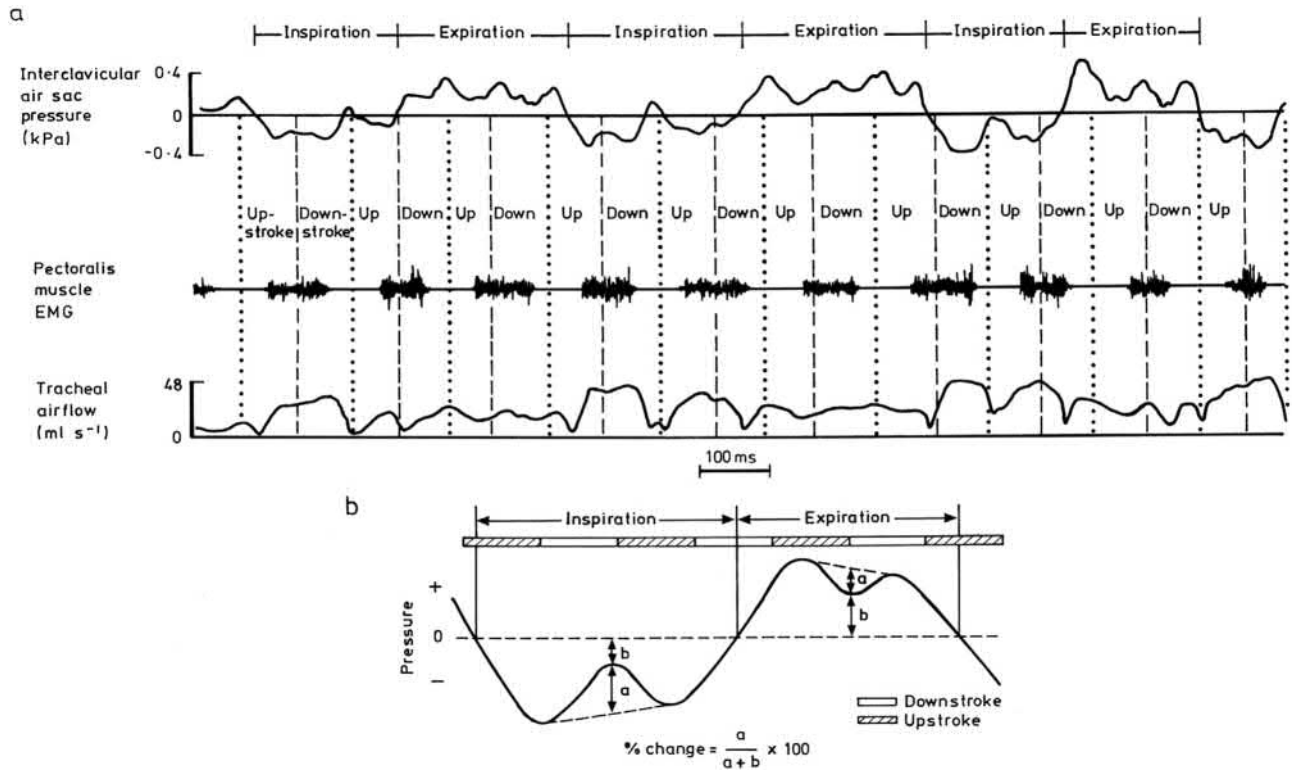

FIGURE 46.28 (A) The relationships between interclavicular air sac pressure, tracheal airflow, and electromyogram (EMG) of a pectoral muscle during flight of a black-billed magpie, *Pica pica,* in a wind tunnel. As the flow signal is not directional, inspiration is taken as that period during which pressure is subatmospheric (below 0) and expiration is that period during which pressure is above atmospheric (above 0). The EMG of the pectoral muscle indicates the upstrokes and downstrokes of the wings. When a downstroke occurs during inspiration, the subatmospheric pressure is driven up toward or above zero and when upstroke occurs during expiration, the supraatmospheric pressure is reduced toward zero. (B) Diagram to indicate how the average changes in air sac pressure shown in (A) were quantified in terms of the percentage change in pressure caused during inspiration or expiration by downstroke or upstroke of the wings, respectively. *(A) from Boggs (1997); with permission. (B) From Boggs et al. (1997a).*

upstrokes of the wings do have compressive and expansive effects, respectively, on the thoracoabdominal cavity, most probably by way of inertial mechanisms. It was only possible to quantify the effect of these influences when the movements of the wings were opposing the action of the respiratory muscles (Figure 46.28B). Thus, the average change in air sac pressure caused when a downstroke occurred during inspiration was 94%, whereas the average change caused by an upstroke occurring during expiration was 41%. The corresponding average changes in flow and volume were 75 and 23% and 35 and 11%, respectively. The conclusion is, therefore, that when the effects of the wings and the respiratory muscles are acting together (i.e., when downstroke occurs during expiration and upstroke during inspiration), ventilation of the lung is substantially enhanced. With the normal 3:1 ratio between f_{wb} and f_{resp}, the pattern of phasic coordination means that there are two upstrokes during inspiration (cf. Figure 46.27B) and two downstrokes during expiration, thus giving a net assistance to inspiration during the former and a net assistance to expiration during the latter. When they spontaneously switch to a 2:1 ratio, they shorten inspiratory time to ensure that upstroke occurs during most of inspiration and that downstroke corresponds with the transition to expiration (Boggs et al., 1997b).

46.8.2 Respiratory water loss

As indicated above, during flight, ventilation rates will naturally increase to meet the demand for additional gas exchange. Water vapor will inevitably be exhaled during respiration, so the higher ventilation rate may increase respiratory water loss. Ambient air temperature, in particular, may increase the risk of hyperthermia, thus further increasing ventilation frequency and rates of respiratory water loss (Carmi et al., 1992; Klaassen et al., 2020). Water may also be lost through excretion, at least during the early phases of flights (Giladi et al., 1997). Nevertheless, Carmi et al. (1993) demonstrated that when at rest or during flight, birds have an ability to maintain plasma volume, despite significant reductions in M_b which are largely the result of water loss. This is of obvious significance during flight, particularly during long-distance migratory flights, when a reduction in plasma volume would result in an increase in

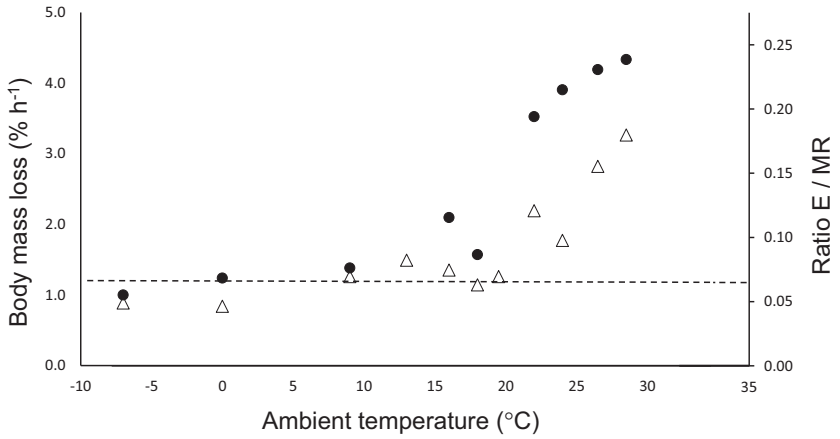

FIGURE 46.29 Data showing the rate of loss of body mass and the ratio of the rate of evaporative cooling to the metabolic rate (E/MR) as a function of ambient temperature in two starlings, *Sturnus vulgaris,* flying in a wind tunnel at between 9 and 14 m/s. *Redrawn from Torre-Bueno (1978b), J. Exp. Biol. 75.*

viscosity of the blood which, in turn, would increase the workload of the heart.

Experiments on birds in captivity and flying in wind tunnels indicate that during flapping flight at T_a above 18°C for the budgerigar and 15°C for the pigeon, water is lost at a greater rate than it is produced metabolically (i.e., the birds are dehydrating; Tucker, 1968b; Giladi and Pinshow, 1999). The starling is in apparent water balance only at T_a below 7°C (Figure 46.29; Torrre-Bueno, 1978b); however, because of the uncertainty regarding the rate of metabolic water production during flight, the author points out that the critical temperature may lie between 0 and 12°C. Only below a T_a of 0°C was the hovering hummingbird *Amazilia fimbriata* apparently in water balance (Berger and Hart, 1972).

Torre-Bueno (1978b) suggested that, during migrations, birds may ascend to altitudes where the air is cool enough to enable a greater proportion of heat to be dissipated by nonevaporative means, thus keeping them in water balance. However, while the air gets cooler with increasing altitude, it also gets less dense and will increase the *P*o required during flapping flight (Pennycuick, 2008; Carmi et al., 1992), thereby limiting the effect of the cooler atmosphere and/or resulting in an increasing ventilation rate. Despite the potential importance of water balance, there are few studies of dehydration in wild migrant birds. Landys et al. (2000) measured the hydration state of Bar-tailed Godwits (*Limosa lapponica*) in "arriving" and "early-refueling" migrants (individuals that had a chance to take a drink) in the Netherlands. The percentage body water (around 58%) was not significantly different between the two groups and suggested they were fully hydrated despite their long flights. Using the model of Klaassen et al. (1999), they determined that they would only be fully hydrated if they had an extremely low body drag coefficient (0.05, see Pennycuick et al., 1996a,b) and did not fly significantly above 3000m (Figure 46.30).

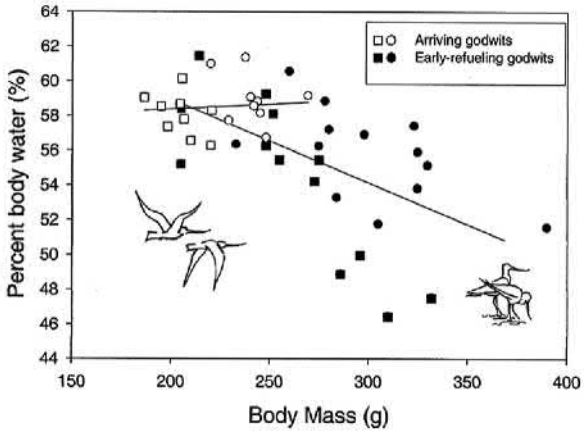

FIGURE 46.30 Percentage of body water plotted against body mass in migratory Bar-tailed Godwits, either on immediate arrival (open symbols) or early after refueling (filled symbols). Squares are males and circles are females. There is no evidence of dehydration for the arriving migrants. *Redrawn from Landys et al. (2000), The Condor 102.*

Many species do occasionally fly at quite high altitudes (Alerstam and Gudmundsson, 1999; Liechti and Schaller, 1999), but it is mostly considered that they do this to take advantage of favorable tailwind conditions. Due to the frictional drag effect of the Earth's surface, wind strength is almost always greater as altitude increases within the Troposphere. Thus, it may be worth climbing higher altitudes during tailwinds, to gain the added advantage of increasing ground speeds and, potentially, a lower overall cost of the journey (Pennycuick, 1978). In a similar study to that of the Bar-tailed Godwit, Senner et al. (2018) studied Black-tailed Godwits (*Limosa limosa*) migrating between the Netherlands and sub-Saharan West Africa. The mean average altitude for 24 migratory flights was 1385 m, with a mean maximum altitude of 3372 m, which is close to the predicted optimal height for maximum range in the Bar-tailed Godwit (Landys et al., 2000). While over 40% of flights recorded altitudes greater than 4000 m, within flight,

patterns were dynamic and the best correlates with a rapid gain in altitude were either high temperatures, or strong tailwinds, or both. Surprisingly, high ground temperature was the strongest predictor of high altitudes, indicating that it was the primary strategic factor. Air temperature at flight altitudes averaged 10.2°C, while average ground temperature was 18.8°C (with maxima above 40°C). Thus, at the highest ground temperatures, the birds may also be trying to avoid excessive T_b, rather than just respiratory water loss (see temperature control 8.3).

Smaller species of birds exhibit higher maximum climb rates while on migration (Hedenström and Alerstam, 1992) and should have a biomechanical and physiological advantage when climbing to higher flight altitudes (Bishop, 2005). However, Carmi et al. (1992) used program 1 from Pennycuick (1989) to calculate *P*i and concluded that smaller species might be better off staying below 1000 m, under low to moderate air temperatures, provided the birds have an effective countercurrent heat exchanger in their respiratory passages (Schmidt-Nielsen et al., 1970). These authors emphasize the importance of efficient $O_{2,ext}$ and the temperature of the exhaled air (T_{exp}) in water conservation during flight. The greater the $O_{2,ext}$, the lower the V_I for a given $\dot{V}_{O_2}$, which favors lower altitudes. The lower the T_{exp}, the less water will be lost in expired air, which favors higher altitudes, if it was not for the added flight costs. However, the best of both worlds might be for migrants to fly at lower altitude at night (when it is cooler) and to rest during the day, especially in warmer climates. Studies of the behavior of primarily nocturnal migrants in the desert areas of Israel indicate that only tailwind speed is closely related to the altitude at which the birds fly (Bruderer and Liechti, 1995), although the majority of flights were below 3500 m (Bruderer et al., 1995). The change to night time flight activity, from normal day time foraging, has been shown to be an abrupt shift on the night of the migration for European Blackbird, *Turdus merula* (Zúñiga et al., 2016).

46.8.3 Temperature control

Birds during flapping flight will produce a lot of heat and coupled with the excellent insulative properties of their feathers; this may make them susceptible to rising T_b during locomotion. If the rate of heat generated exceeds the rate of heat loss for a significant period of time, then T_b will rise and could, in theory, reach critical values under adverse condition. Eider ducks (*Somateria mollissima*) are relatively large seabirds with good insulation and a high cost of flight. Studies show that even during migration they only fly for around 15% of the day (Guillemette et al., 2016) and that they stop regularly during this period. They perform 14 flights per day, with an average duration of only 15.7 min and a rate of T_b increase of 4°C per hour. Higher values of heat storage index (up to 12°C/h) were associated with shorter maximum flight durations, as were higher absolute T_b (overall maximum T_b or 42.6°C). Birds spent 36% of their day cooling down while resting on the water (Guillemette et al., 2017), which is a significant investment of time and was not related to feeding behavior. The authors conclude that hyperthermia in Eiders is the predominant factor determining their short migratory flight durations and their stop-and-go strategy.

The tendency toward hyperthermia will be exacerbated by higher T_a and, as discussion in Section 46.8.2, may stimulate evaporative heat loss via the respiratory system. Thus, the hyperventilation that occurs in starlings during forward flapping flight (Torre Bueno, 1978a) is not simply due to the associated increase in the $\dot{V}_{O_2}$, but could also be the result of the typical small increase in T_b above the resting value that occurs in many birds. However, at relatively low T_a (<23°C), T_b does not tend to change with varying T_a at constant speed in Starlings, White-necked Ravens, and Pigeons flying in a wind tunnel (Torre-Bueno, 1976; Hudson and Bernstein, 1981; Hirth et al., 1987). Above a T_a of 23°C, T_b does increase with increasing T_a in the same three species. In the raven, V_I

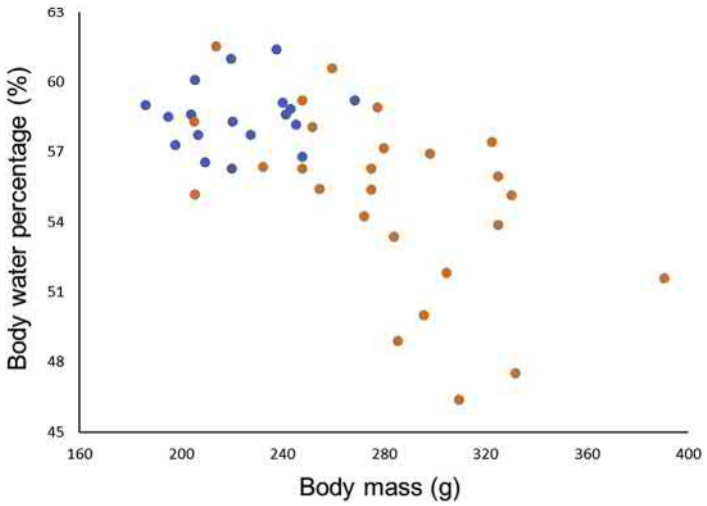

FIGURE 46.31 The relationship between ambient temperature and steady-state oxygen extraction of fish crows, Corvus ossifragus, while at rest and while flying in a wind tunnel. *From Berstein (1976).*

increases with increasing T_b so that, in this species and in the Fish Crow flying at constant speed, V_I progressively rises above that required by the metabolic demands of the bird as T_a increases above about 23°C. Thus, $O_{2,ext}$ falls from a value of 0.19 at a T_a of 20°C to 0.13 at a T_a of 25°C in the flying Fish Crow (Figure 46.31). The increased hyperventilation at higher T_a would tend to cause a lowering of the PCO_2 and induce hypocapnia (see Torre-Bueno, 1978a) and, thus, alkalosis of the blood. It has been demonstrated that the White-necked Raven resorted to so-called compound ventilation when flying at high T_a. A high frequency, shallow ventilatory component is superimposed upon a deeper, lower-frequency component and may serve to reduce hypocapnia during thermal panting (Hudson and Bernstein, 1978).

The physiological significance of the hyperthermia during flapping flight, even at low T_a, is uncertain, although Torre-Bueno (1976) concluded that birds adjust their insulation and rate of heat loss to allow a certain increase in T_b during flight in order to improve muscle efficiency and to increase maximal work output. However, at higher altitudes where oxygen availability may become limiting, increased blood temperature will shift the oxygen saturation curve for Hb to the right and could reduce oxygen uptake at the lungs (Meir and Milsom, 2013). Whatever the significance of the increase in core temperature during flapping flight, brain temperature is maintained at a lower level. In fact, even in birds under resting, thermoneutral conditions, there is approximately a 1°C difference between brain and T_b (Bernstein et al., 1979a). This difference is maintained as kestrels (*Falco sparverius*) become hyperthermic during flapping flight and may even increase (Figure 46.32). The structure that appears to be largely responsible for this phenomenon is the *rete mirabile ophthalmicum* (RMO) (Kilgore et al., 1979; Bernstein et al., 1979a,b), which is closely associated with the circulatory system of the eye. Warm arterial blood from the body is thought to be cooled by the countercurrent exchange with venous blood returning from the relatively cool eye, evaporative surfaces of the upper respiratory tract, and the beak (Midtgård, 1983).

The covering of the bill is highly vascularized and its role in heat exchange and thermoregulation has only recently been appreciated (review Tattersall et al., 2017). The latter authors conclude that the avian bill shows dynamic changes in blood flow and, therefore, rates of heat exchange and that they conform to Allen's rule in which beak size is generally smaller in cooler environments (Symonds and Tattersall, 2010). Bill size may also be correlated with seasonal and local climate conditions. Scott et al. (2008) demonstrated that three species of waterfowl are capable of "dumping" heat using the bill as a thermal window, in a similar fashion to that of their webbed feet. Many tropical species of birds have relatively large bills and Tattersall et al. (2009) showed that the Toco Toucan's (*Ramphastos toco*) massive bill can act as a transient

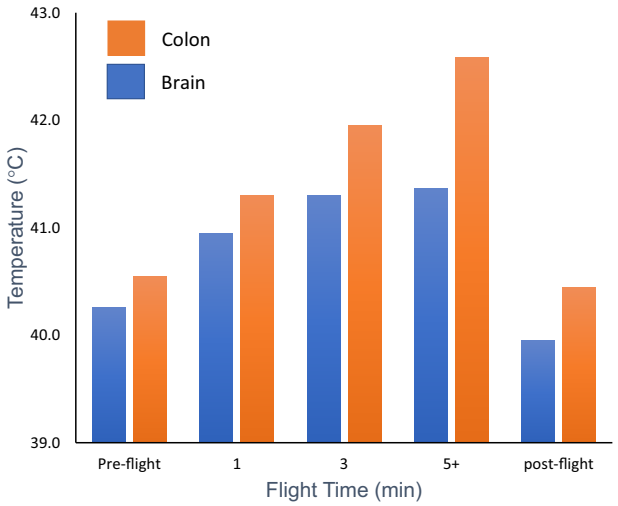

FIGURE 46.32 Mean (± 2 SE) temperatures in the colon and brain of American kestrels, Falco sparverius, before, during and after flying at a speed of 10 m s^{-1} and at an ambient temperature of 23°C. Data at 5+ min were obtained as mean values over the period between 5 min and 15 min after the onset of flight and represent steady-state values. Postflight values are those obtained after reestablishment of steady-state following each flight. *Redrawn from Bernstein et al. (1979a), Am. J. Physiol. 237.*

thermal radiator, accounting for 30–60% of total heat loss while at rest. At an air speed of 6 m/s and T_a or 21°C, maximum heat loss can reach a value of up to 10 W, or 400% of resting heat production, or around 10–20% of estimated flight costs. Similar findings were found for the Yellow-billed Hornbill (*Tockus leucomelas*) of South Africa, which revealed significant heat loss across the bill in T_a between 30 and 40°C (Figure 46.33, van de Ven et al., 2016). Thus, rates of heat exchange from larger billed species are comparable with those via hyperventilation and respiratory losses, at least at low to medium T_a. Even at a T_a of 30°C, respiratory heat loss is only approximately 20% of total heat loss for the budgerigar and fish crow (Tucker, 1968b; Bernstein, 1976) and 30% for the white-necked raven and pigeon (Hudson and Bernstein, 1981; Biesel and Nachtigall, 1987). So, most metabolic heat must be dissipated by means other than active respiratory evaporation. Indeed, herring gulls may lose up to 80% of total heat production through their webbed feet during flight (Baudinette et al., 1976). In the pigeon, the value is probably less, but nonetheless significant, at 50–65% (Martineau and Larochelle, 1988).

In warmer climates, smaller birds should have an advantage with regard to nonrespiratory, or passive heat dissipation (conduction, radiation, and convection), due to their large surface area to volume ratio. However, as T_a approaches T_b, then reliance on respiratory evaporation will increase. In the hummingbird *A. fimbriata,* maximum respiratory heat losses are 40% of the total at a T_a of 35°C (Berger and Hart, 1972). Above this temperature, heat dissipation from the eyes, shoulder, and feet of all but the smaller species of hummingbirds are greatly reduced and behavioral thermoregulation becomes increasingly

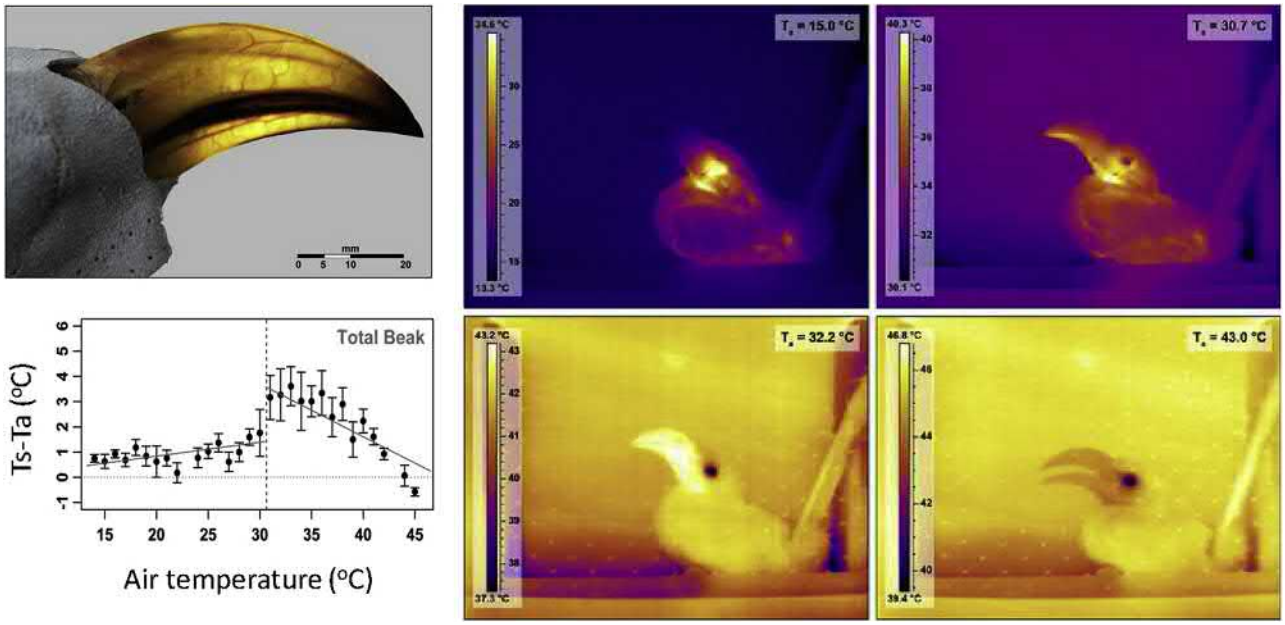

FIGURE 46.33 Regulation of Heat Exchange across the Yellow-billed Hornbill Beak (A) backlit image revealing the vasculature of the beak (B) Difference between the temperature of the air and the beak surface (Ts−Ta) (C) Thermal images of a female hornbill at different temperatures. In particular, at Ta= 32.2°C the bill is much hotter than the rest of the body and is maximizing heat loss, while at Ta = 43°C the bill is relatively cooler and is open to allow for respiratory heat loss. *From van de Ven et al. (2016).*

important via the use of thermal refugia (Powers et al., 2017). Larger species, such as the Blue-throated hummingbird (*Lampornis clemenciae*, 8 g), appeared to have the least tolerance to high T_a and were inactive when they had no capacity for nonrespiratory heat loss. In colder climates, or when flying at higher altitudes with reduced T_a, it might be anticipated that even larger species of birds should have sufficient ability to regulate to an optimal T_b and to maximize flight muscle performance and oxygen delivery. Bar-headed geese (*A. indicus*) exhibit quite stable abdominal T_b (grand flight mean 39.9°C, with minimum 37.3°C to maximum 42.8°C) during their high-altitude autumn migration across the Qinghai−Tibetan Plateau, from the breeding sites in Mongolia to the overwintering sites in India and South eastern Tibet (Parr et al., 2019a,b). In general, T_b did not change in a consistent relationship with absolute altitude, or rate of change in altitude, or heart rate, suggesting that for a substantial part of the migration the birds were able to thermoregulate T_b within a relatively narrow range. The hypothesis that bar-headed geese may strategically regulate at a lower T_b when migrating at higher altitudes, in order to improve lung oxygen uptake due to the thermal sensitivity of their hemoglobin−oxygen binding curve (Meir and Milsom, 2013), was not supported by the findings of Bishop et al. (2015) or Parr et al. (2019a,b).

Nevertheless, there has been much interest in the concept of the heat dissipation limit (HDL) theory (review Speakman and Krol, 2010), in which a limit to the locomotor performance of endotherms is determined by the maximum ability to dissipate heat loads and avoidance of hyperthermia. M_b scaling exponents for the FMRs of birds (0.658) and mammals (0.647) are consistent with the predicted theoretical value of 0.63 (Speakman and Krol, 2010). Experiments on wild birds have used feather clipping to provide a thermal window on the ventral surface of Blue Tits (*Cyanistes caeruleus*; Nord and Nilsson, 2019) and female Tree Swallows (*Tachycineta bicolor*; Tapper et al., 2020). While feeding their chicks, feather-clipped Blue Tits lost less M_b than controls while maintaining a lower T_b and raising larger chicks. Female Tree Swallows were able to feed their chicks at higher rates than controls when conditions were hot. Both these studies and that of the migratory Eider duck (Guillemette et al., 2017) provide experimental support for the HDL theory, at least in a species-specific−dependent context.

46.9 Migration and long-distance flight performance

46.9.1 Preparation for migration

As discussed by Fry and Ferguson-Lees (1972), it is a reasonable expectation that there will be correlated physiological adaptations associated with the extra power required to fly due to the laying down of fat as fuel for long-distance flights. Their work indicated that early in the fattening process of the yellow wagtail (*Motacilla flava*) the flight muscles showed a small hypertrophy. Other studies have also found muscle hypertrophy during fattening for both the pectoralis muscles (Marsh, 1984; Driedzic et al., 1993; Bishop et al., 1996; Jehl, 1997) and the cardiac muscles of birds (Driedzic et al., 1993; Bishop et al., 1996; Jehl, 1997). Thus, as protein as well as lipid is metabolized during long duration flights, it is also replaced during

stopovers, so the increase in M_b before a migration and during stopovers should be described as "fueling" rather than "fattening" (Piersma, 1998).

There has to be a close relationship between the amounts of fuel and flight muscle that are deposited before migration as the greater the fuel load, the greater the mass of flight muscle required to carry that load. A study by Piersma (1998) indicates that the proportions of fat-free tissue and fat that are deposited before long-distance (>1500 km) migration of shore birds vary between similar-sized species depending on the duration and nature of their impending flights. Just before departure, the pectoral muscles and heart tend to hypertrophy, whereas the stomach, intestine, and liver tend to atrophy. Figure 46.34 indicates that the greater fat deposition and atrophy of the visceral organs (such as the liver) are most pronounced in those species that have the longest migrations and

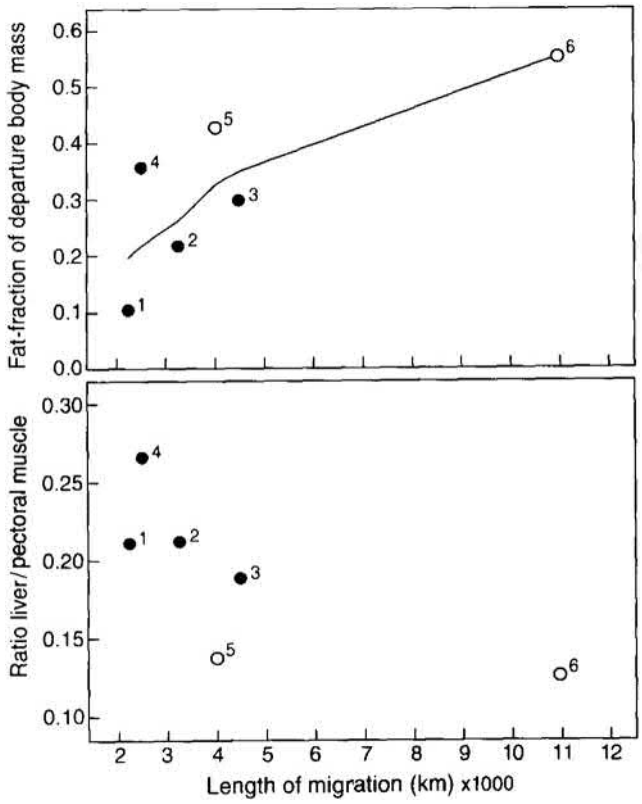

FIGURE 46.34 Fat loads and relative organ sizes before departure of 6 species of long-distance migrants (A) The amount of fat as a fraction of body mass in relation to the distance of the migration to be undertaken (B) The ratio of liver mass to pectoral muscle mass in relation to the distance of migration. Closed circles indicate species that would be able to make stopovers during their migration and open circles indicate subspecies that would not. (1) Golden plover, Pluvialis apricaria (2) Ruff, Philomachus pugnax (3) Bar-tailed godwit, Limosa lapponica lapponica (4) Red knot, Calidris canutus islandica (5) Bristle-thighed curlew, Numenius tahitiensis (6) Bar-tailed godwit, Limosa lapponica baueri. *From Piersma (1998).*

especially in those that have little or no opportunity for an emergency landing (e.g., by flying over an ocean). Of particular interest are the two subspecies of bar-tailed godwit. Although the distances of their migrations are vastly different (4500 km vs. 11,000 km), they both have high fat fractions and low liver to pectoral muscle mass ratios. What they have in common is their inability to make emergency landings during their migrations.

Bishop et al. (1998) compared the development of a captive population of barnacle geese with that of the wild migratory population in order to investigate to what link extent some of the migratory specializations of the cardiac and locomotory muscles might be determined by developmental processes and to what extent they might be modulated by differences in relative levels of activity. Postflight increases in the masses of the pectoralis muscles, of both wild and captive geese, tend to show an appropriate amount of hypertrophy in response to changes in M_b (Figure 46.35A and B). Regression equations were calculated for both the wild adult premigratory geese (pectoralis mass $= 0.5\ M_b^{0.86}$, $r^2 = 0.93$) and captive adult geese (pectoralis mass $= 0.3\ M_b^{0.92}$, $r^2 = 0.90$). The M_b exponents (or slopes) of the two regression equations are not significantly different between the two populations, although the coefficients are slightly smaller in the captive geese. Thus, approximately, 92% of the pectoralis muscle mass of premigratory barnacle geese appears to be almost independent of the experience of flight per se. Indeed, wild adult barnacle geese showed no increase in the amount of time they spent flying before their autumn and spring migrations (Portugal et al., 2012) and Portugal et al. (2009) found that hypertrophy of the pectoralis muscles of captive barnacle geese actually began even before their M_b increased.

Gaunt et al. (1990) studied the flight muscle changes of the eared grebe (*Podiceps nigricollis*) during a staging period at Mono Lake, California, where the food resources were not limiting. Following a postbreeding moult at the lake, the birds become flightless and their flight muscles show a slight atrophy, but due to an abundance of food, the birds put on a large amount of fat and M_b greatly increases. Just prior to departure for the winter grounds, the birds metabolize much of the fat and it is at this time that the flight muscles hypertrophy. In this example, flight muscle atrophy occurs when the birds have plenty of food, while subsequent hypertrophy occurs while the birds are actually reducing in M_b. Marsh and Storer (1981) had originally suggested that the correlation between flight muscle mass and M_b in Cooper's hawk (*Accipiter cooperii*) was a natural analog of "power" training during flight. Subsequent studies have found no obvious mechanistic link between hypertrophy of the flight muscle and M_b, although the authors did associate increased wing flapping with the flight muscle hypertrophy. Dietz et al. (1999) found that two

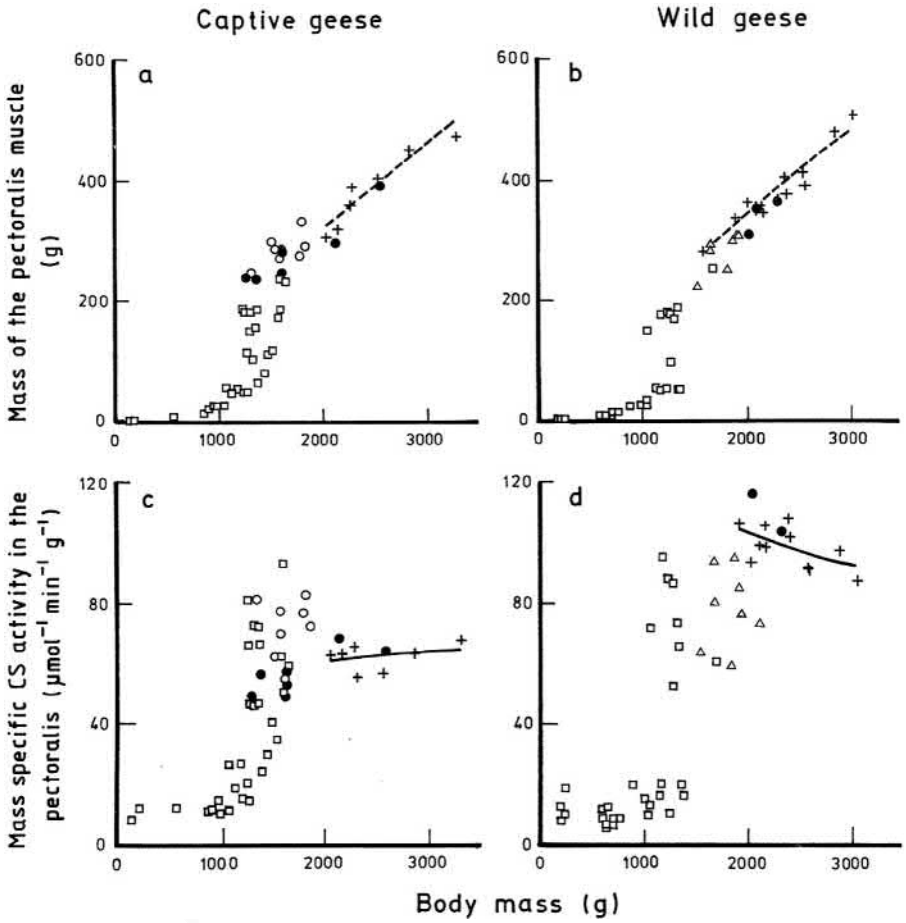

FIGURE 46.35 Scatter diagram of the masses of the pectoral muscles (g) and the mass-specific activity of citrate synthase (CS) in the pectoral muscles (μmol min-1 g wet wt-1) of captive (a and c) and wild (b and d) barnacle geese, Branta leucopsis, plotted against body mass (g). Goslings of 1−7 weeks of age (□), goslings of 12−20 weeks of age (●), adults at 7 weeks after the population hatch date (Δ) and premigratory adults >10 weeks post-hatch (+). *From Bishop et al. (1998).*

subspecies of red knots (*Calidris canutus*), which were kept under a constant photoperiod, showed similar increases in pectoral muscle hypertrophy (44%) during premigratory fattening and that this represented between 29 and 39% of the total mass increase. This suggested that there was no direct photoperiodic control and that the mechanism was likely to be endogenous, possibly with some kind of circannual regulation. It still remains an outside possibility that the relatively infrequent bouts of wing flapping and occasional take-offs exhibited by captive birds might provide a sufficient mechanistic link by which the birds are able to maintain the flight muscle to M_b relationship. However, as mentioned above, Portugal et al. (2012) showed that wild migratory barnacle geese did not show any change in the time spent flying during a 3-week premigratory period, thus, ruling out any overt evidence for flight training prior to the actual migration.

Figure 46.35C and D show the change in maximum mass-specific CS activity in the same barnacle geese (Bishop et al., 1998) for the data on pectoralis muscle mass (Figure 46.35A and B). There is little difference between the two populations up to 7 weeks of age. Specific activities of CS in the pectoralis muscles of the two wild 11.5-week-old juveniles are, at 103 and 116 μmol of substrate/min g, outside the range of that for the 12-week-old captive birds (55−59 μmol of substrate/min g) and the captive adult birds (56−58 μmol of substrate/min g) but similar to the range of wild adult birds (92−106 μmol/min g). The main conclusion from these results is that the captive adults have mass-specific values of activity for CS (mean = 62.1 ± 1.7 μmol/min g) which do not scale with M_b ($CS = 20\ M_b^{0.14}$, $r^2 = 0.11$) and are substantially below those of the wild premigratory birds (mean = 98.6 ± 1.9 μmol/min g, $P < .0001$). Results from captive goslings aged between 12 and 20 weeks also appear to be closely associated with the regression line resulting from the data from captive adult geese.

Peak values for the activity of CS in the pectoralis muscles of wild barnacle geese are found in the premigratory birds, although there is a tendency for the mass-specific activity to decline with increasing M_b ($CS = 862\ M_b^{-0.28}$, $r^2 = 0.33$). Thus, the activity of CS in the pectoralis of adult captive geese, and captive goslings over 11 weeks of age, is only around 60% of that measured in

wild geese. In addition, CS activity in the pectoralis muscles of a group of postmoulting, wild, adult geese was similar to that of long-term captive birds. Thus, it is suggested that the rise in the activity of CS in the premigratory birds may be a reaction to the increase in flight activity per se, while the rise in CS activity during development of the goslings up to fledging could be primarily under endogenous control. In addition, heart ventricular mass is reduced in captive and postmolt wild adults compared to that in wild premigratory birds and is qualitatively similar to the reduction shown in the aerobic capacity of the pectoralis muscle. It is suggested that this reduction in ventricular mass is also likely to be a direct result of the lower activity levels experienced by captive birds (Bishop et al., 1998).

One of the factors which may be important in the development of the aerobic capability of the pectoral muscles of barnacle geese is thyroxine (T_4). Circulating levels of T_4 show a similar developmental profile as mass and mass-specific activity of CS of the pectoral muscles (Bishop, 1997). While artificially accelerating the increase in circulating T_4 did not have a significant effect on either relative mass or on the mass-specific CS activity of these muscles (Deaton et al., 1997), hypothyroidism during development, induced by administration of the drug methimazole, did result in the retardation of their growth, mass-specific CS activity, fractional volume of mitochondria, and capillarity (Deaton et al., 1998). There was no such effect on the mass of the muscles of the leg.

If the mass-specific CS values for the pectoralis muscles of premigratory geese are generalized to the whole muscle, then the largest birds will have the lowest mass-specific aerobic capacity despite requiring the highest relative Po (Pennycuick, 1989). Consequently, during sustained flight, the larger birds may have to fly nearer to their minimum power speeds than smaller geese. This conclusion is also supported by the data on the heart ventricular mass (Bishop et al., 1996), which indicates that there is a tendency for relative M_h to decline slightly with increasing M_b. Thus, given that maximum oxygen consumption is likely to be closely correlated with M_h (Bishop and Butler, 1995; Bishop, 1997, 1999, 2005), it is suggested that during premigratory fattening, Pi available is likely to scale relative to M_b with an exponent value considerably lower than that of the Po exponent theoretically required ($M_b^{1.59}$) for flight performance to be maintained at a similar level according to aerodynamic theory (Rayner, 1990). However, a number of studies have questioned whether the allometric exponent for the scaling of Pi with increasing M_b is similar to that predicted for Po. Tucker (1972) measured the rate of oxygen consumption, from a single gull flying in a wind tunnel at 10.8 m/s, on 13 different occasions and with M_b naturally varying from 0.328 to 0.420 kg. He determined that the cost of carrying the extra M_b was quite small, with an M_b exponent of only $M_b^{0.325}$ but 95% confidence limits of 0.05−0.6. A very similar result was reported by Kvist et al. (2001) using the DLW technique to determine the energy expenditure of red knots flying in a wind tunnel on different days while they naturally put on M_b during the autumn. They calculated an M_b exponent of only $M_b^{0.35}$, with 95% confidence limits of 0.08−0.62. Subsequently, quite low exponents of $M_b^{0.55}$ and $M_b^{0.58}$ were also calculated for flying rose colored starlings, *Sturnus roseus*, and barn swallows, *Hirundo rustica*, respectively, also using DLW (Engel et al., 2006a; Schmidt-Wellenburg et al., 2007). Kvist et al. (2001) suggest that birds may be able to change the mechanochemical conversion efficiency of their flight muscles as they fuel up for the migration. However, it might be expected that birds should maximize muscle efficiency at all times.

46.9.2 Migratory behavior

When migrating, it might be more appropriate for the bird to minimize the time of migration, rather than the energy consumed, particularly if it is important for it to arrive at its destination before most of its competitors (Alerstam and Lindström, 1990). In this case, the optimal flight speed will be greater than U_{mr}. In an analysis of data in the literature for 48 species during migration, Welham (1992) concluded that lighter species do, indeed, fly faster than U_{mr}, but heavier species tend to fly slower. However, in an even more comprehensive study of 138 species (Alerstam et al., 2007), this apparent allometric compression of the expected speed range could be partially explained through the lack of geometric similarity with increases in M_b (e.g., Λ of the wings scales positively). Flight speed was found to be strongly influenced by wing loading and phylogenetic relationships, but some of the variation could not be fully accounted for.

It is now possible to track individual birds of many different species on their migratory flights, some of which cover many thousands of kilometers over land and sea. One of the fastest flights recorded is that of great snipe (*Gallinago media*), despite the fact that it is mostly conducted over land (Klaassen et al., 2011). This species made nonstop flights from Sweden to Central Africa and back again, covering between 4000 and 6800 km at estimated air speeds of 16−26 m/s. Bar-tailed godwit (*L. lapponica*) makes an even longer nonstop flight, largely over the Central Pacific Ocean, while traveling between Alaska to New Zealand (Gill et al., 2009). They averaged 10,153 km in 7.8 days, equivalent to an air speed of around 15 m/s. Other species of wading birds have also been shown to make impressive and rapid migratory flights (Minton et al., 2011; Niles et al., 2012; Johnson et al., 2012) in which they have to greatly increase their M_b greatly before departure (Gudmundsson et al., 1991). More specialized pelagic species of seabird, such as those within the orders

Procellariiformes and Charadriiformes, regularly make quite long foraging trips during the breeding season. In the winter months, they frequently disperse around the oceans of the world on massive migrations, such as that of sooty shearwater, *Puffinus griseus* (Figure 46.36; Shaffer et al., 2006) and Arctic tern, *Sterna paradisaea* (Egevang et al., 2010).

It has been suggested that some species of birds, such as geese, may be able to reduce induced drag by flying in V-formation (Lissaman and Scholenberger, 1970; Hummel, 1995). This would entail their maintaining positions so that the tips of the wings on the inside of the V are close to the centers of the trailing vortices from the wings on the outside of the bird ahead (Hainsworth, 1987). Assuming a fixed wing at maximum span, Hainsworth (1987) found considerable variability in wing tip spacing (WTS) of between −128 and 289 cm, both between and within formations of Canada geese (*B. canadensis*), but found that the median WTS for 55 geese (−19.8 cm) was close to the theoretical optimum (−16 cm) and corresponded to an estimated saving in induced power of 36%. Even so, in order to achieve such savings with beating wings, there would have to be a high degree of synchrony in wingbeat frequencies, as there is little variation in depth (the distance between adjacent birds' body centers, parallel to the flight path) between individuals (Hainsworth, 1988). This author found close synchrony (a difference of <0.1 beat/s) to be present in 48% of the birds he studied and, because of the calm conditions at the time, concluded that this probably represents an upper limit. Indeed, even when not taking wingbeat frequency into account, Cutts and Speakman (1994) calculated mean saving in induced power for 54 skeins of pink-footed geese (*Anser brachyrhynchus*) to be only 14% and concluded that the relationship between depth and WTS supported the communication hypothesis (Gould and Heppner, 1974). This contends that the birds position themselves so as to avoid collisions and to maintain flock unity. Although, not on migration, Weimerskirch et al. (2001) studied the flight performance and heart rate of great white pelicans (*Pelecanus onocrotalus*) while they were flying alone and when they were flying in V-formation. Mean wingbeat frequency was reduced by up to 50% for pelicans flying behind the first two birds in formation, as a result of an increase in the time spent gliding. Heat rate was reduced by 14% for pelicans in formation compared to birds flying alone. If we apply the allometric trend that $\dot{V}_{O_2}$ is proportional to f_h^2 (Bishop and Spivey, 2013), then this would suggest that the mean energetic saving for flying in V-formation was around 27% relative to unaccompanied flight (which is close to the theoretical predictions of Hainsworth, 1987).

46.10 Flight at high altitude

The majority of avian migratory flights occur below 1 km above the ground (Bruderer et al., 2018; Liechti and Schaller, 1999; Berthold, 1993) and reduce in frequency of occurrence with increasing altitudes above this. Thus, migrations where birds climb to higher altitudes to avoid high ground temperatures (Senner et al., 2018), or to select for favorable wind directions (Bruderer and Liechti, 1995), or where traditional flyways route birds over large mountain

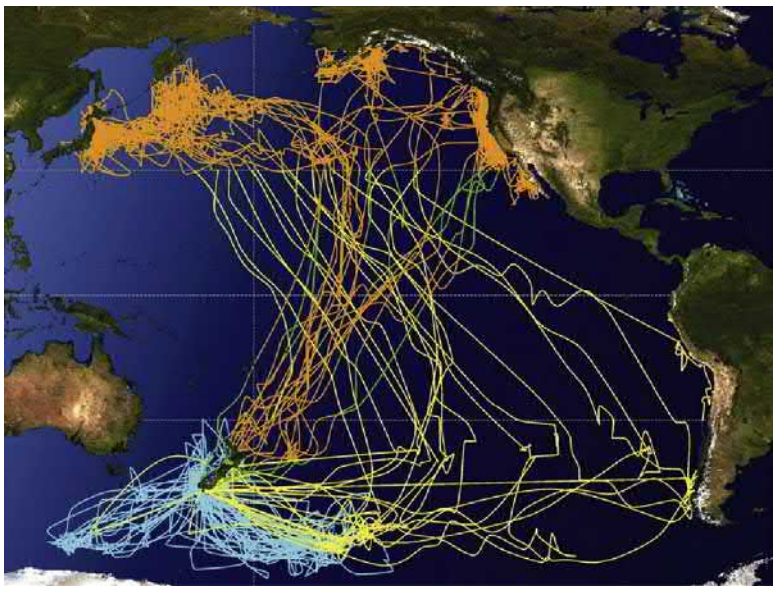

FIGURE 46.36 Geolocation tracks of sooty shearwater, Puffinus griseus, migrations originating from breeding colonies in New Zealand. Interpolated geolocation tracks of 19 sooty shearwaters during breeding (light blue) and subsequent migration pathways (yellow, start of migration and northward transit; orange, wintering grounds and southward transit). *From Shaffer et al. (2006).*

barriers (Hawkes et al., 2011), are of particular interest. Early studies indicated that most small passerines migrating at night fly below 2 km above sea level (Lack, 1960; Nisbet, 1963), although it was demonstrated by Bruderer and Liechti (1995) that wind direction may cause the majority of birds crossing the Negev desert in the south of Israel to fly above 1.8 km in spring, but with 90% below 3.5 km. Occasionally, when a low-level jet offered tailwinds that were particularly strong, birds flying over Israel reached heights between 5 and 9 km (Liechti and Schaller, 1999), and with ground speeds >25 m/s and up to 50 m/s. Even more rarely, some opportunistic observations of various species of birds have been reported at similarly extreme high altitudes (>6km). A flock of 30 swans (probably whooper, *Cygnus cygnus*) was located by radar off the west coast of Scotland at an altitude of 8−8.5 km, where the temperature was −48°C (Stewart, 1978; Elkins, 1979), but it is unclear how these birds managed to reach such high altitudes (Pennycuick et al., 1996a). Bar-headed geese, *A. indicus*, were reported as flying at altitudes of over 8 km (where partial pressure of oxygen (PO_2) is, around 6.7 kPa, approximately one-third of the sea-level value) during their migration across the Himalayas (Swan, 1961). However, these anecdotal observations of larger species performing flapping flight at extreme altitudes are very rare and have almost no environmental context (Bishop et al., 2015). The highest altitudes for flapping flight recorded directly by animal borne devices are for bar-headed goose at 7290 m (Hawkes et al., 2013) and Ruddy Shelduck at 6800 m (Parr et al., 2017). There are also a number of montane bird species that are resident at very high altitudes, such as the Red-billed Chough (*Pyrrhocorax pyrrhocorax*) and Yellow-billed Chough (*Pyrrhocorax graculus*), the latter of which has been recorded nesting at 6500 m (Rahn and Ar, 1974). Thus, birds can certainly fly at altitudes at which nonacclimatized mammals find walking difficult (Tucker, 1968a; review Parr et al., 2019a,b).

46.10.1 Physiology and adaptation

There have been relatively few physiological studies on birds flying at such high altitudes, either real or simulated. Tucker (1968a) trained a budgerigar wearing a $\dot{V}_{O_2}$ mask to fly in a hypobaric wind tunnel for 30s at the equivalent of 6100 m. Two particular aspects of flying at high altitude (low air temperature and evaporative water loss) have already been mentioned. Other aspects are the effect of the decrease in the air density and in PO_2 with increasing altitude, which will have both physiological and biomechanical influences on flight performance. Thus, for small European passerine migrants, air speed increases by 1 m/s/km for flap-gliding species and 1.4 m/s/km for flap-bounding species, while f_w increased by 0.4 and 1.1 Hz/km, respectively (Schmaljohann and Liechti, 2009). Pennycuick (1975) argues that, as birds fly higher, they must fly faster in order to obtain sufficient lift from the wings. However, as air speed increases with height, so does the power required to maintain it. At the same time, the capacity for gas exchange will decrease as the value for PO_2 declines and the blood hemoglobin begins to desaturate. Thus, there must be a particular altitude at which the bird can only just obtain O_2 at a rate sufficient to maintain even its minimum power speed, at which point it will not be able to climb any higher under its own power.

Gudmundsson et al. (1995) studied the migration of brent geese (*Branta bernicla*) from Iceland to Greenland and tracked them by satellite as they flew up and across the Greenland ice cap. These authors concluded that the brent geese (fitted with 60 g satellite transmitters) were not able to fly continuously over the Greenland ice cap (mean height of 2135 m) and had to make frequent and long rests during the climb. Gudmundsson et al. (1995) suggested that this evidence supported the biomechanical predictions of Pennycuick (1989) that these relatively large birds were up against the limit of the biomechanical power available from the flight muscles due to negative scaling of wingbeat frequency with respect to M_b. Certainly, smaller species of birds are able to sustain higher rates of climb and to carry larger relative fat loads for fueling migratory flights (Hedenstrom and Alerstam, 1992), so it is within the larger species where we may expect to see this limitation most easily. However, the analyses of Bishop and Butler (1995) and Bishop (1997, 2005) suggest that the limit to the sustained climbing performance of birds, such as shown by the brent geese, is also likely to be related to the mass-specific biomechanical performance of the cardiac muscle and its negative scaling with body size. As geese have both FG and FOG fiber types in their flight muscles (Rosser and George, 1986a), the net effect is that during "prolonged" flight activity the mass of the pectoralis muscle is effectively reduced to that of the "aerobic" FOG fibers. Thus, the maximum sustained power output (P_{ms}) available becomes proportional to the ability of the cardiovascular and respiratory system to supply the working (aerobic) muscle tissue. With an additional contribution from the FG fibers, the brent geese would have the potential to perform short flights up the steeper slopes using anaerobic power, but the birds would require regular stops (as was observed).

Due to its iconic migration over the Himalayan mountains and across the Tibetan−Qinghai plateau (Figure 46.37), the bar-headed goose has been the subject

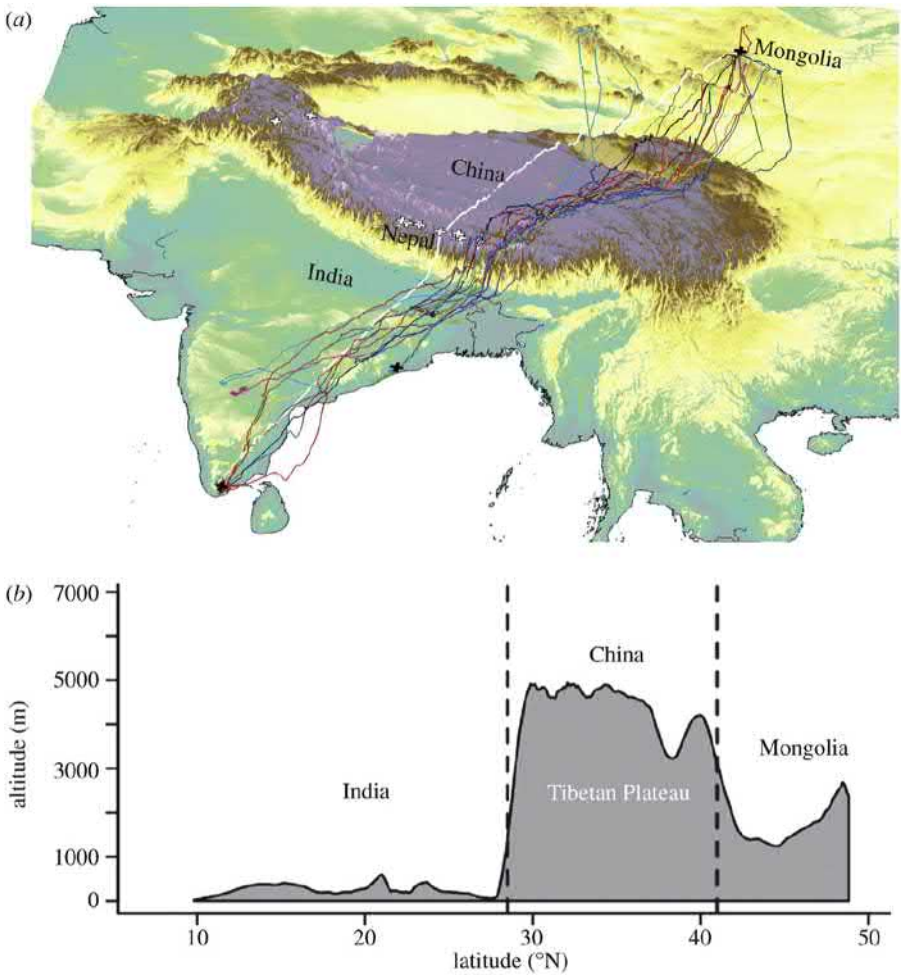

FIGURE 46.37 Satellite tracks of migrating bar-headed geese, Anser indicus: (A) three-dimensional map showing release locations (black crosses) of bar-headed geese in India (n = 2 sites) and Mongolia (n = 1 site). Coloured lines represent 16 individual geese, and coloured background shading indicates elevation. Solid thick white line shows the great circle route. White crosses show locations of the mountains peaks over 8000 m in elevation. (B) Cross-section of land elevation underlying the route of the northwards migration, based on the arithmetic mean of all flights. *From Hawkes et al. (2013).*

of a number of studies concerned with the physiological adaptations for flying at high altitude (reviewed in Butler, 2010; Scott, 2011; Scott et al., 2015; Butler, 2016; Lague, 2017; Parr et al., 2019a,b). Unlike Pekin ducks, bar-headed geese do not significantly increase their Hct and [Hb] when exposed to simulated high altitude (Black and Tenney, 1980). This means that there is no increase in the viscosity of the blood, thus preventing a possible reduction in its circulation. This is more than counterbalanced by the higher affinity for oxygen (low P_{50}) of the Hb of the goose (P_{50} for blood of the bar-headed goose at pH 7.5 is approximately 5kPa compared with 7.5 kPa for the duck), which allows the maintenance of a higher CaO_2 (and hence $(C_aO_2 - C_{\bar{v}}O_2)$) at high altitudes than in the duck (see also Meir and Milsom, 2013).

A comparison between the bar-headed goose and the plain-dwelling greylag goose, *Anser anser*, indicates that their Hb differs by only four amino acid substitutions, one of which (α^{119} Pro→Ala) may, by altering the contact between the α1 and β1 chains, confer a small increase in the O_2 affinity of the Hb from the bar-headed goose (Perutz, 1983), and this is then amplified by the interaction with inositol pentaphosphate (Rollema and Bauer, 1979). The complementary substitution (β55- Leu→Ser) at the same position may have a similar effect on the P_{50} of the Hb of the Andean goose *Cloephaga melanoptera* (Weber et al., 1993). A comparative analysis of eight species of high and low altitude Andean waterfowl species investigated the potential convergence in the functional binding properties of their Hbs (Natarajan et al., 2015). Their results showed that multiple mutations and historical paths can lead to similar functional changes. A similar comparative analysis of Andean waterfowl studying their pectoralis muscle enzyme biochemistry (Dawson et al., 2020) indicated that most species had decreased glycolytic capacity (e.g., LDH and PK) and increased myoglobin concentration and lipid

β-oxidation capacity (e.g., HAD activity); however, some metabolic changes required longer evolutionary time to emerge than others. HEX activity only increased in newly established high-altitude taxa, while only the longest established species exhibited an increase in ATP synthase activity (Figure 46.38). Acute or temporary movements to high altitude in typically lowland-living species may have different acclimation effects to those of long-term evolutionary adaptions.

It is clear from the data of Black and Tenney (1980) that the respiratory system of bar-headed geese is able to maintain a very small difference between the PO_2 of inspired air (P_IO_2) and that in the arterial blood (PaO_2), when at simulated high altitudes. For example, when at sea level, $P_IO_2 - PaO_2$ in bar-headed geese is approximately 7 kPa, whereas at a simulated altitude of 10.67 km, it is only 0.5 kPa. The associated stimulation of hyperventilation results in a large increase in respiratory minute volume ($\dot{V}_I$) that helps to maintain such a small difference between P_IO_2 and PaO_2. However, it also causes a decline in $PaCO_2$ and, therefore, an increase in arterial pH and the bird becomes hypocapnic and alkalotic. Scott and Milsom (2007) showed that the increase in $\dot{V}_I$ in bar-headed geese was the result of a larger increase in tidal volume and a correspondingly lower increase in respiratory frequency than that of the low-land living greylag goose (*A. anser*) or Pekin duck.

In a number of mammals (dog, monkey, rat, and human) the hypocapnia induced by hyperventilation causes a reduction in cerebral blood flow. This is not the case in ducks and bar-headed geese (Grubb et al., 1977; Faraci and Fedde, 1986). Also, hypoxia causes a greater increase in cerebral blood flow in ducks than it does in dogs, rats, and human (Grubb et al., 1978). At high altitude, of course, both of these factors occur together (hypocapnic hypoxia), and under these conditions, hypocapnia appears to attenuate the increase in cerebral blood flow caused by hypoxia (Grubb et al., 1979). However, these authors found that

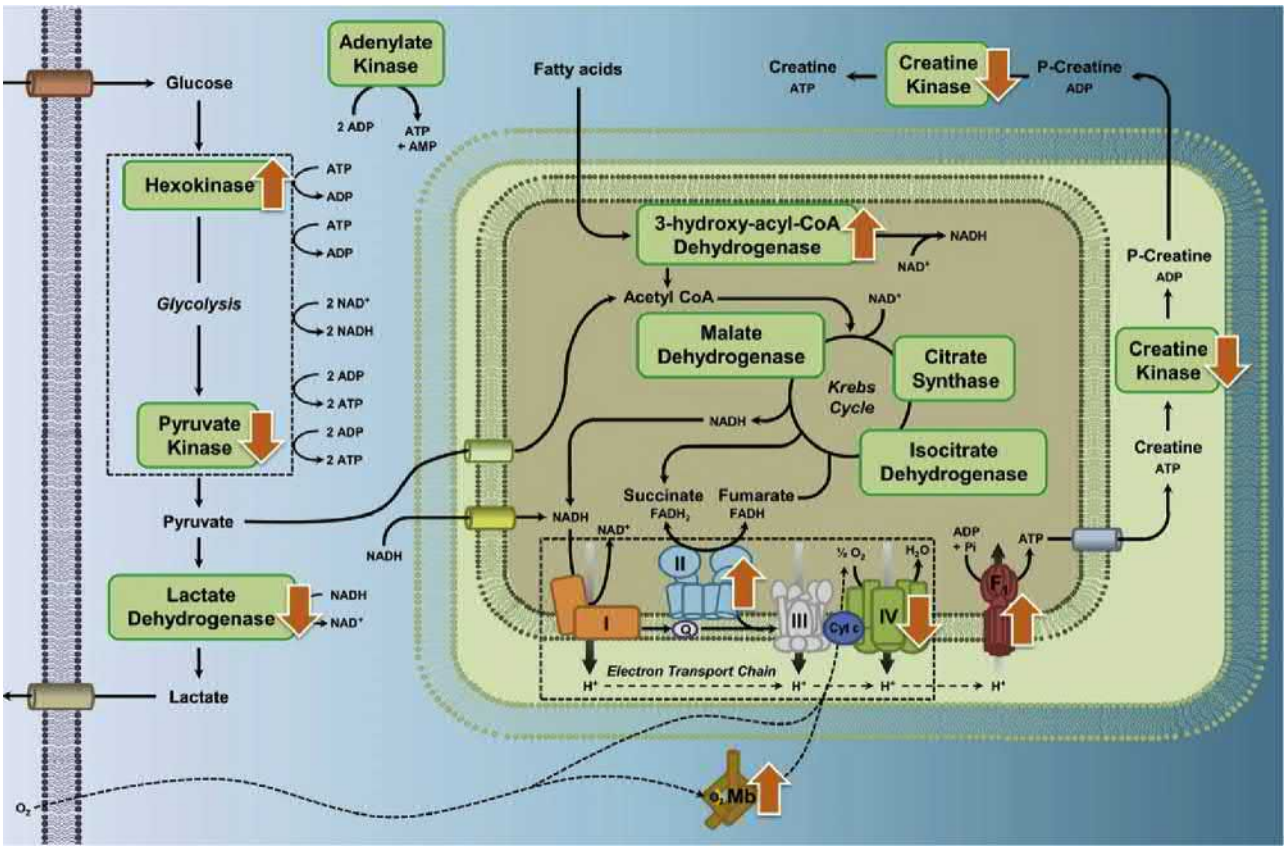

FIGURE 46.38 Enzyme pathway diagram illustrating highlighting differences in metabolic enzyme activity and myoglobin content in high-altitude waterfowl compared to their close low-altitude relatives. There were increases in the activities of hexokinase, ATP synthase, HOAD, and mitochondrial complex II (succinate dehydrogenase). There were decreases in activities of pyruvate kinase, lactate dehydrogenase, creatine kinase and complex IV (cytochrome c oxidase). There were no changes in activity for the enzymes citrate synthase, isocitrate dehydrogenase, malate dehydrogenase, complex I (NADH-ubiquinone oxidoreductase), and adenylate kinase. *From Dawson et al. (2020).*

blood oxygen flow is similar at a given O_2 content in both normocapnic and hypocapnic ducks. This is because during hypocapnia and alkalosis, there is a leftward shift of the O_2 equilibrium curve, as a result of the Bohr effect, so that a given O_2 content is achieved at a lower PO_2. In fact, in bar-headed geese, the alkalosis during severe hypoxia is greater than that in Pekin ducks which, together with the higher affinity of their Hb for O_2, means that at a given (low) PaO_2, CaO_2 is much (at least two times) greater in the geese (Faraci et al., 1984a). In addition, the pulmonary vasoconstrictor response to hypoxia is smaller in the bar-headed goose than in other birds and mammals (Faraci et al., 1984b). Thus, similar (or even greater) O_2 deliveries to the brain and heart can be achieved in hypoxic bar-headed geese at lower cerebral and coronary blood flows than in hypoxic ducks. Indeed, this species of goose is able to maintain, or even to increase, its perfusion of all tissues during severe hypocapnic hypoxia (Faraci et al., 1985).

Delivery of O_2 to the locomotory muscles is also influenced by the architecture of the capillaries. Capillary density and capillary:fiber ratio are greater in the skeletal muscle (gastrocnemius) of bar-headed geese than in that of Canada geese (Snyder et al., 1984), and this is a genetic adaptation that is not dependent on exposure to low atmospheric oxygen during development. Perhaps surprisingly, there was only a 24% increase in the capillary:fiber ration of the bar-headed goose flight muscle compared with that of the barnacle goose and no significant difference in capillary density (Scott et al., 2009). All of these factors are, no doubt, very important features when the bar-headed geese need to fly at higher altitudes. Scott and Milsom (2006) suggested that adaptations to decrease the value for hemoglobin P_{50} and to increase tissue diffusion capacity might be the most beneficial for high flying birds.

It has been suggested that the more effective lungs of birds, compared with those of mammals, may contribute significantly to the ability of birds better to tolerate high altitude (Scheid, 1985). However, Shams and Scheid (1989) concluded that, although the parabronchial lung of birds does confer an advantage at a PO_2 equivalent to that at the top of Mount Everest, the major difference between birds and mammals is the ability of the former to tolerate lower $PaCO_2$, thus enabling the respiratory system to maintain PaO_2 at as high a level as possible. In a subsequent paper, the same authors (Shams and Scheid, 1993) reported that when hypoxia is accompanied by the appropriate hypobaria (reduced atmospheric pressure), V_I and PaO_2 are slightly, but significantly, greater. Although the authors have no explanation for these differences, they would allow a bird at the elevation of Mount Everest to gain another 700 m in height before the "increase" in PaO_2 was eliminated. Gas exchange across the RMO is thought to enhance the supply of oxygen to the brain (Bernstein et al., 1984), and improvement in gas transport as a result of acclimatization to high altitude (Weinstein et al., 1985) may be other ways in which birds are adapted for survival and activity at high altitudes.

Despite all of these apparent adaptations to life at high altitude, there is very little accurate information with regard to the heights that bar-headed geese typically fly at during their migrations. Hawkes et al. (2011) tracked bar-headed geese flying north out of India and climbing up and through the Himalayan mountains, on their way to breed in China and Mongolia (Figure 46.39). The birds typically climbed between 4 and 6 km in 7−8 h in a single day, with regular sustained climb rates of between 0.2 and 0.6 m/s. Over the whole migratory period, the data suggested that bar-headed geese normally minimize flight altitude by traveling through the mountain valleys and only flying as high as the terrain dictates (Hawkes et al., 2013). Maximum altitudes reached were 7290 and 6540 m, for southbound and northbound geese, respectively, but with 95% of locations recorded <5489 m. Arlene Blum (1980) reports seeing bar-headed geese flying over the summit ridge of Annapurna I at >7622 m and took photos of them. Clearly, it is possible that occasional rare flights to very high altitudes could occur, but it is likely that these flights are only possible if assisted by favorable wind conditions in the mountains, or whether they are sustained entirely by the various physiological adaptations for flight at high altitude.

Experiments on bar-headed geese running on a treadmill under hypoxic conditions, similar to those at the top of Mount Everest, indicated possible severe limitations to oxygen uptake (Fedde et al., 1989). Under normoxic conditions, running at 0.6 m/s and at a two-degree incline caused a doubling of $\dot{V}_{O_2}$ and of cardiac output. Under the severe hypoxic conditions of only 7% atmospheric O_2, there was a decline in resting $\dot{V}_{O_2}$ and, surprisingly, $\dot{V}_{O_2}$ did not increase significantly during the subsequent 6 min of exercise. Cardiac output also apparently remained unchanged during exercise, although there was a significant reduction in V_S. The authors suggest that there may be a hypoxic depression of cardiac contractility, but clearly this cannot occur when the birds are flying at high altitude. It may be that the birds used in this study were stressed by the surgical techniques associated with the cannulations and so on (cf. Woakes and Butler, 1986). Certainly, their resting heart rate was almost 3x higher than that of resting barnacle geese (Butler and Woakes, 1980; Ward et al., 2002). In a similar study of bar-headed geese (Hawkes et al., 2014), they obtained similar blood gas and metabolite values to those of Fedde et al. (1989) but significantly

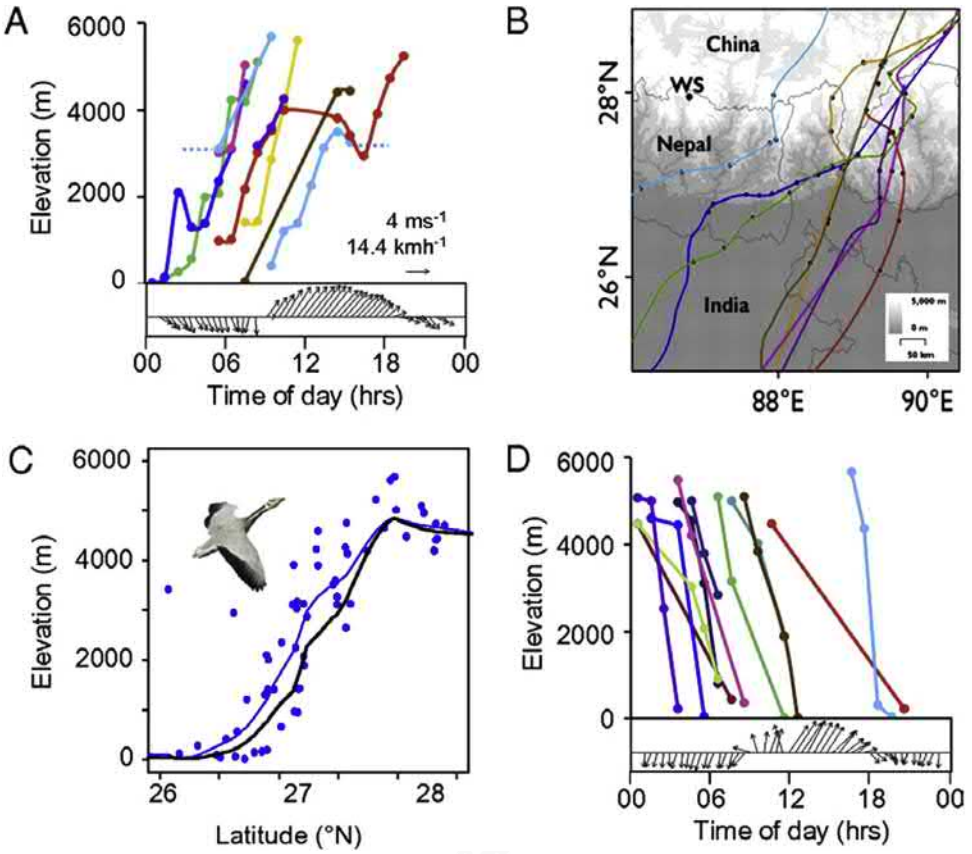

FIGURE 46.39 Timing of migrations with 30-min average wind speed and direction from the Nepal Climate Observatory at Pyramid station for bar-headed geese, Anser indicus, migrating (A) northward (n = 8) and (D) southward (n = 12) over the Himalaya. Arrows show cardinal direction (north pointing up to 0°) in which the wind was blowing and arrow length (indicated in A) is proportional to wind speed in A and D. (B) Map showing the northward migration routes; weather station (WS) location is indicated. (C) Elevation of the mean northward track across the Himalaya (for all crossing locations from all eight geese), blue circles show individual data points and blue line shows Lowess smoother for mean ground elevation under the track (black line). *From Hawkes et al. (2011).*

lower resting heart rates during normoxia and hypoxia. They also used accelerometry to assess the biomechanical cost of locomotion and found that the requirement for oxygen was not different between running in hypoxia and in normoxia. Finally, it was noted that, while lactate levels had risen significantly in the geese running in hypoxia (Hawkes et al., 2014), it could only account for a maximum of 10% of the locomotory costs after 6 min of running, which was not compatible with the 50% reduction in $\dot{V}_{O_2}$ measured in the severely hypoxic geese (Fedde et al., 1989). Put together, these results suggest that there was a problem with the experimental determination of $\dot{V}_{O_2}$ by Fedde et al. (1989) under hypoxic conditions during running, and that the maximum running speeds of bar-headed geese are not significantly affected by severe hypoxia (Hawkes et al., 2014).

These recent studies of bar-headed geese in the wild (Takekawa et al., 2009; Hawkes et al., 2011, 2013) are beginning to reveal the true nature of their migration across the Himalayan Mountains and Tibetan–Qinghai plateau. Technological approaches are allowing the simultaneous recording of altitude, heart rate, and accelerometry during their migratory flights (Figure 46.40; Bishop et al., 2015). These data indicate that even a comparatively gentle climb rate of around 0.1 m/s, between an altitude of 3600 to 4000 m, required a heart rate of well over 400 beats/min, compared to a maximum heart rate of around 500 beats/min (Ward et al., 2002). However, overall the mean heart rates are remarkably low and indicate that there is still much to discover with regard to the maximum flight performance of these high-flying birds.

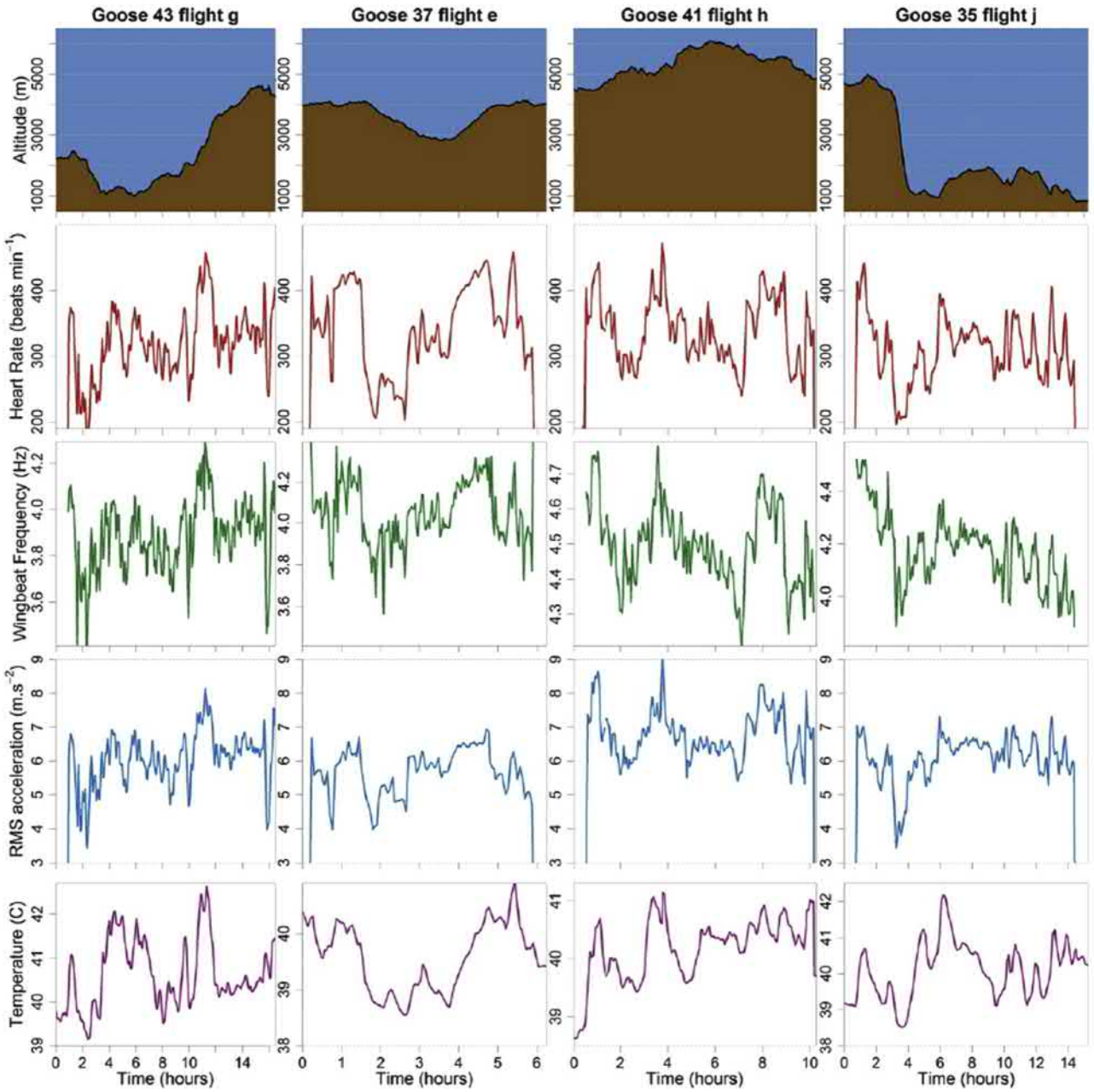

FIGURE 46.40 Examples of simultaneous recordings of altitude (row 1), heart rate (row 2), wingbeat frequency (row 3), root mean squared vertical body acceleration (row 4) and abdominal body acceleration (row 5) from wild bar-headed geese on their autumnal migration. P43 travelled South from Mongolia and ascended onto the Tibetan Plateau (column 1); goose P37 (column 2) and goose P41 (column 3) were traversing the Tibetan Plateau; goose P35 (column 4) crossed the Himalayas and descended into India. *From Bishop et al. (2015).*

Acknowledgments

The authors wish to thank BBSRC, NERC, NSERC, The Royal Society, and the Leverhulme Trust for financial support for their recent and past work on this topic.

References

Alerstam, T., Lindström, A., 1990. Optimal bird migration: the relative importance of time, energy, and safety. In: Gwinner, E. (Ed.), Bird Migration. Springer-Verlag, Berlin/Heidelberg/New York, pp. 331–351.

Alerstam, T., Gudmundsson, G.A., Larsson, B., 1993. Flight tracks and speeds of Antarctic and Atlantic seabirds: radar and optical measurements. Phil. Trans. Roy. Soc. Lond. B 340, 55–67.

Alerstam, T., Gudmunddson, G.A., 1999. Migration patterns of Tundra birds: tracking radar observations along the northeast passage. Arctic 52, 346–371.

Alerstam, T., Rosén, M., Bäckman, J., Ericson, P.G.P., Hellgren, O., 2007. Flight speeds among bird species: allometric and phylogenetic effects. PLoS Biol. 5, e197.

Alexander, R.M.N., 1997. The U, J and L of bird flight. Nature 399, 13.

Alexander, R.M.N., 2005. Models and the scaling of energy costs for locomotion. J. Exp. Biol. 208, 1645–1652.

Alexander, R.M.N., Bennett-Clark, H.C., 1977. Storage of elastic strain energy in muscle and other tissues. Nature 265, 114–117.

Altimiras, J., Lindgren, I., Giraldo-Deck, L.M., Matthei, A., Garitano-Zavala, Á., 2017. Aerobic performance in tinamous is limited by their small heart. A novel hypothesis in the evolution of flight. Sci. Rep. 7 https://doi.org/10.1038/s4198-017-16297-2.

Altshuler, D.L., Dudley, R., Heredia, S.M., McGuire, J.A., 2010. Allometry of hummingbird lifting performance. J. Exp. Biol. 213, 725–734.

Askew, G.N., Ellerby, D.J., 2007. The mechanical power requirements of avian flight. Biol. Lett. 3, 445–448.

Askew, G.N., Marsh, R.L., 2001. The mechanical power output of the pectoralis muscle of blue-breasted quail (*Coturnix chinensis*): the in vivo length cycle and its implications for muscle performance. J. Exp. Biol. 204, 3587–3600.

Askew, G.N., Tregear, R.T., Ellington, C.P., 2010. The scaling of myofibrillar actomyosin ATPase activity in apid bee flight muscle in relation to hovering flight energetics. J. Exp. Biol. 213, 1195–1206.

Balasch, J., Palomeque, J., Palacios, L., Musquera, S., Jimenez, M., 1973. Hematological values of some great flying and aquatic- diving birds. Comp. Biochem. Physiol. A 49, 137–145.

Banzett, R.B., Nations, C.S., Wang, N., Butler, J.P., Lehr, J.L., 1992. Mechanical independence of wingbeat and breathing in starlings. Respir. Physiol. 89, 27–36.

Battley, P.F., Piersma, T., Dietz, M.W., Tang, S., Dekinga, A., Hulsman, K., 2000. Empirical evidence for differential organ reductions during trans-oceanic bird flight. Proc. R. Soc. B. 267, 191–195.

Baudinette, R.V., Schmidt-Nielsen, K., 1974. Energy cost of gliding flight in herring gulls. Nature 248, 83–84.

Baudinette, R.V., Loveridge, J.P., Wilson, K.J., Mills, C.D., Schmidt-Nielsen, K., 1976. Heat loss from feet of herring gulls at rest and during flight. Am. J. Physiol. 230, 920–924.

Berger, M., 1985. Sauerstoffverbrauch von Kolibris (*Colibri corus*- und *C. thalassinus*) beim Horizontalflug. In: Nachtigall, W. (Ed.), BIONA Report 3. Gustav Fischer, Stuttgart, pp. 307–314.

Berger, M., Hart, J.S., 1972. Die Atmung beim Kolibri *Amazilia fimbriata* während des Schwirrfluges bei verschiedenen Umgebungstemperaturen. J. Comp. Physiol. 81, 363–380.

Berger, M., Hart, J.S., 1974. Physiology and energetics of flight. In: Farner, D.S., King, J.R. (Eds.), Avian Biology, vol. IV. Academic Press, New York and London, pp. 415–477.

Berger, M., Roy, O.Z., Hart, J.S., 1970. The co-ordination between respiration and wing beats. Z. vergl. Physiol. 66, 190–200.

Bernstein, M.H., 1976. Ventilation and respiratory evaporation in the flying crow, *Corvus ossifragus*. Respir. Physiol. 26, 371–382.

Bernstein, M.H., Curtis, M.B., Hudson, D.M., 1979a. Independence of brain and body temperatures in flying American kestrels, *Falco sparverius*. Am. J. Physiol. 237, 58–62.

Bernstein, M.H., Duran, H.L., Pinshow, B., 1984. Extrapulmonary gas exchange enhances brain oxygen in pigeons. Science 226, 564–566.

Bernstein, M.H., Sandoval, I., Curtis, M.B., Hudson, D.M., 1979b. Brain temperature in pigeons: effects of anterior respiratory bypass. J. Comp. Physiol. 129, 115–118.

Bernstein, M.H., Thomas, S.P., Schmidt-Nielsen, K., 1973. Power input during flight of the fish crow, *Corvus ossifragus*. J. Exp. Biol. 58, 401–410.

Berthold, P., 1993. Bird Migration: A General Survey. Oxford University Press, Oxford, p. 239.

Bevan, R.M., Butler, P.J., Woakes, A.J., Prince, P.A., 1995b. The energy expenditure of free-ranging back-browed albatrosses. Phil. Trans. Roy. Soc. Lond. B 350, 119–131.

Bevan, R.M., Woakes, A.J., Butler, P.J., 1994. The use of heart rate to estimate oxygen consumption of free-ranging black-browed albatrosses *Diomedea melanophrys*. J. Exp. Biol. 193, 119–137.

Bevan, R.M., Woakes, A.J., Butler, P.J., Croxall, J.P., 1995a. Heart rate and oxygen consumption of exercising gentoo penguins. Physiol. Zool. 68, 855–877.

Biebach, H., 1998. Phenotypic organ flexibility in Garden Warblers Sylvia borin during long-distance migration. J. Avian Biol. 29, 529–535.

Biesel, W., Nachtigall, W., 1987. Pigeon flight in a wind tunnel. IV. Thermoregulation and water homeostasis. J. Comp. Physiol. B 157, 117–128.

Biewener, A.A., Dial, K.P., Goslow Jr., G.E., 1992. Pectoralis muscle force and power output during flight in the starling. J. Exp. Biol. 164, 1–18.

Bishop, C.M., 1997. Heart mass and the maximum cardiac output of birds and mammals: implications for estimating the maximum aerobic power input of flying animals. Phil. Trans. Roy. Soc. Lond. B 352, 447–456.

Bishop, C.M., 1999. Maximum oxygen consumption and aerobic scope of birds and mammals: getting to the heart of the matter. Proc. R. Soc. 266, 2275–2281.

Bishop, C.M., 2005. Circulatory variables and the flight performance of birds. J. Exp. Biol. 208, 1695–1708.

Bishop, C.M., Butler, P.J., 1995. Physiological modelling of oxygen consumption in birds during flight. J. Exp. Biol. 198, 2153–2163.

Bishop, C.M., Butler, P.J., Egginton, S., El Haj, A.J., Gabrielsen, G.W., 1995. Development of metabolic enzyme activity in locomotor and cardiac muscles of the migratory barnacle goose. Am. J. Physiol. 269, R64–R72.

Bishop, C.M., Butler, P.J., El Haj, A.J., Egginton, S., Loonen, M.J.J.E., 1996. The morphological development of the locomotor and cardiac muscles of the migratory barnacle goose (*Branta leucopsis*). J. Zool. London 239, 1–15.

Bishop, C.M., Butler, P.J., El Haj, A.J., Egginton, S., 1998. Comparative development of captive and migratory populations. Physiol. Zool. 71, 198–207.

Bishop, C.M., Spivey, R.J., 2013. Integration of exercise response and allometric scaling in endotherms. J. Theor. Biol. 323, 11–19.

Bishop, C.M., Spivey, R.J., Hawkes, L.A., Batbayar, N., Chua, B., Frappell, P.B., Milsom, W.K., Natsagdorj, T., Newman, S.H., Scott, G.R., Takekawa, J.Y., Wikelski, M., Butler, P.J., 2015. The roller coaster flight strategy of bar-headed geese conserves energy during Himalayan migrations. Science 347, 250–254.

Black, C.P., Tenney, S.M., 1980. Oxygen transport during progressive hypoxia in high-altitude and sea-level waterfowl. Respir. Physiol. 39, 217–239.

Blackburn, T.M., Gaston, K.J., 1994. The distribution of body sizes of the World's bird species. Oikos 70, 127–130.

Blem, C.R., 1976. Patterns of lipid storage and utilization in birds. Am. Zool. 16, 671–684.

Blum, A., 1980. Annapurna: a Woman's Place. Sierra Club Books, USA, p. 247.

Boggs, D.F., 1997. Coordinated control of respiratory pattern during locomotion in birds. Am. Zool. 37, 41–53.

Boggs, D.F., Dial, K.P., 1993. Neuromuscular organization and regional EMG activity of the pectoralis in the pigeon. J. Morphol. 218, 43–57.

Boggs, D.F., Jenkins Jr., F.A., Dial, K.P., 1997a. The effects of wingbeat cycle on respiration in black-billed magpies *Pica pica*. J. Exp. Biol. 200, 1403–1412.

Boggs, D.F., Seveyka, J.J., Kilgore Jr., D.L., Dial, K.P., 1997b. Coordination of respiratory cycles with wingbeat cycles in black-billed magpie (*Pica pica*). J. Exp. Biol. 200, 1413–1420.

Bonen, A., Chabowski, A., Luiken, J.J.F.P., Glatz, J.F.C., 2007. Mechanisms and regulation of protein-mediated cellular fatty acid uptake: molecular, biochemical and physiological evidence. Physiology 22, 15–28.

Bowlin, M.S., Henningsson, P., Muigres, F.T., Vleugels, R.H.E., Liechti, F., Hedenström, A., 2010. The effects of geolocator drag and weight on the flight ranges of small migrants. Meth. Ecol. Evol. 1, 398–402.

Brobeck, J.R., DuBois, A.B., 1980. Energy exchange. In: Mountcastle, V.B. (Ed.), Medical Physiology, vol. 2, pp. 1351–1365 (St Louis).

Bromley, R.G., Jarvis, R.L., 1993. The energetics of migration and reproduction of dusky Canada geese. Condor 95, 193–210.

Bruderer, B., Liechti, F., 1995. Variation in density and height distribution of nocturnal migration in the south of Israel. Isr. J. Zool. 41, 477–487.

Bruderer, B., Peter, D., Korner-Nievergelt, F., 2018. Vertical distribution of bird migration between the Baltic sea and the Sahara. J. Ornithol. 159, 315–336.

Bruderer, B., Underhill, L., Liechti, F., 1995. Altitude choice of night migrants in a desert area predicted by meteorological factors. Ibis 137, 44–55.

Bundle, M.W., Hansen, K.S., Dial, K.P., 2007. Does the metabolic rate-flight speed relationship vary among geometrically similar birds of different mass? J. Exp. Biol. 210, 1075–1083.

Butler, P.J., 1991. Exercise in birds. J. Exp. Biol. 160, 233–262.

Butler, P.J., 2016. The physiological basis of bird flight. Phil. Trans. R. Soc. B 371. https://doi.org/10.1098/rstb.2015.0384.

Butler, P.J., 2010. High fliers: the physiology of bar-headed geese. Comp. Biochem. Physiol. A 156, 325–329.

Butler, P.J., Woakes, A.J., 1980. Heart rate, respiratory frequency and wing beat frequency of free flying barnacle geese *Branta leucopsis*. J. Exp. Biol. 85, 213–226.

Butler, P.J., Woakes, A.J., 1990. The physiology of bird flight. In: Gwinner, E. (Ed.), Bird Migration: Physiology and Ecophysiology. Springer-Verlag, Berlin/Heidelberg, pp. 300–318.

Butler, P.J., West, N.H., Jones, D.R., 1977. Respiratory and cardiovascular responses of the pigeon to sustained, level flight a wind-tunnel. J. Exp. Biol. 71, 7–26.

Butler, P.J., Woakes, A.J., Bishop, C.M., 1998. Behaviour and physiology of Svalbard barnacle geese, *Branta leucopsis* during their autumn migration. J. Avian Biol. 29, 536–545.

Butler, P.J., Green, J.A., Boyd, I.L., Speakman, J.R., 2004. Measuring metabolic rate in the field: the pros and cons of the doubly labelled water and heart rate methods. Funct. Ecol. 18, 168–183.

Caldow, R.W.G., Furness, R.W., 1993. A histochemical comparison of fibre types in the M. pectoralis and M. supracoracoideus of the great skua *Catharacta skua* and the herring gull *Larus argentatus* with reference to kleptoparasitic capabilities. J. Zool. London 229, 91–103.

Carlsson, M., Wahrenberg, V., Carlsson, M.S., Andersson, R., Carlsson, T., 2020. Gross and delta efficiencies during uphill running and cycling among elite triathletes. Eur. J. Appl. Physiol. 120, 961–968.

Carmi, N., Pinshow, B., Horowitz, M., Bernstein, M.H., 1993. Birds conserve plasma volume during thermal and flight-incurred dehydration. Physiol. Zool. 66, 829–846.

Carmi, N., Pinshow, B., Porter, W.P., Jaeger, J., 1992. Water and energy limitations on flight duration in small migrating birds. Auk 109, 268–276.

Carpenter, F.L., 1975. Bird hematocrits: effects of high altitude and strength of flight. Comp. Biochem. Physiol. A 50, 415–417.

Chai, P., Dudley, R., 1995. Limits to vertebrate locomotor energetics suggested by hummingbirds hovering in heliox. Nature 377, 722–725.

Chai, P., Dudley, R., 1996. Limits to flight energetics of hummingbirds hovering in hypodense and hypoxic gas mixtures. J. Exp. Biol. 199, 2285–2295.

Chai, P., Millard, D., 1997. Flight and size constraints: hovering performance of large hummingbirds under maximal loading. J. Exp. Biol. 200, 2757–2763.

Chin, D.D., Lentink, D., 2016. Flapping wing aerodynamics: from insects to vertebrates. J. Exp. Biol. 219, 920–932.

Choi, I., Ricklefs, R.E., Shea, R.E., 1993. Skeletal muscle growth, enzyme activities and the development of thermogenesis: a comparison between altricial and precocial birds. Physiol. Zool. 66, 455–473.

Clark, C.J., Dudley, R., 2010. Hovering and forward flight energetics in Anna's and Allen's hummingbirds. Physiol. Biochem. Zool. 83, 654–662.

Cooke, S.J., Hinch, S.G., Wikelski, M., Andrews, R.D., Kuchel, L.J., Wolcott, T.G., Butler, P.J., 2004. Biotelemetry: a mechanistic approach to ecology. Trends Ecol. Evol. 19, 334–343.

Crabtree, B., Newsholme, E.A., 1972. The activities of phosphorylase, hexokinase, phosphofructokinase, lactate dehydrogenase and glycerol 3-phosphate dehydrogenase in muscles from vertebrate and invertebrates. Biochem. J. 126, 49–58.

Crile, G., Quiring, D.P., 1940. A record of the body weight and certain organ and gland-weights of 3690 animals. Ohio J. Sci. XL 219–259.

Cutts, C.J., Speakman, J.R., 1994. Energy savings in formation flight of pink-footed geese. J. Exp. Biol. 189, 251–261.

Dakin, R., Segre, P.S., Straw, A.D., Altshuler, D.L., 2018. Morphology, muscle capacity, skill, and maneuvering ability in hummingbirds. Science 359, 653–657.

Deaton, K.E., Bishop, C.M., Butler, P.J., 1997. The effect of thyroid hormones on the aerobic development of locomotor and cardiac muscles in the barnacle goose. J. Comp. Physiol. 167, 319–327.

Deaton, K.E., Bishop, C.M., Butler, P.J., 1998. Tissue-specific effects of hypothyroidism on postnatal muscle development in the goose. J. Exp. Biol. 201, 827–836.

Dawson, N.J., Alza, L., Nandal, G., Scott, G.R., McCracken, K.G., 2020. Convergent changes in muscle metabolism depend on duration of high-altitude ancestry across Andean waterfowl. eLife 9, e56259.

Deetjen, M.E., Chin, D.D., Lentink, D., 2020. The aerodynamic force platform as an ergometer. J. Exp. Biol. 223 https://doi.org/10.1242/jeb.220475.

Dial, K.P., 1992a. Activity patterns of the wing muscles of the pigeon (*Columba livia*) during different modes of flight. J. Exp. Zool. 262, 357–373.

Dial, K.P., 1992b. Avian forelimb muscles and nonsteady flight: can birds fly without using the muscles in their wings? Auk 109, 874–885.

Dial, K.P., 2003. Wing-assisted incline running and the evolution of flight. Science 299, 402–404.

Dial, K.P., Biewener, A.A., 1993. Pectoralis muscle force and power output during different modes of flight in pigeons (*Columba livia*). J. Exp. Biol. 176, 31–54.

Dial, K.P., Biewener, A.A., Tobalske, B.W., Warrick, D.R., 1997. Mechanical power output of bird flight. Nature 390, 67–70.

Dial, K.P., Kaplan, S.R., Goslow, G.E.J., Jenkins, F.A.J., 1987. Structure and neural control of the pectoralis in pigeons: implications for flight mechanics. Anat. Rec. 218, 284–287.

Dial, K.P., Kaplan, S.R., Goslow, G.E.J., 1988. A functional analysis of the primary upstroke and downstroke muscles in the domestic pigeon (*Columba livia*) during flight. J. Exp. Biol. 134, 1–16.

Dial, K.P., Goslow, G.E.J., Jenkins, F.A.J., 1991. The functional anatomy of the shoulder in the european starling (*Sturnus vulgaris*). J. Morphol. 207, 327–344.

Dick, M.F., Guglielmo, C.G., 2019a. Dietary polyunsaturated fatty acids influence flight muscle oxidative capacity, but not endurance flight performance in a migratory songbird. Am. J. Physiol. 316, R362–R375.

Dick, M.F., Guglielmo, C.G., 2019b. Flight muscle protein damage during endurance flight is related to energy expenditure but not dietary polyunsaturated fatty acids in a migratory bird. J. Exp. Biol. 222, jeb.187708.

Dietz, M.W., Piersma, T., Dekinga, A., 1999. Body-building without power training: endogenously regulated pectoral muscle hypertrophy in confined shorebirds. J. Exp. Biol. 202, 2831–2837.

Driedzic, W.R., Crowe, H.L., Hicklin, P.W., Sephton, D.H., 1993. Adaptations in pectoralis muscle, heart mass, and energy metabolism during premigratory fattening in semipalmated sandpipers (*Calidris pusilla*). Can. J. Zool. 71, 1602–1608.

Dudley, R., 1998. Atmospheric oxygen, giant paleozoic insects and the evolution of aerial locomotor performance. J. Exp. Biol. 201, 1043–1050.

Duijins, S., Niles, L.J., Dey, A., Aubry, Y., Friis, C., Koch, S., Anderson, A.M., Smith, P.A., 2017. Body condition explains migratory performance of a long-distance migrant. Proc. R. Soc. B 284. https://doi.org/10.1098/rspb.2017.1374.

Duriez, O., Kato, A., Tromp, C., Dell'Omo, G., Vyssotski, A.L., Sarrazin, F., Ropert-Coudert, Y., 2014. How cheap is soaring flight in raptors? A preliminary investigation in freely-flying vultures. PloS One 9, e84887.

Efrat, R., Hatzofe, O., Nathan, R., 2019. Landscape-dependent time versus energy optimizations in pelicans migrating through a large ecological barrier. Funct. Ecol. 33, 2161–2171.

Egevang, C., Stenhouse, I.J., Phillips, R.A., Petersen, A., Fox, J.W., Silk, J.R.D., 2010. Tracking of Arctic terns *Sterna paradisaea* reveals longest animal migration. Proc. Natl. Acad. Sci. U. S. A. 107, 2078–2081.

Elkins, N., 1979. High altitude flight by swans. Br. Birds 72, 238–239.

Ellington, C.P., 1984. The aerodynamics of hovering insect flight. VI. Lift and power requirements. Phil. Trans. Soc. Lond. B 305, 145–181.

Ellington, C.P., 1991. Limitations on animal flight performance. J. Exp. Biol. 160, 71–91.

Elliott, K.H., Le Vaillant, M., Kato, A., Speakman, J.R., Ropert-Coudert, Y., 2013. Accelerometry predicts daily energy expenditure in a bird with high activity levels. Biol. Lett. 9 https://doi.org/10.1098/rsbl.2012.0919.

Ellis, H.I., 1984. Energetics of free-ranging seabirds. In: Whittow, C.G., Rahn, H. (Eds.), Seabird Energetics, vol. 261. Plenum, New York, pp. 203–234, 73–79.

Engel, S., Biebach, H., Visser, G.H., 2006a. Metabolic costs of avian flight in relation to flight velocity: a study in rose coloured starlings (*Sturnus roseus*). J. Comp. Physiol. B 176, 415–427.

Engel, S., Suthers, R.A., Biebach, H., Visser, G.H., 2006b. Respiratory water loss during rest and flight in European starlings (*Sturnus vulgaris*). Comp. Biochem. Physiol. A 145, 423–432.

Faraci, F.M., Fedde, M.R., 1986. Regional circulatory responses to hypocapnia and hypercapnia in bar-headed geese. Am. J. Physiol. 250, R499–R504.

Faraci, F.M., Kilgore Jr., D.L., Fedde, M.R., 1984a. Oxygen delivery to the heart and brain during hypoxia: Pekin duck vs. bar-headed goose. Am. J. Physiol. 247, R69–R75.

Faraci, F.M., Kilgore Jr., D.L., Fedde, M.R., 1984b. Attenuated pulmonary pressor response to hypoxia in bar-headed geese. Am. J. Physiol. 247, R402–R403.

Faraci, F.M., Kilgore Jr., D.L., Fedde, M.R., 1985. Blood flow distribution during hypocapnic hypoxia in Pekin ducks and bar-headed geese. Respir. Physiol. 61, 21–30.

Fedde, M.R., Orr, J.A., Shams, H., Scheid, P., 1989. Cardiopulmonary function in exercising bar-headed geese during normoxia and hypoxia. Respir. Physiol. 77, 239–262.

Fry, C.H., Ferguson-Lees, I.F., 1972. Flight muscle hypertrophy and ecophysiological variation of yellow wagtail (*Motacilla flava*) races at Lake Chad. J. Zool. London 167, 293–306.

Funk, G.D., Milsom, W.K., Steeves, J.D., 1992a. Coordination of wingbeat and respiration in the Canada goose. I. Passive wing flapping. J. Appl. Physiol. 73, 1014–1024.

Funk, G.D., Sholomenko, G.N., Valenzuela, I.J., Steeves, J.D., Milsom, W.K., 1993. Coordination of wing beat and respiration in Canada geese during free flight. J. Exp. Biol. 175, 317–323.

Funk, G.D., Steeves, J.D., Milsom, W.K., 1992b. Coordination of wingbeat and respiration in birds. II. ''Fictive'' flight. J. Appl. Physiol. 73, 1025–1033.

Gaunt, A.S., Hikida, R.S., Jehl Jr., J.R., Fenbert, L., 1990. Rapid atrophy and hypertrophy of an avian flight muscle. Auk 107, 649–659.

George, J.C., Berger, A.J., 1966. Avian Myology. Academic.Press, London/New York.

Gerson, A.R., Guglielmo, C.G., 2011a. Flight at low ambient humidity increases protein catabolism in migratory birds. Science 333, 1434–1436.

Gerson, A.R., Guglielmo, C.G., 2011b. House sparrows (*Passer domesticus*) increase protein catabolism in response to water restriction. Am. J. Physiol. 300, R925–R930.

Gessaman, J.A., 1980. An evaluation of heart rate as an indirect measure of daily energy metabolism of the American kestrel. Comp. Biochem. Physiol. A 65, 273–289.

Gessaman, J.A., Nagy, K.A., 1988. Transmitter loads affect the flight speed and metabolism of homing pigeons. Condor 90, 662–668.

Gibb, R., Shoji, A., Fayet, A.L., Perrins, C.M., Guilford, T., Freeman, R., 2017. J. R. Soc. Interface 14. https://doi.org/10.1098/rsif.2017.0262.

Giladi, I., Pinshow, B., 1999. Evaporative and excretory water loss during free flight in pigeons. J. Comp. Physiol. B 169, 311–318.

Giladi, I., Goldstein, D.L., Pinshow, B., Gerstberger, R., 1997. Renal function and plasma levels of arginine vasotocin during free flight in pigeons. J. Exp. Biol. 200, 3203–3211.

Gill, R.E., Tibbitts, T.L., Douglas, D.C., Handel, C.M., Mulcahy, D.M., Gottschalck, J.C., Warnock, N., McCaffery, B.J., Battley, P.F., Piersma, T., 2009. Extreme endurance flights by landbirds crossing the Pacific Ocean: ecological corridor rather than barrier? Proc. R. Soc. B. 276, 447–457.

Gillooly, J.F., Allen, A.P., 2007. Linking global patterns in biodiversity to evolutionary dynamics using metabolic theory. Ecology 88, 1890–1894.

Glatz, J.F.C., Schapp, F.G., Binas, B., Bonen, A., van der Vusse, G.J., Luiken, J.J.F.P., 2003. Cytoplasmic fatty acid-binding protein facilitates fatty acid utilization by skeletal muscle. Acta Physiol. Scand. 178, 367–371.

Glazier, D.S., 2008. Effects of metabolic level on the body size scaling of metabolic rate in birds and mammals. Proc. R. Soc. B 275. https://doi.org/10.1098/rspb.2008.0118.

Goslow, G.E.J., Dial, K.P., 1990. Active stretch-shorten contractions of the M. Pectoralis in the European starling (*Sturnus vulgaris*): evidence from electromyography and contractile properties. Neth. J. Zool. 40, 106–114. Is a spring. Science 241, 1495–1498.

Gould, L.L., Heppner, F., 1974. The vee formation of Canada geese. Auk 91, 494–506.

Green, J.A., 2011. The heart rate method for estimating metabolic rate: review and recommendations. Comp. Biochem. Physiol. A 158, 287–304.

Greenewalt, C.H., 1962. Dimensional relationships for flying animals. Smithsonian Misc. Collect. 144, 1–46.

Greenewalt, C.H., 1975. The flight of birds. Trans. Am. Phil. 65, 1–67.

Groom, D.J.E., Toledo, M.C.B., Powers, D.R., Tobalske, B.W., Welch Jr., K.C., 2018. Integrating morphology and kinematics in the scaling of hummingbird hovering metabolic rate and efficiency. Proc. R. Soc. B 285. https://doi.org/10.1098/rspb.2017.2011.

Grubb, B.R., 1983. Allometric relations of cardiovascular function in birds. Am. J. Physiol. 245, H567–H572.

Grubb, B., Mills, C.B., Colacino, J.M., Schmidt-Nielsen, K., 1977. Effect of arterial carbon dioxide on cerebral blood flow in ducks. Am. J. Physiol. 232, H596–H601.

Grubb, B., Colacino, J.M., Schmidt-Nielsen, K., 1978. Cerebral blood flow in birds: effect of hypoxia. Am. J. Physiol. 234, H230–H234.

Grubb, B., Jones, J.H., Schmidt-Nielsen, K., 1979. Avian cerebral blood flow: influence of the Bohr effect on oxygen supply. Am. J. Physiol. 236, H744–H749.

Gudmundsson, G.A., Benvenuti, S., Alterstam, T., Papi, F., Lilliendahl, K., Åkesson, S., 1995. Examining the limits of flight and orientation performance: satellite tracking of brent geese migrating across the Greenland ice-cap. Proc. Roy. Soc. Lond. B. 261, 73–79.

Gudmundsson, G.A., Lindström, Å., Alerstam, T., 1991. Optimal fat loads and long-distance flights by migrating knots *Calidris canutus*, sanderlings *C. alba* and turnstones *Arenaria interpres*. Ibis 133, 140–152.

Guglielmo, C.G., 2010. Move that fatty acid: fuel selection and transport in migratory birds and bats. Integr. Comp. Biol. 50, 366-345.

Guglielmo, C.G., 2018. Obese super athletes: fat-fueled migration in birds and bats. J. Exp. Biol. 221, jeb165753.

Guglielmo, C.G., Gerson, A.R., Price, E.R., Hays, Q.R., 2017. The effects of dietary macronutrients on flight ability, energetics, and fuel metabolism of yellow-rumped warblers *Setphaga coronata*. J. Avian Biol. 48, 133–148.

Guglielmo, C.G., Haunerland, N.H., Williams, T.D., 1998. Fatty acid binding protein, a major protein in the flight muscle of migrating western sandpipers. Comp. Biochem. Physiol. B 119, 549–555.

Guglielmo, C.G., Haunerland, N.H., Hochachka, P.W., Williams, T.D., 2002. Seasonal dynamics of flight muscle fatty acid binding protein and catabolic enzymes in a migratory bird. Am. J. Physiol. 282, R1405–R1413.

Guglielmo, C.G., McGuire, L.P., Gerson, A.R., Seewagen, C.L., 2011. Simple, rapid and non-invasive measurement of fat, lean, and total water masses of live birds using quantitative magnetic resonance. J. Ornithol. 152, S75–S85.

Guigueno, M.L., Shoji, A., Elliott, K.H., Aris-Brosou, S., 2019. Flight costs in volant vertebrates: a phylogenetically-controlled meta-analysis of birds and bats. Comp. Biochem. Physiol. A 235, 193–201.

Guillemette, M., Polymeropoulos, E.T., Portugal, S.J., Pelletier, D., 2017. It takes time to be cool: on the relationship between hyperthermia and body cooling in a migrating seaduck. Front. Physiol. 8 https://doi.org/10.3389/fphys.2017.00532.

Guillemette, M., Woakes, A.J., Larochelle, J., Polymeropoulos, E.T., Granbois, J.-M., Butler, P.J., Pelletier, D., Frappell, P.B., Portugal, S.J., 2016. Does hyperthermia constrain flight duration in a short-distance migrant? Phil. Trans. R. Soc. B 371. https://doi.org/10.1098/rstb.2015.0386.

Hails, C.J., 1979. A comparison of flight energetics in hirundines and other birds. Comp. Biochem. Physiol. A 63, 581–585.

Hainsworth, F.R., 1987. Precision and dynamics of positioning by Canada geese flying on formation. J. Exp. Biol. 128, 445–462.

Hainsworth, F.R., 1988. Wing movements and positioning for aerodynamic benefit by Canada geese flying in formation. Can. J. Zool. 67, 585–589.

Halsey, L.G., Portugal, S.J., Smith, J.A., Murn, C.P., Wilson, R.P., 2009. Recording raptor behaviour on the wing via accelerometry. J. Field Ornithol. 80, 171–177.

Halsey, L.G., Shepard, E.L.C., Wilson, R.P., 2011. Assessing the development and application of the accelerometry technique for estimating energy expenditure. Comp. Biochem. Physiol. A 158, 305–314.

Hambly, C., Harper, E.J., Speakman, J.R., 2002. Cost of flight in the zebra finch (*Taenopygia guttata*): a novel approach based on elimination of 13C labelled bicarbonate. J. Comp. Physiol. B 172, 529–539.

Hambly, C., Pinshow, B., Wiersma, P., Verhulst, S., Piertney, S.B., Harper, E.J., Speakman, J.R., 2004. Comparison of the cost of short flights in a nectarivorous and non-nectarivorous bird. J. Exp. Biol. 207, 3959–3968.

Hart, J.S., Roy, O.Z., 1966. Respiratory and cardiac responses to flight in pigeons. Physiol. Zool. 39, 291–306.

Hartman, F.A., 1961. Locomotor mechanisms of birds. Smithsonian Misc. Collect. 143, 1–91.

Hawkes, L.A., Balachandran, S., Batbayar, N., Butler, P.J., Chua, B., Douglas, D.C., Frappell, P.B., Hou, Y., Milsom, W.K., Newman, S.H., Prosser, D.J., Sathiyaselvam, P., Scott, G.R., Takekawa, J.K., Natsagdorj, T., Wikelski, M., Witt, M.J., Yan, B., Bishop, C.M., 2013. The paradox of extreme high-altitude migration in bar-headed geese *Anser indicus*. Proc. R. Soc. B. 280 https://doi.org/10.1098/rspb.2012.2114.

Hawkes, L.A., Balachandran, S., Batbayar, N., Butler, P.J., Frappell, P.B., Milsom, W.K., Natsagdorj, T., Newman, S.H., Scott, G.R., Sathiyaselvam, P., Takekawa, J.K., Wikelski, M., Bishop, C.M., 2011. The trans-Himalayan flights of bar-headed geese (*Anser indicus*). Proc. Natl. Acad. Sci. U. S. A. 108, 9516–9519.

Hawkes, L.A., Butler, P.J., Frappell, P.B., Meir, J.U., Milsom, W.K., Scott, G.R., Bishop, C.M., 2014. Maximum running speed of captive Bar-headed Geese is unaffected by severe hypoxia. PloS One 9, e94015.

Hedenström, A., 2008. Adaptations to migration in birds: behavioural strategies, morphology and scaling effects. Phil. Trans. R. Soc. B. 363, 287–299.

Hedenström, A., Alerstam, T., 1992. Climbing performance of migrating birds as a basis for estimating limits for fuel-carrying capacity and muscle work. J. Exp. Biol. 164, 19–38.

Hedenström, A., Alerstam, T., 1995. Optimal flight speed of birds. Phil. Trans. Roy. Soc. Lond. B 348, 471–487.

Hedenström, A., Norevik, G., Warfvinge, K., Andersson, A., Bäckman, J., Åkesson, S., 2016. Annual 10-month aerial life phase in the Common Swift *Apus apus*. Curr. Biol. 26, 3066–3070.

Hedh, L., Guglielmo, C.G., Johansson, L.C., Deakin, J.E., Voigt, C.C., Hedenström, A., 2020. Measuring power input, power output and energy conversion efficiency in un-instrumented flying birds. J. Exp. Biol. 223, jeb223545.

Henningsson, P., Muijres, F.T., Hedenström, A., 2011. Time-resolved vortex wake of a common swift flying over a range of flight speeds. J. R. Soc. Interface 8, 807–816.

Hickson, R.C., Galassi, T.M., Dougherty, K.A., 1983. Repeated development and regression of exercise-induced cardiac hypertrophy in rats. J. Appl. Physiol. 54, 794–797.

Hirth, K.D., Biesel, W., Nachtigall, W., 1987. Pigeon flight in a wind tunnel. III. Regulation of body temperature. J. Comp. Physiol. B 157, 111–116.

Hudson, D.M., Bernstein, M.H., 1978. Respiratory ventilation during steady-state flight in the white-necked raven, *Corvus cryptoleucus*. Fed. SAVE Proc. 37, 472.

Hudson, D.M., Bernstein, M.H., 1981. Temperature regulation and heat balance in flying white-necked ravens, *Corvus cryptoleucus*. J. Exp. Biol. 90, 267–281.

Hudson, D.M., Bernstein, M.H., 1983. Gas exchange and energy cost of flight in the white-necked raven, *Corvus cryptoleucus*. J. Exp. Biol. 103, 121–130.

Hummel, D., 1995. Formation flight as an energy-saving mechanism. Isr. J. Zool. 41, 261–278.

Jackson, B.E., Dial, K.P., 2011. Scaling of mechanical power output during burst escape flight in the Corvidae. J. Exp. Biol. 214, 452–461.

Jehl Jr., J.R., 1997. Cyclical changes in body composition in the annual cycle and migration of the Eared Grebe, *Podiceps nigricollis*. J. Avian Biol. 28, 132–142.

Jenkins Jr., F.A., Dial, K.P., Goslow Jr., G.E., 1988. A cineradiographic analysis of bird flight: the wishbone in starlings is a spring. Science 241, 1495–1498.

Jenni, L., Jenni-Eiermann, S., 1998. Fuel supply and metabolic constraints in migrating birds. J. Avian Biol. 29, 521–528.

Jenni-Eiermann, S., Jenni, L., 1991. Metabolic responses to flight and fasting in night-migrating passerines. J. Comp. Physiol. B 161, 465–474.

Jenni-Eiermann, S., Jenni, L., 1992. High plasma triglyceride levels in small birds during migratory flight: a new pathway for fuel supply during endurance locomotion at very high mass-specific metabolic rates? Physiol. Zool. 65, 112–123.

Johansson, L.C., Maeda, M., Henningsson, P., Hedenström, A., 2018. Mechanical power curve measured in the wake of a pied flycatchers indicates modulation of parasite power across flight speeds. J. R. Soc. Interface 15. https://doi.org/10.1098/rsif.2017.0814.

Johnson, O.W., Fielding, L., Fisher, J.P., Gold, R.S., Goodwill, R.H., Bruner, A.E., Furey, J.F., Brusseau, P.A., Brusseau, N.H., Johnson, P.M., Jukema, J., Prince, L.L., Tenney, M.J., Fox, J.W., 2012. New insight concerning transoceanic migratory pathways of Pacific golden-plovers (*Pluvialis fulva*): the Japan stopover and other linkages as revealed by geolocators. Wader Study Group Bull. 119, 1–8.

Jouventin, P., Weimerskirch, H., 1990. Satellite tracking of Wandering albatrosses. Nature 343, 746–748.

Joyce, W., White, D.W., Raven, P.B., Wang, T., 2019. Weighing the evidence for using vascular conductance, not resistance, in comparative cardiovascular physiology. J. Exp. Biol. 222 https://doi.org/10.1242/jeb.197426.

Jurgens, K.D., Bartels, H., Bartels, R., 1981. Blood oxygen transport and organ weights of small bats and small nonflying mammals. Respir. Physiol. 45, 243–260.

Kampe, G., Crawford Jr., E.C., 1993. Oscillatory mechanics of the respiratory system of pigeons. Respir. Physiol. 18, 188–193.

Kaplan, S.R., Goslow, G.E.J., 1989. Neuromuscular organization of the pectoralis of the pigeon (*Columbia livia*): implications for motor control. Anat. Rec. 224, 426–430.

Kessler, A.E., Batbayar, N., Natsagdorj, T., Batsuur, D., Smith, A.T., 2013. Satellite telemetry reveals long-distance migration in the Asian great bustard Otis tarda dybowskii. J. Avian Biol. 44, 311–320.

Kiens, B., 2006. Skeletal muscle lipid metabolism in exercise and insulin resistance. Physiol. Rev. 86, 205–243.

Kilgore Jr., D.L., Boggs, D.F., Birchard, G.F., 1979. Role of the *rete mirable ophthalmicum* in maintaining the body-to-brain temperature difference in pigeons. J. Comp. Physiol. 129, 119–122.

Kirby, J.S., Stattersfield, A.J., Butchart, S.H.M., Evans, M.I., Grimmett, R.F.A., Jones, V.R., O'Sullivan, J., Tucker, G.M., Newton, I., 2008. Key conservation issues for migratory land- and waterbird species on the world's major flyways. Bird. Conserv. Int. 18, S49–S73.

Klaassen, M., Kvist, A., Lindström, A., 1999. How body water and fuel stores affect long distance flight in migrating birds. Proceedings 22 Int. Ornithol. Congr., Durban 1450–1467.

Klaassen, R.H.G., Alerstam, T., Carlsson, P., Fox, J.W., Lindström, 2011. Great flights by great snipes: long and fast non-stop migration over benign habitats. Biol. Lett. 7, 833–835.

Klaassen, M., Kvist, A., Lindström, A., 2000. Flight costs and fuel composition of a bird migrating in a wind tunnel. Condor 102, 444–451.

Klein Heerenbrink, M., Johansson, L.C., Hedenström, A., 2015. Power of the wingbeat: modelling the effects of flapping wings in vertebrate flight. Proc. R. Soc. A 471, 20140952. https://doi.org/10.1098/rspa.2014.0952.

Koteja, P., 1987. On the relation between basal and maximum metabolic rate in mammals. Comp. Biochem. Physiol. A 87, 205–208.

Ksepka, D.T., 2014. Flight performance of the largest volant bird. Proc. Natl. Acad. Sci. U. S. A. 111, 10624–10629.

Kunz, T.H., Gauthreaux jr., S.A., Hristov, N.I., Horn, J.W., Jones, G., Kalko, E.K.V., Larkin, R.P., McCracken, G.F., Swartz, S.M., Srygley, R.B., Dudley, R., Westbrook, J.K., Wikelski, M., 2008. Aeroecology: probing and modeling the aerosphere. Integr. Comp. Biol. 48, 1–11.

Krüger, K., Prinzinger, R., Schuchmann, K.-L., 1982. Torpor and metabolism in hummingbirds. Comp. Biochem. Physiol. A 73, 679–689.

Kvist, A., Klaassen, M., Lindström, Å., 1998. Energy expenditure in relation to flight speed: what is the power of mass loss rate estimates? J. Avian Biol. 29, 485–498.

Kvist, A., Lindström, Å., Green, M., Piersma, T., Visser, G.H., 2001. Nature 413, 730–732.

Lack, D., 1960. Migration across the North Sea studied by radar. Part 2. The spring departure 1956–59. Ibis 102, 27–59.

Laguë, S.L., 2017. High-altitude champions: birds that live and migrate at altitude. J. Appl. Physiol. 123, 942–950.

Landys, M.M., Piersma, T., Visser, G.H., Jukema, J., Wijker, A., 2000. Water balance during real and simulated long-distance migratory flight in the bar-tailed godwit. Condor 102, 645–652.

Lasiewski, R.C., 1963. Oxygen consumption of torpid, resting, active and flying hummingbirds. Physiol. Zool. 36, 122–140.

Lasiewski, R.C., Calder Jr., W.A., 1971. Apreliminary allometric analysis of respiratory variables in resting birds. Respir. Physiol. 11, 152–166.

Lentink, D., Müller, U.K., Stamhuis, E.J., de Kat, R., van Gestel, W., Veldhuis, L.L.M., Henningsson, P., Hedenström, A., Videler, J.J., van Leeuwen, J.L., 2007. How swifts control their glide performance with morphing wings. Nature 446, 1082–1085.

Liechti, F., Schaller, E., 1999. The use of low-level jets by migrating birds. Naturwissenschaften 86, 549–551.

Liechti, F., Witvliet, W., Weber, R., Bächler, E., 2013. First evidence of a 200-day non-stop flight in a bird. Nat. Comms. 4, 2554. https://doi.org/10.1038/ncomms3554.

Lifson, N., Gordon, G.B., McClintock, R., 1955. Measurement of total carbon dioxide production by means of D^2O^{18}. J. Appl. Physiol. 7, 704–710.

Lifson, N., Gordon, G.B., Visscher, M.B., Nier, A.O., 1949. The fate of utilized molecular oxygen and the source of the oxygen of respiratory carbon dioxide, studied with the aid of heavy oxygen. J. Biol. Chem. 180, 803–811.

Lissaman, P.B.S., Shollenberger, C.A., 1970. Formation flight of birds. Science 168, 1003–1005.

Lundgren, B.O., Kiessling, K.-H., 1985. Seasonal variation in catabolic enzyme activities in breast muscle of some migratory birds. Oecologia 66, 468–471.

Lundgren, B.O., Kiessling, K.-H., 1986. Catabolic enzyme activities in the pectoralis muscle of premigratory and migratory juvenile reed warblers *Acrocephalus scirpaceus*. Oecologia 68, 529–532.

Lusk, G., 1919. The Elements of the Science of Nutrition. W. B. Saunders, Philadelphia/London.

Magnan, A., 1922. Les caracteristiques des oiseaux suivant le mode de vol. Ann. Sci. Nat. 5, 125–334.

Maillet, D., Weber, J.-M., 2007. Relationship between n-3 PUFA content and energy metabolism in the flight muscles of a migrating shorebird: evidence from natural doping. J. Exp. Biol. 210, 314–420.

Mainguy, S.K., Thomas, V.G., 1985. Comparisons of body reserve buildup and use in several groups of Canada geese. Can. J. Zool. 63, 1765–1772.

Marden, J.H., 1987. Maximum lift production during takeoff in flying animals. J. Exp. Biol. 130, 235–258.

Marden, J.H., 1994. From damselflies to pterosaurs: how burst and sustainable flight performance scale with size. Am. J. Physiol. 266, R1077–R1084.

Marey, E.J., 1890. Le Vol des Oiseaux. Masson, Paris.

Martineau, L., Larochelle, J., 1988. The cooling power of pigeon legs. J. Exp. Biol. 136, 193–208.

Marsh, R.L., 1981. Catabolic enzyme activities in relation to premigratory fattening and muscle hypertrophy in the gray catbird *Dumetella carolinensis*. J. Comp. Physiol. 141, 417–423.

Marsh, R.L., 1984. Adaptations of the gray catbird *Dumatella carolinensis* to long-distance migration: flight muscle hypertrophy associated with elevated body mass. Physiol. Zool. 57, 105–117.

Marsh, R.L., Storer, R.W., 1981. Correlation of flight muscle size and body mass in Cooper's Hawks: a natural analogue of power training. J. Exp. Biol. 91, 363–368.

Marsh, R.L., Wickler, S.J., 1982. The role of muscle development in the transition to endothermy in nestling bank swallows *Riparia riparia*. J. Comp. Physiol. 149, 99–105.

Masman, D., Klaassen, M., 1987. Energy expenditure duringfree flight in trained and free-living Eurasian kestrels (*Falco tinnunculus*). Auk 104, 603–616.

Mathieu-Costello, O., 1991. Morphometric analysis of capillary geometry in pigeon pectoralis muscle. Am. J. Anat. 191, 74–84.

Mathieu-Costello, O., Suarez, R.K., Hochachka, P.W., 1992. Capillary-to-fiber geometry and mitochondrial density in hummingbird flight muscle. Respir. Physiol. 89, 113–132.

McClelland, G.B., 2004. Fat to the fire: the regulation of lipid oxidation with exercise and environmental stress. Comp. Biochem. Physiol. B 139, 443–460.

McFarlan, J.T., Bonen, A., Guglielmo, C.G., 2009. Seasonal upregulation of fatty acid transporters in flight muscles of migratory white-throated sparrows (*Zonotrichia albicollis*). J. Exp. Biol. 212, 2934–2940.

McWilliams, S.R., Pierce, B., Wittenzellner, A., Langlois, L., Engel, S., Speakman, J.R., Fatica, O., DeMoranville, K., Goymann, W., Trost, L., Bryla, A., Dzialo, M., Sadowska, E., Bauchinger, U., 2020. The energy savings-oxidative cost tradeoff for migratory birds during endurance flight. eLife 9. e60626.

Meir, J.U., Milsom, W.K., 2013. High thermal sensitivity of blood enhances oxygen delivery in the high-flying bar-headed goose. J. Exp. Biol. 216, 2172–2175.

Meyers, R.A., 1993. Gliding flight in the American kestrel (*Falco sparverius*): an electromyographic study. J. Morphol. 215, 213–224.

Meyers, R.A., 1997. Anatomy and histochemistry of spread-wing posture in birds. I. Wing drying posture in the double-crested cormorant, *Phalacrocorax auritus*. J. morph. 233, 67–76.

Meyers, R.A., Mathias, E., 1997. Anatomy and histochemistry of spread-wing posture in birds. 2. Gliding flight in the California Gull, *Larus californicus*: a paradox of fast fibers and posture. J. Morphol. 233, 237–247.

Meyers, R.A., Stakebake, E.F., 2005. Anatomy and histochemistry of spread-wing posture in birds. 3. Immunohistochemistry of flight muscles and the "shoulder lock" in albatrosses. J. Morphol. 263, 12–29.

Midtgård, U., 1983. Scaling of the brain and the eye cooling system in birds: a morphometric analysis of the *Rete ophthalmicum*. J. Exp. Zool. 225, 197–207.

Minton, C., Gosbell, K., Johns, P., Christie, M., Klaasen, M., Hassell, C., Boyle, A., Jessop, R., Fox, J., 2011. Geolocator studies on ruddy turnstones *Arenaria interpres* and greater sandplovers *Charadrius leschenaultii* in the East Asian-Australasia flyway reveal widely different migration strategies. Wader Study Group Bull. 118, 87–96.

Mitchell, G.W., Guglielmo, C.G., Hobson, K.A., 2015. Measurement of whole body CO_2 production in birds using real-time laser-derived measurements of hydrogen (δ^2H) and oxygen ($\delta^{18}O$) isotope concentrations in water vapor from breath. Physiol. Biochem. Zool. 88, 599–606.

Morris, C.R., Nelson, F.E., Askew, G.N., 2010. The metabolic power requirements of flight and estimations of flight muscle efficiency in the cockatiel (*Nymphicus hollandicus*). J. Exp. Biol. 213, 2788–2796.

Muijres, F.T., Bowlin, M.S., Johansson, L.C., Hedenström, A., 2012a. Vortex wake, downwash distribution, aerodynamic performance and wingbeat kinematics in slow-flying pied flycatchers. J. R. Soc. Interface 9, 292–303.

Muijres, F.T., Johansson, L.C., Bowlin, M.S., Winter, Y., Hedenström, A., 2012b. Comparing aerodynamic efficiency in birds and bats suggests better flight performance in birds. PloS One 7, e37335.

Nachtigall, W., 1995. Impositions of energy balance in prolonged flight: wind tunnel measurements with ''model birds''. Isr. J. Zool. 41, 279–295.

Nagy, K.A., 1980. CO_2 Production in animals: analysis of potential errors in the doubly labeled water method. Am. J. Physiol. 238, R466–R473.

Nagy, K.A., 1983. The Doubly Labeled Water ($^3HH^{18}O$) Method: A Guide to its Use. University of California at Los Angeles, p. 45. Publication No. 12-1417.

Natarajan, C., Projecto-Garcia, J., Moriyama, H., Weber, R.E., Munoz-Fuentes, V., Green, A.J., Kopuchian, C., Tubaro, P.L., Alza, L., Bulgarella, M., Smith, M.M., Wilson, R.E., Fago, A., McCracken, K.G., Storz, J.F., 2015. Convergent evolution of hemoglobin function in high-altitude Andean waterfowl involves limited parallelism at the molecular sequence level. PLoS Genet. 11, e1005681.

Nespolo, R.F., González-Lagos, C., Solano-Iguaran, J.J., Elfwing, M., Garitano-Zavala, A., Mañosa, S., Alonso, J.C., Altimiras, J., 2018. Aerobic power and flight capacity in birds: a phylogenetic test of the heart-size hypothesis. J. Exp. Biol. 221, jeb175208.

Newsholme, E.A., Leech, A.R., 1983. Biochemistry for the Medical Sciences. Wiley, Chichester/New York.

Niles, L.J., Burger, J., Porter, R.R., Dey, A.D., Koch, S., Harrington, B., Laquinto, K., Boarman, M., 2012. Migration pathways, migration speeds and non-breeding areas used by northern hemisphere wintering red knots *Calidris canutus* of the subspecies *rufa*. Wader Study Group Bull. 119, 1–9.

Nisbet, I.C.T., 1963. Measurements with radar of the height of nocturnal migration over Cape Cod, Massachusetts. Bird Band 34, 57–67.

Nisbet, I.C.T., Drury Jr., W.H., Baird, J., 1963. Weight loss during migration, Part I: deposition and consumption of fat by the blackpoll warbler *Dendroica striata*. Bird Band 34, 107–159.

Nolet, B.A., Butler, P.J., Masman, D., Woakes, A.J., 1992. Estimation of daily energy expenditure from heart rate and doubly labeled water in exercising geese. Physiol. Zool. 65, 1188–1216.

Norberg, U.M., 1990. Vertebrate Flight. Mechanics, Physiology, Morphology, Ecology and Evolution. Springer-Verlag, Berlin/Heidelberg.

Nord, A., Nilsson, J.A., 2019. Heat dissipation rate constrains reproductive investment in a wild bird. Funct. Ecol. 33, 250–259.

Obrecht, H.H., Pennycuick, C.J., Fuller, M.R., 1988. Wind tunnel experiments to assess the effect of back-mounted radio transmitters on bird body drag. J. Exp. Biol. 135, 265–273.

Parr, N., Bearhop, S., Douglas, D.C., Takekawa, J.Y., Prosser, D.J., Newman, S.H., Perry, W.M., Perry, W.M., Balachandran, S., Witt, M.J., Hou, Y., Luo, Z., Hawkes, L.A., 2017. High altitude flights by ruddy shelduck Tadorna ferruginea during trans-Himalayan migrations. J. Avian Biol. 48, 1310–1315.

Parr, N., Bishop, C.M., Batbayar, N., Butler, P.J., Chua, B., Milsom, W.K., Scott, G.R., Hawkes, L.A., 2019a. Tackling the Tibetan Plateau in a down suit: insights into thermoregulation by bar-headed geese during migration. J. Exp. Biol. 222, jeb203695.

Parr, N., Wilkes, M., Hawkes, L.A., 2019b. Insights from avian physiology and high altitude. High Alt. Med. Biol. 20, 427–437.

Pasquis, P., Lacaisse, A., Dejours, P., 1970. Maximal oxygen uptake in four species of small mammals. Respir. Physiol. 9, 298–309.

Pennycuick, C.J., 1968. Power requirements for horizontal flight in the pigeon *Columba livia*. J. Exp. Biol. 49, 527–555.

Pennycuick, C.J., 1969. The mechanics of bird migration. Ibis 111, 525–556.

Pennycuick, C.J., 1975. In: Farner, D.S., King, J.R., Parkes, K.C. (Eds.), Mechanics of Flight, vol. V. Academic Press, New York, pp. 1–75.

Pennycuick, C.J., 1978. Fifteen testable predictions about bird flight. Oikos 30, 165–176.

Pennycuick, C.J., 1982. The flight of petrels and albatrosses (Procellariiformes), observed in South Georgia and its vicinity. Phil. Trans. Roy. Soc. Lond. B 300, 75–106.

Pennycuick, C.J., 1989. Bird Flight Performance: a Practical Calculation Manual. Oxford Univ. Press, Oxford.

Pennycuick, C.J., 1990. Predicting wingbeat frequency and wavelength of birds. J. Exp. Biol. 150, 171–185.

Pennycuick, C.J., 1992. Newton Rules Biology: a Physical Approach to Biological Problems. Oxford Univ. Press, Oxford/New York/Tokyo.

Pennycuick, C.J., 1996. Stress and strain in the flight muscles as constraints on the evolution of flying animals. J. Biomech. 29, 577–581.

Pennycuick, C.J., 1997. Actual and ''optimum'' flight speeds: field data reassessed. J. Exp. Biol. 200, 2355–2361.

Pennycuick, C.J., 2008. Modelling the Flying Bird. Theoretical Ecology Series. Academic Press. Elsevier Inc., USA, p. 480.

Pennycuick, C.M., Einarsson, O., Bradbury, T.A.M., Owen, M., 1996a. Migrating whooper swans (Cygnus Cygnus): satellite tracks and flight performance calculations. J. Avian Biol. 27, 118–134.

Pennycuick, C.J., Fuller, M.R., McAllister, L., 1989. Climbing performance of Harris hawks (*Parabuteo unicinctus*) with added load: implications for muscle mechanics and for radiotracking. Science 177, 222–228 J. Exp. Biol. 142, 17–29.

Pennycuick, C.J., Klaassen, M., Kvist, A., Lindström, Å., 1996b. Wingbeat frequency and the body drag anomaly: wind-tunnel observations on a thrush nightingale (*Luscinia luscinia*) and a teal (*Anas crecca*). J. Exp. Biol. 199, 2757–2765.

Perutz, M.F., 1983. Species adaptation in a protein molecule. Mol. Biol. Evol. 1, 1–28.

Peters, G.W., Steiner, D.A., Rigoni, J.A., Mascilli, A.D., Schnepp, R.W., Thomas, S.P., 2005. Cardiorespiratory adjustments of homing pigeons to steady wind tunnel flight. J. Exp. Biol. 208, 3109–3120.

Piersma, T., 1988. Breast muscle atrophy and constraints on foraging during the flightless period of wing moulting great crested grebes. Ardea 76, 96–106.

Piersma, T., 1998. Phenotypic flexibility during migration: optimization of organ sizes contingent on the risks and rewards of fueling and flight? J. Avian Biol. 29, 511–520.

Piersma, T., Jukema, J., 1990. Budgeting the flight of a long-distance migrant: changes in nutrient reserve levels of bar-tailed godwits at successive spring staging sites. Ardea 78, 315–337.

Portugal, S.J., Green, J.A., White, C.R., Guillemette, M., Butler, P.J., 2012. Wild geese do not increase flight behavior prior to migration. Biol. Lett. 8, 469–472.

Portugal, S.J., Thorpe, S.K.S., Green, J.A., Myatt, J.P., Butler, P.J., 2009. Testing the use/disuse hypothesis: pectoral and leg muscle changes in captive barnacle geese *Branta leucopsis* during wing moult. J. Exp. Biol. 212, 2403–2410.

Powers, D.R., Langland, K.M., Wethington, S.M., Powers, S.D., Graham, C.H., Tobalske, B.W., 2017. Hovering in the heat: effects of environmental temperature on heat regulation in foraging hummingbirds. R. Soc. Open Sci. 4 https://doi.org/10.1098/rsos.171056.

Price, E.R., 2010. Dietary lipid composition and avian migratory flight performance: development of a theoretical framework for avian fat storage. Comp. Biochem. Physiol., A 157, 297–309.

Prinzinger, R., Hänssler, I., 1980. Metabolism–weight relationship in some small non-passerine birds. Experientia 36, 1299–1300.

Prum, R.O., Berv, J.S., Dornburg, A., Field, D.J., Townsend, J.P., Lemmon, E.M., Lemmon, A.R., 2015. A comprehensive phylogeny of birds (Aves) using targeted next-generation DNA sequencing. Nature 526, 569–573.

Qasem, L., Cardew, A., Wilson, A., Griffiths, I., Halsey, L.G., Shepard, E.L.C., Gleiss, A.C., Wilson, R., 2012. Tri-axial dynamic acceleration as a proxy for animal energy expenditure; should we be summing values or calculating the vector? PloS One 7, e31187.

Rahn, H., Ar, A., 1974. The avian egg: incubation time and water loss. Condor 76, 147–152.

Rall, J.A., 1985. Energetic aspects of skeletal muscle contraction: implications of fiber types. Exerc. Sport Sci. Rev. 13, 33–74.

Rattenborg, N.C., Voirin, B., Cruz, S.M., Tisdale, R., Dell'Omo, G., Lipp, H.-P., Wikelski, M., Vyssotski, A.L., 2016. Evidence that birds sleep in mid-flight. Nat. Comms. 7 https://doi.org/10.1038/ncomms12468.

Rayner, J.M.V., 1979. A new approach to animal flight mechanics. J. Exp. Biol. 80, 17–54.

Rayner, J.M.V., 1985a. Bounding and undulating flight in birds. J. Theor. Biol. 117, 47–77.

Rayner, J.M.V., 1988. Form and function in avian flight. In: Johnston, R.F. (Ed.), Current Ornithology, vol. 5. Plenum, New York, pp. 1–66.

Rayner, J.M.V., 1990. The mechanics of flight and bird performance. In: Gwinner, E. (Ed.), Bird Migration. Springer-Verlag, Berlin/Heidelberg, pp. 283–299.

Rayner, J.M.V., 1993. On aerodynamics and the energetics of vertebrate flapping flight. Contemp. Math. 141, 351–399.

Rayner, J.M.V., 1994. Aerodynamic corrections for the flight of birds and bats in wind tunnels. J. Zool. London 234, 537–563.

Richardson, P.L., 2011. How do albatrosses fly around the world without flapping their wings? Prog. Oceanogr. 88, 46–58.

Rohwer, S., Ricklefs, R.E., Rohwer, V.G., Copple, M.M., 2009. Allometry of the duration of flight feather molt in birds. PLoS Biol. 7, e1000132.

Rollema, H.S., Bauer, C., 1979. The interaction of inositol pentaphosphate with the hemoglobins of highland and lowland geese. J. Biol. Chem. 254, 12038–12043.

Ropert-Coudert, Y., Wilson, R.P., 2005. Trends and perspectives in animal-attached remote sensing. Front. Ecol. Environ. 3, 437–444.

Rosén, M., Hedenström, A., 2001. Gliding flight in a jackdaw: a wind tunnel study. J. Exp. Biol. 204, 1153–1166.

Rosser, B.W.C., George, J.C., 1986a. The avian pectoralis: histochemical characterization and distribution of muscle fiber types. Can. J. Zool. 64, 1174–1185.

Rosser, B.W.C., George, J.C., 1986b. Slow muscle fibres in the pectoralis of the Turkey vulture (*Cathartes aura*):An adaptation for soaring flight. Zool. Anz. 217, 252–258.

Rosser, B.W.C., Waldbillig, D.M., Wick, M., Bandman, E., 1994. Muscle fiber types in the pectoralis of the white pelican, a soaring bird. Acta Zool. 75, 329–336.

Rothe, H.J., Biesel, W., Nachtigall, W., 1987. Pigeon flight in a wind tunnel. II.Gas exchange and power requirements. J. Comp. Physiol. B 157, 99–109.

Rotics, S., Kaatz, M., Resheff, Y.S., Turjeman, S.F., Zurell, D., Sapir, N., Eggers, U., Flack, A., Fiedler, W., Jeltsch, F., Wikelski, M., Nathan, R., 2016. The challenges of the first migration: movement and behaviour of juvenile vs. adult white storks with insights regarding juvenile mortality. J. Anim. Ecol. 85, 938–947.

Safi, K., Kranstauber, B., Weinzieri, R., Griffin, L., Rees, E.C., Cabot, D., Cruz, S., Proano, C., Takekawa, J.Y., Newmann, S.H., Waldenstrom, J., Bengtsson, D., Kays, R., Wikelski, M., Bohrer, G., 2013. Flying with the wind: scale dependency of speed and direction measurements in modelling wind support in avian flight. Movement Ecol. 1, 4.

Sakamoto, K.Q., Takahashi, A., Iwata, T., Yamamoto, T., Yamamoto, M., Trathan, P.N., 2013. Heart rate and estimated energy expenditure of flapping and gliding in black-browed albatrosses. J. Exp. Biol. 216, 3175–3182.

Sapir, N., Dudley, R., 2012. Backward flight in hummingbirds employs unique kinematic adjustments and entails low metabolic cost. J. Exp. Biol. 215, 3603–3611.

Sapir, N., Wikelski, M., McCue, M.D., Pinshow, B., Nathan, R., 2010. Flight modes in migrating European bee-eaters: heart rate may indicate low metabolic rate during soaring and gliding. PloS One 5, e13956.

Sato, K., Daunt, F., Watanuki, Y., Takahashi, A., Wanless, S., 2008. A new method to quantify prey acquisition in diving seabirds using wing stroke frequency. J. Exp. Biol. 211, 58–65.

Sato, K., Sakamoto, K.Q., Watanuki, Y., Takahashi, A., Katsumata, N., Bost, C.A., Weimerskirch, H., 2009. Scaling of soaring seabirds and implications for flight abilities of giant pterosaurs. PloS One 4, e5400.

Scheid, P., 1985. Significance of lung structure for performance at high altitude. In: Ilyichev, V.D., Gavrilov, V.M. (Eds.), ACTA XVII, Congressus Internationalis Ornithologici, Moscow, pp. 976–977.

Schmaljohann, H., Liechti, F., 2009. Adjustments of wingbeat frequency and air speed to air density to air density in free-flying migratory birds. J. Exp. Biol. 212, 3633–3642.

Schmaljohann, H., Liechti, F., Bruderer, B., 2007. Songbird migration across the Sahara: the non-stop hypothesis rejected! Proc. R. Soc. B 274, 735–739.

Schmidt-Nielsen, K., 1972. Locomotion: energy cost of swimming, flying, and running. Science 177, 222–228.

Schmidt-Nielsen, K., 1984. Scaling: Why Is Animal Size So Important? Cambridge Univ. Press.

Schmidt-Nielsen, K., 1997. Animal Physiology: Adaptation and Environment, fifth ed. Cambridge Univ. Press.

Schmidt-Nielsen, K., Hainsworth, F.R., Murrish, D.E., 1970. Counter-current heat exchange in the respiration passages: effect on water and heat balance. Respir. Physiol. 9, 263–276.

Schmidt-Wellenburg, C.A., Biebach, H., Daan, S., Visser, G.H., 2007. Energy expenditure and wing beat frequency in relation to body mass in free flying barn swallows (*Hirundo rustica*). J. Comp. Physiol. B. 177, 327–337.

Schwenk, R.W., Holloway, G.P., Luiken, J.J.F.P., Bonen, A., Glatz, J.F.C., 2010. Fatty acid transport across the cell membrane: regulation by fatty acid transporters. Prostagl. Leukot. Essent. Fat. Acids 82, 149–154.

Scott, G.R., 2011. Elevated performance: the unique physiology of birds that fly at high altitudes. J. Exp. Biol. 214, 2455–2462.

Scott, G.R., Milsom, W.K., 2006. Flying high: a theoretical analysis of the factors limiting exercise performance in birds at altitude. Respir. Physiol. Neurobiol. 154, 284–301.

Scott, G.R., Milsom, W.K., 2007. Control of breathing and adaptation to high altitude in the bar-headed goose. Am. J. Physiol. 293, R379–R391.

Scott, G.R., Cadena, V., Tattersall, G.J., Milsom, W.K., 2008. Body temperature depression and peripheral heat loss accompany the metabolic and ventilatory responses to hypoxia in low and high altitude birds. J. Exp. Biol. 211, 1326–1335.

Scott, G.R., Egginton, S., Richards, J.G., Milsom, W.K., 2009. Evolution of muscle phenotype for extreme high altitude flight in the bar-headed goose. Proc. R. Soc. B. 276, 3645–3653.

Scott, G.R., Hawkes, L.A., Frappell, P.B., Butler, P.J., Bishop, C.M., Milsom, W.K., 2015. How bar-headed geese fly over the himalayas. Physiology 30, 107–115.

Sekercioglu, C.H., 2007. Conservation ecology: area trumps mobility in fragment bird extinctions. Curr. Biol. 17, R283–R286.

Senner, N.R., Stager, M., Verhoeven, M.A., Cheviron, Z.A., Piersma, T., Bouten, W., 2018. Proc. R. Soc. B 285. https://doi.org/10.1098/rspb.2018.0569.

Shaffer, S.A., Tremblay, Y., Weimerskirch, H., Scott, D., Thompson, D.R., Sagar, P.M., Moller, H., Taylor, G.A., Foley, D.G., Block, B.A., Costa, D.P., 2006. Migratory shearwaters integrate oceanic resources across the Pacific Ocean in an endless summer. Proc. Natl. Acad. Sci. U. S. A. 103, 12799–12802.

Shams, H., Scheid, P., 1989. Efficiency of parabronchial gas exchange in deep hypoxia: measurements in the resting duck. Resp. Physiol. 77, 135–146.

Shams, H., Scheid, P., 1993. Effects of hypobaria on parabronchial gas exchange in normoxic and hypoxic ducks. Respir. Physiol. 91, 155–163.

Shankar, A., Powers, D.R., Daválos, L.M., Graham, C.H., 2020. The allometry of daily energy expenditure in hummingbirds: an energy budget approach. J. Anim. Ecol. 89, 1254–1261.

Snyder, G.K., 1990. Capillarity and diffusion distances in skeletal-muscles in birds. J. Comp. Physiol. B. 160, 583–591.

Snyder, G.K., Byers, R.L., Kayar, S.R., 1984. Effects of hypoxia on tissue capillarity in geese. Respir. Physiol. 58, 151–160.

Speakman, J.R., 1990. Principles, problems and a paradox with the measurement of energy expenditure of free-living subjects using double-labelled water. Stat. Med. 9, 1365–1380.

Speakman, J.R., 1998. The history and theory of the doubly labeled water technique. Am. J. Clin. Nutr. 68 (Suppl. l), 932S–938S.

Speakman, J.R., Król, E., 2010. Maximal heat dissipation capacity and hyperthermia risk: neglected key factors in the ecology of endotherms. J. Anim. Ecol. 79, 726–746.

Speakman, J.R., Racey, P.A., 1988. Consequences of non-steady-state CO_2 production for accuracy of the doubly labeled water technique: the importance of recapture interval. Comp. Biochem. Physiol. A 90, 337–340.

Spedding, G.R., 1986. The wake of a jackdaw (*Corvus monedula*) in slow flight. J. Exp. Biol. 125, 287–307.

Spedding, G.R., 1987. The wake of a kestrel (*Falco tinnunculus*) in flapping flight. J. Exp. Biol. 127, 59–78.

Spedding, G.R., 1994. On the significance of unsteady effects in the aerodynamic performance of flying animals. Contemp. Math. 141, 401–419 (T).

Spedding, G.R., Rayner, J.M.V., Pennycuick, C.J., 1984. Momentum and energy in the wake of a pigeon (*Columba livia*) in slow flight. J. Exp. Biol. 111, 81–102.

Spedding, G.R., Rosén, M., Hedenström, A., 2003. A family of vortex wakes generated by a thrush nightingale in free flight in a wind tunnel over its entire natural range of flight speeds. J. Exp. Biol. 206, 2313–2344.

Spivey, R.J., Bishop, C.M., 2013. Interpretation of body-mounted accelerometry in flying animals and estimation of biomechanical power. J. R. Soc. Interface 10, 20130404.

Spivey, R.J., Stansfield, S., Bishop, C.M., 2014. Analysing the intermittent flapping flight of a Manx Shearwater, *Puffinus puffinus*, and its sporadic use of a wave-meandering wing-sailing flight strategy. Prog. Oceanogr. 125, 62–73.

Stewart, A.G., 1978. Swans flying at 8,000 metres. Br. Birds 71, 459–460.

Stickland, N.C., 1977. Succinic dehydrogenase distribution in the pectoralis muscle of several East African birds. Acta Zool. 58, 41–44.

Suarez, R.K., Brown, G.S., Hochachka, P.W., 1986. Metabolic sources of energy for hummingbird flight. Am. J. Physiol. 251, 537–542.

Suarez, R.K., Lighton, J.R.B., Moyes, C.D., Brown, G.S., Gass, C.L., Hochachka, P.W., 1990. Fuel selection in rufous hummingbirds: ecological implications of metabolic biochemistry. Proc. Natl. Acad. Sci. U. S. A. 87, 9207–9210.

Suarez, R.K., Welch, K.C., 2017. Sugar metabolism in hummingbirds and nectar bats. *Nutrient*s 9. https://doi.org/10.3390/nu9070743.

Swan, L.W., 1961. The ecology of the high himalayas. Sci. Am. 205, 68–78.

Symonds, M.R.E., Tattersall, G.J., 2010. Geographic variation in bill size across bird species provides evidence for Allen's rule. Am. Nat. 176 https://doi.org/10.1086/653666.

Takekawa, J.Y., Heath, S.R., Douglas, D.C., Perry, W.M., Javed, S., Newman, S.H., Suwal, R.N., Rahmani, A.R., Choudhury, B.C., Prosser, D.J., Yan, B., Hou, Y., Batbayar, N., Natsagdorj, T., Bishop, C.M., Butler, P.J., Frappell, P.B., Milsom, W.K., Scott, G.R., Hawkes, L.A., Wikelski, M., 2009. Geographic variation in bar-headed geese *Anser indicus*: connectivity of wintering areas and breeding grounds across a broad front. Wildfowl 59, 102–125.

Talesara, G.L., Goldspink, G., 1978. A combined histochemical and biochemical study of myofibrillar ATPase in pectoral, leg and cardiac muscle of several species of bird. Histochem. J. 10, 695–710.

Tapper, S., Nocera, J.J., Burness, G., 2020. Heat dissipation capacity influences reproductive performance in an aerial insectivore. J. Exp. Biol. 223 https://doi.org/10.1242/jeb.222232.

Tatner, P., Bryant, D.M., 1989. Doubly-labeled water technique for measuring energy expenditure. In: Bridges, C.R., Butler, P.J. (Eds.), Techniques in Comparative Respiratory Physiology: an Experimental Approach. Cambridge Univ. Press.

Tattersall, G.J., Arnaout, B., Abe, A.S., 2009. Heat exchange from the Toucan bill reveals a controllable vascular thermal radiator. Science 325, 468–470.

Tattersall, G.J., Arnaout, B., Symonds, M.R.E., 2017. The evolution of the avian bill as a thermoregulatory organ. Biol. Rev. 92, 1630–1656.

Taylor, C.R., 1994. Relating mechanics and energetics during exercise. Adv. Vet. Sci. Comp. Med. 38, 181–215.

Tobalske, B.W., 1995. Neuromuscular control and kinematics of intermittent flight in the European starling (*Sturnus vulgaris*). J. Exp. Biol. 198, 1259–1273.

Tobalske, B.W., 1996. Scaling of muscle composition, wing morphology, and intermittent flight behavior in woodpeckers. Auk 113, 151–177.

Tobalske, B.W., Dial, K.P., 1994. Neuromuscular control and kinematics of intermittent flight in budgerigars (*Melopsittacus undulatus*). J. Exp. Biol. 187, 1–18.

Tobalske, B.W., Dial, K.P., 1996. Flight kinematics of black- billed magpies and pigeons over a wide range of speeds. J. Exp. Biol. 199, 263–280.

Tobalske, B.W., Hearn, J.W.D., Warrick, D.R., 2009. Aerodynamics of intermittent bounds in flying birds. Exp. Fluid 46, 963–973.

Tobalske, B.W., Hedrick, T.L., Dial, K.P., Biewener, A.A., 2003. Comparative power curves in bird flight. Nature 421, 363–366.

Tobalske, B.W., Olson, N.E., Dial, K.P., 1997. Flight style of the black-billed magpie: variation in wing kinematics, neuromuscular control and muscle composition. J. Exp. Zool. 279, 313–329.

Torre-Bueno, J.R., 1976. Temperature regulation and heat dissipation during flight in birds. J. Exp. Biol. 65, 471–482.

Torre-Bueno, J.R., 1978a. Respiration during flight in birds. In: Piiper, J. (Ed.), Respiratory Function in Birds, Adult and Embryonic. Springer-Verlag, Berlin/Heidelberg/New York, pp. 89–94.

Torre-Bueno, J.R., 1978b. Evaporative cooling and water balance during flight in birds. J. Exp. Biol. 75, 231–236.

Torre-Bueno, J.R., Larochelle, J., 1978. The metabolic cost of flight in unrestrained birds. J. Exp. Biol. 75, 223–229.

Tucker, V.A., 1966. Oxygen consumption of a flying bird. Science 154, 150–151.

Tucker, V.A., 1968a. Respiratory physiology of house sparrows in relation to high-altitude flight. J. Exp. Biol. 48, 55–66.

Tucker, V.A., 1968b. Respiratory exchange and evaporative water loss in the flying budgerigar. J. Exp. Biol. 48, 67–87.

Tucker, V.A., 1970. Energetic cost of locomotion in animals. Comp. Biochem. Physiol. 34, 841–846.

Tucker, V.A., 1972. Metabolism during flight in the laughing gull, *Larus atricilla*. Am. J. Physiol. 222, 237–245.

Tucker, V.A., 1973. Bird metabolism during flight: evaluation of a theory. J. Exp. Biol. 58, 689–709.

Tucker, V.A., Tucker, A.E., Akers, K., Enderson, J.H., 2000. Curved flight paths and sideways vision in Peregrine Falcons (*Falco peregrinus*). J. Exp. Biol. 203, 3755–3763.

Usherwood, J.R., 2016. Physiological, aerodynamic and geometric constraints of flapping account for bird gaits, and bounding and flap-gliding flight strategies. J. Theor. Biol. 408, 42–52.

Usherwood, J.R., Hedrick, T.L., Biewener, A.A., 2003. The aerodynamics of avian take-off from direct pressure measurements in Canada geese (*Branta canadensis*). J. Exp. Biol. 206, 4051–4056.

Usherwood, J.R., Hedrick, T.L., McGowan, C.P., Biewener, A.A., 2005. Dynamic pressure maps for wings and tails of pigeons in slow, flapping flight, and their energetic implications. J. Exp. Biol. 208, 355–369.

Villers, A., Millon, A., Jiguet, F., Lett, J.-M., Attie, C., Morales, M.B., Bretagnolle, V., 2010. Migration of wild and captive-bred Little Bustards *Tetrax tetrax*: releasing birds from Spain threatens attempts to conserve declining French populations. Ibis 152, 254–261.

Van den Berg, C., Rayner, J.M.V., 1995. The moment of inertia of bird wings and the inertial power requirement for flapping flight. J. Exp. Biol. 198, 1655–1664.

Van de Ven, T.M.F.N., Martin, R.O., Vink, T.J.F., McKechnie, A.E., Cunningham, S.J., 2016. Regulation of heat exchange across the hornbill beak: functional similarities with toucans? PLoS ONE 11 (5). https://doi.org/10.1371/journal.pone.0154768. e0154768.

Van Walsum, T.A., Perna, A., Bishop, C.M., Murn, C.P., Collins, P.M., Wilson, R.P., Halsey, L.G., 2020. Exploring the relationship between flapping behaviour and accelerometer signal during ascending flight, and a new approach to calibration. Ibis 162, 13–26.

Vazquez, R.J., 1994. The automating skeletal and muscular mechanisms of the avian wing (Aves). Zoomorphologie 114, 59–71.

von Busse, R., Waldman, R., Swartz, S., Voigt, C., Breurer, K., 2014. The aerodynamic cost of flight in bats – comparing theory with measurement. J. R. Soc. Interface 11. https://doi.org/10.1098/rsif.2014.0147.

Wang, T., Joyce, W., Hicks, J.W., 2019. Similitude in the cardiorespiratory responses to exercise across vertebrates. Curr. Opin. Physiol. 10, 137–145.

Wang, Y., Tobalske, B.W., Cheng, B., Deng, X., 2018. Gravitation-enabled forward acceleration during flap-bounding flight in birds. J. Bionic Eng. 15, 505–515.

Ward, S., Bishop, C.M., Woakes, A.J., Butler, P.J., 2002. Heart rate and the rate of oxygen consumption of flying and walking barnacle geese (*Branta leucopsis*) and bar-headed geese (*Anser indicus*). J. Exp. Biol. 205, 3347–3356.

Ward, S., Möller, U., Rayner, J.M.V., Jackson, D.M., Bilo, D., Nachtigall, W., Speakman, J.R., 2001. Metabolic power, mechanical power and efficiency during wind tunnel flight by the European starling *Sturnus vulgaris*. J. Exp. Biol. 204, 3311–3322.

Ward, S., Möller, U., Rayner, J.M.V., Jackson, D.M., Nachtigall, W., Speakman, J.R., 2004. Metabolic power of European starlings *Sturnus vulgaris* during flight in a wind tunnel, estimated heat transfer modelling, doubly labelled water and mask respirometry. J. Exp. Biol. 207, 4291–4298.

Warrick, D.R., Tobalske, B.W., Powers, D.R., 2009. Lift production in the hovering hummingbird. Proc. R. Soc. B. 276, 3747–3752.

Warrick, D.R., Hedrick, T., Fernandez, M.J., Tobalske, B., Biewener, A., 2012. Hummingbird flight. Curr. Biol. 22, R472–R475.

Wascher, C.A.F., Scheiber, I.B.R., Weils, B.M., Kotrschal, K., 2009. Heart rate responses to agonistic encounters in graylag geese, Anser anser. An. Beh. J. Comp. psychol. 77, 955–961.

Weber, R.E., Jessen, T.-H., Malte, H., Tame, J., 1993. Mutant hemoglobins (α119-Ala and β55-Ser): functions related to high-altitude respiration in geese. J. Appl. Physiol. 75 (6), 2646–2655.

Weber, J.-M., 2009. The physiology of long-distance migration: extending the limits of endurance. J. Exp. Biol. 212, 593–597.

Weber, J.-M., Roberts, T.J., Vock, R., Weibel, E.R., Taylor, C.R., 1996. Design of the oxygen and substrate pathways III: partitioning energy provision from carbohydrates. J. Exp. Biol. 199, 1659–1666.

Weibel, E.R., Taylor, C.R., Hoppeler, H., 1991. The concept of symmorphosis: a testable hypothesis of structure-function relationship. Proc. Natl. Acad. Sci. U. S. A. 88, 10357–10361.

Weimerskirch, H., Bishop, C., Jeanniard-du-Dot, T., Prudor, A., Sachs, G., 2016. Frigate birds track atmospheric conditions over months-long transoceanic flights. Science 353, 74–78.

Weimerskirch, H., Chastel, O., Barbraud, C., Tostain, O., 2003. Frigatebirds ride high on thermals. Nature 421, 333–334.

Weimerskirch, H., Martin, J., Clerquin, Y., Alexandre, P., Jiraskova, S., 2001. Energy saving in flight formation. Nature 413, 697–698.

Weinstein, Y., Bernstein, M.H., Bickler, P.E., Gonzales, D.V., Samaniego, F.C., Escobedo, M.A., 1985. Blood respiratory properties in pigeons at high altitudes: effects of acclimation. Am. J. Physiol. 249, R765–R775.

Welch Jr., K.C., Altshuler, D.L., 2009. Fiber type homogeneity of the flight musculature in small birds. Comp. Biochem. Physiol. B 152, 324–331.

Welham, C.V., 1992. Flight speeds of migrating birds: a test of maximum range speed predictions from three aerodynamic equations. Behav. Ecol. 5, 1–8.

Wells, D.J., 1993a. Muscle Performance in Hovering Hummingbirds.

Wells, D.J., 1993b. Ecological correlates of hovering flight of hummingbirds. J. Exp. Biol. 178, 59–70.

Williams, H.J., Shepard, E.L.C., Holton, M.D., Alarcón, P.A.E., Wilson, R.P., Lambertucci, S.A., 2020. Physical limits of flight performance in the heaviest soaring bird. Proc. Natl. Acad. Sci. U. S. A. 117, 17884–17890.

Wilson, R.P., White, C.R., Quintana, F., Halsey, L.G., Liebsch, N., Martin, G.R., Butler, P.J., 2006. Moving towards acceleration for estimates of activity-specific metabolic rate in free-living animals: the case of the cormorant. J. Anim. Ecol. 75, 1081–1090.

Wilson, R.P., Borger, L., Holton, M.D., Scantlebury, D.M., Gomez-Laich, A., Quintana, F., Rosell, F., Graf, P.M., Williams, H., Gunner, R., Hopkins, L., Marks, N., Geraldi, N.R., Duarte, C.M., Scott, R., Strano, M.S., Robotka, H., Eizaguirre, C., Fahlman, A., Shepard, E.L.C., 2019. J. Anim. Ecol. 89, 161–172.

Witter, M.S., Cuthill, I.C., 1993. The ecological costs of avian fat storage. Phil. Trans. Roy. Soc. Lond. B 340, 73–92.

White, C.R., Blackburn, T.M., Seymour, R.S., 2009. Phylogenetically informed analysis of the allometry of mammalian basal metabolic rate supports neither geometric nor quarter-power scaling. Evolution 63, 2658–2667.

White, C.R., Blackburn, T.M., Martin, G.R., Butler, P.J., 2007. Basal metabolic rate of birds is associated with habitat temperature and precipitation, not primary productivity. Proc. R. Soc. B 274. https://doi.org/10.1098/rspb.2006.3727.

Woakes, A.J., Butler, P.J., 1986. Respiratory, circulatory and metabolic adjustments during swimming in the tufted duck, *Aythya fuligula*. J. Exp. Biol. 120, 215–231.

Woakes, A.J., Butler, P.J., Bevan, R.M., 1995. Implantable data logging system for heart rate and body temperature: its application to the estimation of field metabolic rates in Antarctic predators. Med. Biol. Eng. Comput. 33, 145–151.

Wolf, L.L., Hainsworth, F.R., 1971. Time and energy budgets of territorial hummingbirds. Ecology 52, 980–988.

Wolff, D., 2006. Nectar sugar composition and volumes of 47 species of Gentianales from a southern Ecuardorian montane forest. Ann. Bot. (Lond.) 97, 767–777.

Young, K.G., Vanderboor, C.M., Regnault, T.R.H., Guglielmo, C.G., 2020. Species-specific metabolic responses of songbird, shorebird, and murine cultured myotubes to n-3 polyunsaturated fatty acids. Am. J. Physiol. (Submitted August 2020).

Zúñiga, D., Falconer, J., Fudickar, A.M., Jensen, W., Schmidt, A., Wikelski, M., Partecke, J., 2016. Abrupt switch to migratory night flight in a wild migratory songbird. Sci. Rep. 6 https://doi.org/10.1038/srep34207.

Chapter 47

Physiological challenges of migration

Scott R. McWilliams[1], Marilyn Ramenofsky[2] and Barbara J. Pierce[3]

[1]*Department of Natural Resources Science, University of Rhode Island, Kingston, RI, United States;* [2]*Department of Neurobiology, Physiology and Behavior, University of California, Davis, CA, United States;* [3]*Department of Biology, Sacred Heart University, Fairfield, CT, United States*

Abbreviations

ACTH Adrenocorticotropic hormone
AGRP Agouti-related peptide
AR Androgen receptor
AVT Arginine vasotocin
C-fos Fos Proto-Oncogene, an early immediate gene
CART Cocaine - and amphetamine-regulated transcript protein
CCK Cholecystokinin
CCO Cytochrome-c oxidase
CK Creatine kinase
CPT Carnitine palmitoyltransferase
CS Citrate synthase
DHT Dihydrotestosterone
DIO2 Type II iodothyronine deiodinase
DIO3 Type III iodothyronine deiodinase
ELHS Emergency life history stage
FFA Free fatty acids
FSH Follicle-stimulating hormone
GH Growth Hormone
GnIH Gonadotropin-inhibitory hormone
GnRH Gonadotropin-releasing hormone
GR Glucocorticoid receptor
GtH Gonadotropin
HOAD Hydroxyacyl CoA dehydrogenase
HPA Hypothalamic-pituitary-adrenal axis
HPG Hypothalamic-pituitary-gonad axis
ICV Intracerebroventricular
IGF-1 Insulin-like growth factor-1
IP Intraperitoneal
LH Luteinizing hormone
MDH Malate dehydrogenase
MR Mineralocorticoid receptor
MSH Melanocyte-stimulating hormone
NPY Neuropeptide Y
PFK Phosphofructokinase
PK Pyruvate kinase
POMC Proopiomelanocortin
PPAR Perixisome proliferator-activated nuclear receptors
PSM Plant secondary metabolites
PUFA Polyunsaturated fatty acids
PRL Prolactin
T Testosterone
T3 Triiodothyronine
T4 Thyroxine
TSH Thyroid-stimulating hormone
VA opsin Vertebrate ancient opsin photopigment

47.1 Introduction

Approximately 19% of the ~10,000 species of birds in the world migrate on a regular basis (Kirby et al., 2008), and this is closer to 50% of species if only birds that breed at latitudes above 35° north and south are considered (Newton and Dale, 1996a, 1996b). The physiological feat of migration has been equated to such athletic feats in mammals as running 130 consecutive marathons (semipalmated sandpiper, *Calidris pusilla,* migrates ~ 5000−7500 km nonstop; Anderson et al., 2019) or completing three trips to the moon and back in a lifetime (arctic tern, *Sterna paradisaea,* migrates ~80,000 km a year over a 30 year lifespan; Egevang et al., 2010). The strategies migratory birds use to complete these annual peregrinations vary among bird species with some birds completing their long-distance migration in one, nonstop flight while most fly intermittently, taking advantage of stopover sites along their routes to rest and refuel. Regardless of strategy, all avian migrants face the same physiological challenges while aloft, albeit to different extents, including: (1) burn fat at a very high rate while fasting and combatting the negative effects of lipid peroxidation, (2) maintain adequate hydration while not drinking and losing water due to elevated breathing rates, (3) obtain adequate oxygen while oxidizing fat for fuel, and especially when flying at high altitudes with low-oxygen content, (4) avoid becoming too hot (heat gained from metabolism and the environment) or too cold (heat loss to the environment), and (5) meeting these challenges under a seasonal time constraint. Additionally, birds that stop to rest

Sturkie's Avian Physiology. https://doi.org/10.1016/B978-0-12-819770-7.00017-7

and refuel at stopover sites have the added physiological challenge of rapidly regaining energy stores with initially reduced gut size and function. Clearly, the physiological challenges associated with long-distance flight are significant and require specialized morphological and physiological adaptations and acclimatizations.

The energy costs of bird flight are substantial and have been the focus of ornithological research since the 1960's when Greenewalt (1960) recorded hummingbirds flying in front of a fan and examined changes in flight speed with changes in fan speeds. The ability of researchers to fly birds in a controlled environment led to significant breakthroughs not only in the field of aerodynamics but in the understanding of the physiology of flight as well. For example, classic studies of birds flying in wind-tunnels have shown that forward flapping flight is energetically more costly than running or swimming per gram body mass (Butler, 1991; Bishop and Butler, 2015). Importantly, the advantage of flying on migration, instead of running and swimming, is revealed when travel distance is considered. Specifically, energy required per gram body mass to travel a given distance (i.e., the cost of transport) is considerably less for a flying migrant compared to a running or swimming migrant (Tucker, 1970; Schmidt-Nielsen, 1972; Bishop and Butler, 2015). With an increase in technology and the ability to track migrating birds throughout the globe, we now know the physiology of migratory flights of free-living birds to be a highly complex, synergistic process between an organism and its ever-changing environment.

In this chapter, we will review, within the context of the migration life history of birds, the neuroendocrine and physiological adaptations that allow birds to meet the challenges of long-duration flights, the preparations they implement to begin their journeys, and the in-flight adjustments they make in order to successfully complete their journeys. We will conclude with a discussion about the flexible phenotypes of birds in relation to how they physiologically respond to the challenges of migratory flight in a dynamic seasonal environment, and some of the important mysteries that remain in terms of the physiology of birds during migration.

47.2 Adaptations of birds for long-duration migratory flights

Flapping flight requires both lift to stay aloft and thrust to move forward through the air (Tobalske, 2016). Birds have evolved feathers and wings that enable them to fly because their collective shape produces lift as air flows over and around them. Combine feathers and wings with a skeletal system that is both strong yet light (hollow bones), and a muscular system that provides the power and endurance, and you have the anatomical skeletal-muscular foundation for the evolution of long-distance migration of birds. Bishop and Butler (2015) provide a thorough description of the biomechanics of bird flight, and how the muscles of birds produce the power required for flight, in general, and the long-duration flapping flight used by birds in migration, in particular. Most pertinent to our review of the physiology of long-distance migration in birds is that (a) self-powered flight is the most demanding form of locomotion in terms of its energy cost per unit time—thus, fuel storage and use is critical; (b) on the other hand, flight is much more efficient than running or swimming. In short, the cost of transport for a flyer (in units of energy required for a bird of a given mass to travel a given distance) is appreciably less than that of a runner or a swimmer—thus, overcoming the fuel storage and use challenges of long-duration flapping flight allows migratory birds to travel far for their size.

47.2.1 Cardiovascular and respiratory general adaptations

The energetic costs of flapping flight have driven adaptive responses in the cardiovascular and respiratory systems of birds. In general, birds have larger hearts, lower resting heart rates, higher exercising heart rates, and higher $\dot{V}O_2$ max than nonflying mammals of similar size (Bishop and Butler, 2015). Adaptations in the vascular system of birds such as increased number of capillaries in each muscle fiber along with mitochondria that are in closer proximity to capillaries allows for efficient exchange of respiratory gasses (Powell, 2015). In addition, the structure of the avian respiratory system contributes to a bird's ability to efficiently exchange large volumes of gas as is needed during flight. Taken together the design of air sacs increases ventilation, the increased surface area in the lungs, unidirectional flow across the respiratory surface, and increased cross-current gas exchange with the blood all contribute to a bird's ability to obtain oxygen, supply oxygen to active tissue, and remove carbon dioxide from the blood at a greater rate than mammals of similar size (Dzialowski and Crossley, 2015; Scott et al., 2015). In general, birds are also more tolerant of hypoxia than mammals at least in part because of differences in their sensitivity to hypocapnia (low-partial pressure of arterial blood carbon dioxide (Scott et al., 2015)). Hypocapnia sensitivity of cerebral blood vessels is one of the main mechanisms in which mammals limit hyperventilation, thereby decreasing oxygen delivery to the brain, and likely limiting overall energetic output (Ogoh and Ainslie, 2009; Ainslie and Ogoh, 2010). Migratory bird insensitivity to hypocapnia especially in cerebral blood vessels allows for extreme hyperventilatory rates without blood flow interference to the brain (Faraci, 1991). In turn, this hyperventilation allows for decreased arteriole partial pressure of carbon dioxide subsequently increasing arteriole partial pressure of oxygen due to the Bohr effect (Powell, 2015). Thus, birds are able to maintain

high-oxygen delivery to tissues even in low-oxygen environments such as those at high altitudes. Additional vascular adaptations that enable birds to meet the high-oxygen demands of long-duration flight while retaining essential blood solute concentrations include an overall higher hematocrit level and greater hemoglobin concentrations (Minias et al., 2013; Bishop and Butler, 2015) compared to nonmigratory birds or mammals and the maintenance of plasma levels throughout a long flight regardless of body mass changes (Carmi et al., 1993). Monthly comparison of hematocrit of White-crowned sparrows (*Zonotrichia leucophrys gambelli*) revealed that migrant subspecies were consistently greater than residents, a difference that increased 10−15% further during both seasonal stages of migration (Krause et al., 2016). Interestingly, recent experiments that directly manipulated hematocrit in short-distance migratory Yellow-rumped warblers (*Setophaga coronata*) found that birds with elevated hematocrit performed better at simulated high altitudes (in a wind tunnel) but not at lower altitudes (Yap et al., 2018); many more such manipulative experiments are needed to better understand how variation in hematocrit affects migratory flight performance.

47.2.2 Metabolism and damage control

Mitochondria generate the cellular energy required by birds (and all animals) to fuel their basal metabolism as well as that required for all activity including flapping flight (Bottje, 2015). Associated with this role as powerhouse of the cell, mitochondria are also the major site for generation of reactive species (RS)—thus an effective antioxidant protection system has evolved to reduce or avoid the negative physiological effects of RS production, the components of which are shared by all eukaryotes (Bottje, 2015; Cooper-Mullin and McWilliams, 2016; Skrip and McWilliams, 2016). Most pertinent to our review of the physiology of long-distance migration in birds is that (a) increased metabolism, like that required for long-duration flapping flight, is associated with increased RS production which may overwhelm the antioxidant system and cause oxidative imbalance or "stress" and thus damage to, for example, lipids, proteins, and DNA in cells; (b) repair of damaged structures is energetically expensive—thus, understanding how the antioxidant system of migrating birds contends with RS production is as important as understanding how the power for long-duration flight is generated.

How birds overcome the potential constraints of redox imbalance (so-called "oxidative stress") associated with their relatively high baseline and active metabolic rates has been the subject of much conjecture (Buttemer et al., 2010; Munshi-South and Wilkinson, 2010; Jimenez et al., 2019), although recently a key adaptation of the master antioxidant response of birds has been revealed (Castiglione et al., 2020). The transcription factor NF-E2-related factor 2 (NRF2) is the major cellular pathway for regulating the antioxidant response of metazoans against oxidative imbalance within cells. Under steady-state conditions, KEAP1 binds NRF2 and keeps it at low levels in the cell. Under conditions of increased metabolic rate and thus RS production, KEAP1 repression is relaxed allowing NRF2 to accumulate, bind to an antioxidant response element, and activate expression of a host of antioxidant target genes. Castiglione et al. (2020) demonstrate that a mutation in the KEAP1 coding sequence, likely caused by intrachromosomal rearrangement, in the Neoaves ancestor has led to constitutive activation of the NRF2 master antioxidant response in living birds, and this enhanced response lowers the risk of macromolecular oxidative damage and thus a decrease in oxidative stress.

47.2.3 Immunity

The avian immune system is broadly similar between mammals and birds although most of what we know about "birds" is based on studies of domesticated chickens (reviewed in Schat et al., 2014; Kaiser and Balic, 2015). Birds and mammals have both an innate and adaptive immune response and the latter includes both cell-mediated (T-cell dependent, developed in the thymus) and humoral (B-cell dependent, developed in the Bursa of Fabricius) immune responses—note that in mammals, the B-cells are derived from bone marrow. Given the high costs of maintaining the immune system (Klasing, 2004; Hasselquest and Nilsson, 2012), birds during migration may reduce immune function to spare these costs (Hasselquest, 2007; Buehler and Piersma, 2008) or since they may encounter more pathogens they may instead upregulate immune function (Møller and Erritzøe, 1998; Buehler et al., 2010) or they could reallocate resources and so maintain immune function (Lee, 2006). The balance of evidence to date at least in terms of innate immune function suggests that it may be compromised during migration in birds (Owen and Moore, 2006; Hegemann et al., 2012; Nebel et al., 2012; Eikenaar and Hegemann, 2016) although many more such studies are needed.

47.2.4 Sensory systems and navigation

Migratory birds must be able to orient and navigate during migration, and birds have evolved several key sensory mechanisms that enable successful navigation (for example, see Mouritsen, 2015). However, this topic is beyond the scope of this chapter. Several recent reviews provide excellent entry into this realm of bird migration physiology (Berthold et al., 2003; Wiltschko and Wiltschko, 2009; Mouritsen, 2018; Muheim et al., 2018).

47.2.5 Endocrine system and the environment

Migration represents the morphological, behavioral, and physiological adaptations to seasonal environments—locations with transient resources sufficient to support breeding at one time of the year and another at a distance for survival, thus creating seasonal movements in spring and autumn. To take advantage of seasonal productivity in support of breeding and rearing young (Baker, 1938; Perrins, 1970), migratory species must maintain synchrony with the environment by relying on environmental cues in conjunction with endogenous rhythms to coordinate patterns of movement and stasis.

The endocrine system is the crucial link integrating the environmental cues with behavioral and physiological cycles that contribute to seasonal migrations. Whereas, the endocrine regulation of reproduction of Aves has been thoroughly studied, less focus and progress has been made on migration. To understand why, it is valuable to consider what migration is. It is a complicated biological process with a variety of forms extending from obligate migration that occurs on a strict time table relying on seasonally reliable resources necessary for breeding and survival to facultative forms, i.e., nomadic and irruptive movements of species that respond reactively to resources that vary unpredictably (Watts et al., 2018). Furthermore, migrations occur over multiple seasons and generations incorporating great distances, various environments, habitats, and climate. Together such variables make for a difficult system to study in its entirety. One approach that has contributed to understanding the relationship of the environment and endocrine systems is Finite State Machine Theory (Jacobs and Wingfield, 2000; Ramenofsky and Wingfield, 2007) by focusing on the unique conditions of each life history stage. For example, the life history of a calendar migrant includes two migration stages—vernal and autumnal—that occur at separate times of the year under differing environmental conditions and regulated by unique neuroendocrine mechanisms. Each stage is composed of three sequential phases—(1) development, the initiation of molecular, biochemical, and genetic processes; (2) mature capability, where all morphological, physiological, and behavioral traits are expressed and actual migration begins; and (3) termination, the disorganization of the migratory traits and beginning of the next life history stage (Figure 47.1). Each phase is regulated by the environmental-endocrine nexus that affects its timing and progression. Current knowledge of the mechanisms regulating the two stages are not thoroughly defined but presenting migration in this format provides an integrated focus for future studies.

47.3 Endocrinology of migration

47.3.1 Vernal stage

47.3.1.1 Synchronization with the environment: initial predictive cue

Though not thoroughly known for all migratory species, a general consensus from many is the cue response to the vernal increase in daylength or photostimulation (Rani and Kumar, 2014; Hahn et al., 2015). The mechanism involves coincidence of the light phase of the photoperiod occurring during the peak of the circadian rhythm of photosensitivity that takes place for most species between 12 and 15 h after dawn. The reaction resides in the extraretinal photoreceptors of the basal hypothalamus in association with the putative photopigments VA opsin and Rod opsin which are

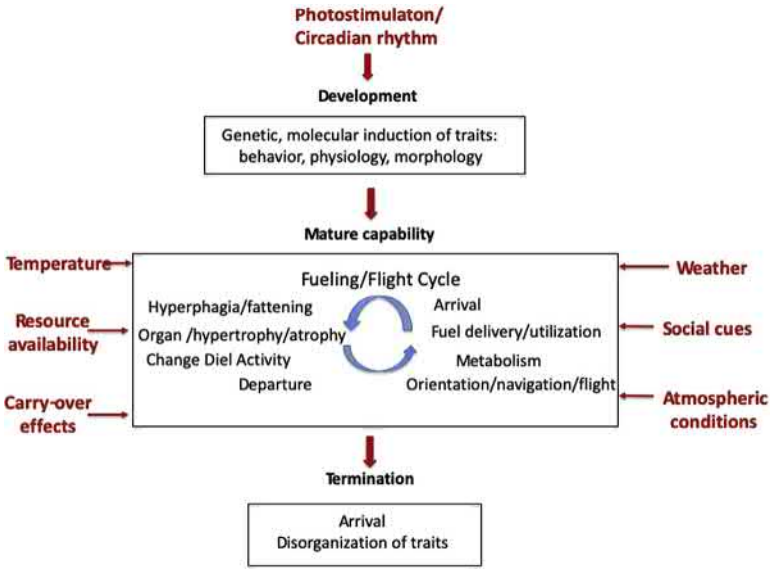

FIGURE 47.1 Three phases of the migration life history stage. Initial predictive cue of photostimulation induces the development phase and continues its effect throughout the entire stage. Local environmental and conditional cues (*red font*) affect the rate of progression through the substages of mature expression and termination.

co-expressed in the gonadotropin-releasing hormone (GnRH) and arginine vasotocin neurons (Follett et al., 1974, 1998; Meddle et al., 1997; Rastogi et al., 2013). Evidence of photostimulation was demonstrated in the First-day Release Model in which activation of the early immediate gene (*c-fos*) was detected 18 h after dawn of the first long day indicating cellular activity in the basal tuberal hypothalamus of Japanese quail (*Coturnix c. Japonica*) (Meddle et al., 1997). As a result, plasma levels of luteinizing hormone from the anterior pituitary could be detected at 22 h after dawn that in turn induced synthesis and secretion of testosterone from the gonads affecting both migration and breeding life history stages. Given that one cue, photostimulation, initiates both migration and breeding life history stages, the question becomes how are they separated to occur sequentially? Photostimulating white-crowned sparrows with low-penetration green light Wang et al. (2013) was able to separate photoperiodic responses of the migration and breeding stages. Birds developed migratory traits of mass increase, fattening, and nocturnal migratory restlessness but without gonadal recrudescence. Separation of the neuroendocrine control over initiation of migration and breeding have further support from the electrolytic lesion studies in the distinct locations of the hypothalamus in both White-throated, *Zonotrichia albicollis*, and white-crowned sparrows that demonstrated separate pathways for migratory fattening and restlessness versus gonadal development (Kuenzel and Helms, 1967; Stetson and Erickson, 1972; Yokoyama, 1976). Taken together these results suggest separate locations for photoreception and transduction for the two stages: one regulating the migratory life history and the other a more attenuated response of gonadal development and eventual breeding.

47.3.1.2 Developmental phase: hyperphagia and fattening

The initial response to photostimulation is increased food intake—hyperphagia—that leads to elevated body mass and fat stores providing fuel, lipid, and protein to support migratory flight (Ramenofsky, 1990; Lindström and Piersma, 1993). Unlike other homeostatic processes, the alterations of body mass during migration is regarded as rheostasis where the *set point* of body mass is defended but fluctuates throughout the fueling flight cycles of the stage (Mrosovsky, 1990; Jenni et al., 2000; Cornelius et al., 2013; Boswell and Dunn, 2015). The hormone action of these processes is not thoroughly understood for most migratory species but the basic principles are drawn from migratory European quail (*Coturnix coturnix*) and domesticated fowl that focus on the gene expression of opposing sets of neurons of the central melanocortin system in the arcuate nucleus of the mediobasal hypothalamus and considered the control center for body weight (Boswell, 2005; Boswell and Dunn, 2015) (Figure 47.2). Two neuropeptides synthesized in the arcuate nucleus—neuropeptide Y (NPY) and agouti-relate protein (AGRP)—act to promote feeding and mass gain. Opposing these actions are the interconnected neurons that express pro-opiomelanocortin (POMC) and cocaine-and amphetamine-regulated transcript (CART) genes. Given its basal position in the hypothalamus, the arcuate nucleus sits adjacent to the third ventricle and median eminence where the neurons are exposed to circulating levels of proteins, metabolites, and hormones that provide peripheral information. The arcuate nucleus expresses receptors for such metabolic compounds as cholecystokinin (CCK), ghrelin, corticosterone, insulin, and leptin and may serve as interpreters of metabolic state with regulatory capacity to promote or inhibit food intake via the NPY, AGRP or POMC, and CART pathways. Empirical studies using intracerebroventricular (ICV) injections into White-crowned sparrows report that while NPY stimulated food intake, the octapeptide CCK inhibited offering further support for the diverse pathways of control for feeding in a migratory bird (Richardson et al., 1992, 1993).

47.3.1.3 Thyroid hormones

Thyroid hormones play broad regulatory roles in avian physiology including metabolism, thermoregulation, breeding, molt, and migration (Groscolas and Leloup, 1986; Jenni-Eiermann et al., 2002; Zeng et al., 2013). In older literature, migratory fattening and restlessness were associated with elevated activity of the thyroid gland (Wingfield et al., 1990). Additionally, measurements of

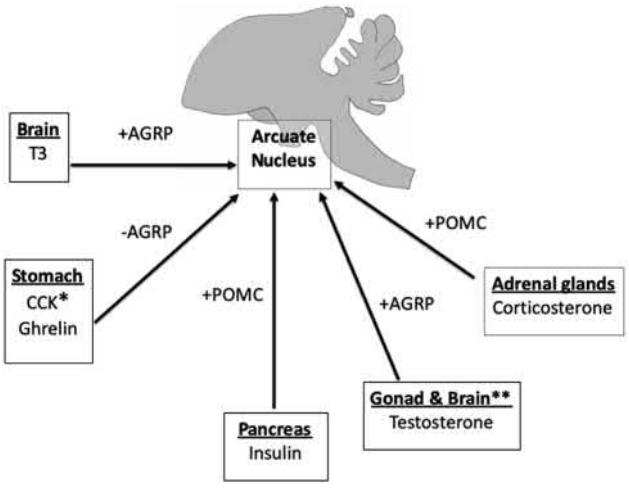

FIGURE 47.2 Suggested model for the endocrine influences on food intake via neuropeptides in the arcuate nucleus of the avian hypothalamus, * Synthesized both in gut and brain, ** possible pathway. *Adapted from Boswell and Dunn (2015).*

plasma levels of thyroxine (T4) and triiodothyronine (T3) were increased during the early stages of vernal migration (Chandola and Pathak, 1980; Smith, 1982; Pant and Chandola-Saklani, 1993). More recently, chemical inhibition of thyroid hormone disrupted prenuptial molt, fattening, mass gain, flight muscle hypertrophy, expression of migratory restlessness, and gonadal recrudescence while administration of T4 reversed these effects (Pérez et al., 2016, 2018). These results indicate a major role for thyroid hormones across the vernal stage.

Regarding photostimulation, thyroid hormones are considered central to molecular mechanisms regulating breeding (Rani and Kumar, 2014, Boswell and Dunn, 2017; Pérez et al., 2018). For a number of seasonally breeding birds, photoperiod is linked to release of thyroid-stimulating hormone (TSH) from the pars tuberalis of the pituitary gland. TSH stimulates expression of the biosynthetic enzyme Type II iodothyronine deiodinase to direct conversion of T4 to the biologically active T3 in the mediobasal hypothalamus that, in turn, stimulates release of GnRH from the median eminence to initiate breeding (Hahn et al., 2015; Nishiwaki-Ohkawa and Yoshimura, 2016). Evidence is accruing in Siberian hamsters and domestic chicks that the hypothalamic T3 may also exert effects on food intake and fattening through the AGRP neurons of the arcuate nucleus (Boswell and Dunn, 2017) (Figure 47.2). Whether these effects take place with photostimulation during migration are unknown but currently under investigation in a First-day Release Model with acute photostimulation of short-day white-crowned sparrows that will test directly whether long-day exposure induces expression of AGRP and increases food intake in the vernal stage.

47.3.1.4 Testosterone

Additionally, testosterone is implicated in regulating spring fattening. In a number of species, low levels of testosterone circulating during the winter stage are necessary for expression of hyperphagia and fattening in both sexes in the vernal but not the autumnal stages (Schwabl and Farner, 1989; Wingfield et al., 1990; Deviche, 1995; Ramenofsky and Nemeth, 2014), a condition challenged by others (Weise, 1967; Boswell et al., 1993). The mechanism by which testosterone could influence migratory fattening is through the androgen receptor (AR) on the arcuate nucleus stimulating the AGRP/NPY/feeding center pathways, as documented in mammals (Diano et al., 1997) (Figure 47.2). The timing of this effect is not known but could vary across migratory species.

47.3.1.5 Insulin and glucagon

The pancreas is the source of 3 proteins, insulin, glucagon, and pancreatic polypeptide; the former two are considered major regulators of food intake in birds acting directly and/or through their effects on carbohydrate and lipid metabolism (Hazelwood, 2000). Only a few studies have investigated these in migrating birds (Goodridge, 1964; Totzke et al., 1997; Cornelius et al., 2013). What is known is that insulin and glucagon have opposite effects on plasma glucose that in turn may influence food intake. Surprisingly, intramuscular injections of either glucagon or insulin decreased feeding in captive white-crowned sparrows (Boswell et al., 1995). Plasma glucose is exceedingly high in birds even though plasma insulin falls within the normal range suggesting peripheral insensitivity to insulin (Sweazea et al., 2006). ICV administration of insulin increased feeding indicating a marked diversion from mammals and suggesting central control of food intake by insulin (Boswell et al., 1995). Besides its effect on carbohydrate metabolism, glucagon has a biphasic effect on lipid production. At elevated levels, glucagon promotes lipolysis enhancing release of free fatty acids (FFAs), a source of energy, into the circulation. At lower range, this is reversed with increased lipogenesis and fat storage (Goodridge, 1964). Testing the effects of metabolites on feeding reported a predominant sensitivity to lipid as opposed to carbohydrate, a reasonable conclusion given the major role that lipid plays during migration (Boswell et al., 1995). Taken together, it is suggestive that glucagon levels cycle throughout migration with lowest levels occurring during the migratory fattening to support lipogenesis countered by elevated levels during flight promoting lipolysis making fatty acids available for oxidation (Goodridge, 1964). More comprehensive studies on the pancreatic peptides are needed.

47.3.1.6 Glucocorticoids (Box 47.1)

Corticosterone in birds has long been associated with hyperphagia, fattening, and stress physiology in migrants, but results across numerous studies and species have not revealed consistent patterns (Landys et al., 2006; Ramenofsky, 2011; Wagner et al., 2014; Eikenaar, 2017). One of two views contributing to these divisions is the Migration Modulation Hypothesis (Holberton et al., 1996) that addresses stress physiology with the hypothesis that neotropical migrants would not show the expected stress response to capture and handling with two predictions: (1). baseline levels of corticosterone remain elevated during migration to promote hyperphagia and lipogenesis, (2). suppression of the stress response to avoid the deleterious effects of catabolism on flight muscle (Long and Holberton, 2004). The alternative view is that most migrants display a robust stress response throughout migration with plasma levels varying seasonally across the stages and in healthy birds within physiological range (Level B (Box 47.1)). Corticosterone concentration is

BOX 47.1 Aligning corticosterone, physiological state, and allostasis.

Corticosterone, the predominant adrenal steroid of birds, is associated with many aspects of the migration life history stage including behavior, metabolism, and allostasis—measure of energy requirements over time (Blas, 2015; Ramenofsky, 2011; Landys-Ciannelli et al., 2002; Romero et al., 1997). Corticosterone acts in concert with other metabolic hormones such as CCK and insulin by regulating availability of energy in the forms of circulating FFAs and glucose to maintain homeostasis (Eikenaar, 2017). To fully appreciate the multiple functions and levels of control of corticosterone, we refer to the hypothalamus-pituitary-adrenal (HPA) axis by considering its actions at three physiological states and hormone levels. Level A is considered the basic homeostasis that maintains life (Romero et al., 2009). Level B involves the activation of the HPA for fluctuations in response to predictable, daily or seasonal demands for energy, allostatic load, across the annual life history stages. Level C, further activation of the HPA that tend to be transitory as the individual reacts to an acute and unpredictable event or stressor. The induced behavioral response is to move away or adopt an emergency life history stage (ELHS) to alleviate effects of the stress (Romero and Wingfield, 2016). To assess function of the HPA axis, two measurements of circulating corticosterone are collected: the first is the baseline measure collected within the first 3 min of capture and reflecting the current and unprovoked energetic state of the organism. The second sample is the acute or Level C collected at the peak of the response to capture and handling indicating the maximal response of the corticosterone synthesis and secretion (Figure 47.3).

regulated by the enzyme 11β-hydroxy steroid dehydrogenase, and it acts through two cellular receptors, the high-affinity mineralocorticoid receptor (MR) and low-affinity glucocorticoid receptor (GR). Considering these multiple levels of control, corticosterone is regarded as a pleiotropic hormone with multiple effects acting in permissive roles with critical metabolic compounds that affect energy balance and allostasis including: insulin, insulin-like growth factor-1, adipose tissue lipoprotein lipase, low-density lipoprotein, FFA, NPY action (Savard et al., 1991; Remage-Healey and Romero, 2001; Landys et al., 2004a, 2006; Blas, 2015; Mishra et al., 2017), and growth hormone (GH) (Tsipoura et al., 1999). All of which contribute to the complexity and often confusion over corticosterone's action. Taking a more comprehensive view of the interactions of hormones and metabolic compounds in terms of allostasis and stress at each substage may provide a more complete assessment of the role of this steroid in migration.

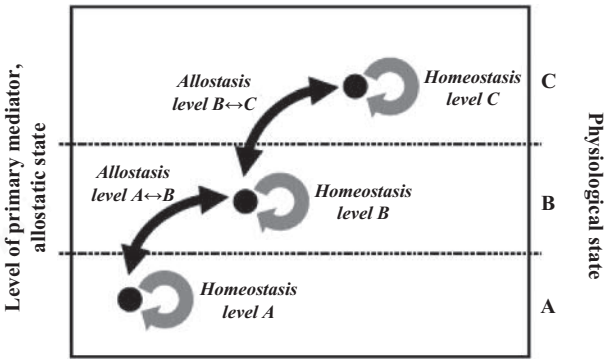

FIGURE 47.3 Description of state levels of corticosterone in relation to homeostasis, allostasis, and physiological state. *With permission from Landys et al. (2006).*

47.3.1.7 Leptin

The protein hormone leptin is known as a strong regulator of energy balance in mammals synthesized almost exclusively in the adipose tissue and signaling presence or deposition of fat—positive energy balance (Zhang et al., 1997). Thus it is considered a hormone with autocrine, paracrine, and endocrine functions promoting homeostasis of energy stores and has been coined an *adipostat* in mammals regulating food intake according to energy balance—fat content (Friedman-Einat et al., 2014; Friedman-Einat and Seroussi, 2019). Recent identification in birds of a leptin ortholog and characterization of leptin activity has questioned whether it functions either as a hormone or an *adipostat*. The leptin ortholog shows no expression in adipose tissue but is found in brain, adrenal gland, and gonad. So far, the avian leptin receptor LEPR is expressed only in the pituitary. Given these diversions from mammals, it is unlikely that avian leptin is acting as an homeostatic adipostat and offers preliminary support for the Rheostasis Model during migration that would allow for greater range of body mass and fat stores (Cornelius et al., 2013; Friedman-Einat et al., 2014; Watts et al., 2018).

47.3.1.8 Ghrelin

Acting in opposition to leptin, this 28-amino-acid peptide is secreted from the stomach and other digestive organs of birds when body condition is low. Ghrelin is reported to be a GH-releasing factor in chickens and mammals that relays information to the arcuate nucleus of nutritional state. In rats, both intraperitoneal (IP) and ICV injections of ghrelin increased food intake. This effect is most apparent during fasting with ghrelin acting on the NPY/agouti-related peptide (AGRP) neurons in the arcuate nucleus (Nakazato et al., 2001). In quail, plasma ghrelin was elevated in fasted

birds but dropped once feeding commenced. The results obtained with injections were less clear; at low concentrations, IP injections enhanced feeding but at greater dosages both IP and ICV injections decreased feeding suggesting a biphasic effect. Other studies in which ghrelin was administered reported that food intake in neonatal chicks was inhibited (Kaiya et al., 2009). Although presently controversial in domestic fowl, these results suggest that ghrelin could regulate feeding during migration, particularly when birds are lean, as they would be following flight. In a recent study, lean Garden warblers, *Silvia borin* captured in the morning upon arrival at a stopover site on the Mediterranean Island of Ponza measured elevated plasma levels of the acylated ghrelin (Goymann et al., 2017). After refueling throughout the day in captivity, injections of the unacylated form of ghrelin decreased food intake and increased migratory restlessness at night pointing to either a biphasic effect on behavior of hormone concentration or different responses to the chemical forms of the hormone. By contrast, plasma ghrelin was not associated with nocturnal departure in fully fattened European blackbirds (*Turdus merula*) at an autumn stopover (Eikenaar et al., 2018b). These outcomes may represent species or seasonal differences calling for a more complete understanding of ghrelin's role during migration.

47.3.1.9 Prolactin

Understanding prolactin's role in migratory feeding and fattening has been problematic. Administration of this pituitary protein increases fattening in a number of migratory species (Meier and Farner, 1964; Yokoyama, 1976). Also, central effects of prolactin have been identified in specific sites of the hypothalamus of migratory and nonmigratory birds (Yokoyama, 1976; Buntin et al., 1993). Prolactin levels, like other pituitary hormones, vary seasonally as photostimulation induces secretion of vasoactive intestinal peptide, the stimulatory hypothalamic neuropeptide that induces production and secretion of prolactin from the pituitary (Figure 47.4). This information led to the hypothesis that prolactin could be acting in conjunction with gonadal steroids and corticosterone that were also elevated with photostimulation to induce migratory fattening and restlessness. However, questions have been raised in a number of migrants as the photoinduced peak of prolactin corresponds only weakly with onset of feeding, fattening, and migratory restlessness (Hall and Gwinner, 1987; Schwabl et al., 1988; Holberton and Dufty, 2005). Timing of peak prolactin levels appears to align its function with the autumnal stages of refractoriness and postnuptial molt (Dawson et al., 2001). So, even though prolactin injections increase fattening in birds, prolactin function in relation to migratory fattening is far from resolved.

47.3.1.10 Hormones of flight muscle hypertrophy

In addition to fueling, the pectoralis flight muscles undergo hypertrophy in numerous migratory species (Fry et al., 1972; Driedzic et al., 1993; Jehl, 1997; Bauchinger et al., 2005; Banerjee and Chaturvedi, 2016) during migration that entails increased size of the muscle fibers serving to enhance contractile force and flight performance (Marsh, 1984; Gaunt et al., 1990; Evans et al., 1992; Vezina et al., 2021) (Ramenofsky et al., in prep). Though not well

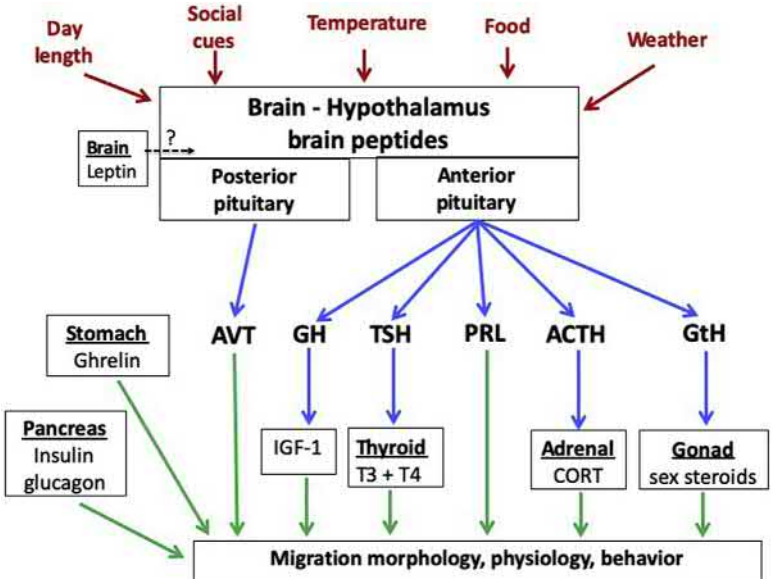

FIGURE 47.4 Flow chart of the environmental cues on the neuroendocrine—endocrine system influencing migratory morphology, physiology and behavior. *Red arrows*—environmental cues influence the activity of hypothalamic brain peptides, *Blue arrows*—pituitary hormones regulated by the brain peptides affect peripheral endocrine glands. *Green arrows*—hormones of the endocrine glands regulate migratory functions. Role of leptin at present is uncertain (Friedman-Einat and Seroussi, 2019).

understood in migratory birds, anabolic steroids—testosterone and 5α-dihydrotestosterone (DHT)—are likely candidates for regulating phenotypic changes given reports of AR gene increasing expression in flight muscles of Golden-collared manakin (*Manacus vitellinus*) during sexual displays (Fuxjager et al., 2012). Furthermore, elevations of androgen signaling via DHT, AR mRNA and the androgen dependent gene, insulin-like growth factor 1, showed increased levels of expression in White-crowned sparrows at spring departure when flight muscles were enlarging (Pradhan et al., 2018). Regulation of muscle hypertrophy could be a function of vernal photostimulation that activates androgen secretion and gonadal recrudescence (Blanchard and Erickson, 1949; Wingfield et al., 1990; Bauchinger et al., 2007). Or it is possible that testosterone secreted during the winter stage has an early priming effect on muscle as it does on fattening (Wingfield et al., 1990), something that is unknown at present. Nevertheless, the circulating levels of androgen are low as birds prepare for vernal departure suggesting intramuscular cell signaling pathways may direct muscle remodeling and thus avoiding the systemic and behavioral effects if levels of androgen were elevated at this substage (Bauchinger et al., 2007; Pradhan et al., 2018). In addition to androgen, corticosterone is implicated in flight muscle hypertrophy at vernal departure. Elevation of baseline corticosterone was associated with increased expression of the high-affinity MRs expression in White-crowned sparrows (Pradhan et al., 2019). This relationship is thought to promote the anabolic stimulation of the muscle fibers, contributing to hypertrophy. Such effects are not known for the autumnal stage.

In addition to the phenotypic changes orchestrated by the endocrine system, integral components of the muscle fibers alter during this vernal substage. Myosin heavy chain (MyHC) expression is associated with the muscle's mechanical capabilities (Reiser et al., 1996). Changes in the expression of the MyHC isoform during the development phase may represent an adaptation for upgrading the muscle mechanics for impending long-distance flight (Velten et al., 2016). Again, hormonal mechanisms regulating these molecular processes are not known but deserve further study during the autumnal stage.

47.3.1.11 Mature expression—hormones of the fueling and flight cycle

Stopover in both the vernal and autumnal stages provides the clearest example of the fueling and flight cycle as flight temporarily ceases upon arrival for rest, fueling, and then departure (Delingat et al., 2006, 2009) offering an excellent opportunity for tracking metabolic hormones. During the 4500 km journey from Africa to a stopover site along the northern Dutch coast in spring, Bar-tail godwits (*Limosa lapponica*) cease travel for approximately one month to rest, continue prenuptial molt and refuel before continuing northward to the breeding grounds. One indication that baseline corticosterone levels align with allostatic load was noted initially by Landys-Ciannelli et al. (2002). Birds arrived in lean condition having lost on average 55.3% from their African departure body mass with elevated baseline levels of corticosterone suggesting a heightened allostatic load resulting from the "wear and tear" of a long continuous flight. Similarly, elevated baseline levels are reported in recently arrived Semipalmated sandpipers at a vernal stopover in Delaware Bay (Tsipoura et al., 1999), Gray Catbirds (*Dumetella carolinensis*) along the Gulf Coast of the United States (DeSimone et al., 2020), and Garden warblers on the Mediterranean Island of Ponza (J. Wingfield and M. Ramenofsky, in preparation). Measurements of body mass of the sandpipers throughout the period of arrival varied over a range of 10 g indicating the different stages of recovery of birds across the flock. Over this period plasma GH was negatively correlated with mass. Given the lipolytic functions of GH, the data suggest hormone action would supply fatty acids to meet the energetic demands of flight and arrival until sufficient refueling achieved positive energy balance observed in the heavier birds of the flock (Tsipoura et al., 1999). During the refueling phase of the godwits, the baseline corticosterone declined 55% from arrival. The corticosterone response levels of both the refueling and arriving birds were similar, however the peak for the arriving birds reached their maxima more rapidly suggesting a heightened sensitivity of negative feedback possibly related to allostasis and/or CNS functions required for flight (Landys-Ciannelli et al., 2002; Eikenaar et al., 2013; Romero and Wingfield, 2016). Once refueling achieved positive energy balance, godwits became aphagic while digestive organs atrophy to conserve body mass and metabolic costs for the ensuing flight (Piersma, 1998; McWilliams and Karasov, 2001). Baseline corticosterone increased around the time of departure and has been associated with the upregulation of HPA for regulating metabolic and behavioral functions for impending flight and organ remodeling (Reneerkens et al., 2002b; Eikenaar et al., 2013, 2018a; Pradhan et al., 2019). However, such upregulation was not identified in the short-hop migrant, Gray catbird (DeSimone et al., 2020) suggesting a divergence in preparation for flight depending upon species and migratory strategy. Nonetheless, studies of both captive and free-living migrants offer further support for the association of corticosterone with expression of migratory flight in the vernal and autumnal stages (Schwabl et al., 1991; Ramenofsky et al., 1999; Landys et al., 2004b; Falsone et al., 2009; Eikenaar et al., 2014; Ramenofsky and Wingfield, 2017). Taken together the results from these studies offer insight into the effects

of corticosterone and GH, providing endocrine support for the behavioral and metabolic processes during flight, at arrival, and preparation for departure during stopover.

47.3.1.12 Termination: arrival biology

Reaching the breeding grounds heralds the termination phase that includes the substage of arrival biology (Wingfield et al., 2004). This substage requires flexibility and coordination of morphology, behavior, and physiology given the quixotic environmental conditions birds may face in early spring. Observational studies note that migratory behavior changes as birds approach breeding areas and begin to search widely for optimal habitats (Hahn et al., 1995). Studies of captive birds, report changes in intensity of migratory restlessness and orientation near the conclusion of the migratory period, suggesting transition to more wandering and searching behaviors expressed even in captivity (Helms, 1963; Wiltschko et al., 1980; Ramenofsky et al., 2003). Elevated corticosterone during arrival has been proposed to support these behaviors (Ramenofsky, 2011, 2012; Romero and Wingfield, 2016) providing examples of the pleiotropic effects of corticosterone influenced by its multiple sites of control at the enzymatic, receptor, and state levels.

Field studies document that winter conditions may prevail at high altitudes and latitudes after birds arrive with storms likely forcing delay of the onset of breeding (Morton, 2002). In these cases, migrants retain elevated levels of corticosterone that promote escape to refuges until conditions on the breeding grounds improve (Reneerkens et al., 2002a; Hahn et al., 2004; Ramenofsky and Wingfield, 2007; Cornelius et al., 2013; Ramenofsky and Wingfield, 2017).

Throughout the vernal stage, hypothalamic-pituitary-gonad (HPG) axis function progresses with increasing levels of gonadotrophin (GtH), testosterone, and DHT, so males are ready to breed once females arrive and environmental conditions allow (Wingfield and Farner, 1978a; O'Reilly and Wingfield, 1995; Ramenofsky and Wingfield, 2006; Covino et al., 2015, 2017; Lymburnera et al., 2016). For females, the story differs as the final stages of oogenesis, yolk deposition, egg laying, and behaviors regulated by estrogen and progesterone are held in check under the regulation of the hypothalamic peptide gonadotropin-inhibiting hormone (GnIH) (Tsutsui et al., 2000; Bentley et al., 2009). This peptide is thought to act as a "brake" on reproduction by its central effects on sexual behavior and hypophysiotropic control of steroidogenesis and ovulation (Wingfield et al., 2016). Under extreme conditions, interactions of elevated corticosterone and GnIH may serve to extend the more mobile or nomadic phase of arrival biology until conditions improve sufficiently for GnIH levels to decline and activation of the breeding stage to proceed. Regulation of GnIH function is not well understood, but environmental conditions appear to play a major role guiding synchronization of egg laying with the potential peak of food abundance (Perrins, 1970; Ramenofsky and Wingfield, 2017). Onset of breeding marks the termination of the vernal migratory stage.

47.3.2 Autumnal stage

47.3.2.1 Development phase

In many ways, autumnal migration appears similar to that of the vernal stage, as it can be divided into the same three phases. The traits are similar that include hyperphagia, fattening, organ remodeling, fueling flight cycles, etc. But major differences exist that provide important clues to the endocrine regulation and biological significance of each stage. For example, the recognized mechanisms that regulate activation of the vernal stage are not operating in the autumnal stage. Daylength is decreasing rather than increasing and many migrants are known to be photorefractory with a loss of responsiveness of reproductive development to long photoperiods (Dawson et al., 2001). The HPG regresses with circulating levels of GtHs and gonadal hormones decline to basal precluding further breeding attempts late in the season. For most species, both baseline and response levels of corticosterone have dropped from elevated breeding titers.

47.3.2.2 Thyroid hormones

A number of seminal studies of captive birds have identified that the rate of increase of vernal photoperiods during photostimulation exert latent effects on the timing of photorefractoriness followed by the autumnal events of postnuptial molt and migration (Farner and Follett, 1966; Gavrilov and Dolnik, 1974; Dolnik, 1980; Moore et al., 1982, 1983). Thyroid hormones are considered central by playing organizational roles for both vernal and autumnal stages during photostimulation (Dawson et al., 2001; Pérez et al., 2016, 2018). Timing of the thyroid organizational effects is considered the basis for the separate pathways of control for the two stages (Wilson and Reinert, 1996, 1999). A further understanding is now needed for the hormonal and genomic mechanisms underlying the potential roles for thyroid hormones during autumnal migration.

47.3.2.3 Androgen

Unlike in spring, plasma levels of androgen in the autumn are basal and probably not capable of activating feeding centers in the hypothalamus. Furthermore castration during the previous winter months had no effect on autumnal fattening in white-crowned sparrows (Wingfield et al., 1990). However, both androgen and estrogen are

synthesized locally in the brain and affect autumnal behavior (Soma et al., 2002; Pradhan et al., 2010). So, it is possible that neurosteroids (steroid synthesized in the brain) could influence the arcuate nucleus via AGRP as in spring (Boswell and Dunn, 2015) to affect autumnal hyperphagia and fattening. Whether the molecular pathways associated with vernal flight muscle hypertrophy operate during the autumnal stage are unknown at present but represent intriguing possibilities.

47.3.2.4 Glucagon

One of a very few studies investigating glucagon in migratory birds during the autumnal stage in comparison with winter identified a decrease in plasma levels of glucagon and FFA in captive Red-winged blackbirds (*Agelaius phoeniceus*) while fattening for autumnal migration (Hintz, 2000). Although a surprising result, Goodridge (1964) suggested previously that seasonal patterns of circulating levels of glucagon could contribute to fluctuations in adiposity with elevated levels promoting lipolysis to mobilize energy to fuel such activities as thermogenesis during winter months and lower titers to enhance fat storage for migration. Further studies are needed to more clearly define the roles of glucagon during the autumn stage.

47.3.2.5 Mature expression—hormones of the fueling and flight cycle

Field studies focusing on the transition from breeding to autumnal departure identified that birds express individual schedules that vary according to investment and timing of breeding, molt, social interactions, age, body condition as well as local weather and wind direction (Runfeldt and Wingfield, 1985; Morton and Pereyra, 1994; Bonier et al., 2007; Sjoberg et al., 2015; Chmura et al., 2020). This asynchrony across individuals deviates markedly from the highly synchronous schedules birds express in spring driven by the initial predictive cues and strong selective pressure for birds to arrive on the breeding grounds as early as feasibly possible for reproductive advantage (Smith and Moore, 2005). Investigating the differences may help to further identify the regulatory distinctions of the two stages but very few studies have focused on seasonal comparisons at time of departure (Wingfield and Farner, 1978a).

Among the overland migrant populations of White-crowned Sparrow, body mass and fat scores reached their annual peak just prior to departure, a time when plasma levels of baseline and response corticosterone are comparable with the vernal and autumnal values but at significantly lower levels than the annual peaks reached upon arrival on the breeding grounds and during early stages of breeding (Wingfield and Farner, 1978a; 1978b; O'Reilly and Wingfield, 1995; Krause et al., 2021). By contrast, in trans-hemispheric migrant Barn swallow (*Hirundo rustica*), the baseline levels of corticosteron prior to spring departure exceeded the values in autumn, while the response levels of autumn rose above vernal values (Raja-Aho et al., 2013). Body condition of spring birds was poor compared to autumn leading to question the role of corticosterone at the time of departure. Given the disparate results across the two species it is clear that additional studies of the physiological condition and endocrine state of birds at departure in the vernal and autumnal stages require further investigations.

47.3.2.6 Stopover: arrival

As in spring, the autumnal stopover substage provides advantageous views of the behavioral, physiological, and endocrinological states upon arrival and at departure. A pattern of elevated baseline and response corticosterone levels has been recorded in some but not all migratory species with greater titers measured in vernal than in autumnal stages (O'Reilly and Wingfield, 2003; Romero et al., 1997; Loshchagina et al., 2018; Bauer et al., 2019). When seasonal differences are detected it is suggested that allostatic load of vernal migration for these species exceeds that of autumn. Impending breeding, unpredictable and unfavorable climatic conditions and less reliable sources of food are some of the issues migrants face at higher altitudes and latitudes in spring. In species that cross extreme barriers (oceans and deserts) with routes that are comparable in both seasons, the baseline levels corticosterone may not vary to any great extent. However another mechanism for differential regulation of corticosterone is presented in Dark-eyed junco sampled during spring and autumn stopovers (Bauer et al., 2019). Neither baseline nor response corticosterone varied seasonally but negative feedback was weaker in spring than autumn suggesting a greater response to environmental purturbations. Surprisingly, these findings diverge from the increased sensitivity to capture in the spring arriving Bar-tailed godwits in comparison with refueling birds and possibly suggests a species or migratory strategy difference.

Thus, a more consistent theme arising from a variety of species captured during autumnal migration indicate only moderate elevations of baseline corticosterone, suggesting an allostatic load that falls substantially below stress-induced values Level C (Schwabl et al., 1991; Gwinner et al., 1992; Falsone et al., 2009). At such titers, corticosterone may serve to support metabolic processes supplying energy required for endurance flight in terms of protein-mediated transport of fatty acids into flight muscle and high-oxidative capacity (Lundgren and Kiessling, 1985; McFarlan et al., 2009; Price et al., 2010). Yet, a few extreme cases are reported of birds captured in flight in nearly starved condition with depleted stores of fat, atrophied flight muscle, and baseline corticosterone titers that

reach well into the realm of the acute response to stress Level C (Box 47.1). Fat stores are considered key regulators of systemic protein catabolism that can affect allostatic load, plasma corticosterone, and potentially survival (Schwabl et al., 1991; Jenni and Jenni-Eiermann, 1992; Schwilch et al., 2002; Falsone et al., 2009). Such elevated baseline levels indicate that an individual has entered the ELHS in which corticosterone metabolically promotes protein catabolism and directs a change in behavior from landing to foraging enabling recovery as long as sufficient resources can be accessed (Romero and Wingfield, 2016).

47.3.2.7 Stopover: departure

At departure from stopover sites, birds are metabolically ready for flight with elevated body mass, fat deposits, circulating triglyceride levels, and hypertrophied flight muscle (Sandberg et al., 2002; Fusani et al., 2009; Goymann et al., 2010; Covino and Holberton, 2011). Additionally, baseline levels of corticosterone correspond with orientation at take off and environmental cues conducive for flight namely favorable winds (Lohmus et al., 2003; Eikenaar and Schmaljohann, 2015; Eikenaar et al., 2017b, 2018a). In captive migrants, expression of nocturnal migratory restlessness coincides with increased baseline corticosterone (Ramenofsky and Wingfield, 2017). Taken together, departure involves the interactions of the environment, endocrine system, physiological state, and motivation to fly. The causal relationship of these variables remains to be elucidated fully.

47.3.2.8 Termination—arrival

Generally, arrival at the overwintering sites marks the end of autumnal migration with the loss of such traits as hyperphagia, fattening, flight muscle hypertrophy, and nocturnal restlessness (Romero et al., 1997; Ramenofsky, 2011). For the most part overwintering sites provide sufficient resources for survival but competition for access to roosts sites, quality food, and protection from predators can be intense given presence of resident birds as well as potential influx of breeding birds from the opposite hemisphere (Newton, 2008). Unlike the vernal stage, autumnal arrival is less synchronized, more facultative, and birds may not settle for weeks (Watts et al., 2018). To avoid competition, some cohorts arrive early or continue movement to locate in areas where food is more abundant and environmental conditions less harsh, as noted in the differential migration patterns (Ketterson and Nolan, 1976; Terrill, 1990; Newton, 2008). Given the degree of competition for resources at this stage, it is surprising that levels of androgen and corticosterone levels are basal (Wingfield and Farner, 1978a, b; Romero et al., 1997; Krause et al., 2021). However, the prospects that neurosteroids may be influencing behavior is a possibility but unknown to date. Also, involvement of the metabolic hormones is unclear emphasizing the need for more research during the autumnal stage.

47.3.3 Conclusions to endocrine system

Comparing vernal and autumnal life history stages of migration offers insight into the adaptations of each providing a fuller appreciation of the migratory processes as a whole. In general, there are common traits that support movement in either season that include an engine (muscle) for power, fuel supplies, oriented movement, and a clock (Piersma et al., 2005; Ramenofsky and Wingfield, 2007; Dingle, 2014). Specifically, the two stages and their substages diverge in terms of the environmental conditions encountered, types of available resources, reproductive states, endocrine status, age groups participating, and in many cases the migratory routes. These differences are the most revealing as they convey individual and/or population responses to the selective pressures of the environment, season, fitness, and survival supporting the premise that the two migratory stages are distinct adaptations. But before any conclusions can be fully drawn, more thorough coverage of the endocrinology of the autumnal stage is needed in addition to the studies that track plasma levels of hormones over the course of each stage. Together these points emphasize more work is needed that focuses on the molecular and genomic aspects of the endocrine system, receptor expression, and the metabolic enzymes all playing key roles in determining hormone action during both the vernal and autumnal stages as reported by (Sharma et al., 2018). Such integrative studies will provide a more complete understanding of how the environment influences migration and how individuals will cope with the challenges of climate change.

47.4 Physiological aspects of migratory preparation and long-duration flight: fueling/flight cycle

47.4.1 Introduction

Given that the vernal and autumnal migration stages occur at separate times of the year under differing environmental conditions and evidence to date suggests that the two stages are regulated by unique neuroendocrine mechanisms, we would expect some important differences in the physiology of birds during the two migration stages. In general, physiological ecologists who study migration in birds pay attention to the season in which birds are studied, but few studies have focused on how the physiology of migratory birds differs between vernal and autumnal migration. This paucity of information about the mechanistic underpinnings of physiology during the two migration stages has led us to

organize the following section around several themes (feeding and diet selection, fuel storage and fat quality, fuel use and oxidative balance) that we assume to be relatively common to both migration stages, but that may be produced by different gene-to-physiology-to-behavior mechanisms.

47.4.2 Feeding

47.4.2.1 Hyperphagia

During spring and fall migration, migratory birds increase their daily food intake (e.g., hyperphagia) in an effort to increase energy stores (fattening) to fuel their migratory flights (Odum, 1960; King and Farner, 1965). These periods of intensive feeding and fattening can last a few days to several weeks (Schaub and Jenni, 2001; Chernetsov and Mukhin, 2006; O'Neal et al., 2018), and the duration is influenced by a variety of ultimate and proximate factors such as migration strategy (e.g., long-distance, short-distance), weather, food availability, predation risk, endogenous cycles, and physiological state (Jenni and Schaub, 2003; Fusani et al., 2009; Goymann et al., 2010; Guillemette et al., 2012; Hou and Welch, 2016). For many species, the total duration of migration is composed mostly of time spent at stopovers and not in flight itself (Wikelski et al., 2003). Thus, much of the hyperphagic periods of most birds are at stopover sites. For several species of dabbling ducks, for example, the average stopover duration was 28 days and was heavily correlated with habitat quality and the availability of food (O'neal et al., 2018). In contrast, the primary predictor of stopover duration in several species of songbirds was dependent upon the amount of fat reserves when all other factors such as weather, predation, and food availability were equal or controlled (Fusani et al., 2009; Goymann et al., 2010; Smith and McWilliams, 2014) although this generalization is based almost entirely on correlational rather than empirical experiments (Smith and McWilliams, 2014).

47.4.2.2 Balancing the energy costs of hyperphagia

Hyperphagia can inherently increase daily energy expenditure (DEE) due to the additional time required to search for and process food as well as maintain more metabolically active tissue (reviewed in Lindström, 2003). Hyperphagic birds must compensate for increased foraging costs in order to rapidly gain body stores. Thus, migratory birds exhibit behavioral and physiological adjustments during hyperphagia that help to promote fattening while keeping their DEE similar to or below nonhyperphagic periods. For example, premigratory common eiders, *Somateria mollissima*, foraged three times more than postmigration periods yet their DEE remained the same because they reduced their heart rate during inactive times and decreased their time spent flying (Guillemette et al., 2012). Several species of migratory birds ranging in size from hummingbirds (Carpenter and Hixon, 1988) to small passerines (Wojciechowski and Pinshow, 2009) to large geese (Butler and Woakes, 2001) reduce their body temperature and so reduce energy expenditure prior to migratory flight regardless of food availability, weather conditions, or degree of fat storage.

47.4.2.3 Fasting and refeeding during migration

During migration, many birds alternate between short-term fasting while flying and intense refeeding at stop over sites. This cycle of alternating feeding and fasting influences gut morphometrics, fattening rates, and subsequently the pace of migration (Karasov and McWilliams, 2005). It is well established that the guts of migrating birds atrophy after just 1 or 2 days of fasting, and this decreased digestive capacity influences the rate at which birds can increase feeding rate and uptake of nutrients upon arrival at stopover sites (Diamond et al., 1986; Karasov and Pinshow, 2000; McWilliams and Karasov, 2005). Thus, the phenotypic flexibility in the gut of migratory birds plays a significant role in their ability to immediately refeed and fatten. Several species of migratory birds increase gut length, mass, and volume in response to increases in food intake in preparation for migratory flight (Dykstra and Karasov, 1992; McWilliams et al., 1999; McWilliams and Karasov, 2001, McWilliams and Karasov, 2005). However, digestive enzyme activity and nutrient uptake per unit of tissue did not change with an increase in food intake in several species of fasted passerines (reviewed in McWilliams and Karasov, 2005). Thus, the relevant phenotypic flexibility seems to be primarily in the size of the gut and not the chemical aspects of digestive efficiency. The digestive organ sizes of fasted birds appear to increase within one to six days upon increasing food intake (Dekinga et al., 2001; McWilliams and Karasov, 2001) and the activity of digestive enzymes, nutrient transporters, and absorption rates take 2–3 days to recover after fasting (Karasov and Hume, 1997; Karasov and Pinshow, 2000). This delay in recovery can impact the overall time it takes for a bird to become ready to migrate and thus slow the overall pace of migration.

47.4.2.4 Diet selection during migration

Many migratory bird species display seasonal shifts in diets associated with migration. For example, several passerines switch from a primarily insectivorous diet to a more frugivorous diet (Herrera, 1984; Bairlein and Gwinner, 1994; Parrish, 1997, 2000), and some artic nesting

shorebirds switch from a diet of primarily terrestrial invertebrates to aquatic invertebrates during fall migration (Schwemmer et al., 2016). This dietary flexibility has been attributed in part to the changes in food availability linked with season (Martin and Karr, 1986; Tsipoura and Burger, 1999). For example, migratory songbirds locally congregated where fruit abundance was high (Smith and McWilliams, 2014), they consistently chose foraging sites with higher fruit availability than insect availability during migration (Martin and Karr, 1986), and migrating shorebirds chose stopover sites along the shores of the eastern United States in conjunction with horseshoe crab spawning (Tsipoura and Berger, 1999). However, food abundance does not entirely explain diet switching in birds during migration as a multitude of factors play into diet choice (see Murphy, 1994 for complete review) including the need to rapidly satisfy the elevated daily energy and nutrient demands associated with migration while eating foods that are typically nutritionally unbalanced.

Birds seem capable of discriminating between foods based on relatively small differences in key nutrients, and these nutrient-based preferences may change with nutrient demands although the evidence for this is less convincing. As an example, four species of tanagers, Blue Dacnis, *Dacnis cayana*, Flame-crested tanager, *Tachyphonus cristatus*, Green Honeycreeper, *Chlorophanes spiza,* and Short-billed tanager, *Cyanerpes nitidus*, were shown to detect differences of 1% in sugar concentration and 2% in lipid concentration in available diets (Schaefer et al., 2003). In addition, these tanagers were able to distinguish between diets that differed in protein type (casein vs. bovine serum albumin) while protein concentration remained constant (Schaefer et al., 2003). Furthermore, white-crowned sparrows preferred semisynthetic diets that differed only in certain amino acids, and their preferences for sulfur amino acids needed for feather growth increased during times of molt (Murphy and King, 1987). Yellow-rumped warblers offered several diets that varied in nutrient and energy content ate a combination of available diets that allowed them to satisfy both their energy and protein demands during nonmigratory as well as migratory periods (Marshall et al., 2016). Whether or not birds have preferences for specific amino acids during the migratory period has not yet been determined. Likewise, many species of migratory birds prefer diets containing certain types of fats (i.e., unsaturated over saturated) and certain amounts or ratios of fatty acids in their diets (Pierce and McWilliams, 2014). There is some evidence that these bird preferences for specific fats remain similar across seasons. For example, red-eyed vireos, *Vireo olivaceous*, preferred diets with more 18:1n9 than diets with more 18:0 or 16:0, and this diet preference did not change between nonmigratory and migratory periods (Pierce and McWilliams, 2005). In sum, migratory birds can discriminate between diets based on certain nutritionally relevant components such as carbohydrates, amino acids, and fatty acids, although whether these nutrient preferences change with nutrient demands is not well documented.

Plant secondary metabolites (PSMs) may influence diet choice in migratory birds somewhat independently of the nutrient composition of foods. PSMs have been shown to increase fruit consumption in some passerines (Cipollini and Stiles, 1993; Bairlein and Simons, 1995) while decreasing consumption in others (Cipollini and Levey, 1997; Levey and Cipollini, 1998). Cedar waxwings, *Bombycilla cedrorum*, chose to eat the energy-rich fruit of *Viburnum opulus*, only when catkin proteins were simultaneously available as a protein source to help produce buffers against the acidic high-PSM fruits (Witmer, 2001). In addition, dietary PSM increased energy intake, intestinal mass, and BMR of rufous-collard sparrows, *Zonotrichia capensis*, but not the common diuca-finch, *Diuca diuca* (Barceló et al., 2016). The impact of the wide diversity of PSM on the diet choices of birds during migration and their ability to regain fuel stores remains a fruitful but largely unexplored question.

47.4.3 Fuel storage

47.4.3.1 Fats are the primary fuel

Birds fuel their high-intensity endurance exercise such as migratory flights primarily by metabolizing fat along with a small amount of protein (McWilliams et al., 2004; Guglielmo, 2010, 2018; Jenni-Eiermann, 2017). Migratory birds use primarily fat to fuel their long-duration flights because fat provides substantially more energy than an equal mass of either carbohydrate or protein (Blem, 1990) which makes it an ideal fuel for weight-economizing migratory birds (Bishop and Butler, 2015; Braun, 2015). Thus, in preparation for long-duration flights birds store appreciable energy mostly as fat (90+% of body mass increase) as well as key nutrients including protein (Jenni and Jenni-Eiermann, 1998; McWilliams et al., 2004; Bishop and Butler, 2015; Guglielmo, 2018) and antioxidants (Skrip et al., 2015a; Cooper-Mullin and McWilliams, 2016). The resulting hypertrophy of muscles and accumulation of substantial visceral, subcutaneous, and intramuscular fat stores has been long-known and well-studied (Blem, 1976, 1990; Bishop and Butler, 2015).

Given that storage of energy and key nutrients is necessary for all migratory birds, and especially those that travel long distances without the opportunity to stopover (Piersma, 1998), there is a type of "limiting factor" worth mentioning here—there are clear limits to how much storage mass can be carried for birds that also must fly. In general, the scaling of energy required to fly to that available from the muscles given their size declines as body size

increases (Pennycuick, 1975). This means that birds as heavy as ostriches cannot become airborne even if they had the largest of wings (Norberg, 1990; Marden, 1994). Such biomechanical constraints (i.e., high-wing loading expressed as grams body mass/cm^2 wing area) associated with flight have been invoked to explain why, for example, swans and ducks require a running takeoff to become airborne and fly (Lovvorn and Jones, 1994), the flightlessness of steamer ducks (Livezey and Humphrey, 1986), and why there are relatively few bird species that fly and eat only plants due to gut size limitations of herbivory (Dudley and Vermeij, 1992; McWilliams, 1999). However, such biomechanical constraints also apply to individuals that dramatically increase their energy and nutrient reserves or gut mass during key times of the annual cycle such as migration (Guillemette, 1994; Piersma, 1998; McWilliams, 1999), while not changing the size of their flight apparatus. For example, the accumulation of large body reserves during the prelaying period results in some female common eider unable to take off (Guillemette and Ouellet, 2005). Such thresholds for flightlessness seem best explained by biomechanical models that integrate wing morphology, muscle mass, and maximum power output required for take off (Marden, 1994). Thus, limitations associated with the power requirements of flapping flight constrain the extent of energy and nutrient storage that can be accumulated especially for larger birds.

47.4.3.2 Physiological challenges associated with fatty acids as fuels

Fats may be ideal fuels for weight-economizing migratory birds because of their high-energy density; however, the metabolism of stored fats requires protein-mediated transport at most every step of the way from adipocyte to mitochondria (Figure 47.5) which can inhibit the very high rates of fat metabolism required for flight (McWilliams et al., 2004; Guglielmo, 2018). Birds are able to enhance their use of stored fats during migratory flights in several important ways (McWilliams et al., 2004; Price, 2010; Guglielmo, 2018). First, they may change the "quality" of their fat stores to enhance the rate of mobilization and oxidation. Fatty acid composition of stored fat changes in birds during migration primarily in response to diet and to preferential metabolism of certain fatty acids (Pierce and McWilliams, 2005; Pierce and McWilliams, 2014) and such changes in fat quality can affect flight performance during long-duration flights (Price, 2010; Guglielmo, 2018; Carter et al., 2020; McWilliams et al., 2020). Second, birds may increase the membrane proteins involved in transporting lipids into cells from the carriers in the blood plasma and the activity of cellular enzymes and so increase the oxidative capacity to use fatty acids (Guglielmo, 2010, 2018). Third, the acquisition of fat stores in birds during migration is associated with a coincident increase in antioxidant capacity to protect against oxidative damage caused by fat storage and use during long-duration flights (Skrip et al., 2015a; Cooper-Mullin and McWilliams, 2016; Skrip and McWilliams, 2016).

47.4.3.3 Fat quality is dynamic, affected mostly by diet, and changes seasonally during migration

The fatty acid composition of natural foods eaten by birds in migration can be quite variable (Pierce and McWilliams, 2014), migratory birds discriminate between foods based

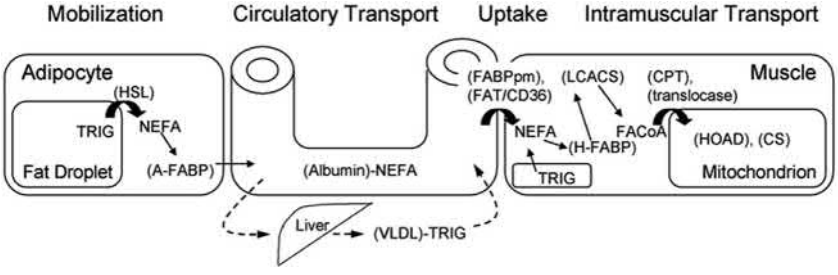

FIGURE 47.5 Lipid transport and oxidation in a bird during exercise while postabsorptive (from Price, 2010). Adipocyte triacylglycerol (TRIG) is hydrolyzed to nonesterified fatty acids (NEFAs) and glycerol through the action of hormone sensitive lipase (HSL). The extremely low-aqueous solubility of fatty acids requires the action of soluble protein carriers at every step of transport. These lipid transporters as well as key enzymes are shown in parentheses. Transport of NEFA within the adipocyte is accomplished by adipocyte fatty acid binding protein (A-FABP). Once exported from the adipocyte, NEFA are bound by plasma albumin and carried to the muscles. In addition to using fat stores as a source of fatty acids, the liver can synthesize many fatty acids de novo or use plasma NEFA to, by esterification to glycerol, produce TRIG packaged into very low-density lipoprotein (VLDL) for release into circulation. Note that the use of plasma VLDL as a source of fatty acids for working muscles requires hydrolysis by lipoprotein lipase (LPL, not shown) at the capillary endothelium (Ramenofsky, 1990; McWilliams et al., 2004). Uptake of fatty acids from circulation into muscle is facilitated by two important fatty acid transport proteins, fatty acid translocase (FAT/CD36) and a plasma membrane fatty acid binding protein (FABPpm). Once in the muscle cells, NEFAs are bound and intracellularly transported by heart-type fatty acid binding protein (H- FABP) which also serves to increase the rate of removal of NEFA from the membrane surface. In addition to these fatty acids sourced from adipocytes and liver, TRIG can also be directly stored within muscle and be hydrolyzed to NEFA and glycerol. Intracellular NEFA are converted by long chain acyl-CoA synthetase (LCACS) to acyl Co-A (FACoA). Uptake of FACoA into the muscle mitochondrion requires several biochemical conversions carried out by two forms of carnitine palmitoyltransferase (CPT) as well as a translocase. Once in the mitochondrial matrix, FACoA enters the β-oxidation pathway and citric acid cycle where key enzymes, including 3-hydroxyacyl-CoA dehydrogenase (HOAD) and citrate synthase (CS), lead to the aerobic production of CO_2, H_2O, and ATP.

on fatty acid composition (Bairlein, 1991; Zurovchak, 1997; Boyles, 2011; Pierce and McWilliams, 2014; Rios et al., 2014), and fatty acid composition of diet primarily determines that of stored fat at least for the mid-chain length fatty acids (e.g., 16:1 and 18:1, no. carbons:no. double bonds) and the essential fatty acids (e.g., 18:2n-6, 18:3n-3 along with their dominate elongation products, 20:4n-6 and 22:6n-3, respectively) with selective metabolism of certain fatty acids playing a possibly important but minor role (Blem, 1976; Pierce et al., 2005; Price and Guglielmo, 2009; Price, 2010). Note that conventional fatty acid nomenclature includes reference to the position of the double bonds relative to the methyl end of the molecule (e.g., n-6 refers to the first double bond at the sixth carbon from this end; n-6 is also referred to as omega-6 or ω-6) because the methyl end is not subject to elongation and desaturation and determines nutritional essentiality (Klasing, 1998). The implication is that migratory birds can select diets so as to achieve a certain fatty acid composition of their stored fat and muscle membranes and thereby satisfy the changing energy and nutritional demands across seasons, including that associated with endurance exercise during migration (Heitmeyer and Fredrickson, 1990; Conway et al., 1994; Bairlein, 1996; Maillet and Weber, 2006; Weber, 2009). Interestingly, behavioral preferences for certain dietary fatty acids (i.e., 18:1 and 18:2 over 18:0) were consistent across migration and nonmigration periods of the annual cycle (Pierce et al., 2004) and more recent studies suggest that migratory birds consistently prefer a 2:1 ratio of 18:1 to 18:2 (Boyles, 2011; Pierce and McWilliams, 2014). In sum, any observed seasonal changes in fatty acid composition of migratory birds are likely due primarily to diet and not to some endogenous seasonal change in diet preference for certain fatty acids or selective metabolism, although many more such studies are clearly needed.

In contrast to the composition of fat stores, the fatty acid composition of muscle and mitochondrial membranes is less affected by diet (Abbott et al., 2012). However, the apparently more consistent membrane composition conceals the fact that 95% of relevant membrane-bound fatty acids (i.e., 16:0, 18:2n-6) turn over on average every 10−17 days in volant birds, and at a faster rate than those in fat stores (Carter et al., 2019). Some studies have measured fatty acid composition of whole plasma [e.g., (Jensen et al., 2020)] or plasma fractions [i.e., NEFA, neutral lipids, phospholipids (Guglielmo et al., 2002c)] although we ignore such information here because seasonal changes in fatty acid composition of circulating lipids primarily reflect changes in feeding rate and diet composition rather than what is necessarily used during migratory flights when birds are fasting and must rely on stored fats (Guglielmo et al., 2002b, 2002c).

Seasonal changes in the fatty acid composition of fat stores in free-living migratory birds suggest that only a few fatty acids may be ecologically relevant and affect exercise performance (Pierce and McWilliams, 2014; Guglielmo, 2018), although given the wide variety of diets eaten by free-living birds during migration, and the relatively few such studies, such interspecific comparisons produce somewhat complicated trends (Table 47.1). In general, the 16- and 18-carbon fatty acids predominate (usually >75% of lipid stores) and the most common forms are usually the saturated 16:0 (no double bonds) and the monounsaturated 18:1n-9. During migration, 16:0 and 18:1n-9 still predominate although 16:1n-7 and two polyunsaturated fatty acids (PUFAs) considered essential for birds, mostly linoleic acid (18:2n-6) and small amounts of alpha-linolenic acid (18:3n-3), are often moderately abundant (up to 40%, but usually <20%) in the fat stores of landbirds. The fatty acid composition of fat stores of marine birds, mostly shorebirds (Napolitano and Ackman, 1990; Egeler and Williams, 2000; Maillet and Weber, 2006; Guglielmo, 2018) and waterfowl (Thomas and George, 1975; Heitmeyer and Fredrickson, 1990) studied to date, also includes much 16:0 and 18:1n-9 but can include up to ca. 20% of longer-chain 18:2n-6 and smaller amounts of 18:3n-3 PUFA (Table 47.1).

Seasonal changes in the fatty acid composition of flight muscle membrane phospholipids in free-living migratory birds confirm that only a few fatty acids may be ecologically relevant and affect exercise performance although much more information is needed (Pierce and McWilliams, 2005; Price, 2010; Guglielmo, 2018). Muscle membrane phospholipids are usually comprised of more saturated fatty acids (notably 16:0 and 18:0), less long-chain monounsaturated fatty acids (notably 18:1n-9), and more longer-chain PUFA (notably 18:2n-6, 20:4n-6, and 20:5n-3, 22:6n-3) compared to the fatty acid composition of fat stores (e.g., western sandpipers *Calidris mauri* (Egeler and Williams, 2000; Guglielmo et al., 2002c), white-throated sparrows (Klaiman et al., 2009), and semipalmated sandpipers (Maillet and Weber, 2006). Fatty acid composition of muscle membrane phospholipids changed seasonally in the two species studied to date (Table 47.1) with n-3 PUFAs (mostly 22:6n-3) decreasing and n-6 PUFAs (mostly 20:4n-6) coincidentally increasing in white-throated sparrows (Klaiman et al., 2009), whereas in western sandpipers, the n-3 PUFAs (mostly 22:5n-3 and 22:6n-3) increased and n-6 PUFAs (mostly 20:4n-6) coincidentally decreased (Guglielmo et al., 2002c), and there was a modest increase in 18:0 during migration in both species. Klaiman et al. (2009) suggest that these differences between species in the reciprocal change in long-chain n-3 and n-6 fatty acids in muscle phospholipids during migration were because of diet changes (to more enriched n-3

TABLE 47.1 Fatty acid composition (%) of subcutaneous fat (including neutral lipids) or whole carcass or muscle phospholipids (structural membranes) for migratory birds captured during both the nonmigration (i.e., breeding or winter) and migration (fall or spring migration) period of the annual cycle.

		Fatty acid composition of tissue(s)							Hypothesized patterns					
Species	Season	14:0	16:0	16:1	18:0	18:1n-9	18:2n-6	18:3n-3	% unsaturated	18:1 / 18:2	16:1&18:1 / 18:2	n-6[a] / n-3	Tissue	Source
Slate-colored Junco[b] (*Junco hyemalis*)	Spring migration	0.6	19.2	3.1	7.3	33.7	31.1		67.9	1.1	1.2		Whole animal	1
			↑			↑	↓		-	-	-			
	Winter	0.7	14.3	3.1	6.2	27.5	41.8		72.4	0.7	0.7		Whole animal	1
White-crowned Sparrow (*Zonotrichia leucophrys*)	Spring migration	31.8	16.6	4.2	5.8	24.4	10.6	1.6	39.2	2.3	2.7	6.6	Whole animal	2
		↑	-	-	-	-	↓	-	-	-	-	-		
	Winter	1.5	22.3	2.8	11.6	31.1	29.3	1.0	63.2	1.1	1.2	29.3	Whole animal	2
Wood Thrush (*Hylocichla mustelina*)	Fall migration		15.2	2.4	7.6	61.6	7.6	1.3	71.6	8.1	8.4	2.6	Whole animal	3
			↓		↓	↑	↓	↓	-	-	-	-		
	Breeding		24.0	4.7	13.8	34.4	12.0[c]	3.9	55.0	2.9	3.3	2.3	Whole animal	3
Red-eyed Vireo (*Vireo olivaceous*)	Fall migration		17.5	28.0	2.5	32.8	16.1	0.2	76.9	2.0	3.8	80.5	Subcutaneous fat	4
			↓	↑		↓		↓	-	-	-	-		
	Breeding		29.9	2.1	6.9	39.7	14.4	4.2	56.2	2.8	2.9	3.4	Subcutaneous fat	4
White-throated Sparrow (*Zonotrichia albicollis*)	Fall & Spring migration[d]		13.5	2.1	5.9	34.0	38.0	4.1	74.1	1.0	1.1	9.3	Subcutaneous fat	5
			↓	↓			↑		↑	↓	↓			
	Winter		21.5	5.0	7.2	32.8	24.9	3.4	62.7	1.5	1.7	7.3	Subcutaneous fat	5
	Fall & Spring migration[d]		18.0		25.5	6.0	15.0[e]	23.0[f]	51.5	0.4	0.4	0.9	Muscle phospholipids	5
					↑		↑	↓				↑		
	Winter		22.1		22.0	5.9	8.1[e]	27.9[f]	50.0	0.7	0.7	0.5	Muscle phospholipids	5
Western Sandpiper[g] (*Calidris mauri*)	Spring migration	4.0	33.8	11.5	10.9	29.6	2.2	1.9	47.3	13.5	18.7	1.0	Subcutaneous fat	6
			↓		↓	↑			↑	-	-	-		
	Winter	6.0	36.3	8.1	17.6	18.7	2.0	2.0	34.8	9.3	13.4	0.9	Subcutaneous fat	6
Western Sandpiper[g]	Spring migration		13.8	0.6	25.7	11.9	22.3[h]	20.3[i]	59.6	6.6	6.9	1.6[j]	Muscle phospholipids	7
					↑	↑	↓	↑						
	Winter		16.4	0.2	21.4	10.4	29.2[h]	14.6[i]	61.0	8.6	8.8	2.4	Muscle phospholipids	7
Canada Goose (*Branta canadensis*)	Spring migration	0.3	24.7	4.1	4.9	45.7	19.1	0.9	68.9	2.4	2.6	22.3	Subcutaneous fat	8
						↓	↑		-	-	-	-		
	Breeding	0.2	24.3	2.5	5.1	54.5	12.8	0.6	69.8	4.3	4.5	23.3	Subcutaneous fat	8
Mallard	Spring migration	1.0	17.1	2.9	6.0	51.9	19.1	2.1	74.9	2.7	2.9	9.1	Peritoneal fat	9
			↓	↓		↑			-	-	-	-		
	Winter	1.3	21.0	3.4	7.0	44.8	18.8	3.4	68.3	2.4	2.6	5.5	Peritoneal fat	9

Only studies that measured fatty acid composition in two or more seasons (e.g., migration, nonmigration periods) are included. Fatty acid nomenclature is number of carbon atoms to number of double bonds, and the location of the first double bond from the methyl end of the fatty acid (e.g., 18:2n-6 has 18 carbons in its backbone, two double bonds, and the first double bond is at the sixth carbon from the methyl end). Fatty acids that were sometimes detected but represent <3% across all studies are excluded (i.e., 18:1n-7, 20:0, 20:3n-6, 20:5n-3, 22:5n-3) except where noted. Given the fatty acid composition of tissues, several hypotheses have been proposed to explain the pattern of change in composition during

Continued

TABLE 47.1 Fatty acid composition (%) of subcutaneous fat (including neutral lipids) or whole carcass or muscle phospholipids (structural membranes) for migratory birds captured during both the nonmigration (i.e., breeding or winter) and migration (fall or spring migration) period of the annual cycle.—cont'd

migration. Arrows denote significant changes in fatty acid composition during migration as reported by the original authors (lack of an arrow or dash indicates no significant difference between migration vs. nonmigration periods for a given species). Dashes between migration versus nonmigration rows for a given species indicate no statistical comparison was reported in the original study.

[1] Bower and Helms, 1968.
[2] Morton and Liebman, 1974.
[3] Conway et al., 1994.
[4] Pierce and McWilliams, 2005.
[5] Klaiman et al., 2009.
[6] Egeler and Williams, 2000.
[7] Guglielmo et al. (2002a, b, c).
[8] Thomas and George, 1975.
[9] Heitmeyer and Fredrickson, 1990.

[a] Combined n-6 fatty acids (18:2n-6, 20:4n-6) and n-3 fatty acids (18:3n-3, 20:5n-3, 22:5n-3, 22:6n-3).
[b] Proportion of 18:3n-3 was not reported by season.
[c] in addition, 20:4n-6, another long-chain n-6 PUFA, comprised 3.9% and 2.0% of total fatty acid composition in breeding versus fall migration periods, respectively.
[d] Birds were sampled in both a fall and spring migration period, but combined here (average presented) because differences between these migration periods were relatively uncommon (exceptions for common fatty acids (>2% of total lipids): 18:0 and 18:2n-6 in muscle phospholipids, 18:3n-3 in adipose, and 18:2n-6 in intramuscular neutral lipids were different between fall versus spring migration).
[e] In addition, 20:4n-6, another long-chain n-6 PUFA, comprised 8.1% and 7.5% of total fatty acid composition in winter versus migration (fall and spring) periods, respectively.
[f] Proportion of 22:6n-3, another long-chain n-3 PUFA, is presented because 18:3n-3 comprised <0.5% of total fatty acid composition.
[g] Males and females were separately measured during winter (December in Panama), spring migration (May in British Columbia), and fall migration (July in British Columbia), but the sexes were averaged here. Fatty acid composition of stored fat (Egeler and Williams, 2000) and pectoralis muscle phospholipids (Guglielmo et al., 2002a, b, c) during spring and fall migration were not significantly different so only fall migration is presented.
[h] Proportion of 20:4n-6, another long-chain n-6 PUFA, is presented because 18:2n-6 comprised <1.9% of total fatty acid composition and unlike 20:4n-6 did not change seasonally.
[i] proportion of the combined longer-chain n-3 PUFAs (i.e., 20:5 + 22:5 + 22:6) is presented because 18:3n-3 comprised <0.5% of total fatty acid composition. Significant seasonal changes were detected in only 22:5n-3 and 22:6n-3, and not 18:3n-3 or 20:5n-3.
[j] The n-6/n-3 ratio for birds in fall migration was similar to that during spring migration (presented here), but was significantly lower (1.0) than during winter.

marine prey for sandpipers, to more enriched n-6 seeds for sparrows). Clearly more such studies are needed to determine if the general pattern of reciprocal change in long-chain n-3 and n-6 PUFAs in flight muscle membrane phospholipids is robust across birds species with different migration strategies that inhabit terrestrial and/or marine ecosystems.

47.4.3.4 Physiology of protein storage and flight muscle preparation

Lean mass typically accounts for approximately one quarter of the body mass gain in passerine birds prior to migration (Klaassen and Biebach, 1994; Klaassen et al., 1997; Bauchinger and Biebach, 2001) and on average ~50% of body mass gain in several species of waders (reviewed in Lindström and Piersma, 1993). Much of the lean mass gain observed in free-living birds has been attributed to increases in the size of the gut and organs associated with flight, i.e., heart and pectoralis (flight) muscle (Marsh, 1984; Dietz et al., 1999; reviewed in Lindström and Piersma, 1993; McWilliams et al., 2004). Several hypotheses have been put forth to explain the increase in lean mass and muscle hypertrophy prior to migration including the increased power needed for flight with a larger body mass (Marsh, 1984), as a source for gluconeogenesis (Jenni and Jenni-Eiermann, 1998; Guglielmo et al., 2017) and a storage mechanism for water (Gerson and Guglielmo, 2011) (see Protein Use section below). For pectoralis (flight) muscle in particular, studies suggest the increase in size of the pectoralis muscle is the result of a concomitant increase in body size (Marsh, 1981), a result of power training before flight (Marsh and Storer, 1981), or of an endogenously regulated process that occurs independent of training or size changes (Evans et al., 1992; Bishop et al., 1998; Dietz et al., 1999).

In addition to an overall mass increase in flight muscle, the mass-specific activities of key catabolic enzymes related to the oxidation of fatty acids, overall aerobic/anaerobic capacity, burst power, and glycolytic capacity increase in flight muscle prior to migration (Marsh, 1981; Lundgren and Kiessling, 1985; Banerjee and Chaturvedi, 2016). For example, hydroxyacyl-CoA-dehydrogenase (HOAD) concentration almost doubles in the flight muscle of gray catbirds (Marsh, 1981), and CS and HOAD activity increases in reed warblers, *Acrocephalus scirpaceus*, during fattening prior to migration (Lundgren and Kiessling, 1985). Additionally, Evans et al. (1992) showed that the percentage volume of mitochondria in muscle fibers in Dunlin, *Calidris alpina*, and Sanderlings, *Calidris alba*, increased from winter to spring migration suggesting an increased aerobic capacity of the flight muscle in preparation for migration. Banerjee and Chaturvedi (2016) concluded that the pectoral muscle of premigratory, red-headed buntings, *Emberiza bruniceps*, showed significant increases in aerobic and anaerobic capacity (CS, CCO, and MDH activity), increased fatty acid oxidation capacity [increased carnitine palmitoyltransferase (CPT) and HOAD activity], increased glycolytic capacity (increased PFK and PK activity), and increased burst power (CK activity) compared to nonmigratory buntings (Banerjee and Chaturvedi, 2016). Thus, although the dynamics of fat stores are more extreme than that of body protein, the turnover and dynamics of body protein has important functional significance (Bauchinger and McWilliams, 2012; Bauchinger and McWilliams, 2010; Carter et al., 2019).

47.4.4 Fuel use

47.4.4.1 Patterns of change in fatty acid composition of birds during migratory stage: proposed hypotheses

Understanding how the fatty acid composition of fat stores in free-living birds changes during migration periods provides a foundation upon which to generate ecologically relevant hypotheses, informed by comparative physiology, about how fatty acid composition can affect exercise performance of migratory birds. Given that specific unsaturated fatty acids are preferentially used and more rapidly mobilized during metabolism over saturated fatty acids (Leyton et al., 1987; Raclot and Groscolas, 1995; McKenzie et al., 1998; McKenzie, 2001; Raclot, 2003; Price et al., 2008), which compensates for their relatively lower energy content and potential for ATP production (Weber, 2009; Price, 2010), one proposed hypothesis is that the proportion of unsaturated fatty acids in fat stores will increase during migration. Both studies that directly tested this hypothesis (Table 47.1) found the predicted increase in unsaturation of fat stores (Egeler and Williams, 2000; Klaiman et al., 2009), and three of the other six species studied (wood thrush, *Hylocichla mustelina*, red-eyed vireos, and mallard, *Anas platyrhynchos*) support this hypothesis. Two of the three species (slate-colored junco, *Junco hyemalis*, Canada goose, *Branta canadensis*) had a relatively similar proportion of unsaturated fatty acids in their fat stores (Table 47.1) which led Guglielmo (2018) to conclude that the most general pattern observed to date was that the proportion of unsaturated fatty acids in fat stores of migratory birds increased or stayed the same during migration (the only exception thus far is the white-crowned sparrow which had unusually high proportions of 14:0 in its fat stores during migration).

The other alternative hypotheses that have been proposed to explain the patterns in the fatty acid composition of birds during migration have focused on the essential fatty acids (18:2n-6 and 18:3n-3) and their elongation products (e.g., 20:4n-6 and 22:6n-3,

respectively). Blem (1980) suggested that the ratio of 18:1 to 18:2 was higher in migratory birds. Results from five of the eight species studied to date (slate-colored junco, white-crowned sparrow, wood thrush, western sandpiper, and mallard) support this alternative hypothesis (Table 47.1). Pierce and McWilliams (2005) noted that the ratio of long-chain monounsaturated fatty acids (16:1, 18:1) to an essential long-chain PUFA (18:2) increased during migratory periods for most of the six species studied up to that point in time. Results from six of the eight species presented in Table 47.1 support this alternative hypothesis (Canada goose and white-throated sparrows were the exceptions). The potential importance of a certain ratio of n-3 and n-6 PUFAs to physiological function is long standing and is known to be strongly influenced by diet (Hulbert et al., 2005). For four of the species studied, n-3 PUFAs during both migration and nonmigration periods were <2% of all fatty acids in the whole animal (junco, white-crowned sparrow) or in separated fat stores (western sandpiper, Canada goose), and none of these four species showed the expected increase in n-6/n-3 ratio during the migration period (Table 47.1). For the other four species with more substantial n-3 fatty acids in their tissues (whole animal for wood thrush, fat stores for red-eyed vireo, white-throated sparrow, and mallard), the ratio of n-6/n-3 PUFAs consistently increased during migration compared to nonmigration periods (Table 47.1). As noted above, the changes in muscle phospholipids of birds during migration are modest compared to those observed in fat stores. The general pattern from the two studies conducted to date of reciprocal change between n-6 and n-3 PUFAs in muscle phospholipids and to a lesser extent 18:0 and 16:0 (but not fat stores; Table 47.1), provides little to no consistent support for any of the proposed hypotheses above.

Thus, the principle pattern that emerges from these few studies (Table 47.1) is that (1) there are seasonal changes in fatty acid composition of fat stores and muscle phospholipids that are associated with migration. For fat stores, the observed changes include (a) the proportion of unsaturated fatty acids either remain the same or increase during migration and (b) in particular, the relative amounts of the n-6 and n-3 PUFAs increase during migration (at least for those bird species with >2% n-3 PUFAs in their fat stores). For muscle phospholipids, reciprocal changes between primarily n-6 and n-3 PUFAs occur during migration although the direction of change differs between the two species studied to date. (2) These seasonal changes in fatty acid composition of fat stores and muscle phospholipids seem primarily driven by seasonal changes in diet, and the extent to which diet affects membrane composition is more modest than that of fat stores. Clearly, more studies are needed that systematically measure fatty acid composition of both fat stores (neutral lipids) and membranes (phospholipids) in several tissues [e.g., (McCue et al., 2009)] in a wide variety of migratory birds during migratory and nonmigratory seasons before these trends are confirmed and considered broadly applicable.

47.4.4.2 The oxidative costs of burning fat as fuel

Regulating oxidative balance is important for all air-breathing organisms such as birds because reactive prooxidant molecules can cause considerable cellular damage and affect health, longevity, and performance (Halliwell and Gutteridge, 1999), and PUFAs are especially susceptible to lipid peroxidation (Hulbert et al., 2007; Montgomery et al., 2012). This has led to a rich literature relating variation in membrane fatty acid composition to size-related variation in metabolic rate in mammals and birds (Hulbert and Else, 1999, 2000) and in turn to variation in reactive species (RS) production, life span, and aging (Harman, 1956; Speakman, 2005; Speakman and Selman, 2011; Speakman and Garratt, 2013; Herborn et al., 2016). In this context, birds have often been portrayed as exceptional vertebrates in that they display relatively high-metabolic rates, with the associated increased RS production, yet they are remarkably long-lived compared to mammals (Buttemer et al., 2010; Munshi-South and Wilkinson, 2010; Barja, 2014; Jimenez et al., 2019). Furthermore, birds use of fats as their primary fuel during high-intensity endurance exercise such as migratory flights (Jenni and Jenni-Eiermann, 1998; Guglielmo, 2010) has potential acute oxidative costs because fats, and especially PUFAs, are highly susceptible to oxidative damage (Cooper-Mullin and McWilliams, 2016; Skrip and McWilliams, 2016). As noted earlier, an important adaptation in Neoaves has led to the constitutive activation of the NRF2 master antioxidant response which lowers the risk of macromolecular oxidative damage in birds other than the fowl (e.g., chicken, ducks, geese (Castiglione et al., 2020). This constitutive activation of the antioxidant response may require birds to maintain a more robust and costly endogenous antioxidant system, although consumption of dietary antioxidants could reduce or alleviate these costs.

One of the challenges of studying how the antioxidant system of birds responds to the physiological challenges of migration is that the primary instigator of the oxidative challenge, increased RS production with increased metabolism, is not yet measurable in whole organisms (Costantini, 2014; Cooper-Mullin and McWilliams, 2016; Skrip and McWilliams, 2016). This must be inferred from measurements of key components of the antioxidant system (e.g., upregulation of antioxidant enzymes implies a response to increased RS production) and ideally simultaneous measures of RS-associated damage (e.g., upregulation

of lipid peroxidation products implies increased RS production that are insufficiently quenched by the antioxidant system). Another challenge of studying phenotypic flexibility in the antioxidant system of migratory birds is that the major site for generation of RS is the mitochondria which will vary in density and activity across tissues (Costantini, 2019) as well as with exercise and age (Cooper-Mullin and McWilliams, 2016). In addition, RS can act as both damaging molecules, as discussed above, and also as signaling molecules that can stimulate the endogenous antioxidant system (Halliwell and Gutteridge, 1999; Costantini, 2014, 2019). There are also a multitude of tests available to probe the response of the antioxidant system to ecologically relevant challenges which too often complicates comparisons across studies (Costantini, 2016, 2019; Skrip and McWilliams, 2016). Consequently, integrative studies (from mitochondria to cells to tissues to whole organism) that are also comparative (e.g., multiple tissues within the same individuals, migration state vs. nonmigration periods, multiple species that differ in migration strategy) are required to fully understand the antioxidant system of migratory birds within an ecological context. Given such integrative and comparative studies of migratory birds are largely lacking, evidence to date provides a more piecemeal view of how the antioxidant system of migratory birds changes during migration.

Does fattening and storage of oxidatively vulnerable PUFAs in preparation for migration increase RS production and an associated antioxidant response? Blackpoll warblers, *Dendroica striata*, and red-eyed vireos at a New England stopover site during fall migration (Skrip et al., 2015a), and garden warblers and barn swallows at a Mediterranean coastal stopover site during spring migration (Costantini et al., 2007), simultaneously increased their fat stores, nonenzymatic antioxidant capacity (plasma OXY), and oxidative damage (plasma d-ROMs) suggesting that fattening may incur oxidative costs and that the balance of capacity and damage may be condition-dependent. Captive-reared Northern wheatears, *Oenanthe pileata*, that were photostimulated into "migration state" in fall and that were rapidly refueling and hyperphagic increased their nonenzymatic antioxidant capacity (plasma OXY), consistent with the field studies described above, but not lipid peroxidation (red blood cell MDA) compared to control (*ad libitum*-fed) birds (Eikenaar et al., 2016). Several experimental and field studies suggest that the quality of fats consumed and stored in migratory birds affects circulating markers of oxidative damage. For example, European starlings, *Sturnus vulgaris*, fed for many months on diets with more or less n-6 PUFA had fuel stores composed of more or less n-6 PUFA, and those composed of more n-6 PUFA had consistently higher levels of plasma markers of oxidative damage (McWilliams et al., 2020). White-throated sparrows that consumed diets with more PUFA had increased circulating oxidative damage (d-ROMs) although when given choices between diets that differed only in available antioxidants (vitamin E) these birds did not prefer antioxidant-rich diets when consuming more dietary PUFA (Alan and McWilliams, 2013). Common blackbirds captured at a stopover site in northern Germany had a higher plasma fatty acid peroxidation index, higher nonenzymatic antioxidant capacity (OXY), but similar lipid peroxidation compared to sympatric resident blackbirds (Eikenaar et al., 2017a). The lack of correspondence between plasma fatty acid composition and that of fat stores and cell membranes in the same individuals (as described earlier) may explain why oxidative damage did not change with plasma peroxidation index in this latter study. Hudsonian godwits, *Limosa haemastica*, preparing for a very long-duration migratory flight increased total antioxidant capacity and reduced oxidative damage (TBARS) but did not change metabolic enzyme activity (Gutiérrez et al., 2019). In sum, migratory birds seem to build some component of their antioxidant capacity concomitantly with fat stores and increased oxidative damage may be an inevitable consequence of increasing (or maintaining more) fat stores, especially if they are composed of mostly PUFA.

During migratory flight, do birds upregulate antioxidant capacity and thus avoid the energetically expensive repair of damaged structures? In two recent reviews, Cooper-Mullin and McWilliams, 2016 and Skrip and McWilliams, 2016 reported that free-living birds during migration, or captive birds that flew for certain periods of time, often exhibit an increase in damage to lipids and/or proteins despite an often upregulated antioxidant system composed of antioxidant enzymes, nonenzymatic sacrificial molecules, and dietary antioxidants. For example, homing pigeons, *Columba livia*, that flew further (200 km) had more oxidative damage and less serum nonenzymatic antioxidant capacity than those that flew less far (60 km) when blood was sampled w/in 15 min of returning to the roost (Costantini et al., 2008). European robins, *Erithacus rubecula,* caught during nocturnal migratory flight had elevated markers of circulating oxidative damage to proteins (protein carbonyls) compared to resting robins even though the former also had higher circulating levels of glutathione peroxidase (GPx), an enzymatic antioxidant (Jenni-Eiermann and Jenni, 1991; Jenni-Eiermann et al., 2014). In contrast, migratory common blackbirds had higher nonenzymatic antioxidant capacity (OXY) but similar lipid peroxidation compared to sympatric resident blackbirds (Eikenaar et al., 2017a). Captive zebra finches, *Taeniopygia guttata*, flown for 2 h/day for many weeks increased the coordination between the enzymatic (GPx) and nonenzymatic (OXY) components of the antioxidant system while oxidative damage remained low and similar to sedentary finches (Cooper-Mullin et al., 2019). Plasma

markers of oxidative damage did not change in European starlings over the course of daily flying for several weeks, nor before and after a single long flight, in part because of upregulation of components of their antioxidant system (Frawley et al., 2021; McWilliams et al., 2020). Thus, upregulation of the antioxidant system and, at least in one case, increased coordination of key components of the antioxidant system occurs during repeated long-duration flights, and in some but not all cases, this seems to avoid the potential increase in oxidative damage with exercise. These studies also provide an important reminder that the response of individuals to an oxidative challenge involves an interacting, multicomponent antioxidant system (Costantini, 2019).

Given that some oxidative damage may occur during a migratory flight or enforced exercise, are migratory birds able to recover from this damage in an appropriately short period of time? Migratory birds at stopover sites seem to be able to in part recover from any oxidative damage that may have occurred during migration. For example, European robins that rested during the day had lower protein damage levels (protein carbonyls) than those caught during active nocturnal flight presumably because they had time to remove or repair damaged proteins (Jenni-Eiermann and Jenni, 1991). Individual Garden Warblers sampled repeatedly at a spring stopover reduced circulating lipid peroxidation levels over time (Skrip et al., 2015a). Thus, if oxidative damage occurs, then migratory birds seem capable of repairing this damage in a relatively reasonable amount of time (i.e., days not weeks) given their usual stopover durations, although many more such studies are needed that track recovery of individuals after long-duration flights.

Does consumption of dietary antioxidants affect the upregulation of the endogenous antioxidant system associated with migratory flights? In theory, the costs of upregulating the endogenous antioxidant system could be reduced if dietary antioxidants could quench RS producing during flight (Costantini et al., 2010a; Pamplona and Costantini, 2011; Costantini, 2014). Recent experimental evidence demonstrated for the first time that an ingested fat-soluble dietary antioxidant (Vitamin E) was absorbed and transported to the mitochondria in the flight muscles of a songbird within 22.5 h, but only if the birds were regularly flying each day (Cooper-Mullin et al., 2021). Thus, actively migrating songbirds that ingest dietary antioxidants during the day at a stopover, in this case fat-soluble antioxidants, would have these available in their mitochondria to protect against RS produced during subsequent nocturnal flight(s). Several experimental studies have directly manipulated the amount and type of dietary antioxidant(s) available to migratory birds, or captive birds exposed to regular exercise, and then measured the response of the antioxidant system often in relation to some ecologically relevant challenge (e.g., flight, high-PUFA diets). For example, European starlings fed diets supplemented or not with anthocyanins had similar plasma nonenzymatic antioxidant capacity (OXY) and oxidative damage (d-ROMs), but circulating uric acid was higher in individuals fed the low-antioxidant diet (Frawley et al., 2021). Likewise, zebra finches fed more or less anthocyanins and exercised (daily 2-h flying for months) or not had similar plasma nonenzymatic antioxidant capacity (OXY), antioxidant enzyme activity in liver (GPx, catalase, superoxide dismutase) and oxidative damage (d-ROMs); plasma uric acid was not measured in this study (Skrip et al., 2016). The suggestion from these studies is that when birds consume too little dietary antioxidants, this may not directly affect upregulation of antioxidant enzymes but may increase protein catabolism and thus circulating uric acid when flying for long durations and/or consuming high-PUFA diets. There is also evidence that consumption and physiological use of dietary antioxidants in birds may depend on their nutritional needs, energy demands, and type of dietary antioxidant (Costantini et al., 2010b; Beaulieu and Schaefer, 2013). Clearly, much more work is needed to adequately understand the role of dietary antioxidants in enabling migratory birds to maintain oxidative balance.

47.4.4.3 Carry over effects from winter to breeding

For the many birds that breed in seasonal environments, migration to more benign areas during winter has evolved along with the need to acquire energy and nutrient stores to fuel migration and, in the spring, also prepare for breeding. Life-history theory predicts that major annual cycle events such as breeding and migration are separated in time (and often space) to effectively distribute the total costs over time and to maximize the benefit-to-cost ratio given seasonal changes in resources (Lack, 1954; Dingle, 1996). However, such temporally separated events are not thereby independent in that, for example, condition of animals during one annual cycle event (e.g., in winter or on migration) can affect subsequent events (e.g., migration, reproduction). These so-called carry-over effects (Marra et al., 1998; Holmes, 2007; Harrison et al., 2011; Mitchell et al., 2011; Drake et al., 2013; Paxton and Moore, 2015) reveal links between annual cycle events that affect populations and individual fitness (Harrison et al., 2011). It has long been recognized that the extent of nutrient acquisition during spring, often prior to initiating migration, largely determines reproductive success in many waterfowl species (Ryder, 1970; Drent and Daan, 1980; Alisauskas and Ankney, 1992). As such, waterfowl provide many examples of the importance of carry-over effects (Harrison et al., 2011), the acquisition and storage of nutrient reserves at

one time or place (e.g., during the nonbreeding period) that are then used as resources at a later time and place (e.g., for breeding) (Warren et al., 2013; Sedinger and Alisauskas, 2014). Knowing the location and timing of nutrient storage during the nonbreeding period often has important conservation implications (Raveling and Heitmeyer, 1989; Abraham et al., 2005; Stafford et al., 2014; Alisauskas and Devink, 2015). Despite the importance of carry-over effects especially in migratory animals, a major gap in our understanding of these effects involves identifying the proximate causal links. All previous work has focused on how energy in the form of fat, protein, or carbohydrate stores may provide such linkages, whereas no previous studies have focused on antioxidants even though they have been proposed as an important currency that underpins life history tradeoffs (Catoni et al., 2008; Alonso-Alvarez et al., 2010) and potentially carry-over effects (Harrison et al., 2011).

Dietary antioxidants are likely an important, yet understudied, currency for carry-over effects in birds especially during spring migration for primarily three reasons. First, dietary antioxidants play important roles during the reproductive season in that breeding effort of birds promotes oxidative damage (Alonso-Alvarez et al., 2010) and domestic fowl supplemented with dietary fat-soluble antioxidants gain fitness advantages (Koutsos et al., 2003; Royle et al., 2003; McGraw et al., 2005; Williamson et al., 2006). Additionally, developing egg embryos are protected from external oxidative challenges if the females are able to deposit antioxidants in the yolk (Watson et al., 2018). Consistent with this important role of dietary antioxidants during reproduction, European starlings fed high-anthocyanin diets during spring had more elevated testosterone and more sustained breeding behaviors compared to individuals fed less antioxidants (Carbeck et al., 2018). Second, the increased metabolic rate associated with long-duration migratory flights produces pro-oxidants that must be quenched to avoid damage (Costantini, 2008; Costantini et al., 2007, 2008), and for spring migrating birds, this may reduce the antioxidant capacity available for subsequent reproduction. Importantly, dietary anthocyanins can support the metabolic function of glucocorticoids (corticosterone) and so control potential negative effects of excessive secretion of these hormones especially during long-duration flights (Casagrande et al., 2020). Third, fat-soluble antioxidants can be deposited in fat stores and so migratory birds could strategically store antioxidants prior to departure (Costantini et al., 2007), and balance their use during migratory flights so as to retain enough for investment into eggs that can subsequently enhance offspring survival and fitness (Blount et al., 2003; McGraw et al., 2005; Skrip et al., 2016). Clearly, much more study is needed to determine how female migratory birds contend with the oxidative costs of migratory flights in spring while also preparing for subsequent breeding and egg laying.

47.4.4.4 Fat quality matters

In theory, selectively eating and hence storing certain long-chain unsaturated fatty acids may be advantageous because (1) such fatty acids may be preferentially mobilized and metabolized more quickly (fuel hypothesis); (2) such fatty acids may affect composition and key functions of lipid-rich cell membranes (membrane hypothesis); and (3) such fatty acids may stimulate key facets of aerobic metabolism such as stimulating expression of genes involved in fatty acid oxidation (signal hypothesis) (Figure 47.6). Below we briefly discuss aspects of each of these hypotheses and how they may relate to the observed effect on exercise performance of migratory birds. Other reviews should be consulted for more thorough discussion of these hypotheses and the evidence (Weber, 2009; Guglielmo, 2010; Price, 2010; Pierce and McWilliams, 2014; Guglielmo, 2018). Although we separately describe these three hypotheses for convenience, they are not mutually exclusive.

The fuel hypothesis states that enhanced exercise performance occurs because certain fatty acids are more quickly mobilized and metabolized, and this can occur in several ways (Figure 47.5): selective mobilization from adipocytes, enhanced transport to target tissues, selective uptake by and transport within muscle cells, and/or enhanced oxidation and production of ATP (McWilliams et al., 2004, Price, 2010; Guglielmo, 2018). Several studies across taxa have shown that mobilization of shorter chain SFAs and fatty acids with more double bonds (e.g., 18:2n-6) was more rapid from fat stores in rats, fish, and birds (Raclot and Groscolas, 1995; Sidell et al., 1995; Hulbert et al., 2005; Price et al., 2008; Guglielmo, 2018). Isotope tracer studies that track ingested nutrients to breath CO_2 confirm that long-chain unsaturated fatty acids are oxidized more rapidly than their saturated counterparts (e.g., 18:1 vs. 18:0) (McCue et al., 2010). Once mobilized from fat stores, fatty acids require solubilization and intracellular translocation by the family of fatty acid binding proteins (FABPs) such that an increase in the number and action of FABPs present in the cell membranes and cytosols of muscle cells increases oxidative capacity (Guglielmo et al., 1998, Guglielmo et al., 2002a; McFarlan et al., 2009; Guglielmo, 2010, 2018). Furthermore, within flight muscle cells, the rate of CPT catalysis (Figure 47.5) was relatively higher for fatty acids with more double bonds compared to their saturated forms (e.g., 18:2 and 18:3 vs. 18:0) (Price et al., 2011; Guglielmo, 2018). This evidence supports the fuel hypothesis in that certain fatty acids such as 18:2n-6

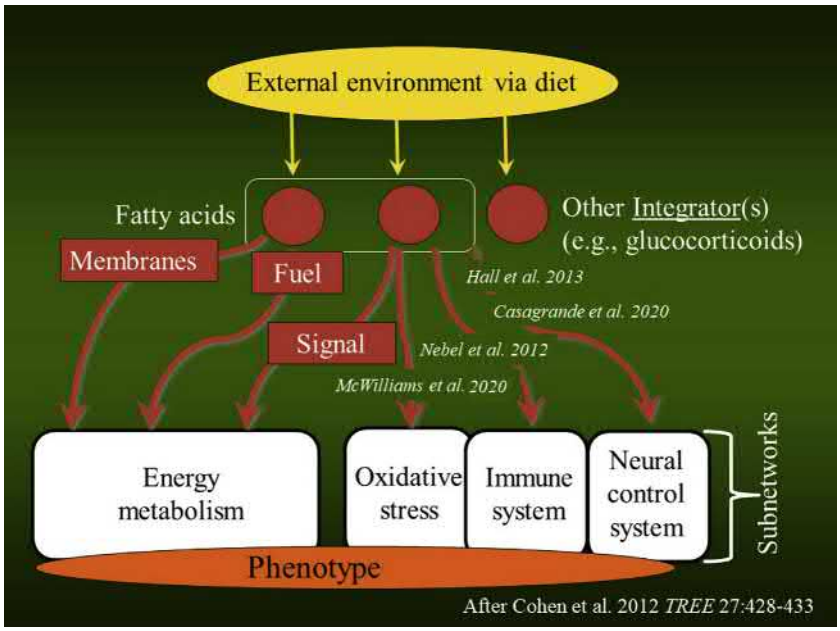

FIGURE 47.6 A simplified schematic of a physiological regulatory network that indicates how certain dietary fatty acids serve as key "integrators" that interact with multiple systems (subnetworks) and each other, thereby ensuring an appropriate match between phenotype and environmental conditions. Dietary fatty acids have been shown to influence the immune system (Nebel et al., 2012), neurogenesis (Hall et al., 2013), and neuroendocrine control of metabolism (Casagrande et al., 2020), and oxidative status (McWilliams et al., 2020). The three hypotheses (membrane, fuel, and signal), and the evidence that supports or refutes them are described in the text. *After Cohen et al. (2012).*

are metabolized more quickly at many steps of fatty acid oxidation although whether this is primarily responsible for enhanced exercise performance during migration periods is not yet clear (Guglielmo, 2010; Price, 2010) and discussed in the next section.

The membrane hypothesis states that the fatty acid composition of membrane phospholipids can effect key aspects of membrane structure and function (Hulbert and Else, 1999; 2000; Hulbert et al., 2005) and thus exercise performance of an organism (Valencak et al., 2003; Maillet and Weber, 2006; Maillet and Weber, 2007; Weber, 2009; Price, 2010). As described above, fatty acid composition of diet influences the phospholipid composition of muscle membranes in vertebrates, and this effect of diet on membrane composition is especially strong for dietary n-3 and n-6 compared to other fatty acids (e.g., shorter-chained saturated fatty acids (Hulbert et al., 2005; Maillet and Weber, 2006; 2007). Accordingly, the fatty acid composition of cell and subcellular membrane phospholipids converged with that of diet in migrating shorebirds that consumed marine invertebrates laden with n-3 PUFAs (Maillet and Weber, 2006, 2007). An increase in membrane PUFAs has potential functional importance for exercising animals in that (1) n-3 and/or n-6 PUFAs increase the fluidity and permeability of cell membranes (Stillwell and Wassall, 2003; Weber, 2009) and (2) n-3 and/or n-6 PUFAs are known to influence the activity of membrane-bound proteins and enzymes (e.g., UCP and -ATPases) which could affect efficiency of aerobic respiration (Hulbert and Else, 2000; Infante et al., 2001; Hulbert et al., 2005; Maillet and Weber, 2006, 2007; Gerson et al., 2008).

The signal hypothesis states that certain dietary fatty acids (most notably the n-3 and n-6 PUFAs) directly act as natural ligands for receptors that regulate the expression of genes associated with lipid metabolism (McClelland, 2004; Bordoni et al., 2006; Maillet and Weber, 2006; 2007; Weber, 2009). In particular, PUFA directly bind to and regulate the activity of peroxisome proliferator-activated nuclear receptors (PPARs) which are well known to stimulate expression of genes involved in fatty acid oxidation (Hochachka and Somero, 2002; Pawar et al., 2002; Zhang et al., 2004; Narkar et al., 2008; Weber, 2009), although the specific mechanism of action depends on the type of PPAR (Feige et al., 2006). PPAR α and β stimulate fatty acid oxidation and transport whereas PPAR γ is involved in lipid storage and adipocyte differentiation (Desvergne and Wahli, 1999; Nagahuedi et al., 2009). PPARs exhibit high affinity for n-3 PUFAs (Bordoni et al., 2006) and the upregulation of rate-limiting enzymes involved in aerobic metabolism by certain fatty acids such as 18:2n-6 (Sidell et al., 1995; Egginton, 1996; McKenzie, 2001) enables more rapid production of ATP during exercise (Guglielmo et al., 1998, 2002a; McWilliams et al., 2004). The effects of PUFAs on gene expression depend largely on the cellular concentration of PUFA, although it is not yet clear if a specific amount or ratio of dietary n-3 and n-6 fatty acids is optimal (Bordoni et al., 2006). The direct binding of certain dietary PUFAs to PPARs that then activate genes regulating lipid metabolism provides an example of "natural doping" whereby exercising animals can eat certain PUFAs, upregulate key aspects of lipid metabolism, and so enhance their exercise performance (Maillet and Weber, 2006, 2007, Weber, 2009). Such natural doping on n-3

PUFAs has been proposed for semipalmated sandpipers as they pause at key stopover sites during fall migration (Maillet and Weber, 2007). Whether this is a most interesting but unusual case in migratory birds deserves further investigations. In addition, these same essential PUFAs are used to build eicosanoids (e.g., prostaglandins, thromboxanes, leukotrienes, and lipoxins) that act locally on the cells that produce them or are nearby, and in this sense they are classified as hormones with signaling properties. At present, the importance of eicosanoids in birds during migration has not been directly studied and only proposed as an explanation (Klaiman et al., 2009; Carter et al., 2020), although their involvement in regulating a wide variety of physiological systems (e.g., immunity, development and growth, thermoregulation, and oviposition) suggests some attention may be worthwhile.

47.4.4.5 Testing the fuel, membrane, and signal hypotheses

Empirical evidence somewhat supports all of these alternative hypotheses although the weight of evidence to date seems to favor the fuel or signal hypotheses. The fuel hypothesis has been invoked to explain how fatty acid composition affects performance in rats, lizards, fish, and more recently migratory birds (Leyton et al., 1987; Geiser and Learmonth, 1994; Raclot and Groscolas, 1995; McKenzie et al., 1998; Wagner et al., 2004; Pierce et al., 2005; Price et al., 2008; Price and Guglielmo, 2009; Petersson et al., 2010). Our own recent work and that of colleagues has confirmed that songbirds with stored fat composed of more n-6 PUFA have improved exercise performance during short-term intense exercise (Pierce et al., 2005; Price and Guglielmo, 2009; Price, 2010). Price and Guglielmo (2009) used a cleverly designed sequence of feeding and fasting protocols to produce white-throated sparrows with fat stores and muscle membranes composed of different fatty acids. Consequently, they were able to demonstrate that the enhanced exercise performance of sparrows was associated with the fatty acid composition of fat stores rather than muscle membranes. The implied mechanism for the enhanced performance, in this case higher peak metabolic rates, included both faster mobilization rates of n-6 fatty acids from adipose as well as selective uptake of fatty acids into muscle cells and intramyocyte transport (Price and Guglielmo, 2009; Price, 2010). As correctly pointed out by Price (2010), a crucial untested assumption of this proposed mechanism for producing higher peak metabolic rates is that rate of fatty acid supply, and not some other factor such as oxygen supply or oxidative capacity, is the physiological limitation responsible for these whole-animal changes in exercise performance. In vivo studies that examine *selective* uptake and intracellular transport rates of certain fatty acids in muscle cells during exercise would be quite informative, especially if combined with diet and feeding regime manipulations that allow the effect of fatty acid composition of fat stores to be isolated from that of the other mechanisms.

Birds during migration, however, may be optimizing energy efficiency rather than maximizing metabolic rate and so may not need to maximize rate of fatty acid supply, as is often assumed. Energy efficiency in this case refers to flying further for a given amount of fuel energy or flying as far but expending less fuel energy. A possible mechanism for such enhanced efficiency that is consistent with the fuel hypothesis includes, for example, the documented higher transport rates of unsaturated fatty acids reducing the energy needed for transport of fatty acids (Price, 2010). Evidence in support of this enhanced flight efficiency idea comes from a study of European starlings from a migratory population in southern Germany that were fed for many months specially formulated diets that differed only in the amount of n-6 and n-3 fatty acids—the fatty acid composition of their fat stores was likewise different as expected. During the fall migration period, and after several weeks of flight-training in a wind tunnel, starlings composed of more n-6 (and n-3) PUFA used substantially less energy (ca. 11%) to fly the same distance (260 km) and duration (6 h) than those composed of more monounsaturated fatty acids (McWilliams and Pierce, 2006; McWilliams et al., 2020). This experimentally demonstrated that migratory birds can enhance fuel economy when composed of more n-6 PUFAs, a result consistent with the fuel hypothesis although it does not by itself definitively refute the other proposed hypotheses. As discussed further below, this energy savings gained during a long flight by starlings composed of more n-6 PUFA came at the long-term cost of higher oxidative damage in the n-6 PUFA-fed birds (McWilliams et al., 2020). This may explain why migratory birds seasonally shift their diet to increase consumption of n-3 and/or n-6 PUFAs during migration but then reduce their consumption of long-chain PUFAs during nonmigration periods.

Several lines of evidence suggest a link between the n-3 and/or n-6 PUFA content in membrane phospholipids and exercise performance. For example, maximal running speed in 36 species of mammal was strongly related to the n-6 PUFA content of their muscle membrane phospholipids (Ruf et al., 2006), n-6 PUFA in muscle membranes of rats was positively associated with their exercise performance (Ayre and Hulbert, 1997), and regular exercise increased PUFA content of muscle membranes in humans (Andersson et al., 2000). Also, PUFA-rich membranes have been found in various muscle types having high-aerobic capacity such as the pectoralis muscle in hummingbirds and the shaker muscle in rattlesnakes (Infante et al., 2001). Along with high levels of n-3 PUFAs, these muscle membranes had increased Ca^{2+}-ATPase activity

which may play a significant role in metabolism during exercise (Infante et al., 2001; Ruf et al., 2006). Furthermore, the activity of Na+/K+ -ATPase enzyme in the tissue membranes of birds and mammals has been correlated with the amount of 22:6n-3 in the membrane suggesting a causal link between certain types of PUFA and metabolic rate (Wu et al., 2001, 2004; Turner et al., 2003).

Studies of migratory birds provide some evidence in support of the membrane hypothesis in terms of effects of diet composition on membrane composition and in turn on cellular-level fat metabolism, although the evidence was not consistent (e.g., Maillet and Weber, 2007; Nagahuedi et al., 2009; Guglielmo, 2010; Dick and Guglielmo, 2019). Most studies to date that related membrane composition to whole-animal performance refuted the membrane hypothesis. For example, as discussed above, when Price and Guglielmo (2009) used a sequence of feeding and fasting protocols to produce white-throated sparrows with fat stores and muscle membranes composed of different fatty acids, they found that the enhanced performance (i.e., peak metabolic rate) was associated with the fatty acid composition of fat stores rather than muscle membranes. Dick and Guglielmo (2019) used diet manipulations to produce groups of yellow-rumped warblers that differed in the MUFA, n-3, and n-6 composition of flight muscle membranes. They found effects of membrane composition on activity of several flight muscle oxidative enzymes in warblers but not on multiple whole-animal performance measures including BMR, peak metabolic rate, and energy expenditure and duration of wind tunnel flights. Carter et al. (2020) fed European Starlings one of two diets that differed primarily in 18:2n-6 (reciprocally replaced with 16:0) and this in turn produced starlings with corresponding differences in fatty acid composition of fat stores and muscle membranes that were consistent over the 4-month experiment (Carter et al., 2020). Carter et al. (2020) found effects of membrane composition on activity of several flight muscle oxidative enzymes (Carter et al., 2021) but also on multiple whole-animal performance measures including BMR, peak metabolic rate, and rate of energy expenditure during >2-h wind tunnel flights. Specifically, birds with higher concentrations of 18:2n-6 in membranes and fat stores had higher BMR and peak metabolic rates, although this pattern was evident early in the fall and not later in the fall experiment. The change through time in performance measures but not membrane composition led Carter et al. (2020) to conclude that their results were most consistent with the signal hypothesis rather than the membrane hypothesis. Thus, evidence to date supports the membrane hypothesis in the sense that key metabolic enzymes and other suborganismal measures are affected by fatty acid composition of membranes; however, these studies have not consistently found the predicted effects on whole-animal exercise performance given differences in membrane composition alone.

The natural doping hypothesis proposes that birds (in this case shorebirds) during migration enhance their exercise performance by selecting high n-3 diets (marine prey such as *Corophium volutator* in the case of semipalmated sandpipers) and thereby (a) incorporate these PUFAs into membrane phospholipids and affect membrane function (membrane hypothesis), and (b) (signal hypothesis) binding of n-3 PUFAs to PPARs that then activate the expression and activity of key genes and enzymes that instigate the metabolic pathways involved in enhancing the oxidative metabolism of fatty acids (Maillet and Weber, 2006, 2007, Weber, 2009). Some support for the mechanisms proposed by the signal hypothesis comes from recent studies of Gray catbirds sampled throughout their annual cycle. During premigratory fattening periods, catbirds had increased mRNA expression of certain PPARs and key target genes (Corder et al., 2016; DeMoranville et al., 2019), and these PPAR isoforms from catbirds were activated by certain fatty acids (i.e., 18:1, 20:5n-3) tested on mammal cell lines (Hamiliton et al., 2018). Whether dietary n-3 fatty acids (and n-6 PUFA) act as important natural ligands and so determine these seasonal changes in PPAR expression in migratory catbirds remains unknown (Corder et al., 2016; DeMoranville et al., 2019). In one of the most comprehensive and relevant tissue-to-whole animal experimental studies of migratory birds to date, yellow-rumped warblers fed more n-3 PUFAs and that had membranes composed of more n-3 PUFA *decreased* PPAR-β mRNA abundance, activity of muscle oxidative enzymes, and overall oxidative capacity, and this was not associated with any whole-animal performance effects, in direct opposition to the natural doping, signal hypothesis (Dick and Guglielmo, 2019). The potential to enhance whole-animal performance as proposed by the signal hypothesis may also pertain to the essential n-6 PUFAs. As noted earlier, Carter et al. (2020) concluded that the results from their study of European starlings that were fed and composed of more n-6 PUFAs, and then flown for long durations in a wind tunnel, were most consistent with the signal hypothesis. These same starlings composed of more 18:2n-6 increased the expression of PPARα in the liver and LPL in the pectoralis; however, this occurred only in starlings that flew daily for 2 weeks in the wind tunnel and not untrained birds fed the same diet, and no such effect of diet was observed on the expression of other PPAR transcription factors, PGC-1 coactivators, and key metabolic genes (i.e., CD36, MCAD, CS, PLIN2, and avUCP) in the pectoralis muscle and the liver (DeMoranville et al., 2020). The dependency of the signaling effect of n-6 PUFA on flight training suggests something more complex than a simple direct diet influence.

The three proposed hypotheses (fuel, membrane, and signal) are not mutually exclusive, and each has garnered some support. Given that the use of fats as fuel requires storage, protein transport at many steps of the ways, up- and downregulation of metabolic enzymes (Figure 47.5), and that dietary fatty acids affect the composition of stored fat as well as membranes and can act as signaling molecules, we should not be surprised that this multifaceted fat metabolism system can be affected by diet and exercise in multiple ways. We know from both experimental and correlative studies that the fatty acid composition of diet largely determines that of fat stores and muscle membranes and that there is seasonal variation in the composition of the fat stores and membranes. Thus, the study of how dietary fatty acids affect fat metabolism at large as well as exercise performance in birds during migration presents a very tractable and ecologically relevant opportunity to test these various hypotheses. Especially intriguing and potentially informative are recent transcriptomic analyses (Dick, 2017) that revealed upregulation of key fatty acid metabolism pathways in captive yellow-rumped warblers in fall (vs. winter) while 45 other metabolic pathways were downregulated including those related to muscle growth, inflammation and immune function, and hormone signaling. The extreme challenges of migration may require such metabolic tradeoffs (Guglielmo, 2018), as has also been suggested in terms of an energy savings-oxidative cost tradeoff for birds during migration (McWilliams et al., 2020).

47.4.4.6 Fatty acid transport really matters

Metabolizing fatty acids at very high rates is quite difficult compared to the alternative, more soluble, carbohydrate and protein fuels used predominately by mammals during exercise (Guglielmo, 2010, 2018). As discussed in the next section, fatty acid oxidation in the flight muscles of migratory birds is enhanced by increasing the activity of key mitochondrial enzymes (e.g., HOAD and CPT) although the primary metabolic limitation seems more related to fatty acid transport through the circulation and its uptake by muscle cells (Guglielmo, 2010, 2018). The hypothesized mechanisms for effective and adequately rapid transport of fatty acids from fat stores into muscle cells in migratory birds has been extensively discussed elsewhere (McWilliams et al., 2004; Guglielmo, 2018) and above. In brief, migratory birds in general and birds during active migration, in particular, rely somewhat on augmented circulatory pathways to enhance fatty acid utilization, but the more important determinants of fatty acid flux seems to occur at the muscle cell level—specifically, protein-mediated transport of fatty acids across the muscle cell membrane [e.g., fatty acid translocase (FAT/CD36), plasma membrane fatty acid binding protein (FABPpm)] and within cells [e.g., heart-type fatty acid binding protein (H-FABP)] seems most likely to limit the overall rate of fatty acid metabolism in migratory birds (Figure 47.5). See Bishop and Butler (2015) for a more thorough treatment of this topic.

47.4.4.7 Protein use during flight and water balance

It is well established that birds catabolize lean mass as a protein source during flight with significant reductions in pectoralis muscle, leg muscle, digestive organs, and liver masses among other organs (Åkesson et al., 1992; Bauchinger and Biebach, 1998, 2001; Battley et al., 2000). Unlike lipids and carbohydrates, birds have no specific storage form for proteins (except very small endogenous amino acid pools). Proteins are stored in functional tissue such as flight muscle, digestive organs including the liver, and even skin (Marsh, 1984; Bauchinger and Biebach, 1998; Battley et al., 2000). Thus, the use of protein during flight causes a concomitant loss of structure and/or function. In red knots, *Calidris tenuirostris*, all organs (flight muscle, leg muscle, intestines, liver, kidney, stomach, heart, spleen, and skin) except brain and lungs decreased in mass during their long-duration flight from Australia to China (Battley et al., 2000). This lean mass loss in organs coincided with a 40% decrease in mass-specific BMR after migration suggesting a significant functional consequence in the organs contributing to BMR (Battley et al., 2000).

Several hypotheses explain why birds utilize protein during long-duration flights including the need for proteins as an adaptive reduction in muscle mass to conserve energy (Pennycuick, 1998), as intermediaries in the citric acid (Kreb's) cycle (Jenni and Jenni-Eiermann, 1998; Jenni-Eiermann, 2017), in tissue maintenance and repair (Lindström and Piersma, 1993; Guglielmo et al., 2001), and as a water source (Gerson and Guglielmo, 2011; Jenni-Eiermann, 2017; Groom et al., 2019). It is well understood that exercising mammals use proteins as a fuel source for gluconeogenesis and as intermediaries in the citric acid cycle (Aragón, 1981; Dohm, 1986). Jenni and Jenni-Eiermann (1998) concluded that the use of protein for the maintenance of citric acid cycle intermediaries is important in permitting the high rates of fatty acid oxidation required to meet the increased metabolic demands of long-duration flight in migratory birds. Guglielmo et al. (2001) found elevated plasma creatine kinase (CK) in migrating western sandpipers, and bar-tailed godwits as compared to nonmigrants in the same year suggesting that birds undergo a moderate amount of flight-induced muscle damage during migration and therefore must repair this damage before continuing their migration. However, the extent to which this damage impacts the recovery time at stopover sites and ultimately the pace of migration is still unclear.

Models of water use during flight suggest that water may be an important factor in limiting flight duration (Carmi et al., 1992; Klaassen, 1996). Protein catabolism provides 5.9 times more water per kilojoule than lipid catabolism (Jenni and Jenni-Eiermann, 1998) and thus can provide an invaluable source of water for fasting, flying birds (Gerson and Guglielmo, 2011; Jenni-Eiermann, 2017; Groom et al., 2019). The rate of protein catabolism during flight has been shown to be directly related to ambient relative humidity. Gerson and Guglielmo (2011) found that Swainson's thrushes *Catharus ustulatus* flown in a wind-tunnel at moderately low-ambient humidity had greater lean mass loss, increased metabolic water production, and higher uric acid levels (indicative of protein catabolism) than birds flown in moderately high humidity. Additionally, Groom et al. (2019) found that lean mass loss in birds exposed to low and high-ambient humidity was independent of metabolic rate in Swainson's thrushes with flown birds having similar protein catabolism as birds at rest. Birds have been shown to be effective at controlling blood plasma volumes regardless of thermal dehydration or dehydration incurred during flight (Carmi et al., 1993). Gerson and Guglielmo (2011) suggest that birds may utilize the protein-for-water strategy in an effort to maintain osmotic homeostasis since the plasma osmolarity of the thrushes was unaffected by ambient humidity during flight.

Although several species of birds have been shown to be sensitive to dehydration in ambient temperatures below 20°C in wind-tunnel studies (Torre-Bueno, 1978; Giladi and Pinshow, 1999; Engel et al., 2006), studies of trans-Saharan migrants suggest that energy savings may supersede any limitations set by water loss as migrants fly at higher ambient temperatures and lower humidity than expected given our current understanding from wind tunnel studies (Schmaljohann et al., 2008, 2009). Notably, access to drinking water may be a factor in a bird's decision to depart a stopover site and continue migration. For example, Garden warblers at a spring migration stopover site in the Mediterranean Sea that were captured with large fat stores and then given no access to water, were more likely to depart that night (i.e., had the greatest zugunruhe activity) compared to warblers with similar fat loads and access to water as well as those with less fat loads regardless of access to water (Skrip et al., 2015b). The degree to which freely available water influences departure of birds from a stopover site deserves further study, especially given the impact of climate change on worldwide water distribution.

The amount of protein used during long flights and the sources of these proteins appears to also be influenced in part by the level of fat storage, at least in passerines. Garden warblers, pied flycatchers *Ficedula hypoleuca*, Willow warblers *Phylloscopus trochilus*, and Barn swallows consumed protein primarily from flight muscle when fat stores comprised greater than 20% of total dry body mass. However, when fat stores reached critically low levels (i.e., 5–10% of total dry body mass), protein catabolism greatly increased and the protein mass of all organs decreased with significant reductions in the digestive organs as well as flight muscle masses (Schwilch et al., 2002). This pattern of protein use suggests an adaptive response in birds to the interaction of fuel use, energy requirements, and flight capability. When fat stores are adequate, reduction in flight muscle coincides with reductions in overall body mass (thus conserving energy) without compromising flight capability. However, when fat stores are nearing depletion, protein requirements increase and so birds rely more heavily on protein stores in nonuse organs such as the digestive tract as well as flight muscle. Although this is an adaptive response to meeting the energetic needs of the bird during flight, it appears to be at the detriment of flight capability.

47.4.4.8 Rebuilding protein stores after flight

The loss of proteins from structural and functional tissue during flight naturally requires that birds replenish what has been lost prior to their next flight. Birds arriving at a stopover site replenish protein reserves first before storing fat (Atkinson et al., 2007). For example, mass gain in red knots at Delaware Bay, USA, comprised ~15% fat when birds were below 133 g and ~84% fat above 133 g suggesting that birds have a critical body mass level where they must first rebuild protein stores before they are able to begin refattening (Atkinson et al., 2007). Since much of the protein used during flight is taken from digestive organs, fasted birds must rebuild their guts before returning to maximum digestive capacity and food intake (McWilliams and Karasov, 2001; Gannes, 2002; Pierce and McWilliams, 2004; Muñoz-Garcia et al., 2012). Passerine birds require 1–3 days for their digestive system to fully recover from fasting (Karasov and Pinshow, 2000; McWilliams and Karasov, 2001; Gannes, 2002) and this recovery may be diet-dependent (Pierce and McWilliams, 2004; Muñoz-Garcia et al., 2012). For example, fasted and food restricted white-throated sparrows fed a fruit diet (low protein) were unable to increase food intake rates to pre-fasted levels and thus regain body stores in three days of refeeding whereas sparrows fed a grain diet (high protein) were able to fully recover food intakes to prefast levels and regain energy stores in 24 h (Pierce and McWilliams, 2004). Munoz-Garcia et al. (2012) fed blackcaps, *Sylvia atricapilla*, diets containing 3% (low) and 20% (high) protein with labeled leucine to determine the extent to which these birds relied on dietary (exogenous) or endogenous sources of protein to rebuild their guts. Blackcaps fed a low-protein diet incorporated less exogenous protein into their tissue than blackcaps fed the high-protein diet. Interestingly, blackcaps incorporated more

exogenous protein into their gut than their pectoral muscle but were unable to rebuild their intestines at a similar rate as the blackcaps fed a high-protein diet (Muñoz-Garcia et al., 2012). However, the rate of rebuilding of protein stores (i.e., gut tissue) in migrating blackcaps was influenced by the availability of drinking water when the water content of food was low (Mizrahy et al., 2011). Blackcaps with limited access to drinking water and fed food with low-water content had no increase in lean mass nor fat mass during a simulated stopover period whereas birds provided with unlimited access to drinking water and/or food with high-water content were able to gain lean and fat mass (Mizrahy et al., 2011). This finding, along with that of Skrip et al. (2015) discussed above, suggests that freely available water at stopover sites may play a much larger role than previously thought in enabling birds to rebuild energy and protein stores and complete migration. A full understanding of the interaction between the protein-for-water strategy and the availability of drinking water at stopover sites deserves further investigation.

47.4.5 Temperature regulation during flight

Much of what is known about the body temperature fluctuations of birds during flight has been from wind tunnel studies of captive birds in short duration flights (Aulie, 1971; Torre-Bueno, 1976; Hudson and Bernstein, 1981). For example, pigeons increase their core body temperature (hyperthermia) during short-duration wind tunnel flights at ambient temperatures between 25 and 29C (Aulie, 1971), and this hyperthermia seems to limit the length of flight bouts in pigeons and European starlings (Aulie, 1971; Torre-Bueno, 1976). More recently, studies on wild birds using implanted data loggers have found that hyperthermia may play a much greater role in limiting the duration of migratory flights than previously assumed (Guillemette et al., 2016, 2017); however, this may only be relevant for the larger aquatic species with continuous, fast-flapping flight (Guillemette et al., 2017). Common eiders allow their body temperatures to rise on average 1C by the end of a typical flight and spend a significant portion (36%) of their daily time budget behaviorally cooling their body temperatures from previous flight bouts (Guillemette et al., 2017). Thus, eiders are heat dumping in between migratory flights. Less is known about temperature regulation to avoid hyperthermia during migratory flight in passerines as there are no studies to our knowledge that have used data loggers to track migratory temperature fluctuations in songbirds. Given the few studies to date on free-living birds, it would be beneficial to investigate the role of hyperthermia in regulating the duration of flight in migratory birds, especially in light of climate change.

47.4.6 Flight at high altitude

Birds are preadapted to low-oxygen conditions since the design of their respiratory and circulatory systems makes their oxygen uptake highly efficient, although several aspects of their physiology enable regular flying at high altitude during migration (see Bishop and Butler, 2015 for a thorough treatment of this topic). For example, birds such as bar-headed geese, *Anser indicus*, that fly regularly at high altitudes produce more hemoglobin, more red blood cells, and more myoglobin (the hemoglobin equivalent in muscle cells) as they prepare for migration which enhances their blood's capacity to bind and transport oxygen (Scott and Milsom, 2006). In addition, relatively larger lungs, and more and deeper penetrating blood capillaries in their heart and flight muscles compared to other geese further facilitates oxygen transport. Bar-headed geese also have a special form of an enzyme (nicknamed COX) involved in energy production within their muscle cells (Scott et al., 2011).

47.5 Beyond systems

Migration is one of the most complicated life history stages given the diverse habitats traversed, distances covered, multiple routes, and daily fluctuations of climatic conditions to which birds are exposed in vernal and autumnal stages. To be successful, this life history stage requires flexibility of morphology, physiology, and behavior in tight coordination with environmental information that initially regulates preparation for the stage and subsequently influences the timing, duration, and amplitude or intensity of the response throughout the fueling and flight cycle and eventually termination. The endocrine system plays major roles integrating environmental information with the molecular and cellular physiology as presented here. But, questions remain including: (1) how does seasonal variation of resources and routes affect fueling and flight, (2) does the endocrine status of vernal and autumnal migrants affect their responses to the conditions of specific habitats *en route*, and (3) are the apparent seasonal differences in the endocrine pathways exerting similar effects on fueling or are there multiple ways in which such regulatory systems have evolved?

A fundamental aspect of the life history of migratory birds is the ability to flexibly modify their physiology to satisfy the changing demands associated with migration. Such physiological flexibility is possible only because the network structure of molecules and regulatory relationships that maintain and adjust homeostasis (i.e., the Physiological Regulatory Network, PRN *structure*) can remain the same while the concentrations and relative strengths of the

relationships (i.e., the PRN *state*) can change depending on conditions (e.g., age, seasons, and migration; Cohen et al., 2012). In this chapter, we have outlined key components of the PRN *structure* (e.g., Figure 47.6) and how the PRN *state* is adjusted within individuals during migration. However, our review also makes clear that there remain major gaps in our understanding of both (a) the network of specific molecules and regulatory relationships that maintain and adjust homeostasis (i.e., PRN *structure*) and especially (b) how the concentrations of key molecules and the relative strengths of certain regulatory relationships change with the context and the conditions of vernal and autumnal migration (i.e., PRN *states*). For example, the biochemical mechanisms involved in using fats as fuel, or those responsible for maintaining redox homeostasis and limiting oxidative damage, are usually considered distinct physiological systems (i.e., separate PRN *structures*) that dynamically respond to changing conditions. However, we have emphasized here that there are physiological linkages between fat metabolism and oxidative status that require a more systems-level, integrative approach to fully understand how migratory birds respond to their changing environment(s), and the conditions of vernal and autumnal migration. Furthermore, phenotypic flexibility of physiological traits requires that the capacity of a physiological system is matched to the prevailing demand but can be modulated in response to changes in demand as to provide some limited excess capacity ("enough but not too much") (Diamond, 1991; Hammond and Diamond, 1997; McWilliams and Karasov, 2014). The level of so-called "spare capacity" and the full extent of phenotypic flexibility and its required time course provide important insights into constraints on whole-animal performance, diet diversity, and ecological niche (Piersma and Gils, 2011; McWilliams and Karasov, 2014). Given this systems-level perspective, the following related questions remain outstanding: (1) for a given physiological system (e.g., fat metabolism, oxidative status, and immune function), what is the PRN *structure* for migratory birds and how does PRN *state* change within individuals during migration, (2) what are the key physiological linkages between these systems that influence the limits to animal performance, and (3) what is the time course for such phenotypic flexibility of key physiological traits given that birds during migration are often time-limited?

References

Abbott, S.K., Else, P.L., Atkins, T.A., Hulbert, A.J., 2012. Fatty acid composition of membrane bilayers: importance of diet polyunsaturated fat balance. Biochim. Biophys. Acta 1818, 1309–1317.

Abraham, K.F., Jefferies, R.L., Alisauskas, R.T., 2005. The dynamics of landscape change and snow geese in mid-continent North America. Global Change Biol. 11, 841–855.

Ainslie, P.N., Ogoh, S., 2010. Regulation of cerebral blood flow in mammals during chronic hypoxia: a matter of balance. Exp. Physiol. 95, 251–262.

Åkesson, S., Karlsson, L., Pettersson, J., Walinder, G., 1992. Body composition and migration strategies: a comparison between robins (*Erithacus rubecula*) from two stop-over sites in Sweden. Vogelwarte 36, 188–195.

Alan, R.R., McWilliams, S.R., 2013. Oxidative stress, circulating antioxidants, and dietary preferences in songbirds. Comp. Biochem. Physiol. 164B, 185–193.

Alisauskas, R.T., Ankney, C.D., 1992. The cost of egg laying and its relationship to nutrient reserves in waterfowl. In: Batt, B.D.J., Afton, A.D., Anderson, M.G., Ankney, C.D., Johnson, D.H., Kadlec, J.A., Krapu, G.L. (Eds.), Ecology and Management of Breeding Waterfowl. University of Minnesota Press, Minneapolis.

Alisauskas, R.T., Devink, J.-M., 2015. Breeding costs, nutrient reserves, and cross-seasonal effects. In: Savard, J.-P.L., Derksen, D.V., Esler, D., Eadie, J.M. (Eds.), Ecology and Conservation of North American Sea Ducks. CRC Press, Boca Raton, FL.

Alonso-Alvarez, C., Perez-Rodriguez, L., Garcia, J.T., Vinuela, J., Mateo, R., 2010. Age and breeding effort as sources of individual variability in oxidative stress markers in a bird species. Physiol. Biochem. Zool. 83, 110–118.

Anderson, A.M., Duijns, S., Smith, P.A., Friis, C., Nol, E., 2019. Migration distance and body condition influence shorebird migration strategies and stopover decisions during southbound migration. Front. Ecol. Evol. 7.

Andersson, A., Sjodin, A., Hedman, A., Olsson, R., Vessby, B., 2000. Fatty acid profile of skeletal muscle phospholipids in trained and untrained young men. Am. J. Physiol. Endocrinol. Metabol. 279, 744–751.

Aragón, J.J., 1981. Replenishment of citric acid cycle intermediates by the purine nucleotide cycle in rat skeletal musle. In: RW Estabroook, P.S. (Ed.), Biological Cycles: Current Topics in Cellular Regulation. Academic Press, London.

Atkinson, P.W., Baker, A.J., Bennett, K.A., Clark, N.A., Clark, J.A., Cole, K.B., Dekinga, A., Dey, A., Gillings, S., González, P.M., 2007. Rates of mass gain and energy deposition in red knot on their final spring staging site is both time-and condition-dependent. J. Appl. Ecol. 44, 885–895.

Aulie, A., 1971. Body temperatures in pigeons and budgerigars during sustained flight. Comp. Biochem. Physiol. Physiol. 39, 173–176.

Ayre, K.J., Hulbert, A.J., 1997. Dietary fatty acid profile affects endurance in rats. Lipids 32, 1265–1270.

Bairlein, F., 1991. Nutritional adaptations to fat deposition in the long-distance migratory Garden Warbler (*Sylvia borin*). In: Proceedings of the 20th International Ornithological Congress. Christ-church, NZ.

Bairlein, F., 1996. Fruit-eating in birds and its nutritional consequences. Comp. Biochem. Physiol. 113A, 215–224.

Bairlein, F., Gwinner, E., 1994. Nutritional mechanisms and temporal control of migratory energy accumulation in birds. Annu. Rev. Nutr. 14, 187–215.

Bairlein, F., Simons, D., 1995. Nutritional adaptations in migrating birds. Israel J. Ecol. Evol. 41, 357–367.

Baker, J.R., 1938. The evolution of breeding seasons. In: Debeer, G.R. (Ed.), Evolution: Essays on Aspects of Evolutionary Biology. Clarendon Press, Oxford, U.K.

Banerjee, S., Chaturvedi, C.M., 2016. Migratory preparation associated alterations in pectoralis muscle biochemistry and proteome in Palearctic–Indian emberizid migratory finch, red-headed bunting, *Emberiza bruniceps*. Comp. Biochem. Physiol. D 17, 9–25.

Barceló, G., Ríos, J.M., Maldonado, K., Sabat, P., 2016. Energetic costs and implications of the intake of plant secondary metabolites on digestive and renal morphology in two austral passerines. J. Comp. Physiol. B 186, 625–637.

Barja, G., 2014. The mitochondrial free radical theory of aging. Prog. Mol. Biol. Transl. Sci. 127, 1–27.

Battley, P.F., Piersma, T., Dietz, M.W., Tang, S., Dekinga, A., Hulsman, K., 2000. Empirical evidence for differential organ reductions during trans–oceanic bird flight. Proc. R. Soc. Lond. Ser. B Biol. Sci. 267, 191–195.

Bauchinger, U., Biebach, H., 1998. The role of protein during migration in passerine birds. Biol. Conserv. della Fauna 102, 299–305.

Bauchinger, U., Biebach, H., 2001. Differential catabolism of muscle protein in garden warblers (*Sylvia borin*): flight and leg muscle act as a protein source during long-distance migration. J. Comp. Physiol. B 171, 293–301.

Bauchinger, U., McWilliams, S.R., 2010. Extent of phenotypic flexibility during long-distance flight is determined by tissue-specific turnover rates: a new hypothesis. J. Avian Biol. 41, 1–7.

Bauchinger, U., McWilliams, S.R., 2012. Tissue-specific mass changes during fasting: the protein turnover hypothesis. In: McCue, M. (Ed.), The comparative physiology of fasting and starvation. Springer-Verlag, Berlin, pp. 193–206.

Bauchinger, U., Van't hof, T., Biebach, H., 2007. Testicular development during long-distance spring migration. Horm. Behav. 51, 295–305.

Bauchinger, U., Wohlmann, A., Biebach, H., 2005. Flexible remodeling of organ size during spring migration of the garden warbler (*Sylvia borin*). Zoology 108, 97–106.

Bauer, C.M., Graham, J.L., Greives, T.J., 2019. Corticosterone negative feedback is weaker during spring vs. autumn migration in a songbird (Junco hyemalis). Gen. Comp. Endocrinol. 280, 36–42.

Beaulieu, M., Schaefer, H.M., 2013. Rethinking the role of dietary antioxidants through the lens of self-medication. Anim. Behav. 86, 17–24.

Bentley, G.E., Ubuka, T., Mcguire, N.L., Calisi, R., Perfito, N., Kriegsfeld, L.J., Wingfield, J.C., Tsutsui, K., 2009. Gonadotrophin-inhibitory hormone: a multifunctional neuropeptide. J. Neuroendocrinol. 21, 276–281.

Berthold, P., Gwinner, E., Sonnenschein, E. (Eds.), 2003. Avian Migration. Spring-Verlag, Berlin, Germany.

Bishop, C.M., Butler, P.J., 2015. Flight. In: Scanes, C.G. (Ed.), Sturkie's Avian Physiology, sixth ed. Academic Press, London.

Bishop, C.M., Butler, P.J., El Haj, A.J., Egginton, S., 1998. Comparative development in captive and migratory populations of the barnacle goose. Physiol. Zool. 71, 198–207.

Blanchard, B.D., Erickson, M.M., 1949. The Cycle of the Gambel Sparrow, vol. 47. University of California Publications in Zoology, pp. 255–318.

Blas, J., 2015. Stress in birds. In: Scanes, C.G. (Ed.), Sturkie's Avian Physiology, sixth ed. Academic Press, London, pp. 769–805.

Blem, C.R., 1976. Patterns of lipid storage and utilization in birds. Am. Zool. 16, 671–684.

Blem, C.R., 1980. The energetics of migration. In: Gauthreaux Jr., S.A. (Ed.), Animal Migration, Orientation, and Navigation. Academic Press, New York.

Blem, C.R., 1990. Avian energy storage. In: Power, M. (Ed.), Current Ornithology. Plenum Press, New York.

Blount, J.D., Metcalfe, N.B., Arnold, K.E., Surai, P.F., Devevey, G.L., Monaghan, P., 2003. Neonatal nutrition, adult antioxidant defences and sexual attractiveness in the zebra finch. Proc. Roy. Soc. B 270, 1691–1696.

Bonier, F., Martin, P.R., Jensen, J.P., Butler, L.K., Ramenofsky, M., Wingfield, J.C., 2007. Pre-migratory life history stages of juvenile arctic birds: costs, constraints, and trade-offs. Ecology 88, 2729–2735.

Bordoni, A., Nunzio, M.D., Danesi, F., Biagi, P.L., 2006. Polyunsaturated fatty acids: from diet to binding to PPARS and other nuclear receptors. Genes Nutr. 1, 95–106.

Boswell, T., 2005. Regulation of energy balance in birds by the neuroendocrine hypothalamus. J. Poultry Sci. 42, 161–181.

Boswell, T., Dunn, I.C., 2015. Regulation of the avian central melanocortin system and the role of leptin. Gen. Comp. Endocrinol. 221, 278–283.

Boswell, T., Dunn, I.C., 2017. Regulation of agouti-related protein and pro-opiomelanocortin gene expression in the avian arcuate nucleus. Front. Endocrinol. 8, 75–86.

Boswell, T., Hall, M.R., Goldsmith, A.R., 1993. Annual cycles of migratory fattening, reproduction and moult in European quail (*Coturnix coturnix*). J. Zool. Lond. 231, 627–644.

Boswell, T., Richardson, R.D., Seeley, R.J., Ramenofsky, M., Wingfield, J.C., Friedman, M.I., Woods, S.C., 1995. Regulation of food intake by metabolic fuels in white-crowned sparrows. Am. J. Physiol. Regul. Integr. Comp. Physiol. 269, R1462–R1468.

Bottje, W., 2015. Mitochondrial physiology. In: Scanes, C.G. (Ed.), Sturkie's Avian Physiology, sixth ed. Academic Press, London.

Bower, E.B., Helms, C.W., 1968. Seasonal variation in fatty acids of the slate-colored junco (*Junco hyemalis*). Physiol. Zool. 41 (2), 157–168.

Boyles, M., 2011. Seasonal Diet Preferences for Fatty Acids Differ between Species of Migratory Passerine, are Affected by Antioxidant Level, and Relate to the Fatty Acid Composition of Wild Fruits (Masters in Environmental Science). University of Rhode Island.

Braun, E.J., 2015. Physiological challenges of migration. In: Scanes, C.G. (Ed.), Sturkie's Avian Physiology, sixth ed. Academic Press, London.

Buehler, D.M., Piersma, T., 2008. Traveling on a budget: predictions and ecological relevance for bottlenecks in the annual cycle of long-distance migrants. Phil. Trans. Biol. Sci. 363, 247–266.

Buehler, D.M., Tieleman, B.I., Piersma, T., 2010. How do migratory species stay healthy over the annual cycle? A conceptual model for immune function and for resistance to disease. Integr. Comp. Biol. 50, 346–357.

Buntin, J.D., Ruzycki, E., Witebsky, J., 1993. Prolactin receptors in dove brain: autoradiographic analysis of binding characteristics in discrete brain regions and accessibility to blood-borne prolactin. Neuroendocrinology 57, 738.

Butler, P., 1991. Exercise in birds. J. Exp. Biol. 160, 233–262.

Butler, P.J., Woakes, A.J., 2001. Seasonal hypothermia in a large migrating bird: saving energy for fat deposition? J. Exp. Biol. 204, 1361–1367.

Buttemer, W.A., Abele, D., Costantinit, D., 2010. From bivalves to birds: oxidative stress and longevity. Funct. Ecol. 24, 971–983.

Carbeck, K.M., DeMoranville, K.J., D'amelio, P.B., Goymann, W., Trost, L., Pierce, B., Bryla, A., Dzialo, M., Bauchinger, U., McWilliams, S.R., 2018. Environmental cues and dietary antioxidants affect breeding behavior and testosterone of male European starlings (*Sturnus vulgaris*). Horm. Behav. 103, 36–44.

Carmi, N., Pinshow, B., Horowitz, M., Bernstein, M.H., 1993. Birds conserve plasma volume during thermal and flight-incurred dehydration. Physiol. Zool. 66, 829–846.

Carmi, N., Pinshow, B., Porter, W.P., Jaeger, J., 1992. Water and energy limitations on flight duration in small migrating birds. Auk 109, 268–276.

Carpenter, F.L., Hixon, M.A., 1988. A new function for torpor: fat conservation in a wild migrant hummingbird. Condor 90, 373–378.

Carter, W.A., Bauchinger, U., McWilliams, S.R., 2019. The importance of isotopic turnover for understanding key aspects of animal ecology and nutrition. Diversity 11, 1–20.

Carter, W.A., DeMoranville, K.J., Pierce, B.J., McMilliams, S.R., 2021. Dietary linoleic acid, antioxidants, and flight training influence the activity of oxidative enzymes in European Starlings (*Sturnus vulgaris*). J. Comp. Physiol. B Biochem. Syst. Environ. Physiol. 191, 357–370.

Carter, W.A., DeMoranville, K.J., Pierce, B.J., McWilliams, S.R., 2020. The effects of dietary linoleic acid and hydrophilic antioxidants on basal, peak, and sustained metabolism in flight-trained European starlings. Ecol. Evol. 10, 1552–1566.

Carter, W.A., Whiteman, J.P., Cooper-Mullin, C., Newsome, S.D., McWilliams, S.R., 2019. Dynamics of individual fatty acids in muscle fat stores and membranes of a songbird and its functional and ecological importance. Physiol. Biochem. Zool. 92, 239–251.

Casagrande, S., Demoranville, K.J., Trost, L., Pierce, B.J., Bryla, A., Dzialo, M., Sadowska, E.T., Bauchinger, U., McWilliams, S.R., 2020. Dietary antioxidants attenuate the endocrine stress response during long-duration flight of a migratory bird. Proc. Roy. Soc. B 287, 20200744.

Castiglione, G.M., Xu, Z., Zhou, L., Duh, E., 2020. Adaptation of the master antioxidant response connects metabolism, lifespan and feather development pathways in birds. Nat. Commun. 11, 2476.

Catoni, C., Peters, A., Schaefer, H.M., 2008. Life history trade-offs are influenced by the diversity, availability and interactions of dietary antioxidants. Anim. Behav. 76, 1107–1119.

Chandola, A., Pathak, V., 1980. Premigratory increase in circulating triiodothyronine/thyroxine ratio in the red-headed bunting (*Emberiza brunicaps*). Gen. Comp. Endocrinol. 42, 39–46.

Chernetsov, N., Mukhin, A., 2006. Spatial behavior Of European robins during migratory stopovers: a telemetry study. Wilson J. Ornithol. 118, 364–373, 10.

Chmura, H.E., Krause, J.S., Perez, J.H., Ramenofsky, M., Wingfield, J.C., 2020. Autumn migratory departure is influenced by reproductive timing and weather in an Arctic passerine. J. Ornith. 161, 779–791.

Cipollini, M.L., Levey, D.J., 1997. Secondary metabolites of fleshy vertebrate-dispersed fruits: adaptive hypotheses and implications for seed dispersal. Am. Nat. 150, 346–372.

Cipollini, M.L., Stiles, E.W., 1993. Fruit rot, antifungal defense, and palatability of fleshy fruits for frugivorous birds. Ecology 74, 751–762.

Cohen, A.A., Martin, L.B., Wingfield, J.C., Mcwilliams, S.R., Dunne, J.A., 2012. Physiological regulatory networks: ecological roles and evolutionary constraints. Trends Ecol. Evol. 27, 428–435.

Conway, C.J., Eddleman, W.R., Simpson, K.L., 1994. Seasonal changes in fatty acid composition of the wood thrush. Condor 96, 791–794.

Cooper-Mullin, C., Carter, W.A., Amato, R.S., Podlesak, D., McWilliams, S.R., 2021. Dietary antioxidants reach the mitochondria in the flight muscles of birds but only if they exercise. PLoS One 16(6), e0253264.

Cooper-Mullin, C., Carter, W.A., McWilliams, S.R., 2019. Acute effects of intense exercise on the antioxidant system in birds: does exercise training help? J. Exp. Biol. 222.

Cooper-Mullin, C., McWilliams, S.R., 2016. The role of the antioxidant system during intense endurance exercise: lessons from migrating birds. J. Exp. Biol. 219, 3684–3695.

Corder, K.R., Demoranville, K.J., Russell, D.E., Huss, J.M., Schaeffer, P.J., 2016. Annual life-stage regulation of lipid metabolism and storage and associated with PPARs in a migrant species: the gray catbird (*Dumetella carolinensis*). J. Exp. Biol. 219, 3391–3398.

Cornelius, J.M., Boswell, T., Jenni-Eiermann, S., Breuner, C., Ramenofsky, M., 2013. Contribution of endocrinology to the migration life history of birds. Gen. Comp. Endocrinol. 190, 47–60.

Costantini, D., 2008. Oxidative stress in ecology and evolution: lessons from avian studies. Ecol. Lett. 11, 1238–1251.

Costantini, D., 2014. Oxidative Stress and Hormesis in Evolutionary Ecology and Physiology: A Marriage between Mechanistic and Evolutionary Approaches. Springer-Verlag, Berlin, Heidelberg.

Costantini, D., 2016. Oxidative stress ecology and the d-ROMs test: facts, misfacts and an appraisal of a decade's work. Behav. Ecol. Sociobiol. 70, 809–820.

Costantini, D., 2019. Understanding diversity in oxidative status and oxidative stress: the opportunities and challenges ahead. J. Exp. Biol. 222.

Costantini, D., Cardinale, M., Carere, C., 2007. Oxidative damage and anti-oxidant capacity in two migratory bird species at a stop-over site. Comp. Biochem. Physiol. 144C, 363–371.

Costantini, D., Dell'Ariccia, G., Lipp, H.-P., 2008. Long flights and age affect oxidative status of homing pigeons (*Columba livia*). J. Exp. Biol. 211, 377–381.

Costantini, D., Metcalfe, N.B., Monaghan, P., 2010a. Ecological processes in a hormetic framework. Ecol. Lett. 13, 1435–1447.

Costantini, D., Rowe, M., Butler, M.W., Mcgraw, K.J., 2010b. From molecules to living systems: historical and contemporary issues in oxidative stress and antioxidant ecology. Funct. Ecol. 24, 950–959.

Covino, K.M., Holberton, R.L., 2011. The influence of energetic condition on flight initiation and orientation of migratory songbirds in the Gulf of Maine region. Auk 128, 313–320.

Covino, K.M., Jawor, J.M., Kelly, J.F., Moore, F.R., 2017. Overlapping life-history stages in migrating songbirds: variation in circulating testosterone and testosterone production capacity. J. Ornithol. 158, 203–212.

Covino, K.M., Morris, S.R., Moore, F.R., 2015. Patterns of testosterone in three Nearctic–Neotropical migratory songbirds during spring passage. Gen. Comp. Endocrinol. 224, 186–193.

Dawson, A., King, V.M., Bentley, G.E., Ball, G.F., 2001. Photoperiodic control of seasonality in birds. J. Biol. Rhythm. 16, 365–380.

Dekinga, A., Dietz, M.W., Koolhaas, A., Piersma, T., 2001. Time course and reversibility of changes in the gizzards of red knots alternately eating hard and soft food. J. Exp. Biol. 204, 2167–2173.

Delingat, J., Dierschke, V., Schmaljohann, H., Bairlein, F., 2009. Diurnal patterns of body mass change during stopover in a migrating songbird, the northern wheatear *Oenanthe oenanthe*. J. Avian Biol. 40, 625–634.

Delingat, J., Dierschke, V., Schmaljohann, H., Mendel, B., Bairlein, F., 2006. Daily stopovers as optimal migration strategy in a long-distance migrating passerine: the Northern Wheatear *Oenanthe oenanthe*. Ardea 94, 593–605.

DeMoranville, K.J., Carter, W.A., Pierce, B.J., McWilliams, S.R., 2020. Flight training in a migratory bird drives metabolic gene expression in the flight muscle but not liver, and dietary fat quality influences select genes. Am. J. Physiol. Regul. Integr. Comp. Physiol. 319, R637–R652.

DeMoranville, K.J., Corder, K.R., Hamilton, A., Russell, D.E., Huss, J.M., Schaeffer, P.J., 2019. PPAR expression, muscle size and metabolic rates across the gray catbird's annual cycle are greatest in preparation for fall migration. J. Exp. Biol. 222, 1–11.

DeSimone, J.G., Ramirez, M.G., Elowe, C.R., Griego, M.S., Breuner, C.W., Gerson, A.R., 2020. Developing a Stopover-CORT hypothesis: corticosterone predicts body composition and refueling rate in Gray Catbirds during migratory stopover. Horm. Behav. 124, 104776.

Desvergne, B., Wahli, W., 1999. Peroxisome proliferator-activated receptors: nuclear control of metabolism. Endocr. Rev. 20, 649–688.

Deviche, P., 1995. Androgen regulation of avian premigratory hyperphagia and fattening: from eco-physiology to neuroendocrinology. Am. Zool. 35, 234–245.

Diamond, J., 1991. Evolutionary design of intestinal nutrient absorption: enough but not too much. News Physiol. Sci. 6, 92–96.

Diamond, J.M., Karasov, W.H., Phan, D., Carpenter, F.L., 1986. Digestive physiology is a determinant of foraging bout frequency in hummingbirds. Nature 320, 62–63.

Diano, S., Naftolin, F., Horvath, T.L., 1997. Gonadal steroids target AMPA glutamate receptor-containing neurons in the rat hypothalamus, septum and amygdala: a morphological and biochemical study. Endocrinology 138, 778–789.

Dick, M.F., 2017. The Long Haul: Migratory Flight Preparation and Performance in Songbirds (Ph.D. dissertation). University of Western Ontario.

Dick, M.F., Guglielmo, C.G., 2019. Dietary polyunsaturated fatty acids influence flight muscle oxidative capacity but not endurance flight performance in a migratory songbird. Am. J. Physiol. Regul. Integr. Comp. Physiol. 316, R362–R375.

Dietz, M.W., Piersma, T., Dekinga, A., 1999. Body-building without power training: endogenously regulated pectoral muscle hypertrophy in confined shorebirds. J. Exp. Biol. 202, 2831–2837.

Dingle, H., 1996. Migration: The Biology of Life on the Move. Oxford University Press, New York.

Dingle, H., 2014. Migration, the Biology of Life on the Move. Oxford University Press, New York.

Dohm, G.L., 1986. 5 protein as a fuel far endurance exercise. Exerc. Sport Sci. Rev. 14, 143–174.

Dolnik, V.R., 1980. Regulyatsiya okonchaniya linki inachala osennei migratsii u molodykh zyablikov (*Fringilla coelebs*). Zool. Zh. 59, 91–98.

Drake, A., Rock, C., Quinlan, S.P., Green, D.J., 2013. Carry-over effects of winter habitat vary with age and sex in yellow warblers *Setophaga petechia*. J. Avian Biol. 44, 321–330.

Drent, R., Daan, S., 1980. Prudent parent: energetic adjustments in avian breeding. Ardea 68, 225–252.

Driedzic, W.R., Crowe, H.L., Hicklin, P.W., Sephton, D.H., 1993. Adaptations in pectoralis muscle, heart mass, and energy metabolism during premigratory fattening in semipalmated sandpipers (*Calidris pusilla*). Can. J. Zool. 71, 1602–1608.

Dudley, R., Vermeij, G.J., 1992. Do the power requirements of flapping flight constrain folivory in flying animals? Funct. Ecol. 6, 101–104.

Dykstra, C.R., Karasov, W.H., 1992. Changes in gut structure and function of house wrens (*Troglodytes aedon*) in response to increased energy demands. Physiol. Zool. 65, 422–442.

Dzialowski, E.M., Crossley II, D.A., 2015. The cardiovascular system. In: Scanes, C.G. (Ed.), Sturkie's Avian Physiology, sixth ed. Academic Press, London.

Egeler, O., Williams, T.D., 2000. Seasonal, age, and sex-related variation in fatty-acid composition of depot fat in relation to migration in western sandpipers. Auk 117, 110–119.

Egevang, C., Stenhouse, I.J., Phillips, R.A., Petersen, A., Fox, J.W., Silk, J.R., 2010. Tracking of Arctic terns *Sterna paradisaea* reveals longest animal migration. Proc. Natl. Acad. Sci. U.S.A. 107, 2078–2081.

Egginton, S., 1996. Effect of temperature on optimal susbtrate for B-oxidation. J. Fish. Biol. 49.

Eikenaar, C., 2017. Endocrine regulation of fueling by hyperphagia in migratory birds. J. Comp. Physiol. 203, 439–445.

Eikenaar, C., Ballstaedt, E., Hessler, S., Klinner, T., Muller, F., Schmaljohann, H., 2018a. Cues, corticosterone and departure decisions in a partial migrant. Gen. Comp. Endocrinol. 261, 59–66.

Eikenaar, C., Fritzsch, A., Bairlein, F., 2013. Corticosterone and migratory fueling in Northern wheatears facing different barrier crossings. Gen. Comp. Endocrinol. 186, 181–186.

Eikenaar, C., Hegemann, A., 2016. Migratory common blackbirds have lower innate immune function during autumn migration than resident conspecifics. Biol. Lett. 12, 20160078.

Eikenaar, C., Hesslera, S., Ballstaedta, E., Schmaljohann, H., Kaiya, H., 2018b. Ghrelin, corticosterone and the resumption of migration from stopover, an automated telemetry study. Physiol. Behav. 194, 450–455.

Eikenaar, C., Jonsson, J., Fritzsch, A., Wang, H.-L., Isaksson, C., 2016. Migratory refueling affects non-enzymatic antioxidant capacity, but does not increase lipid peroxidation. Physiol. Behav. 158, 26–32.

Eikenaar, C., Kallstig, E., Andersson, M.N., Herrera-Duenas, A., Isaksson, C., 2017a. Oxidative challenges of avian migration: a comparative field study on a partial migrant. Physiol. Biochem. Zool. 90, 223–229.

Eikenaar, C., Klinner, T., Stowe, M., 2014. Corticosterone predicts nocturnal restlessness in a long-distance migrant. Horm. Behav. 66, 324–329.

Eikenaar, C., Muller, F., Leutgeb, C., Hessler, S., Lebus, K., Taylor, P.D., Schmaljohann, H., 2017b. Corticosterone and timing of migratory departure in a songbird. Proc. R. Soc. B 284, 20162300.

Eikenaar, C., Schmaljohann, H., 2015. Wind conditions experienced during the day predict nocturnal restleness in a migratory songbird. Ibis 157, 125–132.

Engel, S., Biebach, H., Visser, G.H., 2006. Water and heat balance during flight in the rose-colored starling (*Sturnus roseus*). Physiol. Biochem. Zool. 79, 763–774.

Evans, P.R., Davidson, N.C., Uttley, J.D., Evans, R.D., 1992. Premigratory hypertrophy of flight muscle: an ultrastructure study. Ornis Scand. 23, 238–243.

Falsone, K., Jenni-Eiermann, S., Jenni, L., 2009. Corticosterone in migrating songbirds during endurance flight. Horm. Behav. 56, 548–556.

Faraci, F.M., 1991. Adaptations to hypoxia in birds: how to fly high. Annu. Rev. Physiol. 53, 59–70.

Farner, D.S., Follett, B.K., 1966. Light and other environmental factors affecting avian reproduction. J. Anim. Sci. (Sofia) 25, 90–115.

Feige, J.N., Gelman, L., Michalik, L., Devergne, B., Wahli, W., 2006. From molecular action to physiological outputs: peroxisome proliferator-activated receptors are nuclear receptors at the crossroads of key cellular functions. Prog. Lipid Res. 45, 120–159.

Follett, B.K., King, V.M., Meddle, S.L., 1998. Rhythms and photoperiodsm in birds. In: Lumsden, P.J., Millar, A.J. (Eds.), Biological Rhythms and Photperiodsm in Plants. BIOS Scientiic Publishers Ltd, Oxford.

Follett, B.K., Mattocks JR., P.W., Farner, D.S., 1974. Circadian function in the photoperiodic induction of gonadotropin secretion in the white-crowned sparrow, *Zonotrichia leucophrys gambelii*. Proc. Natl. Acad. Sci. U.S.A. 71, 1666–1669.

Frawley, A.E., DeMoranville, K.J., Carbeck, K.M., Trost, L., Bryla, A., Dzialo, M., Sadowska, E.T., Bauchinger, U., Pierce, B.J., McWilliams, S.R., 2021. Season, anthocyanin supplementation, and flight training have mixed effects on the antioxidant system of migratory European Starlings. Ornithology 138, 1–16.

Friedman-Einat, M., Cogburn, L.A., Yosefi, S., Hen, G., Shinder, D., Shirak, A., Seroussi, E., 2014. Discovery and characterization of the first genuine avian leptin gene in the rock dove (*Columba livia*). Endocrinology 155, 3376–3384.

Friedman-Einat, M., Seroussi, E., 2019. Avian leptin: bird's-eye view of the evolution of vertebrate energy-balance control. Trends Endocrinol. Metabol. 30, 819–832.

Fry, C.H., Ferguson-Lees, I.J., Dowsett, R.J., 1972. Flight muscle hypertrophy and ecophysiological variation of yellow Wagtail *motacilla-Flava* races at lake Chad. J. Zool. 167, 293–306.

Fusani, L., Cardinale, M., Carere, C., Goymann, W., 2009. Stopover decision during migration: physiological conditions predict nocturnal restlessness in wild passerines. Biol. Lett. 5, 302–305.

Fuxjager, M.J., Barske, J., Du, S., Day, L.B., Schlinger, B.A., 2012. Androgens regulate gene expression in avian skeletal muscles. PLoS One 7, e51482.

Gannes, L.Z., 2002. Mass change pattern of blackcaps refueling during spring migration: evidence for physiological limitations to food assimilation. Condor 104, 231–239.

Gaunt, A.S., Hikida, R.S., Jehl, J.R., Fenbert, L., 1990. Rapid atrophy and hypertrophy of an avian flight muscle. Auk 107, 649–659.

Gavrilov, V.M., Dolnik, V.R., 1974. Bioenergetika i regulyatsiya poslebrachnoi i postyuvenaloi linek u zyablikov (*Fringilla coelebs coelebs* L.). Tr. Zool. Inst. Akad. Nauk SSSR 55, 254–267.

Geiser, F., Learmonth, R.P., 1994. Dietary fats, selected body temperature and tissue fatty acid composition of agamid lizards (*Amphibolurus nuchalis*). J. Comp. Physiol. 164B, 55–61.

Gerson, A., Brown, J.C., Thomas, R., Bernards, M.A., Staples, J.F., 2008. Effects of dietary polyunsaturated fatty acids on mitochondrial metabolism in mammalian hibernation. J. Exp. Biol. 211, 2689–2699.

Gerson, A.R., Guglielmo, C.G., 2011. Flight at low ambient humidity increases protein catabolism in migratory birds. Science 333, 1434–1436.

Giladi, I., Pinshow, B., 1999. Evaporative and excretory water loss during free flight in pigeons. J. Comp. Physiol. B 169, 311–318.

Goodridge, A.G., 1964. The effect of insulin, glucagon and prolactin on lipid synthesis and related metabolic activity in migratory and non-migratory finches. Comp. Biochem. Physiol. A 13, 1–26.

Goymann, W., Lupi, S., Kaiya, H., Cardinale, M., Fusani, L., 2017. Ghrelin affects stop-over decisions and food-intake in a long-distance migrant. Proc. Natl. Acad. Sci. Unit. States Am. 114, 1946–1951.

Goymann, W., Spina, F., Ferri, A., Fusani, L., 2010. Body fat influences departure from stopover sites in migratory birds: evidence from whole-island telemetry. Biol. Lett. 6, 478–481.

Greenewalt, C.H., 1960. Hummingbirds. Dover Publications, New York.

Groom, D.J.E., Deakin, J.E., Lauzau, M.C., Gerson, A.R., 2019. The role of humidity and metabolic status on lean mass catabolism in migratory Swainson's thrushes (*Catharus ustulatus*). Proc. Biol. Sci. 286, 20190859.

Groscolas, R., Leloup, J., 1986. The endocrine control of reproduction oand moult in male and female Empereor *Aptenodytes forsteri* and Adelie *Pygoscelis adeliae* Penguins. Gen. Comp. Endocrinol. 63, 264–274.

Guglielmo, C., 2010. Move that fatty acid: fuel selection and transport in migratory birds and bats. Integr. Comp. Biol. 50, 336–345.

Guglielmo, C., 2018. Obese super athletes: fat-fueled migration in birds and bats. J. Exp. Biol. 221, jeb165753.

Guglielmo, C., Haunerland, N.H., Williams, T.D., 1998. Fatty acid binding protein, a major protein in the flight muscle of migrating western sandpipers. Comp. Biochem. Physiol. 119, 549–555.

Guglielmo, C.G., Gerson, A.R., Price, E.R., Hays, Q.R., 2017. The effects of dietary macronutrients on flight ability, energetics, and fuel metabolism of yellow-rumped warblers *Setophaga coronata*. J. Avian Biol. 48, 133–148.

Guglielmo, C.G., Haunerland, N.H., Hochachka, P.W., Williams, T.D., 2002a. Seasonal dynamics of flight muscle fatty acid binding protein and catabolic enzymes in a long-distance migrant shorebird. Am. J. Physiol. 282, R1405–R1413.

Guglielmo, C.G., O'hara, P.D., Williams, T.D., 2002b. Extrinsic and intrinsic sources of variation in plasma lipid metabolites of free-living western sandpipers (*Calidris mauri*). Auk 119, 437–445.

Guglielmo, C.G., Piersma, T., Williams, T.D., 2001. A sport-physiological perspective on bird migration: evidence for flight-induced muscle damage. J. Exp. Biol. 204, 2683–2690.

Guglielmo, C.G., Williams, T.D., Zwingelstein, G., Brichon, G., Weber, J.-M., 2002c. Plasma and muscle phospholipids are involved in the metabolic response to long-distance migration in a shorebird. J. Comp. Physiol. 172B, 409–417.

Guillemette, M., 1994. Digestive-rate constraint in wintering Common Eider (*Somateria mollissim*a): implications for flying capabilities. Auk 111, 900–909.

Guillemette, M., Ouellet, J.-F., 2005. Temporary flightlessness in pre-laying Common Eiders *Somateria mollissima*: are females constrained by excessive wing-loading or by minimal flight muscle ratio? Ibis 147, 293–300.

Guillemette, M., Polymeropoulos, E.T., Portugal, S.J., Pelletier, D., 2017. It takes time to be cool: on the relationship between hyperthermia and body cooling in a migrating seaduck. Front. Physiol. 8, 532.

Guillemette, M., Richman, S.E., Portugal, S.J., Butler, P.J., 2012. Behavioural compensation reduces energy expenditure during migration hyperphagia in a large bird. Funct. Ecol. 26, 876–883.

Guillemette, M., Woakes, A.J., Larochelle, J., Polymeropoulos, E.T., Granbois, J.-M., Butler, P.J., Pelletier, D., Frappell, P.B., Portugal, S.J., 2016. Does hyperthermia constrain flight duration in a short-distance migrant? Phil. Trans. Biol. Sci. 371, 20150386.

Gutiérrez, J.S., Sabat, P., Castañeda, L.E., Contreras, C., Navarrete, L., Peña-Villalobos, I., Navedo, J.G., 2019. Oxidative status and metabolic profile in a long-lived bird preparing for extreme endurance migration. Sci. Rep. 9, 17616.

Gwinner, E., Zeman, M., Schwabl-Benzinger, I., Jenni-Eiermann, S., Jenni, L., Schwabl, H., 1992. Corticosterone levels of passerine birds during migratory flight. Naturwissenschaften 79, 276–278.

Hahn, T.P., Brazeal, K.R., Schultz, E.M., Chmura, H.E., Cornelius, J.M., Watts, H.E., Macdougall-Shackelton, S.A., 2015. Annual schedules. In: Scanes, C.G. (Ed.), Sturkie's Avian Physiology, sixth ed. Elsevier, Boston.

Hahn, T.P., Sockman, K.W., Breuner, C.W., Morton, M.L., 2004. Facultatiive altitudinal movements by mountain white-crowned sparrows (*Zonotrichia leucophrys oriantha*) in the Sierra Nevada. Auk 121, 1269–1281.

Hahn, T.P., Wingfield, J.C., Mullen, R., Deviche, P.J., 1995. Endocrine bases of spatial and temporal opportunism in arctic-breeding birds. Am. Zool. 35, 259–273.

Hall, Z.J., Bauchinger, U., Gerson, A.R., Price, E.R., Langlois, L.A., Boyles, M., Pierce, B., McWilliams, S.R., Sherry, D.F., MacDougal-Shackleton, S.A., 2013. Site-specific regulation of adult neurogenesis by dietary fatty acid content, vitamin E and flight exercise in European starlings. Eur. J. Neurosci. 2013, 1–8.

Hall, M.R., Gwinner, E., 1987. Annual cycles in moult, body mass, luteininzing hormone, prolactinand gonadal steroids during the development of sexual maturity in the white stork (*Ciconia ciconia*). J. Zool, Lond 211, 467–486.

Halliwell, B., Gutteridge, J.M., 1999. Free Radicals in Biology and Medicine. Clarendon Press, Oxford.

Hamiliton, A., Ly, J., Robinson, J.R., Corder, K.R., Demoranville, K.J., Schaeffer, P.J., Huss, J.M., 2018. Conserved transcriptional activity and ligand responsiveness of avian PPARs: potential role in regulating lipid metabolism in migratory birds. Gen. Comp. Endocrinol. 268, 110–120.

Hammond, K.A., Diamond, J., 1997. Maximal sustained energy budgets in humans and animals. Nature 386, 457–462.

Harman, D., 1956. Aging: a theory based on free radical and radiation chemistry. J. Gerontol. 11, 298–300.

Harrison, X.A., Blount, J.D., Inger, R., Norris, D.R., Bearhop, S., 2011. Carry-over effects as drivers of fitness differences in animals. J. Anim. Ecol. 80, 4–18.

Hasselquest, D., 2007. Comparative immunoecology in birds: hypotheses and tests. J. Ornithol. 148, S571–S582.

Hasselquest, D., Nilsson, J.A., 2012. Physiological mechanisms mediating costs of immune responses: what can we learn from studies of birds? Anim. Behav. 83, 1303–1312.

Hazelwood, R.L., 2000. Pancreas. In: Whittlow, G. (Ed.), Sturkie's Avian Physiology. Academic Press, New York.

Hegemann, A., Matson, K.D., Both, C., Tielman, B.I., 2012. Immune function in a free-living bird varies over the annual cycle, but seasonal patterns differ between years. Oecologia 170, 605–618.

Heitmeyer, M.E., Fredrickson, L.H., 1990. Fatty acid composition of wintering female mallards in relation to nutrient use. J. Wildl. Manag. 54, 54–61.

Helms, C.W., 1963. The annual cycle and Zugunruhe in birds. Proc. Int. Ornithol. Congr. 13, 925–939.

Herborn, K.A., Daunt, F., Heidinger, B.J., Granroth-Wildling, H.M.V., Burthe, S.J., Newell, M.A., Monaghan, P., 2016. Age, oxidative stress exposure and fitness in a long-lived seabird. Funct. Ecol. 30, 913–921.

Herrera, C.M., 1984. Selective Pressures on Fruit Seediness: Differential Predation of Fly Larvae on the Fruits of Berberis Hispanica. Oikos, pp. 166–170.

Hintz, J.V., 2000. The hormonal regulation of premigratory fat deposition and winter fattening in red-winged blackbirds. Mol. Integr. Physiol. 125, 239–249.

Hochachka, P.W., Somero, G.N., 2002. Biochemical Adaptation - Mechanisms and Process in Physiological Evolution. Oxford University Press, New York.

Holberton, R., Dufty, A.M., 2005. Hormones and variation in life history strategies of migratory and nonmigratory birds. In: Greenberg, R., Marra, P.P. (Eds.), Birds of Two Worlds, the Ecology and Evolution of Migration. Johns Hopkins University Press, Baltimore, London.

Holberton, R.L., Parrish, J.D., Wingfield, J.C., 1996. Modulation of the adrenocortical stress response in neotropical migrants during autumn migration. Auk 113, 558–564.

Holmes, R.T., 2007. Understanding population change in migratory songbirds: long-term and experimental studies of Neotropical migrants in breeding and wintering areas. Ibis 149, 2–13.

Hou, L., Welch, K.C., 2016. Premigratory ruby-throated hummingbirds, Archilochus colubris, exhibit multiple strategies for fuelling migration. Anim. Behav. 121, 87–99.

Hudson, D.M., Bernstein, M.H., 1981. Temperature regulation and heat balance in flying white-necked ravens, *Corvus cryptoleucus*. J. Exp. Biol. 90, 267–281.

Hulbert, A.J., Else, P.L., 1999. Membranes as possible pacemakers of metabolism. J. Theor. Biol. 199, 257–274.

Hulbert, A.J., Else, P.L., 2000. Mechanisms underlying the cost of living in animals. Annu. Rev. Physiol. 62, 207–235.

Hulbert, A.J., Pamplona, R., Buffenstein, R., Buttemer, W.A., 2007. Life and death: metabolic rate, membrane composition, and life span of animals. Physiol. Rev. 87, 1175–1213.

Hulbert, A.J., Turner, N., Storlien, L.H., Else, P.L., 2005. Dietary fats and membrane function: implications for metabolism and disease. Biol. Rev. 80, 155–169.

Infante, J.P., Kirwan, R.C., Brenna, J.T., 2001. High levels of docosahexaenoic acid (22:6n-3)-containing phospholipids in high-frequency contraction muscles of hummingbirds and rattlesnakes. Comp. Biochem. Physiol. 130B, 291–298.

Jacobs, J.D., Wingfield, J.C., 2000. Endocrine control of life-cycle stages: a constraint on response to the environment? Condor 102, 35–51.

Jehl, J.R., 1997. Cyclical changes in body composition in the annual cycle and migration of the Eared Grebe *Podiceps nigricollis*. J. Avian Biol. 28, 132–142.

Jenni-Eiermann, S., 2017. Energy metabolism during endurance flight and the post-flight recovery phase. J. Comp. Physiol. 203, 431–438.

Jenni-Eiermann, S., Jenni, L., 1991. Metabolic responses to flight and fasting in night migrating passerines. J. Comp. Physiol. 161, 465–474.

Jenni-Eiermann, S., Jenni, L., Piersma, T., 2002. Temporal uncoupling of thyroid hormones in Red Knots: T3 peaks in cold weather, T4 during moult. J. Ornithol. 143, 331–340.

Jenni-Eiermann, S., Jenni, L., Smith, S., Costantini, D., 2014. Oxidative stress in endurance flight: an unconsidered factor in bird migration. PLoS One 9, e97650.

Jenni, L., Jenni-Eiermann, S., 1992. Metabolic patterns of feeding overnight fasted and flying night migrants during autumn migration. Ornis Scand. 23, 251–259.

Jenni, L., Jenni-Eiermann, S., 1998. Fuel supply and metabolic constraints in migrating birds. J. Avian Biol. 29, 521–528.

Jenni, L., Jenni-Eiermann, S., Spina, F., Schwabl, H., 2000. Regulation of protein breakdown and adrenocortical response to stress in birds during migratory flight. Am. J. Physiol. Regul. Integr. Comp. Physiol. 278, R1182–R1189.

Jenni, L., Schaub, M., 2003. Behavioural and Physiological Reactions to Environmental Variation in Bird Migration: A Review. *Avian migration*. Springer.

Jensen, J.K., Isaksson, C., Eikenaar, C., Andersson, M.N., 2020. Migrant blackbirds, *Turdus merula*, have higher plasma levels of polyunsaturated fatty acids compared to residents, but not enhanced fatty acid unsaturation index. Ecol. Evol. 2020, 1–11.

Jimenez, A.G., O'Connor, E.S., Elliott, K.H., 2019. Muscle myonuclear domain, but not oxidative stress, decreases with age in a long-lived seabird with high activity costs. J. Exp. Biol. 222 (18), jeb211185.

Kaiser, P., Balic, A., 2015. The Avian Immune System. In: Scanes, C.G. (Ed.), Sturkie's Avian Physiology, sixth ed. Academic Press, London.

Kaiya, H., Furuse, M., Miyazato, M., Kangawa, K., 2009. Current knowledge of the roles of ghrelin in regulating food intake and energy balance in birds. Gen. Comp. Endocrinol. 163, 33–38.

Karasov, W.H., Hume, I., 1997. Vertebrate gastrointestinal system. In: Dantzler, W. (Ed.), Handbook of Physiology Section 12: Comparative Physiology. Oxford University Press, New York, NY.

Karasov, W.H., McWilliams, S.R., 2005. Digestive constraints in mammalian and avian ecology. In: Starck, J.M., Wang, T. (Eds.), Physiological and Ecological Adaptations to Feeding in Vertebrates. Science Publishers Inc, Enfield, New Hampshire, pp. 87–112.

Karasov, W.H., Pinshow, B., 2000. Test for physiological limitation to nutrient assimilation in a long-distance passerine migrant at a springtime stopover site. Physiol. Biochem. Zool. 73, 335–343.

Ketterson, E.D., Nolan Jr., V., 1976. Geographic variation and its climatic correlates in the sex ratio of eastern-wintering dark-eyed Juncos (*Junco hyemalis hyemalis*). Ecology 57, 679–693.

King, J.S., Farner, D.S., 1965. Studies of fat deposition in migratory birds. Ann. N. Y. Acad. Sci. 131, 422–440.

Kirby, J.S., Stattersfield, A.J., Butchart, S.H.M., Evans, M.I., Grimmett, R.F.A., Jones, V.R., O'Sullivan, J., Tucker, G.M., Newton, I., 2008. Key conservation issues for migratory land- and waterbird species on the world's major flyways. Bird Conserv. Int. 18, S49–S73.

Klaassen, M., 1996. Metabolic constraints on long-distance migration in birds. J. Exp. Biol. 199, 57–64.

Klaassen, M., Biebach, H., 1994. Energetics of fattening and starvation in the long-distance migratory garden warbler, *Sylvia borin*, during the migratory phase. J. Comp. Physiol. B 164, 362–371.

Klaassen, M., Lindström, Å., Zijlstra, R., 1997. Composition of fuel stores and digestive limitations to fuel deposition rate in the long-distance migratory thrush nightingale, *Luscinia luscinia*. Physiol. Zool. 70, 125–133.

Klaiman, J.M., Price, E.R., Guglielmo, C.G., 2009. Fatty acid composition of pectoralis muscle membrane, intramuscular fat stores and adipose tissue of migrant and wintering white-throated sparrows (*Zonotrichia albicollis*). J. Exp. Biol. 212, 3865–3872.

Klasing, K., 2004. The costs of immunity. Acta Zool. Sin. 50, 961–969.

Klasing, K.C., 1998. Comparative Avian Nutrition. CAB International, New York.

Koutsos, E.A., Clifford, A.J., Calvert, C.C., Klasing, K.C., 2003. Maternal carotenoid status modifies the incorporation of dietary carotenoids into immune tissues of growing chickens (*Gallus gallus domesticus*). J. Nutr. 133, 1132–1138.

Krause, J., Nemeth, Z., Perez, J., Chmura, H.E., Ramenofsky, M., Wingfield, J.C., 2016. Annual hematocrit profiles in two sub-species of White-crowned Sparrows: a migrant and resident comparison. Physiol. Biochem. Zool. 89, 51–60.

Krause, J.S., Németh, Z., Pérez, J.H., Chmura, H.E., Word, K.R., Lau, H.J., Swanson, R.E., Cheah, J.C., Quach, L.N., Meddle, S.L., Wingfield, J.C., Ramenofsky, M., 2021. Annual regulation of adrenocortical function in migrant and resident subspecies of white-crowned sparrow. Horm. Behav. 127, 104884.

Kuenzel, W.J., Helms, C.W., 1967. Obesity produced in a migratory bird by hypothalamic lesions. Bioscience 17, 395–396.

Lack, D., 1954. The Natural Regulation of Animal Numbers. Oxford University Press, London.

Landys-Ciannelli, M.M., Ramenofsky, M., Piersma, T., Jukema, J., Wingfield, J.C., Group, C.R., 2002. Baseline and stress-induced plasma corticosterone during long-distance migration in the bar-tailed godwit, Limosa lapponica. Physiol. Biochem. Zool. 75, 101–110.

Landys, M.M., Ramenofsky, M., Guglielmo, C.G., Wingfield, J.C., 2004a. The low-affinity glucocorticoid receptor regulates feeding and lipid breakdown in the migratory Gambel's white-crowned sparrow *Zonotrichia leucophrys gambelii*. J. Exp. Biol. 207, 143–154.

Landys, M.M., Ramenofsky, M., Wingfield, J.C., 2006. Actions of glucocorticoids at a seasonal baseline as compared to stress-related levels in the regulation of periodic life processes. Gen. Comp. Endocrinol. 148, 132–149.

Landys, M.M., Wingfield, J.C., Ramenofsky, M., 2004b. Plasma corticosterone increases during migratory restlessness in the captive white-crowned sparrow *Zonotrichia leucophrys gambelii*. Horm. Behav. 46, 574–581.

Lee, K.A., 2006. Linking immune defenses and life history at the levels of the individual and the species. Integr. Comp. Biol. 46, 1000–1015.

Levey, D.J., Cipollini, M.L., 1998. Glycoalkaloid in ripe fruit deters consumption by cedar waxwings. Auk 115, 359–367.

Leyton, J., Drury, P.J., Crawford, M.A., 1987. Differential oxidation of saturated and unsaturated fatty acids in vivo in the rat. Br. J. Nutr. 57, 383–393.

Lindström, Å., 2003. Fuel Deposition Rates in Migrating Birds: Causes, Constraints and Consequences. In: Berthold, P., Gwinner, E., Sonnenschein, E. (Eds.), Avian Migration. Springer, Berlin, pp. 307–320.

Lindström, Å., Piersma, T., 1993. Mass changes in migrating birds: the evidence for fat and protein storage re-examined. Ibis 135, 70–78.

Livezey, B.C., Humphrey, P.S., 1986. Flightlessness in steamer-ducks (Anatidae: *Tachyeres*): its morphological bases and a probable evolution. Evolution 40, 540–558.

Lohmus, M., Sandberg, R., Holberton, R.L., Moore, F.R., 2003. Corticosterone levels in relation to migratory readiness in Red-Eyed Vireos (*Vireo olivaceus*). Behav. Ecol. Sociobiol. 54, 233–239.

Long, J.A., Holberton, R.L., 2004. Corticosterone secretion energetic condition and a test of the migration modulation hypothesis in the hermit thrush (*Catharus guttatus*) a short disttance migrant. Auk 1094–1102.

Loshchagina, J., Tsveya, A., Naidenkoc, S., 2018. Baseline and stress-induced corticosterone levels are higher during spring than autumn migration in European robins. Horm. Behav. 98, 96–101.

Lovvorn, J.R., Jones, D.R., 1994. Biomechanical conflicts between adaptations for diving and aerial flight in estuarine birds. Estuaries 17, 62–75.

Lundgren, B.O., Kiessling, K.-H., 1985. Seasonal variation in catabolic enzyme activities in breast muscle of some migratory birds. Oecologia 66, 468–471.

Lymburnera, A.L., Kellya, T.R., Hobsona, K.A., MacDougall-Shackleton, E.A., MacDougall-Shackleton, S.A., 2016. Testosterone, migration distance, and migratory timing in song sparrows. Horm. Behav. 85, 102–107.

Maillet, M., Weber, J.-M., 2006. Performance-enhancing role of dietary fatty acids in a long-distance migrant shorebird: the semipalmated sandpiper. J. Exp. Biol. 209, 2686–2695.

Maillet, M., Weber, J.-M., 2007. Relationship between n-3 PUFA content and energy metabolism in the flight muscles of a migrating shorebird: evidence for natural doping. J. Exp. Biol. 210, 413–420.

Marden, J.H., 1994. From damselflies to pterosaurs: how burst and sustainable flight performance scale with size. Am. J. Physiol. 266R, 1077–1084.

Marra, P.P., Hobson, K.A., Holmes, R.T., 1998. Linking winter and summer events in a migratory bird by using stable-carbon isotopes. Science 282, 1884–1886.

Marsh, R.L., 1981. Catabolic enzyme activities in relation to premigratory fattening and muscle hypertrophy in the gray catbird (*Dumetella carolinensis*). J. Comp. Physiol. 141, 417–423.

Marsh, R.L., 1984. Adaptations of the gray catbird, *Dumetella carolinensis* to long-distance migration: flight muscle hypertophy associated with elevated body mass. Physiol. Zool. 57, 105–117.

Marsh, R.L., Storer, R.W., 1981. Correlation of flight-muscle size and body mass in Cooper's hawks: a natural analogue of power training. J. Exp. Biol. 91, 363–368.

Marshall, T.J., Dick, M.F., Guglielmo, C.G., 2016. Seasonal dietary shifting in yellow-rumped warblers is unrelated to macronutrient targets. Comp. Biochem. Physiol. Mol. Integr. Physiol. 192, 57–63.

Martin, T.E., Karr, J.R., 1986. Patch utilization by migrating birds: resource oriented? Ornis Scand. 165–174.

McClelland, G.B., 2004. Fat to the fire: the regulation of lipid oxidation with exercise and environmental stress. Comp. Biochem. Physiol. 139B, 443–460.

McCue, M.D., Amitai, O., Khozin-Goldberg, I., McWilliams, S.R., Pinshow, B., 2009. Effect of dietary fatty acid composition on fatty acid profiles of polar and neutral lipid tissue fractions in zebra finches, *Taeniopygia guttata*. Comp. Biochem. Physiol. 154A, 165–172.

McCue, M.D., Sivan, O., McWilliams, S.R., Pinshow, B., 2010. Tracking the oxidative kinetics of carbohydrates, amino acids, and fatty acids in the house sparrow using exhaled $13CO_2$. J. Exp. Biol. 213, 782–789.

McFarlan, J.T., Bonen, A., Guglielmo, C.G., 2009. Seasonal upregulation of fatty acid transporters in flight muscles of migratory white-throated sparrows (*Zonotrichia albicollis*). J. Exp. Biol. 212, 2934–2940.

McGraw, K.J., Adkins-Regan, E., Parker, R.S., 2005. Maternally derived carotenoid pigments affect offspring survival, sex ratio, and sexual attractiveness in a colorful songbird. Naturwissenschaften 92, 375–380.

McKenzie, D.J., 2001. Effects of dietary fatty acids on the respiratory and cardiovascular physiology of fish. Comp. Biochem. Physiol. 128A, 607–621.

McKenzie, D.J., Higgs, D.A., Dosanjh, B.S., Deacon, G., Randall, D.J., 1998. Dietary fatty acid composition influences swimming performance in Atlantic salmon (*Salmo salar*) in seawater. Fish Physiol. Biochem. 19, 111–122.

McWilliams, S.R., 1999. Digestive strategies of avian herbivores. In: Adams, N., Slotow, R. (Eds.), Proceedings of the 22nd International Ornithological Congress. University of Natal, Durban, South Africa.

McWilliams, S.R., Caviedes-Vidal, E., Karasov, W.H., 1999. Digestive adjustments in cedar waxwings to high feeding rate. J. Exp. Zool. 283, 394–407.

McWilliams, S.R., Guglielmo, C., Pierce, B.J., Klaassen, M., 2004. Flying, fasting, and feeding in birds during migration: a nutritional and physiological ecology perspective. J. Avian Biol. 35, 377–393.

McWilliams, S.R., Karasov, W.H., 2001. Phenotypic flexibility in digestive system structure and function in migratory birds and its ecological significance. Comp. Biochem. Physiol. Mol. Integr. Physiol. 128, 577–591.

McWilliams, S.R., Karasov, W.H., 2005. Migration takes guts. In: Birds of Two Worlds: The Ecology and Evolution of Migration. Smithsonian Institution Press, Washington, DC, pp. 67–78.

McWilliams, S.R., Karasov, W.H., 2014. Spare capacity and phenotypic flexibility in the digestive system of a migratory bird: defining the limits of animal design. Proc. Roy. Soc. B 281, 20150308.

McWilliams, S., Pierce, B.J., 2006. Diet, body composition, and exercise performance: why birds during migration should be careful about what they eat. Physiologist 49, C1–C57 (Comparative Physiology 2006: Integrating Diversity) Abstract.

McWilliams, S.R., Pierce, B.J., Witenzellner, A., Langlois, L., Engel, S., Speakman, J., Fatica, O., DeMoranville, K.J., Goymann, W., Trost, L., Bryla, A., Dzialo, M., Sadowska, E.T., Bauchinger, U., 2020. The energy savings-oxidative cost trade-off for migratory birds during endurance flight. eLife 9:e60626.

Meddle, S.L., King, V.M., Follett, B.K., Wingfield, J.C., Ramenofsky, M., Foidart, A., Balthazart, J., 1997. Copulation activates Fos-like immunoreactivity in the male quail forebrain. Behav. Brain Res. 85, 143–159.

Meier, A.H., Farner, D.S., 1964. A possible endocrine basis for premigratory fattening in the white-crowned sparrow, *Zonotrichia leucophrys gambelii* (nuttall). Gen. Comp. Endocrinol. 102, 584–595.

Minias, P., Kaczmarek, K., Włodarczyk, R., Janiszewski, T., 2013. Hemoglobin concentrations in waders vary with their strategies of migration: a comparative analysis. Comp. Biochem. Physiol. Mol. Integr. Physiol. 165, 7–12.

Mishra, I., Singh, D., Kumar, V., 2017. Daily levels and rhythm in circulating corticosterone and insulin are altered with photostimulated seasonal states in night-migratory blackheaded buntings. Horm. Behav. 94, 114–123.

Mitchell, G.W., Guglielmo, C.G., Wheelwright, N.T., Freeman-Gallant, C.R., Norris, D.R., 2011. Early life events carry over to influence pre-migratory condition in a free-living songbird. PLoS One 6, e28838.

Mizrahy, O., Bauchinger, U., Aamidor, S., McWilliams, S.R., Pinshow, B., 2011. Availability of water affects renewal of tissues in migratory blackcaps during stopover. Integr. Comp. Biol. 51, 374–384.

Møller, A.P., Erritzøe, J., 1998. Host immune defence and migration in birds. Evol. Ecol. 12, 945–953.

Montgomery, M.K., Hulbert, A.J., Buttemer, W.A., 2012. Metabolic rate and membrane fatty acid composition in birds: a comparison between long-living parrots and short-living fowl. J. Comp. Physiol. 182B, 127–137.

Moore, M.C., Donham, R.S., Farner, D.S., 1982. Physiological preparation for autumnal migration in white-crowned sparrows. Condor 84, 410–419.

Moore, M.C., Farner, D.S., Donham, R.S., Matt, K.S., 1983. Endocrine and photoperiodic relationships during photorefractoriness postnuptial molt and onset of migration in *Zonotrichia leucophrys gambelii*. In: Proceedings XVIII International Ornithological Congress, Moscow, vol. 2, pp. 946–952.

Morton, M.L., 2002. The mountain white-crowned sparrow: migration and reproduction at high altitude. In: Rottenberry, J.T. (Ed.), Studies in Avian Biol. Cooper Ornithological Society, Lawrence, Kansas.

Morton, M.L., Liebman, H.A., 1974. Seasonal variations in fatty acids of a migratory bird with and without a controlled diet. Comp. Biochem. Physiol. Part A: Physiol. 48 (2), 329–335.

Morton, M.L., Pereyra, M.E., 1994. Autumnal migration departure schedules in mountain white-crowned sparrows. Condor 96, 1020–1029.

Mouritsen, H., 2015. Magnetoreception in birds and its use for long-distance migration. In: Scanes, C.G. (Ed.), Sturkie's Avian Physiology, sixth ed. Academic Press, London.

Mouritsen, H., 2018. Long-distance navigation and magnetoreception in migratory animals. Nature 558, 50–59.

Mrosovsky, N., 1990. Rheostasis: The Physiology of Change. Oxford University Press, New York.

Muheim, R., Schmaljohann, H., Alerstam, T., 2018. Feasibility of sun and magnetic compass mechanisms in avian long-distance migration. Movement Ecol. 6, 8.

Muñoz-Garcia, A., Aamidor, S.E., McCue, M.D., McWilliams, S.R., Pinshow, B., 2012. Allocation of endogenous and dietary protein in the reconstitution of the gastrointestinal tract in migratory blackcaps at stopover sites. J. Exp. Biol. 215, 1069–1075.

Munshi-South, J., Wilkinson, G.S., 2010. Bats and birds: exceptional longevity despite high metabolic rates. Ageing Res. Rev. 9, 12–19.

Murphy, M.E., 1994. Dietary complementation by wild birds: considerations for field studies. J. Biosci. 19, 355–368.

Murphy, M.E., King, J.R., 1987. Dietary discrimination by molting white-crowned sparrows given diets differing only in sulfur amino acid concentration. Physiol. Zool. 60, 279–289.

Nagahuedi, S., Popesku, J.T., Trudeau, V.L., Weber, J.-M., 2009. Mimicking the natural doping of migrant sandpipers in sedentary quails: effects of dietary n-3 fatty acids on muscle membranes and PPAR expression. J. Exp. Biol. 212, 1106–1114.

Nakazato, M., Murakami, N., Date, Y., Kojima, M., Matsuo, H., Kangawa, K., 2001. A role for ghrelin in the central regulation of feeding. Nature 409, 194e198.

Napolitano, G.E., Ackman, R.G., 1990. Anatomical distribution of lipids and their fatty acids in the semipalmated sandpiper *Calidris pusilla* L. from Shepody Bay, New Brunswick, Canada. J. Exp. Mar. Biol. Ecol. 114, 113–124.

Narkar, V.A., Downes, M., Yu, R.T., Embler, E., Wang, Y.-X., Banayo, E., Mihaylova, M.M., Nelson, M.C., Zou, Y., Juguilon, H., Kang, H., Shaw, R.J., Evans, R.M., 2008. AMPK and PPAR-delta agonists are exercise mimetics. Cell 134, 405–415.

Nebel, S., Bauchinger, U., Buehler, D.M., Langlois, L.A., Boyles, M., Gerson, A.R., Price, E.R., McWilliams, S.R., Guglielmo, C.G., 2012. Constitutive immune function in European starlings *Sturnus vulgaris* is decreased in response to endurance flight in a wind tunnel. J. Exp. Biol. 215, 272–278.

Newton, I., 2008. The Migration Ecology of Birds. Academic Press, London.

Newton, I., Dale, L., 1996a. Relationship between migration and latitude among west European birds. J. Animal Ecol. 65, 137–146.

Newton, I., Dale, L., 1996. Bird migration at different latitudes in Eastern North America. The Auk 113 (3), 626–635.

Nishiwaki-Ohkawa, T., Yoshimura, T., 2016. Molecular basis for regulating seasonal reproduction in vertebrates. J. Endocrinol. 229, R117–R127.

Norberg, U.M., 1990. Vertebrate Flight. Springer-Verlag, Berlin, Germany.

O'Reilly, K.M., Wingfield, J.C., 1995. Spring and autumn migration in arctic shorebirds - same distance, different strategies. Am. Zool. 35, 222–233.

O'Neal, B.J., Stafford, J.D., Larkin, R.P., Michel, E.S., 2018. The effect of weather on the decision to migrate from stopover sites by autumn-migrating ducks. Movement Ecol. 6, 23.

Odum, E.P., 1960. Premigratory hyperphagia in birds. Am. J. Clin. Nutr. 8, 621–629.

Ogoh, S., Ainslie, P.N., 2009. Cerebral blood flow during exercise: mechanisms of regulation. J. Appl. Physiol. 107, 1370–1380.

O'Reilly, K.M., Wingfield, J.C., 2003. Seasonal, age, and sex differences in weight, fat reserves, and plasma corticosterone in Western Sandpipers. Condor 105, 13–26.

Owen, J.C., Moore, F.R., 2006. Seasonal differences in immunological condition of three species of thrushes. Condor 108, 389–398.

Pamplona, R., Costantini, D., 2011. Molecular and structural antioxidant defenses against oxidative stress in animals. Am. J. Physiol. Integr. Compar. Physiol. 301, R843–R863.

Pant, K., Chandola-Saklani, A., 1993. A role for thyroid hormones in the development of premigratory disposition in Redheaded Bunting, *Emberiza bruniceps*. J. Comp. Physiol. 163B, 389–394.

Parrish, J.D., 1997. Patterns of frugivory and energetic condition in Nearctic landbirds during autumn migration. Condor 99, 681–697.

Parrish, J.D., 2000. Behavioral, energetic, and conservation implications of foraging plasticity during migration. Stud. Avian Biol. 20, 53–70.

Pawar, A., Xu, J., Jerks, E., Mangelsdorf, D.J., Jump, D.B., 2002. Fatty acid regulation of liver X receptors (LXR) and peroxisome proliferator-activated receptor α (PPARα) in HEK293 cells. J. Biol. Chem. 277, 39243–39250.

Paxton, K.L., Moore, F.R., 2015. Carry-over effects of winter habitat quality on en route timing and condition of a migratory passerine during spring migration. J. Avian Biol. 46, 495–506.

Pennycuick, C., 1998. Computer simulation of fat and muscle burn in long-distance bird migration. J. Theor. Biol. 191, 47–61.

Pennycuick, C.J., 1975. Mechanics of flight. In: Farner, D.S., King, J.R. (Eds.), Avian Biology. Academic Press, London.

Pérez, J.H., Furlow, J.D., Wingfield, J.C., Ramenofsky, M., 2016. Regulation of vernal migration in Gambel's white-crowned sparrows: role of thyroxine and triiodothyronine. Horm. Behav. 84, 50–56.

Pérez, J.P., Meddle, S.L., Wingfield, J.C., Ramenofsky, M., 2018. Effects of thyroid hormone manipulation on pre-nuptial molt, luteinizing hormone

and testicular growth in male white-crowned sparrows (*Zonotrichia leuchophrys gambelii*). Gen. Comp. Endocrinol. 255, 12–18.

Perrins, C.M., 1970. The timing of birds' breeding seasons. Ibis 112, 242–255.

Petersson, A., Pickova, J., Brannas, E., 2010. Swimming performance at different temperatures and fatty acid composition of Arctic charr (*Salvelinus alpinus*) fed palm and rapeseed oils. Aquaculture 300, 176–181.

Pierce, B.J., McWilliams, S.R., 2004. Diet quality and food limitation affect the dynamics of body composition and digestive organs in a migratory songbird (*Zonotrichia albicollis*). Physiol. Biochem. Zool. 77, 471–483.

Pierce, B.J., McWilliams, S.R., 2005. Seasonal changes in composition of lipid stores in migratory birds: causes and consequences. Condor 107, 271–281.

Pierce, B., McWilliams, S.R., 2014. The fat of the matter: how dietary fatty acids can affect exercise performance. Integr. Comp. Biol. 54, 903–912.

Pierce, B.J., McWilliams, S.R., O'Connor, T., Place, A.R., Guglielmo, C., 2005. Effect of dietary fatty acid composition on depot fat and exercise performance in a migrating songbird, the red-eyed vireo. J. Exp. Biol. 208, 1277–1285.

Pierce, B.J., McWilliams, S.R., Place, A.R., Huguenin, M.A., 2004. Diet preferences for specific fatty acids and their effect on composition of fat reserves in migratory Red-eyed Vireos (*Vireo olivaceous*). Comp. Biochem. Physiol. 138A, 503–514.

Piersma, T., 1998. Phenotypic flexibility during migration: optimization of organ size contingent on the risks and rewards of fueling and flight? J. Avian Biol. 29, 511–520.

Piersma, T., Gils, J.A.V., 2011. The Flexible Phenotype: A Body-Centred Integration of Ecology, Physiology, and Behaviour. Oxford University Press, New York.

Piersma, T., Perez-Tris, J., Mouritsen, H., Bauchinger, U., Bairlein, F., 2005. Is there a "migratory syndrome" common to all migrant birds?. In: Bird Hormones and Bird Migrations: Analyzing Hormones in Droppings and Egg Yolks and Assessing Adaptations in Long-Distance Migration, vol. 1046, pp. 282–293.

Powell, F., 2015. Respiration. In: Scanes, C.G. (Ed.), Sturkie's Avian Physiology, sixth ed. Academic Press, London.

Pradhan, D.S., Ma, C., Schlinger, B.A., Soma, K.K., Ramenofsky, M., 2018. Preparing to migrate: expression of androgen signaling molecules and insulin-like growth factor-1 in skeletal muscles of Gambel's white-crowend sparrows. J. Comp. Physiol. 205, 113–123.

Pradhan, D.S., Newman, A.E.M., Wacker, D.W., Wingfield, J.C., Schlinger, B.A., Soma, K.K., 2010. Aggressive interactions rapidly increase androgen synthesis in the brain during the non-breeding season. Horm. Behav. 57, 381–389.

Pradhan, D.S., Van Ness, R., Jalabert, C., Hamden, J.E., Austin, S.H., Soma, K.K., Ramenofsky, M., Schlinger, B.A., 2019. Phenotypic flexibility of glucocorticoid signaling in skeletal muscles of a songbird preparing to migrate. Horm. Behav. 116, 104586.

Price, E.R., McFarlan, J.T., Guglielmo, C.G., 2010. Preparing for migration: the effects of photoperiod and exercise on muscle oxidative enzymes, lipid transporters, and phospholipids in White-crowned Sparrows. Physiol. Biochem. Zool. 83, 252–262.

Price, E., Staples, J.F., Milligan, C.L., Guglielmo, C.G., 2011. Carnitine palmitoyl transferase activity and whole muscle oxidation rates vary with fatty acid substrate in avian flight muscles. J. Comp. Physiol. 181B, 565–573.

Price, E.R., 2010. Dietary lipid composition and avian migratory flight performance: development of a theoretical framework for avian fat storage. Comp. Biochem. Physiol. 157A, 297–309.

Price, E.R., Guglielmo, C.G., 2009. The effect of muscle phospholipid fatty acid composition on exercise performance: a direct test in the migratory white-throated sparrow. Am. J. Physiol. 297R, R775–R782.

Price, E.R., Krokfors, A., Guglielmo, C.G., 2008. Selective mobilization of fatty acids from adipose tissue in migratory birds. J. Exp. Biol. 211, 29–34.

Raclot, T., 2003. Selective mobilization of fatty acids from adipose tissue triacylglycerols. Prog. Lipid Res. 42, 257–288.

Raclot, T., Groscolas, R., 1995. Selective mobilization of adipose tissue fatty acids during energy depletion in the rat. J. Lipid Res. 36, 2164–2173.

Raja-Aho, S., Lehikoinen, E., Suorsa, P., Nikinmaa, M.V., Vosloo, D., Eeva, T., 2013. Corticosterone secretion patterns prior to spring and autumn migration differ in free-living barn swallows (*Hirundo rustica* L.). Oecologia 173, 689–697.

Ramenofsky, M., 1990. Fat storage and fat metabolism in relation to bird migration. In: Gwinner, E. (Ed.), Physiology and Ecophysiological Aspects of Bird Migration. Springer, Berlin.

Ramenofsky, M., 2011. Hormones in migration and reproductive cycles of birds. In: Norris, D., Lopez, K.H. (Eds.), Hormones and Reproduction of Vertebrates. Academic Press.

Ramenofsky, M., Agatsuma, R., Barga, M., Cameron, R., Harm, J., Landys, M., Ramfar, T., 2003. Migratory behavior: new insights from captive studies. In: Berthold, P., Gwinner, E., Sonnenschein, E. (Eds.), Avian Migration. Springer, Berlin.

Ramenofsky, M., Cornelius, J.M., Helm, B., 2012. Physiological and behavioral responses of migrants to environmental cues. J. Ornithol. 153, S181–S191.

Ramenofsky, M., Nemeth, Z., 2014. Regulatory mechanisms for the development of the migratory phenotype: roles for photoperiod and the gonad. Horm. Behav. 66, 148–158.

Ramenofsky, M., Savard, R., Greenwood, M.R.C., 1999. Seasonal and diel transitions in physiology and behavior in the migratory dark-eyed junco. Compar. Biochem. Physiol.-Mol. Integr. Physiol. 122, 385–397.

Ramenofsky, M., Wingfield, J.C., 2006. Behavioral and Physiological Conflicts in Migrants: The Transition between Migration and Breeding, pp. 135–145.

Ramenofsky, M., Wingfield, J.C., 2007. Regulation of migration. Bioscience 57, 135–143.

Ramenofsky, M., Wingfield, J.C., 2017. Regulation of complex behavioral transitions: migration to breeding. Anim. Behav. 124, 299–306.

Rani, S., Kumar, V., 2014. Photoperiodic regulation of seasonal reproduction in higher vertebrates. IJEB 52, 413–419.

Rastogi, A., Kumari, A., Rani, S., Kumar, V., 2013. Neural Correlates of migration: activation of hypothalamic clock(s) in and out of migratory state in the Blackheaded Bunting (*Emberiza melanocephal*). PLoS One 8, e70065.

Raveling, D.G., Heitmeyer, M.E., 1989. Relationships of population size and recruitment of pintails to habitat conditions and harvest. J. Wildl. Manag. 53, 1088–1103.

Reiser, P.J., Greaser, M.L., Moss, R.L., 1996. Contractile properties and protein isoforms of single fibres from the chicken pectoralis red strip muscle. J. Physiol. (Lond.) 493, 553–562.

Remage-Healey, L., Romero, L.M., 2001. Corticosterone and insulin interact to regulate glucose and triglyceride levels during stress in a bird. Am. J. Physiol. 281, R994–R1003.

Reneerkens, J., Morrison, R.I.G., Ramenofsky, M., Piersma, T., Wingfield, J.C., 2002a. Baseline and stress-induced levels of corticosterone during different life cycle substages in a shorebird on the high arctic breeding grounds. Physiol. Biochem. Zool. 75, 200–208.

Reneerkens, J., Piersma, T., Ramenofsky, M., 2002b. An experimental test of the relationship between temporal variability of feeding opportunities and baseline levels of corticosterone in a shorebird. J. Exp. Zool. 293, 81–88.

Richardson, R.D., Boswell, T., Weatherford, S.C., Wingfield, J.C., Woods, S.C., 1992. Central and peripheral regulators of food-intake in the white-crowned sparrow. Appetite 19, 212.

Richardson, R.D., Boswell, T., Weatherford, S.C., Wingfield, J.C., Woods, S.C., 1993. Cholecystokinin octapeptide decreases food-intake in white-crowned sparrows. Am. J. Physiol. 264, R852–R856.

Rios, J.M., Barcelo, G.F., Narvaez, C., Maldonado, K., Sabat, P., 2014. Feeding and digestive responses to fatty acid intake in two South American passerines with different food habits. J. Comp. Physiol. B 184, 729–739.

Romero, L.M., Dickens, M.J., Cyr, N.E., et al., 2009. The reactive scope model - A new model integrating homeostasis, allostasis, and stress. Horm. Behav. 55.

Romero, L.M., Ramenofsky, M., Wingfield, J.C., 1997. Season and migration alters the corticosterone response to capture and handling in an Arctic migrant, the white-crowned sparrow (*Zonotrichia leucophrys gambelii*). Compar. Biochem. Physiol. C-Pharmacol. Toxicol. Endocrinol. 116, 171–177.

Romero, L.M., Wingfield, J.C., 2016. Tempests, Poxes, Predators and People: Stress in Wild Animals and How They Cope. Oxford University Press, Oxford, U.K.

Royle, N.J., Surai, P.F., Hartley, I.R., 2003. The effect of variation in dietary intake on maternal deposition of antioxidants in zebra finch eggs. Funct. Ecol. 17, 472–481.

Ruf, T., Valencak, T., Tataruch, F., Arnold, W., 2006. Running speed in mammals increases with muscle n-6 polyunsaturated fatty acid content. PLoS One 1, e65.

Runfeldt, S., Wingfield, J.C., 1985. Experimentally prolonged sexual-activity in female sparrows delays termination of reproductive activity in their untreated mates. Anim. Behav. 33, 403–410.

Ryder, J.P., 1970. A possible factor in the evolution of clutch size in Ross's Goose. Wilson Bull. 82, 5–13.

Sandberg, R., Moore, F.R., Backman, J., Lohmus, M., 2002. Orientation of nocturnally migrating Swainson's thrush at dawn and dusk: importance of energetic condition and geomagnetic cues. Auk 119, 201–209.

Savard, R., Ramenofsky, M., Greenwood, M.R.C., 1991. A north-temperate migratory bird - a model for the fate of lipids during exercise of long duration. Can. J. Physiol. Pharmacol. 69, 1443–1447.

Schaefer, H.M., Schmidt, V., Bairlein, F., 2003. Discrimination abilities for nutrients: which difference matters for choosy birds and why? Anim. Behav. 65, 531–541.

Schat, K.A., Kaspers, B., Kaiser, P. (Eds.), 2014. Avian Immunology. Elsevier, New York, NY.

Schaub, M., Jenni, L., 2001. Stopover durations of three warbler species along their autumn migration route. Oecologia 128, 217–227.

Schmaljohann, H., Bruderer, B., Liechti, F., 2008. Sustained bird flights occur at temperatures far beyond expected limits. Anim. Behav. 76, 1133–1138.

Schmaljohann, H., Liechti, F., Bruderer, B., 2009. Trans-Sahara migrants select flight altitudes to minimize energy costs rather than water loss. Behav. Ecol. Sociobiol. 63, 1609–1619.

Schmidt-Nielsen, K., 1972. Locomotion: energy cost of swimming, flying, and running. Science 177, 222–228.

Schwabl, H., Bairlein, F., Gwinner, E., 1991. Basal and stress-induced corticosterone levels of garden warblers, *Sylvia borin*, during migration. J. Comp. Physiol. B Biochem. Syst. Environ. Physiol. 161, 576–580.

Schwabl, H., Farner, D.S., 1989. Endocrine and environmental control of vernal migration in male White-crowned Sparrows, *Zonotrichia leucophrys gambelii*. Physol. Zool. 62, 1–10.

Schwabl, H., Schwabl-Benzinger, I., Goldsmith, A.R., Farner, D.S., 1988. Effects of ovariectomy on long-day-induced premigratory fat deposition, plasma levels of luteinizing hormone and prolactin, and molt in White-crowned Sparows. *Zonotrichia leucophrys gambelii*. Gen. Comp. Endocrinol. 71, 398–405.

Schwemmer, P., Voigt, C.C., Corman, A.M., Adler, S., Garthe, S., 2016. Body mass change and diet switch tracked by stable isotopes indicate time spent at a stopover site during autumn migration in dunlins *Calidris alpina alpina*. J. Avian Biol. 47, 806–814.

Schwilch, R., Grattarola, A., Spina, F., Jenni, L., 2002. Protein loss during long-distance migratory flight in passerine birds: adaptation and constraint. J. Exp. Biol. 205, 687–695.

Scott, G.R., Hawkes, L.A., Frappell, P.B., Butler, P.J., Bishop, C.M., Milsom, W.K., 2015. How bar-headed geese fly over the Himalayas. Physiology 30, 107–115.

Scott, G.R., Milsom, W.K., 2006. Flying high: a theoretical analysis of the factors limiting exercise performance in birds at altitude. Respir. Physiol. Neurobiol. 154, 284–301.

Scott, G.R., Schulte, P.M., Egginton, S., Scott, A.L.M., Richards, J.G., Milsom, W.K., 2011. Molecular evolution of the cytochrome C oxidase underlies high-altitude adaptation in the bar-headed goose. Mol. Biol. Evol. 28, 351–363.

Sedinger, J.S., Alisauskas, R.T., 2014. Cross-seasonal effect and the dynamics of waterfowl populations. Wildfowl 99, 836–840.

Sharma, A., Singh, D., Malik, S., Gupta, N.J., Rani, S., Kumar, V., 2018. Difference in control between spring and autumn migration in birds: insight from seasonal changes in hypothalamic gene expression in captive buntings. Proc. R. Soc. B 285.

Sidell, B.D., Crockett, E.L., Driedzic, W.R., 1995. Antarctic fish tissues preferentially catabolize monoenoic fatty acids. J. Exp. Zool. 271, 73–81.

Sjoberg, S., Alerstam, T., Akesson, S., Schulz, A., Weidauer, A., Coppack, T., Muheim, R., 2015. Weather and fuel reserves determine departure and flight decitions in passerines migrating across the Baltic Sea. Anim. Behav. 104, 59–68.

Skrip, M., Bauchinger, U., Goymann, W., Fusani, L., Cardinale, M., Alan, R., Mcwilliams, S.R., 2015a. Migrating songbirds on stopover prepare for, and recover from, oxidative challenges posed by long-distance flight. Ecol. Evol. 5, 3198–3209.

Skrip, M.M., Bauchinger, U., Goymann, W., Fusani, L., Mcwilliams, S.R., 2015b. Access to water affects the condition dependency of nocturnal restlessness in Garden Warblers on a Mediterranean island stopover. J. Ornithol. 156, 425–432.

Skrip, M., McWilliams, S.R., 2016. Oxidative balance in birds: an atoms-to-organisms-to-ecology primer for ornithologists. J. Field Ornithol. 87, 1–20.

Skrip, M.M., Seeram, N.P., Yuan, T., Ma, H., McWilliams, S.R., 2016. Dietary antioxidants and flight exercise in female birds affect allocation of nutrients to eggs: how carry-over effects work. J. Exp. Biol. 219, 2716–2725.

Smith, J.P., 1982. Changes in blood levels of thyroid hormones in two species of passerine birds. Condor 84, 160–167.

Smith, A.D., McWilliams, S.R., 2014. What to do when stopping over: behavioral decisions of a migrating songbird during stopover are dictated by initial change in their body condition and mediated by key environmental conditions. Behav. Ecol. 25, 1423–1435.

Smith, R.J., Moore, F.R., 2005. Arrival timing and seasonal reproductive performance in a long-distance migratory landbird. Behav. Ecol. Sociobiol. 57, 231–239.

Soma, K.K., Wissman, A.M., Brenowitz, E.A., Wingfield, J.C., 2002. Dehydroepiandrosterone (DHEA) increases territorial song and the size of an associated brain region in a male songbird. Horm. Behav. 41, 203–212.

Speakman, J.R., 2005. Body size, energy metabolism and lifespan. J. Exp. Biol. 208, 1717–1730.

Speakman, J.R., Garratt, M., 2013. Oxidative stress as a cost of reproduction: beyond the simplistic trade-off model. Bioessays 36, 93–106.

Speakman, J.R., Selman, C., 2011. The free-radical damage theory: accumulating evidence against a simple link of oxidative stress to ageing and lifespan. Bioessays 33, 255–259.

Stafford, J.D., Janke, A.K., Anteau, M.J., Pearse, A.T., Fox, A.D., Elmberg, J., Straub, J.N., Eichholz, M.W., Arzel, C., 2014. Spring migration of waterfowl in the northern hemisphere: a conservation perspective. Wildfowl 4, 70–85.

Stetson, M.H., Erickson, J.E., 1972. Hormonal control of photoperiodically induced fat deposition in White-crowned Sparrows. Gen. Comp. Endocrinol. 19, 355–362.

Stillwell, W., Wassall, S.R., 2003. Docosahexaenoic acid: membrane properties of a unique fatty acid. Chem. Phys. Lipids 126, 1–27.

Sweazea, K.L., McMurtry, J.P., Braun, E.J., 2006. Inhibition of lipolysis does not affect insulin sensitivity to glucose uptake in the mourning dove. Comp. Biochem. Physiol. B 144, 387–394.

Terrill, S.B., 1990. Ecophysiological aspects of movements by migrants in the wintering quarters. In: Gwinner, E. (Ed.), Bird Migration: Physiology and Ecophysiology. Springer-verlag, Berlin.

Thomas, V.G., George, J.C., 1975. Plasma and depot fat fatty acids in Canada Geese in relation to diet, migration, and reproduction. Physiol. Zool. 48, 157–167.

Tobalske, B.W., 2016. Avian flight. In: Lovette, I.J., Fitzpatrick, J.W. (Eds.), Handbook of Bird Biology, third ed. John Wiley & Sons, Ltd, West Sussex, U.K.

Torre-Bueno, J.R., 1976. Temperature regulation and heat dissipation during flight in birds. J. Exp. Biol. 65, 471–482.

Torre-Bueno, J.R., 1978. Evaporative cooling and water balance during flight in birds. J. Exp. Biol. 75, 231–236.

Totzke, U., Hubinger, A., Bairlein, F., 1997. A role for pancreatic hormones in the regulation of autumnal fat deposition of the garden warbler (*Sylvia borin*)? Gen. Comp. Endocrinol. 107, 166–171.

Tsipoura, N., Burger, J., 1999. Shorebird diet during spring migration stopover on Delaware Bay. Condor 101, 635–644.

Tsipoura, N., Scanes, C.G., Burger, J., 1999. Corticosterone and growth hormone levels in shorebirds during spring and fall migration stopover. J Exp BIology 284, 645–651.

Tsutsui, K., Saigoh, E., Ukena, K., Teranishi, H., Fujisawa, Y., Kikuchi, M., Ishii, S., Sharp, P.J., 2000. A novel avian hypothalamic peptide inhibiting gonadotropin release. Biochem. Biophys. Comm. 275, 661–667.

Tucker, V.A., 1970. Energetic cost of locomotion in animals. Comp. Biochem. Physiol. 34, 841–846.

Turner, N., Else, P.L., Hulbert, A.J., 2003. Docosahexaenoic acid (DHA) content of membranes determines molecular activity of the sodium pump: implications for disease states and metabolism. Naturwissenschaften 90, 521–523.

Valencak, T.G., Arnold, W., Tataruch, F., Ruf, T., 2003. High content of polyunsaturated fatty acids in muscle phospholipids of a fast runner, the European brown hare (*Lepus europaeus*). J. Comp. Physiol. 173B, 695–702.

Velten, B.P., Welch JR., K.C., Ramenofsky, M., 2016. Altered expression of pectoral myosin heavy chain isoforms corresponds to migration status in the White-crowned Sparrow (*Zonotrichia leucophrys gambelii*). Roy. Soc. Open Sci. 3, 160775.

Wagner, D.N., Green, D.J., Cooper, J.M., Love, O.P., Williams, T.D., 2014. Variation in plasma corticosterone in migratory songbirds: a test of the migration-modulation hypothesis. Physiol. Biochem. Zool. 87, 695–703.

Vezina, F., O'Connor, R.S., Le Pogam, A., De Jesus, A.D., Love, O.P., Jimenez, G., 2021. Snow buntings preparing for migration increase muscle fiber size and myonuclear domain in parallel with a major gain in fat mass. J Av Biol 52 (5).

Wagner, G.N., Balfry, S.K., Higgs, D.A., Lall, S.P., Farrell, A.P., 2004. Dietary fatty acid composition affects the repeat swimming performance of Atlantic salmon in seawater. Comp. Biochem. Physiol. 137A, 567–576.

Wang, G., Ramenofsky, M., Wingfield, J.C., 2013. Apparent dissociation of photoperiodic time measurement between vernal migration and breeding under dim green light conditions in Gambel's white-crowned sparrow *Zonotrichia leucophrys gambelii*. Curr. Zool. 59, 349–359.

Warren, J.M., Cutting, K.A., Koons, D.A., 2013. Body condition dynamics and the cost-of-delay hypothesis in a temperate-breeding duck. J. Avian Biol. 44, 1–8.

Watson, H., Salmon, P., Isaksson, C., 2018. Maternally derived yolk antioxidants buffer the developing avian embryo against oxidatives stress induced by hyperoxia. J. Exp. Biol. 221, jeb179465.

Watts, H.E., Cornelius, J.M., Fudickar, A.M., Pérez, J., Ramenofsky, M., 2018. Understanding variation in migratory movements: a mechanistic approach. Gen. Comp. Endocrinol. 256, 112–122.

Weber, J.-M., 2009. The physiology of long-distance migration: extending the limits of endurance metabolism. J. Exp. Biol. 212, 593–597.

Weise, G.M., 1967. Castration and spring migration in the white-throated sparrow. Condor 69, 49–68.

Wikelski, M., Tarlow, E.M., Raim, A., Diehl, R.H., Larkin, R.P., Visser, G.H., 2003. Costs of migration in free-flying songbirds. Nature 423, 704.

Williamson, K.A., Surai, P.F., Graves, J.A., 2006. Yolk antioxidants and mate attractiveness in the Zebra Finch. Funct. Ecol. 20, 354–359.

Wilson, F.E., Reinert, B.D., 1996. Programming in seasonally breeding male American tree sparrows (*Spizella arborea*). Gen. Comp. Endocrinol. 103, 82–92.

Wilson, F.E., Reinert, B.D., 1999. Time of thyroidectomy variably affects seasonality in female American tree sparrows (*Spizella arborea*). Gen. Comp. Endocrinol. 114, 425–430.

Wiltschko, R., Wiltschko, W., 2009. Avian navigation. Auk 126, 717–743.

Wiltschko, W., Wiltschko, R., Emlen, S.R., Demong, N.J., 1980. Nocturnal activity and orientation behavior during spring migration and early summer in the indigo bunting, *Passerina cyanea*. J. Comp. Physiol. 137, 4740.

Wingfield, J.C., Farner, D.S., 1978a. The annual cycle of plasma irLH and steroid hormones in feral populations of the white-crowned sparrow, *Zonotrichia leucophrys gambelii*. Biol. Reprod. 19, 1046–1056.

Wingfield, J.C., Farner, D.S., 1978b. Endocrinology of a natural breeding population of the White-crowned sparrow, *Zonotrichia leucophrys pugetensis*. Physiol. Zool. 51, 188–205.

Wingfield, J.C., Owen-Ashley, N.T., Benowitz-Fredericks, Z.M., Lynn, S., Hahn, T.P., Wada, H., Breuner, C.M., Meddle, S.L., Romero, L.M., 2004. Arctic Spring: the arrival biology of migrant birds. Acta Zool. Sin. 50, 948–960.

Wingfield, J.C., Perfito, N., Calisi, R., Bentley, G.E., Ubuka, T., Mukai, M., O'Brien, S., Tsutsui, K., 2016. Putting the brakes on reproduction: implications for conservation, global climate change and biomedicine. Gen. Comp. Endocrinol. 227, 16–26.

Wingfield, J.C., Schwabl, H., Mattocks Jr., P.W., 1990. Endocrine mechanisms of migration. In: Gwinner, E. (Ed.), Bird Migration. Springer-Verlag, Berlin.

Witmer, M.C., 2001. Nutritional interactions and fruit removal: cedar waxwing consumption of *Viburnum opulus* fruits in spring. Ecology 82, 3120–3130.

Wojciechowski, M.S., Pinshow, B., 2009. Heterothermy in small, migrating passerine birds during stopover: use of hypothermia at rest accelerates fuel accumulation. J. Exp. Biol. 212, 3068–3075.

Wu, B.J., Else, P.L., Storlien, L.H., Hulbert, A.J., 2001. Molecular activity of Na+/K+-ATPase from different sources is related to the packing of membrane lipids. J. Exp. Biol. 204, 4271–4280.

Wu, B.J., Hulbert, A.J., Storlien, L.H., Else, P.L., 2004. Membrane lipids and sodium pumps of cattle and crocodiles: an experimental test of the membrane pacemaker theory of metabolism. Am. J. Physiol. 287, R633–R641.

Yap, K.N., Dick, M.F., Guglielmo, C.G., Williams, T.D., 2018. Effects of experimental manipulation of hematocrit on avian flight performance in high-and low-altitude conditions. J. Exp. Biol. 221, jeb191056.

Yokoyama, K., 1976. Hypothalamic and hormonal control of photoperiodically induced vernal functions in the White-crowned sparrow, *Zonotrichia leucophrys gambelii*. I. The effects of hypothalamic lesions and exogenous hormones. Cell Tissue Res. 174, 391–416.

Zeng, W.-H., Lin, L., Lui, J.-S., Xu, Z.-J., Li, M., 2013. Geographicaal variation in basal thermogenesis in little buntings: relation to celular thermogenesis and thyroid hormone concentrations. Comp. Biochem. Physiol. A 164, 483–490.

Zhang, F., Basinski, M.B., Beals, J.M., Briggs, S.L., Churgay, L.M., Clawson, D.K., Dimarchi, R.D., Furman, T.C., Hale, J.E., Hsiung, H.M., Schoner, B.E., Smith, D.P., Zhang, X.Y., Wery, J.P., Schevitz, R.W., 1997. Crystal structure of the obese protein leptin-E100. Nature 387, 206–209.

Zhang, J., Phillips, D.I.W., Wang, C., Byrne, C.D., 2004. Human skeletal muscle PPARα expression correlates with fat metabolism gene expression but not BMI or insulin sensitivity. Am. J. Physiol. 286, E168–E175.

Zurovchak, J.G., 1997. Nutritional Role of High-Lipid Fruits in the Diet of Migrant Thrushes (Ph.D. dissertation). Rutgers University.

Chapter 48

Actions of toxicants and endocrine disrupting chemicals in birds

Mary Ann Ottinger[1] and Karen D.M. Dean[2]
[1]Department of Biology and Biochemistry, University of Houston, Houston, TX, United States; [2]University of Lethbridge, Lethbridge, AB, Canada

Abbreviations

(ACHase) acetylcholine esterase
(AhR) aryl hydrocarbon receptor
(AOP) Adverse Outcomes Pathway
(AR) androgen receptor
(BPA) bisphenol A
(DDE) dichlorodiphenyldichloroethylene
(DDT) dichlorodiphenyltrichloroethane
(E_2) estradiol
(ED15) embryonic day 15
(ED17) embryonic day 17
(EDCs) endocrine disrupting chemicals
(EDSP) Endocrine Disruptor Screening Program
(EDSTAC) Endocrine Disruptor Screening and Testing Advisory Committee
(EDTA) Endocrine Disrupters Testing and Assessment
(EPA) Environmental Protection Agency
(EROD) ethoxyresorufin-*O*-dealkylase activity
(F1) first generation
(F2) second generation
(FIFRA) The Federal Insecticide, Fungicide, and Rodenticide Act
(GnRH) gonadotropin-releasing hormone
(GnRH-I) gonadotropin-releasing hormone-I
(HPG axis) hypothalamic−-pituitary−gonadal axis
(JQTT) Japanese quail two-generation test
(LD_{50}) median lethal dose for 50% of the population
(OECD) Organization for Economic Cooperation and Development
(PAHs) polycyclic aromatic hydrocarbons
(PBDEs) polybrominated biphenyls
(PCB 126) 3,3',4,4',5-pentachlorobiphenyl
(PCBs) polychlorinated biphenyls
(PCBs) polychlorinated biphenyl congeners
(PFASs) perfluoroalkyl
(POA-SL) preoptic-septal region
(T3) triiodothyronine
(T4) thyroxine
(TCDD) 2,3,7,8-tetrachlorodibenzo-*p*-dioxin
(TEF) toxic equivalency factor
(TEQ) toxic equivalency
(USEPA) United States Environmental Protection Agency
(USGS) United States Geological Service

48.1 Introduction

The use of chemicals has been critical in crop production, pest control, health and beauty products, and industrial systems crucial in our global economies. Nonrenewable energy sources, plastics, and industrially produced compounds have been essential to our lifestyle and are key in the efficiency of production systems, packaging, and storage. Not surprisingly, as we learn more about the chemical components used in many of these processes, in storage and production, and for control of pests and our environment, adverse effects have come to light. One of the earliest findings indicative of potential adverse effects of industrial chemicals and pesticides was the thinning of eggs in bald eagles in response to exposure to dichlorodiphenyltrichloroethane (DDT), which dramatically illustrates the potency of these chemicals in wild birds (Felton et al., 2015). Since that time, there has been extensive research aimed at assessing the actions and risks associated with exposure to environmental chemicals across vertebrate and invertebrate species. Workshops, including the Wingspread Meetings and research publications have documented a range of impacts of endocrine disruptors and other toxicants in laboratory studies and in field populations of avian species (Basu, 2015; Berg et al., 1999; Bowerman et al., 2007; Brunstrom et al., 1991; Cesh et al., 2010; Cohen-Barnhouse et al., 2011; Corbitt et al., 2007; Custer et al., 2010a, 2012b; Custer and Read, 2006; Hotchkiss et al., 2008; Kavlock et al., 2005; Rattner, 2009; Rattner et al., 2000, 2001, 2010; Safe et al., 1985; Levengood et al., 2007). Many of these environmental chemicals persist in and move through the environment, with secondary metabolites and degradants that are also

Sturkie's Avian Physiology. https://doi.org/10.1016/B978-0-12-819770-7.00036-0

biologically potent. Further, multiple chemicals generally coexist in the environment, meaning that most vertebrates are exposed to a mixture of chemicals at any point in time (Vermeulen et al., 2020). Exposure to complex mixtures vary in wild populations depending on location; migratory birds also may encounter very different chemical mixtures at their wintering grounds compared to nesting area.

It is important to distinguish between a primary toxic effect from environmental chemicals versus adverse impacts from endocrine disruption, which often is nonlethal (details provided later in this review). Some early studies began to distinguish toxic from endocrine disruption and characterize the actions as well as physiological targets of EDCs. Although the characterization of exposure effects has focused on single compounds, it is also clear that wild birds are exposed to a complex mixture of environmental chemicals, which often include toxic compounds, metals, and EDCs. Research is needed to understand possible synergisms of the compounds in these complex mixtures. The potential for deleterious results has been supported by observations of endocrine related effects to organisms in areas in which dioxin, PCB, or other chemicals occurred. Furthermore, the exposure of wildlife to environmentally relevant levels is often at sublethal concentrations, making the determination of effects of EDCs a challenge, especially when attempting to separate other interacting factors in the animal's environment that also impact fitness and overall health. Additional environmental factors impacting wild populations include environmental conditions, habitat loss, food availability, disease, or exposure to complex mixtures of chemicals.

It is therefore important to develop reliable and sensitive measures that are appropriate for the endocrine or organ system that are the targets of the EDCs. This chapter will consider EDCs and their actions target physiological systems, particularly reproductive and metabolic endocrine systems of birds. In addition to physiological targets of EDCs that are found across vertebrates, termed conserved mechanisms, birds also have unique adaptations for migration, flight, and reproductive strategies, such as precocial or altricial developmental stages in chicks at hatch. Further, birds living in varied habitats, climates, and resources have developed a range of reproductive strategies, as well as other adaptations for flight, migration; all with associated metabolic and reproductive modifications. Some of these unique characteristics of birds may also affect their vulnerability to exposure to environmental chemicals. It is important to identify specific physiological measures that reflect EDC exposure and utilize these measurement end points as metrics to assess effects. Testing provides the basis for risk assessment and injury quantification criteria that take these unique characteristics of birds into consideration. As more compounds are characterized as endocrine disruptors, it has become clear that there are thousands of these chemicals in the environment. As such, these chemicals have been considered in terms of broad categories, often with studies conducted on representative chemicals for a category. Influence diagrams, AOPs, and the one health framework help to describe molecular/cellular mechanisms of action and relate these adverse impacts to effects of exposure for the organism and potentially to the population. Compiling this information becomes essential in developing reliable testing paradigms for the commercial, industrial, and personal applications of chemicals that migrate into the environment.

48.2 Environmental chemicals: utilities and hazards?

48.2.1 Chemical sources and production

A number of factors must be considered when evaluating the cost/benefit for production and use of environmental chemicals. The productivity of modern agricultural systems is outstanding, in part due to the use of chemical treatments that limit pests and make applications, storage, and preparation more efficient. The use of chemicals has dramatically increased as our knowledge of chemistry and biochemistry has enabled the development of designer chemicals for specific applications. In recent years as we have become more aware of the adverse impacts of some of these chemicals on nontarget species or systems, we have seen the emergence of "green chemicals" (see https://www.epa.gov/greenchemistry), designed with the intent of lessened adverse impacts on nontarget organisms and attenuated presence in the environment. However, many of these chemicals are effective because they specifically interact with endocrine-related processes or other physiological functions in pest species. For example, an effective pesticide for gypsy moths is tebufenozide, which is an ecdysone inhibitor that acts on the timing of molting in larvae. Because these compounds were developed specifically to act on physiological targets in insects, coincident effects on other vertebrate classes are generally regarded as minimal risk compared to the benefit of pest management. However, as we have seen in the past, there are sometimes unexpected adverse impacts due to spills, or chemical overuse resulting from chemical resistance by the target pest species. One of the challenges of characterizing the potential risk and impacts of environmental chemicals to wildlife, and birds in particular distinguishing between toxic physiological effects and endocrine disruption. Moreover, wildlife populations are generally exposed to multiple chemicals that exist in the environment that may also include metals and other contaminants. These complex mixtures will also be discussed in the context of physiological targets of single compounds and

actions of simultaneous exposure to a suite of chemicals. Additionally, the assessment of adverse effects of EDCs has presented some unique challenges as discussed below.

48.2.2 Assessing the safety of chemicals

The US Environmental Protection Agency formed the Endocrine Disruptor Screening and Testing Advisory Committee (EDSTAC), a committee of scientists and stakeholders that was charged by the EPA to provide recommendations on how to implement its Endocrine Disruptor Screening Program (EDSP). The EDSP is critical for assessing the potential for EDCs to impact vertebrate species with the added benefit that identifying EDCs with adverse effects in vertebrates and banning them from use would then prevent human exposure. Upon recommendations from the EDSTAC (Harvey and Everett, 2006), the EPA expanded the EDSP using the Administrator's discretionary authority to include the androgen and thyroid hormonal systems as well as the reproductive endocrine systems of wildlife (see http://www.epa.gov/endo/pubs/edspoverview/edstac.htm). Following broader international concerns and the creation of similar programs in other countries, the Organization for Economic Cooperation and Development established the Endocrine Disrupters Testing and Assessment Task Force in 1998 within its Test Guidelines Program, with the charge of developing an internationally harmonized testing strategy for the screening and testing of EDCs. Additional international collaborative efforts have been initiated through professional societies and workshops focused on the effects of exposure to environmental chemicals across vertebrates.

48.2.2.1 Assessing multigenerational impacts in the Japanese quail model

To address possible effects specifically due to EDC exposure in birds, the Japanese Quail (*Coturnix japonica*) Two Generation Test was developed to detect potential disruption of the endocrine system by EDCs at varied stages of the lifecycle; this and other tests will be reviewed later in this chapter. One of the primary challenges, given the diversity of chemicals considered potential EDCs is to ascertain risk across vertebrate classes. Additionally, the incidence of EDCs is global, including areas that have been considered relatively pristine (Kakimoto et al., 2018; Santamans et al., 2017). Because birds have a broad range of life histories and unique developmental characteristics, there are differential sensitivities across avian species with changing lifetime vulnerability. Further, migratory birds have enormous metabolic demands (Seegar et al., 2015). As such, EDCs that impact metabolic and in particular the thyroid systems pose risk to migratory avian species. Not only to ensure adequate growth and fattening before migration but also adequate feather replacement or development of subadult or adult plumage for young-of-the-year prior to migration. Furthermore, sexual differentiation of reproductive and other endocrine systems is unique to birds, being driven by primarily estradiol-mediated mechanisms. Migratory birds are once again subject to particular stressors during reproductive periods, such as switching rapid from physiology and energetics associated with long-distance flight to egg production, song production, nest building, territorial defenses, and parental behavior, all of which rely on functioning endocrine pathways and feedback loops. Developmentally, songbirds and other passerine species are altricial, while ducks, quail, and other ground dwelling species are generally precocial. This developmental difference appears to relate to the extent and timing of sensitivity to EDCs because precocial species are fully functional and relatively independent at hatch. They undergo sexual differentiation in ovo; similarly, other physiological systems are also well developed at hatch as compared to altricial birds that require intensive parental care. These developmental differences can be greatly impacted by the degree of maternal transfer of environmental toxicants. Lipophilic compounds such as PCBs are primarily sequestered in egg yolk, which is used in the latter part of in ovo development and in the first few days posthatch. The exact timing of the transfer of EDCs into the developing embryo could greatly impact brain, neuroendocrine function, and gonadal development, and this can vary with the degree of development at hatch. Finally, the potential for adverse effects of EDCs on long- or short-lived birds is unknown especially in the context that long-lived birds tend to have small clutches and raise fewer chicks per year compared to short-lived birds (Holmes and Ottinger, 2003; Ottinger et al., 2009a; Ottinger, 2005).

48.2.2.2 Effects of environmental chemical impacts in wild birds

Historically, there are many studies in wild birds that document cases of exposures with higher concentrations of toxicants originating from chemical applications and industrial spills. Often these occurrences were associated with high mortality; thereby prompting federal and regional responses aimed at protecting human and wildlife health. However, less is known about nonlethal impacts of EDCs on wild birds and the potential for adverse effects translating even to the level of a risk to the population. The deleterious effects of DDT were recognized as adverse effects of a pesticide exerting endocrine disruption of an estrogen dependent process in bald eagles, resulting in egg shell thinning (Lundholm, 1997). As a consequence, embryonic eagles failed to develop to hatch. In addition, there are extensively documented cases, such as incidences of avian impacts from the Great Lakes, PCBs released into the

Housatonic and Hudson Rivers and the Gulf of Mexico Macondo Oil Spill that indicate impacts on birds (Best et al., 2010; Bowerman et al., 2007; Burger, 2018; Champoux et al., 2020; Custer et al., 2010a; Darnerud, 2003; Franceschini et al., 2008). Data from some extraordinary datasets are emerging from long-term monitoring and research programs, such as the Great Lakes region, Chesapeake Bay Programs, and The Gulf of Mexico (Gulf of Mexico Avian Monitoring Program https://gomamn.org); many of these studies have considered physiological and reproductive impacts of exposure to chemicals found in those areas (Deepwater Horizon Natural Resource Damage Assessment Trustees, 2016). Laboratory studies have provided additional insights into potential mechanisms of action of EDCs as well as periods of sensitivity throughout the life cycle. Information from many of these studies will be discussed below in order to put the proposed two-generation test into the context of testing in avian species. Furthermore, it is important to consider unique characteristics of the avian physiology with emphasis on sexual differentiation, hormonal modulation of endocrine and behavioral components of reproduction, and functional impacts of EDCs on neuroendocrine regulatory systems, especially considering potential adverse outcomes.

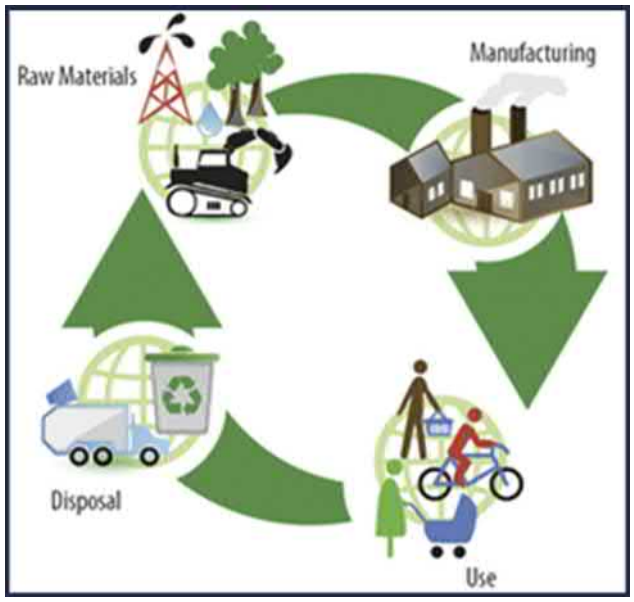

FIGURE 48.1 Diagrammatic representation of the life cycle of industrial compounds; once manufactured, they are used and then disposed allowing reentry into the environment. *From: Environmental Protection Agency "Risk Management Sustainability Technology" http://www.epa.gov/nrmrl/std/lifecycle.html.*

48.3 Life cycle of chemicals: endocrine disrupting chemicals in the environment

48.3.1 Parent compounds and their metabolites in the environment

There are many sources of chemical contaminants, including EDCs in the environment, and there are excellent resources available to search for information and distribution about many of these compounds. For example, the United States Geological Service (USGS) has a Contaminant Exposure and Effects—Terrestrial Vertebrates Database provides a searchable database containing over 20,000 records that provide information on taxonomy and chronology of ecotoxicological exposure and effects as well as geographic location of contaminants (see http://www.pwrc.usgs.gov/contaminants-online/pages/ceetv/ceetvintro.htm). In considering the use and fate of environmental chemicals, it is important to consider the life cycle of a chemical or compound (Figure 48.1). The fate of a compound in the environment relates to both the movement in soil, water, and air as well as the metabolism of the parent or original chemical. Some chemicals enter directly into the air as a consequence of the manufacturing process, such as in the case of airborne chemicals through smoke stacks or steam. Moreover, chemicals in the environment become metabolized with exposure to air, sun, heat, and microbial metabolism. Metabolites of parent compounds are often bioactive and, in some cases, impact different physiological targets with even greater toxicity than the parent compound. Alternatively and more frequently, chemicals are manufactured for a specific purpose such as in the case of DDT, which as an effective insecticide became ubiquitous in the environment with wide use as a pesticide and in the battle against malaria-carrying mosquitos (Asawasinsopon et al., 2006; Borga et al., 2007; Braune et al., 2005; Rattner, 2009). As may be seen in Figure 48.2, DDT applied to fields as an insecticide then migrates into the water via rain events and runoff into waterways and ultimately into the groundwater. In the rivers and streams, DDT becomes part of the food chain by ingestion into invertebrates, which are eaten by fish and eventually by organisms higher on the food chain. This brings to attention the effects, meaning. In this example, effects were observed in bald eagles and more recently in herons at Lake Michigan on egg shell thinning (Lundholm, 1997; Rattner, 2009). The life cycle of DDT also includes metabolism into dichlorodiphenyldichloroethylene (DDE), an antiandrogenic compound in vertebrates (Bowerman et al., 2007; Quinn et al., 2008). Although banned in the United States in 1972 as well as in many parts of the world, significant concentrations of DDT and its metabolites are found in agricultural areas and in wildlife living and breeding in proximity to areas that had wide use of DDT as an insecticide (Weseloh et al., 1990; Mora et al., 2016). Further, the use of DDT continues in some countries battling persistent malaria-carrying mosquitos, including providing mosquito netting impregnated with DDT to families with

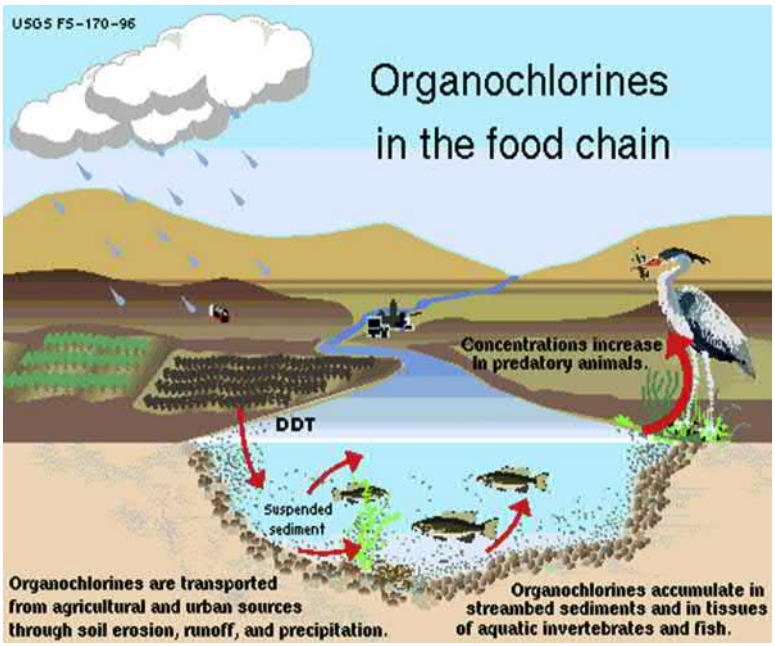

FIGURE 48.2 The life cycle of DDT in the environment from application on fields, transport to aquatic environments, uptake by invertebrates and fish that are eaten by higher vertebrates higher on the food chain. *From U.S. Department of the Interior-USGS Fact Sheet 170–96; https://pubs.usgs.gov/fs/1996/0170/report.pdf.*

young children. Alternative chemicals related to DDT have also been developed to address the need for effective pesticides, including dicofol and methoxychlor, both of which have been linked to adverse impacts in birds and transfer into the eggs of exposed females (Wiemeyer et al., 2001; Kamata et al., 2010).

48.3.2 Environmental contamination by industrial chemicals and mixtures

In the case of industrial compounds, such as crude oil, lubricants, plastics, flame retardants, and nanofibers, there may be purposeful or inadvertent release into the environment, especially at the time of usage or disposal. This is the case with the release of polychlorinated biphenyls (PCBs) into the environment, which occurred both as a consequence of the manufacturing practices for electrical transformers containing Aroclors® and affected the Housatonic River in western Massachusetts (Custer and Read, 2006; Custer et al., 2012a; Barnthouse et al., 2003). Similarly, General Electric's Hudson Falls and Fort Edward plants discharged PCBs into the upper Hudson River from 1947 until 1952 (http://www.darrp.noaa.gov/northeast/hudson/index.html). This, in combination with leakage of these compounds from the manufacturing process for capacitors resulted in long-term contamination of the river and continued persistence of PCBs in the environment (Erickson et al., 2005; Butcher and Garvey, 2004; Cho et al., 2002; Foley, 1992; Man et al., 2011). Not only do PCBs have a very long half-life in the environment, they also remain chemically stable in the sediment and become available when the sediment is disturbed. Further, measurements in tree swallow and sandpiper eggs, respectively, revealed that there were two mixtures present in the Hudson River environs; reflecting both released congeners and other congeners associated with metabolism (Echols et al., 2004; Nichols et al., 2004). As such, there are dynamics in the environment including rainfall events as well as climate change that will impact the movement and potential for exposure across living organisms.

As initially discussed above, it is most common to have mixtures of chemicals occurring in the environment, which in turn become incorporated into the body burden carried by all vertebrates, including humans and wildlife. As such, there is a growing literature focused on understanding exposure and persistence of these chemical mixtures in the environment and retention in the body, generally in the fatty tissue as many of these chemicals are lipophilic compounds. In addition, it is unclear how the compounds that constitute the complex mixture interact, specifically do these compounds have synergistic actions? Further, metals are often in these mixtures but rarely considered as a component; thereby not included in an assessment of risk from exposure.

48.4 Classes of endocrine disrupting chemicals and their physiological actions

As mentioned earlier, the Environmental Protection Agency (EPA) formed a federal advisory committee, the

Endocrine Disruptor Screening and Testing Advisory Committee in 1996 to consider the specific risks from exposure to EDCs and recommend appropriate regulatory measures (see http://www.epa.gov/endo/pubs/edspoverview/edstac.htm). Over two years, EDSTAC considered the complexities of potential and recognized EDCs, risks to vertebrate and invertebrate organisms, and recommended a series of testing paradigms to be developed and verified (see http://www.epa.gov/endo/pubs/edspoverview/finalrpt.htm for EDSTAC final report). These tests would include screening and testing, utilizing cell-based screens and bioassays sensitive to endocrine disruption of the reproductive and thyroid endocrine systems. The tests were separated into Tier 1 containing in vitro high-throughput screens to allow rapid assessment and identification of endocrine active compounds and in vivo specific assays to target known EDC mechanisms of action (Table 48.1) primarily focused on estrogenic, androgenic, or thyroid active compounds (Table 48.2). Tier 1 assays serve to identify compounds for in depth tests in Tier 2 multigenerational tests, to capture periods of vulnerability to EDC effects (Touart, 2004). There are a range of two-generation tests, including the medaka multigeneration test, Japanese quail two-generation test (JQTT), mysid two-generation toxicity test, and larval amphibian growth and development test. All tests are reviewed by expert panels (FIFRA Science Advisory Panels) for use in regulatory oversight of current and emerging chemicals. Further review and updated regulatory guidelines continue as more is learned about the actions, risks, target organisms, and of EDCs.

48.4.1 Categorizing endocrine disruptors according to structure and function

Many factors impact the passage and life cycle of chemicals in the environment and affect the potential for exposure to living organisms. Moreover, individuals are generally exposed to multiple environmental chemicals concurrently and all living organisms carry some chemical contaminant burden within their body. There have been attempts to organize potential and proven EDCs into classes of chemicals, grouped by mechanism of action, physiological target, and relative activity including capacity for toxicity. These groupings are based on

TABLE 48.1 List of assays proposed by the endocrine screening and testing advisory committee.

Assay	Reason for inclusion
Estrogen receptor binding or transcriptional activation assay	An in vitro test to detect chemicals that may affect the endocrine system by binding to the estrogen receptor.
Estrogen receptor transcriptional activation assay	An in vitro test to detect chemicals that may affect the endocrine system by binding to the estrogen receptor.
Androgen receptor binding assay	An in vitro test to detect chemicals that may affect the endocrine system by binding to the androgen receptor.
In vitro steroidogenesis assay	An in vitro test to detect chemicals that interfere with the synthesis of the sex steroid hormones
Placental aromatase assay	An assay to detect interference with aromatase.
Uterotrophic assay	An in vivo assay to detect estrogenic chemicals.
Hershberger assay	An in vivo assay to detect androgenic and antiandrogenic chemicals.
Pubertal male	An in vivo assay to detect chemicals that act on androgen or through the hypothalamic–pituitary–gonadal (HPG) axis that controls the estrogen and androgen hormone systems. It is also enhanced to detect chemicals that interfere with the thyroid system. This assay could in part substitute for the female pubertal assay.
Pubertal female assay	An in vivo assay to detect chemicals that act on estrogen or through the HPG axis that controls the estrogen and androgen hormone systems. It is also enhanced to detect chemicals that interfere with the thyroid system.
Amphibian metamorphosis assay	An in vivo assay for detection of chemicals that interfere with the thyroid hormone system.
Fish screening assay	An in vivo assay for detection chemicals that interfere with the HPG axes.

Assays recommended for consideration for the Tier 1 screening battery.
From EPA publication October 21, 2009; Tier 1 Screening Battery; http://www.epa.gov/endo/pubs/assayvalidation/tier1battery.htm.

TABLE 48.2 The mechanism considered in the selection of screening tests; tests focus on known and potential mechanisms of action for compounds having endocrine disrupting activity

	Modes of action							
	Receptor binding				Steroidogenesis			
Screening assays	E[b]	Anti-E	A[b]	Anti-A	E[b]	A[b]	HPG[c] Axis	HPT[c] Axis
In vitro								
Estrogen receptor binding[a]	■	■[d]						
ERα transcriptional activation	■							
Androgen receptor binding[a]			■	■				
Steroidogenesis H295R					■	■		
Aromatase recombinant					■			
In vivo								
Uterotrophic	■							
Hershberger			■	■		■		
Pubertal male			■	■		■	■	■
Pubertal female	■	■[d]			■		■	■
Amphibian metamorphosis								■
Fish short-term reproduction (male and female)	■	■[d]	■	■	■	■	■	

Complementary Modes of Action among Screening Assays in the EDSP Tier 1 Battery.
[a]*Estrogen and Androgen Receptor binding.*
[b]*Estrogen and Androgen.*
[c]*Hypothalamic–pituitary–gonadal or–thyroidal axis.*
[d]*Assays are expected to detect antiestrogens, but this was not established during the validation process since no estrogen receptor antagonists were tested.*
From http://www.epa.gov/endo/pubs/assayvalidation/tier1battery.htm.

structure-function relationships and when available, on experimental findings in the literature for a specific or similar compound (Le Page et al., 2011; Newbold et al., 2008; Safe et al., 1998; Watanabe et al., 2002; Zacharewski, 1998; Foster, 1998; Kavlock and Ankley, 1996). A great deal of emphasis has gone into understanding the actions of xenoestrogens because much of the initial recognition of endocrine disruption from antiestrogenic effects of DDT and subsequently compounds and mixtures that are androgen active, either having androgen like activity or antiandrogenic actions. In addition, many compounds including polybrominated biphenyls, triphenyl phosphate, PCBs, and others target the thyroid axis as well as metabolic function; with variable effects in field birds (Marteinson and Fernie, 2019; Nossen et al., 2016; Ruuskanen et al., 2019). The perfluoroalkyls are gaining increasing attention as EDCs and emerging as a contaminant impacting birds (Guigueno and Fernie, 2017; Guigueno et al., 2019; Vorkamp et al., 2019), and evidence that polycyclic aromatic hydrocarbons (PAHs) from crude oil can impact the adrenal axis (Lattin and Romero, 2014; Lattin et al., 2014). Finally, there is increasing recognition that environmental chemicals are inherently stressors, with a wide range of other actions on the immune response, growth, epigenetic actions associated with alterations at the genetic level, and lifetime effects on metabolism and overall fitness. Therefore, it is critical to continue to refine the detection and characterization of environmental chemicals and complex mixtures.

Analysis of the chemical structure of a compound provides valuable insight into the potential actions and physiological targets. In the case of PCBs, there is increasing toxicity associated with the number of and molecular placement of chlorine atoms. Extremely toxic compounds, such as dioxins, particularly 2,3,7,8-tetrachlorodibenzodioxin, provide a "yardstick" for comparison of toxic effects from other toxicants with the same mode of action (activation of the AhR). As pointed out earlier, it is challenging to discern frank toxicity from endocrine disruption, given the complexity of the endocrine systems, variation among individuals and plethora of compensatory physiology mechanism. Therefore, it has become important to utilize approaches, such as AOP (details provided below) that describe the suite of effects associated with exposure to a compound or mixture.

Because the presumed targets of EDCs have been the reproductive axis and more specifically via interaction with steroid hormone receptors, many of the strategies for high-throughput screening have utilized cell-based systems that detect interactions with these steroids (Fisher, 2004; Hartig et al., 2002; Kase et al., 2009; Kusk et al., 2011; D'ursi et al., 2005). However, these in vitro approaches must be integrated with information about physiological and toxicological effects. As a consequence, computer-based predictive models have been developed that provide a rapid method for ascertaining potential endocrine activity based on structure-function and known mechanisms of action (Wambaugh et al., 2013; Knudsen et al., 2013; Kavlock et al., 2012; Martin et al., 2009; Dix et al., 2007; Basu, 2015). As more information becomes available, these approaches provide a powerful technique for assessing the potential for emerging chemicals to be endocrine disruptors.

48.4.2 Mechanisms of action of endocrine disrupting chemicals in vertebrates

There is an extensive literature that clearly demonstrates the interaction of EDCs and steroid hormone receptors, particularly xenoestrogens, androgens, and thyroid hormone active compounds (Kusk et al., 2011; Zhang and Trudeau, 2006; Masuyama et al., 2002). There are conserved mechanisms of action found for birds, mammals, and other vertebrates in response to EDC exposure. In addition to extensive databases and mechanism-based models, a number of investigations have explored the mechanisms of endocrine disrupting activity, in mammals, birds, and other taxa (Stoker et al., 2000; Zacharewski, 1998; Watanabe et al., 2002; Le Page et al., 2011; Janer et al., 2005; Gore, 2010; Harvey and Everett, 2006). A number of EDCs are estrogen mimics, interacting with estradiol receptors and/or with estrogen responsive systems as agonists or antagonists (Watson et al., 2014; Hall and Korach, 2002; Marino et al., 2012; Felton et al., 2015; Jimenez et al., 2007). Conversely, DDE, trenbolone, and others having potent androgenic or antiandrogenic actions (Hartig et al., 2007; Manikkam et al., 2013; Soto and Sonnenschein, 2010; Guerrero-Bosagna and Skinner, 2009; Prins, 2008; Skinner, 2007; Maffini et al., 2006; Bigsby et al., 1999; Santti et al., 1998; Quinn et al., 2007a,b). Many of the assays developed have taken advantage of the mechanisms revealed by these studies, as for example, the vitellogenic effects of EDCs in fish (Wang et al., 2011; Larkin et al., 2002). It is also important to recognize that there are effects of EDC exposure, which may reflect some direct toxicological effects of these compounds in addition to endocrine effects (Fucic et al., 2012; Carro et al., 2013a,b; Quinn et al., 2007b). Furthermore, induction of cancer in reproductive organs has also been linked to EDC exposure (Ohlson and Hardell, 2000; Fucic et al., 2012). There are additional specific vulnerabilities associated with unique characteristics of birds that must be considered in order to accurately assess potential for adverse outcomes from exposure, which will be discussed in more detail later in this chapter.

48.4.3 Interactions of endocrine disrupting chemicals and specific receptors

Interactions with receptors depend on the structural characteristics of the EDC. In the case of PCBs, the toxicity and relative impacts relate to the number and location of chlorine molecules on the ring structure (Figure 48.3, Fischer et al., 1998; Hennig et al., 2002). Primary effects of EDCs rely on the ability to interact with steroid or thyroid hormone receptors, which then exert competitive inhibition or antagonistic effects; or in some cases may be stimulatory with agonistic effects. The up- or down-regulation of cellular processes via interaction with these receptors then has the capacity to alter a host of physiological functions that are modulated through steroid hormone or thyroid hormones. Although less is known about the potential for EDCs to act on the stress axis, a stressed individual would be predicted to be more vulnerable to other insults such as those from EDC exposure (Burger, 2018; Fairbrother et al., 2004; Fairhurst et al., 2017; Fernie et al., 2005a; Grasman, 2002; Grasman et al., 1998; Franceschini et al., 2008; Perez et al., 2017a,b,c). Studies on the effect of crude oil on the hypothalamic–pituitary–adrenal (HPA) axis (Lattin and Romero, 2014; Lattin et al., 2014), suggest that PAHs can directly impact the adrenal gland, reducing the ability of house sparrows (*Passer domesticus*) to mount a stress response and also reduce glucocorticoid receptor density.

Data are emerging that demonstrate effects of EDCs on multiple growth and differentiation factors, which in turn affect the ontogeny of that organ system as well as impact function in the mature individual (Thackaberry et al., 2005; Walker and Catron, 2000; Head et al., 2008). For example, effect of EDCs on the ryanodine receptor has been shown to impact calcium signaling, which in turn alters neural function, neurodevelopment, and neurodegenerative processes (Pessah et al., 2010). EDCs have the potential to affect immune function both short- and long-term in individuals and can be especially potent if there are other environmental stressors (Schug et al., 2011; Ottinger et al., 2005a; Quinn et al., 2007a, Lavoie et al., 2010). At a more cellular level, dioxins, PAHs, and other EDCs have been shown to affect oxidative damage processes, with potential to impact mitochondrial function (Pereira et al., 2013). As such, the impacts of EDCs on endocrine function should not only consider "cross-talk" effects of the thyroid, stress, immune, reproductive, and growth axes with other physiological systems, but should also consider the additive impacts of environmental stressors other than EDCs.

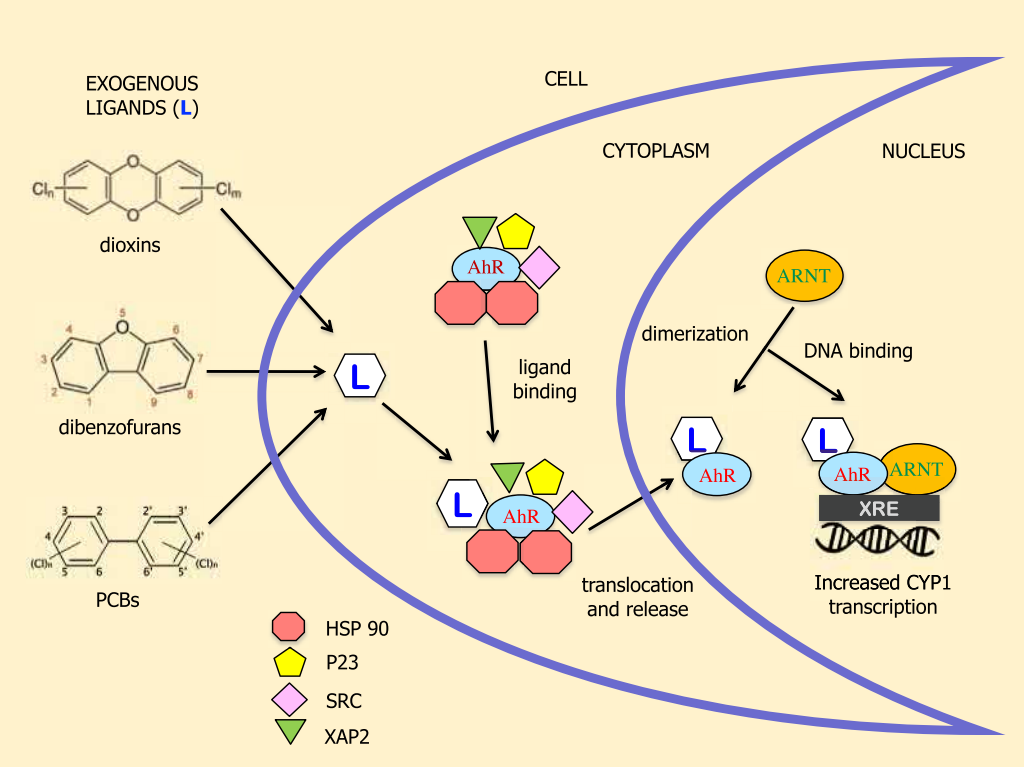

FIGURE 48.3 Aryl hydrocarbon Receptor (AhR) signaling pathway is comprised of interaction of endocrine disrupting chemicals with affinity to AhR, translocation of the complex to the nucleus, dimerization, and binding of the aryl hydrocarbon nuclear translocator complex to the xenobiotic response element on the DNA ultimately leading to increased transcription of CYP mRNA for translation to CYP enzymes.

48.4.4 Discerning endocrine disrupting chemical impacts in field birds

Effects of toxicants that affect wild populations of birds have often been associated with spills and critical exposures that gained attention due to the death of a number of individuals, such as the Deepwater Horizon or *Exxon Valdez* oil spills. Conversely, it is often difficult to detect nonlethal effects in wild populations due to the lack of curated data that includes individuals and associated metadata for the presence of environmental chemicals in the environs. Brown pelicans (*Pelecanus occidentalis*) studied along the Louisiana coastline (Gulf of Mexico) prior to and during DWH oil spill suffered from habitat destruction, including loss of preferred nesting sites in shrubby vegetation resulting in reproductive losses in 2010 following the DWH spill (Walter et al., 2013). When considered on its own, this is likely to be construed as a reproductive loss due to stressors on nesting pairs; however, in study along the coast of the Gulf of Mexico that was unrelated to oil spill damage, researchers found that nestling feather corticosterone levels were lower in chicks raised in the preferred elevated nest sites (Lamb et al., 2016), indicating that there may be further physiological and epigenetic effects to offspring from the oil itself, and the consequences of habitat destruction caused by the spill. As such, it is sometimes difficult to separate impacts of environmental chemicals from other stressors. Further, tracking data for birds, especially through migration is gradually becoming more available, as are more sensitive methods for detecting endocrine disruption. This will provide more complete metadata that will help inform the sum total of challenges faced by an individual as well as the population. Moreover, large data sets on wild birds are already available from the USGS Bird Banding lab and from annual surveys for species and individuals and other databases in eBird (https://ebird.org/home; The Cornell Lab of Ornithology). In addition, there are a number of monitoring studies and programs with short- and long-term data on the status of avian populations. Consolidating these monitoring data can provide valuable information on populations and health metrics for natural resources managers (Ottinger et al., 2019) and in combination with metadata on environmental chemicals, can provide potential risk estimates from effects of exposure over an individual's lifetime.

48.4.5 Establishing reliable and sensitive measures of adverse impacts

It is a challenge to develop reliable and sensitive measurement endpoints that can serve as indices of exposure in

birds, especially those that are field-friendly. It is particularly useful to select endpoints that are bioindicators; this requires understanding the association of an adverse impact on the individual and risk to populations as a whole. Exposure to steroid hormones or EDCs disrupt embryonic development including organ development, sexual differentiation, reproduction and immune function, reproductive behavior, and metabolic processes (Best et al., 2010; Berg et al., 1999; Darnerud, 2003; Ottinger et al., 2005a,b; Fernie et al., 2005a; Franceschini et al., 2008; Fox and Grasman, 1999). Biomedical and epidemiological data reveal clear linkages between EDC exposure, particularly early events and later disease and possibly epigenetic effects. In addition, field studies correlated EDC exposure to immunosuppression in a number of taxa, demonstrating that the effects of these compounds have conserved mechanisms and impact a range of species, including invertebrates. Laboratory studies have been successful in establishing clear effects of various classes of EDCs on a number of physiological systems (Berg et al., 1998; Halldin et al., 2005). Because many of the initially identified EDCs of concern, such as methoxychlor, dioxin, and some PCBs, have estrogenic activity. However, at any one time, wildlife species are actually exposed to many different types of EDCs (e.g., androgenic, thyroid active) as well as other toxicants; these mixtures often contain chemicals with potentially different mechanisms of action (e.g., metals) (Levengood et al., 2007; Hotchkiss et al., 2008). As a result of this complexity, it has been difficult to develop comprehensive risk assessment models. Furthermore, as mentioned above, some EDCs such as DDE are androgen receptor blockers, whereas other compounds such as trenbolone are androgenic (Mura et al., 2009; Panzica et al., 2007; Quinn et al., 2007a, 2008). As in mammals, EDCs are physiologically active on the reproductive endocrine system as well as on a variety of pathways, including not only steroid sensitive pathways but also pathways involving thyroid, metabolic, stress, and immune systems (Crump et al., 2016; Head et al., 2008; Fairbrother et al., 2004; Fernie et al., 2005a; Fox and Grasman, 1999; McNabb and Fox, 2003; Kavlock and Ankley, 1996; Knudsen et al., 2009; Qasimi et al., 2018; Quinn et al., 2007a,b). Complexities of differential EDC sensitivity among species and even within a species to different classes of EDCs, as well as differential exposure add another layer of complexity that must be considered for all wildlife, not just birds.

48.5 Methods for assessing risk

48.5.1 Predicting impact: toxic equivalency factor and toxic equivalent quotient

There is a large body of literature on the role of the AhR in response to exposure to toxicants. The signaling pathway showing activation of the AhR by dioxin or dioxin-like compounds has been well characterized; initial interaction of an EDC with the AhR triggers a cascade leading to translocation into the nucleus. After dimerization, the aryl hydrocarbon nuclear translocator complex binds to the xenobiotic response element on the DNA with transcription of mRNA for translation into CYP proteins (Figure 48.3). This AhR response to dioxin-like compounds has become an accepted toxicological measure for environmental chemicals to estimate the toxic equivalency factor (TEF) for a compound. An arithmetic calculation of added TEFs provides an estimate of toxicity potential for a mixture or compound that is termed the toxic equivalent (TEQ). The standard for comparison is dioxin (2,3,7,8-tetrachlorodibenzo-p-dioxin; Figure 48.4). Structure and functional data derived from the literature and other information relative to the functional similarities compared to dioxin are used to ascertain the relative toxicity against dioxin (van den Berg et al., 2013). For example, the structure and functional comparison for polychlorinated biphenyl 126 (PCB 126) compared to dioxin is shown in Figure 48.4. This TEQ for PCB 126 only accounts for dioxin-related activity and does not consider separate nondioxin or endocrine disrupting activity. That said, in birds as well as other vertebrates experience, a range of adverse physiological outcomes have been documented with exposure to dioxin (Hervé et al., 2010; Hsu et al., 2007; Kuil et al., 1998; Watanabe et al., 2009). Further, some dioxin-like EDCs do activate the AhR in a species-specific manner across as a relative measure among avian species (Head et al., 2008). These studies have demonstrated a wide variation in the vulnerability of avian species to toxicants, with molecular differences at the level of the AhR ligand-binding domain structure, and that these changes function across avian species (Farmahin et al., 2012; Karchner et al., 2006; Manning et al., 2012; Zhang et al., 2013). It is clear that as in mammals, EDCs can exert wide-ranging effects of

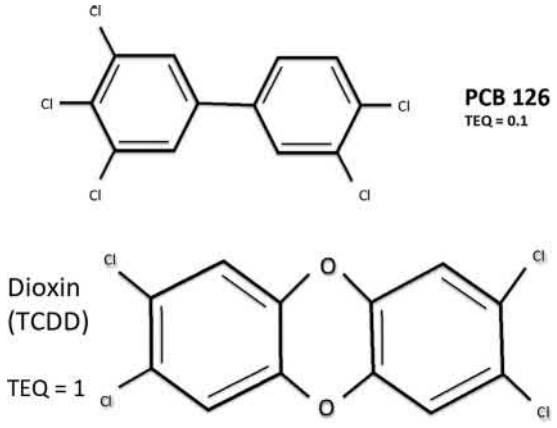

FIGURE 48.4 Structures of polychlorinated biphenyl 126 (PCB 126) with a toxic equivalency quotient (TEQ) of 0.1 compared to dioxin with a TEQ of 1.

these compounds and mixtures on endocrine processes in birds, with the potential for lifetime effects that will impact fitness of the individual and ultimately have a potential population fitness level impact.

48.6 Frameworks for visualizing risk and effects from endocrine disrupting chemical exposure

48.6.1 Visualizing predicting risk through influence diagrams and adverse outcomes pathways

A number of approaches have been developed to conceptualize the myriad of effects associated with sublethal toxicity with the overall intent to span molecular and cellular effects to the whole organism and eventual population level impacts. A comprehensive approach has been developed and termed AOPs. This approach has been conceptualized and applied for specific compounds in birds as well as applied to aquatic species (Lalone et al., 2013; Villeneuve et al., 2014; Ankley et al., 2010; Currie et al., 2005; Doering et al., 2018). Subsequent studies will utilize this and other approaches will underpin assessing the risks associated to establish probable outcomes with exposure to EDCs and establish data-based models for the potential for population level effects. In addition, it will be critical to integrate data collected from these and future studies to further refine the mechanisms that are responsible for both short- and long-term impacts to individuals and ultimately potentially for adverse outcomes to wildlife and human populations (Ottinger et al., 2013; Villeneuve et al., 2014; Zawatski and Lee, 2013). Influence diagrams and AOPs (Hotchkiss et al., 2008) are both important tools for conceptualizing effects of EDCs including fundamental actions and molecular targets and linking impacts to organism and population levels. As reviewed below, both approaches are extremely useful to gaining an understanding of the mechanisms and actions of environmental chemicals as well as insights useful for assessing potential risk. Additionally, both influence diagrams and AOPs can be customized for species and taxa.

48.6.1.1 Influence diagrams

Developing an *influence diagram* that captures exposure risks and potential impacts for field birds is challenging due to many uncertainties, such as consistency and doses of exposures, presence of complex mixtures of compounds, climate change, weather events, anthropogenic factors including habitat loss and resource availability. It is helpful to visualize primary stressors as well as their downstream effects in order to understand interactions and drivers impacting field birds. Influence diagrams visualize impacts from the Gulf of Mexico Macondo Oil Spill to birds in the Gulf and coastal environs (Figure 48.5A and B). These diagrams bring to light both potential toxicity as well as the lesser understood nonlethal physiological impacts on wild birds and adverse effects translating to population level risk. In birds, one of the most commonly observed impacts of oil exposure is feather fouling. Extreme levels of feather fouling may lead to loss of buoyancy and thermoregulatory ability, then death (Perry et al., 1978; Lambert et al., 1982; O'Hara and Morandin, 2010). Lesser oil coverage will likely cause birds to begin preening feathers to remove oil. Not only will these birds likely spend less time foraging during this period and find thermoregulation more energetically expensive (Jenssen, 1994; Walton et al., 1997; Burger and Tshipoura, 1998; Mathewson et al., 2018), they will also inadvertently expose themselves and incubating eggs to the toxic effects of oil. Through the mechanical process of preening oil may be swallowed, fumes may be inhaled, skin can become irritated and oil may be transferred to a nest. This oil will reach organ systems and activate liver detoxification pathways causing anemia, cardiac and gastrointestinal tract damage, loss of liver and kidney function, immune and adrenal dysfunction, and oxidative damage (Bursian et al., 2017; Dean et al., 2017; Harr et al., 2017a,b,c; Horak et al., 2017; Maggini et al., 2017a; Pritsos et al., 2017; Bianchini and Morrissey, 2018). Not only will the mechanical damage to feathers reduce flight efficiency (Maggini et al., 2017b,c; Perez et al., 2017a,b), organ damage and anemia will further reduce an individual's chance of survival. The EDC effects of PAHs on adult birds are not well understood, but they can result in loss of breeding success, nest abandonment, reduced parental care, and adrenal dysfunction (Peakall et al., 1981; Fry et al., 1986; Eppley and Rubega, 1990; Fowler et al., 1995; Walton et al., 1997; Lattin and Romero, 2014; Lattin et al., 2014).

Information from both laboratory and field research are considered in building the influence diagram to include outcomes and potential risks, including those for which additional testing is warranted. All aspects are critical in order to conduct an informed risk analysis. A further example of an influence diagram shown in Figure 48.7 presents a more detailed focus on physiological responses to selected environmental stressors. In this influence diagram, each of the selected environmental stressors are linked to one or more physiological responses, which in turn interact. Effects of these stressors translate into responses that can be monitored via specific metrics or measures. Furthermore, this influence diagram incorporates unique physiological characteristics and responses of birds; migration and exposure to different geographic regions are additional potential sources of stress.

There are a number of examples of well-documented environmental contamination events that impact birds.

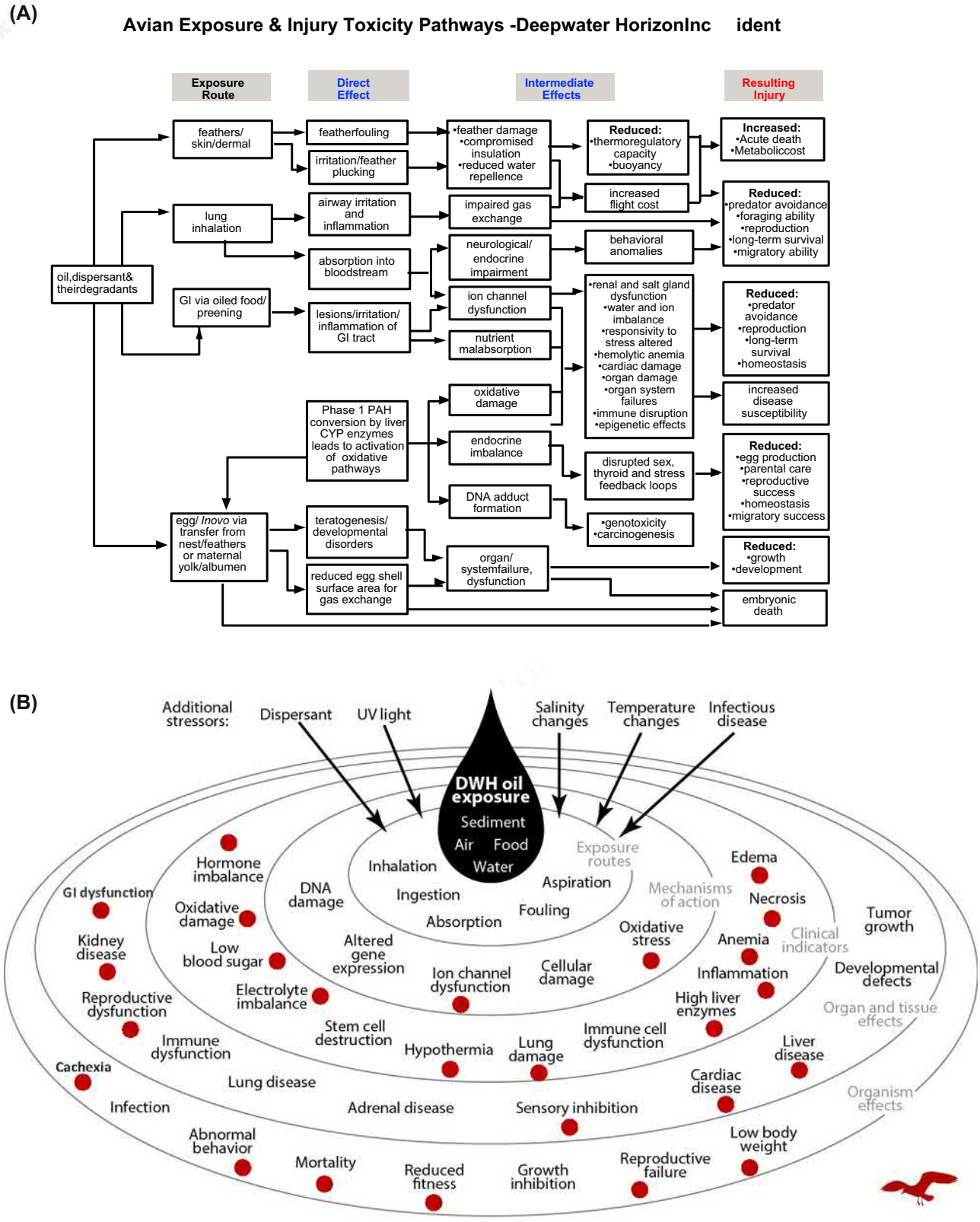

FIGURE 48.5 (A) and (B): Influence diagrams showing alternate depictions of potential routes of exposure, direct and intermediate effects, responses, and fate for birds exposed to toxicants associated with the Deepwater Horizon Oil Spill. (A). This diagram depicts how exposure routes, mechanisms of action, clinical indicators, organ and tissue effects, and organism effects (shown in light gray) in birds can be broadly linked. Oil toxicity will manifest differently in each exposed individual, leading to different combinations of the outcomes listed in this diagram. The diagram includes information from DWH NRDA studies, as well as from the literature. *(A) Adapted from illustration by Milton et al. (2003); Hooper, M.J (US Geological Survey) and Ottinger et al. (2019); In Gulf of Mexico Avian Monitoring Network Strategic Avian Monitoring Plan. eds.: Wilson, RR, Fournier AMV, Gleason JS, Lyons JE, Woodrey M. Mississippi State University, Research Bulletin 1228, 2019), depicts the multiple downstream physiological and behavioral impacts of oil on exposed birds. (B). Diagram adapted from the Deepwater Horizon Final Programmatic Damage Assessment Plan Chapter 4: Injury to Natural Resources (https://www.gulfspillrestoration.noaa.gov/sites/default/files/wp-content/uploads/Chapter-4_Injury_to_Natural_Resources_508.pdf). Reproduced with permission from Abt Associates Takeshita et al. (2016), Lipton et al. (2017).*

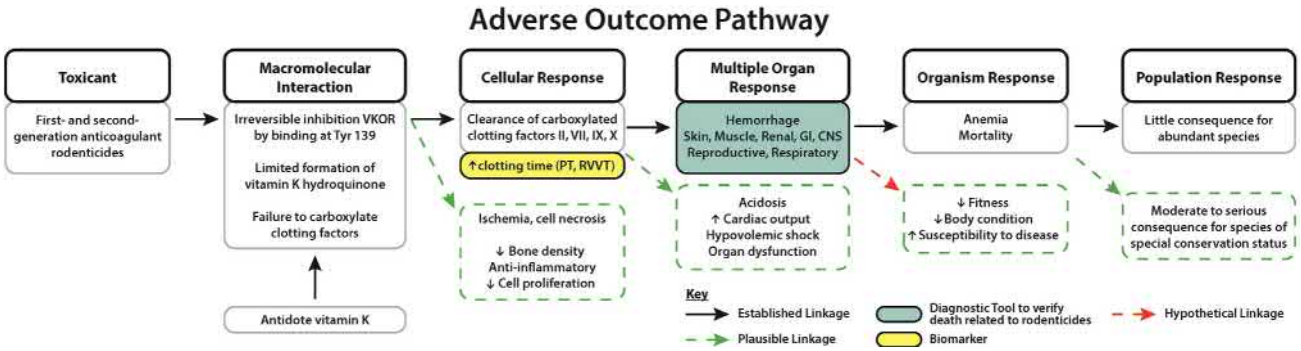

FIGURE 48.6 The Adverse Outcome Pathway visualizes effects of exposure to anticoagulant rodenticides, showing molecular and cellular mechanisms of action on physiological targets, leading to a sequential cascade impacting multiple organs leading to adverse impacts to the individual organism and eventually to the population. *Reprinted with permission from Rattner et al., 2014. Copyright 2014 American Chemical Society.*

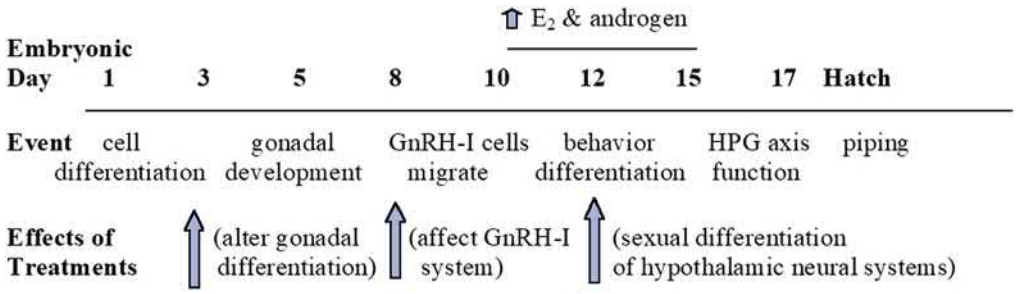

FIGURE 48.7 Stages in Embryonic Development. Diagram shows timing of developmental events during embryogenesis with indications of endogenous endocrine change and potential periods of vulnerability.

These include industrial chemical contamination in the Great Lakes and effects on eagles and other vertebrate species, dioxins released into the Tittabawassee River, PCB congeners released into the Housatonic and Hudson Rivers, and impacts of the *Exxon Valdez* and Gulf of Mexico Deepwater Horizon oil spills on birds and other taxa (Custer et al., 2010a,d, 2012a,b; Custer and Read, 2006; Franceschini et al., 2008; Levengood et al., 2007; Esler et al., 2018). It is important to synthesize data on these incidents of localized or widespread chemical contamination; influence diagrams can provide an effective way to diagrammatically visualize the impacts and risks to wild birds and ultimately assess the potential for population level effects.

48.6.1.2 Adverse outcomes pathways

Similarly, the AOP allows visualization of the actions of EDCs at the molecular and mechanistic level, and relates these actions to subsequent effects on physiological systems, and to the organism, and potentially population level effects. An example of an AOP is shown in Figure 48.6 (Rattner et al., 2014) visualizes the entire cascade of impacts from rodenticide exposure going from molecular and cellular responses on the left and the impacts of these responses to organ function and eventually the adverse outcomes to both the individual organism and the population. These examples of AOPs demonstrate not only the mechanisms of action by compounds on physiological targets but also the flow down effects to impair the fitness of the bird, ultimately leading to individual and potential population decline.

48.6.2 The one health concept

The *one health concept* brings together the powerful interrelationship between human and wildlife health with ecosystem health. The initial concept of One Health focused on disease transfer from wildlife to human populations (Destoumieus-Garzon et al., 2018). More recently, it is recognized that resilience to environmental stressors, including disease, align with the health of the ecosystem (Lerner and Berg, 2017; Rabinowitz et al., 2018). As such, the definition of One Health has broadened to consider environmental factors and ecohealth as essential components of the health of wildlife with resources and tools to promote implementation of multidisciplinary and multisector collaborations (Vesterinen et al., 2019). This broadened definition of the One Health concept requires this multidimensional approach incorporating factors such as health, stressors, disease incidence, societal pressures, and environmental factors. This includes selecting key

health measures, metrics to assess the impacts of stressors, such as habitat loss, anthropogenic stress, environmental toxicants, disease, climate change, among others. More specific measures of health for people, wildlife, and birds could include overall physical health, immune, metabolic, and endocrine function as well as nutrition/food availability. possible contributing factors, such as environmental toxicants, taxa specific resource availability, and species-specific characteristics, including lifespan and habitat requirements. Finally, the challenge of integrating societal needs with maintaining healthy vulture populations is key for implementing a successful one health framework as a roadmap for optimizing the health of human and wildlife populations and ensuring ecosystem health.

48.7 Why are birds unique?

Birds have specific attributes that distinguish them from other vertebrate classes (Table 48.3). These characteristics underpin differences in vulnerability to EDCs and contribute to the unique responses observed in birds compared to other vertebrate classes. Most obviously birds have feathers. These are not only adapted for flight and thermoregulation but also they provide a means by which sexual selection can occur. In birds cues for mate choice generally come in three forms: colorful male plumage to attract females, courtship displays, and in the case of songbirds, song production. EDC exposure from sewage effluent were associated with more complex song and reduced immune response in male starlings feeding in filter beds (Markman et al., 2008) and American kestrels experimentally exposed to dietary PCBs showed plumage changes in males and their offspring (Borolotti et al., 2003). Impacts on male selection cues could have repercussions for population and species health. On top of the energetic costs of daily flight and consequent plumage maintenance, large numbers of bird species face the additional energetic demands of seasonal migration which requires energy utilization that is focused on migration, seasonal changes in metabolism, and adequate feather replacement. These migration-related metabolic changes are dynamic and critical to survival, and are also vulnerable to effects from exposure to environmental chemicals and endocrine modulators (Broggi et al., 2003; Hallanger et al., 2011; Hurlbert and Haskell, 2003; Majewski et al., 2005; Perez et al., 2017a,b,c; Vyas et al., 1995; Wilson and Reinert, 1999). As such, both seasonality and exposure to environmental contaminants alter thyroid hormone system responses (McNabb, 2005; Nost et al., 2012; Ross et al., 2011; Webb and McNabb, 2008; Wilson and Reinert, 1999).

The metabolic cost of migration must be balanced with seasonal changes in reproductive physiology. Female birds have one functional ovary (the left), while males have two functional internal testes. Both sets of gonads undergo seasonal changes in size and functionality, presumably to maintain reduced body weight for flight. However, the

TABLE 48.3 Unique characteristics of avian species that influence response to endocrine disrupting chemicals.

- Growth and Metabolism
  - High-body temperature (105°F) with high-metabolic rate
  - Rapid growth rate
  - Seasonal metabolic changes associated with migration
  - Seasonal shift in mobilization of lipid reserves
  - Differential developmental patterns in altricial versus precocial birds
  - Thyroid system critical for premigratory fattening
- Reproductive system
  - Female has one functional ovary
  - Altered gonadal differentiation results in ovotestes
  - Eggs have hard shells
- Hormones and behavior
  - Males adversely impacted by xenoestrogens and androgenic compounds
  - Females less sensitive to xenoestrogens
  - Biparental care is common, particular in species with altricial young
- Sexual differentiation
  - Males are the homogametic sex (ZZ); females (ZW)
  - Hypothalamic–pituitary–gonadal axis relies on relative exposure to estradiol and testosterone
    - Males experience relatively higher exposure to testosterone
    - Females experience relatively higher exposure to estradiol
  - Song system differentiation occurs in passerines with potential role of steroids
  - dimorphic plumage involved in mate selection
- Lifespan
  - Long-lived birds produce few offspring annually over many years
  - Social learning is common in long-lived species.

energetic cost to the female bird also includes production of high-nutrient value eggs. Associated with the single ovary is the shell gland, which not only produces the hard shell unique to birds, but "plumps" the egg to ensure sufficient nutrients are available for the entire developmental period. Eggshell thinning was in fact the first reported effects of EDCs in birds; however, many environmental toxicants transferred from the maternal system to the egg yolk and albumen have direct impacts on embryonic development.

Avian species rely on genetic-based sexual differentiation with well-characterized developmental events occurring during ontogeny. The genetic basis for sex determination is reversed from that of mammals in that the male is the homozygotic sex (ZZ) and the female is the heterozygotic (ZW), providing a "different" substrate on which the effects of EDCs on sexual differentiation can act (Adkins-Regan et al., 1995; Ottinger and vom Saal, 2002; Ottinger et al., 2009a,b). Chicks hatch in one of two primary developmental states: precocial chicks are mobile and aside from thermoregulation, they are relatively independent and altricial chicks which require intensive parental care with feeding and care until they fledge from the nest. The differential pattern in development of precocial and altricial chicks impacts the maturation of thyroid and metabolic endocrine systems with precocial birds relatively functionally mature at hatch and altricial birds still undergoing maturation (Schwabl, 1996a, 1996b; McNabb, 2007; McNabb and Fox, 2003; Wada et al., 2009; Webb and McNabb, 2008; Wilson and Reinert, 1999). Many of these unique characteristics, including breeding characteristics, neural mechanisms, and lifetime impacts will be discussed below in the context of ascertaining the specific physiological and behavioral impacts associated with EDC exposure.

48.7.1 Altricial versus precocial birds: ontogeny and vulnerable life stages

Of the two developmental strategies that occur in birds, the most heavily studied in toxicology has been the precocial birds, as the direct influences of maternal contaminant deposition on development can be more readily quantified. Altricial chicks require extensive posthatch parental care, whereas precocial chicks are well developed at hatch, and therefore lend themselves to in ovo toxicity tests. However, altricial species have particular life history stages that are more vulnerable to EDCs. The neural circuitry of the song system, unique to song birds that are also altricial, is steroid-dependent with elements that are sexually differentiated primarily posthatch, and remains plastic throughout the life cycle, showing seasonal regression and hormone-induced seasonal neurogenesis (Adkins-Regan and Watson, 1990; Adkins-Regan et al., 1990; Adkins-Regan and Ascenzi, 1990; Wade and Arnold, 2004; Fusani and Gahr, 2006; Ball and Balthazart, 2010). This neuroplasticity contributes to an apparent lifelong vulnerability yet potential resilience to EDC exposure (Iwaniuk et al., 2006; Markman et al., 2008; Rochester et al., 2010; Rochester and Millam, 2009). Adverse effects of EDCs have also been observed in finches and the dark-eyed junco (Hoogesteijn et al., 2008; Satre et al., 2009). Species with altricial young often have biparental parental care, which is modulated by hormones that modulate specific neural systems (Angelier et al., 2016; Hartman et al., 2019; Smiley, 2019; Smiley et al., 2020).

Precocial birds, such as Japanese quail (*Coturnix japonica),* have often been the subject for toxicological studies and regulatory testing. They are well developed at hatch, with sexual differentiation of the reproductive endocrine and functional competency of other physiological systems already relatively complete (Adkins-Regan, 2009; Balthazart et al., 2009; Ottinger et al., 2005b; Ottinger and Dean, 2011). These studies have shown that the male Japanese quail is exquisitely sensitive to exogenous steroids, with both estradiol and androgen treatments resulting in impaired male reproductive behavior. As such, estradiol (E_2) is very useful as a positive control and as a means of comparison for the relative activity of EDCs with varying impacts on endocrine, neural, and behavioral components of reproduction (Berg et al., 2001; Halldin et al., 1999; Berg et al., 1998; Adkins-Regan and Watson, 1990; Panzica et al., 2007). Japanese quail have a 17-day incubation period and during development, each level of the reproductive [hypothalamic−pituitary−gonadal (HPG)] axis develops and begins to function as early as embryonic day 5 (gonadal differentiation), embryonic days 12−14 (hypothalamus and pituitary gland), and later in embryonic development (accessory structures). Gonadal function is initiated as early as embryonic day 5, with differential patterns of circulating steroid hormones in males and females (Figure 48.7).

Estradiol is a critical element in sexual differentiation in quail. During embryonic development, females have relatively high concentrations of estradiol/androgen whereas males have a relative low estradiol/androgen ratio. Moreover, there are sex-related differences in the patterns of plasma steroid levels during embryonic development. In female embryos, plasma E_2 rose until hatch and decreased, posthatch (Ottinger et al., 2008; Ottinger et al., 2005a). In males, plasma androgen peaked at embryonic days 14−17 (ED14-E17), during the 17-day incubation period, and declined posthatch. In addition, yolk steroid hormone content reflects embryonic steroid hormone levels. These steroid hormones are present and available to the embryo during sexual differentiation of multiple organ and endocrine systems throughout incubation. Once the embryonic gonads and adrenal glands begin to produce steroid hormones, circulating concentrations rise to make the gender-related pattern in changes more evident, especially during

the last half of embryonic development. Both sexes experience increased steroid hormones after embryonic days 10−12 in males and embryonic days 10−16 in females. Sexual differentiation of endocrine and behavioral components of reproduction occurs during this time, organizing the HPG axis and sex-specific behaviors (Adkins-Regan and Watson, 1990; Ottinger et al., 2005a). There is a large literature that links steroid hormones, brain regions that modulate reproductive behavior, onset of reproduction during maturation, and adult reproductive function. The primary hypothalamic hormone that regulates the HPG axis is gonadotropin-releasing hormone-I (GnRH-I), which is produced by the cell bodies located in the preoptic septal region of the hypothalamus. Hypothalamic GnRH-I levels rise between embryonic days 10−15; followed by a sharp drop that appears associated with activation of the function of the HPG axis and feedback regulation of GnRH-I (Li et al., 1991). Both the endocrine and behavioral components of reproduction in Japanese quail are sexually differentiated during embryonic development.

In concert with the changing steroid hormones during embryonic development, the adrenal axis and the thyroid axis develop and achieve function. Circulating concentrations of adrenal and thyroid hormones rise during embryogenesis to peak at about the time of hatching in precocial birds, with a slight delay in this pattern for altricial birds. Additionally, the steroid hormones circulating during embryonic development also impact the immune system, with circulating testosterone in males inducing regression in the bursal tissue in males (Grasman, 2010; Lavoie et al., 2007; Lavoie and Grasman, 2007). Clear effects of EDCs have been observed for the immune system, especially for the response of the bursa, which is exquisitely sensitive to steroid hormones during embryonic development. Additionally, it has been well documented that the thyroid axis is also a primary target for many EDCs, including PCBs, flame retardants, and other compounds. Effects of EDCs exerted during embryonic development may also impair the thyroid axis, which is critical for hatching as well as in overall metabolic function (McNabb and Fox, 2003).

48.7.2 Maternal deposition of compounds

Maternal deposition of steroids and EDCs into the egg is a primary mode of exposure to the avian embryo. There is increasing recognition of the important role of maternally deposited steroid hormones, as well as corticosterone and thyroid hormones (Adkins-Regan et al., 1995; Almasi et al., 2012a,b; Hayward and Wingfield, 2004). Mounting data point to both direct and epigenetic effects of maternally deposited hormones, which vary according to the condition of the female, health, reproductive status, and stressors. These steroids can affect viability as well as developmental characteristics of the chicks (Lipar et al., 1999; Schwabl, 1993, 1996a,b). Deposition of EDCs is layered on top of these endogenously produced hormones from the hen. Moreover, most maternally transferred compounds and EDCs are lipid soluble, thereby deposited primarily into the egg yolk; whereas, water-soluble compounds such as atrazine may be more evenly distributed throughout the egg compartments. There is significant deposition of EDCs into the eggs of field birds (Custer et al., 2010a,b,c,d). Similarly, laboratory studies have demonstrated that EDCs, including exogenous estradiol, methoxychlor, and soy phytoestrogens (see Figure 48.8 for phytoestrogens) all readily transfer from the hen into the egg and partition in the egg compartment according to lipid solubility (Lin et al., 2004; Ottinger et al., 2005b).

48.7.3 Posthatch growth and maturation

Posthatch growth and maturation are periods that are vulnerable to interference from EDCs. Steroid hormones continue to decline from the late embryonic and posthatch levels associated with sexual differentiation to remain at low-quiescent concentrations until the onset of sexual maturation. During sexual maturation, reproductive endocrine and behavioral responses are initiated earlier in males so that they mature by six−eight weeks of age (Ottinger and Brinkley, 1978, 1979). Females begin to mature slightly later than males with onset of egg production by 8−10 weeks of age. This dimorphism is reflected in hypothalamic GnRH-I levels, which increase in males earlier than females (Ottinger et al., 2004). Organizational effects of steroids in quail are also reflected morphologically in the sexually dimorphic preoptic region of the quail, which is larger in males and testosterone sensitive in the adult; high levels of aromatase metabolize testosterone to estradiol, which is essential for sexual behavior). Because this area in known to be important in modulating courtship and mating behavior, a number of studies have focused on the neural systems contained in this area in Japanese quail; this area is potentially vulnerable to the effects of EDCs (Panzica et al., 2007). In addition, the preoptic-septal region (POA-SL) contains many of the GnRH cell bodies; these cells project to the median eminence of the hypothalamus, making the POA-SL critical in the regulation of both endocrine and behavioral components of reproduction. All these characteristics of the HPG axis and sexually dimorphic neuroendocrine systems are vulnerable to EDC exposure, especially during organization of the reproductive axis during embryonic sexual differentiation.

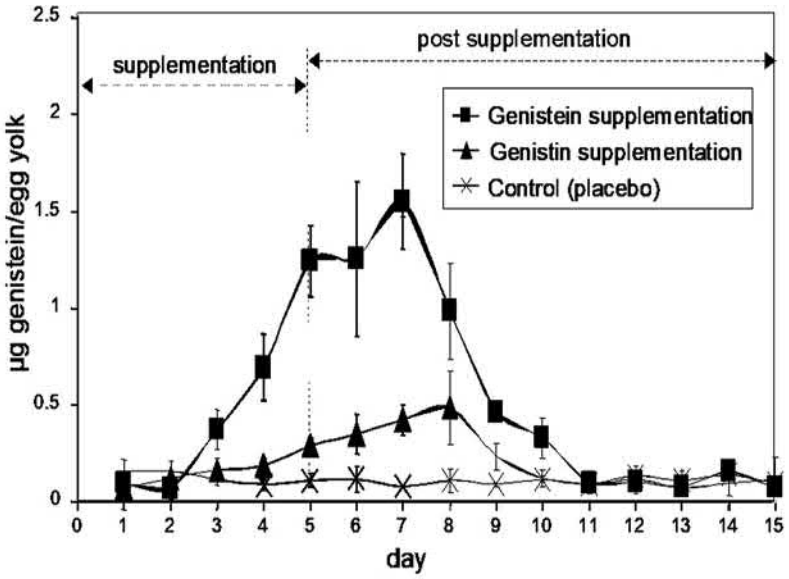

FIGURE 48.8 Maternal deposition of the phytoestrogen, genistein by the quail hen into eggs.

Concentrations of Genistein in Japanese Quail egg yolks supplemented with genistein (aglycone), genistin (glucoside) or placebo capsules. Data points represent average of 4 replicates for treatment groups and 2 replicates for the control group. Modified from Lin et al, 2004.

48.8 Investigating endocrine disrupting chemical effects in an avian model: the Japanese quail two-generation test

Laboratory tests provide important information about EDC actions and impacts in birds and have used several experimental approaches. Most studies on the actions of steroid hormones have used egg injection, with treatment with known concentrations in order to understand the role of steroids in ontogeny and sexual differentiation. Many of the studies on EDC effects have used a similar approach, and these studies have been conducted in domestic chick embryos, mallard duck, and Japanese quail. The US EPA oversees the safety of chemicals in use by industry, agricultural practices, recreational application, and individual residences. The JQTT provides a multigenerational test to assess the impacts of EDCs on all life stages, both separately and as a continuum. Current testing for registration of chemicals may require select Ecological Effects Studies, including: Avian Acute Oral Toxicity, Avian Subacute Dietary Toxicity, Avian Reproduction, the JQTT, and Simulated or Actual Field Testing (http://www.epa.gov/oppefed1/ecorisk_ders/toera_analysis_eco.htm) to ascertain safety for birds. These tests are conducted on a variety of species according to the test and are conducted in tandem with tests in other vertebrate and invertebrate species.

As discussed in the introduction to this chapter, EDCs may be difficult to detect nonlethal effects that have more subtle and long-term impacts on organisms. As a result, a series of testing protocols have been developed to address potential effects vertebrates and invertebrates over the life cycle. These two generation testing protocols consider a range of measurement end points to assess effects and potential risks to selected organisms. In birds, there is consideration of a multigeneration test using Japanese quail, which contains each primary phase in the life cycle with isolated exposure at that phase as well as cumulative exposure over the multiple life stages. Initial exposure in the current testing protocol occurs in proven breeders followed by continuous exposure to first generation (F1) offspring to evaluation of their second generation (F2) offspring as the final step in the testing protocol. As will be described below, there are a number of measures considered to assess health, toxicity effects, and endocrine disruption. The general list of measurement endpoints include: measures of health and overt toxicity (food consumption, body weights, secondary sex characteristics, activity, chick health, growth and maturation, lethargy, morbidity, or other clinical signs of toxicity, mortality); reproductive measures (sexual differentiation, sexual maturation, egg production, egg quality, fertility, embryo death, hatchability, chick survival and condition, sex ratio, reproductive behavior and reproductive hormones, testes

histology and sperm counts, cloacal gland size, and foam); endocrine and physiological endpoints (weight and histology of liver, testes, thyroid, adrenals, gonads, and brain, fecal steroid hormones, serum hormones and vitellogenin, glandular thyroid hormone). The reasoning for use of these end points in assessing EDCs is briefly discussed below to provide a more complete overview of the responses of the endocrine and physiological systems to EDCs.

48.8.1 Pertinent endpoints for assessing potential endocrine disruption

The selection of endpoints depends on the dosing regimen (i.e., amount of compound administered and the timing of administration), projected dose response, the window of exposure (i.e., life-stage), projected mechanisms of action, potential endocrine activity or induction of vitellogenin or other biochemical responses, and mode of exposure are all critical variables in evaluating potential EDCs. As more information becomes available on EDC actions, it will be possible to use the structure proposed by the AOPs framework to help elucidate both the targeted physiological systems vulnerable to a chemical/chemical class and the potential for significant impacts to avian species. This approach is not currently integrated into the testing paradigm, but may prove useful for providing structure to interpreting the observations and findings. For example, the developing embryo is much more sensitive to the effects of EDCs than the adult, and developmental defects (i.e., permanent central and peripheral disruption) often persist into maturation and adult life stages. Conversely, adult exposure does not generally have as much impact or effects appear to be more transient, especially in precocial species. Advances in our understanding of molecular mechanisms have revealed that EDCs often exert epigenetic effects. This has changed our understanding of both the activational and organizational effects of EDCs, allowing for the possibility that exposure can cause lasting effects in multiple generations (Skinner et al., 2011; Hochberg et al., 2011). Therefore, it is extremely important to understand the physiology of the model (i.e., Japanese quail) and the species-specific endocrine mechanisms behind the selection of endpoints.

Laboratory studies conducted under controlled conditions filter out some of the confounding factors encountered in field studies, thereby allowing insights into the mechanisms of action of EDCs, and distinguishing sensitive life stages. As such, EDCs may interfere with endogenous processes critical for sexual differentiation, maturation, breeding, and parental behavior. It is against this backdrop that exogenous EDCs act, with variations in specific mechanism(s) of action and targets for a particular compound. Although an emphasis of EDC studies has been on the reproductive axis, it is clear that the thyroid, immune, and stress axes are also targets of endocrine disruption. Toxicological effects are also observed with higher dose exposures to EDCs and some measures of activation of the liver detoxification processes in the form ethoxyresorufin-O-dealkylase (EROD) activity measurements are excellent indicators of exposure. Elegant studies have also shown that subtle differences in the amino acid sequence of the AhR ligand-binding domain contribute to observed variations in the sensitivity of wild birds species to EDCs (Head et al., 2008; Head and Kennedy, 2007a,b).

48.8.2 Survival

Survival is a basic endpoint or determinant of injury for acute and chronic toxicity testing of compounds. Determining the median lethal dose that will kill 50% of the population being tested (LD50) is an important value for traditional toxicology studies. In dietary studies, survival must be monitored in order to assess health effects. In the context of endocrine disruption studies, it is unlikely that the doses will approach lethal concentrations because circulating concentrations of endogenous hormones are in the pico- or femtograms. Nonetheless, sublethal treatments are important in ascertaining potential risk from endocrine disruption. For example, 50 μg/kg/day of bisphenol A has been determined to be a safe exposure by classic toxicology testing (Myers et al., 2009). However, doses 100 to 1000 times lower than that have been shown to induce feminization of the gonads in Japanese quail, with no changes in survivability among groups (Oshima et al., 2012). As such, monitoring survival following exposure to toxic chemicals provides information about potential risk and species vulnerabilities.

48.8.3 Food consumption and body weight

Food consumption is a basic measure of the general health; changes in food intake can indicate acute or chronic toxic effects of a compound. Additionally, if the route of chemical exposure is through the feed, it is important to monitor the consumption carefully to determine the exact exposure. It is also important to measure the stability of treatment compounds. Reduced food consumption has been associated with EDC exposure in Japanese quail (Yamashita et al., 2011). Similarly, body weight is closely linked with food intake and overall health and can be indicative of toxicological effects. For example, perchlorate, a thyroid hormone system disruptor, significantly reduced the growth (measured in body mass) of zebra finches dosed for the first two weeks of life (Rainwater et al., 2008). These birds also exhibited altered begging and fledging behaviors indicating that other endpoints may be linked to altered body weight, depending on the mechanism of disruption.

48.8.4 Accessory sex characteristics; sexual maturation

A number of secondary sex characteristics are gender-specific and provide excellent hormone-dependent response indices. In many species, including the Japanese quail, male and female plumage differs; with these sexual dimorphisms generally emerging during sexual maturation and in seasonal and migratory species, during the breeding season. Ultimately, the male has a rust hued chest, which is even in color; females have a buff colored chest with small dark areas in a dappled pattern. In general, feather color, especially that in more brightly colored species such as blue birds, and depends on dietary carotenoids as well as relate to overall health. In addition, males often have sexually dimorphic characteristics that are testosterone-dependent. The male Japanese quail cloacal gland produces a glycoproteinaceous secretion, termed cloacal gland foam that is critical for sperm transfer to the female (Ottinger and Brinkley, 1979). Measurements of the cloacal gland area have provided a reliable correlated measure for the sexual maturation and reproductive status of an individual male and the foam produced can be estimated on a scale of one to five or a similar ordinal subjective measurement scale. Since Japanese quail are ground dwellers and males establish territories during breeding season, cloacal gland foam provides a marker delineating their territory; the foam has been called the "topping on the dropping" (Schleidt and Shalter, 1973). Monitoring the effects of EDCs on sexual maturation provides insight into the mechanisms of action. In males, monitoring for presence of cloacal gland foam in males provides an initial indicator of testicular activity and production of androgens. Further, depending on an EDC's action(s), there may be differential effects in males and females with males maturing slightly earlier than females. By five–six weeks of age, testicular activity initiates and begins to produce increasing concentrations of testosterone leading to increasing expression of reproductive endocrine function, courtship and mating behavior whereas females initiate egg production by 9–10 weeks of age.

48.8.5 Behavioral indicators

Although the Japanese quail female exhibits a range of sex-specific behaviors, these behaviors are not readily quantifiable. Males and females both exhibit aggressive behavior, which can be quantified (Ramenofsky, 1985). Male courtship and mating behavior provide excellent bioindicators of reproductive competency. Sexual behaviors are steroid hormone-dependent, meaning that there must be sufficient circulating concentrations of androgens to enable the expression of male sexual behavior. Moreover, male sexual behavior is an exquisitely sensitive endpoint for embryonic exposure to estrogenic and highly active androgen active compounds. A three-minute test is conducted in which a receptive female (control diet female that is from the same population; nonexperimental) is introduced into the male's home cage. Latency to mount, mount attempts, and cloacal contacts by the male are recorded. An individual may be tested on three successive days if it is important to determine the effects of experience on behavioral responses. Interpretation of the outcomes of behavioral testing relates to the potential mechanisms of action of compounds under testing. More specifically, the female quail requires exposure to estradiol during embryonic development and is masculinized by exposure to androgens between embryonic days 12–18. Conversely, males are demasculinized as evidenced by impaired male sexual behavior as adults, if they have been exposed to either estrogens or androgens during this critical period. As such, the male Japanese quail is exquisitely sensitive to exposure to EDCs during sexual differentiation.

As such, behavior is a sensitive measure of endocrine disruption; however, behavioral measures that are easily implemented in field work or even in the laboratory are challenging. It is known from laboratory studies that EDCs does impair male sexual behavior in male quail and that diminished behavioral responses often parallel effects on other physiological responses (Mura et al., 2009; Ottinger et al., 2013; Panzica et al., 2007). Additionally, seabirds exposed to oil prior to or during breeding season have been observed to avoid breeding, abandon nests, and exhibit reduced parental care (Fry et al., 1986; Eppley and Rubega, 1990; Walter et al., 2013); however, the degree to which these are endocrine impacts or as a result of other physiological impacts remains unclear. As such, more work is needed to link endocrine and neuroendocrine impacts to assess behavioral impairment related to EDC exposure as well as developing clear behavioral metrics that are utilizable in field and laboratory studies. Behavioral measures also provide useful indicators of effects, including sensory deficits, stress responses, and impaired reproductive function. Finally, behavioral measures may prove to be very revealing in song birds in which the neural circuitry is steroid-dependent and in distinguishing EDC effects on altricial versus precocial birds.

48.8.6 Egg production, shell quality, fertility, and embryo viability

As early as the 1960s, exposure to DDT and DDE was linked to eggshell thinning and population decline in many wild bird species (Rattner, 2009). Egg production and onset of laying are important measures of reproductive function in birds, and are easily monitored by checking cages daily

and marking eggs. EDC exposure has related to reduced egg production as well as delayed onset of egg production by acting on the gonads, gametes, or sperm-host glands, potentially resulting in decreased fertilization success. Similarly, the fertilized egg may not develop properly due to interference from an EDC and the embryo may not survive beyond the first few hours or days of development. During this time, the uptake of yolk (white and yellow yolk) is minimal and as such reflects primarily a toxic effect of a compound or specific effects impairing the function of homeobox genes and disruption of cellular lineages contributing to the formation of organ systems, such as in the case of heart effects (Carro et al., 2013b). Eggshell thickness, strength, and gross abnormalities can affect embryo viability.

Later embryonic effects and lethality are more likely to relate to disruption of essential physiological systems, such as impacting the thyroid endocrine axis and other systems essential for the development and synchronization of endocrine and other physiological systems. A combination of early and late embryo mortality is a stronger indicator of toxicity that either alone. Moreover, there are distinct strain differences in Japanese quail, and there is an extensive literature that deals with a variety of physiological responses in Japanese quail that have been selected for multiple generations (Blohowiak et al., 1984; Bursian et al., 1983; Marks, 1996; Marks and Siegel, 1980). The Japanese quail chick begins to pip at embryonic day 15 in preparation for hatching at embryonic day 17. Once pipped, the chick is able to vocalize and often there is synchronizing in hatching of chicks in proximity. Pipping is followed by the chick pecking a hole, similar to an escape hatch, and requires a great deal of energy. The hatching success of chicks has been shown to be highly sensitive to chemical perturbation, and thus hatchability is an important endpoint in EDC studies.

48.8.7 Neuroendocrine systems regulating reproduction, metabolism, and stress

Embryonic exposures to steroids or compounds that are estrogen or androgen active result in impaired behavior in male behavior in adult quail (Ottinger et al., 2005a, 2008, 2009b; Panzica et al., 2007). Further, it has been shown that specific neural systems, including neurotransmitters (norepinephrine, dopamine, serotonergic) and neuropeptides (vasotocinergic) are modified in response to embryonic exposure to steroid hormones and to EDCs. Assessing the effects of embryonic exposure to EDCs on neurotransmitters and neuropeptides can provide information about direct effects of these compounds on regulatory systems that modulate reproductive, thyroid, and adrenal endocrine axes. GnRH-I neurons are located in the preoptic/lateral septal region of the hypothalamus. Although redundant, this system may be vulnerable to endocrine disruption (Ottinger et al., 2009b). Impact to neurotransmitter systems such as acetylcholine esterase has been used as a measure of toxicant exposure (Rattner et al., 1986).

48.8.8 Songbirds

Songbirds and other altricial birds also show impacts of EDC exposure on avian brain morphology (Iwaniuk et al., 2006; Millam et al., 2001). Further, there is a large literature about the impacts on steroid hormones on the sexual differentiation and function of the nuclei that direct and modulate song control in songbirds (Wade et al., 2004; Grisham et al., 2008; Arnold and Itoh, 2011; Wade and Arnold, 2004; Gilbert et al., 2007). Because of the neuroplasticity in songbirds, EDC effects may be more transient in songbirds; however, there are insufficient data to ascertain if this is the case. Nonetheless, there are clearly documentations of EDC effects on brain regions that modulate singing and other behaviors that are steroid dependent in both precocial and altricial birds.

48.8.9 Metabolic and thyroid systems

In addition, metabolic systems have been investigated in detail in birds, especially for domestic poultry. The thyroid system in birds has proven vulnerable to specific types of endocrine disruption in which this endocrine system is a target. Specifically, PCBs, flame retardants, and other classes of EDCs have been implicated in having thyroid system actions that impact birds, both in the laboratory and in field birds (Scanes and McNabb, 2003; McNabb and Fox, 2003; McNabb, 2005; Chen et al., 2008; Webb and McNabb, 2008; Fernie et al., 2005b). It is not clear if histological methods provide a sensitive method for revealing these EDC effects; however, impaired production and release of thyroid hormones would be observed in abnormal thyroid gland follicles size and distribution and in differences in circulating thyroxine (T4) and the more bioactive form, triiodothyronine (T3). Finally, the HPA is another endocrine system potentially responsive to EDC challenges. Measuring corticosterone in feathers may be an interesting technique to determine if long-term stress has occurred using a noninvasive technique. Seasonality and migration also complicate responses by birds to EDCs. Birds often exhibit seasonal patterns in reproduction and species that migrate often show complete regression of the reproductive axis with cessation of function followed by restimulation of the reproductive system, or seasonal recrudescence for the next breeding cycle. Initial stimulation of reproductive function in birds relies on environmental triggers, termed zeitgebers and in the case of temperate zone species; this environmental cue is often photoperiod. Birds are generally long day breeders due to their relatively short incubation and relatively quick maturation times for their offspring. As such, most photoperiodic birds become

reproductive with day length longer than 12 h. There is a very large literature on this subject that deals with the neural mechanisms, response via the eyes and pineal gland, and the hypothalamic response to regulate reproductive function; review of this literature is beyond the scope of this chapter, but it is important to recognize seasonal variations in energy demands due to reproduction, migration, and environmental challenges especially as EDCs impact critical endocrine systems involved in these seasonal and adaptive responses.

48.8.10 Histopathology

Many organ systems are highly sensitive to hormonal perturbations, particularly if exposed during development. This includes reproductive organ (i.e., testes/ovaries/oviduct) weight, gross disruption of organ morphology, and microscopic disruption (i.e., disrupted follicular function or spermatogenesis). Thyroid glands, liver, bursa, and other organs should be examined, depending on the projected target(s) for the EDC. Because sexual differentiation of the avian female involves regression of one of the two primordial ovaries with its accompanying oviduct, the presence/regression of the right ovary and oviduct provides initial information about appropriate sexual differentiation of the female reproductive axis. There are sperm-host glands in the oviduct of the avian female, in which sperm may reside for some weeks; however, there are no data available for a potential impact of EDCs on these glands. The ovary in the ovulating female should multiple follicles in varied stages of recruitment and maturation. Histological analyses will provide information as to the status of ovarian function and linking ovarian morphology to these components of ovarian function provides insight into potential EDC targets and actions. Early exposure to EDCs in males can impact gonadal development in a genetic male; however, there is less information about this type of long-term impacts. In some studies, EDC exposure resulted into transient presence of ovotestes, which are found in the hatchling but generally does not persist into the adult. Liver histology can provide information on any abnormalities associated with toxic effects. In addition, the activation of detoxification enzymes are excellent markers for initiation of these enzyme systems. Measurement of the EROD activity on liver subsamples can provide supporting evidence for histopathology findings.

There is a link between embryonic exposure to PCBs and cardiac malformations (Carro et al., 2013a,b) and kidney histology can provide information about toxicological impacts of EDCs due to the critical role of the kidneys in detoxification and elimination of water-soluble toxicants. Pathophysiological measurements of the bursa provide a powerful tool to assess endocrine disruption affecting the immune system. The bursa of Fabricius is exquisitely sensitive to steroid hormones, especially during development with testosterone having an immunosuppressive effect (Ottinger et al., 2005b). As shown in Table 48.4, embryonic exposure to trenbolone acetate resulted in persistent effects on bursal morphology with fewer, smaller follicles (Quinn et al., 2007a). Conversely, estradiol

TABLE 48.4 Summary of significant ($P < .05$) effects of trenbolone acetate and p,p- dichlorodiphenyldichloroethylene on immune, reproductive, and behavioral measures in Japanese quail.

Endpoint group	Endpoint	Trenbolone acetate (androgen)	p,p-dichlorodiphenyldichloroethylene (antiandrogen)
Immune measures	Bursa-body weight index	Decreased	Increased
	Bursal follicle number	Decreased in hatchlings and adults	Decreased in chicks
	Bursal follicle size	Increased at 0.05 µm g/g, decreased at 50 µg/g	NA
	Spleen-body weight index	NA	NA
	Humoral response to chukar red blood cells	NA	NA
	Cell-mediated response to phytohemagglutinin	NA	NA
	Hatchling plasma immunoglobulin G	Increased at only 0.05 and 0.5 µg/g	NA
	Hatchling total leukocyte counts	NA	Increased in chicks
	Hatchling differential leukocyte counts	Increased heterophil: Lymphocyte ratio	NA

Continued

TABLE 48.4 Summary of significant ($P < .05$) effects of trenbolone acetate and p,p- dichlorodiphenyldichloroethylene on immune, reproductive, and behavioral measures in Japanese quail.—cont'd

Endpoint group	Endpoint	Trenbolone acetate (androgen)	p,p-dichlorodiphenyldichloroethylene (antiandrogen)
Physiological reproductive measures	Gonad-body weight indices	NA	NA
	Testes morphology	NA	NA
	Ovarian follicle count	NA	NA
	Proctodeal foam gland weight	Decreased	NA
	Onset of puberty	Prolonged in males	Shortened in females
	Sperm penetration of perivitelline layer	NA	NA
Male copulatory behavior	Number of attempts to mount female	Decreased	Decreased
	Number of successful copulations	Decreased	NA
	Time to initial mount attempt	NA	NA
	Time to achieve first successful copulation	NA	Increased

"NA" denotes measures that were not affected by treatments.
Adapted from Quinn and Ottinger (2006). Reprinted with permission, The J. Poultry Sci. 43, 1–11, Japan Poultry Science Association, Tsukuba, Ibaraki, Japan.

treatment resulted in larger bursal size (Table 48.5); there was evidence of histopathology in treated individuals (Quinn et al., 2009). Many of these studies have also found a consistent relationship between bursal morphology and immune response. As such, bursal histopathology appears to be a reliable measure of impact to the immune system, especially assessing impacts during embryonic treatment and the persistence of these effects into adulthood.

TABLE 48.5 Summary of responses to estradiol or trenbolone with day of egg injection from the studies reviewed above.

	Hatchling effects summary[a]			
Endpoint	Estradiol ED4	Estradiol ED11	Trenbolone ED4	Trenbolone ED11
Embryo mortality	↑	–	↑	↑
Hatchability	↓	–	↓	↓
Body Mass	–	–	–	–
Male—androgen	–	↑↓	(↓)	↓
Female—estradiol	–	↑	(↑↓)	↓
Bursa mass	↓	-	↓	↑
Aromatase	(↑)	↑	–	–
Norepinephrine	–	(↑)	–	–
Dopamine	–	↑	–	–
Serotonin	–	–	–	–
5 HT	–	–	–	–
GnRH-I	–	–	–	–

[a](↑) or (↓) means effect/trend was nonsignificant, (↑↓) means a nonmonotonic dose response was observed.

48.9 Conclusions

Estradiol and estrogen active compounds are potent endocrine disruptors early in embryonic development, particularly in precocial chicks and throughout the lifespan of altricial birds, including songbirds. Effects in females may be due to direct effects on the ovary as well as on other physiological systems. Moreover, males are exquisitely sensitive to impacts from xenoestrogens, with impaired endocrine and behavioral components of reproduction, altered immune responses, and modifications in other physiological systems. Androgen active and EDCs that impact thyroid system function alter reproductive, metabolic, and immune responses. Further, EDC impacts on stress responses place individuals at risk from multiple environmental challenges. It is clear that early exposure has greater overall impacts on precocial species, which have relatively developed and functional physiological systems at hatch. Altricial birds follow a longer-term developmental pattern with seasonal recrudescence of the song system in tandem with reproductive function; thereby differing in the timing and relative vulnerability to EDC exposure throughout their lifespan. Nonetheless, there are distinct and documented effects of EDCs in birds that must be considered for effective conservation of field populations of birds and to protect these populations from adverse effects from these environmental compounds, often with severe and persistent injury. Further, there are some well-documented cases of environmental contamination in which adverse impacts on birds have experienced significant injury to the population over a long span of time, especially with persistent environmental chemicals such as DDT and PCBs. These long-term cases provide a rich set of data that are valuable in constructing both influence diagrams and AOPs. The One Health concept provides an integrative framework to structure a because these datasets contain valuable long-term monitoring and research programs, which consider physiological and reproductive impacts of exposure to chemicals found in those areas. These cases of environmental contamination and documented outcomes provide information that can be used to develop both influence diagrams and AOPs, which will help identify metrics for assessment and give managers tools to assess the status of avian populations and evaluate the success of restoration projects.

Acknowledgments

Research from the Ottinger lab supported by EPA grants #R826134010 (Star Grant) and R-82877801; Battelle contract for EPA-EDSTAC validation studies, NRI #92−37203 and NSF #9817024; MAES, University of Maryland, College Park; Fish and Wildlife Service and Hudson River NRDA Trustees. The conclusions and opinions presented here are those of the authors, they do not represent the official position of any of the funding agencies, the Hudson River Trustees, or the United States.

References

Adkins-Regan, E., 2009. Hormones and sexual differentiation of avian social behavior. Dev. Neurosci. 31, 342−350.

Adkins-Regan, E., Ascenzi, M., 1990. Sexual differentiation of behavior in the zebra finch: effect of early gonadectomy or androgen treatment. Horm. Behav. 24, 114−127.

Adkins-Regan, E., Watson, J.T., 1990. Sexual dimorphism in the avian brain is not limited to the song system of songbirds: a morphometric analysis of the brain of the quail (*Coturnix japonica*). Brain Res. 514, 320−326.

Adkins-Regan, E., Abdelnabi, M., Mobarak, M., Ottinger, M.A., 1990. Sex steroid levels in developing and adult male and female zebra finches (*Poephila guttata*). Gen. Comp. Endocrinol. 78, 93−109.

Adkins-Regan, E.K., Ottinger, M.A., Park, J., 1995. Maternal transfer of estradiol to egg yolks alters sexual differentiation of avian offspring. J. Exp. Zool. 271, 466−470.

Almasi, B., Rettenbacher, S., Muller, C., Brill, S., Wagner, H., Jenni, L., 2012a. Maternal corticosterone is transferred into the egg yolk. Gen. Comp. Endocrinol. 178, 139−144.

Almasi, B., Roulin, A., Korner-Nievergelt, F., Jenni-Eiermann, S., Jenni, L., 2012b. Coloration signals the ability to cope with elevated stress hormones: effects of corticosterone on growth of barn owls are associated with melanism. J. Evol. Biol. 25, 1189−1199.

Angelier, F., Wingfield, J.C., Tartu, S., Chastel, O., 2016. Does prolactin mediate parental and life-history decisions in response to environmental conditions in a birds? A review. Horm. Behav. 77, 18−29.

Ankley, G.T., Bennett, R.S., Erickson, R.J., Hoff, D.J., Hornung, M.W., Johnson, R.D., Mount, D.R., Nichols, J.W., Russom, C.L., Schmieder, P.K., Serrrano, J.A., Tietge, J.E., Villeneuve, D.L., 2010. Adverse outcome pathways: a conceptual framework to support ecotoxicology research and risk assessment. Environ. Toxicol. Chem. 29, 730−741.

Arnold, A.P., Itoh, Y., 2011. Factors causing sex differences in birds. Avian Biol. Res. 4, 44−51.

Asawasinsopon, R., Prapamontol, T., Prakobvitayakit, O., Vaneesorn, Y., Mangklabruks, A., Hock, B., 2006. Plasma levels of DDT and their association with reproductive hormones in adult men from Northern Thailand. Sci. Total Environ. 355, 98−105.

Ball, G.F., Balthazart, J., 2010. Seasonal and hormonal modulation of neurotransmitter systems in the song control circuit. J. Chem. Neuroanat. 39, 82−95.

Balthazart, J., Taziaux, M., Holloway, K., Ball, G.F., Cornil, C.A., 2009. Behavioral effects of brain-derived estrogens in birds. In: Vaudry, H., Roubos, E.W., Coast, G.M., Vallarino, M. (Eds.), Trends in Comparative Endocrinology and Neurobiology.

Barnthouse, L.W., Glaser, D., Young, J., 2003. Effects of historic PCB exposures on the reproductive success of the Hudson River striped bass population. Environ. Sci. Technol. 37, 223−228.

Basu, N., 2015. Applications and implications of neurochemical biomarkers in environmental toxicology. Environ. Toxicol. Chem. 34 (1), 22−29. https://doi.org/10.1002/etc.2783.

Berg, C., Halldin, K., Brunstrom, B., Brandt, I., 1998. Methods for studying xenoestrogenic effects in birds. Toxicol. Lett. 102−103, 671−676.

Berg, C., Halldin, K., Fridolfsson, A.K., Brandt, I., Brunstrom, B., 1999. The avian egg as a test system for endocrine disrupters: effects of diethylstilbestrol and ethynylestradiol on sex organ development. Sci. Total Environ. 233, 57–66.

Berg, C., Halldin, K., Brunstrom, B., 2001. Effects of bisphenol A and tetrabromobisphenol A on sex organ development in quail and chicken embryos. Environ. Toxicol. Chem. 20, 2836–2840.

Best, D.A., Elliott, K.H., Bowerman, W.W., Shieldcastle, M., Postupalsky, S., Kubiak, T.J., Tillitt, D.E., Elliott, J.E., 2010. Productivity, embryo and eggshell characteristics, and contaminants in bald eagles from the Great Lakes, USA, 1986 to 2000. Environ. Toxicol. Chem. 29, 1581–1592.

Bianchini, K., Morrissey, C.A., 2018. Polycyclic aromatic hydrocarbon exposure impairs pre-migratory fuelling in captively-dosed Sanderling (*Calidris alba*). Ecotoxicol. Environ. Saf. 161, 383–391.

Bigsby, R., Chapin, R.E., Daston, G.P., Davis, B.J., Gorski, J., Gray, L.E., Howdeshell, K.L., Zoeller, R.T., Vom Saal, F.S., 1999. Evaluating the effects of endocrine disruptors on endocrine function during development. Environ. Health Perspect. 107 (Suppl. 4), 613–618.

Blohowiak, C.C., Dunnington, E.A., Marks, H.L., Siegel, P.B., 1984. Body size, reproductive behavior, and fertility in three genetic lines of Japanese quail. Poultry Sci. 63, 847–854.

Borga, K., Hop, H., Skaare, J.U., Wolkers, H., Gabrielsen, G.W., 2007. Selective bioaccumulation of chlorinated pesticides and metabolites in Arctic seabirds. Environ. Pollut. 145, 545–553.

Borolotti, G.R., Fernie, K.J., Smits, J.E., 2003. Carotenoid concentration and coloration of American Kestrels (*Falco sparverius*) disrupted by experimental exposure to PCBs. Funct. Ecol. 17, 651–657. https://doi.org/10.1046/j.1365-2435.2003.00778.x.

Bowerman, W.W., Bryan JR., A.L., Robinette, J.R., Wing, J.M., Wiley, F.E., Murugasan, S., 2007. Concentrations of p,p′-DDE in plasma of nestling Wood Storks from Georgia. Chemosphere 68, 1506–1510.

Braune, B.M., Outridge, P.M., Fisk, A.T., Muir, D.C.G., Helm, P.A., Hobbs, K., Hoekstra, P.F., Kuzyk, Z.A., Kwan, M., Letcher, R.J., Lockhart, W.L., Norstrom, R.J., Stern, G.A., Stirling, I., 2005. Persistent organic pollutants and mercury in marine biota of the Canadian Arctic: an overview of spatial and temporal trends. Sci. Total Environ. 351–352, 4–56.

Broggi, J., Koivula, K., Lahti, K., Orell, M., 2003. Seasonality in daily body mass variation in a hoarding boreal passerine. Oecologia 137, 627–633.

Brunstrom, B., Hakansson, H., Lundberg, K., 1991. Effects of a technical PCB preparation and fractions thereof on ethoxyresorufin O-deethylase activity, vitamin-A levels and thymic development in the mink (Mustela-vison). Pharmacol. Toxicol. 69, 421–426.

Burger, J., February 9, 2018. Productivity of waterbirds in potentially impacted areas of Louisiana in 2011 following the Deepwater Horizon oil spill. Environ. Monit. Assess. 190 (3), 131. https://doi.org/10.1007/s10661-017-6428-y.

Burger, J., Tsipoura, N., 1998. Experimental oiling of sanderlings (*Calidris alba*): behavior and weight changes. Environ. Toxicol. Chem. 17 (6), 1154–1158.

Bursian, S.J., Polin, D., Olson, B.A., Shull, L.R., Marks, H.L., Siegel, H.S., 1983. Microsomal enzyme induction, egg production, and reproduction in three lines of Japanese quail fed polybrominated biphenyls. J. Toxicol. Environ. Health 12, 291–307.

Bursian, S.J., Dean, K.M., Harr, K.E., Kennedy, L., Link, J.E., Maggini, I., Pritsos, C., Pritsos, K.L., Schmidt, R.E., Guglielmo, C.G., 2017. Effect of oral exposure to artificially weathered Deepwater Horizon crude oil on blood chemistries, hepatic antioxidant enzyme activities, organ weights and histopathology in western sandpipers (*Calidris mauri*). Ecotoxicol. Environ. Saf. 146, 91–97. https://doi.org/10.1016/j.ecoenv.2017.03.045.

Butcher, J.B., Garvey, E.A., 2004. PCB loading from sediment in the Hudson River: congener signature analysis of pathways. Environ. Sci. Technol. 38, 3232–3238.

Carro, T., Dean, K., Ottinger, M.A., 2013a. Effects of an environmentally relevant polychlorinated biphenyl (PCB) mixture on embryonic survival and cardiac development in the domestic chicken. Environ. Toxicol. Chem. 32, 1325–1331.

Carro, T., Taneyhill, L.A., Ann Ottinger, M., 2013b. The effects of an environmentally relevant 58-congener polychlorinated biphenyl (PCB) mixture on cardiac development in the chick embryo. Environ. Toxicol. Chem. 32, 1317–1324.

Cesh, L.S., Elliott, K.H., Quade, S., Mckinney, M.A., Maisoneuve, F., Garcelon, D.K., Sandau, C.D., Letcher, R.J., Williams, T.D., Elliott, J.E., 2010. Polyhalogenated aromatic hydrocarbons and metabolites: relation to circulating thyroid hormone and retinol in nestling bald eagles (*Haliaeetus leucocephalus*). Environ. Toxicol. Chem. 29 (6), 1301–1310. https://doi.org/10.1002/etc.165, 2010 Oct;29(10):2388.

Champoux, L., Rail, J.F., Houde, M., Giraudo, M., Lacaze, E., Franci, C.D., Fairhurst, G.D., Hobson, K.A., Brousseau, P., Guillemette, M., Pelletier, D., Montevecchi, W.A., Lair, S., Verrault, J., Soos, C., 2020. An investigation of physiological effects of the Deepwater Horizon oil spill on a long-distance migratory seabird, the northern gannet. Mar. Pollut. Bull. 153, 110953. https://doi.org/10.1016/j.marpolbul.2020.110953.

Chen, Y., Sible, J.C., McNabb, F.M.A., 2008. Effects of maternal exposure to ammonium perchlorate on thyroid function and the expression of thyroid-responsive genes in Japanese quail embryos. Gen. Comp. Endocrinol. 159, 196–207.

Cho, Y.C., Sokol, R.C., Rhee, G.Y., 2002. Kinetics of polychlorinated biphenyl dechlorination by Hudson River, New York, USA, sediment microorganisms. Environ. Toxicol. Chem. 21, 715–719.

Cohen-Barnhouse, A.M., Zwiernik, M.J., Link, J.E., Fitzgerald, S.D., Kennedy, S.W., Giesy, J.P., Wiseman, S., Jones, P.D., Newsted, J.L., Kay, D., Bursian, S.J., 2011. Developmental and posthatch effects of in ovo exposure to 2,3,7,8-TCDD, 2,3,4,7,8-PECDF, and 2,3,7,8-TCDF in Japanese quail (*Coturnix japonica*), common pheasant (*Phasianus colchicus*), and white leghorn chicken (Gallus gallus domesticus) embryos. Environ. Toxicol. Chem. 30, 1659–1668.

Corbitt, C., Satre, D., Adamson, L.A., Cobbs, G.A., Bentley, G.E., 2007. Dietary phytoestrogens and photoperiodic response in a male songbird, the Dark-eyed Junco (*Junco hyemalis*). Gen. Comp. Endocrinol. 154, 16–21.

Crump, D., Chiu, S., Williams, K.L., 2016. Bisphenol S alters embryonic viability, development, gallbladder size, and messenger RNA expression in chicken embryos exposed via egg injection. Environ. Toxicol. Chem. 35 (6), 1541–1549. https://doi.org/10.1002/etc.3313.

Currie, R.A., Orphanides, G., Moggs, J.G., 2005. Mapping molecular responses to xenoestrogens through gene ontology and pathway analysis of toxicogenomic data. Reprod. Toxicol. 20, 433–440.

Custer, C.M., Read, L.B., 2006. Polychlorinated biphenyl congener patterns in tree swallows (Tachycineta bicolor) nesting in the Housatonic River Watershed, Western Massachusetts, USA, using a novel statistical approach. Environ. Pollut. 142, 235–245.

Custer, C.M., Custer, T.W., Dummer, P.M., 2010a. Patterns of organic contaminants in eggs of an insectivorous, an omnivorous, and a piscivorous bird nesting on the Hudson River, New York, USA. Environ. Toxicol. Chem. 29, 2286–2296.

Custer, C.M., Gray, B.R., Custer, T.W., 2010b. Effects of egg order on organic and inorganic element concentrations and egg characteristics in tree swallows, Tachycineta bicolor. Environ. Toxicol. Chem. 29, 909–921.

Custer, T.W., Custer, C.M., Gray, B.R., 2010c. Polychlorinated biphenyls, dioxins, furans, and organochlorine pesticides in belted kingfisher eggs from the upper Hudson River basin, New York, USA. Environ. Toxicol. Chem. 29, 99–110.

Custer, T.W., Custer, C.M., Gray, B.R., 2010d. Polychlorinated biphenyls, dioxins, furans, and organochlorine pesticides in spotted sandpiper eggs from the upper Hudson River basin, New York. Ecotoxicology 19, 391–404.

Custer, C.M., Custer, T.W., Hines, J.E., 2012a. Adult tree swallow survival on the polychlorinated biphenyl-contaminated Hudson River, New York, USA, between 2006 and 2010. Environ. Toxicol. Chem. 31, 1788–1792.

Custer, C.M., Custer, T.W., Schoenfuss, H.L., Poganski, B.H., Solem, L., 2012b. Exposure and effects of perfluoroalkyl compounds on tree swallows nesting at Lake Johanna in East Central Minnesota, USA. Reprod. Toxicol. 33, 556–562.

D'ursi, P., Salvi, E., Fossa, P., Milanesi, L., Rovida, E., 2005. Modelling the interaction of steroid receptors with endocrine disrupting chemicals. BMC Bioinf. 6 (Suppl. 4), S10.

Darnerud, P.O., 2003. Toxic effects of brominated flame retardants in man and in wildlife. Environ. Int. 29, 841–853.

Dean, K.M., Bursian, S.J., Cacela, D., Carney, M.W., Cunningham, F.L., Dorr, B., Hanson-Dorr, K.C., Healy, K.A., Horak, K.E., Link, J.E., Lipton, I., Mcfadden, A.K., Mckernan, M.A., Harr, K.E., 2017. Changes in white cell estimates and plasma chemistry measurements following oral or external dosing of double-crested cormorants, *Phalacocorax auritus*, with artificially weathered MC252 oil. Ecotoxicol. Environ. Saf. 146, 40–51. https://doi.org/10.1016/j.ecoenv.2017.08.007.

Deepwater Horizon Natural Resource Damage Assessment Trustees, 2016. Deepwater Horizon Oil Spill: Final Programmatic Damage Assessment and Restoration Plan and Final Programmatic Environmental Impact Statement. Available: http://www.gulfspillrestoration.noaa.gov/restoration-planning/gulf-plan.

Destoumieus-Garzon, D., Mavingui, P., Boetsch, G., Bossier, J., Darroet, F., Duboz, P., Fritsch, C., Giraudous, P., Le Roux, F., Morand, S., Paillard, C., Pontier, D., Sueur, C., Voituron, Y., February 12, 2018. The One Health concept: 10 years old and a long road ahead. Front. Vet. Sci. 5, 14. https://doi.org/10.3389/fvets.2018.00014.

Dix, D.J., Houck, K.A., Martin, M.T., Richard, A.M., Setzer, R.W., Kavlock, R.J., 2007. The ToxCast program for prioritizing toxicity testing of environmental chemicals. Toxicol. Sci. 95, 5–12.

Doering, J.A., Wiseman, S., Giesy, J.P., Hecker, M.A., 2018. Cross-species quantitative adverse outcome pathway for activation of the aryl hydrocarbon receptor leading to early life stage mortality in birds and fishes. Environ. Sci. Technol. 52 (13), 7524–7533. https://doi.org/10.1021/acs.est.8b01438.

Echols, K.R., Tillitt, D.E., Nichols, J.W., Secord, A.L., Mccarty, J.P., 2004. Accumulation of PCB congeners in nestling tree swallows (Tachycineta bicolor) on the Hudson River, New York. Environ. Sci. Technol. 38, 6240–6246.

Eppley, Z.A., Rubega, M.A., 1990. Indirect effects of an oil spill: reproductive failure in a population of South Polar skuas following the 'Bahia Paraiso' oil spill in Antarctica. Mar. Ecol. Prog. Ser. 67, 1–6.

Erickson, M.J., Turner, C.L., Thibodeaux, L.J., 2005. Field observation and modeling of dissolved fraction sediment-water exchange coefficients for PCBs in the Hudson River. Environ. Sci. Technol. 39, 549–556.

Esler, D., Brenda, E., Ballachev, B.E., Matkin, C., Cushing, D., Kaler, R., Bodkin, J., Monson, D., Esslinger, G., Kloecker, K., 2018. Timelines and mechanisms of wildlife population recovery following the Exxon Valdez oil spill. Deep Sea Res. Part II Top. Stud. Oceanogr. 147, 36–42.

Fairbrother, A., Smits, J., Grasman, K.A., 2004. Avian immunotoxicology. J. Toxicol. Environ. Health B Crit. Rev. 7, 105–137.

Fairhurst, G.D., Champoux, L., Hobson, K.A., Rail, J.-F., Verreault, J., Guillemette, M., Montevecchi, W.A., Brousseau, P., Soos, C., 2017. Feather corticosterone during non-breeding correlates with multiple measures of physiology during subsequent breeding in a migratory seabird. Comp. Biochem. Physiol. Mol. Integr. Physiol. 208, 1–13. https://doi.org/10.1016/j.cbpa.2017.02.024.

Farmahin, R., Wu, D., Crump, D., Herve, J.C., Jones, S.P., Hahn, M.E., Karchner, S.I., Giesy, J.P., Bursian, S.J., Zwiernik, M.J., Kennedy, S.W., 2012. Sequence and in vitro function of chicken, ring-necked pheasant, and Japanese quail AHR1 predict in vivo sensitivity to dioxins. Environ. Sci. Technol. 46, 2967–2975.

Felton, R.G., Steiner, C.C., Durrant, B.S., Keisler, D.H., Milnes, M.R., Tubbs, C.W., 2015. Identification of California condor estrogen receptors 1 and 2 and their activation by endocrine disrupting chemicals. Endocrinology 156 (12), 4448–4457. https://doi.org/10.1210/en.2015-1448.

Fernie, K.J., Mayne, G., Shutt, J.L., Pekarik, C., Grasman, K.A., Letcher, R.J., Drouillard, K., 2005a. Evidence of immunomodulation in nestling American kestrels (*Falco sparverius*) exposed to environmentally relevant PBDEs. Environ. Pollut. 138, 485–493.

Fernie, K.J., Shutt, J.L., Mayne, G., Hoffman, D., Letcher, R.J., Drouillard, K.G., Ritchie, I.J., 2005b. Exposure to polybrominated diphenyl ethers (PBDEs): changes in thyroid, vitamin A, glutathione homeostasis, and oxidative stress in American kestrels (*Falco sparverius*). Toxicol. Sci. 88, 375–383.

Fischer, L.J., Seegal, R.F., Ganey, P.E., Pessah, I.N., Kodavanti, P.R., 1998. Symposium overview: toxicity of non-coplanar PCBs. Toxicol. Sci. 41, 49–61.

Fisher, J.S., 2004. Are all EDC effects mediated via steroid hormone receptors? Toxicology 205, 33–41.

Foley, R.E., 1992. Organochlorine residues in New York waterfowl harvested by hunters in 1983–1984. Environ. Monit. Assess. 21, 37–48.

Foster, W.G., 1998. Endocrine disruptors and development of the reproductive system in the fetus and children: is there cause for concern? Can. J. Public Health 89 (Suppl. 1), S37–S41. S52, S41-6.

Fowler, G.S., Wingfield, J.C., Boersma, P.D., 1995. Hormonal and reproductive effects of low levels of petroleum fouling in magellanic penguins (*Spheniscus magellanicus*). Auk 112, 382–389.

Fox, L.L., Grasman, K.A., 1999. Effects of PCB 126 on primary immune organ development in chicken embryos. J. Toxicol. & Environ. Health A 58, 233–244.

Franceschini, M.D., Custer, C.M., Custer, T.W., Reed, J.M., Romero, L.M., 2008. Corticosterone stress response IN tree swallows nesting near polychlorinated biphenyl- and dioxin-contaminated rivers. Environ. Toxicol. Chem. 27, 2326–2331.

Fry, D.M., Swenson, J., Addiego, L.A., Grau, C.R., Kang, A., 1986. Reduced reproduction of wedge-tailed shearwaters exposed to weathered Santa Barbara crude oil. Arch. Environ. Contam. Toxicol. 15, 453–463.

Fucic, A., Gamulin, M., Ferencic, Z., Katic, J., Krayer Von Krauss, M., Bartonova, A., Merlo, D.F., 2012. Environmental exposure to xenoestrogens and oestrogen related cancers: reproductive system, breast, lung, kidney, pancreas, and brain. Environ. Health 11 (Suppl. 1), S8.

Fusani, L., Gahr, M., 2006. Hormonal influence on song structure and organization: the role of estrogen. Neuroscience 138, 939–946.

Gilbert, L., Bulmer, E., Arnold, K.E., Graves, J.A., 2007. Yolk androgens and embryo sex: maternal effects or confounding factors? Horm. Behav. 51, 231–238.

Gore, A.C., 2010. Neuroendocrine targets of endocrine disruptors. Hormones (Basel) 9, 16–27.

Grasman, K.A., 2002. Assessing immunological function in toxicological studies of avian wildlife. Integr. Comp. Biol. 42, 34–42.

Grasman, K.A., 2010. In vivo functional tests for assessing immunotoxicity in birds. Methods Mol. Biol. 598, 387–398.

Grasman, K.A., Scanlon, P.F., Fox, G.A., 1998. Reproductive and physiological effects of environmental contaminants in fish-eating birds of the Great Lakes: a review of historical trends. Environ. Monit. Assess. 53, 117–145.

Grisham, W., Lee, J., Park, S.H., Mankowski, J.L., Arnold, A.P., 2008. A dose–response study of estradiol's effects on the developing zebra finch song system. Neurosci. Lett. 445, 158–161.

Guerrero-Bosagna, C.M., Skinner, M.K., 2009. Epigenetic transgenerational effects of endocrine disruptors on male reproduction. Semin. Reprod. Med. 27, 403–408.

Guigueno, M.F., Fernie, K.J., 2017. Birds and flame retardants: a review of the toxic effects on birds of historical and novel flame retardants. Environ. Res. 154, 398–424. https://doi.org/10.1016/j.envres.2016.12.033.

Guigueno, M.F., Head, J.A., Letcher, R.J., Karouna-Renier, N., Peters, L., Hanas, A.M., Fernie, K.J., 2019. Early life exposure to triphenyl phosphate: effects on thyroid function, growth, and resting metabolic rate of Japanese quail (*Coturnix japonica*) chicks. Environ. Pollut. 253, 899–908. https://doi.org/10.1016/j.envpol.2019.05.110.

Hall, J.M., Korach, K.S., 2002. Analysis of the molecular mechanisms of human estrogen receptors alpha and beta reveals differential specificity in target promoter regulation by xenoestrogens. J. Biol. Chem. 277, 44455–44461.

Hallanger, I.G., Warner, N.A., Ruus, A., Evenset, A., Christensen, G., Herzke, D., Gabrielsen, G.W., Borga, K., 2011. Seasonality in contaminant accumulation in Arctic marine pelagic food webs using trophic magnification factor as a measure of bioaccumulation. Environ. Toxicol. Chem. 30, 1026–1035.

Halldin, K., Berg, C., Brandt, I., Brunstrom, B., 1999. Sexual behavior in Japanese quail as a test end point for endocrine disruption: effects of in ovo exposure to ethinylestradiol and diethylstilbestrol. Environ. Health Perspect. 107, 861–866.

Halldin, K., Axelsson, J., Brunström, B., 2005. Effects of endocrine modulators on sexual differentiation and reproductive function in male Japanese quail. Brain Res. Bull. 65, 211–218.

Harr, K.E., Reavill, D.R., Bursian, S.J., Cacela, D., Cunningham, F.L., Dean, K.M., Dorr, B.S., Hanson-Dorr, K.C., Healy, K., Horak, K., Link, J.E., Shriner, S., Schmidt, R.E., 2017a. Organ weights and histopathology of double-crested cormorants (*Phalacrocorax auritus*) dosed orally or dermally with artificially weathered Mississippi Canyon 252 crude oil. Ecotoxicol. Environ. Saf. 146, 52–61. https://doi.org/10.1016/j.ecoenv.2017.07.011.

Harr, K.E., Cunningham, F.L., Pritsos, C.A., Pritsos, K.L., Muthumalage, T., Dorr, B.S., Horak, K.E., Hanson-Dorr, K.C., Dean, K.M., Cacela, D., Mcfadden, A.K., Link, J.E., Healy, K.A., Tuttle, P., Bursian, S.J., 2017b. Weathered MC252 crude oil-induced anemia and abnormal erythroid morphology in double-crested cormorants (*Phalacrocorax auritus*) with light microscopic and ultrastructural description of Heinz bodies. Ecotoxicol. Environ. Saf. 146, 29–39. https://doi.org/10.1016/j.ecoenv.2017.07.030.

Harr, K.E., Rishniw, M., Rupp, T.L., Cacela, D., Dean, K.M., Dorr, B.S., Hanson-Dorr, K.C., Healy, K., Horak, K., Link, J.E., Revill, D., Bursian, S.J., Cunningham, F.L., 2017c. Dermal exposure to weathered MC252 crude oil results in echocardiographically identifiable systolic myocardial dysfunction in double-crested cormorants (*Phalacrocorax auritus*). Ecotoxicol. Environ. Saf. 146, 76–82. https://doi.org/10.1016/j.ecoenv.2017.04.010.

Hartig, P.C., Bobseine, K.L., Britt, B.H., Cardon, M.C., Lambright, C.R., Wilson, V.S., Gray Jr., L.E., 2002. Development of two androgen receptor assays using adenoviral transduction of MMTV-luc reporter and/or hAR for endocrine screening. Toxicol. Sci. 66, 82–90.

Hartig, P.C., Cardon, M.C., Lambright, C.R., Bobseine, K.L., Gray Jr., L.E., Wilson, V.S., 2007. Substitution of synthetic chimpanzee androgen receptor for human androgen receptor in competitive binding and transcriptional activation assays for EDC screening. Toxicol. Lett. 174, 89–97.

Hartman, C.A., Ackerman, J.T., Herzog, M.P., 2019. Mercury exposure and altered parental nesting behavior in a wild songbird. Environ. Sci. Technol. 53 (9), 5396–5405. https://doi.org/10.1021/acs.est.8b07227.

Harvey, P.W., Everett, D.J., 2006. Regulation of endocrine-disrupting chemicals: critical overview and deficiencies in toxicology and risk assessment for human health. Best Pract. Res. Clin. Endocrinol. Metabol. 20, 145–165.

Hayward, L.S., Wingfield, J.C., 2004. Maternal corticosterone is transferred to avian yolk and may alter offspring growth and adult phenotype. Gen. Comp. Endocrinol. 135, 365–371.

Head, J.A., Kennedy, S.W., 2007a. Differential expression, induction, and stability of CYP1A4 and CYP1A5 mRNA in chicken and herring gull embryo hepatocytes. Comp. Biochem. Physiol. C Toxicol. Pharmacol. 145, 617–624.

Head, J.A., Kennedy, S.W., 2007b. Same-sample analysis of ethoxyresorufin-O-deethylase activity and cytochrome P4501A mRNA abundance in chicken embryo hepatocytes. Anal. Biochem. 360, 294–302.

Head, J.A., Hahn, M.E., Kennedy, S.W., 2008. Key amino acids in the aryl hydrocarbon receptor predict dioxin sensitivity in avian species. Environ. Sci. Technol. 42, 7535–7541.

Hennig, B., Meerarani, P., Slim, R., Toborek, M., Daugherty, A., Silverstone, A.E., Robertson, L.W., 2002. Proinflammatory properties of coplanar PCBs: in vitro and in vivo evidence. Toxicol. Appl. Pharmacol. 181, 174–183.

Hervé, J.C., Crump, D., Giesy, J.P., Zwiernik, M.J., Bursian, S.J., Kennedy, S.W., 2010. Ethoxyresorufin O-deethylase induction by Tcdd, PeCDF and TCDF in ring-necked pheasant and Japanese quail hepatocytes: time-dependent effects on concentration–response curves. Toxicol. Vitro 24, 1301–1305.

Hochberg, Z., Feil, R., Constancia, M., Fraga, M., Junien, C., Carel, J.C., Boileau, P., LE Bouc, Y., Deal, C.L., Lillycrop, K., Scharfmann, R., Sheppard, A., Skinner, M., Szyf, M., Waterland, R.A., Waxman, D.J., Whitelaw, E., Ong, K., Albertsson-Wikland, K., 2011. Child health, developmental plasticity, and epigenetic programming. Endocr. Rev. 32, 159–224.

Holmes, D.J., Ottinger, M.A., 2003. Birds as long-lived animal models for the study of aging. Exp. Gerontol. 38, 1365–1375.

Hoogesteijn, A.L., Kollias, G.V., Quimby, F.W., De Caprio, A.P., Winkler, D.W., Devoogd, T.J., 2008. Development of a brain nucleus involved in song production in zebra finches (*Taeniopygia guttata*) is disrupted by Aroclor 1248. Environ. Toxicol. Chem. 27, 2071–2075.

Horak, K.E., Bursian, S.J., Ellis, C.K., Dean, K.M., Link, J.E., HANSON-Dorr, K.C., Cunningham, F.L., Harr, K.E., Pritsos, C.A., Pritsos, K.L., Healy, K.A., Cacela, D., Shriner, S.A., 2017. Toxic effects of orally ingested oil from the Deepwater Horizon spill on laughing gulls. Ecotoxicol. Environ. Saf. 146, 83–90. https://doi.org/10.1016/j.ecoenv.2017.07.018.

Hotchkiss, A.K., Rider, C.V., Blystone, C.R., Wilson, V.S., Hartig, P.C., Ankley, G.T., Foster, P.M., Gray, C.L., Gray, L.E., 2008. Fifteen years after "Wingspread"–environmental endocrine disrupters and human and wildlife health: where we are today and where we need to go. Toxicol. Sci. 105, 235–259.

Hsu, P.C., Pan, M.H., Li, L.A., Chen, C.J., Tsai, S.S., Guo, Y.L., 2007. Exposure in utero to 2,2′,3,3′,4,6′-hexachlorobiphenyl (PCB 132) impairs sperm function and alters testicular apoptosis-related gene expression in rat offspring. Toxicol. Appl. Pharmacol. 221, 68–75.

Hurlbert, A.H., Haskell, J.P., 2003. The effect of energy and seasonality on avian species richness and community composition. Am. Nat. 161, 83–97.

Iwaniuk, A.N., Koperski, D.T., Cheng, K.M., Elliott, J.E., Smith, L.K., Wilson, L.K., Wylie, D.R.W., 2006. The effects of environmental exposure to DDT on the brain of a songbird: changes in structures associated with mating and song. Behav. Brain Res. 173, 1–10.

Janer, G., Sternberg, R.M., Leblanc, G.A., Porte, C., 2005. Testosterone conjugating activities in invertebrates: are they targets for endocrine disruptors? Aquat. Toxicol. 71, 273–282.

Jenssen, B.M., 1994. Effects of oil pollution, chemically treated oil, and cleaning on the thermal balance of birds. Environ. Pollut. 86, 207–215.

Jimenez, B., Mori, G., Concejero, M.A., Merino, R., Casini, S., Fossi, M.C., 2007. Vitellogenin and zona radiata proteins as biomarkers of endocrine disruption in peregrine falcon (*Falco peregrinus*). Chemosphere 67 (9), S375–S378. https://doi.org/10.1016/j.chemosphere.2006.05.131.

Kakimoto, K., Akutsu, K., Nagayoshi, H., Konishi, Y., Kajimura, K., Tsukue, N., Yoshino, T., Matsumoto, F., Nakano, T., Tang, N., Hayakawa, K., Toriba, A., 2018. Persistent organic pollutants in red-crowned cranes (*Grus japonensis*) from Hokkaido, Japan. Ecotoxicol. Environ. Saf. 147, 367–372. https://doi.org/10.1016/j.ecoenv.2017.08.060.

Kamata, R., Shiraishi, F., Nakajima, D., Takahashi, S., Shimizu, A., 2010. Evaluation of the impact of in-ovo exposure to dicofol on avian reproduction. Environ. Toxicol. Chem. 29 (10), 2316–2322. https://doi.org/10.1002/etc.274.

Karchner, S.I., Franks, D.G., Kennedy, S.W., Hahn, M.E., 2006. The molecular basis for differential dioxin sensitivity in birds: role of the aryl hydrocarbon receptor. Proc. Natl. Acad. Sci. U. S. A. 103, 6252–6257.

Kase, R., Hansen, P.D., Fischer, B., Manz, W., Heininger, P., Reifferscheid, G., 2009. Integral assessment of estrogenic potentials in sediment-associated samples: part 2: study of estrogen and anti-estrogen receptor-binding potentials of sediment-associated chemicals under different salinity conditions using the salinity-adapted enzyme-linked receptor assay. Environ. Sci. Pollut. Res. Int. 16, 54–64.

Kavlock, R.J., Ankley, G.T., 1996. A perspective on the risk assessment process for endocrine-disruptive effects on wildlife and human health. Risk Anal. 16, 731–739.

Kavlock, R., Ankley, G.T., Collette, T., Francis, E., Hammerstrom, K., Fowle, J., Tilson, H., Toth, G., Schmieder, P., Veith, G.D., Weber, E., Wolf, D.C., Young, D., 2005. Computational toxicology: framework, partnerships, and program development: September 29–30, 2003, Research Triangle Park, North Carolina. Reprod. Toxicol. 19, 265–280.

Kavlock, R., Chandler, K., Houck, K., Hunter, S., Judson, R., Kleinstreuer, N., Knudsen, T., Martin, M., Padilla, S., Reif, D., Richard, A., Rotroff, D., Sipes, N., Dix, D., 2012. Update on EPA's ToxCast program: providing high throughput decision support tools for chemical risk management. Chem. Res. Toxicol. 25, 1287–1302.

Knudsen, T.B., Martin, M.T., Kavlock, R.J., Judson, R.S., Dix, D.J., Singh, A.V., 2009. Profiling the activity of environmental chemicals in prenatal developmental toxicity studies using the U.S. EPA's ToxRefDB. Reprod. Toxicol. 28, 209–219.

Knudsen, T., Martin, M., Chandler, K., Kleinstreuer, N., Judson, R., Sipes, N., 2013. Predictive models and computational toxicology. Methods Mol. Biol. 947, 343–374.

Kuil, C.W., Brouwer, A., Van Der Saag, P.T., Van Der Burg, B., 1998. Interference between progesterone and dioxin signal transduction pathways. Different mechanisms are involved in repression by the progesterone receptor A and B isoforms. J. Biol. Chem. 273, 8829–8834.

Kusk, K.O., Kruger, T., Long, M., Taxvig, C., Lykkesfeldt, A.E., Frederiksen, H., Andersson, A.M., Andersen, H.R., Hansen, K.M., Nellemann, C., Bonefeld-Jorgensen, E.C., 2011. Endocrine potency of wastewater: contents of endocrine disrupting chemicals and effects measured by in vivo and in vitro assays. Environ. Toxicol. Chem. 30, 413–426.

Lalone, C.A., Villeneuve, D.L., Burgoon, L.D., Russom, C.L., Helgen, H.W., Berninger, J.P., Tietge, J.E., Severson, M.N., Cavallin, J.E., Ankley, G.T., 2013. Molecular target sequence similarity as a basis for species extrapolation to assess the ecological risk of chemicals with known modes of action. Aquat. Toxicol. 144–145, 141–154.

Lamb, J.S., O'Reilly, K.M., Jodice, P.G., 2016. Physical condition and stress levels during early development reflect feeding rates and predict pre- and post-fledging survival in a nearshore seabird. Conserv. Physiol. 4 (1), cow060. https://doi.org/10.1093/conphys/cow060.

Lambert, G., Peakall, D.B., Philogene, B.J.R., Engelhardt, R.R., 1982. Effect of oil and oil dispersant mixtures on the basal metabolic rate of ducks. Bull. Environ. Contam. Toxicol. 29, 520–524.

Larkin, P., Folmar, L.C., Hemmer, M.J., Poston, A.J., Lee, H.S., Denslow, N.D., 2002. Array technology as a tool to monitor exposure of fish to xenoestrogens. Mar. Environ. Res. 54, 395–399.

Lattin, C.R., Romero, L.M., 2014. Chronic exposure to a low dose of ingested petroleum disrupts corticosterone receptor signalling in a tissue-specific manner in the house sparrow (*Passer domesticus*). Conserv. Physiol. 2, cou058.

Lattin, C.R., Ngai, H.M., Romero, L.M., 2014. Evaluating the stress response as a bioindicator of sub-lethal effects of crude oil exposure in wild house sparrows (*Passer domesticus*). PloS One 9, e102106.

Lavoie, E.T., Grasman, K.A., 2007. Effects of in ovo exposure to PCBs 126 and 77 on mortality, deformities and post-hatch immune function in chickens. J. Toxicol. Environ. Health 70, 547–558.

Lavoie, E.T., Wiley, F., Grasman, K.A., Tillitt, D.E., Sikarskie, J.G., Bowerman, W.W., 2007. Effect of in Ovo exposure to an organochlorine mixture extracted from double crested cormorant eggs (*Phalacrocorax auritus*) and PCB 126 on immune function of juvenile chickens. Arch. Environ. Contam. Toxicol. 53, 655–661.

Lavoie, R.A., Champoux, L., Rail, J.-F., Lean, D.R.S., 2010. Organochlorines, brominated flame retardants and mercury levels in six seabird species from the Gulf of St. Lawrence (Canada): relationships with feeding ecology, migration and molt. Environ. Pollut. 158, 2189–2199.

Le Page, Y., Vosges, M., Servili, A., Brion, F., Kah, O., 2011. Neuroendocrine effects of endocrine disruptors in teleost fish. J. Toxicol. Environ. Health B Crit. Rev. 14, 370–386.

Lerner, H., Berg, C., 2017. A comparison of three holistic approaches to health: one Health, EcoHealth, and planetary health. Front Vet Sci 4, 163. https://doi.org/10.3389/fvets.2017.00163.eCollection.

Levengood, J.M., Wiedenmann, L., Custer, T.W., Schaeffer, D.J., Matson, C.W., Melancon, M.J., Hoffman, D.J., Scott, J.W., Talbott, J.L., Bordson, G.O., Bickham, J.W., Rattner, B.A., Golden, N.H., 2007. Contaminant exposure and biomarker response in embryos of black-crowned night-herons (*Nycticorax nycticorax*) nesting near lake calumet, Illinois. J. Great Lake. Res. 33, 791–805.

Li, Q.C., Alston-Mills, B., Ottinger, M.A., 1991. Avian LHRH during embryonic development: measurement by competitive ELISA with a monoclonal antibody. Gen. Comp. Endocrinol. 82, 444–450.

Lin, F., Wu, J., Abdelnabi, M.A., Ottinger, M.A., Giusti, M.M., 2004. Effects of dose and glycosylation on the transfer of genistein into the eggs of the Japanese quail (*Coturnix japonica*). J. Agric. Food Chem. 52, 2397–2403.

Lipar, J.L., Ketterson, E.D., Nolan JR., V., Casto, J.M., 1999. Egg yolk layers vary in the concentration of steroid hormones in two avian species. Gen. Comp. Endocrinol. 115, 220–227.

Lipton, J., Morris, J., Takeshita, R., Dean, K., Gielazyn, M., Ricker, R., Tuttle, P., 2017. Toxicological effects of Deepwater Horizon oil: cross-taxonomic synthesis. In: 19th International Symposium on Pollutant Responses in Marine Organisms (PRIMO), Matsuyama, Japan. June 30–July 3.

Lundholm, C.D., 1997. DDE-induced eggshell thinning in birds: effects of p,p′-DDE on the calcium and prostaglandin metabolism of the eggshell gland. Comp. Biochem. Physiol. C Pharmacol. Toxicol. Endocrinol. 118, 113–128.

Maffini, M.V., Rubin, B.S., Sonnenschein, C., Soto, A.M., 2006. Endocrine disruptors and reproductive health: the case of bisphenol-A. Mol. Cell. Endocrinol. 254–255, 179–186.

Maggini, I., Kennedy, L.V., Bursian, S.J., Dean, K.M., Gerson, A.R., Harr, K.E., Link, J.E., Pritsos, C.A., Pritsos, K.L., Guglielmo, C.G., 2017a. Toxicological and thermoregulatory effects of feather contamination with artificially weathered MC 252 oil in western sandpipers (Calidris mauri). Ecotoxicol. Environ. Saf. 146, 118–128. https://doi.org/10.1016/j.ecoenv.2017.04.025.

Maggini, I., Kennedy, L.V., Elliott, K.H., Dean, K.M., Maccurdy, R., Macmillan, A., Pritsos, C.A., Guglielmo, C.G., 2017b. Trouble on takeoff: crude oil on feathers reduces escape performance of shorebirds. Ecotoxicol. Environ. Saf. 146, 111–117. https://doi.org/10.1016/j.ecoenv.2017.05.018.

Maggini, I., Kennedy, L.V., Macmillan, A., Elliott, K.H., Dean, K., Guglielmo, C.G., 2017c. Light oiling of feathers increases flight energy expenditure in a migratory shorebird. J. Exp. Biol. 220 (Pt 13), 2372–2379. https://doi.org/10.1242/jeb.158220.

Majewski, P., Adamska, I., Pawlak, J., Baranska, A., Skwarlo-Sonta, K., 2005. Seasonality of pineal gland activity and immune functions in chickens. J. Pineal Res. 39, 66–72.

Man, Y.B., Chow, K.L., Wang, H.S., Lau, K.Y., Sun, X.L., Wu, S.C., Cheung, K.C., Chung, S.S., Wong, M.H., 2011. Health risk assessment of organochlorine pesticides with emphasis on DDTs and HCHs in abandoned agricultural soils. J. Environ. Monit. 13, 2250–2259.

Manikkam, M., Tracey, R., Guerrero-Bosagna, C., Skinner, M.K., 2013. Plastics derived endocrine disruptors (Bpa, Dehp and DBP) induce epigenetic transgenerational inheritance of obesity, reproductive disease and sperm epimutations. PloS One 8, e55387.

Manning, G.E., Farmahin, R., Crump, D., Jones, S.P., Klein, J., Konstantinov, A., Potter, D., Kennedy, S.W., 2012. A luciferase reporter gene assay and aryl hydrocarbon receptor 1 genotype predict the LD50 of polychlorinated biphenyls in avian species. Toxicol. Appl. Pharmacol. 263, 390–401.

Marino, M., Pellegrini, M., La Rosa, P., Acconcia, F., 2012. Susceptibility of estrogen receptor rapid responses to xenoestrogens: physiological outcomes. Steroids 77, 910–917.

Markman, S., Leitner, S., Catchpole, C., Barnsley, S., Muller, C.T., Pascoe, D., Buchanan, K.L., 2008. Pollutants increase song complexity and the volume of the brain area HVC in a songbird. PloS One 3 (2), e1674. https://doi.org/10.1371/journal.pone.0001674.

Marks, H.L., 1996. Long-term selection for body weight in Japanese quail under different environments. Poultry Sci. 75, 1198–1203.

Marks, H.L., Siegel, H.S., 1980. Divergent selection in Japanese quail for the plasma cholesterol response to ACTH. Poultry Sci. 59, 1700–1705.

Marteinson, S.C., Fernie, K.J., 2019. Is the current-use flame retardant, DBE-DBCH, a potential obesogen? Effects on body mass, fat content and associated behaviors in American kestrels. Ecotoxicol. Environ. Saf. 169, 770–777. https://doi.org/10.1016/j.ecoenv.2018.11.104.

Martin, M.T., Judson, R.S., Reif, D.M., Kavlock, R.J., Dix, D.J., 2009. Profiling chemicals based on chronic toxicity results from the U.S. EPA ToxRef Database. Environ. Health Perspect. 117, 392–399.

Masuyama, H., Inoshita, H., Hiramatsu, Y., Kudo, T., 2002. Ligands have various potential effects on the degradation of pregnane X receptor by proteasome. Endocrinology 143, 55–61.

Mathewson, P.D., Hanson-Dorr, K.C., Porter, W.P., Bursian, S.J., Dean, K.M., Healy, K.C., Horak, K.E., Link, J.E., Harr, K.E., Dorr, B.S., 2018. Experimental and modeled thermoregulatory costs of repeated sublethal oil exposure in the double-crested cormorant, *Phalacrocorax auritus*. Mar. Pollut. Bull. 135, 216–223.

McNabb, F.M.A., 2005. Biomarkers for the assessment of avian thyroid disruption by chemical contaminants. Avian Poultry Biol. Rev. 16, 3–10.

McNabb, F.M., 2007. The hypothalamic-pituitary-thyroid (HPT) axis in birds and its role in bird development and reproduction. Crit. Rev. Toxicol. 37, 163–193.

McNabb, F.M., Fox, G.A., 2003. Avian thyroid development in chemically contaminated environments: is there evidence of alterations in thyroid function and development? Evol. Dev. 5, 76–82.

Millam, J.R., Craig-Veit, C.B., Quaglino, A.E., Erichsen, A.L., Famula, T.R., Fry, D.M., 2001. Posthatch oral estrogen exposure impairs adult reproductive performance of zebra finch in a sex-specific manner. Horm. Behav. 40, 542–549.

Milton, S., Lutz, P., Shigenaka, G., 2003. Oil Toxicity and Im- Pacts on Sea Turtles. Oil and Sea Turtles: Biology, Planning, and Response. NOAA National Ocean Service, pp. 35–47.

Mora, M.A., Durgin, B., Hudson, L.B., Jones, E., 2016. Temporal and latitudinal trends of p,p′-DDE in eggs and carcasses of North American birds from 1980 to 2005. Environ. Toxicol. Chem. 35 (6), 1340–1348. https://doi.org/10.1002/etc.3360.

Mura, E., Barale, C., Quinn Jr., M.J., Panzica, G., Ottinger, M.A., Viglietti-Panzica, C., 2009. Organizational effects of DDE on brain vasotocin system in male Japanese quail. Neurotoxicology 30, 479–484.

Myers, J.P., Vom Saal, F.S., Akingbemi, B.T., Arizono, K., Belcher, S., Colborn, T., Chahoud, I., Crain, D.A., Farabollini, F., Guillette JR., L.J., Hassold, T., Ho, S.M., Hunt, P.A., Iguchi, T., Jobling, S., Kanno, J., Laufer, H., Marcus, M., Mclachlan, J.A., Nadal, A., Oehlmann, J., Olea, N., Palanza, P., Parmigiani, S., Rubin, B.S., Schoenfelder, G., Sonnenschein, C., Soto, A.M., Talsness, C.E., Taylor, J.A., Vandenberg, L.N., Vandenbergh, J.G., Vogel, S., Watson, C.S., Welshons, W.V., Zoeller, R.T., 2009. Why public health agencies cannot depend on good laboratory practices as a criterion for selecting data: the case of bisphenol A. Environ. Health Perspect. 117, 309–315.

Newbold, R.R., Padilla-Banks, E., Jefferson, W.N., Heindel, J.J., 2008. Effects of endocrine disruptors on obesity. Int. J. Androl. 31, 201–208.

Nichols, J.W., Echols, K.R., Tillitt, D.E., Secord, A.L., Mccarty, J.P., 2004. Bioenergetics-based modeling of individual PCB congeners in nestling tree swallows from two contaminated sites on the upper Hudson River, New York. Environ. Sci. Technol. 38, 6234–6239.

Nost, T.H., Helgason, L.B., Harju, M., Heimstad, E.S., Gabrielsen, G.W., Jenssen, B.M., 2012. Halogenated organic contaminants and their correlations with circulating thyroid hormones in developing Arctic seabirds. Sci. Total Environ. 414, 248–256.

Nossen, I., Ciesielski, T.M., Dimmen, M.V., Jensen, H., Ringsby, T.H., Polder, A., Ronning, B., Jenssen, B.M., Styrishave, B., 2016. Steroids in house sparrows (Passer domesticus): Effects of POPs and male quality signalling. Sci. Total Environ. 547, 295–304. https://doi.org/10.1016/j.scitotenv.2015.12.113.

O'hara, P.D., Morandin, L.A., 2010. Effects of sheens associated with offshore oil and gas development on the feather microstructure of pelagic seabirds. Mar. Pollut. Bull. 60 (5), 672–678.

Ohlson, C.G., Hardell, L., 2000. Testicular cancer and occupational exposures with a focus on xenoestrogens in polyvinyl chloride plastics. Chemosphere 40, 1277–1282.

Oshima, A., Yamashita, R., Nakamura, K., Wada, M., Shibuya, K., 2012. In ovo exposure to nonylphenol and bisphenol A resulted in dose-independent feminization of male gonads in Japanese quail (*Coturnix japonica*) embryos. Environ. Toxicol. Chem. 31, 1091–1097.

Ottinger, M.A., 2005. Avian Species Comparison Study—A Protocol Development Study for the Avian 2-Generation Tier II Assay, Report to the Endocrine Disruptor Methods Validation Advisory Committee. College Park, MD.

Ottinger, M.A., Brinkley, H.J., 1978. Testosterone and sex-related behavior and morphology: relationship during maturation and in the adult Japanese quail. Horm. Behav. 11, 175–182.

Ottinger, M.A., Brinkley, H.J., 1979. Testosterone and sex related physical characteristics during the maturation of the male Japanese quail (coturnix coturnix japonica). Biol. Reprod. 20, 905–909.

Ottinger, M.A., Dean, K.M., 2011. Neuroendocrine impacts of endocrine-disrupting chemicals in birds: life stage and species sensitivities. J. Toxicol. Environ. Health B Crit. Rev. 14, 413–422.

Ottinger, M.A., vom Saal, F.S., 2002. Impact of environmental endocrine disruptors on sexual differentiation in birds and mammals. In: Pfaff, D., Arnold, A., Etgen, A., Rubin, R. (Eds.), Hormones and Behavior in Higher Vertebrates, vol. 4. Academic Press, pp. 325–383.

Ottinger, M.A., Abdelnabi, M., Li, Q., Chen, K., Thompson, N., Harada, N., Viglietti-Panzica, C., Panzica, G.C., 2004. The Japanese quail: a model for studying reproductive aging of hypothalamic systems. Exp. Gerontol. 39, 1679–1693.

Ottinger, M.A., Quinn Jr., M.J., Lavoie, E., Abdelnabi, M.A., Thompson, N., Hazelton, J.L., Wu, J.M., Beavers, J., Jaber, M., 2005a. Consequences of endocrine disrupting chemicals on reproductive endocrine function in birds: establishing reliable end points of exposure. Domest. Anim. Endocrinol. 29, 411–419.

Ottinger, M.A., Wu, J.M., Hazelton, J.L., Abdelnabi, M.A., Thompson, N., Quinn Jr., M.L., Donoghue, D., Schenck, F., Ruscio, M., Beavers, J., Jaber, M., 2005b. Assessing the consequences of the pesticide methoxychlor: neuroendocrine and behavioral measures as indicators of biological impact of an estrogenic environmental chemical. Brain Res. Bull. 65, 199–209.

Ottinger, M.A., Lavoie, E., Thompson, N., Barton, A., Whitehouse, K., Barton, M., Abdelnabi, M., Quinn Jr., M., Panzica, G., Viglietti-Panzica, C., 2008. Neuroendocrine and behavioral effects of embryonic exposure to endocrine disrupting chemicals in birds. Brain Res. Rev. 57, 376–385.

Ottinger, M.A., Lavoie, E.T., Abdelnabi, M., Quinn, M.J., Marcell, A., Dean, K., 2009a. An overview of dioxin-like compounds, PCB, and pesticide exposures associated with sexual differentiation of neuroendocrine systems, fluctuating asymmetry, and behavioral effects in birds. J. Environ. Sci. Health Part C Environ. Carcinog. Ecotoxicol. Rev. 27, 286–300.

Ottinger, M.A., Lavoie, E.T., Thompson, N., Bohannon, M., Dean, K., Quinn, M.J., 2009b. Is the gonadotropin releasing hormone system vulnerable to endocrine disruption in birds? Gen. Comp. Endocrinol. 163, 104–108.

Ottinger, M.A., Carro, T., Bohannon, M., Baltos, L., Marcell, A.M., Mckernan, M., Dean, K.M., Lavoie, E., Abdelnabi, M., 2013. Assessing effects of environmental chemicals on neuroendocrine systems: potential mechanisms and functional outcomes. Gen. Comp. Endocrinol. 190, 194–202.

Ottinger, M.A., Maness, T., Grace, J.K., Wilson, R.R., Jodice, P.G.R., 2019. Avian health assessments. In: Wilson, R.R., Fournier, A.M.V., Gleason, J.S., Lyons, J.E. (Eds.), Research Bulletin, Gulf of Mexico Avian Monitoring Network Strategic Avian Monitoring Plan, vol. 1228. Woodrey. Mississippi State University.

Panzica, G.C., Viglietti-Panzica, C., Mura, E., Quinn Jr., M.J., Lavoie, E., Palanza, P., Ottinger, M.A., 2007. Effects of xenoestrogens on the differentiation of behaviorally-relevant neural circuits. Front. Neuroendocrinol. 28, 179–200.

Peakall, D.B., Tremblay, J., Kinter, W.B., Miller, D.S., 1981. Endocrine dysfunction in seabirds caused by ingested oil. Environ. Res. 24, 6–14.

Pereira, S.P., Pereira, G.C., Pereira, C.V., Carvalho, F.S., Cordeiro, M.H., Mota, P.C., Ramalho-Santos, J., Moreno, A.J., Oliveira, P.J., 2013. Dioxin-induced acute cardiac mitochondrial oxidative damage and increased activity of ATP-sensitive potassium channels in Wistar rats. Environ. Pollut. 180, 281–290.

Perez, C.R., Moye, J.K., Cacela, D., Dean, K.M., Pritsos, C.A., 2017a. Homing pigeons externally exposed to Deepwater Horizon crude oil change flight performance and behavior. Environ. Pollut. 230, 530–539. https://doi.org/10.1016/j.envpol.2017.07.008.

Perez, C.R., Moye, J.K., Cacela, D., Dean, K.M., Pritsos, C.A., 2017b. Low level exposure to crude oil impacts avian flight performance: the Deepwater Horizon oil spill effect on migratory birds. Ecotoxicol. Environ. Saf. 146, 98–103. https://doi.org/10.1016/j.ecoenv.2017.05.028.

Perez, C.R., Moye, J.K., Cacela, D., Dean, K.M., Pritsos, C.A., 2017c. Body mass change in flying homing pigeons externally exposed to Deepwater Horizon crude oil. Ecotoxicol. Environ. Saf. 146, 104–110. https://doi.org/10.1016/j.ecoenv.2017.05.012.

Perry, M.C., Ferrigno, F., Settle, F.H., 1978. Rehabilitation of birds oiled on two mid-Atlantic estuaries. Proc. Annu. Conf. Southeast. Assoc. Fish Wildl. Agencies 32, 318–325.

Pessah, I.N., Cherednichenko, G., Lein, P.J., 2010. Minding the calcium store: ryanodine receptor activation as a convergent mechanism of PCB toxicity. Pharmacol. Ther. 125, 260–285.

Prins, G.S., 2008. Endocrine disruptors and prostate cancer risk. Endocr. Relat. Canc. 15, 649–656.

Pritsos, K.L., Perez, C.R., Muthumalage, T., Dean, K.M., Cacela, D., Hanson-Dorr, K., Cunningham, R., Bursian, S.J., Link, J.E., Shriner, S., Horak, K., Pritsos, C.A., 2017. Dietary intake of Deepwater Horizon oil-injected live food fish by double-crested cormorants resulted in oxidative stress. Ecotoxicol. Environ. Saf. 146, 62–67. https://doi.org/10.1016/j.ecoenv.2017.06.067.

Qasimi, M.I., Nagaoka, K., Watanabe, G., 2018. Feeding of phytosterols reduced testosterone production by modulating GnRH and GnIH expression in the brain and testes of male Japanese quail (*Coturnix coturnix* japonica). Poultry Sci. 97 (3), 1066–1072. https://doi.org/10.3382/ps/pex370.

Quinn Jr., M.J., Lavoie, E.T., Ottinger, M.A., 2007a. Reproductive toxicity of trenbolone acetate in embryonically exposed Japanese quail. Chemosphere 66, 1191–1196.

Quinn, M.J., Mckernan, M., Lavoie, E.T., Ottinger, M.A., 2007b. Immunotoxicity of trenbolone acetate in Japanese quail. J. Toxicol. Environ. Health 70, 88–93.

Quinn Jr., M.J., Summitt, C.L., Ottinger, M.A., 2008. Consequences of in ovo exposure to p,p′-DDE on reproductive development and function in Japanese quail. Horm. Behav. 53, 249–253.

Quinn, M.J. Jr., Ottinger, M.A., 2006. Embryonic effects of androgen active endocrine disrupting chemicals on avian immune and reproductive systems. J. Poult. Sci. 43, 1–11.

Quinn Jr., M.J., Mckernan, M., Lavoie, E.T., Ottinger, M.A., 2009. Effects of estradiol on the development of the bursa of Fabricius in Japanese quail. J. Exp. Zool. A Ecol. Genet. Physiol. 311, 91–95.

Rabinowitz, P.M., Pappaioanou, M., Bardosh, K.L., Conti, L., 2018. A planetary vision for one health. BMJ Glob. Health 3 (5), 3001137. https://doi.org/10.1136/bmjgh-2018-001137.

Rainwater, T.R., Wood, M.B., Millam, J.R., Hooper, M.J., 2008. Effects of perchlorate on growth and behavior of a granivorous passerine, the zebra finch (*Taeniopygia guttata*). Arch. Environ. Contam. Toxicol. 54, 516–524.

Ramenofsky, M., 1985. Acute changes in plasma steroids and agonistic behavior in male Japanese quail. Gen. Comp. Endocrinol. 60, 116–128.

Rattner, B.A., 2009. History of wildlife toxicology. Ecotoxicology 18, 773–783.

Rattner, B.A., Clarke, R.N., Ottinger, M.A., 1986. Depression of plasma luteinizing hormone concentration in quail by the anticholinesterase insecticide parathion. Comp. Biochem. Physiol., C 83, 451–453.

Rattner, B.A., Hoffman, D.J., Melancon, M.J., Olsen, G.H., Schmidt, S.R., Parsons, K.C., 2000. Organochlorine and metal contaminant exposure and effects in hatching black-crowned night herons (*Nycticorax nycticorax*) in Delaware Bay. Arch. Environ. Contam. Toxicol. 39, 38–45.

Rattner, B.A., Mcgowan, P.C., Hatfield, J.S., Hong, C.S., Chu, S.G., 2001. Organochlorine contaminant exposure and reproductive success of black-crowned night-herons (*Nycticorax nycticorax*) nesting in Baltimore Harbor, Maryland. Arch. Environ. Contam. Toxicol. 41, 73–82.

Rattner, B.A., Horak, K.E., Warner, S.E., Johnston, J.J., 2010. Acute toxicity of diphacinone in Northern bobwhite: effects on survival and blood clotting. Ecotoxicol. Environ. Saf. 73, 1159–1164.

Rattner, B.A., Lazarus, R.S., Elliott, J.E., Shore, R.F., van den Brink, N., 2014. Adverse outcome pathway and risks of anticoagulant rodenticides to predatory wildlife. Environ. Sci. Technol. 48 (15), 8433–8445. https://doi.org/10.1021/es501740n.

Rochester, J.R., Millam, J.R., 2009. Phytoestrogens and avian reproduction: exploring the evolution and function of phytoestrogens and possible role of plant compounds in the breeding ecology of wild birds. Comp. Biochem. Physiol. Mol. Integr. Physiol. 154, 279–288.

Rochester, J.R., Forstmeier, W., Millam, J.R., 2010. Post-hatch oral estrogen in zebra finches (*Taeniopygia guttata*): is infertility due to disrupted testes morphology or reduced copulatory behavior? Physiol. Behav. 101, 13–21.

Ross, A.W., Helfer, G., Russell, L., Darras, V.M., Morgan, P.J., 2011. Thyroid hormone signalling genes are regulated by photoperiod in the hypothalamus of F344 rats. PloS One 6.

Ruuskanen, S., Epsin, S., Sanchez-Virosta, P., Sarraude, T., Hsu, B.-Y., Pajunen, P., Costa, R.A., Eens, M., Hargitai, R., Torok, J., Eeva, T., 2019. Transgenerational endocrine disruption: does elemental pollution affect egg or nestling thyroid hormone levels in a wild songbird? Environ. Pollut. 247, 725–735. https://doi.org/10.1016/j.envpol.2019.01.088.

Safe, S., Bandiera, S., Sawyer, T., Robertson, L., Safe, L., Parkinson, A., Thomas, P.E., Ryan, D.E., Reik, L.M., Levin, W., et al., 1985. PCBs: structure-function relationships and mechanism of action. Environ. Health Perspect. 60, 47–56.

Safe, S., Wang, F., Porter, W., Duan, R., Mcdougal, A., 1998. Ah receptor agonists as endocrine disruptors: antiestrogenic activity and mechanisms. Toxicol. Lett. 102–103, 343–347.

Santamans, A.C., Boluda, R., Picazo, A., Gil, C., Ramos-Mira, J., Tejedo, P., Pertierra, L.R., Benayas, J., Camacho, A., August 16, 2017. Soil features in rookeries of Antarctic penguins reveal sea to land biotransport of chemical pollutants. PloS One 12 (8), e0181901. https://doi.org/10.1371/journal.pone.0181901.

Santti, R., Makela, S., Strauss, L., Korkman, J., Kostian, M.L., 1998. Phytoestrogens: potential endocrine disruptors in males. Toxicol. Ind. Health 14, 223–237.

Satre, D., Reichert, M., Corbitt, C., 2009. Effects of vinclozolin, an antiandrogen, on affiliative behavior in the Dark-eyed Junco, Junco hyemalis. Environ. Res. 109, 400–404.

Scanes, C.G., McNabb, F.M.A., 2003. Avian models for research in toxicology and endocrine disruption. Avian Poultry Biol. Rev. 14, 21–52.

Schleidt, W.M., Shalter, M.D., 1973. Stereotypy of a fixed action pattern during ontogeny in *Coturnix coturnix coturnix*. Z. Tierpsychol. 33, 35–37.

Schug, T.T., Janesick, A., Blumberg, B., Heindel, J.J., 2011. Endocrine disrupting chemicals and disease susceptibility. J. Steroid Biochem. Mol. Biol. 127, 204–215.

Schwabl, H., 1993. Yolk is a source of maternal testosterone for developing birds. Proc. Natl. Acad. Sci. U. S. A. 90, 11446–11450.

Schwabl, H., 1996a. Environment modifies the testosterone levels of a female bird and its eggs. J. Exp. Zool. 276, 157–163.

Schwabl, H., 1996b. Maternal testosterone in the avian egg enhances postnatal growth. Comp. Biochem. Physiol. A Physiol. 114, 271–276.

Seegar, W.S., Yates, M.A., Doney, G.E., Jenny, J.P., Seegar, T.C.M., Perkins, C., Giovanni, M., 2015. Migrating Tundra Peregrine Falcons accumulate polycyclic aromatic hydrocarbons along Gulf of Mexico following Deepwater Horizon oil spill. Ecotoxicology 24 (5), 1102–1111. https://doi.org/10.1007/s10646-015-1450-8.

Skinner, M.K., 2007. Endocrine disruptors and epigenetic transgenerational disease etiology. Pediatr. Res. 61, 48R–50R.

Skinner, M.K., Manikkam, M., Guerrero-Bosagna, C., 2011. Epigenetic transgenerational actions of endocrine disruptors. Reprod. Toxicol. 31, 337–343.

Smiley, K.O., 2019. Prolactin and avian parental care: new insights and unanswered questions. Horm. Behav. 111, 114–130. https://doi.org/10.1016/j.yhbeh.2019.02.012.

Smiley, K.O., Buntin, J.D., Corbitt, C., Deviche, P., 2020. Central prolactin binding site densities change seasonally in an adult male passerine bird (Junco hyemalis). J. Chem. Neuroanat. 106, 101786. https://doi.org/10.1016/j.jchemneu.2020.101786.

Soto, A.M., Sonnenschein, C., 2010. Environmental causes of cancer: endocrine disruptors as carcinogens. Nat. Rev. Endocrinol. 6, 363–370.

Stoker, T.E., Parks, L.G., Gray, L.E., Cooper, R.L., 2000. Endocrine-disrupting chemicals: prepubertal exposures and effects on sexual maturation and thyroid function in the male rat. A focus on the EDSTAC recommendations. Endocrine Disrupter Screening and Testing Advisory Committee. Crit. Rev. Toxicol. 30, 197–252.

Takeshita, R., J. Morris, J., Dean, K., Gielazyn, M., Ricker, R., Tuttle, P., Lipton, J., 2016. Identifying and characterizing Deepwater Horizon oil's toxic effects across taxa. In: 37th Annual Meeting of the Society of Environmental Toxicology and Chemistry (SETAC), Orlando, FL. November 6–10.

Thackaberry, E.A., Nunez, B.A., Ivnitski-Steele, I.D., Friggins, M., Walker, M.K., 2005. Effect of 2,3,7,8-tetrachlorodibenzo-p-dioxin on murine heart development: alteration in fetal and postnatal cardiac growth, and postnatal cardiac chronotropy. Toxicol. Sci. 88, 242–249.

Touart, L.W., 2004. Factors considered in using birds for evaluating endocrine-disrupting chemicals. ILAR J. 45, 462–468.

Van den Berg, M., Denison, M.S., Birnbaum, L.S., Devito, M.J., Fiedler, H., Falandysz, J., Rose, M., Schrenk, D., Safe, S., Tohyama, C., Tritscher, A., Tysklind, M., Peterson, R.E., 2013. Polybrominated dibenzo-p-dioxins, dibenzofurans, and biphenyls: inclusion in the toxicity equivalency factor concept for dioxin-like compounds. Toxicol. Sci. 133, 197–208.

Vermeulen, R., Schymanski, E., Barbasi, A.-L., Miller, G.W., 2020. The exposome and health: where chemistry meets biology. Science 367, 392–396.

Vesterinen, H.M., Dutcher, T.V., Errecaborde, K.M., Mahero, M.W., Macy, K.W., Prasamphanich, O.-O., Kassenborg, H., Yulizar, E., Fauzi, R.P., Budayanti, N.S., Suwandono, A., Artama, W.T., Valeri, L., Pelican, K.M., 2019. Strengthening multi-sectoral collaboration on critical health issues: one Health systems mapping and analysis resource toolkit (OH-SMART) for operationalizing one health. PloS One 14 (7), e0219197. https://doi.org/10.1371/journal.pone.0219197.

Villeneuve, D., Volz, D.C., Embry, M.R., Ankley, G.T., Belanger, S.E., Leonard, M., Schirmer, K., Tanguay, R., Truong, L., Wehmas, L., 2014. Investigating Alternatives to the fish early-life stage test: a strategy for discovering and annotating adverse outcome pathways for early fish development. Environ. Toxicol. Chem. 33 (1), 158–169.

Vorkamp, K., Falk, K., Moller, S., Bossi, R., Riget, F.F., Sorensen, P.B., 2019. Perfluoroalkyl substances (PFASs) and polychlorinated naphthalenes (PCNs) add to the chemical cocktail in peregrine falcon eggs. Sci. Total Environ. 648, 894–901. https://doi.org/10.1016/j.scitotenv.2018.08.090.

Vyas, N.B., Hill, E.F., Sauer, J.R., Kuenzel, W.J., 1995. Acephate affects migratory orientation of the white-throated sparrow (*Zonotrichia albicollis*). Environ. Toxicol. Chem. 14 (11), 1961–1965.

Wada, H., Cristol, D.A., McNabb, F.M.A., Hopkins, W.A., 2009. Suppressed adrenocortical responses and thyroid hormone levels in birds near a mercury-contaminated river. Environ. Sci. Technol. 43, 6031–6038.

Wade, J., Arnold, A.P., 2004. Sexual differentiation of the zebra finch song system. Ann. N. Y. Acad. Sci. 1016, 540–559.

Wade, J., Peabody, C., Coussens, P., Tempelman, R.J., Clayton, D.F., Liu, L., Arnold, A.P., Agate, R., 2004. A cDNA microarray from the telencephalon of juvenile male and female zebra finches. J. Neurosci. Methods 138, 199–206.

Walker, M.K., Catron, T.F., 2000. Characterization of cardiotoxicity induced by 2,3,7, 8-tetrachlorodibenzo-p-dioxin and related chemicals during early chick embryo development. Toxicol. Appl. Pharmacol. 167, 210–221.

Walter, S.T., Carloss, M.R., Hess, T.J., Leberg, P.L., 2013. Hurricane, habitat degradation, and land loss effects on Brown Pelican nesting colonies. J. Coast Res. 29, 187–195.

Walton, P., Turner, C.M.R., Austin, G., Burns, M.D., Monaghan, P.M., 1997. Sub-lethal effects of an oil pollution incident on breeding kittiwakes *Rissa tridactyla*. Mar. Ecol. Prog. Ser. 155, 261–268.

Wambaugh, J.F., Setzer, R.W., Reif, D.M., Gangwal, S., Mitchell-Blackwood, J., Arnot, J.A., Joliet, O., Frame, A., Rabinowitz, J., Knudsen, T.B., Judson, R.S., Egeghy, P., Vallero, D., Cohen Hubal, E.A., 2013. High-throughput models for exposure-based chemical prioritization in the ExpoCast project. Environ. Sci. Technol. 47, 8479–8488.

Wang, J., Shi, X., Du, Y., Zhou, B., 2011. Effects of xenoestrogens on the expression of vitellogenin (vtg) and cytochrome P450 aromatase (cyp19a and b) genes in zebrafish (*Danio rerio*) larvae. J. Environ. Sci. Health A Tox. Hazard Subst. Environ. Eng. 46, 960–967.

Watanabe, H., Iguchi, T., Morohashi, K., 2002. Endocrine disruptors and nuclear receptors. Nihon Rinsho 60, 397–403.

Watanabe, M.X., Jones, S.P., Iwata, H., Kim, E.-Y., Kennedy, S.W., 2009. Effects of co-exposure to 2,3,7,8-tetrachlorodibenzo-p-dioxin and perfluorooctane sulfonate or perfluorooctanoic acid on expression of cytochrome P450 isoforms in chicken (Gallus gallus) embryo hepatocyte cultures. Comp. Biochem. Physiol. C Toxicol. Pharmacol. 149, 605–612.

Watson, C.S., Hu, G., Paulucci-Holthauzen, A.A., 2014. Rapid actions of xenoestrogens disrupt normal estrogenic signaling. Steroids 81, 36–42.

Webb, C.M., McNabb, F.M.A., 2008. Polychlorinated biphenyl effects on avian hepatic enzyme induction and thyroid function. Gen. Comp. Endocrinol. 155, 650–657.

Weseloh, D.V., Mineau, P., Struger, J., 1990. Geographical distribution of contaminants and productivity measures of herring gulls in the Great Lakes: Lake Erie and connecting channels 1978/79. Sci. Total Environ. 91, 141–159.

Wiemeyer, S.N., Clark Jr., D.R., Spann, J.W., Belisle, A.A., Bunck, C.M., 2001. Dicofol residues in eggs and carcasses of captive American kestrels. Environ. Toxicol. Chem. 20 (12), 2848–2851. https://doi.org/10.1897/1551-5028(2001)020<2848:drieac>2.0.co;2.

Wilson, F.E., Reinert, B.D., 1999. Long days and thyroxine program american tree sparrows for seasonality: evidence for temporal flexibility of the breeding season of euthyroid females. Gen. Comp. Endocrinol. 113, 136–145.

Yamashita, R., Oshima, A., Hasegawa-Baba, Y., Wada, M., Shibuya, K., 2011. Endocrine disrupting effects of low dose 17 beta-estradiol (E2) on the Japanese quail (*Coturnix japonica*) were detected by modified one-generation reproduction study. J. Toxicol. Sci. 36, 43–54.

Zacharewski, T., 1998. Identification and assessment of endocrine disruptors: limitations of in vivo and in vitro assays. Environ. Health Perspect. 106 (Suppl. 2), 577–582.

Zawatski, W., Lee, M.M., 2013. Male pubertal development: are endocrine-disrupting compounds shifting the norms? J. Endocrinol. 218, R1–R12.

Zhang, D., Trudeau, V.L., 2006. Integration of membrane and nuclear estrogen receptor signaling. Comp. Biochem. Physiol. Mol. Integr. Physiol. 144, 306–315.

Zhang, R., Manning, G.E., Farmahin, R., Crump, D., Zhang, X., Kennedy, S.W., 2013. Relative potencies of aroclor mixtures derived from avian in vitro bioassays: comparisons with calculated toxic equivalents. Environ. Sci. Technol. 47, 8852–8861.

Chapter 49

Blood supplement

Colin G. Scanes
Department of Biological Sciences, University of Wisconsin Milwaukee, Milwaukee, WI, United States

Tables 49.1–49.5.

TABLE 49.1 Summary of blood concentrations of erythrocytes, leukocytes, and thrombocytes, together with hemoglobin concentration and hematocrit in avian species.

	HCT or PCV %	Hb g dL^{-1}	RBC #x 10^6 mm^{-3}	Leukocytes #x 10^3 mm^{-3}	Thrombocytes #x 10^3 mm^{-3}	References
Species						
Palaeognathae						
Elegant crested tinamou (*Eudromia elegans*)	33.8					Black et al. (2013)
Emu (*Dromaius novaehollandiae*)	37.0	11.8	1.6	15.7		Patodkar et al. (2008)
Greater rhea (*Rhea americana*)	49.4			8.9		Uhart et al. (2006)
Lesser rhea (*Pterocnemia pennata*)	48	17.8	2.2	14.1		Reissig et al. (2002)
Ostrich (*Struthio camelus*)	44.15	11.2	1.95	10.0	25.85	Mean: Mushi et al. (1999), Bonadiman et al. (2009)
Red-legged tinamou (*Crypturellus erythropus*)	34.3	22	1.87	9.55		Smith (2003)
Order *Accipitriformes*						
Family Accipitridae						
African fish eagle (*Haliaeetus vocifer*)	43.2	22.3	2.04			Hollamby et al. (2004)
African harrier-hawk (*Polyboroides typus*)	46.7	24.2	2.29			Cooper (1975)
African hawk-eagle (*Aquila spilogaster*)	40.1	21.9	2.31			Cooper (1975)
African white-backed vulture (*Gyps africanus*)	44.3	19.7	2.5	16.7		Naidoo et al. (2008)
Augur buzzard (*Buteo augur*)	30.8	18.4	1.74			Cooper (1975)
Bald eagle (*Haliaeetus leucocephalus*)	47.5	15.3	3	11.3		Mean: Elliott et al. (1974), Hoffmanet al. (1981)

Continued

Sturkie's Avian Physiology. https://doi.org/10.1016/B978-0-12-819770-7.00007-4

TABLE 49.1 Summary of blood concentrations of erythrocytes, leukocytes, and thrombocytes, together with hemoglobin concentration and hematocrit in avian species.—cont'd

	HCT or PCV %	Hb g dL^{-1}	RBC #x 10^6 mm^{-3}	Leukocytes #x 10^3 mm^{-3}	Thrombocytes #x 10^3 mm^{-3}	References
Bearded vulture (*Gypaetus barbatus*)	47	16.4	2.9	9.7		Hernández and Margalida (2010)
Black kite (*Milvus migrans*)	42.5	20.3	1.93	19.0		Mean: Cooper (1975), Ferrer et al. (1987), Powers et al. (1994)
Black-shouldered kite (*Elanus axillaris*)	48.5	19.6	2.00			Cooper (1975)
Black sparrowhawk (*Accipiter melanoleucus*)	41.8	24.4	2.33			Cooper (1975)
Black vulture (*Coragyps atratus*)	48.4	10.5	1.8	16.5	14.1	Barbara et al. (2017)
Booted eagle (*Hieraaetus pennatus*)	43					Ferrer et al. (1987)
Cape vulture (*Gyps coprotheres*)	46		2.8	44.5		Van Heerden et al. (1987)
Cinereous vulture (*Aegypius monachus*)	43	18.3	2.4	19.6	33.9	Seok et al. (2017)
Common buzzard (*Buteo buteo*)	41			31.5		Ferrer et al. (1987), Powers et al. (1994)
Cooper's hawk (*Accipiter cooperi*)	49.9		3.75			Gessaman et al. (1986)
Crested serpent eagle (*Spilornis cheela*)	44.9		2.6	22.0		Elliott et al. (1974), Chan et al. (2012)
Eastern imperial eagle (*Aquila heliaca*)	40					Ferrer et al. (1987)
Egyptian vulture (*Neophron percnopterus*)	42.5	13.7	2.3	16.0		Polo et al. (1992)
Eurasian griffon (*Gyps fulvus*)	45	15.1	2.6	13.2		Polo et al. (1992)
European honey buzzard (*Pernis apivorus*)				10.5		Cited in Powers et al. (1994)
Gabar goshawk (*Micronisus gabar*)	32.8	16.4	1.72			Cooper (1975)
Galapagos hawk (*Buteo galapagoensis*)	43					Dem et al. (2012)
Golden eagle (*Aquila chrysaetos*)	39	13.8	2.1	19.7		Mean: Elliott et al. (1974), Polo et al. (1992)
Griffon vulture (*Gyps fulvus*)	47	15.2	2.5	13.2	10.5	Polo et al. (1992), Giambelluca et al. (2017)
Harpy eagle (*Harpia harp*)	34.2	8.8	1.5	15.3		Oliveira et al. (2014)
Harris's hawk (*Parabuteo unicinctus*)				13.0		Cited in Powers et al. (1994)
Hooded vulture (*Necrosyrtes monachus*)	41.4	20.4	2.4	22.4		Mean: Elliott et al. (1974), Cooper (1975)

Continued

TABLE 49.1 Summary of blood concentrations of erythrocytes, leukocytes, and thrombocytes, together with hemoglobin concentration and hematocrit in avian species.—cont'd

	HCT or PCV %	Hb g dL^{-1}	RBC #x 10^6 mm^{-3}	Leukocytes #x 10^3 mm^{-3}	Thrombocytes #x 10^3 mm^{-3}	References
Lizard buzzard (*Kaupifalco monogrammicus*)	44.7	24.8	2.7			Cooper (1975)
Long-crested eagle (*Lophaetus occipitalis*)	41.0	13.2	4.01			Cooper (1975)
Marsh harrier (*Circus aeruginosus*)	34.7			21.0		Lavin et al. (1992); Cited in Powers et al. (1994)
Montagu's harrier (*Circus pygargus*)	51	13.5	3.1	12.3		Lavin et al. (1993)
Northern goshawk (*Accipiter gentilis*)				8.7		Hanauska-Brown and Roloff (2003)
Ornate hawk-eagle (*Spizaetus ornatus*)	40.0		1.8	33.0		Elliott et al. (1974)
Pale chanting goshawk (*Melierax canorus*)	32.0	16.4	1.59			Cooper (1975)
Red kite (*Milvus milvus*)				12.0		Cited in Powers et al. (1994)
Red-tailed hawk (*Buteo jamaicensis*)	39.4		2.45			Rehder et al. (1982)
Savanna hawk (*Buteogallus meridionalis*)	52.5		3.0	31.0		Elliott et al. (1974)
Sharp-shinned hawk (*Accipiter striatus*)	49.1			12.9		Polo et al. (1992)
South American snail kite (*Rostrhamus sociabilis*)	42	14.0	2.8			Mean: Gessaman et al. (1986), Powers et al. (1994)
Spanish imperial eagle (*Aquila adalberti*)	43.5	14.2	2.29	15.1		Gee et al. (1981)
Steppe eagle (*Aquila nipalensis*)	35.0	17.8	2.12			Cooper (1975)
Swamp harrier (*Circus approximans*)	39			20.7		Calculated from
Tawny eagle (*Aquila rapax*)	38.1	15.1	2.30			Youl (2009)
Wahlberg's eagle (*Aquila wahlbergi*)	32.5	16.9	1.53			Mean: Cooper (1975), Fourie and Hattingh (1983)
White-bellied sea eagle (*Haliaeetus leucogaster*)	55		3.2	22.0		Cooper (1975)
White-tailed sea eagle (*Haliaeetus albicilla*)				19.5		Elliott et al. (1974)
Family *Cathartidae*						Cited in Powers et al. (1994)
Andean condor (*Vultur gryphus*)	42	13.5	2.4			Gee et al. (1981)
California condor (*Gymnogyps californianus*)	44			15.7		Dujowich et al. (2005)

Continued

TABLE 49.1 Summary of blood concentrations of erythrocytes, leukocytes, and thrombocytes, together with hemoglobin concentration and hematocrit in avian species.—cont'd

	HCT or PCV %	Hb g dL^{-1}	RBC #x 10^6 mm^{-3}	Leukocytes #x 10^3 mm^{-3}	Thrombocytes #x 10^3 mm^{-3}	References
King vulture (*Sarcoramphus papa*)	43		3.8			Elliott et al. (1974)
Secretary bird (*Sagittarius serpentarius*)	37.5	22.3	1.5			Cooper (1975)
Order *Anseriformes*						
Andean goose (*Chloephaga melanoptera*)	35.3	10.8				Lague et al. (2017)
Bar-headed goose (*Anser indicus*)	31	9.75				Lague et al. (2017)
Black duck (*Anas superciliosa*)	40.2	13.0	2.8	19.7		Mulley (1979)
Bufflehead (*Bucephala albeola*)	54.3		2.6			Kocan (1972)
Canvasback duck (*Aythya valisineria*)	52.2		2.6			Kocan (1972)
Common pochard (*Aythya ferina*)	43.7	14.6	3.2			Balasch et al. (1974)
Eurasian teal (*Anas crecca*)	38.2	12.4	4.2	6.7		Elarabany (2018)
Ferruginous ducks (*Aythya nyroca*)	46.3			3.9		Avni-Magen et al. (2016)
Lesser scaup (*Aythya af nis*)	57.1		2.4			Kocan (1972)
Maccoa duck (*Oxyura maccoa*)	37.9	15.1	3.1			Fourie and Hattingh (1983)
Mallard (*Anas platyrhynchos*)	42	16.4	3.0			Shave and Howard (1976), Butler and Jones (1997)
Maned duck or Australian wood duck (*Chenonetta jubata*)	45.5	14.9	2.8	25.1		Mulley (1980), Driver (1981)
Mottled duck (*Anas fulvigula*)	38	12.5		18.0		Ratliff et al. (2017)
Northern shoveler (*Anas clypeata*)	46.2	15.1	5.7	6.0		Elarabany (2018)
Red-billed teal (*Anas erythrorhyncha*)	44.6	14.0	3.5			Fourie and Hattingh (1983)
Ring-necked duck (*Aythya collaris*)	49.1		2.5			Kocan (1972)
Tufted duck (*Aythya fuligula*)		18.4				Butler and Jones (1997)
Yellow-billed duck (*Anas undulata*)	40.7	13.4	3.2			Fourie and Hattingh (1983)
Wood duck (*Chenonetta jubata*)	45.5	14.9	2.8	23.6		Mulley (1980)
Aleutian Canada goose (*Branta canadensis leucopareia*)	42	13.2	2.6			Gee et al. (1981)

Continued

TABLE 49.1 Summary of blood concentrations of erythrocytes, leukocytes, and thrombocytes, together with hemoglobin concentration and hematocrit in avian species.—cont'd

	HCT or PCV %	Hb g dL^{-1}	RBC #x 10^6 mm^{-3}	Leukocytes #x 10^3 mm^{-3}	Thrombocytes #x 10^3 mm^{-3}	References
Egyptian goose (*Alopochen aegyptiacus*)	43.7	14.9	3.2			Fourie and Hattingh (1983)
Embden goose (*Anser anser*)	38	11.4	2.6			Gee et al. (1981)
Nene goose (*Branta sandvicensis*)	46	15.5	2.6			Gee et al. (1981)
Snow goose (*Anser caerulescens*)	45.8	14.2	2.24	19.7		Williams and Trainer (1971)
Spur-winged goose (*Plectropterus gambensis*)	42.2	13.4	2.8			Fourie and Hattingh (1983)
Tule white-fronted goose (*Anser albifrons*)	43	15.0	2.9			Gee et al. (1981)
Black-necked swan (*Cygnus melanocoryphus*)	35.5	12.0		11.75		Norambuena and Bozinovic (2009)
Mute swan (*Cygnus olor*)	34.5	12.7	2.07	16.2		Dolka et al. (2014)
Trumpeter swan (*Cygnus buccinators*)	45			12.6		Olsen et al. (2002)
Tundra swan (*Cygnus columbianus*)				19.1		Milani et al. (2012)
Order *Apodiformes*						
Alpine swift (*Apus melba*)	51.1	18.6	4.0			Palomeque et al. (1980)
Pallid swift (*Apus pallidus*)	54.5	18.3	5.3			Palomeque et al. (1980)
Swift (*Apus apus*)	50	17.8	4.7			Palomeque et al. (1980)
Anna's hummingbird (*Calypte anna*)	55.3	18.2	6.1			Carey and Morton (1976)
Order *Caprimulgiformes*						
Tawny frogmouth (*Podargus strigoides*)	41		2.3	12.9		McCracken (2003)
Order *Charadriiformes*						
Family *Alcidae*						
Ancient murrelet (*Synthliboramphus antiquus*)	40			4.1		Newman et al. (1997)
Cassin's auklet (*Ptychoramphus aleuticus*)	34		9.2			Newman et al. (1997)
Common murre or common guillemot (*Uria aalge*)	39			9.3		Newman et al. (1997)
Crested auklet (*Aethia cristatella*)	40			2.5		Newman et al. (1997)
Horned puffin (*Fratercula corniculata*)	44			4.3		Newman et al. (1997)

Continued

TABLE 49.1 Summary of blood concentrations of erythrocytes, leukocytes, and thrombocytes, together with hemoglobin concentration and hematocrit in avian species.—cont'd

	HCT or PCV %	Hb g dL^{-1}	RBC #x 10^6 mm^{-3}	Leukocytes #x 10^3 mm^{-3}	Thrombocytes #x 10^3 mm^{-3}	References
Little auk (*Plautus alle*)	56.8	17.0	3.5			Newman et al. (1997)
Marbled murrelet (*Brachyramphus marmoratus*)	41			5.7		Kostelecka-Myrcha (1987)
Parakeet auklet (*Aethia psittacula*)	42			5.0		Newman et al. (1997)
Pigeon guillemot (*Cepphus columba*)	47			4.0		Newman et al. (1997)
Rhinoceros auklet (*Cerorhinca monocerata*)	44.6	12.3				Newman et al. (1999)
Tufted puffin (*Fratercula cirrhata*)	41			4.0		Newman et al. (1997)
Family *Burhinidae*						
Double-striped thick-knee (*Burhinus bistriatus*)	49.3	13.6	3.6	9.5		Ball (2003)
Stone curlew (Bur*hinus oedicnemus*)	47	14.4	2.9	7.9		Samour et al. (1998)
Spotted thick-knee (*Burhinus capensis*)	46	13.3	2.1	13.6		Samour et al. (1998)
Family *Charadriidae*						
Killdeer (*Charadrius vociferus*)	46.6	14.0	4.0	8.2		Ball (2003)
Piping plover (*Charadrius melodus*)	49.1			3.8		Ball (2003)
Two-banded plover (*Charadrius falklandicus*)	50.9					D'Amico et al. (2017)
Family (*Haematopodidae*)						
American oystercatcher (*Haematopus palliates*)	46.1			8.7		Carlson-Bremer et al. (2010), Fallon et al. (2018)
Family *Jacanidae*						
Wattled jacana (*Jacana jacana*)	48.7			5.1		Ball (2003)
Family Laridae						
Black-headed gull (*Chroicocephalus ridibundus* or *Larus ridibundus*)	43.9	15.9	3.2			Balasch et al. (1974)
Black-legged kittiwake (*Rissa tridactyla*)	41			4.2		Newman et al. (1997)
Black skimmer (*Rynchops niger*)	44.6	17	2.7			Fallon et al. (2018)
European herring gull (*Larus argentatus*)	42.1	14.4	2.5	15.5		Balasch et al. (1974)
Glaucous-winged gull (*Larus glaucescens*)	38			5.1		Newman et al. (1997)

Continued

TABLE 49.1 Summary of blood concentrations of erythrocytes, leukocytes, and thrombocytes, together with hemoglobin concentration and hematocrit in avian species.—cont'd

	HCT or PCV %	Hb g dL^{-1}	RBC #x 10^6 mm^{-3}	Leukocytes #x 10^3 mm^{-3}	Thrombocytes #x 10^3 mm^{-3}	References
Great black-backed gull (*Larus marinus*)	41	12.9	2.1	15.7		Averbeck (1992)
Kelp gull (*Larus dominicanus*)	43.4	13.5	3.6	10.0		Myrcha and Kostelecka-Myrcha (1980), Doussang et al. (2015)
Family *Recurvirostridae*						
American avocet (*Recurvirostra americana*)	46.2	13.4	3.5	8.3		Ball (2003)
Black-winged stilt (*Himantopus himantopus*)	50.3	15.0	3.45	7.8		Ball (2003)
Family *Scolopacidae*						
Red knot (*Calidris canutus rufa*)	51					D'Amico et al. (2010)
Family *Stercorariidae*						
Brown skua (*Stercorarius antarcticus* or *S. lönnbergi*)	42.3	14.0	3.4			Myrcha and Kostelecka-Myrcha (1980)
Great skua (*Stercorarius skua*)	44					Bearhop et al. (1999a,b)
Family *Sternidae*						
Antarctic tern (*Sterna vittata*)	47.9	14.4	3.8			Myrcha and Kostelecka-Myrcha (1980)
Arctic tern (*Sterna paradisaea*)	46.0	14.4	3.1			Kostelecka-Myrcha (1987)
Common tern (*Sterna hirundo*)	48.1			10		Fiorello et al. (2009)
Sooty tern (*Sterna fuscata*)	47			21.2		Work (1996)
Order *Coliiformes*						
Blue-naped mousebird (*Urocolius macrourus*)	53.1	18.8	4.5	12.8		Calculated from Pye (2003)
Speckled mousebird (*Colius striatus*)	42.4	13.2	2.4	8.7		Pye (2003)
Order *Columbiformes*						
African-collared dove (*Streptopelia roseogrisea*)		15	5.5	35	32	Lashev et al. (2009)
Collared dove (*Streptopelia decaocto*)		13	5.3	23	30	Lashev et al. (2009)
Domestic pigeon (*Columba livia*)	50.5	16.7	4.0	24	34	Mean: Balasch et al. (1974), Kalomenopoulou and Koliakos (1989), Lashev et al. (2009)
Laughing dove (*Spilopelia senegalensis*)	38.9	13.8	2.3			Fourie and Hattingh (1983)

Continued

TABLE 49.1 Summary of blood concentrations of erythrocytes, leukocytes, and thrombocytes, together with hemoglobin concentration and hematocrit in avian species.—cont'd

	HCT or PCV %	Hb g dL^{-1}	RBC #x 10^6 mm^{-3}	Leukocytes #x 10^3 mm^{-3}	Thrombocytes #x 10^3 mm^{-3}	References
Mourning dove (*Zenaida macroura*)	48.5					Harms and Harms (2012), Harmes et al. (2016)
Nicobar pigeon (*Caloenas nicobarica*)	50.7	17.0	3.4	4.3		Peinado et al. (1992a)
Pheasant pigeon (*Otidiphaps nobilis*)	41.7	13.9	2.6	6.9		Peinado et al. (1992a)
Pink-headed fruit dove (*Ptilinopus porphyreus*)	46.8	13.8	2.5	10.0		Schultz (2003)
Rock pigeon (*Columba livia*)	47	15	2.5	12.3		Gayathri et al. (2004)
Speckled pigeon (*Columba guinea*)	50	19.4	3.9			Fourie and Hattingh (1983)
Spotted dove (*Streptopelia chinensis*)		17.0				Lill (2011)
Southern crowned or Scheepmaker's crowned pigeon (*Goura scheepmakeri*)	42	12.7	2.3	19.4		Peinado et al. (1992a)
Tambourine dove (*Turtur tympanistria*)	35.6	14.6	2.3			Fourie and Hattingh (1983)
Victoria crowned pigeon (*Goura victoria*)	37.6	12.3	2.3	10.8		Peinado et al. (1992a)
Western or common crowned pigeon (*Goura cristata*)	34.3	10.8	2.2	17.7		Peinado et al. (1992a)
White-winged dove (*Zenaida asiatica*)				16.0		Small et al. (2005)
Order *Coraciiformes*						
Northern ground hornbill (*Bucorvus abyssinicus*)	45.9	13.8	2.4	15.8		Dutton (2003)
Blue-crowned motmot (*Momotus momota*)	40.7	12.7	4.0	13.3		Dutton (2003)
Great hornbill (*Buceros bicornis*)	47.9	16.1	2.5	11.6		Dutton (2003)
Green wood hoopoe (*Phoeniculus purpureus*)	54.2	16.5	4.1	6.6		Dutton (2003)
Hoopoe (*Upupa epops*)	46.6	16.2	3.7	10.0		Dutton (2003)
Lilac-breasted roller (*Coracias caudatus*)	47.4	14.7	3.4	9.9		Dutton (2003)
Micronesian king fisher (*Todiramphus cinnamominus*)	47	16.1	3.3	8.2		Dutton (2003)
Southern carmine bee-eater (*Merops nubicoides*)	51.1	15.9		6.30		Dutton (2003)

Continued

TABLE 49.1 Summary of blood concentrations of erythrocytes, leukocytes, and thrombocytes, together with hemoglobin concentration and hematocrit in avian species.—cont'd

	HCT or PCV %	Hb g dL^{-1}	RBC #x 10^6 mm^{-3}	Leukocytes #x 10^3 mm^{-3}	Thrombocytes #x 10^3 mm^{-3}	References
Order *Cuculiformes*						
Greater roadrunner (*Geococcyx californianus*)	40.7	11.5	2.4	12.7		Abou-Madi (2003)
Guira cuckoo (*Guira guira*)	48.7	16.6	3.2	6.8		Abou-Madi (2003)
Order *Falconiformes*						
***Family* Falconidae**						
American kestrel (*Falco sparverius*)	43.0			9.8		Franson et al. (1983), Dressen et al. (1999)
Crested caracara (*Polyborus plancus*)	48		3.1	24.1		Elliott et al. (1974)
Collared forest falcon (*Micrastur semitorquatus*)	35.5		2.4	26.4		Elliott et al. (1974)
Common kestrel (*Falco tinnunculus*)	24.7		2.47	6.02		Shen et al. (2008)
Greater kestrel (*Falco rupicoloides*)	44.2	14.1	2.8			Fourie and Hattingh (1983)
Gyr falcons (*Falco rusticolus*)	41.5	14.1				Raghav et al. (2015)
Lanner falcon (*Falco biarmicus*)	46.75	19.2	3.0			Mean: Cooper (1975), Fourie and Hattingh (1983)
Peregrine falcon (*Falco peregrinus*)	41	14.6	2.8	12.6		Mean: Gee et al. (1981), Samour et al. (1996)
Saker falcon (*Falco cherrug*)	47	15.9	2.6	5.7		Samour et al. (1996)
Order *Galliformes*						
Attwater's prairie chicken (*Tympanuchus cupido attwateri*)	44.8			13.7		West and Haines (2002)
Black-fronted piping-guan (*Aburria jacutinga*)	38.4	12.9	2.2	8.5	6.4	Motta et al. (2013)
Bobwhite quail (*Colinus virginianus*)	38.5	12.9	3.22	18.1		Mean: Bond and Gilbert (1958), Gee et al. (1981), Hill and Murray (1987), Johnson et al. (2007), Quinn et al. (2009)
Chicken (*Gallus gallus*)	31.0	13.5	3.0			Mean: Fourie and Hattingh (1983), Borges et al. (2004) Andretta et al. (2011)
Chukar (*Alectoris chukar*)	38	11.6	2.6	24		Straková et al. (2010)
Common quail (*Coturnix coturnix*)	38.0	13.2	3.6			Pages and Planas (1983)

Continued

TABLE 49.1 Summary of blood concentrations of erythrocytes, leukocytes, and thrombocytes, together with hemoglobin concentration and hematocrit in avian species.—cont'd

	HCT or PCV %	Hb g dL^{-1}	RBC #x 10^6 mm^{-3}	Leukocytes #x 10^3 mm^{-3}	Thrombocytes #x 10^3 mm^{-3}	References
Greater sage grouse (*Centrocercus urophasianus*)	53			5.1		Mean: Dunbar et al. (2005), Dyer et al. (2009)
Grey partridge (*Perdix perdix*)	39	11.2	2.2	17.4		Straková et al. (2010)
Helmeted guineafowl (*Numida meleagris*)	39.7	15.3	2.8	14.3		Mean: Balasch et al. (1973), Fallaw et al. (1976), Fourie and Hattingh (1983), Straková et al. (2010)
Japanese quail (*Coturnix japonica*)	33	14.3	4.1	30	65	Mean: Belleville et al. (1982), Fourie and Hattingh (1983), Schindler et al. (1987), Nirmalan and Robinson (1971)
Natal spurfowl or Natal francolin (*Pternistis natalensis* or *Francolinus natalensis*)	31.7	11.4	3.3			Fourie and Hattingh (1983)
Peacock (*Pavo cristatus*)	36.9	12	2.1			Balasch et al. (1973)
Pheasant (*Phasianus colchicus*)	37.3	11.3	2.6	13.5		Balasch et al. (1973), Straková et al. (2010)
Jungle fowl (*Gallus gallus*)	40.2	12.2	2.6			Mean: Balasch et al. (1973), Adnan and Amin Babjee (1985), Aengwanich and Tanomtong (2007)
Red grouse (*Lagopus lagopus*)	46.7	14.4	3.7	6.7		Wilson and Wilson (1978)
Red-necked spurfowl or Red-necked francolin (*Pternistis afer* or *Francolinus afer*)	32.5	12.2	3.2			Fourie and Hattingh (1983)
Rock partridge (*Alectoris graeca*)	43	14.9	2.8			Balasch et al. (1973)
Turkey (*Meleagris gallopavo*)	34.7	13.7	1.6	17.3		Schmidt et al. (2009a), Straková et al. (2010)
Order *Gaviiformes*						
Common loon (*Gavia immer*)	47			17		Haefele et al. (2005)
Red-throated loon (*Gavia stellata*)	54	20.7	3.1			Bond and Gilbert (1958)
Order *Gruiformes*						
Blue crane (*Anthropoides paradiseus*)	34.0	14.7	2.1			Fourie and Hattingh (1983)
Common crane (*Grus grus*)	42.7	14.6	2.4	21.9	10.6	Puerta et al. (1990)
Florida sandhill crane (*Grus canadensis pratensis*)	44	12.6	2.2			Gee et al. (1981)

Continued

TABLE 49.1 Summary of blood concentrations of erythrocytes, leukocytes, and thrombocytes, together with hemoglobin concentration and hematocrit in avian species.—cont'd

	HCT or PCV %	Hb g dL^{-1}	RBC #x 10^6 mm^{-3}	Leukocytes #x 10^3 mm^{-3}	Thrombocytes #x 10^3 mm^{-3}	References
Greater sandhill crane (*Grus canadensis tabida*)	41	14.5	2.6			Gee et al. (1981)
Mississippi sandhill crane (*Grus canadensis pulla*)	44	13.7	2.5			Gee et al. (1981)
Siberian crane (*Grus leucogeranus*)	45			10.8		Carpenter (2003)
Wattled crane (*Bugeranus carunculatus*)	45			12.7		Carpenter (2003)
Whooping crane (*Grus americana*)	42		2.2	18.2		Carpenter (2003)
Coot (*Fulica americana*)	43.5	17.0				Mean: Bond and Gilbert (1958), Rubio et al. (2012)
Guam rail (*Gallirallus owstoni*)	45		2.7	3.9		Fontenot et al. (2006)
Red-knobbed coot or crested coot (*Fulica cristata*)	37.4					Rubio et al. (2012)
Family *Otididae*						
Great bustard (*Otis tarda*)	51	13.0	3.0	33		Jimenez et al. (1991)
Houbara bustard (*Chlamydotis undulate*)	43	13.6	1.9	7.9	4.1	Howlett et al. (2002)
Heuglin's bustard (*Neotis heuglinii*)	43	12.5	2.2	4.2	5.1	D'Aloia et al. (1996)
Kori bustard (*Ardeotis kori*)	47	14.1	2.3	7.3	5.5	Howlett et al. (1995)
Little black bustard (*Eupodotis afra*)	44	14.6	2.7	7.8	10.5	D'Aloia et al. (1996)
Red-crested bustard (*Lophotis ruficrista*)	50	14.2	2.9	10.7	9.2	Howlett et al. (2002)
White-bellied bustard (*Eupodotis senegalensis*)	45.5	14.7	2.4	12.3	7.6	Mean: D'Aloia et al. (1996), Howlett et al. (2002)
Purple swamphen (*Porphyrio porphyrio*)	47.6	15.9	2.8	5.2		Celdrán et al. (1994)
Order *Passeriformes*						
***Family* Acanthizidae**						
Brown thornbill (*Acanthiza pusilla*)	44.8	16.3	3.0			Breuer et al. (1995)
Family Corvidae						
American crow (*Corvus brachyrhynchos*)				12.7		Nemeth et al. (2011)
Blue jay (*Cyanocitta cristata*)	45.7	15.3	3.5			Mean: Carey and Morton (1976), Garvin et al. (2003)

Continued

TABLE 49.1 Summary of blood concentrations of erythrocytes, leukocytes, and thrombocytes, together with hemoglobin concentration and hematocrit in avian species.—cont'd

	HCT or PCV %	Hb g dL^{-1}	RBC #x 10^6 mm^{-3}	Leukocytes #x 10^3 mm^{-3}	Thrombocytes #x 10^3 mm^{-3}	References
Clark's nutcracker (*Nucifraga columbiana*)	49.3	14.8	4.5			Carey and Morton (1976)
Fish crow (*Corvus ossifragus*)				18		Nemeth et al. (2011)
Indian house crow (*Corvus splendens*)	29.5	11.1	1.8			Cooper (1996)
Pied crow (*Corvus albus*)	40.9	14.5	2.9	26.0		Fourie and Hattingh (1983), Ihedioha et al. (2011)
Raven (*Corvus corax*)	40.7	16.1	3.2			Balasch et al. (1974)
Family *Estrildidae*						
Canyon towhee (*Melozone fusca*)	44.1	15.1	3.8			Carey and Morton (1976)
Chipping sparrow (*Spizella passerina*)	53.1	16.2	5.1			Carey and Morton (1976)
Dark-eyed junco (*Junco hyemalis*)	51.9	16.2	4.4			Carey and Morton (1976)
Green-tailed towhee (*Pipilo chlorurus*)	50.0	15.6	3.3			Carey and Morton (1976)
Gouldian finch (*Chloebia gouldi*)	52.8			7.5		Gentz (2003)
Grey-headed junco (*Junco caniceps*)	49.7	16.6	4.2			Carey and Morton (1976)
Field sparrow (*Spizella pusilla*)	51.0	16.1	3.3			Carey and Morton (1976)
Lincoln's sparrow (*Melospiza lincolnii*)	50.9	15.8	3.7			Carey and Morton (1976)
Red-browed finch (*Neochmia temporalis*)	49.9	12.6	2.9			Breuer et al. (1995)
Red-headed finch (*Amadina erythrocephala*)	41.2	15.9	3.4			Fourie and Hattingh (1983)
Rock bunting (*Emberiza cia*)	49.9	14.8	5.2	8.6		Llacuna et al. (1996)
Song sparrow (*Melospiza melodia*)	53.3	16.6	3.3			Carey and Morton (1976)
White-throated sparrow (*Zonotrichia albicollis*)	47.2	12.8	3.4			Carey and Morton (1976)
White-crowned sparrow (*Zonotrichia leucophrys*)	51.3	16.4	3.8			Carey and Morton (1976)
Family *Eurylamidae*						
Green broadbill (*Calyptomena viridis*)	49.4	13.9	5.955			Gentz (2003)
Family *Fringillidae*						
American goldfinch (*Carduelis tristis*)	56.3	17.0	4.2			Carey and Morton (1976)

Continued

TABLE 49.1 Summary of blood concentrations of erythrocytes, leukocytes, and thrombocytes, together with hemoglobin concentration and hematocrit in avian species.—cont'd

	HCT or PCV %	Hb g dL^{-1}	RBC #x 10^6 mm^{-3}	Leukocytes #x 10^3 mm^{-3}	Thrombocytes #x 10^3 mm^{-3}	References
European greenfinch (*Carduelis chloris*)	51.0			14.0		Sepp et al. (2010)
Lesser goldfinch (*Carduelis psaltria*)	52.5	17.0				Carey and Morton (1976)
Pine siskin (*Carduelis pinus*)	53.5	17.8	4.35			Carey and Morton (1976)
Cassin's finch (*Haemorhous cassinii*)	56.0	20.9	3.54			Carey and Morton (1976)
House finch (*Haemorhous mexicanus*)	50.8	18.4				Carey and Morton (1976)
Purple finch (*Haemorhous purpureus*)	51.9	17.0				Carey and Morton (1976)
Family *Hirundinidae*						
Welcome swallow (*Hirundo neoxena*)		19.5				Lill (2011)
Family *Icteridae*						
Boat-tailed grackle (*Quiscalus major*)	46.5					Harms and Harms (2012), Harmes et al. (2016)
Common grackle (*Quiscalus quiscula*)	43.5	16.3				Hill and Murray (1987)
Red-winged blackbird (*Agelaius phoeniceus*)	47.5	15.7				Hill and Murray (1987)
Family *Meliphagidae*						
Red wattlebird (*Anthochaera carunculata*)		17.8				Lill (2011)
Noisy miner (*Manorina melanocephala*)		16.9				Lill (2011)
Family *Mimidae*						
Gray catbird (*Dumetella carolinensis*)	48.0					Hatch et al. (2010)
Floreana mockingbird or Charles mockingbird (*Nesomimus trifasciatus*)	44.5	18.8				Deem et al. (2011)
Family *Maluridae*						
Superb fairywren (*Malurus cyaneus*)	44.9	14.5	2.9			Breuer et al. (1995)
Family *Paridae*						
Great tit (*Parus major*)	48.6	15.7	5.4	4.3		Llacuna et al. (1996), Hauptmanová et al. (2002)
Black-capped chickadee (*Poecile atricapillus*)	48.1	12.6	3.3			Carey and Morton (1976)
Mountain chickadee (*Poecile gambeli*)	51.4	15.7	4.1			Carey and Morton (1976)

Continued

TABLE 49.1 Summary of blood concentrations of erythrocytes, leukocytes, and thrombocytes, together with hemoglobin concentration and hematocrit in avian species.—cont'd

	HCT or PCV %	Hb g dL^{-1}	RBC #x 10^6 mm^{-3}	Leukocytes #x 10^3 mm^{-3}	Thrombocytes #x 10^3 mm^{-3}	References
Siberian tit (*Poecile cinctus*)				14.3		Krams et al. (2010)
Family *Parulidae*						
American yellow warbler (*Setophaga petechia*)	50.2	13.5	3.5			Carey and Morton (1976)
Orange-crowned warbler (*Oreothlypis celata*)	57.2	17.7	5.3			Carey and Morton (1976)
MacGillivray's warbler (*Geothlypis tolmiei*)	58.4	19.4	3.5			Carey and Morton (1976)
Magnolia warbler (*Setophaga magnolia*)		14.9	3.3			Carey and Morton (1976)
Nashville warbler (*Oreothlypis ruficapilla*)	43.1	12.7	3.3			Carey and Morton (1976)
Townsend's warbler (*Setophaga townsendi*)	50.8	18.4	4.9			Carey and Morton (1976)
Wilson's warbler (*Cardellina pusilla*)	54.1	16.7	4.8			Carey and Morton (1976)
Yellow-rumped warbler (*Setophaga coronata*)	50.6	16.6	4.5			Carey and Morton (1976)
Family *Passeridae*						
Cape sparrow (*Passer melanurus*)	39.1	12.5	3.2			Fourie and Hattingh (1983)
House sparrow (*Passer domesticus*)	46.1	12.3	4.1	18.9		Mean Puerta et al., 1995, Harms and Harms (2012), Harmes et al. (2016)
Family *Petroicidae*						
Eastern yellow robin (*Eopsaltria australis*)	45.3	15.3	2.4			Breuer et al. (1995)
Family *Pycnonotidae*						
Common bulbul (*Pycnonotus barbatus*)	45.0	14.3	3.0			Fourie and Hattingh (1983)
Family *Sturnidae*						
Common starling (*Sturnus vulgaris*)	47.7	15.4	4.4			Hill and Murray (1987), Pages and Planas (1983)
Common hill mynah (*Gracula religiosa*)	47.1	12.3	3.5	23.9		Archawaranon (2005)
Superb starling (*Lamprotornis superbus*)	49.4	15.7	4.2	9.3		Carey and Morton (1976)
Family *Tharaupidae*						
Darwin's small ground finch (*Geospiza fuliginosa*)	58.3					Clark et al. (2018)
Family *Turdidae*						
American robin (*Turdus migratorius*)	51.5	16.2	3.4			Carey and Morton (1976)

Continued

TABLE 49.1 Summary of blood concentrations of erythrocytes, leukocytes, and thrombocytes, together with hemoglobin concentration and hematocrit in avian species.—cont'd

	HCT or PCV %	Hb g dL^{-1}	RBC #x 10^6 mm^{-3}	Leukocytes #x 10^3 mm^{-3}	Thrombocytes #x 10^3 mm^{-3}	References
Blackbird (*Turdus merula*)	47.6	13.7	4.3	14.8		Llacuna et al. (1996)
Hermit thrush (*Catharus guttatus*)	51.2	15.7	5.0			Carey and Morton (1976)
Pale-breasted thrush (*Turdus leucomelas*)	43.3	14.7		15.8		Lobato et al. (2011)
Swainson's thrush (*Catharus ustulatus*)	58.4	18.0	3.32			Carey and Morton (1976)
Family *Zosteropidae*						
Grey-breasted white eye (*Zosterops lateralis*)		15.5				Lill (2011)
Order *Pelecaniformes*						
***Family* Ardeidae**						
Black-crowned night heron (*Nycticorax nycticorax*)	44.8	13.6	2.9	8.3		Celdrán et al. (1994)
Cattle egret (*Bubulcus ibis*)	45.6	12.6	2.75	6.4		Celdrán et al. (1994)
Great egret (*Ardea alba*)	45.9	15.9	2.6			Fallon et al. (2018)
Grey heron (*Ardea cinerea*)	40.0	13.2	2.5			Fourie and Hattingh (1983)
Little egret (*Egretta garzetta*)	47.7	11.3	2.8	6.1		Fontenelle (2001)
Purple heron (*Ardea purpurea*)	43.9	12.9	2.5	9.4		Celdrán et al. (1994)
Family *Ciconiidae*						
Black stork (*Ciconia nigra*)	42	11.5	2.2	64.7	90.9	Puerta et al. (1989)
Greater adjutant (*Leptoptilos dubius*)	38.0	13.6	1.6	8.7		Salakij et al. (2004)
Lesser adjutant (*Leptoptilos javanicus*)	41.3	13.9	1.9	9.4		Salakij et al. (2004)
Maguari stork (*Ciconia maguari*)	46	16.1	2.3	9.8		Fontenelle (2001)
Oriental white stork (*Ciconia boyciana*)	50	14.1	2.4	13.5		Han et al. (2016)
Painted stork (*Mycteria leucocephala*)	42.4	17.7	3.2	3.9	12.9	Aengwanich et al. (2002)
White stork (*Ciconia ciconia*)	36	11.1	1.9	62.1	66.6	Puerta et al. (1989)
Family *Fregatidae*						
Great frigatebird (*Fregata minor*)	52.7	12.6		7.0		Work (1996), Valle et al. (2018)
Puna ibis (*Plegadis ridgwayi*)	42	16.8	3.0	3.9		Coke et al. (2004)

Continued

TABLE 49.1 Summary of blood concentrations of erythrocytes, leukocytes, and thrombocytes, together with hemoglobin concentration and hematocrit in avian species.—cont'd

	HCT or PCV %	Hb g dL^{-1}	RBC #x 10^6 mm^{-3}	Leukocytes #x 10^3 mm^{-3}	Thrombocytes #x 10^3 mm^{-3}	References
Southern giant petrel (*Macronectes giganteus*)	47			4.0		Uhart et al. (2003)
White ibis (*Threskiornis melanocephalus*)	46	18.7	2.8	14.9	16.2	Aengwanich and Tanomtong (2004)
Family *Pelecanidae*						
Black-faced spoonbill (*Platalea minor*)	45.1		2.5	15.0		Chou et al. (2008)
Brown pelican (*Pelecanus occidentalis*)	45.9	15.7	2.7			Balasch et al. (1974), Fallon et al. (2018)
Grey heron (*Ardea cinerea*)	40.0	13.2	2.5			Fourie and Hattingh (1983)
Pink-backed pelican (*Pelecanus rufescens*)	43			18.5		Weber (2003)
Family *Sulidae*						
Black-faced cormorant (*Leucocarbo fuscescens*)	43.4	14.5	2.2	1.8		Melrose and Nicol (1992)
Brown booby (*Sula leucogaster*)	45			10.3		Work (1999)
Great cormorant (*Phalacrocorax carbo*)	43.5	13.8	2.9			Balasch et al. (1974)
Flightless cormorant (*Phalacrocorax harrisi*)	49.2			8.0		Travis et al. (2006a)
Guanay cormorant (*Phalacrocorax bougainvillii*)	45			12.1		Weber (2003)
Imperial cormorant (*Phalacrocorax atriceps*)	49.9		3.7	12.1		Gallo et al. (2013)
Northern gannet (*Morus bassanus*)	41	14.0	2.6			Balasch et al. (1974)
Pelagic cormorant (*Phalacrocorax pelagicus*)	30			3.1		Newman et al. (1997)
Red-footed booby (*Sula sula*)	48			9.9		Work (1996)
Family *Threskiornithidae*						
Black-faced spoonbill (*Platalea minor*)	45.1		2.5	15.0		Chou et al. (2008)
Eurasian spoonbill (*Platalea leucorodia*)	46.4	15.9	3.0	9.4		Celdrán et al. (1994)
Glossy ibis (*Plegadis falcinellus*)	49.0	17.1	3.5	9.1		Celdrán et al. (1994)
Northern bald ibis (*Geronticus ermita*)	44	3.1		3.4		Dutton et al. (2002)
Puna ibis (*Plegadis ridgwayi*)	42	16.8	3.0	3.9		Coke et al. (2004)
Scarlet ibis (*Eudocimus ruber*)	46	16.1	2.3	9.8		Fontenelle (2001)

Continued

TABLE 49.1 Summary of blood concentrations of erythrocytes, leukocytes, and thrombocytes, together with hemoglobin concentration and hematocrit in avian species.—cont'd

	HCT or PCV %	Hb g dL^{-1}	RBC #x 10^6 mm^{-3}	Leukocytes #x 10^3 mm^{-3}	Thrombocytes #x 10^3 mm^{-3}	References
Black-headed ibis (*Threskiornis melanocephalus*)	46	18.7	2.8	14.9	16.2	Aengwanich and Tanomtong (2004)
Order *Phaethontiformes*						
Red-tailed tropicbird (*Phaeton rubricauda*)	50			6.8		Work (1996)
Order *Phoenicopteriformes*						
Chilean flamingo (*Phoenicopterus chiliensis*)	46	16.9	2.8	6.6		Peinado et al. (1992b)
Greater flamingo (*Phoenicopterus tuber roseus*)	49	18.0	2.9	6.2		Peinado et al. (1992b)
Rosy flamingo (*Phoenicopterus ruber*)	45	15.4	2.4	10.1		Peinado et al. (1992b)
Lesser flamingo (*Phoeniconaias minor*)	46	15.4	2.2	17.5		Peinado et al. (1992b), Nyariki et al. (2018)
Order *Procellariiformes*						
Cory's shearwater (*Calonectris diomedea*)	47.6			33.8	63.8	Bried et al. (2011)
Galápagos petrel (*Pterodroma phaeopygia*)	49			10.9		Work (1996)
Hawaiian dark-rumped petrel (*Pterodroma phaeopygia*)	49			10.9		Work (1996)
Laysan albatross (*Diomedea immutabilis*)	38			22.4		Work (1996)
Manx shearwater (*Puffinus puffinus*)	48	14.8	2.9	5.4		Stoskopf (2003)
Northern fulmar (*Fulmarus glacialis*)	32			3.4		Newman et al. (1997)
Waved albatross (*Phoebastria* irrorata)	38.2			5.9		Padilla et al. (2003)
Wedge-tailed shearwater (*Puffinus pacificus*)	48			18.2		Work (1996)
Wilson's petrel (*Oceanites oceanicus*)	50.0	17.0	4.0			Mean: Myrcha and Kostelecka-Myrcha (1980), Quillfeldt et al. (2004)
Order *Psittaciformes*						
Amazon parrot (*Amazona aestiva*)	38.7	13.2				Valéria et al. (2008)
Baudin's cockatoo (*Calyptorhynchus baudinii*)	45	13.4		17.1		Le Souëf et al. (2013)
Blue-fronted Amazon parrot (*Amazona aestiva*)	46.5	11.7	2.1	23.9		Deem et al. (2005), Silva et al. (2014)

Continued

TABLE 49.1 Summary of blood concentrations of erythrocytes, leukocytes, and thrombocytes, together with hemoglobin concentration and hematocrit in avian species.—cont'd

	HCT or PCV %	Hb g dL^{-1}	RBC #x 10^6 mm^{-3}	Leukocytes #x 10^3 mm^{-3}	Thrombocytes #x 10^3 mm^{-3}	References
Budgerigar (*Melopsittacus undulatus*)	47.6	16.3	5.1	5.5		Harper and Lowe (1998)
Carnaby's cockatoo (*Calyptorhynchus latirostris*)	45	13.7		16.7		Le Souëf et al. (2013)
Cuban Amazon parrot (*Amazona leucocephala leucocephala*)	56	22	3.1	6.6		Tell and Citino (1992)
Golden conure or arara juba (*Guaruba guarouba*)	46	12.8	3.6	11.9	26.3	Prioste et al. (2012)
Hispaniolan Amazon parrot (*Amazona ventralis*)	51.6			10.6		Guzman et al. (2008)
Hyacinth macaw (*Anodorhynchus hyacinthinus*)	50			13.5		Calle and Stewart (1987)
Kakapo (*Strigops habroptilus*)	40.5	14.0		18.4		Low et al. (2006)
Kea (*Nestor notabilis*)	49.8			11.3		Calculated from Youl (2009)
Macaw (*Ara rubrogenys*)	49.5	12.0	3.6	10.1		García del Campo et al. (1991)
Monk parakeet or quaker parrot (*Myiopsitta monachus*)	50	14.6	3.3	6.0		Rettenmund et al. (2014), Godwin et al. (1982)
Red-capped parrot (*Pionopsitta pileata*)	46.7	15.8	2.1	8.7		Schmidt et al. (2009b)
Spix's macaw (*Cyanopsitta spixii*)	46.8		2.9	9.2		Foldenauer et al. (2007)
St Vincent parrot (*Amazona guildingii*)	40		1.9	8.7		Deem et al. (2008)
Vinaceous Amazon parrot (*Amazona vinacea*)	45.5	15.4	2.3	9.2		Schmidt et al. (2009b)
Order *Sphenisciformes*						
Adélie penguin (*Pygoscelis adeliae*)	48.1	25.2		15.9		Ibañez et al. (2015)
African penguin (*Spheniscus demersus*)	46			21.1		Mazzaro et al. (2013)
Chinstrap penguin (*Pygoscelis antarctica*)	46.3	18.1	1.9			Myrcha and Kostelecka-Myrcha (1980), Butler and Jones (1997)
Emperor penguin (*Aptenodytes forsteri*)		16.8				Butler and Jones (1997)
Galápagos penguin (*Spheniscus mendiculus*)	43.5			31.5		Travis et al. (2006b)
Gentoo penguin (*Pygoscelis papua*)	47.7	23.7	2.2	11.2		Hawkey et al. (1989), Ibañez et al. (2015)

Continued

TABLE 49.1 Summary of blood concentrations of erythrocytes, leukocytes, and thrombocytes, together with hemoglobin concentration and hematocrit in avian species.—cont'd

	HCT or PCV %	Hb g dL^{-1}	RBC #x 10^6 mm^{-3}	Leukocytes #x 10^3 mm^{-3}	Thrombocytes #x 10^3 mm^{-3}	References
Humboldt penguin (*Spheniscus humboldti*)	49.4			23.2		Wallace et al. (1995)
Jackass penguin (*Spheniscus demersus*)	46.5	17.1	1.7	4.3		Stoskopf et al. (1980), Parsons et al. (2015)
King penguin (*Aptenodytes patagonicus*)	47.8	16.7	1.5	14.3		Cranfield (2003)
Little penguin (*Eudyptula minor*)	41	8.7	1.7			Nicol et al. (1988)
Magellanic penguin (*Spheniscus magellanicus*)	42	13.9	2.0			Hawkey et al. (1989)
Rockhopper penguin (*Eudyptes chrysocome*)	45	16.4	2.4			Hawkey et al. (1989)
Order *Strigiformes*						
African grass owl (*Tyto capensis*)	39.6	12.7	2.2			Fourie and Hattingh (1983)
African wood owl (*Strix woodfordii*)	31.0		1.7			Cooper (1975)
Barn owl (*Tyto alba*)	43.1	13.8	2.8	18.4		Mean: Elliott et al. (1974), Cooper (1975), Fourie and Hattingh (1983), Szabo et al. (2014)
Barred owl (*Strix varia*)	39.7	17.2	2.9	17.7		Elliott et al. (1974)
Burrowing owl (*Athene cunicularia*)	45.1	15.9	2.2	8.9		Aguilar (2003)
Collared scops owl (*Otus lettia*)	39.1					Chan et al. (2012)
Eastern screech owl (*Otus asio*)	49.1.	12.2	4.2	18.1		Elliott et al. (1974) or Aguilar (2003)
Eagle owl (*Bubo bubo*)	37.8	11.2	1.9	14.6		Aguilar (2003)
Great grey owl (*Strix nebulosa*)	42.2	7.9		15.0		Aguilar (2003)
Great-horned owl (*Bubo virginianus*)	32	7.7	2.2			Bond and Gilbert (1958)
Malay fish owl (*Ketupa ketupu*)	47.5		2.6	13.2		Elliott et al. (1974)
Nepal brown wood owl (*Strix leptogrammica*)	37.5		2.1	39.6		Elliott et al. (1974)
Short-eared owl (*Asio flaammeus*)	42	12.0	3.0	14.3		Elliott et al. (1974) or Aguilar (2003)
Snowy owl (*Nyctea scandiaca*)	38.2	12.6	2.8	28.1		Elliott et al. (1974) or Aguilar (2003)
Spectacled owl (*Pulsatrix perspicillata*)	38.9	12.7	1.5	11.4		Aguilar (2003)
Spotted eagle-owl (*Bubo africanus*)	36.8	16.4	1.9			Mean: Cooper (1975), Fourie and Hattingh (1983)

Continued

TABLE 49.1 Summary of blood concentrations of erythrocytes, leukocytes, and thrombocytes, together with hemoglobin concentration and hematocrit in avian species.—cont'd

	HCT or PCV %	Hb g dL^{-1}	RBC #x 10^6 mm^{-3}	Leukocytes #x 10^3 mm^{-3}	Thrombocytes #x 10^3 mm^{-3}	References
Striped owl (*Rhinoptynx clamator*)	47.0		2.6	26.9		Elliott et al. (1974)
Verreaux's eagle-owl (*Bubo lacteus*)	36.0	17.9	1.3			Cooper (1975)
Order *Trogoniformes*						
Crested quetzal (*Pharomachrus antisianus*)	40	12.9	1.4	8.8		Neiffer (2003)
Golden-headed quetzal (*Pharomachrus auriceps*)	52.3	17.1	3.5	5.5		Neiffer (2003)
Javan trogon (*Apalharpactes reinwardtii*)	50			12.5		Neiffer (2003)
White-tailed trogon (*Trogon chionurus*)	47.5			3.8		Neiffer (2003)

TABLE 49.2 Erythrocyte characteristics in avian species.

	MCV	Erythrocyte		Nucleus		
		Length	Width	Length	Width	References
Emu (*Dromaius novahollandiae*)	226					Calculated from Mushi et al., 1999; Bonadiman et al., 2009
Greater rhea (*Rhea americana*)	220					Calculated from Uhart et al., 2006
Lesser rhea (*Pterocnemia pennata*)	217					Reissig et al., 2002
Ostrich (*Struthio camelus*)	229	16.2	11.3	5.4	3.6	Mean: Mushi et al., 1999; Bonadiman et al., 2009
Red-legged tinamou (*Crypturellus erythropus*)	183					Calculated from Smith, 2003
Order *Accipitriformes*						
Family *Accipitridae*						
African fish eagle (*Haliaeetus vocifer*)	203					Calculated from Cooper, 1975
African harrier-hawk (*Polyboroides typus*)	204					Calculated from Cooper, 1975
African hawk-eagle (*Aquila spilogaster*)	174					Calculated from Cooper, 1975
African white-backed vulture (*Gyps africanus*)	197					Naidoo et al., 2008
Augur buzzard (*Buteo augur*)	177					Calculated from Cooper, 1975
Bald eagle (*Haliaeetus leucocephalus*)	167					Elliot et al., 1974
Bearded vulture (*Gypaetus barbatus*)	161					Hernández and Margalida, 2010
Black kite (*Milvusmigrans*)	210					Calculated from Cooper, 1975
Black sparrowhawk (*Accipiter melanoleucus*)	179					Calculated from Cooper, 1975
Black-shouldered kite (*Elanus axillaris*)	242					Calculated from Cooper, 1975

Continued

TABLE 49.2 Erythrocyte characteristics in avian species.—cont'd

	MCV	Erythrocyte		Nucleus		
		Length	Width	Length	Width	References
Black vulture (*Coragyps atratus*)	302					Barbara et al., 2017
Cape vulture (*Gyps coprotheres*)	164					Van Heerden et al., 1987
Cinereous vulture (*Aegypius monachus*)	179					Seok et al., 2017
Cooper's hawk (*Accipiter cooperi*)	133					Calculated from Gessaman et al., 1986
Crested serpent eagle (*Spilornis cheela*)	181					Elliot et al., 1974
Egyptian vulture (*Neophronpercnopterus*)	188	15.1	7.9	6.7	2.4	Polo et al., 1992
Eurasian griffon (*Gyps fulvus*)	170	14.1	7.7	6.8	2.5	Polo et al., 1992
Gabar goshawk (*Micronisus* gabar)	191					Calculated from Cooper, 1975
Golden eagle (*Aquila chrysaetos*)		14.7	8.2	6.8	2.7	Mean: Elliot et al., 1974; Polo et al., 1992
Griffon vulture (*Gyps fulvus*)	188	14.1	7.7	6.8	2.5	Polo et al., 1992; Giambelluca et al., 2017
Harpy eagle (*Harpia harp*)	230					Oliveira et al., 2014
Hooded vulture (*Necrosyrtes monachus*)	184					Elliot et al., 1974; Calculated from Cooper, 1975
Lizard buzzard (*Kaupifalco monogrammicus*)	170					Calculated from Cooper, 1975
Long-crested eagle (*Lophaetus occipitalis*)	180					Calculated from Cooper, 1975
Montagu's harrier (*Circus pygargus*)	166	13.4	7.8	6.5	2.3	Lavin et al., 1993
Ornate hawk-eagle (*Spizaetus ornatus*)	102					Elliot et al., 1974
Pale chanting goshawk (*Melierax canorus*)	222					Calculated from Cooper, 1975
Red-tailed hawk (*Buteo jamaicensis*)	210					Calculated from Rehder et al., 1982
Savanna hawk (*Buteogallus meridionalis*)	161					Elliot et al., 1974
South American snail kite (*Rostrhamus sociabilis*)	173					Calculated from Gee et al., 1981
Spanish imperial eagle (*Aquila adalberti*)	150	14.9	8.0	7.4	2.6	García-Montijano et al., 2002; Polo et al., 1992
Steppe eagle (*Aquila nipalensis*)	190					Calculated from Cooper, 1975
Tawny eagle (*Aquila rapax*)	165	14.3	7.6			Mean: Calculated from Cooper, 1975; Fourie and Hattingh, 1983
Wahlberg's eagle (*Aquila wahlbergi*)	166					Cooper, 1975
White-bellied sea eagle (*Haliaeetus leucogaster*)	212					Elliot et al., 1974
Family *Cathartidae*						
Andean condor (*Vultur gryphus*)	175					Calculated from Gee et al., 1981
King vulture (*Sarcoramphus papa*)	123					Elliot et al., 1974
Secretary bird (*Sagittarius serpentarius*)	248					Calculated from Cooper, 1975

Continued

TABLE 49.2 Erythrocyte characteristics in avian species.—cont'd

	MCV	Erythrocyte		Nucleus		
		Length	Width	Length	Width	References
Anseriformes						
Common pochard (*Aythya ferina*)	134					Balasch et al., 1974
Black duck (*Anas superciliosa*)	145					Mulley, 1979
Buffiehead (*Bucephala albeola*)	206					Calculated from Kocan, 1972
Canvasback duck (*Aythya valisineria*)	204					Calculated from Kocan, 1972
Eurasian teal (*Anas crecca*)	91.5					Elarabany, 2018
Maccoa duck (*Oxyura maccoa*)	121	12.2	6.2			Fourie and Hattingh, 1983
Mallard (*Anas platyrhynchos*)	162	12.5	6.8	6.0	2.7	Shave and Howard, 1971; Driver, 1981
Maned duck (*Chenonetta jubata*)	163					Calculated from Mulley, 1980
Northern shoveler (*Anas clypeata*)	88.1					Elarabany, 2018
Red-billed teal (*Anas erythrorhyncha*)	127					Fourie and Hattingh, 1983
Ring-neck duck (*Aythya collaris*)	196					Calculated from Kocan, 1972
Red-billed teal (*Anas erythrorhyncha*)	127	12.5	7.5			Fourie and Hattingh, 1983
Wood duck (*Chenonetta jubata*)	164					Mulley, 1980
Yellow-billed duck (*Anas undulata*)	128	12.5	7.4			Fourie and Hattingh, 1983
Canada goose (*Branta canadensis*)	161					Calculated from Gee et al., 1981
Egyptian goose (*Alopochen aegyptiacus*)	138	13.1	7.5			Fourie and Hattingh, 1983
Embden goose (*Anser anser*)	146					Calculated from Gee et al., 1981
Nene goose (*Branta sandvicensis*)	177					Calculated from Gee et al., 1981
Snow goose (*Anser caerulescens*)	204					Calculated from Williams and Trainer, 1971
Spur-winged goose (*Plectropterus gambensis*)	153	12.9	7.8			Fourie and Hattingh, 1983
Tule white-fronted goose (*Anser albifrons*)	148					Calculated from Williams and Trainer, 1971
Mute Swan (*Cygnus olor*)	170					Dolka et al., 2014
Black-necked swan (*Cygnus melanocoryphus*)	208					Norambuena and Bozinovic, 2009
Order *Caprimulgiformes*						
Alpine swift (*Apus melba*)	126	13.8	7.0	2.4		Palomeque et al., 1980
Anna's hummingbird (*Calypte anna*)	91					Calculated from Carey and Morton, 1976
Pallid swift (*Apus pallidus*)	104	13.4	6.8	2.5		Palomeque et al., 1980
Swift (*Apus apus*)	109	13.6	6.9	2.2		Palomeque et al., 1980
Tawny frogmouth (*Podargus strigoides*)	181					Calculated from McCracken, 2003
Order *Charadriiformes*						
Family *Alcidae*						
Antarctic tern (*Sterna vittata*)	127	12.0	6.3			Myrcha and Kostelecka-Myrcha, 1980
Arctic tern (*Sterna paradisaea*)	152	12.7	6.6			Kostelecka-Myrcha, 1987
Little auk (*Plautus alle*)	167	12.8	6.8			Kostelecka-Myrcha, 1987

Continued

TABLE 49.2 Erythrocyte characteristics in avian species.—cont'd

	MCV	Erythrocyte		Nucleus		
		Length	Width	Length	Width	References
Family *Burhinidae*						
Double-striped thick-knee (*Burhinus bistriatus*)	154					Ball, 2003
Stone curlew (*Burhinus oedicnemus*)	167					Samour et al., 1998
Spotted thick-knee (*Burhinus capensis*)	175					Samour et al., 1998
Family *Charadriidae*						
Killdeer (*Charadrius vociferus*)	117					Ball, 2003
Family *Laridae*						
Black-headed gull (*Larus ridibundus*)	144					Balasch et al., 1974
European herring gull (*Larus argentatus*)	173	12.2	7.0			Mean: Balasch et al., 1974; Averbeck, 1992
Great black-backed gull (*Larus marinus*)	200	12.4	7.1			Averbeck, 1992
Kelp gull (*Larus dominicanus*)	107	12.6	6.6			Myrcha and Kostelecka-Myrcha, 1980
Family *Recurvirostridae*						
American avocet (*Recurvirostra americana*)	135					Ball, 2003
Black-winged stilt (*Himantopus himantopus*)	149					Ball, 2003
Brown skua (*Stercorarius antarcticus*) or *Stercorarius lönnbergi*	124					Myrcha and Kostelecka-Myrcha, 1980
Great skua (*Stercorarius skua*)	169					Bearhop et al., 1999
Family *Sternidae*						
Antarctic tern (*Sterna vittata*)	127	12.0	6.6			Myrcha and Kostelecka-Myrcha, 1980
Arctic tern (*Sterna paradisaea*)	152	12.7	6.6			Kostelecka-Myrcha, 1987
Order *Coliiformes*						
Blue-naped mousebird (*Urocolius macrourus*)	117					Calculated from Pye, 2003
Speckled mousebird (*Colius striatus*)	179					Calculated from Pye, 2003
White-backed mousebird (*Colius colius*)	127					Calculated from Pye, 2003
Order *Columbiformes*						
Laughing dove (*Spilopelia senegalensis*)	162	12.5	6.2	6.6	2.5	Fourie and Hattingh, 1983
Nicobar pigeon (*Caloenas nicobarica*)	150	13.9	7.3	6.3	2.9	Peinado et al., 1992a
Pheasant pigeon (*Otidip- haps nobilis*)	159	13.5	7.6			Peinado et al., 1992a
Pink-headed fruit pigeon (*Ptilinopus porphyreus*)	140					Schultz, 2003
Rock pigeon (*Columba livia*)	135	11.7	6.6	6.8	3.3	Balasch et al., 1974; Gayathri et al., 2004
Pigeon domestic	147	11.9	6.4			Fourie and Hattingh, 1983
Southern crowned or Scheepmaker's crowned pigeon (*Goura scheepmakeri*)	183	13.3	8.1	5.8	2.9	Peinado et al., 1992a
Speckled pigeon (*Columba guinea*)	125	12.5	7.6			Fourie and Hattingh, 1983

Continued

TABLE 49.2 Erythrocyte characteristics in avian species.—cont'd

	MCV	Erythrocyte		Nucleus		
		Length	Width	Length	Width	References
Tambourine dove (*Turtur tympanistria*)	108	12.5				Fourie and Hattingh, 1983
Victoria crowned pigeon (*Goura victoria*)	169	13.6	8.1	5.8	2.9	Peinado et al., 1992a
Western or common crowned pigeon (*Goura cristata*)	159	14.1	6.1	6.1	2.9	Peinado et al., 1992a
Order *Cuculiformes*						
Greater roadrunner (Geococcyx californianus)	188					Abou-Madi, 2003
Guira cuckoo (Guira guira) Coraciiformes	151					Abou-Madi, 2003
Order *Coraciiformes*						
Northern ground hornbill (*Bucorvus abyssinicus*)	199					Dutton, 2003
Blue-crowned motmot (*Momotus momota*)	130					Dutton, 2003
Great hornbill (*Buceros bicornis*)	194					Dutton, 2003
Green wood hoopoe (*Phoeniculus purpureus*)	155					Dutton, 2003
Hoopoe (*Upupa epops*)	131					Dutton, 2003
Lilac-breasted roller (*Coracias caudatus*)	132					Dutton, 2003
Micronesian kingfisher (*Todiramphus cinnamominus*)	147					Dutton, 2003
Order *Falconiformes*						
Family *Falconidae*						
Collared forest falcon (*Micrastur semitorquatus)*	146					Elliot et al., 1974
Common kestrel (*Falco tinnunculus*)	169					Shen et al., 2008
Greater kestrel or white-eyed kestrel (*Falco rupicoloides)*	158	13.1	7.4			Fourie and Hattingh, 1983
Lanner falcon (*Falco biarmicusis*)	151	12.8	7.8			Mean: Cooper, 1975; Fourie and Hattingh, 1983
Peregrine falcon (*Falco perigrinus*)	150					Calculated from Gee et al., 1981
Saker falcon (Falco cherrug)	183					Samour et al., 1996
Southern crested caracara (*Polyborus plancus*)	155					Elliot et al., 1974
Order *Galliformes*						
Black-fronted piping-guan (*Penelope jacutinga*)	174					Calculated from Motta et al., 2013
Bobwhite quail (*Colinus virginianus*)	121					Calculated from Bond and Gilbert, 1958; Gee et al., 1981; Johnson et al., 2007
Chicken (*Gallus gallus*)	127	12.5	7.5			Fourie and Hattingh, 1983
Common quail (*Coturnix coturnix*)	66	12.5	6.2			Fourie and Hattingh, 1983

Continued

TABLE 49.2 Erythrocyte characteristics in avian species.—cont'd

	MCV	Erythrocyte		Nucleus		
		Length	Width	Length	Width	References
Grouse (*Lagopus lagopus*)	126					Calculated from Wilson and Wilson, 1978
Helmeted guineafowl (*Numida meleagris*)	140	14.5	8.0			Fourie and Hattingh, 1983
Horned guan *(Oreophasis derbianus)*	166					Cornejo et al., 2014
Japanese quail (*Coturnix japonica*)	80					Calculated from Belleville et al., 1982; Fourie and Hattingh, 1983; Schindler et al., 1987; Nirmalan and Robinson, 1971
Jungle fowl (*Gallus gallus*)	154					Calculated from Balasch et al., 1973; Adnan and Amin Babjee, 1985; Aengwanich and Tanomtong, 2007
Natal Spurfowl or Natal Francolin (*Pternistis natalensis* or *Francolinusnatalensis*)	95	12.5	7.5			Fourie and Hattingh, 1983
Peacock (*Pavo cristatus*)	176					Calculated from Balasch et al., 1973
Pheasant (*Phasianus colchicus*)	143					Calculated from Balasch et al., 1973
Red-necked spurfowl or red-necked francolin (*Pternistis afer* or *Francolinus afer*)	100	12.6	7.6			Calculated from Wilson and Wilson, 1978
Rock partridge (*Alectoris graeca*)	154					Balasch et al., 1973
Gruiformes						
Blue crane (*Anthropoides paradiseus*)	160	13.9	8.7			Fourie and Hattingh, 1983
Sandhill crane (*Grus canadensis*)	180					Carpenter, 2003
Whooping crane (*Grus americana*)	204					Carpenter, 2003
Guam rail (*Gallirallus owstoni*)	167					Calculated from Fontenot et al., 2006
Purple swamphen (*Porphyrio porphyrio*)	170					Celdrán et al., 1994
Family *Otididae*						
Great bustard (*Otis tarda*)	179					Jimenez et al., 1991
Heuglin's bustard (*Neotis heuglinii*)	198					D'Aloia et al., 1996
Houbara bustard (*Chlamydotis undulata*)	232					Howlett et al., 2002
Kori bustard (*Ardeotis kori*)	208	13.5				Howlett et al., 1995
Little black bustard (*Eupodotis afra*)	170					D'Aloia et al., 1996
Red-crested bustard (*Lophotis rucrasta*)	176					Howlett et al., 2002
Rufous-crested bustard (*Eupodotis rucrista*)	176					Howlett et al., 2002
White-bellied bustard (*Eupodotis senegalensis*)	171					Howlett et al., 1995
Passeriformes						
Family *Acanthizidae*						
Brown thornbill (*Acanthiza pusilla*)	156					Breuer et al., 1995
Family *Corvidae*						

Continued

TABLE 49.2 Erythrocyte characteristics in avian species.—cont'd

	MCV	Erythrocyte		Nucleus		
		Length	Width	Length	Width	References
American crow (*Corvus brachyrhynchos*)	120					Gentz, 2003
Blue jay (*Cyanocitta cristata*)	130					Calculated from Carey and Morton, 1976; Garvin et al., 2003
Clark's nutcracker (*Nucifraga columbiana*)	110					Calculated from Carey and Morton, 1976
Indian house crow (*Corvus splendens*)	166					Calculated from Cooper, 1996.
Pied crow (*Corvus albus*)	152	12.5	6.9			Fourie and Hattingh, 1983
Raven (*Corvus corax*)	128					Balasch et al., 1974
Family *Emberizidae*						
Red-crested cardinal (*Paroaria coronata*)	134					Calculated from Carey and Morton, 1976
Family *Eurylamidae*						
Green broadbill (*Calyptomena viridis*)	122					Calculated from Carey and Morton, 1976
Family *Estrildidae*						
Canyon towhee (*Melozone fusca*)	116					Calculated from Carey and Morton, 1976
Chipping sparrow (*Spizella oronate*)	104					Calculated from Carey and Morton, 1976
Dark-eyed junco (*Junco hyemalis*)	119					Calculated from Carey and Morton, 1976
Green-tailed towhee (*Pipilo chlorurus*)	152					Calculated from Carey and Morton, 1976
Grey-headed junco (*Junco caniceps*)	118					Calculated from Carey and Morton, 1976
Field sparrow (*Spizella pusilla*)	154					Calculated from Carey and Morton, 1976
Lincoln's sparrow (*Melospiza lincolnii*)	137					Calculated from Carey and Morton, 1976
Red-browed firetail (*Neochmia temporalis*)	182					Breuer et al., 1995
Red-headed finch (*Amadina erythrocephala*)	119	11.6	6.8			Fourie and Hattingh, 1983
Rock bunting (*Emberiza cia*)	97					Llacuna et al., 1996
Song sparrow (*Melospiza melodia*)	161					Calculated from Carey and Morton, 1976
White-throated sparrow (*Zonotrichia albicollis*)	139					Calculated from Carey and Morton, 1976
White-crowned sparrow (*Zonotrichia leucophrys*)	134					Calculated from Carey and Morton, 1976
Family *Fringillidae*						
American goldfinch (*Carduelis tristis*)	133					Calculated from Carey and Morton, 1976
Pine siskin (*Carduelis pinus*)	123					Calculated from Carey and Morton, 1976

Continued

TABLE 49.2 Erythrocyte characteristics in avian species.—cont'd

	MCV	Erythrocyte		Nucleus		
		Length	Width	Length	Width	References
Cassin's finch (*Haemorhous cassinii*)	158					Calculated from Carey and Morton, 1976
Family *Icteridae*						
Venezuelan troupial (*Icterus icterus*)	154					Gentz, 2003
Family *Irenidae*						
Asian fairy-bluebird (*Irena puella*)	118					Gentz, 2003
Family *Maluridae*						
Superb fairywren (*Malurus cyaneus*)	172					Breuer et al., 1995
Family *Meliphagidae*						
Blue-faced honeyeater (*Entomyzon cyanotis*)	117					Gentz, 2003
Family *Muscicapidae*						
Silver-eared mesia (*Leiothrix argentauris*)	186					Gentz, 2003
Family *Paridae*						
Great tit (*Parus major*)	93					Llacuna et al., 1996; Hauptmanová et al., 2002
Black-capped chickadee (*Poecile atricapillus*)	146					Calculated from Carey and Morton, 1976
Mountain chickadee (*Poecile gambeli*)	125					Calculated from Carey and Morton, 1976
Family *Parulidae*						
American yellow warbler (*Setophaga petechialia*)	142					Calculated from Carey and Morton, 1976
Orange-crowned warbler (*Oreothlypis celata*)	107					Calculated from Carey and Morton, 1976
MacGillivray's warbler (*Geothlypis tolmiei*)	165					Calculated from Carey and Morton, 1976
Nashville warbler (*Oreothlypis rucapilla*)	129					Calculated from Carey and Morton, 1976
Townsend's warbler (*Setophaga townsendi*)	103					Calculated from Carey and Morton, 1976
Wilson's warbler (*Cardellina pusilla*)	113					Calculated from Carey and Morton, 1976
Yellow-rumped warbler (*Setophaga oronate*)	113					Calculated from Carey and Morton, 1976
Family *Passeridae*						
Cape sparrow (*Passer melanurus*)	121	11.3	5.2			Fourie and Hattingh, 1983
House sparrow (*Passer domesticus*)	110					Calculated from Puerta et al., 1995; Harms and Harms, 2012
Family *Petroicidae*						
Eastern yellow robin (*Eopsaltria australis*)	201					Breuer et al., 1995
Family *Pittidae*						
Hooded pitta (*Pitta sordida*)	114					Gentz, 2003

Continued

TABLE 49.2 Erythrocyte characteristics in avian species.—cont'd

	MCV	Erythrocyte		Nucleus		
		Length	Width	Length	Width	References
Family *Ploceidae*						
Southern red bishop (*Euplectes orix*)	133					Gentz, 2003
Family *Pycnonotidae*						
Common bulbul (*Pycnonotus barbatus*)	150	12.5	6.9			Fourie and Hattingh, 1983
Family *Sturnidae*						
Common hill mynah (*Gracula religiosa*)	125					Archawaranon, 2005
Common starling (*Sturnus vulgaris*)	106					Calculated from Pages and Planas, 1983
Superb starling (*Lamprotornis superbus*)	127					Gentz, 2003
Family *Turdidae*						
American robin (*Turdus migratorius*)	149					Calculated from Carey and Morton, 1976
Blackbird (*Turdus merula*)	111					Calculated from Carey and Morton, 1976
Hermit thrush (*Catharus guttatus*)	102					Calculated from Carey and Morton, 1976
Swainson's thrush (*Catharus ustulatus*)	176					Calculated from Carey and Morton, 1976
Order *Pelecaniformes*						
Black-headed ibis (*Threskiouris melanocephalus*)	174					Aengwanich and Tanomtong, 2004
Black stork (*Ciconia nigra*)	191					Calculated from Puerta et al., 1989
Brown pelican (*Pelecanus occidentalis*)	160					Balasch et al., 1974
Greater adjutant (*Leptoptilos dubius*)	233.1	16.4	8.8			Salakij et al., 2004
Grey heron (*Ardea cinerea*)	160					Fourie and Hattingh, 1983
Lesser adjutant (*Leptoptilos javanicus*)	223	15.5	7.3			Salakij et al., 2004
Oriental white stork (*Ciconia boyciana*)	207					Han et al., 2016
Painted stork (*Mycteria leucocephala*)	139					Aengwanich et al., 2002
Puna ibis (*Plegadis ridgwayi*)	140					Coke et al., 2004
White ibis (*Threskiouris melanocephalus*)	174					Aengwanich and Tanomtong, 2004
Black-faced cormorant (*Leucocarbo fuscescens*)	198					Melrose and Nicoll, 1992
Imperial cormorant (*Phalacrocorax actriceps*)	134					Calculated from Gallo et al., 2013
Great cormorant (*Phalacrocorax carbo*)	151					Balasch et al., 1974
Northern gannet (*Sula bassanus*)	156					Balasch et al., 1974
White stork (*Ciconia ciconia*)	189					Calculated from Puerta et al., 1989

Continued

TABLE 49.2 Erythrocyte characteristics in avian species.—cont'd

	MCV	Erythrocyte		Nucleus		
		Length	Width	Length	Width	References
Order *Phoenicopteriformes*						
Chilean flamingo (*Phoe- nicopterus chiliensis*)	164	15.2	8.0	6.8	2.7	
Greater flamingo (*Phoe- nicopterus tuber roseus*)	169	15.1	8.3	5.9	2.6	
Rosy flamingo (*Phoenicopterus ruber ruber*)	187	14.8	8.2	6.7	2.6	
Lesser flamingo (*Phoeni- conais minor*)	209	15.1	8.1	7.1	2.6	
Order *Procellariiformes*						
Wilson's petrel (*Oceanites oceanicus*)	125	11.8	6.4			Myrcha and Kostelecka-Myrcha, 1980
Manx shearwater (*Puf nus puffinus*)	167.2					Stoskopf, 2003
Order *Psittaciformes*						
Blue-fronted amazons (*Amazona aestiva*)	215					Silva et al., 2014
Budgerigar (*Melopsittacus undulatus*)	95					Harper and Lowe, 1998
Cuban amazon parrot (*Amazona leu- cocephala leucocephala*)	181					Calculated from Tell and Citino, 1992
Golden conures or ararajubas (*Guar- uba guarouba*)	132					Prioste et al., 2012
Macaw (*Ara rubrogenys*)	137					Calculated from García del Campo et al., 1991
Monk parakeet or quaker parrot (*Myo- psitta monachus*)	150					Godwin et al., 1982
Red-capped parrot (*Pionopsitta pileata*)	222					Calculated from Schmidt et al., 2009b
Spix's macaw (*Cyanopsitta spixii*)	161					Calculated from
St Vincent parrot (*Amazona guildingii*)	210					Foldenauer et al., 2007
Vinaceous amazon parrot (*Amazona vinacea*)	198					Calculated from Deem et al., 2008
Sphenisciformes						
Adélie penguin (*Pygoscelis adeliae*)		14.9	10.8			Bonatto et al., 2008
Chinstrap penguin (*Pygoscelis antarcticus*)	244	15.5	11.4			Calculated from Myrcha and Kostelecka-Myrcha, 1980 or Bonatto et al., 2008
Galápagos penguin (*Spheniscus mendiculus*)	195					Travis et al., 2006
Gentoo penguin (*Pygoscelis papua*)	206	15.3	10.9			Hawkey et al., 1989; Bonatto et al., 2008
Jackass penguin (*Spheniscus demersus*)	250					Cranfeld, 2003; Parsons et al., 2015

Continued

TABLE 49.2 Erythrocyte characteristics in avian species.—cont'd

	MCV	Erythrocyte		Nucleus		
		Length	Width	Length	Width	References
King penguin (*Aptenodytes patagonicus*)	241					Cranfeld, 2003
Little penguin (*Eudyptula minor*)	229	18.8	9.2			Nicol *et al.*, 1988
Magellanic penguin (*Spheniscus magellanicus*)	215					Hawkey et al., 1989
Rockhopper penguin (*Eudyptes chrysocome*)	195					Hawkey et al., 1989
Strigiformes						
African grass owl (*Tyto capensis*)	183	12.5	7.6			Fourie and Hattingh, 1983
African wood owl (*Strix woodfordii*)	177					Cooper, 1975
Barn owl (*Tyto alba*)	186	15.0	7.5			Mean: Cooper, 1975; Fourie and Hattingh, 1983
Barred owl (*Strix varia*)	139					Elliot et al., 1974
Burrowing owl (*Athene cunicularia*)	200					Aguilar, 2003
Common barn owl (*Tyto alba*)	152					Elliot et al., 1974
Eagle owl (*Bubo bubo*)	233					Aguilar, 2003
Eastern screech owl (*Otus asio*)	117					Elliot et al., 1974
Great horned owl (*Bubo virginianus*)	213					Aguilar, 2003
Malay fishing owl (*Ketupa ketupu*)	188					Elliot et al., 1974
Nepal brown wood owl (*Strix leptogrammica*)	181					Elliot et al., 1974
Short-eared owl (*Asio ammeus*)	140					Elliot et al., 1974
Snowy owl (*Nyctea scandiaca*)	136					Elliot et al., 1974
Spectacled owl (*Pulsatrix perspicillata*)	260					Aguilar, 2003
Spotted eagle-owl (*Bubo africanus*)	188	12.5	10.0			Mean: Cooper, 1975; Fourie and Hattingh, 1983
Striped owl (*Rhinoptynx clamator*)	157					Elliot et al., 1974
Verreaux's eagle owl (*Bubo lacteus*)	286					Cooper, 1975
Trogoniformes						
Crested quetzal (*Pharomachrus antisianus*)	285					Neiffer, 2003
Golden-headed quetzal (*Pharomachrus auriceps*)	152					Neiffer, 2003
White-tailed trogon (*Trogon chionurus*)	193					Neiffer, 2003

TABLE 49.3 Summary of differential count of leukocytes in avian species.

	Heterocytes %	Lymphocytes %	Monocytes %	Eosinophils %	Basophils %	References
Emu (*Dromaius novaehollandiae*)	63.2	32.1	1.2	2.5	0.8	Patodkar et al. (2008)
Greater rhea (*Rhea americana*)	65.2	18.9	7.1	7.7	0	Uhart et al. (2006)
Ostrich (*Struthio camelus*)	66.8	27.0	1.6	1.4	3.03	Mean: Mushi et al. (1999), Bonadiman et al. (2009)
Red-legged tinamou (*Crypturellus erythropus*)	57.4	39.4	2.9	<0.4	<0.4	Smith (2003)
Order *Accipitriformes*						
***Family* Accipitridae**						
African white-backed vulture (*Gyps africanus*)	82.0	7.4	11.5	5.5	0	Naidoo et al. (2008)
Bearded vulture (*Gypaetus barbatus*)	70.4	23.7	2.7	2.8	0.6	Hernández and Margalida (2010)
Black kite (*Milvus migrans*)	32.0	40.0	1.0	24.1	2.9	Cited in Powers et al. (1994)
Black vulture (*Coragyps atratus*)	72.3	15.5	4.3	7.2	0.7	Barbara et al. (2017)
Cinereous vulture (*Aegypius monachus*)	84.8	9.6	0.7	4.8	0.1	Seok et al. (2017)
Common buzzard (*Buteo buteo*)	30.1	50.2	2.0	12.2	4.1	Cited in Powers et al. (1994)
Egyptian vulture (*Neophron percnopterus*)	69.7	27.2	0.5	2.0	0.4	Polo et al. (1992)
Eurasian griffon (*Gyps fulvus*)	57.8	40.7	0.5	0.9	0	Polo et al. (1992)
European honey buzzard (*Pernis apivorus*)	29.8	55.3	1.25	9.0	4.8	Cited in Powers et al. (1994)
Golden eagle (*Aquila chrysaetos*)	58.8	34.2	4.3	2.3	0	Polo et al. (1992)
Griffon vulture (*Gyps fulvus*)	57.8	40.7	0.5	0.9	0	Polo et al. (1992)
Harpy eagle (*Harpia harp*)	66.0	18.5	2.9	11.6	1.0	Oliveira et al. (2014)
Imperial eagle (*Aquila heliaca*)	44.0	40.3	1.3	11.8	2.3	Cited in Powers et al. (1994)

Continued

TABLE 49.3 Summary of differential count of leukocytes in avian species.—cont'd

	Heterocytes %	Lymphocytes %	Monocytes %	Eosinophils %	Basophils %	References
Marsh harrier (*Circus aeruginosus*)	33.0	53.7	6.5	4.0	4.0	Cited in Powers et al. (1994)
Montagu's harrier (*Circus pygargus*)	70.7	16.6	2.5	12.3	0	Lavin et al. (1993)
Northern goshawk (*Accipiter gentilis*)	37.1	42.5	3.8	16.6	0	Hanauska-Brown et al. (2003)
Red kite (*Milvus milvus*)	19.5	48.8	0.75	28.3	2.8	Cited in Powers et al. (1994)
Sharp-shinned hawk (*Accipiters triatus*)	27.0	63.5	1.6	7.7	0.4	Powers et al. (1994)
Spanish imperial eagle (*Aquila adalberti*)	60.0	33.1	3.15	4.8	0	Mean: Polo et al. (1992), García-Montijano et al. (2002)
Swamp harrier (*Circus approximans*)	86.5	5.25	3.25	4.25	0.5	Calculated from Youl (2009)
Tawny eagle (*Aquila rapax*)	57.3	30.0	0.8	10	2	Cited in Powers et al. (1994)
White-tailed sea-eagle (*Haliaeetus albicilla*)	32.3	55.0	2.0	9.5	3.3	Cited in Powers et al. (1994)
Family *Cathartidae*						
Andean condor (*Vultur gryphus*)	42.8	42.0	1.8	11	2.5	Cited in Powers et al. (1994)
California condor (*Gymnogyps californianus*)	68.1	22.9	3.2	5.1	1.3	Dujowich et al. (2005)
Order *Anseriformes*						
Black duck (*Anas superciliosa*)	24.7	66.1	7.4	1.1	0.8	Mulley (1979)
Black-necked swan (*Cygnus melanocoryphus*)	26.6	61.2	2.1	8.9	1.3	Norambuena and Bozinovic (2009)
Canada goose (*Branta canadensis*)	39	46	6	7	2	Cited in Sturkie (1986)
Eurasian teal (*Anas crecca*)	60.6	32	4.4	3.0	0	Elarabany (2018)
Ferruginous ducks (*Aythya nyroca*)	77	16	2	3	2	Avni-Magen et al. (2016)

Continued

TABLE 49.3 Summary of differential count of leukocytes in avian species.—cont'd

	Heterocytes %	Lymphocytes %	Monocytes %	Eosinophils %	Basophils %	References
Mallard (*Anas platyrhynchos*)	50.4	39.3	2.2	5.5	2.7	Driver (1981)
Mottled duck (*Anas fulvigula*)	47.1	35.1	4.3	10.6	2.9	Ratliff et al. (2017)
Mute swan (*Cygnus olor*)	39.0	55.3	2.2	1.1	2.4	Dolka et al. (2014)
Northern shoveler (*Anas clypeata*)	64.5	27.7	4.0	3.75	0	Elarabany (2018)
Snow goose (*Anser caerulescens*)	34.9	61.0	0.8	0.6	2.5	Williams and Trainer (1971)
Trumpeter swan (*Cygnus buccinators*)	26.6	61.2	2.1	8.9	1.3	Olsen et al. (2002)
Tundra swan (*Cygnus columbianus*)	67.2	28.0	0.4	3.2	1.2	Milani et al. (2012)
Upland geese (*Chloephaga picta*)	28.5	66.3				Gladbach et al. (2010)
Wood duck (*Chenonetta jubata*)	84.5	13.3	1.65	0.5	0.4	Mulley (1980)
Order *Apodiformes*						
Anna's hummingbirds (*Calypte anna*)/black-chinned bummingbirds (*Archilochus alexandri*)	35.4	52.8	3.1	2.35	6.42	Safra et al. (2018)
Order *Caprimulgiformes*						
Tawny frogmouth (*Podargus strigoides*)	41.1	45.5	3.8	7.2	2.5	McCracken (2003)
Order *Charadriiformes*						
***Family* Burhinidae**						
Double-striped thick-knee (*Burhinus bistriatus*)	51.4	32.6	7.8	4.5	3.7	Calculated from Ball (2003)
Spotted thick-knee (*Burhinus capensis*)	43.8	35.2	5.6	11.8	3.5	Samour et al. (1998)
Stone-curlew (*Burhinus oedicnemus*)	76.2	6.9	5.9	8.7	2.41	Samour et al. (1998)
Family *Charadriidae*						
Killdeer (*Charadrius vociferus*)	35.9	48.4	8.2	2.2	3.1	Calculated from Ball (2003)

Continued

TABLE 49.3 Summary of differential count of leukocytes in avian species.—cont'd

	Heterocytes %	Lymphocytes %	Monocytes %	Eosinophils %	Basophils %	References
Piping plover (*Charadrius melodus*)	37.8	39	14.6	4.5	3.4	Calculated from Ball (2003)
Two-banded plover (*Charadrius falklandicus*)	28.5	49.7	6.9	13.7	1.2	D'Amico et al. (2017)
Family *Haematopodidae*						
American oystercatchers (*Haematopus palliates*)	46.1	36.0	1.6	13.9	2.5	Carlson-Bremer et al. (2010)
Family *Jacanidae*						
Wattled jacana (*Jacana jacana*)	62.1	20.9	1.1	4.1	11.8	Calculated from Ball (2003)
Family *Laridae*						
European herring gull (*Larus argentatus*)	35.5	60.9	1.3	0.9	2.0	Averbeck (1992)
Great black-backed gull (*Larus marinus*)	35.2	61.0	1.4	0.7	2.0	Averbeck (1992)
Kelp gulls (*Larus dominicanus*)	68.9	22.6	4.7	2.8	0.9	Doussang et al. (2015)
Family *Recurvirostridae*						
American avocet (*Recurvirostra americana*)	65.5	30.4	1.1	1.7	1.3	Calculated from Ball (2003)
Black-winged stilt (*Himantopus himantopus*)	41.6	47.8	5.0	2.9	2.6	Calculated from Ball (2003)
Family *Scolopacidae*						
Red knot (*Calidris canutus rufa*)	40.6	49.8	6.4	0.4	2.5	D'Amico et al. (2010)
Common tern (*Sterna hirundo*)	38	51	5.6	9.1	0.1	Fiorello et al. (2009)
Sooty tern (*Sterna fuscata*)	24.7	67.3	0.8	5.8	1.3	Work (1996)
Order *Coliiformes*						
Blue-naped mousebird (*Urocolius macrourus*)	48.7	37.2	3.4	6.5	4.2	Calculated from Pye (2003)
Speckled mousebird (*Colius striatus*)	39.2	43.6	6.2	6.5	4.5	Calculated from Pye (2003)
White-backed mousebird (*Colius colius*)	23.8	58	3.2	10.2	4.8	Calculated from Pye (2003)

Continued

TABLE 49.3 Summary of differential count of leukocytes in avian species.—cont'd

	Heterocytes %	Lymphocytes %	Monocytes %	Eosinophils %	Basophils %	References
Order *Columbiformes*						
African collared dove (*Streptopelia roseogrisea*)	44.5	47.7	1.2	3.5	2.4	Lashev et al. (2009)
Collared dove (*Streptopelia decaocto*)	41.7	53.5	0.5	2.1	1.5	Lashev et al. (2009)
Domestic pigeon (*Columba livia*)	38.8	57.8	0.7	1.5	0.9	Lashev et al. (2009)
Mourning dove (Zenaida macroura)	19	41	9	10	0	Harmes et al. (2016)
Nicobar pigeon (*Caloenas nicobarica*)	52.2	37.4	2.1	2.7	0	Peinado et al. (1992a)
Pheasant pigeon (*Otidiphaps nobilis*)	54.1	42.5	1.6	0.6	1.2	Peinado et al. (1992a)
Pink-headed fruit pigeon (*Ptilinopus porphyreus*)	29.7	57.5	5.5	5.3	2.1	Schultz (2003)
Southern crowned or Scheepmaker's crowned pigeon (*Goura scheepmakeri*)	56	37	2	3	2	Peinado et al. (1992a)
Victoria crowned pigeon (*Goura victoria*)	52.8	44.6	0.7	2.5	0.3	Peinado et al. (1992a)
Western or common crowned pigeon (*Goura cristata*)	66.0	30.3	1.0	2.4	0.2	Peinado et al. (1992a)
White-winged dove (*Zenaida asiatica*)	27.2	64.9	2.5	3.2	2.3	Small et al. (2005)
Order *Coraciiformes*						
Northern ground hornbill (*Bucorvus abyssinicus*)	51.4	28.5	6.6	11.6	1.9	Calculated from Dutton (2003)
Blue-crowned motmot (*Momotus momota*)	39	36	7.4	14.4	3.2	Calculated from Dutton (2003)
Great hornbill (*Buceros bicornis*)	51.5	36	6.7	3.2	2.6	Calculated from Dutton (2003)
Green wood hoopoe (*Phoeniculus purpureus*)	37.1	35.7	3.7	5.3	18.2	Calculated from Dutton (2003)

Continued

TABLE 49.3 Summary of differential count of leukocytes in avian species.—cont'd

	Heterocytes %	Lymphocytes %	Monocytes %	Eosinophils %	Basophils %	References
Hoopoe (*Upupa epops*)	43.2	41.8	8.2	4	2.7	Calculated from Dutton (2003)
Lilac-breasted roller (*Coracias caudatus*)	47.5	36.5	9.4	3.6	3.0	Calculated from Dutton (2003)
Micronesian kingfisher (*Todiramphus cinnamominus*)	30.7	45.9	10.9	5.7	6.8	Calculated from Dutton (2003)
Southern carmine bee-eater (*Merops nubicoides*)	39.9	43.7	7.1	5.2	4.2	Calculated from Dutton (2003)
Greater roadrunner (*Geococcyx californianus*)	45.3	31.7	6.1	14.2	2.7	
Guira cuckoo (*Guira guira*)	41.9	19.6	14.4	14.4	9.8	
Order *Falconiformes*						
American kestrel (*Falco sparverius*)	47.9	46.9	2.1	1.0	2.1	Dressen et al. (1999)
Common falcon (*Falco tinnunculus*)	22.1	40.7	1.6	34	2.6	Cited in Powers et al. (1994)
Peregrine falcon (*Falco peregrinus*)	35.9	43.8	2	18.3	0	Samour et al. (1996)
Saker falcons (*Falco cherrug*)	73.1	22.1	3.5	0	1.3	Samour et al. (1996)
Order *Galliformes*						
Attwater's prairie chickens (*Tympanuchus cupido attwateri*)	53.1	40.2	2.4	1.5	2.6	West and Haines (2002)
Black-fronted piping-guan (*Aburria jacutinga*)	19.4	73.2	1.7	5.1	0.6	Motta et al. (2013)
Chukar (*Alectoris chukar*)	33.2	64.7	0.2	1.3	0.2	Straková et al. (2010)
Common or ring-neck pheasant (*Phasianus colchicus*)	30.8	56.95	4.25	2.65	5.8	Cited in Sturkie (1986), Straková et al. (2010)
Greater sage grouse (*Centrocercus urophasianus*)	36	62	1.0	0.2	1	Dunbar et al. (2005)
Grey partridge (*Perdix perdix*)	22.0	77.8	1.1	0.5	0.1	Straková et al. (2010)

Continued

TABLE 49.3 Summary of differential count of leukocytes in avian species.—cont'd

	Heterocytes %	Lymphocytes %	Monocytes %	Eosinophils %	Basophils %	References
Helmeted guinea-fowl (*Numida meleagris*)	18	80.9	0.7	0.3	0.1	Straková et al. (2010)
Horned guan (*Oreophasis derbianus*)	57	37	3.0	3.2	0	Cornejo et al. (2014)
Japanese quail (*Coturnix japonica*)	27.55	68.4	2.1	1.95	0.3	Schindler et al. (1987), Straková et al. (2010)
Jungle fowl (*Gallus gallus*)	36.4	52.9	5.3	3.9	3.1	Mean: Adnan and Amin Babjee (1985), Aengwanich and Tanomtong (2007)
Rock partridge (*Alectoris graeca*)	33	57.5	4.7	2.2	2.7	Dǒnmez and Sur (2008)
Red grouse (*Lagopus lagopus*)	31.4	62.4	3.0	2.0	1.3	Wilson and Wilson (1978)
Turkey (*Meleagris gallopavo*)	29.2	64.4	2.3	0.7	3.4	Schmidt et al. (2009a), Straková et al. (2010)
Order *Gaviiformes*						
Common loon (*Gavia immer*)	32				0	Haefele et al. (2005)
Order *Gruiformes*						
***Family* Gruidae**						
Common crane (*Grus grus*)	55.4	35.8	3.4	3.7	1.9	Puerta et al. (1990)
Red-crowned crane (*Grus japonensis*)	41	48	6.0	5.0	0	Carpenter (2003)
Sandhill crane (*Grus canadensis*)	37	58	2.3	2.0	2.6	Carpenter (2003)
Siberian crane (*Grus leucogeranus*)	53	39	3.0	5.0	0	Carpenter (2003)
Wattled crane (*Bugeranus carunculatus*)	48	39	5	8	0	Carpenter (2003)
Whooping crane (*Grus americana*)	56	41	2	1	0	Carpenter (2003)
Family *Rallidae*						
Common coot (*Fulica atra*)	26.7	67.8	2.2	1.9	0.5	Rubeo et al. (2012)

Continued

TABLE 49.3 Summary of differential count of leukocytes in avian species.—cont'd

	Heterocytes %	Lymphocytes %	Monocytes %	Eosinophils %	Basophils %	References
Red-knobbed coot (*Fulica cristata*)	18.1	78.5	2.2	0.8	0.7	Rubeo et al. (2012)
Guam rail (*Gallirallus owstoni*)	32.8	50.0	6.1	8.6	2.3	Fontenot et al. (2006)
Family *Otididae*						
Great bustard (*Otis tarda*)	68.2	18.2	5.5	8.2	0	Jimenez et al. (1991)
Heuglin's bustard (*Neotis heuglinii*)	37.5	46.3	9.9	2.9	3.3	D'Aloia et al. (1996)
Houbara bustard (*Chlamydotis undulata*)	40.9	52.5	4.1	0.5	2.1	Howlett et al. (2002)
Kori bustard (*Ardeotis kori*)	54.2	30.1	8.2	4.8	2.7	Howlett et al. (1995)
Little black bustard (*Eupodotis afra*)	37.3	46.7	8.7	2.2	5.1	D'Aloia et al. (1996)
Purple swamphen (*Porphyrio porphyrio*)	61.2	36.2	1.6	1.0	0.2	Celdrán et al. (1994)
Red-crested bustard (*Lophotis ruficrista*)	25.9	58.5	9.3	5.0	1.2	Howlett et al. (2002)
Rufous-crested bustard (*Eupodotis ruficrista*)	25.9	58.5	9.3	5.0	1.2	Howlett et al. (2002)
White-bellied bustard (*Eupodotis senegalensis*)	40.0	46.1	7.9	1.1	4.6	Howlett et al. (2002)
Order *Passeriformes*						
African pied crow (*Corvus albus*)	67.9	28.5	1.3	1.6	0.4	Ihedioha et al. (2011)
Asian fairy-bluebird (*Irena puella*)	23.7	52.7	5.5	5.6	12.5	Gentz (2003)
Blackbird (*Agelaius phoeniceus*)	30.0	55.0	8.0	3.0	2.5	From Sturkie, 1986
Boat-tailed grackle (*Quiscalus major*)	36.75	34.5	17	9.5	3	Harmes et al. (2016)
Blue-faced honeyeater (*Entomyzon cyanotis*)	41.3	49.8	4.4	1.2	3.3	Gentz (2003)
Captive hill mynah (*Gracula religiosa*)	43.6	48.4	4.4	3.9	0.53	Archawaranon (2005)

Continued

TABLE 49.3 Summary of differential count of leukocytes in avian species.—cont'd

	Heterocytes %	Lymphocytes %	Monocytes %	Eosinophils %	Basophils %	References
Common crow (*Corvus brachyrhynchos*)	27.5	34.4	2.1	24.0	12.0	Gentz (2003)
European greenfinch (*Carduelis chloris*)	21	55	2.5			Sepp et al. (2010)
Floreana mockingbird (*Mimus trifasciatus*)	16.9	72.2	1.3	8.8	0.2	Deem et al. (2011)
Gouldian finch (*Chloebia gouldi*)	16.5	52.4	3.4	17.8	10	Gentz (2003)
Green broadbill (*Calyptomena viridis*)	35.1	49.4	5.1	4.8	5.6	Gentz (2003)
Great tit (*Parus major*)	19.6	68.5	1.0	5.6	5.6	Hauptmanova et al. (2002)
Hooded pitta (*Pitta sordida*)	27	44.1	12.2	11.9	4.8	Gentz (2003)
House sparrow (*Passer domesticus*)	26	65	8	3	0	Harmes et al. (2016)
Red-crested cardinal (*Paroaria coronata*)	31.7	48.6	8.5	3.9	7.3	Gentz (2003)
Rufous-collared sparrows (*Zonotrichia capensis*)	23.1	76.1	2.5	1.0	2.4	Ruiz et al. (2002)
Siberian tit (*Poecile cinctus*)	6.9	81.3	0	8.9	0	Krams et al. (2010)
Silver-eared mesia (*Leiothrix argentauris*)	20.5	46.7	4.0	17.6	11.2	Gentz (2003)
Southern red bishop (*Euplectes orix*)	22.3	60.1	7.1	2.5	8	Gentz (2003)
Superb starling (*Lamprotornis superbus*)	17.2	59.9	6.1	8.1	8.8	Gentz (2003)
Venezuelan troupial (*Icterus icterus*)	23.3	52.1	5.8	1.2	17.5	Gentz (2003)
Order *Pelecaniformes*						
***Family* Ardeidae**						
Black-crowned night heron (*Nycticorax nycticorax*)	68.9	29.4	0.8	0.8	0.0	Celdrán et al. (1994)
Cattle egret (*Bubulcus ibis*)	56.2	41.3	1.0	0.9	0.6	Fontenelle (2001)

Continued

TABLE 49.3 Summary of differential count of leukocytes in avian species.—cont'd

	Heterocytes %	Lymphocytes %	Monocytes %	Eosinophils %	Basophils %	References
Little egret (*Egretta garzetta*)	65.1	31.8	1.8	0.6	0.5	Celdrán et al. (1994)
Purple heron (*Ardea purpurea*)	55.5	40.3	2.5	1.2	0.5	Celdrán et al. (1994)
Family *Ciconiidae*						
Painted stork (*Mycteria leucocephala*)	10.6	76.1	0	12	1	Aengwanich et al. (2002)
Greater adjutant (*Leptoptilos dubius*)	47.5	31.5	1.0	13.5	6.5	Salakij et al. (2004)
Lesser adjutant (*Leptoptilos javanicus*)	54.8	34.0	0.3	8.3	2.4	Salakij et al. (2004)
Maguari stork (*Ciconia maguari*)	55.1	24.3	3.3	13.6	3.7	Fontenelle (2001)
Family *Frigatidae*						
Great frigatebird (*Fregata minor*)	48.0	24.8	0.8	22.8	0.5	Work (1996)
Family *Pelecanidae*						
Brown pelican (*Pelecanus occidentalis*)	60.9	23.6	4.2	7.4	4	Calculated from Weber (2003)
Pink-backed pelican (*Pelecanus rufescens*)	66.9	19.5	5.3	5.1	3.1	Calculated from Weber (2003)
Family *Phalacrocoracidae*						
Black-faced cormorant (*Leucocarbo fuscescens*)	33	49	2.2	20.8	0.1	Melrose and Nicol (1992)
Flightless cormorant (*Phalacrocorax harrisi*)	36.6	40.0	7.3	3.1	0.5	Travis et al. (2006a)
Guanay cormorant (*Phalacrocorax bougainvillii*)	64.4	25.2	3.4	8.7	0	Weber (2003)
Imperial cormorant (*Phalacrocorax atriceps*)	48.6	43.6	2	8	0	Gallo et al. (2013)
Pelagic cormorant (*Phalacrocorax pelagicus*)	61	27	12	4	2	Newman et al. (1997)
Family *Sulidae*						
Brown booby (*Sula leucogaster*)	70.2	11.8	3.7	12.4	2.1	Work (1999)
Red-footed booby (*Sula sula*)	57.8	32.8	1.9	5.8	1.6	Work (1996)

Continued

TABLE 49.3 Summary of differential count of leukocytes in avian species.—cont'd

	Heterocytes %	Lymphocytes %	Monocytes %	Eosinophils %	Basophils %	References
Family *Threskiornithidae*						
Eurasian spoonbill (*Platalea leucorodia*)	57.5	39.3	2.1	0.8	0.3	Celdrán et al. (1994)
Black-headed ibis (*Threskiornis melanocephalus*)	8.5	89.7	0.5	0.9	0.3	Aengwanich and Tanomtong (2004)
Glossy ibis (*Plegadis falcinellus*)	57.2	40.1	1.1	0.8	0.9	Celdrán et al. (1994)
Northern bald ibis (*Geronticus ermita*)	63.2	30.9	2.9	0	3.0	Dutton et al. (2002)
Puna ibis (*Plegadis ridgwayi*)	21.0	62.0	7	1	12	Coke et al. (2004)
Scarlet ibis (*Eudocimus ruber*)	62.1	27.6	0	5.5	4.8	Fontenelle (2001)
Order *Phaethontiformes*						
Red-tailed tropicbird (*Phaeton rubricauda*)	49.4	30.6	1.8	17.3	1.0	Work (1996)
Order *Phoenicopteriformes*						
Chilean flamingo (*Phoenicopterus chiliensis*)	31.4	65.3	1.7	1.2	0	Peinado et al. (1992b)
Greater flamingo (*Phoenicopterus tuber roseus*)	37.6	59.5	0.3	1.9	0.7	Peinado et al. (1992b)
Rosy flamingo (*Phoenicopterus ruber ruber*)	36.0	61.0	0.5	1.0	2.0	Peinado et al. (1992b)
Lesser flamingo (*Phoeniconaias minor*)	21.0	71.6	2.2	4.0	0.3	Peinado et al. (1992b), Nyariki et al. (2018)
Order *Procellariiformes*						
Cory's shearwater (*Calonectris diomedea*)	37.9	17.0	1.8	43.6	0	Bried et al. (2011)
Hawaiian dark-rumped petrel (*Pterodroma phaeopygia*)	31.1	39.8	0.9	18.1	10.1	Work (1996)
Laysan albatross (*Diomedea immutabilis*)	47.9	21.9	0.1	25.0	5.0	Work (1996)
Northern fulmar (*Fulmarus glacialis*)	29	56	2	13	0	Newman et al. (1997)

Continued

TABLE 49.3 Summary of differential count of leukocytes in avian species.—cont'd

	Heterocytes %	Lymphocytes %	Monocytes %	Eosinophils %	Basophils %	References
Southern giant petrel (*Macronectes giganteus*)	52.4	32.5	5.0	10.0	0.15	Uhart et al. (2003)
Waved albatross (*Phoebastria irrorata*)	66.1	30.5	1.7	1.7	0	Padilla et al. (2003)
Wedge-tailed shearwater (*Puffinus pacificus*)	22.0	71.1	2.5	2.6	1.7	Work (1996)
Order *Psittaciformes*						
Baudin's cockatoo (*Calyptorhynchus baudinii*)	73.9	22.4	3.7	0	0	Le Souëf et al. (2013)
Blue-fronted Amazon parrots (*Amazona aestiva*)	89.8	27.3	2.0	0.8	0.1	Deem et al. (2005), Silva et al. (2014)
Budgerigar (*Melopsittacus undulatus*)	39.7	48.0	9.1	0.6	2.7	Harper and Lowe (1998)
Carnaby's cockatoo (*Calyptorhynchus latirostris*)	71.3	14.2	14.4	0	0	Le Souëf et al. (2013)
Cuban Amazon parrot (*Amazona leucocephala leucocephala*)	16	84	0	1	0	Tell and Citino (1992)
Golden conure or ararajubas (*Guaruba guarouba*)	52.8	46.0	0.9	0.1	0.2	Prioste et al. (2012)
Hispaniolan Amazon parrot (*Amazona ventralis*)	48.1	37.7	9.4	0.9	1.4	Guzman et al. (2008)
Hyacinth macaw (*Anodorhynchus hyacinthinus*)	75	22.6	0.9	0.6	0.8	Calle and Stewart (1987)
Kakapo (*Strigops habroptilus*)	80.1	16.3	0.8	1.6	0.9	Low et al. (2006)
Macaw (*Ara rubrogenys*)	42.2	49.9	4.5	0.8	2.4	García del Campo et al. (1991)
Monk parakeet or quaker parrot (*Myiopsitta monachus*)	11.5	82	2.5	0.5	1.5	Godwin et al. (1982)
Red-capped parrot (*Pionopsitta pileata*)	45.7	44.7	2.5	1.5	1.5	Schmidt et al. (2009b)

Continued

TABLE 49.3 Summary of differential count of leukocytes in avian species.—cont'd

	Heterocytes %	Lymphocytes %	Monocytes %	Eosinophils %	Basophils %	References
St Vincent parrot (*Amazona guildingii*)	58.9	41.1	1.1	0	0	Deem et al. (2008)
Spix's macaw (*Cyanopsitta spixii*)	56.4	41.1	3.1	0.6	0	Foldenauer et al. (2007)
Vinaceous Amazon parrot (*Amazona vinacea*)	39.3	56.8	1.0	1.7	1.2	Schmidt et al. (2009b)
Order *Sphenisciformes*						
Adélie penguin (*Pygoscelis adeliae*)	65.3	23.9	3.9	4.5	2.5	Paris Zinsmeister and Van der Heyden (1987)
African penguin (*Spheniscus demersus*)	57.0	41.4	1.6	0	0	Mazzaro et al. (2013)
Chinstrap penguin (*Pygoscelis antarctica*)	61.6	37.1	2.3	0	0.3	Paris Zinsmeister and Van der Heyden (1987)
Galápagos penguins (*Spheniscus mendiculus*)	57.6	31.5	2.4	8.0	0.4	Travis et al. (2006b)
Gentoo penguin (*Pygoscelis papua*)	48.1	45.5	1.6	4.2	0.4	Zinsmeister and Van Der Hyden (1987), Hawkey et al. (1989)
Jackass penguin (*Spheniscus demersus*)	60.1	36.4	2.5	0.9	0.3	Stoskopf et al. (1980), Parson et al. (2015)
Humboldt penguin (*Spheniscus humboldti*)	52.6	34.9	3.4	0	1.7	Wallace et al. (1995)
King penguin (*Aptenodytes patagonicus*)	39.5	48.9	4.6	1.6	5.4	Canfield (2003)
Magellanic penguin (*Spheniscus magellanicus*)	31	60	1.2	6.4	0.12	Hawkey et al. (1989)
Rockhopper penguin (*Eudyptes chrysocome*)	29	63	1.8	6.4	0.6	Hawkey et al. (1989)
Order *Strigiformes*						
Barn owl (*Tyto alba*)	56.5	40.3	1.8	1.0	0.6	Szabo et al. (2014)

Continued

TABLE 49.3 Summary of differential count of leukocytes in avian species.—cont'd

	Heterocytes %	Lymphocytes %	Monocytes %	Eosinophils %	Basophils %	References
Barred owl (*Strix varia*)	43.7	37.9	4.6	6.8	6.9	Calculated from Aguilar (2003)
Burrowing owl (*Athene cunicularia*)	42.4	36.3	5.3	10.3	5.6	Calculated from Aguilar (2003)
Common barn owl (*Tyto alba*)	51.3	33.7	3.7	8.5	2.8	Calculated from Aguilar (2003)
Eagle owl (*Bubo bubo*)	50	38.1	5.3	10.4	5.6	Calculated from Aguilar (2003)
Eastern screech owl (*Otis asio*)	37.3	35.9	6.6	15.4	4.7	Calculated from Aguilar (2003)
Great grey owl (*Strix nebulosa*)	25.2	63.4	4.1	5.9	1.3	Calculated from Aguilar (2003)
Great horned owl (*Bubo virginianus*)	50.4	29.7	6.5	10.6	2.9	Calculated from Aguilar (2003)
Short-eared owl (*Asio flammeus*)	53.3	34.9	8.7	1	2.1	Calculated from Aguilar (2003)
Snowy owl (*Nyctea scandiacus*)	47.9	39.3	4.9	4.9	3	Calculated from Aguilar (2003)
Spectacled owl (*Pulsatrix perspicillata*)	41.1	39.7	3.7	11.5	4.1	Calculated from Aguilar (2003)
Order *Trogoniformes*						
Crested quetzal (*Pharomachrus antisianus*)	70	26	4	0	0	Neiffer (2003)
Golden-headed quetzal (*Pharomachrus auriceps*)	33.2	52.2	8.6	5.1	1.1	Neiffer (2003)
Javan trogon (*Apalharpactes reinwardtii*)	59.9	21.0	6.0	7.0	6.0	Neiffer (2003)
White-tailed trogon (*Trogon chionurus*)	19.1	35	0.4	0	48.7	Neiffer (2003)

TABLE 49.4 Summary of plasma/serum concentrations of ions in avian species (for glucose concentrations see supplementary materials for carbohydrate chapter).

	Na^+	Cl^-	K^+	Ca^{++}	P	References
Elegant-crested tinamou (*Eudromia elegans*)	165.4	123.1	2.15			Black et al. (2013)
Greater rhea (*Rhea americana*)	162		4.5	3.8	2.0	Uhart et al. (2006)
Lesser rhea (*Pterocnemia pennata*)	162		4.5	3.2		Reissig et al. (2002)
Ostrich (*Struthio camelus*)	144		3.6	-	-	Bonadiman et al. (2009)
Order *Accipitriformes*						
***Family* Accipitridae**						
African fish eagle (*Haliaeetus vocifer*)	153	115	1.6	2.4	0.74	Hollamby et al. (2004)
African white-backed vulture (*Gyps africanus*)	154		1.4	1.7		Naidoo et al. (2008)
Bearded vulture (*Gypaetus barbatus*)				2.4	0.9	Hernández and Margalida (2010)
Black kite (*Milvus migrans*)				2.3		Ferrer et al. (1987)
Cape vulture (*Gyps coprotheres*)	157	117	1.2	2.7	0.8	Van Heerden et al. (1987)
Cinereous vulture (*Aegypius monachus*)	144		3.5			Seok et al. (2017)
Common buzzard (*Buteo buteo*)				2.3		Ferrer et al. (1987)
Eastern imperial eagle (*Aquila heliaca*)				2.3		Ferrer et al. (1987)
Egyptian vulture (*Neophron percnopterus*)	152	100	1.6	2.7	2.3	Polo et al. (1992)
Galapagos hawk (*Buteo galapagoensis*)	152	121	2.0	2.0	0.8	Deem et al. (2012)
Golden eagle (*Aquila chrysaetos*)	162	107	2.2	2.7	1.5	Polo et al. (1992)
Griffon vulture (*Gyps fulvus*)	155	98	2.1	3.5	1.5	Polo et al. (1992)
Northern goshawk (*Accipiter gentilis*)	159		3.0	1.2	1.2	Hanauska-Brown et al. (2003)
South American snail kite (*Rostrhamus sociabilis*)	154	115	2.8	2.3	1.5	Gee et al. (1981)
Spanish imperial eagle (*Aquila adalberti*)	156	104	2.6	2.6	1.5	Mean: Polo et al. (1992), García-Montijano et al. (2002)
Swamp harrier (*Circus approximans*)	157	124	2.8	2.5	2.3	Calculated from Youl (2009)
Family *Cathartidae*						
Andean condor (*Vultur gryphus*)	147	111	2.9	2.2	0.7	Gee et al. (1981)
California condor (*Gymnogyps californianus*)	146	115	3.0	2.9	0.7	Dujowich et al. (2005)
Order *Anseriformes*						
Aleutian Canada goose (*Branta canadensis leucopareia*)	147	105	3.4	2.6	0.9	Gee et al. (1981)
Black duck (*Anas superciliosa*)					1.4	Mulley (1979)
Common pochard (*Aythya ferina*)	150	120	2.1			Balasch et al. (1974)
Common eider (*Somateria mollissima*)	151	109	3.0			Hollmén et al. (2001)
Embden goose (*Anser anser*)	140	101	3.1	2.6	1.2	Gee et al. (1981)
Emperor geese (*Chen canagica*)					1.1	Franson et al. (2009)
Eurasian teal (*Anas crecca*)	131		3.42			Elarabany (2018)
Ferruginous ducks (*Aythya nyroca*)	142		2.8			Avni-Magen et al. (2016)
Harlequin duck (*Histrionicus histrionicus*)			2.7	2.3		Stoskopf et al. (2010)
Mottled duck (*Anas fulvigula*)	146					Ratliff et al. (2017)
Mute swan (*Cygnus olor*)	144		6.8	2.7	1.6	Dolka et al. (2014)

Continued

TABLE 49.4 Summary of plasma/serum concentrations of ions in avian species (for glucose concentrations see supplementary materials for carbohydrate chapter).—cont'd

	Na^+	Cl^-	K^+	Ca^{++}	P	References
Nene goose (*Branta sandvicensis*)	166	99	2.5	2.6	0.8	Gee et al. (1981)
Northern shoveler (*Anas clypeata*)	109		3.1			Elarabany (2018)
Tule white-fronted goose (*Anser albifrons*)	146	112	3.3	2.5	1.2	Gee et al. (1981)
Order *Caprimulgiformes*						
Tawny frogmouth (*Podargus strigoides*)	155	111	3.2	2.3	1.3	
Order *Charadriiformes*						
American avocet (*Recurvirostra americana*)	155	115	3.2	2.2	0.8	Ball (2003)
American oystercatcher (*Haematopus palliates*)	151		3.2	2.1	0.8	Carlson-Bremer et al. (2010)
Black-headed gull (*Larus ridibundus*)	160	119	1.6			Balasch et al. (1974)
Black-winged stilt (*Himantopus himantopus*)	147	113		2.2	0.7	Ball (2003)
Common black-headed gull (*Larus ridibundus*)	160	119	1.6			Balasch et al. (1974)
Common murre (*Uria aalge*)	155	114	3.6			Frankfurter et al. (2012)
Double-striped thick-knee (*Burhinus bistriatus*)	153	121	2.7	2.2	1.9	Ball (2003)
European herring gull (*Larus argentatus*)	157	121	1.8			Balasch et al. (1974)
Kelp gulls (*Larus dominicanus*)				1.0	2.2	Doussang et al. (2015)
Killdeer (*Charadrius vociferus*)				2.3	0.8	Ball (2003)
Piping plover (*Charadrius melodus*)				2.7		Ball (2003)
Sooty tern (*Sterna fuscata*)				2.3	1.3	Work (1996)
South polar skua (*Stercorarius maccormicki*)						Deguirmendjian Rosa et al. (1992)
Wattled jacana (*Jacana jacana*)				3.3	1.1	Ball (2003)
Order *Ciconiiformes*						
Northern bald ibis (*Geronticus ermita*)				2.3		Dutton et al. (2002)
Puna Ibis (*Plegadis ridgwayi*)	143	115	3.5	2.3	1.0	Coke et al. (2004)
Order *Coliiformes*						
Blue-naped mousebird (*Urocolius macrourus*)	187	124	1.9	2.0	1.5	Calculated from Pye (2003)
Speckled mousebird (*Colius striatus*)				2.2	1.7	Calculated from Pye (2003)
White-backed mousebird (*Colius colius*)				4.4		Calculated from Pye (2003)
Order *Columbiformes*						
Pigeon (*Columba livia*)	160	117	2.1			Balasch et al. (1974)
Nicobar pigeon (*Caloenas nicobarica*)	150	107	2.4	2.5	4.4	Mean: Peinado et al. (1992a), Schultz (2003)
Pheasant pigeon (*Otidiphaps nobilis*)		130		4.0	4.4	Peinado et al. (1992a)
Pink-headed fruit dove (*Ptilinopus porphyreus*)	162	120	2.6	2.5	1.8	Schultz (2003)
Western or common crowned pigeon (*Goura cristata*)		101		2.2	2.2	Peinado et al. (1992a)
Victoria crowned pigeon (*Goura victoria*)		105		2.4	1.8	Peinado et al. (1992a)
Southern crowned or Scheepmaker's crowned pigeon (*Goura scheepmakeri*)		100				Peinado et al. (1992a)

Continued

TABLE 49.4 Summary of plasma/serum concentrations of ions in avian species (for glucose concentrations see supplementary materials for carbohydrate chapter).—cont'd

	Na^+	Cl^-	K^+	Ca^{++}	P	References
Order *Coraciiformes*						
Northern ground hornbill (*Bucorvus abyssinicus*)	154	117	3.1	2.3	1.2	Calculated from Dutton (2003)
Blue-crowned motmot (*Momotus momota*)	158	120	2	2.5	1.7	Calculated from Dutton (2003)
Great hornbill (*Buceros bicornis*)	153	111	4.5	2.2	1.5	Calculated from Dutton (2003)
Green wood hoopoe (*Phoeniculus purpureus*)	159	111	1.9	2.3	1.2	Calculated from Dutton (2003)
Hoopoe (*Upupa epops*)	183	125	2.9	2.1	2.6	Calculated from Dutton (2003)
Lilac-breasted roller (*Coracias caudatus*)	158	118	2.9	2.2	0.9	Calculated from Dutton (2003)
Micronesian kingfisher (*Todiramphus cinnamominus*)	160	127	3.1	2.2	0.8	Calculated from Dutton (2003)
Southern Carmine Bee-eater (*Merops nubicoides*)	157	111	4.4	1.9	0.7	Calculated from Dutton (2003)
Order *Cuculiformes*						
Greater roadrunner (*Geococcyx californianus*)	157	121	2.7	2.5	1.2	Abou-Madi (2003)
Guira cuckoo (*Guira guira*)				2.4	2.9	Abou-Madi (2003)
Order *Falconiformes*						
American kestrel (*Falco sparverius*)	158	108	2.2	1.8	3.0	Dressen et al. (1999)
Artic peregrine falcon (*Falco peregrinus tundrius*)				1.8	0.9	Gee et al. (1981)
Gyr falcons (*Falco rusticolus*)	147		3.3			Raghav et al. (2015)
Order *Galliformes*						
Attwater's prairie chicken (*Tympanuchus cupido attwateri*)				3.4	5.5	West and Haines (2002)
Black-fronted piping-guan (*Aburria jacutinga*)				2.7	2.7	Motta et al. (2013)
Bobwhite quail (*Colinus virginianus*)	161	115	3.9	2.6	1.6	Mean: Gee et al. (1981), Johnson et al. (2007)
Chukar partridge (*Alectoris chukar*)	155	117	9.1	2.1	2.1	Ozek and Bahtiyarca (2004)
Greater sage grouse (*Centrocercus urophasianus*)				5.3	2.3	Dunbar et al. (2005)
Guinea fowl (*Numida meleagris*)	161	122	2.2			Mean: Balasch et al. (1973), Drew (2003)
Peacock (*Pavo cristatus*)	159	114	3.6			Balasch et al. (1973)
Pheasant (*Phasianus colchicus*)	155	120	3.3			Balasch et al. (1973)
Rock partridge (*Alectoris graeca*)	154	113	3.2			Balasch et al. (1973)
Red jungle fowl (*Gallus gallus*) (Java)	157	119	3.5			Balasch et al. (1973)
Turkey (*Meleagris gallopavo*)				2.0		Drew (2003)
Wattled curassow (*Crax globulosa*)	161		4.3	2.9		Drew (2003)
Gruiformes						
***Family* Gruidae**						
Florida sandhill crane (*Grus canadensis pratensis*)	149	109	3.4	2.4	1.2	Gee et al. (1981)

Continued

TABLE 49.4 Summary of plasma/serum concentrations of ions in avian species (for glucose concentrations see supplementary materials for carbohydrate chapter).—cont'd

	Na^+	Cl^-	K^+	Ca^{++}	P	References
Greater sandhill crane (*Grus canadensis tabida*	147	107	3.5	2.4	1.2	Gee et al. (1981)
Mississippi sandhill crane (*Grus canadensis pulla*)	147	103	3.6	2.4	1.2	Gee et al. (1981)
Red-crowned crane (*Grus japonensis*)	148	107	2.8	2.7	1.1	Carpenter (2003)
Siberian crane (*Grus leucogeranus*)	149	109	2.9	2.6	1.2	Carpenter (2003)
Wattled crane (*Bugeranus carunculatus*)	146	108	3.2	2.7	0.9	Carpenter (2003)
Whooping crane (*Grus americana*)	147	107	3.4	2.3	0.9	Gee et al. (1981)
Family *Rallidae*						
Guam rail (*Gallirallus owstoni*)		120	1.8	3.0	1.1	Fontenot et al. (2006) (*units corrected)
Takahē (*Porphyrio hochstetteri*)	146	108	4.2	2.7	1.1	Calculated from Youl (2009)
Family *Otididae*						
Great bustard (*Otis tarda*)	162		2.7	5.0	0.9	Barrera et al. (1992)
Houbara bustard (*Chlamydotis undulate*)	149	113	3.7	2.5	0.8	D'Aloia et al. (1996a)
Kori bustard (*Ardeotis kori*)	154	115	2.9		1.3	D'Aloia et al. (1996b)
White-bellied bustard (*Eupodotis senegalensis*)				2.4		Bailey et al. (1998b)
Order *Passeriformes*						
American crow (*Corvus brachyrhynchos*)	152	120	4.4	2.0	1.1	Gentz, 2003
Asian fairy-bluebird (*Irena puella*)	158	121	2.3	2.1	1.6	Genz (2003)
Black-capped chickadees (*Poecile atricapillus*)	158	122				Van Hemert and Handel (2016)
Blue-faced honeyeater (*Entomyzon cyanotis*)	162			2.5	2.4	Genz (2003)
Green broadbill (*Calyptomena viridis*)	146			2.3	1.6	Genz (2003)
Hooded pitta (*Pitta sordida*)				3.0	2.5	Genz (2003)
House sparrow (*Passer domesticus*)	155					Khalilieh et al. (2012)
Raven (*Corvus corax*)	162	132				Balasch et al. (1974)
Red-crested cardinal (*Paroaria coronata*)			2.4	1.9	2.0	Genz (2003)
Silver-eared mesia (*Leiothrix argentauris*)				2.5	2.5	Genz (2003)
Superb starling (*Lamprotornis superbus*)		122		2.0	0.7	Genz (2003)
Venezuelan troupial (*Icterus icterus*)	163	122	2.8	2.4	3.1	Genz (2003)
Order *Pelecaniformes*						
Brown pelican (*Pelecanus occidentalis*)	151	114	4.1	2.2	1.3	Balasch et al. (1974), Wolf et al. (1985)
Pink-backed pelican (*Pelecanus rufescens*)	149	109	3.3	2.3	0.8	Weber (2003)
Black-faced cormorant (*Leucocarbo fuscescens*)	142	112	5.9	2.6	2.6	Melrose and Nicol (1992)
Flightless cormorant (*Phalacrocorax harrisi*)	150	109		2.2	4.4	Travis et al. (2006a)
Great cormorant (*Phalacrocorax carbo*)	154	119	2.5			Balasch et al. (1974)
Great frigatebird (*Fregata minor*)	142	122	3.8	3.9	3.4	Work (1996), Valle et al. (2018)

Continued

TABLE 49.4 Summary of plasma/serum concentrations of ions in avian species (for glucose concentrations see supplementary materials for carbohydrate chapter).—cont'd

	Na^+	Cl^-	K^+	Ca^{++}	P	References
Guanay cormorant (*Phalacrocorax bougainvillii*)	160	114	3.4	2.3	0.8	Weber (2003)
Imperial shag (*Phalacrocorax atriceps*)				2.3	1.4	Gallo et al. (2013)
Brown booby (*Sula leucogaster*)				2.7	1.3	Work (1999)
Northern gannet (*Morus bassanus* or *Sula bassanus*)	153	124	3.0			Balasch et al. (1974)
Puna ibis (*Plegadis ridgwayi*)	143	115	3.5	2.3		Coke et al. (2004)
Order *Phaethontiformes*						
Red-tailed tropicbird (*Phaeton rubricauda*)						Work (1996)
Order *Phoenicopteriformes*						
Chilean flamingo (*Phoenicopterus chiliensis*)	153	116	2.2	2.7		Norton (2003)
American flamingo (*Phoenicopterus ruber*)	157	117	3.2	2.3	1.4	Norton (2003)
Order *Podicipediformes*						
Western grebe (*Aechmophorus occidentalis*)	154	118	3.9			Frankfurter et al. (2012)
Order *Procellariiformes*						
Hawaiian dark-rumped petrel (*Pterodroma phaeopygia*)				1.7	0.3	Work (1996)
Laysan albatross (*Diomedea immutabilis*)				2.7	2.0	Work (1996)
Northern fulmar (*Fulmarus glacialis*)	153		4.5			Frankfurter et al. (2012)
Southern giant petrel (*Macronectes giganteus*)	154	121	<1.5	2.3	0.8	Uhart et al. (2003)
Waved albatross (*Phoebastria irrorata*)	153	118	3.7	2.5	1.1	Padilla et al. (2003)
Wedge-tailed Shearwater (*Puffinus pacificus*)				2.2	0.5	Work (1996)
Order *Psittaciformes*						
Amazon parrot (*Amazona aestiva*)	147		3.5	0.8	0.6	Valéria et al. (2008)
Baudin's cockatoo (*Calyptorhynchus baudinii*)	145.8	116.7	5.4			Le Souëf et al. (2013)
Blue-fronted Amazon parrot (*Amazona aestiva*)	152		6.1	1.7	6.9	Deem et al. (2005)
Carnaby's cockatoo (*Calyptorhynchus latirostris*)	146.6	113.7	5.4			Le Souëf et al. (2013)
Galah (*Eolophus roseicapilla*)	106		10.3	1.7	1.0	McDonald et al. (2010)
Kakapo (*Strigops habroptilus*)	148		4.5	2.4		Low et al. (2006)
Kea (*Nestor notabilis*)	145	113	4.4	2.1		Calculated from Youl (2009)
Long-billed corella (*Cacatua tenuirostris*)	108		8.0	1.8	7.0	McDonald et al. (2010)
Spix's macaw (*Cyanopsitta spixii*)					0.8	Foldenauer et al. (2007)
Monk or quaker parrots (*Myiopsitta monachus*)	144		3.5			Rettenmund et al. (2014)
St Vincent parrot (*Amazona guildingii*)	144		3.1	2.0	1.2	Deem et al. (2008)
Sulphur-crested cockatoo (*Cacatua galerita*)	95		8.3	1.7	5.7	McDonald et al. (2010)

Continued

TABLE 49.4 Summary of plasma/serum concentrations of ions in avian species (for glucose concentrations see supplementary materials for carbohydrate chapter).—cont'd

	Na^+	Cl^-	K^+	Ca^{++}	P	References
Order *Pteroclidiformes*						
Pin-tailed Sandgrouse (*Pterocles alchata*)	147	111	2.5	2.5	0.7	Lierz and Fenske (2004)
Order *Sphenisciformes*						
Adélie penguin (*Pygoscelis adeliae*)	147	121	3.8	2.6	4.5	Aquilera et al. (1993), Parsons et al. (2015) Ibañez et al. (2015)
African penguin (*Spheniscus demersus*)	155	116	5.2			Mazzaro et al. (2013)
Chinstrap penguin (*Pygoscelis antarcticus*)	156	117	3.5	1.6	1.7	Aquilera et al. (1993, 1992), Ibañez et al. (2015)
Galápagos penguin (*Spheniscus mendiculus*)	156	118	3.9	2.5	1.6	Travis et al. (2006b)
Gentoo penguin (*Pygoscelis papua*)	149	108	3.3	1.6	1.8	Aquilera et al. (1993), Ibañez et al. (2015)
Humboldt penguin (*Spheniscus humboldti*)	154		3.5	3.5	1.4	Wallace et al. (1995)
Jackass penguin (*Spheniscus demersus*)	150	111	4.5	2.7	1.3	Cranfield (2003)
King penguin (*Aptenodytes patagonicus*)	157	110	3.0	2.7	1.2	Cranfield (2003)
Rockhopper penguin (*Eudyptes chrysocome*)	155	118	4.3	1.7	2.0	Mean: Karesh et al. (1999), Maxime and Hassani (2014)
Order *Strigiformes*						
Barn owl (*Tyto alba*)	153	118	2.8	2.2	1.2	Aguilar (2003)
Barred owl (*Strix varia*)	150	110	3.3	2.4	1.4	Aguilar (2003)
Burrowing owl (*Athene cunicularia*)	150	111	3.2	2.2	1.4	Aguilar (2003)
Eagle owl (*Bubo bubo*)	166	132	2.8	2.4	2.8	Aguilar (2003)
Great horned owl (*Bubo virginianus*)	159	121	2.5	2.4	1.9	Aguilar (2003)
Great grey owl (*Strix nebulosa*)	152	119	3.5	2.4	1.9	Aguilar (2003)
Short-eared owl (*Asio flaammeus*)	157	136	2.9	2.3	2.6	Aguilar (2003)
Screech owl (*Otus asio*)	152	116	3.0	2.2	1.4	Aguilar (2003)
Snowy owl (*Nyctea scandiaca*)	152	117	2.8	2.3	1.3	Aguilar (2003)
Spectacled owl (*Pulsatrix perspicillata*)	156	119	2.6	3.0	1.8	Aguilar (2003)
Order *Trogoniformes*						
Crested quetzal (*Pharomachrus antisianus*)				4.3		Neiffer (2003)
Golden-headed quetzal (*Pharomachrus auriceps*)	158	121	2.4	2.3	1.1	Neiffer (2003)
Javan trogon (*Apalharpactes reinwardtii*)				2.9	1.2	Neiffer (2003)
White-tailed trogon (*Trogon chionurus*)				2.2	0.4	Neiffer (2003)

TABLE 49.5 Summary of plasma/serum concentrations of proteins, uric acid, and urea in avian species.

	Protein g L^{-1}	Albumin g L^{-1}	Globulin g L^{-1}	Uric acid mM	BUN/ urea mM	References
Elegant-crested tinamou (*Eudromia elegans*)	51.9	29.2	22.2	0.29		Black et al. (2013)
Emu (*Dromaius novaehollandiae*)	40.5	17	22	0.3	0.42	Mean: Okotie-Eboh et al. (1992), Smith (2003)
Ostrich (*Struthio camelus*)	46.5	16.9	29.6	0.4		Mean: Smith (2003), Bonadiman et al. (2009)
Greater rhea (*Rhea americana*)	48.2	25.8	22.5	0.3		Uhart et al. (2006)
Order *Accipitriformes*						
African fish eagle (*Haliaeetus vocifer*)	48			1.0		Hollamby et al. (2004)
African white-backed vulture (*Gyps africanus*)	33.5	11.7	21.8	0.65		Naidoo et al. (2008)
Bald eagle (*Haliaeetus leucocephalus*)	41					Elliott et al. (1974)
Bearded vulture (*Gypaetus barbatus*)	40			0.2		Hernández and Margalida (2010)
Black kite (*Milvus migrans*)	37	12	24		1.20	Ferrer et al. (1987)
Booted eagle (*Hieraaetus pennatus*)	38	8	29		1.47	Ferrer et al. (1987)
Cape vulture (*Gyps coprotheres*)	37.8	19.2	18.6			Van Heerden et al. (1987)
Cinereous vulture (*Aegypius monachus*)	41	18.9	22.1	0.32		Seok et al. (2017)
Common buzzard (*Buteo buteo*)	38	10	28	0.83	3.75	Ferrer et al. (1987), Garcia-Rodriguez et al. (1987)
Crested serpent eagle (*Spilornis cheela*)	51.5	14.9	32.9	0.38	0.64	Elliott et al. (1974), Chan et al. (2012)
Eastern imperial eagle (*Aquila heliaca*)	33	10	22		1.67	Ferrer et al. (1987)
Egyptian vulture (*Neophron percnopterus*)	39	15.3	20.4	0.2	1.6	Polo et al. (1992)
Galapagos hawk (*Buteo galapagoensis*)	33	12.5	21	1.1		Deem et al. (2012)
Golden eagle (*Aquila chrysaetos*)	33.5	9.5	17.1	0.3	1.8	Mean: Elliott et al. (1974), Polo et al. (1992)
Griffon vulture (*Gyps fulvus*)	39	17.7	25.8	0.3	1.3	Polo et al. (1992)
Hooded vulture (*Necrosyrtes monachus*)	42					Elliott et al. (1974)
Marsh harrier (*Circus aeruginosus*)	34.7					Lavin et al. (1992)
Northern goshawk (*Accipiter gentilis*)	27	11	16	0.75		Hanauska-Brown et al. (2003)
Ornate hawk-eagle (*Spizaetus ornatus*)	48					Elliott et al. (1974)
South American snail kite (*Rostrhamus sociabilis*)	37	13	23	0.67	2.3	Gee et al. (1981)

Continued

TABLE 49.5 Summary of plasma/serum concentrations of proteins, uric acid, and urea in avian species.—cont'd

	Protein g L^{-1}	Albumin g L^{-1}	Globulin g L^{-1}	Uric acid mM	BUN/ urea mM	References
Spanish imperial eagle (*Aquila adalberti*)	38	10.7	19.2	0.19	1.6	Mean; Polo et al. (1992), García-Montijano et al. (2002)
Swainson's hawk (*Buteo swainsoni*)				0.39	2.45	
Swamp harrier (*Circus approximans*)	33	14	19	0.31		Calculated from Youl (2009)
White-bellied sea eagle (*Haliaeetus leucogaster*)	50					Elliott et al. (1974)
Family *Cathartidae*						
Andean condor (*Vultur gryphus*)	37	13	23	0.53	1.7	Gee et al. (1981)
California condor (*Gymnogyps californianus*)	30	11	22	0.30		Dujowich et al. (2005)
King vulture (*Sarcoramphus papa*)	41					Elliott et al. (1974)
Anseriformes						
Aleutian Canada goose (*Branta canadensis leucopariea*)	48	20	28	0.49	0.5	Gee et al. (1981)
Black brant (*Branta bernicla*)	36.3	14.5	21.8	0.4		Franson et al. (2017)
Black duck (*Anas superciliosa*)	43.2	30.4	5.4	0.09		Mulley (1979)
Black-necked swan (*Cygnus melanocoryphus*)	55.1	21.9	33.2	0.75	0.52	Artachoa et al. (2007)
Common eider (*Somateria mollissima*)	39.4	18.6	20.8		0.4	Hollmén et al. (2001)
Common pochard (*Aythya ferina*)	17.9	8.0	7.4		0.6	Balasch et al. (1974)
Coscoroba swan (*Coscoroba coscoroba*)					0.15	Pérez Calabuig et al. (2010)
Embden goose (Anser anser)	44	17	27	0.45	0.7	Gee et al. (1981)
Emperor geese (*Chen canagica*)	48			0.42	0.34	Franson et al. (2009)
Eurasian teal (*Anas crecca*)	71	13.3		0.28	3.6	Elarabany (2018)
Ferruginous duck (*Aythya nyroca*)	40	23	17	0.22		Avni-Magen et al. (2016)
Harlequin duck (*Histrionicus histrionicus*)	34	13	21			Stoskopf et al. (2010)
Mallard (*Anas platyrhynchos*)	43.1	17.7		0.6		Driver (1981)
Mute swan (*Cygnus olor*)	45.7	15.2	30.5	0.33	1.7	Dolka et al. (2014)
Nene goose (*Branta sandvicensis*)	44	18	26	0.48	0.3	Gee et al. (1981)
Northern shoveler (*Anas clypeata*)	70	13.2		0.38	3.4	Elarabany (2018)
Pekin or domestic duck (*Anas platyrhynchos*)	30			0.17		Zhang et al. (2005)

Continued

TABLE 49.5 Summary of plasma/serum concentrations of proteins, uric acid, and urea in avian species.—cont'd

	Protein g L^{-1}	Albumin g L^{-1}	Globulin g L^{-1}	Uric acid mM	BUN/ urea mM	References
Trumpeter swan (*Cygnus buccinators*)	48 3	14	34	0.26	0.75	Olsen et al. (2002)
Tule white-fronted goose (*Anser albifrons*)	44	17	27	0.64	0.5	Gee et al. (1981)
Tundra swan (*Cygnus columbianus*)	35	13	22	0.48	0.5	Milani et al. (2012)
Order *Caprimulgiformes*						
Tawny frogmouth (*Podargus strigoides*)	35	20	15		0.47	McCracken (2003)
Order *Charadriiformes*						
American oystercatcher (*Haematopus palliates*)	40	17.7	21.2	0.4		Carlson-Bremer et al. (2010)
American avocet (*Recurvirostra americana*)	30	12	18		0.44	Ball (2003)
Black-headed gull (*Chroicocephalus ridibundus* or *Larus ridibundus*)	36.7	19.6	17.1		1.9	Balasch et al. (1974)
Black-winged stilt (*Himantopus himantopus*)	36	22	13		0.42	Ball (2003)
Double-striped thick-knee (*Burhinus bistriatus*)	35	14	18		0.44	Ball (2003)
European herring gull (*Larus argentatus*)	34.8	16.0	14.6	0.4	1.05	Balasch et al. (1974), Totzke et al. (1999)
Kelp gulls (*Larus dominicanus*)	54			0.5	0.6	Doussang et al. (2015)
Killdeer (*Charadrius vociferus*)	29	11	16		0.45	Ball (2003)
Piping plover (*Charadrius melodus*)	45	13	32		0.30	Ball (2003)
Red knot (*Calidris canutus rufa*)	35	20	14.8			D'Amico et al. (2010)
Sooty tern (*Sterna fuscata*)	33	15	18	0.7		Work (1996)
South polar skua (*Stercorarius maccormicki*)	28	8.2	19.8			Deguirmendjian Rosa et al. (1992)
Spotted thick-knee (*Burhinus capensis*)	36.0	14.0	22.0		1.2	Samour et al. (1998)
Stone curlew (*Burhinus oedicnemus*)	39.8	10.5	29.8		0.8	Samour et al. (1998)
Wattled jacana (*Jacana jacana*)	42	21	24		0.4	Ball (2003)
Order *Coliiformes*						
Blue-naped mousebird (*Urocolius macrourus*)	37.5				0.3	Calculated from Pye (2003)
Speckled mousebird (*Colius striatus*)	37	12	24		0.4	Calculated from Pye (2003)

Continued

TABLE 49.5 Summary of plasma/serum concentrations of proteins, uric acid, and urea in avian species.—cont'd

	Protein g L^{-1}	Albumin g L^{-1}	Globulin g L^{-1}	Uric acid mM	BUN/ urea mM	References
Order *Columbiformes*						
Rock pigeon (*Columba livia*)	28.7	9	24	0.3	1.2	Mean: Balasch et al. (1974), Lumeij (1987), Gayathri et al. (2004), Roman et al. (2013)
Nicobar pigeon (*Caloenas nicobarica*)	32.6	14.8	6.9	0.61	1.0	Peinado et al. (1992a)
Pheasant pigeon (*Otidiphaps nobilis*)	32.7	15.4	13.3	0.78	0.9	Peinado et al. (1992a)
Pink-headed fruit dove (*Ptilinopus porphyreus*)	36	15	18	0.41	0.54	Schultz (2003)
Western or common crowned pigeon (*Goura cristata*)	44.6	21.8	17.4	0.41	1.4	Peinado et al. (1992a)
Victoria crowned pigeon (*Goura victoria*)	35.8	17.4	11.9	0.31	1.7	Peinado et al. (1992a)
Southern crowned or Scheepmaker's crowned pigeon (*Goura scheepmakeri*)	40.5	20.4	13.3		1.6	Peinado et al. (1992a)
Order *Coraciiformes*						
Northern ground hornbill (*Bucorvus abyssinicus*)	34	19	15	0.83	0.57	Calculated from Dutton (2003)
Blue-crowned Motmot (*Momotus momota*)	43	23	20	1.0	0.5	Calculated from Dutton (2003)
Great hornbill (*Buceros bicornis*)	40	21	20	1.67	0.45	Calculated from Dutton (2003)
Green wood hoopoe (*Phoeniculus purpureus*)	30	10	15	1.17	1.10	Calculated from Dutton (2003)
Hoopoe (*Upupa epops*)	36	15	7	1.33	0.89	Calculated from Dutton (2003)
Lilac-breasted Roller (*Coracias caudatus*)	33	18	15	0.50	0.43	Calculated from Dutton (2003)
Micronesian kingfisher (*Todiramphus cinnamominus*)	36	19	19	1.33	0.65	Calculated from Dutton (2003)
Southern carmine bee-eater (*Merops nubicoides*)	32	23	9	0.83	0.68	Calculated from Dutton (2003)
Order *Cuculiformes*						
Greater roadrunner (*Geococcyx californianus*)	34	15	18	1.2	0.4	Abou-Madi (2003)
Guira cuckoo (*Guira guira*)				0.5	0.6	Abou-Madi (2003)
Order *Falconiformes*						
American kestrels (*Falco sparverius*)	32	10	12	0.53	1.0	Dressen et al. (1999)
Artic peregrine falcon (*Falco peregrinus tundrius*)	33	9	24	0.68	1.2	Gee et al. (1981)
Collared forest falcon (*Micrastur semitorquatus*)	45					Elliott et al. (1974)

Continued

TABLE 49.5 Summary of plasma/serum concentrations of proteins, uric acid, and urea in avian species.—cont'd

	Protein g L^{-1}	Albumin g L^{-1}	Globulin g L^{-1}	Uric acid mM	BUN/ urea mM	References
Lesser kestrel (*Falco naumanni*)				0.90	4.0	Rodríguez (2011)
Southern crested caracara (*Polyborus plancus*)	38					Elliott et al. (1974)
Order *Galliformes*						
Attwater's prairie chicken (*Tympanuchus cupido attwateri*)	32.6	15.6	17.8	0.52		West and Haines (2002)
Black-fronted piping-guan (*Aburria jacutinga*)				0.91	1.38	Motta et al. (2013)
Bobwhite quail (*Colinus virginianus*)	37.6	16.5	17	0.6	1.6	Gee et al. (1981), Hill and Murray (1987), Johnson et al. (2007)
Chukar partridge (*Alectoris chukar*)	42			0.2		Ozek and Bahtiyarca (2004)
Greater sage grouse (*Centrocercus urophasianus*)	52.1	21	31.1	0.31	1.3	Mean: Dunbar et al. (2005), Dyer et al. (2009)
Grouse (*Lagopus lagopus*)	39.4	19.7	17.9	0.36		Wilson and Wilson (1978), Korhonen (1987)
Guinea fowl (*Numida meleagris*)	44.3			0.3	0.7	Balasch et al. (1973)
Jungle Fowl (*Gallus gallus*)	44.3			0.15	1.02	Mean: Balasch et al. (1973), Adnan and Amin Babjee (1985)
Peacock (*Pavo cristatus*)	43.6			0.2	2.8	Balasch et al. (1973)
Pheasant (*Phasianus colchicus*)	49.0			0.3	0.9	Balasch et al. (1973)
Rock partridge (*Alectoris graeca*)	35.2			0.4	0.43	Balasch et al. (1973)
Turkey (*Meleagris gallopavo*)	46.2	16	30.2	0.60		Mean: Drew (2003), Schmidt et al. (2009a)
Wattled curassow (*Crax globulosa*)	40				0.59	Drew (2003)
Order *Gruiformes*						
***Family* Gruidae**						
Common crane (*Grus grus*)	49			0.17	1.18	Puerta et al. (1990)
Florida sandhill crane (*Grus canadensis pratensis*)	39	14	24	0.74	0.5	Gee et al. (1981)
Greater sandhill crane (*Grus canadensis tabida*)	39	16	23	0.45	0.3	Gee et al. (1981)
Mississippi sandhill crane (*Grus canadensis pulla*)	39	14	25	0.41	0.3	Gee et al. (1981)
Red-crowned crane (*Grus japonensis*)	33	12	21		0.46	Calculated from Carpenter (2003)
Siberian crane (*Grus leucogeranus*)	37	14	23		0.54	Calculated from Carpenter (2003)
Wattled crane (*Bugeranus carunculatus*)	31	11	20		0.46	Calculated from Carpenter (2003)
Whooping crane (*Grus americana*)	38	15	23	0.48	0.5	Gee et al. (1981)

Continued

TABLE 49.5 Summary of plasma/serum concentrations of proteins, uric acid, and urea in avian species.—cont'd

	Protein g L^{-1}	Albumin g L^{-1}	Globulin g L^{-1}	Uric acid mM	BUN/ urea mM	References
Family *Rallidae*						
Common coot (*Fulica atra*)				0.13	1.45	Rubio et al. (2012)
Red-knobbed coot (*Fulica cristata*)				0.44		Rubio et al. (2012)
Guam rail (*Gallirallus owstoni*)	47.5	20	21	0.34		Fontenot et al. (2006)
Takahē (Porphyrio hochstetteri)	40.9	13.8	27.3	0.5		Calculated from Youl (2009)
Family *Otididae*						
Great bustard (*Otis tarda*)	35					Barrera et al. (1992)
Buff-crested bustard (*Eupoditis ruficrista*)	32.8	12.9	19.6	0.53		Bailey et al. (1998a)
Houbara bustard (*Chlamydotis undulate*)	33.3	14.8	17.9	0.58		D'Aloia et al. (1996a)
Kori bustard (*Ardeotis kori*)	29.6	15.9	13	0.47		D'Aloia et al. (1996b)
White-bellied bustard (*Eupodotis senegalensis*)	30	12	18	0.41		Bailey et al. (1998b)
Order *Passeriformes*						
Abert's towhee (*Melozone aberti*)				1.8		Davis et al. (2013)
American crow (*Corvus brachyrhynchos*)	37	18	18	0.5	0.7	Gentz (2003)
Asian fairy-bluebird (*Irena puella*)	38	18	17	0.8	0.6	Gentz (2003)
Blackbird (*Turdus merula*)	39	17	17.9			Llacuna et al. (1996)
Black-capped chickadees (*Poecile atricapillus*)	26	18.5	7.5	1.1		Van Hemert and Handel (2016)
Blue jay (*Cyanocitta cristata*)	41					Garvin et al. (2003)
Common grackle (*Quiscalus quiscula*)	31.7	14.5	17.2	0.77	1.7	Hill and Murray (1987)
Common starling (*Sturnus vulgaris*)	28	17	11	0.77	1.4	Hill and Murray (1987)
Garden warbler (*Sylvia borin*)	38				1.1	Jenni-Eiermann and Jenni (1994)
Great tit (*Parus major*)	25	9.3	8.3			Llacuna et al. (1996)
Green broadbill (*Calyptomena viridis*)	49				0.5	Gentz (2003)
Hooded pitta (*Pitta sordida*)	43			1.0	0.7	Gentz (2003)
House sparrow (*Passer domesticus*)	32			1.0		Puerta et al. (1995), Lattin et al. (2015)
(African) pied crow (*Corvus albus*)	31.3	13.2	18.1	1.3	1.1	Ihedioha et al. (2011)
Pied flycatchers (*Ficedula hypoleuca*)					1.63	Kern et al. (2005)

Continued

TABLE 49.5 Summary of plasma/serum concentrations of proteins, uric acid, and urea in avian species.—cont'd

	Protein g L^{-1}	Albumin g L^{-1}	Globulin g L^{-1}	Uric acid mM	BUN/ urea mM	References
Raven (*Corvus corax*)	38	18	19.1		1.0	Balasch et al. (1974)
Red wing blackbirds (*Agelaius phoeniceus*)	28	13	15	1.08	1.85	Hill and Murray (1987)
Red-crested cardinal (*Paroaria coronata*)	44	16	29		0.7	Gentz (2003)
Rock bunting (*Emberiza cia*)	22	11	7.2			Llacuna et al. (1996)
Silver-eared mesia (*Leiothrix argentauris*)	27			1.0	0.6	Gentz (2003)
Southern red bishop (*Euplectes orix*)	31				1.1	Gentz (2003)
Superb starling (*Lamprotornis superbus*)	35	12	24	1.0	0.8	Gentz (2003)
Venezuelan troupial (*Icterus icterus*)	38	20	19	0.3	0.6	Gentz (2003)
Order *Pelecaniformes*						
Black stork (*Ciconia nigra*)	35			0.76	2.1	Puerta et al. (1989)
Black-crowned night heron (*Nycticorax nycticorax*)	34	14.6	19.4	0.38	1.8	Fontenelle (2001)
Black-faced cormorant (*Leucocarbo fuscescens*)	39	15	24	1.3	0.7	Melrose and Nicol (1992)
Brown booby (*Sula leucogaster*)	40	16	24	1.2		Work (1999)
Brown pelican (*Pelecanus occidentalis*)	34.2	14.1	19.4	0.4	1.4	Mean: Balasch et al. (1974), Wolf et al. (1985)
Cattle egret (*Bubulcus ibis*)	34	16.3	17.7	0.23	1.6	Fontenelle (2001)
Flightless cormorant (*Phalacrocorax harrisi*)	39.8	16.8	23	1.3		Travis et al. (2006a)
Great cormorant (*Phalacrocorax carbo*)	32.2	11.5	16.7		1.5	Balasch et al. (1974)
Great frigatebird (Fregata minor)	41.4	16.5	23.5	0.3		Work (1996), Valle et al. (2018)
Imperial cormorant (*Phalacrocorax atriceps*)	38.4	18.3	20.1	0.27	1.29	Gallo et al. (2013)
Little egret (*Egretta garzetta*)	33	16.5	16.5	0.47	1.6	Fontenelle (2001)
Northern bald ibis (*Geronticus ermita*)	36	10	26	0.7		Dutton et al. (2002)
Northern gannet (*Morus bassanus* or *Sula bassanus*)	45	20.1	18.5		1.6	Balasch et al. (1974)
Oriental white stork (*Ciconia boyciana*)	45	15	30			Han et al. (2016)
Pink-backed pelican (*Pelecanus rufescens*)	41	14	27		0.37	Weber (2003)
Puna ibis (*Plegadis ridgwayi*)	38	15	24	0.5	0.35	Coke et al. (2004)
Red-footed booby (*Sula sula*)	30	13	17	0.8		Work (1996)

Continued

TABLE 49.5 Summary of plasma/serum concentrations of proteins, uric acid, and urea in avian species.—cont'd

	Protein g L^{-1}	Albumin g L^{-1}	Globulin g L^{-1}	Uric acid mM	BUN/ urea mM	References
White stork (*Ciconia ciconia*)	45			0.85	2.4	Puerta et al. (1989)
Order *Phaethontiformes*						
Red-tailed tropicbird (*Phaeton rubricauda*)	26.5	12.5	14	0.7		Work (1996)
Order *Procellariiformes*						
Hawaiian dark-rumped petrel (*Pterodroma phaeopygia*)	31	15	17	0.4		Work (1996)
Laysan albatross (*Diomedea immutabilis*)	47	18	30	0.2		Work (1996)
Waved albatross (*Phoebastria irrorata*)	45	18	28	0.3		Padilla et al. (2003)
Wedge-tailed shearwater (*Puffinus pacificus*)	31	15	18	0.6		Work (1996)
Wilson's storm petrel (*Oceanites oceanicus*)	27	9	18			Quillfeldt et al. (2004)
Order *Psittaciformes*						
African grey (*Psittacus erithacus*)	39.5					Lumeij (1987)
Baudin's cockatoo (*Calyptorhynchus baudinii*)	29.5			0.23		Le Souëf et al. (2013)
Blue-fronted Amazon parrot (*Amazona aestiva*)	26	9	18	0.2		Deem et al. (2005)
Blue and gold macaw (*Ara ararauna*)	34.5					Lumeij (1987)
Budgerigar (*Melopsittacus undulatus*)	2.5					Lumeij (1987)
Carnaby's cockatoo (*Calyptorhynchus latirostris*)	29.3			0.29		Le Souëf et al. (2013)
Cuban Amazon parrots (*Amazona leucocephala leucocephala*)	39			0.17	0.28	Tell and Citino (1992)
Kakapo (*Strigops habroptilus*)	45.8	12.4	14.1	0.2	0.9	Low et al. (2006)
Kea (*Nestor notabilis*)	26.3			0.1		Calculated from Youl (2009)
Macaw (*Ara rubrogenys*)	32			0.3	1.0	García del Campo et al. (1991)
Monk parakeet or quaker parrot (*Myopsitta monachus*)	44					Godwin et al. (1982)
Red-capped parrot (*Pionopsitta pileata*)	36					Schmidt et al. (2009a,b)
Spix's macaws (*Cyanopsitta spixii*)	38.3	21	8.2	0.3		Foldenauer et al. (2007)
St Vincent parrots (*Amazona guildingii*)	33.5	17.4	10.1			Deem et al. (2008)
Vinaceous Amazon parrot (*Amazona vinacea*)	40					Schmidt et al. (2009a,b)

Continued

TABLE 49.5 Summary of plasma/serum concentrations of proteins, uric acid, and urea in avian species.—cont'd

	Protein g L^{-1}	Albumin g L^{-1}	Globulin g L^{-1}	Uric acid mM	BUN/ urea mM	References
Order *Pteroclidiformes*						
Pin-tailed sandgrouse (*Pterocles alchata*)	32.9	10.7	22.2	0.27	0.6	Lierz and Fenske (2004)
Order *Sphenisciformes*						
Penguins (*Spheniscus* genus)	39	21	18			Cray et al. (2011)
Adélie penguin (*Pygoscelis adeliae*)	42.4	21.4	22.5	0.75	2.2	Aquilera et al. (1993), Ibañez et al. (2015)
African penguin (*Spheniscus demersus*)		19			0.62	Mazzaro et al. (2013)
Chinstrap penguin (*Pygoscelis antarcticus*)	40.2	17.3	22.9	0.4	1.3	Mean: Aquilera et al. (1993), Ferreret al. (1994), Deguirmendjian Rosa et al. (1992), Ibañez et al. (2015)
Galápagos penguin (*Spheniscus mendiculus*)	56	12.2	43.8	1.1		Travis et al. (2006a,b)
Gentoo penguin (*Pygoscelis papua*)	48.6	17.7	30.9	0.7	1.5	Calculated from Aquilera et al. (1993), Deguirmendjian Rosa et al. (1992), Ibañez et al. (2015)
Humboldt penguin (*Spheniscus humboldti*)	55.8	14.8	41.2	0.4	1.2	Wallace et al. (1995)
Jackass penguin (*Spheniscus demersus*)	55.5	21	34	0.67	0.67	Stoskopf et al. (1980), Cranfeld (2003)
King penguin (*Aptenodytes patagonicus*)	52	18	34	0.63	0.67	Calculated from Cranfeld (2003)
Rockhopper penguin (*Eudyptes chrysocome*)	35.8	13.6	22.2	0.32		Karesh et al. (1999)
Order *Strigiformes*						
Barred owl (*Strix varia*)	49	20.3	25	0.65	1.5	Elliott et al. (1974)
Burrowing owl (*Athene cunicularia*)	38	15.2	19	0.56	2.17	Aguilar (2003)
Collared scops owl (*Otus lettia*)	47.1	14.9	32.2	0.52	1.47	Chan et al. (2012)
Common barn owl (*Tyto alba*)	36.5	16.2	16	0.47	0.84	Elliott et al. (1974), Aguilar (2003)
Eagle owl (*Bubo bubo*)	38	17.2	21	0.73	1	Aguilar (2003)
Great horned owl (*Bubo virginianus*)	39	17.2	24	0.70	1	Aguilar (2003)
Great grey owl (*Strix nebulosa*)	34	15.2	20	0.99	0.84	Aguilar (2003)
Malay fishing owl (*Ketupa ketupu*)	48		21			Elliott et al. (1974)
Nepal brown wood owl (*Strix leptogrammica*)	38.5		19			Elliott et al. (1974)
Screech owl (*Otus asio*)	37	19.2	17.8	0.48	1.5	Aguilar (2003)
Short-eared owl (*Asio flammeus*)	35.5	15.2	20.3	0.34	0.67	Elliott et al. (1974), Aguilar (2003)

References

Abou-Madi, N., 2003. Cuculiformes (cuckoos, roadrunners). In: Fowler, M.E., Miller, R.E. (Eds.), Zoo and Wild Animal Medicine, fth ed. Saunders, St. Louis, MO, pp. 211–213.

Adnan, S., Amin Babjee, S.M., 1985. Haematology of the Malaysian jungle fowl (*Gallus gallus spadiceus*). Pertanika 8, 123–126.

Aengwanich, W., Tanomtong, A., 2007. Blood cell characteristics and hematological values of free ranging red jungle fowl (*Gallus gallus*) in Northeastern, Thailand. J. Biol. Sci. 7, 689–692.

Aengwanich, W., Tanomtong, A., 2004. Hematological and serum biochemical values of white ibis (*Threskiouris melanocephalus*). Asean Biodiv. 823–828 (Accessed 01.02.13.). http://rdo.psu.ac.th/sjstweb/journal/26-6/06white-ibis-hematological.pdf.

Aengwanich, W., Tanomtong, A., Pattanarungson Rattapant, P., Suchint, S., 2002. Blood cell characteristic, hematological and serum biochemistry values of Painted Stork (*Mycteria leucocephala*). Songklanakarin J. Sci. Technol. 24, 473–479.

Aguilar, R.F., 2003. Strigiformes (owls). In: Fowler, M.E., Miller, R.E. (Eds.), Zoo and Wild Animal Medicine, fifth ed. Saunders, St. Louis, MO, pp. 213–223.

Andretta, I., Kipper, M., Lehnen, C.R., Hauschild, L., Vale, M.M., Lovatto, P.A., 2011. Meta-analytical study of productive and nutritional interactions of mycotoxins in broilers. Poultry Sci. 90, 1934–1940.

Aquilera, E., Moreno, J., Ferrer, M., 1993. Blood chemistry values in three *Pygoscelis* penguins. Comp. Biochem. Physiol. 105A, 471–473.

Archawaranon, M., 2005. Hematological investigations of captive hill Mynah Gracula religiosa in Thailand. Int. J. Poultry Sci. 4, 679–682.

Artachoa, P., Soto-Gamboa, M., Verdugoc, C., Nespoloa, R.F., 2007. Blood biochemistry reveals malnutrition in black-necked swans (*Cygnus melanocoryphus*) living in a conservation priority area. Comp. Biochem. Physiol. 146, 283–290.

Averbeck, C., 1992. Haematology and blood biochemistry of healthy and clinically abnormal great black-backed gulls (*Larus marinus*) and herring gulls (*Larus argentatus*). Avian Pathol. 21, 215–223.

Avni-Magen, N., Gancz, A.Y., Beaufrère, H., Lublin, A., Eshar, D., 2016. Selected hematologic and plasma biochemistry analysis of ferruginous ducks (*Aythya nyroca*) in Israel. J. Zoo Wildl. Med. 47, 354–358.

Bailey, T.A., Wernery, U., Howlett, J.C., Naldo, J., Samour, J.H., 1998a. Age related plasma chemistry in the buff-crested bustard (*Eupoditis rucrista gindiana*). J. Vet. Med. 45, 635–640.

Bailey, T.A., Wernery, U., Naldo, J., Howlett, J., Samour, J.H., 1998b. Normal blood chemistry and age-related changes in the white-bellied bustard (*Eupodotis senegalensis*), with some clinical observations. Comp. Haematol. Int. 8, 61–65.

Balasch, J., Palacios, L., Musquera, S., Palomeque, J., Jiménez, M., Alemany, M., 1973. Comparative hematological values of several galliformes. Poultry Sci. 52, 1531–1534.

Balasch, J., Palomeque, J., Palcios, L., Muscquera, S., Jimenez, M., 1974. Hematological values of some great flying and aquatic-diving birds. Comp. Biochem. Physiol. 49A, 137–145.

Ball, R.L., 2003. Charadriiformes (gulls, shorebirds). In: Fowler, M.E., Miller, R.E. (Eds.), Zoo and Wild Animal Medicine, fifth ed. Saunders, St. Louis, MO, pp. 136–141.

Barbara, J.C.A., Ferreira, V.L., Guida, F.J.V., Prioste, F.E.S., Matushima, E.R., Raso, T.F., 2017. Hematologic reference intervals for wild Black vultures (*Coragyps atratus*). Vet. Clin. Pathol. 46, 575–579.

Barrera, R., Jimenez, A., Sanchez, J., Cuenca, R., Rodriguez, J., Andres, S., Mane, M.C., 1992. Blood biochemistry in the great bustard Otis tarda. Misc. Zool. Barc. 14, 244–247.

Bearhop, S., Grif ths, R., Orr, K., Furness, R.W., 1999a. Mean corpuscular volume (MCV) as a measure of condition in birds. Ecology. Lett. 2, 352–356.

Bearhop, S., Grif ths, R., Orr, K., Furness, R.W., 1999b. The normal haematology of great skuas (*Catharacta skua*) in the wild. Comp. Haematol. Int. 9, 107–109.

Belleville, J., Cornillon, B., Paul, J., Baguet, J., Clendinnen, G., Roy, R., 1982. Haemostasis, blood coagulation and brinolysis in the Japanese quail. Comp. Biochem. Physiol. 71A, 219–230.

Black, P.A., Macek, M., Tieber, A., Weber, M., 2013. Reference values for hematology, plasma biochemical analysis, plasma protein electrophoresis, and aspergillus serology in elegant-crested tinamou (*Eudromia elegans*). J. Avian Med. Surg. 27, 1–6.

Bonadiman, S.F., Stratievsky, G.C., Machado, J.A., Albernaz, A.P., Rabelo, G.R., DaMatta, R.A., 2009. Leukocyte ultrastructure, hematological and serum biochemical profiles of ostriches (*Struthio camelus*). Poultry Sci. 88, 2298–2306.

Bond, C.F., Gilbert, P.W., 1958. Comparative study of blood volume in representative aquatic and nonaquatic birds. Am. J. Physiol. 194, 519–521.

Borges, S.A., Silva, A.V.F.d., Majorka, A., Hooge, D.M., Cummings, K.R., 2004. Physiological responses of broiler chickens to heat stress and dietary electrolyte balance (sodium plus potassium minus chloride milliequivalents per kilogram). Poultry Sci. 83, 1551–1558.

Bried, J., Célérier, A., Maurel, L., Bonadonna, F., 2011. New haematological data in Cory's shearwater, *Calonectris diomedia* (*Aves, Procellariiformes*). Ital. J. Zool. 78, 279–286.

Breuer, K., Lill, A., Baldwin, J., 1995. Hematological and body-mass changes in small Passerines overwintering in South-East Australia. Aust. J. Zool. 43, 31–38.

Butler, P.J., Jones, D.R., 1997. Physiology of diving of birds and mammals. Physiol. Rev. 77, 837–899.

Calle, P.P., Stewart, C.A., 1987. Hematologic and serum chemistry values of captive hyacinth macaws (*Anodorhynchus hyacinthinus*). J. Zoo Wildl. Med. 18, 98–99.

Canfield, M.A., 2003. Sphenisciformes. In: Fowler, M.E., Miller, R.E. (Eds.), Zoo and Wild Animal Medicine, 3th ed. Saunders, St. Louis, MO, pp. 82–88.

Carey, C., Morton, M.L., 1976. Aspects of circulatory physiology of montane and lowland birds. Comp. Biochem. Physiol. 54, 61–74.

Carlson-Bremer, D., Norton, T.M., Gilardi, K.V., Dierenfeld, E.S., Winn, B., Sanders, F.J., Cray, C., Oliva, M., Chen, T.C., Gibbs, S.E., Sepúlveda, M.S., Johnson, C.K., 2010. Health assessment of American oystercatchers (*Haematopus palliatus palliatus*) in Georgia and South Carolina. J. Wildl. Dis. 46, 772–780.

Carpenter, J.W., 2003. Gruiformes (cranes, limplets, rails, gallinules, coots, bustards). In: Fowler, M.E., Miller, R.E. (Eds.), Zoo and Wild Animal Medicine, fifth ed. Saunders, St. Louis, MO, pp. 171–180.

Celdrán, J., Polo, F.J., Peinado, V.I., Viscor, G., Palomeque, J., 1994. Haematology of captive herons, egrets, spoonbill, ibis and gallinule. Comp. Biochem. Physiol. 107A, 337–341.

Chan, F.T., Lin, P.I., Chang, G.R., Wang, H.C., Hsu, T.H., 2012. Hematocrit and plasma chemistry values in adult collared scops owls (*Otus lettia*) and crested serpent eagles (*Spilornis cheela hoya*). J. Vet. Med. Sci. 74, 893–898.

Chou, S.J., Shieh, Y.C., Yu, C.Y., 2008. Hematologic and biochemistry values for black-faced spoonbills (*Platalea minor*) with and recovering from botulism. J. Wildl. Dis. 44, 781−784.

Clark, T.D., Kleindorfer, S., Dudaniec, R.Y., 2018. Baseline and stress-induced blood properties of male and female Darwin's small ground finch (*Geospiza fuliginosa*) of the Galapagos Islands. Gen. Comp. Endocrinol. 259, 199−206.

Coke, R.L., West, G.D., Hoover, J.P., 2004. Hematology and plasma biochemistry of captive puna ibis (*Plegadis ridgwayi*). J. Wildl. Dis. 40, 141−144.

Cooper, J.E., 1975. Haematological investigation of East African birds of prey. J. Wildl. Dis. 11, 389−394.

Cooper, J.E., 1996. Health studies on the Indian house crow *(Corvus splendens*). Avian Pathol 25, 281−286.

Cornejo, J., Richardson, D., Perez, J.G., Brightsmith, D.J., Bonar, C.J., Heatley, J.J., 2014. Hematological and plasma biochemical reference values of the horned guan, *Oreophasis derbianus*. J. Zoo Wildl. Med. 45, 15−22.

Cranfield, M.R., 2003. *Sphenisciformes* (penguins). In: Fowler, M.E., Miller, R.E. (Eds.), Zoo and Wild Animal Medicine, fifth ed. Saunders, St. Louis, MO, pp. 103−110.

Cray, C., Wack, A., Arheart, K.L., 2011. Invalid measurement of plasma albumin using Bromocresol Green methodology in penguins (*Spheniscus species*). J. Avian Med. Surg. 25, 14−22.

D'Aloia, M.-A.E., Samour, J.H., Howlett, J.C., Bailey, T.A., Naldo, J., 1996a. Normal blood chemistry of the Houbara bustard (*Chlamydotis undulata*). Avian Pathol. 25, 167−173.

D'Aloia, M.-A.E., Samour, J.H., Bailey, T.A., Naldo, J., Howlett, J.C., 1996b. Normal blood chemistry of the kori bustard (*Ardeotis kori*). Avian Pathol. 25, 161−165.

D'Amico, V.L., Bertellotti, M., Baker, A.J., González, P.M., 2010. Hematologic and plasma biochemistry values for endangered red knots (*Calidris canutus rufa*) at wintering and migratory sites in Argentina. J. Wildl. Dis. 46, 644−648.

D'Amico, V.L., Palacios, M.G., Baker, A.J., González, P.M., Madrid, E., Bertellotti, M., 2017. Physiological parameters and their response to handling stress in a neotropical migratory shorebird during the non-breeding season. J. Wildl. Dis. 53, 437−446.

Davies, S., Rodriguez, N., Sweazea, K.L., Deviche, P., 2013. The effect of acute stress and long-term corticosteroid administration on plasma metabolites in an urban and desert songbird. Physiol. Biochem. Zool. 86, 47−60.

Deem, S.L., Noss, A.J., Cuéllar, R.L., Karesh, W.B., 2005. Health evaluation of free-ranging and captive blue-fronted Amazon parrots (*Amazona aestiva*) in the Gran Chaco, Bolivia. J. Zoo Wildl. Med. 36, 598−605.

Deem, S.L., Ladwig, E., Cray, C., Karesh, W.B., Amato, G., 2008. Health assessment of the ex situ population of St Vincent parrots (*Amazona guildingii*) in St Vincent and the Grenadines. J. Avian Med. Surg. 22, 114−122.

Deem, S.L., Parker, P.G., Cruz, M.B., Merkel, J., Hoeck, P.E., 2011. Comparison of blood values and health status of Floreana Mockingbirds (*Mimus trifasciatus*) on the islands of Champion and Gardner-by- Floreana, Galápagos Islands. J. Wildl. Dis. 47, 94−106.

Deem, S.L., Rivera-Parra, J.L., Parker, P.G., 2012. Health evaluation of Galapagos hawks (*Buteo galapagoensis*) on Santiago Island, Galapagos. J. Wildl. Dis. 48, 39−46.

Deguirmendjian Rosa, C., Rosa, R., Rodregues, E., Bacila, M., 1992. Blood constituents and electrophoretic patterns in antarctic birds: penguins and skuas. Comp. Biochem. Physiol. A. 104, 117−123.

Dolka, B., Włodarczyk, R., Zbikowski, A., Dolka, I., Szeleszczuk, P., Kluciński, W., 2014. Hematological parameters in relation to age, sex and biochemical values for mute swans (*Cygnus olor*). Vet. Res. Commun. 38, 93−100.

Dönmez, H.H., Sur, E., 2008. Hematology and enzyme histochemistry of the peripheral blood leucocytes in rock partridges (*Alectoris graeca*). Poultry Sci. 87, 56−60.

Doussang, D., Merino, V., Moreno, L., Islas, A., Barrientos, C., Mathieu, C., Cerda, F., López, J., Ortega, R., González-Acuña, D., 2015. Hematologic and biochemical parameters of kelp gulls (*Larus dominicanus*) captured in the city of Talcahuano, Chile. J. Zoo Wildl. Med. 46, 447−455.

Dressen, P.J., Wimsatt, J., Burkhard, M.J., 1999. The Effects of isoflurane anesthesia on hematologic and plasma biochemical values of American Kestrels (*Falco sparverius*). J. Avian Med. Surg. 13, 173−179.

Drew, M.L., 2003. *Galliformes* (pheasants, grouse, quail, turkeys, chacalacas, currasows, hoatzin). In: Fowler, M.E., Miller, R.E. (Eds.), Zoo and Wild Animal Medicine, fifth ed. Saunders, St. Louis, MO, pp. 161−171.

Driver, E.A., 1981. Hematological and blood chemical values of mallard, *Anas p. platyrhynchos*, drakes before, during and after remise. J. Wildl. Dis. 17, 413−420.

Dujowich, M., Mazet, J.K., Zuba, J.R., 2005. Hematologic and biochemical reference ranges for captive California condors (*Gymnogyps californianus*). J. Zoo Wildl. Med. 36, 590−597.

Dunbar, M.R., Gregg, M.A., Giordano, M.R., Davis, D.M., Byrne, M.W., Crawford, J.A., Tornquist, S.J., 2005. Normal hematologic and biochemical values for prelaying greater sage grouse (*Centrocercus urophasianus*) and their influence on chick survival. J. Zoo Wildl. Med. 36, 422−429.

Dutton, C.J., Allchurch, A.F., Cooper, J.E., 2002. Comparison of hematologic and biochemical reference ranges between captive populations of northern bald ibises (*Geronticus ermita*). J. Wildl. Dis. 38, 583−588.

Dutton, C.J., 2003. Coraciiformes (kingfishers, motmots, bee-eaters, hoopoes, hornbills). In: Fowler, M.E., Miller, R.E. (Eds.), Zoo and Wild Animal Medicine, 3th ed. Saunders, St. Louis, MO, pp. 254−260.

Dyer, K.J., Perryman, B.L., Holcombe, D.W., 2009. Fitness and nutritional assessment of greater sage grouse (*Centrocercus urophasianus*) using hematologic and serum chemistry parameters through a cycle of seasonal habitats in northern Nevada. J. Zoo Wildl. Med. 40, 18−28.

Elarabany, N., 2018. A comparative study of some haematological and biochemical parameters between two species from the Anatidae family within migration season. J. Basic Appl. Zool. 79, 31.

Elliott, R.H., Smith, E., Bush, M., 1974. Preliminary report on hematology of birds of prey. J. Zoo Anim. Med. 5, 11−16.

Fallaw, S.A., Jones, J.E., Hughes, B.L., 1976. Hematocrit, erythrocyte, and hemoglobin values for male and female guineas at various ages. Poultry Sci. 55, 814−816.

Fallon, J.A., Smith, E.P., Schoch, N., Paruk, J.D., Adams, E.A., Evers, D.C., Jodice, P.G.R., Perkins, C., Schulte, S., Hopkins, W.A., 2018. Hematological indices of injury to lightly oiled birds from the Deepwater Horizon oil spill. Environ. Toxicol. Chem. 37, 451−461.

Ferrer, M., García-Rodríguez, T., Carrillo, J.C., Castroviejo, J., 1987. Hematocrit and blood chemistry values in captive raptors (*Gyps Fulvus, Buteo Buteo, Milvus migrans, Aquila Heliaca*). Comp. Biochem.Physiol. A 87, 1123−1127.

Ferrer, M., Amat, J.A., Vinuela, J., 1994. Blood chemistry values in chinstrap penguins (P*ygoscelis Antarctica*) during the Antarctic summer. Comp. Biochem. Physiol. 107A, 81−84.

Fiorello, C.V., Nisbet, I.C., Hatch, J.J., Corsiglia, C., Pokras, M.A., 2009. Hematology and absence of hemoparasites in breeding common terns (*Sterna hirundo*) from Cape Cod, Massachusetts. J. Zoo Wildl. Med. 40, 409−413.

Foldenauer, U., Borjal, R.J., Deb, A., Arif, A., Taha, A.S., Watson, R.W., Steinmetz, H., Bürkle, M., Hammer, S., 2007. Hematologic and plasma biochemical values of Spix's macaws (*Cyanopsitta spixii*). J. Avian Med. Surg. 21, 275−282.

Fontenelle, J.H., 2001. Cicioniiformes. In: Fowler, M.E., Cubas, Z.S. (Eds.), Biology, Medicine, and Surgery of South American Animals. Iowa State Press, Ames, IA, pp. 84−87.

Fontenot, D.K., Terrell, S.P., Malakoot, K., Medina, S., 2006. Health assessment of the Guam rail (*Gallirallus owstoni*) population in the Guam Rail recovery program. J. Avian Med. Surg. 20, 225−233.

Fourie, F.R., Hattingh, J., 1983. Comparative haematology of some South African birds. Comp. Biochem. Physiol. 74A, 443−448.

Frankfurter, G., Ziccardi, M.H., Massey, J.G., 2012. Effects of freshwater housing and uid types on aquatic bird serum electrolyte concentrations. J. Zoo Wildl. Med. 43, 852−857.

Franson, J.C., Sileo, L., Pattee, O.H., Moore, J.F., 1983. Effects of chronic dietary lead in American kestrels (Falco sparverius). J. Wildl. Dis. 19, 110−113.

Franson, J.C., Hoffman, D.J., Schmutz, J.A., 2009. Plasma biochemistry values in emperor geese (*Chen canagica*) in Alaska: comparisons among age, sex, incubation, and molt. J. Zoo Wildl. Med. 40, 321−327.

Franson, J.C., Flint, P.L., Schmutz, J.A., 2017. Reference intervals for serum biochemistries of molting Pacific black brant (*Branta bernicla nigricans*) in Northern Alaska, USA. J. Wildl. Dis. 53, 417−419.

Gallo, L., Qunitana, F., Svagelj, W.S., Uhart, M., 2013. Hematology and blood chemistry values in free-living imperial cormorants (*Phalacrocorax atriceps*). Avian Dis. 57, 737−743.

García del Campo, A.L., Huecas, V., Fernández, A., Puerta, M.L., 1991. Hematology and blood chemistry of macaws, *Ara rubrogenys*. Comp. Biochem. Physiol. A 100, 943−944.

García-Montijano, M., García, A., Lemus, J.A., Montesinos, A., Canales, R., Luaces, I., Pereira, P., 2002. Blood chemistry, protein electrophoresis, and hematologic values of captive Spanish imperial eagles (*Aquila adalberti*). J. Zoo Wildl. Med. 33, 112−117.

García-Rodríguez, T., Ferrer, M., Recio, F., Castroviejo, J., 1987. Circadian rhythms of determined blood chemistry values in buzzards and eagle owls. Comp. Biochem. Physiol. 88A, 663−669.

Garvin, M.C., Homer, B.L., Ellis, E.C., 2003. Pathogenicity of *Haemoproteus danilewskyi*, Kruse 1891 in blue jays (*Cyanocitta cristata*). J. Wildl. Dis. 39, 161−169.

Gayathri, K.L., Shenoy, K.B., Hegde, S.N., 2004. Blood pro les of pigeons (*Columba livia*) during growth and breeding. Comp. Biochem. Physiol. 138A, 187−192.

Gee, C.F., Carpenter, J.W., Hensler, B.L., 1981. Species differences in hematological values of captive cranes, geese, raptors, and quail. J. Wildl. Manage. 45, 463−483.

Gessaman, J.A., Johnson, J.A., Hoffman, S.W., 1986. Hematocrits and erythrocyte numbers for Cooper's and sharp-shinned Hawks. Condor 88, 95−96.

Gentz, E.J., 2003. *Passeriformes* (songbirds, perching birds). In: Fowler, M.E., Miller, R.E. (Eds.), Zoo and Wild Animal Medicine, fifth ed. Saunders, St. Louis, MO, pp. 267−275.

Giambelluca, S., Cammarata, M., Dara, S., Orefice, T., Camiña-Cardenal, A., Vazzana, I., 2017. The impact of captivity on some haematological parameters of griffon vultures (*Gyps fulvus*). Vet. Ital. 53, 243−249.

Gladbach, A., Gladbach, D.J., Quillfeldt, P., 2010. Variations in leucocyte profiles and plasma biochemistry are related to different aspects of parental investment in male and female Upland geese *Chloephaga picta leucoptera*. Comp. Biochem. Physiol. A 156, 269−277.

Godwin, J.S., Jacobson, E.R., Gaskin, J.M., 1982. Effects of Pacheco's parrot disease virus on hematologic and blood chemistry values of quaker parrots (*Myopsitta monachus*). J. Wildl. Dis. 13, 127−132.

Guzman, D.S., Mitchell, M.A., Gaunt, S.D., Beaufrère, H., Tully Jr., T.N., 2008. Comparison of hematologic values in blood samples with lithium heparin or dipotassium ethylenediaminetetraacetic acid anticoagulants in Hispaniolan Amazon parrots (*Amazona Ventralis*). J. Avian Med. Surg. 22, 108−113.

Haefele, H.J., Sidor, I., Evers, D.C., Hoyt, D.E., Pokras, M.A., 2005. Hematologic and physiologic reference Ranges for free-ranging adult and young common loons (*Gavia immer*). J. Zoo Wildl. Med. 36, 385−390.

Han, J.I., Jang, H.J., Na, K.J., 2016. Hematologic and serum biochemical reference intervals of the Oriental white stork (*Ciconia boyciana*) and the application of an automatic hematologic analyzer. J. Vet. Sci. 17, 399−405.

Hanauska-Brown, D., Roloff, G.J., 2003. Blood chemistry, cytology, and body condition in adult Northern Goshawks (*Accipiter gentilis*). J. Raptor Res. 37, 299−306.

Hauptmanová, K., Literák, I., Bártová, L., 2002. Haematology and leucocytozoonosis of great tits (*Parus major* L.) during Winter. Acta Vet. Brno 71, 199−204.

Harms, C.A., Harms, R.V., 2012. Venous blood gas and lactate values of mourning doves (*Zenaida macroura*), boat-tailed grackles (*Quiscalus major*), and house sparrows (*Passer domesticus*) after capture by mist net, banding, and venipuncture. J. Zoo Wildl. Med. 43, 77−84.

Harms, C.A., Jinks, M.R., Harms, R.V., 2016. Blood gas, lactate, and hematology effects of venipuncture timing and location after mist-net capture of mourning doves (*Zenaida macroura*), boat tailed grackles (*Quiscalus major*), and house sparrows (*Passer domesticus*). J. Wildl. Dis. 52 (2 Suppl. l), S54−S64.

Harper, E.J., Lowe, B., 1998. Hematology values in a colony of budgerigars (*Melopsittacus undulatus*) and changes associated with aging. J. Nutr. 128, 395−405.

Hatch, M.I., Smith, R.J., Owen, J.C., 2010. Arrival timing and hematological parameters in gray catbirds (*Dumetella carolinensis*). J. Ornithol. 151, 545−552.

Hawkey, C.M., Horsley, D.T., Keymer, I.F., 1989. Haematology of wild *penguins* (*Spenisciformes*) in the Falkland Islands. Avian Pathol. 18, 495−502.

Hernández, M., Margalida, A., 2010. Hematology and blood chemistry reference values and age-related changes in wild bearded vultures (*Gypaetus barbatus*). J. Wildl. Dis. 46, 390−400.

Hill, E.F., Murray, H.C., 1987. Seasonal variation in diagnostic enzymes and biochemical constituents of captive Northern Bobwhites and passerines. Comp. Biochem. Physiol. B 87, 933−940.

Hoffman, D.J., Pattee, O.H., Wiemeyer, S.N., Mulhern, B., 1981. Effects of lead shot ingestion on delta-aminolevulinic acid dehydratase activity, hemoglobin concentration, and serum chemistry in bald eagles. J. Wildl. Dis. 17, 423–431.

Hollamby, S., Afema-Azikuru, J., Sikarskie, J.G., Kaneene, J.B., Stuht, J.N., Fitzgerald, S.D., Bowerman, W.W., Cameron, K., Gandolf, A.R., Hui, G.N., Dranzoa, C., Rumbeiha, W.K., 2004. Clinical pathology and morphometrics of African fish eagles in Uganda. J. Wildl. Dis. 40, 523–532.

Hollmén, T., Franson, J.C., Hario, M., Sankari, S., Kilpi, M., Lindström, K., 2001. Use of serum biochemistry to evaluate nutritional status and health of incubating common eiders (*Somateria mollissima*) in Finland. Physiol. Biochem. Zool. 74, 333–342.

Howlett, J.C., Samour, J.H., D'Aloia, M.A., Bailey, T.A., Naldo, J.L., 1995. Normal haematology of captive adult Kori bustards. Comp. Haematol. Int. 5, 102–105.

Howlett, J.C., Bailey, T.A., Samour, J.H., Naldo, J.L., D'Aloia, M.A., 2002. Age-related hematologic changes in captive-reared houbara, white-bellied, and rufous-crested bustards. J. Wildl. Dis. 38, 804–816.

Ibañez, A.E., Najle, R., Larsen, K., Pari, M., Figueroa, A., Montalti, D., 2015. Haematological values of three Antarctic penguins: gentoo (*Pygoscelis papua*), Adélie (*P. adeliae*) and chinstrap (*P. antarcticus*). Polar Res. 34 (1), 25718.

Ihedioha, J.I., Okorie-Kanu, C.O., Ugwu, C.P., 2011. The blood picture and serum biochemistry pro le of the African pied crow (*Corvus albus*). Comp. Clin. Pathol. 20, 239.

Jenni-Eiermann, S., Jenni, L., 1994. Plasma metabolite levels predict individual body-mass changes in a small long-distance migrant, the garden-warbler. Auk 111, 888–899.

Jimenez, A., Barrera, R., Sanchez, J., Cuenca, R., Rodriguez, J., Andres, S., Cinta Mañe, M., 1991. Clinical haematology of the great bustard (*Otis tarda*). Avian Pathol. 20, 675–680.

Johnson, M.S., Quinn, M.J., Bazar, M.A., Gust, K.A., Escalon, B.L., Perkins, E.J., 2007. Subacute toxicity of oral 2,6-dinitrotoluene and 1,3,5-trinitro-1,3,5-triazine (RDX) exposure to the northern bobwhite (*Colinus virginianus*). Environ. Toxicol. Chem. 26, 1481–1487.

Kalomenopoulou, M., Koliakos, G., 1989. Total body haematocrit iron kinetics and erythrocyte life span in pigeons (*Columba livia*). Comp. Biochem. Physiol. 92, 215–218.

Karesh, W.B., Uhart, M.M., Frere, E., Gandini, P., Braselton, W.E., Puche, H., Cook, R.A., 1999. Health evaluation of free-ranging rockhopper penguins (*Eudyptes chrysocomes*) in Argentina. J. Zoo Wildl. Med. 30, 25–31.

Kern, M., Bacon, W., Long, D., Cowie, R.J., 2005. Blood metabolite and corticosterone levels in breeding adult Pied Flycatchers. Condor 107, 665–677.

Khalilieh, A., McCue, M.D., Pinshow, B., 2012. Physiological responses to food deprivation in the house sparrow, a species not adapted to prolonged fasting. Am. J. Physiol. 303, R551–R561.

Kocan, R.M., 1972. Some physiologic blood values of wild diving ducks. J. Wildl. Dis. 8, 115–118.

Korhonen, K., 1987. The effect of short-term fasting on certain blood parameters and on glycogen storage in pectoral muscles of willow grouse (*Lagopus l. Lagopus* L.). Comp. Biochem. Physiol. 88A, 677–682.

Kostelecka-Myrcha, A., 1987. Respiratory function of a unit of blood volume in the little auk (*Plautus alle*) and the Arctic Tern (*Sterna paradisaea*). Comp. Biochem. Physiol. A. 86, 117–120.

Krams, I., Cirule, D., Krama, T., Hukkanen, M., Rytkonen, S., Orell, M., Iezhova, T., Rantala, M.J., Tummeleht, L., 2010. Effect of forest management on haematological parameters, blood parasites, and reproductive success of the Siberian tit (*Poecile cinctus*). Ann. Zool. Fennici. 47, 335–346.

Lague, S.L., Chua, B., Alza, L., Scott, G.R., Frappell, P.B., Zhong, Y., Farrell, A.P., McCracken, K.G., Wang, Y., Milsom, W.K., 2017. Divergent respiratory and cardiovascular responses to hypoxia in bar-headed geese and Andean birds. J. Exp. Biol. 220, 4186–4194.

Lashev, L., Hubenov, H., Nikolov, Y., Lasheva, V., Mihailov, R., 2009. Comparison of some haematological parameters in three bird species from the *Columbidae* family. Vet. arhiv. 79, 409–414.

Lattin, C.R., Durant, S.E., Romero, L.M., 2015. Wounding alters blood chemistry parameters and skin mineralocorticoid receptors in house sparrows (*Passer domesticus*). J. Exp. Zool. A 323, 322–330.

Lavin, S., Cuenca, R., Marco, I., Velarde, R., Viñas, L., 1992. Hematology and blood chemistry of the marsh harrier (*Circus aeruginosus*). Comp. Biochem. Physiol. 103 A, 493–495.

Lavin, S., Cuenca, R., Marco, I., Pastor, J., Vinas, L., 1993. Hematological values of Montagu's harrier (*Circus pygargus*). Comp. Biochem. Physiol. 105A, 103–104.

Le Souëf, A.T., Holyoake, C.S., Vitali, S.D., Warren, K.S., 2013. Hematologic and plasma biochemical reference values for three species of black cockatoos (*Calyptorhynchus* species). J. Avian Med. Surg. 27, 14–22.

Lierz, M., Fenske, M., 2004. Plasma chemistry reference values in pin-tailed Sandgrouse (*Pterocles alchata*). Vet. Record 154, 210–211.

Lill, A., 2011. Sources of variation in blood glucose concentrations of free-living birds. Avian Biol. Res. https://doi.org/10.3184/175815511X13073729328092, 2011.

Llacuna, S., Gorriz, A., Riera, M., Nadal, J., 1996. Effects of air pollution on hematological parameters in passerine birds. Arch. Environ. Contam. Toxicol. 31, 148–152.

Lobato, D.N.C., Braga, E.M., Belo, N. de O., Antonini, Y.(, 2011. Hematological and parasitological health conditions of the pale-breasted thrush (*Turdus leucomelas*) (*Passeriformes: Turdidae*) in southeastern Brazil. Zoologia 28, 771–776.

Low, M., Eason, D., Elliott, G., McInnes, K., Paul-Murphy, J., 2006. Hematologic and biochemical reference ranges for the kakapo (*Strigops habroptilus*): generation and interpretation in a field-based wildlife recovery program. J. Avian Med. Surg. 20, 80–88.

Lumeij, J.T., 1987. The diagnostic value of plasma proteins and non-protein nitrogen substances in birds. Vet. Quart. 9, 262–268.

Maxime, V., Hassani, S., 2014. Blood oxygen- and carbon dioxide- carrying properties in captive penguins: effects of moulting and inter-species comparison. Comp. Biochem. Physiol. 168A, 76–81.

Mazzaro, L.M., Meegan, J., Sarran, D., Romano, T.A., Bonato, V., Shibing Deng, J., Lawrence Dunn, L., 2013. Molt-associated changes in hematologic and plasma biochemical values and stress hormone levels in African penguins (*Spheniscus demersus*). J. Avian Med. Surg. 27, 285–293.

McCracken, H., 2003. Caprimulgiformes (goatsuckers). In: Fowler, M.E., Miller, R.E. (Eds.), Zoo and Wild Animal Medicine, 3th ed. Saunders, St. Louis, MO, pp. 224–231.

McDonald, D.L., Jaensch, S., Harrison, G.J., Gelis, S., Brennan, D., Bernardo, D., 2010. Health and nutritional status of wild Australian Psittacine birds: an evaluation of plasma and hepatic mineral levels, plasma biochemical values, and fecal micro ora. J. Avian Med. Surg. 24, 288–298.

Melrose, W.D., Nicol, S.C., 1992. Haematology, red cell metabolism and blood chemistry of the black-faced cormorant Leucocarbo fuscescens. Comp. Biochem. Physiol. 102, 67–70.

Milani, J.F., Wilson, H., Ziccardi, M., LeFebvre, R., Scott, C., 2012. Hematology, plasma chemistry, and bacteriology of wild Tundra swans (*Cygnus columbianus*) in Alaska. J. Wildl. Dis. 48, 212–215.

Motta, R.O.C., Marques, M.V.R., Ferreira, F.C., Andery, D.A., Horta, R.S., Peixoto, R.B., Lacorte, G.A., Moreira, P.A., Leme, F.O.P., Melo, M.M., Martins, N.R.S., Martins Braga, E., 2013. Does haemosporidian infection affect hematological and biochemical profiles of the endangered black-fronted piping-guan (*Aburria jacutinga*)? Peer J. https://doi.org/10.7717/peerj.45.

Mulley, R.C., 1979. Haematology and blood chemistry of the black duck, *Anas. superciliosa*. J. Wildl. Dis. 15, 437–441.

Mulley, R.C., 1980. Haematology of the wood duck, *Chenonetta jubata*. J. Wildl. Dis. 16, 271–273.

Mushi, E.Z., Binta, M.G., Chabo, R.G., Isa, J.F.W., Kapaata, R.W., 1999. Selected hematologic values of farmed ostriches (*Struthio camelus*) in Botswana. J. Vet. Diagn. Invest. 11, 372–374.

Myrcha, A., Kostelecka-Myrcha, A., 1980. Hematological studies on Antarctic birds. I. hematological indices of some of the birds studied in Australian summer. Pol. Polar Res. http://polish.polar.pan.pl/ppr01/1980_2-3_169-173.pdf.

Naidoo, V., Diekmann, M., Wolters, K., Swan, G.E., 2008. Establishment of selected baseline blood chemistry and hematologic parameters in captive and wild-caught African white-backed vultures (*Gyps africanus*). J. Wildl. Dis. 44, 649–654.

Neiffer, D.L., 2003. Trogoniformes (trogons). In: Fowler, M.E., Miller, R.E. (Eds.), Zoo and Wild Animal Medicine, 3th ed. Saunders, St. Louis, MO, pp. 245–253.

Nemeth, N.M., Thomsen, B.V., Spraker, T.R., Benson, J.M., Bosco-Lauth, A.M., Oesterle, P.T., Bright, J.M., Muth, J.P., Campbell, T.W., Gidlewski, T.L., Bowen, R.A., 2011. Clinical and pathologic responses of American crows (*Corvus brachyrhynchos*) and fish crows (*Cossifragus*) to experimental west nile virus infection. Vet. Pathol. 48, 1061–1074.

Newman, S.H., Piatt, J.F., White, J., 1997. Hematogical and plasma chemical reference ranges of Alaskan seabirds: their ecological signi cance and clinical importance. Colon. Waterbirds 20, 492–504.

Newman, S.H., Mazet, J.K., Ziccardi, M.H., Lieske, C.L., Fauquier, D.A., Gardner, I.A., Zinkl, J.G., Christopher, M.M., 1999. Haematological changes and anaemia associated with captivity and petroleum exposure in seabirds. Comp. Haematol. Int. 9, 60–67.

Nicol, S.C., Melrose, W., Stahel, C.D., 1988. Haematology and metabolism of the blood of the little penguin, *Eudyptula minor*. Comp. Biochem. Physiol. 89A, 383–386.

Nirmalan, G.P., Robinson, G.A., 1971. Haematology of the Japanese quail (*Coturnix cortunix japonica*). Brit. Poult. Sci. 12, 475–481.

Norambuena, M.C., Bozinovic, F., 2009. Health and nutritional status of a perturbed black-necked swan (*Cygnus melanocoryphus*) population: diet quality. J. Zoo Wildl. Med. 40, 607–616.

Norton, T.M., 2003. Phoenicopteriformes (flamingos). In: Fowler, M.E., Miller, R.E. (Eds.), Zoo and Wild Animal Medicine, fifth ed. Saunders, St. Louis, MO, pp. 129–135.

Nyariki, T.M., Gathumbi, P.K., Bebora, L.C., Muchemi, G.M., Maina, E.W., Gakuya, F.M., Kariuki, E.K., Ngatia, T.A., 2018. Hematologic values of healthy and sick free-ranging Lesser flamingos (*Phoeniconaias minor*) in Kenya. J. Wildl. Dis. Sep 20.

Okotie-Eboh, G., Bailey, C.A., Hicks, K.D., Kubena, L.F., 1992. Reference serum biochemical values for emus and ostriches. Am. J. Vet. Res. 53, 1765–1768.

Oliveira, J.O., Nascimento, I.A., Ribeiro, V.O., Cortes, L.A., Fernandes, R.D., Santos, L.C., Moraes, W., Cubas, Z.S., 2014. Haematological values for captive harpy eagle (*Harpia harp*). Pesqui. Vet. Brasil. 34, 805–809.

Olsen, G.H., Rininger, D.L., Ets, M.K., Sladen, W.J.L., 2002. Baseline hematology and clinical chemistry results from captive-raised trumpeter swans. Waterbirds 25, 375–379.

Ozek, K., Bahtiyarca, Y., 2004. Effects of sex and protein and energy levels in the diet on the blood parameters of the chukar partridge (*Alectoris chukar*). Br. Poult. Sci. 45, 290–293.

Padilla, L.R., Huyvaert, K.P., Merkel, J., Miller, R.E., Parker, P.G., 2003. Hematology, plasma chemistry, serology, and chlamydophila status of the waved albatross (*Phoebastria irrorata*) on the Galapagos Islands. J. Zoo Wildl. Med. 34, 278–283.

Pages, T., Planas, J., 1983. Muscle myoglobin and flying habits in birds. Comp. Biochem. Physiol. 74A, 289–294.

Palomeque, J., Rodriguez, J.D., Palacios, L., Planas, J., 1980. Blood respiratory properties of swifts. Comp. Biochem. Physiol. A 67, 91–95.

Paris Zinsmeister, V.A., Van der Heyden, N., 1987. Hematological parameters of the penguin genus Pygoscelis of Antarctica (Adélie, gentoo, and chinstrap). Antarctic J 22, 223–224.

Parsons, N.J., Schaefer, A.M., van der Spuy, S.D., Gous, T.A., 2015. Establishment of baseline haematology and biochemistry parameters in wild adult African penguins (*Spheniscus demersus*). J. S. Afr. Vet. Assoc. 86, e1–e8.

Patodkar, V.R., Somkuwar, A.P., Rahane, S.D., Shejal, M.A., Belhekar, D.R., 2008. Effect of sex on haematological parameters in emu (*Dromaius novahollandiae*). Vet. World 1, 171–172.

Peinado, V.I., Polo, F.J., Celdrán, J.F., Viscor, G., Palomeque, J., 1992a. Hematology and plasma chemistry in endangered pigeons. J. Zoo Wildl. Med. 23, 65–71.

Peinado, V.I., Polo, F.J., Viscor, G., Palomeque, J., 1992b. Haematology and blood chemistry values for several amingo species. Avian Pathol. 21, 55–64.

Pérez Calabuig, C., Ferrer, M., Muriel, R., 2010. Blood Chemistry of wild Brazilian coscoroba swans during molt. J. Wildl. Dis. 46, 591–595.

Polo, F.J., Celdrán, J.F., Peinado, V.I., Viscor, G., Palomeque, J., 1992. Hematological values for four species of prey. Condor 94, 1007–1013.

Powers, L.V., Pokras, M., Rio, K., Viverette, C., Goodrich, L., 1994. Hematology and occurrence of hemoparasites in migrating sharp-shinned hawks (*Accipiter striatus*) during fall migration. J. Raptor Res. 28, 178–185.

Prioste, F.E., Zwarg, T., Teixeira, R.H., Vanstreels, R.E., Rocha, A., Matushima, E.R., 2012. Hematologic reference values for clinically healthy captive golden conures (*Guaruba guarouba*). Avian Dis. 56, 701–703.

Puerta, M.L., Munõz Pulido, R., Huecas, V., Abelenda, M., 1989. Hematology and blood chemistry of chicks of white and black storks (*Ciconia ciconia* and *Ciconia nigra*). Comp. Biochem. Physiol. A 94, 201–204.

Puerta, M.L., Alonso, J.C., Huecas, V., Alonso, J.A., Abelenda, M., Munoz-Pulido, R., 1990. Hematology and blood chemistry of wintering common cranes. Condor 92, 210–214.

Puerta, M., Nava, M.P., Venero, C., Veiga, J.P., 1995. Hematology and plasma chemistry of house sparrows (*Passer domesticus*) along the summer months and after testosterone treatment. Comp. Biochem. Physiol. A 110, 303−307.

Pye, G.W., 2003. Apodiformes and Coliiformes (swifts, swiftlets, mousebirds). In: Fowler, M.E., Miller, R.E. (Eds.), Zoo and Wild Animal Medicine, 7th ed. Saunders, St. Louis, MO, pp. 239−244.

Quillfeldt, P., Masello, J.F., Möstl, E., 2004. Blood chemistry in relation to nutrition and ectoparasite load in Wilson's storm-petrels Oceanites oceanicus. Polar Biol. 27, 168−176.

Quinn Jr., M.J., Bazar, M.A., McFarlandm, C.A., Perkins, E.J., Gust, K.A., Johnson, M.S., 2009. Sublethal effects of subacute exposure to RDX (1,3,5-trinitro-1,3,5-triazine) in the northern bobwhite (*Colinus virginianus*). Environ. Toxicol. Chem. 28, 1266−1270.

Ratliff, C., Gentry, J., Kusmierczyk, J., Hartke, K.M., Acierno, M.J., Musser, J.M., Russell, K.E., Heatley, J.J., 2017. Venous blood gas, electrolyte, and hematologic analytes of the mottled duck, *Anas fulvigula*. J. Wildl. Dis. 53, 159−164.

Rehder, N.B., Bird, D.M., Lague, P.C., MacKay, C., 1982. Variation in selected hematological parameters in captive red-tailed hawks. J. Wildl. Dis. 18, 105−109.

Reissig, E.C., Robles, C.A., Sager, R., 2002. Hematology and serum chemistry values of the lesser rhea (*Pterocnemia pennata*) raised in Patagonian farms (Argentina). J. Zoo Wildl. Med. 33, 328−331.

Rettenmund, C.L., Heatley, J.J., Russell, K.E., 2014. Comparison of two analyzers to determine selected venous blood analytes of Quaker parrots (*Myiopsitta monachus*). J. Zoo Wildl. Med. 45, 256−262.

Rodríguez, A., Negro, J.J., Figuerola, J., 2011. Sources of variation for nutritional condition indices of the plasma of migratory lesser kestrels in the breeding grounds. Comp. Biochem. Physiol. 160 (A), 453−460.

Roman, Y., Bomsel-Demontoy, M.-C., Levrier, J., Chaste-Duvernoy, D., Jalme, M.S., 2013. Plasma protein electrophoresis in birds: comparison of a semiautomated agarose gel system with an automated capillary system. J. Avian Med. Surg. 27, 99−108.

Ruiz, G., Rosenmann, M., Fernando Novoa, F., Sabat, P., 2002. Hematological parameters and stress index in Rufous-collared sparrows dwelling in urban environments. Condor 104, 162−166.

Rubio, M.D., Ildefonso, N., Agüera, E.I., Almaraz, P., De Miguel, R.J., Escribano, B.M., 2012. Plasma biochemistry and haematology of crested coots (*Fulica cristata*) and common coots (*Fulica atra*) from Spain. Comp. Clin. Pathol. 23, 385−391.

Safra, N., Christopher, M.M., Ernest, H.B., Bandivadekar, R., Tell, L.A., 2018. Leukocyte reference intervals for free-ranging hummingbirds in Northern California, USA. J. Wildl. Dis. 54, 607−611.

Salakij, C., Salakij, J., Nirachara Rochanapat, N., Pitakkingthong, D., 2004. Hematology, morphology and cytochemistry of blood cells in lesser adjutant (*Leptoptilos javanicus*) and greater adjutant (*Leptoptilos dubius*). Kasetsart J./Nat. Sci. 38, 400−408.

Samour, J.H., D'Aloia, M.-A., Howlett, J.C., 1996. Normal haematology of captive saker falcons (*Falco cherrug*). Comp. Haematol. Int. 6, 50−52.

Samour, J.H., Howell, J.C., Silvarose, C., Bailey, T.A., Wernery, U., 1998. Normal haematology and blood chemistry of captive stone curlews (*Burhinus oedicnemus*). Comp. Haematol. Int. 8, 219−224.

Schindler, S.L., Gildersleeve, R.P., Thaxton, J.P., McRee, D.I., 1987. Blood volume recovery in hemorrhaged Japanese quail. Comp. Biochem. Physiol. 88A, 95−100.

Schmidt, E.M., Paulillo, Antonio, C., Martins, G.R.V., Lapera, I.M., Testi, A.J.P., Nardi Leonildo Junior, N.L., Denadai, J., Fagliari, J.J., 2009a. Hematology of the bronze Turkey (*Meleagris gallopavo*): variations with age and gender. Int. J. Poult. Sci. 8, 752−754.

Schmidt, E.M.S., Lange, R.R., Ribas, J.M., Daciuk, B.M., Montiani-Ferreira, F., Paulillo, A.C., 2009b. Hematology of the red-capped parrot (*Pionopsitta pileata*) and vinaceous Amazon parrot (*Amazona vinacea*) in captivity. J. Zoo Wildl. Med. 40, 15−17.

Schultz, D.J., 2003. *Columbiformes* (pigeons, doves). In: Fowler, M.E., Miller, R.E. (Eds.), Zoo and Wild Animal Medicine, fifth ed. Saunders, St. Louis, MO, pp. 180−187.

Seok, S.H., Jeong, D.H., Park, S.J., Lee, S.Y., Lee, H.C., Yeon, S.C., 2017. Hematological and plasma biochemical values of cinereous vulture (*Aegypius monachus*). J. Zoo Wildl. Med. 48, 514−517.

Sepp, T., Sild, E., Hõrak, P., 2010. Hematological condition indexes in green finches: effects of captivity and diurnal variation. Physiol. Biochem. Zool. 83, 276−282.

Shave, H.J., Howard, V., 1976. A hematologic survey of captive waterfowl. J. Wildl. Dis. 12, 195−201.

Shen, X., Zhang, Z., Jia, B., Tu, Y., Tian, Y., 2008. Blood cell morphology, some hematological and serum biochemistry values of common kestrel (*Falco tinnunculus*). J. Sustain. Dev. 1, 123−128.

Silva, C.R., Putarov, T.C., Fruhvald, E., Destro, F.C., Marques Filho, W.C., Thomazini, C.M., Barbosa, T.S., Orsi, R.O., Siqueira, E.R., 2014. Action of Brazilian propolis on hematological and serum biochemical parameters of Blue-fronted Amazons (*Amazona aestiva*, Linnaeus, 1758) in captivity. Poultry Sci. 93, 1688−1694.

Small, M.F., Baccus, J.T., Mink, J.N., Roberson, J.A., 2005. Hematologic responses in captive white-winged doves (*Zenaida asiatica*), induced by various radiotransmitter attachments. J. Wildl. Dis. 41, 387−394.

Smith, D.A., 2003. *Tinamiformes* (Tinamous) and *Struthioniformes, Rheiiformes, Cassuariformes* (ostriches, emus, cassowaries, and kiwis). In: Fowler, M.E., Miller, R.E. (Eds.), Zoo and Wild Animal Medicine, fifth ed. Saunders, St. Louis, MO, pp. 94−104.

Straková, E., Suchý, P., Kábelová, R., Vitula, F., Herzig, I., 2010. Values of selected haematological indicators in six species of feathered game. Acta Vet. Brno 79, S3−S8.

Stoskopf, M.K., 2003. *Gaviiformes* (loons), *Podicidiformes* (grebes) and *Procellariiformes* (albatrosses, fulmars, petrels, storm petrels, and shearwaters). In: Fowler, M.E., Miller, R.E. (Eds.), Zoo and Wild Animal Medicine, fifth ed. Saunders, St. Louis, MO, pp. 110−117.

Stoskopf, M.K., Yarbrough, B.A., Beall, F.B., 1980. Baseline hematology of the African blackfooted penguin. In: Montali, R. (Ed.), The Comparative Pathology of Zoo Animals. Smithsonian Press, Washington, D.C, pp. 647−652.

Stoskopf, M.K., Mulcahy, D.L., Esler, D., 2010. Evaluation of a portable automated serum chemistry analyzer for eld assessment of Harlequin ducks. Histrionicus histrionicus. Vet. Med. Internat. https://doi.org/10.4061/2010/418596.

Sturkie, P.D., 1986. Body fluids: blood. In: Sturkie, P.D. (Ed.), Avian Physiology. Springer-Verlag, New York, pp. 102−120.

Szabo, Z., Klein, A., Jakab, C., 2014. Hematologic and plasma biochemistry reference intervals of healthy adult barn owls (*Tyto alba*). Avian Dis. 58, 228−231.

Tell, L.A., Citino, S.B., 1992. Hematological and serum chemistry reference intervals for Cuban Amazon parrots (*Amazona leucocephala leucocephala*). J. Zoo. Wildlife Med. 23, 65−71.

Totzke, U., Fenske, M., Huppop, O., Raabe, H., Schach, N., 1999. The influence of fasting on blood and plasma composition of herring gulls (*Larus argentatus*). Physiol. Biochem. Zool. 72, 426–437.

Travis, E.K., Vargas, F.H., Merkel, J., Gottdenker, N., Miller, R.E., Parker, P.G., 2006a. Hematology, plasma chemistry, and serology of the ightless cormorant (*Phalacrocorax harrisi*) in the Galpagos Islands, Ecuador. J. Wildlife Dis. 42, 133–141.

Travis, E.K., Vargas, F.H., Merkel, J., Gottdenker, N., Miller, R.E., Parker, P.G., 2006b. Hematology, serum chemistry, and serology of Galápagos penguins (*Spheniscus mendiculus*) in the Galápagos Islands, Ecuador. J. Wildl. Dis. 42, 625–632.

Uhart, M.M., Quintana, F., Karesh, W.B., Braselton, W.E., 2003. Hematology, plasma biochemistry, and serosurvey for selected infectious agents in southern giant petrels from Patagonia, Argentina. J. Wildl. Dis. 39, 359–365.

Uhart, M., Aprile, G., Beldomenico, P., Solís, G., Marull, C., Beade, M., Carminati, A., Moreno, D., 2006. Evaluation of the health of free-ranging greater rheas (*Rhea americana*) in Argentina. Vet. Record 158, 297–303.

Valéria, V.P., Fantoni, D.T., Otsuk, D.A., Auler Jr., J.O.C., 2008. Blood-gas and electrolyte values for Amazon parrots (*Amazona aestiva*). Pesq. Vet. Bras. 28, 108–112.

Valle, C.A., Ulloa, C., Deresienski, D., Regalado, C., Muñoz-Pérez, J.P., Garcia, J., Hardesty, B.D., Skehel, A., Lewbart, G.A., 2018. Health status of great frigatebirds (*Fregata minor*) determined by haematology, biochemistry, blood gases, and physical examination. Conserv. Physiol. 6, coy034.

Van Heerden, J., Dauth, J., Komen, J., Myer, E., 1987. Serum biochemical and haematological parameters in the Cape vulture *Gyps coprotheres*. J. South Afr. Vet. Assoc. 58, 145–146.

Van Hemert, C., Handel, C.M., 2016. Blood serum chemistry of wild Alaskan black-capped chickadees (*Poecile atricapillus*) with avian keratin disorder. J. Wildl. Dis. 52, 927–930.

Wallace, R.S., Teare, J.A., Diebold, E., Michaels, M., Willis, M.J., 1995. Hematology and plasma chemistry values in free-ranging Humboldt penguins (*Spheniscus humboldti*) in Chile. Zoo Biol. 14, 311–316.

Weber, M., 2003. *Pelecaniformes* (pelicans, tropicbirds, cormorants, frigatebirds, anhingas, gannets). In: Fowler, M.E., Miller, R.E. (Eds.), Zoo and Wild Animal Medicine, fifth ed. Saunders, St. Louis, MO, pp. 118–122.

West, G.D., Haines, V.L., 2002. Hematology and serum biochemistry values of captive Attwater's Prairie Chickens (*Tympanuchus cupido attwateri*). J. Zoo Wildl. Med. 33, 122–124.

Williams, J.I., Trainer, D.O., 1971. A hematological study of snow, blue, and Canada geese. J. Wildl. Dis. 7, 258–265.

Wilson, G.R., Wilson, L.P., 1978. Haematology, weight and condition of captive red grouse (Lagopus lagopus scoticus) infected with caecal threadworm (*Trichostrongylus tenuis*). Res. Vet. Sci. 25, 331–336.

Wolf, S.H., Schreiber, R.W., Kahana, L., Torres, J.J., 1985. Seasonal and age-related variation in the blood composition of the brown pelican (*Pelecanes occidentalis*). Comp. Biochem. Physiol. 82A, 837–846.

Work, T.M., 1996. Weights, hematology, and serum chemistry of seven species of free ranging tropic pelagic seabirds. J. Wildl. Dis. 32, 643–657.

Work, T.M., 1999. Weights, hematology, and serum chemistry of free-ranging Brown *Boobies* (*Sula leucogaster*) in Johnston Atoll, central Paci c. J. Zoo Wildl. Med. 30, 81–84.

Youl, J.M., 2009. Lead Exposure in Free-Ranging Kea (Nestor Notabilis), Takahe (Porphyrio Hochstetteri) and Australasian Harriers (Circus Approximans). Master's Thesis. Massey University, New Zealand.

Zhang, C.L., Niu, Z.Y., Hou, S.S., Liu, F.Z., Huang, W., Xie, M., 2005. The effect of force-feeding, fasting and glucose saturated water intake on the contents of some biochemical parameters in plasma of Peking ducks. Int. J. Poult. Sci. 4, 202–205.

Further reading

Angel, C.R., 1995. Serum vitamin D metabolites, thyroxine, and chemistries of ostriches, emus, rheas and cassowaries. Proc. Assoc. Am. Phys. 233–240.

Boismenu, C., Gauthier, G., Larochelle, J., 1992. Physiology of prolonged fasting in greater snow geese (*Chen caerulescens atlantica*). Auk 109, 511–552.

Bonatto, C.C., Magalhães, B.S., Branco, J.O., Durigon, E.L., Silva, L.P., 2008. Shape and size of red blood cells from the Pygoscelid penguins of Antarctica using atomic force microscopy. Polar Biol. https://doi.org/10.1007/s00300-008-0554-5.

Gregory, T.R., 2001a. The bigger the C-Value, the larger the cell: genome size and red blood cell size in vertebrates. Blood Cells Mol. Dis. 27, 830–843.

Gregory, T.R., 2001b. Coincidence, coevolution, or causation? DNA content, cell size, and the C-value enigma. Biol. Rev. Camb. Philos. Soc. 76, 65–101.

Gregory, T.R., 2001c. Animal Genome Size Database. http://www.genomesize.com/cellsize/birds.htm.

Gulliver, G., 1875. Observations on the sizes and shapes of the red corpuscles of the blood of vertebrates, with drawings of them to a uniform scale, and extended and revised tables of measurements. Proc. Zool. Soc. Lond. 474–495.

Sarasola, J.H., Negro, J.J., Travaini, A., 2004. Nutritional condition and serum biochemistry for free-living Swainson's Hawks wintering in central Argentina. Comp. Biochem. Physiol. 137A, 697–701.

van As, P., Elferink, M.G., Closter, A.M., Vereijken, A., Bovenhuis, H., Crooijmans, R.P., Decuypere, E., Groenen, M.A., 2010. The use of blood gas parameters to predict ascites susceptibility in juvenile broilers. Poultry Sci. 89, 1684–1691.

Verstappen, F.A., Lumeij, J.T., Bronneberg, R.G., 2002. Plasma chemistry reference values in ostriches. J. Wildl. Dis. 38, 154–159.

Chapter 50

Carbohydrate supplementary materials

Colin G. Scanes
Department of Biological Sciences, University of Wisconsin Milwaukee, Milwaukee, WI, United States

Tables 50.1 −50.2.

TABLE 50.1 Circulating concentration of glucose in avian species.

Taxa[a] genus, species	Plasma/Serum glucose		References
	mg/dL	mmoles L^{-1}	
Order Accipitriformes			
Family Accipitridae			
African Fish Eagle (*Haliaeetus vocifer*)	223	12.4	Hollamby et al. (2004)
Bald Eagle (*Haliaeetus leucocephalus*)	315.5	17.6	Hoffman et al. (1981)
Black Kite (*Milvus migrans*)	350	19.4	Ferrer et al. (1987)
Bonelli's Eagle (*Hieraaetus fasciatus*)	353	19.6	Ferrer et al. (1987)
Booted Eagle (*Hieraaetus pennatus*)	292	16.2	Ferrer et al. (1987)
Bearded Vulture (*Gypaetus barbatus*)	239	13.3	Hernández and Margalida (2010)
Cape Griffon (*Gyps coprotheres*)	236	13.1	Van Heerden et al. (1987)
Cinereous vulture (*Aegypius monachus*)	308	17.1	Seok et al. (2017)
Crested serpent eagle (*Spilornis cheela*)	326	18.1	Chan et al. (2012)
Common Buzzard (*Buteo buteo*)	362	20.1	Ferrer et al. (1987), Garcia- Rodriguez et al. (1987)
Egyptian Vulture (*Neophron percnopterus*)	319	16.5	Polo et al. (1992), Dobado-Berrios et al. (1998)
Eurasian Griffon (*Gyps fulvus*)	275	15.3	Mean: Ferrer et al. (1987), Polo et al. (1992)
Galapagos Hawk (*Buteo galapagoensis*)	273	15.1	Deem et al. (2012)
Golden Eagle (*Aquila chrysaetos*)	368	18.6	Mean: O'Donnell et al. (1978), Polo et al. (1992)
Hen Harrier (*Circus cyaneus*)	369	20.5	O'Donnell et al. (1978)
Marsh Harrier (*Circus aeruginosus*)	196	10.9	Lavin et al. (1992a)
Northern Goshawk (*Accipiter gentilis*)	496	27.6	Stout et al. (2010)
Red-tailed Hawk (*Buteo jamaicencis*)	346	19.2	O'Donnell et al. (1978)
Snail Kite (*Rostrhamus sociabilis*)	336	18.7	Gee et al. (1981)
Spanish Imperial Eagle (*Aquila adalberti*)	317	17.6	Mean: Ferrer et al. (1987), Polo et al. (1992), García-Montijano et al. (2002)
Swamp Harrier (*Circus approximans*)	349	19.4	Calculated from Youl (2009)

Continued

Sturkie's Avian Physiology. https://doi.org/10.1016/B978-0-12-819770-7.00032-3

TABLE 50.1 Circulating concentration of glucose in avian species.—cont'd

Taxa[a] genus, species	Plasma/Serum glucose		References
	mg/dL	mmoles L^{-1}	
Family *Cathartidae*			
California Condor (*Gymnogyps californianus*)	302	16.8	Dujowich et al. (2005)
Andean Condor (*Vultur gryphus*)	337	18.7	Gee et al. (1981)
Order *Anseriformes*			
Black brant (*Branta bernicla*)	277	15.4	Franson et al. (2017)
Black-necked Swan (*Cygnus melanocoryphus*)	134	7.4	Artachoa et al. (2007)
Coscoroba Swan (*Coscoroba coscoroba*)	115	6.4	Pérez Calabuig et al. (2010)
Common Pochard (*Aythya ferina*)	274	15.2	Balasch et al. (1974)
Common Eider (*Somateria mollissima*)	209	11.6	Hollmén et al. (2001)
Canada Goose (*Branta canadensis*)	236	13.1	Mori and George (1978), Gee et al. (1981)
Embden Goose (*Anser anser*)	222	12.3	Gee et al. (1981)
Emperor Goose (*Anser canagica*)	235	13.1	Franson et al. (2009)
Eurasian teal (*Anas crecca*)	136	7.6	Elarabany (2018)
Ferruginous ducks (*Aythya nyroca*)	209	11.6	Avni-Magen et al. (2016)
Harlequin Duck (*Histrionicus histrionicus*)	331	18.4	Stoskopf et al. (2010)
Hawaian Goose (*Branta sandvicensis*)	232	12.9	Gee et al. (1981)
Mallard (*Anas platyrhynchos*)	205	11.1	Mean: Driver (1981), Fairbrother et al. (1990)
Mute Swan (*Cygnus olor*)	146	8.1	Miksik and Hodný (1992), Dolka et al. (2014)
Northern Shoveler (*Anas clypeata*)	188	10.5	Elarabany (2018)
Pacific Black Duck (*Anas superciliosa*)	176	9.8	Mulley (1979)
Snow Goose (*Anser caerulescens*)	175	9.8	Boismenu et al. (1992)
Tule White-fronted Goose (*Anser albifrons*)	232	12.9	Gee et al. (1981)
Tundra Swan (*Cygnus columbianus*)	294	16.3	Milani et al. (2012)
Trumpeter Swan (*Cygnus buccinators*)	134	7.5	Olsen et al. (2002)
Order *Apodiformes*			
Anna's Hummingbird (*Calypte anna*)	286	15.9	Beuchat and Chong (1998)
Costa's Hummingbird (*Calypte costae*)	315	17.5	Beuchat and Chong (1998)
Ruby-throated Hummingbird (*Archilochus colubris*)	306	17.0	Beuchat and Chong (1998)
Order *Caprimulgiformes*			
Tawny Frogmouth (*Podargus strigoides*)	351	19.5	McCracken (2003)
Order *Charadriiformes*			
Family Alcidae			
Ancient Murrelet (*Synthliboramphus antiquus*)	272	15.1	Newman et al. (1997)
Cassin's Auklet (*Ptychoramphus aleuticus*)	245	13.6	Newman et al. (1997)
Common Murre (*Uria aalge*)	313	17.4	Newman et al. (1997)
Crested Auklet (*Aethia cristatella*)	238	13.2	Newman et al. (1997)
Horned Puffin (*Fratercula corniculata*)	317	17.6	Newman et al. (1997)
Marbled Murrelet (*Brachyramphus marmoratus*)	229	12.7	Newman et al. (1997)

Continued

TABLE 50.1 Circulating concentration of glucose in avian species.—cont'd

Taxa[a] genus, species	Plasma/Serum glucose		References
	mg/dL	mmoles L^{-1}	
Parakeet Auklet (*Aethia psittacula*)	299	16.6	Newman et al. (1997)
Pigeon Guillemot (*Cepphus columba*)	322	17.9	Newman et al. (1997)
Tufted Puffin (*Fratercula cirrhata*)	279	15.5	Newman et al. (1997)
Family Burhinidae			
Double-striped Thick-knee (*Burhinus bistriatus*)	251	13.9	Ball (2003)
Family Charadriidae			
Killdeer (*Charadrius vociferus*)	359	19.9	Ball (2003)
Piping Plover (*Charadrius melodus*)	341	18.9	Ball (2003)
Two-banded plover (*Charadrius falklandicus*)	281	15.6	D'Amico et al. (2017)
Family Haematopodidae			
American Oystercatcher (*Haematopus palliates*)	337	18.7	Carlson-Bremer et al. (2010)
Family Jacanidae			
Wattled Jacana (*Jacana jacana*)	326	18.1	Ball (2003)
Family Laridae			
Black-legged Kittiwake (*Rissa tridactyla*)	265	14.7	Balasch et al. (1974)
Common Black-headed Gull (*Larus ridibundus*)	331	18.4	Mean: Newman et al. (1997), Mostaghni et al. (2005)
Glaucous-winged Gull (*Larus glaucescens*)	320	17.8	Newman et al. (1997)
European Herring Gull (*Larus argentatus*)	468	22.9	Mean: Balasch et al. (1974), Fox et al. (2007)
Yellow-legged Gull (*Larus cachinnans*)	366	20.3	Alonso-Alvarez and Ferrer (2001)
Whiskered tern (Chlidonias hybrida)	363	20.2	Minias (2014)
Family Recurvirostridae			
American Avocet (*Recurvirostra americana*)	266	14.8	Ball (2003)
Black-winged Stilt (*Himantopus himantopus*)	275	15.3	Ball (2003)
Family Scolopacidae			
Bar-tailed Godwit (*Limosa lapponica*)	250	13.9	Landy et al. (2005)
Red Knot (*Calidris canutus*)	323	17.9	D'Amico et al. (2010)
Family Stercorariidae			
South Polar Skua (*Stercorarius maccormicki*)	353	19.6	Deguirmendjian et al. (1993)
Family Sternidae			
Sooty Tern (*Sterna fuscata*)	267	14.8	Work (1996)
Order Ciconiiformes			
Family Ardeidae			
Black-crowned Night-heron (*Nycticorax nycticorax*)	303	15.0	Mean: Fontenelle (2001), Hoffman et al. (2009)
Cattle Egret (*Bubulcus ibis*)	265	14.7	Fontenelle (2001)
Great Egret (*Egretta alba*)	251	13.9	Hoffman et al. (2005)
Little Egret (*Egretta garzetta*)	302	16.8	Fontenelle (2001)
Snowy Egret (*Egretta thula*)	283	15.7	Hoffman et al. (2009)
Family Ciconiidae			

Continued

TABLE 50.1 Circulating concentration of glucose in avian species.—cont'd

Taxa[a] genus, species	Plasma/Serum glucose		References
	mg/dL	mmoles L^{-1}	
Painted Stork (*Mycteria leucocephala*)	270	15	Aengwanich et al. (2002)
Oriental white stork (*Ciconia boyciana*)	243	13.5	Han et al. (2016)
Family Threskiornithidae			
Black-faced Spoonbill (*Platalea minor*)	243	13.5	Chou et al. (2008)
Northern Bald Ibis (*Geronticus eremita*)	252	14.0	Dutton et al. (2002)
Puna Ibis (*Plegadis ridgwayi*)	302	16.8	Coke et al. (2004)
White Ibis (*Threskiouris melanocephalus*)	226	12.6	Aengwanich and Tanomtong (2004)
Order *Coliiformes*			
Blue-naped Mousebird (*Urocolius macrourus*)	317	17.6	Calculated from Pye (2003)
Speckled Mousebird (*Colius striatus*)	282	15.6	Pye (2003), Lobban et al. (2009)
Order *Columbiformes*			
Mourning Dove (*Zenaida macroura*)	340	18.9	Smith et al. (2011).
Ring-necked Turtle-dove (*Streptopelia roseogrisea*)	238	13.2	Lea et al. (1992)
Rock Pigeon (*Columba livia*)	279	15.5	Gayathri et al. (2004)
Nicobar Pigeon (*Caloenas nicobarica*)	289.8	16.1	Peinado et al. (1992a)
Pheasant Pigeon (*Otidiphaps nobilis*)	354.6	19.7	Peinado et al. (1992a)
Pink-headed Fruit Dove (*Ptilinopus porphyreus*)	290.7	16.1	Schultz (2003)
Southern Crowned or Scheep Maker's crowned Pigeon (*Goura scheepmakeri*)	351	19.5	Peinado et al. (1992a)
Victoria Crowned Pigeon (*Goura victoria*)	255.6	14.2	Peinado et al. (1992a)
Western Crowned Pigeon (*Goura cristata*)	250	13.9	Peinado et al. (1992a)
Order *Coraciiformes*			
Abyssinian Ground Hornbill or Northern Ground Hornbill (*Bucorvus abyssinicus*)	271	15.1	Dutton (2003)
Blue-crowned Motmot (*Momotus momota*)	347	19.3	Dutton (2003)
Great Hornbill (*Buceros bicornis*)	232	12.9	Dutton (2003)
Green Wood Hoopoe (*Phoeniculus purpureus*)	378	21.0	Dutton (2003)
Hoopoe (*Upupa epops*)	307	17.1	Dutton (2003)
Lilac-breasted Roller (*Coracias caudatus*)	331	18.4	Dutton (2003)
Micronesian King sher (*Todiramphus cinnamominus*)	324	18.0	Dutton (2003)
Southern Carmine Bee-eater (*Merops nubicoides*)	360	20.0	Dutton (2003)
Order *Cuculiformes*			
Greater Roadrunner (*Geococcyx californianus*)	387	21.5	Abou-Madi (2003)
Guira Cuckoo (*Guira guira*)	356	19.8	Abou-Madi (2003)
Order *Falconiformes*			
***Family* Falconidae**			
American Kestrel (*Falco sparverius*)	305	16.9	Dressen et al. (1999)

Continued

TABLE 50.1 Circulating concentration of glucose in avian species.—cont'd

Taxa[a] genus, species	Plasma/Serum glucose		References
	mg/dL	mmoles L^{-1}	
Common Kestrel (*Falco tinnunculus*)	393	21.8	Ferrer et al. (1987)
Gyr falcons (*Falco rusticolus*)	321	17.8	Raghav et al. (2015)
Peregrine Falcon (*Falco perigrinus*)	316	17.6	Gee et al. (1981)
Prairie Falcon (*Falco mexicanus*)	414	23.0	O'Donnell et al. (1978)
Order *Galliformes*			
Attwater's Prairie Chicken (*Tympanuchus cupido*)	180	10.0	West et al. (2002)
Black-fronted Piping-guan (*Penelope jacutinga*)	298	16.5	Motta et al. (2013)
Bobwhite Quail (*Colinus virginianus*)	336	20.1	Mean: Gee et al. (1981), Hill and Murray (1987), Johnson et al. (2007)
Chicken or Domestic Fowl (*Gallus gallus*)	235	13.1	Mean: Dupont et al., 2008
Chukar (*Alectoris chukar*)	296	16.6	Mean: Ozek and Bahtiyarca (2004), Naza et al. (2011)
Grouse (*Lagopus lagopus*)	270	15.0	Korhonen (1987)
Helmeted Guineafowl (*Numida meleagris*)	309	17.1	Balasch et al. (1973), Weideman et al. (2012)
Horned Guan (*Oreophasis derbianus*)	280	15.5	Cornejo et al. (2014)
Japanese Quail (*Coturnix japonica*)	292	16.2	Calculated from data in Itoh et al. (1998) and Scholtz et al. (2009)
Peacock (*Pavo cristatus*)	316	17.5	Balasch et al. (1973)
Red Jungle Fowl (*Gallus gallus*)	239	13.3	Mean: Balasch et al. (1973), Zulkifli et al. (1999), Soleimani and Zulki i, 2010
Red-legged Partridge (*Alectoris rufa*)	356	19.8	Lloyd and Gibson (2006)
Ring-necked Pheasant (*Phasianus colchicus*)	290	16.1	Mean: Balasch et al. (1973), Lloyd and Gibson (2006), Naza et al. (2012)
Rock Partridge (*Alectoris graeca*)	293	16.3	Mean: Balasch et al. (1973), Ozbey and Esen (2007)
Sage Grouse (*Centrocercus urophasianus*)	328	18.2	Dunbar et al. (2005), Dyer et al. (2009)
Turkey (*Meleagris gallopavo*)	355	19.7	Lisano and Kennamer (1977)
Western Capercaillie (*Tetrao urogallus*)	396	22.0	Lavin et al. (1992b)
Order *Gaviformes*			
Great Northern Diver (*Gavia immer*)	189	10.5	Haefele et al. (2005)
Order *Gruiformes*			
***Family* Gruidae**			
Florida Sandhill Crane (*Grus canadensis pratensis*)	229	12.7	Gee et al. (1981)
Greater Sandhill Crane (*Grus canadensis tabida*)	264	14.7	Gee et al. (1981)
Mississippi Sandhill Crane (*Grus canadensis pulla*)	216	12.0	Gee et al. (1981)
Red-crowned Crane (*Grus japonensis*)	267	14.8	Carpenter (2003)
Siberian Crane (*Grus leucogeranus*)	266	14.7	Carpenter (2003)
Wattled Crane (*Bugeranus carunculatus*)	266	14.7	Carpenter (2003)

Continued

TABLE 50.1 Circulating concentration of glucose in avian species.—cont'd

Taxa[a] genus, species	Plasma/Serum glucose		References
	mg/dL	mmoles L^{-1}	
White-napes cranes (*Grus vipio*).	231	12.8	Rayhel et al. (2015)
Whooping Crane (*Grus americana*)	232	12.9	Gee et al. (1981)
***Family* Rallidae**			
Guam Rail (*Gallirallus owstoni*)	276	15.3	Fontenot et al. (2006) (units corrected)
Takahe (*Porphyrio hochstetteri*)	194	10.8	Calculated from Youl (2009)
***Family* Otididae**			
Buff-crested Bustard (*Lophotis gindiana*)	366	20.4	Bailey et al. (1998a)
Houbara Bustard (*Chlamydotis undulate*)	304	16.9	Bailey et al. (1999)
Kori Bustard (*Ardeotis kori*)	248	13.8	Mean: D'Aloia et al. (1996), Bailey et al. (1999)
White-Bellied Bustard (*Eupodotis senegalensis*)	344	19.1	Bailey et al. (1998b)
Order *Musophagiformes*			
Knysna Turaco (*Tauraco corythaix*)	227	12.6	Lobban et al. (2009)
Order *Passeriformes*			
American Goldfinches (*Carduelis tristis*)	405	22.5	Marsh and Dawson (1982)
African Pied Crow (*Corvus albus*)	295	16.4	Ihedioha et al. (2011)
Abert's Towhee (*Melozone aberti*)	324	18.0	Davies et al. (2013)
American Common Crow (*Corvus brachyrhynchos*)	366	21.4	Gentz (2003)
American Robin (*Turdus migratorius*)	338	18.8	Gerson and Guglielmo (2013)
Asian Fairy-bluebird (*Irena puella*)	294	16.3	Gentz (2003)
Black-capped Chickadee (*Poecile atricapillus*)	133	15.5	Mean of Bairlein (1983), Van Hemert and Handel (2016)
Blue-faced Honeyeater (*Entomyzon cyanotis*)	357	19.8	Gentz (2003)
Cape White-eye (*Zosterops virens*)	279	15.5	Lobban et al. (2009)
Common Grackle (*Quiscalus quiscula*)	319	17.7	Hill and Murray (1987), Martinez del Rio et al. (1988)
Common mynahs (*Acridotheres tristis*)	336	18.7	Jahantigh et al. (2019)
Common Starling (*Sturnus vulgaris*)	350	19.5	Hill and Murray (1987), Martinez del Rio et al. (1988), Remage-Healy and Romero (2000)
Curve-Billed Thrashers *Toxostoma curvirostre*	279	15.5	Fokidis et al. (2011), 2012
Darwin's small ground finch (*Geospiza fuliginosa*)	248	13.8	Clark et al. (2018)
Garden Warbler (*Silva borin*)	246	13.7	Bairlein (1983), Jenni-Eiermann and Jenni (1994), Totzke et al. (1998)
Green Broadbill (*Calyptomena viridis*)	281	15.6	Gentz (2003)
Gray Catbird (*Dumetella carolinensis*)	378	21.0	Malcarney et al. (1994)
Hooded Pitta (*Pitta sordida*)	136	7.6	Gentz (2003)
Horned lark (*Eremophila alpestris*)	445	24.7	Swain (1992)
House Sparrow (*Passer domesticus*)	308	17.1	Khalilieh et al. (2012)
Malachite sunbirds (*Nectarinia famosa*)	274	15.2	Downs et al. (2010)

Continued

TABLE 50.1 Circulating concentration of glucose in avian species.—cont'd

Taxa[a] genus, species	Plasma/Serum glucose		References
	mg/dL	mmoles L^{-1}	
Pale-bellied tyrant-manakin (*Neopelma pallescens*)	301	16.7	Azeredo et al. (2016)
Pied Flycatchers (*Ficedula hypoleuca*)	391	21.7	Kern et al. (2005)
Purple headed Glossy Starling (*Lamprotornis purpureiceps*)	294	16.3	Malcarney et al. (1994)
Raven (*Corvus corax*)	360	20.0	Balasch et al. (1974)
Red-crested Cardinal (*Paroaria coronata*)	401	22.3	Gentz (2003)
Red-winged Blackbird (*Agelaius phoeniceus*)	341	19.0	Hill and Murray (1987), Martinez del Rio et al. (1988)
Red-winged Starling (*Onychognathus morio*)	247	13.7	Lobban et al. (2009)
Rook (*Corvus frugilegus*)	236	13.	Miksik and Hodný (1992)
Rufous-collared Sparrow (*Zonotrichia capensis*)	240	13.3	Ruiz et al. (2002)
Silver-eared Mesia (*Leiothrix argentauris*)	444	24.7	Gentz (2003)
Southern Red Bishop (*Euplectes orix*)	309	17.2	Gentz (2003)
Superb Starling (*Lamprotornis superbus*)	335	18.6	Gentz (2003)
Venezuelan Troupial (*Icterus icterus*)	375	20.8	Gentz (2003)
Vesper sparrow (*Pooecetes gramineus*)	370	20.7	Swain (1987)
White-crowned Sparrow (*Zonotrichia leucophrys*)	448	24.9	Boswell et al. (1997)
Order *Pelicaniformes*			
***Family* Pelecanidae**			
Brown Pelican (*Pelecanes occidentalis*)	243	13.5	Wolf et al. (1985), Balasch et al. (1974)
Pink-backed Pelican (*Pelecanus rufescens*)	219	12.2	Weber (2003)
***Family* Frigatidae**			
Great Frigatebird (*Fregata minor*)	123	6.8	Work (1996)
***Family* Phaethontidae**			
Red-tailed Tropicbird (*Phaethon rubricauda*)	231	12.8	Work (1996)
Family Phalacrocoracidae			
Flightless Cormorant (*Phalacrocorax harrisi*)	128	10.8	Mean of Travis et al. (2006a), Valle et al. (2018)
Great Cormorant (*Phalacrocorax carbo*)	238	13.2	Balasch et al. (1974)
Guanay Cormorant (*Phalacrocorax bougainvillii*)	271	15.1	Weber (2003)
Imperial Shag (*Phalacrocorax actriceps*)	195	10.8	Gallo et al. (2013)
Pelagic Cormorant (*Phalacrocorax pelagicus*)	223	12.4	Newman et al. (1997)
***Family* Sulidae**			
Brown booby (*Sula leucogaster*)	264	14.7	Work (1999)
Northern Gannet (*Sula bassana*)	216	12.0	Balasch et al. (1974)
Red-foot Booby (*Sula sula*)	179	9.9	Work (1996)
Order *Phoenicopteriformes*			
Chilean Flamingo (*Phoenicopterus chiliensis*)	203	11.3	Peinado et al. (1992a,b)

Continued

TABLE 50.1 Circulating concentration of glucose in avian species.—cont'd

Taxa[a] genus, species	Plasma/Serum glucose		References
	mg/dL	mmoles L^{-1}	
Greater flamingo (*Phoenicopterus* tuber)	202	11.2	Peinado et al. (1992a,b)
Rosy Flamingo (*Phoenicopterus ruber*)	205	11.4	Peinado et al. (1992a,b)
Lesser Flamingo (*Phoeniconais minor*)	166	9.2	Peinado et al. (1992a,b)
Order *Procellariiformes*			
Galápagos Petrel (*Pterodroma phaeopygia*)	329	18.3	Work (1996)
Laysan Albatross (*Diomedea immutabilis*)	125	7.0	Work (1996)
Northern Fulmar (*Fulmarus glacialis*)	229	12.6	Newman et al. (1997)
Southern Giant Petrel (*Macronectes giganteus*)	284	15.8	Uhart et al. (2003)
Wedge-tailed Shearwater (*Puf nus paci cus*)	248	13.8	Work (1996)
Waved Albatross (*Diomedia irrorata*)	229	12.7	Padilla et al. (2003)
Order *Psittaciformes*			
African Gray Parrot (*Psittacus erithacus*)	248	13.8	Lumeij and Overduin (1990), Polo et al. (1998)
Yellow-crowned Amazon (*Amazona ochrocephala*)	252	14.0	Polo et al. (1998)
Baudin's cockatoo (*Calyptorhynchus baudinii*)	315	17.5	Le Souëf et al. (2013)
Blue-fronted Amazon Parrot (*Amazona aestiva*)	252	14.0	Deem et al. (2005)
Budgerigar (*Melopsittacus undulates*)	348	19.3	Scope et al. (2005)
Carnaby's cockatoo (*Calyptorhynchus latirostris*)	328	18.2	Le Souëf et al. (2013)
Cuban Amazon Parrot (*Amazona leucocephala*)	251	13.9	Tell and Citino (1992)
Kakapo (*Strigops habroptilus*)	223	12.4	Low et al. (2006)
Kea (*Nestor notabilis*)	281	15.6	Calculated from Youl (2009)
Macaw (*Ara rubrogenys*)	295	16.4	García del Campo et al. (1991)
Palm Cockatoo (*Probosciger aterrimus*)	281	15.6	Polo et al. (1998)
Quaker parrots (*Myiopsitta monachus*)	272	15.1	Rettenmund et al. (2014)
Red-fronted Macaw (*Ara rubrogenys*)	295	16.4	García del Campo et al. (1991)
Spix's Macaw (*Cyanopsitta spixii*)	324	18.0	Foldenauer et al. (2007)
St Vincent Parrot (*Amazona guildingii*)	212	11.8	Deem et al. (2008)
Thick-billed Parrot (*Rhynchopsitta pachyrhyncha*)	278	15.4	Waldoch et al. (2009)
White Cockatoo (*Cacatua alba*)	235	13.1	Polo et al. (1998)
Hyacinthine Macaw (*Anodorhynchus hyacinthinus*)	261	14.5	Polo et al. (1998)
Blue and yellow Macaw (*Ara ararauna*)	272	15.1	Polo et al. (1998)
Green-winged Macaw (*Ara chlorptera*)	288	16.0	Polo et al. (1998)
Scarlet Macaw (*Ara macao*)	248	13.8	Polo et al. (1998)
Red Lory (*Eos bornea*)	337	18.7	Polo et al. (1998)
Rose-ringed Parakeet (*Psittacula krameri*)	222	12.3	Anan and Maitra (1995)
Order *Pteroclidiformes*			
Pin-tailed Sandgrouse (*Pterocles alchata*)	392	21.8	Lierz and Fenske (2004)

Continued

TABLE 50.1 Circulating concentration of glucose in avian species.—cont'd

Taxa[a] genus, species	Plasma/Serum glucose		References
	mg/dL	mmoles L^{-1}	
Order *Sphenisciformes*			
Adélie Penguin (*Pygoscelis adeliae*)	299	15.2	Mean of Aquilera et al. (1993), Vleck and Vleck (2002), Parsons et al. (2015), Ibañez et al. (2015)
African penguins (*Spheniscus demersus*)	225	12.5	Mazzaro et al. (2013)
Chinstrap Penguin (*Pygoscelis Antarctica*)	279	15.5	Aquilera et al. (1993), Ferrer et al. (1994), Ibañez et al., 2015
Emperor Penguin (*Aptenodytes forsteri*)	281	15.6	Groscolas and Rodriguez (1981)
Galápagos Penguin (*Spheniscus mendiculus*)	218	12.1	Travis et al. (2006b)
Gentoo penguin (*Pygoscelis papua*)	236	13.1	Aquilera et al. (1993), Ibañez et al., 2015
Humboldt Penguin (*Spheniscus humboldti*)	227	12.6	Wallace et al. (1995)
Jackass Penguin (*Spheniscus demersus*)	196	10.9	Cray et al. (2010)
King Penguin (*Aptenodytes patagonicus*)	207	11.5	Bernard et al. (2002)
Rockhopper Penguin (*Eudyptes chrysomes*)	233	12.9	Karesh et al. (1999)
Order *Strigiformes*			
Barn Owl (*Tyto alba*)	263	14.6	Ferrer et al. (1987), Myers and Klasing (1999)
Barred Owl (*Strix varia*)	297	16.5	Aguilar (2003)
Burrowing Owl (*Athene cunicularia*)	329	18.3	Aguilar (2003)
Collared scops owl (*Otus lettia*)	361	20.1	Chan et al. (2012)
Eagle Owl (*Bubo bubo*)	386	21.5	Mean: Ferrer et al. (1987), Garcia-Rodriguez et al. (1987)
Eastern Screech Owl (*Megascops asio*)	335	18.6	Aguilar (2003)
Great Gray Owl (*Strix nebulosa*)	316	17.6	Aguilar (2003)
Great Horned Owl (*Bubo virginianus*)	375	20.8	O'Donnell et al. (1978)
Short-eared Owl (*Asio ammeus*)	293	16.3	Aguilar (2003)
Snowy Owl (*Bubo scandiacus*)	339	18.8	Aguilar (2003)
Spectacled Owl (*Pulsatrix perspicillata*)	326	18.1	Aguilar (2003)
Order *Trogoniformes*			
Crested Quetzal (*Pharomachrus antisianus*)	288	16.0	Neiffer (2003)
Golden-headed Quetzal (*Pharomachrus auriceps*)	245	13.6	Neiffer (2003)
Javan Trogon (*Apalharpactes reinwardtii*)	332	18.4	Neiffer (2003)
White-tailed Trogon (*Trogon chionurus*)	339	18.8	Neiffer (2003)
Paleognathae			
Cassowary (*Casuarius* sp.)	185	10.2	Angel (1995)
Elegant crested tinamou (*Eudromia elegans*)	331	18.4	Black et al. (2013)
Emu (*Dromaius novaehollandiae*)	160	8.9	Mean: Okotie-Eboh et al. (1992), Angel (1995)
Greater Rhea (*Rhea americana*)	212	11.8	Uhart et al. (2006)
Ostrich (*Struthio camelus*)	229	12.7	Calculated from data in Palomeque et al. (1991), Verstappen et al. (2002), Okotie-Eboh et al. (1992)

[a]*Classifcation based on the del Hoyo, J., Elliott, A., Sargatal, J. (Eds.), 1992–2013. Handbook of the Birds of the World. 17 Volumes, Lynx Ediciones, Barcelona but with families Accipitridae and Cathartidae placed into a separate Order Accipitriformes following the Tree of Life.*

TABLE 50.2 Mammalian lactate concentrations

Species	Lactate mmoles/L	Reference
Baboon[a] (5–7 week old)	1.0	Levitsky et al., 1984
Bottlenose dolphins (*Tursiops truncatus*)	2.5	Williams et al., 1993
California sea lion (*Zalophus californianus*)	2.1	Marinkovich et al., 2019
Cat	1.63	Redavid et al., 2012
Cattle	2.0	Omole et al., 2001
Dog	1.4	Allen and Holm, 2008
Harbor seal (*Phoca vitulina*)	0.8	Davis, 1983
Horse	1.2	Delesalle et al., 2007
Human	0.94	Edwards, 1938
Japanese monkey (*Macaca fuscata*)	2.08	Kimura, 2014
Moose (A*lces alces*)	9.2	Haga et al., 2009
Northern elephant seal (*Mirounga angustirostris*)	1.28	Marinkovich et al., 2019
Pacific harbor seal (*Phoca vitulina richardsi*)	1.64	Marinkovich et al., 2019
Rat (*Rattus norvegicus*)	1.7	Rezaei et al., 2017
Rabbit	6.1	Langlois et al., 1999
Rhesus macaque (*Macaca mulatta*)	2.77	Hobbs et al., 2010
Tammar wallaby (*Macropus eugenii*)	0.83	Baudinette et al., 1992
Tasmanian devil (*Sarcophilus harrisii*)	0.60	Nicol and Maskrey, 1986
White rhinoceros (*Ceratotherium simum*)	2.88	Buss et al., 2015
White whale (*Delphinapterus leucas*)	0.79	Shaffer et al., 1997
Mean 2.17 + (20) 0.46 p = 0.068 cf birds		

[a]*species not stated.*

References

Abou-Madi, N., 2003. *Cuculiformes* (cuckoos, roadrunners). In: Fowler, M.E., Miller, R.E. (Eds.), Zoo and Wild Animal Medicine, fifth ed. Saunders, St. Louis, MO, pp. 211–213.

Aengwanich, W., Tanomtong, A., 2004. Hematological and serum biochemical values of white ibis (*Threskiornis melanocephalus*). Asean biodivers 823–828 (Accessed 10.04.12). http://www.aseanbiodiversity.info/Abstract/53004145.pdf.

Aengwanich, W., Tanomtong, A., Pattanarungson, R., Simaraks, S., 2002. Blood cell characteristic, hematological and serum biochemistry values of painted stork (*Mycteria leucocephala*). Songklanakarin J. Sci. Technol. 24, 473–480.

Aguilar, R.F., 2003. Strigiformes (owls). In: Fowler, M.E., Miller, R.E. (Eds.), Zoo and Wild Animal Medicine, 5th. Saunders, St. Louis, MO, pp. 213–223.

Allen, S.E., Holm, J.L., 2008. Lactate: physiology and clinical utility. J. Vet. Emerg. Crit. Care 18, 123–132.

Alonso-Alvarez, C., Ferrer, M., 2001. A biochemical study of fasting, subfeeding, and recovery processes in yellow-legged gulls. Physiol. Biochem. Zool. 74, 703–713.

Anan, K.K., Maitra, S.K., 1995. Impact of quinalphos on blood glucose and acetyl choline activity in the brain and pancreas in a rose ringed parakeet (*Psittacula krameri borealis* Newmann). Arch. Environ. Contam. Toxicol. 29, 20–23.

Angel, C.R., 1995. Serum vitamin D metabolites, thyroxine and chemistries of ostriches, emus, rheas and cassowaries. Assoc. Avian Vet. Conf. Proc. 233–240.

Aquilera, E., Moreno, J., Ferrer, M., 1993. Blood chemistry values in three P*ygoscelis* penguins. Comp. Biochem. Physiol. 105A, 471–473.

Artachoa, P., Soto- Gamboa, M., Verdugoc, C., Nespoloa, R.F., 2007. Blood biochemistry reveals malnutrition in black-necked swans (*Cygnus melanocoryphus*) living in a conservation priority area. Comp. Biochem. Physiol. 146 (A), 283–290.

Avni-Magen, N., Gancz, A.Y., Beaufrère, H., Lublin, A., Eshar, D., 2016. Selected hematologic and plasma biochemistry analysis of ferruginous ducks (*Aythya nyroca*) in Israel. J. Zoo Wildl. Med. 47, 354–358.

Azeredo, L.M.M., Oliveira, T.C., Lopez, L.C.S., 2016. Blood metabolites as predictors to evaluate the body condition of *Neopelma pallescens* (Passeriformes: *Pipridae*) in northeastern Brazil. Zoologia (Curitiba) 33, e20160043.

Bailey, T.A., Wernery, U., Howlett, J.C., Naldo, J., Samour, J.H., 1998a. Age related plasma chemistry in the buff-crested bustard (*Eupodotis ruficrista gindiana*). J. Vet. Med. 45, 635–640.

Bailey, T.A., Wernery, U., Naldo, J., Howlett, J., Samour, J.H., 1998b. Normal blood chemistry and age-related changes in the white-bellied bustard *(Eupodotis senegalensis)*, with some clinical observations. Comp Haematol. Int. 8, 61–65.

Bailey, T.A., Wernery, U., Howlett, J., Naldo, J., Samour, J.H., 1999. Age related plasma chemistry changes in houbara and kori bustards in the United Arab Emirates. J. Wildl. Dis. 35, 31–37.

Bairlein, F., 1983. Seasonal variations of serum glucose levels in a migratory songbird, *Sylvia borin*. Comp. Biochem. Physiol. 76A, 397–399.

Balasch, J., Palacios, L., Musquera, S., Palomeque, J., Jiménez, M., Ale- many, M., 1973. Comparative hematological values of several *galliformes*. Poultry Sci. 52, 1531–1534.

Balasch, J., Palomeque, J., Palcios, L., Muscquera, S., Jimenez, M., 1974. Hematological values of some great flying and aquatic-diving birds. Comp. Biochem. Physiol. 49A, 137–145.

Ball, R.L., 2003. *Charadriiformes* (gulls, shorebirds). In: Fowler, M.E., Miller, R.E. (Eds.), Zoo and Wild Animal Medicine, fifth ed. Saunders, St. Louis, MO, pp. 136–141.

Baudinette, R.V., Snyder, G.K., Frappell, P.B., 1992. Energetic cost of locomotion in the tammar wallaby. Am. J. Physiol. 262, R771–R778.

Bernard, S.F., Fayolle, C., Robin, J.P., Groscolas, R., 2002. Glycerol and NEFA kinetics in long-term fasting king penguins: phase II versus phase III. J. Exp. Biol. 205, 2745–2754.

Beuchat, C.A., Chong, C.R., 1998. Hyperglycemia in hummingbirds and its consequences for hemoglobin glycation. Comp. Biochem. Physiol. A. Mol. Integr. Physiol. 120, 409–416.

Black, P.A., Macek, M., Tieber, A., Weber, M., 2013. Reference values for hematology, plasma biochemical analysis, plasma protein electrophoresis, and aspergillus serology in elegant-crested tinamou (*Eudromia elegans*). J. Avian Med. Surg. 27, 1–6.

Boismenu, C., Gauthier, G., Larochelle, J., 1992. Physiology of prolonged fasting in greater snow geese (*Chen caerulescens atlantica*). Auk 109, 511–552.

Boswell, T., Lehman, T.L., Ramenofsky, M., 1997. Effects of plasma glucose manipulations on food intake in white-crowned sparrows. Comp. Biochem. Physiol. 118A, 721–726.

Buss, P., Olea-Polpeka, F., Meyer, L., Hofmeyr, J., Mathebula, N., Kruger, M., Angela Brüns, A., Martin, L., Miller, M., 2015. Evaluation of cardiorespiratory, blood gas, and lactate values during extended immobilization of white rhinoceros (*Ceratotherium simum*). J. Zoo Wildl. Med. 46, 224–233.

Carlson-Bremer, D., Norton, T.M., Gilardi, K.V., Dierenfeld, E.S., Winn, B., Sanders, F.J., Cray, C., Oliva, M., Chen, T.C., Gibbs, S.E., Sepúlveda, M.S., Johnson, C.K., 2010. Health assessment of American Oystercatchers (*Haematopus palliatus palliatus*) in Georgia and South Carolina. J. Wildl. Dis. 46, 772–780.

Carpenter, J.W., 2003. *Gruiformes* (cranes, limplets, rails, gallinules, coots, bustards). In: Fowler, M.E., Miller, R.E. (Eds.), Zoo and Wild Animal Medicine, fifth ed. Saunders, St. Louis, MO, pp. 171–180.

Chan, F.T., Lin, P.I., Chang, G.R., Wang, H.C., Hsu, T.H., 2012. Hematocrit and plasma chemistry values in adult collared scops owls (*Otus lettia*) and crested serpent eagles (*Spilornis cheela hoya*). J. Vet. Med. Sci. 74, 893–898.

Chou, S.J., Shieh, Y.C., Yu, C.Y., 2008. Hematologic and biochemistry values for black-faced spoonbills (*Platalea minor*) with and recovering from botulism. J. Wildl. Dis. 44, 781–784.

Clark, T.D., Kleindorfer, S., Dudaniec, R.Y., 2018. Baseline and stress-induced blood properties of male and female Darwin's small ground finch (*Geospiza fuliginosa*) of the Galapagos Islands. Gen. Comp. Endocrinol. 259, 199–206.

Coke, R.L., West, G.D., Hoover, J.P., 2004. Hematology and plasma biochemistry of captive puna ibis (*Plegadis ridgwayi*). J. Wildl. Dis. 40, 141–144.

Cornejo, J., Richardson, D., Perez, J.G., Brightsmith, D.J., Bonar, C.J., Heatley, J.J., 2014. Hematological and plasma biochemical reference values of the horned guan, *Oreophasis derbianus*. J. Zoo Wildl. Med. 45, 15–22.

Cray, C., Stremme, D.W., Arheart, K.L., 2010. Postprandial biochemistry changes in penguins (*Spheniscus demersus*) including hyperuricemia. J. Zoo Wildl. Med. 41, 325–326.

Davies, S., Rodriguez, N., Sweazea, K.L., Deviche, P., 2013. The effect of acute stress and long-term corticosteroid administration on plasma metabolites in an urban and desert songbird. Physiol. Biochem. Zool. 86, 47–60.

Deem, S.L., Ladwig, E., Cray, C., Karesh, W.B., Amato, G., 2008. Health assessment of the *ex situ* population of St Vincent parrots (Amazona guildingii) in St Vincent and the Grenadines. J. Avian Med. Surg. 22, 114–122.

Deem, S.L., Noss, A.J., Cuéllar, R.L., Karesh, W.B., 2005. Health evaluation of free-ranging and captive blue-fronted Amazon parrots (*Amazona aestiva*) in the Gran Chaco, Bolivia. J. Zoo Wildl. Med. 36, 598–605.

Deem, S.L., Rivera-Parra, J.L., Parker, P.G., 2012. Health evaluation of Galapagos Hawk (*Buteo Galapagoensis*) on Santiago island, Galapagos. J. Wildlife Dis. 48, 39–46.

Deguirmendjian, C., Rosa, R., Rodrigues, E., Bacila, M., 1993. Blood constituents and electrophoretic patterns in Antarctic birds: penguins and skuas. Comp. Biochem. Physiol. 104A, 117–123.

Delesalle, C., Dewulf, J., Lefebvre, R.A., Schuurkes, J.A.J., Proot, J., Lefere, L., Deprez, P., 2007. Determination of lactate concentrations in blood plasma and peritoneal fluid in horses with colic by an Accusport analyzer. J. Vet. Intern. Med. 21, 293-301.

Dobado-Berrios, P.M., Tella, J.L., Ceballos, O., Donazar, J.A., 1998. Effects of age and captivity on plasma chemistry values of the Egyptian vulture. Condor 100, 719–725.

Dolka, B., Włodarczyk, R., Zbikowski, A., Dolka, I., Szeleszczuk, P., Kluciński, W., 2014. Hematological parameters in relation to age, sex and biochemical values for mute swans (*Cygnus olor*). Vet. Res. Commun. Electronic publication.

Downs, C.T., Wellmann, A.E., Brown, A., 2010. Diel variations in plasma concentrations of glucose of Malachite sunbirds (*Nectarinia famosa*). J. Ornithol. 151, 235–239.

Dressen, P.J., Wimsatt, J., Burkhard, M.J., 1999. The effects of Isoflurane anesthesia on hematologic and plasma biochemical values of American Kestrels (*Falco sparverius*). J. Avian Med. Surg. 13, 173–179.

Driver, E.A., 1981. Hematological and blood chemical values of mallard, *Anas p. platyrhynchos*, drakes before, during and after remise. J. Wildl. Dis. 17, 413–420.

Dujowich, M., Mazet, J.K., Zuba, J.R., 2005. Hematologic and biochemical reference ranges for captive California Condors (*Gymnogyps californianus*). J. Zoo Wildl. Med. 36, 590–597.

Dunbar, M.R., Gregg, M.A., Giordano, M.R., Davis, D.M., Byrne, M.W., Crawford, J.A., Tornquist, S.J., 2005. Normal hematologic and biochemical values for prelaying greater sage grouse (*Centrocercus urophasianus*) and their influence on chick survival. J. Zoo Wildl. Med. 36, 422–429.

Dupont, J., Tesseraud, S., Derouet, M., Collin, A., Rideau, N., Crochet, S., Godet, E., Cailleau-Audouin, E., Métayer-Coustard, S., Duclos, M.J., Gespach, C., Porter, T.E., Cogburn, L.A., Simon, J., 2008. Insulin immuno-neutralization in chicken: effects on insulin signaling and gene expression in liver and muscle. J. Endocrinol. 197, 531–542.

Dutton, C.J., 2003. *Coraciiformes* (king Fishers, motmots, bee-eaters, hoopoes, hornbills). In: Fowler, M.E., Miller, R.E. (Eds.), Zoo and Wild Animal Medicine, fifth ed. Saunders, St. Louis, MO, pp. 254–260.

Dutton, C.J., Allchurch, A.F., Cooper, J.E., 2002. Comparison of hematologic and biochemical reference ranges between captive populations of northern bald ibises (*Geronticus eremita*). J. Wildl. Dis. 38, 583–588.

Dyer, K.J., Perryman, B.L., Holcombe, D.W., 2009. Fitness and nutritional assessment of greater sage grouse (*Centrocercus urophasianus*) using hematologic and serum chemistry parameters through a cycle of seasonal habitats in Northern Nevada. J. Zoo Wildl. Med. 40, 18–28.

D'Aloia, M.-A.E., Samour, J.H., Bailey, T.A., Naldo, J., Howlett, J.C., 1996. Normal blood chemistry of the kori bustard (*Ardeotis kori*). Avian Pathol. 25, 161–165.

D'Amico, V.L., Bertellotti, M., Baker, A.J., González, P.M., 2010. Hematologic and plasma biochemistry values for endangered red knots (*Calidris canutus rufa*) at wintering and migratory sites in Argentina. J. Wildl. Dis. 46, 644–648.

D'Amico, V.L., Palacios, M.G., Baker, A.J., González, P.M., Madrid, E., Bertellotti, M., 2017. Physiological parameters and their response to handling stress in a neotropical migratory shorebird during the non-breeding season. J. Wildl. Dis. 53, 437–446.

Edwards, 1938. A simplified estimation of lactate in normal human blood. J. Biol. Chem. 125, 571–583.

Elarabany, N., 2018. A comparative study of some haematological and biochemical parameters between two species from the *Anatidae* family within migration season. J. Basic Appl. Zool. 79, 31.

Fairbrother, A., Craig, M.A., Walker, K., O'Loughlin, D., 1990. Changes in mallard (*Anas platyrhynchos*) serum chemistry due to age, sex, and reproductive condition. J. Wildl. Dis. 26, 67–77.

Ferrer, M., Garcia-Rodriguez, T., Carrillo, J.C., Castroviejo, J., 1987. Hematocrit and blood chemistry values in captive raptors (*Gyps fulvus*, *Buteo buteo*, *Milvus migrans*, *Aquila heliaca*). Comp. Biochem. Physiol. 87A, 1123–1127.

Ferrer, M., Amat, J.A., Vinuela, J., 1994. Blood chemistry values in chinstrap penguins (P*ygoscelis Antarctica*) during the Antarctic summer. Comp. Biochem. Physiol. 107A, 81–84.

Fokidis, H.B., Hurley, L., Rogowski, C., Sweazea, K., Deviche, P., 2011. Effects of captivity and body condition on plasma corticosterone, locomotor behavior, and plasma metabolites in Curve-Billed Thrashers. Physiol. Biochem. Zool. 84, 595–606.

Fokidis, H.B., des Roziers, M.B., Sparr, R., Rogowski, C., Sweazea, K., Deviche, P., 2012. Unpredictable food availability induces metabolic and hormonal changes independent of food intake in a sedentary songbird. J. Exp. Biol. 215, 2920–2930.

Foldenauer, U., Borjal, R.J., Deb, A., Arif, A., Taha, A.S., Watson, R.W., Steinmetz, H., Bürkle, M., Hammer, S., 2007. Hematologic and plasma biochemical values of Spix's macaws (*Cyanopsitta spixii*). J. Avian Med. Surg. 21, 275–282.

Fontenelle, J.H., 2001. Cicioniiformes. In: Fowler, M.E., Cubas, Z.S. (Eds.), Biology, Medicine, and Surgery of South American Animals. Iowa State Press, Ames, IA, pp. 84–87.

Fontenot, D.K., Terrell, S.P., Malakoot, K., Medina, S., 2006. Health assessment of the Guam Rail (*Gallirallus owstoni*) population in the Guam Rail recovery program. J. Avian Med. Surg. 20, 225–233.

Fox, G.A., Jeffrey, D.A., Williams, K.S., Kennedy, S.W., Grasman, K.A., 2007. Health of herring gulls (*Larus argentatus*) in relation to breeding location in the early 1990s. I. Biochem. measures. J. Toxicol. Environ. Health A. 70, 1443–1470.

Franson, J.C., Hoffman, D.J., Schmutz, J.A., 2009. Plasma biochemistry values in emperor geese (*Chen canagica*) in Alaska: comparisons among age, sex, incubation, and molt. J. Zoo Wildl. Med. 40, 321–327.

Franson, J.C., Flint, P.L., Schmutz, J.A., 2017. Reference intervals for serum biochemistries of molting Pacific black brant (*Branta bernicla nigricans*) in Northern Alaska, USA. J. Wildl. Dis. 53, 417–419.

Gallo, L., Qunitana, F., Svagelj, W.S., Uhart, M., 2013. Hematology and blood chemistry values in free-living Imperial Cormorants (*Phalacrocorax atriceps*). Avian Dis. 57, 737–743.

García del Campo, A.L., Huecas, V., Fernández, A., Puerta, M.L., 1991. Hematology and blood chemistry of macaws, Ara rubrogenys. Comp. Biochem. Physiol. 100 A, 943–944.

Garcıá-Montijano, M., García, A., Luaces, I., Lemus, J.A., Montesinos, A., Canales, R., Pereira, P., 2002. Blood chemistry, protein electrophoresis, and hematologic values of captive Spanish imperial eagles (*Aquila adalberti*). J. Zoo Wildl. Med. 33, 112–117.

Garcia-Rodriguez, T., Ferrer, M., Recio, F., Castroviejo, J., 1987. Circadian rhythms of determined blood chemistry values in buzzards and eagle owls. Comp. Biochem. Physiol. 88A, 663–669.

Gayathri, K.L., Shenoy, K.B., Hegde, S.N., 2004. Blood profile of pigeons (*Columba livia*) during growth and breeding. Comp. Biochem. Physiol. A 138, 187–192.

Gee, C.F., Carpenter, J.W., Hensler, B.L., 1981. Species differences in hematological values of captive cranes, geese, raptors, and quail. J. Wildl. Manag. 45, 463–483.

Gentz, E.J., 2003. *Passeriformes* (songbirds, perching birds). In: Fowler, M.E., Miller, R.E. (Eds.), Zoo and Wild Animal Medicine, fifth ed. Saunders, St. Louis, MO, pp. 267–275.

Gerson, A.R., Guglielmo, C.G., 2013. Energetics and metabolite profiles during early flight in American robins (*Turdus migratorius*). J. Comp. Physiol. B. 183, 983–991.

Groscolas, R., Rodriguez, A., 1981. Glucose metabolism in fed and fasted emperor penguins (*Aptenodytes forsteri*). Comp. Biochem. Physiol. 70A, 191–198.

Haefele, H.J., Sidor, I., Evers, D.C., Hoyt, D.E., Pokras, M.A., 2005. Hematologic and physiologic reference ranges for free-ranging adult and young Common Loons (*Gavia immer*). J. Zoo Wildl. Med. 36, 385–390.

Haga, H.A., Wenger, S., Hvarnes, S., Os, O., Rolandsen, C.M., Solberg, E.J., 2009. Plasma lactate concentrations in free-ranging moose (*Alces alces*) immobilized with etorphine. Vet. Anaesth. Analg. 6, 555–561.

Han, J.I., Jang, H.J., Na, K.J., 2016. Hematologic and serum biochemical reference intervals of the Oriental white stork (*Ciconia boyciana*) and

the application of an automatic hematologic analyzer. J. Vet. Sci. 17, 399–405.

Hernández, M., Margalida, A., 2010. Hematology and blood chemistry reference values and age-related changes in wild Bearded Vultures (*Gypaetus barbatus*). J. Wildl. Dis. 46, 390–400.

Hill, E.F., Murray, H.C., 1987. Seasonal variation in diagnostic enzymes and biochemical constituents of captive Northern Bobwhites and passerines. Comp. Biochem. Physiol. B 87, 933–940.

Hobbs, T.R., O'Malley, J.P., Khouangsathiene, S., Dubay, C.J., 2010. Comparison of lactate, base excess, bicarbonate, and pH as predictors of mortality after severe trauma in rhesus macaques (*Macaca mulatta*). Comp. Med. 60, 233–239.

Hoffman, D.J., Pattee, O.H., Wiemeyer, S.N., Mulhern, B., 1981. Effects of lead shot ingestion on delta-aminolevulinic acid dehydratase activity, hemoglobin concentration, and serum chemistry in bald eagles. J. Wildl. Dis. 17, 423–431.

Hoffman, D.J., Spalding, M.G., Frederick, P.C., 2005. Subchronic effects of methylmercury on plasma and organ biochemistries in great egret nestlings. Environ. Toxicol. Chem. 24, 3078–3084.

Hoffman, D.J., Henny, C.J., Hill, E.F., Grove, R.A., Kaiser, J.L., Stebbins, K.R., 2009. Mercury and drought along the Lower Carson River, Nevada: III. Effects on blood and organ biochemistry and histopathology of snowy egrets and black-crowned night-herons on Lahontan Reservoir, 2002–2006. J. Toxicol. Environ. Health A. 72, 1223–1241.

Hollamby, S., Afema-Azikuru, J., Sikarskie, J.G., Kaneene, J.B., Stuht, J.N., Fitzgerald, S.D., Bowerman, W.W., Cameron, K., Gandolf, A.R., Hui, G.N., Dranzoa, C., Rumbeiha, W.K., 2004. Clinical pathology and morphometrics of African fish eagles in Uganda. J. Wildl. Dis. 40, 523–532.

Hollmén, T., Franson, J.C., Hario, M., Sankari, S., Kilpi, M., Lindström, K., 2001. Use of serum biochemistry to evaluate nutritional status and health of incubating common eiders (*Somateria mollissima*) in Finland. Physiol. Biochem. Zool. 74, 333–342.

Ibañez, A.E., Najle, R., Larsen, K., Pari, M., Figueroa, A., Montalti, D., 2015. Haematological values of three Antarctic penguins: gentoo (*Pygoscelis papua*), Adélie (*P. adeliae*) and chinstrap (*P. antarcticus*). Polar Res. 34 (1), 25718.

Ihedioha, J.I., Okorie-Kanu, C.O., Ugwu, C.P., 2011. The blood picture and serum biochemistry pro le of the African pied crow (*Corvus albus*). Comp. Clin. Pathol. 20, 239.

Itoh, N., Makita, T., Koiwa, M., 1998. Characteristics of blood chemical parameters in male and female quails. J. Vet. Med. Sci. 60, 1035–1037.

Jahantigh, M., Zaeemi, M., Razmyar, J., Mohammad Azizzadeh, M., 2019. Plasma biochemical and lipid panel reference intervals in common mynahs (*Acridotheres tristis*). J. Avian Med. Surg. 33, 15–21.

Jenni-Eiermann, S., Jenni, L., 1994. Plasma metabolite levels predict individual body-mass changes in a small long-distance migrant, the garden-warbler. Auk 111, 888–899.

Johnson, M.S., Quinn Jr., M.J., Bazar, M.A., Gust, K.A., Escalon, B.L., Perkins, E.J., 2007. Subacute toxicity of oral 2,6-dinitrotoluene and 1,3,5-trinitro-1,3,5-triazine (RDX) exposure to the Northern Bobwhite (*Colinus virginianus*). Environ. Toxicol. Chem. 26, 1481–1487.

Karesh, W.B., Uhart, M.M., Frere, E., Gandini, P., Braselton, W.E., Puche, H., Cook, R.A., 1999. Health evaluation of free-ranging rockhopper penguins (*Eudyptes chrysocomes)* in Argentina. J. Zoo Wildl. Med. 30, 25–31.

Kern, M., Bacon, W., Long, D., Cowie, R.J., 2005. Blood metabolite and corticosterone levels in breeding adult Pied Flycatchers. Condor 107, 665–677.

Khalilieh, A., McCue, M.D., Pinshow, B., 2012. Physiological responses to food deprivation in the house sparrow, a species not adapted to prolonged fasting. Am. J. Physiol. 303, R551–R561.

Kimura, T., 2014. The early diagnostic and prognostic values of blood lactate concentrations in Japanese monkeys with acute gastric dilatation. Vet. Sci. Dev. 4, 5155.

Korhonen, K., 1987. The effect of short-term fasting on certain blood parameters and on glycogen storage in pectoral muscles of willow grouse (*Lagopus l. Lagopus* L.). Comp. Biochem. Physiol. 88A, 677–682.

Landys, M.M., Piersma, T., Guglielmo, C.G., Jukema, J., Ramenof- sky, M., Wing eld, J.C., 2005. Metabolic profile of long-distance migratory flight and stopover in a shorebird. Proc. Biol. Sci. 272, 295–302.

Langlois, I., Planché, A., Boysen, S.R., Abeysekara, S., Zello, G.A., 1999. Blood concentrations of d- and l-lactate in healthy rabbits. Am. J. Vet. Res. 60, 521–524.

Lavin, S., Cuenca, R., Marco, I., Velarde, R., Viñas, L., 1992a. Hematology and blood chemistry of the marsh harrier (*Circus aeruginosus*). Comp. Biochem. Physiol. 103 A, 493–495.

Lavin, S., Cuenca, R., Marco, I., Velarde, R., Vinas, L., 1992b. Haematology and blood biochemistry of capercaillie (*Tetrao urogallus*). Avian Pathol. 21, 711–715.

Le Souëf, A.T., Holyoake, C.S., Vitali, S.D., Warren, K.S., 2013. Hematologic and plasma biochemical reference values for three species of black cockatoos (*Calyptorhynchus* species). J. Avian Med. Surg. 27, 14–22.

Lea, R.W., Klandorf, H., Harvey, S., Hall, T.R., 1992. Thyroid and adrenal function in the ring dove (*Streptopelia risoria*) during food deprivation and a breeding cycle. Gen. Comp. Endocrinol. 86, 138–146.

Levitsky, L.L., Paton, J.B., Fisher, D.E., Delannoy, C.W., 1984. Splanchnic uptake and release of energy substrates in the fasting baboon infant. Pediatr. Res. 18, 1316–1320.

Lierz, M., Fenske, M., 2004. Plasma chemistry reference values in pin-tailed Sandgrouse (*Pterocles alchata*). Vet. Rec. 154, 210–211.

Lisano, M.E., Kennamer, J.E., 1977. Values for several blood parameters in eastern wild turkeys. Poultry Sci. 56, 157–166.

Lloyd, S., Gibson, J.S., 2006. Haematology and biochemistry in healthy young pheasants and red-legged partridges and effects of spironucleosis on these parameters. Avian Pathol. 35, 335–340.

Lobban, K., Downs, C.T., Brown, M., 2009. Diel variations in plasma glucose concentration in some South African avian frugivores. Emu 110, 66–70.

Low, M., Eason, D., Elliot, G., McInnes, K., Paul-Murphy, J., 2006. Hematological and biochemical reference ranges for kakapo (*Strigops haproptilus*): generation and interpretation in a field based wildlife recovery program. J. Avian Med. Surg. 20, 80–88.

Lumeij, T.J., Overduin, L.M., 1990. Plasma chemistry reference in psittaciformes. Avian Pathol. 19, 235–244.

Malcarney, H.I., Martinez del Rio, C., Apanius, V., 1994. Sucrose intolerance in birds: simple non-lethal diagnostic methods and consequences for assimilation of complex carbohydrates. Auk 111, 170–177.

Marinkovich, M., Wack, R.W., Field, C.L., Whoriskey, S.T., Kass, P.H., Gjeltema, J., 2019. Evaluation of serial blood lactate and the use of a point-of-care lactate meter in live-stranded pinnipeds. J. Zoo Wildl. Med. 50, 137–146.

Marsh, R.L., Dawson, W.R., 1982. Substrate metabolism in seasonally acclimatized American goldfinches. Am. J. Physiol. 242, R563–R569.

Martinez del Rio, C., Stevens, B.R., Daneke, D., Andreadis, P.T., 1988. Physiological correlates of preference and aversion for sugars in three species of birds. Physiol. Zool. 61, 222–229.

Mazzaro, L.M., Meegan, J., Sarran, D., Romano, T.A., Bonato, V., Shibing Deng, J., Lawrence Dunn, L., 2013. Molt-associated changes in hematologic and plasma biochemical values and stress hormone levels in African penguins (*Spheniscus demersus*). J. Avian. Med. Surg. 27, 285–293.

McCracken, 2003. *Caprimulgiformes* (goatsuckers). In: Fowler, M.E., Miller, R.E. (Eds.), Zoo and Wild Animal Medicine, fifth ed. Saunders, St. Louis, MO, pp. 224–231.

Miksik, I., Hodný, Z., 1992. Glycated hemoglobin in mute swan (*Cygnus olor*) and rook (*Corvus frugilegus*). Comp. Biochem. Physiol. 103B, 553–559.

Milani, J.F., Wilson, H., Ziccardi, M., LeFebvre, R., Scott, C., 2012. Hematology, plasma chemistry, and bacteriology of wild Tundra swans (*Cygnus columbianus*) in Alaska. J. Wildl. Dis. 48, 212–215.

Minias, P., 2014. High glucose concentrations are associated with symptoms of mild anaemia in whiskered terns: consequences for assessing physiological quality in birds. J. Ornithol. 155, 1067–1070.

Mori, J.C., George, J.C., 1978. Seasonal changes in serum levels of certain metabolites, uric acid and calcium in the migratory Canada goose (*Branta canadensis interior*). Comp. Biochem. Physiol. 59B, 263–269.

Mostaghni, K., Badiei, K., Nili, H., Fazeli, A., 2005. Haematological and biochemical parameters and the serum concentrations of phosphorus, lead, cadmium and chromium in flamingo (*Phoenicopterus ruber*) and black-headed gull (*Larus ridibundus*) in Iran. Comp. Clin. Pathol. 14, 146–148.

Motta, R.O., Romero Marques, M.V., Ferreira Junior, F.C., Andery Dde, A., Horta, R.S., Peixoto, R.B., Lacorte, G.A., Moreira Pde, A., Paes Leme Fde, O., Melo, M.M., Martins, N.R., Braga, E.M., 2013. Does haemosporidian infection affect hematological and biochemical pro- les of the endangered Black-fronted piping-guan (*Aburria jacutinga*)? Peer J 1, e45.

Mulley, R.C., 1979. Haematology and blood chemistry of the black duck *Anas superciliosa*. J. Wildl. Dis. 15, 437–441.

Myers, M.R., Klasing, K.C., 1999. Low glucokinase activity and high rates of gluconeogenesis contribute to hyperglycemia in barn owls (*Tyto alba*) after a glucose challenge. J. Nutr. 129, 1896–1904.

Naza, S., Mosleh, N., Ranjbar, V.R., Khordadmehr, M., 2011. Reference values of serum biochemical parameters in adult male and female Iranian Chukar partridge (*Alectoris Chukar*). Aust. J. Bas. Appl. Sci. 5, 252–256.

Naza, S., Mosleh, N., Ranjbar, V.R., Khordadmehr, M., 2012. Refer- ence values of serum biochemical parameters in adult male and female ring-necked pheasants (*Phasianus colchicus*). Comp. Clin. Pathol. 21, 981–984.

Neiffer, D.L., 2003. *Trogoniformes* (trogons). In: Fowler, M.E., Miller, R.E. (Eds.), Zoo and Wild Animal Medicine, fifth ed. Saunders, St. Louis, MO, pp. 245–253.

Newman, S.H., Piatt, J.F., White, J., 1997. Hematogical and plasma chemical reference ranges of Alaskan seabirds: their ecological significance and clinical importance. Colon. Waterbirds 20, 492–504.

Nicol, S., Maskrey, M., 1986. Arterial blood acid-base regulation in the *Tasmanian devil*, *Sarcophilus harrisii*, during exercise. Physiol. Zool. 59, 212–219.

Okotie-Eboh, G., Bailey, C.A., Hicks, K.D., Kubena, L.F., 1992. Reference serum biochemical values for emus and ostriches. Am. J. Vet. Res. 53, 1765–1768.

Olsen, G.H., Rininger, D.L., Ets, M.K., Sladen, W.J.L., 2002. Baseline hematology and clinical chemistry results from captive-raised Trumpeter Swans. Waterbirds 25, 375–379.

Omole, O.O., Nappert, G., Naylor, J.M., Zello, 2001. Both L- and D-lactate contribute to metabolic acidosis in diarrheic calves. J. Nutr. 131, 2128–2131.

Ozbey, O., Esen, F., 2007. The effects of breeding systems and stocking density on some blood parameters of rock partridges (*Alectoris graeca*). Poultry Sci. 86, 420–422.

Ozek, K., Bahtiyarca, Y., 2004. Effects of sex and protein and energy levels in the diet on the blood parameters of the chukar partridge (*Alectoris chukar*). Br. Poultry Sci. 45, 290–293.

O'Donnell, J.A., Garbett, R., Morzenti, A., 1978. Normal fasting plasma glucose levels in some birds of prey. J. Wildl. Dis. 14, 479–481.

Padilla, L.R., Huyvaert, K.P., Merkel, J., Miller, R.E., Parker, P.G., 2003. Hematology, plasma chemistry, serology, and Chlamydophila status of the waved albatross (*Phoebastria irrorata*) on the Galapagos Islands. J. Zoo Wildl. Med. 34, 278–283.

Palomeque, J., Pintó, O., Viscor, G., 1991. Hematological and blood chemistry values of the Masai ostrich (*Struthio camelus*). J. Wildl. Dis. 27, 34–40.

Parsons, N.J., Schaefer, A.M., van der Spuy, S.D., Gous, T.A., 2015. Establishment of baseline haematology and biochemistry parameters in wild adult African penguins (*Spheniscus demersus*). J. S. Afr. Vet. Assoc. 86, e1–e8.

Peinado, V.I., Polo, F.J., Celdrán, J.F., Viscor, G., Palomeque, J., 1992a. Hematology and plasma chemistry in endangered pigeons. J. Zoo Wildl. Med. 23, 65–71.

Peinado, V.I., Polo, F.J., Viscor, G., Palomeque, J., 1992b. Haematology and blood chemistry values for several flamingo species. Avian Pathol. 21, 55–64.

Pérez Calabuig, C., Ferrer, M., Muriel, R., 2010. Blood chemistry of wild Brazilian Coscoroba swans during molt. J. Wildl. Dis. 46, 591–595.

Polo, F.J., Celdrán, J.F., Peinado, V.I., Viscor, G., Palomeque, J., 1992. Hematological values for four species of prey. Condor 94, 1007–1013.

Polo, F.J., Peinado, V.I., Viscor, G., Palomeque, J., 1998. Hematologic and plasma chemistry values in captive Psittacine birds. Avian Dis. 42, 523–535.

Pye, G.W., 2003. *Apodiformes* and *Coliiformes* (swifts, swiftlets, mousebirds). In: Fowler, M.E., Miller, R.E. (Eds.), Zoo and Wild Animal Medicine, fifth ed. Saunders, St. Louis, MO, pp. 239–245.

Raghav, R., Middleton, R., Ahamed, R., Arjunan, R., Caliendo, V., 2015. Analysis of arterial and venous blood gases in healthy gyr falcons (*Falco rusticolus*) under anesthesia. J. Avian Med. Surg. 29, 290–298.

Rayhel, L., Aitken-Palmer, C., Joyner, P., Cray, C., Lizárraga, C.A., Ackerman, B., Crowe, C., 2015. Hematology and biochemistry in captive white-napes cranes (*Grus vipio*). J. Zoo Wildl. Med. 46, 747–754.

Redavid, L.A., Sharp, C.R., Mitchell, M.A., Beckel, N.F., 2012. Plasma lactate measurements in healthy cats. J. Vet. Emerg. Crit. Care 22, 580–587.

Remage-Healy, L., Romero, L.M., 2000. Daily and seasonal variation in response to stress in captive starlings (*Sturnus vulgaris*): glucose. Gen. Comp. Endocrinol. 119, 60–68.

Rettenmund, C.L., Heatley, J.J., Russell, K.E., 2014. Comparison of two analyzers to determine selected venous blood analytes of Quaker parrots (*Myiopsitta monachus*). J. Zoo Wildl. Med. 45, 256–262.

Rezaei, S., Agha-Alinejad, H., Molanouri Shamsi, M., Jafari, M., Azevedo Voltarelli, F., Naderi, A., Earnest, C., 2017. Evaluation of efforts in untrained Wistar rats following exercise on forced running wheel at maximal lactate steady state. J. Exerc. Nutrition Biochem. 21, 26–32.

Ruiz, G., Rosenmann, M., Fernando Novoa, F., Sabat, P., 2002. Hematological parameters and stress index in Rufous-collared sparrows dwelling in urban environments. Condor 104, 162–166.

Scanes, C.G., 2014. Comparison of circulating concentrations of glucose in vertebrate and invertebrate taxa: Evolutionary and physiological implications. Trends Comp. Biochem. Physiol. 18, 15–60.

Scholtz, N., Halle, I., Flachowsky, G., Sauerwein, H., 2009. Serum chemistry reference values in adult Japanese quail (*Coturnix coturnix* japonica) including sex-related differences. Poultry Sci. 88, 1186–1190.

Schultz, D.J., 2003. *Columbiformes* (pigeons, doves). In: Fowler, M.E., Miller, R.E. (Eds.), Zoo and Wild Animal Medicine, fifth ed. Saunders, St. Louis, MO, pp. 180–187.

Scope, A., Frommlet, F., Schwendenwein, I., 2005. Circadian and seasonal variability and influence of sex and race on eight clinical chemistry parameters in budgerigars (*Melopsittacus undulatus*, Shaw 1805). Res. Vet. Sci. 78, 85–91.

Seok, S.H., Jeong, D.H., Park, S.J., Lee, S.Y., Lee, H.C., Yeon, S.C., 2017. Hematological and plasma biochemical values of cinereous vulture (*Aegypius monachus*). J. Zoo Wildl. Med. 48, 514–517.

Shaffer, S.A., Costa, D.P., Williams, T.M., Ridgway, S.H., 1997. Diving and swimming performance of white whales, *Delphinapterus leucas*: an assessment of plasma lactate and blood gas levels and respiratory rates. J. Exp. Biol. 200, 3091–3099.

Simon, J., Nicole Rideau, N., Taouis, M., Dupont, J., 2011. Plasma insulin levels are rather similar in chicken and rat. Gen. Comp. Endocrinol. 171, 267–268.

Smith, C.L., Toomey, M., Walker, B.R., Braun, E.J., Wolf, B.O., McGraw, K., Sweazea, K.L., 2011. Naturally high plasma glucose levels in mourning doves (*Zenaida macroura*) do not lead to high levels of reactive oxygen species in the vasculature. Zoology (Jena) 114, 171–176.

Soleimani, A.F., Zulki i, I., 2010. Effects of high ambient temperature on blood parameters in red jungle fowl, village fowl and broiler chickens. J. Anim. Vet. Adv. 9, 1201–1207.

Stoskopf, M.K., Mulcahy, D.M., Esler, D., 2010. Evaluation of a portable automated serum chemistry analyzer for field assessment of harlequin ducks, Histrionicus histrionicus. Vet. Med. Int. 2010, 418596.

Stout, J.D., Brinker, D.F., Driscoll, C.P., Davison, S., Murphy, L.A., 2010. Serum biochemistry values, plasma mineral levels, and whole blood heavy metal measurements in wild northern goshawks (*Accipiter gentilis*). J. Zoo Wildl. Med. 41, 649–655.

Swain, D.W., 1987. Overnight changes in circulating energy substrate concentrations in the vesper sparrow (*Pooecetes gramineus*). Comp. Biochem. Physiol. 86A, 439–441.

Swain, S.D., 1992. Energy profiles during fasting in horned larks (*Eremophila alpestris*). Physiol. Zool. 63, 568–582.

Tell, L.A., Citino, S.B., 1992. Hematological and serum chemistry reference intervals for Cuban Amazon parrots (*Amazona leucocephala leucocephala*). J. Zoo Wildl. Med. 23, 65–71.

Totzke, U., Hübinger, A., Bairlein, F., 1998. Glucose utilization rate and pancreatic hormone response to oral glucose loads are influenced by the migratory condition and fasting in the garden warbler (*Sylvia borin*). J. Endocrinol. 158, 191–196.

Travis, E.K., Vargas, F.H., Merkel, J., Gottdenker, N., Miller, R.E., Parker, P.G., 2006a. Hematology, plasma chemistry, and serology of the flightless cormorant (*Phalacrocorax harrisi*) in the Galapagos Islands, Ecuador. J. Wildl. Dis. 42, 133–141.

Travis, E.K., Vargas, F.H., Merkel, J., Gottdenker, N., Miller, R.E., Parker, P.G., 2006b. Hematology, serum chemistry, and serology of Galápagos penguins (*Spheniscus mendiculus*) in the Galápagos Islands, Ecuador. J. Wildl. Dis. 42, 625–632.

Uhart, M., Aprile, G., Beldomenico, P., Solís, G., Marull, C., Beade, M., Carminati, A., Moreno, D., 2006. Evaluation of the health of free-ranging greater rheas (Rhea americana) in Argentina. Vet. Rec. 158, 297–303.

Uhart, M.M., Quintana, F., Karesh, W.B., Braselton, W.E., 2003. Hematology, plasma biochemistry, and serosurvey for selected infectious agents in southern giant petrels from Patagonia, Argentina. J. Wildl. Dis. 39, 359–365.

Valle, C.A., Ulloa, C., Deresienski, D., Regalado, C., Muñoz-Pérez, J.P., Garcia, J., Hardesty, B.D., Skehel, A., Lewbart, G.A., 2018. Health status of great frigatebirds (*Fregata minor*) determined by haematology, biochemistry, blood gases, and physical examination. Conserv. Physiol. 6, coy034.

Van Heerden, J., Dauth, J., Komen, J., Myer, E., 1987. Serum biochemical and haematological parameters in the Cape vulture *Gyps coprotheres*. J. S. Afr. Vet. Assoc. 58, 145–146.

Van Hemert, C., Handel, C.M., 2016. Blood serum chemistry of wild Alaskan black-capped chickadees (*Poecile atricapillus*) with avian keratin disorder. J. Wildl. Dis. 52, 927–930.

Verstappen, F.A., Lumeij, J.T., Bronneberg, R.G., 2002. Plasma chemistry reference values in ostriches. J. Wildl. Dis. 38, 154–159.

Vleck, C.M., Vleck, D., 2002. Physiological condition and reproductive consequences in Adélie penguins. Integr. Comp. Biol. 42, 76–83.

Waldoch, J., Wack, R., Christopher, M., 2009. Avian plasma chemistry analysis using diluted samples. J. Zoo Wildl. Med. 40, 667–674.

Wallace, R.S., Teare, J.A., Diebold, E., Michaels, M., Willis, M.J., 1995. Hematology and plasma chemistry values in free-ranging Humboldt penguins (*Spheniscus humboldti*) in Chile. Zoo Biol. 14, 311–316.

Weber, M., 2003. *Pelecaniformes* (pelicans, tropicbirds, cormorants, frigatebirds, anhingas, gannets). In: Fowler, M.E., Miller, R.E. (Eds.), Zoo and Wild Animal Medicine, fth ed. Saunders, St. Louis, MO, pp. 118–122.

Weideman, M.A., Chivandi, E., Erlwanger, K.H., 2012. Glucose tolerance and lipid absorption in Guinea fowl (*Numida meleagris*) and domestic fowl (*Gallus gallus* var.*domesticus*). Asian J. Anim. Vet. Adv. 7, 653–663.

West, G.D., Haines, V.L., 2002. Hematology and serum biochemistry values of captive Attwater's prairie chickens (*Tympanuchus cupido attwateri*). J. Zoo Wildl. Med. 33, 122–124.

Williams, T.M., Friedl, W.A., Haun, J.E., 1993. The physiology of bottlenose dolphins (*Tursiops truncatus*): heart rate, metabolic rate and plasma lactate concentration during exercise. J. Exp. Biol. 179, 31–46.

Wolf, S.H., Schreiber, R.W., Kahana, L., Torres, J.J., 1985. Seasonal and age related variation in the blood composition of the brown pelican (*Pelecanus occidentalis*). Comp. Biochem. Physiol. 82A, 837–846.

Work, T.M., 1996. Weights, hematology, and serum chemistry of seven species of free-ranging tropical pelagic seabirds. J. Wildl. Dis. 32, 643–657.

Work, T.M., 1999. Weights, hematology, and serum chemistry of free-ranging brown boobies (*Sula leucogaster*) in Johnston Atoll, Central Pacific. J. Zoo Wildl. Med. 30, 81–84.

Youl, J.M., 2009. Lead Exposure in Free-Ranging Kea (Nestor Notabilis), Takahe (Porphyrio Hochstetteri) and Australasian Harriers (Circus Approximans). Master's Thesis. Massey University, New Zealand.

Zulkifli, I., Dass, R.T., Che Norma, M.T., 1999. Acute heat-stress effects on physiology and fear-related behaviour in red jungle fowl and domestic fowl. Can. J. Anim. Sci. 79, 165–170.

Further reading

Davis, R.W., 1983. Lactate and glucose metabolism in the resting and diving harbor seal (*Phoca vitulina*). J. Comp. Physiol. 153, 275–288.

Index

Note: 'Page numbers followed by "*f*" indicate figures and "*t*" indicate tables.'

C

D

E

F

G

H

I

J

K

L

M

N

O

P

Q

R

S

U